
REVIEW OF PARTICLE PHYSICS*

Particle Data Group

Abstract

This biennial *Review* summarizes much of particle physics. Using data from previous editions, plus 2778 new measurements from 645 papers, we list, evaluate, and average measured properties of gauge bosons, leptons, quarks, mesons, and baryons. We also summarize searches for hypothetical particles such as Higgs bosons, heavy neutrinos, and supersymmetric particles. All the particle properties and search limits are listed in Summary Tables. We also give numerous tables, figures, formulae, and reviews of topics such as the Standard Model, particle detectors, probability, and statistics. Among the 108 reviews are many that are new or heavily revised including those on CKM quark-mixing matrix, V_{ud} & V_{us} , V_{cb} & V_{ub} , top quark, muon anomalous magnetic moment, extra dimensions, particle detectors, cosmic background radiation, dark matter, cosmological parameters, and big bang cosmology.

A booklet is available containing the Summary Tables and abbreviated versions of some of the other sections of this full *Review*. All tables, listings, and reviews (and errata) are also available on the Particle Data Group website: <http://pdg.lbl.gov>.

Particle Data Group

C. Amsler,¹ M. Doser,² M. Antonelli,³ D.M. Asner,⁴ K.S. Babu,⁵ H. Baer,⁶ H.R. Band,⁷ R.M. Barnett,⁸ E. Bergren,⁸ J. Beringer,⁸ G. Bernardi,⁹ W. Bertl,¹⁰ H. Bichsel,¹¹ O. Biebel,¹² P. Bloch,² E. Blucher,¹³ S. Blusk,¹⁴ R.N. Cahn,⁸ M. Carena,^{15,13,16} C. Caso,^{17*} A. Ceccucci,² D. Chakraborty,¹⁸ M.-C. Chen,¹⁹ R.S. Chivukula,²⁰ G. Cowan,²¹ O. Dahl,⁸ G. D'Ambrosio,²² T. Damour,²³ A. de Gouvêa,²⁴ T. DeGrand,²⁵ B. Dobrescu,¹⁵ M. Drees,²⁶ D.A. Edwards,²⁷ S. Eidelman,²⁸ V.D. Elvira,¹⁵ J. Erler,²⁹ V.V. Ezhela,³⁰ J.L. Feng,¹⁹ W. Fetscher,³¹ B.D. Fields,³² B. Foster,³³ T.K. Gaisser,³⁴ L. Garren,¹⁵ H.-J. Gerber,³¹ G. Gerbier,³⁵ T. Gherghetta,³⁶ G.F. Giudice,² M. Goodman,³⁷ C. Grab,³¹ A.V. Gritsan,³⁸ J.-F. Grivaz,³⁹ D.E. Groom,⁸ M. Grünwald,⁴⁰ A. Gurtu,^{41,2} T. Gutsche,⁴² H.E. Haber,⁴³ K. Hagiwara,⁴⁴ C. Hagmann,⁴⁵ K.G. Hayes,⁴⁶ J.J. Hernández-Rey,^{47†} K. Hikasa,⁴⁸ I. Hinchliffe,⁸ A. Höcker,² J. Huston,²⁰ P. Igo-Kemenes,⁴⁹ J.D. Jackson,⁸ K.F. Johnson,⁶ T. Junk,¹⁵ D. Karlen,⁵⁰ B. Kayser,¹⁵ D. Kirkby,¹⁹ S.R. Klein,⁵¹ I.G. Knowles,⁵² C. Kolda,⁵³ R.V. Kowalewski,⁵⁰ P. Kreitz,⁵⁴ B. Krusche,⁵⁵ Yu.V. Kuyanov,³⁰ Y. Kwon,⁵⁶ O. Lahav,⁵⁷ P. Langacker,⁵⁸ A. Liddle,⁵⁹ Z. Ligeti,⁸ C.-J. Lin,⁸ T.M. Liss,⁶⁰ L. Littenberg,⁶¹ J.C. Liu,⁵⁴ K.S. Lugovsky,³⁰ S.B. Lugovsky,³⁰ H. Mahlke,⁶² M.L. Manganò,² T. Mannel,⁶³ A.V. Manohar,⁶⁴ W.J. Marciano,⁶¹ A.D. Martin,⁶⁵ A. Masoni,⁶⁶ D. Milstead,⁶⁷ R. Miquel,⁶⁸ K. Mönig,⁶⁹ H. Murayama,^{70,71,8} K. Nakamura,⁴⁴ M. Narain,⁷² P. Nason,⁷³ S. Navas,^{74†} P. Nevski,⁶¹ Y. Nir,⁷⁵ K.A. Olive,⁷⁶ L. Pape,³¹ C. Patrignani,¹⁷ J.A. Peacock,⁵² A. Piepke,⁷⁷ G. Punzi,⁷⁸ A. Quadt,⁷⁹ S. Raby,⁸⁰ G. Raffelt,⁸¹ B.N. Ratcliff,⁵⁴ B. Renk,⁸² P. Richardson,⁶⁵ S. Roesler,² S. Rolli,⁸³ A. Romaniouk,⁸⁴ L.J. Rosenberg,¹¹ J.L. Rosner,¹³ C.T. Sachrajda,⁸⁵ Y. Sakai,⁴⁴ S. Sarkar,⁸⁶ F. Sauli,² O. Schneider,⁸⁷ D. Scott,⁸⁸ W.G. Seligman,⁸⁹ M.H. Shaevitz,⁹⁰ T. Sjöstrand,⁹¹ J.G. Smith,²⁵ G.F. Smoot,⁸ S. Spanier,⁵⁴ H. Spieler,⁸ A. Stahl,⁹² T. Stanev,³⁴ S.L. Stone,¹⁴ T. Sumiyoshi,⁹³ M. Tanabashi,⁹⁴ J. Terning,⁹⁵ M. Titov,⁹⁶ N.P. Tkachenko,³⁰ N.A. Törnqvist,⁹⁷ D. Tovey,⁹⁸ G.H. Trilling,⁸ T.G. Trippe,⁸ G. Valencia,⁹⁹ K. van Bibber,⁴⁵ M.G. Vincter,⁴ P. Vogel,¹⁰⁰ D.R. Ward,¹⁰¹ T. Watari,¹⁰² B.R. Webber,¹⁰¹ G. Weiglein,⁶⁵ J.D. Wells,¹⁰³ M. Whalley,⁶⁵ A. Wheeler,⁵⁴ C.G. Wohl,⁸ L. Wolfenstein,¹⁰⁴ J. Womersley,¹⁰⁵ C.L. Woody,⁶¹ R.L. Workman,¹⁰⁶ A. Yamamoto,⁴⁴ W.-M. Yao,⁸ O.V. Zenin,³⁰ J. Zhang,¹⁰⁷ R.-Y. Zhu,¹⁰⁸ P.A. Zyla⁸

Technical Associates: G. Harper,⁸ V.S. Lugovsky,³⁰ P. Schaffner⁸

1. *Physik-Institut, Universität Zürich, CH-8057 Zürich, Switzerland*
2. *CERN, European Organization for Nuclear Research, CH-1211 Genève 23, Switzerland*
3. *Lab. Nazionali di Frascati dell'INFN, CP 13, via E. Fermi, 40, I-00044 Frascati (Roma), Italy*
4. *Department of Physics, Carleton University, 1125 Colonel By Drive, Ottawa, ON K1S 5B6, Canada*
5. *Department of Physics, Oklahoma State University, Stillwater, OK 74078, USA*
6. *Department of Physics, Florida State University, Tallahassee, FL 32306, USA*
7. *Department of Physics, University of Wisconsin, Madison, WI 53706, USA*
8. *Physics Division, Lawrence Berkeley National Laboratory, 1 Cyclotron Road, Berkeley, CA 94720, USA*
9. *LPNHE, IN2P3-CNRS et Universités de Paris 6 et 7, F-75252 Paris, France*
10. *Paul Scherrer Institut, CH-5232 Villigen PSI, Switzerland*
11. *Department of Physics, University of Washington, Seattle, WA 98195, USA*
12. *Ludwig-Maximilians-Universität, Department für Physik, Schellingstr. 4, D-80799 München, Germany*
13. *Department of Physics, University of Chicago, Chicago, IL 60637-1433, USA*
14. *Department of Physics, Syracuse University, Syracuse, NY, 13244-1130, USA*
15. *Fermi National Accelerator Laboratory, P.O. Box 500, Batavia, IL 60510, USA*
16. *Enrico Fermi Institute, University of Chicago, 5640 Ellis Av., Chicago, IL 60637, USA*
17. *Dipartimento di Fisica e INFN, Università di Genova, I-16146 Genova, Italy*
18. *Department of Physics, Northern Illinois University, DeKalb, IL 60115, USA*
19. *Department of Physics and Astronomy, University of California, Irvine, CA 92697-4576, USA*
20. *Michigan State University, Dept. of Physics and Astronomy, East Lansing, MI 48824-2320, USA*
21. *Department of Physics, Royal Holloway, University of London, Egham, Surrey TW20 0EX, UK*
22. *INFN - Sezione di Napoli Complesso Universitario Monte Sant'Angelo, Via Cintia, 80126 Napoli, Italy*
23. *Institut des Hautes Etudes Scientifiques, F-91440 Bures-sur-Yvette, France*
24. *Department of Physics and Astronomy, Northwestern University, Evanston, IL 60208, USA*
25. *Department of Physics, University of Colorado at Boulder, Boulder, CO 80309, USA*
26. *Universität Bonn, Physikalisches Institut, Nussallee 12, D-53115 Bonn, Germany*
27. *Deutsches Elektronen-Synchrotron DESY, Notkestraße 85, D-22603 Hamburg, Germany*
28. *Budker Institute of Nuclear Physics, RU-630090, Novosibirsk, Russia*
29. *Departamento de Física Teórica, Instituto de Física, Universidad Nacional Autónoma de México, México D.F. 04510, México*
30. *COMPAS Group, Institute for High Energy Physics, RU-142284, Protvino, Russia*
31. *Institute for Particle Physics, ETH Zürich, CH-8093 Zürich, Switzerland*
32. *Department of Astronomy, University of Illinois, 1002 W. Green St., Urbana, IL 61801, USA*

* Deceased

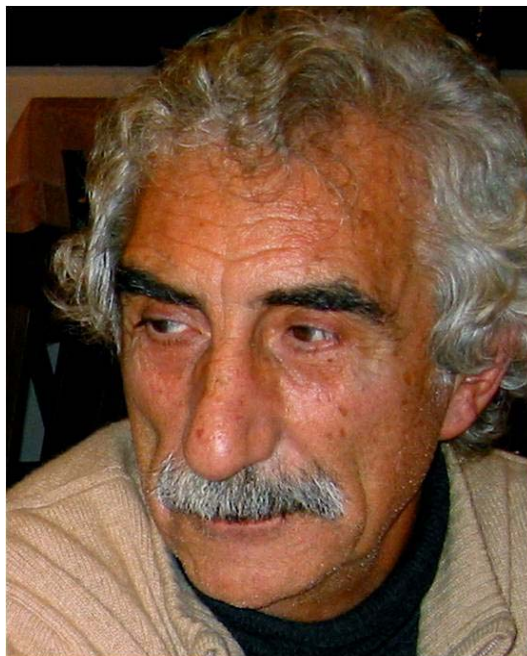
† J.J. Hernández-Rey and S. Navas acknowledge support from MICINN, Spain (FPA2005-25354-E and FPA2007-29104-E)

33. *Denys Wilkinson Building, Department of Physics, University of Oxford, Oxford, OX1 3RH, UK*
34. *Bartol Research Institute, University of Delaware, Newark, DE 19716, USA*
35. *CEA/Saclay, DSM/IRFU, BP 2, F-91191 Gif s Yvette, France*
36. *School of Physics, University of Melbourne, Victoria, 3010 Australia*
37. *Argonne National Laboratory, 9700 S. Cass Ave., Argonne, IL 60439-4815, USA*
38. *Johns Hopkins University, Baltimore, Maryland 21218, USA*
39. *LAL, IN2P3-CNRS et Univ. de Paris 11, F-91898 Orsay CEDEX, France*
40. *Dept. Subatomic Physics, University of Ghent, Proeftuinstraat 86, B-9000 Ghent, Belgium*
41. *Tata Institute of Fundamental Research, Mumbai (Bombay) 400 005, India*
42. *Institut für Theoretische Physik, Universität Tübingen, Auf der Morgenstelle 14, D-72076 Tübingen, Germany*
43. *Santa Cruz Institute for Particle Physics, University of California, Santa Cruz, CA 95064, USA*
44. *KEK, High Energy Accelerator Research Organization, Oho, Tsukuba-shi, Ibaraki-ken 305-0801, Japan*
45. *Lawrence Livermore National Laboratory, 7000 East Ave., Livermore, CA 94550, USA*
46. *Department of Physics, Hillsdale College, Hillsdale, MI 49242, USA*
47. *IFIC — Instituto de Física Corpuscular, Universitat de València — C.S.I.C., E-46071 Valencia, Spain*
48. *Department of Physics, Tohoku University, Aoba-ku, Sendai 980-8578, Japan*
49. *Physikalisches Institut, Universität Heidelberg, Philosophenweg 12, D-69120 Heidelberg, Germany*
50. *University of Victoria, Victoria, BC V8W 3P6, Canada*
51. *Nuclear Science Division, Lawrence Berkeley National Laboratory, 1 Cyclotron Road, Berkeley, CA 94720, USA*
52. *Institute for Astronomy, University of Edinburgh, Royal Observatory, Blackford Hill, Edinburgh, EH9 3JZ, Scotland, UK*
53. *Department of Physics, University of Notre Dame, 225 Niewland Hall, Notre Dame, IN 46556, USA*
54. *Stanford Linear Accelerator Center, P.O. box 4349, Stanford, CA 94309, USA*
55. *Institute of Physics, University of Basel, CH-4056 Basel, Switzerland*
56. *Yonsei University, Department of Physics, 134 Sinchon-dong, Sudaemoon-gu, Seoul 120-749, South Korea*
57. *Department of Physics and Astronomy, University College London, Gower Street, London WC1E 6BT, UK*
58. *School of Natural Science, Institute for Advanced Study, Princeton, NJ 08540, USA*
59. *Astronomy Centre, University of Sussex, Falmer, Brighton BN1 9QH, UK*
60. *Department of Physics, University of Illinois, 1110 W. Green Street, Urbana, IL 61801, USA*
61. *Physics Department, Brookhaven National Laboratory, Upton, NY 11973, USA*
62. *Laboratory of Elementary-Particle Physics, Cornell University, Ithaca, NY 14853, USA*
63. *University Siegen, Fachbereich für Physik, Siegen, Germany*
64. *Department of Physics, University of California at San Diego, La Jolla, CA 92093, USA*
65. *Institute for Particle Physics Phenomenology, Department of Physics, University of Durham, Durham DH1 3LE, UK*
66. *INFN Sezione di Cagliari, Cittadella Universitaria de Monserrato, Casella postale 170, I-09042 Monserrato (CA), Italy*
67. *Fysikum, Stockholms Universitet, AlbaNova University Centre, SE-106 91 Stockholm, Sweden*
68. *Institució Catalana de Recerca i Estudis Avançats, Institut de Física d'Altes Energies, E-08193 Bellaterra (Barcelona), Spain*
69. *DESY-Zeuthen, D-15735 Zeuthen, Germany*
70. *Institute for the Physics and Mathematics of the Universe, University of Tokyo, Kashiwa, 277-8568, Japan*
71. *Department of Physics, University of California, Berkeley, CA 94720, USA*
72. *Brown University, Department of Physics, 182 Hope Street, Providence, RI 02912, USA*
73. *INFN, Sez. di Milano-Bicocca, Piazza della Scienza, 3, I-20126 Milano, Italy*
74. *Dpto. de Física Teórica y del Cosmos & C.A.F.P.E., Universidad de Granada, 18071 Granada, Spain*
75. *Weizmann Institute of Science, Department of Particle Physics, P.O. Box 26 Rehovot 76100, Israel*
76. *School of Physics and Astronomy, University of Minnesota, Minneapolis, MN 55455, USA*
77. *Department of Physics and Astronomy University of Alabama, 206 Gallalee Hall, Box 870324, Tuscaloosa, AL 35487-0324, USA*
78. *INFN and Dipartimento di Fisica, Università di Pisa, I-56127 Pisa, Italy*
79. *Georg-August-Universität Göttingen, II. Physikalisches Institut, Friedrich-Hund-Platz 1, D-37077 Göttingen, Germany*
80. *Department of Physics, The Ohio State University, 191 W. Woodruff Ave., Columbus, OH 43210, USA*
81. *Max-Planck-Institut für Physik (Werner-Heisenberg-Institut), Föhringer Ring 6, D-80805 München, Germany*
82. *Institut für Physik, Johannes-Gutenberg Universität Mainz, D-55099 Mainz, Germany*
83. *Tufts University, Robinson Hall, Medford, MA 02155, USA*
84. *Moscow Engineering and Physics Institute, 31, Kashirskoye shosse, 115409 Moscow, Russia*
85. *School of Physics and Astronomy, University of Southampton, Highfield, Southampton S017 1BJ, UK*
86. *Rudolf Peierls Centre for Theoretical Physics, University of Oxford, 1 Keble Road, Oxford OX1 3NP, UK*
87. *Ecole Polytechnique Fédérale de Lausanne (EPFL), CH-1015 Lausanne, Switzerland*
88. *Department of Physics and Astronomy, University of British Columbia, Vancouver, BC V6T 1Z1, Canada*

89. *Columbia University, Nevis Labs, PO Box 137, Irvington, NY 10533, USA*
90. *Department of Physics, Columbia University, 538 West 120th St., New York, NY 10027, USA*
91. *Department of Theoretical Physics, Lund University, S-223 62 Lund, Sweden*
92. *III. Physikalisches Institut, Physikzentrum, RWTH Aachen University, 52056 Aachen, Germany*
93. *High Energy Physics Laboratory, Tokyo Metropolitan University, Tokyo, 192-0397, Japan*
94. *Department of Physics, Nagoya University, Chikusa-ku, Nagoya, 464-8602, Japan*
95. *Department of Physics, University of California, Davis, CA 95616, USA*
96. *CEA/Saclay, B.P.2, Orme des Merisiers, F-91191 Gif-sur-Yvette Cedex, France*
97. *Department of Physical Sciences, POB 64 FIN-00014 University of Helsinki, Finland*
98. *Department of Physics and Astronomy, University of Sheffield, Sheffield S3 7RH, UK*
99. *Department of Physics, Iowa State University, Ames, IA 50011, USA*
100. *California Institute of Technology, Kellogg Radiation Laboratory 106-38, Pasadena, CA 91125, USA*
101. *Cavendish Laboratory, J.J. Thomson Avenue, Cambridge CB3 0HE, UK*
102. *Department of Physics, University of Tokyo, Tokyo 113-0033, Japan*
103. *Michigan Center for Theoretical Physics, Physics Dept., 2477 Randall Laboratory, University of Michigan, Ann Arbor, MI 48109, USA*
104. *Department of Physics, Carnegie Mellon University, Pittsburgh, PA 15213, USA*
105. *STFC Rutherford Appleton Laboratory, Didcot, OX11 0QX, UK*
106. *Department of Physics, George Washington University Virginia Campus, Ashburn, VA 20147-2604, USA*
107. *IHEP, Chinese Academy of Sciences, Beijing 100049, P.R. China*
108. *California Institute of Technology, Physics Department, 256-48, Pasadena, CA 91125, USA*

We dedicate this edition of the Review of Particle Physics
to the memory of Carlo Caso, a long-time member of the Particle Data Group

Carlo Caso (1940–2007)



For many years, Carlo Caso was an esteemed member of the Particle Data Group. He joined the Group as LEP was starting, and was responsible along with Atul Gurtu for all aspects of the W and Z boson sections. They created the organization of the sections, brought in all the data, carried out fits to the data, and wrote vital reviews. The gauge bosons were at the forefront throughout that era, and the community benefited greatly from their insight and their service.

Carlo's wisdom helped guide the Particle Data Group as a whole. He was always a gentleman and gave freely of his experience and expertise in many ways. Above all, he was a friend to all of us and we will miss him dearly.

Leonardo Rossi of the ATLAS Experiment wrote about Carlo's larger career and, with his permission, we reproduce his comments here.

"Our friend and colleague Carlo Caso passed away on July 7th, after several months of courageous fight against cancer.

"Carlo spent most of his scientific career at CERN, taking an active part in the experimental programme of the laboratory. His long and fruitful involvement in particle physics started in the sixties, in the Genoa group led by G. Tomasini. He then made several experiments using the CERN liquid hydrogen bubble chambers -first the 2000HBC and later BEBC- to study various facets of the production and decay of meson and baryon resonances. He later made his own group and joined the NA27 Collaboration to exploit the EHS Spectrometer with a rapid cycling bubble chamber as vertex detector. Amongst their many achievements, they were the first to measure, with excellent precision, the lifetime of the charmed D mesons. At the start of the LEP era, Carlo and his group moved to the DELPHI experiment, participating in the construction and running of the HPC electromagnetic calorimeter. In DELPHI he contributed significantly to beauty physics measurements and Higgs searches.

"After LEP, his interest turned to LHC and he became an enthusiastic supporter of the ATLAS experiment. He led the Genoa group engaged in the design and construction of the pixel detector and made significant contributions to this effort. He also maintained an active interest in the overall ATLAS experiment and its Collaboration life, and served as Chairman of the ATLAS Publication Committee. It is very sad that Carlo did not live long enough to enjoy the LHC data.

"In parallel with his research, Carlo played an important role as a teacher. Full Professor of Experimental Physics in Genoa, he was able to motivate many students around him. He taught them to love physics, to ask questions and not to be satisfied with a superficial answer. His door was always open and discussions with him were always pleasant and inspiring."

The full text of Rossi's comments may be found at:

<http://aenews.cern.ch/article.php?issueno=200709&date=September%2%A02007&id=ATL-ENEWS-2007-049>.

HIGHLIGHTS OF THE 2008 EDITION OF THE REVIEW OF PARTICLE PHYSICS

- 645 new papers with 2778 new measurements.
- Latest from B -meson physics: 182 papers with 859 measurements: CP violation, B_s mixing, determination of V_{cb} , and V_{ub} CKM elements, new b -hadron states, *etc.*
- Significant improvements in $K^+ \rightarrow 3\pi$ Dalitz slope parameters, $K_{\ell 3}^+$ branching ratios, and K_L form factor measurements.
- Many new results in the sections on strongly-decaying mesons: 152 papers with 816 measurements, including new charmonium-like states properties and review.
- First good evidence for $D^0 - \overline{D}^0$ mixing. Major update to the review on this subject.
- Substantial improvement in D_s^+ branching fractions.
- The Table of Astrophysical Constants and Parameters has been extensively revised and modernized.
- 108 reviews (most are revised or new).
- Major update of the reviews on:
 - Higgs Bosons;
 - CKM Quark Mixing Matrix;
 - Supersymmetry (part II, experiment);
 - Axions.
- New sections in Particle Detector review on Hadron Calorimeters and on Gaseous Detectors, with subsections on energy loss and charge transport in gases, Multi-Wire Chambers, Micro-Pattern Gas Detectors, TPC's and TRD's.
- Cosmic ray review: Latest measurements of the highest energy cosmic rays from the Auger detector.
- New section on diffractive deep inelastic scattering in the "Structure functions" review.
- New CPT Invariance Test in Neutral Kaon Decay review.

See pdgLive.lbl.gov for online access to PDG database.

See pdg.lbl.gov/AtomicNuclearProperties for Atomic Properties of Materials.

COLOR VERSIONS OF MANY FIGURES AVAILABLE AT END OF BOOK.

TABLE OF CONTENTS

HIGHLIGHTS	7		
INTRODUCTION		Astrophysics and Cosmology	
1. Overview	13	18. Experimental tests of gravitational theory (rev.)	212
2. Particle Listings responsibilities	13	19. Big-Bang cosmology (rev.)	217
3. Consultants	14	20. Big-Bang nucleosynthesis (rev.)	228
4. Naming scheme for hadrons	15	21. The cosmological parameters (rev.)	232
5. Procedures	15	22. Dark matter (rev.)	241
5.1 Selection and treatment of data	15	23. Cosmic microwave background (rev.)	246
5.2 Averages and fits	16	24. Cosmic rays (rev.)	254
5.2.1 Treatment of errors	16	Experimental Methods and Colliders	
5.2.2 Unconstrained averaging	16	25. Accelerator physics of colliders	261
5.2.3 Constrained fits	17	26. High-energy collider parameters (rev.)	264
5.3 Rounding	18	27. Passage of particles through matter (rev.)	267
5.4 Discussion	18	28. Particle detectors (rev.)	281
History plots (rev.)	20	29. Radioactivity and radiation protection (rev.)	312
Online particle physics information (rev.)	21	30. Commonly used radioactive sources	315
PARTICLE PHYSICS SUMMARY TABLES		Mathematical Tools or Statistics, Monte Carlo, Group Theory	
Gauge and Higgs bosons	31	31. Probability (rev.)	316
Leptons	34	32. Statistics (rev.)	320
Quarks	37	33. Monte Carlo techniques (rev.)	330
Mesons	38	34. Monte Carlo particle numbering scheme (rev.)	333
Baryons	76	35. Clebsch-Gordan coefficients, spherical harmonics, and d functions	337
Searches (Supersymmetry, Compositeness, <i>etc.</i>)	91	36. SU(3) isoscalar factors and representation matrices	338
Tests of conservation laws	93	37. SU(n) multiplets and Young diagrams	339
REVIEWS, TABLES, AND PLOTS		Kinematics, Cross-Section Formulae, and Plots	
Constants, Units, Atomic and Nuclear Properties		38. Kinematics (rev.)	340
1. Physical constants (rev.)	103	39. Cross-section formulae for specific processes (rev.)	345
2. Astrophysical constants (rev.)	104	40. Plots of cross sections and related quantities (rev.)	353
3. International System of Units (SI)	106		
4. Periodic table of the elements (rev.)	107		
5. Electronic structure of the elements	108		
6. Atomic and nuclear properties of materials (rev.)	110		
7. Electromagnetic relations	112		
8. Naming scheme for hadrons	114		
Standard Model and Related Topics			
9. Quantum chromodynamics	116		
10. Electroweak model and constraints on new physics (rev.)	125		
11. The Cabibbo-Kobayashi-Maskawa quark-mixing matrix (rev.)	145		
12. CP violation (rev.)	153		
13. Neutrino Mass, Mixing, and Flavor Change (rev.)	163		
14. Quark model (rev.)	172		
15. Grand Unified Theories	180		
16. Structure functions (rev.)	188		
17. Fragmentation functions in e^+e^- annihilation and lepton-nucleon DIS (rev.)	202		

(Continued on next page.)

PARTICLE LISTINGS*

Illustrative key and abbreviations	373
Gauge and Higgs bosons	
(γ , gluon, graviton, W , Z , Higgs, Axions)	385
Leptons	
(e , μ , τ , Heavy-charged lepton searches, Neutrino properties, Number of neutrino types Double- β decay, Neutrino mixing, Heavy-neutral lepton searches)	479
Quarks	
(u , d , s , c , b , t , b' , t' (4^{th} generation), Free quarks)	551
Mesons	
Light unflavored (π , ρ , a , b) (η , ω , f , ϕ , h)	583
Other light unflavored	698
Strange (K , K^*)	704
Charmed (D , D^*)	766
Charmed, strange (D_s , D_s^* , D_{sJ})	816
Bottom (B , V_{cb}/V_{ub} , B^* , B_J^*)	833
Bottom, strange (B_s , B_s^* , B_{sJ}^*)	968
Bottom, charmed (B_c)	976
$c\bar{c}$ (η_c , $J/\psi(1S)$, χ_c , ψ)	977
$b\bar{b}$ (χ , χ_b)	1042
Non- $q\bar{q}$ candidates	1057
Baryons	
N	1061
Δ	1104
Exotic	1124
Λ	1126
Σ	1142
Ξ	1166
Ω	1179
Charmed (Λ_c , Σ_c , Ξ_c , Ω_c)	1182
Doubly charmed (Ξ_{cc})	1201
Bottom (Λ_b , Σ_b , Σ_b^* , Ξ_b , b -baryon admixture)	1202
Miscellaneous searches	
Monopoles	1209
Supersymmetry	1211
Technicolor	1258
Compositeness	1265
Extra Dimensions	1272
Searches for WIMPs and Other Particles	1282
INDEX	1291
COLOR FIGURES	1309

MAJOR REVIEWS IN THE PARTICLE LISTINGS

Gauge and Higgs bosons	
The Mass of the W Boson (rev.)	386
Triple Gauge Couplings	389
Anomalous W/Z Quartic Couplings	392
The Z Boson (rev.)	393
Anomalous $ZZ\gamma$, $Z\gamma\gamma$, and ZZV Couplings	411
Searches for Higgs Bosons (rev.)	414
The W' Searches (rev.)	443
The Z' Searches (rev.)	446
The Leptoquark Quantum Numbers (new)	452
Axions and Other Very Light Bosons (new)	459
Leptons	
Muon Anomalous Magnetic Moment (new.)	485
Muon Decay Parameters (rev.)	485
τ Branching Fractions (rev.)	493
τ -Lepton Decay Parameters (rev.)	493
Number of Light Neutrino Types (rev.)	523
Neutrinoless Double- β Decay (rev.)	525
Solar Neutrinos Review (rev.)	531
Quarks	
Quark Masses (rev.)	551
The Top Quark (rev.)	563
Free Quark Searches	577
Mesons	
Note on Scalar Mesons (rev.)	594
The $\eta(1405)$, $\eta(1475)$, $f_1(1420)$, and $f_1(1510)$ (rev.)	641
Rare Kaon Decays (rev.)	706
$K_{\ell 3}^{\pm}$ and $K_{\ell 3}^0$ Form Factors (rev.)	717
CPT Invariance Tests in Neutral Kaon Decay (new)	721
CP Violation in $K_S \rightarrow 3\pi$	727
V_{ud} , V_{us} , Cabibbo Angle, and CKM Unitarity (rev.)	733
CP -Violation in K_L Decays (rev.)	741
Dalitz-Plot Analysis Formalism	771
Review of Charm Dalitz-Plot Analyses (rev.)	774
$D^0-\bar{D}^0$ Mixing (rev.)	783
Production and Decay of b -flavored Hadrons (rev.)	833
Polarization in B Decays (rev.)	910
$B^0-\bar{B}^0$ Mixing (rev.)	914
Determination of V_{cb} and V_{ub} (rev.)	951
Branching Ratios of $\psi(2S)$ and $\chi_{c0,1,2}$ (rev.)	997
Baryons	
Baryon Decay Parameters	1071
N and Δ Resonances	1075
Pentaquarks (new)	1124
Radiative Hyperon Decays	1167
Charmed Baryons (rev.)	1182
Λ_c^+ Branching Fractions	1185
Miscellaneous searches	
Supersymmetry (rev.)	1211
Dynamical Electroweak Symmetry Breaking (rev.)	1258
Searches for Quark & Lepton Compositeness	1265
Extra Dimensions (rev.)	1272

*The divider sheets give more detailed indices for each main section of the Particle Listings.

INTRODUCTION

1. Overview	13
2. Particle Listings responsibilities	13
3. Consultants	14
4. Naming scheme for hadrons	15
5. Procedures	15
5.1 Selection and treatment of data	15
5.2 Averages and fits	16
5.2.1 Treatment of errors	16
5.2.2 Unconstrained averaging	16
5.2.3 Constrained fits	17
5.3 Rounding	18
5.4 Discussion	18
History plots	20

ONLINE PARTICLE PHYSICS INFORMATION

1. Particles & Properties Data	21
2. Collaborations & Experiments	21
3. Conferences	21
4. Current Notices & Announcement Services	22
5. Directories: Research Institutions, People, Libraries, Publishers, Scholarly Societies	22
6. E-Prints/Pre-Prints, Papers & Reports	23
7. Particle Physics Journals & Reviews	23
8. Particle Physics Education Sites	25
9. Physics Job Sites	27
10. Software Repositories	28
11. Specialized Subject Pages	28



INTRODUCTION

1. Overview

The *Review of Particle Physics* and the abbreviated version, the *Particle Physics Booklet*, are reviews of the field of Particle Physics. This complete *Review* includes a compilation/evaluation of data on particle properties, called the “Particle Listings.” These Listings include 2,778 new measurements from 645 papers, in addition to the 24,559 measurements from 7,104 papers that first appeared in previous editions [1].

Both books include Summary Tables with our best values and limits for particle properties such as masses, widths or lifetimes, and branching fractions, as well as an extensive summary of searches for hypothetical particles. In addition, we give a long section of “Reviews, Tables, and Plots” on a wide variety of theoretical and experimental topics, a quick reference for the practicing particle physicist.

The *Review* and the *Booklet* are published in even-numbered years. This edition is an updating through January 2008 (and, in some areas, well into 2008). As described in the section “Using Particle Physics Databases” following this introduction, the content of this *Review* is available on the World-Wide Web, and is updated between printed editions (<http://pdg.lbl.gov/>).

The Summary Tables give our best values of the properties of the particles we consider to be well established, a summary of search limits for hypothetical particles, and a summary of experimental tests of conservation laws.

The Particle Listings contain all the data used to get the values given in the Summary Tables. Other measurements considered recent enough or important enough to mention, but which for one reason or another are not used to get the best values, appear separately just beneath the data we do use for the Summary Tables. The Particle Listings also give information on unconfirmed particles and on particle searches, as well as short “reviews” on subjects of particular interest or controversy.

The Particle Listings were once an archive of all published data on particle properties. This is no longer possible because of the large quantity of data. We refer interested readers to earlier editions for data now considered to be obsolete.

We organize the particles into six categories:

- Gauge and Higgs bosons
- Leptons
- Quarks
- Mesons
- Baryons
- Searches for monopoles, supersymmetry, compositeness, extra dimensions, *etc.*

The last category only includes searches for particles that do not belong to the previous groups; searches for heavy charged leptons and massive neutrinos, by contrast, are with the leptons.

In Sec. 2 of this Introduction, we list the main areas of responsibility of the authors, and also list our large number of consultants, without whom we would not have been able to produce this *Review*. In Sec. 4, we mention briefly the naming scheme for hadrons. In Sec. 5, we discuss our procedures for choosing among measurements of particle properties and for obtaining best values of the properties

from the measurements.

The accuracy and usefulness of this *Review* depend in large part on interaction between its users and the authors. We appreciate comments, criticisms, and suggestions for improvements of any kind. Please send them to the appropriate author, according to the list of responsibilities in Sec. 2 below, or to the LBNL addresses below.

To order a copy of the *Review* or the *Particle Physics Booklet* from North and South America, Australia, and the Far East, send email to PDG@LBL.GOV

or via the web at:

(<http://pdg.lbl.gov/pdgmail>)

or write to:

Particle Data Group, MS 50R6008
Lawrence Berkeley National Laboratory
Berkeley, CA 94720-8166, USA

From all other areas, see

(<http://weblib.cern.ch/publreq.php>)

or write to

CERN Scientific Information Service
CH-1211 Geneva 23
Switzerland

2. Particle Listings responsibilities

* Asterisk indicates the people to contact with questions or comments about Particle Listings sections.

Gauge and Higgs bosons

γ	C. Grab, D.E. Groom*
Gluons	R.M. Barnett,* A.V. Manohar
Graviton	D.E. Groom*
W, Z	A. Gurtu,* M. Gr�unewald*
Higgs bosons	K. Hikasa, G. Weiglein*
Heavy bosons	M. Tanabashi, T. Watari*
Axions	G. Raffelt*

Leptons

Neutrinos	M. Goodman, R. Miquel,* K. Nakamura, K.A. Olive, A. Piepke, P. Vogel
e, μ	J. Beringer,* C. Grab
τ	K.G. Hayes, K. M�onig*

Quarks

Quarks	R.M. Barnett,* A.V. Manohar
Top quark	J. Beringer,* K. Hagiwara
b', t'	K. Hagiwara, W.-M. Yao*
Free quark	J. Beringer*

Mesons

π, η	J. Beringer,* C. Grab
Unstable mesons	C. Amsler, M. Doser,* S. Eidelman,* T. Gutsche, J.J. Hern�andez-Rey, A. Masoni, H. Mahlke, S. Navas, C. Patrignani, N.A. T�ornqvist
K (stable)	G. D’Ambrosio, C.-J. Lin*
D (stable)	D.M. Asner, S. Blusk, C.G. Wohl*
B (stable)	Y. Kwon, G. Punzi, J.G. Smith, W.-M. Yao*

Baryons

Stable baryons	C. Grab, C.G. Wohl*
Unstable baryons	C.G. Wohl,* R.L. Workman
Charmed baryons	S. Blusk, C.G. Wohl*
Bottom baryons	Y. Kwon, J.G. Smith, G. Punzi, W.-M. Yao*

Miscellaneous searches

Monopole	D.E. Groom*
Supersymmetry	A. de Gouvêa, G. Weiglein,* K.A. Olive, L. Pape
Technicolor	M. Tanabashi, J. Terning*
Compositeness	M. Tanabashi, J. Terning*
Extra Dimensions	T. Gherghetta*, C. Kolda
WIMPs and Other	K. Hikasa,*

3. Consultants

The Particle Data Group benefits greatly from the assistance of some 700 physicists who are asked to verify every piece of data entered into this *Review*. Of special value is the advice of the PDG Advisory Committee which meets annually and thoroughly reviews all aspects of our operation. The members of the 2008 committee are:

H. Aihara (Tokyo), Chair
 G. Brooijmans (Columbia)
 D. Harris (FNAL)
 P. Janot (CERN)
 G. Perez (Stony Brook)

We have especially relied on the expertise of the following people for advice on particular topics:

- M.N. Achasov (BINP, Novosibirsk)
- S.I. Alekhin (COMPAS Group, IHEP, Protvino)
- M. Arenton (University of Virginia)
- M. Artuso (Syracuse University)
- E. Barberio (University of Melbourne, Australia)
- S. Biagi (Liverpool University)
- I.I. Bigi (Notre Dame University)
- A. Belyaev (University of Southampton)
- M. Billing (Cornell University)
- V.E. Blinov (BINP, Novosibirsk)
- A.E. Bondar (BINP, Novosibirsk)
- B. Brau (UC Santa Barbara)
- J. Brodzicka (Niewodniczanski I.N.P.)
- T. Browder (University of Hawaii)
- O. Bruening (CERN)
- V. Buescher (Bonn University)
- A. Buras (Munich U.)
- G. Cavoto (University of Rome, Italy)
- M. Chanowitz (LBNL)
- H.-C. Cheng (UC Davis)
- M. Cherry (Louisiana State University)
- D. Cinabro (Wayne State University)
- F. Close (Oxford University)
- P. Colas (DAPNIA, CEA)
- J.S. Conway (UC Davis)
- J. Cumalat (Colorado U.)
- A. Das (University of Rochester)
- D. Denisov (FNAL)
- L. Demortier (Rockefeller University)
- V. Dmitrasinovic (VINCA INS, Belgrade)
- A. Donnachie (University of Manchester)
- V.P. Druzhinin (BINP, Novosibirsk)
- M. Dubrovin (Wayne State U.)
- E. Dudas (CPHT; Orsay, LPT)
- A. Duperrin (CPPM, Marseille)
- R. Erbacher (UC Davis)
- M. Erdmann (RWTH Aachen)
- A. Ereditato (Bern University)
- G. Fanourakis (INP-Demokritos, Athens)
- M. Fidecaro (CERN)
- W. Fischer (BNL)
- P. Franzini (Rome U. & INFN, Frascati)
- S.J. Freedman (UC Berkeley & LBNL)
- E. Frlez (University of Virginia)
- D. Froidevaux (CERN)
- L.K. Gibbons (Cornell University)
- I. Giomataris (CEA, Saclay)
- R. Godang (University of South Alabama)
- B. Golob (U. Ljubljana)
- G. Gomez-Ceballos (MIT)
- M.C. Gonzalez-Garcia (Stony Brook and IFIC Valencia)
- K. Hatakeyama (Rockefeller University)
- F. Harris (University of Hawaii)
- J. Hauptman (Iowa State University)
- C.P. Hays (Oxford University)
- U. Heintz (Boston University)
- S. Heinemeyer (Cantabria Institute of Physics)
- J. Heinrich (University of Pennsylvania)
- A. Hoang (Max-Planck-Institut, Germany)
- T. Iijima (KEK)
- G. Isidori (INFN, Frascati)
- E. James (Fermilab)
- W. Johns (Vanderbilt U.)
- J. Jowett (CERN)
- R.W. Kadel (LBNL)
- A. Kagan (University of Cincinnati)
- K. Kampf (PSI)
- T. Kaneko (KEK, Tsukuba U.)
- S.G. Karshenboim (VNIIM, St-Petersburg)
- J.E. Kim (Seoul National University)
- R. Klanner (DESY)
- J. Konigsberg (University of Florida)
- S. Kretzer (BNL)
- P.P. Krokovny (KEK)
- S.-I. Kurokawa (KEK)
- H. Lacker (LAL-Orsay)
- K. Lesko (LBNL)
- E.B. Levichev (BINP, Novosibirsk)
- W. Lewis (Los Alamos National Lab)
- H.-W. Lin (TJNAF, Newport News)
- E. Linder (LBNL)
- E. Lisi (INFN Bari)
- W. Lockman (U.C. Santa Cruz)
- F. Di Lodovico (University of Lodon)
- O. Long (UC Riverside)
- V. Luth (SLAC)
- G.R. Lynch (LBNL)
- M. Manley (Kent State U.)
- P. Massarotti (Naples U.&INFN)
- B. Meadows (U. of Cincinnati)
- P.J. Mohr (NIST)

- R. Moore (FNAL)
- M. Neubert (Cornell University)
- J. Nico (NIST)
- S. Olsen (University of Hawaii)
- M. Paulini (Carnegie Mellon University)
- M.R. Pennington (University of Durham)
- A. Pich (IFIC, Valencia)
- T. Plehn (University of Edinburgh)
- S.A. Prell (Iowa State University)
- M.V. Purohit (U. South Carolina)
- E. de Rafael (CPT, Marseille)
- P. Raimondi (INFN, Frascati)
- B.L. Roberts (Boston University)
- G. Rolandi (CERN)
- M. Ross (FNAL)
- P. Roudeau (LAL, Orsay)
- F. Sannino (University of Southern Denmark)
- M. Schmitt (Northwestern University)
- C. Schwanda (Vienna)
- C. Schwanenberger (University of Manchester)
- A.J. Schwartz (University of Cincinnati)
- J.T. Seeman (SLAC)
- F. Sefkow (DESY)
- E. Shabalina (University of Illinois at Chicago)
- S. Sharpe (University of Washington)
- M.R. Shepherd (Indiana U.)
- R.E. Shrock (SUNY, Stony Brook)
- Yu.M. Shatunov (BINP, Novosibirsk)
- T. Siedenbuck (CERN)
- P. Sikivie (University of Florida)
- B.A. Shwartz (BINP, Novosibirsk)
- M.S. Sozzi (Pisa, Scuola Normale Superiore)
- A. Stocchi (Orsay, LAL)
- S.I. Striganov (COMPAS Group, IHEP, Protvino)
- Z. Sullivan (ANL & Southern Methodist U.)
- W.M. Sun (Cornell U.)
- B.N. Taylor (NIST)
- J. Thaler (LBNL)
- M. Palutan (INFN, Frascati)
- D. Peterson (Cornell)
- T. Plehn (University of Edinburgh)
- R. Settles (CERN)
- T. Tait (ANL)
- K. Tollefson (Michigan State University)
- K. Trabelsi (KEK)
- R.D. Tripp (LBNL)
- R. Van Kooten (Indiana University)
- R. Voss (CERN)
- L.-T. Wang (Princeton University)
- C. Weiser (University of Freiburg, Germany)
- M. Wobisch (Louisiana Tech University)
- D. Wood (Northeastern University)
- C.Z. Yuan (IHEP, Beijing)
- A.M. Zaitsev (IHEP, Protvino)
- P. Zerwas (DESY)
- C. Zhang (IHEP, Beijing)

4. Naming scheme for hadrons

We introduced in the 1986 edition [2] a new naming scheme for the hadrons. Changes from older terminology affected mainly the heavier mesons made of u , d , and s quarks. Otherwise, the only important change to known hadrons was that the F^\pm became the D_s^\pm . None of the lightest pseudoscalar or vector mesons changed names, nor did the $c\bar{c}$ or $b\bar{b}$ mesons (we do, however, now use χ_c for the $c\bar{c}$ χ states), nor did any of the established baryons. The Summary Tables give both the new and old names whenever a change has occurred.

The scheme is described in “Naming Scheme for Hadrons” (p. 112) of this *Review*.

We give here our conventions on type-setting style. Particle symbols are italic (or slanted) characters: e^- , p , Λ , π^0 , K_L , D_s^+ , b . Charge is indicated by a superscript: B^- , Δ^{++} . Charge is not normally indicated for p , n , or the quarks, and is optional for neutral isosinglets: η or η^0 . Antiparticles and particles are distinguished by charge for charged leptons and mesons: τ^+ , K^- . Otherwise, distinct antiparticles are indicated by a bar (overline): $\bar{\nu}_\mu$, \bar{l} , \bar{p} , \bar{K}^0 , and $\bar{\Sigma}^+$ (the antiparticle of the Σ^-).

5. Procedures

5.1. Selection and treatment of data : The Particle Listings contain all relevant data known to us that are published in journals. With very few exceptions, we do not include results from preprints or conference reports. Nor do we include data that are of historical importance only (the Listings are not an archival record). We search every volume of 20 journals through our cutoff date for relevant data. We also include later published papers that are sent to us by the authors (or others).

In the Particle Listings, we clearly separate measurements that are used to calculate or estimate values given in the Summary Tables from measurements that are not used. We give explanatory comments in many such cases. Among the reasons a measurement might be excluded are the following:

- It is superseded by or included in later results.
- No error is given.
- It involves assumptions we question.
- It has a poor signal-to-noise ratio, low statistical significance, or is otherwise of poorer quality than other data available.
- It is clearly inconsistent with other results that appear to be more reliable. Usually we then state the criterion, which sometimes is quite subjective, for selecting “more reliable” data for averaging. See Sec. 5.4.
- It is not independent of other results.
- It is not the best limit (see below).
- It is quoted from a preprint or a conference report.

In some cases, *none* of the measurements is entirely reliable and no average is calculated. For example, the masses of many of the baryon resonances, obtained from partial-wave analyses, are quoted as estimated ranges thought to probably include the true values, rather than as averages with errors. This is discussed in the Baryon Particle Listings.

For upper limits, we normally quote in the Summary Tables the strongest limit. We do not average or combine

upper limits except in a very few cases where they may be re-expressed as measured numbers with Gaussian errors.

As is customary, we assume that particle and antiparticle share the same spin, mass, and mean life. The Tests of Conservation Laws table, following the Summary Tables, lists tests of *CPT* as well as other conservation laws.

We use the following indicators in the Particle Listings to tell how we get values from the tabulated measurements:

- OUR AVERAGE—From a weighted average of selected data.
- OUR FIT—From a constrained or overdetermined multi-parameter fit of selected data.
- OUR EVALUATION—Not from a direct measurement, but evaluated from measurements of related quantities.
- OUR ESTIMATE—Based on the observed range of the data. Not from a formal statistical procedure.
- OUR LIMIT—For special cases where the limit is evaluated by us from measured ratios or other data. Not from a direct measurement.

An experimentalist who sees indications of a particle will of course want to know what has been seen in that region in the past. Hence we include in the Particle Listings all reported states that, in our opinion, have sufficient statistical merit and that have not been disproved by more reliable data. However, we promote to the Summary Tables only those states that we feel are well established. This judgment is, of course, somewhat subjective and no precise criteria can be given. For more detailed discussions, see the minireviews in the Particle Listings.

5.2. Averages and fits: We divide this discussion on obtaining averages and errors into three sections: (1) treatment of errors; (2) unconstrained averaging; (3) constrained fits.

5.2.1. Treatment of errors: In what follows, the “error” δx means that the range $x \pm \delta x$ is intended to be a 68.3% confidence interval about the central value x . We treat this error as if it were Gaussian. Thus when the error is Gaussian, δx is the usual one standard deviation (1σ). Many experimenters now give statistical and systematic errors separately, in which case we usually quote both errors, with the statistical error first. For averages and fits, we then add the two errors in quadrature and use this combined error for δx .

When experimenters quote asymmetric errors $(\delta x)^+$ and $(\delta x)^-$ for a measurement x , the error that we use for that measurement in making an average or a fit with other measurements is a continuous function of these three quantities. When the resultant average or fit \bar{x} is less than $x - (\delta x)^-$, we use $(\delta x)^-$; when it is greater than $x + (\delta x)^+$, we use $(\delta x)^+$. In between, the error we use is a linear function of x . Since the errors we use are functions of the result, we iterate to get the final result. Asymmetric output errors are determined from the input errors assuming a linear relation between the input and output quantities.

In fitting or averaging, we usually do not include correlations between different measurements, but we try to select data in such a way as to reduce correlations. Correlated errors are, however, treated explicitly when there are a number of results of the form $A_i \pm \sigma_i \pm \Delta$ that have identical systematic errors Δ . In this case, one can first average the $A_i \pm \sigma_i$ and then combine the resulting statistical

error with Δ . One obtains, however, the same result by averaging $A_i \pm (\sigma_i^2 + \Delta_i^2)^{1/2}$, where $\Delta_i = \sigma_i \Delta [\sum (1/\sigma_j^2)]^{1/2}$. This procedure has the advantage that, with the modified systematic errors Δ_i , each measurement may be treated as independent and averaged in the usual way with other data. Therefore, when appropriate, we adopt this procedure. We tabulate Δ and invoke an automated procedure that computes Δ_i before averaging and we include a note saying that there are common systematic errors.

Another common case of correlated errors occurs when experimenters measure two quantities and then quote the two and their difference, *e.g.*, m_1 , m_2 , and $\Delta = m_2 - m_1$. We cannot enter all of m_1 , m_2 and Δ into a constrained fit because they are not independent. In some cases, it is a good approximation to ignore the quantity with the largest error and put the other two into the fit. However, in some cases correlations are such that the errors on m_1 , m_2 and Δ are comparable and none of the three values can be ignored. In this case, we put all three values into the fit and invoke an automated procedure to increase the errors prior to fitting such that the three quantities can be treated as independent measurements in the constrained fit. We include a note saying that this has been done.

5.2.2. Unconstrained averaging: To average data, we use a standard weighted least-squares procedure and in some cases, discussed below, increase the errors with a “scale factor.” We begin by assuming that measurements of a given quantity are uncorrelated, and calculate a weighted average and error as

$$\bar{x} \pm \delta\bar{x} = \frac{\sum_i w_i x_i}{\sum_i w_i} \pm (\sum_i w_i)^{-1/2}, \quad (1)$$

where

$$w_i = 1/(\delta x_i)^2.$$

Here x_i and δx_i are the value and error reported by the i th experiment, and the sums run over the N experiments. We then calculate $\chi^2 = \sum w_i (\bar{x} - x_i)^2$ and compare it with $N - 1$, which is the expectation value of χ^2 if the measurements are from a Gaussian distribution.

If $\chi^2/(N - 1)$ is less than or equal to 1, and there are no known problems with the data, we accept the results.

If $\chi^2/(N - 1)$ is very large, we may choose not to use the average at all. Alternatively, we may quote the calculated average, but then make an educated guess of the error, a conservative estimate designed to take into account known problems with the data.

Finally, if $\chi^2/(N - 1)$ is greater than 1, but not greatly so, we still average the data, but then also do the following:

(a) We increase our quoted error, $\delta\bar{x}$ in Eq. (1), by a scale factor S defined as

$$S = [\chi^2/(N - 1)]^{1/2}. \quad (2)$$

Our reasoning is as follows. The large value of the χ^2 is likely to be due to underestimation of errors in at least one of the experiments. Not knowing which of the errors are underestimated, we assume they are all underestimated by the same factor S . If we scale up all the input errors by this factor, the χ^2 becomes $N - 1$, and of course the output error $\delta\bar{x}$ scales up by the same factor. See Ref. 3.

When combining data with widely varying errors, we modify this procedure slightly. We evaluate S using only the

experiments with smaller errors. Our cutoff or ceiling on δx_i is arbitrarily chosen to be

$$\delta_0 = 3N^{1/2} \delta \bar{x},$$

where $\delta \bar{x}$ is the unscaled error of the mean of all the experiments. Our reasoning is that although the low-precision experiments have little influence on the values \bar{x} and $\delta \bar{x}$, they can make significant contributions to the χ^2 , and the contribution of the high-precision experiments thus tends to be obscured. Note that if each experiment has the same error δx_i , then $\delta \bar{x}$ is $\delta x_i/N^{1/2}$, so each δx_i is well below the cutoff. (More often, however, we simply exclude measurements with relatively large errors from averages and fits: new, precise data chase out old, imprecise data.)

Our scaling procedure has the property that if there are two values with comparable errors separated by much more than their stated errors (with or without a number of other values of lower accuracy), the scaled-up error $\delta \bar{x}$ is approximately half the interval between the two discrepant values.

We emphasize that our scaling procedure for *errors* in no way affects central values. And if you wish to recover the unscaled error $\delta \bar{x}$, simply divide the quoted error by S .

(b) If the number M of experiments with an error smaller than δ_0 is at least three, and if $\chi^2/(M-1)$ is greater than 1.25, we show in the Particle Listings an ideogram of the data. Figure 1 is an example. Sometimes one or two data points lie apart from the main body; other times the data split into two or more groups. We extract no numbers from these ideograms; they are simply visual aids, which the reader may use as he or she sees fit.

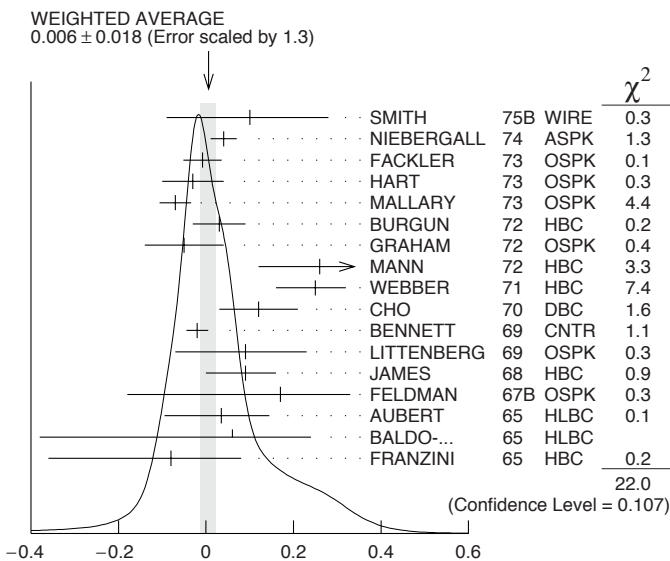


Figure 1: A typical ideogram. The arrow at the top shows the position of the weighted average, while the width of the shaded pattern shows the error in the average after scaling by the factor S . The column on the right gives the χ^2 contribution of each of the experiments. Note that the next-to-last experiment, denoted by the incomplete error flag (\perp), is not used in the calculation of S (see the text).

Each measurement in an ideogram is represented by a Gaussian with a central value x_i , error δx_i , and area

proportional to $1/\delta x_i$. The choice of $1/\delta x_i$ for the area is somewhat arbitrary. With this choice, the center of gravity of the ideogram corresponds to an average that uses weights $1/\delta x_i$ rather than the $(1/\delta x_i)^2$ actually used in the averages. This may be appropriate when some of the experiments have seriously underestimated systematic errors. However, since for this choice of area the height of the Gaussian for each measurement is proportional to $(1/\delta x_i)^2$, the peak position of the ideogram will often favor the high-precision measurements at least as much as does the least-squares average. See our 1986 edition [2] for a detailed discussion of the use of ideograms.

5.2.3. Constrained fits: In some cases, such as branching ratios or masses and mass differences, a constrained fit may be needed to obtain the best values of a set of parameters. For example, most branching ratios and rate measurements are analyzed by making a simultaneous least-squares fit to all the data and extracting the partial decay fractions P_i , the partial widths Γ_i , the full width Γ (or mean life), and the associated error matrix.

Assume, for example, that a state has m partial decay fractions P_i , where $\sum P_i = 1$. These have been measured in N_r different ratios R_r , where, e.g., $R_1 = P_1/P_2$, $R_2 = P_1/P_3$, etc. [We can handle any ratio R of the form $\sum \alpha_i P_i / \sum \beta_i P_i$, where α_i and β_i are constants, usually 1 or 0. The forms $R = P_i P_j$ and $R = (P_i P_j)^{1/2}$ are also allowed.] Further assume that *each* ratio R has been measured by N_k experiments (we designate each experiment with a subscript k , e.g., R_{1k}). We then find the best values of the fractions P_i by minimizing the χ^2 as a function of the $m-1$ independent parameters:

$$\chi^2 = \sum_{r=1}^{N_r} \sum_{k=1}^{N_k} \left(\frac{R_{rk} - R_r}{\delta R_{rk}} \right)^2, \quad (3)$$

where the R_{rk} are the measured values and R_r are the fitted values of the branching ratios.

In addition to the fitted values \bar{P}_i , we calculate an error matrix $\langle \delta \bar{P}_i \delta \bar{P}_j \rangle$. We tabulate the diagonal elements of $\delta \bar{P}_i = \langle \delta \bar{P}_i \delta \bar{P}_i \rangle^{1/2}$ (except that some errors are scaled as discussed below). In the Particle Listings, we give the complete correlation matrix; we also calculate the fitted value of each ratio, for comparison with the input data, and list it above the relevant input, along with a simple unconstrained average of the same input.

Three comments on the example above:

(1) There was no connection assumed between measurements of the full width and the branching ratios. But often we also have information on partial widths Γ_i as well as the total width Γ . In this case we must introduce Γ as a parameter in the fit, along with the P_i , and we give correlation matrices for the widths in the Particle Listings.

(2) We try to pick those ratios and widths that are as independent and as close to the original data as possible. When one experiment measures all the branching fractions and constrains their sum to be one, we leave one of them (usually the least well-determined one) out of the fit to make the set of input data more nearly independent. We now do allow for correlations between input data.

(3) We calculate scale factors for both the R_r and P_i when the measurements for any R give a larger-than-expected contribution to the χ^2 . According to Eq. (3), the

double sum for χ^2 is first summed over experiments $k = 1$ to N_k , leaving a single sum over ratios $\chi^2 = \sum \chi_r^2$. One is tempted to define a scale factor for the ratio r as $S_r^2 = \chi_r^2 / \langle \chi_r^2 \rangle$. However, since $\langle \chi_r^2 \rangle$ is not a fixed quantity (it is somewhere between N_k and N_{k-1}), we do not know how to evaluate this expression. Instead we define

$$S_r^2 = \frac{1}{N_k} \sum_{k=1}^{N_k} \frac{(R_{rk} - \bar{R}_r)^2}{\langle (R_{rk} - \bar{R}_r)^2 \rangle}. \quad (4)$$

With this definition the expected value of S_r^2 is one. We can show that

$$\langle (R_{rk} - \bar{R}_r)^2 \rangle = (\delta R_{rk})^2 - (\delta \bar{R}_r)^2, \quad (5)$$

where $\delta \bar{R}_r$ is the fitted error for ratio r .

The fit is redone using errors for the branching ratios that are scaled by the larger of S_r and unity, from which new and often larger errors $\delta \bar{P}'_i$ are obtained. The scale factors we finally list in such cases are defined by $S_i = \delta \bar{P}'_i / \delta \bar{P}_i$. However, in line with our policy of not letting S affect the central values, we give the values of \bar{P}_i obtained from the original (unscaled) fit.

There is one special case in which the errors that are obtained by the preceding procedure may be changed. When a fitted branching ratio (or rate) \bar{P}_i turns out to be less than three standard deviations ($\delta \bar{P}'_i$) from zero, a new smaller error $(\delta \bar{P}'_i)^-$ is calculated on the low side by requiring the area under the Gaussian between $\bar{P}_i - (\delta \bar{P}'_i)^-$ and \bar{P}_i to be 68.3% of the area between zero and \bar{P}_i . A similar correction is made for branching fractions that are within three standard deviations of one. This keeps the quoted errors from overlapping the boundary of the physical region.

5.3. Rounding: While the results shown in the Particle Listings are usually exactly those published by the experiments, the numbers that appear in the Summary Tables (means, averages and limits) are subject to a set of rounding rules.

The basic rule states that if the three highest order digits of the error lie between 100 and 354, we round to two significant digits. If they lie between 355 and 949, we round to one significant digit. Finally, if they lie between 950 and 999, we round up to 1000 and keep two significant digits. In all cases, the central value is given with a precision that matches that of the error. So, for example, the result (coming from an average) 0.827 ± 0.119 would appear as 0.83 ± 0.12 , while 0.827 ± 0.367 would turn into 0.8 ± 0.4 .

Rounding is not performed if a result in a Summary Table comes from a single measurement, without any averaging. In that case, the number of digits published in the original paper is kept, unless we feel it inappropriate. Note that, even for a single measurement, when we combine statistical and systematic errors in quadrature, rounding rules apply to the result of the combination. It should be noted also that most of the limits in the Summary Tables come from a single source (the best limit) and, therefore, are not subject to rounding.

Finally, we should point out that in several instances, when a group of results come from a single fit to a set of data, we have chosen to keep two significant digits for all the results. This happens, for instance, for several properties of the W and Z bosons and the τ lepton.

5.4. Discussion: The problem of averaging data containing discrepant values is nicely discussed by Taylor in Ref. 4. He considers a number of algorithms that attempt to incorporate inconsistent data into a meaningful average. However, it is difficult to develop a procedure that handles simultaneously in a reasonable way two basic types of situations: (a) data that lie apart from the main body of the data are incorrect (contain unreported errors); and (b) the opposite—it is the main body of data that is incorrect. Unfortunately, as Taylor shows, case (b) is not infrequent. He concludes that the choice of procedure is less significant than the initial choice of data to include or exclude.

We place much emphasis on this choice of data. Often we solicit the help of outside experts (consultants). Sometimes, however, it is simply impossible to determine which of a set of discrepant measurements are correct. Our scale-factor technique is an attempt to address this ignorance by increasing the error. In effect, we are saying that present experiments do not allow a precise determination of this quantity because of unresolvable discrepancies, and one must await further measurements. The reader is warned of this situation by the size of the scale factor, and if he or she desires can go back to the literature (via the Particle Listings) and redo the average with a different choice of data.

Our situation is less severe than most of the cases Taylor considers, such as estimates of the fundamental constants like \hbar , *etc.* Most of the errors in his case are dominated by systematic effects. For our data, statistical errors are often at least as large as systematic errors, and statistical errors are usually easier to estimate. A notable exception occurs in partial-wave analyses, where different techniques applied to the same data yield different results. In this case, as stated earlier, we often do not make an average but just quote a range of values.

A brief history of early Particle Data Group averages is given in Ref. 3. Figure 2 shows some histories of our values of a few particle properties. Sometimes large changes occur. These usually reflect the introduction of significant new data or the discarding of older data. Older data are discarded in favor of newer data when it is felt that the newer data have smaller systematic errors, or have more checks on systematic errors, or have made corrections unknown at the time of the older experiments, or simply have much smaller errors. Sometimes, the scale factor becomes large near the time at which a large jump takes place, reflecting the uncertainty introduced by the new and inconsistent data. By and large, however, a full scan of our history plots shows a dull progression toward greater precision at central values quite consistent with the first data points shown.

We conclude that the reliability of the combination of experimental data and our averaging procedures is usually good, but it is important to be aware that fluctuations outside of the quoted errors can and do occur.

ACKNOWLEDGMENTS

The publication of the *Review of Particle Physics* is supported by the Director, Office of Science, Office of High Energy and Nuclear Physics, the Division of High Energy Physics of the U.S. Department of Energy under Contract No. DE-AC02-05CH11231; by the U.S. National Science Foundation under Agreement No. PHY-0652989; by the European Laboratory for Particle Physics (CERN); by an implementing arrangement between the governments of Japan (Monbusho) and the United States (DOE) on

cooperative research and development; and by the Italian National Institute of Nuclear Physics (INFN).

We thank all those who have assisted in the many phases of preparing this *Review*. We particularly thank the many who have responded to our requests for verification of data entered in the Listings, and those who have made suggestions or pointed out errors.

REFERENCES

1. The previous edition was Particle Data Group: W.-M. Yao *et al.*, *J. Phys.* **G33**, 1 (2006).
2. Particle Data Group: M. Aguilar-Benitez *et al.*, *Phys. Lett.* **170B** (1986).
3. A.H. Rosenfeld, *Ann. Rev. Nucl. Sci.* **25**, 555 (1975).
4. B.N. Taylor, "Numerical Comparisons of Several Algorithms for Treating Inconsistent Data in a Least-Squares Adjustment of the Fundamental Constants," U.S. National Bureau of Standards NBSIR 81-2426 (1982).

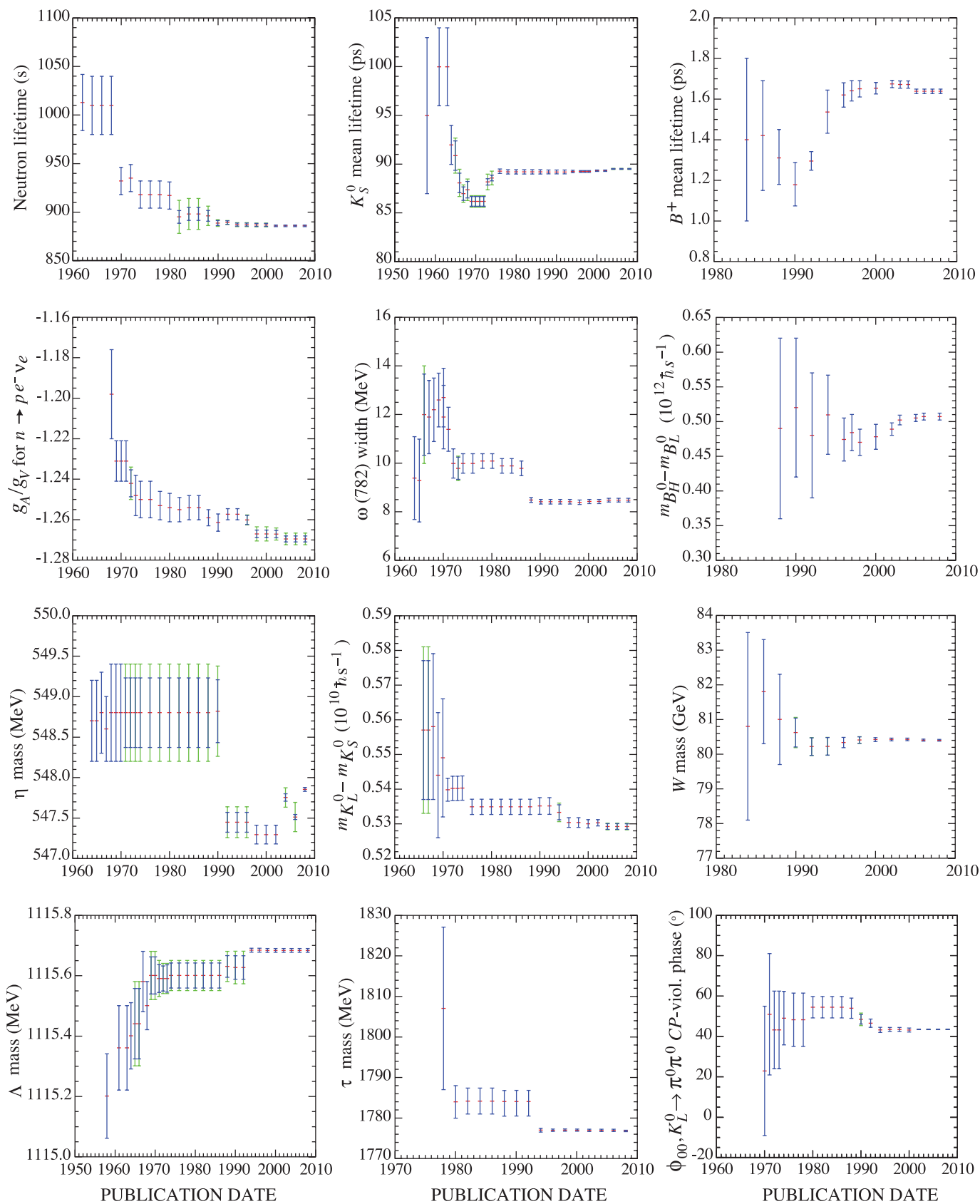


Figure 2: A historical perspective of values of a few particle properties tabulated in this *Review* as a function of date of publication of the *Review*. A full error bar indicates the quoted error; a thick-lined portion indicates the same but without the “scale factor.”

ONLINE PARTICLE PHYSICS INFORMATION

Revised August 2007 by A. Wheeler (SLAC)

This annotated list provides a highly selective set of online resources that are useful to the particle physics community. It describes the scope, size, and organization of the resources so that efficient choices can be made amongst many sites which may appear similar. A resource is excluded if it provides information primarily of interest to only one institution. Because this list must be fixed in print, it is important to consult the updated version of this compilation which includes newly added resources and hypertext links to more complete information at:

<http://www.slac.stanford.edu/library/pdg/>

My thanks to Piotr Zyla, Particle Data Group, Pat Kreitz, Travis Brooks, Nicole Thomas, Lesley Wolf, SLAC Research Library, and the many particle physics Web site and database maintainers who have all given me their generous assistance. Please send comments and corrections to e-mail wheeler@slac.stanford.edu.

1. Particles & Properties Data:

- REVIEW OF PARTICLE PHYSICS (RPP): A biennial comprehensive review summarizing much of the known data about the field of particle physics produced by the international Particle Data Group (PDG). Includes compilations and evaluation of data on particle properties, summary tables with best values and limits for particle properties, extensive summaries of searches for hypothetical particles, and a long section of reviews, tables, and plots on a wide variety of theoretical and experimental topics of interest to particle physicists and astrophysicists. The linked table of contents provides access to particle listings, reviews, summary tables, errata, indices, *etc.* The current printed version is W.-M. Yao, *et al.*, J. Phys. **G33**, 1 (2006).
- PARTICLE PHYSICS BOOKLET: Although this booklet is produced in print only and has no online access, it is included in this guide because it is one of the most useful summary sets of physics data available. Its small size and ease of ordering from the Particle Data Group make it one of the most useful and frequently used tools for particle physicists. This pocket-sized 300-page booklet contains data abstracted from the most recent edition of the full Review of Particle Physics. Includes summary tables and abbreviated versions of some of the other sections. Contains useful plots and figures. Order a copy from the PDG Products Web page.
- COMPUTER-READABLE FILES: Currently available from the PDG: Tables of masses, widths, and PDG Monte Carlo particle numbers and cross-section data, including hadronic total and elastic cross sections vs laboratory momenta, and total center-of mass energy. The PDG Monte Carlo particle numbering scheme has been updated for the recent edition of the RPP and is also available as a MobileDB database. Palm Pilot products include physical constants, astrophysical constants and particle properties. These files are updated in even-numbered years coinciding with the production of the *Review of Particle Properties*:
http://pdg.lbl.gov/2008/html/computer_read.html
- PARTICLE PHYSICS DATA SYSTEM: This site contains an indexed bibliography of particle physics (1895–1995), a database of computerized numerical data extracted from experimental publications, and an index of papers (1895–present) that contain experimental data or data analyses. The Web interface permits simple searching for compilations of integrated cross-section data. The search interface for numerical data on observables in reactions (ReacData or RD) is under construction. Maintained by the COMPAS group at IHEP:
<http://wwwppds.ihep.su:8001/ppds.html>
- HEPDATA: REACTION DATA DATABASE: A part of the HEPDATA databases at University of Durham/RAL, this database is compiled by the Durham Database Group (UK) with help from the COMPAS Group (Russia) for the PDG. Contains numerical values of HEP reaction data such as total and differential cross sections, fragmentation functions, structure functions, and polarization measurements from a wide range of experiments.

Updated at regular intervals. Provides data reviews which contain precompiled reviewed data such as ‘Structure Functions in DIS,’ ‘Single Photon Production in Hadronic Interactions,’ and ‘Drell-Yan Cross Sections.’

<http://durpdg.dur.ac.uk/HEPDATA/REAC>

- NIST PHYSICS LABORATORY: This unit of the National Institute of Standards and Technology provides measurement services and research for electronic, optical, and radiation technologies. Three sub-pages, on Physical Reference Data, on Constants, Units & Uncertainty, and on Measurements & Calibrations, are extremely useful. Additional links to other physical properties and data of tangential interest to particle physics are also available from this page:

<http://physics.nist.gov/>

2. Collaborations & Experiments:

- EXPERIMENTS Database: Contains more than 2,200 past, present, and future experiments in elementary particle physics. Lists both accelerator and non-accelerator experiments. Includes official experiment name and number, location, spokespersons, and collaboration lists. Simple searches by participant, title, experiment number, institution, date approved, accelerator, or detector, return a result that fully describes the experiment, including a complete list of authors, title, description of the experiment’s goals and methods, and a link to the experiment’s Web page if available. Publication lists distinguish articles in refereed journals, theses, technical or instrumentation papers, and those which make the Topcite at 50+ subsequent citations or more:

<http://www.slac.stanford.edu/spires/experiments/>

- COSMIC RAY/GAMMA RAY/NEUTRINO AND SIMILAR EXPERIMENTS: This is an extensive collection of experimental Web sites organized by focus of study and also by location. Additional sections link to educational materials, organizations and related Web sites, *etc.* Maintained at the Max Planck Institute for Nuclear Physics by Konrad Bernlöhner:

<http://www.mpi-hd.mpg.de/hfm/CosmicRay/CosmicRaySites.html>

3. Conferences:

- CONFERENCES: Database of more than 12,300 past, present and future conferences, schools, and meetings of interest to high-energy physics and related fields. Covers 1973 to the future. The current year lists more than 600 events. Search or browse by title, acronym, date, location. Includes information about published proceedings, links to submitted papers from the SPIRES-HEP database, and links to the conference Web site when available. Links to a form with which one can submit a new conference or edit an existing one:

<http://www.slac.stanford.edu/spires/conferences/additions.shtml>

to submit a new conference. Can also search for any conferences occurring by day, month, quarter, or year:

<http://www.slac.stanford.edu/spires/conferences/>

- CERN & HEP EVENTS: A list of current and upcoming conferences, schools, workshops, *etc.*, of interest to high-energy physicists. Organized by year and then by date. Covers from 1993 to 2010. Includes about 275 current and future events:

<http://events.web.cern.ch/events/>

- EUROPHYSICS MEETINGS LIST: Maintained by the European Physical Society, this lists in chronological order all the current and future meetings, workshops, schools, *etc.*, organized or sponsored by EPS or organized in conjunction with an EPS-sponsored group:

<http://www.eps.org/conferences>

- PHYSICSWEB EVENTS: Part of the Institute of Physics (IOP) Web site, this site contains approximately a hundred entries for

the current year's meetings, workshops, exhibitions and schools. Fills a gap by covering smaller conferences and workshops around the world. Searchable by type of event *e.g.*: school, workshop, or by date or free text words. Provides a Web form and email address for adding a conference and for signing up to receive email notices of new events added:

<http://physicsweb.org/events/>

4. Current Notices & Announcement Services:

- See also the conference and event sites above for links to email notification services or event submission forms.
- E-PRINT ARCHIVES LISTSERV NOTICES: The Cornell-based E-Print Archives provides daily notices of preprints in the fields of physics, mathematics, nonlinear sciences, computer science, quantitative biology, and statistics which have been submitted to the archives as full text electronic documents. Use the Web-accessible listings:

<http://arXiv.org/>

or subscribe:

<http://arXiv.org/help/subscribe>

- HEPJOBS DATABASE: Maintained by Fermilab and SLAC libraries, this database lists jobs in the fields of core interest to the particle physics and astroparticle physics communities. Use this page to post a job or to receive email notices of new job listings:

<http://www.slac.stanford.edu/spires/jobs/>

- INTERACTIONS.ORG: Provides an email newsletter covering particle physics news and resources from particle physics laboratories worldwide. Subscribe to Interactions.org Newswire:

<http://www.interactions.org/cms/>

- NASA ASTROPHYSICS DATA SYSTEM: This page provides access to the tables of contents of the most recent issues of selected journals in the field. It permits the user to select which titles are shown and eliminates the ones the user has already read:

http://adsabs.harvard.edu/custom_toc.html

- PREPRINTS IN PARTICLES AND FIELDS (PPF): A weekly listing averaging 250 new preprints in particle physics and related fields. Contains bibliographic listings for and, in the Web version, full text links to, the new preprints received by and cataloged into the SPIRES High-Energy Physics (HEP) database. Includes that week's titles from the e-print archives as well as preprints and articles received from other sources. Directions for subscribing to an email version can be found on the page listing the most recent week's preprints:

<http://www.slac.stanford.edu/library/documents/newppf.html>

5. Directories:

5.1. Directories—Research Institutions:

- HEP and Astrophysics INSTITUTIONS: SPIRES database of over 6,500 high-energy physics and astroparticle physics institutes, laboratories, and university departments in which research on particle physics is performed. Covers six continents and over a hundred countries. Provides an alphabetical list by country or an interface that is searchable by name, acronym, location, *etc.* Includes address, phone and fax numbers, e-mail address, and Web links where available. Has links to the recent HEP papers from each institution. Maintained by SLAC, DESY and Fermilab libraries. To search the Institutions database:

<http://www.slac.stanford.edu/spires/institutions/>

- HEP INSTITUTES: Contains almost a thousand institutional addresses used in the CERN Library catalog. Includes, where available, the following: phone and fax numbers, e-mail addresses, and Web links. Provides free text searching and result sorting by organization, country, or town:

<http://cdsweb.cern.ch/collection/HEP%20Institutes>

- TOP 500 HEP AND ASTROPHYSICS INSTITUTIONS BY COUNTRY: Lists the 500 major HEP-related organizations and universities that have published the most papers in the past five years, as identified from the SPIRES HEP Database. Provides active links to the home pages and full INSTITUTIONS database records. Listed by country, and then alphabetically by institution:

<http://www.slac.stanford.edu/spires/inst/major.shtml>

5.2. Directories—People:

- HEPNAMES: Searchable worldwide database of over 40,000 people associated with particle physics, astroparticle physics, synchrotron radiation, and related fields. Provides e-mail addresses, country in which the person is currently working, and a SPIRES HEP database search for their papers. If the person has supplied the following information, it lists the countries in which they did their undergraduate and graduate work, their URL, and their graduate students. It also provides listings of Nobel Laureates, country statistics, Lab Directors, *etc.*:

<http://www.slac.stanford.edu/spires/hepnames/>

- HEP VIRTUAL PHONEBOOK: A list of links to phonebooks and directories of high-energy physics sites and collaborations around the world organized by site. Often provides links to more specialized phone or e-mail listings, such as a department within a university, visiting scientists, or postdocs. Some phonebooks may require passwords or other authentication to access. Maintained by HEPiC, and many linked phonebooks are still active, however, this Web site was last updated in 2003:

<http://www.hep.net/sites/directories.html>

5.3. Directories—Libraries:

- Argonne National Laboratory (ANL) Library:
<http://www.library.anl.gov/>
- Brookhaven National Laboratory (BNL) Library:
http://www.bnl.gov/isd/reslib/main_e.asp
- (CERN) European Organization for Nuclear Research Library:
<http://library.cern.ch/>
- Deutsches Elektronen-Synchrotron (DESY) Library:
<http://library.desy.de/>
- Fermi National Accelerator Laboratory (Fermilab) Library:
<http://bss.fnal.gov/library/index.html>
- Idaho National Laboratory (INL) Technical Library:
<http://www.inl.gov/library/>
- (KEK) National Laboratory for High Energy Physics Library:
<http://www-lib.kek.jp/top-e.html>
- Lawrence Berkeley National Laboratory (LBNL) Library:
<http://www-library.lbl.gov/library/public/tmLib/aboutus/LibDefault.htm>
- Lawrence Livermore National Laboratory (LLNL) Library:
<http://www.llnl.gov/library/>
- Los Alamos National Laboratory (LANL) Library:
<http://lib-www.lanl.gov/>
- Oak Ridge National Laboratory (ORNL) Library:
<http://www.ornl.gov/Library/library-home.html>
- Pacific Northwest National Laboratory (PNL) Library:
<http://libraryweb.pnl.gov/index.stm>
- Sandia National Laboratory Technical Library:
<http://infoserve.sandia.gov/>
- Stanford Linear Accelerator Center (SLAC) Library:
<http://www.slac.stanford.edu/library>
- Thomas Jefferson National Accelerator Facility (JLab) Library:
<http://www.jlab.org/IR/library/index.html>

5.4. Directories—Publishers:

- **DIRECTORY OF PUBLISHERS AND VENDORS:** International directory of publishers and vendors used by libraries. Organized by publisher name, by subject (*e.g.* Science, Mathematics, and Technology), and by location. Also provides an email directory. Has not been updated since 2004:

<http://www.acqweb.org/pubr.html>

5.5. Directories—Scholarly Societies:

- **American Association for the Advancement of Science:**

<http://www.aaas.org/>

- **American Association of Physics Teachers:**

<http://www.aapt.org/>

- **American Astronomical Society:**

<http://www.aas.org>

- **American Institute of Physics:**

<http://www.aip.org/>

- **American Mathematical Society:**

<http://www.ams.org/>

- **American Physical Society:**

<http://www.aps.org>

- **European Physical Society:**

<http://www.eps.org/>

- **IEEE Nuclear and Plasma Sciences Society:**

<http://ewh.ieee.org/soc/nps/aboutnpss.htm>

- **Institute of Physics:**

<http://www.iop.org/>

- **International Union of Pure and Applied Physics:**

<http://www.iupap.org/>

- **Japan Society of Applied Physics:**

<http://www.jsap.or.jp/english/>

- **Physical Society of Japan:**

<http://wwwsoc.nii.ac.jp/jps/>

- **Physical Society of the Republic of China:**

<http://psroc.phys.ntu.edu.tw/english/index.html>

- **SCHOLARLY SOCIETIES PROJECT:** Directory of more than 4,000 scholarly and technical societies with links to their Web sites. Permits searching by subject, country, language, founding dates, and more. Includes acronyms and indicates when a Web site contains both its native language and an English-language version and when it has a permanent URL. Provides direct links to society meeting and conference announcement lists, standards, and full text journals. Maintained by the University of Waterloo:

<http://www.scholarly-societies.org/>

6. E-Prints/Pre-Prints, Papers, & Reports:

- **CERN ARTICLES & PREPRINTS:** The CERN document server contains records of more than 700,000 CERN and non-CERN articles, preprints, theses. Includes records for CERN Yellow Reports, internal and technical notes, and official CERN committee documents. Provides access to full text of the documents for about 50 percent of the entries and to the references when available:

<http://cdsweb.cern.ch/?c=Articles+%26+Preprints&as=0>

- **ECONF:** Electronic Conference Proceedings Archive: This site offers a fully electronic, Web-accessible archive for the proceedings of scientific conferences in High-Energy Physics and related fields.

Conference editors can use the site tools to prepare and post an electronic version of their proceedings. Librarians and other indexers can download metadata from each proceedings. Researchers can browse an entire proceedings via a table of contents or search for papers through a link to the SPIRES HEP Database which indexes the EConf contents:

<http://www.slac.stanford.edu/econf/>

- **HEP DATABASE (SPIRES):** Contains over 700,000 bibliographic records for particle physics articles, including journal papers, preprints, e-prints, technical reports, conference papers and theses. Comprehensively indexed with multiple links to full text as well as links to author and institutional information. Covers 1974 to the present with substantial older materials added. Updated daily with links to electronic texts, Durham Reaction Data, *Review of Particle Properties*, *etc.* Searchable by citation, by all authors and authors' affiliations, title, topic, report number, citation (footnotes), e-print archive number, date, journal, *etc.* A joint project of the SLAC and DESY libraries with the collaboration of Fermilab, Durham University (UK), KEK, Kyoto University, and many other research institutions and scholarly societies:

<http://www.slac.stanford.edu/spires/hep/>

- **JACoW:** This Joint Accelerator Conference Website is organized by the editorial boards of the Asian, European and American Particle Accelerator Conferences and the COOL, CYCLOTRONS, DIPAC, FEL, ICALEPCS, ICAP, ICFA ABDW, LINAC, RuPAC and SRF conferences. It contains the full text of all the papers of these accelerator conferences. Search by conference name, author, title, keyword or full text of the paper:

<http://www.JACoW.org/>

- **KISS (KEK INFORMATION SERVICE SYSTEM) FOR PREPRINTS:** KEK Library preprint and technical report database. Contains bibliographic records of preprints and technical reports held in the KEK library with links to the full text images of more than 100,000 papers scanned from their worldwide collection of preprints. Particularly useful for older scanned preprints:

http://www-lib.kek.jp/KISS/kiss_prepri.html

- **arXiv.org E-PRINT ARCHIVE:** The arXiv.org is an automated electronic repository of full text papers in physics, mathematics, computer, statistics, nonlinear sciences, cosmology and quantitative biology. Papers, called pre-prints or e(electronic)-prints, are usually sent by their authors to arXiv in advance of submission to a journal for publication. Primarily covers 1991 to the present but authors are encouraged to post older papers retroactively. Permits searching by author, title, and keyword in abstract. Allows limiting by subfield archive or by date:

<http://arXiv.org>

- **NASA ASTROPHYSICS DATA SYSTEM:** The ADS Abstract Service provides a search interface for four bibliographic databases covering: Astronomy and Astrophysics, Instrumentation, Physics and Geophysics, Science Education, and arXiv Preprints. Contains abstracts from articles and monographs as well as conference proceedings:

http://adsabs.harvard.edu/ads_abstracts.html

- **DIRECTORY OF MATHEMATICS PREPRINT AND E-PRINT SERVERS:** Provides the current home page and email contacts for mathematical preprint and e-print servers throughout the world:

<http://www.ams.org/global-preprints/>

7. Particle Physics Journals & Reviews:

7.1. Online Journals and Tables of Contents: Please note, some of these journals, publishers, and reviews may limit access to subscribers. If you encounter access problems, check with your institution's library.

- **ADVANCES IN THEORETICAL AND MATHEMATICAL PHYSICS (ATMP):** Advances in Theoretical and Mathematical Physics is a publication of the International Press, publishing papers on all areas in which theoretical physics and mathematics interact with each other:
<http://www.intlpress.com/ATMP/>
- **AMERICAN JOURNAL OF PHYSICS:** A monthly publication of the American Association of Physics Teachers on instructional and cultural aspects of physical science:
<http://ojps.aip.org/ajp>
- **APPLIED PHYSICS LETTERS:** Weekly publication of short (3 pages maximum) articles:
<http://ojps.aip.org/aplo/>
- **ASTROPHYSICAL JOURNAL:** Published by the American Astronomical Society (AAS). See also AAS entry under Journal Publishers (below):
<http://www.journals.uchicago.edu/ApJ/>
- **CLASSICAL AND QUANTUM GRAVITY:** Published by the Institute of Physics (IOP) covering the fields of gravitation and spacetime theory:
<http://www.iop.org/Journals/cq>
- **EUROPEAN PHYSICAL JOURNAL A: HADRONS AND NUCLEI:** This journal merges *Il Nuovo Cimento A* and *Zeitschrift fur Physik A* and covers physics and astronomy:
<http://www.springeronline.com/sgw/cda/frontpage/0,11855,4-40109-70-1123848-0,00.html>
- **EUROPEAN PHYSICAL JOURNAL C: PARTICLES AND FIELDS:** This journal is the successor to *Zeitschrift fur Physik C*, covering physics and astronomy:
<http://www.springeronline.com/sgw/cda/frontpage/0,11855,4-40109-70-1126563-0,00.html>
- **INTERNATIONAL JOURNAL OF MODERN PHYSICS C: PHYSICS AND COMPUTERS:** Includes both review and research articles:
<http://ejournals.wspc.com.sg/ijmpc/ijmpc.shtml>
- **INTERNATIONAL JOURNAL OF MODERN PHYSICS D: GRAVITATION, ASTROPHYSICS AND COSMOLOGY:** Includes both review and research articles:
<http://ejournals.wspc.com.sg/ijmpd/ijmpd.shtml>
- **INTERNATIONAL JOURNAL OF MODERN PHYSICS E: NUCLEAR PHYSICS:** Includes both review and research articles:
<http://ejournals.wspc.com.sg/ijmpe/ijmpe.shtml>
- **JAPANESE JOURNAL OF APPLIED PHYSICS:** Part 1 covers papers, short notes, and review papers. Part 2 publishes letters including a special *Express Letters* section:
<http://www.ipap.jp/jjap/index.htm>
- **JOURNAL OF COSMOLOGY AND ASTROPARTICLE PHYSICS:** An electronic peer-reviewed journal created by the International School for Advanced Studies (SISSA) and the Institute of Physics. Authors are encouraged to submit media files to enhance the online versions of articles:
<http://jcap.sissa.it/>
- **JOURNAL OF HIGH ENERGY PHYSICS:** Open Access. Electronic and print available. Like *ATMP*, this is a refereed journal written, run, and distributed by electronic means. It accepts email submission notices and “fetches” the submitted paper from the arXiv.org E-print archives:
<http://jhep.sissa.it/>
- **JOURNAL OF PHYSICS G: NUCLEAR AND PARTICLE PHYSICS:** Published by IOP:
<http://www.iop.org/EJ/journal/0954-3899>
- **JOURNAL OF THE PHYSICAL SOCIETY OF JAPAN: JPSJ ONLINE:**
<http://jpsj.ipap.jp/>
- **MODERN PHYSICS LETTERS A:** This journal contains research papers in gravitation, cosmology, nuclear physics, and particles and fields. *Brief Review* section for short reports on new findings and developments:
<http://www.worldscinet.com/mpla/mpla.shtml>
- **MODERN PHYSICS LETTERS B:** This journal contains research papers in condensed matter physics, statistical physics, applied physics and High Tc Superconductivity. *Brief Review* section for short reports on new findings and developments:
<http://www.worldscinet.com/mplb/mplb.shtml>
- **NEW JOURNAL OF PHYSICS:** Open Access. Co-owned by the Institute of Physics and the Deutsche Physikalische Gesellschaft, this journal is funded by article charges from authors of published papers and by scholarly societies, *NJP* is available in a free, electronic form:
<http://www.iop.org/EJ/journal/1367-2630/1>
- **NUCLEAR INSTRUMENTS AND METHODS IN PHYSICS RESEARCH A: ACCELERATORS, SPECTROMETERS, DETECTORS, AND ASSOCIATED EQUIPMENT:** This journal was formerly part of *Nuclear Instruments and Methods in Physics Research*. This journal covers instrumentation and large scale facilities:
<http://www.sciencedirect.com/science/journal/01689002>
- **NUCLEAR PHYSICS A: NUCLEAR AND HADRONIC PHYSICS:**
<http://www.sciencedirect.com/science/journal/03759474>
- **NUCLEAR PHYSICS B: PARTICLE PHYSICS, FIELD THEORY, STATISTICAL SYSTEMS, AND MATHEMATICAL PHYSICS:**
<http://www.sciencedirect.com/science/journal/05503213>
- **NUCLEAR PHYSICS B: PROCEEDINGS SUPPLEMENTS:** Publishes proceedings of international conferences and topical meetings in high-energy physics and related areas:
<http://www.sciencedirect.com/science/journal/09205632>
- **PHYSICAL REVIEW D: PARTICLES, FIELDS, GRAVITATION, AND COSMOLOGY:**
<http://prd.aps.org/>
- **PHYSICAL REVIEW SPECIAL TOPICS – ACCELERATORS AND BEAMS:**
<http://prst-ab.aps.org/>
- **PHYSICS LETTERS B: Nuclear and Particle Physics:**
<http://www.sciencedirect.com/science/journal/03702693>
- **PHYSICS—USPEKHI:** English edition of *Uspekhi Fizicheskikh Nauk*:
<http://ufn.ioc.ac.ru/>
- **PROGRESS IN PARTICLE AND NUCLEAR PHYSICS:**
<http://www.sciencedirect.com/science/journal/01466410>
- **PROGRESS OF THEORETICAL PHYSICS:** Covers all fields of theoretical physics. A supplement is published roughly quarterly containing either long original or review papers or collections of papers on specific topics:
<http://www2.yukawa.kyoto-u.ac.jp/ptpwww/>

7.2. Journals – Publishers & Repositories:

- NASA ASTROPHYSICS DATA SYSTEM: Provides free electronic access to back issues of the *Astrophysical Journal*, *Astrophysical Journal Letters*, and the *Astrophysical Journal Supplement Series* and to many other titles. Often a journal allows the ADS to provide free, full text access after a delay of some period of time which can be several years:
<http://adsabs.harvard.edu/>
- AIP JOURNAL CENTER: The American Institute of Physics' top-level page for their electronic journals may be found at:
<http://www.aip.org/ojs/service.html>
- AMERICAN PHYSICAL SOCIETY: The top-level page for the APS research journals. From this page one can access their *Physical Review* Online Archive (PROLA) search engine which is free to users:
<http://publish.aps.org/>
- ELSEVIER SCIENCE: This Web site lists all Elsevier journal titles alphabetically and also enables browsing by subject field. "Astronomy, Astrophysics and Space Science" (20 titles) or "Physics" (175 titles):
http://www.elsevier.com/wps/find/journal_browse.cws_home
- EUROPEAN PHYSICAL SOCIETY: This is the top-level page listing the society's journals:
<http://www.eps.org/publications>
- INSTITUTE OF PHYSICS (IOP): Journals: Information: A list of the IOP journals organized by subject. A page organized by title is also available linked to this page:
<http://www.iop.org/EJ/S/3/418/main/-list=subject>
- SPRINGER PUBLISHING: Physics: From this link, one can reach a subject list of Springer journals in physics through the list of subdisciplines on the Subject Menu:
<http://www.springer.com/west/home/physics?SGWID=4-10100-0-0-0>
- SPRINGER PUBLISHING: Astronomy, Astrophysics & Space Science: From this link, one can reach a subject list of Springer journals in Astronomy, Astrophysics & Space Science through the list of subdisciplines on the Subject Menu:
<http://www.springer.com/west/home/astronomy?SGWID=4-123-0-0-0>

7.3. Review Publications:

- HEP Reviews: SPIRES guide to the Review Literature in HEP, reviewed and compiled by SPIRES database staff. The guide indexes by topic the review papers that have a significant number of citations in the SPIRES-HEP database. These papers include all of those with at least 100 citations by June 2004, but other papers are added as well. The guide is updated annually:
<http://www.slac.stanford.edu/spires/reviews/>
- LIVING REVIEWS IN RELATIVITY: A peer-refereed, solely online physics journal publishing invited reviews covering all areas of relativity. Provided as a free service to the scientific community by the Max-Planck-Institut für Gravitationsphysik. Published in yearly volumes, although articles appear throughout the year. Hyperlinks are kept checked and active and reviews are updated frequently:
<http://relativity.livingreviews.org/sitecontents.html>
- NET ADVANCE OF PHYSICS: A free electronic service providing review articles and tutorials in an encyclopedic format. Covers all areas of physics. Includes e-prints, book announcements, full text of electronic books, and other resources with hypertext links when available. Welcomes contributions of original review articles:
<http://web.mit.edu/redingtn/www/netadv/welcome.html>

- PHYSICS REPORTS: A review section for *Physics Letters A* and *Physics Letters B*. Each report deals with one subject. The reviews are specialized in nature, more extensive than a literature survey but normally less than book length:
<http://www.sciencedirect.com/science/journal/03701573>
- REPORTS ON PROGRESS IN PHYSICS: Covers all areas of physics and is published monthly. All papers are free for 30 days from the date of online publication:
<http://www.iop.org/EJ/journal/0034-4885/1>
- REVIEWS OF MODERN PHYSICS:
<http://rmp.aps.org/>

8. Particle Physics Education Sites:

8.1. Particle Physics Education: General Sites:

- ARGONNE NATIONAL LABORATORY K-12 PROGRAMS: Includes links to a variety of information and programs such as ArthmAttack, NEWTON, and the Rube Goldberg Machine Contest:
http://www.dep.anl.gov/p_k-12/
 - CONTEMPORARY PHYSICS EDUCATION PROJECT (CPEP): Provides charts, brochures, Web links, and classroom activities. Online interactive courses include: Fundamental Particles and Interactions; Plasma Physics and Fusion; and Nuclear Science:
<http://www.cpepweb.org/>
 - FERMLAB EDUCATION OFFICE: Outstanding collection of resources from the "grandmother" of all physics lab educational programs. Sections are organized for students and educators by grade level and for general visitors:
<http://www-ed.fnal.gov/>
 - PARTICLE PHYSICS EDUCATION SITES: This rich site maintained by the Particle Data Group provides links to many other educational sites. Organizes the links by subject, level, and type of educational experience:
<http://particleadventure.org/other/othersites.html>
 - PHYSICAL SCIENCE: EDUCATIONAL HOTLISTS: Created by the outstanding Franklin Institute Science Museum, these hotlists contain a pre-screened list of resources for science educators, students, and enthusiasts. The criteria for inclusion is that a site stimulates creative thinking and learning about science. The excellent Physical Science list contains useful links for physics, physicists, optics, material science, applied design and engineering, sites for museums, "doing science," and inventors and engineers:
<http://sln.fi.edu/tfi/hotlists/hotlists.html>
 - PHYSLINK.COM: EDUCATION: This site provides sub-lists of online resources in the following areas: History of Physics and Astronomy, Essays on the interface between science, art, religion and philosophy, Astronomy, Graduate School and Student Advice, Software (reviews), References and Learning Sites for Educators, Youth Science, and New Theories:
<http://www.physlink.com/Education/Index.cfm>
- ### 8.2. Particle Physics Education: Background Knowledge:
- ALBERT EINSTEIN ONLINE: A meta-Einstein site with links to dozens of resources by and about this scientist. The site is organized into the following categories: Overviews, Moments (recollections of Einstein by others), Physics, Writings, Quotes, Pictures, and Miscellaneous:
<http://www.westegg.com/einstein/>
 - ANTIMATTER: MIRROR OF THE UNIVERSE: Find out what antimatter is, where it is made, the history behind its discovery, and how it is a part of our lives. This award-winning site, sponsored by the European Organization for Nuclear Research (CERN),

explains to big kids and little kids alike the truth (and fiction) about antimatter. Features colorful photos and illustrations, a Kids Corner, and CERN physicists answering your questions on antimatter:

<http://livefromcern.web.cern.ch/livefromcern/antimatter/>

- **BIG BANG SCIENCE—EXPLORING THE ORIGINS OF MATTER:** In clear, concise, yet elegant language, this Web site, produced by the Particle Physics and Astronomy Research Council of the UK (PPARC), explains what physicists are looking for with their giant instruments called accelerators and particle detectors. Includes a brief history on how scientists came to define what is fundamental in the universe. Big Bang Science focuses on CERN particle detectors and on United Kingdom scientists' contribution to the search for the fundamental building blocks of matter. In addition to information on the how and why of particle physics, this site also shows particle physics as an international collaborative endeavor:

<http://hepwww.rl.ac.uk/pub/bigbang/part1.html>

- **Stanford Linear Accelerator Center:** This Stanford Linear Accelerator Center Web site explains basic particle physics, linear and synchrotron accelerators, electron gamma showers, cosmic rays, and the experiments conducted at SLAC, including real-world applications. Intended for the general public as well as teachers and students:

<http://www2.slac.stanford.edu/vvc/>

- **THE WORLD OF BEAMS:** A site to visit if you wish to know a little or a lot about laser beams, particle beams, and other kinds of beams. Includes interactive tutorials, such as: What are Beams?, Working with Beams, and Beam Research and Technology. A good resource for physical science units involving energy, structure and properties of matter, and motion and forces for Grades 8-12. The information here is also helpful if you plan to tour any of the national laboratories listed in the "Libraries" section of this guide:

http://bc1.lbl.gov/CBP_pages/educational/WoB/home.htm

8.3. *Particle Physics Education: Particle Physics Lessons and Activities:*

- **CONTEMPORARY PHYSICS EDUCATION PROJECT (CPEP):** This site is especially designed to help teachers bring four areas of physics to their students in an accessible and engaging format. Provides charts, brochures, Web links, and classroom activities. Online interactive courses include: Fundamental Particles and Interactions (includes lesson plans), Plasma Physics and Fusion, and Nuclear Science (includes lesson plans and simple experiments):

<http://www.cpepweb.org/>

- **FERMILAB EDUCATION OFFICE:** Outstanding collection of resources from the "grandmother" of all physics lab educational programs. Thoughtful unit and lesson plans in both physics and the environment (Fermilab is located on a rare, protected prairie in Illinois). Sections are organized by grade level:

<http://www-ed.fnal.gov/>

- **GLAST CLASSROOM MATERIALS:** The Gamma Ray Large Area Space Telescope (GLAST) project and the National Aeronautics and Space Administration (NASA)'s Education and Public Outreach Office have developed this colorful, in depth, and engaging Web site teaching about the origin and structure of the universe and the fundamental relationship between energy and matter:

<http://glast.sonoma.edu/teachers/teachers.html>

- **JEFFERSON LAB SCIENCE EDUCATION:** This well-organized, visually attractive Web site from the Thomas Jefferson National Accelerator Facility, supports science and math education in K-12 classrooms. Features hands-on physics activities, math games, and puzzles. Check out the All About Atoms slide show and the interactive Table of Elements:

<http://education.jlab.org/>

- **THE PARTICLE ADVENTURE:** One of the most popular Web sites for learning the fundamentals of matter and force. Created by the Particle Data Group of Lawrence Berkeley National Laboratory. An award-winning, interactive tour of the atom, with visits to quarks, neutrinos, antimatter, extra dimensions, dark matter, accelerators and particle detectors. Simple elegant graphics and translations into eleven languages:

<http://ParticleAdventure.org>

- **QUARKNET:** QuarkNet brings the excitement of particle physics research to high school teachers and their students. Teachers join research groups at sixty universities and labs across the country. These research groups are part of particle physics experiments at CERN, Fermilab, or SLAC. Students learn fundamental physics as they participate in inquiry-oriented investigations and analyze live, online data. QuarkNet is supported in part by the National Science Foundation and the U.S. Department of Energy:

<http://QuarkNet.fnal.gov>

8.4. *Particle Physics Education: Astronomy Lessons and Experiments:*

- **HANDS-ON UNIVERSE:** Enables students in middle and high schools to investigate the night sky without having to stay out late. Created by a collaboration of teachers and students including the Lawrence Hall of Science at the U.C. Berkeley, it uses high quality astronomical images to explore central concepts in math, science, and technology. Students analyze real images with image-processing software similar to that used by professional astronomers:

<http://www.handsonuniverse.org>

- **IMAGINE THE UNIVERSE:** Created by the Laboratory for High-Energy Astrophysics at NASA/Goddard Space Flight Center, this site features astronomy and astrophysics lesson plans for age 14 and up, teachers' guides, classroom posters, and links to other classroom resources. Activities are linked to National Standards for Science and Math. Lessons include: What is Your Cosmic Connection to the Elements?, Life Cycle of Stars, and Gamma-Ray Bursts. Also included in the Teacher's Corner are links to math/science lesson plans for grades 6-12. The Multimedia Theatre Archive provides more than a dozen movies with free downloadable viewing software:

<http://imagine.gsfc.nasa.gov>

- **SPACE TODAY ONLINE:** This news magazine covers space from Earth to the edge of the universe. The site provides news, history, encyclopedia-like explanations of terms, activities, people and events, historical summaries, and an outstanding collection of images covering all aspects of space:

<http://www.spacetoday.org/STO.html>

- **WINDOWS TO THE UNIVERSE:** Provides a rich array of material for exploring earth, space, physics, geology, and chemistry in K-12 classrooms. Includes numerous, thorough lesson plans on topics ranging from the solar system to atmosphere and weather to physics and chemistry. Student-centered activities such as Building a Magnetometer or Create Your Own Cloud are simple, yet highly engaging:

<http://www.windows.ucar.edu/>

8.5. *Particle Physics Education: Ask-a-Scientist Sites:*

- **ASK A SCIENTIST SERVICE:** Questions are answered by volunteer scientists throughout the world. Service provided by the Newton BBS through Argonne National Lab. Submission form permits very age-specific information to be included with the question so that the answer can be targeted to the questioner's level of knowledge:

<http://www.newton.dep.anl.gov/>

- **ASK THE EXPERTS:** Submit questions via a form to scientists at PhysLink.com. Questions are answered free. Submission

form warns that they won't answer questions from homework assignments or help design something for a science fair or competition. Has links to commonly asked questions and to a list of the most active scientists who provide answers:

<http://www.physlink.com/Education/AskExperts/Index.cfm>

- **MAD SCIENTIST'S NETWORK: ASK A QUESTION:** Scientists at this Web site respond to hundreds of questions a week. Be sure to check out their extensive archive of answered questions and use their Science Fair Links for ideas for projects. Also note questions they decline to answer:

<http://www.madsci.org/submit.html>

8.6. *Particle Physics Education: Experiments, Demos, & Fun*

- **ALL ABOUT LIGHT:** From Fermilab, this offers a delightful collection of pages giving classical, relativistic, and quantum explanations of light:

<http://www.fnal.gov/pub/inquiring/more/light/index.html>

- **CANTEACH: PHYSICAL SCIENCE:** Canadian elementary teachers have put together a list of investigations and hands-on physics experiments for elementary level. These well-written physical science lesson plans feature such activities as Making a Pinhole Camera, Air Takes Space, Acid and Basic Test, Growing Crystals, Potential and Kinetic Energy, and Evaporation Painting:

<http://www.canteach.ca/elementary/physical.html>

- **HELPING YOUR CHILD LEARN SCIENCE:** A wonderful introduction and set of tools for parents of elementary-age children compiled by the U.S. Department of Education. Provides ideas, home experiments, community-based science activities, and more:

<http://www.ed.gov/pubs/parents/Science/index.html>

- **INSULTINGLY STUPID MOVIE PHYSICS:** An entertaining and educational site to learn how many movie special effects violate the laws of physics. Includes a rating system for movie reviews. Heavy on text, with few graphics. Equations are included. A good way to emphasize, at the high school level, the immutability of the laws of physics in the real world. Provides instructions on how to use movie physics in the classroom and a bibliography:

<http://www.intuitior.com/moviephysics>

- **PHYSICS/PHYS/SCI DEMOS:** This Web site provides over fifty physics demonstrations on the topics of density, motion, force, angular measurement, waves and sound, electricity and magnetism, optics and nuclear physics. Some of the demos feature photographs. Most of the demos are original, although a few were taken from the TV program, *Newton's Apple*. The high school teacher who created this site has won both a Presidential Award for Excellence in Mathematics and Science Teaching and the 2003 Classroom Connect Internet Educator of the Year Award:

<http://www.darylscience.com/DemoPhys.html>

8.7. *Particle Physics Education: Physics History and Diversity Sites:*

- **AIP CENTER FOR HISTORY OF PHYSICS:** This site, produced by the American Institute of Physics, aims to preserve and make known the history of modern physics and allied fields including astronomy, geophysics, and optics. Of interest to teachers and students is the Exhibit Hall, with award-winning exhibits including photos and facts about Marie Curie, Einstein, the discovery of the electron, and the invention of the transistor:

<http://www.aip.org/history>

- **A CENTURY OF PHYSICS:** This is the top-level page for a timeline from the American Physical Society providing a comprehensive history of major physical science developments with a selection of other events from society, art, politics and literature. Links on this page provide a physical timeline, an index, a search system, and reproductions of the posters and images:

<http://timeline.aps.org/APS/>

- **CONTRIBUTIONS OF 20TH CENTURY WOMEN TO PHYSICS:** A great resource for that history of science paper, this archive features descriptions of important contributions to science made by 83 women in the 20th century. Provides historical essays and links to additional documentation such as primary source materials:

<http://cwp.library.ucla.edu>

- **EDUCATION AND OUTREACH COMMITTEE ON THE STATUS OF WOMEN IN PHYSICS:** Interested in inspiring a young woman to pursue physics? This American Physical Society site features Physics in Your Future, which conveys the exciting possibilities of a career in physics to middle and high school girls. Copies of this four-color booklet are available at no charge to students and their parents, educators, guidance counselors, and groups who work with young women. Available online in PDF:

<http://www.aps.org/programs/women/index.cfm>

- **NOBEL LAUREATES IN PHYSICS 1901-PRESENT:** Maintained by SLAC, this site provides very comprehensive information on physics laureates. Links to the Nobel Foundation's pages on each laureate. Also lists the location(s) of the laureate's prize-winning work, where, if appropriate, the laureate is currently working, and where she or he was working when the work was done. Links to books, related Web sites, and to the HEP Database for in-depth bibliography. An interesting Quick Facts section provides great trivia about some of the prize winners:

<http://www.slac.stanford.edu/library/nobel/index.html>

- **PHYSLINK.COM HISTORY OF PHYSICS AND ASTRONOMY:** This site, which is a compendium of other history of physics, astronomy and science sites, organizes that historical world into: general guides, histories of physics, of astronomy and space exploration, and of mathematics, online archives, museums and exhibits, and famous scientists. Serves as a guide to some of the most well known people and events in the physical sciences:

<http://www.physlink.com/Education/History.cfm>

8.8. *Particle Physics Education: Art in Physics:*

Note: This modest collection of physics art links is provided for high school art, photography, and literature teachers who may be interested in the intersections between science and technology and art and literature, or who wish to take an interdisciplinary approach to the curriculum in collaborating with their science department colleagues.

- **HIDDEN CATHEDRALS—SCIENCE OR ART?:** This page provides roughly seventeen dramatic color images of the inner workings of particle detectors at the European Organisation for Nuclear Research (CERN) which is the world's largest particle physics center:

<http://public.web.cern.ch/public/about/how/art/art.html>

- **PHYSICS ICONS:** A video by Chip Dalby, SLAC InfoMedia Solutions, showing particle physics as delicate, experiential art. This meditation on the shifting nature of physics iconography was featured in the New York Museum of Modern Art's P.S.1 exhibit, *Signatures of the Invisible*:

<http://www-project.slac.stanford.edu/streaming-media/Sub-Movies.html>

9. Physics Job Sites:

- **AIP Education and Employment Statistics:** The latest data regarding education and employment trends in physics and related science fields:

<http://www.aip.org/statistics>

- **AIP Employment and Industry:** American Institute of Physics career network for physics, engineering and related physical sciences:

<http://www.aip.org/careersvc/>

- **APS Careers in Physics:** The American Physical Society Jobs/careers page:

<http://www.aps.org/jobs/>

- Careers with Physics: Advice and resources from the UK Institute of Physics:

http://www.iop.org/activity/careers/Careers/Resources/Career_resources/page_3964.html

- CERN Jobs Portal: Human resources portal for CERN:

<http://humanresources.web.cern.ch/humanresources/external/general/HN-recruitment/default.asp>

- HEPJobs Database: Maintained by Fermilab and SLAC libraries, this database lists jobs in the fields of core interest to the particle physics and astroparticle physics communities. Use this page to post a job or to receive e-mail notices of new job listings:

<http://www.slac.stanford.edu/spires/jobs/>

- Physicsweb.org: Listing of physics openings for all degree levels:

<http://physicsweb.org/jobs/>

- SPIEWorks: Maintained by the International Society for Optical Engineering. Includes job listings for related science and engineering posts, with a search function, as well as a list of conferences and some tips:

<http://www.spieworks.com/employment/>

10. Software Repositories:

- CERNLIB: CERN PROGRAM LIBRARY: A large collection of general purpose libraries and modules offered in both source code and object code forms from the CERN central computing division. Provides programs applicable to a wide range of physics research problems such as general mathematics, data analysis, detectors simulation, data-handling, *etc.* Also includes links to commercial, free, and other software:

<http://wwwasd.web.cern.ch/wwwasd/index.html>

- FREEHEP: A collection of software and information about software useful in high-energy physics. Searching can be done by title, subject, date acquired, date updated, or by browsing an alphabetical list of all packages:

<http://www.freehep.org/>

- FERMITOOLS: Fermilab's software tools program provides a repository of Fermilab-developed software packages of value to the HEP community. Permits searching for packages by title or subject category:

<http://www.fnal.gov/fermitools/>

- HEPIC: SOFTWARE & TOOLS USED IN HEP RESEARCH: A meta-level site with links to other sites of HEP-related software and computing tools:

<http://www.hep.net/resources/software.html>

- GRID PHYSICS NETWORK: The GriPhyN Project is developing grid technologies for scientific and engineering projects that collect and analyze distributed, petabyte-scale datasets. Provides links to project information such as documents, education, workspace, virtual data toolkits, Chimera and Sphinx, as well as people, activities, news, and related projects:

<http://www.griphyn.org/>

- PARTICLE PHYSICS DATA GRID: The Web site for the U.S. collaboration of federal laboratories and universities to build a worldwide distributed computing model for current and future particle and nuclear physics experiments:

<http://www.ppdg.net/>

11. Specialized Subject Pages:

11.1. *Subject Pages*

- CAMBRIDGE RELATIVITY: PUBLIC HOME PAGE: These pages focus on the non-technical learner and explain aspects of relativity such as: cosmology, black holes, cosmic strings, inflation, and quantum gravity. Provides links to movies, research-level home pages and to Stephen Hawking's Web site:

<http://www.damtp.cam.ac.uk/user/gr/public/>

- THE OFFICIAL STRING THEORY WEB SITE: Outstanding compilation of information about string theory includes: basics, mathematics, experiments, cosmology, black holes, people (including interviews with string theorists), history, theater, links to other Web sites and a discussion forum:

<http://superstringtheory.com/>

- SUPERSTRINGS: An online introduction to superstring theory for the advanced student. Includes further links:

<http://www.sukidog.com/jpierre/strings/>

- THE ULTIMATE NEUTRINO PAGE: This page provides a gateway to an extremely useful compilation of experimental data and results:

<http://cupp.oulu.fi/neutrino/>

SUMMARY TABLES OF PARTICLE PHYSICS

Gauge and Higgs Bosons	31
Leptons	34
Quarks	37
Mesons	38
Baryons	77
Miscellaneous searches*	91
Tests of conservation laws	93
Meson Quick Reference Table	75
Baryon Quick Reference Table	76

* There are also search limits in the Summary Tables for the Gauge and Higgs Bosons, the Leptons, the Quarks, and the Mesons.



Gauge & Higgs Boson Summary Table

SUMMARY TABLES OF PARTICLE PROPERTIES

Extracted from the Particle Listings of the
Review of Particle Physics
 C. Amsler *et al.*, PL **B667**, 1 (2008)
 Available at <http://pdg.lbl.gov>

Particle Data Group

C. Amsler, M. Doser, M. Antonelli, D.M. Asner, K.S. Babu, H. Baer, H.R. Band, R.M. Barnett, E. Bergren, J. Beringer, G. Bernardi, W. Bertl, H. Bichsel, O. Biebel, P. Bloch, E. Blucher, S. Blusk, R.N. Cahn, M. Carena, C. Caso, A. Ceccucci, D. Chakraborty, M.-C. Chen, R.S. Chivukula, G. Cowan, O. Dahl, G. D'Ambrosio, T. Damour, A. de Gouvêa, T. DeGrand, B. Dobrescu, M. Drees, D.A. Edwards, S. Eidelman, V.D. Elvira, J. Erler, V.V. Ezhela, J.L. Feng, W. Fetscher, B.D. Fields, B. Foster, T.K. Gaisser, L. Garren, H.-J. Gerber, G. Gerbier, T. Gherghetta, G.F. Giudice, M. Goodman, C. Grab, A.V. Gritsan, J.-F. Grivaz, D.E. Groom, M. Grünewald, A. Gurtu, T. Gutsche, H.E. Haber, K. Hagiwara, C. Hagmann, K.G. Hayes, J.J. Hernández-Rey, K. Hikasa, I. Hinchliffe, A. Höcker, J. Huston, P. Igo-Kemenes, J.D. Jackson, K.F. Johnson, T. Junk, D. Karlen, B. Kayser, D. Kirkby, S.R. Klein, I.G. Knowles, C. Kolda, R.V. Kowalewski, P. Kreitz, B. Krusche, Yu.V. Kuyanov, Y. Kwon, O. Lahav, P. Langacker, A. Liddle, Z. Ligeti, C.-J. Lin, T.M. Liss, L. Littenberg, J.C. Liu, K.S. Lugovsky, S.B. Lugovsky, H. Mahlke, M.L. Mangano, T. Mannel, A.V. Manohar, W.J. Marciano, A.D. Martin, A. Masoni, D. Milstead, R. Miquel, K. Mönig, H. Murayama, K. Nakamura, M. Narain, P. Nason, S. Navas, P. Nevski, Y. Nir, K.A. Olive, L. Pape, C. Patrignani, J.A. Peacock, A. Piepke, G. Punzi, A. Quadt, S. Raby, G. Raffelt, B.N. Ratcliff, B. Renk, P. Richardson, S. Roesler, S. Rolli, A. Romaniouk, L.J. Rosenberg, J.L. Rosner, C.T. Sachrajda, Y. Sakai, S. Sarkar, F. Sauli, O. Schneider, D. Scott, W.G. Seligman, M.H. Shaevitz, T. Sjöstrand, J.G. Smith, G.F. Smoot, S. Spanier, H. Spieler, A. Stahl, T. Stanev, S.L. Stone, T. Sumiyoshi, M. Tanabashi, J. Terning, M. Titov, N.P. Tkachenko, N.A. Törnqvist, D. Tovey, G.H. Trilling, T.G. Trippe, G. Valencia, K. van Bibber, M.G. Vinciter, P. Vogel, D.R. Ward, T. Watari, B.R. Webber, G. Weiglein, J.D. Wells, M. Whalley, A. Wheeler, C.G. Wohl, L. Wolfenstein, J. Womersley, C.L. Woody, R.L. Workman, A. Yamamoto, W.-M. Yao, O.V. Zenin, J. Zhang, R.-Y. Zhu, P.A. Zyla

Technical Associates:

G. Harper, V.S. Lugovsky, P. Schaffner

©Regents of the University of California
 (Approximate closing date for data: January 15, 2008)

GAUGE AND HIGGS BOSONS

γ

$$I(J^{PC}) = 0,1(1^{--})$$

Mass $m < 1 \times 10^{-18}$ eV
 Charge $q < 5 \times 10^{-30}$ e
 Mean life $\tau = \text{Stable}$

**g
or gluon**

$$I(J^P) = 0(1^-)$$

Mass $m = 0$ [a]
 SU(3) color octet

W

$$J = 1$$

Charge = ± 1 e
 Mass $m = 80.398 \pm 0.025$ GeV
 $m_Z - m_W = 10.4 \pm 1.6$ GeV
 $m_{W^+} - m_{W^-} = -0.2 \pm 0.6$ GeV
 Full width $\Gamma = 2.141 \pm 0.041$ GeV
 $\langle N_{\pi^\pm} \rangle = 15.70 \pm 0.35$
 $\langle N_{K^\pm} \rangle = 2.20 \pm 0.19$
 $\langle N_p \rangle = 0.92 \pm 0.14$
 $\langle N_{\text{charged}} \rangle = 19.39 \pm 0.08$

W^- modes are charge conjugates of the modes below.

W⁺ DECAY MODES	Fraction (Γ_i/Γ)	Confidence level	ρ (MeV/c)
$\ell^+ \nu$	[b] (10.80 ± 0.09) %		–
$e^+ \nu$	(10.75 ± 0.13) %		40199
$\mu^+ \nu$	(10.57 ± 0.15) %		40199
$\tau^+ \nu$	(11.25 ± 0.20) %		40179
hadrons	(67.60 ± 0.27) %		–
$\pi^+ \gamma$	< 8	$\times 10^{-5}$	95% 40199
$D_s^+ \gamma$	< 1.3	$\times 10^{-3}$	95% 40175
cX	(33.4 ± 2.6) %		–
$c\bar{s}$	(31 $\begin{smallmatrix} +13 \\ -11 \end{smallmatrix}$) %		–
invisible	[c] (1.4 ± 2.8) %		–

Z

$$J = 1$$

Charge = 0
 Mass $m = 91.1876 \pm 0.0021$ GeV [d]
 Full width $\Gamma = 2.4952 \pm 0.0023$ GeV
 $\Gamma(\ell^+ \ell^-) = 83.984 \pm 0.086$ MeV [b]
 $\Gamma(\text{invisible}) = 499.0 \pm 1.5$ MeV [e]
 $\Gamma(\text{hadrons}) = 1744.4 \pm 2.0$ MeV
 $\Gamma(\mu^+ \mu^-)/\Gamma(e^+ e^-) = 1.0009 \pm 0.0028$
 $\Gamma(\tau^+ \tau^-)/\Gamma(e^+ e^-) = 1.0019 \pm 0.0032$ [f]

Average charged multiplicity

$$\langle N_{\text{charged}} \rangle = 20.76 \pm 0.16 \quad (S = 2.1)$$

Couplings to leptons

$$g_V^\ell = -0.03783 \pm 0.00041$$

$$g_A^\ell = -0.50123 \pm 0.00026$$

$$g_V^{\nu\ell} = 0.5008 \pm 0.0008$$

$$g_V^{\nu e} = 0.53 \pm 0.09$$

$$g_V^{\nu\mu} = 0.502 \pm 0.017$$

Asymmetry parameters [g]

$$A_e = 0.1515 \pm 0.0019$$

$$A_\mu = 0.142 \pm 0.015$$

$$A_\tau = 0.143 \pm 0.004$$

$$A_s = 0.90 \pm 0.09$$

$$A_c = 0.670 \pm 0.027$$

$$A_b = 0.923 \pm 0.020$$

Charge asymmetry (%) at Z pole

$$A_{FB}^{(0\ell)} = 1.71 \pm 0.10$$

$$A_{FB}^{(0u)} = 4 \pm 7$$

$$A_{FB}^{(0s)} = 9.8 \pm 1.1$$

$$A_{FB}^{(0c)} = 7.07 \pm 0.35$$

$$A_{FB}^{(0b)} = 9.92 \pm 0.16$$

Gauge & Higgs Boson Summary Table

Z DECAY MODES	Fraction (Γ_i/Γ)	Scale factor/ Confidence level	p (MeV/c)
e^+e^-	(3.363 \pm 0.004) %		45594
$\mu^+\mu^-$	(3.366 \pm 0.007) %		45594
$\tau^+\tau^-$	(3.370 \pm 0.008) %		45559
$\ell^+\ell^-$	[b] (3.3658 \pm 0.0023) %		—
invisible	(20.00 \pm 0.06) %		—
hadrons	(69.91 \pm 0.06) %		—
$(u\bar{u}+c\bar{c})/2$	(11.6 \pm 0.6) %		—
$(d\bar{d}+s\bar{s}+b\bar{b})/3$	(15.6 \pm 0.4) %		—
$c\bar{c}$	(12.03 \pm 0.21) %		—
$b\bar{b}$	(15.12 \pm 0.05) %		—
$b\bar{b}b\bar{b}$	(3.6 \pm 1.3) $\times 10^{-4}$		—
$g\bar{g}g$	< 1.1	% CL=95%	—
$\pi^0\gamma$	< 5.2	$\times 10^{-5}$ CL=95%	45594
$\eta\gamma$	< 5.1	$\times 10^{-5}$ CL=95%	45592
$\omega\gamma$	< 6.5	$\times 10^{-4}$ CL=95%	45590
$\eta'(958)\gamma$	< 4.2	$\times 10^{-5}$ CL=95%	45589
$\gamma\gamma$	< 5.2	$\times 10^{-5}$ CL=95%	45594
$\gamma\gamma\gamma$	< 1.0	$\times 10^{-5}$ CL=95%	45594
$\pi^\pm W^\mp$	[h] < 7	$\times 10^{-5}$ CL=95%	10150
$\rho^\pm W^\mp$	[h] < 8.3	$\times 10^{-5}$ CL=95%	10125
$J/\psi(1S)X$	(3.51 \pm 0.23 \pm 0.25) $\times 10^{-3}$	S=1.1	—
$\psi(2S)X$	(1.60 \pm 0.29) $\times 10^{-3}$		—
$\chi_{c1}(1P)X$	(2.9 \pm 0.7) $\times 10^{-3}$		—
$\chi_{c2}(1P)X$	< 3.2	$\times 10^{-3}$ CL=90%	—
$T(1S)X + T(2S)X$ $+ T(3S)X$	(1.0 \pm 0.5) $\times 10^{-4}$		—
$T(1S)X$	< 4.4	$\times 10^{-5}$ CL=95%	—
$T(2S)X$	< 1.39	$\times 10^{-4}$ CL=95%	—
$T(3S)X$	< 9.4	$\times 10^{-5}$ CL=95%	—
$(D^0/\bar{D}^0)X$	(20.7 \pm 2.0) %		—
$D^\pm X$	(12.2 \pm 1.7) %		—
$D^*(2010)^\pm X$	[h] (11.4 \pm 1.3) %		—
$D_{s1}(2536)^\pm X$	(3.6 \pm 0.8) $\times 10^{-3}$		—
$D_{sJ}(2573)^\pm X$	(5.8 \pm 2.2) $\times 10^{-3}$		—
$D^*(2629)^\pm X$	searched for		—
B^+X	(6.10 \pm 0.14) %		—
B_s^0X	(1.56 \pm 0.13) %		—
B_c^+X	searched for		—
A_c^+X	(1.54 \pm 0.33) %		—
Ξ_c^0X	seen		—
Ξ_c^-X	seen		—
b -baryon X	(1.38 \pm 0.22) %		—
anomalous γ + hadrons	[j] < 3.2	$\times 10^{-3}$ CL=95%	—
$e^+e^-\gamma$	[i] < 5.2	$\times 10^{-4}$ CL=95%	45594
$\mu^+\mu^-\gamma$	[i] < 5.6	$\times 10^{-4}$ CL=95%	45594
$\tau^+\tau^-\gamma$	[i] < 7.3	$\times 10^{-4}$ CL=95%	45559
$\ell^+\ell^-\gamma\gamma$	[j] < 6.8	$\times 10^{-6}$ CL=95%	—
$q\bar{q}\gamma\gamma$	[j] < 5.5	$\times 10^{-6}$ CL=95%	—
$\nu\bar{\nu}\gamma\gamma$	[j] < 3.1	$\times 10^{-6}$ CL=95%	45594
$e^\pm\mu^\mp$	LF [h] < 1.7	$\times 10^{-6}$ CL=95%	45594
$e^\pm\tau^\mp$	LF [h] < 9.8	$\times 10^{-6}$ CL=95%	45576
$\mu^\pm\tau^\mp$	LF [h] < 1.2	$\times 10^{-5}$ CL=95%	45576
pe	L,B < 1.8	$\times 10^{-6}$ CL=95%	45589
$p\mu$	L,B < 1.8	$\times 10^{-6}$ CL=95%	45589

Higgs Bosons — H^0 and H^\pm , Searches for

The limits for H_1^0 and A_0 refer to the m_h^{\max} benchmark scenario for the supersymmetric parameters.

H^0 Mass $m > 114.4$ GeV, CL = 95%

H_1^0 in Supersymmetric Models ($m_{H_1^0} < m_{H_2^0}$)

Mass $m > 92.8$ GeV, CL = 95%

 A^0 Pseudoscalar Higgs Boson in Supersymmetric Models [k]

Mass $m > 93.4$ GeV, CL = 95% $\tan\beta > 0.4$

H^\pm Mass $m > 79.3$ GeV, CL = 95%

See the Particle Listings for a Note giving details of Higgs Bosons.

Heavy Bosons Other Than Higgs Bosons, Searches for

Additional W Bosons

W' with standard couplings decaying to $e\nu$

Mass $m > 1.000 \times 10^3$ GeV, CL = 95%

W_R — right-handed W

Mass $m > 715$ GeV, CL = 90% (electroweak fit)

Additional Z Bosons

Z'_{SM} with standard couplings

Mass $m > 923$ GeV, CL = 95% ($p\bar{p}$ direct search)

Mass $m > 1500$ GeV, CL = 95% (electroweak fit)

Z_{LR} of $SU(2)_L \times SU(2)_R \times U(1)$ (with $g_L = g_R$)

Mass $m > 630$ GeV, CL = 95% ($p\bar{p}$ direct search)

Mass $m > 860$ GeV, CL = 95% (electroweak fit)

Z_χ of $SO(10) \rightarrow SU(5) \times U(1)_\chi$ (with $g_\chi = e/\cos\theta_W$)

Mass $m > 822$ GeV, CL = 95% ($p\bar{p}$ direct search)

Mass $m > 781$ GeV, CL = 95% (electroweak fit)

Z_ψ of $E_6 \rightarrow SO(10) \times U(1)_\psi$ (with $g_\psi = e/\cos\theta_W$)

Mass $m > 822$ GeV, CL = 95% ($p\bar{p}$ direct search)

Mass $m > 475$ GeV, CL = 95% (electroweak fit)

Z_η of $E_6 \rightarrow SU(3) \times SU(2) \times U(1) \times U(1)_\eta$ (with $g_\eta = e/\cos\theta_W$)

Mass $m > 891$ GeV, CL = 95% ($p\bar{p}$ direct search)

Mass $m > 619$ GeV, CL = 95% (electroweak fit)

Scalar Leptoquarks

Mass $m > 256$ GeV, CL = 95% (1st generation, pair prod.)

Mass $m > 298$ GeV, CL = 95% (1st gener., single prod.)

Mass $m > 251$ GeV, CL = 95% (2nd gener., pair prod.)

Mass $m > 73$ GeV, CL = 95% (2nd gener., single prod.)

Mass $m > 229$ GeV, CL = 95% (3rd gener., pair prod.)

(See the Particle Listings for assumptions on leptoquark quantum numbers and branching fractions.)

Axions (A^0) and Other Very Light Bosons, Searches for

The standard Peccei-Quinn axion is ruled out. Variants with reduced couplings or much smaller masses are constrained by various data.

The Particle Listings in the full Review contain a Note discussing axion searches.

The best limit for the half-life of neutrinoless double beta decay with Majoron emission is $> 7.2 \times 10^{24}$ years (CL = 90%).

Gauge & Higgs Boson Summary Table

NOTES

In this Summary Table:

When a quantity has "(S = ...)" to its right, the error on the quantity has been enlarged by the "scale factor" S , defined as $S = \sqrt{\chi^2/(N-1)}$, where N is the number of measurements used in calculating the quantity. We do this when $S > 1$, which often indicates that the measurements are inconsistent. When $S > 1.25$, we also show in the Particle Listings an ideogram of the measurements. For more about S , see the Introduction.

A decay momentum p is given for each decay mode. For a 2-body decay, p is the momentum of each decay product in the rest frame of the decaying particle. For a 3-or-more-body decay, p is the largest momentum any of the products can have in this frame.

[a] Theoretical value. A mass as large as a few MeV may not be precluded.

[b] ℓ indicates each type of lepton (e , μ , and τ), not sum over them.

[c] This represents the width for the decay of the W boson into a charged particle with momentum below detectability, $p < 200$ MeV.

[d] The Z -boson mass listed here corresponds to a Breit-Wigner resonance parameter. It lies approximately 34 MeV above the real part of the position of the pole (in the energy-squared plane) in the Z -boson propagator.

[e] This partial width takes into account Z decays into $\nu\bar{\nu}$ and any other possible undetected modes.

[f] This ratio has not been corrected for the τ mass.

[g] Here $A \equiv 2g_V g_A / (g_V^2 + g_A^2)$.

[h] The value is for the sum of the charge states or particle/antiparticle states indicated.

[i] See the Z Particle Listings for the γ energy range used in this measurement.

[j] For $m_{\gamma\gamma} = (60 \pm 5)$ GeV.

[k] The limits assume no invisible decays.

Lepton Summary Table

LEPTONS

e

$$J = \frac{1}{2}$$

Mass $m = (548.57990943 \pm 0.00000023) \times 10^{-6}$ u
 Mass $m = 0.510998910 \pm 0.00000013$ MeV
 $|m_{e^+} - m_{e^-}|/m < 8 \times 10^{-9}$, CL = 90%
 $|q_{e^+} + q_{e^-}|/e < 4 \times 10^{-8}$
 Magnetic moment anomaly
 $(g-2)/2 = (1159.6521811 \pm 0.0000007) \times 10^{-6}$
 $(g_{e^+} - g_{e^-}) / g_{\text{average}} = (-0.5 \pm 2.1) \times 10^{-12}$
 Electric dipole moment $d = (0.07 \pm 0.07) \times 10^{-26}$ ecm
 Mean life $\tau > 4.6 \times 10^{26}$ yr, CL = 90% [a]

 μ

$$J = \frac{1}{2}$$

Mass $m = 0.1134289256 \pm 0.0000000029$ u
 Mass $m = 105.658367 \pm 0.000004$ MeV
 Mean life $\tau = (2.197019 \pm 0.000021) \times 10^{-6}$ s (S = 1.1)
 $\tau_{\mu^+}/\tau_{\mu^-} = 1.00002 \pm 0.00008$
 $c\tau = 658.650$ m
 Magnetic moment anomaly $(g-2)/2 = (11659208 \pm 6) \times 10^{-10}$
 $(g_{\mu^+} - g_{\mu^-}) / g_{\text{average}} = (-0.11 \pm 0.12) \times 10^{-8}$
 Electric dipole moment $d = (3.7 \pm 3.4) \times 10^{-19}$ ecm

Decay parameters [b]

$\rho = 0.7509 \pm 0.0010$
 $\eta = 0.001 \pm 0.024$ (S = 2.0)
 $\delta = 0.7495 \pm 0.0012$
 $\xi P_{\mu} = 1.0007 \pm 0.0035$ [c]
 $\xi P_{\mu} \delta / \rho > 0.99682$, CL = 90% [c]
 $\xi' = 1.00 \pm 0.04$
 $\xi'' = 0.7 \pm 0.4$
 $\alpha/A = (0 \pm 4) \times 10^{-3}$
 $\alpha'/A = (0 \pm 4) \times 10^{-3}$
 $\beta/A = (4 \pm 6) \times 10^{-3}$
 $\beta'/A = (1 \pm 5) \times 10^{-3}$
 $\overline{\eta} = 0.02 \pm 0.08$

μ^+ modes are charge conjugates of the modes below.

μ^- DECAY MODES	Fraction (Γ_i/Γ)	Confidence level	P (MeV/c)
$e^- \overline{\nu}_e \nu_{\mu}$	$\approx 100\%$		53
$e^- \overline{\nu}_e \nu_{\mu} \gamma$	[d] $(1.4 \pm 0.4) \%$		53
$e^- \overline{\nu}_e \nu_{\mu} e^+ e^-$	[e] $(3.4 \pm 0.4) \times 10^{-5}$		53
Lepton Family number (LF) violating modes			
$e^- \nu_e \overline{\nu}_{\mu}$	LF [f] < 1.2 %	90%	53
$e^- \gamma$	LF < 1.2 $\times 10^{-11}$	90%	53
$e^- e^+ e^-$	LF < 1.0 $\times 10^{-12}$	90%	53
$e^- 2\gamma$	LF < 7.2 $\times 10^{-11}$	90%	53

 τ

$$J = \frac{1}{2}$$

Mass $m = 1776.84 \pm 0.17$ MeV
 $(m_{\tau^+} - m_{\tau^-})/m_{\text{average}} < 2.8 \times 10^{-4}$, CL = 90%
 Mean life $\tau = (290.6 \pm 1.0) \times 10^{-15}$ s
 $c\tau = 87.11$ μm
 Magnetic moment anomaly > -0.052 and < 0.013 , CL = 95%
 $\text{Re}(d_{\tau}) = -0.22$ to 0.45×10^{-16} ecm, CL = 95%
 $\text{Im}(d_{\tau}) = -0.25$ to 0.008×10^{-16} ecm, CL = 95%

Weak dipole moment

$\text{Re}(d_{\tau}^W) < 0.50 \times 10^{-17}$ ecm, CL = 95%
 $\text{Im}(d_{\tau}^W) < 1.1 \times 10^{-17}$ ecm, CL = 95%

Weak anomalous magnetic dipole moment

$\text{Re}(\alpha_{\tau}^W) < 1.1 \times 10^{-3}$, CL = 95%
 $\text{Im}(\alpha_{\tau}^W) < 2.7 \times 10^{-3}$, CL = 95%

Decay parameters

See the τ Particle Listings for a note concerning τ -decay parameters.

$\rho(e \text{ or } \mu) = 0.745 \pm 0.008$
 $\rho(e) = 0.747 \pm 0.010$
 $\rho(\mu) = 0.763 \pm 0.020$
 $\xi(e \text{ or } \mu) = 0.985 \pm 0.030$
 $\xi(e) = 0.994 \pm 0.040$
 $\xi(\mu) = 1.030 \pm 0.059$
 $\eta(e \text{ or } \mu) = 0.013 \pm 0.020$
 $\eta(\mu) = 0.094 \pm 0.073$
 $(\delta\xi)(e \text{ or } \mu) = 0.746 \pm 0.021$
 $(\delta\xi)(e) = 0.734 \pm 0.028$
 $(\delta\xi)(\mu) = 0.778 \pm 0.037$
 $\xi(\pi) = 0.993 \pm 0.022$
 $\xi(\rho) = 0.994 \pm 0.008$
 $\xi(a_1) = 1.001 \pm 0.027$
 $\xi(\text{all hadronic modes}) = 0.995 \pm 0.007$

τ^+ modes are charge conjugates of the modes below. " h^{\pm} " stands for π^{\pm} or K^{\pm} . " e " stands for e or μ . "Neutrals" stands for γ 's and/or π^0 's.

τ^- DECAY MODES	Fraction (Γ_i/Γ)	Scale factor/ Confidence level	P (MeV/c)
Modes with one charged particle			
particle $^- \geq 0$ neutrals $\geq 0K^0 \nu_{\tau}$ ("1-prong")	$(85.36 \pm 0.08) \%$	S=1.3	-
particle $^- \geq 0$ neutrals $\geq 0K_L^0 \nu_{\tau}$	$(84.73 \pm 0.08) \%$	S=1.4	-
$\mu^- \overline{\nu}_{\mu} \nu_{\tau}$	[g] $(17.36 \pm 0.05) \%$		885
$\mu^- \overline{\nu}_{\mu} \nu_{\tau} \gamma$	[e] $(3.6 \pm 0.4) \times 10^{-3}$		885
$e^- \overline{\nu}_e \nu_{\tau}$	[g] $(17.85 \pm 0.05) \%$		888
$e^- \overline{\nu}_e \nu_{\tau} \gamma$	[e] $(1.75 \pm 0.18) \%$		888
$h^- \geq 0K^0 \nu_{\tau}$	$(12.13 \pm 0.07) \%$	S=1.1	883
$h^- \nu_{\tau}$	$(11.60 \pm 0.06) \%$	S=1.1	883
$\pi^- \nu_{\tau}$	[g] $(10.91 \pm 0.07) \%$	S=1.1	883
$K^- \nu_{\tau}$	[g] $(6.95 \pm 0.23) \times 10^{-3}$	S=1.1	820
$h^- \geq 1$ neutrals ν_{τ}	$(37.08 \pm 0.11) \%$	S=1.2	-
$h^- \geq 1\pi^0 \nu_{\tau} (\text{ex. } K^0)$	$(36.54 \pm 0.11) \%$	S=1.2	-
$h^- \pi^0 \nu_{\tau}$	$(25.95 \pm 0.10) \%$	S=1.1	878
$\pi^- \pi^0 \nu_{\tau}$	[g] $(25.52 \pm 0.10) \%$	S=1.1	878
$\pi^- \pi^0$ non- $\rho(770) \nu_{\tau}$	$(3.0 \pm 3.2) \times 10^{-3}$		878
$K^- \pi^0 \nu_{\tau}$	[g] $(4.28 \pm 0.15) \times 10^{-3}$		814
$h^- \geq 2\pi^0 \nu_{\tau}$	$(10.84 \pm 0.12) \%$	S=1.3	-
$h^- 2\pi^0 \nu_{\tau}$	$(9.49 \pm 0.11) \%$	S=1.2	862
$h^- 2\pi^0 \nu_{\tau} (\text{ex. } K^0)$	$(9.33 \pm 0.12) \%$	S=1.2	862
$\pi^- 2\pi^0 \nu_{\tau} (\text{ex. } K^0)$	[g] $(9.27 \pm 0.12) \%$	S=1.2	862
$\pi^- 2\pi^0 \nu_{\tau} (\text{ex. } K^0),$	$< 9 \times 10^{-3}$	CL=95%	862
scalar $\pi^- 2\pi^0 \nu_{\tau} (\text{ex. } K^0),$	$< 7 \times 10^{-3}$	CL=95%	862
vector $K^- 2\pi^0 \nu_{\tau} (\text{ex. } K^0)$	[g] $(6.3 \pm 2.3) \times 10^{-4}$		796
$h^- \geq 3\pi^0 \nu_{\tau}$	$(1.35 \pm 0.07) \%$	S=1.1	-
$h^- \geq 3\pi^0 \nu_{\tau} (\text{ex. } K^0)$	$(1.26 \pm 0.07) \%$	S=1.1	-
$h^- 3\pi^0 \nu_{\tau}$	$(1.18 \pm 0.08) \%$		836
$\pi^- 3\pi^0 \nu_{\tau} (\text{ex. } K^0)$	[g] $(1.04 \pm 0.07) \%$		836
$K^- 3\pi^0 \nu_{\tau} (\text{ex. } K^0),$	[g] $(4.7 \pm 2.1) \times 10^{-4}$		765
η $h^- 4\pi^0 \nu_{\tau} (\text{ex. } K^0)$	$(1.6 \pm 0.4) \times 10^{-3}$		800
$h^- 4\pi^0 \nu_{\tau} (\text{ex. } K^0, \eta)$	[g] $(1.0 \pm 0.4) \times 10^{-3}$		800
$K^- \geq 0\pi^0 \geq 0K^0 \geq 0\gamma \nu_{\tau}$	$(1.57 \pm 0.04) \%$	S=1.1	820
$K^- \geq 1(\pi^0 \text{ or } K^0 \text{ or } \gamma) \nu_{\tau}$	$(8.74 \pm 0.32) \times 10^{-3}$		-
Modes with K^0 's			
$K_S^0 (\text{partides})^- \nu_{\tau}$	$(9.2 \pm 0.4) \times 10^{-3}$	S=1.4	-
$h^- \overline{K}^0 \nu_{\tau}$	$(10.0 \pm 0.5) \times 10^{-3}$	S=1.8	812
$\pi^- \overline{K}^0 \nu_{\tau}$	[g] $(8.4 \pm 0.4) \times 10^{-3}$	S=2.0	812
$\pi^- \overline{K}^0$	$(5.4 \pm 2.1) \times 10^{-4}$		812
(non- $K^*(892)^-$) ν_{τ}			
$K^- K^0 \nu_{\tau}$	[g] $(1.58 \pm 0.16) \times 10^{-3}$		737
$K^- K^0 \geq 0\pi^0 \nu_{\tau}$	$(3.16 \pm 0.23) \times 10^{-3}$		737
$h^- \overline{K}^0 \pi^0 \nu_{\tau}$	$(5.5 \pm 0.4) \times 10^{-3}$		794
$\pi^- \overline{K}^0 \pi^0 \nu_{\tau}$	[g] $(3.9 \pm 0.4) \times 10^{-3}$		794
$\overline{K}^0 \rho^- \nu_{\tau}$	$(2.2 \pm 0.5) \times 10^{-3}$		612
$K^- K^0 \pi^0 \nu_{\tau}$	[g] $(1.58 \pm 0.20) \times 10^{-3}$		685

Lepton Summary Table

$\pi^- \bar{K}^0 \geq 1\pi^0 \nu_\tau$	$(3.2 \pm 1.0) \times 10^{-3}$				$X^- (S=-1) \nu_\tau$	$(2.85 \pm 0.07) \%$	S=1.3	-	
$\pi^- \bar{K}^0 \pi^0 \pi^0 \nu_\tau$	$(2.6 \pm 2.4) \times 10^{-4}$		763		$K^*(892)^- \geq 0 \text{ neutrals} \geq 0 K_S^0 \nu_\tau$	$(1.42 \pm 0.18) \%$	S=1.4	665	
$K^- K^0 \pi^0 \pi^0 \nu_\tau$	$< 1.6 \times 10^{-4}$	CL=95%	619		$K^*(892)^- \nu_\tau$	$(1.20 \pm 0.07) \%$	S=1.8	665	
$\pi^- K^0 \bar{K}^0 \nu_\tau$	$(1.7 \pm 0.4) \times 10^{-3}$	S=1.6	682		$K^*(892)^- \nu_\tau \rightarrow \pi^- \bar{K}^0 \nu_\tau$	$(7.8 \pm 0.5) \times 10^{-3}$		-	
$\pi^- K_S^0 K_S^0 \nu_\tau$	[g] $(2.4 \pm 0.5) \times 10^{-4}$		682		$K^*(892)^0 K^- \geq 0 \text{ neutrals} \nu_\tau$	$(3.2 \pm 1.4) \times 10^{-3}$		542	
$\pi^- K_S^0 K_S^0 \nu_\tau$	[g] $(1.2 \pm 0.4) \times 10^{-3}$	S=1.7	682		$K^*(892)^0 K^- \nu_\tau$	$(2.1 \pm 0.4) \times 10^{-3}$		542	
$\pi^- K^0 \bar{K}^0 \pi^0 \nu_\tau$	$(3.1 \pm 2.3) \times 10^{-4}$		614		$\bar{K}^*(892)^0 \pi^- \geq 0 \text{ neutrals} \nu_\tau$	$(3.8 \pm 1.7) \times 10^{-3}$		655	
$\pi^- K_S^0 K_S^0 \pi^0 \nu_\tau$	$< 2.0 \times 10^{-4}$	CL=95%	614		$\bar{K}^*(892)^0 \pi^- \nu_\tau$	$(2.2 \pm 0.5) \times 10^{-3}$		655	
$\pi^- K_S^0 K_S^0 \pi^0 \nu_\tau$	$(3.1 \pm 1.2) \times 10^{-4}$		614		$(\bar{K}^*(892) \pi^-) \nu_\tau \rightarrow \pi^- \bar{K}^0 \pi^0 \nu_\tau$	$(1.0 \pm 0.4) \times 10^{-3}$		-	
$K^0 h^+ h^- h^- \geq 0 \text{ neutrals} \nu_\tau$	$< 1.7 \times 10^{-3}$	CL=95%	760		$K_1(1270)^- \nu_\tau$	$(4.7 \pm 1.1) \times 10^{-3}$		433	
$K^0 h^+ h^- h^- \nu_\tau$	$(2.3 \pm 2.0) \times 10^{-4}$		760		$K_1(1400)^- \nu_\tau$	$(1.7 \pm 2.6) \times 10^{-3}$	S=1.7	335	
Modes with three charged particles									
$h^- h^- h^+ \geq 0 \text{ neutrals} \geq 0 K_S^0 \nu_\tau$	$(15.18 \pm 0.08) \%$	S=1.4	861		$K^*(1410)^- \nu_\tau$	$(1.5 \pm 1.0) \times 10^{-3}$		326	
$h^- h^- h^+ \geq 0 \text{ neutrals} \nu_\tau$ (ex. $K_S^0 \rightarrow \pi^+ \pi^-$) ("3-prong")	$(14.56 \pm 0.08) \%$	S=1.3	861		$K_0^*(1430)^- \nu_\tau$	$< 5 \times 10^{-4}$	CL=95%	326	
$h^- h^- h^+ \nu_\tau$	$(9.80 \pm 0.08) \%$	S=1.4	861		$K_2^*(1430)^- \nu_\tau$	$< 3 \times 10^{-3}$	CL=95%	317	
$h^- h^- h^+ \nu_\tau$ (ex. K^0)	$(9.45 \pm 0.07) \%$	S=1.3	861		$\eta \pi^- \nu_\tau$	$< 1.4 \times 10^{-4}$	CL=95%	797	
$h^- h^- h^+ \nu_\tau$ (ex. K^0, ω)	$(9.42 \pm 0.07) \%$	S=1.3	861		$\eta \pi^- \pi^0 \nu_\tau$	[g] $(1.81 \pm 0.24) \times 10^{-3}$		778	
$\pi^- \pi^+ \pi^- \nu_\tau$	$(9.32 \pm 0.07) \%$	S=1.2	861		$\eta \pi^- \pi^0 \pi^0 \nu_\tau$	$(1.5 \pm 0.5) \times 10^{-4}$		746	
$\pi^- \pi^+ \pi^- \nu_\tau$ (ex. K^0)	$(9.03 \pm 0.06) \%$	S=1.2	861		$\eta K^- \nu_\tau$	[g] $(2.7 \pm 0.6) \times 10^{-4}$		719	
$\pi^- \pi^+ \pi^- \nu_\tau$ (ex. K^0), non-axial vector	$< 2.4 \%$	CL=95%	861		$\eta K^*(892)^- \nu_\tau$	$(2.9 \pm 0.9) \times 10^{-4}$		511	
$\pi^- \pi^+ \pi^- \nu_\tau$ (ex. K^0, ω)	[g] $(8.99 \pm 0.06) \%$	S=1.2	861		$\eta K^- \pi^0 \nu_\tau$	$(1.8 \pm 0.9) \times 10^{-4}$		665	
$h^- h^- h^+ \geq 1 \text{ neutrals} \nu_\tau$	$(5.38 \pm 0.07) \%$	S=1.2	-		$\eta \bar{K}^0 \pi^- \nu_\tau$	$(2.2 \pm 0.7) \times 10^{-4}$		661	
$h^- h^- h^+ \geq 1\pi^0 \nu_\tau$ (ex. K^0)	$(5.08 \pm 0.06) \%$	S=1.1	-		$\eta \pi^+ \pi^- \pi^- \geq 0 \text{ neutrals} \nu_\tau$	$< 3 \times 10^{-3}$	CL=90%	744	
$h^- h^- h^+ \pi^0 \nu_\tau$	$(4.75 \pm 0.06) \%$	S=1.2	834		$\eta \pi^- \pi^+ \pi^- \nu_\tau$	$(2.3 \pm 0.5) \times 10^{-4}$		744	
$h^- h^- h^+ \pi^0 \nu_\tau$ (ex. K^0)	$(4.56 \pm 0.06) \%$	S=1.2	834		$\eta a_1(1260)^- \nu_\tau \rightarrow \eta \pi^- \rho^0 \nu_\tau$	$< 3.9 \times 10^{-4}$	CL=90%	-	
$h^- h^- h^+ \pi^0 \nu_\tau$ (ex. K^0, ω)	$(2.79 \pm 0.08) \%$	S=1.2	834		$\eta \eta \pi^- \nu_\tau$	$< 1.1 \times 10^{-4}$	CL=95%	637	
$\pi^- \pi^+ \pi^- \pi^0 \nu_\tau$	$(4.61 \pm 0.06) \%$	S=1.1	834		$\eta \eta \pi^- \pi^0 \nu_\tau$	$< 2.0 \times 10^{-4}$	CL=95%	559	
$\pi^- \pi^+ \pi^- \pi^0 \nu_\tau$ (ex. K^0)	$(4.48 \pm 0.06) \%$	S=1.1	834		$\eta'(958) \pi^- \nu_\tau$	$< 7.4 \times 10^{-5}$	CL=90%	620	
$\pi^- \pi^+ \pi^- \pi^0 \nu_\tau$ (ex. K^0, ω)	[g] $(2.70 \pm 0.08) \%$	S=1.2	834		$\eta'(958) \pi^- \pi^0 \nu_\tau$	$< 8.0 \times 10^{-5}$	CL=90%	591	
$h^- h^- h^+ \geq 2\pi^0 \nu_\tau$ (ex. K^0)	$(5.16 \pm 0.33) \times 10^{-3}$		-		$\phi \pi^- \nu_\tau$	$(3.4 \pm 0.6) \times 10^{-5}$		585	
$h^- h^- h^+ 2\pi^0 \nu_\tau$	$(5.04 \pm 0.32) \times 10^{-3}$		797		$\phi K^- \nu_\tau$	$(3.70 \pm 0.33) \times 10^{-5}$	S=1.3	445	
$h^- h^- h^+ 2\pi^0 \nu_\tau$ (ex. K^0)	$(4.94 \pm 0.32) \times 10^{-3}$		797		$f_1(1285) \pi^- \nu_\tau$	$(4.1 \pm 0.8) \times 10^{-4}$		408	
$h^- h^- h^+ 2\pi^0 \nu_\tau$ (ex. K^0, ω, η)	[g] $(9 \pm 4) \times 10^{-4}$		797		$f_1(1285) \pi^- \nu_\tau \rightarrow \eta \pi^- \pi^+ \pi^- \nu_\tau$	$(1.3 \pm 0.4) \times 10^{-4}$		-	
$h^- h^- h^+ 3\pi^0 \nu_\tau$	[g] $(2.3 \pm 0.6) \times 10^{-4}$	S=1.2	749		$\pi(1300)^- \nu_\tau \rightarrow (\rho \pi)^- \nu_\tau \rightarrow (3\pi)^- \nu_\tau$	$< 1.0 \times 10^{-4}$	CL=90%	-	
$K^- h^+ h^- \geq 0 \text{ neutrals} \nu_\tau$	$(6.24 \pm 0.24) \times 10^{-3}$	S=1.5	794		$\pi(1300)^- \nu_\tau \rightarrow ((\pi \pi) S\text{-wave} \pi)^- \nu_\tau \rightarrow (3\pi)^- \nu_\tau$	$< 1.9 \times 10^{-4}$	CL=90%	-	
$K^- h^+ \pi^- \nu_\tau$ (ex. K^0)	$(4.27 \pm 0.19) \times 10^{-3}$	S=2.4	794		$h^- \omega \geq 0 \text{ neutrals} \nu_\tau$	$(2.40 \pm 0.09) \%$	S=1.2	708	
$K^- h^+ \pi^- \pi^0 \nu_\tau$ (ex. K^0)	$(8.7 \pm 1.2) \times 10^{-4}$	S=1.1	763		$h^- \omega \nu_\tau$	[g] $(1.99 \pm 0.08) \%$	S=1.3	708	
$K^- \pi^+ \pi^- \geq 0 \text{ neutrals} \nu_\tau$	$(4.78 \pm 0.21) \times 10^{-3}$	S=1.3	794		$K^- \omega \nu_\tau$	$(4.1 \pm 0.9) \times 10^{-4}$		610	
$K^- \pi^+ \pi^- \geq 0\pi^0 \nu_\tau$ (ex. K^0)	$(3.68 \pm 0.19) \times 10^{-3}$	S=1.4	794		$h^- \omega \pi^0 \nu_\tau$	[g] $(4.1 \pm 0.4) \times 10^{-3}$		684	
$K^- \pi^+ \pi^- \nu_\tau$	$(3.41 \pm 0.16) \times 10^{-3}$	S=1.8	794		$h^- \omega 2\pi^0 \nu_\tau$	$(1.4 \pm 0.5) \times 10^{-4}$		644	
$K^- \pi^+ \pi^- \nu_\tau$ (ex. K^0)	[g] $(2.87 \pm 0.16) \times 10^{-3}$	S=2.1	794		$h^- 2\omega \nu_\tau$	$< 5.4 \times 10^{-7}$	CL=90%	250	
$K^- \rho^0 \nu_\tau \rightarrow K^- \pi^+ \pi^- \nu_\tau$	$(1.4 \pm 0.5) \times 10^{-3}$		-		$2h^- h^+ \omega \nu_\tau$	$(1.20 \pm 0.22) \times 10^{-4}$		641	
$K^- \pi^+ \pi^- \pi^0 \nu_\tau$	$(1.35 \pm 0.14) \times 10^{-3}$		763		Lepton Family number (LF), Lepton number (L), or Baryon number (B) violating modes				
$K^- \pi^+ \pi^- \pi^0 \nu_\tau$ (ex. K^0)	$(8.1 \pm 1.2) \times 10^{-4}$		763		L means lepton number violation (e.g. $\tau^- \rightarrow e^+ \pi^- \pi^-$). Following common usage, LF means lepton family number and not lepton number violation (e.g. $\tau^- \rightarrow e^- \pi^+ \pi^-$). B means baryon number violation.				
$K^- \pi^+ \pi^- \pi^0 \nu_\tau$ (ex. K^0, η)	[g] $(7.5 \pm 1.2) \times 10^{-4}$		763		$e^- \gamma$	LF $< 1.1 \times 10^{-7}$	CL=90%	888	
$K^- \pi^+ \pi^- \pi^0 \nu_\tau$ (ex. K^0, ω)	$(3.7 \pm 0.9) \times 10^{-4}$		763		$\mu^- \gamma$	LF $< 6.8 \times 10^{-8}$	CL=90%	885	
$K^- \pi^+ K^- \geq 0 \text{ neut.} \nu_\tau$	$< 9 \times 10^{-4}$	CL=95%	685		$e^- \pi^0$	LF $< 8.0 \times 10^{-8}$	CL=90%	883	
$K^- K^+ \pi^- \geq 0 \text{ neut.} \nu_\tau$	$(1.46 \pm 0.06) \times 10^{-3}$	S=1.6	685		$\mu^- \pi^0$	LF $< 1.1 \times 10^{-7}$	CL=90%	880	
$K^- K^+ \pi^- \nu_\tau$	[g] $(1.40 \pm 0.05) \times 10^{-3}$	S=1.7	685		$e^- K_S^0$	LF $< 5.6 \times 10^{-8}$	CL=90%	819	
$K^- K^+ \pi^- \pi^0 \nu_\tau$	[g] $(6.1 \pm 2.5) \times 10^{-5}$	S=1.4	618		$\mu^- K_S^0$	LF $< 4.9 \times 10^{-8}$	CL=90%	815	
$K^- K^+ K^- \geq 0 \text{ neut.} \nu_\tau$	$< 2.1 \times 10^{-3}$	CL=95%	472		$e^- \eta$	LF $< 9.2 \times 10^{-8}$	CL=90%	804	
$K^- K^+ K^- \nu_\tau$	$(1.58 \pm 0.18) \times 10^{-5}$		472		$\mu^- \eta$	LF $< 6.5 \times 10^{-8}$	CL=90%	800	
$K^- K^+ K^- \nu_\tau$ (ex. ϕ)	$< 2.5 \times 10^{-6}$	CL=90%	-		$e^- \rho^0$	LF $< 6.3 \times 10^{-8}$	CL=90%	719	
$K^- K^+ K^- \pi^0 \nu_\tau$	$< 4.8 \times 10^{-6}$	CL=90%	345		$\mu^- \rho^0$	LF $< 6.8 \times 10^{-8}$	CL=90%	715	
$\pi^- K^+ \pi^- \geq 0 \text{ neut.} \nu_\tau$	$< 2.5 \times 10^{-3}$	CL=95%	794		$e^- \omega$	LF $< 1.1 \times 10^{-7}$	CL=90%	716	
$e^- e^- e^+ \bar{\nu}_e \nu_\tau$	$(2.8 \pm 1.5) \times 10^{-5}$		888		$\mu^- \omega$	LF $< 8.9 \times 10^{-8}$	CL=90%	711	
$\mu^- e^- e^+ \bar{\nu}_\mu \nu_\tau$	$< 3.6 \times 10^{-5}$	CL=90%	885		$e^- K^*(892)^0$	LF $< 7.8 \times 10^{-8}$	CL=90%	665	
Modes with five charged particles									
$3h^- 2h^+ \geq 0 \text{ neutrals} \nu_\tau$	$(1.02 \pm 0.04) \times 10^{-3}$	S=1.1	794		$\mu^- K^*(892)^0$	LF $< 5.9 \times 10^{-8}$	CL=90%	659	
(ex. $K_S^0 \rightarrow \pi^- \pi^+$) ("5-prong")					$e^- \bar{K}^*(892)^0$	LF $< 7.7 \times 10^{-8}$	CL=90%	665	
$3h^- 2h^+ \nu_\tau$ (ex. K^0)	[g] $(8.39 \pm 0.35) \times 10^{-4}$	S=1.1	794		$\mu^- \bar{K}^*(892)^0$	LF $< 1.0 \times 10^{-7}$	CL=90%	659	
$3h^- 2h^+ \pi^0 \nu_\tau$ (ex. K^0)	[g] $(1.78 \pm 0.27) \times 10^{-4}$		746		$e^- \eta'(958)$	LF $< 1.6 \times 10^{-7}$	CL=90%	630	
$3h^- 2h^+ 2\pi^0 \nu_\tau$	$< 3.4 \times 10^{-6}$	CL=90%	687		$\mu^- \eta'(958)$	LF $< 1.3 \times 10^{-7}$	CL=90%	625	
Miscellaneous other allowed modes									
$(5\pi)^- \nu_\tau$	$(7.6 \pm 0.5) \times 10^{-3}$		800		$e^- \phi$	LF $< 7.3 \times 10^{-8}$	CL=90%	596	
$4h^- 3h^+ \geq 0 \text{ neutrals} \nu_\tau$	$< 3.0 \times 10^{-7}$	CL=90%	682		$\mu^- \phi$	LF $< 1.3 \times 10^{-7}$	CL=90%	590	
("7-prong")					$e^- e^+ e^-$	LF $< 3.6 \times 10^{-8}$	CL=90%	888	
$4h^- 3h^+ \nu_\tau$	$< 4.3 \times 10^{-7}$	CL=90%	682		$e^- \mu^+ \mu^-$	LF $< 3.7 \times 10^{-8}$	CL=90%	882	
$4h^- 3h^+ \pi^0 \nu_\tau$	$< 2.5 \times 10^{-7}$	CL=90%	612		$e^+ \mu^- \mu^-$	LF $< 2.3 \times 10^{-8}$	CL=90%	882	
					$\mu^- e^+ e^-$	LF $< 2.7 \times 10^{-8}$	CL=90%	885	

Lepton Summary Table

$\mu^+ e^- e^-$	LF	< 2.0	$\times 10^{-8}$	CL=90%	885
$\mu^- \mu^+ \mu^-$	LF	< 3.2	$\times 10^{-8}$	CL=90%	873
$e^- \pi^+ \pi^-$	LF	< 1.2	$\times 10^{-7}$	CL=90%	877
$e^+ \pi^- \pi^-$	L	< 2.0	$\times 10^{-7}$	CL=90%	877
$\mu^- \pi^+ \pi^-$	LF	< 2.9	$\times 10^{-7}$	CL=90%	866
$\mu^+ \pi^- \pi^-$	L	< 7	$\times 10^{-8}$	CL=90%	866
$e^- \pi^+ K^-$	LF	< 3.2	$\times 10^{-7}$	CL=90%	813
$e^- \pi^- K^+$	LF	< 1.6	$\times 10^{-7}$	CL=90%	813
$e^+ \pi^- K^-$	L	< 1.8	$\times 10^{-7}$	CL=90%	813
$e^- K_S^0 K_S^0$	LF	< 2.2	$\times 10^{-6}$	CL=90%	736
$e^- K^+ K^-$	LF	< 1.4	$\times 10^{-7}$	CL=90%	738
$e^+ K^- K^-$	L	< 1.5	$\times 10^{-7}$	CL=90%	738
$\mu^- \pi^+ K^-$	LF	< 2.6	$\times 10^{-7}$	CL=90%	800
$\mu^- \pi^- K^+$	LF	< 3.2	$\times 10^{-7}$	CL=90%	800
$\mu^+ \pi^- K^-$	L	< 2.2	$\times 10^{-7}$	CL=90%	800
$\mu^- K_S^0 K_S^0$	LF	< 3.4	$\times 10^{-6}$	CL=90%	696
$\mu^- K^+ K^-$	LF	< 2.5	$\times 10^{-7}$	CL=90%	699
$\mu^+ K^- K^-$	L	< 4.4	$\times 10^{-7}$	CL=90%	699
$e^- \pi^0 \pi^0$	LF	< 6.5	$\times 10^{-6}$	CL=90%	878
$\mu^- \pi^0 \pi^0$	LF	< 1.4	$\times 10^{-5}$	CL=90%	867
$e^- \eta \eta$	LF	< 3.5	$\times 10^{-5}$	CL=90%	699
$\mu^- \eta \eta$	LF	< 6.0	$\times 10^{-5}$	CL=90%	653
$e^- \pi^0 \eta$	LF	< 2.4	$\times 10^{-5}$	CL=90%	798
$\mu^- \pi^0 \eta$	LF	< 2.2	$\times 10^{-5}$	CL=90%	784
$\bar{p} \gamma$	L,B	< 3.5	$\times 10^{-6}$	CL=90%	641
$\bar{p} \pi^0$	L,B	< 1.5	$\times 10^{-5}$	CL=90%	632
$\bar{p} 2\pi^0$	L,B	< 3.3	$\times 10^{-5}$	CL=90%	604
$\bar{p} \eta$	L,B	< 8.9	$\times 10^{-6}$	CL=90%	475
$\bar{p} \pi^0 \eta$	L,B	< 2.7	$\times 10^{-5}$	CL=90%	360
$\Lambda \pi^-$	L,B	< 7.2	$\times 10^{-8}$	CL=90%	525
$\bar{\Lambda} \pi^-$	L,B	< 1.4	$\times 10^{-7}$	CL=90%	525
e^- light boson	LF	< 2.7	$\times 10^{-3}$	CL=95%	-
μ^- light boson	LF	< 5	$\times 10^{-3}$	CL=95%	-

Heavy Charged Lepton Searches

 L^\pm – charged leptonMass $m > 100.8$ GeV, CL = 95% ^[h] Decay to νW . L^\pm – stable charged heavy leptonMass $m > 102.6$ GeV, CL = 95%

Neutrino Properties

See the note on “Neutrino properties listings” in the Particle Listings.

Mass $m < 2$ eV (tritium decay)Mean life/mass, $\tau/m > 300$ s/eV, CL = 90% (reactor)Mean life/mass, $\tau/m > 7 \times 10^9$ s/eV (solar)Mean life/mass, $\tau/m > 15.4$ s/eV, CL = 90% (accelerator)Magnetic moment $\mu < 0.74 \times 10^{-10} \mu_B$, CL = 90% (reactor)

Number of Neutrino Types

Number $N = 2.984 \pm 0.008$ (Standard Model fits to LEP data)Number $N = 2.92 \pm 0.05$ ($S = 1.2$) (Direct measurement of invisible Z width)

Neutrino Mixing

The following values are obtained through data analyses based on the 3-neutrino mixing scheme described in the review “Neutrino mass, mixing, and flavor change” by B. Kayser in this Review.

$$\sin^2(2\theta_{12}) = 0.86^{+0.03}_{-0.04}$$

$$\Delta m_{21}^2 = (8.0 \pm 0.3) \times 10^{-5} \text{ eV}^2$$

The ranges below for $\sin^2(2\theta_{23})$ and Δm_{32}^2 correspond to the projections onto the appropriate axes of the 90% CL contour in the $\sin^2(2\theta_{23})$ - Δm_{32}^2 plane.

$$\sin^2(2\theta_{23}) > 0.92$$

$$\Delta m_{32}^2 = 1.9 \text{ to } 3.0 \times 10^{-3} \text{ eV}^2 \text{ [i]}$$

$$\sin^2(2\theta_{13}) < 0.19, \text{ CL} = 90\%$$

Heavy Neutral Leptons, Searches for

For excited leptons, see Compositeness Limits below.

Stable Neutral Heavy Lepton Mass Limits

Mass $m > 45.0$ GeV, CL = 95% (Dirac)Mass $m > 39.5$ GeV, CL = 95% (Majorana)

Neutral Heavy Lepton Mass Limits

Mass $m > 90.3$ GeV, CL = 95%(Dirac ν_L coupling to e, μ, τ ; conservative case(τ))Mass $m > 80.5$ GeV, CL = 95%(Majorana ν_L coupling to e, μ, τ ; conservative case(τ))

NOTES

In this Summary Table:

When a quantity has “(S = ...)” to its right, the error on the quantity has been enlarged by the “scale factor” S, defined as $S = \sqrt{\chi^2/(N-1)}$, where N is the number of measurements used in calculating the quantity. We do this when $S > 1$, which often indicates that the measurements are inconsistent. When $S > 1.25$, we also show in the Particle Listings an ideogram of the measurements. For more about S, see the Introduction.

A decay momentum p is given for each decay mode. For a 2-body decay, p is the momentum of each decay product in the rest frame of the decaying particle. For a 3-or-more-body decay, p is the largest momentum any of the products can have in this frame.

[a] This is the best limit for the mode $e^- \rightarrow \nu \gamma$. The best limit for “electron disappearance” is 6.4×10^{24} yr.

[b] See the “Note on Muon Decay Parameters” in the μ Particle Listings for definitions and details.

[c] P_μ is the longitudinal polarization of the muon from pion decay. In standard $V-A$ theory, $P_\mu = 1$ and $\rho = \delta = 3/4$.

[d] This only includes events with the γ energy > 10 MeV. Since the $e^- \bar{\nu}_e \nu_\mu$ and $e^- \bar{\nu}_e \nu_\mu \gamma$ modes cannot be clearly separated, we regard the latter mode as a subset of the former.

[e] See the relevant Particle Listings for the energy limits used in this measurement.

[f] A test of additive vs. multiplicative lepton family number conservation.

[g] Basis mode for the τ .

[h] L^\pm mass limit depends on decay assumptions; see the Full Listings.

[i] The sign of Δm_{32}^2 is not known at this time. The range quoted is for the absolute value.

Quark Summary Table

QUARKS

The u -, d -, and s -quark masses are estimates of so-called "current-quark masses," in a mass-independent subtraction scheme such as $\overline{\text{MS}}$ at a scale $\mu \approx 2$ GeV. The c - and b -quark masses are the "running" masses in the $\overline{\text{MS}}$ scheme. For the b -quark we also quote the 1S mass. These can be different from the heavy quark masses obtained in potential models.

u	$I(J^P) = \frac{1}{2}(\frac{1}{2}^+)$
Mass $m = 1.5$ to 3.3 MeV [a]	Charge = $\frac{2}{3} e$ $I_z = +\frac{1}{2}$
$m_u/m_d = 0.35$ to 0.60	
d	$I(J^P) = \frac{1}{2}(\frac{1}{2}^+)$
Mass $m = 3.5$ to 6.0 MeV [a]	Charge = $-\frac{1}{3} e$ $I_z = -\frac{1}{2}$
$m_s/m_d = 17$ to 22	
$\overline{m} = (m_u + m_d)/2 = 2.5$ to 5.0 MeV	
s	$I(J^P) = 0(\frac{1}{2}^+)$
Mass $m = 104^{+26}_{-34}$ MeV [a]	Charge = $-\frac{1}{3} e$ Strangeness = -1
$(m_s - (m_u + m_d)/2)/(m_d - m_u) = 30$ to 50	
c	$I(J^P) = 0(\frac{1}{2}^+)$
Mass $m = 1.27^{+0.07}_{-0.11}$ GeV	Charge = $\frac{2}{3} e$ Charm = $+1$
b	$I(J^P) = 0(\frac{1}{2}^+)$
	Charge = $-\frac{1}{3} e$ Bottom = -1
Mass $m = 4.20^{+0.17}_{-0.07}$ GeV ($\overline{\text{MS}}$ mass)	
t	$I(J^P) = 0(\frac{1}{2}^+)$
	Charge = $\frac{2}{3} e$ Top = $+1$
Mass $m = 171.2 \pm 2.1$ GeV [b] (direct observation of top events)	
DECAY MODES	Fraction (Γ_i/Γ) Confidence level (MeV/c) ^p
$W q (q = b, s, d)$	—
$W b$	—
$\ell \nu_\ell$ anything	[c,d] (9.4 ± 2.4) %
$\gamma q (q = u, c)$	[e] < 5.9 × 10 ⁻³ 95% —
$\Delta T = 1$ weak neutral current (TI) modes	
$Z q (q = u, c)$	TI [f] < 13.7 % 95% —

b' (4th Generation) Quark, Searches for

Mass $m > 190$ GeV, CL = 95% ($p\bar{p}$, quasi-stable b')
 Mass $m > 199$ GeV, CL = 95% ($p\bar{p}$, neutral-current decays)
 Mass $m > 128$ GeV, CL = 95% ($p\bar{p}$, charged-current decays)
 Mass $m > 46.0$ GeV, CL = 95% ($e^+ e^-$, all decays)

t' (4th Generation) Quark, Searches for

Mass $m > 256$ GeV, CL = 95% ($p\bar{p}$, $t'\bar{t}'$ prod., $t' \rightarrow W q$)

Free Quark Searches

All searches since 1977 have had negative results.

NOTES

- [a] The ratios m_u/m_d and m_s/m_d are extracted from pion and kaon masses using chiral symmetry. The estimates of u and d masses are not without controversy and remain under active investigation. Within the literature there are even suggestions that the u quark could be essentially massless. The s -quark mass is estimated from SU(3) splittings in hadron masses.
- [b] Based on published top mass measurements using data from Tevatron Run-I and Run-II. Including also the most recent unpublished results from Run-II, the Tevatron Electroweak Working Group reports a top mass of $172.6 \pm 0.8 \pm 1.1$ GeV. See the note "The Top Quark" in the Quark Particle Listings of this Review.
- [c] ℓ means e or μ decay mode, not the sum over them.
- [d] Assumes lepton universality and W -decay acceptance.
- [e] This limit is for $\Gamma(t \rightarrow \gamma q)/\Gamma(t \rightarrow W b)$.
- [f] This limit is for $\Gamma(t \rightarrow Z q)/\Gamma(t \rightarrow W b)$.

Meson Summary Table

LIGHT UNFLAVORED MESONS ($S = C = B = 0$)

For $I = 1$ (π, b, ρ, a): $u\bar{d}, (u\bar{u}-d\bar{d})/\sqrt{2}, d\bar{u}$;
for $I = 0$ ($\eta, \eta', h, h', \omega, \phi, f, f'$): $c_1(u\bar{u} + d\bar{d}) + c_2(s\bar{s})$

 π^\pm

$$I^G(J^{PC}) = 1^-(0^-)$$

Mass $m = 139.57018 \pm 0.00035$ MeV ($S = 1.2$)
Mean life $\tau = (2.6033 \pm 0.0005) \times 10^{-8}$ s ($S = 1.2$)
 $c\tau = 7.8045$ m

$\pi^\pm \rightarrow \ell^\pm \nu \gamma$ form factors [a]

$F_V = 0.017 \pm 0.008$
 $F_A = 0.0115 \pm 0.0005$ ($S = 1.2$)
 $R = 0.059^{+0.009}_{-0.008}$

π^- modes are charge conjugates of the modes below.

For decay limits to particles which are not established, see the appropriate Search sections (Massive Neutrino Peak Search Test, A^0 (axion), and Other Light Boson (X^0) Searches, etc.).

π^\pm DECAY MODES	Fraction (Γ_i/Γ)	Confidence level	ρ (MeV/c)
$\mu^+ \nu_\mu$	[b] (99.98770 \pm 0.00004) %		30
$\mu^+ \nu_\mu \gamma$	[c] (2.00 \pm 0.25) $\times 10^{-4}$		30
$e^+ \nu_e$	[b] (1.230 \pm 0.004) $\times 10^{-4}$		70
$e^+ \nu_e \gamma$	[c] (1.61 \pm 0.23) $\times 10^{-7}$		70
$e^+ \nu_e \pi^0$	(1.036 \pm 0.006) $\times 10^{-8}$		4
$e^+ \nu_e e^+ e^-$	(3.2 \pm 0.5) $\times 10^{-9}$		70
$e^+ \nu_e \nu \bar{\nu}$	< 5 $\times 10^{-6}$	90%	70
Lepton Family number (LF) or Lepton number (L) violating modes			
$\mu^+ \bar{\nu}_e$	L [d] < 1.5 $\times 10^{-3}$	90%	30
$\mu^+ \nu_e$	LF [d] < 8.0 $\times 10^{-3}$	90%	30
$\mu^- e^+ e^+ \nu$	LF < 1.6 $\times 10^{-6}$	90%	30

 π^0

$$I^G(J^{PC}) = 1^-(0^-)$$

Mass $m = 134.9766 \pm 0.0006$ MeV ($S = 1.1$)
 $m_{\pi^\pm} - m_{\pi^0} = 4.5936 \pm 0.0005$ MeV
Mean life $\tau = (8.4 \pm 0.6) \times 10^{-17}$ s ($S = 3.0$)
 $c\tau = 25.1$ nm

For decay limits to particles which are not established, see the appropriate Search sections (A^0 (axion) and Other Light Boson (X^0) Searches, etc.).

π^0 DECAY MODES	Fraction (Γ_i/Γ)	Scale factor/ Confidence level	ρ (MeV/c)
2γ	(98.798 \pm 0.032) %	S=1.1	67
$e^+ e^- \gamma$	(1.198 \pm 0.032) %	S=1.1	67
γ positronium	(1.82 \pm 0.29) $\times 10^{-9}$		67
$e^+ e^+ e^- e^-$	(3.14 \pm 0.30) $\times 10^{-5}$		67
$e^+ e^-$	(6.46 \pm 0.33) $\times 10^{-8}$		67
4γ	< 2 $\times 10^{-8}$	CL=90%	67
$\nu \bar{\nu}$	[e] < 2.7 $\times 10^{-7}$	CL=90%	67
$\nu_e \bar{\nu}_e$	< 1.7 $\times 10^{-6}$	CL=90%	67
$\nu_\mu \bar{\nu}_\mu$	< 1.6 $\times 10^{-6}$	CL=90%	67
$\nu_\tau \bar{\nu}_\tau$	< 2.1 $\times 10^{-6}$	CL=90%	67
$\gamma \nu \bar{\nu}$	< 6 $\times 10^{-4}$	CL=90%	67
Charge conjugation (C) or Lepton Family number (LF) violating modes			
3γ	C < 3.1 $\times 10^{-8}$	CL=90%	67
$\mu^+ e^-$	LF < 3.8 $\times 10^{-10}$	CL=90%	26
$\mu^- e^+$	LF < 3.4 $\times 10^{-9}$	CL=90%	26
$\mu^+ e^- + \mu^- e^+$	LF < 1.72 $\times 10^{-8}$	CL=90%	26

 η

$$I^G(J^{PC}) = 0^+(0^-)$$

Mass $m = 547.853 \pm 0.024$ MeV [f]
Full width $\Gamma = 1.30 \pm 0.07$ keV [g]

C-nonconserving decay parameters

$\pi^+ \pi^- \pi^0$ Left-right asymmetry = $(0.09 \pm 0.17) \times 10^{-2}$
 $\pi^+ \pi^- \pi^0$ Sextant asymmetry = $(0.18 \pm 0.16) \times 10^{-2}$
 $\pi^+ \pi^- \pi^0$ Quadrant asymmetry = $(-0.17 \pm 0.17) \times 10^{-2}$
 $\pi^+ \pi^- \gamma$ Left-right asymmetry = $(0.9 \pm 0.4) \times 10^{-2}$
 $\pi^+ \pi^- \gamma$ β (D-wave) = -0.02 ± 0.07 ($S = 1.3$)

Dalitz plot parameter

$\pi^0 \pi^0 \pi^0$ $\alpha = -0.031 \pm 0.004$

 η DECAY MODES

	Fraction (Γ_i/Γ)	Scale factor/ Confidence level	ρ (MeV/c)
Neutral modes			
neutral modes	(71.91 \pm 0.34) %	S=1.2	-
2γ	[g] (39.31 \pm 0.20) %	S=1.1	274
$3\pi^0$	(32.56 \pm 0.23) %	S=1.1	179
$\pi^0 2\gamma$	(4.4 \pm 1.5) $\times 10^{-4}$	S=2.0	257
$\pi^0 \pi^0 \gamma \gamma$	< 1.2 $\times 10^{-3}$	CL=90%	238
4γ	< 2.8 $\times 10^{-4}$	CL=90%	274
invisible	< 6 $\times 10^{-4}$	CL=90%	-
Charged modes			
charged modes	(28.06 \pm 0.34) %	S=1.2	-
$\pi^+ \pi^- \pi^0$	(22.73 \pm 0.28) %	S=1.2	174
$\pi^+ \pi^- \gamma$	(4.60 \pm 0.16) %	S=2.1	236
$e^+ e^- \gamma$	(6.8 \pm 0.8) $\times 10^{-3}$	S=1.7	274
$\mu^+ \mu^- \gamma$	(3.1 \pm 0.4) $\times 10^{-4}$		253
$e^+ e^-$	< 7.7 $\times 10^{-5}$	CL=90%	274
$\mu^+ \mu^-$	(5.8 \pm 0.8) $\times 10^{-6}$		253
$e^+ e^- e^+ e^-$	< 6.9 $\times 10^{-5}$	CL=90%	274
$\pi^+ \pi^- e^+ e^-$	(4.2 \pm 1.2) $\times 10^{-4}$		235
$\pi^+ \pi^- 2\gamma$	< 2.0 $\times 10^{-3}$		236
$\pi^+ \pi^- \pi^0 \gamma$	< 5 $\times 10^{-4}$	CL=90%	174
$\pi^0 \mu^+ \mu^- \gamma$	< 3 $\times 10^{-6}$	CL=90%	210

**Charge conjugation (C), Parity (P),
Charge conjugation \times Parity (CP), or
Lepton Family number (LF) violating modes**

$\pi^0 \gamma$	C < 9 $\times 10^{-5}$	CL=90%	257
$\pi^+ \pi^-$	P, CP < 1.3 $\times 10^{-5}$	CL=90%	236
$\pi^0 \pi^0$	P, CP < 3.5 $\times 10^{-4}$	CL=90%	238
$\pi^0 \pi^0 \gamma$	C < 5 $\times 10^{-4}$	CL=90%	238
$\pi^0 \pi^0 \pi^0 \gamma$	C < 6 $\times 10^{-5}$	CL=90%	179
3γ	C < 1.6 $\times 10^{-5}$	CL=90%	274
$4\pi^0$	P, CP < 6.9 $\times 10^{-7}$	CL=90%	40
$\pi^0 e^+ e^-$	C [h] < 4 $\times 10^{-5}$	CL=90%	257
$\pi^0 \mu^+ \mu^-$	C [h] < 5 $\times 10^{-6}$	CL=90%	210
$\mu^+ e^- + \mu^- e^+$	LF < 6 $\times 10^{-6}$	CL=90%	264

 **$f_0(600)$ [i]
or σ**

$$I^G(J^{PC}) = 0^+(0^+)$$

Mass $m = (400-1200)$ MeV
Full width $\Gamma = (600-1000)$ MeV

 $f_0(600)$ DECAY MODES

	Fraction (Γ_i/Γ)	ρ (MeV/c)
$\pi \pi$	dominant	-
$\gamma \gamma$	seen	-

Meson Summary Table

 $\rho(770)$ [1]

$$I^G(J^{PC}) = 1^+(1^{--})$$

Mass $m = 775.49 \pm 0.34$ MeV
 Full width $\Gamma = 149.4 \pm 1.0$ MeV
 $\Gamma_{ee} = 7.04 \pm 0.06$ keV

$\rho(770)$ DECAY MODES	Fraction (Γ_i/Γ)	Scale factor/ Confidence level	ρ (MeV/c)
$\pi^+\pi^-$	~ 100 %		363
$\rho(770)^\pm$ decays			
$\pi^\pm\gamma$	$(4.5 \pm 0.5) \times 10^{-4}$	S=2.2	375
$\pi^\pm\eta$	$< 6 \times 10^{-3}$	CL=84%	153
$\pi^\pm\pi^+\pi^-\pi^0$	$< 2.0 \times 10^{-3}$	CL=84%	254
$\rho(770)^0$ decays			
$\pi^+\pi^-\gamma$	$(9.9 \pm 1.6) \times 10^{-3}$		362
$\pi^0\gamma$	$(6.0 \pm 0.8) \times 10^{-4}$		376
$\eta\gamma$	$(3.00 \pm 0.21) \times 10^{-4}$		194
$\pi^0\pi^0\gamma$	$(4.5 \pm 0.8) \times 10^{-5}$		363
$\mu^+\mu^-$	[k] $(4.55 \pm 0.28) \times 10^{-5}$		373
e^+e^-	[k] $(4.71 \pm 0.05) \times 10^{-5}$		388
$\pi^+\pi^-\pi^0$	$(1.01^{+0.54}_{-0.36} \pm 0.34) \times 10^{-4}$		323
$\pi^+\pi^-\pi^+\pi^-$	$(1.8 \pm 0.9) \times 10^{-5}$		251
$\pi^+\pi^-\pi^0\pi^0$	$< 4 \times 10^{-5}$	CL=90%	257

 $\omega(782)$

$$I^G(J^{PC}) = 0^-(1^{--})$$

Mass $m = 782.65 \pm 0.12$ MeV ($S = 1.9$)
 Full width $\Gamma = 8.49 \pm 0.08$ MeV
 $\Gamma_{ee} = 0.60 \pm 0.02$ keV

$\omega(782)$ DECAY MODES	Fraction (Γ_i/Γ)	Scale factor/ Confidence level	ρ (MeV/c)
$\pi^+\pi^-\pi^0$	$(89.2 \pm 0.7) \%$		327
$\pi^0\gamma$	$(8.92 \pm 0.24) \%$	S=1.1	380
$\pi^+\pi^-$	$(1.53^{+0.11}_{-0.13}) \%$	S=1.2	366
neutrals (excluding $\pi^0\gamma$)	$(1.5^{+7.4}_{-1.0}) \times 10^{-3}$		–
$\eta\gamma$	$(4.6 \pm 0.4) \times 10^{-4}$	S=1.1	200
$\pi^0 e^+ e^-$	$(7.7 \pm 0.9) \times 10^{-4}$	S=1.1	380
$\pi^0 \mu^+ \mu^-$	$(9.6 \pm 2.3) \times 10^{-5}$		349
$e^+ e^-$	$(7.16 \pm 0.12) \times 10^{-5}$	S=1.1	391
$\pi^+\pi^-\pi^0\pi^0$	$< 2 \%$	CL=90%	262
$\pi^+\pi^-\gamma$	$< 3.6 \times 10^{-3}$	CL=95%	366
$\pi^+\pi^-\pi^+\pi^-$	$< 1 \times 10^{-3}$	CL=90%	256
$\pi^0\pi^0\gamma$	$(6.7 \pm 1.1) \times 10^{-5}$		367
$\eta\pi^0\gamma$	$< 3.3 \times 10^{-5}$	CL=90%	162
$\mu^+\mu^-$	$(9.0 \pm 3.1) \times 10^{-5}$		377
3γ	$< 1.9 \times 10^{-4}$	CL=95%	391
Charge conjugation (C) violating modes			
$\eta\pi^0$	C $< 1 \times 10^{-3}$	CL=90%	162
$3\pi^0$	C $< 3 \times 10^{-4}$	CL=90%	330

 $\eta'(958)$

$$I^G(J^{PC}) = 0^+(0^{--})$$

Mass $m = 957.66 \pm 0.24$ MeV
 Full width $\Gamma = 0.205 \pm 0.015$ MeV ($S = 1.2$)
 c C-violating decay parameter = 0.015 ± 0.018

 $\eta'(958)$ DECAY MODES

	Fraction (Γ_i/Γ)	Scale factor/ Confidence level	ρ (MeV/c)
$\pi^+\pi^-\eta$	$(44.6 \pm 1.4) \%$	S=1.2	232
$\rho^0\gamma$ (including non-resonant)	$(29.4 \pm 0.9) \%$	S=1.1	165
$\pi^+\pi^-\pi^-\gamma$			
$\pi^0\pi^0\eta$	$(20.7 \pm 1.2) \%$	S=1.2	238
$\omega\gamma$	$(3.02 \pm 0.31) \%$		159
$\gamma\gamma$	$(2.10 \pm 0.12) \%$	S=1.2	479
$3\pi^0$	$(1.54 \pm 0.26) \times 10^{-3}$		430
$\mu^+\mu^-\gamma$	$(1.03 \pm 0.26) \times 10^{-4}$		467
$\pi^+\pi^-\pi^0$	$< 5 \%$	CL=90%	427
$\pi^0\rho^0$	$< 4 \%$	CL=90%	110
$\pi^+\pi^+\pi^-\pi^-$	$< 1 \%$	CL=90%	372
$\pi^+\pi^+\pi^-\pi^0$ neutrals	$< 1 \%$	CL=95%	–
$\pi^+\pi^+\pi^-\pi^-\pi^0$	$< 1 \%$	CL=90%	298
6π	$< 1 \%$	CL=90%	211
$\pi^+\pi^-e^+e^-$	$< 6 \times 10^{-3}$	CL=90%	458
$\gamma e^+ e^-$	$< 9 \times 10^{-4}$	CL=90%	479
$\pi^0\gamma\gamma$	$< 8 \times 10^{-4}$	CL=90%	469
$4\pi^0$	$< 5 \times 10^{-4}$	CL=90%	379
e^+e^-	$< 2.1 \times 10^{-7}$	CL=90%	479
invisible	$< 1.4 \times 10^{-3}$	CL=90%	–

**Charge conjugation (C), Parity (P),
 Lepton family number (LF) violating modes**

$\pi^+\pi^-$	P, CP	$< 2.9 \times 10^{-3}$	CL=90%	458
$\pi^0\pi^0$	P, CP	$< 9 \times 10^{-4}$	CL=90%	459
$\pi^0 e^+ e^-$	C	[h] $< 1.4 \times 10^{-3}$	CL=90%	469
$\eta e^+ e^-$	C	[h] $< 2.4 \times 10^{-3}$	CL=90%	322
3γ	C	$< 1.0 \times 10^{-4}$	CL=90%	479
$\mu^+\mu^-\pi^0$	C	[h] $< 6.0 \times 10^{-5}$	CL=90%	445
$\mu^+\mu^-\eta$	C	[h] $< 1.5 \times 10^{-5}$	CL=90%	273
$e\mu$	LF	$< 4.7 \times 10^{-4}$	CL=90%	473

 $f_0(980)$ [1]

$$I^G(J^{PC}) = 0^+(0^{++})$$

Mass $m = 980 \pm 10$ MeV
 Full width $\Gamma = 40$ to 100 MeV

 $f_0(980)$ DECAY MODES

	Fraction (Γ_i/Γ)	ρ (MeV/c)
$\pi^+\pi^-$	dominant	471
$K\bar{K}$	seen	†
$\gamma\gamma$	seen	490

 $a_0(980)$ [1]

$$I^G(J^{PC}) = 1^-(0^{++})$$

Mass $m = 984.7 \pm 1.2$ MeV ($S = 1.5$)
 Full width $\Gamma = 50$ to 100 MeV

 $a_0(980)$ DECAY MODES

	Fraction (Γ_i/Γ)	ρ (MeV/c)
$\eta\pi$	dominant	322
$K\bar{K}$	seen	†
$\gamma\gamma$	seen	492

 $\phi(1020)$

$$I^G(J^{PC}) = 0^-(1^{--})$$

Mass $m = 1019.455 \pm 0.020$ MeV ($S = 1.1$)
 Full width $\Gamma = 4.26 \pm 0.04$ MeV ($S = 1.4$)

Meson Summary Table

$\phi(1020)$ DECAY MODES	Fraction (Γ_i/Γ)	Scale factor/ Confidence level	ρ (MeV/c)
$K^+ K^-$	(49.2 \pm 0.6) %	S=1.2	127
$K_L^0 K_S^0$	(34.0 \pm 0.5) %	S=1.1	110
$\rho\pi^+ + \pi^+\pi^-\pi^0$	(15.25 \pm 0.35) %	S=1.1	-
$\eta\gamma$	(1.304 \pm 0.025) %	S=1.1	363
$\pi^0\gamma$	(1.26 \pm 0.06) $\times 10^{-3}$		501
$e^+ e^-$	(2.97 \pm 0.04) $\times 10^{-4}$	S=1.1	510
$\mu^+ \mu^-$	(2.86 \pm 0.19) $\times 10^{-4}$		499
$\eta e^+ e^-$	(1.15 \pm 0.10) $\times 10^{-4}$		363
$\pi^+\pi^-$	(7.3 \pm 1.3) $\times 10^{-5}$		490
$\omega\pi^0$	(5.2 \pm 1.3 -1.1) $\times 10^{-5}$		171
$\omega\gamma$	< 5 %	CL=84%	209
$\rho\gamma$	< 1.2 $\times 10^{-5}$	CL=90%	215
$\pi^+\pi^-\gamma$	(4.1 \pm 1.3) $\times 10^{-5}$		490
$f_0(980)\gamma$	(3.22 \pm 0.19) $\times 10^{-4}$	S=1.1	39
$\pi^0\pi^0\gamma$	(1.07 \pm 0.06) $\times 10^{-4}$		492
$\pi^+\pi^-\pi^+\pi^-$	(3.9 \pm 2.8 -2.2) $\times 10^{-6}$		410
$\pi^+\pi^+\pi^-\pi^-\pi^0$	< 4.6 $\times 10^{-6}$	CL=90%	342
$\pi^0 e^+ e^-$	(1.12 \pm 0.28) $\times 10^{-5}$		501
$\pi^0\eta\gamma$	(8.3 \pm 0.5) $\times 10^{-5}$		346
$a_0(980)\gamma$	(7.6 \pm 0.6) $\times 10^{-5}$		34
$\eta'(958)\gamma$	(6.23 \pm 0.21) $\times 10^{-5}$		60
$\eta\pi^0\pi^0\gamma$	< 2 $\times 10^{-5}$	CL=90%	293
$\mu^+\mu^-\gamma$	(1.4 \pm 0.5) $\times 10^{-5}$		499
$\rho\gamma\gamma$	< 5 $\times 10^{-4}$	CL=90%	215
$\eta\pi^+\pi^-$	< 1.8 $\times 10^{-5}$	CL=90%	288
$\eta\mu^+\mu^-$	< 9.4 $\times 10^{-6}$	CL=90%	321

$$h_1(1170) \quad I^G(J^{PC}) = 0^-(1^+ -)$$

Mass $m = 1170 \pm 20$ MeV
Full width $\Gamma = 360 \pm 40$ MeV

$h_1(1170)$ DECAY MODES	Fraction (Γ_i/Γ)	ρ (MeV/c)
$\rho\pi$	seen	307

$$b_1(1235) \quad I^G(J^{PC}) = 1^+(1^+ -)$$

Mass $m = 1229.5 \pm 3.2$ MeV ($S = 1.6$)
Full width $\Gamma = 142 \pm 9$ MeV ($S = 1.2$)

$b_1(1235)$ DECAY MODES	Fraction (Γ_i/Γ)	Confidence level	ρ (MeV/c)
$\omega\pi$	dominant		348
[D/S amplitude ratio = 0.277 \pm 0.027]			
$\pi^\pm\gamma$	(1.6 \pm 0.4) $\times 10^{-3}$		607
$\eta\rho$	seen		†
$\pi^+\pi^+\pi^-\pi^0$	< 50 %	84%	535
$(K\bar{K})^\pm\pi^0$	< 8 %	90%	248
$K_S^0 K_L^0 \pi^\pm$	< 6 %	90%	235
$K_S^0 K_S^0 \pi^\pm$	< 2 %	90%	235
$\phi\pi$	< 1.5 %	84%	147

$$a_1(1260)^{[m]} \quad I^G(J^{PC}) = 1^-(1^+ +)$$

Mass $m = 1230 \pm 40$ MeV $^{[n]}$
Full width $\Gamma = 250$ to 600 MeV

$a_1(1260)$ DECAY MODES	Fraction (Γ_i/Γ)	ρ (MeV/c)
$(\rho\pi)_{S\text{-wave}}$	seen	353
$(\rho\pi)_{D\text{-wave}}$	seen	353
$(\rho(1450)\pi)_{S\text{-wave}}$	seen	†
$(\rho(1450)\pi)_{D\text{-wave}}$	seen	†
$\sigma\pi$	seen	-
$f_0(980)\pi$	not seen	189
$f_0(1370)\pi$	seen	†
$f_2(1270)\pi$	seen	†
$K\bar{K}^*(892) + \text{c.c.}$	seen	†
$\pi\gamma$	seen	608

$$f_2(1270) \quad I^G(J^{PC}) = 0^+(2^+ +)$$

Mass $m = 1275.1 \pm 1.2$ MeV ($S = 1.1$)
Full width $\Gamma = 185.0^{+2.9}_{-2.4}$ MeV ($S = 1.5$)

$f_2(1270)$ DECAY MODES	Fraction (Γ_i/Γ)	Scale factor/ Confidence level	ρ (MeV/c)
$\pi\pi$	(84.8 \pm 2.4 -1.2) %	S=1.2	623
$\pi^+\pi^-\pi^0$	(7.1 \pm 1.4 -2.7) %	S=1.3	562
$K\bar{K}$	(4.6 \pm 0.4) %	S=2.7	403
$2\pi^+ 2\pi^-$	(2.8 \pm 0.4) %	S=1.2	559
$\eta\eta$	(4.0 \pm 0.8) $\times 10^{-3}$	S=2.1	326
$4\pi^0$	(3.0 \pm 1.0) $\times 10^{-3}$		564
$\gamma\gamma$	(1.41 \pm 0.13) $\times 10^{-5}$		638
$\eta\pi\pi$	< 8 $\times 10^{-3}$	CL=95%	477
$K^0 K^- \pi^+ + \text{c.c.}$	< 3.4 $\times 10^{-3}$	CL=95%	293
$e^+ e^-$	< 6 $\times 10^{-10}$	CL=90%	638

$$f_1(1285) \quad I^G(J^{PC}) = 0^+(1^+ +)$$

Mass $m = 1281.8 \pm 0.6$ MeV ($S = 1.6$)
Full width $\Gamma = 24.3 \pm 1.1$ MeV ($S = 1.4$)

$f_1(1285)$ DECAY MODES	Fraction (Γ_i/Γ)	Scale factor/ Confidence level	ρ (MeV/c)
4π	(33.1 \pm 2.1 -1.8) %	S=1.3	568
$\pi^0\pi^0\pi^+\pi^-$	(22.0 \pm 1.4 -1.2) %	S=1.3	566
$2\pi^+ 2\pi^-$	(11.0 \pm 0.7 -0.6) %	S=1.3	563
$\rho^0\pi^+\pi^-$	(11.0 \pm 0.7 -0.6) %	S=1.3	336
$\rho^0\rho^0$	seen		†
$4\pi^0$	< 7 $\times 10^{-4}$	CL=90%	568
$\eta\pi\pi$	(52 \pm 16) %		482
$a_0(980)\pi$ [ignoring $a_0(980) \rightarrow K\bar{K}$]	(36 \pm 7) %		234
$\eta\pi\pi$ [excluding $a_0(980)\pi$]	(16 \pm 7) %		482
$K\bar{K}\pi$	(9.0 \pm 0.4) %	S=1.1	308
$K\bar{K}^*(892)$	not seen		†
$\gamma\rho^0$	(5.5 \pm 1.3) %	S=2.8	406
$\phi\gamma$	(7.4 \pm 2.6) $\times 10^{-4}$		236

$$\eta(1295) \quad I^G(J^{PC}) = 0^+(0^- +)$$

Mass $m = 1294 \pm 4$ MeV ($S = 1.6$)
Full width $\Gamma = 55 \pm 5$ MeV

$\eta(1295)$ DECAY MODES	Fraction (Γ_i/Γ)	ρ (MeV/c)
$\eta\pi^+\pi^-$	seen	487
$a_0(980)\pi$	seen	244
$\eta\pi^0\pi^0$	seen	490
$\eta(\pi\pi)_{S\text{-wave}}$	seen	-

$$\pi(1300) \quad I^G(J^{PC}) = 1^-(0^- +)$$

Mass $m = 1300 \pm 100$ MeV $^{[n]}$
Full width $\Gamma = 200$ to 600 MeV

$\pi(1300)$ DECAY MODES	Fraction (Γ_i/Γ)	ρ (MeV/c)
$\rho\pi$	seen	404
$\pi(\pi\pi)_{S\text{-wave}}$	seen	-

$$a_2(1320) \quad I^G(J^{PC}) = 1^-(2^+ +)$$

Mass $m = 1318.3 \pm 0.6$ MeV ($S = 1.2$)
Full width $\Gamma = 107 \pm 5$ MeV $^{[n]}$

Meson Summary Table

$a_2(1320)$ DECAY MODES	Fraction (Γ_i/Γ)	Scale factor/ Confidence level	ρ (MeV/c)
3π	(70.1 \pm 2.7) %	S=1.2	624
$\eta\pi$	(14.5 \pm 1.2) %		535
$\omega\pi\pi$	(10.6 \pm 3.2) %	S=1.3	366
$K\bar{K}$	(4.9 \pm 0.8) %		437
$\eta'(958)\pi$	(5.3 \pm 0.9) $\times 10^{-3}$		288
$\pi^\pm\gamma$	(2.68 \pm 0.31) $\times 10^{-3}$		652
$\gamma\gamma$	(9.4 \pm 0.7) $\times 10^{-6}$		659
e^+e^-	< 6 $\times 10^{-9}$	CL=90%	659

 $f_0(1370)$ [l]

$$J^G(J^{PC}) = 0^+(0^{++})$$

Mass $m = 1200$ to 1500 MeV
Full width $\Gamma = 200$ to 500 MeV

$f_0(1370)$ DECAY MODES	Fraction (Γ_i/Γ)	ρ (MeV/c)
$\pi\pi$	seen	672
4π	seen	617
$4\pi^0$	seen	617
$2\pi^+2\pi^-$	seen	612
$\pi^+\pi^-2\pi^0$	seen	615
$\rho\rho$	dominant	†
$2(\pi\pi)_{s\text{-wave}}$	seen	-
$\pi(1300)\pi$	seen	†
$a_1(1260)\pi$	seen	35
$\eta\eta$	seen	411
$K\bar{K}$	seen	475
$K\bar{K}\eta\pi$	not seen	†
6π	not seen	508
$\omega\omega$	not seen	†
$\gamma\gamma$	seen	685
e^+e^-	not seen	685

 $\pi_1(1400)$ [o]

$$J^G(J^{PC}) = 1^-(1^{-+})$$

Mass $m = 1351 \pm 30$ MeV (S = 2.0)
Full width $\Gamma = 313 \pm 40$ MeV

$\pi_1(1400)$ DECAY MODES	Fraction (Γ_i/Γ)	ρ (MeV/c)
$\eta\pi^0$	seen	555
$\eta\pi^-$	seen	554

 $\eta(1405)$ [p]

$$J^G(J^{PC}) = 0^+(0^{-+})$$

Mass $m = 1409.8 \pm 2.5$ MeV [n] (S = 2.2)
Full width $\Gamma = 51.1 \pm 3.4$ MeV [n] (S = 2.0)

$\eta(1405)$ DECAY MODES	Fraction (Γ_i/Γ)	Confidence level	ρ (MeV/c)
$K\bar{K}\pi$	seen		425
$\eta\pi\pi$	seen		563
$a_0(980)\pi$	seen		342
$\eta(\pi\pi)_{s\text{-wave}}$	seen		-
$f_0(980)\eta$	seen		†
4π	seen		639
$\rho\rho$	<58 %	99.85%	†
$K^*(892)K$	seen		125

 $f_1(1420)$ [q]

$$J^G(J^{PC}) = 0^+(1^{++})$$

Mass $m = 1426.4 \pm 0.9$ MeV (S = 1.1)
Full width $\Gamma = 54.9 \pm 2.6$ MeV

$f_1(1420)$ DECAY MODES	Fraction (Γ_i/Γ)	ρ (MeV/c)
$K\bar{K}\pi$	dominant	438
$K\bar{K}^*(892) + c.c.$	dominant	163
$\eta\pi\pi$	possibly seen	573
$\phi\gamma$	seen	349

 $\omega(1420)$ [r]

$$J^G(J^{PC}) = 0^-(1^{--})$$

Mass m (1400–1450) MeV
Full width Γ (180–250) MeV

$\omega(1420)$ DECAY MODES	Fraction (Γ_i/Γ)	ρ (MeV/c)
$\rho\pi$	dominant	486
$\omega\pi\pi$	seen	444
$b_1(1235)\pi$	seen	125
e^+e^-	seen	710

 $a_0(1450)$ [l]

$$J^G(J^{PC}) = 1^-(0^{++})$$

Mass $m = 1474 \pm 19$ MeV
Full width $\Gamma = 265 \pm 13$ MeV

$a_0(1450)$ DECAY MODES	Fraction (Γ_i/Γ)	ρ (MeV/c)
$\pi\eta$	seen	627
$\pi\eta'(958)$	seen	411
$K\bar{K}$	seen	547
$\omega\pi\pi$	seen	484

 $\rho(1450)$ [s]

$$J^G(J^{PC}) = 1^+(1^{--})$$

Mass $m = 1465 \pm 25$ MeV [n]
Full width $\Gamma = 400 \pm 60$ MeV [n]

$\rho(1450)$ DECAY MODES	Fraction (Γ_i/Γ)	ρ (MeV/c)
$\pi\pi$	seen	720
4π	seen	669
e^+e^-	seen	732
$\eta\rho$	possibly seen	310
$a_2(1320)\pi$	not seen	55
$K\bar{K}$	not seen	541
$K\bar{K}^*(892) + c.c.$	possibly seen	229
$\eta\gamma$	possibly seen	630

 $\eta(1475)$ [p]

$$J^G(J^{PC}) = 0^+(0^{-+})$$

Mass $m = 1476 \pm 4$ MeV (S = 1.3)
Full width $\Gamma = 85 \pm 9$ MeV (S = 1.5)

$\eta(1475)$ DECAY MODES	Fraction (Γ_i/Γ)	ρ (MeV/c)
$K\bar{K}\pi$	dominant	477
$K\bar{K}^*(892) + c.c.$	seen	245
$a_0(980)\pi$	seen	393
$\gamma\gamma$	seen	738

 $f_0(1500)$ [o]

$$J^G(J^{PC}) = 0^+(0^{++})$$

Mass $m = 1505 \pm 6$ MeV (S = 1.3)
Full width $\Gamma = 109 \pm 7$ MeV

$f_0(1500)$ DECAY MODES	Fraction (Γ_i/Γ)	Scale factor	ρ (MeV/c)
$\pi\pi$	(34.9 \pm 2.3) %	1.2	741
$\pi^+\pi^-$	seen		740
$2\pi^0$	seen		741
4π	(49.5 \pm 3.3) %	1.2	691
$4\pi^0$	seen		691
$2\pi^+2\pi^-$	seen		687
$\eta\eta$	(5.1 \pm 0.9) %	1.4	516
$\eta\eta'(958)$	(1.9 \pm 0.8) %	1.7	†
$K\bar{K}$	(8.6 \pm 1.0) %	1.1	568
$\gamma\gamma$	not seen		753

 $f_2'(1525)$

$$J^G(J^{PC}) = 0^+(2^{++})$$

Mass $m = 1525 \pm 5$ MeV [n]
Full width $\Gamma = 73_{-5}^{+6}$ MeV [n]

Meson Summary Table

$f_2'(1525)$ DECAY MODES	Fraction (Γ_i/Γ)	ρ (MeV/c)
$K\bar{K}$	(88.7 \pm 2.2) %	581
$\eta\eta$	(10.4 \pm 2.2) %	530
$\pi\pi$	(8.2 \pm 1.5) $\times 10^{-3}$	750
$\gamma\gamma$	(1.11 \pm 0.14) $\times 10^{-6}$	763

$$\pi_1(1600) [^a] \quad I^G(J^{PC}) = 1^-(1^-+)$$

Mass $m = 1662^{+15}_{-11}$ MeV ($S = 1.2$)
Full width $\Gamma = 234 \pm 50$ MeV ($S = 1.7$)

$\pi_1(1600)$ DECAY MODES	Fraction (Γ_i/Γ)	ρ (MeV/c)
$\pi\pi\pi$	not seen	803
$\rho^0\pi^-$	not seen	641
$f_2(1270)\pi^-$	not seen	319
$b_1(1235)\pi$	seen	357
$\eta'(958)\pi^-$	seen	544
$f_1(1285)\pi$	seen	315

$$\eta_2(1645) \quad I^G(J^{PC}) = 0^+(2^-+)$$

Mass $m = 1617 \pm 5$ MeV
Full width $\Gamma = 181 \pm 11$ MeV

$\eta_2(1645)$ DECAY MODES	Fraction (Γ_i/Γ)	ρ (MeV/c)
$a_2(1320)\pi$	seen	242
$K\bar{K}\pi$	seen	580
$K^*\bar{K}$	seen	404
$\eta\pi^+\pi^-$	seen	685
$a_0(980)\pi$	seen	496
$f_2(1270)\eta$	not seen	†

$$\omega(1650) [^t] \quad I^G(J^{PC}) = 0^-(1^-+)$$

Mass $m = 1670 \pm 30$ MeV
Full width $\Gamma = 315 \pm 35$ MeV

$\omega(1650)$ DECAY MODES	Fraction (Γ_i/Γ)	ρ (MeV/c)
$\rho\pi$	seen	646
$\omega\pi\pi$	seen	617
$\omega\eta$	seen	500
e^+e^-	seen	835

$$\omega_3(1670) \quad I^G(J^{PC}) = 0^-(3^-+)$$

Mass $m = 1667 \pm 4$ MeV
Full width $\Gamma = 168 \pm 10$ MeV [n]

$\omega_3(1670)$ DECAY MODES	Fraction (Γ_i/Γ)	ρ (MeV/c)
$\rho\pi$	seen	645
$\omega\pi\pi$	seen	615
$b_1(1235)\pi$	possibly seen	361

$$\pi_2(1670) \quad I^G(J^{PC}) = 1^-(2^-+)$$

Mass $m = 1672.4 \pm 3.2$ MeV [n] ($S = 1.4$)
Full width $\Gamma = 259 \pm 9$ MeV [n] ($S = 1.3$)

$\pi_2(1670)$ DECAY MODES	Fraction (Γ_i/Γ)	Confidence level	ρ (MeV/c)
3π	(95.8 \pm 1.4) %		809
$f_2(1270)\pi$	(56.3 \pm 3.2) %		329
$\rho\pi$	(31 \pm 4) %		648
$\sigma\pi$	(10.9 \pm 3.4) %		—
$(\pi\pi)$ s-wave	(8.7 \pm 3.4) %		—
$K\bar{K}^*(892) + \text{c.c.}$	(4.2 \pm 1.4) %		455
$\omega\rho$	(2.7 \pm 1.1) %		304
$\gamma\gamma$	< 2.8 $\times 10^{-7}$	90%	836
$\rho(1450)\pi$	< 3.6 $\times 10^{-3}$	97.7%	148
$b_1(1235)\pi$	< 1.9 $\times 10^{-3}$	97.7%	366
$f_1(1285)\pi$	possibly seen		323
$a_2(1320)\pi$	not seen		292

$$\phi(1680) \quad I^G(J^{PC}) = 0^-(1^-+)$$

Mass $m = 1680 \pm 20$ MeV [n]
Full width $\Gamma = 150 \pm 50$ MeV [n]

$\phi(1680)$ DECAY MODES	Fraction (Γ_i/Γ)	ρ (MeV/c)
$K\bar{K}^*(892) + \text{c.c.}$	dominant	462
$K_S^0 K\pi$	seen	621
$K\bar{K}$	seen	680
e^+e^-	seen	840
$\omega\pi\pi$	not seen	623

$$\rho_3(1690) \quad I^G(J^{PC}) = 1^+(3^-+)$$

Mass $m = 1688.8 \pm 2.1$ MeV [n]
Full width $\Gamma = 161 \pm 10$ MeV [n] ($S = 1.5$)

$\rho_3(1690)$ DECAY MODES	Fraction (Γ_i/Γ)	Scale factor	ρ (MeV/c)
4π	(71.1 \pm 1.9) %		790
$\pi^\pm\pi^+\pi^-\pi^0$	(67 \pm 22) %		787
$\omega\pi$	(16 \pm 6) %		655
$\pi\pi\pi$	(23.6 \pm 1.3) %		834
$K\bar{K}\pi$	(3.8 \pm 1.2) %		629
$K\bar{K}$	(1.58 \pm 0.26) %	1.2	685
$\eta\pi^+\pi^-$	seen		727
$\rho(770)\eta$	seen		520
$\pi\pi\rho$	seen		633
Excluding 2ρ and $a_2(1320)\pi$.			
$a_2(1320)\pi$	seen		307
$\rho\rho$	seen		334

$$\rho(1700) [^s] \quad I^G(J^{PC}) = 1^+(1^-+)$$

Mass $m = 1720 \pm 20$ MeV [n] ($\eta\rho^0$ and $\pi^+\pi^-$ modes)
Full width $\Gamma = 250 \pm 100$ MeV [n] ($\eta\rho^0$ and $\pi^+\pi^-$ modes)

$\rho(1700)$ DECAY MODES	Fraction (Γ_i/Γ)	ρ (MeV/c)
$2(\pi^+\pi^-)$	large	803
$\rho\pi\pi$	dominant	653
$\rho^0\pi^+\pi^-$	large	650
$\rho^\pm\pi^\mp\pi^0$	large	652
$a_1(1260)\pi$	seen	404
$h_1(1170)\pi$	seen	447
$\pi(1300)\pi$	seen	349
$\rho\rho$	seen	372
$\pi^+\pi^-$	seen	849
$\pi\pi$	seen	849
$K\bar{K}^*(892) + \text{c.c.}$	seen	496
$\eta\rho$	seen	545
$a_2(1320)\pi$	not seen	334
$K\bar{K}$	seen	704
e^+e^-	seen	860
$\pi^0\omega$	seen	674

Meson Summary Table

 $f_0(1710)$ ^[u]

$$I^G(J^{PC}) = 0^+(0^{++})$$

Mass $m = 1724 \pm 7$ MeV ($S = 1.5$)
 Full width $\Gamma = 137 \pm 8$ MeV ($S = 1.1$)

$f_0(1710)$ DECAY MODES	Fraction (Γ_i/Γ)	ρ (MeV/c)
$K\bar{K}$	seen	707
$\eta\eta$	seen	666
$\pi\pi$	seen	852
$\omega\omega$	seen	362

 $\pi(1800)$

$$I^G(J^{PC}) = 1^-(0^{-+})$$

Mass $m = 1816 \pm 14$ MeV ($S = 2.3$)
 Full width $\Gamma = 208 \pm 12$ MeV

$\pi(1800)$ DECAY MODES	Fraction (Γ_i/Γ)	ρ (MeV/c)
$\pi^+\pi^-\pi^-$	seen	881
$f_0(600)\pi^-$	seen	—
$f_0(980)\pi^-$	seen	634
$f_0(1370)\pi^-$	seen	371
$f_0(1500)\pi^-$	not seen	254
$\rho\pi^-$	not seen	735
$\eta\eta\pi^-$	seen	664
$a_0(980)\eta$	seen	473
$a_2(1320)\eta$	not seen	†
$f_2(1270)\pi$	not seen	445
$f_0(1300)\pi$	not seen	—
$f_0(1500)\pi^-$	seen	254
$\eta\eta'(958)\pi^-$	seen	380
$K_0^*(1430)K^-$	seen	†
$K^*(892)K^-$	not seen	573

 $\phi_3(1850)$

$$I^G(J^{PC}) = 0^-(3^{--})$$

Mass $m = 1854 \pm 7$ MeV
 Full width $\Gamma = 87^{+28}_{-23}$ MeV ($S = 1.2$)

$\phi_3(1850)$ DECAY MODES	Fraction (Γ_i/Γ)	ρ (MeV/c)
$K\bar{K}$	seen	785
$K\bar{K}^*(892) + c.c.$	seen	602

 $\pi_2(1880)$

$$I^G(J^{PC}) = 1^-(2^{-+})$$

Mass $m = 1895 \pm 16$ MeV
 Full width $\Gamma = 235 \pm 34$ MeV

 $f_2(1950)$

$$I^G(J^{PC}) = 0^+(2^{++})$$

Mass $m = 1944 \pm 12$ MeV ($S = 1.5$)
 Full width $\Gamma = 472 \pm 18$ MeV

$f_2(1950)$ DECAY MODES	Fraction (Γ_i/Γ)	ρ (MeV/c)
$K^*(892)\bar{K}^*(892)$	seen	387
$\pi^+\pi^-$	seen	962
4π	seen	925
$\eta\eta$	seen	803
$K\bar{K}$	seen	837
$\gamma\gamma$	seen	972

 $f_2(2010)$

$$I^G(J^{PC}) = 0^+(2^{++})$$

Mass $m = 2011^{+60}_{-80}$ MeV
 Full width $\Gamma = 202 \pm 60$ MeV

$f_2(2010)$ DECAY MODES	Fraction (Γ_i/Γ)	ρ (MeV/c)
$\phi\phi$	seen	†
$K\bar{K}$	seen	876

 $a_4(2040)$

$$I^G(J^{PC}) = 1^-(4^{++})$$

Mass $m = 2001 \pm 10$ MeV
 Full width $\Gamma = 313 \pm 31$ MeV

 $a_4(2040)$ DECAY MODES

DECAY MODES	Fraction (Γ_i/Γ)	ρ (MeV/c)
$K\bar{K}$	seen	870
$\pi^+\pi^-\pi^0$	seen	977
$\rho\pi$	seen	844
$f_2(1270)\pi$	seen	583
$\omega\pi^-\pi^0$	seen	822
$\omega\rho$	seen	628
$\eta\pi^0$	seen	920
$\eta'(958)\pi$	seen	764

 $f_4(2050)$

$$I^G(J^{PC}) = 0^+(4^{++})$$

Mass $m = 2018 \pm 11$ MeV ($S = 2.1$)
 Full width $\Gamma = 237 \pm 18$ MeV ($S = 1.9$)

 $f_4(2050)$ DECAY MODES

DECAY MODES	Fraction (Γ_i/Γ)	ρ (MeV/c)
$\omega\omega$	seen	637
$\pi\pi$	(17.0 ± 1.5) %	1000
$K\bar{K}$	($6.8^{+3.4}_{-1.8}$) $\times 10^{-3}$	880
$\eta\eta$	(2.1 ± 0.8) $\times 10^{-3}$	848
$4\pi^0$	< 1.2 %	964
$a_2(1320)\pi$	seen	567

 $f_2(2300)$

$$I^G(J^{PC}) = 0^+(2^{++})$$

Mass $m = 2297 \pm 28$ MeV
 Full width $\Gamma = 149 \pm 40$ MeV

 $f_2(2300)$ DECAY MODES

DECAY MODES	Fraction (Γ_i/Γ)	ρ (MeV/c)
$\phi\phi$	seen	529
$K\bar{K}$	seen	1037
$\gamma\gamma$	seen	1149

 $f_2(2340)$

$$I^G(J^{PC}) = 0^+(2^{++})$$

Mass $m = 2339 \pm 60$ MeV
 Full width $\Gamma = 319^{+80}_{-70}$ MeV

 $f_2(2340)$ DECAY MODES

DECAY MODES	Fraction (Γ_i/Γ)	ρ (MeV/c)
$\phi\phi$	seen	573
$\eta\eta$	seen	1033

STRANGE MESONS ($S = \pm 1, C = B = 0$)

$$K^+ = u\bar{s}, K^0 = d\bar{s}, \bar{K}^0 = \bar{d}s, K^- = \bar{u}s, \text{ similarly for } K^{*s}$$

 K^\pm

$$I(J^P) = \frac{1}{2}(0^-)$$

Mass $m = 493.677 \pm 0.016$ MeV ^[v] ($S = 2.8$)
 Mean life $\tau = (1.2380 \pm 0.0021) \times 10^{-8}$ s ($S = 1.9$)
 $c\tau = 3.712$ m

Slope parameter g ^[w]

(See Particle Listings for quadratic coefficients and alternative parametrization related to $\pi\pi$ scattering)

$$K^\pm \rightarrow \pi^\pm \pi^+ \pi^- \quad g = -0.21134 \pm 0.00017$$

$$K^\pm \rightarrow \pi^\pm \pi^0 \pi^0 \quad g = 0.626 \pm 0.007$$

$$(g_+ - g_-) / (g_+ + g_-) = (-1.5 \pm 2.2) \times 10^{-4}$$

$$(g_+ - g_-) / (g_+ + g_-) = (1.8 \pm 1.8) \times 10^{-4}$$

 K^\pm decay form factors ^[a,x]

Assuming μ -e universality

$$\lambda_+(K_{\mu 3}^+) = \lambda_+(K_{e 3}^+) = (2.96 \pm 0.06) \times 10^{-2}$$

$$\lambda_0(K_{\mu 3}^+) = (1.96 \pm 0.12) \times 10^{-2}$$

Meson Summary Table

Not assuming μ - e universality

$$\lambda_+(K_{e3}^+) = (2.96 \pm 0.06) \times 10^{-2}$$

$$\lambda_+(K_{\mu 3}^+) = (2.96 \pm 0.17) \times 10^{-2}$$

$$\lambda_0(K_{\mu 3}^+) = (1.96 \pm 0.13) \times 10^{-2}$$

K_{e3} form factor quadratic fit

$$\lambda'_+(K_{e3}^+) \text{ linear coeff.} = (2.48 \pm 0.17) \times 10^{-2}$$

$$\lambda''_+(K_{e3}^+) \text{ quadratic coeff.} = (0.19 \pm 0.09) \times 10^{-2}$$

$$K_{e3}^+ |f_S/f_+| = (-0.3^{+0.8}_{-0.7}) \times 10^{-2}$$

$$K_{e3}^+ |f_T/f_+| = (-1.2 \pm 2.3) \times 10^{-2}$$

$$K_{\mu 3}^+ |f_S/f_+| = (0.2 \pm 0.6) \times 10^{-2}$$

$$K_{\mu 3}^+ |f_T/f_+| = (-0.1 \pm 0.7) \times 10^{-2}$$

$$K^+ \rightarrow e^+ \nu_e \gamma |F_A + F_V| = 0.148 \pm 0.010$$

$$K^+ \rightarrow \mu^+ \nu_\mu \gamma |F_A + F_V| = 0.165 \pm 0.013$$

$$K^+ \rightarrow e^+ \nu_e \gamma |F_A - F_V| < 0.49$$

$$K^+ \rightarrow \mu^+ \nu_\mu \gamma |F_A - F_V| = -0.24 \text{ to } 0.04, \text{ CL} = 90\%$$

Charge Radius

$$\langle r \rangle = 0.560 \pm 0.031 \text{ fm}$$

CP violation parameters

$$\Delta(K_{\pi\mu\mu}^\pm) = -0.02 \pm 0.12$$

T violation parameters

$$K^+ \rightarrow \pi^0 \mu^+ \nu_\mu \quad P_T = (-1.7 \pm 2.5) \times 10^{-3}$$

$$K^+ \rightarrow \mu^+ \nu_\mu \gamma \quad P_T = (-0.6 \pm 1.9) \times 10^{-2}$$

$$K^+ \rightarrow \pi^0 \mu^+ \nu_\mu \quad \text{Im}(\xi) = -0.006 \pm 0.008$$

K^- modes are charge conjugates of the modes below.

K^+ DECAY MODES	Fraction (Γ_i/Γ)	Scale factor/ Confidence level	p (MeV/c)
Leptonic and semileptonic modes			
$K^+ \rightarrow e^+ \nu_e$	(1.55 ± 0.07) × 10 ⁻⁵		247
$K^+ \rightarrow \mu^+ \nu_\mu$	(63.54 ± 0.14) %	S=1.3	236
$K^+ \rightarrow \pi^0 e^+ \nu_e$ Called K_{e3}^+ .	(5.08 ± 0.05) %	S=2.1	228
$K^+ \rightarrow \pi^0 \mu^+ \nu_\mu$ Called $K_{\mu 3}^+$.	(3.35 ± 0.04) %	S=1.9	215
$K^+ \rightarrow \pi^0 \pi^0 e^+ \nu_e$	(2.2 ± 0.4) × 10 ⁻⁵		206
$K^+ \rightarrow \pi^+ \pi^- e^+ \nu_e$	(4.09 ± 0.10) × 10 ⁻⁵		203
$K^+ \rightarrow \pi^+ \pi^- \mu^+ \nu_\mu$	(1.4 ± 0.9) × 10 ⁻⁵		151
$K^+ \rightarrow \pi^0 \pi^0 \pi^0 e^+ \nu_e$	< 3.5 × 10 ⁻⁶	CL=90%	135
Hadronic modes			
$K^+ \rightarrow \pi^+ \pi^0$	(20.68 ± 0.13) %	S=1.6	205
$K^+ \rightarrow \pi^+ \pi^0 \pi^0$	(1.761 ± 0.022) %	S=1.1	133
$K^+ \rightarrow \pi^+ \pi^+ \pi^-$	(5.59 ± 0.04) %	S=1.5	125
Leptonic and semileptonic modes with photons			
$K^+ \rightarrow \mu^+ \nu_\mu \gamma$	[y,z] (6.2 ± 0.8) × 10 ⁻³		236
$K^+ \rightarrow \mu^+ \nu_\mu \gamma$ (SD ⁺)	[a,aa] < 3.0 × 10 ⁻⁵	CL=90%	-
$K^+ \rightarrow \mu^+ \nu_\mu \gamma$ (SD ⁺ INT)	[a,aa] < 2.7 × 10 ⁻⁵	CL=90%	-
$K^+ \rightarrow \mu^+ \nu_\mu \gamma$ (SD ⁻ + SD ⁻ INT)	[a,aa] < 2.6 × 10 ⁻⁴	CL=90%	-
$K^+ \rightarrow e^+ \nu_e \gamma$ (SD ⁺)	[a,aa] (1.52 ± 0.23) × 10 ⁻⁵		-
$K^+ \rightarrow e^+ \nu_e \gamma$ (SD ⁻)	[a,aa] < 1.6 × 10 ⁻⁴	CL=90%	-
$K^+ \rightarrow \pi^0 e^+ \nu_e \gamma$	[y,z] (2.56 ± 0.16) × 10 ⁻⁴		228
$K^+ \rightarrow \pi^0 e^+ \nu_e \gamma$ (SD)	[a,aa] < 5.3 × 10 ⁻⁵	CL=90%	228
$K^+ \rightarrow \pi^0 \mu^+ \nu_\mu \gamma$	[y,z] (1.5 ± 0.4) × 10 ⁻⁵		215
$K^+ \rightarrow \pi^0 \pi^0 e^+ \nu_e \gamma$	< 5 × 10 ⁻⁶	CL=90%	206
Hadronic modes with photons or $\ell\bar{\ell}$ pairs			
$K^+ \rightarrow \pi^+ \pi^0 \gamma$	[y,z] (2.75 ± 0.15) × 10 ⁻⁴		205
$K^+ \rightarrow \pi^+ \pi^0 \gamma$ (DE)	[z,bb] (4.3 ± 0.7) × 10 ⁻⁶		205
$K^+ \rightarrow \pi^+ \pi^0 \pi^0 \gamma$	[y,z] (7.6 $^{+5.6}_{-3.0}$) × 10 ⁻⁶		133
$K^+ \rightarrow \pi^+ \pi^+ \pi^- \gamma$	[y,z] (1.04 ± 0.31) × 10 ⁻⁴		125
$K^+ \rightarrow \pi^+ \gamma \gamma$	[z] (1.10 ± 0.32) × 10 ⁻⁶		227
$K^+ \rightarrow \pi^+ 3\gamma$	[z] < 1.0 × 10 ⁻⁴	CL=90%	227
$K^\pm \rightarrow \pi^\pm e^\pm e^- \gamma$	(1.19 ± 0.13) × 10 ⁻⁸		227

Leptonic modes with $\ell\bar{\ell}$ pairs

$K^+ \rightarrow e^+ \nu_e \nu\bar{\nu}$	< 6	× 10 ⁻⁵	CL=90%	247
$K^+ \rightarrow \mu^+ \nu_\mu \nu\bar{\nu}$	< 6.0	× 10 ⁻⁶	CL=90%	236
$K^+ \rightarrow e^+ \nu_e e^+ e^-$	(2.48 ± 0.20)	× 10 ⁻⁸		247
$K^+ \rightarrow \mu^+ \nu_\mu e^+ e^-$	(7.06 ± 0.31)	× 10 ⁻⁸		236
$K^+ \rightarrow e^+ \nu_e \mu^+ \mu^-$	(1.7 ± 0.5)	× 10 ⁻⁸		223
$K^+ \rightarrow \mu^+ \nu_\mu \mu^+ \mu^-$	< 4.1	× 10 ⁻⁷	CL=90%	185

Lepton Family number (LF), Lepton number (L), $\Delta S = \Delta Q$ (SQ)

violating modes, or $\Delta S = 1$ weak neutral current (S1) modes					
$K^+ \rightarrow \pi^+ \pi^+ e^- \bar{\nu}_e$	SQ	< 1.2	× 10 ⁻⁸	CL=90%	203
$K^+ \rightarrow \pi^+ \pi^+ \mu^- \bar{\nu}_\mu$	SQ	< 3.0	× 10 ⁻⁶	CL=95%	151
$K^+ \rightarrow \pi^+ e^+ e^-$	S1	(2.88 ± 0.13)	× 10 ⁻⁷		227
$K^+ \rightarrow \pi^+ \mu^+ \mu^-$	S1	(8.1 ± 1.4)	× 10 ⁻⁸	S=2.7	172
$K^+ \rightarrow \pi^+ \nu\bar{\nu}$	S1	(1.5 $^{+1.3}_{-0.9}$)	× 10 ⁻¹⁰		227
$K^+ \rightarrow \pi^+ \pi^0 \nu\bar{\nu}$	S1	< 4.3	× 10 ⁻⁵	CL=90%	205
$K^+ \rightarrow \mu^- \nu e^+ e^+$	LF	< 2.0	× 10 ⁻⁸	CL=90%	236
$K^+ \rightarrow \mu^+ \nu_e$	LF	[d] < 4	× 10 ⁻³	CL=90%	236
$K^+ \rightarrow \pi^+ \mu^+ e^-$	LF	< 1.3	× 10 ⁻¹¹	CL=90%	214
$K^+ \rightarrow \pi^+ \mu^- e^+$	LF	< 5.2	× 10 ⁻¹⁰	CL=90%	214
$K^+ \rightarrow \pi^- \mu^+ e^+$	L	< 5.0	× 10 ⁻¹⁰	CL=90%	214
$K^+ \rightarrow \pi^- e^+ e^+$	L	< 6.4	× 10 ⁻¹⁰	CL=90%	227
$K^+ \rightarrow \pi^- \mu^+ \mu^+$	L	[d] < 3.0	× 10 ⁻⁹	CL=90%	172
$K^+ \rightarrow \mu^+ \bar{\nu}_e$	L	[d] < 3.3	× 10 ⁻³	CL=90%	236
$K^+ \rightarrow \pi^0 e^+ \bar{\nu}_e$	L	< 3	× 10 ⁻³	CL=90%	228
$K^+ \rightarrow \pi^+ \gamma$	[cc] < 2.3	× 10 ⁻⁹	CL=90%	227	

K^0

$$I(J^P) = \frac{1}{2}(0^-)$$

50% K_S , 50% K_L

$$\text{Mass } m = 497.614 \pm 0.024 \text{ MeV} \quad (S = 1.6)$$

$$m_{K^0} - m_{K^\pm} = 3.937 \pm 0.028 \text{ MeV} \quad (S = 1.8)$$

Mean Square Charge Radius

$$\langle r^2 \rangle = -0.077 \pm 0.010 \text{ fm}^2$$

T-violation parameters in K^0 - \bar{K}^0 mixing [x]

$$\text{Asymmetry } A_T \text{ in } K^0$$
- \bar{K}^0 mixing = (6.6 ± 1.6) × 10⁻³

CPT-violation parameters [x]

$$\text{Re } \delta = (2.3 \pm 2.7) \times 10^{-4}$$

$$\text{Im } \delta = (0.4 \pm 2.1) \times 10^{-5}$$

$$\text{Re}(y), K_{e3} \text{ parameter} = (0.4 \pm 2.5) \times 10^{-3}$$

$$\text{Re}(x_-), K_{e3} \text{ parameter} = (-2.9 \pm 2.0) \times 10^{-3}$$

$$|m_{K^0} - m_{\bar{K}^0}| / m_{\text{average}} < 8 \times 10^{-19}, \text{ CL} = 90\% \text{ [dd]}$$

$$(\Gamma_{K^0} - \Gamma_{\bar{K}^0}) / m_{\text{average}} = (8 \pm 8) \times 10^{-18}$$

Tests of $\Delta S = \Delta Q$

$$\text{Re}(x_+), K_{e3} \text{ parameter} = (-0.9 \pm 3.0) \times 10^{-3}$$

K_S^0

$$I(J^P) = \frac{1}{2}(0^-)$$

Mean life $\tau = (0.8953 \pm 0.0005) \times 10^{-10}$ s (S = 1.1) Assuming CPT

Mean life $\tau = (0.8958 \pm 0.0005) \times 10^{-10}$ s Not assuming CPT
 $c\tau = 2.6842$ cm Assuming CPT

CP-violation parameters [ee]

$$\text{Im}(\eta_{+-0}) = -0.002 \pm 0.009$$

$$\text{Im}(\eta_{000}) = (-0.1 \pm 1.6) \times 10^{-2}$$

$$|\eta_{000}| = |A(K_S^0 \rightarrow 3\pi^0)/A(K_L^0 \rightarrow 3\pi^0)| < 0.018, \text{ CL} = 90\%$$

$$\text{CP asymmetry } A \text{ in } \pi^+ \pi^- e^+ e^- = (-1 \pm 4)\%$$

Meson Summary Table

K_S^0 DECAY MODES	Fraction (Γ_i/Γ)	Confidence level	P (MeV/c)
Hadronic modes			
$\pi^0 \pi^0$	$(30.69 \pm 0.05) \%$		209
$\pi^+ \pi^-$	$(69.20 \pm 0.05) \%$		206
$\pi^+ \pi^- \pi^0$	$(3.5 \pm 1.1) \times 10^{-7}$		133
Modes with photons or $\ell\bar{\ell}$ pairs			
$\pi^+ \pi^- \gamma$	[y, \bar{y}] $(1.79 \pm 0.05) \times 10^{-3}$		206
$\pi^+ \pi^- e^+ e^-$	$(4.69 \pm 0.30) \times 10^{-5}$		206
$\pi^0 \gamma \gamma$	[f] $(4.9 \pm 1.8) \times 10^{-8}$		231
$\gamma \gamma$	$(2.71 \pm 0.06) \times 10^{-6}$		249
Semileptonic modes			
$\pi^\pm e^\mp \nu_e$	[gg] $(7.04 \pm 0.08) \times 10^{-4}$		229
CP violating (CP) and $\Delta S = 1$ weak neutral current ($S1$) modes			
$3\pi^0$	CP	$< 1.2 \times 10^{-7}$	90% 139
$\mu^+ \mu^-$	S1	$< 3.2 \times 10^{-7}$	90% 225
$e^+ e^-$	S1	$< 1.4 \times 10^{-7}$	90% 249
$\pi^0 e^+ e^-$	S1 [ff]	$(3.0 \pm 1.5) \times 10^{-9}$	230
$\pi^0 \mu^+ \mu^-$	S1	$(2.9 \pm 1.5) \times 10^{-9}$	177

 K_L^0

$$I(J^P) = \frac{1}{2}(0^-)$$

$$m_{K_L} - m_{K_S}$$

$$= (0.5292 \pm 0.0009) \times 10^{10} \text{ h s}^{-1} \quad (S = 1.2) \quad \text{Assuming } CPT$$

$$= (3.483 \pm 0.006) \times 10^{-12} \text{ MeV} \quad \text{Assuming } CPT$$

$$= (0.5290 \pm 0.0015) \times 10^{10} \text{ h s}^{-1} \quad (S = 1.1) \quad \text{Not assuming } CPT$$

$$\text{Mean life } \tau = (5.116 \pm 0.020) \times 10^{-8} \text{ s}$$

$$c\tau = 15.34 \text{ m}$$

Slope parameter g [w]

(See Particle Listings for quadratic coefficients)

$$K_L^0 \rightarrow \pi^+ \pi^- \pi^0: g = 0.678 \pm 0.008 \quad (S = 1.5)$$

 K_L decay form factors [x]Linear parametrization assuming μ - e universality

$$\lambda_+(K_{\mu 3}^0) = \lambda_+(K_{e 3}^0) = (2.82 \pm 0.04) \times 10^{-2} \quad (S = 1.1)$$

$$\lambda_0(K_{\mu 3}^0) = (1.38 \pm 0.18) \times 10^{-2} \quad (S = 2.2)$$

Quadratic parametrization assuming μ - e universality

$$\lambda'_+(K_{\mu 3}^0) = \lambda'_+(K_{e 3}^0) = (2.40 \pm 0.12) \times 10^{-2} \quad (S = 1.2)$$

$$\lambda''_+(K_{\mu 3}^0) = \lambda''_+(K_{e 3}^0) = (0.20 \pm 0.05) \times 10^{-2} \quad (S = 1.2)$$

$$\lambda_0(K_{\mu 3}^0) = (1.16 \pm 0.09) \times 10^{-2} \quad (S = 1.2)$$

Pole parametrization assuming μ - e universality

$$M_V^\mu(K_{\mu 3}^0) = M_V^e(K_{e 3}^0) = 878 \pm 6 \text{ MeV} \quad (S = 1.1)$$

$$M_S^\mu(K_{\mu 3}^0) = 1252 \pm 90 \text{ MeV} \quad (S = 2.6)$$

$$K_{e 3}^0 \quad |f_S/f_+| = (1.5 \pm 1.4) \times 10^{-2}$$

$$K_{e 3}^0 \quad |f_T/f_+| = (5 \pm 4) \times 10^{-2}$$

$$K_{\mu 3}^0 \quad |f_T/f_+| = (12 \pm 12) \times 10^{-2}$$

$$K_L \rightarrow \ell^+ \ell^- \gamma, K_L \rightarrow \ell^+ \ell^- \ell'^+ \ell'^-: \alpha_{K^*} = -0.205 \pm 0.022 \quad (S = 1.8)$$

$$K_L^0 \rightarrow \ell^+ \ell^- \gamma, K_L^0 \rightarrow \ell^+ \ell^- \ell'^+ \ell'^-: \alpha_{DIP} = -1.69 \pm 0.08 \quad (S = 1.7)$$

$$K_L \rightarrow \pi^+ \pi^- e^+ e^-: a_1/a_2 = -0.737 \pm 0.014 \text{ GeV}^2$$

$$K_L \rightarrow \pi^0 2\gamma: a_V = -0.54 \pm 0.12 \quad (S = 2.8)$$

CP-violation parameters [e^e]

$$A_L = (0.332 \pm 0.006) \%$$

$$|\eta_{00}| = (2.222 \pm 0.012) \times 10^{-3} \quad (S = 1.7)$$

$$|\eta_{+-}| = (2.233 \pm 0.012) \times 10^{-3} \quad (S = 1.7)$$

$$|\epsilon| = (2.229 \pm 0.012) \times 10^{-3} \quad (S = 1.7)$$

$$|\eta_{00}/\eta_{+-}| = 0.9951 \pm 0.0008 [hh] \quad (S = 1.6)$$

$$\text{Re}(\epsilon'/\epsilon) = (1.65 \pm 0.26) \times 10^{-3} [hh] \quad (S = 1.6)$$

Assuming CPT

$$\phi_{+-} = (43.51 \pm 0.05)^\circ \quad (S = 1.1)$$

$$\phi_{00} = (43.52 \pm 0.05)^\circ \quad (S = 1.1)$$

$$\phi_\epsilon = \phi_{sw} = (43.51 \pm 0.05)^\circ \quad (S = 1.1)$$

Not assuming CPT

$$\phi_{+-} = (43.4 \pm 0.7)^\circ \quad (S = 1.3)$$

$$\phi_{00} = (43.7 \pm 0.8)^\circ \quad (S = 1.2)$$

$$\phi_\epsilon = (43.5 \pm 0.7)^\circ \quad (S = 1.3)$$

CP asymmetry A in $K_L^0 \rightarrow \pi^+ \pi^- e^+ e^- = (13.7 \pm 1.5) \%$

$$\beta_{CP} \text{ from } K_L^0 \rightarrow e^+ e^- e^+ e^- = -0.19 \pm 0.07$$

$$\gamma_{CP} \text{ from } K_L^0 \rightarrow e^+ e^- e^+ e^- = 0.01 \pm 0.11 \quad (S = 1.6)$$

$$j \text{ for } K_L^0 \rightarrow \pi^+ \pi^- \pi^0 = 0.0012 \pm 0.0008$$

$$f \text{ for } K_L^0 \rightarrow \pi^+ \pi^- \pi^0 = 0.004 \pm 0.006$$

$$|\eta_{+-\gamma}| = (2.35 \pm 0.07) \times 10^{-3}$$

$$\phi_{+-\gamma} = (44 \pm 4)^\circ$$

$$|\epsilon'_{+-\gamma}|/\epsilon < 0.3, \text{ CL} = 90\%$$

$$|\bar{g}_{E1}| \text{ for } K_L^0 \rightarrow \pi^+ \pi^- \gamma < 0.21, \text{ CL} = 90\%$$

T-violation parameters

$$\text{Im}(\xi) \text{ in } K_{\mu 3}^0 = -0.007 \pm 0.026$$

CPT invariance tests

$$\phi_{00} - \phi_{+-} = (0.2 \pm 0.4)^\circ$$

$$\text{Re}(\frac{2}{3}\eta_{+-} + \frac{1}{3}\eta_{00}) - \frac{A}{2} = (-3 \pm 35) \times 10^{-6}$$

 $\Delta S = -\Delta Q$ in $K_{e 3}^0$ decay

$$\text{Re } x = -0.002 \pm 0.006$$

$$\text{Im } x = 0.0012 \pm 0.0021$$

K_L^0 DECAY MODES	Fraction (Γ_i/Γ)	Scale factor / Confidence level	P (MeV/c)
Semileptonic modes			
$\pi^\pm e^\mp \nu_e$	[gg] $(40.55 \pm 0.12) \%$	S=1.8	229
Called $K_{e 3}^0$.			
$\pi^\pm \mu^\mp \nu_\mu$	[gg] $(27.04 \pm 0.07) \%$	S=1.1	216
Called $K_{\mu 3}^0$.			
$(\pi \mu \text{atom}) \nu$	$(1.05 \pm 0.11) \times 10^{-7}$		188
$\pi^0 \pi^\pm e^\mp \nu$	[gg] $(5.20 \pm 0.11) \times 10^{-5}$		207
$\pi^\pm e^\mp \nu e^+ e^-$	[gg] $(1.28 \pm 0.04) \times 10^{-5}$		229
Hadronic modes, including Charge conjugation \times Parity Violating (CPV) modes			
$3\pi^0$	$(19.52 \pm 0.12) \%$	S=1.7	139
$\pi^+ \pi^- \pi^0$	$(12.54 \pm 0.05) \%$		133
$\pi^+ \pi^-$	CPV [ii] $(1.966 \pm 0.010) \times 10^{-3}$	S=1.6	206
$\pi^0 \pi^0$	CPV $(8.65 \pm 0.06) \times 10^{-4}$	S=1.8	209
Semileptonic modes with photons			
$\pi^\pm e^\mp \nu_e \gamma$	[$y, gg, j\bar{j}$] $(3.80 \pm 0.08) \times 10^{-3}$		229
$\pi^\pm \mu^\mp \nu_\mu \gamma$	$(5.65 \pm 0.23) \times 10^{-4}$		216
Hadronic modes with photons or $\ell\bar{\ell}$ pairs			
$\pi^0 \pi^0 \gamma$	$< 5.6 \times 10^{-6}$	CL=90%	209
$\pi^+ \pi^- \gamma$	[$y, j\bar{j}$] $(4.15 \pm 0.15) \times 10^{-5}$	S=2.8	206
$\pi^+ \pi^- \gamma (\text{DE})$	$(2.84 \pm 0.11) \times 10^{-5}$	S=2.0	206
$\pi^0 2\gamma$	[$j\bar{j}$] $(1.32 \pm 0.14) \times 10^{-6}$	S=3.6	231
$\pi^0 \gamma e^+ e^-$	$(1.62 \pm 0.17) \times 10^{-8}$		230
Other modes with photons or $\ell\bar{\ell}$ pairs			
2γ	$(5.47 \pm 0.04) \times 10^{-4}$	S=1.2	249
3γ	$< 2.4 \times 10^{-7}$	CL=90%	249
$e^+ e^- \gamma$	$(9.50 \pm 0.35) \times 10^{-6}$	S=1.7	249
$\mu^+ \mu^- \gamma$	$(3.59 \pm 0.11) \times 10^{-7}$	S=1.3	225
$e^+ e^- \gamma \gamma$	[$j\bar{j}$] $(5.95 \pm 0.33) \times 10^{-7}$		249
$\mu^+ \mu^- \gamma \gamma$	[$j\bar{j}$] $(1.0 \pm 0.8) \times 10^{-8}$		225

Meson Summary Table

Charge conjugation \times Parity (CP) or Lepton Family Number (LF) violating modes, or $\Delta S = 1$ weak neutral current (SI) modes

$\mu^+ \mu^-$	SI	$(6.84 \pm 0.11) \times 10^{-9}$	225
$e^+ e^-$	SI	$(9 \pm 4) \times 10^{-12}$	249
$\pi^+ \pi^- e^+ e^-$	SI [ll]	$(3.11 \pm 0.19) \times 10^{-7}$	206
$\pi^0 \pi^0 e^+ e^-$	SI	$< 6.6 \times 10^{-9}$	CL=90% 209
$\mu^+ \mu^- e^+ e^-$	SI	$(2.69 \pm 0.27) \times 10^{-9}$	225
$e^+ e^- e^+ e^-$	SI	$(3.56 \pm 0.21) \times 10^{-8}$	249
$\pi^0 \mu^+ \mu^-$	CP, SI [kk]	$< 3.8 \times 10^{-10}$	CL=90% 177
$\pi^0 e^+ e^-$	CP, SI [kk]	$< 2.8 \times 10^{-10}$	CL=90% 230
$\pi^0 \nu \bar{\nu}$	CP, SI [ll]	$< 2.1 \times 10^{-7}$	CL=90% 231
$\pi^0 \pi^0 \nu \bar{\nu}$	SI	$< 4.7 \times 10^{-5}$	CL=90% 209
$e^\pm \mu^\mp$	LF [gg]	$< 4.7 \times 10^{-12}$	CL=90% 238
$e^\pm e^\pm \mu^\mp \mu^\mp$	LF [gg]	$< 4.12 \times 10^{-11}$	CL=90% 225
$\pi^0 \mu^\pm e^\mp$	LF [gg]	$< 6.2 \times 10^{-9}$	CL=90% 217

$K^*(892)$ $I(J^P) = \frac{1}{2}(1^-)$

$K^*(892)^\pm$ mass $m = 891.66 \pm 0.26$ MeV
 Mass $m = 895.5 \pm 0.8$ MeV
 $K^*(892)^0$ mass $m = 896.00 \pm 0.25$ MeV ($S = 1.4$)
 $K^*(892)^\pm$ full width $\Gamma = 50.8 \pm 0.9$ MeV
 Full width $\Gamma = 46.2 \pm 1.3$
 $K^*(892)^0$ full width $\Gamma = 50.3 \pm 0.6$ MeV ($S = 1.1$)

$K^*(892)$ DECAY MODES	Fraction (Γ_i/Γ)	Confidence level	ρ (MeV/c)
$K\pi$	~ 100 %		289
$K^0\gamma$	$(2.31 \pm 0.20) \times 10^{-3}$		307
$K^\pm\gamma$	$(9.9 \pm 0.9) \times 10^{-4}$		309
$K\pi\pi$	$< 7 \times 10^{-4}$	95%	223

$K_1(1270)$ $I(J^P) = \frac{1}{2}(1^+)$

Mass $m = 1272 \pm 7$ MeV [n]
 Full width $\Gamma = 90 \pm 20$ MeV [n]

$K_1(1270)$ DECAY MODES	Fraction (Γ_i/Γ)	ρ (MeV/c)
$K\rho$	(42 ± 6) %	45
$K_0^*(1430)\pi$	(28 ± 4) %	†
$K^*(892)\pi$	(16 ± 5) %	302
$K\omega$	(11.0 ± 2.0) %	†
$Kf_0(1370)$	(3.0 ± 2.0) %	†
γK^0	seen	539

$K_1(1400)$ $I(J^P) = \frac{1}{2}(1^+)$

Mass $m = 1403 \pm 7$ MeV
 Full width $\Gamma = 174 \pm 13$ MeV ($S = 1.6$)

$K_1(1400)$ DECAY MODES	Fraction (Γ_i/Γ)	ρ (MeV/c)
$K^*(892)\pi$	(94 ± 6) %	402
$K\rho$	(3.0 ± 3.0) %	292
$Kf_0(1370)$	(2.0 ± 2.0) %	†
$K\omega$	(1.0 ± 1.0) %	284
$K_0^*(1430)\pi$	not seen	†
γK^0	seen	613

$K^*(1410)$ $I(J^P) = \frac{1}{2}(1^-)$

Mass $m = 1414 \pm 15$ MeV ($S = 1.3$)
 Full width $\Gamma = 232 \pm 21$ MeV ($S = 1.1$)

$K^*(1410)$ DECAY MODES	Fraction (Γ_i/Γ)	Confidence level	ρ (MeV/c)
$K^*(892)\pi$	> 40 %	95%	410
$K\pi$	(6.6 ± 1.3) %		612
$K\rho$	< 7 %	95%	305
γK^0	seen		619

$K_0^*(1430)$ [mm] $I(J^P) = \frac{1}{2}(0^+)$

Mass $m = 1425 \pm 50$ MeV
 Full width $\Gamma = 270 \pm 80$ MeV

$K_0^*(1430)$ DECAY MODES	Fraction (Γ_i/Γ)	ρ (MeV/c)
$K\pi$	(93 ± 10) %	619

$K_2^*(1430)$ $I(J^P) = \frac{1}{2}(2^+)$

$K_2^*(1430)^\pm$ mass $m = 1425.6 \pm 1.5$ MeV ($S = 1.1$)
 $K_2^*(1430)^0$ mass $m = 1432.4 \pm 1.3$ MeV
 $K_2^*(1430)^\pm$ full width $\Gamma = 98.5 \pm 2.7$ MeV ($S = 1.1$)
 $K_2^*(1430)^0$ full width $\Gamma = 109 \pm 5$ MeV ($S = 1.9$)

$K_2^*(1430)$ DECAY MODES	Fraction (Γ_i/Γ)	Scale factor / Confidence level	ρ (MeV/c)
$K\pi$	(49.9 ± 1.2) %		619
$K^*(892)\pi$	(24.7 ± 1.5) %		419
$K^*(892)\pi\pi$	(13.4 ± 2.2) %		372
$K\rho$	(8.7 ± 0.8) %	$S=1.2$	318
$K\omega$	(2.9 ± 0.8) %		311
$K^+\gamma$	$(2.4 \pm 0.5) \times 10^{-3}$	$S=1.1$	627
$K\eta$	$(1.5 \pm 3.4) \times 10^{-3}$	$S=1.3$	486
$K\omega\pi$	$< 7.2 \times 10^{-4}$	CL=95%	100
$K^0\gamma$	$< 9 \times 10^{-4}$	CL=90%	626

$K^*(1680)$ $I(J^P) = \frac{1}{2}(1^-)$

Mass $m = 1717 \pm 27$ MeV ($S = 1.4$)
 Full width $\Gamma = 322 \pm 110$ MeV ($S = 4.2$)

$K^*(1680)$ DECAY MODES	Fraction (Γ_i/Γ)	ρ (MeV/c)
$K\pi$	(38.7 ± 2.5) %	781
$K\rho$	$(31.4 \pm 4.7) \times 10^{-2}$ %	570
$K^*(892)\pi$	$(29.9 \pm 2.2) \times 10^{-2}$ %	618

$K_2(1770)$ [nn] $I(J^P) = \frac{1}{2}(2^-)$

Mass $m = 1773 \pm 8$ MeV
 Full width $\Gamma = 186 \pm 14$ MeV

$K_2(1770)$ DECAY MODES	Fraction (Γ_i/Γ)	ρ (MeV/c)
$K\pi\pi$		794
$K_2^*(1430)\pi$	dominant	288
$K^*(892)\pi$	seen	654
$Kf_2(1270)$	seen	55
$K\phi$	seen	441
$K\omega$	seen	607

$K_3^*(1780)$ $I(J^P) = \frac{1}{2}(3^-)$

Mass $m = 1776 \pm 7$ MeV ($S = 1.1$)
 Full width $\Gamma = 159 \pm 21$ MeV ($S = 1.3$)

$K_3^*(1780)$ DECAY MODES	Fraction (Γ_i/Γ)	Confidence level	ρ (MeV/c)
$K\rho$	(31 ± 9) %		613
$K^*(892)\pi$	(20 ± 5) %		656
$K\pi$	(18.8 ± 1.0) %		813
$K\eta$	(30 ± 13) %		719
$K_2^*(1430)\pi$	< 16 %	95%	291

Meson Summary Table

 $K_2(1820)$ $[00]$

$$I(J^P) = \frac{1}{2}(2^-)$$

Mass $m = 1816 \pm 13$ MeV
 Full width $\Gamma = 276 \pm 35$ MeV

$K_2(1820)$ DECAY MODES	Fraction (Γ_i/Γ)	ρ (MeV/c)
$K_2^*(1430)\pi$	seen	327
$K^*(892)\pi$	seen	681
$K f_2(1270)$	seen	186
$K\omega$	seen	638

 $K_4^*(2045)$

$$I(J^P) = \frac{1}{2}(4^+)$$

Mass $m = 2045 \pm 9$ MeV ($S = 1.1$)
 Full width $\Gamma = 198 \pm 30$ MeV

$K_4^*(2045)$ DECAY MODES	Fraction (Γ_i/Γ)	ρ (MeV/c)
$K\pi$	$(9.9 \pm 1.2)\%$	958
$K^*(892)\pi\pi$	$(9 \pm 5)\%$	802
$K^*(892)\pi\pi\pi$	$(7 \pm 5)\%$	768
$\rho K\pi$	$(5.7 \pm 3.2)\%$	741
$\omega K\pi$	$(5.0 \pm 3.0)\%$	738
$\phi K\pi$	$(2.8 \pm 1.4)\%$	594
$\phi K^*(892)$	$(1.4 \pm 0.7)\%$	363

CHARMED MESONS ($C = \pm 1$)

$D^+ = c\bar{d}$, $D^0 = c\bar{u}$, $\bar{D}^0 = \bar{c}u$, $D^- = \bar{c}d$, similarly for D^{*s}

 D^\pm

$$I(J^P) = \frac{1}{2}(0^-)$$

Mass $m = 1869.62 \pm 0.20$ MeV ($S = 1.1$)
 Mean life $\tau = (1040 \pm 7) \times 10^{-15}$ s
 $c\tau = 311.8 \mu\text{m}$

c-quark decays

$\Gamma(c \rightarrow \ell^+ \text{anything})/\Gamma(c \rightarrow \text{anything}) = 0.096 \pm 0.004$ [$\rho\rho$]
 $\Gamma(c \rightarrow D^*(2010)^+ \text{anything})/\Gamma(c \rightarrow \text{anything}) = 0.255 \pm 0.017$

CP-violation decay-rate asymmetries

$A_{CP}(K_S^0 \pi^\pm) = -0.009 \pm 0.009$
 $A_{CP}(K^\mp 2\pi^\pm) = -0.005 \pm 0.010$
 $A_{CP}(K^\mp \pi^\pm \pi^\pm \pi^0) = 0.010 \pm 0.013$
 $A_{CP}(K_S^0 \pi^\pm \pi^0) = 0.003 \pm 0.009$
 $A_{CP}(K_S^0 \pi^\pm \pi^+ \pi^-) = 0.001 \pm 0.013$
 $A_{CP}(K_S^0 K^\pm) = 0.07 \pm 0.06$
 $A_{CP}(K^\pm K^- \pi^\pm) = 0.006 \pm 0.007$
 $A_{CP}(K^\pm K^*0) = 0.005 \pm 0.017$
 $A_{CP}(\phi \pi^\pm) = -0.001 \pm 0.015$
 $A_{CP}(\pi^+ \pi^- \pi^\pm) = -0.02 \pm 0.04$
 $A_{CP}(K_S^0 K^\pm \pi^+ \pi^-) = -0.04 \pm 0.07$

T-violation decay-rate asymmetry

$A_T(K_S^0 K^\pm \pi^+ \pi^-) = 0.02 \pm 0.07$

 $D^+ \rightarrow \bar{K}^*(892)^0 \ell^+ \nu_\ell$ form factors

$r_V = 1.62 \pm 0.08$ ($S = 1.5$)
 $r_2 = 0.83 \pm 0.05$
 $r_3 = 0.0 \pm 0.4$
 $\Gamma_L/\Gamma_T = 1.13 \pm 0.08$
 $\Gamma_+/ \Gamma_- = 0.22 \pm 0.06$ ($S = 1.6$)

Most decay modes (other than the semileptonic modes) that involve a neutral K meson are now given as K_S^0 modes, not as \bar{K}^0 modes. Nearly always it is a K_S^0 that is measured, and interference between Cabibbo-allowed and doubly Cabibbo-suppressed modes can invalidate the assumption that $2\Gamma(K_S^0) = \Gamma(\bar{K}^0)$.

 D^+ DECAY MODES

	Fraction (Γ_i/Γ)	Scale factor/ Confidence level	ρ (MeV/c)
Inclusive modes			
e^+ anything	$(16.0 \pm 0.4)\%$		—
K^- anything	$(25.7 \pm 1.4)\%$		—
\bar{K}^0 anything + K^0 anything	$(61 \pm 5)\%$		—
K^+ anything	$(5.9 \pm 0.8)\%$		—
$K^*(892)^-$ anything	$(6 \pm 5)\%$		—
$\bar{K}^*(892)^0$ anything	$(23 \pm 5)\%$		—
$K^*(892)^0$ anything	$< 6.6\%$	CL=90%	—
η anything	$(6.3 \pm 0.7)\%$		—
η' anything	$(1.04 \pm 0.18)\%$		—
ϕ anything	$(1.03 \pm 0.12)\%$		—

Leptonic and semileptonic modes

$e^+ \nu_e$	$< 2.4 \times 10^{-5}$	CL=90%	935
$\mu^+ \nu_\mu$	$(4.4 \pm 0.7) \times 10^{-4}$		932
$\tau^+ \nu_\tau$	$< 2.1 \times 10^{-3}$		90
$\bar{K}^0 e^+ \nu_e$	$(8.6 \pm 0.5)\%$		869
$\bar{K}^0 \mu^+ \nu_\mu$	$(9.3 \pm 0.8)\%$	S=1.1	865
$K^- \pi^+ e^+ \nu_e$	$(4.1 \pm 0.6)\%$	S=1.1	864
$\bar{K}^*(892)^0 e^+ \nu_e$	$(3.66 \pm 0.21)\%$		722
$\bar{K}^*(892)^0 \rightarrow K^- \pi^+$			
$K^- \pi^+ e^+ \nu_e$ nonresonant	$< 7 \times 10^{-3}$	CL=90%	864
$K^- \pi^+ \mu^+ \nu_\mu$	$(3.9 \pm 0.5)\%$		851
$\bar{K}^*(892)^0 \mu^+ \nu_\mu$	$(3.6 \pm 0.3)\%$		717
$\bar{K}^*(892)^0 \rightarrow K^- \pi^+$			
$K^- \pi^+ \mu^+ \nu_\mu$ nonresonant	$(2.1 \pm 0.5) \times 10^{-3}$		851
$K^- \pi^+ \pi^0 \mu^+ \nu_\mu$	$< 1.6 \times 10^{-3}$	CL=90%	825
$\pi^0 e^+ \nu_e$	$(4.4 \pm 0.7) \times 10^{-3}$		930
$\rho^0 e^+ \nu_e$	$(2.2 \pm 0.4) \times 10^{-3}$		774
$\rho^0 \mu^+ \nu_\mu$	$(2.4 \pm 0.4) \times 10^{-3}$		770
$\omega e^+ \nu_e$	$(1.6 \pm 0.7) \times 10^{-3}$		771
$\phi e^+ \nu_e$	$< 2.01\%$	CL=90%	657
$\phi \mu^+ \nu_\mu$	$< 2.04\%$	CL=90%	651
$\eta \ell^+ \nu_\ell$	$< 7 \times 10^{-3}$	CL=90%	855
$\eta'(958) \mu^+ \nu_\mu$	$< 1.1\%$	CL=90%	684

Fractions of some of the following modes with resonances have already appeared above as submodes of particular charged-particle modes.

$\bar{K}^*(892)^0 e^+ \nu_e$	$(5.49 \pm 0.31)\%$	S=1.2	722
$\bar{K}^*(892)^0 \mu^+ \nu_\mu$	$(5.4 \pm 0.4)\%$	S=1.1	717
$\bar{K}_S^0(1430)^0 \mu^+ \nu_\mu$	$< 2.5 \times 10^{-4}$		380
$\bar{K}^*(1680)^0 \mu^+ \nu_\mu$	$< 1.5 \times 10^{-3}$		105

Hadronic modes with a \bar{K} or $\bar{K}\bar{K}$

$K_S^0 \pi^+$	$(1.45 \pm 0.04)\%$	S=1.3	863
$K_L^0 \pi^+$	$(1.46 \pm 0.05)\%$		863
$K^- \pi^+ \pi^+$	[qq] $(9.22 \pm 0.21)\%$	S=1.1	846
$(K^- \pi^+)_{S\text{-wave}} \pi^+$	$(7.54 \pm 0.26)\%$		846
$\bar{K}^*(892)^0 \pi^+$	$(1.22 \pm 0.09)\%$		714
$\bar{K}^*(892)^0 \rightarrow K^- \pi^+$			
$\bar{K}_S^0(1430)^0 \pi^+$	[rr] $(3.0 \pm 0.8) \times 10^{-4}$		371
$\bar{K}_S^0(1430)^0 \rightarrow K^- \pi^+$			
$\bar{K}^*(1680)^0 \pi^+$	[rr] $(1.6 \pm 0.6) \times 10^{-3}$		58
$\bar{K}^*(1680)^0 \rightarrow K^- \pi^+$			
$K_S^0 \pi^+ \pi^0$	[qq] $(6.8 \pm 0.5)\%$	S=1.9	845
$K_S^0 \rho^+$	$(4.6 \pm 1.0)\%$		677
$\bar{K}^*(892)^0 \pi^+$	$(1.3 \pm 0.6)\%$		714
$\bar{K}^*(892)^0 \rightarrow K_S^0 \pi^0$			
$K_S^0 \pi^+ \pi^0$ nonresonant	$(9 \pm 7) \times 10^{-3}$		845
$K^- \pi^+ \pi^+ \pi^0$	[qq] $(6.00 \pm 0.20)\%$	S=1.2	816
$\bar{K}^*(892)^0 \rho^+$ total,	$(1.3 \pm 0.8)\%$		422
$\bar{K}^*(892)^0 \rightarrow K^- \pi^+$			
$\bar{K}_1(1400)^0 \pi^+$	$(1.8 \pm 0.7)\%$		390
$\bar{K}_1(1400)^0 \rightarrow K^- \pi^+ \pi^0$			
$K^- \rho^+ \pi^+$ total	$(2.9 \pm 1.0) \times 10^{-3}$		613
$K^- \rho^+ \pi^+$ 3-body	$(1.0 \pm 0.4)\%$		613
$\bar{K}^*(892)^0 \pi^+ \pi^0$ total,	$(4.2 \pm 0.6)\%$		690
$\bar{K}^*(892)^0 \rightarrow K^- \pi^+$			

Meson Summary Table

$\bar{K}^*(892)^0 \pi^+ \pi^0$ 3-body, $\bar{K}^*(892)^0 \rightarrow K^- \pi^+$	(2.7 ± 0.8) %		690
$K^*(892)^- \pi^+ \pi^+$ 3-body, $K^*(892)^- \rightarrow K^- \pi^0$	(6 ± 3) × 10 ⁻³		688
$K^- \pi^+ \pi^0$ nonresonant	[ss] (1.1 ± 0.5) %		816
$K_S^0 \pi^+ \pi^-$	[qq] (3.02 ± 0.12) %	S=1.3	814
$K_S^0 a_1(1260)^+$, $a_1(1260)^+ \rightarrow \pi^+ \pi^+ \pi^-$	(1.8 ± 0.3) %		328
$\bar{K}_1(1400)^0 \pi^+$, $\bar{K}_1(1400)^0 \rightarrow K_S^0 \pi^+ \pi^-$	(1.8 ± 0.7) %		390
$K^*(892)^- \pi^+ \pi^+$ 3-body, $K^*(892)^- \rightarrow K_S^0 \pi^-$	(1.3 ± 0.6) %		688
$K_S^0 \rho^0 \pi^+$ total	(1.8 ± 0.6) %		611
$K_S^0 \rho^0 \pi^+$ 3-body	(2.1 ± 2.2) × 10 ⁻³		611
$K_S^0 \pi^+ \pi^-$ nonresonant	(3.6 ± 1.8) × 10 ⁻³		814
$K^- 3\pi^+ \pi^-$	[qq] (5.6 ± 0.5) × 10 ⁻³	S=1.1	772
$\bar{K}^*(892)^0 \pi^+ \pi^+ \pi^-$, $\bar{K}^*(892)^0 \rightarrow K^- \pi^+$	(1.2 ± 0.4) × 10 ⁻³		645
$\bar{K}^*(892)^0 \rho^0 \pi^+$, $\bar{K}^*(892)^0 \rightarrow K^- \pi^+$	(2.3 ± 0.4) × 10 ⁻³		239
$K^- \rho^0 \pi^+ \pi^+$	(1.69 ± 0.28) × 10 ⁻³		524
$K^- 3\pi^+ \pi^-$ nonresonant	(3.9 ± 2.9) × 10 ⁻⁴		772
$K^+ 2K_S^0$	(4.5 ± 2.1) × 10 ⁻³		545
$K^+ K^- K_S^0 \pi^+$	(2.3 ± 0.5) × 10 ⁻⁴		436

Fractions of some of the following modes with resonances have already appeared above as submodes of particular charged-particle modes.

$K_S^0 a_1(1260)^+$	(3.5 ± 0.6) %		329
$K_S^0 a_2(1320)^+$	< 1.5 × 10 ⁻³	CL=90%	200
$\bar{K}^*(892)^0 \rho^+$ total	[ss] (2.0 ± 1.2) %		422
$\bar{K}^*(892)^0 \rho^+$ S-wave	[ss] (1.5 ± 1.5) %		422
$\bar{K}^*(892)^0 \rho^+$ P-wave	< 1 × 10 ⁻³	CL=90%	422
$\bar{K}^*(892)^0 \rho^+$ D-wave	(9 ± 6) × 10 ⁻³		422
$\bar{K}^*(892)^0 \rho^+$ D-wave longitudinal	< 7 × 10 ⁻³	CL=90%	422
$\bar{K}_1(1270)^0 \pi^+$	< 7 × 10 ⁻³	CL=90%	487
$\bar{K}_1(1400)^0 \pi^+$	(3.8 ± 1.3) %		390
$\bar{K}^*(892)^0 \pi^+ \pi^0$ total	(6.3 ± 0.8) %		690
$\bar{K}^*(892)^0 \pi^+ \pi^0$ 3-body	[ss] (4.0 ± 1.2) %		690
$K^*(892)^- \pi^+ \pi^+$ total	—		689
$K^*(892)^- \pi^+ \pi^+$ 3-body	(1.4 ± 0.9) %		689
$\bar{K}^*(892)^0 a_1(1260)^+$	(9.1 ± 1.8) × 10 ⁻³		†

Pionic modes

$\pi^+ \pi^0$	(1.24 ± 0.07) × 10 ⁻³		925
$\pi^+ \pi^+ \pi^-$	(3.21 ± 0.19) × 10 ⁻³		909
$\rho^0 \pi^+$	(8.2 ± 1.5) × 10 ⁻⁴		767
$\pi^+ (\pi^+ \pi^-)$ S-wave	(1.80 ± 0.16) × 10 ⁻³		909
$\sigma \pi^+$, $\sigma \rightarrow \pi^+ \pi^-$	(1.35 ± 0.12) × 10 ⁻³		—
$f_0(980) \pi^+$, $f_0(980) \rightarrow \pi^+ \pi^-$	(1.54 ± 0.33) × 10 ⁻⁴		669
$f_0(1370) \pi^+$, $f_0(1370) \rightarrow \pi^+ \pi^-$	(8 ± 4) × 10 ⁻⁵		—
$f_2(1270) \pi^+$, $f_2(1270) \rightarrow \pi^+ \pi^-$	(5.0 ± 0.9) × 10 ⁻⁴		485
$\rho(1450)^0 \pi^+$, $\rho(1450)^0 \rightarrow \pi^+ \pi^-$	< 8 × 10 ⁻⁵	CL=95%	338
$f_0(1500) \pi^+$, $f_0(1500) \rightarrow \pi^+ \pi^-$	(1.1 ± 0.4) × 10 ⁻⁴		—
$f_0(1710) \pi^+$, $f_0(1710) \rightarrow \pi^+ \pi^-$	< 5 × 10 ⁻⁵	CL=95%	—
$f_0(1790) \pi^+$, $f_0(1790) \rightarrow \pi^+ \pi^-$	< 6 × 10 ⁻⁵	CL=95%	—
$(\pi^+ \pi^+)$ S-wave π^-	< 1.2 × 10 ⁻⁴	CL=95%	909
$\pi^+ \pi^+ \pi^-$ nonresonant	< 1.1 × 10 ⁻⁴	CL=95%	909
$\pi^+ 2\pi^0$	(4.6 ± 0.4) × 10 ⁻³		910
$\pi^+ \pi^+ \pi^- \pi^0$	(1.14 ± 0.08) %		883
$\eta \pi^+$, $\eta \rightarrow \pi^+ \pi^- \pi^0$	(7.7 ± 0.7) × 10 ⁻⁴		848
$\omega \pi^+$, $\omega \rightarrow \pi^+ \pi^- \pi^0$	< 3 × 10 ⁻⁴	CL=90%	763
$3\pi^+ 2\pi^-$	(1.63 ± 0.16) × 10 ⁻³	S=1.1	845

Fractions of some of the following modes with resonances have already appeared above as submodes of particular charged-particle modes.

$\eta \pi^+$	(3.39 ± 0.29) × 10 ⁻³		848
$\omega \pi^+$	< 3.4 × 10 ⁻⁴	CL=90%	764
$\eta \rho^+$	< 7 × 10 ⁻³	CL=90%	655
$\eta'(958) \pi^+$	(5.1 ± 1.0) × 10 ⁻³		681
$\eta'(958) \rho^+$	< 5 × 10 ⁻³	CL=90%	349

Hadronic modes with a $K\bar{K}$ pair

$K^+ K_S^0$	(2.89 ± 0.17) × 10 ⁻³		793
$K^+ K^- \pi^+$	[qq] (9.63 ± 0.31) × 10 ⁻³	S=1.3	744
$\phi \pi^+$, $\phi \rightarrow K^+ K^-$	(3.06 ± 0.34) × 10 ⁻³		647
$K^+ \bar{K}^*(892)^0$, $\bar{K}^*(892)^0 \rightarrow K^- \pi^+$	(2.90 ± 0.32) × 10 ⁻³		613
$K^+ \bar{K}_0^*(1430)^0$, $\bar{K}_0^*(1430)^0 \rightarrow K^- \pi^+$	(3.6 ± 0.4) × 10 ⁻³		—
$K_S^0 K_S^0 \pi^+$	—		741
$K^*(892)^+ K_S^0$, $K^*(892)^+ \rightarrow K_S^0 \pi^+$	(5.3 ± 2.3) × 10 ⁻³		611
$K^+ K^- \pi^+ \pi^0$	—		682
$\phi \pi^+ \pi^0$, $\phi \rightarrow K^+ K^-$	(1.1 ± 0.5) %		619
$\phi \rho^+$, $\phi \rightarrow K^+ K^-$	< 7 × 10 ⁻³	CL=90%	258
$K^+ K^- \pi^+ \pi^0$ non- ϕ	(1.5 ± 0.6) %		682
$K^+ K_S^0 \pi^+ \pi^-$	(1.69 ± 0.18) × 10 ⁻³		678
$K_S^0 K^- \pi^+ \pi^+$	(2.32 ± 0.18) × 10 ⁻³		678
$K^+ K^- \pi^+ \pi^+ \pi^-$	(2.3 ± 1.2) × 10 ⁻⁴		600

Fractions of the following modes with resonances have already appeared above as submodes of particular charged-particle modes.

$\phi \pi^+$	(6.2 ± 0.7) × 10 ⁻³		647
$\phi \pi^+ \pi^0$	(2.3 ± 1.0) %		619
$\phi \rho^+$	< 1.5 %	CL=90%	259
$K^+ \bar{K}^*(892)^0$	(4.4 ± 0.5) × 10 ⁻³		613
$K^*(892)^+ K_S^0$	(1.6 ± 0.7) %		612

Doubly Cabibbo-suppressed modes

$K^+ \pi^0$	(2.37 ± 0.32) × 10 ⁻⁴		864
$K^+ \pi^+ \pi^-$	(6.2 ± 0.7) × 10 ⁻⁴		846
$K^+ \rho^0$	(2.4 ± 0.6) × 10 ⁻⁴		679
$K^*(892)^0 \pi^+$, $K^*(892)^0 \rightarrow$ $K^+ \pi^-$	(2.9 ± 0.6) × 10 ⁻⁴		714
$K^+ f_0(980)$, $f_0(980) \rightarrow$ $\pi^+ \pi^-$	(5.6 ± 3.4) × 10 ⁻⁵		—
$K_2^*(1430)^0 \pi^+$, $K_2^*(1430)^0 \rightarrow$ $K^+ \pi^-$	(5.0 ± 3.4) × 10 ⁻⁵		—
$K^+ K^+ K^-$	(8.7 ± 2.0) × 10 ⁻⁵		550

 $\Delta C = 1$ weak neutral current (C1) modes, or Lepton Family number (LF) or Lepton number (L) violating modes

$\pi^+ e^+ e^-$	C1	< 7.4 × 10 ⁻⁶	CL=90%	930
$\pi^+ \phi$, $\phi \rightarrow e^+ e^-$	[tt]	(2.7 ± 3.6) × 10 ⁻⁶ -1.8		—
$\pi^+ \mu^+ \mu^-$	C1	< 3.9 × 10 ⁻⁶	CL=90%	918
$\rho^+ \mu^+ \mu^-$	C1	< 5.6 × 10 ⁻⁴	CL=90%	757
$K^+ e^+ e^-$	[uu]	< 6.2 × 10 ⁻⁶	CL=90%	870
$K^+ \mu^+ \mu^-$	[uu]	< 9.2 × 10 ⁻⁶	CL=90%	856
$\pi^+ e^\pm \mu^\mp$	LF [gg]	< 3.4 × 10 ⁻⁵	CL=90%	927
$K^+ e^\pm \mu^\mp$	LF [gg]	< 6.8 × 10 ⁻⁵	CL=90%	866
$\pi^- e^+ e^+$	L	< 3.6 × 10 ⁻⁶	CL=90%	930
$\pi^- \mu^+ \mu^+$	L	< 4.8 × 10 ⁻⁶	CL=90%	918
$\pi^- e^+ \mu^+$	L	< 5.0 × 10 ⁻⁵	CL=90%	927
$\rho^- \mu^+ \mu^+$	L	< 5.6 × 10 ⁻⁴	CL=90%	757
$K^- e^+ e^+$	L	< 4.5 × 10 ⁻⁶	CL=90%	870
$K^- \mu^+ \mu^+$	L	< 1.3 × 10 ⁻⁵	CL=90%	856
$K^- e^+ \mu^+$	L	< 1.3 × 10 ⁻⁴	CL=90%	866
$K^*(892)^- \mu^+ \mu^+$	L	< 8.5 × 10 ⁻⁴	CL=90%	703

D⁰

$$I(J^P) = \frac{1}{2}(0^-)$$

$$\text{Mass } m = 1864.84 \pm 0.17 \text{ MeV} \quad (S = 1.1)$$

$$m_{D^\pm} - m_{D^0} = 4.78 \pm 0.10 \text{ MeV} \quad (S = 1.1)$$

$$\text{Mean lifetime } \tau = (410.1 \pm 1.5) \times 10^{-15} \text{ s}$$

$$c\tau = 122.9 \text{ } \mu\text{m}$$

$$|m_{D_1^0} - m_{D_2^0}| = (2.37^{+0.66}_{-0.71}) \times 10^{10} \text{ } \hbar \text{ s}^{-1}$$

$$(\Gamma_{D_1^0} - \Gamma_{D_2^0})/\Gamma = 2\gamma = (1.56^{+0.36}_{-0.38}) \times 10^{-2}$$

$$|q/p| = 0.86 \pm 0.31$$

$$A_\Gamma = (1.4 \pm 2.7) \times 10^{-3}$$

$$\Gamma(K^+ \ell^- \bar{\nu}_\ell \text{ (via } \bar{D}^0)) / \Gamma(K^- \ell^+ \nu_\ell) < 0.005, \text{ CL} = 90\%$$

$$\Gamma(K^+ \pi^- \text{ via } \bar{D}^0) / \Gamma(K^- \pi^+) < 4.0 \times 10^{-4}, \text{ CL} = 95\%$$

$$\Gamma(K_S^0 \pi^+ \pi^- \text{ in } D^0 \rightarrow \bar{D}^0) / \Gamma(K_S^0 \pi^+ \pi^-) < 0.0063, \text{ CL} = 95\%$$

Meson Summary Table

CP-violation decay-rate asymmetries

$$\begin{aligned}
A_{CP}(K^+K^-) &= (0.1 \pm 0.5) \times 10^{-2} \quad (S = 1.4) \\
A_{CP}(K_S^0 K_S^0) &= -0.23 \pm 0.19 \\
A_{CP}(\pi^+ \pi^-) &= (0.0 \pm 0.5) \times 10^{-2} \\
A_{CP}(\pi^0 \pi^0) &= 0.00 \pm 0.05 \\
A_{CP}(\pi^+ \pi^- \pi^0) &= 0.004 \pm 0.013 \\
A_{CP}(K_S^0 \phi) &= -0.03 \pm 0.09 \\
A_{CP}(K_S^0 \pi^0) &= 0.001 \pm 0.013 \\
A_{CP}(K_S^0 \pi^\pm) \text{ in } D^0 \rightarrow K^- \pi^+, \bar{D}^0 \rightarrow K^+ \pi^- &= -0.004 \pm 0.010 \\
A_{CP}(K_S^0 \pi^\mp) &= 0.022 \pm 0.032 \\
A_{CP}(K_S^0 \pi^\pm \pi^0) &= 0.002 \pm 0.009 \\
A_{CP}(K_S^0 \pi^\mp \pi^0) &= 0.00 \pm 0.05 \\
A_{CP}(K_S^0 \pi^+ \pi^-) &= -0.009 \pm_{-0.061}^{+0.026} \\
A_{CP}(K^*(892)^\mp \pi^\pm \rightarrow K_S^0 \pi^+ \pi^-) \text{ in } D^0 \rightarrow K^{*-} \pi^+, \bar{D}^0 \rightarrow K^{*+} \pi^- &< 3.5 \times 10^{-4}, \text{ CL} = 95\% \\
A_{CP}(K^*(892)^\pm \pi^\mp \rightarrow K_S^0 \pi^+ \pi^-) \text{ in } D^0 \rightarrow K^{*+} \pi^-, \bar{D}^0 \rightarrow K^{*-} \pi^+ &< 7.8 \times 10^{-4}, \text{ CL} = 95\% \\
A_{CP}(K_S^0 \rho^0 \rightarrow K_S^0 \pi^+ \pi^-) \text{ in } D^0 \rightarrow \bar{K}^0 \rho^0, \bar{D}^0 \rightarrow K^0 \rho^0 &< 4.8 \times 10^{-4}, \text{ CL} = 95\% \\
A_{CP}(K_S^0 \omega \rightarrow K_S^0 \pi^+ \pi^-) \text{ in } D^0 \rightarrow \bar{K}^0 \omega, \bar{D}^0 \rightarrow K^0 \omega &< 9.2 \times 10^{-4}, \text{ CL} = 95\% \\
A_{CP}(K_S^0 f_0(980) \rightarrow K_S^0 \pi^+ \pi^-) \text{ in } D^0 \rightarrow \bar{K}^0 f_0(980), \bar{D}^0 \rightarrow K^0 f_0(980) &< 6.8 \times 10^{-4}, \text{ CL} = 95\% \\
A_{CP}(K_S^0 f_2(1270) \rightarrow K_S^0 \pi^+ \pi^-) \text{ in } D^0 \rightarrow \bar{K}^0 f_2(1270), \bar{D}^0 \rightarrow K^0 f_2(1270) &< 13.5 \times 10^{-4}, \text{ CL} = 95\% \\
A_{CP}(K_S^0 f_0(1370) \rightarrow K_S^0 \pi^+ \pi^-) \text{ in } D^0 \rightarrow \bar{K}^0 f_0(1370), \bar{D}^0 \rightarrow K^0 f_0(1370) &< 25.5 \times 10^{-4}, \text{ CL} = 95\% \\
A_{CP}(K_0^*(1430)^\mp \pi^\pm \rightarrow K_S^0 \pi^+ \pi^-) \text{ in } D^0 \rightarrow K_0^{*+}(1430) \pi^-, \bar{D}^0 \rightarrow K_0^{*-}(1430) \pi^+ &< 9.0 \times 10^{-4}, \text{ CL} = 95\% \\
A_{CP}(K_2^*(1430)^\mp \pi^\pm \rightarrow K_S^0 \pi^+ \pi^-) \text{ in } D^0 \rightarrow K_2^{*+}(1430) \pi^-, \bar{D}^0 \rightarrow K_2^{*-}(1430) \pi^+ &< 6.5 \times 10^{-4}, \text{ CL} = 95\% \\
A_{CP}(K^*(1680)^\mp \pi^\pm \rightarrow K_S^0 \pi^+ \pi^-) \text{ in } D^0 \rightarrow K^*(1680) \pi^-, \bar{D}^0 \rightarrow K^*(1680) \pi^+ &< 28.4 \times 10^{-4}, \text{ CL} = 95\% \\
A_{CP}(K^- \pi^+ \pi^+ \pi^-) \text{ in } D^0 \rightarrow K^- \pi^+ \pi^+ \pi^-, \bar{D}^0 \rightarrow K^+ \pi^- \pi^- \pi^+ &= 0.007 \pm 0.010 \\
A_{CP}(K^\pm \pi^\mp \pi^+ \pi^-) &= -0.02 \pm 0.04 \\
A_{CP}(K^+ K^- \pi^+ \pi^-) &= -0.08 \pm 0.07
\end{aligned}$$

T-violation decay-rate asymmetry

$$A_T(K^+ K^- \pi^+ \pi^-) = 0.01 \pm 0.07$$

CPT-violation decay-rate asymmetry

$$A_{CPT}(K^\mp \pi^\pm) = 0.008 \pm 0.008$$

Most decay modes (other than the semileptonic modes) that involve a neutral K meson are now given as K_S^0 modes, not as \bar{K}^0 modes. Nearly always it is a K_S^0 that is measured, and interference between Cabibbo-allowed and doubly Cabibbo-suppressed modes can invalidate the assumption that $2\Gamma(K_S^0) = \Gamma(\bar{K}^0)$.

D^0 DECAY MODES	Fraction (Γ_i/Γ)	Scale factor/ Confidence level	p (MeV/c)
Topological modes			
0-prongs	[$\nu\nu$] (15 \pm 6) %		—
2-prongs	(71 \pm 6) %		—
4-prongs	[ww] (14.6 \pm 0.5) %		—
6-prongs	(1.2 $\pm_{-0.7}^{+1.3}$) $\times 10^{-3}$		—
Inclusive modes			
e^+ anything	[xx] (6.53 \pm 0.17) %		—
μ^+ anything	(6.7 \pm 0.6) %		—
K^- anything	(54.7 \pm 2.8) %	S=1.3	—
\bar{K}^0 anything + K^0 anything	(47 \pm 4) %		—
K^+ anything	(3.4 \pm 0.4) %		—
$K^*(892)^-$ anything	(15 \pm 9) %		—
$\bar{K}^*(892)^0$ anything	(9 \pm 4) %		—
$K^*(892)^+$ anything	< 3.6 %	CL=90%	—
$K^*(892)^0$ anything	(2.8 \pm 1.3) %		—
η anything	(9.5 \pm 0.9) %		—
η' anything	(2.48 \pm 0.27) %		—
ϕ anything	(1.05 \pm 0.11) %		—

Semileptonic modes

$K^- e^+ \nu_e$	(3.58 \pm 0.06) %	S=1.1	867
$K^- \mu^+ \nu_\mu$	(3.31 \pm 0.13) %		864
$K^*(892)^- e^+ \nu_e$	(2.18 \pm 0.16) %		719
$K^*(892)^- \mu^+ \nu_\mu$	(2.01 \pm 0.25) %		714
$K^- \pi^0 e^+ \nu_e$	(1.6 $\pm_{-0.5}^{+1.3}$) %		861
$\bar{K}^0 \pi^- e^+ \nu_e$	(2.7 $\pm_{-0.7}^{+0.9}$) %		860
$K^- \pi^+ \pi^- e^+ \nu_e$	(2.8 $\pm_{-1.1}^{+1.4}$) $\times 10^{-4}$		843
$K_1(1270)^- e^+ \nu_e$	(7.6 $\pm_{-3.1}^{+4.2}$) $\times 10^{-4}$		498
$K^- \pi^+ \pi^- \mu^+ \nu_\mu$	< 1.2 $\times 10^{-3}$	CL=90%	821
$(\bar{K}^*(892) \pi)^- \mu^+ \nu_\mu$	< 1.4 $\times 10^{-3}$	CL=90%	692
$\pi^- e^+ \nu_e$	(2.83 \pm 0.17) $\times 10^{-3}$		927
$\pi^- \mu^+ \nu_\mu$	(2.37 \pm 0.24) $\times 10^{-3}$		924
$\rho^- e^+ \nu_e$	(1.9 \pm 0.4) $\times 10^{-3}$		771

Hadronic modes with one \bar{K}

$K^- \pi^+$	(3.89 \pm 0.05) %	S=1.1	861
$K_S^0 \pi^0$	(1.22 \pm 0.06) %	S=1.2	860
$K_L^0 \pi^0$	(10.0 \pm 0.7) $\times 10^{-3}$		860
$K_S^0 \pi^+ \pi^-$	[qq] (2.99 \pm 0.17) %	S=1.1	842
$K_S^0 \rho^0$	(7.7 $\pm_{-0.8}^{+0.6}$) $\times 10^{-3}$		674
$K_S^0 \omega, \omega \rightarrow \pi^+ \pi^-$	(2.2 \pm 0.6) $\times 10^{-4}$		670
$K_S^0 f_0(980), f_0(980) \rightarrow \pi^+ \pi^-$	(1.40 $\pm_{-0.22}^{+0.30}$) $\times 10^{-3}$		549
$K_S^0 f_2(1270), f_2(1270) \rightarrow \pi^+ \pi^-$	(1.3 $\pm_{-0.7}^{+1.2}$) $\times 10^{-4}$		262
$K_S^0 f_0(1370), f_0(1370) \rightarrow \pi^+ \pi^-$	(2.5 $\pm_{-0.7}^{+0.6}$) $\times 10^{-3}$		†
$K^*(892)^- \pi^+, K^*(892)^- \rightarrow K_S^0 \pi^-$	(1.97 \pm 0.13) %		711
$K^*(892)^+ \pi^-, K^*(892)^+ \rightarrow [yy]$	(1.0 $\pm_{-0.4}^{+1.3}$) $\times 10^{-4}$		711
$K_0^*(1430)^- \pi^+, K_0^*(1430)^- \rightarrow K_S^0 \pi^-$	(2.9 $\pm_{-0.4}^{+0.7}$) $\times 10^{-3}$		378
$K_2^*(1430)^- \pi^+, K_2^*(1430)^- \rightarrow K_S^0 \pi^-$	(3.3 $\pm_{-1.1}^{+2.2}$) $\times 10^{-4}$		367
$K^*(1680)^- \pi^+, K^*(1680)^- \rightarrow K_S^0 \pi^-$	(7 \pm_{-5}^{+6}) $\times 10^{-4}$		46
$K_S^0 \pi^+ \pi^-$ nonresonant	(2.7 $\pm_{-1.7}^{+6.1}$) $\times 10^{-4}$		842
$K^- \pi^+ \pi^0$	[qq] (13.9 \pm 0.5) %	S=1.6	844
$K^- \rho^+$	(10.8 \pm 0.7) %		675
$K^- \rho(1700)^+, \rho(1700)^+ \rightarrow \pi^+ \pi^0$	(7.9 \pm 1.7) $\times 10^{-3}$		†
$K^*(892)^- \pi^+, K^*(892)^- \rightarrow K^- \pi^0$	(2.22 $\pm_{-0.19}^{+0.36}$) %		711
$\bar{K}^*(892)^0 \pi^0, \bar{K}^*(892)^0 \rightarrow K^- \pi^+$	(1.88 \pm 0.23) %		711
$K_0^*(1430)^- \pi^+, K_0^*(1430)^- \rightarrow K^- \pi^0$	(4.6 \pm 2.1) $\times 10^{-3}$		378
$\bar{K}_0^*(1430)^0 \pi^0, \bar{K}_0^*(1430)^0 \rightarrow K^- \pi^+$	(5.7 $\pm_{-1.5}^{+4.5}$) $\times 10^{-3}$		379
$K^*(1680)^- \pi^+, K^*(1680)^- \rightarrow K^- \pi^0$	(1.8 \pm 0.7) $\times 10^{-3}$		46
$K^- \pi^+ \pi^0$ nonresonant	(1.11 $\pm_{-0.19}^{+0.53}$) %		844
$K_S^0 \pi^0 \pi^0$	—		843
$\bar{K}^*(892)^0 \pi^0, \bar{K}^*(892)^0 \rightarrow K_S^0 \pi^0$	(6.7 $\pm_{-1.8}^{+1.5}$) $\times 10^{-3}$		711
$K_S^0 \pi^0 \pi^0$ nonresonant	(4.5 \pm 1.1) $\times 10^{-3}$		843
$K^- \pi^+ \pi^+ \pi^-$	[qq] (8.10 \pm 0.20) %	S=1.3	813
$K^- \pi^+ \rho^0$ total	(6.76 \pm 0.33) %		609
$K^- \pi^+ \rho^0$ 3-body	(5.1 \pm 2.3) $\times 10^{-3}$		609
$\bar{K}^*(892)^0 \rho^0, \bar{K}^*(892)^0 \rightarrow K^- \pi^+$	(1.00 \pm 0.22) %		416
$K^- a_1(1260)^+, a_1(1260)^+ \rightarrow \pi^+ \pi^+ \pi^-$	(3.6 \pm 0.6) %		327
$\bar{K}^*(892)^0 \pi^+ \pi^-$ total, $\bar{K}^*(892)^0 \rightarrow K^- \pi^+$	(1.5 \pm 0.4) %		685

Meson Summary Table

$\bar{K}^*(892)^0 \pi^+ \pi^-$ 3-body, $\bar{K}^*(892)^0 \rightarrow K^- \pi^+$	(9.7 ± 2.1) × 10 ⁻³	685	$3K_S^0$	(9.6 ± 1.4) × 10 ⁻⁴	539
$K_1(1270)^- \pi^+$, [ss]	(2.9 ± 0.3) × 10 ⁻³	484	$K^+ K^- K^- \pi^+$	(2.22 ± 0.32) × 10 ⁻⁴	434
$K_1(1270)^- \rightarrow K^- \pi^+ \pi^-$			$K^+ K^- \bar{K}^*(892)^0$,	(4.4 ± 1.7) × 10 ⁻⁵	†
$K^- \pi^+ \pi^+ \pi^-$ nonresonant	(1.88 ± 0.26) %	813	$\bar{K}^*(892)^0 \rightarrow K^- \pi^+$		
$K_S^0 \pi^+ \pi^- \pi^0$ [qq]	(5.4 ± 0.6) %	813	$K^- \pi^+ \phi, \phi \rightarrow K^+ K^-$	(4.0 ± 1.7) × 10 ⁻⁵	422
$K_S^0 \eta, \eta \rightarrow \pi^+ \pi^- \pi^0$	(8.6 ± 1.4) × 10 ⁻⁴	772	$\phi \bar{K}^*(892)^0$,	(1.06 ± 0.20) × 10 ⁻⁴	†
$K_S^0 \omega, \omega \rightarrow \pi^+ \pi^- \pi^0$	(9.8 ± 1.8) × 10 ⁻³	670	$\phi \rightarrow K^+ K^-$,		
$K^*(892)^- \rho^+$,	(2.1 ± 0.8) %	416	$\bar{K}^*(892)^0 \rightarrow K^- \pi^+$		
$K^*(892)^- \rightarrow K_S^0 \pi^-$			$K^+ K^- K^- \pi^+$ nonresonant	(3.3 ± 1.5) × 10 ⁻⁵	434
$K_1(1270)^- \pi^+$,			$K_S^0 K_S^0 K^\pm \pi^\mp$	(6.3 ± 1.3) × 10 ⁻⁴	427
$K_1(1270)^- \rightarrow K_S^0 \pi^- \pi^0$ [ss]	(2.2 ± 0.6) × 10 ⁻³	484			
$\bar{K}^*(892)^0 \pi^+ \pi^-$ 3-body, $\bar{K}^*(892)^0 \rightarrow K_S^0 \pi^0$	(2.4 ± 0.5) × 10 ⁻³	685	Pionic modes		
$K_S^0 \pi^+ \pi^- \pi^0$ nonresonant	(1.1 ± 1.2) %	813	$\pi^+ \pi^-$	(1.397 ± 0.027) × 10 ⁻³	922
$K^- \pi^+ \pi^+ \pi^- \pi^0$	(4.2 ± 0.4) %	771	$\pi^0 \pi^0$	(8.0 ± 0.8) × 10 ⁻⁴	923
$\bar{K}^*(892)^0 \pi^+ \pi^- \pi^0$,	(1.2 ± 0.6) %	643	$\pi^+ \pi^- \pi^0$	(1.44 ± 0.06) %	S=1.8 907
$\bar{K}^*(892)^0 \rightarrow K^- \pi^+$			$\rho^+ \pi^-$	(9.8 ± 0.4) × 10 ⁻³	764
$K^- \pi^+ \omega, \omega \rightarrow \pi^+ \pi^- \pi^0$	(2.7 ± 0.5) %	605	$\rho^0 \pi^0$	(3.73 ± 0.22) × 10 ⁻³	764
$\bar{K}^*(892)^0 \omega$,	(6.5 ± 2.4) × 10 ⁻³	410	$\rho^- \pi^+$	(4.97 ± 0.23) × 10 ⁻³	764
$\bar{K}^*(892)^0 \rightarrow K^- \pi^+$,			$\rho(1450)^+ \pi^-, \rho(1450)^+ \rightarrow$	(1.6 ± 2.0) × 10 ⁻⁵	-
$\bar{K}^*(892)^0 \rightarrow \pi^+ \pi^- \pi^0$			$\pi^+ \pi^0$		
$K_S^0 \eta \pi^0$	(5.6 ± 1.2) × 10 ⁻³	721	$\rho(1450)^0 \pi^0, \rho(1450)^0 \rightarrow$	(4.3 ± 1.9) × 10 ⁻⁵	-
$K_S^0 a_0(980), a_0(980) \rightarrow \eta \pi^0$	(6.7 ± 2.1) × 10 ⁻³	-	$\pi^+ \pi^-$	(2.6 ± 0.4) × 10 ⁻⁴	-
$\bar{K}^*(892)^0 \eta, \bar{K}^*(892)^0 \rightarrow$	(1.6 ± 0.5) × 10 ⁻³	-	$\rho(1700)^+ \pi^-, \rho(1700)^+ \rightarrow$	(5.9 ± 1.4) × 10 ⁻⁴	-
$K_S^0 \pi^0$			$\pi^+ \pi^0$		
$K_S^0 2\pi^+ 2\pi^-$	(2.84 ± 0.31) × 10 ⁻³	768	$\rho(1700)^0 \pi^0, \rho(1700)^0 \rightarrow$	(7.2 ± 1.7) × 10 ⁻⁴	-
$K_S^0 \rho^0 \pi^+ \pi^-$, no $K^*(892)^-$	(1.1 ± 0.7) × 10 ⁻³	-	$\pi^+ \pi^-$	(4.6 ± 1.1) × 10 ⁻⁴	-
$K^*(892)^- \pi^+ \pi^+ \pi^-$,	(5 ± 8) × 10 ⁻⁴	642	$\rho(1700)^- \pi^+, \rho(1700)^- \rightarrow$	(4.6 ± 1.1) × 10 ⁻⁴	-
$K^*(892)^- \rightarrow K_S^0 \pi^-$,			$\pi^+ \pi^-$	(3.6 ± 0.8) × 10 ⁻⁵	-
no ρ^0			$f_0(980) \pi^0, f_0(980) \rightarrow$	(1.18 ± 0.21) × 10 ⁻⁴	-
$K^*(892)^- \rho^0 \pi^+$,	(1.7 ± 0.7) × 10 ⁻³	230	$\pi^+ \pi^-$	(5.3 ± 2.1) × 10 ⁻⁵	-
$K^*(892)^- \rightarrow K_S^0 \pi^-$			$f_0(1370) \pi^0, f_0(1370) \rightarrow$	(5.6 ± 1.5) × 10 ⁻⁵	-
$K_S^0 2\pi^+ 2\pi^-$ nonresonant	< 1.3 × 10 ⁻³ CL=90%	768	$\pi^+ \pi^-$	(4.5 ± 1.5) × 10 ⁻⁵	-
$K^- 3\pi^+ 2\pi^-$	(2.2 ± 0.6) × 10 ⁻⁴	713	$\pi^+ \pi^-$	(1.90 ± 0.20) × 10 ⁻⁴	-
			$f_2(1270) \pi^0, f_2(1270) \rightarrow$	(1.90 ± 0.20) × 10 ⁻⁴	-
			$\pi^+ \pi^-$	(1.21 ± 0.35) × 10 ⁻⁴	907
			$\pi^+ \pi^- \pi^0$ nonresonant	(1.21 ± 0.35) × 10 ⁻⁴	907
			$3\pi^0$	< 3.5 × 10 ⁻⁴ CL=90%	908
			$2\pi^+ 2\pi^-$	(7.44 ± 0.21) × 10 ⁻³ S=1.1	880
			$a_1(1260)^+ \pi^-, a_1^+ \rightarrow$	(4.47 ± 0.31) × 10 ⁻³	-
			$\pi^+ \pi^- \pi^+$ total	(3.22 ± 0.25) × 10 ⁻³	-
			$a_1(1260)^+ \pi^-, a_1^+ \rightarrow$	(1.9 ± 0.5) × 10 ⁻⁴	-
			$\rho^0 \pi^+ S$ -wave	(6.2 ± 0.7) × 10 ⁻⁴	-
			$\rho^0 \pi^+ D$ -wave	(1.82 ± 0.13) × 10 ⁻³	518
			$a_1(1260)^+ \pi^-, a_1^+ \rightarrow$	(8.2 ± 3.2) × 10 ⁻⁵	-
			$\sigma \pi^+$	(4.8 ± 0.6) × 10 ⁻⁴	-
			$2\rho^0$ total	(1.25 ± 0.10) × 10 ⁻³	-
			$2\rho^0$, parallel helicities	(1.49 ± 0.12) × 10 ⁻³	-
			$2\rho^0$, perpendicular helicities	(6.1 ± 0.9) × 10 ⁻⁴	-
			$2\rho^0$, longitudinal helicities	(1.8 ± 0.5) × 10 ⁻⁴	-
			Resonant $(\pi^+ \pi^-) \pi^+ \pi^-$		
			3-body total		
			$\sigma \pi^+ \pi^-$		
			$f_0(980) \pi^+ \pi^-, f_0 \rightarrow$		
			$\pi^+ \pi^-$		
			$f_2(1270) \pi^+ \pi^-, f_2 \rightarrow$	(3.6 ± 0.6) × 10 ⁻⁴	-
			$\pi^+ \pi^- 2\pi^0$	(1.00 ± 0.09) %	882
			$\eta \pi^0$	[zz] (5.7 ± 1.4) × 10 ⁻⁴	846
			$\omega \pi^0$	[zz] < 2.6 × 10 ⁻⁴ CL=90%	761
			$2\pi^+ 2\pi^- \pi^0$	(4.2 ± 0.5) × 10 ⁻³	844
			$\eta \pi^+ \pi^-$	[zz] < 1.9 × 10 ⁻³ CL=90%	827
			$\omega \pi^+ \pi^-$	[zz] (1.6 ± 0.5) × 10 ⁻³	738
			$3\pi^+ 3\pi^-$	(4.2 ± 1.2) × 10 ⁻⁴	795
			Hadronic modes with three K's		
$K_S^0 K^+ K^-$	(4.72 ± 0.32) × 10 ⁻³	544	Hadronic modes with a $K\bar{K}$ pair		
$K_S^0 a_0(980)^0, a_0^0 \rightarrow K^+ K^-$	(3.1 ± 0.4) × 10 ⁻³	-	$K^+ K^-$	(3.93 ± 0.08) × 10 ⁻³	791
$K^- a_0(980)^+, a_0^+ \rightarrow K^+ K_S^0$	(6.3 ± 1.9) × 10 ⁻⁴	-	$2K_S^0$	(3.8 ± 0.7) × 10 ⁻⁴	789
$K^+ a_0(980)^-, a_0^- \rightarrow K^- K_S^0$	< 1.2 × 10 ⁻⁴ CL=95%	-	$K_S^0 K^- \pi^+$	(3.5 ± 0.5) × 10 ⁻³ S=1.1	739
$K_S^0 f_0(980), f_0 \rightarrow K^+ K^-$	< 1.0 × 10 ⁻⁴ CL=95%	-	$\bar{K}^*(892)^0 K_S^0, \bar{K}^*(892)^0 \rightarrow$	< 6 × 10 ⁻⁴ CL=90%	608
$K_S^0 \phi, \phi \rightarrow K^+ K^-$	(2.17 ± 0.15) × 10 ⁻³	520	$K^- \pi^+$		
$K_S^0 f_0(1400), f_0 \rightarrow K^+ K^-$	(1.8 ± 1.1) × 10 ⁻⁴	-	$K_S^0 K^+ \pi^-$	(2.7 ± 0.5) × 10 ⁻³	739
			$K^*(892)^0 K_S^0, K^*(892)^0 \rightarrow$	< 3.0 × 10 ⁻⁴ CL=90%	608
			$K^+ \pi^-$		

Fractions of many of the following modes with resonances have already appeared above as submodes of particular charged-particle modes. (Modes for which there are only upper limits and $\bar{K}^*(892)\rho$ submodes only appear below.)

Meson Summary Table

$K^+ K^- \pi^0$		$(3.29 \pm 0.14) \times 10^{-3}$	743
$K^*(892)^+ K^-, K^*(892)^+ \rightarrow$		$(1.47 \pm 0.07) \times 10^{-3}$	-
$K^*(892)^- K^+, K^*(892)^- \rightarrow$		$(5.1 \pm 0.5) \times 10^{-4}$	-
$(K^+ \pi^0)_{S\text{-wave}} K^-$		$(2.34 \pm 0.17) \times 10^{-3}$	743
$(K^- \pi^0)_{S\text{-wave}} K^+$		$(1.3 \pm 0.4) \times 10^{-4}$	743
$f_0(980) \pi^0, f_0 \rightarrow K^+ K^-$		$(3.5 \pm 0.6) \times 10^{-4}$	-
$\phi \pi^0, \phi \rightarrow K^+ K^-$		$(6.1 \pm 0.6) \times 10^{-4}$	-
$K_S^0 K_S^0 \pi^0$		$< 5.9 \times 10^{-4}$	740
$K^+ K^- \pi^+ \pi^-$	[aaa]	$(2.43 \pm 0.12) \times 10^{-3}$	677
$\phi \pi^+ \pi^-$ 3-body, $\phi \rightarrow$		$(2.4 \pm 2.4) \times 10^{-5}$	614
$\phi \rho^0, \phi \rightarrow K^+ K^-$		$(7.1 \pm 0.6) \times 10^{-4}$	250
$K^+ K^- \rho^0$ 3-body		$(5 \pm 7) \times 10^{-5}$	302
$f_0(980) \pi^+ \pi^-, f_0 \rightarrow K^+ K^-$		$(3.6 \pm 0.9) \times 10^{-4}$	-
$K^*(892)^0 K^\mp \pi^\pm$ 3-body, [bbb]		$(2.7 \pm 0.6) \times 10^{-4}$	531
$K^{*0} \rightarrow K^\pm \pi^\mp$			
$K^*(892)^0 K^*(892)^0, K^{*0} \rightarrow$		$(7 \pm 5) \times 10^{-5}$	272
$K_1(1270)^\pm K^\mp$		$(8.0 \pm 1.8) \times 10^{-4}$	-
$K_1(1270)^\pm \rightarrow K^\pm \pi^+ \pi^-$			
$K_1(1400)^\pm K^\mp$		$(5.4 \pm 1.2) \times 10^{-4}$	-
$K_1(1400)^\pm \rightarrow K^\pm \pi^+ \pi^-$			
$K_S^0 K_S^0 \pi^+ \pi^-$		$(1.30 \pm 0.24) \times 10^{-3}$	673
$K_S^0 K^- \pi^+ \pi^+ \pi^-$		$< 1.5 \times 10^{-4}$	595
$K^+ K^- \pi^+ \pi^- \pi^0$		$(3.1 \pm 2.0) \times 10^{-3}$	600

Fractions of most of the following modes with resonances have already appeared above as submodes of particular charged-particle modes.

$\phi \pi^0$		$(7.6 \pm 0.5) \times 10^{-4}$	645
$\phi \eta$		$(1.4 \pm 0.5) \times 10^{-4}$	489
$\phi \omega$		$< 2.1 \times 10^{-3}$	238

Radiative modes

$\rho^0 \gamma$		$< 2.4 \times 10^{-4}$	771
$\omega \gamma$		$< 2.4 \times 10^{-4}$	768
$\phi \gamma$		$(2.5 \pm_{-0.6}^{+0.7}) \times 10^{-5}$	654
$\bar{K}^*(892)^0 \gamma$		$< 7.6 \times 10^{-4}$	719

Doubly Cabibbo suppressed (DC) modes or $\Delta C = 2$ forbidden via mixing (C2M) modes

$K^+ \ell^- \bar{\nu}_\ell$ via \bar{D}^0		$< 1.8 \times 10^{-4}$	CL=90%	-
K^+ or $K^*(892)^+$ $e^- \bar{\nu}_e$ via \bar{D}^0		$< 6 \times 10^{-5}$	CL=90%	-
$K^+ \pi^-$	DC	$(1.48 \pm 0.07) \times 10^{-4}$		861
$K^+ \pi^-$ via DCS		$(1.31 \pm 0.08) \times 10^{-4}$		-
$K^+ \pi^-$ via \bar{D}^0		$< 1.6 \times 10^{-5}$	CL=95%	861
$K_S^0 \pi^+ \pi^-$ in $D^0 \rightarrow \bar{D}^0$		$< 1.9 \times 10^{-4}$	CL=95%	-
$K^*(892)^+ \pi^-, K^*(892)^+ \rightarrow K_S^0 \pi^+$	DC	$(1.0 \pm_{-0.4}^{+1.3}) \times 10^{-4}$		711
$K^+ \pi^- \pi^0$	DC	$(3.05 \pm 0.17) \times 10^{-4}$		844
$K^+ \pi^- \pi^0$ via \bar{D}^0		$< 8 \times 10^{-5}$	CL=95%	-
$K^+ \pi^- \pi^+ \pi^-$	DC	$(2.62 \pm_{-0.19}^{+0.21}) \times 10^{-4}$		813
$K^+ \pi^- \pi^+ \pi^-$ via \bar{D}^0		$< 4 \times 10^{-4}$	CL=90%	812
μ^- anything via \bar{D}^0		$< 4 \times 10^{-4}$	CL=90%	-

 $\Delta C = 1$ weak neutral current (C1) modes, Lepton Family number (LF) violating modes, or Lepton number (L) violating modes

$\gamma \gamma$	C1	$< 2.7 \times 10^{-5}$	CL=90%	932
$e^+ e^-$	C1	$< 1.2 \times 10^{-6}$	CL=90%	932
$\mu^+ \mu^-$	C1	$< 1.3 \times 10^{-6}$	CL=90%	926
$\pi^0 e^+ e^-$	C1	$< 4.5 \times 10^{-5}$	CL=90%	928
$\pi^0 \mu^+ \mu^-$	C1	$< 1.8 \times 10^{-4}$	CL=90%	915
$\eta e^+ e^-$	C1	$< 1.1 \times 10^{-4}$	CL=90%	852
$\eta \mu^+ \mu^-$	C1	$< 5.3 \times 10^{-4}$	CL=90%	838
$\pi^+ \pi^- e^+ e^-$	C1	$< 3.73 \times 10^{-4}$	CL=90%	922
$\rho^0 e^+ e^-$	C1	$< 1.0 \times 10^{-4}$	CL=90%	771
$\pi^+ \pi^- \mu^+ \mu^-$	C1	$< 3.0 \times 10^{-5}$	CL=90%	894
$\rho^0 \mu^+ \mu^-$	C1	$< 2.2 \times 10^{-5}$	CL=90%	754
$\omega e^+ e^-$	C1	$< 1.8 \times 10^{-4}$	CL=90%	768
$\omega \mu^+ \mu^-$	C1	$< 8.3 \times 10^{-4}$	CL=90%	751
$K^- K^+ e^+ e^-$	C1	$< 3.15 \times 10^{-4}$	CL=90%	791
$\phi e^+ e^-$	C1	$< 5.2 \times 10^{-5}$	CL=90%	654
$K^- K^+ \mu^+ \mu^-$	C1	$< 3.3 \times 10^{-5}$	CL=90%	710
$\phi \mu^+ \mu^-$	C1	$< 3.1 \times 10^{-5}$	CL=90%	631
$\bar{K}^0 e^+ e^-$	[uu]	$< 1.1 \times 10^{-4}$	CL=90%	866

$\bar{K}^0 \mu^+ \mu^-$		[uu]	$< 2.6 \times 10^{-4}$	CL=90%	852
$K^- \pi^+ e^+ e^-$	C1	$< 3.85 \times 10^{-4}$	CL=90%	861	
$\bar{K}^*(892)^0 e^+ e^-$		[uu]	$< 4.7 \times 10^{-5}$	CL=90%	719
$K^- \pi^+ \mu^+ \mu^-$	C1	$< 3.59 \times 10^{-4}$	CL=90%	829	
$\bar{K}^*(892)^0 \mu^+ \mu^-$		[uu]	$< 2.4 \times 10^{-5}$	CL=90%	700
$\pi^+ \pi^- \pi^0 \mu^+ \mu^-$	C1	$< 8.1 \times 10^{-4}$	CL=90%	863	
$\mu^\pm e^\mp$	LF	[gg]	$< 8.1 \times 10^{-7}$	CL=90%	929
$\pi^0 e^\pm \mu^\mp$	LF	[gg]	$< 8.6 \times 10^{-5}$	CL=90%	924
$\eta e^\pm \mu^\mp$	LF	[gg]	$< 1.0 \times 10^{-4}$	CL=90%	848
$\pi^+ \pi^- e^\pm \mu^\mp$	LF	[gg]	$< 1.5 \times 10^{-5}$	CL=90%	911
$\rho^0 e^\pm \mu^\mp$	LF	[gg]	$< 4.9 \times 10^{-5}$	CL=90%	767
$\omega e^\pm \mu^\mp$	LF	[gg]	$< 1.2 \times 10^{-4}$	CL=90%	764
$K^- K^+ e^\pm \mu^\mp$	LF	[gg]	$< 1.8 \times 10^{-4}$	CL=90%	754
$\phi e^\pm \mu^\mp$	LF	[gg]	$< 3.4 \times 10^{-5}$	CL=90%	648
$\bar{K}^0 e^\pm \mu^\mp$	LF	[gg]	$< 1.0 \times 10^{-4}$	CL=90%	863
$K^- \pi^+ e^\pm \mu^\mp$	LF	[gg]	$< 5.53 \times 10^{-4}$	CL=90%	848
$\bar{K}^*(892)^0 e^\pm \mu^\mp$	LF	[gg]	$< 8.3 \times 10^{-5}$	CL=90%	714
$\pi^- \pi^- e^+ \mu^+ + \text{c.c.}$	L	$< 1.12 \times 10^{-4}$	CL=90%	922	
$\pi^- \pi^- \mu^+ \mu^+ + \text{c.c.}$	L	$< 2.9 \times 10^{-5}$	CL=90%	894	
$K^- \pi^- e^+ \mu^+ + \text{c.c.}$	L	$< 2.06 \times 10^{-4}$	CL=90%	861	
$K^- \pi^- \mu^+ \mu^+ + \text{c.c.}$	L	$< 3.9 \times 10^{-4}$	CL=90%	829	
$K^- K^- e^+ \mu^+ + \text{c.c.}$	L	$< 1.52 \times 10^{-4}$	CL=90%	791	
$K^- K^- \mu^+ \mu^+ + \text{c.c.}$	L	$< 9.4 \times 10^{-5}$	CL=90%	710	
$\pi^- \pi^- e^+ \mu^+ + \text{c.c.}$	L	$< 7.9 \times 10^{-5}$	CL=90%	911	
$K^- \pi^- e^+ \mu^+ + \text{c.c.}$	L	$< 2.18 \times 10^{-4}$	CL=90%	848	
$K^- K^- e^+ \mu^+ + \text{c.c.}$	L	$< 5.7 \times 10^{-5}$	CL=90%	754	

 $D^*(2007)^0$

$$I(J^P) = \frac{1}{2}(1^-)$$

I, J, P need confirmation.

$$\text{Mass } m = 2006.97 \pm 0.19 \text{ MeV} \quad (S = 1.1)$$

$$m_{D^{*0}} - m_{D^0} = 142.12 \pm 0.07 \text{ MeV}$$

$$\text{Full width } \Gamma < 2.1 \text{ MeV, CL} = 90\%$$

$\bar{D}^*(2007)^0$ modes are charge conjugates of modes below.

 $D^*(2007)^0$ DECAY MODES

	Fraction (Γ_i/Γ)	ρ (MeV/c)
$D^0 \pi^0$	$(61.9 \pm 2.9) \%$	43
$D^0 \gamma$	$(38.1 \pm 2.9) \%$	137

 $D^*(2010)^\pm$

$$I(J^P) = \frac{1}{2}(1^-)$$

I, J, P need confirmation.

$$\text{Mass } m = 2010.27 \pm 0.17 \text{ MeV} \quad (S = 1.1)$$

$$m_{D^*(2010)^+} - m_{D^+} = 140.64 \pm 0.10 \text{ MeV} \quad (S = 1.1)$$

$$m_{D^*(2010)^+} - m_{D^0} = 145.421 \pm 0.010 \text{ MeV} \quad (S = 1.1)$$

$$\text{Full width } \Gamma = 96 \pm 22 \text{ keV}$$

$D^*(2010)^-$ modes are charge conjugates of the modes below.

 $D^*(2010)^\pm$ DECAY MODES

	Fraction (Γ_i/Γ)	ρ (MeV/c)
$D^0 \pi^+$	$(67.7 \pm 0.5) \%$	39
$D^+ \pi^0$	$(30.7 \pm 0.5) \%$	38
$D^+ \gamma$	$(1.6 \pm 0.4) \%$	136

 $D_1(2420)^0$

$$I(J^P) = \frac{1}{2}(1^+)$$

I, J, P need confirmation.

$$\text{Mass } m = 2422.3 \pm 1.3 \text{ MeV} \quad (S = 1.2)$$

$$m_{D_1^0} - m_{D^{*+}} = 411.7 \pm 0.8$$

$$\text{Full width } \Gamma = 20.4 \pm 1.7 \text{ MeV}$$

$\bar{D}_1(2420)^0$ modes are charge conjugates of modes below.

 $D_1(2420)^0$ DECAY MODES

	Fraction (Γ_i/Γ)	ρ (MeV/c)
$D^*(2010)^+ \pi^-$	seen	355
$D^0 \pi^+ \pi^-$	seen	426
$D^+ \pi^-$	not seen	474
$D^{*0} \pi^+ \pi^-$	not seen	281

Meson Summary Table

 $D_2^*(2460)^0$

$$I(J^P) = \frac{1}{2}(2^+)$$

 $J^P = 2^+$ assignment strongly favored.

Mass $m = 2461.1 \pm 1.6$ MeV ($S = 1.3$)

$m_{D_2^{*0}} - m_{D^+} = 593.9 \pm 0.8$

Full width $\Gamma = 43 \pm 4$ MeV ($S = 1.8$)

 $\bar{D}_2^*(2460)^0$ modes are charge conjugates of modes below.

$D_2^*(2460)^0$ DECAY MODES	Fraction (Γ_i/Γ)	ρ (MeV/c)
$D^+ \pi^-$	seen	505
$D^*(2010)^+ \pi^-$	seen	389
$D^0 \pi^+ \pi^-$	not seen	462
$D^{*0} \pi^+ \pi^-$	not seen	324

 $D_2^*(2460)^\pm$

$$I(J^P) = \frac{1}{2}(2^+)$$

 $J^P = 2^+$ assignment strongly favored.

Mass $m = 2460.1^{+2.6}_{-3.5}$ MeV ($S = 1.5$)

$m_{D_2^*(2460)^\pm} - m_{D_2^*(2460)^0} = 2.4 \pm 1.7$ MeV

Full width $\Gamma = 37 \pm 6$ MeV ($S = 1.4$)

 $D_2^*(2460)^\mp$ modes are charge conjugates of modes below.

$D_2^*(2460)^\pm$ DECAY MODES	Fraction (Γ_i/Γ)	ρ (MeV/c)
$D^0 \pi^+$	seen	508
$D^{*0} \pi^+$	seen	391
$D^\pm \pi^+ \pi^-$	not seen	457
$D^{*\pm} \pi^+ \pi^-$	not seen	320

**CHARMED, STRANGE MESONS
($C = S = \pm 1$)**

$$D_s^+ = c\bar{s}, D_s^- = \bar{c}s, \text{ similarly for } D_s^{* \pm}$$

 D_s^\pm

$$I(J^P) = 0(0^-)$$

Mass $m = 1968.49 \pm 0.34$ MeV ($S = 1.3$)

$m_{D_s^\pm} - m_{D^\pm} = 98.87 \pm 0.30$ MeV ($S = 1.4$)

Mean life $\tau = (500 \pm 7) \times 10^{-15}$ s ($S = 1.3$)

$c\tau = 149.9 \mu\text{m}$

CP-violating decay-rate asymmetries

$A_{CP}(K^\pm K_S^0) = 0.049 \pm 0.023$

$A_{CP}(K^+ K^- \pi^\pm) = 0.003 \pm 0.014$

$A_{CP}(K^+ K^- \pi^\pm \pi^0) = -0.06 \pm 0.04$

$A_{CP}(K_S^0 K^\mp 2\pi^\pm) = -0.01 \pm 0.04$

$A_{CP}(\pi^+ \pi^- \pi^\pm) = 0.02 \pm 0.05$

$A_{CP}(\pi^\pm \eta) = -0.08 \pm 0.05$

$A_{CP}(\pi^\pm \eta') = -0.06 \pm 0.04$

$A_{CP}(K^\pm \pi^0) = 0.02 \pm 0.29$

$A_{CP}(K_S^0 \pi^\pm) = 0.27 \pm 0.11$

$A_{CP}(K^\pm \pi^+ \pi^-) = 0.11 \pm 0.07$

$A_{CP}(K^\pm \eta) = -0.20 \pm 0.18$

$A_{CP}(K^\pm \eta'(958)) = -0.2 \pm 0.4$

T-violating decay-rate asymmetry

$A_T(K_S^0 K^\pm \pi^+ \pi^-) = -0.04 \pm 0.07$ [ccc]

 D_s^\pm form factors

$r_2 = 1.32 \pm 0.24$ ($S = 1.2$)

$r_V = 1.72 \pm 0.21$

$\Gamma_L/\Gamma_T = 0.72 \pm 0.18$

Unless otherwise noted, the branching fractions for modes with a resonance in the final state include all the decay modes of the resonance. D_s^- modes are charge conjugates of the modes below.

D_s^\pm DECAY MODES	Fraction (Γ_i/Γ)	Confidence level	ρ (MeV/c)
Inclusive modes			
K^- anything	$(13^{+14}_{-12})\%$		—
\bar{K}^0 anything + K^0 anything	$(39 \pm 28)\%$		—
K^+ anything	$(20^{+18}_{-14})\%$		—
(non- $K \bar{K}$) anything	$(64 \pm 17)\%$		—
η anything	[ddd] $(24 \pm 4)\%$		—
η' anything	$(8.7 \pm 2.1)\%$		—
ϕ anything	$(16.1 \pm 1.6)\%$		—
e^+ anything	$(8^{+6}_{-5})\%$		—
Leptonic and semileptonic modes			
$e^+ \nu_e$	$< 1.3 \times 10^{-4}$	90%	984
$\mu^+ \nu_\mu$	$(6.2 \pm 0.6) \times 10^{-3}$		981
$\tau^+ \nu_\tau$	$(6.6 \pm 0.6)\%$		182
$\phi \ell^+ \nu_\ell$	[eee] $(2.36 \pm 0.26)\%$		720
$\eta \ell^+ \nu_\ell + \eta'(958) \ell^+ \nu_\ell$	[eee] $(3.9 \pm 0.7)\%$		—
$\eta \ell^+ \nu_\ell$	[eee] $(2.9 \pm 0.6)\%$		908
$\eta'(958) \ell^+ \nu_\ell$	[eee] $(1.02 \pm 0.33)\%$		751
Hadronic modes with a $K \bar{K}$ pair			
$K^+ K_S^0$	$(1.49 \pm 0.09)\%$		850
$K^+ K^- \pi^+$	[qq] $(5.50 \pm 0.28)\%$		805
$\phi \pi^+$	[fff,ggg] $(4.38 \pm 0.35)\%$		712
$\phi \pi^+, \phi \rightarrow K^+ K^-$	[fff] $(2.18 \pm 0.33)\%$		712
$K^+ \bar{K}^*(892)^0, \bar{K}^{*0} \rightarrow$	$(2.6 \pm 0.4)\%$		416
$K^- \pi^+$			
$f_0(980) \pi^+, f_0 \rightarrow K^+ K^-$	$(6.0 \pm 2.4) \times 10^{-3}$		732
$K^+ \bar{K}_0^*(1430)^0, \bar{K}_0^* \rightarrow$	$(5.1 \pm 2.5) \times 10^{-3}$		218
$K^0 \bar{K}^0 \pi^+$			802
$K^*(892)^+ \bar{K}^0$	[ggg] $(5.3 \pm 1.2)\%$		683
$K^+ K^- \pi^+ \pi^0$	$(5.6 \pm 0.5)\%$		748
$\phi \rho^+, \phi \rightarrow K^+ K^-$	$(4.0^{+1.1}_{-1.2})\%$		400
$\phi \pi^+ \pi^0$ 3-body, $\phi \rightarrow$	$< 1.5\%$	90%	686
$K^+ K^-$			
$K^+ K^- \pi^+ \pi^0$ non- ϕ	$< 11\%$	90%	748
$K_S^0 K^- \pi^+ \pi^+$	$(1.64 \pm 0.12)\%$		744
$K^*(892)^+ \bar{K}^*(892)^0$	[ggg] $(7.0 \pm 2.5)\%$		417
$K^0 K^- 2\pi^+$ (non- $K^* \bar{K}^{*0}$)	$< 3.5\%$	90%	744
$K^+ K_S^0 \pi^+ \pi^-$	$(9.6 \pm 1.3) \times 10^{-3}$		744
$K^+ K^- \pi^+ \pi^+ \pi^-$	$(8.8 \pm 1.6) \times 10^{-3}$		673
$\phi \pi^+ \pi^+ \pi^-, \phi \rightarrow K^+ K^-$	$(5.9 \pm 1.1) \times 10^{-3}$		640
$K^+ K^- \rho^0 \pi^+$ non- ϕ	$< 2.6 \times 10^{-4}$	90%	249
$\phi \rho^0 \pi^+, \phi \rightarrow K^+ K^-$	$(6.6 \pm 1.3) \times 10^{-3}$		181
$\phi a_1(1260)^+, \phi \rightarrow$	$(7.5 \pm 1.3) \times 10^{-3}$		†
$K^+ K^-, a_1^+ \rightarrow \rho^0 \pi^+$			
$K^+ K^- \pi^+ \pi^+ \pi^-$ nonresonant	$(9 \pm 7) \times 10^{-4}$		673
$K_S^0 K_S^0 \pi^+ \pi^+ \pi^-$	$(8.4 \pm 3.5) \times 10^{-4}$		669
Hadronic modes without K's			
$\pi^+ \pi^0$	$< 6 \times 10^{-4}$	90%	975
$\pi^+ \pi^+ \pi^-$	$(1.11 \pm 0.08)\%$		959
$\rho^0 \pi^+$	not seen		825
$\pi^+ (\pi^+ \pi^-)_{S\text{-wave}}$	[hhh] $(9.7 \pm 1.1) \times 10^{-3}$		959
$f_2(1270) \pi^+, f_2 \rightarrow \pi^+ \pi^-$	$(1.1 \pm 0.6) \times 10^{-3}$		559
$\rho(1450)^0 \pi^+, \rho^0 \rightarrow \pi^+ \pi^-$	$(7 \pm 6) \times 10^{-4}$		421
$\pi^+ \pi^+ \pi^- \pi^0$	$< 14\%$	90%	935
$\eta \pi^+$	[ggg] $(1.58 \pm 0.21)\%$		902
$\omega \pi^+$	[ggg] $(2.5 \pm 0.9) \times 10^{-3}$		822
$3\pi^+ 2\pi^-$	$(8.0 \pm 0.9) \times 10^{-3}$		899
$\pi^+ \pi^+ \pi^- \pi^0 \pi^0$	—		902
$\eta \rho^+$	[ggg] $(13.0 \pm 2.2)\%$		724
$\eta \pi^+ \pi^0$ 3-body	[ggg] $< 5\%$	90%	886
$3\pi^+ 2\pi^- \pi^0$	$(4.9 \pm 3.2)\%$		856
$\eta'(958) \pi^+$	[ggg] $(3.8 \pm 0.4)\%$		743
$3\pi^+ 2\pi^- 2\pi^0$	—		803
$\eta'(958) \rho^+$	[ggg] $(12.2 \pm 2.0)\%$		465
$\eta'(958) \pi^+ \pi^0$ 3-body	[ggg] $< 1.8\%$	90%	720

Meson Summary Table

Modes with one or three K 's			
$K^+ \pi^0$	$(8.2 \pm 2.2) \times 10^{-4}$		917
$K_S^0 \pi^+$	$(1.25 \pm 0.15) \times 10^{-3}$		916
$K^+ \eta$	$(1.41 \pm 0.31) \times 10^{-3}$		835
$K^+ \eta'(958)$	$(1.6 \pm 0.5) \times 10^{-3}$		646
$K^+ \pi^+ \pi^-$	$(6.9 \pm 0.5) \times 10^{-3}$		900
$K^+ \rho^0$	$(2.7 \pm 0.5) \times 10^{-3}$		745
$K^+ \rho(1450)^0, \rho^0 \rightarrow \pi^+ \pi^-$	$(7.4 \pm 2.6) \times 10^{-4}$		-
$K^*(892)^0 \pi^+, K^{*0} \rightarrow$	$(1.50 \pm 0.26) \times 10^{-3}$		775
$K^*(1410)^0 \pi^+, K^{*0} \rightarrow$	$(1.30 \pm 0.31) \times 10^{-3}$		-
$K^*(1430)^0 \pi^+, K^{*0} \rightarrow$	$(5 \pm 4) \times 10^{-4}$		-
$K^+ \pi^+ \pi^-$ nonresonant	$(1.1 \pm 0.4) \times 10^{-3}$		900
$K_S^0 \pi^+ \pi^+ \pi^-$	$(3.0 \pm 1.1) \times 10^{-3}$		870
$K^+ K^+ K^-$	$(4.9 \pm 1.7) \times 10^{-4}$		628
$\phi K^+, \phi \rightarrow K^+ K^-$	$< 2.8 \times 10^{-4}$	90%	607
Doubly Cabibbo-suppressed modes			
$K^+ K^+ \pi^-$	$(2.9 \pm 1.1) \times 10^{-4}$		805
Baryon-antibaryon mode			
$p \bar{n}$	$(1.3 \pm 0.4) \times 10^{-3}$		295
$\Delta C = 1$ weak neutral current (C1) modes, Lepton family number (LF), or Lepton number (L) violating modes			
$\pi^+ e^+ e^-$	$[uu] < 2.7 \times 10^{-4}$	90%	979
$\pi^+ \mu^+ \mu^-$	$[uu] < 2.6 \times 10^{-5}$	90%	968
$K^+ e^+ e^-$	$CI < 1.6 \times 10^{-3}$	90%	922
$K^+ \mu^+ \mu^-$	$CI < 3.6 \times 10^{-5}$	90%	909
$K^*(892)^+ \mu^+ \mu^-$	$CI < 1.4 \times 10^{-3}$	90%	765
$\pi^+ e^\pm \mu^\mp$	$LF [gg] < 6.1 \times 10^{-4}$	90%	976
$K^+ e^\pm \mu^\mp$	$LF [gg] < 6.3 \times 10^{-4}$	90%	919
$\pi^- e^+ e^+$	$L < 6.9 \times 10^{-4}$	90%	979
$\pi^- \mu^+ \mu^+$	$L < 2.9 \times 10^{-5}$	90%	968
$\pi^- e^+ \mu^+$	$L < 7.3 \times 10^{-4}$	90%	976
$K^- e^+ e^+$	$L < 6.3 \times 10^{-4}$	90%	922
$K^- \mu^+ \mu^+$	$L < 1.3 \times 10^{-5}$	90%	909
$K^- e^+ \mu^+$	$L < 6.8 \times 10^{-4}$	90%	919
$K^*(892)^- \mu^+ \mu^+$	$L < 1.4 \times 10^{-3}$	90%	765

$D_s^{*\pm}$	$I(J^P) = 0(??)$
J^P is natural, width and decay modes consistent with 1^- .	
Mass $m = 2112.3 \pm 0.5$ MeV ($S = 1.1$)	
$m_{D_s^{*+}} - m_{D_s^{*-}} = 143.8 \pm 0.4$ MeV	
Full width $\Gamma < 1.9$ MeV, CL = 90%	
D_s^{*-} modes are charge conjugates of the modes below.	

D_s^{*+} DECAY MODES	Fraction (Γ_i/Γ)	ρ (MeV/c)
$D_s^+ \gamma$	$(94.2 \pm 0.7) \%$	139
$D_s^+ \pi^0$	$(5.8 \pm 0.7) \%$	48

$D_{s0}^*(2317)^\pm$	$I(J^P) = 0(0^+)$ J, P need confirmation.
J^P is natural, low mass consistent with 0^+ .	
Mass $m = 2317.8 \pm 0.6$ MeV ($S = 1.1$)	
$m_{D_{s0}^*(2317)^\pm} - m_{D_s^\pm} = 349.3 \pm 0.6$ MeV ($S = 1.1$)	
Full width $\Gamma < 3.8$ MeV, CL = 95%	
$D_{s0}^*(2317)^-$ modes are charge conjugates of modes below.	

$D_{s0}^*(2317)^\pm$ DECAY MODES	Fraction (Γ_i/Γ)	ρ (MeV/c)
$D_{s0}^+ \pi^0$	seen	298
$D_{s0}^+ \pi^0 \pi^0$	not seen	205

$D_{s1}(2460)^\pm$	$I(J^P) = 0(1^+)$
Mass $m = 2459.6 \pm 0.6$ MeV ($S = 1.1$)	
$m_{D_{s1}(2460)^\pm} - m_{D_s^\pm} = 347.2 \pm 0.8$ MeV ($S = 1.2$)	
$m_{D_{s1}(2460)^\pm} - m_{D_s^\pm} = 491.1 \pm 0.7$ MeV ($S = 1.1$)	
Full width $\Gamma < 3.5$ MeV, CL = 95%	

$D_{s1}(2460)^-$ modes are charge conjugates of the modes below.

$D_{s1}(2460)^+$ DECAY MODES	Fraction (Γ_i/Γ)	Scale factor/ Confidence level	ρ (MeV/c)
$D_{s1}^{*+} \pi^0$	$(48 \pm 11) \%$		297
$D_{s1}^{*+} \gamma$	$(18 \pm 4) \%$		442
$D_{s1}^{*+} \pi^+ \pi^-$	$(4.3 \pm 1.3) \%$	$S=1.1$	363
$D_{s1}^{*+} \gamma$	$< 8 \%$	CL=90%	323
$D_{s0}^*(2317)^+ \gamma$	$(3.7 \pm 5.1) \%$		138

 $D_{s1}(2536)^\pm$

$I(J^P) = 0(1^+)$
 J, P need confirmation.

Mass $m = 2535.35 \pm 0.34 \pm 0.5$ MeV

Full width $\Gamma < 2.3$ MeV, CL = 90%

$D_{s1}(2536)^-$ modes are charge conjugates of the modes below.

$D_{s1}(2536)^+$ DECAY MODES	Fraction (Γ_i/Γ)	ρ (MeV/c)
$D^*(2010)^+ K^0$	seen	149
$D^*(2007)^0 K^+$	seen	168
$D^+ K^0$	not seen	382
$D^0 K^+$	not seen	391
$D_s^{*+} \gamma$	possibly seen	388
$D_s^{*+} \pi^+ \pi^-$	seen	437

 $D_{s2}(2573)^\pm$

$I(J^P) = 0(??)$

J^P is natural, width and decay modes consistent with 2^+ .

Mass $m = 2572.6 \pm 0.9$ MeV

Full width $\Gamma = 20 \pm 5$ MeV ($S = 1.3$)

$D_{s2}(2573)^-$ modes are charge conjugates of the modes below.

$D_{s2}(2573)^+$ DECAY MODES	Fraction (Γ_i/Γ)	ρ (MeV/c)
$D^0 K^+$	seen	435
$D^*(2007)^0 K^+$	not seen	244

BOTTOM MESONS ($B = \pm 1$)

$B^+ = u\bar{b}, B^0 = d\bar{b}, \bar{B}^0 = \bar{d}b, B^- = \bar{u}b$, similarly for B^{*} 's

B-particle organization

Many measurements of B decays involve admixtures of B hadrons. Previously we arbitrarily included such admixtures in the B^\pm section, but because of their importance we have created two new sections: " B^\pm/B^0 Admixture" for $\Upsilon(4S)$ results and " $B^\pm/B^0/B_s^0/b$ -baryon Admixture" for results at higher energies. Most inclusive decay branching fractions and χ_b at high energy are found in the Admixture sections. B^0 - \bar{B}^0 mixing data are found in the B^0 section, while B_s^0 - \bar{B}_s^0 mixing data and B - \bar{B} mixing data for a B^0/B_s^0 admixture are found in the B_s^0 section. CP -violation data are found in the B^\pm, B^0 , and B^\pm/B^0 Admixture sections. b -baryons are found near the end of the Baryon section.

The organization of the B sections is now as follows, where bullets indicate particle sections and brackets indicate reviews.

- B^\pm
mass, mean life, CP violation, branching fractions
- B^0
mass, mean life, B^0 - \bar{B}^0 mixing, CP violation, branching fractions
- B^\pm/B^0 Admixtures
 CP violation, branching fractions

Meson Summary Table

- $B^\pm/B^0/B_s^0/b$ -baryon Admixtures
mean life, production fractions, branching fractions
 - B^*
mass
 - $B_1(5721)^0$
mass
 - $B_2^*(5747)^0$
mass
 - B_s^0
mass, mean life, $B_s^0\bar{B}_s^0$ mixing, CP violation,
branching fractions
 - B_s^*
mass
 - $B_{s1}(5830)^0$
mass
 - $B_{s2}^0(5840)^0$
mass
 - B_c^\pm
mass, mean life, branching fractions
- At end of Baryon Listings:
- Λ_b
mass, mean life, branching fractions
 - Σ_b
mass
 - Σ_b^*
mass
 - Ξ_b^0, Ξ_b^-
mass
 - b -baryon Admixture
mean life, branching fractions

B^\pm

$$I(J^P) = \frac{1}{2}(0^-)$$

I, J, P need confirmation. Quantum numbers shown are quark-model predictions.

$$\begin{aligned} \text{Mass } m_{B^\pm} &= 5279.15 \pm 0.31 \text{ MeV} \\ \text{Mean life } \tau_{B^\pm} &= (1.638 \pm 0.011) \times 10^{-12} \text{ s} \\ c\tau &= 491.1 \text{ } \mu\text{m} \end{aligned}$$

CP violation

$$\begin{aligned} A_{CP}(B^+ \rightarrow J/\psi(1S)K^+) &= 0.017 \pm 0.016 \quad (S = 1.2) \\ A_{CP}(B^+ \rightarrow J/\psi(1S)\pi^+) &= 0.09 \pm 0.08 \\ A_{CP}(B^+ \rightarrow J/\psi\rho^+) &= -0.11 \pm 0.14 \\ A_{CP}(B^+ \rightarrow J/\psi K^*(892)^+) &= -0.048 \pm 0.033 \\ A_{CP}(B^+ \rightarrow \eta_c K^+) &= -0.16 \pm 0.08 \\ A_{CP}(B^+ \rightarrow \psi(2S)K^+) &= -0.025 \pm 0.024 \\ A_{CP}(B^+ \rightarrow \psi(2S)K^*(892)^+) &= 0.08 \pm 0.21 \\ A_{CP}(B^+ \rightarrow \chi_{c1}(1P)\pi^+) &= 0.07 \pm 0.18 \\ A_{CP}(B^+ \rightarrow \chi_{c0}K^+) &= -0.07 \pm 0.20 \\ A_{CP}(B^+ \rightarrow \chi_{c1}K^+) &= -0.009 \pm 0.033 \\ A_{CP}(B^+ \rightarrow \chi_{c1}K^*(892)^+) &= 0.5 \pm 0.5 \\ A_{CP}(B^+ \rightarrow \bar{D}^0\pi^+) &= -0.008 \pm 0.008 \\ A_{CP}(B^+ \rightarrow D_{CP(+1)}\pi^+) &= 0.035 \pm 0.024 \\ A_{CP}(B^+ \rightarrow D_{CP(-1)}\pi^+) &= 0.017 \pm 0.026 \\ A_{CP}(B^+ \rightarrow \bar{D}^0 K^+) &= 0.07 \pm 0.04 \\ r_B(B^+ \rightarrow D^0 K^+) &= 0.14 \pm 0.06 \\ \delta_B(B^+ \rightarrow D^0 K^+) &= 135 \pm 26 \text{ degrees} \\ r_B(B^+ \rightarrow DK^{*+}) &= 0.56^{+0.24}_{-0.18} \\ \delta_B(B^+ \rightarrow DK^{*+}) &= 243 \pm 50 \text{ degrees} \\ A_{CP}(B^+ \rightarrow [K^-\pi^+]_D K^+) &= 0.9^{+0.8}_{-0.6} \\ A_{CP}(B^+ \rightarrow [K^-\pi^+]_{\bar{D}} K^*(892)^+) &= -0.2 \pm 0.6 \\ A_{CP}(B^+ \rightarrow [K^-\pi^+]_D \pi^+) &= 0.30^{+0.30}_{-0.26} \\ A_{CP}(B^+ \rightarrow [\pi^+\pi^-\pi^0]_D K^+) &= -0.02 \pm 0.15 \\ A_{CP}(B^+ \rightarrow D_{CP(+1)}K^+) &= 0.22 \pm 0.14 \quad (S = 1.4) \\ A_{CP}(B^+ \rightarrow D_{CP(-1)}K^+) &= -0.09 \pm 0.10 \end{aligned}$$

$$\begin{aligned} A_{CP}(B^+ \rightarrow \bar{D}^{*0}\pi^+) &= -0.014 \pm 0.015 \\ A_{CP}(B^+ \rightarrow (D_{CP(+1)}^*)^0\pi^+) &= -0.02 \pm 0.05 \\ A_{CP}(B^+ \rightarrow (D_{CP(-1)}^*)^0\pi^+) &= -0.09 \pm 0.05 \\ A_{CP}(B^+ \rightarrow D^{*0}K^+) &= -0.09 \pm 0.09 \\ r_B^*(B^+ \rightarrow D^{*0}K^+) &= 0.17 \pm 0.08 \\ \delta_B^*(B^+ \rightarrow D^{*0}K^+) &= 299 \pm 31 \text{ degrees} \\ A_{CP}(B^+ \rightarrow D_{CP(+1)}^{*0}K^+) &= -0.15 \pm 0.16 \\ A_{CP}(B^+ \rightarrow D_{CP(-1)}^{*0}K^+) &= 0.13 \pm 0.31 \\ A_{CP}(B^+ \rightarrow D_{CP(+1)}K^*(892)^+) &= -0.08 \pm 0.21 \\ A_{CP}(B^+ \rightarrow D_{CP(-1)}K^*(892)^+) &= -0.3 \pm 0.4 \\ A_{CP}(B^+ \rightarrow D^{*+}\bar{D}^{*0}) &= -0.15 \pm 0.11 \\ A_{CP}(B^+ \rightarrow D^{*+}\bar{D}^0) &= -0.06 \pm 0.13 \\ A_{CP}(B^+ \rightarrow D^+\bar{D}^{*0}) &= 0.13 \pm 0.18 \\ A_{CP}(B^+ \rightarrow D^+\bar{D}^0) &= -0.13 \pm 0.14 \\ A_{CP}(B^+ \rightarrow K_S^0\pi^+) &= 0.009 \pm 0.029 \quad (S = 1.2) \\ A_{CP}(B^+ \rightarrow K^+\pi^0) &= 0.027 \pm 0.032 \\ A_{CP}(B^+ \rightarrow \eta'K^+) &= 0.016 \pm 0.019 \\ A_{CP}(B^+ \rightarrow \eta'K^*(892)^+) &= 0.30^{+0.33}_{-0.37} \\ A_{CP}(B^+ \rightarrow \eta K^+) &= -0.27 \pm 0.09 \\ A_{CP}(B^+ \rightarrow \eta K^*(892)^+) &= 0.02 \pm 0.06 \\ A_{CP}(B^+ \rightarrow \eta K_0^*(1430)^+) &= 0.05 \pm 0.13 \\ A_{CP}(B^+ \rightarrow \eta K_2^*(1430)^+) &= -0.45 \pm 0.30 \\ A_{CP}(B^+ \rightarrow \omega K^+) &= 0.02 \pm 0.05 \\ A_{CP}(B^+ \rightarrow K^*(892)^+\pi^0) &= 0.04 \pm 0.29 \\ A_{CP}(B^+ \rightarrow K^{*0}\pi^+) &= -0.08 \pm 0.10 \quad (S = 1.8) \\ A_{CP}(B^+ \rightarrow K^+\pi^-\pi^+) &= 0.023 \pm 0.031 \quad (S = 1.2) \\ A_{CP}(B^+ \rightarrow f_0(980)K^+) &= -0.04^{+0.08}_{-0.07} \quad (S = 1.1) \\ A_{CP}(B^+ \rightarrow f_2(1270)K^+) &= -0.59 \pm 0.22 \\ A_{CP}(B^+ \rightarrow X_0(1550)K^+) &= -0.04 \pm 0.07 \\ A_{CP}(B^+ \rightarrow \rho^0 K^+) &= 0.31^{+0.11}_{-0.09} \\ A_{CP}(B^+ \rightarrow K_0^*(1430)^0\pi^+) &= 0.00 \pm 0.07 \quad (S = 2.4) \\ A_{CP}(B^+ \rightarrow K^0\rho^+) &= (-0.12 \pm 0.17) \times 10^{-6} \\ A_{CP}(B^+ \rightarrow \rho\bar{\Lambda}\pi^0) &= 0.01 \pm 0.17 \\ A_{CP}(B^+ \rightarrow \rho^0 K^*(892)^+) &= 0.20 \pm 0.31 \\ A_{CP}(B^+ \rightarrow K^*(892)^+ f_0(980)) &= -0.34 \pm 0.21 \\ A_{CP}(B^+ \rightarrow a_1^+ K^0) &= 0.12 \pm 0.11 \\ A_{CP}(B^+ \rightarrow K^*(892)^0\rho^+) &= -0.01 \pm 0.16 \\ A_{CP}(B^+ \rightarrow K^0 K^+) &= 0.12 \pm 0.18 \\ A_{CP}(B^+ \rightarrow b_1^0 K^+) &= -0.46 \pm 0.20 \\ A_{CP}(B^+ \rightarrow K^+ K_S^0 K_S^0) &= -0.04 \pm 0.11 \\ A_{CP}(B^+ \rightarrow K^+ K^- \pi^+) &= 0.00 \pm 0.10 \\ A_{CP}(B^+ \rightarrow K^+ K^- K^+) &= -0.017 \pm 0.030 \\ A_{CP}(B^+ \rightarrow K^{*+} K^+ K^-) &= 0.11 \pm 0.09 \\ A_{CP}(B^+ \rightarrow K^{*+} \pi^+ \pi^-) &= 0.07 \pm 0.08 \\ A_{CP}(B^+ \rightarrow \phi K^+) &= -0.01 \pm 0.06 \\ A_{CP}(B^+ \rightarrow \phi K^*(892)^+) &= -0.01 \pm 0.08 \\ A_{CP}(B^+ \rightarrow \phi K^+ \gamma) &= -0.26 \pm 0.15 \\ A_{CP}(B^+ \rightarrow \eta K^+ \gamma) &= -0.13 \pm 0.08 \\ A_{CP}(B^+ \rightarrow \pi^+ \pi^0) &= 0.01 \pm 0.06 \\ A_{CP}(B^+ \rightarrow \pi^+ \pi^- \pi^+) &= -0.01 \pm 0.08 \\ A_{CP}(B^+ \rightarrow \rho^0 \pi^+) &= -0.07 \pm 0.13 \\ A_{CP}(B^+ \rightarrow f_2(1270)\pi^+) &= 0.00 \pm 0.25 \\ A_{CP}(B^+ \rightarrow \rho^+ \pi^0) &= 0.02 \pm 0.11 \\ A_{CP}(B^+ \rightarrow \rho^+ \rho^0) &= -0.08 \pm 0.13 \\ A_{CP}(B^+ \rightarrow b_1^0 \pi^+) &= 0.05 \pm 0.16 \\ A_{CP}(B^+ \rightarrow \omega \pi^+) &= -0.04 \pm 0.06 \\ A_{CP}(B^+ \rightarrow \omega \rho^+) &= 0.04 \pm 0.18 \\ A_{CP}(B^+ \rightarrow \eta \pi^+) &= -0.16 \pm 0.07 \quad (S = 1.1) \\ A_{CP}(B^+ \rightarrow \eta' \pi^+) &= 0.21 \pm 0.15 \\ A_{CP}(B^+ \rightarrow \eta \rho^+) &= 0.01 \pm 0.16 \\ A_{CP}(B^+ \rightarrow \eta' \rho^+) &= -0.04 \pm 0.28 \\ A_{CP}(B^+ \rightarrow \rho \bar{\rho} \pi^+) &= 0.00 \pm 0.04 \\ A_{CP}(B^+ \rightarrow \rho \bar{\rho} K^+) &= -0.16 \pm 0.07 \\ A_{CP}(B^+ \rightarrow \rho \bar{\rho} K^*(892)^+) &= 0.32 \pm 0.14 \\ A_{CP}(B^+ \rightarrow \rho \bar{\Lambda} \gamma) &= 0.17 \pm 0.17 \\ A_{CP}(B^+ \rightarrow K^+ \ell^+ \ell^-) &= -0.07 \pm 0.22 \\ A_{CP}(B^+ \rightarrow K^{*+} \ell^+ \ell^-) &= 0.03 \pm 0.23 \\ \gamma(B^+ \rightarrow D^*(*) K^*(*)^+) &= (57 \pm 17)^\circ \end{aligned}$$

Meson Summary Table

B^- modes are charge conjugates of the modes below. Modes which do not identify the charge state of the B are listed in the B^\pm/B^0 ADMIXTURE section.

The branching fractions listed below assume 50% $B^0\bar{B}^0$ and 50% B^+B^- production at the $\Upsilon(4S)$. We have attempted to bring older measurements up to date by rescaling their assumed $\Upsilon(4S)$ production ratio to 50:50 and their assumed D, D_s, D^* , and ψ branching ratios to current values whenever this would affect our averages and best limits significantly.

Indentation is used to indicate a subchannel of a previous reaction. All resonant subchannels have been corrected for resonance branching fractions to the final state so the sum of the subchannel branching fractions can exceed that of the final state.

For inclusive branching fractions, e.g., $B \rightarrow D^\pm$ anything, the values usually are multiplicities, not branching fractions. They can be greater than one.

B^+ DECAY MODES	Fraction (Γ_i/Γ)	Scale factor/ Confidence level (MeV/c)	ρ
Semileptonic and leptonic modes			
$\ell^+ \nu_\ell$ anything	[iii] (10.99 \pm 0.28) %	–	–
$e^+ \nu_e X_C$	(10.8 \pm 0.4) %	–	–
$D \ell^+ \nu_\ell$ anything	(10.4 \pm 0.8) %	–	–
$\bar{D}^0 \ell^+ \nu_\ell$	[iii] (2.27 \pm 0.11) %	2310	–
$\bar{D}^0 \tau^+ \nu_\tau$	(7 \pm 4) $\times 10^{-3}$	1911	–
$\bar{D}^*(2007)^0 \ell^+ \nu_\ell$	[iii] (6.07 \pm 0.29) %	2258	–
$\bar{D}^*(2007)^0 \tau^+ \nu_\tau$	(2.2 \pm 0.6) %	1839	–
$D^- \pi^+ \ell^+ \nu_\ell$	(4.2 \pm 0.5) $\times 10^{-3}$	2306	–
$\bar{D}_0^*(2420)^0 \ell^+ \nu_\ell \times$ $B(\bar{D}_0^{*0} \rightarrow D^+ \pi^-)$	(2.4 \pm 0.7) $\times 10^{-3}$	–	–
$\bar{D}_2^*(2460)^0 \ell^+ \nu_\ell \times$ $B(\bar{D}_2^{*0} \rightarrow D^+ \pi^-)$	(2.2 \pm 0.5) $\times 10^{-3}$	2066	–
$D^{(*)} n \pi \ell^+ \nu_\ell$ ($n \geq 1$)	(1.99 \pm 0.28) %	–	–
$D^{*-} \pi^+ \ell^+ \nu_\ell$	(6.1 \pm 0.6) $\times 10^{-3}$	2254	–
$\bar{D}_1(2420)^0 \ell^+ \nu_\ell \times B(\bar{D}_1^0 \rightarrow$ $D^{*+} \pi^-)$	(4.0 \pm 0.7) $\times 10^{-3}$	2084	–
$\bar{D}_1'(2430)^0 \ell^+ \nu_\ell \times$ $B(\bar{D}_1'^0 \rightarrow D^{*+} \pi^-)$	< 7 $\times 10^{-4}$	CL=90%	–
$\bar{D}_2^*(2460)^0 \ell^+ \nu_\ell \times$ $B(\bar{D}_2^{*0} \rightarrow D^{*+} \pi^-)$	(1.8 \pm 0.7) $\times 10^{-3}$	2066	–
$\pi^0 \ell^+ \nu_\ell$	(7.7 \pm 1.2) $\times 10^{-5}$	2638	–
$\eta \ell^+ \nu_\ell$	< 1.01 $\times 10^{-4}$	CL=90%	2611
$\eta' \ell^+ \nu_\ell$	(2.7 \pm 1.0) $\times 10^{-4}$	2553	–
$\omega \ell^+ \nu_\ell$	[iii] (1.3 \pm 0.6) $\times 10^{-4}$	2582	–
$\rho^0 \ell^+ \nu_\ell$	[iii] (1.28 \pm 0.18) $\times 10^{-4}$	2583	–
$\rho \bar{p} e^+ \nu_e$	< 5.2 $\times 10^{-3}$	CL=90%	2467
$e^+ \nu_e$	< 9.8 $\times 10^{-6}$	CL=90%	2640
$\mu^+ \nu_\mu$	< 1.7 $\times 10^{-6}$	CL=90%	2639
$\tau^+ \nu_\tau$	(1.4 \pm 0.4) $\times 10^{-4}$	2341	–
$e^+ \nu_e \gamma$	< 2.0 $\times 10^{-4}$	CL=90%	2640
$\mu^+ \nu_\mu \gamma$	< 5.2 $\times 10^{-5}$	CL=90%	2639
Inclusive modes			
$D^0 X$	(8.6 \pm 0.7) %	–	–
$\bar{D}^0 X$	(79 \pm 4) %	–	–
$D^+ X$	(2.5 \pm 0.5) %	–	–
$D^- X$	(9.9 \pm 1.2) %	–	–
$D_s^+ X$	(7.9 \pm 1.4 – 1.3) %	–	–
$D_s^- X$	(1.10 \pm 0.45 – 0.32) %	–	–
$A_c^+ X$	(2.1 \pm 0.9 – 0.6) %	–	–
$\bar{A}_c^- X$	(2.8 \pm 1.1 – 0.9) %	–	–
$\bar{c} X$	(97 \pm 4) %	–	–
$c X$	(23.4 \pm 2.2 – 1.8) %	–	–
$\bar{c} c X$	(120 \pm 6) %	–	–
D, D*, or D_s modes			
$\bar{D}^0 \pi^+$	(4.84 \pm 0.15) $\times 10^{-3}$	2308	–
$D_{CP(+1)} \pi^+$	[jii] (1.96 \pm 0.34) $\times 10^{-3}$	–	–
$D_{CP(-1)} \pi^+$	[jii] (1.8 \pm 0.4) $\times 10^{-3}$	–	–
$\bar{D}^0 \rho^+$	(1.34 \pm 0.18) %	2237	–
$\bar{D}^0 K^+$	(4.02 \pm 0.21) $\times 10^{-4}$	2280	–
$D_{CP(+1)} K^+$	[jii] (1.81 \pm 0.27) $\times 10^{-4}$	–	–
$D_{CP(-1)} K^+$	[jii] (1.73 \pm 0.23) $\times 10^{-4}$	–	–
$[K^- \pi^+]_D \pi^+$	[kkk] (1.7 \pm 0.5) $\times 10^{-5}$	–	–
$[\pi^+ \pi^- \pi^0]_D K^-$	(4.6 \pm 0.9) $\times 10^{-6}$	–	–

$\bar{D}^0 K^*(892)^+$	(5.3 \pm 0.4) $\times 10^{-4}$	2213	–
$D_{CP(-1)} K^*(892)^+$	[jii] (1.7 \pm 0.7) $\times 10^{-4}$	–	–
$D_{CP(+1)} K^*(892)^+$	[jii] (5.2 \pm 1.2) $\times 10^{-4}$	–	–
$\bar{D}^0 K^+ \bar{K}^0$	(5.5 \pm 1.6) $\times 10^{-4}$	2189	–
$\bar{D}^0 K^+ \bar{K}^*(892)^0$	(7.5 \pm 1.7) $\times 10^{-4}$	2071	–
$\bar{D}^0 \pi^+ \pi^+ \pi^-$	(1.1 \pm 0.4) %	2289	–
$\bar{D}^0 \pi^+ \pi^+ \pi^-$ nonresonant	(5 \pm 4) $\times 10^{-3}$	2289	–
$\bar{D}^0 \pi^+ \rho^0$	(4.2 \pm 3.0) $\times 10^{-3}$	2207	–
$\bar{D}^0 a_1(1260)^+$	(4 \pm 4) $\times 10^{-3}$	2123	–
$\bar{D}^0 \omega \pi^+$	(4.1 \pm 0.9) $\times 10^{-3}$	2206	–
$D^*(2010)^- \pi^+ \pi^+$	(1.35 \pm 0.22) $\times 10^{-3}$	2247	–
$D^- \pi^+ \pi^+$	(1.02 \pm 0.16) $\times 10^{-3}$	2299	–
$D^+ K^0$	< 5.0 $\times 10^{-6}$	CL=90%	2278
$\bar{D}^*(2007)^0 \pi^+$	(5.19 \pm 0.26) $\times 10^{-3}$	2256	–
$\bar{D}^*(2007)^0 \omega \pi^+$	(4.5 \pm 1.2) $\times 10^{-3}$	2149	–
$\bar{D}^*(2007)^0 \rho^+$	(9.8 \pm 1.7) $\times 10^{-3}$	2181	–
$\bar{D}^*(2007)^0 K^+$	(4.16 \pm 0.33) $\times 10^{-4}$	2227	–
$\bar{D}^*(2007)^0 K^* (892)^+$	(8.1 \pm 1.4) $\times 10^{-4}$	2156	–
$\bar{D}^*(2007)^0 K^+ \bar{K}^0$	< 1.06 $\times 10^{-3}$	CL=90%	2132
$\bar{D}^*(2007)^0 K^+ K^*(892)^0$	(1.5 \pm 0.4) $\times 10^{-3}$	2008	–
$\bar{D}^*(2007)^0 \pi^+ \pi^+ \pi^-$	(1.03 \pm 0.12) %	2236	–
$\bar{D}^*(2007)^0 a_1(1260)^+$	(1.9 \pm 0.5) %	2062	–
$\bar{D}^*(2007)^0 \pi^- \pi^+ \pi^0$	(1.8 \pm 0.4) %	2219	–
$\bar{D}^{*0} 3\pi^+ 2\pi^-$	(5.7 \pm 1.2) $\times 10^{-3}$	2196	–
$D^*(2010)^+ \pi^0$	< 1.7 $\times 10^{-4}$	CL=90%	2255
$D^*(2010)^+ K^0$	< 9.0 $\times 10^{-6}$	CL=90%	2225
$D^*(2010)^- \pi^+ \pi^+ \pi^0$	(1.5 \pm 0.7) %	2235	–
$D^*(2010)^- \pi^+ \pi^+ \pi^+ \pi^-$	(2.6 \pm 0.4) $\times 10^{-3}$	2217	–
$\bar{D}^{*0} \pi^+$	[iii] (5.9 \pm 1.3) $\times 10^{-3}$	–	–
$\bar{D}_1^*(2420)^0 \pi^+$	(1.5 \pm 0.6) $\times 10^{-3}$	S=1.3	2081
$\bar{D}_1(2420)^0 \pi^+ \times B(\bar{D}_1^0 \rightarrow$ $\bar{D}^0 \pi^+ \pi^-)$	(1.9 \pm 0.5 – 0.6) $\times 10^{-4}$	2081	–
$\bar{D}_2^*(2462)^0 \pi^+$	(3.4 \pm 0.8) $\times 10^{-4}$	–	–
$\times B(\bar{D}_2^{*0} \rightarrow D^- \pi^+)$	–	–	–
$\bar{D}_0^*(2400)^0 \pi^+$	(6.1 \pm 1.9) $\times 10^{-4}$	2113	–
$\times B(\bar{D}_0^{*0} \rightarrow D^- \pi^+)$	–	–	–
$\bar{D}_1(2421)^0 \pi^+$	(6.8 \pm 1.5) $\times 10^{-4}$	–	–
$\times B(\bar{D}_1^0 \rightarrow D^{*-} \pi^+)$	–	–	–
$\bar{D}_2^*(2462)^0 \pi^+$	(1.8 \pm 0.5) $\times 10^{-4}$	–	–
$\times B(\bar{D}_2^{*0} \rightarrow D^{*-} \pi^+)$	–	–	–
$\bar{D}_1'(2427)^0 \pi^+$	(5.0 \pm 1.2) $\times 10^{-4}$	–	–
$\times B(\bar{D}_1'^0 \rightarrow D^{*-} \pi^+)$	–	–	–
$\bar{D}_1(2420)^0 \pi^+ \times B(\bar{D}_1^0 \rightarrow$ $\bar{D}^{*0} \pi^+ \pi^-)$	< 6 $\times 10^{-6}$	CL=90%	2081
$\bar{D}_1^*(2420)^0 \rho^+$	< 1.4 $\times 10^{-3}$	CL=90%	1995
$\bar{D}_2^*(2460)^0 \pi^+$	< 1.3 $\times 10^{-3}$	CL=90%	2063
$\bar{D}_2^*(2460)^0 \pi^+ \times B(\bar{D}_2^{*0} \rightarrow$ $\bar{D}^{*0} \pi^+ \pi^-)$	< 2.2 $\times 10^{-5}$	CL=90%	2063
$\bar{D}_2^*(2460)^0 \rho^+$	< 4.7 $\times 10^{-3}$	CL=90%	1976
$\bar{D}^0 D_s^+$	(1.03 \pm 0.17) %	1815	–
$D_{s0}(2317)^+ \bar{D}^0 \times$ $B(D_{s0}(2317)^+ \rightarrow D_s^+ \pi^0)$	(7.5 \pm 2.2 – 1.7) $\times 10^{-4}$	1605	–
$D_{s0}(2317)^+ \bar{D}^0 \times$ $B(D_{s0}(2317)^+ \rightarrow D_s^{*+} \gamma)$	< 7.6 $\times 10^{-4}$	CL=90%	1605
$D_{s0}(2317)^+ \bar{D}^*(2007)^0 \times$ $B(D_{s0}(2317)^+ \rightarrow D_s^+ \pi^0)$	(9 \pm 7) $\times 10^{-4}$	1511	–
$D_{sJ}(2457)^+ \bar{D}^0$	(3.1 \pm 1.0 – 0.9) $\times 10^{-3}$	–	–
$D_{sJ}(2457)^+ \bar{D}^0 \times$ $B(D_{sJ}(2457)^+ \rightarrow D_s^+ \gamma)$	(4.8 \pm 1.3 – 1.1) $\times 10^{-4}$	–	–
$D_{sJ}(2457)^+ \bar{D}^0 \times$ $B(D_{sJ}(2457)^+ \rightarrow$ $D_s^+ \pi^+ \pi^-)$	< 2.2 $\times 10^{-4}$	CL=90%	–
$D_{sJ}(2457)^+ \bar{D}^0 \times$ $B(D_{sJ}(2457)^+ \rightarrow D_s^+ \pi^0)$	< 2.7 $\times 10^{-4}$	CL=90%	–
$D_{sJ}(2457)^+ \bar{D}^0 \times$ $B(D_{sJ}(2457)^+ \rightarrow D_s^{*+} \gamma)$	< 9.8 $\times 10^{-4}$	CL=90%	–
$D_{sJ}(2457)^+ \bar{D}^*(2007)^0$	(1.20 \pm 0.30) %	–	–
$D_{sJ}(2457)^+ \bar{D}^*(2007)^0 \times$ $B(D_{sJ}(2457)^+ \rightarrow D_s^+ \gamma)$	(1.4 \pm 0.7 – 0.6) $\times 10^{-3}$	–	–
$\bar{D}^0 D_{s1}(2536)^+ \times$ $B(D_{s1}(2536)^+ \rightarrow$ $D^*(2007)^0 K^+)$	(2.2 \pm 0.7) $\times 10^{-4}$	1447	–

Meson Summary Table

$K^*(1410)^0 \pi^+$	< 4.5	$\times 10^{-5}$	CL=90%	2448	$f_0(1370) \pi^+ \times B(f_0(1370) \rightarrow \pi^+ \pi^-)$	< 3.0	$\times 10^{-6}$	CL=90%	2460
$K^*(1680)^0 \pi^+$	< 1.2	$\times 10^{-5}$	CL=90%	2358	$f_0(600) \pi^+ \times B(f_0(600) \rightarrow \pi^+ \pi^-)$	< 4.1	$\times 10^{-6}$	CL=90%	–
$K^- \pi^+ \pi^+$	< 1.8	$\times 10^{-6}$	CL=90%	2609	$\pi^+ \pi^- \pi^+$ nonresonant	< 4.6	$\times 10^{-6}$	CL=90%	2630
$K_1(1400)^0 \pi^+$	< 2.6	$\times 10^{-3}$	CL=90%	2451	$\pi^+ \pi^0 \pi^0$	< 8.9	$\times 10^{-4}$	CL=90%	2631
$K^0 \pi^+ \pi^0$	< 6.6	$\times 10^{-5}$	CL=90%	2609	$\rho^+ \pi^0$	(1.09 \pm 0.14)	$\times 10^{-5}$		2581
$K^0 \rho^+$	(8.0 \pm 1.5)	$\times 10^{-6}$		2558	$\pi^+ \pi^- \pi^+ \pi^0$	< 4.0	$\times 10^{-3}$	CL=90%	2621
$K^*(892)^+ \pi^+ \pi^-$	(7.5 \pm 1.0)	$\times 10^{-5}$		2556	$\rho^+ \rho^0$	(1.8 \pm 0.4)	$\times 10^{-5}$	S=1.5	2523
$K^*(892)^+ \rho^0$	< 6.1	$\times 10^{-6}$	CL=90%	2504	$\rho^+ f_0(980) \times B(f_0(980) \rightarrow \pi^+ \pi^-)$	< 1.9	$\times 10^{-6}$	CL=90%	2487
$K^*(892)^+ f_0(980)$	(5.2 \pm 1.3)	$\times 10^{-6}$		2468	$a_1(1260)^+ \pi^0$	(2.6 \pm 0.7)	$\times 10^{-5}$		2494
$a_1^+ K^0$	(3.5 \pm 0.7)	$\times 10^{-5}$		–	$a_1(1260)^0 \pi^+$	(2.0 \pm 0.6)	$\times 10^{-5}$		2494
$K^*(892)^0 \rho^+$	(9.2 \pm 1.5)	$\times 10^{-6}$		2504	$b_1^0 \pi^+ \times B(b_1^0 \rightarrow \omega \pi^0)$	(6.7 \pm 2.0)	$\times 10^{-6}$		–
$K^*(892)^+ K^*(892)^0$	< 7.1	$\times 10^{-5}$	CL=90%	2484	$\omega \pi^+$	(6.9 \pm 0.5)	$\times 10^{-6}$		2580
$K_1(1400)^+ \rho^0$	< 7.8	$\times 10^{-4}$	CL=90%	2387	$\omega \rho^+$	(1.06 \pm 0.26)	$\times 10^{-5}$		2522
$K_2^*(1430)^+ \rho^0$	< 1.5	$\times 10^{-3}$	CL=90%	2381	$\eta \pi^+$	(4.4 \pm 0.4)	$\times 10^{-6}$	S=1.1	2609
$K^+ \bar{K}^0$	(1.36 \pm 0.27)	$\times 10^{-6}$		2593	$\eta' \pi^+$	(2.7 \pm 1.0)	$\times 10^{-6}$	S=2.1	2551
$\bar{K}^0 K^+ \pi^0$	< 2.4	$\times 10^{-5}$	CL=90%	2578	$\eta' \rho^+$	(8.7 \pm 3.9)	$\times 10^{-6}$		2492
$K^+ K_S^0 K_S^0$	(1.15 \pm 0.13)	$\times 10^{-5}$		2521	$\eta \rho^+$	(5.4 \pm 1.9)	$\times 10^{-6}$	S=1.6	2553
$K_S^0 K_S^0 \pi^+$	< 3.2	$\times 10^{-6}$	CL=90%	2577	$\phi \pi^+$	< 2.4	$\times 10^{-7}$	CL=90%	2539
$K^+ K^- \pi^+$	(5.0 \pm 0.7)	$\times 10^{-6}$		2578	$\phi \rho^+$	< 1.6	$\times 10^{-5}$		2480
$K^+ K^- \pi^+$ nonresonant	< 7.5	$\times 10^{-5}$	CL=90%	2578	$a_0(980)^0 \pi^+ \times B(a_0(980)^0 \rightarrow \eta \pi^0)$	< 5.8	$\times 10^{-6}$	CL=90%	–
$K^+ \bar{K}^*(892)^0$	< 1.1	$\times 10^{-6}$	CL=90%	2540	$a_0(980)^+ \pi^0 \times B(a_0^+ \rightarrow \eta \pi^+)$	< 1.4	$\times 10^{-6}$	CL=90%	–
$K^+ \bar{K}_0^0(1430)^0$	< 2.2	$\times 10^{-6}$	CL=90%	2421	$\pi^+ \pi^+ \pi^+ \pi^-$	< 8.6	$\times 10^{-4}$	CL=90%	2608
$K^+ K^+ \pi^-$	< 1.3	$\times 10^{-6}$	CL=90%	2578	$\rho^0 a_1(1260)^+$	< 6.2	$\times 10^{-4}$	CL=90%	2433
$K^+ K^+ \pi^-$ nonresonant	< 8.79	$\times 10^{-5}$	CL=90%	2578	$\rho^0 a_2(1320)^+$	< 7.2	$\times 10^{-4}$	CL=90%	2410
$b_1^0 K^+ \times B(b_1^0 \rightarrow \omega \pi^0)$	(9.1 \pm 2.0)	$\times 10^{-6}$		–	$\pi^+ \pi^+ \pi^+ \pi^- \pi^0$	< 6.3	$\times 10^{-3}$	CL=90%	2592
$K^{*+} \pi^+ K^-$	< 1.18	$\times 10^{-5}$	CL=90%	2524	$a_1(1260)^+ a_1(1260)^0$	< 1.3	%	CL=90%	2335
$K^{*+} K^+ \pi^-$	< 6.1	$\times 10^{-6}$	CL=90%	2524	Charged particle (h^\pm) modes				
$K^+ K^- K^+$	(3.37 \pm 0.22)	$\times 10^{-5}$	S=1.4	2522	$h^\pm = K^\pm \text{ or } \pi^\pm$				
$K^+ \phi$	(8.3 \pm 0.7)	$\times 10^{-6}$		2516	$h^+ \pi^0$	(1.6 \pm 0.7)	$\times 10^{-5}$		2636
$f_0(980) K^+ \times B(f_0(980) \rightarrow K^+ K^-)$	< 2.9	$\times 10^{-6}$	CL=90%	2524	ωh^+	(1.38 \pm 0.27)	$\times 10^{-5}$		2580
$a_2(1320) K^+ \times B(a_2(1320) \rightarrow K^+ K^-)$	< 1.1	$\times 10^{-6}$	CL=90%	2449	$h^+ X^0$ (Familon)	< 4.9	$\times 10^{-5}$	CL=90%	–
$f_2'(1525) K^+ \times B(f_2'(1525) \rightarrow K^+ K^-)$	< 4.9	$\times 10^{-6}$	CL=90%	2392	Baryon modes				
$X_0(1550) K^+ \times B(X_0(1550) \rightarrow K^+ K^-)$	(4.3 \pm 0.7)	$\times 10^{-6}$		–	$p \bar{p} \pi^+$	(1.62 \pm 0.20)	$\times 10^{-6}$		2439
$\phi(1680) K^+ \times B(\phi(1680) \rightarrow K^+ K^-)$	< 8	$\times 10^{-7}$	CL=90%	2344	$p \bar{p} \pi^+ \pi^+$ nonresonant	< 5.3	$\times 10^{-5}$	CL=90%	2439
$f_0(1710) K^+ \times B(f_0(1710) \rightarrow K^+ K^-)$	(1.7 \pm 1.0)	$\times 10^{-6}$		2329	$p \bar{p} \pi^+ \pi^+ \pi^-$	< 5.2	$\times 10^{-4}$	CL=90%	2370
$K^+ K^- K^+$ nonresonant	(2.8 \pm 0.9)	$\times 10^{-5}$	S=3.3	2522	$p \bar{p} K^+$	(5.9 \pm 0.5)	$\times 10^{-6}$	S=1.5	2348
$K^*(892)^+ K^+ K^-$	(3.6 \pm 0.5)	$\times 10^{-5}$		2466	$\Theta(1710)^{++} \bar{p} \times B(\Theta(1710)^{++} \rightarrow p K^+)$	< 9.1	$\times 10^{-8}$	CL=90%	–
$K^*(892)^+ \phi$	(1.05 \pm 0.15)	$\times 10^{-5}$	S=1.4	2460	$f_J(2220) K^+ \times B(f_J(2220) \rightarrow [nnn])$	< 4.1	$\times 10^{-7}$	CL=90%	2135
$K_1(1400)^+ \phi$	< 1.1	$\times 10^{-3}$	CL=90%	2339	$\rho \bar{\rho}$	< 1.5	$\times 10^{-6}$	CL=90%	2322
$K_2^*(1430)^+ \phi$	< 3.4	$\times 10^{-3}$	CL=90%	2332	$p \bar{p} K^+$ nonresonant	< 8.9	$\times 10^{-5}$	CL=90%	2348
$K^+ \phi \phi$	(4.9 \pm 2.4)	$\times 10^{-6}$	S=2.9	2306	$p \bar{p} K^*(892)^+$	(6.6 \pm 2.3)	$\times 10^{-6}$	S=1.3	2215
$\eta' \eta' K^+$	< 2.5	$\times 10^{-5}$	CL=90%	–	$f_J(2220) K^{*+} \times B(f_J(2220) \rightarrow p \bar{p})$	< 7.7	$\times 10^{-7}$	CL=90%	2059
$K^*(892)^+ \gamma$	(4.03 \pm 0.26)	$\times 10^{-5}$		2564	$\rho \bar{\rho}$	< 3.2	$\times 10^{-7}$	CL=90%	2430
$K_1(1270)^+ \gamma$	(4.3 \pm 1.3)	$\times 10^{-5}$		2486	$\rho \bar{\rho} \gamma$	(2.5 \pm 0.5)	$\times 10^{-6}$		2430
$\eta K^+ \gamma$	(9.4 \pm 1.1)	$\times 10^{-6}$		2588	$\rho \bar{\rho} \pi^0$	(3.0 \pm 0.7)	$\times 10^{-6}$		2402
$\eta' K^+ \gamma$	< 4.2	$\times 10^{-6}$	CL=90%	–	$\rho \bar{\Sigma}(1385)^0$	< 4.7	$\times 10^{-7}$	CL=90%	2362
$\phi K^+ \gamma$	(3.5 \pm 0.6)	$\times 10^{-6}$		2516	$\Delta^+ \bar{\Lambda}$	< 8.2	$\times 10^{-7}$	CL=90%	–
$K^+ \pi^- \pi^+ \gamma$	(2.76 \pm 0.22)	$\times 10^{-5}$	S=1.2	2609	$\rho \bar{\Sigma} \gamma$	< 4.6	$\times 10^{-6}$	CL=90%	2413
$K^*(892)^0 \pi^+ \gamma$	(2.0 \pm 0.7)	$\times 10^{-5}$		2562	$\rho \bar{\Lambda} \pi^+ \pi^-$	< 2.0	$\times 10^{-4}$	CL=90%	2367
$K^+ \rho^0 \gamma$	< 2.0	$\times 10^{-5}$	CL=90%	2559	$\Lambda \bar{\Lambda} \pi^+$	< 2.8	$\times 10^{-6}$	CL=90%	2358
$K^+ \pi^- \pi^+ \gamma$ nonresonant	< 9.2	$\times 10^{-6}$	CL=90%	2609	$\Lambda \bar{\Lambda} K^+$	(2.9 \pm 1.0)	$\times 10^{-6}$		2251
$K^0 \pi^+ \pi^0 \gamma$	(4.6 \pm 0.5)	$\times 10^{-5}$		2609	$\bar{\Delta}^0 p$	< 1.38	$\times 10^{-6}$	CL=90%	2402
$K_1(1400)^+ \gamma$	< 1.5	$\times 10^{-5}$	CL=90%	2453	$\Delta^+ \pi^+ \bar{p}$	< 1.4	$\times 10^{-7}$	CL=90%	2402
$K_2^*(1430)^+ \gamma$	(1.4 \pm 0.4)	$\times 10^{-5}$		2447	$D^+ \rho \bar{p}$	< 1.5	$\times 10^{-5}$	CL=90%	1860
$K^*(1680)^+ \gamma$	< 1.9	$\times 10^{-3}$	CL=90%	2360	$D^*(2010)^+ \rho \bar{p}$	< 1.5	$\times 10^{-5}$	CL=90%	1786
$K_3^*(1780)^+ \gamma$	< 3.9	$\times 10^{-5}$	CL=90%	2341	$\bar{\Lambda}_c^- \rho \pi^+$	(2.1 \pm 0.6)	$\times 10^{-4}$		1980
$K_4^*(2045)^+ \gamma$	< 9.9	$\times 10^{-3}$	CL=90%	2244	$\bar{\Lambda}_c^- \Delta(1232)^{++}$	< 1.9	$\times 10^{-5}$	CL=90%	1928
Light unflavored meson modes					$\bar{\Lambda}_c^- \Delta_X(1600)^{++}$	(5.9 \pm 1.9)	$\times 10^{-5}$		–
$\rho^+ \gamma$	(8.8 \pm 2.9)	$\times 10^{-7}$		2583	$\bar{\Lambda}_c^- \Delta_X(2420)^{++}$	(4.7 \pm 1.6)	$\times 10^{-5}$		–
$\pi^+ \pi^0$	(5.7 \pm 0.5)	$\times 10^{-6}$	S=1.4	2636	$(\bar{\Lambda}_c^- p)_s \pi^+$	[ooo] (3.9 \pm 1.3)	$\times 10^{-5}$		–
$\pi^+ \pi^+ \pi^-$	(1.62 \pm 0.15)	$\times 10^{-5}$		2630	$\bar{\Lambda}_c^- p \pi^+ \pi^0$	(1.8 \pm 0.6)	$\times 10^{-3}$		1935
$\rho^0 \pi^+$	(8.7 \pm 1.1)	$\times 10^{-6}$		2581	$\bar{\Lambda}_c^- \rho \pi^+ \pi^+ \pi^-$	(2.3 \pm 0.7)	$\times 10^{-3}$		1880
$\pi^+ f_0(980) \times B(f_0(980) \rightarrow \pi^+ \pi^-)$	< 3.0	$\times 10^{-6}$	CL=90%	2547	$\bar{\Lambda}_c^- \rho \pi^+ \pi^+ \pi^- \pi^0$	< 1.34	%	CL=90%	1822
$\pi^+ f_2(1270)$	(8.2 \pm 2.5)	$\times 10^{-6}$		2484					
$\rho(1450)^0 \pi^+$	< 2.3	$\times 10^{-6}$	CL=90%	2434					

Meson Summary Table

$\Lambda_c^+ \Lambda_c^- K^+$	(7 ± 4) × 10 ⁻⁴	-
$\Sigma_c(2455)^0 \rho$	(3.7 ± 1.3) × 10 ⁻⁵	1938
$\Sigma_c(2520)^0 \rho$	< 2.7 × 10 ⁻⁵	CL=90% 1904
$\Sigma_c(2455)^0 \rho \pi^0$	(4.4 ± 1.8) × 10 ⁻⁴	1896
$\Sigma_c(2455)^0 \rho \pi^- \pi^+$	(4.4 ± 1.7) × 10 ⁻⁴	1845
$\Sigma_c(2455)^- \rho \pi^+ \pi^+$	(2.8 ± 1.2) × 10 ⁻⁴	1845
$\Lambda_c(2593)^- / \Lambda_c(2625)^- \rho \pi^+$	< 1.9 × 10 ⁻⁴	CL=90% -
$\Xi_c^0 \Lambda_c^+ \times B(\Xi_c^0 \rightarrow \Xi^+ \pi^-)$	(5.6 ^{+2.7} _{-2.4}) × 10 ⁻⁵	1143
$\Xi_c^0 \Lambda_c^+ \times B(\Xi_c^0 \rightarrow \Lambda K^+ \pi^-)$	(4.0 ± 1.6) × 10 ⁻⁵	1143

Lepton Family number (LF) or Lepton number (L) violating modes, or $\Delta B = 1$ weak neutral current (BI) modes

$\pi^+ \ell^+ \ell^-$	BI	< 1.2 × 10 ⁻⁷	CL=90%	2638
$\pi^+ e^+ e^-$	BI	< 1.8 × 10 ⁻⁷	CL=90%	2638
$\pi^+ \mu^+ \mu^-$	BI	< 2.8 × 10 ⁻⁷	CL=90%	2633
$\pi^+ \nu \bar{\nu}$	BI	< 1.0 × 10 ⁻⁴	CL=90%	2638
$K^+ \ell^+ \ell^-$	BI [iii]	(4.4 ^{+0.8} _{-0.7}) × 10 ⁻⁷	S=1.1	2616
$K^+ e^+ e^-$	BI	(4.9 ± 1.0) × 10 ⁻⁷		2616
$K^+ \mu^+ \mu^-$	BI	(3.9 ^{+1.0} _{-0.9}) × 10 ⁻⁷		2612
$K^+ \bar{\nu} \nu$	BI	< 1.4 × 10 ⁻⁵	CL=90%	2616
$\rho^+ \nu \bar{\nu}$	BI	< 1.5 × 10 ⁻⁴	CL=90%	2583
$K^*(892)^+ \ell^+ \ell^-$	BI [iii]	(7 ± 5) × 10 ⁻⁷		2564
$K^*(892)^+ \nu \bar{\nu}$	BI	< 1.4 × 10 ⁻⁴	CL=90%	-
$K^*(892)^+ e^+ e^-$	BI	(8 ± 8) × 10 ⁻⁷		2564
$K^*(892)^+ \mu^+ \mu^-$	BI	(8 ⁺⁶ ₋₄) × 10 ⁻⁷		2560
$\pi^+ e^+ \mu^-$	LF	< 6.4 × 10 ⁻³	CL=90%	2637
$\pi^+ e^- \mu^+$	LF	< 6.4 × 10 ⁻³	CL=90%	2637
$\pi^+ e^\pm \mu^\mp$	LF	< 1.7 × 10 ⁻⁷	CL=90%	2637
$K^+ e^+ \mu^-$	LF	< 9.1 × 10 ⁻⁸	CL=90%	2615
$K^+ e^- \mu^+$	LF	< 1.3 × 10 ⁻⁷	CL=90%	2615
$K^+ e^\pm \mu^\mp$	LF	< 9.1 × 10 ⁻⁸	CL=90%	2615
$K^+ \mu^\pm \tau^\mp$	LF	< 7.7 × 10 ⁻⁵	CL=90%	2298
$K^*(892)^+ e^+ \mu^-$	LF	< 1.3 × 10 ⁻⁶	CL=90%	2563
$K^*(892)^+ e^- \mu^+$	LF	< 9.9 × 10 ⁻⁷	CL=90%	2563
$K^*(892)^+ e^\pm \mu^\mp$	LF	< 1.4 × 10 ⁻⁷	CL=90%	2563
$\pi^- e^+ e^+$	L	< 1.6 × 10 ⁻⁶	CL=90%	2638
$\pi^- \mu^+ \mu^+$	L	< 1.4 × 10 ⁻⁶	CL=90%	2633
$\pi^- e^+ \mu^+$	L	< 1.3 × 10 ⁻⁶	CL=90%	2637
$\rho^- e^+ e^+$	L	< 2.6 × 10 ⁻⁶	CL=90%	2583
$\rho^- \mu^+ \mu^+$	L	< 5.0 × 10 ⁻⁶	CL=90%	2578
$\rho^- e^+ \mu^+$	L	< 3.3 × 10 ⁻⁶	CL=90%	2582
$K^- e^+ e^+$	L	< 1.0 × 10 ⁻⁶	CL=90%	2616
$K^- \mu^+ \mu^+$	L	< 1.8 × 10 ⁻⁶	CL=90%	2612
$K^- e^+ \mu^+$	L	< 2.0 × 10 ⁻⁶	CL=90%	2615
$K^*(892)^- e^+ e^+$	L	< 2.8 × 10 ⁻⁶	CL=90%	2564
$K^*(892)^- \mu^+ \mu^+$	L	< 8.3 × 10 ⁻⁶	CL=90%	2560
$K^*(892)^- e^+ \mu^+$	L	< 4.4 × 10 ⁻⁶	CL=90%	2563

B⁰

$$I(J^P) = \frac{1}{2}(0^-)$$

I, J, P need confirmation. Quantum numbers shown are quark-model predictions.

$$\text{Mass } m_{B^0} = 5279.53 \pm 0.33 \text{ MeV}$$

$$m_{B^0} - m_{B^\pm} = 0.37 \pm 0.24 \text{ MeV}$$

$$\text{Mean life } \tau_{B^0} = (1.530 \pm 0.009) \times 10^{-12} \text{ s}$$

$$c\tau = 458.7 \mu\text{m}$$

$$\tau_{B^+} / \tau_{B^0} = 1.071 \pm 0.009 \quad (\text{direct measurements})$$

B⁰- \bar{B}^0 mixing parameters

$$\chi_d = 0.1878 \pm 0.0024$$

$$\Delta m_{B^0} = m_{B_H^0} - m_{B_L^0} = (0.507 \pm 0.005) \times 10^{12} \hbar \text{ s}^{-1}$$

$$= (3.337 \pm 0.033) \times 10^{-10} \text{ MeV}$$

$$x_d = \Delta m_{B^0} / \Gamma_{B^0} = 0.776 \pm 0.008$$

$$\text{Re}(\lambda_{CP} / |\lambda_{CP}|) \text{Re}(z) = 0.01 \pm 0.05$$

$$\Delta\Gamma \text{Re}(z) = -0.007 \pm 0.004$$

$$\text{Re}(z) = 0.00 \pm 0.12$$

$$\text{Im}(z) = -0.015 \pm 0.008$$

CP violation parameters

$$\text{Re}(\epsilon_{B^0}) / (1 + |\epsilon_{B^0}|^2) = (-0.1 \pm 1.4) \times 10^{-3}$$

$$A_{T/CP} = 0.005 \pm 0.018$$

$$A_{CP}(B^0 \rightarrow D^*(2010)^+ D^-) = -0.06 \pm 0.09 \quad (S = 1.7)$$

$$\mathbf{A}_{CP}(B^0 \rightarrow K^+ \pi^-) = -0.101 \pm 0.015$$

$$A_{CP}(B^0 \rightarrow \eta' K^*(892)^0) = -0.08 \pm 0.25$$

$$\mathbf{A}_{CP}(B^0 \rightarrow \eta K^*(892)^0) = 0.19 \pm 0.05$$

$$A_{CP}(B^0 \rightarrow K^0 K^0) = (-0.6 \pm 0.7) \times 10^{-6}$$

$$A_{CP}(B^0 \rightarrow \eta K_S^0(1430)^0) = 0.06 \pm 0.13$$

$$A_{CP}(B^0 \rightarrow \eta K_S^0(1430)^0) = -0.07 \pm 0.19$$

$$A_{CP}(B^0 \rightarrow \rho^+ K^-) = -0.08 \pm 0.24 \quad (S = 1.7)$$

$$A_{CP}(B^0 \rightarrow K^+ \pi^- \pi^0) = 0.07 \pm 0.11$$

$$A_{CP}(B^0 \rightarrow K^*(892)^+ \pi^-) = -0.05 \pm 0.14$$

$$A_{CP}(B^0 \rightarrow K^*(892)^0 \rho^0) = 0.09 \pm 0.19$$

$$A_{CP}(B^0 \rightarrow a_1^- K^+) = -0.16 \pm 0.12$$

$$A_{CP}(B^0 \rightarrow K^*(892)^0 \pi^+ \pi^-) = 0.07 \pm 0.05$$

$$A_{CP}(B^0 \rightarrow K^*(892)^0 K^+ K^-) = 0.01 \pm 0.05$$

$$A_{CP}(B^0 \rightarrow K^*(892)^0 \phi) = -0.01 \pm 0.06$$

$$A_{CP}(B^0 \rightarrow K^*(892)^0 K^- \pi^+) = 0.2 \pm 0.4$$

$$A_{CP}(B^0 \rightarrow \phi(K\pi)_0^0) = 0.17 \pm 0.15$$

$$A_{CP}(B^0 \rightarrow \phi K_S^0(1430)^0) = -0.12 \pm 0.15$$

$$A_{CP}(B^0 \rightarrow \rho^+ \pi^-) = 0.08 \pm 0.12 \quad (S = 2.0)$$

$$A_{CP}(B^0 \rightarrow \rho^- \pi^+) = -0.16 \pm 0.23 \quad (S = 1.7)$$

$$A_{CP}(B^0 \rightarrow \rho^0 \pi^0) = -0.5 \pm 0.5$$

$$A_{CP}(B^0 \rightarrow a_1(1260)^\pm \pi^\mp) = -0.07 \pm 0.07$$

$$A_{CP}(B^0 \rightarrow b_1 \pi^+) = -0.05 \pm 0.10$$

$$A_{CP}(B^0 \rightarrow K^*(1430) \gamma) = -0.08 \pm 0.15$$

$$A_{CP}(B^0 \rightarrow p \bar{p} K^*(892)^0) = 0.11 \pm 0.14$$

$$A_{CP}(B^0 \rightarrow p \bar{p} \pi^-) = -0.02 \pm 0.10$$

$$A_{CP}(B^0 \rightarrow b_1 K^+) = -0.07 \pm 0.12$$

$$C_{D^*(2010)^- D^+} (B^0 \rightarrow D^*(2010)^- D^+) = 0.23 \pm 0.13$$

$$S_{D^*(2010)^- D^+} (B^0 \rightarrow D^*(2010)^- D^+) = -0.55 \pm 0.21$$

$$C_{D^*(2010)^+ D^-} (B^0 \rightarrow D^*(2010)^+ D^-) = 0.01 \pm 0.26 \quad (S = 2.0)$$

$$S_{D^*(2010)^+ D^-} (B^0 \rightarrow D^*(2010)^+ D^-) = -0.74 \pm 0.19$$

$$C_{D^{*+} D^{*-}} (B^0 \rightarrow D^{*+} D^{*-}) = 0.02 \pm 0.10$$

$$\mathbf{S}_{D^{*+} D^{*-}} (B^0 \rightarrow D^{*+} D^{*-}) = -0.67 \pm 0.18$$

$$C_+ (B^0 \rightarrow D^{*+} D^{*-}) = -0.05 \pm 0.14$$

$$\mathbf{S}_+ (B^0 \rightarrow D^{*+} D^{*-}) = -0.72 \pm 0.20$$

$$C_- (B^0 \rightarrow D^{*+} D^{*-}) = 0.2 \pm 0.7$$

$$S_- (B^0 \rightarrow D^{*+} D^{*-}) = -1.8 \pm 1.1$$

$$C(B^0 \rightarrow D^*(2010)^+ D^*(2010)^- K_S^0) = 0.01 \pm 0.29$$

$$S(B^0 \rightarrow D^*(2010)^+ D^*(2010)^- K_S^0) = 0.1 \pm 0.4$$

$$C_{D^+ D^-} (B^0 \rightarrow D^+ D^-) = -0.4 \pm 0.5 \quad (S = 3.1)$$

$$\mathbf{S}_{D^+ D^-} (B^0 \rightarrow D^+ D^-) = -0.81 \pm 0.29 \quad (S = 1.1)$$

$$C_{J/\psi(1S) \pi^0} (B^0 \rightarrow J/\psi(1S) \pi^0) = -0.11 \pm 0.20$$

$$S_{J/\psi(1S) \pi^0} (B^0 \rightarrow J/\psi(1S) \pi^0) = -0.69 \pm 0.25$$

$$C_{D_{CP}^*(*) h^0} (B^0 \rightarrow D_{CP}^*(*) h^0) = -0.23 \pm 0.16$$

$$S_{D_{CP}^*(*) h^0} (B^0 \rightarrow D_{CP}^*(*) h^0) = -0.56 \pm 0.24$$

$$S_{K_S^0 K_S^0} (B^0 \rightarrow K_S^0 K_S^0) = -1.3 \pm 0.8$$

$$C_{K_S^0 K_S^0} (B^0 \rightarrow K_S^0 K_S^0) = -0.4 \pm 0.4$$

$$C_{\eta'(958) K} (B^0 \rightarrow \eta'(958) K_S^0) = -0.04 \pm 0.20 \quad (S = 2.5)$$

$$S_{\eta'(958) K} (B^0 \rightarrow \eta'(958) K_S^0) = 0.43 \pm 0.17 \quad (S = 1.5)$$

$$C_{\eta' K^0} (B^0 \rightarrow \eta' K^0) = -0.09 \pm 0.08 \quad (S = 1.5)$$

$$\mathbf{S}_{\eta' K^0} (B^0 \rightarrow \eta' K^0) = 0.61 \pm 0.07$$

$$C_{\omega K_S^0} (B^0 \rightarrow \omega K_S^0) = -0.25 \pm 0.31 \quad (S = 1.6)$$

$$S_{\omega K_S^0} (B^0 \rightarrow \omega K_S^0) = 0.35 \pm 0.29$$

$$C_{f_0(980) K_S^0} (B^0 \rightarrow f_0(980) K_S^0) = -0.03 \pm 0.26 \quad (S = 1.9)$$

$$S_{f_0(980) K_S^0} (B^0 \rightarrow f_0(980) K_S^0) = -0.02 \pm 0.21 \quad (S = 1.1)$$

$$C_{K_S K_S} (B^0 \rightarrow K_S K_S) = -0.15 \pm 0.16 \quad (S = 1.1)$$

$$S_{K_S K_S} (B^0 \rightarrow K_S K_S) = -0.4 \pm 0.5 \quad (S = 2.5)$$

$$C_{K^+ K^- K_S^0} (B^0 \rightarrow K^+ K^- K_S^0) = 0.07 \pm 0.08$$

$$\mathbf{S}_{K^+ K^- K_S^0} (B^0 \rightarrow K^+ K^- K_S^0) = -0.74 ^{+0.12} _{-0.10}$$

$$C_{K^+ K^- K_S^0} (B^0 \rightarrow K^+ K^- K_S^0 \text{ inclusive}) = 0.01 \pm 0.09$$

Meson Summary Table

$S_{K^+K^-K_S^0}(B^0 \rightarrow K^+K^-K_S^0 \text{ inclusive}) = -0.65 \pm 0.12$

$C_{\phi K_S^0}(B^0 \rightarrow \phi K_S^0) = -0.01 \pm 0.12$

$S_{\phi K_S^0}(B^0 \rightarrow \phi K_S^0) = 0.39 \pm 0.17$

$C_{K_S^0\pi^0}(B^0 \rightarrow K_S^0\pi^0) = 0.14 \pm 0.11$

$S_{K_S^0\pi^0}(B^0 \rightarrow K_S^0\pi^0) = 0.38 \pm 0.19$

$C(B^0 \rightarrow K_S^0\pi^0\pi^0) = 0.2 \pm 0.5$

$S(B^0 \rightarrow K_S^0\pi^0\pi^0) = 0.7 \pm 0.7$

$C_{K_S^0\pi^0\gamma}(B^0 \rightarrow K_S^0\pi^0\gamma) = 0.0 \pm 0.4 \quad (S = 2.1)$

$S_{K_S^0\pi^0\gamma}(B^0 \rightarrow K_S^0\pi^0\gamma) = -0.01 \pm 0.30$

$C_{K^*(892)^0\gamma}(B^0 \rightarrow K^*(892)^0\gamma) = -0.12 \pm 0.30 \quad (S = 1.8)$

$S_{K^*(892)^0\gamma}(B^0 \rightarrow K^*(892)^0\gamma) = -0.27 \pm 0.26$

$C(B^0 \rightarrow \rho^0\gamma) = 0.4 \pm 0.5$

$S(B^0 \rightarrow \rho^0\gamma) = -0.8 \pm 0.7$

$C_{\pi\pi}(B^0 \rightarrow \pi^+\pi^-) = -0.38 \pm 0.17 \quad (S = 2.6)$

$S_{\pi\pi}(B^0 \rightarrow \pi^+\pi^-) = -0.61 \pm 0.08$

$C_{\pi^0\pi^0}(B^0 \rightarrow \pi^0\pi^0) = -0.48 \pm 0.30$

$C_{\rho\pi}(B^0 \rightarrow \rho^+\pi^-) = 0.01 \pm 0.14 \quad (S = 1.9)$

$S_{\rho\pi}(B^0 \rightarrow \rho^+\pi^-) = 0.01 \pm 0.09$

$\Delta C_{\rho\pi}(B^0 \rightarrow \rho^+\pi^-) = 0.37 \pm 0.08$

$\Delta S_{\rho\pi}(B^0 \rightarrow \rho^+\pi^-) = -0.05 \pm 0.10$

$C_{\rho^0\pi^0}(B^0 \rightarrow \rho^0\pi^0) = -0.1 \pm 0.7$

$S_{\rho^0\pi^0}(B^0 \rightarrow \rho^0\pi^0) = 0.1 \pm 0.4$

$C_{a_1\pi}(B^0 \rightarrow a_1(1260)^+\pi^-) = -0.10 \pm 0.17$

$S_{a_1\pi}(B^0 \rightarrow a_1(1260)^+\pi^-) = 0.37 \pm 0.22$

$\Delta C_{a_1\pi}(B^0 \rightarrow a_1(1260)^+\pi^-) = 0.26 \pm 0.17$

$\Delta S_{a_1\pi}(B^0 \rightarrow a_1(1260)^+\pi^-) = -0.14 \pm 0.22$

$C(B^0 \rightarrow b_1^-K^+) = -0.22 \pm 0.24$

$\Delta C(B^0 \rightarrow b_1^-K^+) = -1.04 \pm 0.24$

$C_{\rho^0 K_S^0}(B^0 \rightarrow \rho^0 K_S^0) = 0.6 \pm 0.5$

$S_{\rho^0 K_S^0}(B^0 \rightarrow \rho^0 K_S^0) = 0.2 \pm 0.6$

$C_{\rho\rho}(B^0 \rightarrow \rho^+\rho^-) = -0.05 \pm 0.13$

$S_{\rho\rho}(B^0 \rightarrow \rho^+\rho^-) = -0.06 \pm 0.17$

$|\lambda|(B^0 \rightarrow c\bar{c}K^0) = 0.988 \pm 0.020$

$|\lambda|(B^0 \rightarrow J/\psi K^*(892)^0) < 0.25, \text{ CL} = 95\%$

$\cos 2\beta(B^0 \rightarrow J/\psi K^*(892)^0) = 1.7_{-0.9}^{+0.7} \quad (S = 1.6)$

$\cos 2\beta(B^0 \rightarrow [K_S^0\pi^+\pi^-]_{D^{(*)}} h^0) = 1.0_{-0.7}^{+0.6} \quad (S = 1.8)$

$(S_+ + S_-)/2(B^0 \rightarrow D^{*+}\pi^+) = -0.037 \pm 0.012$

$(S_- - S_+)/2(B^0 \rightarrow D^{*-}\pi^+) = -0.006 \pm 0.016$

$(S_+ + S_-)/2(B^0 \rightarrow D^-\pi^+) = -0.046 \pm 0.023$

$(S_- - S_+)/2(B^0 \rightarrow D^-\pi^+) = -0.022 \pm 0.021$

$(S_+ + S_-)/2(B^0 \rightarrow D^-\rho^+) = -0.024 \pm 0.032$

$(S_- - S_+)/2(B^0 \rightarrow D^-\rho^+) = -0.10 \pm 0.06$

$\sin(2\beta) = 0.678 \pm 0.025$

$C_{J/\psi K^0}(B^0 \rightarrow J/\psi K^0) = -0.018 \pm 0.025$

$S_{J/\psi K^0}(B^0 \rightarrow J/\psi K^0) = 0.642 \pm 0.035$

$\sin(2\beta_{\text{eff}})(B^0 \rightarrow \phi K^0) = 0.22 \pm 0.30$

$\sin(2\beta_{\text{eff}})(B^0 \rightarrow K^+K^-K_S^0) = 0.77_{-0.12}^{+0.13}$

$\sin(2\beta_{\text{eff}})(B^0 \rightarrow [K_S^0\pi^+\pi^-]_{D^{(*)}} h^0) = 0.45 \pm 0.28$

$|\lambda|(B^0 \rightarrow [K_S^0\pi^+\pi^-]_{D^{(*)}} h^0) = 1.01 \pm 0.08$

$|\sin(2\beta + \gamma)| > 0.40, \text{ CL} = 90\%$

$\alpha = (96 \pm 10)^\circ$

\bar{B}^0 modes are charge conjugates of the modes below. Reactions indicate the weak decay vertex and do not include mixing. Modes which do not identify the charge state of the B are listed in the B^\pm/B^0 ADMIXTURE section.

The branching fractions listed below assume 50% $B^0\bar{B}^0$ and 50% B^+B^- production at the $\Upsilon(4S)$. We have attempted to bring older measurements up to date by rescaling their assumed $\Upsilon(4S)$ production ratio to 50:50 and their assumed D, D_s, D^* , and ψ branching ratios to current values whenever this would affect our averages and best limits significantly.

Indentation is used to indicate a subchannel of a previous reaction. All resonant subchannels have been corrected for resonance branching fractions to the final state so the sum of the subchannel branching fractions can exceed that of the final state.

For inclusive branching fractions, e.g., $B \rightarrow D^\pm \text{anything}$, the values usually are multiplicities, not branching fractions. They can be greater than one.

B^0 DECAY MODES	Fraction (Γ_i/Γ)	Scale factor / Confidence level	p (MeV/c)
$\ell^+ \nu_\ell \text{anything}$	[iii] (10.33±0.28) %		–
$e^+ \nu_e X_c$	(10.1 ± 0.4) %		–
$D \ell^+ \nu_\ell \text{anything}$	(9.6 ± 0.9) %		–
$D^- \ell^+ \nu_\ell$	[iii] (2.17±0.12) %		2309
$D^- \tau^+ \nu_\tau$	(1.0 ± 0.4) %		1909
$D^*(2010)^- \ell^+ \nu_\ell$	[iii] (5.16±0.11) %		2257
$D^*(2010)^- \tau^+ \nu_\tau$	(1.6 ± 0.5) %	S=1.2	1837
$\bar{D}^0 \pi^- \ell^+ \nu_\ell$	(4.3 ± 0.6) × 10 ⁻³		2308
$D_0^*(2400)^- \ell^+ \nu_\ell \times$ $B(D_0^{*-} \rightarrow \bar{D}^0 \pi^-)$	(2.0 ± 0.9) × 10 ⁻³		–
$D_2^*(2460)^- \ell^+ \nu_\ell \times$ $B(D_2^{*-} \rightarrow \bar{D}^0 \pi^-)$	(2.2 ± 0.6) × 10 ⁻³		2067
$\bar{D}^{(*)} n \pi \ell^+ \nu_\ell (n \geq 1)$	(2.4 ± 0.5) %		–
$\bar{D}^{*0} \pi^- \ell^+ \nu_\ell$	(4.9 ± 0.8) × 10 ⁻³		2256
$D_1(2420)^- \ell^+ \nu_\ell \times$ $B(D_1^- \rightarrow \bar{D}^{*0} \pi^-)$	(5.4 ± 2.1) × 10 ⁻³		–
$D_1'(2430)^- \ell^+ \nu_\ell \times$ $B(D_1'^- \rightarrow \bar{D}^{*0} \pi^-)$	< 5.0 × 10 ⁻³	CL=90%	–
$D_2^*(2460)^- \ell^+ \nu_\ell \times$ $B(D_2^{*-} \rightarrow \bar{D}^{*0} \pi^-)$	< 3.0 × 10 ⁻³	CL=90%	2067
$\rho^- \ell^+ \nu_\ell$	[iii] (2.47±0.33) × 10 ⁻⁴		2583
$\pi^- \ell^+ \nu_\ell$	[iii] (1.36±0.09) × 10 ⁻⁴		2638
Inclusive modes			
$K^\pm \text{anything}$	(78 ± 8) %		–
$D^0 X$	(8.1 ± 1.5) %		–
$\bar{D}^0 X$	(47.4 ± 2.8) %		–
$D^+ X$	< 3.9 %	CL=90%	–
$D^- X$	(36.9 ± 3.3) %		–
$D_s^+ X$	(10.3 $_{-1.8}^{+2.1}$) %		–
$D_s^- X$	< 2.6 %	CL=90%	–
$\Lambda_c^+ X$	< 3.1 %	CL=90%	–
$\bar{\Lambda}_c^- X$	(5.0 $_{-1.5}^{+2.1}$) %		–
$\bar{c} X$	(95 ± 5) %		–
$c X$	(24.6 ± 3.1) %		–
$\bar{c} X$	(119 ± 6) %		–
D, D*, or D_s modes			
$D^- \pi^+$	(2.68±0.13) × 10 ⁻³		2306
$D^- \rho^+$	(7.7 ± 1.3) × 10 ⁻³		2235
$D^- K^0 \pi^+$	(4.9 ± 0.9) × 10 ⁻⁴		2259
$D^- K^*(892)^+$	(4.5 ± 0.7) × 10 ⁻⁴		2211
$D^- \omega \pi^+$	(2.8 ± 0.6) × 10 ⁻³		2204
$D^- K^+$	(2.0 ± 0.6) × 10 ⁻⁴		2279
$D^- K^+ \bar{K}^0$	< 3.1 × 10 ⁻⁴	CL=90%	2188
$D^- K^+ \bar{K}^*(892)^0$	(8.8 ± 1.9) × 10 ⁻⁴		2070
$\bar{D}^0 \pi^+ \pi^-$	(8.4 ± 0.9) × 10 ⁻⁴		2301
$D^*(2010)^- \pi^+$	(2.76±0.13) × 10 ⁻³		2255
$D^- \pi^+ \pi^+ \pi^-$	(8.0 ± 2.5) × 10 ⁻³		2287
$(D^- \pi^+ \pi^+ \pi^-) \text{ nonresonant}$	(3.9 ± 1.9) × 10 ⁻³		2287
$D^- \pi^+ \rho^0$	(1.1 ± 1.0) × 10 ⁻³		2206
$D^- a_1(1260)^+$	(6.0 ± 3.3) × 10 ⁻³		2121
$D^*(2010)^- \pi^+ \pi^0$	(1.5 ± 0.5) %		2247
$D^*(2010)^- \rho^+$	(6.8 ± 0.9) × 10 ⁻³		2180
$D^*(2010)^- K^+$	(2.14±0.16) × 10 ⁻⁴		2226
$D^*(2010)^- K^0 \pi^+$	(3.0 ± 0.8) × 10 ⁻⁴		2205
$D^*(2010)^- K^*(892)^+$	(3.3 ± 0.6) × 10 ⁻⁴		2155

Meson Summary Table

$D^*(2010)^- K^+ \bar{K}^0$	< 4.7	$\times 10^{-4}$	CL=90%	2131	$D^- D_{sJ}(2573)^+ \times$	< 1	$\times 10^{-4}$	CL=90%	1414
$D^*(2010)^- K^+ \bar{K}^*(892)^0$	(1.29±0.33)	$\times 10^{-3}$		2007	$B(D_{sJ}(2573)^+ \rightarrow D^0 K^+)$				
$D^*(2010)^- \pi^+ \pi^+ \pi^-$	(7.0 ±0.8)	$\times 10^{-3}$	S=1.3	2235	$D^*(2010)^- D_{sJ}(2573)^+ \times$	< 2	$\times 10^{-4}$	CL=90%	1303
$(D^*(2010)^- \pi^+ \pi^+ \pi^-)$ non-resonant	(0.0 ±2.5)	$\times 10^{-3}$		2235	$B(D_{sJ}(2573)^+ \rightarrow D^0 K^+)$				
$D^*(2010)^- \pi^+ \rho^0$	(5.7 ±3.2)	$\times 10^{-3}$		2150	$D_s^+ \pi^-$	(1.53±0.35)	$\times 10^{-5}$		2270
$D^*(2010)^- a_1(1260)^+$	(1.30±0.27)	%		2061	$D_s^{*+} \pi^-$	(3.0 ±0.7)	$\times 10^{-5}$		2215
$D^*(2010)^- \pi^+ \pi^+ \pi^- \pi^0$	(1.76±0.27)	%		2218	$D_s^+ \rho^-$	< 6	$\times 10^{-4}$	CL=90%	2197
$D^{*-} 3\pi^+ 2\pi^-$	(4.7 ±0.9)	$\times 10^{-3}$		2195	$D_s^{*+} \rho^-$	< 6	$\times 10^{-4}$	CL=90%	2138
$D^*(2010)^- \rho \bar{\rho} \pi^+$	(6.5 ±1.6)	$\times 10^{-4}$		1707	$D_s^+ a_0^-$	< 1.9	$\times 10^{-5}$	CL=90%	-
$D^*(2010)^- \rho \bar{\pi}$	(1.5 ±0.4)	$\times 10^{-3}$		1785	$D_s^{*+} a_0^-$	< 3.6	$\times 10^{-5}$	CL=90%	-
$\bar{D}^*(2010)^- \omega \pi^+$	(2.89±0.30)	$\times 10^{-3}$		2148	$D_s^+ a_1(1260)^-$	< 2.2	$\times 10^{-3}$	CL=90%	2080
$D_1(2430)^0 \omega \times$	(4.1 ±1.6)	$\times 10^{-4}$		1992	$D_s^{*+} a_1(1260)^-$	< 1.8	$\times 10^{-3}$	CL=90%	2015
$B(D_1(2430)^0 \rightarrow D^{*-} \pi^+)$					$D_s^+ a_2^-$	< 1.9	$\times 10^{-4}$	CL=90%	-
$\bar{D}^{*-} \pi^+$	[III] (2.1 ±1.0)	$\times 10^{-3}$		-	$D_s^{*+} a_2^-$	< 2.0	$\times 10^{-4}$	CL=90%	-
$D_1(2420)^- \pi^+ \times B(D_1^- \rightarrow D^- \pi^+ \pi^-)$	(8.9 $\pm_{-3.5}^{+2.3}$)	$\times 10^{-5}$		-	$D_s^- K^+$	(2.9 ±0.5)	$\times 10^{-5}$		2242
$D_1(2420)^- \pi^+ \times B(D_1^- \rightarrow D^{*-} \pi^+ \pi^-)$	< 3.3	$\times 10^{-5}$	CL=90%	-	$D_s^{*-} K^+$	(2.2 ±0.6)	$\times 10^{-5}$		2185
$\bar{D}_2^*(2460)^- \pi^+ \times B(D_2^{*0}(2460)^- \rightarrow D^0 \pi^-)$	(2.15±0.35)	$\times 10^{-4}$		2064	$D_s^- K^*(892)^+$	< 8	$\times 10^{-4}$	CL=90%	2172
$\bar{D}_0^*(2400)^- \pi^+ \times B(D_0^{*0}(2400)^- \rightarrow D^0 \pi^-)$	(6.0 ±3.0)	$\times 10^{-5}$		2090	$D_s^{*-} K^*(892)^+$	< 9	$\times 10^{-4}$	CL=90%	2112
$D_2^*(2460)^- \pi^+ \times B((D_2^*)^- \rightarrow D^{*-} \pi^+ \pi^-)$	< 2.4	$\times 10^{-5}$	CL=90%	-	$D_s^- \pi^+ K^0$	< 5	$\times 10^{-3}$	CL=90%	2222
$\bar{D}_2^*(2460)^- \rho^+$	< 4.9	$\times 10^{-3}$	CL=90%	1977	$D_s^- \pi^+ K^0$	< 2.6	$\times 10^{-3}$	CL=90%	2164
$D^0 \bar{D}^0$	< 6	$\times 10^{-5}$	CL=90%	1868	$D_s^- \pi^+ K^*(892)^0$	< 3.1	$\times 10^{-3}$	CL=90%	2138
$D^{*0} \bar{D}^0$	< 2.9	$\times 10^{-4}$	CL=90%	1794	$D_s^{*-} \pi^+ K^*(892)^0$	< 1.7	$\times 10^{-3}$	CL=90%	2076
$D^- D^+$	(2.11±0.31)	$\times 10^{-4}$	S=1.2	1864	$\bar{D}^0 K^0$	(5.2 ±0.7)	$\times 10^{-5}$		2280
$D^- D_s^+$	(7.4 ±0.7)	$\times 10^{-3}$		1812	$\bar{D}^0 K^+ \pi^-$	(8.8 ±1.7)	$\times 10^{-5}$		2261
$D^*(2010)^- D_s^+$	(8.3 ±1.1)	$\times 10^{-3}$		1735	$\bar{D}^0 K^*(892)^0$	(4.2 ±0.6)	$\times 10^{-5}$		2213
$D^- D_s^{*+}$	(7.6 ±1.6)	$\times 10^{-3}$		1731	$D_2^*(2460)^- K^+ \times$	(1.8 ±0.5)	$\times 10^{-5}$		2031
$D^*(2010)^- D_s^{*+}$	(1.79±0.14)	%		1649	$B(D_2^*(2460)^- \rightarrow \bar{D}^0 \pi^-)$				
$D_{s0}(2317)^- K^+ \times B(D_{s0}(2317)^- \rightarrow D_s^- \pi^0)$	(4.4 ±1.4)	$\times 10^{-5}$		2097	$\bar{D}^0 K^+ \pi^-$ non-resonant	< 3.7	$\times 10^{-5}$	CL=90%	-
$D_{s0}(2317)^- \pi^+ \times B(D_{s0}(2317)^- \rightarrow D_s^- \pi^0)$	< 2.5	$\times 10^{-5}$	CL=90%	2128	$\bar{D}^0 \pi^0$	(2.61±0.24)	$\times 10^{-4}$		2308
$D_{sJ}(2457)^- K^+ \times B(D_{sJ}(2457)^- \rightarrow D_s^- \pi^0)$	< 9.4	$\times 10^{-6}$	CL=90%	-	$\bar{D}^0 \rho^0$	(3.2 ±0.5)	$\times 10^{-4}$		2237
$D_{sJ}(2457)^- \pi^+ \times B(D_{sJ}(2457)^- \rightarrow D_s^- \pi^0)$	< 4.0	$\times 10^{-6}$	CL=90%	-	$\bar{D}^0 f_2$	(1.2 ±0.4)	$\times 10^{-4}$		-
$D_s^- D_s^+$	< 3.6	$\times 10^{-5}$	CL=90%	1759	$\bar{D}^0 \eta$	(2.02±0.35)	$\times 10^{-4}$	S=1.6	2274
$D_s^- D_s^+$	< 1.3	$\times 10^{-4}$	CL=90%	1674	$\bar{D}^0 \eta'$	(1.25±0.23)	$\times 10^{-4}$	S=1.1	2198
$D_s^- D_s^{*+}$	< 2.4	$\times 10^{-4}$	CL=90%	1583	$\bar{D}^0 \omega$	(2.59±0.30)	$\times 10^{-4}$		2235
$D_{s0}(2317)^+ D^- \times B(D_{s0}(2317)^+ \rightarrow D_s^+ \pi^0)$	(9.9 $\pm_{-3.4}^{+4.2}$)	$\times 10^{-4}$	S=1.5	1602	$D^0 \phi$	< 1.16	$\times 10^{-5}$	CL=90%	2182
$D_{s0}(2317)^+ D^- \times B(D_{s0}(2317)^+ \rightarrow D_s^{*+} \gamma)$	< 9.5	$\times 10^{-4}$	CL=90%	-	$D^0 K^+ \pi^-$	< 1.9	$\times 10^{-5}$	CL=90%	2261
$D_{s0}(2317)^+ D^*(2010)^- \times B(D_{s0}(2317)^+ \rightarrow D_s^+ \pi^0)$	(1.5 ±0.6)	$\times 10^{-3}$		1509	$D^0 K^*(892)^0$	< 1.1	$\times 10^{-5}$	CL=90%	2213
$D_{sJ}(2457)^+ D^- \times B(D_{sJ}(2457)^+ \rightarrow D_s^+ \pi^0)$	(3.5 ±1.1)	$\times 10^{-3}$		-	$\bar{D}^{*0} \gamma$	< 2.5	$\times 10^{-5}$	CL=90%	2258
$D_{sJ}(2457)^+ D^- \times B(D_{sJ}(2457)^+ \rightarrow D_s^+ \gamma)$	(6.7 $\pm_{-1.4}^{+1.7}$)	$\times 10^{-4}$		-	$\bar{D}^*(2007)^0 \pi^0$	(1.7 ±0.4)	$\times 10^{-4}$	S=1.5	2256
$D_{sJ}(2457)^+ D^- \times B(D_{sJ}(2457)^+ \rightarrow D_s^{*+} \gamma)$	< 6.0	$\times 10^{-4}$	CL=90%	-	$\bar{D}^*(2007)^0 \rho^0$	< 5.1	$\times 10^{-4}$	CL=90%	2182
$D_{sJ}(2457)^+ D^- \times B(D_{sJ}(2457)^+ \rightarrow D_s^+ \gamma)$	< 2.0	$\times 10^{-4}$	CL=90%	-	$\bar{D}^*(2007)^0 \eta$	(1.8 ±0.6)	$\times 10^{-4}$	S=1.8	2220
$D_{sJ}(2457)^+ D^- \times B(D_{sJ}(2457)^+ \rightarrow D_s^{*+} \gamma)$	< 3.6	$\times 10^{-4}$	CL=90%	-	$\bar{D}^*(2007)^0 \eta'$	(1.23±0.35)	$\times 10^{-4}$		2141
$D_{sJ}(2457)^+ D^- \times B(D_{sJ}(2457)^+ \rightarrow D_s^+ \gamma)$	< 6.0	$\times 10^{-4}$	CL=90%	-	$\bar{D}^*(2007)^0 \pi^+ \pi^-$	(6.2 ±2.2)	$\times 10^{-4}$		2248
$D_{sJ}(2457)^+ D^- \times B(D_{sJ}(2457)^+ \rightarrow D_s^{*+} \gamma)$	< 2.0	$\times 10^{-4}$	CL=90%	-	$\bar{D}^*(2007)^0 K^0$	(3.6 ±1.2)	$\times 10^{-5}$		2227
$D_{sJ}(2457)^+ D^- \times B(D_{sJ}(2457)^+ \rightarrow D_s^+ \gamma)$	< 3.6	$\times 10^{-4}$	CL=90%	-	$\bar{D}^*(2007)^0 K^*(892)^0$	< 6.9	$\times 10^{-5}$	CL=90%	2157
$D_{sJ}(2457)^+ D^- \times B(D_{sJ}(2457)^+ \rightarrow D_s^+ \gamma)$	< 3.6	$\times 10^{-4}$	CL=90%	-	$D^*(2007)^0 K^*(892)^0$	< 4.0	$\times 10^{-5}$	CL=90%	2157
$D^*(2010)^- D_{sJ}(2457)^+$	(9.3 ±2.2)	$\times 10^{-3}$		-	$D^*(2007)^0 \pi^+ \pi^+ \pi^- \pi^-$	(2.7 ±0.5)	$\times 10^{-3}$		2219
$D_{sJ}(2457)^+ D^*(2010) \times B(D_{sJ}(2457)^+ \rightarrow D_s^+ \gamma)$	(2.3 $\pm_{-0.7}^{+0.9}$)	$\times 10^{-3}$		-	$D^*(2010)^+ D^*(2010)^-$	(8.2 ±0.9)	$\times 10^{-4}$		1711
$D^- D_{s1}(2536)^+ \times B(D_{s1}(2536)^+ \rightarrow D^{*0} K^+)$	(1.7 ±0.6)	$\times 10^{-4}$		1444	$\bar{D}^*(2007)^0 \omega$	(2.7 ±0.8)	$\times 10^{-4}$	S=1.5	2180
$D^*(2010)^- D_{s1}(2536)^+ \times B(D_{s1}(2536)^+ \rightarrow D^{*0} K^+)$	(3.3 ±1.1)	$\times 10^{-4}$		1336	$D^*(2010)^+ D^-$	(6.1 ±1.5)	$\times 10^{-4}$	S=1.6	1790
$D^- D_{s1}(2536)^+ \times B(D_{s1}(2536)^+ \rightarrow D^{*+} K^0)$	(2.6 ±1.1)	$\times 10^{-4}$		1444	$\bar{D}^*(2007)^0 \bar{D}^*(2007)^0$	< 9	$\times 10^{-5}$	CL=90%	1715
$D^{*-} D_{s1}(2536)^+ \times B(D_{s1}(2536)^+ \rightarrow D^{*+} K^0)$	(5.0 ±1.7)	$\times 10^{-4}$		1336	$D^- D^0 K^+$	(1.7 ±0.4)	$\times 10^{-3}$		1574
					$D^- D^*(2007)^0 K^+$	(4.6 ±1.0)	$\times 10^{-3}$		1478
					$D^*(2010)^- D^0 K^+$	(3.1 $\pm_{-0.5}^{+0.6}$)	$\times 10^{-3}$		1479
					$D^*(2010)^- D^*(2007)^0 K^+$	(1.18±0.20)	%		1366
					$D^- D^+ K^0$	< 1.7	$\times 10^{-3}$	CL=90%	1568
					$D^*(2010)^- D^+ K^0 + D^- D^*(2010)^+ K^0$	(6.5 ±1.6)	$\times 10^{-3}$		1473
					$D^*(2010)^- D^*(2010)^+ K^0$	(7.8 ±1.1)	$\times 10^{-3}$		1360
					$D^* - D_{s1}(2536)^+ \times B(D_{s1}(2536)^+ \rightarrow D^{*+} K^0)$	(8.0 ±2.4)	$\times 10^{-4}$		1336
					$\bar{D}^0 D^0 K^0$	< 1.4	$\times 10^{-3}$	CL=90%	1574
					$\bar{D}^0 D^*(2007)^0 K^0 + \bar{D}^*(2007)^0 D^0 K^0$	< 3.7	$\times 10^{-3}$	CL=90%	1478
					$\bar{D}^*(2007)^0 D^*(2007)^0 K^0$	< 6.6	$\times 10^{-3}$	CL=90%	1365
					$(\bar{D} + \bar{D}^*)(D + D^*)K$	(4.3 ±0.7)	%		-
					Charmonium modes				
					$\eta_c K^0$	(8.9 ±1.6)	$\times 10^{-4}$		1753
					$\eta_c K^*(892)^0$	(9.6 ±3.3)	$\times 10^{-4}$	S=1.1	1648
					$J/\psi(1S) K^0$	(8.71±0.32)	$\times 10^{-4}$		1683
					$J/\psi(1S) K^+ \pi^-$	(1.2 ±0.6)	$\times 10^{-3}$		1652
					$J/\psi(1S) K^*(892)^0$	(1.33±0.06)	$\times 10^{-3}$		1571
					$J/\psi(1S) \eta_c K_S^0$	(8 ±4)	$\times 10^{-5}$		1508

Meson Summary Table

$\eta f_0(980) \times B(f_0(980) \rightarrow \pi^+ \pi^-)$	< 4	$\times 10^{-7}$	CL=90%	2518
$\omega \eta$	< 1.9	$\times 10^{-6}$	CL=90%	2552
$\omega \eta'$	< 2.2	$\times 10^{-6}$	CL=90%	2491
$\omega \rho^0$	< 1.5	$\times 10^{-6}$	CL=90%	2522
$\omega f_0(980)$	< 1.5	$\times 10^{-6}$	CL=90%	2487
$\omega \omega$	< 4.0	$\times 10^{-6}$	CL=90%	2521
$\phi \pi^0$	< 2.8	$\times 10^{-7}$	CL=90%	2539
$\phi \eta$	< 6	$\times 10^{-7}$	CL=90%	2511
$\phi \eta'$	< 5	$\times 10^{-7}$	CL=90%	2448
$\phi \rho^0$	< 1.3	$\times 10^{-5}$	CL=90%	2480
$\phi \omega$	< 1.2	$\times 10^{-6}$	CL=90%	2479
$\phi \phi$	< 1.5	$\times 10^{-6}$	CL=90%	2435
$a_0(980)^\pm \pi^\mp \times B(a_0(980)^\pm \rightarrow \eta \pi^\pm)$	< 3.1	$\times 10^{-6}$	CL=90%	-
$a_0(1450)^\pm \pi^\mp \times B(a_0(1450)^\pm \rightarrow \eta \pi^\pm)$	< 2.3	$\times 10^{-6}$	CL=90%	-
$\pi^+ \pi^- \pi^0$	< 7.2	$\times 10^{-4}$	CL=90%	2631
$\rho^0 \pi^0$	(1.8 \pm 0.5)	$\times 10^{-6}$		2581
$\rho^\mp \pi^\pm$ [gg]	(2.28 \pm 0.25)	$\times 10^{-5}$		2581
$\pi^+ \pi^- \pi^+ \pi^-$	< 2.3	$\times 10^{-4}$	CL=90%	2621
$\rho^0 \rho^0$	(1.1 \pm 0.4)	$\times 10^{-6}$		2523
$\rho^0 f_0(980) \times B(f_0(980) \rightarrow \pi^+ \pi^-)$	< 5.3	$\times 10^{-7}$	CL=90%	2488
$f_0(980) f_0(980) \times B(f_0(980) \rightarrow \pi^+ \pi^-)^2$	< 1.6	$\times 10^{-7}$	CL=90%	2451
$a_1(1260)^\mp \pi^\pm$ [gg]	(3.3 \pm 0.5)	$\times 10^{-5}$		2494
$b_1^\mp \pi^\pm \times B(b_1^\mp \rightarrow \omega \pi^\mp)$	(1.09 \pm 0.15)	$\times 10^{-5}$		-
$a_2(1320)^\mp \pi^\pm$ [gg]	< 3.0	$\times 10^{-4}$	CL=90%	2473
$\pi^+ \pi^- \pi^0 \pi^0$	< 3.1	$\times 10^{-3}$	CL=90%	2622
$\rho^+ \rho^-$	(2.42 \pm 0.31)	$\times 10^{-5}$		2523
$a_1(1260)^0 \pi^0$	< 1.1	$\times 10^{-3}$	CL=90%	2495
$\omega \pi^0$	< 1.2	$\times 10^{-6}$	CL=90%	2580
$\pi^+ \pi^+ \pi^- \pi^- \pi^0$	< 9.0	$\times 10^{-3}$	CL=90%	2609
$a_1(1260)^+ \rho^-$	< 6.1	$\times 10^{-5}$	CL=90%	2433
$a_1(1260)^0 \rho^0$	< 2.4	$\times 10^{-3}$	CL=90%	2433
$\pi^+ \pi^+ \pi^+ \pi^- \pi^- \pi^-$	< 3.0	$\times 10^{-3}$	CL=90%	2592
$a_1(1260)^+ a_1(1260)^-$	< 2.8	$\times 10^{-3}$	CL=90%	2336
$\pi^+ \pi^+ \pi^+ \pi^- \pi^- \pi^- \pi^0$	< 1.1	%	CL=90%	2572
Baryon modes				
$p \bar{p}$	< 1.1	$\times 10^{-7}$	CL=90%	2467
$\rho \bar{p} \pi^+ \pi^-$	< 2.5	$\times 10^{-4}$	CL=90%	2406
$\rho \bar{p} K^0$	(2.7 \pm 0.4)	$\times 10^{-6}$		2347
$\Theta(1540)^+ \bar{p} \times B(\Theta(1540)^+ \rightarrow p K_S^0)$	[sss] < 5	$\times 10^{-8}$	CL=90%	2318
$f_J(2220) K^0 \times B(f_J(2220) \rightarrow p \bar{p})$	< 4.5	$\times 10^{-7}$	CL=90%	2135
$\rho \bar{p} K^*(892)^0$	(1.5 \pm 0.6)	$\times 10^{-6}$		2216
$f_J(2220) K_S^0 \times B(f_J(2220) \rightarrow p \bar{p})$	< 1.5	$\times 10^{-7}$	CL=90%	-
$\rho \bar{\Lambda} \pi^-$	(3.2 \pm 0.4)	$\times 10^{-6}$		2401
$\rho \bar{\Sigma}^-(1385)^-$	< 2.6	$\times 10^{-7}$	CL=90%	2363
$\Delta^0 \bar{\Lambda}$	< 9.3	$\times 10^{-7}$	CL=90%	2364
$\rho \bar{\Lambda} K^-$	< 8.2	$\times 10^{-7}$	CL=90%	2308
$\rho \bar{\Sigma}^0 \pi^-$	< 3.8	$\times 10^{-6}$	CL=90%	2383
$\bar{\Lambda} \Lambda$	< 3.2	$\times 10^{-7}$	CL=90%	2392
$\Delta^0 \bar{\Delta}^0$	< 1.5	$\times 10^{-3}$	CL=90%	2335
$\Delta^{++} \bar{\Delta}^{--}$	< 1.1	$\times 10^{-4}$	CL=90%	2335
$\bar{D}^0 \rho \bar{p}$	(1.14 \pm 0.09)	$\times 10^{-4}$		1862
$D_s^- \bar{\Lambda} p$	(2.9 \pm 0.9)	$\times 10^{-5}$		1710
$\bar{D}^*(2007)^0 \rho \bar{p}$	(1.03 \pm 0.13)	$\times 10^{-4}$		1788
$D^- \rho \bar{p} \pi^+$	(3.38 \pm 0.32)	$\times 10^{-4}$		1786
$D^{*-} \rho \bar{p} \pi^+$	(4.8 \pm 0.5)	$\times 10^{-4}$		1707
$\Theta_c \bar{p} \pi^+ \times B(\Theta_c \rightarrow D^- p)$	< 9	$\times 10^{-6}$	CL=90%	-
$\Theta_c \bar{p} \pi^+ \times B(\Theta_c \rightarrow D^{*-} p)$	< 1.4	$\times 10^{-5}$	CL=90%	-
$\bar{\Sigma}_c^- \Delta^{++}$	< 1.0	$\times 10^{-3}$	CL=90%	1839
$\bar{\Lambda}_c^- p \pi^+ \pi^-$	(1.3 \pm 0.4)	$\times 10^{-3}$		1934
$\bar{\Lambda}_c^- p$	(2.1 \pm 0.7 / -0.5)	$\times 10^{-5}$		2021
$\bar{\Lambda}_c^- p \pi^0$	< 5.9	$\times 10^{-4}$	CL=90%	1982
$\bar{\Lambda}_c^- p \pi^+ \pi^- \pi^0$	< 5.07	$\times 10^{-3}$	CL=90%	1882
$\bar{\Lambda}_c^- p \pi^+ \pi^- \pi^+ \pi^-$	< 2.74	$\times 10^{-3}$	CL=90%	1821
$\Lambda_c^+ \bar{p} \pi^+ \pi^-$	(1.12 \pm 0.32)	$\times 10^{-3}$		1934
$\Lambda_c^+ \bar{p} \pi^+ \pi^-$ (nonresonant)	(6.4 \pm 1.9)	$\times 10^{-4}$		1934
$\bar{\Sigma}_c^-(2520)^- p \pi^+$	(1.2 \pm 0.4)	$\times 10^{-4}$		1860
$\bar{\Sigma}_c^-(2520)^0 p \pi^-$	< 3.8	$\times 10^{-5}$	CL=90%	1860

$\bar{\Sigma}_c^-(2455)^0 p \pi^-$	(1.5 \pm 0.5)	$\times 10^{-4}$		1895	
$\bar{\Sigma}_c^-(2455)^- p \pi^+$	(2.2 \pm 0.7)	$\times 10^{-4}$		1895	
$\bar{\Lambda}_c^- \Lambda_c^+$	< 6.2	$\times 10^{-5}$	CL=90%	1319	
$\bar{\Lambda}_c^-(2593)^- / \bar{\Lambda}_c^-(2625)^- p$	< 1.1	$\times 10^{-4}$	CL=90%	-	
$\bar{\Xi}_c^- \Lambda_c^+ \times B(\bar{\Xi}_c^- \rightarrow \Xi^+ \pi^- \pi^-)$	(9 \pm 5 / -4)	$\times 10^{-5}$		1147	
$\Lambda_c^+ \Lambda_c^- K^0$	(8 \pm 5)	$\times 10^{-4}$		-	
Lepton Family number (LF) violating modes, or $\Delta B = 1$ weak neutral current (BI) modes					
$\gamma \gamma$	BI	< 6.2	$\times 10^{-7}$	CL=90%	2640
$e^+ e^-$	BI	< 1.13	$\times 10^{-7}$	CL=90%	2640
$e^+ e^- \gamma$	BI	< 1.2	$\times 10^{-7}$	CL=90%	2640
$\mu^+ \mu^-$	BI	< 1.5	$\times 10^{-8}$	CL=90%	2638
$\mu^+ \mu^- \gamma$	BI	< 1.6	$\times 10^{-7}$	CL=90%	2638
$\tau^+ \tau^-$	BI	< 4.1	$\times 10^{-3}$	CL=90%	1952
$\pi^0 \ell^+ \ell^-$	BI	< 1.2	$\times 10^{-7}$	CL=90%	2638
$\pi^0 \nu \bar{\nu}$	BI	< 2.2	$\times 10^{-4}$	CL=90%	2638
$\pi^0 e^+ e^-$	BI	< 1.4	$\times 10^{-7}$	CL=90%	2638
$\pi^0 \mu^+ \mu^-$	BI	< 5.1	$\times 10^{-7}$	CL=90%	2634
$K^0 \ell^+ \ell^-$	BI [iii]	(2.9 \pm 1.6 / -1.3)	$\times 10^{-7}$		2616
$K^0 \nu \bar{\nu}$	BI	< 1.6	$\times 10^{-4}$	CL=90%	2616
$\rho^0 \nu \bar{\nu}$	BI	< 4.4	$\times 10^{-4}$	CL=90%	2583
$K^0 e^+ e^-$	BI	(1.3 \pm 1.6 / -1.1)	$\times 10^{-7}$		2616
$K^0 \mu^+ \mu^-$	BI	(5.7 \pm 2.2 / -1.8)	$\times 10^{-7}$		2612
$K^*(892)^0 \ell^+ \ell^-$	BI [iii]	(9.5 \pm 1.8)	$\times 10^{-7}$		2564
$K^*(892)^0 e^+ e^-$	BI	(1.04 \pm 0.35 / -0.31)	$\times 10^{-6}$		2564
$K^*(892)^0 \mu^+ \mu^-$	BI	(1.10 \pm 0.29 / -0.26)	$\times 10^{-6}$		2560
$K^*(892)^0 \nu \bar{\nu}$	BI	< 3.4	$\times 10^{-4}$	CL=90%	2564
$\phi \nu \bar{\nu}$	BI	< 5.8	$\times 10^{-5}$	CL=90%	2541
$e^\pm \mu^\mp$	LF [gg]	< 9.2	$\times 10^{-8}$	CL=90%	2639
$\pi^0 e^\pm \mu^\mp$	LF	< 1.4	$\times 10^{-7}$	CL=90%	2637
$K^0 e^\pm \mu^\mp$	LF	< 2.7	$\times 10^{-7}$	CL=90%	2615
$K^*(892)^0 e^+ \mu^-$	LF	< 5.3	$\times 10^{-7}$	CL=90%	2563
$K^*(892)^0 e^- \mu^+$	LF	< 3.4	$\times 10^{-7}$	CL=90%	2563
$K^*(892)^0 e^\pm \mu^\mp$	LF	< 5.8	$\times 10^{-7}$	CL=90%	2563
$e^\pm \tau^\mp$	LF [gg]	< 1.1	$\times 10^{-4}$	CL=90%	2341
$\mu^\pm \tau^\mp$	LF [gg]	< 3.8	$\times 10^{-5}$	CL=90%	2339
invisible	BI	< 2.2	$\times 10^{-4}$	CL=90%	-
$\nu \bar{\nu} \gamma$	BI	< 4.7	$\times 10^{-5}$	CL=90%	2640

 B^\pm/B^0 ADMIXTURE**CP violation**

$$A_{CP}(B \rightarrow K^*(892)\gamma) = -0.010 \pm 0.028$$

$$A_{CP}(B \rightarrow s\gamma) = 0.01 \pm 0.04$$

$$A_{CP}(b \rightarrow (s+d)\gamma) = -0.11 \pm 0.12$$

$$A_{CP}(b \rightarrow X_s \ell^+ \ell^-) = -0.22 \pm 0.26$$

The branching fraction measurements are for an admixture of B mesons at the $T(4S)$. The values quoted assume that $B(T(4S) \rightarrow B\bar{B}) = 100\%$.

For inclusive branching fractions, e.g., $B \rightarrow D^\pm$ anything, the treatment of multiple D 's in the final state must be defined. One possibility would be to count the number of events with one-or-more D 's and divide by the total number of B 's. Another possibility would be to count the total number of D 's and divide by the total number of B 's, which is the definition of average multiplicity. The two definitions are identical if only one D is allowed in the final state. Even though the "one-or-more" definition seems sensible, for practical reasons inclusive branching fractions are almost always measured using the multiplicity definition. For heavy final state particles, authors call their results inclusive branching fractions while for light particles some authors call their results multiplicities. In the B sections, we list all results as inclusive branching fractions, adopting a multiplicity definition. This means that inclusive branching fractions can exceed 100% and that inclusive partial widths can exceed total widths, just as inclusive cross sections can exceed total cross section.

\bar{B} modes are charge conjugates of the modes below. Reactions indicate the weak decay vertex and do not include mixing.

Meson Summary Table

B DECAY MODES	Fraction (Γ_i/Γ)	Scale factor/ Confidence level (MeV/c)	p			
Semileptonic and leptonic modes						
$B \rightarrow e^+ \nu_e$ anything	[ttf] (10.74 ± 0.16) %		—			
$B \rightarrow \bar{p} e^+ \nu_e$ anything	< 5.9 × 10 ⁻⁴	CL=90%	—			
$B \rightarrow \mu^+ \nu_\mu$ anything	[ttt] (10.74 ± 0.16) %		—			
$B \rightarrow \ell^+ \nu_\ell$ anything	[iii,ttt] (10.74 ± 0.16) %		—			
$B \rightarrow D^- \ell^+ \nu_\ell$ anything	[iii] (2.8 ± 0.9) %		—			
$B \rightarrow \bar{D}^0 \ell^+ \nu_\ell$ anything	[iii] (7.2 ± 1.4) %		—			
$B \rightarrow D \tau^+ \nu_\tau$	(8.6 ± 2.7) × 10 ⁻³		1911			
$B \rightarrow D^{*-} \ell^+ \nu_\ell$ anything	[uuu] (6.7 ± 1.3) × 10 ⁻³		—			
$B \rightarrow D^* \tau^+ \nu_\tau$	(1.62 ± 0.33) %		—			
$B \rightarrow \bar{D}^{*+} \ell^+ \nu_\ell$	[iii,uvw] (2.7 ± 0.7) %		—			
$B \rightarrow \bar{D}_1(2420) \ell^+ \nu_\ell$ anything	(3.8 ± 1.3) × 10 ⁻³	S=2.4	—			
$B \rightarrow D \pi \ell^+ \nu_\ell$ anything + $D^* \pi \ell^+ \nu_\ell$ anything	(2.6 ± 0.5) %	S=1.5	—			
$B \rightarrow D \pi \ell^+ \nu_\ell$ anything	(1.5 ± 0.6) %		—			
$B \rightarrow D^* \pi \ell^+ \nu_\ell$ anything	(1.9 ± 0.4) %		—			
$B \rightarrow \bar{D}_s^*(2460) \ell^+ \nu_\ell$ anything	(4.4 ± 1.6) × 10 ⁻³		—			
$B \rightarrow D^{*-} \pi^+ \ell^+ \nu_\ell$ anything	(1.00 ± 0.34) %		—			
$B \rightarrow D_s^- \ell^+ \nu_\ell$ anything	[iii] < 7 × 10 ⁻³	CL=90%	—			
$B \rightarrow D_s^- \ell^+ \nu_\ell K^+$ anything	[iii] < 5 × 10 ⁻³	CL=90%	—			
$B \rightarrow D_s^- \ell^+ \nu_\ell K^0$ anything	[iii] < 7 × 10 ⁻³	CL=90%	—			
$B \rightarrow \ell^+ \nu_\ell$ charm	(10.57 ± 0.15) %		—			
$B \rightarrow X_u \ell^+ \nu_\ell$	(2.33 ± 0.22) × 10 ⁻³		—			
$B \rightarrow \pi \ell \nu_\ell$	(1.35 ± 0.10) × 10 ⁻⁴		2638			
$B \rightarrow K^+ \ell^+ \nu_\ell$ anything	[iii] (6.2 ± 0.5) %		—			
$B \rightarrow K^- \ell^+ \nu_\ell$ anything	[iii] (10 ± 4) × 10 ⁻³		—			
$B \rightarrow K^0 / \bar{K}^0 \ell^+ \nu_\ell$ anything	[iii] (4.5 ± 0.5) %		—			
D, D*, or D_s modes						
$B \rightarrow D^\pm$ anything	(23.5 ± 1.3) %		—			
$B \rightarrow D^0 / \bar{D}^0$ anything	(62.5 ± 2.9) %	S=1.3	—			
$B \rightarrow D^*(2010)^\pm$ anything	(22.5 ± 1.5) %		—			
$B \rightarrow D^*(2007)^0$ anything	(26.0 ± 2.7) %		—			
$B \rightarrow D^\pm$ anything	[gg] (8.5 ± 0.8) %		—			
$B \rightarrow D_s^{*\pm}$ anything	(6.5 ± 1.0) %		—			
$B \rightarrow D_s^\pm \bar{D}^*$	(3.5 ± 0.6) %		—			
$B \rightarrow D^*(*) \bar{D}^*(*) K^0 + D^*(*) \bar{D}^*(*) K^\pm$	[gg,www] (7.1 ± 2.7 / -1.7) %		—			
$b \rightarrow c \bar{c} s$	(22 ± 4) %		—			
$B \rightarrow D_s^*(*) \bar{D}^*(*)$	[gg,www] (4.0 ± 0.4) %		—			
$B \rightarrow D^* D^*(2010)^\pm$	[gg] < 5.9 × 10 ⁻³	CL=90%	1711			
$B \rightarrow D D^*(2010)^\pm + D^* D^\pm$	[gg] < 5.5 × 10 ⁻³	CL=90%	—			
$B \rightarrow D D^\pm$	[gg] < 3.1 × 10 ⁻³	CL=90%	1866			
$B \rightarrow D_s^*(*) \bar{D}^*(*) X (n \pi^+)$	[gg,www] (9 ± 5 / -4) %		—			
$B \rightarrow D^*(2010) \gamma$	< 1.1 × 10 ⁻³	CL=90%	2257			
$B \rightarrow D^+ \pi^-, D_s^{*+} \pi^-, D_s^+ \pi^0, D_s^{*+} \pi^0, D_s^+ \eta, D_s^{*+} \eta, D_s^+ \rho^0, D_s^{*+} \rho^0, D_s^+ \omega, D_s^{*+} \omega$	[gg] < 4 × 10 ⁻⁴	CL=90%	—			
$B \rightarrow D_{s1}(2536)^+ \text{ anything}$	< 9.5 × 10 ⁻³	CL=90%	—			
Charmonium modes						
$B \rightarrow J/\psi(1S)$ anything	(1.094 ± 0.032) %	S=1.1	—			
$B \rightarrow J/\psi(1S)$ (direct) anything	(7.8 ± 0.4) × 10 ⁻³	S=1.1	—			
$B \rightarrow \psi(2S)$ anything	(3.07 ± 0.21) × 10 ⁻³		—			
$B \rightarrow \chi_{c1}(1P)$ anything	(3.86 ± 0.27) × 10 ⁻³		—			
$B \rightarrow \chi_{c1}(1P)$ (direct) anything	(3.16 ± 0.25) × 10 ⁻³		—			
$B \rightarrow \chi_{c2}(1P)$ anything	(1.3 ± 0.4) × 10 ⁻³	S=1.9	—			
$B \rightarrow \chi_{c2}(1P)$ (direct) anything	(1.65 ± 0.31) × 10 ⁻³		—			
$B \rightarrow \eta_c(1S)$ anything	< 9 × 10 ⁻³	CL=90%	—			
$B^0 \rightarrow X(3872) K \times B(X \rightarrow D^0 \bar{D}^0 \pi^0)$	(1.2 ± 0.4) × 10 ⁻⁴		1141			
$B \rightarrow K X(3945) \times B(X(3945) \rightarrow \omega J/\psi)$	[xxx] (7.1 ± 3.4) × 10 ⁻⁵		1083			
K or K* modes						
$B \rightarrow K^\pm$ anything	[gg] (78.9 ± 2.5) %		—			
$B \rightarrow K^+$ anything	(66 ± 5) %		—			
$B \rightarrow K^-$ anything	(13 ± 4) %		—			
$B \rightarrow K^0 / \bar{K}^0$ anything	[gg] (64 ± 4) %		—			
$B \rightarrow K^*(892)^\pm$ anything	(18 ± 6) %		—			
$B \rightarrow K^*(892)^0 / \bar{K}^*(892)^0$ anything	[gg] (14.6 ± 2.6) %		—			
$B \rightarrow K^*(892) \gamma$	(4.2 ± 0.6) × 10 ⁻⁵		2564			
$B \rightarrow \eta K \gamma$	(8.5 ± 1.8 / -1.6) × 10 ⁻⁶		2588			
$B \rightarrow K_1(1400) \gamma$	< 1.27 × 10 ⁻⁴	CL=90%	2453			
$B \rightarrow K_2^*(1430) \gamma$	(1.7 ± 0.6 / -0.5) × 10 ⁻⁵		2447			
$B \rightarrow K_2(1770) \gamma$	< 1.2 × 10 ⁻³	CL=90%	2342			
$B \rightarrow K_3^*(1780) \gamma$	< 3.7 × 10 ⁻⁵	CL=90%	2341			
$B \rightarrow K_4^*(2045) \gamma$	< 1.0 × 10 ⁻³	CL=90%	2244			
$B \rightarrow K \eta'(958)$	(8.3 ± 1.1) × 10 ⁻⁵		2528			
$B \rightarrow K^*(892) \eta'(958)$	(4.1 ± 1.1) × 10 ⁻⁶		2472			
$B \rightarrow K \eta$	< 5.2 × 10 ⁻⁶	CL=90%	2588			
$B \rightarrow K^*(892) \eta$	(1.8 ± 0.5) × 10 ⁻⁵		2534			
$B \rightarrow K \phi \phi$	(2.3 ± 0.9) × 10 ⁻⁶		2306			
$B \rightarrow \bar{b} \rightarrow \bar{s} \gamma$	(3.56 ± 0.25) × 10 ⁻⁴		—			
$B \rightarrow \bar{b} \rightarrow \bar{s} \text{ gluon}$	< 6.8 %		—			
$B \rightarrow \eta$ anything	< 4.4 × 10 ⁻⁴	CL=90%	—			
$B \rightarrow \eta'$ anything	(4.2 ± 0.9) × 10 ⁻⁴		—			
Light unflavored meson modes						
$B \rightarrow \rho \gamma$	(1.36 ± 0.30) × 10 ⁻⁶		2583			
$B \rightarrow \rho / \omega \gamma$	(1.28 ± 0.21) × 10 ⁻⁶		—			
$B \rightarrow \pi^\pm$ anything	[gg,yyy] (358 ± 7) %		—			
$B \rightarrow \pi^0$ anything	(235 ± 11) %		—			
$B \rightarrow \eta$ anything	(17.6 ± 1.6) %		—			
$B \rightarrow \rho^0$ anything	(21 ± 5) %		—			
$B \rightarrow \omega$ anything	< 81 %	CL=90%	—			
$B \rightarrow \phi$ anything	(3.43 ± 0.12) %		—			
$B \rightarrow \phi K^*(892)$	< 2.2 × 10 ⁻⁵	CL=90%	2460			
Baryon modes						
$B \rightarrow \Lambda_c^+ / \bar{\Lambda}_c^-$ anything	(4.5 ± 1.2) %		—			
$B \rightarrow \bar{\Lambda}_c^- e^+$ anything	< 2.3 × 10 ⁻³	CL=90%	—			
$B \rightarrow \bar{\Lambda}_c^- p$ anything	(2.6 ± 0.8) %		—			
$B \rightarrow \bar{\Lambda}_c^- p e^+ \nu_e$	< 1.0 × 10 ⁻³	CL=90%	2021			
$B \rightarrow \bar{\Sigma}_c^-$ anything	(4.2 ± 2.4) × 10 ⁻³		—			
$B \rightarrow \bar{\Sigma}_c^0$ anything	< 9.6 × 10 ⁻³	CL=90%	—			
$B \rightarrow \bar{\Sigma}_c^+$ anything	(4.6 ± 2.4) × 10 ⁻³		—			
$B \rightarrow \bar{\Sigma}_c^0 N (N = p \text{ or } n)$	< 1.5 × 10 ⁻³	CL=90%	1938			
$B \rightarrow \Xi_c^0$ anything × $B(\Xi_c^0 \rightarrow \Xi^- \pi^+)$	(1.93 ± 0.30) × 10 ⁻⁴	S=1.1	—			
$B \rightarrow \Xi_c^+$ anything × $B(\Xi_c^+ \rightarrow \Xi^- \pi^+ \pi^+)$	(4.5 ± 1.3 / -1.2) × 10 ⁻⁴		—			
$B \rightarrow p / \bar{p}$ anything	[gg] (8.0 ± 0.4) %		—			
$B \rightarrow p / \bar{p}$ (direct) anything	[gg] (5.5 ± 0.5) %		—			
$B \rightarrow \Lambda / \bar{\Lambda}$ anything	[gg] (4.0 ± 0.5) %		—			
$B \rightarrow \Xi^- / \bar{\Xi}^+$ anything	[gg] (2.7 ± 0.6) × 10 ⁻³		—			
$B \rightarrow$ baryons anything	(6.8 ± 0.6) %		—			
$B \rightarrow p \bar{p}$ anything	(2.47 ± 0.23) %		—			
$B \rightarrow \Lambda \bar{\Lambda} / \bar{\Lambda} p$ anything	[gg] (2.5 ± 0.4) %		—			
$B \rightarrow \Lambda \bar{\Lambda}$ anything	< 5 × 10 ⁻³	CL=90%	—			
Lepton Family number (LF) violating modes or $\Delta B = 1$ weak neutral current (BI) modes						
$B \rightarrow s e^+ e^-$	BI (4.7 ± 1.3) × 10 ⁻⁶		—			
$B \rightarrow s \mu^+ \mu^-$	BI (4.3 ± 1.2) × 10 ⁻⁶		—			
$B \rightarrow s \ell^+ \ell^-$	BI [iii] (4.5 ± 1.0) × 10 ⁻⁶		—			
$B \rightarrow \pi \ell^+ \ell^-$	< 9.1 × 10 ⁻⁸	CL=90%	2638			
$B \rightarrow K e^+ e^-$	BI (3.8 ± 0.8 / 0.7) × 10 ⁻⁷		2617			
$B \rightarrow K^*(892) e^+ e^-$	BI (1.13 ± 0.27) × 10 ⁻⁶		2564			

Meson Summary Table

$B \rightarrow K \mu^+ \mu^-$	$B1$	$(4.2 \pm_{-0.8}^{+0.9}) \times 10^{-7}$	2612
$B \rightarrow K^*(892) \mu^+ \mu^-$	$B1$	$(1.03 \pm_{-0.23}^{+0.26}) \times 10^{-6}$	2560
$B \rightarrow K \ell^+ \ell^-$	$B1$	$(3.9 \pm 0.7) \times 10^{-7}$	S=1.2 2617
$B \rightarrow K^*(892) \ell^+ \ell^-$	$B1$	$(9.4 \pm 1.8) \times 10^{-7}$	S=1.1 2564
$B \rightarrow s e^\pm \mu^\mp$	LF	$[gg] < 2.2 \times 10^{-5}$	CL=90% -
$B \rightarrow \pi e^\pm \mu^\mp$	LF	$< 9.2 \times 10^{-8}$	CL=90% 2637
$B \rightarrow \rho e^\pm \mu^\mp$	LF	$< 3.2 \times 10^{-6}$	CL=90% 2582
$B \rightarrow K e^\pm \mu^\mp$	LF	$< 3.8 \times 10^{-8}$	CL=90% 2616
$B \rightarrow K^*(892) e^\pm \mu^\mp$	LF	$< 5.1 \times 10^{-7}$	CL=90% 2563

 $B^\pm/B^0/B_s^0/b$ -baryon ADMIXTURE

These measurements are for an admixture of bottom particles at high energy (LEP, Tevatron, $Sp\bar{P}S$).

$$\text{Mean life } \tau = (1.568 \pm 0.009) \times 10^{-12} \text{ s}$$

$$\text{Mean life } \tau = (1.72 \pm 0.10) \times 10^{-12} \text{ s} \quad \text{Charged } b\text{-hadron admixture}$$

$$\text{Mean life } \tau = (1.58 \pm 0.14) \times 10^{-12} \text{ s} \quad \text{Neutral } b\text{-hadron admixture}$$

$$\tau_{\text{charged } b\text{-hadron}}/\tau_{\text{neutral } b\text{-hadron}} = 1.09 \pm 0.13$$

$$|\Delta\tau_b|/\tau_{b,\bar{b}} = -0.001 \pm 0.014$$

The branching fraction measurements are for an admixture of B mesons and baryons at energies above the $\Upsilon(4S)$. Only the highest energy results (LEP, Tevatron, $Sp\bar{P}S$) are used in the branching fraction averages. In the following, we assume that the production fractions are the same at the LEP and at the Tevatron.

For inclusive branching fractions, e.g., $B \rightarrow D^\pm$ anything, the values usually are multiplicities, not branching fractions. They can be greater than one.

The modes below are listed for a \bar{b} initial state. b modes are their charge conjugates. Reactions indicate the weak decay vertex and do not include mixing.

\bar{b} DECAY MODES	Fraction (Γ_i/Γ)	Scale factor/ Confidence level	p (MeV/c)
-----------------------	--------------------------------	-----------------------------------	----------------

PRODUCTION FRACTIONS

The production fractions for weakly decaying b -hadrons at high energy have been calculated from the best values of mean lives, mixing parameters, and branching fractions in this edition by the Heavy Flavor Averaging Group (HFAG) as described in the note “ B^0/\bar{B}^0 Mixing” in the B^0 Particle Listings. The production fractions in b -hadronic Z decay are also listed at the end of the section. Values assume

$$B(\bar{b} \rightarrow B^+) = B(\bar{b} \rightarrow B^0)$$

$$B(\bar{b} \rightarrow B^+) + B(\bar{b} \rightarrow B^0) + B(\bar{b} \rightarrow B_s^0) + B(b \rightarrow b\text{-baryon}) = 100 \%$$

The notation for production fractions varies in the literature ($f_d, d_{B^0}, f(b \rightarrow \bar{B}^0), B(b \rightarrow \bar{B}^0)$). We use our own branching fraction notation here, $B(\bar{b} \rightarrow B^0)$.

B^+	$(39.9 \pm 1.1) \%$	-
B^0	$(39.9 \pm 1.1) \%$	-
B_s^0	$(11.0 \pm 1.2) \%$	-
b -baryon	$(9.2 \pm 1.9) \%$	-
B_C	-	-

DECAY MODES**Semileptonic and leptonic modes**

ν anything	$(23.1 \pm 1.5) \%$	-
$\ell^+ \nu_\ell$ anything	[iii] $(10.69 \pm 0.22) \%$	-
$e^+ \nu_e$ anything	$(10.86 \pm 0.35) \%$	-
$\mu^+ \nu_\mu$ anything	$(10.95 \pm_{-0.25}^{+0.29}) \%$	-
$D^- \ell^+ \nu_\ell$ anything	[iii] $(2.3 \pm 0.4) \%$	S=1.8 -
$D^- \pi^+ \ell^+ \nu_\ell$ anything	$(4.9 \pm 1.9) \times 10^{-3}$	-
$D^- \pi^- \ell^+ \nu_\ell$ anything	$(2.6 \pm 1.6) \times 10^{-3}$	-
$\bar{D}^0 \ell^+ \nu_\ell$ anything	[iii] $(6.84 \pm 0.35) \%$	-
$\bar{D}^0 \pi^- \ell^+ \nu_\ell$ anything	$(1.07 \pm 0.27) \%$	-
$\bar{D}^0 \pi^+ \ell^+ \nu_\ell$ anything	$(2.3 \pm 1.6) \times 10^{-3}$	-
$D^{*-} \ell^+ \nu_\ell$ anything	[iii] $(2.75 \pm 0.19) \%$	-
$D^{*-} \pi^- \ell^+ \nu_\ell$ anything	$(6 \pm 7) \times 10^{-4}$	-
$D^{*-} \pi^+ \ell^+ \nu_\ell$ anything	$(4.8 \pm 1.0) \times 10^{-3}$	-
$\bar{D}_j^0 \ell^+ \nu_\ell$ anything \times $B(\bar{D}_j^0 \rightarrow D^{*+} \pi^-)$	[iii,zzz] $(2.6 \pm 0.9) \times 10^{-3}$	-
$D_j^- \ell^+ \nu_\ell$ anything \times $B(D_j^- \rightarrow D^0 \pi^-)$	[iii,zzz] $(7.0 \pm 2.3) \times 10^{-3}$	-

$\bar{D}_2^*(2460)^0 \ell^+ \nu_\ell$ anything $\times B(\bar{D}_2^*(2460)^0 \rightarrow$ $D^{*-} \pi^+)$	$< 1.4 \times 10^{-3}$	CL=90% -
$D_2^*(2460)^- \ell^+ \nu_\ell$ anything $\times B(D_2^*(2460)^- \rightarrow$ $D^0 \pi^-)$	$(4.2 \pm_{-1.8}^{+1.5}) \times 10^{-3}$	-
$\bar{D}_2^*(2460)^0 \ell^+ \nu_\ell$ anything $\times B(\bar{D}_2^*(2460)^0 \rightarrow$ $D^- \pi^+)$	$(1.6 \pm 0.8) \times 10^{-3}$	-
charmless $\ell \bar{\nu}_\ell$	[iii] $(1.7 \pm 0.5) \times 10^{-3}$	-
$\tau^+ \nu_\tau$ anything	$(2.41 \pm 0.23) \%$	-
$D^{*-} \tau \nu_\tau$ anything	$(9 \pm 4) \times 10^{-3}$	-
$\bar{c} \rightarrow \ell^- \bar{\nu}_\ell$ anything	[iii] $(8.02 \pm 0.19) \%$	-
$c \rightarrow \ell^+ \nu$ anything	$(1.6 \pm_{-0.5}^{+0.4}) \%$	-

Charmed meson and baryon modes

\bar{D}^0 anything	$(59.6 \pm 2.9) \%$	-
$D^0 D_s^\pm$ anything	[gg] $(9.1 \pm_{-2.8}^{+3.9}) \%$	-
$D^\mp D_s^\pm$ anything	[gg] $(4.0 \pm_{-1.8}^{+2.3}) \%$	-
$\bar{D}^0 D^0$ anything	[gg] $(5.1 \pm_{-1.8}^{+2.0}) \%$	-
$D^0 D^\pm$ anything	[gg] $(2.7 \pm_{-1.6}^{+1.8}) \%$	-
$D^\pm D^\mp$ anything	[gg] $< 9 \times 10^{-3}$	CL=90% -
D^- anything	$(23.1 \pm 1.7) \%$	-
$D^*(2010)^+$ anything	$(17.3 \pm 2.0) \%$	-
$D_1(2420)^0$ anything	$(5.0 \pm 1.5) \%$	-
$D^*(2010)^\mp D_s^\pm$ anything	[gg] $(3.3 \pm_{-1.3}^{+1.6}) \%$	-
$D^0 D^*(2010)^\pm$ anything	[gg] $(3.0 \pm_{-0.9}^{+1.1}) \%$	-
$D^*(2010)^\pm D^\mp$ anything	[gg] $(2.5 \pm_{-1.0}^{+1.2}) \%$	-
$D^*(2010)^\pm D^*(2010)^\mp$ anything	[gg] $(1.2 \pm 0.4) \%$	-
$\bar{D} D$ anything	$(10 \pm_{-10}^{+11}) \%$	-
$D_2^*(2460)^0$ anything	$(4.7 \pm 2.7) \%$	-
D_s^- anything	$(15.0 \pm 2.1) \%$	-
D_s^+ anything	$(10.1 \pm 3.1) \%$	-
Λ_c^+ anything	$(9.7 \pm 2.9) \%$	-
\bar{c}/c anything	[yyy] $(116.2 \pm 3.2) \%$	-

Charmonium modes

$J/\psi(1S)$ anything	$(1.16 \pm 0.10) \%$	-
$\psi(2S)$ anything	$(4.8 \pm 2.4) \times 10^{-3}$	-
$\chi_{c1}(1P)$ anything	$(1.3 \pm 0.4) \%$	-

K or K* modes

$\bar{3}\gamma$	$(3.1 \pm 1.1) \times 10^{-4}$	-
$\bar{3}\bar{\nu}$	$< 6.4 \times 10^{-4}$	CL=90% -
K^\pm anything	$(74 \pm 6) \%$	-
K_S^0 anything	$(29.0 \pm 2.9) \%$	-

Pion modes

π^\pm anything	$(397 \pm 21) \%$	-
π^0 anything	[yyy] $(278 \pm 60) \%$	-
ϕ anything	$(2.82 \pm 0.23) \%$	-

Baryon modes

$\rho/\bar{\rho}$ anything	$(13.1 \pm 1.1) \%$	-
----------------------------	---------------------	---

Other modes

charged anything	[yyy] $(497 \pm 7) \%$	-
hadron ⁺ hadron ⁻	$(1.7 \pm_{-0.7}^{+1.0}) \times 10^{-5}$	-
charmless	$(7 \pm 21) \times 10^{-3}$	-

Baryon modes

$\Lambda/\bar{\Lambda}$ anything	$(5.9 \pm 0.6) \%$	-
b -baryon anything	$(10.2 \pm 2.8) \%$	-

 $\Delta B = 1$ weak neutral current ($B1$) modes

$\mu^+ \mu^-$ anything	$B1$ $< 3.2 \times 10^{-4}$	CL=90% -
------------------------	-----------------------------	----------

Meson Summary Table

 B^*

$$I(J^P) = \frac{1}{2}(1^-)$$

I, J, P need confirmation. Quantum numbers shown are quark-model predictions.

$$\begin{aligned} \text{Mass } m_{B^*} &= 5325.1 \pm 0.5 \text{ MeV} \\ m_{B^*} - m_B &= 45.78 \pm 0.35 \text{ MeV} \end{aligned}$$

B^* DECAY MODES	Fraction (Γ_i/Γ)	ρ (MeV/c)
$B\gamma$	dominant	45

 $B_1(5721)^0$

$$I(J^P) = \frac{1}{2}(1^+)$$

I, J, P need confirmation.

$$\begin{aligned} B_1(5721)^0 \text{ MASS} &= 5720.7 \pm 2.7 \text{ MeV} \\ m_{B_1^0} - m_{B^+} &= 441.5 \pm 2.7 \text{ MeV} \end{aligned}$$

$B_1(5721)^0$ DECAY MODES	Fraction (Γ_i/Γ)	ρ (MeV/c)
$B^{*+}\pi^-$	dominant	-

 $B_2^*(5747)^0$

$$I(J^P) = \frac{1}{2}(2^+)$$

I, J, P need confirmation.

$$\begin{aligned} B_2^*(5747)^0 \text{ MASS} &= 5746.9 \pm 2.9 \text{ MeV} \\ m_{B_2^{*0}} - m_{B_1^0} &= 26.2 \pm 3.2 \text{ MeV} \end{aligned}$$

$B_2^*(5747)^0$ DECAY MODES	Fraction (Γ_i/Γ)	ρ (MeV/c)
$B^+\pi^-$	dominant	428
$B^{*+}\pi^-$	dominant	-

BOTTOM, STRANGE MESONS ($B = \pm 1, S = \mp 1$)

$$B_s^0 = s\bar{b}, \bar{B}_s^0 = \bar{s}b, \text{ similarly for } B_s^{*s}$$

 B_s^0

$$I(J^P) = 0(0^-)$$

I, J, P need confirmation. Quantum numbers shown are quark-model predictions.

$$\begin{aligned} \text{Mass } m_{B_s^0} &= 5366.3 \pm 0.6 \text{ MeV} \\ \text{Mean life } \tau &= (1.470_{-0.027}^{+0.026}) \times 10^{-12} \text{ s} \\ c\tau &= 441 \mu\text{m} \end{aligned}$$

 B_s^0 - \bar{B}_s^0 mixing parameters

$$\begin{aligned} \Delta m_{B_s^0} = m_{B_s^0 H} - m_{B_s^0 L} &= (17.77 \pm 0.12) \times 10^{12} \hbar \text{ s}^{-1} \\ &= (117.0 \pm 0.8) \times 10^{-10} \text{ MeV} \end{aligned}$$

$$\begin{aligned} x_s = \Delta m_{B_s^0} / \Gamma_{B_s^0} &= 26.1 \pm 0.5 \\ \chi_s &= 0.49927 \pm 0.00003 \end{aligned}$$

CP violation parameters in B_s^0

$$\begin{aligned} \text{Re}(\epsilon_{B_s^0}) / (1 + |\epsilon_{B_s^0}|^2) &= (-0.75 \pm 2.52) \times 10^{-3} \\ \text{CP Violation phase } \beta_s \text{ in the } B_s^0 \text{ System} &= 0.35_{-0.24}^{+0.20} \end{aligned}$$

These branching fractions all scale with $B(\bar{D} \rightarrow B_s^0)$, the LEP B_s^0 production fraction. The first four were evaluated using $B(\bar{D} \rightarrow B_s^0) = (10.7 \pm 1.2)\%$ and the rest assume $B(\bar{D} \rightarrow B_s^0) = 12\%$.

The branching fraction $B(B_s^0 \rightarrow D_s^- \ell^+ \nu_\ell \text{ anything})$ is not a pure measurement since the measured product branching fraction $B(\bar{D} \rightarrow B_s^0) \times B(B_s^0 \rightarrow D_s^- \ell^+ \nu_\ell \text{ anything})$ was used to determine $B(\bar{D} \rightarrow B_s^0)$, as described in the note on " B^0 - \bar{B}^0 Mixing"

For inclusive branching fractions, e.g., $B \rightarrow D^\pm \text{ anything}$, the values usually are multiplicities, not branching fractions. They can be greater than one.

 B_s^0 DECAY MODES

B_s^0 DECAY MODES	Fraction (Γ_i/Γ)	Scale factor/ Confidence level	ρ (MeV/c)
D_s^- anything	(93 \pm 25) %		-
$D_s^- \ell^+ \nu_\ell$ anything	[aaaa] (7.9 \pm 2.4) %		-
$D_s^- \pi^+$	(3.2 \pm 0.9) $\times 10^{-3}$	S=1.3	2320
$D_s^- \pi^+ \pi^+ \pi^-$	(8.4 \pm 3.3) $\times 10^{-3}$		2301
$D_s^-(*) + D_s^-(*)^-$	(4.9 \pm 2.9) %	S=1.2	-
$D_s^+ D_s^-$	(1.1 \pm 0.4) %		1823
$D_s^{*+} D_s^-$	< 12.1 %	CL=90%	1742
$D_s^{*+} D_s^{*-}$	< 25.7 %	CL=90%	1655
$J/\psi(1S)\phi$	(9.3 \pm 3.3) $\times 10^{-4}$		1587
$J/\psi(1S)\pi^0$	< 1.2 $\times 10^{-3}$	CL=90%	1786
$J/\psi(1S)\eta$	< 3.8 $\times 10^{-3}$	CL=90%	1733
$\psi(2S)\phi$	(4.8 \pm 2.2) $\times 10^{-4}$		1119
$\pi^+ \pi^-$	< 1.7 $\times 10^{-6}$	CL=90%	2680
$\pi^0 \pi^0$	< 2.1 $\times 10^{-4}$	CL=90%	2680
$\eta \pi^0$	< 1.0 $\times 10^{-3}$	CL=90%	2653
$\eta \eta$	< 1.5 $\times 10^{-3}$	CL=90%	2627
$\rho^0 \rho^0$	< 3.20 $\times 10^{-4}$	CL=90%	2569
$\phi \rho^0$	< 6.17 $\times 10^{-4}$	CL=90%	2526
$\phi \phi$	(1.4 \pm 0.8) $\times 10^{-5}$		2482
$\pi^+ K^-$	< 5.6 $\times 10^{-6}$	CL=90%	2659
$K^+ K^-$	(3.3 \pm 0.9) $\times 10^{-5}$		2637
$\bar{K}^*(892)^0 \rho^0$	< 7.67 $\times 10^{-4}$	CL=90%	2550
$\bar{K}^*(892)^0 K^*(892)^0$	< 1.681 $\times 10^{-3}$	CL=90%	2531
$\phi K^*(892)^0$	< 1.013 $\times 10^{-3}$	CL=90%	2507
$\rho \bar{\rho}$	< 5.9 $\times 10^{-5}$	CL=90%	2514
$\gamma \gamma$	< 5.3 $\times 10^{-5}$	CL=90%	2683
$\phi \gamma$	< 1.2 $\times 10^{-4}$	CL=90%	2586

Lepton Family number (LF) violating modes or $\Delta B = 1$ weak neutral current (B1) modes

$\mu^+ \mu^-$	B1	< 4.7 $\times 10^{-8}$	CL=90%	2681
$e^+ e^-$	B1	< 5.4 $\times 10^{-5}$	CL=90%	2683
$e^\pm \mu^\mp$	LF [gg]	< 6.1 $\times 10^{-6}$	CL=90%	2682
$\phi(1020) \mu^+ \mu^-$	B1	< 3.2 $\times 10^{-6}$	CL=90%	2582
$\phi \nu \bar{\nu}$	B1	< 5.4 $\times 10^{-3}$	CL=90%	2586

 B_s^*

$$I(J^P) = 0(1^-)$$

I, J, P need confirmation. Quantum numbers shown are quark-model predictions.

$$\begin{aligned} \text{Mass } m &= 5412.8 \pm 1.3 \text{ MeV} \quad (S = 1.2) \\ m_{B_s^*} - m_{B_s} &= 46.5 \pm 1.2 \text{ MeV} \quad (S = 1.1) \end{aligned}$$

B_s^* DECAY MODES	Fraction (Γ_i/Γ)	ρ (MeV/c)
$B_s \gamma$	dominant	-

 $B_{s1}(5830)^0$

$$I(J^P) = \frac{1}{2}(1^+)$$

I, J, P need confirmation.

$$\begin{aligned} \text{Mass } m &= 5829.4 \pm 0.7 \text{ MeV} \\ m_{B_{s1}^0} - m_{B^{*+}} &= 504.41 \pm 0.25 \text{ MeV} \end{aligned}$$

$B_{s1}(5830)^0$ DECAY MODES	Fraction (Γ_i/Γ)	ρ (MeV/c)
$B^{*+} K^-$	dominant	-

Meson Summary Table

$B_{s2}^*(5840)^0$	$I(J^P) = \frac{1}{2}(2^+)$ <i>I, J, P need confirmation.</i>	Radiative decays		
	Mass $m = 5839.7 \pm 0.6$ MeV $m_{B_{s2}^0} - m_{B_{s1}^0} = 10.5 \pm 0.6$ MeV	$\gamma\gamma$	$(2.4^{+1.1}_{-0.9}) \times 10^{-4}$	1490
$B_{s2}^*(5840)^0$ DECAY MODES	Fraction (Γ_i/Γ)	Charge conjugation (C), Parity (P), Lepton family number (LF) violating modes		
$B^+ K^-$	dominant	$\pi^+ \pi^-$	$P, CP < 8.7 \times 10^{-4}$	90% 1484
		$\pi^0 \pi^0$	$P, CP < 5.6 \times 10^{-4}$	90% 1484
		$K^+ K^-$	$P, CP < 7.6 \times 10^{-4}$	90% 1406
		$K_S^0 K_S^0$	$P, CP < 4.2 \times 10^{-4}$	90% 1405

BOTTOM, CHARMED MESONS ($B = C = \pm 1$)

$B_c^+ = c\bar{b}, B_c^- = \bar{c}b$, similarly for B_c^* 's

B_c^\pm	$I(J^P) = 0(0^-)$ <i>I, J, P need confirmation.</i>	$J/\psi(1S)$		$I^G(J^{PC}) = 0^-(1^{--})$
	Quantum numbers shown are quark-model predictions. Mass $m = 6.276 \pm 0.004$ GeV Mean life $\tau = (0.46 \pm 0.07) \times 10^{-12}$ s	Mass $m = 3096.916 \pm 0.011$ MeV Full width $\Gamma = 93.2 \pm 2.1$ keV $\Gamma_{ee} = 5.55 \pm 0.14 \pm 0.02$ keV	$J/\psi(1S)$ DECAY MODES	
B_c^- modes are charge conjugates of the modes below.		hadrons	(87.7 \pm 0.5) %	p (MeV/c)
		virtual $\gamma \rightarrow$ hadrons	(13.50 \pm 0.30) %	—
		$e^+ e^-$	(5.94 \pm 0.06) %	1548
		$\mu^+ \mu^-$	(5.93 \pm 0.06) %	1545

B_c^+ DECAY MODES $\times B(\bar{b} \rightarrow B_c)$	Fraction (Γ_i/Γ)	Confidence level	p (MeV/c)
The following quantities are not pure branching ratios; rather the fraction $\Gamma_i/\Gamma \times B(\bar{b} \rightarrow B_c)$.			
$J/\psi(1S) \ell^+ \nu_\ell$ anything	$(5.2^{+2.4}_{-2.1}) \times 10^{-5}$	—	—
$J/\psi(1S) \pi^+$	$< 8.2 \times 10^{-5}$	90%	2371
$J/\psi(1S) \pi^+ \pi^+ \pi^-$	$< 5.7 \times 10^{-4}$	90%	2351
$J/\psi(1S) a_1(1260)$	$< 1.2 \times 10^{-3}$	90%	2170
$D^*(2010)^+ \bar{D}^0$	$< 6.2 \times 10^{-3}$	90%	2467

$c\bar{c}$ MESONS

$\eta_c(1S)$	$I^G(J^{PC}) = 0^+(0^{-+})$	$\eta_c(1S)$ DECAY MODES		p (MeV/c)
	Mass $m = 2980.3 \pm 1.2$ MeV ($S = 1.7$) Full width $\Gamma = 26.7 \pm 3.0$ MeV ($S = 2.0$)	Fraction (Γ_i/Γ)	Confidence level	

Decays involving hadronic resonances				
$\eta'(958) \pi\pi$	(4.1 \pm 1.7) %			1321
$\rho\rho$	(2.0 \pm 0.7) %			1272
$K^*(892)^0 K^- \pi^+ + c.c.$	(2.0 \pm 0.7) %			1275
$K^*(892) \bar{K}^*(892)$	(9.2 \pm 3.4) $\times 10^{-3}$			1194
$K^* \bar{K}^* \pi^+ \pi^-$	(1.5 \pm 0.8) %			1071
$\phi K^+ K^-$	(2.9 \pm 1.4) $\times 10^{-3}$			1102
$\phi\phi$	(2.7 \pm 0.9) $\times 10^{-3}$			1087
$\phi 2(\pi^+ \pi^-)$	$< 4.7 \times 10^{-3}$	90%		1249
$a_0(980) \pi$	< 2 %	90%		1324
$a_2(1320) \pi$	< 2 %	90%		1194
$K^*(892) \bar{K} + c.c.$	< 1.28 %	90%		1308
$f_2(1270) \eta$	< 1.1 %	90%		1143
$\omega\omega$	$< 3.1 \times 10^{-3}$	90%		1268
$\omega\phi$	$< 1.7 \times 10^{-3}$	90%		1183
$f_2(1270) f_2(1270)$	(1.0 $^{+0.4}_{-0.5}$) %			771
$f_2(1270) f_2'(1525)$	(8 \pm 4) $\times 10^{-3}$			508
Decays into stable hadrons				
$K \bar{K} \pi$	(7.0 \pm 1.2) %			1379
$\eta\pi\pi$	(4.9 \pm 1.8) %			1427
$\pi^+ \pi^- K^+ K^-$	(1.5 \pm 0.6) %			1343
$K^+ K^- 2(\pi^+ \pi^-)$	(10 \pm 4) $\times 10^{-3}$			1252
$2(K^+ K^-)$	(1.5 \pm 0.7) $\times 10^{-3}$			1053
$2(\pi^+ \pi^-)$	(1.20 \pm 0.30) %			1457
$3(\pi^+ \pi^-)$	(2.0 \pm 0.7) %			1405
$\rho\bar{\rho}$	(1.3 \pm 0.4) $\times 10^{-3}$			1158
$\Lambda\bar{\Lambda}$	(1.04 \pm 0.31) $\times 10^{-3}$			988
$K \bar{K} \eta$	< 3.1 %	90%		1263
$\pi^+ \pi^- \rho\bar{\rho}$	< 1.2 %	90%		1024

$J/\psi(1S)$		$I^G(J^{PC}) = 0^-(1^{--})$		
Mass $m = 3096.916 \pm 0.011$ MeV Full width $\Gamma = 93.2 \pm 2.1$ keV $\Gamma_{ee} = 5.55 \pm 0.14 \pm 0.02$ keV		$J/\psi(1S)$ DECAY MODES		Scale factor/ Confidence level
hadrons	(87.7 \pm 0.5) %			p (MeV/c)
virtual $\gamma \rightarrow$ hadrons	(13.50 \pm 0.30) %			—
$e^+ e^-$	(5.94 \pm 0.06) %			1548
$\mu^+ \mu^-$	(5.93 \pm 0.06) %			1545
Decays involving hadronic resonances				
$\rho\pi$	(1.69 \pm 0.15) %		$S=2.4$	1448
$\rho^0 \pi^0$	(5.6 \pm 0.7) $\times 10^{-3}$			1448
$a_2(1320) \rho$	(1.09 \pm 0.22) %			1123
$\omega \pi^+ \pi^+ \pi^- \pi^-$	(8.5 \pm 3.4) $\times 10^{-3}$			1392
$\omega \pi^+ \pi^- \pi^0$	(4.0 \pm 0.7) $\times 10^{-3}$			1418
$\omega \pi^+ \pi^-$	(8.6 \pm 0.7) $\times 10^{-3}$	$S=1.1$		1435
$\omega f_2(1270)$	(4.3 \pm 0.6) $\times 10^{-3}$			1142
$K^*(892)^0 \bar{K}_2^*(1430)^0 + c.c.$	(6.0 \pm 0.6) $\times 10^{-3}$			1012
$K^*(892)^0 \bar{K}_2^*(1770)^0 + c.c. \rightarrow$ $K^*(892)^0 K^- \pi^+ + c.c.$	(6.9 \pm 0.9) $\times 10^{-4}$			—
$\omega K^*(892) \bar{K} + c.c.$	(6.1 \pm 0.9) $\times 10^{-3}$			1097
$K^+ \bar{K}^*(892)^- + c.c.$	(5.12 \pm 0.30) $\times 10^{-3}$			1373
$K^+ \bar{K}^*(892)^- + c.c. \rightarrow$ $K^+ K^- \pi^0 + c.c.$	(1.97 \pm 0.20) $\times 10^{-3}$			—
$K^+ \bar{K}^*(892)^- + c.c. \rightarrow$ $K^+ K^- \pi^+ \pi^- + c.c.$	(3.0 \pm 0.4) $\times 10^{-3}$			—
$K^0 \bar{K}^*(892)^0 + c.c.$	(4.39 \pm 0.31) $\times 10^{-3}$			1373
$K^0 \bar{K}^*(892)^0 + c.c. \rightarrow$ $K^0 K^\pm \pi^\mp + c.c.$	(3.2 \pm 0.4) $\times 10^{-3}$			—
$K_1(1400)^\pm K^\mp$	(3.8 \pm 1.4) $\times 10^{-3}$			1170
$\bar{K}^*(892)^0 K^+ \pi^- + c.c.$	seen			1343
$\omega \pi^0 \pi^0$	(3.4 \pm 0.8) $\times 10^{-3}$			1436
$b_1(1235)^\pm \pi^\mp$	[gg] (3.0 \pm 0.5) $\times 10^{-3}$			1300
$\omega K^\pm K_S^0 \pi^\mp$	[gg] (3.4 \pm 0.5) $\times 10^{-3}$			1210
$b_1(1235)^0 \pi^0$	(2.3 \pm 0.6) $\times 10^{-3}$			1300
$\eta K^\pm K_S^0 \pi^\mp$	[gg] (2.2 \pm 0.4) $\times 10^{-3}$			1278
$\phi K^*(892) \bar{K} + c.c.$	(2.18 \pm 0.23) $\times 10^{-3}$			969
$\omega K \bar{K}$	(1.6 \pm 0.5) $\times 10^{-4}$			1268
$\omega f_0(1710) \rightarrow \omega K \bar{K}$	(4.8 \pm 1.1) $\times 10^{-4}$			878
$\phi 2(\pi^+ \pi^-)$	(1.66 \pm 0.23) $\times 10^{-3}$			1318
$\Delta(1232)^{++} \bar{p} \pi^-$	(1.6 \pm 0.5) $\times 10^{-3}$			1030
$\omega \eta$	(1.74 \pm 0.20) $\times 10^{-3}$		$S=1.6$	1394
$\phi K \bar{K}$	(1.83 \pm 0.24) $\times 10^{-3}$		$S=1.5$	1179
$\phi f_0(1710) \rightarrow \phi K \bar{K}$	(3.6 \pm 0.6) $\times 10^{-4}$			875
$\Delta(1232)^{++} \bar{\Delta}(1232)^{--}$	(1.10 \pm 0.29) $\times 10^{-3}$			938
$\Sigma(1385)^- \bar{\Sigma}(1385)^+ (or c.c.)$	[gg] (1.03 \pm 0.13) $\times 10^{-3}$			697
$\phi f_2'(1525)$	(8 \pm 4) $\times 10^{-4}$		$S=2.7$	871
$\phi \pi^+ \pi^-$	(9.4 \pm 0.9) $\times 10^{-4}$		$S=1.2$	1365
$\phi \pi^0 \pi^0$	(5.6 \pm 1.6) $\times 10^{-4}$			1366
$\phi K^\pm K_S^0 \pi^\mp$	[gg] (7.2 \pm 0.8) $\times 10^{-4}$			1114
$\omega f_1(1420)$	(6.8 \pm 2.4) $\times 10^{-4}$			1062
$\phi \eta$	(7.5 \pm 0.8) $\times 10^{-4}$		$S=1.5$	1320
$\Xi(1530)^- \Xi^+$	(5.9 \pm 1.5) $\times 10^{-4}$			600
$p K^- \bar{\Sigma}(1385)^0$	(5.1 \pm 3.2) $\times 10^{-4}$			646
$\omega \pi^0$	(4.5 \pm 0.5) $\times 10^{-4}$		$S=1.4$	1446
$\phi \eta'(958)$	(4.0 \pm 0.7) $\times 10^{-4}$		$S=2.1$	1192
$\phi f_0(980)$	(3.2 \pm 0.9) $\times 10^{-4}$		$S=1.9$	1182
$\phi f_0(980) \rightarrow \phi \pi^+ \pi^-$	(1.8 \pm 0.4) $\times 10^{-4}$			—
$\phi f_0(980) \rightarrow \phi \pi^0 \pi^0$	(1.7 \pm 0.7) $\times 10^{-4}$			—
$\Xi(1530)^0 \Xi^0$	(3.2 \pm 1.4) $\times 10^{-4}$			608
$\Sigma(1385)^- \bar{\Sigma}^+ (or c.c.)$	[gg] (3.1 \pm 0.5) $\times 10^{-4}$			855
$\phi f_1(1285)$	(2.6 \pm 0.5) $\times 10^{-4}$		$S=1.1$	1032
$\eta \pi^+ \pi^-$	(4.0 \pm 1.7) $\times 10^{-4}$			1487

Meson Summary Table

$\chi_{c0}(1P)$		$J^G(J^{PC}) = 0^+(0^{++})$	
Mass $m = 3414.75 \pm 0.31$ MeV			
Full width $\Gamma = 10.2 \pm 0.7$ MeV			
$\chi_{c0}(1P)$ DECAY MODES	Fraction (Γ_i/Γ)	Scale factor/ Confidence level	ρ (MeV/c)
Hadronic decays			
$2(\pi^+\pi^-)$	$(2.23 \pm 0.20) \%$		1679
$f_0(980)f_0(980)$	$(6.9 \pm 2.2) \times 10^{-4}$		1398
$\pi^+\pi^-K^+K^-$	$(1.79 \pm 0.16) \%$		1580
$f_0(980)f_0(980)$	$(1.7 \pm 1.1) \times 10^{-4}$		1398
$f_0(980)f_0(2200)$	$(8.3 \pm 2.1) \times 10^{-4}$		595
$f_0(1370)f_0(1370)$	$< 2.8 \times 10^{-4}$	CL=90%	1019
$f_0(1370)f_0(1500)$	$< 1.8 \times 10^{-4}$	CL=90%	920
$f_0(1370)f_0(1710)$	$(7.0 \pm 3.7) \times 10^{-4}$		718
$f_0(1500)f_0(1370)$	$< 1.4 \times 10^{-4}$	CL=90%	920
$f_0(1500)f_0(1500)$	$< 5 \times 10^{-5}$	CL=90%	805
$f_0(1500)f_0(1710)$	$< 7 \times 10^{-5}$	CL=90%	553
$\rho^0\pi^+\pi^-$	$(8.7 \pm 2.8) \times 10^{-3}$		1607
$3(\pi^+\pi^-)$	$(1.20 \pm 0.18) \%$		1633
$K^+\bar{K}^*(892)^0\pi^- + c.c.$	$(7.2 \pm 1.6) \times 10^{-3}$		1523
$K_1(1270)^+K^- + c.c. \rightarrow$	$(6.5 \pm 2.0) \times 10^{-3}$		-
$\pi^+\pi^-K^+K^-$			-
$K_1(1400)^+K^- + c.c. \rightarrow$	$< 2.8 \times 10^{-3}$	CL=90%	-
$\pi^+\pi^-K^+K^-$			-
$K^*(892)^0\bar{K}^*(892)^0$	$(1.8 \pm 0.6) \times 10^{-3}$		1456
$K_0^*(1430)^0\bar{K}_0^*(1430)^0 \rightarrow$	$(1.02 \pm 0.38) \times 10^{-3}$		-
$\pi^+\pi^-K^+K^-$			-
$K_0^*(1430)^0\bar{K}_2^*(1430)^0 + c.c. \rightarrow$	$(8.3 \pm 2.1) \times 10^{-4}$		-
$\pi^+\pi^-K^+K^-$			-
$\pi\pi$	$(7.3 \pm 0.6) \times 10^{-3}$		1702
$\eta\eta$	$(2.4 \pm 0.4) \times 10^{-3}$		1617
$\eta\pi^+\pi^-$	$< 1.1 \times 10^{-3}$	CL=90%	1651
$\eta\eta'$	$< 5 \times 10^{-4}$	CL=90%	1521
$\eta'\eta'$	$(1.7 \pm 0.4) \times 10^{-3}$		1414
$\omega\omega$	$(2.3 \pm 0.7) \times 10^{-3}$		1517
K^+K^-	$(5.7 \pm 0.6) \times 10^{-3}$		1634
$K_S^0K_S^0$	$(2.82 \pm 0.28) \times 10^{-3}$		1633
$\pi^+\pi^-\eta$	$< 2.1 \times 10^{-4}$		1651
$\pi^+\pi^-\eta'$	$< 4 \times 10^{-4}$		1560
$\bar{K}^0K^+\pi^- + c.c.$	$< 9.8 \times 10^{-5}$		1610
$K^+K^-\pi^0$	$< 6 \times 10^{-5}$		1611
$K^+K^-\eta$	$< 2.4 \times 10^{-4}$		1512
$K^+K^-K_S^0K_S^0$	$(1.5 \pm 0.5) \times 10^{-3}$		1331
$K^+K^-K^+K^-$	$(2.81 \pm 0.30) \times 10^{-3}$		1333
$K^+K^-\phi$	$(1.01 \pm 0.26) \times 10^{-3}$		1381
$K_S^0K_S^0\pi^+\pi^-$	$(5.9 \pm 1.1) \times 10^{-3}$		1579
$\phi\phi$	$(9.3 \pm 2.0) \times 10^{-4}$		1370
$\rho\bar{\rho}$	$(2.15 \pm 0.19) \times 10^{-4}$		1426
$\rho\bar{\rho}\pi^0$	$(5.8 \pm 1.2) \times 10^{-4}$		1379
$\rho\bar{\rho}\eta$	$(3.8 \pm 1.1) \times 10^{-4}$		1187
$\pi^+\pi^-\rho\bar{\rho}$	$(2.1 \pm 0.7) \times 10^{-3}$	S=1.4	1320
$K_S^0K_S^0\rho\bar{\rho}$	$< 8.8 \times 10^{-4}$	CL=90%	884
$\rho\bar{\rho}\pi^-$	$(1.17 \pm 0.32) \times 10^{-3}$		1376
$\Lambda\bar{\Lambda}$	$(4.4 \pm 1.5) \times 10^{-4}$		1292
$\Lambda\bar{\Lambda}\pi^+\pi^-$	$< 4.0 \times 10^{-3}$	CL=90%	1153
$K^+\bar{\Lambda} + c.c.$	$(1.05 \pm 0.20) \times 10^{-3}$		1132
$\Xi^-\bar{\Xi}^+$	$< 1.03 \times 10^{-3}$	CL=90%	1081
Radiative decays			
$\gamma J/\psi(1S)$	$(1.28 \pm 0.11) \%$		303
$\gamma\gamma$	$(2.35 \pm 0.23) \times 10^{-4}$		1707

$\chi_{c1}(1P)$		$J^G(J^{PC}) = 0^+(1^{++})$	
Mass $m = 3510.66 \pm 0.07$ MeV (S = 1.5)			
Full width $\Gamma = 0.89 \pm 0.05$ MeV			

$\chi_{c1}(1P)$ DECAY MODES		Fraction (Γ_i/Γ)	Scale factor/ Confidence level	ρ (MeV/c)
Hadronic decays				
$3(\pi^+\pi^-)$		$(5.8 \pm 1.4) \times 10^{-3}$	S=1.2	1683
$2(\pi^+\pi^-)$		$(7.6 \pm 2.6) \times 10^{-3}$		1728
$\pi^+\pi^-K^+K^-$		$(4.5 \pm 1.0) \times 10^{-3}$		1632
$\pi^+\pi^-\eta$		$(5.2 \pm 0.6) \times 10^{-3}$		1701
$\pi^+\pi^-\eta'$		$(2.5 \pm 0.5) \times 10^{-3}$		-
$\rho^0\pi^+\pi^-$		$(3.9 \pm 3.5) \times 10^{-3}$		1657
$K^+K^-\eta$		$(3.5 \pm 1.1) \times 10^{-4}$		1566
$K^0K^+\pi^- + c.c.$		$(7.7 \pm 0.7) \times 10^{-3}$		1661
$K^+K^-\pi^0$		$(2.01 \pm 0.28) \times 10^{-3}$		1662
$\eta\pi^+\pi^-$		$(5.8 \pm 1.1) \times 10^{-3}$		1701
$a_0(980)^+\pi^- + c.c. \rightarrow \eta\pi^+\pi^-$		$(2.0 \pm 0.7) \times 10^{-3}$		-
$f_2(1270)\eta$		$(3.0 \pm 0.9) \times 10^{-3}$		1468
$K^+\bar{K}^*(892)^0\pi^- + c.c.$		$(3.2 \pm 2.1) \times 10^{-3}$		1577
$K^*(892)^0\bar{K}^*(892)^0$		$(1.6 \pm 0.4) \times 10^{-3}$		1512
$K^*(892)^0\bar{K}^0 + c.c.$		$(1.1 \pm 0.4) \times 10^{-3}$		1602
$K^*(892)^+K^- + c.c.$		$(1.6 \pm 0.7) \times 10^{-3}$		1602
$K_S^*(1430)^0\bar{K}^0 + c.c. \rightarrow$		$< 9 \times 10^{-4}$	CL=90%	-
$K_S^0K^+\pi^- + c.c.$				-
$K_S^*(1430)^+K^- + c.c. \rightarrow$		$< 2.4 \times 10^{-3}$	CL=90%	-
$K_S^0K^+\pi^- + c.c.$				-
$\pi^+\pi^-K_S^0K_S^0$		$(7.6 \pm 3.2) \times 10^{-4}$		1630
$K^+K^-K_S^0K_S^0$		$< 5 \times 10^{-4}$	CL=90%	1390
$K^+K^-K^+K^-$		$(5.8 \pm 1.2) \times 10^{-4}$		1393
$K^+K^-\phi$		$(4.5 \pm 1.7) \times 10^{-4}$		1440
$\rho\bar{\rho}$		$(6.6 \pm 0.5) \times 10^{-5}$		1484
$\rho\bar{\rho}\pi^0$		$(1.2 \pm 0.5) \times 10^{-4}$		1438
$\rho\bar{\rho}\eta$		$< 1.6 \times 10^{-4}$	CL=90%	1254
$\pi^+\pi^-\rho\bar{\rho}$		$(5.0 \pm 1.9) \times 10^{-4}$		1381
$K_S^0K_S^0\rho\bar{\rho}$		$< 4.5 \times 10^{-4}$	CL=90%	968
$\Lambda\bar{\Lambda}$		$(2.4 \pm 1.0) \times 10^{-4}$		1355
$\Lambda\bar{\Lambda}\pi^+\pi^-$		$< 1.5 \times 10^{-3}$	CL=90%	1223
$K^+\bar{\Lambda}$		$(3.4 \pm 1.0) \times 10^{-4}$		1203
$\Xi^-\bar{\Xi}^+$		$< 3.4 \times 10^{-4}$	CL=90%	1155
$\pi^+\pi^- + K^+K^-$		$< 2.1 \times 10^{-3}$		-
$K_S^0K_S^0$		$< 7 \times 10^{-5}$	CL=90%	1683
Radiative decays				
$\gamma J/\psi(1S)$		$(36.0 \pm 1.9) \%$		389

$h_c(1P)$		$J^G(J^{PC}) = 1^-(1^{+-})$	
Mass $m = 3525.93 \pm 0.27$ MeV (S = 1.5)			
Full width $\Gamma < 1$ MeV			
$h_c(1P)$ DECAY MODES	Fraction (Γ_i/Γ)	ρ (MeV/c)	
$J/\psi(1S)\pi\pi$	not seen	313	
$\eta_c\gamma$	seen	503	

$\chi_{c2}(1P)$		$J^G(J^{PC}) = 0^+(2^{++})$	
Mass $m = 3556.20 \pm 0.09$ MeV			
Full width $\Gamma = 2.03 \pm 0.12$ MeV			

$\chi_{c2}(1P)$ DECAY MODES	Fraction (Γ_i/Γ)	Confidence level	ρ (MeV/c)
Hadronic decays			
$2(\pi^+\pi^-)$	$(1.14 \pm 0.12) \%$		1751
$\pi^+\pi^-K^+K^-$	$(9.4 \pm 1.1) \times 10^{-3}$		1656
$3(\pi^+\pi^-)$	$(8.6 \pm 1.8) \times 10^{-3}$		1707
$K^+\bar{K}^*(892)^0\pi^- + c.c.$	$(2.3 \pm 1.3) \times 10^{-3}$		1602
$K^*(892)^0\bar{K}^*(892)^0$	$(2.6 \pm 0.5) \times 10^{-3}$		1538
$\phi\phi$	$(1.54 \pm 0.30) \times 10^{-3}$		1457
$\omega\omega$	$(2.0 \pm 0.7) \times 10^{-3}$		1597
$\pi\pi$	$(2.17 \pm 0.25) \times 10^{-3}$		1773
$\rho^0\pi^+\pi^-$	$(4.1 \pm 1.8) \times 10^{-3}$		1681
$\pi^+\pi^-\eta$	$(5.5 \pm 1.5) \times 10^{-4}$		1724
$\pi^+\pi^-\eta'$	$(5.7 \pm 2.1) \times 10^{-4}$		1636
$\eta\eta$	$< 5 \times 10^{-4}$	90%	1692
K^+K^-	$(7.9 \pm 1.4) \times 10^{-4}$		1708
$K_S^0K_S^0$	$(6.5 \pm 0.8) \times 10^{-4}$		1707
$\bar{K}^0K^+\pi^- + c.c.$	$(1.40 \pm 0.21) \times 10^{-3}$		1685
$K^+K^-\pi^0$	$(3.5 \pm 0.9) \times 10^{-4}$		1686

Meson Summary Table

$K^+ K^- \eta$	$< 4 \times 10^{-4}$	90%	1592
$\eta \pi^+ \pi^-$	$< 1.7 \times 10^{-3}$	90%	1724
$\eta \eta'$	$< 2.6 \times 10^{-4}$	90%	1600
$\eta' \eta'$	$< 3.5 \times 10^{-4}$	90%	1498
$\pi^+ \pi^- K_S^0 K_S^0$	$(2.5 \pm 0.6) \times 10^{-3}$		1655
$K^+ K^- K_S^0 K_S^0$	$< 4 \times 10^{-4}$	90%	1418
$K^+ K^- K^+ K^-$	$(1.84 \pm 0.24) \times 10^{-3}$		1421
$K^+ K^- \phi$	$(1.63 \pm 0.34) \times 10^{-3}$		1468
$K_S^0 K_S^0 \rho \bar{\rho}$	$< 7.9 \times 10^{-4}$	90%	1007
$\rho \bar{\rho}$	$(6.7 \pm 0.5) \times 10^{-5}$		1510
$\rho \bar{\rho} \pi^0$	$(4.9 \pm 1.0) \times 10^{-4}$		1465
$\rho \bar{\rho} \eta$	$(2.1 \pm 0.8) \times 10^{-4}$		1285
$\pi^+ \pi^- \rho \bar{\rho}$	$(1.32 \pm 0.34) \times 10^{-3}$		1410
$\rho \bar{\rho} \pi^-$	$(1.2 \pm 0.4) \times 10^{-3}$		1463
$\Lambda \bar{\Lambda}$	$(2.7 \pm 1.3) \times 10^{-4}$		1385
$\Lambda \bar{\Lambda} \pi^+ \pi^-$	$< 3.5 \times 10^{-3}$	90%	1255
$K^+ \bar{p} \Lambda + c.c.$	$(9.6 \pm 1.9) \times 10^{-4}$		1236
$\Xi^- \Xi^+$	$< 3.7 \times 10^{-4}$	90%	1189
$J/\psi(1S) \pi^+ \pi^- \pi^0$	$< 1.5 \%$	90%	185

Radiative decays

$\gamma J/\psi(1S)$	$(20.0 \pm 1.0) \%$	430
$\gamma \gamma$	$(2.43 \pm 0.18) \times 10^{-4}$	1778

 $\eta_c(2S)$

$$I^G(J^{PC}) = 0^+(0^-+)$$

Quantum numbers are quark model predictions.

Mass $m = 3637 \pm 4$ MeV ($S = 1.7$)Full width $\Gamma = 14 \pm 7$ MeV

$\eta_c(2S)$ DECAY MODES	Fraction (Γ_i/Γ)	Confidence level	ρ (MeV/c)
hadrons	not seen		–
$K \bar{K} \pi$	seen		1729
$2\pi^+ 2\pi^-$	not seen		1792
$K^+ K^- \pi^+ \pi^-$	not seen		1700
$2K^+ 2K^-$	not seen		1470
$\rho \bar{\rho}$	not seen		1558
$\gamma \gamma$	$< 5 \times 10^{-4}$	90%	1819

 $\psi(2S)$

$$I^G(J^{PC}) = 0^-(1^-+)$$

Mass $m = 3686.09 \pm 0.04$ MeV ($S = 1.6$)Full width $\Gamma = 317 \pm 9$ keV $\Gamma_{e^+ e^-} = 2.38 \pm 0.04$ keV

$\psi(2S)$ DECAY MODES	Fraction (Γ_i/Γ)	Scale factor/ Confidence level	ρ (MeV/c)
hadrons	$(97.85 \pm 0.13) \%$		–
virtual $\gamma \rightarrow$ hadrons	$(1.73 \pm 0.14) \%$	$S=1.5$	–
$e^+ e^-$	$(7.52 \pm 0.17) \times 10^{-3}$		1843
$\mu^+ \mu^-$	$(7.5 \pm 0.8) \times 10^{-3}$		1840
$\tau^+ \tau^-$	$(3.0 \pm 0.4) \times 10^{-3}$		490

Decays into $J/\psi(1S)$ and anything

$J/\psi(1S)$ anything	$(57.4 \pm 0.9) \%$		–
$J/\psi(1S)$ neutrals	$(23.5 \pm 0.4) \%$		–
$J/\psi(1S) \pi^+ \pi^-$	$(32.6 \pm 0.5) \%$		477
$J/\psi(1S) \pi^0 \pi^0$	$(16.84 \pm 0.33) \%$		481
$J/\psi(1S) \eta$	$(3.16 \pm 0.07) \%$		199
$J/\psi(1S) \pi^0$	$(1.26 \pm 0.13) \times 10^{-3}$	$S=1.3$	528

Hadronic decays

$3(\pi^+ \pi^-) \pi^0$	$(3.5 \pm 1.6) \times 10^{-3}$		1746
$2(\pi^+ \pi^-) \pi^0$	$(2.9 \pm 1.0) \times 10^{-3}$	$S=4.6$	1799
$\rho a_2(1320)$	$(2.6 \pm 0.9) \times 10^{-4}$		1500
$\rho \bar{\rho}$	$(2.74 \pm 0.12) \times 10^{-4}$		1586
$\Delta^{++} \bar{\Delta}^{--}$	$(1.28 \pm 0.35) \times 10^{-4}$		1371
$\Lambda \bar{\Lambda} \pi^0$	$< 1.2 \times 10^{-4}$	CL=90%	1412
$\Lambda \bar{\Lambda} \eta$	$< 4.9 \times 10^{-5}$	CL=90%	1197
$\Lambda \bar{p} K^+$	$(1.00 \pm 0.14) \times 10^{-4}$		1327
$\Lambda \bar{p} K^+ \pi^+ \pi^-$	$(1.8 \pm 0.4) \times 10^{-4}$		1167
$\Lambda \bar{\Lambda} \pi^+ \pi^-$	$(2.8 \pm 0.6) \times 10^{-4}$		1346
$\Lambda \bar{\Lambda}$	$(2.8 \pm 0.5) \times 10^{-4}$		1467
$\Sigma^+ \bar{\Sigma}^-$	$(2.6 \pm 0.8) \times 10^{-4}$		1408
$\Sigma^0 \bar{\Sigma}^0$	$(2.2 \pm 0.4) \times 10^{-4}$	$S=1.5$	1405
$\Sigma(1385)^+ \bar{\Sigma}(1385)^-$	$(1.1 \pm 0.4) \times 10^{-4}$		1218

$\Xi^- \Xi^+$	$(1.8 \pm 0.6) \times 10^{-4}$	$S=2.8$	1284
$\Xi^0 \Xi^0$	$(2.8 \pm 0.9) \times 10^{-4}$		1291
$\Xi(1530)^0 \Xi(1530)^0$	$< 8.1 \times 10^{-5}$	CL=90%	1025
$\Omega^- \bar{\Omega}^+$	$< 7.3 \times 10^{-5}$	CL=90%	774
$\pi^0 \rho \bar{\rho}$	$(1.33 \pm 0.17) \times 10^{-4}$		1543
$\eta \rho \bar{\rho}$	$(6.0 \pm 1.2) \times 10^{-5}$		1373
$\omega \rho \bar{\rho}$	$(6.9 \pm 2.1) \times 10^{-5}$		1247
$\phi \rho \bar{\rho}$	$< 2.4 \times 10^{-5}$	CL=90%	1109
$\pi^+ \pi^- \rho \bar{\rho}$	$(6.0 \pm 0.4) \times 10^{-4}$		1491
$\rho \bar{\rho} \pi^-$ or c.c.	$(2.48 \pm 0.17) \times 10^{-4}$		–
$\rho \bar{\rho} \pi^- \pi^0$	$(3.2 \pm 0.7) \times 10^{-4}$		1492
$2(\pi^+ \pi^- \pi^0)$	$(4.7 \pm 1.5) \times 10^{-3}$		1776
$\eta \pi^+ \pi^-$	$< 1.6 \times 10^{-4}$	CL=90%	1791
$\eta \pi^+ \pi^- \pi^0$	$(9.5 \pm 1.7) \times 10^{-4}$		1778
$2(\pi^+ \pi^-) \eta$	$(1.2 \pm 0.6) \times 10^{-3}$		1758
$\eta' \pi^+ \pi^- \pi^0$	$(4.5 \pm 2.1) \times 10^{-4}$		–
$\omega \pi^+ \pi^-$	$(7.3 \pm 1.2) \times 10^{-4}$	$S=2.1$	1748
$b_1^\pm \pi^\mp$	$(4.0 \pm 0.6) \times 10^{-4}$	$S=1.1$	1635
$b_1^0 \pi^0$	$(2.4 \pm 0.6) \times 10^{-4}$		–
$\omega f_2(1270)$	$(2.2 \pm 0.4) \times 10^{-4}$		1515
$\pi^+ \pi^- K^+ K^-$	$(7.5 \pm 0.9) \times 10^{-4}$	$S=1.9$	1726
$\rho^0 K^+ K^-$	$(2.2 \pm 0.4) \times 10^{-4}$		1616
$K^*(892)^0 \bar{K}_2^*(1430)^0$	$(1.9 \pm 0.5) \times 10^{-4}$		1418
$K^+ K^- \pi^+ \pi^- \eta$	$(1.3 \pm 0.7) \times 10^{-3}$		1574
$K^+ K^- 2(\pi^+ \pi^-) \pi^0$	$(1.00 \pm 0.31) \times 10^{-3}$		1611
$K^+ K^- 2(\pi^+ \pi^-)$	$(1.8 \pm 0.9) \times 10^{-3}$		1654
$K_1(1270)^\pm K^\mp$	$(1.00 \pm 0.28) \times 10^{-3}$		1581
$K_S^0 K_S^0 \pi^+ \pi^-$	$(2.2 \pm 0.4) \times 10^{-4}$		1724
$\rho^0 \rho \bar{\rho}$	$(5.0 \pm 2.2) \times 10^{-5}$		1251
$K^+ \bar{K}^*(892)^0 \pi^- + c.c.$	$(6.7 \pm 2.5) \times 10^{-4}$		1674
$2(\pi^+ \pi^-)$	$(2.4 \pm 0.6) \times 10^{-4}$	$S=2.2$	1817
$\rho^0 \pi^+ \pi^-$	$(2.2 \pm 0.6) \times 10^{-4}$	$S=1.4$	1750
$K^+ K^- \pi^+ \pi^- \pi^0$	$(1.26 \pm 0.09) \times 10^{-3}$		1694
$\omega f_0(1710) \rightarrow \omega K^+ K^-$	$(5.9 \pm 2.2) \times 10^{-5}$		–
$K^*(892)^0 K^- \pi^+ \pi^0 + c.c.$	$(8.6 \pm 2.2) \times 10^{-4}$		–
$K^*(892)^+ K^- \pi^+ \pi^- + c.c.$	$(9.6 \pm 2.8) \times 10^{-4}$		–
$K^*(892)^+ K^- \rho^0 + c.c.$	$(7.3 \pm 2.6) \times 10^{-4}$		–
$K^*(892)^0 K^- \rho^+ + c.c.$	$(6.1 \pm 1.8) \times 10^{-4}$		–
$\eta K^+ K^-$	$< 1.3 \times 10^{-4}$	CL=90%	1664
$\omega K^+ K^-$	$(1.85 \pm 0.25) \times 10^{-4}$	$S=1.1$	1614
$3(\pi^+ \pi^-)$	$(3.5 \pm 2.0) \times 10^{-4}$	$S=2.8$	1774
$\rho \bar{\rho} \pi^+ \pi^- \pi^0$	$(7.3 \pm 0.7) \times 10^{-4}$		1435
$K^+ K^-$	$(6.3 \pm 0.7) \times 10^{-5}$		1776
$K_S^0 K_L^0$	$(5.4 \pm 0.5) \times 10^{-5}$		1775
$\pi^+ \pi^- \pi^0$	$(1.68 \pm 0.26) \times 10^{-4}$	$S=1.4$	1830
$\rho(2150) \pi \rightarrow \pi^+ \pi^- \pi^0$	$(1.9 \pm 1.2) \times 10^{-4}$		–
$\rho(770) \pi \rightarrow \pi^+ \pi^- \pi^0$	$(3.2 \pm 1.2) \times 10^{-5}$	$S=1.8$	–
$\pi^+ \pi^-$	$(8 \pm 5) \times 10^{-5}$		1838
$K_1(1400)^\pm K^\mp$	$< 3.1 \times 10^{-4}$	CL=90%	1532
$K^+ K^- \pi^0$	$< 2.96 \times 10^{-5}$	CL=90%	1754
$K^+ \bar{K}^*(892)^- + c.c.$	$(1.7 \pm 0.8) \times 10^{-5}$		1698
$K^*(892)^0 \bar{K}_2^0 + c.c.$	$(1.09 \pm 0.20) \times 10^{-4}$		1697
$\phi \pi^+ \pi^-$	$(1.17 \pm 0.29) \times 10^{-4}$	$S=1.7$	1690
$\phi f_0(980) \rightarrow \pi^+ \pi^-$	$(6.8 \pm 2.4) \times 10^{-5}$	$S=1.1$	–
$2(K^+ K^-)$	$(6.0 \pm 1.4) \times 10^{-5}$		1499
$\phi K^+ K^-$	$(7.0 \pm 1.6) \times 10^{-5}$		1546
$2(K^+ K^-) \pi^0$	$(1.10 \pm 0.28) \times 10^{-4}$		1440
$\phi \eta$	$(2.8 \pm 1.0) \times 10^{-5}$		1654
$\phi \eta'$	$(3.1 \pm 1.6) \times 10^{-5}$		1555
$\omega \eta'$	$(3.2 \pm 2.5) \times 10^{-5}$		1623
$\omega \pi^0$	$(2.1 \pm 0.6) \times 10^{-5}$		1757
$\rho \eta'$	$(1.9 \pm 1.7) \times 10^{-5}$		1625
$\rho \eta$	$(2.2 \pm 0.6) \times 10^{-5}$	$S=1.1$	1717
$\omega \eta$	$< 1.1 \times 10^{-5}$	CL=90%	1715
$\phi \pi^0$	$< 4 \times 10^{-6}$	CL=90%	1699
$\eta_c \pi^+ \pi^- \pi^0$	$< 1.0 \times 10^{-3}$	CL=90%	–
$\rho \bar{\rho} K^+ K^-$	$(2.7 \pm 0.7) \times 10^{-5}$		1118
$\Lambda n K_S^0 + c.c.$	$(8.1 \pm 1.8) \times 10^{-5}$		1324
$\phi f_2'(1525)$	$(4.4 \pm 1.6) \times 10^{-5}$		1321
$\Theta(1540) \bar{\Theta}(1540) \rightarrow K_S^0 \rho K^- \bar{n} + c.c.$	$< 8.8 \times 10^{-6}$	CL=90%	–
$\Theta(1540) K^- \bar{n} \rightarrow K_S^0 \rho K^- \bar{n}$	$< 1.0 \times 10^{-5}$	CL=90%	–
$\Theta(1540) K_S^0 \bar{p} \rightarrow K_S^0 \bar{p} K^+ n$	$< 7.0 \times 10^{-6}$	CL=90%	–

Meson Summary Table

$\bar{D}(1540) K^+ n \rightarrow K_S^0 \bar{p} K^+ n$	< 2.6	$\times 10^{-5}$	CL=90%	-
$\bar{D}(1540) K_S^0 p \rightarrow K_S^0 p K^- \bar{n}$	< 6.0	$\times 10^{-6}$	CL=90%	-
$K_S^0 K_S^0$	< 4.6	$\times 10^{-6}$		1775
Radiative decays				
$\gamma \chi_{c0}(1P)$	(9.4 \pm 0.4) %			261
$\gamma \chi_{c1}(1P)$	(8.8 \pm 0.4) %			171
$\gamma \chi_{c2}(1P)$	(8.3 \pm 0.4) %			128
$\gamma \eta_c(1S)$	(3.0 \pm 0.5) $\times 10^{-3}$			638
$\gamma \eta_c(2S)$	< 2.0	$\times 10^{-3}$	CL=90%	48
$\gamma \pi^0$	< 5.4	$\times 10^{-3}$	CL=95%	1841
$\gamma \eta'(958)$	(1.36 \pm 0.24) $\times 10^{-4}$			1719
$\gamma f_2(1270)$	(2.1 \pm 0.4) $\times 10^{-4}$			1622
$\gamma f_0(1710) \rightarrow \gamma \pi \pi$	(3.0 \pm 1.3) $\times 10^{-5}$			-
$\gamma f_0(1710) \rightarrow \gamma K \bar{K}$	(6.0 \pm 1.6) $\times 10^{-5}$			-
$\gamma \gamma$	< 1.4	$\times 10^{-4}$	CL=90%	1843
$\gamma \eta$	< 9	$\times 10^{-5}$	CL=90%	1802
$\gamma \eta \pi^+ \pi^-$	(8.7 \pm 2.1) $\times 10^{-4}$			1791
$\gamma \eta(1405) \rightarrow \gamma K \bar{K} \pi$	< 9	$\times 10^{-5}$	CL=90%	1569
$\gamma \eta(1405) \rightarrow \eta \pi^+ \pi^-$	(3.6 \pm 2.5) $\times 10^{-5}$			-
$\gamma \eta(1475) \rightarrow K \bar{K} \pi$	< 1.4	$\times 10^{-4}$	CL=90%	-
$\gamma \eta(1475) \rightarrow \eta \pi^+ \pi^-$	< 8.8	$\times 10^{-5}$	CL=90%	-
$\gamma 2(\pi^+ \pi^-)$	(4.0 \pm 0.6) $\times 10^{-4}$			1817
$\gamma K^{*0} K^+ \pi^- + c.c.$	(3.7 \pm 0.9) $\times 10^{-4}$			1674
$\gamma K^{*0} \bar{K}^{*0}$	(2.4 \pm 0.7) $\times 10^{-4}$			1613
$\gamma K_S^0 K^+ \pi^- + c.c.$	(2.6 \pm 0.5) $\times 10^{-4}$			1753
$\gamma K^+ K^- \pi^+ \pi^-$	(1.9 \pm 0.5) $\times 10^{-4}$			1726
$\gamma \rho \bar{\rho}$	(2.9 \pm 0.6) $\times 10^{-5}$			1586
$\gamma \pi^+ \pi^- \rho \bar{\rho}$	(2.8 \pm 1.4) $\times 10^{-5}$			1491
$\gamma 2(\pi^+ \pi^-) K^+ K^-$	< 2.2	$\times 10^{-4}$	CL=90%	1654
$\gamma 3(\pi^+ \pi^-)$	< 1.7	$\times 10^{-4}$	CL=90%	1774
$\gamma K^+ K^- K^+ K^-$	< 4	$\times 10^{-5}$	CL=90%	1499

 $\psi(3770)$

$$I^G(J^{PC}) = 0^-(1^{--})$$

Mass $m = 3772.92 \pm 0.35$ MeV (S = 1.1)

Full width $\Gamma = 27.3 \pm 1.0$ MeV

$\Gamma_{ee} = 0.265 \pm 0.018$ keV (S = 1.3)

In addition to the dominant decay mode to $D\bar{D}$, $\psi(3770)$ was found to decay into the final states containing the J/ψ (BAI 05, ADAM 06). ADAMS 06 and HUANG 06a searched for various decay modes with light hadrons and found a statistically significant signal for the decay to $\phi \eta$ only (ADAMS 06).

$\psi(3770)$ DECAY MODES	Fraction (Γ_i/Γ)	Scale factor/ Confidence level	p (MeV/c)
$D\bar{D}$	(85.3 \pm 3.2) %		285
$D^0 \bar{D}^0$	(48.7 \pm 3.2) %		285
$D^+ D^-$	(36.1 \pm 2.8) %		251
$J/\psi \pi^+ \pi^-$	(1.93 \pm 0.28) $\times 10^{-3}$		560
$J/\psi \pi^0 \pi^0$	(8.0 \pm 3.0) $\times 10^{-4}$		564
$J/\psi \eta$	(9 \pm 4) $\times 10^{-4}$		359
$J/\psi \pi^0$	< 2.8	$\times 10^{-4}$	CL=90% 603
$\gamma \chi_{c0}$	(7.3 \pm 0.9) $\times 10^{-3}$		-
$\gamma \chi_{c1}$	(2.9 \pm 0.6) $\times 10^{-3}$		-
$\gamma \chi_{c2}$	< 9	$\times 10^{-4}$	CL=90% -
$e^+ e^-$	(9.7 \pm 0.7) $\times 10^{-6}$	S=1.2	1886
$K_S^0 K_L^0$	< 1.2	$\times 10^{-5}$	CL=90% 1820
$2(\pi^+ \pi^-)$	< 1.12	$\times 10^{-3}$	CL=90% 1861
$2(\pi^+ \pi^-) \pi^0$	< 1.06	$\times 10^{-3}$	CL=90% 1843
$\omega \pi^+ \pi^-$	< 6.0	$\times 10^{-4}$	CL=90% 1794
$3(\pi^+ \pi^-)$	< 9.1	$\times 10^{-3}$	1819
$3(\pi^+ \pi^-) \pi^0$	< 1.37	%	1792
$\eta \pi^+ \pi^-$	< 1.24	$\times 10^{-3}$	CL=90% 1836
$\rho^0 \pi^+ \pi^-$	< 6.9	$\times 10^{-3}$	CL=90% 1796
$\eta 3\pi$	< 1.34	$\times 10^{-3}$	CL=90% 1824
$\eta 2(\pi^+ \pi^-)$	< 2.43	%	1804
$\eta' 3\pi$	< 2.44	$\times 10^{-3}$	CL=90% 1740
$K^+ K^- \pi^+ \pi^-$	< 9.0	$\times 10^{-4}$	CL=90% 1772
$\phi \pi^+ \pi^-$	< 4.1	$\times 10^{-4}$	CL=90% 1737
$\phi \pi^0$	not seen		1746
$\phi \eta$	(3.1 \pm 0.7) $\times 10^{-4}$		1703
$4(\pi^+ \pi^-)$	< 1.67	%	CL=90% 1757
$4(\pi^+ \pi^-) \pi^0$	< 3.06	%	CL=90% 1720
$\phi f_0(980)$	< 4.5	$\times 10^{-4}$	CL=90% 1600
$K^+ K^- \pi^+ \pi^- \pi^0$	< 2.36	$\times 10^{-3}$	CL=90% 1741
$K^+ K^- \rho^0 \pi^0$	< 8	$\times 10^{-4}$	CL=90% 1624
$K^+ K^- \rho^+ \pi^-$	< 1.46	%	CL=90% 1622

$\omega K^+ K^-$	< 3.4	$\times 10^{-4}$	CL=90%	1664
$\phi \pi^+ \pi^- \pi^0$	< 3.8	$\times 10^{-3}$	CL=90%	1722
$K^{*0} K^- \pi^+ \pi^0 + c.c.$	< 1.62	%	CL=90%	1693
$K^{*+} K^- \pi^+ \pi^- + c.c.$	< 3.23	%	CL=90%	1692
$K^+ K^- 2(\pi^+ \pi^-)$	< 1.03	%	CL=90%	1702
$K^+ K^- 2(\pi^+ \pi^-) \pi^0$	< 3.60	%	CL=90%	1660
$\eta K^+ K^-$	< 4.1	$\times 10^{-4}$	CL=90%	1711
$\rho^0 K^+ K^-$	< 5.0	$\times 10^{-3}$	CL=90%	1665
$2(K^+ K^-)$	< 6.0	$\times 10^{-4}$	CL=90%	1551
$\phi K^+ K^-$	< 7.5	$\times 10^{-4}$	CL=90%	1597
$2(K^+ K^-) \pi^0$	< 2.9	$\times 10^{-4}$	CL=90%	1493
$2(K^+ K^-) \pi^+ \pi^-$	< 3.2	$\times 10^{-3}$	CL=90%	1425
$K^{*0} K^- \pi^+ + c.c.$	< 9.7	$\times 10^{-3}$	CL=90%	1721
$\rho \bar{\rho} \pi^0$	< 1.2	$\times 10^{-3}$		1595
$\rho \bar{\rho} \pi^+ \pi^-$	< 5.8	$\times 10^{-4}$	CL=90%	1544
$\Lambda \bar{\Lambda}$	< 1.2	$\times 10^{-4}$	CL=90%	1521
$\rho \bar{\rho} \pi^+ \pi^- \pi^0$	< 1.85	$\times 10^{-3}$	CL=90%	1490
$\omega \rho \bar{\rho}$	< 2.9	$\times 10^{-4}$	CL=90%	1309
$\Lambda \bar{\Lambda} \pi^0$	< 1.2	$\times 10^{-3}$	CL=90%	1468
$\rho \bar{\rho} 2(\pi^+ \pi^-)$	< 2.6	$\times 10^{-3}$	CL=90%	1425
$\eta \rho \bar{\rho}$	< 5.4	$\times 10^{-4}$	CL=90%	1430
$\rho^0 \rho \bar{\rho}$	< 1.7	$\times 10^{-3}$	CL=90%	1313
$\rho \bar{\rho} K^+ K^-$	< 3.2	$\times 10^{-4}$	CL=90%	1185
$\phi \rho \bar{\rho}$	< 1.3	$\times 10^{-4}$	CL=90%	1178
$\Lambda \bar{\Lambda} \pi^+ \pi^-$	< 2.5	$\times 10^{-4}$	CL=90%	1404
$\Lambda \bar{\Lambda} K^+$	< 2.8	$\times 10^{-4}$	CL=90%	1387
$\Lambda \bar{\Lambda} K^+ \pi^+ \pi^-$	< 6.3	$\times 10^{-4}$	CL=90%	1234
$\pi^+ \pi^- \pi^0$	not seen			1874
$\rho \pi$	not seen			1804
$\omega \pi^0$	not seen			1803
$\rho \eta$	not seen			1763
$\omega \eta$	not seen			1762
$\rho \eta'$	not seen			1674
$\omega \eta'$	not seen			1672
$\phi \eta'$	not seen			1606
$K^{*0} \bar{K}^0$	not seen			1744
$K^{*+} K^-$	not seen			1745
$b_1 \pi$	not seen			1683

 $X(3872)$

$$I^G(J^{PC}) = 0^?(?^{?+})$$

Quantum numbers not established.

Mass $m = 3872.2 \pm 0.8$ MeV (S = 2.5)

$m_{X(3872)^\pm} - m_{J/\psi} = 775 \pm 4$ MeV

Full width $\Gamma = 3.0^{+2.1}_{-1.7}$ MeV

$X(3872)$ DECAY MODES	Fraction (Γ_i/Γ)	p (MeV/c)
$\pi^+ \pi^- J/\psi(1S)$	seen	650
$\rho^0 J/\psi(1S)$	seen	†
$D^0 \bar{D}^0$	not seen	520
$D^+ D^-$	not seen	503
$D^0 \bar{D}^0 \pi^0$	seen	121

 $\psi(4040)$ [cccc]

$$I^G(J^{PC}) = 0^-(1^{--})$$

Mass $m = 4039 \pm 1$ MeV

Full width $\Gamma = 80 \pm 10$ MeV

$\Gamma_{ee} = 0.86 \pm 0.07$ keV

Meson Summary Table

$\psi(4040)$ DECAY MODES	Fraction (Γ_i/Γ)	Confidence level	P (MeV/c)
$e^+ e^-$	$(1.07 \pm 0.16) \times 10^{-5}$		2019
$D^0 \bar{D}^0$	seen		775
$D^*(2007)^0 \bar{D}^0 + c.c.$	seen		575
$D^*(2007)^0 \bar{D}^*(2007)^0$	seen		225
$J/\psi \pi^+ \pi^-$	< 4	$\times 10^{-3}$	90%
$J/\psi \pi^0 \pi^0$	< 2	$\times 10^{-3}$	90%
$J/\psi \eta$	< 7	$\times 10^{-3}$	90%
$J/\psi \pi^0$	< 2	$\times 10^{-3}$	90%
$J/\psi \pi^+ \pi^- \pi^0$	< 2	$\times 10^{-3}$	90%
$\chi_{c1} \gamma$	< 1.1	%	90%
$\chi_{c2} \gamma$	< 1.7	%	90%
$\chi_{c1} \pi^+ \pi^- \pi^0$	< 1.1	%	90%
$\chi_{c2} \pi^+ \pi^- \pi^0$	< 3.2	%	90%
$\phi \pi^+ \pi^-$	< 3	$\times 10^{-3}$	90%

 $\psi(4160)$ [cccc]

$$I^G(J^{PC}) = 0^-(1^{--})$$

Mass $m = 4153 \pm 3$ MeV
 Full width $\Gamma = 103 \pm 8$ MeV
 $\Gamma_{ee} = 0.83 \pm 0.07$ keV

$\psi(4160)$ DECAY MODES	Fraction (Γ_i/Γ)	Confidence level	P (MeV/c)
$e^+ e^-$	$(8.1 \pm 0.9) \times 10^{-6}$		2076
$J/\psi \pi^+ \pi^-$	< 3	$\times 10^{-3}$	90%
$J/\psi \pi^0 \pi^0$	< 3	$\times 10^{-3}$	90%
$J/\psi K^+ K^-$	< 2	$\times 10^{-3}$	90%
$J/\psi \eta$	< 8	$\times 10^{-3}$	90%
$J/\psi \pi^0$	< 1	$\times 10^{-3}$	90%
$J/\psi \eta'$	< 5	$\times 10^{-3}$	90%
$J/\psi \pi^+ \pi^- \pi^0$	< 1	$\times 10^{-3}$	90%
$\psi(2S) \pi^+ \pi^-$	< 4	$\times 10^{-3}$	90%
$\chi_{c1} \gamma$	< 7	$\times 10^{-3}$	90%
$\chi_{c2} \gamma$	< 1.3	%	90%
$\chi_{c1} \pi^+ \pi^- \pi^0$	< 2	$\times 10^{-3}$	90%
$\chi_{c2} \pi^+ \pi^- \pi^0$	< 8	$\times 10^{-3}$	90%
$\phi \pi^+ \pi^-$	< 2	$\times 10^{-3}$	90%

 $X(4260)$

$$I^G(J^{PC}) = ?^?(1^{--})$$

Mass $m = 4263^{+8}_{-9}$ MeV ($S = 1.1$)
 Full width $\Gamma = 95 \pm 14$ MeV

$X(4260)$ DECAY MODES	Fraction (Γ_i/Γ)	P (MeV/c)
$J/\psi \pi^+ \pi^-$	seen	976
$J/\psi \pi^0 \pi^0$	[dddd] seen	978
$J/\psi K^+ K^-$	[dddd] seen	530
$J/\psi \eta$	[dddd] not seen	886
$J/\psi \pi^0$	[dddd] not seen	999
$J/\psi \eta'$	[dddd] not seen	569
$J/\psi \pi^+ \pi^- \pi^0$	[dddd] not seen	939
$J/\psi \eta \eta$	[dddd] not seen	339
$\psi(2S) \pi^+ \pi^-$	[dddd] not seen	470
$\psi(2S) \eta$	[dddd] not seen	167
$\chi_{c0} \omega$	[dddd] not seen	284
$\chi_{c1} \gamma$	[dddd] not seen	686
$\chi_{c2} \gamma$	[dddd] not seen	648
$\chi_{c1} \pi^+ \pi^- \pi^0$	[dddd] not seen	571
$\chi_{c2} \pi^+ \pi^- \pi^0$	[dddd] not seen	524
$\phi \pi^+ \pi^-$	[dddd] not seen	1999
$D \bar{D}$	not seen	1032

 $\psi(4415)$ [cccc]

$$I^G(J^{PC}) = 0^-(1^{--})$$

Mass $m = 4421 \pm 4$ MeV
 Full width $\Gamma = 62 \pm 20$ MeV
 $\Gamma_{ee} = 0.58 \pm 0.07$ keV

$\psi(4415)$ DECAY MODES	Fraction (Γ_i/Γ)	Confidence level	P (MeV/c)
hadrons	dominant		—
$(D^0 D^- \pi^+)_{non-res}$	< 2.3 %	90%	—
$D \bar{D}_2^*(2460) \rightarrow D^0 D^- \pi^+$	(10 ± 4) %		—
$e^+ e^-$	$(9.4 \pm 3.2) \times 10^{-6}$		2210

 $b\bar{b}$ MESONS **$\Upsilon(1S)$**

$$I^G(J^{PC}) = 0^-(1^{--})$$

Mass $m = 9460.30 \pm 0.26$ MeV ($S = 3.3$)
 Full width $\Gamma = 54.02 \pm 1.25$ keV
 $\Gamma_{ee} = 1.340 \pm 0.018$ keV

$\Upsilon(1S)$ DECAY MODES	Fraction (Γ_i/Γ)	Confidence level	P (MeV/c)
$\tau^+ \tau^-$	(2.60 ± 0.10) %		4384
$e^+ e^-$	(2.38 ± 0.11) %		4730
$\mu^+ \mu^-$	(2.48 ± 0.05) %		4729

Hadronic decays

$\eta'(958)$ anything	(2.94 ± 0.24) %		—
$J/\psi(1S)$ anything	$(6.5 \pm 0.7) \times 10^{-4}$		4223
χ_{c0} anything	< 5	$\times 10^{-3}$	90%
χ_{c1} anything	$(2.3 \pm 0.7) \times 10^{-4}$		—
χ_{c2} anything	$(3.4 \pm 1.0) \times 10^{-4}$		—
$\psi(2S)$ anything	$(2.7 \pm 0.9) \times 10^{-4}$		—
$\rho \pi$	< 2	$\times 10^{-4}$	90%
$\pi^+ \pi^-$	< 5	$\times 10^{-4}$	90%
$K^+ K^-$	< 5	$\times 10^{-4}$	90%
$p \bar{p}$	< 5	$\times 10^{-4}$	90%
$\pi^0 \pi^+ \pi^-$	< 1.84	$\times 10^{-5}$	90%
\bar{d} anything	$(2.86 \pm 0.28) \times 10^{-5}$		—

Radiative decays

$\gamma \pi^+ \pi^-$	$(6.3 \pm 1.8) \times 10^{-5}$		4728
$\gamma \pi^0 \pi^0$	$(1.7 \pm 0.7) \times 10^{-5}$		4728
$\gamma \pi^0 \eta$	< 2.4	$\times 10^{-6}$	90%
$K^+ K^-$ with $2 < m_{K^+ K^-} < 3$ GeV	$(1.14 \pm 0.13) \times 10^{-5}$		—
$\gamma p \bar{p}$ with $2 < m_{p \bar{p}} < 3$ GeV	< 6	$\times 10^{-6}$	90%
$\gamma 2h^+ 2h^-$	$(7.0 \pm 1.5) \times 10^{-4}$		4720
$\gamma 3h^+ 3h^-$	$(5.4 \pm 2.0) \times 10^{-4}$		4703
$\gamma 4h^+ 4h^-$	$(7.4 \pm 3.5) \times 10^{-4}$		4679
$\gamma \pi^+ \pi^- K^+ K^-$	$(2.9 \pm 0.9) \times 10^{-4}$		4686
$\gamma 2\pi^+ 2\pi^-$	$(2.5 \pm 0.9) \times 10^{-4}$		4720
$\gamma 3\pi^+ 3\pi^-$	$(2.5 \pm 1.2) \times 10^{-4}$		4703
$\gamma 2\pi^+ 2\pi^- K^+ K^-$	$(2.4 \pm 1.2) \times 10^{-4}$		4658
$\gamma \pi^+ \pi^- p \bar{p}$	$(1.5 \pm 0.6) \times 10^{-4}$		4604
$\gamma 2\pi^+ 2\pi^- p \bar{p}$	$(4 \pm 6) \times 10^{-5}$		4563
$\gamma 2K^+ 2K^-$	$(2.0 \pm 2.0) \times 10^{-5}$		4601
$\gamma \eta'(958)$	< 1.9	$\times 10^{-6}$	90%
$\gamma \eta$	< 1.0	$\times 10^{-6}$	90%
$\gamma f_0(980)$	< 3	$\times 10^{-5}$	90%
$\gamma f_2'(1525)$	$(3.7 \pm 1.1) \times 10^{-5}$		4607
$\gamma f_2(1270)$	$(1.01 \pm 0.09) \times 10^{-4}$		4644
$\gamma \eta(1405)$	< 8.2	$\times 10^{-5}$	90%
$\gamma f_0(1500)$	< 1.5	$\times 10^{-5}$	90%
$\gamma f_0(1710)$	< 2.6	$\times 10^{-4}$	90%
$\gamma f_0(1710) \rightarrow \gamma K^+ K^-$	< 7	$\times 10^{-6}$	90%
$\gamma f_0(1710) \rightarrow \gamma \pi^0 \pi^0$	< 1.4	$\times 10^{-6}$	90%
$\gamma f_0(1710) \rightarrow \gamma \eta \eta$	< 1.8	$\times 10^{-6}$	90%
$\gamma f_4(2050)$	< 5.3	$\times 10^{-5}$	90%
$\gamma f_0(2200) \rightarrow \gamma K^+ K^-$	< 2	$\times 10^{-4}$	90%
$\gamma f_J(2220) \rightarrow \gamma K^+ K^-$	< 8	$\times 10^{-7}$	90%
$\gamma f_J(2220) \rightarrow \gamma \pi^+ \pi^-$	< 6	$\times 10^{-7}$	90%
$\gamma f_J(2220) \rightarrow \gamma p \bar{p}$	< 1.1	$\times 10^{-6}$	90%
$\gamma \eta(2225) \rightarrow \gamma \phi \phi$	< 3	$\times 10^{-3}$	90%
γX	[eeee] < 3	$\times 10^{-5}$	90%
$\gamma X \bar{X}$	[ffff] < 1	$\times 10^{-3}$	90%
$\gamma X \rightarrow \gamma + \geq 4$ prongs	[gggg] < 1.78	$\times 10^{-4}$	95%

Meson Summary Table

Other decays	Fraction (Γ_i/Γ)	Confidence level	ρ (MeV/c)
invisible	$< 2.5 \times 10^{-3}$	90%	-

$\chi_{b0}(1P)$ ^[hhhh]	$J^G(JPC) = 0^+(0^{++})$ J needs confirmation.
Mass $m = 9859.44 \pm 0.42 \pm 0.31$ MeV	

$\chi_{b0}(1P)$ DECAY MODES	Fraction (Γ_i/Γ)	Confidence level	ρ (MeV/c)
$\gamma T(1S)$	$< 6\%$	90%	391

$\chi_{b1}(1P)$ ^[hhhh]	$J^G(JPC) = 0^+(1^{++})$ J needs confirmation.
Mass $m = 9892.78 \pm 0.26 \pm 0.31$ MeV	

$\chi_{b1}(1P)$ DECAY MODES	Fraction (Γ_i/Γ)	ρ (MeV/c)
$\gamma T(1S)$	$(35 \pm 8)\%$	423

$\chi_{b2}(1P)$ ^[hhhh]	$J^G(JPC) = 0^+(2^{++})$ J needs confirmation.
Mass $m = 9912.21 \pm 0.26 \pm 0.31$ MeV	

$\chi_{b2}(1P)$ DECAY MODES	Fraction (Γ_i/Γ)	ρ (MeV/c)
$\gamma T(1S)$	$(22 \pm 4)\%$	442

$T(2S)$	$J^G(JPC) = 0^-(1^{--})$
Mass $m = 10.02326 \pm 0.00031$ GeV	
Full width $\Gamma = 31.98 \pm 2.63$ keV	
$\Gamma_{ee} = 0.612 \pm 0.011$ keV	

$T(2S)$ DECAY MODES	Fraction (Γ_i/Γ)	Scale factor/ Confidence level	ρ (MeV/c)
$T(1S)\pi^+\pi^-$	$(18.8 \pm 0.6)\%$		475
$T(1S)\pi^0\pi^0$	$(9.0 \pm 0.8)\%$		480
$\tau^+\tau^-$	$(2.00 \pm 0.21)\%$		4686
$\mu^+\mu^-$	$(1.93 \pm 0.17)\%$	S=2.2	5011
e^+e^-	$(1.91 \pm 0.16)\%$		5012
$T(1S)\pi^0$	$< 1.1 \times 10^{-3}$	CL=90%	531
$T(1S)\eta$	$< 2 \times 10^{-3}$	CL=90%	126
$J/\psi(1S)$ anything	$< 6 \times 10^{-3}$	CL=90%	4533
\bar{d} anything	$(3.4 \pm 0.6) \times 10^{-5}$		-
hadrons	$(94 \pm 11)\%$		-

Radiative decays

$\gamma\chi_{b1}(1P)$	$(6.9 \pm 0.4)\%$		130
$\gamma\chi_{b2}(1P)$	$(7.15 \pm 0.35)\%$		110
$\gamma\chi_{b0}(1P)$	$(3.8 \pm 0.4)\%$		162
$\gamma f_0(1710)$	$< 5.9 \times 10^{-4}$	CL=90%	4863
$\gamma f_2'(1525)$	$< 5.3 \times 10^{-4}$	CL=90%	4896
$\gamma f_2(1270)$	$< 2.41 \times 10^{-4}$	CL=90%	4931
$\gamma\eta_b(1S)$	$< 5.1 \times 10^{-4}$	CL=90%	697
$\gamma X \rightarrow \gamma + \geq 4$ prongs	$[ijii] < 1.95 \times 10^{-4}$	CL=95%	-

$\chi_{b0}(2P)$ ^[hhhh]	$J^G(JPC) = 0^+(0^{++})$ J needs confirmation.
Mass $m = 10.2325 \pm 0.0004 \pm 0.0005$ GeV	

$\chi_{b0}(2P)$ DECAY MODES	Fraction (Γ_i/Γ)	ρ (MeV/c)
$\gamma T(2S)$	$(4.6 \pm 2.1)\%$	207
$\gamma T(1S)$	$(9 \pm 6) \times 10^{-3}$	743

$\chi_{b1}(2P)$ ^[hhhh]	$J^G(JPC) = 0^+(1^{++})$ J needs confirmation.
Mass $m = 10.25546 \pm 0.00022 \pm 0.00050$ GeV	
$m_{\chi_{b1}(2P)} - m_{\chi_{b0}(2P)} = 23.5 \pm 1.0$ MeV	

$\chi_{b1}(2P)$ DECAY MODES	Fraction (Γ_i/Γ)	Scale factor	ρ (MeV/c)
$\omega T(1S)$	$(1.63^{+0.38}_{-0.34})\%$		135
$\gamma T(2S)$	$(21 \pm 4)\%$	1.5	230
$\gamma T(1S)$	$(8.5 \pm 1.3)\%$	1.3	764
$\pi\pi\chi_{b1}(1P)$	$(8.6 \pm 3.1) \times 10^{-3}$		238

$\chi_{b2}(2P)$ ^[hhhh]	$J^G(JPC) = 0^+(2^{++})$ J needs confirmation.
Mass $m = 10.26865 \pm 0.00022 \pm 0.00050$ GeV	
$m_{\chi_{b2}(2P)} - m_{\chi_{b1}(2P)} = 13.5 \pm 0.6$ MeV	

$\chi_{b2}(2P)$ DECAY MODES	Fraction (Γ_i/Γ)	ρ (MeV/c)
$\omega T(1S)$	$(1.10^{+0.34}_{-0.30})\%$	194
$\gamma T(2S)$	$(16.2 \pm 2.4)\%$	242
$\gamma T(1S)$	$(7.1 \pm 1.0)\%$	777
$\pi\pi\chi_{b2}(1P)$	$(6.0 \pm 2.1) \times 10^{-3}$	229

$T(3S)$	$J^G(JPC) = 0^-(1^{--})$
Mass $m = 10.3552 \pm 0.0005$ GeV	
Full width $\Gamma = 20.32 \pm 1.85$ keV	
$\Gamma_{ee} = 0.443 \pm 0.008$ keV	

$T(3S)$ DECAY MODES	Fraction (Γ_i/Γ)	Scale factor/ Confidence level	ρ (MeV/c)
$T(2S)$ anything	$(10.6 \pm 0.8)\%$		296
$T(2S)\pi^+\pi^-$	$(2.8 \pm 0.6)\%$	S=2.2	177
$T(2S)\pi^0\pi^0$	$(2.00 \pm 0.32)\%$		190
$T(2S)\gamma\gamma$	$(5.0 \pm 0.7)\%$		327
$T(1S)\pi^+\pi^-$	$(4.48 \pm 0.21)\%$		813
$T(1S)\pi^0\pi^0$	$(2.06 \pm 0.28)\%$		816
$T(1S)\eta$	$< 2.2 \times 10^{-3}$	CL=90%	677
$\tau^+\tau^-$	$(2.29 \pm 0.30)\%$		4863
$\mu^+\mu^-$	$(2.18 \pm 0.21)\%$	S=2.1	5177
e^+e^-	seen		5178

Radiative decays

$\gamma\chi_{b2}(2P)$	$(13.1 \pm 1.6)\%$	S=3.4	86
$\gamma\chi_{b1}(2P)$	$(12.6 \pm 1.2)\%$	S=2.4	99
$\gamma\chi_{b0}(2P)$	$(5.9 \pm 0.6)\%$	S=1.4	122
$\gamma\chi_{b0}(1P)$	$(3.0 \pm 1.1) \times 10^{-3}$		484
$\gamma\eta_b(2S)$	$< 6.2 \times 10^{-4}$	CL=90%	-
$\gamma\eta_b(1S)$	$< 4.3 \times 10^{-4}$	CL=90%	1001
$\gamma X \rightarrow \gamma + \geq 4$ prongs	$[ijii] < 2.2 \times 10^{-4}$	CL=95%	-

$T(4S)$ or $T(10580)$	$J^G(JPC) = 0^-(1^{--})$
Mass $m = 10.5794 \pm 0.0012$ GeV	
Full width $\Gamma = 20.5 \pm 2.5$ MeV	
$\Gamma_{ee} = 0.272 \pm 0.029$ keV (S = 1.5)	

$T(4S)$ DECAY MODES	Fraction (Γ_i/Γ)	Confidence level	ρ (MeV/c)
$B\bar{B}$	$> 96\%$	95%	328
B^+B^-	$(51.6 \pm 0.6)\%$		334
D^+ anything + c.c.	$(18.3 \pm 2.6)\%$		-
$B^0\bar{B}^0$	$(48.4 \pm 0.6)\%$		328
$J/\psi K_S^0(J/\psi, \eta_c) K_S^0$	$< 4 \times 10^{-7}$	90%	-
non- $B\bar{B}$	$< 4\%$	95%	-
e^+e^-	$(1.57 \pm 0.08) \times 10^{-5}$		5290
$J/\psi(1S)$ anything	$< 1.9 \times 10^{-4}$	95%	-
D^{*+} anything + c.c.	$< 7.4\%$	90%	5099
ϕ anything	$(7.1 \pm 0.6)\%$		5240
$\phi\eta$	$< 2.5 \times 10^{-6}$	90%	5226
$T(1S)$ anything	$< 4 \times 10^{-3}$	90%	1053
$T(1S)\pi^+\pi^-$	$(9.0 \pm 1.5) \times 10^{-5}$		1026
$T(2S)\pi^+\pi^-$	$(8.8 \pm 1.9) \times 10^{-5}$		468
\bar{d} anything	$< 1.3 \times 10^{-5}$	90%	-

Meson Summary Table

7(10860)

$$J^G(J^{PC}) = 0^-(1^{--})$$

Mass $m = 10.865 \pm 0.008$ GeV ($S = 1.1$)

Full width $\Gamma = 110 \pm 13$ MeV

$\Gamma_{ee} = 0.31 \pm 0.07$ keV ($S = 1.3$)

7(10860) DECAY MODES	Fraction (Γ_i/Γ)	Confidence level	p (MeV/c)
e^+e^-	$(2.8 \pm 0.7) \times 10^{-6}$		5432
$B\bar{B}X$	$(59 \pm 14)\%$		—
$B\bar{B}$	$< 13.8\%$	90%	1280
$B\bar{B}^* + \text{c.c.}$	$(14 \pm 6)\%$		—
$B^*\bar{B}^*$	$(44 \pm 11)\%$		—
$B\bar{B}^{(*)}\pi$	$< 19.7\%$	90%	—
$B\bar{B}\pi\pi$	$< 8.9\%$	90%	441
$B_s^{(*)}\bar{B}_s^{(*)}(X)$	$(19.3 \pm 2.9)\%$		—
$\mathcal{T}(1S)\pi^+\pi^-$	$(5.3 \pm 0.6) \times 10^{-3}$		1288
$\mathcal{T}(2S)\pi^+\pi^-$	$(7.8 \pm 1.3) \times 10^{-3}$		763
$\mathcal{T}(3S)\pi^+\pi^-$	$(4.8 \pm 1.9) \times 10^{-3}$		416
$\mathcal{T}(1S)K^+K^-$	$(6.1 \pm 1.8) \times 10^{-4}$		933

Inclusive Decays.

These decay modes are submodes of one or more of the decay modes above.

ϕ anything	$(13.8 \pm 2.4) \pm 1.7\%$	—
D^0 anything + c.c.	$(108 \pm 8)\%$	—
D_s anything + c.c.	$(47 \pm 6)\%$	—
J/ψ anything	$(2.06 \pm 0.21)\%$	—

7(11020)

$$J^G(J^{PC}) = 0^-(1^{--})$$

Mass $m = 11.019 \pm 0.008$ GeV

Full width $\Gamma = 79 \pm 16$ MeV

$\Gamma_{ee} = 0.130 \pm 0.030$ keV

7(11020) DECAY MODES	Fraction (Γ_i/Γ)	p (MeV/c)
e^+e^-	$(1.6 \pm 0.5) \times 10^{-6}$	5510

NOTES

In this Summary Table:

When a quantity has “(S = ...)” to its right, the error on the quantity has been enlarged by the “scale factor” S, defined as $S = \sqrt{\chi^2/(N-1)}$, where N is the number of measurements used in calculating the quantity. We do this when $S > 1$, which often indicates that the measurements are inconsistent. When $S > 1.25$, we also show in the Particle Listings an ideogram of the measurements. For more about S, see the Introduction.

A decay momentum p is given for each decay mode. For a 2-body decay, p is the momentum of each decay product in the rest frame of the decaying particle. For a 3-or-more-body decay, p is the largest momentum any of the products can have in this frame.

- [a] See the “Note on $\pi^\pm \rightarrow \ell^\pm \nu \gamma$ and $K^\pm \rightarrow \ell^\pm \nu \gamma$ Form Factors” in the π^\pm Particle Listings for definitions and details.
- [b] Measurements of $\Gamma(e^+ \nu_e)/\Gamma(\mu^+ \nu_\mu)$ always include decays with γ 's, and measurements of $\Gamma(e^+ \nu_e \gamma)$ and $\Gamma(\mu^+ \nu_\mu \gamma)$ never include low-energy γ 's. Therefore, since no clean separation is possible, we consider the modes with γ 's to be subreactions of the modes without them, and let $[\Gamma(e^+ \nu_e) + \Gamma(\mu^+ \nu_\mu)]/\Gamma_{\text{total}} = 100\%$.
- [c] See the π^\pm Particle Listings for the energy limits used in this measurement; low-energy γ 's are not included.
- [d] Derived from an analysis of neutrino-oscillation experiments.
- [e] Astrophysical and cosmological arguments give limits of order 10^{-13} ; see the π^0 Particle Listings.
- [f] Due to a new measurement in the average, this is 0.45 MeV larger than the mass we gave in our 2002 edition, 547.30 ± 0.12 MeV.
- [g] Due to removing an old measurement from the average, this is 0.11 keV larger than the width we gave in our 2002 edition, 1.18 ± 0.11 keV. See the $\Gamma(2\gamma)$ data block in the Data Listings.
- [h] C parity forbids this to occur as a single-photon process.
- [i] See the “Note on scalar mesons” in the $f_0(1370)$ Particle Listings. The interpretation of this entry as a particle is controversial.

[j] See the “Note on $\rho(770)$ ” in the $\rho(770)$ Particle Listings.

[k] The $\omega\rho$ interference is then due to $\omega\rho$ mixing only, and is expected to be small. If $e\mu$ universality holds, $\Gamma(\rho^0 \rightarrow \mu^+ \mu^-) = \Gamma(\rho^0 \rightarrow e^+ e^-) \times 0.99785$.

[l] See the “Note on scalar mesons” in the $f_0(1370)$ Particle Listings.

[m] See the “Note on $a_1(1260)$ ” in the $a_1(1260)$ Particle Listings in PDG 06, Journal of Physics, G **33** 1 (2006).

[n] This is only an educated guess; the error given is larger than the error on the average of the published values. See the Particle Listings for details.

[o] See the “Note on non- $q\bar{q}$ mesons” in the Particle Listings in PDG 06, Journal of Physics, G **33** 1 (2006).

[p] See the “Note on the $\eta(1405)$ ” in the $\eta(1405)$ Particle Listings.

[q] See the “Note on the $f_1(1420)$ ” in the $\eta(1405)$ Particle Listings.

[r] See also the $\omega(1650)$ Particle Listings.

[s] See the “Note on the $\rho(1450)$ and the $\rho(1700)$ ” in the $\rho(1700)$ Particle Listings.

[t] See also the $\omega(1420)$ Particle Listings.

[u] See the “Note on $f_0(1710)$ ” in the $f_0(1710)$ Particle Listings in 2004 edition of *Review of Particle Physics*.

[v] See the note in the K^\pm Particle Listings.

[w] The definition of the slope parameter g of the $K \rightarrow 3\pi$ Dalitz plot is as follows (see also “Note on Dalitz Plot Parameters for $K \rightarrow 3\pi$ Decays” in the K^\pm Particle Listings):

$$|M|^2 = 1 + g(s_3 - s_0)/m_{\pi^+}^2 + \dots$$

[x] For more details and definitions of parameters see the Particle Listings.

[y] Most of this radiative mode, the low-momentum γ part, is also included in the parent mode listed without γ 's.

[z] See the K^\pm Particle Listings for the energy limits used in this measurement.

[aa] Structure-dependent part.

[bb] Direct-emission branching fraction.

[cc] Violates angular-momentum conservation.

[dd] Derived from measured values of ϕ_{+-} , ϕ_{00} , $|\eta|$, $|m_{K_L^0} - m_{K_S^0}|$, and $\tau_{K_S^0}$, as described in the introduction to “Tests of Conservation Laws.”

[ee] The CP -violation parameters are defined as follows (see also “Note on CP Violation in $K_S \rightarrow 3\pi$ ” and “Note on CP Violation in K_L^0 Decay” in the Particle Listings):

$$\eta_{+-} = |\eta_{+-}| e^{i\phi_{+-}} = \frac{A(K_L^0 \rightarrow \pi^+ \pi^-)}{A(K_S^0 \rightarrow \pi^+ \pi^-)} = \epsilon + \epsilon'$$

$$\eta_{00} = |\eta_{00}| e^{i\phi_{00}} = \frac{A(K_L^0 \rightarrow \pi^0 \pi^0)}{A(K_S^0 \rightarrow \pi^0 \pi^0)} = \epsilon - 2\epsilon'$$

$$\delta = \frac{\Gamma(K_L^0 \rightarrow \pi^- \ell^+ \nu) - \Gamma(K_L^0 \rightarrow \pi^+ \ell^- \nu)}{\Gamma(K_L^0 \rightarrow \pi^- \ell^+ \nu) + \Gamma(K_L^0 \rightarrow \pi^+ \ell^- \nu)}$$

$$\text{Im}(\eta_{+-0})^2 = \frac{\Gamma(K_S^0 \rightarrow \pi^+ \pi^- \pi^0)^{CP \text{ viol.}}}{\Gamma(K_L^0 \rightarrow \pi^+ \pi^- \pi^0)}$$

$$\text{Im}(\eta_{000})^2 = \frac{\Gamma(K_S^0 \rightarrow \pi^0 \pi^0 \pi^0)}{\Gamma(K_L^0 \rightarrow \pi^0 \pi^0 \pi^0)}$$

where for the last two relations CPT is assumed valid, i.e., $\text{Re}(\eta_{+-0}) \simeq 0$ and $\text{Re}(\eta_{000}) \simeq 0$.

[ff] See the K_S^0 Particle Listings for the energy limits used in this measurement.

[gg] The value is for the sum of the charge states or particle/antiparticle states indicated.

[hh] $\text{Re}(\epsilon'/\epsilon) = \epsilon'/\epsilon$ to a very good approximation provided the phases satisfy CPT invariance.

[ii] This mode includes gammas from inner bremsstrahlung but not the direct emission mode $K_L^0 \rightarrow \pi^+ \pi^- \gamma(\text{DE})$.

[jj] See the K_L^0 Particle Listings for the energy limits used in this measurement.

[kk] Allowed by higher-order electroweak interactions.

[ll] Violates CP in leading order. Test of direct CP violation since the indirect CP -violating and CP -conserving contributions are expected to be suppressed.

Meson Summary Table

- [*mm*] See the “Note on $f_0(1370)$ ” in the $f_0(1370)$ Particle Listings and in the 1994 edition.
- [*nn*] See the note in the $L(1770)$ Particle Listings in Reviews of Modern Physics **56** S1 (1984), p. S200. See also the “Note on $K_2(1770)$ and the $K_2(1820)$ ” in the $K_2(1770)$ Particle Listings .
- [*oo*] See the “Note on $K_2(1770)$ and the $K_2(1820)$ ” in the $K_2(1770)$ Particle Listings .
- [*pp*] This result applies to $Z^0 \rightarrow c\bar{c}$ decays only. Here ℓ^+ is an average (not a sum) of e^+ and μ^+ decays.
- [*qq*] The branching fraction for this mode may differ from the sum of the submodes that contribute to it, due to interference effects. See the relevant papers in the Particle Listings.
- [*rr*] These subfractions of the $K^- \pi^+ \pi^+$ mode are uncertain: see the Particle Listings.
- [*ss*] The two experiments measuring this fraction are in serious disagreement. See the Particle Listings.
- [*tt*] This is *not* a test for the $\Delta C=1$ weak neutral current, but leads to the $\pi^+ e^+ e^-$ final state.
- [*uu*] This mode is not a useful test for a $\Delta C=1$ weak neutral current because both quarks must change flavor in this decay.
- [*vv*] This value is obtained by subtracting the branching fractions for 2-, 4- and 6-prongs from unity.
- [*ww*] This is the sum of our $K^- \pi^+ \pi^+ \pi^-$, $K^- \pi^+ \pi^+ \pi^- \pi^0$, $\bar{K}^0 2\pi^+ 2\pi^-$, $2\pi^+ 2\pi^-$, $2\pi^+ 2\pi^- \pi^0$, $K^+ K^- \pi^+ \pi^-$, and $K^+ K^- \pi^+ \pi^- \pi^0$, branching fractions.
- [*xx*] The branching fractions for the $K^- e^+ \nu_e$, $K^*(892)^- e^+ \nu_e$, $\pi^- e^+ \nu_e$, and $\rho^- e^+ \nu_e$ modes add up to 6.24 ± 0.18 %.
- [*yy*] This is a doubly Cabibbo-suppressed mode.
- [*zz*] This branching fraction includes all the decay modes of the resonance in the final state.
- [*aaa*] The experiments on the division of this charge mode amongst its submodes disagree, and the submode branching fractions here add up to considerably more than the charged-mode fraction.
- [*bbb*] However, these upper limits are in serious disagreement with values obtained in another experiment.
- [*ccc*] See the Particle Listings for the (complicated) definition of this quantity.
- [*ddd*] This fraction includes η from η' decays.
- [*eee*] For now, we average together measurements of the $X e^+ \nu_e$ and $X \mu^+ \nu_\mu$ branching fractions. This is the *average*, not the *sum*.
- [*fff*] We decouple the $D_s^+ \rightarrow \phi \pi^+$ branching fraction obtained from mass projections (and used to get some of the other branching fractions) from the $D_s^+ \rightarrow \phi \pi^+$, $\phi \rightarrow K^+ K^-$ branching fraction obtained from the Dalitz-plot analysis of $D_s^+ \rightarrow K^+ K^- \pi^+$. That is, the ratio of these two branching fractions is not exactly the $\phi \rightarrow K^+ K^-$ branching fraction 0.491.
- [*ggg*] This branching fraction includes all the decay modes of the final-state resonance.
- [*hhh*] This comes from a K -matrix parametrization of the $\pi^+ \pi^-$ S -wave and is a sum over the $f_0(980)$, $f_0(1300)$, $f_0(1200-1600)$, $f_0(1500)$, and $f_0(1750)$. Not all of these correspond to particles in our Tables.
- [*iii*] An ℓ indicates an e or a μ mode, not a sum over these modes.
- [*jjj*] An $CP(\pm 1)$ indicates the $CP=+1$ and $CP=-1$ eigenstates of the $D^0-\bar{D}^0$ system.
- [*kkk*] D denotes D^0 or \bar{D}^0 .
- [*lll*] \bar{D}^{*} represents an excited state with mass $2.2 < M < 2.8$ GeV/ c^2 .
- [*mmm*] $X(3872)^+$ is a hypothetical charged partner of the $X(3872)$.
- [*nnn*] $\Theta(1710)^{++}$ is a possible narrow pentaquark state and $G(2220)$ is a possible glueball resonance.
- [*ooo*] $(\bar{A}_c^- p)_s$ denotes a low-mass enhancement near 3.35 GeV/ c^2 .
- [*ppp*] Stands for the possible candidates of $K^*(1410)$, $K_0^*(1430)$ and $K_2^*(1430)$.
- [*qqq*] B^0 and B_s^0 contributions not separated. Limit is on weighted average of the two decay rates.
- [*rrr*] This decay refers to the coherent sum of resonant and nonresonant $J^P = 0^+ K \pi$ components with $1.60 < m_{K\pi} < 2.15$ GeV/ c^2 .
- [*sss*] $\Theta(1540)^+$ denotes a possible narrow pentaquark state.
- [*ttt*] These values are model dependent.
- [*uuu*] Here “anything” means at least one particle observed.
- [*vvv*] D^{**} stands for the sum of the $D(1^1P_1)$, $D(1^3P_0)$, $D(1^3P_1)$, $D(1^3P_2)$, $D(2^1S_0)$, and $D(2^1S_1)$ resonances.
- [*www*] $D^{(*)}\bar{D}^{(*)}$ stands for the sum of $D^*\bar{D}^*$, $D^*\bar{D}$, $D\bar{D}^*$, and $D\bar{D}$.
- [*xxx*] $X(3945)$ denotes a near-threshold enhancement in the $\omega J/\psi$ mass spectrum.
- [*yyy*] Inclusive branching fractions have a multiplicity definition and can be greater than 100%.
- [*zzz*] D_j represents an unresolved mixture of pseudoscalar and tensor D^{**} (P -wave) states.
- [*aaa*] Not a pure measurement. See note at head of B_s^0 Decay Modes.
- [*bbb*] Includes $p\bar{p}\pi^+\pi^-\gamma$ and excludes $p\bar{p}\eta$, $p\bar{p}\omega$, $p\bar{p}\eta'$.
- [*cccc*] J^{PC} known by production in e^+e^- via single photon annihilation. I^G is not known; interpretation of this state as a single resonance is unclear because of the expectation of substantial threshold effects in this energy region.
- [*ddd*] See COAN 06 for details.
- [*eeee*] X = pseudoscalar with $m < 7.2$ GeV
- [*fff*] $X\bar{X}$ = vectors with $m < 3.1$ GeV
- [*gggg*] $1.5 \text{ GeV} < m_X < 5.0 \text{ GeV}$
- [*hhhh*] Spectroscopic labeling for these states is theoretical, pending experimental information.
- [*iiii*] $1.5 \text{ GeV} < m_X < 5.0 \text{ GeV}$
- [*jjjj*] $1.5 \text{ GeV} < m_X < 5.0 \text{ GeV}$

Meson Summary Table

See also the table of suggested $q\bar{q}$ quark-model assignments in the Quark Model section.

• Indicates particles that appear in the preceding Meson Summary Table. We do not regard the other entries as being established.

LIGHT UNFLAVORED ($S = C = B = 0$)		STRANGE ($S = \pm 1, C = B = 0$)		CHARMED, STRANGE ($C = S = \pm 1$)		$c\bar{c}$ $I^G(J^{PC})$	
$I^G(J^{PC})$	$I^G(J^{PC})$		$I(J^P)$		$I(J^P)$		
• π^\pm 1 ⁻ (0 ⁻)	• $\phi(1680)$ 0 ⁻ (1 ⁻ -)	• K^\pm 1/2(0 ⁻)	• K^\pm 1/2(0 ⁻)	• D_s^\pm 0(0 ⁻)	• $\eta_c(1S)$ 0 ⁺ (0 ⁻ +	• $J/\psi(1S)$ 0 ⁻ (1 ⁻ -)	
• π^0 1 ⁻ (0 ⁻ +	• $\rho_3(1690)$ 1 ⁺ (3 ⁻ -)	• K^0 1/2(0 ⁻)	• K^0 1/2(0 ⁻)	• $D_s^{*\pm}$ 0(? [?])	• $\chi_{c0}(1P)$ 0 ⁺ (0 ⁺ +	• $\chi_{c0}(1P)$ 0 ⁺ (0 ⁺ +	
• η 0 ⁺ (0 ⁻ +	• $\rho(1700)$ 1 ⁺ (1 ⁻ -)	• K_S^0 1/2(0 ⁻)	• K_S^0 1/2(0 ⁻)	• $D_{s0}^*(2317)^\pm$ 0(0 ⁺)	• $\chi_{c1}(1P)$ 0 ⁺ (1 ⁺ +	• $\chi_{c1}(1P)$ 0 ⁺ (1 ⁺ +	
• $f_0(600)$ 0 ⁺ (0 ⁺ +	• $a_2(1700)$ 1 ⁻ (2 ⁺ +	• K_L^0 1/2(0 ⁻)	• K_L^0 1/2(0 ⁻)	• $D_{s1}(2460)^\pm$ 0(1 ⁺)	• $h_c(1P)$? [?] (1 ⁺ -)	• $h_c(1P)$? [?] (1 ⁺ -)	
• $\rho(770)$ 1 ⁺ (1 ⁻ -)	• $f_0(1710)$ 0 ⁺ (0 ⁺ +	• $K_0^*(800)$ 1/2(0 ⁺)	• $K_0^*(800)$ 1/2(0 ⁺)	• $D_{s1}(2536)^\pm$ 0(1 ⁺)	• $\chi_{c2}(1P)$ 0 ⁺ (2 ⁺ +	• $\chi_{c2}(1P)$ 0 ⁺ (2 ⁺ +	
• $\omega(782)$ 0 ⁻ (1 ⁻ -)	• $\eta(1760)$ 0 ⁺ (0 ⁻ +	• $K^*(892)$ 1/2(1 ⁻)	• $K^*(892)$ 1/2(1 ⁻)	• $D_{s2}(2573)^\pm$ 0(? [?])	• $\eta_c(2S)$ 0 ⁺ (0 ⁻ +	• $\eta_c(2S)$ 0 ⁺ (0 ⁻ +	
• $\eta'(958)$ 0 ⁺ (0 ⁻ +	• $\pi(1800)$ 1 ⁻ (0 ⁻ +	• $K_1(1270)$ 1/2(1 ⁺)	• $K_1(1270)$ 1/2(1 ⁺)	• $D_{s1}(2700)^\pm$ 0(1 ⁻)	• $\psi(2S)$ 0 ⁻ (1 ⁻ -)	• $\psi(2S)$ 0 ⁻ (1 ⁻ -)	
• $f_0(980)$ 0 ⁺ (0 ⁺ +	• $f_2(1810)$ 0 ⁺ (2 ⁺ +	• $K_1(1400)$ 1/2(1 ⁺)	• $K_1(1400)$ 1/2(1 ⁺)		• $\psi(3770)$ 0 ⁻ (1 ⁻ -)	• $\psi(3770)$ 0 ⁻ (1 ⁻ -)	
• $a_0(980)$ 1 ⁻ (0 ⁺ +	• $X(1835)$? [?] (? ⁻ +	• $K^*(1410)$ 1/2(1 ⁻)	• $K^*(1410)$ 1/2(1 ⁻)		• $X(3872)$ 0 [?] (? [?] ?)	• $X(3872)$ 0 [?] (? [?] ?)	
• $\phi(1020)$ 0 ⁻ (1 ⁻ -)	• $\phi_3(1850)$ 0 ⁻ (3 ⁻ -)	• $K_0^*(1430)$ 1/2(0 ⁺)	• $K_0^*(1430)$ 1/2(0 ⁺)	BOTTOM ($B = \pm 1$)			
• $h_1(1170)$ 0 ⁻ (1 ⁺ -)	• $\eta_2(1870)$ 0 ⁺ (2 ⁻ +	• $K_2^*(1430)$ 1/2(2 ⁺)	• $K_2^*(1430)$ 1/2(2 ⁺)	• B^\pm 1/2(0 ⁻)	• $\chi_{c2}(2P)$ 0 ⁺ (2 ⁺ +	• $\chi_{c2}(2P)$ 0 ⁺ (2 ⁺ +	
• $b_1(1235)$ 1 ⁺ (1 ⁺ -)	• $\pi_2(1880)$ 1 ⁻ (2 ⁻ +	• $K(1460)$ 1/2(0 ⁻)	• $K(1460)$ 1/2(0 ⁻)	• B^0 1/2(0 ⁻)	• $X(3940)$? [?] (? [?] ?)	• $X(3940)$? [?] (? [?] ?)	
• $a_1(1260)$ 1 ⁻ (1 ⁺ +	• $\rho(1900)$ 1 ⁺ (1 ⁻ -)	• $K_2(1580)$ 1/2(2 ⁻)	• $K_2(1580)$ 1/2(2 ⁻)	• B^\pm/B^0 ADMIXTURE		• $\psi(4040)$ 0 ⁻ (1 ⁻ -)	
• $f_2(1270)$ 0 ⁺ (2 ⁺ +	• $f_2(1910)$ 0 ⁺ (2 ⁺ +	• $K(1630)$ 1/2(? [?])	• $K(1630)$ 1/2(? [?])	• $B^\pm/B^0/B_s^0/b$ -baryon ADMIXTURE		• $\psi(4160)$ 0 ⁻ (1 ⁻ -)	
• $f_1(1285)$ 0 ⁺ (1 ⁺ +	• $f_2(1950)$ 0 ⁺ (2 ⁺ +	• $K_1(1650)$ 1/2(1 ⁺)	• $K_1(1650)$ 1/2(1 ⁺)	• V_{cb} and V_{ub} CKM Matrix Elements		• $X(4260)$? [?] (1 ⁻ -)	
• $\eta(1295)$ 0 ⁺ (0 ⁻ +	• $\rho_3(1990)$ 1 ⁺ (3 ⁻ -)	• $K^*(1680)$ 1/2(1 ⁻)	• $K^*(1680)$ 1/2(1 ⁻)	• B^* 1/2(1 ⁻)	• $X(4360)$? [?] (1 ⁻ -)	• $X(4360)$? [?] (1 ⁻ -)	
• $\pi(1300)$ 1 ⁻ (0 ⁻ +	• $f_2(2010)$ 0 ⁺ (2 ⁺ +	• $K_2(1770)$ 1/2(2 ⁻)	• $K_2(1770)$ 1/2(2 ⁻)	• B_s^* 1/2(1 ⁻)	• $\psi(4415)$ 0 ⁻ (1 ⁻ -)	• $\psi(4415)$ 0 ⁻ (1 ⁻ -)	
• $a_2(1320)$ 1 ⁻ (2 ⁺ +	• $f_0(2020)$ 0 ⁺ (0 ⁺ +	• $K_3^*(1780)$ 1/2(3 ⁻)	• $K_3^*(1780)$ 1/2(3 ⁻)	• B_s^* (5732) ?(? [?])			
• $f_0(1370)$ 0 ⁺ (0 ⁺ +	• $a_4(2040)$ 1 ⁻ (4 ⁺ +	• $K_2(1820)$ 1/2(2 ⁻)	• $K_2(1820)$ 1/2(2 ⁻)	• $B_1(5721)^0$ 1/2(1 ⁺)	$b\bar{b}$		
• $h_1(1380)$? ⁻ (1 ⁺ -)	• $f_4(2050)$ 0 ⁺ (4 ⁺ +	• $K(1830)$ 1/2(0 ⁻)	• $K(1830)$ 1/2(0 ⁻)	• $B_2^*(5747)^0$ 1/2(2 ⁺)	• $\eta_b(1S)$ 0 ⁺ (0 ⁻ +	• $\eta_b(1S)$ 0 ⁺ (0 ⁻ +	
• $\pi_1(1400)$ 1 ⁻ (1 ⁻ +	• $\pi_2(2100)$ 1 ⁻ (2 ⁻ +	• $K_0^*(1950)$ 1/2(0 ⁺)	• $K_0^*(1950)$ 1/2(0 ⁺)	BOTTOM, STRANGE ($B = \pm 1, S = \mp 1$)		• $\mathcal{T}(1S)$ 0 ⁻ (1 ⁻ -)	
• $\eta(1405)$ 0 ⁺ (0 ⁻ +	• $f_0(2100)$ 0 ⁺ (0 ⁺ +	• $K_2^*(1980)$ 1/2(2 ⁺)	• $K_2^*(1980)$ 1/2(2 ⁺)	• B_s^0 0(0 ⁻)	• $\chi_{b0}(1P)$ 0 ⁺ (0 ⁺ +	• $\chi_{b0}(1P)$ 0 ⁺ (0 ⁺ +	
• $f_1(1420)$ 0 ⁺ (1 ⁺ +	• $f_2(2150)$ 0 ⁺ (2 ⁺ +	• $K_4^*(2045)$ 1/2(4 ⁺)	• $K_4^*(2045)$ 1/2(4 ⁺)	• B_s^* 0(1 ⁻)	• $\chi_{b1}(1P)$ 0 ⁺ (1 ⁺ +	• $\chi_{b1}(1P)$ 0 ⁺ (1 ⁺ +	
• $\omega(1420)$ 0 ⁻ (1 ⁻ -)	• $\rho(2150)$ 1 ⁺ (1 ⁻ -)	• $K_2(2250)$ 1/2(2 ⁻)	• $K_2(2250)$ 1/2(2 ⁻)	• $B_{s1}(5830)^0$ 1/2(1 ⁺)	• $\chi_{b2}(1P)$ 0 ⁺ (2 ⁺ +	• $\chi_{b2}(1P)$ 0 ⁺ (2 ⁺ +	
• $f_2(1430)$ 0 ⁺ (2 ⁺ +	• $\phi(2170)$ 0 ⁻ (1 ⁻ -)	• $K_3(2320)$ 1/2(3 ⁺)	• $K_3(2320)$ 1/2(3 ⁺)	• $B_{s2}^*(5840)^0$ 1/2(2 ⁺)	• $\mathcal{T}(2S)$ 0 ⁻ (1 ⁻ -)	• $\mathcal{T}(2S)$ 0 ⁻ (1 ⁻ -)	
• $a_0(1450)$ 1 ⁻ (0 ⁺ +	• $f_0(2200)$ 0 ⁺ (0 ⁺ +	• $K_5(2380)$ 1/2(5 ⁻)	• $K_5(2380)$ 1/2(5 ⁻)	• $B_{sJ}^*(5850)$?(? [?])	• $\mathcal{T}(1D)$ 0 ⁻ (2 ⁻ -)	• $\mathcal{T}(1D)$ 0 ⁻ (2 ⁻ -)	
• $\rho(1450)$ 1 ⁺ (1 ⁻ -)	• $f_j(2220)$ 0 ⁺ (2 ⁺ +	• $K_4(2500)$ 1/2(4 ⁻)	• $K_4(2500)$ 1/2(4 ⁻)		• $\chi_{b0}(2P)$ 0 ⁺ (0 ⁺ +	• $\chi_{b0}(2P)$ 0 ⁺ (0 ⁺ +	
• $\eta(1475)$ 0 ⁺ (0 ⁻ +	or 4 ⁺ +	• $K(3100)$? [?] (? [?] ?)	• $K(3100)$? [?] (? [?] ?)	BOTTOM, CHARMED ($B = C = \pm 1$)		• $\chi_{b1}(2P)$ 0 ⁺ (1 ⁺ +	
• $f_0(1500)$ 0 ⁺ (0 ⁺ +	• $\eta(2225)$ 0 ⁺ (0 ⁻ +	CHARMED ($C = \pm 1$)		• B_c^\pm 0(0 ⁻)	• $\mathcal{T}(3S)$ 0 ⁻ (1 ⁻ -)	• $\mathcal{T}(3S)$ 0 ⁻ (1 ⁻ -)	
• $f_1(1510)$ 0 ⁺ (1 ⁺ +	• $\rho_3(2250)$ 1 ⁺ (3 ⁻ -)	• D^\pm 1/2(0 ⁻)	• D^\pm 1/2(0 ⁻)		• $\mathcal{T}(4S)$ 0 ⁻ (1 ⁻ -)	• $\mathcal{T}(4S)$ 0 ⁻ (1 ⁻ -)	
• $f_2'(1525)$ 0 ⁺ (2 ⁺ +	• $f_2(2300)$ 0 ⁺ (2 ⁺ +	• $D^*(2007)^0$ 1/2(1 ⁻)	• $D^*(2007)^0$ 1/2(1 ⁻)		• $\mathcal{T}(10860)$ 0 ⁻ (1 ⁻ -)	• $\mathcal{T}(10860)$ 0 ⁻ (1 ⁻ -)	
• $f_2(1565)$ 0 ⁺ (2 ⁺ +	• $f_4(2300)$ 0 ⁺ (4 ⁺ +	• $D^*(2010)^\pm$ 1/2(1 ⁻)	• $D^*(2010)^\pm$ 1/2(1 ⁻)		• $\mathcal{T}(11020)$ 0 ⁻ (1 ⁻ -)	• $\mathcal{T}(11020)$ 0 ⁻ (1 ⁻ -)	
• $\rho(1570)$ 1 ⁺ (1 ⁻ -)	• $f_0(2330)$ 0 ⁺ (0 ⁺ +	• $D_0^*(2400)^0$ 1/2(0 ⁺)	• $D_0^*(2400)^0$ 1/2(0 ⁺)		NON- $q\bar{q}$ CANDIDATES		
• $h_1(1595)$ 0 ⁻ (1 ⁺ -)	• $f_2(2340)$ 0 ⁺ (2 ⁺ +	• $D_0^*(2400)^\pm$ 1/2(0 ⁺)	• $D_0^*(2400)^\pm$ 1/2(0 ⁺)		Non- $q\bar{q}$ candidates		
• $\pi_1(1600)$ 1 ⁻ (1 ⁻ +	• $\rho_5(2350)$ 1 ⁺ (5 ⁻ -)	• $D_1(2420)^0$ 1/2(1 ⁺)	• $D_1(2420)^0$ 1/2(1 ⁺)				
• $a_1(1640)$ 1 ⁻ (1 ⁺ +	• $a_6(2450)$ 1 ⁻ (6 ⁺ +	• $D_1(2420)^\pm$ 1/2(? [?])	• $D_1(2420)^\pm$ 1/2(? [?])				
• $f_2(1640)$ 0 ⁺ (2 ⁺ +	• $f_6(2510)$ 0 ⁺ (6 ⁺ +	• $D_1(2430)^0$ 1/2(1 ⁺)	• $D_1(2430)^0$ 1/2(1 ⁺)				
• $\eta_2(1645)$ 0 ⁺ (2 ⁻ +	OTHER LIGHT		• $D_2^*(2460)^0$ 1/2(2 ⁺)	• $D_2^*(2460)^0$ 1/2(2 ⁺)			
• $\omega(1650)$ 0 ⁻ (1 ⁻ -)	Further States		• $D_2^*(2460)^\pm$ 1/2(2 ⁺)	• $D_2^*(2460)^\pm$ 1/2(2 ⁺)			
• $\omega_3(1670)$ 0 ⁻ (3 ⁻ -)		• $D^*(2640)^\pm$ 1/2(? [?])	• $D^*(2640)^\pm$ 1/2(? [?])				
• $\pi_2(1670)$ 1 ⁻ (2 ⁻ -)							

Baryon Summary Table

This short table gives the name, the quantum numbers (where known), and the status of baryons in the Review. Only the baryons with 3- or 4-star status are included in the main Baryon Summary Table. Due to insufficient data or uncertain interpretation, the other entries in the short table are not established baryons. The names with masses are of baryons that decay strongly. For Λ , Δ , and Ξ resonances, the πN partial wave is indicated by the symbol $L_{2l,2J}$, where L is the orbital angular momentum (S, P, D, \dots), l is the isospin, and J is the total angular momentum. For Λ and Σ resonances, the $\bar{K}N$ partial wave is labeled $L_{l,2J}$. The nucleon is a pole in the P_{11} wave, and similar comments apply to the Λ and Σ .

p	P_{11}	****	$\Delta(1232)$	P_{33}	****	Σ^+	P_{11}	****	Ξ^0	P_{11}	****	Λ_c^+	****
n	P_{11}	****	$\Delta(1600)$	P_{33}	***	Σ^0	P_{11}	****	Ξ^-	P_{11}	****	$\Lambda_c(2595)^+$	***
$N(1440)$	P_{11}	****	$\Delta(1620)$	S_{31}	****	Σ^-	P_{11}	****	$\Xi(1530)$	P_{13}	****	$\Lambda_c(2625)^+$	***
$N(1520)$	D_{13}	****	$\Delta(1700)$	D_{33}	****	$\Sigma(1385)$	P_{13}	****	$\Xi(1620)$	*		$\Lambda_c(2765)^+$	*
$N(1535)$	S_{11}	****	$\Delta(1750)$	P_{31}	*	$\Sigma(1480)$		*	$\Xi(1690)$	***		$\Lambda_c(2880)^+$	***
$N(1650)$	S_{11}	****	$\Delta(1900)$	S_{31}	**	$\Sigma(1560)$		**	$\Xi(1820)$	D_{13}	***	$\Lambda_c(2940)^+$	***
$N(1675)$	D_{15}	****	$\Delta(1905)$	F_{35}	****	$\Sigma(1580)$	D_{13}	*	$\Xi(1950)$	***		$\Sigma_c(2455)$	****
$N(1680)$	F_{15}	****	$\Delta(1910)$	P_{31}	****	$\Sigma(1620)$	S_{11}	**	$\Xi(2030)$	***		$\Sigma_c(2520)$	***
$N(1700)$	D_{13}	***	$\Delta(1920)$	P_{33}	***	$\Sigma(1660)$	P_{11}	***	$\Xi(2120)$	*		$\Sigma_c(2800)$	***
$N(1710)$	P_{11}	***	$\Delta(1930)$	D_{35}	***	$\Sigma(1670)$	D_{13}	****	$\Xi(2250)$	**		Ξ_c^+	***
$N(1720)$	P_{13}	****	$\Delta(1940)$	D_{33}	*	$\Sigma(1690)$		**	$\Xi(2370)$	**		Ξ_c^0	***
$N(1900)$	P_{13}	**	$\Delta(1950)$	F_{37}	****	$\Sigma(1750)$	S_{11}	***	$\Xi(2500)$	*		$\Xi_c^{'+}$	***
$N(1990)$	F_{17}	**	$\Delta(2000)$	F_{35}	**	$\Sigma(1770)$	P_{11}	*				Ξ_c^0	***
$N(2000)$	F_{15}	**	$\Delta(2150)$	S_{31}	*	$\Sigma(1775)$	D_{15}	****	Ω^-	****		$\Xi_c(2645)$	***
$N(2080)$	D_{13}	**	$\Delta(2200)$	G_{37}	*	$\Sigma(1840)$	P_{13}	*	$\Omega(2250)^-$	***		$\Xi_c(2790)$	***
$N(2090)$	S_{11}	*	$\Delta(2300)$	H_{39}	**	$\Sigma(1880)$	P_{11}	**	$\Omega(2380)^-$	**		$\Xi_c(2815)$	***
$N(2100)$	P_{11}	*	$\Delta(2350)$	D_{35}	*	$\Sigma(1915)$	F_{15}	****	$\Omega(2470)^-$	**		$\Xi_c(2930)$	*
$N(2190)$	G_{17}	****	$\Delta(2390)$	F_{37}	*	$\Sigma(1940)$	D_{13}	***				$\Xi_c(2980)$	***
$N(2200)$	D_{15}	**	$\Delta(2400)$	G_{39}	**	$\Sigma(2000)$	S_{11}	*				$\Xi_c(3055)$	**
$N(2220)$	H_{19}	****	$\Delta(2420)$	$H_{3,11}$	****	$\Sigma(2030)$	F_{17}	****				$\Xi_c(3080)$	***
$N(2250)$	G_{19}	****	$\Delta(2750)$	$l_{3,13}$	**	$\Sigma(2070)$	F_{15}	*				$\Xi_c(3123)$	*
$N(2600)$	$l_{1,11}$	***	$\Delta(2950)$	$K_{3,15}$	**	$\Sigma(2080)$	P_{13}	**				Ω_c^0	***
$N(2700)$	$K_{1,13}$	**				$\Sigma(2100)$	G_{17}	*				$\Omega_c(2770)^0$	***
			Λ	P_{01}	****	$\Sigma(2250)$		***					
			$\Lambda(1405)$	S_{01}	****	$\Sigma(2455)$		**				Ξ_{cc}^+	*
			$\Lambda(1520)$	D_{03}	****	$\Sigma(2620)$		**					
			$\Lambda(1600)$	P_{01}	***	$\Sigma(3000)$		*				Λ_b^0	***
			$\Lambda(1670)$	S_{01}	****	$\Sigma(3170)$		*				Σ_b	***
			$\Lambda(1690)$	D_{03}	****							Σ_b^*	***
			$\Lambda(1800)$	S_{01}	***							Ξ_b^0, Ξ_b^-	***
			$\Lambda(1810)$	P_{01}	***								
			$\Lambda(1820)$	F_{05}	****								
			$\Lambda(1830)$	D_{05}	****								
			$\Lambda(1890)$	P_{03}	****								
			$\Lambda(2000)$		*								
			$\Lambda(2020)$	F_{07}	*								
			$\Lambda(2100)$	G_{07}	****								
			$\Lambda(2110)$	F_{05}	***								
			$\Lambda(2325)$	D_{03}	*								
			$\Lambda(2350)$	H_{09}	***								
			$\Lambda(2585)$		**								

**** Existence is certain, and properties are at least fairly well explored.

*** Existence ranges from very likely to certain, but further confirmation is desirable and/or quantum numbers, branching fractions, etc. are not well determined.

** Evidence of existence is only fair.

* Evidence of existence is poor.

Baryon Summary Table

N BARYONS ($S = 0, I = 1/2$)

$$p, N^+ = uud; \quad n, N^0 = udd$$

p

$$I(J^P) = \frac{1}{2}(\frac{1}{2}^+)$$

Mass $m = 1.00727646688 \pm 0.00000000013$ u

Mass $m = 938.27203 \pm 0.00008$ MeV [a]

$|m_p - m_{\bar{p}}|/m_p < 2 \times 10^{-9}$, CL = 90% [b]

$|\frac{q_p}{m_p} - \frac{q_{\bar{p}}}{m_{\bar{p}}}| = 0.99999999991 \pm 0.00000000009$

$|q_p + q_{\bar{p}}|/e < 2 \times 10^{-9}$, CL = 90% [b]

$|q_p + q_e|/e < 1.0 \times 10^{-21}$ [c]

Magnetic moment $\mu = 2.792847351 \pm 0.000000028 \mu_N$

$(\mu_p + \mu_{\bar{p}}) / \mu_p = (-2.6 \pm 2.9) \times 10^{-3}$

Electric dipole moment $d < 0.54 \times 10^{-23}$ e cm

Electric polarizability $\alpha = (12.0 \pm 0.6) \times 10^{-4}$ fm³

Magnetic polarizability $\beta = (1.9 \pm 0.5) \times 10^{-4}$ fm³

Charge radius = 0.875 ± 0.007 fm

Mean life $\tau > 2.1 \times 10^{29}$ years, CL = 90% ($p \rightarrow$ invisible mode)

Mean life $\tau > 10^{31}$ to 10^{33} years [d] (mode dependent)

See the "Note on Nucleon Decay" in our 1994 edition (Phys. Rev. **D50**, 1173) for a short review.

The "partial mean life" limits tabulated here are the limits on τ/B_i , where τ is the total mean life and B_i is the branching fraction for the mode in question. For N decays, p and n indicate proton and neutron partial lifetimes.

p DECAY MODES	Partial mean life (10 ³⁰ years)	Confidence level	p (MeV/c)
Antilepton + meson			
$N \rightarrow e^+ \pi$	> 158 (n), > 1600 (p)	90%	459
$N \rightarrow \mu^+ \pi$	> 100 (n), > 473 (p)	90%	453
$N \rightarrow \nu \pi$	> 112 (n), > 25 (p)	90%	459
$p \rightarrow e^+ \eta$	> 313	90%	309
$p \rightarrow \mu^+ \eta$	> 126	90%	297
$n \rightarrow \nu \eta$	> 158	90%	310
$N \rightarrow e^+ \rho$	> 217 (n), > 75 (p)	90%	149
$N \rightarrow \mu^+ \rho$	> 228 (n), > 110 (p)	90%	113
$N \rightarrow \nu \rho$	> 19 (n), > 162 (p)	90%	149
$p \rightarrow e^+ \omega$	> 107	90%	143
$p \rightarrow \mu^+ \omega$	> 117	90%	105
$n \rightarrow \nu \omega$	> 108	90%	144
$N \rightarrow e^+ K$	> 17 (n), > 150 (p)	90%	339
$p \rightarrow e^+ K_S^0$	> 120	90%	337
$p \rightarrow e^+ K_L^0$	> 51	90%	337
$N \rightarrow \mu^+ K$	> 26 (n), > 120 (p)	90%	329
$p \rightarrow \mu^+ K_S^0$	> 150	90%	326
$p \rightarrow \mu^+ K_L^0$	> 83	90%	326
$N \rightarrow \nu K$	> 86 (n), > 670 (p)	90%	339
$n \rightarrow \nu K_S^0$	> 51	90%	338
$p \rightarrow e^+ K^*(892)^0$	> 84	90%	45
$N \rightarrow \nu K^*(892)$	> 78 (n), > 51 (p)	90%	45
Antilepton + mesons			
$p \rightarrow e^+ \pi^+ \pi^-$	> 82	90%	448
$p \rightarrow e^+ \pi^0 \pi^0$	> 147	90%	449
$n \rightarrow e^+ \pi^- \pi^0$	> 52	90%	449
$p \rightarrow \mu^+ \pi^+ \pi^-$	> 133	90%	425
$p \rightarrow \mu^+ \pi^0 \pi^0$	> 101	90%	427
$n \rightarrow \mu^+ \pi^- \pi^0$	> 74	90%	427
$n \rightarrow e^+ K^0 \pi^-$	> 18	90%	319
Lepton + meson			
$n \rightarrow e^- \pi^+$	> 65	90%	459
$n \rightarrow \mu^- \pi^+$	> 49	90%	453
$n \rightarrow e^- \rho^+$	> 62	90%	150
$n \rightarrow \mu^- \rho^+$	> 7	90%	114
$n \rightarrow e^- K^+$	> 32	90%	340
$n \rightarrow \mu^- K^+$	> 57	90%	330

Lepton + mesons

$p \rightarrow e^- \pi^+ \pi^+$	> 30	90%	448
$n \rightarrow e^- \pi^+ \pi^0$	> 29	90%	449
$p \rightarrow \mu^- \pi^+ \pi^+$	> 17	90%	425
$n \rightarrow \mu^- \pi^+ \pi^0$	> 34	90%	427
$p \rightarrow e^- \pi^+ K^+$	> 75	90%	320
$p \rightarrow \mu^- \pi^+ K^+$	> 245	90%	279

Antilepton + photon(s)

$p \rightarrow e^+ \gamma$	> 670	90%	469
$p \rightarrow \mu^+ \gamma$	> 478	90%	463
$n \rightarrow \nu \gamma$	> 28	90%	470
$p \rightarrow e^+ \gamma \gamma$	> 100	90%	469
$n \rightarrow \nu \gamma \gamma$	> 219	90%	470

Three (or more) leptons

$p \rightarrow e^+ e^+ e^-$	> 793	90%	469
$p \rightarrow e^+ \mu^+ \mu^-$	> 359	90%	457
$p \rightarrow e^+ \nu \nu$	> 17	90%	469
$n \rightarrow e^+ e^- \nu$	> 257	90%	470
$n \rightarrow \mu^+ e^- \nu$	> 83	90%	464
$n \rightarrow \mu^+ \mu^- \nu$	> 79	90%	458
$p \rightarrow \mu^+ e^+ e^-$	> 529	90%	463
$p \rightarrow \mu^+ \mu^+ \mu^-$	> 675	90%	439
$p \rightarrow \mu^+ \nu \nu$	> 21	90%	463
$p \rightarrow e^- \mu^+ \mu^+$	> 6	90%	457
$n \rightarrow 3\nu$	> 0.0005	90%	470

Inclusive modes

$N \rightarrow e^+$ anything	> 0.6 (n, p)	90%	—
$N \rightarrow \mu^+$ anything	> 12 (n, p)	90%	—
$N \rightarrow e^+ \pi^0$ anything	> 0.6 (n, p)	90%	—

$\Delta B = 2$ dinucleon modes

The following are lifetime limits per iron nucleus.

$pp \rightarrow \pi^+ \pi^+$	> 0.7	90%	—
$pn \rightarrow \pi^+ \pi^0$	> 2	90%	—
$nn \rightarrow \pi^+ \pi^-$	> 0.7	90%	—
$nn \rightarrow \pi^0 \pi^0$	> 3.4	90%	—
$pp \rightarrow e^+ e^+$	> 5.8	90%	—
$pp \rightarrow e^+ \mu^+$	> 3.6	90%	—
$pp \rightarrow \mu^+ \mu^+$	> 1.7	90%	—
$pn \rightarrow e^+ \bar{\nu}$	> 2.8	90%	—
$pn \rightarrow \mu^+ \bar{\nu}$	> 1.6	90%	—
$nn \rightarrow \nu_e \bar{\nu}_e$	> 0.000049	90%	—
$pn \rightarrow$ invisible	> 2.1×10^{-5}	90%	—
$pp \rightarrow$ invisible	> 0.00005	90%	—

\bar{p} DECAY MODES

\bar{p} DECAY MODES	Partial mean life (years)	Confidence level	p (MeV/c)
$\bar{p} \rightarrow e^- \gamma$	> 7×10^5	90%	469
$\bar{p} \rightarrow \mu^- \gamma$	> 5×10^4	90%	463
$\bar{p} \rightarrow e^- \pi^0$	> 4×10^5	90%	459
$\bar{p} \rightarrow \mu^- \pi^0$	> 5×10^4	90%	453
$\bar{p} \rightarrow e^- \eta$	> 2×10^4	90%	309
$\bar{p} \rightarrow \mu^- \eta$	> 8×10^3	90%	297
$\bar{p} \rightarrow e^- K_S^0$	> 900	90%	337
$\bar{p} \rightarrow \mu^- K_S^0$	> 4×10^3	90%	326
$\bar{p} \rightarrow e^- K_L^0$	> 9×10^3	90%	337
$\bar{p} \rightarrow \mu^- K_L^0$	> 7×10^3	90%	326
$\bar{p} \rightarrow e^- \gamma \gamma$	> 2×10^4	90%	469
$\bar{p} \rightarrow \mu^- \gamma \gamma$	> 2×10^4	90%	463
$\bar{p} \rightarrow e^- \omega$	> 200	90%	143

Baryon Summary Table

n			
$I(J^P) = \frac{1}{2}(\frac{1}{2}^+)$			
Mass $m = 1.0086649156 \pm 0.0000000006$ u			
Mass $m = 939.56536 \pm 0.00008$ MeV [a]			
$m_n - m_p = 1.2933317 \pm 0.0000005$ MeV $= 0.0013884487 \pm 0.0000000006$ u			
Mean life $\tau = 885.7 \pm 0.8$ s $c\tau = 2.655 \times 10^8$ km			
Magnetic moment $\mu = -1.9130427 \pm 0.0000005$ μ_N			
Electric dipole moment $d < 0.29 \times 10^{-25}$ ecm, CL = 90%			
Mean-square charge radius $\langle r_n^2 \rangle = -0.1161 \pm 0.0022$ fm ² (S = 1.3)			
Electric polarizability $\alpha = (11.6 \pm 1.5) \times 10^{-4}$ fm ³			
Magnetic polarizability $\beta = (3.7 \pm 2.0) \times 10^{-4}$ fm ³			
Charge $q = (-0.4 \pm 1.1) \times 10^{-21}$ e			
Mean $n\bar{n}$ -oscillation time $> 8.6 \times 10^7$ s, CL = 90% (free n)			
Mean $n\bar{n}$ -oscillation time $> 1.3 \times 10^8$ s, CL = 90% [e] (bound n)			
Decay parameters [f]			
$p e^- \bar{\nu}_e$	$\lambda \equiv g_A / g_V = -1.2695 \pm 0.0029$	(S = 2.0)	
"	$A = -0.1173 \pm 0.0013$	(S = 2.3)	
"	$B = 0.9807 \pm 0.0030$		
"	$C = -0.2377 \pm 0.0026$		
"	$a = -0.103 \pm 0.004$		
"	$\phi_{AV} = (180.06 \pm 0.07)^\circ$	[g]	
"	$D = (-4 \pm 6) \times 10^{-4}$		
n DECAY MODES	Fraction (Γ_i/Γ)	Confidence level	ρ (MeV/c)
$p e^- \bar{\nu}_e$	100	%	1
$p e^- \bar{\nu}_e \gamma$	[h] $(3.13 \pm 0.35) \times 10^{-3}$		1
Charge conservation (Q) violating mode			
$p \nu_e \bar{\nu}_e$	Q	$< 8 \times 10^{-27}$	68% 1
$N(1440) P_{11}$			
$I(J^P) = \frac{1}{2}(\frac{1}{2}^+)$			
Breit-Wigner mass = 1420 to 1470 (≈ 1440) MeV			
Breit-Wigner full width = 200 to 450 (≈ 300) MeV			
$p_{\text{beam}} = 0.61$ GeV/c $4\pi\lambda^2 = 31.0$ mb			
Re(pole position) = 1350 to 1380 (≈ 1365) MeV			
$-2\text{Im}(\text{pole position}) = 160$ to 220 (≈ 190) MeV			
$N(1440)$ DECAY MODES	Fraction (Γ_i/Γ)	ρ (MeV/c)	
$N\pi$	0.55 to 0.75	398	
$N\pi\pi$	30-40 %	347	
$\Delta\pi$	20-30 %	147	
$N\rho$	< 8 %	†	
$N(\pi\pi)_{S\text{-wave}}^{I=0}$	5-10 %	-	
$p\gamma$	0.035-0.048 %	414	
$p\gamma$, helicity=1/2	0.035-0.048 %	414	
$n\gamma$	0.009-0.032 %	413	
$n\gamma$, helicity=1/2	0.009-0.032 %	413	
$N(1520) D_{13}$			
$I(J^P) = \frac{1}{2}(\frac{3}{2}^-)$			
Breit-Wigner mass = 1515 to 1525 (≈ 1520) MeV			
Breit-Wigner full width = 100 to 125 (≈ 115) MeV			
$p_{\text{beam}} = 0.74$ GeV/c $4\pi\lambda^2 = 23.5$ mb			
Re(pole position) = 1505 to 1515 (≈ 1510) MeV			
$-2\text{Im}(\text{pole position}) = 105$ to 120 (≈ 110) MeV			
$N(1520)$ DECAY MODES	Fraction (Γ_i/Γ)	ρ (MeV/c)	
$N\pi$	0.55 to 0.65	457	
$N\eta$	$(2.3 \pm 0.4) \times 10^{-3}$	154	
$N\pi\pi$	40-50 %	414	
$\Delta\pi$	15-25 %	230	
$N\rho$	15-25 %	†	
$N(\pi\pi)_{S\text{-wave}}^{I=0}$	< 8 %	-	
$p\gamma$	0.46-0.56 %	470	
$p\gamma$, helicity=1/2	0.001-0.034 %	470	
$p\gamma$, helicity=3/2	0.44-0.53 %	470	
$n\gamma$	0.30-0.53 %	470	
$n\gamma$, helicity=1/2	0.04-0.10 %	470	
$n\gamma$, helicity=3/2	0.25-0.45 %	470	
$N(1535) S_{11}$			
$I(J^P) = \frac{1}{2}(\frac{1}{2}^-)$			
Breit-Wigner mass = 1525 to 1545 (≈ 1535) MeV			
Breit-Wigner full width = 125 to 175 (≈ 150) MeV			
$p_{\text{beam}} = 0.76$ GeV/c $4\pi\lambda^2 = 22.5$ mb			
Re(pole position) = 1490 to 1530 (≈ 1510) MeV			
$-2\text{Im}(\text{pole position}) = 90$ to 250 (≈ 170) MeV			
$N(1535)$ DECAY MODES	Fraction (Γ_i/Γ)	ρ (MeV/c)	
$N\pi$	35-55 %	468	
$N\eta$	45-60 %	186	
$N\pi\pi$	1-10 %	426	
$\Delta\pi$	< 1 %	244	
$N\rho$	< 4 %	†	
$N(\pi\pi)_{S\text{-wave}}^{I=0}$	< 3 %	-	
$N(1440)\pi$	< 7 %	†	
$p\gamma$	0.15-0.35 %	481	
$p\gamma$, helicity=1/2	0.15-0.35 %	481	
$n\gamma$	0.004-0.29 %	480	
$n\gamma$, helicity=1/2	0.004-0.29 %	480	
$N(1650) S_{11}$			
$I(J^P) = \frac{1}{2}(\frac{1}{2}^-)$			
Breit-Wigner mass = 1645 to 1670 (≈ 1655) MeV			
Breit-Wigner full width = 145 to 185 (≈ 165) MeV			
$p_{\text{beam}} = 0.97$ GeV/c $4\pi\lambda^2 = 16.2$ mb			
Re(pole position) = 1640 to 1670 (≈ 1655) MeV			
$-2\text{Im}(\text{pole position}) = 150$ to 180 (≈ 165) MeV			
$N(1650)$ DECAY MODES	Fraction (Γ_i/Γ)	ρ (MeV/c)	
$N\pi$	0.60 to 0.95	551	
$N\eta$	3-10 %	354	
ΛK	3-11 %	179	
$N\pi\pi$	10-20 %	517	
$\Delta\pi$	1-7 %	349	
$N\rho$	4-12 %	†	
$N(\pi\pi)_{S\text{-wave}}^{I=0}$	< 4 %	-	
$N(1440)\pi$	< 5 %	156	
$p\gamma$	0.04-0.18 %	562	
$p\gamma$, helicity=1/2	0.04-0.18 %	562	
$n\gamma$	0.003-0.17 %	561	
$n\gamma$, helicity=1/2	0.003-0.17 %	561	
$N(1675) D_{15}$			
$I(J^P) = \frac{1}{2}(\frac{5}{2}^-)$			
Breit-Wigner mass = 1670 to 1680 (≈ 1675) MeV			
Breit-Wigner full width = 130 to 165 (≈ 150) MeV			
$p_{\text{beam}} = 1.01$ GeV/c $4\pi\lambda^2 = 15.4$ mb			
Re(pole position) = 1655 to 1665 (≈ 1660) MeV			
$-2\text{Im}(\text{pole position}) = 125$ to 150 (≈ 135) MeV			

Baryon Summary Table

N(1675) DECAY MODES	Fraction (Γ_i/Γ)	ρ (MeV/c)
$N\pi$	0.35 to 0.45	564
$N\eta$	(0.0 \pm 1.0) %	376
ΛK	<1 %	216
$N\pi\pi$	50–60 %	532
$\Delta\pi$	50–60 %	366
$N\rho$	< 1–3 %	†
$p\gamma$	0.004–0.023 %	575
$p\gamma$, helicity=1/2	0.0–0.015 %	575
$p\gamma$, helicity=3/2	0.0–0.011 %	575
$n\gamma$	0.02–0.12 %	574
$n\gamma$, helicity=1/2	0.006–0.046 %	574
$n\gamma$, helicity=3/2	0.01–0.08 %	574

N(1680) F_{15}

$$I(J^P) = \frac{1}{2}(\frac{5}{2}^+)$$

Breit-Wigner mass = 1680 to 1690 (\approx 1685) MeV
 Breit-Wigner full width = 120 to 140 (\approx 130) MeV
 $p_{\text{beam}} = 1.02$ GeV/c $4\pi\lambda^2 = 15.0$ mb
 Re(pole position) = 1665 to 1680 (\approx 1675) MeV
 $-2\text{Im}(\text{pole position}) = 110$ to 135 (\approx 120) MeV

N(1680) DECAY MODES	Fraction (Γ_i/Γ)	ρ (MeV/c)
$N\pi$	0.65 to 0.70	571
$N\eta$	(0.0 \pm 1.0) %	386
$N\pi\pi$	30–40 %	539
$\Delta\pi$	5–15 %	374
$N\rho$	3–15 %	†
$N(\pi\pi)_{S\text{-wave}}^{J=0}$	5–20 %	–
$p\gamma$	0.21–0.32 %	581
$p\gamma$, helicity=1/2	0.001–0.011 %	581
$p\gamma$, helicity=3/2	0.20–0.32 %	581
$n\gamma$	0.021–0.046 %	581
$n\gamma$, helicity=1/2	0.004–0.029 %	581
$n\gamma$, helicity=3/2	0.01–0.024 %	581

N(1700) D_{13}

$$I(J^P) = \frac{1}{2}(\frac{3}{2}^-)$$

Breit-Wigner mass = 1650 to 1750 (\approx 1700) MeV
 Breit-Wigner full width = 50 to 150 (\approx 100) MeV
 $p_{\text{beam}} = 1.05$ GeV/c $4\pi\lambda^2 = 14.5$ mb
 Re(pole position) = 1630 to 1730 (\approx 1680) MeV
 $-2\text{Im}(\text{pole position}) = 50$ to 150 (\approx 100) MeV

N(1700) DECAY MODES	Fraction (Γ_i/Γ)	ρ (MeV/c)
$N\pi$	5–15 %	581
$N\eta$	(0.0 \pm 1.0) %	402
ΛK	<3 %	255
$N\pi\pi$	85–95 %	550
$N\rho$	<35 %	†
$p\gamma$	0.01–0.05 %	591
$p\gamma$, helicity=1/2	0.0–0.024 %	591
$p\gamma$, helicity=3/2	0.002–0.026 %	591
$n\gamma$	0.01–0.13 %	590
$n\gamma$, helicity=1/2	0.0–0.09 %	590
$n\gamma$, helicity=3/2	0.01–0.05 %	590

N(1710) P_{11}

$$I(J^P) = \frac{1}{2}(\frac{1}{2}^+)$$

Breit-Wigner mass = 1680 to 1740 (\approx 1710) MeV
 Breit-Wigner full width = 50 to 250 (\approx 100) MeV
 $p_{\text{beam}} = 1.07$ GeV/c $4\pi\lambda^2 = 14.2$ mb
 Re(pole position) = 1670 to 1770 (\approx 1720) MeV
 $-2\text{Im}(\text{pole position}) = 80$ to 380 (\approx 230) MeV

N(1710) DECAY MODES	Fraction (Γ_i/Γ)	ρ (MeV/c)
$N\pi$	10–20 %	588
$N\eta$	(6.2 \pm 1.0) %	412
$N\omega$	(13.0 \pm 2.0) %	†
ΛK	5–25 %	269
$N\pi\pi$	40–90 %	557
$\Delta\pi$	15–40 %	394
$N\rho$	5–25 %	†
$N(\pi\pi)_{S\text{-wave}}^{J=0}$	10–40 %	–
$p\gamma$	0.002–0.05 %	598
$p\gamma$, helicity=1/2	0.002–0.05 %	598
$n\gamma$	0.0–0.02 %	597
$n\gamma$, helicity=1/2	0.0–0.02 %	597

N(1720) P_{13}

$$I(J^P) = \frac{1}{2}(\frac{3}{2}^+)$$

Breit-Wigner mass = 1700 to 1750 (\approx 1720) MeV
 Breit-Wigner full width = 150 to 300 (\approx 200) MeV
 $p_{\text{beam}} = 1.09$ GeV/c $4\pi\lambda^2 = 13.9$ mb
 Re(pole position) = 1660 to 1690 (\approx 1675) MeV
 $-2\text{Im}(\text{pole position}) = 115$ to 275 MeV

N(1720) DECAY MODES	Fraction (Γ_i/Γ)	ρ (MeV/c)
$N\pi$	10–20 %	594
$N\eta$	(4.0 \pm 1.0) %	422
ΛK	1–15 %	283
$N\pi\pi$	>70 %	564
$N\rho$	70–85 %	73
$p\gamma$	0.003–0.10 %	604
$p\gamma$, helicity=1/2	0.003–0.08 %	604
$p\gamma$, helicity=3/2	0.001–0.03 %	604
$n\gamma$	0.002–0.39 %	603
$n\gamma$, helicity=1/2	0.0–0.002 %	603
$n\gamma$, helicity=3/2	0.001–0.39 %	603

N(2190) G_{17}

$$I(J^P) = \frac{1}{2}(\frac{7}{2}^-)$$

Breit-Wigner mass = 2100 to 2200 (\approx 2190) MeV
 Breit-Wigner full width = 300 to 700 (\approx 500) MeV
 $p_{\text{beam}} = 2.07$ GeV/c $4\pi\lambda^2 = 6.21$ mb
 Re(pole position) = 2050 to 2100 (\approx 2075) MeV
 $-2\text{Im}(\text{pole position}) = 400$ to 520 (\approx 450) MeV

N(2190) DECAY MODES	Fraction (Γ_i/Γ)	ρ (MeV/c)
$N\pi$	10–20 %	888
$N\eta$	(0.0 \pm 1.0) %	791

N(2220) H_{19}

$$I(J^P) = \frac{1}{2}(\frac{9}{2}^+)$$

Breit-Wigner mass = 2200 to 2300 (\approx 2250) MeV
 Breit-Wigner full width = 350 to 500 (\approx 400) MeV
 $p_{\text{beam}} = 2.21$ GeV/c $4\pi\lambda^2 = 5.74$ mb
 Re(pole position) = 2130 to 2200 (\approx 2170) MeV
 $-2\text{Im}(\text{pole position}) = 400$ to 560 (\approx 480) MeV

N(2220) DECAY MODES	Fraction (Γ_i/Γ)	ρ (MeV/c)
$N\pi$	10–20 %	924

N(2250) G_{19}

$$I(J^P) = \frac{1}{2}(\frac{9}{2}^-)$$

Breit-Wigner mass = 2200 to 2350 (\approx 2275) MeV
 Breit-Wigner full width = 230 to 800 (\approx 500) MeV
 $p_{\text{beam}} = 2.27$ GeV/c $4\pi\lambda^2 = 5.56$ mb
 Re(pole position) = 2150 to 2250 (\approx 2200) MeV
 $-2\text{Im}(\text{pole position}) = 350$ to 550 (\approx 450) MeV

Baryon Summary Table

$N(2250)$ DECAY MODES	Fraction (Γ_i/Γ)	ρ (MeV/c)
$N\pi$	5–15 %	938

 $N(2600)$ $I_{1,1}$

$$I(J^P) = \frac{1}{2}(\frac{11}{2}^-)$$

Breit-Wigner mass = 2550 to 2750 (\approx 2600) MeV
 Breit-Wigner full width = 500 to 800 (\approx 650) MeV
 $p_{\text{beam}} = 3.12 \text{ GeV}/c$ $4\pi\lambda^2 = 3.86 \text{ mb}$

$N(2600)$ DECAY MODES	Fraction (Γ_i/Γ)	ρ (MeV/c)
$N\pi$	5–10 %	1126

Δ BARYONS ($S=0, I=3/2$)

$$\Delta^{++} = uuu, \quad \Delta^+ = uud, \quad \Delta^0 = udd, \quad \Delta^- = ddd$$

 $\Delta(1232)$ P_{33}

$$I(J^P) = \frac{3}{2}(\frac{3}{2}^+)$$

Breit-Wigner mass (mixed charges) = 1231 to 1233 (\approx 1232) MeV
 Breit-Wigner full width (mixed charges) = 116 to 120 (\approx 118) MeV
 $p_{\text{beam}} = 0.30 \text{ GeV}/c$ $4\pi\lambda^2 = 94.8 \text{ mb}$
 Re(pole position) = 1209 to 1211 (\approx 1210) MeV
 $-2\text{Im}(\text{pole position}) = 98 \text{ to } 102$ (\approx 100) MeV

$\Delta(1232)$ DECAY MODES	Fraction (Γ_i/Γ)	ρ (MeV/c)
$N\pi$	100 %	229
$N\gamma$	0.52–0.60 %	259
$N\gamma$, helicity=1/2	0.11–0.13 %	259
$N\gamma$, helicity=3/2	0.41–0.47 %	259

 $\Delta(1600)$ P_{33}

$$I(J^P) = \frac{3}{2}(\frac{3}{2}^+)$$

Breit-Wigner mass = 1550 to 1700 (\approx 1600) MeV
 Breit-Wigner full width = 250 to 450 (\approx 350) MeV
 $p_{\text{beam}} = 0.87 \text{ GeV}/c$ $4\pi\lambda^2 = 18.6 \text{ mb}$
 Re(pole position) = 1500 to 1700 (\approx 1600) MeV
 $-2\text{Im}(\text{pole position}) = 200 \text{ to } 400$ (\approx 300) MeV

$\Delta(1600)$ DECAY MODES	Fraction (Γ_i/Γ)	ρ (MeV/c)
$N\pi$	10–25 %	513
$N\pi\pi$	75–90 %	477
$\Delta\pi$	40–70 %	303
$N\rho$	<25 %	†
$N(1440)\pi$	10–35 %	82
$N\gamma$	0.001–0.02 %	525
$N\gamma$, helicity=1/2	0.0–0.02 %	525
$N\gamma$, helicity=3/2	0.001–0.005 %	525

 $\Delta(1620)$ S_{31}

$$I(J^P) = \frac{3}{2}(\frac{1}{2}^-)$$

Breit-Wigner mass = 1600 to 1660 (\approx 1630) MeV
 Breit-Wigner full width = 135 to 150 (\approx 145) MeV
 $p_{\text{beam}} = 0.93 \text{ GeV}/c$ $4\pi\lambda^2 = 17.2 \text{ mb}$
 Re(pole position) = 1590 to 1610 (\approx 1600) MeV
 $-2\text{Im}(\text{pole position}) = 115 \text{ to } 120$ (\approx 118) MeV

$\Delta(1620)$ DECAY MODES	Fraction (Γ_i/Γ)	ρ (MeV/c)
$N\pi$	20–30 %	534
$N\pi\pi$	70–80 %	499
$\Delta\pi$	30–60 %	328
$N\rho$	7–25 %	†
$N\gamma$	0.004–0.044 %	545
$N\gamma$, helicity=1/2	0.004–0.044 %	545

 $\Delta(1700)$ D_{33}

$$I(J^P) = \frac{3}{2}(\frac{3}{2}^-)$$

Breit-Wigner mass = 1670 to 1750 (\approx 1700) MeV
 Breit-Wigner full width = 200 to 400 (\approx 300) MeV
 $p_{\text{beam}} = 1.05 \text{ GeV}/c$ $4\pi\lambda^2 = 14.5 \text{ mb}$
 Re(pole position) = 1620 to 1680 (\approx 1650) MeV
 $-2\text{Im}(\text{pole position}) = 160 \text{ to } 240$ (\approx 200) MeV

$\Delta(1700)$ DECAY MODES	Fraction (Γ_i/Γ)	ρ (MeV/c)
$N\pi$	10–20 %	581
$N\pi\pi$	80–90 %	550
$\Delta\pi$	30–60 %	386
$N\rho$	30–55 %	†
$N\gamma$	0.12–0.26 %	591
$N\gamma$, helicity=1/2	0.08–0.16 %	591
$N\gamma$, helicity=3/2	0.025–0.12 %	591

 $\Delta(1905)$ F_{35}

$$I(J^P) = \frac{3}{2}(\frac{5}{2}^+)$$

Breit-Wigner mass = 1865 to 1915 (\approx 1890) MeV
 Breit-Wigner full width = 270 to 400 (\approx 330) MeV
 $p_{\text{beam}} = 1.42 \text{ GeV}/c$ $4\pi\lambda^2 = 9.89 \text{ mb}$
 Re(pole position) = 1825 to 1835 (\approx 1830) MeV
 $-2\text{Im}(\text{pole position}) = 265 \text{ to } 300$ (\approx 280) MeV

$\Delta(1905)$ DECAY MODES	Fraction (Γ_i/Γ)	ρ (MeV/c)
$N\pi$	0.09 to 0.15	704
$N\pi\pi$	85–95 %	680
$\Delta\pi$	<25 %	531
$N\rho$	>60 %	397
$N\gamma$	0.01–0.03 %	712
$N\gamma$, helicity=1/2	0.0–0.1 %	712
$N\gamma$, helicity=3/2	0.004–0.03 %	712

 $\Delta(1910)$ P_{31}

$$I(J^P) = \frac{3}{2}(\frac{1}{2}^+)$$

Breit-Wigner mass = 1870 to 1920 (\approx 1910) MeV
 Breit-Wigner full width = 190 to 270 (\approx 250) MeV
 $p_{\text{beam}} = 1.46 \text{ GeV}/c$ $4\pi\lambda^2 = 9.54 \text{ mb}$
 Re(pole position) = 1830 to 1880 (\approx 1855) MeV
 $-2\text{Im}(\text{pole position}) = 200 \text{ to } 500$ (\approx 350) MeV

$\Delta(1910)$ DECAY MODES	Fraction (Γ_i/Γ)	ρ (MeV/c)
$N\pi$	15–30 %	717
$N\gamma$	0.0–0.2 %	725
$N\gamma$, helicity=1/2	0.0–0.2 %	725

 $\Delta(1920)$ P_{33}

$$I(J^P) = \frac{3}{2}(\frac{3}{2}^+)$$

Breit-Wigner mass = 1900 to 1970 (\approx 1920) MeV
 Breit-Wigner full width = 150 to 300 (\approx 200) MeV
 $p_{\text{beam}} = 1.48 \text{ GeV}/c$ $4\pi\lambda^2 = 9.37 \text{ mb}$
 Re(pole position) = 1850 to 1950 (\approx 1900) MeV
 $-2\text{Im}(\text{pole position}) = 200 \text{ to } 400$ (\approx 300) MeV

$\Delta(1920)$ DECAY MODES	Fraction (Γ_i/Γ)	ρ (MeV/c)
$N\pi$	5–20 %	723
ΣK	(2.10 ± 0.30) %	431

Baryon Summary Table

 $\Delta(1930) D_{35}$

$$I(J^P) = \frac{3}{2}(\frac{5}{2}^-)$$

Breit-Wigner mass = 1900 to 2020 (\approx 1960) MeV
 Breit-Wigner full width = 220 to 500 (\approx 360) MeV
 $p_{\text{beam}} = 1.56 \text{ GeV}/c$ $4\pi\lambda^2 = 8.76 \text{ mb}$
 Re(pole position) = 1840 to 1960 (\approx 1900) MeV
 $-2\text{Im}(\text{pole position}) = 175 \text{ to } 360$ (\approx 270) MeV

$\Delta(1930)$ DECAY MODES	Fraction (Γ_i/Γ)	ρ (MeV/c)
$N\pi$	0.05 to 0.15	748
$N\gamma$	0.0-0.02 %	755
$N\gamma$, helicity=1/2	0.0-0.01 %	755
$N\gamma$, helicity=3/2	0.0-0.01 %	755

 $\Delta(1950) F_{37}$

$$I(J^P) = \frac{3}{2}(\frac{7}{2}^+)$$

Breit-Wigner mass = 1915 to 1950 (\approx 1930) MeV
 Breit-Wigner full width = 235 to 335 (\approx 285) MeV
 $p_{\text{beam}} = 1.50 \text{ GeV}/c$ $4\pi\lambda^2 = 9.21 \text{ mb}$
 Re(pole position) = 1870 to 1890 (\approx 1880) MeV
 $-2\text{Im}(\text{pole position}) = 220 \text{ to } 260$ (\approx 240) MeV

$\Delta(1950)$ DECAY MODES	Fraction (Γ_i/Γ)	ρ (MeV/c)
$N\pi$	0.35 to 0.45	729
$N\pi\pi$		706
$\Delta\pi$	20-30 %	560
$N\rho$	<10 %	442
$N\gamma$	0.08-0.13 %	737
$N\gamma$, helicity=1/2	0.03-0.055 %	737
$N\gamma$, helicity=3/2	0.05-0.075 %	737

 $\Delta(2420) H_{3,11}$

$$I(J^P) = \frac{3}{2}(\frac{11}{2}^+)$$

Breit-Wigner mass = 2300 to 2500 (\approx 2420) MeV
 Breit-Wigner full width = 300 to 500 (\approx 400) MeV
 $p_{\text{beam}} = 2.64 \text{ GeV}/c$ $4\pi\lambda^2 = 4.68 \text{ mb}$
 Re(pole position) = 2260 to 2400 (\approx 2330) MeV
 $-2\text{Im}(\text{pole position}) = 350 \text{ to } 750$ (\approx 550) MeV

$\Delta(2420)$ DECAY MODES	Fraction (Γ_i/Γ)	ρ (MeV/c)
$N\pi$	5-15 %	1023

Λ BARYONS

($S = -1, I = 0$)

$$\Lambda^0 = uds$$

 Λ

$$I(J^P) = 0(\frac{1}{2}^+)$$

Mass $m = 1115.683 \pm 0.006 \text{ MeV}$
 $(m_\Lambda - m_\pi) / m_\Lambda = (-0.1 \pm 1.1) \times 10^{-5}$ ($S = 1.6$)
 Mean life $\tau = (2.631 \pm 0.020) \times 10^{-10} \text{ s}$ ($S = 1.6$)
 $(\tau_\Lambda - \tau_{\bar{\Lambda}}) / \tau_\Lambda = -0.001 \pm 0.009$
 $c\tau = 7.89 \text{ cm}$
 Magnetic moment $\mu = -0.613 \pm 0.004 \mu_N$
 Electric dipole moment $d < 1.5 \times 10^{-16} \text{ ecm}$, CL = 95%

Decay parameters

$p\pi^-$	$\alpha_- = 0.642 \pm 0.013$
"	$\phi_- = (-6.5 \pm 3.5)^\circ$
"	$\gamma_- = 0.76$ [f]
"	$\Delta_- = (8 \pm 4)^\circ$ [f]
$n\pi^0$	$\alpha_0 = 0.65 \pm 0.04$
$p e^- \bar{\nu}_e$	$g_A/g_V = -0.718 \pm 0.015$ [f]

 Λ DECAY MODES

	Fraction (Γ_i/Γ)	ρ (MeV/c)
$p\pi^-$	(63.9 \pm 0.5 %) %	101
$n\pi^0$	(35.8 \pm 0.5 %) %	104
$n\gamma$	(1.75 \pm 0.15) $\times 10^{-3}$	162
$p\pi^- \gamma$	[f] (8.4 \pm 1.4) $\times 10^{-4}$	101
$p e^- \bar{\nu}_e$	(8.32 \pm 0.14) $\times 10^{-4}$	163
$p\mu^- \bar{\nu}_\mu$	(1.57 \pm 0.35) $\times 10^{-4}$	131

 $\Lambda(1405) S_{01}$

$$I(J^P) = 0(\frac{1}{2}^-)$$

Mass $m = 1406 \pm 4 \text{ MeV}$
 Full width $\Gamma = 50 \pm 2 \text{ MeV}$
 Below $\bar{K}N$ threshold

$\Lambda(1405)$ DECAY MODES	Fraction (Γ_i/Γ)	ρ (MeV/c)
$\Sigma\pi$	100 %	157

 $\Lambda(1520) D_{03}$

$$I(J^P) = 0(\frac{3}{2}^-)$$

Mass $m = 1519.5 \pm 1.0 \text{ MeV}$ [K]
 Full width $\Gamma = 15.6 \pm 1.0 \text{ MeV}$ [K]
 $p_{\text{beam}} = 0.39 \text{ GeV}/c$ $4\pi\lambda^2 = 82.8 \text{ mb}$

$\Lambda(1520)$ DECAY MODES	Fraction (Γ_i/Γ)	ρ (MeV/c)
$N\bar{K}$	45 \pm 1%	243
$\Sigma\pi$	42 \pm 1%	268
$\Lambda\pi\pi$	10 \pm 1%	259
$\Sigma\pi\pi$	0.9 \pm 0.1%	169
$\Lambda\gamma$	0.85 \pm 0.15%	350

 $\Lambda(1600) P_{01}$

$$I(J^P) = 0(\frac{1}{2}^+)$$

Mass $m = 1560 \text{ to } 1700$ (\approx 1600) MeV
 Full width $\Gamma = 50 \text{ to } 250$ (\approx 150) MeV
 $p_{\text{beam}} = 0.58 \text{ GeV}/c$ $4\pi\lambda^2 = 41.6 \text{ mb}$

$\Lambda(1600)$ DECAY MODES	Fraction (Γ_i/Γ)	ρ (MeV/c)
$N\bar{K}$	15-30 %	343
$\Sigma\pi$	10-60 %	338

 $\Lambda(1670) S_{01}$

$$I(J^P) = 0(\frac{1}{2}^-)$$

Mass $m = 1660 \text{ to } 1680$ (\approx 1670) MeV
 Full width $\Gamma = 25 \text{ to } 50$ (\approx 35) MeV
 $p_{\text{beam}} = 0.74 \text{ GeV}/c$ $4\pi\lambda^2 = 28.5 \text{ mb}$

$\Lambda(1670)$ DECAY MODES	Fraction (Γ_i/Γ)	ρ (MeV/c)
$N\bar{K}$	20-30 %	414
$\Sigma\pi$	25-55 %	394
$\Lambda\eta$	10-25 %	69

 $\Lambda(1690) D_{03}$

$$I(J^P) = 0(\frac{3}{2}^-)$$

Mass $m = 1685 \text{ to } 1695$ (\approx 1690) MeV
 Full width $\Gamma = 50 \text{ to } 70$ (\approx 60) MeV
 $p_{\text{beam}} = 0.78 \text{ GeV}/c$ $4\pi\lambda^2 = 26.1 \text{ mb}$

$\Lambda(1690)$ DECAY MODES	Fraction (Γ_i/Γ)	ρ (MeV/c)
$N\bar{K}$	20-30 %	433
$\Sigma\pi$	20-40 %	410
$\Lambda\pi\pi$	\sim 25 %	419
$\Sigma\pi\pi$	\sim 20 %	358

Baryon Summary Table

$\Lambda(1800) S_{01}$		$I(J^P) = 0(\frac{1}{2}^-)$
Mass $m = 1720$ to 1850 (≈ 1800) MeV		
Full width $\Gamma = 200$ to 400 (≈ 300) MeV		
$\rho_{\text{beam}} = 1.01$ GeV/c $4\pi\lambda^2 = 17.5$ mb		
$\Lambda(1800)$ DECAY MODES	Fraction (Γ_i/Γ)	ρ (MeV/c)
$N\bar{K}$	25–40 %	528
$\Sigma\pi$	seen	494
$\Sigma(1385)\pi$	seen	349
$N\bar{K}^*(892)$	seen	†

$\Lambda(1810) P_{01}$		$I(J^P) = 0(\frac{1}{2}^+)$
Mass $m = 1750$ to 1850 (≈ 1810) MeV		
Full width $\Gamma = 50$ to 250 (≈ 150) MeV		
$\rho_{\text{beam}} = 1.04$ GeV/c $4\pi\lambda^2 = 17.0$ mb		
$\Lambda(1810)$ DECAY MODES	Fraction (Γ_i/Γ)	ρ (MeV/c)
$N\bar{K}$	20–50 %	537
$\Sigma\pi$	10–40 %	501
$\Sigma(1385)\pi$	seen	357
$N\bar{K}^*(892)$	30–60 %	†

$\Lambda(1820) F_{05}$		$I(J^P) = 0(\frac{5}{2}^+)$
Mass $m = 1815$ to 1825 (≈ 1820) MeV		
Full width $\Gamma = 70$ to 90 (≈ 80) MeV		
$\rho_{\text{beam}} = 1.06$ GeV/c $4\pi\lambda^2 = 16.5$ mb		
$\Lambda(1820)$ DECAY MODES	Fraction (Γ_i/Γ)	ρ (MeV/c)
$N\bar{K}$	55–65 %	545
$\Sigma\pi$	8–14 %	509
$\Sigma(1385)\pi$	5–10 %	366

$\Lambda(1830) D_{05}$		$I(J^P) = 0(\frac{5}{2}^-)$
Mass $m = 1810$ to 1830 (≈ 1830) MeV		
Full width $\Gamma = 60$ to 110 (≈ 95) MeV		
$\rho_{\text{beam}} = 1.08$ GeV/c $4\pi\lambda^2 = 16.0$ mb		
$\Lambda(1830)$ DECAY MODES	Fraction (Γ_i/Γ)	ρ (MeV/c)
$N\bar{K}$	3–10 %	553
$\Sigma\pi$	35–75 %	516
$\Sigma(1385)\pi$	>15 %	374

$\Lambda(1890) P_{03}$		$I(J^P) = 0(\frac{3}{2}^+)$
Mass $m = 1850$ to 1910 (≈ 1890) MeV		
Full width $\Gamma = 60$ to 200 (≈ 100) MeV		
$\rho_{\text{beam}} = 1.21$ GeV/c $4\pi\lambda^2 = 13.6$ mb		
$\Lambda(1890)$ DECAY MODES	Fraction (Γ_i/Γ)	ρ (MeV/c)
$N\bar{K}$	20–35 %	599
$\Sigma\pi$	3–10 %	560
$\Sigma(1385)\pi$	seen	423
$N\bar{K}^*(892)$	seen	236

$\Lambda(2100) G_{07}$		$I(J^P) = 0(\frac{7}{2}^-)$
Mass $m = 2090$ to 2110 (≈ 2100) MeV		
Full width $\Gamma = 100$ to 250 (≈ 200) MeV		
$\rho_{\text{beam}} = 1.68$ GeV/c $4\pi\lambda^2 = 8.68$ mb		

$\Lambda(2100)$ DECAY MODES	Fraction (Γ_i/Γ)	ρ (MeV/c)
$N\bar{K}$	25–35 %	751
$\Sigma\pi$	~ 5 %	705
$\Lambda\eta$	<3 %	617
ΞK	<3 %	491
$\Lambda\omega$	<8 %	443
$N\bar{K}^*(892)$	10–20 %	515

$\Lambda(2110) F_{05}$		$I(J^P) = 0(\frac{5}{2}^+)$
Mass $m = 2090$ to 2140 (≈ 2110) MeV		
Full width $\Gamma = 150$ to 250 (≈ 200) MeV		
$\rho_{\text{beam}} = 1.70$ GeV/c $4\pi\lambda^2 = 8.53$ mb		
$\Lambda(2110)$ DECAY MODES	Fraction (Γ_i/Γ)	ρ (MeV/c)
$N\bar{K}$	5–25 %	757
$\Sigma\pi$	10–40 %	711
$\Lambda\omega$	seen	455
$\Sigma(1385)\pi$	seen	591
$N\bar{K}^*(892)$	10–60 %	525

$\Lambda(2350) H_{09}$		$I(J^P) = 0(\frac{9}{2}^+)$
Mass $m = 2340$ to 2370 (≈ 2350) MeV		
Full width $\Gamma = 100$ to 250 (≈ 150) MeV		
$\rho_{\text{beam}} = 2.29$ GeV/c $4\pi\lambda^2 = 5.85$ mb		
$\Lambda(2350)$ DECAY MODES	Fraction (Γ_i/Γ)	ρ (MeV/c)
$N\bar{K}$	~ 12 %	915
$\Sigma\pi$	~ 10 %	867

Σ BARYONS
 $(S = -1, I = 1)$
 $\Sigma^+ = u u s, \quad \Sigma^0 = u d s, \quad \Sigma^- = d d s$

Σ^+		$I(J^P) = 1(\frac{1}{2}^+)$
Mass $m = 1189.37 \pm 0.07$ MeV ($S = 2.2$)		
Mean life $\tau = (0.8018 \pm 0.0026) \times 10^{-10}$ s		
$c\tau = 2.404$ cm		
$(\tau_{\Sigma^+} - \tau_{\Sigma^-}) / \tau_{\Sigma^+} = (-0.6 \pm 1.2) \times 10^{-3}$		
Magnetic moment $\mu = 2.458 \pm 0.010 \mu_N$ ($S = 2.1$)		
$\Gamma(\Sigma^+ \rightarrow n\ell^+\nu) / \Gamma(\Sigma^- \rightarrow n\ell^-\bar{\nu}) < 0.043$		

Decay parameters

$p\pi^0$	$\alpha_0 = -0.980^{+0.017}_{-0.015}$
"	$\phi_0 = (36 \pm 34)^\circ$
"	$\gamma_0 = 0.16$ [1]
"	$\Delta_0 = (187 \pm 6)^\circ$ [1]
$n\pi^+$	$\alpha_+ = 0.068 \pm 0.013$
"	$\phi_+ = (167 \pm 20)^\circ$ ($S = 1.1$)
"	$\gamma_+ = -0.97$ [1]
"	$\Delta_+ = (-73^{+133}_{-10})^\circ$ [1]
$p\gamma$	$\alpha_\gamma = -0.76 \pm 0.08$

Baryon Summary Table

Σ^+ DECAY MODES	Fraction (Γ_i/Γ)	Confidence level	ρ (MeV/c)
$p\pi^0$	(51.57±0.30) %		189
$n\pi^+$	(48.31±0.30) %		185
$p\gamma$	(1.23±0.05) × 10 ⁻³		225
$n\pi^+\gamma$	[J] (4.5 ± 0.5) × 10 ⁻⁴		185
$\Lambda e^+\nu_e$	(2.0 ± 0.5) × 10 ⁻⁵		71

$\Delta S = \Delta Q$ (SQ) violating modes or
 $\Delta S = 1$ weak neutral current (S1) modes

$n e^+ \nu_e$	SQ	< 5	× 10 ⁻⁶	90%	224
$n \mu^+ \nu_\mu$	SQ	< 3.0	× 10 ⁻⁵	90%	202
$p e^+ e^-$	S1	< 7	× 10 ⁻⁶		225
$p \mu^+ \mu^-$	S1	(9 ± ₋₈ ⁹)	× 10 ⁻⁸		121

$$\Sigma^0 \quad I(J^P) = 1(\frac{1}{2}^+)$$

Mass $m = 1192.642 \pm 0.024$ MeV
 $m_{\Sigma^-} - m_{\Sigma^0} = 4.807 \pm 0.035$ MeV (S = 1.1)
 $m_{\Sigma^0} - m_\Lambda = 76.959 \pm 0.023$ MeV
Mean life $\tau = (7.4 \pm 0.7) \times 10^{-20}$ s
 $c\tau = 2.22 \times 10^{-11}$ m
Transition magnetic moment $|\mu_{\Sigma\Lambda}| = 1.61 \pm 0.08 \mu_N$

Σ^0 DECAY MODES	Fraction (Γ_i/Γ)	Confidence level	ρ (MeV/c)
$\Lambda\gamma$	100 %		74
$\Lambda\gamma\gamma$	< 3 %	90%	74
$\Lambda e^+ e^-$	[J] 5 × 10 ⁻³		74

$$\Sigma^- \quad I(J^P) = 1(\frac{1}{2}^+)$$

Mass $m = 1197.449 \pm 0.030$ MeV (S = 1.2)
 $m_{\Sigma^-} - m_{\Sigma^+} = 8.08 \pm 0.08$ MeV (S = 1.9)
 $m_{\Sigma^-} - m_\Lambda = 81.766 \pm 0.030$ MeV (S = 1.2)
Mean life $\tau = (1.479 \pm 0.011) \times 10^{-10}$ s (S = 1.3)
 $c\tau = 4.434$ cm
Magnetic moment $\mu = -1.160 \pm 0.025 \mu_N$ (S = 1.7)
 Σ^- charge radius = 0.78 ± 0.10 fm

Decay parameters

$n\pi^-$	$\alpha_- = -0.068 \pm 0.008$
"	$\phi_- = (10 \pm 15)^\circ$
"	$\gamma_- = 0.98$ [f]
"	$\Delta_- = (249 \pm_{-120}^{12})^\circ$ [f]
$n e^- \bar{\nu}_e$	$g_A/g_V = 0.340 \pm 0.017$ [f]
"	$f_2(0)/f_1(0) = 0.97 \pm 0.14$
"	$D = 0.11 \pm 0.10$
$\Lambda e^- \bar{\nu}_e$	$g_V/g_A = 0.01 \pm 0.10$ [f] (S = 1.5)
"	$g_{WM}/g_A = 2.4 \pm 1.7$ [f]

Σ^- DECAY MODES	Fraction (Γ_i/Γ)	ρ (MeV/c)
$n\pi^-$	(99.848±0.005) %	193
$n\pi^-\gamma$	[J] (4.6 ± 0.6) × 10 ⁻⁴	193
$n e^- \bar{\nu}_e$	(1.017±0.034) × 10 ⁻³	230
$n \mu^- \bar{\nu}_\mu$	(4.5 ± 0.4) × 10 ⁻⁴	210
$\Lambda e^- \bar{\nu}_e$	(5.73 ± 0.27) × 10 ⁻⁵	79

$$\Sigma(1385) P_{13} \quad I(J^P) = 1(\frac{3}{2}^+)$$

$\Sigma(1385)^+$ mass $m = 1382.8 \pm 0.4$ MeV (S = 2.0)
 $\Sigma(1385)^0$ mass $m = 1383.7 \pm 1.0$ MeV (S = 1.4)
 $\Sigma(1385)^-$ mass $m = 1387.2 \pm 0.5$ MeV (S = 2.2)
 $\Sigma(1385)^+$ full width $\Gamma = 35.8 \pm 0.8$ MeV
 $\Sigma(1385)^0$ full width $\Gamma = 36 \pm 5$ MeV
 $\Sigma(1385)^-$ full width $\Gamma = 39.4 \pm 2.1$ MeV (S = 1.7)
Below $\bar{K}N$ threshold

$\Sigma(1385)$ DECAY MODES	Fraction (Γ_i/Γ)	Confidence level	ρ (MeV/c)
$\Lambda\pi$	(87.0±1.5) %		208
$\Sigma\pi$	(11.7±1.5) %		129
$\Lambda\gamma$	(1.3±0.4) %		241
$\Sigma^-\gamma$	< 2.4 × 10 ⁻⁴	90%	173

$$\Sigma(1660) P_{11} \quad I(J^P) = 1(\frac{1}{2}^+)$$

Mass $m = 1630$ to 1690 (≈ 1660) MeV
Full width $\Gamma = 40$ to 200 (≈ 100) MeV
 $\rho_{\text{beam}} = 0.72$ GeV/c $4\pi\lambda^2 = 29.9$ mb

$\Sigma(1660)$ DECAY MODES	Fraction (Γ_i/Γ)	ρ (MeV/c)
$N\bar{K}$	10–30 %	405
$\Lambda\pi$	seen	440
$\Sigma\pi$	seen	387

$$\Sigma(1670) D_{13} \quad I(J^P) = 1(\frac{3}{2}^-)$$

Mass $m = 1665$ to 1685 (≈ 1670) MeV
Full width $\Gamma = 40$ to 80 (≈ 60) MeV
 $\rho_{\text{beam}} = 0.74$ GeV/c $4\pi\lambda^2 = 28.5$ mb

$\Sigma(1670)$ DECAY MODES	Fraction (Γ_i/Γ)	ρ (MeV/c)
$N\bar{K}$	7–13 %	414
$\Lambda\pi$	5–15 %	448
$\Sigma\pi$	30–60 %	394

$$\Sigma(1750) S_{11} \quad I(J^P) = 1(\frac{1}{2}^-)$$

Mass $m = 1730$ to 1800 (≈ 1750) MeV
Full width $\Gamma = 60$ to 160 (≈ 90) MeV
 $\rho_{\text{beam}} = 0.91$ GeV/c $4\pi\lambda^2 = 20.7$ mb

$\Sigma(1750)$ DECAY MODES	Fraction (Γ_i/Γ)	ρ (MeV/c)
$N\bar{K}$	10–40 %	486
$\Lambda\pi$	seen	507
$\Sigma\pi$	< 8 %	456
$\Sigma\eta$	15–55 %	98

$$\Sigma(1775) D_{15} \quad I(J^P) = 1(\frac{5}{2}^-)$$

Mass $m = 1770$ to 1780 (≈ 1775) MeV
Full width $\Gamma = 105$ to 135 (≈ 120) MeV
 $\rho_{\text{beam}} = 0.96$ GeV/c $4\pi\lambda^2 = 19.0$ mb

$\Sigma(1775)$ DECAY MODES	Fraction (Γ_i/Γ)	ρ (MeV/c)
$N\bar{K}$	37–43%	508
$\Lambda\pi$	14–20%	525
$\Sigma\pi$	2–5%	475
$\Sigma(1385)\pi$	8–12%	327
$\Lambda(1520)\pi$	17–23%	201

$$\Sigma(1915) F_{15} \quad I(J^P) = 1(\frac{5}{2}^+)$$

Mass $m = 1900$ to 1935 (≈ 1915) MeV
Full width $\Gamma = 80$ to 160 (≈ 120) MeV
 $\rho_{\text{beam}} = 1.26$ GeV/c $4\pi\lambda^2 = 12.8$ mb

$\Sigma(1915)$ DECAY MODES	Fraction (Γ_i/Γ)	ρ (MeV/c)
$N\bar{K}$	5–15 %	618
$\Lambda\pi$	seen	623
$\Sigma\pi$	seen	577
$\Sigma(1385)\pi$	< 5 %	443

Baryon Summary Table

$\Sigma(1940) D_{13}$		
$I(J^P) = 1(\frac{3}{2}^-)$		
Mass $m = 1900$ to 1950 (≈ 1940) MeV		
Full width $\Gamma = 150$ to 300 (≈ 220) MeV		
$p_{\text{beam}} = 1.32$ GeV/c $4\pi\lambda^2 = 12.1$ mb		
$\Sigma(1940)$ DECAY MODES	Fraction (Γ_i/Γ)	ρ (MeV/c)
$N\bar{K}$	<20 %	637
$\Lambda\pi$	seen	640
$\Sigma\pi$	seen	595
$\Sigma(1385)\pi$	seen	463
$\Lambda(1520)\pi$	seen	355
$\Delta(1232)\bar{K}$	seen	410
$N\bar{K}^*(892)$	seen	322

$\Sigma(2030) F_{17}$		
$I(J^P) = 1(\frac{7}{2}^+)$		
Mass $m = 2025$ to 2040 (≈ 2030) MeV		
Full width $\Gamma = 150$ to 200 (≈ 180) MeV		
$p_{\text{beam}} = 1.52$ GeV/c $4\pi\lambda^2 = 9.93$ mb		
$\Sigma(2030)$ DECAY MODES	Fraction (Γ_i/Γ)	ρ (MeV/c)
$N\bar{K}$	17–23 %	702
$\Lambda\pi$	17–23 %	700
$\Sigma\pi$	5–10 %	657
ΞK	<2 %	422
$\Sigma(1385)\pi$	5–15 %	532
$\Lambda(1520)\pi$	10–20 %	430
$\Delta(1232)\bar{K}$	10–20 %	498
$N\bar{K}^*(892)$	<5 %	439

$\Sigma(2250)$		
$I(J^P) = 1(?)^?$		
Mass $m = 2210$ to 2280 (≈ 2250) MeV		
Full width $\Gamma = 60$ to 150 (≈ 100) MeV		
$p_{\text{beam}} = 2.04$ GeV/c $4\pi\lambda^2 = 6.76$ mb		
$\Sigma(2250)$ DECAY MODES	Fraction (Γ_i/Γ)	ρ (MeV/c)
$N\bar{K}$	<10 %	851
$\Lambda\pi$	seen	842
$\Sigma\pi$	seen	803

Ξ BARYONS

$(S = -2, I = 1/2)$

$$\Xi^0 = uss, \quad \Xi^- = dss$$

Ξ^0		
$I(J^P) = \frac{1}{2}(\frac{1}{2}^+)$		
P is not yet measured; + is the quark model prediction.		
Mass $m = 1314.86 \pm 0.20$ MeV		
$m_{\Xi^-} - m_{\Xi^0} = 6.85 \pm 0.21$ MeV		
Mean life $\tau = (2.90 \pm 0.09) \times 10^{-10}$ s		
$c\tau = 8.71$ cm		
Magnetic moment $\mu = -1.250 \pm 0.014 \mu_N$		
Decay parameters		
$\Lambda\pi^0$	$\alpha = -0.411 \pm 0.022$ ($S = 2.1$)	
"	$\phi = (21 \pm 12)^\circ$	
"	$\gamma = 0.85$ [I]	
"	$\Delta = (218^{+12}_{-19})^\circ$ [I]	
$\Lambda\gamma$	$\alpha = -0.73 \pm 0.17$	
$\Lambda e^+ e^-$	$\alpha = -0.8 \pm 0.2$	
$\Sigma^0\gamma$	$\alpha = -0.63 \pm 0.09$	
$\Sigma^+ e^- \bar{\nu}_e$	$g_1(0)/f_1(0) = 1.21 \pm 0.05$	
$\Sigma^+ e^- \bar{\nu}_e$	$f_2(0)/f_1(0) = 2.0 \pm 1.3$	

Ξ^0 DECAY MODES	Fraction (Γ_i/Γ)	Confidence level	ρ (MeV/c)
$\Lambda\pi^0$	$(99.525 \pm 0.012) \%$		135
$\Lambda\gamma$	$(1.17 \pm 0.07) \times 10^{-3}$		184
$\Lambda e^+ e^-$	$(7.6 \pm 0.6) \times 10^{-6}$		184
$\Sigma^0\gamma$	$(3.33 \pm 0.10) \times 10^{-3}$		117
$\Sigma^+ e^- \bar{\nu}_e$	$(2.53 \pm 0.08) \times 10^{-4}$		120
$\Sigma^+ \mu^- \bar{\nu}_\mu$	$(4.6^{+1.8}_{-1.4}) \times 10^{-6}$		64
$\Delta S = \Delta Q$ (SQ) violating modes or $\Delta S = 2$ forbidden (S2) modes			
$\Sigma^- e^+ \nu_e$	$SQ < 9$	$\times 10^{-4}$	90% 112
$\Sigma^- \mu^+ \nu_\mu$	$SQ < 9$	$\times 10^{-4}$	90% 49
$\rho\pi^-$	$S2 < 8$	$\times 10^{-6}$	90% 299
$\rho e^- \bar{\nu}_e$	$S2 < 1.3$	$\times 10^{-3}$	323
$\rho\mu^- \bar{\nu}_\mu$	$S2 < 1.3$	$\times 10^{-3}$	309

Ξ^-		
$I(J^P) = \frac{1}{2}(\frac{1}{2}^+)$		
P is not yet measured; + is the quark model prediction.		
Mass $m = 1321.71 \pm 0.07$ MeV		
Mean life $\tau = (1.639 \pm 0.015) \times 10^{-10}$ s		
$c\tau = 4.91$ cm		
Magnetic moment $\mu = -0.6507 \pm 0.0025 \mu_N$		
Decay parameters		
$\Lambda\pi^-$	$\alpha = -0.458 \pm 0.012$ ($S = 1.8$)	
$[\alpha(\Xi^-)\alpha_-(\Lambda) - \alpha(\Xi^+)\alpha_+(\bar{\Lambda})] / [\text{sum}] = (0 \pm 7) \times 10^{-4}$		
"	$\phi = (-2.1 \pm 0.8)^\circ$	
"	$\gamma = 0.89$ [I]	
"	$\Delta = (175.9 \pm 1.5)^\circ$ [I]	
$\Lambda e^- \bar{\nu}_e$	$g_A/g_V = -0.25 \pm 0.05$ [I]	

Ξ^- DECAY MODES	Fraction (Γ_i/Γ)	Confidence level	ρ (MeV/c)
$\Lambda\pi^-$	$(99.887 \pm 0.035) \%$		140
$\Sigma^- \gamma$	$(1.27 \pm 0.23) \times 10^{-4}$		118
$\Lambda e^- \bar{\nu}_e$	$(5.63 \pm 0.31) \times 10^{-4}$		190
$\Lambda\mu^- \bar{\nu}_\mu$	$(3.5^{+3.5}_{-2.2}) \times 10^{-4}$		163
$\Sigma^0 e^- \bar{\nu}_e$	$(8.7 \pm 1.7) \times 10^{-5}$		123
$\Sigma^0 \mu^- \bar{\nu}_\mu$	< 8	$\times 10^{-4}$	90% 70
$\Xi^0 e^- \bar{\nu}_e$	< 2.3	$\times 10^{-3}$	90% 7
$\Delta S = 2$ forbidden (S2) modes			
$n\pi^-$	$S2 < 1.9$	$\times 10^{-5}$	90% 304
$n e^- \bar{\nu}_e$	$S2 < 3.2$	$\times 10^{-3}$	90% 327
$n\mu^- \bar{\nu}_\mu$	$S2 < 1.5$	%	90% 314
$\rho\pi^- \pi^-$	$S2 < 4$	$\times 10^{-4}$	90% 223
$\rho\pi^- e^- \bar{\nu}_e$	$S2 < 4$	$\times 10^{-4}$	90% 305
$\rho\pi^- \mu^- \bar{\nu}_\mu$	$S2 < 4$	$\times 10^{-4}$	90% 251
$\rho\mu^- \mu^-$	$L < 4$	$\times 10^{-8}$	90% 272

$\Xi(1530) P_{13}$			
$I(J^P) = \frac{1}{2}(\frac{3}{2}^+)$			
$\Xi(1530)^0$ mass $m = 1531.80 \pm 0.32$ MeV ($S = 1.3$)			
$\Xi(1530)^-$ mass $m = 1535.0 \pm 0.6$ MeV			
$\Xi(1530)^0$ full width $\Gamma = 9.1 \pm 0.5$ MeV			
$\Xi(1530)^-$ full width $\Gamma = 9.9^{+1.7}_{-1.9}$ MeV			
$\Xi(1530)$ DECAY MODES	Fraction (Γ_i/Γ)	Confidence level	ρ (MeV/c)
$\Xi\pi$	100 %		158
$\Xi\gamma$	<4 %	90%	202

Baryon Summary Table

 $\Xi(1690)$

$$I(J^P) = \frac{1}{2}(?^?)$$

Mass $m = 1690 \pm 10$ MeV [k]
 Full width $\Gamma < 30$ MeV

$\Xi(1690)$ DECAY MODES	Fraction (Γ_i/Γ)	ρ (MeV/c)
$\Lambda\bar{K}$	seen	240
$\Sigma\bar{K}$	seen	70
$\Xi\pi$	seen	311
$\Xi^-\pi^+\pi^-$	possibly seen	213

 $\Xi(1820) D_{13}$

$$I(J^P) = \frac{1}{2}(\frac{3}{2}^-)$$

Mass $m = 1823 \pm 5$ MeV [k]
 Full width $\Gamma = 24^{+15}_{-10}$ MeV [k]

$\Xi(1820)$ DECAY MODES	Fraction (Γ_i/Γ)	ρ (MeV/c)
$\Lambda\bar{K}$	large	402
$\Sigma\bar{K}$	small	324
$\Xi\pi$	small	421
$\Xi(1530)\pi$	small	237

 $\Xi(1950)$

$$I(J^P) = \frac{1}{2}(?^?)$$

Mass $m = 1950 \pm 15$ MeV [k]
 Full width $\Gamma = 60 \pm 20$ MeV [k]

$\Xi(1950)$ DECAY MODES	Fraction (Γ_i/Γ)	ρ (MeV/c)
$\Lambda\bar{K}$	seen	522
$\Sigma\bar{K}$	possibly seen	460
$\Xi\pi$	seen	519

 $\Xi(2030)$

$$I(J^P) = \frac{1}{2}(\geq \frac{5}{2}^?)$$

Mass $m = 2025 \pm 5$ MeV [k]
 Full width $\Gamma = 20^{+15}_{-5}$ MeV [k]

$\Xi(2030)$ DECAY MODES	Fraction (Γ_i/Γ)	ρ (MeV/c)
$\Lambda\bar{K}$	$\sim 20\%$	585
$\Sigma\bar{K}$	$\sim 80\%$	529
$\Xi\pi$	small	574
$\Xi(1530)\pi$	small	416
$\Lambda\bar{K}\pi$	small	499
$\Sigma\bar{K}\pi$	small	428

Ω BARYONS (S = -3, I = 0)

$$\Omega^- = sss$$

 Ω^-

$$I(J^P) = 0(\frac{3}{2}^+)$$

$J^P = \frac{3}{2}^+$ is the quark-model prediction; and $J = 3/2$ is fairly well established.

Mass $m = 1672.45 \pm 0.29$ MeV
 $(m_{\Omega^-} - m_{\bar{\Omega}^+}) / m_{\Omega^-} = (-1 \pm 8) \times 10^{-5}$
 Mean life $\tau = (0.821 \pm 0.011) \times 10^{-10}$ s
 $c\tau = 2.461$ cm
 $(\tau_{\Omega^-} - \tau_{\bar{\Omega}^+}) / \tau_{\Omega^-} = -0.002 \pm 0.040$
 Magnetic moment $\mu = -2.02 \pm 0.05 \mu_N$

Decay parameters

ΛK^-	$\alpha = 0.0180 \pm 0.0024$
$\Lambda K^-, \bar{\Lambda} K^+$	$(\alpha + \bar{\alpha}) / (\alpha - \bar{\alpha}) = -0.02 \pm 0.13$
$\Xi^0 \pi^-$	$\alpha = 0.09 \pm 0.14$
$\Xi^- \pi^0$	$\alpha = 0.05 \pm 0.21$

Ω⁻ DECAY MODES

	Fraction (Γ_i/Γ)	Confidence level	ρ (MeV/c)
ΛK^-	(67.8 ± 0.7) %		211
$\Xi^0 \pi^-$	(23.6 ± 0.7) %		294
$\Xi^- \pi^0$	(8.6 ± 0.4) %		289
$\Xi^- \pi^+ \pi^-$	$(4.3^{+3.4}_{-1.3}) \times 10^{-4}$		189
$\Xi(1530)^0 \pi^-$	$(6.4^{+5.1}_{-2.0}) \times 10^{-4}$		17
$\Xi^0 e^- \bar{\nu}_e$	$(5.6 \pm 2.8) \times 10^{-3}$		319
$\Xi^- \gamma$	$< 4.6 \times 10^{-4}$	90%	314

ΔS = 2 forbidden (S2) modes

$\Lambda \pi^-$	S2	$< 2.9 \times 10^{-6}$	90%	449
-----------------	----	------------------------	-----	-----

 $\Omega(2250)^-$

$$I(J^P) = 0(?^?)$$

Mass $m = 2252 \pm 9$ MeV
 Full width $\Gamma = 55 \pm 18$ MeV

Ω(2250)⁻ DECAY MODES

	Fraction (Γ_i/Γ)	ρ (MeV/c)
$\Xi^- \pi^+ K^-$	seen	532
$\Xi(1530)^0 K^-$	seen	437

CHARMED BARYONS (C = +1)

$$\Lambda_c^+ = udc, \quad \Sigma_c^{++} = uuc, \quad \Sigma_c^+ = udc, \quad \Sigma_c^0 = ddc,$$

$$\Xi_c^+ = usc, \quad \Xi_c^0 = dsc, \quad \Omega_c^0 = ssc$$

 Λ_c^+

$$I(J^P) = 0(\frac{1}{2}^+)$$

J is not well measured; $\frac{1}{2}$ is the quark-model prediction.

Mass $m = 2286.46 \pm 0.14$ MeV
 Mean life $\tau = (200 \pm 6) \times 10^{-15}$ s ($S = 1.6$)
 $c\tau = 59.9 \mu\text{m}$

Decay asymmetry parameters

$\Lambda\pi^+$	$\alpha = -0.91 \pm 0.15$
$\Sigma^+ \pi^0$	$\alpha = -0.45 \pm 0.32$
$\Lambda\ell^+ \nu_\ell$	$\alpha = -0.86 \pm 0.04$
$(\alpha + \bar{\alpha}) / (\alpha - \bar{\alpha})$ in $\Lambda_c^+ \rightarrow \Lambda\pi^+, \bar{\Lambda}_c^- \rightarrow \bar{\Lambda}\pi^-$	-0.07 ± 0.31
$(\alpha + \bar{\alpha}) / (\alpha - \bar{\alpha})$ in $\Lambda_c^+ \rightarrow \Lambda e^+ \nu_e, \bar{\Lambda}_c^- \rightarrow \bar{\Lambda} e^- \bar{\nu}_e$	0.00 ± 0.04

Nearly all branching fractions of the Λ_c^+ are measured relative to the $pK^- \pi^+$ mode, but there are no model-independent measurements of this branching fraction. We explain how we arrive at our value of $B(\Lambda_c^+ \rightarrow pK^- \pi^+)$ in a Note at the beginning of the branching-ratio measurements in the Listings. When this branching fraction is eventually well determined, all the other branching fractions will slide up or down proportionally as the true value differs from the value we use here.

Λ_c⁺ DECAY MODES

	Fraction (Γ_i/Γ)	Scale factor / Confidence level	ρ (MeV/c)
Hadronic modes with a p: S = -1 final states			
$p\bar{K}^0$	(2.3 ± 0.6) %		873
$pK^-\pi^+$	[m] (5.0 ± 1.3) %		823
$p\bar{K}^*(892)^0$	[n] (1.6 ± 0.5) %		685
$\Delta(1232)^{++} K^-$	(8.6 ± 3.0) × 10 ⁻³		710
$\Lambda(1520)\pi^+$	[n] (1.8 ± 0.6) %		627
$pK^-\pi^+$ nonresonant	(2.8 ± 0.8) %		823
$p\bar{K}^0 \pi^0$	(3.3 ± 1.0) %		823
$p\bar{K}^0 \eta$	(1.2 ± 0.4) %		568
$p\bar{K}^0 \pi^+ \pi^-$	(2.6 ± 0.7) %		754
$pK^-\pi^+ \pi^0$	(3.4 ± 1.0) %		759
$pK^*(892)^-\pi^+$	[n] (1.1 ± 0.5) %		580
$p(K^-\pi^+)$ nonresonant π^0	(3.6 ± 1.2) %		759
$\Delta(1232)K^*(892)$	seen		419
$pK^-\pi^+ \pi^+ \pi^-$	(1.1 ± 0.8) × 10 ⁻³		671
$pK^-\pi^+ \pi^0 \pi^0$	(8 ± 4) × 10 ⁻³		678

Baryon Summary Table

Hadronic modes with a p : $S = 0$ final states			
$p\pi^+\pi^-$		$(3.5 \pm 2.0) \times 10^{-3}$	927
$p f_0(980)$	[n]	$(2.8 \pm 1.9) \times 10^{-3}$	622
$p\pi^+\pi^+\pi^-\pi^-$		$(1.8 \pm 1.2) \times 10^{-3}$	852
pK^+K^-		$(7.7 \pm 3.5) \times 10^{-4}$	616
$p\phi$	[n]	$(8.2 \pm 2.7) \times 10^{-4}$	590
pK^+K^- non- ϕ		$(3.5 \pm 1.7) \times 10^{-4}$	616
Hadronic modes with a hyperon: $S = -1$ final states			
$\Lambda\pi^+$		$(1.07 \pm 0.28) \%$	864
$\Lambda\pi^+\pi^0$		$(3.6 \pm 1.3) \%$	844
$\Lambda\rho^+$		$< 5 \%$	CL=95% 635
$\Lambda\pi^+\pi^+\pi^-$		$(2.6 \pm 0.7) \%$	807
$\Sigma(1385)^+\pi^+\pi^-, \Sigma^{*+} \rightarrow$		$(7 \pm 4) \times 10^{-3}$	688
$\Lambda\pi^+$			
$\Sigma(1385)^-\pi^+\pi^+, \Sigma^{*-} \rightarrow$		$(5.5 \pm 1.7) \times 10^{-3}$	688
$\Lambda\pi^-\rho^0$		$(1.1 \pm 0.5) \%$	523
$\Lambda\pi^+\rho^0, \Sigma^{*+} \rightarrow \Lambda\pi^+$		$(3.7 \pm 3.1) \times 10^{-3}$	363
$\Lambda\pi^+\pi^+\pi^-$ nonresonant		$< 8 \times 10^{-3}$	CL=90% 807
$\Lambda\pi^+\pi^+\pi^-\pi^0$ total		$(1.8 \pm 0.8) \%$	757
$\Lambda\pi^+\eta$	[n]	$(1.8 \pm 0.6) \%$	691
$\Sigma(1385)^+\eta$	[n]	$(8.5 \pm 3.3) \times 10^{-3}$	570
$\Lambda\pi^+\omega$	[n]	$(1.2 \pm 0.5) \%$	517
$\Lambda\pi^+\pi^+\pi^-\pi^0$, no η or ω		$< 7 \times 10^{-3}$	CL=90% 757
$\Lambda K^+\bar{K}^0$		$(4.7 \pm 1.5) \times 10^{-3}$	S=1.2 443
$\Xi(1690)^0 K^+, \Xi^{*0} \rightarrow \Lambda\bar{K}^0$		$(1.3 \pm 0.5) \times 10^{-3}$	286
$\Sigma^0\pi^+$		$(1.05 \pm 0.28) \%$	825
$\Sigma^+\pi^0$		$(1.00 \pm 0.34) \%$	827
$\Sigma^+\eta$		$(5.5 \pm 2.3) \times 10^{-3}$	713
$\Sigma^+\pi^+\pi^-$		$(3.6 \pm 1.0) \%$	804
$\Sigma^+\rho^0$		$< 1.4 \%$	CL=95% 575
$\Sigma^-\pi^+\pi^+$		$(1.9 \pm 0.8) \%$	799
$\Sigma^0\pi^+\pi^0$		$(1.8 \pm 0.8) \%$	803
$\Sigma^0\pi^+\pi^+\pi^-$		$(8.3 \pm 3.1) \times 10^{-3}$	763
$\Sigma^+\pi^+\pi^-\pi^0$		—	767
$\Sigma^+\omega$	[n]	$(2.7 \pm 1.0) \%$	569
$\Sigma^+K^+K^-$		$(2.8 \pm 0.8) \times 10^{-3}$	349
$\Sigma^+\phi$	[n]	$(3.2 \pm 1.0) \times 10^{-3}$	295
$\Xi(1690)^0 K^+, \Xi^{*0} \rightarrow$		$(8.2 \pm 3.1) \times 10^{-4}$	286
Σ^+K^-			
$\Sigma^+K^+K^-$ nonresonant		$< 7 \times 10^{-4}$	CL=90% 349
$\Xi^0 K^+$		$(3.9 \pm 1.4) \times 10^{-3}$	653
$\Xi^- K^+\pi^+$		$(5.1 \pm 1.4) \times 10^{-3}$	565
$\Xi(1530)^0 K^+$	[n]	$(2.6 \pm 1.0) \times 10^{-3}$	473
Hadronic modes with a hyperon: $S = 0$ final states			
ΛK^+		$(5.0 \pm 1.6) \times 10^{-4}$	781
$\Lambda K^+\pi^+\pi^-$		$< 4 \times 10^{-4}$	CL=90% 637
$\Sigma^0 K^+$		$(4.2 \pm 1.3) \times 10^{-4}$	735
$\Sigma^0 K^+\pi^+\pi^-$		$< 2.1 \times 10^{-4}$	CL=90% 574
$\Sigma^+ K^+\pi^-$		$(1.7 \pm 0.7) \times 10^{-3}$	670
$\Sigma^+ K^*(892)^0$	[n]	$(2.8 \pm 1.1) \times 10^{-3}$	470
$\Sigma^- K^+\pi^+$		$< 1.0 \times 10^{-3}$	CL=90% 664
Doubly Cabibbo-suppressed modes			
$pK^+\pi^-$		$< 2.3 \times 10^{-4}$	CL=90% 823
Semileptonic modes			
$\Lambda\ell^+\nu_\ell$	[o]	$(2.0 \pm 0.6) \%$	871
$\Lambda e^+\nu_e$		$(2.1 \pm 0.6) \%$	871
$\Lambda\mu^+\nu_\mu$		$(2.0 \pm 0.7) \%$	867
Inclusive modes			
e^+ anything		$(4.5 \pm 1.7) \%$	—
$p e^+$ anything		$(1.8 \pm 0.9) \%$	—
p anything		$(50 \pm 16) \%$	—
p anything (no Λ)		$(12 \pm 19) \%$	—
n anything		$(50 \pm 16) \%$	—
n anything (no Λ)		$(29 \pm 17) \%$	—
Λ anything		$(35 \pm 11) \%$	S=1.4
Σ^\pm anything	[p]	$(10 \pm 5) \%$	—
3prongs		$(24 \pm 8) \%$	—
$\Delta C = 1$ weak neutral current (C1) modes, or Lepton number (L) violating modes			
$p\mu^+\mu^-$	C1	$< 3.4 \times 10^{-4}$	CL=90% 937
$\Sigma^-\mu^+\mu^+$	L	$< 7.0 \times 10^{-4}$	CL=90% 812

 $\Lambda_c(2595)^+$

$$I(J^P) = 0(\frac{1}{2}^-)$$

The spin-parity follows from the fact that $\Sigma_c(2455)\pi$ decays, with little available phase space, are dominant. This assumes that $J^P = 1/2^+$ for the $\Sigma_c(2455)$.

$$\text{Mass } m = 2595.4 \pm 0.6 \text{ MeV} \quad (S = 1.1)$$

$$m - m_{\Lambda_c^+} = 308.9 \pm 0.6 \text{ MeV} \quad (S = 1.1)$$

$$\text{Full width } \Gamma = 3.6_{-1.3}^{+2.0} \text{ MeV}$$

$\Lambda_c^+\pi\pi$ and its submode $\Sigma_c(2455)\pi$ — the latter just barely — are the only strong decays allowed to an excited Λ_c^+ having this mass; and the submode seems to dominate.

 $\Lambda_c(2595)^+$ DECAY MODES

	Fraction (Γ_i/Γ)	p (MeV/c)
$\Lambda_c^+\pi^+\pi^-$	[q] $\approx 67 \%$	124
$\Sigma_c(2455)^{++}\pi^-$	$24 \pm 7 \%$	28
$\Sigma_c(2455)^0\pi^+$	$24 \pm 7 \%$	28
$\Lambda_c^+\pi^+\pi^-$ 3-body	$18 \pm 10 \%$	124
$\Lambda_c^+\pi^0$	[r] not seen	261
$\Lambda_c^+\gamma$	not seen	291

 $\Lambda_c(2625)^+$

$$I(J^P) = 0(\frac{3}{2}^-)$$

J^P has not been measured; $\frac{3}{2}^-$ is the quark-model prediction.

$$\text{Mass } m = 2628.1 \pm 0.6 \text{ MeV} \quad (S = 1.5)$$

$$m - m_{\Lambda_c^+} = 341.7 \pm 0.6 \text{ MeV} \quad (S = 1.6)$$

$$\text{Full width } \Gamma < 1.9 \text{ MeV, CL} = 90\%$$

$\Lambda_c^+\pi\pi$ and its submode $\Sigma(2455)\pi$ are the only strong decays allowed to an excited Λ_c^+ having this mass.

 $\Lambda_c(2625)^+$ DECAY MODES

	Fraction (Γ_i/Γ)	Confidence level	p (MeV/c)
$\Lambda_c^+\pi^+\pi^-$	[q] $\approx 67\%$		184
$\Sigma_c(2455)^{++}\pi^-$	< 5	90%	102
$\Sigma_c(2455)^0\pi^+$	< 5	90%	102
$\Lambda_c^+\pi^+\pi^-$ 3-body	large		184
$\Lambda_c^+\pi^0$	[r] not seen		293
$\Lambda_c^+\gamma$	not seen		319

 $\Lambda_c(2880)^+$

$$I(J^P) = 0(\frac{5}{2}^+)$$

There is some good evidence that indeed $J^P = 5/2^+$

$$\text{Mass } m = 2881.53 \pm 0.35 \text{ MeV}$$

$$m - m_{\Lambda_c^+} = 595.1 \pm 0.4 \text{ MeV}$$

$$\text{Full width } \Gamma = 5.8 \pm 1.1 \text{ MeV}$$

 $\Lambda_c(2880)^+$ DECAY MODES

	Fraction (Γ_i/Γ)	p (MeV/c)
$\Lambda_c^+\pi^+\pi^-$	seen	471
$\Sigma_c(2455)^0, ++\pi^\pm$	seen	376
$\Sigma_c(2520)^0, ++\pi^\pm$	seen	317
pD^0	seen	316

Baryon Summary Table

 $\Lambda_c(2940)^+$

$$I(J^P) = 0(?^?)$$

Mass $m = 2939.3^{+1.4}_{-1.5}$ MeV
 Full width $\Gamma = 17^{+8}_{-6}$ MeV

$\Lambda_c(2940)^+$ DECAY MODES	Fraction (Γ_i/Γ)	ρ (MeV/c)
ρD^0	seen	420
$\Sigma_c(2455)^0, ++ \pi^\pm$	seen	-

 $\Sigma_c(2455)$

$$I(J^P) = 1(\frac{1}{2}^+)$$

J^P has not been measured; $\frac{1}{2}^+$ is the quark-model prediction.

$\Sigma_c(2455)^{++}$ mass $m = 2454.02 \pm 0.18$ MeV
 $\Sigma_c(2455)^+$ mass $m = 2452.9 \pm 0.4$ MeV
 $\Sigma_c(2455)^0$ mass $m = 2453.76 \pm 0.18$ MeV
 $m_{\Sigma_c^{++}} - m_{\Lambda_c^+} = 167.56 \pm 0.11$ MeV
 $m_{\Sigma_c^+} - m_{\Lambda_c^+} = 166.4 \pm 0.4$ MeV
 $m_{\Sigma_c^0} - m_{\Lambda_c^+} = 167.30 \pm 0.11$ MeV
 $m_{\Sigma_c^{++}} - m_{\Sigma_c^0} = 0.27 \pm 0.11$ MeV ($S = 1.1$)
 $m_{\Sigma_c^+} - m_{\Sigma_c^0} = -0.9 \pm 0.4$ MeV
 $\Sigma_c(2455)^{++}$ full width $\Gamma = 2.23 \pm 0.30$ MeV
 $\Sigma_c(2455)^+$ full width $\Gamma < 4.6$ MeV, CL = 90%
 $\Sigma_c(2455)^0$ full width $\Gamma = 2.2 \pm 0.4$ MeV ($S = 1.4$)

$\Lambda_c^+ \pi$ is the only strong decay allowed to a Σ_c having this mass.

$\Sigma_c(2455)$ DECAY MODES	Fraction (Γ_i/Γ)	ρ (MeV/c)
$\Lambda_c^+ \pi$	$\approx 100\%$	94

 $\Sigma_c(2520)$

$$I(J^P) = 1(\frac{3}{2}^+)$$

J^P has not been measured; $\frac{3}{2}^+$ is the quark-model prediction.

$\Sigma_c(2520)^{++}$ mass $m = 2518.4 \pm 0.6$ MeV ($S = 1.4$)
 $\Sigma_c(2520)^+$ mass $m = 2517.5 \pm 2.3$ MeV
 $\Sigma_c(2520)^0$ mass $m = 2518.0 \pm 0.5$ MeV
 $m_{\Sigma_c(2520)^{++}} - m_{\Lambda_c^+} = 231.9 \pm 0.6$ MeV ($S = 1.5$)
 $m_{\Sigma_c(2520)^+} - m_{\Lambda_c^+} = 231.0 \pm 2.3$ MeV
 $m_{\Sigma_c(2520)^0} - m_{\Lambda_c^+} = 231.6 \pm 0.5$ MeV ($S = 1.1$)
 $m_{\Sigma_c(2520)^{++}} - m_{\Sigma_c(2520)^0} = 0.3 \pm 0.6$ MeV ($S = 1.2$)
 $\Sigma_c(2520)^{++}$ full width $\Gamma = 14.9 \pm 1.9$ MeV
 $\Sigma_c(2520)^+$ full width $\Gamma < 17$ MeV, CL = 90%
 $\Sigma_c(2520)^0$ full width $\Gamma = 16.1 \pm 2.1$ MeV

$\Lambda_c^+ \pi$ is the only strong decay allowed to a Σ_c having this mass.

$\Sigma_c(2520)$ DECAY MODES	Fraction (Γ_i/Γ)	ρ (MeV/c)
$\Lambda_c^+ \pi$	$\approx 100\%$	180

 $\Sigma_c(2800)$

$$I(J^P) = 1(?^?)$$

$\Sigma_c(2800)^{++}$ mass $m = 2801^{+4}_{-6}$ MeV
 $\Sigma_c(2800)^+$ mass $m = 2792^{+14}_{-5}$ MeV
 $\Sigma_c(2800)^0$ mass $m = 2802^{+7}_{-6}$ MeV
 $m_{\Sigma_c(2800)^{++}} - m_{\Lambda_c^+} = 514^{+4}_{-6}$ MeV
 $m_{\Sigma_c(2800)^+} - m_{\Lambda_c^+} = 505^{+14}_{-5}$ MeV
 $m_{\Sigma_c(2800)^0} - m_{\Lambda_c^+} = 515^{+4}_{-7}$ MeV
 $\Sigma_c(2800)^{++}$ full width $\Gamma = 75^{+22}_{-17}$ MeV
 $\Sigma_c(2800)^+$ full width $\Gamma = 62^{+60}_{-40}$ MeV
 $\Sigma_c(2800)^0$ full width $\Gamma = 61^{+28}_{-18}$ MeV

 $\Xi_c(2800)$ DECAY MODESFraction (Γ_i/Γ) ρ (MeV/c)

$\Lambda_c^+ \pi$	seen	443
-------------------	------	-----

 Ξ_c^+

$$I(J^P) = \frac{1}{2}(\frac{1}{2}^+)$$

J^P has not been measured; $\frac{1}{2}^+$ is the quark-model prediction.

Mass $m = 2467.9 \pm 0.4$ MeV
 Mean life $\tau = (442 \pm 26) \times 10^{-15}$ s ($S = 1.3$)
 $c\tau = 132$ μm

 Ξ_c^+ DECAY MODESFraction (Γ_i/Γ)Confidence level (ρ (MeV/c))

No absolute branching fractions have been measured.
The following are branching ratios relative to $\Xi^- \pi^+ \pi^+$.

Cabibbo-favored ($S = -2$) decays

$\rho K_S^0 K_S^0$	[s]	0.087 ± 0.022	767
$\Lambda \bar{K}^0 \pi^+$		—	852
$\Sigma(1385)^+ \bar{K}^0$	[n,s]	1.0 ± 0.5	746
$\Lambda K^- \pi^+ \pi^+$	[s]	0.323 ± 0.033	787
$\Lambda \bar{K}^*(892)^0 \pi^+$	[n,s]	< 0.2	90% 608
$\Sigma(1385)^+ K^- \pi^+$	[n,s]	< 0.3	90% 678
$\Sigma^+ K^- \pi^+$	[s]	0.94 ± 0.11	811
$\Sigma^+ \bar{K}^*(892)^0 \pi^+$	[n,s]	0.81 ± 0.15	658
$\Sigma^0 K^- \pi^+ \pi^+$	[s]	0.29 ± 0.16	735
$\Xi^0 \pi^+$	[s]	0.55 ± 0.16	877
$\Xi^- \pi^+ \pi^+$	[s]	DEFINED AS 1	851
$\Xi(1530)^0 \pi^+$	[n,s]	< 0.1	90% 750
$\Xi^0 \pi^+ \pi^0$	[s]	2.34 ± 0.68	856
$\Xi^0 \pi^+ \pi^+ \pi^-$	[s]	1.74 ± 0.50	818
$\Xi^0 e^+ \nu_e$	[s]	2.3 ± 0.7 -0.9	884
$\Omega^- K^+ \pi^+$	[s]	0.07 ± 0.04	399

Cabibbo-suppressed decays

$\rho K^- \pi^+$	[s]	0.21 ± 0.03	944
$\rho \bar{K}^*(892)^0 \pi^+$	[n,s]	0.12 ± 0.02	828
$\Sigma^+ K^+ K^-$	[s]	0.15 ± 0.07	580
$\Sigma^+ \phi$	[n,s]	< 0.11	90% 549
$\Xi(1690)^0 K^+, \Xi(1690)^0 \rightarrow \Sigma^+ K^-$	[s]	< 0.05	90% 501

 Ξ_c^0

$$I(J^P) = \frac{1}{2}(\frac{1}{2}^+)$$

J^P has not been measured; $\frac{1}{2}^+$ is the quark-model prediction.

Mass $m = 2471.0 \pm 0.4$ MeV
 $m_{\Xi_c^0} - m_{\Xi_c^+} = 3.1 \pm 0.5$ MeV
 Mean life $\tau = (112^{+13}_{-10}) \times 10^{-15}$ s
 $c\tau = 33.6$ μm

Decay asymmetry parameters

$$\Xi^- \pi^+ \quad \alpha = -0.6 \pm 0.4$$

No absolute branching fractions have been measured. Several measurements of ratios of fractions may be found in the Listings that follow.

 Ξ_c^0 DECAY MODESFraction (Γ_i/Γ) ρ (MeV/c)

$\rho K^- K^- \pi^+$	seen	676
$\rho K^- \bar{K}^*(892)^0$	seen	413
$\rho K^- K^- \pi^+$ no $\bar{K}^*(892)^0$	seen	676
ΛK_S^0	seen	906
$\Lambda \bar{K}^0 \pi^+ \pi^-$	seen	787
$\Lambda K^- \pi^+ \pi^+ \pi^-$	seen	703
$\Xi^- \pi^+$	seen	875
$\Xi^- \pi^+ \pi^+ \pi^-$	seen	816
$\Omega^- K^+$	seen	523
$\Xi^- e^+ \nu_e$	seen	882
$\Xi^- \ell^+$ anything	seen	-

Baryon Summary Table

$\Xi_c^{'+}$	$I(J^P) = \frac{1}{2}(\frac{1}{2}^+)$
J^P has not been measured; $\frac{1}{2}^+$ is the quark-model prediction.	
Mass $m = 2575.7 \pm 3.1$ MeV	
$m_{\Xi_c^{'+}} - m_{\Xi_c^+} = 107.8 \pm 3.0$ MeV	
The $\Xi_c^{'+} - \Xi_c^+$ mass difference is too small for any strong decay to occur.	

$\Xi_c^{'+}$ DECAY MODES	Fraction (Γ_i/Γ)	ρ (MeV/c)
$\Xi_c^+ \gamma$	seen	106

$\Xi_c^{'0}$	$I(J^P) = \frac{1}{2}(\frac{1}{2}^+)$
J^P has not been measured; $\frac{1}{2}^+$ is the quark-model prediction.	
Mass $m = 2578.0 \pm 2.9$ MeV	
$m_{\Xi_c^{'0}} - m_{\Xi_c^0} = 107.0 \pm 2.9$ MeV	
The $\Xi_c^{'0} - \Xi_c^0$ mass difference is too small for any strong decay to occur.	

$\Xi_c^{'0}$ DECAY MODES	Fraction (Γ_i/Γ)	ρ (MeV/c)
$\Xi_c^0 \gamma$	seen	105

$\Xi_c(2645)$	$I(J^P) = \frac{1}{2}(\frac{3}{2}^+)$
J^P has not been measured; $\frac{3}{2}^+$ is the quark-model prediction.	
$\Xi_c(2645)^+$ mass $m = 2646.6 \pm 1.4$ MeV ($S = 1.6$)	
$\Xi_c(2645)^0$ mass $m = 2646.1 \pm 1.2$ MeV	
$m_{\Xi_c(2645)^+} - m_{\Xi_c^0} = 175.6 \pm 1.4$ MeV ($S = 1.7$)	
$m_{\Xi_c(2645)^0} - m_{\Xi_c^+} = 178.2 \pm 1.1$ MeV	
$\Xi_c(2645)^+$ full width $\Gamma < 3.1$ MeV, CL = 90%	
$\Xi_c(2645)^0$ full width $\Gamma < 5.5$ MeV, CL = 90%	
$\Xi_c \pi$ is the only strong decay allowed to a Ξ_c resonance having this mass.	

$\Xi_c(2645)$ DECAY MODES	Fraction (Γ_i/Γ)	ρ (MeV/c)
$\Xi_c^0 \pi^+$	seen	102
$\Xi_c^+ \pi^-$	seen	107

$\Xi_c(2790)$	$I(J^P) = \frac{1}{2}(\frac{1}{2}^-)$
J^P has not been measured; $\frac{1}{2}^-$ is the quark-model prediction.	
$\Xi_c(2790)^+$ mass = 2789.2 ± 3.2 MeV	
$\Xi_c(2790)^0$ mass = 2791.9 ± 3.3 MeV	
$m_{\Xi_c(2790)^+} - m_{\Xi_c^+} = 318.2 \pm 3.2$ MeV	
$m_{\Xi_c(2790)^0} - m_{\Xi_c^0} = 324.0 \pm 3.3$ MeV	
$\Xi_c(2790)^+$ width < 15 MeV, CL = 90%	
$\Xi_c(2790)^0$ width < 12 MeV, CL = 90%	

$\Xi_c(2790)$ DECAY MODES	Fraction (Γ_i/Γ)	ρ (MeV/c)
$\Xi_c' \pi$	seen	159

$\Xi_c(2815)$	$I(J^P) = \frac{1}{2}(\frac{3}{2}^-)$
J^P has not been measured; $\frac{3}{2}^-$ is the quark-model prediction.	
$\Xi_c(2815)^+$ mass $m = 2816.5 \pm 1.2$ MeV	
$\Xi_c(2815)^0$ mass $m = 2818.2 \pm 2.1$ MeV	
$m_{\Xi_c(2815)^+} - m_{\Xi_c^+} = 348.6 \pm 1.2$ MeV	
$m_{\Xi_c(2815)^0} - m_{\Xi_c^0} = 347.2 \pm 2.1$ MeV	
$\Xi_c(2815)^+$ full width $\Gamma < 3.5$ MeV, CL = 90%	
$\Xi_c(2815)^0$ full width $\Gamma < 6.5$ MeV, CL = 90%	

The $\Xi_c \pi \pi$ modes are consistent with being entirely via $\Xi_c(2645) \pi$.

$\Xi_c(2815)$ DECAY MODES	Fraction (Γ_i/Γ)	ρ (MeV/c)
$\Xi_c^+ \pi^+ \pi^-$	seen	196
$\Xi_c^0 \pi^+ \pi^-$	seen	191

$\Xi_c(2980)$	$I(J^P) = \frac{1}{2}(?)$
$\Xi_c(2980)^+$ $m = 2974 \pm 5$ MeV ($S = 2.3$)	
$\Xi_c(2980)^0$ $m = 2974 \pm 4$ MeV	
$\Xi_c(2980)^+$ width $\Gamma = 33 \pm 8$ MeV ($S = 1.3$)	
$\Xi_c(2980)^0$ width $\Gamma = 31 \pm 11$ MeV	

$\Xi_c(2980)$ DECAY MODES	Fraction (Γ_i/Γ)	ρ (MeV/c)
$\Lambda_c^+ \bar{K} \pi$	seen	244
$\Sigma_c(2455) \bar{K}$	seen	151
$\Lambda_c^+ \bar{K}$	not seen	421

$\Xi_c(3080)$	$I(J^P) = \frac{1}{2}(?)$
$\Xi_c(3080)^+$ $m = 3077.0 \pm 0.4$ MeV	
$\Xi_c(3080)^0$ $m = 3079.9 \pm 1.4$ MeV ($S = 1.3$)	
$\Xi_c(3080)^+$ width $\Gamma = 5.8 \pm 1.0$ MeV	
$\Xi_c(3080)^0$ width $\Gamma = 5.6 \pm 2.2$ MeV	

$\Xi_c(3080)$ DECAY MODES	Fraction (Γ_i/Γ)	ρ (MeV/c)
$\Lambda_c^+ \bar{K} \pi$	seen	415
$\Sigma_c(2455) \bar{K}$	seen	342
$\Sigma_c(2455) \bar{K} + \Sigma_c(2520) \bar{K}$	seen	-
$\Lambda_c^+ \bar{K}$	not seen	536
$\Lambda_c^+ \bar{K} \pi^+ \pi^-$	not seen	143

Ω_c^0	$I(J^P) = 0(\frac{1}{2}^+)$
J^P has not been measured; $\frac{1}{2}^+$ is the quark-model prediction.	
Mass $m = 2697.5 \pm 2.6$ MeV ($S = 1.2$)	
Mean life $\tau = (69 \pm 12) \times 10^{-15}$ s	
$c\tau = 21 \mu\text{m}$	
No absolute branching fractions have been measured.	

Ω_c^0 DECAY MODES	Fraction (Γ_i/Γ)	ρ (MeV/c)
$\Sigma^+ K^- K^- \pi^+$	seen	691
$\Xi^0 K^- \pi^+$	seen	903
$\Xi^- K^- \pi^+ \pi^+$	seen	832
$\Omega^- e^+ \nu_e$	seen	830
$\Omega^- \pi^+$	seen	822
$\Omega^- \pi^+ \pi^0$	seen	798
$\Omega^- \pi^- \pi^+ \pi^+$	seen	754

$\Omega_c(2770)^0$	$I(J^P) = 0(\frac{3}{2}^+)$
J^P has not been measured; $\frac{3}{2}^+$ is the quark-model prediction.	
Mass $m = 2768.3 \pm 3.0$ MeV ($S = 1.2$)	
$m_{\Omega_c(2770)^0} - m_{\Omega_c^0} = 70.8 \pm 1.5$ MeV	
The $\Omega_c(2770)^0 - \Omega_c^0$ mass difference is too small for any strong decay to occur.	

$\Omega_c(2770)^0$ DECAY MODES	Fraction (Γ_i/Γ)	ρ (MeV/c)
$\Omega_c^0 \gamma$	presumably 100%	70

Baryon Summary Table

BOTTOM BARYONS ($B = -1$)

$$\Lambda_b^0 = udb, \Xi_b^0 = usb, \Xi_b^- = dsb$$

Λ_b^0

$$I(J^P) = 0(\frac{1}{2}^+)$$

$I(J^P)$ not yet measured; $0(\frac{1}{2}^+)$ is the quark model prediction.

$$\text{Mass } m = 5620.2 \pm 1.6 \text{ MeV}$$

$$m_{\Lambda_b} - m_{p^0} = 339.2 \pm 1.4 \text{ MeV}$$

$$\text{Mean life } \tau = (1.383_{-0.048}^{+0.049}) \times 10^{-12} \text{ s}$$

$$c\tau = 415 \mu\text{m}$$

These branching fractions are actually an average over weakly decaying b -baryons weighted by their production rates in Z decay (or high-energy $p\bar{p}$), branching ratios, and detection efficiencies. They scale with the LEP b -baryon production fraction $B(b \rightarrow b\text{-baryon})$ and are evaluated for our value $B(b \rightarrow b\text{-baryon}) = (9.2 \pm 1.8)\%$.

The branching fractions $B(b\text{-baryon} \rightarrow \Lambda \ell^- \bar{\nu}_\ell \text{ anything})$ and $B(\Lambda_b^0 \rightarrow \Lambda_c^+ \ell^- \bar{\nu}_\ell \text{ anything})$ are not pure measurements because the underlying measured products of these with $B(b \rightarrow b\text{-baryon})$ were used to determine $B(b \rightarrow b\text{-baryon})$, as described in the note "Production and Decay of b -Flavored Hadrons."

For inclusive branching fractions, e.g., $B \rightarrow D^\pm \text{ anything}$, the values usually are multiplicities, not branching fractions. They can be greater than one.

Λ_b^0 DECAY MODES	Fraction (Γ_i/Γ)	Confidence level	ρ (MeV/c)
$J/\psi(1S)\Lambda$	$(4.7 \pm 2.8) \times 10^{-4}$		1741
$\Lambda_c^+ \pi^-$	$(8.8 \pm 3.2) \times 10^{-3}$		2343
$\Lambda_c^+ a_1(1260)^-$	seen		2153
$\Lambda_c^+ \ell^- \bar{\nu}_\ell \text{ anything}$	[t] $(9.9 \pm 2.6)\%$		—
$\Lambda_c^+ \ell^- \bar{\nu}_\ell$	$(5.0_{-1.4}^{+1.9})\%$		2345
$\Lambda_c^+ \pi^+ \pi^- \ell^- \bar{\nu}_\ell$	$(5.6 \pm 3.1)\%$		2335
$p h^-$	[u] $< 2.3 \times 10^{-5}$	90%	2730
$p \pi^-$	$< 5.0 \times 10^{-5}$	90%	2730
$p K^-$	$< 5.0 \times 10^{-5}$	90%	2709
$\Lambda \gamma$	$< 1.3 \times 10^{-3}$	90%	2699

Σ_b

$$I(J^P) = 1(\frac{1}{2}^+)$$

I, J, P need confirmation.

$$\text{Mass } m(\Sigma_b^+) = 5807.8 \pm 2.7 \text{ MeV}$$

$$\text{Mass } m(\Sigma_b^-) = 5815.2 \pm 2.0 \text{ MeV}$$

Σ_b DECAY MODES	Fraction (Γ_i/Γ)	ρ (MeV/c)
$\Lambda_b^0 \pi$	dominant	128

Σ_b^*

$$I(J^P) = 1(\frac{3}{2}^+)$$

I, J, P need confirmation.

$$\text{Mass } m(\Sigma_b^{*+}) = 5829.0 \pm 3.4 \text{ MeV}$$

$$\text{Mass } m(\Sigma_b^{*-}) = 5836.4 \pm 2.8 \text{ MeV}$$

$$m_{\Sigma_b^*} - m_{\Sigma_b} = 21.2 \pm 2.0 \text{ MeV}$$

Σ_b^* DECAY MODES	Fraction (Γ_i/Γ)	ρ (MeV/c)
$\Lambda_b^0 \pi$	dominant	156

Ξ_b^0, Ξ_b^-

$$I(J^P) = \frac{1}{2}(\frac{1}{2}^+)$$

I, J, P need confirmation.

$$\text{Mass } m = 5792.4 \pm 3.0 \text{ MeV}$$

$$\text{Mean life } \tau = (1.42_{-0.24}^{+0.28}) \times 10^{-12} \text{ s}$$

Ξ_b DECAY MODES	Fraction (Γ_i/Γ)	Scale factor	ρ (MeV/c)
$\Xi_b^- \rightarrow \Xi^- \ell^- \bar{\nu}_\ell X \times B(\bar{b} \rightarrow \Xi_b^-)$	$(3.9 \pm 1.2) \times 10^{-4}$	1.4	—
$\Xi_b^- \rightarrow J/\psi \Xi^- \times B(\bar{b} \rightarrow \Xi_b^-)$	$(1.3 \pm 1.0) \times 10^{-4}$		—
$\Xi_b^- \rightarrow B(\bar{b} \rightarrow \Lambda_b)$			

b -baryon ADMIXTURE ($\Lambda_b, \Xi_b, \Sigma_b, \Omega_b$)

$$\text{Mean life } \tau = (1.319_{-0.038}^{+0.039}) \times 10^{-12} \text{ s}$$

These branching fractions are actually an average over weakly decaying b -baryons weighted by their production rates in Z decay (or high-energy $p\bar{p}$), branching ratios, and detection efficiencies. They scale with the LEP b -baryon production fraction $B(b \rightarrow b\text{-baryon})$ and are evaluated for our value $B(b \rightarrow b\text{-baryon}) = (9.2 \pm 1.8)\%$.

The branching fractions $B(b\text{-baryon} \rightarrow \Lambda \ell^- \bar{\nu}_\ell \text{ anything})$ and $B(\Lambda_b^0 \rightarrow \Lambda_c^+ \ell^- \bar{\nu}_\ell \text{ anything})$ are not pure measurements because the underlying measured products of these with $B(b \rightarrow b\text{-baryon})$ were used to determine $B(b \rightarrow b\text{-baryon})$, as described in the note "Production and Decay of b -Flavored Hadrons."

For inclusive branching fractions, e.g., $B \rightarrow D^\pm \text{ anything}$, the values usually are multiplicities, not branching fractions. They can be greater than one.

b -baryon ADMIXTURE DECAY MODES ($\Lambda_b, \Xi_b, \Sigma_b, \Omega_b$)

Decay Mode	Fraction (Γ_i/Γ)	ρ (MeV/c)
$p \mu^- \bar{\nu}_\ell \text{ anything}$	$(5.3 \pm \frac{2.3}{2.0})\%$	—
$p \ell \bar{\nu}_\ell \text{ anything}$	$(5.1 \pm 1.4)\%$	—
$p \text{ anything}$	$(64 \pm 23)\%$	—
$\Lambda \ell^- \bar{\nu}_\ell \text{ anything}$	$(3.5 \pm 0.8)\%$	—
$\Lambda/\bar{\Lambda} \text{ anything}$	$(36 \pm 9)\%$	—
$\Xi^- \ell^- \bar{\nu}_\ell \text{ anything}$	$(6.0 \pm 1.8) \times 10^{-3}$	—

NOTES

This Summary Table only includes established baryons. The Particle Listings include evidence for other baryons. The masses, widths, and branching fractions for the resonances in this Table are Breit-Wigner parameters, but pole positions are also given for most of the N and Δ resonances.

For most of the resonances, the parameters come from various partial-wave analyses of more or less the same sets of data, and it is not appropriate to treat the results of the analyses as independent or to average them together. Furthermore, the systematic errors on the results are not well understood. Thus, we usually only give ranges for the parameters. We then also give a best guess for the mass (as part of the name of the resonance) and for the width. The *Note on N and Δ Resonances* and the *Note on Λ and Σ Resonances* in the Particle Listings review the partial-wave analyses.

When a quantity has "($S = \dots$)" to its right, the error on the quantity has been enlarged by the "scale factor" S , defined as $S = \sqrt{\chi^2/(N-1)}$, where N is the number of measurements used in calculating the quantity. We do this when $S > 1$, which often indicates that the measurements are inconsistent. When $S > 1.25$, we also show in the Particle Listings an ideogram of the measurements. For more about S , see the Introduction.

A decay momentum p is given for each decay mode. For a 2-body decay, p is the momentum of each decay product in the rest frame of the decaying particle. For a 3-or-more-body decay, p is the largest momentum any of the products can have in this frame. For any resonance, the *nominal* mass is used in calculating p . A dagger ("†") in this column indicates that the mode is forbidden when the nominal masses of resonances are used, but is in fact allowed due to the nonzero widths of the resonances.

- The masses of the p and n are most precisely known in u (unified atomic mass units). The conversion factor to MeV, $1 \text{ u} = 931.494043 \pm 0.000080 \text{ MeV}$, is less well known than are the masses in u.
- These two results are not independent, and both use the more precise measurement of $|q_p/m_p|/(q_p/m_p)$.
- The limit is from neutrality-of-matter experiments; it assumes $q_n = q_p + q_e$. See also the charge of the neutron.
- The first limit is for $p \rightarrow \text{anything} + \text{"disappearance" modes of a bound proton}$. The second entry, a rough range of limits, assumes the dominant decay modes are among those investigated. For antiprotons the best limit, inferred from the observation of cosmic ray \bar{p} 's is $\tau_{\bar{p}} > 10^7 \text{ yr}$, the cosmic-ray storage time, but this limit depends on a number of assumptions. The best direct observation of stored antiprotons gives $\tau_{\bar{p}}/B(\bar{p} \rightarrow e^- \gamma) > 7 \times 10^5 \text{ yr}$.
- There is some controversy about whether nuclear physics and model dependence complicate the analysis for bound neutrons (from which the best limit comes). The first limit here is from reactor experiments with free neutrons.
- The parameters g_A, g_V , and g_{WM} for semileptonic modes are defined by $\bar{B}_f[\gamma_\lambda(g_V + g_A \gamma_5) + i(g_{WM}/m_{B_i}) \sigma_{\lambda\nu} q^\nu] B_i$, and ϕ_{AV} is defined by

Baryon Summary Table

$g_A/g_V = |g_A/g_V| e^{i\phi_{AV}}$. See the "Note on Baryon Decay Parameters" in the neutron Particle Listings.

[g] Time-reversal invariance requires this to be 0° or 180° .

[h] This limit is for γ energies between 35 and 100 keV.

[i] The decay parameters γ and Δ are calculated from α and ϕ using

$$\gamma = \sqrt{1-\alpha^2} \cos\phi, \quad \tan\Delta = -\frac{1}{\alpha} \sqrt{1-\alpha^2} \sin\phi.$$

See the "Note on Baryon Decay Parameters" in the neutron Particle Listings.

[j] See the Listings for the pion momentum range used in this measurement.

[k] The error given here is only an educated guess. It is larger than the error on the weighted average of the published values.

[l] A theoretical value using QED.

[m] See the note on " Λ_c^+ Branching Fractions" in the Λ_c^+ Particle Listings.

[n] This branching fraction includes all the decay modes of the final-state resonance.

[o] An ℓ indicates an e or a μ mode, not a sum over these modes.

[p] The value is for the sum of the charge states or particle/antiparticle states indicated.

[q] Assuming isospin conservation, so that the other third is $\Lambda_c^+ \pi^0 \pi^0$.

[r] A test that the isospin is indeed 0, so that the particle is indeed a Λ_c^+ .

[s] No absolute branching fractions have been measured. The value here is the branching *ratio* relative to $\Xi^- \pi^+ \pi^+$.

[t] Not a pure measurement. See note at head of Λ_b^0 Decay Modes.

[u] Here h^- means π^- or K^- .

SEARCHES FOR MONOPOLES, SUPERSYMMETRY, TECHNICOLOR, COMPOSITENESS, EXTRA DIMENSIONS, etc.

Magnetic Monopole Searches

Isolated supermassive monopole candidate events have not been confirmed. The most sensitive experiments obtain negative results.

Best cosmic-ray supermassive monopole flux limit:

$$< 1.0 \times 10^{-15} \text{ cm}^{-2}\text{sr}^{-1}\text{s}^{-1} \quad \text{for } 1.1 \times 10^{-4} < \beta < 0.1$$

Supersymmetric Particle Searches

Limits are based on the Minimal Supersymmetric Standard Model.

Assumptions include: 1) $\tilde{\chi}_1^0$ (or $\tilde{\gamma}$) is lightest supersymmetric particle; 2) R -parity is conserved; 3) With the exception of \tilde{t} and \tilde{b} , all scalar quarks are assumed to be degenerate in mass and $m_{\tilde{q}_R} = m_{\tilde{q}_L}$. 4) Limits for sleptons refer to the \tilde{L}_R states. 5) Gaugino mass unification at the GUT scale.

See the Particle Listings for a Note giving details of supersymmetry.

$\tilde{\chi}_i^0$ — neutralinos (mixtures of $\tilde{\gamma}$, \tilde{Z}^0 , and \tilde{H}_i^0)

Mass $m_{\tilde{\chi}_1^0} > 46$ GeV, CL = 95%

[all $\tan\beta$, all m_0 , all $m_{\tilde{\chi}_2^0} - m_{\tilde{\chi}_1^0}$]

Mass $m_{\tilde{\chi}_2^0} > 62.4$ GeV, CL = 95%

[$1 < \tan\beta < 40$, all m_0 , all $m_{\tilde{\chi}_3^0} - m_{\tilde{\chi}_1^0}$]

Mass $m_{\tilde{\chi}_3^0} > 99.9$ GeV, CL = 95%

[$1 < \tan\beta < 40$, all m_0 , all $m_{\tilde{\chi}_4^0} - m_{\tilde{\chi}_1^0}$]

Mass $m_{\tilde{\chi}_4^0} > 116$ GeV, CL = 95%

[$1 < \tan\beta < 40$, all m_0 , all $m_{\tilde{\chi}_2^0} - m_{\tilde{\chi}_1^0}$]

$\tilde{\chi}_i^\pm$ — charginos (mixtures of \tilde{W}^\pm and \tilde{H}_i^\pm)

Mass $m_{\tilde{\chi}_1^\pm} > 94$ GeV, CL = 95%

[$\tan\beta < 40$, $m_{\tilde{\chi}_1^\pm} - m_{\tilde{\chi}_1^0} > 3$ GeV, all m_0]

\tilde{e} — scalar electron (selectron)

Mass $m > 73$ GeV, CL = 95% [all $m_{\tilde{e}_R} - m_{\tilde{\chi}_1^0}$]

$\tilde{\mu}$ — scalar muon (smuon)

Mass $m > 94$ GeV, CL = 95%

[$1 \leq \tan\beta \leq 40$, $m_{\tilde{\mu}_R} - m_{\tilde{\chi}_1^0} > 10$ GeV]

$\tilde{\tau}$ — scalar tau (stau)

Mass $m > 81.9$ GeV, CL = 95%

[$m_{\tilde{\tau}_R} - m_{\tilde{\chi}_1^0} > 15$ GeV, all θ_τ]

\tilde{q} — scalar quark (squark)

These limits include the effects of cascade decays, evaluated assuming a fixed value of the parameters μ and $\tan\beta$. The limits are weakly sensitive to these parameters over much of parameter space. Limits assume GUT relations between gaugino masses and the gauge coupling.

Mass $m > 379$ GeV, CL = 95% [tan β = 2, $\mu < 0$, $A = 0$]

\tilde{b} — scalar bottom (sbottom)

Mass $m > 89$ GeV, CL = 95% [$m_{\tilde{b}_1} - m_{\tilde{\chi}_1^0} > 8$ GeV, all θ_b]

\tilde{t} — scalar top (stop)

Mass $m > 95.7$ GeV, CL = 95%

[$\tilde{t} \rightarrow c\tilde{\chi}_1^0$, all θ_t , $m_{\tilde{t}} - m_{\tilde{\chi}_1^0} > 10$ GeV]

\tilde{g} — gluino

The limits summarised here refer to the high-mass region ($m_{\tilde{g}} \gtrsim 5$ GeV), and include the effects of cascade decays, evaluated assuming a fixed value of the parameters μ and $\tan\beta$.

The limits are weakly sensitive to these parameters over much of parameter space. Limits assume GUT relations between gaugino masses and the gauge coupling,

Mass $m > 308$ GeV, CL = 95% [any $m_{\tilde{q}}$]

Mass $m > 390$ GeV, CL = 95% [$m_{\tilde{q}} = m_{\tilde{g}}$]

Technicolor

Searches for a color-octet techni- ρ constrain its mass to be greater than 260 to 480 GeV, depending on allowed decay channels. Similar bounds exist on the color-octet techni- ω .

Quark and Lepton Compositeness, Searches for

Scale Limits Λ for Contact Interactions (the lowest dimensional interactions with four fermions)

If the Lagrangian has the form

$$\pm \frac{g^2}{2\Lambda^2} \bar{\psi}_L \gamma_\mu \psi_L \bar{\psi}_L \gamma^\mu \psi_L$$

(with $g^2/4\pi$ set equal to 1), then we define $\Lambda \equiv \Lambda_{LL}^\pm$. For the full definitions and for other forms, see the Note in the Listings on Searches for Quark and Lepton Compositeness in the full Review and the original literature.

$\Lambda_{LL}^+(eeee) > 8.3$ TeV, CL = 95%

$\Lambda_{LL}^-(eeee) > 10.3$ TeV, CL = 95%

$\Lambda_{LL}^+(ee\mu\mu) > 8.5$ TeV, CL = 95%

$\Lambda_{LL}^-(ee\mu\mu) > 7.3$ TeV, CL = 95%

$\Lambda_{LL}^+(ee\tau\tau) > 5.4$ TeV, CL = 95%

$\Lambda_{LL}^-(ee\tau\tau) > 7.2$ TeV, CL = 95%

$\Lambda_{LL}^+(\ell\ell\ell\ell) > 9.0$ TeV, CL = 95%

$\Lambda_{LL}^-(\ell\ell\ell\ell) > 9.5$ TeV, CL = 95%

$\Lambda_{LL}^+(eeuu) > 23.3$ TeV, CL = 95%

$\Lambda_{LL}^-(eeuu) > 12.5$ TeV, CL = 95%

$\Lambda_{LL}^+(eedd) > 11.1$ TeV, CL = 95%

$\Lambda_{LL}^-(eedd) > 26.4$ TeV, CL = 95%

$\Lambda_{LL}^+(eccc) > 1.0$ TeV, CL = 95%

$\Lambda_{LL}^-(eccc) > 2.1$ TeV, CL = 95%

$\Lambda_{LL}^+(eebb) > 5.6$ TeV, CL = 95%

$\Lambda_{LL}^-(eebb) > 4.9$ TeV, CL = 95%

$\Lambda_{LL}^+(\mu\mu qq) > 2.9$ TeV, CL = 95%

$\Lambda_{LL}^-(\mu\mu qq) > 4.2$ TeV, CL = 95%

$\Lambda(\ell\nu\ell\nu) > 3.10$ TeV, CL = 90%

$\Lambda(e\nu qq) > 2.81$ TeV, CL = 95%

$\Lambda_{LL}^+(qqqq) > 2.7$ TeV, CL = 95%

$\Lambda_{LL}^-(qqqq) > 2.4$ TeV, CL = 95%

$\Lambda_{LL}^+(\nu\nu qq) > 5.0$ TeV, CL = 95%

$\Lambda_{LL}^-(\nu\nu qq) > 5.4$ TeV, CL = 95%

Excited Leptons

The limits from $\ell^{*+}\ell^{*-}$ do not depend on λ (where λ is the $\ell\ell^*$ transition coupling). The λ -dependent limits assume chiral coupling.

$e^{\pm*}$ — excited electron

Mass $m > 103.2$ GeV, CL = 95% (from e^*e^*)

Mass $m > 255$ GeV, CL = 95% (from e^*e^*)

Mass $m > 310$ GeV, CL = 95% (if $\lambda_\gamma = 1$)

Searches Summary Table

$\mu^{*\pm}$ — excited muon

Mass $m > 103.2$ GeV, CL = 95% (from $\mu^* \mu^*$)

Mass $m > 221$ GeV, CL = 95% (from $\mu \mu^*$)

$\tau^{*\pm}$ — excited tau

Mass $m > 103.2$ GeV, CL = 95% (from $\tau^* \tau^*$)

Mass $m > 185$ GeV, CL = 95% (from $\tau \tau^*$)

ν^* — excited neutrino

Mass $m > 102.6$ GeV, CL = 95% (from $\nu^* \nu^*$)

Mass $m > 190$ GeV, CL = 95% (from $\nu \nu^*$)

q^* — excited quark

Mass $m > 45.6$ GeV, CL = 95% (from $q^* q^*$)

Mass m (from $q^* X$)

Color Sextet and Octet Particles

Color Sextet Quarks (q_6)

Mass $m > 84$ GeV, CL = 95% (Stable q_6)

Color Octet Charged Leptons (ℓ_8)

Mass $m > 86$ GeV, CL = 95% (Stable ℓ_8)

Color Octet Neutrinos (ν_8)

Mass $m > 110$ GeV, CL = 90% ($\nu_8 \rightarrow \nu g$)

Extra Dimensions

Please refer to the Extra Dimensions section of the full *Review* for a discussion of the model-dependence of these bounds, and further constraints.

Constraints on the fundamental gravity scale

$M_H > 1.1$ TeV, CL = 95% (dim-8 operators; $p\bar{p} \rightarrow e^+ e^-, \gamma\gamma$)

$M_D > 1.1$ TeV, CL = 95% ($e^+ e^- \rightarrow G\gamma$; 2-flat dimensions)

$M_D > 3\text{--}1000$ TeV (astrophys. and cosmology; 2-flat dimensions; limits depend on technique and assumptions)

Constraints on the radius of the extra dimensions, for the case of two-flat dimensions of equal radii

$r < 90\text{--}660$ nm (astrophysics; limits depend on technique and assumptions)

$r < 0.22$ mm, CL = 95% (direct tests of Newton's law; cited in Extra Dimensions review)

TESTS OF CONSERVATION LAWS

Updated June 2008 by L. Wolfenstein (Carnegie-Mellon University), T.G. Trippe (LBNL), and C.-J. Lin (LBNL).

In keeping with the current interest in tests of conservation laws, we collect together a Table of experimental limits on all weak and electromagnetic decays, mass differences, and moments, and on a few reactions, whose observation would violate conservation laws. The Table is given only in the full *Review of Particle Physics*, not in the Particle Physics Booklet. For the benefit of Booklet readers, we include the best limits from the Table in the following text. Limits in this text are for CL=90% unless otherwise specified. The Table is in two parts: “Discrete Space-Time Symmetries,” *i.e.*, C , P , T , CP , and CPT ; and “Number Conservation Laws,” *i.e.*, lepton, baryon, hadronic flavor, and charge conservation. The references for these data can be found in the the Particle Listings in the *Review*. A discussion of these tests follows.

CPT INVARIANCE

General principles of relativistic field theory require invariance under the combined transformation CPT . The simplest tests of CPT invariance are the equality of the masses and lifetimes of a particle and its antiparticle. The best test comes from the limit on the mass difference between K^0 and \bar{K}^0 . Any such difference contributes to the CP -violating parameter ϵ . Assuming CPT invariance, ϕ_ϵ , the phase of ϵ should be very close to 44° . (See the review “ CP Violation in K_L decay” in this edition.) In contrast, if the entire source of CP violation in K^0 decays were a $K^0 - \bar{K}^0$ mass difference, ϕ_ϵ would be $44^\circ + 90^\circ$.

Assuming that there is no other source of CPT violation than this mass difference, it is possible to deduce that[1]

$$m_{\bar{K}^0} - m_{K^0} \approx \frac{2(m_{K_L^0} - m_{K_S^0}) |\eta| (\frac{2}{3}\phi_{+-} + \frac{1}{3}\phi_{00} - \phi_{SW})}{\sin \phi_{SW}},$$

where $\phi_{SW} = (43.51 \pm 0.05)^\circ$, the superweak angle. Using our best values of the CP -violation parameters, we get $|(m_{\bar{K}^0} - m_{K^0})/m_{K^0}| \leq 0.8 \times 10^{-18}$ at CL=90%. Limits can also be placed on specific CPT -violating decay amplitudes. Given the small value of $(1 - |\eta_{00}/\eta_{+-}|)$, the value of $\phi_{00} - \phi_{+-}$ provides a measure of CPT violation in $K_L^0 \rightarrow 2\pi$ decay. Results from CERN [1] and Fermilab [2] indicate no CPT -violating effect.

CP AND T INVARIANCE

Given CPT invariance, CP violation and T violation are equivalent. The original evidence for CP violation came from the measurement of $|\eta_{+-}| = |A(K_L^0 \rightarrow \pi^+\pi^-)/A(K_S^0 \rightarrow \pi^+\pi^-)| = (2.233 \pm 0.012) \times 10^{-3}$. This could be explained in terms of $K^0 - \bar{K}^0$ mixing, which also leads to the asymmetry $[\Gamma(K_L^0 \rightarrow \pi^-e^+\nu) - \Gamma(K_L^0 \rightarrow \pi^+e^-\bar{\nu})]/[\text{sum}] = (0.334 \pm 0.007)\%$. Evidence for CP violation in the kaon decay amplitude comes from the measurement of $(1 - |\eta_{00}/\eta_{+-}|)/3 = \text{Re}(\epsilon'/\epsilon) = (1.65 \pm 0.26) \times 10^{-3}$. In the Standard Model much larger CP -violating effects are expected. The first of these, which is associated with $B - \bar{B}$ mixing, is the parameter $\sin(2\beta)$ now measured

quite accurately to be 0.678 ± 0.025 . A number of other CP -violating observables are being measured in B decays; direct evidence for CP violation in the B decay amplitude comes from the asymmetry $[\Gamma(\bar{B}^0 \rightarrow K^-\pi^+) - \Gamma(B^0 \rightarrow K^+\pi^-)]/[\text{sum}] = -0.101 \pm 0.015$. Direct tests of T violation are much more difficult; a measurement by CPLEAR of the difference between the oscillation probabilities of K^0 to \bar{K}^0 and \bar{K}^0 to K^0 is related to T violation [3]. Other searches for CP or T violation involve effects that are expected to be unobservable in the Standard Model. The most sensitive are probably the searches for an electric dipole moment of the neutron, measured to be $< 2.9 \times 10^{-26}$ e cm, and the electron $(0.07 \pm 0.07) \times 10^{-26}$ e cm. A nonzero value requires both P and T violation.

CONSERVATION OF LEPTON NUMBERS

Present experimental evidence and the standard electroweak theory are consistent with the absolute conservation of three separate lepton numbers: electron number L_e , muon number L_μ , and tau number L_τ , except for the effect of neutrino mixing associated with neutrino masses. Searches for violations are of the following types:

a) $\Delta L = 2$ for one type of charged lepton. The best limit comes from the search for neutrinoless double beta decay $(Z, A) \rightarrow (Z + 2, A) + e^- + e^-$. The best laboratory limit is $t_{1/2} > 1.9 \times 10^{25}$ yr (CL=90%) for ^{76}Ge .

b) Conversion of one charged-lepton type to another. For purely leptonic processes, the best limits are on $\mu \rightarrow e\gamma$ and $\mu \rightarrow 3e$, measured as $\Gamma(\mu \rightarrow e\gamma)/\Gamma(\mu \rightarrow \text{all}) < 1.2 \times 10^{-11}$ and $\Gamma(\mu \rightarrow 3e)/\Gamma(\mu \rightarrow \text{all}) < 1.0 \times 10^{-12}$. For semileptonic processes, the best limit comes from the coherent conversion process in a muonic atom, $\mu^- + (Z, A) \rightarrow e^- + (Z, A)$, measured as $\Gamma(\mu^- \text{Ti} \rightarrow e^- \text{Ti})/\Gamma(\mu^- \text{Ti} \rightarrow \text{all}) < 4.3 \times 10^{-12}$. Of special interest is the case in which the hadronic flavor also changes, as in $K_L \rightarrow e\mu$ and $K^+ \rightarrow \pi^+e^-\mu^+$, measured as $\Gamma(K_L \rightarrow e\mu)/\Gamma(K_L \rightarrow \text{all}) < 4.7 \times 10^{-12}$ and $\Gamma(K^+ \rightarrow \pi^+e^-\mu^+)/\Gamma(K^+ \rightarrow \text{all}) < 1.3 \times 10^{-11}$. Limits on the conversion of τ into e or μ are found in τ decay and are much less stringent than those for $\mu \rightarrow e$ conversion, *e.g.*, $\Gamma(\tau \rightarrow \mu\gamma)/\Gamma(\tau \rightarrow \text{all}) < 6.8 \times 10^{-8}$ and $\Gamma(\tau \rightarrow e\gamma)/\Gamma(\tau \rightarrow \text{all}) < 1.1 \times 10^{-7}$.

c) Conversion of one type of charged lepton into another type of charged antilepton. The case most studied is $\mu^- + (Z, A) \rightarrow e^+ + (Z - 2, A)$, the strongest limit being $\Gamma(\mu^- \text{Ti} \rightarrow e^+ \text{Ca})/\Gamma(\mu^- \text{Ti} \rightarrow \text{all}) < 3.6 \times 10^{-11}$.

d) Neutrino oscillations. If neutrinos have mass, then it is expected even in the standard electroweak theory that the lepton numbers are not separately conserved, as a consequence of lepton mixing analogous to Cabibbo quark mixing. However, if the only source of lepton-number violation is the mixing of low-mass neutrinos then processes such as $\mu \rightarrow e\gamma$ are expected to have extremely small unobservable probabilities. For small neutrino masses, the lepton-number violation would be observed first in neutrino oscillations, which have been the subject of extensive experimental searches. Strong evidence for neutrino mixing has come from atmospheric and solar neutrinos. The

Tests of Conservation Laws

SNO experiment has detected the total flux of neutrinos from the sun measured via neutral current interactions and found it greater than the flux of ν_e . This confirms previous indications of a deficit of ν_e and can be explained by oscillations with $\Delta(m^2) = (8.0 \pm 0.3) \times 10^{-5} \text{ eV}^2$. Evidence for such oscillations for reactor $\bar{\nu}$ has been found by the KAMLAND detector. In addition, underground detectors observing neutrinos produced by cosmic rays in the atmosphere have found a factor of 2 deficiency of upward going ν_μ compared to downward. This provides compelling evidence for ν_μ disappearance, for which the most probable explanation is $\nu_\mu \rightarrow \nu_\tau$ oscillations with nearly maximal mixing and $\Delta(m^2)$ of the order 0.0019–0.0030 eV^2 .

CONSERVATION OF HADRONIC FLAVORS

In strong and electromagnetic interactions, hadronic flavor is conserved, *i.e.* the conversion of a quark of one flavor (d, u, s, c, b, t) into a quark of another flavor is forbidden. In the Standard Model, the weak interactions violate these conservation laws in a manner described by the Cabibbo-Kobayashi-Maskawa mixing (see the section “Cabibbo-Kobayashi-Maskawa Mixing Matrix”). The way in which these conservation laws are violated is tested as follows:

(a) $\Delta S = \Delta Q$ rule. In the strangeness-changing semileptonic decay of strange particles, the strangeness change equals the change in charge of the hadrons. Tests come from limits on decay rates such as $\Gamma(\Sigma^+ \rightarrow ne^+\nu)/\Gamma(\Sigma^+ \rightarrow \text{all}) < 5 \times 10^{-6}$, and from a detailed analysis of $K_L \rightarrow \pi e \nu$, which yields the parameter x , measured to be $(\text{Re } x, \text{Im } x) = (-0.002 \pm 0.006, 0.0012 \pm 0.0021)$. Corresponding rules are $\Delta C = \Delta Q$ and $\Delta B = \Delta Q$.

(b) Change of flavor by two units. In the Standard Model this occurs only in second-order weak interactions. The classic example is $\Delta S = 2$ via $K^0 - \bar{K}^0$ mixing, which is directly measured by $m(K_L) - m(K_S) = (0.5292 \pm 0.0009) \times 10^{10} \hbar s^{-1}$. The $\Delta B = 2$ transitions in the B^0 and B_s^0 systems via mixing are also well established. The measured mass differences between the eigenstates are $(m_{B_H^0} - m_{B_L^0}) = (0.507 \pm 0.005) \times 10^{12} \hbar s^{-1}$ and $(m_{B_{sH}^0} - m_{B_{sL}^0}) = (17.77 \pm 0.12) \times 10^{12} \hbar s^{-1}$. There is now strong evidence of $\Delta C = 2$ transition in the charm sector with the mass difference $m_{D_H^0} - m_{D_L^0} = (2.37^{+0.66}_{-0.71}) \times 10^{10} \hbar s^{-1}$. All results are consistent with the second-order calculations in the Standard Model.

(c) Flavor-changing neutral currents. In the Standard Model the neutral-current interactions do not change flavor. The low rate $\Gamma(K_L \rightarrow \mu^+ \mu^-)/\Gamma(K_L \rightarrow \text{all}) = (6.84 \pm 0.11) \times 10^{-9}$ puts limits on such interactions; the nonzero value for this rate is attributed to a combination of the weak and electromagnetic interactions. The best test should come from

$K^+ \rightarrow \pi^+ \nu \bar{\nu}$, which occurs in the Standard Model only as a second-order weak process with a branching fraction of $(0.4 \text{ to } 1.2) \times 10^{-10}$. Recent results, including observation of two events, yields $\Gamma(K^+ \rightarrow \pi^+ \nu \bar{\nu})/\Gamma(K^+ \rightarrow \text{all}) = (1.5^{+1.3}_{-0.9}) \times 10^{-10}$ [4]. Limits for charm-changing or bottom-changing neutral currents are much less stringent: $\Gamma(D^0 \rightarrow \mu^+ \mu^-)/\Gamma(D^0 \rightarrow \text{all}) < 1.3 \times 10^{-6}$ and $\Gamma(B^0 \rightarrow \mu^+ \mu^-)/\Gamma(B^0 \rightarrow \text{all}) < 1.5 \times 10^{-8}$. One cannot isolate flavor-changing neutral current (FCNC) effects in non leptonic decays. For example, the FCNC transition $s \rightarrow d + (\bar{u} + u)$ is equivalent to the charged-current transition $s \rightarrow u + (\bar{u} + d)$. Tests for FCNC are therefore limited to hadron decays into lepton pairs. Such decays are expected only in second-order in the electroweak coupling in the Standard Model.

References

1. R. Carosi *et al.*, Phys. Lett. **B237**, 303 (1990).
2. A. Alavi-Harati *et al.*, Phys. Rev. **D67**, 012005 (2003); B. Schwingerheuer *et al.*, Phys. Rev. Lett. **74**, 4376 (1995).
3. A. Angelopoulos *et al.*, Phys. Lett. **B444**, 43 (1998); L. Wolfenstein, Phys. Rev. Lett. **83**, 911 (1999).
4. V.V. Anisimovsky *et al.*, Phys. Rev. Lett. **93**, 031801 (2004).

TESTS OF DISCRETE SPACE-TIME SYMMETRIES

CHARGE CONJUGATION (C) INVARIANCE

$\Gamma(\pi^0 \rightarrow 3\gamma)/\Gamma_{\text{total}}$	$< 3.1 \times 10^{-8}$, CL = 90%
η C-nonconserving decay parameters	
$\pi^+ \pi^- \pi^0$ left-right asymmetry parameter	$(0.09 \pm 0.17) \times 10^{-2}$
$\pi^+ \pi^- \pi^0$ sextant asymmetry parameter	$(0.18 \pm 0.16) \times 10^{-2}$
$\pi^+ \pi^- \pi^0$ quadrant asymmetry parameter	$(-0.17 \pm 0.17) \times 10^{-2}$
$\pi^+ \pi^- \gamma$ left-right asymmetry parameter	$(0.9 \pm 0.4) \times 10^{-2}$
$\pi^+ \pi^- \gamma$ parameter β (D-wave)	-0.02 ± 0.07 (S = 1.3)
$\Gamma(\eta \rightarrow \pi^0 \gamma)/\Gamma_{\text{total}}$	$< 9 \times 10^{-5}$, CL = 90%
$\Gamma(\eta \rightarrow \pi^0 \pi^0 \gamma)/\Gamma_{\text{total}}$	$< 5 \times 10^{-4}$, CL = 90%
$\Gamma(\eta \rightarrow \pi^0 \pi^0 \pi^0 \gamma)/\Gamma_{\text{total}}$	$< 6 \times 10^{-5}$, CL = 90%
$\Gamma(\eta \rightarrow 3\gamma)/\Gamma_{\text{total}}$	$< 1.6 \times 10^{-5}$, CL = 90%
$\Gamma(\eta \rightarrow \pi^0 e^+ e^-)/\Gamma_{\text{total}}$	[a] $< 4 \times 10^{-5}$, CL = 90%
$\Gamma(\eta \rightarrow \pi^0 \mu^+ \mu^-)/\Gamma_{\text{total}}$	[a] $< 5 \times 10^{-6}$, CL = 90%
$\Gamma(\omega(782) \rightarrow \eta \pi^0)/\Gamma_{\text{total}}$	$< 1 \times 10^{-3}$, CL = 90%
$\Gamma(\omega(782) \rightarrow 3\pi^0)/\Gamma_{\text{total}}$	$< 3 \times 10^{-4}$, CL = 90%
c decay parameter of $\eta'(958)$	0.015 \pm 0.018
asymmetry parameter for $\eta'(958) \rightarrow \pi^+ \pi^- \gamma$ decay	-0.01 \pm 0.04
$\Gamma(\eta'(958) \rightarrow \pi^0 e^+ e^-)/\Gamma_{\text{total}}$	[a] $< 1.4 \times 10^{-3}$, CL = 90%
$\Gamma(\eta'(958) \rightarrow \eta e^+ e^-)/\Gamma_{\text{total}}$	[a] $< 2.4 \times 10^{-3}$, CL = 90%
$\Gamma(\eta'(958) \rightarrow 3\gamma)/\Gamma_{\text{total}}$	$< 1.0 \times 10^{-4}$, CL = 90%
$\Gamma(\eta'(958) \rightarrow \mu^+ \mu^- \pi^0)/\Gamma_{\text{total}}$	[a] $< 6.0 \times 10^{-5}$, CL = 90%
$\Gamma(\eta'(958) \rightarrow \mu^+ \mu^- \eta)/\Gamma_{\text{total}}$	[a] $< 1.5 \times 10^{-5}$, CL = 90%
$\Gamma(J/\psi(1S) \rightarrow \gamma \gamma)/\Gamma_{\text{total}}$	$< 2.2 \times 10^{-5}$, CL = 90%

Tests of Conservation Laws

PARITY (P) INVARIANCE

e electric dipole moment	$(0.07 \pm 0.07) \times 10^{-26}$ ecm
μ electric dipole moment	$(3.7 \pm 3.4) \times 10^{-19}$ ecm
$\text{Re}(d_\tau = \tau$ electric dipole moment)	-0.22 to 0.45×10^{-16} ecm, CL = 95%
$\Gamma(\eta \rightarrow \pi^+ \pi^-)/\Gamma_{\text{total}}$	$<1.3 \times 10^{-5}$, CL = 90%
$\Gamma(\eta \rightarrow \pi^0 \pi^0)/\Gamma_{\text{total}}$	$<3.5 \times 10^{-4}$, CL = 90%
$\Gamma(\eta \rightarrow 4\pi^0)/\Gamma_{\text{total}}$	$<6.9 \times 10^{-7}$, CL = 90%
$\Gamma(\eta'(958) \rightarrow \pi^+ \pi^-)/\Gamma_{\text{total}}$	$<2.9 \times 10^{-3}$, CL = 90%
$\Gamma(\eta'(958) \rightarrow \pi^0 \pi^0)/\Gamma_{\text{total}}$	$<9 \times 10^{-4}$, CL = 90%
$\Gamma(\eta_c(1S) \rightarrow \pi^+ \pi^-)/\Gamma_{\text{total}}$	$<8.7 \times 10^{-4}$, CL = 90%
$\Gamma(\eta_c(1S) \rightarrow \pi^0 \pi^0)/\Gamma_{\text{total}}$	$<5.6 \times 10^{-4}$, CL = 90%
$\Gamma(\eta_c(1S) \rightarrow K^+ K^-)/\Gamma_{\text{total}}$	$<7.6 \times 10^{-4}$, CL = 90%
$\Gamma(\eta_c(1S) \rightarrow K_S^0 K_S^0)/\Gamma_{\text{total}}$	$<4.2 \times 10^{-4}$, CL = 90%
p electric dipole moment	$<0.54 \times 10^{-23}$ ecm
n electric dipole moment	$<0.29 \times 10^{-25}$ ecm, CL = 90%
Λ electric dipole moment	$<1.5 \times 10^{-16}$ ecm, CL = 95%

TIME REVERSAL (T) INVARIANCE

e electric dipole moment	$(0.07 \pm 0.07) \times 10^{-26}$ ecm
μ electric dipole moment	$(3.7 \pm 3.4) \times 10^{-19}$ ecm
μ decay parameters	
transverse e^+ polarization normal to plane of μ spin, e^+ momentum	$(-2 \pm 8) \times 10^{-3}$
α'/A	$(0 \pm 4) \times 10^{-3}$
β'/A	$(1 \pm 5) \times 10^{-3}$
$\text{Re}(d_\tau = \tau$ electric dipole moment)	-0.22 to 0.45×10^{-16} ecm, CL = 95%
P_T in $K^+ \rightarrow \pi^0 \mu^+ \nu_\mu$	$(-1.7 \pm 2.5) \times 10^{-3}$
P_T in $K^+ \rightarrow \mu^+ \nu_\mu \gamma$	$(-0.6 \pm 1.9) \times 10^{-2}$
$\text{Im}(\xi)$ in $K^+ \rightarrow \pi^0 \mu^+ \nu_\mu$ decay (from transverse μ pol.)	-0.006 ± 0.008
asymmetry A_T in $K^0 \bar{K}^0$ mixing	$(6.6 \pm 1.6) \times 10^{-3}$
$\text{Im}(\xi)$ in $K_{\mu 3}^0$ decay (from transverse μ pol.)	-0.007 ± 0.026
$A_T(K_S^0 K^\pm \pi^+ \pi^-)$ in D^\pm	0.02 ± 0.07
$A_T(K^+ K^- \pi^+ \pi^-)$ in D^0, \bar{D}^0	0.01 ± 0.07
$A_T(K_S^0 K^\pm \pi^+ \pi^-)$ in D_S^\pm	[b] -0.04 ± 0.07
p electric dipole moment	$<0.54 \times 10^{-23}$ ecm
n electric dipole moment	$<0.29 \times 10^{-25}$ ecm, CL = 90%
$n \rightarrow pe^- \bar{\nu}_e$ decay parameters	
ϕ_{AV} , phase of g_A relative to g_V	[c] $(180.06 \pm 0.07)^\circ$
triple correlation coefficient D	$(-4 \pm 6) \times 10^{-4}$
Λ electric dipole moment	$<1.5 \times 10^{-16}$ ecm, CL = 95%
triple correlation coefficient D for $\Sigma^- \rightarrow ne^- \bar{\nu}_e$	0.11 ± 0.10

CP INVARIANCE

$\text{Re}(d_\tau^W)$	$<0.50 \times 10^{-17}$ ecm, CL = 95%
$\text{Im}(d_\tau^W)$	$<1.1 \times 10^{-17}$ ecm, CL = 95%
$\Gamma(\eta \rightarrow \pi^+ \pi^-)/\Gamma_{\text{total}}$	$<1.3 \times 10^{-5}$, CL = 90%
$\Gamma(\eta \rightarrow \pi^0 \pi^0)/\Gamma_{\text{total}}$	$<3.5 \times 10^{-4}$, CL = 90%
$\Gamma(\eta \rightarrow 4\pi^0)/\Gamma_{\text{total}}$	$<6.9 \times 10^{-7}$, CL = 90%
$\Gamma(\eta'(958) \rightarrow \pi^+ \pi^-)/\Gamma_{\text{total}}$	$<2.9 \times 10^{-3}$, CL = 90%
$\Gamma(\eta'(958) \rightarrow \pi^0 \pi^0)/\Gamma_{\text{total}}$	$<9 \times 10^{-4}$, CL = 90%
$K^\pm \rightarrow \pi^\pm \pi^+ \pi^-$ rate difference/average	$(0.08 \pm 0.12)\%$
$K^\pm \rightarrow \pi^\pm \pi^0 \pi^0$ rate difference/average	$(0.0 \pm 0.6)\%$
$K^\pm \rightarrow \pi^\pm \pi^0 \gamma$ rate difference/average	$(0.9 \pm 3.3)\%$
$K^\pm \rightarrow \pi^\pm \pi^+ \pi^- (g_+ - g_-) / (g_+ + g_-)$	$(-1.5 \pm 2.2) \times 10^{-4}$
$K^\pm \rightarrow \pi^\pm \pi^0 \pi^0 (g_+ - g_-) / (g_+ + g_-)$	$(1.8 \pm 1.8) \times 10^{-4}$
$\Delta(K_{\pi\mu\mu}^\pm) = \frac{\Gamma(K_{\pi\mu\mu}^+) - \Gamma(K_{\pi\mu\mu}^-)}{\Gamma(K_{\pi\mu\mu}^+) + \Gamma(K_{\pi\mu\mu}^-)}$	-0.02 ± 0.12
$A_S = [\Gamma(K_S^0 \rightarrow \pi^- e^+ \nu_e) - \Gamma(K_S^0 \rightarrow \pi^+ e^- \bar{\nu}_e)] / \text{SUM}$	$(2 \pm 10) \times 10^{-3}$
$\text{Im}(\eta_{+-0}) = \text{Im}(A(K_S^0 \rightarrow \pi^+ \pi^- \pi^0, CP\text{-violating}) / A(K_L^0 \rightarrow \pi^+ \pi^- \pi^0))$	-0.002 ± 0.009
$\text{Im}(\eta_{000}) = \text{Im}(A(K_S^0 \rightarrow \pi^0 \pi^0 \pi^0) / A(K_L^0 \rightarrow \pi^0 \pi^0 \pi^0))$	$(-0.1 \pm 1.6) \times 10^{-2}$

$ \eta_{000} = A(K_S^0 \rightarrow 3\pi^0)/A(K_L^0 \rightarrow 3\pi^0) $	<0.018 , CL = 90%
CP asymmetry A in $K_S^0 \rightarrow \pi^+ \pi^- e^+ e^-$	$(-1 \pm 4)\%$
$\Gamma(K_S^0 \rightarrow 3\pi^0)/\Gamma_{\text{total}}$	$<1.2 \times 10^{-7}$, CL = 90%
linear coefficient j for $K_L^0 \rightarrow \pi^+ \pi^- \pi^0$	0.0012 ± 0.0008
quadratic coefficient f for $K_L^0 \rightarrow \pi^+ \pi^- \pi^0$	0.004 ± 0.006
$ \epsilon'_{+-\gamma} /\epsilon$ for $K_L^0 \rightarrow \pi^+ \pi^- \gamma$	<0.3 , CL = 90%
$ \bar{g}_{E1} $ for $K_L^0 \rightarrow \pi^+ \pi^- \gamma$	<0.21 , CL = 90%
$\Gamma(K_L^0 \rightarrow \pi^0 \mu^+ \mu^-)/\Gamma_{\text{total}}$	[d] $<3.8 \times 10^{-10}$, CL = 90%
$\Gamma(K_L^0 \rightarrow \pi^0 e^+ e^-)/\Gamma_{\text{total}}$	[d] $<2.8 \times 10^{-10}$, CL = 90%
$\Gamma(K_L^0 \rightarrow \pi^0 \nu \bar{\nu})/\Gamma_{\text{total}}$	[e] $<2.1 \times 10^{-7}$, CL = 90%
$A_{CP}(K_S^0 \pi^\pm)$ in D^\pm	-0.009 ± 0.009
$A_{CP}(K^\mp 2\pi^\pm)$ in D^\pm	-0.005 ± 0.010
$A_{CP}(K^\mp \pi^\pm \pi^\pm \pi^0)$ in D^\pm	0.010 ± 0.013
$A_{CP}(K_S^0 \pi^\pm \pi^0)$ in D^\pm	0.003 ± 0.009
$A_{CP}(K_S^0 \pi^\pm \pi^+ \pi^-)$ in D^\pm	0.001 ± 0.013
$A_{CP}(K_S^0 K^\pm)$ in D^\pm	0.07 ± 0.06
$A_{CP}(K^+ K^- \pi^\pm)$ in D^\pm	0.006 ± 0.007
$A_{CP}(K^\pm K^*0)$ in D^\pm	0.005 ± 0.017
$A_{CP}(\phi \pi^\pm)$ in D^\pm	-0.001 ± 0.015
$A_{CP}(\pi^+ \pi^- \pi^\pm)$ in D^\pm	-0.02 ± 0.04
$A_{CP}(K_S^0 K^\pm \pi^+ \pi^-)$ in D^\pm	-0.04 ± 0.07
$A_{CP}(K^+ K^-)$ in D^0, \bar{D}^0	$(0.1 \pm 0.5) \times 10^{-2}$ ($S = 1.4$)
$A_{CP}(K_S^0 K_S^0)$ in D^0, \bar{D}^0	-0.23 ± 0.19
$A_{CP}(\pi^+ \pi^-)$ in D^0, \bar{D}^0	$(0.0 \pm 0.5) \times 10^{-2}$
$A_{CP}(\pi^0 \pi^0)$ in D^0, \bar{D}^0	0.00 ± 0.05
$A_{CP}(\pi^+ \pi^- \pi^0)$ in D^0, \bar{D}^0	0.004 ± 0.013
$A_{CP}(K_S^0 \phi)$ in D^0, \bar{D}^0	-0.03 ± 0.09
$A_{CP}(K_S^0 \pi^0)$ in D^0, \bar{D}^0	0.001 ± 0.013
$A_{CP}(K^\pm \pi^\mp)$ in D^0, \bar{D}^0	0.022 ± 0.032
$A_{CP}(K^\mp \pi^\pm \pi^0)$ in D^0, \bar{D}^0	0.002 ± 0.009
$A_{CP}(K^\pm \pi^\mp \pi^0)$ in D^0, \bar{D}^0	0.00 ± 0.05
$A_{CP}(K_S^0 \pi^+ \pi^-)$ in D^0, \bar{D}^0	$-0.009 \pm_{-0.061}^{0.026}$
$A_{CP}(K^*(892)^\mp \pi^\pm \rightarrow K_S^0 \pi^+ \pi^-)$ in D^0	$<3.5 \times 10^{-4}$, CL = 95%
$A_{CP}(K^*(892)^\pm \pi^\mp \rightarrow K_S^0 \pi^+ \pi^-)$ in D^0	$<7.8 \times 10^{-4}$, CL = 95%
$A_{CP}(K_S^0 \rho^0 \rightarrow K_S^0 \pi^+ \pi^-)$ in D^0, \bar{D}^0	$<4.8 \times 10^{-4}$, CL = 95%
$A_{CP}(K_S^0 \omega \rightarrow K_S^0 \pi^+ \pi^-)$ in D^0, \bar{D}^0	$<9.2 \times 10^{-4}$, CL = 95%
$A_{CP}(K_S^0 f_0(980) \rightarrow K_S^0 \pi^+ \pi^-)$ in D^0, \bar{D}^0	$<6.8 \times 10^{-4}$, CL = 95%
$A_{CP}(K_S^0 f_2(1270) \rightarrow K_S^0 \pi^+ \pi^-)$ in D^0, \bar{D}^0	$<13.5 \times 10^{-4}$, CL = 95%
$A_{CP}(K_S^0 f_0(1370) \rightarrow K_S^0 \pi^+ \pi^-)$ in D^0, \bar{D}^0	$<25.5 \times 10^{-4}$, CL = 95%
$A_{CP}(K_S^*(1430)^\mp \pi^\pm \rightarrow K_S^0 \pi^+ \pi^-)$ in D^0, \bar{D}^0	$<9.0 \times 10^{-4}$, CL = 95%
$A_{CP}(K_S^*(1430)^\mp \pi^\pm \rightarrow K_S^0 \pi^+ \pi^-)$ in D^0, \bar{D}^0	$<6.5 \times 10^{-4}$, CL = 95%
$A_{CP}(K^*(1680)^\mp \pi^\pm \rightarrow K_S^0 \pi^+ \pi^-)$ in D^0, \bar{D}^0	$<28.4 \times 10^{-4}$, CL = 95%
$A_{CP}(K^\pm \pi^\mp \pi^+ \pi^-)$ in D^0, \bar{D}^0	-0.02 ± 0.04
$A_{CP}(K^+ K^- \pi^+ \pi^-)$ in D^0, \bar{D}^0	-0.08 ± 0.07
$A_{CP}(K^\pm K_S^0)$ in $D_S^\pm \rightarrow K^\pm K_S^0$	0.049 ± 0.023
$A_{CP}(K^+ K^- \pi^\pm)$ in $D_S^\pm \rightarrow K^+ K^- \pi^\pm$	0.003 ± 0.014
$A_{CP}(K^+ K^- \pi^\pm \pi^0)$ in $D_S^\pm \rightarrow K^+ K^- \pi^\pm \pi^0$	-0.06 ± 0.04
$A_{CP}(K_S^0 K^\mp 2\pi^\pm)$ in $D_S^\pm \rightarrow K_S^0 K^- 2\pi^+$	-0.01 ± 0.04
$A_{CP}(\pi^+ \pi^- \pi^\pm)$ in $D_S^\pm \rightarrow \pi^+ \pi^- \pi^\pm$	0.02 ± 0.05
$A_{CP}(\pi^\pm \eta)$ in $D_S^\pm \rightarrow \pi^\pm \eta$	-0.08 ± 0.05
$A_{CP}(\pi^\pm \eta')$ in $D_S^\pm \rightarrow \pi^\pm \eta'$	-0.06 ± 0.04
$A_{CP}(K^\pm \pi^0)$ in $D_S^\pm \rightarrow K^\pm \pi^0$	0.02 ± 0.29
$A_{CP}(K_S^0 \pi^\pm)$ in $D_S^\pm \rightarrow K_S^0 \pi^\pm$	0.27 ± 0.11
$A_{CP}(K^\pm \eta)$ in $D_S^\pm \rightarrow K^\pm \eta$	-0.20 ± 0.18
$A_{CP}(K^\pm \eta'(958))$ in $D_S^\pm \rightarrow K^\pm \eta'(958)$	-0.2 ± 0.4
$A_{CP}(B^+ \rightarrow J/\psi(1S) K^+)$	0.017 ± 0.016 ($S = 1.2$)
$A_{CP}(B^+ \rightarrow J/\psi(1S) \pi^+)$	0.09 ± 0.08
$A_{CP}(B^+ \rightarrow J/\psi K^*(892)^+)$	-0.048 ± 0.033
$A_{CP}(B^+ \rightarrow \psi(2S) K^+)$	-0.025 ± 0.024
$A_{CP}(B^+ \rightarrow \psi(2S) K^*(892)^+)$	0.08 ± 0.21

Tests of Conservation Laws

$A_{CP}(B^+ \rightarrow \chi_{c1} K^+)$	-0.009 ± 0.033	$A_{CP}(B^0 \rightarrow \rho^+ \pi^-)$	0.08 ± 0.12 (S = 2.0)
$A_{CP}(B^+ \rightarrow \chi_{c1} K^*(892)^+)$	0.5 ± 0.5	$A_{CP}(B^0 \rightarrow \rho^- \pi^+)$	-0.16 ± 0.23 (S = 1.7)
$A_{CP}(B^+ \rightarrow \bar{D}^0 \pi^+)$	-0.008 ± 0.008	$A_{CP}(B^0 \rightarrow K^*(1430) \gamma)$	-0.08 ± 0.15
$A_{CP}(B^+ \rightarrow D_{CP(+1)} \pi^+)$	0.035 ± 0.024	$A_{CP}(B^0 \rightarrow \rho \bar{p} K^*(892)^0)$	0.11 ± 0.14
$A_{CP}(B^+ \rightarrow D_{CP(-1)} \pi^+)$	0.017 ± 0.026	$A_{CP}(B^0 \rightarrow \rho \bar{\Lambda} \pi^-)$	-0.02 ± 0.10
$A_{CP}(B^+ \rightarrow \bar{D}^0 K^+)$	0.07 ± 0.04	$C_{D^*(2010)-D^+}(B^0 \rightarrow D^*(2010)-D^+)$	0.23 ± 0.13
$A_{CP}(B^+ \rightarrow [K^- \pi^+]_D K^+)$	$0.9^{+0.8}_{-0.6}$	$S_{D^*(2010)-D^+}(B^0 \rightarrow D^*(2010)-D^+)$	-0.55 ± 0.21
$A_{CP}(B^+ \rightarrow [K^- \pi^+]_{\bar{D}} K^*(892)^+)$	-0.2 ± 0.6	$C_{D^*(2010)+D^-}(B^0 \rightarrow D^*(2010)+D^-)$	0.01 ± 0.26 (S = 2.0)
$A_{CP}(B^+ \rightarrow [K^- \pi^+]_D \pi^+)$	$0.30^{+0.30}_{-0.26}$	$S_{D^*(2010)+D^-}(B^0 \rightarrow D^*(2010)+D^-)$	-0.74 ± 0.19
$A_{CP}(B^+ \rightarrow [\pi^+ \pi^- \pi^0]_D K^+)$	-0.02 ± 0.15	$C_{D^{*+}D^{*-}}(B^0 \rightarrow D^{*+}D^{*-})$	0.02 ± 0.10
$A_{CP}(B^+ \rightarrow D_{CP(+1)} K^+)$	0.22 ± 0.14 (S = 1.4)	$S_{D^{*+}D^{*-}}(B^0 \rightarrow D^{*+}D^{*-})$	-0.67 ± 0.18
$A_{CP}(B^+ \rightarrow D_{CP(-1)} K^+)$	-0.09 ± 0.10	$C_+(B^0 \rightarrow D^{*+}D^{*-})$	-0.05 ± 0.14
$A_{CP}(B^+ \rightarrow \bar{D}^{*0} \pi^+)$	-0.014 ± 0.015	$S_+(B^0 \rightarrow D^{*+}D^{*-})$	-0.72 ± 0.20
$A_{CP}(B^+ \rightarrow (D_{CP(+1)}^*)^0 \pi^+)$	-0.02 ± 0.05	$C_-(B^0 \rightarrow D^{*+}D^{*-})$	0.2 ± 0.7
$A_{CP}(B^+ \rightarrow (D_{CP(-1)}^*)^0 \pi^+)$	-0.09 ± 0.05	$S_-(B^0 \rightarrow D^{*+}D^{*-})$	-1.8 ± 1.1
$A_{CP}(B^+ \rightarrow D^{*0} K^+)$	-0.09 ± 0.09	$C_{D^+D^-}(B^0 \rightarrow D^+D^-)$	-0.4 ± 0.5 (S = 3.1)
$A_{CP}(B^+ \rightarrow D_{CP(+1)}^{*0} K^+)$	-0.15 ± 0.16	$S_{D^+D^-}(B^0 \rightarrow D^+D^-)$	-0.81 ± 0.29 (S = 1.1)
$A_{CP}(B^+ \rightarrow D_{CP(-1)}^{*0} K^+)$	0.13 ± 0.31	$C_{J/\psi(1S)\pi^0}(B^0 \rightarrow J/\psi(1S)\pi^0)$	-0.11 ± 0.20
$A_{CP}(B^+ \rightarrow D_{CP(+1)} K^*(892)^+)$	-0.08 ± 0.21	$S_{J/\psi(1S)\pi^0}(B^0 \rightarrow J/\psi(1S)\pi^0)$	-0.69 ± 0.25
$A_{CP}(B^+ \rightarrow D_{CP(-1)} K^*(892)^+)$	-0.3 ± 0.4	$C_{\eta'(958)K}(B^0 \rightarrow \eta'(958)K_S^0)$	-0.04 ± 0.20 (S = 2.5)
$A_{CP}(B^+ \rightarrow K_S^0 \pi^+)$	0.009 ± 0.029 (S = 1.2)	$S_{\eta'(958)K}(B^0 \rightarrow \eta'(958)K_S^0)$	0.43 ± 0.17 (S = 1.5)
$A_{CP}(B^+ \rightarrow K^+ \pi^0)$	0.027 ± 0.032	$C_{\omega K_S^0}(B^0 \rightarrow \omega K_S^0)$	-0.25 ± 0.31 (S = 1.6)
$A_{CP}(B^+ \rightarrow \eta' K^+)$	0.016 ± 0.019	$S_{\omega K_S^0}(B^0 \rightarrow \omega K_S^0)$	0.35 ± 0.29
$A_{CP}(B^+ \rightarrow \eta K^+)$	-0.27 ± 0.09	$C_{f_0(980)K_S^0}(B^0 \rightarrow f_0(980)K_S^0)$	-0.03 ± 0.26 (S = 1.9)
$A_{CP}(B^+ \rightarrow \eta K^*(892)^+)$	0.02 ± 0.06	$S_{f_0(980)K_S^0}(B^0 \rightarrow f_0(980)K_S^0)$	-0.02 ± 0.21 (S = 1.1)
$A_{CP}(B^+ \rightarrow \omega K^+)$	0.02 ± 0.05	$C_{K_S K_S K_S}(B^0 \rightarrow K_S K_S K_S)$	-0.15 ± 0.16 (S = 1.1)
$A_{CP}(B^+ \rightarrow K^*(892)^+ \pi^0)$	0.04 ± 0.29	$S_{K_S K_S K_S}(B^0 \rightarrow K_S K_S K_S)$	-0.4 ± 0.5 (S = 2.5)
$A_{CP}(B^+ \rightarrow K^{*0} \pi^+)$	-0.08 ± 0.10 (S = 1.8)	$C_{K^+K^-K_S^0}(B^0 \rightarrow K^+K^-K_S^0)$	0.07 ± 0.08
$A_{CP}(B^+ \rightarrow K^+ \pi^- \pi^+)$	0.023 ± 0.031 (S = 1.2)	$S_{K^+K^-K_S^0}(B^0 \rightarrow K^+K^-K_S^0)$	$-0.74^{+0.12}_{-0.10}$
$A_{CP}(B^+ \rightarrow f_0(980) K^+)$	$-0.04^{+0.08}_{-0.07}$ (S = 1.1)	$C_{\phi K_S^0}(B^0 \rightarrow \phi K_S^0)$	-0.01 ± 0.12
$A_{CP}(B^+ \rightarrow \rho^0 K^+)$	$0.31^{+0.11}_{-0.09}$	$S_{\phi K_S^0}(B^0 \rightarrow \phi K_S^0)$	0.39 ± 0.17
$A_{CP}(B^+ \rightarrow K_0^*(1430)^0 \pi^+)$	0.00 ± 0.07 (S = 2.4)	$C_{K_S^0 \pi^0}(B^0 \rightarrow K_S^0 \pi^0)$	0.14 ± 0.11
$A_{CP}(B^+ \rightarrow \rho \bar{\Lambda} \pi^0)$	0.01 ± 0.17	$S_{K_S^0 \pi^0}(B^0 \rightarrow K_S^0 \pi^0)$	0.38 ± 0.19
$A_{CP}(B^+ \rightarrow \rho^0 K^*(892)^+)$	0.20 ± 0.31	$C_{K_S^0 \pi^0 \gamma}(B^0 \rightarrow K_S^0 \pi^0 \gamma)$	0.0 ± 0.4 (S = 2.1)
$A_{CP}(B^+ \rightarrow K^0 K^+)$	0.12 ± 0.18	$S_{K_S^0 \pi^0 \gamma}(B^0 \rightarrow K_S^0 \pi^0 \gamma)$	-0.01 ± 0.30
$A_{CP}(B^+ \rightarrow K^+ K_S^0 K_S^0)$	-0.04 ± 0.11	$C_{K^*(892)^0 \gamma}(B^0 \rightarrow K^*(892)^0 \gamma)$	-0.12 ± 0.30 (S = 1.8)
$A_{CP}(B^+ \rightarrow K^+ K^- K^+)$	-0.017 ± 0.030	$S_{K^*(892)^0 \gamma}(B^0 \rightarrow K^*(892)^0 \gamma)$	-0.27 ± 0.26
$A_{CP}(B^+ \rightarrow \phi K^+)$	-0.01 ± 0.06	$C_{\pi \pi}(B^0 \rightarrow \pi^+ \pi^-)$	-0.38 ± 0.17 (S = 2.6)
$A_{CP}(B^+ \rightarrow \phi K^*(892)^+)$	-0.01 ± 0.08	$S_{\pi \pi}(B^0 \rightarrow \pi^+ \pi^-)$	-0.61 ± 0.08
$A_{CP}(B^+ \rightarrow \eta K^+ \gamma)$	-0.13 ± 0.08	$C_{\pi^0 \pi^0}(B^0 \rightarrow \pi^0 \pi^0)$	-0.48 ± 0.30
$A_{CP}(B^+ \rightarrow \pi^+ \pi^0)$	0.01 ± 0.06	$C_{\rho \pi}(B^0 \rightarrow \rho^+ \pi^-)$	0.01 ± 0.14 (S = 1.9)
$A_{CP}(B^+ \rightarrow \pi^+ \pi^- \pi^+)$	-0.01 ± 0.08	$S_{\rho \pi}(B^0 \rightarrow \rho^+ \pi^-)$	0.01 ± 0.09
$A_{CP}(B^+ \rightarrow \rho^0 \pi^+)$	-0.07 ± 0.13	$\Delta C_{\rho \pi}(B^0 \rightarrow \rho^+ \pi^-)$	0.37 ± 0.08
$A_{CP}(B^+ \rightarrow f_2(1270) \pi^+)$	0.00 ± 0.25	$\Delta S_{\rho \pi}(B^0 \rightarrow \rho^+ \pi^-)$	-0.05 ± 0.10
$A_{CP}(B^+ \rightarrow \rho^+ \pi^0)$	0.02 ± 0.11	$C_{\rho^0 \pi^0}(B^0 \rightarrow \rho^0 \pi^0)$	-0.1 ± 0.7
$A_{CP}(B^+ \rightarrow \rho^+ \rho^0)$	-0.08 ± 0.13	$S_{\rho^0 \pi^0}(B^0 \rightarrow \rho^0 \pi^0)$	0.1 ± 0.4
$A_{CP}(B^+ \rightarrow \omega \pi^+)$	-0.04 ± 0.06	$C_{\rho \rho}(B^0 \rightarrow \rho^+ \rho^-)$	-0.05 ± 0.13
$A_{CP}(B^+ \rightarrow \omega \rho^+)$	0.04 ± 0.18	$S_{\rho \rho}(B^0 \rightarrow \rho^+ \rho^-)$	-0.06 ± 0.17
$A_{CP}(B^+ \rightarrow \eta \pi^+)$	-0.16 ± 0.07 (S = 1.1)	$ \lambda (B^0 \rightarrow J/\psi K^*(892)^0)$	<0.25 , CL = 95%
$A_{CP}(B^+ \rightarrow \eta' \pi^+)$	0.21 ± 0.15	$(S_+ + S_-)/2(B^0 \rightarrow D^{*-} \pi^+)$	-0.037 ± 0.012
$A_{CP}(B^+ \rightarrow \eta \rho^+)$	0.01 ± 0.16	$(S_- - S_+)/2(B^0 \rightarrow D^{*-} \pi^+)$	-0.006 ± 0.016
$A_{CP}(B^+ \rightarrow \rho \bar{p} \pi^+)$	0.00 ± 0.04	$(S_+ + S_-)/2(B^0 \rightarrow D^- \pi^+)$	-0.046 ± 0.023
$A_{CP}(B^+ \rightarrow \rho \bar{p} K^+)$	-0.16 ± 0.07	$(S_- - S_+)/2(B^0 \rightarrow D^- \pi^+)$	-0.022 ± 0.021
$A_{CP}(B^+ \rightarrow \rho \bar{p} K^*(892)^+)$	0.32 ± 0.14	$A_{CP}(B \rightarrow K^*(892) \gamma)$	-0.010 ± 0.028
$A_{CP}(B^+ \rightarrow \rho \bar{\Lambda} \gamma)$	0.17 ± 0.17	$A_{CP}(B \rightarrow s \gamma)$	0.01 ± 0.04
$\text{Re}(\epsilon_{B^0})/(1+ \epsilon_{B^0} ^2)$	$(-0.1 \pm 1.4) \times 10^{-3}$	$A_{CP}(b \rightarrow X_S \ell^+ \ell^-)$	-0.22 ± 0.26
$A_{T/CP}$	0.005 ± 0.018	$\Gamma(\eta_C(1S) \rightarrow \pi^+ \pi^-)/\Gamma_{\text{total}}$	$<8.7 \times 10^{-4}$, CL = 90%
$A_{CP}(B^0 \rightarrow D^*(2010)+D^-)$	-0.06 ± 0.09 (S = 1.7)	$\Gamma(\eta_C(1S) \rightarrow \pi^0 \pi^0)/\Gamma_{\text{total}}$	$<5.6 \times 10^{-4}$, CL = 90%
$A_{CP}(B^0 \rightarrow K^+ \pi^-)$	-0.101 ± 0.015	$\Gamma(\eta_C(1S) \rightarrow K^+ K^-)/\Gamma_{\text{total}}$	$<7.6 \times 10^{-4}$, CL = 90%
$A_{CP}(B^0 \rightarrow \eta K^*(892)^0)$	0.19 ± 0.05	$\Gamma(\eta_C(1S) \rightarrow K_S^0 K_S^0)/\Gamma_{\text{total}}$	$<4.2 \times 10^{-4}$, CL = 90%
$A_{CP}(B^0 \rightarrow \rho^+ K^-)$	-0.08 ± 0.24 (S = 1.7)		
$A_{CP}(B^0 \rightarrow K^+ \pi^- \pi^0)$	0.07 ± 0.11		
$A_{CP}(B^0 \rightarrow K^*(892)^+ \pi^-)$	-0.05 ± 0.14		
$A_{CP}(B^0 \rightarrow K^*(892)^0 \pi^+ \pi^-)$	0.07 ± 0.05		
$A_{CP}(B^0 \rightarrow K^*(892)^0 K^+ K^-)$	0.01 ± 0.05		
$A_{CP}(B^0 \rightarrow K^*(892)^0 \phi)$	-0.01 ± 0.06		
$A_{CP}(B^0 \rightarrow K^*(892)^0 K^- \pi^+)$	0.2 ± 0.4		
$A_{CP}(B^0 \rightarrow \phi(K \pi)_0^0)$	0.17 ± 0.15		

Unless otherwise stated, limits are given at the 90% confidence level, while errors are given as ± 1 standard deviation.

Tests of Conservation Laws

$[\alpha_-(A) + \alpha_+(\bar{A})] / [\alpha_-(A) - \alpha_+(\bar{A})]$	0.012 ± 0.021
$\frac{[\alpha(\Xi^-)\alpha_-(A) - \alpha(\Xi^+)\alpha_+(\bar{A})]}{[\alpha(\Xi^-)\alpha_-(A) + \alpha(\Xi^+)\alpha_+(\bar{A})]}$	$(0 \pm 7) \times 10^{-4}$
$(\alpha + \bar{\alpha})/(\alpha - \bar{\alpha})$ in $\Omega^- \rightarrow \Lambda K^-, \bar{\Omega}^+ \rightarrow \bar{\Lambda} K^+$	-0.02 ± 0.13
$(\alpha + \bar{\alpha})/(\alpha - \bar{\alpha})$ in $\Lambda_C^+ \rightarrow \Lambda \pi^+, \bar{\Lambda}_C^- \rightarrow \bar{\Lambda} \pi^-$	-0.07 ± 0.31
$(\alpha + \bar{\alpha})/(\alpha - \bar{\alpha})$ in $\Lambda_C^+ \rightarrow \Lambda e^+ \nu_e, \bar{\Lambda}_C^- \rightarrow \bar{\Lambda} e^- \bar{\nu}_e$	0.00 ± 0.04

CP VIOLATION OBSERVED

Re(ϵ)	$(1.596 \pm 0.013) \times 10^{-3}$
charge asymmetry in K_{S3}^0 decays	
A_L = weighted average of $A_L(\mu)$ and $A_L(e)$	$(0.332 \pm 0.006)\%$
$A_L(\mu) = [\Gamma(\pi^+ \mu^+ \nu_\mu) - \Gamma(\pi^+ \mu^- \bar{\nu}_\mu)]/\text{sum}$	$(0.304 \pm 0.025)\%$
$A_L(e) = [\Gamma(\pi^+ e^+ \nu_e) - \Gamma(\pi^+ e^- \bar{\nu}_e)]/\text{sum}$	$(0.334 \pm 0.007)\%$
parameters for $K_L^0 \rightarrow 2\pi$ decay	
$ \eta_{00} = A(K_L^0 \rightarrow 2\pi^0) / A(K_S^0 \rightarrow 2\pi^0) $	$(2.222 \pm 0.012) \times 10^{-3}$ (S = 1.7)
$ \eta_{+-} = A(K_L^0 \rightarrow \pi^+ \pi^-) / A(K_S^0 \rightarrow \pi^+ \pi^-) $	$(2.233 \pm 0.012) \times 10^{-3}$ (S = 1.7)
$ \epsilon = (2 \eta_{+-} + \eta_{00})/3$	$(2.229 \pm 0.012) \times 10^{-3}$ (S = 1.7)
$ \eta_{00}/\eta_{+-} $	[f] 0.9951 ± 0.0008 (S = 1.6)
Re(ϵ'/ϵ) = $(1 - \eta_{00}/\eta_{+-})/3$	[f] $(1.65 \pm 0.26) \times 10^{-3}$ (S = 1.6)

Assuming CPT

ϕ_{+-} , phase of η_{+-}	$(43.51 \pm 0.05)^\circ$ (S = 1.1)
ϕ_{00} , phase of η_{00}	$(43.52 \pm 0.05)^\circ$ (S = 1.1)
$\phi_e = (2\phi_{+-} + \phi_{00})/3$	$(43.51 \pm 0.05)^\circ$ (S = 1.1)

Not assuming CPT

ϕ_{+-} , phase of η_{+-}	$(43.4 \pm 0.7)^\circ$ (S = 1.3)
ϕ_{00} , phase of η_{00}	$(43.7 \pm 0.8)^\circ$ (S = 1.2)
$\phi_e = (2\phi_{+-} + \phi_{00})/3$	$(43.5 \pm 0.7)^\circ$ (S = 1.3)

CP asymmetry A in $K_L^0 \rightarrow \pi^+ \pi^- e^+ e^-$

β_{CP} from $K_L^0 \rightarrow e^+ e^- e^+ e^-$	-0.19 ± 0.07
γ_{CP} from $K_L^0 \rightarrow e^+ e^- e^+ e^-$	0.01 ± 0.11 (S = 1.6)

parameters for $K_L^0 \rightarrow \pi^+ \pi^- \gamma$ decay

$ \eta_{+-\gamma} = A(K_L^0 \rightarrow \pi^+ \pi^- \gamma, CP \text{ violating}) / A(K_S^0 \rightarrow \pi^+ \pi^- \gamma) $	$(2.35 \pm 0.07) \times 10^{-3}$
$\phi_{+-\gamma}$ = phase of $\eta_{+-\gamma}$	$(44 \pm 4)^\circ$
$\Gamma(K_L^0 \rightarrow \pi^+ \pi^-) / \Gamma_{\text{total}}$	[g] $(1.966 \pm 0.010) \times 10^{-3}$ (S = 1.6)
$\Gamma(K_L^0 \rightarrow \pi^0 \pi^0) / \Gamma_{\text{total}}$	$(8.65 \pm 0.06) \times 10^{-4}$ (S = 1.8)
$A_{CP}(B^0 \rightarrow K^+ \pi^-)$	-0.101 ± 0.015
Parameters for $B^0 \rightarrow J/\psi K_S^0$	
$\sin(2\beta)$	0.678 ± 0.025

CPT INVARIANCE

$(m_{W^+} - m_{W^-}) / m_{\text{average}}$	-0.002 ± 0.007
$(m_{e^+} - m_{e^-}) / m_{\text{average}}$	$< 8 \times 10^{-9}$, CL = 90%
$ q_{e^+} + q_{e^-} /e$	$< 4 \times 10^{-8}$
$(g_{e^+} - g_{e^-}) / g_{\text{average}}$	$(-0.5 \pm 2.1) \times 10^{-12}$
$(\tau_{\mu^+} - \tau_{\mu^-}) / \tau_{\text{average}}$	$(2 \pm 8) \times 10^{-5}$
$(g_{\mu^+} - g_{\mu^-}) / g_{\text{average}}$	$(-0.11 \pm 0.12) \times 10^{-8}$
$(m_{\tau^+} - m_{\tau^-}) / m_{\text{average}}$	$< 2.8 \times 10^{-4}$, CL = 90%
$(m_{\pi^+} - m_{\pi^-}) / m_{\text{average}}$	$(2 \pm 5) \times 10^{-4}$
$(\tau_{\pi^+} - \tau_{\pi^-}) / \tau_{\text{average}}$	$(6 \pm 7) \times 10^{-4}$
$(m_{K^+} - m_{K^-}) / m_{\text{average}}$	$(-0.6 \pm 1.8) \times 10^{-4}$
$(\tau_{K^+} - \tau_{K^-}) / \tau_{\text{average}}$	$(0.11 \pm 0.09)\%$ (S = 1.2)
$K^\pm \rightarrow \mu^\pm \nu_\mu$ rate difference/average	$(-0.5 \pm 0.4)\%$
$K^\pm \rightarrow \pi^\pm \pi^0$ rate difference/average	[h] $(0.8 \pm 1.2)\%$
δ in $K^0 - \bar{K}^0$ mixing	
real part of δ	$(2.3 \pm 2.7) \times 10^{-4}$
imaginary part of δ	$(0.4 \pm 2.1) \times 10^{-5}$
Re(γ), K_{e3} parameter	$(0.4 \pm 2.5) \times 10^{-3}$

Re(x_-), K_{e3} parameter	$(-2.9 \pm 2.0) \times 10^{-3}$
$ m_{K^0} - m_{\bar{K}^0} / m_{\text{average}}$	[i] $< 8 \times 10^{-19}$, CL = 90%
$(\Gamma_{K^0} - \Gamma_{\bar{K}^0}) / m_{\text{average}}$	$(8 \pm 8) \times 10^{-18}$
phase difference $\phi_{00} - \phi_{+-}$	$(0.2 \pm 0.4)^\circ$
$\text{Re}(\frac{2}{3}\eta_{+-} + \frac{1}{3}\eta_{00}) - \frac{A_{CP}}{2}$	$(-3 \pm 35) \times 10^{-6}$
$A_{CP} \mathcal{T}(K^\pm \pi^\pm)$ in D^0, \bar{D}^0	0.008 ± 0.008
$ m_{D^0} - m_{\bar{D}^0} / m_{D^0}$	[j] $< 2 \times 10^{-9}$, CL = 90%
$(\frac{q_{D^0}}{m_{D^0}} - \frac{q_{\bar{D}^0}}{m_{\bar{D}^0}}) / \frac{q_{D^0}}{m_{D^0}}$	$(-9 \pm 9) \times 10^{-11}$
$ q_D + q_{\bar{D}} /e$	[j] $< 2 \times 10^{-9}$, CL = 90%
$(\mu_D + \mu_{\bar{D}}) / \mu_D$	$(-2.6 \pm 2.9) \times 10^{-3}$
$(m_n - m_{\bar{n}}) / m_n$	$(9 \pm 5) \times 10^{-5}$
$(m_\Lambda - m_{\bar{\Lambda}}) / m_\Lambda$	$(-0.1 \pm 1.1) \times 10^{-5}$ (S = 1.6)
$(\tau_\Lambda - \tau_{\bar{\Lambda}}) / \tau_\Lambda$	-0.001 ± 0.009
$(\tau_{\Sigma^+} - \tau_{\Sigma^-}) / \tau_{\Sigma^+}$	$(-0.6 \pm 1.2) \times 10^{-3}$
$(\mu_{\Sigma^+} + \mu_{\Sigma^-}) / \mu_{\Sigma^+}$	0.014 ± 0.015
$(m_{\Xi^-} - m_{\Xi^+}) / m_{\Xi^-}$	$(-3 \pm 9) \times 10^{-5}$
$(\tau_{\Xi^-} - \tau_{\Xi^+}) / \tau_{\Xi^-}$	-0.01 ± 0.07
$(\mu_{\Xi^-} + \mu_{\Xi^+}) / \mu_{\Xi^-} $	$+0.01 \pm 0.05$
$(m_{\Omega^-} - m_{\bar{\Omega}^+}) / m_{\Omega^-}$	$(-1 \pm 8) \times 10^{-5}$
$(\tau_{\Omega^-} - \tau_{\bar{\Omega}^+}) / \tau_{\Omega^-}$	-0.002 ± 0.040

TESTS OF NUMBER CONSERVATION LAWS

LEPTON FAMILY NUMBER

Lepton family number conservation means separate conservation of each of L_e, L_μ, L_τ .

$\Gamma(Z \rightarrow e^\pm \mu^\mp) / \Gamma_{\text{total}}$	[k] $< 1.7 \times 10^{-6}$, CL = 95%
$\Gamma(Z \rightarrow e^\pm \tau^\mp) / \Gamma_{\text{total}}$	[k] $< 9.8 \times 10^{-6}$, CL = 95%
$\Gamma(Z \rightarrow \mu^\pm \tau^\mp) / \Gamma_{\text{total}}$	[k] $< 1.2 \times 10^{-5}$, CL = 95%
$\sigma(e^+ e^- \rightarrow e^\pm \tau^\mp) / \sigma(e^+ e^- \rightarrow \mu^\pm \mu^-)$	$< 8.9 \times 10^{-6}$, CL = 95%
$\sigma(e^+ e^- \rightarrow \mu^\pm \tau^\mp) / \sigma(e^+ e^- \rightarrow \mu^\pm \mu^-)$	$< 4.0 \times 10^{-6}$, CL = 95%
limit on $\mu^- \rightarrow e^-$ conversion	
$\sigma(\mu^- 32S \rightarrow e^- 32S) / \sigma(\mu^- 32S \rightarrow \nu_\mu 32P^*)$	$< 7 \times 10^{-11}$, CL = 90%
$\sigma(\mu^- \text{Ti} \rightarrow e^- \text{Ti}) / \sigma(\mu^- \text{Ti} \rightarrow \text{capture})$	$< 4.3 \times 10^{-12}$, CL = 90%
$\sigma(\mu^- \text{Pb} \rightarrow e^- \text{Pb}) / \sigma(\mu^- \text{Pb} \rightarrow \text{capture})$	$< 4.6 \times 10^{-11}$, CL = 90%
limit on muonium \rightarrow antimuonium conversion $R_g = G_C / G_F$	< 0.0030 , CL = 90%
$\Gamma(\mu^- \rightarrow e^- \nu_e \bar{\nu}_\mu) / \Gamma_{\text{total}}$	[l] $< 1.2 \times 10^{-2}$, CL = 90%
$\Gamma(\mu^- \rightarrow e^- \gamma) / \Gamma_{\text{total}}$	$< 1.2 \times 10^{-11}$, CL = 90%
$\Gamma(\mu^- \rightarrow e^- e^+ e^-) / \Gamma_{\text{total}}$	$< 1.0 \times 10^{-12}$, CL = 90%
$\Gamma(\mu^- \rightarrow e^- 2\gamma) / \Gamma_{\text{total}}$	$< 7.2 \times 10^{-11}$, CL = 90%
$\Gamma(\tau^- \rightarrow e^- \gamma) / \Gamma_{\text{total}}$	$< 1.1 \times 10^{-7}$, CL = 90%
$\Gamma(\tau^- \rightarrow \mu^- \gamma) / \Gamma_{\text{total}}$	$< 6.8 \times 10^{-8}$, CL = 90%
$\Gamma(\tau^- \rightarrow e^- \pi^0) / \Gamma_{\text{total}}$	$< 8.0 \times 10^{-8}$, CL = 90%
$\Gamma(\tau^- \rightarrow \mu^- \pi^0) / \Gamma_{\text{total}}$	$< 1.1 \times 10^{-7}$, CL = 90%
$\Gamma(\tau^- \rightarrow e^- K_S^0) / \Gamma_{\text{total}}$	$< 5.6 \times 10^{-8}$, CL = 90%
$\Gamma(\tau^- \rightarrow \mu^- K_S^0) / \Gamma_{\text{total}}$	$< 4.9 \times 10^{-8}$, CL = 90%
$\Gamma(\tau^- \rightarrow e^- \eta) / \Gamma_{\text{total}}$	$< 9.2 \times 10^{-8}$, CL = 90%
$\Gamma(\tau^- \rightarrow \mu^- \eta) / \Gamma_{\text{total}}$	$< 6.5 \times 10^{-8}$, CL = 90%
$\Gamma(\tau^- \rightarrow e^- \rho^0) / \Gamma_{\text{total}}$	$< 6.3 \times 10^{-8}$, CL = 90%
$\Gamma(\tau^- \rightarrow \mu^- \rho^0) / \Gamma_{\text{total}}$	$< 6.8 \times 10^{-8}$, CL = 90%
$\Gamma(\tau^- \rightarrow e^- \omega) / \Gamma_{\text{total}}$	$< 1.1 \times 10^{-7}$, CL = 90%
$\Gamma(\tau^- \rightarrow \mu^- \omega) / \Gamma_{\text{total}}$	$< 8.9 \times 10^{-8}$, CL = 90%
$\Gamma(\tau^- \rightarrow e^- K^*(892)^0) / \Gamma_{\text{total}}$	$< 7.8 \times 10^{-8}$, CL = 90%
$\Gamma(\tau^- \rightarrow \mu^- K^*(892)^0) / \Gamma_{\text{total}}$	$< 5.9 \times 10^{-8}$, CL = 90%
$\Gamma(\tau^- \rightarrow e^- \bar{K}^*(892)^0) / \Gamma_{\text{total}}$	$< 7.7 \times 10^{-8}$, CL = 90%
$\Gamma(\tau^- \rightarrow \mu^- \bar{K}^*(892)^0) / \Gamma_{\text{total}}$	$< 1.0 \times 10^{-7}$, CL = 90%
$\Gamma(\tau^- \rightarrow e^- \eta'(958)) / \Gamma_{\text{total}}$	$< 1.6 \times 10^{-7}$, CL = 90%
$\Gamma(\tau^- \rightarrow \mu^- \eta'(958)) / \Gamma_{\text{total}}$	$< 1.3 \times 10^{-7}$, CL = 90%
$\Gamma(\tau^- \rightarrow e^- \phi) / \Gamma_{\text{total}}$	$< 7.3 \times 10^{-8}$, CL = 90%

Tests of Conservation Laws

$\Gamma(\tau^- \rightarrow \mu^- \phi)/\Gamma_{\text{total}}$	$<1.3 \times 10^{-7}$, CL = 90%
$\Gamma(\tau^- \rightarrow e^- e^+ e^-)/\Gamma_{\text{total}}$	$<3.6 \times 10^{-8}$, CL = 90%
$\Gamma(\tau^- \rightarrow e^- \mu^+ \mu^-)/\Gamma_{\text{total}}$	$<3.7 \times 10^{-8}$, CL = 90%
$\Gamma(\tau^- \rightarrow e^+ \mu^- \mu^-)/\Gamma_{\text{total}}$	$<2.3 \times 10^{-8}$, CL = 90%
$\Gamma(\tau^- \rightarrow \mu^- e^+ e^-)/\Gamma_{\text{total}}$	$<2.7 \times 10^{-8}$, CL = 90%
$\Gamma(\tau^- \rightarrow \mu^+ e^- e^-)/\Gamma_{\text{total}}$	$<2.0 \times 10^{-8}$, CL = 90%
$\Gamma(\tau^- \rightarrow \mu^- \mu^+ \mu^-)/\Gamma_{\text{total}}$	$<3.2 \times 10^{-8}$, CL = 90%
$\Gamma(\tau^- \rightarrow e^- \pi^+ \pi^-)/\Gamma_{\text{total}}$	$<1.2 \times 10^{-7}$, CL = 90%
$\Gamma(\tau^- \rightarrow \mu^- \pi^+ \pi^-)/\Gamma_{\text{total}}$	$<2.9 \times 10^{-7}$, CL = 90%
$\Gamma(\tau^- \rightarrow e^- \pi^+ K^-)/\Gamma_{\text{total}}$	$<3.2 \times 10^{-7}$, CL = 90%
$\Gamma(\tau^- \rightarrow e^- \pi^- K^+)/\Gamma_{\text{total}}$	$<1.6 \times 10^{-7}$, CL = 90%
$\Gamma(\tau^- \rightarrow e^- K_S^0 K_S^0)/\Gamma_{\text{total}}$	$<2.2 \times 10^{-6}$, CL = 90%
$\Gamma(\tau^- \rightarrow e^- K^+ K^-)/\Gamma_{\text{total}}$	$<1.4 \times 10^{-7}$, CL = 90%
$\Gamma(\tau^- \rightarrow \mu^- \pi^+ K^-)/\Gamma_{\text{total}}$	$<2.6 \times 10^{-7}$, CL = 90%
$\Gamma(\tau^- \rightarrow \mu^- \pi^- K^+)/\Gamma_{\text{total}}$	$<3.2 \times 10^{-7}$, CL = 90%
$\Gamma(\tau^- \rightarrow \mu^- K_S^0 K_S^0)/\Gamma_{\text{total}}$	$<3.4 \times 10^{-6}$, CL = 90%
$\Gamma(\tau^- \rightarrow \mu^- K^+ K^-)/\Gamma_{\text{total}}$	$<2.5 \times 10^{-7}$, CL = 90%
$\Gamma(\tau^- \rightarrow e^- \pi^0 \pi^0)/\Gamma_{\text{total}}$	$<6.5 \times 10^{-6}$, CL = 90%
$\Gamma(\tau^- \rightarrow \mu^- \pi^0 \pi^0)/\Gamma_{\text{total}}$	$<1.4 \times 10^{-5}$, CL = 90%
$\Gamma(\tau^- \rightarrow e^- \eta \eta)/\Gamma_{\text{total}}$	$<3.5 \times 10^{-5}$, CL = 90%
$\Gamma(\tau^- \rightarrow \mu^- \eta \eta)/\Gamma_{\text{total}}$	$<6.0 \times 10^{-5}$, CL = 90%
$\Gamma(\tau^- \rightarrow e^- \pi^0 \eta)/\Gamma_{\text{total}}$	$<2.4 \times 10^{-5}$, CL = 90%
$\Gamma(\tau^- \rightarrow \mu^- \pi^0 \eta)/\Gamma_{\text{total}}$	$<2.2 \times 10^{-5}$, CL = 90%
$\Gamma(\tau^- \rightarrow e^- \text{light boson})/\Gamma_{\text{total}}$	$<2.7 \times 10^{-3}$, CL = 95%
$\Gamma(\tau^- \rightarrow \mu^- \text{light boson})/\Gamma_{\text{total}}$	$<5 \times 10^{-3}$, CL = 95%

LEPTON FAMILY NUMBER VIOLATION IN NEUTRINOS

Solar Neutrinos

$\sin^2(2\theta_{12})$

$0.86^{+0.03}_{-0.04}$

Δm_{21}^2

$(8.0 \pm 0.3) \times 10^{-5} \text{ eV}^2$

Atmospheric Neutrinos

The ranges below for $\sin^2(2\theta_{23})$ and Δm_{32}^2 correspond to the projections onto the appropriate axes of the 90% CL contour in the $\sin^2(2\theta_{23})$ - Δm_{32}^2 plane.

$\sin^2(2\theta_{23})$

>0.92

Δm_{32}^2

$[m] 1.9 \text{ to } 3.0 \times 10^{-3} \text{ eV}^2$

$\Gamma(\pi^+ \rightarrow \mu^+ \nu_e)/\Gamma_{\text{total}}$	$<8.0 \times 10^{-3}$, CL = 90%
$\Gamma(\pi^+ \rightarrow \mu^- e^+ e^+ \nu)/\Gamma_{\text{total}}$	$<1.6 \times 10^{-6}$, CL = 90%
$\Gamma(\pi^0 \rightarrow \mu^+ e^-)/\Gamma_{\text{total}}$	$<3.8 \times 10^{-10}$, CL = 90%
$\Gamma(\pi^0 \rightarrow \mu^- e^+)/\Gamma_{\text{total}}$	$<3.4 \times 10^{-9}$, CL = 90%
$\Gamma(\pi^0 \rightarrow \mu^+ e^- + \mu^- e^+)/\Gamma_{\text{total}}$	$<1.72 \times 10^{-8}$, CL = 90%
$\Gamma(\eta \rightarrow \mu^+ e^- + \mu^- e^+)/\Gamma_{\text{total}}$	$<6 \times 10^{-6}$, CL = 90%
$\Gamma(\eta(958) \rightarrow e \mu)/\Gamma_{\text{total}}$	$<4.7 \times 10^{-4}$, CL = 90%
$\Gamma(K^+ \rightarrow \mu^- \nu e^+ e^+)/\Gamma_{\text{total}}$	$<2.0 \times 10^{-8}$, CL = 90%
$\Gamma(K^+ \rightarrow \mu^+ \nu_e)/\Gamma_{\text{total}}$	$<4 \times 10^{-3}$, CL = 90%
$\Gamma(K^+ \rightarrow \pi^+ \mu^+ e^-)/\Gamma_{\text{total}}$	$<1.3 \times 10^{-11}$, CL = 90%
$\Gamma(K^+ \rightarrow \pi^+ \mu^- e^+)/\Gamma_{\text{total}}$	$<5.2 \times 10^{-10}$, CL = 90%
$\Gamma(K_L^0 \rightarrow e^\pm \mu^\mp)/\Gamma_{\text{total}}$	[k] $<4.7 \times 10^{-12}$, CL = 90%
$\Gamma(K_L^0 \rightarrow e^\pm \mu^\pm \mu^\mp)/\Gamma_{\text{total}}$	[k] $<4.12 \times 10^{-11}$, CL = 90%
$\Gamma(K_L^0 \rightarrow \pi^0 \mu^\pm e^\mp)/\Gamma_{\text{total}}$	[k] $<6.2 \times 10^{-9}$, CL = 90%
$\Gamma(D^+ \rightarrow \pi^+ e^\pm \mu^\mp)/\Gamma_{\text{total}}$	[k] $<3.4 \times 10^{-5}$, CL = 90%
$\Gamma(D^+ \rightarrow K^+ e^\pm \mu^\mp)/\Gamma_{\text{total}}$	[k] $<6.8 \times 10^{-5}$, CL = 90%
$\Gamma(D^0 \rightarrow \mu^\pm e^\mp)/\Gamma_{\text{total}}$	[k] $<8.1 \times 10^{-7}$, CL = 90%
$\Gamma(D^0 \rightarrow \pi^0 e^\pm \mu^\mp)/\Gamma_{\text{total}}$	[k] $<8.6 \times 10^{-5}$, CL = 90%
$\Gamma(D^0 \rightarrow \eta e^\pm \mu^\mp)/\Gamma_{\text{total}}$	[k] $<1.0 \times 10^{-4}$, CL = 90%
$\Gamma(D^0 \rightarrow \pi^+ \pi^- e^\pm \mu^\mp)/\Gamma_{\text{total}}$	[k] $<1.5 \times 10^{-5}$, CL = 90%
$\Gamma(D^0 \rightarrow \rho^0 e^\pm \mu^\mp)/\Gamma_{\text{total}}$	[k] $<4.9 \times 10^{-5}$, CL = 90%
$\Gamma(D^0 \rightarrow \omega e^\pm \mu^\mp)/\Gamma_{\text{total}}$	[k] $<1.2 \times 10^{-4}$, CL = 90%
$\Gamma(D^0 \rightarrow K^- K^+ e^\pm \mu^\mp)/\Gamma_{\text{total}}$	[k] $<1.8 \times 10^{-4}$, CL = 90%
$\Gamma(D^0 \rightarrow \phi e^\pm \mu^\mp)/\Gamma_{\text{total}}$	[k] $<3.4 \times 10^{-5}$, CL = 90%
$\Gamma(D^0 \rightarrow \bar{K}^0 e^\pm \mu^\mp)/\Gamma_{\text{total}}$	[k] $<1.0 \times 10^{-4}$, CL = 90%
$\Gamma(D^0 \rightarrow K^- \pi^+ e^\pm \mu^\mp)/\Gamma_{\text{total}}$	[k] $<5.53 \times 10^{-4}$, CL = 90%
$\Gamma(D^0 \rightarrow \bar{K}^*(892)^0 e^\pm \mu^\mp)/\Gamma_{\text{total}}$	[k] $<8.3 \times 10^{-5}$, CL = 90%
$\Gamma(D_S^+ \rightarrow \pi^+ e^\pm \mu^\mp)/\Gamma_{\text{total}}$	[k] $<6.1 \times 10^{-4}$, CL = 90%
$\Gamma(D_S^+ \rightarrow K^+ e^\pm \mu^\mp)/\Gamma_{\text{total}}$	[k] $<6.3 \times 10^{-4}$, CL = 90%
$\Gamma(K^+ \mu^\pm \tau^\mp)/\Gamma_{\text{total}}$	$<77 \times 10^{-6}$, CL = 90%
$\Gamma(B^+ \rightarrow \pi^+ e^+ \mu^-)/\Gamma_{\text{total}}$	$<6.4 \times 10^{-3}$, CL = 90%
$\Gamma(B^+ \rightarrow \pi^+ e^- \mu^+)/\Gamma_{\text{total}}$	$<6.4 \times 10^{-3}$, CL = 90%
$\Gamma(B^+ \rightarrow \pi^+ e^\pm \mu^\mp)/\Gamma_{\text{total}}$	$<1.7 \times 10^{-7}$, CL = 90%
$\Gamma(B^+ \rightarrow K^+ e^+ \mu^-)/\Gamma_{\text{total}}$	$<9.1 \times 10^{-8}$, CL = 90%
$\Gamma(B^+ \rightarrow K^+ e^- \mu^+)/\Gamma_{\text{total}}$	$<1.3 \times 10^{-7}$, CL = 90%
$\Gamma(B^+ \rightarrow K^+ e^\pm \mu^\mp)/\Gamma_{\text{total}}$	$<9.1 \times 10^{-8}$, CL = 90%
$\Gamma(B^+ \rightarrow K^+ \mu^\pm \tau^\mp)/\Gamma_{\text{total}}$	$<7.7 \times 10^{-5}$, CL = 90%

$\Gamma(B^+ \rightarrow K^*(892)^+ e^+ \mu^-)/\Gamma_{\text{total}}$	$<1.3 \times 10^{-6}$, CL = 90%
$\Gamma(B^+ \rightarrow K^*(892)^+ e^- \mu^+)/\Gamma_{\text{total}}$	$<9.9 \times 10^{-7}$, CL = 90%
$\Gamma(B^+ \rightarrow K^*(892)^+ e^\pm \mu^\mp)/\Gamma_{\text{total}}$	$<1.4 \times 10^{-7}$, CL = 90%
$\Gamma(B^0 \rightarrow e^\pm \mu^\mp)/\Gamma_{\text{total}}$	[k] $<9.2 \times 10^{-8}$, CL = 90%
$\Gamma(B^0 \rightarrow \pi^0 e^\pm \mu^\mp)/\Gamma_{\text{total}}$	$<1.4 \times 10^{-7}$, CL = 90%
$\Gamma(B^0 \rightarrow K^0 e^\pm \mu^\mp)/\Gamma_{\text{total}}$	$<2.7 \times 10^{-7}$, CL = 90%
$\Gamma(B^0 \rightarrow K^*(892)^0 e^+ \mu^-)/\Gamma_{\text{total}}$	$<5.3 \times 10^{-7}$, CL = 90%
$\Gamma(B^0 \rightarrow K^*(892)^0 e^- \mu^+)/\Gamma_{\text{total}}$	$<3.4 \times 10^{-7}$, CL = 90%
$\Gamma(B^0 \rightarrow K^*(892)^0 e^\pm \mu^\mp)/\Gamma_{\text{total}}$	$<5.8 \times 10^{-7}$, CL = 90%
$\Gamma(B^0 \rightarrow \mu^\pm \tau^\mp)/\Gamma_{\text{total}}$	[k] $<1.1 \times 10^{-4}$, CL = 90%
$\Gamma(B^0 \rightarrow \mu^\pm \tau^\mp)/\Gamma_{\text{total}}$	[k] $<3.8 \times 10^{-5}$, CL = 90%
$\Gamma(B \rightarrow s e^\pm \mu^\mp)/\Gamma_{\text{total}}$	[k] $<2.2 \times 10^{-5}$, CL = 90%
$\Gamma(B \rightarrow \pi e^\pm \mu^\mp)/\Gamma_{\text{total}}$	$<9.2 \times 10^{-8}$, CL = 90%
$\Gamma(B \rightarrow \rho e^\pm \mu^\mp)/\Gamma_{\text{total}}$	$<3.2 \times 10^{-6}$, CL = 90%
$\Gamma(B \rightarrow K e^\pm \mu^\mp)/\Gamma_{\text{total}}$	$<3.8 \times 10^{-8}$, CL = 90%
$\Gamma(B \rightarrow K^*(892) e^\pm \mu^\mp)/\Gamma_{\text{total}}$	$<5.1 \times 10^{-7}$, CL = 90%
$\Gamma(B_S^0 \rightarrow e^\pm \mu^\mp)/\Gamma_{\text{total}}$	[k] $<6.1 \times 10^{-6}$, CL = 90%
$\Gamma(e^\pm \tau^\mp)/\Gamma_{\text{total}}$	$<8.3 \times 10^{-6}$, CL = 90%
$\Gamma(\mu^\pm \tau^\mp)/\Gamma_{\text{total}}$	$<2.0 \times 10^{-6}$, CL = 90%
$\Gamma(J/\psi(1S) \rightarrow e^\pm \mu^\mp)/\Gamma_{\text{total}}$	$<1.1 \times 10^{-6}$, CL = 90%
$\Gamma(J/\psi(1S) \rightarrow e^\pm \tau^\mp)/\Gamma_{\text{total}}$	$<8.3 \times 10^{-6}$, CL = 90%
$\Gamma(J/\psi(1S) \rightarrow \mu^\pm \tau^\mp)/\Gamma_{\text{total}}$	$<2.0 \times 10^{-6}$, CL = 90%

TOTAL LEPTON NUMBER

Violation of total lepton number conservation also implies violation of lepton family number conservation.

$\Gamma(Z \rightarrow \nu e)/\Gamma_{\text{total}}$	$<1.8 \times 10^{-6}$, CL = 95%
$\Gamma(Z \rightarrow \nu \mu)/\Gamma_{\text{total}}$	$<1.8 \times 10^{-6}$, CL = 95%
limit on $\mu^- \rightarrow e^+$ conversion	
$\sigma(\mu^- 32S \rightarrow e^+ 32Si^*) / \sigma(\mu^- 32S \rightarrow \nu_\mu 32P^*)$	$<9 \times 10^{-10}$, CL = 90%
$\sigma(\mu^- 127I \rightarrow e^+ 127Sb^*) / \sigma(\mu^- 127I \rightarrow \text{anything})$	$<3 \times 10^{-10}$, CL = 90%
$\sigma(\mu^- \text{Ti} \rightarrow e^+ \text{Ca}) / \sigma(\mu^- \text{Ti} \rightarrow \text{capture})$	$<3.6 \times 10^{-11}$, CL = 90%
$\Gamma(\tau^- \rightarrow e^+ \pi^- \pi^-)/\Gamma_{\text{total}}$	$<2.0 \times 10^{-7}$, CL = 90%
$\Gamma(\tau^- \rightarrow \mu^+ \pi^- \pi^-)/\Gamma_{\text{total}}$	$<7 \times 10^{-8}$, CL = 90%
$\Gamma(\tau^- \rightarrow e^+ \pi^- K^-)/\Gamma_{\text{total}}$	$<1.8 \times 10^{-7}$, CL = 90%
$\Gamma(\tau^- \rightarrow e^+ K^- K^-)/\Gamma_{\text{total}}$	$<1.5 \times 10^{-7}$, CL = 90%
$\Gamma(\tau^- \rightarrow \mu^+ \pi^- K^-)/\Gamma_{\text{total}}$	$<2.2 \times 10^{-7}$, CL = 90%
$\Gamma(\tau^- \rightarrow \mu^+ K^- K^-)/\Gamma_{\text{total}}$	$<4.4 \times 10^{-7}$, CL = 90%
$\Gamma(\tau^- \rightarrow \bar{p} \gamma)/\Gamma_{\text{total}}$	$<3.5 \times 10^{-6}$, CL = 90%
$\Gamma(\tau^- \rightarrow \bar{p} \pi^0)/\Gamma_{\text{total}}$	$<1.5 \times 10^{-5}$, CL = 90%
$\Gamma(\tau^- \rightarrow \bar{p} 2\pi^0)/\Gamma_{\text{total}}$	$<3.3 \times 10^{-5}$, CL = 90%
$\Gamma(\tau^- \rightarrow \bar{p} \eta)/\Gamma_{\text{total}}$	$<8.9 \times 10^{-6}$, CL = 90%
$\Gamma(\tau^- \rightarrow \bar{p} \pi^0 \eta)/\Gamma_{\text{total}}$	$<2.7 \times 10^{-5}$, CL = 90%
$\Gamma(\tau^- \rightarrow \Lambda \pi^-)/\Gamma_{\text{total}}$	$<7.2 \times 10^{-8}$, CL = 90%
$\Gamma(\tau^- \rightarrow \bar{\Lambda} \pi^-)/\Gamma_{\text{total}}$	$<1.4 \times 10^{-7}$, CL = 90%
$t_{1/2}(^{76}\text{Ge} \rightarrow ^{76}\text{Se} + 2 e^-)$	$>1.9 \times 10^{25} \text{ yr}$, CL = 90%
$\Gamma(\pi^+ \rightarrow \mu^+ \bar{\nu}_e)/\Gamma_{\text{total}}$	[n] $<1.5 \times 10^{-3}$, CL = 90%
$\Gamma(K^+ \rightarrow \pi^- \mu^+ e^+)/\Gamma_{\text{total}}$	$<5.0 \times 10^{-10}$, CL = 90%
$\Gamma(K^+ \rightarrow \pi^- e^+ e^+)/\Gamma_{\text{total}}$	$<6.4 \times 10^{-10}$, CL = 90%
$\Gamma(K^+ \rightarrow \pi^- \mu^+ \mu^+)/\Gamma_{\text{total}}$	[n] $<3.0 \times 10^{-9}$, CL = 90%
$\Gamma(K^+ \rightarrow \mu^+ \bar{\nu}_e)/\Gamma_{\text{total}}$	[n] $<3.3 \times 10^{-3}$, CL = 90%
$\Gamma(K^+ \rightarrow \pi^0 e^+ \bar{\nu}_e)/\Gamma_{\text{total}}$	$<3 \times 10^{-3}$, CL = 90%
$\Gamma(D^+ \rightarrow \pi^- e^+ e^+)/\Gamma_{\text{total}}$	$<3.6 \times 10^{-6}$, CL = 90%
$\Gamma(D^+ \rightarrow \pi^- \mu^+ \mu^+)/\Gamma_{\text{total}}$	$<4.8 \times 10^{-6}$, CL = 90%
$\Gamma(D^+ \rightarrow \pi^- e^+ \mu^+)/\Gamma_{\text{total}}$	$<5.0 \times 10^{-5}$, CL = 90%
$\Gamma(D^+ \rightarrow \rho^- \mu^+ \mu^+)/\Gamma_{\text{total}}$	$<5.6 \times 10^{-4}$, CL = 90%
$\Gamma(D^+ \rightarrow K^- e^+ e^+)/\Gamma_{\text{total}}$	$<4.5 \times 10^{-6}$, CL = 90%
$\Gamma(D^+ \rightarrow K^- \mu^+ \mu^+)/\Gamma_{\text{total}}$	$<1.3 \times 10^{-5}$, CL = 90%
$\Gamma(D^+ \rightarrow K^- e^+ \mu^+)/\Gamma_{\text{total}}$	$<1.3 \times 10^{-4}$, CL = 90%
$\Gamma(D^+ \rightarrow K^*(892)^- \mu^+ \mu^+)/\Gamma_{\text{total}}$	$<8.5 \times 10^{-4}$, CL = 90%
$\Gamma(D^0 \rightarrow \pi^- \pi^- e^+ e^+ + \text{c.c.})/\Gamma_{\text{total}}$	$<1.12 \times 10^{-4}$, CL = 90%
$\Gamma(D^0 \rightarrow \pi^- \pi^- \mu^+ \mu^+ + \text{c.c.})/\Gamma_{\text{total}}$	$<2.9 \times 10^{-5}$, CL = 90%
$\Gamma(D^0 \rightarrow K^- \pi^- e^+ e^+ + \text{c.c.})/\Gamma_{\text{total}}$	$<2.06 \times 10^{-4}$, CL = 90%
$\Gamma(D^0 \rightarrow K^- \pi^- \mu^+ \mu^+ + \text{c.c.})/\Gamma_{\text{total}}$	$<3.9 \times 10^{-4}$, CL = 90%
$\Gamma(D^0 \rightarrow K^- K^- e^+ e^+ + \text{c.c.})/\Gamma_{\text{total}}$	$<1.52 \times 10^{-4}$, CL = 90%
$\Gamma(D^0 \rightarrow K^- K^- \mu^+ \mu^+ + \text{c.c.})/\Gamma_{\text{total}}$	$<9.4 \times 10^{-5}$, CL = 90%

Tests of Conservation Laws

$\Gamma(D^0 \rightarrow \pi^- \pi^- e^+ \mu^+ + \text{c.c.})/\Gamma_{\text{total}}$	$< 7.9 \times 10^{-5}$, CL = 90%
$\Gamma(D^0 \rightarrow K^- \pi^- e^+ \mu^+ + \text{c.c.})/\Gamma_{\text{total}}$	$< 2.18 \times 10^{-4}$, CL = 90%
$\Gamma(D^0 \rightarrow K^- K^- e^+ \mu^+ + \text{c.c.})/\Gamma_{\text{total}}$	$< 5.7 \times 10^{-5}$, CL = 90%
$\Gamma(D_S^+ \rightarrow \pi^- e^+ e^+)/\Gamma_{\text{total}}$	$< 6.9 \times 10^{-4}$, CL = 90%
$\Gamma(D_S^+ \rightarrow \pi^- \mu^+ \mu^+)/\Gamma_{\text{total}}$	$< 2.9 \times 10^{-5}$, CL = 90%
$\Gamma(D_S^+ \rightarrow \pi^- e^+ \mu^+)/\Gamma_{\text{total}}$	$< 7.3 \times 10^{-4}$, CL = 90%
$\Gamma(D_S^+ \rightarrow K^- e^+ e^+)/\Gamma_{\text{total}}$	$< 6.3 \times 10^{-4}$, CL = 90%
$\Gamma(D_S^+ \rightarrow K^- \mu^+ \mu^+)/\Gamma_{\text{total}}$	$< 1.3 \times 10^{-5}$, CL = 90%
$\Gamma(D_S^+ \rightarrow K^- e^+ \mu^+)/\Gamma_{\text{total}}$	$< 6.8 \times 10^{-4}$, CL = 90%
$\Gamma(D_S^+ \rightarrow K^*(892)^- \mu^+ \mu^+)/\Gamma_{\text{total}}$	$< 1.4 \times 10^{-3}$, CL = 90%
$\Gamma(B^+ \rightarrow \pi^- e^+ e^+)/\Gamma_{\text{total}}$	$< 1.6 \times 10^{-6}$, CL = 90%
$\Gamma(B^+ \rightarrow \pi^- \mu^+ \mu^+)/\Gamma_{\text{total}}$	$< 1.4 \times 10^{-6}$, CL = 90%
$\Gamma(B^+ \rightarrow \pi^- e^+ \mu^+)/\Gamma_{\text{total}}$	$< 1.3 \times 10^{-6}$, CL = 90%
$\Gamma(B^+ \rightarrow \rho^- e^+ e^+)/\Gamma_{\text{total}}$	$< 2.6 \times 10^{-6}$, CL = 90%
$\Gamma(B^+ \rightarrow \rho^- \mu^+ \mu^+)/\Gamma_{\text{total}}$	$< 5.0 \times 10^{-6}$, CL = 90%
$\Gamma(B^+ \rightarrow \rho^- e^+ \mu^+)/\Gamma_{\text{total}}$	$< 3.3 \times 10^{-6}$, CL = 90%
$\Gamma(B^+ \rightarrow K^- e^+ e^+)/\Gamma_{\text{total}}$	$< 1.0 \times 10^{-6}$, CL = 90%
$\Gamma(B^+ \rightarrow K^- \mu^+ \mu^+)/\Gamma_{\text{total}}$	$< 1.8 \times 10^{-6}$, CL = 90%
$\Gamma(B^+ \rightarrow K^- e^+ \mu^+)/\Gamma_{\text{total}}$	$< 2.0 \times 10^{-6}$, CL = 90%
$\Gamma(B^+ \rightarrow K^*(892)^- e^+ e^+)/\Gamma_{\text{total}}$	$< 2.8 \times 10^{-6}$, CL = 90%
$\Gamma(B^+ \rightarrow K^*(892)^- \mu^+ \mu^+)/\Gamma_{\text{total}}$	$< 8.3 \times 10^{-6}$, CL = 90%
$\Gamma(B^+ \rightarrow K^*(892)^- e^+ \mu^+)/\Gamma_{\text{total}}$	$< 4.4 \times 10^{-6}$, CL = 90%
$\Gamma(\Xi^- \rightarrow p \mu^- \mu^-)/\Gamma_{\text{total}}$	$< 4 \times 10^{-8}$, CL = 90%
$\Gamma(\Lambda_c^+ \rightarrow \Sigma^- \mu^+ \mu^+)/\Gamma_{\text{total}}$	$< 7.0 \times 10^{-4}$, CL = 90%

BARYON NUMBER

$\Gamma(Z \rightarrow p e)/\Gamma_{\text{total}}$	$< 1.8 \times 10^{-6}$, CL = 95%
$\Gamma(Z \rightarrow p \mu)/\Gamma_{\text{total}}$	$< 1.8 \times 10^{-6}$, CL = 95%
$\Gamma(\tau^- \rightarrow \bar{p} \gamma)/\Gamma_{\text{total}}$	$< 3.5 \times 10^{-6}$, CL = 90%
$\Gamma(\tau^- \rightarrow \bar{p} \pi^0)/\Gamma_{\text{total}}$	$< 1.5 \times 10^{-5}$, CL = 90%
$\Gamma(\tau^- \rightarrow \bar{p} 2\pi^0)/\Gamma_{\text{total}}$	$< 3.3 \times 10^{-5}$, CL = 90%
$\Gamma(\tau^- \rightarrow \bar{p} \eta)/\Gamma_{\text{total}}$	$< 8.9 \times 10^{-6}$, CL = 90%
$\Gamma(\tau^- \rightarrow \bar{p} \pi^0 \eta)/\Gamma_{\text{total}}$	$< 2.7 \times 10^{-5}$, CL = 90%
$\Gamma(\tau^- \rightarrow \Lambda \pi^-)/\Gamma_{\text{total}}$	$< 7.2 \times 10^{-8}$, CL = 90%
$\Gamma(\tau^- \rightarrow \bar{\Lambda} \pi^-)/\Gamma_{\text{total}}$	$< 1.4 \times 10^{-7}$, CL = 90%
p mean life	$> 2.1 \times 10^{29}$ years, CL = 90%

A few examples of proton or bound neutron decay follow. For limits on many other nucleon decay channels, see the Baryon Summary Table.

$\tau(N \rightarrow e^+ \pi)$	$> 158 (n), > 1600 (p) \times 10^{30}$ years, CL = 90%
$\tau(N \rightarrow \mu^+ \pi)$	$> 100 (n), > 473 (p) \times 10^{30}$ years, CL = 90%
$\tau(N \rightarrow e^+ K)$	$> 17 (n), > 150 (p) \times 10^{30}$ years, CL = 90%
$\tau(N \rightarrow \mu^+ K)$	$> 26 (n), > 120 (p) \times 10^{30}$ years, CL = 90%
limit on $n\bar{n}$ oscillations (free n)	$> 0.86 \times 10^8$ s, CL = 90%
limit on $n\bar{n}$ oscillations (bound n)	$[o] > 1.2 \times 10^8$ s, CL = 90%

ELECTRIC CHARGE (Q)

$e \rightarrow \nu_e \gamma$ and astrophysical limits	$[p] > 4.6 \times 10^{26}$ yr, CL = 90%
$\Gamma(n \rightarrow p \nu_e \bar{\nu}_e)/\Gamma_{\text{total}}$	$< 8 \times 10^{-27}$, CL = 68%

$\Delta S = \Delta Q$ RULE

Violations allowed in second-order weak interactions.

$\Gamma(K^+ \rightarrow \pi^+ \pi^+ e^- \bar{\nu}_e)/\Gamma_{\text{total}}$	$< 1.2 \times 10^{-8}$, CL = 90%
$\Gamma(K^+ \rightarrow \pi^+ \pi^+ \mu^- \bar{\nu}_\mu)/\Gamma_{\text{total}}$	$< 3.0 \times 10^{-6}$, CL = 95%
Re(x_+), K_{e3} parameter	$(-0.9 \pm 3.0) \times 10^{-3}$
$x = A(\bar{K}^0 \rightarrow \pi^- \ell^+ \nu)/A(K^0 \rightarrow \pi^- \ell^+ \nu) = A(\Delta S = -\Delta Q)/A(\Delta S = \Delta Q)$	
real part of x	-0.002 ± 0.006
imaginary part of x	0.0012 ± 0.0021
$\Gamma(\Sigma^+ \rightarrow n \ell^+ \nu)/\Gamma(\Sigma^- \rightarrow n \ell^- \bar{\nu})$	< 0.043
$\Gamma(\Sigma^+ \rightarrow n e^+ \nu_e)/\Gamma_{\text{total}}$	$< 5 \times 10^{-6}$, CL = 90%
$\Gamma(\Sigma^+ \rightarrow n \mu^+ \nu_\mu)/\Gamma_{\text{total}}$	$< 3.0 \times 10^{-5}$, CL = 90%
$\Gamma(\Xi^0 \rightarrow \Sigma^- e^+ \nu_e)/\Gamma_{\text{total}}$	$< 9 \times 10^{-4}$, CL = 90%
$\Gamma(\Xi^0 \rightarrow \Sigma^- \mu^+ \nu_\mu)/\Gamma_{\text{total}}$	$< 9 \times 10^{-4}$, CL = 90%

$\Delta S = 2$ FORBIDDEN

Allowed in second-order weak interactions.

$\Gamma(\Xi^0 \rightarrow p \pi^-)/\Gamma_{\text{total}}$	$< 8 \times 10^{-6}$, CL = 90%
$\Gamma(\Xi^0 \rightarrow p e^- \bar{\nu}_e)/\Gamma_{\text{total}}$	$< 1.3 \times 10^{-3}$
$\Gamma(\Xi^0 \rightarrow p \mu^- \bar{\nu}_\mu)/\Gamma_{\text{total}}$	$< 1.3 \times 10^{-3}$
$\Gamma(\Xi^- \rightarrow n \pi^-)/\Gamma_{\text{total}}$	$< 1.9 \times 10^{-5}$, CL = 90%
$\Gamma(\Xi^- \rightarrow n e^- \bar{\nu}_e)/\Gamma_{\text{total}}$	$< 3.2 \times 10^{-3}$, CL = 90%
$\Gamma(\Xi^- \rightarrow n \mu^- \bar{\nu}_\mu)/\Gamma_{\text{total}}$	$< 1.5 \times 10^{-2}$, CL = 90%
$\Gamma(\Xi^- \rightarrow p \pi^- \pi^-)/\Gamma_{\text{total}}$	$< 4 \times 10^{-4}$, CL = 90%
$\Gamma(\Xi^- \rightarrow p \pi^- e^- \bar{\nu}_e)/\Gamma_{\text{total}}$	$< 4 \times 10^{-4}$, CL = 90%
$\Gamma(\Xi^- \rightarrow p \pi^- \mu^- \bar{\nu}_\mu)/\Gamma_{\text{total}}$	$< 4 \times 10^{-4}$, CL = 90%
$\Gamma(\Omega^- \rightarrow \Lambda \pi^-)/\Gamma_{\text{total}}$	$< 2.9 \times 10^{-6}$, CL = 90%

$\Delta S = 2$ VIA MIXING

Allowed in second-order weak interactions, e.g. mixing.

$m_{K_L^0 - K_S^0}$	$(0.5292 \pm 0.0009) \times 10^{10} \text{ h s}^{-1}$ ($S = 1.2$)
$m_{K_L^0 - K_S^0}$	$(3.483 \pm 0.006) \times 10^{-12} \text{ MeV}$

$\Delta C = 2$ VIA MIXING

Allowed in second-order weak interactions, e.g. mixing.

$ m_{D_1^0 - D_2^0} = x\Gamma$	$(2.37_{-0.71}^{+0.66}) \times 10^{10} \text{ h s}^{-1}$
$(\Gamma_{D_1^0} - \Gamma_{D_2^0})/\Gamma = 2y$	$(1.56_{-0.38}^{+0.36}) \times 10^{-2}$

$\Delta B = 2$ VIA MIXING

Allowed in second-order weak interactions, e.g. mixing.

χ_d	0.1878 ± 0.0024
$\Delta m_{B^0} = m_{B_H^0} - m_{B_L^0}$	$(0.507 \pm 0.005) \times 10^{12} \text{ h s}^{-1}$
$\chi_d = \Delta m_{B^0}/\Gamma_{B^0}$	0.776 ± 0.008
$\Delta m_{B_S^0} = m_{B_{SH}^0} - m_{B_{SL}^0}$	$(17.77 \pm 0.12) \times 10^{12} \text{ h s}^{-1}$
$\chi_s = \Delta m_{B_S^0}/\Gamma_{B_S^0}$	26.1 ± 0.5
χ_s	0.49927 ± 0.00003

$\Delta S = 1$ WEAK NEUTRAL CURRENT FORBIDDEN

Allowed by higher-order electroweak interactions.

$\Gamma(K^+ \rightarrow \pi^+ e^+ e^-)/\Gamma_{\text{total}}$	$(2.88 \pm 0.13) \times 10^{-7}$
$\Gamma(K^+ \rightarrow \pi^+ \mu^+ \mu^-)/\Gamma_{\text{total}}$	$(8.1 \pm 1.4) \times 10^{-8}$ ($S = 2.7$)
$\Gamma(K^+ \rightarrow \pi^+ \nu \bar{\nu})/\Gamma_{\text{total}}$	$(1.5_{-0.9}^{+1.3}) \times 10^{-10}$
$\Gamma(K^+ \rightarrow \pi^+ \pi^0 \nu \bar{\nu})/\Gamma_{\text{total}}$	$< 4.3 \times 10^{-5}$, CL = 90%
$\Gamma(K_L^0 \rightarrow \mu^+ \mu^-)/\Gamma_{\text{total}}$	$< 3.2 \times 10^{-7}$, CL = 90%
$\Gamma(K_L^0 \rightarrow e^+ e^-)/\Gamma_{\text{total}}$	$< 1.4 \times 10^{-7}$, CL = 90%
$\Gamma(K_S^0 \rightarrow \pi^0 e^+ e^-)/\Gamma_{\text{total}}$	$[q] (3.0_{-1.2}^{+1.5}) \times 10^{-9}$
$\Gamma(K_S^0 \rightarrow \pi^0 \mu^+ \mu^-)/\Gamma_{\text{total}}$	$(2.9_{-1.2}^{+1.5}) \times 10^{-9}$
$\Gamma(K_L^0 \rightarrow \mu^+ \mu^-)/\Gamma_{\text{total}}$	$(6.84 \pm 0.11) \times 10^{-9}$
$\Gamma(K_L^0 \rightarrow e^+ e^-)/\Gamma_{\text{total}}$	$(9_{-4}^{+6}) \times 10^{-12}$
$\Gamma(K_L^0 \rightarrow \pi^+ \pi^- e^+ e^-)/\Gamma_{\text{total}}$	$[r] (3.11 \pm 0.19) \times 10^{-7}$
$\Gamma(K_L^0 \rightarrow \pi^0 \pi^0 e^+ e^-)/\Gamma_{\text{total}}$	$< 6.6 \times 10^{-9}$, CL = 90%
$\Gamma(K_L^0 \rightarrow \mu^+ \mu^- e^+ e^-)/\Gamma_{\text{total}}$	$(2.69 \pm 0.27) \times 10^{-9}$
$\Gamma(K_L^0 \rightarrow e^+ e^- e^+ e^-)/\Gamma_{\text{total}}$	$(3.56 \pm 0.21) \times 10^{-8}$
$\Gamma(K_L^0 \rightarrow \pi^0 \mu^+ \mu^-)/\Gamma_{\text{total}}$	$< 3.8 \times 10^{-10}$, CL = 90%
$\Gamma(K_L^0 \rightarrow \pi^0 e^+ e^-)/\Gamma_{\text{total}}$	$< 2.8 \times 10^{-10}$, CL = 90%
$\Gamma(K_L^0 \rightarrow \pi^0 \nu \bar{\nu})/\Gamma_{\text{total}}$	$< 2.1 \times 10^{-7}$, CL = 90%
$\Gamma(K_L^0 \rightarrow \pi^0 \pi^0 \nu \bar{\nu})/\Gamma_{\text{total}}$	$< 4.7 \times 10^{-5}$, CL = 90%
$\Gamma(\Sigma^+ \rightarrow p e^+ e^-)/\Gamma_{\text{total}}$	$< 7 \times 10^{-6}$
$\Gamma(\Sigma^+ \rightarrow p \mu^+ \mu^-)/\Gamma_{\text{total}}$	$(9_{-8}^{+9}) \times 10^{-8}$

Tests of Conservation Laws

$\Delta C = 1$ WEAK NEUTRAL CURRENT FORBIDDEN

Allowed by higher-order electroweak interactions.

$\Gamma(D^+ \rightarrow \pi^+ e^+ e^-)/\Gamma_{\text{total}}$	$< 7.4 \times 10^{-6}$, CL = 90%
$\Gamma(D^+ \rightarrow \pi^+ \mu^+ \mu^-)/\Gamma_{\text{total}}$	$< 3.9 \times 10^{-6}$, CL = 90%
$\Gamma(D^+ \rightarrow \rho^+ \mu^+ \mu^-)/\Gamma_{\text{total}}$	$< 5.6 \times 10^{-4}$, CL = 90%
$\Gamma(D^0 \rightarrow \gamma\gamma)/\Gamma_{\text{total}}$	$< 2.7 \times 10^{-5}$, CL = 90%
$\Gamma(D^0 \rightarrow e^+ e^-)/\Gamma_{\text{total}}$	$< 1.2 \times 10^{-6}$, CL = 90%
$\Gamma(D^0 \rightarrow \mu^+ \mu^-)/\Gamma_{\text{total}}$	$< 1.3 \times 10^{-6}$, CL = 90%
$\Gamma(D^0 \rightarrow \pi^0 e^+ e^-)/\Gamma_{\text{total}}$	$< 4.5 \times 10^{-5}$, CL = 90%
$\Gamma(D^0 \rightarrow \pi^0 \mu^+ \mu^-)/\Gamma_{\text{total}}$	$< 1.8 \times 10^{-4}$, CL = 90%
$\Gamma(D^0 \rightarrow \eta e^+ e^-)/\Gamma_{\text{total}}$	$< 1.1 \times 10^{-4}$, CL = 90%
$\Gamma(D^0 \rightarrow \eta \mu^+ \mu^-)/\Gamma_{\text{total}}$	$< 5.3 \times 10^{-4}$, CL = 90%
$\Gamma(D^0 \rightarrow \pi^+ \pi^- e^+ e^-)/\Gamma_{\text{total}}$	$< 3.73 \times 10^{-4}$, CL = 90%
$\Gamma(D^0 \rightarrow \rho^0 e^+ e^-)/\Gamma_{\text{total}}$	$< 1.0 \times 10^{-4}$, CL = 90%
$\Gamma(D^0 \rightarrow \pi^+ \pi^- \mu^+ \mu^-)/\Gamma_{\text{total}}$	$< 3.0 \times 10^{-5}$, CL = 90%
$\Gamma(D^0 \rightarrow \rho^0 \mu^+ \mu^-)/\Gamma_{\text{total}}$	$< 2.2 \times 10^{-5}$, CL = 90%
$\Gamma(D^0 \rightarrow \omega e^+ e^-)/\Gamma_{\text{total}}$	$< 1.8 \times 10^{-4}$, CL = 90%
$\Gamma(D^0 \rightarrow \omega \mu^+ \mu^-)/\Gamma_{\text{total}}$	$< 8.3 \times 10^{-4}$, CL = 90%
$\Gamma(D^0 \rightarrow K^- K^+ e^+ e^-)/\Gamma_{\text{total}}$	$< 3.15 \times 10^{-4}$, CL = 90%
$\Gamma(D^0 \rightarrow \phi e^+ e^-)/\Gamma_{\text{total}}$	$< 5.2 \times 10^{-5}$, CL = 90%
$\Gamma(D^0 \rightarrow K^- K^+ \mu^+ \mu^-)/\Gamma_{\text{total}}$	$< 3.3 \times 10^{-5}$, CL = 90%
$\Gamma(D^0 \rightarrow \phi \mu^+ \mu^-)/\Gamma_{\text{total}}$	$< 3.1 \times 10^{-5}$, CL = 90%
$\Gamma(D^0 \rightarrow K^- \pi^+ e^+ e^-)/\Gamma_{\text{total}}$	$< 3.85 \times 10^{-4}$, CL = 90%
$\Gamma(D^0 \rightarrow K^- \pi^+ \mu^+ \mu^-)/\Gamma_{\text{total}}$	$< 3.59 \times 10^{-4}$, CL = 90%
$\Gamma(D^0 \rightarrow \pi^+ \pi^- \pi^0 \mu^+ \mu^-)/\Gamma_{\text{total}}$	$< 8.1 \times 10^{-4}$, CL = 90%
$\Gamma(D_S^+ \rightarrow K^+ e^+ e^-)/\Gamma_{\text{total}}$	$< 1.6 \times 10^{-3}$, CL = 90%
$\Gamma(D_S^+ \rightarrow K^+ \mu^+ \mu^-)/\Gamma_{\text{total}}$	$< 3.6 \times 10^{-5}$, CL = 90%
$\Gamma(D_S^+ \rightarrow K^*(892)^+ \mu^+ \mu^-)/\Gamma_{\text{total}}$	$< 1.4 \times 10^{-3}$, CL = 90%
$\Gamma(\Lambda_C^+ \rightarrow p \mu^+ \mu^-)/\Gamma_{\text{total}}$	$< 3.4 \times 10^{-4}$, CL = 90%

$\Delta B = 1$ WEAK NEUTRAL CURRENT FORBIDDEN

Allowed by higher-order electroweak interactions.

$\Gamma(B^+ \rightarrow \pi^+ \ell^+ \ell^-)/\Gamma_{\text{total}}$	$< 1.2 \times 10^{-7}$, CL = 90%
$\Gamma(B^+ \rightarrow \pi^+ e^+ e^-)/\Gamma_{\text{total}}$	$< 1.8 \times 10^{-7}$, CL = 90%
$\Gamma(B^+ \rightarrow \pi^+ \mu^+ \mu^-)/\Gamma_{\text{total}}$	$< 2.8 \times 10^{-7}$, CL = 90%
$\Gamma(B^+ \rightarrow \pi^+ \nu \bar{\nu})/\Gamma_{\text{total}}$	$< 1.0 \times 10^{-4}$, CL = 90%
$\Gamma(B^+ \rightarrow K^+ \ell^+ \ell^-)/\Gamma_{\text{total}}$	[s] $(4.4^{+0.8}_{-0.7}) \times 10^{-7}$ (S = 1.1)
$\Gamma(B^+ \rightarrow K^+ e^+ e^-)/\Gamma_{\text{total}}$	$(4.9 \pm 1.0) \times 10^{-7}$
$\Gamma(B^+ \rightarrow K^+ \mu^+ \mu^-)/\Gamma_{\text{total}}$	$(3.9^{+1.0}_{-0.9}) \times 10^{-7}$
$\Gamma(B^+ \rightarrow K^+ \nu \bar{\nu})/\Gamma_{\text{total}}$	$< 1.4 \times 10^{-5}$, CL = 90%
$\Gamma(B^+ \rightarrow \rho^+ \nu \bar{\nu})/\Gamma_{\text{total}}$	$< 1.5 \times 10^{-4}$, CL = 90%
$\Gamma(B^+ \rightarrow K^*(892)^+ \ell^+ \ell^-)/\Gamma_{\text{total}}$	[s] $(7 \pm 5) \times 10^{-7}$
$\Gamma(B^+ \rightarrow K^*(892)^+ \nu \bar{\nu})/\Gamma_{\text{total}}$	$< 1.4 \times 10^{-4}$, CL = 90%
$\Gamma(B^+ \rightarrow K^*(892)^+ e^+ e^-)/\Gamma_{\text{total}}$	$(8 \pm 8) \times 10^{-7}$
$\Gamma(B^+ \rightarrow K^*(892)^+ \mu^+ \mu^-)/\Gamma_{\text{total}}$	$(8^{+6}_{-4}) \times 10^{-7}$
$\Gamma(B^0 \rightarrow \gamma\gamma)/\Gamma_{\text{total}}$	$< 6.2 \times 10^{-7}$, CL = 90%
$\Gamma(B^0 \rightarrow e^+ e^-)/\Gamma_{\text{total}}$	$< 1.13 \times 10^{-7}$, CL = 90%
$\Gamma(B^0 \rightarrow e^+ e^- \gamma)/\Gamma_{\text{total}}$	$< 1.2 \times 10^{-7}$, CL = 90%
$\Gamma(B^0 \rightarrow \mu^+ \mu^-)/\Gamma_{\text{total}}$	$< 1.5 \times 10^{-8}$, CL = 90%
$\Gamma(B^0 \rightarrow \mu^+ \mu^- \gamma)/\Gamma_{\text{total}}$	$< 1.6 \times 10^{-7}$, CL = 90%
$\Gamma(B^0 \rightarrow \tau^+ \tau^-)/\Gamma_{\text{total}}$	$< 4.1 \times 10^{-3}$, CL = 90%
$\Gamma(B^0 \rightarrow \pi^0 \ell^+ \ell^-)/\Gamma_{\text{total}}$	$< 1.2 \times 10^{-7}$, CL = 90%
$\Gamma(B^0 \rightarrow \pi^0 \nu \bar{\nu})/\Gamma_{\text{total}}$	$< 2.2 \times 10^{-4}$, CL = 90%
$\Gamma(B^0 \rightarrow \pi^0 e^+ e^-)/\Gamma_{\text{total}}$	$< 1.4 \times 10^{-7}$, CL = 90%
$\Gamma(B^0 \rightarrow \pi^0 \mu^+ \mu^-)/\Gamma_{\text{total}}$	$< 5.1 \times 10^{-7}$, CL = 90%
$\Gamma(B^0 \rightarrow K^0 \ell^+ \ell^-)/\Gamma_{\text{total}}$	[s] $(2.9^{+1.6}_{-1.3}) \times 10^{-7}$
$\Gamma(B^0 \rightarrow K^0 \nu \bar{\nu})/\Gamma_{\text{total}}$	$< 1.6 \times 10^{-4}$, CL = 90%
$\Gamma(B^0 \rightarrow \rho^0 \nu \bar{\nu})/\Gamma_{\text{total}}$	$< 4.4 \times 10^{-4}$, CL = 90%
$\Gamma(B^0 \rightarrow K^0 e^+ e^-)/\Gamma_{\text{total}}$	$(1.3^{+1.6}_{-1.1}) \times 10^{-7}$
$\Gamma(B^0 \rightarrow K^0 \mu^+ \mu^-)/\Gamma_{\text{total}}$	$(5.7^{+2.2}_{-1.8}) \times 10^{-7}$
$\Gamma(B^0 \rightarrow K^*(892)^0 \ell^+ \ell^-)/\Gamma_{\text{total}}$	[s] $(9.5 \pm 1.8) \times 10^{-7}$
$\Gamma(B^0 \rightarrow K^*(892)^0 e^+ e^-)/\Gamma_{\text{total}}$	$(1.04^{+0.35}_{-0.31}) \times 10^{-6}$
$\Gamma(B^0 \rightarrow K^*(892)^0 \mu^+ \mu^-)/\Gamma_{\text{total}}$	$(1.10^{+0.29}_{-0.26}) \times 10^{-6}$
$\Gamma(B^0 \rightarrow K^*(892)^0 \nu \bar{\nu})/\Gamma_{\text{total}}$	$< 3.4 \times 10^{-4}$, CL = 90%
$\Gamma(B^0 \rightarrow \phi \nu \bar{\nu})/\Gamma_{\text{total}}$	$< 5.8 \times 10^{-5}$, CL = 90%
$\Gamma(B^0 \rightarrow \text{invisible})/\Gamma_{\text{total}}$	$< 2.2 \times 10^{-4}$, CL = 90%

Unless otherwise stated, limits are given at the 90% confidence level, while errors are given as ± 1 standard deviation.

$\Gamma(B^0 \rightarrow \nu \bar{\nu} \gamma)/\Gamma_{\text{total}}$	$< 4.7 \times 10^{-5}$, CL = 90%
$\Gamma(B \rightarrow s e^+ e^-)/\Gamma_{\text{total}}$	$(4.7 \pm 1.3) \times 10^{-6}$
$\Gamma(B \rightarrow s \mu^+ \mu^-)/\Gamma_{\text{total}}$	$(4.3 \pm 1.2) \times 10^{-6}$
$\Gamma(B \rightarrow s \ell^+ \ell^-)/\Gamma_{\text{total}}$	[s] $(4.5 \pm 1.0) \times 10^{-6}$
$\Gamma(B \rightarrow K e^+ e^-)/\Gamma_{\text{total}}$	$(3.8^{+0.8}_{-0.7}) \times 10^{-7}$
$\Gamma(B \rightarrow K^*(892) e^+ e^-)/\Gamma_{\text{total}}$	$(1.13 \pm 0.27) \times 10^{-6}$
$\Gamma(B \rightarrow K \mu^+ \mu^-)/\Gamma_{\text{total}}$	$(4.2^{+0.9}_{-0.8}) \times 10^{-7}$
$\Gamma(B \rightarrow K^*(892) \mu^+ \mu^-)/\Gamma_{\text{total}}$	$(1.03^{+0.26}_{-0.23}) \times 10^{-6}$
$\Gamma(B \rightarrow K \ell^+ \ell^-)/\Gamma_{\text{total}}$	$(3.9 \pm 0.7) \times 10^{-7}$ (S = 1.2)
$\Gamma(B \rightarrow K^*(892) \ell^+ \ell^-)/\Gamma_{\text{total}}$	$(9.4 \pm 1.8) \times 10^{-7}$ (S = 1.1)
$\Gamma(\bar{b} \rightarrow \mu^+ \mu^- \text{anything})/\Gamma_{\text{total}}$	$< 3.2 \times 10^{-4}$, CL = 90%
$\Gamma(B_S^0 \rightarrow \gamma\gamma)/\Gamma_{\text{total}}$	$< 5.3 \times 10^{-5}$, CL = 90%
$\Gamma(B_S^0 \rightarrow \mu^+ \mu^-)/\Gamma_{\text{total}}$	$< 4.7 \times 10^{-8}$, CL = 90%
$\Gamma(B_S^0 \rightarrow e^+ e^-)/\Gamma_{\text{total}}$	$< 5.4 \times 10^{-5}$, CL = 90%
$\Gamma(B_S^0 \rightarrow \phi(1020) \mu^+ \mu^-)/\Gamma_{\text{total}}$	$< 3.2 \times 10^{-6}$, CL = 90%
$\Gamma(B_S^0 \rightarrow \phi \nu \bar{\nu})/\Gamma_{\text{total}}$	$< 5.4 \times 10^{-3}$, CL = 90%

$\Delta T = 1$ WEAK NEUTRAL CURRENT FORBIDDEN

Allowed by higher-order electroweak interactions.

$$\Gamma(t \rightarrow Z q (q=u,c))/\Gamma_{\text{total}} \quad [t] \quad < 13.7 \times 10^{-2}, \text{ CL} = 95\%$$

NOTES

In this Summary Table:

When a quantity has “(S = ...)” to its right, the error on the quantity has been enlarged by the “scale factor” S, defined as $S = \sqrt{\chi^2/(N-1)}$, where N is the number of measurements used in calculating the quantity. We do this when $S > 1$, which often indicates that the measurements are inconsistent. When $S > 1.25$, we also show in the Particle Listings an ideogram of the measurements. For more about S, see the Introduction.

- [a] C parity forbids this to occur as a single-photon process.
- [b] See the Particle Listings for the (complicated) definition of this quantity.
- [c] Time-reversal invariance requires this to be 0° or 180° .
- [d] Allowed by higher-order electroweak interactions.
- [e] Violates CP in leading order. Test of direct CP violation since the indirect CP -violating and CP -conserving contributions are expected to be suppressed.
- [f] $\text{Re}(\epsilon'/\epsilon) = \epsilon'/\epsilon$ to a very good approximation provided the phases satisfy CPT invariance.
- [g] This mode includes gammas from inner bremsstrahlung but not the direct emission mode $K_L^0 \rightarrow \pi^+ \pi^- \gamma$ (DE).
- [h] Neglecting photon channels. See, e.g., A. Pais and S.B. Treiman, Phys. Rev. **D12**, 2744 (1975).
- [i] Derived from measured values of ϕ_{+-} , ϕ_{00} , $|\eta|$, $|m_{K_L^0} - m_{K_S^0}|$, and $\tau_{K_S^0}$, as described in the introduction to “Tests of Conservation Laws.”
- [j] These two results are not independent, and both use the more precise measurement of $|q_{\bar{p}}/m_{\bar{p}}|/(q_p/m_p)$.
- [k] The value is for the sum of the charge states or particle/antiparticle states indicated.
- [l] A test of additive vs. multiplicative lepton family number conservation.
- [m] The sign of Δm_{32}^2 is not known at this time. The range quoted is for the absolute value.
- [n] Derived from an analysis of neutrino-oscillation experiments.
- [o] There is some controversy about whether nuclear physics and model dependence complicate the analysis for bound neutrons (from which the best limit comes). The first limit here is from reactor experiments with free neutrons.
- [p] This is the best limit for the mode $e^- \rightarrow \nu \gamma$. The best limit for “electron disappearance” is 6.4×10^{24} yr.
- [q] See the K_S^0 Particle Listings for the energy limits used in this measurement.
- [r] See the K_L^0 Particle Listings for the energy limits used in this measurement.
- [s] An ℓ indicates an e or a μ mode, not a sum over these modes.
- [t] This limit is for $\Gamma(t \rightarrow Z q)/\Gamma(t \rightarrow W b)$.

REVIEWS, TABLES, AND PLOTS

Constants, Units, Atomic and Nuclear Properties

1. Physical constants (rev.)	103
2. Astrophysical constants (rev.)	104
3. International System of Units (SI)	106
4. Periodic table of the elements (rev.)	107
5. Electronic structure of the elements	108
6. Atomic and nuclear properties of materials (rev.)	110
7. Electromagnetic relations	112
8. Naming scheme for hadrons	114

Standard Model and Related Topics

9. Quantum chromodynamics	116
10. Electroweak model and constraints on new physics (rev.)	125
11. The Cabibbo-Kobayashi-Maskawa quark-mixing matrix (rev.)	145
12. CP violation (rev.)	153
13. Neutrino Mass, Mixing, & Flavor Change (rev.)	163
14. Quark model (rev.)	172
15. Grand Unified Theories	180
16. Structure functions (rev.)	188
17. Fragmentation functions in e^+e^- annihilation and lepton-nucleon DIS (rev.)	202

Astrophysics and cosmology

18. Experimental tests of gravitational theory (rev.)	212
19. Big-Bang cosmology (rev.)	217
20. Big-Bang nucleosynthesis (rev.)	228
21. The cosmological parameters (rev.)	232
22. Dark matter (rev.)	241
23. Cosmic microwave background (rev.)	246
24. Cosmic rays (rev.)	254

Experimental Methods and Colliders

25. Accelerator physics of colliders	261
26. High-energy collider parameters (rev.)	264
27. Passage of particles through matter (rev.)	267
28. Particle detectors (rev.)	281
29. Radioactivity and radiation protection (rev.)	312
30. Commonly used radioactive sources	315

Mathematical Tools or Statistics, Monte Carlo,

Group Theory	
31. Probability (rev.)	316
32. Statistics (rev.)	320
33. Monte Carlo techniques (rev.)	330
34. Monte Carlo particle numbering scheme (rev.)	333
35. Clebsch-Gordan coefficients, spherical harmonics, and d functions	337
36. $SU(3)$ isoscalar factors and representation matrices	338
37. $SU(n)$ multiplets and Young diagrams	339

Kinematics, Cross-Section Formulae, and Plots

38. Kinematics (rev.)	340
39. Cross-section formulae for specific proc. (rev.)	345
40. Plots of cross sections and related quantities (rev.)	353

MAJOR REVIEWS IN THE PARTICLE LISTINGS

Gauge and Higgs bosons

The Mass of the W Boson (rev.)	386
Triple Gauge Couplings	389
Anomalous W/Z Quartic Couplings	392
The Z Boson (rev.)	393
Anomalous $ZZ\gamma$, $Z\gamma\gamma$, and ZZV Couplings	411
Searches for Higgs Bosons (rev.)	414
The W' Searches (rev.)	443
The Z' Searches (rev.)	446
The Leptoquark Quantum Numbers (new)	452
Axions and Other Very Light Bosons (new)	459

Leptons

Muon Anomalous Magnetic Moment (rev.)	485
Muon Decay Parameters (rev.)	485
τ Branching Fractions (rev.)	493
τ -Lepton Decay Parameters (rev.)	493
Number of Light Neutrino Types (rev.)	523
Neutrinoless Double- β Decay (rev.)	525
Solar Neutrinos Review (rev.)	531

Quarks

Quark Masses (rev.)	551
The Top Quark (rev.)	563
Free Quark Searches	577

Mesons

Note on Scalar Mesons (rev.)	594
The $\eta(1405)$, $\eta(1475)$, $f_1(1420)$, and $f_1(1510)$ (rev.)	641
Rare Kaon Decays (rev.)	706
$K_{\ell 3}^{\pm}$ and $K_{\ell 3}^0$ Form Factors (rev.)	717
CPT Invariance Tests in Neutral Kaon Decay (new)	721
CP Violation in $K_S \rightarrow 3\pi$	727
V_{ud} , V_{us} , Cabibbo Angle, and CKM Unitarity (new)	733
CP -Violation in K_L Decays (rev.)	741
Dalitz-Plot Analysis Formalism	771
Review of Charm Dalitz-Plot Analyses (rev.)	774
$D^0-\bar{D}^0$ Mixing (rev.)	783
Production and Decay of b -flavored Hadrons (rev.)	833
Polarization in B Decays (rev.)	910
$B^0-\bar{B}^0$ Mixing (rev.)	914
Determination of V_{cb} and V_{ub} (rev.)	951
Branching Ratios of $\psi(2S)$ and $\chi_{c0,1,2}$ (rev.)	997

Baryons

Baryon Decay Parameters	1071
N and Δ Resonances	1075
Pentaquarks (new)	1124
Radiative Hyperon Decays	1167
Charmed Baryons (rev.)	1182
Λ_c^+ Branching Fractions	1185

Miscellaneous searches

Supersymmetry (rev.)	1211
Dynamical Electroweak Symmetry Breaking (rev.)	1258
Searches for Quark & Lepton Compositeness	1265
Extra Dimensions (rev.)	1272

Additional Reviews and Notes related to specific particles are located in the Particle Listings.



1. PHYSICAL CONSTANTS

Table 1.1. Reviewed 2007 by P.J. Mohr and B.N. Taylor (NIST). Based mainly on the “CODATA Recommended Values of the Fundamental Physical Constants: 2006” by P.J. Mohr, B.N. Taylor, and D.B. Newell (to be published in Rev. Mod. Phys. and J. Phys. Chem. Ref. Data). The last group of constants (beginning with the Fermi coupling constant) comes from the Particle Data Group. The figures in parentheses after the values give the 1-standard-deviation uncertainties in the last digits; the corresponding fractional uncertainties in parts per 10⁹ (ppb) are given in the last column. This set of constants (aside from the last group) is recommended for international use by CODATA (the Committee on Data for Science and Technology). The full 2006 CODATA set of constants may be found at <http://physics.nist.gov/constants>.

Quantity	Symbol, equation	Value	Uncertainty (ppb)
speed of light in vacuum	c	299 792 458 m s ⁻¹	exact*
Planck constant	h	6.626 068 96(33) × 10 ⁻³⁴ J s	50
Planck constant, reduced	$\hbar \equiv h/2\pi$	1.054 571 628(53) × 10 ⁻³⁴ J s = 6.582 118 99(16) × 10 ⁻²² MeV s	50 25
electron charge magnitude	e	1.602 176 487(40) × 10 ⁻¹⁹ C = 4.803 204 27(12) × 10 ⁻¹⁰ esu	25, 25
conversion constant	$\hbar c$	197.326 9631(49) MeV fm	25
conversion constant	$(\hbar c)^2$	0.389 379 304(19) GeV ² mbarn	50
electron mass	m_e	0.510 998 910(13) MeV/c ² = 9.109 382 15(45) × 10 ⁻³¹ kg	25, 50
proton mass	m_p	938.272 013(23) MeV/c ² = 1.672 621 637(83) × 10 ⁻²⁷ kg = 1.007 276 466 77(10) u = 1836.152 672 47(80) m_e	25, 50 0.10, 0.43
deuteron mass	m_d	1875.612 793(47) MeV/c ²	25
unified atomic mass unit (u)	(mass ¹² C atom)/12 = (1 g)/(N _A mol)	931.494 028(23) MeV/c ² = 1.660 538 782(83) × 10 ⁻²⁷ kg	25, 50
permittivity of free space	$\epsilon_0 = 1/\mu_0 c^2$	8.854 187 817 ... × 10 ⁻¹² F m ⁻¹	exact
permeability of free space	μ_0	4π × 10 ⁻⁷ N A ⁻² = 12.566 370 614 ... × 10 ⁻⁷ N A ⁻²	exact
fine-structure constant	$\alpha = e^2/4\pi\epsilon_0\hbar c$	7.297 352 5376(50) × 10 ⁻³ = 1/137.035 999 679(94) [†]	0.68, 0.68
classical electron radius	$r_e = e^2/4\pi\epsilon_0 m_e c^2$	2.817 940 2894(58) × 10 ⁻¹⁵ m	2.1
(e ⁻ Compton wavelength)/2π	$\lambda_e = \hbar/m_e c = r_e \alpha^{-1}$	3.861 592 6459(53) × 10 ⁻¹³ m	1.4
Bohr radius ($m_{\text{nucleus}} = \infty$)	$a_\infty = 4\pi\epsilon_0 \hbar^2 / m_e e^2 = r_e \alpha^{-2}$	0.529 177 208 59(36) × 10 ⁻¹⁰ m	0.68
wavelength of 1 eV/c particle	$\hbar c / (1 \text{ eV})$	1.239 841 875(31) × 10 ⁻⁶ m	25
Rydberg energy	$\hbar c R_\infty = m_e e^4 / 2(4\pi\epsilon_0)^2 \hbar^2 = m_e c^2 \alpha^2 / 2$	13.605 691 93(34) eV	25
Thomson cross section	$\sigma_T = 8\pi r_e^2 / 3$	0.665 245 8558(27) barn	4.1
Bohr magneton	$\mu_B = e\hbar/2m_e$	5.788 381 7555(79) × 10 ⁻¹¹ MeV T ⁻¹	1.4
nuclear magneton	$\mu_N = e\hbar/2m_p$	3.152 451 2326(45) × 10 ⁻¹⁴ MeV T ⁻¹	1.4
electron cyclotron freq./field	$\omega_{\text{cycl}}^e / B = e/m_e$	1.758 820 150(44) × 10 ¹¹ rad s ⁻¹ T ⁻¹	25
proton cyclotron freq./field	$\omega_{\text{cycl}}^p / B = e/m_p$	9.578 833 92(24) × 10 ⁷ rad s ⁻¹ T ⁻¹	25
gravitational constant [‡]	G_N	6.674 28(67) × 10 ⁻¹¹ m ³ kg ⁻¹ s ⁻² = 6.708 81(67) × 10 ⁻³⁹ $\hbar c$ (GeV/c ²) ⁻²	1.0 × 10 ⁵ 1.0 × 10 ⁵
standard gravitational accel.	g_N	9.806 65 m s ⁻²	exact
Avogadro constant	N_A	6.022 141 79(30) × 10 ²³ mol ⁻¹	50
Boltzmann constant	k	1.380 6504(24) × 10 ⁻²³ J K ⁻¹ = 8.617 343(15) × 10 ⁻⁵ eV K ⁻¹	1700 1700
molar volume, ideal gas at STP	$N_A k (273.15 \text{ K}) / (101 325 \text{ Pa})$	22.413 996(39) × 10 ⁻³ m ³ mol ⁻¹	1700
Wien displacement law constant	$b = \lambda_{\text{max}} T$	2.897 7685(51) × 10 ⁻³ m K	1700
Stefan-Boltzmann constant	$\sigma = \pi^2 k^4 / 60 \hbar^3 c^2$	5.670 400(40) × 10 ⁻⁸ W m ⁻² K ⁻⁴	7000
Fermi coupling constant**	$G_F / (\hbar c)^3$	1.166 37(1) × 10 ⁻⁵ GeV ⁻²	9000
weak-mixing angle	$\sin^2 \hat{\theta}(M_Z) (\overline{\text{MS}})$	0.231 19(14) ^{††}	6.5 × 10 ⁵
W [±] boson mass	m_W	80.398(25) GeV/c ²	3.6 × 10 ⁵
Z ⁰ boson mass	m_Z	91.1876(21) GeV/c ²	2.3 × 10 ⁴
strong coupling constant	$\alpha_s(m_Z)$	0.1176(20)	1.7 × 10 ⁷
$\pi = 3.141 592 653 589 793 238$		$e = 2.718 281 828 459 045 235$	$\gamma = 0.577 215 664 901 532 861$
1 in ≡ 0.0254 m 1 G ≡ 10 ⁻⁴ T		1 eV = 1.602 176 487(40) × 10 ⁻¹⁹ J	kT at 300 K = [38.681 685(68)] ⁻¹ eV
1 Å ≡ 0.1 nm 1 dyne ≡ 10 ⁻⁵ N		1 eV/c ² = 1.782 661 758(44) × 10 ⁻³⁶ kg	0 °C ≡ 273.15 K
1 barn ≡ 10 ⁻²⁸ m ² 1 erg ≡ 10 ⁻⁷ J 2.997 924 58 × 10 ⁹ esu = 1 C		1 atmosphere ≡ 760 Torr ≡ 101 325 Pa	

* The meter is the length of the path traveled by light in vacuum during a time interval of 1/299 792 458 of a second.

† At $Q^2 = 0$. At $Q^2 \approx m_W^2$ the value is $\sim 1/128$.

‡ Absolute lab measurements of G_N have been made only on scales of about 1 cm to 1 m.

** See the discussion in Sec. 10, “Electroweak model and constraints on new physics.”

†† The corresponding $\sin^2 \theta$ for the effective angle is 0.23149(13).

2. ASTROPHYSICAL CONSTANTS AND PARAMETERS

Table 2.1. Revised May 2008 by E. Bergren and D.E. Groom (LBNL). The figures in parentheses after some values give the one standard deviation uncertainties in the last digit(s). Physical constants are from Ref. 1. While every effort has been made to obtain the most accurate current values of the listed quantities, the table does not represent a critical review or adjustment of the constants, and is not intended as a primary reference. The values and uncertainties for the cosmological parameters depend on the exact data sets, priors, and basis parameters used in the fit. Many of the parameters reported in this table are derived parameters or have non-Gaussian likelihoods. The quoted errors may be highly correlated with those of other parameters, so care must be taken in propagating them. Unless otherwise specified, cosmological parameters are best fits of a spatially-flat Λ CDM cosmology with a power-law initial spectrum to WMAP 3-year data alone [2]. For more information see Ref. 3 and the original papers.

Quantity	Symbol, equation	Value	Reference, footnote
speed of light	c	299 792 458 m s ⁻¹	exact[4]
Newtonian gravitational constant	G_N	6.674 3(7) $\times 10^{-11}$ m ³ kg ⁻¹ s ⁻²	[1]
Planck mass	$\sqrt{\hbar c/G_N}$	1.220 89(6) $\times 10^{19}$ GeV/c ² = 2.176 44(11) $\times 10^{-8}$ kg	[1]
Planck length	$\sqrt{\hbar G_N/c^3}$	1.616 24(8) $\times 10^{-35}$ m	[1]
standard gravitational acceleration	g_N	9.806 65 m s ⁻²	exact[1]
jansky (flux density)	Jy	10 ⁻²⁶ W m ⁻² Hz ⁻¹	definition
tropical year (equinox to equinox) (2007)	yr	31 556 925.2 s $\approx \pi \times 10^7$ s	[5]
sidereal year (fixed star to fixed star) (2007)		31 558 149.8 s $\approx \pi \times 10^7$ s	[5]
mean sidereal day (2007) (time between vernal equinox transits)		23 ^h 56 ^m 04 ^s .090 53	[5]
astronomical unit	AU, A	149 597 870 700(3) m	[6]
parsec (1 AU/1 arc sec)	pc	3.085 677 6 $\times 10^{16}$ m = 3.262 ... ly	[7]
light year (deprecated unit)	ly	0.306 6 ... pc = 0.946 053 ... $\times 10^{16}$ m	
Schwarzschild radius of the Sun	$2G_N M_\odot/c^2$	2.953 250 077 0(2) km	[8]
Solar mass	M_\odot	1.988 4(2) $\times 10^{30}$ kg	[9]
Solar equatorial radius	R_\odot	6.9551(3) $\times 10^8$ m	[10]
Solar luminosity	L_\odot	3.842 7(1 4) $\times 10^{26}$ W	[11]
Schwarzschild radius of the Earth	$2G_N M_\oplus/c^2$	8.870 055 881 mm	[12]
Earth mass	M_\oplus	5.972 2(6) $\times 10^{24}$ kg	[13]
Earth mean equatorial radius	R_\oplus	6.378 137 $\times 10^6$ m	[5]
luminosity conversion (deprecated)	L	3.02 $\times 10^{28} \times 10^{-0.4 M_{\text{bol}}}$ W (M_{bol} = absolute bolometric magnitude = bolometric magnitude at 10 pc)	[14]
flux conversion (deprecated)	\mathcal{F}	2.52 $\times 10^{-8} \times 10^{-0.4 m_{\text{bol}}}$ W m ⁻² (m_{bol} = apparent bolometric magnitude)	from above
ABsolute monochromatic magnitude	AB	-2.5 log ₁₀ f_ν - 56.10 (for f_ν in W m ⁻² Hz ⁻¹) = -2.5 log ₁₀ f_ν + 8.90 (for f_ν in Jy)	[15]
Solar velocity around center of Galaxy	Θ_0	220(20) km s ⁻¹	[16]
Solar distance from Galactic center	R_0	8.0(5) kpc	[17]
local disk density	ρ_{disk}	3-12 $\times 10^{-24}$ g cm ⁻³ \approx 2-7 GeV/c ² cm ⁻³	[18]
local halo density	ρ_{halo}	2-13 $\times 10^{-25}$ g cm ⁻³ \approx 0.1-0.7 GeV/c ² cm ⁻³	[19]
present day CMB temperature	T_0	2.725(1) K	[20]
present day CMB dipole amplitude		3.358(17) mK	[21]
Solar velocity with respect to CMB		369(2) km/s towards $(\ell, b) = (263.86(4)^\circ, 48.24(10)^\circ)$	[21]
Local Group velocity with respect to CMB	v_{LG}	627(22) km s ⁻¹ towards $(\ell, b) = (276(3)^\circ, 30(3)^\circ)$	[22]
entropy density/Boltzmann constant	s/k	2 889.2 $(T/2.725)^3$ cm ⁻³	[14]
number density of CMB photons	n_γ	410.5 $(T/2.725)^3$ cm ⁻³	[23]
present day Hubble expansion rate	H_0	100 h km s ⁻¹ Mpc ⁻¹ = $h \times (9.777\,752 \text{ Gyr})^{-1}$	[24]
present day normalized Hubble expansion rate [‡]	h	0.73(3)	[2,3]
Hubble length	c/H_0	0.925 063 $\times 10^{26}$ h ⁻¹ m \approx 1.27 $\times 10^{26}$ m	
scale factor for cosmological constant	$c^2/3H_0^2$	2.852 $\times 10^{51}$ h ⁻² m ²	
critical density of the Universe	$\rho_c = 3H_0^2/8\pi G_N$	2.775 366 27 $\times 10^{11}$ h ² M _☉ Mpc ⁻³ = 1.878 35(19) $\times 10^{-29}$ h ² g cm ⁻³ = 1.053 68(11) $\times 10^{-5}$ h ² (GeV/c ²) cm ⁻³	[24]
pressureless matter density of the Universe [‡]	$\Omega_m = \rho_m/\rho_c$	0.128(8) h ⁻² \approx 0.24 (WMAP3) 0.132(4) h ⁻² \Rightarrow 0.27(2) (ALL mean)	[2,3]
baryon density of the Universe [‡]	$\Omega_b = \rho_b/\rho_c$	0.0223(7) h ⁻² \approx 0.0425	[2,3]
dark matter density of the universe [‡]	$\Omega_{\text{dm}} = \Omega_m - \Omega_b$	0.105(8) h ⁻² \approx 0.20	[2]
dark energy density of the Universe [‡]	Ω_Λ	0.73(3)	[25]
Hubble length	c/H_0	0.925 063 $\times 10^{26}$ h ⁻¹ m \approx 1.27 $\times 10^{26}$ m	
radiation density of the Universe [‡]	$\Omega_\gamma = \rho_\gamma/\rho_c$	2.471 $\times 10^{-5}$ $(T/2.725)^4$ h ⁻² \approx 4.6 $\times 10^{-5}$	[23]
neutrino density of the Universe [‡]	Ω_ν	0.0005 < $\Omega_\nu h^{-2}$ < 0.023 \Rightarrow 0.001 < Ω_ν < 0.05	[26]
total energy density of the Universe [‡]	$\Omega_{\text{tot}} = \Omega_m + \dots + \Omega_\Lambda$	1.011(12)	[2,27]

Quantity	Symbol, equation	Value	Reference, footnote
baryon-to-photon ratio [‡]	$\eta = n_b/n_\gamma$	$6.12(19) \times 10^{-10}$	[28]
number density of baryons [‡]	n_b	$(1.9 \times 10^{-7} < n_b < 2.7 \times 10^{-7}) \text{ cm}^{-3}$ (95% CL)	from η
dark energy equation of state parameter [‡]	w	-0.97(7)	[2]
fluctuation amplitude at $8h^{-1}$ Mpc scale [‡]	σ_8	0.76(5)	[2,3]
scalar spectral index from power-law fit to data [‡]	n_s	0.958(16)	[2,3]
running spectral index slope at $k_0 = 0.05 \text{ Mpc}^{-1}$ [‡]	$dn_s/d \ln k$	-0.05 ± 0.03	[2,29]
tensor-to-scalar field perturbations ratio at $k_0 = 0.002 \text{ Mpc}^{-1}$ [‡]	$r = T/S$	< 0.65 at 95% C.L.	[2,3]
reionization optical depth [‡]	τ	0.09(3)	[2,3]
age of Universe at reionization [‡]	t_{reion}	365 Myr	[2,3]
age of the Universe [‡]	t_0	13.73(15) Gyr	[2]

[‡] See caption for caveats.

References:

- P. J. Mohr, B.N. Taylor, & D.B. Newell, *CODATA Recommended Values of the Fundamental Constants: 2006*, Rev. Mod. Phys. (to be published); physics.nist.gov/constants.
- D.N. Spergel *et al.*, *Astrophys. J. Supp.* **170**, 377 (2007). Post-deadline WMAP5 values have not been used. In any case, they usually vary no more than 1σ from the WMAP3 values.
- O. Lahav & A.R. Liddle, “The Cosmological Parameters,” this *Review*.
- B.W. Petley, *Nature* **303**, 373 (1983).
- The Astronomical Almanac for the year 2007*, U.S. Government Printing Office, Washington, and The Stationery Office, London (2005).
- With the range measurements of the Mars Global Surveyor and Odyssey in 1999–2007 now added to the Viking ranges of 1976–82, the value of the AU is determined to be $149\,597\,870\,700 \pm 2$ meters. While the AU is approximately equal to the semi-major axis of the Earth’s orbit, it is not exactly so. Nor is it exactly the mean earth-sun distance. There are a number of reasons for this: 1) the Earth’s orbit is not exactly Keplerian due to relativity and to perturbations from other planets; 2) the adopted value for the Gaussian gravitational constant k is not exactly equal to the earth’s mean motion; and 3) the mean distance in a Keplerian orbit is not equal to the semi-major axis; instead, it is $\langle r \rangle = a(1 + e^2/2)$, where e is the eccentricity. For an observer far above Earth’s orbital plane at rest in the inertial frame of the Solar System, terrestrial clocks would appear to run slower than local clocks because of (a) time dilation from Earth’s orbital motion and (b) gravitational redshift at the Earth’s surface and in the Sun’s potential well. The last contribution is twice as big as the time dilation. The clock rates differ by 1.5 parts in 10^8 . These effects complicate the measurement and definition of the AU and $G_N M_\odot$ (Discussion courtesy of Myles Standish, JPL).
- The distance at which 1 AU subtends 1 arc sec: 1 AU divided by $\pi/648\,000$.
- Product of $2/c^2$ and the heliocentric gravitational constant $G_N M_\odot = A^3 k^2 / 86400^2$, where k is the Gaussian gravitational constant, 0.017 202 098 95 (exact) [5]. The value and error for A given in this table are used.
- Obtained from the heliocentric gravitational constant [5] and G_N [1]. The error is the 100 ppm standard deviation of G_N .
- T. M. Brown & J. Christensen-Dalsgaard, *Astrophys. J.* **500**, L195 (1998). Many values for the Solar radius have been published, most of which are consistent with this result.
- $4\pi A^2 \times (1366.4 \pm 0.5) \text{ W m}^{-2}$ [30]. Assumes isotropic irradiance.
- Schwarzschild radius of the Sun (above) scaled by the Earth/Sun mass ratio given in Ref. 5.
- Obtained from the geocentric gravitational constant [5] and G_N [1]. The error is the 100 ppm standard deviation of G_N .
- E.W. Kolb & M.S. Turner, *The Early Universe*, Addison-Wesley (1990); The IAU (Commission 36) has recommended $3.055 \times 10^{28} \text{ W}$ for the zero point. Based on newer Solar measurements, the value and significance given in the table seems more appropriate.
- J. B. Oke & J. E. Gunn, *Astrophys. J.* **266**, 713 (1983). Note that in the definition of AB the sign of the constant is wrong.
- F.J. Kerr & D. Lynden-Bell, *Mon. Not. R. Astr. Soc.* **221**, 1023–1038 (1985). “On the basis of this review these [$R_0 = 8.5 \pm 1.1 \text{ kpc}$ and $\Theta_0 = 220 \pm 20 \text{ km s}^{-1}$] were adopted by resolution of IAU Commission 33 on 1985 November 21 at Delhi.” We retain this value for Θ_0 but list a more modern value for R_0 .
- M.J. Reid, *Annu. Rev. Astron. Astrophys.* **31**, 345–372 (1993); M. Shen & Z. Zhu, *Chin. Astron. Astrophys.* **7**, 120 (2007). In Fig. 2 they present a summary of a dozen modern values for R_0 . All but one are within Reid’s error band.
- G. Gilmore, R.F.G. Wyse, & K. Kuijken, *Ann. Rev. Astron. Astrophys.* **27**, 555 (1989).
- E.I. Gates, G. Gyuk, & M.S. Turner (*Astrophys. J.* **449**, L133 (1995)) find the local halo density to be $9.2_{-3.1}^{+3.8} \times 10^{-25} \text{ g cm}^{-3}$, but also comment that previously published estimates are in the range $1\text{--}10 \times 10^{-25} \text{ g cm}^{-3}$. The value $0.3 \text{ GeV}/c^2$ has been taken as “standard” in several papers setting limits on WIMP mass limits, *e.g.* in M. Mori *et al.*, *Phys. Lett.* **B289**, 463 (1992).
- J. Mather *et al.*, *Astrophys. J.* **512**, 511 (1999). This paper gives $T_0 = (2.725 \pm 0.002) \text{ K}$ at 95%CL. We take 0.001 as the one-standard deviation uncertainty.
- G. Hinshaw, *et al.*, *Astrophys. J. Supp.* **170**, 288 (2007).
- D. Scott & G.F. Smoot, “Cosmic Microwave Background,” this *Review*.
- $n_\gamma = \frac{2\zeta(3)}{\pi^2} \left(\frac{kT}{hc}\right)^3$ and $\rho_\gamma = \frac{\pi^2 (kT)^4}{15 (hc)^3}$.
- Conversion using length of sidereal year.
- Ω_Λ from fits to various data sets is given in Table 12 in Ref. 2. The (meaningless) weighted average from the not-independent data sets is 0.727 ± 0.012 . This is almost the WMAP + SDSS LRG fit, which we quote with a 50% more conservative error. The extended error band includes results obtained with all of the data sets.
- The lower limit follows from neutrino mixing results combined with the assumptions that there are three light neutrinos ($m < 45 \text{ GeV}$) and that the lightest neutrino is substantially less massive than the others. Limits set from analyses of WMAP, large-scale structure, and other data are in the $\Omega_\nu < 0.02$ range. If the limit obtained from tritium decay experiments ($m_\nu < 2 \text{ eV}$) is taken seriously, then one can only conclude that $\Omega_\nu < 0.1$.
- From WMAP 3-year + SNLS data. WMAP 3-year data plus the HST Key Project constraint on H_0 implies $\Omega_{\text{tot}} = 1.014 \pm 0.017$ [2].
- Calculated from ρ_c , Ω_b , and n_γ .
- From WMAP 3-year data alone, assuming no tensors. If other data are included, results from -0.058 to -0.066 are obtained. Inclusion of tensors in the model results in values from -0.082 to -0.090 [2].
- R.C. Willson & A.V. Mordvinov, *Geophys. Res. Lett.* **30**, 1119 (2003); C. Frölich, *Space Sci. Rev.* **125**, 53–65 (2006).

3. INTERNATIONAL SYSTEM OF UNITS (SI)

See “The International System of Units (SI),” NIST Special Publication **330**, B.N. Taylor, ed. (USGPO, Washington, DC, 1991); and “Guide for the Use of the International System of Units (SI),” NIST Special Publication **811**, 1995 edition, B.N. Taylor (USGPO, Washington, DC, 1995).

Physical quantity	Name of unit	Symbol
<i>Base units</i>		
length	meter	m
mass	kilogram	kg
time	second	s
electric current	ampere	A
thermodynamic temperature	kelvin	K
amount of substance	mole	mol
luminous intensity	candela	cd
<i>Derived units with special names</i>		
plane angle	radian	rad
solid angle	steradian	sr
frequency	hertz	Hz
energy	joule	J
force	newton	N
pressure	pascal	Pa
power	watt	W
electric charge	coulomb	C
electric potential	volt	V
electric resistance	ohm	Ω
electric conductance	siemens	S
electric capacitance	farad	F
magnetic flux	weber	Wb
inductance	henry	H
magnetic flux density	tesla	T
luminous flux	lumen	lm
illuminance	lux	lx
celsius temperature	degree celsius	$^{\circ}\text{C}$
activity (of a radioactive source)*	becquerel	Bq
absorbed dose (of ionizing radiation)*	gray	Gy
dose equivalent*	sievert	Sv

SI prefixes

10^{24}	yotta	(Y)
10^{21}	zetta	(Z)
10^{18}	exa	(E)
10^{15}	peta	(P)
10^{12}	tera	(T)
10^9	giga	(G)
10^6	mega	(M)
10^3	kilo	(k)
10^2	hecto	(h)
10	deca	(da)
10^{-1}	deci	(d)
10^{-2}	centi	(c)
10^{-3}	milli	(m)
10^{-6}	micro	(μ)
10^{-9}	nano	(n)
10^{-12}	pico	(p)
10^{-15}	femto	(f)
10^{-18}	atto	(a)
10^{-21}	zepto	(z)
10^{-24}	yocto	(y)

*See our section 29, on “Radioactivity and radiation protection,” p. 312.

Table 4.1. Revised 2008 by C.G. Wohl (LBNL), D.E. Groom (LBNL), and E. Bergren. Atomic weights of stable elements are adapted from the Commission on Isotopic Abundances and Atomic Weights, "Atomic Weights of the Elements 2007," <http://www.chem.qmul.ac.uk/iupac/AtWt/>. The atomic number (top left) is the number of protons in the nucleus. The atomic mass (bottom) of a stable elements is weighted by isotopic abundances in the Earth's surface. If the element has no stable isotope, the atomic mass (in parentheses) of the most stable isotope currently known is given. In this case the mass is from <http://www.nndc.bnl.gov/amdc/masstable/Ame2003/mass.mas03> and the longest-lived isotope is from www.nndc.bnl.gov/ensdf/za_form.jsp. The exceptions are Th, Pa, and U, which do have characteristic terrestrial compositions. Atomic masses are relative to the mass of ¹²C, defined to be exactly 12 unified atomic mass units (u) (approx. g/mole). Relative isotopic abundances often vary considerably, both in natural and commercial samples; this is reflected in the number of significant figures given. As of early 2008 element 112 has not been assigned a name, and there are no confirmed elements with *Z* > 112.

PERIODIC TABLE OF THE ELEMENTS																					
1 1A H Hydrogen 1.00794																	18 VIII A He Helium 4.002602				
3 Li Lithium 6.941	4 IIA Be Beryllium 9.012182															13 IIIA B Boron 10.811	14 IVA C Carbon 12.0107	15 VA N Nitrogen 14.0067	16 VIA O Oxygen 15.9994	17 VIIA F Fluorine 18.9984032	10 Ne Neon 20.1797
11 Na Sodium 22.98976928	12 Mg Magnesium 24.3050	3 IIIB	4 IVB	5 VB	6 VIB	7 VIIB	8 VIII	9 VIII	10 VIII	11 IB	12 IIB	13 Al Aluminum 26.9815386	14 Si Silicon 28.0855	15 P Phosph. 30.973762	16 S Sulfur 32.065	17 Cl Chlorine 35.453	18 Ar Argon 39.948				
19 K Potassium 39.0983	20 Ca Calcium 40.078	21 Sc Scandium 44.955912	22 Ti Titanium 47.867	23 V Vanadium 50.9415	24 Cr Chromium 51.9961	25 Mn Manganese 54.938045	26 Fe Iron 55.845	27 Co Cobalt 58.933195	28 Ni Nickel 58.6934	29 Cu Copper 63.546	30 Zn Zinc 65.38	31 Ga Gallium 69.723	32 Ge German. 72.64	33 As Arsenic 74.92160	34 Se Selenium 78.96	35 Br Bromine 79.904	36 Kr Krypton 83.798				
37 Rb Rubidium 85.4678	38 Sr Strontium 87.62	39 Y Yttrium 88.90585	40 Zr Zirconium 91.224	41 Nb Niobium 92.90638	42 Mo Molybd. 95.96	43 Tc Technet. (97.90722)	44 Ru Ruthen. 101.07	45 Rh Rhodium 102.90550	46 Pd Palladium 106.42	47 Ag Silver 107.8682	48 Cd Cadmium 112.411	49 In Indium 114.818	50 Sn Tin 118.710	51 Sb Antimony 121.760	52 Te Tellurium 127.60	53 I Iodine 126.90447	54 Xe Xenon 131.293				
55 Cs Cesium 132.9054519	56 Ba Barium 137.327	57-71 Lanthanides	72 Hf Hafnium 178.49	73 Ta Tantalum 180.94788	74 W Tungsten 183.84	75 Re Rhenium 186.207	76 Os Osmium 190.23	77 Ir Iridium 192.217	78 Pt Platinum 195.084	79 Au Gold 196.966569	80 Hg Mercury 200.59	81 Tl Thallium 204.3833	82 Pb Lead 207.2	83 Bi Bismuth 208.98040	84 Po Polonium (208.98243)	85 At Astatine (209.98715)	86 Rn Radon (222.01758)				
87 Fr Francium (223.01974)	88 Ra Radium (226.02541)	89-103 Actinides	104 Rf Rutherford. (267.122)	105 Db Dubnium (268.125)	106 Sg Seaborg. (271.133)	107 Bh Bohrium (270.134)	108 Hs Hassium (269.134)	109 Mt Meitner. (276.151)	110 Ds Darmstadt. (281.162)	111 Rg Roentgen. (280.164)	112										

Lanthanide series	57 La Lanthan. 138.90547	58 Ce Cerium 140.116	59 Pr Praseodym. 140.90765	60 Nd Neodym. 144.242	61 Pm Prometh. (144.91275)	62 Sm Samarium 150.36	63 Eu Europium 151.964	64 Gd Gadolin. 157.25	65 Tb Terbium 158.92535	66 Dy Dyspros. 162.500	67 Ho Holmium 164.93032	68 Er Erbium 167.259	69 Tm Thulium 168.93421	70 Yb Ytterbium 173.054	71 Lu Lutetium 174.9668
Actinide series	89 Ac Actinium (227.02775)	90 Th Thorium 232.03806	91 Pa Protactin. 231.03588	92 U Uranium 238.02891	93 Np Neptunium (237.04817)	94 Pu Plutonium (244.06420)	95 Am Americ. (243.06138)	96 Cm Curium (247.07035)	97 Bk Berkelium (247.07031)	98 Cf Californ. (251.07959)	99 Es Einstein. (252.0830)	100 Fm Fermium (257.09510)	101 Md Mendelev. (258.09843)	102 No Nobelium (259.1010)	103 Lr Lawrenc. (262.110)

5. ELECTRONIC STRUCTURE OF THE ELEMENTS

Table 5.1. Reviewed 2005 by C.G. Wohl (LBNL). The electronic configurations and the ionization energies are from the NIST database, “Ground Levels and Ionization Energies for the Neutral Atoms,” W.C. Martin, A. Musgrove, S. Kotochigova, and J.E. Sansonetti (2003), <http://physics.nist.gov> (select “Physical Reference Data”). The electron configuration for, say, iron indicates an argon electronic core (see argon) plus six $3d$ electrons and two $4s$ electrons. The ionization energy is the least energy necessary to remove to infinity one electron from an atom of the element.

	Element	Electron configuration ($3d^5 =$ five $3d$ electrons, <i>etc.</i>)	Ground state $2S+1L_J$	Ionization energy (eV)
1	H Hydrogen	$1s$	$^2S_{1/2}$	13.5984
2	He Helium	$1s^2$	1S_0	24.5874
3	Li Lithium	(He) $2s$	$^2S_{1/2}$	5.3917
4	Be Beryllium	(He) $2s^2$	1S_0	9.3227
5	B Boron	(He) $2s^2 2p$	$^2P_{1/2}$	8.2980
6	C Carbon	(He) $2s^2 2p^2$	3P_0	11.2603
7	N Nitrogen	(He) $2s^2 2p^3$	$^4S_{3/2}$	14.5341
8	O Oxygen	(He) $2s^2 2p^4$	3P_2	13.6181
9	F Fluorine	(He) $2s^2 2p^5$	$^2P_{3/2}$	17.4228
10	Ne Neon	(He) $2s^2 2p^6$	1S_0	21.5645
11	Na Sodium	(Ne) $3s$	$^2S_{1/2}$	5.1391
12	Mg Magnesium	(Ne) $3s^2$	1S_0	7.6462
13	Al Aluminum	(Ne) $3s^2 3p$	$^2P_{1/2}$	5.9858
14	Si Silicon	(Ne) $3s^2 3p^2$	3P_0	8.1517
15	P Phosphorus	(Ne) $3s^2 3p^3$	$^4S_{3/2}$	10.4867
16	S Sulfur	(Ne) $3s^2 3p^4$	3P_2	10.3600
17	Cl Chlorine	(Ne) $3s^2 3p^5$	$^2P_{3/2}$	12.9676
18	Ar Argon	(Ne) $3s^2 3p^6$	1S_0	15.7596
19	K Potassium	(Ar) $4s$	$^2S_{1/2}$	4.3407
20	Ca Calcium	(Ar) $4s^2$	1S_0	6.1132
21	Sc Scandium	(Ar) $3d 4s^2$	$^2D_{3/2}$	6.5615
22	Ti Titanium	(Ar) $3d^2 4s^2$	3F_2	6.8281
23	V Vanadium	(Ar) $3d^3 4s^2$	$^4F_{3/2}$	6.7462
24	Cr Chromium	(Ar) $3d^5 4s$	7S_3	6.7665
25	Mn Manganese	(Ar) $3d^5 4s^2$	$^6S_{5/2}$	7.4340
26	Fe Iron	(Ar) $3d^6 4s^2$	5D_4	7.9024
27	Co Cobalt	(Ar) $3d^7 4s^2$	$^4F_{9/2}$	7.8810
28	Ni Nickel	(Ar) $3d^8 4s^2$	3F_4	7.6398
29	Cu Copper	(Ar) $3d^{10} 4s$	$^2S_{1/2}$	7.7264
30	Zn Zinc	(Ar) $3d^{10} 4s^2$	1S_0	9.3942
31	Ga Gallium	(Ar) $3d^{10} 4s^2 4p$	$^2P_{1/2}$	5.9993
32	Ge Germanium	(Ar) $3d^{10} 4s^2 4p^2$	3P_0	7.8994
33	As Arsenic	(Ar) $3d^{10} 4s^2 4p^3$	$^4S_{3/2}$	9.7886
34	Se Selenium	(Ar) $3d^{10} 4s^2 4p^4$	3P_2	9.7524
35	Br Bromine	(Ar) $3d^{10} 4s^2 4p^5$	$^2P_{3/2}$	11.8138
36	Kr Krypton	(Ar) $3d^{10} 4s^2 4p^6$	1S_0	13.9996
37	Rb Rubidium	(Kr) $5s$	$^2S_{1/2}$	4.1771
38	Sr Strontium	(Kr) $5s^2$	1S_0	5.6949
39	Y Yttrium	(Kr) $4d 5s^2$	$^2D_{3/2}$	6.2173
40	Zr Zirconium	(Kr) $4d^2 5s^2$	3F_2	6.6339
41	Nb Niobium	(Kr) $4d^4 5s$	$^6D_{1/2}$	6.7589
42	Mo Molybdenum	(Kr) $4d^5 5s$	7S_3	7.0924
43	Tc Technetium	(Kr) $4d^5 5s^2$	$^6S_{5/2}$	7.28
44	Ru Ruthenium	(Kr) $4d^7 5s$	5F_5	7.3605
45	Rh Rhodium	(Kr) $4d^8 5s$	$^4F_{9/2}$	7.4589
46	Pd Palladium	(Kr) $4d^{10}$	1S_0	8.3369
47	Ag Silver	(Kr) $4d^{10} 5s$	$^2S_{1/2}$	7.5762
48	Cd Cadmium	(Kr) $4d^{10} 5s^2$	1S_0	8.9938

49	In	Indium	(Kr) $4d^{10}5s^2$	$5p$		$^2P_{1/2}$	5.7864
50	Sn	Tin	(Kr) $4d^{10}5s^2$	$5p^2$		3P_0	7.3439
51	Sb	Antimony	(Kr) $4d^{10}5s^2$	$5p^3$		$^4S_{3/2}$	8.6084
52	Te	Tellurium	(Kr) $4d^{10}5s^2$	$5p^4$		3P_2	9.0096
53	I	Iodine	(Kr) $4d^{10}5s^2$	$5p^5$		$^2P_{3/2}$	10.4513
54	Xe	Xenon	(Kr) $4d^{10}5s^2$	$5p^6$		1S_0	12.1298
55	Cs	Cesium	(Xe)	$6s$		$^2S_{1/2}$	3.8939
56	Ba	Barium	(Xe)	$6s^2$		1S_0	5.2117
57	La	Lanthanum	(Xe)	$5d$	$6s^2$	$^2D_{3/2}$	5.5769
58	Ce	Cerium	(Xe) $4f$	$5d$	$6s^2$	1G_4	5.5387
59	Pr	Praseodymium	(Xe) $4f^3$		$6s^2$	$^4I_{9/2}$	5.473
60	Nd	Neodymium	(Xe) $4f^4$		$6s^2$	5I_4	5.5250
61	Pm	Promethium	(Xe) $4f^5$		$6s^2$	$^6H_{5/2}$	5.582
62	Sm	Samarium	(Xe) $4f^6$		$6s^2$	7F_0	5.6437
63	Eu	Europium	(Xe) $4f^7$		$6s^2$	$^8S_{7/2}$	5.6704
64	Gd	Gadolinium	(Xe) $4f^7$	$5d$	$6s^2$	9D_2	6.1498
65	Tb	Terbium	(Xe) $4f^9$		$6s^2$	$^6H_{15/2}$	5.8638
66	Dy	Dysprosium	(Xe) $4f^{10}$		$6s^2$	5I_8	5.9389
67	Ho	Holmium	(Xe) $4f^{11}$		$6s^2$	$^4I_{15/2}$	6.0215
68	Er	Erbium	(Xe) $4f^{12}$		$6s^2$	3H_6	6.1077
69	Tm	Thulium	(Xe) $4f^{13}$		$6s^2$	$^2F_{7/2}$	6.1843
70	Yb	Ytterbium	(Xe) $4f^{14}$		$6s^2$	1S_0	6.2542
71	Lu	Lutetium	(Xe) $4f^{14}5d$		$6s^2$	$^2D_{3/2}$	5.4259
72	Hf	Hafnium	(Xe) $4f^{14}5d^2$		$6s^2$	3F_2	6.8251
73	Ta	Tantalum	(Xe) $4f^{14}5d^3$		$6s^2$	$^4F_{3/2}$	7.5496
74	W	Tungsten	(Xe) $4f^{14}5d^4$		$6s^2$	5D_0	7.8640
75	Re	Rhenium	(Xe) $4f^{14}5d^5$		$6s^2$	$^6S_{5/2}$	7.8335
76	Os	Osmium	(Xe) $4f^{14}5d^6$		$6s^2$	5D_4	8.4382
77	Ir	Iridium	(Xe) $4f^{14}5d^7$		$6s^2$	$^4F_{9/2}$	8.9670
78	Pt	Platinum	(Xe) $4f^{14}5d^9$		$6s$	3D_3	8.9588
79	Au	Gold	(Xe) $4f^{14}5d^{10}6s$			$^2S_{1/2}$	9.2255
80	Hg	Mercury	(Xe) $4f^{14}5d^{10}6s^2$			1S_0	10.4375
81	Tl	Thallium	(Xe) $4f^{14}5d^{10}6s^2$		$6p$	$^2P_{1/2}$	6.1082
82	Pb	Lead	(Xe) $4f^{14}5d^{10}6s^2$		$6p^2$	3P_0	7.4167
83	Bi	Bismuth	(Xe) $4f^{14}5d^{10}6s^2$		$6p^3$	$^4S_{3/2}$	7.2855
84	Po	Polonium	(Xe) $4f^{14}5d^{10}6s^2$		$6p^4$	3P_2	8.414
85	At	Astatine	(Xe) $4f^{14}5d^{10}6s^2$		$6p^5$	$^2P_{3/2}$	
86	Rn	Radon	(Xe) $4f^{14}5d^{10}6s^2$		$6p^6$	1S_0	10.7485
87	Fr	Francium	(Rn)		$7s$	$^2S_{1/2}$	4.0727
88	Ra	Radium	(Rn)		$7s^2$	1S_0	5.2784
89	Ac	Actinium	(Rn)	$6d$	$7s^2$	$^2D_{3/2}$	5.17
90	Th	Thorium	(Rn)	$6d^2$	$7s^2$	3F_2	6.3067
91	Pa	Protactinium	(Rn) $5f^2$	$6d$	$7s^2$	$^4K_{11/2}^*$	5.89
92	U	Uranium	(Rn) $5f^3$	$6d$	$7s^2$	$^5L_6^*$	6.1941
93	Np	Neptunium	(Rn) $5f^4$	$6d$	$7s^2$	$^6L_{11/2}^*$	6.2657
94	Pu	Plutonium	(Rn) $5f^6$		$7s^2$	7F_0	6.0260
95	Am	Americium	(Rn) $5f^7$		$7s^2$	$^8S_{7/2}$	5.9738
96	Cm	Curium	(Rn) $5f^7$	$6d$	$7s^2$	9D_2	5.9914
97	Bk	Berkelium	(Rn) $5f^9$		$7s^2$	$^6H_{15/2}$	6.1979
98	Cf	Californium	(Rn) $5f^{10}$		$7s^2$	5I_8	6.2817
99	Es	Einsteinium	(Rn) $5f^{11}$		$7s^2$	$^4I_{15/2}$	6.42
100	Fm	Fermium	(Rn) $5f^{12}$		$7s^2$	3H_6	6.50
101	Md	Mendelevium	(Rn) $5f^{13}$		$7s^2$	$^2F_{7/2}$	6.58
102	No	Nobelium	(Rn) $5f^{14}$		$7s^2$	1S_0	6.65
103	Lr	Lawrencium	(Rn) $5f^{14}$		$7s^2$	$^2P_{1/2}^?$	4.9?
104	Rf	Rutherfordium	(Rn) $5f^{14}6d^2$		$7s^2?$	$^3F_2?$	6.0?

* The usual LS coupling scheme does not apply for these three elements. See the introductory note to the NIST table from which this table is taken.

6. ATOMIC AND NUCLEAR PROPERTIES OF MATERIALS

Table 6.1 Abridged from pdg.lbl.gov/AtomicNuclearProperties by D. E. Groom (2007). See web pages for more detail about entries in this table including chemical formulae, and for several hundred other entries. Quantities in parentheses are for NTP (20°C and 1 atm), and square brackets indicate quantities evaluated at STP. Boiling points are at 1 atm. Refractive indices n are evaluated at the sodium D line blend (589.2 nm); values $\gg 1$ in brackets are for $(n - 1) \times 10^6$ (gases).

Material	Z	A	$\langle Z/A \rangle$	Nucl.coll. length λ_T {g cm ⁻² }	Nucl.inter. length λ_I {g cm ⁻² }	Rad.len. X_0 {g cm ⁻² }	$dE/dx _{\min}$ { MeV g ⁻¹ cm ² }	Density {g cm ⁻³ } {(gℓ ⁻¹)}	Melting point (K)	Boiling point (K)	Refract. index (@ Na D)
H ₂	1	1.00794(7)	0.99212	42.8	52.0	63.04	(4.103)	0.071(0.084)	13.81	20.28	1.11[132.]
D ₂	1	2.01410177803(8)	0.49650	51.3	71.8	125.97	(2.053)	0.169(0.168)	18.7	23.65	1.11[138.]
He	2	4.002602(2)	0.49967	51.8	71.0	94.32	(1.937)	0.125(0.166)		4.220	1.02[35.0]
Li	3	6.941(2)	0.43221	52.2	71.3	82.78	1.639	0.534	453.6	1615.	
Be	4	9.012182(3)	0.44384	55.3	77.8	65.19	1.595	1.848	1560.	2744.	
C diamond	6	12.0107(8)	0.49955	59.2	85.8	42.70	1.725	3.520			2.42
C graphite	6	12.0107(8)	0.49955	59.2	85.8	42.70	1.742	2.210			
N ₂	7	14.0067(2)	0.49976	61.1	89.7	37.99	(1.825)	0.807(1.165)	63.15	77.29	1.20[298.]
O ₂	8	15.9994(3)	0.50002	61.3	90.2	34.24	(1.801)	1.141(1.332)	54.36	90.20	1.22[271.]
F ₂	9	18.9984032(5)	0.47372	65.0	97.4	32.93	(1.676)	1.507(1.580)	53.53	85.03	[195.]
Ne	10	20.1797(6)	0.49555	65.7	99.0	28.93	(1.724)	1.204(0.839)	24.56	27.07	1.09[67.1]
Al	13	26.9815386(8)	0.48181	69.7	107.2	24.01	1.615	2.699	933.5	2792.	
Si	14	28.0855(3)	0.49848	70.2	108.4	21.82	1.664	2.329	1687.	3538.	3.95
Cl ₂	17	35.453(2)	0.47951	73.8	115.7	19.28	(1.630)	1.574(2.980)	171.6	239.1	[773.]
Ar	18	39.948(1)	0.45059	75.7	119.7	19.55	(1.519)	1.396(1.662)	83.81	87.26	1.23[281.]
Ti	22	47.867(1)	0.45961	78.8	126.2	16.16	1.477	4.540	1941.	3560.	
Fe	26	55.845(2)	0.46557	81.7	132.1	13.84	1.451	7.874	1811.	3134.	
Cu	29	63.546(3)	0.45636	84.2	137.3	12.86	1.403	8.960	1358.	2835.	
Ge	32	72.64(1)	0.44053	86.9	143.0	12.25	1.370	5.323	1211.	3106.	
Sn	50	118.710(7)	0.42119	98.2	166.7	8.82	1.263	7.310	505.1	2875.	
Xe	54	131.293(6)	0.41129	100.8	172.1	8.48	(1.255)	2.953(5.483)	161.4	165.1	1.39[701.]
W	74	183.84(1)	0.40252	110.4	191.9	6.76	1.145	19.300	3695.	5828.	
Pt	78	195.084(9)	0.39983	112.2	195.7	6.54	1.128	21.450	2042.	4098.	
Au	79	196.966569(4)	0.40108	112.5	196.3	6.46	1.134	19.320	1337.	3129.	
Pb	82	207.2(1)	0.39575	114.1	199.6	6.37	1.122	11.350	600.6	2022.	
U	92	[238.02891(3)]	0.38651	118.6	209.0	6.00	1.081	18.950	1408.	4404.	
Air (dry, 1 atm)			0.49919	61.3	90.1	36.62	(1.815)	(1.205)		78.80	
Shielding concrete			0.50274	65.1	97.5	26.57	1.711	2.300			
Borosilicate glass (Pyrex)			0.49707	64.6	96.5	28.17	1.696	2.230			
Lead glass			0.42101	95.9	158.0	7.87	1.255	6.220			
Standard rock			0.50000	66.8	101.3	26.54	1.688	2.650			
Methane (CH ₄)			0.62334	54.0	73.8	46.47	(2.417)	(0.667)	90.68	111.7	[444.]
Ethane (C ₂ H ₆)			0.59861	55.0	75.9	45.66	(2.304)	(1.263)	90.36	184.5	
Propane (C ₃ H ₈)			0.58962	55.3	76.7	45.37	(2.262)	0.493(1.868)	85.52	231.0	
Butane (C ₄ H ₁₀)			0.59497	55.5	77.1	45.23	(2.278)	(2.489)	134.9	272.6	
Octane (C ₈ H ₁₈)			0.57778	55.8	77.8	45.00	2.123	0.703	214.4	398.8	
Paraffin (CH ₃ (CH ₂) _n ≈23CH ₃)			0.57275	56.0	78.3	44.85	2.088	0.930			
Nylon (type 6, 6/6)			0.54790	57.5	81.6	41.92	1.973	1.18			
Polycarbonate (Lexan)			0.52697	58.3	83.6	41.50	1.886	1.20			
Polyethylene ([CH ₂ CH ₂] _n)			0.57034	56.1	78.5	44.77	2.079	0.89			
Polyethylene terephthalate (Mylar)			0.52037	58.9	84.9	39.95	1.848	1.40			
Polyimide film (Kapton)			0.51264	59.2	85.5	40.58	1.820	1.42			
Polymethylmethacrylate (acrylic)			0.53937	58.1	82.8	40.55	1.929	1.19			1.49
Polypropylene			0.55998	56.1	78.5	44.77	2.041	0.90			
Polystyrene ([C ₆ H ₅ CHCH ₂] _n)			0.53768	57.5	81.7	43.79	1.936	1.06			1.59
Polytetrafluoroethylene (Teflon)			0.47992	63.5	94.4	34.84	1.671	2.20			
Polyvinyltoluene			0.54141	57.3	81.3	43.90	1.956	1.03			1.58
Aluminum oxide (sapphire)			0.49038	65.5	98.4	27.94	1.647	3.970	2327.	3273.	1.77
Barium fluoride (BaF ₂)			0.42207	90.8	149.0	9.91	1.303	4.893	1641.	2533.	1.47
Bismuth germanate (BGO)			0.42065	96.2	159.1	7.97	1.251	7.130	1317.		2.15
Carbon dioxide gas (CO ₂)			0.49989	60.7	88.9	36.20	1.819	(1.842)			[449.]
Solid carbon dioxide (dry ice)			0.49989	60.7	88.9	36.20	1.787	1.563	Sublimes at 194.7 K		
Cesium iodide (CsI)			0.41569	100.6	171.5	8.39	1.243	4.510	894.2	1553.	1.79
Lithium fluoride (LiF)			0.46262	61.0	88.7	39.26	1.614	2.635	1121.	1946.	1.39
Lithium hydride (LiH)			0.50321	50.8	68.1	79.62	1.897	0.820	965.		
Lead tungstate (PbWO ₄)			0.41315	100.6	168.3	7.39	1.229	8.300	1403.		2.20
Silicon dioxide (SiO ₂ , fused quartz)			0.49930	65.2	97.8	27.05	1.699	2.200	1986.	3223.	1.46
Sodium chloride (NaCl)			0.55509	71.2	110.1	21.91	1.847	2.170	1075.	1738.	1.54
Sodium iodide (NaI)			0.42697	93.1	154.6	9.49	1.305	3.667	933.2	1577.	1.77
Water (H ₂ O)			0.55509	58.5	83.3	36.08	1.992	1.000(0.756)	273.1	373.1	1.33
Silica aerogel			0.50093	65.0	97.3	27.25	1.740	0.200	(0.03 H ₂ O, 0.97 SiO ₂)		

Material	Dielectric constant ($\kappa = \epsilon/\epsilon_0$) () is $(\kappa-1)\times 10^6$ for gas	Young's modulus [10^6 psi]	Coeff. of thermal expansion [10^{-6} cm/cm- $^{\circ}$ C]	Specific heat [cal/g- $^{\circ}$ C]	Electrical resistivity [$\mu\Omega$ cm(@ $^{\circ}$ C)]	Thermal conductivity [cal/cm- $^{\circ}$ C-sec]
H ₂	(253.9)	—	—	—	—	—
He	(64)	—	—	—	—	—
Li	—	—	56	0.86	8.55(0 $^{\circ}$)	0.17
Be	—	37	12.4	0.436	5.885(0 $^{\circ}$)	0.38
C	—	0.7	0.6-4.3	0.165	1375(0 $^{\circ}$)	0.057
N ₂	(548.5)	—	—	—	—	—
O ₂	(495)	—	—	—	—	—
Ne	(127)	—	—	—	—	—
Al	—	10	23.9	0.215	2.65(20 $^{\circ}$)	0.53
Si	11.9	16	2.8-7.3	0.162	—	0.20
Ar	(517)	—	—	—	—	—
Ti	—	16.8	8.5	0.126	50(0 $^{\circ}$)	—
Fe	—	28.5	11.7	0.11	9.71(20 $^{\circ}$)	0.18
Cu	—	16	16.5	0.092	1.67(20 $^{\circ}$)	0.94
Ge	16.0	—	5.75	0.073	—	0.14
Sn	—	6	20	0.052	11.5(20 $^{\circ}$)	0.16
Xe	—	—	—	—	—	—
W	—	50	4.4	0.032	5.5(20 $^{\circ}$)	0.48
Pt	—	21	8.9	0.032	9.83(0 $^{\circ}$)	0.17
Pb	—	2.6	29.3	0.038	20.65(20 $^{\circ}$)	0.083
U	—	—	36.1	0.028	29(20 $^{\circ}$)	0.064

7. ELECTROMAGNETIC RELATIONS

Revised September 2005 by H.G. Spieler (LBNL).

Quantity	Gaussian CGS	SI
Conversion factors:		
Charge:	$2.997\,924\,58 \times 10^9$ esu	$= 1\text{ C} = 1\text{ A s}$
Potential:	$(1/299.792\,458)$ statvolt (ergs/esu)	$= 1\text{ V} = 1\text{ J C}^{-1}$
Magnetic field:	10^4 gauss = 10^4 dyne/esu	$= 1\text{ T} = 1\text{ N A}^{-1}\text{m}^{-1}$
	$\mathbf{F} = q(\mathbf{E} + \frac{\mathbf{v}}{c} \times \mathbf{B})$	$\mathbf{F} = q(\mathbf{E} + \mathbf{v} \times \mathbf{B})$
	$\nabla \cdot \mathbf{D} = 4\pi\rho$ $\nabla \times \mathbf{H} - \frac{1}{c} \frac{\partial \mathbf{D}}{\partial t} = \frac{4\pi}{c} \mathbf{J}$ $\nabla \cdot \mathbf{B} = 0$ $\nabla \times \mathbf{E} + \frac{1}{c} \frac{\partial \mathbf{B}}{\partial t} = 0$	$\nabla \cdot \mathbf{D} = \rho$ $\nabla \times \mathbf{H} - \frac{\partial \mathbf{D}}{\partial t} = \mathbf{J}$ $\nabla \cdot \mathbf{B} = 0$ $\nabla \times \mathbf{E} + \frac{\partial \mathbf{B}}{\partial t} = 0$
Constitutive relations:	$\mathbf{D} = \mathbf{E} + 4\pi\mathbf{P}$, $\mathbf{H} = \mathbf{B} - 4\pi\mathbf{M}$	$\mathbf{D} = \epsilon_0\mathbf{E} + \mathbf{P}$, $\mathbf{H} = \mathbf{B}/\mu_0 - \mathbf{M}$
Linear media:	$\mathbf{D} = \epsilon\mathbf{E}$, $\mathbf{H} = \mathbf{B}/\mu$ 1 1	$\mathbf{D} = \epsilon\mathbf{E}$, $\mathbf{H} = \mathbf{B}/\mu$ $\epsilon_0 = 8.854\,187 \dots \times 10^{-12}$ F m ⁻¹ $\mu_0 = 4\pi \times 10^{-7}$ N A ⁻²
	$\mathbf{E} = -\nabla V - \frac{1}{c} \frac{\partial \mathbf{A}}{\partial t}$ $\mathbf{B} = \nabla \times \mathbf{A}$	$\mathbf{E} = -\nabla V - \frac{\partial \mathbf{A}}{\partial t}$ $\mathbf{B} = \nabla \times \mathbf{A}$
	$V = \sum_{\text{charges}} \frac{q_i}{r_i} = \int \frac{\rho(\mathbf{r}')}{ \mathbf{r} - \mathbf{r}' } d^3x'$ $\mathbf{A} = \frac{1}{c} \oint \frac{I d\boldsymbol{\ell}}{ \mathbf{r} - \mathbf{r}' } = \frac{1}{c} \int \frac{\mathbf{J}(\mathbf{r}')}{ \mathbf{r} - \mathbf{r}' } d^3x'$	$V = \frac{1}{4\pi\epsilon_0} \sum_{\text{charges}} \frac{q_i}{r_i} = \frac{1}{4\pi\epsilon_0} \int \frac{\rho(\mathbf{r}')}{ \mathbf{r} - \mathbf{r}' } d^3x'$ $\mathbf{A} = \frac{\mu_0}{4\pi} \oint \frac{I d\boldsymbol{\ell}}{ \mathbf{r} - \mathbf{r}' } = \frac{\mu_0}{4\pi} \int \frac{\mathbf{J}(\mathbf{r}')}{ \mathbf{r} - \mathbf{r}' } d^3x'$
	$\mathbf{E}'_{\parallel} = \mathbf{E}_{\parallel}$ $\mathbf{E}'_{\perp} = \gamma(\mathbf{E}_{\perp} + \frac{1}{c} \mathbf{v} \times \mathbf{B})$ $\mathbf{B}'_{\parallel} = \mathbf{B}_{\parallel}$ $\mathbf{B}'_{\perp} = \gamma(\mathbf{B}_{\perp} - \frac{1}{c} \mathbf{v} \times \mathbf{E})$	$\mathbf{E}'_{\parallel} = \mathbf{E}_{\parallel}$ $\mathbf{E}'_{\perp} = \gamma(\mathbf{E}_{\perp} + \mathbf{v} \times \mathbf{B})$ $\mathbf{B}'_{\parallel} = \mathbf{B}_{\parallel}$ $\mathbf{B}'_{\perp} = \gamma(\mathbf{B}_{\perp} - \frac{1}{c^2} \mathbf{v} \times \mathbf{E})$
	$\frac{1}{4\pi\epsilon_0} = c^2 \times 10^{-7} \text{ N A}^{-2} = 8.987\,55 \dots \times 10^9 \text{ m F}^{-1}$; $\frac{\mu_0}{4\pi} = 10^{-7} \text{ N A}^{-2}$; $c = \frac{1}{\sqrt{\mu_0\epsilon_0}} = 2.997\,924\,58 \times 10^8 \text{ m s}^{-1}$	

7.1. Impedances (SI units)

ρ = resistivity at room temperature in $10^{-8} \Omega \text{ m}$:
 ~ 1.7 for Cu ~ 5.5 for W
 ~ 2.4 for Au ~ 73 for SS 304
 ~ 2.8 for Al ~ 100 for Nichrome
 (Al alloys may have double the Al value.)

For alternating currents, instantaneous current I , voltage V , angular frequency ω :

$$V = V_0 e^{j\omega t} = ZI. \quad (7.1)$$

Impedance of self-inductance L : $Z = j\omega L$.

Impedance of capacitance C : $Z = 1/j\omega C$.

Impedance of free space: $Z = \sqrt{\mu_0/\epsilon_0} = 376.7 \Omega$.

High-frequency surface impedance of a good conductor:

$$Z = \frac{(1+j)\rho}{\delta}, \quad \text{where } \delta = \text{skin depth}; \quad (7.2)$$

$$\delta = \sqrt{\frac{\rho}{\pi\nu\mu}} \approx \frac{6.6 \text{ cm}}{\sqrt{\nu \text{ (Hz)}}} \quad \text{for Cu}. \quad (7.3)$$

7.2. Capacitors, inductors, and transmission Lines

The capacitance between two parallel plates of area A spaced by the distance d and enclosing a medium with the dielectric constant ϵ is

$$C = K\epsilon A/d, \quad (7.4)$$

where the correction factor K depends on the extent of the fringing field. If the dielectric fills the capacitor volume without extending beyond the electrodes, the correction factor $K \approx 0.8$ for capacitors of typical geometry.

The inductance at high frequencies of a straight wire whose length ℓ is much greater than the wire diameter d is

$$L \approx 2.0 \left[\frac{\text{nH}}{\text{cm}} \right] \cdot \ell \left(\ln \left(\frac{4\ell}{d} \right) - 1 \right). \quad (7.5)$$

For very short wires, representative of vias in a printed circuit board, the inductance is

$$L(\text{in nH}) \approx \ell/d. \quad (7.6)$$

A transmission line is a pair of conductors with inductance L and capacitance C . The characteristic impedance $Z = \sqrt{L/C}$ and the phase velocity $v_p = 1/\sqrt{LC} = 1/\sqrt{\mu\epsilon}$, which decreases with the inverse square root of the dielectric constant of the medium. Typical coaxial and ribbon cables have a propagation delay of about 5 ns/cm. The impedance of a coaxial cable with outer diameter D and inner diameter d is

$$Z = 60 \Omega \cdot \frac{1}{\sqrt{\epsilon_r}} \ln \frac{D}{d}, \quad (7.7)$$

where the relative dielectric constant $\epsilon_r = \epsilon/\epsilon_0$. A pair of parallel wires of diameter d and spacing $a > 2.5d$ has the impedance

$$Z = 120 \Omega \cdot \frac{1}{\sqrt{\epsilon_r}} \ln \frac{2a}{d}. \quad (7.8)$$

This yields the impedance of a wire at a spacing h above a ground plane,

$$Z = 60 \Omega \cdot \frac{1}{\sqrt{\epsilon_r}} \ln \frac{4h}{d}. \quad (7.9)$$

A common configuration utilizes a thin rectangular conductor above a ground plane with an intermediate dielectric (microstrip). Detailed calculations for this and other transmission line configurations are given by Gunston.*

7.3. Synchrotron radiation (CGS units)

For a particle of charge e , velocity $v = \beta c$, and energy $E = \gamma mc^2$, traveling in a circular orbit of radius R , the classical energy loss per revolution δE is

$$\delta E = \frac{4\pi}{3} \frac{e^2}{R} \beta^3 \gamma^4. \quad (7.10)$$

For high-energy electrons or positrons ($\beta \approx 1$), this becomes

$$\delta E \text{ (in MeV)} \approx 0.0885 [E(\text{in GeV})]^4/R(\text{in m}). \quad (7.11)$$

For $\gamma \gg 1$, the energy radiated per revolution into the photon energy interval $d(\hbar\omega)$ is

$$dI = \frac{8\pi}{9} \alpha \gamma F(\omega/\omega_c) d(\hbar\omega), \quad (7.12)$$

where $\alpha = e^2/\hbar c$ is the fine-structure constant and

$$\omega_c = \frac{3\gamma^3 c}{2R} \quad (7.13)$$

is the critical frequency. The normalized function $F(y)$ is

$$F(y) = \frac{9}{8\pi} \sqrt{3} y \int_y^\infty K_{5/3}(x) dx, \quad (7.14)$$

where $K_{5/3}(x)$ is a modified Bessel function of the third kind. For electrons or positrons,

$$\hbar\omega_c \text{ (in keV)} \approx 2.22 [E(\text{in GeV})]^3/R(\text{in m}). \quad (7.15)$$

Fig. 7.1 shows $F(y)$ over the important range of y .

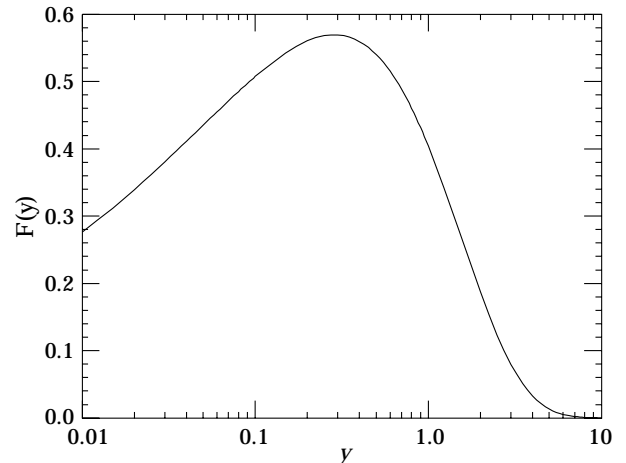


Figure 7.1: The normalized synchrotron radiation spectrum $F(y)$.

For $\gamma \gg 1$ and $\omega \ll \omega_c$,

$$\frac{dI}{d(\hbar\omega)} \approx 3.3\alpha (\omega R/c)^{1/3}, \quad (7.16)$$

whereas for

$$\gamma \gg 1 \text{ and } \omega \gtrsim 3\omega_c,$$

$$\frac{dI}{d(\hbar\omega)} \approx \sqrt{\frac{3\pi}{2}} \alpha \gamma \left(\frac{\omega}{\omega_c} \right)^{1/2} e^{-\omega/\omega_c} \left[1 + \frac{55}{72} \frac{\omega_c}{\omega} + \dots \right]. \quad (7.17)$$

The radiation is confined to angles $\lesssim 1/\gamma$ relative to the instantaneous direction of motion. For $\gamma \gg 1$, where Eq. (7.12) applies, the mean number of photons emitted per revolution is

$$N_\gamma = \frac{5\pi}{\sqrt{3}} \alpha \gamma, \quad (7.18)$$

and the mean energy per photon is

$$\langle \hbar\omega \rangle = \frac{8}{15\sqrt{3}} \hbar\omega_c. \quad (7.19)$$

When $\langle \hbar\omega \rangle \gtrsim O(E)$, quantum corrections are important.

* M.A.R. Gunston. Microwave Transmission Line Data, Noble Publishing Corp., Atlanta (1997) ISBN 1-884932-57-6, TK6565.T73G85.

See J.D. Jackson, *Classical Electrodynamics*, 3rd edition (John Wiley & Sons, New York, 1998) for more formulae and details. (Note that earlier editions had ω_c twice as large as Eq. (7.13).

8. NAMING SCHEME FOR HADRONS

Revised 2004 by M. Roos (University of Finland) and C.G. Wohl (LBNL).

8.1. Introduction

We introduced in the 1986 edition [1] a new naming scheme for the hadrons. Changes from older terminology affected mainly the heavier mesons made of the light (u , d , and s) quarks. Old and new names were listed alongside until 1994. Names also change from edition to edition because some characteristic like mass or spin changes. The Summary Tables give both the new and old names whenever a change occurred.

8.2. “Neutral-flavor” mesons ($S=C=B=T=0$)

Table 8.1 shows the names for mesons having the strangeness and all heavy-flavor quantum numbers equal to zero. The scheme is designed for all ordinary non-exotic mesons, but it will work for many exotic types too, if needed.

Table 8.1: Symbols for mesons with the strangeness and all heavy-flavor quantum numbers equal to zero.

J^{PC}	$\begin{cases} 0^{-+} \\ 2^{-+} \\ \vdots \end{cases}$	$\begin{cases} 1^{+-} \\ 3^{+-} \\ \vdots \end{cases}$	$\begin{cases} 1^{--} \\ 2^{--} \\ \vdots \end{cases}$	$\begin{cases} 0^{++} \\ 1^{++} \\ \vdots \end{cases}$	
$q\bar{q}$ content	$2^{S+1}L_J$	${}^1(L\text{ even})_J$	${}^1(L\text{ odd})_J$	${}^3(L\text{ even})_J$	${}^3(L\text{ odd})_J$
$u\bar{d}, u\bar{u} - d\bar{d}, d\bar{u}$ ($I=1$)	π	b	ρ	a	
$d\bar{d} + u\bar{u}$ and/or $s\bar{s}$ } ($I=0$)	η, η'	h, h'	ω, ϕ	f, f'	
$c\bar{c}$	η_c	h_c	ψ^\dagger	χ_c	
$b\bar{b}$	η_b	h_b	Υ	χ_b	
$t\bar{t}$	η_t	h_t	θ	χ_t	

[†]The J/ψ remains the J/ψ .

First, we assign names to those states with quantum numbers compatible with being $q\bar{q}$ states. The rows of the Table give the possible $q\bar{q}$ content. The columns give the possible parity/charge-conjugation states,

$$PC = -+, ++, --, \text{ and } ++;$$

these combinations correspond one-to-one with the angular-momentum state $2^{S+1}L_J$ of the $q\bar{q}$ system being

$${}^1(L\text{ even})_J, {}^1(L\text{ odd})_J, {}^3(L\text{ even})_J, \text{ or } {}^3(L\text{ odd})_J.$$

Here S , L , and J are the spin, orbital, and total angular momenta of the $q\bar{q}$ system. The quantum numbers are related by $P = (-1)^{L+1}$, $C = (-1)^{L+S}$, and G parity $= (-1)^{L+S+I}$, where of course the C quantum number is only relevant to neutral mesons.

The entries in the Table give the meson names. The spin J is added as a subscript except for pseudoscalar and vector mesons, and the mass is added in parentheses for mesons that decay strongly. However, for the lightest meson resonances, we omit the mass.

Measurements of the mass, quark content (where relevant), and quantum numbers I , J , P , and C (or G) of a meson thus fix its symbol. Conversely, these properties may be inferred unambiguously from the symbol.

If the main symbol cannot be assigned because the quantum numbers are unknown, X is used. Sometimes it is not known whether a meson is mainly the isospin-0 mix of $u\bar{u}$ and $d\bar{d}$ or is mainly $s\bar{s}$. A prime (or pair ω , ϕ) may be used to distinguish two such mixing states.

We follow custom and use spectroscopic names such as $\Upsilon(1S)$ as the primary name for most of those ψ , Υ , and χ states whose spectroscopic identity is known. We use the form $\Upsilon(9460)$ as an alternative, and as the primary name when the spectroscopic identity is not known.

Names are assigned for $t\bar{t}$ mesons, although the top quark is evidently so heavy that it is expected to decay too rapidly for bound states to form.

Gluonium states or other mesons that are not $q\bar{q}$ states are, if the quantum numbers are *not* exotic, to be named just as are the $q\bar{q}$ mesons. Such states will probably be difficult to distinguish from $q\bar{q}$ states and will likely mix with them, and we make no attempt to distinguish those “mostly gluonium” from those “mostly $q\bar{q}$.”

An “exotic” meson with J^{PC} quantum numbers that a $q\bar{q}$ system cannot have, namely $J^{PC} = 0^{--}, 0^{+-}, 1^{-+}, 2^{+-}, 3^{-+}, \dots$, would use the same symbol as does an ordinary meson with all the same quantum numbers as the exotic meson except for the C parity. But then the J subscript may still distinguish it; for example, an isospin-0 1^{-+} meson could be denoted ω_1 .

8.3. Mesons with nonzero S , C , B , and/or T

Since the strangeness or a heavy flavor of these mesons is nonzero, none of them are eigenstates of charge conjugation, and in each of them one of the quarks is heavier than the other. The rules are:

1. The main symbol is an upper-case italic letter indicating the heavier quark as follows:

$$s \rightarrow \bar{K} \quad c \rightarrow D \quad b \rightarrow \bar{B} \quad t \rightarrow T.$$

We use the convention that *the flavor and the charge of a quark have the same sign*. Thus the strangeness of the s quark is negative, the charm of the c quark is positive, and the bottom of the b quark is negative. In addition, I_3 of the u and d quarks are positive and negative, respectively. The effect of this convention is as follows: *Any flavor carried by a charged meson has the same sign as its charge*. Thus the K^+ , D^+ , and B^+ have positive strangeness, charm, and bottom, respectively, and all have positive I_3 . The D_s^+ has positive charm *and* strangeness. Furthermore, the $\Delta(\text{flavor}) = \Delta Q$ rule, best known for the kaons, applies to every flavor.

2. If the lighter quark is not a u or a d quark, its identity is given by a subscript. The D_s^+ is an example.
3. If the spin-parity is in the “normal” series, $J^P = 0^+, 1^-, 2^+, \dots$, a superscript “*” is added.
4. The spin is added as a subscript except for pseudoscalar or vector mesons.

8.4. Ordinary (3-quark) baryons

The symbols N , Δ , Λ , Σ , Ξ , and Ω used for more than 30 years for the baryons made of light quarks (u , d , and s quarks) tell the isospin and quark content, and the same information is conveyed by the symbols used for the baryons containing one or more heavy quarks (c and b quarks). The rules are:

1. Baryons with *three* u and/or d quarks are N 's (isospin 1/2) or Δ 's (isospin 3/2).
2. Baryons with *two* u and/or d quarks are Λ 's (isospin 0) or Σ 's (isospin 1). If the third quark is a c , b , or t quark, its identity is given by a subscript.
3. Baryons with *one* u or d quark are Ξ 's (isospin 1/2). One or two subscripts are used if one or both of the remaining quarks are heavy: thus Ξ_c , Ξ_{cc} , Ξ_b , *etc.**
4. Baryons with *no* u or d quarks are Ω 's (isospin 0), and subscripts indicate any heavy-quark content.
5. A baryon that decays strongly has its mass as part of its name. Thus p , Σ^+ , Ω^+ , Λ_c^+ , *etc.*, but $\Delta(1232)^0$, $\Sigma(1385)^-$, $\Xi_c(2645)^+$, *etc.*

In short, the number of u plus d quarks together with the isospin determine the main symbol, and subscripts indicate any content of heavy quarks. A Σ always has isospin 1, an Ω always has isospin 0, *etc.*

8.5. Exotic baryons

In 2003, several experiments reported finding a strangeness $S = +1$, charge $Q = +1$ baryon, and one experiment reported finding an $S = -2$, $Q = -2$ baryon; see the “Exotic Baryons” section of the Data Listings. Baryons with such quantum numbers cannot be made from three quarks, and thus they are exotic. The $S = +1$ baryon, which once would have been called a Z , was quickly dubbed the $\Theta(1540)^+$, and we propose to name the $S = -2$ baryon the $\Phi(1860)$.

Footnote and Reference:

- * Sometimes a prime is necessary to distinguish two Ξ_c 's in the same $SU(n)$ multiplet. See the “Note on Charmed Baryons” in the Charmed Baryon Listings.
1. Particle Data Group: M. Aguilar-Benitez *et al.*, Phys. Lett. **170B** (1986).

9. QUANTUM CHROMODYNAMICS AND ITS COUPLING

9.1. The QCD Lagrangian

Revised September 2005 by I. Hinchliffe (LBNL).

Quantum Chromodynamics (QCD), the gauge field theory which describes the strong interactions of colored quarks and gluons, is one of the components of the $SU(3) \times SU(2) \times U(1)$ Standard Model. A quark of specific flavor (such as a charm quark) comes in 3 colors; gluons come in eight colors; hadrons are color-singlet combinations of quarks, anti-quarks, and gluons. The Lagrangian describing the interactions of quarks and gluons is (up to gauge-fixing terms)

$$L_{\text{QCD}} = -\frac{1}{4} F_{\mu\nu}^{(a)} F^{(a)\mu\nu} + i \sum_q \bar{\psi}_q^i \gamma^\mu (D_\mu)_{ij} \psi_q^j - \sum_q m_q \bar{\psi}_q^i \psi_{qi}, \quad (9.1)$$

$$F_{\mu\nu}^{(a)} = \partial_\mu A_\nu^a - \partial_\nu A_\mu^a - g_s f_{abc} A_\mu^b A_\nu^c, \quad (9.2)$$

$$(D_\mu)_{ij} = \delta_{ij} \partial_\mu + i g_s \sum_a \frac{\lambda_{ij}^a}{2} A_\mu^a, \quad (9.3)$$

where g_s is the QCD coupling constant, and the f_{abc} are the structure constants of the $SU(3)$ algebra (the λ matrices and values for f_{abc} can be found in “ $SU(3)$ Isoscalar Factors and Representation Matrices,” Sec. 36 of this *Review*). The $\psi_q^i(x)$ are the 4-component Dirac spinors associated with each quark field of (3) color i and flavor q , and the $A_\mu^a(x)$ are the (8) Yang-Mills (gluon) fields. A complete list of the Feynman rules which derive from this Lagrangian, together with some useful color-algebra identities, can be found in Ref. 1.

The principle of “asymptotic freedom” determines that the renormalized QCD coupling is small only at high energies, and it is only in this domain that high-precision tests—similar to those in QED—can be performed using perturbation theory. Nonetheless, there has been in recent years much progress in understanding and quantifying the predictions of QCD in the nonperturbative domain, for example, in soft hadronic processes and on the lattice [2]. This short review will concentrate on QCD at short distances (large momentum transfers), where perturbation theory is the standard tool. It will discuss the processes that are used to determine the coupling constant of QCD. Other recent reviews of the coupling constant measurements may be consulted for a different perspective [3–6].

9.2. The QCD coupling and renormalization scheme

The renormalization scale dependence of the effective QCD coupling $\alpha_s = g_s^2/4\pi$ is controlled by the β -function:

$$\mu \frac{\partial \alpha_s}{\partial \mu} = 2\beta(\alpha_s) = -\frac{\beta_0}{2\pi} \alpha_s^2 - \frac{\beta_1}{4\pi^2} \alpha_s^3 - \frac{\beta_2}{64\pi^3} \alpha_s^4 - \dots, \quad (9.4a)$$

$$\beta_0 = 11 - \frac{2}{3} n_f, \quad (9.4b)$$

$$\beta_1 = 51 - \frac{19}{3} n_f, \quad (9.4c)$$

$$\beta_2 = 2857 - \frac{5033}{9} n_f + \frac{325}{27} n_f^2, \quad (9.4d)$$

where n_f is the number of quarks with mass less than the energy scale μ . The expression for the next term in this series (β_3) can be found in Ref. 8. In solving this differential equation for α_s , a constant of integration is introduced. This constant is the fundamental constant of QCD that must be determined from experiment in addition to the quark masses. The most sensible choice for this constant is the value of α_s at a fixed-reference scale μ_0 . It has become standard to choose $\mu_0 = M_Z$. The value at other values of μ can be obtained from $\log(\mu^2/\mu_0^2) = \int_{\alpha_s(\mu_0)}^{\alpha_s(\mu)} \frac{d\alpha}{\beta(\alpha)}$. It is also convenient to introduce the dimensional parameter Λ , since this provides a parameterization of the μ dependence of α_s . The definition of Λ is arbitrary. One way to define it (adopted here) is to write a solution of Eq. (9.4) as an expansion in inverse powers of $\ln(\mu^2)$:

$$\alpha_s(\mu) = \frac{4\pi}{\beta_0 \ln(\mu^2/\Lambda^2)} \left[1 - \frac{2\beta_1}{\beta_0^2} \frac{\ln[\ln(\mu^2/\Lambda^2)]}{\ln(\mu^2/\Lambda^2)} + \frac{4\beta_1^2}{\beta_0^4 \ln^2(\mu^2/\Lambda^2)} \right. \\ \left. \times \left(\left(\ln[\ln(\mu^2/\Lambda^2)] - \frac{1}{2} \right)^2 + \frac{\beta_2 \beta_0}{8\beta_1^2} - \frac{5}{4} \right) \right]. \quad (9.5)$$

This solution illustrates the *asymptotic freedom* property: $\alpha_s \rightarrow 0$ as $\mu \rightarrow \infty$ and shows that QCD becomes strongly coupled at $\mu \sim \Lambda$.

Consider a “typical” QCD cross section which, when calculated perturbatively [7], starts at $\mathcal{O}(\alpha_s)$:

$$\sigma = A_1 \alpha_s + A_2 \alpha_s^2 + \dots \quad (9.6)$$

The coefficients A_1, A_2 come from calculating the appropriate Feynman diagrams. In performing such calculations, various divergences arise, and these must be regulated in a consistent way. This requires a particular renormalization scheme (RS). The most commonly used one is the modified minimal subtraction ($\overline{\text{MS}}$) scheme [9]. This involves continuing momentum integrals from 4 to $4-2\epsilon$ dimensions, and then subtracting off the resulting $1/\epsilon$ poles and also $(\ln 4\pi - \gamma_E)$, which is an artifact of continuing the dimension. (Here γ_E is the Euler-Mascheroni constant.) To preserve the dimensionless nature of the coupling, a mass scale μ must also be introduced: $g \rightarrow \mu^\epsilon g$. The finite coefficients A_i ($i \geq 2$) thus obtained depend implicitly on the renormalization convention used and explicitly on the scale μ .

The first two coefficients (β_0, β_1) in Eq. (9.4) are independent of the choice of RS. In contrast, the coefficients of terms proportional to α_s^n for $n > 3$ are RS-dependent. The form given above for β_2 is in the $\overline{\text{MS}}$ scheme.

The fundamental theorem of RS dependence is straightforward. Physical quantities, such as the cross section calculated to all orders in perturbation theory, do not depend on the RS. It follows that a truncated series *does* exhibit RS dependence. In practice, QCD cross sections are known to leading order (LO), or to next-to-leading order (NLO), or in some cases, to next-to-next-to-leading order (NNLO); and it is only the latter two cases, which have reduced RS dependence, that are useful for precision tests. At NLO the RS dependence is completely given by one condition which can be taken to be the value of the renormalization scale μ . At NNLO this is not sufficient, and μ is no longer equivalent to a choice of scheme; both must now be specified. One, therefore, has to address the question of what is the “best” choice for μ within a given scheme, usually $\overline{\text{MS}}$. There is no definite answer to this question—higher-order corrections do not “fix” the scale, rather they render the theoretical predictions less sensitive to its variation.

One should expect that choosing a scale μ characteristic of the typical energy scale (E) in the process would be most appropriate. In general, a poor choice of scale generates terms of order $\ln(E/\mu)$ in the A_i 's. Various methods have been proposed including choosing the scale for which the next-to-leading-order correction vanishes (“Fastest Apparent Convergence [10]”); the scale for which the next-to-leading-order prediction is stationary [11], (*i.e.*, the value of μ where $d\sigma/d\mu = 0$); or the scale dictated by the effective charge scheme [12] or by the BLM scheme [13]. By comparing the values of α_s that different reasonable schemes give, an estimate of theoretical errors can be obtained. It has also been suggested to replace the perturbation series by its Padé approximant [14]. Results obtained using this method have, in certain cases, a reduced scale dependence [15,16]. One can also attempt to determine the scale from data by allowing it to vary and using a fit to determine it. This method can allow a determination of the error due to the scale choice and can give more confidence in the end result [17]. In many of the cases discussed below this scale uncertainty is the dominant error.

An important corollary is that if the higher-order corrections are naturally small, then the additional uncertainties introduced by the μ dependence are likely to be small. There are some processes, however, for which the choice of scheme *can* influence the extracted value of $\alpha_s(M_Z)$. There is no resolution to this problem other than to try to calculate even more terms in the perturbation series. It is important to note that, since the perturbation series is an asymptotic expansion, there is a limit to the precision with which any theoretical quantity can be calculated. In some processes, the highest-order perturbative terms may be comparable in size to nonperturbative corrections (sometimes called higher-twist or renormalon effects, for a discussion see Ref. 18); an estimate of these terms and their uncertainties is required if a value of α_s is to be extracted.

Cases occur where there is more than one large scale, say μ_1 and μ_2 . In these cases, terms appear of the form $\log(\mu_1/\mu_2)$. If the ratio μ_1/μ_2 is large, these logarithms can render naive perturbation theory unreliable and a modified perturbation expansion that takes these terms into account must be used. A few examples are discussed below.

In the cases where the higher-order corrections to a process are known and are large, some caution should be exercised when quoting the value of α_s . In what follows, we will attempt to indicate the size of the theoretical uncertainties on the extracted value of α_s . There are two simple ways to determine this error. First, we can estimate it by comparing the value of $\alpha_s(\mu)$ obtained by fitting data using the QCD formula to highest known order in α_s , and then comparing it with the value obtained using the next-to-highest-order formula (μ is chosen as the typical energy scale in the process). The corresponding Λ 's are then obtained by evolving $\alpha_s(\mu)$ to $\mu = M_Z$ using Eq. (9.4) to the same order in α_s as the fit. Alternatively, we can vary the value of μ over a reasonable range, extracting a value of Λ for each choice of μ . This method is by its nature imprecise, since “reasonable” involves a subjective judgment. In either case, if the perturbation series is well behaved, the resulting error on $\alpha_s(M_Z)$ will be small.

In the above discussion we have ignored quark-mass effects, *i.e.*, we have assumed an idealized situation where quarks of mass greater than μ are neglected completely. In this picture, the β -function coefficients change by discrete amounts as flavor thresholds (a quark of mass M) are crossed when integrating the differential equation for α_s . Now imagine an experiment at energy scale μ ; for example, this could be $e^+e^- \rightarrow$ hadrons at center-of-mass energy μ . If $\mu \gg M$, the mass M is negligible and the process is well described by QCD with n_f massless flavors and its parameter $\alpha_{(n_f)}$ up to terms of order M^2/μ^2 . Conversely if $\mu \ll M$, the heavy quark plays no role and the process is well described by QCD with $n_f - 1$ massless flavors and its parameter $\alpha_{(n_f-1)}$ up to terms of order μ^2/M^2 . If $\mu \sim M$, the effects of the quark mass are process-dependent and cannot be absorbed into the running coupling. The values of $\alpha_{(n_f)}$ and $\alpha_{(n_f-1)}$ are related so that a physical quantity calculated in both “theories” gives the same result [19]. This implies, for $\mu = M$

$$\alpha_{(n_f)}(M) = \alpha_{(n_f-1)}(M) - \frac{11}{72\pi^2} \alpha_{(n_f-1)}^3(M) + \mathcal{O}(\alpha_{(n_f-1)}^4) \quad (9.7)$$

which is almost identical to the naive result $\alpha_{(n_f)}(M) = \alpha_{(n_f-1)}(M)$. Here M is the mass of the value of the running quark mass defined in the $\overline{\text{MS}}$ scheme (see the note on “Quark Masses” in the Particle Listings for more details), *i.e.*, where $M_{\overline{\text{MS}}}(M) = M$.

It also follows that, for a relationship such as Eq. (9.5) to remain valid for all values of μ , Λ must also change as flavor thresholds are crossed, the value corresponds to an effective number of massless quarks: $\Lambda \rightarrow \Lambda^{(n_f)}$ [19,20]. The formulae are given in the 1998 edition of this review.

Experiments such as those from deep-inelastic scattering involve a range of energies. After fitting to their measurements to QCD, the resulting fit can be expressed as a value of $\alpha_s(M_Z)$.

Determinations of α_s result from fits to data using NLO and NNLO: LO fits are not useful and their values will not be used in the following. Care must be exercised when comparing results from NLO and NNLO. In order to compare the values of α_s from various experiments, they must be evolved using the renormalization group to a common scale. For convenience, this is taken to be the mass of the Z boson. The extrapolation is performed using same order in perturbation theory as was used in the analysis. This evolution uses third-order perturbation theory and can introduce additional errors particularly if extrapolation from very small scales is used. The variation in the charm and bottom quark masses ($M_b = 4.3 \pm 0.2$ GeV and $M_c = 1.3 \pm 0.3$ GeV are used [21]) can also introduce errors. These result in a fixed value of $\alpha_s(2 \text{ GeV})$ giving an uncertainty in $\alpha_s(M_Z) = \pm 0.001$ if only perturbative evolution is used. There could be additional errors from nonperturbative effects that enter at low energy.

9.3. QCD in deep-inelastic scattering

The original and still one of the most powerful quantitative tests of perturbative QCD is the breaking of Bjorken scaling in deep-inelastic lepton-hadron scattering. The review “Structure Functions,” (Sec. 16 of this *Review*) describes the basic formalism and reviews the data. α_s is obtained together with the structure functions. The global fit from MRST04 [41] of (Sec. 16) gives $\alpha_s(M_Z) = 0.1205 \pm 0.004$ from NLO and $\alpha_s(M_Z) = 0.1167 \pm 0.004$ from NNLO. Other fits are consistent with these values but cannot be averaged as they use overlapping data sets. The good agreement between the NLO and NNLO fits indicates that the theoretical uncertainties are under control.

Nonsinglet structure functions offer in principle the most precise test of the theory and cleanest way to extract α_s , since the Q^2 evolution is independent of the gluon distribution, which is much more poorly constrained. The CCFR collaboration fit to the Gross-Llewellyn Smith sum rule [23] whose value at leading order is determined by baryon number and which is known to order α_s^3 [24,25] (NNLO); estimates of the order α_s^4 term are available [26].

$$\int_0^1 dx \left(F_3^{\overline{p}p}(x, Q^2) + F_3^{\nu p}(x, Q^2) \right) = 3 \left[1 - \frac{\alpha_s}{\pi} \left(1 + 3.58 \frac{\alpha_s}{\pi} + 19.0 \left(\frac{\alpha_s}{\pi} \right)^2 \right) - \Delta HT \right], \quad (9.8)$$

where the higher-twist contribution ΔHT is estimated to be $(0.09 \pm 0.045)/Q^2$ in [24,27] and to be somewhat smaller by [28]. The CCFR collaboration [29], combines their data with that from other experiments [30] and gives $\alpha_s(\sqrt{3} \text{ GeV}) = 0.28 \pm 0.035$ (expt.) ± 0.05 (sys) ${}_{-0.03}^{+0.035}$ (theory). The error from higher-twist terms (assumed to be $\Delta HT = 0.05 \pm 0.05$) dominates the theoretical error. If the higher twist result of [28] is used, the central value increases to 0.31 in agreement with the fit of [31]. This value corresponds to $\alpha_s(M_Z) = 0.118 \pm 0.011$. Fits of the Q^2 evolution [32] of $x F_3$ using the CCFR data using NNLO and estimates of NNNLO QCD and higher twist terms enables the effect of these terms to be studied.

The spin-dependent structure functions, measured in polarized lepton-nucleon scattering, can also be used to determine α_s . Note that these experiments measure asymmetries and rely on measurements of unpolarized data to extract the spin-dependent structure functions. Here the values of $Q^2 \sim 2.5 \text{ GeV}^2$ are small, particularly for the E143 data [33], and higher-twist corrections are important. A fit [34] by an experimental group using the measured spin dependent structure functions for several experiments [33,35] as well as their own data has been made. When data from HERMES [36] and SMC are included [37] $\alpha_s(M_Z) = 0.120 \pm 0.009$ is obtained: this is used in the final average.

α_s can also be determined from the Bjorken spin sum rule [38]; a fit gives $\alpha_s(M_Z) = 0.118 {}_{-0.024}^{+0.010}$ [39]; consistent with an earlier determination [40], the larger error being due to the extrapolation into the (unmeasured) small x region. Theoretically, the sum rule is preferable as the perturbative QCD result is known to higher order and these terms are important at the low Q^2 involved. It has been shown that the theoretical errors associated with the choice of scale are considerably reduced by the use of Padé approximants [15], which results in $\alpha_s(1.7 \text{ GeV}) = 0.328 \pm 0.03$ (expt.) ± 0.025 (theory) corresponding to $\alpha_s(M_Z) = 0.116 {}_{-0.005}^{+0.003}$ (expt.) ± 0.003 (theory). No error is included from the extrapolation into the region of x that is unmeasured. Should data become available at smaller values of x so that this extrapolation could be more tightly constrained. This result is not used in the final average.

9.4. QCD in decays of the τ lepton

The semi-leptonic branching ratio of the tau ($\tau \rightarrow \nu_\tau +$ hadrons, R_τ) is an inclusive quantity. It is related to the contribution of hadrons to the imaginary part of the W self energy ($\text{Im}\Pi(s)$). It is sensitive to a range of energies since it involves an integral

$$R_\tau \sim \int_0^{m_\tau^2} \frac{ds}{m_\tau^2} \left(1 - \frac{s}{m_\tau^2} \right)^2 \left((1 + 2s/m_\tau^2) \text{Im}\Pi(1) + \text{Im}\Pi(0) \right) \quad (9.9)$$

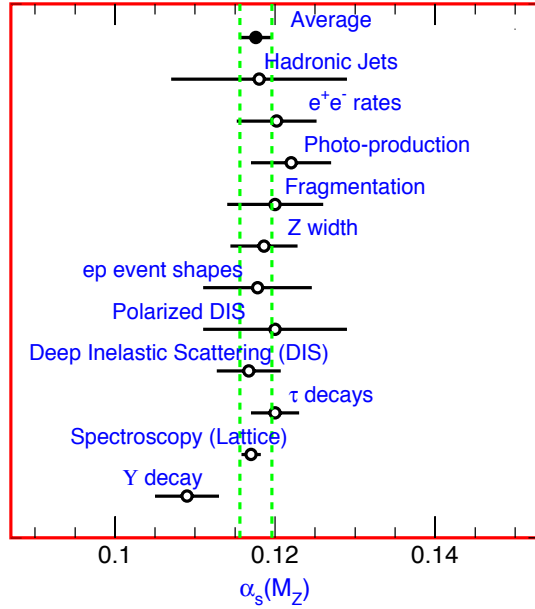


Figure 9.1: Summary of the value of $\alpha_s(M_Z)$ from various processes. The values shown indicate the process and the measured value of α_s extrapolated to $\mu = M_Z$. The error shown is the *total* error including theoretical uncertainties. The average quoted in this report which comes from these measurements is also shown. See text for discussion of errors.

where $Im\Pi(1)$ denotes the vector part and $Im\Pi(0)$ the scalar part. Since the scale involved is low, one must take into account nonperturbative (higher-twist) contributions which are suppressed by powers of the τ mass.

$$R_\tau = 3.058 \left[1 + \delta_{EW} + \frac{\alpha_s(m_\tau)}{\pi} + 5.2 \left(\frac{\alpha_s(m_\tau)}{\pi} \right)^2 + 26.4 \left(\frac{\alpha_s(m_\tau)}{\pi} \right)^3 + a \frac{m^2}{m_\tau^2} + b \frac{m\psi\bar{\psi}}{m_\tau^4} + c \frac{\psi\bar{\psi}\psi\bar{\psi}}{m_\tau^6} + \dots \right]. \quad (9.10)$$

$\delta_{EW} = 0.0010$ is the electroweak correction. Here $a, b,$ and c are dimensionless constants and m is a light quark mass. The term of order $1/m_\tau^2$ is a kinematical effect due to the light quark masses and is consequently very small. The nonperturbative terms are estimated using sum rules [41]. In total, they are estimated to be -0.014 ± 0.005 [42,43]. This estimate relies on there being no term of order Λ^2/m_τ^2 (note that $\frac{\alpha_s(m_\tau)}{\pi} \sim (\frac{0.5 \text{ GeV}}{m_\tau})^2$). The $a, b,$ and c can be determined from the data [44] by fitting to moments of the $\Pi(s)$ and separately to the final states accessed by the vector and axial parts of the W coupling. The values so extracted [45,46] are consistent with the theoretical estimates. If the nonperturbative terms are omitted from the fit, the extracted value of $\alpha_s(m_\tau)$ decreases by ~ 0.02 .

For $\alpha_s(m_\tau) = 0.35$ the perturbative series for R_τ is $R_\tau \sim 3.058(1 + 0.112 + 0.064 + 0.036)$. The size (estimated error) of the nonperturbative term is 20% (7%) of the size of the order α_s^3 term. The perturbation series is not very well convergent; if the order α_s^3 term is omitted, the extracted value of $\alpha_s(m_\tau)$ increases by 0.05. The order α_s^4 term has been estimated [47] and attempts made to resum the entire series [48,49]. These estimates can be used to obtain an estimate of the errors due to these unknown terms [50,51]. Another approach to estimating this α_s^4 term gives a contribution that is slightly larger than the α_s^3 term [52].

R_τ can be extracted from the semi-leptonic branching ratio from the relation $R_\tau = 1/B(\tau \rightarrow e\nu\bar{\nu}) - 1.97256$; where $B(\tau \rightarrow e\nu\bar{\nu})$ is measured directly or extracted from the lifetime, the muon mass, and the muon lifetime assuming universality of lepton couplings. Using the average lifetime of 290.6 ± 1.1 fs and a τ mass of 1776.99 ± 0.29 MeV from the PDG fit gives $R_\tau = 3.645 \pm 0.020$. The direct

measurement of $B(\tau \rightarrow e\nu\bar{\nu})$ can be combined with $B(\tau \rightarrow \mu\nu\bar{\nu})$ to give $B(\tau \rightarrow e\nu\bar{\nu}) = 0.1785 \pm 0.0005$ which gives $R_\tau = 3.629 \pm 0.015$. Averaging these yields $\alpha_s(m_\tau) = 0.338 \pm 0.004$ using the experimental error alone. We assign a theoretical error equal to 40% of the contribution from the order α_s^3 term and all of the nonperturbative contributions. This then gives $\alpha_s(m_\tau) = 0.34 \pm 0.03$ for the final result. This corresponds to $\alpha_s(M_Z) = 0.120 \pm 0.003$. This result is consistent with that obtained by using the moments [53] of the integrand and is used in the average below.

9.5. QCD in high-energy hadron collisions

There are many ways in which perturbative QCD can be tested in high-energy hadron colliders. The quantitative tests are only useful if the process in question has been calculated beyond leading order in QCD perturbation theory. The production of hadronic jets with large transverse momentum in hadron-hadron collisions provides a direct probe of the scattering of quarks and gluons: $qq \rightarrow qq, qg \rightarrow qq, gg \rightarrow gg, \text{ etc.}$ Higher-order QCD calculations of the jet rates [54] and shapes are in impressive agreement with data [55]. This agreement has led to the proposal that these data could be used to provide a determination of α_s [56]. A set of structure functions is assumed and jet data are fitted over a very large range of transverse momenta to the QCD prediction for the underlying scattering process that depends on α_s . The evolution of the coupling over this energy range (40 to 250 GeV) is therefore tested in the analysis. CDF obtains $\alpha_s(M_Z) = 0.1178 \pm 0.0001$ (stat.) ± 0.0085 (syst.) [57]. Estimation of the theoretical errors is not straightforward. The structure functions used depend implicitly on α_s and an iteration procedure must be used to obtain a consistent result; different sets of structure functions yield different correlations between the two values of α_s . CDF includes a scale error of 4% and a structure function error of 5% in the determination of α_s . Ref. 56 estimates the error from unknown higher order QCD corrections to be ± 0.005 . Combining these then gives $\alpha_s(M_Z) = 0.118 \pm 0.011$ which is used in the final average. For additional comments on comparisons between these data and theory see Ref. 4. Data are also available on the angular distribution of jets; these are also in agreement with QCD expectations [58,59].

QCD corrections to Drell-Yan type cross sections (*i.e.*, the production in hadron collisions by quark-antiquark annihilation of lepton pairs of invariant mass Q from virtual photons, or of real W or Z bosons), are known [60]. These $\mathcal{O}(\alpha_s)$ QCD corrections are sizable at small values of Q . The correction to W and Z production, as measured in $p\bar{p}$ collisions at $\sqrt{s} = 0.63$ TeV and $\sqrt{s} = 1.8, 1.96$ TeV, is of order 30%. The NNLO corrections to this process are known [61].

The production of W and Z bosons and photons at large transverse momentum can also be used to test QCD. The leading-order QCD subprocesses are $q\bar{q} \rightarrow Vg$ and $qg \rightarrow Vq$ ($V = W, Z, \gamma$). If the parton distributions are taken from other processes and a value of α_s assumed, then an absolute prediction is obtained. Conversely, the data can be used to extract information on quark and gluon distributions and on the value of α_s . The next-to-leading-order QCD corrections are known for photons [62,63], and for W/Z production [64], and so a precision test is possible. Data exist on photon production from the CDF and DØ collaborations [65,66] and from fixed target experiments [67]. Detailed comparisons with QCD predictions [68] may indicate an excess of the data over the theoretical prediction at low value of transverse momenta, although other authors [69] find smaller excesses.

The UA2 collaboration [70] extracted a value of $\alpha_s(M_W) = 0.123 \pm 0.018$ (stat.) ± 0.017 (syst.) from the measured ratio $R_W = \frac{\sigma(W + 1\text{jet})}{\sigma(W + 0\text{jet})}$. The result depends on the algorithm used to define a jet, and the dominant systematic errors due to fragmentation and corrections for underlying events (the former causes jet energy to be lost, the latter causes it to be increased) are connected to the algorithm. There is also dependence on the parton distribution functions, and hence, α_s appears explicitly in the formula for R_W , and implicitly in the distribution functions. The UA2 result is not used in the final average. Data from CDF and DØ on the $W p_t$ distribution [71] are in agreement with QCD but are not able to determine α_s with sufficient precision to have any weight in a global average.

In the region of low p_t , the fixed order perturbation theory is not applicable; one must sum terms of order $\alpha_s^n \ln^n(p_t/M_W)$ [72]. Data from DØ [73] on the p_t distribution of Z bosons agree well with these predictions.

The production rates of b quarks in $p\bar{p}$ have been used to determine α_s [74]. The next-to-leading-order QCD production processes [75] have been used. By selecting events where the b quarks are back-to-back in azimuth, the next-to-leading-order calculation can be used to compare rates to the measured value and a value of α_s extracted. The errors are dominated by the measurement errors, the choice of μ and the scale at which the structure functions are evaluated, and uncertainties in the choice of structure functions. The last were estimated by varying the structure functions used. The result is $\alpha_s(M_Z) = 0.113^{+0.009}_{-0.013}$, which is not included in the final average, as the measured $b\bar{b}$ cross section is not in very good agreement with perturbative QCD [76] and it is therefore difficult to interpret this result. Recent improvements in the theoretical understanding [77] and measurements from CDF [78] now show good agreement between the measured cross-sections and the QCD predictions but there is no extraction of α_s using these.

9.6. QCD in heavy-quarkonium decay

Under the assumption that the hadronic and leptonic decay widths of heavy $Q\bar{Q}$ resonances can be factorized into a nonperturbative part—dependent on the confining potential—and a calculable perturbative part, the ratios of partial decay widths allow measurements of α_s at the heavy-quark mass scale. The most precise data come from the decay widths of the $1^{--} J/\psi(1S)$ and Υ resonances. The total decay width of the Υ is predicted by perturbative QCD [79,80]

$$\begin{aligned} R_\mu(\Upsilon) &= \frac{\Gamma(\Upsilon \rightarrow \text{hadrons})}{\Gamma(\Upsilon \rightarrow \mu^+\mu^-)} \\ &= \frac{10(\pi^2 - 9)\alpha_s^3(M_b)}{9\pi\alpha_{\text{em}}^2} \\ &\quad \times \left[1 + \frac{\alpha_s}{\pi} \left(-14.05 + \frac{3\beta_0}{2} \left(1.161 + \ln\left(\frac{2M_b}{M_\Upsilon}\right) \right) \right) \right]. \end{aligned} \quad (9.11)$$

Data are available for the Υ , Υ' , Υ'' , and J/ψ . The result is very sensitive to α_s and the data are sufficiently precise ($R_\mu(\Upsilon) = 37.28 \pm 0.75$) [81] that the theoretical errors will dominate. There are theoretical corrections to this formula due to the relativistic nature of the $Q\bar{Q}$ system which have been calculated [80] to order v^2/c^2 . These corrections are more severe for the J/ψ . There are also nonperturbative corrections arising from annihilation from higher Fock states (“color octet” contribution) which can only be estimated [82]; again these are more severe for the J/ψ . The Υ gives $\alpha_s(M_b) = 0.183 \pm 0.01$, where the error includes that from the “color octet” term and the choice of scale which together dominate. The ratio of widths $\frac{\Upsilon \rightarrow \gamma\gamma\gamma}{\Upsilon \rightarrow ggg}$ has been measured by the CLEO collaboration and can be used to determine $\alpha_s(M_b) = 0.189 \pm 0.01 \pm 0.01$. The error is dominated by theoretical uncertainties associated with the scale choice; the uncertainty due to the “color octet” piece is not present in this case [83]. The theoretical uncertainties due to the production of photons in fragmentation [84] are small [85]. Higher order QCD calculations of the photon energy distribution are available [86]; this distribution could now be used to further test the theory. The width $\Gamma(\Upsilon \rightarrow e^+e^-)$ can also be used to determine α_s by using moments of the quantity $R_b(s) = \frac{\sigma(e^+e^- \rightarrow b\bar{b})}{\sigma(e^+e^- \rightarrow \mu^+\mu^-)}$

defined by $M_n = \int_0^\infty \frac{R_b(s)}{s^{n+1}} ds$ [87]. At large values of n , M_n is dominated by $\Gamma(\Upsilon \rightarrow e^+e^-)$. Higher order corrections are available and the method gives $\alpha_s(M_b) = 0.220 \pm 0.027$ [88]. The dominant error is theoretical and is dominated by the choice of scale and by uncertainties in Coulomb corrections that have been resummed in Ref. 89. These various Υ decay measurements can be combined and give $\alpha_s(M_b) = 0.185 \pm 0.01$ corresponding to $\alpha_s(M_Z) = 0.109 \pm 0.004$ which is used in the final average [83]. The mass of charmonium can also be used for determination of α_s after taking into account

effects of analytic continuation (π^2 -terms summation), and Coulomb summation [90].

9.7. Perturbative QCD in e^+e^- collisions

The total cross section for $e^+e^- \rightarrow \text{hadrons}$ is obtained (at low values of \sqrt{s}) by multiplying the muon-pair cross section by the factor $R = 3\Sigma_q e_q^2$. The higher-order QCD corrections to this quantity have been calculated, and the results can be expressed in terms of the factor:

$$R = R^{(0)} \left[1 + \frac{\alpha_s}{\pi} + C_2 \left(\frac{\alpha_s}{\pi} \right)^2 + C_3 \left(\frac{\alpha_s}{\pi} \right)^3 + \dots \right], \quad (9.12)$$

where $C_2 = 1.411$ and $C_3 = -12.8$ [91].

$R^{(0)}$ can be obtained from the formula for $d\sigma/d\Omega$ for $e^+e^- \rightarrow f\bar{f}$ by integrating over Ω . The formula is given in Sec. 39.2 of this *Review*. This result is only correct in the zero-quark-mass limit. The $\mathcal{O}(\alpha_s)$ corrections are also known for massive quarks [92]. The principal advantage of determining α_s from R in e^+e^- annihilation is that there is no dependence on fragmentation models, jet algorithms, *etc.*

A measurement by CLEO [93] at $\sqrt{s} = 10.52$ GeV yields $\alpha_s(10.52 \text{ GeV}) = 0.20 \pm 0.01 \pm 0.06$, which corresponds to $\alpha_s(M_Z) = 0.130 \pm 0.005 \pm 0.03$. A comparison of the theoretical prediction of Eq. (9.12) (corrected for the b -quark mass), with all the available data at values of \sqrt{s} between 20 and 65 GeV, gives [94] $\alpha_s(35 \text{ GeV}) = 0.146 \pm 0.030$. The size of the order α_s^3 term is of order 40% of that of the order α_s^2 and 3% of the order α_s . If the order α_s^3 term is not included, a fit to the data yields $\alpha_s(35 \text{ GeV}) = 0.142 \pm 0.030$, indicating that the theoretical uncertainty is smaller than the experimental error.

Measurements of the ratio of hadronic to leptonic width of the Z at LEP and SLC, Γ_h/Γ_μ probe the same quantity as R . Using the average of $\Gamma_h/\Gamma_\mu = 20.767 \pm 0.025$ gives $\alpha_s(M_Z) = 0.1226 \pm 0.0038$ [95]. In performing this extraction it is necessary to include the electroweak corrections to the Z width. As these must be calculated beyond leading order, they depend on the top top-quark and Higgs masses. The latter is not yet measured and is inferred from global fits to the electroweak data. There are additional theoretical errors arising from the choice of QCD scale. While this method has small theoretical uncertainties from QCD itself, it relies sensitively on the electroweak couplings of the Z to quarks [96]. The presence of new physics which changes these couplings via electroweak radiative corrections would invalidate the value of $\alpha_s(M_Z)$. An illustration of the sensitivity can be obtained by comparing this value with the one obtained from the global fits [95] of the various precision measurements at LEP/SLC and the W and top masses: $\alpha_s(M_Z) = 0.1186 \pm 0.0027$. The difference between these two values may be accounted for by systematic uncertainties as large as ± 0.003 [95], therefore $\alpha_s(M_Z) = 0.1186 \pm 0.0042$ will be used in the final average.

An alternative method of determining α_s in e^+e^- annihilation is from measuring quantities that are sensitive to the relative rates of two-, three-, and four-jet events. A review should be consulted for more details [97] of the issues mentioned briefly here. In addition to simply counting jets, there are many possible choices of such “shape variables”: thrust [98], energy-energy correlations [99], average jet mass, *etc.* All of these are infrared safe, which means they can be reliably calculated in perturbation theory. The starting point for all these quantities is the multijet cross section. For example, at order α_s , for the process $e^+e^- \rightarrow q\bar{q}g$: [100]

$$\frac{1}{\sigma} \frac{d^2\sigma}{dx_1 dx_2} = \frac{2\alpha_s}{3\pi} \frac{x_1^2 + x_2^2}{(1-x_1)(1-x_2)}, \quad (9.13)$$

$$x_i = \frac{2E_i}{\sqrt{s}} \quad (9.14)$$

where x_i are the center-of-mass energy fractions of the final-state (massless) quarks. A distribution in a “three-jet” variable, such as those listed above, is obtained by integrating this differential cross

section over an appropriate phase space region for a fixed value of the variable. The order α_s^2 corrections to this process have been computed, as well as the 4-jet final states such as $e^+e^- \rightarrow q\bar{q}q\bar{q}$ [101].

There are many methods used by the e^+e^- experimental groups to determine α_s from the event topology. The jet-counting algorithm, originally introduced by the JADE collaboration [102], has been used by many other groups. Here, particles of momenta p_i and p_j are combined into a pseudo-particle of momentum $p_i + p_j$ if the invariant mass of the pair is less than $y_0\sqrt{s}$. The process is iterated until all pairs of particles or pseudoparticles have a mass-measure that exceeds $y_0\sqrt{s}$; the remaining number is then defined to be the jet multiplicity. The remaining number is then defined to be the number of jets in the event, and can be compared to the QCD prediction. The Durham algorithm is slightly different: in combining a pair of partons, it uses $M^2 = 2\min(E_i^2, E_j^2)(1 - \cos\theta_{ij})$ for partons of energies E_i and E_j separated by angle θ_{ij} [103].

There are theoretical ambiguities in the way this process is carried out. Quarks and gluons are massless, whereas the observed hadrons are not, so that the massive jets that result from this scheme cannot be compared directly to the jets of perturbative QCD. Different recombination schemes have been tried, for example combining 3-momenta and then rescaling the energy of the cluster so that it remains massless. These schemes result in the same data giving slightly different values [104,105] of α_s . These differences can be used to determine a systematic error. In addition, since what is observed are hadrons rather than quarks and gluons, a model is needed to describe the evolution of a partonic final state into one involving hadrons, so that detector corrections can be applied. The QCD matrix elements are combined with a parton-fragmentation model. This model can then be used to correct the data for a direct comparison with the parton calculation. The different hadronization models that are used [106–109] model the dynamics that are controlled by nonperturbative QCD effects which we cannot yet calculate. The fragmentation parameters of these Monte Carlos are tuned to get agreement with the observed data. The differences between these models contribute to the systematic errors. The systematic errors from recombination schemes and fragmentation effects dominate over the statistical and other errors of the LEP/SLD experiments.

The scale M at which $\alpha_s(M)$ is to be evaluated is not clear. The invariant mass of a typical jet (or $\sqrt{sy_0}$) is probably a more appropriate choice than the e^+e^- center-of-mass energy. While there is no justification for doing so, if the value is allowed to float in the fit to the data, the fit improves and the data tend to prefer values of order $\sqrt{s}/10$ GeV for some variables [105,110]; the exact value depends on the variable that is fitted.

The perturbative QCD formulae can break down in special kinematical configurations. For example, the thrust (T) distribution contains terms of the type $\alpha_s \ln^2(1 - T)$. The higher orders in the perturbation expansion contain terms of order $\alpha_s^n \ln^m(1 - T)$. For $T \sim 1$ (the region populated by 2-jet events), the perturbation expansion is unreliable. The terms with $n \leq m$ can be summed to all orders in α_s [111]. If the jet recombination methods are used higher-order terms involve $\alpha_s^n \ln^m(y_0)$, these too can be resummed [112]. The resummed results give better agreement with the data at large values of T . Some caution should be exercised in using these resummed results because of the possibility of overcounting; the showering Monte Carlos that are used for the fragmentation corrections also generate some of these leading-log corrections. Different schemes for combining the order α_s^2 and the resummations are available [113]. These different schemes result in shifts in α_s of order ± 0.002 . The use of the resummed results improves the agreement between the data and the theory; for more details see Ref. 114. An average of results at the Z resonance from SLD [105], OPAL [115], L3 [116], ALEPH [117], and DELPHI [118], using the combined α_s^2 and resummation fitting to a large set of shape variables, gives $\alpha_s(M_Z) = 0.122 \pm 0.007$. The errors in the values of $\alpha_s(M_Z)$ from these shape variables are totally dominated by the theoretical uncertainties associated with the choice of scale, and the effects of hadronization Monte Carlos on the different quantities fitted.

Estimates are available for the nonperturbative corrections to the mean value of $1 - T$ [119]. These are of order $1/E$ and involve a single parameter to be determined from experiment. These corrections can then be used as an alternative to those modeled by the fragmentation Monte Carlos. The DELPHI collaboration has fitted its data using an additional parameter to take into account these $1/E$ effects [120] and quotes for the $\overline{\text{MS}}$ scheme $\alpha_s = 0.1217 \pm 0.0046$ and a significant $1/E$ term. This term vanishes in the RGI/ECH scheme and the data are well described by pure perturbation theory with consistent $\alpha_s = 0.1201 \pm 0.0020$.

Studies have been carried out at energies between ~ 130 GeV [121] and ~ 200 GeV [122]. These can be combined to give $\alpha_s(130 \text{ GeV}) = 0.114 \pm 0.008$ and $\alpha_s(189 \text{ GeV}) = 0.1104 \pm 0.005$. The dominant errors are theoretical and systematic and, most of these are in common at the two energies. These data and those at the Z resonance and below provide clear confirmation of the expected decrease in α_s as the energy is increased.

The LEP QCD working group [123] uses all LEP data Z mass and higher energies to perform a global fit using a large number of shape variables. It determines $\alpha_s(M_Z) = 0.1202 \pm 0.0003$ (stat) ± 0.0049 (syst), (result quoted in Ref. 6) the error being dominated by theoretical uncertainties which are the most difficult to quantify.

Similar studies on event shapes have been undertaken at lower energies at TRISTAN, PEP/PETRA, and CLEO. A combined result from various shape parameters by the TOPAZ collaboration gives $\alpha_s(58 \text{ GeV}) = 0.125 \pm 0.009$, using the fixed order QCD result, and $\alpha_s(58 \text{ GeV}) = 0.132 \pm 0.008$ (corresponding to $\alpha_s(M_Z) = 0.123 \pm 0.007$), using the same method as in the SLD and LEP average [124]. The measurements of event shapes at PEP/PETRA are summarized in earlier editions of this note. A recent reevaluation of the JADE data [125] obtained using resummed QCD results with modern models of jet fragmentation and by averaging over several shape variables gives $\alpha_s(22 \text{ GeV}) = 0.151 \pm 0.004$ (expt) $\frac{+0.014}{-0.012}$ (theory) which is used in the final average. These results also attempt to constrain the non-perturbative parameters and show a remarkable agreement with QCD even at low energies [126]. An analysis by the TPC group [127] gives $\alpha_s(29 \text{ GeV}) = 0.160 \pm 0.012$, using the same method as TOPAZ.

The CLEO collaboration fits to the order α_s^2 results for the two jet fraction at $\sqrt{s} = 10.53$ GeV, and obtains $\alpha_s(10.53 \text{ GeV}) = 0.164 \pm 0.004$ (expt.) ± 0.014 (theory) [128]. The dominant systematic error arises from the choice of scale (μ), and is determined from the range of α_s that results from fit with $\mu = 10.53$ GeV, and a fit where μ is allowed to vary to get the lowest χ^2 . The latter results in $\mu = 1.2$ GeV. Since the quoted result corresponds to $\alpha_s(1.2 \text{ GeV}) = 0.35$, it is by no means clear that the perturbative QCD expression is reliable and the resulting error should, therefore, be treated with caution. A fit to many different variables as is done in the LEP/SLC analyses would give added confidence to the quoted error.

All these measurements are consistent with the LEP average quoted above which has the smallest statistical error; the systematic errors being mostly theoretical are likely to be strongly correlated between the measurements. The value of $\alpha_s(M_Z) = 0.1202 \pm 0.005$ is used in the final average.

The four jet final states can be used to measure the color factors of QCD, related to the relative strength of the couplings of quarks and gluons to each other. While these factors are not free parameters, the agreement between the measurements and expectations provides more evidence for the validity of QCD. The results are summarized in Ref. 129.

9.8. Scaling violations in fragmentation functions

Measurements of the fragmentation function $d_i(z, E)$, (the probability that a hadron of type i be produced with energy zE in e^+e^- collisions at $\sqrt{s} = 2E$) can be used to determine α_s . (Detailed definitions and a discussion of the properties of fragmentation functions can be found in Sec. 17 of this Review). As in the case of scaling violations in structure functions, perturbative QCD predicts

only the E dependence. Hence, measurements at different energies are needed to extract a value of α_s . Because the QCD evolution mixes the fragmentation functions for each quark flavor with the gluon fragmentation function, it is necessary to determine each of these before α_s can be extracted.

The ALEPH collaboration has used data from energies ranging from $\sqrt{s} = 22$ GeV to $\sqrt{s} = 91$ GeV. A flavor tag is used to discriminate between different quark species, and the longitudinal and transverse cross sections are used to extract the gluon fragmentation function [130]. The result obtained is $\alpha_s(M_Z) = 0.126 \pm 0.007$ (expt.) ± 0.006 (theory) [131]. The theory error is due mainly to the choice of scale. The OPAL collaboration [132] has also extracted the separate fragmentation functions. DELPHI [133] has also performed a similar analysis using data from other experiments at lower energy with the result $\alpha_s(M_Z) = 0.124 \pm 0.007$ (expt.) ± 0.009 (theory). The larger theoretical error is due to the larger range of scales that were used in the fit. These results can be combined to give $\alpha_s(M_Z) = 0.125 \pm 0.005$ (expt.) ± 0.008 (theory).

A global analysis [134] uses data on the production of π, K, p , and \bar{p} from SLC [135], DELPHI [136], OPAL [137], ALEPH [138], and lower-energy data from the TPC collaboration [139]. A flavor tag and a three-jet analysis is used to disentangle the quark and gluon fragmentation functions. The value $\alpha_s(M_Z) = 0.1172^{+0.0055+0.0017}_{-0.0069-0.0025}$ is obtained. The second error is a theoretical one arising from the choice of scale. The fragmentation functions resulting from this fit are consistent with a recent fit of [140].

It is unclear how to combine the measurements discussed in the two previous paragraphs as much of the data used are common to both. If the theoretical errors dominate then a simple average is appropriate as the methods are different. For want of a better solution, the naive average of $\alpha_s(M_Z) = 0.1201 \pm 0.006$ is used in the average value quoted below.

9.9. Photon structure functions

e^+e^- can also be used to study photon-photon interactions, which can be used to measure the structure function of a photon [141], by selecting events of the type $e^+e^- \rightarrow e^+e^- + \text{hadrons}$ which proceeds via two photon scattering. If events are selected where one of the photons is almost on mass shell and the other has a large invariant mass Q , then the latter probes the photon structure function at scale Q ; the process is analogous to deep inelastic scattering where a highly virtual photon is used to probe the proton structure. This process was included in earlier versions of this *Review* which can be consulted for details on older measurements [142–145]. A review of the data can be found in [146]. Data are available from LEP [147–151] and from TRISTAN [152,153] which extend the range of Q^2 to of order 300 GeV² and x as low as 2×10^{-3} and show Q^2 dependence of the structure function that is consistent with QCD expectations. There is evidence for a hadronic (non-perturbative) component to the photon structure function that complicates attempts to extract a value of α_s from the data.

Ref. 154 uses data from PETRA, TRISTAN, and LEP to perform a combined fit. The higher data from LEP extend to higher Q^2 (< 780 GeV²) and enable a measurement: $\alpha_s(m_Z) = 0.1198 \pm 0.0054$ which now is competitive with other results.

Experiments at HERA can also probe the photon structure function by looking at jet production in γp collisions; this is analogous to the jet production in hadron-hadron collisions which is sensitive to hadron structure functions. The data [155] are consistent with theoretical models [156].

9.10. Jet rates in ep collisions

At lowest order in α_s , the ep scattering process produces a final state of (1+1) jets, one from the proton fragment and the other from the quark knocked out by the process $e + \text{quark} \rightarrow e + \text{quark}$. At next order in α_s , a gluon can be radiated, and hence a (2+1) jet final state produced. By comparing the rates for these (1+1) and (2+1) or (2+1) and (3+1) jet processes, a value of α_s can be obtained. A NLO

QCD calculation is available [157]. The basic methodology is similar to that used in the jet counting experiments in e^+e^- annihilation discussed above. Unlike those measurements, the ones in ep scattering are not at a fixed value of Q^2 . In addition to the systematic errors associated with the jet definitions, there are additional ones since the structure functions enter into the rate calculations. A summary of the measurements from HERA can be found in Ref. 158, which clearly demonstrates the evidence for the evolution of $\alpha_s(Q^2)$ with Q^2 . Results from H1 [159] $\alpha_s(M_Z) = 0.1175 \pm 0.0057$ (expt.) ± 0.0053 (theor.) and ZEUS [160] $\alpha_s(M_Z) = 0.1179 \pm 0.0040$ (expt.) ± 0.005 (theor.) can be combined to give $\alpha_s(M_Z) = 0.1178 \pm 0.0033$ (expt.) ± 0.006 (theor.) which is used in the final average. The theoretical errors arise from scale choice, structure functions, and hadronization correction.

Photoproduction of two or more jets via processes such as $\gamma + g \rightarrow q\bar{q}$ can also be observed at HERA. The process is similar to jet production in hadron-hadron collisions. Agreement with perturbative QCD is excellent and ZEUS [161] quotes $\alpha_s(M_Z) = 0.1224 \pm 0.0020$ (expt.) ± 0.0050 (theory) which is used in the average below.

9.11. QCD in diffractive events

In approximately 10% of the deep-inelastic scattering events at HERA a rapidity gap is observed [162]; that is events are seen where there are almost no hadrons produced in the direction of the incident proton. This was unexpected; QCD based models of the final state predicted that the rapidity interval between the quark that is hit by the electron and the proton remnant should be populated approximately evenly by the hadrons. Similar phenomena have been observed at the Tevatron in W and jet production. For a review see Ref. 163.

9.12. Lattice QCD

Lattice gauge theory can be used to calculate, using non-perturbative methods, a physical quantity that can be measured experimentally. The value of this quantity can then be used to determine the QCD coupling that enters in the calculation. The main theoretical difference between this approach and those discussed above is that, in the previous cases, precise calculations are restricted to high energy phenomena where perturbation theory can be applied due to the smallness of α_s in the appropriate energy regime. Lattice calculations enable reliable calculations to be done without this restriction. It is important to emphasize that this is exactly the same methodology used in the cases discussed above. The main quantitative difference is that the experimental measurements involved, such as the masses of \mathcal{T} states, are so precise that their uncertainties have almost no impact on the final comparisons. A discussion of the uncertainties that enter into the QCD tests and determination of α_s is therefore almost exclusively a discussion of the techniques used in the calculations. In addition to α_s , other physical quantities such as the masses of the light quarks can be obtained. For a review of the methodology, see Ref. 164 [165]. For example, the energy levels of a $Q\bar{Q}$ system can be determined and then used to extract α_s . The masses of the $Q\bar{Q}$ states depend only on the quark mass and on α_s . Until a few years ago, calculations have not been performed for three light quark flavors. Results for zero ($n_f = 0$, quenched approximation) and two light flavors were extrapolated to $n_f = 3$. This major limitation has now been removed and a qualitative improvement in the calculations has occurred. Using the mass differences of \mathcal{T} and \mathcal{T}' and \mathcal{T}'' and χ_b , Mason *et al.* [167] extract a value of $\alpha_s(M_Z) = 0.1170 \pm 0.0012$. Many other quantities such as the pion decay constant, and the masses of the B_s meson and Ω baryon are used and the overall consistency is excellent.

There have also been investigations of the running of α_s [173]. These show remarkable agreement with the two loop perturbative result of Eq. (9.5).

There are several sources of error in these estimates of $\alpha_s(M_Z)$. The experimental error associated with the measurements of the particle masses is negligible. The limited statistics of the Monte-Carlo calculation which can be improved only with more computational resources is one dominant error. The conversion from the lattice coupling constant to the $\overline{\text{MS}}$ constant is obtained using a perturbative

expansion where one coupling expanded as a power series in the other. The series is known to third order and this leads to the second largest uncertainty [166]. Extra degrees of freedom introduced by calculating (using staggered fermions) on a lattice have to be removed: see Ref. 174 for a discussion of this point and the possible uncertainties related to it. The use of Wilson fermions involves a different systematic. Results from Ref. 175 using this method with two light quark flavors are $\alpha_s(M_Z) = 0.112 \pm 0.003$, which illustrates the tendency for results using Wilson fermions to be systematically lower than those from staggered fermions.

In this review, we will use only the new result [166] of $\alpha_s(M_Z) = 0.1170 \pm 0.0012$, which is consistent with the value $\alpha_s(M_Z) = 0.121 \pm 0.003$ used in the last version of this review [167].

In addition to the strong coupling constant other quantities can be determined including the light quark masses [168]. Of particular interest are the decay constants of charmed and bottom mesons. These are required, for example, to facilitate the extraction of CKM elements from measurements of charm and bottom decay rates [169,170]. Some of these quantities such as the D -meson decay constant have been found to be in excellent agreement with experiment [171].

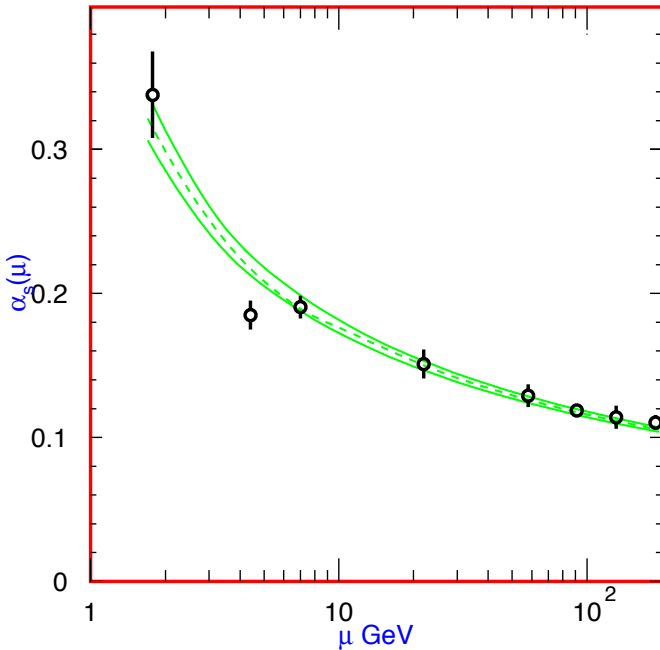


Figure 9.2: Summary of the values of $\alpha_s(\mu)$ at the values of μ where they are measured. The lines show the central values and the $\pm 1\sigma$ limits of our average. The figure clearly shows the decrease in $\alpha_s(\mu)$ with increasing μ . The data are, in increasing order of μ , τ width, Υ decays, deep inelastic scattering, e^+e^- event shapes at 22 GeV from the JADE data, shapes at TRISTAN at 58 GeV, Z width, and e^+e^- event shapes at 135 and 189 GeV.

9.13. Conclusions

The need for brevity has meant that many other important topics in QCD phenomenology have had to be omitted from this review. One should mention in particular the study of exclusive processes (form factors, elastic scattering, ...), the behavior of quarks and gluons in nuclei, the spin properties of the theory, and QCD effects in hadron spectroscopy.

We have focused on those high-energy processes which currently offer the most quantitative tests of perturbative QCD. Figure 9.1 shows the values of $\alpha_s(M_Z)$ deduced from the various experiments. Figure 9.2 shows the values and the values of Q where they are measured. This figure clearly shows the experimental evidence for the variation of $\alpha_s(Q)$ with Q .

An average of the values in Fig. 9.1 gives $\alpha_s(M_Z) = 0.1176$, with a total χ^2 of 9 for eleven fitted points, showing good consistency among the data. The error on this average, assuming that all of the errors in the contributing results are uncorrelated, is ± 0.0009 , and may be an underestimate. Almost all of the values used in the average are dominated by systematic, usually theoretical, errors. Only some of these, notably from the choice of scale, are correlated. The error on the lattice gauge theory result is the smallest and then there are several results with comparable small errors: these are the ones from τ decay, deep inelastic scattering, Υ decay and the Z^0 width. Omitting the lattice-QCD result from the average changes it to $\alpha_s(M_Z) = 0.1185$ or 1σ . All of the results that dominate the average are from NNLO. The NLO results have little weight, there are no LO results used. Almost all of the results have errors that are dominated by theoretical issues, either from unknown higher order perturbative corrections or estimates of non-perturbative contributions. It is therefore prudent to be conservative and quote our average value as $\alpha_s(M_Z) = 0.1176 \pm 0.002$. Note that the average has moved by less than 1σ from the last version of this review. Future experiments can be expected to improve the measurements of α_s somewhat.

The value of α_s at any scale corresponding to our average can be obtained from <http://www-theory.lbl.gov/~ianh/alpha/alpha.html> which uses Eq. (9.5) to interpolate.

References:

1. R.K. Ellis *et al.*, "QCD and Collider Physics" (Cambridge 1996).
2. For reviews see, for example, A.S. Kronfeld and P.B. Mackenzie, *Ann. Rev. Nucl. and Part. Sci.* **43**, 793 (1993); H. Wittig, *Int. J. Mod. Phys.* **A12**, 4477 (1997).
3. For example see, P. Gambino, *International Conference on Lepton Photon Interactions*, Fermilab, USA, (2003); J. Butterworth *International Conference on Lepton Photon Interactions*, Upsala, Sweden, (2005).
4. G Salam at *International Conference on Lepton Photon Interactions*, Upsala, Sweden, (2005).
5. S. Bethke, [hep-ex/0407021](https://arxiv.org/abs/hep-ex/0407021), *Nucl. Phys.* **B135**, 345 (2004); S. Bethke, *J. Phys.* **G26**, R27 (2000).
6. R.W.L. Jones *et al.*, *JHEP* **12**, 7 (2003).
7. See, for example, J. Collins "Renormalization: an introduction to renormalization, the renormalization group and the operator product expansion," (Cambridge University Press, Cambridge, 1984). "QCD and Collider Physics" (Cambridge 1996).
8. S.A. Larin *et al.*, *Phys. Lett.* **B400**, 379 (1997).
9. W.A. Bardeen *et al.*, *Phys. Rev.* **D18**, 3998 (1978).
10. G. Grunberg, *Phys. Lett.* **95B**, 70 (1980); *Phys. Rev.* **D29**, 2315 (1984).
11. P.M. Stevenson, *Phys. Rev.* **D23**, 2916 (1981); and *Nucl. Phys.* **B203**, 472 (1982).
12. S. Brodsky and H.J. Lu, SLAC-PUB-6389 (Nov. 1993).
13. S. Brodsky *et al.*, *Phys. Rev.* **D28**, 228 (1983).
14. M.A. Samuel *et al.*, *Phys. Lett.* **B323**, 188 (1994); M.A. Samuel *et al.*, *Phys. Rev. Lett.* **74**, 4380 (1995).
15. J. Ellis *et al.*, *Phys. Rev.* **D54**, 6986 (1996).
16. P.N. Burrows *et al.*, *Phys. Lett.* **B382**, 157 (1996).
17. P. Abreu *et al.*, *Z. Phys.* **C54**, 55 (1992).
18. A.H. Mueller, *Phys. Lett.* **B308**, 355 (1993).
19. W. Bernreuther, *Ann. Phys.* **151**, 127 (1983); Erratum *Nucl. Phys.* **B513**, 758 (1998); S.A. Larin *et al.*, *Nucl. Phys.* **B438**, 278 (1995).
20. K.G. Chetyrkin *et al.*, *Phys. Rev. Lett.* **79**, 2184 (1997); K.G. Chetyrkin *et al.*, *Nucl. Phys.* **B510**, 61 (1998).
21. See the Review on the "Quark Mass" in the Particle Listings for *Review of Particle Physics*.
22. A.D. Martin *et al.*, *Phys. Lett.* **B604**, 61 (2004).
23. D. Gross and C.H. Llewellyn Smith, *Nucl. Phys.* **B14**, 337 (1969).
24. J. Chyla and A.L. Kataev, *Phys. Lett.* **B297**, 385 (1992).
25. S.A. Larin and J.A.M. Vermaseren, *Phys. Lett.* **B259**, 345 (1991).
26. A.L. Kataev and V.V. Starchenko, *Mod. Phys. Lett.* **A10**, 235 (1995).

27. V.M. Braun and A.V. Kolesnichenko, Nucl. Phys. **B283**, 723 (1987).
28. M. Dasgupta and B. Webber, Phys. Lett. **B382**, 273 (1993).
29. J. Kim *et al.*, Phys. Rev. Lett. **81**, 3595 (1998).
30. D. Allasia *et al.*, Z. Phys. **C28**, 321 (1985);
K. Varvell *et al.*, Z. Phys. **C36**, 1 (1987);
V.V. Ammosov *et al.*, Z. Phys. **C30**, 175 (1986);
P.C. Bosetti *et al.*, Nucl. Phys. **B142**, 1 (1978).
31. A.L. Kataev *et al.*, Nucl. Phys. **A666 & 667**, 184 (2000); Nucl. Phys. **B573**, 405 (2000).
32. A.L. Kataev *et al.*, hep-ph/0106221;
A.L. Kataev *et al.*, Nucl. Phys. Proc. Suppl. **116**, 105 (2003) hep-ph/0211151.
33. K. Abe *et al.*, Phys. Rev. Lett. **74**, 346 (1995); Phys. Lett. **B364**, 61 (1995); Phys. Rev. Lett. **75**, 25 (1995);
P.L. Anthony *et al.*, Phys. Rev. **D54**, 6620 (1996).
34. B. Adeva *et al.*, Phys. Rev. **D58**, 112002 (1998), Phys. Lett. **B420**, 180 (1998).
35. D. Adams *et al.*, Phys. Lett. **B329**, 399 (1995); Phys. Rev. **D56**, 5330 (1998); Phys. Rev. **D58**, 1112001 (1998);
K. Ackerstaff *et al.*, Phys. Lett. **B464**, 123 (1999).
36. P.L. Anthony *et al.*, Phys. Lett. **B463**, 339 (1999); Phys. Lett. **B493**, 19 (2000).
37. J. Blümlein and H. Böttcher, Nucl. Phys. **B636**, 225 (2002).
38. J.D. Bjorken, Phys. Rev. **148**, 1467 (1966).
39. G. Altarelli *et al.*, Nucl. Phys. **B496**, 337 (1997).
40. J. Ellis and M. Karliner, Phys. Lett. **B341**, 397 (1995).
41. M.A. Shifman *et al.*, Nucl. Phys. **B147**, 385 (1979).
42. S. Narison and A. Pich, Phys. Lett. **B211**, 183 (1988);
E. Braaten *et al.*, Nucl. Phys. **B373**, 581 (1992).
43. M. Neubert, Nucl. Phys. **B463**, 511 (1996).
44. F. Le Diberder and A. Pich, Phys. Lett. **B289**, 165 (1992).
45. R. Barate *et al.*, Z. Phys. **C76**, 1 (1997); Z. Phys. **C76**, 15 (1997);
K. Ackerstaff *et al.*, Eur. Phys. J. **C7**, 571 (1999).
46. T. Coan *et al.*, Phys. Lett. **B356**, 580 (1995).
47. A.L. Kataev and V.V. Starshenko, Mod. Phys. Lett. **A10**, 235 (1995).
48. F. Le Diberder and A. Pich, Phys. Lett. **B286**, 147 (1992).
49. C.J. Maxwell and D.J. Tong, Nucl. Phys. **B481**, 681 (1996).
50. G. Altarelli, Nucl. Phys. **B40**, 59 (1995);
G. Altarelli *et al.*, Z. Phys. **C68**, 257 (1995).
51. S. Narison, Nucl. Phys. **B40**, 47 (1995).
52. S. Narison, hep-ph/0508259.
53. S. Menke, hep-ex/0106011.
54. S.D. Ellis *et al.*, Phys. Rev. Lett. **64**, 2121 (1990);
F. Aversa *et al.*, Phys. Rev. Lett. **65**, 401 (1990);
W.T. Giele *et al.*, Phys. Rev. Lett. **73**, 2019 (1994);
S. Frixione *et al.*, Nucl. Phys. **B467**, 399 (1996).
55. F. Abe *et al.*, Phys. Rev. Lett. **77**, 438 (1996);
B. Abbott *et al.*, Phys. Rev. Lett. **86**, 1707 (2001).
56. W.T. Giele *et al.*, Phys. Rev. **D53**, 120 (1996).
57. T. Affolder *et al.*, Phys. Rev. Lett. **88**, 042001 (2002).
58. UA1 Collaboration: G. Arnison *et al.*, Phys. Lett. **B177**, 244 (1986).
59. F. Abe *et al.*, Phys. Rev. Lett. **77**, 533 (1996);
ibid., erratum Phys. Rev. Lett. **78**, 4307 (1997);
B. Abbott, Phys. Rev. Lett. **80**, 666 (1998);
S. Abachi *et al.*, Phys. Rev. **D53**, 6000 (1996).
60. G. Altarelli *et al.*, Nucl. Phys. **B143**, 521 (1978).
61. R. Hamberg *et al.*, Nucl. Phys. **B359**, 343 (1991).
62. P. Aurenche *et al.*, Phys. Rev. **D42**, 1440 (1990);
P. Aurenche *et al.*, Phys. Lett. **140B**, 87 (1984);
P. Aurenche *et al.*, Nucl. Phys. **B297**, 661 (1988).
63. H. Baer *et al.*, Phys. Lett. **B234**, 127 (1990).
64. H. Baer and M.H. Reno, Phys. Rev. **D43**, 2892 (1991);
P.B. Arnold and M.H. Reno, Nucl. Phys. **B319**, 37 (1989).
65. F. Abe *et al.*, Phys. Rev. Lett. **73**, 2662 (1994).
66. B. Abbott *et al.*, Phys. Rev. Lett. **84**, 2786 (2001);
V.M. Abazov *et al.*, Phys. Rev. Lett. **87**, 251805 (2001).
67. G. Alverson *et al.*, Phys. Rev. **D48**, 5 (1993).
68. L. Apanasevich *et al.*, Phys. Rev. **D59**, 074007 (1999); Phys. Rev. Lett. **81**, 2642 (1998).
69. W. Vogelsang and A. Vogt, Nucl. Phys. **B453**, 334 (1995);
P. Aurenche *et al.*, Eur. Phys. J. **C9**, 107 (1999).
70. J. Alitti *et al.*, Phys. Lett. **B263**, 563 (1991).
71. S. Abachi *et al.*, Phys. Rev. Lett. **75**, 3226 (1995);
J. Womersley, private communication;
J. Huston, in the *Proceedings to the 29th International Conference on High-Energy Physics (ICHEP98)*, Vancouver, Canada (23–29 Jul 1998) hep-ph/9901352.
72. R.K. Ellis and S. Veseli, Nucl. Phys. **B511**, 649 (1998);
C.T. Davies *et al.*, Nucl. Phys. **B256**, 413 (1985);
G. Parisi and R. Petronzio, Nucl. Phys. **B154**, 427 (1979);
J.C. Collins *et al.*, Nucl. Phys. **B250**, 199 (1985).
73. DØ Collaboration: B. Abbott *et al.*, Phys. Rev. **D61**, 032004 (2000);
T. Affolder *et al.*, FERMILAB-PUB-99/220.
74. C. Albajar *et al.*, Phys. Lett. **B369**, 46 (1996).
75. M.L. Mangano *et al.*, Nucl. Phys. **B373**, 295 (1992).
76. D. Acosta *et al.*, Phys. Rev. **D65**, 052005 (2002).
77. M. Cacciari *et al.*, JHEP **0407**, 033 (2004).
78. D. Acosta *et al.*, Phys. Rev. D **71**, 032001 (2005).
79. R. Barbieri *et al.*, Phys. Lett. **95B**, 93 (1980);
P.B. Mackenzie and G.P. Lepage, Phys. Rev. Lett. **47**, 1244 (1981).
80. G.T. Bodwin *et al.*, Phys. Rev. **D51**, 1125 (1995).
81. *The Review of Particle Physics*, D.E. Groom *et al.*, Eur. Phys. J. **C15**, 1 (2000) and 2001 off-year partial update for the 2002 edition available on the PDG WWW pages (URL: <http://pdg.lbl.gov/>).
82. M. Gremm and A. Kapustin, Phys. Lett. **B407**, 323 (1997).
83. I. Hinchliffe and A.V. Manohar, Ann. Rev. Nucl. Part. Sci. **50**, 643 (2000).
84. S. Catani and F. Hautmann, Nucl. Phys. **B** (Proc. Supp.), vol. **39BC**, 359 (1995).
85. B. Nemati *et al.*, Phys. Rev. **D55**, 5273 (1997).
86. M. Kramer, Phys. Rev. **D60**, 111503 (1999).
87. M. Voloshin, Int. J. Mod. Phys. **A10**, 2865 (1995).
88. M. Jamin and A. Pich, Nucl. Phys. **B507**, 334 (1997).
89. J.H. Kuhn *et al.*, Nucl. Phys. **B534**, 356 (1998).
90. A.H. Hoang and M. Jamin, Phys. Lett. **B594**, 127 (2004).
91. S.G. Gorishny *et al.*, Phys. Lett. **B259**, 144 (1991);
L.R. Surguladze and M.A. Samuel, Phys. Rev. Lett. **66**, 560 (1991).
92. K.G. Chetyrkin and J.H. Kuhn, Phys. Lett. **B308**, 127 (1993).
93. R. Ammar *et al.*, Phys. Rev. **D57**, 1350 (1998).
94. D. Haidt, in *Directions in High Energy Physics*, vol. 14, p. 201, ed. P. Langacker (World Scientific, 1995).
95. LEP electroweak working group, presented at the *International Europhysics Conference on High Energy Physics, EPS05*, Lisbon Portugal (July 2005);
D. Abbaneo, *et al.*, LEPEWWG/2003-01.
96. A. Blondel and C. Verzegrassi, Phys. Lett. **B311**, 346 (1993);
G. Altarelli *et al.*, Nucl. Phys. **B405**, 3 (1993).
97. G. Dissertori *et al.*, “Quantum Chromodynamics: High Energy Experiments and Theory” (Oxford University Press, 2003).
98. E. Farhi, Phys. Rev. Lett. **39**, 1587 (1977).
99. C.L. Basham *et al.*, Phys. Rev. **D17**, 2298 (1978).
100. J. Ellis *et al.*, Nucl. Phys. **B111**, 253 (1976);
ibid., erratum Nucl. Phys. **B130**, 516 (1977);
P. Hoyer *et al.*, Nucl. Phys. **B161**, 349 (1979).
101. R.K. Ellis *et al.*, Phys. Rev. Lett. **45**, 1226 (1980);
Z. Kunszt and P. Nason, ETH-89-0836 (1989).
102. S. Bethke *et al.*, Phys. Lett. **B213**, 235 (1988), Erratum *ibid.*, B523, 681 (1988).
103. S. Bethke *et al.*, Nucl. Phys. **B370**, 310 (1992).
104. M.Z. Akrawy *et al.*, Z. Phys. **C49**, 375 (1991).
105. K. Abe *et al.*, Phys. Rev. Lett. **71**, 2578 (1993); Phys. Rev. **D51**, 962 (1995).
106. B. Andersson *et al.*, Phys. Reports **97**, 33 (1983).

107. A. Ali *et al.*, Nucl. Phys. **B168**, 409 (1980);
A. Ali and F. Barreiro, Phys. Lett. **118B**, 155 (1982).
108. B.R. Webber, Nucl. Phys. **B238**, 492 (1984);
G. Marchesini *et al.*, Phys. Comm. **67**, 465 (1992).
109. T. Sjostrand and M. Bengtsson, Comp. Phys. Comm. **43**, 367 (1987);
T. Sjostrand, CERN-TH-7112/93 (1993).
110. O. Adriani *et al.*, Phys. Lett. **B284**, 471 (1992);
M. Akrawy *et al.*, Z. Phys. **C47**, 505 (1990);
B. Adeva *et al.*, Phys. Lett. **B248**, 473 (1990);
D. Decamp *et al.*, Phys. Lett. **B255**, 623 (1991).
111. S. Catani *et al.*, Phys. Lett. **B263**, 491 (1991).
112. S. Catani *et al.*, Phys. Lett. **B269**, 432 (1991); G. Dissertori and M. Schmelling, Phys. Lett. B **361**, 167 (1995);
S. Catani *et al.*, Phys. Lett. **B272**, 368 (1991);
N. Brown and J. Stirling, Z. Phys. **C53**, 629 (1992).
113. S. Catani *et al.*, Phys. Lett. **B269**, 432 (1991); Phys. Lett. **B295**, 269 (1992); Nucl. Phys. **B607**, 3 (1993); Phys. Lett. **B269**, 432 (1991).
114. M. Dasgupta and G. P. Salam, J. Phys. **G30**, R143 (2004).
115. P.D. Acton *et al.*, Z. Phys. **C55**, 1 (1992); Z. Phys. **C58**, 386 (1993).
116. O. Adriani *et al.*, Phys. Lett. **B284**, 471 (1992).
117. D. Decamp *et al.*, Phys. Lett. **B255**, 623 (1992); Phys. Lett. **B257**, 479 (1992).
118. P. Abreu *et al.*, Z. Phys. **C59**, 21 (1993); Phys. Lett. **B456**, 322 (1999);
M. Acciarri *et al.*, Phys. Lett. **B404**, 390 (1997).
119. Y.L. Dokshitzer and B.R. Webber Phys. Lett. **B352**, 451 (1995);
Y.L. Dokshitzer *et al.*, Nucl. Phys. **B511**, 396 (1997);
Y.L. Dokshitzer *et al.*, JHEP **9801**, 011 (1998).
120. J. Abdallah *et al.*, [DELPHI Collaboration], Eur. Phys. J. **C29**, 285 (2003).
121. D. Buskulic *et al.*, Z. Phys. **C73**, 409 (1997); Z. Phys. **C73**, 229 (1997).
122. H. Stenzel *et al.* [ALEPH Collaboration], CERN-OPEN-99-303(1999);
DELPHI Collaboration: Eur. Phys. J. **C14**, 557 (2000);
M. Acciarri *et al.* [L3 Collaboration], Phys. Lett. **B489**, 65 (2000);
OPAL Collaboration, PN-403 (1999); all submitted to *International Conference on Lepton Photon Interactions*, Stanford, USA (Aug. 1999);
M. Acciarri *et al.* OPAL Collaboration], Phys. Lett. **B371**, 137 (1996); Z. Phys. **C72**, 191 (1996);
K. Akerstaff *et al.*, Z. Phys. **C75**, 193 (1997);
ALEPH Collaboration: ALEPH 98-025 (1998).
123. <http://lepqcd.web.cern.ch/LEPQCD/annihilations/Welcome.html>.
124. Y. Ohnishi *et al.*, Phys. Lett. **B313**, 475 (1993).
125. P.A. Movilla Fernandez *et al.*, Eur. Phys. J. **C1**, 461 (1998), hep-ex/020501; S. Kluth *et al.*, hep-ex/0305023; J. Schieck *et al.*, hep-ex/0408122;
O. Biebel *et al.*, Phys. Lett. **B459**, 326 (1999).
126. S. Kluth *et al.*, [JADE Collaboration], hep-ex/0305023.
127. D.A. Bauer *et al.*, SLAC-PUB-6518.
128. L. Gibbons *et al.*, CLNS 95-1323 (1995).
129. S. Kluth, Nucl. Phys. Proc. Suppl. **133**, 36 (2004).
130. P. Nason and B.R. Webber, Nucl. Phys. **B421**, 473 (1994).
131. D. Buskulic *et al.*, Phys. Lett. **B357**, 487 (1995);
ibid., erratum Phys. Lett. **B364**, 247 (1995).
132. R. Akers *et al.*, Z. Phys. **C68**, 203 (1995).
133. P. Abreu *et al.*, Phys. Lett. **B398**, 194 (1997).
134. B.A. Kniehl *et al.*, Phys. Rev. Lett. **85**, 5288 (2000).
135. K. Abe *et al.*, [SLD Collab.], Phys. Rev. **D59**, 052001 (1999).
136. P. Abreu *et al.*, [DELPHI Collab.], Eur. Phys. J. **C5**, 585 (1998).
137. G. Abbiendi *et al.*, [OPAL Collab.], Eur. Phys. J. **C11**, 217 (1999).
138. D. Buskulic *et al.*, [ALEPH Collab.], Z. Phys. **C66**, 355 (1995);
R. Barate *et al.*, Eur. Phys. J. **C17**, 1 (2000).
139. H. Aihara, *et al.*, LBL-23737 (1988) (Unpublished).
140. L. Bourhis *et al.*, Eur. Phys. J. **C19**, 89 (2001).
141. E. Witten, Nucl. Phys. **B120**, 189 (1977).
142. C. Berger *et al.*, Nucl. Phys. **B281**, 365 (1987).
143. H. Aihara *et al.*, Z. Phys. **C34**, 1 (1987).
144. M. Althoff *et al.*, Z. Phys. **C31**, 527 (1986).
145. W. Bartel *et al.*, Z. Phys. **C24**, 231 (1984).
146. M. Erdmann, *International Conference on Lepton Photon Interactions*, Rome Italy (Aug. 2001) R. Nisius, hep-ex/0210059.
147. K. Akerstaff *et al.*, Phys. Lett. **B412**, 225 (1997); Phys. Lett. **B411**, 387 (1997).
148. G. Abbiendi *et al.*, [OPAL Collaboration], Eur. Phys. J. **C18**, 15 (2000).
149. R. Barate *et al.*, Phys. Lett. **B458**, 152 (1999).
150. M. Acciarri *et al.*, Phys. Lett. **B436**, 403 (1998); Phys. Lett. **B483**, 373 (2000).
151. P. Abreu *et al.*, Z. Phys. **C69**, 223 (1996).
152. K. Muramatsu *et al.*, Phys. Lett. **B332**, 477 (1994).
153. S.K. Sahu *et al.*, Phys. Lett. **B346**, 208 (1995).
154. S. Albino *et al.*, Phys. Rev. Lett. **89**, 122004 (2002).
155. C. Adloff *et al.*, Eur. Phys. J. **C13**, 397 (2000);
J. Breitweg *et al.*, Eur. Phys. J. **C11**, 35 (1999).
156. S. Frixione, Nucl. Phys. **B507**, 295 (1997);
B.W. Harris and J.F. Owens, Phys. Rev. **D56**, 4007 (1997);
M. Klasen and G. Kramer, Z. Phys. **C72**, 107 (1996).
157. D. Graudenz, Phys. Rev. **D49**, 3921 (1994);
J.G. Korner *et al.*, Int. J. Mod. Phys. **A4**, 1781, (1989);
S. Catani and M. Seymour, Nucl. Phys. **B485**, 291 (1997);
M. Dasgupta and B.R. Webber, Eur. Phys. J. **C1**, 539 (1998);
E. Mirkes and D. Zeppenfeld, Phys. Lett. **B380**, 205 (1996);
Z. Nagy and Z. Trocsanyi, Phys. Rev. Lett. **87**, 082001 (2001).
C. Glasman, at DIS2005 Madison, Wisconsin (2005).
159. T. Kluge (H1 collaboration) at DIS2005, Madison, Wisconsin (2005) C. Adloff *et al.*, Eur. Phys. J. **C19**, 289 (2001).
160. ZEUS Collaboration: DESY-05-019, hep-ex/0502007.
161. ZEUS Collaboration: S. Chekanov *et al.*, Phys. Lett. **B558**, 41 (2003);
E. Tassi at DIS2001 Conference, Bologna (April 2001).
162. M. Derrick *et al.*, Phys. Lett. **B**, 369 (1996);
T. Ahmed *et al.*, Nucl. Phys. **B435**, 3 (1995).
163. D.M. Janson *et al.*, hep-ex/9905537.
164. P. Weisz, Nucl. Phys. (Proc. Supp.) **B47**, 71 (1996).
165. P. E. L. Rakow, Nucl. Phys. (Proc. Supp.) **B140**, 34 (2005).
166. Q. Mason *et al.*, Phys. Rev. Lett. **95**, 052002 (2005).
167. C. T. H. Davies *et al.*, Phys. Rev. Lett. **92**, 022001 (2004).
168. C. Aubin *et al.*, Phys. Rev. **D70**, 031504 (2004).
169. C. Aubin *et al.*, Phys. Rev. Lett. **94**, 011601 (2005).
170. A. Gray *et al.*, [HPQCD Collaboration], hep-lat/0507015.
171. C. Aubin *et al.*, hep-lat/0506030.
172. A.X. El-Khadra *et al.*, Phys. Rev. Lett. **69**, 729 (1992);
A.X. El-Khadra *et al.*, FNAL 94-091/T (1994);
A.X. El-Khadra *et al.*, hep-ph/9608220.
173. G. de Divitiis *et al.*, Nucl. Phys. **B437**, 447 (1995).
174. S. Durr, hep-lat/0509026.
175. M. Gockeler *et al.*, hep-ph/0502212.

10. ELECTROWEAK MODEL AND CONSTRAINTS ON NEW PHYSICS

Revised November 2007 by J. Erler (U. Mexico) and P. Langacker (Institute for Advanced Study).

- 10.1 Introduction
- 10.2 Renormalization and radiative corrections
- 10.3 Cross-section and asymmetry formulae
- 10.4 Precision flavor physics
- 10.5 W and Z decays
- 10.6 Experimental results
- 10.7 Constraints on new physics

10.1. Introduction

The standard electroweak model (SM) is based on the gauge group [1] $SU(2) \times U(1)$, with gauge bosons W_μ^i , $i = 1, 2, 3$, and B_μ for the $SU(2)$ and $U(1)$ factors, respectively, and the corresponding gauge coupling constants g and g' . The left-handed fermion fields $\psi_i = \begin{pmatrix} \nu_i \\ \ell_i^- \end{pmatrix}$ and $\begin{pmatrix} u_i \\ d_i^- \end{pmatrix}$ of the i^{th} fermion family transform as doublets under $SU(2)$, where $d_i^- \equiv \sum_j V_{ij} d_j$, and V is the Cabibbo-Kobayashi-Maskawa mixing matrix. (Constraints on V and tests of universality are discussed in Ref. 2 and in the Section on “The CKM Quark-Mixing Matrix.” The extension of the formalism to allow an analogous leptonic mixing matrix is discussed in the Section on “Neutrino Mass, Mixing, and Flavor Change.”) The right-handed fields are $SU(2)$ singlets. In the minimal model there are three fermion families and a single complex Higgs doublet $\phi \equiv \begin{pmatrix} \phi^+ \\ \phi^0 \end{pmatrix}$.

After spontaneous symmetry breaking the Lagrangian for the fermion fields is

$$\begin{aligned} \mathcal{L}_F = & \sum_i \bar{\psi}_i \left(i \not{\partial} - m_i - \frac{g m_i H}{2M_W} \right) \psi_i \\ & - \frac{g}{2\sqrt{2}} \sum_i \bar{\psi}_i \gamma^\mu (1 - \gamma^5) (T^+ W_\mu^+ + T^- W_\mu^-) \psi_i \\ & - e \sum_i q_i \bar{\psi}_i \gamma^\mu \psi_i A_\mu \\ & - \frac{g}{2 \cos \theta_W} \sum_i \bar{\psi}_i \gamma^\mu (g_V^i - g_A^i \gamma^5) \psi_i Z_\mu . \end{aligned} \quad (10.1)$$

$\theta_W \equiv \tan^{-1}(g'/g)$ is the weak angle; $e = g \sin \theta_W$ is the positron electric charge; and $A \equiv B \cos \theta_W + W^3 \sin \theta_W$ is the (massless) photon field. $W^\pm \equiv (W^1 \mp iW^2)/\sqrt{2}$ and $Z \equiv -B \sin \theta_W + W^3 \cos \theta_W$ are the massive charged and neutral weak boson fields, respectively. T^+ and T^- are the weak isospin raising and lowering operators. The vector and axial-vector couplings are

$$g_V^i \equiv t_{3L}(i) - 2q_i \sin^2 \theta_W , \quad (10.2a)$$

$$g_A^i \equiv t_{3L}(i) , \quad (10.2b)$$

where $t_{3L}(i)$ is the weak isospin of fermion i (+1/2 for u_i and ν_i ; -1/2 for d_i and e_i) and q_i is the charge of ψ_i in units of e .

The second term in \mathcal{L}_F represents the charged-current weak interaction [3,4]. For example, the coupling of a W to an electron and a neutrino is

$$-\frac{e}{2\sqrt{2} \sin \theta_W} \left[W_\mu^- \bar{\nu} \gamma^\mu (1 - \gamma^5) \nu + W_\mu^+ \bar{\nu} \gamma^\mu (1 - \gamma^5) e \right] . \quad (10.3)$$

For momenta small compared to M_W , this term gives rise to the effective four-fermion interaction with the Fermi constant given (at tree level, *i.e.*, lowest order in perturbation theory) by $G_F/\sqrt{2} = g^2/8M_W^2$. CP violation is incorporated in the SM by a single observable phase in V_{ij} . The third term in \mathcal{L}_F describes electromagnetic interactions (QED), and the last is the weak neutral-current interaction.

In Eq. (10.1), m_i is the mass of the i^{th} fermion ψ_i . For the quarks these are the current masses. For the light quarks, as described in the note on “Quark Masses” in the Quark Listings, $\hat{m}_u \approx 1.5\text{--}3$ MeV, $\hat{m}_d \approx 3\text{--}7$ MeV, and $\hat{m}_s = 95 \pm 25$ MeV. These are running $\overline{\text{MS}}$ masses evaluated at the scale $\mu = 2$ GeV. (In this Section we denote quantities defined in the $\overline{\text{MS}}$ scheme by a caret;

the exception is the strong coupling constant, α_s , which will always correspond to the $\overline{\text{MS}}$ definition and where the caret will be dropped.) For the heavier quarks we use QCD sum rule constraints [5] and recalculate their masses in each call of our fits to account for their direct α_s dependence. We find, $\hat{m}_c(\mu = \hat{m}_c) = 1.274_{-0.045}^{+0.036}$ GeV and $\hat{m}_b(\mu = \hat{m}_b) = 4.196 \pm 0.028$ GeV, with a correlation of 28%. The top quark “pole” mass, $m_t = 170.9 \pm 1.8$ GeV, is an average [6] of published and preliminary CDF and DØ results from run I and II. We are working, however, with $\overline{\text{MS}}$ masses in all expressions to minimize theoretical uncertainties, and therefore convert this result to the top quark $\overline{\text{MS}}$ mass,

$$\hat{m}_t(\mu = \hat{m}_t) = m_t \left[1 - \frac{4}{3} \frac{\alpha_s}{\pi} + \mathcal{O}(\alpha_s^2) \right],$$

using the three-loop formula [7]. This introduces an additional uncertainty which we estimate to 0.6 GeV (the size of the three-loop term). We are assuming that the kinematic mass extracted from the collider events corresponds within this uncertainty to the pole mass. Using the BLM optimized [8] version of the two-loop perturbative QCD formula [9] (as we did in previous editions of this *Review*) gives virtually identical results. Thus, we will use $m_t = 170.9 \pm 1.8 \pm 0.6$ GeV $\approx 170.9 \pm 1.9$ GeV (together with $M_H = 117$ GeV) for the numerical values quoted in Sec. 10.2–Sec. 10.4. In the presence of right-handed neutrinos, Eq. (10.1) gives rise also to Dirac neutrino masses. The possibility of Majorana masses is discussed in the Section on “Neutrino Mass, Mixing, and Flavor Change.”

H is the physical neutral Higgs scalar which is the only remaining part of ϕ after spontaneous symmetry breaking. The Yukawa coupling of H to ψ_i , which is flavor diagonal in the minimal model, is $g m_i/2M_W$. In non-minimal models there are additional charged and neutral scalar Higgs particles [10].

10.2. Renormalization and radiative corrections

The SM has three parameters (not counting the Higgs boson mass, M_H , and the fermion masses and mixings). A particularly useful set is:

- (a) The fine structure constant $\alpha = 1/137.035999679(94)$, determined from the e^\pm anomalous magnetic moment, the quantum Hall effect, and other measurements [11]. In most electroweak renormalization schemes, it is convenient to define a running α dependent on the energy scale of the process, with $\alpha^{-1} \sim 137$ appropriate at very low energy. (The running has also been observed [12] directly.) For scales above a few hundred MeV this introduces an uncertainty due to the low-energy hadronic contribution to vacuum polarization. In the modified minimal subtraction ($\overline{\text{MS}}$) scheme [13] (used for this *Review*), and with $\alpha_s(M_Z) = 0.120$ for the QCD coupling at M_Z , we have $\hat{\alpha}(m_\tau)^{-1} = 133.452 \pm 0.016$ and $\hat{\alpha}(M_Z)^{-1} = 127.925 \pm 0.016$. The latter corresponds to a quark sector contribution (without the top) to the conventional (on-shell) QED coupling, $\alpha(M_Z) = \frac{\alpha}{1 - \Delta\alpha(M_Z)}$, of $\Delta\alpha_{\text{had}}^{(5)}(M_Z) \approx 0.02786 \pm 0.00012$. These values are updated from Ref. 14 with $\Delta\alpha_{\text{had}}^{(5)}(M_Z)$ slightly moved upwards and its uncertainty decreased by 40% (mostly due to a more precise $\hat{\alpha}(m_c)$). Its correlation with $\hat{\alpha}(M_Z)$, as well as the non-linear α_s dependence of $\hat{\alpha}(M_Z)$ and the resulting correlation with the input variable α_s , are fully taken into account in the fits. This is done by using as actual input (fit constraint) instead of $\Delta\alpha_{\text{had}}^{(5)}(M_Z)$ the analogous low-energy contribution by the three light quarks, $\Delta\alpha_{\text{had}}^{(3)}(1.8 \text{ GeV}) = 56.91 \pm 0.96 \times 10^{-4}$, and by calculating the perturbative and heavy quark contributions to $\hat{\alpha}(M_Z)$ in each call of the fits according to Ref. 14. The uncertainty is from e^+e^- annihilation data below 1.8 GeV and τ decay data, from isospin breaking effects (affecting the interpretation of the τ data); from uncalculated higher order perturbative and non-perturbative QCD corrections; and from the $\overline{\text{MS}}$ quark masses. Such a short distance mass definition (unlike the pole mass) is free from non-perturbative and renormalon uncertainties. Various recent evaluations of $\Delta\alpha_{\text{had}}^{(5)}$

are summarized in Table 10.1, where the relation between the on-shell and $\overline{\text{MS}}$ definitions is given by

$$\Delta\hat{\alpha}(M_Z) - \Delta\alpha(M_Z) = \frac{\alpha}{\pi} \left(\frac{100}{27} - \frac{1}{6} - \frac{7}{4} \ln \frac{M_Z^2}{M_W^2} \right) \approx 0.0072$$

to leading order, where the first term is from fermions and the other two are from W^\pm loops which are usually excluded from the on-shell definition. Most of the older results relied on $e^+e^- \rightarrow$ hadrons cross-section measurements up to energies of 40 GeV, which were somewhat higher than the QCD prediction, suggested stronger running, and were less precise. The most recent results typically assume the validity of perturbative QCD (PQCD) at scales of 1.8 GeV and above, and are in reasonable agreement with each other. (Evaluations in the on-shell scheme utilize resonance data from BES [33] as further input.) There is, however, some discrepancy between analyzes based on $e^+e^- \rightarrow$ hadrons cross-section data and those based on τ decay spectral functions [34–36]. The latter imply lower central values for the extracted M_H of $\mathcal{O}(10$ GeV). The discrepancy originates from the kinematic region $\sqrt{s} \gtrsim 0.6$ GeV. However, at least some of it appears to be experimental. The dominant $e^+e^- \rightarrow \pi^+\pi^-$ cross-section was measured with the CMD-2 [37] and SND [38] detectors at the VEPP-2M e^+e^- collider at Novosibirsk and the results are (after an initial discrepancy due to a flaw in the Monte Carlo event generator used by SND) in good agreement with each other. As an alternative to cross-section scans, one can use the high statistics radiative return events [39] at e^+e^- accelerators operating at resonances such as the Φ or the $\Upsilon(4S)$. The method is systematics dominated. The energy dependence of the $\pi^+\pi^-$ radiative return results from the Φ obtained by the KLOE collaboration [40] differ significantly from what is observed at VEPP-2M. Likewise, the BaBar collaboration [41] studied multi-hadron events radiatively returned from the $\Upsilon(4S)$ and found only partial agreement with previous results. For a recent review on these e^+e^- data, see Ref. 42. All measurements including older data [43] are accounted for in the fits on the basis of results in Refs. [24,34,42,44]. Further improvement of this dominant theoretical uncertainty in the interpretation of precision data will require better measurements of the cross-section for $e^+e^- \rightarrow$ hadrons below the charmonium resonances, as well as in the threshold region of the heavy quarks (to improve the precision in $\hat{m}_c(\hat{m}_c)$ and $\hat{m}_b(\hat{m}_b)$).

- (b) The Fermi constant, $G_F = 1.166367(5) \times 10^{-5} \text{ GeV}^{-2}$, determined from the muon lifetime formula [45,46],

$$\tau_\mu^{-1} = \frac{G_F^2 m_\mu^5}{192\pi^3} F \left(\frac{m_e^2}{m_\mu^2} \right) \left(1 + \frac{3}{5} \frac{m_\mu^2}{M_W^2} \right) \times \left[1 + \left(\frac{25}{8} - \frac{\pi^2}{2} \right) \frac{\alpha(m_\mu)}{\pi} + C_2 \frac{\alpha^2(m_\mu)}{\pi^2} \right], \quad (10.4a)$$

where

$$F(x) = 1 - 8x + 8x^3 - x^4 - 12x^2 \ln x, \quad (10.4b)$$

$$C_2 = \frac{156815}{5184} - \frac{518}{81} \pi^2 - \frac{895}{36} \zeta(3) + \frac{67}{720} \pi^4 + \frac{53}{6} \pi^2 \ln(2), \quad (10.4c)$$

and

$$\alpha(m_\mu)^{-1} = \alpha^{-1} - \frac{2}{3\pi} \ln \left(\frac{m_\mu}{m_e} \right) + \frac{1}{6\pi} \approx 136. \quad (10.4d)$$

The $\mathcal{O}(\alpha^2)$ corrections to μ decay have been completed in Ref. 46. The remaining uncertainty in G_F is from the experimental uncertainty which has recently been halved by the MuLan [47] and FAST [48] collaborations.

- (c) The Z boson mass, $M_Z = 91.1876 \pm 0.0021$ GeV, determined from the Z lineshape scan at LEP 1 [49].

Table 10.1: Recent evaluations of the on-shell $\Delta\alpha_{\text{had}}^{(5)}(M_Z)$. For better comparison we adjusted central values and errors to correspond to a common and fixed value of $\alpha_s(M_Z) = 0.120$. References quoting results without the top quark decoupled are converted to the five flavor definition. Ref. [25] uses $A_{\text{QCD}} = 380 \pm 60$ MeV; for the conversion we assumed $\alpha_s(M_Z) = 0.118 \pm 0.003$.

Reference	Result	Comment
Martin, Zeppenfeld [15]	0.02744 ± 0.00036	PQCD for $\sqrt{s} > 3$ GeV
Eidelman, Jegerlehner [16]	0.02803 ± 0.00065	PQCD for $\sqrt{s} > 40$ GeV
Geshkenbein, Morgunov [17]	0.02780 ± 0.00006	$\mathcal{O}(\alpha_s)$ resonance model
Burkhardt, Pietrzyk [18]	0.0280 ± 0.0007	PQCD for $\sqrt{s} > 40$ GeV
Swartz [19]	0.02754 ± 0.00046	use of fitting function
Aleman <i>et al.</i> [20]	0.02816 ± 0.00062	incl. τ decay data
Krasnikov, Rodenberg [21]	0.02737 ± 0.00039	PQCD for $\sqrt{s} > 2.3$ GeV
Davier & Höcker [22]	0.02784 ± 0.00022	PQCD for $\sqrt{s} > 1.8$ GeV
Kühn & Steinhauser [23]	0.02778 ± 0.00016	complete $\mathcal{O}(\alpha_s^2)$
Erlar [14]	0.02779 ± 0.00020	conv. from $\overline{\text{MS}}$ scheme
Davier & Höcker [24]	0.02770 ± 0.00015	use of QCD sum rules
Groote <i>et al.</i> [25]	0.02787 ± 0.00032	use of QCD sum rules
Martin <i>et al.</i> [26]	0.02741 ± 0.00019	includes new BES data
Burkhardt, Pietrzyk [27]	0.02763 ± 0.00036	PQCD for $\sqrt{s} > 12$ GeV
de Troconiz, Yndurain [28]	0.02754 ± 0.00010	PQCD for $s > 2$ GeV ²
Jegerlehner [29]	0.02765 ± 0.00013	conv. from MOM scheme
Hagiwara <i>et al.</i> [30]	0.02757 ± 0.00023	PQCD for $\sqrt{s} > 11.09$ GeV
Burkhardt, Pietrzyk [31]	0.02760 ± 0.00035	incl. KLOE data
Hagiwara <i>et al.</i> [32]	0.02770 ± 0.00022	incl. selected KLOE data

Table 10.2: Notations used to indicate the various schemes discussed in the text. Each definition of $\sin^2 \theta_W$ leads to values that differ by small factors depending on m_t and M_H . Approximate values are also given for illustration.

Scheme	Notation and Value
On-shell	$s_W^2 = \sin^2 \theta_W \approx 0.2231$
NOV	$s_{M_Z}^2 = \sin^2 \theta_W \approx 0.2311$
$\overline{\text{MS}}$	$\hat{s}_Z^2 = \sin^2 \theta_W \approx 0.2312$
$\overline{\text{MS}}$ ND	$\hat{s}_{\text{ND}}^2 = \sin^2 \theta_W \approx 0.2314$
Effective angle	$\hat{s}_f^2 = \sin^2 \theta_W \approx 0.2315$

With these inputs, $\sin^2 \theta_W$ and the W boson mass, M_W , can be calculated when values for m_t and M_H are given; conversely (as is done at present), M_H can be constrained by $\sin^2 \theta_W$ and M_W . The value of $\sin^2 \theta_W$ is extracted from Z pole observables and neutral-current processes [49–52], and depends on the renormalization prescription. There are a number of popular schemes [53–60] leading to values which differ by small factors depending on m_t and M_H . The notation for these schemes is shown in Table 10.2.

- (i) The on-shell scheme [53] promotes the tree-level formula $\sin^2 \theta_W = 1 - M_W^2/M_Z^2$ to a definition of the renormalized $\sin^2 \theta_W$ to all orders in perturbation theory, *i.e.*, $\sin^2 \theta_W \rightarrow s_W^2 \equiv 1 - M_W^2/M_Z^2$:

$$M_W = \frac{A_0}{s_W(1 - \Delta r)^{1/2}}, \quad (10.5a)$$

$$M_Z = \frac{M_W}{c_W}, \quad (10.5b)$$

where $c_W \equiv \cos \theta_W$, $A_0 = (\pi\alpha/\sqrt{2}G_F)^{1/2} = 37.28057(8)$ GeV, and Δr includes the radiative corrections relating α , $\alpha(M_Z)$, G_F , M_W , and M_Z . One finds $\Delta r \sim \Delta r_0 - \rho_t / \tan^2 \theta_W$, where $\Delta r_0 = 1 - \alpha/\hat{\alpha}(M_Z) = 0.06649(12)$ is due to the running of α , and $\rho_t = 3G_F m_t^2 / 8\sqrt{2}\pi^2 = 0.00915(m_t/170.9 \text{ GeV})^2$ represents the dominant (quadratic) m_t dependence. There are additional contributions to Δr from bosonic loops, including those which depend logarithmically on M_H . One has $\Delta r = 0.0369 \mp 0.0007 \pm 0.00012$, where the second uncertainty is from $\alpha(M_Z)$. Thus the value of s_W^2 extracted from M_Z includes an uncertainty (∓ 0.00023) from the currently allowed range of m_t . This scheme is simple conceptually. However, the relatively large ($\sim 3\%$) correction from ρ_t causes large spurious contributions in higher orders.

- (ii) A more precisely determined quantity $s_{M_Z}^2$ [54] can be obtained from M_Z by removing the (m_t, M_H) dependent term from Δr [55], *i.e.*,

$$s_{M_Z}^2 c_{M_Z}^2 \equiv \frac{\pi\alpha(M_Z)}{\sqrt{2}G_F M_Z^2}. \quad (10.6)$$

Using $\alpha(M_Z)^{-1} = 128.91 \pm 0.02$ yields $s_{M_Z}^2 = 0.23108 \mp 0.00005$. The small uncertainty in $s_{M_Z}^2$ compared to other schemes is because the m_t dependence has been removed by definition. However, the m_t uncertainty reemerges when other quantities (*e.g.*, M_W or other Z pole observables) are predicted in terms of M_Z .

Both s_W^2 and $s_{M_Z}^2$ depend not only on the gauge couplings but also on the spontaneous-symmetry breaking, and both definitions are awkward in the presence of any extension of the SM which perturbs the value of M_Z (or M_W). Other definitions are motivated by the tree-level coupling constant definition $\theta_W = \tan^{-1}(g'/g)$.

- (iii) In particular, the modified minimal subtraction ($\overline{\text{MS}}$) scheme introduces the quantity $\sin^2 \hat{\theta}_W(\mu) \equiv \hat{g}'^2(\mu)/[\hat{g}^2(\mu) + \hat{g}'^2(\mu)]$, where the couplings \hat{g} and \hat{g}' are defined by modified minimal subtraction and the scale μ is conveniently chosen to be M_Z for many electroweak processes. The value of $\hat{s}_Z^2 = \sin^2 \hat{\theta}_W(M_Z)$ extracted from M_Z is less sensitive than s_W^2 to m_t (by a factor of $\tan^2 \theta_W$), and is less sensitive to most types of new physics than s_W^2 or $s_{M_Z}^2$. It is also very useful for comparing with the predictions of grand unification. There are actually several variant definitions of $\sin^2 \hat{\theta}_W(M_Z)$, differing according to whether or how finite $\alpha \ln(m_t/M_Z)$ terms are decoupled (subtracted from the couplings). One cannot entirely decouple the $\alpha \ln(m_t/M_Z)$ terms from all electroweak quantities because $m_t \gg m_b$ breaks SU(2) symmetry. The scheme that will be adopted here decouples the $\alpha \ln(m_t/M_Z)$ terms from the γ - Z mixing [13,56], essentially eliminating any $\ln(m_t/M_Z)$ dependence in the formulae for asymmetries at the Z pole when written in terms of \hat{s}_Z^2 . (A similar definition is used for $\hat{\alpha}$.) The various definitions are related by

$$\hat{s}_Z^2 = c(m_t, M_H) s_W^2 = \bar{c}(m_t, M_H) s_{M_Z}^2, \quad (10.7)$$

where $c = 1.0352 \pm 0.0008$ and $\bar{c} = 1.0012 \mp 0.0003$. The quadratic m_t dependence is given by $c \sim 1 + \rho_t / \tan^2 \theta_W$ and $\bar{c} \sim 1 - \rho_t / (1 - \tan^2 \theta_W)$, respectively. The expressions for M_W and M_Z in the $\overline{\text{MS}}$ scheme are

$$M_W = \frac{A_0}{\hat{s}_Z(1 - \Delta\hat{r}_W)^{1/2}}, \quad (10.8a)$$

$$M_Z = \frac{M_W}{\hat{\rho}^{1/2}\hat{c}_Z}, \quad (10.8b)$$

and one predicts $\Delta\hat{r}_W = 0.06962 \pm 0.00003 \pm 0.00012$. $\Delta\hat{r}_W$ has no quadratic m_t dependence, because shifts in M_W are absorbed into the observed G_F , so that the error in $\Delta\hat{r}_W$ is dominated by $\Delta r_0 = 1 - \alpha/\hat{\alpha}(M_Z)$ which induces the second quoted uncertainty. The quadratic m_t dependence has been shifted into $\hat{\rho} \sim 1 + \rho_t$, where including bosonic loops, $\hat{\rho} = 1.01023 \pm 0.00022$. Quadratic

M_H effects are deferred to two-loop order, while the leading logarithmic M_H effects are dominant only for large M_H values which are currently disfavored by the precision data. As an illustration, the shift in M_W due to a large M_H (for fixed M_Z) is given by

$$\Delta_H M_W = -\frac{11}{96} \frac{\alpha}{\pi} \frac{M_W}{c_W^2 - s_W^2} \ln \frac{M_H^2}{M_W^2} + \mathcal{O}(\alpha^2). \quad (10.9)$$

- (iv) A variant $\overline{\text{MS}}$ quantity \hat{s}_{ND}^2 (used in the 1992 edition of this *Review*) does not decouple the $\alpha \ln(m_t/M_Z)$ terms [57]. It is related to \hat{s}_Z^2 by

$$\hat{s}_Z^2 = \hat{s}_{\text{ND}}^2 / \left(1 + \frac{\hat{\alpha}}{\pi} d\right), \quad (10.10a)$$

$$d = \frac{1}{3} \left(\frac{1}{\hat{s}^2} - \frac{8}{3} \right) \left[\left(1 + \frac{\alpha_s}{\pi}\right) \ln \frac{m_t}{M_Z} - \frac{15\alpha_s}{8\pi} \right], \quad (10.10b)$$

Thus, $\hat{s}_Z^2 - \hat{s}_{\text{ND}}^2 \sim -0.0002$ for $m_t = 172.7$ GeV.

- (v) Yet another definition, the effective angle [58–60] \bar{s}_f^2 for the Z vector coupling to fermion f , is described in Sec. 10.3.

Experiments are at a level of precision that complete $\mathcal{O}(\alpha)$ radiative corrections must be applied. For neutral-current and Z pole processes, these corrections are conveniently divided into two classes:

1. QED diagrams involving the emission of real photons or the exchange of virtual photons in loops, but not including vacuum polarization diagrams. These graphs often yield finite and gauge-invariant contributions to observable processes. However, they are dependent on energies, experimental cuts, *etc.*, and must be calculated individually for each experiment.
2. Electroweak corrections, including $\gamma\gamma$, γZ , ZZ , and WW vacuum polarization diagrams, as well as vertex corrections, box graphs, *etc.*, involving virtual W 's and Z 's. Many of these corrections are absorbed into the renormalized Fermi constant defined in Eq. (10.4). Others modify the tree-level expressions for Z pole observables and neutral-current amplitudes in several ways [50]. One-loop corrections are included for all processes. In addition, certain two-loop corrections are also important. In particular, two-loop corrections involving the top quark modify ρ_t in $\hat{\rho}$, Δr , and elsewhere by

$$\rho_t \rightarrow \rho_t [1 + R(M_H, m_t)\rho_t/3]. \quad (10.11)$$

$R(M_H, m_t)$ is best described as an expansion in M_Z^2/m_t^2 . The unsuppressed terms were first obtained in Ref. 61, and are known analytically [62]. Contributions suppressed by M_Z^2/m_t^2 were first studied in Ref. 63 with the help of small and large Higgs mass expansions, which can be interpolated. These contributions are about as large as the leading ones in Refs. 61 and 62. The complete two-loop calculation of Δr (without further approximation) has been performed in Refs. 64 and 65 for fermionic and purely bosonic diagrams, respectively. Similarly, the electroweak two-loop calculation for the relation between \bar{s}_f^2 and s_W^2 is complete [66] including the recently obtained purely bosonic contribution [67]. For M_H above its lower direct limit, $-17 < R \leq -13$.

Mixed QCD-electroweak contributions to gauge boson self-energies of order $\alpha\alpha_s m_t^2$ [68] and $\alpha\alpha_s^2 m_t^2$ [69] increase the predicted value of m_t by 6%. This is, however, almost entirely an artifact of using the pole mass definition for m_t . The equivalent corrections when using the $\overline{\text{MS}}$ definition $\hat{m}_t(\hat{m}_t)$ increase m_t by less than 0.5%. The subleading $\alpha\alpha_s$ corrections [70] are also included. Further three-loop corrections of order $\alpha\alpha_s^2$ [71], $\alpha^3 m_t^6$ [72,73], and $\alpha^2\alpha_s m_t^4$ (for $M_H = 0$) [72], are rather small. The same is true for $\alpha^3 M_H^4$ [74] corrections unless M_H approaches 1 TeV. Also known are the singlet contributions (pure gluonic intermediate states) of order $\alpha\alpha_s^2$ [75] and $\alpha\alpha_s^3$ [76]. Very recently, the corresponding non-singlet contributions have been computed as well [77].

The leading electroweak two-loop terms for the $Z \rightarrow b\bar{b}$ -vertex of $\mathcal{O}(\alpha^2 m_t^4)$ have been obtained in Refs. 61 and 62, and the mixed QCD-electroweak contributions in Refs. 78 and 79. The $\mathcal{O}(\alpha\alpha_s)$ -vertex corrections involving massless quarks [80] add coherently, resulting in a sizable effect and shift the extracted $\alpha_s(M_Z)$ by $\approx +0.0007$.

Throughout this *Review* we utilize electroweak radiative corrections from the program GAPP [81], which works entirely in the $\overline{\text{MS}}$ scheme, and which is independent of the package ZFITTER [60].

10.3. Cross-section and asymmetry formulae

It is convenient to write the four-fermion interactions relevant to ν -hadron, ν - e , and parity violating e -hadron neutral-current processes in a form that is valid in an arbitrary gauge theory (assuming massless left-handed neutrinos). One has

$$-\mathcal{L}^{\nu\text{Hadron}} = \frac{G_F}{\sqrt{2}} \bar{\nu} \gamma^\mu (1 - \gamma^5) \nu \times \sum_i \left[\epsilon_L(i) \bar{q}_i \gamma_\mu (1 - \gamma^5) q_i + \epsilon_R(i) \bar{q}_i \gamma_\mu (1 + \gamma^5) q_i \right], \quad (10.12)$$

$$-\mathcal{L}^{\nu e} = \frac{G_F}{\sqrt{2}} \bar{\nu}_\mu \gamma^\mu (1 - \gamma^5) \nu_\mu \bar{e} \gamma_\mu (g_V^{\nu e} - g_A^{\nu e} \gamma^5) e \quad (10.13)$$

(for ν_e - e or $\bar{\nu}_e$ - e , the charged-current contribution must be included), and

$$-\mathcal{L}^{e\text{Hadron}} = -\frac{G_F}{\sqrt{2}} \times \sum_i \left[C_{1i} \bar{e} \gamma_\mu \gamma^5 e \bar{q}_i \gamma^\mu q_i + C_{2i} \bar{e} \gamma_\mu e \bar{q}_i \gamma^\mu \gamma^5 q_i \right]. \quad (10.14)$$

(One must add the parity-conserving QED contribution.)

The SM expressions for $\epsilon_{L,R}(i)$, $g_{V,A}^{\nu e}$, and C_{ij} are given in Table 10.3. Note, that $g_{V,A}^{\nu e}$ and the other quantities are coefficients of effective four-Fermi operators, which differ from the quantities defined in Eq. (10.2) in the radiative corrections and in the presence of possible physics beyond the SM.

A precise determination of the on-shell s_W^2 , which depends only very weakly on m_t and M_H , is obtained from deep inelastic scattering (DIS) of neutrinos from (approximately) isoscalar targets [82]. The ratio $R_\nu \equiv \sigma_{\nu N}^{NC} / \sigma_{\nu N}^{CC}$ of neutral- to charged-current cross-sections has been measured to 1% accuracy by the CDHS [83] and CHARM [84] collaborations at CERN. The CCFR [85] collaboration at Fermilab has obtained an even more precise result, so it is important to obtain theoretical expressions for R_ν and $R_{\bar{\nu}} \equiv \sigma_{\bar{\nu} N}^{NC} / \sigma_{\bar{\nu} N}^{CC}$ to comparable accuracy. Fortunately, most of the uncertainties from the strong interactions and neutrino spectra cancel in the ratio. The largest theoretical uncertainty is associated with the c -threshold, which mainly affects σ^{CC} . Using the slow rescaling prescription [86] the central value of $\sin^2 \theta_W$ from CCFR varies as $0.0111(m_c [\text{GeV}] - 1.31)$, where m_c is the effective mass which is numerically close to the $\overline{\text{MS}}$ mass $\hat{m}_c(\hat{m}_c)$, but their exact relation is unknown at higher orders. For $m_c = 1.31 \pm 0.24$ GeV (determined from ν -induced dimuon production [87]) this contributes ± 0.003 to the total uncertainty $\Delta \sin^2 \theta_W \sim \pm 0.004$. (The experimental uncertainty is also ± 0.003 .) This uncertainty largely cancels, however, in the Paschos-Wolfenstein ratio [88],

$$R^- = \frac{\sigma_{\nu N}^{NC} - \sigma_{\bar{\nu} N}^{NC}}{\sigma_{\nu N}^{CC} - \sigma_{\bar{\nu} N}^{CC}}. \quad (10.15)$$

It was measured by Fermilab's NuTeV collaboration [89] for the first time, and required a high-intensity and high-energy anti-neutrino beam.

Table 10.3: Standard Model expressions for the neutral-current parameters for ν -hadron, ν - e , and e -hadron processes. At tree level, $\rho = \kappa = 1$, $\lambda = 0$. If radiative corrections are included, $\rho_{\nu N}^{NC} = 1.0079$, $\hat{\kappa}_{\nu N}(\langle Q^2 \rangle = -20 \text{ GeV}^2) = 0.9971$, $\hat{\kappa}_{\nu N}(\langle Q^2 \rangle = -35 \text{ GeV}^2) = 0.9964$, $\lambda_{uL} = -0.0031$, $\lambda_{dL} = -0.0025$, and $\lambda_{dR} = 2 \lambda_{uR} = 7.5 \times 10^{-5}$. For ν - e scattering, $\rho_{\nu e} = 1.0125$ and $\hat{\kappa}_{\nu e} = 0.9964$ (at $\langle Q^2 \rangle = 0$). For atomic parity violation and the SLAC polarized electron experiment, $\rho'_{eq} = 0.9875$, $\rho_{eq} = 1.0004$, $\hat{\kappa}'_{eq} = 1.0025$, $\hat{\kappa}_{eq} = 1.0298$, $\lambda_{1d} = -2 \lambda_{1u} = 3.6 \times 10^{-5}$, $\lambda_{2u} = -0.0121$ and $\lambda_{2d} = 0.0026$. The dominant m_t dependence is given by $\rho \sim 1 + \rho_t$, while $\hat{\kappa} \sim 1$ ($\overline{\text{MS}}$) or $\kappa \sim 1 + \rho_t / \tan^2 \theta_W$ (on-shell).

Quantity	Standard Model Expression
$\epsilon_L(u)$	$\rho_{\nu N}^{NC} \left(\frac{1}{2} - \frac{2}{3} \hat{\kappa}_{\nu N} \hat{s}_Z^2 \right) + \lambda_{uL}$
$\epsilon_L(d)$	$\rho_{\nu N}^{NC} \left(-\frac{1}{2} + \frac{1}{3} \hat{\kappa}_{\nu N} \hat{s}_Z^2 \right) + \lambda_{dL}$
$\epsilon_R(u)$	$\rho_{\nu N}^{NC} \left(-\frac{2}{3} \hat{\kappa}_{\nu N} \hat{s}_Z^2 \right) + \lambda_{uR}$
$\epsilon_R(d)$	$\rho_{\nu N}^{NC} \left(\frac{1}{3} \hat{\kappa}_{\nu N} \hat{s}_Z^2 \right) + \lambda_{dR}$
$g_V^{\nu e}$	$\rho_{\nu e} \left(-\frac{1}{2} + 2 \hat{\kappa}_{\nu e} \hat{s}_Z^2 \right)$
$g_A^{\nu e}$	$\rho_{\nu e} \left(-\frac{1}{2} \right)$
C_{1u}	$\rho'_{eq} \left(-\frac{1}{2} + \frac{4}{3} \hat{\kappa}'_{eq} \hat{s}_Z^2 \right) + \lambda_{1u}$
C_{1d}	$\rho'_{eq} \left(\frac{1}{2} - \frac{2}{3} \hat{\kappa}'_{eq} \hat{s}_Z^2 \right) + \lambda_{1d}$
C_{2u}	$\rho_{eq} \left(-\frac{1}{2} + 2 \hat{\kappa}_{eq} \hat{s}_Z^2 \right) + \lambda_{2u}$
C_{2d}	$\rho_{eq} \left(\frac{1}{2} - 2 \hat{\kappa}_{eq} \hat{s}_Z^2 \right) + \lambda_{2d}$

A simple zeroth-order approximation is

$$R_\nu = g_L^2 + g_R^2 r, \quad (10.16a)$$

$$R_{\bar{\nu}} = g_L^2 + \frac{g_R^2}{r}, \quad (10.16b)$$

$$R^- = g_L^2 - g_R^2, \quad (10.16c)$$

where

$$g_L^2 \equiv \epsilon_L(u)^2 + \epsilon_L(d)^2 \approx \frac{1}{2} - \sin^2 \theta_W + \frac{5}{9} \sin^4 \theta_W, \quad (10.17a)$$

$$g_R^2 \equiv \epsilon_R(u)^2 + \epsilon_R(d)^2 \approx \frac{5}{9} \sin^4 \theta_W, \quad (10.17b)$$

and $r \equiv \sigma_{\bar{\nu} N}^{CC} / \sigma_{\nu N}^{CC}$ is the ratio of $\bar{\nu}$ and ν charged-current cross-sections, which can be measured directly. (In the simple parton model, ignoring hadron energy cuts, $r \approx (\frac{1}{3} + \epsilon) / (1 + \frac{1}{3}\epsilon)$, where $\epsilon \sim 0.125$ is the ratio of the fraction of the nucleon's momentum carried by anti-quarks to that carried by quarks.) In practice, Eq. (10.16) must be corrected for quark mixing, quark sea effects, c -quark threshold effects, non-isoscalarity, W - Z propagator differences, the finite muon mass, QED and electroweak radiative corrections. Details of the neutrino spectra, experimental cuts, x and Q^2 dependence of structure functions, and longitudinal structure functions enter only at the level of these corrections and therefore lead to very small uncertainties. The CCFR group quotes $s_W^2 = 0.2236 \pm 0.0041$ for $(m_t, M_H) = (175, 150)$ GeV with very little sensitivity to (m_t, M_H) .

The NuTeV collaboration found $s_W^2 = 0.2277 \pm 0.0016$ (for the same reference values), which was 3.0σ higher than the SM prediction. NuTeV also measured [90] the difference between the strange and anti-strange quark momentum distributions, $S^- \equiv \int_0^1 dx x [s(x) - \bar{s}(x)] = 0.00196 \pm 0.00135$, from dimuon events utilizing the first complete next-to-leading order QCD description [91] and

parton distribution functions (PDFs) according to Ref. 92. The magnitude of the central value agrees with the published result [93] but differs in sign. Since S^- is only marginally (at the 1.5σ level) consistent with zero, the initial result (which assumed a symmetric strange quark distribution) needs to be adjusted. The effect of $S^- \neq 0$ on the NuTeV value for s_W^2 has been studied in Ref. 93, and the S^- above translates into a shift $\delta s_W^2 = -0.0014 \pm 0.0010$. Most of the s_W^2 dependence and the NuTeV discrepancy reside in g_L^2 (initially 2.7σ low), which we adjust correspondingly by $\delta g_L^2 = +0.00094 \pm 0.00065$ to arrive at $g_L^2 = 0.3010 \pm 0.0015$. The right-handed coupling, $g_R^2 = 0.0308 \pm 0.0011$ (which is 0.7σ high) and the other ν -DIS data are expected to exhibit shifts as well, but these ought to be less significant since their relative experimental uncertainties are larger. Moreover, the dimuon data simultaneously affect the effective mass m_e and thus the interpretation of all ν -DIS data. In view of these developments and caveats, we consider the NuTeV result and the other ν -DIS data as preliminary until a re-analysis using PDFs including all experimental and theoretical information and correlations has been completed. This is also because of the following three categories [94] of effects within the SM that could cause or contribute to the remaining 1.9σ deviation in g_L^2 . (i) One possibility is that the PDFs violate isospin symmetry at levels much stronger than generally expected [95]. A minimum χ^2 set of PDFs generalized in this sense [96] shows a reduction in the NuTeV discrepancy in s_W^2 by 0.0015. But isospin symmetry violating PDFs are currently not well constrained and within uncertainties the NuTeV anomaly could be accounted for in full or conversely made larger [96]. (ii) Nuclear physics effects by themselves appear too small to explain the NuTeV anomaly [97]. In particular, while nuclear shadowing corrections are likely to affect the interpretation of the NuTeV result [98] at some level, the NuTeV collaboration argues that their data are dominated by values of Q^2 at which nuclear shadowing is expected to be relatively small. The model of Ref. 99 indicates that nuclear shadowing effects differ for CC and NC cross-sections as well as ν and $\bar{\nu}$ (both would affect the extraction of s_W^2), but also that $R_{\bar{\nu}}$ is affected more than R_{ν} , while the anomaly is in the latter. Overall, the model predicts a shift in s_W^2 by ~ 0.001 with a sign corresponding to a reduction of the discrepancy. (iii) The extracted s_W^2 may also shift at the level of the quoted uncertainty when analyzed using the most recent set of QED and electroweak radiative corrections [100,101], as well as QCD corrections to the structure functions [102]. However, their precise impact can be estimated only after the NuTeV data have been analyzed with a new set of PDFs including these new radiative corrections while simultaneously allowing isospin breaking and asymmetric strange seas. A step in this direction was taken in Ref. 103 in which QED induced isospin violations were shown to reduce the discrepancy in s_W^2 by $5\text{--}10 \times 10^{-4}$. Remaining one- and two-loop radiative corrections have been estimated [101] to induce uncertainties in the extracted s_W^2 of ± 0.0004 and ± 0.0003 , respectively. It is well conceivable that various effects add up to bring the NuTeV data in line with the SM prediction. It is likely that the overall uncertainties in g_L^2 and g_R^2 will increase, but at the same time the older ν -DIS results may become more precise when analyzed with better PDFs than were available at the time.

The cross-section in the laboratory system for $\nu_{\mu}e \rightarrow \nu_{\mu}e$ or $\bar{\nu}_{\mu}e \rightarrow \bar{\nu}_{\mu}e$ elastic scattering is

$$\frac{d\sigma_{\nu,\bar{\nu}}}{dy} = \frac{G_F^2 m_e E_{\nu}}{2\pi} \left[(g_V^{\nu e} \pm g_A^{\nu e})^2 + (g_V^{\bar{\nu}e} \mp g_A^{\bar{\nu}e})^2 (1-y)^2 - (g_V^{\nu e 2} - g_A^{\nu e 2}) \frac{y m_e}{E_{\nu}} \right], \quad (10.18)$$

where the upper (lower) sign refers to $\nu_{\mu}(\bar{\nu}_{\mu})$, and $y \equiv T_e/E_{\nu}$ (which runs from 0 to $(1 + m_e/2E_{\nu})^{-1}$) is the ratio of the kinetic energy of the recoil electron to the incident ν or $\bar{\nu}$ energy. For $E_{\nu} \gg m_e$ this yields a total cross-section

$$\sigma = \frac{G_F^2 m_e E_{\nu}}{2\pi} \left[(g_V^{\nu e} \pm g_A^{\nu e})^2 + \frac{1}{3} (g_V^{\bar{\nu}e} \mp g_A^{\bar{\nu}e})^2 \right]. \quad (10.19)$$

The most accurate leptonic measurements [104–107] of $\sin^2 \theta_W$ are from the ratio $R \equiv \sigma_{\nu_{\mu}e}/\sigma_{\bar{\nu}_{\mu}e}$ in which many of the systematic uncertainties cancel. Radiative corrections (other than m_t effects) are small compared to the precision of present experiments and

have negligible effect on the extracted $\sin^2 \theta_W$. The most precise experiment (CHARM II) [106] determined not only $\sin^2 \theta_W$ but $g_{V,A}^{\nu e}$ as well. The cross-sections for $\nu_e e$ and $\bar{\nu}_e e$ may be obtained from Eq. (10.18) by replacing $g_{V,A}^{\nu e}$ by $g_{V,A}^{\nu e} + 1$, where the 1 is due to the charged-current contribution [107,108].

The SLAC polarized-electron experiment [109] measured the parity-violating asymmetry

$$A = \frac{\sigma_R - \sigma_L}{\sigma_R + \sigma_L}, \quad (10.20)$$

where $\sigma_{R,L}$ is the cross-section for the deep-inelastic scattering of a right- or left-handed electron: $e_{R,L}N \rightarrow eX$. In the quark parton model

$$\frac{A}{Q^2} = a_1 + a_2 \frac{1 - (1-y)^2}{1 + (1-y)^2}, \quad (10.21)$$

where $Q^2 > 0$ is the momentum transfer and y is the fractional energy transfer from the electron to the hadrons. For the deuteron or other isoscalar targets, one has, neglecting the s -quark and anti-quarks,

$$a_1 = \frac{3G_F}{5\sqrt{2}\pi\alpha} \left(C_{1u} - \frac{1}{2}C_{1d} \right) \approx \frac{3G_F}{5\sqrt{2}\pi\alpha} \left(-\frac{3}{4} + \frac{5}{3}\sin^2 \theta_W \right), \quad (10.22a)$$

$$a_2 = \frac{3G_F}{5\sqrt{2}\pi\alpha} \left(C_{2u} - \frac{1}{2}C_{2d} \right) \approx \frac{9G_F}{5\sqrt{2}\pi\alpha} \left(\sin^2 \theta_W - \frac{1}{4} \right). \quad (10.22b)$$

In another polarized-electron scattering experiment on deuterons, but in the quasi-elastic kinematic regime, the SAMPLE experiment [110] at MIT-Bates extracted the combination $C_{2u} - C_{2d}$ at Q^2 values of 0.1 GeV^2 and 0.038 GeV^2 . What was actually determined were nucleon form factors from which the quoted results were obtained by the removal of a multi-quark radiative correction. Other linear combinations of the C_{iq} have been determined in polarized-lepton scattering at CERN in μ -C DIS, at Mainz in e -Be (quasi-elastic), and at Bates in e -C (elastic). See the review articles in Refs. 51 and 111 for more details. Recent polarized electron asymmetry experiments, *i.e.*, SAMPLE, the PVA4 experiment at Mainz, and the HAPPEX and G0 experiments at Jefferson Lab, have focussed on the strange quark content of the nucleon. These are reviewed in Ref. 112, where it is shown that they can also provide significant constraints on C_{1u} and C_{1d} which complement those from atomic parity violation.

There are now precise experiments measuring atomic parity violation (APV) in cesium [114,115] (at the 0.4% level [114]), thallium [116], lead [117], and bismuth [118]. The uncertainties associated with atomic wave functions are quite small for cesium [119], and have been reduced to about 0.4%. In the past, the semi-empirical value of the tensor polarizability added another source of theoretical uncertainty [120]. The ratio of the off-diagonal hyperfine amplitude to the polarizability has now been measured directly by the Boulder group [121]. Combined with the precisely known hyperfine amplitude [122] one finds excellent agreement with the earlier results, reducing the overall theory uncertainty to only 0.5% (while slightly increasing the experimental error). An earlier 2.3 σ deviation from the SM (see the year 2000 edition of this *Review*) is now seen at the 1σ level, after the contributions from the Breit interaction have been reevaluated [123], and after the subsequent inclusion of other large and previously underestimated effects [124] (*e.g.*, from QED radiative corrections), and an update of the SM calculation [125] resulted in a vanishing net effect. The theoretical uncertainties are 3% for thallium [126] but larger for the other atoms. The electroweak physics is contained in the “weak charges”, which at tree level are defined by

$$Q_W = -2[C_{1u}(2Z + N) + C_{1d}(Z + 2N)] \approx Z(1 - 4\sin^2 \theta_W) - N. \quad (10.23)$$

The Boulder experiment in cesium also observed the parity-violating weak corrections to the nuclear electromagnetic vertex (the anapole moment [127]).

In the future it could be possible to reduce the theoretical wave function uncertainties by taking the ratios of parity violation in different isotopes [113,128]. There would still be some residual uncertainties from differences in the neutron charge radii, however [129].

Experiments in hydrogen and deuterium are another possibility for reducing the uncertainties [130].

The forward-backward asymmetry for $e^+e^- \rightarrow \ell^+\ell^-$, $\ell = \mu$ or τ , is defined as

$$A_{FB} \equiv \frac{\sigma_F - \sigma_B}{\sigma_F + \sigma_B}, \quad (10.24)$$

where $\sigma_F(\sigma_B)$ is the cross-section for ℓ^- to travel forward (backward) with respect to the e^- direction. A_{FB} and R , the total cross-section relative to pure QED, are given by

$$R = F_1, \quad (10.25)$$

$$A_{FB} = 3F_2/4F_1, \quad (10.26)$$

where

$$F_1 = 1 - 2\chi_0 g_V^e g_V^\ell \cos\delta_R + \chi_0^2 (g_V^{e2} + g_A^{e2}) (g_V^{\ell 2} + g_A^{\ell 2}), \quad (10.27a)$$

$$F_2 = -2\chi_0 g_A^e g_A^\ell \cos\delta_R + 4\chi_0^2 g_A^e g_A^\ell g_V^e g_V^\ell, \quad (10.27b)$$

$$\tan\delta_R = \frac{M_Z \Gamma_Z}{M_Z^2 - s}, \quad (10.28)$$

$$\chi_0 = \frac{G_F}{2\sqrt{2}\pi\alpha} \frac{sM_Z^2}{[(M_Z^2 - s)^2 + M_Z^2\Gamma_Z^2]^{1/2}}, \quad (10.29)$$

and \sqrt{s} is the CM energy. Eq. (10.27) is valid at tree level. If the data are radiatively corrected for QED effects (as described above), then the remaining electroweak corrections can be incorporated [131,132] (in an approximation adequate for existing PEP, PETRA, and TRISTAN data, which are well below the Z pole) by replacing χ_0 by $\chi(s) \equiv (1 + \rho_t)\chi_0(s)\alpha/\alpha(s)$, where $\alpha(s)$ is the running QED coupling, and evaluating g_V in the \overline{MS} scheme. Reviews and formulae for $e^+e^- \rightarrow$ hadrons may be found in Ref. 133.

At LEP 1 and SLC, there were high-precision measurements of various Z pole observables [49,134–139], as summarized in Table 10.5. These include the Z mass and total width, Γ_Z , and partial widths $\Gamma(f\bar{f})$ for $Z \rightarrow f\bar{f}$ where fermion $f = e, \mu, \tau$, hadrons, b , or c . It is convenient to use the variables $M_Z, \Gamma_Z, R_{\ell_i} \equiv \Gamma(\text{had})/\Gamma(\ell_i^+\ell_i^-)$ ($\ell_i = e, \mu, \tau$), $\sigma_{\text{had}} \equiv 12\pi\Gamma(e^+e^-)\Gamma(\text{had})/M_Z^2\Gamma_Z^2$, $R_b \equiv \Gamma(b\bar{b})/\Gamma(\text{had})$, and $R_c \equiv \Gamma(c\bar{c})/\Gamma(\text{had})$, most of which are weakly correlated experimentally. ($\Gamma(\text{had})$ is the partial width into hadrons.) The three values for R_{ℓ_i} are not inconsistent with lepton universality (although R_τ is somewhat low), but we use the general analysis in which the three observables are treated as independent. Similar remarks apply to A_{FB}^{0,ℓ_i} below ($A_{FB}^{0,\tau}$ is somewhat high). $\mathcal{O}(\alpha^3)$ QED corrections introduce a large anti-correlation ($\sim 30\%$) between Γ_Z and σ_{had} . The anti-correlation between R_b and R_c is $\sim 18\%$ [49]. The R_{ℓ_i} are insensitive to m_t except for the $Z \rightarrow b\bar{b}$ vertex and final state corrections and the implicit dependence through $\sin^2\theta_W$. Thus, they are especially useful for constraining α_s . The width for invisible decays [49], $\Gamma(\text{inv}) = \Gamma_Z - 3\Gamma(\ell^+\ell^-) - \Gamma(\text{had}) = 499.0 \pm 1.5$ MeV, can be used to determine the number of neutrino flavors much lighter than $M_Z/2$, $N_\nu = \Gamma(\text{inv})/\Gamma^{\text{theory}}(\nu\bar{\nu}) = 2.985 \pm 0.009$ for $(m_t, M_H) = (170.9, 117)$ GeV.

There were also measurements of various Z pole asymmetries. These include the polarization or left-right asymmetry

$$A_{LR} \equiv \frac{\sigma_L - \sigma_R}{\sigma_L + \sigma_R}, \quad (10.30)$$

where $\sigma_L(\sigma_R)$ is the cross-section for a left-(right)-handed incident electron. A_{LR} was measured precisely by the SLD collaboration at the SLC [135], and has the advantages of being extremely sensitive to $\sin^2\theta_W$ and that systematic uncertainties largely cancel. In addition, the SLD collaboration extracted the final-state couplings A_b, A_c [49], A_s [136], A_τ , and A_μ [137] from left-right forward-backward asymmetries, using

$$A_{LR}^{FB}(f) = \frac{\sigma_{LF}^f - \sigma_{LB}^f - \sigma_{RF}^f + \sigma_{RB}^f}{\sigma_{LF}^f + \sigma_{LB}^f + \sigma_{RF}^f + \sigma_{RB}^f} = \frac{3}{4}A_f, \quad (10.31)$$

where, for example, σ_{LF} is the cross-section for a left-handed incident electron to produce a fermion f traveling in the forward hemisphere. Similarly, A_τ was measured at LEP 1 [49] through the negative total τ polarization, \mathcal{P}_τ , and A_e was extracted from the angular distribution of \mathcal{P}_τ . An equation such as (10.31) assumes that initial state QED corrections, photon exchange, γ - Z interference, the tiny electroweak boxes, and corrections for $\sqrt{s} \neq M_Z$ are removed from the data, leaving the pure electroweak asymmetries. This allows the use of effective tree-level expressions,

$$A_{LR} = A_e P_e, \quad (10.32)$$

$$A_{FB} = \frac{3}{4}A_f \frac{A_e + P_e}{1 + P_e A_e}, \quad (10.33)$$

where

$$A_f \equiv \frac{2\overline{g}_V^f \overline{g}_A^f}{\overline{g}_V^f{}^2 + \overline{g}_A^f{}^2}, \quad (10.34)$$

and

$$\overline{g}_V^f = \sqrt{\rho_f} (t_{3L}^{(f)} - 2q_f \kappa_f \sin^2\theta_W), \quad (10.34b)$$

$$\overline{g}_A^f = \sqrt{\rho_f} t_{3L}^{(f)}. \quad (10.34c)$$

P_e is the initial e^- polarization, so that the second equality in Eq. (10.31) is reproduced for $P_e = 1$, and the Z pole forward-backward asymmetries at LEP 1 ($P_e = 0$) are given by $A_{FB}^{(0,f)} = \frac{3}{4}A_e A_f$ where $f = e, \mu, \tau, b, c, s$ [138], and q , and where $A_{FB}^{(0,q)}$ refers to the hadronic charge asymmetry. Corrections for t -channel exchange and s/t -channel interference cause $A_{FB}^{(0,e)}$ to be strongly anti-correlated with R_e ($\sim 37\%$). The correlation between $A_{FB}^{(0,b)}$ and $A_{FB}^{(0,c)}$ amounts to 15%. The initial state coupling, A_e , was also determined through the left-right charge asymmetry [139] and in polarized Bhabha scattering at the SLC [137]. The forward-backward asymmetry, A_{FB} , for e^+e^- final states in $p\bar{p}$ collisions has been measured by CDF [140] and a value for \overline{s}_Z^2 has been extracted. By varying the invariant mass and the scattering angle (and assuming the electron couplings), the effective Z couplings to light quarks, $\overline{g}_{V,A}^{u,d}$, resulted, as well, but with large uncertainties and mutual correlations. Similar analyses have also been reported by the H1 and Zeus collaborations at HERA [141] and by the LEP collaborations [49].

The electroweak radiative corrections have been absorbed into corrections $\rho_f - 1$ and $\kappa_f - 1$, which depend on the fermion f and on the renormalization scheme. In the on-shell scheme, the quadratic m_t dependence is given by $\rho_f \sim 1 + \rho_t$, $\kappa_f \sim 1 + \rho_t/\tan^2\theta_W$, while in \overline{MS} , $\hat{\rho}_f \sim \hat{\kappa}_f \sim 1$, for $f \neq b$ ($\hat{\rho}_b \sim 1 - \frac{4}{3}\rho_t$, $\hat{\kappa}_b \sim 1 + \frac{2}{3}\rho_t$). In the \overline{MS} scheme the normalization is changed according to $G_F M_Z^2/2\sqrt{2}\pi \rightarrow \hat{\alpha}/4s_Z^2 c_Z^2$. (If one continues to normalize amplitudes by $G_F M_Z^2/2\sqrt{2}\pi$, as in the 1996 edition of this *Review*, then $\hat{\rho}_f$ contains an additional factor of $\hat{\rho}$.) In practice, additional bosonic and fermionic loops, vertex corrections, leading higher order contributions, *etc.*, must be included. For example, in the \overline{MS} scheme one has $\hat{\rho}_\ell = 0.9981$, $\hat{\kappa}_\ell = 1.0013$, $\hat{\rho}_b = 0.9874$, and $\hat{\kappa}_b = 1.0065$. It is convenient to define an effective angle $\overline{s}_Z^2 \equiv \sin^2\theta_{WF} \equiv \hat{\kappa}_f \hat{s}_Z^2 = \kappa_f s_W^2$, in terms of which \overline{g}_V^f and \overline{g}_A^f are given by $\sqrt{\rho_f}$ times their tree-level formulae. Because \overline{g}_V^f is very small, not only $A_{LR}^0 = A_e$, $A_{FB}^{(0,\ell)}$, and \mathcal{P}_τ , but also $A_{FB}^{(0,b)}$, $A_{FB}^{(0,c)}$, $A_{FB}^{(0,s)}$, and the hadronic asymmetries are mainly sensitive to \overline{s}_Z^2 . One finds that $\hat{\kappa}_f$ ($f \neq b$) is almost independent of (m_t, M_H) , so that one can write

$$\overline{s}_Z^2 \sim \hat{s}_Z^2 + 0.00029. \quad (10.35)$$

Thus, the asymmetries determine values of \overline{s}_Z^2 and \hat{s}_Z^2 almost independent of m_t , while the κ 's for the other schemes are m_t dependent.

LEP 2 [142] ran at several energies above the Z pole up to ~ 209 GeV. Measurements were made of a number of observables, including the cross-sections for $e^+e^- \rightarrow f\bar{f}$ for $f = q, \mu^-, \tau^-$, the differential cross-sections and A_{FB} for μ and τ ; R and A_{FB} for b and c ; W branching ratios; and $WW, WW\gamma, ZZ$, single W , and single

Z cross-sections. They are in agreement with the SM predictions, with the exceptions of the total hadronic cross-section (1.7σ high), R_b (2.1σ low), and $A_{FB}(b)$ (1.6σ low). Also, the SM Higgs boson was excluded below a mass of 114.4 GeV at the 95% CL [143].

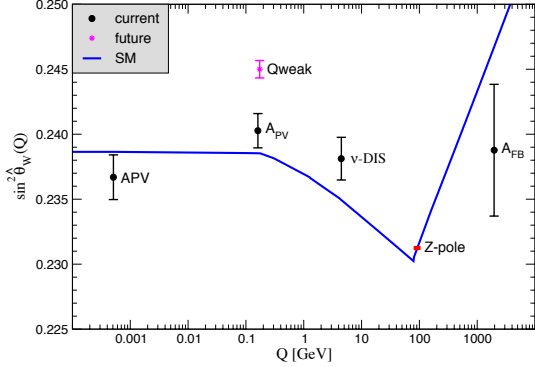


Figure 10.1: Scale dependence of the weak mixing angle defined in the $\overline{\text{MS}}$ scheme [146]. The minimum of the curve corresponds to $Q = M_W$, below which we switch to an effective theory with the W^\pm bosons integrated out, and where the β -function for the weak mixing angle changes sign. At the location of the W boson mass and each fermion mass, there are also discontinuities arising from scheme dependent matching terms which are necessary to ensure that the various effective field theories within a given loop order describe the same physics. However, in the $\overline{\text{MS}}$ scheme these are very small numerically and barely visible in the figure provided one decouples quarks at $Q = \hat{m}_q(\hat{m}_q)$. The width of the curve reflects the theory uncertainty from strong interaction effects which is at the level of $\pm 7 \times 10^{-5}$ [146]. Color version at end of book.

The Z boson properties are extracted assuming the SM expressions for the γ - Z interference terms. These have also been tested experimentally by performing more general fits [142,144] to the LEP 1 and LEP 2 data. Assuming family universality this approach introduces three additional parameters relative to the standard fit [49], describing the γ - Z interference contribution to the total hadronic and leptonic cross-sections, $j_{\text{had}}^{\text{tot}}$ and j_ℓ^{tot} , and to the leptonic forward-backward asymmetry, j_ℓ^{fb} . For example,

$$j_{\text{had}}^{\text{tot}} \sim g_V^\ell g_V^{\text{had}} = 0.277 \pm 0.065, \quad (10.36)$$

which is in good agreement with the SM expectation [49] of 0.21 ± 0.01 . These are valuable tests of the SM; but it should be cautioned that new physics is not expected to be described by this set of parameters, since (i) they do not account for extra interactions beyond the standard weak neutral-current, and (ii) the photonic amplitude remains fixed to its SM value.

Strong constraints on anomalous triple and quartic gauge couplings have been obtained at LEP 2 and at the Tevatron, as are described in the Gauge & Higgs Boson Particle Listings.

The parity violating left-right asymmetry, A_{PV} , in fixed target polarized Møller scattering, $e^-e^- \rightarrow e^-e^-$, is defined as in Eq. (10.30) but with the opposite sign. It has been measured at low $Q^2 = 0.026 \text{ GeV}^2$ in the SLAC E158 experiment [145], with the result $A_{PV} = -1.31 \pm 0.14(\text{stat.}) \pm 0.10(\text{syst.}) \times 10^{-7}$. Expressed in terms of the weak mixing angle in the $\overline{\text{MS}}$ scheme, this yields $\hat{s}^2(Q^2) = 0.2403 \pm 0.0013$, and established the running of the weak mixing (see Fig. 10.1) at the level of 6.4 standard deviations. In a similar experiment and at about the same Q^2 , Qweak at Jefferson Lab [147] will be able to measure $\sin^2 \theta_W$ in polarized ep scattering with a relative precision of 0.3%. These experiments will provide the most precise determinations of the weak mixing angle off the Z peak and will be sensitive to various types of physics beyond the SM.

10.4. W and Z decays

The partial decay width for gauge bosons to decay into massless fermions $f_1 \bar{f}_2$ (the numerical values include the small electroweak radiative corrections and final state mass effects) is

$$\Gamma(W^+ \rightarrow e^+ \nu_e) = \frac{G_F M_W^3}{6\sqrt{2}\pi} \approx 226.20 \pm 0.10 \text{ MeV}, \quad (10.44a)$$

$$\Gamma(W^+ \rightarrow u_i \bar{d}_j) = \frac{CG_F M_W^3}{6\sqrt{2}\pi} |V_{ij}|^2 \approx (705.97 \pm 0.31) |V_{ij}|^2 \text{ MeV}, \quad (10.44b)$$

$$\Gamma(Z \rightarrow \psi_i \bar{\psi}_i) = \frac{CG_F M_Z^3}{6\sqrt{2}\pi} [g_V^{i2} + g_A^{i2}] \quad (10.44c)$$

$$\approx \begin{cases} 300.10 \pm 0.09 \text{ MeV} (u\bar{u}), & 167.18 \pm 0.02 \text{ MeV} (\nu\bar{\nu}), \\ 382.89 \pm 0.08 \text{ MeV} (d\bar{d}), & 83.97 \pm 0.03 \text{ MeV} (e^+e^-), \\ 376.01 \pm 0.05 \text{ MeV} (b\bar{b}). \end{cases}$$

For leptons $C = 1$, while for quarks $C = 3 \left(1 + \alpha_s(M_V)/\pi + 1.409\alpha_s^2/\pi^2 - 12.77\alpha_s^3/\pi^3\right)$, where the 3 is due to color and the factor in parentheses represents the universal part of the QCD corrections [148] for massless quarks [149]. We also included the leading $\mathcal{O}(\alpha_s^4)$ contribution to hadronic Z decays [150]. The $Z \rightarrow f\bar{f}$ widths contain a number of additional corrections: universal (non-singlet) top quark mass contributions [151]; fermion mass effects and further QCD corrections proportional to $\hat{m}_q^2(M_Z^2)$ [152] which are different for vector and axial-vector partial widths; and singlet contributions starting from two-loop order which are large, strongly top quark mass dependent, family universal, and flavor non-universal [153]. All QCD effects are known and included up to three-loop order. The QED factor $1 + 3\alpha q_f^2/4\pi$, as well as two-loop order $\alpha\alpha_s$ and α^2 self-energy corrections [154] are also included. Working in the on-shell scheme, *i.e.*, expressing the widths in terms of $G_F M_{W,Z}^3$, incorporates the largest radiative corrections from the running QED coupling [53,155]. Electroweak corrections to the Z widths are then incorporated by replacing $g_{V,A}^{i2}$ by $\overline{g}_{V,A}^{i2}$. Hence, in the on-shell scheme the Z widths are proportional to $\rho_i \sim 1 + \rho_i$. The $\overline{\text{MS}}$ normalization accounts also for the leading electroweak corrections [58]. There is additional (negative) quadratic m_t dependence in the $Z \rightarrow b\bar{b}$ vertex corrections [156] which causes $\Gamma(b\bar{b})$ to decrease with m_t . The dominant effect is to multiply $\Gamma(b\bar{b})$ by the vertex correction $1 + \delta\rho_{b\bar{b}}$, where $\delta\rho_{b\bar{b}} \sim 10^{-2} \left(-\frac{1}{2} \frac{m_t^2}{M_Z^2} + \frac{1}{5}\right)$. In practice, the corrections are included in ρ_b and κ_b , as discussed before.

For 3 fermion families the total widths are predicted to be

$$\Gamma_Z \approx 2.4952 \pm 0.0004 \text{ GeV}, \quad (10.45)$$

$$\Gamma_W \approx 2.0902 \pm 0.0009 \text{ GeV}. \quad (10.46)$$

We have assumed $\alpha_s(M_Z) = 0.1200$. An uncertainty in α_s of ± 0.0017 introduces an additional uncertainty of 0.05% in the hadronic widths, corresponding to $\pm 0.8 \text{ MeV}$ in Γ_Z . These predictions are to be compared with the experimental results $\Gamma_Z = 2.4952 \pm 0.0023 \text{ GeV}$ [49] and $\Gamma_W = 2.141 \pm 0.041 \text{ GeV}$ (see the Gauge & Higgs Boson Particle Listings for more details).

10.5. Precision flavor physics

In addition to cross-sections, asymmetries, parity violation, W and Z decays, there are a large number of experiments and observables testing the flavor structure of the SM. These are addressed elsewhere in this *Review*, and generally not included in this Section. However, we identify three precision observables with sensitivity to similar types of new physics as the other processes discussed here. The branching fraction of the flavor changing transition $b \rightarrow s\gamma$ is of comparatively low precision, but since it is a loop-level process (in the SM) its sensitivity to new physics (and SM parameters, such as heavy quark masses) is enhanced. The τ -lepton lifetime and leptonic branching ratios are primarily sensitive to α_s and not affected significantly by many types of new physics. However, having an independent and

reliable low-energy measurement of α_s in a global analysis allows the comparison with the Z lineshape determination of α_s which shifts easily in the presence of new physics contributions. By far the most precise observable discussed here is the anomalous magnetic moment of the muon (the electron magnetic moment is measured to even greater precision, but its new physics sensitivity is suppressed by terms proportional to m_e^2/M_Z^2). Its combined experimental and theoretical uncertainty is comparable to typical new physics contributions.

The CLEO [157], Belle [158], and BaBar [159] collaborations reported precise measurements of the process $b \rightarrow s\gamma$. We extrapolated these results to the full photon spectrum which is defined according to the recommendation in Ref. 160. The results for the branching fractions are then given by,

$$\begin{aligned} \text{CLEO} &: 3.34 \times 10^{-4} [1 \pm 0.134 \pm 0.076 \pm 0.038 \pm 0.048 \pm 0.006], \\ \text{Belle} &: 3.59 \times 10^{-4} [1 \pm 0.091_{-0.084}^{+0.081} \pm 0.025 \pm 0.020 \pm 0.006], \\ \text{BaBar} &: 4.01 \times 10^{-4} [1 \pm 0.080 \pm 0.091 \pm 0.079 \pm 0.026 \pm 0.006], \\ \text{BaBar} &: 3.57 \times 10^{-4} [1 \pm 0.055_{-0.122}^{+0.168} \pm 0.000 \pm 0.026 \pm 0.000], \end{aligned}$$

where the first two errors are the statistical and systematic uncertainties (taken uncorrelated). In the case of CLEO, a 3.8% component from the model error of the signal efficiency is moved from the systematic error to the model (third) error. The fourth error accounts for the extrapolation from the finite photon energy cutoff [160–162] (2.0 GeV, 1.815 GeV, and 1.9 GeV, respectively, for CLEO, Belle, and BaBar) to the full theoretical branching ratio. For this we use the results of Ref. 160 for $m_b = 4.70$ GeV which is in good agreement with the more recent Ref. 162. The uncertainty reflects the difference due to choosing $m_b = 4.80$ GeV, instead. The last error is from the correction (0.962 ± 0.006) for the $b \rightarrow d\gamma$ component which is common to all inclusive measurements, but absent for the exclusive BaBar measurement in the last line. The last three errors are taken as 100% correlated, resulting in the correlation matrix in Table 10.4. It is advantageous [163] to normalize the result with respect to the semi-leptonic branching fraction, $\mathcal{B}(b \rightarrow X e \nu) = 0.1024 \pm 0.0015$, yielding,

$$R = \frac{\mathcal{B}(b \rightarrow s\gamma)}{\mathcal{B}(b \rightarrow X e \nu)} = (3.55 \pm 0.30 \pm 0.39) \times 10^{-3}. \quad (10.47)$$

In the fits we use the variable $\ln R = -5.64 \pm 0.14$ to assure an approximately Gaussian error [164]. The second uncertainty in Eq. (10.47) is an 11% theory uncertainty (excluding parametric errors such as from α_s) in the SM prediction which is based on the next-to-leading order calculations of Refs. 163 and 165.

Table 10.4: Correlation matrix for measurements of the $b \rightarrow s\gamma$ transition.

CLEO	1.000	0.092	0.176	0.048
Belle	0.092	1.000	0.136	0.026
BaBar (inclusive)	0.176	0.136	1.000	0.029
BaBar (exclusive)	0.048	0.026	0.029	1.000

The extraction of α_s from the τ lifetime and leptonic branching ratios is standing out from other determinations, because of a variety of independent reasons: (i) the τ -scale is low, so that upon extrapolation to the Z scale (where it can be compared to the theoretically clean Z lineshape determinations) the α_s error shrinks by about an order of magnitude; (ii) yet, this scale is high enough that perturbation theory and the operator product expansion (OPE) can be applied; (iii) these observables are fully inclusive and thus free of fragmentation and hadronization effects that would have to be modeled or measured; (iv) OPE breaking effects are most problematic near the branch cut but there they are suppressed by a double zero at $s = m_c^2$; (v) there are enough data [35] to constrain non-perturbative effects both within and breaking the OPE; (vi) a complete three-loop order QCD calculation is available; (vii) large effects associated with the QCD β -function can be

resummed [166] (in what has become known as contour improvement) and these have been computed to even four-loop precision [167]. The largest uncertainty is from the missing perturbative four and higher loop coefficients (appearing in the Adler- D function). The corresponding effects are highly non-linear so that this uncertainty is itself α_s dependent, updated in each call of the fits, and leading to an asymmetric error. The second largest uncertainty is from the missing perturbative five and higher loop coefficients of the QCD β -function; this induces an uncertainty in the contour improvement which is fully correlated with the renormalization group extrapolation from the τ to the Z scale. The third largest error is from the experimental uncertainty in the lifetime, $\tau_\tau = 290.93 \pm 0.48$ fs, which is from the two leptonic branching ratios and the direct τ_τ . Because of the poor convergence of perturbation theory for strange quark final states, we used for these the experimentally measured branching ratio. Included are also various smaller uncertainties from other sources. In total we obtain a 2% determination of $\alpha_s(M_Z) = 0.1225_{-0.0022}^{+0.0025}$ which updates the result of Ref. 5. For more details, see Ref. 35 where even 1–1.5% uncertainties are advocated (mainly by means of additional assumptions regarding the perturbative four-loop error).

The world average of the muon anomalous magnetic moment**,

$$a_\mu^{\text{exp}} = \frac{g_\mu - 2}{2} = (1165920.80 \pm 0.63) \times 10^{-9}, \quad (10.48)$$

is dominated by the 1999, 2000, and 2001 data runs of the E821 collaboration at BNL [168]. The QED contribution has been calculated to four loops [169] (fully analytically to three loops [170,171]), and the leading logarithms are included to five loops [172,173]. The estimated SM electroweak contribution [174–176], $a_\mu^{\text{EW}} = (1.52 \pm 0.03) \times 10^{-9}$, which includes leading two-loop [175] and three-loop [176] corrections, is at the level of the current uncertainty.

The limiting factor in the interpretation of the result is the uncertainty from the two-loop hadronic contribution. *E.g.*, Ref. 44 uncertainly the value $a_\mu^{\text{had}} = (69.08 \pm 0.44) \times 10^{-9}$ which is dominated by CMD-2 [37] and SND [38] $e^+e^- \rightarrow$ hadrons cross-section data and excludes data from τ decays and KLOE [40]. This value suggests a 3.3 σ discrepancy between Eq. (10.48) and the SM prediction. Updating an alternative analysis [34] the author of Ref. 44 also quotes $a_\mu^{\text{had}} = (71.03 \pm 0.52) \times 10^{-9}$ using τ decay data and isospin symmetry (CVC). This result implies no conflict (0.9 σ) with Eq. (10.48). Thus, there is also a discrepancy between the 2π and 4π spectral functions obtained from the two methods. For example, if one uses the e^+e^- data and CVC to predict the branching ratio for $\tau^- \rightarrow \nu_\tau \pi^- \pi^0$ decays one obtains $24.52 \pm 0.31\%$ [36] (this does not include the SND data) while the average of the measured branching ratios by DELPHI [177], ALEPH, CLEO, L3, and OPAL [34] yields $25.43 \pm 0.09\%$, which is 2.8 σ higher. It is important to understand the origin of this difference, but three observations point to the conclusion that at least some of it is experimental: (i) The $\tau^- \rightarrow \nu_\tau 2\pi^- \pi^+ \pi^0$ spectral function also disagrees with the corresponding e^+e^- data by 3.6 σ , which translates to a 20% effect [44] and seems too large to arise from isospin violation. (ii) Isospin violating corrections have been studied in detail in Ref. 178 and found to be largely under control. The largest effect is due to higher-order electroweak corrections [45] but introduces a negligible uncertainty [179]. (iii) Ref. 180 shows on the basis of a QCD sum rule that the spectral functions derived from τ decay data are consistent with values of $\alpha_s(M_Z) \gtrsim 0.120$, in agreement with what we find from the global fit in Sec. 10.6, while the spectral functions from e^+e^- annihilation are consistent only for somewhat lower (disfavored)

** In what follows, we summarize the most important aspects of $g_\mu - 2$, and give some details about the evaluation in our fits. For more details see the dedicated contribution by A. Höcker and W. Marciano in this *Review*. There are some small numerical differences (at the level of 0.1 standard deviation), which are well understood and mostly arise because internal consistency of the fits requires the calculation of all observables from analytical expressions and common inputs and fit parameters, so that an independent evaluation is necessary for this Section. Note, that in the spirit of a global analysis based on all available information we have chosen here to average in the τ decay and radiative return (KLOE) data, as well.

values. On the other hand, Ref. 181 reevaluated the long-distance electromagnetic radiative corrections to $\tau^- \rightarrow \pi^- \pi^0 \nu$; a model estimate suggests a modest improvement of the conflict. Nevertheless, a_μ^{had} has been evaluated in Refs. 32 and 182 excluding the τ decay data with results which are generally in good agreement with each other and other e^+e^- based analyzes. It is argued [182] that CVC breaking effects (*e.g.*, through a relatively large mass difference between the ρ^\pm and ρ^0 vector mesons) may be larger than expected. (This may also be relevant in the context of the NuTeV discrepancy discussed above [182].) Experimentally [35], this mass difference is indeed larger than expected, but then one would also expect a significant width difference which is contrary to observation [35]. Fortunately, due to the suppression at large s (from where the conflicts originate) these problems are less pronounced as far as a_μ^{had} is concerned. In the following we view all differences in spectral functions as (systematic) fluctuations and average the results.

An additional uncertainty is induced by the hadronic three-loop light-by-light scattering contribution. Two recent and inherently different model calculations yield $a_\mu^{\text{LBS}} = (+1.36 \pm 0.25) \times 10^{-9}$ [183] and $a_\mu^{\text{LBS}} = +1.37^{+0.15}_{-0.27} \times 10^{-9}$ [184] which are higher than previous evaluations [185,186]. The sign of this effect is opposite [185] to the one quoted in the 2002 edition of this *Review*, and has subsequently been confirmed by two other groups [186]. There is also the upper bound $a_\mu^{\text{LBS}} < 1.59 \times 10^{-9}$ [184] but this requires an ad hoc model assumption, too. Other hadronic effects at three-loop order contribute [187], $a_\mu^{\text{had}} \left[\left(\frac{\alpha}{\pi} \right)^3 \right] = (-1.00 \pm 0.06) \times 10^{-9}$. Correlations with the two-loop hadronic contribution and with $\Delta\alpha(M_Z)$ (see Sec. 10.2) were considered in Ref. 171, which also contains analytic results for the perturbative QCD contribution.

The SM prediction is

$$a_\mu^{\text{theory}} = (1165918.81 \pm 0.38) \times 10^{-9}, \quad (10.49)$$

where the error is from the hadronic uncertainties excluding parametric ones such as from α_s and the heavy quark masses. We estimate its correlation with $\Delta\alpha(M_Z)$ to 17%. The overall 2.7 σ discrepancy between the experimental and theoretical values could be due to fluctuations (the E821 result is statistics dominated) or underestimates of the theoretical uncertainties. On the other hand, $g_\mu - 2$ is also affected by many types of new physics, such as supersymmetric models with large $\tan\beta$ and moderately light superparticle masses [188]. Thus, the deviation could also arise from physics beyond the SM.

Table 10.5: Principal Z pole and other observables, compared with the SM best fit predictions (see text). The LEP 1 averages of the ALEPH, DELPHI, L3, and OPAL results include common systematic errors and correlations [49]. The heavy flavor results of LEP 1 and SLD are based on common inputs and correlated, as well [49]. The first $\bar{\kappa}_\ell^2(A_{FB}^{(0,q)})$ is the effective angle extracted from the hadronic charge asymmetry, which has some (neglected) correlation with $A_{FB}^{(0,b)}$; the second $\bar{\kappa}_\ell^2(A_{FB}^{(0,q)})$ is from the lepton asymmetry from CDF [140]. The values of $\Gamma(\ell^+\ell^-)$, $\Gamma(\text{had})$, and $\Gamma(\text{inv})$ are not independent of Γ_Z , the R_ℓ , and σ_{had} . The first M_W value is from UA2, CDF, and DØ [189]; the second one is from LEP 2 [142]. The first M_W and M_Z are correlated, but the effect is negligible due to the tiny M_Z error. The three values of A_e are (i) from A_{LR} for hadronic final states [135]; (ii) from A_{LR} for leptonic final states and from polarized Bhabba scattering [137]; and (iii) from the angular distribution of the τ polarization. The two A_τ values are from SLD and the total τ polarization, respectively. g_L^2 , which has been adjusted to account for an asymmetric strange sea (see Sec. 10.3), and g_R^2 are from NuTeV [89] and have a very small (-1.7%) residual anti-correlation. The older ν -DIS results from CDHS [83], CHARM [84], and CCFR [85] are included, as well, but not shown in the Table. The world averages for $g_{V,A}^{\nu e}$ are dominated by the CHARM II [106] results, $g_V^{\nu e} = -0.035 \pm 0.017$ and $g_A^{\nu e} = -0.503 \pm 0.017$. A_{PV} is the parity violating asymmetry in Møller scattering. The errors in Q_W , DIS, $b \rightarrow s\gamma$, and $g_\mu - 2$ are the total (experimental plus theoretical) uncertainties. The τ_τ value is the τ lifetime world average computed

by combining the direct measurements with values derived from the leptonic branching ratios [5]; the theory uncertainty is included in the SM prediction. In all other SM predictions, the uncertainty is from M_Z , M_H , m_t , m_b , m_c , $\hat{\alpha}(M_Z)$, and α_s , and their correlations have been accounted for. The SM errors in Γ_Z , $\Gamma(\text{had})$, R_ℓ , and σ_{had} are largely dominated by the uncertainty in α_s . The column denoted Pull gives the standard deviations for the principal fit with M_H free, while the column denoted Deviation is for $M_H = 117$ GeV fixed.

Quantity	Value	Standard Model	Pull	Dev.
m_t [GeV]	$170.9 \pm 1.8 \pm 0.6$	171.1 ± 1.9	-0.1	-0.8
M_W [GeV]	80.428 ± 0.039	80.375 ± 0.015	1.4	1.7
	80.376 ± 0.033		0.0	0.5
M_Z [GeV]	91.1876 ± 0.0021	91.1874 ± 0.0021	0.1	-0.1
Γ_Z [GeV]	2.4952 ± 0.0023	2.4968 ± 0.0010	-0.7	-0.5
$\Gamma(\text{had})$ [GeV]	1.7444 ± 0.0020	1.7434 ± 0.0010	-	-
$\Gamma(\text{inv})$ [MeV]	499.0 ± 1.5	501.59 ± 0.08	-	-
$\Gamma(\ell^+\ell^-)$ [MeV]	83.984 ± 0.086	83.988 ± 0.016	-	-
σ_{had} [nb]	41.541 ± 0.037	41.466 ± 0.009	2.0	2.0
R_e	20.804 ± 0.050	20.758 ± 0.011	0.9	1.0
R_μ	20.785 ± 0.033	20.758 ± 0.011	0.8	0.9
R_τ	20.764 ± 0.045	20.803 ± 0.011	-0.9	-0.8
R_b	0.21629 ± 0.00066	0.21584 ± 0.00006	0.7	0.7
R_c	0.1721 ± 0.0030	0.17228 ± 0.00004	-0.1	-0.1
$A_{FB}^{(0,e)}$	0.0145 ± 0.0025	0.01627 ± 0.00023	-0.7	-0.6
$A_{FB}^{(0,\mu)}$	0.0169 ± 0.0013		0.5	0.7
$A_{FB}^{(0,\tau)}$	0.0188 ± 0.0017		1.5	1.6
$A_{FB}^{(0,b)}$	0.0992 ± 0.0016	0.1033 ± 0.0007	-2.5	-2.0
$A_{FB}^{(0,c)}$	0.0707 ± 0.0035	0.0738 ± 0.0006	-0.9	-0.7
$A_{FB}^{(0,s)}$	0.0976 ± 0.0114	0.1034 ± 0.0007	-0.5	-0.4
$\bar{\kappa}_\ell^2(A_{FB}^{(0,q)})$	0.2324 ± 0.0012	0.23149 ± 0.00013	0.8	0.6
	0.2238 ± 0.0050		-1.5	-1.6
A_e	0.15138 ± 0.00216	0.1473 ± 0.0011	1.9	2.4
	0.1544 ± 0.0060		1.2	1.4
	0.1498 ± 0.0049		0.5	0.7
A_μ	0.142 ± 0.015		-0.4	-0.3
A_τ	0.136 ± 0.015		-0.8	-0.7
	0.1439 ± 0.0043		-0.8	-0.5
A_b	0.923 ± 0.020	0.9348 ± 0.0001	-0.6	-0.6
A_c	0.670 ± 0.027	0.6679 ± 0.0005	0.1	0.1
A_s	0.895 ± 0.091	0.9357 ± 0.0001	-0.4	-0.4
g_L^2	0.3010 ± 0.0015	0.30386 ± 0.00018	-1.9	-1.8
g_R^2	0.0308 ± 0.0011	0.03001 ± 0.00003	0.7	0.7
$g_V^{\nu e}$	-0.040 ± 0.015	-0.0397 ± 0.0003	0.0	0.0
$g_A^{\nu e}$	-0.507 ± 0.014	-0.5064 ± 0.0001	0.0	0.0
A_{PV}	$(-1.31 \pm 0.17) \cdot 10^{-7}$	$(-1.54 \pm 0.02) \cdot 10^{-7}$	1.3	1.2
$Q_W(\text{Cs})$	-72.62 ± 0.46	-73.16 ± 0.03	1.2	1.2
$Q_W(\text{TI})$	-116.4 ± 3.6	-116.76 ± 0.04	0.1	0.1
$\frac{\Gamma(b \rightarrow s\gamma)}{\Gamma(b \rightarrow X e \nu)}$	$(3.55^{+0.53}_{-0.46}) \cdot 10^{-3}$	$(3.19 \pm 0.08) \cdot 10^{-3}$	0.8	0.7
$\frac{1}{2}(g_\mu - 2 - \frac{\alpha}{\pi})$	$4511.07(74) \cdot 10^{-9}$	$4509.08(10) \cdot 10^{-9}$	2.7	2.7
τ_τ [fs]	290.93 ± 0.48	291.80 ± 1.76	-0.4	-0.4

10.6. Experimental results

The values of the principal Z pole observables are listed in Table 10.5, along with the SM predictions for $M_Z = 91.1874 \pm 0.0021$ GeV, $M_H = 77_{-22}^{+28}$ GeV, $m_t = 171.1 \pm 1.9$ GeV, $\alpha_s(M_Z) = 0.1217 \pm 0.0017$, and $\hat{\alpha}(M_Z)^{-1} = 127.909 \pm 0.019$ ($\Delta\alpha_{\text{had}}^{(5)} \approx 0.02799 \pm 0.00014$). The predictions result from a global least-square (χ^2) fit to all data using the minimization package MINUIT [190] and the electroweak library GAPP [81]. In most cases, we treat all input errors (the uncertainties of the values) as Gaussian. The reason is not that we assume that theoretical and systematic errors are intrinsically bell-shaped (which they are not) but because in most cases the input errors are combinations of many different (including statistical) error sources, which should yield approximately Gaussian *combined* errors by the large number theorem. Thus, it suffices if either the statistical components dominate or there are many components of similar size. An exception is the theory dominated error on the τ lifetime, which we recalculate in each χ^2 -function call since it depends itself on α_s yielding an asymmetric (and thus non-Gaussian) error bar. Sizes and shapes of the output errors (the uncertainties of the predictions and the SM fit parameters) are fully determined by the fit, and 1σ errors are defined to correspond to $\Delta\chi^2 = \chi^2 - \chi_{\text{min}}^2 = 1$, and do not necessarily correspond to the 68.3% probability range or the 39.3% probability contour (for 2 parameters).

Table 10.6: Principal SM fit result including mutual correlations (all masses in GeV).

M_Z	91.1874 ± 0.0021	1.00	-0.02	0.00	0.00	-0.01	0.00	0.11
$\hat{m}_t(\hat{m}_t)$	161.3 ± 1.8	-0.02	1.00	0.00	0.00	-0.07	-0.01	0.49
$\hat{m}_b(\hat{m}_b)$	4.196 ± 0.028	0.00	0.00	1.00	0.28	-0.04	0.01	0.05
$\hat{m}_c(\hat{m}_c)$	$1.274_{-0.045}^{+0.036}$	0.00	0.00	0.28	1.00	0.08	0.03	0.15
$\alpha_s(M_Z)$	0.1217 ± 0.0017	-0.01	-0.07	-0.04	0.08	1.00	-0.01	-0.06
$\Delta\alpha_{\text{had}}^{(3)}$ (1.8 GeV)	0.00574 ± 0.00010	0.00	-0.01	0.01	0.03	-0.01	1.00	-0.18
M_H	77_{-22}^{+28}	0.11	0.49	0.05	0.15	-0.06	-0.18	1.00

The values and predictions of m_t [6], M_W [142,189]; deep inelastic [89], ν_μ - e [104–106], and polarized Møller scattering [145]; the Q_W for cesium [114,115] and thallium [116]; the $b \rightarrow s\gamma$ observable [157–159]; the muon anomalous magnetic moment [168]; and the τ lifetime are also listed in Table 10.5. The values of M_W and m_t differ from those in the Particle Listings because they include recent preliminary results. The agreement is generally very good. Despite the discrepancies discussed in the following, the goodness of the fit to all data is very reasonable with a $\chi^2/\text{d.o.f.} = 49.4/42$. The probability of a larger χ^2 is 20%. Only the final result for $g_\mu - 2$ from BNL and $A_{FB}^{(0,b)}$ from LEP 1 are currently showing large (2.7 σ and 2.5 σ) deviations. In addition, g_L^2 from NuTeV, the hadronic peak cross-section, σ_{had} (LEP 1), and the A_{LR}^0 (SLD) from hadronic final states differ by about 2 standard deviations. $R_b = \Gamma(b\bar{b})/\Gamma(\text{had})$ whose measured value deviated in the past by as much as 3.7 σ from the SM prediction, is now in agreement.

A_b can be extracted from $A_{FB}^{(0,b)}$ when $A_e = 0.1501 \pm 0.0016$ is taken from a fit to leptonic asymmetries (using lepton universality). The result, $A_b = 0.881 \pm 0.017$, is 3.1 σ below the SM prediction,[†] and also 1.6 σ below $A_b = 0.923 \pm 0.020$ obtained from $A_{LR}^{FB}(b)$ at SLD. Thus, it appears that at least some of the problem in $A_{FB}^{(0,b)}$ is experimental.

[†] Alternatively, one can use $A_\ell = 0.1481 \pm 0.0027$, which is from LEP 1 alone and in excellent agreement with the SM, and obtain $A_b = 0.893 \pm 0.022$ which is 1.9 σ low. This illustrates that some of the discrepancy is related to the one in A_{LR} .

Note, however, that the uncertainty in $A_{FB}^{(0,b)}$ is strongly statistics dominated. The combined value, $A_b = 0.899 \pm 0.013$ deviates by 2.8 σ . It would be extremely difficult to account for this 3.9% deviation by new physics radiative corrections since about a 20% correction to $\hat{\kappa}_b$ would be necessary to account for the central value of A_b . If this deviation is due to new physics, it is most likely of tree-level type affecting preferentially the third generation. Examples include the decay of a scalar neutrino resonance [191], mixing of the b quark with heavy exotics [192], and a heavy Z' with family-nonuniversal couplings [193]. It is difficult, however, to simultaneously account for R_b , which has been measured on the Z peak and off-peak [194] at LEP 1. An average of R_b measurements at LEP 2 at energies between 133 and 207 GeV is 2.1 σ below the SM prediction, while $A_{FB}^{(b)}$ (LEP 2) is 1.6 σ low [142].

The left-right asymmetry, $A_{LR}^0 = 0.15138 \pm 0.00216$ [135], based on all hadronic data from 1992–1998 differs 1.9 σ from the SM expectation of 0.1473 ± 0.0011 . The combined value of $A_\ell = 0.1513 \pm 0.0021$ from SLD (using lepton-family universality and including correlations) is also 1.9 σ above the SM prediction; but there is now experimental agreement between this SLD value and the LEP 1 value, $A_\ell = 0.1481 \pm 0.0027$, obtained from a fit to $A_{FB}^{(0,\ell)}$, $A_e(\mathcal{P}_\tau)$, and $A_\tau(\mathcal{P}_\tau)$, again assuming universality.

The observables in Table 10.5, as well as some other less precise observables, are used in the global fits described below. In all fits, the errors include full statistical, systematic, and theoretical uncertainties. The correlations on the LEP 1 lineshape and τ polarization, the LEP/SLD heavy flavor observables, the SLD lepton asymmetries, and the deep inelastic and ν - e scattering observables, are included. The theoretical correlations between $\Delta\alpha_{\text{had}}^{(5)}$ and $g_\mu - 2$, and between the charm and bottom quark masses, are also accounted for.

The data allow a simultaneous determination of M_Z , M_H , m_t , and the strong coupling $\alpha_s(M_Z)$. (\hat{m}_c , \hat{m}_b , and $\Delta\alpha_{\text{had}}^{(3)}$ are also allowed to float in the fits, subject to the theoretical constraints [5,14] described in Sec. 10.1–Sec. 10.2. These are correlated with α_s .) α_s is determined mainly from R_ℓ , Γ_Z , σ_{had} , and τ_τ and is only weakly correlated with the other variables. The global fit to all data, including the CDF/DØ average $m_t = 170.9 \pm 1.9$ GeV, yields the result in Table 10.6 (the $\overline{\text{MS}}$ top quark mass given there corresponds to $m_t = 171.1 \pm 1.9$ GeV). The weak mixing angle is determined to

$$\hat{s}_Z^2 = 0.23119 \pm 0.00014, \quad s_W^2 = 0.22308 \pm 0.00030,$$

where the larger error in the on-shell scheme is due to the stronger sensitivity to m_t , while the corresponding effective angle is related by Eq. (10.35), *i.e.*, $\overline{s}_Z^2 = 0.23149 \pm 0.00013$.

As described at the beginning of Sec. 10.2 and the paragraph following Eq. (10.48) in Sec. 10.5, there is considerable stress in the experimental e^+e^- spectral functions and also conflict when these are compared with τ decay spectral functions. These are below or above the 2 σ level (depending on what is actually compared) but not much larger than the deviations of some other quantities

entering our analyzes. The number and size of these deviations are not inconsistent with what one would expect to happen as a result of random fluctuations. It is nevertheless instructive to study the effect of doubling the uncertainty in $\Delta\alpha_{\text{had}}^{(3)}(1.8 \text{ GeV}) = 56.91 \pm 0.96 \times 10^{-4}$, (see the beginning of Sec. 10.2) on the extracted Higgs mass. The result, $M_H = 75_{-22}^{+29} \text{ GeV}$, demonstrates that the uncertainty in $\Delta\alpha_{\text{had}}$ is currently of only secondary importance. Note also, that the uncertainty of about ± 0.0001 in $\Delta\alpha_{\text{had}}^{(3)}(1.8 \text{ GeV})$ corresponds to a shift of $\mp 5 \text{ GeV}$ in M_H or about one fifth of its total uncertainty. The hadronic contribution to $\alpha(M_Z)$ is correlated with $g_\mu - 2$ (see Sec. 10.5). The measurement of the latter is higher than the SM prediction, and its inclusion in the fit favors a larger $\alpha(M_Z)$ and a lower M_H (currently by about 3 GeV).

Table 10.7: Values of \hat{s}_Z^2 , s_W^2 , α_s , and M_H [in GeV] for various (combinations of) observables. Unless indicated otherwise, the top quark mass, $m_t = 170.9 \pm 1.9 \text{ GeV}$, is used as an additional constraint in the fits. The (†) symbol indicates a fixed parameter.

Data	\hat{s}_Z^2	s_W^2	$\alpha_s(M_Z)$	M_H
All data	0.23119(14)	0.22308(30)	0.1217(17)	77_{-22}^{+28}
All indirect (no m_t)	0.23123(16)	0.22297(36)	0.1217(17)	104_{-53}^{+130}
Z pole (no m_t)	0.23121(17)	0.22312(59)	0.1198(28)	92_{-46}^{+117}
LEP 1 (no m_t)	0.23152(21)	0.22377(67)	0.1213(30)	173_{-95}^{+241}
SLD + M_Z	0.23067(30)	0.22216(54)	0.1217 (†)	25_{-15}^{+23}
$A_{FB}^{(b,c)} + M_Z$	0.23193(28)	0.22489(75)	0.1217 (†)	326_{-136}^{+224}
$M_W + M_Z$	0.23095(28)	0.22265(55)	0.1217 (†)	49_{-26}^{+37}
M_Z	0.23133(7)	0.22337(21)	0.1217 (†)	117 (†)
polarized Møller	0.2331(14)	0.2252(14)	0.1217 (†)	117 (†)
DIS (isoscalar)	0.2345(17)	0.2267(17)	0.1217 (†)	117 (†)
Q_W (APV)	0.2291(19)	0.2212(19)	0.1217 (†)	117 (†)
elastic $\nu_\mu(\bar{\nu}_\mu)e$	0.2310(77)	0.2232(77)	0.1217 (†)	117 (†)
SLAC eD	0.222(18)	0.213(19)	0.1217 (†)	117 (†)
elastic $\nu_\mu(\bar{\nu}_\mu)p$	0.211(33)	0.203(33)	0.1217 (†)	117 (†)

The weak mixing angle can be determined from Z pole observables, M_W , and from a variety of neutral-current processes spanning a very wide Q^2 range. The results (for the older low-energy neutral-current data see [50,51]) shown in Table 10.7 are in reasonable agreement with each other, indicating the quantitative success of the SM. The largest discrepancy is the value $\hat{s}_Z^2 = 0.23193 \pm 0.00028$ from the forward-backward asymmetries into bottom and charm quarks, which is 2.6 σ above the value 0.23119 ± 0.00014 from the global fit to all data. Similarly, $\hat{s}_Z^2 = 0.23067 \pm 0.00030$ from the SLD asymmetries (in both cases when combined with M_Z) and $\hat{s}_Z^2 = 0.2345 \pm 0.0017$ from DIS are 1.7 σ low and 1.9 σ high, respectively. The SLD result has the additional difficulty (within the SM) of implying very low and excluded [143] Higgs masses. This is also true for $\hat{s}_Z^2 = 0.23095 \pm 0.00028$ from M_W and M_Z and — as a consequence — for the global fit. We have therefore included in Table 10.5 an additional column (denoted Deviation) indicating the deviations if $M_H = 117 \text{ GeV}$ is fixed. The minimum $\chi^2/\text{d.o.f.} = 51.2/41$ (with a probability of 13% for a larger χ^2) is thus worse than for our principal fit.

The extracted Z pole value of $\alpha_s(M_Z)$ is based on a formula with negligible theoretical uncertainty (± 0.0005 in $\alpha_s(M_Z)$) if one assumes the exact validity of the SM. One should keep in mind, however, that this value, $\alpha_s = 0.1198 \pm 0.0028$, is very sensitive to such types of new physics as non-universal vertex corrections. In contrast, the value derived from τ decays, $\alpha_s(M_Z) = 0.1225_{-0.0022}^{+0.0025}$, is theory dominated but less sensitive to new physics. The two values

are in remarkable agreement with each other. They are also in perfect agreement with other recent values, such as from jet-event shapes at LEP [195] (0.1202 ± 0.0050) and the recent average from HERA [196] (0.1198 ± 0.0032), but the τ decay result is somewhat higher than the value, 0.1170 ± 0.0012 , from the most recent unquenched lattice calculation of Ref. 197. For more details and other determinations, see our Section 9 on “Quantum Chromodynamics” in this *Review*.

The data indicate a preference for a small Higgs mass. There is a strong correlation between the quadratic m_t and logarithmic M_H terms in $\hat{\rho}$ in all of the indirect data except for the $Z \rightarrow b\bar{b}$ vertex. Therefore, observables (other than R_b) which favor m_t values higher than the Tevatron range favor lower values of M_H . This effect is enhanced by R_b , which has little direct M_H dependence but favors the lower end of the Tevatron m_t range. M_W has additional M_H dependence through $\Delta\hat{r}_W$ which is not coupled to m_t^2 effects. The strongest individual pulls toward smaller M_H are from M_W and A_{LR}^0 , while $A_{FB}^{(0,b)}$ and the NuTeV results favor high values. The difference in χ^2 for the global fit is $\Delta\chi^2 = \chi^2(M_H = 1000 \text{ GeV}) - \chi_{\text{min}}^2 = 96$. Hence, the data overwhelmingly favor a small value of M_H , as in supersymmetric extensions of the SM. The central value of the global fit result, $M_H = 77_{-22}^{+28} \text{ GeV}$, is below the direct lower bound, $M_H \geq 114.4 \text{ GeV}$ (95% CL) [143].

The 90% central confidence range from all precision data is

$$42 \text{ GeV} \leq M_H \leq 124 \text{ GeV} . \quad (10.50)$$

Including the results of the direct searches [143] as an extra contribution to the likelihood function drives the 95% upper limit to $M_H \leq 161 \text{ GeV}$. As two further refinements, we account for (i) theoretical uncertainties from uncalculated higher order contributions by allowing the T parameter (see next subsection) subject to the constraint $T = 0 \pm 0.02$, (ii) the M_H dependence of the correlation matrix which gives slightly more weight to lower Higgs masses [198]. The resulting limits at 95 (90, 99)% CL are, respectively,

$$M_H \leq 167 \text{ (155, 195) GeV} . \quad (10.51)$$

One can also carry out a fit to the indirect data alone, *i.e.*, without including the constraint, $m_t = 170.9 \pm 1.9 \text{ GeV}$, obtained by CDF and DØ. (The indirect prediction is for the $\overline{\text{MS}}$ mass, $\hat{m}_t(\hat{m}_t) = 164.7_{-7.4}^{+9.6} \text{ GeV}$, which is in the end converted to the pole mass). One obtains $m_t = 174.7_{-7.8}^{+10.0} \text{ GeV}$, in perfect agreement with the direct CDF/DØ average. The tendency for a light Higgs boson also persists when the CDF/DØ constraint on m_t is removed, in which case Eq. (10.50) reads, $37 \text{ GeV} \leq M_H \leq 409 \text{ GeV}$. The relations between M_H and m_t for various observables are shown in Fig. 10.2.

Using $\alpha(M_Z)$ and \hat{s}_Z^2 as inputs, one can predict $\alpha_s(M_Z)$ assuming grand unification. One predicts [199] $\alpha_s(M_Z) = 0.130 \pm 0.001 \pm 0.01$ for the simplest theories based on the minimal supersymmetric extension of the SM, where the first (second) uncertainty is from the inputs (thresholds). This is slightly larger, but consistent with the experimental $\alpha_s(M_Z) = 0.1217 \pm 0.0017$ from the Z lineshape and the τ lifetime, as well as with other determinations. Non-supersymmetric unified theories predict the low value $\alpha_s(M_Z) = 0.073 \pm 0.001 \pm 0.001$. See also the note on “Supersymmetry” in the Searches Particle Listings.

One can also determine the radiative correction parameters Δr : from the global fit one obtains $\Delta r = 0.0356 \pm 0.0009$ and $\Delta\hat{r}_W = 0.06944 \pm 0.00025$. M_W measurements [142,189] (when combined with M_Z) are equivalent to measurements of $\Delta r = 0.0343 \pm 0.0017$, which is 1.0 σ below the result from all other data, $\Delta r = 0.0363 \pm 0.0012$. Fig. 10.3 shows the 1 σ contours in the $M_W - m_t$ plane from the direct and indirect determinations, as well as the combined 90% CL region. The indirect determination uses M_Z from LEP 1 as input, which is defined assuming an s dependent decay width. M_W then corresponds to the s dependent width definition, as well, and can be directly compared with the results from the Tevatron and LEP 2 which have been obtained using the same definition. The difference to a constant width definition is formally only of $\mathcal{O}(\alpha^2)$, but is strongly enhanced since the decay channels add up coherently. It is about 34 MeV for M_Z and 27 MeV for M_W . The residual difference between working consistently with one or the other definition is about 3 MeV, *i.e.*, of typical size for non-enhanced $\mathcal{O}(\alpha^2)$ corrections [64–67].

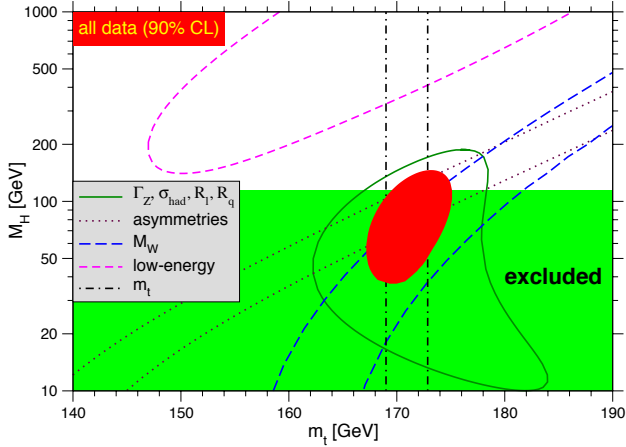


Figure 10.2: One-standard-deviation (39.35%) uncertainties in M_H as a function of m_t for various inputs, and the 90% CL region ($\Delta\chi^2 = 4.605$) allowed by all data. $\alpha_s(M_Z) = 0.120$ is assumed except for the fits including the Z lineshape data. The 95% direct lower limit from LEP 2 is also shown. Color version at end of book.

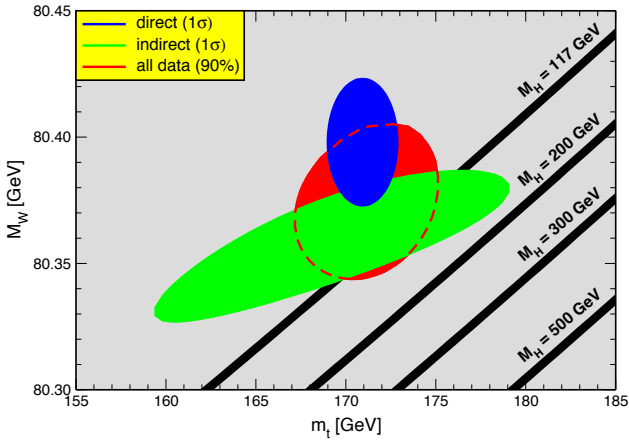


Figure 10.3: One-standard-deviation (39.35%) region in M_W as a function of m_t for the direct and indirect data, and the 90% CL region ($\Delta\chi^2 = 4.605$) allowed by all data. The SM prediction as a function of M_H is also indicated. The widths of the M_H bands reflect the theoretical uncertainty from $\alpha(M_Z)$. Color version at end of book.

Most of the parameters relevant to ν -hadron, ν - e , e -hadron, and e^+e^- processes are determined uniquely and precisely from the data in “model-independent” fits (*i.e.*, fits which allow for an arbitrary electroweak gauge theory). The values for the parameters defined in Eqs. (10.12)–(10.14) are given in Table 10.8 along with the predictions of the SM. The agreement is reasonable, except for the value of g_L^2 , which reflect the discrepancy in the NuTeV results. (The ν -hadron results without the NuTeV data can be found in the 1998 edition of this *Review*, and the fits using the original NuTeV data uncorrected for the strange quark asymmetry in the 2006 edition.). The off Z pole e^+e^- results are difficult to present in a model-independent way because Z propagator effects are non-negligible at TRISTAN, PETRA, PEP, and LEP 2 energies. However, assuming e - μ - τ universality, the low-energy lepton asymmetries imply [133] $4(g_A^e)^2 = 0.99 \pm 0.05$, in good agreement with the SM prediction $\simeq 1$.

Table 10.8: Values of the model-independent neutral-current parameters, compared with the SM predictions. There is a second $g_{V,A}^{\nu e}$ solution, given approximately by $g_{V,A}^{\nu e} \leftrightarrow g_{A,V}^{\nu e}$, which is eliminated by e^+e^- data under the assumption that the neutral current is dominated by the exchange of a single Z boson. The ϵ_L , as well as the ϵ_R , are strongly correlated and non-Gaussian, so that for implementations we recommend the parametrization using g_i^2 and $\theta_i = \tan^{-1}[\epsilon_i(u)/\epsilon_i(d)]$, $i = L$ or R . The analysis of more recent low-energy experiments in polarized electron scattering performed in Ref. 112 is included by means of an additional constraint on the linear combination, $7C_{1u} + 3C_{1d} = -0.254 \pm 0.034$, which reproduces the results [112] on C_{1u} and C_{1d} (including their correlation) almost exactly. In the SM predictions, the uncertainty is from M_Z , M_H , m_t , m_b , m_c , $\hat{\alpha}(M_Z)$, and α_s .

Quantity	Experimental Value	SM	Correlation		
$\epsilon_L(u)$	0.328 ± 0.015	0.3460(1)			
$\epsilon_L(d)$	-0.440 ± 0.011	-0.4291(1)			non-
$\epsilon_R(u)$	$-0.175^{+0.013}_{-0.004}$	-0.1549(1)			Gaussian
$\epsilon_R(d)$	$-0.023^{+0.072}_{-0.048}$	0.0775			
g_L^2	0.3012 ± 0.0013	0.3039(2)	-0.12	-0.22	-0.01
g_R^2	0.0310 ± 0.0010	0.0300		-0.02	-0.03
θ_L	2.50 ± 0.033	2.4630(1)			0.26
θ_R	$4.58^{+0.41}_{-0.28}$	5.1765			
$g_V^{\nu e}$	-0.040 ± 0.015	-0.0397(3)			-0.05
$g_A^{\nu e}$	-0.507 ± 0.014	-0.5064(1)			
$C_{1u} + C_{1d}$	0.1526 ± 0.0013	0.1528(1)	0.49	-0.14	-0.01
$C_{1u} - C_{1d}$	-0.514 ± 0.015	-0.5298(3)		-0.27	-0.02
$C_{2u} + C_{2d}$	-0.23 ± 0.57	-0.0095			-0.30
$C_{2u} - C_{2d}$	-0.077 ± 0.044	-0.0623(5)			

10.7. Constraints on new physics

The Z pole, W mass, and low-energy data can be used to search for and set limits on deviations from the SM. In particular, the combination of these indirect data with the direct CDF and DØ average for m_t allows one to set stringent limits on new physics. We will mainly discuss the effects of exotic particles (with heavy masses $M_{\text{new}} \gg M_Z$ in an expansion in M_Z/M_{new}) on the gauge boson self-energies. (Brief remarks are made on new physics which is not of this type.) Most of the effects on precision measurements can be described by three gauge self-energy parameters S , T , and U . We will define these, as well as related parameters, such as ρ_0 , ϵ_i , and $\hat{\epsilon}_i$, to arise from new physics only. *I.e.*, they are equal to zero ($\rho_0 = 1$) exactly in the SM, and do not include any contributions from m_t or M_H , which are treated separately. Our treatment differs from most of the original papers.

Many extensions of the SM are described by the ρ_0 parameter,

$$\rho_0 \equiv M_W^2 / (M_Z^2 \hat{c}_Z^2 \hat{\rho}), \quad (10.52)$$

which describes new sources of SU(2) breaking that cannot be accounted for by the SM Higgs doublet or m_t effects. In the presence of $\rho_0 \neq 1$, Eq. (10.52) generalizes Eq. (10.8b) while Eq. (10.8a) remains unchanged. Provided that the new physics which yields $\rho_0 \neq 1$ is a small perturbation which does not significantly affect the radiative corrections, ρ_0 can be regarded as a phenomenological parameter which multiplies G_F in Eqs. (10.12)–(10.14), (10.29), and Γ_Z in Eq. (10.44). There are enough data to determine ρ_0 , M_H , m_t , and α_s , simultaneously. From the global fit,

$$\rho_0 = 1.0004^{+0.0008}_{-0.0004}, \quad (10.53)$$

$$114.4 \text{ GeV} \leq M_H \leq 215 \text{ GeV}, \quad (10.54)$$

$$m_t = 171.2 \pm 1.9 \text{ GeV}, \quad (10.55)$$

$$\alpha_s(M_Z) = 0.1215 \pm 0.0017, \quad (10.56)$$

where the lower limit on M_H is the direct search bound. (If the direct limit is ignored one obtains $M_H = 76^{+111}_{-38}$ GeV and $\rho_0 = 1.0000^{+0.0011}_{-0.0007}$.) The error bar in Eq. (10.53) is highly asymmetric: at the 2σ level one has $\rho_0 = 1.0004^{+0.0027}_{-0.0007}$ with no meaningful bound on M_H . The result in Eq. (10.53) is slightly above but consistent with the SM expectation, $\rho_0 = 1$. It can be used to constrain higher-dimensional Higgs representations to have vacuum expectation values of less than a few percent of those of the doublets. Indeed, the relation between M_W and M_Z is modified if there are Higgs multiplets with weak isospin $> 1/2$ with significant vacuum expectation values. In order to calculate to higher orders in such theories one must define a set of four fundamental renormalized parameters which one may conveniently choose to be α , G_F , M_Z , and M_W , since M_W and M_Z are directly measurable. Then \hat{s}_Z^2 and ρ_0 can be considered dependent parameters.

Eq. (10.53) can also be used to constrain other types of new physics. For example, non-degenerate multiplets of heavy fermions or scalars break the vector part of weak SU(2) and lead to a decrease in the value of M_Z/M_W . A non-degenerate SU(2) doublet ($\begin{smallmatrix} f_1 \\ f_2 \end{smallmatrix}$) yields a positive contribution to ρ_0 [200] of

$$\frac{CG_F}{8\sqrt{2}\pi^2} \Delta m^2, \quad (10.57)$$

where

$$\Delta m^2 \equiv m_1^2 + m_2^2 - \frac{4m_1^2 m_2^2}{m_1^2 - m_2^2} \ln \frac{m_1}{m_2} \geq (m_1 - m_2)^2, \quad (10.58)$$

and $C = 1$ (3) for color singlets (triplets). Thus, in the presence of such multiplets, one has

$$\frac{3G_F}{8\sqrt{2}\pi^2} \sum_i \frac{C_i}{3} \Delta m_i^2 = \rho_0 - 1, \quad (10.59)$$

where the sum includes fourth-family quark or lepton doublets, ($\begin{smallmatrix} t' \\ b' \end{smallmatrix}$) or ($\begin{smallmatrix} E^0 \\ E^- \end{smallmatrix}$), and scalar doublets such as ($\begin{smallmatrix} \tilde{t} \\ \tilde{b} \end{smallmatrix}$) in Supersymmetry (in the absence of $L - R$ mixing). This implies

$$\sum_i \frac{C_i}{3} \Delta m_i^2 \leq (98 \text{ GeV})^2 \quad (10.60)$$

at 95% CL. The corresponding constraints on non-degenerate squark and slepton doublets are even stronger, $\sum_i C_i \Delta m_i^2 / 3 \leq (66 \text{ GeV})^2$. This is due to the supersymmetric Higgs mass bound, $m_{h^0} < 150 \text{ GeV}$, and the very strong correlation between m_{h^0} and ρ_0 (91%).

Non-degenerate multiplets usually imply $\rho_0 > 1$. Similarly, heavy Z' bosons decrease the prediction for M_Z due to mixing and generally lead to $\rho_0 > 1$ [201]. On the other hand, additional Higgs doublets which participate in spontaneous symmetry breaking [202], heavy lepton doublets involving Majorana neutrinos [203], and the vacuum expectation values of Higgs triplets or higher-dimensional representations can contribute to ρ_0 with either sign. Allowing for the presence of heavy degenerate chiral multiplets (the S parameter, to be discussed below) affects the determination of ρ_0 from the data, at present leading to a smaller value (for fixed M_H).

A number of authors [204–209] have considered the general effects on neutral-current and Z and W boson observables of various types of heavy (*i.e.*, $M_{\text{new}} \gg M_Z$) physics which contribute to the W and Z self-energies but which do not have any direct coupling to the ordinary fermions. In addition to non-degenerate multiplets, which break the vector part of weak SU(2), these include heavy degenerate multiplets of chiral fermions which break the axial generators. The

effects of one degenerate chiral doublet are small, but in Technicolor theories there may be many chiral doublets and therefore significant effects [204].

Such effects can be described by just three parameters, S , T , and U at the (electroweak) one-loop level. (Three additional parameters are needed if the new physics scale is comparable to M_Z [210]. Further generalizations, including effects relevant to LEP 2, are described in Ref. 211.) T is proportional to the difference between the W and Z self-energies at $Q^2 = 0$ (*i.e.*, vector SU(2)-breaking), while S ($S+U$) is associated with the difference between the Z (W) self-energy at $Q^2 = M_{Z,W}^2$ and $Q^2 = 0$ (axial SU(2)-breaking). Denoting the contributions of new physics to the various self-energies by Π_{ij}^{new} , we have

$$\hat{\alpha}(M_Z)T \equiv \frac{\Pi_{WW}^{\text{new}}(0)}{M_W^2} - \frac{\Pi_{ZZ}^{\text{new}}(0)}{M_Z^2}, \quad (10.61a)$$

$$\begin{aligned} \frac{\hat{\alpha}(M_Z)}{4\hat{s}_Z^2 \hat{c}_Z^2} S \equiv & \frac{\Pi_{ZZ}^{\text{new}}(M_Z^2) - \Pi_{ZZ}^{\text{new}}(0)}{M_Z^2} \\ & - \frac{\hat{c}_Z^2 - \hat{s}_Z^2}{\hat{c}_Z \hat{s}_Z} \frac{\Pi_{Z\gamma}^{\text{new}}(M_Z^2)}{M_Z^2} - \frac{\Pi_{\gamma\gamma}^{\text{new}}(M_Z^2)}{M_Z^2}, \end{aligned} \quad (10.61b)$$

$$\begin{aligned} \frac{\hat{\alpha}(M_Z)}{4\hat{s}_Z^2} (S+U) \equiv & \frac{\Pi_{WW}^{\text{new}}(M_W^2) - \Pi_{WW}^{\text{new}}(0)}{M_W^2} \\ & - \frac{\hat{c}_Z}{\hat{s}_Z} \frac{\Pi_{Z\gamma}^{\text{new}}(M_Z^2)}{M_Z^2} - \frac{\Pi_{\gamma\gamma}^{\text{new}}(M_Z^2)}{M_Z^2}. \end{aligned} \quad (10.61c)$$

S , T , and U are defined with a factor proportional to $\hat{\alpha}$ removed, so that they are expected to be of order unity in the presence of new physics. In the $\overline{\text{MS}}$ scheme as defined in Ref. 56, the last two terms in Eq. (10.61b) and Eq. (10.61c) can be omitted (as was done in some earlier editions of this *Review*). These three parameters are related to other parameters (S_i , h_i , \hat{e}_i) defined in Refs. [56,205,206] by

$$\begin{aligned} T &= h_V = \hat{e}_1 / \alpha, \\ S &= h_{AZ} = S_Z = 4\hat{s}_Z^2 \hat{e}_3 / \alpha, \\ U &= h_{AW} - h_{AZ} = S_W - S_Z = -4\hat{s}_Z^2 \hat{e}_2 / \alpha. \end{aligned} \quad (10.62)$$

A heavy non-degenerate multiplet of fermions or scalars contributes positively to T as

$$\rho_0 - 1 = \frac{1}{1 - \alpha T} - 1 \simeq \alpha T, \quad (10.63)$$

where ρ_0 is given in Eq. (10.59). The effects of non-standard Higgs representations cannot be separated from heavy non-degenerate multiplets unless the new physics has other consequences, such as vertex corrections. Most of the original papers defined T to include the effects of loops only. However, we will redefine T to include all new sources of SU(2) breaking, including non-standard Higgs, so that T and ρ_0 are equivalent by Eq. (10.63).

A multiplet of heavy degenerate chiral fermions yields

$$S = C \sum_i \left(t_{3L}(i) - t_{3R}(i) \right)^2 / 3\pi, \quad (10.64)$$

where $t_{3L,R}(i)$ is the third component of weak isospin of the left-(right)-handed component of fermion i and C is the number of colors. For example, a heavy degenerate ordinary or mirror family would contribute $2/3\pi$ to S . In Technicolor models with QCD-like dynamics, one expects [204] $S \sim 0.45$ for an iso-doublet of techni-fermions, assuming $N_{TC} = 4$ techni-colors, while $S \sim 1.62$ for a full techni-generation with $N_{TC} = 4$; T is harder to estimate because it is model dependent. In these examples one has $S \geq 0$. However, the QCD-like models are excluded on other grounds (flavor changing neutral-currents, and too-light quarks and pseudo-Goldstone bosons [212]). In particular, these estimates do not apply to models of walking Technicolor [212], for which S can be smaller or even negative [213]. Other situations in which $S < 0$, such as loops involving scalars or Majorana particles, are also possible [214]. The simplest origin of $S < 0$ would probably be an additional heavy

Z' boson [201], which could mimic $S < 0$. Supersymmetric extensions of the SM generally give very small effects. See Refs. 164 and 215 and the note on “Supersymmetry” in the Searches Particle Listings for a complete set of references.

Most simple types of new physics yield $U = 0$, although there are counter-examples, such as the effects of anomalous triple gauge vertices [206].

The SM expressions for observables are replaced by

$$\begin{aligned} M_Z^2 &= M_{Z0}^2 \frac{1 - \alpha T}{1 - G_F M_{Z0}^2 S / 2\sqrt{2}\pi}, \\ M_W^2 &= M_{W0}^2 \frac{1}{1 - G_F M_{W0}^2 (S + U) / 2\sqrt{2}\pi}, \end{aligned} \quad (10.65)$$

where M_{Z0} and M_{W0} are the SM expressions (as functions of m_t and M_H) in the $\overline{\text{MS}}$ scheme. Furthermore,

$$\begin{aligned} \Gamma_Z &= \frac{1}{1 - \alpha T} M_Z^3 \beta_Z, \\ \Gamma_W &= M_W^3 \beta_W, \\ A_i &= \frac{1}{1 - \alpha T} A_{i0}, \end{aligned} \quad (10.66)$$

where β_Z and β_W are the SM expressions for the reduced widths Γ_{Z0}/M_{Z0}^3 and Γ_{W0}/M_{W0}^3 , M_Z and M_W are the physical masses, and A_i (A_{i0}) is a neutral-current amplitude (in the SM).

The data allow a simultaneous determination of \hat{s}_Z^2 (from the Z pole asymmetries), S (from M_Z), U (from M_W), T (mainly from Γ_Z), α_s (from R_ℓ , σ_{had} , and τ_τ), and m_t (from CDF and $D\mathcal{O}$), with little correlation among the SM parameters:

$$\begin{aligned} S &= -0.10 \pm 0.10 (-0.08), \\ T &= -0.08 \pm 0.11 (+0.09), \\ U &= 0.15 \pm 0.11 (+0.01), \end{aligned} \quad (10.67)$$

and $\hat{s}_Z^2 = 0.23124 \pm 0.00016$, $\alpha_s(M_Z) = 0.1221 \pm 0.0018$, $m_t = 171.0 \pm 1.9$ GeV, where the uncertainties are from the inputs. The central values assume $M_H = 117$ GeV, and in parentheses we show the difference to assuming $M_H = 300$ GeV instead. As can be seen, the SM parameters (U) can be determined with no (little) M_H dependence. On the other hand, S , T , and M_H cannot be obtained simultaneously, because the Higgs boson loops themselves are resembled approximately by oblique effects. Eqs. (10.67) show that negative (positive) contributions to the S (T) parameter can weaken or entirely remove the strong constraints on M_H from the SM fits. Specific models in which a large M_H is compensated by new physics are reviewed in Ref. 216. The parameters in Eqs. (10.67), which by definition are due to new physics only, are in reasonable agreement with the Standard Model values of zero. Fixing $U = 0$ (as is done in Fig. 10.4) moves S and T to even closer agreement,

$$\begin{aligned} S &= -0.04 \pm 0.09 (-0.07), \\ T &= 0.02 \pm 0.09 (+0.09). \end{aligned} \quad (10.68)$$

The plot of T vs. S produced by the LEP Electroweak Working Group [49] shows larger values**, $S = 0.07$ and $T = 0.13$, based on the Z -pole data and M_W . We almost exactly reproduce their values for the same inputs. The lower values reported here are due to the inclusion of the low-energy data, such as atomic parity violation and neutrino scattering, as well as allowing α_s to float and a different evaluation of $\Delta\alpha^{(5)}(M_Z)$. Our results are consistent with those in Ref. 217.

Using Eq. (10.63) the value of ρ_0 corresponding to T in Eq. (10.67) is $0.9994 \pm 0.0009 (+0.0007)$, while the one corresponding to Eq. (10.68)

** The latest figure dates back to the summer of 2006 and does not contain the first results on M_W from Run II at the Tevatron. We have adjusted the values, $S = 0.04$ and $T = 0.08$, which can be read off the figure, to include the Run II M_W result and to correspond to $M_H = 117$ GeV and the Tevatron $m_t = 170.9$ GeV.

is $1.0002 \pm 0.0007 (+0.0007)$. The values of the $\hat{\epsilon}$ parameters defined in Eq. (10.62) are

$$\begin{aligned} \hat{\epsilon}_3 &= -0.0009 \pm 0.0008 (-0.0006), \\ \hat{\epsilon}_1 &= -0.0006 \pm 0.0009 (+0.0007), \\ \hat{\epsilon}_2 &= -0.0013 \pm 0.0009 (-0.0001). \end{aligned} \quad (10.69)$$

Unlike the original definition, we defined the quantities in Eqs. (10.69) to vanish identically in the absence of new physics and to correspond directly to the parameters S , T , and U in Eqs. (10.67). There is a strong correlation (87%) between the S and T parameters. The allowed region in $S - T$ is shown in Fig. 10.4. From Eqs. (10.67) one obtains $S \leq 0.06 (-0.02)$ and $T \leq 0.10 (0.19)$ at 95% CL for $M_H = 117$ GeV (300 GeV). If one fixes $M_H = 600$ GeV and requires the constraint $S \geq 0$ (as is appropriate in QCD-like Technicolor models) then $S \leq 0.09$ (Bayesian) or $S \leq 0.07$ (frequentist). This rules out simple Technicolor models with many techni-doublets and QCD-like dynamics.

An extra generation of ordinary fermions is excluded at the 6σ level on the basis of the S parameter alone, corresponding to $N_F = 2.71 \pm 0.22$ for the number of families. This result assumes that there are no new contributions to T or U and therefore that any new families are degenerate. This restriction can be relaxed by allowing T to vary as well, since $T > 0$ is expected from a non-degenerate extra family. Fixing $S = 2/3\pi$, the global fit favors a fourth family contribution to T of 0.232 ± 0.045 . However, the quality of the fit deteriorates ($\Delta\chi^2 = 6.8$ relative to the SM fit with M_H fixed to the same value of 117 GeV) so that this tuned T scenario is also disfavored (roughly at the 99% CL). A more detailed analysis is required if the extra neutrino (or the extra down-type quark) is close to its direct mass limit [218]. This can drive S to small or even negative values but at the expense of too-large contributions to T . These results are in agreement with a fit to the number of light neutrinos, $N_\nu = 2.986 \pm 0.007$ (which favors a larger value for $\alpha_s(M_Z) = 0.1237 \pm 0.0021$ mainly from R_ℓ and τ_τ , as well as a very low M_H). However, the S parameter fits are valid even for a very heavy fourth family neutrino.

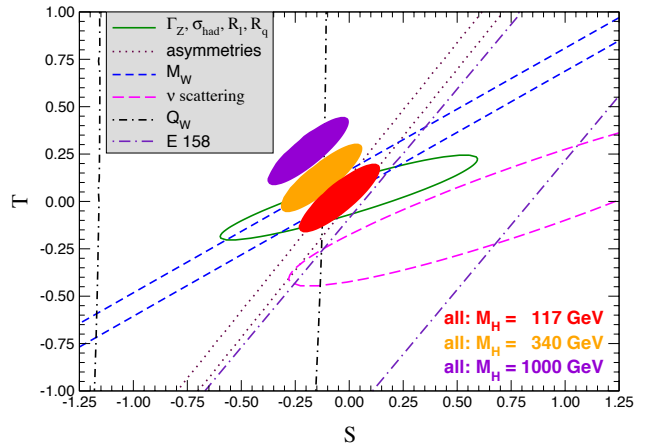


Figure 10.4: 1σ constraints (39.35%) on S and T from various inputs combined with M_Z . S and T represent the contributions of new physics only. (Uncertainties from m_t are included in the errors.) The contours assume $M_H = 117$ GeV except for the central and upper 90% CL contours allowed by all data, which are for $M_H = 340$ GeV and 1000 GeV, respectively. Data sets not involving M_W are insensitive to U . Due to higher order effects, however, $U = 0$ has to be assumed in all fits. α_s is constrained using the τ lifetime as additional input in all fits. Color version at end of book.

There is no simple parametrization that is powerful enough to describe the effects of every type of new physics on every possible observable. The S , T , and U formalism describes many types of heavy physics which affect only the gauge self-energies, and it can be applied to all precision observables. However, new physics which couples directly to ordinary fermions, such as heavy Z' bosons [201] or mixing with exotic fermions [219] cannot be fully parametrized in the S , T , and U framework. It is convenient to treat these types of new physics by parameterizations that are specialized to that particular class of theories (*e.g.*, extra Z' bosons), or to consider specific models (which might contain, *e.g.*, Z' bosons and exotic fermions with correlated parameters). Constraints on various types of new physics are reviewed in Refs. [51,125,220,221].

Fits to Supersymmetric models are described in Refs. 164 and 222. Models involving strong dynamics (such as (extended) Technicolor) for electroweak breaking are considered in Ref. 223. The effects of compactified extra spatial dimensions at the TeV scale are reviewed in Ref. 224, and constraints on Little Higgs models in Ref. 225. Limits on new four-Fermi operators and on leptoquarks using LEP 2 and lower energy data are given in Ref. 142.

An alternate formalism [226] defines parameters, $\epsilon_1, \epsilon_2, \epsilon_3, \epsilon_b$ in terms of the specific observables $M_W/M_Z, \Gamma_{\ell\ell}, A_{FB}^{(0,\ell)}$, and R_b . The definitions coincide with those for $\hat{\epsilon}_i$ in Eqs. (10.61) and (10.62) for physics which affects gauge self-energies only, but the ϵ 's now parametrize arbitrary types of new physics. However, the ϵ 's are not related to other observables unless additional model dependent assumptions are made. Another approach [227] parametrizes new physics in terms of gauge-invariant sets of operators. It is especially powerful in studying the effects of new physics on non-Abelian gauge vertices. The most general approach introduces deviation vectors [220]. Each type of new physics defines a deviation vector, the components of which are the deviations of each observable from its SM prediction, normalized to the experimental uncertainty. The length (direction) of the vector represents the strength (type) of new physics.

Table 10.9: 95% CL lower mass limits (in GeV) from low energy and Z pole data on various extra Z' gauge bosons, appearing in models of unification and string theory. More general parametrizations are described in Ref. 228 and Ref. 232. ρ_0 free indicates a completely arbitrary Higgs sector, while $\rho_0 = 1$ restricts to Higgs doublets and singlets with still unspecified charges. The CDF and DØ bounds [233] from searches for $\bar{p}p \rightarrow e^+e^-$ and the LEP 2 $e^+e^- \rightarrow f\bar{f}$ bounds [142] (assuming $\theta = 0$) are listed in the last three columns, respectively (the Tevatron bounds would be weakened if there are open supersymmetric or exotic decay channels [234]).

Z'	ρ_0 free	$\rho_0 = 1$	CDF	DØ	LEP 2
Z_χ	551	545	822	640	673
Z_ψ	151	146	822	650	481
Z_η	379	365	891	680	434
Z_{LR}	570	564	729(Z_I)	575(Z_I)	804
Z_{SM}	822	809	923	780	1787
Z_{string}	582	578	—	—	—

One of the best motivated kinds of physics beyond the SM besides Supersymmetry are extra Z' bosons [228]. They do not spoil the observed approximate gauge coupling unification, and appear copiously in many Grand Unified Theories (GUTs), most Superstring models [229], as well as in dynamical symmetry breaking [223] and Little Higgs models [225]. For example, the SO(10) GUT contains an extra U(1) as can be seen from its maximal subgroup, $SU(5) \times U(1)_\chi$. Similarly, the E_6 GUT contains the subgroup $SO(10) \times U(1)_\psi$. The Z_ψ possesses only axial-vector couplings to the ordinary fermions, and its mass is generally less constrained. The Z_η boson is the linear combination $\sqrt{3/8}Z_\chi - \sqrt{5/8}Z_\psi$.

The Z_{LR} boson occurs in left-right models with gauge group $SU(3)_C \times SU(2)_L \times SU(2)_R \times U(1)_{B-L} \subset SO(10)$, and the inert Z_I emerges in an alternative E_6 breaking pattern [230]. The sequential Z_{SM} boson is defined to have the same couplings to fermions as the SM Z boson. Such a boson is not expected in the context of gauge theories unless it has different couplings to exotic fermions than the ordinary Z boson. However, it serves as a useful reference case when comparing constraints from various sources. It could also play the role of an excited state of the ordinary Z boson in models with extra dimensions at the weak scale [224]. Finally, we consider a Superstring motivated Z_{string} boson appearing in a specific model [231]. The potential Z' boson is in general a superposition of the SM Z and the new boson associated with the extra U(1). The mixing angle θ satisfies,

$$\tan^2 \theta = \frac{M_{Z_1^0}^2 - M_Z^2}{M_{Z'}^2 - M_{Z_1^0}^2},$$

where $M_{Z_1^0}$ is the SM value for M_Z in the absence of mixing. Note, that $M_Z < M_{Z_1^0}$, and that the SM Z couplings are changed by the mixing. The couplings of the heavier Z' may also be modified by kinetic mixing [228,235]. If the Higgs U(1)' quantum numbers are known, there will be an extra constraint,

$$\theta = C \frac{g_2 M_Z^2}{g_1 M_{Z'}^2}, \quad (10.70)$$

where $g_{1,2}$ are the U(1) and U(1)' gauge couplings with $g_2 = \sqrt{\frac{5}{3}} \sin \theta_W \sqrt{\lambda} g_1$ and $g_1 = \sqrt{g^2 + g'^2}$. $\lambda \sim 1$ (which we assume) if the GUT group breaks directly to $SU(3) \times SU(2) \times U(1) \times U(1)'$. C is a function of vacuum expectation values. For minimal Higgs sectors it can be found in Ref. 201. Table 10.9 shows the 95% CL lower mass limits obtained from a somewhat earlier data set [236] for ρ_0 free and $\rho_0 = 1$, respectively. In cases of specific minimal Higgs sectors where C is known, the Z' mass limits are generally pushed into the TeV region. The limits on $|\theta|$ are typically $< \text{few} \times 10^{-3}$. For more details see [228,236,237] and the note on “The Z' Searches” in the Gauge & Higgs Boson Particle Listings. Also listed in Table 10.9 are the direct lower limits on Z' production from the Tevatron [233] and LEP 2 bounds [142]. The final LEP 1 value for σ_{had} , some previous values for $Q_W(\text{Cs})$, NuTeV, and $A_{FB}^{0,b}$ (for family-nonuniversal couplings [238]) modify the results and might even suggest the possible existence of a Z' [193,239].

Acknowledgments:

This work was supported in part by DGAPA–UNAM contract PAPIIT IN115207, by the Friends of the IAS, and by NSF grant PHT-0503584.

References:

1. S. Weinberg, Phys. Rev. Lett. **19**, 1264 (1967); A. Salam, p. 367 of *Elementary Particle Theory*, ed. N. Svartholm (Almqvist and Wiksells, Stockholm, 1969); S.L. Glashow, J. Iliopoulos, and L. Maiani, Phys. Rev. **D2**, 1285 (1970).
2. CKMfitter Group: J. Charles *et al.*, Eur. Phys. J. **C41**, 1 (2005).
3. For reviews, see G. Barbiellini and C. Santoni, Riv. Nuovo Cimento **9(2)**, 1 (1986); E.D. Commins and P.H. Bucksbaum, *Weak Interactions of Leptons and Quarks*, (Cambridge Univ. Press, Cambridge, 1983); W. Fetscher and H.J. Gerber, p. 657 of Ref. 4; J. Deutsch and P. Quin, p. 706 of Ref. 4; J.M. Conrad, M.H. Shaevitz, and T. Bolton, Rev. Mod. Phys. **70**, 1341 (1998); N. Severijns, M. Beck, and O. Naviliat-Cuncic, Rev. Mod. Phys. **78**, 991 (2006).
4. *Precision Tests of the Standard Electroweak Model*, ed. P. Langacker (World Scientific, Singapore, 1995).
5. J. Erler and M. Luo, Phys. Lett. **B558**, 125 (2003).
6. CDF, DØ, and the Tevatron Electroweak Working Group, hep-ex/0703034.

7. K. Melnikov and T. v. Ritbergen, Phys. Lett. **B482**, 99 (2000).
8. S.J. Brodsky, G.P. Lepage, and P.B. Mackenzie, Phys. Rev. **D28**, 228 (1983).
9. N. Gray *et al.*, Z. Phys. **C48**, 673 (1990).
10. For reviews, see the note on "Searches for Higgs Bosons" in the Gauge and Higgs Boson Listings; J. Gunion *et al.*, *The Higgs Hunter's Guide*, (Addison-Wesley, Redwood City, 1990); M. Sher, Phys. Reports **179**, 273 (1989); M. Carena and H.E. Haber, Prog. Part. Nucl. Phys. **50**, 63 (2003); L. Reina, hep-ph/0512377.
11. CODATA Recommended Values of the Fundamental Physical Constants: 2006, P.J. Mohr, B.N. Taylor, and D.B. Newell (to be published).
12. For a review, see S. Mele, hep-ex/0610037.
13. S. Fanchiotti, B. Kniehl, and A. Sirlin, Phys. Rev. **D48**, 307 (1993) and references therein.
14. J. Erler, Phys. Rev. **D59**, 054008 (1999).
15. A.D. Martin and D. Zeppenfeld, Phys. Lett. **B345**, 558 (1995).
16. S. Eidelman and F. Jegerlehner, Z. Phys. **C67**, 585 (1995).
17. B.V. Geshkenbein and V.L. Morgunov, Phys. Lett. **B340**, 185 (1995); B.V. Geshkenbein and V.L. Morgunov, Phys. Lett. **B352**, 456 (1995).
18. H. Burkhardt and B. Pietrzyk, Phys. Lett. **B356**, 398 (1995).
19. M.L. Swartz, Phys. Rev. **D53**, 5268 (1996).
20. R. Alemany, M. Davier, and A. Höcker, Eur. Phys. J. **C2**, 123 (1998).
21. N.V. Krasnikov and R. Rodenberg, Nuovo Cimento **111A**, 217 (1998).
22. M. Davier and A. Höcker, Phys. Lett. **B419**, 419 (1998).
23. J.H. Kühn and M. Steinhauser, Phys. Lett. **B437**, 425 (1998).
24. M. Davier and A. Höcker, Phys. Lett. **B435**, 427 (1998).
25. S. Groote *et al.*, Phys. Lett. **B440**, 375 (1998).
26. A.D. Martin, J. Outhwaite, and M.G. Ryskin, Phys. Lett. **B492**, 69 (2000).
27. H. Burkhardt and B. Pietrzyk, Phys. Lett. **B513**, 46 (2001).
28. J.F. de Troconiz and F.J. Yndurain, Phys. Rev. **D65**, 093002 (2002).
29. F. Jegerlehner, Nucl. Phys. Proc. Suppl. **126**, 325 (2004).
30. K. Hagiwara *et al.*, Phys. Rev. **D69**, 093003 (2004).
31. H. Burkhardt and B. Pietrzyk, Phys. Rev. **D72**, 057501 (2005).
32. K. Hagiwara *et al.*, Phys. Lett. **B649**, 173 (2007).
33. BES: J.Z. Bai *et al.*, Phys. Rev. Lett. **88**, 101802 (2002); G.S. Huang, hep-ex/0105074.
34. M. Davier *et al.*, Eur. Phys. J. **C31**, 503 (2003).
35. ALEPH: S. Schael *et al.*, Phys. Reports **421**, 191 (2005).
36. M. Davier, A. Höcker, and Z. Zhang, Rev. Mod. Phys. **78**, 1043 (2006).
37. CMD-2: R.R. Akhmetshin *et al.*, Phys. Lett. **B578**, 285 (2004); CMD-2: V.M. Aulchenko *et al.*, JETP Lett. **82**, 743 (2005); CMD-2: R.R. Akhmetshin *et al.*, JETP Lett. **84**, 413 (2006); CMD-2: R. R. Akhmetshin *et al.*, Phys. Lett. **B648**, 28 (2007).
38. SND: M.N. Achasov *et al.*, Sov. Phys. JETP **103**, 380 (2006).
39. A.B. Arbuzov *et al.*, JHEP **9812**, 009 (1998); S. Binner, J.H. Kühn, and K. Melnikov, Phys. Lett. **B459**, 279 (1999).
40. KLOE: F. Ambrosino *et al.*, 0707.4078 [hep-ex].
41. BABAR: B. Aubert *et al.*, Phys. Rev. **D70**, 072004 (2004); BABAR: B. Aubert *et al.*, Phys. Rev. **D71**, 052001 (2005); BABAR: B. Aubert *et al.*, Phys. Rev. **D73**, 052003 (2006); BABAR: B. Aubert *et al.*, 0708.2461 [hep-ex].
42. V.P. Druzhinin, 0710.3455 [hep-ex].
43. See *e.g.*, CMD and OLYA: L.M. Barkov *et al.*, Nucl. Phys. **B256**, 365 (1985).
44. M. Davier, Nucl. Phys. Proc. Suppl. **169**, 288 (2007).
45. W.J. Marciano and A. Sirlin, Phys. Rev. Lett. **61**, 1815 (1988).
46. T. van Ritbergen and R.G. Stuart, Phys. Rev. Lett. **82**, 488 (1999).
47. MuLan: D.B. Chitwood *et al.*, Phys. Rev. Lett. **99**, 032001 (2007).
48. FAST: A. Barczyk *et al.*, 0707.3904 [hep-ex].
49. ALEPH, DELPHI, L3, OPAL, SLD, LEP Electroweak Working Group, SLD Electroweak and Heavy Flavour Groups: S. Schael *et al.*, Phys. Reports **427**, 257 (2006); for updates see <http://lepewwg.web.cern.ch/LEPEWWG/>.
50. Earlier analyses include U. Amaldi *et al.*, Phys. Rev. **D36**, 1385 (1987); G. Costa *et al.*, Nucl. Phys. **B297**, 244 (1988); Deep inelastic scattering is considered by G.L. Fogli and D. Haidt, Z. Phys. **C40**, 379 (1988); P. Langacker and M. Luo, Phys. Rev. **D44**, 817 (1991); For more recent analyses, see Ref. 51.
51. P. Langacker, p. 883 of Ref. 4; J. Erler and P. Langacker, Phys. Rev. **D52**, 441 (1995).
52. J. Erler and M.J. Ramsey-Musolf, Prog. Part. Nucl. Phys. **54**, 351 (2005); Neutrino scattering is reviewed by J.M. Conrad *et al.* in Ref. 3; Nonstandard neutrino interactions are surveyed in Z. Berezhiani and A. Rossi, Phys. Lett. **B535**, 207 (2002); S. Davidson *et al.*, JHEP **0303**, 011 (2003).
53. A. Sirlin, Phys. Rev. **D22**, 971 (1980); A. Sirlin, Phys. Rev. **D29**, 89 (1984); D.C. Kennedy *et al.*, Nucl. Phys. **B321**, 83 (1989); D.C. Kennedy and B.W. Lynn, Nucl. Phys. **B322**, 1 (1989); D.Yu. Bardin *et al.*, Z. Phys. **C44**, 493 (1989); W. Hollik, Fortsch. Phys. **38**, 165 (1990); For reviews, see the articles by W. Hollik, pp. 37 and 117, and W. Marciano, p. 170 in Ref. 4. Extensive references to other papers are given in Ref. 50.
54. V.A. Novikov, L.B. Okun, and M.I. Vysotsky, Nucl. Phys. **B397**, 35 (1993).
55. W. Hollik in Ref. 53 and references therein.
56. W.J. Marciano and J.L. Rosner, Phys. Rev. Lett. **65**, 2963 (1990).
57. G. Degrossi, S. Fanchiotti, and A. Sirlin, Nucl. Phys. **B351**, 49 (1991).
58. G. Degrossi and A. Sirlin, Nucl. Phys. **B352**, 342 (1991).
59. P. Gambino and A. Sirlin, Phys. Rev. **D49**, 1160 (1994).
60. ZFITTER: D. Bardin *et al.*, Comput. Phys. Commun. **133**, 229 (2001) and references therein; ZFITTER: A.B. Arbuzov *et al.*, Comput. Phys. Commun. **174**, 728 (2006).
61. R. Barbieri *et al.*, Phys. Lett. **B288**, 95 (1992) and *ibid.*, **312**, 511(E) (1993); R. Barbieri *et al.*, Nucl. Phys. **B409**, 105 (1993).
62. J. Fleischer, O.V. Tarasov, and F. Jegerlehner, Phys. Lett. **B319**, 249 (1993).
63. G. Degrossi, P. Gambino, and A. Vicini, Phys. Lett. **B383**, 219 (1996); G. Degrossi, P. Gambino, and A. Sirlin, Phys. Lett. **B394**, 188 (1997).
64. A. Freitas *et al.*, Phys. Lett. **B495**, 338 (2000) and *ibid.*, **570**, 260(E) (2003); M. Awramik and M. Czakon, Phys. Lett. **B568**, 48 (2003).
65. A. Freitas *et al.*, Nucl. Phys. **B632**, 189 (2002) and *ibid.*, **666**, 305(E) (2003); M. Awramik and M. Czakon, Phys. Rev. Lett. **89**, 241801 (2002); A. Onishchenko and O. Veretin, Phys. Lett. **B551**, 111 (2003).
66. M. Awramik *et al.*, Phys. Rev. Lett. **93**, 201805 (2004); W. Hollik, U. Meier, and S. Uccirati, Nucl. Phys. **B731**, 213 (2005).
67. M. Awramik, M. Czakon, and A. Freitas, Phys. Lett. **B642**, 563 (2006); M. Awramik, M. Czakon and A. Freitas, JHEP **0611**, 048 (2006); W. Hollik, U. Meier, and S. Uccirati, Nucl. Phys. **B765**, 154 (2007).

68. A. Djouadi and C. Verzegnassi, Phys. Lett. **B195**, 265 (1987); A. Djouadi, Nuovo Cimento **100A**, 357 (1988).
69. K.G. Chetyrkin, J.H. Kühn, and M. Steinhauser, Phys. Lett. **B351**, 331 (1995); L. Avdeev *et al.*, Phys. Lett. **B336**, 560 (1994) and *ibid.*, **B349**, 597(E) (1995).
70. B.A. Kniehl, J.H. Kühn, and R.G. Stuart, Phys. Lett. **B214**, 621 (1988); B.A. Kniehl, Nucl. Phys. **B347**, 86 (1990); F. Halzen and B.A. Kniehl, Nucl. Phys. **B353**, 567 (1991); A. Djouadi and P. Gambino, Phys. Rev. **D49**, 4705 (1994); A. Djouadi and P. Gambino, Phys. Rev. **D49**, 3499 (1994) and *ibid.*, **53**, 4111(E) (1996).
71. K.G. Chetyrkin, J.H. Kühn, and M. Steinhauser, Phys. Rev. Lett. **75**, 3394 (1995).
72. J.J. van der Bij *et al.*, Phys. Lett. **B498**, 156 (2001).
73. M. Faisst *et al.*, Nucl. Phys. **B665**, 649 (2003).
74. R. Boughezal, J.B. Tausk, and J.J. van der Bij, Nucl. Phys. **B713**, 278 (2005); R. Boughezal, J.B. Tausk, and J.J. van der Bij, Nucl. Phys. **B725**, 3 (2005).
75. A. Anselm, N. Dombey, and E. Leader, Phys. Lett. **B312**, 232 (1993).
76. Y. Schröder and M. Steinhauser, Phys. Lett. **B622**, 124 (2005).
77. K.G. Chetyrkin *et al.*, Phys. Rev. Lett. **97**, 102003 (2006); R. Boughezal and M. Czakon, Nucl. Phys. **B755**, 221 (2006).
78. J. Fleischer *et al.*, Phys. Lett. **B293**, 437 (1992); K.G. Chetyrkin, A. Kwiatkowski, and M. Steinhauser, Mod. Phys. Lett. **A8**, 2785 (1993).
79. R. Harlander, T. Seidensticker, and M. Steinhauser, Phys. Lett. **B426**, 125 (1998); J. Fleischer *et al.*, Phys. Lett. **B459**, 625 (1999).
80. A. Czarnecki and J.H. Kühn, Phys. Rev. Lett. **77**, 3955 (1996).
81. J. Erler, hep-ph/0005084.
82. For reviews, see F. Perrier, p. 385 of Ref. 4; J.M. Conrad *et al.* in Ref. 3.
83. CDHS: H. Abramowicz *et al.*, Phys. Rev. Lett. **57**, 298 (1986); CDHS: A. Blondel *et al.*, Z. Phys. **C45**, 361 (1990).
84. CHARM: J.V. Allaby *et al.*, Phys. Lett. **B177**, 446 (1986); CHARM: J.V. Allaby *et al.*, Z. Phys. **C36**, 611 (1987).
85. CCFR: C.G. Arroyo *et al.*, Phys. Rev. Lett. **72**, 3452 (1994); CCFR: K.S. McFarland *et al.*, Eur. Phys. J. **C1**, 509 (1998).
86. R.M. Barnett, Phys. Rev. **D14**, 70 (1976); H. Georgi and H.D. Politzer, Phys. Rev. **D14**, 1829 (1976).
87. LAB-E: S.A. Rabinowitz *et al.*, Phys. Rev. Lett. **70**, 134 (1993).
88. E.A. Paschos and L. Wolfenstein, Phys. Rev. **D7**, 91 (1973).
89. NuTeV: G. P. Zeller *et al.*, Phys. Rev. Lett. **88**, 091802 (2002).
90. NuTeV: D. Mason *et al.*, presented at DIS 2006, Tsukuba.
91. S. Kretzer, D. Mason, and F. Olness, Phys. Rev. **D65**, 074010 (2002).
92. J. Pumplin *et al.*, JHEP **0207**, 012 (2002); S. Kretzer *et al.*, Phys. Rev. Lett. **93**, 041802 (2004).
93. NuTeV: G.P. Zeller *et al.*, Phys. Rev. **D65**, 111103 (2002) and *ibid.*, **D67**, 119902(E) (2003).
94. For reviews including discussions of possible new physics explanations, see S. Davidson *et al.*, JHEP **0202**, 037 (2002); J.T. Londergan, Eur. Phys. J. **A32**, 415 (2007).
95. E. Sather, Phys. Lett. **B274**, 433 (1992); E.N. Rodionov, A.W. Thomas, and J.T. Londergan, Mod. Phys. Lett. **A9**, 1799 (1994).
96. A.D. Martin *et al.*, Eur. Phys. J. **C35**, 325 (2004).
97. S. Kumano, Phys. Rev. **D66**, 111301 (2002); S.A. Kulagin, Phys. Rev. **D67**, 091301 (2003); M. Hirai, S. Kumano, and T. H. Nagai, Phys. Rev. **D71**, 113007 (2005).
98. G.A. Miller and A.W. Thomas, Int. J. Mod. Phys. A **20**, 95 (2005).
99. S.J. Brodsky, I. Schmidt, and J.J. Yang, Phys. Rev. **D70**, 116003 (2004).
100. K.P.O. Diener, S. Dittmaier, and W. Hollik, Phys. Rev. **D69**, 073005 (2004); A.B. Arbuzov, D.Y. Bardin, and L.V. Kalinovskaya, JHEP **0506**, 078 (2005).
101. K.P.O. Diener, S. Dittmaier, and W. Hollik, Phys. Rev. **D72**, 093002 (2005).
102. B.A. Dobrescu and R.K. Ellis, Phys. Rev. **D69**, 114014 (2004).
103. A.D. Martin *et al.*, Eur. Phys. J. **C39**, 155 (2005).
104. CHARM: J. Dorenbosch *et al.*, Z. Phys. **C41**, 567 (1989).
105. CALO: L.A. Ahrens *et al.*, Phys. Rev. **D41**, 3297 (1990).
106. CHARM II: P. Vilain *et al.*, Phys. Lett. **B335**, 246 (1994).
107. For a review, see J. Panman, p. 504 of Ref. 4.
108. ILM: R.C. Allen *et al.*, Phys. Rev. **D47**, 11 (1993); LSND: L.B. Auerbach *et al.*, Phys. Rev. **D63**, 112001 (2001).
109. SSF: C.Y. Prescott *et al.*, Phys. Lett. **B84**, 524 (1979).
110. E. J. Beise, M. L. Pitt and D. T. Spayde, Prog. Part. Nucl. Phys. **54**, 289 (2005).
111. P. Souder, p. 599 of Ref. 4.
112. R.D. Young *et al.*, Phys. Rev. Lett. **99**, 122003 (2007).
113. For reviews and references to earlier work, see M.A. Bouchiat and L. Pottier, Science **234**, 1203 (1986); B.P. Masterson and C.E. Wieman, p. 545 of Ref. 4.
114. Cesium (Boulder): C.S. Wood *et al.*, Science **275**, 1759 (1997).
115. Cesium (Paris): J. Guéna, M. Lintz, and M.A. Bouchiat, physics/0412017.
116. Thallium (Oxford): N.H. Edwards *et al.*, Phys. Rev. Lett. **74**, 2654 (1995); Thallium (Seattle): P.A. Vetter *et al.*, Phys. Rev. Lett. **74**, 2658 (1995).
117. Lead (Seattle): D.M. Meekhof *et al.*, Phys. Rev. Lett. **71**, 3442 (1993).
118. Bismuth (Oxford): M.J.D. MacPherson *et al.*, Phys. Rev. Lett. **67**, 2784 (1991).
119. V.A. Dzuba, V.V. Flambaum, and O.P. Sushkov, Phys. Lett. **141A**, 147 (1989); S.A. Blundell, J. Sapirstein, and W.R. Johnson, Phys. Rev. Lett. **65**, 1411 (1990); S.A. Blundell, J. Sapirstein, and W.R. Johnson, Phys. Rev. **D45**, 1602 (1992); For reviews, see S.A. Blundell, W.R. Johnson, and J. Sapirstein, p. 577 of Ref. 4; J.S.M. Ginges and V.V. Flambaum, Phys. Reports **397**, 63 (2004); J. Guena, M. Lintz, and M. A. Bouchiat, Mod. Phys. Lett. **A20**, 375 (2005); A. Derevianko and S.G. Porsev, Eur. Phys. J. A **32**, 517 (2007).
120. V.A. Dzuba, V.V. Flambaum, and O.P. Sushkov, Phys. Rev. **A56**, R4357 (1997).
121. S.C. Bennett and C.E. Wieman, Phys. Rev. Lett. **82**, 2484 (1999).
122. M.A. Bouchiat and J. Guéna, J. Phys. (France) **49**, 2037 (1988).
123. A. Derevianko, Phys. Rev. Lett. **85**, 1618 (2000); V.A. Dzuba, C. Harabati, and W.R. Johnson, Phys. Rev. **A63**, 044103 (2001); M.G. Kozlov, S.G. Porsev, and I.I. Tupitsyn, Phys. Rev. Lett. **86**, 3260 (2001).
124. A.I. Milstein and O.P. Sushkov, Phys. Rev. **A66**, 022108 (2002); W.R. Johnson, I. Bednyakov, and G. Soff, Phys. Rev. Lett. **87**, 233001 (2001); V.A. Dzuba, V.V. Flambaum, and J.S. Ginges, Phys. Rev. **D66**, 076013 (2002); M.Y. Kuchiev and V.V. Flambaum, Phys. Rev. Lett. **89**, 283002 (2002); A.I. Milstein, O.P. Sushkov, and I.S. Terekhov, Phys. Rev. Lett. **89**, 283003 (2002); V.V. Flambaum and J.S.M. Ginges, Phys. Rev. **A72**, 052115 (2005).
125. J. Erler, A. Kurylov, and M.J. Ramsey-Musolf, Phys. Rev. **D68**, 016006 (2003).
126. V.A. Dzuba *et al.*, J. Phys. **B20**, 3297 (1987).
127. Ya.B. Zel'dovich, Sov. Phys. JETP **6**, 1184 (1958); For recent discussions, see V.V. Flambaum and D.W. Murray,

- Phys. Rev. **C56**, 1641 (1997);
W.C. Haxton and C.E. Wieman, Ann. Rev. Nucl. Part. Sci. **51**, 261 (2001).
128. J.L. Rosner, Phys. Rev. **D53**, 2724 (1996).
129. S.J. Pollock, E.N. Fortson, and L. Willets, Phys. Rev. **C46**, 2587 (1992);
B.Q. Chen and P. Vogel, Phys. Rev. **C48**, 1392 (1993).
130. R.W. Dunford and R.J. Holt, J. Phys. **G34**, 2099 (2007).
131. B.W. Lynn and R.G. Stuart, Nucl. Phys. **B253**, 216 (1985).
132. *Physics at LEP*, ed. J. Ellis and R. Peccei, CERN 86-02, Vol. 1.
133. PETRA: S.L. Wu, Phys. Reports **107**, 59 (1984);
C. Kiesling, *Tests of the Standard Theory of Electroweak Interactions*, (Springer-Verlag, New York, 1988);
R. Marshall, Z. Phys. **C43**, 607 (1989);
Y. Mori *et al.*, Phys. Lett. **B218**, 499 (1989);
D. Haidt, p. 203 of Ref. 4.
134. For reviews, see D. Schaile, p. 215, and A. Blondel, p. 277 of Ref. 4.
135. SLD: K. Abe *et al.*, Phys. Rev. Lett. **84**, 5945 (2000).
136. SLD: K. Abe *et al.*, Phys. Rev. Lett. **85**, 5059 (2000).
137. SLD: K. Abe *et al.*, Phys. Rev. Lett. **86**, 1162 (2001).
138. DELPHI: P. Abreu *et al.*, Z. Phys. **C67**, 1 (1995);
OPAL: K. Ackerstaff *et al.*, Z. Phys. **C76**, 387 (1997).
139. SLD: K. Abe *et al.*, Phys. Rev. Lett. **78**, 17 (1997).
140. CDF: D. Acosta *et al.*, Phys. Rev. **D71**, 052002 (2005).
141. H1: A. Aktas *et al.*, Phys. Lett. **B632**, 35 (2006);
H1 and ZEUS: K. Wichmann *et al.*, 0707.2724 [hep-ex].
142. ALEPH, DELPHI, L3, OPAL, and LEP Electroweak Working Group: J. Alcazar *et al.*, hep-ex/0612034.
143. ALEPH, DELPHI, L3, OPAL, and the LEP Working Group for Higgs Boson Searches: D. Abbaneo *et al.*, Phys. Lett. **B565**, 61 (2003).
144. A. Leike, T. Riemann, and J. Rose, Phys. Lett. **B273**, 513 (1991);
T. Riemann, Phys. Lett. **B293**, 451 (1992).
145. E158: P.L. Anthony *et al.*, Phys. Rev. Lett. **95**, 081601 (2005);
the implications are discussed in A. Czarnecki and W.J. Marciano, Int. J. Mod. Phys. A **15**, 2365 (2000).
146. J. Erler and M.J. Ramsey-Musolf, Phys. Rev. **D72**, 073003 (2005);
for the scale dependence of the weak mixing angle defined in a mass-dependent renormalization scheme, see A. Czarnecki and W.J. Marciano, Int. J. Mod. Phys. A **15**, 2365 (2000).
147. Qweak: W.T.H. van Oers, 0708.1972 [nucl-ex];
the implications are discussed in Ref. 125.
148. A comprehensive report and further references can be found in K.G. Chetyrkin, J.H. Kühn, and A. Kwiatkowski, Phys. Reports **277**, 189 (1996).
149. J. Schwinger, *Particles, Sources, and Fields*, Vol. II, (Addison-Wesley, New York, 1973);
K.G. Chetyrkin, A.L. Kataev, and F.V. Tkachev, Phys. Lett. **B85**, 277 (1979);
M. Dine and J. Sapirstein, Phys. Rev. Lett. **43**, 668 (1979);
W. Celmaster and R.J. Gonsalves, Phys. Rev. Lett. **44**, 560 (1980);
S.G. Gorishnii, A.L. Kataev, and S.A. Larin, Phys. Lett. **B212**, 238 (1988);
S.G. Gorishnii, A.L. Kataev, and S.A. Larin, Phys. Lett. **B259**, 144 (1991);
L.R. Surguladze and M.A. Samuel, Phys. Rev. Lett. **66**, 560 (1991) and *ibid.*, 2416(E).
150. A.L. Kataev and V.V. Starshenko, Mod. Phys. Lett. **A10**, 235 (1995).
151. W. Bernreuther and W. Wetzel, Z. Phys. **11**, 113 (1981);
W. Bernreuther and W. Wetzel, Phys. Rev. **D24**, 2724 (1982);
B.A. Kniehl, Phys. Lett. **B237**, 127 (1990);
K.G. Chetyrkin, Phys. Lett. **B307**, 169 (1993);
A.H. Hoang *et al.*, Phys. Lett. **B338**, 330 (1994);
S.A. Larin, T. van Ritbergen, and J.A.M. Vermaseren, Nucl. Phys. **B438**, 278 (1995).
152. T.H. Chang, K.J.F. Gaemers, and W.L. van Neerven, Nucl. Phys. **B202**, 407 (1980);
J. Jersak, E. Laermann, and P.M. Zerwas, Phys. Lett. **B98**, 363 (1981);
J. Jersak, E. Laermann, and P.M. Zerwas, Phys. Rev. **D25**, 1218 (1982);
S.G. Gorishnii, A.L. Kataev, and S.A. Larin, Nuovo Cimento **92**, 117 (1986);
K.G. Chetyrkin and J.H. Kühn, Phys. Lett. **B248**, 359 (1990);
K.G. Chetyrkin, J.H. Kühn, and A. Kwiatkowski, Phys. Lett. **B282**, 221 (1992);
K.G. Chetyrkin and J.H. Kühn, Phys. Lett. **B406**, 102 (1997).
153. B.A. Kniehl and J.H. Kühn, Phys. Lett. **B224**, 229 (1990);
B.A. Kniehl and J.H. Kühn, Nucl. Phys. **B329**, 547 (1990);
K.G. Chetyrkin and A. Kwiatkowski, Phys. Lett. **B305**, 285 (1993);
K.G. Chetyrkin and A. Kwiatkowski, Phys. Lett. **B319**, 307 (1993);
S.A. Larin, T. van Ritbergen, and J.A.M. Vermaseren, Phys. Lett. **B320**, 159 (1994);
K.G. Chetyrkin and O.V. Tarasov, Phys. Lett. **B327**, 114 (1994).
154. A.L. Kataev, Phys. Lett. **B287**, 209 (1992).
155. D. Albert *et al.*, Nucl. Phys. **B166**, 460 (1980);
F. Jegerlehner, Z. Phys. **C32**, 425 (1986);
A. Djouadi, J.H. Kühn, and P.M. Zerwas, Z. Phys. **C46**, 411 (1990);
A. Borrelli *et al.*, Nucl. Phys. **B333**, 357 (1990).
156. A.A. Akhundov, D.Yu. Bardin, and T. Riemann, Nucl. Phys. **B276**, 1 (1986);
W. Beenakker and W. Hollik, Z. Phys. **C40**, 141 (1988);
B.W. Lynn and R.G. Stuart, Phys. Lett. **B352**, 676 (1990);
J. Bernabeu, A. Pich, and A. Santamaria, Nucl. Phys. **B363**, 326 (1991).
157. CLEO: S. Chen *et al.*, Phys. Rev. Lett. **87**, 251807 (2001).
158. Belle: P. Koppenburg *et al.*, Phys. Rev. Lett. **93**, 061803 (2004).
159. BaBar: B. Aubert *et al.*, hep-ex/0507001;
BaBar: B. Aubert *et al.*, Phys. Rev. **D72**, 052004 (2005).
160. A.L. Kagan and M. Neubert, Eur. Phys. J. **C7**, 5 (1999).
161. A. Ali and C. Greub, Phys. Lett. **B259**, 182 (1991).
162. I. Bigi and N. Uraltsev, Int. J. Mod. Phys. A **17**, 4709 (2002).
163. A. Czarnecki and W.J. Marciano, Phys. Rev. Lett. **81**, 277 (1998).
164. J. Erler and D.M. Pierce, Nucl. Phys. **B526**, 53 (1998).
165. Y. Nir, Phys. Lett. **B221**, 184 (1989);
K. Adel and Y.P. Yao, Phys. Rev. **D49**, 4945 (1994);
C. Greub, T. Hurth, and D. Wyler, Phys. Rev. **D54**, 3350 (1996);
K.G. Chetyrkin, M. Misiak, and M. Münz, Phys. Lett. **B400**, 206 (1997);
C. Greub and T. Hurth, Phys. Rev. **D56**, 2934 (1997);
M. Ciuchini *et al.*, Nucl. Phys. **B527**, 21 (1998);
M. Ciuchini *et al.*, Nucl. Phys. **B534**, 3 (1998);
F.M. Borzumati and C. Greub, Phys. Rev. **D58**, 074004 (1998);
F.M. Borzumati and C. Greub, Phys. Rev. **D59**, 057501 (1999);
A. Strumia, Nucl. Phys. **B532**, 28 (1998).
166. F. Le Diberder and A. Pich, Phys. Lett. **B286**, 147 (1992).
167. T. van Ritbergen, J.A.M. Vermaseren, and S.A. Larin, Phys. Lett. **B400**, 379 (1997).
168. E821: H.N. Brown *et al.*, Phys. Rev. Lett. **86**, 2227 (2001);
E821: G.W. Bennett, *et al.*, Phys. Rev. Lett. **89**, 101804 (2002);
E821: G.W. Bennett *et al.*, Phys. Rev. Lett. **92**, 161802 (2004).
169. T. Kinoshita and M. Nio, Phys. Rev. **D70**, 113001 (2004);
M. Passera, J. Phys. **G31**, R75 (2005);
T. Kinoshita, Nucl. Phys. Proc. Suppl. **144**, 206 (2005).
170. G. Li, R. Mendel, and M.A. Samuel, Phys. Rev. **D47**, 1723 (1993);
S. Laporta and E. Remiddi, Phys. Lett. **B301**, 440 (1993);
S. Laporta and E. Remiddi, Phys. Lett. **B379**, 283 (1996);
A. Czarnecki and M. Skrzypek, Phys. Lett. **B449**, 354 (1999).

171. J. Erler and M. Luo, Phys. Rev. Lett. **87**, 071804 (2001).
172. A.L. Kataev, Nucl. Phys. Proc. Suppl. **155**, 369 (2006);
T. Kinoshita and M. Nio, Phys. Rev. **D73**, 053007 (2006).
173. For reviews, see V.W. Hughes and T. Kinoshita, Rev. Mod. Phys. **71**, S133 (1999);
A. Czarnecki and W.J. Marciano, Phys. Rev. **D64**, 013014 (2001);
T. Kinoshita, J. Phys. **G29**, 9 (2003);
M. Davier and W.J. Marciano, Ann. Rev. Nucl. Part. Sci. **54**, 115 (2004);
J.P. Miller, E. de Rafael, and B.L. Roberts, Rept. Prog. Phys. **70**, 795 (2007);
F. Jegerlehner, Acta Phys. Polon. **B38**, 3021 (2007).
174. S.J. Brodsky and J.D. Sullivan, Phys. Rev. **D156**, 1644 (1967);
T. Burnett and M.J. Levine, Phys. Lett. **B24**, 467 (1967);
R. Jackiw and S. Weinberg, Phys. Rev. **D5**, 2473 (1972);
I. Bars and M. Yoshimura, Phys. Rev. **D6**, 374 (1972);
K. Fujikawa, B.W. Lee, and A.I. Sanda, Phys. Rev. **D6**, 2923 (1972);
G. Altarelli, N. Cabibbo, and L. Maiani, Phys. Lett. **B40**, 415 (1972);
W.A. Bardeen, R. Gastmans, and B.E. Laurup, Nucl. Phys. **B46**, 315 (1972).
175. T.V. Kukhto *et al.*, Nucl. Phys. **B371**, 567 (1992);
S. Peris, M. Perrottet, and E. de Rafael, Phys. Lett. **B355**, 523 (1995);
A. Czarnecki, B. Krause, and W.J. Marciano, Phys. Rev. **D52**, 2619 (1995);
A. Czarnecki, B. Krause, and W.J. Marciano, Phys. Rev. Lett. **76**, 3267 (1996).
176. G. Degross and G. Giudice, Phys. Rev. **D58**, 053007 (1998).
177. DELPHI: J. Abdallah *et al.*, Eur. Phys. J. **C46**, 1 (2006).
178. V. Cirigliano, G. Ecker, and H. Neufeld, JHEP **0208**, 002 (2002);
K. Maltman and C.E. Wolfe, Phys. Rev. **D73**, 013004 (2006).
179. J. Erler, Rev. Mex. Fis. **50**, 200 (2004).
180. K. Maltman, Phys. Lett. **B633**, 512 (2006).
181. F. Flores-Baez *et al.*, Phys. Rev. **D74**, 071301 (2006).
182. S. Ghozzi and F. Jegerlehner, Phys. Lett. **B583**, 222 (2004).
183. K. Melnikov and A. Vainshtein, Phys. Rev. **D70**, 113006 (2004).
184. J. Erler and G. Toledo Sánchez, Phys. Rev. Lett. **97**, 161801 (2006).
185. M. Knecht and A. Nyffeler, Phys. Rev. **D65**, 073034 (2002).
186. M. Hayakawa and T. Kinoshita, hep-ph/0112102;
J. Bijnens, E. Pallante, and J. Prades, Nucl. Phys. **B626**, 410 (2002);
A recent discussion is in J. Bijnens and J. Prades, Mod. Phys. Lett. **A22**, 767 (2007).
187. B. Krause, Phys. Lett. **B390**, 392 (1997).
188. J.L. Lopez, D.V. Nanopoulos, and X. Wang, Phys. Rev. **D49**, 366 (1994);
for recent reviews, see Ref. 173.
189. UA2: S. Alitti *et al.*, Phys. Lett. **B276**, 354 (1992);
CDF: T. Affolder *et al.*, Phys. Rev. **D64**, 052001 (2001);
DØ: V. M. Abazov *et al.*, Phys. Rev. **D66**, 012001 (2002);
CDF and DØ: Phys. Rev. **D70**, 092008 (2004);
CDF II: T. Aaltonen *et al.*, 0708.3642 [hep-ex].
190. F. James and M. Roos, Comput. Phys. Commun. **10**, 343 (1975).
191. J. Erler, J.L. Feng, and N. Polonsky, Phys. Rev. Lett. **78**, 3063 (1997).
192. D. Choudhury, T.M.P. Tait, and C.E.M. Wagner, Phys. Rev. **D65**, 053002 (2002).
193. J. Erler and P. Langacker, Phys. Rev. Lett. **84**, 212 (2000).
194. DELPHI: P. Abreu *et al.*, Eur. Phys. J. **C10**, 415 (1999).
195. S. Bethke, Phys. Reports **403**, 203 (2004).
196. H1 and ZEUS: C. Glasman *et al.*, 0709.4426 [hep-ex].
197. HPQCD and UKQCD: Q. Mason *et al.*, Phys. Rev. Lett. **95**, 052002 (2005).
198. J. Erler, Phys. Rev. **D63**, 071301 (2001).
199. P. Langacker and N. Polonsky, Phys. Rev. **D52**, 3081 (1995);
J. Bagger, K.T. Matchev, and D. Pierce, Phys. Lett. **B348**, 443 (1995).
200. M. Veltman, Nucl. Phys. **B123**, 89 (1977);
M. Chanowitz, M.A. Furman, and I. Hinchliffe, Phys. Lett. **B78**, 285 (1978);
The two-loop correction has been obtained by J.J. van der Bij and F. Hoogeveen, Nucl. Phys. **B283**, 477 (1987).
201. P. Langacker and M. Luo, Phys. Rev. **D45**, 278 (1992) and references therein.
202. A. Denner, R.J. Guth, and J.H. Kühn, Phys. Lett. **B240**, 438 (1990);
W. Grimus *et al.*, 0711.4022 [hep-ph].
203. S. Bertolini and A. Sirlin, Phys. Lett. **B257**, 179 (1991).
204. M. Peskin and T. Takeuchi, Phys. Rev. Lett. **65**, 964 (1990);
M. Peskin and T. Takeuchi, Phys. Rev. **D46**, 381 (1992);
M. Golden and L. Randall, Nucl. Phys. **B361**, 3 (1991).
205. D. Kennedy and P. Langacker, Phys. Rev. Lett. **65**, 2967 (1990);
D. Kennedy and P. Langacker, Phys. Rev. **D44**, 1591 (1991).
G. Altarelli and R. Barbieri, Phys. Lett. **B253**, 161 (1990).
207. B. Holdom and J. Terning, Phys. Lett. **B247**, 88 (1990).
208. B.W. Lynn, M.E. Peskin, and R.G. Stuart, p. 90 of Ref. 132.
209. An alternative formulation is given by K. Hagiwara *et al.*, Z. Phys. **C64**, 559 (1994), and *ibid.*, **68**, 352(E) (1995);
K. Hagiwara, D. Haidt, and S. Matsumoto, Eur. Phys. J. **C2**, 95 (1998).
210. I. Maksymyk, C.P. Burgess, and D. London, Phys. Rev. **D50**, 529 (1994);
C.P. Burgess *et al.*, Phys. Lett. **B326**, 276 (1994).
211. R. Barbieri *et al.*, Nucl. Phys. **B703**, 127 (2004).
212. K. Lane, hep-ph/0202255.
213. E. Gates and J. Terning, Phys. Rev. Lett. **67**, 1840 (1991);
R. Sundrum and S.D.H. Hsu, Nucl. Phys. **B391**, 127 (1993);
R. Sundrum, Nucl. Phys. **B395**, 60 (1993);
M. Luty and R. Sundrum, Phys. Rev. Lett. **70**, 529 (1993);
T. Appelquist and J. Terning, Phys. Lett. **B315**, 139 (1993);
D.D. Dietrich, F. Sannino, and K. Tuominen, Phys. Rev. **D72**, 055001 (2005);
N.D. Christensen and R. Shrock, Phys. Lett. **B632**, 92 (2006);
M. Harada, M. Kurachi, and K. Yamawaki, Prog. Theor. Phys. **115**, 765 (2006).
214. H. Georgi, Nucl. Phys. **B363**, 301 (1991);
M.J. Dugan and L. Randall, Phys. Lett. **B264**, 154 (1991).
215. R. Barbieri *et al.*, Nucl. Phys. **B341**, 309 (1990).
216. M.E. Peskin and J.D. Wells, Phys. Rev. **D64**, 093003 (2001).
217. Z. Han and W. Skiba, Phys. Rev. **D71**, 075009 (2005).
218. H.J. He, N. Polonsky, and S. Su, Phys. Rev. **D64**, 053004 (2001);
V.A. Novikov *et al.*, Sov. Phys. JETP **76**, 127 (2002);
S.S. Bulanov *et al.*, Yad. Fiz. **66**, 2219 (2003) and references therein;
G.D. Kribs *et al.*, Phys. Rev. **D76**, 075016 (2007).
219. For a review, see D. London, p. 951 of Ref. 4;
a recent analysis is M.B. Popovic and E.H. Simmons, Phys. Rev. **D58**, 095007 (1998);
for collider implications, see T.C. Andre and J.L. Rosner, Phys. Rev. **D69**, 035009 (2004).
220. P. Langacker, M. Luo, and A.K. Mann, Rev. Mod. Phys. **64**, 87 (1992);
M. Luo, p. 977 of Ref. 4.
221. F.S. Merritt *et al.*, p. 19 of *Particle Physics: Perspectives and Opportunities: Report of the DPF Committee on Long Term Planning*, ed. R. Peccei *et al.* (World Scientific, Singapore, 1995).
222. G. C. Cho and K. Hagiwara, Nucl. Phys. **B574**, 623 (2000);
G. Altarelli *et al.*, JHEP **0106**, 018 (2001);
S. Heinemeyer, W. Hollik, and G. Weiglein, Phys. Reports **425**, 265 (2006);
S. P. Martin, K. Tobe, and J. D. Wells, Phys. Rev. **D71**, 073014 (2005);

- G. Marandella, C. Schappacher, and A. Strumia, Nucl. Phys. **B715**, 173 (2005);
S. Heinemeyer *et al.*, JHEP **0608**, 052 (2006);
M.J. Ramsey-Musolf and S. Su, hep-ph/0612057;
J. R. Ellis *et al.*, JHEP **0708**, 083 (2007);
S. Heinemeyer *et al.*, 0710.2972 [hep-ph].
223. R.S. Chivukula and E.H. Simmons, Phys. Rev. **D66**, 015006 (2002);
C.T. Hill and E.H. Simmons, Phys. Reports **381**, 235 (2003);
R.S. Chivukula *et al.*, Phys. Rev. **D70**, 075008 (2004).
224. K. Agashe *et al.*, JHEP **0308**, 050 (2003);
M. Carena *et al.*, Phys. Rev. **D68**, 035010 (2003);
I. Gogoladze and C. Macesanu, Phys. Rev. **D74**, 093012 (2006);
I. Antoniadis, hep-th/0102202;
see also the note on “Extra Dimensions” in the Searches Particle Listings.
225. T. Han, H.E. Logan, and L.T. Wang, JHEP **0601**, 099 (2006);
M. Perelstein, Prog. Part. Nucl. Phys. **58**, 247 (2007).
226. G. Altarelli, R. Barbieri, and S. Jadach, Nucl. Phys. **B369**, 3 (1992) and *ibid.*, **B376**, 444(E) (1992).
227. A. De Rújula *et al.*, Nucl. Phys. **B384**, 3 (1992);
K. Hagiwara *et al.*, Phys. Rev. **D48**, 2182 (1993);
C.P. Burgess *et al.*, Phys. Rev. **D49**, 6115 (1994);
Z. Han and W. Skiba, Phys. Rev. **D71**, 075009 (2005);
G. Cacciapaglia *et al.*, Phys. Rev. **D74**, 033011 (2006);
V. Bernard *et al.*, 0707.4194 [hep-ph].
228. For reviews, see A. Leike, Phys. Reports **317**, 143 (1999);
P. Langacker, 0801.1345 [hep-ph].
229. M. Cvetič and P. Langacker, Phys. Rev. **D54**, 3570 (1996).
230. R.W. Robinett and J.L. Rosner, Phys. Rev. **D26**, 2396 (1982).
231. S. Chaudhuri *et al.*, Nucl. Phys. **B456**, 89 (1995);
G. Cleaver *et al.*, Phys. Rev. **D59**, 055005 (1999).
232. M. Carena *et al.*, Phys. Rev. **D70**, 093009 (2004).
233. CDF: T. Aaltonen *et al.*, Phys. Rev. Lett. **99**, 171802 (2007);
CDF and DØ: A. Lath *et al.*, presented at the XL Rencontres de Moriond 2005, session on *ElectroWeak Interactions and Unified Theories*.
234. J. Kang and P. Langacker, Phys. Rev. **D71**, 035014 (2005).
235. B. Holdom, Phys. Lett. **B166**, 196 (1986).
236. J. Erler and P. Langacker, Phys. Lett. **B456**, 68 (1999).
237. T. Appelquist, B.A. Dobrescu, and A.R. Hopper, Phys. Rev. **D68**, 035012 (2003);
R.S. Chivukula *et al.*, Phys. Rev. **D69**, 015009 (2004).
238. P. Langacker and M. Plümacher, Phys. Rev. **D62**, 013006 (2000).
239. R. Casalbuoni *et al.*, Phys. Lett. **B460**, 135 (1999);
J.L. Rosner, Phys. Rev. **D61**, 016006 (2000).

11. THE CKM QUARK-MIXING MATRIX

Revised February 2008 by A. Ceccucci (CERN), Z. Ligeti (LBNL), and Y. Sakai (KEK).

11.1. Introduction

The masses and mixings of quarks have a common origin in the Standard Model (SM). They arise from the Yukawa interactions with the Higgs condensate,

$$\mathcal{L}_Y = -Y_{ij}^d \overline{Q_{Li}^d} \phi d_{Rj}^d - Y_{ij}^u \overline{Q_{Li}^u} \epsilon \phi^* u_{Rj}^u + \text{h.c.}, \quad (11.1)$$

where $Y^{u,d}$ are 3×3 complex matrices, ϕ is the Higgs field, i, j are generation labels, and ϵ is the 2×2 antisymmetric tensor. Q_L^I are left-handed quark doublets, and d_R^I and u_R^I are right-handed down- and up-type quark singlets, respectively, in the weak-eigenstate basis. When ϕ acquires a vacuum expectation value, $\langle \phi \rangle = (0, v/\sqrt{2})$, Eq. (11.1) yields mass terms for the quarks. The physical states are obtained by diagonalizing $Y^{u,d}$ by four unitary matrices, $V_{L,R}^{u,d}$, as $M_{\text{diag}}^f = V_L^f Y^f V_R^{f\dagger} (v/\sqrt{2})$, $f = u, d$. As a result, the charged-current W^\pm interactions couple to the physical u_{Lj} and d_{Lk} quarks with couplings given by

$$V_{\text{CKM}} \equiv V_L^u V_L^{d\dagger} = \begin{pmatrix} V_{ud} & V_{us} & V_{ub} \\ V_{cd} & V_{cs} & V_{cb} \\ V_{td} & V_{ts} & V_{tb} \end{pmatrix}. \quad (11.2)$$

This Cabibbo-Kobayashi-Maskawa (CKM) matrix [1,2] is a 3×3 unitary matrix. It can be parameterized by three mixing angles and a CP -violating phase. Of the many possible parameterizations, a standard choice has become

$$V = \begin{pmatrix} c_{12}c_{13} & s_{12}c_{13} & s_{13}e^{-i\delta} \\ -s_{12}c_{23} - c_{12}s_{23}s_{13}e^{i\delta} & c_{12}c_{23} - s_{12}s_{23}s_{13}e^{i\delta} & s_{23}c_{13} \\ s_{12}s_{23} - c_{12}c_{23}s_{13}e^{i\delta} & -c_{12}s_{23} - s_{12}c_{23}s_{13}e^{i\delta} & c_{23}c_{13} \end{pmatrix}, \quad (11.3)$$

where $s_{ij} = \sin \theta_{ij}$, $c_{ij} = \cos \theta_{ij}$, and δ is the KM phase [2] responsible for all CP -violating phenomena in flavor-changing processes in the SM. The angles θ_{ij} can be chosen to lie in the first quadrant, so $s_{ij}, c_{ij} \geq 0$.

It is known experimentally that $s_{13} \ll s_{23} \ll s_{12} \ll 1$, and it is convenient to exhibit this hierarchy using the Wolfenstein parameterization. We define [3–5]

$$s_{12} = \lambda = \frac{|V_{us}|}{\sqrt{|V_{ud}|^2 + |V_{us}|^2}}, \quad s_{23} = A\lambda^2 = \lambda \left| \frac{V_{cb}}{V_{us}} \right|, \\ s_{13}e^{i\delta} = V_{ub}^* = A\lambda^3(\rho + i\eta) = \frac{A\lambda^3(\bar{\rho} + i\bar{\eta})\sqrt{1 - A^2\lambda^4}}{\sqrt{1 - \lambda^2[1 - A^2\lambda^4(\bar{\rho} + i\bar{\eta})]}}. \quad (11.4)$$

These relations ensure that $\bar{\rho} + i\bar{\eta} = -(V_{ud}V_{ub}^*)/(V_{cd}V_{cb}^*)$ is phase-convention-independent, and the CKM matrix written in terms of λ , A , $\bar{\rho}$, and $\bar{\eta}$ is unitary to all orders in λ . The definitions of $\bar{\rho}, \bar{\eta}$ reproduce all approximate results in the literature. For example, $\bar{\rho} = \rho(1 - \lambda^2/2 + \dots)$ and we can write V_{CKM} to $\mathcal{O}(\lambda^4)$ either in terms of $\bar{\rho}, \bar{\eta}$ or, traditionally,

$$V = \begin{pmatrix} 1 - \lambda^2/2 & \lambda & A\lambda^3(\rho - i\eta) \\ -\lambda & 1 - \lambda^2/2 & A\lambda^2 \\ A\lambda^3(1 - \rho - i\eta) & -A\lambda^2 & 1 \end{pmatrix} + \mathcal{O}(\lambda^4). \quad (11.5)$$

The CKM matrix elements are fundamental parameters of the SM, so their precise determination is important. The unitarity of the CKM matrix imposes $\sum_i V_{ij}V_{ik}^* = \delta_{jk}$ and $\sum_j V_{ij}V_{kj}^* = \delta_{ik}$. The six vanishing combinations can be represented as triangles in a complex plane, of which the ones obtained by taking scalar products of neighboring rows or columns are nearly degenerate. The areas of all triangles are the same, half of the Jarlskog invariant, J [6], which is a phase-convention-independent measure of CP violation, defined by $\text{Im}[V_{ij}V_{kl}V_{il}^*V_{kj}^*] = J \sum_{m,n} \varepsilon_{ikm} \varepsilon_{jln}$.

The most commonly used unitarity triangle arises from

$$V_{ud}V_{ub}^* + V_{cd}V_{cb}^* + V_{td}V_{tb}^* = 0, \quad (11.6)$$

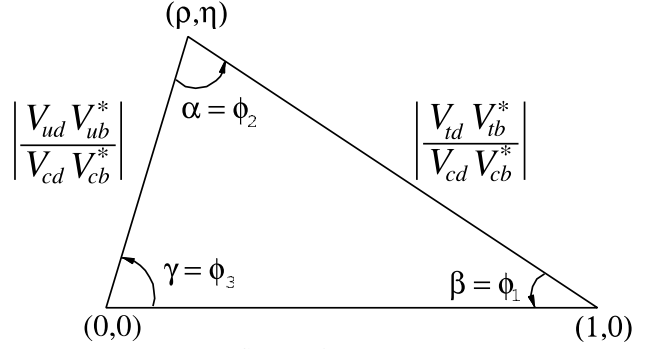


Figure 11.1: Sketch of the unitarity triangle.

by dividing each side by the best-known one, $V_{cd}V_{cb}^*$ (see Fig. 1). Its vertices are exactly $(0,0)$, $(1,0)$, and, due to the definition in Eq. (11.4), $(\bar{\rho}, \bar{\eta})$. An important goal of flavor physics is to overconstrain the CKM elements, and many measurements can be conveniently displayed and compared in the $\bar{\rho}, \bar{\eta}$ plane.

Processes dominated by loop contributions in the SM are sensitive to new physics, and can be used to extract CKM elements only if the SM is assumed. In Sec. 11.2 and 11.3, we describe such measurements assuming the SM, and discuss implications for new physics in Sec. 11.5.

11.2. Magnitudes of CKM elements

11.2.1. $|V_{ud}|$:

The most precise determination of $|V_{ud}|$ comes from the study of superallowed $0^+ \rightarrow 0^+$ nuclear beta decays, which are pure vector transitions. Taking the average of the nine most precise determinations [7] yields [8]

$$|V_{ud}| = 0.97418 \pm 0.00027. \quad (11.7)$$

The error is dominated by theoretical uncertainties stemming from nuclear Coulomb distortions and radiative corrections. A precise determination of $|V_{ud}|$ is also obtained from the measurement of the neutron lifetime. The theoretical uncertainties are very small, but the determination is limited by the knowledge of the ratio of the axial-vector and vector couplings, $g_A = G_A/G_V$ [8]. The PIBETA experiment [9] has improved the measurement of the $\pi^+ \rightarrow \pi^0 e^+ \nu$ branching ratio to 0.6%, and quote $|V_{ud}| = 0.9728 \pm 0.0030$, in agreement with the more precise results listed above. The interest in this measurement is that the determination of $|V_{ud}|$ is very clean theoretically, because it is a pure vector transition and is free from nuclear-structure uncertainties.

11.2.2. $|V_{us}|$:

The product of $|V_{us}|$ and the form factor at $q^2 = 0$, $|V_{us}| f_+(0)$ have been extracted traditionally from $K_L^0 \rightarrow \pi e \nu$ decays in order to avoid isospin-breaking corrections ($\pi^0 - \eta$ mixing) that affect the charged-kaon semileptonic decay, and the complications induced by a second (scalar) form factor present in the muonic decays. The last round of experiments has lead to enough experimental constraints to justify the comparison between different decay modes. Systematic errors related to the experimental quantities, *e.g.*, the lifetime of neutral or charged kaons, and the form factor determinations for electron and muonic decays, differ among decay modes, and the consistency between different determinations enhances the confidence in the final result. For this reason, we follow the prescription [10] to average $K_L^0 \rightarrow \pi e \nu$, $K_L^0 \rightarrow \pi \mu \nu$, $K^\pm \rightarrow \pi^0 e^\pm \nu$, $K^\pm \rightarrow \pi^0 \mu^\pm \nu$ and $K_S^0 \rightarrow \pi e \nu$. The average of these five decay modes yields $|V_{us}| f_+(0) = 0.21668 \pm 0.00045$. Results obtained from each decay mode, and exhaustive references to the experimental data, are listed for instance, in Ref. 8. The form factor value $f_+(0) = 0.961 \pm 0.008$ [11] is still broadly accepted [8] and gives

$$|V_{us}| = 0.2255 \pm 0.0019. \quad (11.8)$$

Lattice gauge theory calculations [12] provide results for $f_+(0)$ in agreement with [11], while other calculations [14] differ by as much as 2%.

Other determinations of $|V_{us}|$ involve leptonic kaon decays, hyperon decays, and τ decays. The calculation of the ratio of the kaon and pion decay constants enables one to extract $|V_{us}/V_{ud}|$ from $K \rightarrow \mu\nu(\gamma)$ and $\pi \rightarrow \mu\nu(\gamma)$, where (γ) indicates that radiative decays are included [15]. The KLOE measurement of the $K^+ \rightarrow \mu^+\nu(\gamma)$ branching ratio [16], combined with the lattice QCD calculation, $f_K/f_\pi = 1.198 \pm 0.010$ [12], leads to $|V_{us}| = 0.2242 \pm 0.0019$, where the accuracy is limited by the knowledge of the ratio of the decay constants. The determination from hyperon decays was updated in [18]. These authors focus on the analysis of the vector form factor, protected from first order $SU(3)$ breaking effects by the Ademollo-Gatto theorem [19], and treat the ratio between the axial and vector form factors g_1/f_1 as experimental input, thus avoiding first order $SU(3)$ breaking effects in the axial-vector contribution. They find $|V_{us}| = 0.2250 \pm 0.0027$, although this does not include an estimate of the theoretical uncertainty due to second-order $SU(3)$ -breaking, contrary to Eq. (11.8). Concerning hadronic τ decays to strange particles, the latest determinations based on ALEPH, OPAL, CLEO, and recent BABAR and Belle data yields $|V_{us}| = 0.2165 \pm 0.0027$ [20].

11.2.3. $|V_{cd}|$:

The magnitude of V_{cd} can be extracted from semileptonic charm decays if theoretical knowledge of the form factors is available. Three-flavor unquenched lattice QCD calculations for $D \rightarrow K\ell\nu$ and $D \rightarrow \pi\ell\nu$ have been published [21]. Using these estimates and the average of recent CLEO-c [22] and Belle [23] measurements of $D \rightarrow \pi\ell\nu$ decays, one obtains $|V_{cd}| = 0.218 \pm 0.007 \pm 0.023$, where the first uncertainty is experimental, and the second is from the theoretical error of the form factor.

This determination is not yet as precise as the one based on neutrino and antineutrino interactions. The difference of the ratio of double-muon to single-muon production by neutrino and antineutrino beams is proportional to the charm cross section off valence d -quarks, and therefore to $|V_{cd}|^2$ times the average semileptonic branching ratio of charm mesons, \mathcal{B}_μ . The method was used first by CDHS [24] and then by CCFR [25,26] and CHARM II [27]. Averaging these results is complicated, not only because it requires assumptions about the scale of the QCD corrections, but also because \mathcal{B}_μ is an effective quantity, which depends on the specific neutrino beam characteristics. Given that no new experimental input is available, we quote the average provided in a previous review, $\mathcal{B}_\mu|V_{cd}|^2 = (0.463 \pm 0.034) \times 10^{-2}$ [28]. Analysis cuts make these experiments insensitive to neutrino energies smaller than 30 GeV. Thus, \mathcal{B}_μ should be computed using only neutrino interactions with visible energy larger than 30 GeV. An appraisal [29] based on charm-production fractions measured in neutrino interactions [30,31] gives $\mathcal{B}_\mu = 0.088 \pm 0.006$. Data from the CHORUS experiment [32] are now sufficiently precise to extract \mathcal{B}_μ directly, by comparing the number of charm decays with a muon to the total number of charmed hadrons found in the nuclear emulsions. Requiring the visible energy to be larger than 30 GeV, CHORUS finds $\mathcal{B}_\mu = 0.085 \pm 0.009 \pm 0.006$. To extract $|V_{cd}|$, we use the average of these two determinations, $\mathcal{B}_\mu = 0.0873 \pm 0.0052$, and obtain

$$|V_{cd}| = 0.230 \pm 0.011. \quad (11.9)$$

11.2.4. $|V_{cs}|$:

The determination of $|V_{cs}|$ from neutrino and antineutrino scattering suffers from the uncertainty of the s -quark sea content. Measurements sensitive to $|V_{cs}|$ from on-shell W^\pm decays were performed at LEP-2. The branching ratios of the W depend on the six CKM matrix elements involving quarks with masses smaller than M_W . The W branching ratio to each lepton flavor is given by $1/\mathcal{B}(W \rightarrow \ell\bar{\nu}_\ell) = 3[1 + \sum_{u,c,d,s,b} |V_{ij}|^2 (1 + \alpha_s(m_W)/\pi)]$. The measurement assuming lepton universality, $\mathcal{B}(W \rightarrow \ell\bar{\nu}_\ell) = (10.83 \pm 0.07 \pm 0.07) \%$ [33], implies $\sum_{u,c,d,s,b} |V_{ij}|^2 = 2.002 \pm 0.027$. This is a precise test of unitarity, but only flavor-tagged measurements determine $|V_{cs}|$. DELPHI measured tagged $W^+ \rightarrow c\bar{s}$ decays, obtaining $|V_{cs}| = 0.94_{-0.26}^{+0.32} \pm 0.13$ [34]. Hereafter, the first error is statistical and the second is systematic, unless mentioned otherwise.

The direct determination of $|V_{cs}|$ is possible from semileptonic D or leptonic D_s decays, using unquenched lattice QCD calculations of

the semileptonic D form factor or the D_s decay constant. For muonic decays, the average of the recent data from BABAR [35], Belle [36], and CLEO-c [37] gives $\mathcal{B}(D_s^+ \rightarrow \mu^+\nu) = (6.26 \pm 0.51) \times 10^{-3}$. For decays with τ leptons, a measurement from CLEO-c is available: $\mathcal{B}(D_s^+ \rightarrow \tau^+\nu) = (6.47 \pm 0.61 \pm 0.26) \times 10^{-2}$ [38]. From each of these two values, determinations of $|V_{cs}|$ can be obtained by using the PDG values for the mass and lifetime of the D_s , the masses of the leptons, and $f_{D_s} = (249 \pm 3 \pm 16) \text{ MeV}$ [39]. The average of these two determinations gives $|V_{cs}| = 1.07 \pm 0.08$, where the error is dominated by the lattice QCD determination of f_{D_s} . In semileptonic D decays, unquenched lattice QCD calculations have predicted the normalization and the shape (dependence on the invariant mass of the lepton pair, q^2) of the form factors in $D \rightarrow K\ell\nu$ and $D \rightarrow \pi\ell\nu$ [21]. Using these theoretical results and the average of recent CLEO-c [22], Belle [23] and BaBar [40] measurements of $B \rightarrow K\ell\nu$ decays, one obtains $|V_{cs}| = 0.99 \pm 0.01 \pm 0.10$, where the first error is experimental and the second one, which is dominant, is from the theoretical error of the form factor. Averaging the determinations from leptonic and semileptonic decays, we quote

$$|V_{cs}| = 1.04 \pm 0.06. \quad (11.10)$$

11.2.5. $|V_{cb}|$:

This matrix element can be determined from exclusive and inclusive semileptonic decays of B mesons to charm. The inclusive determinations use the semileptonic decay rate measurement, together with the leptonic energy and the hadronic invariant-mass spectra. The theoretical foundation of the calculation is the operator product expansion (OPE) [41,42]. It expresses the total rate and moments of differential energy and invariant-mass spectra as expansions in α_s , and inverse powers of the heavy-quark mass. The dependence on m_b , m_c , and the parameters that occur at subleading order is different for different moments, and a large number of measured moments overconstrains all the parameters, and tests the consistency of the determination. The precise extraction of $|V_{cb}|$ requires using a ‘‘threshold’’ quark mass definition [43,44]. Inclusive measurements have been performed using B mesons from Z^0 decays at LEP, and at e^+e^- machines operated at the $\mathcal{T}(4S)$. At LEP, the large boost of B mesons from Z^0 allows the determination of the moments throughout phase space, which is not possible otherwise, but the large statistics available at the B factories leads to more precise determinations. An average of the measurements and a compilation of the references are provided by Kowalewski and Mannel [45]: $|V_{cb}| = (41.6 \pm 0.7) \times 10^{-3}$.

Exclusive determinations are based on semileptonic B decays to D and D^* . In the $m_{b,c} \gg \Lambda_{\text{QCD}}$ limit, all form factors are given by a single Isgur-Wise function [46], which depends on the product of the four velocities, $w = v \cdot v'$, and of the initial and final-state hadrons. Heavy-quark symmetry determines the normalization of the rate at $w = 1$, the maximum momentum transfer to the leptons, and $|V_{cb}|$ is obtained from an extrapolation to $w = 1$. The exclusive determination, $|V_{cb}| = (38.6 \pm 1.3) \times 10^{-3}$ [45], is less precise than the inclusive one, because the theoretical uncertainty in the form factor, and the experimental uncertainty in the rate near $w = 1$, are both about 3%. The $|V_{cb}|$ review quotes a combination with a scaled error as [45]

$$|V_{cb}| = (41.2 \pm 1.1) \times 10^{-3}. \quad (11.11)$$

11.2.6. $|V_{ub}|$:

The determination of $|V_{ub}|$ from inclusive $B \rightarrow X_u\ell\bar{\nu}$ decay suffers from large $B \rightarrow X_c\ell\bar{\nu}$ backgrounds. In most regions of phase space where the charm background is kinematically forbidden, the hadronic physics enters via unknown nonperturbative functions, so-called shape functions. (In contrast, the nonperturbative physics for $|V_{cb}|$ is encoded in a few parameters.) At leading order in Λ_{QCD}/m_b , there is only one shape function, which can be extracted from the photon energy spectrum in $B \rightarrow X_s\gamma$ [47,48], and applied to several spectra in $B \rightarrow X_u\ell\bar{\nu}$. The subleading shape functions are modeled in the current calculations. Phase space cuts for which the rate has only subleading dependence on the shape function are also possible [49]. The measurements of both hadronic and leptonic systems are important

for effective choice of phase space. A different approach is to extend the measurements deeper into the $B \rightarrow X_c \ell \bar{\nu}$ region to reduce the theoretical uncertainties. Analyses of the electron-energy endpoint from CLEO [50], *BABAR* [51], and Belle [52] quote $B \rightarrow X_u e \bar{\nu}$ partial rates for $|\vec{p}_e| \geq 2.0$ GeV and 1.9 GeV, which are well below the charm endpoint. The large and pure $B\bar{B}$ samples at the B factories permit the selection of $B \rightarrow X_u \ell \bar{\nu}$ decays in events where the other B is fully reconstructed [53]. With this full-reconstruction tag method, the four momenta of both the leptonic and the hadronic systems can be measured. It also gives access to a wider kinematic region due to improved signal purity.

To extract $|V_{ub}|$ from an exclusive channel, the form factors have to be known. Experimentally, better signal-to-background ratios are offset by smaller yields. The $B \rightarrow \pi \ell \bar{\nu}$ branching ratio is now known to 6%. Unquenched lattice QCD calculations of the $B \rightarrow \pi \ell \bar{\nu}$ form factor for $q^2 > 16$ GeV² are available [54,55] and yield $|V_{ub}| = (3.4 \pm 0.2_{-0.4}^{+0.6}) \times 10^{-3}$. Light-cone QCD sum rules are applicable for $q^2 < 14$ GeV² [56] and yield similar results. The theoretical uncertainties in extracting $|V_{ub}|$ from inclusive and exclusive decays are different. A combination of the determinations is quoted by the V_{cb} and V_{ub} minireview as [45],

$$|V_{ub}| = (3.93 \pm 0.36) \times 10^{-3}, \quad (11.12)$$

which is dominated by the inclusive measurement. Given the theoretical and experimental progress, it will be interesting to see how the inclusive and exclusive determinations develop.

11.2.7. $|V_{td}|$ and $|V_{ts}|$:

The CKM elements $|V_{td}|$ and $|V_{ts}|$ cannot be measured from tree-level decays of the top quark, so one has to rely on determinations from $B-\bar{B}$ oscillations mediated by box diagrams with top quarks, or loop-mediated rare K and B decays. Theoretical uncertainties in hadronic effects limit the accuracy of the current determinations. These can be reduced by taking ratios of processes that are equal in the flavor $SU(3)$ limit to determine $|V_{td}/V_{ts}|$.

The mass difference of the two neutral B meson mass eigenstates is very well measured, $\Delta m_d = 0.507 \pm 0.005$ ps⁻¹ [57]. For the B_s^0 system, the CDF Collaboration measured $\Delta m_s = (17.77 \pm 0.10 \pm 0.07)$ ps⁻¹ [58] with more than 5σ significance (the $D\bar{D}$ result [59] is compatible and has about 2σ significance). Using the unquenched lattice QCD calculations [60] $f_{B_d} \sqrt{\hat{B}_{B_d}} = (223 \pm 8 \pm 16)$ MeV, $f_{B_s} \sqrt{\hat{B}_{B_s}} = (275 \pm 7 \pm 15)$ MeV, and assuming $|V_{tb}| = 1$, one finds

$$|V_{td}| = (8.1 \pm 0.6) \times 10^{-3}, \quad |V_{ts}| = (38.7 \pm 2.3) \times 10^{-3}. \quad (11.13)$$

The uncertainties are dominated by lattice QCD. Several uncertainties are reduced in the calculation of the ratio $\xi = (f_{B_s} \sqrt{\hat{B}_{B_s}})/(f_{B_d} \sqrt{\hat{B}_{B_d}}) = 1.23 \pm 0.02 \pm 0.03$, and therefore the constraint on $|V_{td}/V_{ts}|$ from $\Delta m_d/\Delta m_s$ is more reliable theoretically. These provide a new theoretically clean and significantly improved constraint

$$|V_{td}/V_{ts}| = (0.209 \pm 0.001 \pm 0.006) \times 10^{-3}. \quad (11.14)$$

The inclusive rate $\mathcal{B}(B \rightarrow X_s \gamma) = (3.55 \pm 0.26) \times 10^{-4}$ extrapolated to $E_\gamma > 1.6$ GeV [61] is also sensitive to $V_{tb}V_{ts}^*$. In addition to t -quark penguins, a large part of the sensitivity comes from charm contributions proportional to $V_{cb}V_{cs}^*$ via the application of 3×3 CKM unitarity (which is used here; any CKM determination from loop processes necessarily assumes the SM). With the recently completed NNLO calculation of $\mathcal{B}(B \rightarrow X_s \gamma)_{E_\gamma > E_0}/\mathcal{B}(B \rightarrow X_c e \bar{\nu})$ [62], we obtain $|V_{ts}/V_{cb}| = (1.04 \pm 0.05)$.

A complementary determination of $|V_{td}/V_{ts}|$ is possible from the ratio of $B \rightarrow \rho \gamma$ and $K^* \gamma$ rates. The ratio of the neutral modes is theoretically cleaner than that of the charged ones, because the poorly known spectator-interaction contribution is expected to be smaller (W -exchange vs. weak annihilation). For now, we average the charged and neutral rates assuming the isospin symmetry and heavy-quark

limit motivated relation, $|V_{td}/V_{ts}|^2 = \xi_\gamma^2 [\Gamma(B^+ \rightarrow \rho^+ \gamma) + 2\Gamma(B^0 \rightarrow \rho^0 \gamma)]/[\Gamma(B^+ \rightarrow K^{*+} \gamma) + \Gamma(B^0 \rightarrow K^{*0} \gamma)] = (2.96 \pm 0.57)\%$ [61]. Here ξ_γ contains the poorly known hadronic physics. Using $\xi_\gamma = 1.2 \pm 0.2$ [63], and combining the experimental and theoretical errors in quadrature, gives $|V_{td}/V_{ts}| = 0.21 \pm 0.04$.

A theoretically clean determination of $|V_{td}V_{ts}^*|$ is possible from $K^+ \rightarrow \pi^+ \nu \bar{\nu}$ decay [64]. Experimentally, only three events have been observed [65], and the rate is consistent with the SM with large uncertainties. Much more data are needed for a precision measurement.

11.2.8. $|V_{tb}|$:

The determination of $|V_{tb}|$ from top decays uses the ratio of branching fractions $R = \mathcal{B}(t \rightarrow Wb)/\mathcal{B}(t \rightarrow Wq) = |V_{tb}|^2/(\sum_q |V_{tq}|^2) = |V_{tb}|^2$, where $q = b, s, d$. The CDF and $D\bar{D}$ measurements performed on data collected during Run II of the Tevatron give $|V_{tb}| > 0.78$ [66] and $|V_{tb}| > 0.89$ [67], respectively, at 95% CL. The direct determination of $|V_{tb}|$ without assuming unitarity is possible from the single top-quark-production cross section. From the average cross sections of $D\bar{D}$ [68] and CDF [69], (3.7 ± 0.8) pb, the lower limit at 95% CL is obtained to be

$$|V_{tb}| > 0.74. \quad (11.15)$$

An attempt at constraining $|V_{tb}|$ from the precision electroweak data was made in [70]. The result, mostly driven by the top-loop contributions to $\Gamma(Z \rightarrow b\bar{b})$, gives $|V_{tb}| = 0.77_{-0.24}^{+0.18}$.

11.3. Phases of CKM elements

As can be seen from Fig. 11.1, the angles of the unitarity triangle are

$$\begin{aligned} \beta = \phi_1 &= \arg\left(-\frac{V_{cd}V_{cb}^*}{V_{td}V_{tb}^*}\right), \\ \alpha = \phi_2 &= \arg\left(-\frac{V_{td}V_{tb}^*}{V_{ud}V_{ub}^*}\right), \\ \gamma = \phi_3 &= \arg\left(-\frac{V_{ud}V_{ub}^*}{V_{cd}V_{cb}^*}\right). \end{aligned} \quad (11.16)$$

Since CP violation involves phases of CKM elements, many measurements of CP -violating observables can be used to constrain these angles and the $\bar{\rho}, \bar{\eta}$ parameters.

11.3.1. ϵ and ϵ' :

The measurement of CP violation in $K^0-\bar{K}^0$ mixing, $|\epsilon| = (2.233 \pm 0.015) \times 10^{-3}$ [71], provides important information about the CKM matrix. In the SM [72]

$$\begin{aligned} |\epsilon| &= \frac{G_F^2 f_K^2 m_K m_W^2}{12\sqrt{2}\pi^2 \Delta m_K} \hat{B}_K \left\{ \eta_c S(x_c) \text{Im}[(V_{cs}V_{cd}^*)^2] \right. \\ &\quad \left. + \eta_t S(x_t) \text{Im}[(V_{ts}V_{td}^*)^2] + 2\eta_{ct} S(x_c, x_t) \text{Im}(V_{cs}V_{cd}^*V_{ts}V_{td}^*) \right\}, \end{aligned} \quad (11.17)$$

where S is an Inami-Lim function [73], $x_q = m_q^2/m_W^2$, and η_i are perturbative QCD corrections. The constraint from ϵ in the $\bar{\rho}, \bar{\eta}$ plane is bounded by approximate hyperbolas. The dominant uncertainties are due to the bag parameter, for which we use $\hat{B}_K = 0.720 \pm 0.039$ from lattice QCD [12], and the parametric uncertainty proportional to $\sigma(A^4)$ from $(V_{ts}V_{td}^*)^2$, which is approximately $\sigma(|V_{cb}|^4)$.

The measurement of ϵ' provides a qualitative test of the CKM mechanism because its nonzero experimental average, $\text{Re}(\epsilon'/\epsilon) = (1.67 \pm 0.23) \times 10^{-3}$ [71], demonstrates the existence of direct CP violation, a prediction of the KM ansatz. While $\text{Re}(\epsilon'/\epsilon) \propto \text{Im}(V_{td}V_{ts}^*)$, this quantity cannot easily be used to extract CKM parameters, because the electromagnetic penguin contributions tend to cancel the gluonic penguins for large m_t [74], thereby significantly increasing the hadronic uncertainties. Most estimates [75–77] can agree with the observed value, indicating that $\bar{\eta}$ is positive. Progress in lattice QCD, in particular finite-volume calculations [78,79], may eventually provide a determination of the $K \rightarrow \pi\pi$ matrix elements.

11.3.2. β / ϕ_1 :

11.3.2.1. Charmonium modes:

CP -violation measurements in B -meson decays provide direct information on the angles of the unitarity triangle, shown in Fig. 11.1. These overconstraining measurements serve to improve the determination of the CKM elements, or to reveal effects beyond the SM.

The time-dependent CP asymmetry of neutral B -decays to a final state f common to B^0 and \bar{B}^0 is given by [80,81]

$$A_f = \frac{\Gamma(\bar{B}^0(t) \rightarrow f) - \Gamma(B^0(t) \rightarrow f)}{\Gamma(\bar{B}^0(t) \rightarrow f) + \Gamma(B^0(t) \rightarrow f)} = S_f \sin(\Delta m_d t) - C_f \cos(\Delta m_d t), \quad (11.18)$$

where

$$S_f = \frac{2 \operatorname{Im} \lambda_f}{1 + |\lambda_f|^2}, \quad C_f = \frac{1 - |\lambda_f|^2}{1 + |\lambda_f|^2}, \quad \lambda_f = \frac{q \bar{A}_f}{p A_f}. \quad (11.19)$$

Here, q/p describes B^0 - \bar{B}^0 mixing and, to a good approximation in the SM, $q/p = V_{tb}^* V_{td} / V_{ub}^* V_{ud} = e^{-2i\beta + \mathcal{O}(\lambda^4)}$ in the usual phase convention. A_f (\bar{A}_f) is the amplitude of the $B^0 \rightarrow f$ ($\bar{B}^0 \rightarrow f$) decay. If f is a CP eigenstate, and amplitudes with one CKM phase dominate the decay, then $|A_f| = |\bar{A}_f|$, $C_f = 0$, and $S_f = \sin(\arg \lambda_f) = \eta_f \sin 2\phi$, where η_f is the CP eigenvalue of f and 2ϕ is the phase difference between the $B^0 \rightarrow f$ and $B^0 \rightarrow \bar{B}^0 \rightarrow f$ decay paths. A contribution of another amplitude to the decay with a different CKM phase makes the value of S_f sensitive to relative strong interaction phases between the decay amplitudes (it also makes $C_f \neq 0$ possible).

The $b \rightarrow c\bar{c}s$ decays to CP eigenstates ($B^0 \rightarrow$ charmonium $K_{S,L}^0$) are the theoretically cleanest examples, measuring $S_f = -\eta_f \sin 2\beta$. The $b \rightarrow s\bar{q}q$ penguin amplitudes have dominantly the same weak phase as the $b \rightarrow c\bar{c}s$ tree amplitude. Since only λ^2 -suppressed penguin amplitudes introduce a new CP -violating phase, amplitudes with a single weak phase dominate, and we expect $|\bar{A}_{\psi K} / A_{\psi K} - 1| < 0.01$. The e^+e^- asymmetric-energy B -factory experiments from BABAR [82] and Belle [83] provide precise measurements. The world average is [61]

$$\sin 2\beta = 0.681 \pm 0.025. \quad (11.20)$$

This measurement has a four-fold ambiguity in β , which can be resolved by a global fit mentioned in Sec. 11.4. Experimentally, the two-fold ambiguity $\beta \rightarrow \pi/2 - \beta$ (but not $\beta \rightarrow \pi + \beta$) can be resolved by a time-dependent angular analysis of $B^0 \rightarrow J/\psi K^{*0}$ [84,85], or a time-dependent Dalitz plot analysis of $B^0 \rightarrow \bar{D}^0 h^0$ ($h^0 = \pi^0, \eta, \omega$) with $\bar{D}^0 \rightarrow K_S^0 \pi^+ \pi^-$ [86,87]. These results indicate that negative $\cos 2\beta$ solutions are very unlikely, in agreement with the global CKM fit result.

The $b \rightarrow c\bar{c}d$ mediated transitions, such as $B^0 \rightarrow J/\psi \pi^0$ and $B^0 \rightarrow D^{(*)+} D^{(*)-}$, also measure approximately $\sin 2\beta$. However, the dominant component of the $b \rightarrow d$ penguin amplitude has a different CKM phase ($V_{tb}^* V_{td}$) than the tree amplitude ($V_{cb}^* V_{cd}$), and its magnitudes are of the same order in λ . Therefore, the effect of penguins could be large, resulting in $S_f \neq -\eta_f \sin 2\beta$ and $C_f \neq 0$. These decay modes have also been measured by BABAR and Belle. The world averages [61], $S_{J/\psi \pi^0} = -0.65 \pm 0.18$, $S_{D^+ D^-} = -0.75 \pm 0.26$, and $S_{D^{*+} D^{*-}} = -0.67 \pm 0.18$, are consistent with $\sin 2\beta$ obtained from $B^0 \rightarrow$ charmonium K^0 decays, and the C_f 's are also consistent with zero, although the uncertainties are sizable.

11.3.2.2. Penguin-dominated modes:

The $b \rightarrow s\bar{q}q$ penguin-dominated decays have the same CKM phase as the $b \rightarrow c\bar{c}s$ tree level decays, up to corrections suppressed by λ^2 , since $V_{tb}^* V_{ts} = -V_{cb}^* V_{cs} [1 + \mathcal{O}(\lambda^2)]$. Therefore, decays such as $B^0 \rightarrow \phi K^0$ and $\eta' K^0$ provide $\sin 2\beta$ measurements in the SM. Any new physics contribution to the amplitude with a different weak phase would give rise to $S_f \neq -\eta_f \sin 2\beta$, and possibly $C_f \neq 0$. Therefore, the main interest in these modes is not simply to measure $\sin 2\beta$, but to search for new physics. Measurements of many other decay modes in this category, such as $B \rightarrow \pi^0 K_S^0$, $K_S^0 K_S^0 K_S^0$, etc., have also been performed by BABAR and Belle. The results and their uncertainties are summarized in Fig. 12.3 and Table 12.1 of Ref. 81.

11.3.3. α / ϕ_2 :

Since α is the angle between $V_{tb}^* V_{td}$ and $V_{ub}^* V_{ud}$, only time-dependent CP asymmetries in $b \rightarrow u\bar{u}d$ -dominated modes can directly measure $\sin 2\alpha$, in contrast to $\sin 2\beta$, where several different transitions can be used. Since $b \rightarrow d$ penguin amplitudes have a different CKM phase than $b \rightarrow u\bar{u}d$ tree amplitudes, and their magnitudes are of the same order in λ , the penguin contribution can be sizable, and makes the α determination complicated. To date, α has been measured in $B \rightarrow \pi\pi$, $\rho\pi$ and $\rho\rho$ decay modes.

11.3.3.1. $B \rightarrow \pi\pi$:

It is now experimentally well established that there is a sizable contribution of $b \rightarrow d$ penguin amplitudes in $B \rightarrow \pi\pi$ decays. Thus, $S_{\pi^+ \pi^-}$ in the time-dependent $B^0 \rightarrow \pi^+ \pi^-$ analysis does not measure $\sin 2\alpha$, but

$$S_{\pi^+ \pi^-} = \sqrt{1 - C_{\pi^+ \pi^-}^2} \sin(2\alpha + 2\Delta\alpha), \quad (11.21)$$

where $2\Delta\alpha$ is the phase difference between $e^{2i\gamma} \bar{A}_{\pi^+ \pi^-}$ and $A_{\pi^+ \pi^-}$. The value of $\Delta\alpha$, hence α , can be extracted using the isospin relations among the amplitudes of $B^0 \rightarrow \pi^+ \pi^-$, $B^0 \rightarrow \pi^0 \pi^0$, and $B^+ \rightarrow \pi^+ \pi^0$ decays [88],

$$\frac{1}{\sqrt{2}} A_{\pi^+ \pi^-} + A_{\pi^0 \pi^0} - A_{\pi^+ \pi^0} = 0, \quad (11.22)$$

and a similar one for the $\bar{A}_{\pi\pi}$'s. This method utilizes the fact that a pair of pions from $B \rightarrow \pi\pi$ decay must be in a zero angular momentum state, and, because of Bose statistics, they must have even isospin. Consequently, $\pi^0 \pi^{\pm}$ is in a pure isospin-2 state, while the penguin amplitudes only contribute to the isospin-0 final state. The latter does not hold for the electroweak penguin amplitudes, but their effect is expected to be small. The isospin analysis uses the world averages [61] $S_{\pi^+ \pi^-} = -0.61 \pm 0.08$, $C_{\pi^+ \pi^-} = -0.38 \pm 0.07$, the branching fractions of all three modes, and the direct CP asymmetry $C_{\pi^0 \pi^0} = -0.48^{+0.31}_{-0.32}$. This analysis leads to 16 mirror solutions for $0 \leq \alpha < 2\pi$. Because of this, and the sizable experimental error of the $B^0 \rightarrow \pi^0 \pi^0$ rate and CP asymmetry, only a loose constraint on α can be obtained at present [89], $0^\circ < \alpha < 7^\circ$, $83^\circ < \alpha < 103^\circ$, $118^\circ < \alpha < 152^\circ$, and $167^\circ < \alpha < 180^\circ$ at 68% CL.

11.3.3.2. $B \rightarrow \rho\rho$:

The decay $B^0 \rightarrow \rho^+ \rho^-$ contains two vector mesons in the final state, which in general is a mixture of CP -even and CP -odd components. Therefore, it was thought that extracting α from this mode would be complicated.

However, the longitudinal polarization fractions (f_L) in $B^+ \rightarrow \rho^+ \rho^0$ and $B^0 \rightarrow \rho^+ \rho^-$ decays were measured to be close to unity [90], which implies that the final states are almost purely CP -even. Furthermore, $\mathcal{B}(B^0 \rightarrow \rho^0 \rho^0) = (0.86 \pm 0.28) \times 10^{-6}$ is much smaller than $\mathcal{B}(B^0 \rightarrow \rho^+ \rho^-) = (24.2^{+3.1}_{-3.2}) \times 10^{-6}$ and $\mathcal{B}(B^+ \rightarrow \rho^+ \rho^0) = (18.2 \pm 3.0) \times 10^{-6}$ [61], which implies that the effect of the penguin diagrams is small. The isospin analysis using the world averages, $S_{\rho^+ \rho^-} = -0.05 \pm 0.17$ and $C_{\rho^+ \rho^-} = -0.06 \pm 0.13$ [61], together with newly measured time-dependent CP violation parameters for these decays, where $B^0 \rightarrow \pi^+ \pi^- \pi^0$ decays are treated as quasi-two-body decays, have been made both by BABAR [93] and the Belle [94]. However, the isospin analysis is rather complicated, and no significant model-independent constraint on α has been obtained.

11.3.3.3. $B \rightarrow \rho\pi$:

The final state in $B^0 \rightarrow \rho^+ \pi^-$ decay is not a CP eigenstate, but this decay proceeds via the same quark-level diagrams as $B^0 \rightarrow \pi^+ \pi^-$, and both B^0 and \bar{B}^0 can decay to $\rho^+ \pi^-$. Consequently, mixing-induced CP violations can occur in four decay amplitudes, $B^0 \rightarrow \rho^{\pm} \pi^{\mp}$ and $\bar{B}^0 \rightarrow \rho^{\pm} \pi^{\mp}$. The measurements of CP violation parameters for these decays, where $B^0 \rightarrow \pi^+ \pi^- \pi^0$ decays are treated as quasi-two-body decays, have been made both by BABAR [93] and the Belle [94]. However, the isospin analysis is rather complicated, and no significant model-independent constraint on α has been obtained.

The time-dependent Dalitz plot analysis of $B^0 \rightarrow \pi^+ \pi^- \pi^0$ decays permits the extraction of α with a single discrete ambiguity, $\alpha \rightarrow \alpha + \pi$, since one knows the variation of the strong phases in

the interference regions of the $\rho^+\pi^-$, $\rho^-\pi^+$, and $\rho^0\pi^0$ amplitudes in the Dalitz plot [95]. The combination of Belle [96] and BABAR [97] measurements gives $\alpha = (120_{-7}^{+11})^\circ$ [89]. This constraint is still moderate, and there are also solutions around 30° and 90° within 2σ significance level.

Combining the above-mentioned three decay modes [89], α is constrained as

$$\alpha = (88_{-5}^{+6})^\circ. \quad (11.23)$$

A different statistical approach [98] gives similar constraint from the combination of these measurements.

11.3.4. γ / ϕ_3 :

By virtue of Eq. (11.16), γ does not depend on CKM elements involving the top quark, so it can be measured in tree-level B decays. This is an important distinction from the measurements of α and β , and implies that the direct measurements of γ are unlikely to be affected by physics beyond the SM.

11.3.4.1. $B^\pm \rightarrow DK^\pm$:

The interference of $B^- \rightarrow D^0 K^-$ ($b \rightarrow c\bar{u}s$) and $B^- \rightarrow \bar{D}^0 K^-$ ($b \rightarrow u\bar{c}s$) transitions can be studied in final states accessible in both D^0 and \bar{D}^0 decays [80]. In principle, it is possible to extract the B and D decay amplitudes, the relative strong phases, and the weak phase γ from the data.

A practical complication is that the precision depends sensitively on the ratio of the interfering amplitudes

$$r_B = \left| A(B^- \rightarrow \bar{D}^0 K^-) / A(B^- \rightarrow D^0 K^-) \right|, \quad (11.24)$$

which is around 0.1–0.2. The original GLW method [99,100] considers D decays to CP eigenstates, such as $B^\pm \rightarrow D_{CP}^{(*)}(\rightarrow \pi^+\pi^-)K^\pm$. To alleviate the smallness of r_B and make the interfering amplitudes (which are products of the B and D decay amplitudes) comparable in magnitude, the ADS method [101] considers final states where Cabibbo-allowed \bar{D}^0 and doubly-Cabibbo-suppressed D^0 decays interfere. Extensive measurements have been made by the B factories using both methods [102].

It was realized that both D^0 and \bar{D}^0 have large branching fractions to certain three-body final states, such as $K_S\pi^+\pi^-$, and the analysis can be optimized by studying the Dalitz plot-dependence of the interferences [103,104]. The best present determination of γ comes from this method. Belle [105] and BABAR [106] obtained $\gamma = 53_{-18}^{+15} \pm 3 \pm 9^\circ$ and $\gamma = 92 \pm 41 \pm 11 \pm 12^\circ$, respectively, where the last uncertainty is due to the D -decay modeling. The error is sensitive to the central value of the amplitude ratio r_B (and r_B^* for the D^*K mode), for which Belle found somewhat larger central values than BABAR. The same values of $r_B^{(*)}$ enter the ADS analyses, and the data can be combined to fit for $r_B^{(*)}$ and γ . The D^0 - \bar{D}^0 -mixing has been neglected in all measurements, but its effect on γ is far below the present experimental accuracy [107], unless D^0 - \bar{D}^0 -mixing is due to CP -violating new physics, in which case it could be included in the analysis [108].

Combining the GLW, ADS, and Dalitz analyses [89], γ is constrained as

$$\gamma = (77_{-32}^{+30})^\circ. \quad (11.25)$$

The likelihood function of γ is not Gaussian, and the 95% CL range is $26^\circ < \gamma < 130^\circ$. Similar results are found in [98]. The error on γ increased from the previous review [109] because of a decrease of $r_B^{(*)}$.

11.3.4.2. $B^0 \rightarrow D^{(*)}\pi^\mp$:

The interference of $b \rightarrow u$ and $b \rightarrow c$ transitions can be studied in $\bar{B}^0 \rightarrow D^{(*)}\pi^-$ ($b \rightarrow c\bar{u}d$) and $\bar{B}^0 \rightarrow B^0 \rightarrow D^{(*)}\pi^-$ ($\bar{b} \rightarrow \bar{u}c\bar{d}$) decays and their CP conjugates, since both B^0 and \bar{B}^0 decay to $D^{(*)}\pi^\mp$ (or $D^\pm\rho^\mp$, etc.). Since there are only tree and no penguin contributions to these decays, in principle, it is possible to extract from the four time-dependent rates the magnitudes of the two hadronic amplitudes, their relative strong phase, and the weak phase between the two-decay paths, which is $2\beta + \gamma$.

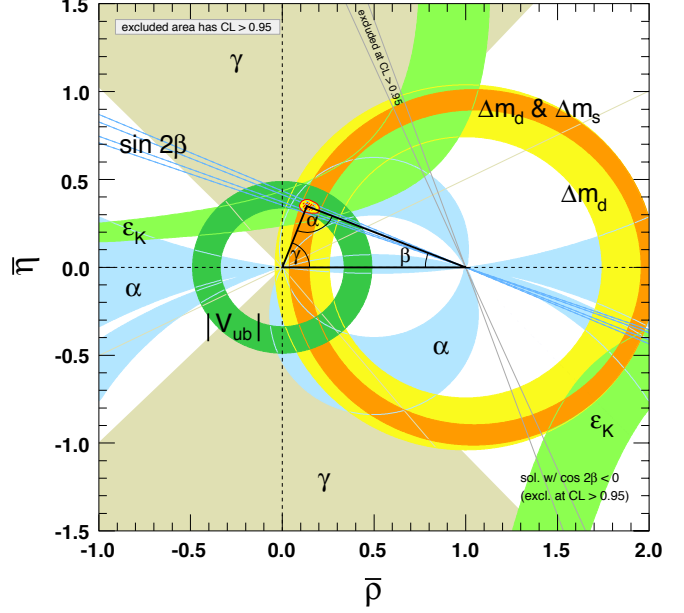


Figure 11.2: Constraints on the $\bar{\rho}, \bar{\eta}$ plane. The shaded areas have 95% CL. Color version at end of book.

A complication is that the ratio of the interfering amplitudes is very small, $r_{D\pi} = A(B^0 \rightarrow D^+\pi^-) / A(\bar{B}^0 \rightarrow D^+\pi^-) = \mathcal{O}(0.01)$ (and similarly for $r_{D^*\pi}$ and $r_{D\rho}$), and therefore it has not been possible to measure it. To obtain $2\beta + \gamma$, $SU(3)$ flavor symmetry and dynamical assumptions have been used to relate $A(\bar{B}^0 \rightarrow D^-\pi^+)$ to $A(\bar{B}^0 \rightarrow D_s^-\pi^+)$, so this measurement is not model-independent at present. Combining the $D^\pm\pi^\mp$, $D^{*\pm}\pi^\mp$ and $D^\pm\rho^\mp$ measurements [110] gives $\sin(2\beta + \gamma) > 0.59$ at 68% CL [89], consistent with the previously discussed results for β and γ . The amplitude ratio is much larger in the analogous $B_s^0 \rightarrow D_s^\pm K^\mp$ decays, so it will be possible at LHCb to measure it and model-independently extract $\gamma - 2\beta_s$ [111] (where $\beta_s = \arg(-V_{ts}V_{tb}^*/V_{cs}V_{cb}^*)$ is related to the phase of B_s mixing).

11.4. Global fit in the Standard Model

Using the independently measured CKM elements mentioned in the previous sections, the unitarity of the CKM matrix can be checked. We obtain $|V_{ud}|^2 + |V_{us}|^2 + |V_{ub}|^2 = 0.9999 \pm 0.0011$ (1st row), $|V_{cd}|^2 + |V_{cs}|^2 + |V_{cb}|^2 = 1.136 \pm 0.125$ (2nd row), $|V_{ud}|^2 + |V_{cd}|^2 + |V_{td}|^2 = 1.002 \pm 0.005$ (1st column), and $|V_{us}|^2 + |V_{cs}|^2 + |V_{ts}|^2 = 1.134 \pm 0.125$ (2nd column), respectively. The uncertainties in the second row and column are dominated by that of $|V_{cs}|$. For the second row, a more stringent check is obtained from the measurement of $\sum_{u,c,d,s,b} |V_{ij}|^2$ in Sec. 11.2.4 minus the sum in the first row above: $|V_{cd}|^2 + |V_{cs}|^2 + |V_{cb}|^2 = 1.002 \pm 0.027$. These provide strong tests of the unitarity of the CKM matrix. The sum of the three angles of the unitarity triangle, $\alpha + \beta + \gamma = (186_{-32}^{+31})^\circ$, is also consistent with the SM expectation.

The CKM matrix elements can be most precisely determined by a global fit that uses all available measurements and imposes the SM constraints (*i.e.*, three generation unitarity). The fit must also use theory predictions for hadronic matrix elements, which sometimes have significant uncertainties. There are several approaches to combining the experimental data. CKMfitter [89,5] and Ref. 112 (which develops [113,114] further) use frequentist statistics, while UTfit [98,115] uses a Bayesian approach. These approaches provide similar results.

The constraints implied by the unitarity of the three generation CKM matrix significantly reduce the allowed range of some of the CKM elements. The fit for the Wolfenstein parameters defined in Eq. (11.4) gives

$$\begin{aligned} \lambda &= 0.2257_{-0.0010}^{+0.0009}, & A &= 0.814_{-0.022}^{+0.021}, \\ \bar{\rho} &= 0.135_{-0.016}^{+0.031}, & \bar{\eta} &= 0.349_{-0.017}^{+0.015}, \end{aligned} \quad (11.26)$$

These values are obtained using the method of Refs. [5,89], and the prescription of Refs. [98,115] gives similar results [116]. The fit results for the magnitudes of all nine CKM elements are

$$V_{\text{CKM}} = \begin{pmatrix} 0.97419 \pm 0.00022 & 0.2257 \pm 0.0010 & 0.00359 \pm 0.00016 \\ 0.2256 \pm 0.0010 & 0.97334 \pm 0.00023 & 0.0415^{+0.0010}_{-0.0011} \\ 0.00874^{+0.00026}_{-0.00037} & 0.0407 \pm 0.0010 & 0.999133^{+0.000044}_{-0.000043} \\ & & (11.27) \end{pmatrix},$$

and the Jarlskog invariant is $J = (3.05^{+0.19}_{-0.20}) \times 10^{-5}$.

Fig. 11.2 illustrates the constraints on the $\bar{\rho}, \bar{\eta}$ plane from various measurements and the global fit result. The shaded 95% CL regions all overlap consistently around the global fit region, though the consistency of $|V_{ub}/V_{cb}|$ and $\sin 2\beta$ is not very good.

11.5. Implications beyond the SM

If the constraints of the SM are lifted, K , B , and D decays and mixings are described by many more parameters than just the four CKM parameters and the W , Z , and quark masses. The most general effective Lagrangian at lowest order contains around a hundred flavor changing operators, and the observable effects of interactions at the weak scale or above are encoded in their coefficients. For example, Δm_d , $\Gamma(B \rightarrow \rho\gamma)$, and $\Gamma(B \rightarrow X_d \ell^+ \ell^-)$ are all proportional to $|V_{td}V_{tb}^*|^2$ in the SM, however, they may receive unrelated contributions from new physics. Similar to the measurements of $\sin 2\beta$ from tree- and loop-dominated modes, such overconstraining measurements of the magnitudes and phases of CKM elements provide excellent sensitivity to new physics. Another very clean test of the SM can come from future measurements of $K_L^0 \rightarrow \pi^0 \nu \bar{\nu}$ and $K^+ \rightarrow \pi^+ \nu \bar{\nu}$. These loop-induced rare decays are sensitive to new physics, and will allow a determination of β independent of its value measured in B decays [117].

Not all CP -violating measurements can be interpreted as constraints on the $\bar{\rho}, \bar{\eta}$ plane. Besides the angles in Eq. (11.16), it is also useful to define $\beta_s = \arg(-V_{ts}V_{tb}^*/V_{cs}V_{cb}^*)$, which is the small, λ^2 -suppressed, angle of a “squashed” unitarity triangle obtained by taking the scalar product of the second and third columns. The angle β_s can be measured via time-dependent CP violation in $B_s^0 \rightarrow J/\psi\phi$, similar to β in $B^0 \rightarrow J/\psi K^0$. Checking if β_s agrees with its SM prediction, $\beta_s = 0.019 \pm 0.001$ [118,89], is an equally important test of the theory. The first flavor-tagged time-dependent CP -asymmetry measurements of $B_s^0 \rightarrow J/\psi\phi$ decay appeared recently [119], disfavoring large negative $\sin 2\beta_s$ values.

In the kaon sector, both CP -violating observables ϵ and ϵ' are tiny, so models in which all sources of CP violation are small were viable before the B -factory measurements. Since the measurement of $\sin 2\beta$, we know that CP violation can be an $\mathcal{O}(1)$ effect, and it is only flavor mixing that is suppressed between the three quark generations. Thus, many models with spontaneous CP violation are excluded. Model-independent statements for the constraints imposed by the CKM measurements on new physics are hard to make, because most models that allow for new flavor physics contain a large number of new parameters. For example, the flavor sector of the MSSM contains 69 CP -conserving parameters and 41 CP -violating phases (*i.e.*, 40 new ones) [120].

In a large class of models, the unitarity of the CKM matrix is maintained, and the dominant new-physics effect is a contribution to the B^0 - \bar{B}^0 -mixing amplitude [121], which can be parameterized as $M_{12} = M_{12}^{\text{SM}}(1 + h_d e^{i\sigma_d})$. While the constraints on h_d and σ_d are significant (before the measurements of γ and α they were not), new physics with a generic weak phase may still contribute to M_{12} at order 20% of the SM. Measurements unimportant for the SM-CKM fit, such as the CP asymmetry in semileptonic decays, play a role in constraining such extensions of the SM [118]. Similar results for the constraints on new physics in K^0 and B_s^0 mixing are discussed in Refs. [115,122].

The CKM elements are fundamental parameters, so they should be measured as precisely as possible. The overconstraining measurements of CP asymmetries, mixing, semileptonic, and rare decays have started to severely constrain the magnitudes and phases of possible new physics contributions to flavor-changing interactions. When new

particles are observed at the LHC, it will be important to know the flavor parameters as precisely as possible to understand the underlying physics.

References:

1. N. Cabibbo, Phys. Rev. Lett. **10**, 531 (1963).
2. M. Kobayashi and T. Maskawa, Prog. Theor. Phys. **49**, 652 (1973).
3. L. Wolfenstein, Phys. Rev. Lett. **51**, 1945 (1983).
4. A. J. Buras *et al.*, Phys. Rev. **D50**, 3433 (1994) [hep-ph/9403384].
5. J. Charles *et al.* [CKMfitter Group], Eur. Phys. J. **C41**, 1 (2005) [hep-ph/0406184].
6. C. Jarlskog, Phys. Rev. Lett. **55**, 1039 (1985).
7. J. C. Hardy and I. S. Towner, Phys. Rev. Lett. **94**, 092502 (2005) [nucl-th/0412050].
8. E. Blucher and W.J. Marciano, “ V_{ud} , V_{us} , the Cabibbo Angle and CKM Unitarity,” in this Review.
9. D. Poganic *et al.*, Phys. Rev. Lett. **93**, 181803 (2004) [hep-ex/0312030].
10. M. Antonelli *et al.* [The FlaviaNet Kaon Working Group], arXiv:0801.1817; see also <http://www.lnf.infn.it/wg/vus>.
11. H. Leutwyler and M. Roos, Z. Phys. **C25**, 91 (1984).
12. A. Juttner, arXiv:0711.1239.
13. E. Blucher *et al.*, hep-ph/0512039.
14. J. Bijnens and P. Talavera, Nucl. Phys. **B669**, 341 (2003) [hep-ph/0303103]; M. Jamin *et al.*, JHEP **402**, 047 (2004) [hep-ph/0401080]; V. Cirigliano *et al.*, JHEP **504**, 6 (2005) [hep-ph/0503108]; C. Dawson *et al.*, PoS **LAT2005**, 337 (2005) [hep-lat/0510018]; N. Tsutsui *et al.* [JLQCD Collaboration], PoS **LAT2005**, 357 (2005) [hep-lat/0510068]; M. Okamoto [Fermilab Lattice Collab.], hep-lat/0412044.
15. W. J. Marciano, Phys. Rev. Lett. **93**, 231803 (2004) [hep-ph/0402299].
16. F. Ambrosino *et al.* [KLOE Collaboration], Phys. Lett. **B632**, 76 (2006) [hep-ex/0509045].
17. C. Bernard *et al.* [MILC Collaboration], PoS **LAT2007**, 090 (2006) [arXiv:0710.1118].
18. N. Cabibbo *et al.*, Ann. Rev. Nucl. and Part. Sci. **53**, 39 (2003) [hep-ph/0307298]; Phys. Rev. Lett. **92**, 251803 (2004) [hep-ph/0307214].
19. M. Ademollo and R. Gatto, Phys. Rev. Lett. **13**, 264 (1964).
20. E. Gamiz *et al.*, PoS **KAON2007**, 008 (2007) [arXiv:0709.0282].
21. C. Aubin *et al.* [Fermilab Lattice, MILC, and HPQCD Collaborations], Phys. Rev. Lett. **94**, 011601 (2005) [hep-ph/0408306].
22. D. Cronin-Hennessy *et al.* [CLEO Collaboration] arXiv:0712.0998.
23. L. Widhalm *et al.* [Belle Collaboration], Phys. Rev. Lett. **97**, 061804 (2006) [hep-ex/0604049].
24. H. Abramowicz *et al.*, Z. Phys. **C15**, 19 (1982).
25. S. A. Rabinowitz *et al.*, Phys. Rev. Lett. **70**, 134 (1993).
26. A. O. Bazarko *et al.* [CCFR Collaboration], Z. Phys. **C65**, 189 (1995) [hep-ex/9406007].
27. P. Vilain *et al.* [CHARM II Collaboration], Eur. Phys. J. **C11**, 19 (1999).
28. F. J. Gilman *et al.*, Phys. Lett. **B592**, 793 (2004).
29. G. D. Lellis *et al.*, Phys. Rept. **399**, 227 (2004) [Erratum *ibid.* **411**, 323 (2005)].
30. N. Ushida *et al.* [Fermilab E531 Collaboration], Phys. Lett. **B206**, 380 (1988).
31. T. Bolton, hep-ex/9708014.
32. A. Kayis-Topaksu *et al.* [CHORUS Collaboration], Phys. Lett. **B626**, 24 (2005).
33. LEP W branching fraction results for this Review of Particle Physics, LEPEWWG/ XSEC/2005-01, <http://lepewwg.web.cern.ch/LEPEWWG/lepww/4f/Winter05/>.
34. P. Abreu *et al.* [DELPHI Collaboration], Phys. Lett. **B439**, 209 (1998).

35. B. Aubert *et al.* [BABAR Collaboration], Phys. Rev. Lett. **98**, 141801 (2007) [hep-ex/0607094].
36. K. Abe *et al.* [Belle Collaboration], arXiv:0709.1340.
37. M. Artuso *et al.* [CLEO Collaboration], Phys. Rev. Lett. **99**, 071802 (2007) [arXiv:0704.0629].
38. K. M. Ecklund *et al.* [CLEO Collaboration], Phys. Rev. Lett. **100**, 161801 (2008) [arXiv:0712.1175].
39. C. Aubin *et al.* [Fermilab, Lattice, MILC, and HPQCD Collaborations], Phys. Rev. Lett. **95**, 122002 (2005) [hep-lat/0506030]; a smaller error was reported recently by, E. Follana *et al.* [HPQCD and UKQCD Collaborations], Phys. Rev. Lett. **100**, 062002 (2008) [arXiv:0706.1726].
40. B. Aubert *et al.* [BABAR Collaboration], Phys. Rev. **D76**, 052005 (2007) [arXiv:0704.0020].
41. I. I. Y. Bigi *et al.*, Phys. Rev. Lett. **71**, 496 (1993) [hep-ph/9304225].
42. A. V. Manohar and M. B. Wise, Phys. Rev. **D49**, 1310 (1994) [hep-ph/9308246].
43. I. I. Y. Bigi *et al.*, Phys. Rev. **D56**, 4017 (1997) [hep-ph/9704245].
44. A. H. Hoang *et al.*, Phys. Rev. **D59**, 074017 (1999) [hep-ph/9811239]; Phys. Rev. Lett. **82**, 277 (1999) [hep-ph/9809423]; A. H. Hoang and T. Teubner, Phys. Rev. **D60**, 114027 (1999) [hep-ph/9904468].
45. R. Kowalewski and T. Mannel, “Determination of V_{cb} and V_{ub} ,” in this *Review*.
46. N. Isgur and M. B. Wise, Phys. Lett. **B237**, 527 (1990); N. Isgur and M. B. Wise, Phys. Lett. **B232**, 113 (1989).
47. M. Neubert, Phys. Rev. **D49**, 3392 (1994) [hep-ph/9311325]; Phys. Rev. **D49**, 4623 (1994) [hep-ph/9312311].
48. I. I. Y. Bigi *et al.*, Int. J. Mod. Phys. **A9**, 2467 (1994) [hep-ph/9312359].
49. C. W. Bauer *et al.*, Phys. Lett. **B479**, 395 (2000) [hep-ph/0002161]; Phys. Rev. **D64**, 113004 (2001) [hep-ph/0107074].
50. A. Bornheim *et al.* [CLEO Collaboration], Phys. Rev. Lett. **88**, 231803 (2002) [hep-ex/0202019].
51. B. Aubert *et al.* [BABAR Collaboration], Phys. Rev. **D73**, 012006 (2006) [hep-ex/0509040].
52. A. Limosani *et al.* [Belle Collaboration], Phys. Lett. **B621**, 28 (2005) [hep-ex/0504046].
53. I. Bizjak *et al.* [Belle Collaboration], Phys. Rev. Lett. **95**, 241801 (2005) [hep-ex/0505088]; B. Aubert *et al.* [BABAR Collaboration], Phys. Rev. Lett. **96**, 221801 (2006) [hep-ex/0601046]; arXiv:0708.3702.
54. M. Okamoto *et al.*, Nucl. Phys. Proc. Supp. **140**, 461 (2005) [hep-lat/0409116].
55. E. Dalgic *et al.*, Phys. Rev. **D73**, 074502 (2006) [Erratum *ibid.* **D75**, 119906 (2007)] [hep-lat/0601021].
56. P. Ball and R. Zwicky, Phys. Rev. **D71**, 014015 (2005) [hep-ph/0406232].
57. O. Schneider, “ B^0 - \bar{B}^0 mixing,” in this *Review*.
58. A. Abulencia *et al.* [CDF Collaboration], Phys. Rev. Lett. **97**, 242003 (2006) [hep-ex/0609040].
59. V. Abazov *et al.* [DØ Collaboration], Phys. Rev. Lett. **97**, 021802 (2006) [hep-ex/0603029].
60. We use following two $N_f = 3$ calculations for f_{B_s} and f_{B_s}/f_{B_d} : M. Wingate *et al.* [HPQCD Collaboration], Phys. Rev. Lett. **92**, 162001 (2004) [hep-ph/0311130]; A. Gray *et al.* [HPQCD Collaboration], Phys. Rev. Lett. **95**, 212001 (2005) [hep-lat/0507015]; C. Bernard *et al.* [Fermilab Lattice and MILC Collaborations], PoS **LAT2007**, 370 (2007).
For $\hat{B}_{B_s}/\hat{B}_{B_d}$, we use following two unquenched calculations: S. Aoki *et al.* [JLQCD Collaboration], Phys. Rev. Lett. **91**, 212001 (2003) [hep-ph/0307039]; V. Gadiyak and Q. Loktik, Phys. Rev. **D72**, 114504 (2005) [hep-ph/0509075]; and \hat{B}_{B_s} value is taken from N. Tantalo, hep-ph/0703241.
61. Heavy Flavor Averaging Group, E. Barberio *et al.*, arXiv:0704.3575, and Summer 2007 updates at <http://www.slac.stanford.edu/xorg/hfag/>.
62. M. Misiak *et al.*, Phys. Rev. Lett. **98**, 022002 (2007) [hep-ph/0609232].
63. B. Grinstein and D. Pirjol, Phys. Rev. **D62**, 093002 (2000) [hep-ph/0002216]; A. Ali *et al.*, Phys. Lett. **B595**, 323 (2004) [hep-ph/0405075]; M. Beneke *et al.*, Nucl. Phys. **B612**, 25 (2001) [hep-ph/0106067]; S. W. Bosch and G. Buchalla, Nucl. Phys. **B621**, 459 (2002) [hep-ph/0106081]; Z. Ligeti and M. B. Wise, Phys. Rev. **D60**, 117506 (1999) [hep-ph/9905277]; D. Becirevic *et al.*, JHEP **305**, 7 (2003) [hep-lat/0301020]; P. Ball *et al.*, Phys. Rev. **D75**, 054004 (2007) [hep-ph/0612081]; W. Wang *et al.*, arXiv:0711.0432; C. D. Lu *et al.*, Phys. Rev. **D76**, 014013 (2007) [hep-ph/0701265].
64. A. J. Buras *et al.*, Phys. Rev. Lett. **95**, 261805 (2005) [hep-ph/0508165].
65. V. V. Anisimovsky *et al.* [E949 Collaboration], Phys. Rev. Lett. **93**, 031801 (2004) [hep-ex/0403036].
66. D. Acosta *et al.* [CDF Collaboration], Phys. Rev. Lett. **95**, 102002 (2005) [hep-ex/0505091].
67. V. M. Abazov *et al.* [DØ Collaboration], arXiv:0801.1326.
68. V. M. Abazov *et al.* [DØ Collaboration], arXiv:0803.0739.
69. CDF note 8968, [CDF Collaboration], contributed to *Lepton Photon Symposium 2007*, http://www-cdf.fnal.gov/physics/new/top/confNotes/cdf8968_STME_pub.pdf.
70. J. Swain and L. Taylor, Phys. Rev. **D58**, 093006 (1998) [hep-ph/9712420].
71. “ K_L^0 meson” particle listing, in this *Review*.
72. G. Buchalla *et al.*, Rev. Mod. Phys. **68**, 1125 (1996) [hep-ph/9512380].
73. T. Inami and C. S. Lim, Prog. Theor. Phys. **65**, 297 (1981) [Erratum *ibid.* **65**, 1772 (1981)].
74. J. M. Flynn and L. Randall, Phys. Lett. **B224**, 221 (1989); G. Buchalla, A. J. Buras, and M. K. Harlander, Nucl. Phys. **B337**, 313 (1990).
75. M. Ciuchini *et al.*, Phys. Lett. **B301**, 263 (1993) [hep-ph/9212203]; A. J. Buras, M. Jamin, and M. E. Lautenbacher, Nucl. Phys. **B408**, 209 (1993) [hep-ph/9303284].
76. S. Bertolini *et al.*, Phys. Rev. **D63**, 056009 (2001) [hep-ph/0002234].
77. A. Pich, hep-ph/0410215.
78. L. Lellouch and M. Luscher, Commun. Math. Phys. **219**, 31 (2001) [hep-lat/0003023].
79. C. h. Kim *et al.*, Nucl. Phys. **B727**, 218 (2005) [hep-lat/0507006].
80. A. B. Carter and A. I. Sanda, Phys. Rev. Lett. **45**, 952 (1980); Phys. Rev. **D23**, 1567 (1981).
81. A more detailed discussion and references can be found in: D. Kirkby and Y. Nir, “ CP violation in meson decays,” in this *Review*.
82. B. Aubert *et al.* [BABAR Collaboration], Phys. Rev. Lett. **99**, 171803 (2007) [hep-ex/0703021].
83. K.-F. Chen *et al.* [Belle Collaboration], Phys. Rev. Lett. **98**, 131802 (2007) [hep-ex/0608039].
84. B. Aubert *et al.* [BABAR Collaboration], Phys. Rev. **D71**, 032005 (2005) [hep-ex/0411016].
85. R. Itoh *et al.* [Belle Collaboration], Phys. Rev. Lett. **95**, 091601 (2005) [hep-ex/0504030].
86. P. Krokovny *et al.* [Belle Collaboration], Phys. Rev. Lett. **97**, 081801 (2006) [hep-ex/0507065].
87. B. Aubert *et al.* [BABAR Collaboration], Phys. Rev. Lett. **99**, 231802 (2007) [arXiv:0708.1544].
88. M. Gronau and D. London, Phys. Rev. Lett. **65**, 3381 (1990).
89. A. Höcker *et al.*, Eur. Phys. J. **C21**, 225 (2001) [hep-ph/0104062]; see also Ref. 5 and updates at <http://ckmfitter.in2p3.fr/>.

90. J. Zhang *et al.* [Belle Collaboration], Phys. Rev. Lett. **91**, 221801 (2003) [[hep-ex/0306007](#)]; A. Somov *et al.* [Belle Collaboration], Phys. Rev. Lett. **96**, 171801 (2006) [[hep-ex/0601024](#)]; B. Aubert *et al.* [BABAR Collaboration], Phys. Rev. Lett. **97**, 261801 (2006) [[hep-ex/0607092](#)]; Phys. Rev. **D76**, 052007 (2007) [[arXiv:0705.2157](#)].
91. B. Aubert *et al.* [BABAR Collaboration], [arXiv:0708.1630](#).
92. A. F. Falk *et al.*, Phys. Rev. **D69**, 011502 (2004) [[hep-ph/0310242](#)].
93. B. Aubert *et al.* [BABAR Collaboration], Phys. Rev. Lett. **91**, 201802 (2003) [[hep-ex/0306030](#)].
94. C. C. Wang *et al.* [Belle Collaboration], Phys. Rev. Lett. **94**, 121801 (2005) [[hep-ex/0408003](#)].
95. H. R. Quinn and A. E. Snyder, Phys. Rev. **D48**, 2139 (1993).
96. A. Kusaka *et al.* [Belle Collaboration], Phys. Rev. Lett. **98**, 221602 (2007) [[hep-ex/0701015](#)].
97. B. Aubert *et al.* [BABAR Collaboration], Phys. Rev. **D76**, 102004 (2007) [[hep-ex/0703008](#)].
98. M. Bona *et al.* [UTfit Collaboration], JHEP **507**, 28 (2005) [[hep-ph/0501199](#)], and updates at <http://www.utfit.org/>.
99. M. Gronau and D. London, Phys. Lett. **B253**, 483 (1991).
100. M. Gronau and D. Wyler, Phys. Lett. **B265**, 172 (1991).
101. D. Atwood *et al.*, Phys. Rev. Lett. **78**, 3257 (1997) [[hep-ph/9612433](#)]; Phys. Rev. **D63**, 036005 (2001) [[hep-ph/0008090](#)].
102. B. Aubert *et al.* [BABAR Collaboration], Phys. Rev. **D71**, 031102 (2005) [[hep-ex/0411091](#)]; Phys. Rev. **D72**, 071103 (2005) [[hep-ex/0507002](#)]; [arXiv:0708.1534](#); Phys. Rev. **D72**, 032004 (2005) [[hep-ex/0504047](#)]; Phys. Rev. **D72**, 071104 (2005) [[hep-ex/0508001](#)]; Phys. Rev. **D76**, 111101 (2007) [[arXiv:0708.0182](#)]; K. Abe *et al.* [Belle Collaboration], Phys. Rev. **D73**, 051106 (2006) [[hep-ex/0601032](#)]; [hep-ex/0508048](#).
103. A. Bondar, talk at the Belle analysis workshop, Novosibirsk, September 2002; A. Poluektov *et al.* [Belle Collaboration], Phys. Rev. **D70**, 072003 (2004) [[hep-ex/0406067](#)].
104. A. Giri *et al.*, Phys. Rev. **D68**, 054018 (2003) [[hep-ph/0303187](#)].
105. A. Poluektov *et al.* [Belle Collaboration], Phys. Rev. **D73**, 112009 (2006) [[hep-ex/0604054](#)].
106. B. Aubert *et al.* [BABAR Collaboration], [hep-ex/0607104](#).
107. Y. Grossman *et al.*, Phys. Rev. **D72**, 031501 (2005) [[hep-ph/0505270](#)].
108. A. Amorim *et al.*, Phys. Rev. **D59**, 056001 (1999) [[hep-ph/9807364](#)].
109. A. Ceccucci *et al.*, J. Phys. **G 33**, 138 (2006).
110. B. Aubert *et al.* [BABAR Collaboration], Phys. Rev. **D71**, 112003 (2005) [[hep-ex/0504035](#)]; Phys. Rev. **D73**, 111101 (2006) [[hep-ex/0602049](#)]; F. J. Ronga *et al.* [Belle Collaboration], Phys. Rev. **D73**, 092003 (2006) [[hep-ex/0604013](#)].
111. R. Aleksan *et al.*, Z. Phys. **C54**, 653 (1992).
112. G. P. Dubois-Felsmann *et al.*, [hep-ph/0308262](#).
113. “The BABAR physics book: Physics at an asymmetric B factory,” (P. F. Harrison and H. R. Quinn, eds.), SLAC-R-0504, 1998.
114. S. Plaszczynski and M. H. Schune, [hep-ph/9911280](#).
115. M. Bona *et al.* [UTfit Collaboration], JHEP **0803**, 049 (2008) [[arXiv:0707.0636](#)].
116. We thank the CKMfitter and UTfit groups for performing fits and making plots using the inputs in our *Review*.
117. G. Buchalla and A. J. Buras, Phys. Lett. **B333**, 221 (1994) [[hep-ph/9405259](#)].
118. S. Laplace *et al.*, Phys. Rev. **D65**, 094040 (2002) [[hep-ph/0202010](#)].
119. T. Aaltonen *et al.* [CDF Collaboration], [arXiv:0712.2397](#); V. M. Abazov *et al.* [DØ Collaboration], [arXiv:0802.2255](#).
120. H. E. Haber, Nucl. Phys. Proc. Supp. **62**, 469 (1998) [[hep-ph/9709450](#)]; Y. Nir, [hep-ph/0109090](#).
121. J. M. Soares and L. Wolfenstein, Phys. Rev. **D47**, 1021 (1993); T. Goto *et al.*, Phys. Rev. **D53**, 6662 (1996) [[hep-ph/9506311](#)]; J. P. Silva and L. Wolfenstein, Phys. Rev. **D55**, 5331 (1997) [[hep-ph/9610208](#)].
122. K. Agashe *et al.*, [hep-ph/0509117](#).

12. CP VIOLATION IN MESON DECAYS

Revised September 2007 by D. Kirkby (UC Irvine) and Y. Nir (Weizmann Institute).

The CP transformation combines charge conjugation C with parity P . Under C , particles and antiparticles are interchanged, by conjugating all internal quantum numbers, *e.g.*, $Q \rightarrow -Q$ for electromagnetic charge. Under P , the handedness of space is reversed, $\vec{x} \rightarrow -\vec{x}$. Thus, for example, a left-handed electron e_L^- is transformed under CP into a right-handed positron, e_R^+ .

If CP were an exact symmetry, the laws of Nature would be the same for matter and for antimatter. We observe that most phenomena are C - and P -symmetric, and therefore, also CP -symmetric. In particular, these symmetries are respected by the gravitational, electromagnetic, and strong interactions. The weak interactions, on the other hand, violate C and P in the strongest possible way. For example, the charged W bosons couple to left-handed electrons, e_L^- , and to their CP -conjugate right-handed positrons, e_R^+ , but to neither their C -conjugate left-handed positrons, e_L^+ , nor their P -conjugate right-handed electrons, e_R^- . While weak interactions violate C and P separately, CP is still preserved in most weak interaction processes. The CP symmetry is, however, violated in certain rare processes, as discovered in neutral K decays in 1964 [1], and observed in recent years in B decays. A K_L meson decays more often to $\pi^- e^+ \bar{\nu}_e$ than to $\pi^+ e^- \nu_e$, thus allowing electrons and positrons to be unambiguously distinguished, but the decay-rate asymmetry is only at the 0.003 level. The CP -violating effects observed in B decays are larger: the CP asymmetry in B^0/\bar{B}^0 meson decays to CP eigenstates like $J/\psi K_S$ is about 0.70 [2,3]. These effects are related to $K^0 - \bar{K}^0$ and $B^0 - \bar{B}^0$ mixing, but CP violation arising solely from decay amplitudes has also been observed, first in $K \rightarrow \pi\pi$ decays [4–6] and more recently in various neutral [7,8] and charged [9,10] B decays. CP violation has not yet been observed in D or B_s meson decays, or in the lepton sector.

In addition to parity and to continuous Lorentz transformations, there is one other spacetime operation that could be a symmetry of the interactions: time reversal T , $t \rightarrow -t$. Violations of T symmetry have been observed in neutral K decays [12], and are expected as a corollary of CP violation if the combined CPT transformation is a fundamental symmetry of Nature [13]. All observations indicate that CPT is indeed a symmetry of Nature. Furthermore, one cannot build a Lorentz-invariant quantum field theory with a Hermitian Hamiltonian that violates CPT . (At several points in our discussion, we avoid assumptions about CPT , in order to identify cases where evidence for CP violation relies on assumptions about CPT .)

Within the Standard Model, CP symmetry is broken by complex phases in the Yukawa couplings (that is, the couplings of the Higgs scalar to quarks). When all manipulations to remove unphysical phases in this model are exhausted, one finds that there is a single CP -violating parameter [14]. In the basis of mass eigenstates, this single phase appears in the 3×3 unitary matrix that gives the W -boson couplings to an up-type antiquark and a down-type quark. (If the Standard Model is supplemented with Majorana mass terms for the neutrinos, the analogous mixing matrix for leptons has three CP -violating phases.) The beautifully consistent and economical Standard-Model description of CP violation in terms of Yukawa couplings, known as the Kobayashi-Maskawa (KM) mechanism [14], agrees with all measurements to date. Furthermore, one can fit the data allowing new physics contributions to loop processes to compete with, or even dominate over, the Standard Model ones [15,16]. Such an analysis provides a model-independent proof that the KM phase is different from zero, and that the matrix of three-generation quark mixing is the dominant source of CP violation in meson decays.

The current level of experimental accuracy and the theoretical uncertainties involved in the interpretation of the various observations leave room, however, for additional subdominant sources of CP violation from new physics. Indeed, almost all extensions of the Standard Model imply that there are such additional sources. Moreover, CP violation is a necessary condition for baryogenesis, the process of dynamically generating the matter-antimatter asymmetry of the Universe [17]. Despite the phenomenological success of the KM

mechanism, it fails (by several orders of magnitude) to accommodate the observed asymmetry [18]. This discrepancy strongly suggests that Nature provides additional sources of CP violation beyond the KM mechanism. (Recent evidence for neutrino masses implies that CP can be violated also in the lepton sector. This situation makes leptogenesis [19], a scenario where CP -violating phases in the Yukawa couplings of the neutrinos play a crucial role in the generation of the baryon asymmetry, a very attractive possibility.) The expectation of new sources motivates the large ongoing experimental effort to find deviations from the predictions of the KM mechanism.

CP violation can be experimentally searched for in a variety of processes, such as meson decays, electric dipole moments of neutrons, electrons and nuclei, and neutrino oscillations. Meson decays probe flavor-changing CP violation. The search for electric dipole moments may find (or constrain) sources of CP violation that, unlike the KM phase, are not related to flavor-changing couplings. Future searches for CP violation in neutrino oscillations might provide further input on leptogenesis.

The present measurements of CP asymmetries provide some of the strongest constraints on the weak couplings of quarks. Future measurements of CP violation in K , D , B , and B_s meson decays will provide additional constraints on the flavor parameters of the Standard Model, and can probe new physics. In this review, we give the formalism and basic physics that are relevant to present and near future measurements of CP violation in meson decays.

Before going into details, we list here the independent CP -violating observables where a signal has been established:

1. Indirect CP violation in $K \rightarrow \pi\pi$ decays [1] and in $K \rightarrow \pi\ell\nu$ decays is given by [20]

$$\epsilon = (2.229 \pm 0.010) \times 10^{-3} e^{i\pi/4}. \quad (12.1)$$

2. Direct CP violation in $K \rightarrow \pi\pi$ decays [4–6] is given by [20]

$$\mathcal{R}e(\epsilon'/\epsilon) = (1.65 \pm 0.26) \times 10^{-3}. \quad (12.2)$$

3. CP violation in the interference of mixing and decay in the $B \rightarrow \psi K^0$ and other related modes is given by (we use K^0 throughout to denote results that combine K_S and K_L modes, but use the sign appropriate to K_S) [2,3]:

$$S_{\psi K^0} = +0.668 \pm 0.026. \quad (12.3)$$

4. CP violation in the interference of mixing and decay in the $B \rightarrow \eta' K^0$ modes is given by [21,22]

$$S_{\eta' K^0} = +0.61 \pm 0.07. \quad (12.4)$$

5. CP violation in the interference of mixing and decay in the $B \rightarrow K^+ K^- K_S$ mode is given by [23,24]

$$S_{(K^+ K^- K_0)_+} = -0.73 \pm 0.10. \quad (12.5)$$

6. CP violation in the interference of mixing and decay in the $B \rightarrow \pi^+ \pi^-$ mode is given by [25,26]

$$S_{\pi^+ \pi^-} = -0.61 \pm 0.08, \quad (12.6)$$

7. Direct CP violation in the $B \rightarrow \pi^+ \pi^-$ mode is given by [25,26]

$$C_{\pi^+ \pi^-} = -0.38 \pm 0.07. \quad (12.7)$$

8. CP violation in the interference of mixing and decay in the $B \rightarrow \psi \pi^0$ mode is given by [27,28]

$$S_{\psi \pi^0} = -0.65 \pm 0.18. \quad (12.8)$$

9. CP violation in the interference of mixing and decay in the $B \rightarrow D^{*+} D^{*-}$ mode is given by [29,30]

$$S_{D^{*+} D^{*-}} = -0.67 \pm 0.18. \quad (12.9)$$

10. Direct *CP* violation in the $\bar{B}^0 \rightarrow K^- \pi^+$ mode is given by [7,8,11]

$$\mathcal{A}_{K^\mp \pi^\pm} = -0.095 \pm 0.013. \quad (12.10)$$

11. Direct *CP* violation in the $B^0 \rightarrow \eta K^{*0}$ mode is given by [31,32]

$$\mathcal{A}_{\eta K^{*0}} = +0.19 \pm 0.05. \quad (12.11)$$

12. Direct *CP* violation in the $B^- \rightarrow K^- \rho^0$ mode is given by [9,10]

$$\mathcal{A}_{\rho^0 K^\mp} = +0.31^{+0.11}_{-0.10}. \quad (12.12)$$

In addition, there is evidence for *CP* violation in neutral *B* decays into final $D^* D$ and $D^* \pi$ modes.

12.1. Formalism

The phenomenology of *CP* violation is superficially different in *K*, *D*, *B*, and B_s decays. This is primarily because each of these systems is governed by a different balance between decay rates, oscillations, and lifetime splitting. However, the underlying mechanisms of *CP* violation are identical for all pseudoscalar mesons.

In this section, we present a general formalism for, and classification of, *CP* violation in the decay of a pseudoscalar meson *M* that might be a charged or neutral *K*, *D*, *B*, or B_s meson. Subsequent sections describe the *CP*-violating phenomenology, approximations, and alternative formalisms that are specific to each system.

12.1.1. Charged- and neutral-meson decays: We define decay amplitudes of *M* (which could be charged or neutral) and its *CP* conjugate \bar{M} to a multi-particle final state *f* and its *CP* conjugate \bar{f} as

$$\begin{aligned} A_f &= \langle f | \mathcal{H} | M \rangle, & \bar{A}_f &= \langle f | \mathcal{H} | \bar{M} \rangle, \\ A_{\bar{f}} &= \langle \bar{f} | \mathcal{H} | M \rangle, & \bar{A}_{\bar{f}} &= \langle \bar{f} | \mathcal{H} | \bar{M} \rangle, \end{aligned} \quad (12.13)$$

where \mathcal{H} is the Hamiltonian governing weak interactions. The action of *CP* on these states introduces phases ξ_M and ξ_f that depend on their flavor content, according to

$$CP|M\rangle = e^{+i\xi_M} |\bar{M}\rangle, \quad CP|f\rangle = e^{+i\xi_f} |\bar{f}\rangle, \quad (12.14)$$

with

$$CP|\bar{M}\rangle = e^{-i\xi_M} |M\rangle, \quad CP|\bar{f}\rangle = e^{-i\xi_f} |f\rangle \quad (12.15)$$

so that $(CP)^2 = 1$. The phases ξ_M and ξ_f are arbitrary and unphysical because of the flavor symmetry of the strong interaction. If *CP* is conserved by the dynamics, $[CP, \mathcal{H}] = 0$, then A_f and $\bar{A}_{\bar{f}}$ have the same magnitude and an arbitrary unphysical relative phase

$$\bar{A}_{\bar{f}} = e^{i(\xi_f - \xi_M)} A_f. \quad (12.16)$$

12.1.2. Neutral-meson mixing: A state that is initially a superposition of M^0 and \bar{M}^0 , say

$$|\psi(0)\rangle = a(0)|M^0\rangle + b(0)|\bar{M}^0\rangle, \quad (12.17)$$

will evolve in time acquiring components that describe all possible decay final states $\{f_1, f_2, \dots\}$, that is,

$$|\psi(t)\rangle = a(t)|M^0\rangle + b(t)|\bar{M}^0\rangle + c_1(t)|f_1\rangle + c_2(t)|f_2\rangle + \dots \quad (12.18)$$

If we are interested in computing only the values of $a(t)$ and $b(t)$ (and not the values of all $c_i(t)$), and if the times *t* in which we are interested are much larger than the typical strong interaction scale, then we can use a much simplified formalism [33]. The simplified time evolution is determined by a 2×2 effective Hamiltonian \mathbf{H} that is not Hermitian, since otherwise the mesons would only oscillate and not decay. Any complex matrix, such as \mathbf{H} , can be written in terms of Hermitian matrices \mathbf{M} and $\mathbf{\Gamma}$ as

$$\mathbf{H} = \mathbf{M} - \frac{i}{2} \mathbf{\Gamma}. \quad (12.19)$$

\mathbf{M} and $\mathbf{\Gamma}$ are associated with $(M^0, \bar{M}^0) \leftrightarrow (M^0, \bar{M}^0)$ transitions via off-shell (dispersive), and on-shell (absorptive) intermediate states, respectively. Diagonal elements of \mathbf{M} and $\mathbf{\Gamma}$ are associated with the flavor-conserving transitions $M^0 \rightarrow M^0$ and $\bar{M}^0 \rightarrow \bar{M}^0$, while off-diagonal elements are associated with flavor-changing transitions $M^0 \leftrightarrow \bar{M}^0$.

The eigenvectors of \mathbf{H} have well-defined masses and decay widths. To specify the components of the strong interaction eigenstates, M^0 and \bar{M}^0 , in the light (M_L) and heavy (M_H) mass eigenstates, we introduce three complex parameters: *p*, *q*, and, for the case that both *CP* and *CPT* are violated in mixing, *z*:

$$\begin{aligned} |M_L\rangle &\propto p\sqrt{1-z}|M^0\rangle + q\sqrt{1+z}|\bar{M}^0\rangle \\ |M_H\rangle &\propto p\sqrt{1+z}|M^0\rangle - q\sqrt{1-z}|\bar{M}^0\rangle, \end{aligned} \quad (12.20)$$

with the normalization $|q|^2 + |p|^2 = 1$ when $z = 0$. (Another possible choice, which is in standard usage for *K* mesons, defines the mass eigenstates according to their lifetimes: K_S for the short-lived and K_L for the long-lived state. The K_L is experimentally found to be the heavier state.)

The real and imaginary parts of the eigenvalues $\omega_{L,H}$ corresponding to $|M_{L,H}\rangle$ represent their masses and decay widths, respectively. The mass and width splittings are

$$\begin{aligned} \Delta m &\equiv m_H - m_L = \mathcal{R}e(\omega_H - \omega_L), \\ \Delta\Gamma &\equiv \Gamma_H - \Gamma_L = -2\mathcal{I}m(\omega_H - \omega_L). \end{aligned} \quad (12.21)$$

Note that here Δm is positive by definition, while the sign of $\Delta\Gamma$ is to be experimentally determined. The sign of $\Delta\Gamma$ has not yet been established for *D*, *B*, and B_s mesons, while $\Delta\Gamma < 0$ is established for *K* mesons. The Standard Model predicts $\Delta\Gamma < 0$ for *B* and B_s mesons (for this reason, $\Delta\Gamma = \Gamma_L - \Gamma_H$, which is still a signed quantity, is often used in the *B* and B_s literature and is the convention used in the PDG experimental summaries). For *D* mesons, non-perturbative contributions are expected to dominate and, consequently, it is difficult to make a definitive prediction for the size and sign of $\Delta\Gamma$.

Solving the eigenvalue problem for \mathbf{H} yields

$$\left(\frac{q}{p}\right)^2 = \frac{\mathbf{M}_{12}^* - (i/2)\mathbf{\Gamma}_{12}^*}{\mathbf{M}_{12} - (i/2)\mathbf{\Gamma}_{12}} \quad (12.22)$$

and

$$z \equiv \frac{\delta m - (i/2)\delta\Gamma}{\Delta m - (i/2)\Delta\Gamma}, \quad (12.23)$$

where

$$\delta m \equiv \mathbf{M}_{11} - \mathbf{M}_{22}, \quad \delta\Gamma \equiv \mathbf{\Gamma}_{11} - \mathbf{\Gamma}_{22} \quad (12.24)$$

are the differences in effective mass and decay-rate expectation values for the strong interaction states M^0 and \bar{M}^0 .

If either *CP* or *CPT* is a symmetry of \mathbf{H} (independently of whether *T* is conserved or violated), then the values of δm and $\delta\Gamma$ are both zero, and hence $z = 0$. We also find that

$$\omega_H - \omega_L = 2\sqrt{\left(\mathbf{M}_{12} - \frac{i}{2}\mathbf{\Gamma}_{12}\right)\left(\mathbf{M}_{12}^* - \frac{i}{2}\mathbf{\Gamma}_{12}^*\right)}. \quad (12.25)$$

If either *CP* or *T* is a symmetry of \mathbf{H} (independently of whether *CPT* is conserved or violated), then $\mathbf{\Gamma}_{12}/\mathbf{M}_{12}$ is real, leading to

$$\left(\frac{q}{p}\right)^2 = e^{2i\xi_M} \Rightarrow \left|\frac{q}{p}\right| = 1, \quad (12.26)$$

where ξ_M is the arbitrary unphysical phase introduced in Eq. (12.15). If, and only if, *CP* is a symmetry of \mathbf{H} (independently of *CPT* and *T*), then both of the above conditions hold, with the result that the mass eigenstates are orthogonal

$$\langle M_H | M_L \rangle = |p|^2 - |q|^2 = 0. \quad (12.27)$$

12.1.3. CP-violating observables : All CP-violating observables in M and \bar{M} decays to final states f and \bar{f} can be expressed in terms of phase-convention-independent combinations of A_f , \bar{A}_f , $A_{\bar{f}}$, and $\bar{A}_{\bar{f}}$, together with, for neutral-meson decays only, q/p . CP violation in charged-meson decays depends only on the combination $|\bar{A}_{\bar{f}}/A_f|$, while CP violation in neutral-meson decays is complicated by $M^0 \leftrightarrow \bar{M}^0$ oscillations, and depends, additionally, on $|q/p|$ and on $\lambda_f \equiv (q/p)(\bar{A}_f/A_f)$.

The decay rates of the two neutral K mass eigenstates, K_S and K_L , are different enough ($\Gamma_S/\Gamma_L \sim 500$) that one can, in most cases, actually study their decays independently. For neutral D , B , and B_s mesons, however, values of $\Delta\Gamma/\Gamma$ (where $\Gamma \equiv (\Gamma_H + \Gamma_L)/2$) are relatively small, and so both mass eigenstates must be considered in their evolution. We denote the state of an initially pure $|M^0\rangle$ or $|\bar{M}^0\rangle$ after an elapsed proper time t as $|M^0_{\text{phys}}(t)\rangle$ or $|\bar{M}^0_{\text{phys}}(t)\rangle$, respectively. Using the effective Hamiltonian approximation, but not assuming CPT is a good symmetry, we obtain

$$\begin{aligned} |M^0_{\text{phys}}(t)\rangle &= (g_+(t) + z g_-(t)) |M^0\rangle - \sqrt{1-z^2} \frac{q}{p} g_-(t) |\bar{M}^0\rangle, \\ |\bar{M}^0_{\text{phys}}(t)\rangle &= (g_+(t) - z g_-(t)) |\bar{M}^0\rangle - \sqrt{1-z^2} \frac{p}{q} g_-(t) |M^0\rangle, \end{aligned} \quad (12.28)$$

where

$$g_{\pm}(t) \equiv \frac{1}{2} \left(e^{-im_H t - \frac{1}{2}\Gamma_H t} \pm e^{-im_L t - \frac{1}{2}\Gamma_L t} \right) \quad (12.29)$$

and $z = 0$ if either CPT or CP is conserved.

Defining $x \equiv \Delta m/\Gamma$ and $y \equiv \Delta\Gamma/(2\Gamma)$, and assuming $z = 0$, one obtains the following time-dependent decay rates:

$$\begin{aligned} \frac{d\Gamma[M^0_{\text{phys}}(t) \rightarrow f]/dt}{e^{-\Gamma t} \mathcal{N}_f} &= \\ & \left(|A_f|^2 + |(q/p)\bar{A}_f|^2 \right) \cosh(y\Gamma t) + \left(|A_f|^2 - |(q/p)\bar{A}_f|^2 \right) \cos(x\Gamma t) \\ & + 2 \operatorname{Re}((q/p)A_f^* \bar{A}_f) \sinh(y\Gamma t) - 2 \operatorname{Im}((q/p)A_f^* \bar{A}_f) \sin(x\Gamma t), \end{aligned} \quad (12.30)$$

$$\begin{aligned} \frac{d\Gamma[\bar{M}^0_{\text{phys}}(t) \rightarrow f]/dt}{e^{-\Gamma t} \mathcal{N}_f} &= \\ & \left(|(p/q)A_f|^2 + |\bar{A}_f|^2 \right) \cosh(y\Gamma t) - \left(|(p/q)A_f|^2 - |\bar{A}_f|^2 \right) \cos(x\Gamma t) \\ & + 2 \operatorname{Re}((p/q)A_f \bar{A}_f^*) \sinh(y\Gamma t) - 2 \operatorname{Im}((p/q)A_f \bar{A}_f^*) \sin(x\Gamma t), \end{aligned} \quad (12.31)$$

where \mathcal{N}_f is a common, time-independent, normalization factor. Decay rates to the CP-conjugate final state \bar{f} are obtained analogously, with $\mathcal{N}_f = \mathcal{N}_{\bar{f}}$ and the substitutions $A_f \rightarrow A_{\bar{f}}$ and $\bar{A}_f \rightarrow \bar{A}_{\bar{f}}$ in Eqs. (12.30,12.31). Terms proportional to $|A_f|^2$ or $|\bar{A}_f|^2$ are associated with decays that occur without any net $M \leftrightarrow \bar{M}$ oscillation, while terms proportional to $|(q/p)\bar{A}_f|^2$ or $|(p/q)A_f|^2$ are associated with decays following a net oscillation. The $\sinh(y\Gamma t)$ and $\sin(x\Gamma t)$ terms of Eqs. (12.30,12.31) are associated with the interference between these two cases. Note that, in multi-body decays, amplitudes are functions of phase-space variables. Interference may be present in some regions but not others, and is strongly influenced by resonant substructure.

When neutral pseudoscalar mesons are produced coherently in pairs from the decay of a vector resonance, $V \rightarrow M^0 \bar{M}^0$ (for example, $\Upsilon(4S) \rightarrow B^0 \bar{B}^0$ or $\phi \rightarrow K^0 \bar{K}^0$), the time-dependence of their subsequent decays to final states f_1 and f_2 has a similar form to Eqs. (12.30,12.31):

$$\begin{aligned} \frac{d\Gamma[V_{\text{phys}}(t_1, t_2) \rightarrow f_1 f_2]/dt}{e^{-\Gamma|\Delta t|} \mathcal{N}_{f_1 f_2}} &= \\ & \left(|a_+|^2 + |a_-|^2 \right) \cosh(y\Gamma\Delta t) + \left(|a_+|^2 - |a_-|^2 \right) \cos(x\Gamma\Delta t) \\ & - 2 \operatorname{Re}(a_+^* a_-) \sinh(y\Gamma\Delta t) + 2 \operatorname{Im}(a_+^* a_-) \sin(x\Gamma\Delta t), \end{aligned} \quad (12.32)$$

where $\Delta t \equiv t_2 - t_1$ is the difference in the production times, t_1 and t_2 , of f_1 and f_2 , respectively, and the dependence on the average decay time and on decay angles has been integrated out. The coefficients in Eq. (12.32) are determined by the amplitudes for no net oscillation from $t_1 \rightarrow t_2$, $\bar{A}_{f_1} A_{f_2}$, and $A_{f_1} \bar{A}_{f_2}$, and for a net oscillation, $(q/p)\bar{A}_{f_1} \bar{A}_{f_2}$ and $(p/q)A_{f_1} A_{f_2}$, via

$$\begin{aligned} a_+ &\equiv \bar{A}_{f_1} A_{f_2} - A_{f_1} \bar{A}_{f_2}, \\ a_- &\equiv -\sqrt{1-z^2} \left(\frac{q}{p} \bar{A}_{f_1} \bar{A}_{f_2} - \frac{p}{q} A_{f_1} A_{f_2} \right) + z (\bar{A}_{f_1} A_{f_2} + A_{f_1} \bar{A}_{f_2}). \end{aligned} \quad (12.33)$$

Assuming CPT conservation, $z = 0$, and identifying $\Delta t \rightarrow t$ and $f_2 \rightarrow f$, we find that Eqs. (12.32) and (12.33) reduce to Eq. (12.30) with $A_{f_1} = 0$, $\bar{A}_{f_1} = 1$, or to Eq. (12.31) with $\bar{A}_{f_1} = 0$, $A_{f_1} = 1$. Indeed, such a situation plays an important role in experiments. Final states f_1 with $A_{f_1} = 0$ or $\bar{A}_{f_1} = 0$ are called tagging states, because they identify the decaying pseudoscalar meson as, respectively, \bar{M}^0 or M^0 . Before one of M^0 or \bar{M}^0 decays, they evolve in phase, so that there is always one M^0 and one \bar{M}^0 present. A tagging decay of one meson sets the clock for the time evolution of the other: it starts at t_1 as purely M^0 or \bar{M}^0 , with time evolution that depends only on $t_2 - t_1$.

When f_1 is a state that both M^0 and \bar{M}^0 can decay into, then Eq. (12.32) contains interference terms proportional to $A_{f_1} \bar{A}_{f_1} \neq 0$ that are not present in Eqs. (12.30,12.31). Even when f_1 is dominantly produced by M^0 decays rather than \bar{M}^0 decays, or vice versa, $A_{f_1} \bar{A}_{f_1}$ can be non-zero owing to doubly-CKM-suppressed decays (with amplitudes suppressed by at least two powers of λ relative to the dominant amplitude, in the language of Section 12.3), and these terms should be considered for precision studies of CP violation in coherent $V \rightarrow M^0 \bar{M}^0$ decays [34].

12.1.4. Classification of CP-violating effects : We distinguish three types of CP-violating effects in meson decays:

I. CP violation in decay is defined by

$$|\bar{A}_{\bar{f}}/A_f| \neq 1. \quad (12.34)$$

In charged meson decays, where mixing effects are absent, this is the only possible source of CP asymmetries:

$$A_{f\pm} \equiv \frac{\Gamma(M^- \rightarrow f^-) - \Gamma(M^+ \rightarrow f^+)}{\Gamma(M^- \rightarrow f^-) + \Gamma(M^+ \rightarrow f^+)} = \frac{|\bar{A}_{f-}/A_{f+}|^2 - 1}{|\bar{A}_{f-}/A_{f+}|^2 + 1}. \quad (12.35)$$

II. CP (and T) violation in mixing is defined by

$$|q/p| \neq 1. \quad (12.36)$$

In charged-current semileptonic neutral meson decays $M, \bar{M} \rightarrow \ell^\pm X$ (taking $|A_{\ell^+ X}| = |\bar{A}_{\ell^- X}|$ and $A_{\ell^- X} = \bar{A}_{\ell^+ X} = 0$, as is the case in the Standard Model, to lowest order in G_F , and in most of its reasonable extensions), this is the only source of CP violation, and can be measured via the asymmetry of “wrong-sign” decays induced by oscillations:

$$\begin{aligned} A_{\text{SL}}(t) &\equiv \frac{d\Gamma/dt[\bar{M}^0_{\text{phys}}(t) \rightarrow \ell^+ X] - d\Gamma/dt[M^0_{\text{phys}}(t) \rightarrow \ell^- X]}{d\Gamma/dt[\bar{M}^0_{\text{phys}}(t) \rightarrow \ell^+ X] + d\Gamma/dt[M^0_{\text{phys}}(t) \rightarrow \ell^- X]} \\ &= \frac{1 - |q/p|^4}{1 + |q/p|^4}. \end{aligned} \quad (12.37)$$

Note that this asymmetry of time-dependent decay rates is actually time-independent.

III. CP violation in interference between a decay without mixing, $M^0 \rightarrow f$, and a decay with mixing, $M^0 \rightarrow \bar{M}^0 \rightarrow f$ (such an effect occurs only in decays to final states that are common to M^0 and \bar{M}^0 , including all CP eigenstates), is defined by

$$\operatorname{Im}(\lambda_f) \neq 0, \quad (12.38)$$

with

$$\lambda_f \equiv \frac{q \bar{A}_f}{p A_f}. \quad (12.39)$$

This form of CP violation can be observed, for example, using the asymmetry of neutral meson decays into final CP eigenstates f_{CP}

$$\mathcal{A}_{f_{CP}}(t) \equiv \frac{d\Gamma/dt[\bar{M}_{\text{phys}}^0(t) \rightarrow f_{CP}] - d\Gamma/dt[M_{\text{phys}}^0(t) \rightarrow f_{CP}]}{d\Gamma/dt[\bar{M}_{\text{phys}}^0(t) \rightarrow f_{CP}] + d\Gamma/dt[M_{\text{phys}}^0(t) \rightarrow f_{CP}]}. \quad (12.40)$$

If $\Delta\Gamma = 0$ and $|q/p| = 1$, as expected to a good approximation for B mesons, but not for K mesons, then $\mathcal{A}_{f_{CP}}$ has a particularly simple form (see Eq. (12.74), below). If, in addition, the decay amplitudes fulfill $|\bar{A}_{f_{CP}}| = |A_{f_{CP}}|$, the interference between decays with and without mixing is the only source of the asymmetry and $\mathcal{A}_{f_{CP}}(t) = \mathcal{I}m(\lambda_{f_{CP}}) \sin(x\Gamma t)$.

Examples of these three types of CP violation will be given in Sections 12.4, 12.5, and 12.6.

12.2. Theoretical Interpretation: General Considerations

Consider the $M \rightarrow f$ decay amplitude A_f , and the CP conjugate process, $\bar{M} \rightarrow \bar{f}$, with decay amplitude $\bar{A}_{\bar{f}}$. There are two types of phases that may appear in these decay amplitudes. Complex parameters in any Lagrangian term that contributes to the amplitude will appear in complex conjugate form in the CP -conjugate amplitude. Thus, their phases appear in A_f and $\bar{A}_{\bar{f}}$ with opposite signs. In the Standard Model, these phases occur only in the couplings of the W^\pm bosons, and hence, are often called ‘‘weak phases.’’ The weak phase of any single term is convention-dependent. However, the difference between the weak phases in two different terms in A_f is convention-independent. A second type of phase can appear in scattering or decay amplitudes, even when the Lagrangian is real. Their origin is the possible contribution from intermediate on-shell states in the decay process. Since these phases are generated by CP -invariant interactions, they are the same in A_f and $\bar{A}_{\bar{f}}$. Usually the dominant rescattering is due to strong interactions; hence the designation ‘‘strong phases’’ for the phase shifts so induced. Again, only the relative strong phases between different terms in the amplitude are physically meaningful.

The ‘weak’ and ‘strong’ phases discussed here appear in addition to the ‘spurious’ CP -transformation phases of Eq. (12.16). Those spurious phases are due to an arbitrary choice of phase convention, and do not originate from any dynamics or induce any CP violation. For simplicity, we set them to zero from here on.

It is useful to write each contribution a_i to A_f in three parts: its magnitude $|a_i|$, its weak phase ϕ_i , and its strong phase δ_i . If, for example, there are two such contributions, $A_f = a_1 + a_2$, we have

$$\begin{aligned} A_f &= |a_1|e^{i(\delta_1+\phi_1)} + |a_2|e^{i(\delta_2+\phi_2)}, \\ \bar{A}_{\bar{f}} &= |a_1|e^{i(\delta_1-\phi_1)} + |a_2|e^{i(\delta_2-\phi_2)}. \end{aligned} \quad (12.41)$$

Similarly, for neutral meson decays, it is useful to write

$$\mathbf{M}_{12} = |\mathbf{M}_{12}|e^{i\phi_M}, \quad \mathbf{\Gamma}_{12} = |\mathbf{\Gamma}_{12}|e^{i\phi_\Gamma}. \quad (12.42)$$

Each of the phases appearing in Eqs. (12.41,12.42) is convention-dependent, but combinations such as $\delta_1 - \delta_2$, $\phi_1 - \phi_2$, $\phi_M - \phi_\Gamma$, and $\phi_M + \phi_1 - \bar{\phi}_1$ (where $\bar{\phi}_1$ is a weak phase contributing to $\bar{A}_{\bar{f}}$) are physical.

It is now straightforward to evaluate the various asymmetries in terms of the theoretical parameters introduced here. We will do so with approximations that are often relevant to the most interesting measured asymmetries.

1. The CP asymmetry in charged meson decays [Eq. (12.35)] is given by

$$\mathcal{A}_{f^\pm} = -\frac{2|a_1 a_2| \sin(\delta_2 - \delta_1) \sin(\phi_2 - \phi_1)}{|a_1|^2 + |a_2|^2 + 2|a_1 a_2| \cos(\delta_2 - \delta_1) \cos(\phi_2 - \phi_1)}. \quad (12.43)$$

The quantity of most interest to theory is the weak phase difference $\phi_2 - \phi_1$. Its extraction from the asymmetry requires, however, that the amplitude ratio $|a_2/a_1|$ and the strong phase difference $\delta_2 - \delta_1$ are known. Both quantities depend on non-perturbative hadronic parameters that are difficult to calculate.

2. In the approximation that $|\mathbf{\Gamma}_{12}/\mathbf{M}_{12}| \ll 1$ (valid for B and B_s mesons), the CP asymmetry in semileptonic neutral-meson decays [Eq. (12.37)] is given by

$$\mathcal{A}_{\text{SL}} = -\left| \frac{\mathbf{\Gamma}_{12}}{\mathbf{M}_{12}} \right| \sin(\phi_M - \phi_\Gamma). \quad (12.44)$$

The quantity of most interest to theory is the weak phase $\phi_M - \phi_\Gamma$. Its extraction from the asymmetry requires, however, that $|\mathbf{\Gamma}_{12}/\mathbf{M}_{12}|$ is known. This quantity depends on long-distance physics that is difficult to calculate.

3. In the approximations that only a single weak phase contributes to decay, $A_f = |a_f|e^{i(\delta_f+\phi_f)}$, and that $|\mathbf{\Gamma}_{12}/\mathbf{M}_{12}| = 0$, we obtain $|\lambda_f| = 1$, and the CP asymmetries in decays to a final CP eigenstate f [Eq. (12.40)] with eigenvalue $\eta_f = \pm 1$ are given by

$$\mathcal{A}_{f_{CP}}(t) = \mathcal{I}m(\lambda_f) \sin(\Delta mt) \quad \text{with} \quad \mathcal{I}m(\lambda_f) = \eta_f \sin(\phi_M + 2\phi_f). \quad (12.45)$$

Note that the phase so measured is purely a weak phase, and no hadronic parameters are involved in the extraction of its value from $\mathcal{I}m(\lambda_f)$.

The discussion above allows us to introduce another classification of CP -violating effects:

1. *Indirect CP violation* is consistent with taking $\phi_M \neq 0$ and setting all other CP violating phases to zero. CP violation in mixing (type II) belongs to this class.
2. *Direct CP violation* cannot be accounted for by just $\phi_M \neq 0$. CP violation in decay (type I) belongs to this class.

As concerns type III CP violation, observing $\eta_{f_1} \mathcal{I}m(\lambda_{f_1}) \neq \eta_{f_2} \mathcal{I}m(\lambda_{f_2})$ (for the same decaying meson and two different final CP eigenstates f_1 and f_2) would establish direct CP violation. The significance of this classification is related to theory. In superweak models [35], CP violation appears only in diagrams that contribute to \mathbf{M}_{12} , hence they predict that there is no direct CP violation. In most models and, in particular, in the Standard Model, CP violation is both direct and indirect. The experimental observation of $\epsilon' \neq 0$ (see Section 12.4) excluded the superweak scenario.

12.3. Theoretical Interpretation: The KM Mechanism

Of all the Standard Model quark parameters, only the Kobayashi-Maskawa (KM) phase is CP -violating. Having a single source of CP violation, the Standard Model is very predictive for CP asymmetries: some vanish, and those that do not are correlated.

To be precise, CP could be violated also by strong interactions. The experimental upper bound on the electric-dipole moment of the neutron implies, however, that θ_{QCD} , the non-perturbative parameter that determines the strength of this type of CP violation, is tiny, if not zero. (The smallness of θ_{QCD} constitutes a theoretical puzzle, known as ‘the strong CP problem.’) In particular, it is irrelevant to our discussion of meson decays.

The charged current interactions (that is, the W^\pm interactions) for quarks are given by

$$-\mathcal{L}_{W^\pm} = \frac{g}{\sqrt{2}} \bar{u}_{Li} \gamma^\mu (V_{\text{CKM}})_{ij} d_{Lj} W_\mu^\pm + \text{h.c.} \quad (12.46)$$

Here $i, j = 1, 2, 3$ are generation numbers. The Cabibbo-Kobayashi-Maskawa (CKM) mixing matrix for quarks is a 3×3 unitary matrix [36]. Ordering the quarks by their masses, *i.e.*, $(u_1, u_2, u_3) \rightarrow (u, c, t)$ and $(d_1, d_2, d_3) \rightarrow (d, s, b)$, the elements of V_{CKM} are written as follows:

$$V_{\text{CKM}} = \begin{pmatrix} V_{ud} & V_{us} & V_{ub} \\ V_{cd} & V_{cs} & V_{cb} \\ V_{td} & V_{ts} & V_{tb} \end{pmatrix}. \quad (12.47)$$

While a general 3×3 unitary matrix depends on three real angles and six phases, the freedom to redefine the phases of the quark mass eigenstates can be used to remove five of the phases, leaving a single physical phase, the Kobayashi-Maskawa phase, that is responsible for all CP violation in meson decays in the Standard Model.

The fact that one can parametrize V_{CKM} by three real and only one imaginary physical parameters can be made manifest by choosing an explicit parametrization. The Wolfenstein parametrization [37,38] is particularly useful:

$$V_{\text{CKM}} = \begin{pmatrix} 1 - \frac{1}{2}\lambda^2 - \frac{1}{8}\lambda^4 & \lambda & A\lambda^3(\rho - i\eta) \\ -\lambda + \frac{1}{2}A^2\lambda^5[1 - 2(\rho + i\eta)] & 1 - \frac{1}{2}\lambda^2 - \frac{1}{8}\lambda^4(1 + 4A^2) & A\lambda^2 \\ A\lambda^3[1 - (1 - \frac{1}{2}\lambda^2)(\rho + i\eta)] & -A\lambda^2 + \frac{1}{2}A\lambda^4[1 - 2(\rho + i\eta)] & 1 - \frac{1}{2}A^2\lambda^4 \end{pmatrix}. \quad (12.48)$$

Here $\lambda \approx 0.23$ (not to be confused with λ_f) plays the role of an expansion parameter, and η represents the CP -violating phase. Terms of $\mathcal{O}(\lambda^6)$ were neglected.

The unitarity of the CKM matrix, $(VV^\dagger)_{ij} = (V^\dagger V)_{ij} = \delta_{ij}$, leads to twelve distinct complex relations among the matrix elements. The six relations with $i \neq j$ can be represented geometrically as triangles in the complex plane. Two of these,

$$\begin{aligned} V_{ud}V_{ub}^* + V_{cd}V_{cb}^* + V_{td}V_{tb}^* &= 0 \\ V_{td}V_{ud}^* + V_{ts}V_{us}^* + V_{tb}V_{ub}^* &= 0, \end{aligned}$$

have terms of equal order, $\mathcal{O}(A\lambda^3)$, and so have corresponding triangles whose interior angles are all $\mathcal{O}(1)$ physical quantities that can, in principle, be independently measured. The angles of the first triangle (see Fig. 12.1) are given by

$$\begin{aligned} \alpha \equiv \varphi_2 &\equiv \arg\left(-\frac{V_{td}V_{tb}^*}{V_{ud}V_{ub}^*}\right) \simeq \arg\left(-\frac{1 - \rho - i\eta}{\rho + i\eta}\right), \\ \beta \equiv \varphi_1 &\equiv \arg\left(-\frac{V_{cd}V_{cb}^*}{V_{td}V_{tb}^*}\right) \simeq \arg\left(\frac{1}{1 - \rho - i\eta}\right), \\ \gamma \equiv \varphi_3 &\equiv \arg\left(-\frac{V_{ud}V_{ub}^*}{V_{cd}V_{cb}^*}\right) \simeq \arg(\rho + i\eta). \end{aligned} \quad (12.49)$$

The angles of the second triangle are equal to (α, β, γ) up to corrections of $\mathcal{O}(\lambda^2)$. The notations (α, β, γ) and $(\varphi_1, \varphi_2, \varphi_3)$ are both in common usage but, for convenience, we only use the first convention in the following.

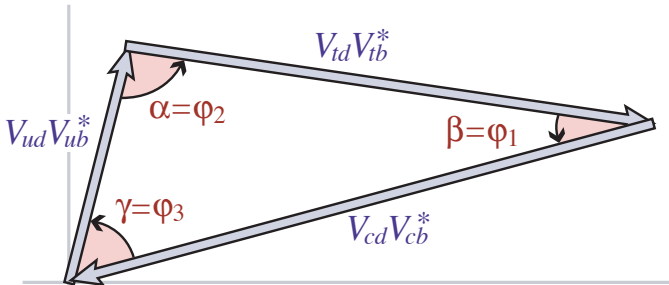


Figure 12.1: Graphical representation of the unitarity constraint $V_{ud}V_{ub}^* + V_{cd}V_{cb}^* + V_{td}V_{tb}^* = 0$ as a triangle in the complex plane.

All unitarity triangles have the same area, commonly denoted by $J/2$ [39]. If CP is violated, J is different from zero and can be taken as the single CP -violating parameter. In the Wolfenstein parametrization of Eq. (12.48), $J \simeq \lambda^6 A^2 \eta$.

12.4. K Decays

CP violation was discovered in $K \rightarrow \pi\pi$ decays in 1964 [1]. The same mode provided the first evidence for direct CP violation [4–6].

The decay amplitudes actually measured in neutral K decays refer to the mass eigenstates K_L and K_S , rather than to the K and \bar{K} states referred to in Eq. (12.13). The final $\pi^+\pi^-$ and $\pi^0\pi^0$ states are CP -even. In the CP limit, $K_S(K_L)$ would be CP -even (odd), and therefore would (would not) decay to two pions. We define CP -violating amplitude ratios for two-pion final states,

$$\eta_{00} \equiv \frac{\langle \pi^0\pi^0 | \mathcal{H} | K_L \rangle}{\langle \pi^0\pi^0 | \mathcal{H} | K_S \rangle}, \quad \eta_{+-} \equiv \frac{\langle \pi^+\pi^- | \mathcal{H} | K_L \rangle}{\langle \pi^+\pi^- | \mathcal{H} | K_S \rangle}. \quad (12.50)$$

Another important observable is the asymmetry of time-integrated semileptonic decay rates:

$$\delta_L \equiv \frac{\Gamma(K_L \rightarrow \ell^+\nu_\ell\pi^-) - \Gamma(K_L \rightarrow \ell^-\bar{\nu}_\ell\pi^+)}{\Gamma(K_L \rightarrow \ell^+\nu_\ell\pi^-) + \Gamma(K_L \rightarrow \ell^-\bar{\nu}_\ell\pi^+)}. \quad (12.51)$$

CP violation has been observed as an appearance of K_L decays to two-pion final states [40],

$$|\eta_{00}| = (2.222 \pm 0.010) \times 10^{-3} \quad |\eta_{+-}| = (2.233 \pm 0.010) \times 10^{-3} \quad (12.52)$$

$$|\eta_{00}/\eta_{+-}| = 0.9950 \pm 0.0008, \quad (12.53)$$

where the phase ϕ_{ij} of the amplitude ratio η_{ij} has been determined both assuming CPT invariance:

$$\phi_{00} = (43.50 \pm 0.06)^\circ, \quad \phi_{+-} = (43.52 \pm 0.05)^\circ, \quad (12.54)$$

and without assuming CPT invariance:

$$\phi_{00} = (43.7 \pm 0.8)^\circ, \quad \phi_{+-} = (43.4 \pm 0.7)^\circ. \quad (12.55)$$

CP violation has also been observed in semileptonic K_L decays [40]

$$\delta_L = (3.32 \pm 0.06) \times 10^{-3}, \quad (12.56)$$

where δ_L is a weighted average of muon and electron measurements, as well as in K_L decays to $\pi^+\pi^-\gamma$ and $\pi^+\pi^-e^+e^-$ [40]. CP violation in $K \rightarrow 3\pi$ decays has not yet been observed [40,41].

Historically, CP violation in neutral K decays has been described in terms of parameters ϵ and ϵ' . The observables η_{00} , η_{+-} , and δ_L are related to these parameters, and to those of Section 12.1, by

$$\begin{aligned} \eta_{00} &= \frac{1 - \lambda_{\pi^0\pi^0}}{1 + \lambda_{\pi^0\pi^0}} = \epsilon - 2\epsilon', \\ \eta_{+-} &= \frac{1 - \lambda_{\pi^+\pi^-}}{1 + \lambda_{\pi^+\pi^-}} = \epsilon + \epsilon', \\ \delta_L &= \frac{1 - |q/p|^2}{1 + |q/p|^2} = \frac{2\text{Re}(\epsilon)}{1 + |\epsilon|^2}, \end{aligned} \quad (12.57)$$

where, in the last line, we have assumed that $|A_{\ell^+\nu_\ell\pi^-}| = |\bar{A}_{\ell^-\bar{\nu}_\ell\pi^+}|$ and $|A_{\ell^-\bar{\nu}_\ell\pi^+}| = |\bar{A}_{\ell^+\nu_\ell\pi^-}| = 0$. (The convention-dependent parameter $\bar{\epsilon} \equiv (1 - q/p)/(1 + q/p)$, sometimes used in the literature, is, in general, different from ϵ but yields a similar expression, $\delta_L = 2\text{Re}(\bar{\epsilon})/(1 + |\bar{\epsilon}|^2)$.) A fit to the $K \rightarrow \pi\pi$ data yields [40]

$$\begin{aligned} |\epsilon| &= (2.229 \pm 0.010) \times 10^{-3}, \\ \text{Re}(\epsilon'/\epsilon) &= (1.65 \pm 0.26) \times 10^{-3}. \end{aligned} \quad (12.58)$$

In discussing two-pion final states, it is useful to express the amplitudes $A_{\pi^0\pi^0}$ and $A_{\pi^+\pi^-}$ in terms of their isospin components via

$$\begin{aligned} A_{\pi^0\pi^0} &= \sqrt{\frac{1}{3}} |A_0| e^{i(\delta_0 + \phi_0)} - \sqrt{\frac{2}{3}} |A_2| e^{i(\delta_2 + \phi_2)}, \\ A_{\pi^+\pi^-} &= \sqrt{\frac{2}{3}} |A_0| e^{i(\delta_0 + \phi_0)} + \sqrt{\frac{1}{3}} |A_2| e^{i(\delta_2 + \phi_2)}, \end{aligned} \quad (12.59)$$

where we parameterize the amplitude $A_I(\bar{A}_I)$ for $K^0(\bar{K}^0)$ decay into two pions with total isospin $I = 0$ or 2 as

$$\begin{aligned} A_I &\equiv \langle (\pi\pi)_I | \mathcal{H} | K^0 \rangle = |A_I| e^{i(\delta_I + \phi_I)}, \\ \bar{A}_I &\equiv \langle (\pi\pi)_I | \mathcal{H} | \bar{K}^0 \rangle = |A_I| e^{i(\delta_I - \phi_I)}. \end{aligned} \quad (12.60)$$

The smallness of $|\eta_{00}|$ and $|\eta_{+-}|$ allows us to approximate

$$\epsilon \simeq \frac{1}{2}(1 - \lambda_{(\pi\pi)_{I=0}}), \quad \epsilon' \simeq \frac{1}{6}(\lambda_{\pi^0\pi^0} - \lambda_{\pi^+\pi^-}). \quad (12.61)$$

The parameter ϵ represents indirect CP violation, while ϵ' parameterizes direct CP violation: $\mathcal{R}e(\epsilon')$ measures CP violation in decay (type I), $\mathcal{R}e(\epsilon)$ measures CP violation in mixing (type II), and $\mathcal{I}m(\epsilon)$ and $\mathcal{I}m(\epsilon')$ measure the interference between decays with and without mixing (type III).

The following expressions for ϵ and ϵ' are useful for theoretical evaluations:

$$\epsilon \simeq \frac{e^{i\pi/4}}{\sqrt{2}} \frac{\mathcal{I}m(\mathbf{M}_{12})}{\Delta m}, \quad \epsilon' \simeq \frac{i}{\sqrt{2}} \left| \frac{A_2}{A_0} \right| e^{i(\delta_2 - \delta_0)} \sin(\phi_2 - \phi_0). \quad (12.62)$$

The expression for ϵ is only valid in a phase convention where $\phi_2 = 0$, corresponding to a real $V_{ud}V_{us}^*$, and in the approximation that also $\phi_0 = 0$. The phase of ϵ , $\arg(\epsilon) \approx \arctan(-2\Delta m/\Delta\Gamma)$, is independent of the electroweak model and is experimentally determined to be about $\pi/4$. The calculation of ϵ benefits from the fact that $\mathcal{I}m(\mathbf{M}_{12})$ is dominated by short distance physics. Consequently, the main source of uncertainty in theoretical interpretations of ϵ are the values of matrix elements, such as $\langle K^0 | (\bar{s}d)_{V-A} (\bar{s}d)_{V-A} | \bar{K}^0 \rangle$. The expression for ϵ' is valid to first order in $|A_2/A_0| \sim 1/20$. The phase of ϵ' is experimentally determined, $\pi/2 + \delta_2 - \delta_0 \approx \pi/4$, and is independent of the electroweak model. Note that, accidentally, ϵ'/ϵ is real to a good approximation.

A future measurement of much interest is that of CP violation in the rare $K \rightarrow \pi\nu\bar{\nu}$ decays. The signal for CP violation is simply observing the $K_L \rightarrow \pi^0\nu\bar{\nu}$ decay. The effect here is that of interference between decays with and without mixing (type III) [42]:

$$\frac{\Gamma(K_L \rightarrow \pi^0\nu\bar{\nu})}{\Gamma(K^+ \rightarrow \pi^+\nu\bar{\nu})} = \frac{1}{2} \left[1 + |\lambda_{\pi\nu\bar{\nu}}|^2 - 2\mathcal{R}e(\lambda_{\pi\nu\bar{\nu}}) \right] \simeq 1 - \mathcal{R}e(\lambda_{\pi\nu\bar{\nu}}), \quad (12.63)$$

where in the last equation we neglect CP violation in decay and in mixing (expected, model-independently, to be of order 10^{-5} and 10^{-3} , respectively). Such a measurement would be experimentally very challenging and theoretically very rewarding [43]. Similar to the CP asymmetry in $B \rightarrow J/\psi K_S$, the CP violation in $K \rightarrow \pi\nu\bar{\nu}$ decay is predicted to be large (that is, the ratio in Eq. (12.63) is neither CKM- nor loop-suppressed) and can be very cleanly interpreted.

Within the Standard Model, the $K_L \rightarrow \pi^0\nu\bar{\nu}$ decay is dominated by an intermediate top quark contribution and, consequently, can be interpreted in terms of CKM parameters [44]. (For the charged mode, $K^+ \rightarrow \pi^+\nu\bar{\nu}$, the contribution from an intermediate charm quark is not negligible, and constitutes a source of hadronic uncertainty.) In particular, $\mathcal{B}(K_L \rightarrow \pi^0\nu\bar{\nu})$ provides a theoretically clean way to determine the Wolfenstein parameter η [45]:

$$\mathcal{B}(K_L \rightarrow \pi^0\nu\bar{\nu}) = \kappa_L [X(m_t^2/m_W^2)]^2 A^4 \eta^2, \quad (12.64)$$

where $\kappa_L \sim 2 \times 10^{-10}$ incorporates the value of the four-fermion matrix element which is deduced, using isospin relations, from $\mathcal{B}(K^+ \rightarrow \pi^0 e^+\nu)$, and $X(m_t^2/m_W^2)$ is a known function of the top mass.

12.5. D Decays

First evidence for $D^0-\bar{D}^0$ mixing has been recently obtained [46,47]. Long-distance contributions make it difficult to calculate the Standard Model prediction for the $D^0-\bar{D}^0$ mixing parameters. Therefore, the goal of the search for $D^0-\bar{D}^0$ mixing is not to constrain the CKM parameters, but rather to probe new physics. Here CP violation plays an important role. Within the Standard Model, the CP -violating effects are predicted to be negligibly small, since the mixing and the relevant decays are described, to an excellent approximation, by physics of the first two generations. Observation of CP violation in $D^0-\bar{D}^0$ mixing (at a level much higher than $\mathcal{O}(10^{-3})$) will constitute an unambiguous signal of new physics. At present, the most sensitive searches involve the $D \rightarrow K^+K^-$ and $D \rightarrow K^\pm\pi^\mp$ modes.

The neutral D mesons decay via a singly-Cabibbo-suppressed transition to the CP eigenstate K^+K^- . Since the decay proceeds via a Standard-Model tree diagram, it is very likely unaffected by new physics and, furthermore, dominated by a single weak phase. It is safe then to assume that direct CP violation plays no role here. In addition, given the experimental constraints [20,48], $x \equiv \Delta m/\Gamma = 0.0084 \pm 0.0033$ and $y \equiv \Delta\Gamma/(2\Gamma) = 0.0069 \pm 0.0021$, we can expand the decay rates to first order in these parameters. Using Eq. (12.30) with these assumptions and approximations yields, for $xt, yt \lesssim \Gamma^{-1}$,

$$\begin{aligned} \Gamma[D_{\text{phys}}^0(t) \rightarrow K^+K^-] &= e^{-\Gamma t} |A_{KK}|^2 [1 - |q/p|(y \cos \phi_D - x \sin \phi_D)\Gamma t], \\ \Gamma[\bar{D}_{\text{phys}}^0(t) \rightarrow K^+K^-] &= e^{-\Gamma t} |A_{KK}|^2 [1 - |p/q|(y \cos \phi_D + x \sin \phi_D)\Gamma t], \end{aligned} \quad (12.65)$$

where ϕ_D is defined via $\lambda_{K^+K^-} = -|q/p|e^{i\phi_D}$. (In the limit of CP conservation, choosing $\phi_D = 0$ is equivalent to defining the mass eigenstates by their CP eigenvalue: $|D_{\mp}\rangle = p|D^0\rangle \pm q|\bar{D}^0\rangle$, with $D_-(D_+)$ being the CP -odd (CP -even) state; that is, the state that does not (does) decay into K^+K^- .) Given the small values of x and y , the time dependencies of the rates in Eq. (12.65) can be recast into purely exponential forms, but with modified decay-rate parameters [49]:

$$\begin{aligned} \Gamma_{D^0 \rightarrow K^+K^-} &= \Gamma \times [1 + |q/p|(y \cos \phi_D - x \sin \phi_D)], \\ \Gamma_{\bar{D}^0 \rightarrow K^+K^-} &= \Gamma \times [1 + |p/q|(y \cos \phi_D + x \sin \phi_D)]. \end{aligned} \quad (12.66)$$

One can define CP -conserving and CP -violating combinations of these two observables (normalized to the true width Γ):

$$\begin{aligned} y_{CP} &\equiv \frac{\Gamma_{\bar{D}^0 \rightarrow K^+K^-} + \Gamma_{D^0 \rightarrow K^+K^-}}{2\Gamma} - 1 \\ &= \frac{|q/p| + |p/q|}{2} y \cos \phi_D - \frac{|q/p| - |p/q|}{2} x \sin \phi_D, \\ A_\Gamma &\equiv \frac{\Gamma_{D^0 \rightarrow K^+K^-} - \Gamma_{\bar{D}^0 \rightarrow K^+K^-}}{2\Gamma} \\ &= \frac{|q/p| - |p/q|}{2} y \cos \phi_D - \frac{|q/p| + |p/q|}{2} x \sin \phi_D. \end{aligned} \quad (12.67)$$

In the limit of CP conservation (and, in particular, within the Standard Model), $y_{CP} = (\Gamma_+ - \Gamma_-)/2\Gamma$ (where $\Gamma_+(\Gamma_-)$ is the decay width of the CP -even (-odd) mass eigenstate) and $A_\Gamma = 0$.

The $K^\pm\pi^\mp$ states are not CP eigenstates, but they are still common final states for D^0 and \bar{D}^0 decays. Since $D^0(\bar{D}^0) \rightarrow K^-\pi^+$ is a Cabibbo-favored (doubly-Cabibbo-suppressed) process, these processes are particularly sensitive to x and/or $y = \mathcal{O}(\lambda^2)$. Taking into account that $|\lambda_{K^-\pi^+}|, |\lambda_{K^+\pi^-}^{-1}| \ll 1$ and $x, y \ll 1$, assuming that there is no direct CP violation (again, these are Standard Model tree-level decays dominated by a single weak phase), and expanding the time-dependent rates for $xt, yt \lesssim \Gamma^{-1}$, one obtains

$$\Gamma[D_{\text{phys}}^0(t) \rightarrow K^+\pi^-] = e^{-\Gamma t} |\bar{A}_{K^-\pi^+}|^2$$

$$\begin{aligned} & \times \left[r_d^2 + r_d \left| \frac{q}{p} \right| (y' \cos \phi_D - x' \sin \phi_D) \Gamma t + \left| \frac{q}{p} \right|^2 \frac{y^2 + x^2}{4} (\Gamma t)^2 \right], \\ \Gamma[\overline{D}_{\text{phys}}^0(t) \rightarrow K^- \pi^+] &= e^{-\Gamma t} |\overline{A}_{K^- \pi^+}|^2 \\ & \times \left[r_d^2 + r_d \left| \frac{p}{q} \right| (y' \cos \phi_D + x' \sin \phi_D) \Gamma t + \left| \frac{p}{q} \right|^2 \frac{y^2 + x^2}{4} (\Gamma t)^2 \right], \end{aligned} \quad (12.68)$$

where

$$\begin{aligned} y' &\equiv y \cos \delta - x \sin \delta, \\ x' &\equiv x \cos \delta + y \sin \delta. \end{aligned} \quad (12.69)$$

The weak phase ϕ_D is the same as that of Eq. (12.65) (a consequence of the absence of direct CP violation), δ is a strong-phase difference for these processes, and $r_d = \mathcal{O}(\tan^2 \theta_c)$ is the amplitude ratio, $r_d = |\overline{A}_{K^- \pi^+}/A_{K^- \pi^+}| = |A_{K^+ \pi^-}/\overline{A}_{K^+ \pi^-}|$, that is, $\lambda_{K^- \pi^+} = r_d(q/p)e^{-i(\delta - \phi_D)}$ and $\lambda_{K^+ \pi^-}^{-1} = r_d(p/q)e^{-i(\delta + \phi_D)}$. By fitting to the six coefficients of the various time-dependences, one can extract r_d , $|q/p|$, $(x^2 + y^2)$, $y' \cos \phi_D$, and $x' \sin \phi_D$. In particular, finding CP violation ($|q/p| \neq 1$ and/or $\sin \phi_D \neq 0$) at a level higher than 10^{-3} would constitute evidence for new physics.

A fit to all data [20], assuming no direct CP violation, yields no evidence for indirect CP violation:

$$\begin{aligned} 1 - |q/p| &= 0.12 \pm 0.23, \\ \phi_D &= -0.07 \pm 0.18. \end{aligned}$$

More details on theoretical and experimental aspects of $D^0 - \overline{D}^0$ mixing can be found in [50].

12.6. B and B_s Decays

The upper bound on the CP asymmetry in semileptonic B decays [51] implies that CP violation in $B^0 - \overline{B}^0$ mixing is a small effect (we use $\mathcal{A}_{\text{SL}}/2 \approx 1 - |q/p|$, see Eq. (12.37)):

$$\mathcal{A}_{\text{SL}} = (-0.4 \pm 5.6) \times 10^{-3} \implies |q/p| = 1.0002 \pm 0.0028. \quad (12.70)$$

The Standard Model prediction is

$$\mathcal{A}_{\text{SL}} = \mathcal{O} \left[(m_c^2/m_t^2) \sin \beta \right] \lesssim 0.001. \quad (12.71)$$

In models where $\mathbf{\Gamma}_{12}/\mathbf{M}_{12}$ is approximately real, such as the Standard Model, an upper bound on $\Delta\Gamma/\Delta m \approx \mathcal{R}e(\mathbf{\Gamma}_{12}/\mathbf{M}_{12})$ provides yet another upper bound on the deviation of $|q/p|$ from one. This constraint does not hold if $\mathbf{\Gamma}_{12}/\mathbf{M}_{12}$ is approximately imaginary. (An alternative parameterization uses $q/p = (1 - \tilde{\epsilon}_B)/(1 + \tilde{\epsilon}_B)$, leading to $\mathcal{A}_{\text{SL}} \simeq 4\mathcal{R}e(\tilde{\epsilon}_B)$.)

The small deviation (less than one percent) of $|q/p|$ from 1 implies that, at the present level of experimental precision, CP violation in B mixing is a negligible effect. Thus, for the purpose of analyzing CP asymmetries in hadronic B decays, we can use

$$\lambda_f = e^{-i\phi_{M(B)}} (\overline{A}_f/A_f), \quad (12.72)$$

where $\phi_{M(B)}$ refers to the phase of \mathbf{M}_{12} appearing in Eq. (12.42) that is appropriate for $B^0 - \overline{B}^0$ oscillations. Within the Standard Model, the corresponding phase factor is given by

$$e^{-i\phi_{M(B)}} = (V_{tb}^* V_{td}) / (V_{ub}^* V_{ud}). \quad (12.73)$$

Some of the most interesting decays involve final states that are common to B^0 and \overline{B}^0 [52,53]. It is convenient to rewrite Eq. (12.40) for B decays as [54–56]

$$\begin{aligned} A_f(t) &= S_f \sin(\Delta m t) - C_f \cos(\Delta m t), \\ S_f &\equiv \frac{2\mathcal{I}m(\lambda_f)}{1 + |\lambda_f|^2}, \quad C_f \equiv \frac{1 - |\lambda_f|^2}{1 + |\lambda_f|^2}, \end{aligned} \quad (12.74)$$

where we assume that $\Delta\Gamma = 0$ and $|q/p| = 1$. An alternative notation in use is $A_f \equiv -C_f$, but this A_f should not be confused with the A_f of Eq. (12.13).

A large class of interesting processes proceed via quark transitions of the form $\overline{b} \rightarrow \overline{q}q'$ with $q' = s$ or d . For $q = c$ or u , there are contributions from both tree (t) and penguin (p^{qu} , where $q_u = u, c, t$ is the quark in the loop) diagrams (see Fig. 12.2) which carry different weak phases:

$$A_f = (V_{qb}^* V_{qq'}) t_f + \sum_{q_u=u,c,t} (V_{qu}^* V_{quq'}) p_f^{q_u}. \quad (12.75)$$

(The distinction between tree and penguin contributions is a heuristic one; the separation by the operator that enters is more precise. For a detailed discussion of the more complete operator product approach, which also includes higher order QCD corrections, see, for example, Ref. 57.) Using CKM unitarity, these decay amplitudes can always be written in terms of just two CKM combinations. For example, for $f = \pi\pi$, which proceeds via $\overline{b} \rightarrow \overline{u}u$ transition, we can write

$$A_{\pi\pi} = (V_{ub}^* V_{ud}) T_{\pi\pi} + (V_{tb}^* V_{td}) P_{\pi\pi}^t, \quad (12.76)$$

where $T_{\pi\pi} = t_{\pi\pi} + p_{\pi\pi}^u - p_{\pi\pi}^c$ and $P_{\pi\pi}^t = p_{\pi\pi}^t - p_{\pi\pi}^c$. CP -violating phases in Eq. (12.76) appear only in the CKM elements, so that

$$\frac{\overline{A}_{\pi\pi}}{A_{\pi\pi}} = \frac{(V_{ub} V_{ud}^*) T_{\pi\pi} + (V_{tb} V_{td}^*) P_{\pi\pi}^t}{(V_{ub}^* V_{ud}) T_{\pi\pi} + (V_{tb}^* V_{td}) P_{\pi\pi}^t}. \quad (12.77)$$

For $f = J/\psi K$, which proceeds via $\overline{b} \rightarrow \overline{c}c$ transition, we can write

$$A_{\psi K} = (V_{cb}^* V_{cs}) T_{\psi K} + (V_{ub}^* V_{us}) P_{\psi K}^u, \quad (12.78)$$

where $T_{\psi K} = t_{\psi K} + p_{\psi K}^c - p_{\psi K}^t$ and $P_{\psi K}^u = p_{\psi K}^u - p_{\psi K}^t$. A subtlety arises in this decay that is related to the fact that B^0 decays into a final $J/\psi K^0$ state while \overline{B}^0 decays into a final $J/\psi \overline{K}^0$ state. A common final state, *e.g.*, $J/\psi K_S$, is reached only via $K^0 - \overline{K}^0$ mixing. Consequently, the phase factor (defined in Eq. (12.42)) corresponding to neutral K mixing, $e^{-i\phi_{M(K)}} = (V_{cd}^* V_{cs}) / (V_{cd} V_{cs}^*)$, plays a role:

$$\frac{\overline{A}_{\psi K_S}}{A_{\psi K_S}} = - \frac{(V_{cb} V_{cs}^*) T_{\psi K} + (V_{ub} V_{us}^*) P_{\psi K}^u}{(V_{cb}^* V_{cs}) T_{\psi K} + (V_{ub}^* V_{us}) P_{\psi K}^u} \times \frac{V_{cd}^* V_{cs}}{V_{cd} V_{cs}^*}. \quad (12.79)$$

For $q = s$ or d , there are only penguin contributions to A_f , that is, $t_f = 0$ in Eq. (12.75). (The tree $\overline{b} \rightarrow \overline{u}u$ transition followed by $\overline{u}u \rightarrow \overline{q}q$ rescattering is included below in the P^u terms.) Again, CKM unitarity allows us to write A_f in terms of two CKM combinations. For example, for $f = \phi K_S$, which proceeds via $\overline{b} \rightarrow \overline{s}s$ transition, we can write

$$\frac{\overline{A}_{\phi K_S}}{A_{\phi K_S}} = - \frac{(V_{cb} V_{cs}^*) P_{\phi K}^c + (V_{ub} V_{us}^*) P_{\phi K}^u}{(V_{cb}^* V_{cs}) P_{\phi K}^c + (V_{ub}^* V_{us}) P_{\phi K}^u} \times \frac{V_{cd}^* V_{cs}}{V_{cd} V_{cs}^*}, \quad (12.80)$$

where $P_{\phi K}^c = p_{\phi K}^c - p_{\phi K}^t$ and $P_{\phi K}^u = p_{\phi K}^u - p_{\phi K}^t$.

Since the amplitude A_f involves two different weak phases, the corresponding decays can exhibit both CP violation in the interference of decays with and without mixing, $S_f \neq 0$, and CP violation in decays, $C_f \neq 0$. (At the present level of experimental precision, the contribution to C_f from CP violation in mixing is negligible, see Eq. (12.70).) If the contribution from a second weak phase is suppressed, then the interpretation of S_f in terms of Lagrangian CP -violating parameters is clean, while C_f is small. If such a second contribution is not suppressed, S_f depends on hadronic parameters and, if the relevant strong phase is large, C_f is large.

A summary of $\overline{b} \rightarrow \overline{q}q'$ modes with $q' = s$ or d is given in Table 12.1. The $\overline{b} \rightarrow \overline{d}d$ transitions lead to final states that are similar to the $\overline{b} \rightarrow \overline{u}u$ transitions and have similar phase dependence. Final states that consist of two-vector mesons ($\psi\phi$ and $\phi\phi$) are not CP eigenstates, and angular analysis is needed to separate the CP -even from the CP -odd contributions.

For $B \rightarrow \pi\pi$ and other $\bar{b} \rightarrow \bar{u}d$ processes, the penguin-to-tree ratio can be estimated using SU(3) relations and experimental data on related $B \rightarrow K\pi$ decays. The result is that the suppression is on the order of 0.2–0.3 and so cannot be neglected. The expressions for $S_{\pi\pi}$ and $C_{\pi\pi}$ to leading order in $R_{PT} \equiv (|V_{tb}V_{td}|P_{\pi\pi}^t)/(|V_{ub}V_{ud}|T_{\pi\pi})$ are:

$$\lambda_{\pi\pi} = e^{2i\alpha} \left[(1 - R_{PT}e^{-i\alpha}) / (1 - R_{PT}e^{+i\alpha}) \right] \Rightarrow$$

$$S_{\pi\pi} \approx \sin 2\alpha + 2 \operatorname{Re}(R_{PT}) \cos 2\alpha \sin \alpha, \quad C_{\pi\pi} \approx 2 \operatorname{Im}(R_{PT}) \sin \alpha. \quad (12.83)$$

Note that R_{PT} is mode-dependent and, in particular, could be different for $\pi^+\pi^-$ and $\pi^0\pi^0$. If strong phases can be neglected, then R_{PT} is real, resulting in $C_{\pi\pi} = 0$. The size of $C_{\pi\pi}$ is an indicator of how large the strong phase is. The present experimental range is $C_{\pi\pi} = -0.38 \pm 0.07$ [20]. As concerns $S_{\pi\pi}$, it is clear from Eq. (12.83) that the relative size or strong phase of the penguin contribution must be known to extract α . This is the problem of penguin pollution.

The cleanest solution involves isospin relations among the $B \rightarrow \pi\pi$ amplitudes [58]:

$$\frac{1}{\sqrt{2}} A_{\pi^+\pi^-} + A_{\pi^0\pi^0} = A_{\pi^+\pi^0}. \quad (12.84)$$

The method exploits the fact that the penguin contribution to $P_{\pi\pi}^t$ is pure $\Delta I = \frac{1}{2}$ (this is not true for the electroweak penguins which, however, are expected to be small), while the tree contribution to $T_{\pi\pi}$ contains pieces which are both $\Delta I = \frac{1}{2}$ and $\Delta I = \frac{3}{2}$. A simple geometric construction then allows one to find R_{PT} and extract α cleanly from $S_{\pi^+\pi^-}$. The key experimental difficulty is that one must measure accurately the separate rates for $B^0, \bar{B}^0 \rightarrow \pi^0\pi^0$.

CP asymmetries in $B \rightarrow \rho\pi$ and $B \rightarrow \rho\rho$ can also be used to determine α . In particular, the $B \rightarrow \rho\rho$ measurements are presently very significant in constraining α . The extraction proceeds via isospin analysis similar to that of $B \rightarrow \pi\pi$. There are, however, several important differences. First, due to the finite width of the ρ mesons, a final $(\rho\rho)_{I=1}$ state is possible [59]. The effect is, however, small, on the order of $(\Gamma_\rho/m_\rho)^2 \sim 0.04$. Second, due to the presence of three helicity states for the two-vector mesons, angular analysis is needed to separate the CP -even and CP -odd components. The theoretical expectation is, however, that the CP -odd component is small. This expectation is supported by experiments which find that the $\rho^+\rho^-$ and $\rho^\pm\rho^0$ modes are dominantly longitudinally polarized. Third, an important advantage of the $\rho\rho$ modes is that the penguin contribution is expected to be small due to different hadronic dynamics. This expectation is confirmed by the smallness of the upper bound on $\mathcal{B}(B^0 \rightarrow \rho^0\rho^0)$. Thus, $S_{\rho^+\rho^-}$ is not far from $\sin 2\alpha$. Finally, both $S_{\rho^0\rho^0}$ and $C_{\rho^0\rho^0}$ are experimentally accessible, which may allow a precision determination of α . The consistency between the range of α determined by the $B \rightarrow \pi\pi, \rho\pi, \rho\rho$ measurements and the range allowed by CKM fits (excluding these direct determinations) provides further support to the Kobayashi-Maskawa mechanism.

An interesting class of decay modes is that of the tree level decays $B^\pm \rightarrow D^{(*)0}K^\pm$. These decays provide golden methods for a clean determination of the angle γ [60–63]. The method uses the decays $B^+ \rightarrow D^0K^+$, which proceeds via the quark transition $\bar{b} \rightarrow \bar{u}c\bar{s}$, and $B^+ \rightarrow \bar{D}^0K^+$, which proceeds via the quark transition $\bar{b} \rightarrow \bar{c}u\bar{s}$, with the D^0 and \bar{D}^0 decaying into a common final state. The decays into common final states, such $(\pi^0 K_S) D K^+$, involve interference effects between the two amplitudes, with sensitivity to the relative phase, $\delta + \gamma$ (δ is the relevant strong phase). The CP -conjugate processes are sensitive to $\delta - \gamma$. Measurements of branching ratios and CP asymmetries allow an extraction of γ and δ from amplitude triangle relations. The extraction suffers from discrete ambiguities but involves no hadronic uncertainties. However, the smallness of the CKM-suppressed $b \rightarrow u$ transitions makes it difficult at present to use the simplest methods [60–62] to determine γ . These difficulties are overcome by performing a Dalitz plot analysis for multi-body D decays [63]. The consistency between the range of γ determined by the $B \rightarrow DK$ measurements and the range allowed by CKM fits

(excluding these direct determinations) provides further support to the Kobayashi-Maskawa mechanism.

For B_s decays, one has to replace Eq. (12.73) with $e^{-i\phi_{M(B_s)}} = (V_{tb}^*V_{ts})/(V_{tb}V_{ts}^*)$. Note that one expects $\Delta\Gamma/\Gamma = \mathcal{O}(0.1)$, and therefore, y should not be put to zero in Eqs. (12.30,12.31), but $|q/p| = 1$ is expected to hold to an even better approximation than for B mesons. The CP asymmetry in $B_s \rightarrow J/\psi\phi$ will determine (with angular analysis to disentangle the CP -even and CP -odd components of the final state) $\sin 2\beta_s$, where

$$\beta_s \equiv \arg \left(-\frac{V_{ts}V_{tb}^*}{V_{cs}V_{cb}^*} \right). \quad (12.85)$$

Other observables, such as the width difference between the neutral B_s -mesons and the semileptonic asymmetry in their decay, are also sensitive to $\phi_{M(B_s)}$. The CDF and D0 experiments are now providing first constraints on these observables.

12.7. Summary and Outlook

CP violation has been experimentally established in neutral K and B meson decays:

1. All three types of CP violation have been observed in $K \rightarrow \pi\pi$ decays:

$$\operatorname{Re}(\epsilon') = \frac{1}{6} \left(\left| \frac{\bar{A}_{\pi^0\pi^0}}{A_{\pi^0\pi^0}} \right| - \left| \frac{\bar{A}_{\pi^+\pi^-}}{A_{\pi^+\pi^-}} \right| \right) = (2.5 \pm 0.4) \times 10^{-6} \text{(I)}$$

$$\operatorname{Re}(\epsilon) = \frac{1}{2} \left(1 - \left| \frac{q}{p} \right| \right) = (1.657 \pm 0.021) \times 10^{-3} \quad \text{(II)}$$

$$\operatorname{Im}(\epsilon) = -\frac{1}{2} \operatorname{Im}(\lambda_{(\pi\pi)_{I=0}}) = (1.572 \pm 0.022) \times 10^{-3}. \quad \text{(III)} \quad (12.86)$$

2. Direct CP violation has been observed, first in $B^0 \rightarrow K^+\pi^-$ decays (and more recently also in $B \rightarrow \pi^+\pi^-$, $B^0 \rightarrow \eta K^{*0}$, and $B^+ \rightarrow \rho^0 K^+$ decays), and CP violation in interference of decays with and without mixing has been observed, first in $B \rightarrow J/\psi K_S$ decays and related modes (as well as other final CP eigenstates: $\eta' K_S$, $K^+K^-K_S$, $J/\psi\pi^0$ and $\pi^+\pi^-$):

$$\mathcal{A}_{K^+\pi^-} = \frac{|\bar{A}_{K^-\pi^+}/A_{K^+\pi^-}|^2 - 1}{|\bar{A}_{K^-\pi^+}/A_{K^+\pi^-}|^2 + 1} = -0.095 \pm 0.013 \quad \text{(I)}$$

$$S_{\psi K} = \operatorname{Im}(\lambda_{\psi K}) = 0.68 \pm 0.03. \quad \text{(III)} \quad (12.87)$$

Searches for additional CP asymmetries are ongoing in B , D , and K decays, and current limits are consistent with Standard Model expectations.

Based on Standard Model predictions, further observation of CP violation in B decays seems promising for the near future, followed later by CP violation observed in B_s decays and in the process $K \rightarrow \pi\nu\bar{\nu}$. Observables that are subject to clean theoretical interpretation, such as $S_{\psi K_S}$ and $\mathcal{B}(K_L \rightarrow \pi^0\nu\bar{\nu})$, are of particular value for constraining the values of the CKM parameters and probing the flavor sector of extensions to the Standard Model. Other probes of CP violation now being pursued experimentally include the electric dipole moments of the neutron and electron, and the decays of tau leptons. Additional processes that are likely to play an important role in future CP studies include top-quark production and decay, and neutrino oscillations.

All measurements of CP violation to date are consistent with the predictions of the Kobayashi-Maskawa mechanism of the Standard Model. Actually, it is now established that the KM mechanism plays a major role in the CP violation measured in meson decays. However, a dynamically-generated matter-antimatter asymmetry of the universe requires additional sources of CP violation, and such sources are naturally generated by extensions to the Standard Model. New sources might eventually reveal themselves as small deviations from the predictions of the KM mechanism in meson decay rates, or

else might not be observable in meson decays at all, but observable with future probes such as neutrino oscillations or electric dipole moments. We cannot guarantee that new sources of *CP* violation will ever be found experimentally, but the fundamental nature of *CP* violation demands a vigorous effort.

A number of excellent reviews of *CP* violation are available [64–70], where the interested reader may find a detailed discussion of the various topics that are briefly reviewed here.

References:

1. J.H. Christenson *et al.*, Phys. Rev. Lett. **13**, 138 (1964).
2. B. Aubert *et al.*, [BABAR Collab.], Phys. Rev. Lett. **87**, 091801 (2001).
3. K. Abe *et al.*, [Belle Collab.], Phys. Rev. Lett. **87**, 091802 (2001).
4. H. Burkhardt *et al.*, [NA31 Collab.], Phys. Lett. **B206**, 169 (1988).
5. V. Fanti *et al.*, [NA48 Collab.], Phys. Lett. **B465**, 335 (1999).
6. A. Alavi-Harati *et al.*, [KTeV Collab.], Phys. Rev. Lett. **83**, 22 (1999).
7. B. Aubert *et al.*, [BABAR Collab.], Phys. Rev. Lett. **93**, 131801 (2004).
8. K. Abe *et al.*, [Belle Collab.], arXiv:hep-ex/0507045.
9. B. Aubert *et al.*, [BABAR Collab.], Phys. Rev. **D72**, 072003 (2005).
10. A. Garmash *et al.*, [Belle Collab.], Phys. Rev. Lett. **96**, 251803 (2006).
11. M. Morello [CDF Collab.], Nucl. Phys. Proc. Suppl. **170**, 39 (2007).
12. See results on the “Time reversal invariance,” within the review on “Tests of Conservation Laws,” in this *Review*.
13. See, for example, R. F. Streater and A. S. Wightman, *CPT, Spin and Statistics, and All That*, reprinted by Addison-Wesley, New York (1989).
14. M. Kobayashi and T. Maskawa, Prog. Theor. Phys. **49**, 652 (1973).
15. J. Charles *et al.*, [CKMfitter Group], Eur. Phys. J. **C41**, 1 (2005), updated results and plots available at: <http://ckmfitter.in2p3.fr>.
16. M. Bona *et al.*, [UTfit Collab.], JHEP **0603**, 080 (2006), updated results and plots available at: <http://babar.roma1.infn.it/ckm/>.
17. A.D. Sakharov, Pisma Zh. Eksp. Teor. Fiz. **5**, 32 (1967) [Sov. Phys. JETP Lett. **5**, 24 (1967)].
18. For a review, see *e.g.* A. Riotto, “Theories of baryogenesis,” arXiv:hep-ph/9807454.
19. M. Fukugita and T. Yanagida, Phys. Lett. **B174**, 45 (1986).
20. E. Barberio *et al.*, [HFAG Collab.], arXiv:0704.3575 [hep-ex], and online update at <http://www.slac.stanford.edu/xorg/hfag>.
21. B. Aubert *et al.*, [BABAR Collab.], Phys. Rev. Lett. **98**, 031801 (2007).
22. K. F. Chen *et al.*, [Belle Collab.], Phys. Rev. Lett. **98**, 031802 (2007).
23. B. Aubert *et al.*, [BABAR Collab.], arXiv:0706.3885 [hep-ex].
24. K. Abe *et al.*, [Belle Collab.], arXiv:hep-ex/0609006.
25. H. Ishino *et al.*, [Belle Collab.], Phys. Rev. Lett. **98**, 211801 (2007).
26. B. Aubert *et al.*, [BABAR Collab.], Phys. Rev. Lett. **99**, 021603 (2007).
27. B. Aubert *et al.*, [BaBar Collab.], Phys. Rev. **D74**, 011101 (2006).
28. S. U. Kataoka *et al.*, [Belle Collab.], Phys. Rev. Lett. **93**, 261801 (2004).
29. H. Miyake *et al.*, [Belle Collab.], Phys. Lett. **B618**, 34 (2005).
30. B. Aubert *et al.*, [BABAR Collab.], Phys. Rev. Lett. **95**, 151804 (2005).
31. B. Aubert *et al.*, [BABAR Collab.], Phys. Rev. Lett. **97**, 201802 (2006).
32. C. H. Wang *et al.*, [Belle Collab.], Phys. Rev. **D75**, 092005 (2007).
33. V. Weisskopf and E. P. Wigner, Z. Phys. **63**, 54 (1930); Z. Phys. **65**, 18 (1930). [See also Appendix A of P.K. Kabir, *The CP Puzzle: Strange Decays of the Neutral Kaon*, Academic Press (1968)].
34. O. Long *et al.*, Phys. Rev. **D68**, 034010 (2003).
35. L. Wolfenstein, Phys. Rev. Lett. **13**, 562 (1964).
36. See the review on “Cabibbo-Kobayashi-Maskawa Mixing Matrix,” in this *Review*.
37. L. Wolfenstein, Phys. Rev. Lett. **51**, 1945 (1983).
38. A.J. Buras, M.E. Lautenbacher, and G. Ostermaier, Phys. Rev. **D50**, 3433 (1994).
39. C. Jarlskog, Phys. Rev. Lett. **55**, 1039 (1985).
40. See the *K*-Meson Listings in this *Review*.
41. See the review on “*CP* violation in $K_S \rightarrow 3\pi$,” in this *Review*.
42. Y. Grossman and Y. Nir, Phys. Lett. **B398**, 163 (1997).
43. L.S. Littenberg, Phys. Rev. **D39**, 3322 (1989).
44. A.J. Buras, Phys. Lett. **B333**, 476 (1994).
45. G. Buchalla and A.J. Buras, Nucl. Phys. **B400**, 225 (1993).
46. B. Aubert *et al.*, [BABAR Collab.], Phys. Rev. Lett. **98**, 211802 (2007).
47. M. Staric *et al.*, [Belle Collab.], Phys. Rev. Lett. **98**, 211803 (2007).
48. See the *D*-Meson Listings in this *Review*.
49. S. Bergmann *et al.*, Phys. Lett. **B486**, 418 (2000).
50. See the review on “ $D^0 - \bar{D}^0$ Mixing” in this *Review*.
51. See the *B*-Meson Listings in this *Review*.
52. A.B. Carter and A.I. Sanda, Phys. Rev. Lett. **45**, 952 (1980); Phys. Rev. **D23**, 1567 (1981).
53. I.I. Bigi and A.I. Sanda, Nucl. Phys. **B193**, 85 (1981).
54. I. Dunietz and J.L. Rosner, Phys. Rev. **D34**, 1404 (1986).
55. Ya.I. Azimov, N.G. Uraltsev, and V.A. Khoze, Sov. J. Nucl. Phys. **45**, 878 (1987) [Yad. Fiz. **45**, 1412 (1987)].
56. I.I. Bigi and A.I. Sanda, Nucl. Phys. **B281**, 41 (1987).
57. G. Buchalla, A.J. Buras, and M.E. Lautenbacher, Rev. Mod. Phys. **68**, 1125 (1996).
58. M. Gronau and D. London, Phys. Rev. Lett. **65**, 3381 (1990).
59. A. F. Falk *et al.*, Phys. Rev. **D69**, 011502 (2004).
60. M. Gronau and D. London, Phys. Lett. **B253**, 483 (1991).
61. M. Gronau and D. Wyler, Phys. Lett. **B265**, 172 (1991).
62. D. Atwood, I. Dunietz, and A. Soni, Phys. Rev. Lett. **78**, 3257 (1997).
63. A. Giri *et al.*, Phys. Rev. **D68**, 054018 (2003).
64. G.C. Branco, L. Lavoura, and J.P. Silva, *CP Violation*, Oxford University Press, Oxford (1999).
65. I.I. Y. Bigi and A.I. Sanda, *CP Violation*, Cambridge Monogr., Part. Phys. Nucl. Phys. Cosmol. **9**, 1 (2000).
66. P.F. Harrison and H.R. Quinn, editors [BABAR Collab.], *The BABAR physics book: Physics at an asymmetric B factory*, SLAC-R-0504.
67. K. Anikeev *et al.*, arXiv:hep-ph/0201071.
68. K. Kleinknecht, “Uncovering *CP* Violation,” Springer tracts in modern physics **195** (2003).
69. J. Hewett *et al.*, arXiv:hep-ph/0503261.
70. A. G. Akeroyd *et al.*, [SuperKEKB Physics Working Group], arXiv:hep-ex/0406071.

13. NEUTRINO MASS, MIXING, AND FLAVOR CHANGE

Revised March 2008 by B. Kayser (Fermilab).

There is now compelling evidence that atmospheric, solar, accelerator, and reactor neutrinos change from one flavor to another. This implies that neutrinos have masses and that leptons mix. In this review, we discuss the physics of flavor change and the evidence for it, summarize what has been learned so far about neutrino masses and leptonic mixing, consider the relation between neutrinos and their antiparticles, and discuss the open questions about neutrinos to be answered by future experiments.

I. The physics of flavor change: If neutrinos have masses, then there is a spectrum of three or more neutrino mass eigenstates, $\nu_1, \nu_2, \nu_3, \dots$, that are the analogues of the charged-lepton mass eigenstates, e, μ , and τ . If leptons mix, the weak interaction coupling the W boson to a charged lepton and a neutrino can couple any charged-lepton mass eigenstate ℓ_α to any neutrino mass eigenstate ν_i . Here, $\alpha = e, \mu$, or τ , and ℓ_e is the electron, *etc.* The amplitude for the decay of a real or virtual W^+ to yield the specific combination $\ell_\alpha^+ + \nu_i$ is $U_{\alpha i}^*$, where U is the unitary leptonic mixing matrix [1]. Thus, the neutrino state created in the decay $W^+ \rightarrow \ell_\alpha^+ + \nu$ is the state

$$|\nu_\alpha\rangle = \sum_i U_{\alpha i}^* |\nu_i\rangle. \quad (13.1)$$

This superposition of neutrino mass eigenstates, produced in association with the charged lepton of “flavor” α , is the state we refer to as the neutrino of flavor α . Assuming CPT invariance, the unitarity of U guarantees that the only charged lepton a ν_α can create in a detector is an ℓ_α , with the same flavor as the neutrino. Eq. (13.1) may be inverted to give

$$|\nu_i\rangle = \sum_\beta U_{\beta i} |\nu_\beta\rangle, \quad (13.2)$$

which expresses the mass eigenstate ν_i as a superposition of the neutrinos of definite flavor.

While there are only three (known) charged lepton mass eigenstates, it may be that there are more than three neutrino mass eigenstates. If, for example, there are four ν_i , then one linear combination of them,

$$|\nu_s\rangle = \sum_i U_{s i}^* |\nu_i\rangle, \quad (13.3)$$

does not have a charged-lepton partner, and consequently does not couple to the Standard Model W boson. Indeed, since the decays $Z \rightarrow \nu_\alpha \bar{\nu}_\alpha$ of the Standard Model Z boson have been found to yield only three distinct neutrinos ν_α of definite flavor [2], ν_s does not couple to the Z boson either. Such a neutrino, which does not have any Standard Model weak couplings, is referred to as a “sterile” neutrino.

Neutrino flavor change is the process $\nu_\alpha \rightarrow \nu_\beta$, in which a neutrino born with flavor α becomes one of a different flavor β while propagating in vacuum or in matter. This process, often referred to as neutrino oscillation, is quantum mechanical to its core. Rather than present a full wave packet treatment [3], we shall give a simpler description that captures all the essential physics. We begin with oscillation in vacuum, and work in the neutrino mass eigenstate basis. Then the neutrino that travels from the source to the detector is one or another of the mass eigenstates ν_i . The amplitude for the oscillation $\nu_\alpha \rightarrow \nu_\beta$, $\text{Amp}(\nu_\alpha \rightarrow \nu_\beta)$, is a coherent sum over the contributions of all the ν_i , given by

$$\text{Amp}(\nu_\alpha \rightarrow \nu_\beta) = \sum_i U_{\alpha i}^* \text{Prop}(\nu_i) U_{\beta i}. \quad (13.4)$$

In the contribution $U_{\alpha i}^* \text{Prop}(\nu_i) U_{\beta i}$ of ν_i to this sum, the factor $U_{\alpha i}^*$ is the amplitude for the neutrino ν_α to be the mass eigenstate ν_i [see Eq. (13.1)], the factor $\text{Prop}(\nu_i)$ is the amplitude for this ν_i to propagate from the source to the detector, and the factor $U_{\beta i}$ is the amplitude for the ν_i to be a ν_β [see Eq. (13.2)]. From elementary quantum mechanics, the propagation amplitude $\text{Prop}(\nu_i)$ is $\exp[-im_i \tau_i]$, where m_i is the mass of ν_i , and τ_i is the proper time that elapses in the ν_i rest frame during its propagation. By Lorentz

invariance, $m_i \tau_i = E_i t - p_i L$, where L is the lab-frame distance between the neutrino source and the detector, t is the lab-frame time taken for the beam to traverse this distance, and E_i and p_i are, respectively, the lab-frame energy and momentum of the ν_i component of the beam.

In the probability $P(\nu_\alpha \rightarrow \nu_\beta) = |\text{Amp}(\nu_\alpha \rightarrow \nu_\beta)|^2$ for the oscillation $\nu_\alpha \rightarrow \nu_\beta$, only the relative phases of the propagation amplitudes $\text{Prop}(\nu_i)$ for different mass eigenstates will have physical consequences. From the discussion above, the relative phase of $\text{Prop}(\nu_i)$ and $\text{Prop}(\nu_j)$, $\delta\phi_{ij}$, is given by

$$\delta\phi_{ij} = (p_i - p_j)L - (E_i - E_j)t. \quad (13.5)$$

In practice, experiments do not measure the transit time t . However, Lipkin has shown [4] that, to an excellent approximation, the t in Eq. (13.5) may be taken to be L/\bar{v} , where

$$\bar{v} = \frac{p_i + p_j}{E_i + E_j} \quad (13.6)$$

is an approximation to the average of the velocities of the ν_i and ν_j components of the beam. Then

$$\delta\phi_{ij} \cong \frac{p_i^2 - p_j^2}{p_i + p_j} L - \frac{E_i^2 - E_j^2}{p_i + p_j} L \cong (m_j^2 - m_i^2) \frac{L}{2E}, \quad (13.7)$$

where, in the last step, we have used the fact that for highly relativistic neutrinos, p_i and p_j are both approximately equal to the beam energy E . We conclude that all the relative phases in $\text{Amp}(\nu_\alpha \rightarrow \nu_\beta)$, Eq. (13.4), will be correct if we take $\text{Prop}(\nu_i) = \exp(-im_i^2 L/2E)$, so that

$$\text{Amp}(\nu_\alpha \rightarrow \nu_\beta) = \sum_i U_{\alpha i}^* e^{-im_i^2 L/2E} U_{\beta i}. \quad (13.8)$$

Squaring, and making judicious use of the unitarity of U , we then find that

$$\begin{aligned} P(\nu_\alpha \rightarrow \nu_\beta) &= \delta_{\alpha\beta} \\ &- 4 \sum_{i>j} \Re(U_{\alpha i}^* U_{\beta i} U_{\alpha j} U_{\beta j}^*) \sin^2[1.27 \Delta m_{ij}^2 (L/E)] \\ &+ 2 \sum_{i>j} \Im(U_{\alpha i}^* U_{\beta i} U_{\alpha j} U_{\beta j}^*) \sin[2.54 \Delta m_{ij}^2 (L/E)]. \end{aligned} \quad (13.9)$$

Here, $\Delta m_{ij}^2 \equiv m_i^2 - m_j^2$ is in eV^2 , L is in km, and E is in GeV. We have used the fact that when the previously omitted factors of \hbar and c are included,

$$\Delta m_{ij}^2 (L/4E) \simeq 1.27 \Delta m_{ij}^2 (\text{eV}^2) \frac{L(\text{km})}{E(\text{GeV})}. \quad (13.10)$$

Assuming that CPT invariance holds,

$$P(\bar{\nu}_\alpha \rightarrow \bar{\nu}_\beta) = P(\nu_\beta \rightarrow \nu_\alpha). \quad (13.11)$$

But, from Eq. (13.9) we see that

$$P(\nu_\beta \rightarrow \nu_\alpha; U) = P(\nu_\alpha \rightarrow \nu_\beta; U^*). \quad (13.12)$$

Thus, when CPT holds,

$$P(\bar{\nu}_\alpha \rightarrow \bar{\nu}_\beta; U) = P(\nu_\alpha \rightarrow \nu_\beta; U^*). \quad (13.13)$$

That is, the probability for oscillation of an antineutrino is the same as that for a neutrino, except that the mixing matrix U is replaced by its complex conjugate. Thus, if U is not real, the neutrino and antineutrino oscillation probabilities can differ by having opposite values of the last term in Eq. (13.9). When CPT holds, any difference between these probabilities indicates a violation of CP invariance.

As we shall see, the squared-mass splittings Δm_{ij}^2 called for by the various reported signals of oscillation are quite different from one another. It may be that one splitting, ΔM^2 , is much bigger than all the others. If that is the case, then for an oscillation experiment with

L/E such that $\Delta M^2 L/E = \mathcal{O}(1)$, Eq. (13.9) simplifies considerably, becoming

$$P(\bar{\nu}_\alpha \rightarrow \bar{\nu}_\beta) \simeq S_{\alpha\beta} \sin^2[1.27 \Delta M^2(L/E)] \quad (13.14)$$

for $\beta \neq \alpha$, and

$$P(\bar{\nu}_\alpha \rightarrow \bar{\nu}_\alpha) \simeq 1 - 4T_\alpha(1 - T_\alpha) \sin^2[1.27 \Delta M^2(L/E)] . \quad (13.15)$$

Here,

$$S_{\alpha\beta} \equiv 4 \left| \sum_{i \text{ Up}} U_{\alpha i}^* U_{\beta i} \right|^2 \quad (13.16)$$

and

$$T_\alpha \equiv \sum_{i \text{ Up}} |U_{\alpha i}|^2 , \quad (13.17)$$

where “ $i \text{ Up}$ ” denotes a sum over only those neutrino mass eigenstates that lie *above* ΔM^2 or, alternatively, only those that lie *below* it. The unitarity of U guarantees that summing over either of these two clusters will yield the same results for $S_{\alpha\beta}$ and for $T_\alpha(1 - T_\alpha)$.

The situation described by Eqs. (13.14)–(13.17) may be called “quasi-two-neutrino oscillation.” It has also been called “one mass scale dominance” [5]. It corresponds to an experiment whose L/E is such that the experiment can “see” only the big splitting ΔM^2 . To this experiment, all the neutrinos above ΔM^2 appear to be a single neutrino, as do all those below ΔM^2 .

The relations of Eqs. (13.14)–(13.17) apply to a three-neutrino spectrum in which one of the two squared-mass splittings is much bigger than the other one. If we denote by ν_3 the neutrino that is by itself at one end of the large splitting ΔM^2 , then $S_{\alpha\beta} = 4|U_{\alpha 3}U_{\beta 3}|^2$ and $T_\alpha = |U_{\alpha 3}|^2$. Thus, oscillation experiments with $\Delta M^2 L/E = \mathcal{O}(1)$ can determine the flavor fractions $|U_{\alpha 3}|^2$ of ν_3 .

The relations of Eqs. (13.14)–(13.17) also apply to the special case where, to a good approximation, only two mass eigenstates, and two corresponding flavor eigenstates (or two linear combinations of flavor eigenstates), are relevant. One encounters this case when, for example, only two mass eigenstates couple significantly to the charged lepton with which the neutrino being studied is produced. When only two mass eigenstates count, there is only a single splitting, Δm^2 , and, omitting irrelevant phase factors, the unitary mixing matrix U takes the form

$$U = \begin{array}{cc} & \begin{array}{cc} \nu_1 & \nu_2 \end{array} \\ \begin{array}{c} \nu_\alpha \\ \nu_\beta \end{array} & \begin{bmatrix} \cos \theta & \sin \theta \\ -\sin \theta & \cos \theta \end{bmatrix} . \end{array} \quad (13.18)$$

Here, the symbols above and to the left of the matrix label the columns and rows, and θ is referred to as the mixing angle. From Eqs. (13.16) and (13.17), we now have $S_{\alpha\beta} = \sin^2 2\theta$ and $4T_\alpha(1 - T_\alpha) = \sin^2 2\theta$, so that Eqs. (13.14) and (13.15) become, respectively,

$$P(\bar{\nu}_\alpha \rightarrow \bar{\nu}_\beta) = \sin^2 2\theta \sin^2[1.27 \Delta m^2(L/E)] \quad (13.19)$$

with $\beta \neq \alpha$, and

$$P(\bar{\nu}_\alpha \rightarrow \bar{\nu}_\alpha) = 1 - \sin^2 2\theta \sin^2[1.27 \Delta m^2(L/E)] . \quad (13.20)$$

Many experiments have been analyzed using these two expressions. Some of these experiments actually have been concerned with quasi-two-neutrino oscillation, rather than a genuinely two-neutrino situation. For these experiments, “ $\sin^2 2\theta$ ” and “ Δm^2 ” have the significance that follows from Eqs. (13.14)–(13.17).

When neutrinos travel through matter (*e.g.*, in the Sun, Earth, or a supernova), their coherent forward-scattering from particles they encounter along the way can significantly modify their propagation [6]. As a result, the probability for changing flavor can be rather different than it is in vacuum [7]. Flavor change that occurs in matter, and that grows out of the interplay between flavor-nonchanging neutrino-matter interactions and neutrino mass and mixing, is known as the Mikheyev-Smirnov-Wolfenstein (MSW) effect.

To a good approximation, one can describe neutrino propagation through matter via a Schrödinger-like equation. This equation governs the evolution of a neutrino state vector with several components, one for each flavor. The effective Hamiltonian in the equation, a matrix \mathcal{H} in neutrino flavor space, differs from its vacuum counterpart by the addition of interaction energies arising from the coherent forward neutrino-scattering. For example, the ν_e - ν_e element of \mathcal{H} includes the interaction energy

$$V = \sqrt{2} G_F N_e , \quad (13.21)$$

arising from W -exchange-induced ν_e forward-scattering from ambient electrons. Here, G_F is the Fermi constant, and N_e is the number of electrons per unit volume. In addition, the ν_e - ν_e , ν_μ - ν_μ , and ν_τ - ν_τ elements of \mathcal{H} all contain a common interaction energy growing out of Z -exchange-induced forward-scattering. However, when one is not considering the possibility of transitions to sterile neutrino flavors, this common interaction energy merely adds to \mathcal{H} a multiple of the identity matrix, and such an addition has no effect on flavor transitions.

The effect of matter is illustrated by the propagation of solar neutrinos through solar matter. When combined with information on atmospheric neutrino oscillation, the experimental bounds on short-distance ($L \lesssim 1$ km) oscillation of reactor $\bar{\nu}_e$ [8] tell us that, if there are no sterile neutrinos, then only two neutrino mass eigenstates, ν_1 and ν_2 , are significantly involved in the evolution of the solar neutrinos. Correspondingly, only two flavors are involved: the ν_e flavor with which every solar neutrino is born, and the effective flavor ν_x — some linear combination of ν_μ and ν_τ — which it may become. The Hamiltonian \mathcal{H} is then a 2×2 matrix in ν_e - ν_x space. Apart from an irrelevant multiple of the identity, for a distance r from the center of the Sun, \mathcal{H} is given by

$$\begin{aligned} \mathcal{H} &= \mathcal{H}_V + \mathcal{H}_M(r) \\ &= \frac{\Delta m_\odot^2}{4E} \begin{bmatrix} -\cos 2\theta_\odot & \sin 2\theta_\odot \\ \sin 2\theta_\odot & \cos 2\theta_\odot \end{bmatrix} + \begin{bmatrix} V(r) & 0 \\ 0 & 0 \end{bmatrix} . \end{aligned} \quad (13.22)$$

Here, the first matrix \mathcal{H}_V is the Hamiltonian in vacuum, and the second matrix $\mathcal{H}_M(r)$ is the modification due to matter. In \mathcal{H}_V , θ_\odot is the solar mixing angle defined by the two-neutrino mixing matrix of Eq. (13.18) with $\theta = \theta_\odot$, $\nu_\alpha = \nu_e$, and $\nu_\beta = \nu_x$. The splitting Δm_\odot^2 is $m_2^2 - m_1^2$, and for the present purpose we *define* ν_2 to be the heavier of the two mass eigenstates, so that Δm_\odot^2 is positive. In $\mathcal{H}_M(r)$, $V(r)$ is the interaction energy of Eq. (13.21) with the electron density $N_e(r)$ evaluated at distance r from the Sun’s center.

From Eqs. (13.19–13.20) (with $\theta = \theta_\odot$), we see that two-neutrino oscillation in vacuum cannot distinguish between a mixing angle θ_\odot and an angle $\theta'_\odot = \pi/2 - \theta_\odot$. But these two mixing angles represent physically different situations. Suppose, for example, that $\theta_\odot < \pi/4$. Then, from Eq. (13.18) we see that if the mixing angle is θ_\odot , the lighter mass eigenstate (defined to be ν_1) is more ν_e than ν_x , while if it is θ'_\odot , then this mass eigenstate is more ν_x than ν_e . While oscillation in vacuum cannot discriminate between these two possibilities, neutrino propagation through solar matter can do so. The neutrino interaction energy V of Eq. (13.21) is of definite, positive sign [9]. Thus, the ν_e - ν_e element of the solar \mathcal{H} , $-(\Delta m_\odot^2/4E) \cos 2\theta_\odot + V(r)$, has a different size when the mixing angle is $\theta'_\odot = \pi/2 - \theta_\odot$ than it does when this angle is θ_\odot . As a result, the flavor content of the neutrinos coming from the Sun can be different in the two cases [10].

Solar and long-baseline reactor neutrino data establish that the behavior of solar neutrinos is governed by a Large-Mixing-Angle (LMA) MSW effect (see Sec. II). Let us estimate the probability $P(\nu_e \rightarrow \nu_e)$ that a solar neutrino that undergoes the LMA-MSW effect in the Sun still has its original ν_e flavor when it arrives at the Earth. We focus on the neutrinos produced by ^8B decay, which are at the high-energy end of the solar neutrino spectrum. At $r \simeq 0$, where the solar neutrinos are created, the electron density $N_e \simeq 6 \times 10^{25}/\text{cm}^3$ [11] yields for the interaction energy V of Eq. (13.21) the value $0.75 \times 10^{-5} \text{ eV}^2/\text{MeV}$. Thus, for Δm_\odot^2 in the favored region, around $8 \times 10^{-5} \text{ eV}^2$, and E a typical ^8B neutrino energy (~ 6 - 7 MeV), \mathcal{H}_M dominates over \mathcal{H}_V . This means that, in first approximation, $\mathcal{H}(r \simeq 0)$ is diagonal. Thus, a ^8B neutrino is born not only in a ν_e flavor eigenstate, but also, again in first approximation, in an eigenstate of the Hamiltonian

$\mathcal{H}(r \simeq 0)$. Since $V > 0$, the neutrino will be in the heavier of the two eigenstates. Now, under the conditions where the LMA-MSW effect occurs, the propagation of a neutrino from $r \simeq 0$ to the outer edge of the Sun is adiabatic. That is, $N_e(r)$ changes sufficiently slowly that we may solve Schrödinger's equation for one r at a time, and then patch together the solutions. This means that our neutrino propagates outward through the Sun as one of the r -dependent eigenstates of the r -dependent $\mathcal{H}(r)$. Since the eigenvalues of $\mathcal{H}(r)$ do not cross at any r , and our neutrino is born in the heavier of the two $r = 0$ eigenstates, it emerges from the Sun in the heavier of the two \mathcal{H}_V eigenstates [12]. The latter is the mass eigenstate we have called ν_2 , given according to Eq. (13.18) by

$$\nu_2 = \nu_e \sin \theta_\odot + \nu_x \cos \theta_\odot . \quad (13.23)$$

Since this is an eigenstate of the vacuum Hamiltonian, the neutrino remains in it all the way to the surface of the Earth. The probability of observing the neutrino as a ν_e on Earth is then just the probability that ν_2 is a ν_e . That is [cf. Eq. (13.23)] [13],

$$P(\nu_e \rightarrow \nu_e) = \sin^2 \theta_\odot . \quad (13.24)$$

We note that for $\theta_\odot < \pi/4$, this ν_e survival probability is less than 1/2. In contrast, when matter effects are negligible, the energy-averaged survival probability in two-neutrino oscillation cannot be less than 1/2 for any mixing angle [see Eq. (13.20)] [14].

II. The evidence for flavor metamorphosis, and what it has taught us: The persuasiveness of the evidence that neutrinos actually do change flavor in nature is summarized in Table 13.1. We discuss the different pieces of evidence, and what, together, they imply.

Table 13.1: The persuasiveness of the evidence for neutrino flavor change. The symbol L denotes the distance travelled by the neutrinos. LSND is the Liquid Scintillator Neutrino Detector experiment, and MiniBooNE is an experiment designed to confirm or refute LSND.

Neutrinos	Evidence for Flavor Change
Atmospheric	Compelling
Accelerator ($L = 250$ and 735 km)	Compelling
Solar	Compelling
Reactor ($L \sim 180$ km)	Compelling
From Stopped μ^+ Decay (LSND)	Unconfirmed by MiniBooNE

The atmospheric neutrinos are produced in the Earth's atmosphere by cosmic rays, and then detected in an underground detector. The flux of cosmic rays that lead to neutrinos with energies above a few GeV is isotropic, so that these neutrinos are produced at the same rate all around the Earth. This can easily be shown to imply that at any underground site, the downward- and upward-going fluxes of multi-GeV neutrinos of a given flavor must be equal. That is, unless some mechanism changes the flux of neutrinos of the given flavor as they propagate, the flux coming down from zenith angle θ_Z must equal that coming up from angle $\pi - \theta_Z$ [15].

The underground Super-Kamiokande (SK) detector finds that for multi-GeV atmospheric muon neutrinos, the θ_Z event distribution looks nothing like the expected $\theta_Z \Leftrightarrow \pi - \theta_Z$ symmetric distribution. For $\cos \theta_Z \gtrsim 0.3$, the observed ν_μ flux coming up from zenith angle $\pi - \theta_Z$ is only about half that coming down from angle θ_Z [16]. Thus, some mechanism does change the ν_μ flux as the neutrinos travel to the detector. Since the upward-going muon neutrinos come from the atmosphere on the opposite side of the Earth from the detector, they travel much farther than the downward-going ones to reach the detector. Thus, if the muon neutrinos are oscillating away into another flavor, the upward-going ones have more distance (hence more time) in which to do so, which would explain why Flux Up < Flux Down.

If atmospheric muon neutrinos are disappearing via oscillation into another flavor, then a significant fraction of accelerator-generated

muon neutrinos should disappear on their way to a sufficiently distant detector. This disappearance has been observed by both the K2K [17] and MINOS [18] experiments. Each of these experiments measures its ν_μ flux in a detector near the neutrino source, before any oscillation is expected, and then measures it again in a detector 250 km from the source in the case of K2K, and 735 km from it in the case of MINOS. In its far detector, MINOS has observed 215 ν_μ events in a data sample where 336 ± 14.4 events would have been expected, in the absence of oscillation, on the basis of the near-detector measurements. Both K2K and MINOS also find that the energy spectrum of surviving muon neutrinos in the far detector is distorted in a way that is consistent with two-neutrino oscillation.

The null results of short-baseline reactor neutrino experiments [8] imply limits on $P(\bar{\nu}_e \rightarrow \bar{\nu}_\mu)$, which, assuming CPT invariance, are also limits on $P(\nu_\mu \rightarrow \nu_e)$. From the latter, we know that the neutrinos into which the atmospheric, K2K, and MINOS muon neutrinos oscillate are not electron neutrinos, except possibly a small fraction of the time. All of the voluminous SK atmospheric neutrino data, corroborating data from other atmospheric neutrino experiments [19,20], K2K accelerator neutrino data, and existing MINOS accelerator neutrino data, are very well described by pure $\nu_\mu \rightarrow \nu_\tau$ quasi-two-neutrino oscillation. The allowed region for the oscillation parameters, Δm_{atm}^2 and $\sin^2 2\theta_{\text{atm}}$, which may be identified respectively with the parameters ΔM^2 and $4T_\mu(1 - T_\mu)$ in Eq. (13.15), is shown in Fig. 13.1. We note that this figure implies that at least one mass eigenstate ν_i must have a mass exceeding 40 meV.

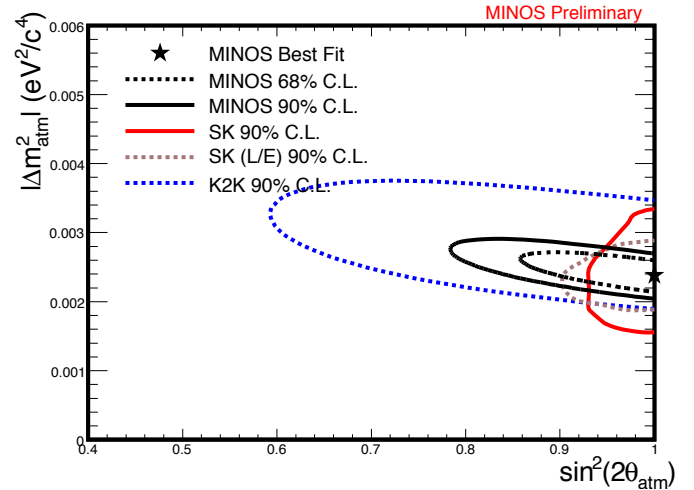


Figure 13.1: The region of the atmospheric oscillation parameters Δm_{atm}^2 and $\sin^2 2\theta_{\text{atm}}$ allowed by the SK, K2K, and MINOS data. The results of two different analyses of the SK ("Super K") data are shown [21]. Color version at end of book.

The neutrinos created in the Sun have been detected on Earth by several experiments, as discussed by K. Nakamura in this *Review*. The nuclear processes that power the Sun make only ν_e , not ν_μ or ν_τ . For years, solar neutrino experiments had been finding that the solar ν_e flux arriving at the Earth is below the one expected from neutrino production calculations. Now, thanks especially to the Sudbury Neutrino Observatory (SNO), we have compelling evidence that the missing ν_e have simply changed into neutrinos of other flavors.

SNO has studied the flux of high-energy solar neutrinos from ^8B decay. This experiment detects these neutrinos via the reactions

$$\nu + d \rightarrow e^- + p + p , \quad (13.25)$$

$$\nu + d \rightarrow \nu + p + n , \quad (13.26)$$

and

$$\nu + e^- \rightarrow \nu + e^- . \quad (13.27)$$

The first of these reactions, charged-current deuteron breakup, can be initiated only by a ν_e . Thus, it measures the flux $\phi(\nu_e)$ of ν_e from ${}^8\text{B}$ decay in the Sun. The second reaction, neutral-current deuteron breakup, can be initiated with equal cross sections by neutrinos of all active flavors. Thus, it measures $\phi(\nu_e) + \phi(\nu_{\mu,\tau})$, where $\phi(\nu_{\mu,\tau})$ is the flux of ν_μ and/or ν_τ from the Sun. Finally, the third reaction, neutrino electron elastic scattering, can be triggered by a neutrino of any active flavor, but $\sigma(\nu_{\mu,\tau} e \rightarrow \nu_{\mu,\tau} e) \simeq \sigma(\nu_e e \rightarrow \nu_e e)/6.5$. Thus, this reaction measures $\phi(\nu_e) + \phi(\nu_{\mu,\tau})/6.5$.

SNO finds from its observed rates for the two deuteron breakup reactions that [22]

$$\frac{\phi(\nu_e)}{\phi(\nu_e) + \phi(\nu_{\mu,\tau})} = 0.340 \pm 0.023 \text{ (stat)} \begin{matrix} +0.029 \\ -0.031 \end{matrix} \text{ (syst)}. \quad (13.28)$$

Clearly, $\phi(\nu_{\mu,\tau})$ is not zero. This non-vanishing $\nu_{\mu,\tau}$ flux from the Sun is “smoking-gun” evidence that some of the ν_e produced in the solar core do indeed change flavor.

Corroborating information comes from the detection reaction $\nu_e^- \rightarrow \nu_e^-$, studied by both SNO and SK [23].

Change of neutrino flavor, whether in matter or vacuum, does not change the total neutrino flux. Thus, unless some of the solar ν_e are changing into sterile neutrinos, the total active high-energy flux measured by the neutral-current reaction (13.26) should agree with the predicted total ${}^8\text{B}$ solar neutrino flux based on calculations of neutrino production in the Sun. This predicted total is $(5.49^{+0.95}_{-0.81}) \times 10^6 \text{ cm}^{-2}\text{s}^{-1}$ or $(4.34^{+0.71}_{-0.61}) \times 10^6 \text{ cm}^{-2}\text{s}^{-1}$, depending on assumptions about the solar heavy element abundances [24]. By comparison, the total active flux measured by reaction (13.26) is $[4.94 \pm 0.21 \text{ (stat)} \begin{matrix} +0.38 \\ -0.34 \end{matrix} \text{ (syst)}] \times 10^6 \text{ cm}^{-2}\text{s}^{-1}$, in good agreement. This agreement provides evidence that neutrino production in the Sun is correctly understood, further strengthens the evidence that neutrinos really do change flavor, and strengthens the evidence that the previously-reported deficits of solar ν_e flux are due to this change of flavor.

The strongly favored explanation of ${}^8\text{B}$ solar neutrino flavor change is the LMA-MSW effect. As pointed out after Eq. (13.24), a ν_e survival probability below 1/2, which is indicated by Eq. (13.28), requires that solar matter effects play a significant role [25]. However, from Eq. (13.22) we see that as the energy E of a solar neutrino decreases, the vacuum (1st) term in the Hamiltonian \mathcal{H} dominates more and more over the matter term. When we go from the ${}^8\text{B}$ neutrinos with typical energies of $\sim 6\text{--}7\text{ MeV}$ to the monoenergetic ${}^7\text{Be}$ neutrinos with energy 0.862 MeV , the matter term becomes fairly insignificant, and the ν_e survival probability is expected to be given by the vacuum oscillation formula of Eq. (13.20). In this formula, θ is to be taken as the vacuum solar mixing angle $\theta_\odot \simeq 35^\circ$ implied by the ${}^8\text{B}$ solar neutrino data via Eqs. (13.28) and (13.24). When averaged over the energy-line shape, the oscillatory factor $\sin^2[1.27 \Delta m^2(L/E)]$ is 1/2, so that from Eq. (13.20) we expect that for the ${}^7\text{Be}$ neutrinos, $P(\nu_e \rightarrow \nu_e) \approx 0.6$.

The Borexino experiment has now provided the first real time detection of the 0.862 MeV ${}^7\text{Be}$ solar neutrinos [26]. Borexino uses a liquid scintillator detector that detects these neutrinos via elastic neutrino-electron scattering. The experiment reports a ${}^7\text{Be}$ ν_e counting rate of $[47 \pm 7 \text{ (stat)} \pm 12 \text{ (syst)}] \text{ counts/day/100 tons}$. Without any flavor change, this rate would have been expected to be $[75 \pm 4] \text{ counts/day/100 tons}$. With the degree of flavor change predicted by our understanding of the ${}^8\text{B}$ data [27] (see rough argument above), the rate would have been expected to be $[49 \pm 4] \text{ counts/day/100 tons}$. The Borexino data are in nice agreement with the latter expectation, and the Borexino Collaboration is vigorously engaged in reducing its uncertainties.

The LMA-MSW interpretation of ${}^8\text{B}$ solar neutrino behavior implies that a substantial fraction of reactor $\bar{\nu}_e$ that travel more than a hundred kilometers should disappear into antineutrinos of other flavors. The KamLAND experiment [28], which studies reactor $\bar{\nu}_e$ that typically travel $\sim 180 \text{ km}$ to reach the detector, confirms this disappearance. In addition, KamLAND finds that the spectrum of the surviving $\bar{\nu}_e$ that do reach the detector is distorted, relative to the

no-oscillation spectrum. As Fig. 13.2 shows, the survival probability $P(\bar{\nu}_e \rightarrow \bar{\nu}_e)$ measured by KamLAND is very well described by the hypothesis of neutrino oscillation. In particular, the measured survival probability displays the signature oscillatory behavior of the two-neutrino expression of Eq. (13.20). Ideally, the data in Fig. 13.2 would be plotted vs. L/E . However, KamLAND detects the $\bar{\nu}_e$ from a number of power reactors, at a variety of distances from the detector, so the distance L travelled by any given $\bar{\nu}_e$ is unknown. Consequently, Fig. 13.2 plots the data vs. L_0/E , where $L_0 = 180 \text{ km}$ is a flux-weighted average travel distance. The oscillation curve and histogram in the figure take the actual distances to the individual reactors into account. Nevertheless, almost two cycles of the sinusoidal structure expected from neutrino oscillation are still plainly visible.

The region allowed by solar neutrino experiments for the two-neutrino vacuum oscillation parameters Δm_\odot^2 and θ_\odot , and that allowed by KamLAND for what we believe to be the same parameters, are shown in Fig. 13.3. From this figure, we see that there is a region of overlap. This is strong evidence that the behavior of both solar neutrinos and reactor antineutrinos has been correctly understood. A joint analysis of KamLAND and solar neutrino data assuming CPT invariance yields $\Delta m_\odot^2 = (7.59 \pm 0.21) \times 10^{-5} \text{ eV}^2$ and $\tan^2 \theta_\odot = 0.47 \begin{matrix} +0.06 \\ -0.05 \end{matrix}$ [28].

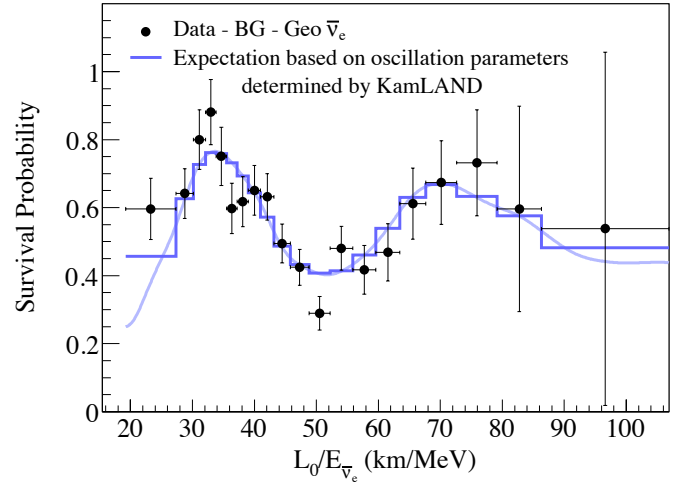


Figure 13.2: Ratio of the background- and geo-neutrino subtracted $\bar{\nu}_e$ spectrum to the no-oscillation expectation as a function of L_0/E [28]. See text for explanation.

That θ_{atm} and θ_\odot are both large, in striking contrast to all quark mixing angles, is very interesting.

The neutrinos studied by the LSND experiment [29] come from the decay $\mu^+ \rightarrow e^+ \nu_e \bar{\nu}_\mu$ of muons at rest. While this decay does not produce $\bar{\nu}_e$, an excess of $\bar{\nu}_e$ over expected background is reported by the experiment. This excess is interpreted as due to oscillation of some of the $\bar{\nu}_\mu$ produced by μ^+ decay into $\bar{\nu}_e$. The related Karlsruhe Rutherford Medium Energy Neutrino (KARMEN) experiment [30] sees no indication for such an oscillation. However, the LSND and KARMEN experiments are not identical; at LSND the neutrino travels a distance $L \approx 30 \text{ m}$ before detection, while at KARMEN it travels $L \approx 18 \text{ m}$. The KARMEN results exclude a portion of the neutrino parameter region favored by LSND, but not all of it. A joint analysis [31] of the results of both experiments finds that a splitting $0.2 \lesssim \Delta m_{\text{LSND}}^2 \lesssim 1 \text{ eV}^2$ and mixing $0.003 \lesssim \sin^2 2\theta_{\text{LSND}} \lesssim 0.03$, or a splitting $\Delta m_{\text{LSND}}^2 \simeq 7 \text{ eV}^2$ and mixing $\sin^2 2\theta_{\text{LSND}} \simeq 0.004$, might explain both experiments.

To confirm or exclude the LSND oscillation signal, the MiniBooNE experiment was launched. MiniBooNE studies ν_μ and $\bar{\nu}_\mu$ that travel a distance L of 540 m and have a typical energy E of 700 MeV , so that L/E is of order 1 km/GeV as in LSND. MiniBooNE’s first results [32], regarding a search for $\nu_\mu \rightarrow \nu_e$ oscillation in a ν_μ beam, do not confirm LSND. For neutrino energies $475 < E < 3000 \text{ MeV}$, there is

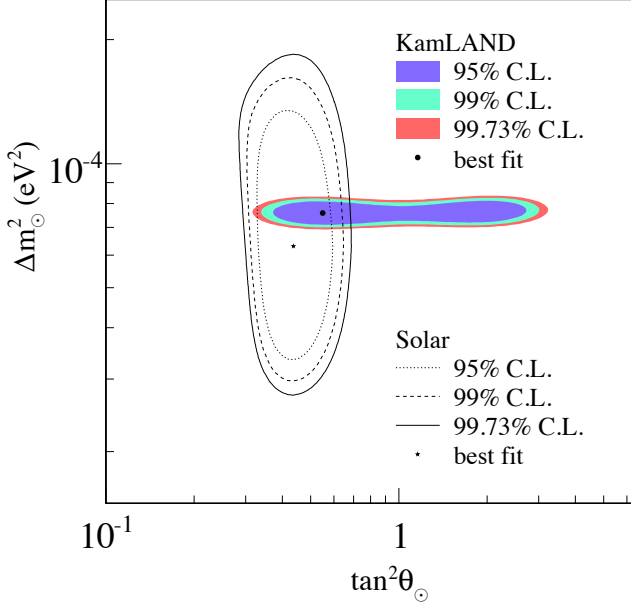


Figure 13.3: Regions allowed by the “solar” neutrino oscillation parameters by KamLAND and by solar neutrino experiments [28]. Color version at end of book.

no significant excess of events above background. A joint analysis of the MiniBooNE data at these energies and the LSND data excludes at 98% CL two-neutrino $\bar{\nu}_\mu \rightarrow \bar{\nu}_e$ oscillation as an explanation of the LSND $\bar{\nu}_e$ excess. To be sure, there is an excess of MiniBooNE ν_e candidate events below 475 MeV. This low-energy excess cannot be explained by two-neutrino oscillation, and its source is being studied. Possibilities include an unidentified background, a Standard Model effect that has been proposed only recently [33], and many-neutrino oscillation with a CP violation that allows the *antineutrino* oscillation reported by LSND to differ from the *neutrino* results reported so far by MiniBooNE [34].

The MiniBooNE detector is illuminated by both the neutrino beam constructed for the purpose, and the beam that is aimed at the MINOS detector. The distance L to MiniBooNE from the neutrino source is 40% larger in the latter beam than in the former. When matter effects may be neglected, the probability of oscillation depends on L and the beam energy E only through L/E [cf. Eq. (13.9)]. Thus, if the low-energy excess seen by MiniBooNE is neutrino oscillation, it should appear at a 40% higher energy in the beam directed at MINOS than in MiniBooNE’s own beam. Whether it does or not is under investigation.

The regions of neutrino parameter space favored or excluded by various neutrino oscillation experiments are shown in Fig. 13.4.

III. Neutrino spectra and mixings: If there are only three neutrino mass eigenstates, ν_1, ν_2 , and ν_3 , then there are only three mass splittings Δm_{ij}^2 , and they obviously satisfy

$$\Delta m_{32}^2 + \Delta m_{21}^2 + \Delta m_{13}^2 = 0. \quad (13.29)$$

However, as we have seen, the Δm^2 values required to explain the flavor changes of the atmospheric, solar, and LSND neutrinos are of three different orders of magnitude. Thus, they cannot possibly obey the constraint of Eq. (13.29). If all of the reported changes of flavor are genuine, then nature must contain at least four neutrino mass eigenstates [35]. As explained in Sec. I, one linear combination of these mass eigenstates would have to be sterile.

If further MiniBooNE results do not confirm the LSND oscillation, then nature may well contain only three neutrino mass eigenstates. The neutrino spectrum then contains two mass eigenstates separated by the splitting Δm_{\odot}^2 needed to explain the solar and KamLAND data, and a third eigenstate separated from the first two by the larger splitting Δm_{atm}^2 called for by the atmospheric, MINOS, and K2K

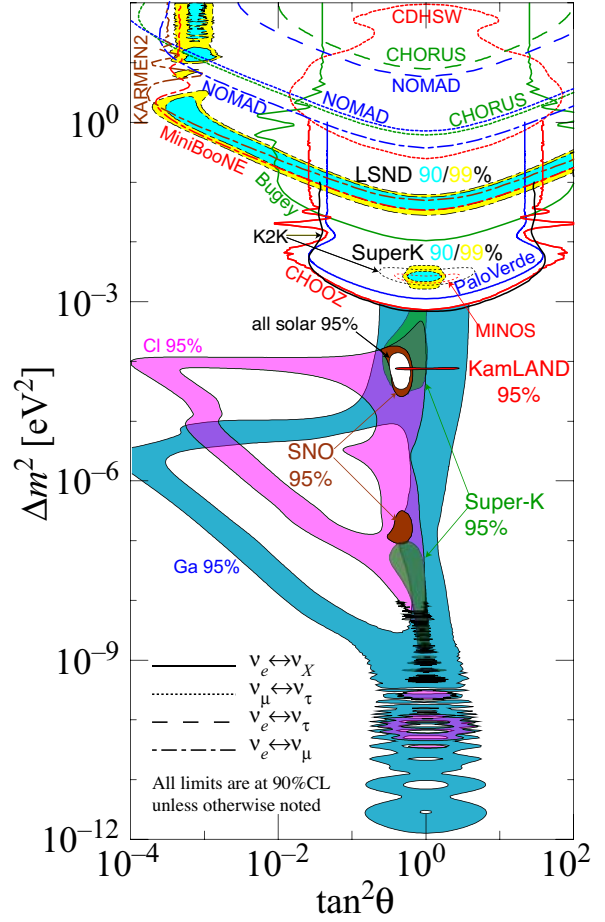


Figure 13.4: The regions of squared-mass splitting and mixing angle favored or excluded by various experiments. This figure was contributed by H. Murayama (University of California, Berkeley). References to the data used in the figure can be found at <http://hitoshi.berkeley.edu/neutrino/>. Color version at end of book.

data. Current experiments do not tell us whether the solar pair — the two eigenstates separated by Δm_{\odot}^2 — is at the bottom or the top of the spectrum. These two possibilities are usually referred to, respectively, as a normal and an inverted spectrum. The study of flavor changes of accelerator-generated neutrinos and antineutrinos that pass through matter can discriminate between these two spectra (see Sec. V). If the solar pair is at the bottom, then the spectrum is of the form shown in Fig. 13.5. There we include the approximate flavor content of each mass eigenstate, the flavor- α fraction of eigenstate ν_i being simply $|\langle \nu_\alpha | \nu_i \rangle|^2 = |U_{\alpha i}|^2$. The flavor content shown assumes that the atmospheric mixing angle is maximal, which gives the best fit to the atmospheric data [16] and, as indicated in Fig. 13.1, to the MINOS data. The content shown also takes into account the now-established LMA-MSW explanation of solar neutrino behavior. For simplicity, it neglects the small, as-yet-unknown ν_e fraction of ν_3 (see below).

When there are only three neutrino mass eigenstates, and the corresponding three familiar neutrinos of definite flavor, the leptonic mixing matrix U can be written as

$$U = \begin{pmatrix} \nu_e \\ \nu_\mu \\ \nu_\tau \end{pmatrix} \begin{pmatrix} & \nu_1 & & \nu_2 & & \nu_3 \\ & c_{12}c_{13} & & s_{12}c_{13} & & s_{13}e^{-i\delta} \\ -s_{12}c_{23} - c_{12}s_{23}s_{13}e^{i\delta} & & c_{12}c_{23} - s_{12}s_{23}s_{13}e^{i\delta} & & s_{23}c_{13} \\ s_{12}s_{23} - c_{12}c_{23}s_{13}e^{i\delta} & & -c_{12}s_{23} - s_{12}c_{23}s_{13}e^{i\delta} & & c_{23}c_{13} \end{pmatrix} \times \text{diag}(e^{i\alpha_1/2}, e^{i\alpha_2/2}, 1). \quad (13.30)$$

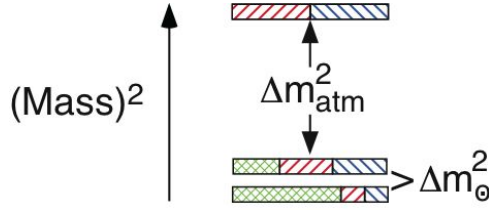


Figure 13.5: A three-neutrino squared-mass spectrum that accounts for the observed flavor changes of solar, reactor, atmospheric, and long-baseline accelerator neutrinos. The ν_e fraction of each mass eigenstate is crosshatched, the ν_μ fraction is indicated by right-leaning hatching, and the ν_τ fraction by left-leaning hatching.

Here, ν_1 and ν_2 are the members of the solar pair, with $m_2 > m_1$, and ν_3 is the isolated neutrino, which may be heavier or lighter than the solar pair. Inside the matrix, $c_{ij} \equiv \cos \theta_{ij}$ and $s_{ij} \equiv \sin \theta_{ij}$, where the three θ_{ij} 's are mixing angles. The quantities δ , α_1 , and α_2 are CP -violating phases. The phases α_1 and α_2 , known as Majorana phases, have physical consequences only if neutrinos are Majorana particles, identical to their antiparticles. Then these phases influence neutrinoless double-beta decay [see Sec. IV] and other processes [36]. However, as we see from Eq. (13.9), α_1 and α_2 do not affect neutrino oscillation, regardless of whether neutrinos are Majorana particles. Apart from the phases α_1 , α_2 , which have no quark analogues, the parametrization of the leptonic mixing matrix in Eq. (13.30) is identical to that [37] advocated for the quark mixing matrix by Ceccucci, Ligeti, and Sakai in their article in this *Review*.

From bounds on the short-distance oscillation of reactor $\bar{\nu}_e$ [8] and other data, at 2σ , $|U_{e3}|^2 \lesssim 0.032$ [38]. (Thus, the ν_e fraction of ν_3 would have been too small to see in Fig. 13.5; this is the reason it was neglected.) From Eq. (13.30), we see that the bound on $|U_{e3}|^2$ implies that $s_{13}^2 \lesssim 0.032$. From Eq. (13.30), we also see that the CP -violating phase δ , which is the sole phase in the U matrix that can produce CP violation in neutrino oscillation, enters U only in combination with s_{13} . Thus, the size of CP violation in oscillation will depend on s_{13} .

Given that s_{13} is small, Eqs. (13.30), (13.15), and (13.17) imply that the atmospheric mixing angle θ_{atm} extracted from ν_μ disappearance measurements is approximately θ_{23} , while Eqs. (13.30) and (13.18) (with $\nu_\alpha = \nu_e$ and $\theta = \theta_\odot$) imply that $\theta_\odot \simeq \theta_{12}$.

IV. The neutrino-antineutrino relation: Unlike quarks and charged leptons, neutrinos may be their own antiparticles. Whether they are depends on the nature of the physics that gives them mass.

In the Standard Model (SM), neutrinos are assumed to be massless. Now that we know they do have masses, it is straightforward to extend the SM to accommodate these masses in the same way that this model accommodates quark and charged lepton masses. When a neutrino ν is assumed to be massless, the SM does not contain the chirally right-handed neutrino field ν_R , but only the left-handed field ν_L that couples to the W and Z bosons. To accommodate the ν mass in the same manner as quark masses are accommodated, we add ν_R to the Model. Then we may construct the ‘‘Dirac mass term’’

$$\mathcal{L}_D = -m_D \bar{\nu}_L \nu_R + h.c. \quad , \quad (13.31)$$

in which m_D is a constant. This term, which mimics the mass terms of quarks and charged leptons, conserves the lepton number L that distinguishes neutrinos and negatively-charged leptons on the one hand from antineutrinos and positively-charged leptons on the other. Since everything else in the SM also conserves L , we then have an L -conserving world. In such a world, each neutrino mass eigenstate ν_i differs from its antiparticle $\bar{\nu}_i$, the difference being that $L(\bar{\nu}_i) = -L(\nu_i)$. When $\bar{\nu}_i \neq \nu_i$, we refer to the $\nu_i - \bar{\nu}_i$ complex as a ‘‘Dirac neutrino.’’

Once ν_R has been added to our description of neutrinos, a ‘‘Majorana mass term,’’

$$\mathcal{L}_M = -m_R \bar{\nu}_R^c \nu_R + h.c. \quad , \quad (13.32)$$

can be constructed out of ν_R and its charge conjugate, ν_R^c . In this term, m_R is another constant. Since both ν_R and $\bar{\nu}_R^c$ absorb ν and create $\bar{\nu}$, \mathcal{L}_M mixes ν and $\bar{\nu}$. Thus, a Majorana mass term does not conserve L . In somewhat the same way that, neglecting CP violation, $K^0 - \bar{K}^0$ mixing causes the neutral kaon mass eigenstates to be the self-conjugate states $(K^0 \pm \bar{K}^0)/\sqrt{2}$, the $\nu - \bar{\nu}$ mixing induced by a Majorana mass term causes the neutrino mass eigenstates to be self-conjugate: $\bar{\nu}_i = \nu_i$. That is, for a given helicity h , $\bar{\nu}_i(h) = \nu_i(h)$. We then refer to ν_i as a ‘‘Majorana neutrino.’’

Suppose the right-handed neutrinos required by Dirac mass terms have been added to the SM. If we insist that this extended SM conserve L , then, of course, Majorana mass terms are forbidden. However, if we do not impose L conservation, but require only the general principles of gauge invariance and renormalizability, then Majorana mass terms like that of Eq. (13.32) are expected to be present. As a result, L is violated, and neutrinos are Majorana particles [39].

In the see-saw mechanism [40], which is the most popular explanation of why neutrinos — although massive — are nevertheless so light, both Dirac and Majorana mass terms are present. Hence, the neutrinos are Majorana particles. However, while half of them are the familiar light neutrinos, the other half are extremely heavy Majorana particles referred to as the N_i , with masses possibly as large as the GUT scale. The N_i may have played a crucial role in baryogenesis in the early universe, as we shall discuss in Sec. V.

How can the theoretical expectation that nature contains Majorana mass terms, so that L is violated and neutrinos are Majorana particles, be confirmed experimentally? The promising approach is to search for neutrinoless double-beta decay ($0\nu\beta\beta$). This is the process $(A, Z) \rightarrow (A, Z+2) + 2e^-$, in which a nucleus containing A nucleons, Z of which are protons, decays to a nucleus containing $Z+2$ protons by emitting two electrons. While $0\nu\beta\beta$ can in principle receive contributions from a variety of mechanisms (R-parity-violating supersymmetric couplings, for example), it is easy to show explicitly that its observation at any non-vanishing rate would imply that nature contains at least one Majorana neutrino mass term [41]. The neutrino mass eigenstates must then be Majorana neutrinos.

Quarks and charged leptons cannot have Majorana mass terms, because such terms mix fermion and antifermion, and $q \leftrightarrow \bar{q}$ or $\ell \leftrightarrow \bar{\ell}$ would not conserve electric charge. Thus, the discovery of $0\nu\beta\beta$ would demonstrate that the physics of neutrino masses is unlike that of the masses of all other fermions.

The dominant mechanism for $0\nu\beta\beta$ is expected to be the one depicted in Fig. 13.6. There, a pair of virtual W bosons are emitted by the parent nucleus, and then these W bosons exchange one or another of the light neutrino mass eigenstates ν_i to produce the outgoing electrons. The $0\nu\beta\beta$ amplitude is then a sum over the contributions of the different ν_i . It is assumed that the interactions at the two leptonic W vertices are those of the SM.

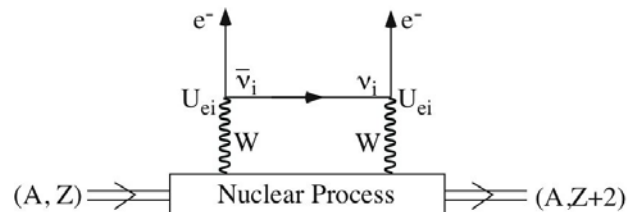


Figure 13.6: The dominant mechanism for $0\nu\beta\beta$. The diagram does not exist unless $\bar{\nu}_i = \nu_i$.

Since the exchanged ν_i is created together with an e^- , the left-handed SM current that creates it gives it the helicity we associate, in common parlance, with an ‘‘antineutrino.’’ That is, the ν_i is almost totally right-handed, but has a small left-handed-helicity component, whose amplitude is of order m_i/E , where E is the ν_i energy. At the vertex where this ν_i is absorbed, the absorbing left-handed SM current can absorb only its small left-handed-helicity component without further suppression. Consequently, the ν_i -exchange contribution to the $0\nu\beta\beta$ amplitude is proportional to m_i . From Fig. 13.6, we see that

this contribution is also proportional to U_{ei}^2 . Thus, summing over the contributions of all the ν_i , we conclude that the amplitude for $0\nu\beta\beta$ is proportional to the quantity

$$\left| \sum_i m_i U_{ei}^2 \right| \equiv | \langle m_{\beta\beta} \rangle | , \quad (13.33)$$

commonly referred to as the “effective Majorana mass for neutrinoless double-beta decay” [42].

To how small an $| \langle m_{\beta\beta} \rangle |$ should a $0\nu\beta\beta$ search be sensitive? In answering this question, it makes sense to assume there are only three neutrino mass eigenstates — if there are more, $| \langle m_{\beta\beta} \rangle |$ might be larger. Suppose that there are just three mass eigenstates, and that the solar pair, ν_1 and ν_2 , is at the top of the spectrum, so that we have an inverted spectrum. If the various ν_i are not much heavier than demanded by the observed splittings Δm_{atm}^2 and Δm_{\odot}^2 , then in $| \langle m_{\beta\beta} \rangle |$, Eq. (13.33), the contribution of ν_3 may be neglected, because both m_3 and $|U_{e3}^2| = s_{13}^2$ are small. From Eqs. (13.33) and (13.30), approximating c_{13} by unity, we then have that

$$| \langle m_{\beta\beta} \rangle | \simeq m_0 \sqrt{1 - \sin^2 2\theta_{\odot} \sin^2 \left(\frac{\Delta\alpha}{2} \right)} . \quad (13.34)$$

Here, m_0 is the average mass of the members of the solar pair, whose splitting will be invisible in a practical $0\nu\beta\beta$ experiment, and $\Delta\alpha \equiv \alpha_2 - \alpha_1$ is a CP -violating phase. Although $\Delta\alpha$ is completely unknown, we see from Eq. (13.34) that

$$| \langle m_{\beta\beta} \rangle | \geq m_0 \cos 2\theta_{\odot} . \quad (13.35)$$

Now, in an inverted spectrum, $m_0 \geq \sqrt{\Delta m_{\text{atm}}^2}$. At 90% CL, $\sqrt{\Delta m_{\text{atm}}^2} > 45 \text{ meV}$ [see Fig. 13.1], while at 95% CL, $\cos 2\theta_{\odot} > 0.25$ [see Fig. 13.3]. Thus, if neutrinos are Majorana particles, and the spectrum is as we have assumed, a $0\nu\beta\beta$ experiment sensitive to $| \langle m_{\beta\beta} \rangle | \gtrsim 10 \text{ meV}$ would have an excellent chance of observing a signal. If the spectrum is inverted, but the ν_i masses are larger than the Δm_{atm}^2 - and Δm_{\odot}^2 -demanded minimum values we have assumed above, then once again $| \langle m_{\beta\beta} \rangle |$ is larger than 10 meV [43], and an experiment sensitive to 10 meV still has an excellent chance of seeing a signal.

If the solar pair is at the bottom of the spectrum, rather than at the top, then $| \langle m_{\beta\beta} \rangle |$ is not as tightly constrained, and can be anywhere from the present bound of 0.3–1.0 eV down to invisibly small [43,44]. For a discussion of the present bounds, see the article by Vogel and Piepke in this *Review* [45].

V. Questions to be answered: The strong evidence for neutrino flavor metamorphosis — hence neutrino mass — opens many questions about the neutrinos. These questions, which hopefully will be answered by future experiments, include the following:

i) How many neutrino species are there? Do sterile neutrinos exist?

This question is being addressed by the MiniBooNE experiment [32]. If MiniBooNE’s final result is positive, the implications will be far-reaching. We will have learned that either there are more than three neutrino species and at least one of these species is sterile, or else there is an even more amazing departure from what has been our picture of the neutrino world.

ii) What are the masses of the mass eigenstates ν_i ?

Assuming there are only three ν_i , we need to find out whether the solar pair, $\nu_{1,2}$, is at the bottom of the spectrum or at its top. This can be done by exploiting matter effects in long-baseline neutrino and antineutrino oscillations. These matter effects will determine the sign one wishes to learn — that of $\{m_3^2 - [(m_2^2 + m_1^2)/2]\}$ — relative to a sign that is already known — that of the interaction energy of Eq. (13.21). Grand unified theories favor a spectrum with the closely spaced solar pair at the bottom [46]. The neutrino spectrum would then resemble the spectra of the quarks, to which grand unified theories relate the neutrinos. A neutrino spectrum with the closely spaced solar pair at the top would be quite un-quark-like, and would

suggest the existence of a new symmetry that leads to the near degeneracy at the top of the spectrum.

While flavor-change experiments can determine a spectral pattern such as the one in Fig. 13.5, they cannot tell us the distance of the entire pattern from the zero of squared-mass. One might discover that distance via study of the β energy spectrum in tritium β decay, if the mass of some ν_i with appreciable coupling to an electron is large enough to be within reach of a feasible experiment. One might also gain some information on the distance from zero by measuring $| \langle m_{\beta\beta} \rangle |$, the effective Majorana mass for neutrinoless double-beta decay [43–45] (see Vogel and Piepke in this *Review*). Finally, one might obtain information on this distance from cosmology or astrophysics. Indeed, from current cosmological data and some cosmological assumptions, it is already concluded that [47]

$$\sum_i m_i < (0.17 - 2.0) \text{ eV} . \quad (13.36)$$

Here, the sum runs over the masses of all the light neutrino mass eigenstates ν_i that may exist and that were in thermal equilibrium in the early universe. The range quoted in Eq. (13.36) reflects the dependence of this upper bound on the underlying cosmological assumptions and on which data are used [47].

If there are just three ν_i , and their spectrum is either the one shown in Fig. 13.5 or its inverted version, then Eq. (13.36) implies that the mass of the heaviest ν_i , Mass [Heaviest ν_i], cannot exceed $(0.07 - 0.7) \text{ eV}$. Moreover, Mass [Heaviest ν_i] obviously cannot be less than $\sqrt{\Delta m_{\text{atm}}^2}$, which in turn is not less than 0.04 eV, as previously noted. Thus, if the cosmological assumptions behind Eq. (13.36) are correct, then

$$0.04 \text{ eV} < \text{Mass [Heaviest } \nu_i] < (0.07 - 0.7) \text{ eV} . \quad (13.37)$$

iii) Are the neutrino mass eigenstates Majorana particles?

The confirmed observation of neutrinoless double-beta decay would establish that the answer is “yes.” If there are only three ν_i , knowledge that the spectrum is inverted and a definitive upper bound on $| \langle m_{\beta\beta} \rangle |$ that is well below 0.01 eV would establish (barring exotic contributions to $0\nu\beta\beta$) that the answer is “no” [see discussion after Eq. (13.35)] [43,44].

iv) What are the mixing angles in the leptonic mixing matrix U ?

The solar mixing angle $\theta_{\odot} \simeq \theta_{12}$ is already rather well determined.

The atmospheric mixing angle $\theta_{\text{atm}} \simeq \theta_{23}$ is constrained by the most stringent analysis to lie, at 90% CL, in the region where $\sin^2 2\theta_{\text{atm}} > 0.92$ [16]. This region is still fairly large: 37° to 53° . A more precise value of $\sin^2 2\theta_{\text{atm}}$, and, in particular, its deviation from unity, can be sought in precision long-baseline ν_{μ} disappearance experiments. If $\sin^2 2\theta_{\text{atm}} \neq 1$, so that $\theta_{\text{atm}} \neq 45^\circ$, one can determine whether it lies below or above 45° with the help of a reactor $\bar{\nu}_e$ experiment [48,49]. Once we know whether the neutrino spectrum is normal or inverted, this determination will tell us whether the heaviest mass eigenstate is more ν_{τ} than ν_{μ} , as naively expected, or more ν_{μ} than ν_{τ} [cf. Eq. (13.30)].

A knowledge of the small mixing angle θ_{13} is important not only to help complete our picture of leptonic mixing, but also because, as Eq. (13.30) made clear, all CP -violating effects of the phase δ are proportional to $\sin \theta_{13}$. Thus, a knowledge of the order of magnitude of θ_{13} would help guide the planning of experiments to probe CP violation. From Eq. (13.30), we recall that $\sin^2 \theta_{13}$ is the ν_e fraction of ν_3 . The ν_3 is the isolated neutrino that lies at one end of the atmospheric squared-mass gap Δm_{atm}^2 , so an experiment seeking to measure θ_{13} should have an L/E that makes it sensitive to Δm_{atm}^2 , and should involve ν_e . Planned approaches include a sensitive search for the disappearance of reactor $\bar{\nu}_e$ while they travel a distance $L \sim 1 \text{ km}$, and an accelerator neutrino search for $\nu_{\mu} \rightarrow \nu_e$ and $\bar{\nu}_{\mu} \rightarrow \bar{\nu}_e$ with a beamline $L >$ several hundred km.

If LSND is confirmed, then (barring the still more revolutionary) the matrix U is at least 4×4 , and contains many more than three angles. A rich program, including short baseline experiments

with multiple detectors, will be needed to learn about both the squared-mass spectrum and the mixing matrix.

Given the large sizes of θ_{atm} and θ_{\odot} , we already know that leptonic mixing is very different from its quark counterpart, where all the mixing angles are small. This difference, and the striking contrast between the tiny neutrino masses and the very much larger quark masses, suggest that the physics underlying neutrino masses and mixing may be very different from the physics behind quark masses and mixing.

v) Does the behavior of neutrinos violate CP?

From Eqs. (13.9), (13.13), and (13.30), we see that if the CP -violating phase δ and the small mixing angle θ_{13} are both non-vanishing, there will be CP -violating differences between neutrino and antineutrino oscillation probabilities. Observation of these differences would establish that CP violation is not a peculiarity of quarks.

The CP -violating difference $P(\nu_{\alpha} \rightarrow \nu_{\beta}) - P(\bar{\nu}_{\alpha} \rightarrow \bar{\nu}_{\beta})$ between “neutrino” and “antineutrino” oscillation probabilities is independent of whether the mass eigenstates ν_i are Majorana or Dirac particles. To study $\nu_{\mu} \rightarrow \nu_e$ with a super-intense but conventionally generated neutrino beam, for example, one would create the beam via the process $\pi^+ \rightarrow \mu^+ \nu_{\mu}$, and detect it via $\nu_i + \text{target} \rightarrow e^- + \dots$. To study $\bar{\nu}_{\mu} \rightarrow \bar{\nu}_e$, one would create the beam via $\pi^- \rightarrow \mu^- \bar{\nu}_{\mu}$, and detect it via $\bar{\nu}_i + \text{target} \rightarrow e^+ + \dots$. Whether $\bar{\nu}_i = \nu_i$ or not, the amplitudes for the latter two processes are proportional to $U_{\mu i}$ and U_{ei}^* , respectively. In contrast, the amplitudes for their $\nu_{\mu} \rightarrow \nu_e$ counterparts are proportional to $U_{\mu i}^*$ and U_{ei} . As this illustrates, Eq. (13.13) relates “neutrino” and “antineutrino” oscillation probabilities even when the neutrino mass eigenstates are their own antiparticles.

The baryon asymmetry of the universe could not have developed without some violation of CP during the universe’s early history. The one known source of CP violation — the complex phase in the quark mixing matrix — could not have produced sufficiently large effects. Thus, perhaps *leptonic* CP violation is responsible for the baryon asymmetry. The see-saw mechanism predicts very heavy Majorana neutral leptons N_i (see Sec. IV), which would have been produced in the Big Bang. Perhaps CP violation in the leptonic decays of an N_i led to the inequality

$$\Gamma(N_i \rightarrow \ell^+ + \dots) \neq \Gamma(N_i \rightarrow \ell^- + \dots) , \quad (13.38)$$

which would have resulted in unequal numbers of ℓ^+ and ℓ^- in the early universe [50]. This leptogenesis could have been followed by nonperturbative SM processes that would have converted the lepton asymmetry, in part, into the observed baryon asymmetry [51].

While the connection between the CP violation that would have led to leptogenesis, and that which we hope to observe in neutrino oscillation, is model-dependent, it is not likely that we have either of these without the other [52], because in the see-saw picture, these two CP violations both arise from the same matrix of coupling constants. This makes the search for CP violation in neutrino oscillation very interesting indeed. Depending on the rough size of θ_{13} , this CP violation may be observable with a very intense conventional neutrino beam, or may require a “neutrino factory,” whose neutrinos come from the decay of stored muons or radioactive nuclei. The detailed study of CP violation may require a neutrino factory in any case.

With a conventional beam, one would seek CP violation, and try to determine whether the mass spectrum is normal or inverted, by studying the oscillations $\nu_{\mu} \rightarrow \nu_e$ and $\bar{\nu}_{\mu} \rightarrow \bar{\nu}_e$. The appearance probability for ν_e in a beam that is initially ν_{μ} can be written for $\sin^2 2\theta_{13} < 0.2$ [53]

$$P(\nu_{\mu} \rightarrow \nu_e) \cong \sin^2 2\theta_{13} T_1 - \alpha \sin 2\theta_{13} T_2 + \alpha \sin 2\theta_{13} T_3 + \alpha^2 T_4 . \quad (13.39)$$

Here, $\alpha \equiv \Delta m_{21}^2 / \Delta m_{31}^2$ is the small ($\sim 1/30$) ratio between the solar and atmospheric squared-mass splittings, and

$$T_1 = \sin^2 2\theta_{23} \frac{\sin^2[(1-x)\Delta]}{(1-x)^2} , \quad (13.40)$$

$$T_2 = \sin \delta \sin 2\theta_{12} \sin 2\theta_{23} \sin \Delta \frac{\sin(x\Delta)}{x} \frac{\sin[(1-x)\Delta]}{(1-x)} , \quad (13.41)$$

$$T_3 = \cos \delta \sin 2\theta_{12} \sin 2\theta_{23} \cos \Delta \frac{\sin(x\Delta)}{x} \frac{\sin[(1-x)\Delta]}{(1-x)} , \quad (13.42)$$

and

$$T_4 = \cos^2 \theta_{23} \sin^2 2\theta_{12} \frac{\sin^2(x\Delta)}{x^2} . \quad (13.43)$$

In these expressions, $\Delta \equiv \Delta m_{31}^2 L / 4E$ is the kinematical phase of the oscillation. The quantity $x \equiv 2\sqrt{2}G_F N_e E / \Delta m_{31}^2$, with G_F the Fermi coupling constant and N_e the electron number density, is a measure of the importance of the matter effect resulting from coherent forward-scattering of electron neutrinos from ambient electrons as the neutrinos travel through the earth from the source to the detector [cf. Sec. I]. In the appearance probability $P(\nu_{\mu} \rightarrow \nu_e)$, the T_1 term represents the oscillation due to the atmospheric-mass-splitting scale, the T_4 term represents the oscillation due to the solar-mass-splitting scale, and the T_2 and T_3 terms are the CP -violating and CP -conserving interference terms, respectively.

The probability for the corresponding antineutrino oscillation, $P(\bar{\nu}_{\mu} \rightarrow \bar{\nu}_e)$, is the same as the probability $P(\nu_{\mu} \rightarrow \nu_e)$ given by Eqs. (13.39)–(13.43), but with the signs in front of both x and $\sin \delta$ reversed: both the matter effect and CP violation lead to a difference between the $\nu_{\mu} \rightarrow \nu_e$ and $\bar{\nu}_{\mu} \rightarrow \bar{\nu}_e$ oscillation probabilities. In view of the dependence of x on Δm_{31}^2 , and in particular on the sign of Δm_{31}^2 , the matter effect can reveal whether the neutrino mass spectrum is normal or inverted. However, to determine the nature of the spectrum, and to establish the presence of CP violation, it obviously will be necessary to disentangle the matter effect from CP violation in the neutrino-antineutrino oscillation probability difference that is actually observed. To this end, complementary measurements will be extremely important. These can take advantage of the differing dependences on the matter effect and on CP violation in $P(\nu_{\mu} \rightarrow \nu_e)$.

vi) Will we encounter the completely unexpected?

The study of neutrinos has been characterized by surprises. It would be surprising if further surprises were not in store. The possibilities include new, non-Standard-Model interactions, unexpectedly large magnetic and electric dipole moments [54], unexpectedly short lifetimes, and violations of CPT invariance, Lorentz invariance, or the equivalence principle.

The questions we have discussed, and other questions about the world of neutrinos, will be the focus of a major experimental program in the years to come.

Acknowledgements

I am grateful to Susan Kayser for her crucial role in the production of this manuscript.

References:

1. This matrix is sometimes referred to as the Maki-Nakagawa-Sakata matrix, or as the Pontecorvo-Maki-Nakagawa-Sakata matrix, in recognition of the pioneering contributions of these scientists to the physics of mixing and oscillation. See Z. Maki, M. Nakagawa, and S. Sakata, *Prog. Theor. Phys.* **28**, 870 (1962); B. Pontecorvo, *Zh. Eksp. Teor. Fiz.* **53**, 1717 (1967) [*Sov. Phys. JETP* **26**, 984 (1968)].
2. D. Karlen in this *Review*.
3. B. Kayser, *Phys. Rev.* **D24**, 110 (1981); F. Boehm and P. Vogel, *Physics of Massive Neutrinos* (Cambridge University Press, Cambridge, 1987) p. 87; C. Giunti, C. Kim, and U. Lee, *Phys. Rev.* **D44**, 3635 (1991); J. Rich, *Phys. Rev.* **D48**, 4318 (1993); H. Lipkin, *Phys. Lett.* **B348**, 604 (1995); W. Grimus and P. Stockinger, *Phys. Rev.* **D54**, 3414 (1996); T. Goldman, [hep-ph/9604357](#); Y. Grossman and H. Lipkin, *Phys. Rev.* **D55**, 2760 (1997); W. Grimus, S. Mohanty, and P. Stockinger, in *Proc. of the 17th Int. Workshop on Weak Interactions and Neutrinos*, eds. C. Dominguez and R. Viollier (World Scientific, Singapore, 2000) p. 355; L. Stodolsky, *Phys. Rev.* **D58**, 036006 (1998); C. Giunti, *Phys. Scripta* **67**, 29 (2003); M. Beuthe, *Phys. Rept.* **375**, 105 (2003) and *Phys. Rev.* **D66**, 013003 (2002), and references therein; H. Lipkin, *Phys. Lett.* **B579**, 355 (2004); H. Lipkin, *Phys. Lett.* **B642**, 366 (2006); C. Giunti and C. Kim, *Fundamentals of Neutrino Physics and Astrophysics* (Oxford University Press, Oxford, 2007), p. 283.

4. H. Lipkin (2006), Ref. 3.
5. G. Fogli, E. Lisi, and G. Scioscia, Phys. Rev. **D52**, 5334 (1995).
6. L. Wolfenstein, Phys. Rev. **D17**, 2369 (1978).
7. S. Mikheyev and A. Smirnov, Yad. Fiz. **42**, 1441 (1985) [Sov. J. Nucl. Phys. **42**, 913 (1986)]; Zh. Eksp. Teor. Fiz. **91**, 7, (1986) [Sov. Phys. JETP **64**, 4 (1986)]; Nuovo Cimento **9C**, 17 (1986).
8. The Bugey Collaboration (B. Achkar *et al.*), Nucl. Phys. **B434**, 503 (1995); The Palo Verde Collaboration (F. Boehm *et al.*), Phys. Rev. **D64**, 112001 (2001); The CHOOZ Collaboration (M. Apollonio *et al.*), Eur. Phys. J. **C27**, 331 (2003).
9. P. Langacker, J. Leveille, and J. Sheiman, Phys. Rev. **D27**, 1228 (1983); The corresponding energy for anti-neutrinos is negative.
10. G. L. Fogli, E. Lisi, and D. Montanino, Phys. Rev. **D54**, 2048 (1996); A. de Gouvêa, A. Friedland, and H. Murayama, Phys. Lett. **B490**, 125 (2000).
11. J. Bahcall, *Neutrino Astrophysics*, (Cambridge Univ. Press, Cambridge, UK 1989).
12. A more quantitative analysis has shown that this is true to better than 90% probability. See H. Nunokawa, S. Parke, and R. Zukanovich Funchal, Phys. Rev. **D74**, 013006 (2006).
13. S. Parke, Phys. Rev. Lett. **57**, 1275 (1986).
14. We thank J. Beacom and A. Smirnov for invaluable conversations on how LMA-MSW works. For an early description, see S. Mikheyev and A. Smirnov, Ref. 7 (first paper).
15. D. Ayres *et al.*, in *Proc. of the 1982 DPF Summer Study on Elementary Particle Physics and Future Facilities*, p. 590; G. Dass and K. Sarma, Phys. Rev. **D30**, 80 (1984); J. Flanagan, J. Learned, and S. Pakvasa, Phys. Rev. **D57**, 2649 (1998); B. Kayser, in *Proc. of the 17th Int. Workshop on Weak Interactions and Neutrinos*, eds. C. Dominguez and R. Viollier (World Scientific, Singapore, 2000) p. 339.
16. The Super-Kamiokande Collaboration (Y. Ashie *et al.*), Phys. Rev. **D71**, 112005 (2005).
17. The K2K Collaboration (M. Ahn *et al.*), Phys. Rev. **D74**, 072003 (2006).
18. The MINOS Collaboration (D. Michael *et al.*), Phys. Rev. Lett. **97**, 191801 (2006).
19. MACRO Collaboration (M. Ambrosio *et al.*), Phys. Lett. **B566**, 35 (2003); MACRO Collaboration, Eur. Phys. J. C, **36**, 323 (2004).
20. M. Sanchez *et al.*, Phys. Rev. **D68**, 113004 (2003); W.W.M. Allison *et al.*, Phys. Rev. **D72**, 052005 (2005).
21. This figure is taken from a talk given by Niki Saoulidou on behalf of the MINOS Collaboration on July 19, 2007. The Super-Kamiokande contours shown are based on Ref. 16 and on The Super-Kamiokande Collaboration (Y. Ashie *et al.*), Phys. Rev. Lett. **93**, 101801 (2004).
22. The SNO Collaboration (B. Aharmim *et al.*), Phys. Rev. **C72**, 055502 (2005).
23. Y. Koshio, in *2003 Electroweak Interactions and Unified Theories (Proceedings of the 38th Rencontres de Moriond)*, ed. J. Trân Thanh Vân (The Gioi, Vietnam, 2003) p. 3; The Super-Kamiokande Collaboration (J. Hosaka *et al.*), Phys. Rev. **D73**, 112001 (2006).
24. J. Bahcall, S. Basu, and A. Serenelli, Astrophys. J. Suppl. **165**, 400 (2006).
25. G. Fogli *et al.*, Phys. Lett. **B583**, 149 (2004).
26. The Borexino Collaboration (C. Arpesella *et al.*), Phys. Lett. **B658**, 101 (2008).
27. J. Bahcall, M.C. Gonzalez-Garcia, and C. Peña-Garay, JHEP **0408**, 16 (2004); G. Fogli *et al.*, Prog. Part. Nucl. Phys. **57**, 742 (2006).
28. The KamLAND Collaboration (S. Abe *et al.*), [arXiv: 0801.4589](https://arxiv.org/abs/0801.4589).
29. The LSND Collaboration (A. Aguilar *et al.*), Phys. Rev. **D64**, 112007 (2001).
30. The KARMEN Collaboration (B. Armbruster *et al.*), Phys. Rev. **D65**, 112001 (2002).
31. E. Church *et al.*, Phys. Rev. **D66**, 013001 (2003).
32. The MiniBooNE Collaboration (A. Aguilar-Arevalo *et al.*), Phys. Rev. Lett. **98**, 231801 (2007).
33. J. Harvey, C. Hill, and R. Hill, Phys. Rev. Lett. **99**, 261601 (2007).
34. G. Karagiorgi *et al.*, Phys. Rev. **D75**, 013011 (2007); See, however, M. Maltoni and T. Schwetz, Phys. Rev. **D76**, 093005 (2007).
35. For an alternative possibility entailing *CPT* violation, see H. Murayama and T. Yanagida, Phys. Lett. **B520**, 263 (2001); G. Barenboim *et al.*, JHEP **0210**, 001 (2002); However, after KamLAND, this alternative is disfavored. M. C. Gonzalez-Garcia, M. Maltoni, and T. Schwetz, Phys. Rev. **D68**, 053007 (2003); G. Barenboim, L. Borissov, and J. Lykken, [hep-ph/0212116 v2](https://arxiv.org/abs/hep-ph/0212116).
36. J. Schechter and J. Valle, Phys. Rev. **D23**, 1666 (1981); J. Nieves and P. Pal, Phys. Rev. **D64**, 076005 (2001); A. de Gouvêa, B. Kayser, and R. Mohapatra, Phys. Rev. **D67**, 053004 (2003).
37. L.-L. Chau and W.-Y. Keung, Phys. Rev. Lett. **53**, 1802 (1984); H. Harari and M. Leurer, Phys. Lett. **B181**, 123 (1986); F.J. Botella and L.-L. Chau, Phys. Lett. **B168**, 97 (1986); H. Fritzsch and J. Plankl, Phys. Rev. **D35**, 1732 (1987).
38. G. Fogli *et al.*, see Ref. 27.
39. We thank Belen Gavela for introducing us to this argument.
40. M. Dell-Mann, P. Ramond, and R. Slansky, in: *Supergravity*, eds. D. Freedman and P. van Nieuwenhuizen (North Holland, Amsterdam, 1979) p. 315; T. Yanagida, in: *Proceedings of the Workshop on Unified Theory and Baryon Number in the Universe*, eds. O. Sawada and A. Sugamoto (KEK, Tsukuba, Japan, 1979); R. Mohapatra and G. Senjanovic, Phys. Rev. Lett. **44**, 912 (1980) and Phys. Rev. **D23**, 165 (1981); P. Minkowski, Phys. Lett. **B67**, 421 (1977).
41. J. Schechter and J. Valle, Phys. Rev. **D25**, 2951 (1982).
42. The physics of Majorana neutrinos and $0\nu\beta\beta$ are discussed in S. Bilenky and S. Petcov, Rev. Mod. Phys. **59**, 671 (1987) [Erratum-*ibid.* **61**, 169 (1987)]; B. Kayser, F. Gibrat-Debu, and F. Perrier, *The Physics of Massive Neutrinos* (World Scientific, Singapore, 1989); B. Kayser, Physica Scripta **T121**, 156 (2005).
43. S. Pascoli and S.T. Petcov, Phys. Lett. **B580**, 280 (2003).
44. Analyses of the possible values of $| < m_{\beta\beta} > |$ have been given by H. Murayama and C. Peña-Garay, Phys. Rev. **D69**, 031301 (2004); S. Pascoli and S. Petcov, Phys. Lett. **B544**, 239 (2002); S. Bilenky, S. Pascoli, and S. Petcov, Phys. Rev. **D64**, 053010 (2001), and Phys. Rev. **D64**, 113003 (2001); H. Klapdor-Kleingrothaus, H. Päs, and A. Smirnov, Phys. Rev. **D63**, 073005 (2001); S. Bilenky *et al.*, Phys. Lett. **B465**, 193 (1999); References in these papers.
45. See also S. Elliott and P. Vogel, Ann. Rev. Nucl. Part. Sci. **52**, 115 (2002), and references therein.
46. C. Albright, Phys. Lett. **B599**, 285 (2004).
47. U. Seljak, A. Slosar, and P. McDonald, JCAP **0610**, 014 (2006); J. Lesgourgues and S. Pastor, Phys. Rept. **429**, 307 (2006).
48. K. Mahn and M. Shaevitz, Int. J. Mod. Phys. **A21**, 3825 (2006).
49. For an alternative approach to determining θ_{atm} , see M. Gonzalez-Garcia, M. Maltoni and A. Smirnov, Phys. Rev. D **70**, 093005 (2004), and references therein.
50. M. Fukugita and T. Yanagida, Phys. Lett. **B174**, 45 (1986).
51. G. 't Hooft, Phys. Rev. Lett. **37**, 8 (1976); V. Kuzmin, V. Rubakov, and M. Shaposhnikov, Phys. Lett. **155B**, 36 (1985).
52. S. Pascoli, S. Petcov, and W. Rodejohann, Phys. Rev. **D68**, 093007 (2003); S. Davidson, S. Pascoli, and S. Petcov, private communications.
53. A. Cervera *et al.*, Nucl. Phys. **B579**, 17 (2000); M. Freund, Phys. Rev. **D64**, 053003 (2001).
54. If the magnetic moments are large, they might possibly tell us whether neutrinos are Majorana or Dirac particles. See S. Davidson, M. Gorbahn, and A. Santamaria, Phys. Lett. **B626**, 151, (2005); N. Bell *et al.*, Phys. Rev. Lett. **95**, 151802 (2005); N. Bell *et al.*, Phys. Lett. **B642**, 377 (2006).

14. QUARK MODEL

Revised December 2007 by C. Amsler (University of Zürich), T. DeGrand (University of Colorado, Boulder), and B. Krusche (University of Basel).

14.1. Quantum numbers of the quarks

Quarks are strongly interacting fermions with spin 1/2 and, by convention, positive parity. Antiquarks have negative parity. Quarks have the additive baryon number 1/3, antiquarks -1/3. Table 14.1 gives the other additive quantum numbers (flavors) for the three generations of quarks. They are related to the charge Q (in units of the elementary charge e) through the generalized Gell-Mann-Nishijima formula

$$Q = I_z + \frac{B + S + C + B + T}{2}, \quad (14.1)$$

where B is the baryon number. The convention is that the *flavor* of a quark (I_z , S , C , B , or T) has the same sign as its *charge* Q . With this convention, any flavor carried by a charged meson has the same sign as its charge, *e.g.*, the strangeness of the K^+ is +1, the bottomness of the B^+ is +1, and the charm and strangeness of the D_s^- are each -1. Antiquarks have the opposite flavor signs.

Table 14.1: Additive quantum numbers of the quarks.

Property \ Quark	d	u	s	c	b	t
Q – electric charge	$-\frac{1}{3}$	$+\frac{2}{3}$	$-\frac{1}{3}$	$+\frac{2}{3}$	$-\frac{1}{3}$	$+\frac{2}{3}$
I – isospin	$\frac{1}{2}$	$\frac{1}{2}$	0	0	0	0
I_z – isospin z-component	$-\frac{1}{2}$	$+\frac{1}{2}$	0	0	0	0
S – strangeness	0	0	-1	0	0	0
C – charm	0	0	0	+1	0	0
B – bottomness	0	0	0	0	-1	0
T – topness	0	0	0	0	0	+1

14.2. Mesons

Mesons have baryon number $B = 0$. In the quark model, they are $q\bar{q}'$ bound states of quarks q and antiquarks \bar{q}' (the flavors of q and q' may be different). If the orbital angular momentum of the $q\bar{q}'$ state is ℓ , then the parity P is $(-1)^{\ell+1}$. The meson spin J is given by the usual relation $|\ell - s| < J < |\ell + s|$, where s is 0 (antiparallel quark spins) or 1 (parallel quark spins). The charge conjugation, or C -parity $C = (-1)^{\ell+s}$, is defined only for the $q\bar{q}$ states made of quarks and their own antiquarks. The C -parity can be generalized to the G -parity $G = (-1)^{I+\ell+s}$ for mesons made of quarks and their own antiquarks (isospin $I_z = 0$), and for the charged $u\bar{d}$ and $d\bar{u}$ states (isospin $I = 1$).

The mesons are classified in J^{PC} multiplets. The $\ell = 0$ states are the pseudoscalars (0^{-+}) and the vectors ($1^{- -}$). The orbital excitations $\ell = 1$ are the scalars (0^{++}), the axial vectors (1^{++}) and (1^{+-}), and the tensors (2^{++}). Assignments for many of the known mesons are given in Tables 14.2 and 14.3. Radial excitations are denoted by the principal quantum number n . The very short lifetime of the t quark makes it likely that bound-state hadrons containing t quarks and/or antiquarks do not exist.

States in the natural spin-parity series $P = (-1)^J$ must, according to the above, have $s = 1$ and hence, $CP = +1$. Thus, mesons with natural spin-parity and $CP = -1$ (0^{+-} , 1^{+-} , 2^{+-} , 3^{+-} , *etc.*) are forbidden in the $q\bar{q}'$ model. The $J^{PC} = 0^{- -}$ state is forbidden as well. Mesons with such *exotic* quantum numbers may exist, but would lie outside the $q\bar{q}'$ model (see section below on exotic mesons).

Following SU(3), the nine possible $q\bar{q}'$ combinations containing the light u , d , and s quarks are grouped into an octet and a singlet of light quark mesons:

$$3 \otimes \bar{3} = 8 \oplus 1. \quad (14.2)$$

A fourth quark such as charm c can be included by extending SU(3) to SU(4). However, SU(4) is badly broken owing to the much heavier c quark. Nevertheless, in an SU(4) classification, the sixteen mesons are grouped into a 15-plet and a singlet:

$$4 \otimes \bar{4} = 15 \oplus 1. \quad (14.3)$$

The *weight diagrams* for the ground-state pseudoscalar (0^{-+}) and vector ($1^{- -}$) mesons are depicted in Fig. 14.1. The light quark mesons are members of nonets building the middle plane in Fig. 14.1(a) and (b).

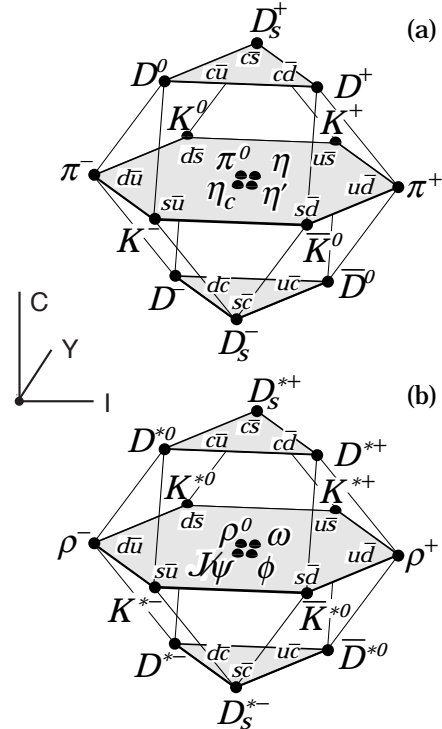


Figure 14.1: SU(4) weight diagram showing the 16-plets for the pseudoscalar (a) and vector mesons (b) made of the u , d , s , and c quarks as a function of isospin I , charm C , and hypercharge $Y = S+B - \frac{C}{3}$. The nonets of light mesons occupy the central planes to which the $c\bar{c}$ states have been added.

Isoscalar states with the same J^{PC} will mix, but mixing between the two light quark isoscalar mesons, and the much heavier charmonium or bottomonium states, are generally assumed to be negligible. In the following, we shall use the generic names a for the $I = 1$, K for the $I = 1/2$, and f and f' for the $I = 0$ members of the light quark nonets. Thus, the physical isoscalars are mixtures of the SU(3) wave function ψ_8 and ψ_1 :

$$f' = \psi_8 \cos \theta - \psi_1 \sin \theta, \quad (14.4)$$

$$f = \psi_8 \sin \theta + \psi_1 \cos \theta, \quad (14.5)$$

where θ is the nonet mixing angle and

$$\psi_8 = \frac{1}{\sqrt{6}}(u\bar{u} + d\bar{d} - 2s\bar{s}), \quad (14.6)$$

$$\psi_1 = \frac{1}{\sqrt{3}}(u\bar{u} + d\bar{d} + s\bar{s}). \quad (14.7)$$

The mixing angle has to be determined experimentally.

Table 14.2: Suggested $q\bar{q}$ quark-model assignments for some of the observed light mesons. Mesons in bold face are included in the Meson Summary Table. The wave functions f and f' are given in the text. The singlet-octet mixing angles from the quadratic and linear mass formulae are also given for the well established nonets. The classification of the 0^{++} mesons is tentative and the mixing angle uncertain due to large uncertainties in some of the masses. Also, the $f_0(1710)$ and $f_0(1370)$ are expected to mix with the $f_0(1500)$. The latter is not in this table as it is hard to accommodate in the scalar nonet. The light scalars $a_0(980)$, $f_0(980)$, and $f_0(600)$ are often considered as meson-meson resonances or four-quark states, and are therefore not included in the table. See the “Note on Scalar Mesons” in the Meson Listings for details and alternative schemes.

$n^{2s+1}\ell_J$	J^{PC}	$l = 1$ $u\bar{d}, \bar{u}d, \frac{1}{\sqrt{2}}(d\bar{d} - u\bar{u})$	$l = \frac{1}{2}$ $u\bar{s}, \bar{d}s; \bar{d}s, -\bar{u}s$	$l = 0$ f'	$l = 0$ f	θ_{quad} [°]	θ_{lin} [°]
1^1S_0	0^{-+}	π	K	η	$\eta'(958)$	-11.5	-24.6
1^3S_1	1^{--}	$\rho(770)$	$K^*(892)$	$\phi(1020)$	$\omega(782)$	38.7	36.0
1^1P_1	1^{+-}	$b_1(1235)$	K_{1B}^\dagger	$h_1(1380)$	$h_1(1170)$		
1^3P_0	0^{++}	$a_0(1450)$	$K_0^*(1430)$	$f_0(1710)$	$f_0(1370)$		
1^3P_1	1^{++}	$a_1(1260)$	K_{1A}^\dagger	$f_1(1420)$	$f_1(1285)$		
1^3P_2	2^{++}	$a_2(1320)$	$K_2^*(1430)$	$f_2'(1525)$	$f_2(1270)$	29.6	28.0
1^1D_2	2^{-+}	$\pi_2(1670)$	$K_2(1770)^\dagger$	$\eta_2(1870)$	$\eta_2(1645)$		
1^3D_1	1^{--}	$\rho(1700)$	$K^*(1680)$		$\omega(1650)$		
1^3D_2	2^{--}		$K_2(1820)$				
1^3D_3	3^{--}	$\rho_3(1690)$	$K_3^*(1780)$	$\phi_3(1850)$	$\omega_3(1670)$	32.0	31.0
1^3F_4	4^{++}	$a_4(2040)$	$K_4^*(2045)$		$f_4(2050)$		
1^3G_5	5^{--}	$\rho_5(2350)$					
1^3H_6	6^{++}	$a_6(2450)$			$f_6(2510)$		
2^1S_0	0^{-+}	$\pi(1300)$	$K(1460)$	$\eta(1475)$	$\eta(1295)$		
2^3S_1	1^{--}	$\rho(1450)$	$K^*(1410)$	$\phi(1680)$	$\omega(1420)$		

† The 1^{++} and 2^{--} isospin $\frac{1}{2}$ states mix. In particular, the K_{1A} and K_{1B} are nearly equal (45°) mixtures of the $K_1(1270)$ and $K_1(1400)$. The physical vector mesons listed under 1^3D_1 and 2^3S_1 may be mixtures of 1^3D_1 and 2^3S_1 , or even have hybrid components.

Table 14.3: $q\bar{q}$ quark-model assignments for the observed heavy mesons. Mesons in bold face are included in the Meson Summary Table.

$n^{2s+1}\ell_J$	J^{PC}	$l = 0$ $c\bar{c}$	$l = 0$ $b\bar{b}$	$l = \frac{1}{2}$ $c\bar{u}, \bar{c}d; \bar{c}u, \bar{c}d$	$l = 0$ $c\bar{s}; \bar{c}s$	$l = \frac{1}{2}$ $b\bar{u}, \bar{b}d; \bar{b}u, \bar{b}d$	$l = 0$ $b\bar{s}; \bar{b}s$	$l = 0$ $b\bar{c}; \bar{b}c$
1^1S_0	0^{-+}	$\eta_c(1S)$	$\eta_b(1S)$	D	D_s^\pm	B	B_s^0	B_c^\pm
1^3S_1	1^{--}	$J/\psi(1S)$	$\Upsilon(1S)$	D^*	$D_s^{*\pm}$	B^*	B_s^*	
1^1P_1	1^{+-}	$h_c(1P)$		$D_1(2420)$	$D_{s1}(2536)^\pm$			
1^3P_0	0^{++}	$\chi_{c0}(1P)$	$\chi_{b0}(1P)$	$D_0^*(2400)$	$D_{s0}^*(2317)^\pm$			
1^3P_1	1^{++}	$\chi_{c1}(1P)$	$\chi_{b1}(1P)$		$D_{s1}(2460)^\pm$			
1^3P_2	2^{++}	$\chi_{c2}(1P)$	$\chi_{b2}(1P)$	$D_2^*(2460)$	$D_{s2}(2573)^\pm$			
1^3D_1	1^{--}	$\psi(3770)$						
2^1S_0	0^{-+}	$\eta_c(2S)$						
2^3S_1	1^{--}	$\psi(2S)$	$\Upsilon(2S)$					
$2^3P_{0,1,2}$	$0^{++}, 1^{++}, 2^{++}$		$\chi_{b0,1,2}(2P)$					

† The masses of these states are considerably smaller than most theoretical predictions. They have also been considered as four-quark states (See the “Note on Non- $q\bar{q}$ Mesons” at the end of the Meson Listings). The $D_{s1}(2460)^\pm$ and $D_{s1}(2536)^\pm$ are mixtures of the 1^{++} states.

These mixing relations are often rewritten to exhibit the $u\bar{u} + d\bar{d}$ and $s\bar{s}$ components which decouple for the “ideal” mixing angle θ_i , such that $\tan \theta_i = 1/\sqrt{2}$ (or $\theta_i=35.3^\circ$). Defining $\alpha = \theta + 54.7^\circ$, one obtains the physical isoscalar in the flavor basis

$$f' = \frac{1}{\sqrt{2}}(u\bar{u} + d\bar{d})\cos\alpha - s\bar{s}\sin\alpha, \quad (14.8)$$

and its orthogonal partner f (replace α by $\alpha - 90^\circ$). Thus for ideal mixing ($\alpha_i = 90^\circ$), the f' becomes pure $s\bar{s}$ and the f pure $u\bar{u} + d\bar{d}$. The mixing angle θ can be derived from the mass relation

$$\tan\theta = \frac{4m_K - m_a - 3m_{f'}}{2\sqrt{2}(m_a - m_K)}, \quad (14.9)$$

which also determines its sign or, alternatively, from

$$\tan^2\theta = \frac{4m_K - m_a - 3m_{f'}}{-4m_K + m_a + 3m_f}. \quad (14.10)$$

Eliminating θ from these equations leads to the sum rule [1]

$$(m_f + m_{f'})(4m_K - m_a) - 3m_f m_{f'} = 8m_K^2 - 8m_K m_a + 3m_a^2. \quad (14.11)$$

This relation is verified for the ground-state vector mesons. We identify the $\phi(1020)$ with the f' and the $\omega(783)$ with the f . Thus

$$\phi(1020) = \psi_8 \cos\theta_V - \psi_1 \sin\theta_V, \quad (14.12)$$

$$\omega(782) = \psi_8 \sin\theta_V + \psi_1 \cos\theta_V, \quad (14.13)$$

with the vector mixing angle $\theta_V = 35^\circ$ from Eq. (14.9), very close to ideal mixing. Thus $\phi(1020)$ is nearly pure $s\bar{s}$. For ideal mixing, Eq. (14.9) and Eq. (14.10) lead to the relations

$$m_K = \frac{m_f + m_{f'}}{2}, \quad m_a = m_f, \quad (14.14)$$

which are satisfied for the vector mesons. However, for the pseudoscalar (and scalar mesons), Eq. (14.11) is satisfied only approximately. Then Eq. (14.9) and Eq. (14.10) lead to somewhat different values for the mixing angle. Identifying the η with the f' one gets

$$\eta = \psi_8 \cos\theta_P - \psi_1 \sin\theta_P, \quad (14.15)$$

$$\eta' = \psi_8 \sin\theta_P + \psi_1 \cos\theta_P. \quad (14.16)$$

Following chiral perturbation theory, the meson masses in the mass formulae (Eq. (14.9) and Eq. (14.10)) should be replaced by their squares. Table 14.2 lists the mixing angle θ_{lin} from Eq. (14.10) and the corresponding θ_{quad} obtained by replacing the meson masses by their squares throughout.

The pseudoscalar mixing angle θ_P can also be measured by comparing the partial widths for radiative J/ψ decay into a vector and a pseudoscalar [2], radiative $\phi(1020)$ decay into η and η' [3], or $\bar{p}p$ annihilation at rest into a pair of vector and pseudoscalar or into two pseudoscalars [4,5]. One obtains a mixing angle between -10° and -20° .

The nonet mixing angles can be measured in $\gamma\gamma$ collisions, *e.g.*, for the 0^{-+} , 0^{++} , and 2^{++} nonets. In the quark model, the amplitude for the coupling of neutral mesons to two photons is proportional to $\sum_i Q_i^2$, where Q_i is the charge of the i -th quark. The 2γ partial width of an isoscalar meson with mass m is then given in terms of the mixing angle α by

$$\Gamma_{2\gamma} = C(5\cos\alpha - \sqrt{2}\sin\alpha)^2 m^3, \quad (14.17)$$

for f' and f ($\alpha \rightarrow \alpha - 90^\circ$). The coupling C may depend on the meson mass. It is often assumed to be a constant in the nonet. For the isovector a , one then finds $\Gamma_{2\gamma} = 9 C m^3$. Thus the members of an ideally mixed nonet couple to 2γ with partial widths in the ratios $f' : a = 25 : 2 : 9$. For tensor mesons, one finds from the ratios of the measured 2γ partial widths for the $f_2(1270)$ and $f_2'(1525)$ mesons a mixing angle α_T of $(81 \pm 1)^\circ$, or $\theta_T = (27 \pm 1)^\circ$, in accord with the linear mass formula. For the pseudoscalars, one finds from the ratios of partial widths $\Gamma(\eta' \rightarrow 2\gamma)/\Gamma(\eta \rightarrow 2\gamma)$ a mixing angle $\theta_P = (-18 \pm 2)^\circ$, while the ratio $\Gamma(\eta' \rightarrow 2\gamma)/\Gamma(\pi^0 \rightarrow 2\gamma)$ leads to $\sim -24^\circ$. SU(3) breaking effects for pseudoscalars are discussed in Ref. 6.

Table 14.4: SU(3) couplings γ^2 for quarkonium decays as a function of nonet mixing angle α , up to a common multiplicative factor C ($\phi \equiv 54.7^\circ + \theta_P$).

Isospin	Decay channel	γ^2
0	$\pi\pi$	$3\cos^2\alpha$
	$K\bar{K}$	$(\cos\alpha - \sqrt{2}\sin\alpha)^2$
	$\eta\eta$	$(\cos\alpha\cos^2\phi - \sqrt{2}\sin\alpha\sin^2\phi)^2$
	$\eta\eta'$	$\frac{1}{2}\sin^2 2\phi (\cos\alpha + \sqrt{2}\sin\alpha)^2$
1	$\eta\pi$	$2\cos^2\phi$
	$\eta'\pi$	$2\sin^2\phi$
	$K\bar{K}$	1
$\frac{1}{2}$	$K\pi$	$\frac{3}{2}$
	$K\eta$	$(\sin\phi - \frac{\cos\phi}{\sqrt{2}})^2$
	$K\eta'$	$(\cos\phi + \frac{\sin\phi}{\sqrt{2}})^2$

The partial width for the decay of a scalar or a tensor meson into a pair of pseudoscalar mesons is model-dependent. Following Ref. 7,

$$\Gamma = C \times \gamma^2 \times |F(q)|^2 \times q. \quad (14.18)$$

C is a nonet constant, q the momentum of the decay products, $F(q)$ a form factor, and γ^2 the SU(3) coupling. The model-dependent form factor may be written as

$$|F(q)|^2 = q^{2\ell} \times \exp\left(-\frac{q^2}{8\beta^2}\right), \quad (14.19)$$

where ℓ is the relative angular momentum between the decay products. The decay of a $q\bar{q}$ meson into a pair of mesons involves the creation of a $q\bar{q}$ pair from the vacuum, and SU(3) symmetry assumes that the matrix elements for the creation of $s\bar{s}$, $u\bar{u}$, and $d\bar{d}$ pairs are equal. The couplings γ^2 are given in Table 14.4, and their dependence upon the mixing angle α is shown in Fig. 14.2 for isoscalar decays. The generalization to unequal $s\bar{s}$, $u\bar{u}$, and $d\bar{d}$ couplings is given in Ref. 7. An excellent fit to the tensor meson decay widths is obtained assuming SU(3) symmetry, with $\beta \simeq 0.5$ GeV/ c , $\theta_V \simeq 26^\circ$ and $\theta_P \simeq -17^\circ$ [7].

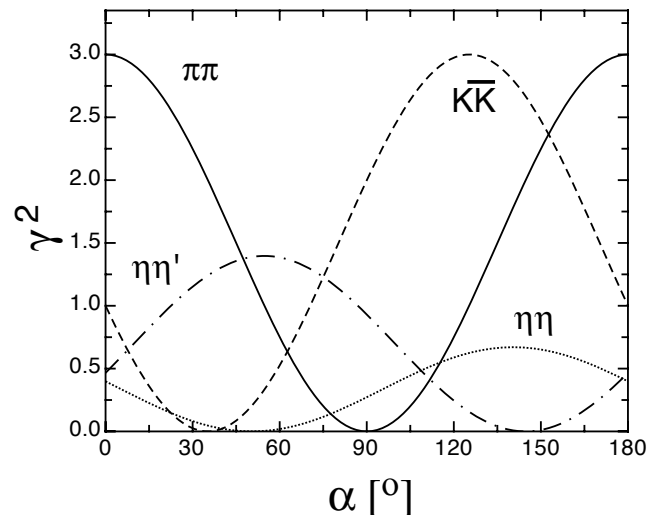


Figure 14.2: SU(3) couplings as a function of mixing angle α for isoscalar decays, up to a common multiplicative factor C and for $\theta_P = -17.3^\circ$.

14.3. Exotic mesons

The existence of a light nonet composed of four quarks with masses below 1 GeV was suggested a long time ago [8]. Coupling two triplets of light quarks u , d , and s , one obtains nine states, of which the six symmetric (uu , dd , ss , $ud + du$, $us + su$, $ds + sd$) form the six dimensional representation $\mathbf{6}$, while the three antisymmetric ($ud - du$, $us - su$, $ds - sd$) form the three dimensional representation $\bar{\mathbf{3}}$ of SU(3):

$$\mathbf{3} \otimes \mathbf{3} = \mathbf{6} \oplus \bar{\mathbf{3}}. \quad (14.20)$$

Combining with spin and color and requiring antisymmetry, one finds that the most deeply bound diquark (and hence the lightest) is the one in the $\bar{\mathbf{3}}$ and spin singlet state. The combination of the diquark with an antiquark in the $\mathbf{3}$ representation then gives a light nonet of four-quark scalar states. Letting the number of strange quarks determine the mass splitting, one obtains a mass inverted spectrum with a light isosinglet ($u\bar{d}\bar{u}\bar{d}$), a medium heavy isodoublet (e.g., $u\bar{d}\bar{s}\bar{d}$) and a heavy isotriplet (e.g., $ds\bar{u}\bar{s}$) + isosinglet (e.g., $us\bar{u}\bar{s}$). It is then tempting to identify the lightest state with the $f_0(600)$, and the heaviest states with the $a_0(980)$, and $f_0(980)$. Then the meson with strangeness $\kappa(800)$ would lie in between.

QCD predicts the existence of extra isoscalar mesons. In the pure gauge theory, they contain only gluons, and are called the glueballs. The ground state glueball is predicted by lattice gauge theories to be 0^{++} , the first excited state 2^{++} . Errors on the mass predictions are large. From Ref. 10 one obtains 1750 (50) (80) MeV for the mass of the lightest 0^{++} glueball from quenched QCD. As an example for the glueball mass spectrum, we show in Fig. 14.3 a recent calculation from the quenched lattice [9]. A mass of 1710 MeV is predicted for the ground state, also with an error of about 100 MeV. Earlier work by other groups produced masses at 1650 MeV [11] and 1550 MeV [12] (see also [13]). The first excited state has a mass of about 2.4 GeV, and the lightest glueball with exotic quantum numbers (2^{+-}) has a mass of about 4 GeV.

These calculations assume that the quark masses are infinite (quenched approximation) and neglect $q\bar{q}$ loops. However, both glue and $q\bar{q}$ states will couple to singlet scalar mesons. Therefore glueballs will mix with nearby $q\bar{q}$ states of the same quantum numbers. For example, the two isoscalar 0^{++} mesons around 1500 MeV will mix with the pure ground state glueball to generate the observed physical states $f_0(1370)$, $f_0(1500)$, and $f_0(1710)$ [7,14]. Lattice calculations are only beginning to include these effects. Unquenched QCD with a coarse lattice suggests that the mass of the singlet scalar meson is very low [15]. However, in quenched QCD, the mass of the 0^{++} glueball strongly depends on lattice spacing, and therefore continuum extrapolation cannot be attempted yet in unquenched lattice simulations for flavor-singlet scalar mesons [16].

The existence of three singlet scalar mesons around 1.5 GeV suggests additional degrees of freedom such as glue, since only two mesons are predicted in this mass range. The $f_0(1500)$ [7,14] or, alternatively, the $f_0(1710)$ [11], have been proposed as candidates for the scalar glueball, both states having considerable mixing also with the $f_0(980)$. Other mixing schemes, in particular with the $f_0(600)$ and the $f_0(980)$, have also been proposed (more details can be found in the “Note on Scalar Mesons” in the Meson Listings and in Ref. 17).

Mesons made of $q\bar{q}$ pairs bound by excited gluons g , the hybrid states $q\bar{q}g$, are also predicted. They should lie in the 1.9 GeV mass region, according to gluon flux tube models [18]. Lattice QCD also predicts the lightest hybrid, an exotic 1^{-+} , at a mass of 1.8 to 1.9 GeV [19]. However, the bag model predicts four nonets, among them an exotic 1^{-+} around or above 1.4 GeV [20,21]. There are so far two candidates for exotic states with quantum numbers 1^{-+} , the $\pi_1(1400)$ and $\pi_1(1600)$, which could be hybrids or four-quark states (see the “Note on Non- $q\bar{q}$ Mesons” in the 2006 issue of this *Review* [22] and in Ref. 17).

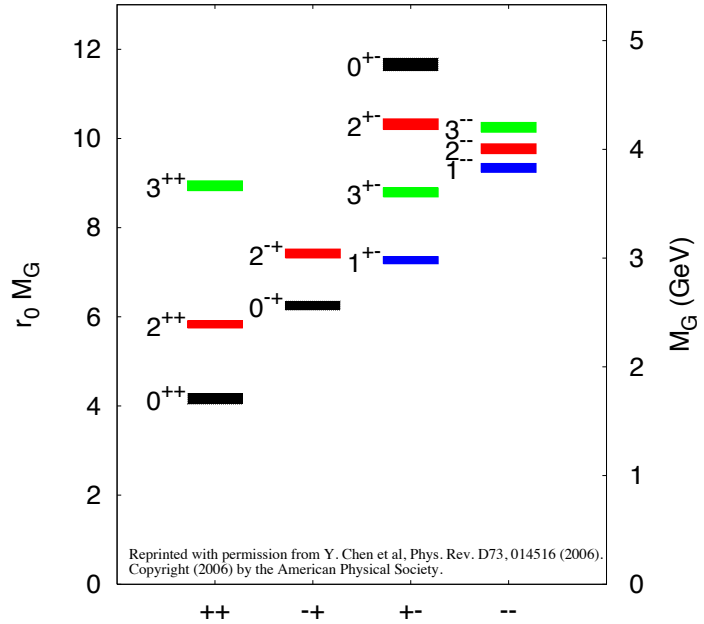


Figure 14.3: Predicted glueball mass spectrum from the lattice, in quenched approximation, (from Ref. 9).

14.4. Baryons: qqq states

Baryons are fermions with baryon number $B = 1$, i.e., in the most general case, they are composed of three quarks plus any number of quark - antiquark pairs. Although recently some experimental evidence for ($qqqq\bar{q}$) pentaquark states has been claimed (see review on Possible Exotic Baryon Resonance), so far all established baryons are 3-quark (qqq) configurations. The color part of their state functions is an SU(3) singlet, a completely antisymmetric state of the three colors. Since the quarks are fermions, the state function must be antisymmetric under interchange of any two equal-mass quarks (up and down quarks in the limit of isospin symmetry). Thus it can be written as

$$|qqq\rangle_A = |\text{color}\rangle_A \times |\text{space, spin, flavor}\rangle_S, \quad (14.21)$$

where the subscripts S and A indicate symmetry or antisymmetry under interchange of any two equal-mass quarks. Note the contrast with the state function for the three nucleons in ${}^3\text{H}$ or ${}^3\text{He}$:

$$|NNN\rangle_A = |\text{space, spin, isospin}\rangle_A. \quad (14.22)$$

This difference has major implications for internal structure, magnetic moments, etc. (For a nice discussion, see Ref. 23.)

The “ordinary” baryons are made up of u , d , and s quarks. The three flavors imply an approximate flavor SU(3), which requires that baryons made of these quarks belong to the multiplets on the right side of

$$\mathbf{3} \otimes \mathbf{3} \otimes \mathbf{3} = \mathbf{10}_S \oplus \mathbf{8}_M \oplus \mathbf{8}_M \oplus \mathbf{1}_A \quad (14.23)$$

(see Sec. 37, on “SU(n) Multiplets and Young Diagrams”). Here the subscripts indicate symmetric, mixed-symmetry, or antisymmetric states under interchange of any two quarks. The $\mathbf{1}$ is a uds state (Λ_1), and the octet contains a similar state (Λ_8). If these have the same spin and parity, they can mix. The mechanism is the same as for the mesons (see above). In the ground state multiplet, the SU(3) flavor singlet Λ_1 is forbidden by Fermi statistics. Section 36, on “SU(3) Isoscalar Factors and Representation Matrices,” shows how relative decay rates in, say, $\mathbf{10} \rightarrow \mathbf{8} \otimes \mathbf{8}$ decays may be calculated.

The addition of the c quark to the light quarks extends the flavor symmetry to SU(4). However, due to the large mass of the c quark, this symmetry is much more strongly broken than the SU(3) of the three light quarks. Figures 14.4(a) and 14.4(b) show the SU(4) baryon multiplets that have as their bottom levels an SU(3) octet, such as the octet that includes the nucleon, or an SU(3) decuplet, such as the decuplet that includes the $\Delta(1232)$. All particles in a given SU(4) multiplet have the same spin and parity. The charmed baryons

are discussed in more detail in the “Note on Charmed Baryons” in the Particle Listings. The addition of a b quark extends the flavor symmetry to $SU(5)$; the existence of baryons with t -quarks is very unlikely due to the short lifetime of the top.

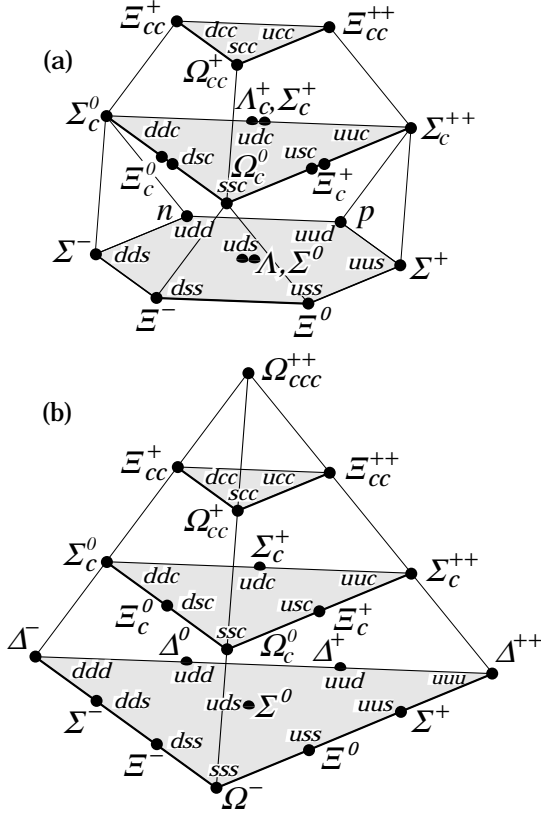


Figure 14.4: $SU(4)$ multiplets of baryons made of $u, d, s,$ and c quarks. (a) The 20-plet with an $SU(3)$ octet. (b) The 20-plet with an $SU(3)$ decuplet.

For the “ordinary” baryons (no c or b quark), flavor and spin may be combined in an approximate flavor-spin $SU(6)$, in which the six basic states are $d \uparrow, d \downarrow, \dots, s \downarrow$ ($\uparrow, \downarrow =$ spin up, down). Then the baryons belong to the multiplets on the right side of

$$6 \otimes 6 \otimes 6 = 56_S \oplus 70_M \oplus 70_M \oplus 20_A. \quad (14.24)$$

These $SU(6)$ multiplets decompose into flavor $SU(3)$ multiplets as follows:

$$56 = {}^4 10 \oplus {}^2 8 \quad (14.25a)$$

$$70 = {}^2 10 \oplus {}^4 8 \oplus {}^2 8 \oplus {}^2 1 \quad (14.25b)$$

$$20 = {}^2 8 \oplus {}^4 1, \quad (14.25c)$$

where the superscript $(2S + 1)$ gives the net spin S of the quarks for each particle in the $SU(3)$ multiplet. The $J^P = 1/2^+$ octet containing the nucleon and the $J^P = 3/2^+$ decuplet containing the $\Delta(1232)$ together make up the “ground-state” 56-plet, in which the orbital angular momenta between the quark pairs are zero (so that the spatial part of the state function is trivially symmetric). The 70 and 20 require some excitation of the spatial part of the state function in order to make the overall state function symmetric. States with nonzero orbital angular momenta are classified in $SU(6) \otimes O(3)$ supermultiplets.

It is useful to classify the baryons into bands that have the same number N of quanta of excitation. Each band consists of a number of supermultiplets, specified by (D, L_N^P) , where D is the dimensionality of the $SU(6)$ representation, L is the total quark orbital angular momentum, and P is the total parity. Supermultiplets contained in bands up to $N = 12$ are given in Ref. 25. The $N = 0$ band,

which contains the nucleon and $\Delta(1232)$, consists only of the $(56, 0_0^+)$ supermultiplet. The $N = 1$ band consists only of the $(70, 1_1^-)$ multiplet and contains the negative-parity baryons with masses below about 1.9 GeV. The $N = 2$ band contains five supermultiplets: $(56, 0_2^+)$, $(70, 0_2^+)$, $(56, 2_2^+)$, $(70, 2_2^+)$, and $(20, 1_2^+)$.

Table 14.5: N and Δ states in the $N=0,1,2$ harmonic oscillator bands. L^P denotes angular momentum and parity, S the three-quark spin and ‘sym’=A,S,M the symmetry of the spatial wave function.

N	sym	L^P	S	$N(I = 1/2)$	$\Delta(I = 3/2)$
2	A	1^+	$1/2$	$1/2^+ 3/2^+$	
2	M	2^+	$3/2$	$1/2^+ 3/2^+ 5/2^+ 7/2^+$	
2	M	2^+	$1/2$	$3/2^+ 5/2^+$	$3/2^+ 5/2^+$
2	M	0^+	$3/2$	$3/2^+$	
2	M	0^+	$1/2$	$1/2^+$	$1/2^+$
2	S	2^+	$3/2$		$1/2^+ 3/2^+ 5/2^+ 7/2^+$
2	S	2^+	$1/2$	$3/2^+ 5/2^+$	
2	S	0^+	$3/2$		$3/2^+$
2	S	0^+	$1/2$	$1/2^+$	
1	M	1^-	$3/2$	$1/2^- 3/2^- 5/2^-$	
1	M	1^-	$1/2$	$1/2^- 3/2^-$	$1/2^- 3/2^-$
0	S	0^+	$3/2$		$3/2^+$
0	S	0^+	$1/2$	$1/2^+$	

Table 14.6: Quark-model assignments for some of the known baryons in terms of a flavor-spin $SU(6)$ basis. Only the dominant representation is listed. Assignments for several states, especially for the $\Lambda(1810)$, $\Lambda(2350)$, $\Xi(1820)$, and $\Xi(2030)$, are merely educated guesses. For assignments of the charmed baryons, see the “Note on Charmed Baryons” in the Particle Listings.

J^P	(D, L_N^P)	S	Octet members	Singlets
$1/2^+$	$(56, 0_0^+)$	$1/2$	$N(939) \Lambda(1116) \Sigma(1193) \Xi(1318)$	
$1/2^+$	$(56, 0_2^+)$	$1/2$	$N(1440) \Lambda(1600) \Sigma(1660) \Xi(?)$	
$1/2^-$	$(70, 1_1^-)$	$1/2$	$N(1535) \Lambda(1670) \Sigma(1620) \Xi(?) \Lambda(1405)$	
$3/2^-$	$(70, 1_1^-)$	$1/2$	$N(1520) \Lambda(1690) \Sigma(1670) \Xi(1820) \Lambda(1520)$	
$1/2^-$	$(70, 1_1^-)$	$3/2$	$N(1650) \Lambda(1800) \Sigma(1750) \Xi(?)$	
$3/2^-$	$(70, 1_1^-)$	$3/2$	$N(1700) \Lambda(?) \Sigma(?) \Xi(?)$	
$5/2^-$	$(70, 1_1^-)$	$3/2$	$N(1675) \Lambda(1830) \Sigma(1775) \Xi(?)$	
$1/2^+$	$(70, 0_2^+)$	$1/2$	$N(1710) \Lambda(1810) \Sigma(1880) \Xi(?) \Lambda(?)$	
$3/2^+$	$(56, 2_2^+)$	$1/2$	$N(1720) \Lambda(1890) \Sigma(?) \Xi(?)$	
$5/2^+$	$(56, 2_2^+)$	$1/2$	$N(1680) \Lambda(1820) \Sigma(1915) \Xi(2030)$	
$7/2^-$	$(70, 3_3^-)$	$1/2$	$N(2190) \Lambda(?) \Sigma(?) \Xi(?) \Lambda(2100)$	
$9/2^-$	$(70, 3_3^-)$	$3/2$	$N(2250) \Lambda(?) \Sigma(?) \Xi(?)$	
$9/2^+$	$(56, 4_4^+)$	$1/2$	$N(2220) \Lambda(2350) \Sigma(?) \Xi(?)$	
Decuplet members				
$3/2^+$	$(56, 0_0^+)$	$3/2$	$\Delta(1232) \Sigma(1385) \Xi(1530) \Omega(1672)$	
$3/2^+$	$(56, 0_2^+)$	$3/2$	$\Delta(1600) \Sigma(?) \Xi(?) \Omega(?)$	
$1/2^-$	$(70, 1_1^-)$	$1/2$	$\Delta(1620) \Sigma(?) \Xi(?) \Omega(?)$	
$3/2^-$	$(70, 1_1^-)$	$1/2$	$\Delta(1700) \Sigma(?) \Xi(?) \Omega(?)$	
$5/2^+$	$(56, 2_2^+)$	$3/2$	$\Delta(1905) \Sigma(?) \Xi(?) \Omega(?)$	
$7/2^+$	$(56, 2_2^+)$	$3/2$	$\Delta(1950) \Sigma(2030) \Xi(?) \Omega(?)$	
$11/2^+$	$(56, 4_4^+)$	$3/2$	$\Delta(2420) \Sigma(?) \Xi(?) \Omega(?)$	

The wave functions of the non-strange baryons in the harmonic oscillator basis are often labeled by $|X^{2S+1}L_{\pi}J^P\rangle$, where S, L, J, P are as above, $X = N$ or Δ , and $\pi = S, M$ or A denotes the symmetry of the spatial wave function. The possible states for the bands with $N=0,1,2$ are given in Table 14.5.

In Table 14.6, quark-model assignments are given for many of the established baryons whose $SU(6)\otimes O(3)$ compositions are relatively unmixed. One must, however, keep in mind that apart from the mixing of the A singlet and octet states, states with same J^P but different L, S combinations can also mix. In the quark model with one-gluon exchange motivated interactions, the size of the mixing is determined by the relative strength of the tensor term with respect to the contact term (see below). The mixing is more important for the decay patterns of the states than for their positions. An example are the lowest lying $(70, 1_{1}^{-})$ states with $J^P=1/2^{-}$ and $3/2^{-}$. The physical states are:

$$|S_{11}(1535)\rangle = \cos(\Theta_S)|N^2P_M1/2^{-}\rangle - \sin(\Theta_S)|N^4P_M1/2^{-}\rangle \quad (14.26)$$

$$|D_{13}(1520)\rangle = \cos(\Theta_D)|N^2P_M3/2^{-}\rangle - \sin(\Theta_D)|N^4P_M3/2^{-}\rangle \quad (14.27)$$

and the orthogonal combinations for $S_{11}(1650)$ and $D_{13}(1700)$. The mixing is large for the $J^P=1/2^{-}$ states ($\Theta_S \approx -32^\circ$), but small for the $J^P=3/2^{-}$ states ($\Theta_D \approx +6^\circ$) [26,29].

All baryons of the ground state multiplets are known. Many of their properties (masses, magnetic moments *etc.*) are in good agreement with the most basic versions of the quark model, including harmonic (or linear) confinement and a spin-spin interaction, which is responsible for the octet - decuplet mass shifts.

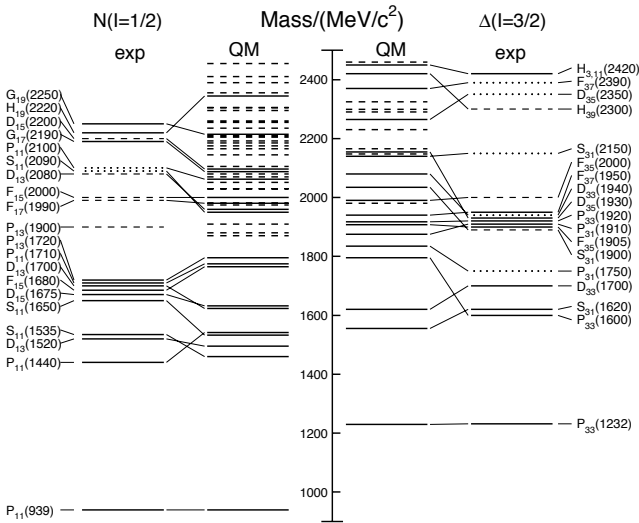


Figure 14.5: Excitation spectrum of the nucleon. Compared are the positions of the excited states identified in experiment, to those predicted by a modern quark model calculation. Left hand side: isospin $I = 1/2$ N -states, right hand side: isospin $I = 3/2$ Δ -states. Experimental: (columns labeled 'exp'), three- and four-star states are indicated by full lines (two-star dashed lines, one-star dotted lines). At the very left and right of the figure, the spectroscopic notation of these states is given. Quark model [27]: (columns labeled 'QM'), all states for the $N=1,2$ bands, low-lying states for the $N=3,4,5$ bands. Full lines: at least tentative assignment to observed states, dashed lines: so far no observed counterparts. Many of the assignments between predicted and observed states are highly tentative.

The situation for the excited states is much less clear. There are two main problems which are illustrated in Fig. 14.5, where the experimentally observed excitation spectrum of the nucleon (N and Δ resonances) is compared to the results of a typical quark model calculation [27]. Many more states are predicted than observed, but on the other hand, states with certain quantum numbers appear in the spectrum at excitation energies much lower than predicted. Up

to an excitation energy of 2.4 GeV, about 45 N states are predicted, but only 12 are established (four- or three-star; see Note on N and Δ Resonances for the rating of the status of resonances) and 7 are tentative (two- or one-star). Even for the $N=1,2$ bands, up to now only half of the predicted states have been observed. This has been known for a long time as the 'missing resonance' problem [26]. On the other hand, the lowest states from the $N=2$ band, the $P_{11}(1440)$, and the $P_{33}(1600)$, appear lower than the negative parity states from the $N=1$ band, and much lower than predicted by most models. Also negative parity Δ states from the $N=3$ band ($S_{31}(1900)$, $D_{33}(1940)$, and $D_{35}(1930)$) are too low in energy. Part of the problem could be experimental. Among the negative parity Δ states, only the D_{35} has three stars and the uncertainty in the position of the $P_{33}(1600)$ is large (1550 - 1700 MeV). For the missing resonance problem, selection rules could play a role [26]. The states are broad and overlapping, and most studies of baryon resonances have been done with pion-induced reactions, so that there is bias in the database against resonances, which couple only weakly to the $N\pi$ channel. Quark model predictions for the couplings to other hadronic channels and to photons are given in Ref. 27. A large experimental effort is ongoing at several electron accelerators to study the baryon resonance spectrum with real and virtual photon-induced meson production reactions. This includes the search for as-yet-unobserved states, as well as detailed studies of the properties of the low lying states (decay patterns, electromagnetic couplings, magnetic moments, *etc.*) (see Ref. 28 for recent reviews).

In quark models, the number of excited states is determined by the effective degrees of freedom, while their ordering and decay properties are related to the residual quark - quark interaction. A recent overview of quark models for baryons is given in Ref. 29. The effective degrees of freedom in the standard nonrelativistic quark model are three equivalent valence quarks with one-gluon exchange-motivated, flavor-independent color-magnetic interactions. A different class of models uses interactions which give rise to a quark - diquark clustering of the baryons (for a review see Ref. 30). If there is a tightly bound diquark, only two degrees of freedom are available at low energies, and thus *fewer* states are predicted. Furthermore, selection rules in the decay pattern may arise from the quantum numbers of the diquark. *More* states are predicted by collective models of the baryon like the algebraic approach in Ref. 31. In this approach, the quantum numbers of the valence quarks are distributed over a Y-shaped string-like configuration, and additional states arise *e.g.*, from vibrations of the strings. *More* states are also predicted in the framework of flux-tube models (see Ref. 32), which are motivated by lattice QCD. In addition to the quark degrees of freedom, flux-tubes responsible for the confinement of the quarks are considered as degrees of freedom. These models include hybrid baryons containing explicit excitations of the gluon fields. However, since all half integral J^P quantum numbers are possible for ordinary baryons, such 'exotics' will be very hard to identify, and probably always mix with ordinary states. So far, the experimentally observed number of states is still far lower even than predicted by the quark-diquark models.

14.5. Dynamics

Many specific quark models exist, but most contain a similar basic set of dynamical ingredients. These include:

- i) A confining interaction, which is generally spin-independent (*e.g.*, harmonic oscillator or linear confinement);
- ii) Different types of spin-dependent interactions:
 - a) commonly used is a color-magnetic flavor-independent interaction modeled after the effects of gluon exchange in QCD (see *e.g.*, Ref. 34). For example, in the S -wave states, there is a spin-spin hyperfine interaction of the form

$$H_{HF} = -\alpha_S M \sum_{i>j} (\vec{\sigma} \lambda_a)_i (\vec{\sigma} \lambda_a)_j, \quad (14.28)$$

where M is a constant with units of energy, λ_a ($a = 1, \dots, 8$) is the set of $SU(3)$ unitary spin matrices, defined in Sec. 36, on "SU(3) Isoscalar Factors and Representation Matrices," and the sum runs over constituent quarks or antiquarks. Spin-orbit interactions, although allowed, seem to be small in general, but a

tensor term is responsible for the mixing of states with the same J^P but different L, S combinations.

b) other approaches include flavor-dependent short-range quark forces from instanton effects (see *e.g.*, Ref. 35). This interaction acts only on scalar, isoscalar pairs of quarks in a relative S -wave state:

$$\langle q^2; S, L, T | W | q^2; S, L, T \rangle = -4g\delta_{S,0}\delta_{L,0}\delta_{T,0}\mathcal{W} \quad (14.29)$$

where \mathcal{W} is the radial matrix element of the contact interaction.

c) a rather different and controversially discussed approach is based on flavor-dependent spin-spin forces arising from one-boson exchange. The interaction term is of the form:

$$H_{HF} \propto \sum_{i < j} V(\vec{r}_{ij}) \lambda_i^F \cdot \lambda_j^F \vec{\sigma}_i \cdot \vec{\sigma}_j \quad (14.30)$$

where the λ_i^F are in flavor space (see *e.g.*, Ref. 36).

- iii) A strange quark mass somewhat larger than the up and down quark masses, in order to split the SU(3) multiplets;
- iv) In the case of spin-spin interactions (ii,c), a flavor-symmetric interaction for mixing $q\bar{q}$ configurations of different flavors (*e.g.*, $u\bar{u} \leftrightarrow d\bar{d} \leftrightarrow s\bar{s}$), in isoscalar channels, so as to reproduce *e.g.*, the $\eta - \eta'$ and $\omega - \Phi$ mesons.

These ingredients provide the basic mechanisms that determine the hadron spectrum in the standard quark model.*

14.6. Lattice Calculations of Hadronic Spectroscopy

Lattice calculations predict the spectrum of bound states in QCD from first principles, beginning with the Lagrangian of full QCD or of various approximations to it. This is typically done using the Euclidean path integral formulation of quantum field theory, where the analog of a partition function for a field theory containing some generic fields $\phi(x)$, with action $S(\phi)$, is

$$Z = \int [d\phi] \exp(-S(\phi)). \quad (14.31)$$

The expectation value of any observable O is

$$\langle O \rangle = \frac{1}{Z} \int [d\phi] O(\phi) \exp(-S(\phi)). \quad (14.32)$$

The theory is regulated by introducing a space-time lattice, with lattice spacing a . This converts the functional integral Eq. (14.31) into an ordinary integral (of very large dimensionality). The integral is replaced by a Monte Carlo sampling over an ensemble of configurations of field variables, using an algorithm which insures that a field configuration is present in the ensemble with a probability proportional to $\exp(-S(\phi_j))$. Then ensemble averages become sample averages,

$$\langle O \rangle = \frac{1}{N} \sum_{j=1}^N O(\phi_j). \quad (14.33)$$

This is all quite similar to the kind of Monte Carlo simulation done by experiments, except that the ensembles of field configurations are created sequentially, as a so-called “Markov chain.”

In QCD, the field variables correspond to gauge fields and quark fields. In a lattice calculation, the lattice spacing (which serves as an ultraviolet cutoff) and the (current) quark masses are inputs; hadron masses and other observables are predicted as a function of those masses. The lattice spacing is unphysical, and it is necessary to extrapolate to the limit of zero lattice spacing. Lattice predictions are for dimensionless ratios of dimensionful parameters (like mass ratios), and predictions of dimensionful quantities require using one experimental input to set the scale. Interpolation or extrapolation of

* However, recently, in a radically different approach [33], it has been suggested that most baryon and meson resonances can be generated by chiral coupled-channel dynamics.

lattice results in the light quark masses involves formulas of chiral perturbation theory.

For conventional hadronic states, lattice calculations use the quark model to construct operators, which are taken as interpolating fields. This does not mean that the hadronic states have minimal quark content: the operators create multi-quark states with particular quantum numbers, but they are connected by quark propagators which include all effects of relativity, and could include the effects of virtual quark-antiquark pairs in the vacuum.

Constituent gluons do not appear naturally in lattice calculations; instead, gauge fields appear as link variables, which allow color to be parallel transported across the lattice in a gauge covariant way. Calculations of glueballs on the lattice use interpolating fields of the form $O_j \sim \exp i \oint \vec{A} \cdot d\vec{l}$ integrated about some path. The fields look like closed tubes of chromoelectric and chromomagnetic flux. Calculations of exotics are done with interpolating fields involving quark and antiquark creation operators joined by flux tubes.

Calculations with heavy quarks typically use Non-Relativistic QCD (NRQCD) or Heavy Quark Effective Theory (HQET), systematic expansions of the QCD Lagrangian in powers of the heavy quark velocity, or the inverse heavy quark mass. Terms in the Lagrangian have obvious quark model analogs, but are derived directly from QCD. The heavy quark potential is a derived quantity, measured in simulations.

Lattice calculations are as specialized as the experiments which produce the data in this book, and it is not easy to give a blanket answer to the question: “How well can lattice calculations predict any specific quantity?” However, let us try:

The cleanest lattice predictions come from measurements of processes in which there is only one particle in the simulation volume. These quantities include masses of hadrons, simple decay constants, like pseudoscalar meson decay constants, and semileptonic form factors (such as the ones appropriate to $B \rightarrow D\nu, K\nu, \pi\nu$). The cleanest predictions for masses are for states which have narrow decay widths and are far below any thresholds to open channels, since the effects of final state interactions are not yet under complete control on the lattice. “Difficult” states for the quark model (such as exotics) are also difficult for the lattice because of the lack of simple operators which couple well to them. Technical issues presently prevent lattice practitioners from directly computing matrix elements for weak decays with more than one strongly interacting particle in the final state.

Good-quality modern lattice calculations will present multi-part error budgets with their predictions. Users are advised to read them carefully! A small part of the uncertainty is statistical, from sample size. Typically, the quoted statistical uncertainty includes uncertainty from a fit: it is rare that a simulation measures one global quantity which is the desired observable. Simulations which include virtual quark-antiquark pairs (also known as “dynamical quarks” or “sea quarks”) are typically done at mass values heavier than the experimental ones, and it is necessary to extrapolate in the quark mass. They are always done at nonzero lattice spacing, and so it is necessary to extrapolate to zero lattice spacing. Some theoretical input is needed to do this. Much of the uncertainty in these extrapolations is systematic, from the choice of fitting function. Other systematics include the number of flavors of dynamical quarks actually simulated, and technical issues with how these dynamical quarks are included. The particular choice of a fiducial mass (to normalize other predictions) is not standardized; there are many possible choices, each with its own set of strengths and weaknesses, and determining it usually requires a second lattice simulation from that used to calculate the quantity under consideration.

A systematic of major historical interest is the “quenched approximation,” in which dynamical quarks are simply left out of the simulation. This was done because the addition of these virtual pairs presented an expensive computational problem. No generally-accepted methodology has ever allowed one to correct for quenching effects, short of redoing all calculations with dynamical quarks. Recent advances in algorithms and computer hardware have rendered it obsolete.

Of course, there is much more to lattice calculations besides spectroscopy; please refer to the mini-review on Quark Masses in the Quarks section of the Listings for more lattice-based phenomenology.

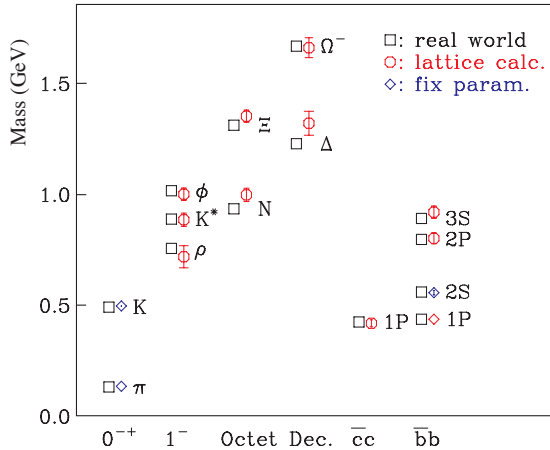


Figure 14.6: A recent calculation of spectroscopy with dynamical u , d , and s quarks. The pion and kaon fix the light quark masses. Only the mass splittings relative to the $1S$ states in the heavy quark sectors are shown. The Υ $1P - 1S$ splitting sets the overall energy scale.

We conclude with a few “representative” pictures of spectroscopy from recent state-of-the-art simulations. They illustrate (better than any discussion) the size of lattice uncertainties.

A recent calculation of spectroscopy with dynamical u , d , and s quarks is shown in Fig. 14.6. The pion and kaon masses are used to set the light quark masses. The Υ $1P - 1S$ splitting is used to set the lattice spacing or equivalently, the overall energy scale in the lattice calculation. This is an updated figure from Ref. 37, using results from Ref. 38 and Ref. 39 (D. Toussaint, private communication).

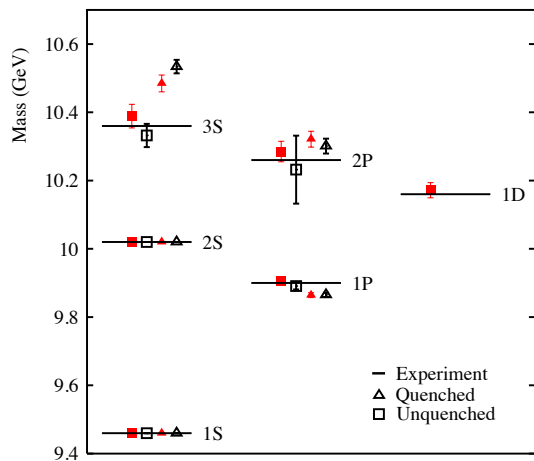


Figure 14.7: The Υ spectrum of radial and orbital levels (adapted from Ref. 40). Closed and open symbols are from coarse and fine lattices (lattice spacing 0.12 and 0.086 fm) respectively. Squares and triangles denote unquenched and quenched results respectively. Lines represent experiment.

Fig. 14.7 shows Upsilon ($b\bar{b}$) spectroscopy from Ref. 40. The calculation uses a discretization of nonrelativistic QCD for its heavy quarks, and includes three flavors of light dynamical fermions. Quenched data are also shown for comparison.

References:

1. J. Schwinger, Phys. Rev. Lett. **12**, 237 (1964).
2. A. Bramon *et al.*, Phys. Lett. **B403**, 339 (1997).
3. A. Aloisio *et al.*, Phys. Lett. **B541**, 45 (2002).
4. C. Amsler *et al.*, Phys. Lett. **B294**, 451 (1992).
5. C. Amsler, Rev. Mod. Phys. **70**, 1293 (1998).
6. T. Feldmann, Int. J. Mod. Phys. **A915**, 159 (2000).
7. C. Amsler and F.E. Close, Phys. Rev. **D53**, 295 (1996).
8. R.L. Jaffe, Phys. Rev. **D 15** 267, 281 (1977).
9. Y. Chen *et al.*, Phys. Rev. **D73**, 014516 (2006).
10. C. Morningstar and M. Peardon, Phys. Rev. **D60**, 034509 (1999).
11. W. J. Lee and D. Weingarten, Phys. Rev. **D61**, 014015 (2000).
12. G. S. Bali, *et. al.* Phys. Lett. **B309**, 378 (1993).
13. C. Michael, AIP Conf. Proc. **432**, 657 (1998).
14. F.E. Close and A. Kirk, Eur. Phys. J. **C21**, 531 (2001).
15. A. Hart *et al.*, Phys. Rev. **D74**, 114504 (2006).
16. C. McNeile, *XXV Int. Symp. on Lattice Field Theory*, Regensburg, 2007, [arXiv:0710.0985v1[hep-lat]].
17. C. Amsler and N.A. Törnqvist, Phys. Rev. **389**, 61 (2004).
18. N. Isgur and J. Paton, Phys. Rev. **D31**, 2910 (1985).
19. P. Lacock *et al.*, Phys. Lett. **B401**, 308 (1997); C. Bernard *et al.*, Phys. Rev. **D56**, 7039 (1997); C. Bernard *et al.*, Phys. Rev. **D68**, 074505 (2003).
20. M. Chanowitz and S. Sharpe, Nucl. Phys. **B222**, 211 (1983).
21. T. Barnes *et al.*, Nucl. Phys. **B224**, 241 (1983).
22. W.-M Yao *et al.*, J. Phys. **G33**, 1 (2006).
23. F.E. Close, in *Quarks and Nuclear Forces* (Springer-Verlag, 1982), p. 56.
24. Particle Data Group, Phys. Lett. **111B** (1982).
25. R.H. Dalitz and L.J. Reinders, in “Hadron Structure as Known from Electromagnetic and Strong Interactions,” *Proceedings of the Hadron ’77 Conference* (Veda, 1979), p. 11.
26. N. Isgur and G. Karl, Phys. Rev. **D18**, 4187 (1978); *ibid.*, **D19**, 2653 (1979); *ibid.*, **D20**, 1191 (1979); K.-T. Chao *et al.*, Phys. Rev. **D23**, 155 (1981).
27. S. Capstick and W. Roberts, Phys. Rev. **D49**, 4570 (1994); *ibid.*, **D57**, 4301 (1998); *ibid.*, **D58**, 074011 (1998); S. Capstick, Phys. Rev. **D46**, 2864 (1992).
28. B. Krusche and S. Schadmand, Prog. Part. Nucl. Phys. **51**, 399 (2003); V.D. Burkert and T.-S.H. Lee, Int. J. Mod. Phys. **E13**, 1035 (2004).
29. S. Capstick and W. Roberts, Prog. Part. Nucl. Phys. **45**, 241 (2000); see also A.J.G. Hey and R.L. Kelly, Phys. Reports **96**, 71 (1983).
30. M. Anselmino *et al.*, Rev. Mod. Phys. **65**, 1199 (1993).
31. R. Bijker *et al.*, Ann. of Phys. **236** 69 (1994).
32. N. Isgur and J. Paton, Phys. Rev. **D31**, 2910 (1985); S. Capstick and P.R. Page, Phys. Rev. **C66**, 065204 (2002).
33. M.F.M Lutz and E.E. Kolomeitsev, Nucl. Phys. **A700**, 193 (2002); M.F.M Lutz and E.E. Kolomeitsev, Nucl. Phys. **A730**, 392 (2004); E.E. Kolomeitsev and M.F.M Lutz, Phys. Lett. **B585**, 243 (2004).
34. A. De Rujula *et al.*, Phys. Rev. **D12**, 147 (1975).
35. W.H. Blask *et al.*, Z. Phys. **A337** 327 (1990); U. Löring *et al.*, Eur. Phys. J. **A10** 309 (2001); U. Löring *et al.*, Eur. Phys. J. **A10** 395 (2001); *ibid.*, **A10** 447 (2001).
36. L.Y. Glozman and D.O. Riska, Phys. Rept. **268** 263 (1996); L.Y. Glozman *et al.*, Phys. Rev. **D58**, 094030 (1998).
37. C. Aubin *et al.* [MILC Collab.], Phys. Rev. **D70**, 094505 (2004) [arXiv:hep-lat/0407028].
38. C. T. H. Davies *et al.* [HPQCD Collaboration], Phys. Rev. Lett. **92**, 022001 (2004) [arXiv:hep-lat/0304004].
39. M. Wingate *et al.*, Phys. Rev. Lett. **92**, 162001 (2004) [arXiv:hep-ph/0311130].
40. A. Gray *et al.*, Phys. Rev. D **72**, 094507 (2005) [arXiv:hep-lat/0507013].

15. GRAND UNIFIED THEORIES

Revised October 2005 by S. Raby (Ohio State University).

15.1. Grand Unification

15.1.1. Standard Model: An Introduction :

In spite of all the successes of the Standard Model [SM], it is unlikely to be the final theory. It leaves many unanswered questions. Why the local gauge interactions $SU(3)_C \times SU(2)_L \times U(1)_Y$, and why 3 families of quarks and leptons? Moreover, why does one family consist of the states $[Q, u^c, d^c; L, e^c]$ transforming as $[(3, 2, 1/3), (\bar{3}, 1, -4/3), (\bar{3}, 1, 2/3); (1, 2, -1), (1, 1, 2)]$, where $Q = (u, d)$, and $L = (\nu, e)$ are $SU(2)_L$ doublets, and u^c, d^c, e^c are charge conjugate $SU(2)_L$ singlet fields with the $U(1)_Y$ quantum numbers given? [We use the convention that electric charge $Q_{EM} = T_{3L} + Y/2$ and all fields are left-handed.] Note the SM gauge interactions of quarks and leptons are completely fixed by their gauge charges. Thus, if we understood the origin of this charge quantization, we would also understand why there are no fractionally charged hadrons. Finally, what is the origin of quark and lepton masses, or the apparent hierarchy of family masses and quark mixing angles? Perhaps if we understood this, we would also know the origin of CP violation, the solution to the strong CP problem, the origin of the cosmological matter-antimatter asymmetry, or the nature of dark matter.

The SM has 19 arbitrary parameters; their values are chosen to fit the data. Three arbitrary gauge couplings: g_3, g, g' (where g, g' are the $SU(2)_L, U(1)_Y$ couplings, respectively) or equivalently, $\alpha_s = (g_3^2/4\pi), \alpha_{EM} = (e^2/4\pi)$ ($e = g \sin \theta_W$), and $\sin^2 \theta_W = (g')^2/(g^2 + (g')^2)$. In addition, there are 13 parameters associated with the 9 charged fermion masses and the four mixing angles in the CKM matrix. The remaining 3 parameters are v, λ [the Higgs VEV (vacuum expectation value) and quartic coupling] (or equivalently, M_Z, m_h^0), and the QCD θ parameter. In addition, data from neutrino oscillation experiments provide convincing evidence for neutrino masses. With 3 light Majorana neutrinos, there are at least 9 additional parameters in the neutrino sector; 3 masses, 3 mixing angles and 3 phases. In summary, the SM has too many arbitrary parameters, and leaves open too many unresolved questions to be considered complete. These are the problems which grand unified theories hope to address.

15.1.2. Charge Quantization :

In the Standard Model, quarks and leptons are on an equal footing; both fundamental particles without substructure. It is now clear that they may be two faces of the same coin; unified, for example, by extending QCD (or $SU(3)_C$) to include leptons as the fourth color, $SU(4)_C$ [1]. The complete Pati-Salam gauge group is $SU(4)_C \times SU(2)_L \times SU(2)_R$, with the states of one family $[(Q, L), (Q^c, L^c)]$ transforming as $[(4, 2, 1), (\bar{4}, 1, \bar{2})]$, where $Q^c = (d^c, u^c), L^c = (e^c, \nu^c)$ are doublets under $SU(2)_R$. Electric charge is now given by the relation $Q_{EM} = T_{3L} + T_{3R} + 1/2(B-L)$, and $SU(4)_C$ contains the subgroup $SU(3)_C \times (B-L)$ where B (L) is baryon (lepton) number. Note ν^c has no SM quantum numbers and is thus completely “sterile.” It is introduced to complete the $SU(2)_R$ lepton doublet. This additional state is desirable when considering neutrino masses.

Although quarks and leptons are unified with the states of one family forming two irreducible representations of the gauge group, there are still 3 independent gauge couplings (two if one also imposes parity, *i.e.*, $L \leftrightarrow R$ symmetry). As a result, the three low-energy gauge couplings are still independent arbitrary parameters. This difficulty is resolved by embedding the SM gauge group into the simple unified gauge group, Georgi-Glashow $SU(5)$, with one universal gauge coupling α_G defined at the grand unification scale M_G [2]. Quarks and leptons still sit in two irreducible representations, as before, with a $\mathbf{10} = [Q, u^c, e^c]$ and $\mathbf{\bar{5}} = [d^c, L]$. Nevertheless, the three low energy gauge couplings are now determined in terms of two independent parameters: α_G and M_G . Hence, there is one prediction.

In order to break the electroweak symmetry at the weak scale and give mass to quarks and leptons, Higgs doublets are needed which can sit in either a $\mathbf{5}_H$ or $\mathbf{\bar{5}}_H$. The additional 3 states are color triplet Higgs scalars. The couplings of these color triplets violate baryon and lepton number, and nucleons decay via the exchange of a single

color triplet Higgs scalar. Hence, in order not to violently disagree with the non-observation of nucleon decay, their mass must be greater than $\sim 10^{10-11}$ GeV. Moreover, in supersymmetric GUTs, in order to cancel anomalies, as well as give mass to both up and down quarks, both Higgs multiplets $\mathbf{5}_H, \mathbf{\bar{5}}_H$ are required. As we shall discuss later, nucleon decay now constrains the color triplet Higgs states in a SUSY GUT to have mass significantly greater than M_G .

Complete unification is possible with the symmetry group $SO(10)$, with one universal gauge coupling α_G , and one family of quarks and leptons sitting in the 16-dimensional spinor representation $\mathbf{16} = [\mathbf{10} + \mathbf{\bar{5}} + \mathbf{1}]$ [3]. The $SU(5)$ singlet $\mathbf{1}$ is identified with ν^c . In Table 15.1 we present the states of one family of quarks and leptons, as they appear in the $\mathbf{16}$. It is an amazing and perhaps even profound fact that all the states of a single family of quarks and leptons can be represented digitally as a set of 5 zeros and/or ones or equivalently as the tensor product of 5 “spin” $1/2$ states with $\pm = |\pm \frac{1}{2}\rangle$ and with the condition that we have an even number of $|-\rangle$ spins. The first three “spins” correspond to $SU(3)_C$ color quantum numbers, while the last two are $SU(2)_L$ weak quantum numbers. In fact, an $SU(3)_C$ rotation just raises one color index and lowers another, thereby changing colors $\{r, b, y\}$. Similarly an $SU(2)_L$ rotation raises one weak index and lowers another, thereby flipping the weak isospin from up to down or vice versa. In this representation, weak hypercharge Y is given by the simple relation $Y = 2/3(\sum \text{color spins}) - (\sum \text{weak spins})$. $SU(5)$ rotations [not in the Standard Model] then raise (or lower) a color index, while at the same time lowering (or raising) a weak index. It is easy to see that such rotations can mix the states $\{Q, u^c, e^c\}$ and $\{d^c, L\}$ among themselves, and ν^c is a singlet. The new $SO(10)$ rotations [not in $SU(5)$] are then given by either raising or lowering any two spins. For example, by lowering the two weak indices, ν^c rotates into e^c , etc.

Table 15.1: The quantum numbers of the $\mathbf{16}$ dimensional representation of $SO(10)$.

State	Y	Color	Weak
ν^c	0	+++	++
e^c	2	+++	--
u_r	1/3	-++	+-
d_r	1/3	-++	-+
u_b	1/3	+ - +	+-
d_b	1/3	+ - +	-+
u_y	1/3	++ -	+-
d_y	1/3	++ -	-+
u_r^c	-4/3	+ - -	++
u_b^c	-4/3	- + -	++
u_y^c	-4/3	- - +	++
d_r^c	2/3	+ - -	--
d_b^c	2/3	- + -	--
d_y^c	2/3	- - +	--
ν	-1	- - -	+-
e	-1	- - -	-+

$SO(10)$ has two inequivalent maximal breaking patterns: $SO(10) \rightarrow SU(5) \times U(1)_X$ and $SO(10) \rightarrow SU(4)_C \times SU(2)_L \times SU(2)_R$. In the first case, we obtain Georgi-Glashow $SU(5)$ if Q_{EM} is given in terms of $SU(5)$ generators alone, or so-called flipped $SU(5)$ [4] if Q_{EM} is partly in $U(1)_X$. In the latter case, we have the Pati-Salam symmetry. If $SO(10)$ breaks directly to the SM at M_G , then we retain the prediction for gauge coupling unification. However, more possibilities for breaking (hence more breaking scales and more parameters) are available in $SO(10)$. Nevertheless with one breaking pattern $SO(10) \rightarrow SU(5) \rightarrow SM$, where the last breaking scale is M_G , the predictions from gauge coupling unification are preserved. The Higgs multiplets in minimal $SO(10)$ are contained in the fundamental

$\mathbf{10}_H = [\mathbf{5}_H, \bar{\mathbf{5}}_H]$ representation. Note, only in SO(10) does the gauge symmetry distinguish quark and lepton multiplets from Higgs multiplets.

Finally, larger symmetry groups have been considered. For example, $E(6)$ has a fundamental representation $\mathbf{27}$, which under SO(10) transforms as a $[\mathbf{16} + \mathbf{10} + \mathbf{1}]$. The breaking pattern $E(6) \rightarrow SU(3)_C \times SU(3)_L \times SU(3)_R$ is also possible. With the additional permutation symmetry $Z(3)$ interchanging the three SU(3)s, we obtain so-called “trification [5],” with a universal gauge coupling. The latter breaking pattern has been used in phenomenological analyses of the heterotic string [6]. However, in larger symmetry groups, such as $E(6)$, $SU(6)$, *etc.*, there are now many more states which have not been observed and must be removed from the effective low-energy theory. In particular, three families of $\mathbf{27}$ s in $E(6)$ contain three Higgs type multiplets transforming as $\mathbf{10}$ s of SO(10). This makes these larger symmetry groups unattractive starting points for model building.

15.1.3. String Theory and Orbifold GUTs :

Orbifold compactification of the heterotic string [7–9], and recent field theoretic constructions known as orbifold GUTs [10], contain grand unified symmetries realized in 5 and 6 dimensions. However, upon compactifying all but four of these extra dimensions, only the MSSM is recovered as a symmetry of the effective four dimensional field theory.¹ These theories can retain many of the nice features of four dimensional SUSY GUTs, such as charge quantization, gauge coupling unification and sometimes even Yukawa unification; while at the same time resolving some of the difficulties of 4d GUTs, in particular problems with unwieldy Higgs sectors necessary for spontaneously breaking the GUT symmetry, problems with doublet-triplet Higgs splitting or rapid proton decay. We will comment further on the corrections to the four dimensional GUT picture due to orbifold GUTs in the following sections.

15.1.4. Gauge coupling unification :

The biggest paradox of grand unification is to understand how it is possible to have a universal gauge coupling g_G in a grand unified theory [GUT], and yet have three unequal gauge couplings at the weak scale with $g_3 > g > g'$. The solution is given in terms of the concept of an effective field theory [EFT] [16]. The GUT symmetry is spontaneously broken at the scale M_G , and all particles not in the SM obtain mass of order M_G . When calculating Green’s functions with external energies $E \gg M_G$, we can neglect the mass of all particles in the loop and hence all particles contribute to the renormalization group running of the universal gauge coupling. However, for $E \ll M_G$, one can consider an effective field theory including only the states with mass $< E \ll M_G$. The gauge symmetry of the EFT is $SU(3)_C \times SU(2)_L \times U(1)_Y$, and the three gauge couplings renormalize independently. The states of the EFT include only those of the SM; 12 gauge bosons, 3 families of quarks and leptons, and one

¹ Also, in recent years there has been a great deal of progress in constructing three and four family models in Type IIA string theory with intersecting D6 branes [11]. Although these models can incorporate SU(5) or a Pati-Salam symmetry group in four dimensions, they typically have problems with gauge coupling unification. In the former case this is due to charged exotics which affect the RG running, while in the latter case the $SU(4) \times SU(2)_L \times SU(2)_R$ symmetry never unifies. Note, heterotic string theory models also exist whose low energy effective 4d field theory is a SUSY GUT [12]. These models have all the virtues and problems of 4d GUTs. Finally, many heterotic string models have been constructed with the standard model gauge symmetry in 4d and no intermediate GUT symmetry in less than 10d. Recently some minimal 3 family supersymmetric models have been constructed [13,14]. These theories may retain some of the symmetry relations of GUTs, however the unification scale would typically be the string scale, of order 5×10^{17} GeV, which is inconsistent with low energy data. A way out of this problem was discovered in the context of the strongly coupled heterotic string, defined in an effective 11 dimensions [15]. In this case the 4d Planck scale (which controls the value of the string scale) now unifies with the GUT scale.

or more Higgs doublets. At M_G , the two effective theories [the GUT itself is most likely the EFT of a more fundamental theory defined at a higher scale] must give identical results; hence we have the boundary conditions $g_3 = g_2 = g_1 \equiv g_G$, where at any scale $\mu < M_G$, we have $g_2 \equiv g$ and $g_1 = \sqrt{5/3} g'$. Then using two low-energy couplings, such as $\alpha_s(M_Z)$, $\alpha_{EM}(M_Z)$, the two independent parameters α_G , M_G can be fixed. The third gauge coupling, $\sin^2 \theta_W$ in this case, is then predicted. This was the procedure up until about 1991 [17,18]. Subsequently, the uncertainties in $\sin^2 \theta_W$ were reduced tenfold. Since then, $\alpha_{EM}(M_Z)$, $\sin^2 \theta_W$ have been used as input to predict α_G , M_G , and $\alpha_s(M_Z)$ [19].

We emphasize that the above boundary condition is only valid when using one-loop-renormalization group [RG] running. With precision electroweak data, however, it is necessary to use two-loop-RG running. Hence, one must include one-loop-threshold corrections to gauge coupling boundary conditions at both the weak and GUT scales. In this case, it is always possible to define the GUT scale as the point where $\alpha_1(M_G) = \alpha_2(M_G) \equiv \bar{\alpha}_G$ and $\alpha_3(M_G) = \bar{\alpha}_G (1 + \epsilon_3)$. The threshold correction ϵ_3 is a logarithmic function of all states with mass of order M_G and $\bar{\alpha}_G = \alpha_G + \Delta$, where α_G is the GUT coupling constant above M_G , and Δ is a one-loop-threshold correction. To the extent that gauge coupling unification is perturbative, the GUT threshold corrections are small and calculable. This presumes that the GUT scale is sufficiently below the Planck scale or any other strong coupling extension of the GUT, such as a strongly coupled string theory.

Supersymmetric grand unified theories [SUSY GUTs] are an extension of non-SUSY GUTs [20]. The key difference between SUSY GUTs and non-SUSY GUTs is the low-energy effective theory. The low-energy effective field theory in a SUSY GUT is assumed to satisfy $N = 1$ supersymmetry down to scales of order the weak scale, in addition to the SM gauge symmetry. Hence, the spectrum includes all the SM states, plus their supersymmetric partners. It also includes one pair (or more) of Higgs doublets; one to give mass to up-type quarks, and the other to down-type quarks and charged leptons. Two doublets with opposite hypercharge Y are also needed to cancel fermionic triangle anomalies. Finally, it is important to recognize that a low-energy SUSY-breaking scale (the scale at which the SUSY partners of SM particles obtain mass) is necessary to solve the gauge hierarchy problem.

Simple non-SUSY SU(5) is ruled out, initially by the increased accuracy in the measurement of $\sin^2 \theta_W$, and by early bounds on the proton lifetime (see below) [18]. However, by now LEP data [19] has conclusively shown that SUSY GUTs is the new Standard Model; by which we mean the theory used to guide the search for new physics beyond the present SM (see Fig. 15.1). SUSY extensions of the SM have the property that their effects decouple as the effective SUSY-breaking scale is increased. Any theory beyond the SM must have this property simply because the SM works so well. However, the SUSY-breaking scale cannot be increased with impunity, since this would reintroduce a gauge hierarchy problem. Unfortunately there is no clear-cut answer to the question, “When is the SUSY-breaking scale too high?” A conservative bound would suggest that the third generation squarks and sleptons must be lighter than about 1 TeV, in order that the one-loop corrections to the Higgs mass from Yukawa interactions remain of order the Higgs mass bound itself.

At present, gauge coupling unification within SUSY GUTs works extremely well. Exact unification at M_G , with two-loop-RG running from M_G to M_Z , and one-loop-threshold corrections at the weak scale, fits to within 3 σ of the present precise low-energy data. A small threshold correction at M_G ($\epsilon_3 \sim -3$ to -4%) is sufficient to fit the low-energy data precisely [22–24].² This may be compared to non-SUSY GUTs, where the fit misses by $\sim 12 \sigma$, and a precise

² This result implicitly assumes universal GUT boundary conditions for soft SUSY-breaking parameters at M_G . In the simplest case, we have a universal gaugino mass $M_{1/2}$, a universal mass for squarks and sleptons m_{16} , and a universal Higgs mass m_{10} , as motivated by SO(10). In some cases, threshold corrections to gauge coupling unification can be exchanged for threshold corrections to soft SUSY parameters. See for example, Ref. 25 and references therein.

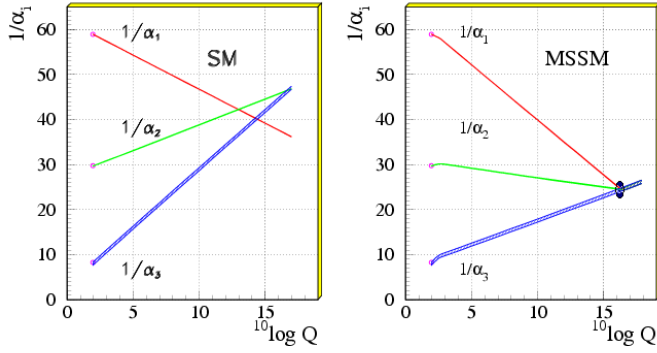


Figure 15.1: Gauge coupling unification in non-SUSY GUTs on the left vs. SUSY GUTs on the right using the LEP data as of 1991. Note, the difference in the running for SUSY is the inclusion of supersymmetric partners of standard model particles at scales of order a TeV (Fig. taken from Ref. 21). Given the present accurate measurements of the three low energy couplings, in particular $\alpha_s(M_Z)$, GUT scale threshold corrections are now needed to precisely fit the low energy data. The dark blob in the plot on the right represents these model dependent corrections.

fit requires new weak-scale states in incomplete GUT multiplets, or multiple GUT-breaking scales.³

Following the analysis of Ref. 24 let us try to understand the need for the GUT threshold correction and its order of magnitude. The renormalization group equations relate the low energy gauge coupling constants $\alpha_i(M_Z)$, $i = 1, 2, 3$ to the value of the unification scale Λ_U and the GUT coupling α_U by the expression

$$\frac{1}{\alpha_i(M_Z)} = \frac{1}{\alpha_U} + \frac{b_i}{2\pi} \log\left(\frac{\Lambda_U}{M_Z}\right) + \delta_i \quad (15.1)$$

where Λ_U is the GUT scale evaluated at one loop and the threshold corrections, δ_i , are given by $\delta_i = \delta_i^{(2)} + \delta_i^{(l)} + \delta_i^{(g)}$ with $\delta_i^{(2)}$ representing two loop running effects, $\delta_i^{(l)}$ the light threshold corrections at the SUSY breaking scale and $\delta_i^{(g)} = \delta_i^{(h)} + \delta_i^{(b)}$ representing GUT scale threshold corrections. Note, in this analysis, the two loop RG running is treated on the same footing as weak and GUT scale threshold corrections. One then obtains the prediction

$$(\alpha_3(M_Z) - \alpha_3^{LO}(M_Z))/\alpha_3^{LO}(M_Z) = -\alpha_3^{LO}(M_Z) \delta_s \quad (15.2)$$

where $\alpha_3^{LO}(M_Z)$ is the leading order one loop RG result and $\delta_s = \frac{1}{7}(5\delta_1 - 12\delta_2 + 7\delta_3)$ is the net threshold correction. [A similar formula applies at the GUT scale with the GUT threshold correction, ϵ_3 , given by $\epsilon_3 = -\bar{\alpha}_G \delta_s^{(g)}$.] Given the experimental inputs [28]:

$$\begin{aligned} \alpha_{em}^{-1}(M_Z) &= 127.906 \pm 0.019 \\ \sin^2\theta_W(M_Z) &= 0.2312 \pm 0.0002 \\ \alpha_3(M_Z) &= 0.1187 \pm 0.0020 \end{aligned} \quad (15.3)$$

and taking into account the light threshold corrections, assuming an ensemble of 10 SUSY spectra [24] (corresponding to the Snowmass benchmark points), we have

$$\alpha_3^{LO}(M_Z) \approx 0.118 \quad (15.4)$$

³ Non-SUSY GUTs with a more complicated breaking pattern can still fit the data. For example, non-SUSY $SO(10) \rightarrow SU(4)_C \times SU(2)_L \times SU(2)_R \rightarrow SM$, with the second breaking scale of order an intermediate scale, determined by light neutrino masses using the see-saw mechanism, can fit the low-energy data for gauge couplings [26], and at the same time survive nucleon decay bounds [27], discussed in the following section.

and

$$\begin{aligned} \delta_s^{(2)} &\approx -0.82 \\ \delta_s^{(l)} &\approx -0.50 + \frac{19}{28\pi} \log\left(\frac{M_{SUSY}}{M_Z}\right). \end{aligned}$$

For $M_{SUSY} = 1$ TeV, we have $\delta_s^{(2)} + \delta_s^{(l)} \approx -0.80$. Since the one loop result $\alpha_3^{LO}(M_Z)$ is very close to the experimental value, we need $\delta_s \approx 0$ or equivalently, $\delta_s^{(g)} \approx 0.80$. This corresponds, at the GUT scale, to $\epsilon_3 \approx -3\%$.⁴

In four dimensional SUSY GUTs, the threshold correction ϵ_3 receives a positive contribution from Higgs doublets and triplets.⁵ Thus a larger, negative contribution must come from the GUT breaking sector of the theory. This is certainly possible in specific $SO(10)$ [29] or $SU(5)$ [30] models, but it is clearly a significant constraint on the 4d GUT sector of the theory. In five or six dimensional orbifold GUTs, on the other hand, the ‘‘GUT scale’’ threshold correction comes from the Kaluza-Klein modes between the compactification scale, M_c , and the effective cutoff scale M_* .⁶ Thus, in orbifold GUTs, gauge coupling unification at two loops is only consistent with the low energy data with a fixed value for M_c and M_* .⁷ Typically, one finds $M_c < M_G = 3 \times 10^{16}$ GeV, where M_G is the 4d GUT scale. Since the grand unified gauge bosons, responsible for nucleon decay, get mass at the compactification scale, the result $M_c < M_G$ for orbifold GUTs has significant consequences for nucleon decay.

A few final comments are in order. We do not consider the scenario of split supersymmetry [33] in this review. In this scenario squarks and sleptons have mass at a scale $\tilde{m} \gg M_Z$, while gauginos and Higgsinos have mass of order the weak scale. Gauge coupling unification occurs at a scale of order 10^{16} GeV, provided that the scale \tilde{m} lies in the range $10^3 - 10^{11}$ GeV [34]. A serious complaint concerning the split SUSY scenario is that it does not provide a solution to the gauge hierarchy problem. Moreover, it is only consistent with grand unification if it also postulates an ‘‘intermediate’’ scale, \tilde{m} , for scalar masses. In addition, it is in conflict with $b - \tau$ Yukawa unification, unless $\tan\beta$ is fine-tuned to be close to 1 [34].⁸

We have also neglected to discuss non-supersymmetric GUTs in four dimensions which still survive once one allows for several scales

⁴ In order to fit the low energy data for gauge coupling constants we require a relative shift in $\alpha_3(M_G)$ of order 3% due to GUT scale threshold corrections. If these GUT scale corrections were not present, however, weak scale threshold corrections of order 9% (due to the larger value of α_3 at M_Z) would be needed to resolve the discrepancy with the data for exact gauge coupling unification at M_G . Leaving out the fact that any consistent GUT necessarily contributes threshold corrections at the GUT scale, it is much more difficult to find the necessary larger corrections at the weak scale. For example, we need $M_{SUSY} \approx 40$ TeV for the necessary GUT scale threshold correction to vanish.

⁵ Note, the Higgs contribution is given by $\epsilon_3 = \frac{3\bar{\alpha}_G}{5\pi} \log\left|\frac{\tilde{M}_t \gamma}{M_G}\right|$ where \tilde{M}_t is the effective color triplet Higgs mass (setting the scale for dimension 5 baryon and lepton number violating operators) and $\gamma = \lambda_b/\lambda_t$ at M_G . Since \tilde{M}_t is necessarily greater than M_G , the Higgs contribution to ϵ_3 is positive.

⁶ In string theory, the cutoff scale is the string scale.

⁷ It is interesting to note that a ratio $M_*/M_c \sim 100$, needed for gauge coupling unification to work in orbifold GUTs is typically the maximum value for this ratio consistent with perturbativity [31]. In addition, in orbifold GUTs brane-localized gauge kinetic terms may destroy the successes of gauge coupling unification. However, for values of $M_*/M_c = M_*\pi R \gg 1$ the unified bulk gauge kinetic terms can dominate over the brane-localized terms [32].

⁸ $b - \tau$ Yukawa unification only works for $\tilde{m} < 10^4$ for $\tan\beta \geq 1.5$. This is because the effective theory between the gaugino mass scale and \tilde{m} includes only one Higgs doublet, as in the standard model. In this case, the large top quark Yukawa coupling tends to increase the ratio λ_b/λ_τ as one runs down in energy below \tilde{m} . This is opposite to what happens in MSSM where the large top quark Yukawa coupling decreases the ratio λ_b/λ_τ [35].

of GUT symmetry breaking [26]. Finally, it has been shown that non-supersymmetric GUTs in warped 5 dimensional orbifolds can be consistent with gauge coupling unification, assuming that the right-handed top quark and the Higgs doublets are composite-like objects with a compositeness scale of order a TeV [36].

15.1.5. Nucleon Decay :

Baryon number is necessarily violated in any GUT [37]. In SU(5), nucleons decay via the exchange of gauge bosons with GUT scale masses, resulting in dimension-6 baryon-number-violating operators suppressed by $(1/M_G^2)$. The nucleon lifetime is calculable and given by $\tau_N \propto M_G^4/(\alpha_G^2 m_p^5)$. The dominant decay mode of the proton (and the baryon-violating decay mode of the neutron), via gauge exchange, is $p \rightarrow e^+ \pi^0$ ($n \rightarrow e^+ \pi^-$). In any simple gauge symmetry, with one universal GUT coupling and scale (α_G , M_G), the nucleon lifetime from gauge exchange is calculable. Hence, the GUT scale may be directly observed via the extremely rare decay of the nucleon. Experimental searches for nucleon decay began with the Kolar Gold Mine, Homestake, Soudan, NUSEX, Frejus, HPW, and IMB detectors [17]. The present experimental bounds come from Super-Kamiokande and Soudan II. We discuss these results shortly. Non-SUSY GUTs are also ruled out by the non-observation of nucleon decay [18]. In SUSY GUTs, the GUT scale is of order 3×10^{16} GeV, as compared to the GUT scale in non-SUSY GUTs, which is of order 10^{15} GeV. Hence, the dimension-6 baryon-violating operators are significantly suppressed in SUSY GUTs [20] with $\tau_p \sim 10^{34-38}$ yrs.

However, in SUSY GUTs, there are additional sources for baryon-number violation—dimension-4 and -5 operators [38]. Although the notation does not change, when discussing SUSY GUTs, all fields are implicitly bosonic superfields, and the operators considered are the so-called F terms, which contain two fermionic components, and the rest scalars or products of scalars. Within the context of SU(5), the dimension-4 and -5 operators have the form $(\mathbf{10} \mathbf{5} \mathbf{5}) \supset (u^c d^c d^c) + (Q L d^c) + (e^c L L)$, and $(\mathbf{10} \mathbf{10} \mathbf{10} \mathbf{5}) \supset (Q Q Q L) + (u^c u^c d^c e^c) + B$ and L conserving terms, respectively. The dimension-4 operators are renormalizable with dimensionless couplings; similar to Yukawa couplings. On the other hand, the dimension-5 operators have a dimensionful coupling of order $(1/M_G)$.

The dimension-4 operators violate baryon number or lepton number, respectively, but not both. The nucleon lifetime is extremely short if both types of dimension-4 operators are present in the low-energy theory. However, both types can be eliminated by requiring R parity. In SU(5), the Higgs doublets reside in a $\mathbf{5}_H$, $\mathbf{5}_H$, and R parity distinguishes the $\mathbf{5}$ (quarks and leptons) from $\mathbf{5}_H$ (Higgs). R parity [39] (or more precisely, its cousin, family reflection symmetry) (see Dimopoulos and Georgi [20] and DRW [40]) takes $F \rightarrow -F$, $H \rightarrow H$ with $F = \{\mathbf{10}, \mathbf{5}\}$, $H = \{\mathbf{5}_H, \mathbf{5}_H\}$. This forbids the dimension-4 operator $(\mathbf{10} \mathbf{5} \mathbf{5})$, but allows the Yukawa couplings of the form $(\mathbf{10} \mathbf{5} \mathbf{5}_H)$ and $(\mathbf{10} \mathbf{10} \mathbf{5}_H)$. It also forbids the dimension-3, lepton-number-violating operator $(\mathbf{5} \mathbf{5}_H) \supset (L H_u)$, with a coefficient with dimensions of mass which, like the μ parameter, could be of order the weak scale and the dimension-5, baryon-number-violating operator $(\mathbf{10} \mathbf{10} \mathbf{10} \mathbf{5}_H) \supset (Q Q Q H_d) + \dots$.

Note, in the MSSM, it is possible to retain R -parity-violating operators at low energy, as long as they violate either baryon number or lepton number only, but not both. Such schemes are natural if one assumes a low-energy symmetry, such as lepton number, baryon number, or a baryon parity [41]. However, these symmetries cannot be embedded in a GUT. Thus, in a SUSY GUT, only R parity can prevent unwanted dimension four operators. Hence, by naturalness arguments, R parity must be a symmetry in the effective low-energy theory of any SUSY GUT. This does not mean to say that R parity is guaranteed to be satisfied in any GUT.

Note also, R parity distinguishes Higgs multiplets from ordinary families. In SU(5), Higgs and quark/lepton multiplets have identical quantum numbers; while in $E(6)$, Higgs and families are unified within the fundamental $\mathbf{27}$ representation. Only in SO(10) are Higgs and ordinary families distinguished by their gauge quantum numbers. Moreover, the $Z(4)$ center of SO(10) distinguishes $\mathbf{10}_s$ from $\mathbf{16}_s$, and can be associated with R parity [42].

In SU(5), dimension-5 baryon-number-violating operators may be forbidden at tree level by additional symmetries. These symmetries are typically broken, however, by the VEVs responsible for the color triplet Higgs masses. Consequently, these dimension-5 operators are generically generated via color triplet Higgsino exchange. Hence, the color triplet partners of Higgs doublets must necessarily obtain mass of order the GUT scale. The dominant decay modes from dimension-5 operators are $p \rightarrow K^+ \bar{\nu}$ ($n \rightarrow K^0 \bar{\nu}$). This is due to a simple symmetry argument; the operators $(Q_i Q_j Q_k L_l)$, $(u_i^c u_j^c d_k^c e_l^c)$ (where $i, j, k, l = 1, 2, 3$ are family indices, and color and weak indices are implicit) must be invariant under SU(3) $_C$ and SU(2) $_L$. As a result, their color and weak doublet indices must be anti-symmetrized. However, since these operators are given by bosonic superfields, they must be totally symmetric under interchange of all indices. Thus, the first operator vanishes for $i = j = k$, and the second vanishes for $i = j$. Hence, a second or third generation member must exist in the final state [40].

Recent Super-Kamiokande bounds on the proton lifetime severely constrain these dimension-6 and dimension-5 operators with $\tau_{(p \rightarrow e^+ \pi^0)} > 5.0 \times 10^{33}$ yrs (79.3 ktyr exposure), $\tau_{(n \rightarrow e^+ \pi^-)} > 5 \times 10^{33}$ yrs (61 ktyr), and $\tau_{(p \rightarrow K^+ \bar{\nu})} > 1.6 \times 10^{33}$ yrs (79.3 ktyr), $\tau_{(n \rightarrow K^0 \bar{\nu})} > 1.7 \times 10^{32}$ yrs (61 ktyr) at (90% CL) based on the listed exposures [43]. These constraints are now sufficient to rule out minimal SUSY SU(5) [44].⁹ Non-minimal Higgs sectors in SU(5) or SO(10) theories still survive [23,30]. The upper bound on the proton lifetime from these theories is approximately a factor of 5 above the experimental bounds. They are, however, being pushed to their theoretical limits. Hence, if SUSY GUTs are correct, nucleon decay should be seen soon.

Is there a way out of this conclusion? Orbifold GUTs and string theories, see Sect. 15.1.3, contain grand unified symmetries realized in higher dimensions. In the process of compactification and GUT symmetry breaking, color triplet Higgs states are removed (projected out of the massless sector of the theory). In addition, the same projections typically rearrange the quark and lepton states so that the massless states which survive emanate from different GUT multiplets. In these models, proton decay due to dimension 5 operators can be severely suppressed or eliminated completely. However, proton decay due to dimension 6 operators may be enhanced, since the gauge bosons mediating proton decay obtain mass at the compactification scale, M_c , which is less than the 4d GUT scale (see the discussion at the end of Section 15.1.4), or suppressed, if the states of one family come from different irreducible representations. Which effect dominates is a model dependent issue. In some complete 5d orbifold GUT models [47,24] the lifetime for the decay $\tau(p \rightarrow e^+ \pi^0)$ can be near the excluded bound of 5×10^{33} years with, however, large model dependent and/or theoretical uncertainties. In other cases, the modes $p \rightarrow K^+ \bar{\nu}$ and $p \rightarrow K^0 \mu^+$ may be dominant [24]. To summarize, in either 4d or orbifold string/field theories, nucleon decay remains a premier signature for SUSY GUTs. Moreover, the observation of nucleon decay may distinguish extra-dimensional orbifold GUTs from four dimensional ones.

Before concluding the topic of baryon-number violation, consider the status of $\Delta B = 2$ neutron- anti-neutron oscillations. Generically, the leading operator for this process is the dimension-9 six-quark operator $G_{(\Delta B=2)} (u^c d^c d^c u^c d^c d^c)$, with dimensionful coefficient $G_{(\Delta B=2)} \sim 1/M^5$. The present experimental bound $\tau_{n-\bar{n}} \geq 0.86 \times 10^8$ sec. at 90% CL [48] probes only up to the scale $M \leq 10^6$ GeV. For $M \sim M_G$, $n-\bar{n}$ oscillations appear to be unobservable for any GUT (for a recent discussion see Ref. 49).

⁹ This conclusion relies on the mild assumption that the three-by-three matrices diagonalizing squark and slepton mass matrices are not so different from their fermionic partners. It has been shown that if this caveat is violated, then dimension five proton decay in minimal SUSY SU(5) may not be ruled out [45].

15.1.6. Yukawa coupling unification :

15.1.6.1. 3rd generation, b - τ or t - b - τ unification:

If quarks and leptons are two sides of the same coin, related by a new grand unified gauge symmetry, then that same symmetry relates the Yukawa couplings (and hence the masses) of quarks and leptons. In SU(5), there are two independent renormalizable Yukawa interactions given by $\lambda_t (\mathbf{10} \mathbf{10} \mathbf{5}_H) + \lambda (\mathbf{10} \mathbf{5} \mathbf{5}_H)$. These contain the SM interactions $\lambda_t (\mathbf{Q} \mathbf{u}^c \mathbf{H}_u) + \lambda (\mathbf{Q} \mathbf{d}^c \mathbf{H}_d + \mathbf{e}^c \mathbf{L} \mathbf{H}_d)$. Hence, at the GUT scale, we have the tree-level relation, $\lambda_b = \lambda_\tau \equiv \lambda$ [35]. In SO(10), there is only one independent renormalizable Yukawa interaction given by $\lambda (\mathbf{16} \mathbf{16} \mathbf{10}_H)$, which gives the tree-level relation, $\lambda_t = \lambda_b = \lambda_\tau \equiv \lambda$ [50,51]. Note, in the discussion above, we assume the minimal Higgs content, with Higgs in $\mathbf{5}$, $\mathbf{5}$ for SU(5) and $\mathbf{10}$ for SO(10). With Higgs in higher-dimensional representations, there are more possible Yukawa couplings. [58–60]

In order to make contact with the data, one now renormalizes the top, bottom, and τ Yukawa couplings, using two-loop-RG equations, from M_G to M_Z . One then obtains the running quark masses $m_t(M_Z) = \lambda_t(M_Z) v_u$, $m_b(M_Z) = \lambda_b(M_Z) v_d$, and $m_\tau(M_Z) = \lambda_\tau(M_Z) v_d$, where $\langle H_u^0 \rangle \equiv v_u = \sin \beta v / \sqrt{2}$, $\langle H_d^0 \rangle \equiv v_d = \cos \beta v / \sqrt{2}$, $v_u/v_d \equiv \tan \beta$, and $v \sim 246$ GeV is fixed by the Fermi constant, G_μ .

Including one-loop-threshold corrections at M_Z , and additional RG running, one finds the top, bottom, and τ -pole masses. In SUSY, b - τ unification has two possible solutions, with $\tan \beta \sim 1$ or 40–50. The small $\tan \beta$ solution is now disfavored by the LEP limit, $\tan \beta > 2.4$ [52].¹⁰ The large $\tan \beta$ limit overlaps the SO(10) symmetry relation.

When $\tan \beta$ is large, there are significant weak-scale threshold corrections to down quark and charged lepton masses, from either gluino and/or chargino loops [54]. Yukawa unification (consistent with low energy data) is only possible in a restricted region of SUSY parameter space with important consequences for SUSY searches [55].

15.1.6.2. Three families:

Simple Yukawa unification is not possible for the first two generations, of quarks and leptons. Consider the SU(5) GUT scale relation $\lambda_b = \lambda_\tau$. If extended to the first two generations, one would have $\lambda_s = \lambda_\mu$, $\lambda_d = \lambda_e$, which gives $\lambda_s/\lambda_d = \lambda_\mu/\lambda_e$. The last relation is a renormalization group invariant, and is thus satisfied at any scale. In particular, at the weak scale, one obtains $m_s/m_d = m_\mu/m_e$, which is in serious disagreement with the data, namely $m_s/m_d \sim 20$ and $m_\mu/m_e \sim 200$. An elegant solution to this problem was given by Georgi and Jarlskog [56]. Of course, a three-family model must also give the observed CKM mixing in the quark sector. Note, although there are typically many more parameters in the GUT theory above M_G , it is possible to obtain effective low-energy theories with many fewer parameters making strong predictions for quark and lepton masses.

It is important to note that grand unification alone is not sufficient to obtain predictive theories of fermion masses and mixing angles. Other ingredients are needed. In one approach additional global family symmetries are introduced (non-abelian family symmetries can significantly reduce the number of arbitrary parameters in the Yukawa matrices). These family symmetries constrain the set of effective higher dimensional fermion mass operators. In addition, sequential breaking of the family symmetry is correlated with the hierarchy of fermion masses. Three-family models exist which fit all the data, including neutrino masses and mixing [57]. In a completely separate approach for SO(10) models, the Standard Model Higgs bosons are contained in the higher dimensional Higgs representations including the $\mathbf{10}$, $\mathbf{126}$ and/or $\mathbf{120}$. Such theories have been shown to make predictions for neutrino masses and mixing angles [58–60].

¹⁰ However, this bound disappears if one takes $M_{SUSY} = 2$ TeV and $m_t = 180$ GeV [53].

15.1.7. Neutrino Masses :

Atmospheric and solar neutrino oscillations require neutrino masses. Adding three “sterile” neutrinos ν^c with the Yukawa coupling $\lambda_\nu (\nu^c \mathbf{L} \mathbf{H}_u)$, one easily obtains three massive Dirac neutrinos with mass $m_\nu = \lambda_\nu v_u$.¹¹ However, in order to obtain a tau neutrino with mass of order 0.1 eV, one needs $\lambda_{\nu\tau}/\lambda_\tau \leq 10^{-10}$. The see-saw mechanism, on the other hand, can naturally explain such small neutrino masses [61,62]. Since ν^c has no SM quantum numbers, there is no symmetry (other than global lepton number) which prevents the mass term $\frac{1}{2} \nu^c M \nu^c$. Moreover, one might expect $M \sim M_G$. Heavy “sterile” neutrinos can be integrated out of the theory, defining an effective low-energy theory with only light active Majorana neutrinos, with the effective dimension-5 operator $\frac{1}{2} (\mathbf{L} \mathbf{H}_u) \lambda_\nu^T M^{-1} \lambda_\nu (\mathbf{L} \mathbf{H}_u)$. This then leads to a 3×3 Majorana neutrino mass matrix $\mathbf{m} = m_\nu^T M^{-1} m_\nu$.

Atmospheric neutrino oscillations require neutrino masses with $\Delta m_\nu^2 \sim 3 \times 10^{-3}$ eV² with maximal mixing, in the simplest two-neutrino scenario. With hierarchical neutrino masses, $m_{\nu\tau} = \sqrt{\Delta m_\nu^2} \sim 0.055$ eV. Moreover, via the “see-saw” mechanism, $m_{\nu\tau} = m_t(m_t)^2/(3M)$. Hence, one finds $M \sim 2 \times 10^{14}$ GeV; remarkably close to the GUT scale. Note we have related the neutrino-Yukawa coupling to the top-quark-Yukawa coupling $\lambda_{\nu\tau} = \lambda_t$ at M_G , as given in SO(10) or SU(4) \times SU(2)_L \times SU(2)_R. However, at low energies they are no longer equal, and we have estimated this RG effect by $\lambda_{\nu\tau}(M_Z) \approx \lambda_t(M_Z)/\sqrt{3}$.

15.1.8. Selected Topics :

15.1.8.1. Magnetic Monopoles:

In the broken phase of a GUT, there are typically localized classical solutions carrying magnetic charge under an unbroken U(1) symmetry [63]. These magnetic monopoles with mass of order M_G/α_G are produced during the GUT phase transition in the early universe. The flux of magnetic monopoles is experimentally found to be less than $\sim 10^{-16}$ cm⁻² s⁻¹ sr⁻¹ [64]. Many more are predicted however, hence the GUT monopole problem. In fact, one of the original motivations for an inflationary universe is to solve the monopole problem by invoking an epoch of rapid inflation after the GUT phase transition [65]. This would have the effect of diluting the monopole density as long as the reheat temperature is sufficiently below M_G . Other possible solutions to the monopole problem include: sweeping them away by domain walls [66], U(1) electromagnetic symmetry breaking at high temperature [67] or GUT symmetry non-restoration [68]. Parenthetically, it was also shown that GUT monopoles can catalyze nucleon decay [69]. A significantly lower bound on the monopole flux can then be obtained by considering X-ray emission from radio pulsars due to monopole capture and the subsequent nucleon decay catalysis [70].

15.1.8.2. Baryogenesis via Leptogenesis:

Baryon-number-violating operators in SU(5) or SO(10) preserve the global symmetry $B-L$. Hence, the value of the cosmological $B-L$ density is an initial condition of the theory, and is typically assumed to be zero. On the other hand, anomalies of the electroweak symmetry violate $B+L$ while also preserving $B-L$. Hence, thermal fluctuations in the early universe, via so-called sphaleron processes, can drive $B+L$ to zero, washing out any net baryon number generated in the early universe at GUT temperatures [71].

One way out of this dilemma is to generate a net $B-L$ dynamically in the early universe. We have just seen that neutrino oscillations suggest a new scale of physics of order 10^{14} GeV. This scale is associated with heavy Majorana neutrinos with mass M . If in the early universe, the decay of the heavy neutrinos is out of equilibrium and violates both lepton number and CP , then a net lepton number may be generated. This lepton number will then be partially converted into baryon number via electroweak processes [72].

¹¹ Note, these “sterile” neutrinos are quite naturally identified with the right-handed neutrinos necessarily contained in complete families of SO(10) or Pati-Salam.

15.1.8.3. GUT symmetry breaking:

The grand unification symmetry is necessarily broken spontaneously. Scalar potentials (or superpotentials) exist whose vacua spontaneously break SU(5) and SO(10). These potentials are ad hoc (just like the Higgs potential in the SM), and, therefore it is hoped that they may be replaced with better motivated sectors. Gauge coupling unification now tests GUT-breaking sectors, since it is one of the two dominant corrections to the GUT threshold correction ϵ_3 . The other dominant correction comes from the Higgs sector and doublet-triplet splitting. This latter contribution is always positive $\epsilon_3 \propto \ln(M_T/M_G)$ (where M_T is an effective color triplet Higgs mass), while the low-energy data requires $\epsilon_3 < 0$. Hence, the GUT-breaking sector must provide a significant (of order -8%) contribution to ϵ_3 to be consistent with the Super-K bound on the proton lifetime [23,29,30,57].

In string theory (and GUTs in extra-dimensions), GUT breaking may occur due to boundary conditions in the compactified dimensions [7,10]. This is still ad hoc. The major benefits are that it does not require complicated GUT-breaking sectors.

15.1.8.4. Doublet-triplet splitting:

The Minimal Supersymmetric Standard Model has a μ problem: why is the coefficient of the bilinear Higgs term in the superpotential μ ($\mathbf{H}_u \mathbf{H}_d$) of order the weak scale when, since it violates no low-energy symmetry, it could be as large as M_G ? In a SUSY GUT, the μ problem is replaced by the problem of *doublet-triplet* splitting—giving mass of order M_G to the color triplet Higgs, and mass μ to the Higgs doublets. Several mechanisms for natural doublet-triplet splitting have been suggested, such as the sliding singlet, missing partner or missing VEV [73], and pseudo-Nambu-Goldstone boson mechanisms. Particular examples of the missing partner mechanism for SU(5) [30], the missing VEV mechanism for SO(10) [23,57], and the pseudo-Nambu-Goldstone boson mechanism for SU(6) [74], have been shown to be consistent with gauge coupling unification and proton decay. There are also several mechanisms for explaining why μ is of order the SUSY-breaking scale [75]. Finally, for a recent review of the μ problem and some suggested solutions in SUSY GUTs and string theory, see Refs. [76,9] and references therein.

Once again, in string theory (and orbifold GUTs), the act of breaking the GUT symmetry via orbifolding projects certain states out of the theory. It has been shown that it is possible to remove the color triplet Higgs while retaining the Higgs doublets in this process. Hence the doublet-triplet splitting problem is finessed. As discussed earlier (see Section 15.1.5), this has the effect of eliminating the contribution of dimension 5 operators to nucleon decay.

15.2. Conclusion

Grand unification of the strong and electroweak interactions requires that the three low energy gauge couplings unify (up to small threshold corrections) at a unique scale, M_G . Supersymmetric grand unified theories provide, by far, the most predictive and economical framework allowing for perturbative unification.

The three pillars of SUSY GUTs are:

- gauge coupling unification at $M_G \sim 3 \times 10^{16}$ GeV;
- low-energy supersymmetry [with a large SUSY desert], and
- nucleon decay.

The first prediction has already been verified (see Fig. 15.1). Perhaps the next two will soon be seen. Whether or not Yukawa couplings unify is more model dependent. Nevertheless, the “digital” 16-dimensional representation of quarks and leptons in SO(10) is very compelling, and may yet lead to an understanding of fermion masses and mixing angles.

In any event, the experimental verification of the first three pillars of SUSY GUTs would forever change our view of Nature. Moreover, the concomitant evidence for a vast SUSY desert would expose a huge lever arm for discovery. For then it would become clear that experiments probing the TeV scale could reveal physics at the GUT scale and perhaps beyond. Of course, some questions will still remain: Why do we have three families of quarks and leptons? How is the

grand unified symmetry and possible family symmetries chosen by Nature? At what scale might stringy physics become relevant? *Etc.*

References:

1. J. Pati and A. Salam, Phys. Rev. **D8**, 1240 (1973);
For more discussion on the standard charge assignments in this formalism, see A. Davidson, Phys. Rev. **D20**, 776 (1979); and R.N. Mohapatra and R.E. Marshak, Phys. Lett. **B91**, 222 (1980).
2. H. Georgi and S.L. Glashow, Phys. Rev. Lett. **32**, 438 (1974).
3. H. Georgi, Particles and Fields, *Proceedings of the APS Div. of Particles and Fields*, ed. C. Carlson, p. 575 (1975);
H. Fritzsch and P. Minkowski, Ann. Phys. **93**, 193 (1975).
4. S.M. Barr, Phys. Lett. **B112**, 219 (1982).
5. A. de Rujula *et al.*, p. 88, *5th Workshop on Grand Unification*, ed. K. Kang *et al.*, World Scientific, Singapore (1984);
See also earlier paper by Y. Achiman and B. Stech, p. 303, “New Phenomena in Lepton-Hadron Physics,” ed. D.E.C. Fries and J. Wess, Plenum, NY (1979).
6. B.R. Greene *et al.*, Nucl. Phys. **B278**, 667 (1986);
ibid., Nucl. Phys. **B292**, 606 (1987);
B.R. Greene *et al.*, Nucl. Phys. **B325**, 101 (1989).
7. P. Candelas *et al.*, Nucl. Phys. **B258**, 46 (1985);
L.J. Dixon *et al.*, Nucl. Phys. **B261**, 678 (1985);
ibid., Nucl. Phys. **B274**, 285 (1986);
L. E. Ibanez *et al.*, Phys. Lett. **B187**, 25 (1987);
ibid., Phys. Lett. **B191**, 282 (1987);
J.E. Kim *et al.*, Nucl. Phys. **B712**, 139 (2005).
8. T. Kobayashi *et al.*, Phys. Lett. **B593**, 262 (2004);
S. Forste *et al.*, Phys. Rev. **D70**, 106008 (2004);
T. Kobayashi *et al.*, Nucl. Phys. **B704**, 3 (2005);
W. Buchmuller *et al.*, Nucl. Phys. **B712**, 139 (2005).
9. E. Witten, [hep-ph/0201018];
M. Dine *et al.*, Phys. Rev. **D66**, 115001 (2002), [hep-ph/0206268].
10. Y. Kawamura, Prog. Theor. Phys. **103**, 613 (2000);
ibid., **105**, 999 (2001);
G. Altarelli *et al.*, Phys. Lett. **B5111**, 257 (2001);
L.J. Hall *et al.*, Phys. Rev. **D64**, 055003 (2001);
A. Hebecker and J. March-Russell, Nucl. Phys. **B613**, 3 (2001);
T. Asaka *et al.*, Phys. Lett. **B523**, 199 (2001);
L.J. Hall *et al.*, Phys. Rev. **D65**, 035008 (2002);
R. Dermisek and A. Mafi, Phys. Rev. **D65**, 055002 (2002);
H.D. Kim and S. Raby, JHEP **0301**, 056 (2003).
11. For a recent review see, R. Blumenhagen *et al.*, “Toward realistic intersecting D-brane models,” hep-th/0502005.
12. G. Aldazabal *et al.*, Nucl. Phys. **B452**, 3 (1995);
Z. Kakushadze and S.H.H. Tye, Phys. Rev. **D54**, 7520 (1996);
Z. Kakushadze *et al.*, Int. J. Mod. Phys. **A13**, 2551 (1998).
13. G. B. Cleaver *et al.*, Int. J. Mod. Phys. **A16**, 425 (2001),
hep-ph/9904301;
ibid., Nucl. Phys. **B593**, 471 (2001) hep-ph/9910230.
14. V. Braun *et al.*, Phys. Lett. **B618**, 252 (2005), hep-th/0501070;
ibid., JHEP **506**, 039 (2005), [hep-th/0502155].
15. E. Witten, Nucl. Phys. **B471**, 135 (1996), [hep-th/9602070].
16. H. Georgi *et al.*, Phys. Rev. Lett. **33**, 451 (1974);
See also the definition of effective field theories by S. Weinberg, Phys. Lett. **91B**, 51 (1980).
17. See talks on proposed and running nucleon decay experiments, and theoretical talks by P. Langacker, p. 131, and W.J. Marciano and A. Sirlin, p. 151, in *The Second Workshop on Grand Unification*, eds. J.P. Leveille *et al.*, Birkhäuser, Boston (1981).
18. W.J. Marciano, p. 190, *Eighth Workshop on Grand Unification*, ed. K. Wali, World Scientific Publishing Co., Singapore (1987).
19. U. Amaldi *et al.*, Phys. Lett. **B260**, 447 (1991);
J. Ellis *et al.*, Phys. Lett. **B260**, 131 (1991);
P. Langacker and M. Luo, Phys. Rev. **D44**, 817 (1991);
P. Langacker and N. Polonsky, Phys. Rev. **D47**, 4028 (1993);
M. Carena *et al.*, Nucl. Phys. **B406**, 59 (1993);
see also the review by S. Dimopoulos *et al.*, Physics Today, 25–33, October (1991).
20. S. Dimopoulos *et al.*, Phys. Rev. **D24**, 1681 (1981);
S. Dimopoulos and H. Georgi, Nucl. Phys. **B193**, 150 (1981);

- L. Ibanez and G.G. Ross, Phys. Lett. **105B**, 439 (1981);
N. Sakai, Z. Phys. **C11**, 153 (1981);
M.B. Einhorn and D.R.T. Jones, Nucl. Phys. **B196**, 475 (1982);
W.J. Marciano and G. Senjanovic, Phys. Rev. **D25**, 3092 (1982).
21. D.I. Kazakov, Lectures given at the European School on High Energy Physics, Aug.-Sept. 2000, Caramulo, Portugal [hep-ph/0012288v2].
 22. V. Lucas and S. Raby, Phys. Rev. **D54**, 2261 (1996) [hep-ph/9601303];
T. Blazek *et al.*, Phys. Rev. **D56**, 6919 (1997) [hep-ph/9611217];
G. Altarelli *et al.*, JHEP **0011**, 040 (2000) [hep-ph/0007254].
 23. R. Dermíšek *et al.*, Phys. Rev. **D63**, 035001 (2001);
K.S. Babu *et al.*, Nucl. Phys. **B566**, 33 (2000).
 24. M. L. Alciati *et al.*, JHEP **0503**, 054 (2005) [hep-ph/0501086].
 25. G. Anderson *et al.*, eConf **C960625**, SUP107 (1996) [hep-ph/9609457].
 26. R.N. Mohapatra and M.K. Parida, Phys. Rev. **D47**, 264 (1993).
 27. D.G. Lee *et al.*, Phys. Rev. **D51**, 229 (1995).
 28. S. Eidelman *et al.* [Particle Data Group], Phys. Lett. **B592**, 1 (2004).
 29. K.S. Babu and S.M. Barr, Phys. Rev. **D48**, 5354 (1993);
V. Lucas and S. Raby, Phys. Rev. **D54**, 2261 (1996);
S.M. Barr and S. Raby, Phys. Rev. Lett. **79**, 4748 (1997) and references therein.
 30. G. Altarelli *et al.*, JHEP **0011**, 040 (2000) See also earlier papers by A. Masiero *et al.*, Phys. Lett. **B115**, 380 (1982);
B. Grinstein, Nucl. Phys. **B206**, 387 (1982).
 31. K.R. Dienes *et al.*, Phys. Rev. Lett. **91**, 061601 (2003).
 32. L. J. Hall *et al.*, Phys. Rev. **D64**, 055003 (2001).
 33. N. Arkani-Hamed and S. Dimopoulos, JHEP **0506**, 073 (2005) [hep-th/0405159].
 34. G. F. Giudice and A. Romanino, Nucl. Phys. **B6999**, 65 (2004) [Erratum: *ibid.*, Nucl. Phys. **B706**, 65 (2005)] [hep-ph/0406088].
 35. M. Chanowitz *et al.*, Nucl. Phys. **B135**, 66 (1978);
For the corresponding SUSY analysis, see M. Einhorn and D.R.T. Jones, Nucl. Phys. **B196**, 475 (1982);
K. Inoue *et al.*, Prog. Theor. Phys. **67**, 1889 (1982);
L. E. Ibanez and C. Lopez, Phys. Lett. **B126**, 54 (1983);
ibid., Nucl. Phys. **B233**, 511 (1984).
 36. K. Agashe *et al.*, [hep-ph/0502222].
 37. M. Gell-Mann *et al.*, in *Supergravity*, eds. P. van Nieuwenhuizen and D.Z. Freedman, North-Holland, Amsterdam, 1979, p. 315.
 38. S. Weinberg, Phys. Rev. **D26**, 287 (1982);
N. Sakai and T. Yanagida, Nucl. Phys. **B197**, 533 (1982).
 39. G. Farrar and P. Fayet, Phys. Lett. **B76**, 575 (1978).
 40. S. Dimopoulos *et al.*, Phys. Lett. **112B**, 133 (1982);
J. Ellis *et al.*, Nucl. Phys. **B202**, 43 (1982).
 41. L.E. Ibanez and G.G. Ross, Nucl. Phys. **B368**, 3 (1992).
 42. For a recent discussion, see C.S. Aulakh *et al.*, Nucl. Phys. **B597**, 89 (2001).
 43. See talks by Matthew Earl, *NNN workshop*, Irvine, February (2000);
Y. Totsuka, *SUSY2K*, CERN, June (2000);
Y. Suzuki, *International Workshop on Neutrino Oscillations and their Origins*, Tokyo, Japan, December (2000), and *Baksan School, Baksan Valley*, Russia, April (2001), hep-ex/0110005;
K. Kobayashi [Super-Kamiokande Collaboration], "Search for nucleon decay from Super-Kamiokande," *Prepared for 27th International Cosmic Ray Conference (ICRC 2001), Hamburg, Germany, 7-15 Aug 2001*. For published results see : Y. Hayato *et al.* (Super-Kamiokande Collab.), Phys. Rev. Lett. **83**, 1529 (1999);
K. Kobayashi *et al.* [Super-Kamiokande Collaboration], [hep-ex/0502026].
 44. T. Goto and T. Nihei, Phys. Rev. **D59**, 115009 (1999) [hep-ph/9808255];
H. Murayama and A. Pierce, Phys. Rev. **D65**, 055009 (2002) hep-ph/0108104.
 45. B. Bajc *et al.*, Phys. Rev. **D66**, 075005 (2002) [hep-ph/0204311].
 46. J. L. Chkareuli and I. G. Gogoladze, Phys. Rev. **D58**, 055011 (1998) [hep-ph/9803335].
 47. L. J. Hall and Y. Nomura, Phys. Rev. **D66**, 075004 (2002);
H. D. Kim *et al.*, JHEP **0505**, 036 (2005).
 48. M. Baldoceolin *et al.*, Z. Phys. **C63**, 409 (1994).
 49. K. S. Babu and R. N. Mohapatra, Phys. Lett. **B518**, 269 (2001) [hep-ph/0108089].
 50. H. Georgi and D.V. Nanopoulos, Nucl. Phys. **B159**, 16 (1979);
J. Harvey *et al.*, Phys. Lett. **B92**, 309 (1980);
ibid., Nucl. Phys. **B199**, 223 (1982).
 51. T. Banks, Nucl. Phys. **B303**, 172 (1988);
M. Olechowski and S. Pokorski, Phys. Lett. **B214**, 393 (1988);
S. Pokorski, Nucl. Phys. (Proc. Supp.) **B13**, 606 (1990);
B. Ananthanarayan *et al.*, Phys. Rev. **D44**, 1613 (1991);
Q. Shafi and B. Ananthanarayan, ICTP Summer School lectures (1991);
S. Dimopoulos *et al.*, Phys. Rev. Lett. **68**, 1984 (1992);
ibid., Phys. Rev. **D45**, 4192 (1992);
G. Anderson *et al.*, Phys. Rev. **D47**, 3702 (1993);
B. Ananthanarayan *et al.*, Phys. Lett. **B300**, 245 (1993);
G. Anderson *et al.*, Phys. Rev. **D49**, 3660 (1994);
B. Ananthanarayan *et al.*, Phys. Rev. **D50**, 5980 (1994).
 52. LEP Higgs Working Group and ALEPH collaboration and DELPHI collaboration and L3 collaboration and OPAL Collaboration, Preliminary results, [hep-ex/0107030] (2001).
 53. M. Carena and H. E. Haber, Prog. in Part. Nucl. Phys. **50**, 63 (2003) [hep-ph/0208209].
 54. L.J. Hall *et al.*, Phys. Rev. **D50**, 7048 (1994);
M. Carena *et al.*, Nucl. Phys. **B419**, 213 (1994);
R. Rattazzi and U. Sarid, Nucl. Phys. **B501**, 297 (1997).
 55. Blazek *et al.*, Phys. Rev. Lett. **88**, 111804 (2002) [hep-ph/0107097];
ibid., Phys. Rev. **D65**, 115004 (2002) [hep-ph/0201081];
K. Tobe and J. D. Wells, Nucl. Phys. **B663**, 123 (2003) [hep-ph/0301015];
D. Auto *et al.*, JHEP **0306**, 023 (2003) [hep-ph/0302155].
 56. H. Georgi and C. Jarlskog, Phys. Lett. **B86**, 297 (1979).
 57. K.S. Babu and R.N. Mohapatra, Phys. Rev. Lett. **74**, 2418 (1995);
V. Lucas and S. Raby, Phys. Rev. **D54**, 2261 (1996);
T. Blažek *et al.*, Phys. Rev. **D56**, 6919 (1997);
R. Barbieri *et al.*, Nucl. Phys. **B493**, 3 (1997);
T. Blazek *et al.*, Phys. Rev. **D60**, 113001 (1999);
ibid., Phys. Rev. **D62**, 055001 (2000);
Q. Shafi and Z. Tavartkiladze, Phys. Lett. **B487**, 145 (2000);
C.H. Albright and S.M. Barr, Phys. Rev. Lett. **85**, 244 (2000);
K.S. Babu *et al.*, Nucl. Phys. **B566**, 33 (2000);
G. Altarelli *et al.*, Ref. 30;
Z. Berezhiani and A. Rossi, Nucl. Phys. **B594**, 113 (2001);
C. H. Albright and S. M. Barr, Phys. Rev. **D64**, 073010 (2001) [hep-ph/0104294];
R. Dermisek and S. Raby, Phys. Lett. **B622**, 327 (2005) [hep-ph/0507045].
 58. G. Lazarides *et al.*, Nucl. Phys. **B181**, 287 (1981);
T. E. Clark *et al.*, Phys. Lett. **B115**, 26 (1982);
K. S. Babu and R. N. Mohapatra, Phys. Rev. Lett. **70**, 2845 (1993) [hep-ph/9209215].
 59. B. Bajc *et al.*, Phys. Rev. Lett. **90**, 051802 (2003) [hep-ph/0210207].
 60. H. S. Goh *et al.*, Phys. Lett. **B570**, 215 (2003) [hep-ph/0303055];
ibid., Phys. Rev. **D68**, 115008 (2003) [hep-ph/0308197];
B. Dutta *et al.*, Phys. Rev. **D69**, 115014 (2004) [hep-ph/0402113];
S. Bertolini and M. Malinsky, [hep-ph/0504241];
K. S. Babu and C. Macesanu, [hep-ph/0505200].
 61. P. Minkowski, Phys. Lett. **B67**, 421 (1977).
 62. T. Yanagida, in *Proceedings of the Workshop on the Unified Theory and the Baryon Number of the Universe*, eds. O. Sawada and A. Sugamoto, KEK report No. 79-18, Tsukuba, Japan, 1979;
S. Glashow, Quarks and leptons, published in Proceedings of the Cargèse Lectures, M. Levy (ed.), Plenum Press, New York, (1980);

- M. Gell-Mann *et al.*, in *Supergravity*, ed. P. van Nieuwenhuizen *et al.*, North-Holland, Amsterdam, (1979), p. 315;
R.N. Mohapatra and G. Senjanovic, *Phys. Rev. Lett.* **44**, 912 (1980).
63. G. 't Hooft, *Nucl. Phys.* **B79**, 276 (1974);
A.M. Polyakov, *Pis'ma Zh. Eksp. Teor. Fiz.* **20**, 430 (1974) [*JETP Lett.* **20**, 194 (1974)];
For a pedagogical introduction, see S. Coleman, in *Aspects of Symmetry*, Selected Erice Lectures, Cambridge University Press, Cambridge, (1985), and P. Goddard and D. Olive, *Rep. Prog. Phys.* **41**, 1357 (1978).
64. I. De Mitri, (MACRO Collab.), *Nucl. Phys. (Proc. Suppl.)* **B95**, 82 (2001).
65. For a review, see A.D. Linde, *Particle Physics and Inflationary Cosmology*, Harwood Academic, Switzerland (1990).
66. G. R. Dvali *et al.*, *Phys. Rev. Lett.* **80**, 2281 (1998) [[hep-ph/9710301](#)].
67. P. Langacker and S. Y. Pi, *Phys. Rev. Lett.* **45**, 1 (1980).
68. G. R. Dvali *et al.*, *Phys. Rev. Lett.* **75**, 4559 (1995) [[hep-ph/9507230](#)].
69. V. Rubakov, *Nucl. Phys.* **B203**, 311 (1982), Institute of Nuclear Research Report No. P-0211, Moscow (1981), unpublished;
C. Callan, *Phys. Rev.* **D26**, 2058 (1982);
F. Wilczek, *Phys. Rev. Lett.* **48**, 1146 (1982);
See also, S. Dawson and A.N. Schellekens, *Phys. Rev.* **D27**, 2119 (1983).
70. K. Freese *et al.*, *Phys. Rev. Lett.* **51**, 1625 (1983).
71. V. A. Kuzmin *et al.*, *Phys. Lett.* **B155**, 36 (1985).
72. M. Fukugita and T. Yanagida, *Phys. Lett.* **B174**, 45 (1986);
See also the recent review by W. Buchmuller *et al.*, [hep-ph/0502169](#) and references therein.
73. S. Dimopoulos and F. Wilczek, *Proceedings Erice Summer School*, ed. A. Zichichi (1981);
K.S. Babu and S.M. Barr, *Phys. Rev.* **D50**, 3529 (1994).
74. R. Barbieri *et al.*, *Nucl. Phys.* **B391**, 487 (1993);
Z. Berezhiani *et al.*, *Nucl. Phys.* **B444**, 61 (1995);
Q. Shafi and Z. Tavartkiladze, *Phys. Lett.* **B522**, 102 (2001).
75. G.F. Giudice and A. Masiero, *Phys. Lett.* **B206**, 480 (1988);
J.E. Kim and H.P. Nilles, *Mod. Phys. Lett.* **A9**, 3575 (1994).
76. L. Randall and C. Csaki, [hep-ph/9508208](#).

16. STRUCTURE FUNCTIONS

Updated September 2007 by B. Foster (University of Oxford), A.D. Martin (University of Durham), and M.G. Vinster (Carleton University).

16.1. Deep inelastic scattering

High-energy lepton-nucleon scattering (deep inelastic scattering) plays a key role in determining the partonic structure of the proton. The process $\ell N \rightarrow \ell' X$ is illustrated in Fig. 16.1. The filled circle in this figure represents the internal structure of the proton which can be expressed in terms of structure functions.

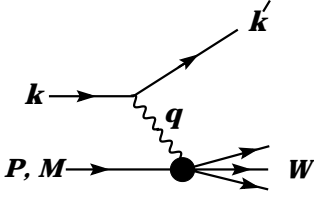


Figure 16.1: Kinematic quantities for the description of deep inelastic scattering. The quantities k and k' are the four-momenta of the incoming and outgoing leptons, P is the four-momentum of a nucleon with mass M , and W is the mass of the recoiling system X . The exchanged particle is a γ , W^\pm , or Z ; it transfers four-momentum $q = k - k'$ to the nucleon.

Invariant quantities:

$\nu = \frac{q \cdot P}{M} = E - E'$ is the lepton's energy loss in the nucleon rest frame (in earlier literature sometimes $\nu = q \cdot P$). Here, E and E' are the initial and final lepton energies in the nucleon rest frame.

$Q^2 = -q^2 = 2(E E' - \vec{k} \cdot \vec{k}') - m_\ell^2 - m_{\ell'}^2$ where $m_\ell(m_{\ell'})$ is the initial (final) lepton mass. If $E E' \sin^2(\theta/2) \gg m_\ell^2, m_{\ell'}^2$, then $\approx 4E E' \sin^2(\theta/2)$, where θ is the lepton's scattering angle with respect to the lepton beam direction.

$x = \frac{Q^2}{2M\nu}$ where, in the parton model, x is the fraction of the nucleon's momentum carried by the struck quark.

$y = \frac{q \cdot P}{k \cdot P} = \frac{\nu}{E}$ is the fraction of the lepton's energy lost in the nucleon rest frame.

$W^2 = (P + q)^2 = M^2 + 2M\nu - Q^2$ is the mass squared of the system X recoiling against the scattered lepton.

$s = (k + P)^2 = \frac{Q^2}{xy} + M^2 + m_\ell^2$ is the center-of-mass energy squared of the lepton-nucleon system.

The process in Fig. 16.1 is called deep ($Q^2 \gg M^2$) inelastic ($W^2 \gg M^2$) scattering (DIS). In what follows, the masses of the initial and scattered leptons, m_ℓ and $m_{\ell'}$, are neglected.

16.1.1. DIS cross sections :

$$\frac{d^2\sigma}{dx dy} = x(s - M^2) \frac{d^2\sigma}{dx dQ^2} = \frac{2\pi M\nu}{E'} \frac{d^2\sigma}{d\Omega_{N\text{rest}} dE'} \quad (16.1)$$

In lowest-order perturbation theory, the cross section for the scattering of polarized leptons on polarized nucleons can be expressed in terms of the products of leptonic and hadronic tensors associated with the coupling of the exchanged bosons at the upper and lower vertices in Fig. 16.1 (see Refs. 1–4)

$$\frac{d^2\sigma}{dx dy} = \frac{2\pi y \alpha^2}{Q^4} \sum_j \eta_j L_j^{\mu\nu} W_{\mu\nu}^j \quad (16.2)$$

For neutral-current processes, the summation is over $j = \gamma, Z$ and γZ representing photon and Z exchange and the interference between

them, whereas for charged-current interactions there is only W exchange, $j = W$. (For transverse nucleon polarization, there is a dependence on the azimuthal angle of the scattered lepton.) $L_{\mu\nu}$ is the lepton tensor associated with the coupling of the exchange boson to the leptons. For incoming leptons of charge $e = \pm 1$ and helicity $\lambda = \pm 1$,

$$\begin{aligned} L_{\mu\nu}^\gamma &= 2 \left(k_\mu k'_\nu + k'_\mu k_\nu - k \cdot k' g_{\mu\nu} - i\lambda \varepsilon_{\mu\nu\alpha\beta} k^\alpha k'^\beta \right), \\ L_{\mu\nu}^{\gamma Z} &= (g_V^e + e\lambda g_A^e) L_{\mu\nu}^\gamma, \quad L_{\mu\nu}^Z = (g_V^e + e\lambda g_A^e)^2 L_{\mu\nu}^\gamma, \\ L_{\mu\nu}^W &= (1 + e\lambda)^2 L_{\mu\nu}^\gamma, \end{aligned} \quad (16.3)$$

where $g_V^e = -\frac{1}{2} + 2\sin^2\theta_W$, $g_A^e = -\frac{1}{2}$.

Although here the helicity formalism is adopted, an alternative approach is to express the tensors in Eq. (16.3) in terms of the polarization of the lepton.

The factors η_j in Eq. (16.2) denote the ratios of the corresponding propagators and couplings to the photon propagator and coupling squared

$$\begin{aligned} \eta_\gamma &= 1 \quad ; \quad \eta_{\gamma Z} = \left(\frac{G_F M_Z^2}{2\sqrt{2}\pi\alpha} \right) \left(\frac{Q^2}{Q^2 + M_Z^2} \right); \\ \eta_Z &= \eta_{\gamma Z}^2 \quad ; \quad \eta_W = \frac{1}{2} \left(\frac{G_F M_W^2}{4\pi\alpha} \frac{Q^2}{Q^2 + M_W^2} \right)^2. \end{aligned} \quad (16.4)$$

The hadronic tensor, which describes the interaction of the appropriate electroweak currents with the target nucleon, is given by

$$W_{\mu\nu} = \frac{1}{4\pi} \int d^4z e^{iq \cdot z} \langle P, S | [J_\mu^\dagger(z), J_\nu(0)] | P, S \rangle, \quad (16.5)$$

where S denotes the nucleon-spin 4-vector, with $S^2 = -M^2$ and $S \cdot P = 0$.

16.2. Structure functions of the proton

The structure functions are defined in terms of the hadronic tensor (see Refs. 1–3)

$$\begin{aligned} W_{\mu\nu} &= \left(-g_{\mu\nu} + \frac{q_\mu q_\nu}{q^2} \right) F_1(x, Q^2) + \frac{\hat{P}_\mu \hat{P}_\nu}{P \cdot q} F_2(x, Q^2) \\ &\quad - i\varepsilon_{\mu\nu\alpha\beta} \frac{q^\alpha P^\beta}{2P \cdot q} F_3(x, Q^2) \\ &\quad + i\varepsilon_{\mu\nu\alpha\beta} \frac{q^\alpha}{P \cdot q} \left[S^\beta g_1(x, Q^2) + \left(S^\beta - \frac{S \cdot q}{P \cdot q} P^\beta \right) g_2(x, Q^2) \right] \\ &\quad + \frac{1}{P \cdot q} \left[\frac{1}{2} (\hat{P}_\mu \hat{S}_\nu + \hat{S}_\mu \hat{P}_\nu) - \frac{S \cdot q}{P \cdot q} \hat{P}_\mu \hat{P}_\nu \right] g_3(x, Q^2) \\ &\quad + \frac{S \cdot q}{P \cdot q} \left[\frac{\hat{P}_\mu \hat{P}_\nu}{P \cdot q} g_4(x, Q^2) + \left(-g_{\mu\nu} + \frac{q_\mu q_\nu}{q^2} \right) g_5(x, Q^2) \right] \end{aligned} \quad (16.6)$$

where

$$\hat{P}_\mu = P_\mu - \frac{P \cdot q}{q^2} q_\mu, \quad \hat{S}_\mu = S_\mu - \frac{S \cdot q}{q^2} q_\mu \quad (16.7)$$

In Ref. [2], the definition of $W_{\mu\nu}$ with $\mu \leftrightarrow \nu$ is adopted, which changes the sign of the $\varepsilon_{\mu\nu\alpha\beta}$ terms in Eq. (16.6), although the formulae given here below are unchanged. Ref. [1] tabulates the relation between the structure functions defined in Eq. (16.6) and other choices available in the literature.

The cross sections for neutral- and charged-current deep inelastic scattering on unpolarized nucleons can be written in terms of the structure functions in the generic form

$$\begin{aligned} \frac{d^2\sigma^i}{dx dy} &= \frac{4\pi\alpha^2}{xyQ^2} \eta^i \left\{ \left(1 - y - \frac{x^2 y^2 M^2}{Q^2} \right) F_2^i \right. \\ &\quad \left. + y^2 x F_1^i \mp \left(y - \frac{y^2}{2} \right) x F_3^i \right\}, \end{aligned} \quad (16.8)$$

where $i = \text{NC}, \text{CC}$ corresponds to neutral-current ($eN \rightarrow eX$) or charged-current ($eN \rightarrow \nu X$ or $\nu N \rightarrow eX$) processes, respectively. For incoming neutrinos, $L_{\mu\nu}^W$ of Eq. (16.3) is still true, but with e, λ corresponding to the outgoing charged lepton. In the last term of Eq. (16.8), the $-$ sign is taken for an incoming e^+ or $\bar{\nu}$ and the $+$ sign for an incoming e^- or ν . The factor $\eta^{\text{NC}} = 1$ for unpolarized e^\pm beams, whereas*

$$\eta^{\text{CC}} = (1 \pm \lambda)^2 \eta_W \quad (16.9)$$

with \pm for ℓ^\pm ; and where λ is the helicity of the incoming lepton and η_W is defined in Eq. (16.4); for incoming neutrinos $\eta^{\text{CC}} = 4\eta_W$. The CC structure functions, which derive exclusively from W exchange, are

$$F_1^{\text{CC}} = F_1^W, \quad F_2^{\text{CC}} = F_2^W, \quad xF_3^{\text{CC}} = xF_3^W. \quad (16.10)$$

The NC structure functions $F_2^\gamma, F_2^{\gamma Z}, F_2^Z$ are, for $e^\pm N \rightarrow e^\pm X$, given by Ref. [5],

$$F_2^{\text{NC}} = F_2^\gamma - (g_V^e \pm \lambda g_A^e) \eta_{\gamma Z} F_2^{\gamma Z} + (g_V^e \pm \lambda g_A^e \pm 2\lambda g_V^e g_A^e) \eta_Z F_2^Z \quad (16.11)$$

and similarly for F_1^{NC} , whereas

$$xF_3^{\text{NC}} = -(g_A^e \pm \lambda g_V^e) \eta_{\gamma Z} xF_3^{\gamma Z} + [2g_V^e g_A^e \pm \lambda(g_V^e \pm g_A^e)] \eta_Z xF_3^Z. \quad (16.12)$$

The polarized cross-section difference

$$\Delta\sigma = \sigma(\lambda_n = -1, \lambda_\ell) - \sigma(\lambda_n = 1, \lambda_\ell), \quad (16.13)$$

where λ_ℓ, λ_n are the helicities (± 1) of the incoming lepton and nucleon, respectively, may be expressed in terms of the five structure functions $g_{1,\dots,5}(x, Q^2)$ of Eq. (16.6). Thus,

$$\begin{aligned} \frac{d^2 \Delta\sigma^i}{dx dy} &= \frac{8\pi\alpha^2}{xyQ^2} \eta^i \left\{ -\lambda_\ell y \left(2 - y - 2x^2 y^2 \frac{M^2}{Q^2} \right) x g_1^i + \lambda_\ell 4x^3 y^2 \frac{M^2}{Q^2} g_2^i \right. \\ &+ 2x^2 y \frac{M^2}{Q^2} \left(1 - y - x^2 y^2 \frac{M^2}{Q^2} \right) g_3^i \\ &\left. - \left(1 + 2x^2 y \frac{M^2}{Q^2} \right) \left[\left(1 - y - x^2 y^2 \frac{M^2}{Q^2} \right) g_4^i + xy^2 g_5^i \right] \right\} \quad (16.14) \end{aligned}$$

with $i = \text{NC}$ or CC as before. The Eq. (16.13) corresponds to the difference of antiparallel minus parallel spins of the incoming particles for e^- or ν initiated reactions, but parallel minus antiparallel for e^+ or $\bar{\nu}$ initiated processes. For longitudinal nucleon polarization, the contributions of g_2 and g_3 are suppressed by powers of M^2/Q^2 . These structure functions give an unsuppressed contribution to the cross section for transverse polarization [1], but in this case the cross-section difference vanishes as $M/Q \rightarrow 0$.

Because the same tensor structure occurs in the spin-dependent and spin-independent parts of the hadronic tensor of Eq. (16.6) in the $M^2/Q^2 \rightarrow 0$ limit, the differential cross-section difference of Eq. (16.14) may be obtained from the differential cross section Eq. (16.8) by replacing

$$F_1 \rightarrow -g_5, \quad F_2 \rightarrow -g_4, \quad F_3 \rightarrow 2g_1, \quad (16.15)$$

and multiplying by two, since the total cross section is the average over the initial-state polarizations. In this limit, Eq. (16.8) and Eq. (16.14) may be written in the form

$$\begin{aligned} \frac{d^2 \sigma^i}{dx dy} &= \frac{2\pi\alpha^2}{xyQ^2} \eta^i \left[Y_+ F_2^i \mp Y_- x F_3^i - y^2 F_L^i \right], \\ \frac{d^2 \Delta\sigma^i}{dx dy} &= \frac{4\pi\alpha^2}{xyQ^2} \eta^i \left[-Y_+ g_4^i \mp Y_- 2x g_1^i + y^2 g_L^i \right], \quad (16.16) \end{aligned}$$

with $i = \text{NC}$ or CC , where $Y_\pm = 1 \pm (1 - y)^2$ and

$$F_L^i = F_2^i - 2x F_1^i, \quad g_L^i = g_4^i - 2x g_5^i. \quad (16.17)$$

In the naive quark-parton model, the analogy with the Callan-Gross relations [6] $F_L^i = 0$, are the Dicus relations [7] $g_L^i = 0$. Therefore, there are only two independent polarized structure functions: g_1 (parity conserving) and g_5 (parity violating), in analogy with the unpolarized structure functions F_1 and F_3 .

16.2.1. Structure functions in the quark-parton model :

In the quark-parton model [8,9], contributions to the structure functions F^i and g^i can be expressed in terms of the quark distribution functions $q(x, Q^2)$ of the proton, where $q = u, \bar{u}, d, \bar{d}$ etc. The quantity $q(x, Q^2) dx$ is the number of quarks (or antiquarks) of designated flavor that carry a momentum fraction between x and $x + dx$ of the proton's momentum in a frame in which the proton momentum is large.

For the neutral-current processes $ep \rightarrow eX$,

$$\begin{aligned} [F_2^\gamma, F_2^{\gamma Z}, F_2^Z] &= x \sum_q [e_q^2, 2e_q g_V^q, g_V^{q2} + g_A^{q2}] (q + \bar{q}), \\ [F_3^\gamma, F_3^{\gamma Z}, F_3^Z] &= \sum_q [0, 2e_q g_A^q, 2g_V^q g_A^q] (q - \bar{q}), \\ [g_1^\gamma, g_1^{\gamma Z}, g_1^Z] &= \frac{1}{2} \sum_q [e_q^2, 2e_q g_V^q, g_V^{q2} + g_A^{q2}] (\Delta q + \Delta \bar{q}), \\ [g_5^\gamma, g_5^{\gamma Z}, g_5^Z] &= \sum_q [0, e_q g_A^q, g_V^q g_A^q] (\Delta q - \Delta \bar{q}), \quad (16.18) \end{aligned}$$

where $g_V^q = \pm \frac{1}{2} - 2e_q \sin^2 \theta_W$ and $g_A^q = \pm \frac{1}{2}$, with \pm according to whether q is a u - or d -type quark respectively. The quantity Δq is the difference $q \uparrow - q \downarrow$ of the distributions with the quark spin parallel and antiparallel to the proton spin.

For the charged-current processes $e^- p \rightarrow \nu X$ and $\bar{\nu} p \rightarrow e^+ X$, the structure functions are:

$$\begin{aligned} F_2^{W^-} &= 2x(u + \bar{d} + \bar{s} + c \dots), \\ F_3^{W^-} &= 2(u - \bar{d} - \bar{s} + c \dots), \\ g_1^{W^-} &= (\Delta u + \Delta \bar{d} + \Delta \bar{s} + \Delta c \dots), \\ g_5^{W^-} &= (-\Delta u + \Delta \bar{d} + \Delta \bar{s} - \Delta c \dots), \quad (16.19) \end{aligned}$$

where only the active flavors are to be kept and where CKM mixing has been neglected. For $e^+ p \rightarrow \bar{\nu} X$ and $\nu p \rightarrow e^- X$, the structure functions F^{W^+}, g^{W^+} are obtained by the flavor interchanges $d \leftrightarrow u, s \leftrightarrow c$ in the expressions for F^{W^-}, g^{W^-} . The structure functions for scattering on a neutron are obtained from those of the proton by the interchange $u \leftrightarrow d$. For both the neutral- and charged-current processes, the quark-parton model predicts $2xF_1^i = F_2^i$ and $g_4^i = 2xg_5^i$.

Neglecting masses, the structure functions g_2 and g_3 contribute only to scattering from transversely polarized nucleons (for which $S \cdot q = 0$), and have no simple interpretation in terms of the quark-parton model. They arise from off-diagonal matrix elements $\langle P, \lambda' | [J_\mu^\dagger(z), J_\nu(0)] | P, \lambda \rangle$, where the proton helicities satisfy $\lambda' \neq \lambda$. In fact, the leading-twist contributions to both g_2 and g_3 are both twist-2 and twist-3, which contribute at the same order of Q^2 . The Wandzura-Wilczek relation [10] expresses the twist-2 part of g_2 in terms of g_1 as

$$g_2^i(x) = -g_1^i(x) + \int_x^1 \frac{dy}{y} g_1^i(y). \quad (16.20)$$

However, the twist-3 component of g_2 is unknown. Similarly, there is a relation expressing the twist-2 part of g_3 in terms of g_4 . A complete set of relations, including M^2/Q^2 effects, can be found in Ref. [11].

16.2.2. Structure functions and QCD :

One of the most striking predictions of the quark-parton model is that the structure functions F_i, g_i scale, i.e., $F_i(x, Q^2) \rightarrow F_i(x)$ in the Bjorken limit that Q^2 and $\nu \rightarrow \infty$ with x fixed [12]. This property is related to the assumption that the transverse momentum of the partons in the infinite-momentum frame of the proton is small. In QCD, however, the radiation of hard gluons from the quarks violates this assumption, leading to logarithmic scaling violations, which are particularly large at small x , see Fig. 16.2. The radiation of gluons produces the evolution of the structure functions. As Q^2 increases, more and more gluons are radiated, which in turn split into $q\bar{q}$ pairs. This process leads both to the softening of the initial quark momentum distributions and to the growth of the gluon density and the $q\bar{q}$ sea as x decreases.

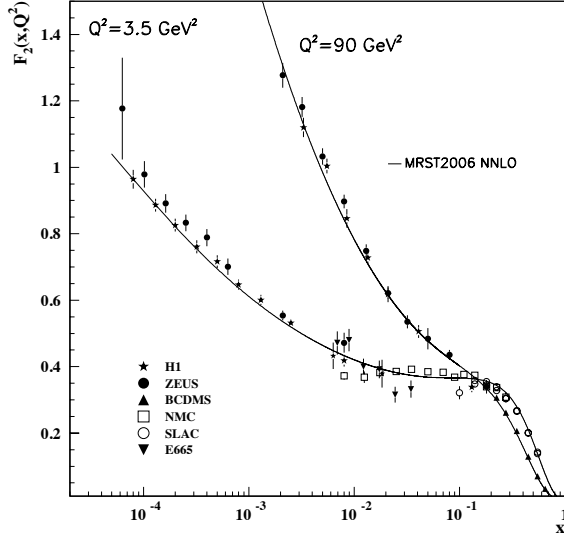


Figure 16.2: The proton structure function F_2^p given at two Q^2 values (3.5 GeV^2 and 90 GeV^2), which exhibit scaling at the ‘pivot’ point $x \sim 0.14$. See the captions in Fig. 16.7 and Fig. 16.10 for the references of the data. Also shown is the MRST2006 parameterization [13] given at the same scales.

In QCD, the above process is described in terms of scale-dependent parton distributions $f_a(x, \mu^2)$, where $a = g$ or q and, typically, μ is the scale of the probe Q . For $Q^2 \gg M^2$, the structure functions are of the form

$$F_i = \sum_a C_i^a \otimes f_a, \quad (16.21)$$

where \otimes denotes the convolution integral

$$C \otimes f = \int_x^1 \frac{dy}{y} C(y) f\left(\frac{x}{y}\right), \quad (16.22)$$

and where the coefficient functions C_i^a are given as a power series in α_s . The parton distribution f_a corresponds, at a given x , to the density of parton a in the proton integrated over transverse momentum k_t up to μ . Its evolution in μ is described in QCD by a DGLAP equation (see Refs. 14–17) which has the schematic form

$$\frac{\partial f_a}{\partial \ln \mu^2} \sim \frac{\alpha_s(\mu^2)}{2\pi} \sum_b (P_{ab} \otimes f_b), \quad (16.23)$$

where the P_{ab} , which describe the parton splitting $b \rightarrow a$, are also given as a power series in α_s . Although perturbative QCD can predict, via Eq. (16.23), the evolution of the parton distribution functions from a particular scale, μ_0 , these DGLAP equations cannot predict them *a priori* at any particular μ_0 . Thus they must be measured at a starting point μ_0 before the predictions of QCD can be compared to the data at other scales, μ . In general, all observables involving a hard hadronic interaction (such as structure functions) can be expressed as a convolution of calculable, process-dependent coefficient functions and these universal parton distributions, e.g. Eq. (16.21).

It is often convenient to write the evolution equations in terms of the gluon, non-singlet (q^{NS}) and singlet (q^S) quark distributions, such that

$$q^{NS} = q_i - \bar{q}_i \quad (\text{or } q_i - q_j), \quad q^S = \sum_i (q_i + \bar{q}_i). \quad (16.24)$$

The non-singlet distributions have non-zero values of flavor quantum numbers, such as isospin and baryon number. The DGLAP evolution equations then take the form

$$\begin{aligned} \frac{\partial q^{NS}}{\partial \ln \mu^2} &= \frac{\alpha_s(\mu^2)}{2\pi} P_{qq} \otimes q^{NS}, \\ \frac{\partial}{\partial \ln \mu^2} \begin{pmatrix} q^S \\ g \end{pmatrix} &= \frac{\alpha_s(\mu^2)}{2\pi} \begin{pmatrix} P_{qq} & 2n_f P_{qg} \\ P_{gq} & P_{gg} \end{pmatrix} \otimes \begin{pmatrix} q^S \\ g \end{pmatrix}, \end{aligned} \quad (16.25)$$

where P are splitting functions that describe the probability of a given parton splitting into two others, and n_f is the number of (active) quark flavors. The leading-order Altarelli-Parisi [16] splitting functions are

$$P_{qq} = \frac{4}{3} \left[\frac{1+x^2}{(1-x)} \right]_+ = \frac{4}{3} \left[\frac{1+x^2}{(1-x)_+} \right] + 2\delta(1-x), \quad (16.26)$$

$$P_{qg} = \frac{1}{2} \left[x^2 + (1-x)^2 \right], \quad (16.27)$$

$$P_{gq} = \frac{4}{3} \left[\frac{1+(1-x)^2}{x} \right], \quad (16.28)$$

$$\begin{aligned} P_{gg} &= 6 \left[\frac{1-x}{x} + x(1-x) + \frac{x}{(1-x)_+} \right] \\ &+ \left[\frac{11}{2} - \frac{n_f}{3} \right] \delta(1-x), \end{aligned} \quad (16.29)$$

where the notation $[F(x)]_+$ defines a distribution such that for any sufficiently regular test function, $f(x)$,

$$\int_0^1 dx f(x) [F(x)]_+ = \int_0^1 dx (f(x) - f(1)) F(x). \quad (16.30)$$

In general, the splitting functions can be expressed as a power series in α_s . The series contains both terms proportional to $\ln \mu^2$ and to $\ln 1/x$. The leading-order DGLAP evolution sums up the $(\alpha_s \ln \mu^2)^n$ contributions, while at next-to-leading order (NLO) the sum over the $\alpha_s (\alpha_s \ln \mu^2)^{n-1}$ terms is included [18,19]. In fact, the NNLO contributions to the splitting functions and the DIS coefficient functions are now also all known [20–22].

In the kinematic region of very small x , it is essential to sum leading terms in $\ln 1/x$, independent of the value of $\ln \mu^2$. At leading order, LLx, this is done by the BFKL equation for the unintegrated distributions (see Refs. [23,24]). The leading-order $(\alpha_s \ln(1/x))^n$ terms result in a power-like growth, $x^{-\omega}$ with $\omega = (12\alpha_s \ln 2)/\pi$, at asymptotic values of $\ln 1/x$. More recently, the next-to-leading $\ln 1/x$ (NLLx) contributions have become available [25,26]. They are so large (and negative) that the result appears to be perturbatively unstable. Methods, based on a combination of collinear and small x resummations, have been developed which reorganize the perturbative series into a more stable hierarchy [27–29]. These studies show that the asymptotic properties of the small x resummations are not significant at today’s energies (which sample $x \gtrsim 10^{-4}$), and that in this domain NNLO DGLAP is a good approximation. Indeed, as yet, there is no firm evidence for any deviation from standard DGLAP evolution in the data for $Q^2 \gtrsim 2 \text{ GeV}^2$. Nor is there any convincing indication that we have entered the ‘non-linear’ regime where the gluon density is so high that gluon-gluon recombination effects become significant.

The precision of the contemporary experimental data demands that at least NLO, and preferably NNLO, DGLAP evolution be used in comparisons between QCD theory and experiment. Beyond the leading order, it is necessary to specify, and to use consistently, both a renormalization and a factorization scheme. Whereas the renormalization scheme used is almost universally the modified minimal subtraction ($\overline{\text{MS}}$) scheme [30,31], there are two popular choices for factorization scheme, in which the form of the correction for each structure function is different. The two most-used factorization schemes are: DIS [32], in which there are no higher-order corrections to the F_2 structure function, and $\overline{\text{MS}}$ [33]. They differ in how the non-divergent pieces are assimilated in the parton distribution functions.

It is usually assumed that the quarks are massless. The effects of the c and b -quark masses have been studied up to NNLO, for example, in Refs. 34–39. An approach using a variable flavor number is now generally adopted, in which evolution with $n_f = 3$ is matched to that with $n_f = 4$ at the charm threshold, with an analogous matching at the bottom threshold.

The discussion above relates to the Q^2 behavior of leading-twist (twist-2) contributions to the structure functions. Higher-twist terms, which involve their own non-perturbative input, exist. These die off

as powers of Q ; specifically twist- n terms are damped by $1/Q^{n-2}$. The higher-twist terms appear to be numerically unimportant for Q^2 above a few GeV^2 , except for x close to 1.

Table 16.1: Lepton-nucleon and related hard-scattering processes and their primary sensitivity to the parton distributions that are probed.

Process	Main Subprocess	PDFs Probed
$\ell^\pm N \rightarrow \ell^\pm X$	$\gamma^* q \rightarrow q$	$g(x \lesssim 0.01), q, \bar{q}$
$\ell^+(\ell^-)N \rightarrow \bar{\nu}(\nu)X$	$W^* q \rightarrow q'$	
$\nu(\bar{\nu})N \rightarrow \ell^-(\ell^+)X$	$W^* q \rightarrow q'$	
$\nu N \rightarrow \mu^+ \mu^- X$	$W^* s \rightarrow c \rightarrow \mu^+$	s
$\ell N \rightarrow \ell Q X$	$\gamma^* Q \rightarrow Q$	$Q = c, b$
	$\gamma^* g \rightarrow Q\bar{Q}$	$g(x \lesssim 0.01)$
$pp \rightarrow \gamma X$	$qg \rightarrow \gamma q$	g
$pN \rightarrow \mu^+ \mu^- X$	$q\bar{q} \rightarrow \gamma^*$	\bar{q}
$pp, pn \rightarrow \mu^+ \mu^- X$	$u\bar{u}, d\bar{d} \rightarrow \gamma^*$	$\bar{u} - \bar{d}$
	$u\bar{d}, d\bar{u} \rightarrow \gamma^*$	
$ep, en \rightarrow e\pi X$	$\gamma^* q \rightarrow q$	
$p\bar{p} \rightarrow W \rightarrow \ell^\pm X$	$ud \rightarrow W$	$u, d, u/d$
$p\bar{p} \rightarrow \text{jet} + X$	$gg, qg, qq \rightarrow 2j$	$q, g(0.01 \lesssim x \lesssim 0.5)$

16.3. Determination of parton distributions

The parton distribution functions (PDFs) can be determined from data for deep inelastic lepton-nucleon scattering and for related hard-scattering processes initiated by nucleons. Table 16.1 (based on Ref. [40]) highlights some processes and their primary sensitivity to PDFs.

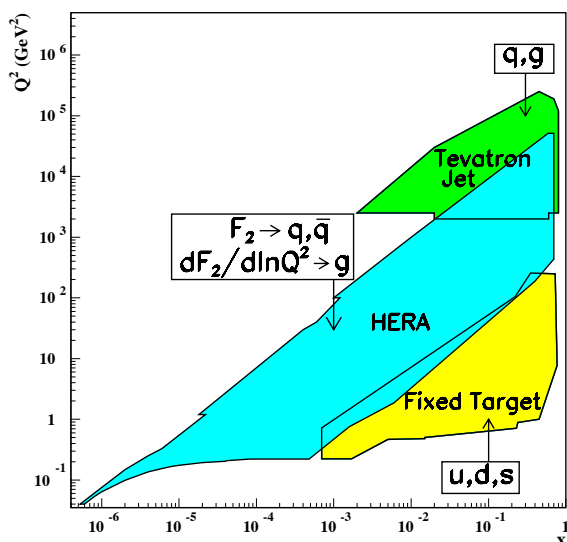


Figure 16.3: Kinematic domains in x and Q^2 probed by fixed-target and collider experiments, shown together with the important constraints they make on the various parton distributions. Color version at end of book.

The kinematic ranges of fixed-target and collider experiments are complementary (as is shown in Fig. 16.3), which enables the determination of PDFs over a wide range in x and Q^2 . Recent determinations of the unpolarized PDFs from NLO global analyses are given in Ref. [41,42], and at NNLO in Ref. [13] (see also Refs. [43,44]). Recent studies of the uncertainties in the PDFs and

observables can be found in Refs. [45,46] and Refs. [47,48] (see also Ref. [49]). The results of one analysis are shown in Fig. 16.4 at scales $\mu^2 = 20$ and 10^4 GeV^2 . The polarized PDFs are obtained through NLO global analyses of measurements of the g_1 structure function in inclusive polarized deep inelastic scattering (for recent examples see Refs. 50–52). The inclusive data do not provide enough observables to determine all polarized PDFs. These polarized PDFs may be fully accessed via flavor tagging in semi-inclusive deep inelastic scattering. Fig. 16.5 shows several global analyses at a scale of 2.5 GeV^2 along with the data from semi-inclusive DIS.

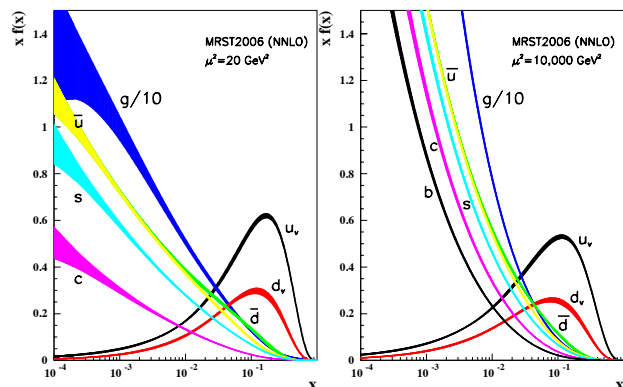


Figure 16.4: Distributions of x times the unpolarized parton distributions $f(x)$ (where $f = u_v, d_v, \bar{u}, \bar{d}, s, c, b, g$) and their associated uncertainties using the NNLO MRST2006 parameterization [13] at a scale $\mu^2 = 20 \text{ GeV}^2$ and $\mu^2 = 10,000 \text{ GeV}^2$. Color version at end of book.

Comprehensive sets of PDFs available as program-callable functions can be obtained from several sources *e.g.*, Refs. [55,56]. As a result of a Les Houches Accord, a PDF package (LHAPDF) exists [57] which facilitates the inclusion of recent PDFs in Monte Carlo/Matrix Element programs in a very compact and efficient format.

16.4. DIS determinations of α_s

Table 16.2 shows the values of $\alpha_s(M_Z^2)$ found in recent fits to DIS and related data in which the coupling is left as a free parameter. There have been several other studies of α_s using subsets of inclusive DIS data, and also from measurements of spin-dependent structure functions, see the Quantum Chromodynamics section of this *Review*.

Table 16.2: The values of $\alpha_s(M_Z^2)$ found in NLO and NNLO fits to DIS and related data. CTEQ [58] and MRST06 [13] are global fits. H1 [59] fit only a subset of the F_2^{ep} data, while Alekhin [43] also includes F_2^{pd} and ZEUS [60] in addition include their charged current and jet data. At NNLO, Alekhin *et al.* [44] include Drell-Yan data in their fit. The experimental errors quoted correspond to different choices of the effective increase $\Delta\chi^2$ from the best fit value of χ^2 .

	$\Delta\chi^2$	$\alpha_s(M_Z^2) \pm \text{expt} \pm \text{theory} \pm \text{model}$
NLO		
CTEQ	100	0.1170 ± 0.0047
ZEUS	50	$0.1183 \pm 0.0028 \pm 0.0008$
MRST06	20	$0.1212 \pm 0.002 \pm 0.003$
H1	1	$0.115 \pm 0.0017 \pm 0.005 \pm 0.0009 \pm 0.0005$
Alekhin	1	$0.1171 \pm 0.0015 \pm 0.0033$
NNLO		
MRST06	20	$0.1191 \pm 0.002 \pm 0.003$
Alekhin	1	0.1128 ± 0.0015

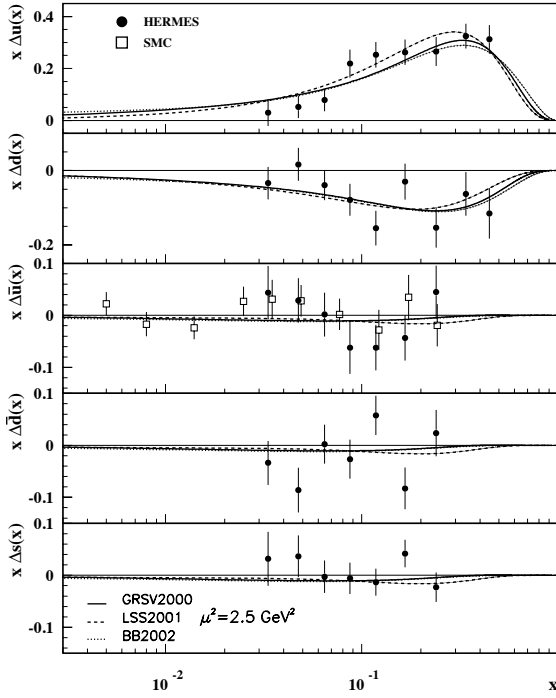


Figure 16.5: Distributions of x times the polarized parton distributions $\Delta q(x)$ (where $q = u, d, \bar{u}, \bar{d}, s$) using the GRSV2000 [50], LSS2001 [51], and BB2002 [52] parameterizations at a scale $\mu^2 = 2.5 \text{ GeV}^2$. Points represent data from semi-inclusive positron (HERMES [53]) and muon (SMC [54]) deep inelastic scattering given at $Q^2 = 2.5 \text{ GeV}^2$. SMC results are extracted under the assumption that $\Delta\bar{u}(x) = \Delta\bar{d}(x)$.

16.5. The hadronic structure of the photon

Besides the *direct* interactions of the photon, it is possible for it to fluctuate into a hadronic state via the process $\gamma \rightarrow q\bar{q}$. While in this state, the partonic content of the photon may be *resolved*, for example, through the process $e^+e^- \rightarrow e^+e^-\gamma^* \rightarrow e^+e^-X$, where the virtual photon emitted by the DIS lepton probes the hadronic structure of the quasi-real photon emitted by the other lepton. The perturbative LO contributions, $\gamma \rightarrow q\bar{q}$ followed by $\gamma^*q \rightarrow q$, are subject to QCD corrections due to the coupling of quarks to gluons.

Often the equivalent-photon approximation is used to express the differential cross section for deep inelastic electron–photon scattering in terms of the structure functions of the transverse quasi-real photon times a flux factor N_γ^T (for these incoming quasi-real photons of transverse polarization)

$$\frac{d^2\sigma}{dx dQ^2} = N_\gamma^T \frac{2\pi\alpha^2}{xQ^4} \left[\left(1 + (1-y)^2\right) F_2^\gamma(x, Q^2) - y^2 F_L^\gamma(x, Q^2) \right],$$

where we have used $F_2^\gamma = 2xF_T^\gamma + F_L^\gamma$. Complete formulae are given, for example, in the comprehensive review of Ref. [61].

The hadronic photon structure function, F_2^γ , evolves with increasing Q^2 from the ‘hadron-like’ behavior, calculable via the vector-meson-dominance model, to the dominating ‘point-like’ behaviour, calculable in perturbative QCD. Due to the point-like coupling, the logarithmic evolution of F_2^γ with Q^2 has a *positive* slope for all values of x , see Fig. 16.14. The ‘loss’ of quarks at large x due to gluon radiation is over-compensated by the ‘creation’ of quarks via the point-like $\gamma \rightarrow q\bar{q}$ coupling. The logarithmic evolution was first predicted in the quark–parton model ($\gamma^*\gamma \rightarrow q\bar{q}$) [62,63], and then in QCD in the limit of large Q^2 [64]. The evolution is now known to NLO (Refs. 65–67). Recent NLO data analyses to determine the parton densities of the photon can be found in Refs. 68–70.

16.6. Diffractive DIS (DDIS)

Some 10% of DIS events are diffractive, $\gamma^*p \rightarrow X + p$, in which the slightly deflected proton and the cluster X of outgoing hadrons are well-separated in rapidity. Besides x and Q^2 , two extra variables are needed to describe a DDIS event: the fraction x_{IP} of the proton’s momentum transferred across the rapidity gap and t , the square of the 4-momentum transfer of the proton. The DDIS data (see Refs. 71–74) are usually analyzed using two levels of factorization. First, the diffractive structure function F_2^D satisfies *collinear factorization*, and can be expressed as the convolution [75]

$$F_2^D = \sum_{a=q,g} C_2^a \otimes f_{a/p}^D, \quad (16.31)$$

with the same coefficient functions as in DIS (see Eq. (16.21)), and where the diffractive parton distributions $f_{a/p}^D$ ($a = q, g$) satisfy DGLAP evolution. Second, *Regge factorization* is assumed [76],

$$f_{a/p}^D(x_{IP}, t, z, \mu^2) = f_{IP/p}(x_{IP}, t) f_{a/IP}(z, \mu^2), \quad (16.32)$$

where $f_{a/IP}$ are the parton densities of the Pomeron, which itself is treated like a hadron, and $z \in [x/x_{IP}, 1]$ is the fraction of the Pomeron’s momentum carried by the parton entering the hard subprocess. The Pomeron flux factor $f_{IP/p}(x_{IP}, t)$ is taken from Regge phenomenology. There are also secondary Reggeon contributions to Eq. (16.32). A sample of the t -integrated diffractive parton densities, obtained in this way, is shown in Fig. 16.6 as Fit A.

Although collinear factorization holds as $\mu^2 \rightarrow \infty$, there are non-negligible corrections for finite μ^2 and small x_{IP} . Besides the *resolved* interactions of the Pomeron, the perturbative QCD Pomeron may also interact *directly* with the hard subprocess, giving rise to an inhomogeneous evolution equation for the diffractive parton densities analogous to the photon case. The results of the MRW analysis [77], which includes these contributions, are also shown in Fig. 16.6. Unlike the inclusive case, the diffractive parton densities cannot be directly used to calculate diffractive hadron–hadron cross sections, since account must first be taken of ‘soft’ rescattering effects.

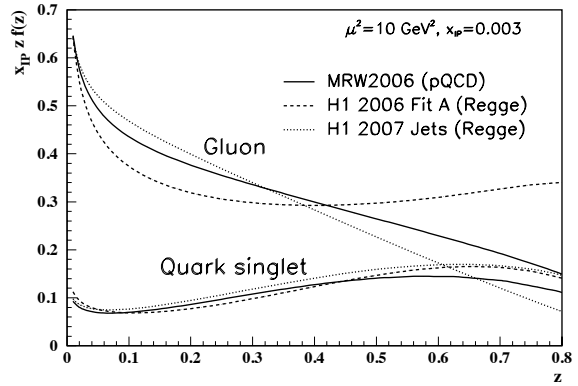


Figure 16.6: Diffractive parton distributions, $x_{IP} z f_{a/p}^D$, obtained from fitting to the H1 data with $Q^2 > 8.5 \text{ GeV}^2$ assuming Regge factorization [74], and using a more perturbative QCD approach [77]. Only the Pomeron contributions are shown and not the secondary Reggeon contributions which are negligible at the value of $x_{IP} = 0.003$ chosen here. Diffractive DIS dijet data [78,79,80] favour a smaller gluon at high z than that in H1 Fit A, more like MRW, as shown by the H1 Jets curve [79].

* The value of η^{CC} deduced from Ref. [1] is found to be a factor of two too small; η^{CC} of Eq. (16.9) agrees with Refs. [2,3].

References:

1. J. Blümlein and N. Kochelev, Nucl. Phys. **B498**, 285 (1997).
2. S. Forte *et al.*, Nucl. Phys. **B602**, 585 (2001).
3. M. Anselmino *et al.*, Z. Phys. **C64**, 267 (1994).
4. M. Anselmino *et al.*, Phys. Rep. **261**, 1 (1995).
5. M. Klein and T. Riemann, Z. Phys. **C24**, 151 (1984).
6. C.G. Callan and D.J. Gross, Phys. Rev. Lett. **22**, 156 (1969).
7. D.A. Dicus, Phys. Rev. **D5**, 1367 (1972).
8. J.D. Bjorken and E.A. Paschos, Phys. Rev. **185**, 1975 (1969).
9. R.P. Feynman, Photon Hadron Interactions (Benjamin, New York, 1972).
10. S. Wandzura and F. Wilczek, Phys. Rev. **B72**, 195 (1977).
11. J. Blümlein and A. Tkabladze, Nucl. Phys. **B553**, 427 (1999).
12. J.D. Bjorken, Phys. Rev. **179**, 1547 (1969).
13. A.D. Martin *et al.*, Phys. Lett. **B652**, 292 (2007).
14. V.N. Gribov and L.N. Lipatov, Sov. J. Nucl. Phys. **15**, 438 (1972).
15. L.N. Lipatov, Sov. J. Nucl. Phys. **20**, 95 (1975).
16. G. Altarelli and G. Parisi, Nucl. Phys. **B126**, 298 (1977).
17. Yu.L. Dokshitzer, Sov. Phys. JETP **46**, 641 (1977).
18. G. Curci *et al.*, Nucl. Phys. **B175**, 27 (1980); W. Furmanski, and R. Petronzio, Phys. Lett. **B97**, 437 (1980).
19. R.K. Ellis *et al.*, QCD and Collider Physics (Cambridge UP, 1996).
20. E.B. Zijlstra and W.L. van Neerven, Phys. Lett. **B272**, 127 (1991); Phys. Lett. **B273**, 476 (1991); Phys. Lett. **B297**, 377 (1992); Nucl. Phys. **B383**, 525 (1992).
21. S. Moch and J.A.M. Vermaseren, Nucl. Phys. **B573**, 853 (2000).
22. S. Moch *et al.*, Nucl. Phys. **B688**, 101 (2004); Nucl. Phys. **B691**, 129 (2004); Phys. Lett. **B606**, 123 (2005); Nucl. Phys. **B724**, 3 (2005).
23. E.A. Kuraev *et al.*, Phys. Lett. **B60**, 50 (1975); Sov. Phys. JETP **44**, 443 (1976); Sov. Phys. JETP **45**, 199 (1977).
24. Ya.Ya. Balitsky and L.N. Lipatov, Sov. J. Nucl. Phys. **28**, 822 (1978).
25. V.S. Fadin, and L.N. Lipatov, Phys. Lett. **B429**, 127 (1998).
26. G. Camici and M. Ciafaloni, Phys. Lett. **B412**, 396 (1997), erratum-Phys. Lett. **B147**, 390 (1997); Phys. Lett. **B430**, 349 (1998).
27. M. Ciafaloni *et al.*, Phys. Rev. **D60**, 114036 (1999); JHEP **0007** 054 (2000).
28. M. Ciafaloni *et al.*, Phys. Lett. **B576**, 143 (2003); Phys. Rev. **D68**, 114003 (2003).
29. G. Altarelli *et al.*, Nucl. Phys. **B621**, 359 (2002); Nucl. Phys. **B674**, 459 (2003).
30. G. 't Hooft and M. Veltman, Nucl. Phys. **B44**, 189 (1972).
31. G. 't Hooft, Nucl. Phys. **B61**, 455 (1973).
32. G. Altarelli *et al.*, Nucl. Phys. **B143**, 521 (1978) and erratum: Nucl. Phys. **B146**, 544 (1978).
33. W.A. Bardeen *et al.*, Phys. Rev. **D18**, 3998 (1978).
34. M.A.G. Aivazis *et al.*, Phys. Rev. **D50**, 3102 (1994).
35. J.C. Collins, Phys. Rev. **D58**, 094002 (1998).
36. A. Chuvakin *et al.*, Phys. Rev. **D61**, 096004 (2000).
37. R.S. Thorne and R.G. Roberts, Phys. Rev. **D57**, 6871 (1998); Phys. Lett. **B421**, 303 (1998); Eur. Phys. J. **C19**, 339 (2001).
38. W.-K. Tung *et al.*, J. Phys. **G28**, 983 (2002); S. Kretzer *et al.*, Phys. Rev. **D69**, 114005 (2004).
39. R.S. Thorne, Phys. Rev. **D73**, 054019 (2006).
40. A.D. Martin *et al.*, Eur. Phys. J. **C4**, 463 (1998).
41. A.D. Martin *et al.*, Phys. Lett. **B604**, 61 (2004).
42. CTEQ, W.-K. Tung *et al.*, JHEP **0702**, 053 (2007); J. Pumplin *et al.*, Phys. Rev. **D75**, 054029 (2007); H.L. Lai *et al.*, JHEP **0704**, 089 (2007).
43. S. Alekhin, JHEP **0302**, 015 (2003).
44. S. Alekhin *et al.*, Phys. Rev. **D74**, 054033 (2006).
45. CTEQ, D. Stump *et al.*, Phys. Rev. **D65**, 014012 (2001).
46. CTEQ, J. Pumplin *et al.*, Phys. Rev. **D65**, 014013 (2001).
47. A.D. Martin *et al.*, Eur. Phys. J. **C28**, 455 (2003).
48. A.D. Martin *et al.*, Eur. Phys. J. **C35**, 325 (2004).
49. L. Del Debbio *et al.*, JHEP **0703**, 039 (2007).
50. M. Glück *et al.*, Phys. Rev. **D63**, 094005 (2001).
51. E. Leader *et al.*, Eur. Phys. J. **C23**, 479 (2002).
52. J. Blümlein and H. Böttcher, Nucl. Phys. **B636**, 225 (2002).
53. HERMES, A. Airpetian *et al.*, Phys. Rev. Lett. **92**, 012005 (2004); A. Airpetian *et al.*, Phys. Rev. **D71**, 012003 (2005).
54. SMC, B. Adeva *et al.*, Phys. Lett. **B420**, 180 (1998).
55. H. Plathow-Besch, CERN PDFLIB, W5051 (2000).
56. <http://durpdg.dur.ac.uk/HEPDATA/PDF>.
57. <http://durpdg.dur.ac.uk/lhapdf/index.html>.
58. J. Pumplin *et al.*, JHEP **0602**, 032 (2006).
59. H1, C. Adloff *et al.*, Eur. Phys. J. **C21**, 33 (2001).
60. ZEUS, S. Chekanov *et al.*, Eur. Phys. J. **C42**, 1 (2005).
61. R. Nisius, Phys. Reports **332**, 165 (2000).
62. T.F. Walsh and P.M. Zerwas, Phys. Lett. **B44**, 195 (1973).
63. R.L. Kingsley, Nucl. Phys. **B60**, 45 (1973).
64. E. Witten, Nucl. Phys. **B120**, 189 (1977).
65. W.A. Bardeen and A.J. Buras, Phys. Rev. **D20**, 166 (1979), erratum Phys. Rev. **D21**, 2041 (1980).
66. M. Fontannaz and E. Pilon, Phys. Rev. **D45**, 382 (1992), erratum Phys. Rev. **D46**, 484 (1992).
67. M. Glück *et al.*, Phys. Rev. **D45**, 3986 (1992).
68. F. Cornet *et al.*, Phys. Rev. **D70**, 093004 (2004).
69. P. Aurenche, *et al.*, Eur. Phys. J. **C44**, 395 (2005).
70. W. Slominski *et al.*, Eur. Phys. J. **C45**, 633 (2006).
71. ZEUS, S. Chekanov *et al.*, Eur. Phys. J. **C38**, 43 (2004).
72. ZEUS, S. Chekanov *et al.*, Nucl. Phys. **B713**, 3 (2005).
73. H1, A. Aktas *et al.*, Eur. Phys. J. **C48**, 749 (2006).
74. H1, A. Aktas *et al.*, Eur. Phys. J. **C48**, 715 (2006).
75. J. C. Collins, Phys. Rev. **D57**, 3051 (1998); Erratum Phys. Rev. **D61**, 019902 (2000).
76. G. Ingelman and P. E. Schlein, Phys. Lett. **B152**, 256 (1985).
77. A. D. Martin, M. G. Ryskin and G. Watt, Phys. Lett. **B644**, 131 (2007).
78. H1, A. Aktas *et al.*, Eur. Phys. J. **C51**, 549 (2007).
79. H1, A. Aktas *et al.*, arXiv:0708.3217.
80. ZEUS, S. Chekanov *et al.*, arXiv:0708.1415.

NOTE: THE FIGURES IN THIS SECTION ARE INTENDED TO SHOW THE REPRESENTATIVE DATA. THEY ARE NOT MEANT TO BE COMPLETE COMPILATIONS OF ALL THE WORLD'S RELIABLE DATA.

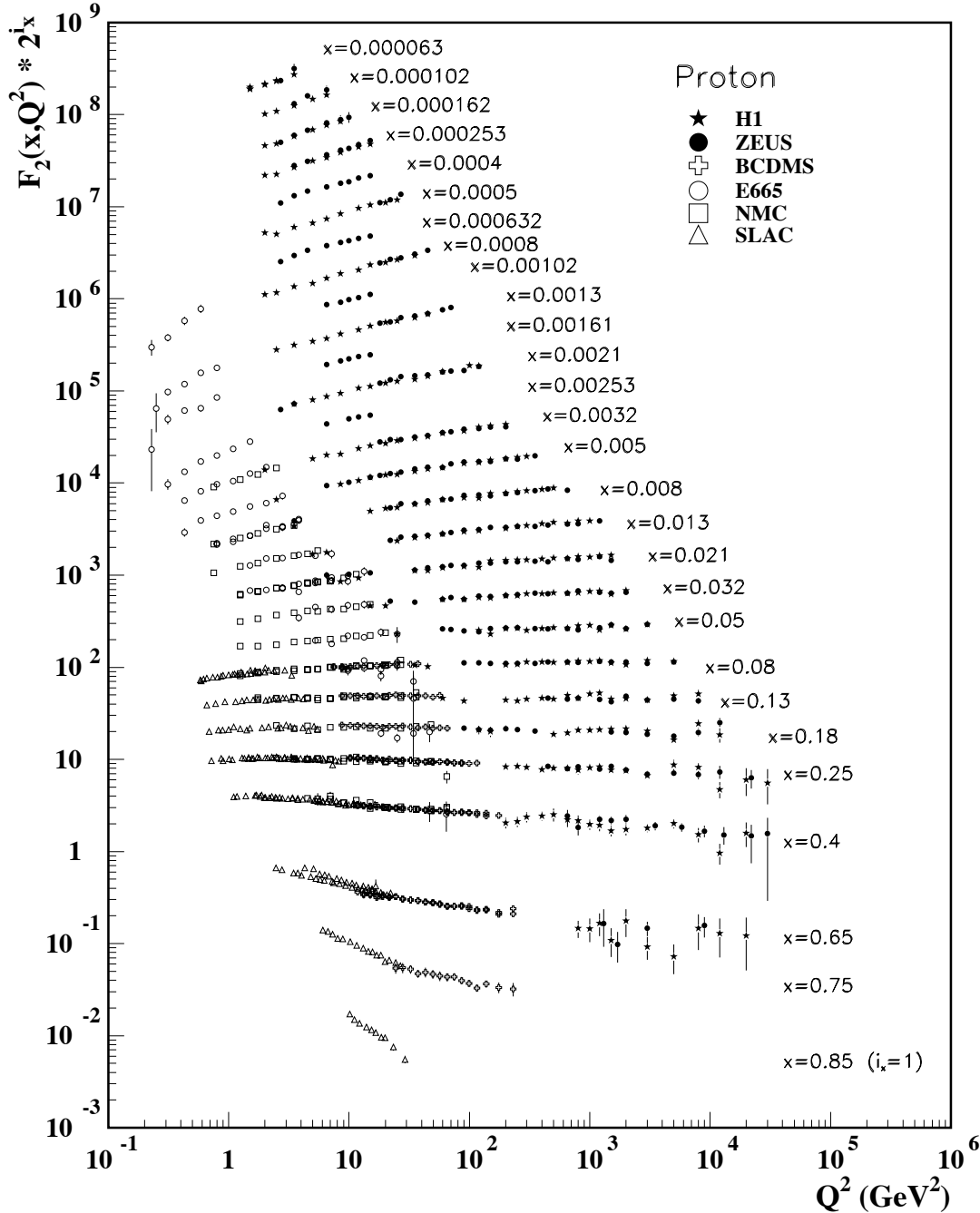


Figure 16.7: The proton structure function F_2^p measured in electromagnetic scattering of positrons on protons (collider experiments ZEUS and H1), in the kinematic domain of the HERA data, for $x > 0.00006$ (*cf.* Fig. 16.10 for data at smaller x and Q^2), and for electrons (SLAC) and muons (BCDMS, E665, NMC) on a fixed target. Statistical and systematic errors added in quadrature are shown. The data are plotted as a function of Q^2 in bins of fixed x . Some points have been slightly offset in Q^2 for clarity. The ZEUS binning in x is used in this plot; all other data are rebinned to the x values of the ZEUS data. For the purpose of plotting, F_2^p has been multiplied by 2^{i_x} , where i_x is the number of the x bin, ranging from $i_x = 1$ ($x = 0.85$) to $i_x = 28$ ($x = 0.000063$). References: **H1**—C. Adloff *et al.*, *Eur. Phys. J.* **C21**, 33 (2001); C. Adloff *et al.*, *Eur. Phys. J.* **C30**, 1 (2003); **ZEUS**—S. Chekanov *et al.*, *Eur. Phys. J.* **C21**, 443 (2001); S. Chekanov *et al.*, *Phys. Rev.* **D70**, 052001 (2004); **BCDMS**—A.C. Benvenuti *et al.*, *Phys. Lett.* **B223**, 485 (1989) (as given in [56]); **E665**—M.R. Adams *et al.*, *Phys. Rev.* **D54**, 3006 (1996); **NMC**—M. Arneodo *et al.*, *Nucl. Phys.* **B483**, 3 (1997); **SLAC**—L.W. Whitlow *et al.*, *Phys. Lett.* **B282**, 475 (1992).

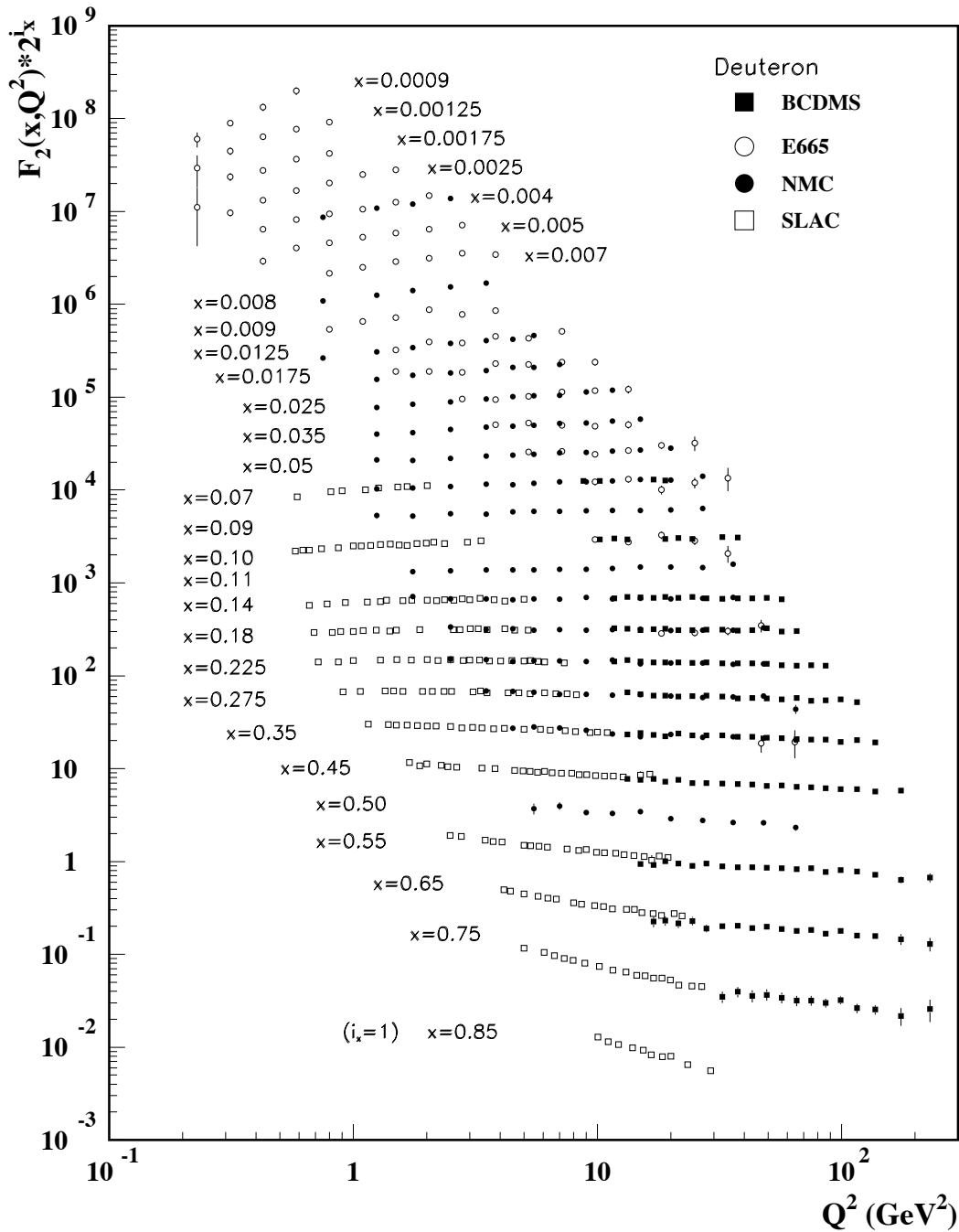


Figure 16.8: The deuteron structure function F_2^d measured in electromagnetic scattering of electrons (SLAC) and muons (BCDMS, E665, NMC) on a fixed target, shown as a function of Q^2 for bins of fixed x . Statistical and systematic errors added in quadrature are shown. For the purpose of plotting, F_2^d has been multiplied by 2^{i_x} , where i_x is the number of the x bin, ranging from 1 ($x = 0.85$) to 29 ($x = 0.0009$). References: **BCDMS**—A.C. Benvenuti *et al.*, Phys. Lett. **B237**, 592 (1990). **E665**, **NMC**, **SLAC**—same references as Fig. 16.7.

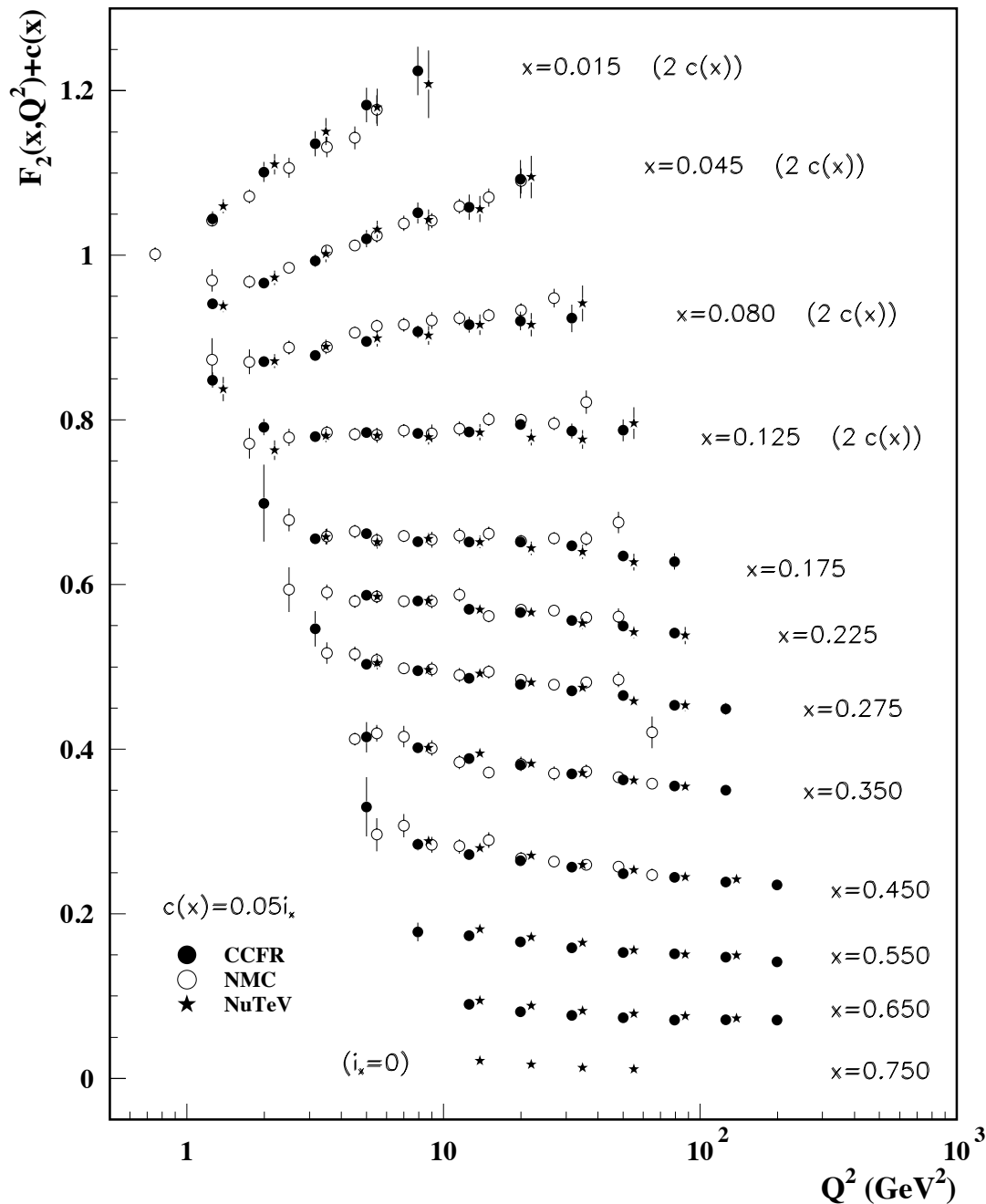


Figure 16.9: The deuteron structure function F_2 measured in deep inelastic scattering of muons on a fixed target (NMC) is compared to the structure function F_2 from neutrino-iron scattering (CCFR and NuTeV) using $F_2^{\mu} = (5/18)F_2^{\nu} - x(s + \bar{s})/6$, where heavy-target effects have been taken into account. The data are shown versus Q^2 , for bins of fixed x . The NMC data have been rebinned to CCFR and NuTeV x values. Statistical and systematic errors added in quadrature are shown. For the purpose of plotting, a constant $c(x) = 0.05i_x$ is added to F_2 , where i_x is the number of the x bin, ranging from 0 ($x = 0.75$) to 7 ($x = 0.175$). For $i_x = 8$ ($x = 0.125$) to 11 ($x = 0.015$), $2c(x)$ has been added. References: NMC—M. Arneodo *et al.*, Nucl. Phys. **B483**, 3 (1997); CCFR/NuTeV—U.K. Yang *et al.*, Phys. Rev. Lett. **86**, 2741 (2001); NuTeV—M. Tzanov *et al.*, Phys. Rev. **D74**, 012008 (2006).

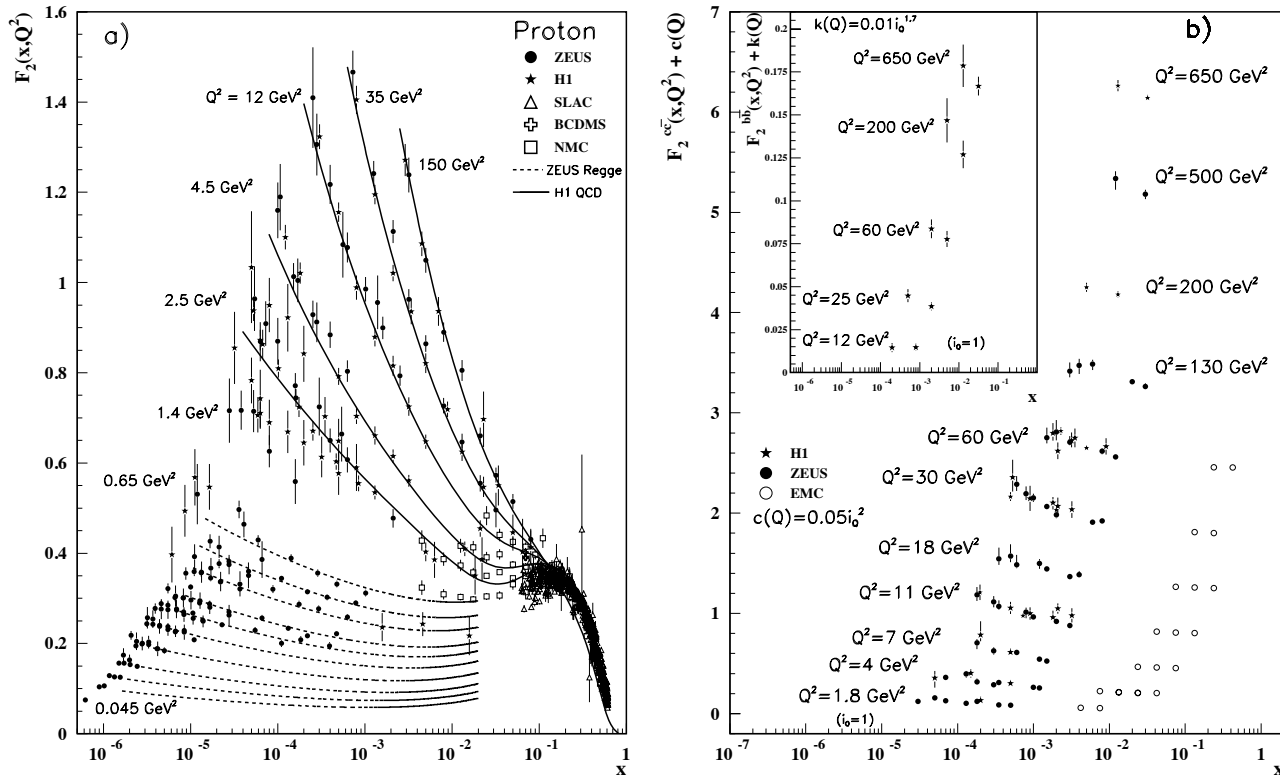


Figure 16.10: a) The proton structure function F_2^p mostly at small x and Q^2 , measured in electromagnetic scattering of positrons (H1, ZEUS), electrons (SLAC), and muons (BCDMS, NMC) on protons. Lines are ZEUS and H1 parameterizations for lower (Regge) and higher (QCD) Q^2 . The width of the bins can be up to 10% of the stated Q^2 . Some points have been slightly offset in x for clarity. References: **ZEUS**—J. Breitweg *et al.*, Phys. Lett. **B407**, 432 (1997); J. Breitweg *et al.*, Eur. Phys. J. **C7**, 609 (1999); J. Breitweg *et al.*, Phys. Lett. **B487**, 53 (2000) (both data and ZEUS Regge parameterization); S. Chekanov *et al.*, Eur. Phys. J. **C21**, 443 (2001); S. Chekanov *et al.*, Phys. Rev. **D70**, 052001 (2004); **H1**—C. Adloff *et al.*, Nucl. Phys. **B497**, 3 (1997); C. Adloff *et al.*, Eur. Phys. J. **C21**, 33 (2001) (both data and H1 QCD parameterization); C. Adloff *et al.*, Eur. Phys. J. **C30**, 1 (2003); A. Aktas *et al.*, Phys. Lett. **B598**, 159 (2004); **BCDMS, NMC, SLAC**—same references as Fig. 16.7.

b) The charm structure function $F_2^{c\bar{c}}(x)$, i.e. that part of the inclusive structure function F_2^p arising from the production of charm quarks, measured in electromagnetic scattering of positrons on protons (H1, ZEUS) and muons on iron (EMC). The H1 points have been slightly offset in x for clarity. For the purpose of plotting, a constant $c(Q) = 0.05i_Q^2$ is added to $F_2^{c\bar{c}}$ where i_Q is the number of the Q^2 bin, ranging from 1 ($Q^2 = 1.8 \text{ GeV}^2$) to 11 ($Q^2 = 650 \text{ GeV}^2$). References: **ZEUS**—J. Breitweg *et al.*, Eur. Phys. J. **C12**, 35 (2000); S. Chekanov *et al.*, Phys. Rev. **D69**, 012004 (2004); **H1**—C. Adloff *et al.*, Z. Phys. **C72**, 593 (1996); C. Adloff *et al.*, Phys. Lett. **B528**, 199 (2002); A. Aktas *et al.*, Eur. Phys. J. **C40**, 349 (2005); A. Aktas *et al.*, Eur. Phys. J. **C45**, 23 (2006); **EMC**—J.J. Aubert *et al.*, Nucl. Phys. **B213**, 31 (1983).

Inset: The bottom quark structure function $F_2^{b\bar{b}}(x)$. For the purpose of plotting, a constant $k(Q) = 0.01i_Q^{1.7}$ is added to $F_2^{b\bar{b}}$ where i_Q is the number of the Q^2 bin, ranging from 1 ($Q^2 = 12 \text{ GeV}^2$) to 5 ($Q^2 = 650 \text{ GeV}^2$). References: **H1**—A. Aktas *et al.*, Eur. Phys. J. **C40**, 349 (2005); A. Aktas *et al.*, Eur. Phys. J. **C45**, 23 (2006).

Statistical and systematic errors added in quadrature are shown for both plots. The data are given as a function of x in bins of Q^2 .

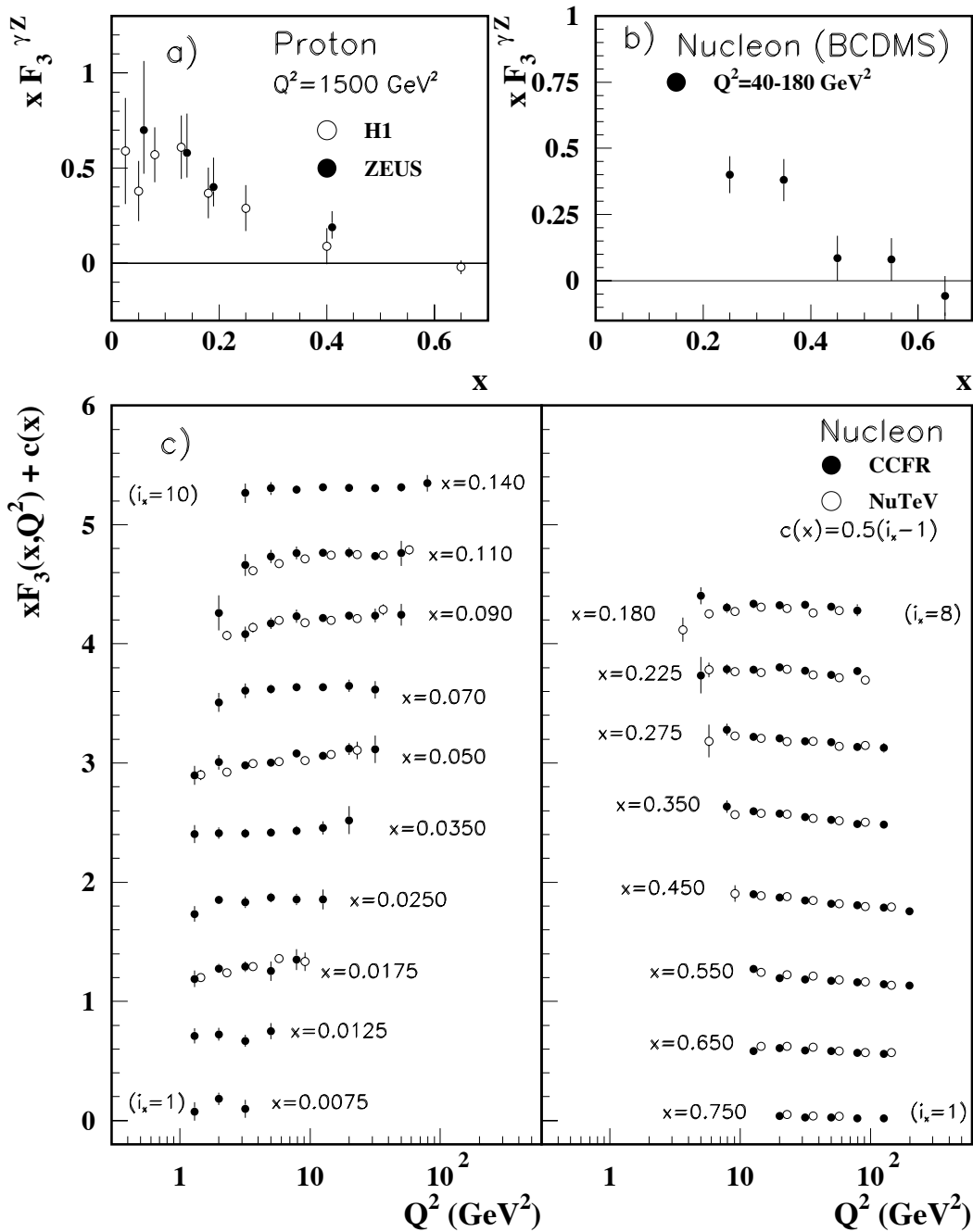


Figure 16.11: The structure function $x F_3^{\gamma Z}$ measured in electroweak scattering of **a)** electrons on protons (H1 and ZEUS) and **b)** muons on carbon (BCDMS). The ZEUS points have been slightly offset in x for clarity. References: **H1**—C. Adloff *et al.*, Eur. Phys. J. **C30**, 1 (2003); **ZEUS**—S. Chekanov *et al.*, Eur. Phys. J. **C28**, 175 (2003); **BCDMS**—A. Argento *et al.*, Phys. Lett. **B140**, 142 (1984). **c)** The structure function $x F_3$ of the nucleon measured in ν -Fe scattering. The data are plotted as a function of Q^2 in bins of fixed x . For the purpose of plotting, a constant $c(x) = 0.5(i_x - 1)$ is added to $x F_3$, where i_x is the number of the x bin as shown in the plot. The NuTeV points have been shifted to the nearest corresponding x bin as given in the plot and slightly offset in Q^2 for clarity. References: **CCFR**—W.G. Seligman *et al.*, Phys. Rev. Lett. **79**, 1213 (1997). **NuTeV**—M. Tzanov *et al.*, Phys. Rev. **D74**, 012008 (2006).

Statistical and systematic errors added in quadrature are shown for all plots.

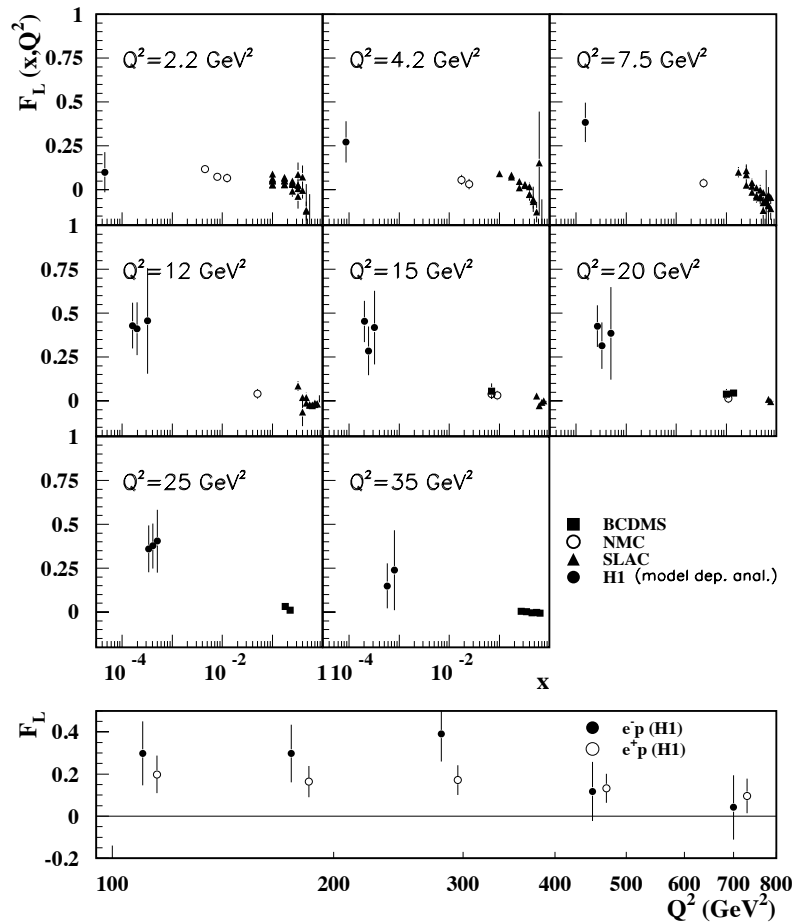


Figure 16.12: Top panel: The longitudinal structure function F_L as a function of x in bins of fixed Q^2 measured on the proton (except for the SLAC data which also contain deuterium data). BCDMS, NMC, and SLAC results are from measurements of R (the ratio of longitudinal to transverse photon absorption cross sections) which are converted to F_L by using the BCDMS parameterization of F_2 (A.C. Benvenuti *et al.*, Phys. Lett. **B223**, 485 (1989)). It is assumed that the Q^2 dependence of the fixed-target data is small within a given Q^2 bin. References: **H1**—C. Adloff *et al.*, Eur. Phys. J. **C21**, 33 (2001); **BCDMS**—A. Benvenuti *et al.*, Phys. Lett. **B223**, 485 (1989); **NMC**—M. Arneodo *et al.*, Nucl. Phys. **B483**, 3 (1997); **SLAC**—L.W. Whitlow *et al.*, Phys. Lett. **B250**, 193 (1990) and numerical values from the thesis of L.W. Whitlow (SLAC-357).

Bottom panel: Higher Q^2 values of the longitudinal structure function F_L as a function of Q^2 given at the measured x for e^+/e^- -proton scattering. Points have been slightly offset in Q^2 for clarity. References: **H1**—C. Adloff *et al.*, Eur. Phys. J. **C30**, 1 (2003).

The H1 results shown in both plots require the assumption of the validity of the QCD form for the F_2 structure function in order to extract F_L . Statistical and systematic errors added in quadrature are shown for both plots.

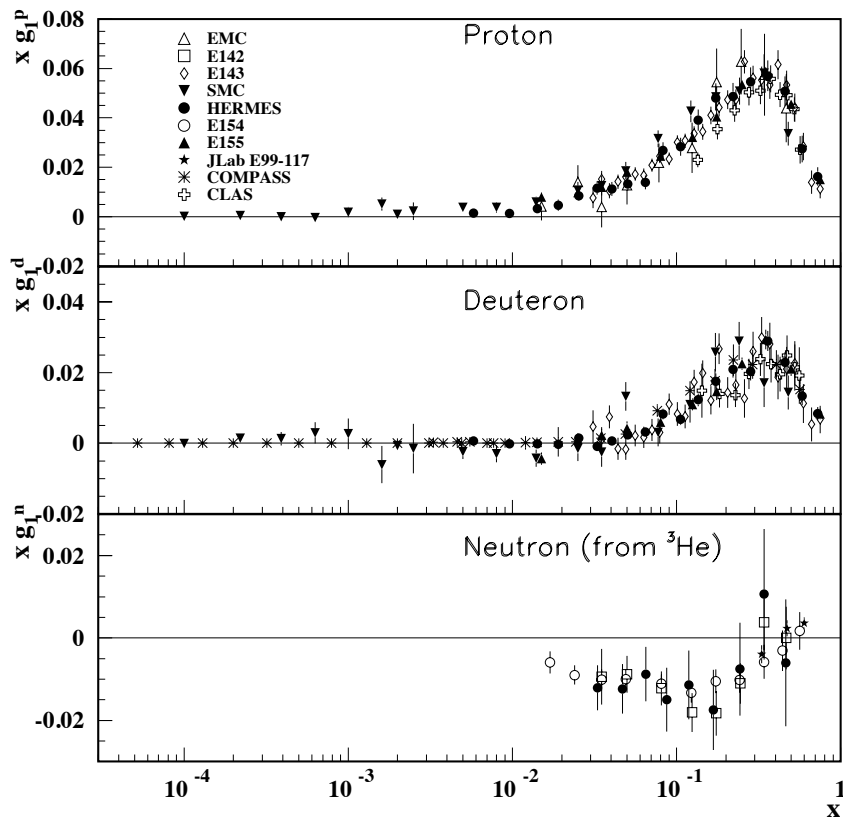


Figure 16.13: The spin-dependent structure function $xg_1(x)$ of the proton, deuteron, and neutron (from ${}^3\text{He}$ target) measured in deep inelastic scattering of polarized electrons/positrons: E142 ($Q^2 \sim 0.3 - 10 \text{ GeV}^2$), E143 ($Q^2 \sim 0.3 - 10 \text{ GeV}^2$), E154 ($Q^2 \sim 1 - 17 \text{ GeV}^2$), E155 ($Q^2 \sim 1 - 40 \text{ GeV}^2$), JLab E99-117 ($Q^2 \sim 2.71 - 4.83 \text{ GeV}^2$), HERMES ($Q^2 \sim 0.18 - 20 \text{ GeV}^2$), CLAS ($Q^2 \sim 1 - 5 \text{ GeV}^2$) and muons: EMC ($Q^2 \sim 1.5 - 100 \text{ GeV}^2$), SMC ($Q^2 \sim 0.01 - 100 \text{ GeV}^2$), COMPASS ($Q^2 \sim 0.001 - 100 \text{ GeV}^2$), shown at the measured Q^2 (except for EMC data given at $Q^2 = 10.7 \text{ GeV}^2$ and E155 data given at $Q^2 = 5 \text{ GeV}^2$). Note that $g_1^n(x)$ may also be extracted by taking the difference between $g_1^d(x)$ and $g_1^p(x)$, but these values have been omitted in the bottom plot for clarity. Statistical and systematic errors added in quadrature are shown. References: **EMC**—J. Ashman *et al.*, Nucl. Phys. **B328**, 1 (1989); **E142**—P.L. Anthony *et al.*, Phys. Rev. **D54**, 6620 (1996); **E143**—K. Abe *et al.*, Phys. Rev. **D58**, 112003 (1998); **SMC**—B. Adeva *et al.*, Phys. Rev. **D58**, 112001 (1998), B. Adeva *et al.*, Phys. Rev. **D60**, 072004 (1999) and Erratum-Phys. Rev. **D62**, 079902 (2000); **HERMES**—A. Airapetian *et al.*, Phys. Rev. **D75**, 012007 (2007) and K. Ackerstaff *et al.*, Phys. Lett. **B404**, 383 (1997); **E154**—K. Abe *et al.*, Phys. Rev. Lett. **79**, 26 (1997); **E155**—P.L. Anthony *et al.*, Phys. Lett. **B463**, 339 (1999) and P.L. Anthony *et al.*, Phys. Lett. **B493**, 19 (2000); **Jlab-E99-117**—X. Zheng *et al.*, Phys. Rev. **C70**, 065207 (2004); **COMPASS**—V.Yu. Alexakhin *et al.*, Phys. Lett. **B647**, 8 (2007) and E.S. Ageev *et al.*, Phys. Lett. **B647**, 330 (2007); **CLAS**—K.V. Dharmawardane *et al.*, Phys. Lett. **B641**, 11 (2006) (which also includes resonance region data not shown on this plot).

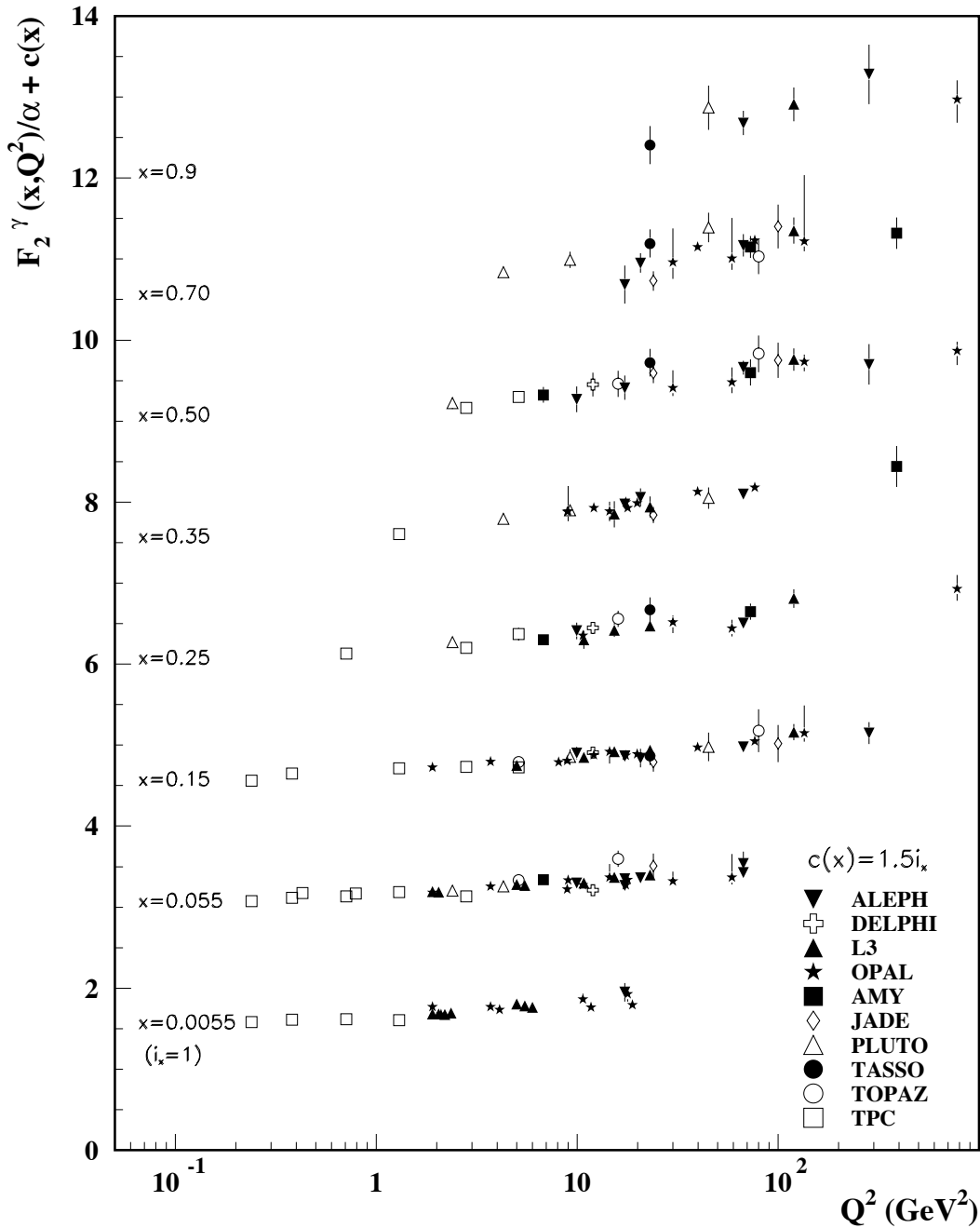


Figure 16.14: The hadronic structure function of the photon F_2^γ divided by the fine structure constant α measured in e^+e^- scattering, shown as a function of Q^2 for bins of x . Data points have been shifted to the nearest corresponding x bin as given in the plot. Some points have been offset in Q^2 for clarity. Statistical and systematic errors added in quadrature are shown. For the purpose of plotting, a constant $c(x) = 1.5i_x$ is added to F_2^γ/α where i_x is the number of the x bin, ranging from 1 ($x = 0.0055$) to 8 ($x = 0.9$). References: **ALEPH**–R. Barate *et al.*, Phys. Lett. **B458**, 152 (1999); A. Heister *et al.*, Eur. Phys. J. **C30**, 145 (2003); **DELPHI**–P. Abreu *et al.*, Z. Phys. **C69**, 223 (1995); **L3**–M. Acciarri *et al.*, Phys. Lett. **B436**, 403 (1998); M. Acciarri *et al.*, Phys. Lett. **B447**, 147 (1999); M. Acciarri *et al.*, Phys. Lett. **B483**, 373 (2000); **OPAL**–A. Ackerstaff *et al.*, Phys. Lett. **B411**, 387 (1997); A. Ackerstaff *et al.*, Z. Phys. **C74**, 33 (1997); G. Abbiendi *et al.*, Eur. Phys. J. **C18**, 15 (2000); G. Abbiendi *et al.*, Phys. Lett. **B533**, 207 (2002) (note that there is overlap of the data samples in these last two papers); **AMY**–S.K. Sahu *et al.*, Phys. Lett. **B346**, 208 (1995); T. Kojima *et al.*, Phys. Lett. **B400**, 395 (1997); **JADE**–W. Bartel *et al.*, Z. Phys. **C24**, 231 (1984); **PLUTO**–C. Berger *et al.*, Phys. Lett. **142B**, 111 (1984); C. Berger *et al.*, Nucl. Phys. **B281**, 365 (1987); **TASSO**–M. Althoff *et al.*, Z. Phys. **C31**, 527 (1986); **TOPAZ**–K. Muramatsu *et al.*, Phys. Lett. **B332**, 477 (1994); **TPC/Two Gamma**–H. Aihara *et al.*, Z. Phys. **C34**, 1 (1987).

17. FRAGMENTATION FUNCTIONS IN e^+e^- ANNIHILATION AND LEPTON-NUCLEON DIS

Revised August 2007 by O. Biebel (Ludwig-Maximilians-Universität, Munich, Germany), D. Milstead (Fysikum, Stockholms Universitet, Sweden), P. Nason (INFN, Sez. di Milano-Bicocca, Milan, Italy), and B.R. Webber (Cavendish Laboratory, Cambridge, UK). An extended version of the 2001 review can be found in Ref. 1.

17.1. Concept of fragmentation

17.1.1. Introduction :

Fragmentation functions are dimensionless functions that describe the final-state single-particle energy distributions in hard scattering processes, like e^+e^- annihilation or deep inelastic lepton-nucleon scattering, or high transverse momentum hadrons in photon-hadron and hadron-hadron collisions. The total e^+e^- fragmentation function for hadrons of type h in annihilation at c.m. energy \sqrt{s} , via an intermediate vector boson $V = \gamma/Z^0$, is defined as

$$F^h(x, s) = \frac{1}{\sigma_{\text{tot}}} \frac{d\sigma}{dx}(e^+e^- \rightarrow V \rightarrow hX), \quad (17.1)$$

where $x = 2E_h/\sqrt{s} \leq 1$ is the scaled hadron energy (in practice, the approximation $x = x_p = 2p_h/\sqrt{s}$ is often used). Its integral with respect to x gives the average multiplicity of those hadrons:

$$\langle n_h(s) \rangle = \int_0^1 dx F^h(x, s), \quad (17.2)$$

Neglecting contributions suppressed by inverse powers of s , the fragmentation function (17.1) can be represented as a sum of contributions from the different parton types $i = u, \bar{u}, d, \bar{d}, \dots, g$:

$$F^h(x, s) = \sum_i \int_x^1 \frac{dz}{z} C_i(s; z, \alpha_S) D_i^h(x/z, s). \quad (17.3)$$

where D_i^h are the parton fragmentation functions. At lowest order in α_S , the coefficient function C_g for gluons is zero, while for quarks $C_i = g_i(s)\delta(1-z)$, where $g_i(s)$ is the appropriate electroweak coupling. In particular, $g_i(s)$ is proportional to the charge-squared of parton i at $s \ll M_Z^2$, when weak effects can be neglected. In higher orders the coefficient functions and parton fragmentation functions are factorization-scheme dependent.

Parton fragmentation functions are analogous to the parton distributions in deep inelastic scattering (see sections on QCD and Structure Functions, 9 and 16 of this *Review*). In both cases, the simplest parton-model approach would predict a scale-independent x distribution. Furthermore, we obtain similar violations of this scaling behavior when QCD corrections are taken into account.

Fragmentation functions in lepton-hadron scattering and e^+e^- annihilation are complementary. Since e^+e^- annihilation results in a neutral off mass-shell photon or Z^0 , fragmentation arising from a pure quark-antiquark system can be studied. Lepton-hadron scattering is a more complicated environment with which it is possible to study the influence on fragmentation functions from initial state QCD radiation, the partonic and spin structure of the hadron target, and the target remnant system.¹

In lepton-hadron scattering, calling p the four momentum of the incoming hadron, and q the four momentum of the exchanged virtual boson, one can construct two independent kinematic invariants. One usually introduces $Q^2 = -q^2$ and defines $x_{\text{Bj}} = Q^2/(2p \cdot q)$. Thus, there is a freedom in the choice of scale used to define a fragmentation function. For e^+e^- , the c.m. energy provides a natural choice of scale as twice the energy of each produced quark. For lepton-hadron interactions, fragmentation scales such as $Q = \sqrt{-q^2}$, or the invariant

mass of the exchanged boson and target nucleon system $W = \sqrt{(p+q)^2} = \sqrt{m_h^2 + 2p \cdot q - Q^2}$ (where m_h is the incoming hadron mass), are typically used. Both W and Q can vary by several orders of magnitudes for a given c.m. energy, thus allowing the study of fragmentation in different environments by a single experiment, *e.g.*, in photoproduction the exchanged photon is quasi-real ($Q^2 \sim 0$) leading to processes akin to hadron-hadron scattering. In deep inelastic scattering (DIS) ($Q^2 \gg 1 \text{ GeV}^2$), using the Quark Parton Model (QPM), the hadronic fragments of the struck quark can be directly compared with quark fragmentation in e^+e^- . Results from lepton-hadron experiments quoted in this report primarily concern fragmentation in the DIS regime. Studies made by lepton-hadron experiments of fragmentation with photoproduction data containing high transverse momentum jets or particles are also reported, when these are directly comparable to DIS and e^+e^- results.

After the lepton-hadron interaction, the transverse momentum of the scattered lepton is balanced by the hadronic system. To remove the transverse momentum imbalance, many fragmentation studies have been performed in frames in which the target hadron and the exchanged boson are collinear. Two frames of reference are typically used which fulfill this condition.

The so-called hadronic c.m. frame (HCMS) is defined as the rest system of the exchanged boson and incoming hadron, with the z^* -axis defined along the direction of the exchanged boson. The $+z^*$ direction defines the so-called current region. Fragmentation measurements performed in the HCMS often use the Feynman- x variable $x_F = 2p_z^*/W$, where p_z^* is the longitudinal momentum of the particle in the HCMS. Since W is the invariant mass of the hadronic final state, x_F ranges between -1 and 1 .

The Breit system [3] is connected to the HCMS by a longitudinal boost such that the time component of q becomes 0, so that $q = (0, 0, 0, -Q)$. In this frame, the target has three momentum $\vec{p} = (0, 0, Q/(2x_{\text{Bj}}))$, as can be easily verified using the definition of x_{Bj} . In the quark parton model, the struck parton has momentum $x_{\text{Bj}} \cdot p$, and thus its longitudinal momentum is $Q/2$, which becomes $-Q/2$ after the collision. As compared with the HCMS, the current region of the Breit frame is more closely matched to the partonic scattering process, and is thus appropriate for direct comparisons of fragmentation functions in DIS with those from e^+e^- annihilation. The variable $x_p = 2p^*/Q$ is used at HERA for measurements of fragmentation functions in the Breit frame, ensuring directly comparable DIS and e^+e^- results.

17.2. Scaling violation

The evolution of the parton fragmentation function $D_i(x, t)$ with increasing scale $t = s$, like that of the parton distribution function $f_i(x, t)$ with $t = s$ (see Sec. 39 of this *Review*), is governed by the DGLAP equation [4]

$$t \frac{\partial}{\partial t} D_i(x, t) = \sum_j \int_x^1 \frac{dz}{z} \frac{\alpha_S}{2\pi} P_{ji}(z, \alpha_S) D_j(x/z, t). \quad (17.4)$$

In analogy to DIS, in some cases an evolution equation for the fragmentation function F itself (Eq. (17.3)) can be derived from Eq. (17.4) [5]. Notice that the splitting function is now P_{ji} rather than P_{ij} since here D_j represents the fragmentation of the final parton. The splitting functions again have perturbative expansions of the form

$$P_{ji}(z, \alpha_S) = P_{ji}^{(0)}(z) + \frac{\alpha_S}{2\pi} P_{ji}^{(1)}(z) + \dots \quad (17.5)$$

where the lowest-order functions $P_{ji}^{(0)}(z)$ are the same as those in deep inelastic scattering, but the higher-order terms [6,7]² are different. The effect of evolution is, however, the same in both cases: as the scale increases, one observes a scaling violation in which the x distribution is shifted towards lower values. This can be seen from Fig. 17.1.

¹ For a comprehensive review of the measurements and models of fragmentation in lepton-hadron scattering, see [2].

² There are misprints in the formulas in the published article [6]. The correct expressions can be found in the preprint version or in Ref. 8.

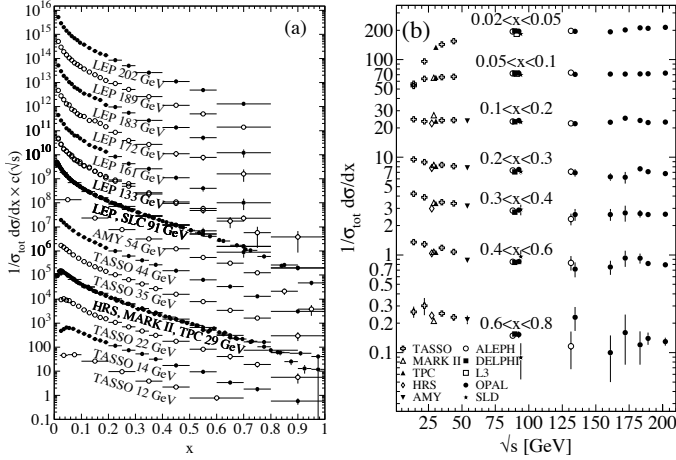


Figure 17.1: The e^+e^- fragmentation function for all charged particles is shown [9–25] (a) for different c.m. energies, \sqrt{s} , versus x and (b) for various ranges of x versus \sqrt{s} . For the purpose of plotting (a), the distributions were scaled by $c(\sqrt{s}) = 10^i$ where i is ranging from $i = 0$ ($\sqrt{s} = 12$ GeV) to $i = 13$ ($\sqrt{s} = 202$ GeV).

The coefficient functions C_i in Eq. (17.3) and the splitting functions P_{ji} contain singularities at $z = 0$ and 1, which have important effects on fragmentation at small and large values of x , respectively. For details see *e.g.*, Ref. 1.

Quantitative results of studies of scaling violation in e^+e^- fragmentation are reported in [26–30]. The values of α_S obtained are consistent with the world average (see review on QCD in Sec. 9 of this *Review*).

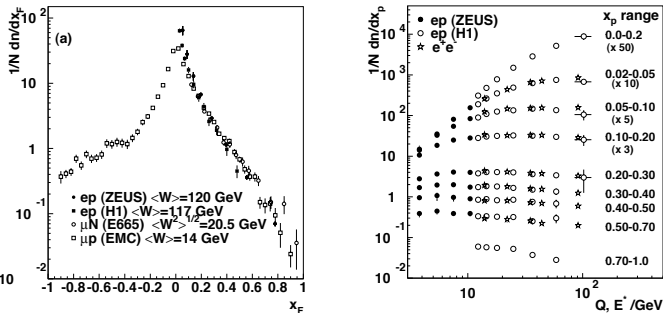


Figure 17.2: (a) The distribution $1/N \cdot dN/dx_F$ for all charged particles in DIS lepton-hadron experiments at different values of W , and measured in the HCMS [31–34]. (b) Scaling violations of the fragmentation function for all charged particles in the current region of the Breit frame of DIS [35,40] and in e^+e^- interactions [24,27]. The data are shown as a function of \sqrt{s} for e^+e^- results, and as a function of Q for the DIS results, each within the same indicated intervals of the scaled momentum x_p . The data for the four lowest intervals of x_p are multiplied by factors 50, 10, 5, and 3, respectively for clarity.

Scaling violations in DIS are shown in Fig. 17.2 for both HCMS and Breit frame. In Fig. 17.2(a), the distribution in terms of $x_F = 2p_z/W$ shows for values of $x_F > 0.15$ a steeper slope in ep data than for the μp data, indicating the scaling violations. At smaller values of x_F in the current jet region, the multiplicity of particles substantially increases with W owing to the increased phase space available for the fragmentation process. The EMC data access both the current region and the region of the fragmenting target remnant system. At higher values of $|x_F|$, owing to the extended nature of the remnant, the multiplicity in the target region far exceeds that in the current region. Owing to acceptance reasons, the remnant hemisphere of the HCMS is only accessible by the lower-energy fixed-target experiments.

Using hadrons from the current hemisphere in the Breit frame, measurements of fragmentation functions and the production properties of particles in ep scattering have been made by [35–40]. Fig. 17.2(b) compares results from ep scattering and e^+e^- experiments, the latter results are halved as they cover both event hemispheres. The agreement between the DIS and e^+e^- results is fairly good. However, processes in DIS which are not present in e^+e^- annihilation, such as boson-gluon fusion and initial state QCD radiation, can depopulate the current region. These effects become most prominent at low values of Q and x_p . When compared with e^+e^- annihilation data at $\sqrt{s} = 5.2, 6.5$ GeV [41], which are not shown here, the DIS particle rates tend to lie below those from e^+e^- annihilation. NLO QCD calculations [42], convoluted with fragmentation functions derived from e^+e^- data, have been tested against the HERA scaling violations data and provide a good description of the data in the kinematical regions in which the calculations are predictive [35,39,43].

17.3. Fragmentation functions for small particle momenta

As in the case of the parton distribution functions, the most common strategy for solving the evolution equations Eq. (17.4) is to take moments (Mellin transforms) with respect to x :

$$\tilde{D}(j, s) = \int_0^1 dx x^{j-1} D(x, s). \quad (17.6)$$

The behavior of $\tilde{D}(j, s)$ away from $j = 1$ determines the form of small- x fragmentation functions. Keeping the first three terms in a Taylor expansion around $j = 1$ gives a simple Gaussian function of j which transforms by inverse Mellin transformation into a Gaussian in the variable $\xi \equiv \ln(1/x)$:

$$xD(x, s) \propto \exp\left[-\frac{1}{2\sigma^2}(\xi - \xi_p)^2\right], \quad (17.7)$$

where the peak position is

$$\xi_p = \frac{1}{4b\alpha_S(s)} \approx \frac{1}{4} \ln\left(\frac{s}{\Lambda^2}\right), \quad (17.8)$$

with $b = (33 - 2n_f)/12\pi$ for n_f quark flavors and the width of the distribution of ξ is ($C_A = 3$)

$$\sigma = \left(\frac{1}{24b} \sqrt{\frac{2\pi}{C_A\alpha_S^3(s)}}\right)^{\frac{1}{2}} \propto \left[\ln\left(\frac{s}{\Lambda^2}\right)\right]^{\frac{3}{4}}. \quad (17.9)$$

Again, one can compute next-to-leading corrections to these predictions. In the method of [44], the corrections are included in an analytical form known as the ‘modified leading logarithmic approximation’ (MLLA). Alternatively they can be used to compute the higher moment corrections to the Gaussian form Eq. (17.7) [45]. Fig. 17.3 shows the ξ distribution for charged particles produced in the current region of the Breit frame in DIS interactions,³ and in e^+e^- annihilation. As expected from Eq. (17.7), Eq. (17.8), and Eq. (17.9), the distributions have a Gaussian shape, with the peak position and area becoming progressively larger with c.m. energy (e^+e^-) and Q^2 (DIS).

The predicted energy dependence Eq. (17.8) of the peak in the ξ distribution is a striking illustration of soft gluon coherence, which is the origin of the suppression of hadron production at small x . Of course, a decrease at very small x is expected on purely kinematical grounds, but this would occur at particle energies proportional to their masses, *i.e.*, at $x \propto m/\sqrt{s}$ and hence $\xi \sim \frac{1}{2} \ln s$. Thus, if the suppression were purely kinematic, the peak position ξ_p would vary twice as rapidly with energy, which is ruled out by the data (see Fig. 17.4). The e^+e^- and DIS data agree well with each other, demonstrating the universality of hadronization. The MLLA prediction describes the data. Measurements of the higher moments of the ξ distribution in e^+e^- [24,49–51] and DIS [39] have also been made and show consistency with each other.

³ Dominant systematic errors used for the results of [39] are according to this reference 10% for $x_p < 0.3$ and increase up to 30% for large x_p .

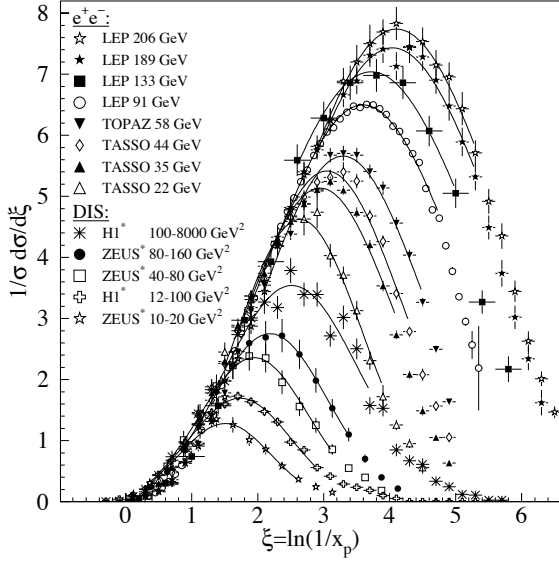


Figure 17.3: Distribution of $\xi = \ln(1/x_p)$ at several c.m. energies (e^+e^-) [9,10,14,17–20,24,46–49] and intervals of Q^2 (DIS) [38,39].³ At each energy only one representative measurement is shown. For clarity some measurements at intermediate c.m. energies (e^+e^-) or Q^2 ranges (DIS) are not shown. The DIS measurements marked with * have been scaled by a factor of 2 for direct comparability with the e^+e^- results. Overlaid are fits of a simple Gaussian function for illustration.

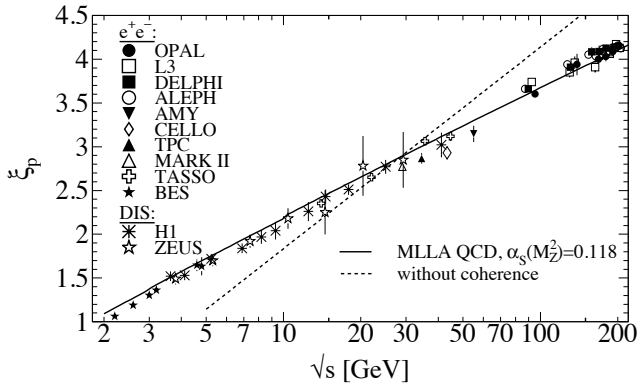


Figure 17.4: Evolution of the peak position, ξ_p , of the ξ distribution with the c.m. energy \sqrt{s} . The MLLA QCD prediction (solid) using $\alpha_S(s = M_Z^2) = 0.118$ and the expectation without gluon coherence (dashed) are superimposed to the data [9,11,14,16–18,20,24,37,38,47,48,50,52–59].

17.3.1. Longitudinal Fragmentation :

In the process $e^+e^- \rightarrow V \rightarrow hX$, the joint distribution in the energy fraction x and the angle θ between the observed hadron h and the incoming electron beam has the general form

$$\frac{1}{\sigma_{\text{tot}}} \frac{d^2\sigma}{dx d\cos\theta} = \frac{3}{8}(1 + \cos^2\theta) F_T(x) + \frac{3}{4}\sin^2\theta F_L(x) + \frac{3}{4}\cos\theta F_A(x), \quad (17.10)$$

where F_T , F_L and F_A are respectively the transverse, longitudinal and asymmetric fragmentation functions. All these functions also depend on the c.m. energy \sqrt{s} . Eq. (17.10) is the most general form of the inclusive single particle production from the decay of a massive vector boson [5]. As their names imply, F_T and F_L represent

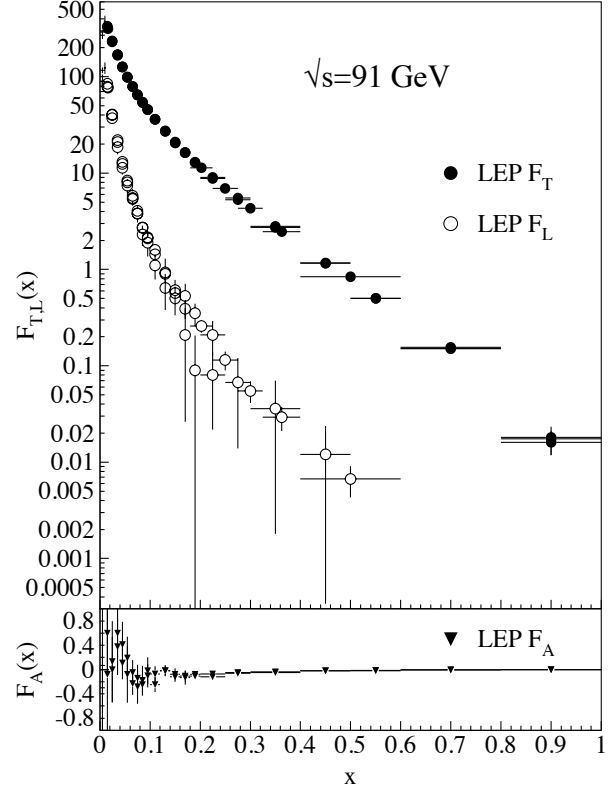


Figure 17.5: Transverse (F_T), longitudinal (F_L), and asymmetric (F_A) fragmentation functions are shown [12,26,60]. Data points with relative errors greater than 100% are omitted.

the contributions from virtual bosons polarized transversely or longitudinally with respect to the direction of motion of the hadron h . F_A is a parity-violating contribution which comes from the interference between vector and axial vector contributions. Integrating over all angles, we obtain the total fragmentation function, $F = F_T + F_L$. Each of these functions can be represented as a convolution of the parton fragmentation functions D_i with appropriate coefficient functions $C_i^{T,L,A}$ as in Eq. (17.3). This representation works in the high energy limit. As $x \cdot \sqrt{s}/2$ approaches hadronic scales $\simeq m_\rho$, power suppressed effects can no longer be neglected, and the fragmentation function formalism no longer accounts correctly for the separation of F_T , F_L , and F_A . In Fig. 17.5, F_T , F_L , and F_A measured at $\sqrt{s} = 91$ GeV are shown.

17.4. Gluon fragmentation

The gluon fragmentation function $D_g(x)$ can be extracted from the longitudinal fragmentation function defined in Eq. (17.10). Since the coefficient functions C_i^L for quarks and gluons are comparable in $\mathcal{O}(\alpha_S)$, F_L can be expressed in terms of F_T and D_g which allows one to obtain D_g from the measured F_L and F_T , see *e.g.*, [1] for details. At NLO, *i.e.*, $\mathcal{O}(\alpha_S^2)$ coefficient functions C_i , quark fragmentation is dominant in F_L over a large part of the kinematic range, see *e.g.*, [61]. This leaves some sensitivity of F_L to D_g , but further constraints will be needed, for instance from hadro-production in deep-inelastic scattering.

D_g can also be deduced from the fragmentation of three-jet events in which the gluon jet is identified, for example, by tagging the other two jets with heavy quark decays. To leading order, the measured distributions of $x = E_{\text{had}}/E_{\text{jet}}$ for particles in gluon jets can be identified directly with the gluon fragmentation functions $D_g(x)$. The experimentally measured gluon fragmentation functions are shown in Fig. 17.6.

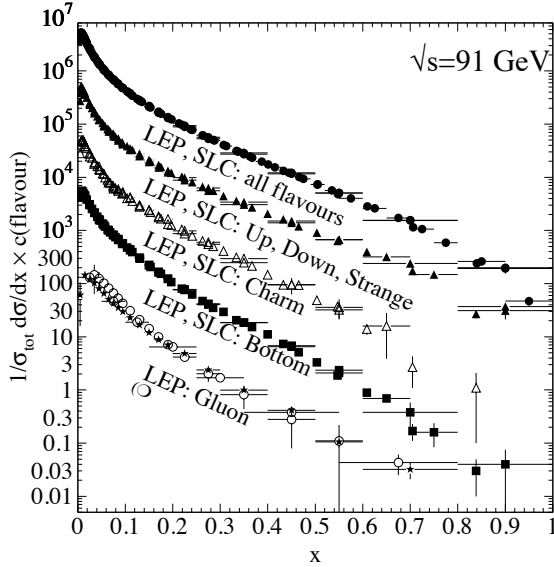


Figure 17.6: Comparison of the charged-particle and the flavor-dependent e^+e^- fragmentation functions obtained at $\sqrt{s} = 91$ GeV. The data [10,12,14,15,19,21] and [22,28,60,62] are shown for the inclusive, light (up, down, strange) quarks, charm quark, bottom quark, and the gluon versus x . For the purpose of plotting, the distributions were scaled by $c(\text{flavour}) = 10^i$, where i is ranging from $i = 0$ (Gluon) to $i = 4$ (all flavours).

17.5. Spin-dependent fragmentation

Measurements of hadron production in polarized lepton-hadron scattering are used principally in the determination of polarized parton densities from DIS interactions with longitudinally polarized targets [63–65]. Since flavor-dependent fragmentation functions derived from the $e^+e^- \rightarrow hX$ can give significantly different flavor contributions [66–71], experiments use string fragmentation in JETSET [72], which is tuned to describe their own identified particle data, and those measured by other low energy DIS experiments.

Polarized scattering presents the possibility to measure the spin transfer from the struck quark to the final hadron, and thus develop spin-dependent fragmentation functions [73,74]. These are useful in the study of the quark transversity distribution [75], which describes the probability of finding a transversely polarized quark with its spin aligned or anti-aligned with the spin of a transversely polarized nucleon. The transversity function is chiral-odd, and therefore not accessible through measurements of inclusive lepton-hadron scattering. Semi-inclusive DIS, in which another chiral-odd observable may be involved, provides a valuable tool to probe transversity. The Collins fragmentation function [76] relates the transverse polarization of the quark to that of the final hadron. It is chiral-odd and naive T-odd, leading to a characteristic single spin asymmetry in the azimuthal angular distribution of the produced hadron in the hadron scattering plane. A number of experiments have measured this asymmetry (see *e.g.*, [77]). However, these studies were unable to distinguish between processes due to transversity in conjunction with the Collins fragmentation with other processes requiring non-polarized fragmentation functions, such as the Sivers mechanism [78]. However, the HERMES and COMPASS collaborations have made early studies of the Collins and Sivers asymmetries using a transversely polarized target [79–81].

17.6. Fragmentation models

Although the scaling violation can be calculated perturbatively, the actual form of the parton fragmentation functions is non-perturbative. Perturbative evolution gives rise to a shower of quarks and gluons (partons). Phenomenological schemes are then used to model the carry-over of parton momenta and flavor to the hadrons. Two of the very popular models are the *string fragmentation* [82,83], implemented in the JETSET [72] and UCLA [84] Monte Carlo event generation programs, and the *cluster fragmentation* of the HERWIG Monte Carlo event generator [85].

17.6.1. String fragmentation: The string-fragmentation scheme considers the color field between the partons, *i.e.*, quarks and gluons, to be the fragmenting entity rather than the partons themselves. The string can be viewed as a color flux tube formed by gluon self-interaction as two colored partons move apart. Energetic gluon emission is regarded as energy-momentum carrying “kinks” on the string. When the energy stored in the string is sufficient, a $q\bar{q}$ pair may be created from the vacuum. Thus, the string breaks up repeatedly into color singlet systems, as long as the invariant mass of the string pieces exceeds the on-shell mass of a hadron. The $q\bar{q}$ pairs are created according to the probability of a tunneling process $\exp(-\pi m_{q,\perp}^2/\kappa)$, which depends on the transverse mass squared $m_{q,\perp}^2 \equiv m_q^2 + p_{q,\perp}^2$ and the string tension $\kappa \approx 1$ GeV/fm. The transverse momentum $p_{q,\perp}$ is locally compensated between quark and antiquark. Due to the dependence on the parton mass, m_q , and/or hadron mass, m_h , the production of strange and, in particular, heavy-quark hadrons is suppressed. The light-cone momentum fraction $z = (E+p_{\parallel})_h/(E+p)_{q\bar{q}}$, where p_{\parallel} is the momentum of the formed hadron h along the direction of the quark q , is given by the string-fragmentation function

$$f(z) \sim \frac{1}{z}(1-z)^a \exp\left(-\frac{bm_{h,\perp}^2}{z}\right), \quad (17.11)$$

where a and b are free parameters. These parameters need to be adjusted to bring the fragmentation into accordance with measured data, *e.g.*, $a = 0.11$ and $b = 0.52$ GeV $^{-2}$ as determined in Ref. 86 (for an overview on tuned parameters see Ref. 87).

17.6.2. Cluster fragmentation: Assuming a local compensation of color based on the *pre-confinement* property of perturbative QCD [88], the remaining gluons at the end of the parton shower evolution are split non-perturbatively into quark-antiquark pairs. Color singlet clusters of typical mass of a couple of GeV are then formed from quark and antiquark of color-connected splittings. These clusters decay directly into two hadrons unless they are either too heavy (relative to an adjustable parameter CLMAX, default value 3.35 GeV), when they decay into two clusters, or too light, in which case a cluster decays into a single hadron, requiring a small rearrangement of energy and momentum with neighboring clusters. The decay of a cluster into two hadrons is assumed to be isotropic in the rest frame of the cluster except if a perturbative-formed quark is involved. A decay channel is chosen based on the phase-space probability, the density of states, and the spin degeneracy of the hadrons. Cluster fragmentation has a compact description with few parameters, due to the phase-space dominance in the hadron formation.

17.7. Fragmentation into identified particles

A great wealth of measurements of e^+e^- fragmentation into identified particles exists. A collection of references to find data on the fragmentation into identified particles is given for Table 40.1. As representatives of all the data, Fig. 17.7 shows fragmentation functions as the scaled momentum spectra of charged particles at several c.m. energies. Heavy flavor particles are dealt with separately in Sect. 17.8.

The measured fragmentation functions are solutions to the DGLAP equation (17.4), but need to be parametrized at some initial scale t_0 (usually 2 GeV 2 for light quarks and gluons). A general parametrization is [90]

$$D_{p \rightarrow h}(x, t_0) = N x^\alpha (1-x)^\beta \left(1 + \frac{\gamma}{x}\right), \quad (17.12)$$

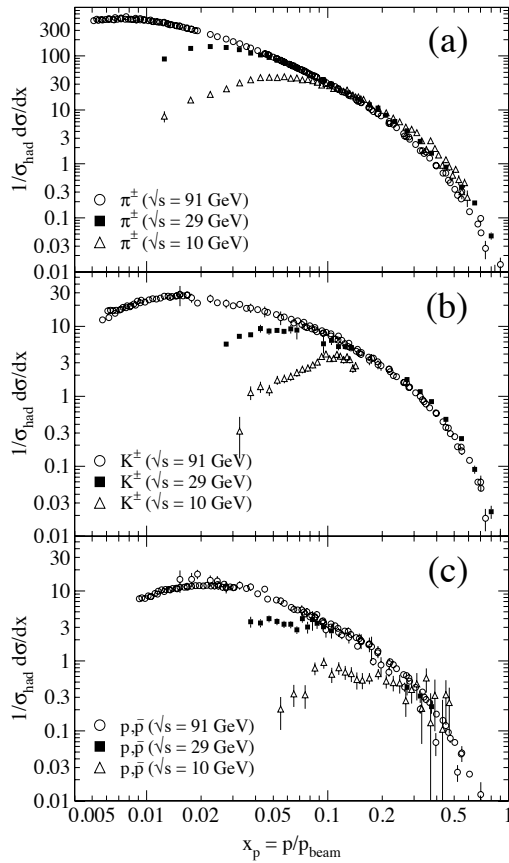


Figure 17.7: Scaled momentum spectra of (a) π^\pm , (b) K^\pm , and (c) p/\bar{p} at $\sqrt{s} = 10, 29$, and 91 GeV are shown [22,25,56,89].

where the normalization N , and the parameters α , β , and γ in general depend on the energy scale t_0 , and also on the type of the parton, p , and the hadron, h . Frequently the term involving γ is left out [66–70]. The parameters of Eq. (17.12), listed in [66–70], were obtained by fitting data on various hadron types for different combinations of partons and hadrons in $p \rightarrow h$ in the range $\sqrt{s} \approx 5 - 200$ GeV.

Many studies have been made of identified particles produced in lepton-hadron scattering, although fewer particle species have been measured than in e^+e^- collisions. References [91–96] and [97–101] are representative of the data from fixed target and ep collider experiments.

Fig. 17.8(a) compares lower-energy fixed-target and HERA data on strangeness production, showing that the HERA spectra have substantially increased multiplicities, albeit with insufficient statistical precision to study scaling violations. The fixed-target data show that the Λ rate substantially exceeds the $\bar{\Lambda}$ rate in the remnant region, owing to the conserved baryon number from the baryon target. Fig. 17.8(b) shows neutral and charged pion fragmentation functions $1/N \cdot dn/dz$, where z is defined as the ratio of the pion energy to that of the exchanged boson, both measured in the laboratory frame. Results are shown from HERMES and the EMC experiments, where HERMES data have been evolved with NLO QCD to $\langle Q^2 \rangle = 25$ GeV² in order to be consistent with the EMC. Each of the experiments uses various kinematic cuts to ensure that the measured particles lie in the region which is expected to be associated with the struck quark. In the DIS kinematic regime accessed at these experiments, and over the range in z shown in Fig. 17.8, the z and x_F variables have similar values [31]. The precision data on identified particles can be used in the study of the quark flavor content of the proton [102].

Data on identified particle production are also useful in studying the universality of jet fragmentation in e^+e^- and DIS. The strangeness

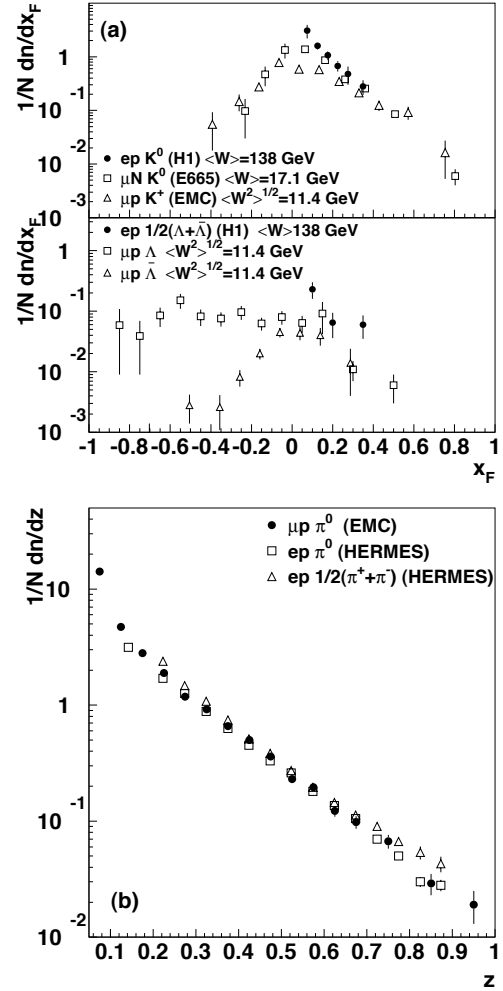


Figure 17.8: (a) $1/N \cdot dn/dx_F$ for identified strange particles in DIS at various values of W [91,94,97]. (b) $1/N \cdot dn/dz$ for measurements of pions from fixed-target DIS experiment [92,95,96].

suppression factor γ_s , as derived principally from tuning the Lund string model [83] within JETSET [72], is typically found to be around 0.3 in e^+e^- experiments [46], although values closer to 0.2 [103] have also been obtained. The converse is true for DIS experiments, with the tendency from HERA [97,99] and recent fixed-target measurements [91] of light strange particle production, to support a stronger suppression ($\gamma_s \approx 0.2$), although values close to 0.3 have also been obtained [104,105].

However, when comparing the description of QCD-based models for lepton-hadron interactions and e^+e^- collisions, it is important to note that the overall description by event generators of inclusively produced hadronic final states is more precise in e^+e^- collisions than lepton-hadron interactions [106]. Predictions of particle rates in lepton-hadron scattering are affected by uncertainties in the modeling of the parton composition of the proton and photon, the extended target remnant, and initial and final state QCD radiation. Furthermore, the tuning of event generators for e^+e^- collisions is typically based on a larger set of parameters and uses more observables [46] than are used when optimizing models for lepton-hadron data [107].

17.8. Heavy quark fragmentation

It was recognized very early [108] that a heavy flavored meson should retain a large fraction of the momentum of the primordial heavy quark, and therefore its fragmentation function should be much harder than that of a light hadron. In the limit of a very heavy quark, one expects the fragmentation function for a heavy quark to go into any heavy hadron to be peaked near 1.

When the heavy quark is produced at a momentum much larger than its mass, one expects important perturbative effects, enhanced by powers of the logarithm of the transverse momentum over the heavy quark mass, to intervene and modify the shape of the fragmentation function. In leading logarithmic order (*i.e.*, including all powers of $\alpha_S \log m_Q/p_T$), the total (*i.e.*, summed over all hadron types) perturbative fragmentation function is simply obtained by solving the leading evolution equation for fragmentation functions, Eq. (17.4), with the initial condition at a scale $\mu^2 = m_Q^2$ given by $D_Q(z, m_Q^2) = \delta(1-z)$ and $D_i(z, m_Q^2) = 0$ for $i \neq Q$ (the notation $D_i(z)$, stands for the probability to produce a heavy quark Q from parton i with a fraction z of the parton momentum).

Several extensions of the leading logarithmic result have appeared in the literature. Next-to-leading-log (NLL) order results for the perturbative heavy quark fragmentation function have been obtained in Ref. 109. At large z , phase space for gluon radiation is suppressed. This exposes large perturbative corrections due to the incomplete cancellation of real gluon radiation and virtual gluon exchange (Sudakov effects), which should be resummed in order to get accurate results. A leading-log (LL) resummation formula has been obtained in [109,110]. Next-to-leading-log resummation has been performed in Ref. 111. Fixed-order calculations of the fragmentation function at order α_S^2 in e^+e^- annihilation have appeared in Ref. 112. This result does not include terms of order $(\alpha_S \log s/m^2)^k$ and $\alpha_S(\alpha_S \log s/m^2)^k$, but it does include correctly all terms up to the order α_S^2 , including terms without any logarithmic enhancements. The result of Ref. 109 for the perturbative initial condition of the heavy quark fragmentation function has been extended to NNLO (next-to-next-to-leading order) in Ref. 113. Other ingredients (*i.e.*, NNLO single inclusive production cross sections for light quarks, and NNLO evolution for fragmentation function) are, however, still missing for a full NNLO analysis of heavy-flavor fragmentation functions.

Inclusion of non-perturbative effects in the calculation of the heavy-quark fragmentation function is done in practice by convolving the perturbative result with a phenomenological non-perturbative form. Among the most popular parameterizations we have the following:

$$\text{Peterson } et al. [114]: D_{np}(z) \propto \frac{1}{z} \left(1 - \frac{1}{z} - \frac{\epsilon}{1-z}\right)^{-2} \quad (17.13)$$

$$\text{Kartvelishvili } et al. [115]: D_{np}(z) \propto z^\alpha(1-z), \quad (17.14)$$

$$\text{Collins\&Spiller [116]: } D_{np}(z) \propto \left(\frac{1-z}{z} + \frac{(2-z)\epsilon_C}{1-z}\right) \times \\ (1+z^2) \left(1 - \frac{1}{z} - \frac{\epsilon_C}{1-z}\right)^{-2} \quad (17.15)$$

$$\text{Colangelo\&Nason [117]: } D_{np}(z) \propto (1-z)^\alpha z^\beta \quad (17.16)$$

$$\text{Bowler [118]: } D_{np}(z) \propto z^{-1} \exp\left(-\frac{bm_{h,\perp}^2}{z}\right) \\ (1-z)^a \exp\left(-\frac{bm_{h,\perp}^2}{z}\right) \quad (17.17)$$

$$\text{Braaten } et al. [119]: \quad (\text{see Eq. (31), (32) in [119]}) \quad (17.18)$$

where ϵ , ϵ_C , a , $bm_{h,\perp}^2$, α , and β are non-perturbative parameters, depending upon the heavy hadron considered. In general, the non-perturbative parameters entering the non-perturbative forms do not have an absolute meaning. They are fitted together with some model of hard radiation, which can be either a shower Monte Carlo, a leading-log or NLL calculation (which may or may not include Sudakov resummation), or a fixed order calculation. In [112], for example, the Peterson *et al.* [114] ϵ parameter for charm and bottom production is fitted from the measured distributions of refs. [120,121] for charm, and of [122] for bottom. If the leading-logarithmic approximation (LLA) is

used for the perturbative part, one finds $\epsilon_c \approx 0.05$ and $\epsilon_b \approx 0.006$; if a second order calculation is used one finds $\epsilon_c \approx 0.035$ and $\epsilon_b \approx 0.0033$; if a NLL calculation is used instead, one finds $\epsilon_c \approx 0.022$ and $\epsilon_b \approx 0.0023$. The larger values found in the LL approximation are consistent with what is obtained in the context of parton shower models [123], as expected. The ϵ parameter for charm and bottom scales roughly with the inverse square of the heavy flavor mass. This behavior can be justified by several arguments [108,124,125]. It can be used to relate the non-perturbative parts of the fragmentation functions of charm and bottom quarks [112,117,126].

17.8.1. Charm quark fragmentation: High statistics data for charmed mesons production near the Υ resonance (excluding decay products of B mesons) have been published [127,128]. They include results for D and D^* , D_s (see also [129,130]) and A_c . Shown in Fig. 17.9(a) are the CLEO and BELLE inclusive cross-sections times branching ratio \mathcal{B} , $s \cdot \mathcal{B} d\sigma/dx_p$, for the production of D^0 and D^{*+} . The variable x_p approximates the light-cone momentum fraction z in Eq. (17.13), but is not identical to it. The two measurements are fairly consistent with each other.

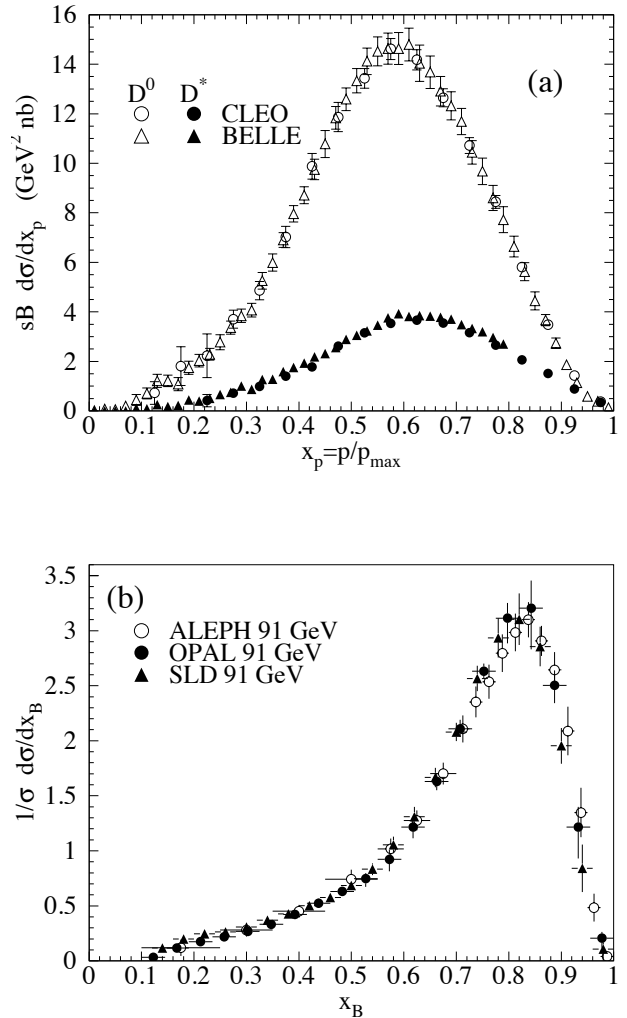


Figure 17.9: (a) Efficiency-corrected inclusive cross-section measurements for the production of D^0 and D^{*+} in e^+e^- annihilation at $\sqrt{s} \approx 10.6$ GeV, excluding B decay products [127,128]. (b) Measured e^+e^- fragmentation function of b quarks into B hadrons at $\sqrt{s} \approx 91$ GeV [131].

The branching ratio \mathcal{B} represents $D^0 \rightarrow K^-\pi^+$ for the D^0 results and for the D^{*+} the product branching fraction: $D^{*+} \rightarrow D^0\pi^+$, $D^0 \rightarrow K^-\pi^+$. Older studies are reported in Refs. [121,132].

Charmed meson spectra on the Z peak have been published by OPAL and ALEPH [86,133]. The relative production fractions of the various hadron species should be process-independent at high energies according to QCD factorization. Combining results near the $T(4S)$ from Refs. [127,128,130,132,134], neglecting the gluon splitting contribution, which is negligible at these energies, we obtain $f(c \rightarrow D^0) = 0.565 \pm 0.032$, $f(c \rightarrow D^+) = 0.246 \pm 0.020$, $f(c \rightarrow D_s^+) = 0.080 \pm 0.017$, $f(c \rightarrow A_c^+) = 0.094 \pm 0.035$, $f(c \rightarrow D^{*0}) = 0.213 \pm 0.024$, $f(c \rightarrow D^{*+}) = 0.224 \pm 0.028$, and $f(c \rightarrow D_s^{*+}) = 0.061 \pm 0.018$, in good agreement with those reported by LEP and SLD (see App. B of Ref. 135). Here, f is the fraction of produced charm quarks that hadronize into the respective hadron, eventually including decays of short-lived resonances.

As is well known, the large (isospin violating) difference in D^+ and D^0 production is well understood as a consequence of the fact that D^* mesons have a mass that is accidentally very near the sum of the D and the pion mass. The small isospin violating mass differences between states of different charge are such that both the D^{*+} and the D^{*0} can decay into the D^0 with large branching fractions, while only the D^{*+} can decay to a D^+ , with a relatively small branching. If we can assume that similar accidents do not happen with higher resonances, we can conclude that D^{*+} and D^{*0} are produced with the same rate, and that D^0 and D^+ not coming from D^* decays are also produced with the same rate. The data are at present consistent with this view within errors, although it would seem to favor a $f(c \rightarrow D^{*+})$ larger than $f(c \rightarrow D^{*0})$. BELLE [128] publishes a ratio $(D^{*+} + D^{*0})/(D^+ + D^0) = 0.527 \pm 0.013 \pm 0.024$, so that the ratio of primary to total D is $0.473 \pm 0.013 \pm 0.024$.

Given the high precision of CLEO's and BELLE's data, it is difficult to obtain good fits of the inclusive cross-sections with the simple parameterizations generally used [114–118], see Ref. 128. It is, however, still possible to obtain good fits to the data using relatively simple forms. In the context of a QCD calculation of the fragmentation function, including NLO initial condition, evolution and coefficient functions, and NLL resummation of Sudakov effects in the initial condition and in the coefficient functions, it was shown in Ref. 136 that a superposition of the form proposed in Ref. 117 and a delta function for the description of D^* 's and primary D mesons yields very good fits to CLEO and BELLE data. In the same work it is shown, however, that one cannot fit simultaneously CLEO/BELLE and ALEPH data in a pure perturbative QCD framework. This fact could be interpreted in terms of power corrections to the coefficient functions, with a suppression $1/Q^2$ (compatible with the result of Ref. 137) or $1/Q$ (similar to the form proposed in Ref. 5).

Charm quark production has also been extensively studied at HERA by the H1 and ZEUS collaborations. Measurements have been made of $D^{*\pm}$, D^\pm , and D_s^\pm mesons [138–142] and the A_c baryon [141]. Various fragmentation quantities have been extracted, some of which are shown in Table 17.1 as measured by H1 and ZEUS, along with averages of these quantities as obtained from e^+e^- data.

17.8.2. Bottom quark fragmentation : Experimental studies of the fragmentation function for b quarks, shown in Fig. 17.9(b), have been performed at LEP and SLD [122,131,144]. Commonly used methods identify the B meson through its semileptonic decay or based upon tracks emerging from the B secondary vertex. The most recent studies [131] fit the B spectrum using a Monte Carlo shower model supplemented with non-perturbative fragmentation functions yielding consistent results.

The experiments measure primarily the spectrum of B mesons. This defines a fragmentation function which includes the effect of the decay of higher mass excitations, like the B^* and B^{**} . In the literature, there is sometimes ambiguity in what is defined to be the bottom fragmentation function. Instead of using what is directly measured (*i.e.*, the B meson spectrum) corrections are applied to account for B^* or B^{**} production in some cases. For a more detailed discussion see [1].

Heavy-flavor production in e^+e^- collisions is the primary source of information for the role of fragmentation effects in heavy-flavor production in hadron-hadron and lepton-hadron collisions. The QCD calculations tend to underestimate the data in certain regions of phase

Table 17.1: Measurements of fragmentation ratios from ep [140,142] and e^+e^- experiments [143]. $R_{u/d}$ is ratio of neutral to charged D -mesons, γ_s is the strangeness suppression factor in charm fragmentation, and P_v^d is the fraction of charged D -mesons produced in a vector state.

$R_{u/d}$	
H1	1.26 ± 0.20 (stat.) ± 0.11 (syst.) ± 0.04 (br. \oplus theo.)
ZEUS	1.22 ± 0.11 (stat.) $^{+0.05}_{-0.02}$ (syst.) ± 0.03 (br.)
e^+e^- av.	1.020 ± 0.069 (stat. \oplus syst.) $^{+0.045}_{-0.047}$ (br.)
γ_s	
H1	0.36 ± 0.10 (stat.) ± 0.01 (syst.) ± 0.08 (br. \oplus theo.)
ZEUS	0.225 ± 0.03 (stat.) $^{+0.018}_{-0.007}$ (syst.) $^{+0.034}_{-0.026}$ (br.)
e^+e^- av.	0.259 ± 0.023 (stat. \oplus syst.) $^{+0.087}_{-0.052}$ (br.)
P_v^d	
H1	0.693 ± 0.045 (stat.) ± 0.004 (syst.) ± 0.009 (br. \oplus theo.)
ZEUS	0.617 ± 0.038 (stat.) $^{+0.017}_{-0.009}$ (syst.) ± 0.017 (br.)
e^+e^- av.	0.614 ± 0.019 (stat. \oplus syst.) $^{+0.023}_{-0.025}$ (br.)

space. Recently, it was also pointed out [145] that the long-standing discrepancy between theoretical calculations and the measured B meson spectrum at the hadron colliders [146] was substantially reduced if a correct use of available information on heavy flavor production from e^+e^- data was made.

Both bottomed- and charmed-mesons spectra have been measured recently at the TEVATRON with unprecedented accuracy [147]. The measured spectra are in good agreement with QCD calculations (including non-perturbative fragmentation effects inferred from e^+e^- data [148]), no longer supporting the previously reported discrepancies [146].

The HERA collaborations have produced a number of measurements of beauty production [139,149]. Compared with LEP data, there is at present insufficient statistical precision to make detailed measurements of the fragmentation properties of b -quarks in lepton-hadron scattering. The data which do exist have been tested against QCD-based models implementing Peterson *et al.* [114] fragmentation.

17.8.3. Gluon splitting into heavy quarks : Besides degrading the fragmentation function by gluon radiation, QCD evolution can also generate soft heavy quarks, increasing in the small x region as s increases. Several theoretical studies are available on the issue of how often $b\bar{b}$ or $c\bar{c}$ pairs are produced indirectly, via a gluon splitting mechanism [150–152]. Experimental results from studies on charm production via gluon splitting and measurements of $g \rightarrow b\bar{b}$ are given in Table 17.2.

In Ref. 151, an explicit calculation of these quantities has been performed. Using these results, charm and bottom multiplicities as reported in Table 17.2 for different values of the masses and of $A_{\text{MS}}^{(5)}$ were computed in Ref. 158. The averaged experimental result for charm, taking correlations into account, $(2.96 \pm 0.38)\%$ [159] is 1–2 standard deviations above the theoretical prediction, preferring lower values of the quark mass and/or a larger value of $A_{\text{MS}}^{(5)}$. However, higher-order corrections may well be substantial at the charm quark mass scale. Better agreement is achieved for bottom.

As reported in Ref. 151, Monte Carlo models are in qualitative agreement with these results, although the spread of the values they obtain is somewhat larger than the theoretical error estimated by the direct calculation. In particular, for charm one finds that while HERWIG [85] and JETSET [72] agree quite well with the theoretical calculation, ARIADNE [160] is higher by roughly a factor of 2, and thus is in better agreement with data. For bottom, agreement between theory, models and data is adequate. For a detailed discussion see Ref. 161.

Table 17.2: Measured fraction of events containing $g \rightarrow c\bar{c}$ and $g \rightarrow b\bar{b}$ subprocesses in Z decays, compared with theoretical predictions. The central/lower/upper values for the theoretical predictions are obtained with $m_c = (1.5 \pm 0.3)$ and $m_b = (4.75 \pm 0.25)$ GeV.

	$\bar{n}_{g \rightarrow c\bar{c}}$ (%)	$\bar{n}_{g \rightarrow b\bar{b}}$ (%)
ALEPH	[133] $3.26 \pm 0.23 \pm 0.42$	[153] $0.2777 \pm 0.042 \pm 0.057$
DELPHI		[154] $0.21 \pm 0.11 \pm 0.09$
L3	[155] $2.45 \pm 0.29 \pm 0.53$	
OPAL	[156] $3.20 \pm 0.21 \pm 0.38$	
SLD		[157] $0.307 \pm 0.071 \pm 0.066$
Theory [151]		
$\Lambda_{\overline{\text{MS}}}^{(5)} = 150 \text{ MeV}$	$1.35^{+0.48}_{-0.30}$	0.20 ± 0.02
$\Lambda_{\overline{\text{MS}}}^{(5)} = 300 \text{ MeV}$	$1.85^{+0.69}_{-0.44}$	0.26 ± 0.03

The discrepancy with the charm prediction may be due to experimental cuts forcing the final state configuration to be more 3-jet like, which increases the charm multiplicity. Calculations that take this possibility into account are given in Ref. 152.

References:

- O. Biebel, P. Nason, and B.R. Webber, Bicocca-FT-01-20, Cavendish-HEP-01/12, MPI-PhE/2001-14, hep-ph/0109282.
- W. Kittel and E.A. De Wolf, *Soft Multihadron Dynamics*, World Scientific, Singapore (2005).
- H.F. Jones, *Nuovo Cimento* **40A**, 1018 (1965); R.P. Feynman, *Photon Hadron Interactions*, W.A. Benjamin, New York (1972); Yu.L. Dokshitzer *et al.*, *Perturbative Quantum Chromodynamics*, ed. A.H. Mueller, World Scientific, Singapore (1989); K.H. Streng, *Z. Phys.* **C2**, 377 (1994).
- V.N. Gribov and L.N. Lipatov, *Sov. J. Nucl. Phys.* **15**, 438 (1972); L.N. Lipatov, *Sov. J. Nucl. Phys.* **20**, 95 (1975); G. Altarelli and G. Parisi, *Nucl. Phys.* **B126**, 298 (1977); Yu.L. Dokshitzer, *Sov. Phys. JETP* **46**, 641 (1977).
- P. Nason and B.R. Webber, *Nucl. Phys.* **B421**, 473 (1994); Erratum *ibid.*, **B480**, 755 (1996).
- W. Furmanski and R. Petronzio, preprint TH.2933-CERN (1980), *Phys. Lett.* **97B**, 437 (1980).
- G. Curci *et al.*, *Nucl. Phys.* **B175**, 27 (1980); E.G. Floratos *et al.*, *Nucl. Phys.* **B192**, 417 (1981); J. Kalinowski *et al.*, *Nucl. Phys.* **B181**, 221 (1981); J. Kalinowski *et al.*, *Nucl. Phys.* **B181**, 253 (1981).
- R.K. Ellis, J. Stirling, and B.R. Webber: *QCD and Collider Physics*, Cambridge University Press, Cambridge (1996).
- ALEPH Collab.: D. Buskulic *et al.*, *Z. Phys.* **C73**, 409 (1997).
- ALEPH Collab.: E. Barate *et al.*, *Phys. Rev.* **294**, 1 (1998).
- AMY Collab.: Y.K. Li *et al.*, *Phys. Rev.* **D41**, 2675 (1990).
- DELPHI Collab.: P. Abreu *et al.*, *Eur. Phys. J.* **C6**, 19 (1999).
- HRS Collab.: D.Bender *et al.*, *Phys. Rev.* **D31**, 1 (1984).
- L3 Collab.: B. Adeva *et al.*, *Phys. Lett.* **B259**, 199 (1991).
- MARK II Collab.: G.S. Abrams *et al.*, *Phys. Rev. Lett.* **64**, 1334 (1990).
- MARK II Collab.: A. Petersen *et al.*, *Phys. Rev.* **D37**, 1 (1988).
- OPAL Collab.: R. Akers *et al.*, *Z. Phys.* **C72**, 191 (1996).
- OPAL Collab.: K. Ackerstaff *et al.*, *Z. Phys.* **C75**, 193 (1997).
- OPAL Collab.: K. Ackerstaff *et al.*, *Eur. Phys. J.* **C7**, 369 (1998).
- OPAL Collab.: G. Abbiendi *et al.*, *Eur. Phys. J.* **C16**, 185 (2000); OPAL Collab.: G. Abbiendi *et al.*, *Eur. Phys. J.* **C27**, 467 (2003).
- OPAL Collab.: G. Abbiendi *et al.*, *Eur. Phys. J.* **C37**, 25 (2004).
- SLD Collab.: K. Abe *et al.*, *Phys. Rev.* **D69**, 072003 (2004).
- TASSO Collab.: R. Brandelik *et al.*, *Phys. Lett.* **B114**, 65 (1982).
- TASSO Collab.: W. Braunschweig *et al.*, *Z. Phys.* **C47**, 187 (1990).
- TPC Collab.: H. Aihara *et al.*, *Phys. Rev. Lett.* **61**, 1263 (1988).
- ALEPH Collab.: D. Barate *et al.*, *Phys. Lett.* **B357**, 487 (1995); Erratum *ibid.*, **B364**, 247 (1995).
- DELPHI Collab.: P. Abreu *et al.*, *Phys. Lett.* **B311**, 408 (1993).
- DELPHI Collab.: P. Abreu *et al.*, *Phys. Lett.* **B398**, 194 (1997).
- DELPHI Collab.: P. Abreu *et al.*, *Eur. Phys. J.* **C13**, 573 (2000); W. de Boer and T. Kußmaul, IEKP-KA/93-8, hep-ph/9309280.
- B.A. Kniehl, G. Kramer, and B. Pötter, *Phys. Rev. Lett.* **85**, 5288 (2001).
- E665 Collab.: M.R. Adams *et al.*, *Phys. Lett.* **B272**, 163 (1991).
- EMC Collab.: M. Arneodo *et al.*, *Z. Phys.* **C35**, 417 (1987).
- H1 Collab.: I. Abt *et al.*, *Z. Phys.* **C63**, 377 (1994).
- ZEUS Collab.: M. Derrick *et al.*, *Z. Phys.* **C70**, 1 (1996).
- ZEUS Collab.: J. Breitweg *et al.*, *Phys. Lett.* **B414**, 428 (1997).
- H1 Collab.: S. Aid *et al.*, *Nucl. Phys.* **B445**, 3 (1995).
- ZEUS Collab.: M. Derrick *et al.*, *Z. Phys.* **C67**, 93 (1995).
- H1 Collab.: C. Adloff *et al.*, *Nucl. Phys.* **B504**, 3 (1997).
- ZEUS Collab.: J. Breitweg *et al.*, *Eur. Phys. J.* **C11**, 251 (1999).
- H1 Collab.: F.D. Aaron *et al.*, *Phys. Lett.* **B654**, 148 (2007).
- MARK II Collab.: J.F. Patrick *et al.*, *Phys. Rev. Lett.* **49**, 1232, (1982).
- D. Graudenz, CERN-TH/96-52.
- P. Dixon *et al.*, *J. Phys.* **G25**, 1453 (1999).
- Yu.L. Dokshitzer *et al.*, *Basics of Perturbative QCD*, Editions Frontières, Paris (1991).
- C.P. Fong and B.R. Webber, *Nucl. Phys.* **B355**, 54 (1992).
- DELPHI Collab.: P. Abreu *et al.*, *Z. Phys.* **C73**, 11 (1996).
- DELPHI Collab.: P. Abreu *et al.*, *Z. Phys.* **C73**, 229 (1997).
- L3 Collab.: P. Achard *et al.*, *Phys. Reports* **399**, 71 (2004).
- TOPAZ Collab.: R. Itoh *et al.*, *Phys. Lett.* **B345**, 335 (1995).
- OPAL Collab.: M.Z. Akrawy *et al.*, *Phys. Lett.* **B247**, 617 (1990).
- TASSO Collab.: W. Braunschweig *et al.*, *Z. Phys.* **C22**, 307 (1990).
- BES Collab.: J.Z. Bai *et al.*, *Phys. Rev.* **D69**, 072002 (2004).
- ALEPH Collab.: D. Buskulic *et al.*, *Z. Phys.* **C55**, 209 (1992).
- ALEPH Collab.: A. Heister *et al.*, *Eur. Phys. J.* **C35**, 457 (2004).
- DELPHI Collab.: P. Abreu *et al.*, *Phys. Lett.* **B275**, 231 (1992).
- DELPHI Collab.: P. Abreu *et al.*, *Eur. Phys. J.* **C5**, 585 (1998).
- DELPHI Collab.: P. Abreu *et al.*, *Phys. Lett.* **B459**, 397 (1999).
- L3 Collab.: M. Acciarri *et al.*, *Phys. Lett.* **B444**, 569 (1998).
- TPC/TWO-GAMMA Collab.: H. Aihara *et al.*, "Charged Hadron Production in e^+e^- Annihilation at $\sqrt{s} = 29 \text{ GeV}$," LBL 23737.
- OPAL Collab.: R. Akers *et al.*, *Z. Phys.* **C86**, 203 (1995).
- J. Binnewies, Hamburg University PhD Thesis, DESY 97-128, hep-ph/9707269.
- ALEPH Collab.: R. Barate *et al.*, *Eur. Phys. J.* **C17**, 1 (2000); OPAL Collab.: R. Akers *et al.*, *Z. Phys.* **C68**, 179 (1995); OPAL Collab.: G. Abbiendi *et al.*, *Eur. Phys. J.* **C11**, 217 (1999).
- COMPASS Collab.: G. Baum *et al.*, CERN-SPSLC-96-14; CERN-SPSLC-P-297.
- HERMES Collab.: A. Airapetian *et al.*, *Phys. Rev.* **D71**, 012003 (2005).
- SMC Collab.: B. Adeva *et al.*, *Phys. Lett.* **B420**, 180, (1998).
- J. Binnewies *et al.*, *Phys. Rev.* **D52**, 4947 (1995); *Z. Phys.* **C65**, 471 (1995).
- B.A. Kniehl *et al.*, *Nucl. Phys.* **B582**, 514 (2000).
- S.Albino *et al.*, *Nucl. Phys.* **B725**, 181, (2005); *ibid.*, **B734**, 50 (2006).

69. S. Kretzer, Phys. Rev. **D62**, 054001 (2000).
70. L. Bourhis *et al.*, Eur. Phys. J. **C19**, 89 (2001).
71. S. Kretzer *et al.*, Eur. Phys. J. **C22**, 269 (2001).
72. T. Sjöstrand and M. Bengtsson, Comp. Phys. Comm. **43**, 367 (1987);
T. Sjöstrand, Comput. Phys. Commun. **82**, 74 (1994).
73. P.J. Mulders and R.D. Tangerman, Nucl. Phys. **B461**, 197 (1996);
Erratum *ibid.*, **B484**, 538 (1997).
74. R. Jacob, Nucl. Phys. **A711**, 35 (2002).
75. J.P. Ralston and D.E. Soper, Nucl. Phys. **B152**, 109 (1979).
76. J. Collins, Nucl. Phys. **B396**, 161 (1993).
77. CLAS Collab.: H. Avakian *et al.*, Phys. Rev. **D69**, 112004 (2004);
HERMES Collab.: A. Airapetian *et al.*, Phys. Rev. Lett. **84**, 4047 (2000);
HERMES Collab.: A. Airapetian *et al.*, Phys. Rev. **D64**, 097101 (2001).
78. D. Sivers, Phys. Rev. **D43**, 261 (1991).
79. HERMES Collab.: A. Airapetian *et al.*, Phys. Rev. Lett. **94**, 012002 (2005).
80. COMPASS Collab.: V.Y. Alexakhin *et al.*, Phys. Rev. Lett. **94**, 202002 (2005).
81. COMPASS Collab.: V.Y. Alexakhin *et al.*, Nucl. Phys. **B765**, 31 (2007).
82. X. Artru and G. Mennessier, Nucl. Phys. **B70**, 93 (1974).
83. B. Andersson *et al.*, Phys. Reports **97**, 31 (1983).
84. S. Chun and C. Buchanan, Phys. Reports **292**, 239 (1998).
85. G. Marchesini *et al.*, Comput. Phys. Commun. **67**, 465 (1992);
G. Corcella *et al.*, JHEP **0101**, 010 (2001).
86. OPAL Collab.: G. Alexander *et al.*, Z. Phys. **C69**, 543 (1996).
87. M. Schmelling, Phys. Script. **51**, 683 (1995).
88. D. Amati and G. Veneziano, Phys. Lett. **B83**, 87 (1979).
89. ALEPH Collab.: D. Buskulic *et al.*, Z. Phys. **C66**, 355 (1995);
ARGUS Collab.: H. Albrecht *et al.*, Z. Phys. **C44**, 547 (1989);
OPAL Collab.: R. Akers *et al.*, Z. Phys. **C63**, 181 (1994);
SLD Collab.: K. Abe *et al.*, Phys. Rev. **D59**, 052001 (1999).
90. B.A. Kniehl *et al.*, Nucl. Phys. **B597**, 337 (2001).
91. E665 Collab.: M.R. Adams *et al.*, Z. Phys. **C61**, 539 (1994).
92. EMC Collab.: J.J. Aubert *et al.*, Z. Phys. **C18**, 189 (1983);
EMC Collab.: M. Arneodo *et al.*, Phys. Lett. **B150**, 458 (1985).
93. EMC Collab.: M. Arneodo *et al.*, Z. Phys. **C33**, 167 (1986).
94. EMC Collab.: M. Arneodo *et al.*, Z. Phys. **C34**, 283 (1987).
95. HERMES Collab.: A. Airapetian *et al.*, Eur. Phys. J. **C21**, 599 (2001).
96. T.P. McPharlin *et al.*, Phys. Lett. **B90**, 479 (1980).
97. H1 Collab.: S. Aid *et al.*, Nucl. Phys. **B480**, 3 (1996).
98. H1 Collab.: C. Adloff *et al.*, Eur. Phys. J. **C18**, 293 (2000);
H1 Collab.: A. Aktas *et al.*, Eur. Phys. J. **C36**, 413 (2004).
99. ZEUS Collab.: M. Derrick *et al.*, Z. Phys. **C68**, 29 (1995);
ZEUS Collab.: J. Breitweg *et al.*, Eur. Phys. J. **C2**, 77 (1998).
100. ZEUS Collab.: S. Chekanov *et al.*, Phys. Lett. **B553**, 141 (2003).
101. ZEUS Collab.: S. Chekanov *et al.*, Nucl. Phys. **B786**, 121 (2007).
102. S. Albino *et al.*, Phys. Rev. **D75**, 034018, (2007).
103. OPAL Collab.: P.D. Acton *et al.*, Phys. Lett. **B305**, 407 (1993).
104. E632 Collab.: D. DeProspero *et al.*, Phys. Rev. **D50**, 6691 (1994).
105. ZEUS Collab.: S. Chekanov *et al.*, Eur. Phys. J. **C51**, 1 (2007).
106. G. Grindhammer *et al.*, in: *Proceedings of the Workshop on Monte Carlo Generators for HERA Physics*, Hamburg, Germany, 1998/1999.
107. N. Brook *et al.*, in: *Proceedings of the Workshop for Future HERA Physics at HERA*, Hamburg, Germany, 1996.
108. V.A. Khoze *et al.*, *Proceedings, Conference on High-Energy Physics, Tbilisi 1976*;
J.D. Bjorken, Phys. Rev. **D17**, 171 (1978).
109. B. Mele and P. Nason, Phys. Lett. **B245**, 635 (1990);
Nucl. Phys. **B361**, 626 (1991).
110. Yu.L. Dokshitzer *et al.*, Phys. Rev. **D53**, 89 (1996).
111. M. Cacciari and S. Catani, Nucl. Phys. **B617**, 253 (2001).
112. P. Nason and C. Oleari, Phys. Lett. **B418**, 199 (1998);
ibid., **B447**, 327 (1999);
Nucl. Phys. **B565**, 245 (2000).
113. K. Melnikov and A. Mitov, Phys. Rev. **D70**, 034027 (2004).
114. C. Peterson *et al.*, Phys. Rev. **D27**, 105 (1983).
115. V.G. Kartvelishvili *et al.*, Phys. Lett. **B78**, 615 (1978).
116. P. Collins and T. Spiller, J. Phys. **G11**, 1289 (1985).
117. G. Colangelo and P. Nason, Phys. Lett. **B285**, 167 (1992).
118. M.G. Bowler, Z. Phys. **C11**, 169 (1981).
119. E. Braaten *et al.*, Phys. Rev. **D51**, 4819 (1995).
120. OPAL Collab.: R. Akers *et al.*, Z. Phys. **C67**, 27 (1995).
121. ARGUS Collab.: H. Albrecht *et al.*, Z. Phys. **C52**, 353 (1991).
122. ALEPH Collab.: D. Buskulic *et al.*, Phys. Lett. **B357**, 699 (1995).
123. J. Chrin, Z. Phys. **C36**, 163 (1987).
124. R.L. Jaffe and L. Randall, Nucl. Phys. **B412**, 79 (1994);
P. Nason and B. Webber, Phys. Lett. **B395**, 355 (1997).
125. M. Cacciari and E. Gardi, Nucl. Phys. **B664**, 299 (2003).
126. L. Randall and N. Rius, Nucl. Phys. **B441**, 167 (1995).
127. CLEO Collab.: M. Artuso *et al.*, Phys. Rev. **D70**, 112001 (2004).
128. BELLE Collab.: R. Seuster *et al.*, Phys. Rev. **D73**, 032002 (2006).
129. CLEO Collab.: R.A. Briere *et al.*, Phys. Rev. **D62**, 112003 (2000).
130. BABAR Collab.: B. Aubert *et al.*, Phys. Rev. **D65**, 0911004 (2002).
131. ALEPH Collab.: A. Heister *et al.*, Phys. Lett. **B512**, 30 (2001);
OPAL Collab.: G. Abbiendi *et al.*, Eur. Phys. J. **C29**, 463 (2003);
SLD Collab.: K. Abe *et al.*, Phys. Rev. **D65**, 092006 (2002);
Erratum *ibid.*, **D66**, 079905 (2002).
132. CLEO Collab.: D. Bortoletto *et al.*, Phys. Rev. **D37**, 1719 (1988).
133. ALEPH Collab.: R. Barate *et al.*, Phys. Lett. **B561**, 213 (2003).
134. ARGUS Collab.: H. Albrecht *et al.*, Z. Phys. **C54**, 1 (1992).
135. LEP Collab. and the LEP and SLD electroweak and heavy flavour working groups, hep-ex/0412015.
136. M. Cacciari *et al.*, JHEP **0604**, 006 (2006).
137. M. Dasgupta and B.R. Webber, Nucl. Phys. **B484**, 247 (1997).
138. H1 Collab.: C. Adloff *et al.*, Nucl. Phys. **B520**, 191 (2001);
H1 Collab.: C. Adloff *et al.*, Phys. Lett. **B528**, 199 (2002);
H1 Collab.: A. Aktas *et al.*, Eur. Phys. J. **C40**, 56 (2005);
H1 Collab.: A. Aktas *et al.*, Eur. Phys. J. **C45**, 23 (2006);
ZEUS Collab.: J. Breitweg *et al.*, Phys. Lett. **B481**, 213 (2000);
ZEUS Collab.: S. Chekanov *et al.*, Phys. Lett. **B545**, 244 (2002);
ZEUS Collab.: S. Chekanov *et al.*, Nucl. Phys. **B672**, 3 (2003);
ZEUS Collab.: S. Chekanov *et al.*, Phys. Lett. **B590**, 143 (2004);
ZEUS Collab.: S. Chekanov *et al.*, Phys. Rev. **D69**, 012004 (2004).
139. H1 Collab.: A. Aktas *et al.*, Phys. Lett. **B621**, 56 (2005).
140. H1 Collab.: A. Aktas *et al.*, Eur. Phys. J. **C38**, 447 (2005).
141. ZEUS Collab.: S. Chekanov *et al.*, Eur. Phys. J. **C44**, 351 (2005).
142. ZEUS Collab.: S. Chekanov *et al.*, JHEP **0707**, 074 (2007).
143. L. Gladilin, hep-ex/9912064.
144. L3 Collab.: B. Adeva *et al.*, Phys. Lett. **B261**, 177 (1991).
145. M. Cacciari and P. Nason, Phys. Rev. Lett. **89**, 122003 (2002).
146. CDF Collab.: F. Abe *et al.*, Phys. Rev. Lett. **71**, 500 (1993);
CDF Collab.: F. Abe *et al.*, Phys. Rev. Lett. **71**, 2396 (1993);
CDF Collab.: F. Abe *et al.*, Phys. Rev. **D50**, 4252 (1994);
CDF Collab.: F. Abe *et al.*, Phys. Rev. Lett. **75**, 1451 (1995);
CDF Collab.: D. Acosta *et al.*, Phys. Rev. **D66**, 032002 (2002);
CDF Collab.: D. Acosta *et al.*, Phys. Rev. **D65**, 052005 (2002);
D0 Collab.: S. Abachi *et al.*, Phys. Rev. Lett. **74**, 3548 (1995);
UA1 Collab.: C. Albajar *et al.*, Phys. Lett. **B186**, 237 (1987);
UA1 Collab.: C. Albajar *et al.*, Phys. Lett. **B256**, 121 (1991);
Erratum *ibid.*, **B272**, 497 (1991).

147. CDF Collab.: D. Acosta *et al.*, Phys. Rev. Lett. **91**, 241804 (2003);
CDF Collab.: D. Acosta *et al.*, Phys. Rev. **D71**, 032001 (2005).
148. M. Cacciari and P. Nason, JHEP **0309**, 006 (2003);
M. Cacciari *et al.*, JHEP **0407**, 033 (2004);
B.A. Kniehl *et al.*, Phys. Rev. Lett. **96**, 012001 (2006).
149. H1 Collab.: C. Adloff *et al.*, Phys. Lett. **B467**, 156 (1999);
H1 Collab.: A. Aktas *et al.*, Eur. Phys. J. **C41**, 453 (2005);
ZEUS Collab.: J. Breitweg *et al.*, Eur. Phys. J. **C18**, 625 (2001);
ZEUS Collab.: S. Chekanov *et al.*, Phys. Lett. **B599**, 173 (2004).
150. A.H. Mueller and P. Nason, Nucl. Phys. **B266**, 265 (1986);
M.L. Mangano and P. Nason, Phys. Lett. **B285**, 160 (1992).
151. M.H. Seymour, Nucl. Phys. **B436**, 163 (1995).
152. D.J. Miller and M.H. Seymour, Phys. Lett. **B435**, 213 (1998).
153. ALEPH Collab.: R. Barate *et al.*, Phys. Lett. **B434**, 437 (1998).
154. DELPHI Collab.: P. Abreu *et al.*, Phys. Lett. **B405**, 202 (1997).
155. L3 Collab.: M. Acciarri *et al.*, Phys. Lett. **B476**, 243 (2000).
156. OPAL Collab.: G. Abbiendi *et al.*, Eur. Phys. J. **C13**, 1 (2000).
157. SLD Collab.: K. Abe *et al.*, SLAC-PUB-8157, hep-ex/9908028.
158. S. Frixione *et al.*, Heavy Quark Production, in A.J. Buras and M. Lindner (eds.), *Heavy flavours II*, World Scientific, Singapore (1998), hep-ph/9702287.
159. A. Giammanco, in: *Proceedings of the XII International Workshop on Deep Inelastic Scattering DIS'2004*, Štrbské Pleso, Slovakia.
160. L. Lönnblad, Comp. Phys. Comm. **71**, 15 (1992).
161. A. Ballestrero *et al.*, CERN-2000-09-B, hep-ph/0006259.

18. EXPERIMENTAL TESTS OF GRAVITATIONAL THEORY

Revised September 2007 by T. Damour (IHES, Bures-sur-Yvette, France).

Einstein's General Relativity, the current "standard" theory of gravitation, describes gravity as a universal deformation of the Minkowski metric:

$$g_{\mu\nu}(x^\lambda) = \eta_{\mu\nu} + h_{\mu\nu}(x^\lambda), \text{ where } \eta_{\mu\nu} = \text{diag}(-1, +1, +1, +1). \quad (18.1)$$

Alternatively, it can be defined as the unique, consistent, local theory of a massless spin-2 field $h_{\mu\nu}$, whose source must then be the total, conserved energy-momentum tensor [1]. General Relativity is classically defined by two postulates. One postulate states that the Lagrangian density describing the propagation and self-interaction of the gravitational field is

$$\mathcal{L}_{\text{Ein}}[g_{\mu\nu}] = \frac{c^4}{16\pi G_N} \sqrt{g} g^{\mu\nu} R_{\mu\nu}(g), \quad (18.2)$$

$$R_{\mu\nu}(g) = \partial_\alpha \Gamma_{\mu\nu}^\alpha - \partial_\nu \Gamma_{\mu\alpha}^\alpha + \Gamma_{\alpha\beta}^\beta \Gamma_{\mu\nu}^\alpha - \Gamma_{\alpha\nu}^\beta \Gamma_{\mu\beta}^\alpha, \quad (18.3)$$

$$\Gamma_{\mu\nu}^\lambda = \frac{1}{2} g^{\lambda\sigma} (\partial_\mu g_{\nu\sigma} + \partial_\nu g_{\mu\sigma} - \partial_\sigma g_{\mu\nu}), \quad (18.4)$$

where G_N is Newton's constant, $g = -\det(g_{\mu\nu})$, and $g^{\mu\nu}$ is the matrix inverse of $g_{\mu\nu}$. A second postulate states that $g_{\mu\nu}$ couples universally, and minimally, to all the fields of the Standard Model by replacing everywhere the Minkowski metric $\eta_{\mu\nu}$. Schematically (suppressing matrix indices and labels for the various gauge fields and fermions and for the Higgs doublet),

$$\begin{aligned} \mathcal{L}_{\text{SM}}[\psi, A_\mu, H, g_{\mu\nu}] = & -\frac{1}{4} \sum \sqrt{g} g^{\mu\alpha} g^{\nu\beta} F_{\mu\nu}^\alpha F_{\alpha\beta}^\alpha \\ & - \sum \sqrt{g} \bar{\psi} \gamma^\mu D_\mu \psi \\ & - \frac{1}{2} \sqrt{g} g^{\mu\nu} \overline{D_\mu H} D_\nu H - \sqrt{g} V(H) \\ & - \sum \lambda \sqrt{g} \bar{\psi} H \psi, \end{aligned} \quad (18.5)$$

where $\gamma^\mu \gamma^\nu + \gamma^\nu \gamma^\mu = 2g^{\mu\nu}$, and where the covariant derivative D_μ contains, besides the usual gauge field terms, a (spin-dependent) gravitational contribution $\Gamma_\mu(x)$ [2]. From the total action follow Einstein's field equations,

$$R_{\mu\nu} - \frac{1}{2} R g_{\mu\nu} = \frac{8\pi G_N}{c^4} T_{\mu\nu}. \quad (18.6)$$

Here $R = g^{\mu\nu} R_{\mu\nu}$, $T_{\mu\nu} = g_{\mu\alpha} g_{\nu\beta} T^{\alpha\beta}$, and $T^{\mu\nu} = (2/\sqrt{g}) \delta \mathcal{L}_{\text{SM}} / \delta g_{\mu\nu}$ is the (symmetric) energy-momentum tensor of the Standard Model matter. The theory is invariant under arbitrary coordinate transformations: $x'^\mu = f^\mu(x^\nu)$. To solve the field equations Eq. (18.6), one needs to fix this coordinate gauge freedom. *E.g.*, the "harmonic gauge" (which is the analogue of the Lorentz gauge, $\partial_\mu A^\mu = 0$, in electromagnetism) corresponds to imposing the condition $\partial_\nu (\sqrt{g} g^{\mu\nu}) = 0$.

In this *Review*, we only consider the classical limit of gravitation (*i.e.* classical matter and classical gravity). Considering quantum matter in a classical gravitational background already poses interesting challenges, notably the possibility that the zero-point fluctuations of the matter fields generate a nonvanishing vacuum energy density ρ_{vac} , corresponding to a term $-\sqrt{g} \rho_{\text{vac}}$ in \mathcal{L}_{SM} [3]. This is equivalent to adding a "cosmological constant" term $+\Lambda g_{\mu\nu}$ on the left-hand side of Einstein's equations Eq. (18.6), with $\Lambda = 8\pi G_N \rho_{\text{vac}}/c^4$. Recent cosmological observations (see the following *Reviews*) suggest a positive value of Λ corresponding to $\rho_{\text{vac}} \approx (2.3 \times 10^{-3} \text{eV})^4$. Such a small value has a negligible effect on the tests discussed below. Quantizing the gravitational field itself poses a very difficult challenge because of the perturbative non-renormalizability of Einstein's Lagrangian. Superstring theory offers a promising avenue toward solving this challenge.

18.1. Experimental tests of the coupling between matter and gravity

The universality of the coupling between $g_{\mu\nu}$ and the Standard Model matter postulated in Eq. (18.5) ("Equivalence Principle") has many observable consequences. First, it predicts that the outcome of a local non-gravitational experiment, referred to local standards, does not depend on where, when, and in which locally inertial frame, the experiment is performed. This means, for instance, that local experiments should neither feel the cosmological evolution of the universe (constancy of the "constants"), nor exhibit preferred directions in spacetime (isotropy of space, local Lorentz invariance). These predictions are consistent with many experiments and observations. The best limit on a possible time variation of the basic coupling constants concerns the fine-structure constant α_{em} , and has been obtained by analyzing a natural fission reactor phenomenon which took place at Oklo, Gabon, two billion years ago [4]. A conservative estimate of the (95% C.L.) Oklo limit on the variability of α_{em} is (see second reference in [4])

$$-0.9 \times 10^{-7} < \frac{\alpha_{\text{em}}^{\text{Oklo}} - \alpha_{\text{em}}^{\text{now}}}{\alpha_{\text{em}}} < 1.2 \times 10^{-7}, \quad (18.7)$$

which corresponds to the following limit on the average time derivative of α_{em}

$$-6.7 \times 10^{-17} \text{yr}^{-1} < \dot{\alpha}_{\text{em}}/\alpha_{\text{em}} < 5.0 \times 10^{-17} \text{yr}^{-1}. \quad (18.8)$$

The second best limit on the variability of α_{em} comes from analyzing isotopic measurements of some meteorites dating back to the formation of the solar system (about 4.6 Gyr ago). The ensuing determination of the lifetime of Rhenium 187 can be interpreted in terms of the following bound: $(\alpha_{\text{em}}^{4.6\text{Gyr}} - \alpha_{\text{em}}^{\text{now}})/\alpha_{\text{em}} = (8 \pm 8) \times 10^{-7}$ [5]. Recent measurements of absorption lines in astronomical spectra also give stringent limits on the variability of α_{em} [6], which disagree with an earlier claim of a non-zero effect [7]. Direct laboratory limits on the time variation of α_{em} (based on monitoring the frequency ratio of several different atomic clocks) are [8]: $\dot{\alpha}_{\text{em}}/\alpha_{\text{em}} = (-0.9 \pm 2.9) \times 10^{-15} \text{yr}^{-1}$, which is less stringent than Eq. (18.8), but less model-dependent. See Ref. 9 for a general review of the issue of "variable constants."

The highest precision tests of the isotropy of space have been performed by looking for possible quadrupolar shifts of nuclear energy levels [10]. The (null) results can be interpreted as testing the fact that the various pieces in the matter Lagrangian Eq. (18.5) are indeed coupled to one and the same external metric $g_{\mu\nu}$ to the 10^{-27} level. For astrophysical constraints on possible Planck-scale violations of Lorentz invariance, see Ref. 11.

The universal coupling to $g_{\mu\nu}$ postulated in Eq. (18.5) implies that two (electrically neutral) test bodies dropped at the same location and with the same velocity in an external gravitational field fall in the same way, independently of their masses and compositions. The universality of the acceleration of free fall has been verified below the 10^{-12} level for laboratory bodies [12], notably earth-core-like and moon-mantle-like bodies [13],

$$(\Delta a/a)_{\text{ECMM}} = (3.6 \pm 5.0) \times 10^{-13}, \quad (18.9)$$

as well as for the gravitational accelerations of the Earth and the Moon toward the Sun [14],

$$(\Delta a/a)_{\text{EarthMoon}} = (-1.0 \pm 1.4) \times 10^{-13}. \quad (18.10)$$

See also Ref. 15 for *short-range* tests of the universality of free-fall.

Finally, Eq. (18.5) also implies that two identically constructed clocks located at two different positions in a static external Newtonian potential $U(\mathbf{x}) = \sum G_N m/r$ exhibit, when intercompared by means of electromagnetic signals, the (apparent) difference in clock rate,

$$\frac{\tau_1}{\tau_2} = \frac{\nu_2}{\nu_1} = 1 + \frac{1}{c^2} [U(\mathbf{x}_1) - U(\mathbf{x}_2)] + O\left(\frac{1}{c^4}\right), \quad (18.11)$$

independently of their nature and constitution. This universal gravitational redshift of clock rates has been verified at the 10^{-4} level by comparing a hydrogen-maser clock flying on a rocket up to an altitude $\sim 10,000$ km to a similar clock on the ground [16]. For more details and references on experimental gravity see, *e.g.*, Refs. 17 and 18.

18.2. Tests of the dynamics of the gravitational field in the weak field regime

The effect on matter of one-graviton exchange, *i.e.*, the interaction Lagrangian obtained when solving Einstein's field equations Eq. (18.6) written in, say, the harmonic gauge at first order in $h_{\mu\nu}$,

$$\square h_{\mu\nu} = -\frac{16\pi G_N}{c^4}(T_{\mu\nu} - \frac{1}{2}T\eta_{\mu\nu}) + O(h^2) + O(hT), \quad (18.12)$$

reads $-(8\pi G_N/c^4)T^{\mu\nu}\square^{-1}(T_{\mu\nu} - \frac{1}{2}T\eta_{\mu\nu})$. For a system of N moving

point masses, with free Lagrangian $L^{(1)} = \sum_{A=1}^N -m_A c^2 \sqrt{1 - \mathbf{v}_A^2/c^2}$, this interaction, expanded to order v^2/c^2 , reads (with $r_{AB} \equiv |\mathbf{x}_A - \mathbf{x}_B|$, $\mathbf{n}_{AB} \equiv (\mathbf{x}_A - \mathbf{x}_B)/r_{AB}$)

$$L^{(2)} = \frac{1}{2} \sum_{A \neq B} \frac{G_N m_A m_B}{r_{AB}} \left[1 + \frac{3}{2c^2}(\mathbf{v}_A^2 + \mathbf{v}_B^2) - \frac{7}{2c^2}(\mathbf{v}_A \cdot \mathbf{v}_B) - \frac{1}{2c^2}(\mathbf{n}_{AB} \cdot \mathbf{v}_A)(\mathbf{n}_{AB} \cdot \mathbf{v}_B) + O\left(\frac{1}{c^4}\right) \right]. \quad (18.13)$$

The two-body interactions (Eq. (18.13)) exhibit v^2/c^2 corrections to Newton's $1/r$ potential induced by spin-2 exchange. Consistency at the “post-Newtonian” level $v^2/c^2 \sim G_N m/rc^2$ requires that one also considers the three-body interactions induced by some of the three-graviton vertices and other nonlinearities (terms $O(h^2)$ and $O(hT)$ in Eq. (18.12)),

$$L^{(3)} = -\frac{1}{2} \sum_{B \neq A \neq C} \frac{G_N^2 m_A m_B m_C}{r_{AB} r_{AC} c^2} + O\left(\frac{1}{c^4}\right). \quad (18.14)$$

All currently performed gravitational experiments in the solar system, including perihelion advances of planetary orbits, the bending and delay of electromagnetic signals passing near the Sun, and very accurate ranging data to the Moon obtained by laser echoes, are compatible with the post-Newtonian results Eqs. (18.12)–(18.14).

Similar to what is done in discussions of precision electroweak experiments, it is useful to quantify the significance of precision gravitational experiments by parameterizing plausible deviations from General Relativity. The addition of a mass-term in Einstein's field equations leads to a score of theoretical difficulties [19] which have not yet received any consensual solution. We shall, therefore, not consider here the ill-defined “mass of the graviton” as a possible deviation parameter from General Relativity (see, however, the phenomenological limits quoted in the Section “Gauge and Higgs Bosons” of this *Review*). Deviations from Einstein's pure spin-2 theory are then defined by adding new, bosonic light or massless, macroscopically coupled fields. The possibility of new gravitational-strength couplings leading (on small, and possibly large, scales) to deviations from Einsteinian (and Newtonian) gravity is suggested by String Theory [20], and by Brane World ideas [21]. For compilations of experimental constraints on Yukawa-type additional interactions, see Refs. [12,22,23] and the Section “Extra Dimensions” in this *Review*. Recent experiments have set limits on non-Newtonian forces below 0.056 mm [24].

Here, we shall focus on the parametrization of long-range deviations from relativistic gravity obtained by adding a massless scalar field φ coupled to the trace of the energy-momentum tensor $T = g_{\mu\nu}T^{\mu\nu}$ [25]. The most general such theory contains an arbitrary function $a(\varphi)$ of the scalar field, and can be defined by the Lagrangian

$$\mathcal{L}_{\text{tot}}[g_{\mu\nu}, \varphi, \psi, A_\mu, H] = \frac{c^4}{16\pi G} \sqrt{g}(R(g) - 2g^{\mu\nu}\partial_\mu\varphi\partial_\nu\varphi) + \mathcal{L}_{\text{SM}}[\psi, A_\mu, H, \tilde{g}_{\mu\nu}], \quad (18.15)$$

where G is a “bare” Newton constant, and where the Standard Model matter is coupled not to the “Einstein” (pure spin-2) metric $g_{\mu\nu}$, but to the conformally related (“Jordan-Fierz”) metric $\tilde{g}_{\mu\nu} = \exp(2a(\varphi))g_{\mu\nu}$. The scalar field equation $\square_g\varphi = -(4\pi G/c^4)a(\varphi)T$ displays $\alpha(\varphi) \equiv \partial a(\varphi)/\partial\varphi$ as the basic (field-dependent) coupling between φ and matter [26]. The one-parameter (ω) Jordan-Fierz-Brans-Dicke theory [25] is the special case $a(\varphi) = \alpha_0\varphi$ leading to a field-independent coupling $\alpha(\varphi) = \alpha_0$ (with $\alpha_0^2 = 1/(2\omega + 3)$).

In the weak-field slow-motion limit appropriate to describing gravitational experiments in the solar system, the addition of φ modifies Einstein's predictions only through the appearance of two “post-Einstein” dimensionless parameters: $\bar{\gamma} = -2\alpha_0^2/(1 + \alpha_0^2)$ and $\bar{\beta} = +\frac{1}{2}\beta_0\alpha_0^2/(1 + \alpha_0^2)$, where $\alpha_0 \equiv \alpha(\varphi_0)$, $\beta_0 \equiv \partial\alpha(\varphi_0)/\partial\varphi_0$, φ_0 denoting the vacuum expectation value of φ . These parameters show up also naturally (in the form $\gamma_{\text{PPN}} = 1 + \bar{\gamma}$, $\beta_{\text{PPN}} = 1 + \bar{\beta}$) in phenomenological discussions of possible deviations from General Relativity [17,27]. The parameter $\bar{\gamma}$ measures the admixture of spin 0 to Einstein's graviton, and contributes an extra term $+\bar{\gamma}(\mathbf{v}_A - \mathbf{v}_B)^2/c^2$ in the square brackets of the two-body Lagrangian Eq. (18.13). The parameter $\bar{\beta}$ modifies the three-body interaction Eq. (18.14) by an overall multiplicative factor $1 + 2\bar{\beta}$. Moreover, the combination $\eta \equiv 4\bar{\beta} - \bar{\gamma}$ parameterizes the lowest order effect of the self-gravity of orbiting masses by modifying the Newtonian interaction energy terms in Eq. (18.13) into $G_{AB}m_A m_B/r_{AB}$, with a body-dependent gravitational “constant” $G_{AB} = G_N[1 + \eta(E_A^{\text{grav}}/m_A c^2 + E_B^{\text{grav}}/m_B c^2) + O(1/c^4)]$, where $G_N = G \exp[2a(\varphi_0)](1 + \alpha_0^2)$ and where E_A^{grav} denotes the gravitational binding energy of body A .

The best current limits on the post-Einstein parameters $\bar{\gamma}$ and $\bar{\beta}$ are (at the 68% confidence level):

$$\bar{\gamma} = (2.1 \pm 2.3) \times 10^{-5}, \quad (18.16)$$

deduced from the additional Doppler shift experienced by radio-wave beams connecting the Earth to the Cassini spacecraft when they passed near the Sun [28], and

$$4\bar{\beta} - \bar{\gamma} = (4.4 \pm 4.5) \times 10^{-4}, \quad (18.17)$$

from Lunar Laser Ranging measurements [14] of a possible polarization of the Moon toward the Sun [29]. More stringent limits on $\bar{\gamma}$ are obtained in models (*e.g.*, string-inspired ones [20]) where scalar couplings violate the Equivalence Principle.

18.3. Tests of the dynamics of the gravitational field in the radiative and/or strong field regimes

The discovery of pulsars (*i.e.*, rotating neutron stars emitting a beam of radio noise) in gravitationally bound orbits [30,31] has opened up an entirely new testing ground for relativistic gravity, giving us an experimental handle on the regime of radiative and/or strong gravitational fields. In these systems, the finite velocity of propagation of the gravitational interaction between the pulsar and its companion generates damping-like terms at order $(v/c)^5$ in the equations of motion [32]. These damping forces are the local counterparts of the gravitational radiation emitted at infinity by the system (“gravitational radiation reaction”). They cause the binary orbit to shrink and its orbital period P_b to decrease. The remarkable stability of pulsar clocks has allowed one to measure the corresponding very small orbital period decay $\dot{P}_b \equiv dP_b/dt \sim -(v/c)^5 \sim -10^{-12}$ in several binary systems, thereby giving us a direct experimental confirmation of the propagation properties of the gravitational field, and, in particular, an experimental confirmation that the speed of propagation of gravity is equal to the velocity of light to better than a part in a thousand. In addition, the surface gravitational potential of a neutron star $h_{00}(R) \simeq 2Gm/c^2R \simeq 0.4$ being a factor $\sim 10^8$ higher than the surface potential of the Earth, and a mere factor 2.5 below the black hole limit ($h_{00} = 1$), pulsar data have allowed one, as we discuss next, to obtain several accurate tests of the strong-gravitational-field regime.

Binary pulsar timing data record the times of arrival of successive electromagnetic pulses emitted by a pulsar orbiting around the

center of mass of a binary system. After correcting for the Earth motion around the Sun and for the dispersion due to propagation in the interstellar plasma, the time of arrival of the N th pulse t_N can be described by a generic, parameterized “timing formula” [33] whose functional form is common to the whole class of tensor-scalar gravitation theories:

$$t_N - t_0 = F[T_N(\nu_p, \dot{\nu}_p, \ddot{\nu}_p); \{p^K\}; \{p^{PK}\}]. \quad (18.18)$$

Here, T_N is the pulsar proper time corresponding to the N th turn given by $N/2\pi = \nu_p T_N + \frac{1}{2}\dot{\nu}_p T_N^2 + \frac{1}{6}\ddot{\nu}_p T_N^3$ (with $\nu_p \equiv 1/P_p$ the spin frequency of the pulsar, *etc.*), $\{p^K\} = \{P_b, T_0, e, \omega_0, x\}$ is the set of “Keplerian” parameters (notably, orbital period P_b , eccentricity e and projected semi-major axis $x = a \sin i/c$), and $\{p^{PK}\} = \{k, \gamma_{\text{timing}}, \dot{P}_b, r, s, \delta_\theta, \dot{e}, \dot{x}\}$ denotes the set of (separately measurable) “post-Keplerian” parameters. Most important among these are: the fractional periastron advance per orbit $k \equiv \dot{\omega} P_b / 2\pi$, a dimensionful time-dilation parameter γ_{timing} , the orbital period derivative \dot{P}_b , and the “range” and “shape” parameters of the gravitational time delay caused by the companion, r and s .

Without assuming any specific theory of gravity, one can phenomenologically analyze the data from any binary pulsar by least-squares fitting the observed sequence of pulse arrival times to the timing formula Eq. (18.18). This fit yields the “measured” values of the parameters $\{\nu_p, \dot{\nu}_p, \ddot{\nu}_p\}$, $\{p^K\}$, $\{p^{PK}\}$. Now, each specific relativistic theory of gravity predicts that, for instance, k , γ_{timing} , \dot{P}_b , r and s (to quote parameters that have been successfully measured from some binary pulsar data) are some theory-dependent functions of the Keplerian parameters and of the (unknown) masses m_1, m_2 of the pulsar and its companion. For instance, in General Relativity, one finds (with $M \equiv m_1 + m_2$, $n \equiv 2\pi/P_b$)

$$\begin{aligned} k^{\text{GR}}(m_1, m_2) &= 3(1 - e^2)^{-1} (G_N M n / c^3)^{2/3}, \\ \gamma_{\text{timing}}^{\text{GR}}(m_1, m_2) &= e n^{-1} (G_N M n / c^3)^{2/3} m_2 (m_1 + 2m_2) / M^2, \\ \dot{P}_b^{\text{GR}}(m_1, m_2) &= - (192\pi/5) (1 - e^2)^{-7/2} \left(1 + \frac{73}{24} e^2 + \frac{37}{96} e^4 \right) \\ &\quad \times (G_N M n / c^3)^{5/3} m_1 m_2 / M^2, \\ r(m_1, m_2) &= G_N m_2 / c^3, \\ s(m_1, m_2) &= n x (G_N M n / c^3)^{-1/3} M / m_2. \end{aligned} \quad (18.19)$$

In tensor-scalar theories, each of the functions $k^{\text{theory}}(m_1, m_2)$, $\gamma_{\text{timing}}^{\text{theory}}(m_1, m_2)$, $\dot{P}_b^{\text{theory}}(m_1, m_2)$, *etc.*, is modified by quasi-static strong field effects (associated with the self-gravities of the pulsar and its companion), while the particular function $\dot{P}_b^{\text{theory}}(m_1, m_2)$ is further modified by radiative effects (associated with the spin 0 propagator) [26,34,35].

Let us summarize the current experimental situation (see Ref. 36 for a more extensive review). In the first discovered binary pulsar PSR1913 + 16 [30,31], it has been possible to measure with accuracy the three post-Keplerian parameters k , γ_{timing} and \dot{P}_b . The three equations $k^{\text{measured}} = k^{\text{theory}}(m_1, m_2)$, $\gamma_{\text{timing}}^{\text{measured}} = \gamma_{\text{timing}}^{\text{theory}}(m_1, m_2)$, $\dot{P}_b^{\text{measured}} = \dot{P}_b^{\text{theory}}(m_1, m_2)$ determine, for each given theory, three curves in the two-dimensional mass plane. This yields *one* (combined radiative/strong-field) test of the specified theory, according to whether the three curves meet at one point, as they should. After subtracting a small ($\sim 10^{-14}$ level in $\dot{P}_b^{\text{obs}} = (-2.4211 \pm 0.0014) \times 10^{-12}$), but significant, Newtonian perturbing effect caused by the Galaxy [37], one finds that General Relativity passes this $(k - \gamma_{\text{timing}} - \dot{P}_b)_{1913+16}$ test with complete success at the 10^{-3} level [31,38,39]

$$\begin{aligned} \left[\frac{\dot{P}_b^{\text{obs}} - \dot{P}_b^{\text{galactic}}}{\dot{P}_b^{\text{GR}}[k^{\text{obs}}, \gamma_{\text{timing}}^{\text{obs}}]} \right]_{1913+16} &= 1.0026 \pm 0.0006(\text{obs}) \pm 0.0021(\text{galactic}) \\ &= 1.0026 \pm 0.0022. \end{aligned} \quad (18.20)$$

Here $\dot{P}_b^{\text{GR}}[k^{\text{obs}}, \gamma_{\text{timing}}^{\text{obs}}]$ is the result of inserting in $\dot{P}_b^{\text{GR}}(m_1, m_2)$ the values of the masses predicted by the two equations $k^{\text{obs}} =$

$k^{\text{GR}}(m_1, m_2)$, $\gamma_{\text{timing}}^{\text{obs}} = \gamma_{\text{timing}}^{\text{GR}}(m_1, m_2)$. This experimental evidence for the reality of gravitational radiation damping forces at the 0.3% level is illustrated in Fig. 18.1, which shows actual orbital phase data (after subtraction of a linear drift).

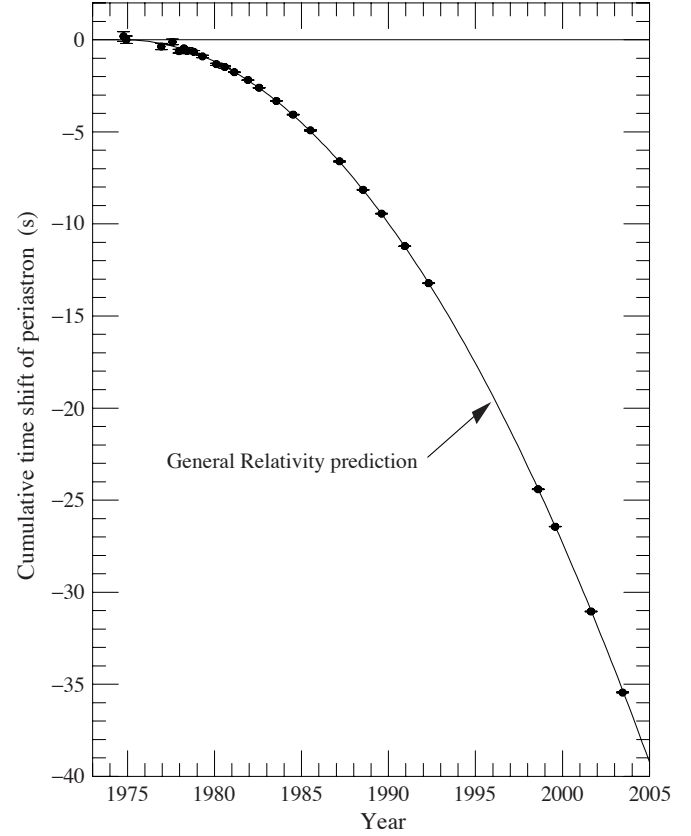


Figure 18.1: Accumulated shift of the times of periastron passage in the PSR 1913+16 system, relative to an assumed orbit with a constant period. The parabolic curve represents the general relativistic prediction, modified by Galactic effects, for orbital period decay from gravitational radiation damping forces. (Figure obtained with permission from Ref. 39.)

The discovery of the binary pulsar PSR1534 + 12 [40] has allowed one to measure the four post-Keplerian parameters k , γ_{timing} , r and s , and thereby to obtain *two* (four observables minus two masses) tests of strong field gravity, without mixing of radiative effects [41]. General Relativity passes these tests within the measurement accuracy [31,41]. The most precise of these new, pure, strong-field tests is the one obtained by combining the measurements of k , γ , and s . Using the most recent data [42], one finds agreement at the 1% level:

$$\left[\frac{s^{\text{obs}}}{s^{\text{GR}}[k^{\text{obs}}, \gamma_{\text{timing}}^{\text{obs}}]} \right]_{1534+12} = 1.000 \pm 0.007. \quad (18.21)$$

It has also been possible to measure the orbital period change of PSR1534 + 12. General Relativity passes the corresponding $(k - \gamma_{\text{timing}} - \dot{P}_b)_{1534+12}$ test with success at the 15% level [42].

The discovery of the binary pulsar PSR J1141 – 6545 [43] (whose companion is probably a white dwarf) has led to the measurement of the three post-Keplerian parameters k , γ_{timing} and \dot{P}_b [44]. As in the PSR 1913 + 16 system, this yields *one* combined radiative/strong-field test of relativistic gravity. One finds that General Relativity passes this $(k - \gamma_{\text{timing}} - \dot{P}_b)_{1141-6545}$ test with success at the 25% level [44].

The discovery of the remarkable *double* binary pulsar PSR J0737 – 3039 A and B [45,46] has led to the measurement of *six* independent timing parameters: five of them are the post-Keplerian parameters k , γ_{timing} , r , s and \dot{P}_b entering the relativistic timing formula of the

fast-spinning pulsar PSR J0737 – 3039 A, while the sixth is the ratio $R = x_B/x_A$ between the projected semi-major axis of the more slowly spinning companion pulsar PSR J0737 – 3039 B, and that of PSR J0737 – 3039 A. [The theoretical prediction for the ratio $R = x_B/x_A$, considered as a function of the (inertial) masses $m_1 = m_A$ and $m_2 = m_B$, is $R^{\text{theory}} = m_1/m_2 + O((v/c)^4)$ [33], independently of the gravitational theory considered. These six measurements give us *four* accurate tests of relativistic gravity [47]: one test is a new, precise confirmation of the reality of gravitational radiation (obtained after only 2.5 years of timing)

$$\left[\frac{\dot{P}_b^{\text{obs}}}{\dot{P}_b^{\text{GR}}[k^{\text{obs}}, R^{\text{obs}}]} \right]_{0737-3039} = 1.003 \pm 0.014, \quad (18.22)$$

while the other three (obtained from combining the measurements of k , γ_{timing} , r , s and R) are new, accurate tests of strong-field gravity. General Relativity passes all those tests with flying colors. The most precise new strong-field confirmation of General Relativity is at the 5×10^{-4} level:

$$\left[\frac{s^{\text{obs}}}{s^{\text{GR}}[k^{\text{obs}}, R^{\text{obs}}]} \right]_{0737-3039} = 0.99987 \pm 0.00050. \quad (18.23)$$

In addition, data from several nearly circular binary systems (made of a neutron star and a white dwarf) have led to strong-field confirmations (at the 5.6×10^{-3} level) of the ‘strong equivalence principle,’ *i.e.*, the fact that neutron stars and white dwarfs fall with the same acceleration in the gravitational field of the Galaxy [48,49].

The constraints on tensor-scalar theories provided by the various binary-pulsar ‘‘experiments’’ have been analyzed in [35,50] and shown to exclude a large portion of the parameter space allowed by solar-system tests.

Finally, measurements over several years of the pulse profiles of various pulsars have detected secular profile changes compatible with the prediction [51] that the general relativistic spin-orbit coupling should cause a secular change in the orientation of the pulsar beam with respect to the line of sight (‘‘geodetic precession’’). Such qualitative confirmations of general-relativistic spin-orbit effects were obtained in PSR 1913+16 [52], PSR B1534+12 [53] and PSR J1141–6545 [54].

The tests considered above have examined the gravitational interaction on scales between a fraction of a millimeter and a few astronomical units. On the other hand, the general relativistic action on light and matter of an external gravitational field on a length scale ~ 100 kpc has been verified to $\sim 30\%$ in some gravitational lensing systems (see, *e.g.*, Ref. 55). Some tests on cosmological scales are also available. In particular, Big Bang Nucleosynthesis (see Section 20 of this *Review*) has been used to set significant constraints on the variability of the gravitational ‘‘constant’’ [56]. For other cosmological tests of the ‘‘constancy of constants,’’ see the review [9].

18.4. Conclusions

All present experimental tests are compatible with the predictions of the current ‘‘standard’’ theory of gravitation: Einstein’s General Relativity. The universality of the coupling between matter and gravity (Equivalence Principle) has been verified around the 10^{-13} level. Solar system experiments have tested the weak-field predictions of Einstein’s theory at the 10^{-4} level (and down to the 2×10^{-5} level for the post-Einstein parameter $\bar{\gamma}$). The propagation properties of relativistic gravity, as well as several of its strong-field aspects, have been verified at the 10^{-3} level in binary pulsar experiments. Recent laboratory experiments have set strong constraints on sub-millimeter modifications of Newtonian gravity.

Several important new developments in experimental gravitation are expected in the near future. The improved lunar laser ranging experiment APOLLO [57] is currently accumulating data with a range accuracy of about one millimeter. The approved European Space Agency’s Atomic Clock Ensemble in Space (ACES) Mission [58] should

provide improved tests of gravitational redshift and of the ‘variability of constants’ by comparing several types of ultrastable clocks in space. The universality of free-fall acceleration should soon be tested to much better than the 10^{-13} level by some satellite experiments: the approved CNES MICROSCOPE [59] mission (10^{-15} level), and the planned (cryogenic) NASA-ESA STEP [60] mission (10^{-18} level). The recently constructed kilometer-size laser interferometers (notably LIGO [61] in the USA and VIRGO [62] and GEO600 [63] in Europe) should soon directly detect gravitational waves arriving on Earth. As the sources of these waves are expected to be extremely relativistic objects with strong internal gravitational fields (*e.g.*, coalescing binary black holes), their detection will allow one to experimentally probe gravity in highly dynamical circumstances. Note finally that arrays of millisecond pulsars are sensitive detectors of (very low frequency) gravitational waves [64–66].

References:

1. S.N. Gupta, Phys. Rev. **96**, 1683 (1954);
R.H. Kraichnan, Phys. Rev. **98**, 1118 (1955);
R.P. Feynman, F.B. Morinigo, and W.G. Wagner, *Feynman Lectures on Gravitation*, ed. by B. Hatfield, (Addison-Wesley, Reading, 1995);
S. Weinberg, Phys. Rev. **138**, B988 (1965);
V.I. Ogievetsky and I.V. Polubarinov, Ann. Phys. (NY) **35**, 167 (1965);
W. Wyss, Helv. Phys. Acta **38**, 469 (1965);
S. Deser, Gen. Rel. Grav. **1**, 9 (1970);
D.G. Boulware and S. Deser, Ann. Phys. (NY) **89**, 193 (1975);
J. Fang and C. Fronsdal, J. Math. Phys. **20**, 2264 (1979);
R.M. Wald, Phys. Rev. **D33**, 3613 (1986);
C. Cutler and R.M. Wald, Class. Quantum Grav. **4**, 1267 (1987);
R.M. Wald, Class. Quantum Grav. **4**, 1279 (1987);
N. Boulanger *et al.*, Nucl. Phys. **B597**, 127 (2001).
2. S. Weinberg, *Gravitation and Cosmology* (John Wiley, New York, 1972).
3. S. Weinberg, Rev. Mod. Phys. **61**, 1 (1989).
4. A.I. Shlyakhter, Nature **264**, 340 (1976);
T. Damour and F. Dyson, Nucl. Phys. **B480**, 37 (1996);
Y. Fujii *et al.*, Nucl. Phys. **B573**, 377 (2000).
5. K.A. Olive *et al.*, Phys. Rev. **D66**, 045022 (2002);
K. A. Olive *et al.*, Phys. Rev. D **69**, 027701 (2004).
6. R. Quast, D. Reimers, and S.A. Levshakov, Astron. Astrophys. **415**, L7 (2004);
R. Srianand *et al.*, Phys. Rev. Lett. **92**, 121302 (2004).
7. J.K. Webb *et al.*, Phys. Rev. Lett. **87**, 091301 (2001);
M.T. Murphy *et al.*, Mon. Not. Roy. Astron. Soc. **327**, 1208 (2001).
8. S. Bize *et al.*, Phys. Rev. Lett. **90**, 150802 (2003);
H. Marion *et al.*, Phys. Rev. Lett. **90**, 150801 (2003);
M. Fischer *et al.*, Phys. Rev. Lett. **92**, 230802 (2004).
9. J.P. Uzan, Rev. Mod. Phys. **75**, 403 (2003).
10. J.D. Prestage *et al.*, Phys. Rev. Lett. **54**, 2387 (1985);
S.K. Lamoreaux *et al.*, Phys. Rev. Lett. **57**, 3125 (1986);
T.E. Chupp *et al.*, Phys. Rev. Lett. **63**, 1541 (1989).
11. T. Jacobson, S. Liberati, and D. Mattingly, Annals Phys. **321**, 150 (2006).
12. Y. Su *et al.*, Phys. Rev. **D50**, 3614 (1994).
13. S. Baessler *et al.*, Phys. Rev. Lett. **83**, 3585 (1999);
E. G. Adelberger, Class. Quantum Grav. **18**, 2397 (2001).
14. J.G. Williams, S.G. Turyshev, and D.H. Boggs, Phys. Rev. Lett. **93**, 261101 (2004).
15. G.L. Smith *et al.*, Phys. Rev. **D61**, 022001 (2000).
16. R.F.C. Vessot and M.W. Levine, Gen. Rel. Grav. **10**, 181 (1978);
R.F.C. Vessot *et al.*, Phys. Rev. Lett. **45**, 2081 (1980).
17. C.M. Will, *Theory and Experiment in Gravitational Physics* (Cambridge University Press, Cambridge, 1993); and Living Rev. Rel. **9**, 3 (2006).
18. T. Damour, in *Gravitation and Quantizations*, ed. B. Julia and J. Zinn-Justin, Les Houches, Session LVII (Elsevier, Amsterdam, 1995), pp. 1–61.
19. H. van Dam and M.J. Veltman, Nucl. Phys. **B22**, 397 (1970);
V.I. Zakharov, Sov. Phys. JETP Lett. **12**, 312 (1970);

- D.G. Boulware and S. Deser, Phys. Rev. **D6**, 3368 (1972);
C. Aragone and J. Chela-Flores, Nuovo Cim. **10A**, 818 (1972);
A.I. Vainshtein, Phys. Lett. **B39**, 393 (1972);
C. Deffayet *et al.*, Phys. Rev. **D65**, 044026 (2002);
M. Porrati, Phys. Lett. **B534**, 209 (2002);
N. Arkani-Hamed, H. Georgi, and M.D. Schwartz, Annals Phys. **305**, 96 (2003);
T. Damour, I.I. Kogan, and A. Papazoglou, Phys. Rev. **D67**, 064009 (2003);
G. Dvali, A. Gruzinov, and M. Zaldarriaga, Phys. Rev. **D68**, 024012 (2003).
20. T.R. Taylor and G. Veneziano, Phys. Lett. **B213**, 450 (1988);
T. Damour and A.M. Polyakov, Nucl. Phys. **B423**, 532 (1994);
S. Dimopoulos and G. Giudice, Phys. Lett. **B379**, 105 (1996);
I. Antoniadis, S. Dimopoulos, and G. Dvali, Nucl. Phys. **B516**, 70 (1998).
21. V.A. Rubakov, Phys. Usp **44**, 871 (2001);
R. Maartens, Living Rev. Rel. **7**, 7 (2004).
22. E. Fischbach and C.L. Talmadge, *The search for Non-Newtonian gravity*, (Springer-Verlag, New York, 1999).
23. E.G. Adelberger, B.R. Heckel, and A.E. Nelson, Ann. Rev. Nucl. Part. Sci. **53**, 77 (2003).
24. D. J. Kapner *et al.*, Phys. Rev. Lett. **98**, 021101 (2007).
25. P. Jordan, *Schwerkraft und Weltall* (Vieweg, Braunschweig, 1955);
M. Fierz, Helv. Phys. Acta **29**, 128 (1956);
C. Brans and R.H. Dicke, Phys. Rev. **124**, 925 (1961).
26. T. Damour and G. Esposito-Farèse, Class. Quantum Grav. **9**, 2093 (1992).
27. A.S. Eddington, *The Mathematical Theory of Relativity*, (Cambridge University Press, Cambridge, 1923);
K. Nordtvedt, Phys. Rev. **169**, 1017 (1968);
C.M. Will, Astrophys. J. **163**, 611 (1971).
28. B. Bertotti, L. Iess, and P. Tortora, Nature, **425**, 374 (2003).
29. K. Nordtvedt, Phys. Rev. **170**, 1186 (1968).
30. R.A. Hulse, Rev. Mod. Phys. **66**, 699 (1994).
31. J.H. Taylor, Rev. Mod. Phys. **66**, 711 (1994).
32. T. Damour and N. Deruelle, Phys. Lett. **A87**, 81 (1981);
T. Damour, C.R. Acad. Sci. Paris **294**, 1335 (1982).
33. T. Damour and N. Deruelle, Ann. Inst. H. Poincaré A, **44**, 263 (1986);
T. Damour and J.H. Taylor, Phys. Rev. **D45**, 1840 (1992).
34. C.M. Will and H.W. Zaglauer, Astrophys. J. **346**, 366 (1989).
35. T. Damour and G. Esposito-Farèse, Phys. Rev. **D54**, 1474 (1996); and Phys. Rev. **D58**, 042001 (1998).
36. I.H. Stairs, Living Rev. Rel. **6** 5 (2003).
37. T. Damour and J.H. Taylor, Astrophys. J. **366**, 501 (1991).
38. J.H. Taylor, Class. Quantum Grav. **10**, S167 (Supplement 1993).
39. J. Weisberg and J.H. Taylor, in *Radio Pulsars, ASP Conference Series* **302**, 93 (2003); [astro-ph/0211217](https://arxiv.org/abs/astro-ph/0211217).
40. A. Wolszczan, Nature **350**, 688 (1991).
41. J.H. Taylor *et al.*, Nature **355**, 132 (1992).
42. I.H. Stairs *et al.*, Astrophys. J. **505**, 352 (1998);
I.H. Stairs *et al.*, Astrophys. J. **581**, 501 (2002).
43. V.M. Kaspi *et al.*, Astrophys. J. **528**, 445 (2000).
44. M. Bailes *et al.*, Astrophys. J. **595**, L49 (2003).
45. M. Burgay *et al.*, Nature **426**, 531 (2003).
46. A. G. Lyne *et al.*, Science **303**, 1153 (2004).
47. M. Kramer *et al.*, Science **314**, 97 (2006).
48. T. Damour and G. Schäfer, Phys. Rev. Lett. **66**, 2549 (1991).
49. I. H. Stairs *et al.*, Astrophys. J. **632**, 1060 (2005).
50. G. Esposito-Farese, [arXiv:gr-qc/0402007](https://arxiv.org/abs/gr-qc/0402007).
51. T. Damour and R. Ruffini, C. R. Acad. Sc. Paris **279**, série A, 971 (1974);
B.M. Barker and R.F. O'Connell, Phys. Rev. **D12**, 329 (1975).
52. M. Kramer, Astrophys. J. **509**, 856 (1998);
J.M. Weisberg and J.H. Taylor, Astrophys. J. **576**, 942 (2002).
53. I.H. Stairs, S.E. Thorsett, and Z. Arzumianian, Phys. Rev. Lett. **93**, 141101 (2004).
54. A.W. Hotan, M. Bailes, and S.M. Ord, Astrophys. J. **624**, 906 (2005).
55. A. Dar, Nucl. Phys. (Proc. Supp.) **B28**, 321 (1992).
56. J. Yang *et al.*, Astrophys. J. **227**, 697 (1979);
T. Rothman and R. Matzner, Astrophys. J. **257**, 450 (1982);
F.S. Accetta, L.M. Krauss, and P. Romanelli, Phys. Lett. **B248**, 146 (1990);
T. Damour and B. Pichon, Phys. Rev. D **59**, 123502 (1999).
57. <http://physics.ucsd.edu/tmurphy/apollo/apollo.html>.
58. <http://www.phys.ens.fr/salomon/horlogesfin.pdf>.
59. P. Touboul *et al.*, C.R.Acad. Sci. Paris **2**, (série IV) 1271 (2001).
60. P.W. Worden, in *Proc. 7th Marcel Grossmann Meeting on General Relativity*, eds. R.J. Jantzen and G. MacKeiser, (World Scientific, Singapore, 1995), p. 1569.
61. <http://www.ligo.caltech.edu>.
62. <http://www.virgo.infn.it>.
63. <http://www.geo600.uni-hannover.de>.
64. V.M. Kaspi, J.H. Taylor, and M.F. Ryba, Astrophys. J. **428**, 713 (1994).
65. A.N. Lommen and D.C. Backer, Bulletin of the American Astronomical Society **33**, 1347 (2001); and Astrophys. J. **562**, 297 (2001).
66. F. A. Jenet *et al.*, Astrophys. J. **653**, 1571 (2006).

19. BIG-BANG COSMOLOGY

Revised September 2007 by K.A. Olive (University of Minnesota) and J.A. Peacock (University of Edinburgh).

19.1. Introduction to Standard Big-Bang Model

The observed expansion of the Universe [1,2,3] is a natural (almost inevitable) result of any homogeneous and isotropic cosmological model based on general relativity. However, by itself, the Hubble expansion does not provide sufficient evidence for what we generally refer to as the Big-Bang model of cosmology. While general relativity is in principle capable of describing the cosmology of any given distribution of matter, it is extremely fortunate that our Universe appears to be homogeneous and isotropic on large scales. Together, homogeneity and isotropy allow us to extend the Copernican Principle to the Cosmological Principle, stating that all spatial positions in the Universe are essentially equivalent.

The formulation of the Big-Bang model began in the 1940s with the work of George Gamow and his collaborators, Alpher and Herman. In order to account for the possibility that the abundances of the elements had a cosmological origin, they proposed that the early Universe which was once very hot and dense (enough so as to allow for the nucleosynthetic processing of hydrogen), and has expanded and cooled to its present state [4,5]. In 1948, Alpher and Herman predicted that a direct consequence of this model is the presence of a relic background radiation with a temperature of order a few K [6,7]. Of course this radiation was observed 16 years later as the microwave background radiation [8]. Indeed, it was the observation of the 3 K background radiation that singled out the Big-Bang model as the prime candidate to describe our Universe. Subsequent work on Big-Bang nucleosynthesis further confirmed the necessity of our hot and dense past. (See the review on BBN—Sec. 20 of this *Review* for a detailed discussion of BBN.) These relativistic cosmological models face severe problems with their initial conditions, to which the best modern solution is inflationary cosmology, discussed in Sec. 19.3.5. If correct, these ideas would strictly render the term ‘Big Bang’ redundant, since it was first coined by Hoyle to represent a criticism of the lack of understanding of the initial conditions.

19.1.1. The Robertson-Walker Universe :

The observed homogeneity and isotropy enable us to describe the overall geometry and evolution of the Universe in terms of two cosmological parameters accounting for the spatial curvature and the overall expansion (or contraction) of the Universe. These two quantities appear in the most general expression for a space-time metric which has a (3D) maximally symmetric subspace of a 4D space-time, known as the Robertson-Walker metric:

$$ds^2 = dt^2 - R^2(t) \left[\frac{dr^2}{1 - kr^2} + r^2 (d\theta^2 + \sin^2 \theta d\phi^2) \right] \quad (19.1)$$

Note that we adopt $c = 1$ throughout. By rescaling the radial coordinate, we can choose the curvature constant k to take only the discrete values $+1$, -1 , or 0 corresponding to closed, open, or spatially flat geometries. In this case, it is often more convenient to re-express the metric as

$$ds^2 = dt^2 - R^2(t) \left[d\chi^2 + S_k^2(\chi) (d\theta^2 + \sin^2 \theta d\phi^2) \right], \quad (19.2)$$

where the function $S_k(\chi)$ is $(\sin \chi, \chi, \sinh \chi)$ for $k = (+1, 0, -1)$. The coordinate r (in Eq. (19.1)) and the ‘angle’ χ (in Eq. (19.2)) are both dimensionless; the dimensions are carried by $R(t)$, which is the cosmological scale factor which determines proper distances in terms of the comoving coordinates. A common alternative is to define a dimensionless scale factor, $a(t) = R(t)/R_0$, where $R_0 \equiv R(t_0)$ is R at the present epoch. It is also sometimes convenient to define a dimensionless or conformal time coordinate, η , by $d\eta = dt/R(t)$. Along constant spatial sections, the proper time is defined by the time coordinate, t . Similarly, for $dt = d\theta = d\phi = 0$, the proper distance is given by $R(t)\chi$. For standard texts on cosmological models see *e.g.*, Refs. [9–14].

19.1.2. The redshift :

The cosmological redshift is a direct consequence of the Hubble expansion, determined by $R(t)$. A local observer detecting light from a distant emitter sees a redshift in frequency. We can define the redshift as

$$z \equiv \frac{\nu_1 - \nu_2}{\nu_2} \simeq \frac{v_{12}}{c}, \quad (19.3)$$

where ν_1 is the frequency of the emitted light, ν_2 is the observed frequency and v_{12} is the relative velocity between the emitter and the observer. While the definition, $z = (\nu_1 - \nu_2)/\nu_2$ is valid on all distance scales, relating the redshift to the relative velocity in this simple way is only true on small scales (*i.e.*, less than cosmological scales) such that the expansion velocity is non-relativistic. For light signals, we can use the metric given by Eq. (19.1) and $ds^2 = 0$ to write

$$\frac{v_{12}}{c} = \dot{R} \delta r = \frac{\dot{R}}{R} \delta t = \frac{\delta R}{R} = \frac{R_2 - R_1}{R_1}, \quad (19.4)$$

where $\delta r(\delta t)$ is the radial coordinate (temporal) separation between the emitter and observer. Thus, we obtain the simple relation between the redshift and the scale factor

$$1 + z = \frac{\nu_1}{\nu_2} = \frac{R_2}{R_1}. \quad (19.5)$$

This result does not depend on the non-relativistic approximation.

19.1.3. The Friedmann-Lemaître equations of motion :

The cosmological equations of motion are derived from Einstein’s equations

$$\mathcal{R}_{\mu\nu} - \frac{1}{2} g_{\mu\nu} \mathcal{R} = 8\pi G_N T_{\mu\nu} + \Lambda g_{\mu\nu}. \quad (19.6)$$

Gliner [15] and Zeldovich [16] seem to have pioneered the modern view, in which the Λ term is taken to the rhs and interpreted as particle-physics processes yielding an effective energy–momentum tensor $T_{\mu\nu}$ for the vacuum of $\Lambda g_{\mu\nu}/8\pi G_N$. It is common to assume that the matter content of the Universe is a perfect fluid, for which

$$T_{\mu\nu} = -p g_{\mu\nu} + (p + \rho) u_\mu u_\nu, \quad (19.7)$$

where $g_{\mu\nu}$ is the space-time metric described by Eq. (19.1), p is the isotropic pressure, ρ is the energy density and $u = (1, 0, 0, 0)$ is the velocity vector for the isotropic fluid in co-moving coordinates. With the perfect fluid source, Einstein’s equations lead to the Friedmann-Lemaître equations

$$H^2 \equiv \left(\frac{\dot{R}}{R} \right)^2 = \frac{8\pi G_N \rho}{3} - \frac{k}{R^2} + \frac{\Lambda}{3}, \quad (19.8)$$

and

$$\frac{\ddot{R}}{R} = \frac{\Lambda}{3} - \frac{4\pi G_N}{3} (\rho + 3p), \quad (19.9)$$

where $H(t)$ is the Hubble parameter and Λ is the cosmological constant. The first of these is sometimes called the Friedmann equation. Energy conservation via $T^{\mu\nu}_{;\mu} = 0$, leads to a third useful equation [which can also be derived from Eq. (19.8) and Eq. (19.9)]

$$\dot{\rho} = -3H(\rho + p). \quad (19.10)$$

Eq. (19.10) can also be simply derived as a consequence of the first law of thermodynamics.

Eq. (19.8) has a simple classical mechanical analog if we neglect (for the moment) the cosmological term Λ . By interpreting $-k/R^2$ as a “total energy,” then we see that the evolution of the Universe is governed by a competition between the potential energy, $8\pi G_N \rho/3$, and the kinetic term $(\dot{R}/R)^2$. For $\Lambda = 0$, it is clear that the Universe must be expanding or contracting (except at the turning point prior to collapse in a closed Universe). The ultimate fate of the Universe is determined by the curvature constant k . For $k = +1$, the Universe will recollapse in a finite time, whereas for $k = 0, -1$, the Universe will expand indefinitely. These simple conclusions can be altered when $\Lambda \neq 0$ or more generally with some component with $(\rho + 3p) < 0$.

19.1.4. Definition of cosmological parameters :

In addition to the Hubble parameter, it is useful to define several other measurable cosmological parameters. The Friedmann equation can be used to define a critical density such that $k = 0$ when $\Lambda = 0$,

$$\begin{aligned} \rho_c &\equiv \frac{3H^2}{8\pi G_N} = 1.88 \times 10^{-26} h^2 \text{ kg m}^{-3} \\ &= 1.05 \times 10^{-5} h^2 \text{ GeV cm}^{-3}, \end{aligned} \quad (19.11)$$

where the scaled Hubble parameter, h , is defined by

$$\begin{aligned} H &\equiv 100 h \text{ km s}^{-1} \text{ Mpc}^{-1} \\ \Rightarrow H^{-1} &= 9.78 h^{-1} \text{ Gyr} \\ &= 2998 h^{-1} \text{ Mpc}. \end{aligned} \quad (19.12)$$

The cosmological density parameter Ω_{tot} is defined as the energy density relative to the critical density,

$$\Omega_{\text{tot}} = \rho / \rho_c. \quad (19.13)$$

Note that one can now rewrite the Friedmann equation as

$$k/R^2 = H^2(\Omega_{\text{tot}} - 1). \quad (19.14)$$

From Eq. (19.14), one can see that when $\Omega_{\text{tot}} > 1$, $k = +1$ and the Universe is closed, when $\Omega_{\text{tot}} < 1$, $k = -1$ and the Universe is open, and when $\Omega_{\text{tot}} = 1$, $k = 0$, and the Universe is spatially flat.

It is often necessary to distinguish different contributions to the density. It is therefore convenient to define present-day density parameters for pressureless matter (Ω_m) and relativistic particles (Ω_r), plus the quantity $\Omega_\Lambda = \Lambda/3H^2$. In more general models, we may wish to drop the assumption that the vacuum energy density is constant, and we therefore denote the present-day density parameter of the vacuum by Ω_v . The Friedmann equation then becomes

$$k/R_0^2 = H_0^2(\Omega_m + \Omega_r + \Omega_v - 1), \quad (19.15)$$

where the subscript 0 indicates present-day values. Thus, it is the sum of the densities in matter, relativistic particles, and vacuum that determines the overall sign of the curvature. Note that the quantity $-k/R_0^2 H_0^2$ is sometimes referred to as Ω_k . This usage is unfortunate: it encourages one to think of curvature as a contribution to the energy density of the Universe, which is not correct.

19.1.5. Standard Model solutions :

Much of the history of the Universe in the standard Big-Bang model can be easily described by assuming that either matter or radiation dominates the total energy density. During inflation or perhaps even today if we are living in an accelerating Universe, domination by a cosmological constant or some other form of dark energy should be considered. In the following, we shall delineate the solutions to the Friedmann equation when a single component dominates the energy density. Each component is distinguished by an equation of state parameter $w = p/\rho$.

19.1.5.1. Solutions for a general equation of state:

Let us first assume a general equation of state parameter for a single component, w which is constant. In this case, Eq. (19.10) can be written as $\dot{\rho} = -3(1+w)\rho\dot{R}/R$ and is easily integrated to yield

$$\rho \propto R^{-3(1+w)}. \quad (19.16)$$

Note that at early times when R is small, the less singular curvature term k/R^2 in the Friedmann equation can be neglected so long as $w > -1/3$. Curvature domination occurs at rather late times (if a cosmological constant term does not dominate sooner). For $w \neq -1$, one can insert this result into the Friedmann equation Eq. (19.8), and if one neglects the curvature and cosmological constant terms, it is easy to integrate the equation to obtain,

$$R(t) \propto t^{2/[3(1+w)]}. \quad (19.17)$$

19.1.5.2. A Radiation-dominated Universe:

In the early hot and dense Universe, it is appropriate to assume an equation of state corresponding to a gas of radiation (or relativistic particles) for which $w = 1/3$. In this case, Eq. (19.16) becomes $\rho \propto R^{-4}$. The ‘‘extra’’ factor of $1/R$ is due to the cosmological redshift; not only is the number density of particles in the radiation background decreasing as R^{-3} since volume scales as R^3 , but in addition, each particle’s energy is decreasing as $E \propto \nu \propto R^{-1}$. Similarly, one can substitute $w = 1/3$ into Eq. (19.17) to obtain

$$R(t) \propto t^{1/2}; \quad H = 1/2t. \quad (19.18)$$

19.1.5.3. A Matter-dominated Universe:

At relatively late times, non-relativistic matter eventually dominates the energy density over radiation (see Sec. 19.3.8). A pressureless gas ($w = 0$) leads to the expected dependence $\rho \propto R^{-3}$ from Eq. (19.16) and, if $k = 0$, we get

$$R(t) \propto t^{2/3}; \quad H = 2/3t. \quad (19.19)$$

19.1.5.4. A Universe dominated by vacuum energy:

If there is a dominant source of vacuum energy, V_0 , it would act as a cosmological constant with $\Lambda = 8\pi G_N V_0$ and equation of state $w = -1$. In this case, the solution to the Friedmann equation is particularly simple and leads to an exponential expansion of the Universe

$$R(t) \propto e^{\sqrt{\Lambda/3}t}. \quad (19.20)$$

A key parameter is the equation of state of the vacuum, $w \equiv p/\rho$: this need not be the $w = -1$ of Λ , and may not even be constant [17,18,19]. There is now much interest in the more general possibility of a dynamically evolving vacuum energy, for which the name ‘dark energy’ has become commonly used. A variety of techniques exist whereby the vacuum density as a function of time may be measured, usually expressed as the value of w as a function of epoch [20,21]. The best current measurement for the equation of state (assumed constant) is $w = -0.967^{+0.073}_{-0.072}$ [22]. Unless stated otherwise, we will assume that the vacuum energy is a cosmological constant with $w = -1$ exactly.

The presence of vacuum energy can dramatically alter the fate of the Universe. For example, if $\Lambda < 0$, the Universe will eventually recollapse independent of the sign of k . For large values of Λ (larger than the Einstein static value needed to halt any cosmological expansion or contraction), even a closed Universe will expand forever. One way to quantify this is the deceleration parameter, q_0 , defined as

$$q_0 = - \left. \frac{R\ddot{R}}{\dot{R}^2} \right|_0 = \frac{1}{2}\Omega_m + \Omega_r + \frac{(1+3w)}{2}\Omega_v. \quad (19.21)$$

This equation shows us that $w < -1/3$ for the vacuum may lead to an accelerating expansion. Astonishingly, it appears that such an effect has been observed in the Supernova Hubble diagram [23–26] (see Fig. 19.1 below); current data indicate that vacuum energy is indeed the largest contributor to the cosmological density budget, with $\Omega_v = 0.759 \pm 0.034$ and $\Omega_m = 0.241 \pm 0.034$ if $k = 0$ is assumed (3-year mean WMAP figure) [22].

The nature of this dominant term is presently uncertain, but much effort is being invested in dynamical models (*e.g.*, rolling scalar fields), under the catch-all heading of ‘‘quintessence.’’

19.2. Introduction to Observational Cosmology

19.2.1. Fluxes, luminosities, and distances :

The key quantities for observational cosmology can be deduced quite directly from the metric.

(1) The *proper* transverse size of an object seen by us to subtend an angle $d\psi$ is its comoving size $d\psi S_k(\chi)$ times the scale factor at the time of emission:

$$d\ell = d\psi R_0 S_k(\chi)/(1+z) . \quad (19.22)$$

(2) The apparent flux density of an object is deduced by allowing its photons to flow through a sphere of current radius $R_0 S_k(\chi)$; but photon energies and arrival rates are redshifted, and the bandwidth $d\nu$ is reduced. The observed photons at frequency ν_0 were emitted at frequency $\nu_0(1+z)$, so the flux density is the luminosity at this frequency, divided by the total area, divided by $1+z$:

$$S_\nu(\nu_0) = \frac{L_\nu([1+z]\nu_0)}{4\pi R_0^2 S_k^2(\chi)(1+z)} . \quad (19.23)$$

These relations lead to the following common definitions:

$$\begin{aligned} \text{angular-diameter distance: } D_A &= (1+z)^{-1} R_0 S_k(\chi) \\ \text{luminosity distance: } D_L &= (1+z) R_0 S_k(\chi) . \end{aligned} \quad (19.24)$$

These distance-redshift relations are expressed in terms of observables by using the equation of a null radial geodesic ($R(t)d\chi = dt$) plus the Friedmann equation:

$$\begin{aligned} R_0 d\chi &= \frac{1}{H(z)} dz = \frac{1}{H_0} \left[(1 - \Omega_m - \Omega_v - \Omega_r)(1+z)^2 \right. \\ &\quad \left. + \Omega_v(1+z)^{3+3w} + \Omega_m(1+z)^3 + \Omega_r(1+z)^4 \right]^{-1/2} dz . \end{aligned} \quad (19.25)$$

The main scale for the distance here is the Hubble length, $1/H_0$.

The flux density is the product of the specific intensity I_ν and the solid angle $d\Omega$ subtended by the source: $S_\nu = I_\nu d\Omega$. Combining the angular size and flux-density relations thus gives the relativistic version of surface-brightness conservation:

$$I_\nu(\nu_0) = \frac{B_\nu([1+z]\nu_0)}{(1+z)^3} , \quad (19.26)$$

where B_ν is surface brightness (luminosity emitted into unit solid angle per unit area of source). We can integrate over ν_0 to obtain the corresponding total or bolometric formula:

$$I_{\text{tot}} = \frac{B_{\text{tot}}}{(1+z)^4} . \quad (19.27)$$

This cosmology-independent form expresses Liouville's Theorem: photon phase-space density is conserved along rays.

19.2.2. Distance data and geometrical tests of cosmology :

In order to confront these theoretical predictions with data, we have to bridge the divide between two extremes. Nearby objects may have their distances measured quite easily, but their radial velocities are dominated by deviations from the ideal Hubble flow, which typically have a magnitude of several hundred km s^{-1} . On the other hand, objects at redshifts $z \gtrsim 0.01$ will have observed recessional velocities that differ from their ideal values by $\lesssim 10\%$, but absolute distances are much harder to supply in this case. The traditional solution to this problem is the construction of the distance ladder: an interlocking set of methods for obtaining relative distances between various classes of object, which begins with absolute distances at the 10 to 100 pc level, and terminates with galaxies at significant redshifts. This is reviewed in the review on Cosmological Parameters—Sec. 21 of this *Review*.

By far the most exciting development in this area has been the use of type Ia Supernovae (SNe), which now allow measurement of relative distances with 5% precision. In combination with Cepheid data from the HST key project on the distance scale, SNe results

are the dominant contributor to the best modern value for H_0 : $72 \text{ km s}^{-1} \text{ Mpc}^{-1} \pm 10\%$ [27]. Better still, the analysis of high- z SNe has allowed the first meaningful test of cosmological geometry to be carried out: as shown in Fig. 19.1 and Fig. 19.2, a combination of supernova data and measurements of microwave-background anisotropies strongly favors a $k=0$ model dominated by vacuum energy. (See the review on Cosmological Parameters—Sec. 21 of this *Review* for a more comprehensive review of Hubble parameter determinations.)

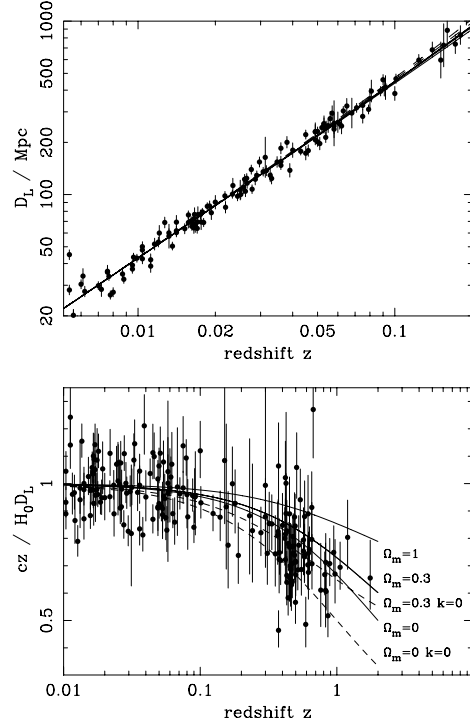


Figure 19.1: The type Ia supernova Hubble diagram [23–25]. The first panel shows that for $z \ll 1$ the large-scale Hubble flow is indeed linear and uniform; the second panel shows an expanded scale, with the linear trend divided out, and with the redshift range extended to show how the Hubble law becomes nonlinear. ($\Omega_r = 0$ is assumed.) Comparison with the prediction of Friedmann-Lemaître models appears to favor a vacuum-dominated Universe.

19.2.3. Age of the Universe :

The most striking conclusion of relativistic cosmology is that the Universe has not existed forever. The dynamical result for the age of the Universe may be written as

$$\begin{aligned} H_0 t_0 &= \int_0^\infty \frac{dz}{(1+z)H(z)} \\ &= \int_0^\infty \frac{dz}{(1+z) [(1+z)^2(1+\Omega_m z) - z(2+z)\Omega_v]^{1/2}} , \end{aligned} \quad (19.28)$$

where we have neglected Ω_r and chosen $w = -1$. Over the range of interest ($0.1 \lesssim \Omega_m \lesssim 1$, $|\Omega_v| \lesssim 1$), this exact answer may be approximated to a few % accuracy by

$$H_0 t_0 \simeq \frac{2}{3} (0.7\Omega_m + 0.3 - 0.3\Omega_v)^{-0.3} . \quad (19.29)$$

For the special case that $\Omega_m + \Omega_v = 1$, the integral in Eq. (19.28) can be expressed analytically as

$$H_0 t_0 = \frac{2}{3\sqrt{\Omega_v}} \ln \frac{1+\sqrt{\Omega_v}}{\sqrt{1-\Omega_v}} \quad (\Omega_m < 1) . \quad (19.30)$$

The most accurate means of obtaining ages for astronomical objects is based on the natural clocks provided by radioactive decay. The use of these clocks is complicated by

a lack of knowledge of the initial conditions of the decay. In the Solar System, chemical fractionation of different elements helps pin down a precise age for the pre-Solar nebula of 4.6 Gyr, but for stars it is necessary to attempt an a priori calculation of the relative abundances of nuclei that result from supernova explosions. In this way, a lower limit for the age of stars in the local part of the Milky Way of about 11 Gyr is obtained [29].

The other major means of obtaining cosmological age estimates is based on the theory of stellar evolution. In principle, the main-sequence turnoff point in the color-magnitude diagram of a globular cluster should yield a reliable age. However, these have been controversial owing to theoretical uncertainties in the evolution model, as well as observational uncertainties in the distance, dust extinction, and metallicity of clusters. The present consensus favors ages for the oldest clusters of about 12 Gyr [30,31].

These methods are all consistent with the age deduced from studies of structure formation, using the microwave background and large-scale structure: $t_0 = 13.73 \pm 0.15$ Gyr [22], where the extra accuracy comes at the price of assuming the Cold Dark Matter model to be true.

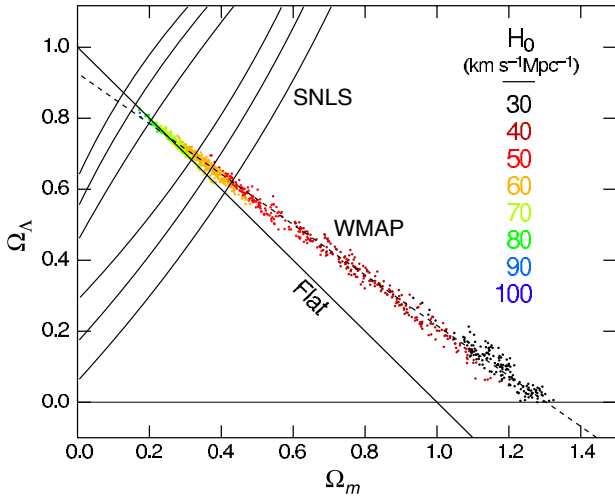


Figure 19.2: Likelihood-based probability densities on the plane Ω_Λ (i.e., Ω_v assuming $w = -1$) vs Ω_m . The colored Monte-Carlo points derive from WMAP [22] and show that the CMB alone requires a flat universe $\Omega_v + \Omega_m \simeq 1$ if the Hubble constant is not too high. The SNe Ia results [28] very nearly constrain the orthogonal combination $\Omega_v - \Omega_m$. The intersection of these constraints is the most direct (but far from the only) piece of evidence favoring a flat model with $\Omega_m \simeq 0.25$. Color version at end of book.

19.2.4. Horizon, isotropy, flatness problems :

For photons, the radial equation of motion is just $c dt = R d\chi$. How far can a photon get in a given time? The answer is clearly

$$\Delta\chi = \int_{t_1}^{t_2} \frac{dt}{R(t)} \equiv \Delta\eta, \quad (19.31)$$

i.e., just the interval of conformal time. We can replace dt by dR/\dot{R} , which the Friedmann equation says is $\propto dR/\sqrt{\rho R^2}$ at early times. Thus, this integral converges if $\rho R^2 \rightarrow \infty$ as $t_1 \rightarrow 0$, otherwise it diverges. Provided the equation of state is such that ρ changes faster than R^{-2} , light signals can only propagate a finite distance between the Big Bang and the present; there is then said to be a particle horizon. Such a horizon therefore exists in conventional Big-Bang models, which are dominated by radiation ($\rho \propto R^{-4}$) at early times.

At late times, the integral for the horizon is largely determined by the matter-dominated phase, for which

$$D_H = R_0 \chi_H \equiv R_0 \int_0^{t(z)} \frac{dt}{R(t)} \simeq \frac{6000}{\sqrt{\Omega_z}} h^{-1} \text{Mpc} \quad (z \gg 1). \quad (19.32)$$

The horizon at the time of formation of the microwave background ('last scattering,' $z \simeq 1100$) was thus of order 100 Mpc in size, subtending an angle of about 1° . Why then are the large number of causally disconnected regions we see on the microwave sky all at the same temperature? The Universe is very nearly isotropic and homogeneous, even though the initial conditions appear not to permit such a state to be constructed.

A related problem is that the $\Omega = 1$ Universe is unstable:

$$\Omega(a) - 1 = \frac{\Omega - 1}{1 - \Omega + \Omega_v a^2 + \Omega_m a^{-1} + \Omega_r a^{-2}}, \quad (19.33)$$

where Ω with no subscript is the total density parameter, and $a(t) = R(t)/R_0$. This requires $\Omega(t)$ to be unity to arbitrary precision as the initial time tends to zero; a universe of non-zero curvature today requires very finely tuned initial conditions.

19.3. The Hot Thermal Universe

19.3.1. Thermodynamics of the early Universe :

As alluded to above, we expect that much of the early Universe can be described by a radiation-dominated equation of state. In addition, through much of the radiation-dominated period, thermal equilibrium is established by the rapid rate of particle interactions relative to the expansion rate of the Universe (see Sec. 19.3.3 below). In equilibrium, it is straightforward to compute the thermodynamic quantities, ρ, p , and the entropy density, s . In general, the energy density for a given particle type i can be written as

$$\rho_i = \int E_i dn_{q_i}, \quad (19.34)$$

with the density of states given by

$$dn_{q_i} = \frac{g_i}{2\pi^2} (\exp[(E_{q_i} - \mu_i)/T_i] \pm 1)^{-1} q_i^2 dq_i, \quad (19.35)$$

where g_i counts the number of degrees of freedom for particle type i , $E_{q_i}^2 = m_i^2 + q_i^2$, μ_i is the chemical potential, and the \pm corresponds to either Fermi or Bose statistics. Similarly, we can define the pressure of a perfect gas as

$$p_i = \frac{1}{3} \int \frac{q_i^2}{E_i} dn_{q_i}. \quad (19.36)$$

The number density of species i is simply

$$n_i = \int dn_{q_i}, \quad (19.37)$$

and the entropy density is

$$s_i = \frac{\rho_i + p_i - \mu_i n_i}{T_i}. \quad (19.38)$$

In the Standard Model, a chemical potential is often associated with baryon number, and since the net baryon density relative to the photon density is known to be very small (of order 10^{-10}), we can neglect any such chemical potential when computing total thermodynamic quantities.

For photons, we can compute all of the thermodynamic quantities rather easily. Taking $g_i = 2$ for the 2 photon polarization states, we have

$$\rho_\gamma = \frac{\pi^2}{15} T^4; \quad p_\gamma = \frac{1}{3} \rho_\gamma; \quad s_\gamma = \frac{4\rho_\gamma}{3T}; \quad n_\gamma = \frac{2\zeta(3)}{\pi^2} T^3, \quad (19.39)$$

with $2\zeta(3)/\pi^2 \simeq 0.2436$. Note that Eq. (19.10) can be converted into an equation for entropy conservation. Recognizing that $\dot{p} = s\dot{T}$, Eq. (19.10) becomes

$$d(sR^3)/dt = 0. \quad (19.40)$$

For radiation, this corresponds to the relationship between expansion and cooling, $T \propto R^{-1}$ in an adiabatically expanding Universe. Note also that both s and n_γ scale as T^3 .

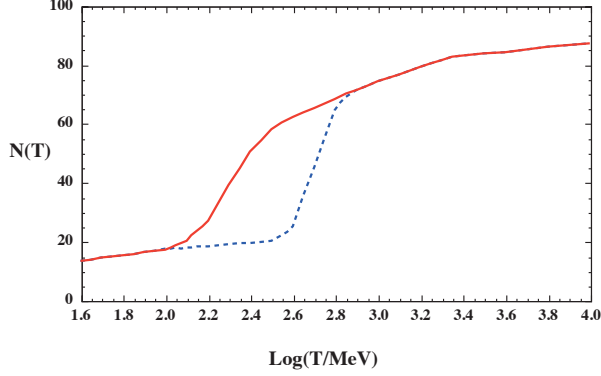


Figure 19.3: The effective numbers of relativistic degrees of freedom as a function of temperature. The sharp drop corresponds to the quark-hadron transition. The solid curve assume a QCD scale of 150 MeV, while the dashed curve assumes 450 MeV.

19.3.2. Radiation content of the Early Universe :

At the very high temperatures associated with the early Universe, massive particles are pair produced, and are part of the thermal bath. If for a given particle species i we have $T \gg m_i$, then we can neglect the mass in Eq. (19.34) to Eq. (19.38), and the thermodynamic quantities are easily computed as in Eq. (19.39). In general, we can approximate the energy density (at high temperatures) by including only those particles with $m_i \ll T$. In this case, we have

$$\rho = \left(\sum_B g_B + \frac{7}{8} \sum_F g_F \right) \frac{\pi^2}{30} T^4 \equiv \frac{\pi^2}{30} N(T) T^4, \quad (19.41)$$

where $g_{B(F)}$ is the number of degrees of freedom of each boson (fermion) and the sum runs over all boson and fermion states with $m \ll T$. The factor of $7/8$ is due to the difference between the Fermi and Bose integrals. Eq. (19.41) defines the effective number of degrees of freedom, $N(T)$, by taking into account new particle degrees of freedom as the temperature is raised. This quantity is plotted in Fig. 19.3 [32].

The value of $N(T)$ at any given temperature depends on the particle physics model. In the standard $SU(3) \times SU(2) \times U(1)$ model, we can specify $N(T)$ up to temperatures of $O(100)$ GeV. The change in N (ignoring mass effects) can be seen in the above table.

Temperature	New Particles	$4N(T)$
$T < m_e$	γ 's + ν 's	29
$m_e < T < m_\mu$	e^\pm	43
$m_\mu < T < m_\pi$	μ^\pm	57
$m_\pi < T < T_c^\dagger$	π 's	69
$T_c < T < m_{\text{strange}}$	π 's + u, \bar{u}, d, \bar{d} + gluons	205
$m_s < T < m_{\text{charm}}$	s, \bar{s}	247
$m_c < T < m_\tau$	c, \bar{c}	289
$m_\tau < T < m_{\text{bottom}}$	τ^\pm	303
$m_b < T < m_{W,Z}$	b, \bar{b}	345
$m_{W,Z} < T < m_{\text{Higgs}}$	W^\pm, Z	381
$m_H < T < m_{\text{top}}$	H^0	385
$m_t < T$	t, \bar{t}	427

$^\dagger T_c$ corresponds to the confinement-deconfinement transition between quarks and hadrons.

At higher temperatures, $N(T)$ will be model-dependent. For example, in the minimal $SU(5)$ model, one needs to add 24 states to $N(T)$ for the X and Y gauge bosons, another 24 from the adjoint Higgs, and another 6 (in addition to the 4 already counted in W^\pm, Z , and H) from the $\bar{5}$ of Higgs. Hence for $T > m_X$ in minimal $SU(5)$, $N(T) = 160.75$. In a supersymmetric model this would at least double, with some changes possibly necessary in the table if the lightest supersymmetric particle has a mass below m_t .

In the radiation-dominated epoch, Eq. (19.10) can be integrated (neglecting the T -dependence of N) giving us a relationship between the age of the Universe and its temperature

$$t = \left(\frac{90}{32\pi^3 G_N N(T)} \right)^{1/2} T^{-2}. \quad (19.42)$$

Put into a more convenient form

$$t T_{\text{MeV}}^2 = 2.4 [N(T)]^{-1/2}, \quad (19.43)$$

where t is measured in seconds and T_{MeV} in units of MeV.

19.3.3. Neutrinos and equilibrium : Due to the expansion of the Universe, certain rates may be too slow to either establish or maintain equilibrium. Quantitatively, for each particle i , as a minimal condition for equilibrium, we will require that some rate Γ_i involving that type be larger than the expansion rate of the Universe or

$$\Gamma_i > H. \quad (19.44)$$

Recalling that the age of the Universe is determined by H^{-1} , this condition is equivalent to requiring that on average, at least one interaction has occurred over the lifetime of the Universe.

A good example for a process which goes in and out of equilibrium is the weak interactions of neutrinos. On dimensional grounds, one can estimate the thermally averaged scattering cross section

$$\langle \sigma v \rangle \sim O(10^{-2}) T^2 / m_W^4 \quad (19.45)$$

for $T \lesssim m_W$. Recalling that the number density of leptons is $n \propto T^3$, we can compare the weak interaction rate, $\Gamma \sim n \langle \sigma v \rangle$, with the expansion rate,

$$H = \left(\frac{8\pi G_N \rho}{3} \right)^{1/2} = \left(\frac{8\pi^3}{90} N(T) \right)^{1/2} T^2 / M_P \quad (19.46)$$

$$\sim 1.66 N(T)^{1/2} T^2 / M_P.$$

The Planck mass $M_P = G_N^{-1/2} = 1.22 \times 10^{19}$ GeV.

Neutrinos will be in equilibrium when $\Gamma_{\text{wk}} > H$ or

$$T > (500 m_W^4 / M_P)^{1/3} \sim 1 \text{ MeV}. \quad (19.47)$$

The temperature at which these rates are equal is commonly referred to as the neutrino decoupling or freeze-out temperature and is defined by $\Gamma(T_d) = H(T_d)$.

At very high temperatures, the Universe is too young for equilibrium to have been established. For $T \gg m_W$, we should write $\langle \sigma v \rangle \sim O(10^{-2}) / T^2$, so that $\Gamma \sim 10^{-2} T$. Thus, at temperatures $T \gtrsim 10^{-2} M_P / \sqrt{N}$, equilibrium will not have been established.

For $T < T_d$, neutrinos drop out of equilibrium. The Universe becomes transparent to neutrinos and their momenta simply redshift with the cosmic expansion. The effective neutrino temperature will simply fall with $T \sim 1/R$.

Soon after decoupling, e^\pm pairs in the thermal background begin to annihilate (when $T \lesssim m_e$). Because the neutrinos are decoupled, the energy released due to annihilation heats up the photon background relative to the neutrinos. The change in the photon temperature can be easily computed from entropy conservation. The neutrino entropy must be conserved separately from the entropy of interacting particles. A straightforward computation yields

$$T_\nu = (4/11)^{1/3} T_\gamma \simeq 1.9 \text{ K}. \quad (19.48)$$

Today, the total entropy density is therefore given by

$$s = \frac{4\pi^2}{30} \left(2 + \frac{21}{4} (T_\nu / T_\gamma)^3 \right) T_\gamma^3 = \frac{4\pi^2}{30} \left(2 + \frac{21}{11} \right) T_\gamma^3 = 7.04 n_\gamma. \quad (19.49)$$

Similarly, the total relativistic energy density today is given by

$$\rho_r = \frac{\pi^2}{30} \left[2 + \frac{21}{4} (T_\nu/T_\gamma)^4 \right] T_\gamma^4 \simeq 1.68 \rho_\gamma. \quad (19.50)$$

In practice, a small correction is needed to this, since neutrinos are not totally decoupled at e^\pm annihilation: the effective number of massless neutrino species is 3.04, rather than 3 [33].

This expression ignores neutrino rest masses, but current oscillation data require at least one neutrino eigenstate to have a mass exceeding 0.05 eV. In this minimal case, $\Omega_\nu h^2 = 5 \times 10^{-4}$, so the neutrino contribution to the matter budget would be negligibly small (which is our normal assumption). However, a nearly degenerate pattern of mass eigenstates could allow larger densities, since oscillation experiments only measure differences in m^2 values. Note that a 0.05-eV neutrino has $kT_\nu = m_\nu$ at $z \simeq 297$, so the above expression for the total present relativistic density is really only an extrapolation. However, neutrinos are almost certainly relativistic at all epochs where the radiation content of the universe is dynamically significant.

19.3.4. Field Theory and Phase transitions :

It is very likely that the Universe has undergone one or more phase transitions during the course of its evolution [34–37]. Our current vacuum state is described by $SU(3)_c \times U(1)_{em}$, which in the Standard Model is a remnant of an unbroken $SU(3)_c \times SU(2)_L \times U(1)_Y$ gauge symmetry. Symmetry breaking occurs when a non-singlet gauge field (the Higgs field in the Standard Model) picks up a non-vanishing vacuum expectation value, determined by a scalar potential. For example, a simple (non-gauged) potential describing symmetry breaking is $V(\phi) = \frac{1}{4} \lambda \phi^4 - \frac{1}{2} \mu^2 \phi^2 + V(0)$. The resulting expectation value is simply $\langle \phi \rangle = \mu/\sqrt{\lambda}$.

In the early Universe, finite temperature radiative corrections typically add terms to the potential of the form $\phi^2 T^2$. Thus, at very high temperatures, the symmetry is restored and $\langle \phi \rangle = 0$. As the Universe cools, depending on the details of the potential, symmetry breaking will occur via a first order phase transition in which the field tunnels through a potential barrier, or via a second order transition in which the field evolves smoothly from one state to another (as would be the case for the above example potential).

The evolution of scalar fields can have a profound impact on the early Universe. The equation of motion for a scalar field ϕ can be derived from the energy-momentum tensor

$$T_{\mu\nu} = \partial_\mu \phi \partial_\nu \phi - \frac{1}{2} g_{\mu\nu} \partial_\rho \phi \partial^\rho \phi - g_{\mu\nu} V(\phi). \quad (19.51)$$

By associating $\rho = T_{00}$ and $p = R^{-2}(t)T_{ii}$ we have

$$\begin{aligned} \rho &= \frac{1}{2} \dot{\phi}^2 + \frac{1}{2} R^{-2}(t) (\nabla \phi)^2 + V(\phi) \\ p &= \frac{1}{2} \dot{\phi}^2 - \frac{1}{6} R^{-2}(t) (\nabla \phi)^2 - V(\phi), \end{aligned} \quad (19.52)$$

and from Eq. (19.10) we can write the equation of motion (by considering a homogeneous region, we can ignore the gradient terms)

$$\ddot{\phi} + 3H\dot{\phi} = -\partial V/\partial \phi. \quad (19.53)$$

19.3.5. Inflation :

In Sec. 19.2.4, we discussed some of the problems associated with the standard Big-Bang model. However, during a phase transition, our assumptions of an adiabatically expanding universe are generally not valid. If, for example, a phase transition occurred in the early Universe such that the field evolved slowly from the symmetric state to the global minimum, the Universe may have been dominated by the vacuum energy density associated with the potential near $\phi \simeq 0$. During this period of slow evolution, the energy density due to radiation will fall below the vacuum energy density, $\rho \ll V(0)$. When this happens, the expansion rate will be dominated by the constant $V(0)$, and we obtain the exponentially expanding solution given in Eq. (19.20). When the field evolves towards the global minimum it will

begin to oscillate about the minimum, energy will be released during its decay, and a hot thermal universe will be restored. If released fast enough, it will produce radiation at a temperature $NT_{R^4} \lesssim V(0)$. In this reheating process, entropy has been created and the final value of RT is greater than the initial value of RT . Thus, we see that, during a phase transition, the relation $RT \sim \text{constant}$ need not hold true. This is the basis of the inflationary Universe scenario [38–40].

If, during the phase transition, the value of RT changed by a factor of $O(10^{29})$, the cosmological problems discussed above would be solved. The observed isotropy would be generated by the immense expansion; one small causal region could get blown up, and hence, our entire visible Universe would have been in thermal contact some time in the past. In addition, the density parameter Ω would have been driven to 1 (with exponential precision). Density perturbations will be stretched by the expansion, $\lambda \sim R(t)$. Thus it will appear that $\lambda \gg H^{-1}$ or that the perturbations have left the horizon, where in fact the size of the causally connected region is now no longer simply H^{-1} . However, not only does inflation offer an explanation for large scale perturbations, it also offers a source for the perturbations themselves through quantum fluctuations.

Early models of inflation were based on a first order phase transition of a Grand Unified Theory [41]. Although these models led to sufficient exponential expansion, completion of the transition through bubble percolation did not occur. Later models of inflation [42,43], also based on Grand Unified symmetry breaking, through second order transitions were also doomed. While they successfully inflated and reheated, and in fact produced density perturbations due to quantum fluctuations during the evolution of the scalar field, they predicted density perturbations many orders of magnitude too large. Most models today are based on an unknown symmetry breaking involving a new scalar field, the inflaton, ϕ .

19.3.6. Baryogenesis :

The Universe appears to be populated exclusively with matter rather than antimatter. Indeed antimatter is only detected in accelerators or in cosmic rays. However, the presence of antimatter in the latter is understood to be the result of collisions of primary particles in the interstellar medium. There is in fact strong evidence against primary forms of antimatter in the Universe. Furthermore, the density of baryons compared to the density of photons is extremely small, $\eta \sim 10^{-10}$.

The production of a net baryon asymmetry requires baryon number violating interactions, C and CP violation and a departure from thermal equilibrium [44]. The first two of these ingredients are expected to be contained in grand unified theories as well as in the non-perturbative sector of the Standard Model, the third can be realized in an expanding universe where as we have seen interactions come in and out of equilibrium.

There are several interesting and viable mechanisms for the production of the baryon asymmetry. While, we can not review any of them here in any detail, we mention some of the important scenarios. In all cases, all three ingredients listed above are incorporated. One of the first mechanisms was based on the out of equilibrium decay of a massive particle such as a superheavy GUT gauge of Higgs boson [45,46]. A novel mechanism involving the decay of flat directions in supersymmetric models is known as the Affleck-Dine scenario [47]. Recently, much attention has been focused on the possibility of generating the baryon asymmetry at the electro-weak scale using the non-perturbative interactions of sphalerons [48]. Because these interactions conserve the sum of baryon and lepton number, $B + L$, it is possible to first generate a lepton asymmetry (*e.g.*, by the out-of-equilibrium decay of a superheavy right-handed neutrino), which is converted to a baryon asymmetry at the electro-weak scale [49]. This mechanism is known as leptobaryogenesis.

19.3.7. Nucleosynthesis :

An essential element of the standard cosmological model is Big-Bang nucleosynthesis (BBN), the theory which predicts the abundances of the light element isotopes D, ^3He , ^4He , and ^7Li . Nucleosynthesis takes place at a temperature scale of order 1 MeV. The nuclear processes lead primarily to ^4He , with a primordial mass fraction of about 24%. Lesser amounts of the other light elements are produced: about 10^{-5} of D and ^3He and about 10^{-10} of ^7Li by number relative to H. The abundances of the light elements depend almost solely on one key parameter, the baryon-to-photon ratio, η . The nucleosynthesis predictions can be compared with observational determinations of the abundances of the light elements. Consistency between theory and observations leads to a conservative range of

$$4.7 \times 10^{-10} < \eta < 6.5 \times 10^{-10}. \quad (19.54)$$

η is related to the fraction of Ω contained in baryons, Ω_b

$$\Omega_b = 3.66 \times 10^7 \eta h^{-2}, \quad (19.55)$$

or $10^{10}\eta = 274\Omega_b h^2$. The WMAP result [22] for $\Omega_b h^2$ of 0.0223 ± 0.0007 translates into a value of $\eta = 6.11 \pm 0.19$. This result can be used to ‘predict’ the light element abundance which can in turn be compared with observation [50]. The resulting D/H abundance is in excellent agreement with that found in quasar absorption systems. It is in reasonable agreement with the helium abundance observed in extra-galactic HII regions (once systematic uncertainties are accounted for), but is in poor agreement with the Li abundance observed in the atmospheres of halo dwarf stars. (See the review on BBN—Sec. 20 of this *Review* for a detailed discussion of BBN or references [51,52].)

19.3.8. The transition to a matter-dominated Universe :

In the Standard Model, the temperature (or redshift) at which the Universe undergoes a transition from a radiation dominated to a matter dominated Universe is determined by the amount of dark matter. Assuming three nearly massless neutrinos, the energy density in radiation at temperatures $T \ll 1$ MeV, is given by

$$\rho_r = \frac{\pi^2}{30} \left[2 + \frac{21}{4} \left(\frac{4}{11} \right)^{4/3} \right] T^4. \quad (19.56)$$

In the absence of non-baryonic dark matter, the matter density can be written as

$$\rho_m = m_N \eta n_\gamma, \quad (19.57)$$

where m_N is the nucleon mass. Recalling that $n_\gamma \propto T^3$ [cf. Eq. (19.39)], we can solve for the temperature or redshift at the matter-radiation equality when $\rho_r = \rho_m$.

$$T_{\text{eq}} = 0.22 m_N \eta \quad \text{or} \quad (1 + z_{\text{eq}}) = 0.22 \eta \frac{m_N}{T_0}, \quad (19.58)$$

where T_0 is the present temperature of the microwave background. For $\eta = 5 \times 10^{-10}$, this corresponds to a temperature $T_{\text{eq}} \simeq 0.1$ eV or $(1 + z_{\text{eq}}) \simeq 425$. A transition this late is very problematic for structure formation (see Sec. 19.4.5).

The redshift of matter domination can be pushed back significantly if non-baryonic dark matter is present. If instead of Eq. (19.57), we write

$$\rho_m = \Omega_m \rho_c \left(\frac{T}{T_0} \right)^3, \quad (19.59)$$

we find that

$$T_{\text{eq}} = 0.9 \frac{\Omega_m \rho_c}{T_0^3} \quad \text{or} \quad (1 + z_{\text{eq}}) = 2.4 \times 10^4 \Omega_m h^2. \quad (19.60)$$

19.4. The Universe at late times

19.4.1. The CMB :

One form of the infamous Olbers’ paradox says that, in Euclidean space, surface brightness is independent of distance. Every line of sight will terminate on matter that is hot enough to be ionized and so scatter photons: $T \gtrsim 10^3$ K; the sky should therefore shine as brightly as the surface of the Sun. The reason the night sky is dark is entirely due to the expansion, which cools the radiation temperature to 2.73 K. This gives a Planck function peaking at around 1 mm to produce the microwave background (CMB).

The CMB spectrum is a very accurate match to a Planck function [53]. (See the review on CBR—Sec. 23 of this *Review*.) The COBE estimate of the temperature is [54]

$$T = 2.725 \pm 0.002 \text{ K}. \quad (19.61)$$

The lack of any distortion of the Planck spectrum is a strong physical constraint. It is very difficult to account for in any expanding universe other than one that passes through a hot stage. Alternative schemes for generating the radiation, such as thermalization of starlight by dust grains, inevitably generate a superposition of temperatures. What is required in addition to thermal equilibrium is that $T \propto 1/R$, so that radiation from different parts of space appears identical.

Although it is common to speak of the CMB as originating at ‘recombination,’ a more accurate terminology is the era of ‘last scattering.’ In practice, this takes place at $z \simeq 1100$, almost independently of the main cosmological parameters, at which time the fractional ionization is very small. This occurred when the age of the Universe was a few hundred thousand years. (See the review on CBR—Sec. 23 of this *Review* for a full discussion of the CMB.)

19.4.2. Matter in the Universe :

One of the main tasks of cosmology is to measure the density of the Universe, and how this is divided between dark matter and baryons. The baryons consist partly of stars, with $0.002 \lesssim \Omega_* \lesssim 0.003$ [55] but mainly inhabit the IGM. One powerful way in which this can be studied is via the absorption of light from distant luminous objects such as quasars. Even very small amounts of neutral hydrogen can absorb rest-frame UV photons (the Gunn-Peterson effect), and should suppress the continuum by a factor $\exp(-\tau)$, where

$$\tau \simeq \left[\frac{n_{\text{HI}}(z)}{(1+z)\sqrt{1+\Omega_m z}} \right] / 10^{-4.62} h \text{ m}^{-3}, \quad (19.62)$$

and this expression applies while the Universe is matter dominated ($z \gtrsim 1$ in the $\Omega_m = 0.3$ $\Omega_v = 0.7$ model). It is possible that this general absorption has now been seen at $z = 6.2$ [56]. In any case, the dominant effect on the spectrum is a ‘forest’ of narrow absorption lines, which produce a mean $\tau = 1$ in the Ly α forest at about $z = 3$, and so we have $\Omega_{\text{HI}} \simeq 10^{-5.5} h^{-1}$. This is such a small number that clearly the IGM is very highly ionized at these redshifts.

The Ly α forest is of great importance in pinning down the abundance of deuterium. Because electrons in deuterium differ in reduced mass by about 1 part in 4000 compared to hydrogen, each absorption system in the Ly α forest is accompanied by an offset deuterium line. By careful selection of systems with an optimal HI column density, a measurement of the D/H ratio can be made. This has now been done in 6 quasars, with relatively consistent results [52]. Combining these determinations with the theory of primordial nucleosynthesis yields a baryon density of $\Omega_b h^2 = 0.021 \pm 0.003$ (95% confidence). (See also the review on BBN—Sec. 20 of this *Review*.)

Ionized IGM can also be detected in emission when it is densely clumped, via bremsstrahlung radiation. This generates the spectacular X-ray emission from rich clusters of galaxies. Studies of this phenomenon allow us to achieve an accounting of the total baryonic material in clusters. Within the central $\simeq 1$ Mpc, the masses in stars, X-ray emitting gas and total dark matter can be determined with reasonable accuracy (perhaps 20% rms), and this allows a minimum baryon fraction to be determined [57,58]:

$$\frac{M_{\text{baryons}}}{M_{\text{total}}} \gtrsim 0.009 + (0.066 \pm 0.003) h^{-3/2}. \quad (19.63)$$

Because clusters are the largest collapsed structures, it is reasonable to take this as applying to the Universe as a whole. This equation implies a minimum baryon fraction of perhaps 12% (for reasonable h), which is too high for $\Omega_m = 1$ if we take $\Omega_b h^2 \simeq 0.02$ from nucleosynthesis. This is therefore one of the more robust arguments in favor of $\Omega_m \simeq 0.3$. (See the review on Cosmological Parameters—Sec. 21 of this *Review*.) This argument is also consistent with the inference on Ω_m that can be made from Fig. 19.2.

This method is much more robust than the older classical technique for weighing the Universe: ‘ $L \times M/L$.’ The overall light density of the Universe is reasonably well determined from redshift surveys of galaxies, so that a good determination of mass M and luminosity L for a single object suffices to determine Ω_m if the mass-to-light ratio is universal.

Galaxy redshift surveys allow us to deduce the galaxy luminosity function, ϕ , which is the comoving number density of galaxies; this may be described by the Schechter function, which is a power law with an exponential cutoff:

$$\phi = \phi^* \left(\frac{L}{L^*} \right)^{-\alpha} e^{-L/L^*} \frac{dL}{L^*}. \quad (19.64)$$

The total luminosity density produced by integrating over the distribution is

$$\rho_L = \phi^* L^* \Gamma(2 - \alpha), \quad (19.65)$$

and this tells us the average mass-to-light ratio needed to close the Universe. Answers vary (principally owing to uncertainties in ϕ^*). In blue light, the total luminosity density is $\rho_L = 2 \pm 0.2 \times 10^8 \text{ h}L_\odot \text{Mpc}^{-3}$ [59,60]. The critical density is $2.78 \times 10^{11} \Omega h^2 M_\odot \text{Mpc}^{-3}$, so the critical M/L for closure is

$$(M/L)_{\text{crit, B}} = 1390 h \pm 10\%. \quad (19.66)$$

Dynamical determinations of mass on the largest accessible scales consistently yield blue M/L values of at least $300h$, but normally fall short of the closure value [61]. This was a long-standing argument against the $\Omega_m = 1$ model, but it was never conclusive because the stellar populations in objects such as rich clusters (where the masses can be determined) differ systematically from those in other regions.

19.4.3. Gravitational lensing :

A robust method for determining masses in cosmology is to use gravitational light deflection. Most systems can be treated as a geometrically thin gravitational lens, where the light bending is assumed to take place only at a single distance. Simple geometry then determines a mapping between the coordinates in the intrinsic source plane and the observed image plane:

$$\alpha(D_L \theta_1) = \frac{D_S}{D_{LS}} (\theta_1 - \theta_S), \quad (19.67)$$

where the angles θ_1, θ_S and α are in general two-dimensional vectors on the sky. The distances D_{LS} etc. are given by an extension of the usual distance-redshift formula:

$$D_{LS} = \frac{R_0 S_k (\chi_S - \chi_L)}{1 + z_S}. \quad (19.68)$$

This is the angular-diameter distance for objects on the source plane as perceived by an observer on the lens.

Solutions of this equation divide into weak lensing, where the mapping between source plane and image plane is one-to-one, and strong lensing, in which multiple imaging is possible. For circularly-symmetric lenses, an on-axis source is multiply imaged into a ‘caustic’ ring, whose radius is the Einstein radius:

$$\begin{aligned} \theta_E &= \left(4GM \frac{D_{LS}}{D_L D_S} \right)^{1/2} \\ &= \left(\frac{M}{10^{11.09} M_\odot} \right)^{1/2} \left(\frac{D_L D_S / D_{LS}}{\text{Gpc}} \right)^{-1/2} \text{ arcsec}. \end{aligned} \quad (19.69)$$

The observation of ‘arcs’ (segments of near-perfect Einstein rings) in rich clusters of galaxies has thus given very accurate masses for the central parts of clusters—generally in good agreement with other indicators, such as analysis of X-ray emission from the cluster IGM [62].

Gravitational lensing has also developed into a particularly promising probe of cosmological structure on 10 to 100 Mpc scales. Weak image distortions manifest themselves as an additional ellipticity of galaxy images (‘shear’), which can be observed by averaging many images together (the corresponding flux amplification is less readily detected). The result is a ‘cosmic shear’ field of order 1% ellipticity, coherent over scales of around 30 arcmin, which is directly related to the cosmic mass field, without any astrophysical uncertainties. For this reason, weak lensing is seen as potentially the cleanest probe of matter fluctuations, next to the CMB. Already, impressive results have been obtained in measuring cosmological parameters, based on survey data from only $\sim 10 \text{ deg}^2$ [63]. The particular current strength of this technique is the ability to measure the amplitude of mass fluctuations; this can be deduced from the CMB only subject to uncertainty over the optical depth due to Thomson scattering after reionization.

19.4.4. Density Fluctuations :

The overall properties of the Universe are very close to being homogeneous; and yet telescopes reveal a wealth of detail on scales varying from single galaxies to large-scale structures of size exceeding 100 Mpc. The existence of these structures must be telling us something important about the initial conditions of the Big Bang, and about the physical processes that have operated subsequently. This motivates the study of the density perturbation field, defined as

$$\delta(\mathbf{x}) \equiv \frac{\rho(\mathbf{x}) - \langle \rho \rangle}{\langle \rho \rangle}. \quad (19.70)$$

A critical feature of the δ field is that it inhabits a universe that is isotropic and homogeneous in its large-scale properties. This suggests that the statistical properties of δ should also be statistically homogeneous—*i.e.*, it is a stationary random process.

It is often convenient to describe δ as a Fourier superposition:

$$\delta(\mathbf{x}) = \sum \delta_{\mathbf{k}} e^{-i\mathbf{k} \cdot \mathbf{x}}. \quad (19.71)$$

We avoid difficulties with an infinite universe by applying periodic boundary conditions in a cube of some large volume V . The cross-terms vanish when we compute the variance in the field, which is just a sum over modes of the power spectrum

$$\langle \delta^2 \rangle = \sum |\delta_{\mathbf{k}}|^2 \equiv \sum P(k). \quad (19.72)$$

Note that the statistical nature of the fluctuations must be isotropic, so we write $P(k)$ rather than $P(\mathbf{k})$. The $\langle \dots \rangle$ average here is a volume average. Cosmological density fields are an example of an ergodic process, in which the average over a large volume tends to the same answer as the average over a statistical ensemble.

The statistical properties of discrete objects sampled from the density field are often described in terms of N -point correlation functions, which represent the excess probability over random for finding one particle in each of N boxes in a given configuration. For the 2-point case, the correlation function is readily shown to be identical to the autocorrelation function of the δ field: $\xi(r) = \langle \delta(x)\delta(x+r) \rangle$.

The power spectrum and correlation function are Fourier conjugates, and thus are equivalent descriptions of the density field (similarly, k -space equivalents exist for the higher-order correlations). It is convenient to take the limit $V \rightarrow \infty$ and use k -space integrals, defining a dimensionless power spectrum as $\Delta^2(k) = d\langle \delta^2 \rangle / d \ln k = V k^3 P(k) / 2\pi^2$:

$$\xi(r) = \int \Delta^2(k) \frac{\sin kr}{kr} d \ln k; \quad \Delta^2(k) = \frac{2}{\pi} k^3 \int_0^\infty \xi(r) \frac{\sin kr}{kr} r^2 dr. \quad (19.73)$$

For many years, an adequate approximation to observational data on galaxies was $\xi = (r/r_0)^{-\gamma}$, with $\gamma \simeq 1.8$ and $r_0 \simeq 5 h^{-1} \text{ Mpc}$. Modern surveys are now able to probe into the large-scale linear regime where traces of the curved primordial spectrum can be detected [70,71,72].

19.4.5. Formation of cosmological structure :

The simplest model for the generation of cosmological structure is gravitational instability acting on some small initial fluctuations (for the origin of which a theory such as inflation is required). If the perturbations are adiabatic (*i.e.*, fractionally perturb number densities of photons and matter equally), the linear growth law for matter perturbations is simple:

$$\delta \propto \begin{cases} a(t)^2 & (\text{radiation domination; } \Omega_r = 1) \\ a(t) & (\text{matter domination; } \Omega_m = 1) . \end{cases} \quad (19.74)$$

For low density universes, the present-day amplitude is suppressed by a factor $g(\Omega)$, where

$$g(\Omega) \simeq \frac{5}{2} \Omega_m \left[\Omega_m^{4/7} - \Omega_v + (1 + \Omega_m/2) \left(1 + \frac{1}{70} \Omega_v \right) \right]^{-1} \quad (19.75)$$

is an accurate fit for models with matter plus cosmological constant. The alternative perturbation mode is isocurvature: only the equation of state changes, and the total density is initially unperturbed. These modes perturb the total entropy density, and thus induce additional large-scale CMB anisotropies [64]. Although the character of perturbations in the simplest inflationary theories are purely adiabatic, correlated adiabatic and isocurvature modes are predicted in many models; the simplest example is the curvaton, which is a scalar field that decays to yield a perturbed radiation density. If the matter content already exists at this time, the overall perturbation field will have a significant isocurvature component. Such a prediction is inconsistent with current CMB data [65], and most analyses of CMB and LSS data assume the adiabatic case to hold exactly.

Linear evolution preserves the shape of the power spectrum. However, a variety of processes mean that growth actually depends on the matter content:

- (1) Pressure opposes gravity effectively for wavelengths below the horizon length while the Universe is radiation dominated. The *comoving* horizon size at z_{eq} is therefore an important scale:

$$D_H(z_{\text{eq}}) = \frac{2(\sqrt{2}-1)}{(\Omega_m z_{\text{eq}})^{1/2} H_0} = \frac{16.0}{\Omega_m h^2} \text{Mpc} . \quad (19.76)$$

- (2) At early times, dark matter particles will undergo free streaming at the speed of light, and so erase all scales up to the horizon—a process that only ceases when the particles go nonrelativistic. For light massive neutrinos, this happens at z_{eq} ; all structure up to the horizon-scale power-spectrum break is in fact erased. Hot(cold) dark matter models are thus sometimes dubbed large(small)-scale damping models.
- (3) A further important scale arises where photon diffusion can erase perturbations in the matter–radiation fluid; this process is named Silk damping.

The overall effect is encapsulated in the transfer function, which gives the ratio of the late-time amplitude of a mode to its initial value (see Fig. 19.4). The overall power spectrum is thus the primordial power-law, times the square of the transfer function:

$$P(k) \propto k^n T_k^2 . \quad (19.77)$$

The most generic power-law index is $n = 1$: the ‘Zeldovich’ or ‘scale-invariant’ spectrum. Inflationary models tend to predict a small ‘tilt’: $|n - 1| \lesssim 0.03$ [13,14]. On the assumption that the dark matter is cold, the power spectrum then depends on 5 parameters: n , h , Ω_b , Ω_{cdm} ($\equiv \Omega_m - \Omega_b$) and an overall amplitude. The latter is often specified as σ_8 , the linear-theory fractional rms in density when a spherical filter of radius $8h^{-1}$ Mpc is applied in linear theory. This scale can be probed directly via weak gravitational lensing, and also via its effect on the abundance of rich galaxy clusters. The favored value is approximately [66,67,22]

$$\sigma_8 \simeq (0.76 \pm 6\%) (\Omega_m/0.24)^{-0.5} . \quad (19.78)$$

A direct measure of mass inhomogeneity is valuable, since the galaxies inevitably are biased with respect to the mass. This means that the

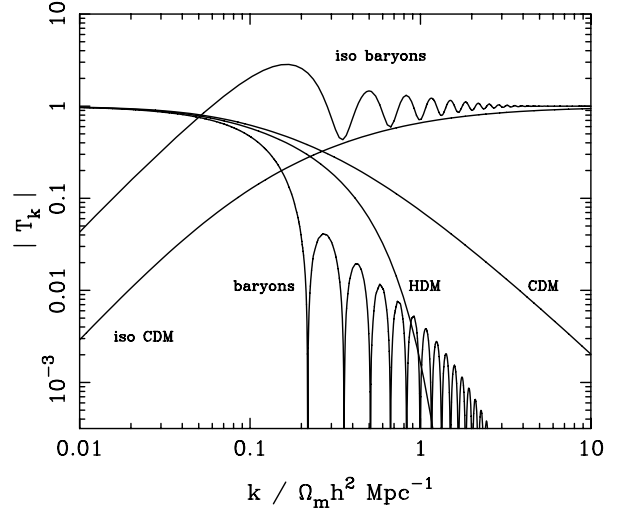


Figure 19.4: A plot of transfer functions for various models. For adiabatic models, $T_k \rightarrow 1$ at small k , whereas the opposite is true for isocurvature models. For dark-matter models, the characteristic wavenumber scales proportional to $\Omega_m h^2$. The scaling for baryonic models does not obey this exactly; the plotted cases correspond to $\Omega_m = 1$, $h = 0.5$.

fractional fluctuations in galaxy number, $\delta n/n$, may differ from the mass fluctuations, $\delta\rho/\rho$. It is commonly assumed that the two fields obey some proportionality on large scales where the fluctuations are small, $\delta n/n = b\delta\rho/\rho$, but even this is not guaranteed [68].

The main shape of the transfer function is a break around the horizon scale at z_{eq} , which depends just on $\Omega_m h$ when wavenumbers are measured in observable units ($h \text{Mpc}^{-1}$). For reasonable baryon content, weak oscillations in the transfer function are also expected, and these BAOs (Baryon Acoustic Oscillations) have been clearly detected [69]. As well as directly measuring the baryon fraction, the scale of the oscillations directly measures the acoustic horizon at decoupling; this can be used as an additional standard ruler for cosmological tests, and the BAO method is likely to be important in future large galaxy surveys. Overall, current power-spectrum data [70,71,72] favor $\Omega_m h \simeq 0.20$ and a baryon fraction of about 0.15 for $n = 1$ (see Fig. 19.5).

In principle, accurate data over a wide range of k could determine both Ωh and n , but in practice there is a strong degeneracy between these. In order to constrain n itself, it is necessary to examine data on anisotropies in the CMB.

19.4.6. CMB anisotropies :

The CMB has a clear dipole anisotropy, of magnitude 1.23×10^{-3} . This is interpreted as being due to the Earth’s motion, which is equivalent to a peculiar velocity for the Milky Way of

$$v_{\text{MW}} \simeq 600 \text{ km s}^{-1} \text{ towards } (\ell, b) \simeq (270^\circ, 30^\circ) . \quad (19.79)$$

All higher-order multipole moments of the CMB are however much smaller (of order 10^{-5}), and interpreted as signatures of density fluctuations at last scattering ($\simeq 1100$). To analyze these, the sky is expanded in spherical harmonics as explained in the review on CBR–Sec. 23 of this *Review*. The dimensionless power per $\ln k$ or ‘bandpower’ for the CMB is defined as

$$\mathcal{T}^2(\ell) = \frac{\ell(\ell+1)}{2\pi} C_\ell . \quad (19.80)$$

This function encodes information from the three distinct mechanisms that cause CMB anisotropies:

- (1) Gravitational (Sachs–Wolfe) perturbations. Photons from high-density regions at last scattering have to climb out of potential wells, and are thus redshifted.
- (2) Intrinsic (adiabatic) perturbations. In high-density regions, the coupling of matter and radiation can compress the radiation also, giving a higher temperature.

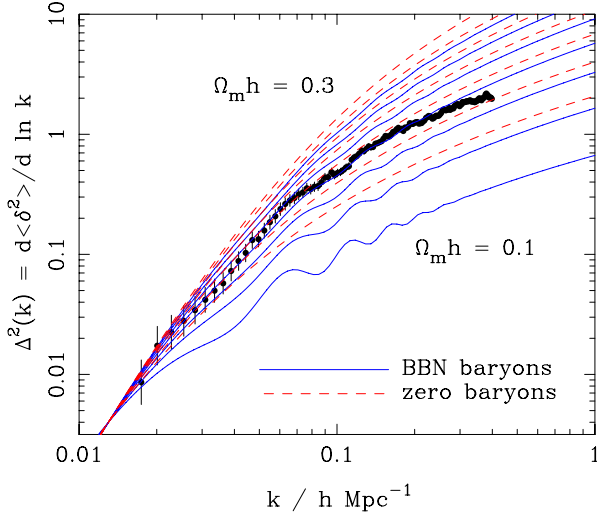


Figure 19.5: The galaxy power spectrum from the 2dFGRS, shown in dimensionless form, $\Delta^2(k) \propto k^3 P(k)$. The solid points with error bars show the power estimate. The window function correlates the results at different k values, and also distorts the large-scale shape of the power spectrum. An approximate correction for the latter effect has been applied. The solid and dashed lines show various CDM models, all assuming $n = 1$. For the case with non-negligible baryon content, a big-bang nucleosynthesis value of $\Omega_b h^2 = 0.02$ is assumed, together with $h = 0.7$. A good fit is clearly obtained for $\Omega_m h \simeq 0.2$. Color version at end of book.

- (3) Velocity (Doppler) perturbations. The plasma has a non-zero velocity at recombination, which leads to Doppler shifts in frequency and hence shifts in brightness temperature.

Because the potential fluctuations obey Poisson's equation, $\nabla^2 \Phi = 4\pi G \rho \delta$, and the velocity field satisfies the continuity equation $\nabla \cdot \mathbf{u} = -\dot{\delta}$, the resulting different powers of k ensure that the Sachs-Wolfe effect dominates on large scales and adiabatic effects on small scales.

The relation between angle and comoving distance on the last-scattering sphere requires the comoving angular-diameter distance to the last-scattering sphere; because of its high redshift, this is effectively identical to the horizon size at the present epoch, D_H :

$$D_H = \frac{2}{\Omega_m H_0} \quad (\Omega_v = 0) \quad (19.81)$$

$$D_H \simeq \frac{2}{\Omega_m^{0.4} H_0} \quad (\text{flat: } \Omega_m + \Omega_v = 1) .$$

These relations show how the CMB is strongly sensitive to curvature: the horizon length at last scattering is $\propto 1/\sqrt{\Omega_m}$, so that this subtends an angle that is virtually independent of Ω_m for a flat model. Observations of a peak in the CMB power spectrum at relatively large scales ($\ell \simeq 225$) are thus strongly inconsistent with zero- Λ models with low density: current CMB data require $\Omega_m + \Omega_v = 1.011 \pm 0.012$ [22]. (See *e.g.*, Fig. 19.2).

In addition to curvature, the CMB encodes information about several other key cosmological parameters. Within the compass of simple adiabatic CDM models, there are 9 of these:

$$\omega_c, \omega_b, \Omega_t, h, \tau, n_s, n_t, r, Q . \quad (19.82)$$

The symbol ω denotes the physical density, Ωh^2 : the transfer function depends only on the densities of CDM (ω_c) and baryons (ω_b). Transcribing the power spectrum at last scattering into an angular power spectrum brings in the total density parameter ($\Omega_t \equiv \Omega_m + \Omega_v = \Omega_c + \Omega_b + \Omega_v$) and h : there is an exact geometrical degeneracy [73] between these that keeps the angular-diameter distance to last scattering invariant, so that models with substantial spatial curvature and large vacuum energy cannot be ruled out without prior knowledge of the Hubble parameter. Alternatively, the CMB alone cannot measure the Hubble parameter.

The other main parameter degeneracy involves the tensor contribution to the CMB anisotropies. These are important at large scales (up to the horizon scales); for smaller scales, only scalar fluctuations (density perturbations) are important. Each of these components is characterized by a spectral index, n , and a ratio between the power spectra of tensors and scalars (r). Finally, the overall amplitude of the spectrum must be specified (Q), together with the optical depth to Compton scattering owing to recent reionization (τ). The tensor degeneracy operates as follows: the main effect of adding a large tensor contribution is to reduce the contrast between low ℓ and the peak at $\ell \simeq 225$ (because the tensor spectrum has no acoustic component). The required height of the peak can be recovered by increasing n_s to increase the small-scale power in the scalar component; this in turn over-predicts the power at $\ell \sim 1000$, but this effect can be counteracted by raising the baryon density [74]. In order to break this degeneracy, additional data are required. For example, an excellent fit to the CMB data is obtained with a scalar-only model with zero curvature and $\omega_b = 0.0223$, $\omega_c = 0.105$, $h = 0.73$, $n_s = 0.96$ [22]. However, this is indistinguishable from a model where tensors dominate at $\ell \lesssim 100$, if we raise ω_b to 0.03 and n_s to 1.2. This baryon density is too high for nucleosynthesis, which disfavors the high-tensor solution [75].

The reason the tensor component is introduced, and why it is so important, is that it is the only non-generic prediction of inflation. Slow-roll models of inflation involve two dimensionless parameters:

$$\epsilon \equiv \frac{M_{\text{P}}^2}{16\pi} (V'/V)^2 \quad \eta \equiv \frac{M_{\text{P}}^2}{8\pi} (V''/V) , \quad (19.83)$$

where V is the inflaton potential, and dashes denote derivatives with respect to the inflation field. In terms of these, the tensor-to-scalar ratio is $r \simeq 12\epsilon$, and the spectral indices are $n_s = 1 - 6\epsilon + 2\eta$ and $n_t = -2\epsilon$. The natural expectation of inflation is that the quasi-exponential phase ends once the slow-roll parameters become significantly non-zero, so that both $n_s \neq 1$ and a significant tensor component are expected. These prediction can be avoided in some models, but it is undeniable that observation of such features would be a great triumph for inflation. Cosmology therefore stands at a fascinating point given that the most recent combination of CMB and LSS data appear to reject the zero-tensor $n_s = 1$ model at around 3σ : $n_s = 0.958 \pm 0.016$ [22]. If we insist on $n_s = 1$, then a very substantial tensor fraction would be required ($r \simeq 0.3$), although the fit is better with $r = 0$. Assuming that no systematic error in this result can be identified, cosmology has passed a critical hurdle; the years ahead will be devoted to the task of breaking the tensor degeneracy — for which the main tool will be the polarization of the CMB [76].

References:

1. V.M. Slipher, *Pop. Astr.* **23**, 21 (1915).
2. K. Lundmark, *MNRAS* **84**, 747 (1924).
3. E. Hubble and M.L. Humason, *Ap. J.* **74**, 43 (1931).
4. G. Gamow, *Phys. Rev.* **70**, 572 (1946).
5. R.A. Alpher *et al.*, *Phys. Rev.* **73**, 803 (1948).
6. R.A. Alpher and R.C. Herman, *Phys. Rev.* **74**, 1737 (1948).
7. R.A. Alpher and R.C. Herman, *Phys. Rev.* **75**, 1089 (1949).
8. A.A. Penzias and R.W. Wilson, *Ap. J.* **142**, 419 (1965).
9. S. Weinberg, *Gravitation and Cosmology*, John Wiley and Sons (1972).
10. P.J.E. Peebles, *Principles of Physical Cosmology* Princeton University Press (1993).
11. G. Börner, *The Early Universe: Facts and Fiction*, Springer-Verlag (1988).
12. E.W. Kolb and M.S. Turner, *The Early Universe*, Addison-Wesley (1990).
13. J.A. Peacock, *Cosmological Physics*, Cambridge Univ. Press (1999).
14. A.R. Liddle and D. Lyth, *Cosmological Inflation and Large-Scale Structure*, Cambridge University Press (2000).
15. E.B. Gliner, *Sov. Phys. JETP* **22**, 378 (1966).
16. Y.B. Zeldovich, (1967), *Sov. Phys. Uspekhi*, **11**, 381 (1968).
17. P.M. Garnavich *et al.*, *Ap. J.* **507**, 74 (1998).
18. S. Perlmutter *et al.*, *Phys. Rev. Lett.* **83**, 670 (1999).

19. I. Maor *et al.*, Phys. Rev. **D65**, 123003 (2002).
20. A. Albrecht *et al.*, astro-ph/0609591.
21. J. Peacock *et al.*, astro-ph/0610906.
22. D.N. Spergel *et al.*, Astrophys. J. Supp. **170**, 377 (2007).
23. A.G. Riess *et al.*, A. J. **116**, 1009 (1998).
24. S. Perlmutter *et al.*, Ap. J. **517**, 565 (1999).
25. A.G. Riess, PASP, **112**, 1284 (2000).
26. J.L. Tonry *et al.*, Ap. J. **594**, 1 (2003).
27. W.L. Freedman *et al.*, Astrophys. J. **553**, 47 (2001).
28. P. Astier *et al.*, A&A, **447** 31 (2006).
29. J.A. Johnson and M. Bolte, Astrophys. J. **554**, 888 (2001).
30. R. Jimenez and P. Padoan, Astrophys. J. **498**, 704 (1998).
31. E. Carretta *et al.*, Astrophys. J. **533**, 215 (2000).
32. M. Srednicki *et al.*, Nucl. Phys. B **310**, 693 (1988).
33. G. Mangano *et al.*, Phys. Lett. **B534**, 8 (2002).
34. A. Linde, Phys. Rev. **D14**, 3345 (1976).
35. A. Linde, Rep. Prog. Phys. **42**, 389 (1979).
36. C.E. Vayonakis, Surveys High Energ. Phys. **5**, 87 (1986).
37. S.A. Bonometto and A. Masiero, Riv. Nuovo Cim. **9N5**, 1 (1986).
38. A. Linde, *Particle Physics And Inflationary Cosmology*, Harwood (1990).
39. K.A. Olive, Phys. Rep. **190**, 3345 (1990).
40. D. Lyth and A. Riotto, Phys. Rep. **314**, 1 (1999).
41. A.H. Guth, Phys. Rev. **D23**, 347 (1981).
42. A.D. Linde, Phys. Lett. **108B**, 389 (1982).
43. A. Albrecht and P.J. Steinhardt, Phys. Rev. Lett. **48**, 1220 (1982).
44. A.D. Sakharov, Sov. Phys. JETP Lett. **5**, 24 (1967).
45. S. Weinberg, Phys. Rev. Lett. **42**, 850 (1979).
46. D. Toussaint *et al.*, Phys. Rev. **D19**, 1036 (1979).
47. I. Affleck and M. Dine, Nucl. Phys. **B249**, 361 (1985).
48. V. Kuzmin *et al.*, Phys. Lett. **B155**, 36 (1985).
49. M. Fukugita and T. Yanagida, Phys. Lett. **B174**, 45 (1986).
50. R.H. Cyburt *et al.*, Phys. Lett. **B567**, 227 (2003).
51. K.A. Olive *et al.*, Phys. Rept. **333**, 389 (2000).
52. J. M. O'meara *et al.*, Ap. J. **649**, L61 (2006).
53. D.J. Fixsen *et al.*, Astrophys. J. **473**, 576 (1996).
54. J.C. Mather *et al.*, Astrophys. J. **512**, 511 (1999).
55. S.M. Cole *et al.*, MNRAS **326**, 255 (2001).
56. R.H. Becker *et al.*, Astr. J. **122**, 2850 (2001).
57. S.D.M. White *et al.*, Nature **366**, 429 (1993).
58. S.W. Allen *et al.*, MNRAS, **334**, L11 (2002).
59. S. Folkes *et al.*, MNRAS **308**, 459 (1999).
60. M.L. Blanton *et al.*, Astr. J. **121**, 2358 (2001).
61. H. Hoekstra *et al.*, Astrophys. J. **548**, L5 (2001).
62. S.W. Allen, MNRAS **296**, 392 (1998).
63. H. Hoekstra *et al.*, Astrophys. J. **647**, 116 (2006).
64. G. Efstathiou and J.R. Bond, MNRAS **218**, 103 (1986).
65. C. Gordon and A. Lewis, Phys. Rev. **D67**, 123513 (2003).
66. M.L. Brown *et al.*, MNRAS, **341**, 1 (2003).
67. P.T.P. Viana, R.C. Nichol, and A.R. Liddle, Astrophys. J. **569**, L75 (2002).
68. A. Dekel and O. Lahav, Astrophys. J. **520**, 24 (1999).
69. W.J. Percival *et al.*, arXiv:0705.3323.
70. W.J. Percival *et al.*, MNRAS **327**, 1297 (2001).
71. S.M. Cole *et al.*, MNRAS **362**, 505 (2005).
72. W.J. Percival *et al.*, Astrophys. J. **657**, 645 (2007).
73. G. Efstathiou and J.R. Bond, MNRAS, **304**, 75 (1999).
74. G.P. Efstathiou *et al.*, MNRAS **330**, L29 (2002).
75. G.P. Efstathiou, MNRAS **332**, 193 (2002).
76. S. Dodelson, *Modern Cosmology*, Academic Press (2003).

20. BIG-BANG NUCLEOSYNTHESIS

Revised October 2007 by B.D. Fields (Univ. of Illinois) and S. Sarkar (Univ. of Oxford).

Big-bang nucleosynthesis (BBN) offers the deepest reliable probe of the early universe, being based on well-understood Standard Model physics [1–4]. Predictions of the abundances of the light elements, D, ^3He , ^4He , and ^7Li , synthesized at the end of the “first three minutes,” are in good overall agreement with the primordial abundances inferred from observational data, thus validating the standard hot big-bang cosmology (see [5] for a review). This is particularly impressive given that these abundances span nine orders of magnitude — from $^4\text{He}/\text{H} \sim 0.08$ down to $^7\text{Li}/\text{H} \sim 10^{-10}$ (ratios by number). Thus BBN provides powerful constraints on possible deviations from the standard cosmology [2], and on new physics beyond the Standard Model [3].

20.1. Theory

The synthesis of the light elements is sensitive to physical conditions in the early radiation-dominated era at temperatures $T \lesssim 1$ MeV, corresponding to an age $t \gtrsim 1$ s. At higher temperatures, weak interactions were in thermal equilibrium, thus fixing the ratio of the neutron and proton number densities to be $n/p = e^{-Q/T}$, where $Q = 1.293$ MeV is the neutron-proton mass difference. As the temperature dropped, the neutron-proton inter-conversion rate, $\Gamma_{n \leftrightarrow p} \sim G_F^2 T^5$, fell faster than the Hubble expansion rate, $H \sim \sqrt{g_* G_N} T^2$, where g_* counts the number of relativistic particle species determining the energy density in radiation. This resulted in departure from chemical equilibrium (“freeze-out”) at $T_{\text{fr}} \sim (g_* G_N / G_F^4)^{1/6} \simeq 1$ MeV. The neutron fraction at this time, $n/p = e^{-Q/T_{\text{fr}}} \simeq 1/6$, is thus sensitive to every known physical interaction, since Q is determined by both strong and electromagnetic interactions while T_{fr} depends on the weak as well as gravitational interactions. Moreover, the sensitivity to the Hubble expansion rate affords a probe of *e.g.*, the number of relativistic neutrino species [6]. After freeze-out, the neutrons were free to β -decay so the neutron fraction dropped to $\simeq 1/7$ by the time nuclear reactions began. A simplified analytic model of freeze-out yields the n/p ratio to an accuracy of $\sim 1\%$ [7,8].

The rates of these reactions depend on the density of baryons (strictly speaking, nucleons), which is usually expressed normalized to the relic blackbody photon density as $\eta \equiv n_B/n_\gamma$. As we shall see, all the light-element abundances can be explained with $\eta_{10} \equiv \eta \times 10^{10}$ in the range 4.7–6.5 (95% CL). With n_γ fixed by the present CMB temperature 2.725 K (see Cosmic Microwave Background review), this can be stated as the allowed range for the baryon mass density today, $\rho_B = (3.2\text{--}4.5) \times 10^{-31}$ g cm $^{-3}$, or as the baryonic fraction of the critical density, $\Omega_B = \rho_B/\rho_{\text{crit}} \simeq \eta_{10} h^{-2}/274 = (0.017\text{--}0.024)h^{-2}$, where $h \equiv H_0/100$ km s $^{-1}$ Mpc $^{-1} = 0.72 \pm 0.08$ is the present Hubble parameter (see Cosmological Parameters review).

The nucleosynthesis chain begins with the formation of deuterium in the process $p(n, \gamma)\text{D}$. However, photo-dissociation by the high number density of photons delays production of deuterium (and other complex nuclei) well after T drops below the binding energy of deuterium, $\Delta_D = 2.23$ MeV. The quantity $\eta^{-1} e^{-\Delta_D/T}$, *i.e.*, the number of photons per baryon above the deuterium photo-dissociation threshold, falls below unity at $T \simeq 0.1$ MeV; nuclei can then begin to form without being immediately photo-dissociated again. Only 2-body reactions, such as $\text{D}(p, \gamma)^3\text{He}$, $^3\text{He}(\text{D}, p)^4\text{He}$, are important because the density has become rather low by this time.

Nearly all the surviving neutrons when nucleosynthesis begins end up bound in the most stable light element ^4He . Heavier nuclei do not form in any significant quantity both because of the absence of stable nuclei with mass number 5 or 8 (which impedes nucleosynthesis via $n^4\text{He}$, $p^4\text{He}$ or $^4\text{He}^4\text{He}$ reactions), and the large Coulomb barriers for reactions such as $\text{T}(^4\text{He}, \gamma)^7\text{Li}$ and $^3\text{He}(^4\text{He}, \gamma)^7\text{Be}$. Hence the primordial mass fraction of ^4He , conventionally referred to as Y_p , can be estimated by the simple counting argument

$$Y_p = \frac{2(n/p)}{1 + n/p} \simeq 0.25. \quad (20.1)$$

There is little sensitivity here to the actual nuclear reaction rates, which are, however, important in determining the other “left-over”

abundances: D and ^3He at the level of a few times 10^{-5} by number relative to H, and $^7\text{Li}/\text{H}$ at the level of about 10^{-10} (when η_{10} is in the range 1–10). These values can be understood in terms of approximate analytic arguments [8,9]. The experimental parameter most important in determining Y_p is the neutron lifetime, τ_n , which normalizes (the inverse of) $\Gamma_{n \leftrightarrow p}$. The experimental uncertainty in τ_n used to be a source of concern, but has recently been reduced substantially: $\tau_n = 885.7 \pm 0.8$ s (see *N* Baryons Listing).

The elemental abundances are calculated using an updated version [10] of the Wagoner code [1]; other modern versions [11] are publicly available [12]. Results appear in Fig. 20.1 as a function of η_{10} . The ^4He curve includes small corrections due to radiative processes at zero and finite temperatures [13], non-equilibrium neutrino heating during e^\pm annihilation [14], and finite nucleon mass effects [15]; the range reflects primarily the 2σ uncertainty in the neutron lifetime. The spread in the curves for D, ^3He , and ^7Li corresponds to the 2σ uncertainties in nuclear cross sections, as estimated by Monte Carlo methods [16–17]. The input nuclear data have been carefully reassessed [10, 18–21], leading to improved precision in the abundance predictions. Polynomial fits to the predicted abundances and the error correlation matrix have been given [17,22]. The boxes in Fig. 20.1 show the observationally inferred primordial abundances with their associated statistical and systematic uncertainties, as discussed below.

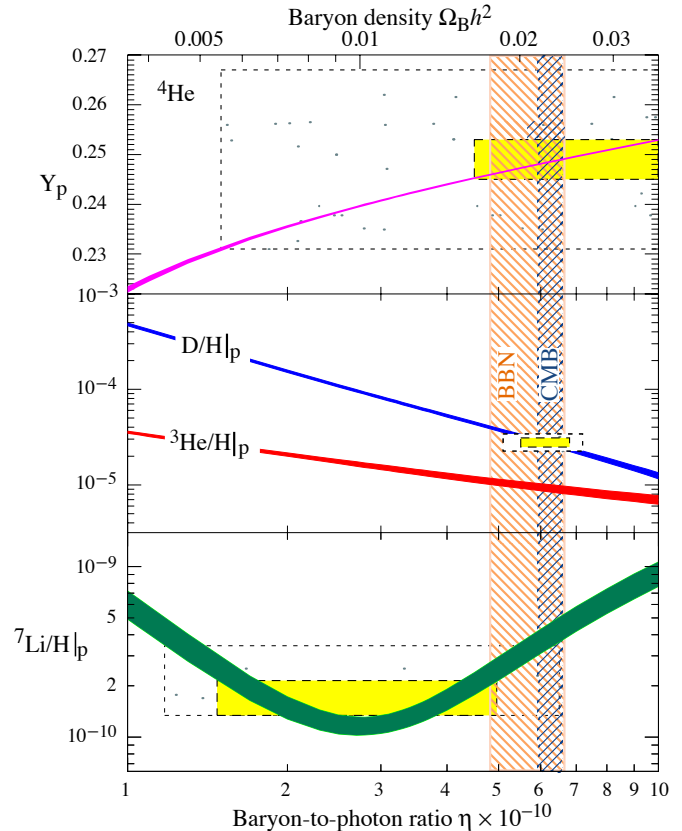


Figure 20.1: The abundances of ^4He , D, ^3He , and ^7Li as predicted by the standard model of big-bang nucleosynthesis — the bands show the 95% CL range. Boxes indicate the observed light element abundances (smaller boxes: $\pm 2\sigma$ statistical errors; larger boxes: $\pm 2\sigma$ statistical and systematic errors). The narrow vertical band indicates the CMB measure of the cosmic baryon density, while the wider band indicates the BBN concordance range (both at 95% CL). Color version at end of book.

20.2. Light Element Abundances

BBN theory predicts the universal abundances of D, ^3He , ^4He , and ^7Li , which are essentially determined by $t \sim 180$ s. Abundances are,

however, observed at much later epochs, after stellar nucleosynthesis has commenced. The ejected remains of this stellar processing can alter the light element abundances from their primordial values, but also produce heavy elements such as C, N, O, and Fe (“metals”). Thus, one seeks astrophysical sites with low metal abundances, in order to measure light element abundances which are closer to primordial. For all of the light elements, systematic errors are an important, and often dominant, limitation to the precision with which primordial abundances can be inferred.

In recent years, high-resolution spectra have revealed the presence of D in high-redshift, low-metallicity quasar absorption systems (QAS), via its isotope-shifted Lyman- α absorption [23–28]. It is believed that there are no astrophysical sources of deuterium [29], so any detection provides a lower limit to primordial D/H, and thus an upper limit on η ; for example, the local interstellar value of $D/H|_p = (1.56 \pm 0.04) \times 10^{-5}$ [30] requires $\eta_{10} \leq 9$. Recent observations find an unexpected scatter of a factor of ~ 2 [31], as well as correlations with heavy element abundances which, suggest interstellar D may suffer stellar processing (astration), but also partly reside in dust particles which evade gas-phase observations. This is supported by a measurement in the lower halo [32] which indicates that the Galactic D abundance has been reduced by a factor of only 1.12 ± 0.13 since its formation. For the high-redshift systems, conventional models of galactic nucleosynthesis (chemical evolution) do not predict either of these effects for D/H [33].

The observed extragalactic D values are bracketed by the non-detection of D in a high-redshift system, $D/H|_p < 6.7 \times 10^{-5}$ at 1σ [34], and low values in some (damped Lyman- α) systems [24,25]. Averaging the six most precise observations of deuterium in QAS gives $D/H = (2.84 \pm 0.14) \times 10^{-5}$, where the error is statistical only [23,27]. However, there remains concern over systematic errors, the dispersion between the values being much larger than is expected from the individual measurement errors ($\chi^2 = 18.1$ for $\nu = 5$ d.o.f.). Increasing the error by a factor $\sqrt{\chi^2/\nu}$ gives, as shown on Fig. 20.1:

$$D/H|_p = (2.84 \pm 0.26) \times 10^{-5}. \quad (20.2)$$

We observe ^4He in clouds of ionized hydrogen (H II regions), the most metal-poor of which are in dwarf galaxies. There is now a large body of data on ^4He and CNO in these systems [35]. These data confirm that the small stellar contribution to helium is positively correlated with metal production. Extrapolating to zero metallicity gives the primordial ^4He abundance [36]

$$Y_p = 0.249 \pm 0.009. \quad (20.3)$$

Here the latter error is a careful (and significantly enlarged) estimate of the systematic uncertainties which dominate, and is based on the scatter in different analyses of the physical properties of the H II regions [35,36]. Other recent extrapolations to zero metallicity give $Y_p = 0.2472 \pm 0.0012$ or 0.2516 ± 0.0011 depending on which set of He I emissivities are used [37], and $Y_p = 0.2477 \pm 0.0029$ [38]. These are consistent (given the systematic errors) with the above estimate [36], which appears in Fig. 20.1.

The systems best suited for Li observations are metal-poor stars in the spheroid (Pop II) of our Galaxy, which have metallicities going down to at least 10^{-4} , and perhaps 10^{-5} of the Solar value [39]. Observations have long shown [40–44] that Li does not vary significantly in Pop II stars with metallicities $\lesssim 1/30$ of Solar — the “Spite plateau” [40]. Precision data suggest a small but significant correlation between Li and Fe [41], which can be understood as the result of Li production from Galactic cosmic rays [42]. Extrapolating to zero metallicity, one arrives at a primordial value $\text{Li}/\text{H}|_p = (1.23 \pm 0.06) \times 10^{-10}$ [43]. One systematic error stems from the differences in techniques to determine the physical parameters (*e.g.*, the temperature) of the stellar atmosphere in which the Li absorption line is formed. Alternative analyses, using methods that give systematically higher temperatures, yield $\text{Li}/\text{H}|_p = (2.19 \pm 0.28) \times 10^{-10}$ [44], $\text{Li}/\text{H}|_p = (2.34 \pm 0.32) \times 10^{-10}$ [45], and $\text{Li}/\text{H}|_p = (1.26 \pm 0.26) \times 10^{-10}$ [46]; the difference with [43] indicates a systematic uncertainty of a factor of ~ 2 . Moreover, it

is possible that the Li in Pop II stars has been partially destroyed, due to mixing of the outer layers with the hotter interior [47]. Such processes can be constrained by the absence of significant scatter in Li-Fe [41], and by observations of the fragile isotope ^6Li [42]. Nevertheless, depletion by a factor as large as ~ 1.8 is possible [48]. Including these systematics, we estimate a primordial Li range, as shown in Fig. 20.1:

$$\text{Li}/\text{H}|_p = (1.7 \pm 0.02_{-0}^{+1.1}) \times 10^{-10}. \quad (20.4)$$

Stellar determination of Li abundances typically sum over both stable isotopes ^6Li and ^7Li . Recent high-precision measurements are sensitive to the tiny isotopic shift in Li absorption (which manifests itself in the shape of the blended, thermally broadened line) and indicate $^6\text{Li}/^7\text{Li} \leq 0.15$ [49]. This confirms that ^7Li is dominant, but surprisingly there is indication of a ^6Li plateau (analogous to the ^7Li plateau) which suggests a significant primordial ^6Li abundance. Caution must however be exercised since convective motions in the star can generate similar asymmetries in the line shape, hence the deduced ^6Li abundance is presently best interpreted as an upper limit [50].

Turning to ^3He , the only data available are from the Solar system and (high-metallicity) H II regions in our Galaxy [51]. This makes inference of the primordial abundance difficult, a problem compounded by the fact that stellar nucleosynthesis models for ^3He are in conflict with observations [52]. Consequently, it is no longer appropriate to use ^3He as a cosmological probe; instead, one might hope to turn the problem around and constrain stellar astrophysics using the predicted primordial ^3He abundance [53].

20.3. Concordance, Dark Matter, and the CMB

We now use the observed light element abundances to assess the theory. We first consider standard BBN, which is based on Standard Model physics alone, so $N_\nu = 3$ and the only free parameter is the baryon-to-photon ratio η . (The implications of BBN for physics beyond the Standard Model will be considered below, §4). Thus, any abundance measurement determines η , while additional measurements overconstrain the theory and thereby provide a consistency check.

First we note that the overlap in the η ranges spanned by the larger boxes in Fig. 20.1 indicates overall concordance. More quantitatively, when we account for theoretical uncertainties as well as the statistical and systematic errors in observations, there is acceptable agreement among the abundances when

$$4.7 \leq \eta_{10} \leq 6.5 \text{ (95\% CL)}. \quad (20.5)$$

However, the agreement is much less satisfactory if we use only the quoted statistical errors in the observations. In particular, as seen in Fig. 20.1, D and ^4He are consistent with each other, but favor a value of η which is higher by a factor of at least 2, and by at least 2σ from that indicated by the ^7Li abundance determined in stars. Furthermore, if the ^6Li plateau [49] reflects a primordial component, it is ~ 1000 times that expected in standard BBN [54]; both these “lithium problems” may indicate new physics (see below).

Even so, the overall concordance is remarkable: using well-established microphysics we have extrapolated back to an age of ~ 1 s to correctly predict light element abundances spanning 9 orders of magnitude. This is a major success for the standard cosmology, and inspires confidence in extrapolation back to still earlier times.

This concordance provides a measure of the baryon content

$$0.017 \leq \Omega_B h^2 \leq 0.024 \text{ (95\% CL)}, \quad (20.6)$$

a result that plays a key role in our understanding of the matter budget of the universe. First we note that $\Omega_B \ll 1$, *i.e.*, baryons cannot close the universe [55]. Furthermore, the cosmic density of (optically) luminous matter is $\Omega_{\text{lum}} \simeq 0.0024 h^{-1}$ [56], so that $\Omega_B \gg \Omega_{\text{lum}}$: most baryons are optically dark, probably in the form of a $\sim 10^6$ K X-ray emitting intergalactic medium [57]. Finally, given that $\Omega_M \sim 0.3$ (see Dark Matter and Cosmological Parameters

reviews), we infer that most matter in the universe is not only dark, but also takes some non-baryonic (more precisely, non-nucleonic) form.

The BBN prediction for the cosmic baryon density can be tested through precision observations of CMB temperature fluctuations (see Cosmic Microwave Background review). One can determine η from the amplitudes of the acoustic peaks in the CMB angular power spectrum [58], making it possible to compare two measures of η using very different physics, at two widely separated epochs. In the standard cosmology, there is no change in η between BBN and CMB decoupling, thus, a comparison of η_{BBN} and η_{CMB} is a key test. Agreement would endorse the standard picture while disagreement could point to new physics during/between the BBN and CMB epochs.

The release of the WMAP results was a landmark event in this test of BBN. As with other cosmological parameter determinations from CMB data, the derived η_{CMB} depends on the adopted priors [59], in particular the form assumed for the power spectrum of primordial density fluctuations. If this is taken to be a scale-free power-law, the three-year WMAP data implies $\Omega_{\text{B}}h^2 = 0.0223 \pm 0.0007$ or $\eta_{10} = 6.11 \pm 0.19$ [60] as shown in Fig. 20.1. Other assumptions for the shape of the power spectrum can lead to baryon densities as low as $\Omega_{\text{B}}h^2 = 0.0175 \pm 0.0007$ [61]. Thus, outstanding uncertainties regarding priors are a source of systematic error which presently exceeds the statistical error in the prediction for η .

It is remarkable that the CMB estimate of the baryon density is consistent with the BBN range quoted in Eq. (20.6), and in very good agreement with the value inferred from recent high-redshift D/H measurements [26] and ${}^4\text{He}$ determinations; together these observations span diverse environments from redshifts $z = 1000$ to the present. However, ${}^7\text{Li}$ is at best marginally consistent with the CMB (and with D), given the error budgets we have quoted. The question then becomes more pressing as to whether this mismatch comes from systematic errors in the observed abundances, and/or uncertainties in stellar astrophysics, or whether there might be new physics at work. Inhomogeneous nucleosynthesis can alter abundances for a given η_{BBN} , but will overproduce ${}^7\text{Li}$ [62]. While entropy generation by some non-standard process could have decreased η between the BBN era and CMB decoupling, however the lack of spectral distortions in the CMB rules out any significant energy injection upto a redshift $z \sim 10^7$ [63].

Bearing in mind the importance of priors, the promise of precision determinations of the baryon density using the CMB motivates using this value as an input to BBN calculations. Within the context of the Standard Model, BBN then becomes a zero-parameter theory, and the light element abundances are completely determined to within the uncertainties in η_{CMB} and the BBN theoretical errors. Comparison with the observed abundances then can be used to test the astrophysics of post-BBN light element evolution [64]. Alternatively, one can consider possible physics beyond the Standard Model (*e.g.*, which might change the expansion rate during BBN) and then use all of the abundances to test such models; this is the subject of our final section.

20.4. Beyond the Standard Model

Given the simple physics underlying BBN, it is remarkable that it still provides the most effective test for the cosmological viability of ideas concerning physics beyond the Standard Model. Although baryogenesis and inflation must have occurred at higher temperatures in the early universe, we do not as yet have ‘standard models’ for these, so BBN still marks the boundary between the established and the speculative in big bang cosmology. It might appear possible to push the boundary back to the quark-hadron transition at $T \sim \Lambda_{\text{QCD}}$ or electroweak symmetry breaking at $T \sim 1/\sqrt{G_{\text{F}}}$; however, so far no observable relics of these epochs have been identified, either theoretically or observationally. Thus, although the Standard Model provides a precise description of physics up to the Fermi scale, cosmology cannot be traced in detail before the BBN era.

Limits on particle physics beyond the Standard Model come mainly from the observational bounds on the ${}^4\text{He}$ abundance. This is proportional to the n/p ratio which is determined when the weak-interaction rates fall behind the Hubble expansion rate at $T_{\text{fr}} \sim 1 \text{ MeV}$. The presence of additional neutrino flavors (or of

any other relativistic species) at this time increases g_* , hence the expansion rate, leading to a larger value of T_{fr} , n/p , and therefore Y_{p} [6,65]. In the Standard Model, the number of relativistic particle species at 1 MeV is $g_* = 5.5 + \frac{7}{4}N_{\nu}$, where 5.5 accounts for photons and e^{\pm} , and N_{ν} is the number of (nearly massless) neutrino flavors (see Big Bang Cosmology review). The helium curves in Fig. 20.1 were computed taking $N_{\nu} = 3$; the computed abundance scales as $\Delta Y_{\text{BBN}} \simeq 0.013 \Delta N_{\nu}$ [7]. Clearly the central value for N_{ν} from BBN will depend on η , which is independently determined (with weaker sensitivity to N_{ν}) by the adopted D or ${}^7\text{Li}$ abundance. For example, if the best value for the observed primordial ${}^4\text{He}$ abundance is 0.249, then, for $\eta_{10} \sim 6$, the central value for N_{ν} is very close to 3. This limit depends sensitively on the adopted light element abundances, particularly Y_{BBN} . A maximum likelihood analysis on η and N_{ν} based on the above ${}^4\text{He}$ and D abundances finds the (correlated) 95% CL ranges to be $4.9 < \eta_{10} < 7.1$ and $1.8 < N_{\nu} < 4.5$ [66]. Similar results were obtained in another study [67] which presented a simpler method [12] to extract such bounds based on χ^2 statistics, given a set of input abundances. Using the CMB determination of η improves the constraints: with a ‘low’ ${}^4\text{He}$, $N_{\nu} = 3$ is barely allowed at 2σ [68], but using the ${}^4\text{He}$ (and D) abundance quoted above gives $5.66 < \eta_{10} < 6.58$ ($\Omega_{\text{B}}h^2 = 0.0226 \pm 0.0017$) and $N_{\nu} = 3.24 \pm 1.2$ at 95% CL [66].

Just as one can use the measured helium abundance to place limits on g_* [65], any changes in the strong, weak, electromagnetic, or gravitational coupling constants, arising *e.g.*, from the dynamics of new dimensions, can be similarly constrained [69], as can be any speed-up of the expansion rate in *e.g.* scalar-tensor theories of gravity [70].

The limits on N_{ν} can be translated into limits on other types of particles or particle masses that would affect the expansion rate of the Universe during nucleosynthesis. For example, consider ‘sterile’ neutrinos with only right-handed interactions of strength $G_{\text{R}} < G_{\text{F}}$. Such particles would decouple at higher temperature than (left-handed) neutrinos, so their number density ($\propto T^3$) relative to neutrinos would be reduced by any subsequent entropy release, *e.g.*, due to annihilations of massive particles that become non-relativistic in between the two decoupling temperatures. Thus (relativistic) particles with less than full strength weak interactions contribute less to the energy density than particles that remain in equilibrium up to the time of nucleosynthesis [71]. If we impose $N_{\nu} < 4$ as an illustrative constraint, then the three right-handed neutrinos must have a temperature $3(T_{\nu_{\text{R}}}/T_{\nu_{\text{L}}})^4 < 1$. Since the temperature of the decoupled ν_{R} ’s is determined by entropy conservation (see Big Bang Cosmology review), $T_{\nu_{\text{R}}}/T_{\nu_{\text{L}}} = [(43/4)/g_*(T_{\text{d}})]^{1/3} < 0.76$, where T_{d} is the decoupling temperature of the ν_{R} ’s. This requires $g_*(T_{\text{d}}) > 24$, so decoupling must have occurred at $T_{\text{d}} > 140 \text{ MeV}$. The decoupling temperature is related to G_{R} through $(G_{\text{R}}/G_{\text{F}})^2 \sim (T_{\text{d}}/3 \text{ MeV})^{-3}$, where 3 MeV is the decoupling temperature for ν_{L} ’s. This yields a limit $G_{\text{R}} \lesssim 10^{-2} G_{\text{F}}$. The above argument sets lower limits on the masses of new Z' gauge bosons in superstring models [72], or in extended technicolor models [73] to which such right-handed neutrinos would be coupled. Similarly a Dirac magnetic moment for neutrinos, which would allow the right-handed states to be produced through scattering and thus increase g_* , can be significantly constrained [74], as can any new interactions for neutrinos which have a similar effect [75]. Right-handed states can be populated directly by helicity-flip scattering if the neutrino mass is large enough, and this was used to infer a bound of $m_{\nu_{\tau}} \lesssim 1 \text{ MeV}$ taking $N_{\nu} < 4$ [76]. If there is mixing between active and sterile neutrinos then the effect on BBN is more complicated [77].

The limit on the expansion rate during BBN can also be translated into bounds on the mass/lifetime of non-relativistic particles which decay during BBN. This results in an even faster speed-up rate, and typically also change the entropy [78]. If the decays include Standard Model particles, the resulting electromagnetic [79–80] and/or hadronic [81] cascades can strongly perturb the light elements, which leads to even stronger constraints. Such arguments were applied to rule out a MeV mass ν_{τ} , which decays during nucleosynthesis [82].

Such arguments have proved very effective in constraining

supersymmetry. For example, if the gravitino is very light and contributes to g_* , the illustrative BBN limit $N_\nu < 4$ requires its mass to exceed ~ 1 eV [83]. Alternatively, much recent interest has focussed on the case in which the next-to-lightest supersymmetric particle is metastable and decays during or after BBN. The constraints on unstable particles discussed above imply stringent bounds on the allowed abundance of such particles [81]; if the metastable particle is charged (*e.g.*, the stau), then it is possible for it to form atom-like electromagnetic bound states with nuclei, and the resulting impact on light elements can be quite complex [84]. Such decays can destroy ${}^7\text{Li}$ and/or produce ${}^6\text{Li}$, leading to a possible supersymmetric solution to the Li problems noted above [85] (see however [86]). In addition, these models impose powerful constraints on supersymmetric inflationary cosmology [80–81]. These can be evaded only if the gravitino is massive enough to decay before BBN, *i.e.*, $m_{3/2} \gtrsim 50$ TeV [87], which would be unnatural, or if it is in fact the LSP and thus stable [80,88]. Similar constraints apply to moduli – very weakly coupled fields in string theory which obtain an electroweak-scale mass from supersymmetry breaking [89].

Finally, we mention that BBN places powerful constraints on the recently suggested possibility that there are new large dimensions in nature, perhaps enabling the scale of quantum gravity to be as low as the electroweak scale [90]. Thus, Standard Model fields may be localized on a ‘brane,’ while gravity alone propagates in the ‘bulk.’ It has been further noted that the new dimensions may be non-compact, even infinite [91], and the cosmology of such models has attracted considerable attention. The expansion rate in the early universe can be significantly modified so BBN is able to set interesting constraints on such possibilities [92].

References:

1. R.V. Wagoner *et al.*, *Astrophys. J.* **148**, 3 (1967).
2. R.A. Malaney, G.J. Mathews, *Phys. Reports* **229**, 145 (1993).
3. S. Sarkar, Rept. on Prog. in Phys. **59**, 1493 (1996).
4. D.N. Schramm, M.S. Turner, *Rev. Mod. Phys.* **70**, 303 (1998).
5. K.A. Olive *et al.*, *Phys. Reports* **333**, 389 (2000).
6. P.J.E. Peebles, *Phys. Rev. Lett.* **16**, 411 (1966).
7. J. Bernstein *et al.*, *Rev. Mod. Phys.* **61**, 25 (1989).
8. S. Mukhanov, *Int. J. Theor. Phys.* **143**, 669 (2004).
9. R. Esmailzadeh *et al.*, *Astrophys. J.* **378**, 504 (1991).
10. R.H. Cyburt *et al.*, *New Astron.* **6**, 215 (2001).
11. L. Kawano, FERMILAB-PUB-92/04-A.
12. <http://www-thphys.physics.ox.ac.uk/users/SubirSarkar/bbn.html>.
13. S. Esposito *et al.*, *Nucl. Phys.* **B568**, 421 (2000).
14. S. Dodelson and M.S. Turner, *Phys. Rev.* **D46**, 3372 (1992).
15. D. Seckel, hep-ph/9305311;
R. Lopez and M.S. Turner, *Phys. Rev.* **D59**, 103502 (1999).
16. M.S. Smith *et al.*, *Astrophys. J. Supp.* **85**, 219 (1993).
17. G. Fiorentini *et al.*, *Phys. Rev.* **D58**, 063506 (1998).
18. K.M. Nollett and S. Burles, *Phys. Rev.* **D61**, 123505 (2000).
19. A. Coc *et al.*, *Astrophys. J.* **600**, 544 (2004).
20. R.H. Cyburt, *Phys. Rev.* **D70**, 023505 (2004).
21. P.D. Serpico *et al.*, *J. Cosmo. Astropart. Phys.* **12**, 010 (2004).
22. K.M. Nollett *et al.*, *Astrophys. J. Lett.* **552**, L1 (2001).
23. J.M. O’Meara *et al.*, *Astrophys. J.* **552**, 718 (2001).
24. S. D’Odorico *et al.*, *Astron. & Astrophys.* **368**, L21 (2001).
25. M. Pettini and D. Bowen, *Astrophys. J.* **560**, 41 (2001).
26. D. Kirkman *et al.*, *Astrophys. J. Supp.* **149**, 1 (2003).
27. J.M. O’Meara *et al.*, *Astrophys. J. Lett.* **649**, 61 (2006).
28. N.H.M. Crighton *et al.*, *MNRAS* **355**, 1042 (2004).
29. R.I. Epstein *et al.*, *Nature* **263**, 198 (1976).
30. B.E. Wood *et al.*, *Astrophys. J.* **609**, 838 (2004).
31. J.L. Linsky *et al.*, *Astrophys. J.* **647**, 1106 (2006).
32. B.D. Savage *et al.*, *Astrophys. J.* **659**, 1222 (2007).
33. B.D. Fields, *Astrophys. J.* **456**, 678 (1996).
34. D. Kirkman *et al.*, *Astrophys. J.* **529**, 655 (2000).
35. Y.I. Izotov *et al.*, *Astrophys. J.* **527**, 757 (1999).
36. K.A. Olive and E. Skillman, *Astrophys. J.* **617**, 29 (2004).
37. Y.I. Izotov *et al.*, *Astrophys. J.* **662**, 15 (2007).
38. M. Peimbert *et al.*, *Astrophys. J.* **667**, 636 (2007).
39. N. Christlieb *et al.*, *Nature* **419**, 904 (2002).
40. M. Spite and F. Spite, *Nature* **297**, 483 (1982).
41. S.G. Ryan *et al.*, *Astrophys. J.* **523**, 654 (1999).
42. E. Vangioni-Flam *et al.*, *New Astron.* **4**, 245 (1999).
43. S.G. Ryan *et al.*, *Astrophys. J. Lett.* **530**, L57 (2000).
44. P. Bonifacio *et al.*, *Astron. & Astrophys.* **390**, 91 (2002).
45. J. Meléndez and I. Ramirez, *Astrophys. J. Lett.* **615**, 33 (2004).
46. P. Bonifacio *et al.*, *Astron. & Astrophys.* **462**, 851 (2007).
47. M.H. Pinsonneault *et al.*, *Astrophys. J.* **574**, 389 (2002).
48. A.J. Korn *et al.*, *Nature* **442**, 657 (2006).
49. M. Asplund *et al.*, *Astrophys. J.* **644**, 229 (2006).
50. R. Cayrel *et al.*, *Astron. & Astrophys.* **473**, L37 (2007).
51. T.M. Bania *et al.*, *Nature* **415**, 54 (2002).
52. K.A. Olive *et al.*, *Astrophys. J.* **479**, 752 (1997).
53. E. Vangioni-Flam *et al.*, *Astrophys. J.* **585**, 611 (2003).
54. E. Vangioni-Flam *et al.*, *Astron. & Astrophys.* **360**, 15 (2000).
55. H. Reeves *et al.*, *Astrophys. J.* **179**, 909 (1973).
56. M. Fukugita and P.J.E. Peebles, *Astrophys. J.* **616**, 643 (2004).
57. R. Cen and J.P. Ostriker, *Astrophys. J.* **514**, 1 (1999).
58. G. Jungman *et al.*, *Phys. Rev.* **D54**, 1332 (1996).
59. M. Tegmark *et al.*, *Phys. Rev.* **D63**, 043007 (2001).
60. D.N. Spergel *et al.*, *Astrophys. J. Supp.* **170**, 377 (2007).
61. P. Hunt and S. Sarkar, *Phys. Rev.* **D76**, 123504 (2007).
62. K. Jedamzik and J.B. Rehm, *Phys. Rev.* **D64**, 023510 (2001).
63. D.J. Fixsen *et al.*, *Astrophys. J.* **473**, 576 (1996).
64. R.H. Cyburt *et al.*, *Phys. Lett.* **B567**, 227 (2003).
65. G. Steigman *et al.*, *Phys. Lett.* **B66**, 202 (1977).
66. R. H. Cyburt *et al.*, *Astropart. Phys.* **23**, 313 (2005).
67. E. Lisi *et al.*, *Phys. Rev.* **D59**, 123520 (1999).
68. V. Barger *et al.*, *Phys. Lett.* **B566**, 8 (2003).
69. E.W. Kolb *et al.*, *Phys. Rev.* **D33**, 869 (1986);
F.S. Accetta *et al.*, *Phys. Lett.* **B248**, 146 (1990);
B.A. Campbell and K.A. Olive, *Phys. Lett.* **B345**, 429 (1995);
K.M. Nollett and R. Lopez, *Phys. Rev.* **D66**, 063507 (2002);
C. Bambi *et al.*, *Phys. Rev.* **D71**, 123524 (2005).
70. A. Coc *et al.*, *Phys. Rev.* **D73**, 083525 (2006).
71. K.A. Olive *et al.*, *Nucl. Phys.* **B180**, 497 (1981).
72. J. Ellis *et al.*, *Phys. Lett.* **B167**, 457 (1986).
73. L.M. Krauss *et al.*, *Phys. Rev. Lett.* **71**, 823 (1993).
74. J.A. Morgan, *Phys. Lett.* **B102**, 247 (1981).
75. E.W. Kolb *et al.*, *Phys. Rev.* **D34**, 2197 (1986);
J.A. Grifols and E. Massó, *Mod. Phys. Lett.* **A2**, 205 (1987);
K.S. Babu *et al.*, *Phys. Rev. Lett.* **67**, 545 (1991).
76. A.D. Dolgov *et al.*, *Nucl. Phys.* **B524**, 621 (1998).
77. K. Enqvist *et al.*, *Nucl. Phys.* **B373**, 498 (1992);
A.D. Dolgov, *Phys. Reports* **370**, 333 (2002).
78. K. Sato and M. Kobayashi, *Prog. Theor. Phys.* **58**, 1775 (1977);
D.A. Dicus *et al.*, *Phys. Rev.* **D17**, 1529 (1978);
R.J. Scherrer and M.S. Turner, *Astrophys. J.* **331**, 19 (1988).
79. D. Lindley, *MNRAS* **188**, 15 (1979), *Astrophys. J.* **294**, 1 (1985).
80. J. Ellis *et al.*, *Nucl. Phys.* **B259**, 175 (1985);
J. Ellis *et al.*, *Nucl. Phys.* **B373**, 399 (1992);
R.H. Cyburt *et al.*, *Phys. Rev.* **D67**, 103521 (2003).
81. M.H. Reno and D. Seckel, *Phys. Rev.* **D37**, 3441 (1988);
S. Dimopoulos *et al.*, *Nucl. Phys.* **B311**, 699 (1989);
K. Kohri *et al.*, *Phys. Rev.* **D71**, 083502 (2005).
82. S. Sarkar and A.M. Cooper, *Phys. Lett.* **B148**, 347 (1984).
83. J.A. Grifols *et al.*, *Phys. Lett.* **B400**, 124 (1997).
84. M. Pospelov *et al.*, *Phys. Rev. Lett.* **98**, 231301 (2007);
R.H. Cyburt *et al.*, *JCAP* **11**, 014 (2006);
M. Kawasaki *et al.*, *Phys. Lett.* **B649**, 436 (2007).
85. K. Jedamzik *et al.*, *J. Cosmo. Astropart. Phys.* **07**, 007 (2006).
86. J. Ellis *et al.*, *Phys. Lett.* **B619**, 30 (2005).
87. S. Weinberg, *Phys. Rev. Lett.* **48**, 1303 (1979).
88. M. Bolz *et al.*, *Nucl. Phys.* **B606**, 518 (2001).
89. G. Coughlan *et al.*, *Phys. Lett.* **B131**, 59 (1983).
90. N. Arkani-Hamed *et al.*, *Phys. Rev.* **D59**, 086004 (1999).
91. L. Randall and R. Sundrum, *Phys. Rev. Lett.* **83**, 3370 (1999).
92. J.M. Cline *et al.*, *Phys. Rev. Lett.* **83**, 4245 (1999);
P. Binetruy *et al.*, *Phys. Lett.* **B477**, 285 (2000).

21. THE COSMOLOGICAL PARAMETERS

Updated September 2007, by O. Lahav (University College London) and A.R. Liddle (University of Sussex).

21.1. Parametrizing the Universe

Rapid advances in observational cosmology are leading to the establishment of the first precision cosmological model, with many of the key cosmological parameters determined to one or two significant figure accuracy. Particularly prominent are measurements of cosmic microwave anisotropies, led by the three-year results from the Wilkinson Microwave Anisotropy Probe (WMAP) [1,2]. However the most accurate model of the Universe requires consideration of a wide range of different types of observation, with complementary probes providing consistency checks, lifting parameter degeneracies, and enabling the strongest constraints to be placed.

The term ‘cosmological parameters’ is forever increasing in its scope, and nowadays includes the parametrization of some functions, as well as simple numbers describing properties of the Universe. The original usage referred to the parameters describing the global dynamics of the Universe, such as its expansion rate and curvature. Also now of great interest is how the matter budget of the Universe is built up from its constituents: baryons, photons, neutrinos, dark matter, and dark energy. We need to describe the nature of perturbations in the Universe, through global statistical descriptions such as the matter and radiation power spectra. There may also be parameters describing the physical state of the Universe, such as the ionization fraction as a function of time during the era since decoupling. Typical comparisons of cosmological models with observational data now feature between five and ten parameters.

21.1.1. The global description of the Universe :

Ordinarily, the Universe is taken to be a perturbed Robertson–Walker space-time with dynamics governed by Einstein’s equations. This is described in detail by Olive and Peacock in this volume. Using the density parameters Ω_i for the various matter species and Ω_Λ for the cosmological constant, the Friedmann equation can be written

$$\sum_i \Omega_i + \Omega_\Lambda = \frac{k}{R^2 H^2}, \quad (21.1)$$

where the sum is over all the different species of matter in the Universe. This equation applies at any epoch, but later in this article we will use the symbols Ω_i and Ω_Λ to refer to the present values. A typical collection would be baryons, photons, neutrinos, and dark matter (given charge neutrality, the electron density is guaranteed to be too small to be worth considering separately).

The complete present state of the homogeneous Universe can be described by giving the present values of all the density parameters and the present Hubble parameter h . These also allow us to track the history of the Universe back in time, at least until an epoch where interactions allow interchanges between the densities of the different species, which is believed to have last happened at neutrino decoupling shortly before nucleosynthesis. To probe further back into the Universe’s history requires assumptions about particle interactions, and perhaps about the nature of physical laws themselves.

21.1.2. Neutrinos :

The standard neutrino sector has three flavors. For neutrinos of mass in the range 5×10^{-4} eV to 1 MeV, the density parameter in neutrinos is predicted to be

$$\Omega_\nu h^2 = \frac{\sum m_\nu}{93 \text{ eV}}, \quad (21.2)$$

where the sum is over all families with mass in that range (higher masses need a more sophisticated calculation). We use units with $c = 1$ throughout. Results on atmospheric and solar neutrino oscillations [3] imply non-zero mass-squared differences between the three neutrino flavors. These oscillation experiments cannot tell us the absolute neutrino masses, but within the simple assumption of a mass hierarchy suggest a lower limit of $\Omega_\nu \approx 0.001$ on the neutrino mass density parameter.

For a total mass as small as 0.1 eV, this could have a potentially observable effect on the formation of structure, as neutrino free-streaming damps the growth of perturbations. Present cosmological observations have shown no convincing evidence of any effects from either neutrino masses or an otherwise non-standard neutrino sector, and impose quite stringent limits, which we summarize in Section 21.3.4. Consequently, the standard assumption at present is that the masses are too small to have a significant cosmological impact, but this may change in the near future.

The cosmological effect of neutrinos can also be modified if the neutrinos have decay channels, or if there is a large asymmetry in the lepton sector manifested as a different number density of neutrinos versus anti-neutrinos. This latter effect would need to be of order unity to be significant, rather than the 10^{-9} seen in the baryon sector, which may be in conflict with nucleosynthesis [4].

21.1.3. Inflation and perturbations :

A complete model of the Universe should include a description of deviations from homogeneity, at least in a statistical way. Indeed, some of the most powerful probes of the parameters described above come from the evolution of perturbations, so their study is naturally intertwined in the determination of cosmological parameters.

There are many different notations used to describe the perturbations, both in terms of the quantity used to describe the perturbations and the definition of the statistical measure. We use the dimensionless power spectrum Δ^2 as defined in Olive and Peacock (also denoted \mathcal{P} in some of the literature). If the perturbations obey Gaussian statistics, the power spectrum provides a complete description of their properties.

From a theoretical perspective, a useful quantity to describe the perturbations is the curvature perturbation \mathcal{R} , which measures the spatial curvature of a comoving slicing of the space-time. A case of particular interest is the Harrison–Zel’dovich spectrum, which corresponds to a constant spectrum $\Delta_{\mathcal{R}}^2$. More generally, one can approximate the spectrum by a power-law, writing

$$\Delta_{\mathcal{R}}^2(k) = \Delta_{\mathcal{R}}^2(k_*) \left[\frac{k}{k_*} \right]^{n-1}, \quad (21.3)$$

where n is known as the spectral index, always defined so that $n = 1$ for the Harrison–Zel’dovich spectrum, and k_* is an arbitrarily chosen scale. The initial spectrum, defined at some early epoch of the Universe’s history, is usually taken to have a simple form such as this power-law, and we will see that observations require n close to one, which corresponds to the perturbations in the curvature being independent of scale. Subsequent evolution will modify the spectrum from its initial form.

The simplest viable mechanism for generating the observed perturbations is the inflationary cosmology, which posits a period of accelerated expansion in the Universe’s early stages [5]. It is a useful working hypothesis that this is the sole mechanism for generating perturbations. Commonly, it is further assumed to be the simplest class of inflationary model, where the dynamics are equivalent to that of a single scalar field ϕ slowly rolling on a potential $V(\phi)$. One aim of cosmology is to verify that this simple picture can match observations, and to determine the properties of $V(\phi)$ from the observational data.

Inflation generates perturbations through the amplification of quantum fluctuations, which are stretched to astrophysical scales by the rapid expansion. The simplest models generate two types, density perturbations which come from fluctuations in the scalar field and its corresponding scalar metric perturbation, and gravitational waves which are tensor metric fluctuations. The former experience gravitational instability and lead to structure formation, while the latter can influence the cosmic microwave background anisotropies. Defining slow-roll parameters, with primes indicating derivatives with respect to the scalar field, as

$$\epsilon = \frac{m_{\text{Pl}}^2}{16\pi} \left(\frac{V'}{V} \right)^2 \quad ; \quad \eta = \frac{m_{\text{Pl}}^2}{8\pi} \frac{V''}{V}, \quad (21.4)$$

which should satisfy $\epsilon, |\eta| \ll 1$, the spectra can be computed using the slow-roll approximation as

$$\Delta_{\mathcal{R}}^2(k) \simeq \frac{8}{3m_{\text{Pl}}^4} \frac{V}{\epsilon} \Big|_{k=aH};$$

$$\Delta_{\text{grav}}^2(k) \simeq \frac{128}{3m_{\text{Pl}}^4} V \Big|_{k=aH}. \quad (21.5)$$

In each case, the expressions on the right-hand side are to be evaluated when the scale k is equal to the Hubble radius during inflation. The symbol ‘ \simeq ’ indicates use of the slow-roll approximation, which is expected to be accurate to a few percent or better.

From these expressions, we can compute the spectral indices

$$n \simeq 1 - 6\epsilon + 2\eta \quad ; \quad n_{\text{grav}} \simeq -2\epsilon. \quad (21.6)$$

Another useful quantity is the ratio of the two spectra, defined by

$$r \equiv \frac{\Delta_{\text{grav}}^2(k_*)}{\Delta_{\mathcal{R}}^2(k_*)}. \quad (21.7)$$

The literature contains a number of definitions of r ; this convention matches that of recent versions of CMBFAST [6] and that used by WMAP [8], while definitions based on the relative effect on the microwave background anisotropies typically differ by tens of percent. We have

$$r \simeq 16\epsilon \simeq -8n_{\text{grav}}, \quad (21.8)$$

which is known as the consistency equation.

In general, one could consider corrections to the power-law approximation, which we discuss later. However, for now we make the working assumption that the spectra can be approximated by power laws. The consistency equation shows that r and n_{grav} are not independent parameters, and so the simplest inflation models give initial conditions described by three parameters, usually taken as $\Delta_{\mathcal{R}}^2$, n , and r , all to be evaluated at some scale k_* , usually the ‘statistical centre’ of the range explored by the data. Alternatively, one could use the parametrization V , ϵ , and η , all evaluated at a point on the putative inflationary potential.

After the perturbations are created in the early Universe, they undergo a complex evolution up until the time they are observed in the present Universe. While the perturbations are small, this can be accurately followed using a linear theory numerical code such as CMBFAST [6]. This works right up to the present for the cosmic microwave background, but for density perturbations on small scales non-linear evolution is important and can be addressed by a variety of semi-analytical and numerical techniques. However the analysis is made, the outcome of the evolution is in principle determined by the cosmological model, and by the parameters describing the initial perturbations, and hence can be used to determine them.

Of particular interest are cosmic microwave background anisotropies. Both the total intensity and two independent polarization modes are predicted to have anisotropies. These can be described by the radiation angular power spectra C_ℓ as defined in the article of Scott and Smoot in this volume, and again provide a complete description if the density perturbations are Gaussian.

21.1.4. The standard cosmological model :

We now have most of the ingredients in place to describe the cosmological model. Beyond those of the previous subsections, there are two parameters which are essential — a measure of the ionization state of the Universe and the galaxy bias parameter. The Universe is known to be highly ionized at low redshifts (otherwise radiation from distant quasars would be heavily absorbed in the ultra-violet), and the ionized electrons can scatter microwave photons altering the pattern of observed anisotropies. The most convenient parameter to describe this is the optical depth to scattering τ (*i.e.*, the probability that a given photon scatters once); in the approximation of instantaneous and complete re-ionization, this could equivalently be described by the redshift of re-ionization z_{ion} . The bias parameter, described fully later, is needed to relate the observed galaxy power spectrum to the predicted dark matter power spectrum. The basic set of cosmological parameters is therefore as shown in Table 21.1. The spatial curvature does not appear in the list, because it can be determined from the other parameters using Eq. (21.1). The total present matter density $\Omega_{\text{m}} = \Omega_{\text{dm}} + \Omega_{\text{b}}$ is usually used in place of the dark matter density.

Table 21.1: The basic set of cosmological parameters. We give values (with some additional rounding) as obtained using a fit of a Λ CDM cosmology with a power-law initial spectrum to WMAP3 data alone [2]. Tensors are assumed zero except in quoting a limit on them. We cannot stress too much that the exact values and uncertainties depend on both the precise datasets used and the choice of parameters allowed to vary, and the effects of varying some assumptions will be shown later in Table 21.2. Limits on the cosmological constant depend on whether the Universe is assumed flat. The density perturbation amplitude is specified by the derived parameter σ_8 . Uncertainties are one-sigma/68% confidence unless otherwise stated.

Parameter	Symbol	Value
Hubble parameter	h	0.73 ± 0.03
Total matter density	Ω_{m}	$\Omega_{\text{m}}h^2 = 0.128 \pm 0.008$
Baryon density	Ω_{b}	$\Omega_{\text{b}}h^2 = 0.0223 \pm 0.0007$
Cosmological constant	Ω_{Λ}	See Ref. 2
Radiation density	Ω_{r}	$\Omega_{\text{r}}h^2 = 2.47 \times 10^{-5}$
Neutrino density	Ω_{ν}	See Sec. 21.1.2
Density perturbation amplitude	σ_8	0.76 ± 0.05
Density perturbation spectral index	n	$n = 0.958 \pm 0.016$
Tensor to scalar ratio	r	$r < 0.65$ (95% conf)
Ionization optical depth	τ	$\tau = 0.089 \pm 0.030$
Bias parameter	b	See Sec. 21.3.4

Most attention to date has been on parameter estimation, where a set of parameters is chosen by hand and the aim is to constrain them. Interest has been growing towards the higher-level inference problem of model selection, which compares different choices of parameter sets. Bayesian inference offers an attractive framework for cosmological model selection, setting a tension between model complexity and ability to fit the data.

As described in Sec. 21.4, models based on these eleven parameters are able to give a good fit to the complete set of high-quality data available at present, and indeed some simplification is possible. Observations are consistent with spatial flatness, and indeed the inflation models so far described automatically generate negligible spatial curvature, so we can set $k = 0$; the density parameters then must sum to one, and so one can be eliminated. The neutrino energy density is often not taken as an independent parameter. Provided the neutrino sector has the standard interactions, the neutrino energy density, while relativistic, can be related to the photon density using thermal physics arguments, and it is currently difficult to see the effect of the neutrino mass, although observations of large-scale structure have already placed interesting upper limits. This reduces the standard parameter set to nine. In addition, there is no observational evidence for the existence of tensor perturbations (though the upper limits are quite weak), and so r could be set to zero. Presently n is in a somewhat controversial position regarding whether it needs to be varied in a fit, or can be set to the Harrison–Zel’dovich value $n = 1$. Parameter estimation [2] suggests $n = 1$ is ruled out at reasonable significance, but Bayesian model selection techniques [9] suggest the data is not conclusive. With n set to one, this leaves seven parameters, which is the smallest set that can usefully be compared to the present cosmological data set. This model (usually with n kept as a parameter) is referred to by various names, including Λ CDM, the concordance cosmology, and the standard cosmological model.

Of these parameters, only Ω_{r} is accurately measured directly. The radiation density is dominated by the energy in the cosmic microwave background, and the COBE FIRAS experiment has determined its temperature to be $T = 2.725 \pm 0.001$ Kelvin [10], corresponding to $\Omega_{\text{r}} = 2.47 \times 10^{-5}h^{-2}$. It typically does not need to be varied in fitting other data. If galaxy clustering data is not included in a fit, then the bias parameter is also unnecessary.

In addition to this minimal set, there is a range of other parameters which might prove important in future as the dataset further improves,

but for which there is so far no direct evidence, allowing them to be set to a specific value. We discuss various speculative options in the next section. For completeness at this point, we mention one other interesting parameter, the helium fraction, which is a non-zero parameter that can affect the microwave anisotropies at a subtle level. Presently, big-bang nucleosynthesis provides the best measurement of this parameter, and it is usually fixed in microwave anisotropy studies, but the data are just reaching a level where allowing its variation may become mandatory.

21.1.5. Derived parameters :

The parameter list of the previous subsection is sufficient to give a complete description of cosmological models which agree with observational data. However, it is not a unique parametrization, and one could instead use parameters derived from that basic set. Parameters which can be obtained from the set given above include the age of the Universe, the present horizon distance, the present microwave background and neutrino background temperatures, the epoch of matter–radiation equality, the epochs of recombination and decoupling, the epoch of transition to an accelerating Universe, the baryon-to-photon ratio, and the baryon to dark matter density ratio. The physical densities of the matter components, $\Omega_i h^2$, are often more useful than the density parameters. The density perturbation amplitude can be specified in many different ways other than the large-scale primordial amplitude, for instance, in terms of its effect on the cosmic microwave background, or by specifying a short-scale quantity, a common choice being the present linear-theory mass dispersion on a scale of $8 h^{-1} \text{Mpc}$, known as σ_8 .

Different types of observation are sensitive to different subsets of the full cosmological parameter set, and some are more naturally interpreted in terms of some of the derived parameters of this subsection than on the original base parameter set. In particular, most types of observation feature degeneracies whereby they are unable to separate the effects of simultaneously varying several of the base parameters.

21.2. Extensions to the standard model

This section discusses some ways in which the standard model could be extended. At present, there is no positive evidence in favor of any of these possibilities, which are becoming increasingly constrained by the data, though there always remains the possibility of trace effects at a level below present observational capability.

21.2.1. More general perturbations :

The standard cosmology assumes adiabatic, Gaussian perturbations. Adiabaticity means that all types of material in the Universe share a common perturbation, so that if the space-time is foliated by constant-density hypersurfaces, then all fluids and fields are homogeneous on those slices, with the perturbations completely described by the variation of the spatial curvature of the slices. Gaussianity means that the initial perturbations obey Gaussian statistics, with the amplitudes of waves of different wavenumbers being randomly drawn from a Gaussian distribution of width given by the power spectrum. Note that gravitational instability generates non-Gaussianity; in this context, Gaussianity refers to a property of the initial perturbations before they evolve significantly.

The simplest inflation models, based on one dynamical field, predict adiabatic fluctuations and a level of non-Gaussianity which is too small to be detected by any experiment so far conceived. For present data, the primordial spectra are usually assumed to be power laws.

21.2.1.1. Non-power-law spectra:

For typical inflation models, it is an approximation to take the spectra as power laws, albeit usually a good one. As data quality improves, one might expect this approximation to come under pressure, requiring a more accurate description of the initial spectra, particularly for the density perturbations. In general, one can write a Taylor expansion of $\ln \Delta_{\mathcal{R}}^2$ as

$$\ln \Delta_{\mathcal{R}}^2(k) = \ln \Delta_{\mathcal{R}}^2(k_*) + (n_* - 1) \ln \frac{k}{k_*} + \frac{1}{2} \frac{dn}{d \ln k} \Big|_* \ln^2 \frac{k}{k_*} + \dots, \quad (21.9)$$

where the coefficients are all evaluated at some scale k_* . The term $dn/d \ln k|_*$ is often called the running of the spectral index [11]. Once non-power-law spectra are allowed, it is necessary to specify the scale k_* at which the spectral index is defined.

21.2.1.2. Isocurvature perturbations:

An isocurvature perturbation is one which leaves the total density unperturbed, while perturbing the relative amounts of different materials. If the Universe contains N fluids, there is one growing adiabatic mode and $N - 1$ growing isocurvature modes. These can be excited, for example, in inflationary models where there are two or more fields which acquire dynamically-important perturbations. If one field decays to form normal matter, while the second survives to become the dark matter, this will generate a cold dark matter isocurvature perturbation.

In general, there are also correlations between the different modes, and so the full set of perturbations is described by a matrix giving the spectra and their correlations. Constraining such a general construct is challenging, though constraints on individual modes are beginning to become meaningful, with no evidence that any other than the adiabatic mode must be non-zero.

21.2.1.3. Non-Gaussianity:

Multi-field inflation models can also generate primordial non-Gaussianity. The extra fields can either be in the same sector of the underlying theory as the inflation, or completely separate, an interesting example of the latter being the curvaton model [12]. Current upper limits on non-Gaussianity are becoming stringent, but there remains much scope to push down those limits and perhaps reveal trace non-Gaussianity in the data. If non-Gaussianity is observed, its nature may favor an inflationary origin, or a different one such as topological defects. A plausible possibility is non-Gaussianity caused by defects forming in a phase transition which ended inflation.

21.2.2. Dark matter properties :

Dark matter properties are discussed in the article by Drees and Gerbier in this volume. The simplest assumption concerning the dark matter is that it has no significant interactions with other matter, and that its particles have a negligible velocity. Such dark matter is described as ‘cold,’ and candidates include the lightest supersymmetric particle, the axion, and primordial black holes. As far as astrophysicists are concerned, a complete specification of the relevant cold dark matter properties is given by the density parameter Ω_{cdm} , though those seeking to directly detect it are as interested in its interaction properties.

Cold dark matter is the standard assumption and gives an excellent fit to observations, except possibly on the shortest scales where there remains some controversy concerning the structure of dwarf galaxies and possible substructure in galaxy halos. For all the dark matter to have a large velocity dispersion, so-called hot dark matter, has long been excluded, as it does not permit galaxies to form; for thermal relics the mass must be above about 1 keV to satisfy this constraint, though relics produced non-thermally, such as the axion, need not obey this limit. However, there remains the possibility that further parameters might need to be introduced to describe dark matter properties relevant to astrophysical observations. Suggestions which have been made include a modest velocity dispersion (warm dark matter) and dark matter self-interactions. There remains the possibility that the dark matter comprises two separate components, *e.g.*, a cold one and a hot one, an example being if massive neutrinos have a non-negligible effect.

21.2.3. Dark energy :

While the standard cosmological model given above features a cosmological constant, in order to explain observations indicating that the Universe is presently accelerating, further possibilities exist under the general heading dark energy.[†] A particularly attractive possibility

[†] Unfortunately this is rather a misnomer, as it is the negative pressure of this material, rather than its energy, that is responsible for giving the acceleration. Furthermore, while generally in physics matter and energy are interchangeable terms, dark matter and dark energy are quite distinct concepts.

(usually called quintessence, though that word is used with various different meanings in the literature) is that a scalar field is responsible, with the mechanism mimicking that of early Universe inflation [13]. As described by Olive and Peacock, a fairly model-independent description of dark energy can be given just using the equation of state parameter w , with $w = -1$ corresponding to a cosmological constant. In general, the function w could itself vary with redshift, though practical experiments devised so far would be sensitive primarily to some average value weighted over recent epochs. For high-precision predictions of microwave background anisotropies, it is better to use a scalar-field description in order to have a self-consistent evolution of the ‘sound speed’ associated with the dark energy perturbations.

A competing possibility is that the observed acceleration is due to a modification of gravity, *i.e.*, the left-hand side of Einstein’s equation rather than the right. Observations of expansion kinematics alone cannot distinguish these two possibilities, but future probes of the growth rate of structure formation may be able to.

Present observations are consistent with a cosmological constant, but it is quite common to see w kept as a free parameter to be added to the set described in the previous section. Most, but not all, researchers assume the weak energy condition $w \geq -1$. In the future, it may be necessary to use a more sophisticated parametrization of the dark energy.

21.2.4. Complex ionization history :

The full ionization history of the Universe is given by specifying the ionization fraction as a function of redshift z . The simplest scenario takes the ionization to be zero from recombination up to some redshift z_{ion} , at which point the Universe instantaneously re-ionizes completely. In that case, there is a one-to-one correspondence between τ and z_{ion} (that relation, however, also depending on other cosmological parameters).

While simple models of the re-ionization process suggest that rapid ionization is a good approximation, observational evidence is mixed, with indications of a high optical depth inferred from the microwave background difficult to reconcile with absorption seen in some high-redshift quasar systems, and also perhaps with the temperature of the intergalactic medium at $z \simeq 3$. Accordingly, a more complex ionization history may need to be considered, and perhaps separate histories for hydrogen and helium, which will necessitate new parameters. Additionally, high-precision microwave anisotropy experiments may require consideration of the level of residual ionization left after recombination, which in principle is computable from the other cosmological parameters.

21.2.5. Varying ‘constants’ :

Variation of the fundamental constants of Nature over cosmological times is another possible enhancement of the standard cosmology. There is a long history of study of variation of the gravitational constant G , and more recently attention has been drawn to the possibility of small fractional variations in the fine-structure constant. There is presently no observational evidence for the former, which is tightly constrained by a variety of measurements. Evidence for the latter has been claimed from studies of spectral line shifts in quasar spectra at redshifts of order two [14], but this is presently controversial and in need of further observational study.

More broadly, one can ask whether general relativity is valid at all epochs under consideration.

21.2.6. Cosmic topology :

The usual hypothesis is that the Universe has the simplest topology consistent with its geometry, for example that a flat Universe extends forever. Observations cannot tell us whether that is true, but they can test the possibility of a non-trivial topology on scales up to roughly the present Hubble scale. Extra parameters would be needed to specify both the type and scale of the topology, for example, a cuboidal topology would need specification of the three principal axis lengths. At present, there is no direct evidence for cosmic topology, though the low values of the observed cosmic microwave quadrupole and octupole have been cited as a possible signature.

21.3. Probes

The goal of the observational cosmologist is to utilize astronomical objects to derive cosmological parameters. The transformation from the observables to the key parameters usually involves many assumptions about the nature of the objects, as well as about the nature of the dark matter. Below we outline the physical processes involved in each probe, and the main recent results. The first two subsections concern probes of the homogeneous Universe, while the remainder consider constraints from perturbations.

We note three types of uncertainties that enter into any errors on the cosmological parameters of interest: (i) due to the assumptions on the cosmological model and its priors (*i.e.*, the number of assumed cosmological parameters and their allowed range); (ii) due to the uncertainty in the astrophysics of the objects (*e.g.*, the mass–temperature relation of galaxy clusters); and (iii) due to instrumental and observational limitations (*e.g.*, the effect of ‘seeing’ on weak gravitational lensing measurements).

21.3.1. Direct measures of the Hubble constant :

In 1929, Edwin Hubble discovered the law of expansion of the Universe by measuring distances to nearby galaxies. The slope of the relation between the distance and recession velocity is defined to be the Hubble constant H_0 . Astronomers argued for decades on the systematic uncertainties in various methods and derived values over the wide range, $40 \text{ km s}^{-1} \text{ Mpc}^{-1} \lesssim H_0 \lesssim 100 \text{ km s}^{-1} \text{ Mpc}^{-1}$.

One of the most reliable results on the Hubble constant comes from the Hubble Space Telescope Key Project [15]. The group has used the empirical period–luminosity relations for Cepheid variable stars to obtain distances to 31 galaxies, and calibrated a number of secondary distance indicators (Type Ia Supernovae, Tully-Fisher, surface brightness fluctuations, and Type II Supernovae) measured over distances of 400 to 600 Mpc. They estimated $H_0 = 72 \pm 3$ (statistical) ± 7 (systematic) $\text{km s}^{-1} \text{ Mpc}^{-1}$.[‡] The major sources of uncertainty in this result are due to the metallicity of the Cepheids and the distance to the fiducial nearby galaxy (called the Large Magellanic Cloud) relative to which all Cepheid distances are measured. Nevertheless, it is remarkable that this result is in such good agreement with the result derived from the WMAP CMB measurements (see Table 21.2).

21.3.2. Supernovae as cosmological probes :

The relation between observed flux and the intrinsic luminosity of an object depends on the luminosity distance d_L , which in turn depends on cosmological parameters. More specifically

$$d_L = (1+z)r_e(z), \quad (21.10)$$

where $r_e(z)$ is the coordinate distance. For example, in a flat Universe

$$r_e(z) = \int_0^z dz'/H(z'). \quad (21.11)$$

For a general dark energy equation of state $w(z) = p_Q(z)/\rho_Q(z)$, the Hubble parameter is, still considering only the flat case,

$$H^2(z)/H_0^2 = (1+z)^3\Omega_m + \Omega_Q \exp[3X(z)], \quad (21.12)$$

where

$$X(z) = \int_0^z [1 + w(z')](1+z')^{-1} dz', \quad (21.13)$$

and Ω_m and Ω_Q are the present density parameters of matter and dark energy components. If a general equation of state is allowed, then one has to solve for $w(z)$ (parametrized, for example, as $w(z) = w = \text{const.}$, or $w(z) = w_0 + w_1 z$) as well as for Ω_Q .

Empirically, the peak luminosity of supernova of Type Ia (SNe Ia) can be used as an efficient distance indicator (*e.g.*, Ref. 16). The favorite theoretical explanation for SNe Ia is the thermonuclear disruption of carbon-oxygen white dwarfs. Although not perfect

[‡] Unless stated otherwise, all quoted uncertainties in this article are one-sigma/68% confidence. It is common for cosmological parameters to have significantly non-Gaussian error distributions.

‘standard candles,’ it has been demonstrated that by correcting for a relation between the light curve shape and the luminosity at maximum brightness, the dispersion of the measured luminosities can be greatly reduced. There are several possible systematic effects which may affect the accuracy of the SNe Ia as distance indicators, for example, evolution with redshift and interstellar extinction in the host galaxy and in the Milky Way, but there is no indication that any of these effects are significant for the cosmological constraints.

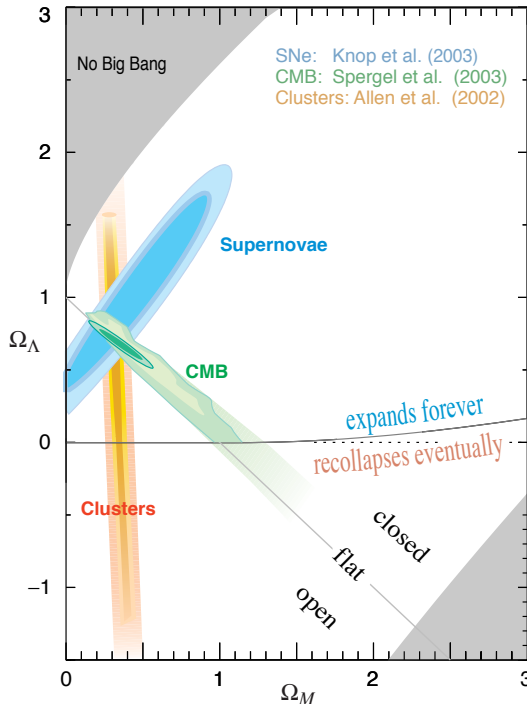


Figure 21.1: This shows the preferred region in the Ω_m – Ω_Λ plane from the compilation of supernovae data in Ref. 18, and also the complementary results coming from some other observations. [Courtesy of the Supernova Cosmology Project.] Color version at end of book.

Two major studies, the ‘Supernova Cosmology Project’ and the ‘High- z Supernova Search Team,’ found evidence for an accelerating Universe [17], interpreted as due to a cosmological constant, or to a more general ‘dark energy’ component. Current results from the Supernova Cosmology Project [18] are shown in Fig. 21.1 (see also Ref. 19). The SNe Ia data alone can only constrain a combination of Ω_m and Ω_Λ . When combined with the CMB data (which indicates flatness, *i.e.*, $\Omega_m + \Omega_\Lambda \approx 1$), the best-fit values are $\Omega_m \approx 0.3$ and $\Omega_\Lambda \approx 0.7$. Most results in the literature are consistent with Einstein’s $w = -1$ cosmological constant case. For example, Wood-Vasey *et al.* [20] combined data from the ESSENCE and SNLS surveys and deduced $w = -1.07 \pm 0.09$ (stat 1σ) ± 0.13 (sys), $\Omega_m = 0.267^{+0.028}_{-0.018}$ (stat 1σ).

Future experiments will aim to set constraints on the cosmic equation of state $w(z)$. However, given the integral relation between the luminosity distance and $w(z)$, it is not straightforward to recover $w(z)$ (*e.g.*, Ref. 21).

21.3.3. Cosmic microwave background :

The physics of the cosmic microwave background (CMB) is described in detail by Scott and Smoot in this volume. Before recombination, the baryons and photons are tightly coupled, and the perturbations oscillate in the potential wells generated primarily by the dark matter perturbations. After decoupling, the baryons are free to collapse into those potential wells. The CMB carries a record of conditions at the time of decoupling, often called primary anisotropies. In addition, it is affected by various processes as it propagates towards

us, including the effect of a time-varying gravitational potential (the integrated Sachs-Wolfe effect), gravitational lensing, and scattering from ionized gas at low redshift.

The primary anisotropies, the integrated Sachs-Wolfe effect, and scattering from a homogeneous distribution of ionized gas, can all be calculated using linear perturbation theory, a widely-used implementation being the CMBFAST code of Seljak and Zaldarriaga [6] (CAMB is a popular alternative, often used embedded in the analysis package CosmoMC [7]). Gravitational lensing is also calculated in this code. Secondary effects such as inhomogeneities in the re-ionization process, and scattering from gravitationally-collapsed gas (the Sunyaev–Zel’dovich effect), require more complicated, and more uncertain, calculations.

The upshot is that the detailed pattern of anisotropies, quantified, for instance, by the angular power spectrum C_ℓ , depends on all of the cosmological parameters. In a typical cosmology, the anisotropy power spectrum [usually plotted as $\ell(\ell+1)C_\ell$] features a flat plateau at large angular scales (small ℓ), followed by a series of oscillatory features at higher angular scales, the first and most prominent being at around one degree ($\ell \approx 200$). These features, known as acoustic peaks, represent the oscillations of the photon-baryon fluid around the time of decoupling. Some features can be closely related to specific parameters—for instance, the location of the first peak probes the spatial geometry, while the relative heights of the peaks probes the baryon density—but many other parameters combine to determine the overall shape.

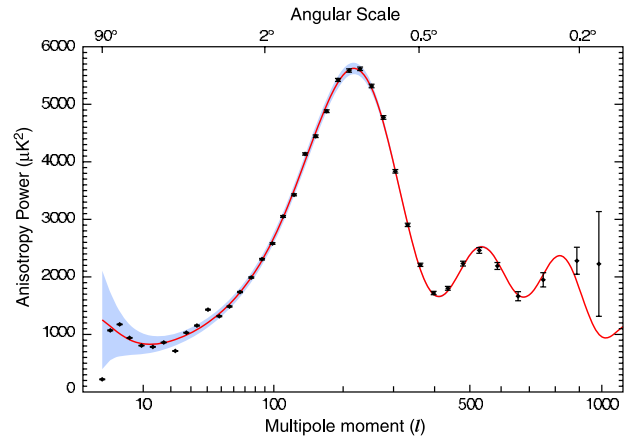


Figure 21.2: The angular power spectrum of the cosmic microwave background temperature from WMAP3. The solid line shows the prediction from the best-fitting Λ CDM model [2]. The error bars on the data points (which are tiny for most of them) indicate the observational errors, while the shaded region indicates the statistical uncertainty from being able to observe only one microwave sky, known as cosmic variance, which is the dominant uncertainty on large angular scales. [Figure courtesy NASA/WMAP Science Team.]

The three-year data release from the WMAP satellite [1], henceforth WMAP3, has provided the most accurate results to date on the spectrum of CMB fluctuations, with a precision determination of the temperature power spectrum up to $\ell \approx 900$, shown in Fig. 21.2, and the best measurements of the spectrum of E -polarization anisotropies and the correlation spectrum between temperature and polarization (those spectra having first been detected by DASI [22]). These are consistent with models based on the parameters we have described, and provide quite accurate determinations of many of them [2]. In this subsection, we will refer to results from WMAP alone, with the following section studying some combinations with other observations. We note that as the parameter fitting is done in a multi-parameter space, one has to assume a ‘prior’ range for each of the parameters (*e.g.*, Hubble constant $0.5 < h < 1$), and there may be some dependence on these assumed priors.

WMAP3 provides an exquisite measurement of the location of the first acoustic peak, which directly probes the spatial geometry and

yields a total density $\Omega_{\text{tot}} \equiv \sum \Omega_i + \Omega_\Lambda$ of

$$\Omega_{\text{tot}} = 1.011 \pm 0.012, \quad (21.14)$$

consistent with spatial flatness and completely excluding significantly curved Universes. (This result does however require constraints on the Hubble parameter from other measurements, in this case the SNLS supernovae; WMAP3 alone constrains Ω_{tot} only weakly, and allows significantly closed Universes if h is small. This result also assumes that the dark energy is a cosmological constant.) WMAP3 also gives a precision measurement of the age of the Universe. It gives a baryon density consistent with, and at much higher precision than, that coming from nucleosynthesis. It affirms the need for both dark matter and dark energy if the data are to be explained. It shows no evidence for dynamics of the dark energy, being consistent with a pure cosmological constant ($w = -1$).

The density perturbations are consistent with a power-law primordial spectrum. There are indications that the spectral slope is less than the Harrison-Zel'dovich value $n = 1$ [2], though the result appears less strong using Bayesian techniques [9]. There is no indication of tensor perturbations, but the upper limit is quite weak.

WMAP3 gives a much lower result for the reionization optical depth τ than did their first year results [23]. The current best-fit value $\tau = 0.089$ is in reasonable agreement with models of how early structure formation induces reionization.

WMAP3 is consistent with other experiments and its dynamic range can be enhanced by including information from small-angle CMB experiments including ACBAR, CBI and VSA. However the WMAP3 dataset on its own is so powerful that these add little constraining power.

21.3.4. Galaxy clustering:

The power spectrum of density perturbations depends on the nature of the dark matter. Within the Cold Dark Matter model, the shape of the power spectrum depends primarily on the primordial power spectrum and on the combination $\Omega_m h$ which determines the horizon scale at matter-radiation equality, with a subdominant dependence on the baryon density. The matter distribution is most easily probed by observing the galaxy distribution, but this must be done with care as the galaxies do not perfectly trace the dark matter distribution. Rather, they are a ‘biased’ tracer of the dark matter. The need to allow for such bias is emphasized by the observation that different types of galaxies show bias with respect to each other. Further, the observed 3D galaxy distribution is in redshift space, *i.e.*, the observed redshift is the sum of the Hubble expansion and the line-of-sight peculiar velocity, leading to linear and non-linear dynamical effects which also depend on the cosmological parameters. On the largest length scales, the galaxies are expected to trace the location of the dark matter, except for a constant multiplier b to the power spectrum, known as the linear bias parameter. On scales smaller than $20 h^{-1}$ Mpc or so, the clustering pattern is ‘squashed’ in the radial direction due to coherent infall, which depends on the parameter $\beta \equiv \Omega_m^{0.6}/b$ (on these shorter scales, more complicated forms of biasing are not excluded by the data). On scales of a few h^{-1} Mpc, there is an effect of elongation along the line of sight (colloquially known as the ‘finger of God’ effect) which depends on the galaxy velocity dispersion σ_p .

21.3.4.1. The galaxy power spectrum:

The 2-degree Field (2dF) Galaxy Redshift Survey is now complete and publicly available.** The power-spectrum analysis of the final 2dFGRS data set of approximately 220,000 galaxies was fitted to a CDM model [24]. It shows evidence for baryon acoustic oscillations, with baryon fraction $\Omega_b/\Omega_m = 0.185 \pm 0.046$ (1- σ uncertainties). The shape of the power spectrum is characterized by $\Omega_m h = 0.168 \pm 0.016$, and in combination with WMAP data gives $\Omega_m = 0.231 \pm 0.021$ (see also Ref. 25). The 2dF power spectrum is compared with the Sloan Digital Sky Survey (SDSS) †† power spectrum [26] in Fig. 21.3. We see agreement in the gross features, but also some discrepancies. Eisenstein *et al.* [27] reported on detection of baryon

acoustic peak in the large-scale correlation function of the SDSS sample of nearly 47,000 Luminous Red Galaxies (LRG). By using the baryon acoustic peak as a ‘standard ruler’ they found, independent of WMAP, that $\Omega_m = 0.273 \pm 0.025$ for a flat Λ CDM model. A combination of the 2dF, the SDSS main and the LRG samples [28] yield from the baryon oscillation signals $\Omega_m = 0.249 \pm 0.018$ and $w = -1.004 \pm 0.089$, assuming a flat universe and constraints from SN Ia and CMB data. Signatures of baryon acoustic oscillations have also been measured [29,30] from samples nearly 600,000 LRGs with photometric redshifts (which are less accurate than spectroscopic redshifts, but easier to obtain for large samples).

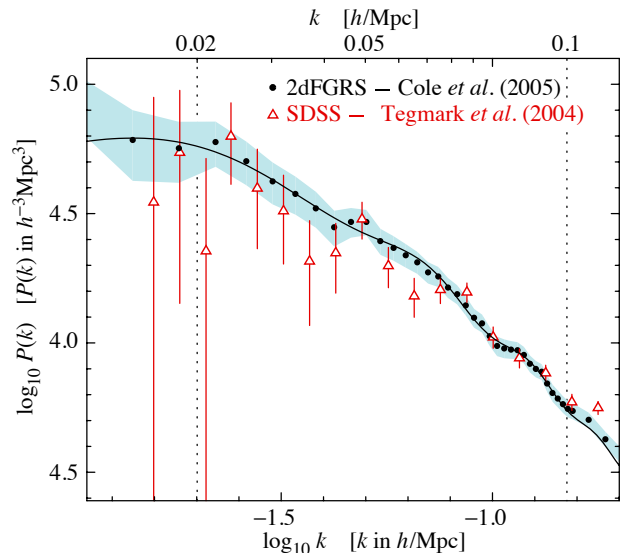


Figure 21.3: The galaxy power spectrum from the 2dF galaxy redshift survey [24] compared with that from SDSS [26], each corrected for its survey geometry. The 2dFGRS power spectrum (with distances measured in redshift space) is shown by solid circles with one-sigma errors shown by the shaded area. The triangles and error bars show the SDSS power spectrum. The solid curve shows a linear-theory Λ CDM model with $\Omega_m h = 0.168$, $\Omega_b/\Omega_m = 0.17$, $h = 0.72$, $n = 1$ and normalization matched to the 2dFGRS power spectrum. The dotted vertical lines indicate the range over which the best-fit model was evaluated. [Figure provided by Shaun Cole and Will Percival; see Ref. 24.]

Combination of the 2dF data with the CMB indicates a ‘biasing’ parameter $b \sim 1$, in agreement with a 2dF-alone analysis of higher-order clustering statistics. However, results for biasing also depend on the length scale over which a fit is done, and the selection of the objects by luminosity, spectral type, or color. In particular, on scales smaller than $10 h^{-1}$ Mpc, different galaxy types are clustered differently. This ‘biasing’ introduces a systematic effect on the determination of cosmological parameters from redshift surveys. Prior knowledge from simulations of galaxy formation could help, but is model-dependent. We also note that the present-epoch power spectrum is not sensitive to dark energy, so it is mainly a probe of the matter density.

21.3.4.2. Limits on neutrino mass from galaxy surveys and other probes:

Large-scale structure data can put an upper limit on the ratio Ω_ν/Ω_m due to the neutrino ‘free streaming’ effect [31,32]. For example, by comparing the 2dF galaxy power spectrum with a four-component model (baryons, cold dark matter, a cosmological constant, and massive neutrinos), it was estimated that $\Omega_\nu/\Omega_m < 0.13$ (95% confidence limit), giving $\Omega_\nu < 0.04$ if a concordance prior of $\Omega_m = 0.3$ is imposed. The latter corresponds to an upper limit of about 2 eV on the total neutrino mass, assuming a prior of $h \approx 0.7$ [33]. Potential systematic effects include biasing of the galaxy distribution and non-linearities of the power spectrum. A similar upper limit of 2 eV was derived from CMB anisotropies alone [2,34,35]. The above

** See <http://www.mso.anu.edu.au/2dFGRS>

†† See <http://www.sdss.edu>

analyses assume that the primordial power spectrum is adiabatic, scale-invariant and Gaussian. Additional cosmological data sets bring down this upper limit [36,37]. An upper limit on the total neutrino mass of 0.17 eV was reported by combining a large number of cosmological probes [38].

Laboratory limits on absolute neutrino masses from tritium beta decay and especially from neutrinoless double-beta decay should, within the next decade, push down towards (or perhaps even beyond) the 0.1 eV level that has cosmological significance.

21.3.5. Clusters of galaxies :

A cluster of galaxies is a large collection of galaxies held together by their mutual gravitational attraction. The largest ones are around 10^{15} solar masses, and are the largest gravitationally-collapsed structures in the Universe. Even at the present epoch they are relatively rare, with only a few percent of galaxies being in clusters. They provide various ways to study the cosmological parameters; here we discuss constraints from the measurements of the cluster number density and the baryon fraction in clusters.

21.3.5.1. Cluster number density:

The first objects of a given kind form at the rare high peaks of the density distribution, and if the primordial density perturbations are Gaussian-distributed, their number density is exponentially sensitive to the size of the perturbations, and hence can strongly constrain it. Clusters are an ideal application in the present Universe. They are usually used to constrain the amplitude σ_8 , as a box of side $8 h^{-1}$ Mpc contains about the right amount of material to form a cluster. The most useful observations at present are of X-ray emission from hot gas lying within the cluster, whose temperature is typically a few keV, and which can be used to estimate the mass of the cluster. A theoretical prediction for the mass function of clusters can come either from semi-analytic arguments or from numerical simulations. At present, the main uncertainty is the relation between the observed gas temperature and the cluster mass, despite extensive study using simulations. Ref. [39] gives

$$\sigma_8 = 0.78^{+0.30}_{-0.06} \quad (95\% \text{ confidence}) \quad (21.15)$$

for $\Omega_m = 0.35$, with highly non-Gaussian error bars, but different authors still find a spread of values. Scaling to lower Ω_m increases σ_8 . This result is somewhat above the values predicted in cosmologies compatible with WMAP3.

The same approach can be adopted at high redshift (which for clusters means redshifts approaching one) to attempt to measure σ_8 at an earlier epoch. The evolution of σ_8 is primarily driven by the value of the matter density Ω_m , with a sub-dominant dependence on the dark energy density. It is generally recognized that such analyses favor a low matter density, though there is not complete consensus on this, and at present this technique for constraining the density is not competitive with the CMB.

21.3.5.2. Cluster baryon fraction:

If clusters are representative of the mass distribution in the Universe, the fraction of the mass in baryons to the overall mass distribution would be $f_b = \Omega_b/\Omega_m$. If Ω_b , the baryon density parameter, can be inferred from the primordial nucleosynthesis abundance of the light elements, the cluster baryon fraction f_b can then be used to constrain Ω_m and h (e.g., Ref. 40). The baryons in clusters are primarily in the form of X-ray-emitting gas that falls into the cluster, and secondarily in the form of stellar baryonic mass. Hence, the baryon fraction in clusters is estimated to be

$$f_b = \frac{\Omega_b}{\Omega_m} \simeq f_{\text{gas}} + f_{\text{gal}}, \quad (21.16)$$

where $f_b = M_b/M_{\text{grav}}$, $f_{\text{gas}} = M_{\text{gas}}/M_{\text{grav}}$, $f_{\text{gal}} = M_{\text{gal}}/M_{\text{grav}}$, and M_{grav} is the total gravitating mass.

This can be used to obtain an approximate relation between Ω_m and h :

$$\Omega_m = \frac{\Omega_b}{f_{\text{gas}} + f_{\text{gal}}} \simeq \frac{\Omega_b}{0.08h^{-1.5} + 0.01h^{-1}}. \quad (21.17)$$

Big Bang Nucleosynthesis gives $\Omega_b h^2 \approx 0.02$, allowing the above relation to be approximated as $\Omega_m h^{0.5} \approx 0.25$ (e.g., Ref. 41). For example, Allen *et al.* [42] derived a density parameter consistent with $\Omega_m = 0.3$ from Chandra observations.

21.3.6. Clustering in the inter-galactic medium :

It is commonly assumed, based on hydrodynamic simulations, that the neutral hydrogen in the inter-galactic medium (IGM) can be related to the underlying mass distribution. It is then possible to estimate the matter power spectrum on scales of a few megaparsecs from the absorption observed in quasar spectra, the so-called Lyman-alpha forest. The usual procedure is to measure the power spectrum of the transmitted flux, and then to infer the mass power spectrum. Photo-ionization heating by the ultraviolet background radiation and adiabatic cooling by the expansion of the Universe combine to give a simple power-law relation between the gas temperature and the baryon density. It also follows that there is a power-law relation between the optical depth τ and ρ_b . Therefore, the observed flux $F = \exp(-\tau)$ is strongly correlated with ρ_b , which itself traces the mass density. The matter and flux power spectra can be related by

$$P_m(k) = b^2(k) P_F(k), \quad (21.18)$$

where $b(k)$ is a bias function which is calibrated from simulations. Croft *et al.* [43] derived cosmological parameters from Keck Telescope observations of the Lyman-alpha forest at redshifts $z = 2 - 4$. Their derived power spectrum corresponds to that of a CDM model, which is in good agreement with the 2dF galaxy power spectrum. A recent study using VLT spectra [44] agrees with the flux power spectrum of Ref. 43. This method depends on various assumptions. Seljak *et al.* [45] pointed out that errors are sensitive to the range of cosmological parameters explored in the simulations, and the treatment of the mean transmitted flux.

21.3.7. Gravitational lensing :

Images of background galaxies get distorted due to the gravitational effect of mass fluctuations along the line of sight. Deep gravitational potential wells such as galaxy clusters generate ‘strong lensing,’ *i.e.*, arcs and arclets, while more moderate fluctuations give rise to ‘weak lensing’. Weak lensing is now widely used to measure the mass power spectrum in random regions of the sky (see Ref. 46 for recent reviews). As the signal is weak, the CCD frame of deformed galaxy shapes (‘shear map’) is analyzed statistically to measure the power spectrum, higher moments, and cosmological parameters.

The shear measurements are mainly sensitive to the combination of Ω_m and the amplitude σ_8 . For example, the weak lensing signal detected by the CFHT Legacy Survey [47] translates into $\sigma_8 = 0.85 \pm 0.06$ for a fiducial $\Omega_m = 0.3$ assuming a Λ CDM model. Earlier results are summarized in Ref. 46. There are various systematic effects in the interpretation of weak lensing, *e.g.*, due to atmospheric distortions during observations, the redshift distribution of the background galaxies, intrinsic correlation of galaxy shapes, and non-linear modeling uncertainties.

21.3.8. Peculiar velocities :

Deviations from the Hubble flow directly probe the mass fluctuations in the Universe, and hence provide a powerful probe of the dark matter. Peculiar velocities are deduced from the difference between the redshift and the distance of a galaxy. The observational difficulty is in accurately measuring distances to galaxies. Even the best distance indicators (e.g., the Tully-Fisher relation) give an error of 15% per galaxy, hence limiting the application of the method at large distances. Peculiar velocities are mainly sensitive to Ω_m , not to Ω_Λ or quintessence. Extensive analyses in the early 1990s (e.g., Ref. 48) suggested a value of Ω_m close to unity. A more recent analysis [49], which takes into account non-linear corrections, gives $\sigma_8 \Omega_m^{0.6} = 0.49 \pm 0.06$ and $\sigma_8 \Omega_m^{0.6} = 0.63 \pm 0.08$ (90% errors) for two independent data sets. While at present cosmological parameters derived from peculiar velocities are strongly affected by random and systematic errors, a new generation of surveys may improve their accuracy. Three promising approaches are the 6dF near-infrared survey of 15,000 peculiar velocities^{‡‡}, supernovae Type Ia, and the kinematic Sunyaev-Zel’dovich effect.

^{‡‡} See <http://www.mso.anu.edu.au/6dFGS/>

21.4. Bringing observations together

Although it contains two ingredients—dark matter and dark energy—which have not yet been verified by laboratory experiments, the Λ CDM model is almost universally accepted by cosmologists as the best description of present data. The basic ingredients are given by the parameters listed in Sec. 21.1.4, with approximate values of some of the key parameters being $\Omega_b \approx 0.04$, $\Omega_{\text{dm}} \approx 0.20$, $\Omega_\Lambda \approx 0.76$, and a Hubble constant $h \approx 0.73$. The spatial geometry is very close to flat (and often assumed to be precisely flat), and the initial perturbations Gaussian, adiabatic, and nearly scale-invariant.

Table 21.2: Parameter constraints reproduced from Spergel *et al.* [2], with some additional rounding. All columns assume the Λ CDM cosmology with a power-law initial spectrum, no tensors, spatial flatness, and a cosmological constant as dark energy. Three different data combinations are shown to highlight the extent to which this choice matters. The first column is WMAP3 alone, the second combines this with 2dF, and the third column shows a combination of all datasets considered in Ref. 2. The perturbation amplitude is specified via the derived parameter σ_8 ; see Ref. 2 for details. Uncertainties are shown at one sigma, and caution is needed in extrapolating them to higher significance levels due to non-Gaussian likelihoods and assumed priors.

	WMAP alone	WMAP + 2dF	WMAP + all
$\Omega_m h^2$	0.128 ± 0.008	0.126 ± 0.005	0.132 ± 0.004
$\Omega_b h^2$	0.0223 ± 0.0007	0.0222 ± 0.0007	0.0219 ± 0.0007
h	0.73 ± 0.03	0.73 ± 0.02	$0.704^{+0.015}_{-0.016}$
n	0.958 ± 0.016	0.948 ± 0.015	0.947 ± 0.015
τ	0.089 ± 0.030	0.083 ± 0.028	$0.073^{+0.027}_{-0.028}$
σ_8	0.76 ± 0.05	0.74 ± 0.04	0.78 ± 0.03

The most powerful single experiment is WMAP3, which on its own supports all these main tenets. Values for some parameters, as given in Spergel *et al.* [2], are reproduced in Table 21.2. This model presumes a flat Universe, and so Ω_Λ is a derived quantity in this analysis, with best-fit value $\Omega_\Lambda = 0.76$.

These constraints can be somewhat strengthened by adding additional datasets, as shown in the Table. However, WMAP3 on its own is sufficiently powerful that inclusion of other datasets only changes things at quite a detailed level. In our view, the most robust present constraints are those from WMAP3 alone.

The baryon density Ω_b is now measured with quite high accuracy from the CMB and large-scale structure, and is consistent with the determination from big bang nucleosynthesis; Fields and Sarkar in this volume quote the range $0.017 \leq \Omega_b h^2 \leq 0.024$.

While Ω_Λ is measured to be non-zero with very high confidence, there is no evidence of evolution of the dark energy density. The WMAP team find the limit $w < -0.82$ at 95% confidence from a compilation of data including SNe Ia data, with the cosmological constant case $w = -1$ giving an excellent fit to the data.

The data provides strong support for the main predictions of the simplest inflation models: spatial flatness and adiabatic, Gaussian, nearly scale-invariant density perturbations. But it is disappointing that there is no sign of primordial gravitational waves, with WMAP3 providing only a weak upper limit $r < 0.65$ at 95% confidence [2] (this assumes no running, and weakens yet further if running is allowed). The spectral index n is placed in an interesting position by WMAP3, with indications that $n < 1$ is required by the data. However, the conclusion that $n = 1$ is ruled out that is suggested by parameter estimation [2] receives much less compelling support in Bayesian model selection analyses [9], and in our view, it is premature to conclude that $n = 1$ is no longer viable.

Tests have been made for various types of non-Gaussianity, a particular example being a parameter f_{NL} which measures a quadratic contribution to the perturbations and is constrained to $-54 < f_{\text{NL}} < 114$ at 95% confidence [2] (this looks weak, but prominent non-Gaussianity requires the product $f_{\text{NL}} \Delta \mathcal{R}$ to be large, and $\Delta \mathcal{R}$ is of order 10^{-5}).

Two parameters which are still uncertain are Ω_m and σ_8 , both of which were revised downwards significantly by WMAP3 to a level where they do not sit well against local measures of σ_8 , particularly those using weak gravitational lensing. However an analysis including Lyman-alpha data with WMAP3 has found that this brings σ_8 up again [38]. It is clear that we have yet to reach the last word on these parameters. It is also worth noting that WMAP3 only probes larger length scales, and the constraint comes from using WMAP to estimate all the parameters of the model needed to determine σ_8 . As such, their constraint depends strongly on the assumed set of cosmological parameters being sufficient.

One parameter which is surprisingly robust is the age of the Universe. There is a useful coincidence that for a flat Universe the position of the first peak is strongly correlated with the age of the Universe. The WMAP3 result is 13.7 ± 0.2 Gyr (assuming a flat Universe). This is in good agreement with the ages of the oldest globular clusters [50] and radioactive dating [51].

21.5. Outlook for the future

The concordance model is now well established, and there seems little room left for any dramatic revision of this paradigm. A measure of the strength of that statement is how difficult it has proven to formulate convincing alternatives. For example, one corner of parameter space that has been explored is the possibility of abandoning the dark energy, and instead considering a mixed dark matter model with $\Omega_m = 1$ and $\Omega_\nu = 0.2$. Such a model fits both the 2dF and WMAP data reasonably well, but only for a Hubble constant $h < 0.5$ [33,52]. However, this model is inconsistent with the HST key project value of h , the results from SNe Ia, cluster number density evolution, and baryon fraction in clusters.

Should there indeed be no major revision of the current paradigm, we can expect future developments to take one of two directions. Either the existing parameter set will continue to prove sufficient to explain the data, with the parameters subject to ever-tightening constraints, or it will become necessary to deploy new parameters. The latter outcome would be very much the more interesting, offering a route towards understanding new physical processes relevant to the cosmological evolution. There are many possibilities on offer for striking discoveries, for example:

- The cosmological effects of a neutrino mass may be unambiguously detected, shedding light on fundamental neutrino properties;
- Compelling detection of deviations from scale-invariance in the initial perturbations would indicate dynamical processes during perturbation generation by, for instance, inflation;
- Detection of primordial non-Gaussianities would indicate that non-linear processes influence the perturbation generation mechanism;
- Detection of variation in the dark energy density (*i.e.*, $w \neq -1$) would provide much-needed experimental input into the question of the properties of the dark energy.

These provide more than enough motivation for continued efforts to test the cosmological model and improve its precision.

Over the coming years, there are a wide range of new observations, which will bring further precision to cosmological studies. Indeed, there are far too many for us to be able to mention them all here, and so we will just highlight a few areas.

The cosmic microwave background observations will improve in several directions. The new frontier is the study of polarization, first detected in 2002 by DASI and for which power spectrum measurements have now been made by WMAP and Boomerang [53]. Dedicated ground-based polarization experiments, such as CBI, QUaD, and Clover promise powerful measures of the polarization spectrum in the next few years, and may be able to separately detect the two modes of

polarization. Another area of development is pushing accurate power spectrum measurements to smaller angular scales, typically achieved by interferometry, which should allow measurements of secondary anisotropy effects, such as the Sunyaev–Zel’dovich effect, whose detection has already been tentatively claimed by CBI. Finally, we mention the Planck satellite, due to launch in 2008, which will make high-precision all-sky maps of temperature and polarization, utilizing a very wide frequency range for observations to improve understanding of foreground contaminants, and to compile a large sample of clusters via the Sunyaev–Zel’dovich effect.

On the supernova side, the most ambitious initiative at present is a proposed satellite mission JDEM (Joint Dark Energy Mission) funded by NASA and DOE. There are several candidates for this mission, including the much-publicized SNAP satellite, but the funding has yet to be secured. An impressive array of ground-based dark energy surveys are also already operational or proposed, including the ESSENCE project, the Dark Energy Survey, LSST, and WFMOS. With large samples, it may be possible to detect evolution of the dark energy density, thus measuring its equation of state and perhaps even its variation.

An exciting new area for the future will be radio surveys of the redshifted 21-cm line of hydrogen. Because of the intrinsic narrowness of this line, by tuning of the bandpass the emission from narrow redshift slices of the Universe will be measured to extremely high redshift, probing the details of the reionization process at redshifts up to perhaps 20. LOFAR is the first instrument able to do this and is at an advanced construction stage. In the medium term, the Square Kilometer Array (SKA) will take these studies to a precision level.

The above future surveys will address fundamental questions of physics well beyond just testing the ‘concordance’ Λ CDM model and minor variations. It would be important to distinguish the imprint of dark energy and dark matter on the geometry from the growth of perturbations, and to test theories of modified gravity as alternatives for fitting the observations to a Dark Energy component.

The development of the first precision cosmological model is a major achievement. However, it is important not to lose sight of the motivation for developing such a model, which is to understand the underlying physical processes at work governing the Universe’s evolution. On that side, progress has been much less dramatic. For instance, there are many proposals for the nature of the dark matter, but no consensus as to which is correct. The nature of the dark energy remains a mystery. Even the baryon density, now measured to an accuracy of a few percent, lacks an underlying theory able to predict it even within orders of magnitude. Precision cosmology may have arrived, but at present many key questions remain unanswered.

Acknowledgements:

Both authors acknowledge PPARC Senior Research Fellowships. We thank Sarah Bridle and Jochen Weller for useful comments on this article, and OL thanks members of the Cambridge Leverhulme Quantitative Cosmology and 2dFGRS Teams for helpful discussions.

References:

- G. Hinshaw *et al.*, *Astrophys. J. Supp.* **170**, 288 (2007);
L. Page *et al.*, *Astrophys. J. Supp.* **170**, 335 (2007);
N. Jarosik *et al.*, *Astrophys. J. Supp.* **170**, 263 (2007).
- D. N. Spergel *et al.*, *Astrophys. J. Supp.* **170**, 377 (2007).
- S. Fukuda *et al.*, *Phys. Rev. Lett.* **85**, 3999 (2000);
Q.R. Ahmad *et al.*, *Phys. Rev. Lett.* **87**, 071301 (2001).
- A.D. Dolgov *et al.*, *Nucl. Phys.* **B632**, 363 (2002).
- For detailed accounts of inflation see E.W. Kolb and M.S. Turner, *The Early Universe*, Addison–Wesley (Redwood City, 1990);
A.R. Liddle and D.H. Lyth, *Cosmological Inflation and Large-Scale Structure*, (Cambridge University Press, 2000).
- U. Seljak and M. Zaldarriaga, *Astrophys. J.* **469**, 1 (1996).
- A. Lewis and S. Bridle, *Phys. Rev.* **D66**, 103511 (2002).
- H.V. Peiris *et al.*, *Astrophys. J. Supp.* **148**, 213 (2003).
- D. Parkinson *et al.*, *Phys. Rev.* **D73**, 123523 (2006).
- J.C. Mather *et al.*, *Astrophys. J.* **512**, 511 (1999).
- A. Kosowsky and M.S. Turner, *Phys. Rev.* **D52**, 1739 (1995).
- D.H. Lyth and D. Wands, *Phys. Lett.* **B524**, 5 (2002);
K. Enqvist and M.S. Sloth, *Nucl. Phys.* **B626**, 395 (2002);
T. Moroi and T. Takahashi, *Phys. Lett.* **B522**, 215 (2001).
- B. Ratra and P.J.E. Peebles, *Phys. Rev.* **D37**, 3406 (1988);
C. Wetterich, *Nucl. Phys.* **B302**, 668 (1988);
T. Padmanabhan, *Phys. Rept.* **380**, 235 (2003);
V. Sahni and A. Starobinsky, *Int. J. Mod. Phys.* **D9**, 373 (2000).
- J.K. Webb *et al.*, *Phys. Rev. Lett.* **82**, 884 (1999);
J.K. Webb *et al.*, *Phys. Rev. Lett.* **87**, 091301 (2001);
J.K. Webb *et al.*, *Astrophys. Sp. Sci.* **283**, 565 (2003);
H. Chand *et al.*, *Astron. Astrophys.* **417**, 853 (2004);
R. Srianand *et al.*, *Phys. Rev. Lett.* **92**, 121302 (2004).
- W.L. Freedman *et al.*, *Astrophys. J.* **553**, 47 (2001).
- A. Filippenko, *astro-ph/0307139*.
- A.G. Riess *et al.*, *Astron. J.* **116**, 1009 (1998);
P. Garnavich *et al.*, *Astrophys. J.* **509**, 74 (1998);
S. Perlmutter *et al.*, *Astrophys. J.* **517**, 565 (1999).
- R.A. Knop *et al.*, *Astrophys. J.* **598**, 102 (2003).
- J.L. Tonry *et al.*, *Astrophys. J.* **594**, 1 (2003);
A.G. Riess *et al.*, *Astrophys. J.* **659**, 98 (2007);
S. Jha, A.G. Riess, and R.P. Kirshner *et al.*, *Astrophys. J.* **659**, 122 (2007).
- Wood-Vasey, W.M. *et al.*, *astro-ph/0701041*.
- I. Maor *et al.*, *Phys. Rev.* **D65**, 123003 (2002).
- J. Kovac *et al.*, *Nature* **420**, 772 (2002).
- D.N. Spergel *et al.*, *Astrophys. J. Supp.* **148**, 175 (2003).
- S. Cole *et al.*, *Mon. Not. Roy. Astr. Soc.* **362**, 505 (2005).
- A. Sanchez *et al.*, *Mon. Not. Roy. Astr. Soc.* **366**, 189 (2006).
- M. Tegmark *et al.*, *Astrophys. J.* **606**, 702 (2004).
- D. Eisenstein *et al.*, *Astrophys. J.* **633**, 560 (2005).
- W.J. Percival *et al.*, *arXiv:0705.3323 [astro-ph]* (2007).
- C. Blake *et al.*, *Mon. Not. Roy. Astr. Soc.* **374**, 1527 (2007).
- N. Padmanabhan *et al.*, *Mon. Not. Roy. Astr. Soc.* **378**, 852 (2007).
- W. Hu *et al.*, *Phys. Rev. Lett.* **80**, 5255 (1998).
- J. Lesgourgues and S. Pastor, *Physics Reports*, **429**, 307 (2006).
- O. Elgaroy and O. Lahav, *JCAP* **0304**, 004 (2003).
- K. Ichikawa *et al.*, *Phys. Rev.* **D71**, 043001 (2005).
- M. Fukugita *et al.*, *Phys Rev D*, **74**, 027302 (2006).
- S. Hannestad, *JCAP* **0305**, 004 (2003).
- O. Elgaroy and O. Lahav, *New J. Physics*, **7**, 61 (2005).
- U. Seljak *et al.*, *JCAP* **0610**, 014 (2006).
- P.T.P. Viana *et al.*, *Mon. Not. Roy. Astr. Soc.*, **346**, 319 (2003).
- S.D.M. White *et al.*, *Nature* **366**, 429 (1993).
- P. Erdogdu *et al.*, *Mon. Not. Roy. Astr. Soc.* **340**, 573 (2003).
- S.W. Allen *et al.*, *Mon. Not. Roy. Astr. Soc.* **342**, 287 (2003).
- R.A.C. Croft *et al.*, *Astrophys. J.* **581**, 20 (2002).
- S. Kim *et al.*, *Mon. Not. Roy. Astr. Soc.* **347**, 355 (2004).
- U. Seljak *et al.*, *Mon. Not. Roy. Astr. Soc.* **342**, L79 (2003);
U. Seljak *et al.*, *Phys. Rev.* **D71**, 103515 (2005).
- P. Schneider, *astro-ph/0306465*;
A. Refregier, *Ann. Rev. Astron. Astrophys.* **41**, 645 (2003).
- H. Hoekstra *et al.*, *Astrophys. J.* **647**, 116 (2006).
- A. Dekel, *Ann. Rev. Astron. Astrophys.* **32**, 371 (1994).
- L. Silberman *et al.*, *Astrophys. J.* **557**, 102 (2001).
- B. Chaboyer and L.M. Krauss, *Science* **299**, 65 (2003).
- R. Cayrel *et al.*, *Nature* **409**, 691 (2001).
- A. Blanchard *et al.*, *Astron. Astrophys.* **412**, 35 (2003).
- C.J. MacTavish *et al.*, *Astrophys. J.* **647**, 833 (2006).

22. DARK MATTER

Revised September 2007 by M. Drees (Bonn University) and G. Gerbier (Saclay, CEA).

22.1. Theory

22.1.1. Evidence for Dark Matter :

The existence of Dark (*i.e.*, non-luminous and non-absorbing) Matter (DM) is by now well established. The earliest [1], and perhaps still most convincing, evidence for DM came from the observation that various luminous objects (stars, gas clouds, globular clusters, or entire galaxies) move faster than one would expect if they only felt the gravitational attraction of other visible objects. An important example is the measurement of galactic rotation curves. The rotational velocity v of an object on a stable Keplerian orbit with radius r around a galaxy scales like $v(r) \propto \sqrt{M(r)/r}$, where $M(r)$ is the mass inside the orbit. If r lies outside the visible part of the galaxy and mass tracks light, one would expect $v(r) \propto 1/\sqrt{r}$. Instead, in most galaxies one finds that v becomes approximately constant out to the largest values of r where the rotation curve can be measured; in our own galaxy, $v \simeq 220$ km/s at the location of our solar system, with little change out to the largest observable radius. This implies the existence of a *dark halo*, with mass density $\rho(r) \propto 1/r^2$, *i.e.*, $M(r) \propto r$; at some point ρ will have to fall off faster (in order to keep the total mass of the galaxy finite), but we do not know at what radius this will happen. This leads to a lower bound on the DM mass density, $\Omega_{\text{DM}} \gtrsim 0.1$, where $\Omega_X \equiv \rho_X/\rho_{\text{crit}}$, ρ_{crit} being the critical mass density (*i.e.*, $\Omega_{\text{tot}} = 1$ corresponds to a flat Universe).

The observation of clusters of galaxies tends to give somewhat larger values, $\Omega_{\text{DM}} \simeq 0.2$ to 0.3 . These observations include measurements of the peculiar velocities of galaxies in the cluster, which are a measure of their potential energy if the cluster is virialized; measurements of the *X-ray* temperature of hot gas in the cluster, which again correlates with the gravitational potential felt by the gas; and—most directly—studies of (weak) gravitational lensing of background galaxies on the cluster.

The currently most accurate, if somewhat indirect, determination of Ω_{DM} comes from global fits of cosmological parameters to a variety of observations; see the Section on Cosmological Parameters for details. For example, using measurements of the anisotropy of the cosmic microwave background (CMB) and of the spatial distribution of galaxies, Ref. 2 finds a density of cold, non-baryonic matter

$$\Omega_{\text{nbm}} h^2 = 0.106 \pm 0.008, \quad (22.1)$$

where h is the Hubble constant in units of 100 km/(s·Mpc). Some part of the baryonic matter density [2],

$$\Omega_{\text{b}} h^2 = 0.022 \pm 0.001, \quad (22.2)$$

may well contribute to (baryonic) DM, *e.g.*, MACHOs [3] or cold molecular gas clouds [4].

The DM density in the “neighborhood” of our solar system is also of considerable interest. This was first estimated as early as 1922 by J.H. Jeans, who analyzed the motion of nearby stars transverse to the galactic plane [1]. He concluded that in our galactic neighborhood, the average density of DM must be roughly equal to that of luminous matter (stars, gas, dust). Remarkably enough, the most recent estimates, based on a detailed model of our galaxy, find quite similar results [5]:

$$\rho_{\text{DM}}^{\text{local}} \simeq 0.3 \frac{\text{GeV}}{\text{cm}^3}; \quad (22.3)$$

this value is known to within a factor of two or so.

22.1.2. Candidates for Dark Matter :

Analyses of structure formation in the Universe [6] indicate that most DM should be “cold,” *i.e.*, should have been non-relativistic at the onset of galaxy formation (when there was a galactic mass inside the causal horizon). This agrees well with the upper bound [2] on the contribution of light neutrinos to Eq. (22.1),

$$\Omega_{\nu} h^2 \leq 0.0076 \quad 95\% \text{ CL}. \quad (22.4)$$

Candidates for non-baryonic DM in Eq. (22.1) must satisfy several conditions: they must be stable on cosmological time scales (otherwise they would have decayed by now), they must interact very weakly with electromagnetic radiation (otherwise they wouldn’t qualify as *dark matter*), and they must have the right relic density. Candidates include primordial black holes, axions, and weakly interacting massive particles (WIMPs).

Primordial black holes must have formed before the era of Big-Bang nucleosynthesis, since otherwise they would have been counted in Eq. (22.2) rather than Eq. (22.1). Such an early creation of a large number of black holes is possible only in certain somewhat contrived cosmological models [7].

The existence of axions [8] was first postulated to solve the strong *CP* problem of QCD; they also occur naturally in superstring theories. They are pseudo Nambu-Goldstone bosons associated with the (mostly) spontaneous breaking of a new global “Peccei-Quinn” (PQ) $U(1)$ symmetry at scale f_a ; see the Section on Axions in this *Review* for further details. Although very light, axions would constitute cold DM, since they were produced non-thermally. At temperatures well above the QCD phase transition, the axion is massless, and the axion field can take any value, parameterized by the “misalignment angle” θ_i . At $T \lesssim 1$ GeV, the axion develops a mass m_a due to instanton effects. Unless the axion field happens to find itself at the minimum of its potential ($\theta_i = 0$), it will begin to oscillate once m_a becomes comparable to the Hubble parameter H . These coherent oscillations transform the energy originally stored in the axion field into physical axion quanta. The contribution of this mechanism to the present axion relic density is [8]

$$\Omega_a h^2 = \kappa_a \left(f_a / 10^{12} \text{ GeV} \right)^{1.175} \theta_i^2, \quad (22.5)$$

where the numerical factor κ_a lies roughly between 0.5 and a few. If $\theta_i \sim \mathcal{O}(1)$, Eq. (22.5) will saturate Eq. (22.1) for $f_a \sim 10^{11}$ GeV, comfortably above laboratory and astrophysical constraints [8]; this would correspond to an axion mass around 0.1 meV. However, if the post-inflationary reheat temperature $T_R > f_a$, cosmic strings will form during the PQ phase transition at $T \simeq f_a$. Their decay will give an additional contribution to Ω_a , which is often bigger than that in Eq. (22.5) [9], leading to a smaller preferred value of f_a , *i.e.*, larger m_a . On the other hand, values of f_a near the Planck scale become possible if θ_i is for some reason very small.

Weakly interacting massive particles (WIMPs) χ are particles with mass roughly between 10 GeV and a few TeV, and with cross sections of approximately weak strength. Within standard cosmology, their present relic density can be calculated reliably if the WIMPs were in thermal and chemical equilibrium with the hot “soup” of Standard Model (SM) particles after inflation. In this case, their density would become exponentially (Boltzmann) suppressed at $T < m_\chi$. The WIMPs therefore drop out of thermal equilibrium (“freeze out”) once the rate of reactions that change SM particles into WIMPs or vice versa, which is proportional to the product of the WIMP number density and the WIMP pair annihilation cross section into SM particles σ_A times velocity, becomes smaller than the Hubble expansion rate of the Universe. After freeze out, the co-moving WIMP density remains essentially constant; if the Universe evolved adiabatically after WIMP decoupling, this implies a constant WIMP number to entropy density ratio. Their present relic density is then approximately given by (ignoring logarithmic corrections) [10]

$$\Omega_\chi h^2 \simeq \text{const.} \cdot \frac{T_0^3}{M_{\text{Pl}}^3 \langle \sigma_A v \rangle} \simeq \frac{0.1 \text{ pb} \cdot c}{\langle \sigma_A v \rangle}. \quad (22.6)$$

Here T_0 is the current CMB temperature, M_{Pl} is the Planck mass, c is the speed of light, σ_A is the total annihilation cross section of a pair of WIMPs into SM particles, v is the relative velocity between the two WIMPs in their cms system, and $\langle \dots \rangle$ denotes thermal averaging. Freeze out happens at temperature $T_F \simeq m_\chi/20$ almost independently of the properties of the WIMP. This means that WIMPs are already non-relativistic when they decouple from the thermal plasma; it also implies that Eq. (22.6) is applicable if $T_R > T_F$. Notice that the 0.1 pb in Eq. (22.6) contains factors of T_0 and M_{Pl} ; it is, therefore, quite

intriguing that it “happens” to come out near the typical size of weak interaction cross sections.

The seemingly most obvious WIMP candidate is a heavy neutrino. However, an $SU(2)$ doublet neutrino will have too small a relic density if its mass exceeds $M_Z/2$, as required by LEP data. One can suppress the annihilation cross section, and hence increase the relic density, by postulating mixing between a heavy $SU(2)$ doublet and some “sterile” $SU(2) \times U(1)_Y$ singlet neutrino. However, one also has to require the neutrino to be stable; it is not obvious why a massive neutrino should not be allowed to decay.

The currently best motivated WIMP candidate is, therefore, the lightest superparticle (LSP) in supersymmetric models [11] with exact R -parity (which guarantees the stability of the LSP). Searches for exotic isotopes [12] imply that a stable LSP has to be neutral. This leaves basically two candidates among the superpartners of ordinary particles, a sneutrino, and a neutralino. Sneutrinos again have quite large annihilation cross sections; their masses would have to exceed several hundred GeV for them to make good DM candidates. This is uncomfortably heavy for the lightest sparticle, in view of naturalness arguments. Moreover, the negative outcome of various WIMP searches (see below) rules out “ordinary” sneutrinos as primary component of the DM halo of our galaxy. (In models with gauge-mediated SUSY breaking, the lightest “messenger sneutrino” could make a good WIMP [13].) The most widely studied WIMP is therefore the lightest neutralino. Detailed calculations [14] show that the lightest neutralino will have the desired thermal relic density Eq. (22.1) in at least four distinct regions of parameter space. χ could be (mostly) a bino or photino (the superpartner of the $U(1)_Y$ gauge boson and photon, respectively), if both χ and some sleptons have mass below ~ 150 GeV, or if m_χ is close to the mass of some sfermion (so that its relic density is reduced through co-annihilation with this sfermion), or if $2m_\chi$ is close to the mass of the CP -odd Higgs boson present in supersymmetric models [15]. Finally, Eq. (22.1) can also be satisfied if χ has a large higgsino or wino component.

Many non-supersymmetric extensions of the Standard Model also contain viable WIMP candidates. Examples are the lightest T -odd particle in “Little Higgs” models with conserved T -parity [16], or “techni-baryons” in scenarios with an additional, strongly interacting (“technicolor” or similar) gauge group [17].

Although thermally produced WIMPs are attractive DM candidates because their relic density naturally has at least the right order of magnitude, non-thermal production mechanisms have also been suggested, *e.g.*, LSP production from the decay of some moduli fields [18], from the decay of the inflaton [19], or from the decay of “ Q -balls” (non-topological solitons) formed in the wake of Affleck-Dine baryogenesis [20]. Although LSPs from these sources are typically highly relativistic when produced, they quickly achieve kinetic (but not chemical) equilibrium if T_R exceeds a few MeV [21] (but stays below $m_\chi/20$). They therefore also contribute to cold DM.

Primary black holes (as MACHOs), axions, and WIMPs are all (in principle) detectable with present or near-future technology (see below). There are also particle physics DM candidates which currently seem almost impossible to detect. These include the gravitino (the spin-3/2 superpartner of the graviton) [22], states from the “hidden sector” thought responsible for supersymmetry breaking [13], and the axino (the spin-1/2 superpartner of the axion) [23].

22.2. Experimental detection of Dark Matter

22.2.1. The case of baryonic matter in our galaxy :

The search for hidden galactic baryonic matter in the form of MAssive Compact Halo Objects (MACHOs) has been initiated following the suggestion that they may represent a large part of the galactic DM and could be detected through the microlensing effect [3]. The MACHO, EROS, and OGLE collaborations have performed a program of observation of such objects by monitoring the luminosity of millions of stars in the Large and Small Magellanic Clouds for several years. EROS concluded that MACHOs cannot contribute more than 8% to the mass of the galactic halo [24], while MACHO observed a signal at 0.4 solar mass and put an upper limit of 40%. Overall,

this strengthens the need for non-baryonic DM, also supported by the arguments developed above.

22.2.2. Axion searches :

Axions can be detected by looking for $a \rightarrow \gamma$ conversion in a strong magnetic field [25]. Such a conversion proceeds through the loop-induced $a\gamma\gamma$ coupling, whose strength $g_{a\gamma\gamma}$ is an important parameter of axion models. Currently two experiments searching for axionic DM are taking data. They both employ high quality cavities. The cavity “Q factor” enhances the conversion rate on resonance, *i.e.*, for $m_a c^2 = \hbar\omega_{\text{res}}$. One then needs to scan the resonance frequency in order to cover a significant range in m_a or, equivalently, f_a . The bigger of the two experiments, the ADMX experiment situated at the LLNL in California [26], started taking data in the first half of 1996. It uses very sophisticated “conventional” electronic amplifiers with very low noise temperature to enhance the conversion signal. Their first published results [27] exclude axions with mass between 1.9 and 3.3 μeV , corresponding to $f_a \simeq 4 \cdot 10^{13}$ GeV, as a major component of the dark halo of our galaxy, if $g_{a\gamma\gamma}$ is near the upper end of the theoretically expected range. Later an about five times better limit was achieved [28] for $1.98 \mu\text{eV} \leq m_a \leq 2.18 \mu\text{eV}$, if a large fraction of the local DM density is due to a single flow of axions with very low velocity dispersion. The ADMX experiment is being upgraded by introducing SQUIDS as first-stage amplifiers; this should increase the sensitivity by about a factor of two.

The smaller “CARRACK” experiment now being developed in Kyoto, Japan [29] uses Rydberg atoms (atoms excited to a very high state, $n \simeq 230$) to detect the microwave photons that would result from axion conversion. This allows almost noise-free detection of single photons. Preliminary results of the CARRACK I experiment [30] exclude axions with mass in a narrow range around 10 μeV as major component of the galactic dark halo for some plausible range of $g_{a\gamma\gamma}$ values. This experiment is being upgraded to CARRACK II, which intends to probe the range between 2 and 50 μeV with sensitivity to all plausible axion models, if axions form most of DM [30].

22.2.3. Basics of direct WIMP search :

As stated above, WIMPs should be gravitationally trapped inside galaxies and should have the adequate density profile to account for the observed rotational curves. These two constraints determine the main features of experimental detection of WIMPs, which have been detailed in the reviews [31].

Their mean velocity inside our galaxy relative to its center is expected to be similar to that of stars, *i.e.*, a few hundred kilometers per second at the location of our solar system. For these velocities, WIMPs interact with ordinary matter through elastic scattering on nuclei. With expected WIMP masses in the range 10 GeV to 10 TeV, typical nuclear recoil energies are of order of 1 to 100 keV.

The shape of the nuclear recoil spectrum results from a convolution of the WIMP velocity distribution, usually taken as a Maxwellian distribution in the galactic rest frame, shifted into the Earth rest frame, with the angular scattering distribution, which is isotropic to first approximation but forward-peaked for high nuclear mass (typically higher than Ge mass) due to the nuclear form factor. Overall, this results in a roughly exponential spectrum. The higher the WIMP mass, the higher the mean value of the exponential. This points to the need for low nuclear energy threshold detectors.

On the other hand, expected interaction rates depend on the product of the local WIMP flux and the interaction cross section. The first term is fixed by the local density of dark matter, taken as 0.3 GeV/cm^3 (see above), the mean WIMP velocity, typically 220 km/s, and the mass of the WIMP. The expected interaction rate then mainly depends on two unknowns, the mass and cross section of the WIMP (with some uncertainty [5] due to the halo model). This is why the experimental observable, which is basically the scattering rate as a function of energy, is usually expressed as a contour in the WIMP mass-cross section plane.

The cross section depends on the nature of the couplings. For non-relativistic WIMPs, one in general has to distinguish spin-independent and spin-dependent couplings. The former can involve scalar and vector WIMP and nucleon currents (vector currents are

absent for Majorana WIMPs, *e.g.*, the neutralino), while the latter involve axial vector currents (and obviously only exist if χ carries spin). Due to coherence effects, the spin-independent cross section scales approximately as the square of the mass of the nucleus, so higher mass nuclei, from Ge to Xe, are preferred for this search. For spin-dependent coupling, the cross section depends on the nuclear spin factor; used target nuclei include ^{19}F , ^{23}Na , ^{73}Ge , ^{127}I , ^{129}Xe , ^{131}Xe , and ^{133}Cs .

Cross sections calculated in MSSM models induce rates of at most $1 \text{ evt day}^{-1} \text{ kg}^{-1}$ of detector, much lower than the usual radioactive backgrounds. This indicates the need for underground laboratories to protect against cosmic ray induced backgrounds, and for the selection of extremely radio-pure materials.

The typical shape of exclusion contours can be anticipated from this discussion: at low WIMP mass, the sensitivity drops because of the detector energy threshold, whereas at high masses, the sensitivity also decreases because, for a fixed mass density, the WIMP flux decreases $\propto 1/m_\chi$. The sensitivity is best for WIMP masses near the mass of the recoiling nucleus.

22.2.4. Status and prospects of direct WIMP searches :

The first searches have been performed with ultra-pure semiconductors installed in pure lead and copper shields in underground environments [32]. Combining a priori excellent energy resolutions and very pure detector material, they produced the first limits on WIMP searches (Heidelberg-Moscow, IGEX, COSME-II, HDMS) [32]. Without positive identification of nuclear recoil events, however, these experiments could only set limits, *e.g.*, excluding sneutrinos as major component of the galactic halo. Still, planned experiments using several tens of kg to a ton of Germanium (many of which were designed for double-beta decay search)—GERDA, MAJORANA—are based on only passive reduction of the external and internal electromagnetic and neutron background by using segmented detectors, minimal detector housing, close electronics, and large liquid nitrogen shields. Their sensitivity to WIMP interactions will depend on their ability to lower the energy threshold sufficiently, while keeping the background rate small.

To make further progress, active background rejection and signal identification questions have to be addressed. This has been the focus of many recent investigations and improvements. Active background rejection in detectors relies on the relatively small ionization in nuclear recoils due to their low velocity. This induces a reduction—quenching—of the ionization/scintillation signal for nuclear recoil signal events relative to e or γ induced backgrounds. Energies calibrated with gamma sources are then called “electron equivalent energies” (eee). This effect has been both calculated and measured [32]. It is exploited in cryogenic detectors described later. In scintillation detectors, it induces in addition a difference in decay times of pulses induced by e/γ events vs nuclear recoils. Due to the limited resolution and discrimination power of this technique at low energies, this effect allows only a statistical background rejection. It has been used in NaI(Tl) (DAMA, LIBRA, NAIAD, Saclay NaI), in CsI(Tl)(KIMS), and Xe (ZEPLIN I) [32]. No observation of nuclear recoils has been reported by these experiments.

Two experimental signatures are predicted for true WIMP signals. One is a strong daily forward/backward asymmetry of the nuclear recoil direction, due to the alternate sweeping of the WIMP cloud by the rotating Earth. Detection of this effect requires gaseous detectors or anisotropic response scintillators (stilbene). The second is a few percent annual modulation of the recoil rate due to the Earth speed adding to or subtracting from the speed of the Sun. This tiny effect can only be detected with large masses; nuclear recoil identification should also be performed, as the much larger background may also be subject to seasonal modulation.

The DAMA experiment operating 100 kg of NaI(Tl) in Gran Sasso has observed, with a statistical significance of 6.3σ , an annually modulated signal with the expected phase, over a period of 7 years with a total exposure of around 100 000 kg·d, in the 2 to 6 keV (eee) energy interval [33]. This effect is attributed to a WIMP signal by the authors. If interpreted within the standard halo model described above, it would require a WIMP with $m_\chi \simeq 50 \text{ GeV}$ and

$\sigma_{\chi p} \simeq 7 \cdot 10^{-6} \text{ pb}$ (central values). This interpretation has, however, several unaddressed implications. In particular, the expected nuclear recoil rate from WIMPs should be of the order of 50% of the total measured rate in the 2–3 keV (eee) bin and 7% in the 4–6 keV (eee) bin. The rather large WIMP signal should be detectable by the pulse shape analysis. Moreover, the remaining, presumably e/γ -induced, background would have to rise with energy; no explanation for this is given by the authors. The extended version of DAMA, LIBRA, is now taking data with 250 kg of NaI(Tl) in Gran Sasso; results are scheduled to be published in 2008.

Annual modulation has also been searched for by NaI-32 (Zaragoza), DEMOS (Ge), and ELEGANTS (NaI) [32]. No signal has been seen in these experiments, but their sensitivity is too low to contradict DAMA. By taking advantage of an efficient pulse shape discrimination at low energies in CsI(Tl) scintillators, KIMS, operating four crystals with a total mass of 34.8 kg in the Yang Yang Lab in Korea, currently provides the best limit on pure proton spin-dependent couplings [39]. The same data also exclude the hypothesis that the modulation observed by DAMA is due to interactions occurring on iodine nuclei, that is the “classical” solution of a 60 GeV WIMP, under identical assumptions of form factors, galaxy halos *etc.*, used by the DAMA Collaboration.

New limits on the spin-independent coupling of WIMPs were obtained by the CDMS collaboration, which has operated Ge cryogenic detectors at the Soudan mine, during two runs involving exposures of respectively 19 and 34 kg·d after cuts [34]. They supercede their own earlier results as well as those of EDELWEISS, also obtained with cryogenic Ge detectors in the deep underground Fréjus lab [35]. The simultaneous measurement of the phonon signal and the ionization signal in such semiconductor detectors permits event by event discrimination between nuclear and electronic recoils down to 5 to 10 keV recoil energy. In addition, advanced rejection techniques allowed CDMS to reject surface detector interactions, which can mimic nuclear recoils. Assuming conventional WIMP halo parameters described above, and spin-independent coupling WIMP interactions, the CDMS limit and DAMA signal are clearly incompatible. Varying the halo parameters, and/or including spin-dependent interactions compatible with the neutrino flux limit from the Sun, does not allow reconciliation of both results without finetuning [36]. The obtained sensitivity of $\sigma_{\chi p} \simeq 1.6 \cdot 10^{-7} \text{ pb}$ for a WIMP mass of 60 GeV tests the upper range of cross sections that can be accommodated in the MSSM [37].

CDMS also provides the best sensitivity for spin-dependent WIMP-neutron interactions thanks to the ^{73}Ge (^{29}Si) content of natural Germanium (Silicon) [38].

Other cryogenic experiments like CRESST and ROSEBUD [40] use the scintillation of CaWO_4 or other inorganic scintillators as second variable for background discrimination, while CUORICINO is using TeO_2 in the purely thermal mode. The cryogenic experimental programs of CDMS II, EDELWEISS II, CRESST II, and CUORICINO [40] intend to increase their sensitivity by a factor of 100, by operating from a few to 40 kg of detectors.

Considerable progress has been made by noble gas detectors in the last few years [41]. In particular, dual (liquid and gas) phase detectors allow to measure both the primary scintillation and the ionization electrons drifted through the liquid and amplified in the gas, which can be used for background rejection.

The best current limit worldwide on spin-independent couplings of WIMPs for all masses above 10 GeV has been obtained by the XENON-10 experiment, a 15-kg dual-phase Xenon TPC with 5.4 kg of fiducial mass run at the Gran Sasso laboratory [42]. Thanks to a very low threshold of 4 keV recoil energy and the high A of Xenon nuclei, a limit of about $\sigma_{\chi p} \simeq 4(9) \cdot 10^{-8} \text{ pb}$ has been set for WIMP mass of 30 (100) GeV, even if all ten events observed in the region of interest are interpreted as being due to WIMP scattering. Since a similar number of background events is expected, no signal has been claimed.

ZEPLIN II, using the same principle and with a total mass of 31 kg, has been operated in the Boulby laboratory and reports a lower sensitivity. XMASS in Japan has operated a single-phase 100

kg detector (few kg fiducial mass) at the SuperKamiokande site, and demonstrated the self-shielding effect to lower the background [32]. They are starting to build an 800 kg (100 kg fiducial mass) detector. These projects will scale up to 100 kg or ton scale with the hope of getting a large gain in sensitivity, provided the background decreases accordingly.

Good progress has also been made with liquid Argon detectors by the WARP group, who operated a 3.2-kg double-phase prototype in Gran Sasso. Thanks to a double-background rejection method based on the asymmetry between scintillating and ionizing pulses and pulse shape discrimination of scintillating pulses, they could achieve very high background rejection, even in the presence of the radioactive isotope ^{39}Ar , although with a final sensitivity still lower than that of CDMS or XENON. The ArDM project will use similar technique with a much larger (1,100 kg) volume. Many other projects (CLEAN, DEAP, HPGS, and SIGN) are emerging with the aim of using Argon, Xenon, or Neon in liquid, double-phase, or high-pressure gas form [41].

There is also continuous work in the development of a low pressure Time Projection Chamber, the only convincing technique to measure the direction of nuclear recoils [43]. DRIFT, a 1 m³ volume detector, has been operated underground, but with high background due to internal radon contamination. A sub-keV energy threshold gaseous detector using Helium 3, the Mimac project, is being investigated for WIMP searches [43]. Other exotic techniques include the superheated droplet detectors SIMPLE and PICASSO, which has obtained interesting limits on spin-dependent couplings; an ultra cold pure ^3He detector (ULTIMA) has been operated with a very small sensitive mass; and a bubble chamber like detector, COUPP, run at Fermilab [41].

Sensitivities down to $\sigma_{\chi p}$ of 10^{-10} pb, as needed to probe large regions of MSSM parameter space [37], can be reached with detectors of typical masses of 1 ton [40], assuming nearly perfect background discrimination capabilities. More and more projects are envisaged such EURECA, (European multi-array, multi-target 1 ton cryogenic set up), ELIXIR (European 1 t liquid Xenon), and LUX (US 300 kg liquid Xenon) [32]. Note that the expected WIMP rate is then 5 evts/ton/year for Ge. The ultimate neutron background will only be identified by its multiple interactions in a finely segmented or multiple-interaction-sensitive detector, and/or by operating detectors containing different target materials within the same set-up. Information on various neutron background calculations and measurements can be found in [44]. With an intermediate mass of 10 to 30 kg, and therefore less efficient multiple interaction detection, a muon veto seems mandatory in most existing underground laboratories.

22.2.5. Status and prospects of indirect WIMP searches :

WIMPs can annihilate and their annihilation products can be detected; these include neutrinos, gamma rays, positrons, antiprotons, and antinuclei [45]. These methods are complementary to direct detection and can explore higher masses and different coupling scenarios. “Smoking gun” signals for indirect detection are neutrinos coming from the center of the Sun or Earth, and monoenergetic photons from the halo.

WIMPs can be slowed down, captured, and trapped in celestial objects like the Earth or the Sun, thus enhancing their density and their probability of annihilation. This is a source of muon neutrinos which can interact in the Earth. Upward going muons can then be detected in large neutrino telescopes such as MACRO, BAKSAN, SuperKamiokande, Baikal, AMANDA, ANTARES, NESTOR, and the future large sensitive area IceCube [45]. The best upper limits, of $\simeq 1000$ muons/km²/year, have been set by SuperKamiokande [46]. However, at least in the framework of the MSSM and with standard halo velocity profiles, only the limits from the Sun, which mostly probe spin-dependent couplings, are competitive with direct WIMP search limits. ANTARES (IceCube) will increase this sensitivity respectively by \simeq one (two) order(s) of magnitude.

WIMP annihilation in the halo can give a continuous spectrum of gamma rays and (at one-loop level) also monoenergetic photon contributions from the $\gamma\gamma$ and γZ channels. These channels also allow

to search for WIMPs for which direct detection experiments have little sensitivity, *e.g.*, almost pure higgsinos. However, the size of this signal depends very strongly on the halo model, but is expected to be most prominent towards the galactic center. Existing limits come from the EGRET satellite below 10 GeV, and from the WHIPPLe ground based telescope above 100 GeV [47]. However, only the planned space mission GLAST will be able to provide competitive SUSY sensitivities in both the continuous and γ line channels. Also, Atmospheric Cherenkov Telescopes like MAGIC, VERITAS, and H.E.S.S. should be able to test some SUSY models, at large WIMP mass, for halo models showing a significant WIMP enhancement at the galactic center [45]. H.E.S.S. has actually observed a featureless spectrum, well described by a power law extending beyond 20 TeV [48]. This is most likely due to an astrophysical source, which thus contributes a large background to searches for photons from WIMP annihilation near the center of our galaxy. At the other end of the mass spectrum, a WIMP mass below 20 MeV would be required to explain the excess of 511 keV gamma rays from an extended region around the galactic center observed by INTEGRAL [49].

Diffuse continuum gammas could also give a signature due to their anisotropic distribution tracking the halo density as seen from Earth. According to [50], a re-analysis of EGRET data shows an excess in the energy spectrum at the GeV range, if one normalizes the experimental spectrum to that expected from model calculations at lower energies, assuming that the cosmic ray spectrum has the same shape (but different normalization) everywhere in our galaxy. The excess can be explained in terms of WIMP annihilation, with WIMP mass near 80 GeV, only if one assumes a rather clumpy halo; this can boost the signal by a large factor, since it scales $\propto \rho_{\text{DM}}^2$. However, this interpretation is still under debate. The observation could also be due to astrophysical sources (*e.g.*, due to a location-dependent shape of the cosmic ray spectrum). Moreover, the measurement should be reproduced by an independent instrument before strong conclusions are drawn.

Antiprotons arise as another WIMP annihilation product in the halo. The signal is expected to be detectable above background only at very low energies. The BESS balloon-borne experiment indeed observed antiprotons below 1 GeV [51]. However, the uncertainties in the calculation of the expected signal and background energy spectra are too large to reach a firm conclusion. Precision measurements by the future experiments BESS, AMS2, and PAMELA – which has actually been launched in June 2006 – may allow to disentangle signal and background [45].

A cosmic-ray positron flux excess at around 8 GeV measured by HEAT [52] has given rise to numerous calculations and conjectures concerning a possible SUSY interpretation. The need for an ad-hoc “boost” of the expected flux to match the observed one, and the failure to reproduce the energy shape by including a component from WIMP annihilation, are illustrative of the difficulty to assign a Dark Matter origin to such measurements.

Last but not least, an antideuteron signal [53], as potentially observable by AMS2 or PAMELA, could constitute a signal for WIMP annihilation in the halo.

An interesting comparison of respective sensitivities to MSSM parameter space of future direct and various indirect searches has been performed with the DARKSUSY tool [54]. A web-based up-to-date collection of results from direct WIMP searches, theoretical predictions, and sensitivities of future experiments can be found in Ref. 55. Also, a new web page, initiated by ILIAS, a European underground science and infrastructure network, allows to make predictions for WIMP signals in various experiments, within a variety of SUSY models. Its long-term goal is to propose an interactive integrated analysis of all relevant data. These should ultimately include not only data from direct and indirect WIMP detection experiments, but also from high-energy colliders such as the LHC. If a positive WIMP signal is found anywhere, such a comprehensive approach will be required to fully unravel the mysteries of dark matter.

References:

1. For a brief but delightful history of DM, see V. Trimble, in *Proceedings of the First International Symposium on Sources of Dark Matter in the Universe*, Bel Air, California, 1994, published by World Scientific, Singapore (ed. D.B. Cline). See also the recent review G. Bertone, D. Hooper, and J. Silk, *Phys. Rep.* **405**, 279 (2005).
2. See *Cosmological Parameters* in this *Review*.
3. B. Paczynski, *Astrophys. J.* **304**, 1 (1986); K. Griest, *Astrophys. J.* **366**, 412 (1991).
4. F. De Paolis *et al.*, *Phys. Rev. Lett.* **74**, 14 (1995).
5. M. Kamionkowski and A. Kinkhabwala, *Phys. Rev.* **D57**, 3256 (1998).
6. See *e.g.*, J.R. Primack, in the *Proceedings of Midrasha Mathematicae in Jerusalem: Winter School in Dynamical Systems*, Jerusalem, Israel, January 1997, *astro-ph/9707285*. There is currently some debate whether cold DM models correctly reproduce the DM density profile near the center of galactic haloes. See *e.g.*, R.A. Swaters *et al.*, *Astrophys. J.* **583**, 732 (2003).
7. B.J. Carr and S.W. Hawking, *MNRAS* **168**, 399 (1974).
8. See *Axions and Other Very Light Bosons* in this *Review*.
9. R.A. Battye and E.P.S. Shellard, *Phys. Rev. Lett.* **73**, 2954 (1994); Erratum-*ibid.* **76**, 2203 (1996).
10. E.W. Kolb and M.E. Turner, *The Early Universe*, Addison-Wesley (1990).
11. For a review, see G. Jungman, M. Kamionkowski, and K. Griest, *Phys. Reports* **267**, 195 (1996).
12. See *Searches for WIMPs and Other Particles* in this *Review*.
13. S. Dimopoulos, G.F. Giudice, and A. Pomarol, *Phys. Lett.* **B389**, 37 (1996).
14. See *e.g.*, J.R. Ellis *et al.*, *Nucl. Phys.* **B652**, 259 (2003); J.R. Ellis *et al.*, *Phys. Lett.* **B565**, 176 (2003); H. Baer *et al.*, *JHEP* **0306**, 054 (2003); A. Bottino *et al.*, *Phys. Rev.* **D68**, 043506 (2003).
15. K. Griest and D. Seckel, *Phys. Rev.* **D43**, 3191 (1991).
16. See *e.g.*, A. Birkedal *et al.*, *Phys. Rev.* **D74**, 035002 (2006).
17. See *e.g.*, S. B. Gudnason, C. Kouvaris and F. Sannino, *Phys. Rev.* **D74**, 095008 (2006).
18. T. Moroi and L. Randall, *Nucl. Phys.* **B570**, 455 (2000).
19. R. Allahverdi and M. Drees, *Phys. Rev. Lett.* **89**, 091302 (2002).
20. M. Fujii and T. Yanagida, *Phys. Lett.* **B542**, 80 (2002).
21. J. Hisano, K. Kohri, and M.M. Nojiri, *Phys. Lett.* **B505**, 169 (2001); X. Chen, M. Kamionkowski, and X. Zhang, *Phys. Rev.* **D64**, 021302 (2001).
22. M. Bolz, W. Buchmüller, and M. Plümacher, *Phys. Lett.* **B443**, 209 (1998).
23. L. Covi *et al.*, *JHEP* **0105**, 033 (2001).
24. MACHO Collab., C. Alcock *et al.*, *Astrophys. J.* **542**, 257 (2000); EROS Collab., *AA* **469**, 387 (2007); OGLE Collab., *AA* **343**, 10 (1999).
25. P. Sikivie, *Phys. Rev. Lett.* **51**, 1415 (1983), Erratum-*ibid.* **52**, 695 (1984).
26. H. Peng *et al.*, *Nucl. Instrum. Methods* **A444**, 569 (2000).
27. S. Asztalos *et al.*, *Phys. Rev.* **D69**, 011101 (2004).
28. L.D. Duffy *et al.*, *Phys. Rev.* **D74**, 012006 (2006).
29. M. Tada *et al.*, *physics/0101028*.
30. K. Yamamoto *et al.*, in *Heidelberg 2000, Dark matter in astro- and particle-physics*, *hep-ph/0101200*.
31. P.F. Smith and J.D. Lewin, *Phys. Reports* **187**, 203 (1990); J.R. Primack, D. Seckel, and B. Sadoulet, *Ann. Rev. Nucl. Part. Sci.* **38** 751 (1988); R.J. Gaitskell, *Ann. Rev. Nucl. and Part. Sci.* **54**, 315 (2004).
32. For recent reviews on non cryogenic detectors, see *e.g.*, A. Morales, *Nucl. Phys. (Proc. Suppl.)* **B138** 135 (2005); *Proceedings of Topics in Astroparticles and Underground Physics TAUP 2005*, *J. Phys. Conf. Ser.* **39**, (2006); *Proceedings of Identification of Dark Matter*. IDM 2004, World Scientific, ed. N. Spooner and V. Kudryavtsev (York, UK, 2004).
33. DAMA Collab., R. Bernabei *et al.*, *Phys. Lett.* **B480**, 23 (2000), and *Riv. Nuovo Cimento* **26**, 1 (2003).
34. CDMS Collab., D.S. Akerib *et al.*, *Phys. Rev. Lett.* **96**, 011302 (2006).
35. EDELWEISS Collab., A. Benoit *et al.*, *Phys. Rev.* **D71**, 122002 (2005).
36. C.J. Copi and L.M. Krauss, *Phys. Rev.* **67**, 103507 (2003); G. Gelmini and P. Gondolo, *Phys. Rev.* **D71**, 123520 (2005); A. Kurylov and M. Kamionkowski, *Phys. Rev.* **D69**, 063503 (2004); C.J. Copi and L.M. Krauss, *New Astron. Rev.* **49**, 185 (2005).
37. For a general introduction to SUSY, see the section devoted in this *Review of Particle Physics*. For a review on cross sections for direct detection, see J. Ellis *et al.*, *Phys. Rev.* **D67**, 123502 (2003) and for a recent update *Phys. Rev.* **D71**, 095007 (2005).
38. CDMS Collab., D.S. Akerib *et al.*, *Phys. Rev. D* **73**, 011102 (2006).
39. KIMS Collab., H.S. Lee *et al.*, *Phys. Rev. Lett.* **99**, 091301 (2007).
40. For a recent review on cryogenic detectors, see *e.g.*, W. Seidel, *Nucl. Phys. (Proc. Suppl.)* **B138** 130 (2005). In addition to the TAUP and IDM Conference Proceedings, see also the *Proceedings of Int. Workshop on Low Temperature Detectors*, LTD10, NIM A (2003).
41. For recent reviews on noble gas detectors, in addition to IDM and TAUP proceedings, see also the *Proceedings of 6th UCLA Symposium on Sources and Detection of Dark Matter and Dark Energy in the Universe*, *New Astron. Rev.* **49** (2005), and the web page of *Symposium on Hunt for Dark Matter*, Fermilab, June 2007, <http://conferences.fnal.gov/dmwksp/>.
42. XENON10 Collab., E. Aprile *et al.*, [arXiv:0706.0039](http://arxiv.org/abs/0706.0039) [*astro-ph*] (2007), submitted to *Phys. Rev. Lett.*
43. Workshop on large TPC for low energy rare event detection, Paris, December 2006, <http://www-tpc-paris.cea.fr/>.
44. These sites gather informations on neutrons from various underground labs: <http://www.physics.ucla.edu/wimps/nBG/nBG.html>; <http://iliac-darkmatter.uni-tuebingen.de/BSNS.WG.html>.
45. L. Bergstrom, Rept. on Prog. in Phys. **63**, 793 (2000); L. Bergstrom *et al.*, *Phys. Rev.* **D59**, 043506 (1999); C. Tao, *Phys. Scripta* **T93**, 82 (2001); Y. Mambrini and C. Muoz, *Journ. of Cosm. And Astrop. Phys.*, **10**, 3(2004).
46. SuperKamiokande Collab., S. Desai *et al.*, *Phys. Rev.* **D70**, 109901 (2004).
47. EGRET Collab., D. Dixon *et al.*, *New Astron.* **3**, 539 (1998).
48. H.E.S.S. Collab., F.A. Aharonian *et al.*, *Phys. Rev. Lett.* **97**, 221102 (2006); Erratum-*ibid.* **97**, 249901 (2006).
49. C. Boehm *et al.*, *Phys. Rev. Lett.* **92**, 101301 (2004).
50. W. de Boer *et al.*, *Astron. Astrophys.* **444** (2005) 51, and *Phys. Lett.* **B636**, 13 (2006).
51. BESS Collab., S. Orito *et al.*, *Phys. Rev. Lett.* **84**, 1078 (2000).
52. HEAT Collab., S. W. Barwick *et al.*, *Astrophys. J.* **482**, L191 (2000).
53. F. Donato, N. Fornengo, and P. Salati, *Phys. Rev.* **D62**, 043003 (2000).
54. DARKSUSY site: <http://www.physto.se/edsjo/darksusy/>.
55. <http://dmtools.brown.edu>.
56. ILIAS web page: <http://pisrv0.pit.physik.uni-tuebingen.de/darkmatter/>.

23. COSMIC MICROWAVE BACKGROUND

Revised August 2007 by D. Scott (University of British Columbia) and G.F. Smoot (UCB/LBNL).

23.1. Introduction

The energy content in radiation from beyond our Galaxy is dominated by the Cosmic Microwave Background (CMB), discovered in 1965 [1]. The spectrum of the CMB is well described by a blackbody function with $T = 2.725$ K. This spectral form is one of the main pillars of the hot Big Bang model for the early Universe. The lack of any observed deviations from a blackbody spectrum constrains physical processes over cosmic history at redshifts $z \lesssim 10^7$ (see earlier versions of this mini-review). However, at the moment, all viable cosmological models predict a very nearly Planckian spectrum, and so are not stringently limited.

Another observable quantity inherent in the CMB is the variation in temperature (or intensity) from one part of the microwave sky to another [2]. Since the first detection of these anisotropies by the COBE satellite [3], there has been intense activity to map the sky at increasing levels of sensitivity and angular resolution by ground-based and balloon-borne measurements. These were joined in 2003 by the first results from NASA's Wilkinson Microwave Anisotropy Probe (WMAP) [4], which were improved upon by analysis of the 3 year WMAP data [5]. Together these observations have led to a stunning confirmation of the 'Standard Model of Cosmology.' In combination with other astrophysical data, the CMB anisotropy measurements place quite precise constraints on a number of cosmological parameters, and have launched us into an era of precision cosmology.

23.2. Description of CMB Anisotropies

Observations show that the CMB contains anisotropies at the 10^{-5} level, over a wide range of angular scales. These anisotropies are usually expressed by using a spherical harmonic expansion of the CMB sky:

$$T(\theta, \phi) = \sum_{\ell m} a_{\ell m} Y_{\ell m}(\theta, \phi).$$

The vast majority of the cosmological information is contained in the temperature 2-point function, *i.e.*, the variance as a function of separation θ . Equivalently, the power per unit $\ln \ell$ is $\ell \sum_m |a_{\ell m}|^2 / 4\pi$.

23.2.1. The Monopole :

The CMB has a mean temperature of $T_\gamma = 2.725 \pm 0.001$ K (1σ) [6], which can be considered as the monopole component of CMB maps, a_{00} . Since all mapping experiments involve difference measurements, they are insensitive to this average level. Monopole measurements can only be made with absolute temperature devices, such as the FIRAS instrument on the COBE satellite [6]. Such measurements of the spectrum are consistent with a blackbody distribution over more than three decades in frequency. A blackbody of the measured temperature corresponds to $n_\gamma = (2\zeta(3)/\pi^2) T_\gamma^3 \simeq 411 \text{ cm}^{-3}$ and $\rho_\gamma = (\pi^2/15) T_\gamma^4 \simeq 4.64 \times 10^{-34} \text{ g cm}^{-3} \simeq 0.260 \text{ eV cm}^{-3}$.

23.2.2. The Dipole :

The largest anisotropy is in the $\ell = 1$ (dipole) first spherical harmonic, with amplitude 3.358 ± 0.017 mK [7]. The dipole is interpreted to be the result of the Doppler shift caused by the solar system motion relative to the nearly isotropic blackbody field, as confirmed by measurements of the radial velocities of local galaxies [8]. The motion of an observer with velocity $\beta \equiv v/c$ relative to an isotropic Planckian radiation field of temperature T_0 produces a Doppler-shifted temperature pattern

$$\begin{aligned} T(\theta) &= T_0(1 - \beta^2)^{1/2} / (1 - \beta \cos \theta) \\ &\simeq T_0 \left(1 + \beta \cos \theta + (\beta^2/2) \cos 2\theta + O(\beta^3) \right). \end{aligned}$$

At every point in the sky, one observes a blackbody spectrum, with temperature $T(\theta)$. The spectrum of the dipole is the differential of a blackbody spectrum, as confirmed by Ref. 9.

The implied velocity for the solar system barycenter is $v = 369 \pm 2 \text{ km s}^{-1}$, assuming a value $T_0 = T_\gamma$, towards $(\ell, b) = (263.86^\circ \pm 0.04^\circ, 48.24^\circ \pm 0.10^\circ)$ [10,7]. Such a solar system motion

implies a velocity for the Galaxy and the Local Group of galaxies relative to the CMB. The derived value is $v_{\text{LG}} = 627 \pm 22 \text{ km s}^{-1}$ towards $(\ell, b) = (276^\circ \pm 3^\circ, 30^\circ \pm 3^\circ)$, where most of the error comes from uncertainty in the velocity of the solar system relative to the Local Group.

The dipole is a frame-dependent quantity, and one can thus determine the 'absolute rest frame' as that in which the CMB dipole would be zero. Our velocity relative to the Local Group, as well as the velocity of the Earth around the Sun, and any velocity of the receiver relative to the Earth, is normally removed for the purposes of CMB anisotropy study.

23.2.3. Higher-Order Multipoles :

The variations in the CMB temperature maps at higher multipoles ($\ell \geq 2$) are interpreted as being mostly the result of perturbations in the density of the early Universe, manifesting themselves at the epoch of the last scattering of the CMB photons. In the hot Big Bang picture, the expansion of the Universe cools the plasma so that by a redshift $z \simeq 1100$ (with little dependence on the details of the model), the hydrogen and helium nuclei can bind electrons into neutral atoms, a process usually referred to as recombination [11]. Before this epoch, the CMB photons are tightly coupled to the baryons, while afterwards they can freely stream towards us.

Theoretical models generally predict that the $a_{\ell m}$ modes are Gaussian random fields to high precision, *e.g.*, standard slow-roll inflation's non-Gaussian contribution is expected to be one or two orders of magnitude below current observational limits [12]. Although non-Gaussianity of various forms is possible in early Universe models, tests show that Gaussianity is an extremely good simplifying approximation [14,15], with only some relatively weak indications of non-Gaussianity or statistical anisotropy at large scales. Such signatures found in existing WMAP data are generally considered to be subtle foreground or instrumental artefacts [13,16].

With the assumption of Gaussian statistics, and if there is no preferred axis, then it is the variance of the temperature field which carries the cosmological information, rather than the values of the individual $a_{\ell m}$ s; in other words the power spectrum in ℓ fully characterizes the anisotropies. The power at each ℓ is $(2\ell + 1)C_\ell / (4\pi)$, where $C_\ell \equiv \langle |a_{\ell m}|^2 \rangle$, and a statistically isotropic sky means that all m s are equivalent. Thus averages over m can be used as estimators of the C_ℓ s to constrain their expectation values, which are the quantities predicted by a theoretical model. For an idealized full-sky observation, the variance of each measured C_ℓ (*i.e.*, the variance of the variance) is $[2/(2\ell + 1)]C_\ell^2$. This sampling uncertainty (known as 'cosmic variance') comes about because each C_ℓ is χ^2 distributed with $(2\ell + 1)$ degrees of freedom for our observable volume of the Universe. For fractional sky coverage, f_{sky} , this variance is increased by $1/f_{\text{sky}}$ and the modes become partially correlated.

It is important to understand that theories predict the expectation value of the power spectrum, whereas our sky is a single realization. Hence the cosmic variance is an unavoidable source of uncertainty when constraining models; it dominates the scatter at lower ℓ s, while the effects of instrumental noise and resolution dominate at higher ℓ s [17].

23.2.4. Angular Resolution and Binning :

There is no one-to-one conversion between multipole ℓ and the angle subtended by a particular spatial scale projected onto the sky. However, a single spherical harmonic $Y_{\ell m}$ corresponds to angular variations of $\theta \sim \pi/\ell$. CMB maps contain anisotropy information from the size of the map (or in practice some fraction of that size) down to the beam-size of the instrument, σ . One can think of the effect of a Gaussian beam as rolling off the power spectrum with the function $e^{-\ell(\ell+1)\sigma^2}$.

For less than full sky coverage, the ℓ modes become correlated. Hence, experimental results are usually quoted as a series of 'band powers', defined as estimators of $\ell(\ell + 1)C_\ell/2\pi$ over different ranges of ℓ . Because of the strong foreground signals in the Galactic Plane, even 'all-sky' surveys, such as COBE and WMAP involve a cut sky. The amount of binning required to obtain uncorrelated estimates of power also depends on the map size.

23.3. Cosmological Parameters

The current ‘Standard Model’ of cosmology contains around 10 free parameters (see The Cosmological Parameters—Sec. 21 of this *Review*). The basic framework is the Friedmann-Robertson-Walker (FRW) metric (*i.e.*, a universe that is approximately homogeneous and isotropic on large scales), with density perturbations laid down at early times and evolving into today’s structures (see Big-Bang cosmology—Sec. 19 of this *Review*). These perturbations can be initially either ‘adiabatic’ (meaning that there is no change to the entropy per particle for each species, *i.e.*, $\delta\rho/\rho$ for matter is $(3/4)\delta\rho/\rho$ for radiation) or ‘isocurvature’ (meaning that, for example, matter perturbations compensate radiation perturbations so that the total energy density remains unperturbed, *i.e.*, $\delta\rho$ for matter is $-\delta\rho$ for radiation). These different modes give rise to distinct phases during growth, with those of the adiabatic scenario being strongly preferred by the data. Models that generate mainly isocurvature type perturbations (such as most topological defect scenarios) are no longer considered to be viable. However, admixtures of adiabatic and isocurvature modes are still allowed.

Within the adiabatic family of models, there is, in principle, a free function describing how the comoving curvature perturbations, \mathcal{R} , vary with length scale. There are physical reasons to anticipate that the variance of these perturbations will be described well by a power-law in scale, *i.e.*, $\langle|\mathcal{R}|^2\rangle \propto k^{n-4}$, where k is wavenumber and n is the usual definition of spectral index. So-called ‘scale-invariant’ initial conditions (meaning gravitational potential fluctuations which are independent of k) correspond to $n = 1$. In inflationary models [18], perturbations are generated by quantum fluctuations, which are set by the energy scale of inflation, together with the slope and higher derivatives of the inflationary potential. One generally expects that the Taylor series expansion of $\ln \mathcal{R}(\ln k)$ has terms of steadily decreasing size. For the simplest models, there are thus 2 parameters describing the initial conditions for density perturbations: the amplitude and slope of the power spectrum. These can be explicitly defined, for example, through:

$$\Delta_{\mathcal{R}}^2 \equiv (k^3/2\pi^2) \langle|\mathcal{R}|^2\rangle = A (k/k_0)^{n-1},$$

with $A \equiv \Delta_{\mathcal{R}}^2(k_0)$ and $k_0 = 0.002 \text{ Mpc}^{-1}$, say. There are many other equally valid definitions of the amplitude parameter (see also Sec. 19 and Sec. 21 of this *Review*), and we caution that the relationships between some of them can be cosmology-dependent. In ‘slow roll’ inflationary models, this normalization is proportional to the combination $V^3/(V')^2$, for the inflationary potential $V(\phi)$. The slope n also involves V'' , and so the combination of A and n can, in principle, constrain potentials.

Inflation generates tensor (gravity wave) modes, as well as scalar (density perturbation) modes. This fact introduces another parameter, measuring the amplitude of a possible tensor component, or equivalently the ratio of the tensor to scalar contributions. The tensor amplitude is $A_{\text{T}} \propto V$, and thus one expects a larger gravity wave contribution in models where inflation happens at higher energies. The tensor power spectrum also has a slope, often denoted n_{T} , but since this seems likely to be extremely hard to measure, it is sufficient for now to focus only on the amplitude of the gravity wave component. It is most common to define the tensor contribution through r , the ratio of tensor to scalar perturbation spectra at small wavenumbers (say $k = 0.002 \text{ Mpc}^{-1}$); however, there are other definitions, for example in terms of the ratio of contributions to C_2 . Different inflationary potentials will lead to different predictions, *e.g.*, for $\lambda\phi^4$ inflation with 50 e-folds, $r = 0.32$, and for $m^2\phi^2$ inflation $r \simeq 0.15$, while other models can have arbitrarily small values of r . In any case, whatever the specific definition, and whether they come from inflation or something else, the ‘initial conditions’ give rise to a minimum of 3 parameters: A , n , and r .

The background cosmology requires an expansion parameter (the Hubble Constant, H_0 , often represented through $H_0 = 100 h \text{ km s}^{-1} \text{ Mpc}^{-1}$) and several parameters to describe the matter and energy content of the Universe. These are usually given in terms of the critical density, *i.e.*, for species ‘x’, $\Omega_{\text{x}} \equiv \rho_{\text{x}}/\rho_{\text{crit}}$, where $\rho_{\text{crit}} \equiv 3H_0^2/8\pi G$. Since physical densities $\rho_{\text{x}} \propto \Omega_{\text{x}} h^2 \equiv \omega_{\text{x}}$ are what govern the physics of the CMB anisotropies, it is these ω s that are best

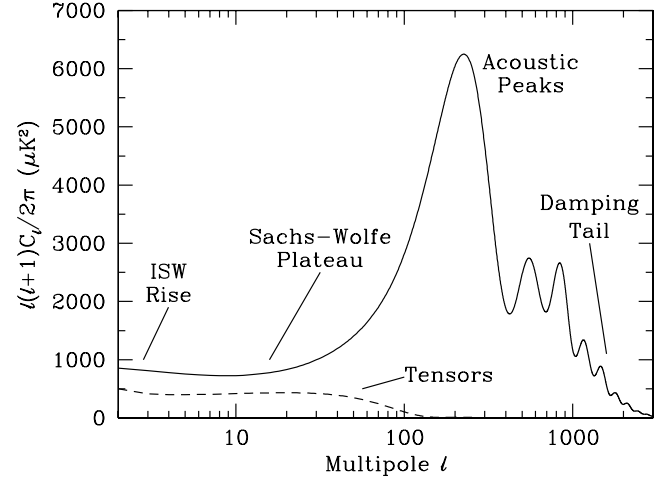


Figure 23.1: The theoretical CMB anisotropy power spectrum, using a standard Λ CDM model from CMBFAST. The x -axis is logarithmic here. The regions, each covering roughly a decade in l , are labeled as in the text: the ISW rise; Sachs-Wolfe plateau; acoustic peaks; and damping tail. Also shown is the shape of the tensor (gravity wave) contribution, with an arbitrary normalization.

constrained by CMB data. In particular CMB observations constrain $\Omega_{\text{B}} h^2$ for baryons and $\Omega_{\text{M}} h^2$ for baryons plus Cold Dark Matter.

The contribution of a cosmological constant Λ (or other form of Dark Energy) is usually included via a parameter which quantifies the curvature, $\Omega_{\text{K}} \equiv 1 - \Omega_{\text{tot}}$, where $\Omega_{\text{tot}} = \Omega_{\text{M}} + \Omega_{\Lambda}$. The radiation content, while in principle a free parameter, is precisely enough determined by the measurement of T_{γ} , and makes a $< 10^{-4}$ contribution to Ω_{tot} today.

The main effect of astrophysical processes on the C_{ℓ} s comes through reionization. The Universe became reionized at some redshift z_{i} , long after recombination, affecting the CMB through the integrated Thomson scattering optical depth:

$$\tau = \int_0^{z_{\text{i}}} \sigma_{\text{T}} n_{\text{e}}(z) \frac{dt}{dz} dz,$$

where σ_{T} is the Thomson cross-section, $n_{\text{e}}(z)$ is the number density of free electrons (which depends on astrophysics), and dt/dz is fixed by the background cosmology. In principle, τ can be determined from the small-scale matter power spectrum, together with the physics of structure formation and feedback processes. However, this is a sufficiently intractable calculation that τ needs to be considered as a free parameter.

Thus, we have 8 basic cosmological parameters: A , n , r , h , $\Omega_{\text{B}} h^2$, $\Omega_{\text{M}} h^2$, Ω_{tot} , and τ . One can add additional parameters to this list, particularly when using the CMB in combination with other data sets. The next most relevant ones might be: $\Omega_{\nu} h^2$, the massive neutrino contribution; w ($\equiv p/\rho$), the equation of state parameter for the Dark Energy; and $dn/d \ln k$, measuring deviations from a constant spectral index. To these 11 one could of course add further parameters describing additional physics, such as details of the reionization process, features in the initial power spectrum, a sub-dominant contribution of isocurvature modes, *etc.*

As well as these underlying parameters, there are other quantities that can be obtained from them. Such derived parameters include the actual Ω s of the various components (*e.g.*, Ω_{M}), the variance of density perturbations at particular scales (*e.g.*, σ_8), the age of the Universe today (t_0), the age of the Universe at recombination, reionization, *etc.*

23.4. Physics of Anisotropies

The cosmological parameters affect the anisotropies through the well understood physics of the evolution of linear perturbations within a background FRW cosmology. There are very effective, fast, and publicly-available software codes for computing the CMB anisotropy, polarization, and matter power spectra, *e.g.*, CMBFAST [19] and CAMB [20]. CMBFAST is the most extensively used code; it has been tested over a wide range of cosmological parameters and is considered to be accurate to better than the 1% level [21].

A description of the physics underlying the C_ℓ s can be separated into 3 main regions, as shown in Fig. 23.1.

23.4.1. The ISW rise, $\ell \lesssim 10$ and Sachs-Wolfe plateau, $10 \lesssim \ell \lesssim 100$:

The horizon scale (or more precisely, the angle subtended by the Hubble radius) at last scattering corresponds to $\ell \simeq 100$. Anisotropies at larger scales have not evolved significantly, and hence directly reflect the ‘initial conditions.’ The combination of gravitational redshift and intrinsic temperature fluctuations leads to $\delta T/T \simeq (1/3)\delta\phi/c^2$, where $\delta\phi$ is the perturbation to the gravitational potential. This is usually referred to as the ‘Sachs-Wolfe’ effect [22].

Assuming that a nearly scale-invariant spectrum of density perturbations was laid down at early times (*i.e.*, $n \simeq 1$, meaning equal power per decade in k), then $\ell(\ell+1)C_\ell \simeq \text{constant}$ at low ℓ s. This effect is hard to see unless the multipole axis is plotted logarithmically (as in Fig. 23.1, but not Fig. 23.2).

Time variation of the potentials (*i.e.*, time-dependent metric perturbations) leads to an upturn in the C_ℓ s in the lowest several multipoles; any deviation from a total equation of state $w = 0$ has such an effect. So the dominance of the Dark Energy at low redshift makes the lowest ℓ s rise above the plateau. This is sometimes called the ‘integrated Sachs-Wolfe effect’ (or ISW rise), since it comes from the line integral of $\dot{\phi}$; it has been confirmed through correlations between the large-angle anisotropies and large-scale structure [23]. Specific models can also give additional contributions at low ℓ (*e.g.*, perturbations in the Dark Energy component itself [24]), but typically these are buried in the cosmic variance.

In principle, the mechanism that produces primordial perturbations could generate scalar, vector, and tensor modes. However, the vector (vorticity) modes decay with the expansion of the Universe. The tensors (transverse trace-free perturbations to the metric) generate temperature anisotropies through the integrated effect of the locally anisotropic expansion of space. Since the tensor modes also redshift away after they enter the horizon, they contribute only to angular scales above about 1° (see Fig. 23.1). Hence some fraction of the low ℓ signal could be due to a gravity wave contribution, although small amounts of tensors are essentially impossible to discriminate from other effects that might raise the level of the plateau. However, the tensors *can* be distinguished using polarization information (see Sec. 23.6).

23.4.2. The acoustic peaks, $100 \lesssim \ell \lesssim 1000$:

On sub-degree scales, the rich structure in the anisotropy spectrum is the consequence of gravity-driven acoustic oscillations occurring before the atoms in the Universe became neutral. Perturbations inside the horizon at last scattering have been able to evolve causally and produce anisotropy at the last scattering epoch, which reflects this evolution. The frozen-in phases of these sound waves imprint a dependence on the cosmological parameters, which gives CMB anisotropies their great constraining power.

The underlying physics can be understood as follows. Before the Universe became neutral, the proton-electron plasma was tightly coupled to the photons, and these components behaved as a single ‘photon-baryon fluid.’ Perturbations in the gravitational potential, dominated by the Dark Matter component, were steadily evolving. They drove oscillations in the photon-baryon fluid, with photon pressure providing most of the restoring force and baryons giving some additional inertia. The perturbations were quite small in amplitude, $O(10^{-5})$, and so evolved linearly. That means each Fourier mode evolved independently, and hence can be described by a driven harmonic oscillator, with frequency determined by the sound speed in the fluid. Thus the fluid density underwent oscillations, giving time

variations in temperature. These combine with a velocity effect which is $\pi/2$ out of phase and has its amplitude reduced by the sound speed.

After the Universe recombined, the radiation decoupled from the baryons and could travel freely towards us. At that point, the phases of the oscillations were frozen-in, and became projected on the sky as a harmonic series of peaks. The main peak is the mode that went through $1/4$ of a period, reaching maximal compression. The even peaks are maximal *under*-densities, which are generally of smaller amplitude because the rebound has to fight against the baryon inertia. The troughs, which do not extend to zero power, are partially filled by the Doppler effect because they are at the velocity maxima.

The physical length scale associated with the peaks is the sound horizon at last scattering, which can be straightforwardly calculated. This length is projected onto the sky, leading to an angular scale that depends on the geometry of space, as well as the distance to last scattering. Hence the angular position of the peaks is a sensitive probe of the spatial curvature of the Universe (*i.e.*, Ω_{tot}), with the peaks lying at higher ℓ in open universes and lower ℓ in closed geometry.

One additional effect arises from reionization at redshift z_i . A fraction of photons (τ) will be isotropically scattered at $z < z_i$, partially erasing the anisotropies at angular scales smaller than those subtended by the Hubble radius at z_i . This corresponds typically to ℓ s above about a few 10s, depending on the specific reionization model. The acoustic peaks are therefore reduced by a factor $e^{-2\tau}$ relative to the plateau.

These peaks were a clear theoretical prediction going back to about 1970 [25]. One can think of them as a snapshot of stochastic standing waves. Since the physics governing them is simple and their structure rich, then one can see how they encode extractable information about the cosmological parameters. Their empirical existence started to become clear around 1994 [26], and the emergence, over the following decade, of a coherent series of acoustic peaks and troughs is a triumph of modern cosmology. This picture has received further confirmation with the recent detection in the power spectrum of galaxies (at redshifts close to zero) of the imprint of these same acoustic oscillations in the baryon component [27].

23.4.3. The damping tail, $\ell \gtrsim 1000$:

The recombination process is not instantaneous, giving a thickness to the last scattering surface. This leads to a damping of the anisotropies at the highest ℓ s, corresponding to scales smaller than that subtended by this thickness. One can also think of the photon-baryon fluid as having imperfect coupling, so that there is diffusion between the two components, and hence the amplitudes of the oscillations decrease with time. These effects lead to a damping of the C_ℓ s, sometimes called Silk damping [28], which cuts off the anisotropies at multipoles above about 2000.

An extra effect at high ℓ s comes from gravitational lensing, caused mainly by non-linear structures at low redshift. The C_ℓ s are convolved with a smoothing function in a calculable way, partially flattening the peaks, generating a power-law tail at the highest multipoles, and complicating the polarization signal [29]. The effects of lensing on the CMB have recently been detected by correlating temperature gradients and small-scale filtered anisotropies from WMAP with lensing potentials traced using radio galaxies [30]. This is an example of a ‘secondary effect,’ *i.e.*, the processing of anisotropies due to relatively nearby structures (see Sec. 23.7.2). Galaxies and clusters of galaxies give several such effects; all are expected to be of low amplitude and typically affect only the highest ℓ s, but they carry additional cosmological information and will be increasingly important as experiments push to higher sensitivity and angular resolution.

23.5. Current Anisotropy Data

There has been a steady improvement in the quality of CMB data that has led to the development of the present-day cosmological model. Probably the most robust constraints currently available come from the combination of the WMAP three year data [15] with smaller scale results from the ACBAR [31], BOOMERANG [32], CBI [33], QUAD [34] and VSA [35] experiments (together with constraints from other cosmological data-sets). We plot power spectrum estimates from these six experiments in Fig. 23.2. Other recent experiments, such as ARCHEOPS [36], DASI [37] and MAXIMA [38] also give powerful

constraints, which are quite consistent with what we describe below. There have been some comparisons among data-sets [39], which indicate very good agreement, both in maps and in derived power spectra (up to systematic uncertainties in the overall calibration for some experiments). This makes it clear that systematic effects are largely under control. However, a fully self-consistent joint analysis of all the current data sets has not been attempted, one of the reasons being that it requires a careful treatment of the overlapping sky coverage.

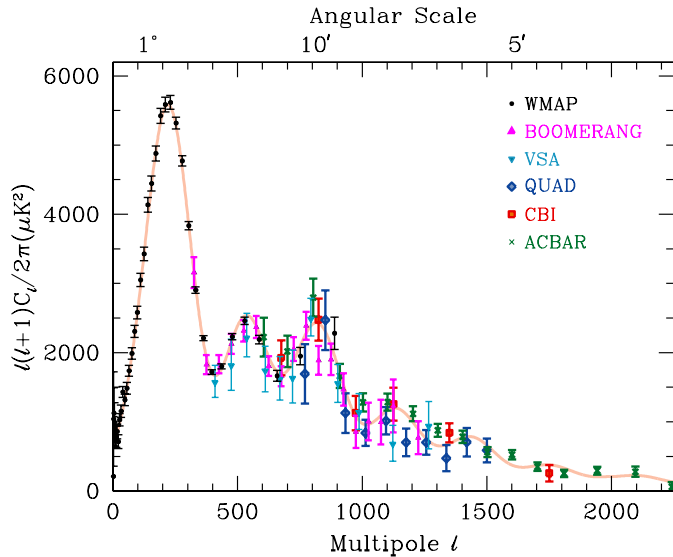


Figure 23.2: Band-power estimates from the WMAP, BOOMERANG, VSA, QUAD, CBI, and ACBAR experiments. Some of the low- ℓ and high- ℓ band-powers which have large error bars have been omitted. Note also that the widths of the ℓ -bands varies between experiments and have not been plotted. This figure represent only a selection of available experimental results, with some other data-sets being of similar quality. The multipole axis here is linear, so the Sachs-Wolfe plateau is hard to see. However, the acoustic peaks and damping region are very clearly observed, with no need for a theoretical curve to guide the eye. Color version at end of book.

Fig. 23.2 shows band-powers from the three year WMAP data [7], together with data from other experiments at higher ℓ . The points are in very good agreement with a ‘ Λ CDM’ type model, as described earlier, with several of the peaks and troughs quite apparent. For details of how these estimates were arrived at, the strength of any correlations between band-powers and other information required to properly interpret them, turn to the original papers.

23.6. CMB Polarization

Since Thomson scattering of an anisotropic radiation field also generates linear polarization, the CMB is predicted to be polarized at the roughly 5% level [40]. Polarization is a spin-2 field on the sky, and the algebra of the modes in ℓ -space is strongly analogous to spin-orbit coupling in quantum mechanics [41]. The linear polarization pattern can be decomposed in a number of ways, with two quantities required for each pixel in a map, often given as the Q and U Stokes parameters. However, the most intuitive and physical decomposition is a geometrical one, splitting the polarization pattern into a part that comes from a divergence (often referred to as the ‘E-mode’) and a part with a curl (called the ‘B-mode’) [42]. More explicitly, the modes are defined in terms of second derivatives of the polarization amplitude, with the Hessian for the E-modes having principle axes in the same sense as the polarization, while the B-mode pattern can be thought of simply as a 45° rotation of the E-mode pattern. Globally one sees that the E-modes have $(-1)^\ell$ parity (like the spherical harmonics), while the B-modes have $(-1)^{\ell+1}$ parity.

The existence of this linear polarization allows for 6 different cross power spectra to be determined from data that measure the

full temperature and polarization anisotropy information. Parity considerations make 2 of these zero, and we are left with 4 potential observables: C_ℓ^{TT} , C_ℓ^{TE} , C_ℓ^{EE} , and C_ℓ^{BB} . Since scalar perturbations have no handedness, the B-mode power spectrum can only be sourced by vectors or tensors. Since inflationary scalar perturbations give only E-modes, while tensors generate roughly equal amounts of E- and B-modes, then the determination of a non-zero B-mode signal is a way to measure the gravity wave contribution (and thus potentially derive the energy scale of inflation), even if it is rather weak. However, one must first eliminate the foreground contributions and other systematic effects down to very low levels.

The oscillating photon-baryon fluid also results in a series of acoustic peaks in the polarization C_ℓ s. The main ‘EE’ power spectrum has peaks that are out of phase with those in the ‘TT’ spectrum, because the polarization anisotropies are sourced by the fluid velocity. The ‘TE’ part of the polarization and temperature patterns comes from correlations between density and velocity perturbations on the last scattering surface, which can be both positive and negative, and is of larger amplitude than the EE signal. There is no polarization ‘Sachs-Wolfe’ effect, and hence no large-angle plateau. However, scattering during a recent period of reionization can create a polarization ‘bump’ at large angular scales.

Because the polarization anisotropies have only a fraction of the amplitude of the temperature anisotropies they took longer to detect. The first measurement of a polarization signal came in 2002 from the DASI experiment [43], which provided a convincing detection, confirming the general paradigm, but of low enough significance that it lent little constraint to models. As well as the E-mode signal, DASI also made a statistical detection of the TE correlation.

In 2003, the WMAP experiment demonstrated that it is able to measure the TE cross-correlation power spectrum with high precision [44], and this was improved upon in the 3-year results, which also included EE measurements [45]. Other recent experimental results include a weak detection of the EE signal from CAPMAP [46], and more significant detections from CBI [47], DASI [48], BOOMERANG [49], and QUAD [34]. In addition, the TE signal has been detected in several multipole bands by BOOMERANG [50] and QUAD [34], and there are statistical detections by CBI [47] and DASI [48]. Some upper limits on C_ℓ^{BB} also exist, but are currently not very constraining.

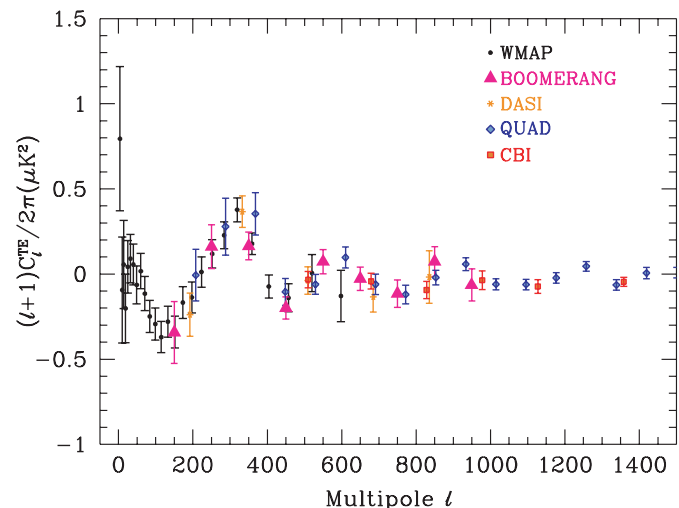


Figure 23.3: Cross power spectrum of the temperature anisotropies and E-mode polarization signal from WMAP [45], together with estimates from BOOMERANG, DASI, QUAD and CBI, which extend to higher ℓ . Note that the BOOMERANG bands are wider in ℓ than those of WMAP, while those of DASI are almost as wide as the features in the power spectrum. Also note that the y -axis here is not multiplied by the additional ℓ , which helps to show both the large and small angular scale features. Color version at end of book.

The results for C_ℓ^{TE} from WMAP [45] are shown in Fig. 23.3, along with data from some other experiments. The measured shape of the

cross-correlation power spectrum provides supporting evidence for the adiabatic nature of the perturbations, as well as directly constraining the thickness of the last scattering surface. Since the polarization anisotropies are generated in this scattering surface, the existence of correlations at angles above about a degree demonstrates that there were super-Hubble fluctuations at the recombination epoch. The sign of this correlation also confirms the adiabatic paradigm.

Fig. 23.4 shows a collection of estimates of C_ℓ^{EE} . Without the benefit of correlating with the temperature anisotropies (*i.e.*, measuring C_ℓ^{TE}), the polarization anisotropies are very weak and challenging to measure. Consequently, the data still require a theoretical power spectrum to guide the eye. Nevertheless, there is a highly significant overall detection which is consistent with expectation, and the new QUAD data convincingly show the peak at $\ell \simeq 400$ (corresponding to the first trough in C_ℓ^{TT}).

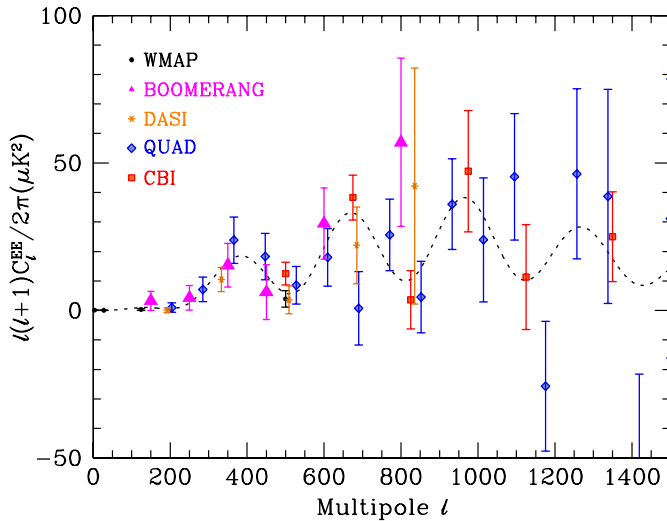


Figure 23.4: Power spectrum of E-mode polarization from several different experiments, plotted along with the theoretical model using parameters which fit the WMAP temperature and polarization data. Color version at end of book.

The most distinctive result from the polarization measurements is at the largest angular scales ($\ell < 10$) in C_ℓ^{TE} , where there is an excess signal compared to that expected from the temperature power spectrum alone. This is precisely the signal anticipated from an early period of reionization, arising from Doppler shifts during the partial scattering at $z < z_i$. This signal is also confirmed in the WMAP C_ℓ^{EE} results at $\ell = 2-6$. The amplitude of the signal indicates that the first stars, presumably the source of the ionizing radiation, formed around $z \simeq 10$ (somewhat lower than the value suggested by the first year WMAP results, although the uncertainty is still quite large). Since this corresponds to scattering optical depth $\tau \simeq 0.1$, then roughly 10% of CMB photons were rescattered at the reionization epoch, with the other 90% last scattering at $z \simeq 1100$.

23.7. Complications

There are a number of issues which complicate the interpretation of CMB anisotropy data, some of which we sketch out below.

23.7.1. Foregrounds :

The microwave sky contains significant emission from our Galaxy and from extra-galactic sources [51]. Fortunately, the frequency dependence of these various sources is in general substantially different from that of the CMB anisotropy signals. The combination of Galactic synchrotron, bremsstrahlung, and dust emission reaches a minimum at a wavelength of roughly 3 mm (or about 100 GHz). As one moves to greater angular resolution, the minimum moves to slightly higher frequencies, but becomes more sensitive to unresolved (point-like) sources.

At frequencies around 100 GHz, and for portions of the sky away from the Galactic Plane, the foregrounds are typically 1 to 10% of the

CMB anisotropies. By making observations at multiple frequencies, it is relatively straightforward to separate the various components and determine the CMB signal to the few per cent level. For greater sensitivity, it is necessary to use the spatial information and statistical properties of the foregrounds to separate them from the CMB.

The foregrounds for CMB polarization are expected to follow a similar pattern, but are less well studied, and are intrinsically more complicated. The three year WMAP data have shown that the polarized foregrounds dominate at large angular scales, and that they must be well characterized in order to be discriminated [52]. Whether it is possible to achieve sufficient separation to detect B-mode CMB polarization is still an open question. However, for the time being, foreground contamination is not a ‘show-stopper’ for CMB experiments.

23.7.2. Secondary Anisotropies :

With increasingly precise measurements of the primary anisotropies, there is growing theoretical and experimental interest in ‘secondary anisotropies.’ Effects which happen at $z \ll 1000$ become more important as experiments push to higher angular resolution and sensitivity.

These secondary effects include gravitational lensing, patchy reionization, and the Sunyaev-Zel’dovich (SZ) effect [53]. The SZ effect is Compton scattering ($\gamma e \rightarrow \gamma' e'$) of the CMB photons by a hot electron gas, which creates spectral distortions by transferring energy from the electrons to the photons. It is particularly important for clusters of galaxies, through which one observes a partially Comptonized spectrum, resulting in a decrement at radio wavelengths and an increment in the submillimeter. This can be used to find and study individual clusters, and to obtain estimates of the Hubble constant. There is also the potential to constrain the equation of state of the Dark Energy through counts of detected clusters as a function of redshift [54]. Many SZ experiments are currently in operation which will probe clusters in this way.

23.7.3. Higher-order Statistics :

Although most of the CMB anisotropy information is contained in the power spectra, there will also be weak signals present in higher-order statistics. These statistics can measure any primordial non-Gaussianity in the perturbations, as well as non-linear growth of the fluctuations on small scales and other secondary effects (plus residual foreground contamination of course). Although there are an infinite variety of ways in which the CMB could be non-Gaussian, there is a generic form to consider for the initial conditions, where a quadratic contribution to the curvature perturbations is parameterized through a dimensionless number f_{NL} . This weakly non-linear component can be constrained through measurements of the bispectrum or Minkowski functionals, for example. The result from the WMAP team is $-54 < f_{NL} < 114$ (95% confidence region) [15], with studies using somewhat different estimators being of similar magnitude [55].

23.8. Constraints on Cosmologies

The clearest outcome of the newer experimental results is that the standard cosmological paradigm is in very good shape. A large amount of high precision data on the power spectrum is adequately fit with fewer than 10 free parameters. The framework is that of FRW models, which have nearly flat geometry, containing Dark Matter and Dark Energy, and with adiabatic perturbations having close to scale invariant initial conditions.

Within this framework, bounds can be placed on the values of the cosmological parameters. Of course, much more stringent constraints can be placed on models which cover a restricted number of parameters, *e.g.*, assuming that $\Omega_{tot} = 1$, $n = 1$ or $r = 0$. More generally, the constraints depend upon the adopted prior probability distributions, even if they are implicit, for example by restricting the parameter freedom or the ranges of parameters (particularly where likelihoods peak near the boundaries), or by using different choices of other data in combination with the CMB. When the data become even more precise, these considerations will be less important, but for now we caution that restrictions on model space and choice of priors need to be kept in mind when adopting specific parameter values and uncertainties.

There are some combinations of parameters that fit the CMB anisotropies almost equivalently. For example, there is a nearly exact geometric degeneracy, where any combination of Ω_M and Ω_Λ that gives the same angular diameter distance to last scattering will give nearly identical C_ℓ s. There are also other less exact degeneracies among the parameters. Such degeneracies can be broken when using the CMB results in combination with other cosmological data sets. Particularly useful are complementary constraints from galaxy clustering, the abundance of galaxy clusters, weak gravitational lensing measurements, Type Ia supernova distances, and the distribution of Lyman α forest clouds. For an overview of some of these other cosmological constraints, see The Cosmological Parameters—Sec. 21 of this *Review*.

The 3-year WMAP data alone, together with weak priors (on h and $\Omega_B h^2$ for example), and within the context of a 6 parameter family of models (which fixes $\Omega_{\text{tot}} = 1$ and $r = 0$), yield the following results [15]: $A = 2.35 \pm 0.13$, $n = 0.958 \pm 0.016$, $h = 0.73 \pm 0.03$, $\Omega_B h^2 = 0.0223 \pm 0.0007$, $\Omega_M h^2 = 0.128 \pm 0.008$ and $\tau = 0.09 \pm 0.03$. The main changes of the 3-year data compared with the first year results are: a lowering of Ω_M (from constraints on the third acoustic peak); a tightening of the confidence interval and decrease in the estimate for τ (driven by the large-angle EE measurements); and a subsequent breaking of the degeneracy between A and τ , which leads to a lowering of A (and hence related quantities such as σ_8) and some evidence (at the roughly 3σ level) for $n < 1$. The WMAP on their own therefore now seem to require a 6-parameter model space, although the significance of the $n \neq 1$ result is still a matter of debate [56].

Other combinations of data, *e.g.*, including other specific CMB measurements, or using large-scale structure data or supernova constraints, lead to consistent results to those given above, sometimes with smaller error bars, and with the precise values depending on data selection [15,57,58]. Note that for h , the CMB data alone provide only a very weak constraint, unless spatial flatness or some other cosmological data are used. For $\Omega_B h^2$, the precise value depends sensitively on how much freedom is allowed in the shape of the primordial power spectrum (see Big-Bang nucleosynthesis—Sec. 20 of this *Review*). The addition of other cosmological data-sets allows for constraints to be placed on further parameters.

For Ω_{tot} , perhaps the best WMAP constraint is 1.011 ± 0.012 , from the combination with Supernova Legacy Survey data [60]. However, similar results come from using independent limits on h [15] or from using large-scale structure data.

The 95% confidence upper limit on r is 0.65 using WMAP alone, tightening to $r < 0.30$ with the addition of the Sloan Digital Sky Survey data for example [61]. This limit depends on how the slope n is restricted and whether $dn/d\ln k \neq 0$ is allowed. Nevertheless, it is clear that the $\lambda\phi^4$ (sometimes called minimally coupled) inflationary model is disfavored by the data, while the $m^2\phi^2$ model (sometimes called mass term) is still allowed [15].

There are also constraints on parameters over and above the basic 8 that we have described, usually requiring extra cosmological data to break degeneracies. For example, the addition of the Dark Energy equation of state w adds the partial degeneracy of being able to fit a ridge in (w, h) space, extending to low values of both parameters. This degeneracy is broken when the CMB is used in combination with independent H_0 limits, or other data. WMAP plus supernova and large-scale structure data yield $w = -1.08 \pm 0.12$, with stronger constraints for flat models.

For the optical depth τ , the best-fit corresponds to a reionization redshift centered on 11 in the best-fit cosmology, and assuming instantaneous reionization. This redshift is not much higher than that suggested from studies of absorption in high- z quasar spectra [62]. The excitement here is that we have direct information from CMB polarization which can be combined with other astrophysical measurements to understand when the first stars formed and brought about the end of the cosmic dark ages.

23.9. Particle Physics Constraints

CMB data are beginning to put limits on parameters which are directly relevant for particle physics models. For example, there is a limit on the neutrino contribution $\Omega_\nu h^2 < 0.0072$ (95% confidence) from a combination of WMAP, galaxy clustering, and supernovae data [15]. This directly implies a limit on neutrino mass, $\sum m_\nu < 0.68$ eV, assuming the usual number density of fermions which decoupled when they were relativistic. Some tighter constraints can be derived using the CMB in combination with other data-sets [63].

The WMAP data, together with other data sets, suggest that $n < 1$, with a best-fitting value about 5% below unity. If borne out, this would be quite constraining for inflationary models. Moreover, this gives a real target for B-mode searches, since the value of r in simple models may be in the range of detectability, *e.g.*, $r \sim 0.15$ for $m^2\phi^2$ inflation if $n \simeq 0.95$. In addition, a combination of the WMAP data with other data-sets appears better fit with models which have a running spectral index, *i.e.*, $dn/d\ln k \neq 0$ [15], although the improvement is not significant at this time.

One other hint of new physics lies in the fact that the quadrupole and possibly some of the other low ℓ modes seem anomalously low compared with the best-fit Λ CDM model [7,64]. This is what might be expected in a universe which has a large-scale cut-off to the power spectrum, or is topologically non-trivial. However, because of cosmic variance, possible foregrounds, apparent correlations between modes (as mentioned in Sec. 23.2), *etc.*, the significance of such low ℓ anomalies is still an open question [13,65].

In addition, it is also possible to put limits on other pieces of physics [66], for example the neutrino chemical potentials, contribution of Warm Dark Matter, decaying particles, time variation of the fine-structure constant, or physics beyond general relativity. Further particle physics constraints will follow as the anisotropy measurements increase in precision.

Careful measurement of the CMB power spectra and non-Gaussianity can in principle put constraints on physics at the highest energies, including ideas of string theory, extra dimensions, colliding branes, *etc.* At the moment any calculation of predictions appears to be far from definitive. However, there is a great deal of activity on implications of string theory for the early Universe, and hence a very real chance that there might be observational implications for specific scenarios.

23.10. Fundamental Lessons

More important than the precise values of parameters is what we have learned about the general features which describe our observable Universe. Beyond the basic hot Big Bang picture, the CMB has taught us that:

- The Universe recombined at $z \simeq 1100$ and started to become ionized again at $z \simeq 10$.
- The geometry of the Universe is close to flat.
- Both Dark Matter and Dark Energy are required.
- Gravitational instability is sufficient to grow all of the observed large structures in the Universe.
- Topological defects were not important for structure formation.
- There are ‘synchronized’ super-Hubble modes generated in the early Universe.
- The initial perturbations were adiabatic in nature.
- The perturbations had close to Gaussian (*i.e.*, maximally random) initial conditions.

It is very tempting to make an analogy between the status of the cosmological ‘Standard Model’ and that of particle physics (see earlier Sections of this *Review*). In cosmology there are about 10 free parameters, each of which is becoming well determined, and with a great deal of consistency between different measurements. However, none of these parameters can be calculated from a fundamental theory, and so hints of the bigger picture, ‘physics beyond the Standard Model,’ are being searched for with ever more ambitious experiments.

Despite this analogy, there are some basic differences. For one thing, many of the cosmological parameters change with cosmic epoch, and so the measured values are simply the ones determined today,

and hence they are not ‘constants,’ like particle masses for example (although they *are* deterministic, so that if one knows their values at one epoch, they can be calculated at another). Moreover, the number of parameters is not as fixed as it is in the particle physics Standard Model; different researchers will not necessarily agree on what the free parameters are, and new ones can be added as the quality of the data improves. In addition, parameters like τ , which come from astrophysics, are in principle calculable from known physical processes. On top of all this, other parameters might be ‘stochastic’ in that they may be fixed only in our observable patch of the Universe or among certain vacuum states in the ‘Landscape’ [68].

In a more general sense, the cosmological ‘Standard Model’ is much further from the underlying ‘fundamental theory,’ which will ultimately provide the values of the parameters from first principles. Nevertheless, any genuinely complete ‘theory of everything’ must include an explanation for the values of these cosmological parameters as well as the parameters of the Standard Model of particle physics.

23.11. Future Directions

Given the significant progress in measuring the CMB sky, which have been instrumental in tying down cosmological parameters, what can we anticipate for the future? There will be a steady improvement in the precision and confidence with which we can determine the appropriate cosmological model and its parameters. We can anticipate that the addition of 5 more years of *WMAP* data (8 years total) will bring improvements from the increased statistical accuracy and from the more detailed treatment of calibration and systematic effects. Ground-based experiments operating at smaller angular scales will also over the next few years provide significantly tighter constraints on the damping tail. The third generation CMB satellite mission, *Planck*, is scheduled for launch in the latter part of 2008, and there are further satellite projects currently being discussed.

Despite the increasing improvement in the results, the addition of the latest experiments has not significantly changed the established cosmological model. It is, therefore, appropriate to ask: what should we expect to come from *Planck* and from other future experiments, including those being discussed as part of the U.S. ‘Beyond Einstein’ and European ‘Cosmic Vision’ initiatives? *Planck* certainly has the advantage of high sensitivity and a full-sky survey. A precise measurement of the third acoustic peak provides a good determination of the matter density; this can only be done by measurements which are accurate relative to the first two peaks (which themselves constrain the curvature and the baryon density). A detailed measurement of the damping tail region will also significantly improve the determination of n and any running of the slope. *Planck* should be capable of measuring C_ℓ^{EE} quite well, providing both a strong check on the cosmological Standard Model and extra constraints that will improve parameter estimation.

A set of cosmological parameters is now known to roughly 10% accuracy, and that may seem sufficient for many people. However, we should certainly demand more of measurements which describe *the entire observable Universe!* Hence a lot of activity in the coming years will continue to focus on determining those parameters with increasing precision. This necessarily includes testing for consistency among different predictions of the cosmological Standard Model, and searching for signals which might require additional physics.

A second area of focus will be the smaller scale anisotropies and ‘secondary effects.’ There is a great deal of information about structure formation at $z \ll 1000$ encoded in the CMB sky. This may involve higher-order statistics as well as spectral signatures, with many new experiments targeting the galaxy cluster SZ effect. Such investigations can also provide constraints on the Dark Energy equation of state, for example. *Planck*, as well as new telescopes aimed at the highest ℓ s, should be able to make a lot of progress in this arena.

A third direction is increasingly sensitive searches for specific signatures of physics at the highest energies. The most promising of these may be the primordial gravitational wave signals in C_ℓ^{BB} , which could be a probe of the $\sim 10^{16}$ GeV energy range. As well as *Planck*, there are several ground- and balloon-based experiments underway which are designed to probe the polarization B-modes. Whether the amplitude of the effect coming from inflation will be detectable is

unclear, but the prize makes the effort worthwhile, and the indications that $n \simeq 0.95$ give some genuine optimism that $r(= T/S)$ may be of order 0.1, and hence within reach soon.

Anisotropies in the CMB have proven to be the premier probe of cosmology and the early Universe. Theoretically the CMB involves well-understood physics in the linear regime, and is under very good calculational control. A substantial and improving set of observational data now exists. Systematics appear to be well understood and not a limiting factor. And so for the next few years we can expect an increasing amount of cosmological information to be gleaned from CMB anisotropies, with the prospect also of some genuine surprises.

References:

1. A.A. Penzias and R. Wilson, *Astrophys. J.* **142**, 419 (1965); R.H. Dicke *et al.*, *Astrophys. J.* **142**, 414 (1965).
2. M. White, D. Scott, and J. Silk, *Ann. Rev. Astron. & Astrophys.* **32**, 329 (1994); W. Hu and S. Dodelson, *Ann. Rev. Astron. & Astrophys.* **40**, 171 (2002).
3. G.F. Smoot *et al.*, *Astrophys. J.* **396**, L1 (1992).
4. C.L. Bennett *et al.*, *Astrophys. J. Supp.* **148**, 1 (2003).
5. N. Jarosik *et al.*, *Astrophys. J. Supp.* **170**, 263 (2007).
6. J.C. Mather *et al.*, *Astrophys. J.* **512**, 511 (1999).
7. G. Hinshaw *et al.*, *Astrophys. J. Supp.* **170**, 288 (2007).
8. S. Courteau *et al.*, *Astrophys. J.* **544**, 636 (2000).
9. D.J. Fixsen *et al.*, *Astrophys. J.* **420**, 445 (1994).
10. D.J. Fixsen *et al.*, *Astrophys. J.* **473**, 576 (1996); A. Kogut *et al.*, *Astrophys. J.* **419**, 1 (1993).
11. S. Seager, D.D. Sasselov, and D. Scott, *Astrophys. J. Supp.* **128**, 407 (2000).
12. N. Bartolo *et al.*, *Phys. Rep.* **402**, 103 (2004).
13. A. de Oliveira-Costa *et al.*, *Phys. Rev.* **D69**, 063516 (2004); K. Land and J. Magueijo, *Monthly Not. Royal Astron. Soc.* **357**, 994 (2005); C.J. Copi *et al.*, *Phys. Rev.* **D75**, 023507 (2007).
14. E. Komatsu *et al.*, *Astrophys. J. Supp.* **148**, 119 (2003).
15. D.N. Spergel *et al.*, *Astrophys. J. Supp.* **170**, 377 (2007).
16. H.K. Eriksen *et al.*, *Astrophys. J.* **660**, L81 (2007); M. Cruz *et al.*, *Astrophys. J.* **655**, 11 (2007); T.R. Jaffe *et al.*, *Astron. & Astrophys.* **460**, 393 (2006).
17. L. Knox, *Phys. Rev.* **D52**, 4307 (1995).
18. A.R. Liddle and D.H. Lyth, *Cosmological Inflation and Large-Scale Structure*, Cambridge University Press (2000).
19. U. Seljak and M. Zaldarriaga, *Astrophys. J.* **469**, 437 (1996).
20. A. Lewis, A. Challinor, and A. Lasenby, *Astrophys. J.* **538**, 473 (2000).
21. U. Seljak *et al.*, *Phys. Rev.* **D68**, 083507 (2003).
22. R.K. Sachs and A.M. Wolfe, *Astrophys. J.* **147**, 73 (1967).
23. R. Crittenden and N. Turok, *Phys. Rev. Lett.* **76**, 575 (1996); A. Cabré *et al.*, *Monthly Not. Royal Astron. Soc.* **372**, L23 (2006); D. McEwen *et al.*, [arXiv:0704.0626](https://arxiv.org/abs/0704.0626).
24. W. Hu and D.J. Eisenstein, *Phys. Rev.* **D59**, 083509 (1999); W. Hu *et al.*, *Phys. Rev.* **D59**, 023512 (1999).
25. P.J.E. Peebles and J.T. Yu, *Astrophys. J.* **162**, 815 (1970); R.A. Sunyaev and Ya.B. Zel’dovich, *Astrophys. & Space Sci.* **7**, 3 (1970).
26. D. Scott, J. Silk, and M. White, *Science* **268**, 829 (1995).
27. D.J. Eisenstein *et al.*, *Astrophys. J.* **633**, 560 (2005); S. Cole *et al.*, *Monthly Not. Royal Astron. Soc.* **362**, 505 (2005); W.J. Percival *et al.*, [arXiv:0705.3323](https://arxiv.org/abs/0705.3323).
28. J. Silk, *Astrophys. J.* **151**, 459 (1968).
29. M. Zaldarriaga and U. Seljak, *Phys. Rev.* **D58**, 023003 (1998); A. Lewis and A. Challinor, *Phys. Rep.* **429**, 1 (2006).
30. K.M. Smith, O. Zahn, and O. Doré, [arXiv:0705.3980](https://arxiv.org/abs/0705.3980).
31. M.C. Runyan *et al.*, *Astrophys. J. Supp.* **149**, 265 (2003); C.L. Kuo *et al.*, *Astrophys. J.* **664**, 687 (2007).
32. S. Masi *et al.*, *Astron. & Astrophys.* **458**, 687 (2006); W.C. Jones *et al.*, *Astrophys. J.* **647**, 823 (2006).

33. T.J. Pearson *et al.*, *Astrophys. J.* **591**, 556 (2003);
A.C.S. Readhead *et al.*, *Astrophys. J.* **609**, 498 (2004);
J.L. Sievers *et al.*, *Astrophys. J.* **660**, 976 (2007).
34. P. Ade *et al.*, [arXiv:0705.2359](https://arxiv.org/abs/0705.2359).
35. P.F. Scott *et al.*, *Monthly Not. Royal Astron. Soc.* **341**, 1076 (2003);
K. Grainge *et al.*, *Monthly Not. Royal Astron. Soc.* **341**, L23 (2003);
C. Dickinson *et al.*, *Monthly Not. Royal Astron. Soc.* **353**, 732 (2004).
36. A. Benoit *et al.*, *Astron. & Astrophys.* **399**, L19 (2003);
M. Tristram *et al.*, *Astron. & Astrophys.* **436**, 785 (2005).
37. N.W. Halverson *et al.*, *Astrophys. J.* **568**, 38 (2002).
38. A.T. Lee *et al.*, *Astrophys. J.* **561**, L1 (2001).
39. M.E. Abroe *et al.*, *Astrophys. J.* **605**, 607 (2004);
N. Rajguru *et al.*, *Monthly Not. Royal Astron. Soc.* **363**, 1125.
40. W. Hu and M. White, *New Astron.* **2**, 323 (1997).
41. W. Hu and M. White, *Phys. Rev.* **D56**, 596 (1997).
42. M. Zaldarriaga and U. Seljak, *Phys. Rev.* **D55**, 1830 (1997);
M. Kamionkowski, A. Kosowsky, and A. Stebbins, *Phys. Rev.* **D55**, 7368 (1997).
43. J. Kovac *et al.*, *Nature*, **420**, 772 (2002).
44. A. Kogut *et al.*, *Astrophys. J. Supp.* **148**, 161 (2003).
45. L. Page *et al.*, *Astrophys. J. Supp.* **170**, 335 (2007).
46. D. Barkats *et al.*, *Astrophys. J.* **619**, L127 (2005).
47. A.C.S. Readhead *et al.*, *Science*, **306**, 836 (2004).
48. E.M. Leitch *et al.*, *Astrophys. J.* **624**, 10 (2005).
49. T.E. Montroy *et al.*, *Astrophys. J.* **647**, 813 (2006).
50. F. Piacentini *et al.*, *Astrophys. J.* **647**, 833 (2006).
51. A. de Oliveira-Costa, M. Tegmark (eds.), *Microwave Foregrounds*,
Astron. Soc. of the Pacific, San Francisco (1999).
52. A. Kogut *et al.*, [arXiv:0704.3991](https://arxiv.org/abs/0704.3991).
53. R.A. Sunyaev and Ya.B. Zel'dovich, *Ann. Rev. Astron. Astrophys.* **18**, 537 (1980);
M. Birkinshaw, *Phys. Rep.* **310**, 98 (1999).
54. J.E. Carlstrom, G.P. Holder, and E.D. Reese, *Ann. Rev. Astron. & Astrophys.* **40**, 643 (2002).
55. P. Creminelli *et al.*, *J. Cosm. & Astropart. Phys.* **3**, 5 (2007).
56. D. Parkinson, P. Mukherjee, and A.R. Liddle, *Phys. Rev.* **D73**, 123523 (2006);
W.H. Kinney *et al.*, *Phys. Rev.* **D74**, 023502 (2006);
M. Bridges, A.N. Lasenby, and M.P. Hobson, *Monthly Not. Royal Astron. Soc.* **369**, 1123 (2006).
57. M. Tegmark *et al.*, *Phys. Rev.* **D74**, 123507 (2006);
C.J. MacTavish *et al.*, *Astrophys. J.* **647**, 799 (2006);
A.G. Sánchez *et al.*, *Monthly Not. Royal Astron. Soc.* **366**, 189 (2006);
M. Viel, M.G. Haehnelt, and A. Lewis, [astro-ph/0604310](https://arxiv.org/abs/astro-ph/0604310);
U. Seljak, A. Slosar, and P. McDonald, *J. Cosm. & Astropart. Phys.* **10**, 014 (2006).
58. D.N. Spergel *et al.*, *Astrophys. J.* **148**, 175 (2003).
59. W.L. Freedman *et al.*, *Astrophys. J.* **553**, 47 (2001).
60. P. Astier *et al.*, *Astron. & Astrophys.* **447**, 31 (2006).
61. M. Tegmark *et al.*, *Astrophys. J.* **606**, 702 (2004).
62. X. Fan *et al.*, *Astrophys. J.* **123**, 1247 (2002).
63. G.L. Fogli *et al.*, *Phys. Rev.* **D75**, 053001 (2007);
A. Goobar *et al.*, *J. Cosm. & Astropart. Phys.* **6**, 019 (2006).
64. G. Hinshaw *et al.*, *Astrophys. J. Supp.* **148**, 135 (2003).
65. G. Efstathiou, *Monthly Not. Royal Astron. Soc.* **346**, L26 (2003).
66. M. Kamionkowski and A. Kosowsky, *Ann. Rev. Nucl. Part. Sci.* **49**, 77 (1999).
67. R. Maartens, *Living Rev. Rel.* **7**, 7 (2004).
68. R. Bousso and J. Polchinski, *JHEP* 0006, 006 (2000);
L. Susskind, *The Davis Meeting On Cosmic Inflation* (2003), [hep-th/0302219](https://arxiv.org/abs/hep-th/0302219).

24. COSMIC RAYS

Revised August 2007 by T.K. Gaisser and T. Stanev (Bartol Research Inst., Univ. of Delaware).

24.1. Primary spectra

The cosmic radiation incident at the top of the terrestrial atmosphere includes all stable charged particles and nuclei with lifetimes of order 10^6 years or longer. Technically, “primary” cosmic rays are those particles accelerated at astrophysical sources, and “secondaries” are those particles produced in interaction of the primaries with interstellar gas. Thus, electrons, protons, and helium, as well as carbon, oxygen, iron, and other nuclei synthesized in stars, are primaries. Nuclei such as lithium, beryllium, and boron (which are not abundant end-products of stellar nucleosynthesis) are secondaries. Antiprotons and positrons are also in large part secondary. Whether a small fraction of these particles may be primary is a question of current interest.

Apart from particles associated with solar flares, the cosmic radiation comes from outside the solar system. The incoming charged particles are “modulated” by the solar wind, the expanding magnetized plasma generated by the Sun, which decelerates and partially excludes the lower energy galactic cosmic rays from the inner solar system. There is a significant anticorrelation between solar activity (which has an alternating eleven-year cycle) and the intensity of the cosmic rays with energies below about 10 GeV. In addition, the lower-energy cosmic rays are affected by the geomagnetic field, which they must penetrate to reach the top of the atmosphere. Thus the intensity of any component of the cosmic radiation in the GeV range depends both on the location and time.

There are four different ways to describe the spectra of the components of the cosmic radiation: (1) By particles per unit rigidity. Propagation (and probably also acceleration) through cosmic magnetic fields depends on gyroradius or *magnetic rigidity*, R , which is gyroradius multiplied by the magnetic field strength:

$$R = \frac{pc}{Ze} = r_L B. \quad (24.1)$$

(2) By particles per energy-per-nucleon. Fragmentation of nuclei propagating through the interstellar gas depends on energy per nucleon, since that quantity is approximately conserved when a nucleus breaks up on interaction with the gas. (3) By nucleons per energy-per-nucleon. Production of secondary cosmic rays in the atmosphere depends on the intensity of nucleons per energy-per-nucleon, approximately independently of whether the incident nucleons are free protons or bound in nuclei. (4) By particles per energy-per-nucleus. Air shower experiments that use the atmosphere as a calorimeter generally measure a quantity that is related to total energy per particle.

The units of differential intensity I are $[\text{m}^{-2} \text{s}^{-1} \text{sr}^{-1} \mathcal{E}^{-1}]$, where \mathcal{E} represents the units of one of the four variables listed above.

The intensity of primary nucleons in the energy range from several GeV to somewhat beyond 100 TeV is given approximately by

$$I_N(E) \approx 1.8 \times 10^4 (E/1 \text{ GeV})^{-\alpha} \frac{\text{nucleons}}{\text{m}^2 \text{ s sr GeV}}, \quad (24.2)$$

where E is the energy-per-nucleon (including rest mass energy), and α ($\equiv \gamma + 1$) = 2.7 is the differential spectral index of the cosmic ray flux and γ is the integral spectral index. About 79% of the primary nucleons are free protons and about 70% of the rest are nucleons bound in helium nuclei. The fractions of the primary nuclei are nearly constant over this energy range (possibly with small but interesting variations). Fractions of both primary and secondary incident nuclei are listed in Table 24.1. Figure 24.1 shows the major components for energies greater than 2 GeV/nucleon.

The composition and energy spectra of nuclei are typically interpreted in the context of propagation models, in which the sources of the primary cosmic radiation are located within the galaxy [13]. The ratio of secondary to primary nuclei is observed to decrease with increasing energy, a fact interpreted to mean that the lifetime of

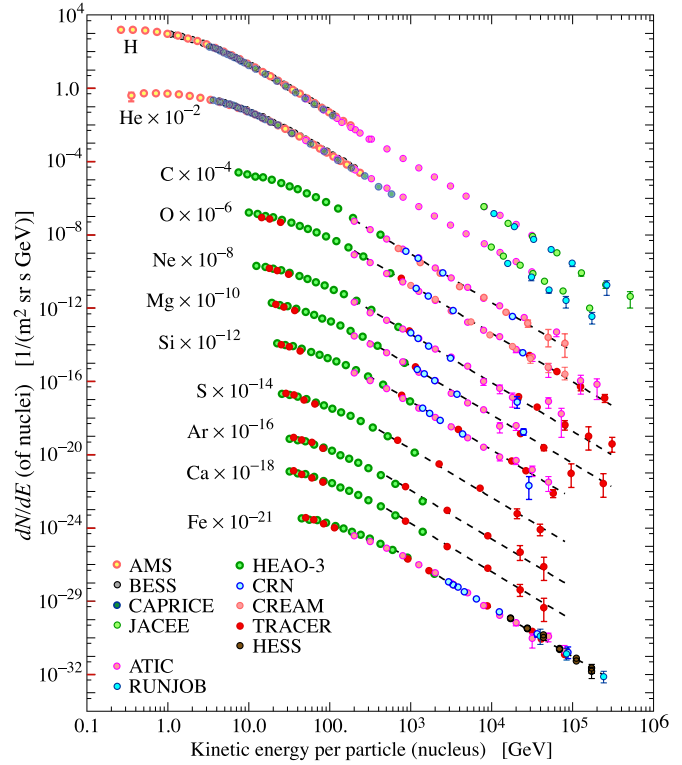


Figure 24.1: Major components of the primary cosmic radiation from Refs. [1–12]. The figure was created by P. Boyle and D. Muller. Color version at end of book.

Table 24.1: Relative abundances F of cosmic-ray nuclei at 10.6 GeV/nucleon normalized to oxygen ($\equiv 1$) [6]. The oxygen flux at kinetic energy of 10.6 GeV/nucleon is $3.26 \times 10^{-6} \text{ cm}^{-2} \text{ s}^{-1} \text{ sr}^{-1} (\text{GeV/nucleon})^{-1}$. Abundances of hydrogen and helium are from Refs. [2,3]. Note that one can not use these values to extend the cosmic ray flux to high energy because the power law spectrum is not fully established yet and that Figure 24.1 is in energy per particle.

Z	Element	F	Z	Element	F
1	H	540	13–14	Al-Si	0.19
2	He	26	15–16	P-S	0.03
3–5	Li-B	0.40	17–18	Cl-Ar	0.01
6–8	C-O	2.20	19–20	K-Ca	0.02
9–10	F-Ne	0.30	21–25	Sc-Mn	0.05
11–12	Na-Mg	0.22	26–28	Fe-Ni	0.12

cosmic rays in the galaxy decreases with energy. Measurements of radioactive “clock” isotopes in the low energy cosmic radiation are consistent with a lifetime in the galaxy of about 15 Myr [14].

The spectrum of electrons and positrons incident at the top of the atmosphere is steeper than the spectra of protons and nuclei, as shown in Fig. 24.2. The positron fraction decreases from ~ 0.2 below 1 GeV [21–23] to ~ 0.1 around 2 GeV and to ~ 0.05 at the highest energies for which it is measured (5–20 GeV) [18]. This behavior refers to measurements made during solar cycles of positive magnetic polarity and at high geomagnetic latitude. Ref. 22 discusses the dependence of the positron fraction on solar cycle and Ref. 23 studies the geomagnetic effects.

The ratio of antiprotons to protons is $\sim 2 \times 10^{-4}$ [24] at around 10–20 GeV, and there is clear evidence [25] for the kinematic suppression at lower energy that is the signature of secondary antiprotons. The

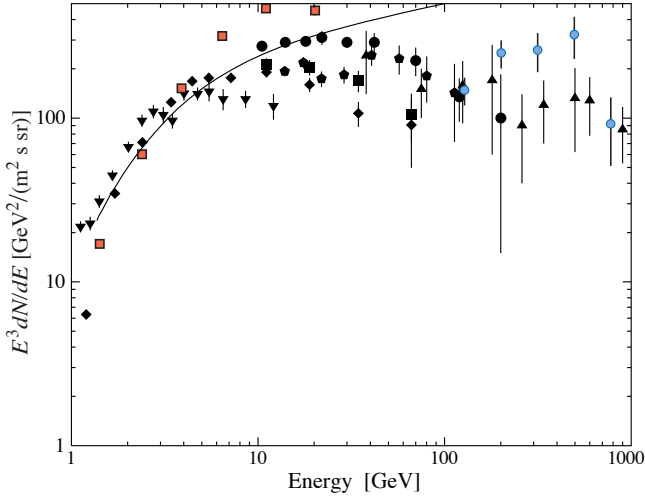


Figure 24.2: Differential spectrum of electrons plus positrons multiplied by E^3 (data from [15–22]). The line shows the proton spectrum multiplied by 0.01.

\bar{p}/p ratio also shows a strong dependence on the phase and polarity of the solar cycle [26] in the opposite sense to that of the positron fraction. There is at this time no evidence for a significant primary component either of positrons or of antiprotons. No antihelium or antideuteron has been found in the cosmic radiation. The best current measured upper limit on the ratio antihelium/helium is approximately 7×10^{-7} [27]. The upper limit on the flux of antideuterons around 1 GeV/nucleon is approximately $2 \times 10^{-4} \text{ m}^2 \text{ s sr GeV/nucleon}$ [28].

24.2. Cosmic rays in the atmosphere

Figure 24.3 shows the vertical fluxes of the major cosmic ray components in the atmosphere in the energy region where the particles are most numerous (except for electrons, which are most numerous near their critical energy, which is about 81 MeV in air). Except for protons and electrons near the top of the atmosphere, all particles are produced in interactions of the primary cosmic rays in the air. Muons and neutrinos are products of the decay of charged mesons, while electrons and photons originate in decays of neutral mesons.

Most measurements are made at ground level or near the top of the atmosphere, but there are also measurements of muons and electrons from airplanes and balloons. Fig. 24.3 includes recent measurements of negative muons [29–32]. Since $\mu^+(\mu^-)$ are produced in association with $\nu_\mu(\bar{\nu}_\mu)$, the measurement of muons near the maximum of the intensity curve for the parent pions serves to calibrate the atmospheric ν_μ beam [33]. Because muons typically lose almost two GeV in passing through the atmosphere, the comparison near the production altitude is important for the sub-GeV range of $\nu_\mu(\bar{\nu}_\mu)$ energies.

The flux of cosmic rays through the atmosphere is described by a set of coupled cascade equations with boundary conditions at the top of the atmosphere to match the primary spectrum. Numerical or Monte Carlo calculations are needed to account accurately for decay and energy-loss processes, and for the energy-dependences of the cross sections and of the primary spectral index γ . Approximate analytic solutions are, however, useful in limited regions of energy [34,35]. For example, the vertical intensity of nucleons at depth X (g cm^{-2}) in the atmosphere is given by

$$I_N(E, X) \approx I_N(E, 0) e^{-X/\Lambda}, \quad (24.3)$$

where Λ is the attenuation length of nucleons in air.

The corresponding expression for the vertical intensity of charged pions with energy $E_\pi \ll \epsilon_\pi = 115 \text{ GeV}$ is

$$I_\pi(E_\pi, X) \approx \frac{Z_{N\pi}}{\lambda_N} I_N(E_\pi, 0) e^{-X/\Lambda} \frac{X E_\pi}{\epsilon_\pi}. \quad (24.4)$$

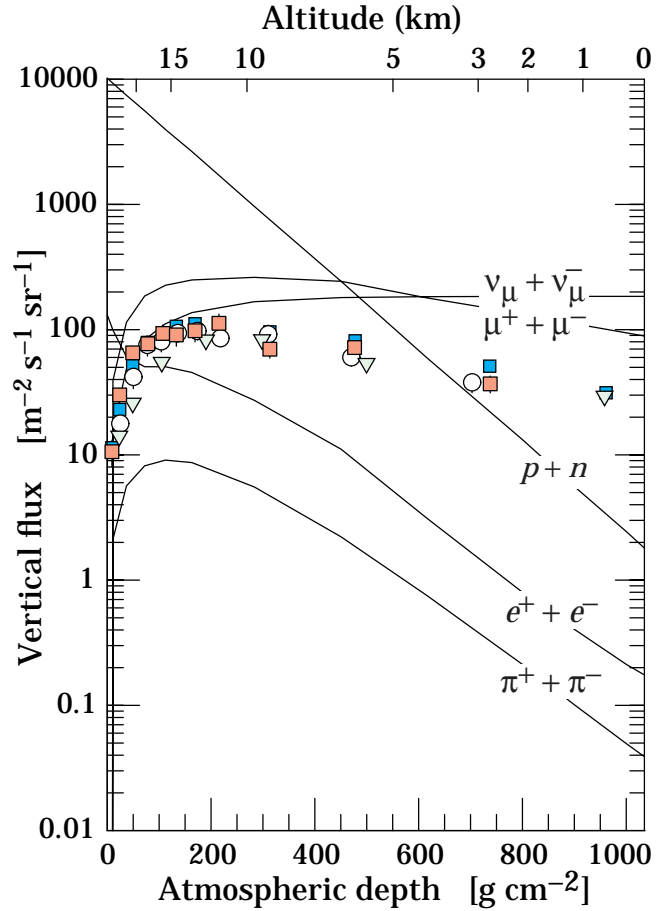


Figure 24.3: Vertical fluxes of cosmic rays in the atmosphere with $E > 1 \text{ GeV}$ estimated from the nucleon flux of Eq. (24.2). The points show measurements of negative muons with $E_\mu > 1 \text{ GeV}$ [29–32].

This expression has a maximum at $X = \Lambda \approx 121 \pm 4 \text{ g cm}^{-2}$ [36], which corresponds to an altitude of 15 kilometers. The quantity $Z_{N\pi}$ is the spectrum-weighted moment of the inclusive distribution of charged pions in interactions of nucleons with nuclei of the atmosphere. The intensity of low-energy pions is much less than that of nucleons because $Z_{N\pi} \approx 0.079$ is small and because most pions with energy much less than the critical energy ϵ_π decay rather than interact.

24.3. Cosmic rays at the surface

24.3.1. Muons: Muons are the most numerous charged particles at sea level (see Fig. 24.3). Most muons are produced high in the atmosphere (typically 15 km) and lose about 2 GeV to ionization before reaching the ground. Their energy and angular distribution reflect a convolution of production spectrum, energy loss in the atmosphere, and decay. For example, 2.4 GeV muons have a decay length of 15 km, which is reduced to 8.7 km by energy loss. The mean energy of muons at the ground is $\approx 4 \text{ GeV}$. For GeV muons there is also a solar activity and a latitude effect that results from the geomagnetic effects. These two effects affect the GeV muon flux at the 10% level. The energy spectrum is almost flat below 1 GeV, steepens gradually to reflect the primary spectrum in the 10–100 GeV range, and steepens further at higher energies because pions with $E_\pi > \epsilon_\pi$ tend to interact in the atmosphere before they decay. Asymptotically ($E_\mu \gg 1 \text{ TeV}$), the energy spectrum of atmospheric muons is one power steeper than the primary spectrum. The integral intensity of vertical muons above 1 GeV/c at sea level is $\approx 70 \text{ m}^{-2} \text{ s}^{-1} \text{ sr}^{-1}$ [37,38], with recent measurements [39–41] tending to give lower normalization by 10–15%. Experimentalists are familiar with this number in the form $I \approx 1 \text{ cm}^{-2} \text{ min}^{-1}$ for horizontal detectors.

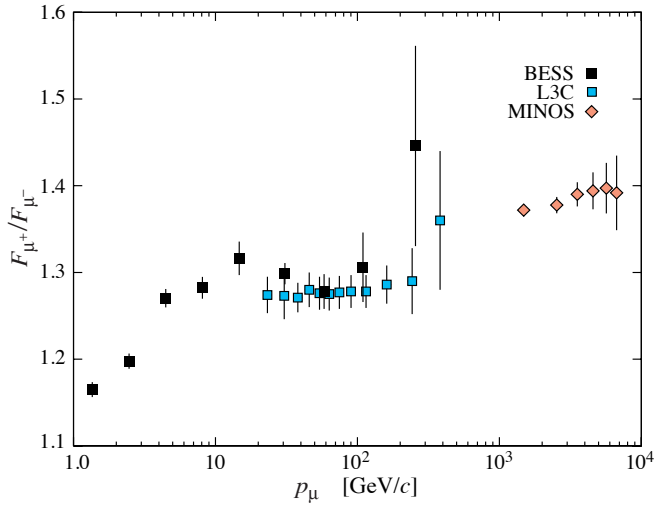


Figure 24.5: Muon charge ratio as a function of the muon momentum from Refs. [40,41,47,48].

The overall angular distribution of muons at the ground is $\propto \cos^2 \theta$, which is characteristic of muons with $E_{\mu} \sim 3$ GeV. At lower energy the angular distribution becomes increasingly steep, while at higher energy it flattens, approaching a $\sec \theta$ distribution for $E_{\mu} \gg \epsilon_{\pi}$ and $\theta < 70^\circ$.

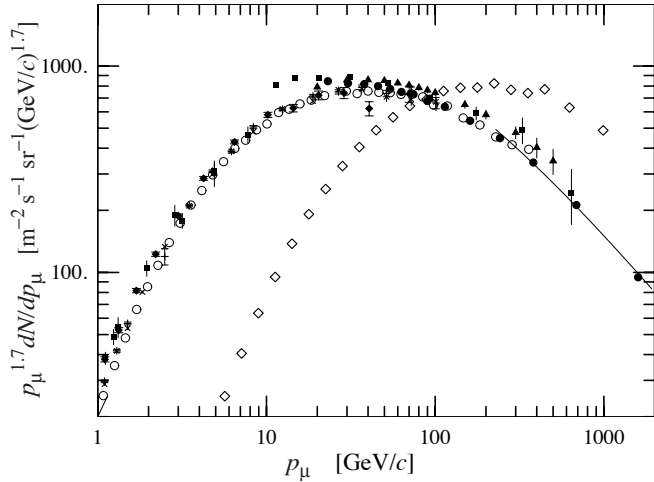


Figure 24.4: Spectrum of muons at $\theta = 0^\circ$ (\blacklozenge [37], \blacksquare [42], \blacktriangledown [43], \blacktriangle [44], \times , $+$ [39], \circ [40] and (blackcircles) [41] and $\theta = 75^\circ$ \diamond [45]). The line plots the result from Eq. (24.5) for vertical showers.

An approximate extrapolation formula valid when muon decay is negligible ($E_{\mu} > 100/\cos \theta$ GeV), and the curvature of the Earth can be neglected ($\theta < 70^\circ$) is

$$\frac{dN_{\mu}}{dE_{\mu} d\Omega} \approx \frac{0.14 E_{\mu}^{-2.7}}{\text{cm}^2 \text{ s sr GeV}} \times \left\{ \frac{1}{1 + \frac{1.1 E_{\mu} \cos \theta}{115 \text{ GeV}}} + \frac{0.054}{1 + \frac{1.1 E_{\mu} \cos \theta}{850 \text{ GeV}}} \right\}, \quad (24.5)$$

where the two terms give the contribution of pions and charged kaons. Eq. (24.5) neglects a small contribution from charm and heavier flavors which is negligible except at very high energy [46].

Figure 24.4 shows the muon energy spectrum at sea level for two angles. At large angles low energy muons decay before reaching the surface and high energy pions decay before they interact, thus the average muon energy increases.

The muon charge ratio reflects the excess of π^+ over π^- and K^+ over K^- in the forward fragmentation region of proton initiated interactions together with the fact that there are more protons than neutrons in the primary spectrum. The increase with energy of μ^+/μ^- shown in Fig. 24.5 reflects the increasing importance of kaons in the TeV range [47], and indicates a significant contribution of associated production by cosmic-ray protons ($p \rightarrow \Lambda + K^+$). The same process is even more important for atmospheric neutrinos at high energy.

24.3.2. Electromagnetic component: At the ground, this component consists of electrons, positrons, and photons primarily from electromagnetic cascades initiated by decay of neutral and charged mesons. Muon decay is the dominant source of low-energy electrons at sea level. Decay of neutral pions is more important at high altitude or when the energy threshold is high. Knock-on electrons also make a small contribution at low energy [49]. The integral vertical intensity of electrons plus positrons is very approximately 30, 6, and $0.2 \text{ m}^{-2} \text{ s}^{-1} \text{ sr}^{-1}$ above 10, 100, and 1000 MeV respectively [38,50], but the exact numbers depend sensitively on altitude, and the angular dependence is complex because of the different altitude dependence of the different sources of electrons [49–51]. The ratio of photons to electrons plus positrons is approximately 1.3 above a GeV and 1.7 below the critical energy [51].

24.3.3. Protons: Nucleons above 1 GeV/c at ground level are degraded remnants of the primary cosmic radiation. The intensity is approximately represented by Eq. (24.3), with the replacement $X \rightarrow X/\cos \theta$ for $\theta < 70^\circ$. At sea level, about 1/3 of the nucleons in the vertical direction are neutrons (up from $\approx 10\%$ at the top of the atmosphere as the n/p ratio approaches equilibrium). The integral intensity of vertical protons above 1 GeV/c at sea level is $\approx 0.9 \text{ m}^{-2} \text{ s}^{-1} \text{ sr}^{-1}$ [38,52].

24.4. Cosmic rays underground

Only muons and neutrinos penetrate to significant depths underground. The muons produce tertiary fluxes of photons, electrons, and hadrons.

24.4.1. Muons: As discussed in Section 27.6 of this *Review*, muons lose energy by ionization and by radiative processes: bremsstrahlung, direct production of e^+e^- pairs, and photonuclear interactions. The total muon energy loss may be expressed as a function of the amount of matter traversed as

$$-\frac{dE_{\mu}}{dX} = a + b E_{\mu}, \quad (24.6)$$

where a is the ionization loss and b is the fractional energy loss by the three radiation processes. Both are slowly varying functions of energy. The quantity $\epsilon \equiv a/b$ (≈ 500 GeV in standard rock) defines a critical energy below which continuous ionization loss is more important than radiative losses. Table 24.2 shows a and b values for standard rock as a function of muon energy. The second column of Table 24.2 shows the muon range in standard rock ($A = 22$, $Z = 11$, $\rho = 2.65 \text{ g cm}^{-3}$). These parameters are quite sensitive to the chemical composition of the rock, which must be evaluated for each experimental location.

Table 24.2: Average muon range R and energy loss parameters calculated for standard rock [53]. Range is given in km-water-equivalent, or 10^5 g cm^{-2} .

E_{μ} GeV	R km.w.e.	a MeV $\text{g}^{-1} \text{cm}^2$	b_{brems}	b_{pair} $10^{-6} \text{ g}^{-1} \text{cm}^2$	b_{nucl}	$\sum b_i$	$\sum b(\text{ice})$
10	0.05	2.17	0.70	0.70	0.50	1.90	1.66
100	0.41	2.44	1.10	1.53	0.41	3.04	2.51
1000	2.45	2.68	1.44	2.07	0.41	3.92	3.17
10000	6.09	2.93	1.62	2.27	0.46	4.35	3.78

The intensity of muons underground can be estimated from the muon intensity in the atmosphere and their rate of energy loss. To the extent that the mild energy-dependence of a and b can be neglected, Eq. (24.6) can be integrated to provide the following relation between the energy $E_{\mu,0}$ of a muon at production in the atmosphere and its average energy E_{μ} after traversing a thickness X of rock (or ice or water):

$$E_{\mu} = (E_{\mu,0} + \epsilon)e^{-bX} - \epsilon. \quad (24.7)$$

Especially at high energy, however, fluctuations are important and an accurate calculation requires a simulation that accounts for stochastic energy-loss processes [54].

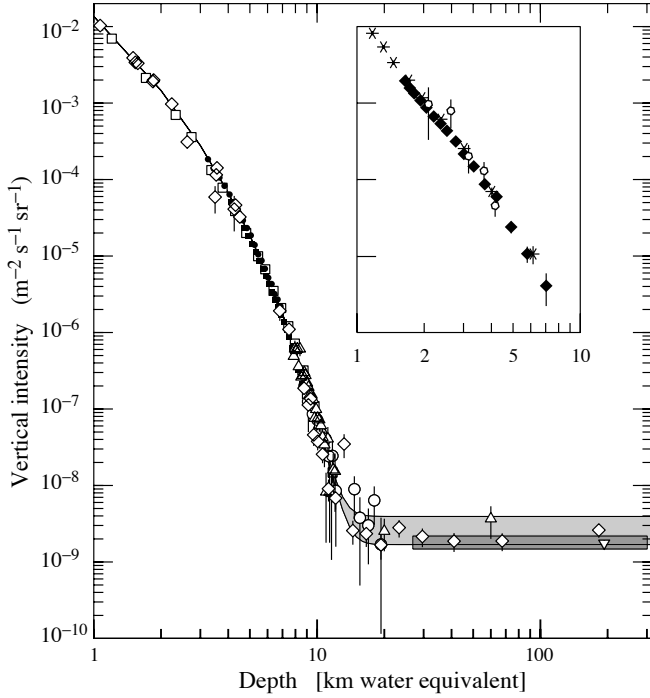


Figure 24.6: Vertical muon intensity vs depth (1 km.w.e. = 10^5 g cm^{-2} of standard rock). The experimental data are from: \diamond : the compilations of Crouch [55], \square : Baksan [59], \circ : LVD [60], \bullet : MACRO [61], \blacksquare : Frejus [62], and \triangle : SNO [63]. The shaded area at large depths represents neutrino-induced muons of energy above 2 GeV. The upper line is for horizontal neutrino-induced muons, the lower one for vertically upward muons.

There are two depth regimes for Eq. (24.7). For $X \ll b^{-1} \approx 2.5$ km water equivalent, $E_{\mu,0} \approx E_{\mu}(X) + aX$, while for $X \gg b^{-1}$ $E_{\mu,0} \approx (\epsilon + E_{\mu}(X)) \exp(bX)$. Thus at shallow depths, the differential muon energy spectrum is approximately constant for $E_{\mu} < aX$, and steepens to reflect the surface muon spectrum for $E_{\mu} > aX$, whereas for $X > 2.5$ km.w.e., the differential spectrum underground is again constant for small muon energies but steepens to reflect the surface muon spectrum for $E_{\mu} > \epsilon \approx 0.5$ TeV. In the deep regime, the shape is independent of depth, although the intensity decreases exponentially with depth. In general the muon spectrum at slant depth X is

$$\frac{dN_{\mu}(X)}{dE_{\mu}} = \frac{dN_{\mu}}{dE_{\mu,0}} \frac{dE_{\mu,0}}{dE_{\mu}} = \frac{dN_{\mu}}{dE_{\mu,0}} e^{bX}, \quad (24.8)$$

where $E_{\mu,0}$ is the solution of Eq. (24.7) in the approximation neglecting fluctuations.

Fig. 24.6 shows the vertical muon intensity versus depth. In constructing this “depth-intensity curve,” each group has taken account of the angular distribution of the muons in the atmosphere, the map of the overburden at each detector, and the properties of the local medium in connecting measurements at various slant

depths and zenith angles to the vertical intensity. Use of data from a range of angles allows a fixed detector to cover a wide range of depths. The flat portion of the curve is due to muons produced locally by charged-current interactions of ν_{μ} . The inset shows the vertical intensity curve for water and ice published in Refs. [56–58]. It is not as steep as the one for rock because of the lower muon energy loss in water.

24.4.2. Neutrinos: Because neutrinos have small interaction cross sections, measurements of atmospheric neutrinos require a deep detector to avoid backgrounds. There are two types of measurements: contained (or semi-contained) events, in which the vertex is determined to originate inside the detector, and neutrino-induced muons. The latter are muons that enter the detector from zenith angles so large (e.g., nearly horizontal or upward) that they cannot be muons produced in the atmosphere. In neither case is the neutrino flux measured directly. What is measured is a convolution of the neutrino flux and cross section with the properties of the detector (which includes the surrounding medium in the case of entering muons).

Contained and semi-contained events reflect neutrinos in the sub-GeV to multi-GeV region, where the product of increasing cross section and decreasing flux is maximum. In the GeV region, the neutrino flux and its angular distribution depend on the geomagnetic location of the detector and, to a lesser extent, on the phase of the solar cycle. Naively, we expect $\nu_{\mu}/\nu_e = 2$ from counting neutrinos of the two flavors coming from the chain of pion and muon decay. This ratio is only slightly modified by the details of the decay kinematics, but the fraction of electron neutrinos gradually decreases above a GeV as parent muons begin to reach the ground before decaying. Experimental measurements have to account for the ratio of $\bar{\nu}/\nu$, which have cross sections different by a factor of 3 in this energy range. In addition, detectors generally have different efficiencies for detecting muon neutrinos and electron neutrinos, which need to be accounted for in comparing measurements with expectation. Fig. 24.7 shows the distributions of the visible energy in the Super-Kamiokande detector [64] for electron-like and muon-like charged current neutrino interactions. Contrary to expectation, the numbers of the two classes of events are similar rather than different by a factor of two. The exposure for the data sample shown here is 1489 days. The falloff of the muon-like events at high energy is a consequence of the poor containment for high energy muons. Corrections for detection efficiencies and backgrounds are, however, insufficient to account for the large difference from the expectation [65,66].

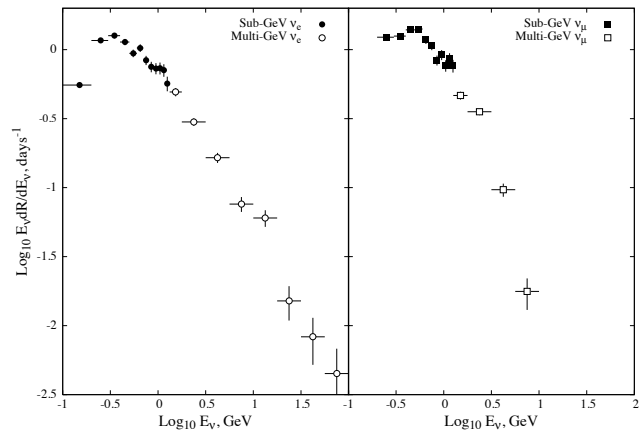


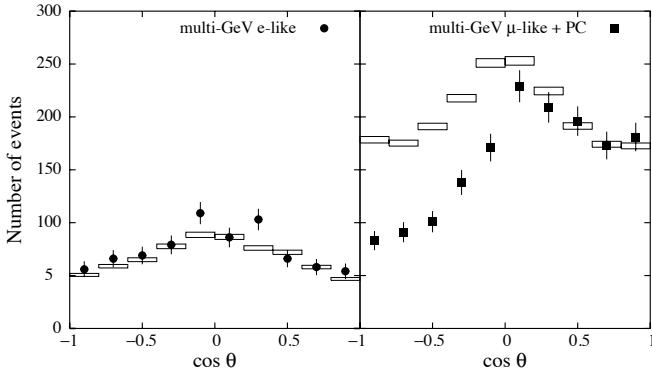
Figure 24.7: Sub-GeV and multi-GeV neutrino interactions from SuperKamiokande [64]. The plot shows the spectra of visible energy in the detector.

Two well-understood properties of atmospheric cosmic rays provide a standard for comparison of the measurements of atmospheric neutrinos. These are the “ $\sec\theta$ effect” and the “east-west effect” [67]. The former refers originally to the enhancement of the flux of > 10 GeV muons (and neutrinos) at large zenith angles, because the parent pions propagate more in the low density upper atmosphere

Table 24.3: Measured fluxes ($10^{-13} \text{ cm}^{-2} \text{ s}^{-1} \text{ sr}^{-1}$) of neutrino-induced muons as a function of the effective minimum muon energy E_μ .

$E_\mu >$	1 GeV	1 GeV	1 GeV	2 GeV	3 GeV	3 GeV
Ref.	CWI [70]	Baksan [71]	MACRO [72]	IMB [73]	Kam [74]	SuperK [75]
F_μ	2.17 ± 0.21	2.77 ± 0.17	2.29 ± 0.15	2.26 ± 0.11	1.94 ± 0.12	1.74 ± 0.07

where decay is enhanced relative to interaction. For neutrinos from muon decay, the enhancement near the horizontal becomes important for $E_\nu > 1 \text{ GeV}$, and arises mainly from the increased pathlength through the atmosphere for muon decay in flight. Fig. 24.8 from Ref. 64 shows a comparison between measurement and expectation for the zenith angle dependence of multi-GeV electron-like (mostly ν_e) and muon-like (mostly ν_μ) events separately. The ν_e show an enhancement near the horizontal and approximate equality for nearly upward ($\cos \theta \approx -1$) and nearly downward ($\cos \theta \approx 1$) events. There is, however, a very significant deficit of upward ($\cos \theta < 0$) ν_μ events, which have long pathlengths comparable to the radius of the Earth. This pattern has been interpreted as evidence for oscillations involving muon neutrinos [68]. (See the article on neutrino properties in this *Review*.) Including three dimensional effects in the calculation of atmospheric neutrinos may change somewhat the expected angular distributions of neutrinos at low energy [69], but it does not change the fundamental expectation of up-down symmetry, which is the basis of the evidence for oscillations.

**Figure 24.8:** Zenith-angle dependence of multi-GeV neutrino interactions from SuperKamiokande [64]. The shaded boxes show the expectation in the absence of any oscillations.

Muons that enter the detector from outside after production in charged-current interactions of neutrinos naturally reflect a higher energy portion of the neutrino spectrum than contained events, because the muon range increases with energy as well as the cross section. The relevant energy range is $\sim 10 < E_\nu < 1000 \text{ GeV}$, depending somewhat on angle. Neutrinos in this energy range show a $\sec \theta$ effect similar to muons (see Eq. (24.5)). This causes the flux of horizontal neutrino-induced muons to be approximately a factor two higher than the vertically upward flux. The upper and lower edges of the horizontal shaded region in Fig. 24.6 correspond to horizontal and vertical intensities of neutrino-induced muons. Table 24.3 gives the measured fluxes of upward-moving neutrino-induced muons averaged over the lower hemisphere. Generally the definition of minimum muon energy depends on where it passes through the detector. The tabulated effective minimum energy estimates the average over various accepted trajectories.

24.5. Air showers

So far we have discussed inclusive or uncorrelated fluxes of various components of the cosmic radiation. An air shower is caused by a single cosmic ray with energy high enough for its cascade to be detectable at the ground. The shower has a hadronic core, which acts as a collimated source of electromagnetic subshowers, generated mostly from $\pi^0 \rightarrow \gamma\gamma$ decays. The resulting electrons and positrons are the most numerous particles in the shower. The number of muons, produced by decays of charged mesons, is an order of magnitude lower. Air showers spread over a large area on the ground, and arrays of detectors operated for long times, are useful for studying cosmic rays with primary energy $E_0 > 100 \text{ TeV}$, where the low flux makes measurements with small detectors in balloons and satellites difficult.

Greisen [76] gives the following approximate expressions for the numbers and lateral distributions of particles in showers at ground level. The total number of muons N_μ with energies above 1 GeV is

$$N_\mu(> 1 \text{ GeV}) \approx 0.95 \times 10^5 \left(N_e / 10^6 \right)^{3/4}, \quad (24.9)$$

where N_e is the total number of charged particles in the shower (not just e^\pm). The number of muons per square meter, ρ_μ , as a function of the lateral distance r (in meters) from the center of the shower is

$$\rho_\mu = \frac{1.25 N_\mu}{2\pi \Gamma(1.25)} \left(\frac{1}{320} \right)^{1.25} r^{-0.75} \left(1 + \frac{r}{320} \right)^{-2.5}, \quad (24.10)$$

where Γ is the gamma function. The number density of charged particles is

$$\rho_e = C_1(s, d, C_2) x^{(s-2)} (1+x)^{(s-4.5)} (1+C_2 x^d). \quad (24.11)$$

Here s , d , and C_2 are parameters in terms of which the overall normalization constant $C_1(s, d, C_2)$ is given by

$$C_1(s, d, C_2) = \frac{N_e}{2\pi r_1^2} [B(s, 4.5 - 2s) + C_2 B(s + d, 4.5 - d - 2s)]^{-1}, \quad (24.12)$$

where $B(m, n)$ is the beta function. The values of the parameters depend on shower size (N_e), depth in the atmosphere, identity of the primary nucleus, *etc.* For showers with $N_e \approx 10^6$ at sea level, Greisen uses $s = 1.25$, $d = 1$, and $C_2 = 0.088$. Finally, x is r/r_1 , where r_1 is the Molière radius, which depends on the density of the atmosphere and hence on the altitude at which showers are detected. At sea level $r_1 \approx 78 \text{ m}$. It increases with altitude as the air density decreases.

The lateral spread of a shower is determined largely by Coulomb scattering of the many low-energy electrons and is characterized by the Molière radius. The lateral spread of the muons (ρ_μ) is larger and depends on the transverse momenta of the muons at production, as well as multiple scattering.

There are large fluctuations in development from shower to shower, even for showers of the same energy and primary mass—especially for small showers, which are usually well past maximum development when observed at the ground. Thus the shower size N_e and primary energy E_0 are only related in an average sense, and even this relation depends on depth in the atmosphere. One estimate of the relation is [77]

$$E_0 \sim 3.9 \times 10^6 \text{ GeV} (N_e / 10^6)^{0.9} \quad (24.13)$$

for vertical showers with $10^{14} < E < 10^{17} \text{ eV}$ at 920 g cm^{-2} (965 m above sea level). As E_0 increases, the shower maximum (on average)

moves down into the atmosphere and the relation between N_e and E_0 changes. Moreover, because of fluctuations, N_e as a function of E_0 is not correctly obtained by inverting Eq. (24.13). At the maximum of shower development, there are approximately 2/3 particles per GeV of primary energy.

There are three types of air shower detectors: shower arrays that study the shower size N_e and the lateral distribution on the ground, Cherenkov detectors that detect the Cherenkov radiation emitted by the charged particles of the shower, and fluorescence detectors that study the nitrogen fluorescence excited by the charged particles in the shower. The fluorescence light is emitted isotropically so the showers can be observed from the side. Detailed simulations and cross-calibrations between different types of detectors are necessary to establish the primary energy spectrum from air-shower experiments.

Figure 24.9 shows the “all-particle” spectrum. The differential energy spectrum has been multiplied by $E^{2.7}$ in order to display the features of the steep spectrum that are otherwise difficult to discern. The steepening that occurs between 10^{15} and 10^{16} eV is known as the *knee* of the spectrum. The feature around 10^{19} eV is called the *ankle* of the spectrum.

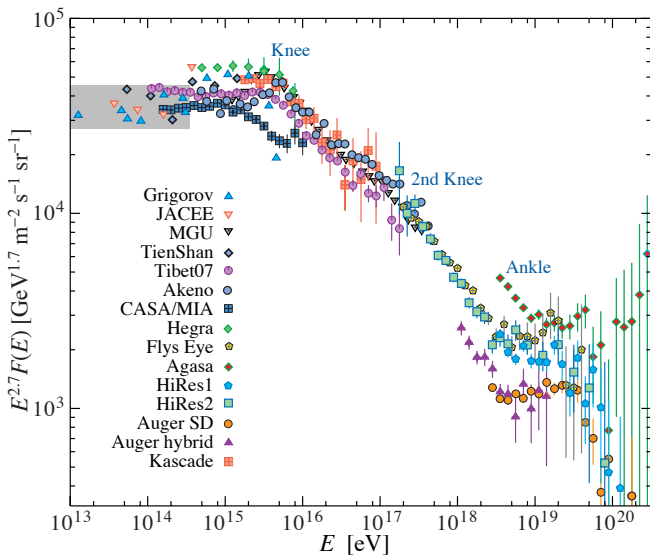


Figure 24.9: The all-particle spectrum from air shower measurements. The shaded area shows the range of the direct cosmic ray spectrum measurements. Color version at end of book.

Measurements with small air shower experiments in the knee region differ by as much as a factor of two, indicative of systematic uncertainties in interpretation of the data. (For a review see Ref. 78.) Newer data sets are listed below. In establishing the spectrum shown in Fig. 24.9, efforts have been made to minimize the dependence of the analysis on the primary composition. Ref. 79 uses an unfolding procedure to obtain the spectra of the individual components, giving a result for the all-particle spectrum between 10^{15} and 10^{17} eV that lies toward the upper range of the data shown in Fig. 24.9. In the energy range above 10^{17} eV, the fluorescence technique [81] is particularly useful, because it can establish the primary energy in a model-independent way by observing most of the longitudinal development of each shower, from which E_0 is obtained by integrating the energy deposition in the atmosphere. The result, however, depends strongly on the light absorption in the atmosphere and the calculation of the detector’s aperture.

Assuming the cosmic ray spectrum below 10^{18} eV is of galactic origin, the *knee* could reflect the fact that most cosmic accelerators in the galaxy have reached their maximum energy. Some types of expanding supernova remnants, for example, are estimated not to be able to accelerate protons above energies in the range of 10^{15} eV.

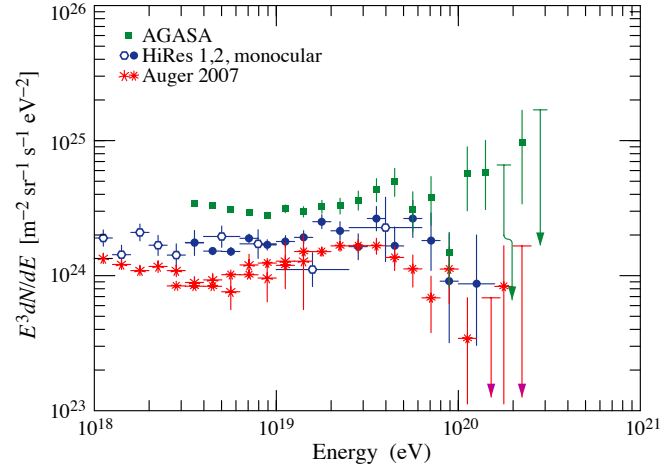


Figure 24.10: Expanded view of the highest energy portion of the cosmic-ray spectrum. ■ [87] (AGASA), ○ [88] (HiRes1,2 monocular), * [89, 90] (Auger). Color version at end of book.

Effects of propagation and confinement in the galaxy [82] also need to be considered.

Concerning the ankle, one possibility is that it is the result of a higher-energy population of particles overtaking a lower-energy population, for example, an extragalactic flux beginning to dominate over the galactic flux (*e.g.*, Ref. 81). Another possibility is that the dip structure in the region of the ankle is due to $\gamma p \rightarrow e^+ + e^-$ energy losses of extragalactic protons on the 2.7 K cosmic microwave radiation (CMB) [84]. This dip structure has been cited as a robust signature of both the protonic and extragalactic nature of the highest energy cosmic rays [83]. If this interpretation is correct, then the end of the galactic cosmic ray spectrum would be at an energy lower than 10^{18} eV, consistent with the maximum expected range of acceleration by supernova remnants. Energy-dependence of the composition from the knee through the ankle holds the key to discriminating between these two viewpoints.

If the cosmic ray flux above the second knee is cosmological in origin, there should be a rapid steepening of the spectrum (called the GZK feature) around 5×10^{19} eV, resulting from the onset of inelastic interactions of UHE cosmic rays with the cosmic microwave background [85,86]. Although all UHECR experiments have detected events of energy above 10^{20} eV [81], [87–89], the spectral shape above the ankle is still not well determined. The AGASA experiment [87] claimed 11 events above 10^{20} eV, while HiRes [88] detected only two. The Auger observatory presented spectra based on its surface detector [89] and on events detected in hybrid mode [90], *i.e.*, with both the surface and the fluorescence detectors. The HiRes and Auger spectra show a significant steepening of the cosmic ray spectrum above $3\text{--}5 \times 10^{19}$ eV, which is consistent with the onset of inelastic interactions with astrophysical photon fields, mostly the CMB [85,86].

Figure 24.10 gives an expanded view of the high energy end of the spectrum, showing only the more recent experiments. (See Ref. 91 for a recent review of all data about 10^{17} eV.) This figure and the previous one have shown the differential flux multiplied by a power of the energy, a procedure that enables one to see structure in the spectrum more clearly, but amplifies small systematic differences in energy assignments into sizable normalization differences. All existing experiments are actually consistent in normalization, if one takes quoted systematic errors in the energy scales into account. However, the continued power law type of flux beyond the GZK cutoff claimed by the AGASA experiment is not supported by the HiRes and Auger data. In November 2007 the Auger Collaboration reported [92] a correlation of the arrival directions of the highest energy cosmic rays with active galactic nuclei (AGN) at distance less than 75 Mpc. Twenty of 27 events with energy above 6×10^{19} eV arrive at an angle less than 3.1° from the position of a nearby AGN.

References:

1. M. Boezio *et al.*, *Astropart. Phys.* **19**, 583 (2003).
2. AMS Collaboration, *Phys. Lett.* **B490**, 27 (2000); *Phys. Lett.* **B494**, 193 (2000).
3. T. Sanuki *et al.*, *Astrophys. J.* **545**, 1135 (2000).
4. S. Haino *et al.*, *Phys. Lett.* **B594**, 35 (2004).
5. CREAM Collaboration, *Proc. 30th Int. Cosmic Ray Conf.*, (Merida, Yucatan, 2007), paper 0301.
6. J.J. Engelmann *et al.*, *Astron. & Astrophys.* **233**, 96 (1990).
7. D. Müller *et al.*, *Ap J*, **374**, 356 (1991).
8. P.J. Boyle *et al.*, *Ap J* submitted. See also P.J. Boyle *et al.*, *Proc. 30th Int. Cosmic Ray Conf.*, (Merida, Yucatan, 2007), paper 1192.
9. A.D. Panov *et al.*, *Bull Russian Acad of Science, Physics*, **71**, 494 (2007).
10. V.A. Derbina *et al.*, *Astrophys. J.* **628**, L41 (2005).
11. K. Asakimori *et al.*(JACEE Collaboration), *Ap J*, **502**, 278 (1998).
12. HESS Collaboration (F. Aharonian *et al.*), *Phys. Rev.* **D75**, 042004 (2007).
13. A.W. Strong *et al.*, *Ann. Rev. Nucl. and Part. Sci.* **157**, 285 (2007).
14. N.E. Yanasak *et al.*, *Ap J*, **563**, 768 (2001).
15. K.K. Tang, *Astrophys. J.* **278**, 881 (1984).
16. D. Müller & J. Tang, *Astrophys. J.* **312**, 183 (1987).
17. J. Nishimura *Advances in Space Research* **19**, 711 (1997).
18. M.A. DuVernois *et al.*, *Astrophys. J.* **559**, 296 (2000).
19. S. Torii *et al.*, *Astrophys. J.* **559**, 973 (2001).
20. K. Yoshida *et al.*, *Proc. 30th Int. Cosmic Ray Conf.*, (Merida, Yucatan, 2007), paper 0892.
21. M. Boezio *et al.*, *Astrophys. J.* **552**, 635 (2000).
22. J. Clem & P. Evenson, *JGR 109 A07107* (2004).
23. J. Alcaraz *et al.*, *Phys. Lett.* **B484**, 10 (2000).
24. A.S. Beach *et al.*, *Phys. Rev. Lett.* **87**, 271101 (2001).
25. A. Yamamoto *et al.*, *Adv. Space Research* (2007) in press.
26. Y. Asaoka *et al.*, *Phys. Rev. Lett.* **88**, 51101 (2002).
27. M. Sasaki *et al.*, *Nucl. Phys.* **B113**, (Proc. Suppl.) 202 (2002).
28. H. Fuke *et al.*, *Phys. Rev. Lett.* **95**, 081101 (2005).
29. R. Bellotti *et al.*, *Phys. Rev.* **D53**, 35 (1996).
30. R. Bellotti *et al.*, *Phys. Rev.* **D60**, 052002 (1999).
31. M. Boezio *et al.*, *Phys. Rev.* **D62**, 032007 (2000).
32. S. Coutu *et al.*, *Phys. Rev.* **D62**, 032001 (2000).
33. T. Sanuki *et al.*, *Phys. Rev.* **D75**, 043005 (2007).
34. T.K. Gaisser, *Cosmic Rays and Particle Physics*, Cambridge University Press (1990).
35. P. Lipari, *Astropart. Phys.* **1**, 195 (1993).
36. E. Mocchiutto *et al.*, in *Proc. 28th Int. Cosmic Ray Conf.*, Tsukuba, 1627 (2003).
37. M.P. De Pascale *et al.*, *J. Geophys. Res.* **98**, 3501 (1993).
38. P.K.F. Grieder, *Cosmic Rays at Earth*, Elsevier Science (2001).
39. J. Kremer *et al.*, *Phys. Rev. Lett.* **83**, 4241 (1999).
40. BESS Collaboration (S. Haino *et al.*), *Phys. Lett.* **B527**, 35 (2004).
41. L3+C Collaboration (P. Archard *et al.*), *Phys. Lett.* **B598**, 15 (2004).
42. O.C. Allkofer, K. Carstensen, and W.D. Dau, *Phys. Lett.* **B36**, 425 (1971).
43. B.C. Rastin, *J. Phys.* **G10**, 1609 (1984).
44. C.A. Ayre *et al.*, *J. Phys.* **G1**, 584 (1975).
45. H. Jokisch *et al.*, *Phys. Rev.* **D19**, 1368 (1979).
46. C.G.S. Costa, *Astropart. Phys.* **16**, 193 (2001).
47. The MINOS Collaboration (P. Adamson *et al.*), *Phys. Rev.* **D76**, 052003 (2007).
48. M. Unger *et al.* (L3 Collab.), *Inter. J. Mod. Phys.* **A20**, 6928 (2005).
49. S. Hayakawa, *Cosmic Ray Physics*, Wiley, Interscience, New York (1969).
50. R.R. Daniel and S.A. Stephens, *Revs. Geophysics & Space Sci.* **12**, 233 (1974).
51. K.P. Beuermann and G. Wibberenz, *Can. J. Phys.* **46**, S1034 (1968).
52. I.S. Diggory *et al.*, *J. Phys.* **A7**, 741 (1974).
53. D.E. Groom, N.V. Mokhov, and S.I. Striganov, "Muon stopping-power and range tables," *Atomic Data and Nuclear Data Tables*, **78**, 183 (2001).
54. P. Lipari and T. Stanev, *Phys. Rev.* **D44**, 3543 (1991).
55. M. Crouch, in *Proc. 20th Int. Cosmic Ray Conf.*, Moscow, **6**, 165 (1987).
56. I.A. Belolaptikov *et al.*, *Astropart. Phys.* **7**, 263 (1997).
57. J. Babson *et al.*, *Phys. Rev.* **D42**, 3613 (1990).
58. P. Desiati *et al.*, in *Proc. 28th Int. Cosmic Ray Conf.*, Tsukuba, 1373 (2003).
59. Yu.M. Andreev, V.I. Gurentzov, and I.M. Kogai, in *Proc. 20th Int. Cosmic Ray Conf.*, Moscow, **6**, 200 (1987).
60. M. Aglietta *et al.*, (LVD Collaboration), *Astropart. Phys.* **3**, 311 (1995).
61. M. Ambrosio *et al.*, (MACRO Collaboration), *Phys. Rev.* **D52**, 3793 (1995).
62. Ch. Berger *et al.*, (Frejus Collaboration), *Phys. Rev.* **D40**, 2163 (1989).
63. C. Waltham *et al.*, in *Proc. 27th Int. Cosmic Ray Conf.*, Hamburg, 991 (2001).
64. SuperKamiokande Collaboration (Y. Ashie *et al.*), *Phys. Rev.* **D71**, 112005 (2005).
65. G. Barr *et al.*, *Phys. Rev.* **D70**, 023006 (2004).
66. M. Honda *et al.*, *Phys. Rev.* **D75**, 096005 (2007).
67. T. Futagami *et al.*, *Phys. Rev. Lett.* **82**, 5194 (1999).
68. Y. Fukuda *et al.*, *Phys. Rev. Lett.* **81**, 1562 (1998).
69. G. Battistoni *et al.*, *Astropart. Phys.* **12**, 315 (2000).
70. F. Reines *et al.*, *Phys. Rev. Lett.* **15**, 429 (1965).
71. M.M. Boliev *et al.*, in *Proc. 3rd Int. Workshop on Neutrino Telescopes* (ed. Milla Baldo Ceolin), 235 (1991).
72. M. Ambrosio *et al.*, (MACRO) *Phys. Lett.* **B434**, 451 (1998). The number quoted for MACRO is the average over 90% of the lower hemisphere, $\cos\theta < -0.1$; see F. Ronga *et al.*, [hep-ex/9905025](#).
73. R. Becker-Szendy *et al.*, *Phys. Rev. Lett.* **69**, 1010 (1992); *Proc. 25th Int. Conf. High-Energy Physics*, Singapore (eds. K.K. Phua and Y. Yamaguchi, World Scientific), 662 (1991).
74. S. Hatakeyama *et al.*, *Phys. Rev. Lett.* **81**, 2016 (1998).
75. Y. Fukuda *et al.*, *Phys. Rev. Lett.* **82**, 2644 (1999).
76. K. Greisen, *Ann. Rev. Nucl. Sci.* **10**, 63 (1960).
77. M. Nagano *et al.*, *J. Phys.* **G10**, 1295 (1984).
78. S.P. Swordy *et al.*, *Astropart. Phys.* **18**, 129 (2002).
79. Cascade collaboration (T. Antoni *et al.*), *Astropart. Phys.* **24**, 1 (2005).
80. M. Amenomori *et al.*, *Proc. 30th Int. Cosmic Ray Conf.*, (Merida, Yucatan, 2007), paper 0277.
81. D.J. Bird *et al.*, *Astrophys. J.* **424**, 491 (1994).
82. V.S. Ptuskin *et al.*, *Astron. & Astrophys.* **268**, 726 (1993).
83. V.S. Berezinsky and S.I. Grigor'eva, *Astron. & Astrophys.* **199**, 1 (1988).
84. V. Berezinsky, A. Gazizov, and S. Grigorieva, *Phys. Rev.* **D74**, 043005 (2006).
85. K. Greisen, *Phys. Rev. Lett.* **16**, 748 (1966).
86. G.T. Zatsepin and V.A. Kuz'min, *Sov. Phys. JETP Lett.* **4**, 78 (1966).
87. The AGASA Collaboration (M. Takeda *et al.*), *Astropart. Phys.* **19**, 447 (2003).
88. R. Abbasi *et al.*, *Phys. Lett.* **B619**, 271 (2005) (see also [astro-ph/0703099](#)).
89. The Auger Collaboration (M. Roth *et al.*), in *Proc. 30th Int. Cosmic Ray Conf.*, Merida, paper 0313 (2007) ([arXiv:0706.2096](#)).
90. The Auger Collaboration (L. Perrone *et al.*), in *Proc. 30th Int. Cosmic Ray Conf.*, Merida, paper 0316 (2007) ([arXiv:0706.2643](#)).
91. D.R. Bergman & J.W. Belz, *J. Phys. G* (in press), [arXiv:0704.3721](#).
92. The Auger Collaboration, *Science* **318**, 938 (2007).

25. ACCELERATOR PHYSICS OF COLLIDERS

Revised August 2005 by K. Desler and D. A. Edwards (DESY).

25.1. Luminosity

The event rate R in a collider is proportional to the interaction cross section σ_{int} and the factor of proportionality is called the *luminosity*:

$$R = \mathcal{L} \sigma_{\text{int}} . \quad (25.1)$$

If two bunches containing n_1 and n_2 particles collide with frequency f , the luminosity is

$$\mathcal{L} = f \frac{n_1 n_2}{4\pi \sigma_x \sigma_y} \quad (25.2)$$

where σ_x and σ_y characterize the Gaussian transverse beam profiles in the horizontal (bend) and vertical directions and to simplify the expression it is assumed that the bunches are identical in transverse profile, that the profiles are independent of position along the bunch, and the particle distributions are not altered during collision. Whatever the distribution at the source, by the time the beam reaches high energy, the normal form is a good approximation thanks to the central limit theorem of probability and the diminished importance of space charge effects.

The beam size can be expressed in terms of two quantities, one termed the *transverse emittance*, ϵ , and the other, the *amplitude function*, β . The transverse emittance is a beam quality concept reflecting the process of bunch preparation, extending all the way back to the source for hadrons and, in the case of electrons, mostly dependent on synchrotron radiation. The amplitude function is a beam optics quantity and is determined by the accelerator magnet configuration. When expressed in terms of σ and β the transverse emittance becomes

$$\epsilon = \pi \sigma^2 / \beta . \quad (25.3)$$

Of particular significance is the value of the amplitude function at the interaction point, β^* . Clearly one wants β^* to be as small as possible; how small depends on the capability of the hardware to make a near-focus at the interaction point.

Eq. (25.2) can now be recast in terms of emittances and amplitude functions as

$$\mathcal{L} = f \frac{n_1 n_2}{4\sqrt{\epsilon_x \beta_x^* \epsilon_y \beta_y^*}} . \quad (25.4)$$

Thus, to achieve high luminosity, all one has to do is make high population bunches of low emittance to collide at high frequency at locations where the beam optics provides as low values of the amplitude functions as possible.

25.2. Beam dynamics

Today's operating HEP colliders are all synchrotrons, and the organization of this section reflects that circumstance.

A major concern of beam dynamics is stability: conservation of adequate beam properties over a sufficiently long time scale. Several time scales are involved, and the approximations used in writing the equations of motion reflect the time scale under consideration. For example, when, in Sec. 25.2.1 below, we write the equations for transverse stability no terms associated with phase stability or synchrotron radiation appear; the time scale associated with the last two processes is much longer than that demanded by the need for transverse stability.

25.2.1. *Betatron oscillations* :

Present-day high-energy accelerators employ alternating gradient focussing provided by quadrupole magnetic fields [1], [2]. The equations of motion of a particle undergoing oscillations with respect to the design trajectory are

$$x'' + K_x(s)x = 0 , \quad y'' + K_y(s)y = 0 , \quad (25.5)$$

with

$$x' \equiv dx/ds , \quad y' \equiv dy/ds \quad (25.6)$$

$$K_x \equiv B'/(B\rho) + \rho^{-2} , \quad K_y \equiv -B'/(B\rho) \quad (25.7)$$

$$B' \equiv \partial B_y / \partial x . \quad (25.8)$$

The independent variable s is path length along the design trajectory. This motion is called a *betatron* oscillation because it was initially studied in the context of that type of accelerator. The functions K_x and K_y reflect the transverse focussing—primarily due to quadrupole fields except for the radius of curvature, ρ , term in K_x for a synchrotron—so each equation of motion resembles that for a harmonic oscillator but with spring constants that are a function of position. No terms relating to synchrotron oscillations appear, because their time scale is much longer and in this approximation play no role.

These equations have the form of Hill's equation and so the solution in one plane may be written as

$$x(s) = A\sqrt{\beta(s)} \cos(\psi(s) + \delta) , \quad (25.9)$$

where A and δ are constants of integration and the phase advances according to $d\psi/ds = 1/\beta$. The dimension of A is the square root of length, reflecting the fact that the oscillation amplitude is modulated by the square root of the amplitude function. In addition to describing the envelope of the oscillation, β also plays the role of an 'instantaneous' λ . The wavelength of a betatron oscillation may be some tens of meters, and so typically values of the amplitude function are of the order of meters rather than on the order of the beam size. The beam optics arrangement generally has some periodicity and the amplitude function is chosen to reflect that periodicity. As noted above, a small value of the amplitude function is desired at the interaction point, and so the focussing optics is tailored in its neighborhood to provide a suitable β^* .

The number of betatron oscillations per turn in a synchrotron is called the *tune* and is given by

$$\nu = \frac{1}{2\pi} \oint \frac{ds}{\beta} . \quad (25.10)$$

Expressing the integration constant A in the solution above in terms of x , x' yields the *Courant-Snyder invariant*

$$A^2 = \gamma(s)x(s)^2 + 2\alpha(s)x(s)x'(s) + \beta(s)x'(s)^2$$

where

$$\alpha \equiv -\beta'/2 , \quad \gamma \equiv \frac{1 + \alpha^2}{\beta} . \quad (25.11)$$

(The Courant-Snyder parameters α , β and γ employ three Greek letters which have other meanings and the significance at hand must often be recognized from context.) Because β is a function of position in the focussing structure, this ellipse changes orientation and aspect ratio from location to location but the area πA^2 remains the same.

As noted above the transverse emittance is a measure of the area in x , x' (or y , y') phase space occupied by an ensemble of particles. The definition used in Eq. (25.3) is the area that encloses 39% of a Gaussian beam.

For electron synchrotrons the equilibrium emittance results from the balance between synchrotron radiation damping and excitation from quantum fluctuations in the radiation rate. The equilibrium is reached in a time small compared with the storage time.

For present-day hadron synchrotrons, synchrotron radiation does not play a similar role in determining the transverse emittance. Rather the emittance during storage reflects the source properties and the abuse suffered by the particles throughout acceleration and storage. Nevertheless it is useful to argue as follows: Though x' and x can serve as canonically conjugate variables at constant energy this definition of the emittance would not be an adiabatic invariant when the energy changes during the acceleration cycle. However, $\gamma(v/c)x'$, where here γ is the Lorentz factor, is proportional to the transverse momentum and so qualifies as a variable conjugate to x . So often one sees a normalized emittance defined according to

$$\epsilon_N = \gamma \frac{v}{c} \epsilon , \quad (25.12)$$

which is an approximate adiabatic invariant, e.g. during acceleration.

25.2.2. Phase stability: The particles in a circular collider also undergo synchrotron oscillations. This is usually referred to as motion in the *longitudinal* degree-of-freedom because particles arrive at a particular position along the accelerator earlier or later than an ideal reference particle. This circumstance results in a finite bunch length, which is related to an energy spread.

For dynamical variables in longitudinal phase space, let us take ΔE and Δt , where these are the energy and time differences from that of the ideal particle. A positive Δt means a particle is behind the ideal particle. The equation of motion is the same as that for a physical pendulum and therefore is nonlinear. But for small oscillations, it reduces to a simple harmonic oscillator:

$$\frac{d^2 \Delta t}{dn^2} = -(2\pi\nu_s)^2 \Delta t \quad (25.13)$$

where the independent variable n is the turn number and ν_s is the number of synchrotron oscillations per turn, analogous to the betatron oscillation tune defined earlier. Implicit in this equation is the approximation that n is a continuous variable. This approximation is valid provided $\nu_s \ll 1$, which is usually well satisfied in practice.

In the high-energy limit, where $v/c \approx 1$,

$$\nu_s = \left[\frac{h\eta eV \cos \phi_s}{2\pi E} \right]^{1/2} . \quad (25.14)$$

There are four as yet undefined quantities in this expression: the harmonic number h , the slip factor η , the maximum energy eV gain per turn from the acceleration system, and the synchronous phase ϕ_s . The frequency of the RF system is normally a relatively high multiple, h , of the orbit frequency. The slip factor relates the fractional change in the orbit period τ to changes in energy according to

$$\frac{\Delta \tau}{\tau} = \eta \frac{\Delta E}{E} . \quad (25.15)$$

At sufficiently high energy, the slip factor just reflects the relationship between path length and energy, since the speed is a constant; η is positive for all the synchrotrons in the “Tables of Collider Parameters” (Sec. 26).

The synchronous phase is a measure of how far up on the RF wave the average particle must ride in order to maintain constant energy to counteract of synchrotron radiation. That is, $\sin \phi_s$ is the ratio of the energy loss per turn to the maximum energy per turn that can be provided by the acceleration system. For hadron colliders built to date, $\sin \phi_s$ is effectively zero. This is not the case for electron storage rings; for example, the electron ring of HERA runs at a synchronous phase of 45° .

Now if one has a synchrotron oscillation with amplitudes $\widehat{\Delta t}$ and $\widehat{\Delta E}$,

$$\Delta t = \widehat{\Delta t} \sin(2\pi\nu_s n) , \quad \Delta E = \widehat{\Delta E} \cos(2\pi\nu_s n) \quad (25.16)$$

then the amplitudes are related according to

$$\widehat{\Delta E} = \frac{2\pi\nu_s E}{\eta\tau} \widehat{\Delta t} . \quad (25.17)$$

The longitudinal emittance ϵ_ℓ may be defined as the phase space area bounded by particles with amplitudes $\widehat{\Delta t}$ and $\widehat{\Delta E}$. In general, the longitudinal emittance for a given amplitude is found by numerical integration. For $\sin \phi_s = 0$, an analytical expression is as follows:

$$\epsilon_\ell = \left[\frac{2\pi^3 E e V h}{\tau^2 \eta} \right]^{1/2} (\widehat{\Delta t})^2 \quad (25.18)$$

Again, a Gaussian is a reasonable representation of the longitudinal profile of a well-behaved beam bunch; if $\sigma_{\Delta t}$ is the standard deviation of the time distribution, then the bunch length can be characterized by

$$\ell = c \sigma_{\Delta t} . \quad (25.19)$$

In the electron case the longitudinal emittance is determined by the synchrotron radiation process just as in the transverse degrees of freedom. For the hadron case the history of acceleration plays a role and because energy and time are conjugate coordinates, the longitudinal emittance is a quasi-invariant.

For HEP bunch length is a significant quantity because if the bunch length becomes larger than β^* the luminosity is adversely affected. This is because β grows parabolically as one proceeds away from the IP and so the beam size increases thus lowering the contribution to the luminosity from such locations. Further discussion and modified expressions for the luminosity may be found in Furman and Zisman [3].

25.2.3. Synchrotron radiation [4]: A relativistic particle undergoing centripetal acceleration radiates at a rate given by the Larmor formula multiplied by the 4th power of the Lorentz factor:

$$P = \frac{1}{6\pi\epsilon_0} \frac{c^2 a^2}{c^3} \gamma^4 . \quad (25.20)$$

Here, $a = v^2/\rho$ is the centripetal acceleration of a particle with speed v undergoing deflection with radius of curvature ρ . In a synchrotron that has a constant radius of curvature within bending magnets, the energy lost due to synchrotron radiation per turn is the above multiplied by the time spent in bending magnets, $2\pi\rho/v$. Expressed in familiar units, this result may be written

$$W = 8.85 \times 10^{-5} E^4 / \rho \text{ MeV per turn} \quad (25.21)$$

for electrons at sufficiently high energy that $v \approx c$. The energy E is in GeV and ρ is in kilometers. The radiation has a broad energy spectrum which falls off rapidly above the *critical energy*, $E_c = (3c/2\rho)\hbar\gamma^3$. Typically, E_c is in the hard x-ray region.

The characteristic time for synchrotron radiation processes is the time during which the energy must be replenished by the acceleration system. If f_0 is the orbit frequency, then the characteristic time is given by

$$\tau_0 = \frac{E}{f_0 W} . \quad (25.22)$$

Oscillations in each of the three degrees of freedom either damp or antidamp depending on the design of the accelerator. For a simple separated-function alternating gradient synchrotron, all three modes damp. The damping time constants are related by Robinson's Theorem, which, expressed in terms of τ_0 , is

$$\frac{1}{\tau_x} + \frac{1}{\tau_y} + \frac{1}{\tau_s} = 2 \frac{1}{\tau_0} . \quad (25.23)$$

Even though all three modes may damp, the emittances do not tend toward zero. Statistical fluctuations in the radiation rate excite synchrotron oscillations and radial betatron oscillations. Thus there is an equilibrium emittance at which the damping and excitation are in balance. The vertical emittance is non-zero due to horizontal-vertical coupling.

Polarization can develop from an initially unpolarized beam as a result of synchrotron radiation. A small fraction $\approx E_c/E$ of the radiated power flips the electron spin. Because the lower energy state is that in which the particle magnetic moment points in the same direction as the magnetic bend field, the transition rate toward this alignment is larger than the rate toward the reverse orientation. An equilibrium polarization of 92% is predicted, and despite a variety of depolarizing processes, polarization above 80% has been observed at a number of facilities.

The radiation rate for protons is of course down by a factor of the fourth power of the mass ratio, and is given by

$$W = 7.8 \times 10^{-3} E^4 / \rho \text{ keV per turn} \quad (25.24)$$

where E is now in TeV and ρ in km. For the LHC, synchrotron radiation presents a significant load to the cryogenic system, and impacts magnet design due to gas desorption and secondary electron emission from the wall of the cold beam tube. The critical energy for the LHC is 44 eV.

25.2.4. Beam-beam tune shift [5] : In a bunch-bunch collision the particles of one bunch see the other bunch as a nonlinear lens. Therefore the focussing properties of the ring are changed in a way that depends on the transverse oscillation amplitude. Hence there is a spread in the frequency of betatron oscillations.

There is an extensive literature on the subject of how large this tune spread can be. In practice, the limiting value is hard to predict. It is consistently larger for electrons because of the beneficial effects of damping from synchrotron radiation.

In order that contributions to the total tune spread arise only at the detector locations, the beams in a multibunch collider are kept apart elsewhere in the collider by a variety of techniques. For equal energy particles of opposite charge circulating in the same vacuum chamber, electrostatic separators may be used assisted by a crossing angle if appropriate. For particles of equal energy and of the same charge, a crossing angle is needed not only for tune spread reasons but to steer the particles into two separate beam pipes. In HERA, because of the large ratio of proton to electron energy, separation can be achieved by bending magnets.

25.2.5. Luminosity lifetime : In electron synchrotrons the luminosity degrades during the store primarily due to particles leaving the phase stable region in longitudinal phase space as a result of quantum fluctuations in the radiation rate and bremsstrahlung. For hadron colliders the luminosity deteriorates due to emittance dilution resulting from a variety of processes. In practice, stores are intentionally terminated when the luminosity drops to the point where a refill will improve the integrated luminosity, while synchrotron radiation facilitates a “topping-up” process in electron-positron rings to provide continuous luminosity.

25.2.6. Luminosity: Achieved and Desired :

Many years ago, the CERN Intersecting Storage Rings set an enviable luminosity record for proton-proton collisions at $1.3 \times 10^{32} \text{ cm}^{-2}\text{s}^{-1}$. Not until the Summer of 2005 was this level matched in a proton-antiproton collider as the Tevatron approached an integrated luminosity of 1 fb^{-1} in its Run II. Thus far, electrons have proved more amenable; KEKB has reached $1.5 \times 10^{34} \text{ cm}^{-2}\text{s}^{-1}$, with the implication of integrated luminosity in the $100 \text{ fb}^{-1}\text{yr}^{-1}$ range.

The luminosity specification for a yet-to-be-built system is a complicated process, involving considerations of organization, funding,

politics and so forth outside the scope of this paper. In the electron world, the $1/s$ dependence of cross sections such as “Higgs-strahlung” plays an important role. In the complex hadron environment, the higher luminosity potential of the LHC helped offset the otherwise totally adverse consequences of the SSC project cancellation. As a historical observation, it is interesting that although improvement directions of present and past facilities could not spelled out in advance, such opportunities have proved to be of critical value to the advance of HEP.

25.3. Prospects

While this update is in preparation, it is interesting to recall that exactly 20 years ago, the Tevatron was entering its commissioning phase as a proton-antiproton collider to provide a c.m.s. energy at the 2 TeV level. Now, the next major step in discovery reach is approaching. The LHC is scheduled to begin operation in 2007, with its proton beams colliding at 14 TeV c.m.s., and at a luminosity two orders of magnitude above that reached in the Tevatron. LHC progress may be followed at the website provided by CERN [6].

A concerted international effort is underway aimed toward the construction of the electron-positron counterpart of the LHC – a linear collider to operate at the 0.5–1.0 TeV c.m.s. level. A recent decision of an International Technical Review Panel decided in favor of the superconducting RF approach for the main linacs [7]. A current goal is to develop the design report by the end of 2006.

References:

1. E. D. Courant and H. S. Snyder, *Ann. Phys.* **3**, 1 (1958). This is the classic article on the alternating gradient synchrotron.
2. A. W. Chao and M. Tigner (eds.), *Handbook of Accelerator Physics and Engineering*, World Science Publishing Co. (Singapore, 2nd printing, 2002.), Sec. 2.1.
3. M. A. Furman and M. S. Zisman, *Handbook of Accelerator Physics and Engineering*, *op cit*, Sec. 4.1.
4. H. Wiedemann, *Handbook of Accelerator Physics and Engineering*, *op cit*, Sec. 3.1.
5. K. Hirata, P. Chen, J. M. Jowett, *Handbook of Accelerator Physics and Engineering*, *op cit*, Secs. 2.6.1, 2.6.2, 2.6.3, respectively.
6. <http://lhc-new-homepage.web.cern.ch/lhc-new-homepage/>.
7. <http://www.interactions.org/linearcollider/gde/>.

HIGH-ENERGY COLLIDER PARAMETERS: e^+e^- Colliders (I)

Updated in early 2008 with numbers received from representatives of the colliders (contact J. Beringer, LBNL). For existing (future) colliders the latest achieved (design) values are given. Quantities are, where appropriate, r.m.s.; H and V indicate horizontal and vertical directions; s.c. stands for superconducting. Parameters for the defunct SPEAR, DORIS, PETRA, PEP, SLC, TRISTAN, and VEPP-2M colliders may be found in our 1996 edition (Phys. Rev. **D54**, 1 July 1996, Part I).

	VEPP-2000 (Novosibirsk)	VEPP-4M (Novosibirsk)	BEPC (China)	BEPC-II (China)	DAΦNE (Frascati)
Physics start date	2008	1994	1989	2008	1999
Physics end date	—	—	2005	—	2008
Maximum beam energy (GeV)	1.0	6	2.2	1.89 (2.3 max)	0.700
Luminosity (10^{30} cm $^{-2}$ s $^{-1}$)	100	20	12.6 at 1.843 GeV/beam 5 at 1.55 GeV/beam	1000	150 (500 achievable)
Time between collisions (μ s)	0.04	0.6	0.8	0.008	0.0027
Full crossing angle (μ rad)	0	0	0	2.2×10^4	$(2.5 \text{ to } 3.2) \times 10^4$
Energy spread (units 10^{-3})	0.64	1	0.58 at 2.2 GeV	0.52	0.40
Bunch length (cm)	4	5	≈ 5	1.3	low current: 1 high current: 3
Beam radius (10^{-6} m)	125 (round)	H : 1000 V : 30	H : 890 V : 37	H : 380 V : 5.7	H : 800 V : 4.8
Free space at interaction point (m)	± 1	± 2	± 2.15	± 0.63	± 0.40
Luminosity lifetime (hr)	continuous	2	7–12	1.5	0.7
Turn-around time (min)	continuous	18	32	26	0.8 (topping up)
Injection energy (GeV)	0.2–1.0	1.8	1.55	1.89	on energy
Transverse emittance ($10^{-9}\pi$ rad-m)	H : 250 V : 250	H : 200 V : 20	H : 660 V : 28	H : 144 V : 2.2	H : 300 V : 1
β^* , amplitude function at interaction point (m)	H : 0.06 – 0.11 V : 0.06 – 0.10	H : 0.75 V : 0.05	H : 1.2 V : 0.05	H : 1.0 V : 0.015	H : 0.25 V : 0.009
Beam-beam tune shift per crossing (units 10^{-4})	H : 750 V : 750	500	350	400	250
RF frequency (MHz)	172	180	199.53	499.8	356
Particles per bunch (units 10^{10})	16	15	20 at 2 GeV 11 at 1.55 GeV	4.8	e^- : 3.3 e^+ : 2.4
Bunches per ring per species	1	2	1	93	120 (incl. 10 bunch gap)
Average beam current per species (mA)	150	80	40 at 2 GeV 22 at 1.55 GeV	910	e^- : 1800 e^+ : 1300
Circumference or length (km)	0.024	0.366	0.2404	0.23753	0.098
Interaction regions	2	1	2	1	2
Magnetic length of dipole (m)	1.2	2	1.6	Outer ring: 1.6 Inner ring: 1.41	1
Length of standard cell (m)	12	7.2	6.6	Outer ring: 6.6 Inner ring: 6.2	12
Phase advance per cell (deg)	H : 738 V : 378	65	≈ 60	60–90 no standard cell	360
Dipoles in ring	8	78	40 + 4 weak	84 + 8 weak	8
Quadrupoles in ring	20	150	68	134+2 s.c.	48
Peak magnetic field (T)	2.4	0.6	0.903 at 2.8 GeV	Outer ring: 0.677 Inner ring: 0.766	1.7

HIGH-ENERGY COLLIDER PARAMETERS: e^+e^- Colliders (II)

Updated in early 2008 with numbers received from representatives of the colliders (contact J. Beringer, LBNL). For existing (future) colliders the latest achieved (design) values are given. Quantities are, where appropriate, r.m.s.; H and V indicate horizontal and vertical directions; s.c. stands for superconducting.

	CESR (Cornell)	CESR-C (Cornell)	KEKB (KEK)	PEP-II (SLAC)	LEP (CERN)	ILC (TBD)
Physics start date	1979	2002	1999	1999	1989	TBD
Physics end date	2002	2008	—	2008	2000	—
Maximum beam energy (GeV)	6	6	$e^- \times e^+ : 8 \times 3.5$	$e^- : 7-12$ (9.0 nominal) $e^+ : 2.5-4$ (3.1 nominal) (nominal $E_{\text{cm}} = 10.5$ GeV)	100 - 104.6	250 (upgrade-able to 500)
Luminosity ($10^{30} \text{ cm}^{-2}\text{s}^{-1}$)	1280 at 5.3 GeV/beam	76 at 2.08 GeV/beam	17120	12069 (design: 3000)	24 at Z^0 100 at > 90 GeV	2×10^4
Time between collisions (μs)	0.014 to 0.22	0.014 to 0.22	0.00590 or 0.00786	0.0042	22	0.3^{\ddagger}
Full crossing angle (μ rad)	± 2000	± 3300	$\pm 11000^{\dagger}$	0	0	14000
Energy spread (units 10^{-3})	0.6 at 5.3 GeV/beam	0.82 at 2.08 GeV/beam	0.7	$e^-/e^+ : 0.61/0.77$	0.7→1.5	1
Bunch length (cm)	1.8	1.2	0.65	$e^-/e^+ : 1.1/1.0$	1.0	0.03
Beam radius (μm)	$H : 460$ $V : 4$	$H : 340$ $V : 6.5$	$H : 110$ $V : 1.9$	$H : 157$ $V : 4.7$	$H : 200 \rightarrow 300$ $V : 2.5 \rightarrow 8$	$H : 0.639$ $V : 0.0057$
Free space at interaction point (m)	± 2.2 (± 0.6 to REC quads)	± 2.2 (± 0.3 to PM quads)	$+0.75/-0.58$ ($+300/-500$) mrad cone	± 0.2 , ± 300 mrad cone	± 3.5	± 3.5
Luminosity lifetime (hr)	2-3	2-3	continuous	continuous	20 at Z^0 10 at > 90 GeV	n/a
Turn-around time (min)	5 (topping up)	1.5 (topping up)	continuous	continuous	50	n/a
Injection energy (GeV)	1.8-6	1.5-6	$e^-/e^+ : 8/3.5$	2.5-12	22	n/a
Transverse emittance (π rad-nm)	$H : 210$ $V : 1$	$H : 120$ $V : 3.5$	$e^- : 24$ (H), 0.61 (V) $e^+ : 18$ (H), 0.56 (V)	$e^- : 48$ (H), 1.5 (V) $e^+ : 24$ (H), 1.5 (V)	$H : 20-45$ $V : 0.25 \rightarrow 1$	$H : 0.02$ $V : 8 \times 10^{-5}$ (at 250 GeV)
β^* , amplitude function at interaction point (m)	$H : 1.0$ $V : 0.018$	$H : 0.94$ $V : 0.012$	$e^- : 0.56$ (H), 0.0059 (V) $e^+ : 0.59$ (H), 0.0065 (V)	$e^- : 0.50$ (H), 0.012 (V) $e^+ : 0.50$ (H), 0.012 (V)	$H : 1.5$ $V : 0.05$	$H : 0.02$ $V : 0.0004$
Beam-beam tune shift per crossing (units 10^{-4})	$H : 250$ $V : 620$	$e^- : 420$ (H), 280 (V) $e^+ : 410$ (H), 270 (V)	$e^- : 750$ (H), 560 (V) $e^+ : 1150$ (H), 1010 (V)	$e^- : 703$ (H), 498 (V) $e^+ : 510$ (H), 727 (V)	830	n/a
RF frequency (MHz)	500	500	508.887	476	352.2	1300
Particles per bunch (units 10^{10})	1.15	4.7	$e^-/e^+ : 6.1/7.5$	$e^-/e^+ : 5.2/8.0$	45 in collision 60 in single beam	2
Bunches per ring per species	9 trains of 5 bunches	8 trains of 3 bunches	1389	1732	4 trains of 1 or 2	2625
Average beam current per species (mA)	340	72	$e^-/e^+ : 1330/1650$	$e^-/e^+ : 1960/3026$	4 at Z^0 4→6 at > 90 GeV	9 (in pulse)
Beam polarization (%)	—	—	—	—	55 at 45 GeV 5 at 61 GeV	$e^- : > 80\%$ $e^+ : > 60\%$
Circumference or length (km)	0.768	0.768	3.016	2.2	26.66	31
Interaction regions	1	1	1	1	4	1
Magnetic length of dipole (m)	1.6-6.6	1.6-6.6	$e^-/e^+ : 5.86/0.915$	$e^-/e^+ : 5.4/0.45$	11.66/pair	n/a
Length of standard cell (m)	16	16	$e^-/e^+ : 75.7/76.1$	15.2	79	n/a
Phase advance per cell (deg)	45-90 (no standard cell)	45-90 (no standard cell)	450	$e^-/e^+ : 60/90$	102/90	n/a
Dipoles in ring	86	84	$e^-/e^+ : 116/112$	$e^-/e^+ : 192/192$	3280+24 inj. + 64 weak	n/a
Quadrupoles in ring	101 + 4 s.c.	101 + 4 s.c.	$e^-/e^+ : 452/452$	$e^-/e^+ : 290/326$	520+288 + 8 s.c.	n/a
Peak magnetic field (T)	0.3 / 0.8 at 8 GeV	0.3 / 0.8 at 8 GeV, 2.1 wigglers at 1.9 GeV	$e^-/e^+ : 0.25/0.72$	$e^-/e^+ : 0.18/0.75$	0.135	n/a

[†]KEKB is operating with crab crossing since February 2007.

[‡]Time between bunch trains: 200ms.

HIGH-ENERGY COLLIDER PARAMETERS: ep , $\bar{p}p$, pp , and Heavy Ion Colliders

Updated in early 2008 with numbers received from representatives of the colliders (contact J. Beringer, LBNL). For existing (future) colliders the latest achieved (design) values are given. Quantities are, where appropriate, r.m.s.; H and V indicate horizontal and vertical directions; s.c. stands for superconducting; pk and ave denote peak and average values.

	HERA (DESY)	TEVATRON* (Fermilab)	RHIC (Brookhaven)				LHC (CERN)	
			2001	2000	2004	2002	2008	2009
Physics start date	1992	1987	2001	2000	2004	2002	2008	2009
Physics end date	2007	—	—				—	
Particles collided	ep	$\bar{p}p$	pp (pol.)	Au Au	Cu Cu	d Au	pp	Pb Pb
Maximum beam energy (TeV)	e : 0.030 p : 0.92	0.980	0.1 60% pol	0.1 TeV/n	0.1 TeV/n	0.1 TeV/n	7.0	2.76 TeV/n
Luminosity (10^{30} cm $^{-2}$ s $^{-1}$)	75	286	35 (pk) 20 (ave)	0.0030 (pk) 0.0012 (ave)	0.020 (pk) 0.0008 (ave)	0.23 (pk) 0.11 (ave)	1.0×10^4	1.0×10^{-3} (5.4×10^{-5}) [†]
Time between collisions (ns)	96	396	107	107	321	107	24.95	99.8 (1347) [†]
Full crossing angle (μ rad)	0	0	0				≈ 300	≤ 100 (0) [†]
Energy spread (units 10^{-3})	e : 0.91 p : 0.2	0.14	0.45	0.75	0.75	0.65	0.113	0.11
Bunch length (cm)	e : 0.83 p : 8.5	p : 50 \bar{p} : 45	100	30	30	25	7.55	7.94
Beam radius (10^{-6} m)	e : 280(H), 50(V) p : 265(H), 50(V)	p : 28 \bar{p} : 16	165 ($\beta^*=1$ m)	145 ($\beta^*=1$ m)	145 ($\beta^*=0.9$ m)	155 ($\beta^*=2$ m)	16.6	15.9 (22.5) [†]
Free space at interaction point (m)	± 2	± 6.5	16				38	38
Initial luminosity decay time, $-L/(dL/dt)$ (hr)	10	6 (average)	3.9	1.5	1.8	1.8	14.9	10.9 - 3.6 [‡] (22 - 7.5) ^{††}
Turn-around time (min)	e : 75, p : 135	150	155	150	145	145	60	
Injection energy (TeV)	e : 0.012 p : 0.040	0.15	0.023	0.011 TeV/n	0.011 TeV/n	0.012 TeV/n	0.450	0.1774 TeV/n
Transverse emittance ($10^{-9}\pi$ rad-m)	e : 20(H), 3.5(V) p : 5(H), 5(V)	p : 3 \bar{p} : 1	28	26	23	28	0.5	0.5
β^* , ampl. function at interaction point (m)	e : 0.6(H), 0.26(V) p : 2.45(H), 0.18(V)	0.28	> 1.0	> 0.8	> 0.9	> 0.85	0.55	0.5 (1.0) [†]
Beam-beam tune shift per crossing (units 10^{-4})	e : 190(H), 450(V) p : 12(H), 9(V)	p : 120 \bar{p} : 120	56	15	30	d: 21 Au: 17	34	—
RF frequency (MHz)	e : 499.7 p : 208.2/52.05	53	accel: 28 store: 28	accel: 28 store: 197	accel: 28 store: 197	accel: 28 store: 197	400.8	400.8
Particles per bunch (units 10^{10})	e : 3 p : 7	p : 26 \bar{p} : 9	13.5	0.11	0.45	d: 10 Au: 0.1	11.5	0.007
Bunches per ring per species	e : 189 p : 180	36	111	103	37	95	2808	592 (62) [†]
Average beam current per species (mA)	e : 40 p : 90	p : 70 \bar{p} : 24	187	112	60	d: 119 Au: 94	584	6.12 (0.641) [†]
Circumference (km)	6.336	6.28	3.834				26.659	
Interaction regions	2 colliding beams 1 fixed target (e beam)	2 high \mathcal{L}	6 total, 2 high \mathcal{L}				2 high \mathcal{L} +1	1 dedicated +2
Magnetic length of dipole (m)	e : 9.185 p : 8.82	6.12	9.45				14.3	
Length of standard cell (m)	e : 23.5 p : 47	59.5	29.7				106.90	
Phase advance per cell (deg)	e : 60 p : 90	67.8	84			d: 84 Au: 93	90	
Dipoles in ring	e : 396 p : 416	774	192 per ring + 12 common				1232 main dipoles	
Quadrupoles in ring	e : 580 p : 280	216	246 per ring				482 2-in-1 24 1-in-1	
Magnet type	e : C-shaped p : s.c., collared, cold iron	s.c. $\cos\theta$ warm iron	s.c. $\cos\theta$ cold iron				s.c. 2 in 1 cold iron	
Peak magnetic field (T)	e : 0.274 p : 5	4.4	3.5				8.3	

* Additional TEVATRON parameters: \bar{p} source accum. rate: 25×10^{10} hr $^{-1}$; max. no. of \bar{p} stored: 3.1×10^{12} (Accumulator), 4.6×10^{12} (Recycler).

[†] Numbers in parentheses refer to settings for "Early" PbPb running.

[‡] For 1 - 3 experiments.

27. PASSAGE OF PARTICLES THROUGH MATTER

Revised April 2008 by H. Bichsel (University of Washington),
D.E. Groom (LBNL), and S.R. Klein (LBNL).

27. PASSAGE OF PARTICLES THROUGH MATTER	267
27.1. Notation	267
27.2. Electronic energy loss by heavy particles	268
27.2.1. Energy loss at low energies	269
27.2.2. Density effect	269
27.2.3. Energetic knock-on electrons (δ rays)	270
27.2.4. Restricted energy loss rates for relativistic ionizing particles	270
27.2.5. Fluctuations in energy loss	270
27.2.6. Energy loss in mixtures and compounds	271
27.2.7. Ionization yields	271
27.3. Multiple scattering through small angles	271
27.4. Photon and electron interactions in matter	272
27.4.1. Radiation length	272
27.4.2. Energy loss by electrons	273
27.4.3. Critical energy	274
27.4.4. Energy loss by photons	274
27.4.5. Bremsstrahlung and pair production at very high energies	275
27.5. Electromagnetic cascades	276
27.6. Muon energy loss at high energy	277
27.7. Cherenkov and transition radiation	278

27.1. Notation

Table 27.1: Summary of variables used in this section. The kinematic variables β and γ have their usual meanings.

Symbol	Definition	Units or Value
α	Fine structure constant ($e^2/4\pi\epsilon_0\hbar c$)	1/137.035 999 11(46)
M	Incident particle mass	MeV/ c^2
E	Incident part. energy γMc^2	MeV
T	Kinetic energy	MeV
$m_e c^2$	Electron mass $\times c^2$	0.510 998 918(44) MeV
r_e	Classical electron radius $e^2/4\pi\epsilon_0 m_e c^2$	2.817 940 325(28) fm
N_A	Avogadro's number	$6.022 1415(10) \times 10^{23}$ mol $^{-1}$
ze	Charge of incident particle	
Z	Atomic number of absorber	
A	Atomic mass of absorber	g mol $^{-1}$
K/A	$4\pi N_A r_e^2 m_e c^2 / A$	0.307 075 MeV g $^{-1}$ cm 2 for $A = 1$ g mol $^{-1}$
I	Mean excitation energy	eV (<i>Nota bene!</i>)
$\delta(\beta\gamma)$	Density effect correction to ionization energy loss	
$\hbar\omega_p$	Plasma energy ($\sqrt{4\pi N_e r_e^3} m_e c^2 / \alpha$)	28.816 $\sqrt{\rho(Z/A)}$ eV ^(a)
N_e	Electron density	(units of r_e) $^{-3}$
w_j	Weight fraction of the j th element in a compound or mixture	
n_j	α number of j th kind of atoms in a compound or mixture	
—	$4\alpha r_e^2 N_A / A$	(716.408 g cm $^{-2}$) $^{-1}$ for $A = 1$ g mol $^{-1}$
X_0	Radiation length	g cm $^{-2}$
E_c	Critical energy for electrons	MeV
$E_{\mu c}$	Critical energy for muons	GeV
E_s	Scale energy $\sqrt{4\pi/\alpha} m_e c^2$	21.2052 MeV
R_M	Molière radius	g cm $^{-2}$

(a) For ρ in g cm $^{-3}$.

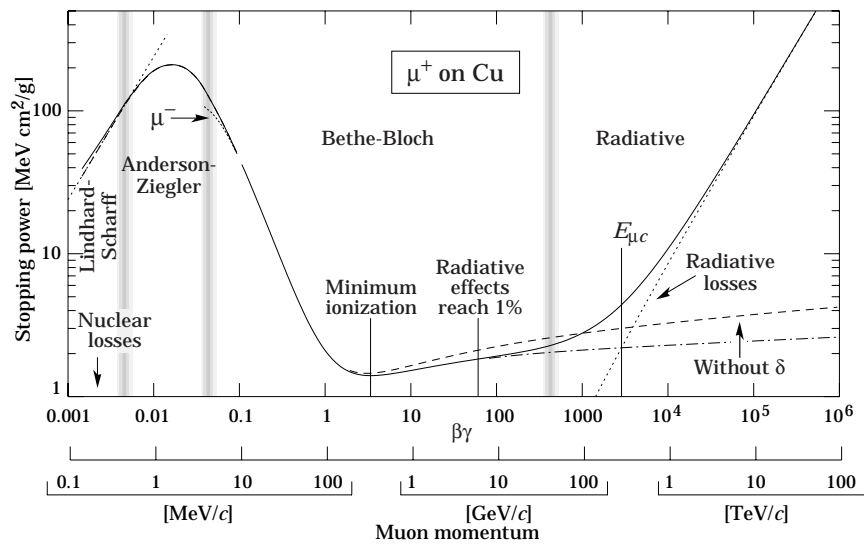


Fig. 27.1: Stopping power ($= \langle -dE/dx \rangle$) for positive muons in copper as a function of $\beta\gamma = p/Mc$ over nine orders of magnitude in momentum (12 orders of magnitude in kinetic energy). Solid curves indicate the total stopping power. Data below the break at $\beta\gamma \approx 0.1$ are taken from ICRU 49 [2], and data at higher energies are from Ref. 1. Vertical bands indicate boundaries between different approximations discussed in the text. The short dotted lines labeled “ μ^- ” illustrate the “Barkas effect,” the dependence of stopping power on projectile charge at very low energies [3].

27.2. Electronic energy loss by heavy particles

[1–22, 24–30, 82]

Moderately relativistic charged particles other than electrons lose energy in matter primarily by ionization and atomic excitation. The mean rate of energy loss (or stopping power) is given by the Bethe-Bloch equation,

$$-\frac{dE}{dx} = K z^2 \frac{Z}{A} \frac{1}{\beta^2} \left[\frac{1}{2} \ln \frac{2m_e c^2 \beta^2 \gamma^2 T_{\max}}{I^2} - \beta^2 - \frac{\delta(\beta\gamma)}{2} \right]. \quad (27.1)$$

Here T_{\max} is the maximum kinetic energy which can be imparted to a free electron in a single collision, and the other variables are defined in Table 27.1. With K as defined in Table 27.1 and A in g mol^{-1} , the units are $\text{MeV g}^{-1}\text{cm}^2$.

In this form, the Bethe-Bloch equation describes the energy loss of pions in a material such as copper to about 1% accuracy for energies between about 6 MeV and 6 GeV (momenta between about 40 MeV/ c and 6 GeV/ c). At lower energies various corrections discussed in Sec. 27.2.1 must be made. At higher energies, radiative effects begin to be important. These limits of validity depend on both the effective atomic number of the absorber and the mass of the slowing particle.

The function as computed for muons on copper is shown by the solid curve in Fig. 27.1, and for pions on other materials in Fig. 27.3. A minor dependence on M at the highest energies is introduced through T_{\max} , but for all practical purposes in high-energy physics dE/dx in a given material is a function only of β . Except in hydrogen, particles of the same velocity have similar rates of energy loss in different materials; there is a slow decrease in the rate of energy loss with increasing Z . The qualitative difference in stopping power behavior at high energies between a gas (He) and the other materials shown in Fig. 27.3 is due to the density-effect correction, $\delta(\beta\gamma)$, discussed below. The stopping power functions are characterized by broad minima whose position drops from $\beta\gamma = 3.5$ to 3.0 as Z goes from 7 to 100. The values of minimum ionization as a function of atomic number are shown in Fig. 27.2.

In practical cases, most relativistic particles (*e.g.*, cosmic-ray muons) have mean energy loss rates close to the minimum, and are said to be minimum ionizing particles, or mip's.

As discussed below, the most probable energy loss in a detector is considerably below the mean given by the Bethe-Bloch equation.

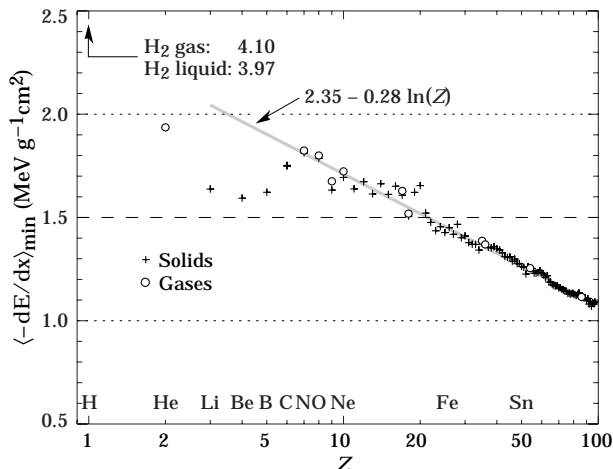


Figure 27.2: Stopping power at minimum ionization for the chemical elements. The straight line is fitted for $Z > 6$. A simple functional dependence on Z is not to be expected, since $(-dE/dx)$ also depends on other variables.

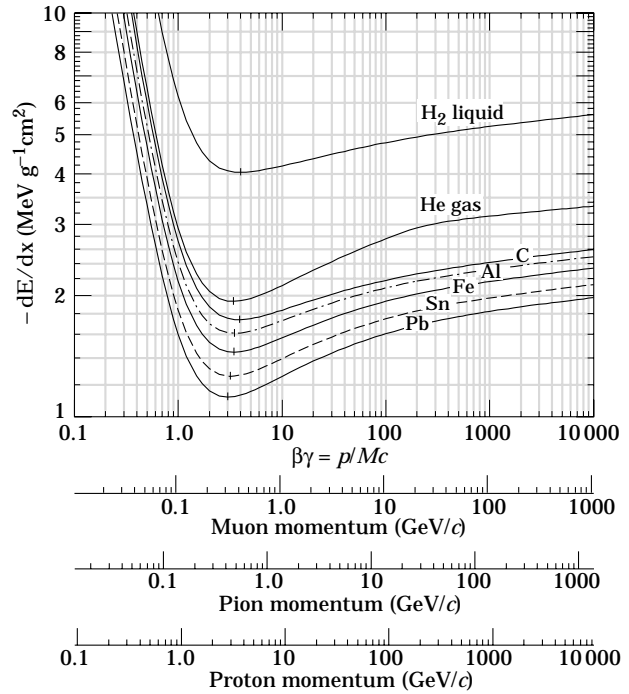


Figure 27.3: Mean energy loss rate in liquid (bubble chamber) hydrogen, gaseous helium, carbon, aluminum, iron, tin, and lead. Radiative effects, relevant for muons and pions, are not included. These become significant for muons in iron for $\beta\gamma \gtrsim 1000$, and at lower momenta for muons in higher- Z absorbers. See Fig. 27.21.

Eq. (27.1) may be integrated to find the total (or partial) “continuous slowing-down approximation” (CSDA) range R for a particle which loses energy only through ionization and atomic excitation. Since dE/dx depends only on β , R/M is a function of E/M or pc/M . In practice, range is a useful concept only for low-energy hadrons ($R \lesssim \lambda_I$, where λ_I is the nuclear interaction length), and for muons below a few hundred GeV (above which radiative effects dominate). R/M as a function of $\beta\gamma = p/Mc$ is shown for a variety of materials in Fig. 27.4.

The mass scaling of dE/dx and range is valid for the electronic losses described by the Bethe-Bloch equation, but not for radiative losses, relevant only for muons and pions.

For a particle with mass M and momentum $M\beta\gamma c$, T_{\max} is given by

$$T_{\max} = \frac{2m_e c^2 \beta^2 \gamma^2}{1 + 2\gamma m_e/M + (m_e/M)^2}. \quad (27.2)$$

In older references [4,5] the “low-energy” approximation $T_{\max} = 2m_e c^2 \beta^2 \gamma^2$, valid for $2\gamma m_e/M \ll 1$, is often implicit. For a pion in copper, the error thus introduced into dE/dx is greater than 6% at 100 GeV.

At energies of order 100 GeV, the maximum 4-momentum transfer to the electron can exceed 1 GeV/ c , where hadronic structure effects significantly modify the cross sections. This problem has been investigated by J.D. Jackson [6], who concluded that for hadrons (but not for large nuclei) corrections to dE/dx are negligible below energies where radiative effects dominate. While the cross section for rare hard collisions is modified, the average stopping power, dominated by many softer collisions, is almost unchanged.

“The determination of the mean excitation energy is the principal non-trivial task in the evaluation of the Bethe stopping-power formula” [7]. Recommended values have varied

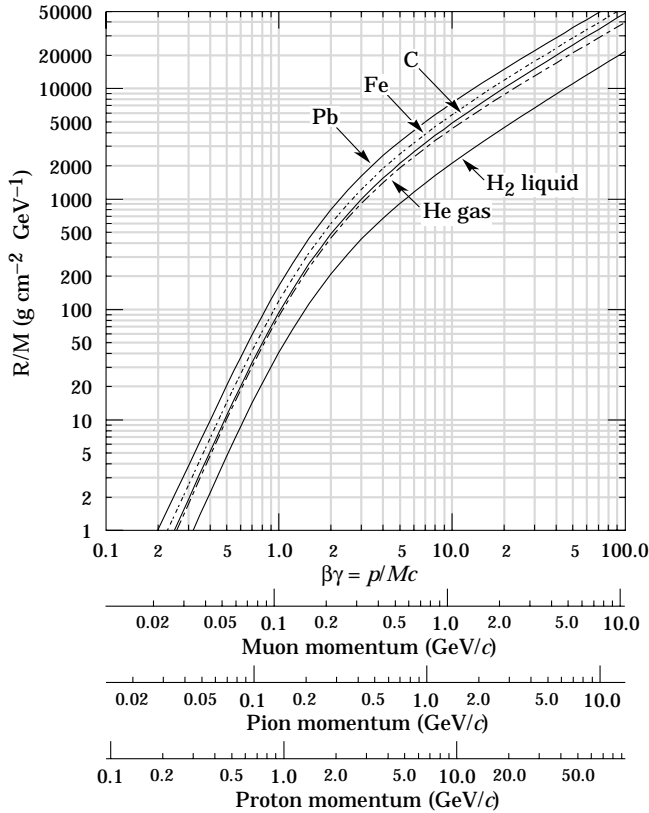


Figure 27.4: Range of heavy charged particles in liquid (bubble chamber) hydrogen, helium gas, carbon, iron, and lead. For example: For a K^+ whose momentum is $700 \text{ MeV}/c$, $\beta\gamma = 1.42$. For lead we read $R/M \approx 396$, and so the range is 195 g cm^{-2} .

substantially with time. Estimates based on experimental stopping-power measurements for protons, deuterons, and alpha particles and on oscillator-strength distributions and dielectric-response functions were given in ICRU 49 [2]. See also ICRU 37 [8]. These values, shown in Fig. 27.5, have since been widely used. Machine-readable versions can also be found [9]. These values are widely used.

27.2.1. Energy loss at low energies: Shell corrections C/Z must be included in the square brackets of Eq. (27.1) [2,8,10,11] to correct for atomic binding having been neglected in calculating some of the contributions to Eq. (27.1). The Barkas form [11] was used in generating Fig. 27.1. For copper it contributes about 1% at $\beta\gamma = 0.3$ (kinetic energy 6 MeV for a pion), and the correction decreases very rapidly with energy.

Eq. (27.1) is based on a first-order Born approximation. Higher-order corrections, again important only at lower energy, are normally included by adding the “Bloch correction” $z^2 L_2(\beta)$ inside the square brackets (Eq.(2.5) in [2]).

An additional “Barkas correction” $zL_1(\beta)$ makes the stopping power for a negative particle somewhat smaller than for a positive particle with the same mass and velocity. In a 1956 paper, Barkas *et al.* noted that negative pions had a longer range than positive pions [3]. The effect has been measured for a number of negative/positive particle pairs, most recently for antiprotons at the CERN LEAR facility [12].

A detailed discussion of low-energy corrections to the Bethe formula is given in ICRU Report 49 [2]. When the corrections are properly included, the accuracy of the Bethe-Bloch treatment is accurate to about 1% down to $\beta \approx 0.05$, or about 1 MeV for protons.

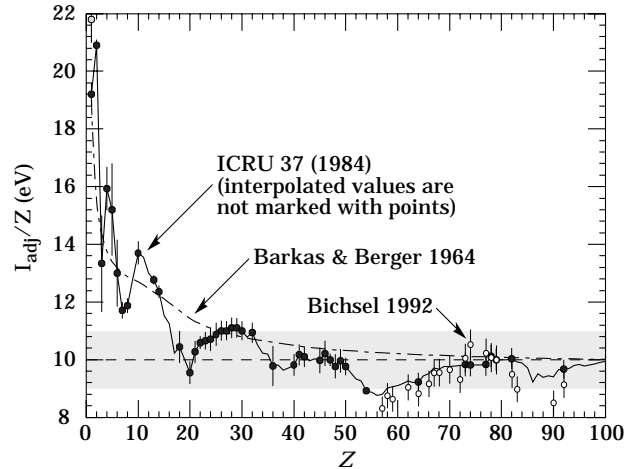


Figure 27.5: Mean excitation energies (divided by Z) as adopted by the ICRU [8]. Those based on experimental measurements are shown by symbols with error flags; the interpolated values are simply joined. The grey point is for liquid H_2 ; the black point at 19.2 eV is for H_2 gas. The open circles show more recent determinations by Bichsel [10]. The dotted curve is from the approximate formula of Barkas [11] used in early editions of this *Review*.

For $0.01 < \beta < 0.05$, there is no satisfactory theory. For protons, one usually relies on the phenomenological fitting formulae developed by Andersen and Ziegler [2,13]. For particles moving more slowly than $\approx 0.01c$ (more or less the velocity of the outer atomic electrons), Lindhard has been quite successful in describing electronic stopping power, which is proportional to β [14]. Finally, we note that at low energies, *e.g.*, for protons of less than several hundred eV, non-ionizing nuclear recoil energy loss dominates the total energy loss [2,14,15].

As shown in ICRU 49 [2] (using data taken from Ref. 13), the nuclear plus electronic proton stopping power in copper is $113 \text{ MeV cm}^2 \text{ g}^{-1}$ at $T = 10 \text{ keV}$, rises to a maximum of $210 \text{ MeV cm}^2 \text{ g}^{-1}$ at $100\text{--}150 \text{ keV}$, then falls to $120 \text{ MeV cm}^2 \text{ g}^{-1}$ at 1 MeV . Above $0.5\text{--}1.0 \text{ MeV}$ the corrected Bethe-Bloch theory is adequate.

27.2.2. Density effect: As the particle energy increases, its electric field flattens and extends, so that the distant-collision contribution to Eq. (27.1) increases as $\ln \beta\gamma$. However, real media become polarized, limiting the field extension and effectively truncating this part of the logarithmic rise [4–5,16–18]. At very high energies,

$$\delta/2 \rightarrow \ln(\hbar\omega_p/I) + \ln \beta\gamma - 1/2, \quad (27.3)$$

where $\delta(\beta\gamma)/2$ is the density effect correction introduced in Eq. (27.1) and $\hbar\omega_p$ is the plasma energy defined in Table 27.1. A comparison with Eq. (27.1) shows that $|dE/dx|$ then grows as $\ln \beta\gamma$ rather than $\ln \beta^2\gamma^2$, and that the mean excitation energy I is replaced by the plasma energy $\hbar\omega_p$. The ionization stopping power as calculated with and without the density effect correction is shown in Fig. 27.1. Since the plasma frequency scales as the square root of the electron density, the correction is much larger for a liquid or solid than for a gas, as is illustrated by the examples in Fig. 27.3.

The density effect correction is usually computed using Sternheimer's parameterization [16]:

$$\delta(\beta\gamma) = \begin{cases} 2(\ln 10)x - \bar{C} & \text{if } x \geq x_1; \\ 2(\ln 10)x - \bar{C} + a(x_1 - x)^k & \text{if } x_0 \leq x < x_1; \\ 0 & \text{if } x < x_0 \text{ (nonconductors);} \\ \delta_0 10^{2(x-x_0)} & \text{if } x < x_0 \text{ (conductors)} \end{cases} \quad (27.4)$$

Here $x = \log_{10} \eta = \log_{10}(p/Mc)$. \bar{C} (the negative of the C used in Ref. 16) is obtained by equating the high-energy case of Eq. (27.4) with the limit given in Eq. (27.3). The other parameters are adjusted to give a best fit to the results of detailed calculations for momenta below $Mc \exp(x_1)$. Parameters for elements and nearly 200 compounds and mixtures of interest are published in a variety of places, notably in Ref. 18. A recipe for finding the coefficients for nontabulated materials is given by Sternheimer and Peierls [20], and is summarized in Ref. 1.

The remaining relativistic rise comes from the $\beta^2\gamma^2$ growth of T_{\max} , which in turn is due to (rare) large energy transfers to a few electrons. When these events are excluded, the energy deposit in an absorbing layer approaches a constant value, the Fermi plateau (see Sec. 27.2.4 below). At extreme energies (e.g., > 332 GeV for muons in iron, and at a considerably higher energy for protons in iron), radiative effects are more important than ionization losses. These are especially relevant for high-energy muons, as discussed in Sec. 27.6.

27.2.3. Energetic knock-on electrons (δ rays): The distribution of secondary electrons with kinetic energies $T \gg I$ is [4]

$$\frac{d^2N}{dTdx} = \frac{1}{2} K z^2 \frac{Z}{A} \frac{1}{\beta^2} \frac{F(T)}{T^2} \quad (27.5)$$

for $I \ll T \leq T_{\max}$, where T_{\max} is given by Eq. (27.2). Here β is the velocity of the primary particle. The factor F is spin-dependent, but is about unity for $T \ll T_{\max}$. For spin-0 particles $F(T) = (1 - \beta^2 T/T_{\max})$; forms for spins 1/2 and 1 are also given by Rossi [4]. For incident electrons, the indistinguishability of projectile and target means that the range of T extends only to half the kinetic energy of the incident particle. Additional formulae are given in Ref. 19. Equation (27.5) is inaccurate for T close to I .

δ rays of even modest energy are rare. For $\beta \approx 1$ particle, for example, on average only one collision with $T_e > 1$ keV will occur along a path length of 90 cm of Ar gas [25].

A δ ray with kinetic energy T_e and corresponding momentum p_e is produced at an angle θ given by

$$\cos \theta = (T_e/p_e)(p_{\max}/T_{\max}), \quad (27.6)$$

where p_{\max} is the momentum of an electron with the maximum possible energy transfer T_{\max} .

27.2.4. Restricted energy loss rates for relativistic ionizing particles: Further insight can be obtained by examining the mean energy deposit by an ionizing particle when energy transfers are restricted to $T \leq T_{\text{cut}} \leq T_{\max}$. The restricted energy loss rate is

$$-\frac{dE}{dx} \Big|_{T < T_{\text{cut}}} = K z^2 \frac{Z}{A} \frac{1}{\beta^2} \left[\frac{1}{2} \ln \frac{2m_e c^2 \beta^2 \gamma^2 T_{\text{cut}}}{I^2} - \frac{\beta^2}{2} \left(1 + \frac{T_{\text{cut}}}{T_{\max}} \right) - \frac{\delta}{2} \right]. \quad (27.7)$$

This form approaches the normal Bethe-Bloch function (Eq. (27.1)) as $T_{\text{cut}} \rightarrow T_{\max}$. It can be verified that the difference between Eq. (27.1) and Eq. (27.7) is equal to $\int_{T_{\text{cut}}}^{T_{\max}} T(d^2N/dTdx)dT$, where $d^2N/dTdx$ is given by Eq. (27.5).

Since T_{cut} replaces T_{\max} in the argument of the logarithmic term of Eq. (27.1), the $\beta\gamma$ term producing the relativistic rise in

the close-collision part of dE/dx is replaced by a constant, and $|dE/dx|_{T < T_{\text{cut}}}$ approaches the constant "Fermi plateau." (The density effect correction δ eliminates the explicit $\beta\gamma$ dependence produced by the distant-collision contribution.) This behavior is illustrated in Fig. 27.6, where restricted loss rates for two examples of T_{cut} are shown in comparison with the full Bethe-Bloch dE/dx and the Landau-Vavilov most probable energy loss (to be discussed in Sec. 27.2.5 below).

27.2.5. Fluctuations in energy loss: For detectors of moderate thickness x (e.g. scintillators or LAr cells),* the energy loss probability distribution $f(\Delta; \beta\gamma, x)$ is adequately described by the highly-skewed Landau (or Landau-Vavilov) distribution [22,23]. The most probable energy loss is [24]

$$\Delta_p = \xi \left[\ln \frac{2mc^2 \beta^2 \gamma^2}{I} + \ln \frac{\xi}{I} + j - \beta^2 - \delta(\beta\gamma) \right], \quad (27.8)$$

where $\xi = (K/2)\langle Z/A \rangle(x/\beta^2)$ MeV for a detector with a thickness x in g cm^{-2} , and $j = 0.200$ [24].[†] While dE/dx is independent of thickness, Δ_p/x scales as $a \ln x + b$. The density correction $\delta(\beta\gamma)$ was not included in Landau's or Vavilov's work, but it was later included by Bichsel [24]. The high-energy behavior of $\delta(\beta\gamma)$ (Eq. (27.3)), is such that

$$\Delta_p \xrightarrow{\beta\gamma \gtrsim 100} \xi \left[\ln \frac{2mc^2 \xi}{(\hbar\omega_p)^2} + j \right]. \quad (27.9)$$

Thus the Landau-Vavilov most probable energy loss, like the restricted energy loss, reaches a Fermi plateau. The Bethe-Bloch dE/dx and Landau-Vavilov-Bichsel Δ_p/x in silicon are shown as a function of muon energy in Fig. 27.6. The case $x/\rho = 1600 \mu\text{m}$ was chosen since it has about the same stopping power as does 3 mm of plastic scintillator. Folding in experimental resolution displaces the peak of the distribution, usually toward a higher value.

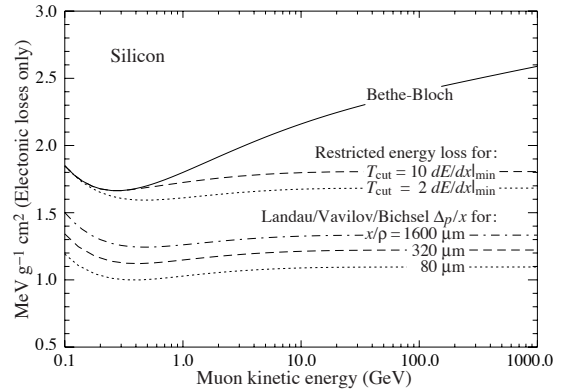


Figure 27.6: Bethe-Bloch dE/dx , two examples of restricted energy loss, and the Landau most probable energy per unit thickness in silicon. The change of Δ_p/x with thickness x illustrates its $a \ln x + b$ dependence. Minimum ionization ($dE/dx|_{\min}$) is $1.664 \text{ MeV g}^{-1} \text{ cm}^2$. Radiative losses are excluded. The incident particles are muons.

The mean of the energy-loss given by the Bethe-Bloch equation, Eq. (27.1), is ill-defined experimentally and is not useful for describing energy loss by single particles. (It finds its application in dosimetry, where only bulk deposit is of relevance.) It rises as $\ln \beta\gamma$ because T_{\max} increases as $\beta^2\gamma^2$. The

* $G \lesssim 0.05\text{--}0.1$, where G is given by Rossi [Ref. 4, Eq. 2.7.10]. It is Vavilov's κ [23].

[†] Rossi [4], Talman [26], and others give somewhat different values for j . The most probable loss is not sensitive to its value.

large single-collision energy transfers that increasingly extend the long tail are rare, making the mean of an experimental distribution consisting of a few hundred events subject to large fluctuations and sensitive to cuts as well as to background. The most probable energy loss should be used.

For very thick absorbers the distribution is less skewed but never approaches a Gaussian. In the case of Si illustrated in Fig. 27.6, the most probable energy loss per unit thickness for $x \approx 35 \text{ g cm}^{-2}$ is very close to the restricted energy loss with $T_{\text{cut}} = 2 dE/dx|_{\text{min}}$.

The Landau distribution fails to describe energy loss in thin absorbers such as gas TPC cells [25] and Si detectors [24], as shown clearly in Fig. 1 of Ref. 25 for an argon-filled TPC cell. Also see Talman [26]. While Δ_p/x may be calculated adequately with Eq. (27.8), the distributions are significantly wider than the Landau width $w = 4\zeta$ [Ref. 24, Fig. 15]. Examples for thin silicon detectors are shown in Fig. 27.7.

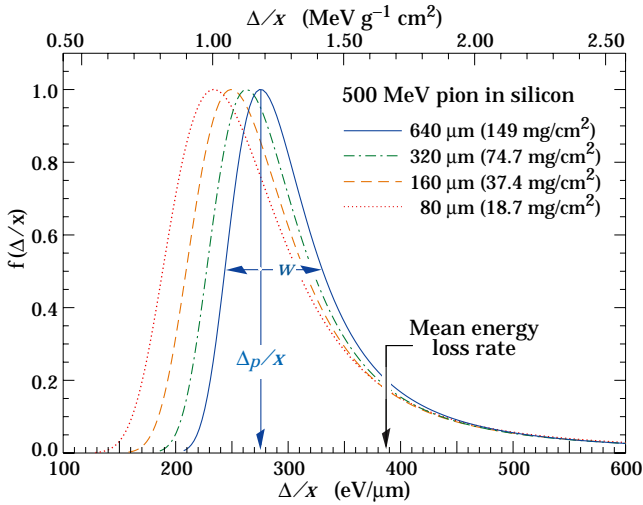


Figure 27.7: Straggling functions in silicon for 500 MeV pions, normalized to unity at the most probable value δ_p/x . The width w is the full width at half maximum.

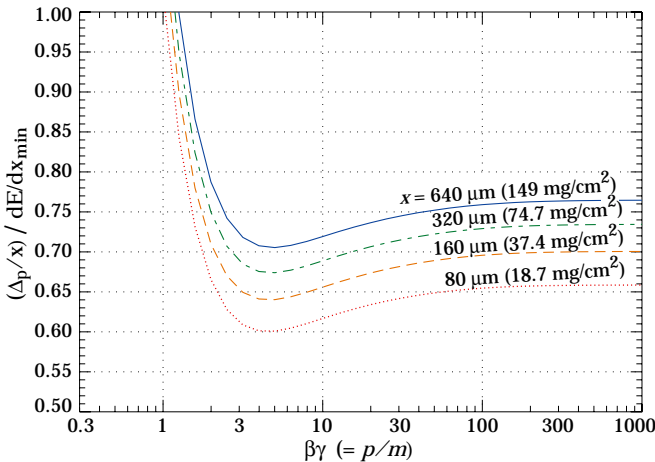


Figure 27.8: Most probable energy loss in silicon, scaled to the mean loss of a minimum ionizing particle, $388 \text{ eV}/\mu\text{m}$ ($1.66 \text{ MeV g}^{-1}\text{cm}^2$).

27.2.6. Energy loss in mixtures and compounds : A mixture or compound can be thought of as made up of thin layers of pure elements in the right proportion (Bragg additivity). In this case,

$$\frac{dE}{dx} = \sum w_j \left. \frac{dE}{dx} \right|_j, \quad (27.10)$$

where $dE/dx|_j$ is the mean rate of energy loss (in MeV g cm^{-2}) in the j th element. Eq. (27.1) can be inserted into Eq. (27.10) to find expressions for $\langle Z/A \rangle$, $\langle I \rangle$, and $\langle \delta \rangle$; for example, $\langle Z/A \rangle = \sum w_j Z_j/A_j = \sum n_j Z_j / \sum n_j A_j$. However, $\langle I \rangle$ as defined this way is an underestimate, because in a compound electrons are more tightly bound than in the free elements, and $\langle \delta \rangle$ as calculated this way has little relevance, because it is the electron density that matters. If possible, one uses the tables given in Refs. 18 and 27, which include effective excitation energies and interpolation coefficients for calculating the density effect correction for the chemical elements and nearly 200 mixtures and compounds. If a compound or mixture is not found, then one uses the recipe for δ given in Ref. 20 (repeated in Ref. 1), and calculates $\langle I \rangle$ according to the discussion in Ref. 7. (Note the “13%” rule!)

27.2.7. Ionization yields : Physicists frequently relate total energy loss to the number of ion pairs produced near the particle’s track. This relation becomes complicated for relativistic particles due to the wandering of energetic knock-on electrons whose ranges exceed the dimensions of the fiducial volume. For a qualitative appraisal of the nonlocality of energy deposition in various media by such modestly energetic knock-on electrons, see Ref. 28. The mean local energy dissipation per local ion pair produced, W , while essentially constant for relativistic particles, increases at slow particle speeds [29]. For gases, W can be surprisingly sensitive to trace amounts of various contaminants [29]. Furthermore, ionization yields in practical cases may be greatly influenced by such factors as subsequent recombination [30].

27.3. Multiple scattering through small angles

A charged particle traversing a medium is deflected by many small-angle scatters. Most of this deflection is due to Coulomb scattering from nuclei, and hence the effect is called multiple Coulomb scattering. (However, for hadronic projectiles, the strong interactions also contribute to multiple scattering.) The Coulomb scattering distribution is well represented by the theory of Molière [31]. It is roughly Gaussian for small deflection angles, but at larger angles (greater than a few θ_0 , defined below) it behaves like Rutherford scattering, with larger tails than does a Gaussian distribution.

If we define

$$\theta_0 = \theta_{\text{plane}}^{\text{rms}} = \frac{1}{\sqrt{2}} \theta_{\text{space}}^{\text{rms}}. \quad (27.11)$$

then it is sufficient for many applications to use a Gaussian approximation for the central 98% of the projected angular distribution, with a width given by [32,33]

$$\theta_0 = \frac{13.6 \text{ MeV}}{\beta c p} z \sqrt{x/X_0} \left[1 + 0.038 \ln(x/X_0) \right]. \quad (27.12)$$

Here p , βc , and z are the momentum, velocity, and charge number of the incident particle, and x/X_0 is the thickness of the scattering medium in radiation lengths (defined below). This value of θ_0 is from a fit to Molière distribution [31] for singly charged particles with $\beta = 1$ for all Z , and is accurate to 11% or better for $10^{-3} < x/X_0 < 100$.

Eq. (27.12) describes scattering from a single material, while the usual problem involves the multiple scattering of a particle traversing many different layers and mixtures. Since it is from a fit to a Molière distribution, it is incorrect to add the individual θ_0 contributions in quadrature; the result is systematically too

small. It is much more accurate to apply Eq. (27.12) once, after finding x and X_0 for the combined scatterer.

Lynch and Dahl have extended this phenomenological approach, fitting Gaussian distributions to a variable fraction of the Molière distribution for arbitrary scatterers [33], and achieve accuracies of 2% or better.

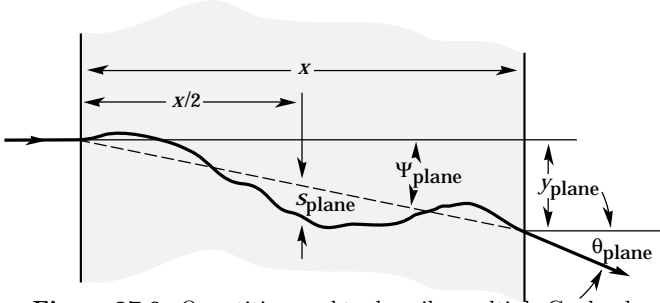


Figure 27.9: Quantities used to describe multiple Coulomb scattering. The particle is incident in the plane of the figure.

The nonprojected (space) and projected (plane) angular distributions are given approximately by [31]

$$\frac{1}{2\pi\theta_0^2} \exp\left(-\frac{\theta_{\text{space}}^2}{2\theta_0^2}\right) d\Omega, \quad (27.13)$$

$$\frac{1}{\sqrt{2\pi}\theta_0} \exp\left(-\frac{\theta_{\text{plane}}^2}{2\theta_0^2}\right) d\theta_{\text{plane}}, \quad (27.14)$$

where θ is the deflection angle. In this approximation, $\theta_{\text{space}}^2 \approx (\theta_{\text{plane},x}^2 + \theta_{\text{plane},y}^2)$, where the x and y axes are orthogonal to the direction of motion, and $d\Omega \approx d\theta_{\text{plane},x} d\theta_{\text{plane},y}$. Deflections into $\theta_{\text{plane},x}$ and $\theta_{\text{plane},y}$ are independent and identically distributed.

Figure 27.9 shows these and other quantities sometimes used to describe multiple Coulomb scattering. They are

$$\psi_{\text{plane}}^{\text{rms}} = \frac{1}{\sqrt{3}} \theta_{\text{plane}}^{\text{rms}} = \frac{1}{\sqrt{3}} \theta_0, \quad (27.15)$$

$$y_{\text{plane}}^{\text{rms}} = \frac{1}{\sqrt{3}} x \theta_{\text{plane}}^{\text{rms}} = \frac{1}{\sqrt{3}} x \theta_0, \quad (27.16)$$

$$s_{\text{plane}}^{\text{rms}} = \frac{1}{4\sqrt{3}} x \theta_{\text{plane}}^{\text{rms}} = \frac{1}{4\sqrt{3}} x \theta_0. \quad (27.17)$$

All the quantitative estimates in this section apply only in the limit of small $\theta_{\text{plane}}^{\text{rms}}$ and in the absence of large-angle scatters. The random variables s , ψ , y , and θ in a given plane are distributed in a correlated fashion (see Sec. 31.1 of this *Review* for the definition of the correlation coefficient). Obviously, $y \approx x\psi$. In addition, y and θ have the correlation coefficient $\rho_{y\theta} = \sqrt{3}/2 \approx 0.87$. For Monte Carlo generation of a joint $(y_{\text{plane}}, \theta_{\text{plane}})$ distribution, or for other calculations, it may be most convenient to work with independent Gaussian random variables (z_1, z_2) with mean zero and variance one, and then set

$$y_{\text{plane}} = z_1 x \theta_0 (1 - \rho_{y\theta}^2)^{1/2} / \sqrt{3} + z_2 \rho_{y\theta} x \theta_0 / \sqrt{3} \\ = z_1 x \theta_0 / \sqrt{12} + z_2 x \theta_0 / 2; \quad (27.18)$$

$$\theta_{\text{plane}} = z_2 \theta_0. \quad (27.19)$$

Note that the second term for y_{plane} equals $x\theta_{\text{plane}}/2$ and represents the displacement that would have occurred had the deflection θ_{plane} all occurred at the single point $x/2$.

For heavy ions the multiple Coulomb scattering has been measured and compared with various theoretical distributions [34].

27.4. Photon and electron interactions in matter

27.4.1. Radiation length : High-energy electrons predominantly lose energy in matter by bremsstrahlung, and high-energy photons by e^+e^- pair production. The characteristic amount of matter traversed for these related interactions is called the radiation length X_0 , usually measured in g cm^{-2} . It is both (a) the mean distance over which a high-energy electron loses all but $1/e$ of its energy by bremsstrahlung, and (b) $\frac{7}{9}$ of the mean free path for pair production by a high-energy photon [35]. It is also the appropriate scale length for describing high-energy electromagnetic cascades. X_0 has been calculated and tabulated by Y.S. Tsai [36]:

$$\frac{1}{X_0} = 4\alpha r_e^2 \frac{N_A}{A} \left\{ Z^2 [L_{\text{rad}} - f(Z)] + Z L'_{\text{rad}} \right\}. \quad (27.20)$$

For $A = 1 \text{ g mol}^{-1}$, $4\alpha r_e^2 N_A / A = (716.408 \text{ g cm}^{-2})^{-1}$. L_{rad} and L'_{rad} are given in Table 27.2. The function $f(Z)$ is an infinite sum, but for elements up to uranium can be represented to 4-place accuracy by

$$f(Z) = a^2 [(1 + a^2)^{-1} + 0.20206 \\ - 0.0369 a^2 + 0.0083 a^4 - 0.002 a^6], \quad (27.21)$$

where $a = \alpha Z$ [37].

Table 27.2: Tsai's L_{rad} and L'_{rad} , for use in calculating the radiation length in an element using Eq. (27.20).

Element	Z	L_{rad}	L'_{rad}
H	1	5.31	6.144
He	2	4.79	5.621
Li	3	4.74	5.805
Be	4	4.71	5.924
Others	> 4	$\ln(184.15 Z^{-1/3})$	$\ln(1194 Z^{-2/3})$

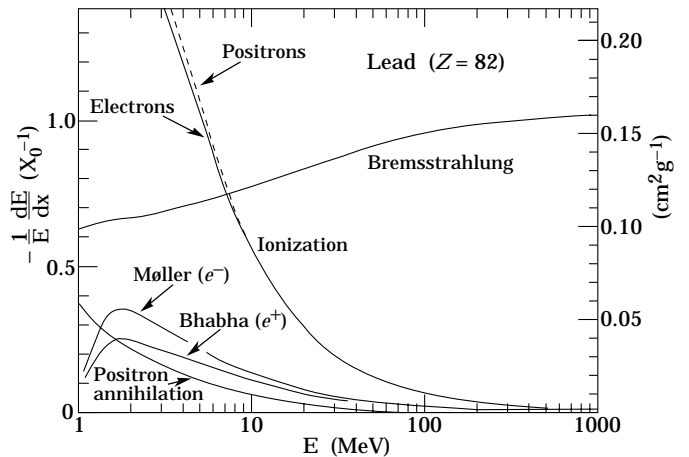


Figure 27.10: Fractional energy loss per radiation length in lead as a function of electron or positron energy. Electron (positron) scattering is considered as ionization when the energy loss per collision is below 0.255 MeV, and as Møller (Bhabha) scattering when it is above. Adapted from Fig. 3.2 from Messel and Crawford, *Electron-Photon Shower Distribution Function Tables for Lead, Copper, and Air Absorbers*, Pergamon Press, 1970. Messel and Crawford use $X_0(\text{Pb}) = 5.82 \text{ g/cm}^2$, but we have modified the figures to reflect the value given in the Table of Atomic and Nuclear Properties of Materials ($X_0(\text{Pb}) = 6.37 \text{ g/cm}^2$).

Although it is easy to use Eq. (27.20) to calculate X_0 , the functional dependence on Z is somewhat hidden. Dahl provides a compact fit to the data [38]:

$$X_0 = \frac{716.4 \text{ g cm}^{-2} A}{Z(Z+1) \ln(287/\sqrt{Z})}. \quad (27.22)$$

Results using this formula agree with Tsai's values to better than 2.5% for all elements except helium, where the result is about 5% low.

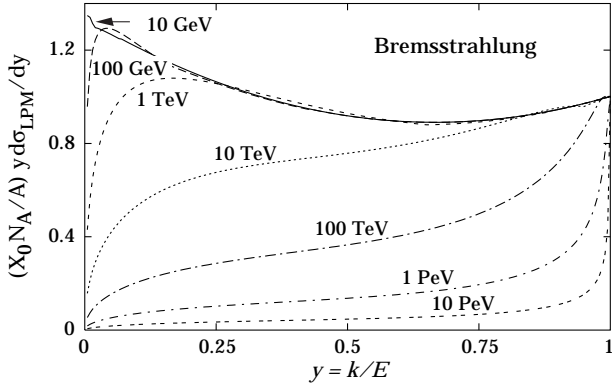


Figure 27.11: The normalized bremsstrahlung cross section $k d\sigma_{LPM}/dk$ in lead versus the fractional photon energy $y = k/E$. The vertical axis has units of photons per radiation length.

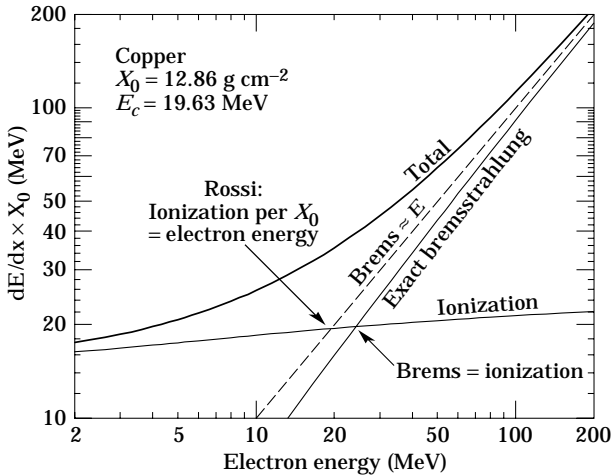


Figure 27.12: Two definitions of the critical energy E_c .

The radiation length in a mixture or compound may be approximated by

$$1/X_0 = \sum w_j/X_j, \quad (27.23)$$

where w_j and X_j are the fraction by weight and the radiation length for the j th element.

27.4.2. Energy loss by electrons: At low energies electrons and positrons primarily lose energy by ionization, although other processes (Møller scattering, Bhabha scattering, e^+ annihilation) contribute, as shown in Fig. 27.10. While ionization loss rates rise logarithmically with energy, bremsstrahlung losses rise nearly linearly (fractional loss is nearly independent of energy), and dominates above a few tens of MeV in most materials

Ionization loss by electrons and positrons differs from loss by heavy particles because of the kinematics, spin, and the identity of the incident electron with the electrons which it ionizes.

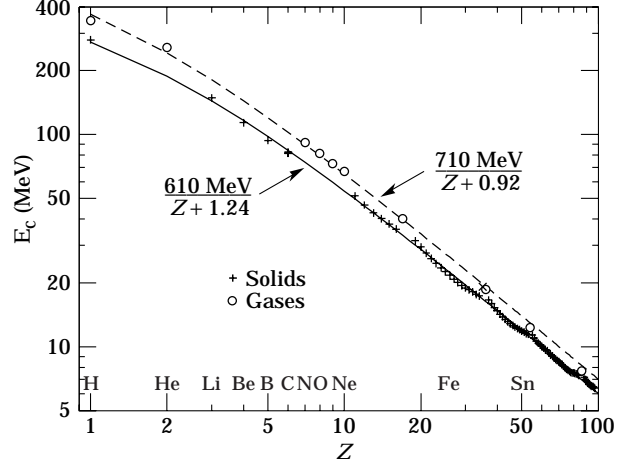


Figure 27.13: Electron critical energy for the chemical elements, using Rossi's definition [4]. The fits shown are for solids and liquids (solid line) and gases (dashed line). The rms deviation is 2.2% for the solids and 4.0% for the gases. (Computed with code supplied by A. Fassó.)

Complete discussions and tables can be found in Refs. 7, 8, and 27.

At very high energies and except at the high-energy tip of the bremsstrahlung spectrum, the cross section can be approximated in the “complete screening case” as [36]

$$\begin{aligned} d\sigma/dk = & (1/k) 4\alpha r_e^2 \left\{ \left(\frac{4}{3} - \frac{4}{3}y + y^2 \right) [Z^2(L_{\text{rad}} - f(Z)) + Z L'_{\text{rad}}] \right. \\ & \left. + \frac{1}{9}(1-y)(Z^2 + Z) \right\}, \end{aligned} \quad (27.24)$$

where $y = k/E$ is the fraction of the electron's energy transferred to the radiated photon. At small y (the “infrared limit”) the term on the second line ranges from 1.7% (low Z) to 2.5% (high Z) of the total. If it is ignored and the first line simplified with the definition of X_0 given in Eq. (27.20), we have

$$\frac{d\sigma}{dk} = \frac{A}{X_0 N_A k} \left(\frac{4}{3} - \frac{4}{3}y + y^2 \right). \quad (27.25)$$

This cross section (times k) is shown by the top curve in Fig. 27.11.

This formula is accurate except in near $y = 1$, where screening may become incomplete, and near $y = 0$, where the infrared divergence is removed by the interference of bremsstrahlung amplitudes from nearby scattering centers (the LPM effect) [39,40] and dielectric suppression [41,42]. These and other suppression effects in bulk media are discussed in Sec. 27.4.5.

With decreasing energy ($E \lesssim 10$ GeV) the high- y cross section drops and the curves become rounded as $y \rightarrow 1$. Curves of this familiar shape can be seen in Rossi [4] (Figs. 2.11.2,3); see also the review by Koch & Motz [43].

Except at these extremes, and still in the complete-screening approximation, the number of photons with energies between k_{min} and k_{max} emitted by an electron travelling a distance $d \ll X_0$ is

$$N_\gamma = \frac{d}{X_0} \left[\frac{4}{3} \ln \left(\frac{k_{\text{max}}}{k_{\text{min}}} \right) - \frac{4(k_{\text{max}} - k_{\text{min}})}{3E} + \frac{k_{\text{max}}^2 - k_{\text{min}}^2}{2E^2} \right]. \quad (27.26)$$

We obtain

$$E_c = \frac{610 \text{ MeV}}{Z + 1.24} \quad (\text{solids and liquids}), \quad = \frac{710 \text{ MeV}}{Z + 0.92} \quad (\text{gases}).$$

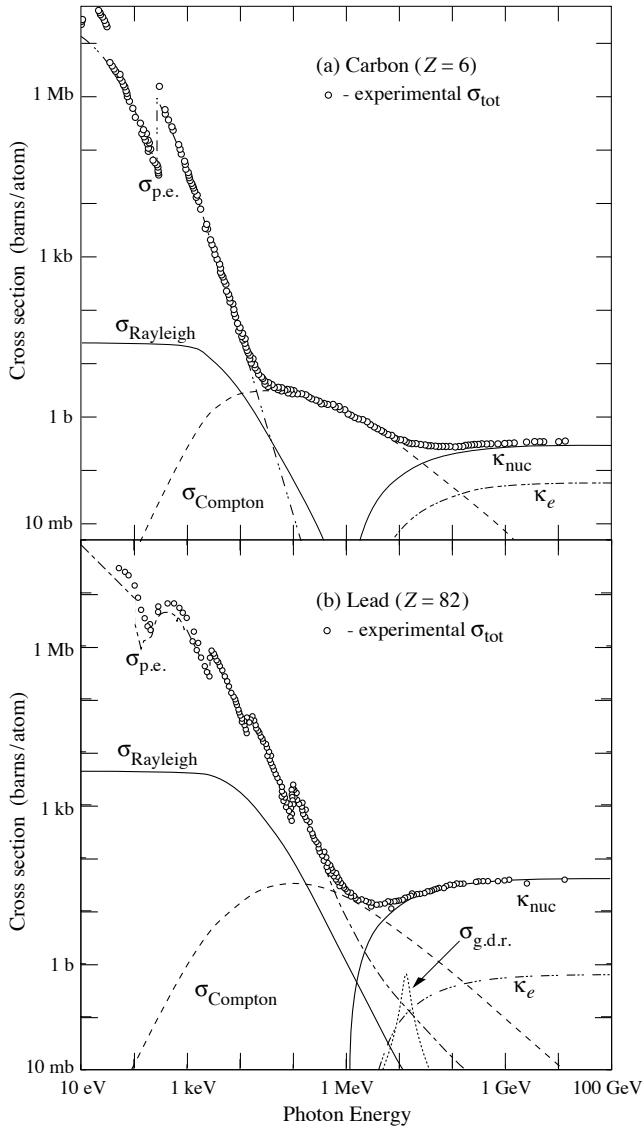


Figure 27.14: Photon total cross sections as a function of energy in carbon and lead, showing the contributions of different processes:

$\sigma_{p.e.}$ = Atomic photoelectric effect (electron ejection, photon absorption)

σ_{Rayleigh} = Rayleigh (coherent) scattering—atom neither ionized nor excited

σ_{Compton} = Incoherent scattering (Compton scattering off an electron)

κ_{nuc} = Pair production, nuclear field

κ_e = Pair production, electron field

$\sigma_{g.d.r.}$ = Photonuclear interactions, most notably the Giant Dipole Resonance [46]. In these interactions, the target nucleus is broken up.

Data from [47]; parameters for $\sigma_{g.d.r.}$ from [48]. Curves for these and other elements, compounds, and mixtures may be obtained from

<http://physics.nist.gov/PhysRefData>. The photon total cross section is approximately flat for at least two decades beyond the energy range shown. Original figures courtesy J.H. Hubbell (NIST).

27.4.3. Critical energy : An electron loses energy by bremsstrahlung at a rate nearly proportional to its energy, while the ionization loss rate varies only logarithmically with the electron energy. The *critical energy* E_c is sometimes defined as the energy at which the two loss rates are equal [44]. Berger and Seltzer [44] also give the approximation $E_c = (800 \text{ MeV})/(Z + 1.2)$. This formula has been widely quoted, and has been given in older editions of this *Review* [45]. Among alternate definitions is that of Rossi [4], who defines the critical energy as the energy at which the ionization loss per radiation length is equal to the electron energy. Equivalently, it is the same as the first definition with the approximation $|dE/dx|_{\text{brems}} \approx E/X_0$. This form has been found to describe transverse electromagnetic shower development more accurately (see below). These definitions are illustrated in the case of copper in Fig. 27.12.

The accuracy of approximate forms for E_c has been limited by the failure to distinguish between gases and solid or liquids, where there is a substantial difference in ionization at the relevant energy because of the density effect. We distinguish these two cases in Fig. 27.13. Fits were also made with functions of the form $a/(Z + b)^\alpha$, but α was found to be essentially unity. Since E_c also depends on A , I , and other factors, such forms are at best approximate.

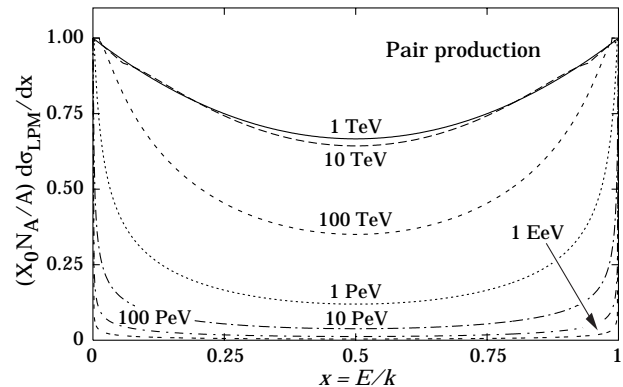


Figure 27.15: The normalized pair production cross section $d\sigma_{LPM}/dy$, versus fractional electron energy $x = E/k$.

27.4.4. Energy loss by photons : Contributions to the photon cross section in a light element (carbon) and a heavy element (lead) are shown in Fig. 27.14. At low energies it is seen that the photoelectric effect dominates, although Compton scattering, Rayleigh scattering, and photonuclear absorption also contribute. The photoelectric cross section is characterized by discontinuities (absorption edges) as thresholds for photoionization of various atomic levels are reached. Photon attenuation lengths for a variety of elements are shown in Fig. 27.16, and data for $30 \text{ eV} < k < 100 \text{ GeV}$ for all elements is available from the web pages given in the caption. Here k is the photon energy.

The increasing domination of pair production as the energy increases is shown in Fig. 27.17. Using approximations similar to those used to obtain Eq. (27.25), Tsai's formula for the differential cross section [36] reduces to

$$\frac{d\sigma}{dx} = \frac{A}{X_0 N_A} \left[1 - \frac{4}{3}x(1-x) \right] \quad (27.27)$$

in the complete-screening limit valid at high energies. Here $x = E/k$ is the fractional energy transfer to the pair-produced electron (or positron), and k is the incident photon energy. The cross section is very closely related to that for bremsstrahlung, since the Feynman diagrams are variants of one another. The

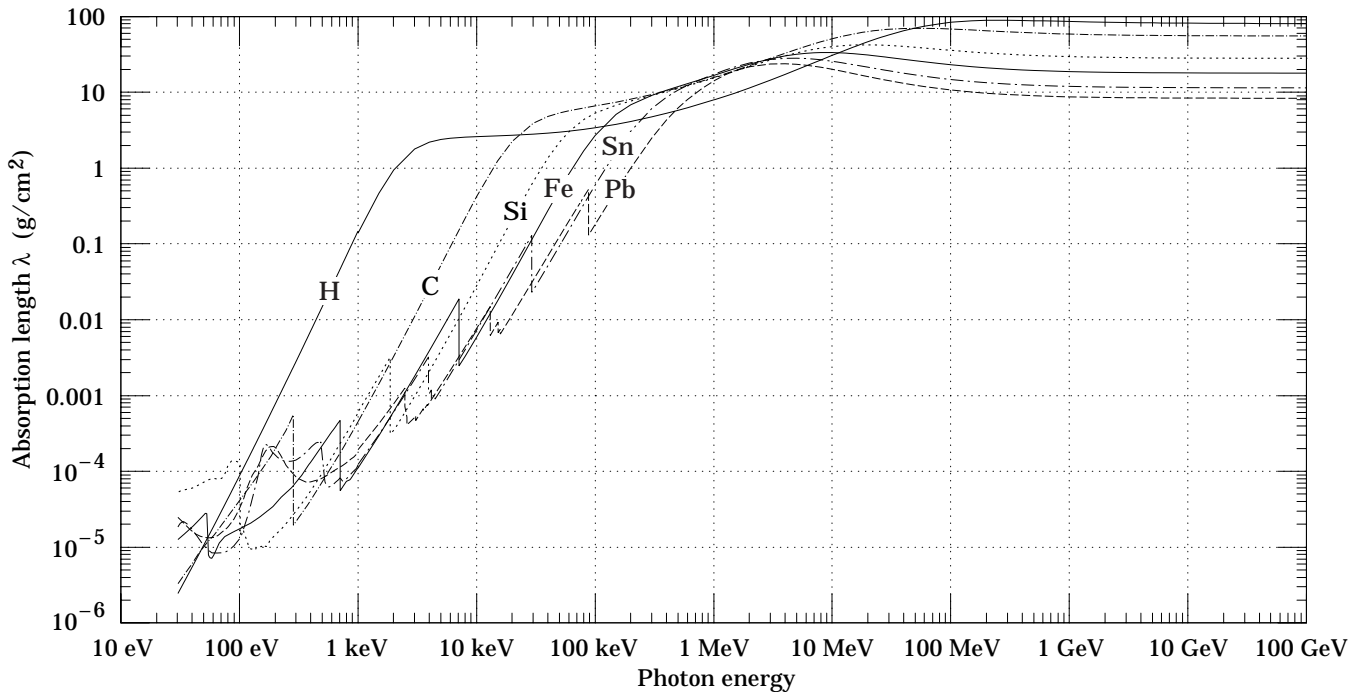


Fig. 27.16: The photon mass attenuation length (or mean free path) $\lambda = 1/(\mu/\rho)$ for various elemental absorbers as a function of photon energy. The mass attenuation coefficient is μ/ρ , where ρ is the density. The intensity I remaining after traversal of thickness t (in mass/unit area) is given by $I = I_0 \exp(-t/\lambda)$. The accuracy is a few percent. For a chemical compound or mixture, $1/\lambda_{\text{eff}} \approx \sum_{\text{elements}} w_Z/\lambda_Z$, where w_Z is the proportion by weight of the element with atomic number Z . The processes responsible for attenuation are given in Fig. 27.10. Since coherent processes are included, not all these processes result in energy deposition. The data for $30 \text{ eV} < E < 1 \text{ keV}$ are obtained from http://www-cxro.lbl.gov/optical_constants (courtesy of Eric M. Gullikson, LBNL). The data for $1 \text{ keV} < E < 100 \text{ GeV}$ are from <http://physics.nist.gov/PhysRefData>, through the courtesy of John H. Hubbell (NIST).

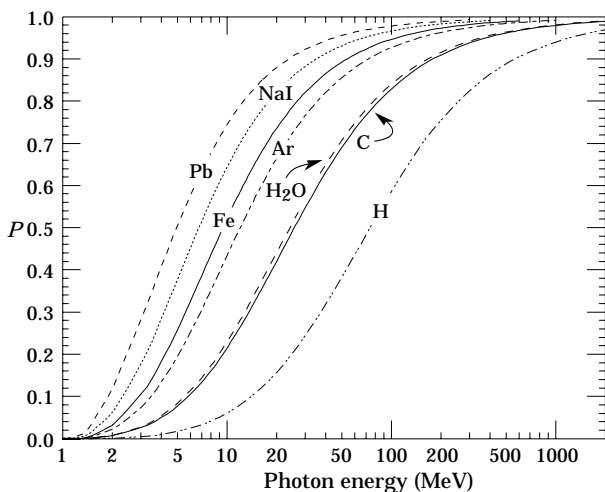


Figure 27.17: Probability P that a photon interaction will result in conversion to an e^+e^- pair. Except for a few-percent contribution from photonuclear absorption around 10 or 20 MeV, essentially all other interactions in this energy range result in Compton scattering off an atomic electron. For a photon attenuation length λ (Fig. 27.16), the probability that a given photon will produce an electron pair (without first Compton scattering) in thickness t of absorber is $P[1 - \exp(-t/\lambda)]$.

cross section is of necessity symmetric between x and $1 - x$, as can be seen by the solid curve in Fig. 27.15. See the review by Motz, Olsen, & Koch for a more detailed treatment [49].

Eq. (27.27) may be integrated to find the high-energy limit for the total e^+e^- pair-production cross section:

$$\sigma = \frac{7}{9}(A/X_0 N_A) . \quad (27.28)$$

Equation Eq. (27.28) is accurate to within a few percent down to energies as low as 1 GeV, particularly for high- Z materials.

27.4.5. Bremsstrahlung and pair production at very high energies : At ultrahigh energies, Eqns. 27.24–27.28 will fail because of quantum mechanical interference between amplitudes from different scattering centers. Since the longitudinal momentum transfer to a given center is small ($\propto k/E(E - k)$), in the case of bremsstrahlung, the interaction is spread over a comparatively long distance called the formation length ($\propto E(E - k)/k$) via the uncertainty principle. In alternate language, the formation length is the distance over which the highly relativistic electron and the photon “split apart.” The interference is usually destructive. Calculations of the “Landau-Pomeranchuk-Migdal” (LPM) effect may be made semi-classically based on the average multiple scattering, or more rigorously using a quantum transport approach [39,40].

In amorphous media, bremsstrahlung is suppressed if the photon energy k is less than $E^2/(E + E_{LPM})$ [40], where*

$$E_{LPM} = \frac{(m_e c^2)^2 \alpha X_0}{4\pi \hbar c \rho} = (7.7 \text{ TeV/cm}) \times \frac{X_0}{\rho} . \quad (27.29)$$

* This definition differs from that of Ref. 50 by a factor of two. E_{LPM} scales as the 4th power of the mass of the incident particle, so that $E_{LPM} = (1.4 \times 10^{10} \text{ TeV/cm}) \times X_0/\rho$ for a muon.

Since physical distances are involved, X_0/ρ , in cm, appears. The energy-weighted bremsstrahlung spectrum for lead, $k d\sigma_{LPM}/dk$, is shown in Fig. 27.11. With appropriate scaling by X_0/ρ , other materials behave similarly.

For photons, pair production is reduced for $E(k - E) > k E_{LPM}$. The pair-production cross sections for different photon energies are shown in Fig. 27.15.

If $k \ll E$, several additional mechanisms can also produce suppression. When the formation length is long, even weak factors can perturb the interaction. For example, the emitted photon can coherently forward scatter off of the electrons in the media. Because of this, for $k < \omega_p E/m_e \sim 10^{-4}$, bremsstrahlung is suppressed by a factor $(km_e/\omega_p E)^2$ [42]. Magnetic fields can also suppress bremsstrahlung.

In crystalline media, the situation is more complicated, with coherent enhancement or suppression possible. The cross section depends on the electron and photon energies and the angles between the particle direction and the crystalline axes [51].

27.5. Electromagnetic cascades

When a high-energy electron or photon is incident on a thick absorber, it initiates an electromagnetic cascade as pair production and bremsstrahlung generate more electrons and photons with lower energy. The longitudinal development is governed by the high-energy part of the cascade, and therefore scales as the radiation length in the material. Electron energies eventually fall below the critical energy, and then dissipate their energy by ionization and excitation rather than by the generation of more shower particles. In describing shower behavior, it is therefore convenient to introduce the scale variables

$$t = x/X_0, \quad y = E/E_c, \quad (27.30)$$

so that distance is measured in units of radiation length and energy in units of critical energy.

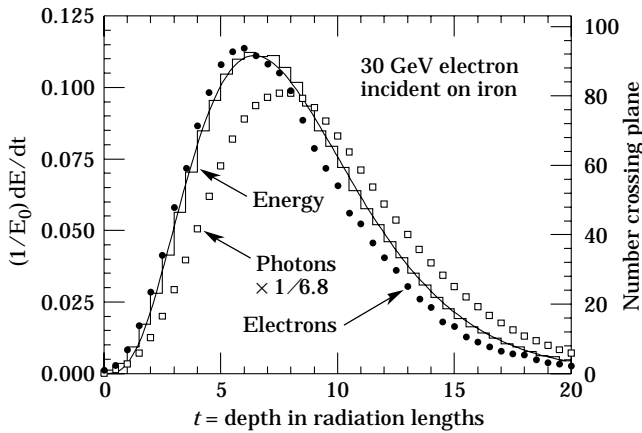


Figure 27.18: An EGS4 simulation of a 30 GeV electron-induced cascade in iron. The histogram shows fractional energy deposition per radiation length, and the curve is a gamma-function fit to the distribution. Circles indicate the number of electrons with total energy greater than 1.5 MeV crossing planes at $X_0/2$ intervals (scale on right) and the squares the number of photons with $E \geq 1.5$ MeV crossing the planes (scaled down to have same area as the electron distribution).

Longitudinal profiles from an EGS4 [52] simulation of a 30 GeV electron-induced cascade in iron are shown in Fig. 27.18. The number of particles crossing a plane (very close to Rossi's Π function [4]) is sensitive to the cutoff energy, here chosen as a total energy of 1.5 MeV for both electrons and photons. The

electron number falls off more quickly than energy deposition. This is because, with increasing depth, a larger fraction of the cascade energy is carried by photons. Exactly what a calorimeter measures depends on the device, but it is not likely to be exactly any of the profiles shown. In gas counters it may be very close to the electron number, but in glass Cherenkov detectors and other devices with “thick” sensitive regions it is closer to the energy deposition (total track length). In such detectors the signal is proportional to the “detectable” track length T_d , which is in general less than the total track length T . Practical devices are sensitive to electrons with energy above some detection threshold E_d , and $T_d = TF(E_d/E_c)$. An analytic form for $F(E_d/E_c)$ obtained by Rossi [4] is given by Fabjan [53]; see also Amaldi [54].

The mean longitudinal profile of the energy deposition in an electromagnetic cascade is reasonably well described by a gamma distribution [55]:

$$\frac{dE}{dt} = E_0 b \frac{(bt)^{a-1} e^{-bt}}{\Gamma(a)} \quad (27.31)$$

The maximum t_{\max} occurs at $(a - 1)/b$. We have made fits to shower profiles in elements ranging from carbon to uranium, at energies from 1 GeV to 100 GeV. The energy deposition profiles are well described by Eq. (27.31) with

$$t_{\max} = (a - 1)/b = 1.0 \times (\ln y + C_j), \quad j = e, \gamma, \quad (27.32)$$

where $C_e = -0.5$ for electron-induced cascades and $C_\gamma = +0.5$ for photon-induced cascades. To use Eq. (27.31), one finds $(a - 1)/b$ from Eq. (27.32) and Eq. (27.30), then finds a either by assuming $b \approx 0.5$ or by finding a more accurate value from Fig. 27.19. The results are very similar for the electron number profiles, but there is some dependence on the atomic number of the medium. A similar form for the electron number maximum was obtained by Rossi in the context of his “Approximation B,” [4] (see Fabjan’s review in Ref. 53), but with $C_e = -1.0$ and $C_\gamma = -0.5$; we regard this as superseded by the EGS4 result.

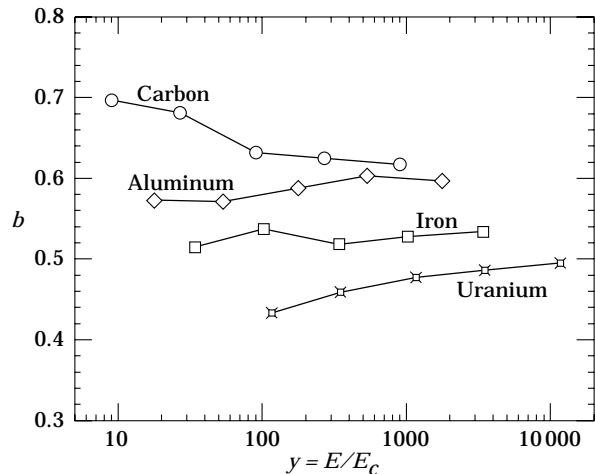


Figure 27.19: Fitted values of the scale factor b for energy deposition profiles obtained with EGS4 for a variety of elements for incident electrons with $1 \leq E_0 \leq 100$ GeV. Values obtained for incident photons are essentially the same.

The “shower length” $X_s = X_0/b$ is less conveniently parameterized, since b depends upon both Z and incident energy, as shown in Fig. 27.19. As a corollary of this Z dependence, the number of electrons crossing a plane near shower maximum is underestimated using Rossi’s approximation for carbon and seriously overestimated for uranium. Essentially the same b

values are obtained for incident electrons and photons. For many purposes it is sufficient to take $b \approx 0.5$.

The gamma function distribution is very flat near the origin, while the EGS4 cascade (or a real cascade) increases more rapidly. As a result Eq. (27.31) fails badly for about the first two radiation lengths; it was necessary to exclude this region in making fits.

Because fluctuations are important, Eq. (27.31) should be used only in applications where average behavior is adequate. Grindhammer *et al.* have developed fast simulation algorithms in which the variance and correlation of a and b are obtained by fitting Eq. (27.31) to individually simulated cascades, then generating profiles for cascades using a and b chosen from the correlated distributions [56].

The transverse development of electromagnetic showers in different materials scales fairly accurately with the *Molière radius* R_M , given by [57,58]

$$R_M = X_0 E_s / E_c, \quad (27.33)$$

where $E_s \approx 21$ MeV (Table 27.1), and the Rossi definition of E_c is used.

In a material containing a weight fraction w_j of the element with critical energy E_{cj} and radiation length X_j , the Molière radius is given by

$$\frac{1}{R_M} = \frac{1}{E_s} \sum \frac{w_j E_{cj}}{X_j}. \quad (27.34)$$

Measurements of the lateral distribution in electromagnetic cascades are shown in Refs. 57 and 58. On the average, only 10% of the energy lies outside the cylinder with radius R_M . About 99% is contained inside of $3.5R_M$, but at this radius and beyond composition effects become important and the scaling with R_M fails. The distributions are characterized by a narrow core, and broaden as the shower develops. They are often represented as the sum of two Gaussians, and Grindhammer [56] describes them with the function

$$f(r) = \frac{2r R^2}{(r^2 + R^2)^2}, \quad (27.35)$$

where R is a phenomenological function of x/X_0 and $\ln E$.

At high enough energies, the LPM effect (Sec. 27.4.5) reduces the cross sections for bremsstrahlung and pair production, and hence can cause significant elongation of electromagnetic cascades [40].

27.6. Muon energy loss at high energy

At sufficiently high energies, radiative processes become more important than ionization for all charged particles. For muons and pions in materials such as iron, this “critical energy” occurs at several hundred GeV. (There is no simple scaling with particle mass, but for protons the “critical energy” is much, much higher.) Radiative effects dominate the energy loss of energetic muons found in cosmic rays or produced at the newest accelerators. These processes are characterized by small cross sections, hard spectra, large energy fluctuations, and the associated generation of electromagnetic and (in the case of photonuclear interactions) hadronic showers [59–67]. As a consequence, at these energies the treatment of energy loss as a uniform and continuous process is for many purposes inadequate.

It is convenient to write the average rate of muon energy loss as [68]

$$-dE/dx = a(E) + b(E) E. \quad (27.36)$$

Here $a(E)$ is the ionization energy loss given by Eq. (27.1), and $b(E)$ is the sum of e^+e^- pair production, bremsstrahlung, and photonuclear contributions. To the approximation that these slowly-varying functions are constant, the mean range x_0 of a muon with initial energy E_0 is given by

$$x_0 \approx (1/b) \ln(1 + E_0/E_{\mu c}), \quad (27.37)$$

where $E_{\mu c} = a/b$. Figure 27.20 shows contributions to $b(E)$ for iron. Since $a(E) \approx 0.002$ GeV g⁻¹ cm², $b(E)E$ dominates the energy loss above several hundred GeV, where $b(E)$ is nearly constant. The rates of energy loss for muons in hydrogen, uranium, and iron are shown in Fig. 27.21 [1].

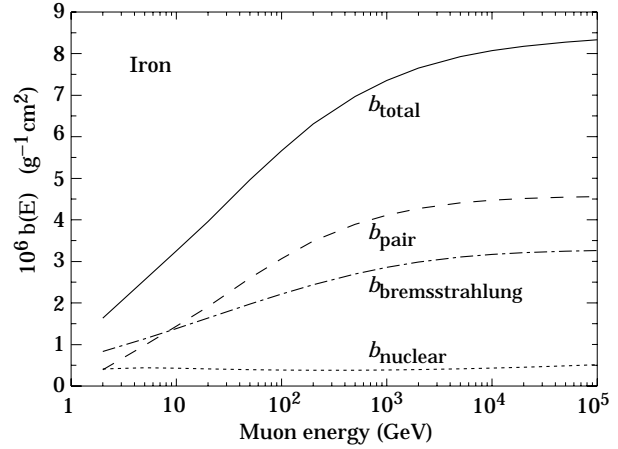


Figure 27.20: Contributions to the fractional energy loss by muons in iron due to e^+e^- pair production, bremsstrahlung, and photonuclear interactions, as obtained from Groom *et al.* [1] except for post-Born corrections to the cross section for direct pair production from atomic electrons.

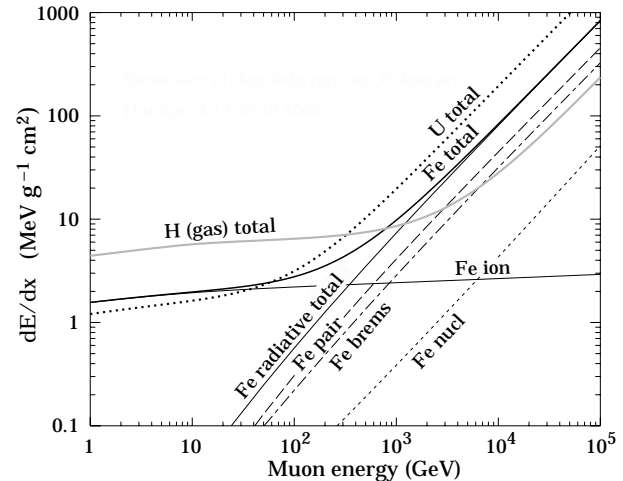


Figure 27.21: The average energy loss of a muon in hydrogen, iron, and uranium as a function of muon energy. Contributions to dE/dx in iron from ionization and the processes shown in Fig. 27.20 are also shown.

The “muon critical energy” $E_{\mu c}$ can be defined more exactly as the energy at which radiative and ionization losses are equal, and can be found by solving $E_{\mu c} = a(E_{\mu c})/b(E_{\mu c})$. This definition corresponds to the solid-line intersection in Fig. 27.12, and is different from the Rossi definition we used for electrons. It serves the same function: below $E_{\mu c}$ ionization losses dominate, and above $E_{\mu c}$ radiative effects dominate. The dependence of $E_{\mu c}$ on atomic number Z is shown in Fig. 27.22.

The radiative cross sections are expressed as functions of the fractional energy loss ν . The bremsstrahlung cross section goes roughly as $1/\nu$ over most of the range, while for the pair production case the distribution goes as ν^{-3} to ν^{-2} [69]. “Hard” losses are therefore more probable in bremsstrahlung,

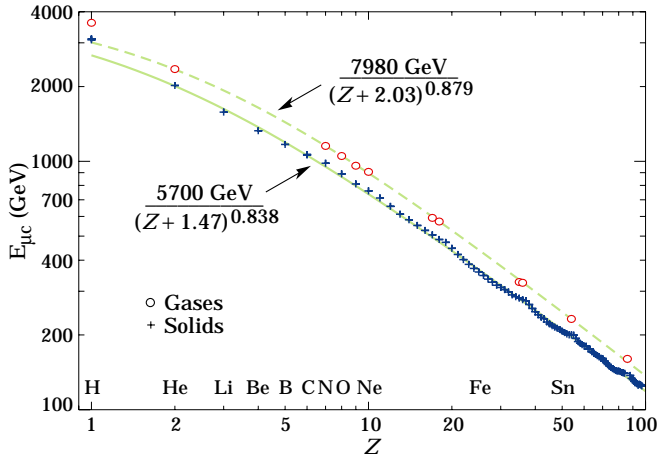


Figure 27.22: Muon critical energy for the chemical elements, defined as the energy at which radiative and ionization energy loss rates are equal [1]. The equality comes at a higher energy for gases than for solids or liquids with the same atomic number because of a smaller density effect reduction of the ionization losses. The fits shown in the figure exclude hydrogen. Alkali metals fall 3–4% above the fitted function, while most other solids are within 2% of the function. Among the gases the worst fit is for radon (2.7% high).

and in fact energy losses due to pair production may very nearly be treated as continuous. The simulated [67] momentum distribution of an incident 1 TeV/c muon beam after it crosses 3 m of iron is shown in Fig. 27.23. The most probable loss is 8 GeV, or 3.4 MeV g⁻¹cm². The full width at half maximum is 9 GeV/c, or 0.9%. The radiative tail is almost entirely due to bremsstrahlung, although most of the events in which more than 10% of the incident energy lost experienced relatively hard photonuclear interactions. The latter can exceed detector resolution [70], necessitating the reconstruction of lost energy. Tables [1] list the stopping power as 9.82 MeV g⁻¹cm² for a 1 TeV muon, so that the mean loss should be 23 GeV (≈ 23 GeV/c), for a final momentum of 977 GeV/c, far below the peak. This agrees with the indicated mean calculated from the simulation. Electromagnetic and hadronic cascades in detector materials can obscure muon tracks in detector planes and reduce tracking efficiency [71].

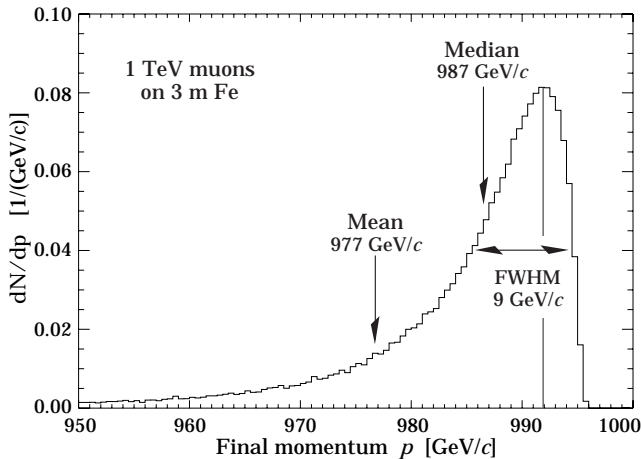


Figure 27.23: The momentum distribution of 1 TeV/c muons after traversing 3 m of iron as calculated with the MARS15 Monte Carlo code [67] by S.I. Striganov [1].

27.7. Cherenkov and transition radiation [72,73,82]

A charged particle radiates if its velocity is greater than the local phase velocity of light (Cherenkov radiation) or if it crosses suddenly from one medium to another with different optical properties (transition radiation). Neither process is important for energy loss, but both are used in high-energy physics detectors.

Cherenkov Radiation. The angle θ_c of Cherenkov radiation, relative to the particle's direction, for a particle with velocity βc in a medium with index of refraction n is

$$\begin{aligned} \cos \theta_c &= (1/n\beta) \\ \text{or } \tan \theta_c &= \sqrt{\beta^2 n^2 - 1} \\ &\approx \sqrt{2(1 - 1/n\beta)} \quad \text{for small } \theta_c, \text{ e.g. in gas} \end{aligned} \quad (27.38)$$

The threshold velocity β_t is $1/n$, and $\gamma_t = 1/(1 - \beta_t^2)^{1/2}$. Therefore, $\beta_t \gamma_t = 1/(2\delta + \delta^2)^{1/2}$, where $\delta = n - 1$. Values of δ for various commonly used gases are given as a function of pressure and wavelength in Ref. 74. For values at atmospheric pressure, see Table 6.1. Data for other commonly used materials are given in Ref. 75.

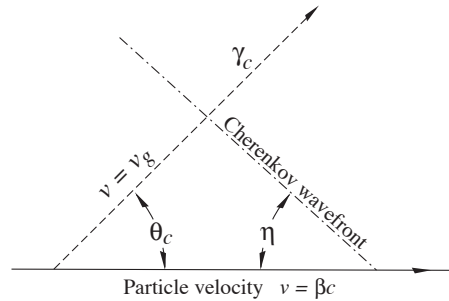


Figure 27.24: Cherenkov light emission and wavefront angles. In a dispersive medium, $\theta_c + \eta \neq 90^\circ$.

Practical Cherenkov radiator materials are dispersive. Let ω be the photon's frequency, and let $k = 2\pi/\lambda$ be its wavenumber. The photons propagate at the group velocity $v_g = d\omega/dk = c/[n(\omega) + \omega(dn/d\omega)]$. In a non-dispersive medium, this simplifies to $v_g = c/n$.

In his classical paper, Tamm [76] showed that for dispersive media the radiation is concentrated in a thin conical shell whose vertex is at the moving charge, and whose opening half-angle η is given by

$$\begin{aligned} \cot \eta &= \left[\frac{d}{d\omega} (\omega \tan \theta_c) \right]_{\omega_0} \\ &= \left[\tan \theta_c + \beta^2 \omega n(\omega) \frac{dn}{d\omega} \cot \theta_c \right]_{\omega_0}, \end{aligned} \quad (27.39)$$

where ω_0 is the central value of the small frequency range under consideration. (See Fig. 27.24.) This cone has a opening half-angle η , and, unless the medium is non-dispersive ($dn/d\omega = 0$), $\theta_c + \eta \neq 90^\circ$. The Cherenkov wavefront 'sideslips' along with the particle [77]. This effect may have timing implications for ring imaging Cherenkov counters [78], but it is probably unimportant for most applications.

The number of photons produced per unit path length of a particle with charge ze and per unit energy interval of the photons is

$$\begin{aligned} \frac{d^2 N}{dE dx} &= \frac{\alpha z^2}{\hbar c} \sin^2 \theta_c = \frac{\alpha^2 z^2}{r_e m_e c^2} \left(1 - \frac{1}{\beta^2 n^2(E)} \right) \\ &\approx 370 \sin^2 \theta_c(E) \text{ eV}^{-1} \text{ cm}^{-1} \quad (z = 1), \end{aligned} \quad (27.40)$$

or, equivalently,

$$\frac{d^2N}{dx d\lambda} = \frac{2\pi\alpha z^2}{\lambda^2} \left(1 - \frac{1}{\beta^2 n^2(\lambda)} \right). \quad (27.41)$$

The index of refraction is a function of photon energy $E = \hbar\omega$, as is the sensitivity of the transducer used to detect the light. For practical use, Eq. (27.40) must be multiplied by the the transducer response function and integrated over the region for which $\beta n(\omega) > 1$. Further details are given in the discussion of Cherenkov detectors in the Particle Detectors section (Sec. 28 of this *Review*).

When two particles are close together (within $\lesssim 1$ wavelength), the electromagnetic fields from the particles may add coherently, affecting the Cherenkov radiation. The radiation from an e^+e^- pair at close separation is suppressed compared to two independent leptons [79].

Coherent radio Cherenkov radiation from electromagnetic showers (containing a net excess of e^- over e^+) is significant [80], and has been used to study cosmic ray air showers [81] and to search for ν_e induced showers.

Transition radiation. The energy radiated when a particle with charge ze crosses the boundary between vacuum and a medium with plasma frequency ω_p is

$$I = \alpha z^2 \gamma \hbar \omega_p / 3, \quad (27.42)$$

where

$$\hbar \omega_p = \sqrt{4\pi N_e r_e^3} m_e c^2 / \alpha = \sqrt{4\pi N_e a_\infty^3} 2 \times 13.6 \text{ eV}. \quad (27.43)$$

Here N_e is the electron density in the medium, r_e is the classical electron radius, and a_∞ is the Bohr radius. For styrene and similar materials, $\sqrt{4\pi N_e a_\infty^3} \approx 0.8$, so that $\hbar \omega_p \approx 20$ eV. The typical emission angle is $1/\gamma$.

The radiation spectrum is logarithmically divergent at low energies and decreases rapidly for $\hbar\omega/\gamma\hbar\omega_p > 1$. About half the energy is emitted in the range $0.1 \leq \hbar\omega/\gamma\hbar\omega_p \leq 1$. For a particle with $\gamma = 10^3$, the radiated photons are in the soft x-ray range 2 to 20 keV. The γ dependence of the emitted energy thus comes from the hardening of the spectrum rather than from an increased quantum yield. For a typical radiated photon energy of $\gamma\hbar\omega_p/4$, the quantum yield is

$$N_\gamma \approx \frac{1}{2} \frac{\alpha z^2 \gamma \hbar \omega_p}{3} \frac{\gamma \hbar \omega_p}{4} \approx \frac{2}{3} \alpha z^2 \approx 0.5\% \times z^2. \quad (27.44)$$

More precisely, the number of photons with energy $\hbar\omega > \hbar\omega_0$ is given by [82]

$$N_\gamma(\hbar\omega > \hbar\omega_0) = \frac{\alpha z^2}{\pi} \left[\left(\ln \frac{\gamma \hbar \omega_p}{\hbar \omega_0} - 1 \right)^2 + \frac{\pi^2}{12} \right], \quad (27.45)$$

within corrections of order $(\hbar\omega_0/\gamma\hbar\omega_p)^2$. The number of photons above a fixed energy $\hbar\omega_0 \ll \gamma\hbar\omega_p$ thus grows as $(\ln \gamma)^2$, but the number above a fixed fraction of $\gamma\hbar\omega_p$ (as in the example above) is constant. For example, for $\hbar\omega > \gamma\hbar\omega_p/10$, $N_\gamma = 2.519 \alpha z^2 / \pi = 0.59\% \times z^2$.

The yield can be increased by using a stack of plastic foils with gaps between. However, interference can be important, and the soft x rays are readily absorbed in the foils. The first problem can be overcome by choosing thicknesses and spacings large compared to the “formation length” $D = \gamma c / \omega_p$, which in practical situations is tens of μm . Other practical problems are discussed in Sec. 28.

References:

1. D.E. Groom, N.V. Mokhov, and S.I. Striganov, “Muon stopping-power and range tables: 10 MeV–100 TeV” *Atomic Data and Nuclear Data Tables* **78**, 183–356 (2001). Since submission of this paper it has become likely that post-Born corrections to the direct pair production cross section should be made. Code used to make Figs. 27.20, 27.21, and 27.12 included these corrections [D.Yu. Ivanov *et al.*, *Phys. Lett.* **B442**, 453 (1998)]. The effect is negligible for except at high Z . (It is less than 1% for iron); More extensive printable and machine-readable tables are given at <http://pdg.lbl.gov/AtomicNuclearProperties/>.
2. “Stopping Powers and Ranges for Protons and Alpha Particles,” ICRU Report No. 49 (1993); Tables and graphs of these data are available at <http://physics.nist.gov/PhysRefData/>.
3. W.H. Barkas, W. Birnbaum, and F.M. Smith, *Phys. Rev.* **101**, 778 (1956).
4. B. Rossi, *High Energy Particles*, Prentice-Hall, Inc., Englewood Cliffs, NJ, 1952.
5. U. Fano, *Ann. Rev. Nucl. Sci.* **13**, 1 (1963).
6. J. D. Jackson, *Phys. Rev.* **D59**, 017301 (1999).
7. S.M. Seltzer and M.J. Berger, *Int. J. of Applied Rad.* **33**, 1189 (1982).
8. “Stopping Powers for Electrons and Positrons,” ICRU Report No. 37 (1984).
9. <http://physics.nist.gov/PhysRefData/XrayMassCoef/tab1.html>.
10. H. Bichsel, *Phys. Rev.* **A46**, 5761 (1992).
11. W.H. Barkas and M.J. Berger, *Tables of Energy Losses and Ranges of Heavy Charged Particles*, NASA-SP-3013 (1964).
12. M. Agnello *et al.*, *Phys. Rev. Lett.* **74**, 371 (1995).
13. H.H. Andersen and J.F. Ziegler, *Hydrogen: Stopping Powers and Ranges in All Elements*. Vol. 3 of *The Stopping and Ranges of Ions in Matter* (Pergamon Press 1977).
14. J. Lindhard, *Kgl. Danske Videnskab. Selskab, Mat.-Fys. Medd.* **28**, No. 8 (1954); J. Lindhard, M. Scharff, and H.E. Schiøtt, *Kgl. Danske Videnskab. Selskab, Mat.-Fys. Medd.* **33**, No. 14 (1963).
15. J.F. Ziegler, J.F. Biersac, and U. Littmark, *The Stopping and Range of Ions in Solids*, Pergamon Press 1985.
16. R.M. Sternheimer, *Phys. Rev.* **88**, 851 (1952).
17. A. Crispin and G.N. Fowler, *Rev. Mod. Phys.* **42**, 290 (1970).
18. R.M. Sternheimer, S.M. Seltzer, and M.J. Berger, “The Density Effect for the Ionization Loss of Charged Particles in Various Substances,” *Atomic Data and Nuclear Data Tables* **30**, 261 (1984). Minor errors are corrected in Ref. 1. Chemical composition for the tabulated materials is given in Ref. 7.
19. For unit-charge projectiles, see E.A. Uehling, *Ann. Rev. Nucl. Sci.* **4**, 315 (1954). For highly charged projectiles, see J.A. Doggett and L.V. Spencer, *Phys. Rev.* **103**, 1597 (1956). A Lorentz transformation is needed to convert these center-of-mass data to knock-on energy spectra.
20. R.M. Sternheimer and R.F. Peierls, *Phys. Rev.* **B3**, 3681 (1971).
21. N.F. Mott and H.S.W. Massey, *The Theory of Atomic Collisions*, Oxford Press, London, 1965.
22. L.D. Landau, *J. Exp. Phys. (USSR)* **8**, 201 (1944).
23. P.V. Vavilov, *Sov. Phys. JETP* **5**, 749 (1957).
24. H. Bichsel, *Rev. Mod. Phys.* **60**, 663 (1988).
25. H. Bichsel, “A method to improve tracking and particle identification in TPCs and silicon detectors,” *Nucl. Inst. & Meth. A* (in press, 2006).
26. R. Talman, *Nucl. Instrum. Methods* **159**, 189 (1979).
27. S.M. Seltzer and M.J. Berger, *Int. J. of Applied Rad.* **35**, 665 (1984). This paper corrects and extends the results of Ref. 7.
28. L.V. Spencer “Energy Dissipation by Fast Electrons,” *Nat’l Bureau of Standards Monograph No. 1* (1959).
29. “Average Energy Required to Produce an Ion Pair,” ICRU Report No. 31 (1979).

30. N. Hadley *et al.*, "List of Poisoning Times for Materials," Lawrence Berkeley Lab Report TPC-LBL-79-8 (1981).
31. H.A. Bethe, Phys. Rev. **89**, 1256 (1953). A thorough review of multiple scattering is given by W.T. Scott, Rev. Mod. Phys. **35**, 231 (1963). However, the data of Shen *et al.*, (Phys. Rev. **D20**, 1584 (1979)) show that Bethe's simpler method of including atomic electron effects agrees better with experiment than does Scott's treatment. For a thorough discussion of simple formulae for single scatters and methods of compounding these into multiple-scattering formulae, see W.T. Scott, Rev. Mod. Phys. **35**, 231 (1963). Detailed summaries of formulae for computing single scatters are given in J.W. Motz, H. Olsen, and H.W. Koch, Rev. Mod. Phys. **36**, 881 (1964).
32. V.L. Highland, Nucl. Instrum. Methods **129**, 497 (1975), and Nucl. Instrum. Methods **161**, 171 (1979).
33. G.R. Lynch and O.I. Dahl, Nucl. Instrum. Methods **B58**, 6 (1991).
34. M. Wong *et al.*, Med. Phys. **17**, 163 (1990).
35. E. Segré, *Nuclei and Particles*, New York, Benjamin (1964) p. 65 ff.
36. Y.S. Tsai, Rev. Mod. Phys. **46**, 815 (1974).
37. H. Davies, H.A. Bethe, and L.C. Maximon, Phys. Rev. **93**, 788 (1954).
38. O.I. Dahl, private communication.
39. L.D. Landau and L.J. Pomeranchuk, Dokl. Akad. Nauk. SSSR **92**, 535 (1953); **92**, 735 (1953). These papers are available in English in L. Landau, *The Collected Papers of L.D. Landau*, Pergamon Press, 1965; A.B. Migdal, Phys. Rev. **103**, 1811 (1956).
40. S. Klein, Rev. Mod. Phys. **71**, 1501 (1999).
41. M. L. Ter-Mikaelian, SSSR **94**, 1033 (1954); M. L. Ter-Mikaelian, *High Energy Electromagnetic Processes in Condensed Media* (John Wiley & Sons, New York, 1972).
42. P. Anthony *et al.*, Phys. Rev. Lett. **76**, 3550 (1996).
43. H. W. Koch and J. W. Motz, Rev. Mod. Phys. **31**, 920 (1959).
44. M.J. Berger and S.M. Seltzer, "Tables of Energy Losses and Ranges of Electrons and Positrons," National Aeronautics and Space Administration Report NASA-SP-3012 (Washington DC 1964).
45. K. Hikasa *et al.*, *Review of Particle Properties*, Phys. Rev. **D46** (1992) S1.
46. B. L. Berman and S. C. Fultz, Rev. Mod. Phys. **47**, 713 (1975).
47. J.S. Hubbell, H. Gimm, and I Øverbø, J. Phys. Chem. Ref. Data **9**, 1023 (1980).
48. A. Veyssiere *et al.*, Nucl. Phys. **A159**, 561 (1970).
49. J. W. Motz, H. A. Olsen, and H. W. Koch, Rev. Mod. Phys. **41**, 581 (1969).
50. P. Anthony *et al.*, Phys. Rev. Lett. **75**, 1949 (1995).
51. U.I. Uggerhoj, Rev. Mod. Phys. **77**, 1131 (2005).
52. W.R. Nelson, H. Hirayama, and D.W.O. Rogers, "The EGS4 Code System," SLAC-265, Stanford Linear Accelerator Center (Dec. 1985).
53. *Experimental Techniques in High Energy Physics*, ed. by T. Ferbel (Addison-Wesley, Menlo Park CA 1987).
54. U. Amaldi, Phys. Scripta **23**, 409 (1981).
55. E. Longo and I. Sestili, Nucl. Instrum. Methods **128**, 283 (1975).
56. G. Grindhammer *et al.*, in *Proceedings of the Workshop on Calorimetry for the Supercollider*, Tuscaloosa, AL, March 13–17, 1989, edited by R. Donaldson and M.G.D. Gilchriese (World Scientific, Teaneck, NJ, 1989), p. 151.
57. W.R. Nelson *et al.*, Phys. Rev. **149**, 201 (1966).
58. G. Bathow *et al.*, Nucl. Phys. **B20**, 592 (1970).
59. H.A. Bethe and W. Heitler, *Proc. Roy. Soc. A* **146**, 83 (1934); H.A. Bethe, *Proc. Cambridge Phil. Soc.* **30**, 542 (1934).
60. A.A. Petrukhin and V.V. Shestakov, Can. J. Phys. **46**, S377 (1968).
61. V.M. Galitskii and S.R. Kel'ner, Sov. Phys. JETP **25**, 948 (1967).
62. S.R. Kel'ner and Yu.D. Kotov, Sov. J. Nucl. Phys. **7**, 237 (1968).
63. R.P. Kokoulin and A.A. Petrukhin, in *Proceedings of the International Conference on Cosmic Rays*, Hobart, Australia, August 16–25, 1971, Vol. **4**, p. 2436.
64. A.I. Nikishov, Sov. J. Nucl. Phys. **27**, 677 (1978).
65. Y.M. Andreev *et al.*, Phys. Atom. Nucl. **57**, 2066 (1994).
66. L.B. Bezrukov and E.V. Bugaev, Sov. J. Nucl. Phys. **33**, 635 (1981).
67. N.V. Mokhov, "The MARS Code System User's Guide," Fermilab-FN-628 (1995); N. V. Mokhov *et al.*, Radiation Protection and Dosimetry, vol. 116, part 2, pp. 99 (2005); Fermilab-Conf-04/053 (2004); N. V. Mokhov *et al.*, in *Proc. of Intl. Conf. on Nuclear Data for Science and Tech.* (Santa Fe, NM, 2004), AIP Conf. Proc. 769, part 2, p. 1618; Fermilab-Conf-04/269-AD (2004); <http://www-ap.fnal.gov/MARS/>.
68. P.H. Barrett *et al.*, Rev. Mod. Phys. **24**, 133 (1952).
69. A. Van Ginneken, Nucl. Instrum. Methods **A251**, 21 (1986).
70. U. Becker *et al.*, Nucl. Instrum. Methods **A253**, 15 (1986).
71. J.J. Eastman and S.C. Loken, in *Proceedings of the Workshop on Experiments, Detectors, and Experimental Areas for the Supercollider*, Berkeley, CA, July 7–17, 1987, edited by R. Donaldson and M.G.D. Gilchriese (World Scientific, Singapore, 1988), p. 542.
72. *Methods of Experimental Physics*, L.C.L. Yuan and C.-S. Wu, editors, Academic Press, 1961, Vol. 5A, p. 163.
73. W.W.M. Allison and P.R.S. Wright, "The Physics of Charged Particle Identification: dE/dx , Cherenkov Radiation, and Transition Radiation," p. 371 in *Experimental Techniques in High Energy Physics*, T. Ferbel, editor, (Addison-Wesley 1987).
74. E.R. Hayes, R.A. Schluter, and A. Tamosaitis, "Index and Dispersion of Some Cherenkov Counter Gases," ANL-6916 (1964).
75. T. Ypsilantis, "Particle Identification at Hadron Colliders", CERN-EP/89-150 (1989), or ECFA 89-124, **2** 661 (1989).
76. I. Tamm, J. Phys. U.S.S.R., **1**, 439 (1939).
77. H. Motz and L. I. Schiff, Am. J. Phys. **21**, 258 (1953).
78. B. N. Ratcliff, Nucl. Instrum & Meth. **A502**, 211 (2003).
79. S. K. Mandal, S. R. Klein, and J. D. Jackson, Phys. Rev. **D72**, 093003 (2005).
80. E. Zas, F. Halzen and T. Stanev, Phys. Rev. **D45**, 362 (1991).
81. H. Falcke *et al.*, Nature **435**, 313 (2005).
82. J.D. Jackson, *Classical Electrodynamics*, 3rd edition, (John Wiley & Sons, New York, 1998).

28. PARTICLE DETECTORS

Revised 2008 (see the various sections for authors).

28. PARTICLE DETECTORS	281
28.1. Summary of detector spatial resolution, temporal resolution, and deadtime	281
28.2. Photon detectors	281
28.2.1. Vacuum photodetectors	282
28.2.1.1. Photomultiplier tubes	282
28.2.1.2. Microchannel plates	283
28.2.1.3. Hybrid photon detectors	283
28.2.2. Gaseous photon detectors	283
28.2.3. Solid-state photon detectors	284
28.3. Organic scintillators	285
28.3.1. Scintillation mechanism	285
28.3.2. Caveats and cautions	286
28.3.3. Scintillating and wavelength-shifting fibers	286
28.4. Inorganic scintillators:	286
28.5. Cherenkov detectors	288
28.5.1. Threshold counters	289
28.5.2. Imaging counters	289
28.6. Cherenkov tracking calorimeters	290
28.7. Gaseous detectors	292
28.7.1. Energy loss and charge transport in gases	292
28.7.2. Multi-Wire Proportional Chambers	294
28.7.3. Micro-pattern Gas Detectors	295
28.7.4. Time-projection chambers	297
28.7.5. Transition radiation detectors (TRD's)	298
28.7.6. Resistive-plate chambers	299
28.8. Silicon semiconductor detectors	300
28.9. Low-noise electronics	301
28.10. Calorimeters	303
28.10.1. Electromagnetic calorimeters	304
28.10.2. Hadronic calorimeters	304
28.10.3. Free electron drift velocities in liquid ionization sensors	306
28.11. Superconducting magnets for collider detectors	307
28.11.1. Solenoid Magnets	307
28.11.2. Properties of collider detector magnets	308
28.11.3. Toroidal magnets	308
28.12. Measurement of particle momenta in a uniform magnetic field	308
References	309

28.1. Summary of detector spatial resolution, temporal resolution, and deadtime

In this section we give various parameters for common detector components. The quoted numbers are usually based on typical devices, and should be regarded only as rough approximations for new designs. More detailed discussions of detectors and their underlying physics can be found in books by Ferbel [1], Grupen [2], Kleinknecht [3], Knoll [4], Green [5], and Leroy & Rancoita [6]. In Table 28.1 are given typical resolutions and deadtimes of common detectors.

Table 28.1: Typical resolutions and deadtimes of common detectors. Revised September 2003 by R. Kadel (LBNL).

Detector Type	Accuracy (rms)	Resolution Time	Dead Time
Bubble chamber	10–150 μm	1 ms	50 ms ^a
Streamer chamber	300 μm	2 μs	100 ms
Proportional chamber	50–300 $\mu\text{m}^{b,c,d}$	2 ns	200 ns
Drift chamber	50–300 μm	2 ns ^e	100 ns
Scintillator	—	100 ps/n ^f	10 ns
Emulsion	1 μm	—	—
Liquid Argon Drift [7]	$\sim 175\text{--}450 \mu\text{m}$	$\sim 200 \text{ ns}$	$\sim 2 \mu\text{s}$
Gas Micro Strip [8]	30–40 μm	< 10 ns	—
Resistive Plate chamber [9]	$\lesssim 10 \mu\text{m}$	1–2 ns	—
Silicon strip	pitch/(3 to 7) ^g	h	h
Silicon pixel	2 μm^i	h	h

^a Multiple pulsing time.

^b 300 μm is for 1 mm pitch.

^c Delay line cathode readout can give $\pm 150 \mu\text{m}$ parallel to anode wire.

^d wirespacing/ $\sqrt{12}$.

^e For two chambers.

^f n = index of refraction.

^g The highest resolution (“7”) is obtained for small-pitch detectors ($\lesssim 25 \mu\text{m}$) with pulse-height-weighted center finding.

^h Limited by the readout electronics [10]. (Time resolution of $\leq 25 \text{ ns}$ is planned for the ATLAS SCT.)

ⁱ Analog readout of 34 μm pitch, monolithic pixel detectors.

28.2. Photon detectors

Updated August 2007 by D. Chakraborty (Northern Illinois U) and T. Sumiyoshi (Tokyo Metro U).

Most detectors in high-energy, nuclear, and astrophysics rely on the detection of photons in or near the visible range, $100 \text{ nm} \lesssim \lambda \lesssim 1000 \text{ nm}$, or $E \approx$ a few eV. This range covers scintillation and Cherenkov radiation as well as the light detected in many astronomical observations.

Generally, photodetection involves generating a detectable electrical signal proportional to the (usually very small) number of incident photons. The process involves three distinct steps:

1. Generation of a primary photoelectron or electron-hole ($e-h$) pair by an incident photon by the photoelectric or photoconductive effect,
2. Amplification of the p.e. signal to detectable levels by one or more multiplicative bombardment steps and/or an avalanche process (usually), and,
3. Collection of the secondary electrons to form the electrical signal.

The important characteristics of a photodetector include the following in statistical averages:

1. Quantum efficiency (QE or ϵ_Q): the number of primary photoelectrons generated per incident photon ($0 \leq \epsilon_Q \leq 1$;

in silicon more than one e - h pair per incident photon can be generated for $\lambda \lesssim 165$ nm),

2. Collection efficiency (CE or ϵ_C): the overall acceptance factor other than the generation of photoelectrons ($0 \leq \epsilon_C \leq 1$),
3. Gain (G): the number of electrons collected for each photoelectron generated,
4. Dark current or dark noise: the electrical signal when there is no photon,
5. Energy resolution: electronic noise (ENC or N_e) and statistical fluctuations in the amplification process compound the Poisson distribution of n_γ photons from a given source:

$$\frac{\sigma(E)}{\langle E \rangle} = \sqrt{\frac{f_N}{n_\gamma \epsilon_Q \epsilon_C} + \left(\frac{N_e}{G n_\gamma \epsilon_Q \epsilon_C} \right)^2}, \quad (28.1)$$

where f_N , or the excess noise factor (ENF), is the contribution to the energy distribution variance due to amplification statistics [11],

6. Dynamic range: the maximum signal available from the detector (this is usually expressed in units of the response to noise-equivalent power, or NEP, which is the optical input power that produces a signal-to-noise ratio of 1),
7. Time dependence of the response: this includes the transit time, which is the time between the arrival of the photon and the electrical pulse, and the transit time spread, which contributes to the pulse rise time and width, and
8. Rate capability: inversely proportional to the time needed, after the arrival of one photon, to get ready to receive the next.

Other important considerations also are highly application-specific. These include the photon flux and wavelength range, the total area to be covered and the efficiency required, the volume available to accommodate the detectors, characteristics of the environment such as chemical composition, temperature, magnetic field, ambient background, as well as ambient radiation of different types and, mode of operation (continuous or triggered), bias (high-voltage) requirements, power consumption, calibration needs, aging, cost, and so on. Several technologies employing different phenomena for the three steps described above, and many variants within each, offer a wide range of solutions to choose from. The salient features of the main technologies and the common variants are described below. Some key characteristics are summarized in Table 28.2.

28.2.1. Vacuum photodetectors: Vacuum photodetectors can be broadly subdivided into three types: photomultiplier tubes, microchannel plates, and hybrid photodetectors.

28.2.1.1. Photomultiplier tubes: A versatile class of photon detectors, vacuum photomultiplier tubes (PMT) has been employed by a vast majority of all particle physics experiments to date [11]. Both “transmission-” and “reflection-type” PMT’s are widely used. In the former, the photocathode material is deposited on the inside of a transparent window through which the photons enter, while in the latter, the photocathode material rests on a separate surface that the incident photons strike. The cathode material has a low work function, chosen for the wavelength band of interest. When a photon hits the cathode and liberates an electron (the photoelectric effect), the latter

Table 28.2: Representative characteristics of some photodetectors commonly used in particle physics. The time resolution of the devices listed here vary in the 10–2000 ps range.

Type	λ (nm)	$\epsilon_Q \epsilon_C$	Gain	Risetime (ns)	Area (mm ²)	1-p.e noise (Hz)	HV (V)	Price (USD)
PMT*	115–1100	0.15–0.25	10^3 – 10^7	0.7–10	10^2 – 10^5	10 – 10^4	500–3000	100–5000
MCP*	100–650	0.01–0.10	10^3 – 10^7	0.15–0.3	10^2 – 10^4	0.1–200	500–3500	10–6000
HPD*	115–850	0.1–0.3	10^3 – 10^4	7	10^2 – 10^5	10 – 10^3	$\sim 2 \times 10^4$	~ 600
GPM*	115–500	0.15–0.3	10^3 – 10^6	$O(0.1)$	$O(10)$	10 – 10^3	300–2000	$O(10)$
APD	300–1700	~ 0.7	10 – 10^8	$O(1)$	10 – 10^3	1 – 10^3	400–1400	$O(100)$
PPD	400–550	0.15–0.3	10^5 – 10^6	~ 1	1–10	$O(10^6)$	30–60	$O(10)$
VLPC	500–600	~ 0.9	$\sim 5 \times 10^4$	~ 10	1	$O(10^4)$	~ 7	~ 1

*These devices often come in multi-anode configurations. In such cases, area, noise, and price are to be considered on a “per readout-channel” basis.

The QE is a strong function of the photon wavelength (λ), and is usually quoted at maximum, together with a range of λ where the QE is comparable to its maximum. Spatial uniformity and linearity with respect to the number of photons are highly desirable in a photodetector’s response.

Optimization of these factors involves many trade-offs and vary widely between applications. For example, while a large gain is desirable, attempts to increase the gain for a given device also increases the ENF and after-pulsing (“echos” of the main pulse). In solid-state devices, a higher QE often requires a compromise in the timing properties. In other types, coverage of large areas by focusing increases the transit time spread.

is accelerated and guided by electric fields to impinge on a secondary-emission electrode, or dynode, which then emits a few (~ 5) secondary electrons. The multiplication process is repeated typically 10 times in series to generate a sufficient number of electrons, which are collected at the anode for delivery to the external circuit. The total gain of a PMT depends on the applied high voltage V as $G = AV^{kn}$, where $k \approx 0.7$ – 0.8 (depending on the dynode material), n is the number of dynodes in the chain, and A a constant (which also depends on n). Typically, G is in the range of 10^5 – 10^6 . Pulse risetimes are usually in the few nanosecond range. With *e.g.* two-level discrimination the effective time resolution can be much better.

A large variety of PMT's, including many just recently developed, covers a wide span of wavelength ranges from infrared (IR) to extreme ultraviolet (XUV) [12]. They are categorized by the window materials, photocathode materials, dynode structures, anode configurations, *etc.* Common window materials are borosilicate glass for IR to near-UV, fused quartz and sapphire (Al_2O_3) for UV, and MgF_2 or LiF for XUV. The choice of photocathode materials include a variety of mostly Cs- and/or Sb-based compounds such as CsI, CsTe, bi-alkali (SbRbCs, SbKCs), multi-alkali (SbNa₂KCs), GaAs(Cs), GaAsP, *etc.* Sensitive wavelengths and peak quantum efficiencies for these materials are summarized in Table 28.3. Typical dynode structures used in PMT's are circular cage, line focusing, box and grid, venetian blind, and fine mesh. In some cases, limited spatial resolution can be obtained by using a mosaic of multiple anodes.

PMT's are vulnerable to magnetic fields—sometimes even the geomagnetic field causes large orientation-dependent gain changes. A high-permeability metal shield is often necessary. However, proximity-focused PMT's, *e.g.* the fine-mesh types, can be used even in a high magnetic field (≥ 1 T) if the electron drift direction is parallel to the field.

28.2.1.2. Microchannel plates: A typical Microchannel plate (MCP) photodetector consists of one or more ~ 2 mm thick glass plates with densely packed $O(10 \mu\text{m})$ -diameter cylindrical holes, or “channels”, sitting between the transmission-type photocathode and anode planes, separated by $O(1 \text{ mm})$ gaps. Instead of discrete dynodes, the inner surface of each cylindrical tube serves as a continuous dynode for the entire cascade of multiplicative bombardments initiated by a photoelectron. Gain fluctuations can be minimized by operating in a saturation mode, whence each channel is only capable of a binary output, but the sum of all channel outputs remains proportional to the number of photons received so long as the photon flux is low enough to ensure that the probability of a single channel receiving more than one photon during a single time gate is negligible. MCP's are thin, offer good spatial resolution, have excellent time resolution (~ 20 ps), and can tolerate random magnetic fields up to 0.1 T and axial fields up to ~ 1 T. However, they suffer from relatively long recovery time per channel and short lifetime. MCP's are widely employed as image-intensifiers, although not so much in HEP or astrophysics.

28.2.1.3. Hybrid photon detectors: Hybrid photon detectors (HPD) combine the sensitivity of a vacuum PMT with the excellent spatial and energy resolutions of a Si sensor [13]. A single photoelectron ejected from the photocathode is accelerated through a potential difference of ~ 20 kV before it impinges on the silicon sensor/anode. The gain nearly equals the maximum number of e - h pairs that could be created from the entire kinetic energy of the accelerated electron: $G \approx eV/w$, where e is the electronic charge, V is the applied potential difference, and $w \approx 3.7$ eV is the mean energy required to create an e - h pair in Si at room temperature. Since the gain is achieved in a single step, one might expect to have the excellent resolution of a simple Poisson statistic with large mean, but in fact it is even better, thanks to the Fano effect discussed in Sec. 28.8.

Low-noise electronics must be used to read out HPD's if one intends to take advantage of the low fluctuations in gain, *e.g.* when counting small numbers of photons. HPD's can have the same $\epsilon_Q \epsilon_C$ and window geometries as PMT's and can be segmented down to $\sim 50 \mu\text{m}$. However, they require rather high

biases and will not function in a magnetic field. The exception is proximity-focused devices (\Rightarrow no (de)magnification) in an axial field. With time resolutions of ~ 10 ps and superior rate capability, proximity-focused HPD's can be an alternative to MCP's. Current applications of HPD's include the CMS hadronic calorimeter and the RICH detector in LHCb. Large-size HPD's with sophisticated focusing may be suitable for future water Cherenkov experiments.

Hybrid APD's (HAPD's) add an avalanche multiplication step following the electron bombardment to boost the gain by a factor of ~ 50 . This affords a higher gain and/or lower electrical bias, but also degrades the signal definition.

Table 28.3: Properties of photocathode and window materials commonly used in vacuum photodetectors [12].

Photocathode material	λ (nm)	Window material	Peak ϵ_Q (λ/nm)
CsI	115–200	MgF_2	0.15 (135)
CsTe	115–240	MgF_2	0.18 (210)
Bi-alkali	300–650	Borosilicate	0.27 (390)
	160–650	Quartz	0.27 (390)
Multi-alkali	300–850	Borosilicate	0.20 (360)
	160–850	Quartz	0.23 (280)
GaAs(Cs)*	160–930	Quartz	0.23 (280)
GaAsP(Cs)	300–750	Borosilicate	0.42 (560)

*Reflection type photocathode is used.

28.2.2. Gaseous photon detectors : In gaseous photomultipliers (GPM) a photoelectron in a suitable gas mixture initiates an avalanche in a high-field region, producing a large number of secondary impact-ionization electrons. In principle the charge multiplication and collection processes are identical to those employed in gaseous tracking detectors such as multiwire proportional chambers, micromesh gaseous detectors (Micromegas), or gas electron multipliers (GEM). These are discussed in Sec. 28.7.3.

The devices can be divided into two types depending on the photocathode material. One type uses solid photocathode materials much in the same way as PMT's. Since it is resistant to gas mixtures typically used in tracking chambers, CsI is a common choice. In the other type, photoionization occurs on suitable molecules vaporized and mixed in the drift volume. Most gases have photoionization work functions in excess of 10 eV, which would limit their sensitivity to wavelengths far too short. However, vapors of TMAE (tetrakis dimethyl-amine ethylene) or TEA (tri-ethyl-amine), which have smaller work functions (5.3 eV for TMAE and 7.5 eV for TEA), are suited for XUV photon detection [14]. Since devices like GEM's offer sub-mm spatial resolution, GPM's are often used as position-sensitive photon detectors. They can be made into flat panels to cover large areas ($O(1 \text{ m}^2)$), can operate in high magnetic fields, and are relatively inexpensive. Many of the ring imaging Cherenkov (RICH) detectors to date have used GPM's for the detection of Cherenkov light [15]. Special care must be taken to suppress the photon-feedback process in GPM's. It is also important to maintain high purity of the gas as minute traces of O_2 can significantly degrade the detection efficiency.

28.2.3. Solid-state photon detectors : In a phase of rapid development, solid-state photodetectors are competing with vacuum- or gas-based devices for many existing applications and making way for a multitude of new ones. Compared to traditional vacuum- and gaseous photodetectors, solid-state devices are more compact, lightweight, rugged, tolerant to magnetic fields, and often cheaper. They also allow fine pixelization, are easy to integrate into large systems, and can operate at low electric potentials, while matching or exceeding most performance criteria. They are particularly well suited for detection of γ - and X-rays. Except for applications where coverage of very large areas or dynamic range is required, solid-state detectors are proving to be the better choice. Some hybrid devices attempt to combine the best features of different technologies while applications of nanotechnology are opening up exciting new possibilities.

Silicon photodiodes (PD) are widely used in high-energy physics as particle detectors and in a great number of applications (including solar cells!) as light detectors. The structure is discussed in some detail in Sec. 28.8. In its simplest form, the PD is a reverse-biased p - n junction. Photons with energies above the indirect bandgap energy (wavelengths shorter than about 1050 nm, depending on the temperature) can create e - h pairs (the photoconductive effect), which are collected on the p and n sides, respectively. Often, as in the PD's used for crystal scintillator readout in CLEO, L3, Belle, BaBar, and GLAST, intrinsic silicon is doped to create a p - i - n structure. The reverse bias increases the thickness of the depleted region; in the case of these particular detectors, to full depletion at a depth of about 100 μm . Increasing the depletion depth decreases the capacitance (and hence electronic noise) and extends the red response. Quantum efficiency can exceed 90%, but falls toward the red because of the increasing absorption length of light in silicon. The absorption length reaches 100 μm at 985 nm. However, since $G = 1$, amplification is necessary. Optimal low-noise amplifiers are slow, but, even so, noise limits the minimum detectable signal in room-temperature devices to several hundred photons.

Very large arrays containing $O(10^7)$ of $O(10 \mu\text{m}^2)$ -sized photodiodes pixelizing a plane are widely used to photograph all sorts of things from everyday subjects at visible wavelengths to crystal structures with X-rays and astronomical objects from infrared to UV. To limit the number of readout channels, these are made into charge-coupled devices (CCD), where pixel-to-pixel signal transfer takes place over thousands of synchronous cycles with sequential output through shift registers [16]. Thus, high spatial resolution is achieved at the expense of speed and timing precision. Custom-made CCD's have virtually replaced photographic plates and other imagers for astronomy and in spacecraft. Typical QE's exceed 90% over much of the visible spectrum, and "thick" CCD's have useful QE up to $\lambda = 1 \mu\text{m}$. Active Pixel Sensor (APS) arrays with a preamplifier on each pixel and CMOS processing afford higher speeds, but are challenged at longer wavelengths. Much R&D is underway to overcome the limitations of both CCD and CMOS imagers.

In avalanche photodiodes (APD), an exponential cascade of impact ionizations initiated by the initial photogenerated e - h pair under a large reverse-bias voltage leads to an avalanche breakdown [17]. As a result, detectable electrical response can be obtained from low-intensity optical signals down to single

photons. Excellent junction uniformity is critical, and a guard ring is generally used as a protection against edge breakdown. Well-designed APD's, such as those used in CMS' crystal-based electromagnetic calorimeter, have achieved $\epsilon_Q \epsilon_C \approx 0.7$ with sub-ns response time. The sensitive wavelength window and gain depend on the semiconductor used. The gain is typically 10–200 in linear and up to 10^8 in Geiger mode of operation. Stability and close monitoring of the operating temperature are important for linear-mode operation, and substantial cooling is often necessary. Position-sensitive APD's use time information at multiple anodes to calculate the hit position.

One of the most promising recent developments in the field is that of devices consisting of large arrays ($O(10^3)$) of tiny APD's packed over a small area ($O(1 \text{ mm}^2)$) and operated in a limited Geiger mode [18]. Among different names used for this class of photodetectors, "PPD" (for "Pixelized Photon Detector") is most widely accepted (formerly "SiPM"). Although each cell only offers a binary output, linearity with respect to the number of photons is achieved by summing the cell outputs in the same way as with a MCP in saturation mode (see above). PPD's are being adopted as the preferred solution for various purposes including medical imaging, *e.g.* positron emission tomography (PET). These compact, rugged, and economical devices allow auto-calibration through decent separation of photoelectron peaks and offer gains of $O(10^6)$ at a moderate bias voltage (~ 50 V). However, the single-photoelectron noise of a PPD, being the logical "or" of $O(10^3)$ Geiger APD's, is rather large: $O(1 \text{ MHz/mm}^2)$ at room temperature. PPD's are particularly well-suited for applications where triggered pulses of several photons are expected over a small area, *e.g.* fiber-guided scintillation light. Intense R&D is expected to lower the noise level and improve radiation hardness, resulting in coverage of larger areas and wider applications. Attempts are being made to combine the fabrication of the sensors and the front-end electronics (ASIC) in the same process with the goal of making PPD's and other finely pixelized solid-state photodetectors extremely easy to use.

Of late, much R&D has been directed to p - i - n diode arrays based on thin polycrystalline diamond films formed by chemical vapor deposition (CVD) on a hot substrate (~ 1000 K) from a hydrocarbon-containing gas mixture under low pressure (~ 100 mbar). These devices have maximum sensitivity in the extreme- to moderate-UV region [19]. Many desirable characteristics, including high tolerance to radiation and temperature fluctuations, low dark noise, blindness to most of the solar radiation spectrum, and relatively low cost make them ideal for space-based UV/XUV astronomy, measurement of synchrotron radiation, and luminosity monitoring at (future) lepton collider(s).

Visible-light photon counters (VLPC) utilize the formation of an impurity band only 50 meV below the conduction band in As-doped Si to generate strong ($G \approx 5 \times 10^4$) yet sharp response to single photons with $\epsilon_Q \approx 0.9$ [20]. The smallness of the band gap considerably reduces the gain dispersion. Only a very small bias (~ 7 V) is needed, but high sensitivity to infrared photons requires cooling below 10 K. The dark noise increases sharply and exponentially with both temperature and bias. The Run 2 DØ detector uses 86000 VLPC's to read the optical signal from its scintillating-fiber tracker and scintillator-strip preshower detectors.

28.3. Organic scintillators

Revised September 2007 by K.F. Johnson (FSU).

Organic scintillators are broadly classed into three types, crystalline, liquid, and plastic, all of which utilize the ionization produced by charged particles (see Sec. 27.2) of this *Review*) to generate optical photons, usually in the blue to green wavelength regions [21]. Plastic scintillators are by far the most widely used. Crystal organic scintillators are practically unused in high-energy physics.

Densities range from 1.03 to 1.20 g cm⁻³. Typical photon yields are about 1 photon per 100 eV of energy deposit [22]. A one-cm-thick scintillator traversed by a minimum-ionizing particle will therefore yield $\approx 2 \times 10^4$ photons. The resulting photoelectron signal will depend on the collection and transport efficiency of the optical package and the quantum efficiency of the photodetector.

Plastic scintillators do not respond linearly to the ionization density. Very dense ionization columns emit less light than expected on the basis of dE/dx for minimum-ionizing particles. A widely used semi-empirical model by Birks posits that recombination and quenching effects between the excited molecules reduce the light yield [23]. These effects are more pronounced the greater the density of the excited molecules. Birks' formula is

$$\frac{d\mathcal{L}}{dx} = \mathcal{L}_0 \frac{dE/dx}{1 + k_B dE/dx}, \quad (28.2)$$

where \mathcal{L} is the luminescence, \mathcal{L}_0 is the luminescence at low specific ionization density, and k_B is Birks' constant, which must be determined for each scintillator by measurement.

Decay times are in the ns range; rise times are much faster. The combination of high light yield and fast response time allows the possibility of sub-ns timing resolution [24]. The fraction of light emitted during the decay "tail" can depend on the exciting particle. This allows pulse shape discrimination as a technique to carry out particle identification. Because of the hydrogen content (carbon to hydrogen ratio ≈ 1) plastic scintillator is sensitive to proton recoils from neutrons. Ease of fabrication into desired shapes and low cost has made plastic scintillators a common detector component. Recently, plastic scintillators in the form of scintillating fibers have found widespread use in tracking and calorimetry [25].

28.3.1. Scintillation mechanism :

Scintillation: A charged particle traversing matter leaves behind it a wake of excited molecules. Certain types of molecules, however, will release a small fraction ($\approx 3\%$) of this energy as optical photons. This process, scintillation, is especially marked in those organic substances which contain aromatic rings, such as polystyrene (PS) and polyvinyltoluene (PVT). Liquids which scintillate include toluene and xylene.

Fluorescence: In fluorescence, the initial excitation takes place via the absorption of a photon, and de-excitation by emission of a longer wavelength photon. Fluors are used as "wavelength shifters" to shift scintillation light to a more convenient wavelength. Occurring in complex molecules, the absorption and emission are spread out over a wide band of photon energies, and have some overlap, that is, there is some fraction of the emitted light which can be re-absorbed [26]. This "self-absorption" is undesirable for detector applications because it causes a shortened attenuation length. The wavelength difference between the major absorption and emission peaks is called the Stokes' shift. It is usually the case that the greater the Stokes' shift, the smaller the self absorption—thus, a large Stokes' shift is a desirable property for a fluor.

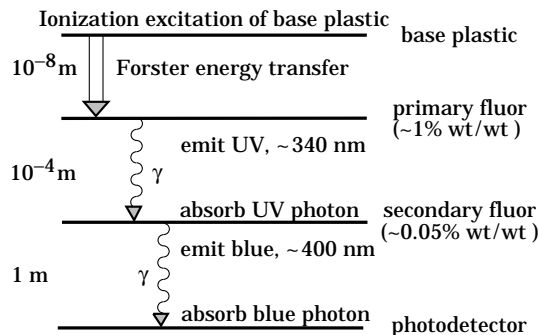


Figure 28.1: Cartoon of scintillation "ladder" depicting the operating mechanism of plastic scintillator. Approximate fluor concentrations and energy transfer distances for the separate sub-processes are shown.

Scintillators: The plastic scintillators used in high-energy physics are binary or ternary solutions of selected fluors in a plastic base containing aromatic rings. (See the appendix in Ref. 27 for a comprehensive list of components.) Virtually all plastic scintillators contain as a base either PVT or PS. PVT-based scintillator can be up to 50% brighter.

Ionization in the plastic base produces UV photons with short attenuation length (several mm). Longer attenuation lengths are obtained by dissolving a "primary" fluor in high concentration (1% by weight) into the base, which is selected to efficiently re-radiate absorbed energy at wavelengths where the base is more transparent.

The primary fluor has a second important function. The decay time of the scintillator base material can be quite long—in pure polystyrene it is 16 ns, for example. The addition of the primary fluor in high concentration can shorten the decay time by an order of magnitude and increase the total light yield. At the concentrations used (1% and greater), the average distance between a fluor molecule and an excited base unit is around 100 Å, much less than a wavelength of light. At these distances the predominant mode of energy transfer from base to fluor is not the radiation of a photon, but a resonant dipole-dipole interaction, first described by Foerster, which strongly couples the base and fluor [28]. The strong coupling sharply increases the speed and the light yield of the plastic scintillators.

Unfortunately, a fluor which fulfills other requirements is usually not completely adequate with respect to emission wavelength or attenuation length, so it is necessary to add yet another wavelshifter (the "secondary" fluor), at fractional percent levels, and occasionally a third (not shown in Fig. 28.1).

External wavelength shifters: Light emitted from a plastic scintillator may be absorbed in a (nonscintillating) base doped with a wave-shifting fluor. Such wavelength shifters are widely used to aid light collection in complex geometries. The wavelength shifter must be insensitive to ionizing radiation and Cherenkov light. A typical wavelength shifter uses an acrylic base because of its good optical qualities, a single fluor to shift the light emerging from the plastic scintillator to the blue-green, and contains ultra-violet absorbing additives to deaden response to Cherenkov light.

28.3.2. Caveats and cautions : Plastic scintillators are reliable, robust, and convenient. However, they possess quirks to which the experimenter must be alert.

Aging and Handling: Plastic scintillators are subject to aging which diminishes the light yield. Exposure to solvent vapors, high temperatures, mechanical flexing, irradiation, or rough handling will aggravate the process. A particularly fragile region is the surface which can “craze”—develop microcracks—which rapidly destroy the capability of plastic scintillators to transmit light by total internal reflection. Crazing is particularly likely where oils, solvents, or *fingerprints* have contacted the surface.

Attenuation length: The Stokes’ shift is not the only factor determining attenuation length. Others are the concentration of fluors (the higher the concentration of a fluor, the greater will be its self-absorption); the optical clarity and uniformity of the bulk material; the quality of the surface; and absorption by additives, such as stabilizers, which may be present.

Afterglow: Plastic scintillators have a long-lived luminescence which does not follow a simple exponential decay. Intensities at the 10^{-4} level of the initial fluorescence can persist for hundreds of ns [21,29].

Atmospheric quenching: Plastic scintillators will decrease their light yield with increasing partial pressure of oxygen. This can be a 10% effect in an artificial atmosphere [30]. It is not excluded that other gases may have similar quenching effects.

Magnetic field: The light yield of plastic scintillators may be changed by a magnetic field. The effect is very nonlinear and apparently not all types of plastic scintillators are so affected. Increases of $\approx 3\%$ at 0.45 T have been reported [31]. Data are sketchy and mechanisms are not understood.

Radiation damage: Irradiation of plastic scintillators creates color centers which absorb light more strongly in the UV and blue than at longer wavelengths. This poorly understood effect appears as a reduction both of light yield and attenuation length. Radiation damage depends not only on the integrated dose, but on the dose rate, atmosphere, and temperature, before, during and after irradiation, as well as the materials properties of the base such as glass transition temperature, polymer chain length, *etc.* Annealing also occurs, accelerated by the diffusion of atmospheric oxygen and elevated temperatures. The phenomena are complex, unpredictable, and not well understood [32]. Since color centers are less intrusive at longer wavelengths, the most reliable method of mitigating radiation damage is to shift emissions at every step to the longest practical wavelengths, *e.g.*, utilize fluors with large Stokes’ shifts (aka the “Better red than dead” strategy).

28.3.3. Scintillating and wavelength-shifting fibers :

The clad optical fiber is an incarnation of scintillator and wavelength shifter (WLS) which is particularly useful [33]. Since the initial demonstration of the scintillating fiber (SCIFI) calorimeter [34], SCIFI techniques have become mainstream [35].

SCIFI calorimeters are fast, dense, radiation hard, and can have leadglass-like resolution. SCIFI trackers can handle high rates and are radiation tolerant, but the low photon yield at the end of a long fiber (see below) forces the use of sensitive photodetectors. WLS scintillator readout of a calorimeter allows a very high level of hermeticity since the solid angle blocked by the fiber on its way to the photodetector is very small. The sensitive region of scintillating fibers can be controlled by splicing them onto clear (non-scintillating/non-WLS) fibers.

A typical configuration would be fibers with a core of polystyrene-based scintillator or WLS (index of refraction

$n = 1.59$), surrounded by a cladding of PMMA ($n = 1.49$) a few microns thick, or, for added light capture, with another cladding of fluorinated PMMA with $n = 1.42$, for an overall diameter of 0.5 to 1 mm. The fiber is drawn from a boule and great care is taken during production to ensure that the intersurface between the core and the cladding has the highest possible uniformity and quality, so that the signal transmission via total internal reflection has a low loss. The fraction of generated light which is transported down the optical pipe is denoted the capture fraction and is about 6% for the single-clad fiber and 10% for the double-clad fiber.

The number of photons from the fiber available at the photodetector is always smaller than desired, and increasing the light yield has proven difficult. A minimum-ionizing particle traversing a high-quality 1 mm diameter fiber perpendicular to its axis will produce fewer than 2000 photons, of which about 200 are captured. Attenuation may eliminate 95% of these photons in a large collider tracker.

A scintillating or WLS fiber is often characterized by its “attenuation length,” over which the signal is attenuated to $1/e$ of its original value. Many factors determine the attenuation length, including the importance of re-absorption of emitted photons by the polymer base or dissolved fluors, the level of crystallinity of the base polymer, and the quality of the total internal reflection boundary. Attenuation lengths of several meters are obtained by high quality fibers. However, it should be understood that the attenuation length is not necessarily a measure of fiber quality. Among other things, it is not constant with distance from the excitation source and it is wavelength dependent. So-called “cladding light” causes some of the distance dependence [36], but not all. The wavelength dependence is usually related to the higher re-absorption of shorter wavelength photons—once absorbed, re-emitted isotropically and lost with 90% probability—and to the lower absorption of longer wavelengths by polystyrene. Experimenters should be aware that measurements of attenuation length by a phototube with a bialkali photocathode, whose quantum efficiency drops below 10% at 480 nm, should not be naïvely compared to measurements utilizing a silicon photodiode, whose quantum efficiency is still rising at 600 nm.

28.4. Inorganic scintillators:

Revised September 2007 by R.-Y. Zhu (California Institute of Technology) and C.L. Woody (BNL).

Inorganic crystals form a class of scintillating materials with much higher densities than organic plastic scintillators (typically $\sim 4\text{--}8\text{ g/cm}^3$) with a variety of different properties for use as scintillation detectors. Due to their high density and high effective atomic number, they can be used in applications where high stopping power or a high conversion efficiency for electrons or photons is required. These include total absorption electromagnetic calorimeters (see Sec. 28.10.1), which consist of a totally active absorber (as opposed to a sampling calorimeter), as well as serving as gamma ray detectors over a wide range of energies. Many of these crystals also have very high light output, and can therefore provide excellent energy resolution down to very low energies (\sim few hundred keV).

Some crystals are intrinsic scintillators in which the luminescence is produced by a part of the crystal lattice itself. However, other crystals require the addition of a dopant, typically fluorescent ions such as thallium (Tl) or cerium (Ce) which is responsible for producing the scintillation light. However, in both cases, the scintillation mechanism is the same. Energy is deposited in the crystal by ionization, either directly by charged particles, or by the conversion of photons into electrons or positrons which subsequently produce ionization.

This energy is transferred to the luminescent centers which then radiate scintillation photons. The efficiency η for the conversion of energy deposit in the crystal to scintillation light can be expressed by the relation [37]

$$\eta = \beta \cdot S \cdot Q . \quad (28.3)$$

where β is the efficiency of the energy conversion process, S is the efficiency of energy transfer to the luminescent center, and Q is the quantum efficiency of the luminescent center. The value of η ranges between 0.1 and ~ 1 depending on the crystal, and is the main factor in determining the intrinsic light output of the scintillator. In addition, the scintillation decay time is primarily determined by the energy transfer and emission process. The decay time of the scintillator is mainly dominated by the decay time of the luminescent center. For example, in the case of thallium doped sodium iodide (NaI(Tl)), the value of η is ~ 0.5 , which results in a light output $\sim 40,000$ photons per MeV of energy deposit. This high light output is largely due to the high quantum efficiency of the thallium ion ($Q \sim 1$), but the decay time is rather slow ($\tau \sim 250$ ns).

Table 28.4 lists the basic properties of some commonly used inorganic crystal scintillators. NaI(Tl) is one of the most common and widely used scintillators, with an emission that is well matched to a bi-alkali photomultiplier tube, but it is highly hygroscopic and difficult to work with, and has a rather low density. CsI(Tl) has high light yield, an emission that is well matched to solid state photodiodes, and is mechanically robust (high plasticity and resistance to cracking). However, it needs careful surface treatment and is slightly hygroscopic. Compared with CsI(Tl), pure CsI has identical mechanical properties, but faster emission at shorter wavelengths and light output approximately an order of magnitude lower. BaF₂ has a fast component with a sub-nanosecond decay time, and is the fastest known scintillator. However, it also has a slow component with a much longer decay time (~ 630 ns). Bismuth germanate (Bi₄Ge₃O₁₂ or BGO) has a high density, and consequently a short radiation length X_0 and Molière radius R_M . BGO's emission is well-matched to the spectral sensitivity of photodiodes, and it is easy to handle and not hygroscopic. Lead tungstate (PbWO₄ or PWO) has a very high density, with a very short X_0 and R_M , but its intrinsic light yield is rather low. Cerium doped lutetium oxyorthosilicate (Lu₂SiO₅:Ce, or LSO:Ce) [38], cerium doped lutetium-yttrium oxyorthosilicate (Lu_{2(1-x)}Y_{2x}SiO₅, LYSO:Ce) [39] and cerium doped gadolinium orthosilicate (Gd₂SiO₅:Ce, or GSO:Ce) [40] are dense crystal scintillators which have a high light yield and a fast decay time. Only properties of LSO:Ce and GSO:Ce are listed in Table 28.4 since the properties of LYSO:Ce are similar to that of LSO:Ce except a little lower density than LSO:Ce depending on the yttrium fraction in LYSO:Ce [41].

Beside the crystals listed in Table 28.4, a number of new crystals are being developed that may have potential applications in high energy or nuclear physics. Of particular interest is the family of yttrium and lutetium perovskites, which include YAP (YAlO₃:Ce) and LuAP (LuAlO₃:Ce) and their mixed compositions. These have been shown to be linear over a large energy range [42], and have the potential for providing extremely good intrinsic energy resolution. In addition, other fluoride crystals such as CeF₃ have been shown to provide excellent energy resolution in calorimeter applications.

Table 28.4 gives the light output of other crystals relative to NaI(Tl) and their dependence to the temperature variations measured for crystal samples of 1.5 X_0 cube with a Tyvek paper wrapping and a full end face coupled to a photodetector [43]. The quantum efficiencies of the photodetector is taken out to facilitate a direct comparison of crystal's light output. However,

the useful signal produced by a scintillator is usually quoted in terms of the number of photoelectrons per MeV produced by a given photodetector. The relationship between the number of photons/MeV produced and photoelectrons/MeV detected involves the factors for the light collection efficiency L and the quantum efficiency QE of the photodetector:

$$N_{\text{p.e.}}/\text{MeV} = L \cdot QE \cdot N_\gamma/\text{MeV} \quad (28.4)$$

L includes the transmission of scintillation light within the crystal (*i.e.*, the bulk attenuation length of the material), reflections and scattering from the surfaces, and the size and shape of the crystal. These factors can vary considerably depending on the sample, but can be in the range of ~ 10 –60%. The internal light transmission depends on the intrinsic properties of the material, e.g. the density and type of the scattering centers and defects that can produce internal absorption within the crystal, and can be highly affected by factors such as radiation damage, as discussed below.

The quantum efficiency depends on the type of photodetector used to detect the scintillation light, which is typically ~ 15 –20% for photomultiplier tubes and $\sim 70\%$ for silicon photodiodes for visible wavelengths. The quantum efficiency of the detector is usually highly wavelength dependent and should be matched to the particular crystal of interest to give the highest quantum yield at the wavelength corresponding to the peak of the scintillation emission. Fig. 28.2 shows the quantum efficiencies of two photodetectors, a Hamamatsu R2059 PMT with bi-alkali cathode and quartz window and a Hamamatsu S8664 avalanche photodiode (APD) as a function of wavelength. Also shown in the figure are emission spectra of three crystal scintillators, BGO, LSO:Ce/LYSO:Ce and CsI(Tl), and the numerical values of the emission weighted quantum efficiency. The area under each emission spectrum is proportional to crystal's light yield, as shown in Table 28.4, where the quantum efficiencies of the photodetector has been taken out. Results with different photodetectors can be significantly different. For example, the response of CsI(Tl) relative to NaI(Tl) with a standard photomultiplier tube with a bi-alkali photocathode, e.g. Hamamatsu R2059, would be 45 rather than 165 because of the photomultiplier's low quantum efficiency at longer wavelengths. For scintillators which emit in the UV, a detector with a quartz window should be used.

One important issue related to the application of a crystal scintillator is its radiation hardness. Stability of its light output, or the ability to track and monitor the variation of its light output in a radiation environment, is required for high resolution and precision calibration [44]. All known crystal scintillators suffer from radiation damage. A common damage phenomenon is the appearance of radiation induced absorption caused by the formation of color centers originated from the impurities or point defects in the crystal. This radiation induced absorption reduces the light attenuation length in the crystal, and hence its light output. For crystals with high defect density, a severe reduction of light attenuation length may cause a distortion of the light response uniformity, leading to a degradation of the energy resolution. Additional radiation damage effects may include a reduced intrinsic scintillation light yield (damage to the luminescent centers) and an increased phosphorescence (afterglow). For crystals to be used in the construction a high precision calorimeter in a radiation environment, its scintillation mechanism must not be damaged and its light attenuation length in the expected radiation environment must be long enough so that its light response uniformity, and thus its energy resolution, does not change [45].

Most of the crystals listed in Table 28.4 have been used in high energy or nuclear physics experiments when the ultimate

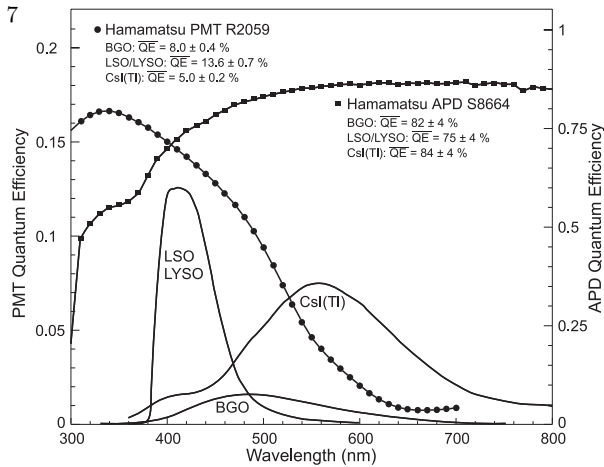


Figure 28.2: The quantum efficiencies of two photodetectors, a Hamamatsu R2059 PMT with bi-alkali cathode and a Hamamatsu S8664 avalanche photodiode (APD), are shown as a function of wavelength. Also shown in the figure are emission spectra of three crystal scintillators, BGO, LSO and CsI(Tl), and the numerical values of the emission weighted quantum efficiency. The area under each emission spectrum is proportional to crystal's light yield.

energy resolution for electrons and photons is desired. Examples are the Crystal Ball NaI(Tl) calorimeter at SPEAR, the L3 BGO calorimeter at LEP, the CLEO CsI(Tl) calorimeter at CESR, the KTeV CsI calorimeter at the Tevatron, the BaBar and BELLE CsI(Tl) calorimeters at PEP-II and KEK. Because of its high density and low cost, PWO calorimeters are widely used by CMS and ALICE at LHC, by CLAS and PrimEx at CEBAF, and are the leading option for PANDA at GSI. Recently, investigations have been made aiming at using LSO:Ce or LYSO:Ce crystals for future high energy or nuclear physics experiments [41].

28.5. Cherenkov detectors

Revised September 2007 by B.N. Ratcliff (SLAC).

Although devices using Cherenkov radiation are often thought of as particle identification (PID) detectors, in practice, they are widely used over a much broader range of applications; including (1) fast particle counters; (2) hadronic particle identification; and (3) tracking detectors performing complete event reconstruction. A few examples of specific applications from each category include; (1) the polarization detector of the SLD [46]; (2) the hadronic PID detectors at the B factory detectors (DIRC in BaBar [9] and the aerogel threshold Cherenkov in Belle [47]); and (3) large water Cherenkov counters such as Super-Kamiokande [49]. Cherenkov counters contain two main elements; (1) a radiator through which the charged particle passes, and (2) a photodetector. As Cherenkov radiation is a weak source of photons, light collection and detection must be as efficient as possible. The presence of the refractive index n and the path length of the particle in the radiator in the Cherenkov relations allows tuning these quantities for a particular experimental application.

Cherenkov detectors utilize one or more of the properties of Cherenkov radiation discussed in the Passages of Particles through Matter section (Sec. 27 of this *Review*): the prompt emission of a light pulse; the existence of a velocity threshold for radiation; and the dependence of the Cherenkov cone half-angle θ_c and the number of emitted photons on the velocity of the particle.

The number of photoelectrons ($N_{p.e.}$) detected in a given device is

$$N_{p.e.} = L \frac{\alpha^2 z^2}{r_e m_e c^2} \int \epsilon(E) \sin^2 \theta_c(E) dE, \quad (28.5)$$

where L is the path length in the radiator, $\epsilon(E)$ is the efficiency for collecting the Cherenkov light and transducing it in photoelectrons, and $\alpha^2/(r_e m_e c^2) = 370 \text{ cm}^{-1} \text{ eV}^{-1}$.

Table 28.4: Properties of several inorganic crystal scintillators. Most of the notation is defined in Sec. 6 of this *Review*.

Parameter:	ρ	MP	X_0^*	R_M^*	dE/dx	λ_I^*	τ_{decay}	λ_{max}	n^{\ddagger}	Relative output [†]	Hygroscopic?	$d(\text{LY})/dT$
Units:	g/cm^3	$^\circ\text{C}$	cm	cm	MeV/cm	cm	ns	nm		%/ $^\circ\text{C}$ [‡]		%/ $^\circ\text{C}$ [‡]
NaI(Tl)	3.67	651	2.59	4.13	4.8	42.9	230	410	1.85	100	yes	-0.2
BGO	7.13	1050	1.12	2.23	9.0	22.8	300	480	2.15	21	no	-0.9
BaF ₂	4.89	1280	2.03	3.10	6.6	30.7	630 ^s 0.9 ^f	300 ^s 220 ^f	1.50	36 ^s 3.4 ^f	no	-1.3 ^s ~0 ^f
CsI(Tl)	4.51	621	1.86	3.57	5.6	39.3	1300	560	1.79	165	slight	0.3
CsI(pure)	4.51	621	1.86	3.57	5.6	39.3	35 ^s 6 ^f	420 ^s 310 ^f	1.95	3.6 ^s 1.1 ^f	slight	-1.3
PbWO ₄	8.3	1123	0.89	2.00	10.2	20.7	30 ^s 10 ^f	425 ^s 420 ^f	2.20	0.083 ^s 0.29 ^f	no	-2.7
LSO(Ce)	7.40	2050	1.14	2.07	9.6	20.9	40	420	1.82	83	no	-0.2
GSO(Ce)	6.71	1950	1.38	2.23	8.9	22.2	600 ^s 56 ^f	430	1.85	3 ^s 30 ^f	no	-0.1

* Numerical values calculated using formulae in this review.

[‡] Refractive index at the wavelength of the emission maximum.

[†] Relative light output measured for samples of 1.5 X_0 cube with a Tyvek paper wrapping and a full end face coupled to a photodetector. The quantum efficiencies of the photodetector is taken out.

[‡] Variation of light yield with temperature evaluated at the room temperature.

f = fast component, s = slow component

The quantities ϵ and θ_c are functions of the photon energy E . However, since the typical energy dependent variation of the index of refraction is modest, a quantity called the *Cherenkov detector quality factor* N_0 can be defined as

$$N_0 = \frac{\alpha^2 z^2}{r_e m_e c^2} \int \epsilon dE, \quad (28.6)$$

so that

$$N_{p.e.} \approx LN_0 \langle \sin^2 \theta_c \rangle. \quad (28.7)$$

We take $z = 1$, the usual case in high-energy physics, in the following discussion.

This definition of the quality factor N_0 is not universal, nor, indeed, very useful for situations where the geometrical photon collection efficiency (ϵ_{coll}) varies substantially for different tracks. In this case, separate factors for photon collection and detection (ϵ_{det}), so that $\epsilon = \epsilon_{\text{coll}}\epsilon_{\text{det}}$, are sometimes included on the right hand side of the equation. A typical value of N_0 for a photomultiplier (PMT) detection system working in the visible and near UV, and collecting most of the Cherenkov light, is about 100 cm^{-1} . Practical counters, utilizing a variety of different photodetectors, have values ranging between about 30 and 180 cm^{-1} . Radiators can be chosen from a variety of transparent materials (Sec. 27 of this *Review* and Table 6.1). In addition to refractive index, the choice requires consideration of factors such as material density, radiation length, transmission bandwidth, absorption length, chromatic dispersion, optical workability (for solids), availability, and cost. Long radiator lengths are required to obtain sufficient numbers of photons when the momenta of the particle species to be separated are high. Recently, the gap in refractive index that has traditionally existed between gases and liquid or solid materials has been partially closed with transparent *silica aerogels* with indices that range between about 1.007 and 1.13.

Cherenkov counters may be classified as either *imaging* or *threshold* types, depending on whether they do or do not make use of Cherenkov angle (θ_c) information. Imaging counters may be used to track particles as well as identify them.

28.5.1.

Threshold counters : Threshold Cherenkov detectors [50], in their simplest form, make a yes/no decision based on whether the particle is above or below the Cherenkov threshold velocity $\beta_t = 1/n$. A straightforward enhancement of such detectors uses the number of observed photoelectrons (or a calibrated pulse height) to discriminate between species or to set probabilities for each particle species [51]. This strategy can increase the momentum range of particle separation by a modest amount (to a momentum some 20% above the threshold momentum of the heavier particle in a typical case).

Careful designs give $\langle \epsilon_{\text{coll}} \rangle \gtrsim 90\%$. For a photomultiplier with a typical alkali cathode, $\int \epsilon_{\text{det}} dE \approx 0.27$, so that

$$N_{p.e.}/L \approx 90 \text{ cm}^{-1} \langle \sin^2 \theta_c \rangle \quad (\text{i.e., } N_0 = 90 \text{ cm}^{-1}). \quad (28.8)$$

Suppose, for example, that n is chosen so that the threshold for species a is p_t ; that is, at this momentum species a has velocity $\beta_a = 1/n$. A second, lighter, species b with the same momentum has velocity β_b , so $\cos \theta_c = \beta_a/\beta_b$, and

$$N_{p.e.}/L \approx 90 \text{ cm}^{-1} \frac{m_a^2 - m_b^2}{p_t^2 + m_a^2}. \quad (28.9)$$

For K/π separation at $p = p_t = 1(5) \text{ GeV}/c$, $N_{p.e.}/L \approx 16(0.8) \text{ cm}^{-1}$ for π 's and (by design) 0 for K 's.

For limited path lengths $N_{p.e.}$ can be small, and a minimum number is required to trigger external electronics. The overall

efficiency of the device is controlled by Poisson fluctuations, which can be especially critical for separation of species where one particle type is dominant. The effective number of photoelectrons is often less than the average number calculated above due to additional equivalent noise from the photodetector. It is common to design for at least 10 photoelectrons for the high velocity particle in order to obtain a robust counter. As rejection of the particle that is below threshold depends on *not* seeing a signal, electronic and other background noise can be important. Physics sources of light production for the below threshold particle, such as decay of the above threshold particle or the production of delta rays in the radiator, often limit the separation attainable, and need to be carefully considered. Well designed, modern multi-channel counters, such as the ACC at Belle [47], can attain good particle separation performance over a substantial momentum range for essentially the full solid angle of the spectrometer.

28.5.2. Imaging counters : The most powerful use of the information available from the Cherenkov process comes from measuring the ring-correlated angles of emission of the individual Cherenkov photons. Since low-energy photon detectors can measure only the position (and, perhaps, a precise detection time) of the individual Cherenkov photons (not the angles directly), the photons must be “imaged” onto a detector so that their angles can be derived [52]. In most cases the optics map the Cherenkov cone onto (a portion of) a distorted circle at the photodetector. Though this imaging process is directly analogous to the familiar imaging techniques used in telescopes and other optical instruments, there is a somewhat bewildering variety of methods used in a wide variety of counter types with different names. Some of the imaging methods used include (1) focusing by a lens; (2) proximity focusing (i.e., focusing by limiting the emission region of the radiation); and (3) focusing through an aperture (a pinhole). In addition, the prompt Cherenkov emission coupled with the speed of modern photon detectors allows the use of time imaging, a method which is used much less frequently in conventional imaging technology. Finally, full tracking (and event reconstruction) can be performed in large water counters by combining the individual space position and time of each photon together with the constraint that Cherenkov photons are emitted from each track at a constant polar angle (Sec. 28.6 of this *Review*).

In a simple model of an imaging PID counter, the fractional error on the particle velocity (δ_β) is given by

$$\delta_\beta = \frac{\sigma_\beta}{\beta} = \tan \theta_c \sigma(\theta_c), \quad (28.10)$$

where

$$\sigma(\theta_c) = \frac{\langle \sigma(\theta_i) \rangle}{\sqrt{N_{p.e.}}} \oplus C, \quad (28.11)$$

where $\langle \sigma(\theta_i) \rangle$ is the average single photoelectron resolution, as defined by the optics, detector resolution and the intrinsic chromaticity spread of the radiator index of refraction averaged over the photon detection bandwidth. C combines a number of other contributions to resolution including, (1) correlated terms such as tracking, alignment, and multiple scattering, (2) hit ambiguities, (3) background hits from random sources, and (4) hits coming from other tracks. In many practical cases, the resolution is limited by these effects.

For a $\beta \approx 1$ particle of momentum (p) well above threshold entering a radiator with index of refraction (n), the number of σ separation (N_σ) between particles of mass m_1 and m_2 is approximately

$$N_\sigma \approx \frac{|m_1^2 - m_2^2|}{2p^2 \sigma(\theta_c) \sqrt{n^2 - 1}}. \quad (28.12)$$

In practical counters, the angular resolution term $\sigma(\theta_c)$ varies between about 0.1 and 5 mrad depending on the size, radiator, and photodetector type of the particular counter. The range of momenta over which a particular counter can separate particle species extends from the point at which the number of photons emitted becomes sufficient for the counter to operate efficiently as a threshold device ($\sim 20\%$ above the threshold for the lighter species) to the value in the imaging region given by the equation above. For example, for $\sigma(\theta_c) = 2\text{mrad}$, a fused silica radiator ($n = 1.474$), or a fluorocarbon gas radiator (C_5F_{12} , $n = 1.0017$), would separate π/K 's from the threshold region starting around $0.15(3)\text{ GeV}/c$ through the imaging region up to about $4.2(18)\text{ GeV}/c$ at better than 3σ .

Many different imaging counters have been built during the last several decades [53]. Among the earliest examples of this class of counters are the very limited acceptance Differential Cherenkov detectors, designed for particle selection in high momentum beam lines. These devices use optical focusing and/or geometrical masking to select particles having velocities in a specified region. With careful design, a velocity resolution of $\sigma_{\beta/\beta} \approx 10^{-4}\text{--}10^{-5}$ can be obtained [50].

Practical multi-track Ring-Imaging Cherenkov detectors (generally called RICH counters) are a more recent development. They have been built in small-aperture and 4π geometries both as PID counters and as stand-alone detectors with complete tracking and event reconstruction as discussed more fully below. PID RICH counters are sometimes further classified by ‘generations’ that differ based on performance, design, and photodetection techniques.

A typical example of a first generation RICH used at the Z factory e^+e^- colliders [54,55] has both liquid (C_6F_{14} , $n = 1.276$) and gas (C_5F_{12} , $n = 1.0017$) radiators, the former being proximity imaged using the small radiator thickness while the latter use mirrors. The phototransducers are a TPC/wire-chamber combination having charge division or pads. They are made sensitive to photons by doping the TPC gas (usually, ethane/methane) with $\sim 0.05\%$ TMAE (tetrakis(dimethylamino)ethylene). Great attention to detail is required, (1) to avoid absorbing the UV photons to which TMAE is sensitive, (2) to avoid absorbing the single photoelectrons as they drift in the long TPC, and (3) to keep the chemically active TMAE vapor from interacting with materials in the system. In spite of their unforgiving operational characteristics, these counters attained good $e/\pi/K/p$ separation over wide momentum ranges during several years of operation. In particular, their π/K separation range extends over momenta from about 0.25 to $20\text{ GeV}/c$.

Later generation counters [53] generally must operate at much higher particle rates than the first generation detectors, and utilize different photon detection bandwidths, with higher readout channel counts, and faster, more forgiving photon detection technology than the TMAE doped TPC's just described. Radiator choices have broadened to include materials such as lithium fluoride, fused silica, and aerogel. Vacuum based photodetection systems (*e.g.*, single or multi anode photomultiplier tubes (PMT), multi channel plate PMTs (MCP-PMT), or hybrid photodiodes (HPD)) have become increasingly common. They handle very high rates, may be used with a wide choice of radiators, and may be sufficiently fast to allow time imaging or the use of time of flight information. Other fast detection systems that use solid cesium iodide (CSI) photocathodes or triethylamine (TEA) doping in proportional chambers are useful with certain radiator types and geometries.

A DIRC (Detector of Internally Reflected Cherenkov light) is a third generation subtype of a RICH first used in the BaBar detector [48]. It ‘inverts’ the usual principle for use of light

from the radiator of a RICH by collecting and imaging the total internally reflected light, rather than the transmitted light. A DIRC utilizes the optical material of the radiator in two ways, simultaneously; first as a Cherenkov radiator, and second, as a light pipe for the Cherenkov light trapped in the radiator by total internal reflection. The DIRC makes use of the fact that the magnitudes of angles are preserved during reflection from a flat surface. This fact, coupled with the high reflection coefficients of the total internal reflection process (> 0.9995 for highly polished SiO_2), and the long attenuation length for photons in high purity fused silica, allows the photons of the ring image to be transported to a detector outside the path of the particle where they may be imaged in up to three dimensions (two in space and one in time). The BaBar DIRC uses 144 fused silica radiator bars ($1.7 \times 3.5 \times 490\text{ cm}$) with the light being focused onto 11 000 conventional PMT's located about 120 cm from the end of the bars by the ‘pinhole’ of the bar end. DIRC performance can be understood using the formula for (N_σ) discussed above. Typically, $N_{\text{p.e.}}$ is rather large (between 15 and 60) and the Cherenkov polar angle is measured to about 2.5 mrad. The momentum range with good π/K separation extends up to about $4\text{ GeV}/c$, matching the B decay momentum spectrum observed in BaBar.

28.6. Cherenkov tracking calorimeters

Written August 2003 by D. Casper (UC Irvine).

In addition to the specialized applications described in the previous section, Cherenkov radiation is also exploited in large, ring-imaging detectors with masses measured in kilotons or greater. Such devices are not subdetector components, but complete experiments with triggering, tracking, vertexing, particle identification and calorimetric capabilities, where the large mass of the transparent dielectric medium serves as an active target for neutrino interactions (or their secondary muons) and rare processes like nucleon decay.

For volumes of this scale, absorption and scattering of Cherenkov light are non-negligible, and a wavelength-dependent factor $e^{-d/L(\lambda)}$ (where d is the distance from emission to the sensor and $L(\lambda)$ is the attenuation length of the medium) must be included in the integral of Eq. (28.5) for the photoelectron yield. The choice of medium is therefore constrained by the refractive index and transparency in the region of photodetector sensitivity; highly-purified water is an inexpensive and effective choice; sea-water, mineral oil, polar ice, and D_2O are also used. Photo-multiplier tubes (PMTs) on either a volume or surface lattice measure the time of arrival and intensity of Cherenkov radiation. Hemispherical PMTs are favored for the widest angular acceptance, and sometimes mounted with reflectors or wavelength-shifting plates to increase the effective photosensitive area. Gains and calibration curves are measured with pulsed laser signals transmitted to each PMT individually via optical fiber or applied to the detector as a whole through one or more diffusing balls.

Volume instrumentation [56] is only cost-effective at low densities, with a spacing comparable to the attenuation (absorption and scattering) length of Cherenkov light in the medium (15–40 m for Antarctic ice and ~ 45 m in the deep ocean). PMTs are deployed in vertical strings as modular units which include pressure housings, front-end electronics and calibration hardware. The effective photocathode coverage of such arrays is less than 1% but still adequate (using timing information and the Cherenkov angular constraint) to reconstruct the direction of TeV muons to 1° or better. The size of such ‘neutrino telescopes’ is limited only by cost once the technical challenges of deployment, power, signal extraction and calibration in an inaccessible and inhospitable environment

are addressed; arrays up to $(1 \text{ km})^3$ in size are under study or development.

Surface instrumentation [57] allows the target volume to be viewed with higher photocathode density by a number of PMTs which scales like $(\text{volume})^{2/3}$. To improve hermeticity and shielding, and to ensure that an outward-going particle's Cherenkov cone illuminates sufficient PMTs for reconstruction, a software-defined fiducial volume begins some distance ($\sim 2 \text{ m}$) inside the photosensor surface. Events originating within the fiducial volume are classified as *fully-contained* if no particles exit the inner detector, or *partially-contained* otherwise. An outer (veto) detector, optically separated from the inner volume and instrumented at reduced density, greatly assists in making this determination and also simplifies the selection of contained events. The maximum size of a pure surface array is limited by the attenuation length ($\sim 100 \text{ m}$ has been achieved for large volumes using reverse-osmosis water purification), pressure tolerance of the PMTs (< 80 meters of water, without pressure housings) and structural integrity of the enclosing cavity, if underground. In practice, these limitations can be overcome by a segmented design involving multiple modules of the nominal maximum size; megaton-scale devices are under study.

Cherenkov detectors are excellent electromagnetic calorimeters, and the number of Cherenkov photons *produced* by an e/γ is nearly proportional to its kinetic energy. For massive particles, the number of photons produced is also related to the energy, but not linearly. For any type of particle, the *visible energy* E_{vis} is defined as the energy of an electron which would produce the same number of Cherenkov photons. The number of photoelectrons *collected* depends on a detector-specific scale factor, with event-by-event corrections for geometry and attenuation. For typical PMTs, in water $N_{\text{p.e.}} \approx 15 \xi E_{\text{vis}}(\text{MeV})$, where ξ is the effective fractional photosensor coverage; for other materials, the photoelectron yield scales with the ratio of $\sin^2 \theta_c$ over density. At solar neutrino energies, the visible energy resolution ($\sim 30\%/\sqrt{\xi E_{\text{vis}}(\text{MeV})}$) is about 20% worse than photoelectron counting statistics would imply. For higher energies, multi-photoelectron hits are likely and the charge collected by each PMT (rather than the number of PMTs firing) must be used; this degrades the energy resolution to approximately $2\%/\sqrt{\xi E_{\text{vis}}(\text{GeV})}$. In addition, the absolute energy scale must be determined with sources of known energy. Using an electron LINAC and/or nuclear sources, 0.5–1.5% has been achieved at solar neutrino energies; for higher energies, cosmic-ray muons, Michel electrons and π^0 from neutrino interactions allow $\sim 3\%$ absolute energy calibration.

A trigger can be formed by the coincidence of PMTs within a window comparable to the detector's light crossing time; the coincidence level thus corresponds to a visible energy threshold. Physics analysis is usually not limited by the hardware trigger, but rather the ability to reconstruct events. The interaction vertex can be estimated using timing and refined by applying the Cherenkov angle constraint to identified ring edges. Multi-ring events are more strongly constrained, and their vertex resolution is 33–50% better than single rings. Vertex resolution depends on the photosensor density and detector size, with smaller detectors performing somewhat better than large ones ($\sim 25 \text{ cm}$ is typical for existing devices). Angular resolution is limited by multiple scattering at solar neutrino energies ($25\text{--}30^\circ$) and improves to a few degrees around $E_{\text{vis}} = 1 \text{ GeV}$.

A non-showering (μ, π^\pm, p) track produces a sharp ring with small contributions from delta rays and other radiated secondaries, while the more diffuse pattern of a showering (e, γ) particle is actually the superposition of many individual rings from charged shower products. Using maximum likelihood techniques and the Cherenkov angle constraint, these two

topologies can be distinguished with an efficiency which depends on the photosensor density and detector size [58]. This particle identification capability has been confirmed by using cosmic-rays and Michel electrons, as well as charged-particle [59] and neutrino [60] beams. Large detectors perform somewhat better than smaller ones with identical photocathode coverage; a misidentification probability of $\sim 0.4\%/\xi$ in the sub-GeV range is consistent with the performance of several experiments for $4\% < \xi < 40\%$. Detection of a delayed coincidence from muon decay offers another, more indirect, means of particle identification; with suitable electronics, efficiency approaches 100% for μ^+ decays but is limited by nuclear absorption (22% probability in water) for μ^- .

Reconstruction of multiple Cherenkov rings presents a challenging pattern recognition problem, which must be attacked by some combination of heuristics, maximum likelihood fitting, Hough transforms and/or neural networks. The problem itself is somewhat ill-defined since, as noted, even a single showering primary produces many closely-overlapping rings. For $\pi^0 \rightarrow \gamma\gamma$ two-ring identification, performance falls off rapidly with increasing π^0 momentum, and selection criteria must be optimized with respect to the analysis-dependent cost-function for $e \leftrightarrow \pi^0$ mis-identification. Two representative cases for $\xi = 39\%$ will be illustrated. In an atmospheric neutrino experiment, where π^0 are relatively rare compared to e^\pm , one can isolate a $> 90\%$ pure 500 MeV/c π^0 sample with an efficiency of $\sim 40\%$. In a ν_e appearance experiment at $E_\nu \leq 1 \text{ GeV}$, where e^\pm are rare compared to π^0 , a 99% pure 500 MeV/c electron sample can be identified with an efficiency of $\sim 70\%$. For constant ξ , a larger detector (with, perforce, a greater number of pixels to sample the light distribution) performs somewhat better at multi-ring separation than a smaller one. For a more detailed discussion of event reconstruction techniques, see Ref. 49.

Table 28.5: Properties of Cherenkov tracking calorimeters. LSND was a hybrid scintillation/Cherenkov detector; the estimated ratio of isotropic to Cherenkov photoelectrons was about 5:1. MiniBooNE's light yield also includes a small scintillation component.

Detector	Fiducial mass (kton)	PMTs (diameter, cm)	ξ	p.e./ MeV	Dates
IMB-1	3.3 H ₂ O	2048 (12.5)	1%	0.25	1982–85
IMB-3	3.3 H ₂ O	2048 (20 +plate)	4.5%	1.1	1987–90
KAM I	0.88/0.78 H ₂ O	1000/948 (50)	20%	3.4	1983–85
KAM II	1.04 H ₂ O	948 (50)	20%	3.4	1986–90
LSND	0.084 oil+scint.	1220 (20)	25%	33	1993–98
SK-1	22.5 H ₂ O	11146 (50)	39%	6	1997–01
SK-2	22.5 H ₂ O	5182 (50)	18%	3	2002–
K2K	0.025 H ₂ O	680 (50)	39%	6	1999–
SNO	1.0 D ₂ O	9456 (20+cone)	55%	9	1999–
MiniBooNE	0.445 oil	1280 (20)	10%	3–4	2002–

28.7. Gaseous detectors

28.7.1. Energy loss and charge transport in gases : Written April 2008 by F. Sauli (CERN) and M. Titov (CEA Saclay).

Gas-filled counters detect and localize the ionization produced by charged particles, generally after charge multiplication. The peculiar statistics of ionization processes, with asymmetries in the ionization trails, affect the coordinate determination deduced from the measurement of drift time or of the center of gravity of the collected charge. For thin gas layers, the width of the energy loss distribution can be larger than the average, requiring multiple sample or truncated mean analysis to achieve particle identification (see Sec. 28.7.4).

The energy loss of charged particles and photons in various materials as a function of energy is discussed in Sec. 27. Table 28.6 provides values of relevant parameters in commonly used gases at NTP for unit charge, minimum-ionizing particles [61–67]. Numbers often differ depending on source, and values in the table should be taken only as approximate. For different conditions and mixtures, and neglecting internal energy transfer processes, one can use gas-density-dependent composition rules.

Table 28.6: Properties of rare and molecular gases at normal temperature and pressure (NTP: 20° C, one atm). E_X , E_I : first excitation and ionization energy; W_I : average energy per ion pair; $dE/dx|_{\min}$, N_P , N_T : differential energy loss, primary and total number of electron-ion pairs per cm, for unit charge, minimum ionizing particles.

Gas	Density, mg cm ⁻³	E_x eV	E_I eV	W_I eV	$dE/dx _{\min}$ keV cm ⁻¹	N_P cm ⁻¹	N_T cm ⁻¹
Ne	0.839	16.7	21.6	30	1.45	13	50
Ar	1.66	11.6	15.7	25	2.53	25	106
Xe	5.495	8.4	12.1	22	6.87	41	312
CH ₄	0.667	8.8	12.6	30	1.61	37	54
C ₂ H ₆	1.26	8.2	11.5	26	2.91	48	112
iC ₄ H ₁₀	2.49	6.5	10.6	26	5.67	90	220
CO ₂	1.84	7.0	13.8	34	3.35	35	100
CF ₄	3.78	10.0	16.0	54	6.38	63	120

When an ionizing particle passes through the gas it creates electron-ion pairs, but often the ejected electrons have sufficient energy to further ionize the medium. On average, the total number of electron-ion pairs (N_T) is between two and three times larger than the number of primaries (N_P) (see Table 28.6).

The probability of releasing an electron of energy E or larger follows an approximate $1/E^2$ dependence (Rutherford law), shown in Fig. 28.3 for argon at NTP (dotted line, left scale). More detailed estimates taking into account the electronic structure of the medium are shown in the figure, for three values of the particle velocity factor $\beta\gamma$ [62]. The dot-dashed line provides, on the right scale, the practical range of electrons of energy E . As an example, there is a 1% probability of creating of an electron of 1 keV or more in 10 mm of argon, substantially increasing the ionization losses. The practical range of 1 keV electrons in argon (dot-dashed line, right scale) is 70 μm ; this contributes to the error in the coordinate determination.

The number of electron-ion pairs per primary interaction, or cluster size, has an exponentially decreasing probability; for argon, there is about 1% probability for primary clusters to contain ten or more electron-ion pairs [63].

Once released in the gas, and under the influence of an applied electric field, electrons and ions drift in opposite directions and diffuse towards the electrodes. The value of drift velocity

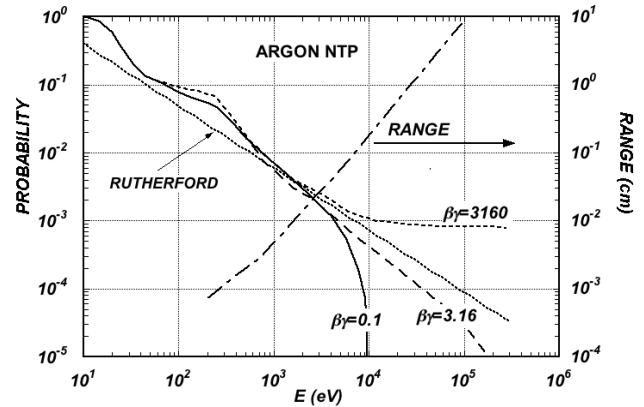


Figure 28.3: Probability of production of an electron of energy equal or larger than E (left scale), and range of electrons in argon at NTP (dot-dashed curve, right scale) [62].

and diffusion depends very strongly on the nature of the gas, namely on the detailed structure of the elastic and inelastic electron-molecule cross-sections. In noble gases, the inelastic cross section is zero below excitation and ionization thresholds. Fast gas mixtures are achieved by adding polyatomic gases (usually CH₄ or CO₂), having large inelastic cross sections at moderate energies, which results in “cooling” electrons into an energy range of the Ramsauer-Townsend minimum (located at ~ 0.5 eV) of the elastic scattering cross-section of argon. The reduction in both the total electron scattering cross-section and the electron energy results in a large increase of electron drift velocity (for a compilation of electron-molecule cross sections see Ref. 64). Another principal role of the polyatomic gas is to absorb the ultraviolet (UV) photons emitted by the excited inert gas atoms. The quenching of UV photons occurs through the photo-decomposition of polyatomic molecules. Extensive collections of experimental data [65] and theoretical calculations based on transport theory [66] permit estimates of drift and diffusion properties in pure gases and their mixtures. In a simple approximation, gas kinetic theory provides the following relation between drift velocity v and mean electron-molecule collision time τ (Townsend’s expression): $v = eE\tau/m$. Examples for commonly used gases at NTP are given in Fig. 28.4 and Fig. 28.5, computed with the program MAGBOLTZ [67] as a function of electric field. For different conditions, the horizontal axis has to be scaled with the gas density, proportional to $1/P$, where P is the pressure. Standard deviations for longitudinal (σ_L) and transverse diffusion (σ_T) are given for one cm of drift, and scale with the square root of distance. Since the collection time is inversely related to the drift velocity, diffusion is smaller in fast-counting gases, as can be seen, for example, in CF₄. In presence of an external magnetic field, the Lorentz force acting on electrons between collisions deflects the drifting swarm and modifies the drift properties. The electron trajectories, velocities and diffusion parameters can be computed with the program mentioned above. A simple theory (the friction force model) provides an expression for the vector drift velocity \mathbf{v} as a function of electric and magnetic field vectors \mathbf{E} and \mathbf{B} , of the Larmor frequency $\omega = eB/m$ and the mean collision time τ between electrons and molecules:

$$\mathbf{v} = \frac{e}{m} \frac{\tau}{1 + \omega^2\tau^2} \left(\mathbf{E} + \frac{\omega\tau}{B}(\mathbf{E} \times \mathbf{B}) + \frac{\omega^2\tau^2}{B^2}(\mathbf{E} \cdot \mathbf{B})\mathbf{B} \right) \quad (28.13)$$

To a good approximation, and for moderate fields, one can assume that the energy of the electrons is not affected by

B , and use for τ the values deduced from the drift velocity at $B = 0$ (Townsend expression). For E perpendicular to B , the drift angle to the electric field vector is $\tan\theta_B = \omega\tau$ and $|\mathbf{v}| = (E/B)(\omega\tau/\sqrt{1+\omega^2\tau^2})$. For parallel electric and magnetic fields, drift velocity and longitudinal diffusion are not affected, while the transverse diffusion can be strongly reduced: $\sigma_T(B) = \sigma_T(B=0)/\sqrt{1+\omega^2\tau^2}$. For example, the large values of $\omega\tau \sim 20$ at 5 T have been measured for Ar/CF₄/iC₄H₁₀ (95:3:2). The dotted line in Fig. 28.5 represents σ_T for the classic P10 mixture Ar/CH₄ (90:10) at 4 T. This reduction is exploited in time projection chambers (Sec. 28.7.4) to improve localization accuracy.

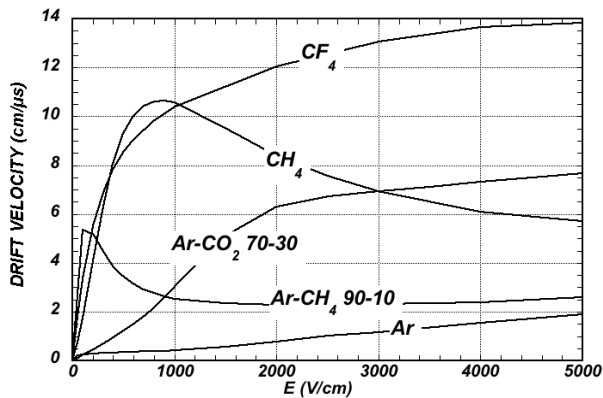


Figure 28.4: Computed electron drift velocity as a function of electric field in several gases at NTP [67].

In mixtures containing electronegative molecules such as oxygen, water or CF₄, electrons can be captured to form negative ions. Capture cross-sections are strongly energy-dependent, and therefore the capture probability is a function of applied field and may differ to a great extent for the same amount of additions other mixtures. As an example, at moderate fields (up to 1 kV/cm) the addition of 0.1% of oxygen to an Ar/CO₂ mixture results in an electron capture probability about twenty times larger than the same addition to Ar/CH₄.

As they experience increasing fields, electrons get enough energy to undergo ionizing collisions with molecules. Above a gas-dependent threshold, the mean free path for ionization λ_i , decreases exponentially with the field; its inverse, $\alpha = 1/\lambda_i$, is the first Townsend coefficient. As most of the avalanche growth occurs very close to the anodes, simple electrostatic consideration show that the largest fraction of the detected signal is due to the motion of ions receding from the wires; the electron component, although very fast, is rarely seen. This determines the characteristic shape of the detected signals in proportional mode, with a fast rise followed by a gradually slower increase. The so-called ion tail that limits the time resolution of the counter is usually removed by differentiation of the signal. In uniform fields, N_0 initial electrons multiply over a length x forming an electron avalanche of size $N = N_0 e^{\alpha x}$; N/N_0 is the gain of the counter. Fig. 28.6 shows examples of Townsend coefficients for several gas mixtures, computed with MAGBOLTZ.

Ions released by ionization or produced in the avalanches drift and diffuse under the influence of the electric field; their drift velocity in the fields encountered in gaseous counters (up to few kV/cm) is typically three orders of magnitude lower than for electrons. The ion mobility μ , the ratio of drift velocity to electric field, is constant for a given ion up to very high fields. For a different temperature and pressure, the mobility can be computed from the expression $\mu(P, T) = \mu(P_0, T_0)(T/P)(P_0/T_0)$.

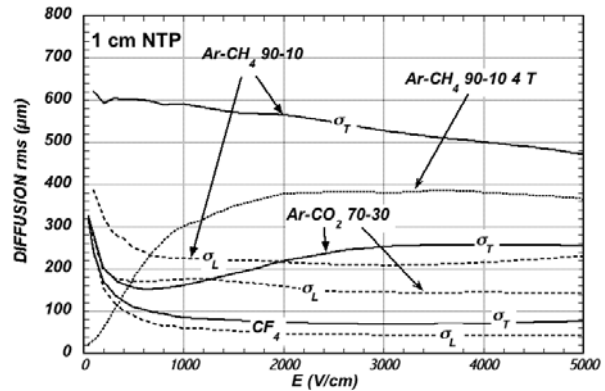


Figure 28.5: Electron longitudinal diffusion (σ_L) (dashed lines) and transverse diffusion (σ_T) (full lines) for 1 cm of drift. The dotted line shows σ_T for the P10 mixture at 4T [67].

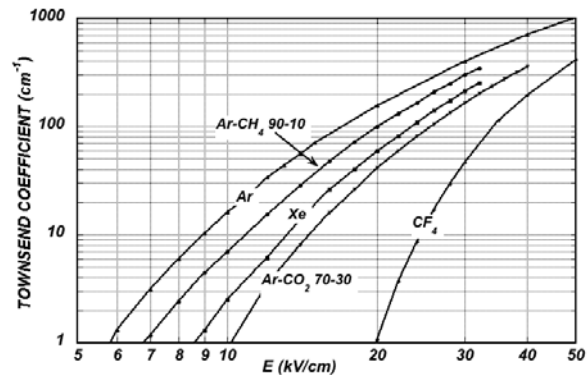


Figure 28.6: Computed first Townsend coefficient α as a function of electric field in several gases at NTP [67].

Values of mobility at NTP (μ_0) for ions in their own and other gases are given in Table 28.7 [68]. For mixtures, due to a very effective charge transfer mechanism, only ions with the lowest ionization potential survive after a short path in the gas. The diffusion of ions follows a simple square root dependence on the drift time, with a coefficient that depends on temperature but not on the ion mass. Accumulation of ions in the gas counters may induce gain reduction and field distortions.

Table 28.7: Mobility of ions in gases at NTP [68].

Gas	Ion	Mobility ($\text{cm}^2 \text{V}^{-1} \text{s}^{-1}$)
He	He ⁺	10.4
Ne	Ne ⁺	4.7
Ar	Ar ⁺	1.54
Ar	CH ₄ ⁺	1.87
Ar	CO ₂ ⁺	1.72
CH ₄	CH ₄ ⁺	2.26
CO ₂	CO ₂ ⁺	1.09

28.7.2. Multi-Wire Proportional Chambers : Written April 2008 by Fabio Sauli (CERN) and Maxim Titov (CEA Saclay).

Single-wire counters that detect the ionization produced in a gas by charged particle energy deposit, followed by charge multiplication and collection around a thin wire, have been used for decades. Good energy resolution is obtained in the streamer mode, and very large saturated pulses can be detected in the Geiger mode. For an overview see *e.g.* Ref. 4.

Multiwire proportional chambers (MWPC's) [69,70], introduced in the late sixties, detect and localize energy deposit by charged particles over large areas. A mesh of parallel anode wires at a suitable potential, inserted between two cathodes, acts (almost) as an independent set of proportional counters (see Fig. 28.7). Electrons released in the gas volume drift towards the anodes and avalanche in the increasing field. Analytical expressions for the electric field can be found in many textbooks; the fields close to the wires $E(r)$ and in the drift region E_D are given by the approximations:

$$E(r) = \frac{CV_0}{2\pi\epsilon_0} \frac{1}{r}; \quad E_D = \frac{CV_0}{2\epsilon_0 s}; \quad C = \frac{2\pi\epsilon_0}{\pi(\ell/s) - \ln(2\pi a/s)}$$

where r is the distance from the center of the anode, s the wire spacing, ℓ and V_0 the distance and difference of potential between anode and cathodes. C the capacitance per unit length of the wires and a the anode wire radius.

Because of electrostatic forces, anode wires are in equilibrium only for a perfect geometry. Small deviations result in forces displacing the wires alternatively below and above the symmetry plane, often with catastrophic results. These displacement forces are countered by the mechanical tension of the wire, up to a maximum stable length L_M [71]:

$$L_M = \frac{s}{CV_0} \sqrt{4\pi\epsilon_0 T_M}$$

The maximum tension T_M depends on the wire diameter and modulus of elasticity. Table 28.8 gives approximate values for tungsten, and the corresponding maximum stable wire length under reasonable assumptions for the operating voltage V_0 [72]. Internal supports and spacers have been used in the construction of longer detectors.

Table 28.8: Maximum tension T_M and stable length L_M for tungsten wires with spacing s .

Wire diameter (μm)	T_M (newton)	s (mm)	L_M (cm)
10	0.16	1	25
20	0.65	2	85

Detection of charge over a predefined threshold on the wires provides the event coordinates with the accuracy of the wire spacing; longitudinal localization can be obtained by measuring the ratio of collected charge at the two ends of resistive wires. Making use of the charge profile induced on segmented cathodes, the so-called center-of gravity (COG) method permits localization of tracks to sub-mm accuracy. Due to the statistics of energy loss and asymmetric ionization clusters, the position accuracy is $50 \mu\text{m}$ rms for tracks perpendicular to the wire plane, but degrades to $\sim 250 \mu\text{m}$ at 30° to the normal [73]. The intrinsic bi-dimensional characteristic of the COG readout has found numerous applications in medical imaging.

Drift chambers, developed in the early '70's, can estimate the position of a track by exploiting the arrival time of electrons at the anodes if the time of the interaction is known. They

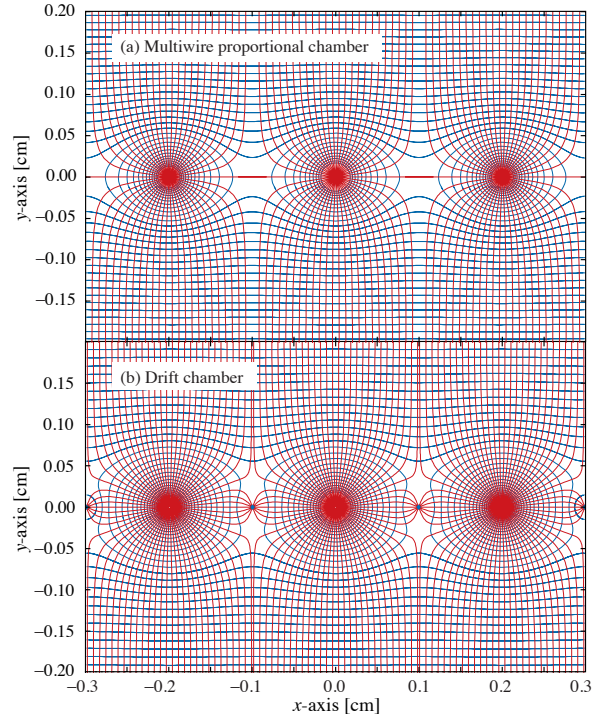


Figure 28.7: Electric field lines and equipotentials in (a) a multiwire proportional chamber and (b) a drift chamber.

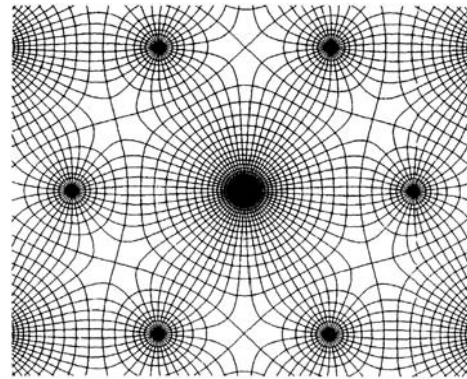


Figure 28.8: Electric field lines and equipotentials in a multiwire drift module. Each anode wire is surrounded by six cathode wires, and each cathode wire is surrounded by three anode wires.

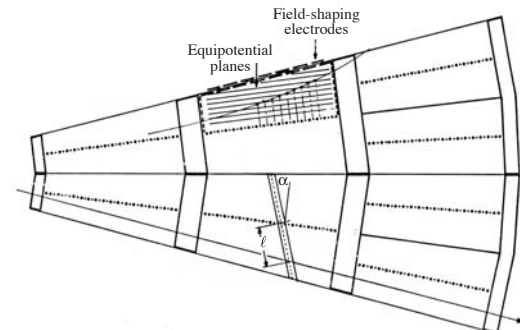


Figure 28.9: Schematics drawing of a JET Chamber sector.

can achieve rms localization accuracies of $50 \mu\text{m}$ or better. The

distance between anode wires, several cm, allows covering large areas at reduced cost. Many designs have been introduced, all aimed at improving performance. In the original design, a thicker wire at proper voltage between anodes (field wire) reduces the field at the middle point between anodes, improving charge collection (Fig. 28.8) [74]. Symmetrically decreasing potentials applied on cathode wires make more uniform and reinforce the drift fields, resulting in a linear space-to-drift-time relation [75]. In some drift chambers design, and with the help of suitable voltages applied to field-shaping electrodes, the electric field structure is adjusted to compensate the distortions.

Sampling the drift time on rows of anodes within the same gas volume, together with longitudinal localization through charge division on wires led to the concept of multiple arrays such as the multi-drift module [76] (Fig. 28.8) and the JET chamber [77] (Fig. 28.9). The time projection chamber [78] combines a measurement of drift time and charge induction on cathodes to obtain excellent tracking for high multiplicity topologies occurring at moderate rates (see Sec. 28.7.4). In all cases, a good knowledge of electron drift velocity and diffusion properties is required. This has to be combined with the knowledge of the electric fields in the structures, computed with commercial or custom-developed software [67,79]. For an overview of detectors exploiting the drift time for coordinate measurement see Refs. 2 and 71. Although very powerful in terms of performance, multi-wire structures have reliability problems when used in harsh or hard-to access environments, as a single broken wire can affect the whole detector. Introduced in the eighties, Straw and drift tube systems make use of large arrays of wire counters encased in individual envelopes, each acting independently [80]. Suitable techniques for low-cost mass production have been developed for the needs of large experiments, as the Transition Radiation Tracker and the Monitored Drift Tubes array for CERN's LHC experiments (for a review see Ref. 81).

The production of positive ions in the avalanches and their slow drift before neutralization result in a rate-dependent accumulation of positive charge in the detector, with consequent field distortion, gain reduction and degradation of spatial resolution. As shown in Fig. 28.10 [82], independently from the avalanche size, the proportional gain drops above a charge production rate around 10^9 electrons per second and mm of wire; for a proportional gain of 10^4 and 100 electrons released per track, this corresponds to a particle flux of $10^3 \text{ s}^{-1} \text{ mm}^{-1}$ (1 kHz/mm² for 1 mm wire spacing). Despite various improvements, position-sensitive detectors based on wire structures are limited by basic diffusion processes and space charge effects in the gas to localization accuracies of 50–100 μm (see for example Ref. 83).

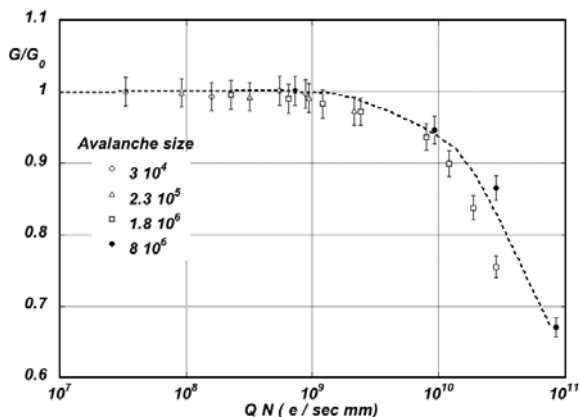


Figure 28.10: Charge rate dependence of normalized gain in a MWPC [82].

Multiwire and drift chambers have been operated with a variety of gas fillings and operating modes, depending on experimental requirements. The so-called “Magic Gas” (a mixture of argon, isobutane and freon) [70] permits very high and saturated gains ($\sim 10^6$), overcoming the electronics limitations of the time, at the cost of reduced survival due to aging processes. With present-day electronics, proportional gains around 10^4 are sufficient for detection of minimum ionizing particles, and noble gases with moderate amounts of polyatomic gases, such as methane or carbon dioxide, are used.

At high radiation fluxes, a fast degradation of detectors due to the formation of polymers deposits (aging) is often observed. The process has been extensively investigated, often with conflicting results; a number of culprits has been identified (organic pollutants, silicone oils); addition of small amounts of water in many (but not all) cases has been demonstrated to extend the lifetime of the detectors. Addition of fluorinated gases (*e.g.*, CF_4) or oxygen results in an etching action that can overcome polymer formation, or even eliminate deposits, but the issue of long-term survival of gas detectors in these gases is controversial [84]. Under optimum operating conditions, a total collected charge of a few coulombs per cm of wire can be reached before degradation, corresponding, for one mm spacing and at a gain of 10^4 , to a total particle flux of $\sim 10^{14}$ MIP's/cm².

A new generation of wireless gaseous detectors, micro-pattern gas detectors, has been developed in the recent years and promises to overcome many of the limitations of MWPC devices—namely the multi-particle resolution and the rate capability. Their operating principles and performances are described in Sec. 28.7.3.

28.7.3. Micro-pattern Gas Detectors : Written October 2007 by M. Titov (CEA Saclay)

Modern photolithographic technology has enabled a series of inventions of novel Micro-Pattern Gas Detector (MPGD) concepts: Micro-Strip Gas Chamber (MSGC) [85], GEM [86], Micromegas [87] and many others [88], revolutionizing cell size limits for many gas detector applications. The MSGC, a concept invented in 1988 by A. Oed, was the first of the micro-structure gas detectors. Consisting of a set of tiny metal strips laid on a thin insulating substrate, and alternatively connected as anodes and cathodes, the MSGC turned out to be easily damaged by discharges induced by heavily ionizing particles and destroying the fragile electrode structure [89]. The more powerful GEM and Micromegas concepts fulfill the needs of high-luminosity colliders with increased reliability in harsh radiation environments. By using fine pitch size compared to classical wire chambers, these detectors offer intrinsic high rate capability (fast signals with risetimes of a few ns and full widths of 20–100 ns), excellent spatial resolution ($\sim 30 \mu\text{m}$), double track resolution ($\sim 500 \mu\text{m}$), and single photo-electron time resolution in the ns range.

The GEM detector was introduced by Fabio Sauli. It consists of a thin-foil copper-Kapton-copper sandwich chemically perforated to obtain a high density of holes. The hole diameter is typically between 25 μm and 150 μm , while the pitch varies between 50 μm and 200 μm . Application of a potential difference between the two sides of the GEM generates the electric fields indicated in Fig. 28.11. Each hole acts as an independent proportional counter; electrons released by the ionization in the gas drift into the hole and multiply in the high electric field (50–70 kV/cm). Most of avalanche electrons are transferred into the gap below the GEM. Distributing the avalanche multiplication among several cascading electrodes allows the multi-GEM detectors to operate at overall gas gain above 10^4 in the presence of highly ionizing particles, while eliminating

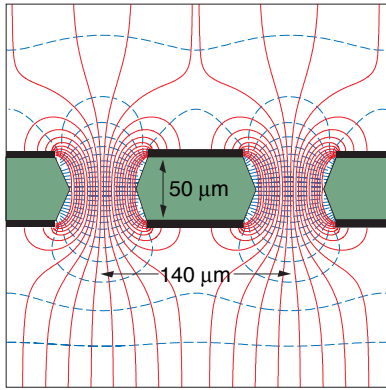


Figure 28.11: Schematic view and typical dimensions of the hole structure in the GEM amplification cell. Electric field lines (solid) and equipotentials (dashed) are shown. On application of a potential difference between the two metal layers electrons released by ionization in the gas volume above the GEM are guided into the holes, where charge multiplication occurs in the high field.

the risk of discharges ($< 10^{-12}$ per hadron). This is the major advantage of the GEM technology [90]. A unique property of the GEM detector is the complete decoupling of the amplification stage (GEM) and the readout electrode (PCB), which operates at unity gain and serves only as a charge collector.

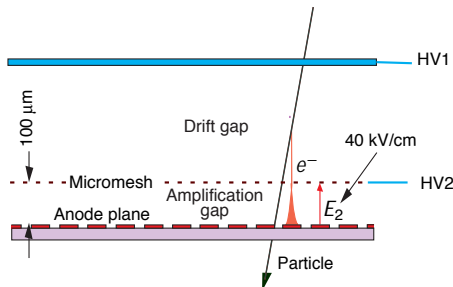


Figure 28.12: Schematic drawing and typical dimensions of the Micromegas detector. Charges produced in the drift gap are drifting to the small amplification region, limited by the mesh and the anode, where they are amplified.

Ioannis Giomataris introduced the micro-mesh gaseous structure (Micromegas), which is a parallel-plate avalanche counter (Fig. 28.12). It consists of a few mm drift region (electric field ~ 1 kV/cm) and a narrow multiplication gap (25–150 μm , 50–70 kV/cm), located between a thin metal grid (micromesh) and the readout electrode (strips/pads of conductor printed on an insulator board). The electric field is homogeneous both in the drift and amplification gaps. Due to the narrow multiplication region in Micromegas, locally small variations of the amplification gap are compensated by an inverse variation of the amplification coefficient and therefore do not induce gain fluctuations. The small amplification gap is a key element in Micromegas operation, giving rise to its excellent spatial resolution: 12 μm accuracy (limited by the micromesh pitch) for MIPs [91], and very good energy resolution ($\sim 12\%$ FWHM with 6 keV x rays).

Over the past decade GEM and Micromegas detectors have become increasingly important. COMPASS is a first high-luminosity experiment at CERN which pioneered the use of large-area ($\sim 40 \times 40 \text{ cm}^2$) GEM and Micromegas detectors for high-rate particle tracking, reaching 25 kHz/mm² in the near-beam area. Both technologies have achieved a tracking

efficiency of close to 100% at gas gains of about 10^4 , a spatial resolution of 70–100 μm and a time resolution of ~ 10 ns. GEM's have entered the LHC program; they will be used for triggering in the LHCb Muon System and in the TOTEM Telescopes. A time projection chamber (TPC) using GEM or Micromegas as a gas amplification device is also one of the main options for high-precision tracking at the International Linear Collider (ILC).

The performance and robustness of MPGD's have encouraged their applications in high-energy and neutrino physics, astrophysics, UV and visible photon detection, nuclear physics and neutron detection domain, radiation therapy and electronic portal imaging devices. A big step in the direction of the industrial manufacturing of large-size MPGD's is the development of the “bulk” Micromegas technology [92]. The basic idea is to build the whole detector in a single process: the anode plane with copper strips, a photo-imageable polyimide film and the woven mesh are laminated together at a high temperature forming a single object. Employing the “bulk” technology, 72 large Micromegas ($34 \times 36 \text{ cm}^2$) planes with an active area of 9 m² are being built for the T2K TPC detector.

Sensitive and low-noise electronics will enlarge the range of the MPGD applications. Recently, GEM and Micromegas were read out by high-granularity (50 μm pitch) CMOS pixel chips assembled directly below the GEM or Micromegas amplification structure and serving as an integrated charge collecting anode [93,94,95]. With this arrangement avalanche electrons are collected on the top metal layer of the CMOS ASIC; every input pixel is then directly connected to the amplification, digitization and sparsification circuits integrated in the underlying active layers of the CMOS technology. GEM coupled to a VLSI pixel array could serve as a highly efficient x-ray polarimeter, which is able to reconstruct simultaneously initial direction and dynamics of photoelectron energy loss for the low energy (< 10 keV) x rays. A fine-pitch GEM matching the pitch of pixel ASIC (50 μm) allows to achieve a superior single-electron avalanche reconstruction accuracy of 4 μm , which makes it suitable candidate for fast gas photo-multipliers. For minimum ionizing particle tracks a spatial resolution down to 20 μm was achieved with Medipix2 and Timepix CMOS chips coupled to GEM devices. Similar performance is expected for Micromegas. An attractive solution for the construction of MPGD's with pixel anode readout is the integration of the Micromegas amplification and CMOS chip by means of the “wafer post-processing” technology. The sub- μm precision of the grid dimensions and avalanche gap size results in a uniform gas gain; the grid hole size, pitch and pattern can be easily adapted to match the geometry of any pixel readout chip.

Recent developments in radiation hardness research with state-of-the-art MPGD's are reviewed in Ref. 96. Better properties of MPGD's, which are rather insensitive to aging compared to wire chambers, can be explained by the separation of multiplication (GEM or parallel plate Micromegas amplification) and anode readout structures, and the lower electric field strength (~ 50 kV/cm) in the multiplication region, compared to the anode wire surface field (~ 250 kV/cm).

28.7.4. Time-projection chambers : Written September 2007 by D. Karlen (U. of Victoria and TRIUMF, Canada)

The Time Projection Chamber (TPC) concept, invented by David Nygren in the late 1970's [78], is the basis for charged particle tracking in a large number of particle and nuclear physics experiments. A uniform electric field drifts tracks of ions produced by charged particles traversing a medium, either gas or liquid, towards a surface segmented into 2D readout pads. The signal amplitudes and arrival times are recorded to provide full 3D measurements of the particle trajectories. The intrinsic 3D segmentation gives the TPC a distinct advantage over other large volume tracking detector designs which record information only in a 2D projection with less overall segmentation, particularly for pattern recognition in events with large numbers of particles.

Gaseous TPC's are often designed to operate within a strong magnetic field (typically parallel to the drift field) so that particle momenta can be estimated from the track curvature. For this application, precise spatial measurements in the plane transverse to the magnetic field are most important. Since the amount of ionization along the length of the track depends on the velocity of the particle, ionization and momentum measurements can be combined to identify the types of particles observed in the TPC. The estimator for the energy deposit by a particle is usually formed as the truncated mean of the energy deposits, using the 50%–70% of the samples with the smallest signals. Variance due to energetic δ -ray production is thus reduced.

Gas amplification of 10^3 – 10^4 at the readout endplate is usually required in order to provide signals with sufficient amplitude for conventional electronics to sense the drifted ionization. Until recently, the gas amplification system used in TPC's have exclusively been planes of anode wires operated in proportional mode placed close to the readout pads. Performance has been recently improved by replacing these wire planes with micro-pattern gas detectors, namely GEM [86] and Micromegas [87] devices. Advances in electronics miniaturization have been important in this development, allowing pad areas to be reduced to the 10 mm^2 scale or less, well matched to the narrow extent of signals produced with micro-pattern gas detectors. Presently, the ultimate in fine segmentation TPC readout are silicon sensors, with $0.05\text{ mm} \times 0.05\text{ mm}$ pixels, in combination with GEM or Micromegas [97]. With such fine granularity it is possible to count the number of ionization clusters along the length of a track which, in principle, can improve the particle identification capability.

Examples of two modern large volume gaseous TPC's are shown in Fig. 28.13 and Fig. 28.14. The particle identification performance is illustrated in Fig. 28.15, for the original TPC in the PEP-4/9 experiment [98].

The greatest challenges for a large TPC arise from the long drift distance, typically 100 times further than in a comparable wire chamber design. In particular, the long drift distance can make the device sensitive to small distortions in the electric field. Distortions can arise from a number of sources, such as imperfections in the TPC construction, deformations of the readout surface, or the presence of ions in the active medium.

For a gaseous TPC operated in a magnetic field, the electron drift velocity v is defined by Eq. (28.13). With a strong magnetic field parallel to the electric field and a gas with a large value of $\omega\tau$ (also favored to reduce transverse diffusion as discussed below), the transverse displacements of the drifting electrons due to electric field distortions are reduced. In this mode of operation, it is essential to precisely map the magnetic field as the electron drift lines closely follow the magnetic field lines. Corrections for electric and/or magnetic field non-uniformities can be determined from control samples of electrons produced by ionizing the gas with UV laser beams, from photoelectrons

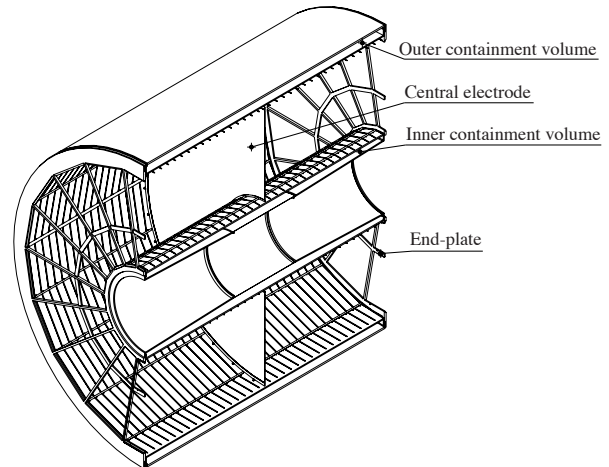


Figure 28.13: The ALICE TPC shown in a cutaway view. The drift volume is 5 m long with a 5 m diameter. Gas amplification is provided by planes of anode wires.

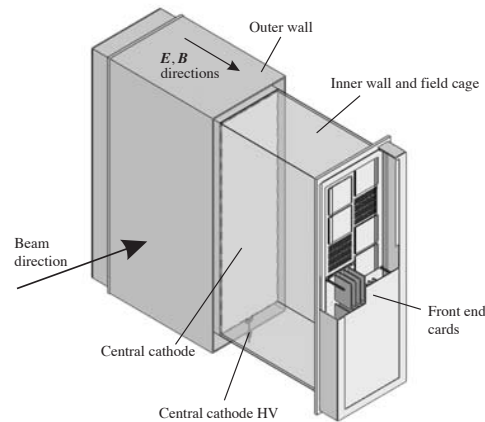


Figure 28.14: One of the 3 TPC modules for the near detector of the T2K experiment. The drift volume is $2\text{ m} \times 2\text{ m} \times 0.8\text{ m}$. Micromegas devices are used for gas amplification and readout.

produced on the cathode, or from tracks emanating from calibration reactions.

The long drift distance means that there is a delay, typically 10 – $100\ \mu\text{s}$ in a large gaseous TPC, for signals to arrive at the endplate. For experiments with shorter intervals between events, this can produce ambiguities in the starting time for the drift of ionization. This can be resolved by matching the TPC data with that from an auxiliary detector providing additional spatial or timing information.

In a gaseous TPC, the motion of positive ions is much slower than the electrons, and so the positive ions produced by many events may exist in the active volume. Of greatest concern is the ions produced in the gas amplification stage. Large gaseous TPC's built until now with wire planes have included a gating grid that prevent the positive ions from escaping into the drift volume in the interval between event triggers. Micro-pattern gas detectors release much less positive ions than wire planes operating at the same gain, which may allow operation of a TPC without a gating grid.

Given the long drift distance in a large TPC, the active medium must remain very pure, as small amounts of contamination can absorb the ionization signal. For example, in a typical large gaseous TPC, O_2 must be kept below a few parts in 10^5 , otherwise a large fraction of the drifting electrons will become

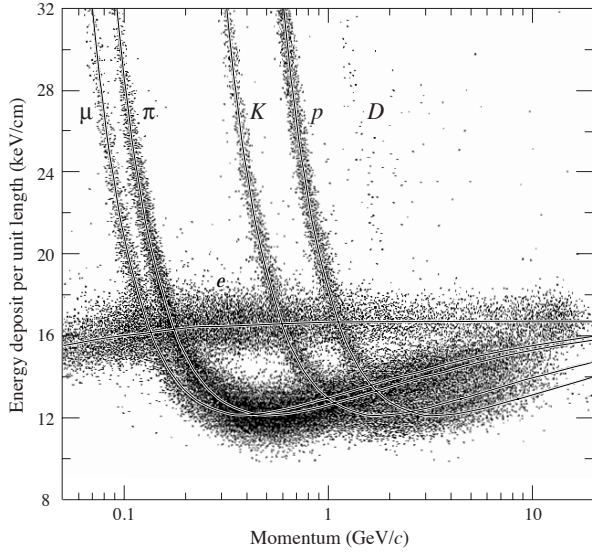


Figure 28.15: The PEP4/9-TPC energy deposit measurements (185 samples, 8.5 atm Ar-CH₄ 80:20). The ionization rate at the Fermi plateau (at high β) is 1.4 times that for the minimum at lower β . This ratio increases to 1.6 at atmospheric pressure.

attached. Special attention must be made in the choice of construction materials in order to avoid the release of other electronegative contaminants.

Diffusion degrades the position information of ionization that drifts a long distance. For a gaseous TPC, the effect can be alleviated by the choice of a gas with low intrinsic diffusion or by operating in a strong magnetic field parallel to the drift field with a gas which exhibits a significant reduction in transverse diffusion with magnetic field. For typical operation without magnetic field, the transverse extent of the electrons, σ_{Dx} , is a few mm after drifting 1 m due to diffusion. With a strong magnetic field, σ_{Dx} can be reduced by as much as a factor of 10,

$$\sigma_{Dx}(B)/\sigma_{Dx}(0) = \frac{1}{\sqrt{1 + \omega^2 \tau^2}} \quad (28.14)$$

where $\omega\tau$ is defined above. The diffusion limited position resolution from the information collected by a single row of pads is

$$\sigma_x = \frac{\sigma_{Dx}}{\sqrt{n}} \quad (28.15)$$

where n is the effective number of electrons collected by the pad row, giving an ultimate single row resolution of order 100 μm .

Diffusion is significantly reduced in a negative-ion TPC [99], which uses a special gas mixture that attaches electrons immediately as they are produced. The drifting negative ions exhibit much less diffusion than electrons. The slow drift velocity and small $\omega\tau$ of negative ions must be compatible with the experimental environment.

The spatial resolution achieved by a TPC is determined by a number of factors in addition to diffusion. Non-uniform ionization along the length of the track is a particularly important factor, and is responsible for the so-called “track angle” and “ $\mathbf{E} \times \mathbf{B}$ ” effects. If the boundaries between pads in a row are not parallel to the track, the ionization fluctuations will increase the variance in the position estimate from that row. For this reason, experiments with a preferred track direction should have pad boundaries aligned with that direction. Traditional TPC’s with wire plane amplification suffer from the effects of non-parallel electric and magnetic fields near the wires that rotate ionization segments, thereby degrading the resolution because of the

non-uniform ionization. Micro-pattern gas detectors exhibit a much smaller $\mathbf{E} \times \mathbf{B}$ effect, since their feature size is much smaller than that of a wire grid.

28.7.5. Transition radiation detectors (TRD’s): Written August 2007 by P. Nevski (BNL), A. Romaniouk (Moscow Eng. & Phys. Inst.)

Transition radiation (TR) x rays are produced when a highly relativistic particle ($\gamma \gtrsim 10^3$) crosses a refractive index interface, as discussed in Sec. 27.7. The x rays, ranging from a few keV to a few dozen keV, are emitted at a characteristic angle $1/\gamma$ from the particle trajectory. Since the TR yield is about 1% per boundary crossing, radiation from multiple surface crossings is used in practical detectors. In the simplest concept, a detector module might consist of low- Z foils followed by a high- Z active layer made of proportional counters filled with a Xe-rich gas mixture. The atomic number considerations follow from the dominant photoelectric absorption cross section per atom going roughly as Z^n/E_x^3 , where n varies between 4 and 5 over the region of interest, and the x-ray energy is E_x .^{*} To minimize self-absorption, materials such as polypropylene, Mylar, carbon, and (rarely) lithium are used as radiators. The TR signal in the active regions is in most cases superimposed upon the particle’s ionization losses. These drop a little faster than Z/A with increasing Z , providing another reason for active layers with high Z .

The TR intensity for a single boundary crossing always increases with γ , but for multiple boundary crossings interference leads to saturation near a Lorentz factor $\gamma_{\text{sat}} = 0.6 \omega_1 \sqrt{\ell_1 \ell_2} / c$ [100,101], where ω_1 is the radiator plasma frequency, ℓ_1 is its thickness, and ℓ_2 the spacing. In most of the detectors used in particle physics the radiator parameters are chosen to provide $\gamma_{\text{sat}} \approx 2000$. Those detectors normally work as threshold devices, ensuring the best electron/pion separation in the momentum range $1 \text{ GeV}/c \lesssim p \lesssim 150 \text{ GeV}/c$.

One can distinguish two design concepts—“thick” and “thin” detectors:

1. The radiator, optimized for a minimum total radiation length at maximum TR yield and total TR absorption, consists of few hundred foils (for instance 300 20 μm thick polypropylene foils). A dominant fraction of the soft TR photons is absorbed in the radiator itself. To increase the average TR photon energy further, part of the radiator far from the active layers is often made of thicker foils. The detector thickness, about 2 cm for Xe-filled gas chambers, is optimized to absorb the shaped x-ray spectrum. A classical detector is composed of several similar modules which respond nearly independently. Such detectors were used in the NA34 [102], NOMAD [103], and are being used in the ALICE [104] experiment.
2. In another TRD concept a fine granular radiator/detector structure exploits the soft part of the TR spectrum more efficiently. This can be achieved, for instance, by distributing small-diameter straw-tube detectors uniformly or in thin layers throughout the radiator material (foils or fibers). Even with a relatively thin radiator stack, radiation below 5 keV is mostly lost in the radiators themselves. However for photon energies above this value the absorption becomes smaller and the radiation can be registered by several consecutive detector layers, thus creating a strong TR build-up effect. Examples of the detectors using this approach can be found in both accelerator (ATLAS [105]) and space (PAMELA [106], AMS [107]) experiments. For example, in the ATLAS TR tracker charged particles cross about 35 effective straw tube

^{*} Photon absorption coefficients for the elements (via a NIST link), and $dE/dx|_{\text{min}}$ and plasma energies for many materials are given in pdg.lbl.gov/AtomicNuclearProperties.

layers embedded in the radiator material. The effective thickness of the Xe gas per straw is about 2.3 mm and the average number of foils per straw is about 40 with an effective foil thickness of about 20 μm .

Both TR photon absorption and the TR build-up significantly affect the detector performance. Although the values mentioned above are typical for most of the plastic radiators used with Xe-based detectors, they vary significantly depending on detector parameters: radiator material, thickness and spacing, the construction of the sensitive chambers, their position, *etc.* Thus careful simulations are usually needed to build a detector optimized for a particular application.

The discrimination between electrons and pions can be based on the charge deposition measured in each detection module, on the number of clusters—energy depositions observed above an optimal threshold (usually in the 5 to 7 keV region), or on more sophisticated methods analyzing the pulse shape as a function of time. The total energy measurement technique is more suitable for thick gas volumes, which absorb most of the TR radiation and where the ionization loss fluctuations are small. The cluster-counting method works better for detectors with thin gas layers, where the fluctuations of the ionization losses are big. Cluster-counting replaces the Landau-Vavilov distribution of background ionization energy losses with the Poisson statistics of δ -electrons, responsible for the distribution tails. The latter distribution is narrower than the Landau-Vavilov distribution.

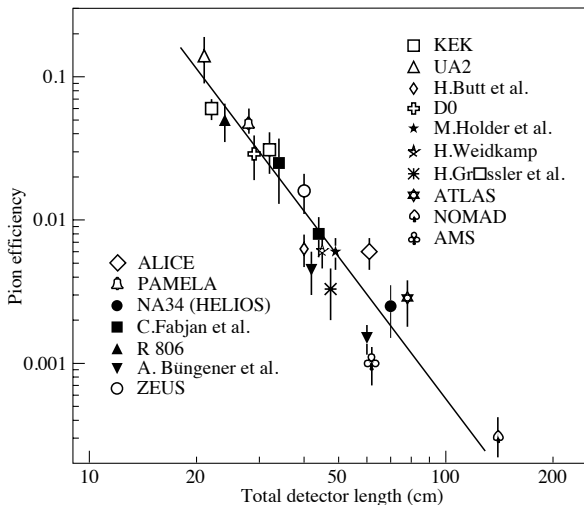


Figure 28.16: Pion efficiency measured (or predicted) for different TRDs as a function of the detector length for a fixed electron efficiency of 90%. The plot is taken from [102] with efficiencies of more recent detectors [105–106] added (ATLAS to PAMELA).

The major factor in the performance of any TRD is its overall length. This is illustrated in Fig. 28.16, which shows, for a variety of detectors, the pion efficiency at a fixed electron efficiency of 90% as a function of the overall detector length. The experimental data, covering a range of particle energies from a few GeV to 40 GeV, are rescaled to an energy of 10 GeV when possible. Phenomenologically, the rejection power against pions increases as $5 \cdot 10^{L/38}$, where the range of validity is $L \approx 20\text{--}100$ cm.

Many recent TRDs combine particle identification with charged-track measurement in the same detector [104,105]. This provides a powerful tool for electron identification even at very high particle densities. Another example of this combination is described in Ref. 108. In this work Si-microstrip detectors operating in a magnetic field are used both for particle and TR

detection. The excellent coordinate resolution of the Si detectors allows spatial separation of the TR photons from particle ionization tracks with relatively modest distances between radiator and detector.

Recent TRDs for particle astrophysics are designed to directly measure the Lorentz factor of high-energy nuclei by using the quadratic dependence of the TR yield on nuclear charge [109,110]. The radiator configuration (ℓ_1, ℓ_2) is tuned to extend the TR yield rise up to $\gamma \lesssim 10^5$ using more energetic part of the TR spectrum (up to 100 keV). Exotic radiator materials such as aluminum and unusual TR detection methods (Compton scattering) are used such cases [109].

28.7.6. Resistive-plate chambers : Revised September 2007 by H.R. Band (U. Wisconsin).

The resistive-plate chamber (RPC) was developed by Santonico and Cardarelli in the early 1980's [111] as a low-cost alternative to large scintillator planes.* Most commonly, an RPC is constructed from two parallel high-resistivity ($10^9\text{--}10^{13}$ $\Omega\text{-cm}$) glass or phenolic (Bakelite)/melamine laminate plates with a few-mm gap between them which is filled with atmospheric-pressure gas. The gas is chosen to absorb UV photons in order to limit transverse growth of discharges. The backs of the plates are coated with a lower-resistivity paint or ink ($\sim 10^5$ Ω/\square), and a high potential (7–12 kV) is maintained between them. The passage of a charged particle initiates an electric discharge, whose size and duration are limited since the current reduces the local potential to below that needed to maintain the discharge. The sensitivity of the detector outside of this region is unaffected. The signal readout is via capacitive coupling to metallic strips on both sides of the detector which are separated from the high voltage coatings by thin insulating sheets. The x and y position of the discharge can be measured if the strips on opposite sides of the gap are orthogonal. When operated in streamer mode, the induced signals on the strips can be quite large (~ 300 mV), making sensitive electronics unnecessary. An example of an RPC structure is shown in Fig. 28.17.

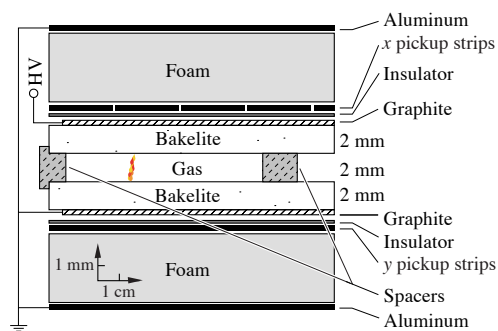


Figure 28.17: Schematic cross section of a typical RPC, in this case the single-gap streamer-mode BaBar RPC.

RPC's have inherent rate limitations since the time needed to re-establish the field after a discharge is proportional to the chamber capacitance and plate resistance. The average charge per streamer is 100–1000 pC. Typically, the efficiency of streamer-mode glass RPC's begins to fall above ~ 0.4 Hz/cm². Because of Bakelite's lower bulk resistivity, Bakelite RPC's can be efficient at 10–100 Hz/cm². The need for higher rate capability led to the development of avalanche-mode RPC's, in which the gas and high voltage have been tuned to limit the

* It was based on earlier work on a spark counter with one high-resistivity plate [112].

growth of the electric discharge, preventing streamer formation. Typical avalanche-mode RPC's have a signal charge of about 10 pC and can be efficient at 1 kHz/cm². The avalanche discharge produces a much smaller induced signal on the pickup strips (~ 1 mV) than streamers, and thus requires a more sophisticated and careful electronic design.

Many variations of the initial RPC design have been built for operation in either mode. Efficiencies of $\gtrsim 92\%$ for single gaps can be improved by the use of two or more gas gaps with shared pickup strips. Non-flammable and more environmentally friendly gas mixtures have been developed. In streamer mode, various mixtures of argon with isobutane and tetrafluoroethane have been used. For avalanche mode operation, a gas mixture of tetrafluoroethane (C₂H₂F₄) with 2–5% isobutane and 0.4–10% sulfur hexafluoride (SF₆) is typical. An example of large-scale RPC use is provided by the muon system being built for the ATLAS detector, where three layers of pairs of RPC's are used to trigger the drift tube arrays between the pairs. The total area is about 10,000 m². These RPC's provide a spatial resolution of 1 cm and a time resolution of 1 ns at an efficiency $\geq 99\%$.

Developments of multiple-gap RPC's [113] lead to RPC designs with much better timing resolution (~ 50 ps) for use in time-of-flight particle identification systems. A pioneering design used by the HARP experiment [114] has two sets of 2 thin gas gaps (0.3 mm) separated by thin (0.7 mm) glass plates. The outer plates are connected to high voltage and ground while the inner plate is electrically isolated and floats to a stable equilibrium potential. The observed RPC intrinsic time resolution of 127 ps may have been limited by amplifier noise. Fonte provides useful review [115] of other RPC designs.

Operational experience with RPC's has been mixed. Several experiments (*e.g.*, L3 and HARP) have reported reliable performance. However, the severe problems experienced with the BaBar RPC's have raised concerns about the long-term reliability of Bakelite RPC's.

Glass RPC's have had fewer problems, as seen by the history of the BELLE chambers. A rapid growth in the noise rate and leakage current in some of the BELLE glass RPC's was observed during commissioning. It was found that water vapor in the input gas was reacting with fluorine (produced by the disassociation of the tetrafluoroethane in the streamers) to produce hydrofluoric acid. The acid etched the glass surfaces, leading to increased noise rates and lower efficiencies. The use of copper gas piping to insure the dryness of the input gas stopped the problem. The BELLE RPC's have now operated reliably for more than 5 years.

Several different failure modes diagnosed in the first-generation BaBar Bakelite RPC's caused the average efficiency of the barrel RPC's to fall from $\gtrsim 90\%$ to 35% in five years. The linseed oil which is used in Bakelite RPC's to coat the inner surface [116] had not been completely cured. Under warm conditions (32° C) and high voltage, oil collected on the spacers between the gaps or formed oil-drop bridges between the gaps. This led to large leakage currents (50–100 μ A in some chambers) which persisted even when the temperature was regulated at 20° C. In addition, the graphite layer used to distribute the high voltage over the Bakelite became highly resistive (100 k Ω /□ \rightarrow 10 M Ω /□), resulting in lowered efficiency in some regions and the complete death of whole chambers.

The BaBar problems and the proposed use of Bakelite RPC's in the LHC detectors prompted detailed studies of RPC aging and have led to improved construction techniques and a better understanding of RPC operational limits. The graphite layer has been improved and should be stable with integrated currents of $\lesssim 600$ mC/cm². Molded gas inlets and improved cleanliness during construction have reduced the noise rate of new chambers.

Unlike glass RPC's, Bakelite RPC's have been found to require humid input gases to prevent drying of the Bakelite (increasing the bulk resistivity) which would decrease the rate capability. Second-generation BaBar RPC's incorporating many of the above improvements have performed reliably for over two years [117].

With many of these problems solved, new-generation RPC's are now being or soon will be used in about a dozen cosmic-ray and HEP detectors. Their comparatively low cost, ease of construction, good time resolution, high efficiency, and moderate spatial resolution make them attractive in many situations, particularly those requiring fast timing and/or large-area coverage.

28.8. Silicon semiconductor detectors

Updated September 2007 by H. Spieler (LBNL).

Semiconductor detectors are widely used in modern high-energy physics experiments. They are the key ingredient of high-resolution vertex and tracking detectors and are also used as photodetectors in scintillation calorimeters. The most commonly used material is silicon, but germanium, gallium-arsenide, CdTe, CdZnTe, and diamond are also useful in some applications. Integrated circuit technology allows the formation of high-density micron-scale electrodes on large (10–15 cm diameter) wafers, providing excellent position resolution. Furthermore, the density of silicon and its small ionization energy result in adequate signals with active layers only 100–300 μ m thick, so the signals are also fast (typically tens of ns). Semiconductor detectors depend crucially on low-noise electronics (see Sec. 28.9), so the detection sensitivity is determined by signal charge and capacitance. For a comprehensive discussion of semiconductor detectors and electronics see Ref. 118.

Silicon detectors are *p-n* junction diodes operated at reverse bias. This forms a sensitive region depleted of mobile charge and sets up an electric field that sweeps charge liberated by radiation to the electrodes. Detectors typically use an asymmetric structure, *e.g.* a highly doped *p* electrode and a lightly doped *n* region, so that the depletion region extends predominantly into the lightly doped volume.

The thickness of the depleted region is

$$W = \sqrt{2\epsilon(V + V_{bi})/Ne} = \sqrt{2\rho\mu\epsilon(V + V_{bi})}, \quad (28.16)$$

where V = external bias voltage

V_{bi} = “built-in” voltage (≈ 0.5 V for resistivities typically used in detectors)

N = doping concentration

e = electronic charge

ϵ = dielectric constant = 11.9 $\epsilon_0 \approx 1$ pF/cm

ρ = resistivity (typically 1–10 k Ω cm)

μ = charge carrier mobility

= 1350 cm² V⁻¹ s⁻¹ for electrons

= 450 cm² V⁻¹ s⁻¹ for holes

or

$W = 0.5 [\mu\text{m}/\sqrt{\Omega\text{-cm}\cdot\text{V}}] \times \sqrt{\rho(V + V_{bi})}$ for *n*-type material, and

$W = 0.3 [\mu\text{m}/\sqrt{\Omega\text{-cm}\cdot\text{V}}] \times \sqrt{\rho(V + V_{bi})}$ for *p*-type material.

The conductive *p* and *n* regions together with the depleted volume form a capacitor with the capacitance per unit area

$$C = \epsilon/W \approx 1 [\text{pF/cm}] / W. \quad (28.17)$$

In strip and pixel detectors the capacitance is dominated by the fringing capacitance. For example, the strip-to-strip fringing capacitance is ~ 1 –1.5 pF cm⁻¹ of strip length at a strip pitch of 25–50 μ m.

Measurements on silicon photodiodes [119] show that for photon energies below 4 eV one electron-hole ($e-h$) pair is formed per incident photon. The mean energy E_i required to produce an $e-h$ pair peaks at 4.4 eV for a photon energy around 6 eV. It assumes a constant value, 3.67 eV at room temperature, above ~ 1.5 keV. It is larger than the bandgap energy because phonon excitation is required for momentum conservation. For minimum-ionizing particles, the most probable charge deposition in a 300 μm thick silicon detector is about 3.5 fC (22000 electrons). Since both electronic and lattice excitations are involved, the variance in the number of charge carriers $N = E/E_i$ produced by an absorbed energy E is reduced by the Fano factor F (about 0.1 in Si). Thus, $\sigma_N = \sqrt{FN}$ and the energy resolution $\sigma_E/E = \sqrt{FE_i/E}$. However, the measured signal fluctuations are usually dominated by electronic noise or energy loss fluctuations in the detector.

Charge collection time decreases with increasing bias voltage, and can be reduced further by operating the detector with “overbias,” *i.e.* a bias voltage exceeding the value required to fully deplete the device. The collection time is limited by velocity saturation at high fields (approaching 10^7 cm/s at $E > 10^4$ V/cm); at an average field of 10^4 V/cm the collection time is about 15 ps/ μm for electrons and 30 ps/ μm for holes. In typical fully-depleted detectors 300 μm thick, electrons are collected within about 10 ns, and holes within about 25 ns.

Position resolution is limited by transverse diffusion during charge collection (typically 5 μm for 300 μm thickness) and by knock-on electrons. Resolutions of 2–4 μm (rms) have been obtained in beam tests. In magnetic fields, the Lorentz drift deflects the electron and hole trajectories and the detector must be tilted to reduce spatial spreading (see “Hall effect” in semiconductor textbooks).

Electrodes can be in the form of cm-scale pads, strips, or μm -scale pixels. Various readout structures have been developed for pixels, *e.g.* CCD’s, DEPFET’s, monolithic pixel devices that integrate sensor and electronics (MAPS), and hybrid pixel devices that utilize separate sensors and readout IC’s connected by two-dimensional arrays of solder bumps. For an overview and further discussion see Ref. 118.

Radiation damage occurs through two basic mechanisms:

1. Bulk damage due to displacement of atoms from their lattice sites. This leads to increased leakage current, carrier trapping, and build-up of space charge that changes the required operating voltage. Displacement damage depends on the nonionizing energy loss and the energy imparted to the recoil atoms, which can initiate a chain of subsequent displacements, *i.e.*, damage clusters. Hence, it is critical to consider both particle type and energy.
2. Surface damage due to charge build-up in surface layers, which leads to increased surface leakage currents. In strip detectors the inter-strip isolation is affected. The effects of charge build-up are strongly dependent on the device structure and on fabrication details. Since the damage is proportional to the absorbed energy (when ionization dominates), the dose can be specified in rad (or Gray) independent of particle type.

The increase in reverse bias current due to bulk damage is $\Delta I_r = \alpha \Phi$ per unit volume, where Φ is the particle fluence and α the damage coefficient ($\alpha \approx 3 \times 10^{-17}$ A/cm for minimum ionizing protons and pions after long-term annealing; $\alpha \approx 2 \times 10^{-17}$ A/cm for 1 MeV neutrons). The reverse bias current depends strongly on temperature

$$\frac{I_R(T_2)}{I_R(T_1)} = \left(\frac{T_2}{T_1}\right)^2 \exp\left[-\frac{E}{2k} \left(\frac{T_1 - T_2}{T_1 T_2}\right)\right] \quad (28.18)$$

where $E = 1.2$ eV, so rather modest cooling can reduce the current substantially (~ 6 -fold current reduction in cooling from room temperature to 0°C).

Displacement damage forms acceptor-like states. These trap electrons, building up a negative space charge, which in turn requires an increase in the applied voltage to sweep signal charge through the detector thickness. This has the same effect as a change in resistivity, *i.e.*, the required voltage drops initially with fluence, until the positive and negative space charge balance and very little voltage is required to collect all signal charge. At larger fluences the negative space charge dominates, and the required operating voltage increases ($V \propto N$). The safe limit on operating voltage ultimately limits the detector lifetime. Strip detectors specifically designed for high voltages have been extensively operated at bias voltages $>500\text{V}$. Since the effect of radiation damage depends on the electronic activity of defects, various techniques have been applied to neutralize the damage sites. For example, additional doping with oxygen increases the allowable charged hadron fluence roughly three-fold [120]. Detectors with columnar electrodes normal to the surface can also extend operational lifetime Ref. 121. The increase in leakage current with fluence, on the other hand, appears to be unaffected by resistivity and whether the material is *n* or *p*-type. At fluences beyond 10^{15} cm^{-2} decreased carrier lifetime becomes critical [122,123].

Strip and pixel detectors have remained functional at fluences beyond 10^{15} cm^{-2} for minimum ionizing protons. At this damage level, charge loss due to recombination and trapping also becomes significant and the high signal-to-noise ratio obtainable with low-capacitance pixel structures extends detector lifetime. The occupancy of the defect charge states is strongly temperature dependent; competing processes can increase or decrease the required operating voltage. It is critical to choose the operating temperature judiciously (-10 to 0°C in typical collider detectors) and limit warm-up periods during maintenance. For a more detailed summary see Ref. 124 and the web-sites of the ROSE and RD50 collaborations at RD48.web.cern.ch/rd48 and RD50.web.cern.ch/rd50.

Currently, the lifetime of detector systems is still limited by the detectors; in the electronics use of standard “deep submicron” CMOS fabrication processes with appropriately designed circuitry has increased the radiation resistance to fluences $> 10^{15}$ cm^{-2} of minimum ionizing protons or pions. For a comprehensive discussion of radiation effects see Ref. 125.

28.9. Low-noise electronics

Revised August 2003 by H. Spieler (LBNL).

Many detectors rely critically on low-noise electronics, either to improve energy resolution or to allow a low detection threshold. A typical detector front-end is shown in Fig. 28.18.

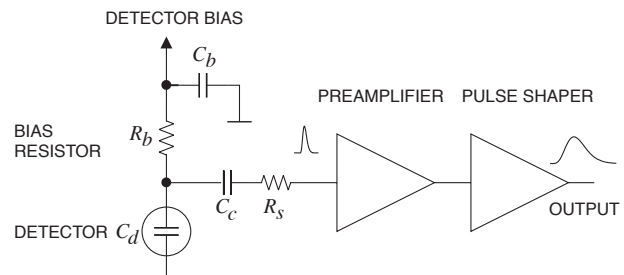


Figure 28.18: Typical detector front-end circuit.

The detector is represented by a capacitance C_d , a relevant model for most detectors. Bias voltage is applied through resistor R_b and the signal is coupled to the preamplifier through

a blocking capacitor C_c . The series resistance R_s represents the sum of all resistances present in the input signal path, *e.g.* the electrode resistance, any input protection networks, and parasitic resistances in the input transistor. The preamplifier provides gain and feeds a pulse shaper, which tailors the overall frequency response to optimize signal-to-noise ratio while limiting the duration of the signal pulse to accommodate the signal pulse rate. Even if not explicitly stated, all amplifiers provide some form of pulse shaping due to their limited frequency response.

The equivalent circuit for the noise analysis (Fig. 28.19) includes both current and voltage noise sources. The leakage current of a semiconductor detector, for example, fluctuates due to electron emission statistics. This “shot noise” i_{nd} is represented by a current noise generator in parallel with the detector. Resistors exhibit noise due to thermal velocity fluctuations of the charge carriers. This noise source can be modeled either as a voltage or current generator. Generally, resistors shunting the input act as noise current sources and resistors in series with the input act as noise voltage sources (which is why some in the detector community refer to current and voltage noise as “parallel” and “series” noise). Since the bias resistor effectively shunts the input, as the capacitor C_b passes current fluctuations to ground, it acts as a current generator i_{nb} and its noise current has the same effect as the shot noise current from the detector. Any other shunt resistances can be incorporated in the same way. Conversely, the series resistor R_s acts as a voltage generator. The electronic noise of the amplifier is described fully by a combination of voltage and current sources at its input, shown as e_{na} and i_{na} .

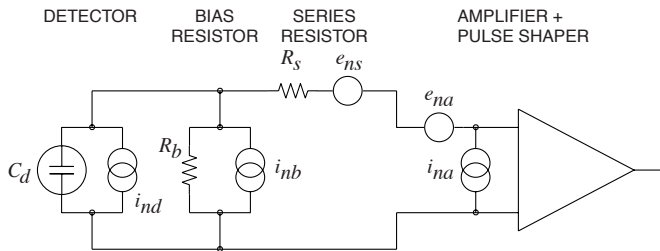


Figure 28.19: Equivalent circuit for noise analysis.

Shot noise and thermal noise have a “white” frequency distribution, *i.e.* the spectral power densities $dP_n/df \propto di_n^2/df \propto de_n^2/df$ are constant with the magnitudes

$$\begin{aligned} i_{nd}^2 &= 2eI_d, \\ i_{nb}^2 &= \frac{4kT}{R_b}, \\ e_{ns}^2 &= 4kTR_s, \end{aligned} \quad (28.19)$$

where e is the electronic charge, I_d the detector bias current, k the Boltzmann constant and T the temperature. Typical amplifier noise parameters e_{na} and i_{na} are of order $\text{nV}/\sqrt{\text{Hz}}$ and $\text{pA}/\sqrt{\text{Hz}}$. Trapping and detrapping processes in resistors, dielectrics and semiconductors can introduce additional fluctuations whose noise power frequently exhibits a $1/f$ spectrum. The spectral density of the $1/f$ noise voltage is

$$e_{nf}^2 = \frac{A_f}{f}, \quad (28.20)$$

where the noise coefficient A_f is device specific and of order 10^{-10} – 10^{-12}V^2 .

A fraction of the noise current flows through the detector capacitance, resulting in a frequency-dependent noise voltage

$i_n/(\omega C_d)$, which is added to the noise voltage in the input circuit. Since the individual noise contributions are random and uncorrelated, they add in quadrature. The total noise at the output of the pulse shaper is obtained by integrating over the full bandwidth of the system. Superimposed on repetitive detector signal pulses of constant magnitude, purely random noise produces a Gaussian signal distribution.

Since radiation detectors typically convert the deposited energy into charge, the system’s noise level is conveniently expressed as an equivalent noise charge Q_n , which is equal to the detector signal that yields a signal-to-noise ratio of one. The equivalent noise charge is commonly expressed in Coulombs, the corresponding number of electrons, or the equivalent deposited energy (eV). For a capacitive sensor

$$Q_n^2 = i_n^2 F_i T_S + e_n^2 F_v \frac{C^2}{T_S} + F_{vf} A_f C^2, \quad (28.21)$$

where C is the sum of all capacitances shunting the input, F_i , F_v , and F_{vf} depend on the shape of the pulse determined by the shaper and T_S is a characteristic time, for example, the peaking time of a semi-gaussian pulse or the sampling interval in a correlated double sampler. The form factors F_i, F_v are easily calculated

$$F_i = \frac{1}{2T_S} \int_{-\infty}^{\infty} [W(t)]^2 dt, \quad F_v = \frac{T_S}{2} \int_{-\infty}^{\infty} \left[\frac{dW(t)}{dt} \right]^2 dt, \quad (28.22)$$

where for time-invariant pulse-shaping $W(t)$ is simply the system’s impulse response (the output signal seen on an oscilloscope) with the peak output signal normalized to unity. For more details see Refs. 126 and 127.

A pulse shaper formed by a single differentiator and integrator with equal time constants has $F_i = F_v = 0.9$ and $F_{vf} = 4$, independent of the shaping time constant. The overall noise bandwidth, however, depends on the time constant, *i.e.* the characteristic time T_S . The contribution from noise currents increases with shaping time, *i.e.*, pulse duration, whereas the voltage noise decreases with increasing shaping time. Noise with a $1/f$ spectrum depends only on the ratio of upper to lower cutoff frequencies (integrator to differentiator time constants), so for a given shaper topology the $1/f$ contribution to Q_n is independent of T_S . Furthermore, the contribution of noise voltage sources to Q_n increases with detector capacitance. Pulse shapers can be designed to reduce the effect of current noise, *e.g.*, mitigate radiation damage. Increasing pulse symmetry tends to decrease F_i and increase F_v (*e.g.*, to 0.45 and 1.0 for a shaper with one CR differentiator and four cascaded integrators). For the circuit shown in Fig. 28.19,

$$\begin{aligned} Q_n^2 &= \left(2eI_d + 4kT/R_b + i_{na}^2 \right) F_i T_S \\ &\quad + (4kTR_s + e_{na}^2) F_v C_d^2 / T_S + F_{vf} A_f C_d^2. \end{aligned} \quad (28.23)$$

As the characteristic time T_S is changed, the total noise goes through a minimum, where the current and voltage contributions are equal. Fig. 28.20 shows a typical example. At short shaping times the voltage noise dominates, whereas at long shaping times the current noise takes over. The noise minimum is flattened by the presence of $1/f$ noise. Increasing the detector capacitance will increase the voltage noise and shift the noise minimum to longer shaping times.

For quick estimates, one can use the following equation, which assumes an FET amplifier (negligible i_{na}) and a simple CR – RC

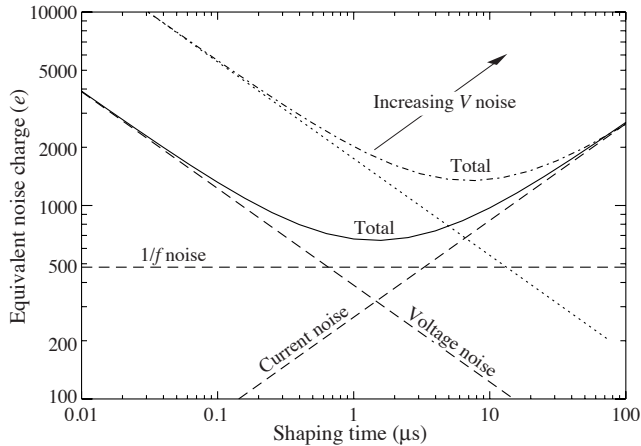


Figure 28.20: Equivalent noise charge *vs* shaping time. Changing the voltage or current noise contribution shifts the noise minimum. Increased voltage noise is shown as an example.

shaper with time constants τ (equal to the peaking time):

$$(Q_n/e)^2 = 12 \left[\frac{1}{\text{nA} \cdot \text{ns}} \right] I_d \tau + 6 \times 10^5 \left[\frac{\text{k}\Omega}{\text{ns}} \right] \frac{\tau}{R_b} + 3.6 \times 10^4 \left[\frac{\text{ns}}{(\text{pF})^2 (\text{nV})^2 / \text{Hz}} \right] e_n^2 \frac{C^2}{\tau}. \quad (28.24)$$

Noise is improved by reducing the detector capacitance and leakage current, judiciously selecting all resistances in the input circuit, and choosing the optimum shaping time constant.

The noise parameters of the amplifier depend primarily on the input device. In field effect transistors, the noise current contribution is very small, so reducing the detector leakage current and increasing the bias resistance will allow long shaping times with correspondingly lower noise. In bipolar transistors, the base current sets a lower bound on the noise current, so these devices are best at short shaping times. In special cases where the noise of a transistor scales with geometry, *i.e.*, decreasing noise voltage with increasing input capacitance, the lowest noise is obtained when the input capacitance of the transistor is equal to the detector capacitance, albeit at the expense of power dissipation. Capacitive matching is useful with field-effect transistors, but not bipolar transistors. In bipolar transistors, the minimum obtainable noise is independent of shaping time, but only at the optimum collector current I_C , which does depend on shaping time.

$$Q_{n,\min}^2 = 4kT \frac{C}{\sqrt{\beta_{DC}}} \sqrt{F_i F_v} \quad \text{at} \quad I_c = \frac{kT}{e} C \sqrt{\beta_{DC}} \sqrt{\frac{F_v}{F_i}} \frac{1}{T_S}, \quad (28.25)$$

where β_{DC} is the DC current gain. For a CR - RC shaper and $\beta_{DC} = 100$,

$$Q_{n,\min}/e \approx 250 \sqrt{C/\text{pF}}. \quad (28.26)$$

Practical noise levels range from $\sim 1e$ for CCD's at long shaping times to $\sim 10^4 e$ in high-capacitance liquid argon calorimeters. Silicon strip detectors typically operate at $\sim 10^3 e$ electrons, whereas pixel detectors with fast readout provide noise of several hundred electrons.

In timing measurements, the slope-to-noise ratio must be optimized, rather than the signal-to-noise ratio alone, so the rise time t_r of the pulse is important. The "jitter" σ_t of the timing distribution is

$$\sigma_t = \frac{\sigma_n}{(dS/dt)_{S_T}} \approx \frac{t_r}{S/N}, \quad (28.27)$$

where σ_n is the rms noise and the derivative of the signal dS/dt is evaluated at the trigger level S_T . To increase dS/dt without incurring excessive noise, the amplifier bandwidth should match the rise-time of the detector signal. The 10 to 90% rise time of an amplifier with bandwidth f_U is $0.35/f_U$. For example, an oscilloscope with 350 MHz bandwidth has a 1 ns rise time. When amplifiers are cascaded, which is invariably necessary, the individual rise times add in quadrature.

$$t_r \approx \sqrt{t_{r1}^2 + t_{r2}^2 + \dots + t_{rn}^2}$$

Increasing signal-to-noise ratio also improves time resolution, so minimizing the total capacitance at the input is also important. At high signal-to-noise ratios, the time jitter can be much smaller than the rise time. The timing distribution may shift with signal level ("walk"), but this can be corrected by various means, either in hardware or software [10].

For a more detailed introduction to detector signal processing and electronics see Ref. 118.

28.10. Calorimeters

A calorimeter is designed to measure the energy deposited in a contained electromagnetic (EM) or hadronic shower. The characteristic interaction distance for an electromagnetic interaction is the radiation length X_0 , which ranges from 13.8 g cm^{-2} in iron to 6.0 g cm^{-2} in uranium.* Similarly, the characteristic nuclear interaction length λ_I varies from 132.1 g cm^{-2} (Fe) to 209 g cm^{-2} (U). In either case, the calorimeter must be many interaction lengths deep, where "many" is determined by physical size, cost, and other factors. EM calorimeters tend to be 15 – $30 X_0$ deep, while hadronic calorimeters are usually compromised at 5 – $8 \lambda_I$. Moreover, in a real experiment there is likely to be an EM calorimeter in front of the hadronic section, and perhaps a more poorly sampling catcher in the back, so the hadronic cascade is contained in a succession of different structures. In all cases there is a premium on high density, to contain the shower as compactly as possible, and, especially in the EM case, high atomic number.

There are homogeneous and sampling calorimeters. In a homogeneous calorimeter the entire volume is sensitive, *i.e.*, contributes signal. Homogeneous calorimeters (usually electromagnetic) may be built with inorganic heavy (high- Z) scintillating crystals such as BGO, CsI, NaI, and PWO, non-scintillating Cherenkov radiators such as lead glass and lead fluoride, or ionizing noble liquids. Properties of commonly used inorganic crystal scintillators can be found in Table 28.4. A sampling calorimeter consists of an active medium which generates signal and a passive medium which functions as an absorber. The active medium may be a scintillator, an ionizing noble liquid, a gas chamber, a semiconductor, or a Cherenkov radiator. The passive medium is usually a material of high density, such as lead, iron, copper, or depleted uranium.

* $\lambda_I \approx 35 \text{ g cm}^{-2} A^{1/3}$; for actual values see pdg.lbl.gov/AtomicNuclearProperties.

28.10.1. Electromagnetic calorimeters : Written August 2003 by R.-Y. Zhu (California Inst. of Technology).

The development of electromagnetic showers is discussed in the section on “Passage of Particles Through Matter” (Sec. 27 of this *Review*).

Formulae are given which approximately describe average showers, but since the physics of electromagnetic showers is well understood, detailed and reliable Monte Carlo simulation is possible. EGS4 [128] and GEANT [129] have emerged as the standards.

The energy resolution σ_E/E of a calorimeter can be parametrized as $a/\sqrt{E} \oplus b \oplus c/E$, where \oplus represents addition in quadrature and E is in GeV. The stochastic term a represents statistics-related fluctuations such as intrinsic shower fluctuations, photoelectron statistics, dead material at the front of the calorimeter, and sampling fluctuations. For a fixed number of radiation lengths, the stochastic term a for a sampling calorimeter is expected to be proportional to $\sqrt{t/f}$, where t is plate thickness and f is sampling fraction [130,131]. While a is at a few percent level for a homogeneous calorimeter, it is typically 10% for sampling calorimeters. The main contributions to the systematic, or constant, term b are detector non-uniformity and calibration uncertainty. In the case of the hadronic cascades discussed below, non-compensation also contributes to the constant term. One additional contribution to the constant term for calorimeters built for modern high-energy physics experiments, operated in a high-beam intensity environment, is radiation damage of the active medium. This can be minimized by developing radiation-hard active media [45] and by frequent *in situ* calibration and monitoring [44,131]. With effort, the constant term b can be reduced to below one percent. The term c is due to electronic noise summed over readout channels within a few Molière radii. The best energy resolution for electromagnetic shower measurement is obtained in total absorption homogeneous calorimeters, *e.g.* calorimeters built with heavy crystal scintillators. These are used when ultimate performance is pursued.

The position resolution depends on the effective Molière radius and the transverse granularity of the calorimeter. Like the energy resolution, it can be factored as $a/\sqrt{E} \oplus b$, where a is a few to 20 mm and b can be as small as a fraction of mm for a dense calorimeter with fine granularity. Electromagnetic calorimeters may also provide direction measurement for electrons and photons. This is important for photon-related physics when there are uncertainties in event origin, since photons do not leave information in the particle tracking system. Typical photon angular resolution is about $45 \text{ mrad}/\sqrt{E}$, which can be provided by implementing longitudinal segmentation [132] for a sampling calorimeter or by adding a preshower detector [133] for a homogeneous calorimeter without longitudinal segmentation.

Novel technologies have been developed for electromagnetic calorimetry. New heavy crystal scintillators, such as PWO, LSO:Ce, and GSO:Ce (see Sec. 28.4), have attracted much attention for homogeneous calorimetry. In some cases, such as PWO, it has received broad applications in high-energy and nuclear physics experiments. The “spaghetti” structure has been developed for sampling calorimetry with scintillating fibers as the sensitive medium. The “accordion” structure has been developed for sampling calorimetry with ionizing noble liquid as the sensitive medium. Table 28.9 provides a brief description of typical electromagnetic calorimeters built recently for high-energy physics experiments. Also listed in this table are calorimeter depths in radiation lengths (X_0) and the achieved energy resolution. Whenever possible, the performance of calorimeters *in situ* is quoted, which is usually in good agreement with prototype test beam results as well as EGS or

GEANT simulations, provided that all systematic effects are properly included. Detailed references on detector design and performance can be found in Appendix C of reference [131] and Proceedings of the International Conference series on Calorimetry in Particle Physics.

Table 28.9: Resolution of typical electromagnetic calorimeters. E is in GeV.

Technology (Exp.)	Depth	Energy resolution	Date
NaI(Tl) (Crystal Ball)	$20X_0$	$2.7\%/E^{1/4}$	1983
$\text{Bi}_4\text{Ge}_3\text{O}_{12}$ (BGO) (L3)	$22X_0$	$2\%/ \sqrt{E} \oplus 0.7\%$	1993
CsI (KTeV)	$27X_0$	$2\%/ \sqrt{E} \oplus 0.45\%$	1996
CsI(Tl) (BaBar)	$16\text{--}18X_0$	$2.3\%/E^{1/4} \oplus 1.4\%$	1999
CsI(Tl) (BELLE)	$16X_0$	1.7% for $E_\gamma > 3.5 \text{ GeV}$	1998
PbWO_4 (PWO) (CMS)	$25X_0$	$3\%/ \sqrt{E} \oplus 0.5\% \oplus 0.2/E$	1997
Lead glass (OPAL)	$20.5X_0$	$5\%/ \sqrt{E}$	1990
Liquid Kr (NA48)	$27X_0$	$3.2\%/ \sqrt{E} \oplus 0.42\% \oplus 0.09/E$	1998
Scintillator/depleted U (ZEUS)	$20\text{--}30X_0$	$18\%/ \sqrt{E}$	1988
Scintillator/Pb (CDF)	$18X_0$	$13.5\%/ \sqrt{E}$	1988
Scintillator fiber/Pb spaghetti (KLOE)	$15X_0$	$5.7\%/ \sqrt{E} \oplus 0.6\%$	1995
Liquid Ar/Pb (NA31)	$27X_0$	$7.5\%/ \sqrt{E} \oplus 0.5\% \oplus 0.1/E$	1988
Liquid Ar/Pb (SLD)	$21X_0$	$8\%/ \sqrt{E}$	1993
Liquid Ar/Pb (H1)	$20\text{--}30X_0$	$12\%/ \sqrt{E} \oplus 1\%$	1998
Liquid Ar/depl. U (DØ)	$20.5X_0$	$16\%/ \sqrt{E} \oplus 0.3\% \oplus 0.3/E$	1993
Liquid Ar/Pb accordion (ATLAS)	$25X_0$	$10\%/ \sqrt{E} \oplus 0.4\% \oplus 0.3/E$	1996

28.10.2. Hadronic calorimeters : [1–6,131] Written April 2008 by D. E. Groom (LBNL).

Most large hadron calorimeters are sampling calorimeters which are parts of complicated 4π detectors at colliding beam facilities. Typically, the basic structure is plates of absorber (Fe, Pb, Cu, or occasionally U or W) alternating with plastic scintillators (plates, tiles, bars), liquid argon (LAr), or gaseous detectors. The ionization is measured directly, as in LAr calorimeters, or via scintillation light observed by photodetectors (usually PMT’s). Waveshifting fibers are often used to solve difficult problems of geometry and light collection uniformity. Silicon sensors are being studied for ILC detectors; in this case $e\text{--}h$ pairs are collected. There are as many variants of these schemes as there are calorimeters, including variations in geometry of the absorber and sensors, *e.g.*, scintillating fibers threading an absorber [134], and the “accordion” LAr detector, with zig-zag absorber plates to minimize channeling effects. Another departure from the traditional sandwich structure is the LAr-tube design shown in Fig. 28.21(a).

A relatively new variant is the use of Cerenkov light in hadron calorimetry. Such a calorimeter is sensitive to e^\pm ’s in the EM showers plus a few relativistic pions. An example is the radiation-hard forward calorimeter in CMS, with iron absorber and quartz fiber readout by PMT’s.

Ideally, the calorimeter is segmented in ϕ and θ (or $\eta = -\ln \tan(\theta/2)$). Fine segmentation, while desirable, is limited by cost, readout complexity, practical geometry, and the transverse size of the cascades. An example, a wedge of the ATLAS central barrel calorimeter, is shown in Fig. 28.21(b).

In an inelastic hadronic collision a significant fraction f_{em} of the energy is removed from further hadronic interaction by the production of secondary π^0 ’s and η ’s, whose decay photons

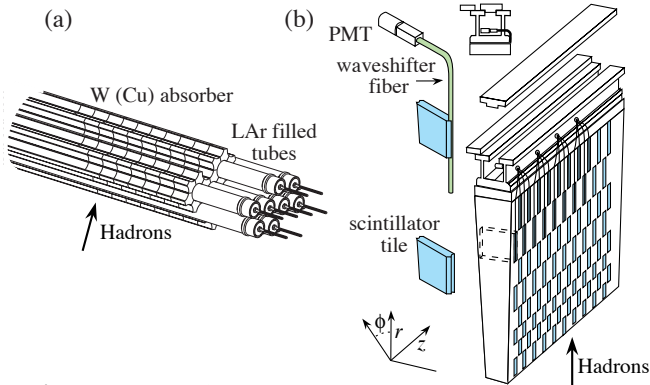


Figure 28.21: (a) ATLAS forward hadronic calorimeter structure (FCal2, 3). Tubes containing LAr are embedded in a mainly tungsten matrix. (b) ATLAS central calorimeter wedge; iron with plastic scintillator tile with wavelength-shifting fiber readout.

generate high-energy electromagnetic (EM) cascades. Charged secondaries (π^\pm , p , ...) deposit energy via ionization and excitation, but also interact with nuclei, producing spallation protons and neutrons, evaporation neutrons, and recoiling nuclei in highly excited states. The charged collision products produce detectable ionization, as do the showering γ -rays from the prompt de-excitation of highly excited nuclei. The recoiling nuclei generate little or no detectable signal. The neutrons lose kinetic energy in elastic collisions over hundreds of ns, gradually thermalize and are captured, with the production of more γ -rays—usually outside the acceptance gate of the electronics. Between endothermic spallation losses, nuclear recoils, and late neutron capture, a significant fraction of the hadronic energy (20%–35%, depending on the absorber and energy of the incident particle) is invisible.

In contrast to EM showers, hadronic cascade processes are characterized by relatively few high-energy particles being produced. The lost energy and the $\pi^0 \rightarrow \gamma\gamma$ fraction f_{em} are highly variable from event to event. Until there is event-by-event knowledge of both the invisible energy loss and EM deposit (to be discussed below), the energy resolution of a hadron calorimeter will remain significantly worse than that of an EM calorimeter.

It has been shown by a simple induction argument and verified by experiment that the decrease in the average value of the hadronic energy fraction ($\langle f_h \rangle = 1 - \langle f_{em} \rangle$) as the projectile energy E increases is fairly well described by the power law [135,136]

$$\langle f_h \rangle \approx (E/E_0)^{m-1} \quad (\text{for } E > E_0), \quad (28.28)$$

up to at least a few hundred GeV. The exponent m depends logarithmically on the mean multiplicity and the mean fractional loss to π^0 production in a single interaction. It is in the range 0.80–0.87, but must be obtained experimentally for each calorimeter configuration. E_0 is roughly the energy for the onset of inelastic collisions. It is 1 GeV or a little less for incident pions.

In a hadron-nucleus collision a large fraction of the incident energy is carried by a “leading particle” with the same quark content as the incident hadron. If the projectile is a charged pion, the leading particle is usually a pion, which can be neutral and hence contributes to the EM sector. This is not true for incident protons. The result is an increased mean hadronic fraction for incident protons: in Eq. (28.29b) $E_0 \approx 2.6$ GeV [135,137].

The EM energy deposit is usually detected more efficiently than the hadronic energy deposit. If the detection efficiency for the EM sector is e and that for the hadronic sector is h , then the ratio of the mean response to a pion to that for an electron is

$$\pi/e = \langle f_{em} \rangle + \langle f_h \rangle h/e = 1 - (1 - h/e)\langle f_h \rangle \quad (28.29a)$$

$$\approx 1 - (1 - h/e)(E/E_0)^{m-1}. \quad (28.29b)$$

If $h \neq e$ the hadronic response is not a linear function of energy. Only the product $(1 - h/e)E_0^{1-m}$ can be obtained by measuring π/e as a function of energy. Since $1 - m$ is small and $E_0 \approx 1$ GeV for the usual pion-induced cascades, this fact is usually ignored and h/e is reported.

The discussion above assumes an idealized calorimeter, with the same structure throughout and without leakage. “Real” calorimeters usually have an EM detector in front and a coarse “catcher” in the back. Complete containment is generally impractical.

By definition, $0 \leq f_{em} \leq 1$. Its variance changes only slowly with energy, but perforce $\langle f_{em} \rangle \rightarrow 1$ as the projectile energy increases. An empirical power law $\sigma_{f_{em}} = (E/E_1)^{1-\ell}$ (where $\ell < 1$) describes the energy dependence adequately and has the right asymptotic properties. For $h/e \neq 1$, fluctuations in f_{em} significantly contribute to the resolution, in particular contributing a larger fraction of the variance at high energies. Since the f_{em} distribution has a tail on the high side, the calorimeter response is non-Gaussian with a high-energy tail if $h/e < 1$. *Noncompensation* ($h/e \neq 1$) thus seriously degrades resolution as well as producing a nonlinear response.

It is clearly desirable to *compensate* the response, *i.e.*, to design the calorimeter such that $h/e = 1$. This is possible only in a sampling calorimeter, where several variables can be chosen or tuned:

1. Decrease the EM sensitivity. Because the EM cross sections increase with Z ,* and the absorber usually has higher $\langle Z \rangle$ than does the sensor, the EM energy deposit rate, relative to minimum ionization, is greater than this ratio in the sensor. Lower- Z inactive cladding, such as the steel cladding on ZEUS U plates, preferentially absorbs low-energy γ 's in EM showers and thus also lowers the electronic response. G10 signal boards in the $D\phi$ calorimeters have the same effect.
2. Increase the hadronic sensitivity. The abundant neutrons have a large n - p scattering cross section, with the production of low-energy scattered protons in hydrogenous sampling materials such as butane-filled proportional counters or plastic scintillator. (When scattering off a nucleus with mass number A , a neutron can at most lose $4/(1+A)^2$ of its kinetic energy.) The down side in the scintillator case is that the signal from a highly-ionizing proton stub can be reduced by as much as 90% by recombination and quenching (Birk's Law, Eq. (28.2)).

Fabjan and Willis proposed that the additional signal generated in the aftermath of fission in ^{238}U absorber plates should compensate nuclear fluctuations [138]. The production of fission fragments due to fast n capture was later observed [139]. However, while a very large amount of energy is released, it is mostly carried by low-velocity fission fragments which produce very little observable signal. The approach seemed promising for awhile. But, for example, the compensation observed with the ZEUS ^{238}U /scintillator calorimeter was the result of the two mechanisms discussed above.

Motivated very much by the work of Brau, Gabriel, Brückmann, and Wigmans [140], several groups built calorimeters which were very nearly compensating. The degree of compensation was sensitive to the acceptance gate width, and so could be somewhat tuned. These included (a) HELIOS with 2.5 mm thick scintillator plates sandwiched between 2 mm thick ^{238}U plates (one of several structures); $\sigma/E = 0.34/\sqrt{E}$ was obtained, (b) ZEUS, 2.6 cm thick scintillator plates between 3.3 mm ^{238}U plates; $\sigma/E = 0.35/\sqrt{E}$, (c) a ZEUS prototype with 10 mm

* The asymptotic pair-production cross section scales roughly as $Z^{0.75}$, and $|dE/dx|$ slowly decreases with increasing Z .

Pb plates and 2.5 mm scintillator sheets; $\sigma/E = 0.44/\sqrt{E}$, and (d) DØ, where the sandwich cell consists of a 4–6 mm thick ^{238}U plate, 2.3 mm LAr, a G-10 signal board, and another 2.3 mm LAr gap.

A more versatile approach to compensation is provided by a *dual-readout calorimeter*, in which the signal is sensed by two readout systems with highly contrasting h/e . Although the concept is more than two decades old [141], it has only recently been implemented by the DREAM collaboration [142]. The test beam calorimeter consisted of copper tubes, each filled with scintillator and quartz fibers. If the two signals Q and S (quartz and scintillator) are both normalized to electrons, then for each event Eq. (28.29) takes the form:

$$\begin{aligned} Q &= E[f_{em} + h/e|_Q(1 - f_{em})] \\ S &= E[f_{em} + h/e|_S(1 - f_{em})] \end{aligned} \quad (28.30)$$

These equations are linear in $1/E$ and f_{em} , and are easily solved for estimators of the *corrected* energy and f_{em} for each event. Both are subject to resolution effects, but effects due to fluctuations in f_{em} are eliminated. The solution for the corrected energy is given by [136]:

$$E = \frac{RS - Q}{R - 1}, \text{ where } R = \frac{1 - h/e|_Q}{1 - h/e|_S} \quad (28.31)$$

R is the energy-independent slope of the event locus on a plot of Q vs S . It can be found either from the fitted slope or by measuring π/e as a function of E . The DREAM collaboration expects to build a “triple-readout calorimeter” in which a neutron signal, proportional to the the missing energy, is measured as well on an event-by-event basis. It is hoped that such a hadronic calorimeter can approach the resolution of an electromagnetic calorimeter.

The fractional resolution can be represented by

$$\frac{\sigma}{E} = \frac{a_1(E)}{\sqrt{E}} \oplus \left| 1 - \frac{h}{e} \right| \left(\frac{E}{E_1} \right)^{1-\ell} \quad (28.32)$$

The coefficient a_1 is expected to have mild energy dependence for a number of reasons. For example, the sampling variance is $(\pi/e)E$ rather than E . $(E/E_1)^{1-\ell}$ is the parameterization of $\sigma_{f_{em}}$ discussed above. At a time when data were of lower quality, a plot of $(\sigma/E)^2$ vs $1/E$ was apparently well-described by a straight line (constant a_1) with a finite intercept—the square of the right term in Eq. (28.32), then called “the constant term.” Modern data show the slight downturn [134].

The average longitudinal distribution rises to a smooth peak about one nuclear interaction length (λ_I) into the calorimeter. It then falls somewhat faster than exponentially. Proton-induced cascades are somewhat shorter and broader than pion-induced cascades. In either case, the falloff distance increases with energy. In Fig. 28.22 experimental results for 90% and 95% containment are shown, as are calculations using Bock’s parameterization [143]. A slightly modified form has been used to fit recent measurements, *e.g.* to fit profiles measured in the ATLAS central barrel wedges [144].

The transverse energy deposit is characterized by a central core dominated by EM cascades, where the neutral meson parents are themselves produced at a variety of angles. There is a wide “skirt” produced by wide-angle hadronic interactions. The energy deposited in an annulus dA is adequately described by an exponential core and a Gaussian halo: $dE/dA = (B_1/r) \exp(-r/a_1) + (B_2/r) \exp(-r^2/a_2)$ [145].

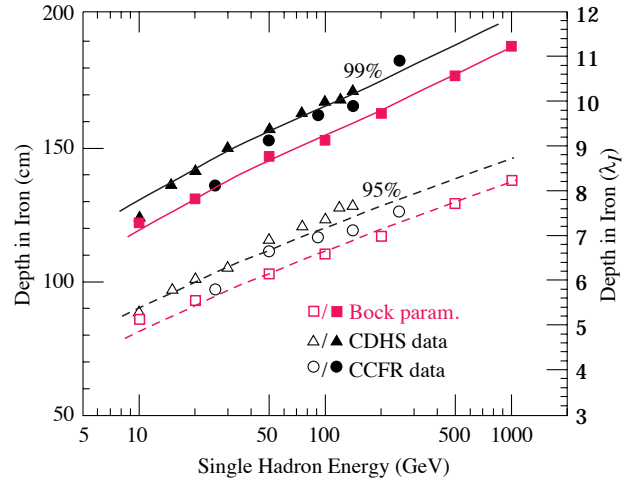


Figure 28.22: Required calorimeter thickness for 95% and 99% hadronic cascade containment in iron, on the basis of data from two large neutrino detectors and Bock’s parameterization [143].

28.10.3. Free electron drift velocities in liquid ionization sensors: Velocities as a function of electric field strength are given in Refs. 146–147 and are plotted in Fig. 28.23. Recent precise measurements of the free electron drift velocity in LAr have been published by W. Walkowiak [148]. The new measurements were motivated by the design of the ATLAS electromagnetic calorimeter and by inconsistencies in the previous literature. Velocities are temperature dependent and are systematically higher than those shown in Fig. 28.23.

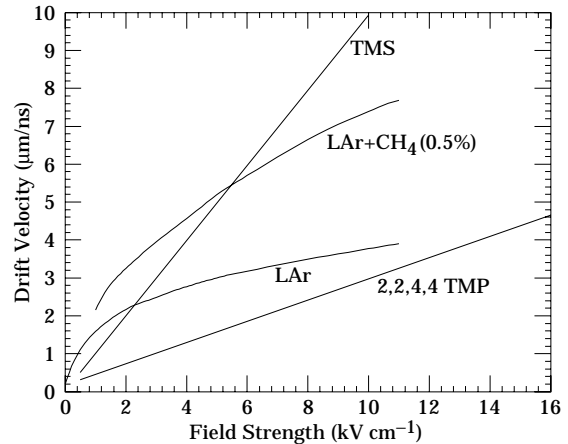


Figure 28.23: Electron drift velocity as a function of field strength for commonly used liquids.

28.11. Superconducting magnets for collider detectors

Revised September 2005 by A. Yamamoto (KEK); revised October 2001 by R.D. Kephart (FNAL)

28.11.1. Solenoid Magnets : In all cases SI unit are assumed, so that the magnetic field, B , is in Tesla, the stored energy, E , is in joules, the dimensions are in meters, and $\mu_0 = 4\pi \times 10^{-7}$.

If the coil thin, (which is the case if it is to superconducting coil), then

$$E \approx (B^2/2\mu_0)\pi R^2 L. \quad (28.38)$$

For a detector in which the calorimetry is outside the aperture of the solenoid, the coil must be thin in terms of radiation and absorption lengths. This usually means that the coil is superconducting and that the vacuum vessel encasing it is of

Table 28.10: Progress of superconducting magnets for particle physics detectors.

Experiment	Laboratory	B [T]	Radius [m]	Length [m]	Energy [MJ]	X/X_0	E/M [kJ/kg]
TOPAZ*	KEK	1.2	1.45	5.4	20	0.70	4.3
CDF	Tsukuba/Fermi	1.5	1.5	5.07	30	0.84	5.4
VENUS*	KEK	0.75	1.75	5.64	12	0.52	2.8
AMY*	KEK	3	1.29	3	40	‡	
CLEO-II	Cornell	1.5	1.55	3.8	25	2.5	3.7
ALEPH*	Saclay/CERN	1.5	2.75	7.0	130	2.0	5.5
DELPHI*	RAL/CERN	1.2	2.8	7.4	109	1.7	4.2
ZEUS*	INFN/DESY	1.8	1.5	2.85	11	0.9	5.5
H1*	RAL/DESY	1.2	2.8	5.75	120	1.8	4.8
BaBar	INFN/SLAC	1.5	1.5	3.46	27	‡	3.6
D0	Fermi	2.0	0.6	2.73	5.6	0.9	3.7
BELLE	KEK	1.5	1.8	4	42	‡	5.3
BES-III†	IHEP	1.0	1.475	3.5	9.5	‡	2.6
ATLAS-CS†	ATLAS/CERN	2.0	1.25	5.3	38	0.66	7.0
ATLAS-BT†	ATLAS/CERN	1	4.7–9.75	26	1080	(Toroid)	
ATLAS-ET†	ATLAS/CERN	1	0.825–5.35	5	2×250	(Toroid)	
CMS†	CMS/CERN	4	6	12.5	2600	‡	12

* No longer in service

† Detector under construction

‡ EM calorimeter is inside solenoid, so small X/X_0 is not a goal

The magnetic field (B) in an ideal solenoid with a flux return iron yoke, in which the magnetic field is < 2 T, is given by

$$B = \mu_0 n I \quad (28.33)$$

where n is the number of turns/meter and I is the current. In an air-core solenoid, the central field is given by

$$B(0,0) = \mu_0 n I \frac{L}{\sqrt{L^2 + 4R^2}}, \quad (28.34)$$

where L is the coil length and R is the coil radius.

In most cases, momentum analysis is made by measuring the circular trajectory of the passing particles according to $p = mv\gamma = qrB$, where p is the momentum, m the mass, q the charge, r the bending radius. The sagitta, s , of the trajectory is given by

$$s = qB\ell^2/8p, \quad (28.35)$$

where ℓ is the path length in the magnetic field. In a practical momentum measurement in colliding beam detectors, it is more effective to increase the magnetic volume than the field strength, since

$$dp/p \propto p/B\ell^2, \quad (28.36)$$

where ℓ corresponds to the solenoid coil radius R .

The energy stored in the magnetic field of any magnet is calculated by integrating B^2 over all space:

$$E = \frac{1}{2\mu_0} \int B^2 dV \quad (28.37)$$

minimum real thickness and fabricated of a material with long radiation length. There are two major contributors to the thickness of a thin solenoid:

- 1) The conductor consisting of the current-carrying superconducting material (usually NbTi/Cu) and the quench protecting stabilizer (usually aluminum) are wound on the inside of a structural support cylinder (usually aluminum also). The coil thickness scales as $B^2 R$, so the thickness in radiation lengths (X_0) is

$$t_{\text{coil}}/X_0 = (R/\sigma_h X_0)(B^2/2\mu_0), \quad (28.39)$$

where t_{coil} is the physical thickness of the coil, X_0 the average radiation length of the coil/stabilizer material, and σ_h is the hoop stress in the coil [151]. $B^2/2\mu_0$ is the magnetic pressure. In large detector solenoids, the aluminum stabilizer and support cylinders dominate the thickness; the superconductor (NbTi/Cu) contributes a smaller fraction. The coil package including the cryostat typically contributes about 2/3 of the total thickness in radiation lengths.

- 2) Another contribution to the material comes from the outer cylindrical shell of the vacuum vessel. Since this shell is susceptible to buckling collapse, its thickness is determined by the diameter, length and the modulus of the material of which it is fabricated. The outer vacuum shell represents about 1/3 of the total thickness in radiation length.

28.11.2. Properties of collider detector magnets :

The physical dimensions, central field stored energy and thickness in radiation lengths normal to the beam line of the superconducting solenoids associated with the major collider are given in Table 28.10 [150]. Fig. 28.24 shows thickness in radiation lengths as a function of B^2R in various collider detector solenoids.

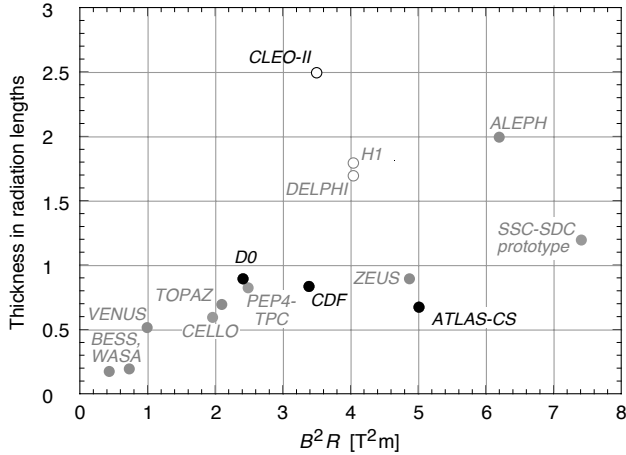


Figure 28.24: Magnet wall thickness in radiation length as a function of B^2R for various detector solenoids. Gray entries are for magnets not listed in Table 28.10. Open circles are for magnets not designed to be “thin.” The SSC-SDC prototype provided important R&D for LHC magnets.

The ratio of stored energy to cold mass (E/M) is a useful performance measure. It can also be expressed as the ratio of the stress, σ_h , to twice the equivalent density, ρ , in the coil [151]:

$$\frac{E}{M} = \frac{\int (B^2/2\mu_0)dV}{\rho V_{\text{coil}}} \approx \frac{\sigma_h}{2\rho} \quad (28.40)$$

The E/M ratio in the coil is approximately equivalent to H ,* the enthalpy of the coil, and it determines the average coil temperature rise after energy absorption in a quench:

$$E/M = H(T_2) - H(T_1) \approx H(T_2) \quad (28.41)$$

where T_2 is the average coil temperature after the full energy absorption in a quench, and T_1 is the initial temperature. E/M ratios of 5, 10, and 20 kJ/kg correspond to ~ 65 , ~ 80 , and ~ 100 K, respectively. The E/M ratios of various detector magnets are shown in Fig. 28.25 as a function of total stored energy. One would like the cold mass to be as small as possible to minimize the thickness, but temperature rise during a quench must also be minimized. An E/M ratio as large as 12 kJ/kg is designed into the CMS solenoid, with the possibility that about half of the stored energy can go to an external dump resistor. Thus the coil temperature can be kept below 80 K if the energy extraction system work well. The limit is set by the maximum temperature that the coil design can tolerate during a quench. This maximum local temperature should be <130 K (50 K + 80 K), so that thermal expansion effects in the coil are manageable.

* The enthalpy, or heat content, is called H in the thermodynamics literature. It is not to be confused with the magnetic field intensity B/μ .

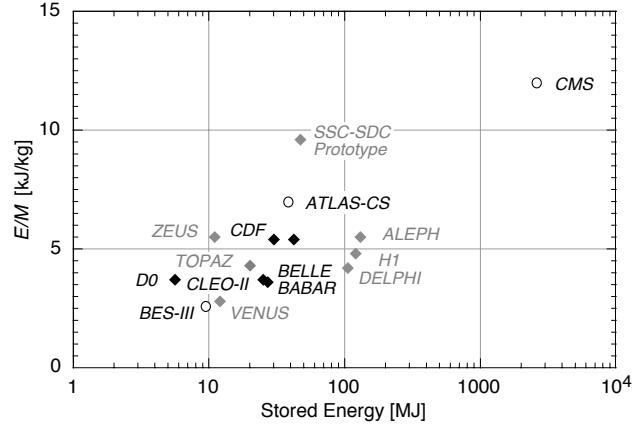


Figure 28.25: Ratio of stored energy to cold mass for thin detector solenoids. Open circles indicate magnets under construction.

28.11.3. Toroidal magnets :

Toroidal coils uniquely provide a closed magnetic field without the necessity of an iron flux-return yoke. Because no field exists at the collision point and along the beam line, there is, in principle, no effect on the beam. On the other hand, the field profile generally has $1/r$ dependence. The particle momentum may be determined by measurements of the deflection angle combined with the sagitta. The deflection (bending) power BL is

$$BL \approx \int_{R_i}^{R_0} \frac{B_i R_i dR}{R \sin \theta} = \frac{B_i R_i}{\sin \theta} \ln(R_0/R_i), \quad (28.42)$$

where R_i is the inner coil radius, R_0 is the outer coil radius, and θ is the angle between the particle trajectory and the beam line axis. The momentum resolution given by the deflection may be expressed as

$$\frac{\Delta p}{p} \propto \frac{p}{BL} \approx \frac{p \sin \theta}{B_i R_i \ln(R_0/R_i)}. \quad (28.43)$$

The momentum resolution is better in the forward/backward (smaller θ) direction. The geometry has been found to be optimal when $R_0/R_i \approx 3-4$. In practical designs, the coil is divided into 6–12 lumped coils in order to have reasonable acceptance and accessibility. This causes the coil design to be much more complex. The mechanical structure needs to sustain the decentering force between adjacent coils, and the peak field in the coil is 3–5 times higher than the useful magnetic field for the momentum analysis [149].

28.12. Measurement of particle momenta in a uniform magnetic field [152,153]

The trajectory of a particle with momentum p (in GeV/ c) and charge ze in a constant magnetic field \vec{B} is a helix, with radius of curvature R and pitch angle λ . The radius of curvature and momentum component perpendicular to \vec{B} are related by

$$p \cos \lambda = 0.3 z B R, \quad (28.44)$$

where B is in tesla and R is in meters.

The distribution of measurements of the curvature $k \equiv 1/R$ is approximately Gaussian. The curvature error for a large number of uniformly spaced measurements on the trajectory of a charged particle in a uniform magnetic field can be approximated by

$$(\delta k)^2 = (\delta k_{\text{res}})^2 + (\delta k_{\text{ms}})^2, \quad (28.45)$$

where δk = curvature error

δk_{res} = curvature error due to finite measurement resolution

δk_{ms} = curvature error due to multiple scattering.

If many (≥ 10) uniformly spaced position measurements are made along a trajectory in a uniform medium,

$$\delta k_{\text{res}} = \frac{\epsilon}{L'^2} \sqrt{\frac{720}{N+4}}, \quad (28.46)$$

where N = number of points measured along track
 L' = the projected length of the track onto the bending plane
 ϵ = measurement error for each point, perpendicular to the trajectory.

If a vertex constraint is applied at the origin of the track, the coefficient under the radical becomes 320.

For arbitrary spacing of coordinates s_i measured along the projected trajectory and with variable measurement errors ϵ_i the curvature error δk_{res} is calculated from:

$$(\delta k_{\text{res}})^2 = \frac{4}{w} \frac{V_{ss}}{V_{ss}V_{s^2s^2} - (V_{ss^2})^2}, \quad (28.47)$$

where V are covariances defined as $V_{s^m s^n} = \langle s^m s^n \rangle - \langle s^m \rangle \langle s^n \rangle$ with $\langle s^m \rangle = w^{-1} \sum (s_i^m / \epsilon_i^2)$ and $w = \sum \epsilon_i^{-2}$.

The contribution due to multiple Coulomb scattering is approximately

$$\delta k_{\text{ms}} \approx \frac{(0.016)(\text{GeV}/c)z}{Lp\beta \cos^2 \lambda} \sqrt{\frac{L}{X_0}}, \quad (28.48)$$

where p = momentum (GeV/c)
 z = charge of incident particle in units of e
 L = the total track length
 X_0 = radiation length of the scattering medium (in units of length; the X_0 defined elsewhere must be multiplied by density)
 β = the kinematic variable v/c .

More accurate approximations for multiple scattering may be found in the section on Passage of Particles Through Matter (Sec. 27 of this *Review*). The contribution to the curvature error is given approximately by $\delta k_{\text{ms}} \approx 8s_{\text{plane}}^{\text{rms}}/L^2$, where $s_{\text{plane}}^{\text{rms}}$ is defined there.

References:

1. *Experimental Techniques in High Energy Physics*, T. Ferbel (ed.) (Addison-Wesley, Menlo Park, CA, 1987).
2. C. Grupen, *Particle Detectors, Cambridge Monographs on Particle Physics, Nuclear Physics and Cosmology*, # 5, Cambridge University Press (1996).
3. K. Kleinknecht, *Detectors for Particle Radiation*, Cambridge University Press (1998).
4. G.F. Knoll, *Radiation Detection and Measurement*, 3rd edition, John Wiley & Sons, New York (1999).
5. D.R. Green, *The Physics of Particle Detectors*, Cambridge Monographs on Particle Physics, Nuclear Physics and Cosmology, # 12, Cambridge University Press (2000).
6. C. Leroy & P.-G. Rancoita, *Principles of Radiation Interaction in Matter and Detection*, (World Scientific, Singapore, 2004).
7. [Icarus Collaboration], ICARUS-TM/2001-09; LGNS-EXP 13/89 add 2-01.
8. E. Albert, *et al.*, Nucl. Instrum. Methods **A409**, 70 (1998).
9. B. Aubert, *et al.*, [BaBar Collaboration], Nucl. Instrum. Methods **A479**, 1 (2002).
10. H. Spieler, IEEE Trans. Nucl. Sci. **NS-29**, 1142 (1982).
11. K. Arisaka, Nucl. Instrum. Methods **A442**, 80 (2000).
12. Hamamatsu K.K. Electron Tube Division, *Photomultiplier Tubes: Basics and Applications*, 2nd edition (2002); Can be found under "Photomultiplier Tube Handbook" at sales.hamamatsu.com/en/products/electron-tube-division/detectors/photomultiplier-tubes-pmts.php.
13. A. Braem *et al.*, Nucl. Instrum. Methods **A518**, 574 (2004).
14. R. Arnold *et al.*, Nucl. Instrum. Methods **A314**, 465 (1992).
15. P. Mangeot *et al.*, Nucl. Instrum. Methods **A216**, 79 (1983);
R. Apsimon *et al.*, IEEE. Trans. Nucl. Sci. **33**, 122 (1986);
R. Arnold *et al.*, Nucl. Instrum. Methods **A270**, 255, 289 (1988);
D. Aston *et al.*, Nucl. Instrum. Methods **A283**, 582 (1989).
16. J. Janesick *Scientific charge-coupled devices*, SPIE Press, Bellingham, WA (2001).
17. R. Haitz *et al.*, J. Appl. Phys. **36**, 3123 (1965);
R. McIntyre, IEEE Trans. Electron Devices **13**, 164 (1966);
H. Dautet *et al.*, Applied Optics, **32**, (21), 3894 (1993);
Perkin-Elmer Optoelectronics, *Avalanche Photodiodes: A User's Guide*.
18. P. Buzhan *et al.*, Nucl. Instrum. Methods **A504**, 48 (2003);
Z. Sadygov *et al.*, Nucl. Instrum. Methods **A504**, 301 (2003);
V. Golovin and V. Saveliev, Nucl. Instrum. Methods **A518**, 560 (2004).
19. M. Landstrass *et al.*, Diam. & Rel. Matter, **2**, 1033 (1993);
R. McKeag and R. Jackman, Diam. & Rel. Matter, **7**, 513 (1998);
R. Brascia *et al.*, Phys. Stat. Sol., **199**, 113 (2003).
20. M. Petrov, M. Stapelbroek, and W. Kleinhans, Appl. Phys. Lett. **51**, 406 (1987);
M. Atac, M. Petrov, IEEE Trans. Nucl. Sci. **36** 163 (1989);
M. Atac *et al.*, Nucl. Instrum. Methods **A314**, 56 (1994).
21. J.B. Birks, *The Theory and Practice of Scintillation Counting*, (Pergamon, London, 1964).
22. D. Clark, Nucl. Instrum. Methods **117**, 295 (1974).
23. J.B. Birks, Proc. Phys. Soc. **A64**, 874 (1951).
24. B. Bengston and M. Moszynski, Nucl. Instrum. Methods **117**, 227 (1974);
J. Bialkowski, *et al.*, Nucl. Instrum. Methods **117**, 221 (1974).
25. C. P. Achenbach, "Active optical fibres in modern particle physics experiments," [arXiv:nucl-ex/0404008v1](https://arxiv.org/abs/nucl-ex/0404008v1).
26. I.B. Berlman, *Handbook of Fluorescence Spectra of Aromatic Molecules*, 2nd edition (Academic Press, New York, 1971).
27. C. Zorn, in *Instrumentation in High Energy Physics*, ed. F. Sauli, (1992, World Scientific, Singapore) pp. 218–279.
28. T. Foerster, Ann. Phys. **2**, 55 (1948).
29. J.M. Fluornoy, Conference on Radiation-Tolerant Plastic Scintillators and Detectors, K.F. Johnson and R.L. Clough editors, Rad. Phys. and Chem., **41** 389 (1993).
30. D. Horstman and U. Holm, *ibid.*, 395.
31. D. Blomker, *et al.*, Nucl. Instrum. Methods **A311**, 505 (1992);
J. Mainusch, *et al.*, Nucl. Instrum. Methods **A312**, 451 (1992).
32. Conference on Radiation-Tolerant Plastic Scintillators and Detectors, K.F. Johnson and R.L. Clough editors, Rad. Phys. and Chem., **41** (1993).
33. S.R. Borenstein and R.C. Strand, IEEE Trans. Nuc. Sci. **NS-31(1)**, 396 (1984).

34. P. Sonderegger, Nucl. Instrum. Methods **A257**, 523 (1987).
35. Achenbach, *ibid.*
36. C.M. Hawkes, *et al.*, Nucl. Instrum. Methods **A292**, 329 (1990).
37. A. Lempicki, *et al.*, Nucl. Instrum. Methods **A333**, 304 (1993);
G. Blasse, *Proceedings of the Crystal 2000 International Workshop on Heavy Scintillators for Scientific and Industrial Applications*, Chamonix, France, Sept. (1992), Edition Frontieres.
38. C. Melcher and J. Schweitzer, Nucl. Instrum. Methods **A314**, 212 (1992).
39. D.W. Cooke *et al.*, *J. Appl. Phys.* **88**, (2000) 7360 (2000);
T. Kimble, M Chou and B.H.T. Chai, in *Proc. IEEE Nuclear Science Symposium Conference* (2002).
40. K. Takagi and T. Fakazawa, *Appl. Phys. Lett.* **42**, 43 (1983).
41. J.M. Chen, R.H. Mao, L.Y. Zhang and R.Y. Zhu, *IEEE Trans. Nuc. Sci.* **NS-54(3)**, 718 (2007) and **NS-54(4)**, 1319 (2007).
42. C. Kuntner, *et al.*, Nucl. Instrum. Methods **A493**, 131 (2002).
43. R.H. Mao, L.Y. Zhang and R.Y. Zhu, presented in *The 9th International Conference on Inorganic Scintillators and their Applications*, Winston-Salem, USA, June (2007), will be published in Nucl. Instrum. Methods.
44. G. Gratta, H. Newman, and R.Y. Zhu, *Ann. Rev. Nucl. and Part. Sci.* **44**, 453 (1994).
45. R.Y. Zhu, Nucl. Instrum. Methods **A413**, 297 (1998).
46. P. Rowson, *et al.*, *Ann. Rev. Nucl. and Part. Sci.* **51**, 345 (2001).
47. A. Abashian, *et al.*, Nucl. Instrum. Methods **A479**, 117 (2002).
48. I. Adam, *et al.*, Nucl. Instrum. Methods **A538**, 281 (2005).
49. M. Shiozawa, [Super-Kamiokande Collaboration], Nucl. Instrum. Methods **A433**, 240 (1999).
50. J. Litt and R. Meunier, *Ann. Rev. Nucl. Sci.* **23**, 1 (1973).
51. D. Bartlett, *et al.*, Nucl. Instrum. Methods **A260**, 55 (1987).
52. B. Ratcliff, Nucl. Instrum. Methods **A502**, 211 (2003).
53. See the RICH Workshop series: Nucl. Instrum. Methods **A343**, 1 (1993); Nucl. Instrum. Methods **A371**, 1 (1996); Nucl. Instrum. Methods **A433**, 1 (1999); Nucl. Instrum. Methods **A502**, 1 (2003); Nucl. Instrum. Methods **A553**, 1 (2005).
54. M. Cavalli-Sforza, *et al.*, "Construction and Testing of the SLC Cherenkov Ring Imaging Detector," *IEEE* **37**, N3:1132 (1990).
55. E.G. Anassontzis, *et al.*, "Recent Results from the DELPHI Barrel Ring Imaging Cherenkov Counter," *IEEE* **38**, N2:417 (1991).
56. H. Blood, *et al.*, FERMILAB-PUB-76-051-EXP.
57. L. Sulak, HUEP-252 Presented at the Workshop on Proton Stability, Madison, Wisc. (1978).
58. K.S. Hirata, *et al.*, *Phys. Lett.* **B205**, 416 (1988).
59. S. Kasuga, *et al.*, *Phys. Lett.* **B374**, 238 (1996).
60. M.H. Ahn, *et al.*, *Phys. Rev. Lett.* **90**, 041801 (2003).
61. L. G. Christophorou, *Atomic and Molecular Radiation Physics* (Wiley, 1971);
I.B. Smirnov, Nucl. Instrum. Methods **A554**, 474 (2005);
J. Berkowitz, *Atomic and Molecular Photo Absorption* (Academic Press, 2002);
<http://pdg.lbl.gov/2007/AtomicNuclearProperties>.
62. H. Bichsel, Nucl. Instrum. Methods **A562**, 154 (2006).
63. H. Fischle *et al.*, Nucl. Instrum. Methods **A301**, 202 (1991).
64. <http://rjd.web.cern.ch/rjd/cgi-bin/cross>.
65. A. Peisert & F. Sauli, "Drift and Diffusion of Electrons in Gases," CERN 84-08 (1984).
66. S. Biagi, Nucl. Instrum. Methods **A421**, 234 (1999).
67. <http://consult.cern.ch/writeup>.
68. E. McDaniel & E. Mason, *The Mobility and Diffusion of Ions in Gases* (Wiley, 1973);
G. Shultz *et al.*, *Rev. Phys. Appl.* **12**, 67(1977).
69. G. Charpak *et al.*, Nucl. Instrum. Methods **A62**, 262 (1968).
70. G. Charpak & F. Sauli, *Ann. Rev. Nucl. Sci.* **34**, 285 (1984).
71. W. Blum & L. Rolandi, *Particle Detection with Drift Chambers* (Springer-Verlag, 1993).
72. F. Sauli, "Principles of Operation of Multiwire Proportional and Drift Chambers," in *Experimental Techniques in High Energy Physics*, T. Ferbel (ed.) (Addison-Wesley, Menlo Park, CA, 1987).
73. G. Charpak *et al.*, Nucl. Instrum. Methods **A167**, 455 (1979).
74. A.H. Walenta *et al.*, Nucl. Instrum. Methods **A92**, 373 (1971).
75. A. Breskin *et al.*, Nucl. Instrum. Methods **A124**, 189 (1975).
76. R. Bouclier *et al.*, Nucl. Instrum. Methods **A265**, 78 (1988).
77. H. Drumm *et al.*, Nucl. Instrum. Methods **A176**, 333 (1980).
78. D.R. Nygren & J.N. Marx, *Phys. Today* 31 Vol. 10 (1978).
79. <http://www.ansoft.com>.
80. P. Beringer *et al.*, Nucl. Instrum. Methods **A254**, 542 (1987).
81. J. Virdee, *Phys. Rep.* 403-404,401(2004).
82. H. Walenta, *Phys. Scripta* **23**, 354 (1981).
83. M. Aleksa *et al.*, Nucl. Instrum. Methods **A446**, 435 (2000).
84. J. Va'vra, Nucl. Instrum. Methods **A515**, 1 (2003);
M. Titov, "Radiation damage and long-term aging in gas detectors," arXiv: [physics/0403055](https://arxiv.org/abs/physics/0403055).
85. A. Oed, Nucl. Instrum. Methods **A263**, 351 (1988).
86. F. Sauli, Nucl. Instrum. Methods **A386**, 531 (1997).
87. Y. Giomataris, *et al.*, Nucl. Instrum. Methods **A376**, 29 (1996).
88. F. Sauli and A. Sharma, *Ann. Rev. Nucl. Part. Sci.* **49**, 341 (1999).
89. Y. Bagaturia, *et al.*, Nucl. Instrum. Methods **A490**, 223 (2002).
90. F. Sauli, <http://gdd.web.cern.ch/GDD/>.
91. J. Derre, *et al.*, Nucl. Instrum. Methods **A459**, 523 (2001).
92. I. Giomataris, *et al.*, Nucl. Instrum. Methods **A560**, 405 (2006).
93. R. Bellazzini, *et al.*, Nucl. Instrum. Methods **A535**, 477 (2004).
94. M. Campbell, *et al.*, Nucl. Instrum. Methods **A540**, 295 (2005).
95. A. Bamberger, *et al.*, Nucl. Instrum. Methods **A573**, 361 (2007).
96. M. Titov, [physics/0403055](https://arxiv.org/abs/physics/0403055); *Proc. of the 42nd Workshop of the INFN ELOISATRON Project*, "Innovative Detectors For Super-Colliders," Erice, Italy, Sept. 28–Oct. 4 (2003).
97. P. Colas *et al.*, Nucl. Instrum. Methods **A535**, 506 (2004);
M. Campbell *et al.*, Nucl. Instrum. Methods **A540**, 295 (2005).
98. H. Aihara *et al.*, *IEEE Trans. NS30*, 63 (1983).

99. C.J. Martoff *et al.*, Nucl. Instrum. Methods **A440**, 355 (2000).
100. X. Artru *et al.*, Phys. Rev. **D12**, 1289 (1975).
101. G.M. Garibian *et al.*, Nucl. Instrum. Methods **125**, 133 (1975).
102. B. Dolgoshein, Nucl. Instrum. Methods **A326**, 434 (1993).
103. G. Bassompierre *et al.*, Nucl. Instrum. Methods **411**, 63 (1998).
104. A. Andronic, ALICE, Nucl. Instrum. Methods **A522**, 40 (2004).
105. T. Akesson *et al.*, ATLAS, Nucl. Instrum. Methods **A412**, 200 (1998).
106. M. Ambriola *et al.*, PAMELA, Nucl. Instrum. Methods **A522**, 77 (2004).
107. Ph. V. Doetinchem *et al.*, AMS, Nucl. Instrum. Methods **A558**, 526 (2006).
108. M. Brigida *et al.*, Nucl. Instrum. Methods **A572**, 440 (2007).
109. M.L. Cherry and G.L. Case, Nucl. Instrum. Methods **A522**, 73 (2004).
110. D. Müller *et al.*, Nucl. Instrum. Methods **A522**, 9 (2004).
111. R. Santonico and R. Cardarelli, Nucl. Instrum. Methods **A187**, 377 (1981).
112. V. V. Parkhomchuck, Yu. N. Pestov, & N. V. Petrovykh, Nucl. Instrum. Methods **93**, 269 (1971).
113. E. Cerron Zeballos *et al.*, Nucl. Instrum. Methods **A374**, 132 (1996).
114. V. Ammosov *et al.*, Nucl. Instrum. Methods **A578**, 119 (2007).
115. P. Fonte, IEEE. Trans. Nucl. Sci. **49**, 881 (2002).
116. M. Abbrescia *et al.*, Nucl. Instrum. Methods **A394**, 13 (1997).
117. F. Anulli *et al.*, Nucl. Instrum. Methods **A552**, 276 (2005).
118. H. Spieler, *Semiconductor Detector Systems*, Oxford Univ. Press, Oxford (2005) ISBN 0-19-852784-5.
119. F. Scholze *et al.*, Nucl. Instrum. Methods **A439**, 208 (2000).
120. G. Lindström *et al.*, Nucl. Instrum. Methods **A465**, 60 (2001).
121. C. Da Via *et al.*, Nucl. Instrum. Methods **A509**, 86 (2003).
122. G. Kramberger *et al.*, Nucl. Instrum. Methods **A481**, 297 (2002).
123. O. Krasel *et al.*, IEEE Trans. Nucl. Sci. **NS-51/6**, 3055 (2004).
124. G. Lindström *et al.*, Nucl. Instrum. Methods **A426**, 1 (1999).
125. A. Holmes-Siedle and L. Adams, *Handbook of Radiation Effects*, 2nd ed., Oxford 2002, ISBN 0-19-850733-X, QC474.H59 2001.
126. V. Radeka, IEEE Trans. Nucl. Sci. **NS-15/3**, 455 (1968); V. Radeka, IEEE Trans. Nucl. Sci. **NS-21**, 51 (1974).
127. F.S. Goulding, Nucl. Instrum. Methods **100**, 493 (1972); F.S. Goulding and D.A. Landis, IEEE Trans. Nucl. Sci. **NS-29**, 1125 (1982).
128. W.R. Nelson, H. Hirayama, and D.W.O. Rogers, "The EGS4 Code System," SLAC-265, Stanford Linear Accelerator Center (Dec. 1985).
129. R. Brun *et al.*, *GEANT3*, CERN DD/EE/84-1 (1987).
130. D. Hitlin *et al.*, Nucl. Instrum. Methods **137**, 225 (1976). See also W. J. Willis and V. Radeka, Nucl. Instrum. Methods **120**, 221 (1974), for a more detailed discussion.
131. R. Wigmans, *Calorimetry: Energy Measurement in Particle Physics*, International Series of Monographs on Physics, vol. 107, Clarendon, Oxford (2000).
132. ATLAS Collaboration, *The ATLAS Liquid Argon Calorimeter Technical Design Report*, CERN/LHCC 96-41 (1996).
133. CMS Collaboration, *The CMS Electromagnetic Calorimeter Technical Design Report*, CERN/LHCC 97-33 (1997).
134. N. Akchurin, *et al.*, Nucl. Instrum. Methods **A399**, 202 (1997).
135. T.A. Gabriel *et al.*, Nucl. Instrum. Methods **A338**, 336-347 (1994).
136. D.E. Groom, Nucl. Instrum. Methods **A572**, 633-653 (2007); Erratum to be published: see [arXiv:physics/0605164v4](https://arxiv.org/abs/physics/0605164v4).
137. N. Akchurin, *et al.*, Nucl. Instrum. Methods **A408**, 380 (1998).
138. C.W. Fabjan *et al.*, Nucl. Instrum. Methods **141**, 61 (1977).
139. C. Leroy, J. Sirois, and R. Wigmans, Nucl. Instrum. Methods **A252**, 4 (1986).
140. J.E. Brau and T.A. Gabriel, Nucl. Instrum. Methods **A238**, 489 (1985); H. Brückmann and H. Kowalski, ZEUS Int. Note 86/026 DESY, Hamburg (1986); R. Wigmans, Nucl. Instrum. Methods **A259**, 389 (1987); R. Wigmans, Nucl. Instrum. Methods **A265**, 273 (1988).
141. P. Mockett, "A review of the physics and technology of high-energy calorimeter devices," *Proc. 11th SLAC Summer Inst. Part. Phys.*, July 1983, SLAC Report No. 267 (July 1983), p. 42, www.slac.stanford.edu/pubs/confproc/ssi83/ssi83-008.html.
142. R. Wigmans, "Quartz Fibers and the Prospects for Hadron Calorimetry at the 1% Resolution Level," *Proc. 7th Inter. Conf. on Calorimetry in High Energy Physics*, Tucson, AZ, Nov. 9-14, 1997, eds. E. Cheu, T. Embry, J. Rutherford, R. Wigmans (World Scientific, River Edge, NJ, 1998), p. 182; N. Akchurin *et al.*, Nucl. Instrum. Methods **A537**, 537 (2005).
143. D. Bintinger, in *Proceedings of the Workshop on Calorimetry for the Supercollider*, Tuscaloosa, AL, March 13-17, 1989, edited by R. Donaldson and M.G.D. Gilchriese (World Scientific, Teaneck, NJ, 1989), p. 91; R.K. Bock, T. Hansl-Kozanecka, and T.P. Shah, Nucl. Instrum. Methods **186**, 533 (1981); Y.A. Kulchitsky and V.B. Vinogradov, Nucl. Instrum. Methods **A455**, 499 (2000).
144. M. Simonyan *et al.*, ATL-TILECAL-PUB-2007-008 and Nucl. Instrum. Methods **A**, to be submitted.
145. D. Acosta *et al.*, Nucl. Instrum. Methods **A316**, 184 (1997).
146. E. Shibamura *et al.*, Nucl. Instrum. Methods **131**, 249 (1975).
147. A.O. Allen, "Drift Mobilities and Conduction Band Energies of Excess Electrons in Dielectric Liquids," NSRDS-NBS-58 (1976).
148. W. Walkowiak, Nucl. Instrum. Methods **A449**, 288 (2000).
149. T. Taylor, Phys. Scr. **23**, 459 (1980).
150. A. Yamamoto, Nucl. Instr. Meth. **A494**, 255 (2003).
151. A. Yamamoto, Nucl. Instr. Meth. **A453**, 445 (2000).
152. R.L. Gluckstern, Nucl. Instrum. Methods **24**, 381 (1963).
153. V. Karimäki, Nucl. Instrum. Methods **A410**, 284 (1998).

29. RADIOACTIVITY AND RADIATION PROTECTION

Revised Sept. 2007 by S. Roesler (CERN) and J.C. Liu (SLAC).

29.1. Definitions

The International Commission on Radiation Units and Measurements (ICRU) recommends the use of SI units. Therefore we list SI units first, followed by cgs (or other common) units in parentheses, where they differ.

- **Activity** (unit: Becquerel):

1 Bq = 1 disintegration per second (= 27 pCi).

- **Absorbed dose** (unit: Gray): The absorbed dose is the energy imparted by ionizing radiation in a volume element of a specified material divided by the mass of this volume element.

1 Gy = 1 J/kg (= 10^4 erg/g = 100 rad)
= 6.24×10^{12} MeV/kg deposited energy.

- **Kerma** (unit: Gray): Kerma is the sum of the initial kinetic energies of all charged particles liberated by indirectly ionizing particles in a volume element of the specified material divided by the mass of this volume element.

- **Exposure** (unit: C/kg of air [= 3880 Roentgen[†]]): The exposure is a measure of photon fluence at a certain point in space integrated over time, in terms of ion charge of either sign produced by secondary electrons in a small volume of air about the point. Implicit in the definition is the assumption that the small test volume is embedded in a sufficiently large uniformly irradiated volume that the number of secondary electrons entering the volume equals the number leaving (so-called charged particle equilibrium).

- **Equivalent dose** (unit: Sievert [= 100 rem (roentgen equivalent in man)]): The equivalent dose H_T in an organ or tissue T is equal to the sum of the absorbed doses $D_{T,R}$ in the organ or tissue caused by different radiation types R weighted with so-called radiation weighting factors w_R :

$$H_T = \sum_R w_R \times D_{T,R} . \quad (29.1)$$

It expresses long-term risks (primarily cancer and leukemia) from low-level chronic exposure. The values for w_R recommended recently by ICRP [1] are given in the following table:

Table 29.1: Radiation weighting factors, w_R .

Radiation type	w_R
Photons	1
Electrons and muons	1
Neutrons, $E_n < 1$ MeV	$2.5 + 18.2 \times \exp[-(\ln E_n)^2/6]$
1 MeV $\leq E_n \leq 50$ MeV	$5.0 + 17.0 \times \exp[-(\ln(2E_n))^2/6]$
$E_n > 50$ MeV	$2.5 + 3.25 \times \exp[-(\ln(0.04E_n))^2/6]$
Protons and charged pions	2
Alpha particles, fission fragments, heavy ions	20

- **Effective dose** (unit: Sievert): The sum of the equivalent doses, weighted by the tissue weighting factors w_T ($\sum_T w_T = 1$) of several organs and tissues T of the body that are considered to be most sensitive [2], is called “effective dose” E :

$$E = \sum_T w_T \times H_T . \quad (29.2)$$

[†] This unit is somewhat historical, but appears on some measuring instruments. One R is the amount of radiation required to liberate positive and negative charges of one electrostatic unit of charge in 1 cm³ of air at standard temperature and pressure (STP)

29.2. Radiation levels [3]

- **Natural annual background**, all sources: Most world areas, whole-body equivalent dose rate $\approx (0.4\text{--}4)$ mSv (40–400 mrem). Can range up to 50 mSv (5 rem) in certain areas. U.S. average ≈ 3.6 mSv, including ≈ 2 mSv (≈ 200 mrem) from inhaled natural radioactivity, mostly radon and radon daughters. (Average is for a typical house and varies by more than an order of magnitude. It can be more than two orders of magnitude higher in poorly ventilated mines. 0.1–0.2 mSv in open areas.)

- **Cosmic ray background** (sea level, mostly muons): $\sim 1 \text{ min}^{-1} \text{ cm}^{-2} \text{ sr}^{-1}$. For more accurate estimates and details, see the Cosmic Rays section (Sec. 24 of this *Review*).

- **Fluence** (per cm²) to deposit one Gy, assuming uniform irradiation: \approx (**charged particles**) $6.24 \times 10^9 / (dE/dx)$, where dE/dx (MeV g⁻¹ cm²), the energy loss per unit length, may be obtained from Figs. 27.3 and 27.4 in Sec. 27 of this *Review*, and pdg.lbl.gov/AtomicNuclearProperties.

$\approx 3.5 \times 10^9 \text{ cm}^{-2}$ minimum-ionizing singly-charged particles in carbon.

\approx (**photons**) $6.24 \times 10^9 / [Ef/\ell]$, for photons of energy E (MeV), attenuation length ℓ (g cm⁻²), and fraction $f \lesssim 1$ expressing the fraction of the photon’s energy deposited in a small volume of thickness $\ll \ell$ but large enough to contain the secondary electrons.

$\approx 2 \times 10^{11} \text{ photons cm}^{-2}$ for 1 MeV photons on carbon ($f \approx 1/2$).

- **Recommended limits of effective dose to radiation workers (whole-body dose):***

EU/Switzerland: 20 mSv yr⁻¹

U.S.: 50 mSv yr⁻¹ (5 rem yr⁻¹)[†]

- **Lethal dose:** The whole-body dose from penetrating ionizing radiation resulting in 50% mortality in 30 days (assuming no medical treatment) is 2.5–4.5 Gy (250–450 rad), as measured internally on body longitudinal center line. Surface dose varies due to variable body attenuation and may be a strong function of energy.

- **Cancer induction by low LET radiation:** The cancer induction probability is about 5% per Sv on average for the entire population [2].

29.3. Prompt neutrons at accelerators

Neutrons dominate the particle environment outside thick shielding (*e.g.*, > 1 m of concrete) for high energy ($>$ a few hundred MeV) electron and hadron accelerators.

29.3.1. Electron beams : At electron accelerators, neutrons are generated via photonuclear reactions from bremsstrahlung photons. Neutron yields from semi-infinite targets per unit electron beam power are plotted in Fig. 29.1 as a function of electron beam energy [4]. In the photon energy range 10–30 MeV, neutron production results from the giant photonuclear resonance mechanism. Neutrons are produced roughly isotropically (within a factor of 2) and with a Maxwellian energy distribution described as:

$$\frac{dN}{dE_n} = \frac{E_n}{T^2} e^{-E_n/T} , \quad (29.3)$$

where T is the nuclear temperature characteristic of the target nucleus, generally in the range of $T = 0.5\text{--}1.0$ MeV. For higher energy photons, the quasi-deuteron and photo-pion production mechanisms become important.

29.3.2. Proton beams : At proton accelerators, neutron yields emitted per incident proton by different target materials are roughly independent [5] of proton energy between 20 MeV and 1 GeV, and are given by the ratio C:Al:Cu:Fe:Sn:Ta:Pb = 0.3 : 0.6 : 1.0 : 1.5 : 1.7. Above 1 GeV, the neutron yield [6] is proportional to E^m , where $0.80 \leq m \leq 0.85$.

A typical neutron spectrum [7] outside a proton accelerator concrete shield is shown in Fig. 29.2. The shape of these spectra are generally characterized as having a low-energy evaporation peak around 1 – 2 MeV, and a high-energy spallation shoulder at around 70 – 80 MeV.

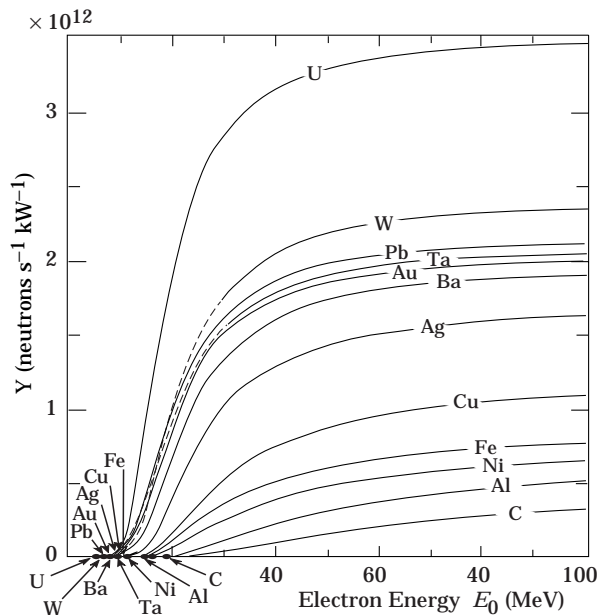


Figure 29.1: Neutron yields from semi-infinite targets, per kW of electron beam power, as a function of electron beam energy, disregarding target self-shielding.

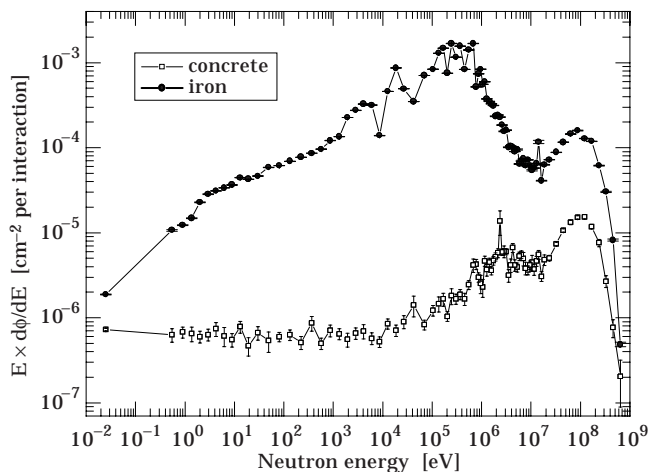


Figure 29.2: Calculated neutron spectrum from 205 GeV/c hadrons (2/3 protons and 1/3 π⁺) on a thick copper target [7]. Spectra are evaluated at 90° to beam and through 80 cm of normal density concrete or 40 cm of iron.

The neutron-attenuation length, is shown in Fig. 29.3 for concrete and mono-energetic broad-beam conditions.

Letaw’s [8] formula for the energy-dependence of the inelastic proton cross-section for $E < 2$ GeV is:

$$\sigma(E) = \sigma_{\text{asympt}} \left[1 - 0.62e^{-E/200} \sin(10.9E^{-0.28}) \right], \quad (29.4)$$

and for $E > 2$ GeV:

$$\sigma_{\text{asympt}} = 45A^{0.7} [1 + 0.016 \sin(5.3 - 2.63 \ln A)], \quad (29.5)$$

where σ is in mb, E is the proton energy in MeV and A is the mass number.

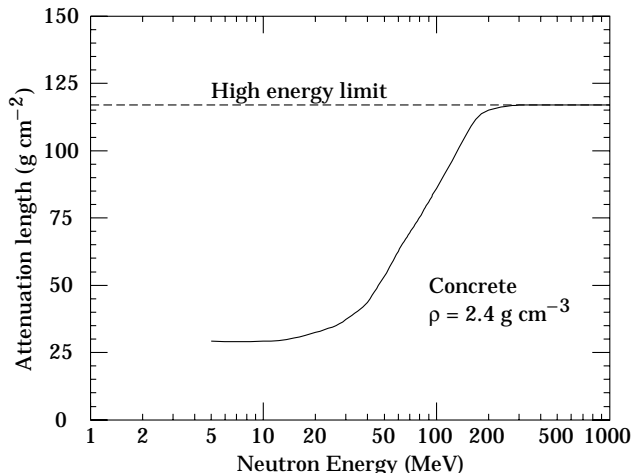


Figure 29.3: The variation of the attenuation length for mono-energetic neutrons in concrete as a function of neutron energy [5].

29.4. Dose conversion factors

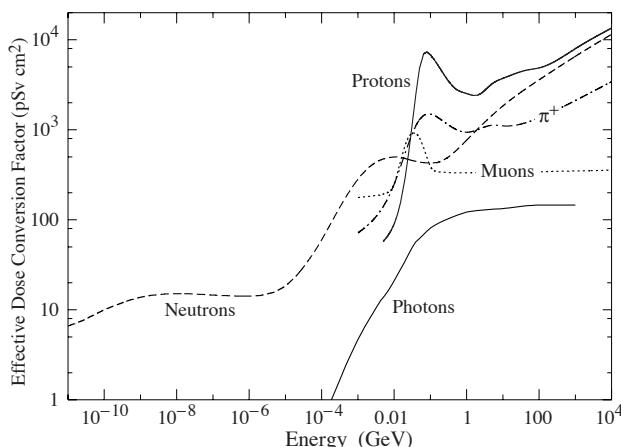


Figure 29.4: Fluence to effective dose conversion factors for anterior-posterior irradiation and various particles [9].

Conversion coefficients from fluence to effective dose are given for anterior-posterior irradiation and various particles in Fig. 29.4 [9]. These factors can be used for converting particle fluence to dose for personnel protection purposes. For example, the effective dose from an anterior-posterior irradiation in a field of 1-MeV neutrons with a fluence of 1 neutron / cm² is about 290 pSv.

29.5. Accelerator-induced activity

The dose rate at 1 m due to spallation-induced activity by high energy hadrons in a 1 g medium atomic weight target can be estimated [10] from the following expression:

$$D = D_0 \Phi \ln[(T + t)/t], \quad (29.6)$$

where T is the irradiation time, t is the decay time since irradiation, Φ is the flux of irradiating hadrons (hadrons cm⁻² s⁻¹), and D_0 has a value of 5.2×10^{-17} [(Sv hr⁻¹)/(hadron cm⁻² s⁻¹)]. This relation is essentially independent of hadron energy above 200 MeV.

Dose due to accelerator-produced induced activity can also be estimated with the use of “ ω factors” [5]. These factors give the dose rate per unit star density (inelastic reaction for $E > 50$ MeV) after a 30-day irradiation and 1-day decay. The ω factor for steel or iron is $\approx 3 \times 10^{-12}$ (Sv cm³/star). This does not include possible contributions from thermal-neutron activation. Induced activity

in concrete can vary widely depending on concrete composition, particularly with the concentration of trace quantities such as sodium. Additional information can be found in Barbier [11].

29.6. Photon sources

The dose rate in air from a gamma point source of C Curies emitting one photon of energy $0.07 < E < 4$ MeV per disintegration at a distance of 30 cm is about $6CE$ (rem/hr), or $60CE$ (mSv/hr), $\pm 20\%$. In general, the dependence of the dose rate from a point source on the distance r follows a $1/r^2$ behaviour

$$D(r) = \frac{D(r_0)}{(r/r_0)^2}. \quad (29.7)$$

The dose rate in air from a semi-infinite uniform photon source of specific activity C ($\mu\text{Ci/g}$) and gamma energy E (MeV) is about $1.07CE$ (rem/hr), or $10.7CE$ (mSv/hr).

Footnotes:

* The ICRP recommendation [2] is 20 mSv yr^{-1} averaged over 5 years, with the dose in any one year $\leq 50 \text{ mSv}$.

† Many laboratories in the U.S. and elsewhere set lower limits.

References:

1. *Recommendation of the International Commission on Radiological Protection*, (2007), (in press).
2. ICRP Publication 60, *1990 Recommendation of the International Commission on Radiological Protection*, Pergamon Press (1991).
3. See E. Pochin, *Nuclear Radiation: Risks and Benefits*, Clarendon Press, Oxford, 1983.
4. W.P. Swanson, *Radiological Safety Aspects of the operation of Electron Linear Accelerators*, IAEA Technical Reports Series No. 188 (1979).
5. R.H. Thomas and G.R. Stevenson, *Radiological Safety Aspects of the Operation of Proton Accelerators*, IAEA Technical Report Series No. 283 (1988).
6. T.A. Gabriel *et al.*, Nucl. Instrum. Methods **A338**, 336 (1994).
7. C. Birattari *et al.*, Nucl. Instrum. Methods **A338**, 534 (1994).
8. J.R. Letaw, R. Silberberg, and C.H. Tsao, *Astrophysical Journal Supplement Series*, **51**, 271 (1983);
For improvements to this formula see Shen Qing-bang, "Systematics of intermediate energy proton nonelastic and neutron total cross section," International Nuclear Data Committee INDC(CPR)-020 (July 1991).
9. M. Pelliccioni, "Overview of fluence-to-effective dose and fluence-to-ambient dose equivalent conversion coefficients for high energy radiation calculated using the FLUKA code," Radiation Protection Dosimetry **88**, 279 (2000).
10. A.H. Sullivan *A Guide To Radiation and Radioactivity Levels Near High Energy Particle Accelerators*, Nuclear Technology Publishing, Ashford, Kent, England (1992).
11. M. Barbier, *Induced Activity*, North-Holland, Amsterdam (1969).

30. COMMONLY USED RADIOACTIVE SOURCES

Table 30.1. Revised November 1993 by E. Browne (LBNL).

Nuclide	Half-life	Particle			Photon	
		Type of decay	Energy (MeV)	Emission prob.	Energy (MeV)	Emission prob.
$^{22}_{11}\text{Na}$	2.603 y	β^+ , EC	0.545	90%	0.511 Annih. 1.275 100%	
$^{54}_{25}\text{Mn}$	0.855 y	EC			0.835 100% Cr K x rays 26%	
$^{55}_{26}\text{Fe}$	2.73 y	EC			Mn K x rays: 0.00590 24.4% 0.00649 2.86%	
$^{57}_{27}\text{Co}$	0.744 y	EC			0.014 9% 0.122 86% 0.136 11% Fe K x rays 58%	
$^{60}_{27}\text{Co}$	5.271 y	β^-	0.316	100%	1.173 100% 1.333 100%	
$^{68}_{32}\text{Ge}$	0.742 y	EC			Ga K x rays 44%	

$\rightarrow ^{68}_{31}\text{Ga}$		β^+ , EC	1.899	90%	0.511 Annih. 1.077 3%	
$^{90}_{38}\text{Sr}$	28.5 y	β^-	0.546	100%		

$\rightarrow ^{90}_{39}\text{Y}$		β^-	2.283	100%		
$^{106}_{44}\text{Ru}$	1.020 y	β^-	0.039	100%		

$\rightarrow ^{106}_{45}\text{Rh}$		β^-	3.541	79%	0.512 21% 0.622 10%	
$^{109}_{48}\text{Cd}$	1.267 y	EC	0.063 e^- 0.084 e^- 0.087 e^-	41% 45% 9%	0.088 3.6% Ag K x rays 100%	
$^{113}_{50}\text{Sn}$	0.315 y	EC	0.364 e^- 0.388 e^-	29% 6%	0.392 65% In K x rays 97%	
$^{137}_{55}\text{Cs}$	30.2 y	β^-	0.514 1.176	94% 6%	0.662 85%	
$^{133}_{56}\text{Ba}$	10.54 y	EC	0.045 e^- 0.075 e^-	50% 6%	0.081 34% 0.356 62% Cs K x rays 121%	
$^{207}_{83}\text{Bi}$	31.8 y	EC	0.481 e^- 0.975 e^- 1.047 e^-	2% 7% 2%	0.569 98% 1.063 75% 1.770 7% Pb K x rays 78%	
$^{228}_{90}\text{Th}$	1.912 y	6α : $3\beta^-$:	5.341 to 8.785 0.334 to 2.246		0.239 44% 0.583 31% 2.614 36%	

$(\rightarrow ^{224}_{88}\text{Ra} \rightarrow ^{220}_{86}\text{Rn} \rightarrow ^{216}_{84}\text{Po} \rightarrow ^{212}_{82}\text{Pb} \rightarrow ^{212}_{83}\text{Bi} \rightarrow ^{212}_{84}\text{Po})$						
$^{241}_{95}\text{Am}$	432.7 y	α	5.443 5.486	13% 85%	0.060 36% Np L x rays 38%	
$^{241}\text{Am/Be}$	432.2 y	6×10^{-5} neutrons (4–8 MeV) and 4×10^{-5} γ 's (4.43 MeV) per Am decay				
$^{244}_{96}\text{Cm}$	18.11 y	α	5.763 5.805	24% 76%	Pu L x rays \sim 9%	
$^{252}_{98}\text{Cf}$	2.645 y	α (97%) Fission (3.1%)	6.076 6.118	15% 82%		

≈ 20 γ 's/fission; 80% < 1 MeV ≈ 4 neutrons/fission; $\langle E_n \rangle = 2.14$ MeV						

“Emission probability” is the probability per decay of a given emission; because of cascades these may total more than 100%. Only principal emissions are listed. EC means electron capture, and e^- means monoenergetic internal conversion (Auger) electron. The intensity of 0.511 MeV e^+e^- annihilation photons depends upon the number of stopped positrons. Endpoint β^\pm energies are listed. In some cases when energies are closely spaced, the γ -ray values are approximate weighted averages. Radiation from short-lived daughter isotopes is included where relevant.

Half-lives, energies, and intensities are from E. Browne and R.B. Firestone, *Table of Radioactive Isotopes* (John Wiley & Sons, New York, 1986), recent *Nuclear Data Sheets*, and *X-ray and Gamma-ray Standards for Detector Calibration*, IAEA-TECDOC-619 (1991).

Neutron data are from *Neutron Sources for Basic Physics and Applications* (Pergamon Press, 1983).

31. PROBABILITY

Revised September 2007 by G. Cowan (RHUL).

31.1. General [1–8]

An abstract definition of probability can be given by considering a set S , called the sample space, and possible subsets A, B, \dots , the interpretation of which is left open. The probability P is a real-valued function defined by the following axioms due to Kolmogorov [9]:

1. For every subset A in S , $P(A) \geq 0$;
2. For disjoint subsets (*i.e.*, $A \cap B = \emptyset$), $P(A \cup B) = P(A) + P(B)$;
3. $P(S) = 1$.

In addition, one defines the conditional probability $P(A|B)$ (read P of A given B) as

$$P(A|B) = \frac{P(A \cap B)}{P(B)}. \quad (31.1)$$

From this definition and using the fact that $A \cap B$ and $B \cap A$ are the same, one obtains *Bayes' theorem*,

$$P(A|B) = \frac{P(B|A)P(A)}{P(B)}. \quad (31.2)$$

From the three axioms of probability and the definition of conditional probability, one obtains the *law of total probability*,

$$P(B) = \sum_i P(B|A_i)P(A_i), \quad (31.3)$$

for any subset B and for disjoint A_i with $\cup_i A_i = S$. This can be combined with Bayes' theorem (Eq. (31.2)) to give

$$P(A|B) = \frac{P(B|A)P(A)}{\sum_i P(B|A_i)P(A_i)}, \quad (31.4)$$

where the subset A could, for example, be one of the A_i .

The most commonly used interpretation of the subsets of the sample space are outcomes of a repeatable experiment. The probability $P(A)$ is assigned a value equal to the limiting frequency of occurrence of A . This interpretation forms the basis of *frequentist statistics*.

The subsets of the sample space can also be interpreted as *hypotheses*, *i.e.*, statements that are either true or false, such as ‘The mass of the W boson lies between 80.3 and 80.5 GeV.’ In the frequency interpretation, such statements are either always or never true, *i.e.*, the corresponding probabilities would be 0 or 1. Using *subjective probability*, however, $P(A)$ is interpreted as the degree of belief that the hypothesis A is true. Subjective probability is used in *Bayesian* (as opposed to frequentist) statistics. Bayes' theorem can be written

$$P(\text{theory}|\text{data}) \propto P(\text{data}|\text{theory})P(\text{theory}), \quad (31.5)$$

where ‘theory’ represents some hypothesis and ‘data’ is the outcome of the experiment. Here $P(\text{theory})$ is the *prior* probability for the theory, which reflects the experimenter's degree of belief before carrying out the measurement, and $P(\text{data}|\text{theory})$ is the probability to have gotten the data actually obtained, given the theory, which is also called the *likelihood*.

Bayesian statistics provides no fundamental rule for obtaining the prior probability; this is necessarily subjective and may depend on previous measurements, theoretical prejudices, *etc.* Once this has been specified, however, Eq. (31.5) tells how the probability for the theory must be modified in the light of the new data to give the *posterior* probability, $P(\text{theory}|\text{data})$. As Eq. (31.5) is stated as a proportionality, the probability must be normalized by summing (or integrating) over all possible hypotheses.

31.2. Random variables

A *random variable* is a numerical characteristic assigned to an element of the sample space. In the frequency interpretation of probability, it corresponds to an outcome of a repeatable experiment. Let x be a possible outcome of an observation. If x can take on any value from a continuous range, we write $f(x;\theta)dx$ as the probability that the measurement's outcome lies between x and $x + dx$. The function $f(x;\theta)$ is called the *probability density function* (p.d.f.), which may depend on one or more parameters θ . If x can take on only discrete values (*e.g.*, the non-negative integers), then $f(x;\theta)$ is itself a probability.

The p.d.f. is always normalized to unit area (unit sum, if discrete). Both x and θ may have multiple components and are then often written as vectors. If θ is unknown, we may wish to estimate its value from a given set of measurements of x ; this is a central topic of *statistics* (see Sec. 32).

The *cumulative distribution function* $F(a)$ is the probability that $x \leq a$:

$$F(a) = \int_{-\infty}^a f(x) dx. \quad (31.6)$$

Here and below, if x is discrete-valued, the integral is replaced by a sum. The endpoint a is expressly included in the integral or sum. Then $0 \leq F(x) \leq 1$, $F(x)$ is nondecreasing, and $P(a < x \leq b) = F(b) - F(a)$. If x is discrete, $F(x)$ is flat except at allowed values of x , where it has discontinuous jumps equal to $f(x)$.

Any function of random variables is itself a random variable, with (in general) a different p.d.f. The *expectation value* of any function $u(x)$ is

$$E[u(x)] = \int_{-\infty}^{\infty} u(x) f(x) dx, \quad (31.7)$$

assuming the integral is finite. For $u(x)$ and $v(x)$, any two functions of x , $E[u+v] = E[u] + E[v]$. For c and k constants, $E[cu+k] = cE[u] + k$.

The n^{th} moment of a random variable is

$$\alpha_n \equiv E[x^n] = \int_{-\infty}^{\infty} x^n f(x) dx, \quad (31.8a)$$

and the n^{th} central moment of x (or moment about the mean, α_1) is

$$m_n \equiv E[(x - \alpha_1)^n] = \int_{-\infty}^{\infty} (x - \alpha_1)^n f(x) dx. \quad (31.8b)$$

The most commonly used moments are the mean μ and variance σ^2 :

$$\mu \equiv \alpha_1, \quad (31.9a)$$

$$\sigma^2 \equiv V[x] \equiv m_2 = \alpha_2 - \mu^2. \quad (31.9b)$$

The mean is the location of the ‘center of mass’ of the p.d.f., and the variance is a measure of the square of its width. Note that $V[cx+k] = c^2V[x]$. It is often convenient to use the *standard deviation* of x , σ , defined as the square root of the variance.

Any odd moment about the mean is a measure of the skewness of the p.d.f. The simplest of these is the dimensionless coefficient of skewness $\gamma_1 = m_3/\sigma^3$.

The fourth central moment m_4 provides a convenient measure of the tails of a distribution. For the Gaussian distribution (see Sec. 31.4), one has $m_4 = 3\sigma^4$. The *kurtosis* is defined as $\gamma_2 = m_4/\sigma^4 - 3$, *i.e.*, it is zero for a Gaussian, positive for a *leptokurtic* distribution with longer tails, and negative for a *platykurtic* distribution with tails that die off more quickly than those of a Gaussian.

Besides the mean, another useful indicator of the “middle” of the probability distribution is the *median*, x_{med} , defined by $F(x_{\text{med}}) = 1/2$, i.e., half the probability lies above and half lies below x_{med} . (More rigorously, x_{med} is a median if $P(x \geq x_{\text{med}}) \geq 1/2$ and $P(x \leq x_{\text{med}}) \geq 1/2$. If only one value exists, it is called ‘the median.’)

Let x and y be two random variables with a *joint* p.d.f. $f(x, y)$. The *marginal* p.d.f. of x (the distribution of x with y unobserved) is

$$f_1(x) = \int_{-\infty}^{\infty} f(x, y) dy, \tag{31.10}$$

and similarly for the marginal p.d.f. $f_2(y)$. The *conditional* p.d.f. of y given fixed x (with $f_1(x) \neq 0$) is defined by $f_3(y|x) = f(x, y)/f_1(x)$, and similarly $f_4(x|y) = f(x, y)/f_2(y)$. From these, we immediately obtain Bayes’ theorem (see Eqs. (31.2) and (31.4)),

$$f_4(x|y) = \frac{f_3(y|x)f_1(x)}{f_2(y)} = \frac{f_3(y|x)f_1(x)}{\int f_3(y|x')f_1(x') dx'}. \tag{31.11}$$

The mean of x is

$$\mu_x = \int_{-\infty}^{\infty} \int_{-\infty}^{\infty} x f(x, y) dx dy = \int_{-\infty}^{\infty} x f_1(x) dx, \tag{31.12}$$

and similarly for y . The *covariance* of x and y is

$$\text{cov}[x, y] = E[(x - \mu_x)(y - \mu_y)] = E[xy] - \mu_x \mu_y. \tag{31.13}$$

A dimensionless measure of the covariance of x and y is given by the *correlation coefficient*,

$$\rho_{xy} = \text{cov}[x, y]/\sigma_x \sigma_y, \tag{31.14}$$

where σ_x and σ_y are the standard deviations of x and y . It can be shown that $-1 \leq \rho_{xy} \leq 1$.

Two random variables x and y are *independent* if and only if

$$f(x, y) = f_1(x)f_2(y). \tag{31.15}$$

If x and y are independent, then $\rho_{xy} = 0$; the converse is not necessarily true. If x and y are independent, $E[u(x)v(y)] = E[u(x)]E[v(y)]$, and $V[x + y] = V[x] + V[y]$; otherwise, $V[x + y] = V[x] + V[y] + 2\text{cov}[x, y]$, and $E[uv]$ does not necessarily factorize.

Consider a set of n continuous random variables $\mathbf{x} = (x_1, \dots, x_n)$ with joint p.d.f. $f(\mathbf{x})$, and a set of n new variables $\mathbf{y} = (y_1, \dots, y_n)$, related to \mathbf{x} by means of a function $\mathbf{y}(\mathbf{x})$ that is one-to-one, i.e., the inverse $\mathbf{x}(\mathbf{y})$ exists. The joint p.d.f. for \mathbf{y} is given by

$$g(\mathbf{y}) = f(\mathbf{x}(\mathbf{y}))|J|, \tag{31.16}$$

where $|J|$ is the absolute value of the determinant of the square matrix $J_{ij} = \partial x_i / \partial y_j$ (the Jacobian determinant). If the transformation from \mathbf{x} to \mathbf{y} is not one-to-one, the \mathbf{x} -space must be broken in to regions where the function $\mathbf{y}(\mathbf{x})$ can be inverted, and the contributions to $g(\mathbf{y})$ from each region summed.

Given a set of functions $\mathbf{y} = (y_1, \dots, y_m)$ with $m < n$, one can construct $n - m$ additional independent functions, apply the procedure above, then integrate the resulting $g(\mathbf{y})$ over the unwanted y_i to find the marginal distribution of those of interest.

To change variables for discrete random variables simply substitute; no Jacobian is necessary because now f is a probability rather than a probability density. If f depends on a set of parameters θ , a change to a different parameter set $\eta(\theta)$ is made by simple substitution; no Jacobian is used.

31.3. Characteristic functions

The characteristic function $\phi(u)$ associated with the p.d.f. $f(x)$ is essentially its Fourier transform, or the expectation value of e^{iux} :

$$\phi(u) = E[e^{iux}] = \int_{-\infty}^{\infty} e^{iux} f(x) dx. \tag{31.17}$$

Once $\phi(u)$ is specified, the p.d.f. $f(x)$ is uniquely determined and vice versa; knowing one is equivalent to the other. Characteristic functions are useful in deriving a number of important results about moments and sums of random variables.

It follows from Eqs. (31.8a) and (31.17) that the n^{th} moment of a random variable x that follows $f(x)$ is given by

$$i^{-n} \frac{d^n \phi}{du^n} \Big|_{u=0} = \int_{-\infty}^{\infty} x^n f(x) dx = \alpha_n. \tag{31.18}$$

Thus it is often easy to calculate all the moments of a distribution defined by $\phi(u)$, even when $f(x)$ cannot be written down explicitly.

If the p.d.f.s $f_1(x)$ and $f_2(y)$ for independent random variables x and y have characteristic functions $\phi_1(u)$ and $\phi_2(u)$, then the characteristic function of the weighted sum $ax + by$ is $\phi_1(au)\phi_2(bu)$. The additional rules for several important distributions (e.g., that the sum of two Gaussian distributed variables also follows a Gaussian distribution) easily follow from this observation.

Let the (partial) characteristic function corresponding to the conditional p.d.f. $f_2(x|z)$ be $\phi_2(u|z)$, and the p.d.f. of z be $f_1(z)$. The characteristic function after integration over the conditional value is

$$\phi(u) = \int \phi_2(u|z)f_1(z) dz. \tag{31.19}$$

Suppose we can write ϕ_2 in the form

$$\phi_2(u|z) = A(u)e^{ig(u)z}. \tag{31.20}$$

Then

$$\phi(u) = A(u)\phi_1(g(u)). \tag{31.21}$$

The cumulants (semi-invariants) κ_n are defined by

$$\phi(u) = \exp \left[\sum_{n=1}^{\infty} \frac{\kappa_n}{n!} (iu)^n \right] = \exp \left(i\kappa_1 u - \frac{1}{2}\kappa_2 u^2 + \dots \right). \tag{31.22}$$

The values κ_n are related to the moments α_n and m_n . The first few relations are

$$\begin{aligned} \kappa_1 &= \alpha_1 (= \mu, \text{ the mean}) \\ \kappa_2 &= m_2 = \alpha_2 - \alpha_1^2 (= \sigma^2, \text{ the variance}) \\ \kappa_3 &= m_3 = \alpha_3 - 3\alpha_1\alpha_2 + 2\alpha_1^3. \end{aligned} \tag{31.23}$$

31.4. Some probability distributions

Table 31.1 gives a number of common probability density functions and corresponding characteristic functions, means, and variances. Further information may be found in Refs. [1–8], [10], and [11], which has particularly detailed tables. Monte Carlo techniques for generating each of them may be found in our Sec. 33.4 and in Ref. 10. We comment below on all except the trivial uniform distribution.

Table 31.1. Some common probability density functions, with corresponding characteristic functions and means and variances. In the Table, $\Gamma(k)$ is the gamma function, equal to $(k - 1)!$ when k is an integer.

Distribution	Probability density function f (variable; parameters)	Characteristic function $\phi(u)$	Mean	Variance σ^2
Uniform	$f(x; a, b) = \begin{cases} 1/(b - a) & a \leq x \leq b \\ 0 & \text{otherwise} \end{cases}$	$\frac{e^{ibu} - e^{iau}}{(b - a)iu}$	$\frac{a + b}{2}$	$\frac{(b - a)^2}{12}$
Binomial	$f(r; N, p) = \frac{N!}{r!(N - r)!} p^r q^{N-r}$ $r = 0, 1, 2, \dots, N; \quad 0 \leq p \leq 1; \quad q = 1 - p$	$(q + pe^{iu})^N$	Np	Npq
Poisson	$f(n; \nu) = \frac{\nu^n e^{-\nu}}{n!}; \quad n = 0, 1, 2, \dots; \quad \nu > 0$	$\exp[\nu(e^{iu} - 1)]$	ν	ν
Normal (Gaussian)	$f(x; \mu, \sigma^2) = \frac{1}{\sigma\sqrt{2\pi}} \exp(-(x - \mu)^2/2\sigma^2)$ $-\infty < x < \infty; \quad -\infty < \mu < \infty; \quad \sigma > 0$	$\exp(i\mu u - \frac{1}{2}\sigma^2 u^2)$	μ	σ^2
Multivariate Gaussian	$f(\mathbf{x}; \boldsymbol{\mu}, V) = \frac{1}{(2\pi)^{n/2} \sqrt{ V }}$ $\times \exp[-\frac{1}{2}(\mathbf{x} - \boldsymbol{\mu})^T V^{-1}(\mathbf{x} - \boldsymbol{\mu})]$ $-\infty < x_j < \infty; \quad -\infty < \mu_j < \infty; \quad V > 0$	$\exp[i\boldsymbol{\mu} \cdot \mathbf{u} - \frac{1}{2}\mathbf{u}^T V \mathbf{u}]$	$\boldsymbol{\mu}$	V_{jk}
χ^2	$f(z; n) = \frac{z^{n/2-1} e^{-z/2}}{2^{n/2} \Gamma(n/2)}; \quad z \geq 0$	$(1 - 2iu)^{-n/2}$	n	$2n$
Student's t	$f(t; n) = \frac{1}{\sqrt{n\pi}} \frac{\Gamma[(n+1)/2]}{\Gamma(n/2)} \left(1 + \frac{t^2}{n}\right)^{-(n+1)/2}$ $-\infty < t < \infty; \quad n$ not required to be integer	—	0 for $n \geq 2$	$n/(n-2)$ for $n \geq 3$
Gamma	$f(x; \lambda, k) = \frac{x^{k-1} \lambda^k e^{-\lambda x}}{\Gamma(k)}; \quad 0 < x < \infty; \quad k$ not required to be integer	$(1 - iu/\lambda)^{-k}$	k/λ	k/λ^2

31.4.1. Binomial distribution :

A random process with exactly two possible outcomes which occur with fixed probabilities is called a *Bernoulli* process. If the probability of obtaining a certain outcome (a “success”) in an individual trial is p , then the probability of obtaining exactly r successes ($r = 0, 1, 2, \dots, N$) in N independent trials, without regard to the order of the successes and failures, is given by the binomial distribution $f(r; N, p)$ in Table 31.1. If r and s are binomially distributed with parameters (N_r, p) and (N_s, p) , then $t = r + s$ follows a binomial distribution with parameters $(N_r + N_s, p)$.

31.4.2. Poisson distribution :

The Poisson distribution $f(n; \nu)$ gives the probability of finding exactly n events in a given interval of x (e.g., space and time) when the events occur independently of one another and of x at an average rate of ν per the given interval. The variance σ^2 equals ν . It is the limiting case $p \rightarrow 0, N \rightarrow \infty, Np = \nu$ of the binomial distribution. The Poisson distribution approaches the Gaussian distribution for large ν .

In an accelerator experiment, for example, an opportunity for any pair of particles to come into collision and produce an event of a given type can be viewed as an independent Bernoulli trial. The total number of trials N may be extremely large, but the number of such events that occur represents in general a tiny fraction, p , of this. Therefore, the number of events is well modeled as a Poisson variable.

31.4.3. Normal or Gaussian distribution :

The normal (or Gaussian) probability density function $f(x; \mu, \sigma^2)$ given in Table 31.1 has mean $E[x] = \mu$ and variance $V[x] = \sigma^2$. Comparison of the characteristic function $\phi(u)$ given in Table 31.1 with Eq. (31.22) shows that all cumulants κ_n beyond κ_2 vanish; this is a unique property of the Gaussian distribution. Some other properties are:

$$P(x \text{ in range } \mu \pm \sigma) = 0.6827,$$

$$P(x \text{ in range } \mu \pm 0.6745\sigma) = 0.5,$$

$$E[|x - \mu|] = \sqrt{2/\pi}\sigma = 0.7979\sigma,$$

$$\text{half-width at half maximum} = \sqrt{2 \ln 2}\sigma = 1.177\sigma.$$

For a Gaussian with $\mu = 0$ and $\sigma^2 = 1$ (the *standard* Gaussian), the cumulative distribution, Eq. (31.6), is related to the error function $\text{erf}(y)$ by

$$F(x; 0, 1) = \frac{1}{2} \left[1 + \text{erf}(x/\sqrt{2})\right]. \tag{31.24}$$

The error function and standard Gaussian are tabulated in many references (e.g., Ref. [11]) and are available in software packages such as ROOT [12] and CERNLIB [13]. For a mean μ and variance σ^2 , replace x by $(x - \mu)/\sigma$. The probability of x in a given range can be calculated with Eq. (32.45).

For x and y independent and normally distributed, $z = ax + by$ follows $f(z; a\mu_x + b\mu_y, a^2\sigma_x^2 + b^2\sigma_y^2)$; that is, the weighted means and variances add.

The Gaussian derives its importance in large part from the *central limit theorem*: If independent random variables x_1, \dots, x_n are distributed according to any p.d.f.s with finite means and variances, then the sum $y = \sum_{i=1}^n x_i$ will have a p.d.f. that approaches a Gaussian for large n . The mean and variance are given by the sums of corresponding terms from the individual x_i . Therefore, the sum of a large number of fluctuations x_i will be distributed as a Gaussian, even if the x_i themselves are not.

(Note that the *product* of a large number of random variables is not Gaussian, but its logarithm is. The p.d.f. of the product is *log-normal*. See Ref. [8] for details.)

For a set of n Gaussian random variables \mathbf{x} with means $\boldsymbol{\mu}$ and corresponding Fourier variables \mathbf{u} , the characteristic function for a one-dimensional Gaussian is generalized to

$$\phi(\mathbf{u}; \boldsymbol{\mu}, V) = \exp \left[i\boldsymbol{\mu} \cdot \mathbf{u} - \frac{1}{2}\mathbf{u}^T V \mathbf{u} \right]. \quad (31.25)$$

From Eq. (31.18), the covariance of x_i and x_j is

$$E[(x_i - \mu_i)(x_j - \mu_j)] = V_{ij}. \quad (31.26)$$

If the components of \mathbf{x} are independent, then $V_{ij} = \delta_{ij}\sigma_i^2$, and Eq. (31.25) is the product of the c.f.s of n Gaussians.

The characteristic function may be inverted to find the corresponding p.d.f.,

$$f(\mathbf{x}; \boldsymbol{\mu}, V) = \frac{1}{(2\pi)^{n/2} \sqrt{|V|}} \exp \left[-\frac{1}{2}(\mathbf{x} - \boldsymbol{\mu})^T V^{-1}(\mathbf{x} - \boldsymbol{\mu}) \right], \quad (31.27)$$

where the determinant $|V|$ must be greater than 0. For diagonal V (independent variables), $f(\mathbf{x}; \boldsymbol{\mu}, V)$ is the product of the p.d.f.s of n Gaussian distributions.

For $n = 2$, $f(\mathbf{x}; \boldsymbol{\mu}, V)$ is

$$f(x_1, x_2; \mu_1, \mu_2, \sigma_1, \sigma_2, \rho) = \frac{1}{2\pi\sigma_1\sigma_2\sqrt{1-\rho^2}} \times \exp \left\{ \frac{-1}{2(1-\rho^2)} \left[\frac{(x_1 - \mu_1)^2}{\sigma_1^2} - \frac{2\rho(x_1 - \mu_1)(x_2 - \mu_2)}{\sigma_1\sigma_2} + \frac{(x_2 - \mu_2)^2}{\sigma_2^2} \right] \right\}. \quad (31.28)$$

The marginal distribution of any x_i is a Gaussian with mean μ_i and variance V_{ii} . V is $n \times n$, symmetric, and positive definite. Therefore, for any vector \mathbf{X} , the quadratic form $\mathbf{X}^T V^{-1} \mathbf{X} = C$, where C is any positive number, traces an n -dimensional ellipsoid as \mathbf{X} varies. If $X_i = x_i - \mu_i$, then C is a random variable obeying the χ^2 distribution with n degrees of freedom, discussed in the following section. The probability that \mathbf{X} corresponding to a set of Gaussian random variables x_i lies outside the ellipsoid characterized by a given value of C ($= \chi^2$) is given by $1 - F_{\chi^2}(C; n)$, where F_{χ^2} is the cumulative χ^2 distribution. This may be read from Fig. 32.1. For example, the “ s -standard-deviation ellipsoid” occurs at $C = s^2$. For the two-variable case ($n = 2$), the point \mathbf{X} lies outside the one-standard-deviation ellipsoid with 61% probability. The use of these ellipsoids as indicators of probable error is described in Sec. 32.3.2.4; the validity of those indicators assumes that $\boldsymbol{\mu}$ and V are correct.

31.4.4. χ^2 distribution :

If x_1, \dots, x_n are independent Gaussian random variables, the sum $z = \sum_{i=1}^n (x_i - \mu_i)^2 / \sigma_i^2$ follows the χ^2 p.d.f. with n degrees of freedom, which we denote by $\chi^2(n)$. More generally, for n correlated Gaussian variables as components of a vector \mathbf{X} with covariance matrix V , $z = \mathbf{X}^T V^{-1} \mathbf{X}$ follows $\chi^2(n)$ as in the previous section. For a set of z_i , each of which follows $\chi^2(n_i)$, $\sum z_i$ follows $\chi^2(\sum n_i)$. For large n , the χ^2 p.d.f. approaches a Gaussian with mean $\mu = n$ and variance $\sigma^2 = 2n$.

The χ^2 p.d.f. is often used in evaluating the level of compatibility between observed data and a hypothesis for the p.d.f. that the data might follow. This is discussed further in Sec. 32.2.2 on tests of goodness-of-fit.

31.4.5. Student’s t distribution :

Suppose that x and x_1, \dots, x_n are independent and Gaussian distributed with mean 0 and variance 1. We then define

$$z = \sum_{i=1}^n x_i^2 \quad \text{and} \quad t = \frac{x}{\sqrt{z/n}}. \quad (31.29)$$

The variable z thus follows a $\chi^2(n)$ distribution. Then t is distributed according to Student’s t distribution with n degrees of freedom, $f(t; n)$, given in Table 31.1.

The Student’s t distribution resembles a Gaussian with wide tails. As $n \rightarrow \infty$, the distribution approaches a Gaussian. If $n = 1$, it is a *Cauchy* or *Breit-Wigner* distribution. The mean is finite only for $n > 1$ and the variance is finite only for $n > 2$, so the central limit theorem is not applicable to sums of random variables following the t distribution for $n = 1$ or 2.

As an example, consider the *sample mean* $\bar{x} = \sum x_i/n$ and the *sample variance* $s^2 = \sum (x_i - \bar{x})^2 / (n - 1)$ for normally distributed x_i with unknown mean μ and variance σ^2 . The sample mean has a Gaussian distribution with a variance σ^2/n , so the variable $(\bar{x} - \mu) / \sqrt{\sigma^2/n}$ is normal with mean 0 and variance 1. The quantity $(n - 1)s^2 / \sigma^2$ is independent of this and follows $\chi^2(n - 1)$. The ratio

$$t = \frac{(\bar{x} - \mu) / \sqrt{\sigma^2/n}}{\sqrt{(n - 1)s^2 / \sigma^2(n - 1)}} = \frac{\bar{x} - \mu}{\sqrt{s^2/n}} \quad (31.30)$$

is distributed as $f(t; n - 1)$. The unknown variance σ^2 cancels, and t can be used to test the probability that the true mean is some particular value μ .

In Table 31.1, n in $f(t; n)$ is not required to be an integer. A Student’s t distribution with non-integral $n > 0$ is useful in certain applications.

31.4.6. Gamma distribution :

For a process that generates events as a function of x (*e.g.*, space or time) according to a Poisson distribution, the distance in x from an arbitrary starting point (which may be some particular event) to the k^{th} event follows a *gamma* distribution, $f(x; \lambda, k)$. The Poisson parameter μ is λ per unit x . The special case $k = 1$ (*i.e.*, $f(x; \lambda, 1) = \lambda e^{-\lambda x}$) is called the *exponential* distribution. A sum of k' exponential random variables x_i is distributed as $f(\sum x_i; \lambda, k')$.

The parameter k is not required to be an integer. For $\lambda = 1/2$ and $k = n/2$, the gamma distribution reduces to the $\chi^2(n)$ distribution.

References:

1. H. Cramér, *Mathematical Methods of Statistics*, (Princeton Univ. Press, New Jersey, 1958).
2. A. Stuart and J.K. Ord, *Kendall’s Advanced Theory of Statistics*, Vol. 1 *Distribution Theory* 6th Ed., (Halsted Press, New York, 1994), and earlier editions by Kendall and Stuart.
3. F.E. James, *Statistical Methods in Experimental Physics*, 2nd ed., (World Scientific, Singapore, 2006).
4. L. Lyons, *Statistics for Nuclear and Particle Physicists*, (Cambridge University Press, New York, 1986).
5. B.R. Roe, *Probability and Statistics in Experimental Physics*, 2nd Ed., (Springer, New York, 2001).
6. R.J. Barlow, *Statistics: A Guide to the Use of Statistical Methods in the Physical Sciences*, (John Wiley, New York, 1989).
7. S. Brandt, *Data Analysis*, 3rd Ed., (Springer, New York, 1999).
8. G. Cowan, *Statistical Data Analysis*, (Oxford University Press, Oxford, 1998).
9. A.N. Kolmogorov, *Grundbegriffe der Wahrscheinlichkeitsrechnung*, (Springer, Berlin 1933); *Foundations of the Theory of Probability*, 2nd Ed., (Chelsea, New York 1956).
10. Ch. Walck, *Hand-book on Statistical Distributions for Experimentalists*, University of Stockholm Internal Report SUF-PFY/96-01, available from www.physto.se/~walck.
11. M. Abramowitz and I. Stegun, eds., *Handbook of Mathematical Functions*, (Dover, New York, 1972).
12. Rene Brun and Fons Rademakers, Nucl. Inst. Meth. A **389**, 81 (1997); see also root.cern.ch.
13. The CERN Program Library (CERNLIB); see cernlib.web.cern.ch/cernlib.

32. STATISTICS

Revised September 2007 by G. Cowan (RHUL).

This chapter gives an overview of statistical methods used in high-energy physics. In statistics, we are interested in using a given sample of data to make inferences about a probabilistic model, *e.g.*, to assess the model's validity or to determine the values of its parameters. There are two main approaches to statistical inference, which we may call frequentist and Bayesian. In frequentist statistics, probability is interpreted as the frequency of the outcome of a repeatable experiment. The most important tools in this framework are parameter estimation, covered in Section 32.1, and statistical tests, discussed in Section 32.2. Frequentist confidence intervals, which are constructed so as to cover the true value of a parameter with a specified probability, are treated in Section 32.3.2. Note that in frequentist statistics one does not define a probability for a hypothesis or for a parameter.

Frequentist statistics provides the usual tools for reporting the outcome of an experiment objectively, without needing to incorporate prior beliefs concerning the parameter being measured or the theory being tested. As such, they are used for reporting most measurements and their statistical uncertainties in high-energy physics.

In Bayesian statistics, the interpretation of probability is more general and includes *degree of belief* (called subjective probability). One can then speak of a probability density function (p.d.f.) for a parameter, which expresses one's state of knowledge about where its true value lies. Bayesian methods allow for a natural way to input additional information, such as physical boundaries and subjective information; in fact they *require* the *prior* p.d.f. as input for the parameters, *i.e.*, the degree of belief about the parameters' values before carrying out the measurement. Using Bayes' theorem Eq. (31.4), the prior degree of belief is updated by the data from the experiment. Bayesian methods for interval estimation are discussed in Sections 32.3.1 and 32.3.2.6

Bayesian techniques are often used to treat systematic uncertainties, where the author's beliefs about, say, the accuracy of the measuring device may enter. Bayesian statistics also provides a useful framework for discussing the validity of different theoretical interpretations of the data. This aspect of a measurement, however, will usually be treated separately from the reporting of the result.

For many inference problems, the frequentist and Bayesian approaches give similar numerical answers, even though they are based on fundamentally different interpretations of probability. For small data samples, however, and for measurements of a parameter near a physical boundary, the different approaches may yield different results, so we are forced to make a choice. For a discussion of Bayesian vs. non-Bayesian methods, see References written by a statistician[1], by a physicist[2], or the more detailed comparison in Ref. [3].

Following common usage in physics, the word "error" is often used in this chapter to mean "uncertainty." More specifically it can indicate the size of an interval as in "the standard error" or "error propagation," where the term refers to the standard deviation of an estimator.

32.1. Parameter estimation

Here we review the frequentist approach to *point estimation* of parameters. An *estimator* $\hat{\theta}$ (written with a hat) is a function of the data whose value, the *estimate*, is intended as a meaningful guess for the value of the parameter θ .

There is no fundamental rule dictating how an estimator must be constructed. One tries, therefore, to choose that estimator which has the best properties. The most important of these are (a) *consistency*, (b) *bias*, (c) *efficiency*, and (d) *robustness*.

(a) An estimator is said to be *consistent* if the estimate $\hat{\theta}$ converges to the true value θ as the amount of data increases. This property is so important that it is possessed by all commonly used estimators.

(b) The *bias*, $b = E[\hat{\theta}] - \theta$, is the difference between the expectation value of the estimator and the true value of the parameter. The expectation value is taken over a hypothetical set of similar experiments in which $\hat{\theta}$ is constructed in the same way. When $b = 0$, the estimator is said to be unbiased. The bias depends on the chosen

metric, *i.e.*, if $\hat{\theta}$ is an unbiased estimator of θ , then $\hat{\theta}^2$ is not in general an unbiased estimator for θ^2 . If we have an estimate \hat{b} for the bias, we can subtract it from $\hat{\theta}$ to obtain a new $\hat{\theta}' = \hat{\theta} - \hat{b}$. The estimate \hat{b} may, however, be subject to statistical or systematic uncertainties that are larger than the bias itself, so that the new $\hat{\theta}'$ may not be better than the original.

(c) *Efficiency* is the inverse of the ratio of the variance $V[\hat{\theta}]$ to its minimum possible value. Under rather general conditions, the minimum variance is given by the Rao-Cramér-Frechet bound,

$$\sigma_{\min}^2 = \left(1 + \frac{\partial b}{\partial \theta}\right)^2 / I(\theta), \quad (32.1)$$

where

$$I(\theta) = E \left[\left(\frac{\partial}{\partial \theta} \sum_i \ln f(x_i; \theta) \right)^2 \right] \quad (32.2)$$

is the *Fisher information*. The sum is over all data, assumed independent, and distributed according to the p.d.f. $f(x; \theta)$, b is the bias, if any, and the allowed range of x must not depend on θ .

The *mean-squared error*,

$$\text{MSE} = E[(\hat{\theta} - \theta)^2] = V[\hat{\theta}] + b^2, \quad (32.3)$$

is a convenient quantity which combines the uncertainties in an estimate due to bias and variance.

(d) *Robustness* is the property of being insensitive to departures from assumptions in the p.d.f., *e.g.*, owing to uncertainties in the distribution's tails.

For some common estimators, the properties above are known exactly. More generally, it is possible to evaluate them by Monte Carlo simulation. Note that they will often depend on the unknown θ .

32.1.1. Estimators for mean, variance and median :

Suppose we have a set of N independent measurements, x_i , assumed to be unbiased measurements of the same unknown quantity μ with a common, but unknown, variance σ^2 . Then

$$\hat{\mu} = \frac{1}{N} \sum_{i=1}^N x_i \quad (32.4)$$

$$\hat{\sigma}^2 = \frac{1}{N-1} \sum_{i=1}^N (x_i - \hat{\mu})^2 \quad (32.5)$$

are unbiased estimators of μ and σ^2 . The variance of $\hat{\mu}$ is σ^2/N and the variance of $\hat{\sigma}^2$ is

$$V[\hat{\sigma}^2] = \frac{1}{N} \left(m_4 - \frac{N-3}{N-1} \sigma^4 \right), \quad (32.6)$$

where m_4 is the 4th central moment of x . For Gaussian distributed x_i , this becomes $2\sigma^4/(N-1)$ for any $N \geq 2$, and for large N , the standard deviation of $\hat{\sigma}^2$ (the "error of the error") is $\sigma/\sqrt{2N}$. Again, if the x_i are Gaussian, $\hat{\mu}$ is an efficient estimator for μ , and the estimators $\hat{\mu}$ and $\hat{\sigma}^2$ are uncorrelated. Otherwise the arithmetic mean (32.4) is not necessarily the most efficient estimator; this is discussed in more detail in Sec. 8.7 [4].

If σ^2 is known, it does not improve the estimate $\hat{\mu}$, as can be seen from Eq. (32.4); however, if μ is known, substitute it for $\hat{\mu}$ in Eq. (32.5) and replace $N-1$ by N to obtain an estimator of σ^2 still with zero bias but smaller variance. If the x_i have different, known variances σ_i^2 , then the weighted average

$$\hat{\mu} = \frac{1}{w} \sum_{i=1}^N w_i x_i \quad (32.7)$$

is an unbiased estimator for μ with a smaller variance than an unweighted average; here $w_i = 1/\sigma_i^2$ and $w = \sum_i w_i$. The standard deviation of $\hat{\mu}$ is $1/\sqrt{w}$.

As an estimator for the median x_{med} , one can use the value \hat{x}_{med} such that half the x_i are below and half above (the sample median). If the sample median lies between two observed values, it is set by convention halfway between them. If the p.d.f. of x has the form $f(x - \mu)$ and μ is both mean and median, then for large N the variance of the sample median approaches $1/[4Nf^2(0)]$, provided $f(0) > 0$. Although estimating the median can often be more difficult computationally than the mean, the resulting estimator is generally more robust, as it is insensitive to the exact shape of the tails of a distribution.

32.1.2. The method of maximum likelihood :

Suppose we have a set of N measured quantities $\mathbf{x} = (x_1, \dots, x_N)$ described by a joint p.d.f. $f(\mathbf{x}; \boldsymbol{\theta})$, where $\boldsymbol{\theta} = (\theta_1, \dots, \theta_n)$ is set of n parameters whose values are unknown. The *likelihood function* is given by the p.d.f. evaluated with the data \mathbf{x} , but viewed as a function of the parameters, *i.e.*, $L(\boldsymbol{\theta}) = f(\mathbf{x}; \boldsymbol{\theta})$. If the measurements x_i are statistically independent and each follow the p.d.f. $f(x; \boldsymbol{\theta})$, then the joint p.d.f. for \mathbf{x} factorizes and the likelihood function is

$$L(\boldsymbol{\theta}) = \prod_{i=1}^N f(x_i; \boldsymbol{\theta}). \quad (32.8)$$

The method of maximum likelihood takes the estimators $\hat{\boldsymbol{\theta}}$ to be those values of $\boldsymbol{\theta}$ that maximize $L(\boldsymbol{\theta})$.

Note that the likelihood function is *not* a p.d.f. for the parameters $\boldsymbol{\theta}$; in frequentist statistics this is not defined. In Bayesian statistics, one can obtain from the likelihood the posterior p.d.f. for $\boldsymbol{\theta}$, but this requires multiplying by a prior p.d.f. (see Sec. 32.3.1).

It is usually easier to work with $\ln L$, and since both are maximized for the same parameter values $\boldsymbol{\theta}$, the maximum likelihood (ML) estimators can be found by solving the *likelihood equations*,

$$\frac{\partial \ln L}{\partial \theta_i} = 0, \quad i = 1, \dots, n. \quad (32.9)$$

Maximum likelihood estimators are important because they are approximately unbiased and efficient for large data samples, under quite general conditions, and the method has a wide range of applicability.

In evaluating the likelihood function, it is important that any normalization factors in the p.d.f. that involve $\boldsymbol{\theta}$ be included. However, we will only be interested in the maximum of L and in ratios of L at different values of the parameters; hence any multiplicative factors that do not involve the parameters that we want to estimate may be dropped, including factors that depend on the data but not on $\boldsymbol{\theta}$.

Under a one-to-one change of parameters from $\boldsymbol{\theta}$ to $\boldsymbol{\eta}$, the ML estimators $\hat{\boldsymbol{\theta}}$ transform to $\boldsymbol{\eta}(\hat{\boldsymbol{\theta}})$. That is, the ML solution is invariant under change of parameter. However, other properties of ML estimators, in particular the bias, are not invariant under change of parameter.

The inverse V^{-1} of the covariance matrix $V_{ij} = \text{cov}[\hat{\theta}_i, \hat{\theta}_j]$ for a set of ML estimators can be estimated by using

$$(\hat{V}^{-1})_{ij} = - \left. \frac{\partial^2 \ln L}{\partial \theta_i \partial \theta_j} \right|_{\hat{\boldsymbol{\theta}}}. \quad (32.10)$$

For finite samples, however, Eq. (32.10) can result in an underestimate of the variances. In the large sample limit (or in a linear model with Gaussian errors), L has a Gaussian form and $\ln L$ is (hyper)parabolic. In this case, it can be seen that a numerically equivalent way of determining s -standard-deviation errors is from the contour given by the $\boldsymbol{\theta}'$ such that

$$\ln L(\boldsymbol{\theta}') = \ln L_{\text{max}} - s^2/2, \quad (32.11)$$

where $\ln L_{\text{max}}$ is the value of $\ln L$ at the solution point (compare with Eq. (32.48)). The extreme limits of this contour on the θ_i axis give

an approximate s -standard-deviation confidence interval for θ_i (see Section 32.3.2.4).

In the case where the size n of the data sample x_1, \dots, x_n is small, the unbinned maximum likelihood method, *i.e.*, use of equation (32.8), is preferred since binning can only result in a loss of information, and hence larger statistical errors for the parameter estimates. The sample size n can be regarded as fixed, or the user can choose to treat it as a Poisson-distributed variable; this latter option is sometimes called “extended maximum likelihood” (see, *e.g.*, [6–8]). If the sample is large, it can be convenient to bin the values in a histogram, so that one obtains a vector of data $\mathbf{n} = (n_1, \dots, n_N)$ with expectation values $\boldsymbol{\nu} = E[\mathbf{n}]$ and probabilities $f(\mathbf{n}; \boldsymbol{\nu})$. Then one may maximize the likelihood function based on the contents of the bins (so i labels bins). This is equivalent to maximizing the likelihood ratio $\lambda(\boldsymbol{\theta}) = f(\mathbf{n}; \boldsymbol{\nu}(\boldsymbol{\theta}))/f(\mathbf{n}; \boldsymbol{\nu})$, or to minimizing the quantity [9]

$$-2 \ln \lambda(\boldsymbol{\theta}) = 2 \sum_{i=1}^N \left[\nu_i(\boldsymbol{\theta}) - n_i + n_i \ln \frac{n_i}{\nu_i(\boldsymbol{\theta})} \right], \quad (32.12)$$

where in bins where $n_i = 0$, the last term in (32.12) is zero. In the limit of zero bin width, maximizing (32.12) is equivalent to maximizing the unbinned likelihood function (32.8).

A benefit of binning is that it allows for a goodness-of-fit test (see Sec. 32.2.2). The minimum of $-2 \ln \lambda$ as defined by Eq. (32.12) follows a χ^2 distribution in the large sample limit. If there are N bins and m fitted parameters, then the number of degrees of freedom for the χ^2 distribution is $N - m$ if the data are treated as Poisson-distributed, and $N - m - 1$ if the n_i are multinomially distributed. If the n_i are Poisson-distributed and the overall normalization $\nu_{\text{tot}} = \sum_i \nu_i$ is taken as an adjustable parameter, then by minimizing Eq. (32.12), one obtains that the area under the fitted function is equal to the sum of the histogram contents, *i.e.*, $\sum_i \nu_i = \sum_i n_i$. This is not the case for parameter estimation methods based on a least-squares procedure with traditional weights (see, *e.g.*, Ref. 8).

32.1.3. The method of least squares :

The *method of least squares* (LS) coincides with the method of maximum likelihood in the following special case. Consider a set of N independent measurements y_i at known points x_i . The measurement y_i is assumed to be Gaussian distributed with mean $F(x_i; \boldsymbol{\theta})$ and known variance σ_i^2 . The goal is to construct estimators for the unknown parameters $\boldsymbol{\theta}$. The likelihood function contains the sum of squares

$$\chi^2(\boldsymbol{\theta}) = -2 \ln L(\boldsymbol{\theta}) + \text{constant} = \sum_{i=1}^N \frac{(y_i - F(x_i; \boldsymbol{\theta}))^2}{\sigma_i^2}. \quad (32.13)$$

The set of parameters $\boldsymbol{\theta}$ which maximize L is the same as those which minimize χ^2 .

The minimum of Equation (32.13) defines the least-squares estimators $\hat{\boldsymbol{\theta}}$ for the more general case where the y_i are not Gaussian distributed as long as they are independent. If they are not independent but rather have a covariance matrix $V_{ij} = \text{cov}[y_i, y_j]$, then the LS estimators are determined by the minimum of

$$\chi^2(\boldsymbol{\theta}) = (\mathbf{y} - \mathbf{F}(\boldsymbol{\theta}))^T V^{-1} (\mathbf{y} - \mathbf{F}(\boldsymbol{\theta})), \quad (32.14)$$

where $\mathbf{y} = (y_1, \dots, y_N)$ is the vector of measurements, $\mathbf{F}(\boldsymbol{\theta})$ is the corresponding vector of predicted values (understood as a column vector in (32.14)), and the superscript T denotes transposed (*i.e.*, row) vector.

In many practical cases, one further restricts the problem to the situation where $F(x_i; \boldsymbol{\theta})$ is a linear function of the parameters, *i.e.*,

$$F(x_i; \boldsymbol{\theta}) = \sum_{j=1}^m \theta_j h_j(x_i). \quad (32.15)$$

Here the $h_j(x)$ are m linearly independent functions, e.g., $1, x, x^2, \dots, x^{m-1}$, or Legendre polynomials. We require $m < N$ and at least m of the x_i must be distinct.

Minimizing χ^2 in this case with m parameters reduces to solving a system of m linear equations. Defining $H_{ij} = h_j(x_i)$ and minimizing χ^2 by setting its derivatives with respect to the θ_i equal to zero gives the LS estimators,

$$\hat{\boldsymbol{\theta}} = (H^T V^{-1} H)^{-1} H^T V^{-1} \mathbf{y} \equiv D \mathbf{y} . \quad (32.16)$$

The covariance matrix for the estimators $U_{ij} = \text{cov}[\hat{\theta}_i, \hat{\theta}_j]$ is given by

$$U = D V D^T = (H^T V^{-1} H)^{-1} , \quad (32.17)$$

or equivalently, its inverse U^{-1} can be found from

$$(U^{-1})_{ij} = \frac{1}{2} \frac{\partial^2 \chi^2}{\partial \theta_i \partial \theta_j} \Big|_{\boldsymbol{\theta} = \hat{\boldsymbol{\theta}}} = \sum_{k,l=1}^N h_i(x_k) (V^{-1})_{kl} h_j(x_l) . \quad (32.18)$$

The LS estimators can also be found from the expression

$$\hat{\boldsymbol{\theta}} = U \mathbf{g} , \quad (32.19)$$

where the vector \mathbf{g} is defined by

$$g_i = \sum_{j,k=1}^N y_j h_i(x_k) (V^{-1})_{jk} . \quad (32.20)$$

For the case of uncorrelated y_i , for example, one can use (32.19) with

$$(U^{-1})_{ij} = \sum_{k=1}^N \frac{h_i(x_k) h_j(x_k)}{\sigma_k^2} , \quad (32.21)$$

$$g_i = \sum_{k=1}^N \frac{y_k h_i(x_k)}{\sigma_k^2} . \quad (32.22)$$

Expanding $\chi^2(\boldsymbol{\theta})$ about $\hat{\boldsymbol{\theta}}$, one finds that the contour in parameter space defined by

$$\chi^2(\boldsymbol{\theta}) = \chi^2(\hat{\boldsymbol{\theta}}) + 1 = \chi_{\min}^2 + 1 \quad (32.23)$$

has tangent planes located at plus-or-minus-one standard deviation $\sigma_{\hat{\theta}}$ from the LS estimates $\hat{\boldsymbol{\theta}}$.

In constructing the quantity $\chi^2(\boldsymbol{\theta})$, one requires the variances or, in the case of correlated measurements, the covariance matrix. Often these quantities are not known *a priori* and must be estimated from the data; an important example is where the measured value y_i represents a counted number of events in the bin of a histogram. If, for example, y_i represents a Poisson variable, for which the variance is equal to the mean, then one can either estimate the variance from the predicted value, $F(x_i; \boldsymbol{\theta})$, or from the observed number itself, y_i . In the first option, the variances become functions of the fitted parameters, which may lead to calculational difficulties. The second option can be undefined if y_i is zero, and in both cases for small y_i , the variance will be poorly estimated. In either case, one should constrain the normalization of the fitted curve to the correct value, i.e., one should determine the area under the fitted curve directly from the number of entries in the histogram (see Ref. 8, Section 7.4). A further alternative is to use the method of maximum likelihood; for binned data this can be done by minimizing Eq. (32.12)

As the minimum value of the χ^2 represents the level of agreement between the measurements and the fitted function, it can be used for assessing the goodness-of-fit; this is discussed further in Section 32.2.2.

32.1.4. Propagation of errors :

Consider a set of n quantities $\boldsymbol{\theta} = (\theta_1, \dots, \theta_n)$ and a set of m functions $\boldsymbol{\eta}(\boldsymbol{\theta}) = (\eta_1(\boldsymbol{\theta}), \dots, \eta_m(\boldsymbol{\theta}))$. Suppose we have estimated $\hat{\boldsymbol{\theta}} = (\hat{\theta}_1, \dots, \hat{\theta}_n)$, using, say, maximum-likelihood or least-squares, and we also know or have estimated the covariance matrix $V_{ij} = \text{cov}[\theta_i, \theta_j]$. The goal of *error propagation* is to determine the covariance matrix for the functions, $U_{ij} = \text{cov}[\hat{\eta}_i, \hat{\eta}_j]$, where $\hat{\boldsymbol{\eta}} = \boldsymbol{\eta}(\hat{\boldsymbol{\theta}})$. In particular, the diagonal elements $U_{ii} = V[\hat{\eta}_i]$ give the variances. The new covariance matrix can be found by expanding the functions $\boldsymbol{\eta}(\boldsymbol{\theta})$ about the estimates $\hat{\boldsymbol{\theta}}$ to first order in a Taylor series. Using this one finds

$$U_{ij} \approx \sum_{k,l} \frac{\partial \eta_i}{\partial \theta_k} \frac{\partial \eta_j}{\partial \theta_l} \Big|_{\hat{\boldsymbol{\theta}}} V_{kl} . \quad (32.24)$$

This can be written in matrix notation as $U \approx A V A^T$ where the matrix of derivatives A is

$$A_{ij} = \frac{\partial \eta_i}{\partial \theta_j} \Big|_{\hat{\boldsymbol{\theta}}} , \quad (32.25)$$

and A^T is its transpose. The approximation is exact if $\boldsymbol{\eta}(\boldsymbol{\theta})$ is linear (it holds, for example, in equation (32.17)). If this is not the case, the approximation can break down if, for example, $\boldsymbol{\eta}(\boldsymbol{\theta})$ is significantly nonlinear close to $\hat{\boldsymbol{\theta}}$ in a region of a size comparable to the standard deviations of $\hat{\boldsymbol{\theta}}$.

32.2. Statistical tests

In addition to estimating parameters, one often wants to assess the validity of certain statements concerning the data's underlying distribution. *Hypothesis tests* provide a rule for accepting or rejecting hypotheses depending on the outcome of a measurement. In *significance tests*, one gives the probability to obtain a level of incompatibility with a certain hypothesis that is greater than or equal to the level observed with the actual data.

32.2.1. Hypothesis tests :

Consider an experiment whose outcome is characterized by a vector of data \mathbf{x} . A *hypothesis* is a statement about the distribution of \mathbf{x} . It could, for example, define completely the p.d.f. for the data (a simple hypothesis), or it could specify only the functional form of the p.d.f., with the values of one or more parameters left open (a composite hypothesis).

A *statistical test* is a rule that states for which values of \mathbf{x} a given hypothesis (often called the null hypothesis, H_0) should be rejected in favor of its complementary alternative H_1 . This is done by defining a region of \mathbf{x} -space called the critical region; if the outcome of the experiment lands in this region, H_0 is rejected, otherwise it is accepted.

Rejecting H_0 if it is true is called an error of the first kind. The probability for this to occur is called the *size* or *significance level* of the test, α , which is chosen to be equal to some pre-specified value. It can also happen that H_0 is false and the true hypothesis is the alternative, H_1 . If H_0 is accepted in such a case, this is called an error of the second kind, which will have some probability β . The quantity $1 - \beta$ is called the *power* of the test to reject H_1 .

In high-energy physics, the components of \mathbf{x} might represent the measured properties of candidate events, and the acceptance region is defined by the cuts that one imposes in order to select events of a certain desired type. That is, H_0 could represent the signal hypothesis, and various alternatives, H_1, H_2, \dots , could represent background processes.

Often rather than using the full set of quantities \mathbf{x} , it is convenient to define a *test statistic*, t , which can be a single number, or in any case a vector with fewer components than \mathbf{x} . Each hypothesis for the distribution of \mathbf{x} will determine a distribution for t , and the acceptance region in \mathbf{x} -space will correspond to a specific range of values of t . In constructing t , one attempts to reduce the volume of data without losing the ability to discriminate between different hypotheses.

In particle physics terminology, the probability to accept the signal hypothesis, H_0 , is the selection efficiency, *i.e.*, one minus the significance level. The efficiencies for the various background processes are given by one minus the power. Often one tries to construct a test to minimize the background efficiency for a given signal efficiency. The *Neyman–Pearson lemma* states that this is done by defining the acceptance region such that, for \mathbf{x} in that region, the ratio of p.d.f.s for the hypotheses H_0 and H_1 ,

$$\lambda(\mathbf{x}) = \frac{f(\mathbf{x}|H_0)}{f(\mathbf{x}|H_1)}, \quad (32.26)$$

is greater than a given constant, the value of which is chosen to give the desired signal efficiency. This is equivalent to the statement that (32.26) represents the test statistic with which one may obtain the highest purity sample for a given signal efficiency. It can be difficult in practice, however, to determine $\lambda(\mathbf{x})$, since this requires knowledge of the joint p.d.f.s $f(\mathbf{x}|H_0)$ and $f(\mathbf{x}|H_1)$.

In the usual case where the likelihood ratio (32.26) cannot be used explicitly, there exist a variety of other multivariate classifiers that effectively separate different types of events. Methods often used in HEP include *neural networks* or *Fisher discriminants* (see Ref. 10). Recently, further classification methods from machine-learning have been applied in HEP analyses; these include *probability density estimation (PDE)* techniques, *kernel-based PDE (KDE or Parzen window)*, *support vector machines*, and *decision trees*. Techniques such as “boosting” and “bagging” can be applied to combine a number of classifiers into a stronger one with greater stability with respect to fluctuations in the training data. Descriptions of these methods can be found in [11–13], and Proceedings of the PHYSTAT conference series [14]. Software for HEP includes the TMVA [15] and StatPatternRecognition [16] packages.

32.2.2. Significance tests :

Often one wants to quantify the level of agreement between the data and a hypothesis without explicit reference to alternative hypotheses. This can be done by defining a statistic t , which is a function of the data whose value reflects in some way the level of agreement between the data and the hypothesis. The user must decide what values of the statistic correspond to better or worse levels of agreement with the hypothesis in question; for many goodness-of-fit statistics, there is an obvious choice.

The hypothesis in question, say, H_0 , will determine the p.d.f. $g(t|H_0)$ for the statistic. The significance of a discrepancy between the data and what one expects under the assumption of H_0 is quantified by giving the p -value, defined as the probability to find t in the region of equal or lesser compatibility with H_0 than the level of compatibility observed with the actual data. For example, if t is defined such that large values correspond to poor agreement with the hypothesis, then the p -value would be

$$p = \int_{t_{\text{obs}}}^{\infty} g(t|H_0) dt, \quad (32.27)$$

where t_{obs} is the value of the statistic obtained in the actual experiment. The p -value should not be confused with the size (significance level) of a test, or the confidence level of a confidence interval (Section 32.3), both of which are pre-specified constants.

The p -value is a function of the data, and is therefore itself a random variable. If the hypothesis used to compute the p -value is true, then for continuous data, p will be uniformly distributed between zero and one. Note that the p -value is not the probability for the hypothesis; in frequentist statistics, this is not defined. Rather, the p -value is the probability, under the assumption of a hypothesis H_0 , of obtaining data at least as incompatible with H_0 as the data actually observed.

When estimating parameters using the method of least squares, one obtains the minimum value of the quantity χ^2 (32.13). This statistic can be used to test the *goodness-of-fit*, *i.e.*, the test provides a measure of the significance of a discrepancy between the data and the hypothesized functional form used in the fit. It may also happen that

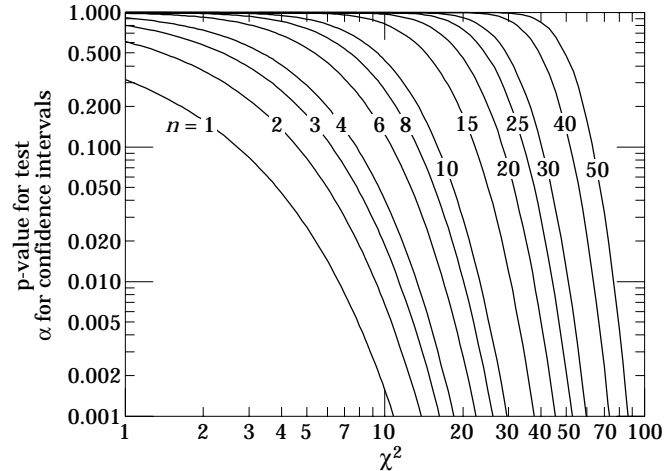


Figure 32.1: One minus the χ^2 cumulative distribution, $1 - F(\chi^2; n)$, for n degrees of freedom. This gives the p -value for the χ^2 goodness-of-fit test as well as one minus the coverage probability for confidence regions (see Sec. 32.3.2.4).

no parameters are estimated from the data, but that one simply wants to compare a histogram, *e.g.*, a vector of Poisson distributed numbers $\mathbf{n} = (n_1, \dots, n_N)$, with a hypothesis for their expectation values $\nu_i = E[n_i]$. As the distribution is Poisson with variances $\sigma_i^2 = \nu_i$, the χ^2 (32.13) becomes *Pearson’s χ^2 statistic*,

$$\chi^2 = \sum_{i=1}^N \frac{(n_i - \nu_i)^2}{\nu_i}. \quad (32.28)$$

If the hypothesis $\boldsymbol{\nu} = (\nu_1, \dots, \nu_N)$ is correct, and if the measured values n_i in (32.28) are sufficiently large (in practice, this will be a good approximation if all $n_i > 5$), then the χ^2 statistic will follow the χ^2 p.d.f. with the number of degrees of freedom equal to the number of measurements N minus the number of fitted parameters. The same holds for the minimized χ^2 from Eq. (32.13) if the y_i are Gaussian.

Alternatively, one may fit parameters and evaluate goodness-of-fit by minimizing $-2 \ln \lambda$ from Eq. (32.12). One finds that the distribution of this statistic approaches the asymptotic limit faster than does Pearson’s χ^2 , and thus computing the p -value with the χ^2 p.d.f. will in general be better justified (see Ref. 9 and references therein).

Assuming the goodness-of-fit statistic follows a χ^2 p.d.f., the p -value for the hypothesis is then

$$p = \int_{\chi^2}^{\infty} f(z; n_d) dz, \quad (32.29)$$

where $f(z; n_d)$ is the χ^2 p.d.f. and n_d is the appropriate number of degrees of freedom. Values can be obtained from Fig. 32.1 or from the CERNLIB routine PROB or the ROOT function TMath::Prob. If the conditions for using the χ^2 p.d.f. do not hold, the statistic can still be defined as before, but its p.d.f. must be determined by other means in order to obtain the p -value, *e.g.*, using a Monte Carlo calculation.

If one finds a χ^2 value much greater than n_d , and a correspondingly small p -value, one may be tempted to expect a high degree of uncertainty for any fitted parameters. Although this may be true for systematic errors in the parameters, it is not in general the case for statistical uncertainties. If, for example, the error bars (or covariance matrix) used in constructing the χ^2 are underestimated, then this will lead to underestimated statistical errors for the fitted parameters. But in such a case, an estimate $\hat{\theta}$ can differ from the true value θ by an amount much greater than its estimated statistical error. The standard deviations of estimators that one finds from, say, Eq. (32.11) reflect how widely the estimates would be distributed if one were to repeat the measurement many times, assuming that the measurement errors used in the χ^2 are also correct. They do not include the systematic error which may result from an incorrect hypothesis or incorrectly estimated measurement errors in the χ^2 .

Since the mean of the χ^2 distribution is equal to n_d , one expects in a “reasonable” experiment to obtain $\chi^2 \approx n_d$. Hence the quantity χ^2/n_d is sometimes reported. Since the p.d.f. of χ^2/n_d depends on n_d , however, one must report n_d as well in order to make a meaningful statement. The p -values obtained for different values of χ^2/n_d are shown in Fig. 32.2.

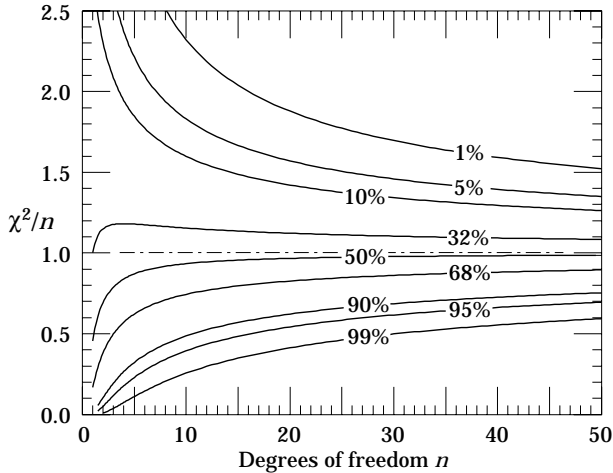


Figure 32.2: The ‘reduced’ χ^2 , equal to χ^2/n , for n degrees of freedom. The curves show as a function of n the χ^2/n that corresponds to a given p -value.

32.3. Confidence intervals and limits

When the goal of an experiment is to determine a parameter θ , the result is usually expressed by quoting, in addition to the point estimate, some sort of interval which reflects the statistical precision of the measurement. In the simplest case, this can be given by the parameter’s estimated value $\hat{\theta}$ plus or minus an estimate of the standard deviation of $\hat{\theta}$, $\sigma_{\hat{\theta}}$. If, however, the p.d.f. of the estimator is not Gaussian or if there are physical boundaries on the possible values of the parameter, then one usually quotes instead an interval according to one of the procedures described below.

In reporting an interval or limit, the experimenter may wish to

- communicate as objectively as possible the result of the experiment;
- provide an interval that is constructed to cover the true value of the parameter with a specified probability;
- provide the information needed by the consumer of the result to draw conclusions about the parameter or to make a particular decision;
- draw conclusions about the parameter that incorporate stated prior beliefs.

With a sufficiently large data sample, the point estimate and standard deviation (or for the multiparameter case, the parameter estimates and covariance matrix) satisfy essentially all of these goals. For finite data samples, no single method for quoting an interval will achieve all of them.

In addition to the goals listed above, the choice of method may be influenced by practical considerations such as ease of producing an interval from the results of several measurements. Of course the experimenter is not restricted to quoting a single interval or limit; one may choose, for example, first to communicate the result with a confidence interval having certain frequentist properties, and then in addition to draw conclusions about a parameter using Bayesian statistics. It is recommended, however, that there be a clear separation between these two aspects of reporting a result. In the remainder of this section, we assess the extent to which various types of intervals achieve the goals stated here.

32.3.1. The Bayesian approach :

Suppose the outcome of the experiment is characterized by a vector of data \mathbf{x} , whose probability distribution depends on an unknown parameter (or parameters) θ that we wish to determine. In Bayesian statistics, all knowledge about θ is summarized by the posterior p.d.f. $p(\theta|\mathbf{x})$, which gives the degree of belief for θ to take on values in a certain region given the data \mathbf{x} . It is obtained by using Bayes’ theorem,

$$p(\theta|\mathbf{x}) = \frac{L(\mathbf{x}|\theta)\pi(\theta)}{\int L(\mathbf{x}|\theta')\pi(\theta') d\theta'} \quad (32.30)$$

where $L(\mathbf{x}|\theta)$ is the likelihood function, *i.e.*, the joint p.d.f. for the data given a certain value of θ , evaluated with the data actually obtained in the experiment, and $\pi(\theta)$ is the prior p.d.f. for θ . Note that the denominator in Eq. (32.30) serves simply to normalize the posterior p.d.f. to unity.

Bayesian statistics supplies no unique rule for determining $\pi(\theta)$; this reflects the experimenter’s subjective degree of belief about θ before the measurement was carried out. By itself, therefore, the posterior p.d.f. is not a good way to report the result of an observation objectively, since it contains both the result (through the likelihood function) and the experimenter’s prior beliefs. Without the likelihood function, someone with different prior beliefs would be unable to substitute these to determine his or her own posterior p.d.f. This is an important reason, therefore, to publish wherever possible the likelihood function or an appropriate summary of it. Often this can be achieved by reporting the ML estimate and one or several low order derivatives of L evaluated at the estimate.

In the single parameter case, for example, an interval (called a Bayesian or credible interval) $[\theta_{lo}, \theta_{up}]$ can be determined which contains a given fraction $1 - \alpha$ of the posterior probability, *i.e.*,

$$1 - \alpha = \int_{\theta_{lo}}^{\theta_{up}} p(\theta|\mathbf{x}) d\theta \quad (32.31)$$

Sometimes an upper or lower limit is desired, *i.e.*, θ_{lo} can be set to zero or θ_{up} to infinity. In other cases, one might choose θ_{lo} and θ_{up} such that $p(\theta|\mathbf{x})$ is higher everywhere inside the interval than outside; these are called *highest posterior density* (HPD) intervals. Note that HPD intervals are not invariant under a nonlinear transformation of the parameter.

The main difficulty with Bayesian intervals is in quantifying the prior beliefs. Sometimes one attempts to construct $\pi(\theta)$ to represent complete ignorance about the parameters by setting it equal to a constant. A problem here is that if the prior p.d.f. is flat in θ , then it is not flat for a nonlinear function of θ , and so a different parametrization of the problem would lead in general to a different posterior p.d.f. In practice, one does not choose a flat prior as a true expression of degree of belief about a parameter; rather, it is used as a recipe to construct an interval, which in the end will have certain frequentist properties.

If a parameter is constrained to be non-negative, then the prior p.d.f. can simply be set to zero for negative values. An important example is the case of a Poisson variable n , which counts signal events with unknown mean s , as well as background with mean b , assumed known. For the signal mean s , one often uses the prior

$$\pi(s) = \begin{cases} 0 & s < 0 \\ 1 & s \geq 0 \end{cases} \quad (32.32)$$

As mentioned above, this is regarded as providing an interval whose frequentist properties can be studied, rather than as representing a degree of belief. In the absence of a clear discovery, (*e.g.*, if $n = 0$ or if in any case n is compatible with the expected background), one usually wishes to place an upper limit on s . Using the likelihood function for Poisson distributed n ,

$$L(n|s) = \frac{(s+b)^n}{n!} e^{-(s+b)} \quad (32.33)$$

along with the prior (32.32) in (32.30) gives the posterior density for s . An upper limit s_{up} at confidence level (or here, rather, credibility level) $1 - \alpha$ can be obtained by requiring

$$1 - \alpha = \int_{-\infty}^{s_{\text{up}}} p(s|n) ds = \frac{\int_{-\infty}^{s_{\text{up}}} L(n|s) \pi(s) ds}{\int_{-\infty}^{\infty} L(n|s) \pi(s) ds}, \quad (32.34)$$

where the lower limit of integration is effectively zero because of the cut-off in $\pi(s)$. By relating the integrals in Eq. (32.34) to incomplete gamma functions, the equation reduces to

$$\alpha = e^{-s_{\text{up}}} \frac{\sum_{m=0}^n (s_{\text{up}} + b)^m / m!}{\sum_{m=0}^n b^m / m!}. \quad (32.35)$$

This must be solved numerically for the limit s_{up} . For the special case of $b = 0$, the sums can be related to the *quantile* $F_{\chi^2}^{-1}$ of the χ^2 distribution (inverse of the cumulative distribution) to give

$$s_{\text{up}} = \frac{1}{2} F_{\chi^2}^{-1}(1 - \alpha; n_d), \quad (32.36)$$

where the number of degrees of freedom is $n_d = 2(n + 1)$. The quantile of the χ^2 distribution can be obtained using the CERNLIB routine CHISIN, or the ROOT function `TMath::ChisquareQuantile`. It so happens that for the case of $b = 0$, the upper limits from Eq. (32.36) coincide numerically with the values of the frequentist upper limits discussed in Section 32.3.2.5. Values for $1 - \alpha = 0.9$ and 0.95 are given by the values ν_{up} in Table 32.3. The frequentist properties of confidence intervals for the Poisson mean obtained in this way are discussed in Refs. [2] and [17].

Bayesian statistics provides a framework for incorporating systematic uncertainties into a result. Suppose, for example, that a model depends not only on parameters of interest θ , but on *nuisance parameters* ν , whose values are known with some limited accuracy. For a single nuisance parameter ν , for example, one might have a p.d.f. centered about its nominal value with a certain standard deviation σ_ν . Often a Gaussian p.d.f. provides a reasonable model for one's degree of belief about a nuisance parameter; in other cases, more complicated shapes may be appropriate. The likelihood function, prior, and posterior p.d.f.s then all depend on both θ and ν , and are related by Bayes' theorem, as usual. One can obtain the posterior p.d.f. for θ alone by integrating over the nuisance parameters, *i.e.*,

$$p(\theta|x) = \int p(\theta, \nu|x) d\nu. \quad (32.37)$$

If the prior joint p.d.f. for θ and ν factorizes, then integrating the posterior p.d.f. over ν is equivalent to replacing the likelihood function by (see Ref. 18),

$$L'(x|\theta) = \int L(x|\theta, \nu) \pi(\nu) d\nu. \quad (32.38)$$

The function $L'(x|\theta)$ can also be used together with frequentist methods that employ the likelihood function such as ML estimation of parameters. The results then have a mixed frequentist/Bayesian character, where the systematic uncertainty due to limited knowledge of the nuisance parameters is built in. Although this may make it more difficult to disentangle statistical from systematic effects, such a hybrid approach may satisfy the objective of reporting the result in a convenient way.

Even if the subjective Bayesian approach is not used explicitly, Bayes' theorem represents the way that people evaluate the impact of a new result on their beliefs. One of the criteria in choosing a method for reporting a measurement, therefore, should be the ease and convenience with which the consumer of the result can carry out this exercise.

32.3.2. Frequentist confidence intervals :

The unqualified phrase “confidence intervals” refers to frequentist intervals obtained with a procedure due to Neyman [19], described below. These are intervals (or in the multiparameter case, regions) constructed so as to include the true value of the parameter with a probability greater than or equal to a specified level, called the *coverage probability*. In this section, we discuss several techniques for producing intervals that have, at least approximately, this property.

32.3.2.1. The Neyman construction for confidence intervals:

Consider a p.d.f. $f(x; \theta)$ where x represents the outcome of the experiment and θ is the unknown parameter for which we want to construct a confidence interval. The variable x could (and often does) represent an estimator for θ . Using $f(x; \theta)$, we can find for a pre-specified probability $1 - \alpha$, and for every value of θ , a set of values $x_1(\theta, \alpha)$ and $x_2(\theta, \alpha)$ such that

$$P(x_1 < x < x_2; \theta) = 1 - \alpha = \int_{x_1}^{x_2} f(x; \theta) dx. \quad (32.39)$$

This is illustrated in Fig. 32.3: a horizontal line segment $[x_1(\theta, \alpha), x_2(\theta, \alpha)]$ is drawn for representative values of θ . The union of such intervals for all values of θ , designated in the figure as $D(\alpha)$, is known as the *confidence belt*. Typically the curves $x_1(\theta, \alpha)$ and $x_2(\theta, \alpha)$ are monotonic functions of θ , which we assume for this discussion.

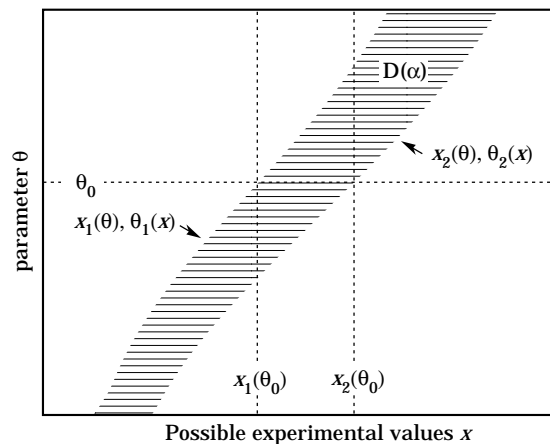


Figure 32.3: Construction of the confidence belt (see text).

Upon performing an experiment to measure x and obtaining a value x_0 , one draws a vertical line through x_0 . The confidence interval for θ is the set of all values of θ for which the corresponding line segment $[x_1(\theta, \alpha), x_2(\theta, \alpha)]$ is intercepted by this vertical line. Such confidence intervals are said to have a *confidence level* (CL) equal to $1 - \alpha$.

Now suppose that the true value of θ is θ_0 , indicated in the figure. We see from the figure that θ_0 lies between $\theta_1(x)$ and $\theta_2(x)$ if and only if x lies between $x_1(\theta_0)$ and $x_2(\theta_0)$. The two events thus have the same probability, and since this is true for any value θ_0 , we can drop the subscript 0 and obtain

$$1 - \alpha = P(x_1(\theta) < x < x_2(\theta)) = P(\theta_2(x) < \theta < \theta_1(x)). \quad (32.40)$$

In this probability statement, $\theta_1(x)$ and $\theta_2(x)$, *i.e.*, the endpoints of the interval, are the random variables and θ is an unknown constant. If the experiment were to be repeated a large number of times, the interval $[\theta_1, \theta_2]$ would vary, covering the fixed value θ in a fraction $1 - \alpha$ of the experiments.

The condition of coverage in Eq. (32.39) does not determine x_1 and x_2 uniquely, and additional criteria are needed. The most common criterion is to choose *central intervals* such that the probabilities excluded below x_1 and above x_2 are each $\alpha/2$. In other cases, one

may want to report only an upper or lower limit, in which case the probability excluded below x_1 or above x_2 can be set to zero. Another principle based on *likelihood ratio ordering* for determining which values of x should be included in the confidence belt is discussed in Sec. 32.3.2.2

When the observed random variable x is continuous, the coverage probability obtained with the Neyman construction is $1 - \alpha$, regardless of the true value of the parameter. If x is discrete, however, it is not possible to find segments $[x_1(\theta, \alpha), x_2(\theta, \alpha)]$ that satisfy Eq. (32.39) exactly for all values of θ . By convention, one constructs the confidence belt requiring the probability $P(x_1 < x < x_2)$ to be *greater than or equal to* $1 - \alpha$. This gives confidence intervals that include the true parameter with a probability greater than or equal to $1 - \alpha$.

32.3.2.2. Relationship between intervals and tests:

An equivalent method of constructing confidence intervals is to consider a test (see Sec. 32.2) of the hypothesis that the parameter's true value is θ (assume one constructs a test for all physical values of θ). One then excludes all values of θ where the hypothesis would be rejected at a significance level less than α . The remaining values constitute the confidence interval at confidence level $1 - \alpha$.

In this procedure, one is still free to choose the test to be used; this corresponds to the freedom in the Neyman construction as to which values of the data are included in the confidence belt. One possibility is use a test statistic based on the *likelihood ratio*,

$$\lambda = \frac{f(x; \theta)}{f(x; \hat{\theta})}, \tag{32.41}$$

where $\hat{\theta}$ is the value of the parameter which, out of all allowed values, maximizes $f(x; \theta)$. This results in the intervals described in Ref. 20 by Feldman and Cousins. The same intervals can be obtained from the Neyman construction described in the previous section by including in the confidence belt those values of x which give the greatest values of λ .

Another technique that can be formulated in the language of statistical tests has been used to set limits on the Higgs mass from measurements at LEP [21,22]. For each value of the Higgs mass, a statistic called CL_s is determined from the ratio

$$CL_s = \frac{p\text{-value of signal plus background hypothesis}}{1 - p\text{-value of hypothesis of background only}}. \tag{32.42}$$

The p -values in Eq. (32.42) are themselves based on a test statistic which depends in general on the signal being tested, *i.e.*, on the hypothesized Higgs mass. Smaller CL_s corresponds to a lesser level of agreement with the signal hypothesis.

In the usual procedure for constructing confidence intervals, one would exclude the signal hypothesis if the probability to obtain a value of CL_s less than the one actually observed is less than α . The LEP Higgs group has in fact followed a more conservative approach, and excludes the signal at a confidence level $1 - \alpha$ if CL_s itself (not the probability to obtain a lower CL_s value) is less than α . This results in a coverage probability that is in general greater than $1 - \alpha$. The interpretation of such intervals is discussed in Refs.[21,22].

32.3.2.3. Profile likelihood and treatment of nuisance parameters:

As mentioned in Section 32.3.1, one may have a model containing parameters that must be determined from data, but which are not of any interest in the final result (nuisance parameters). Suppose the likelihood $L(\theta, \nu)$ depends on parameters of interest θ and nuisance parameters ν . The nuisance parameters can be effectively removed from the problem by constructing the *profile likelihood*, defined by

$$L_p(\theta) = L(\theta, \hat{\nu}(\theta)), \tag{32.43}$$

where $\hat{\nu}(\theta)$ is given by the ν that maximizes the likelihood for fixed θ . The profile likelihood may then be used to construct tests of or intervals for the parameters of interest. This is analogous to use of

the integrated likelihood (32.38) used in the Bayesian approach. For example, one may construct the profile likelihood ratio,

$$\lambda_p(\theta) = \frac{L_p(\theta)}{L(\hat{\theta}, \hat{\nu})}, \tag{32.44}$$

where $\hat{\theta}$ and $\hat{\nu}$ are the ML estimators. The ratio λ_p can be used in place of the likelihood ratio (32.41) for inference about θ . The resulting intervals for the parameters of interest are not guaranteed to have the exact coverage probability for all values of the nuisance parameters, but in cases of practical interest the approximation is found to be very good. Further discussion on use of the profile likelihood can be found in, *e.g.*, Refs.[25,26] and other contributions to the PHYSTAT conferences [14].

32.3.2.4. Gaussian distributed measurements:

An important example of constructing a confidence interval is when the data consists of a single random variable x that follows a Gaussian distribution; this is often the case when x represents an estimator for a parameter and one has a sufficiently large data sample. If there is more than one parameter being estimated, the multivariate Gaussian is used. For the univariate case with known σ ,

$$1 - \alpha = \frac{1}{\sqrt{2\pi}\sigma} \int_{\mu-\delta}^{\mu+\delta} e^{-(x-\mu)^2/2\sigma^2} dx = \text{erf}\left(\frac{\delta}{\sqrt{2}\sigma}\right) \tag{32.45}$$

is the probability that the measured value x will fall within $\pm\delta$ of the true value μ . From the symmetry of the Gaussian with respect to x and μ , this is also the probability for the interval $x \pm \delta$ to include μ . Fig. 32.4 shows a $\delta = 1.64\sigma$ confidence interval unshaded. The choice $\delta = \sigma$ gives an interval called the *standard error* which has $1 - \alpha = 68.27\%$ if σ is known. Values of α for other frequently used choices of δ are given in Table 32.1.

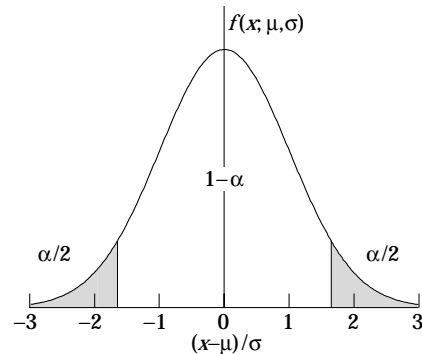


Figure 32.4: Illustration of a symmetric 90% confidence interval (unshaded) for a measurement of a single quantity with Gaussian errors. Integrated probabilities, defined by α , are as shown.

Table 32.1: Area of the tails α outside $\pm\delta$ from the mean of a Gaussian distribution.

α	δ	α	δ
0.3173	1σ	0.2	1.28σ
4.55×10^{-2}	2σ	0.1	1.64σ
2.7×10^{-3}	3σ	0.05	1.96σ
6.3×10^{-5}	4σ	0.01	2.58σ
5.7×10^{-7}	5σ	0.001	3.29σ
2.0×10^{-9}	6σ	10^{-4}	3.89σ

We can set a one-sided (upper or lower) limit by excluding above $x + \delta$ (or below $x - \delta$). The values of α for such limits are half the values in Table 32.1.

In addition to Eq. (32.45), α and δ are also related by the cumulative distribution function for the χ^2 distribution,

$$\alpha = 1 - F(\chi^2; n), \tag{32.46}$$

for $\chi^2 = (\delta/\sigma)^2$ and $n = 1$ degree of freedom. This can be obtained from Fig. 32.1 on the $n = 1$ curve or by using the CERNLIB routine PROB or the ROOT function TMath::Prob.

For multivariate measurements of, say, n parameter estimates $\hat{\theta} = (\hat{\theta}_1, \dots, \hat{\theta}_n)$, one requires the full covariance matrix $V_{ij} = \text{cov}[\hat{\theta}_i, \hat{\theta}_j]$, which can be estimated as described in Sections 32.1.2 and 32.1.3. Under fairly general conditions with the methods of maximum-likelihood or least-squares in the large sample limit, the estimators will be distributed according to a multivariate Gaussian centered about the true (unknown) values θ , and furthermore, the likelihood function itself takes on a Gaussian shape.

The standard error ellipse for the pair $(\hat{\theta}_i, \hat{\theta}_j)$ is shown in Fig. 32.5, corresponding to a contour $\chi^2 = \chi^2_{\min} + 1$ or $\ln L = \ln L_{\max} - 1/2$. The ellipse is centered about the estimated values $\hat{\theta}$, and the tangents to the ellipse give the standard deviations of the estimators, σ_i and σ_j . The angle of the major axis of the ellipse is given by

$$\tan 2\phi = \frac{2\rho_{ij}\sigma_i\sigma_j}{\sigma_j^2 - \sigma_i^2}, \tag{32.47}$$

where $\rho_{ij} = \text{cov}[\hat{\theta}_i, \hat{\theta}_j]/\sigma_i\sigma_j$ is the correlation coefficient.

The correlation coefficient can be visualized as the fraction of the distance σ_i from the ellipse's horizontal centerline at which the ellipse becomes tangent to vertical, *i.e.*, at the distance $\rho_{ij}\sigma_i$ below the centerline as shown. As ρ_{ij} goes to $+1$ or -1 , the ellipse thins to a diagonal line.

It could happen that one of the parameters, say, θ_j , is known from previous measurements to a precision much better than σ_j , so that the current measurement contributes almost nothing to the knowledge of θ_j . However, the current measurement of θ_i and its dependence on θ_j may still be important. In this case, instead of quoting both parameter estimates and their correlation, one sometimes reports the value of θ_i , which minimizes χ^2 at a fixed value of θ_j , such as the PDG best value. This θ_i value lies along the dotted line between the points where the ellipse becomes tangent to vertical, and has statistical error σ_{inner} as shown on the figure, where $\sigma_{\text{inner}} = (1 - \rho_{ij}^2)^{1/2}\sigma_i$. Instead of the correlation ρ_{ij} , one reports the dependency $d\hat{\theta}_i/d\theta_j$ which is the slope of the dotted line. This slope is related to the correlation coefficient by $d\hat{\theta}_i/d\theta_j = \rho_{ij} \times \frac{\sigma_i}{\sigma_j}$.

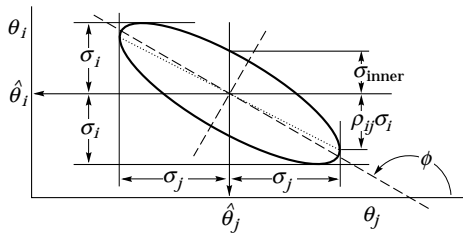


Figure 32.5: Standard error ellipse for the estimators $\hat{\theta}_i$ and $\hat{\theta}_j$. In this case the correlation is negative.

As in the single-variable case, because of the symmetry of the Gaussian function between θ and $\hat{\theta}$, one finds that contours of constant $\ln L$ or χ^2 cover the true values with a certain, fixed probability. That is, the confidence region is determined by

$$\ln L(\theta) \geq \ln L_{\max} - \Delta \ln L, \tag{32.48}$$

or where a χ^2 has been defined for use with the method of least-squares,

$$\chi^2(\theta) \leq \chi^2_{\min} + \Delta\chi^2. \tag{32.49}$$

Table 32.2: $\Delta\chi^2$ or $2\Delta \ln L$ corresponding to a coverage probability $1 - \alpha$ in the large data sample limit, for joint estimation of m parameters.

$(1 - \alpha)$ (%)	$m = 1$	$m = 2$	$m = 3$
68.27	1.00	2.30	3.53
90.	2.71	4.61	6.25
95.	3.84	5.99	7.82
95.45	4.00	6.18	8.03
99.	6.63	9.21	11.34
99.73	9.00	11.83	14.16

Values of $\Delta\chi^2$ or $2\Delta \ln L$ are given in Table 32.2 for several values of the coverage probability and number of fitted parameters.

For finite data samples, the probability for the regions determined by equations (32.48) or (32.49) to cover the true value of θ will depend on θ , so these are not exact confidence regions according to our previous definition. Nevertheless, they can still have a coverage probability only weakly dependent on the true parameter, and approximately as given in Table 32.2. In any case, the coverage probability of the intervals or regions obtained according to this procedure can in principle be determined as a function of the true parameter(s), for example, using a Monte Carlo calculation.

One of the practical advantages of intervals that can be constructed from the log-likelihood function or χ^2 is that it is relatively simple to produce the interval for the combination of several experiments. If N independent measurements result in log-likelihood functions $\ln L_i(\theta)$, then the combined log-likelihood function is simply the sum,

$$\ln L(\theta) = \sum_{i=1}^N \ln L_i(\theta). \tag{32.50}$$

This can then be used to determine an approximate confidence interval or region with Eq. (32.48), just as with a single experiment.

32.3.2.5. Poisson or binomial data:

Another important class of measurements consists of counting a certain number of events, n . In this section, we will assume these are all events of the desired type, *i.e.*, there is no background. If n represents the number of events produced in a reaction with cross section σ , say, in a fixed integrated luminosity \mathcal{L} , then it follows a Poisson distribution with mean $\nu = \sigma\mathcal{L}$. If, on the other hand, one has selected a larger sample of N events and found n of them to have a particular property, then n follows a binomial distribution where the parameter p gives the probability for the event to possess the property in question. This is appropriate, *e.g.*, for estimates of branching ratios or selection efficiencies based on a given total number of events.

For the case of Poisson distributed n , the upper and lower limits on the mean value ν can be found from the Neyman procedure to be

$$\nu_{\text{lo}} = \frac{1}{2} F_{\chi^2}^{-1}(\alpha_{\text{lo}}; 2n), \tag{32.51a}$$

$$\nu_{\text{up}} = \frac{1}{2} F_{\chi^2}^{-1}(1 - \alpha_{\text{up}}; 2(n + 1)), \tag{32.51b}$$

where the upper and lower limits are at confidence levels of $1 - \alpha_{\text{lo}}$ and $1 - \alpha_{\text{up}}$, respectively, and $F_{\chi^2}^{-1}$ is the *quantile* of the χ^2 distribution (inverse of the cumulative distribution). The quantiles $F_{\chi^2}^{-1}$ can be obtained from standard tables or from the CERNLIB routine CHISIN. For central confidence intervals at confidence level $1 - \alpha$, set $\alpha_{\text{lo}} = \alpha_{\text{up}} = \alpha/2$.

It happens that the upper limit from Eq. (32.51a) coincides numerically with the Bayesian upper limit for a Poisson parameter, using a uniform prior p.d.f. for ν . Values for confidence levels of 90% and 95% are shown in Table 32.3.

Table 32.3: Lower and upper (one-sided) limits for the mean ν of a Poisson variable given n observed events in the absence of background, for confidence levels of 90% and 95%.

n	$1 - \alpha = 90\%$		$1 - \alpha = 95\%$	
	ν_{lo}	ν_{up}	ν_{lo}	ν_{up}
0	–	2.30	–	3.00
1	0.105	3.89	0.051	4.74
2	0.532	5.32	0.355	6.30
3	1.10	6.68	0.818	7.75
4	1.74	7.99	1.37	9.15
5	2.43	9.27	1.97	10.51
6	3.15	10.53	2.61	11.84
7	3.89	11.77	3.29	13.15
8	4.66	12.99	3.98	14.43
9	5.43	14.21	4.70	15.71
10	6.22	15.41	5.43	16.96

For the case of binomially distributed n successes out of N trials with probability of success p , the upper and lower limits on p are found to be

$$p_{lo} = \frac{nF_F^{-1}[\alpha_{lo}; 2n, 2(N - n + 1)]}{N - n + 1 + nF_F^{-1}[\alpha_{lo}; 2n, 2(N - n + 1)]}, \quad (32.52a)$$

$$p_{up} = \frac{(n + 1)F_F^{-1}[1 - \alpha_{up}; 2(n + 1), 2(N - n)]}{(N - n) + (n + 1)F_F^{-1}[1 - \alpha_{up}; 2(n + 1), 2(N - n)]}. \quad (32.52b)$$

Here F_F^{-1} is the quantile of the F distribution (also called the Fisher–Snedecor distribution; see Ref. 4).

32.3.2.6. Difficulties with intervals near a boundary:

A number of issues arise in the construction and interpretation of confidence intervals when the parameter can only take on values in a restricted range. An important example is where the mean of a Gaussian variable is constrained on physical grounds to be non-negative. This arises, for example, when the square of the neutrino mass is estimated from $\hat{m}^2 = \hat{E}^2 - \hat{p}^2$, where \hat{E} and \hat{p} are independent, Gaussian-distributed estimates of the energy and momentum. Although the true m^2 is constrained to be positive, random errors in \hat{E} and \hat{p} can easily lead to negative values for the estimate \hat{m}^2 .

If one uses the prescription given above for Gaussian distributed measurements, which says to construct the interval by taking the estimate plus-or-minus-one standard deviation, then this can give intervals that are partially or entirely in the unphysical region. In fact, by following strictly the Neyman construction for the central confidence interval, one finds that the interval is truncated below zero; nevertheless an extremely small or even a zero-length interval can result.

An additional important example is where the experiment consists of counting a certain number of events, n , which is assumed to be Poisson-distributed. Suppose the expectation value $E[n] = \nu$ is equal to $s + b$, where s and b are the means for signal and background processes, and assume further that b is a known constant. Then $\hat{s} = n - b$ is an unbiased estimator for s . Depending on true magnitudes of s and b , the estimate \hat{s} can easily fall in the negative region. Similar to the Gaussian case with the positive mean, the central confidence interval or even the upper limit for s may be of zero length.

The confidence interval is in fact designed not to cover the parameter with a probability of at most α , and if a zero-length interval results, then this is evidently one of those experiments. So although the construction is behaving as it should, a null interval is

an unsatisfying result to report, and several solutions to this type of problem are possible.

An additional difficulty arises when a parameter estimate is not significantly far away from the boundary, in which case it is natural to report a one-sided confidence interval (often an upper limit). It is straightforward to force the Neyman prescription to produce only an upper limit by setting $x_2 = \infty$ in Eq. 32.39. Then x_1 is uniquely determined and the upper limit can be obtained. If, however, the data come out such that the parameter estimate is not so close to the boundary, one might wish to report a central (*i.e.*, two-sided) confidence interval. As pointed out by Feldman and Cousins [20], however, if the decision to report an upper limit or two-sided interval is made by looking at the data (“flip-flopping”), then the resulting intervals will not in general cover the parameter with the probability $1 - \alpha$.

With the confidence intervals suggested in Ref. 20, the prescription determines whether the interval is one- or two-sided in a way which preserves the coverage probability. Interval constructions that have this property and avoid the problem of null intervals are said to be unified. The intervals based on the Feldman-Cousins prescription are of this type. For a given choice of $1 - \alpha$, if the parameter estimate is sufficiently close to the boundary, the method gives a one-sided limit. In the case of a Poisson variable in the presence of background, for example, this would occur if the number of observed events is compatible with the expected background. For parameter estimates increasingly far away from the boundary, *i.e.*, for increasing signal significance, the interval makes a smooth transition from one- to two-sided, and far away from the boundary, one obtains a central interval.

The intervals according to this method for the mean of Poisson variable in the absence of background are given in Table 32.4. (Note that α in Ref. 20 is defined following Neyman [19] as the coverage probability; this is opposite the modern convention used here in which the coverage probability is $1 - \alpha$.) The values of $1 - \alpha$ given here refer to the coverage of the true parameter by the whole interval $[\nu_1, \nu_2]$. In Table 32.3 for the one-sided upper and lower limits, however, $1 - \alpha$ refers to the probability to have individually $\nu_{up} \geq \nu$ or $\nu_{lo} \leq \nu$.

Table 32.4: Unified confidence intervals $[\nu_1, \nu_2]$ for a the mean of a Poisson variable given n observed events in the absence of background, for confidence levels of 90% and 95%.

n	$1 - \alpha = 90\%$		$1 - \alpha = 95\%$	
	ν_1	ν_2	ν_1	ν_2
0	0.00	2.44	0.00	3.09
1	0.11	4.36	0.05	5.14
2	0.53	5.91	0.36	6.72
3	1.10	7.42	0.82	8.25
4	1.47	8.60	1.37	9.76
5	1.84	9.99	1.84	11.26
6	2.21	11.47	2.21	12.75
7	3.56	12.53	2.58	13.81
8	3.96	13.99	2.94	15.29
9	4.36	15.30	4.36	16.77
10	5.50	16.50	4.75	17.82

A potential difficulty with unified intervals arises if, for example, one constructs such an interval for a Poisson parameter s of some yet to be discovered signal process with, say, $1 - \alpha = 0.9$. If the true signal parameter is zero, or in any case much less than the expected background, one will usually obtain a one-sided upper limit on s . In a certain fraction of the experiments, however, a two-sided interval for s will result. Since, however, one typically chooses $1 - \alpha$ to be only 0.9 or 0.95 when searching for a new effect, the value $s = 0$ may be excluded from the interval before the existence of the effect

is well established. It must then be communicated carefully that in excluding $s = 0$ from the interval, one is not necessarily claiming to have discovered the effect.

The intervals constructed according to the unified procedure in Ref. 20 for a Poisson variable n consisting of signal and background have the property that for $n = 0$ observed events, the upper limit decreases for increasing expected background. This is counter-intuitive, since it is known that if $n = 0$ for the experiment in question, then no background was observed, and therefore one may argue that the expected background should not be relevant. The extent to which one should regard this feature as a drawback is a subject of some controversy (see, *e.g.*, Ref. 24).

Another possibility is to construct a Bayesian interval as described in Section 32.3.1. The presence of the boundary can be incorporated simply by setting the prior density to zero in the unphysical region. Priors based on invariance principles (rather than subjective degree of belief) for the Poisson mean are rarely used in high-energy physics. An example one may consider for the Poisson problem is a prior inversely proportional to the mean; here one obtains a posterior that diverges for the case of zero events observed, and finds upper limits which undercover when evaluated by the frequentist definition of coverage [2]. Rather, priors uniform in the Poisson mean have been used, although as previously mentioned, this is generally not done to reflect the experimenter's degree of belief, but rather as a procedure for obtaining an interval with certain frequentist properties. The resulting upper limits have a coverage probability that depends on the true value of the Poisson parameter, and is everywhere greater than the stated probability content. Lower limits and two-sided intervals for the Poisson mean based on flat priors undercover, however, for some values of the parameter, although to an extent that in practical cases may not be too severe [2, 17]. Intervals constructed in this way have the advantage of being easy to derive; if several independent measurements are to be combined then one simply multiplies the likelihood functions (cf. Eq. (32.50)).

An additional alternative is presented by the intervals found from the likelihood function or χ^2 using the prescription of Equations (32.48) or (32.49). As in the case of the Bayesian intervals, the coverage probability is not, in general, independent of the true parameter. Furthermore, these intervals can for some parameter values undercover. The coverage probability can, of course, be determined with some extra effort and reported with the result.

Also as in the Bayesian case, intervals derived from the value of the likelihood function from a combination of independent experiments can be determined simply by multiplying the likelihood functions. These intervals are also invariant under transformation of the parameter; this is not true for Bayesian intervals with a conventional flat prior, because a uniform distribution in, say, θ will not be uniform if transformed to θ^2 . Use of the likelihood function to determine approximate confidence intervals is discussed further in Ref. 23.

In any case, it is important to always report sufficient information so that the result can be combined with other measurements. Often this means giving an unbiased estimator and its standard deviation, even if the estimated value is in the unphysical region.

Regardless of the type of interval reported, the consumer of that result will almost certainly use it to derive some impression about the value of the parameter. This will inevitably be done, either explicitly or intuitively, with Bayes' theorem,

$$p(\theta|\text{result}) \propto L(\text{result}|\theta)\pi(\theta), \quad (32.53)$$

where the reader supplies his or her own prior beliefs $\pi(\theta)$ about the parameter, and the 'result' is whatever sort of interval or other information the author has reported. For all of the intervals discussed, therefore, it is not sufficient to know the result; one must also know the probability to have obtained this result as a function of the parameter, *i.e.*, the likelihood. Contours of constant likelihood, for example, provide this information, and so an interval obtained from $\ln L = \ln L_{\max} - \Delta \ln L$ already takes one step in this direction.

It can also be useful with a frequentist interval to calculate its subjective probability content using the posterior p.d.f. based on one

or several reasonable guesses for the prior p.d.f. If it turns out to be significantly less than the stated confidence level, this warns that it would be particularly misleading to draw conclusions about the parameter's value from the interval alone.

References:

1. B. Efron, *Am. Stat.* **40**, 11 (1986).
2. R.D. Cousins, *Am. J. Phys.* **63**, 398 (1995).
3. A. Stuart, J.K. Ord, and S. Arnold, *Kendall's Advanced Theory of Statistics*, Vol. 2A: *Classical Inference and the Linear Model*, 6th Ed., Oxford Univ. Press (1999), and earlier editions by Kendall and Stuart. The likelihood-ratio ordering principle is described at the beginning of Ch. 23. Chapter 26 compares different schools of statistical inference.
4. F.E. James, *Statistical Methods in Experimental Physics*, 2nd ed., (World Scientific, Singapore, 2007).
5. H. Cramér, *Mathematical Methods of Statistics*, Princeton Univ. Press, New Jersey (1958).
6. L. Lyons, *Statistics for Nuclear and Particle Physicists*, (Cambridge University Press, New York, 1986).
7. R. Barlow, *Nucl. Instrum. Methods* **A297**, 496 (1990).
8. G. Cowan, *Statistical Data Analysis*, (Oxford University Press, Oxford, 1998).
9. For a review, see S. Baker and R. Cousins, *Nucl. Instrum. Methods* **221**, 437 (1984).
10. For information on neural networks and related topics, see *e.g.*, C.M. Bishop, *Neural Networks for Pattern Recognition*, Clarendon Press, Oxford (1995); C. Peterson and T. Rögvaldsson, An Intro. to Artificial Neural Networks, in *Proc. of the 1991 CERN School of Computing*, C. Verkerk (ed.), CERN 92-02 (1992).
11. T. Hastie, R. Tibshirani, and J. Friedman, *The Elements of Statistical Learning* (Springer, New York, 2001).
12. A. Webb, *Statistical Pattern Recognition*, 2nd ed., (Wiley, New York, 2002).
13. L.I. Kuncheva, *Combining Pattern Classifiers*, (Wiley, New York, 2004).
14. Links to the Proceedings of the PHYSTAT conference series (Durham 2002, Stanford 2003, Oxford 2005, and Geneva 2007) can be found at phystat.org.
15. A. Höcker *et al.*, *TMVA Users Guide*, [physics/0703039\(2007\)](http://physics/0703039(2007)); software available from tmva.sf.net.
16. I. Narsky, *StatPatternRecognition: A C++ Package for Statistical Analysis of High Energy Physics Data*, [physics/0507143\(2005\)](http://physics/0507143(2005)); software avail. from sourceforge.net/projects/statpatrec.
17. B.P. Roe and M.B. Woodroffe, *Phys. Rev.* **D63**, 13009 (2001).
18. P.H. Garthwaite, I.T. Jolliffe, and B. Jones, *Statistical Inference*, (Prentice Hall, 1995).
19. J. Neyman, *Phil. Trans. Royal Soc. London, Series A*, **236**, 333 (1937), reprinted in *A Selection of Early Statistical Papers on J. Neyman*, (University of California Press, Berkeley, 1967).
20. G.J. Feldman and R.D. Cousins, *Phys. Rev.* **D57**, 3873 (1998). This paper does not specify what to do if the ordering principle gives equal rank to some values of x . Eq. 21.6 of Ref. 3 gives the rule: all such points are included in the acceptance region (the domain $D(\alpha)$). Some authors have assumed the contrary, and shown that one can then obtain null intervals.
21. T. Junk, *Nucl. Instrum. Methods* **A434**, 435 (1999).
22. A.L. Read, *Modified frequentist analysis of search results (the CL_s method)*, in F. James, L. Lyons, and Y. Perrin (eds.), *Workshop on Confidence Limits*, CERN Yellow Report 2000-005, available through cdsweb.cern.ch.
23. F. Porter, *Nucl. Instrum. Methods* **A368**, 793 (1996).
24. Workshop on Confidence Limits, CERN, 17-18 Jan. 2000, www.cern.ch/CERN/Divisions/EP/Events/CLW/. The proceedings, F. James, L. Lyons, and Y. Perrin (eds.), CERN Yellow Report 2000-005, are available through cdsweb.cern.ch. See also the later Fermilab workshop linked to the CERN web page.
25. N. Reid, *Likelihood Inference in the Presence of Nuisance Parameters*, Proceedings of PHYSTAT2003, L. Lyons, R. Mount, and R. Reitmeyer, eds., eConf C030908, Stanford, 2003.
26. W.A. Rolke, A.M. Lopez, and J. Conrad, *Nucl. Instrum. Methods* **A551**, 493 (2005); physics/0403059.

33. MONTE CARLO TECHNIQUES

Revised September 2007 by G. Cowan (RHUL).

Monte Carlo techniques are often the only practical way to evaluate difficult integrals or to sample random variables governed by complicated probability density functions. Here we describe an assortment of methods for sampling some commonly occurring probability density functions.

33.1. Sampling the uniform distribution

Most Monte Carlo sampling or integration techniques assume a “random number generator,” which generates uniform statistically independent values on the half open interval $[0, 1)$; for reviews see, e.g., [1, 2].

Uniform random number generators are available in software libraries such as CERNLIB [3], CLHEP [4], and ROOT [5]. For example, in addition to a basic congruential generator TRandom (see below), ROOT provides three more sophisticated routines: TRandom1 implements the RANLUX generator [6] based on the method by Lüscher, and allows the user to select different quality levels, trading off quality with speed; TRandom2 is based on the maximally equidistributed combined Tausworthe generator by L’Ecuyer [7]; the TRandom3 generator implements the Mersenne twister algorithm of Matsumoto and Nishimura [8]. All of the algorithms produce a periodic sequence of numbers, and to obtain effectively random values, one must not use more than a small subset of a single period. The Mersenne twister algorithm has an extremely long period of $2^{19937} - 1$.

The performance of the generators can be investigated with tests such as DIEHARD [9] or TestU01 [10]. Many commonly available congruential generators fail these tests and often have sequences (typically with periods less than 2^{32}), which can be easily exhausted on modern computers. A short period is a problem for the TRandom generator in ROOT, which, however, has the advantage that its state is stored in a single 32-bit word. The generators TRandom1, TRandom2, or TRandom3 have much longer periods, with TRandom3 being recommended by the ROOT authors as providing the best combination of speed and good random properties.

33.2. Inverse transform method

If the desired probability density function is $f(x)$ on the range $-\infty < x < \infty$, its cumulative distribution function (expressing the probability that $x \leq a$) is given by Eq. (31.6). If a is chosen with probability density $f(a)$, then the integrated probability up to point a , $F(a)$, is itself a random variable which will occur with uniform probability density on $[0, 1]$. If x can take on any value, and ignoring the endpoints, we can then find a unique x chosen from the p.d.f. $f(s)$ for a given u if we set

$$u = F(x), \tag{33.1}$$

provided we can find an inverse of F , defined by

$$x = F^{-1}(u). \tag{33.2}$$

This method is shown in Fig. 33.1a. It is most convenient when one can calculate by hand the inverse function of the indefinite integral of f . This is the case for some common functions $f(x)$ such as $\exp(x)$, $(1 - x)^n$, and $1/(1 + x^2)$ (Cauchy or Breit-Wigner), although it does not necessarily produce the fastest generator. Standard libraries contain software to implement this method numerically, working from functions or histograms in one or more dimensions, e.g., the UNU.RAN package [11], available in ROOT.

For a discrete distribution, $F(x)$ will have a discontinuous jump of size $f(x_k)$ at each allowed $x_k, k = 1, 2, \dots$. Choose u from a uniform distribution on $(0, 1)$ as before. Find x_k such that

$$F(x_{k-1}) < u \leq F(x_k) \equiv \text{Prob}(x \leq x_k) = \sum_{i=1}^k f(x_i); \tag{33.3}$$

then x_k is the value we seek (note: $F(x_0) \equiv 0$). This algorithm is illustrated in Fig. 33.1b.

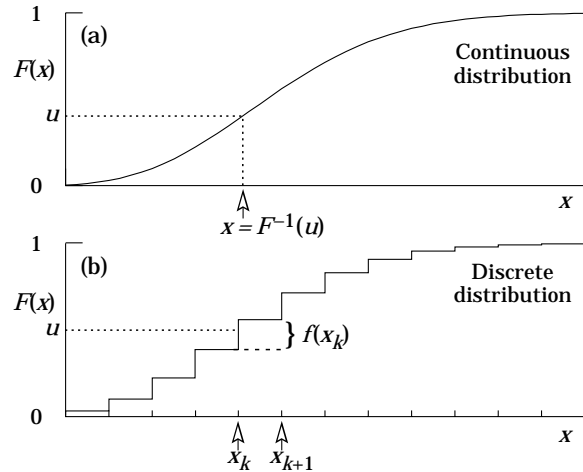


Figure 33.1: Use of a random number u chosen from a uniform distribution $(0, 1)$ to find a random number x from a distribution with cumulative distribution function $F(x)$.

33.3. Acceptance-rejection method (Von Neumann)

Very commonly an analytic form for $F(x)$ is unknown or too complex to work with, so that obtaining an inverse as in Eq. (33.2) is impractical. We suppose that for any given value of x , the probability density function $f(x)$ can be computed, and further that enough is known about $f(x)$ that we can enclose it entirely inside a shape which is C times an easily generated distribution $h(x)$, as illustrated in Fig. 33.2.

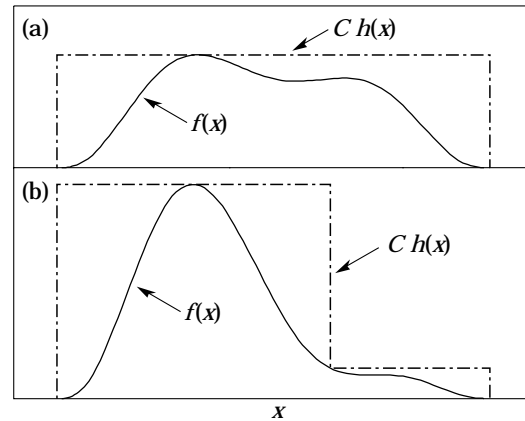


Figure 33.2: Illustration of the acceptance-rejection method. Random points are chosen inside the upper bounding figure, and rejected if the ordinate exceeds $f(x)$. The lower figure illustrates a method to increase the efficiency (see text).

Frequently $h(x)$ is uniform or is a normalized sum of uniform distributions. Note that both $f(x)$ and $h(x)$ must be normalized to unit area, and therefore, the proportionality constant $C > 1$. To generate $f(x)$, first generate a candidate x according to $h(x)$. Calculate $f(x)$ and the height of the envelope $C h(x)$; generate u and test if $u C h(x) \leq f(x)$. If so, accept x ; if not reject x and try again. If we regard x and $u C h(x)$ as the abscissa and ordinate of a point in a two-dimensional plot, these points will populate the entire area $C h(x)$ in a smooth manner; then we accept those which fall under $f(x)$. The efficiency is the ratio of areas, which must equal $1/C$; therefore we must keep C as close as possible to 1.0. Therefore, we try to choose $C h(x)$ to be as close to $f(x)$ as convenience dictates, as in the lower part of Fig. 33.2.

33.4. Algorithms

Algorithms for generating random numbers belonging to many different distributions are given for example by Press [12], Ahrens and Dieter [13], Rubinstein [14], Devroye [15], and Walck [16]. For many distributions, alternative algorithms exist, varying in complexity, speed, and accuracy. For time-critical applications, these algorithms may be coded in-line to remove the significant overhead often encountered in making function calls.

In the examples given below, we use the notation for the variables and parameters given in Table 31.1. Variables named “ u ” are assumed to be independent and uniform on $[0,1]$. Denominators must be verified to be non-zero where relevant.

33.4.1. Exponential decay :

This is a common application of the inverse transform method, and uses the fact that if u is uniformly distributed in $[0,1]$, then $(1-u)$ is as well. Consider an exponential p.d.f. $f(t) = (1/\tau) \exp(-t/\tau)$ that is truncated so as to lie between two values, a and b , and renormalized to unit area. To generate decay times t according to this p.d.f., first let $\alpha = \exp(-a/\tau)$ and $\beta = \exp(-b/\tau)$; then generate u and let

$$t = -\tau \ln(\beta + u(\alpha - \beta)). \quad (33.4)$$

For $(a,b) = (0, \infty)$, we have simply $t = -\tau \ln u$. (See also Sec. 33.4.6.)

33.4.2. Isotropic direction in 3D :

Isotropy means the density is proportional to solid angle, the differential element of which is $d\Omega = d(\cos\theta)d\phi$. Hence $\cos\theta$ is uniform $(2u_1 - 1)$ and ϕ is uniform $(2\pi u_2)$. For alternative generation of $\sin\phi$ and $\cos\phi$, see the next subsection.

33.4.3. Sine and cosine of random angle in 2D :

Generate u_1 and u_2 . Then $v_1 = 2u_1 - 1$ is uniform on $(-1,1)$, and $v_2 = u_2$ is uniform on $(0,1)$. Calculate $r^2 = v_1^2 + v_2^2$. If $r^2 > 1$, start over. Otherwise, the sine (S) and cosine (C) of a random angle (*i.e.*, uniformly distributed between zero and 2π) are given by

$$S = 2v_1v_2/r^2 \quad \text{and} \quad C = (v_1^2 - v_2^2)/r^2. \quad (33.5)$$

33.4.4. Gaussian distribution :

If u_1 and u_2 are uniform on $(0,1)$, then

$$z_1 = \sin 2\pi u_1 \sqrt{-2 \ln u_2} \quad \text{and} \quad z_2 = \cos 2\pi u_1 \sqrt{-2 \ln u_2} \quad (33.6)$$

are independent and Gaussian distributed with mean 0 and $\sigma = 1$.

There are many faster variants of this basic algorithm. For example, construct $v_1 = 2u_1 - 1$ and $v_2 = 2u_2 - 1$, which are uniform on $(-1,1)$. Calculate $r^2 = v_1^2 + v_2^2$, and if $r^2 > 1$ start over. If $r^2 < 1$, it is uniform on $(0,1)$. Then

$$z_1 = v_1 \sqrt{\frac{-2 \ln r^2}{r^2}} \quad \text{and} \quad z_2 = v_2 \sqrt{\frac{-2 \ln r^2}{r^2}} \quad (33.7)$$

are independent numbers chosen from a normal distribution with mean 0 and variance 1. $z'_i = \mu + \sigma z_i$ distributes with mean μ and variance σ^2 .

For a multivariate Gaussian with an $n \times n$ covariance matrix V , one can start by generating n independent Gaussian variables, $\{\eta_j\}$, with mean 0 and variance 1 as above. Then the new set $\{x_i\}$ is obtained as $x_i = \mu_i + \sum_j L_{ij} \eta_j$, where μ_i is the mean of x_i , and L_{ij} are the components of L , the unique lower triangular matrix that fulfils $V = LL^T$. The matrix L can be easily computed by the following recursive relation (Cholesky's method):

$$L_{jj} = \left(V_{jj} - \sum_{k=1}^{j-1} L_{jk}^2 \right)^{1/2}, \quad (33.8a)$$

$$L_{ij} = \frac{V_{ij} - \sum_{k=1}^{j-1} L_{ik} L_{jk}}{L_{jj}}, \quad j = 1, \dots, n; \quad i = j + 1, \dots, n, \quad (33.8b)$$

where $V_{ij} = \rho_{ij} \sigma_i \sigma_j$ are the components of V . For $n = 2$ one has

$$L = \begin{pmatrix} \sigma_1 & 0 \\ \rho \sigma_2 & \sqrt{1 - \rho^2} \sigma_2 \end{pmatrix}, \quad (33.9)$$

and therefore the correlated Gaussian variables are generated as $x_1 = \mu_1 + \sigma_1 \eta_1$, $x_2 = \mu_2 + \rho \sigma_2 \eta_1 + \sqrt{1 - \rho^2} \sigma_2 \eta_2$.

33.4.5. $\chi^2(n)$ distribution :

To generate variable following the χ^2 distribution for n degrees of freedom, use the Gamma distribution with $k = n/2$ and $\lambda = 1/2$ using the method of Sec. 33.4.6.

33.4.6. Gamma distribution :

All of the following algorithms are given for $\lambda = 1$. For $\lambda \neq 1$, divide the resulting random number x by λ .

- If $k = 1$ (the *exponential* distribution), accept $x = -\ln u$. (See also Sec. 33.4.1.)
- If $0 < k < 1$, initialize with $v_1 = (e + k)/e$ (with $e = 2.71828\dots$ being the natural log base). Generate u_1, u_2 . Define $v_2 = v_1 u_1$.

Case 1: $v_2 \leq 1$. Define $x = v_2^{1/k}$. If $u_2 \leq e^{-x}$, accept x and stop, else restart by generating new u_1, u_2 .

Case 2: $v_2 > 1$. Define $x = -\ln([v_1 - v_2]/k)$. If $u_2 \leq x^{k-1}$, accept x and stop, else restart by generating new u_1, u_2 . Note that, for $k < 1$, the probability density has a pole at $x = 0$, so that return values of zero due to underflow must be accepted or otherwise dealt with.

- Otherwise, if $k > 1$, initialize with $c = 3k - 0.75$. Generate u_1 and compute $v_1 = u_1(1 - u_1)$ and $v_2 = (u_1 - 0.5)\sqrt{c/v_1}$. If $x = k + v_2 - 1 \leq 0$, go back and generate new u_1 ; otherwise generate u_2 and compute $v_3 = 64v_3^3 u_2^2$. If $v_3 \leq 1 - 2v_2^2/x$ or if $\ln v_3 \leq 2\{[k-1] \ln[x/(k-1)] - v_2\}$, accept x and stop; otherwise go back and generate new u_1 .

33.4.7. Binomial distribution :

Begin with $k = 0$ and generate u uniform in $[0,1]$. Compute $P_k = (1-p)^n$ and store P_k into B . If $u \leq B$ accept $r_k = k$ and stop. Otherwise, increment k by one; compute the next P_k as $P_k \cdot (p/(1-p)) \cdot (n-k)/(k+1)$; add this to B . Again, if $u \leq B$, accept $r_k = k$ and stop, otherwise iterate until a value is accepted. If $p > 1/2$, it will be more efficient to generate r from $f(r; n, q)$, *i.e.*, with p and q interchanged, and then set $r_k = n - r$.

33.4.8. Poisson distribution :

Iterate until a successful choice is made: Begin with $k = 1$ and set $A = 1$ to start. Generate u . Replace A with uA ; if now $A < \exp(-\mu)$, where μ is the Poisson parameter, accept $n_k = k - 1$ and stop. Otherwise increment k by 1, generate a new u and repeat, always starting with the value of A left from the previous try.

Note that the Poisson generator used in ROOT's `TRandom` classes before version 5.12 (including the derived classes `TRandom1`, `TRandom2`, `TRandom3`) as well as the routine `RNPSSN` from CERNLIB, use a Gaussian approximation when μ exceeds a given threshold. This may be satisfactory (and much faster) for some applications. To do this, generate z from a Gaussian with zero mean and unit standard deviation; then use $x = \max(0, [\mu + z\sqrt{\mu} + 0.5])$ where $[\]$ signifies the greatest integer \leq the expression. The routines from Numerical Recipes [12] and CLHEP's routine `RandPoisson` do not make this approximation (see, *e.g.*, Ref. 17).

33.4.9. Student's t distribution :

Generate u_1 and u_2 uniform in $(0,1)$; then $t = \sin(2\pi u_1)[n(u_2^{-2/n} - 1)]^{1/2}$ follows the Student's t distribution for $n > 0$ degrees of freedom (n not necessarily an integer).

Alternatively, generate x from a Gaussian with mean 0 and $\sigma^2 = 1$ according to the method of 33.4.4. Next generate y , an independent gamma random variate, according to 33.4.6 with $\lambda = 1/2$ and $k = n/2$. Then $z = x/\sqrt{y/n}$ is distributed as a t with n degrees of freedom.

For the special case $n = 1$, the Breit-Wigner distribution, generate u_1 and u_2 ; set $v_1 = 2u_1 - 1$ and $v_2 = 2u_2 - 1$. If $v_1^2 + v_2^2 \leq 1$ accept $z = v_1/v_2$ as a Breit-Wigner distribution with unit area, center at 0.0, and FWHM 2.0. Otherwise start over. For center M_0 and FWHM Γ , use $W = z\Gamma/2 + M_0$.

33.5. Markov Chain Monte Carlo

In applications involving generation of random numbers following a multivariate distribution with a high number of dimensions, the transformation method may not be possible and the acceptance-rejection technique may have too low of an efficiency to be practical. If it is not required to have independent random values, but only that they follow a certain distribution, then Markov Chain Monte Carlo (MCMC) methods can be used. In depth treatments of MCMC can be found, *e.g.*, in the texts by Robert and Casella [18], Liu [19], and the review by Neal [20].

MCMC is particularly useful in connection with Bayesian statistics, where a p.d.f. $p(\boldsymbol{\theta})$ for an n -dimensional vector of parameters $\boldsymbol{\theta} = (\theta_1, \dots, \theta_n)$ is obtained, and one needs the marginal distribution of a subset of the components. Here one samples $\boldsymbol{\theta}$ from $p(\boldsymbol{\theta})$ and simply records the marginal distribution for the components of interest.

A simple and broadly applicable MCMC method is the Metropolis-Hastings algorithm, which allows one to generate multidimensional points $\boldsymbol{\theta}$ distributed according to a target p.d.f. that is proportional to a given function $p(\boldsymbol{\theta})$. It is not necessary to have $p(\boldsymbol{\theta})$ normalized to unit area, which is useful in Bayesian statistics, as posterior probability densities are often determined only up to an unknown normalization constant.

To generate points that follow $p(\boldsymbol{\theta})$, one first needs a proposal p.d.f. $q(\boldsymbol{\theta}; \boldsymbol{\theta}_0)$, which can be (almost) any p.d.f. from which independent random values $\boldsymbol{\theta}$ can be generated, and which contains as a parameter another point in the same space $\boldsymbol{\theta}_0$. For example, a multivariate Gaussian centered about $\boldsymbol{\theta}_0$ can be used. Beginning at an arbitrary starting point $\boldsymbol{\theta}_0$, the Hastings algorithm iterates the following steps:

1. Generate a value $\boldsymbol{\theta}$ using the proposal density $q(\boldsymbol{\theta}; \boldsymbol{\theta}_0)$;
2. Form the Hastings test ratio, $\alpha = \min \left[1, \frac{p(\boldsymbol{\theta})q(\boldsymbol{\theta}_0; \boldsymbol{\theta})}{p(\boldsymbol{\theta}_0)q(\boldsymbol{\theta}; \boldsymbol{\theta}_0)} \right]$;
3. Generate a value u uniformly distributed in $[0, 1]$;
4. If $u \leq \alpha$, take $\boldsymbol{\theta}_1 = \boldsymbol{\theta}$. Otherwise, repeat the old point, *i.e.*, $\boldsymbol{\theta}_1 = \boldsymbol{\theta}_0$.

If one takes the proposal density to be symmetric in $\boldsymbol{\theta}$ and $\boldsymbol{\theta}_0$, then this is the *Metropolis-Hastings* algorithm, and the test ratio becomes $\alpha = \min[1, p(\boldsymbol{\theta})/p(\boldsymbol{\theta}_0)]$. That is, if the proposed $\boldsymbol{\theta}$ is at a value of probability higher than $\boldsymbol{\theta}_0$, the step is taken. If the proposed step is rejected, hop in place.

Methods for assessing and optimizing the performance of the algorithm are discussed in, *e.g.*, [18–20]. One can, for example, examine the autocorrelation as a function of the lag k , *i.e.*, the correlation of a sampled point with that k steps removed. This should decrease as quickly as possible for increasing k .

Generally one chooses the proposal density so as to optimize some quality measure such as the autocorrelation. For certain problems it has been shown that one achieves optimal performance when the acceptance fraction, that is, the fraction of points with $u \leq \alpha$, is around 40%. This can be adjusted by varying the width of the proposal density. For example, one can use for the proposal p.d.f. a multivariate Gaussian with the same covariance matrix as that of the target p.d.f., but scaled by a constant.

References:

1. F. James, *Comp. Phys. Comm.* **60**, 329–344, 1990.
2. P. L'Ecuyer, *Proc. 1997 Winter Simulation Conference*, IEEE Press, Dec. 1997, 127–134.
3. The CERN Program Library (CERNLIB); see cernlib.web.cern.ch/cernlib.
4. Leif Lönnblad, *Comp. Phys. Comm.* **84**, 307 (1994).
5. Rene Brun and Fons Rademakers, *Nucl. Inst. Meth.* **A389**, 81 (1997); see also root.cern.ch.
6. F. James, *Comp. Phys. Comm.* **79**, 111 (1994), based on M. Lüscher, *Comp. Phys. Comm.* **79**, 100 (1994).
7. P. L'Ecuyer, *Mathematics of Computation*, **65**, 213 (1996) and **65**, 225 (1999).
8. M. Matsumoto and T. Nishimura, *ACM Transactions on Modeling and Computer Simulation*, Vol. 8, No. 1, January 1998, 3–30.
9. Much of DIEHARD is described in: G. Marsaglia, *A Current View of Random Number Generators*, keynote address, *Computer Science and Statistics: 16th Symposium on the Interface*, Elsevier (1985).
10. P. L'Ecuyer and R. Simard, *ACM Transactions on Mathematical Software*, 33, 4, Article 1, December 2007.
11. UNURAN is described at statistik.wu-wien.ac.at/software/unuran; see also W. Hörmann, J. Leydold, and G. Derflinger, *Automatic Nonuniform Random Variate Generation*, (Springer, New York, 2004).
12. W.H. Press *et al.*, *Numerical Recipes*, 3rd edition, (Cambridge University Press, New York, 2007).
13. J.H. Ahrens and U. Dieter, *Computing* **12**, 223 (1974).
14. R.Y. Rubinstein, *Simulation and the Monte Carlo Method*, (John Wiley and Sons, Inc., New York, 1981).
15. L. Devroye, *Non-Uniform Random Variate Generation*, (Springer-Verlag, New York, 1986); available online at cg.scs.carleton.ca/~luc/rnbookindex.html.
16. Ch. Walck, *Handbook on Statistical Distributions for Experimentalists*, University of Stockholm Internal Report SUF-PFY/96-01, available from www.physto.se/~walck.
17. J. Heinrich, CDF Note CDF/MEMO/STATISTICS/PUBLIC/8032, 2006.
18. C.P. Robert and G. Casella, *Monte Carlo Statistical Methods*, 2nd ed., (Springer, New York, 2004).
19. J.S. Liu, *Monte Carlo Strategies in Scientific Computing*, (Springer, New York, 2001).
20. R.M. Neal, *Probabilistic Inference Using Markov Chain Monte Carlo Methods*, Technical Report CRG-TR-93-1, Dept. of Computer Science, University of Toronto, available from www.cs.toronto.edu/~radford/res-mcmc.html.

34. MONTE CARLO PARTICLE NUMBERING SCHEME

Revised December 2007 by L. Garren (Fermilab), C.-J. Lin (LBNL), S. Navas (U. Granada), P. Richardson (Durham U.), T. Sjöstrand (Lund U.), and T. Trippé (LBNL).

The Monte Carlo particle numbering scheme presented here is intended to facilitate interfacing between event generators, detector simulators, and analysis packages used in particle physics. The numbering scheme was introduced in 1988 [1] and a revised version [2,3] was adopted in 1998 in order to allow systematic inclusion of quark model states which are as yet undiscovered and hypothetical particles such as SUSY particles. The numbering scheme is used in several event generators, *e.g.* HERWIG and PYTHIA/JETSET, and in the /HEPEVT/ [4] standard interface.

The general form is a 7-digit number:

$$\pm n_r n_L n_{q_1} n_{q_2} n_{q_3} n_J.$$

This encodes information about the particle's spin, flavor content, and internal quantum numbers. The details are as follows:

1. Particles are given positive numbers, antiparticles negative numbers. The PDG convention for mesons is used, so that K^+ and B^+ are particles.
2. Quarks and leptons are numbered consecutively starting from 1 and 11 respectively; to do this they are first ordered by family and within families by weak isospin.
3. In composite quark systems (diquarks, mesons, and baryons) $n_{q_{1-3}}$ are quark numbers used to specify the quark content, while the rightmost digit $n_J = 2J + 1$ gives the system's spin (except for the K_S^0 and K_L^0). The scheme does not cover particles of spin $J > 4$.
4. Diquarks have 4-digit numbers with $n_{q_1} \geq n_{q_2}$ and $n_{q_3} = 0$.
5. The numbering of mesons is guided by the nonrelativistic (L - S decoupled) quark model, as listed in Tables 14.2 and 14.3.
 - a. The numbers specifying the meson's quark content conform to the convention $n_{q_1} = 0$ and $n_{q_2} \geq n_{q_3}$. The special case K_L^0 is the sole exception to this rule.
 - b. The quark numbers of flavorless, light (u, d, s) mesons are: 11 for the member of the isotriplet (π^0, ρ^0, \dots), 22 for the lighter isosinglet (η, ω, \dots), and 33 for the heavier isosinglet (η', ϕ, \dots). Since isosinglet mesons are often large mixtures of $u\bar{u} + d\bar{d}$ and $s\bar{s}$ states, 22 and 33 are assigned by mass and do not necessarily specify the dominant quark composition.
 - c. The special numbers 310 and 130 are given to the K_S^0 and K_L^0 respectively.
 - d. The fifth digit n_L is reserved to distinguish mesons of the same total (J) but different spin (S) and orbital (L) angular momentum quantum numbers. For $J > 0$ the numbers are: (L, S) = ($J - 1, 1$) $n_L = 0$, ($J, 0$) $n_L = 1$, ($J, 1$) $n_L = 2$ and ($J + 1, 1$) $n_L = 3$. For the exceptional case $J = 0$ the numbers are (0,0) $n_L = 0$ and (1,1) $n_L = 1$ (*i.e.* $n_L = L$). See Table 34.1.

Table 34.1: Meson numbering logic. Here qq stands for $n_{q_2} n_{q_3}$.

	$L = J - 1, S = 1$			$L = J, S = 0$			$L = J, S = 1$			$L = J + 1, S = 1$		
J	code	J^{PC}	L	code	J^{PC}	L	code	J^{PC}	L	code	J^{PC}	L
0	—	—	—	00qq1	0 ⁺⁺	0	—	—	—	10qq1	0 ⁺⁺	1
1	00qq3	1 ⁻⁻	0	10qq3	1 ⁺⁻	1	20qq3	1 ⁺⁺	1	30qq3	1 ⁻⁻	2
2	00qq5	2 ⁺⁺	1	10qq5	2 ⁺⁻	2	20qq5	2 ⁻⁻	2	30qq5	2 ⁺⁺	3
3	00qq7	3 ⁻⁻	2	10qq7	3 ⁺⁻	3	20qq7	3 ⁺⁺	3	30qq7	3 ⁻⁻	4
4	00qq9	4 ⁺⁺	3	10qq9	4 ⁺⁻	4	20qq9	4 ⁻⁻	4	30qq9	4 ⁺⁺	5

- e. If a set of physical mesons correspond to a (non-negligible) mixture of basis states, differing in their internal quantum numbers, then the lightest physical state gets the smallest basis state number. For example the $K_1(1270)$ is numbered 10313 ($1^1P_1 K_{1B}$) and the $K_1(1400)$ is numbered 20313 ($1^3P_1 K_{1A}$).

- f. The sixth digit n_r is used to label mesons radially excited above the ground state.
- g. Numbers have been assigned for complete $n_r = 0$ S - and P -wave multiplets, even where states remain to be identified.
- h. In some instances assignments within the $q\bar{q}$ meson model are only tentative; here best guess assignments are made.
- i. Many states appearing in the Meson Listings are not yet assigned within the $q\bar{q}$ model. Here $n_{q_{2-3}}$ and n_J are assigned according to the state's likely flavors and spin; all such unassigned light isoscalar states are given the flavor code 22. Within these groups $n_L = 0, 1, 2, \dots$ is used to distinguish states of increasing mass. These states are flagged using $n = 9$. It is to be expected that these numbers will evolve as the nature of the states are elucidated. Codes are assigned to all mesons which are listed in the one-page table at the end of the Meson Summary Table as long as they have a preferred or established spin. Additional heavy meson states expected from heavy quark spectroscopy are also assigned codes.

6. The numbering of baryons is again guided by the nonrelativistic quark model, see Table 14.6.
 - a. The numbers specifying a baryon's quark content are such that in general $n_{q_1} \geq n_{q_2} \geq n_{q_3}$.
 - b. Two states exist for $J = 1/2$ baryons containing 3 different types of quarks. In the lighter baryon ($\Lambda, \Xi, \Omega, \dots$) the light quarks are in an antisymmetric ($J = 0$) state while for the heavier baryon ($\Sigma^0, \Xi', \Omega', \dots$) they are in a symmetric ($J = 1$) state. In this situation n_{q_2} and n_{q_3} are reversed for the lighter state, so that the smaller number corresponds to the lighter baryon.
 - c. At present most Monte Carlos do not include excited baryons and no systematic scheme has been developed to denote them, though one is foreseen. In the meantime, use of the PDG 96 [5] numbers for excited baryons is recommended.
 - d. For pentaquark states $n = 9$, $n_r n_L n_{q_1} n_{q_2}$ gives the four quark numbers in order $n_r \geq n_L \geq n_{q_1} \geq n_{q_2}$, n_{q_3} gives the antiquark number, and $n_J = 2J + 1$, with the assumption that $J = 1/2$ for the states currently reported.
7. The gluon, when considered as a gauge boson, has official number 21. In codes for glueballs, however, 9 is used to allow a notation in close analogy with that of hadrons.
8. The pomeron and odderon trajectories and a generic reggeon trajectory of states in QCD are assigned codes 990, 9990, and 110 respectively, where the final 0 indicates the indeterminate nature of the spin, and the other digits reflect the expected "valence" flavor content. We do not attempt a complete classification of all reggeon trajectories, since there is currently no need to distinguish a specific such trajectory from its lowest-lying member.
9. Two-digit numbers in the range 21–30 are provided for the Standard Model gauge bosons and Higgs.
10. Codes 81–100 are reserved for generator-specific pseudoparticles and concepts.
11. The search for physics beyond the Standard Model is an active area, so these codes are also standardized as far as possible.
 - a. A standard fourth generation of fermions is included by analogy with the first three.
 - b. The graviton and the boson content of a two-Higgs-doublet scenario and of additional $SU(2) \times U(1)$ groups are found in the range 31–40.
 - c. "One-of-a-kind" exotic particles are assigned numbers in the range 41–80.
 - d. Fundamental supersymmetric particles are identified by adding a nonzero n to the particle number. The superpartner of a boson or a left-handed fermion has $n = 1$ while the superpartner of a right-handed fermion has $n = 2$. When mixing occurs, such as between the winos and charged Higgsinos to give charginos, or between left and right sfermions, the lighter physical state is given the smaller basis state number.
 - e. Technicolor states have $n = 3$, with technifermions treated like ordinary fermions. States which are ordinary color singlets have $n_r = 0$. Color octets have $n_r = 1$. If a state has non-trivial quantum numbers under the topcolor groups

$SU(3)_1 \times SU(3)_2$, the quantum numbers are specified by tech, ij , where i and j are 1 or 2. n_L is then $2i + j$. The colon, V_8 , is a heavy gluon color octet and thus is 3100021.

- f. Excited (composite) quarks and leptons are identified by setting $n = 4$.
- g. Within several scenarios of new physics, it is possible to have colored particles sufficiently long-lived for color-singlet hadronic states to form around them. In the context of supersymmetric scenarios, these states are called R -hadrons, since they carry odd R -parity. R -hadron codes, defined here, should be viewed as templates for corresponding codes also in other scenarios, for any long-lived particle that is either an unflavored color octet or a flavored color triplet. The R -hadron code is obtained by combining the SUSY particle code with a code for the light degrees of freedom, with as many intermediate zeros removed from the former as required to make place for the latter at the end. (To exemplify, a sparticle $n00000n_{\bar{q}}n_{q_1}n_{q_2}n_{q_3}$ combined with quarks q_1 and q_2 obtains code $n00n_{\bar{q}}n_{q_1}n_{q_2}n_{q_3}$.) Specifically, the new-particle spin decouples in the limit of large masses, so that the final n_J digit is defined by the spin state of the light-quark system alone. An appropriate number of n_q digits is used to define the ordinary-quark content. As usual, 9 rather than 21 is used to denote a gluon/gluino in composite states. The sign of the hadron agrees with that of the constituent new particle (a color triplet) where there is a distinct new antiparticle, and else is defined as for normal hadrons. Particle names are R with the flavor content as lower index. A non-exhaustive list of R -hadron codes is given below.
- h. Kaluza-Klein excitations in models with extra dimensions have $n = 5$ or $n = 6$, to distinguish excitations of left- or right-handed fermions or, in case of mixing, the lighter or heavier state (cf. 11d). The nonzero n_r digit gives the radial excitation number, in scenarios where the level spacing allow these to be distinguished. Should the model also contain supersymmetry, excited SUSY states would be denoted by an $n_r > 0$, with $n = 1$ or 2 as usual. Should some colored states be long-lived enough that hadrons would form around them, the coding strategy of 11g applies, with the initial two mn_r digits preserved in the combined code. A non-exhaustive list of codes for the Kaluza-Klein states is given below.

12. Occasionally program authors add their own states. To avoid confusion, these should be flagged by setting $mn_r = 99$.
13. Concerning the non-99 numbers, it may be noted that only quarks, excited quarks, squarks, and diquarks have $n_{q_3} = 0$; only diquarks, baryons (including pentaquarks), and the odderon have $n_{q_1} \neq 0$; and only mesons, the reggeon, and the pomeron have $n_{q_1} = 0$ and $n_{q_2} \neq 0$. Concerning mesons (not antimesons), if n_{q_1} is odd then it labels a quark and an antiquark if even.
14. Nuclear codes are given as 10-digit numbers $\pm 10LZZZAAA I$. For a (hyper)nucleus consisting of n_p protons, n_n neutrons and n_A A 's, $A = n_p + n_n + n_A$ gives the total baryon number, $Z = n_p$ the total charge and $L = n_A$ the total number of strange quarks. I gives the isomer level, with $I = 0$ corresponding to the ground state and $I > 0$ to excitations, see [9], where states denoted m, n, p, q translate to $I = 1 - 4$. As examples, the deuteron is 1000010020 and ^{235}U is 1000922350. To avoid ambiguities, nuclear codes should not be applied to a single hadron, like p , n or A^0 , where quark-contents-based codes already exist.

This text and lists of particle numbers can be found on the WWW [6]. The StdHep Monte Carlo standardization project [7] maintains the list of PDG particle numbers, as well as numbering schemes from most event generators and software to convert between the different schemes.

References:

1. G.P. Yost *et al.*, Particle Data Group, Phys. Lett. **B204**, 1 (1988).
2. I. G. Knowles *et al.*, in "Physics at LEP2", CERN 96-01, vol. 2, p. 103.
3. C. Caso *et al.*, Particle Data Group, Eur. Phys. J. **C3**, 1 (1998).
4. T. Sjöstrand *et al.*, in "Z physics at LEP1", CERN 89-08, vol. 3, p. 327.
5. R.M. Barnett *et al.*, PDG, Phys. Rev. **D54**, 1 (1996).

6. pdg.lbl.gov/2006/mcdata/mc_particle_id_contents.html.
7. L. Garren, StdHep, *Monte Carlo Standardization at FNAL*, Fermilab PM0091 and StdHep WWW site: <http://cepa.fnal.gov/psm/stdhep/>.
8. W.-M. Yao *et al.*, J. Phys. **G33**, 1 (2006).
9. G. Audi *et al.*, Nucl. Phys. **A729**, 3 (2003) See also http://www.nndc.bnl.gov/amdc/web/nubase_en.html.

QUARKS

d	1
u	2
s	3
c	4
b	5
t	6
b'	7
t'	8

LEPTONS

e^-	11
ν_e	12
μ^-	13
ν_μ	14
τ^-	15
ν_τ	16
τ'^-	17
$\nu_{\tau'}$	18

EXCITED PARTICLES

d^*	4000001
u^*	4000002
e^*	4000011
ν_e^*	4000012

GAUGE AND HIGGS BOSONS

g	(9) 21
γ	22
Z^0	23
W^+	24
h^0/H_1^0	25
Z'/Z_2^0	32
Z''/Z_3^0	33
W'/W_2^+	34
H^0/H_2^0	35
A^0/H_3^0	36
H^+	37

DIQUARKS

$(dd)_1$	1103
$(ud)_0$	2101
$(ud)_1$	2103
$(uu)_1$	2203
$(sd)_0$	3101
$(sd)_1$	3103
$(su)_0$	3201
$(su)_1$	3203
$(ss)_1$	3303
$(cd)_0$	4101
$(cd)_1$	4103
$(cu)_0$	4201
$(cu)_1$	4203
$(cs)_0$	4301
$(cs)_1$	4303
$(cc)_1$	4403
$(bd)_0$	5101
$(bd)_1$	5103
$(bu)_0$	5201
$(bu)_1$	5203
$(bs)_0$	5301
$(bs)_1$	5303
$(bc)_0$	5401
$(bc)_1$	5403
$(bb)_1$	5503

TECHNICOLOR PARTICLES

π_{tech}^0	3000111
π_{tech}^+	3000211
$\pi_{\text{tech}}'^0$	3000221
η_{tech}^0	3100221
ρ_{tech}^0	3000113
ρ_{tech}^+	3000213
ω_{tech}^0	3000223
V_8	3100021
$\pi_{\text{tech},22}^1$	3060111
$\pi_{\text{tech},22}^8$	3160111
$\rho_{\text{tech},11}$	3130113
$\rho_{\text{tech},12}$	3140113
$\rho_{\text{tech},21}$	3150113
$\rho_{\text{tech},22}$	3160113

R-HADRONS		SUSY		LIGHT $I = 1$ MESONS		LIGHT $I = 0$ MESONS	
$R_{g\bar{g}}^0$	1000993	PARTICLES		π^0	111	$(u\bar{u}, d\bar{d}, \text{ and } s\bar{s} \text{ Admixtures})$	
$R_{g\bar{d}\bar{d}}^0$	1009113	\tilde{d}_L	1000001	π^+	211	η	221
$R_{g\bar{u}\bar{d}}^+$	1009213	\tilde{u}_L	1000002	$a_0(980)^0$	9000111	$\eta'(958)$	331
$R_{g\bar{u}\bar{u}}^0$	1009223	\tilde{s}_L	1000003	$a_0(980)^+$	9000211	$f_0(600)$	9000221
$R_{g\bar{d}\bar{s}}^0$	1009313	\tilde{c}_L	1000004	$\pi(1300)^0$	100111	$f_0(980)$	9010221
$R_{g\bar{u}\bar{s}}^+$	1009323	\tilde{b}_1	1000005 ^a	$\pi(1300)^+$	100211	$\eta(1295)$	100221
$R_{g\bar{s}\bar{s}}^0$	1009333	\tilde{t}_1	1000006 ^a	$a_0(1450)^0$	10111	$f_0(1370)$	10221
$R_{g\bar{d}\bar{d}\bar{d}}^-$	1091114	\tilde{e}_L	1000011	$a_0(1450)^+$	10211	$\eta(1405)$	9020221
$R_{g\bar{u}\bar{d}\bar{d}}^0$	1092114	$\tilde{\nu}_{eL}$	1000012	$\pi(1800)^0$	9010111	$\eta(1475)$	100331
$R_{g\bar{u}\bar{u}\bar{d}}^+$	1092214	$\tilde{\mu}_L$	1000013	$\pi(1800)^+$	9010211	$f_0(1500)$	9030221
$R_{g\bar{s}\bar{d}\bar{d}}^-$	1093114	$\tilde{\nu}_{\mu L}$	1000014	$\rho(770)^0$	113	$f_0(1710)$	10331
$R_{g\bar{s}\bar{u}\bar{d}}^0$	1093214	$\tilde{\tau}_1$	1000015 ^a	$\rho(770)^+$	213	$\eta(1760)$	9040221
$R_{g\bar{s}\bar{s}\bar{u}}^+$	1093224	$\tilde{\nu}_{\tau L}$	1000016	$b_1(1235)^0$	10113	$f_0(2020)$	9050221
$R_{g\bar{s}\bar{d}\bar{d}\bar{d}}^-$	1093114	\tilde{d}_R	2000001	$b_1(1235)^+$	10213	$f_0(2100)$	9060221
$R_{g\bar{s}\bar{u}\bar{d}\bar{d}}^0$	1093214	\tilde{u}_R	2000002	$a_1(1260)^0$	20113	$f_0(2200)$	9070221
$R_{g\bar{s}\bar{s}\bar{u}\bar{d}}^+$	1093224	\tilde{s}_R	2000003	$a_1(1260)^+$	20213	$\eta(2225)$	9080221
$R_{g\bar{s}\bar{s}\bar{s}\bar{d}}^-$	1093334	\tilde{c}_R	2000004	$\pi_1(1400)^0$	9000113	$\omega(782)$	223
$R_{\tilde{t}_1\bar{d}}^+$	1000612	\tilde{b}_2	2000005 ^a	$\pi_1(1400)^+$	9000213	$\phi(1020)$	333
$R_{\tilde{t}_1\bar{u}}^0$	1000622	\tilde{t}_2	2000006 ^a	$\rho(1450)^0$	100113	$h_1(1170)$	10223
$R_{\tilde{t}_1\bar{s}}^+$	1000632	\tilde{e}_R	2000011	$\rho(1450)^+$	100213	$f_1(1285)$	20223
$R_{\tilde{t}_1\bar{c}}^0$	1000642	$\tilde{\mu}_R$	2000013	$\pi_1(1600)^0$	9010113	$h_1(1380)$	10333
$R_{\tilde{t}_1\bar{b}}^+$	1000652	$\tilde{\tau}_2$	2000015 ^a	$\pi_1(1600)^+$	9010213	$f_1(1420)$	20333
$R_{\tilde{t}_1\bar{d}\bar{d}_1}^0$	1006113	\tilde{g}	1000021	$a_1(1640)^0$	9020113	$\omega(1420)$	100223
$R_{\tilde{t}_1\bar{u}\bar{d}_0}^+$	1006211	$\tilde{\chi}_1^0$	1000022 ^b	$a_1(1640)^+$	9020213	$f_1(1510)$	9000223
$R_{\tilde{t}_1\bar{u}\bar{d}_1}^+$	1006213	$\tilde{\chi}_2^0$	1000023 ^b	$\rho(1700)^0$	30113	$h_1(1595)$	9010223
$R_{\tilde{t}_1\bar{u}\bar{u}_1}^{++}$	1006223	$\tilde{\chi}_1^+$	1000024 ^b	$\rho(1700)^+$	30213	$\omega(1650)$	30223
$R_{\tilde{t}_1\bar{s}\bar{d}_0}^0$	1006311	$\tilde{\chi}_3^0$	1000025 ^b	$\rho(1900)^0$	9030113	$\phi(1680)$	100333
$R_{\tilde{t}_1\bar{s}\bar{d}_1}^0$	1006313	$\tilde{\chi}_4^0$	1000035 ^b	$\rho(1900)^+$	9030213	$f_2(1270)$	225
$R_{\tilde{t}_1\bar{s}\bar{u}_0}^+$	1006321	$\tilde{\chi}_2^+$	1000037 ^b	$\rho(2150)^0$	9040113	$f_2(1430)$	9000225
$R_{\tilde{t}_1\bar{s}\bar{u}_1}^+$	1006323	\tilde{G}	1000039	$\rho(2150)^+$	9040213	$f_2'(1525)$	335
$R_{\tilde{t}_1\bar{s}\bar{s}_1}^0$	1006333			$a_2(1320)^0$	115	$f_2(1565)$	9010225
		KALUZA-KLEIN		$a_2(1320)^+$	215	$f_2(1640)$	9020225
SPECIAL		EXCITATIONS		$\pi_2(1670)^0$	10115	$\eta_2(1645)$	10225
PARTICLES		$d_L^{(1)}$	5100001*	$\pi_2(1670)^+$	10215	$f_2(1810)$	9030225
G (graviton)	39	$u_L^{(1)}$	5100002*	$a_2(1700)^0$	9000115	$\eta_2(1870)$	10335
R^0	41	$e_L^{(1)-}$	5100011*	$a_2(1700)^+$	9000215	$f_2(1910)$	9040225
LQ^c	42	$\nu_{eL}^{(1)}$	5100012*	$\pi_2(2100)^0$	9010115	$f_2(1950)$	9050225
<i>reggeon</i>	110	$d_R^{(1)}$	6100001*	$\pi_2(2100)^+$	9010215	$f_2(2010)$	9060225
<i>pomeron</i>	990	$u_R^{(1)}$	6100002*	$\rho_3(1690)^0$	117	$f_2(2150)$	9070225
<i>odderon</i>	9990	$e_R^{(1)-}$	6100011*	$\rho_3(1690)^+$	217	$f_2(2300)$	9080225
		$\nu_{eR}^{(1)}$	6100012*	$\rho_3(1990)^0$	9000117	$f_2(2340)$	9090225
		$g^{(1)}$	5100021*	$\rho_3(1990)^+$	9000217	$\omega_3(1670)$	227
		$\gamma^{(1)}$	5100022*	$\rho_3(2250)^0$	9010117	$\phi_3(1850)$	337
		$Z^{(1)0}$	5100023*	$\rho_3(2250)^+$	9010217	$f_4(2050)$	229
		$W^{(1)+}$	5100024*	$a_4(2040)^0$	119	$f_J(2220)$	9000229
		$h^{(1)0}$	5100025*	$a_4(2040)^+$	219	$f_4(2300)$	9010229
		$G^{(1)}$	5100039*				

for MC internal
use 81–100

**STRANGE
MESONS**

K_L^0	130
K_S^0	310
K^0	311
K^+	321
$K_0^*(800)^0$	9000311
$K_0^*(800)^+$	9000321
$K_0^*(1430)^0$	10311
$K_0^*(1430)^+$	10321
$K(1460)^0$	100311
$K(1460)^+$	100321
$K(1830)^0$	9010311
$K(1830)^+$	9010321
$K_0^*(1950)^0$	9020311
$K_0^*(1950)^+$	9020321
$K^*(892)^0$	313
$K^*(892)^+$	323
$K_1(1270)^0$	10313
$K_1(1270)^+$	10323
$K_1(1400)^0$	20313
$K_1(1400)^+$	20323
$K^*(1410)^0$	100313
$K^*(1410)^+$	100323
$K_1(1650)^0$	9000313
$K_1(1650)^+$	9000323
$K^*(1680)^0$	30313
$K^*(1680)^+$	30323
$K_2^*(1430)^0$	315
$K_2^*(1430)^+$	325
$K_2(1580)^0$	9000315
$K_2(1580)^+$	9000325
$K_2(1770)^0$	10315
$K_2(1770)^+$	10325
$K_2(1820)^0$	20315
$K_2(1820)^+$	20325
$K_2^*(1980)^0$	9010315
$K_2^*(1980)^+$	9010325
$K_2(2250)^0$	9020315
$K_2(2250)^+$	9020325
$K_3^*(1780)^0$	317
$K_3^*(1780)^+$	327
$K_3(2320)^0$	9010317
$K_3(2320)^+$	9010327
$K_4^*(2045)^0$	319
$K_4^*(2045)^+$	329
$K_4(2500)^0$	9000319
$K_4(2500)^+$	9000329

**CHARMED
MESONS**

D^+	411
D^0	421
$D_0^*(2400)^+$	10411
$D_0^*(2400)^0$	10421
$D^*(2010)^+$	413
$D^*(2007)^0$	423
$D_1(2420)^+$	10413
$D_1(2420)^0$	10423
$D_1(H)^+$	20413
$D_1(2430)^0$	20423
$D_2^*(2460)^+$	415
$D_2^*(2460)^0$	425
D_s^+	431
$D_{s0}^*(2317)^+$	10431
D_s^{*+}	433
$D_{s1}(2536)^+$	10433
$D_{s1}(2460)^+$	20433
$D_{s2}^*(2573)^+$	435

**BOTTOM
MESONS**

B^0	511
B^+	521
B_0^*	10511
B_0^{*+}	10521
B^*	513
B^{*+}	523
$B_1(L)^0$	10513
$B_1(L)^+$	10523
$B_1(H)^0$	20513
$B_1(H)^+$	20523
B_2^0	515
B_2^{*+}	525
B_s^0	531
B_{s0}^*	10531
B_s^*	533
$B_{s1}(L)^0$	10533
$B_{s1}(H)^0$	20533
B_{s2}^*	535
B_c^+	541
B_{c0}^{*+}	10541
B_c^{*+}	543
$B_{c1}(L)^+$	10543
$B_{c1}(H)^+$	20543
B_{c2}^{*+}	545

 $c\bar{c}$ MESONS

$\eta_c(1S)$	441
$\chi_{c0}(1P)$	10441
$\eta_c(2S)$	100441
$J/\psi(1S)$	443
$h_c(1P)$	10443
$\chi_{c1}(1P)$	20443
$\psi(2S)$	100443
$\psi(3770)$	30443
$\psi(4040)$	9000443
$\psi(4160)$	9010443
$\psi(4415)$	9020443
$\chi_{c2}(1P)$	445
$\chi_{c2}(2P)$	100445

 $b\bar{b}$ MESONS

$\eta_b(1S)$	551
$\chi_{b0}(1P)$	10551
$\eta_b(2S)$	100551
$\chi_{b0}(2P)$	110551
$\eta_b(3S)$	200551
$\chi_{b0}(3P)$	210551
$\Upsilon(1S)$	553
$h_b(1P)$	10553
$\chi_{b1}(1P)$	20553
$\Upsilon_1(1D)$	30553
$\Upsilon(2S)$	100553
$h_b(2P)$	110553
$\chi_{b1}(2P)$	120553
$\Upsilon_1(2D)$	130553
$\Upsilon(3S)$	200553
$h_b(3P)$	210553
$\chi_{b1}(3P)$	220553
$\Upsilon(4S)$	300553
$\Upsilon(10860)$	9000553
$\Upsilon(11020)$	9010553
$\chi_{b2}(1P)$	555
$\eta_{b2}(1D)$	10555
$\Upsilon_2(1D)$	20555
$\chi_{b2}(2P)$	100555
$\eta_{b2}(2D)$	110555
$\Upsilon_2(2D)$	120555
$\chi_{b2}(3P)$	200555
$\Upsilon_3(1D)$	557
$\Upsilon_3(2D)$	100557

**LIGHT
BARYONS**

p	2212
n	2112
Δ^{++}	2224
Δ^+	2214
Δ^0	2114
Δ^-	1114

**STRANGE
BARYONS**

Λ	3122
Σ^+	3222
Σ^0	3212
Σ^-	3112
Σ^{*+}	3224 ^d
Σ^{*0}	3214 ^d
Σ^{*-}	3114 ^d
Ξ^0	3322
Ξ^-	3312
Ξ^{*0}	3324 ^d
Ξ^{*-}	3314 ^d
Ω^-	3334

**CHARMED
BARYONS**

Λ_c^+	4122
Σ_c^{++}	4222
Σ_c^+	4212
Σ_c^0	4112
Σ_c^{*++}	4224
Σ_c^{*+}	4214
Σ_c^{*0}	4114
Ξ_c^+	4232
Ξ_c^0	4132
$\Xi_c^{'+}$	4322
$\Xi_c^{'0}$	4312
Ξ_c^{*+}	4324
Ξ_c^{*0}	4314
Ω_c^0	4332
Ω_c^{*0}	4334
Ξ_{cc}^+	4412
Ξ_{cc}^{++}	4422
Ξ_{cc}^{*+}	4414
Ξ_{cc}^{*++}	4424
Ω_{cc}^+	4432
Ω_{cc}^{*+}	4434
Ω_{ccc}^{++}	4444

PENTAQUARKS

Θ^+	9221132
Φ^{--}	9331122

**BOTTOM
BARYONS**

Λ_b^0	5122
Σ_b^-	5112
Σ_b^0	5212
Σ_b^+	5222
Σ_b^{*-}	5114
Σ_b^{*0}	5214
Σ_b^{*+}	5224
Ξ_b^-	5132
Ξ_b^0	5232
$\Xi_b^{'-}$	5312
$\Xi_b^{'0}$	5322
Ξ_b^{*-}	5314
Ξ_b^{*0}	5324
Ω_b^-	5332
Ω_b^{*-}	5334
Ξ_{bc}^0	5142
Ξ_{bc}^+	5242
$\Xi_{bc}^{'0}$	5412
$\Xi_{bc}^{'+}$	5422
Ξ_{bc}^{*0}	5414
Ξ_{bc}^{*+}	5424
Ω_{bc}^0	5342
$\Omega_{bc}^{'0}$	5432
Ω_{bc}^{*0}	5434
Ω_{bcc}^+	5442
Ω_{bcc}^{*+}	5444
Ξ_{bb}^-	5512
Ξ_{bb}^0	5522
Ξ_{bb}^{*-}	5514
Ξ_{bb}^{*0}	5524
Ω_{bb}^-	5532
Ω_{bb}^{*-}	5534
Ω_{bbc}^0	5542
Ω_{bbc}^{*0}	5544
Ω_{bbb}^-	5554

Footnotes to the Tables:

- *) Numbers or names in bold face are new or have changed since the 2006 *Review* [8].
- a) Particularity in the third generation, the left and right sfermion states may mix, as shown. The lighter mixed state is given the smaller number.
- b) The physical $\tilde{\chi}$ states are admixtures of the pure $\tilde{\gamma}$, \tilde{Z}^0 , \tilde{W}^+ , \tilde{H}_1^0 , \tilde{H}_2^0 , and \tilde{H}^+ states.
- c) In this draft we have only provided one generic leptoquark code. More general classifications according to spin, weak isospin and flavor content would lead to a host of states, that could be added as the need arises.
- d) Σ^* and Ξ^* are alternate names for $\Sigma(1385)$ and $\Xi(1530)$.

35. CLEBSCH-GORDAN COEFFICIENTS, SPHERICAL HARMONICS, AND d FUNCTIONS

Note: A square-root sign is to be understood over every coefficient, e.g., for $-8/15$ read $-\sqrt{8/15}$.

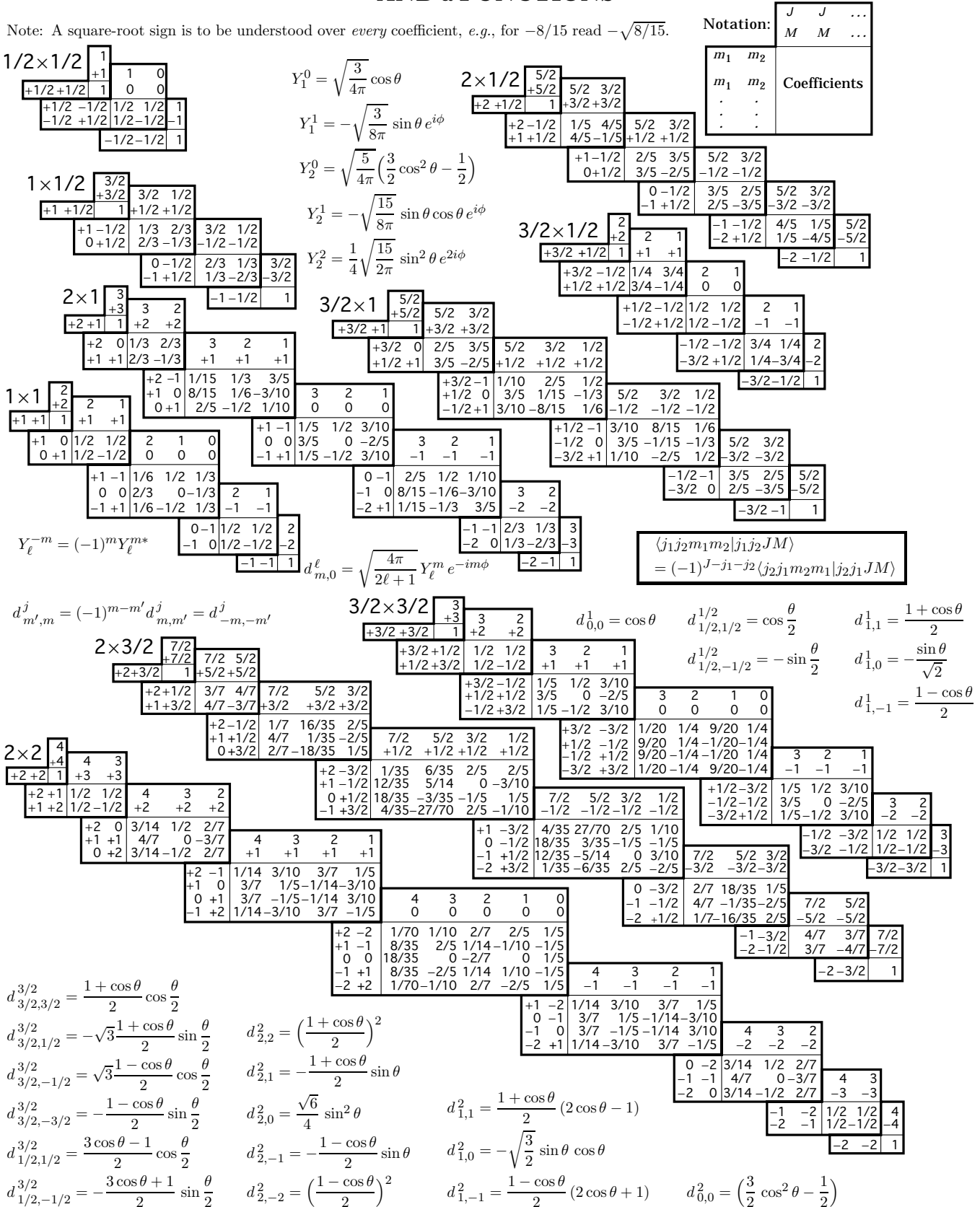


Figure 35.1: The sign convention is that of Wigner (*Group Theory*, Academic Press, New York, 1959), also used by Condon and Shortley (*The Theory of Atomic Spectra*, Cambridge Univ. Press, New York, 1953), Rose (*Elementary Theory of Angular Momentum*, Wiley, New York, 1957), and Cohen (*Tables of the Clebsch-Gordan Coefficients*, North American Rockwell Science Center, Thousand Oaks, Calif., 1974). The coefficients here have been calculated using computer programs written independently by Cohen and at LBNL.

36. SU(3) ISOSCALAR FACTORS AND REPRESENTATION MATRICES

Written by R.L. Kelly (LBNL).

The most commonly used SU(3) isoscalar factors, corresponding to the singlet, octet, and decuplet content of $8 \otimes 8$ and $10 \otimes 8$, are shown at the right. The notation uses particle names to identify the coefficients, so that the pattern of relative couplings may be seen at a glance. We illustrate the use of the coefficients below. See J.J. de Swart, Rev. Mod. Phys. **35**, 916 (1963) for detailed explanations and phase conventions.

A $\sqrt{\quad}$ is to be understood over every integer in the matrices; the exponent 1/2 on each matrix is a reminder of this. For example, the $\Xi \rightarrow \Omega K$ element of the $10 \rightarrow 10 \otimes 8$ matrix is $-\sqrt{6}/\sqrt{24} = -1/2$.

Intramultiplet relative decay strengths may be read directly from the matrices. For example, in decuplet \rightarrow octet + octet decays, the ratio of $\Omega^* \rightarrow \Xi \bar{K}$ and $\Delta \rightarrow N\pi$ partial widths is, from the $10 \rightarrow 8 \times 8$ matrix,

$$\frac{\Gamma(\Omega^* \rightarrow \Xi \bar{K})}{\Gamma(\Delta \rightarrow N\pi)} = \frac{12}{6} \times (\text{phase space factors}). \quad (36.1)$$

Including isospin Clebsch-Gordan coefficients, we obtain, e.g.,

$$\frac{\Gamma(\Omega^{*-} \rightarrow \Xi^0 K^-)}{\Gamma(\Delta^+ \rightarrow p\pi^0)} = \frac{1/2}{2/3} \times \frac{12}{6} \times p.s.f. = \frac{3}{2} \times p.s.f. \quad (36.2)$$

Partial widths for $8 \rightarrow 8 \otimes 8$ involve a linear superposition of 8_1 (symmetric) and 8_2 (antisymmetric) couplings. For example,

$$\Gamma(\Xi^* \rightarrow \Xi\pi) \sim \left(-\sqrt{\frac{9}{20}} g_1 + \sqrt{\frac{3}{12}} g_2 \right)^2. \quad (36.3)$$

The relations between g_1 and g_2 (with de Swart's normalization) and the standard D and F couplings that appear in the interaction Lagrangian,

$$\mathcal{L} = -\sqrt{2} D \text{Tr}(\{\bar{B}, B\}M) + \sqrt{2} F \text{Tr}([\bar{B}, B]M), \quad (36.4)$$

where $[\bar{B}, B] \equiv \bar{B}B - B\bar{B}$ and $\{\bar{B}, B\} \equiv \bar{B}B + B\bar{B}$, are

$$D = \frac{\sqrt{30}}{40} g_1, \quad F = \frac{\sqrt{6}}{24} g_2. \quad (36.5)$$

Thus, for example,

$$\Gamma(\Xi^* \rightarrow \Xi\pi) \sim (F - D)^2 \sim (1 - 2\alpha)^2, \quad (36.6)$$

where $\alpha \equiv F/(D + F)$. (This definition of α is de Swart's. The alternative $D/(D + F)$, due to Gell-Mann, is also used.)

The generators of SU(3) transformations, λ_a ($a = 1, 8$), are 3×3 matrices that obey the following commutation and anticommutation relationships:

$$[\lambda_a, \lambda_b] \equiv \lambda_a \lambda_b - \lambda_b \lambda_a = 2i f_{abc} \lambda_c \quad (36.7)$$

$$\{\lambda_a, \lambda_b\} \equiv \lambda_a \lambda_b + \lambda_b \lambda_a = \frac{4}{3} \delta_{ab} I + 2d_{abc} \lambda_c, \quad (36.8)$$

where I is the 3×3 identity matrix, and δ_{ab} is the Kronecker delta symbol. The f_{abc} are odd under the permutation of any pair of indices, while the d_{abc} are even. The nonzero values are

$1 \rightarrow 8 \otimes 8$

$$(A) \rightarrow (N\bar{K} \ \Sigma\pi \ \Lambda\eta \ \Xi K) = \frac{1}{\sqrt{8}} (2 \ 3 \ -1 \ -2)^{1/2}$$

$8_1 \rightarrow 8 \otimes 8$

$$\begin{pmatrix} N \\ \Sigma \\ \Lambda \\ \Xi \end{pmatrix} \rightarrow \begin{pmatrix} N\pi & N\eta & \Sigma K & \Lambda K \\ N\bar{K} & \Sigma\pi & \Lambda\pi & \Sigma\eta & \Xi K \\ N\bar{K} & \Sigma\pi & \Lambda\eta & \Xi K \\ \Sigma\bar{K} & \Lambda\bar{K} & \Xi\pi & \Xi\eta \end{pmatrix} = \frac{1}{\sqrt{20}} \begin{pmatrix} 9 & -1 & -9 & -1 \\ -6 & 0 & 4 & 4 & -6 \\ 2 & -12 & -4 & -2 \\ 9 & -1 & -9 & -1 \end{pmatrix}^{1/2}$$

$8_2 \rightarrow 8 \otimes 8$

$$\begin{pmatrix} N \\ \Sigma \\ \Lambda \\ \Xi \end{pmatrix} \rightarrow \begin{pmatrix} N\pi & N\eta & \Sigma K & \Lambda K \\ N\bar{K} & \Sigma\pi & \Lambda\pi & \Sigma\eta & \Xi K \\ N\bar{K} & \Sigma\pi & \Lambda\eta & \Xi K \\ \Sigma\bar{K} & \Lambda\bar{K} & \Xi\pi & \Xi\eta \end{pmatrix} = \frac{1}{\sqrt{12}} \begin{pmatrix} 3 & 3 & 3 & -3 \\ 2 & 8 & 0 & 0 & -2 \\ 6 & 0 & 0 & 6 \\ 3 & 3 & 3 & -3 \end{pmatrix}^{1/2}$$

$10 \rightarrow 8 \otimes 8$

$$\begin{pmatrix} \Delta \\ \Sigma \\ \Xi \\ \Omega \end{pmatrix} \rightarrow \begin{pmatrix} N\pi & \Sigma K \\ N\bar{K} & \Sigma\pi & \Lambda\pi & \Sigma\eta & \Xi K \\ \Sigma\bar{K} & \Lambda\bar{K} & \Xi\pi & \Xi\eta \\ \Xi\bar{K} \end{pmatrix} = \frac{1}{\sqrt{12}} \begin{pmatrix} -6 & 6 \\ -2 & 2 & -3 & 3 & 2 \\ 3 & -3 & 3 & 3 \\ 12 \end{pmatrix}^{1/2}$$

$8 \rightarrow 10 \otimes 8$

$$\begin{pmatrix} N \\ \Sigma \\ \Lambda \\ \Xi \end{pmatrix} \rightarrow \begin{pmatrix} \Delta\pi & \Sigma K \\ \Delta\bar{K} & \Sigma\pi & \Sigma\eta & \Xi K \\ \Sigma\pi & \Xi K \\ \Sigma\bar{K} & \Xi\pi & \Xi\eta & \Omega K \end{pmatrix} = \frac{1}{\sqrt{15}} \begin{pmatrix} -12 & 3 \\ 8 & -2 & -3 & 2 \\ -9 & 6 \\ 3 & -3 & -3 & 6 \end{pmatrix}^{1/2}$$

$10 \rightarrow 10 \otimes 8$

$$\begin{pmatrix} \Delta \\ \Sigma \\ \Xi \\ \Omega \end{pmatrix} \rightarrow \begin{pmatrix} \Delta\pi & \Delta\eta & \Sigma K \\ \Delta\bar{K} & \Sigma\pi & \Sigma\eta & \Xi K \\ \Sigma\bar{K} & \Xi\pi & \Xi\eta & \Omega K \\ \Xi\bar{K} & \Omega\eta \end{pmatrix} = \frac{1}{\sqrt{24}} \begin{pmatrix} 15 & 3 & -6 \\ 8 & 8 & 0 & -8 \\ 12 & 3 & -3 & -6 \\ 12 & -12 \end{pmatrix}^{1/2}$$

abc	f_{abc}	abc	d_{abc}	abc	d_{abc}
123	1	118	$1/\sqrt{3}$	355	1/2
147	1/2	146	1/2	366	-1/2
156	-1/2	157	1/2	377	-1/2
246	1/2	228	$1/\sqrt{3}$	448	$-1/(2\sqrt{3})$
257	1/2	247	-1/2	558	$-1/(2\sqrt{3})$
345	1/2	256	1/2	668	$-1/(2\sqrt{3})$
367	-1/2	338	$1/\sqrt{3}$	778	$-1/(2\sqrt{3})$
458	$\sqrt{3}/2$	344	1/2	888	$-1/\sqrt{3}$
678	$\sqrt{3}/2$				

The λ_a 's are

$$\lambda_1 = \begin{pmatrix} 0 & 1 & 0 \\ 1 & 0 & 0 \\ 0 & 0 & 0 \end{pmatrix}, \quad \lambda_2 = \begin{pmatrix} 0 & -i & 0 \\ i & 0 & 0 \\ 0 & 0 & 0 \end{pmatrix}, \quad \lambda_3 = \begin{pmatrix} 1 & 0 & 0 \\ 0 & -1 & 0 \\ 0 & 0 & 0 \end{pmatrix}$$

$$\lambda_4 = \begin{pmatrix} 0 & 0 & 1 \\ 0 & 0 & 0 \\ 1 & 0 & 0 \end{pmatrix}, \quad \lambda_5 = \begin{pmatrix} 0 & 0 & -i \\ 0 & 0 & 0 \\ i & 0 & 0 \end{pmatrix}, \quad \lambda_6 = \begin{pmatrix} 0 & 0 & 0 \\ 0 & 0 & 1 \\ 0 & 1 & 0 \end{pmatrix}$$

$$\lambda_7 = \begin{pmatrix} 0 & 0 & 0 \\ 0 & 0 & -i \\ 0 & i & 0 \end{pmatrix}, \quad \lambda_8 = \frac{1}{\sqrt{3}} \begin{pmatrix} 1 & 0 & 0 \\ 0 & 1 & 0 \\ 0 & 0 & -2 \end{pmatrix}$$

Equation (36.7) defines the Lie algebra of SU(3). A general d -dimensional representation is given by a set of $d \times d$ matrices satisfying Eq. (36.7) with the f_{abc} given above. Equation (36.8) is specific to the defining 3-dimensional representation.

37. $SU(n)$ MULTIPLETS AND YOUNG DIAGRAMMS

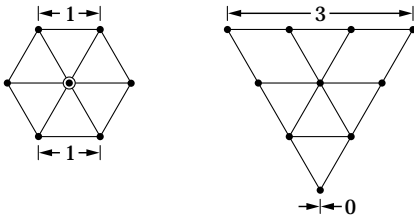
Written by C.G. Wohl (LBNL).

This note tells (1) how $SU(n)$ particle multiplets are identified or labeled, (2) how to find the number of particles in a multiplet from its label, (3) how to draw the Young diagram for a multiplet, and (4) how to use Young diagrams to determine the overall multiplet structure of a composite system, such as a 3-quark or a meson-baryon system.

In much of the literature, the word “representation” is used where we use “multiplet,” and “tableau” is used where we use “diagram.”

37.1. Multiplet labels

An $SU(n)$ multiplet is uniquely identified by a string of $(n-1)$ nonnegative integers: $(\alpha, \beta, \gamma, \dots)$. Any such set of integers specifies a multiplet. For an $SU(2)$ multiplet such as an isospin multiplet, the single integer α is the number of *steps* from one end of the multiplet to the other (*i.e.*, it is one fewer than the number of particles in the multiplet). In $SU(3)$, the two integers α and β are the numbers of steps across the top and bottom levels of the multiplet diagram. Thus the labels for the $SU(3)$ octet and decuplet



are $(1,1)$ and $(3,0)$. For larger n , the interpretation of the integers in terms of the geometry of the multiplets, which exist in an $(n-1)$ -dimensional space, is not so readily apparent.

The label for the $SU(n)$ singlet is $(0, 0, \dots, 0)$. In a flavor $SU(n)$, the n quarks together form a $(1, 0, \dots, 0)$ multiplet, and the n antiquarks belong to a $(0, \dots, 0, 1)$ multiplet. These two multiplets are *conjugate* to one another, which means their labels are related by $(\alpha, \beta, \dots) \leftrightarrow (\dots, \beta, \alpha)$.

37.2. Number of particles

The number of particles in a multiplet, $N = N(\alpha, \beta, \dots)$, is given as follows (note the pattern of the equations).

In $SU(2)$, $N = N(\alpha)$ is

$$N = \frac{(\alpha + 1)}{1} \tag{37.1}$$

In $SU(3)$, $N = N(\alpha, \beta)$ is

$$N = \frac{(\alpha + 1)}{1} \cdot \frac{(\beta + 1)}{1} \cdot \frac{(\alpha + \beta + 2)}{2} \tag{37.2}$$

In $SU(4)$, $N = N(\alpha, \beta, \gamma)$ is

$$N = \frac{(\alpha+1)}{1} \cdot \frac{(\beta+1)}{1} \cdot \frac{(\gamma+1)}{1} \cdot \frac{(\alpha+\beta+2)}{2} \cdot \frac{(\beta+\gamma+2)}{2} \cdot \frac{(\alpha+\beta+\gamma+3)}{3} \tag{37.3}$$

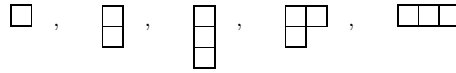
Note that in Eq. (37.3) there is no factor with $(\alpha + \gamma + 2)$: only a *consecutive* sequence of the label integers appears in any factor. One more example should make the pattern clear for any $SU(n)$. In $SU(5)$, $N = N(\alpha, \beta, \gamma, \delta)$ is

$$N = \frac{(\alpha+1)}{1} \cdot \frac{(\beta+1)}{1} \cdot \frac{(\gamma+1)}{1} \cdot \frac{(\delta+1)}{1} \cdot \frac{(\alpha+\beta+2)}{2} \cdot \frac{(\beta+\gamma+2)}{2} \cdot \frac{(\gamma+\delta+2)}{2} \cdot \frac{(\alpha+\beta+\gamma+3)}{3} \cdot \frac{(\beta+\gamma+\delta+3)}{3} \cdot \frac{(\alpha+\beta+\gamma+\delta+4)}{4} \tag{37.4}$$

From the symmetry of these equations, it is clear that multiplets that are conjugate to one another have the same number of particles, but so can other multiplets. For example, the $SU(4)$ multiplets $(3,0,0)$ and $(1,1,0)$ each have 20 particles. Try the equations and see.

37.3. Young diagrams

A Young diagram consists of an array of boxes (or some other symbol) arranged in one or more *left-justified* rows, with each row being *at least as long* as the row beneath. The correspondence between a diagram and a multiplet label is: The top row juts out α boxes to the right past the end of the second row, the second row juts out β boxes to the right past the end of the third row, *etc.* A diagram in $SU(n)$ has at most n rows. There can be any number of “completed” columns of n boxes buttressing the left of a diagram; these don’t affect the label. Thus in $SU(3)$ the diagrams



represent the multiplets $(1,0)$, $(0,1)$, $(0,0)$, $(1,1)$, and $(3,0)$. In any $SU(n)$, the quark multiplet is represented by a single box, the antiquark multiplet by a column of $(n-1)$ boxes, and a singlet by a completed column of n boxes.

37.4. Coupling multiplets together

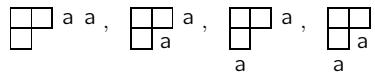
The following recipe tells how to find the multiplets that occur in coupling two multiplets together. To couple together more than two multiplets, first couple two, then couple a third with each of the multiplets obtained from the first two, *etc.*

First a definition: A sequence of the letters a, b, c, \dots is *admissible* if at any point in the sequence at least as many a ’s have occurred as b ’s, at least as many b ’s have occurred as c ’s, *etc.* Thus $abcd$ and $aabcb$ are admissible sequences and abb and acb are not. Now the recipe:

(a) Draw the Young diagrams for the two multiplets, but in one of the diagrams replace the boxes in the first row with a ’s, the boxes in the second row with b ’s, *etc.* Thus, to couple two $SU(3)$ octets (such as the π -meson octet and the baryon octet), we start with $\begin{smallmatrix} \square \\ \square \end{smallmatrix}$ and

$\begin{smallmatrix} a & a \\ b & \end{smallmatrix}$. The *unlettered* diagram forms the *upper left-hand corner* of all the enlarged diagrams constructed below.

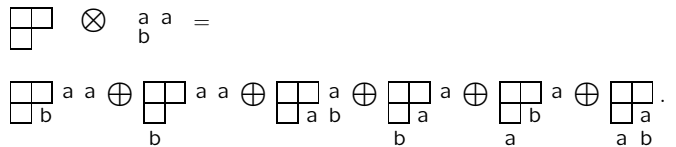
(b) Add the a ’s from the lettered diagram to the right-hand ends of the rows of the unlettered diagram to form all possible legitimate Young diagrams that have no more than one a per column. In general, there will be several distinct diagrams, and all the a ’s appear in each diagram. At this stage, for the coupling of the two $SU(3)$ octets, we have:



(c) Use the b ’s to further enlarge the diagrams already obtained, subject to the same rules. Then throw away any diagram in which the full sequence of letters formed by reading *right to left* in the first row, then the second row, *etc.*, is not admissible.

(d) Proceed as in (c) with the c ’s (if any), *etc.*

The final result of the coupling of the two $SU(3)$ octets is:



Here only the diagrams with admissible sequences of a ’s and b ’s and with fewer than four rows (since $n = 3$) have been kept. In terms of multiplet labels, the above may be written

$$(1, 1) \otimes (1, 1) = (2, 2) \oplus (3, 0) \oplus (0, 3) \oplus (1, 1) \oplus (1, 1) \oplus (0, 0) .$$

In terms of numbers of particles, it may be written

$$8 \otimes 8 = 27 \oplus 10 \oplus \overline{10} \oplus 8 \oplus 8 \oplus 1 .$$

The product of the numbers on the left here is equal to the sum on the right, a useful check. (See also Sec. 14 on the Quark Model.)

38. KINEMATICS

Revised January 2000 by J.D. Jackson (LBNL) and June 2008 by D.R. Tovey (Sheffield).

Throughout this section units are used in which $\hbar = c = 1$. The following conversions are useful: $\hbar c = 197.3$ MeV fm, $(\hbar c)^2 = 0.3894$ (GeV)² mb.

38.1. Lorentz transformations

The energy E and 3-momentum \mathbf{p} of a particle of mass m form a 4-vector $p = (E, \mathbf{p})$ whose square $p^2 \equiv E^2 - |\mathbf{p}|^2 = m^2$. The velocity of the particle is $\boldsymbol{\beta} = \mathbf{p}/E$. The energy and momentum (E^*, \mathbf{p}^*) viewed from a frame moving with velocity $\boldsymbol{\beta}_f$ are given by

$$\begin{pmatrix} E^* \\ p_{\parallel}^* \end{pmatrix} = \begin{pmatrix} \gamma_f & -\gamma_f \beta_f \\ -\gamma_f \beta_f & \gamma_f \end{pmatrix} \begin{pmatrix} E \\ p_{\parallel} \end{pmatrix}, \quad p_T^* = p_T, \quad (38.1)$$

where $\gamma_f = (1 - \beta_f^2)^{-1/2}$ and p_T (p_{\parallel}) are the components of \mathbf{p} perpendicular (parallel) to $\boldsymbol{\beta}_f$. Other 4-vectors, such as the space-time coordinates of events, of course transform in the same way. The scalar product of two 4-momenta $p_1 \cdot p_2 = E_1 E_2 - \mathbf{p}_1 \cdot \mathbf{p}_2$ is invariant (frame independent).

38.2. Center-of-mass energy and momentum

In the collision of two particles of masses m_1 and m_2 the total center-of-mass energy can be expressed in the Lorentz-invariant form

$$\begin{aligned} E_{\text{cm}} &= \left[(E_1 + E_2)^2 - (\mathbf{p}_1 + \mathbf{p}_2)^2 \right]^{1/2}, \\ &= \left[m_1^2 + m_2^2 + 2E_1 E_2 (1 - \beta_1 \beta_2 \cos \theta) \right]^{1/2}, \end{aligned} \quad (38.2)$$

where θ is the angle between the particles. In the frame where one particle (of mass m_2) is at rest (lab frame),

$$E_{\text{cm}} = (m_1^2 + m_2^2 + 2E_{1\text{lab}} m_2)^{1/2}. \quad (38.3)$$

The velocity of the center-of-mass in the lab frame is

$$\boldsymbol{\beta}_{\text{cm}} = \mathbf{p}_{\text{lab}} / (E_{1\text{lab}} + m_2), \quad (38.4)$$

where $\mathbf{p}_{\text{lab}} \equiv \mathbf{p}_{1\text{lab}}$ and

$$\gamma_{\text{cm}} = (E_{1\text{lab}} + m_2) / E_{\text{cm}}. \quad (38.5)$$

The c.m. momenta of particles 1 and 2 are of magnitude

$$p_{\text{cm}} = p_{\text{lab}} \frac{m_2}{E_{\text{cm}}}. \quad (38.6)$$

For example, if a 0.80 GeV/c kaon beam is incident on a proton target, the center of mass energy is 1.699 GeV and the center of mass momentum of either particle is 0.442 GeV/c. It is also useful to note that

$$E_{\text{cm}} dE_{\text{cm}} = m_2 dE_{1\text{lab}} = m_2 \beta_{1\text{lab}} dp_{\text{lab}}. \quad (38.7)$$

38.3. Lorentz-invariant amplitudes

The matrix elements for a scattering or decay process are written in terms of an invariant amplitude $-i\mathcal{M}$. As an example, the S -matrix for $2 \rightarrow 2$ scattering is related to \mathcal{M} by

$$\begin{aligned} \langle p'_1 p'_2 | S | p_1 p_2 \rangle &= I - i(2\pi)^4 \delta^4(p_1 + p_2 - p'_1 - p'_2) \\ &\times \frac{\mathcal{M}(p_1, p_2; p'_1, p'_2)}{(2E_1)^{1/2} (2E_2)^{1/2} (2E'_1)^{1/2} (2E'_2)^{1/2}}. \end{aligned} \quad (38.8)$$

The state normalization is such that

$$\langle p' | p \rangle = (2\pi)^3 \delta^3(\mathbf{p} - \mathbf{p}'). \quad (38.9)$$

38.4. Particle decays

The partial decay rate of a particle of mass M into n bodies in its rest frame is given in terms of the Lorentz-invariant matrix element \mathcal{M} by

$$d\Gamma = \frac{(2\pi)^4}{2M} |\mathcal{M}|^2 d\Phi_n(P; p_1, \dots, p_n), \quad (38.10)$$

where $d\Phi_n$ is an element of n -body phase space given by

$$d\Phi_n(P; p_1, \dots, p_n) = \delta^4(P - \sum_{i=1}^n p_i) \prod_{i=1}^n \frac{d^3 p_i}{(2\pi)^3 2E_i}. \quad (38.11)$$

This phase space can be generated recursively, viz.

$$\begin{aligned} d\Phi_n(P; p_1, \dots, p_n) &= d\Phi_j(q; p_1, \dots, p_j) \\ &\times d\Phi_{n-j+1}(P; q, p_{j+1}, \dots, p_n) (2\pi)^3 dq^2, \end{aligned} \quad (38.12)$$

where $q^2 = (\sum_{i=1}^j E_i)^2 - |\sum_{i=1}^j \mathbf{p}_i|^2$. This form is particularly useful in the case where a particle decays into another particle that subsequently decays.

38.4.1. Survival probability: If a particle of mass M has mean proper lifetime τ ($= 1/\Gamma$) and has momentum (E, \mathbf{p}) , then the probability that it lives for a time t_0 or greater before decaying is given by

$$P(t_0) = e^{-t_0 \Gamma/\gamma} = e^{-M t_0 \Gamma/E}, \quad (38.13)$$

and the probability that it travels a distance x_0 or greater is

$$P(x_0) = e^{-M x_0 \Gamma/|\mathbf{p}|}. \quad (38.14)$$

38.4.2. Two-body decays:

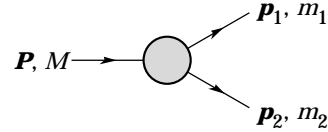


Figure 38.1: Definitions of variables for two-body decays.

In the rest frame of a particle of mass M , decaying into 2 particles labeled 1 and 2,

$$E_1 = \frac{M^2 - m_2^2 + m_1^2}{2M}, \quad (38.15)$$

$$|\mathbf{p}_1| = |\mathbf{p}_2|$$

$$= \frac{[(M^2 - (m_1 + m_2)^2)(M^2 - (m_1 - m_2)^2)]^{1/2}}{2M}, \quad (38.16)$$

and

$$d\Gamma = \frac{1}{32\pi^2} |\mathcal{M}|^2 \frac{|\mathbf{p}_1|}{M^2} d\Omega, \quad (38.17)$$

where $d\Omega = d\phi_1 d(\cos \theta_1)$ is the solid angle of particle 1. The invariant mass M can be determined from the energies and momenta using Eq. (38.2) with $M = E_{\text{cm}}$.

38.4.3. Three-body decays :

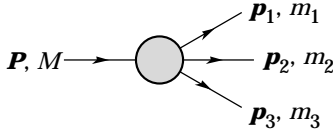


Figure 38.2: Definitions of variables for three-body decays.

Defining $p_{ij} = p_i + p_j$ and $m_{ij}^2 = p_{ij}^2$, then $m_{12}^2 + m_{23}^2 + m_{13}^2 = M^2 + m_1^2 + m_2^2 + m_3^2$ and $m_{12}^2 = (P - p_3)^2 = M^2 + m_3^2 - 2ME_3$, where E_3 is the energy of particle 3 in the rest frame of M . In that frame, the momenta of the three decay particles lie in a plane. The relative orientation of these three momenta is fixed if their energies are known. The momenta can therefore be specified in space by giving three Euler angles (α, β, γ) that specify the orientation of the final system relative to the initial particle [1]. Then

$$d\Gamma = \frac{1}{(2\pi)^5} \frac{1}{16M} |\mathcal{M}|^2 dE_1 dE_2 d\alpha d(\cos\beta) d\gamma. \quad (38.18)$$

Alternatively

$$d\Gamma = \frac{1}{(2\pi)^5} \frac{1}{16M^2} |\mathcal{M}|^2 |\mathbf{p}_1^*| |\mathbf{p}_3| dm_{12} d\Omega_1^* d\Omega_3, \quad (38.19)$$

where $(|\mathbf{p}_1^*|, \Omega_1^*)$ is the momentum of particle 1 in the rest frame of 1 and 2, and Ω_3 is the angle of particle 3 in the rest frame of the decaying particle. $|\mathbf{p}_1^*|$ and $|\mathbf{p}_3|$ are given by

$$|\mathbf{p}_1^*| = \frac{[(m_{12}^2 - (m_1 + m_2)^2)(m_{12}^2 - (m_1 - m_2)^2)]^{1/2}}{2m_{12}}, \quad (38.20a)$$

and

$$|\mathbf{p}_3| = \frac{[(M^2 - (m_{12} + m_3)^2)(M^2 - (m_{12} - m_3)^2)]^{1/2}}{2M}. \quad (38.20b)$$

[Compare with Eq. (38.16).]

If the decaying particle is a scalar or we average over its spin states, then integration over the angles in Eq. (38.18) gives

$$\begin{aligned} d\Gamma &= \frac{1}{(2\pi)^3} \frac{1}{8M} |\overline{\mathcal{M}}|^2 dE_1 dE_2 \\ &= \frac{1}{(2\pi)^3} \frac{1}{32M^3} |\overline{\mathcal{M}}|^2 dm_{12}^2 dm_{23}^2. \end{aligned} \quad (38.21)$$

This is the standard form for the Dalitz plot.

38.4.3.1. Dalitz plot: For a given value of m_{12}^2 , the range of m_{23}^2 is determined by its values when \mathbf{p}_2 is parallel or antiparallel to \mathbf{p}_3 :

$$(m_{23}^2)_{\max} = (E_2^* + E_3^*)^2 - \left(\sqrt{E_2^{*2} - m_2^2} - \sqrt{E_3^{*2} - m_3^2} \right)^2, \quad (38.22a)$$

$$(m_{23}^2)_{\min} = (E_2^* + E_3^*)^2 - \left(\sqrt{E_2^{*2} - m_2^2} + \sqrt{E_3^{*2} - m_3^2} \right)^2. \quad (38.22b)$$

Here $E_2^* = (m_{12}^2 - m_1^2 + m_3^2)/2m_{12}$ and $E_3^* = (M^2 - m_{12}^2 - m_3^2)/2m_{12}$ are the energies of particles 2 and 3 in the m_{12} rest frame. The scatter plot in m_{12}^2 and m_{23}^2 is called a Dalitz plot. If $|\overline{\mathcal{M}}|^2$ is constant, the allowed region of the plot will be uniformly populated with events [see Eq. (38.21)]. A nonuniformity in the plot gives immediate information on $|\overline{\mathcal{M}}|^2$. For example, in the case of $D \rightarrow K\pi\pi$, bands appear when $m_{(K\pi)} = m_{K^*(892)}$, reflecting the appearance of the decay chain $D \rightarrow K^*(892)\pi \rightarrow K\pi\pi$.

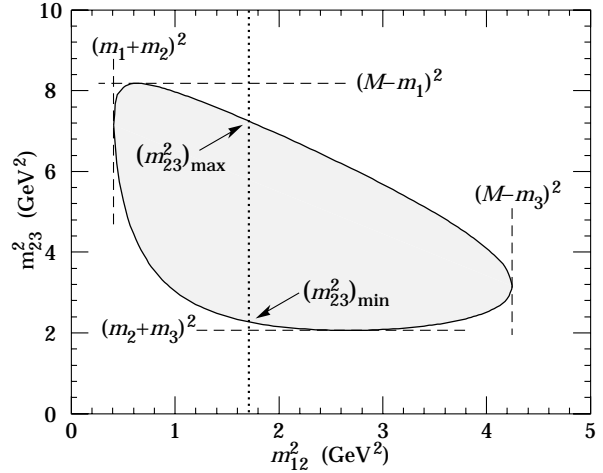


Figure 38.3: Dalitz plot for a three-body final state. In this example, the state is $\pi^+\bar{K}^0 p$ at 3 GeV. Four-momentum conservation restricts events to the shaded region.

38.4.4. Kinematic limits :

38.4.4.1. Three-body decays: In a three-body decay (Fig. 38.2) the maximum of $|\mathbf{p}_3|$, [given by Eq. (38.20)], is achieved when $m_{12} = m_1 + m_2$, i.e., particles 1 and 2 have the same vector velocity in the rest frame of the decaying particle. If, in addition, $m_3 > m_1, m_2$, then $|\mathbf{p}_3|_{\max} > |\mathbf{p}_1|_{\max}, |\mathbf{p}_2|_{\max}$. The distribution of m_{12} values possesses an end-point or maximum value at $m_{12} = M - m_3$. This can be used to constrain the mass difference of a parent particle and one invisible decay product.

38.4.4.2. Sequential two-body decays:

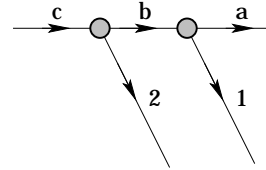


Figure 38.4: Particles participating in sequential two-body decay chain. Particles labeled 1 and 2 are visible while the particle terminating the chain (a) is invisible.

When a heavy particle initiates a sequential chain of two-body decays terminating in an invisible particle, constraints on the masses of the states participating in the chain can be obtained from end-points and thresholds in invariant mass distributions of the aggregated decay products. For the two-step decay chain depicted in Fig. 38.4 the invariant mass distribution of the two visible particles possesses an end-point given by:

$$(m_{12}^{\max})^2 = \frac{(m_c^2 - m_b^2)(m_b^2 - m_a^2)}{m_b^2}, \quad (38.23)$$

provided particles 1 and 2 are massless. If visible particle 1 has non-zero mass m_1 then Eq. (38.23) is replaced by

$$(m_{12}^{\max})^2 = m_1^2 + \frac{(m_c^2 - m_b^2)}{2m_b^2} \times \left(m_1^2 + m_b^2 - m_a^2 + \sqrt{(-m_1^2 + m_b^2 - m_a^2)^2 - 4m_1^2 m_a^2} \right). \quad (38.24)$$

See Refs. 2 and 3 for other cases.

38.4.5. Multibody decays : The above results may be generalized to final states containing any number of particles by combining some of the particles into “effective particles” and treating the final states as 2 or 3 “effective particle” states. Thus, if $p_{ijk\dots} = p_i + p_j + p_k + \dots$, then

$$m_{ijk\dots} = \sqrt{p_{ijk\dots}^2}, \quad (38.25)$$

and $m_{ijk\dots}$ may be used in place of *e.g.*, m_{12} in the relations in Sec. 38.4.3 or Sec. 38.4.4 above.

38.5. Cross sections

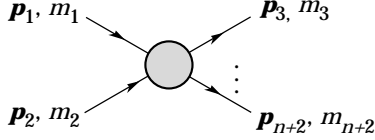


Figure 38.5: Definitions of variables for production of an n -body final state.

The differential cross section is given by

$$d\sigma = \frac{(2\pi)^4 |\mathcal{M}|^2}{4\sqrt{(p_1 \cdot p_2)^2 - m_1^2 m_2^2}} \times d\Phi_n(p_1 + p_2; p_3, \dots, p_{n+2}). \quad (38.26)$$

[See Eq. (38.11).] In the rest frame of m_2 (lab),

$$\sqrt{(p_1 \cdot p_2)^2 - m_1^2 m_2^2} = m_2 p_{1\text{lab}}; \quad (38.27a)$$

while in the center-of-mass frame

$$\sqrt{(p_1 \cdot p_2)^2 - m_1^2 m_2^2} = p_{1\text{cm}} \sqrt{s}. \quad (38.27b)$$

38.5.1. Two-body reactions :

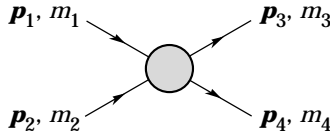


Figure 38.6: Definitions of variables for a two-body final state.

Two particles of momenta p_1 and p_2 and masses m_1 and m_2 scatter to particles of momenta p_3 and p_4 and masses m_3 and m_4 ; the Lorentz-invariant Mandelstam variables are defined by

$$s = (p_1 + p_2)^2 = (p_3 + p_4)^2 = m_1^2 + 2E_1 E_2 - 2\mathbf{p}_1 \cdot \mathbf{p}_2 + m_2^2, \quad (38.28)$$

$$t = (p_1 - p_3)^2 = (p_2 - p_4)^2 = m_1^2 - 2E_1 E_3 + 2\mathbf{p}_1 \cdot \mathbf{p}_3 + m_3^2, \quad (38.29)$$

$$u = (p_1 - p_4)^2 = (p_2 - p_3)^2 = m_1^2 - 2E_1 E_4 + 2\mathbf{p}_1 \cdot \mathbf{p}_4 + m_4^2, \quad (38.30)$$

and they satisfy

$$s + t + u = m_1^2 + m_2^2 + m_3^2 + m_4^2. \quad (38.31)$$

The two-body cross section may be written as

$$\frac{d\sigma}{dt} = \frac{1}{64\pi s} \frac{1}{|\mathbf{p}_{1\text{cm}}|^2} |\mathcal{M}|^2. \quad (38.32)$$

In the center-of-mass frame

$$t = (E_{1\text{cm}} - E_{3\text{cm}})^2 - (p_{1\text{cm}} - p_{3\text{cm}})^2 - 4p_{1\text{cm}} p_{3\text{cm}} \sin^2(\theta_{\text{cm}}/2)$$

$$= t_0 - 4p_{1\text{cm}} p_{3\text{cm}} \sin^2(\theta_{\text{cm}}/2), \quad (38.33)$$

where θ_{cm} is the angle between particle 1 and 3. The limiting values t_0 ($\theta_{\text{cm}} = 0$) and t_1 ($\theta_{\text{cm}} = \pi$) for $2 \rightarrow 2$ scattering are

$$t_0(t_1) = \left[\frac{m_1^2 - m_3^2 - m_2^2 + m_4^2}{2\sqrt{s}} \right]^2 - (p_{1\text{cm}} \mp p_{3\text{cm}})^2. \quad (38.34)$$

In the literature the notation t_{\min} (t_{\max}) for t_0 (t_1) is sometimes used, which should be discouraged since $t_0 > t_1$. The center-of-mass energies and momenta of the incoming particles are

$$E_{1\text{cm}} = \frac{s + m_1^2 - m_2^2}{2\sqrt{s}}, \quad E_{2\text{cm}} = \frac{s + m_2^2 - m_1^2}{2\sqrt{s}}, \quad (38.35)$$

For $E_{3\text{cm}}$ and $E_{4\text{cm}}$, change m_1 to m_3 and m_2 to m_4 . Then

$$p_{i\text{cm}} = \sqrt{E_{i\text{cm}}^2 - m_i^2} \text{ and } p_{1\text{cm}} = \frac{p_{1\text{lab}} m_2}{\sqrt{s}}. \quad (38.36)$$

Here the subscript lab refers to the frame where particle 2 is at rest. [For other relations see Eqs. (38.2)–(38.4).]

38.5.2. Inclusive reactions : Choose some direction (usually the beam direction) for the z -axis; then the energy and momentum of a particle can be written as

$$E = m_T \cosh y, \quad p_x, p_y, p_z = m_T \sinh y, \quad (38.37)$$

where m_T , conventionally called the ‘transverse mass’, is given by

$$m_T^2 = m^2 + p_x^2 + p_y^2. \quad (38.38)$$

and the rapidity y is defined by

$$y = \frac{1}{2} \ln \left(\frac{E + p_z}{E - p_z} \right)$$

$$= \ln \left(\frac{E + p_z}{m_T} \right) = \tanh^{-1} \left(\frac{p_z}{E} \right). \quad (38.39)$$

Note that the definition of the transverse mass in Eq. (38.38) differs from that used by experimentalists at hadron colliders (see Sec. 38.6.1 below). Under a boost in the z -direction to a frame with velocity β , $y \rightarrow y - \tanh^{-1} \beta$. Hence the shape of the rapidity distribution dN/dy is invariant, as are differences in rapidity. The invariant cross section may also be rewritten

$$E \frac{d^3\sigma}{d^3p} = \frac{d^3\sigma}{d\phi dy p_T dp_T} \Rightarrow \frac{d^2\sigma}{\pi dy d(p_T^2)}. \quad (38.40)$$

The second form is obtained using the identity $dy/dp_z = 1/E$, and the third form represents the average over ϕ .

Feynman’s x variable is given by

$$x = \frac{p_z}{p_{z\text{max}}} \approx \frac{E + p_z}{(E + p_z)_{\text{max}}} \quad (p_T \ll |p_z|). \quad (38.41)$$

In the c.m. frame,

$$x \approx \frac{2p_{z\text{cm}}}{\sqrt{s}} = \frac{2m_T \sinh y_{\text{cm}}}{\sqrt{s}} \quad (38.42)$$

and

$$= (y_{\text{cm}})_{\text{max}} = \ln(\sqrt{s}/m). \quad (38.43)$$

The invariant mass M of the two-particle system described in Sec. 38.4.2 can be written in terms of these variables as

$$M^2 = m_1^2 + m_2^2 + 2[E_T(1)E_T(2) \cosh \Delta y - \mathbf{p}_T(1) \cdot \mathbf{p}_T(2)], \quad (38.44)$$

where

$$E_T(i) = \sqrt{|\mathbf{p}_T(i)|^2 + m_i^2}, \quad (38.45)$$

and $\mathbf{p}_T(i)$ denotes the transverse momentum vector of particle i .

For $p \gg m$, the rapidity [Eq. (38.39)] may be expanded to obtain

$$y = \frac{1}{2} \ln \frac{\cos^2(\theta/2) + m^2/4p^2 + \dots}{\sin^2(\theta/2) + m^2/4p^2 + \dots} \approx -\ln \tan(\theta/2) \equiv \eta \quad (38.46)$$

where $\cos \theta = p_z/p$. The pseudorapidity η defined by the second line is approximately equal to the rapidity y for $p \gg m$ and $\theta \gg 1/\gamma$, and in any case can be measured when the mass and momentum of the particle are unknown. From the definition one can obtain the identities

$$\sinh \eta = \cot \theta, \quad \cosh \eta = 1/\sin \theta, \quad \tanh \eta = \cos \theta. \quad (38.47)$$

38.5.3. Partial waves : The amplitude in the center of mass for elastic scattering of spinless particles may be expanded in Legendre polynomials

$$f(k, \theta) = \frac{1}{k} \sum_{\ell} (2\ell + 1) a_{\ell} P_{\ell}(\cos \theta), \quad (38.48)$$

where k is the c.m. momentum, θ is the c.m. scattering angle, $a_{\ell} = (\eta_{\ell} e^{2i\delta_{\ell}} - 1)/2i$, $0 \leq \eta_{\ell} \leq 1$, and δ_{ℓ} is the phase shift of the ℓ^{th} partial wave. For purely elastic scattering, $\eta_{\ell} = 1$. The differential cross section is

$$\frac{d\sigma}{d\Omega} = |f(k, \theta)|^2. \quad (38.49)$$

The optical theorem states that

$$\sigma_{\text{tot}} = \frac{4\pi}{k} \text{Im} f(k, 0), \quad (38.50)$$

and the cross section in the ℓ^{th} partial wave is therefore bounded:

$$\sigma_{\ell} = \frac{4\pi}{k^2} (2\ell + 1) |a_{\ell}|^2 \leq \frac{4\pi(2\ell + 1)}{k^2}. \quad (38.51)$$

The evolution with energy of a partial-wave amplitude a_{ℓ} can be displayed as a trajectory in an Argand plot, as shown in Fig. 38.7.

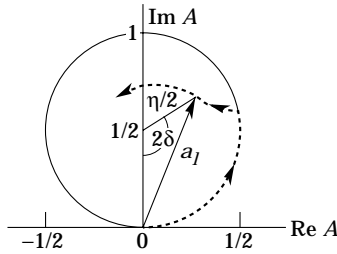


Figure 38.7: Argand plot showing a partial-wave amplitude a_{ℓ} as a function of energy. The amplitude leaves the unitary circle where inelasticity sets in ($\eta_{\ell} < 1$).

The usual Lorentz-invariant matrix element \mathcal{M} (see Sec. 38.3 above) for the elastic process is related to $f(k, \theta)$ by

$$\mathcal{M} = -8\pi\sqrt{s} f(k, \theta), \quad (38.52)$$

so

$$\sigma_{\text{tot}} = -\frac{1}{2p_{\text{lab}} m_2} \text{Im} \mathcal{M}(t = 0), \quad (38.53)$$

where s and t are the center-of-mass energy squared and momentum transfer squared, respectively (see Sec. 38.4.1).

38.5.3.1. Resonances: The Breit-Wigner (nonrelativistic) form for an elastic amplitude a_{ℓ} with a resonance at c.m. energy E_R , elastic width Γ_{el} , and total width Γ_{tot} is

$$a_{\ell} = \frac{\Gamma_{\text{el}}/2}{E_R - E - i\Gamma_{\text{tot}}/2}, \quad (38.54)$$

where E is the c.m. energy. As shown in Fig. 38.8, in the absence of background the elastic amplitude traces a counterclockwise circle with center $ix_{\text{el}}/2$ and radius $x_{\text{el}}/2$, where the elasticity $x_{\text{el}} = \Gamma_{\text{el}}/\Gamma_{\text{tot}}$. The amplitude has a pole at $E = E_R - i\Gamma_{\text{tot}}/2$.

The spin-averaged Breit-Wigner cross section for a spin- J resonance produced in the collision of particles of spin S_1 and S_2 is

$$\sigma_{BW}(E) = \frac{(2J+1)}{(2S_1+1)(2S_2+1)} \frac{\pi}{k^2} \frac{B_{\text{in}} B_{\text{out}} \Gamma_{\text{tot}}^2}{(E - E_R)^2 + \Gamma_{\text{tot}}^2/4}, \quad (38.55)$$

where k is the c.m. momentum, E is the c.m. energy, and B_{in} and B_{out} are the branching fractions of the resonance into the entrance and exit channels. The $2S+1$ factors are the multiplicities of the incident spin states, and are replaced by 2 for photons. This expression is valid only for an isolated state. If the width is not small, Γ_{tot} cannot be treated as a constant independent of E . There are many other forms for σ_{BW} , all of which are equivalent to the one given here in the narrow-width case. Some of these forms may be more appropriate if the resonance is broad.

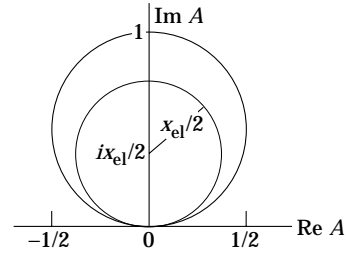


Figure 38.8: Argand plot for a resonance.

The relativistic Breit-Wigner form corresponding to Eq. (38.54) is:

$$a_{\ell} = \frac{-m\Gamma_{\text{el}}}{s - m^2 + im\Gamma_{\text{tot}}}. \quad (38.56)$$

A better form incorporates the known kinematic dependences, replacing $m\Gamma_{\text{tot}}$ by $\sqrt{s}\Gamma_{\text{tot}}(s)$, where $\Gamma_{\text{tot}}(s)$ is the width the resonance particle would have if its mass were \sqrt{s} , and correspondingly $m\Gamma_{\text{el}}$ by $\sqrt{s}\Gamma_{\text{el}}(s)$ where $\Gamma_{\text{el}}(s)$ is the partial width in the incident channel for a mass \sqrt{s} :

$$a_{\ell} = \frac{-\sqrt{s}\Gamma_{\text{el}}(s)}{s - m^2 + i\sqrt{s}\Gamma_{\text{tot}}(s)}. \quad (38.57)$$

For the Z boson, all the decays are to particles whose masses are small enough to be ignored, so on dimensional grounds $\Gamma_{\text{tot}}(s) = \sqrt{s}\Gamma_0/m_Z$, where Γ_0 defines the width of the Z , and $\Gamma_{\text{el}}(s)/\Gamma_{\text{tot}}(s)$ is constant. A full treatment of the line shape requires consideration of dynamics, not just kinematics. For the Z this is done by calculating the radiative corrections in the Standard Model.

38.6. Transverse variables

At hadron colliders, a significant and unknown proportion of the energy of the incoming hadrons in each event escapes down the beam-pipe. Consequently if invisible particles are created in the final state, their net momentum can only be constrained in the plane transverse to the beam direction. Defining the z -axis as the beam direction, this net momentum is equal to the missing transverse energy vector

$$\mathbf{E}_T^{\text{miss}} = -\sum_i \mathbf{p}_T(i), \quad (38.58)$$

where the sum runs over the transverse momenta of all visible final state particles.

38.6.1. Single production with semi-invisible final state :

Consider a single heavy particle of mass M produced in association with visible particles which decays as in Fig. 38.1 to two particles, of which one (labeled particle 1) is invisible. The mass of the parent particle can be constrained with the quantity M_T defined by

$$M_T^2 \equiv [E_T(1) + E_T(2)]^2 - [\mathbf{p}_T(1) + \mathbf{p}_T(2)]^2 = m_1^2 + m_2^2 + 2[E_T(1)E_T(2) - \mathbf{p}_T(1) \cdot \mathbf{p}_T(2)], \quad (38.59)$$

where

$$\mathbf{p}_T(1) = \mathbf{E}_T^{\text{miss}}. \quad (38.60)$$

This quantity is called the ‘transverse mass’ by hadron collider experimentalists but it should be noted that it is quite different from that used in the description of inclusive reactions [Eq. (38.38)]. The distribution of event M_T values possesses an end-point at $M_T^{\text{max}} = M$. If $m_1 = m_2 = 0$ then

$$M_T^2 = 2|\mathbf{p}_T(1)||\mathbf{p}_T(2)|(1 - \cos \phi_{12}), \quad (38.61)$$

where ϕ_{ij} is defined as the angle between particles i and j in the transverse plane.

38.6.2. Pair production with semi-invisible final states :

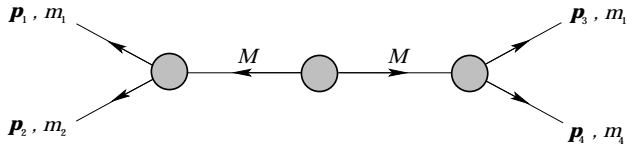


Figure 38.9: Definitions of variables for pair production of semi-invisible final states. Particles 1 and 3 are invisible while particles 2 and 4 are visible.

Consider two identical heavy particles of mass M produced such that their combined center-of-mass is at rest in the transverse plane (Fig. 38.9). Each particle decays to a final state consisting of an invisible particle of fixed mass m_1 together with an additional visible particle. M and m_1 can be constrained with the variables M_{T2} and M_{CT} which are defined in Refs. [4] and [5].

References:

1. See, for example, J.J. Sakurai, *Modern Quantum Mechanics*, Addison-Wesley (1985), p. 172, or D.M. Brink and G.R. Satchler, *Angular Momentum*, 2nd ed., Oxford University Press (1968), p. 20.
2. I. Hinchliffe *et al.*, Phys. Rev. **D55**, 5520 (1997).
3. B.C. Allanach *et al.*, JHEP **0009**, 004 (2000).
4. C.G. Lester and D.J. Summers, Phys. Lett. **B463**, 99 (1999).
5. D.R. Tovey, JHEP **0804**, 034 (2008).

39. CROSS-SECTION FORMULAE FOR SPECIFIC PROCESSES

Revised September 2007 by H. Baer (Florida State University) and R.N. Cahn (LBNL).

PART I: STANDARD MODEL PROCESSES

Setting aside leptoproduction (for which, see Sec. 16 of this *Review*), the cross sections of primary interest are those with light incident particles, e^+e^- , $\gamma\gamma$, $q\bar{q}$, gq , gg , etc., where g and q represent gluons and light quarks. The produced particles include both light particles and heavy ones - t , W , Z , and the Higgs boson H . We provide the production cross sections calculated within the Standard Model for several such processes.

39.1. Resonance Formation

Resonant cross sections are generally described by the Breit-Wigner formula (Sec. 16 of this *Review*).

$$\sigma(E) = \frac{2J+1}{(2S_1+1)(2S_2+1)} \frac{4\pi}{k^2} \left[\frac{\Gamma^2/4}{(E-E_0)^2 + \Gamma^2/4} \right] B_{in} B_{out}, \quad (39.1)$$

where E is the c.m. energy, J is the spin of the resonance, and the number of polarization states of the two incident particles are $2S_1+1$ and $2S_2+1$. The c.m. momentum in the initial state is k , E_0 is the c.m. energy at the resonance, and Γ is the full width at half maximum height of the resonance. The branching fraction for the resonance into the initial-state channel is B_{in} and into the final-state channel is B_{out} . For a narrow resonance, the factor in square brackets may be replaced by $\pi\Gamma\delta(E-E_0)/2$.

39.2. Production of light particles

The production of point-like, spin-1/2 fermions in e^+e^- annihilation through a virtual photon, $e^+e^- \rightarrow \gamma^* \rightarrow f\bar{f}$, at c.m. energy squared s is given by

$$\frac{d\sigma}{d\Omega} = N_c \frac{\alpha^2}{4s} \beta [1 + \cos^2\theta + (1-\beta^2)\sin^2\theta] Q_f^2, \quad (39.2)$$

where β is v/c for the produced fermions in the c.m., θ is the c.m. scattering angle, and Q_f is the charge of the fermion. The factor N_c is 1 for charged leptons and 3 for quarks. In the ultrarelativistic limit, $\beta \rightarrow 1$,

$$\sigma = N_c Q_f^2 \frac{4\pi\alpha^2}{3s} = N_c Q_f^2 \frac{86.8 \text{ nb}}{s(\text{GeV}^2)^2}. \quad (39.3)$$

The cross section for the annihilation of a $q\bar{q}$ pair into a distinct pair $q'\bar{q}'$ through a gluon is completely analogous up to color factors, with the replacement $\alpha \rightarrow \alpha_s$. Treating all quarks as massless, averaging over the colors of the initial quarks and defining $t = -s \sin^2(\theta/2)$, $u = -s \cos^2(\theta/2)$, one finds [1]

$$\frac{d\sigma}{d\Omega}(q\bar{q} \rightarrow q'\bar{q}') = \frac{\alpha_s^2}{9s} \frac{t^2 + u^2}{s^2}. \quad (39.4)$$

Crossing symmetry gives

$$\frac{d\sigma}{d\Omega}(qq' \rightarrow qq') = \frac{\alpha_s^2}{9s} \frac{s^2 + u^2}{t^2}. \quad (39.5)$$

If the quarks q and q' are identical, we have

$$\frac{d\sigma}{d\Omega}(q\bar{q} \rightarrow q\bar{q}) = \frac{\alpha_s^2}{9s} \left[\frac{t^2 + u^2}{s^2} + \frac{s^2 + u^2}{t^2} - \frac{2u^2}{3st} \right], \quad (39.6)$$

and by crossing

$$\frac{d\sigma}{d\Omega}(qq \rightarrow qq) = \frac{\alpha_s^2}{9s} \left[\frac{t^2 + s^2}{u^2} + \frac{s^2 + u^2}{t^2} - \frac{2s^2}{3ut} \right]. \quad (39.7)$$

Annihilation of e^+e^- into $\gamma\gamma$ has the cross section

$$\frac{d\sigma}{d\Omega}(e^+e^- \rightarrow \gamma\gamma) = \frac{\alpha^2}{2s} \frac{u^2 + t^2}{tu}. \quad (39.8)$$

The related QCD process also has a triple-gluon coupling. The cross section is

$$\frac{d\sigma}{d\Omega}(q\bar{q} \rightarrow gg) = \frac{8\alpha_s^2}{27s} (t^2 + u^2) \left(\frac{1}{tu} - \frac{9}{4s^2} \right). \quad (39.9)$$

The crossed reactions are

$$\frac{d\sigma}{d\Omega}(gq \rightarrow qg) = \frac{\alpha_s^2}{9s} (s^2 + u^2) \left(-\frac{1}{su} + \frac{9}{4t^2} \right) \quad (39.10)$$

and

$$\frac{d\sigma}{d\Omega}(gg \rightarrow q\bar{q}) = \frac{\alpha_s^2}{24s} (t^2 + u^2) \left(\frac{1}{tu} - \frac{9}{4s^2} \right). \quad (39.11)$$

Finally,

$$\frac{d\sigma}{d\Omega}(gg \rightarrow gg) = \frac{9\alpha_s^2}{8s} \left(3 - \frac{ut}{s^2} - \frac{su}{t^2} - \frac{st}{u^2} \right). \quad (39.12)$$

39.3. Hadroproduction of heavy quarks

For hadroproduction of heavy quarks $Q = c, b, t$, it is important to include mass effects in the formulae. For $q\bar{q} \rightarrow Q\bar{Q}$, one has

$$\frac{d\sigma}{d\Omega}(q\bar{q} \rightarrow Q\bar{Q}) = \frac{\alpha_s^2}{9s^3} \left[(m_Q^2 - t)^2 + (m_Q^2 - u)^2 + 2m_Q^2 s \right], \quad (39.13)$$

while for $gg \rightarrow Q\bar{Q}$ one has

$$\begin{aligned} \frac{d\sigma}{d\Omega}(gg \rightarrow Q\bar{Q}) = & \frac{\alpha_s^2}{32s} \left[\frac{6}{s^2} (m_Q^2 - t)(m_Q^2 - u) - \frac{m_Q^2(s - 4m_Q^2)}{3(m_Q^2 - t)(m_Q^2 - u)} + \right. \\ & \frac{4}{3} \frac{(m_Q^2 - t)(m_Q^2 - u) - 2m_Q^2(m_Q^2 + t)}{(m_Q^2 - t)^2} \\ & + \frac{4}{3} \frac{(m_Q^2 - t)(m_Q^2 - u) - 2m_Q^2(m_Q^2 + u)}{(m_Q^2 - u)^2} \\ & - \left[3 \frac{(m_Q^2 - t)(m_Q^2 - u) + m_Q^2(u - t)}{s(m_Q^2 - t)} \right. \\ & \left. \left. - 3 \frac{(m_Q^2 - t)(m_Q^2 - u) + m_Q^2(t - u)}{s(m_Q^2 - u)} \right] \right]. \quad (39.14) \end{aligned}$$

39.4. Production of Weak Gauge Bosons

39.4.1. W and Z resonant production :

Resonant production of a single W or Z is governed by the partial widths

$$\Gamma(W \rightarrow \ell_i \bar{\nu}_i) = \frac{\sqrt{2} G_F m_W^3}{12\pi} \quad (39.15)$$

$$\Gamma(W \rightarrow q_i \bar{q}_j) = 3 \frac{\sqrt{2} G_F |V_{ij}|^2 m_W^3}{12\pi} \quad (39.16)$$

$$\Gamma(Z \rightarrow f\bar{f}) = N_c \frac{\sqrt{2} G_F m_Z^3}{6\pi} \times \left[(T_3 - Q_f \sin^2\theta_W)^2 + (Q_f \sin\theta_W)^2 \right]. \quad (39.17)$$

The weak mixing angle is θ_W . The CKM matrix elements are indicated by V_{ij} and N_c is 3 for $q\bar{q}$ final states and 1 for leptonic final states.

The full differential cross section for $f_i \bar{f}_j \rightarrow (W, Z) \rightarrow f'_i \bar{f}'_j$ is given by

$$\begin{aligned} \frac{d\sigma}{d\Omega} &= \frac{N_c^f}{N_c^i} \cdot \frac{1}{256\pi^2 s} \cdot \frac{s^2}{(s-M^2)^2 + s\Gamma^2} \\ &\times \left[(L^2 + R^2)(L'^2 + R'^2)(1 + \cos^2\theta) \right. \\ &\left. + (L^2 - R^2)(L'^2 - R'^2)2 \cos\theta \right] \end{aligned} \quad (39.18)$$

where M is the mass of the W or Z . The couplings for the W are $L = (8G_F m_W^2/\sqrt{2})^{1/2} V_{ij}/\sqrt{2}$; $R = 0$ where V_{ij} is the corresponding CKM matrix element, with an analogous expression for L' and R' . For Z , the couplings are $L = (8G_F m_Z^2/\sqrt{2})^{1/2} (T_3 - \sin^2\theta_W Q)$; $R = -(8G_F m_Z^2/\sqrt{2})^{1/2} \sin^2\theta_W Q$, where T_3 is the weak isospin of the initial left-handed fermion and Q is the initial fermion's electric charge. The expressions for L' and R' are analogous. The color factors $N_c^{i,f}$ are 3 for initial or final quarks and 1 for initial or final leptons.

39.4.2. Production of pairs of weak gauge bosons :

The cross section for $f\bar{f} \rightarrow W^+W^-$ is given in term of the couplings of the left-handed and right-handed fermion f , $\ell = 2(T_3 - Qx_W)$, $r = -2Qx_W$, where T_3 is the third component of weak isospin for the left-handed f , Q is its electric charge (in units of the proton charge), and $x_W = \sin^2\theta_W$:

$$\begin{aligned} \frac{d\sigma}{dt} &= \frac{2\pi\alpha^2}{N_c s^2} \left\{ \left[\left(Q + \frac{\ell+r}{4x_W} \frac{s}{s-m_Z^2} \right)^2 + \left(\frac{\ell+r}{4x_W} \frac{s}{s-m_Z^2} \right)^2 \right] A(s, t, u) \right. \\ &+ \frac{1}{2x_W} \left(Q + \frac{\ell}{2x_W} \frac{s}{s-m_Z^2} \right) (\Theta(-Q)I(s, t, u) - \Theta(Q)I(s, u, t)) \\ &\left. + \frac{1}{8x_W^2} (\Theta(-Q)E(s, t, u) + \Theta(Q)E(s, u, t)) \right\}, \end{aligned} \quad (39.19)$$

where $\Theta(x)$ is 1 for $x > 0$ and 0 for $x < 0$, and where

$$\begin{aligned} A(s, t, u) &= \left(\frac{tu}{m_W^4} - 1 \right) \left(\frac{1}{4} - \frac{m_W^2}{s} + 3\frac{m_W^4}{s^2} \right) + \frac{s}{m_W^2} - 4, \\ I(s, t, u) &= \left(\frac{tu}{m_W^4} - 1 \right) \left(\frac{1}{4} - \frac{m_W^2}{2s} - \frac{m_W^4}{st} \right) + \frac{s}{m_W^2} - 2 + 2\frac{m_W^2}{t}, \\ E(s, t, u) &= \left(\frac{tu}{m_W^4} - 1 \right) \left(\frac{1}{4} + \frac{m_W^2}{t} \right) + \frac{s}{m_W^2}, \end{aligned} \quad (39.20)$$

and s, t, u are the usual Mandelstam variables with $s = (p_f + p_{\bar{f}})^2$, $t = (p_f - p_{W^-})^2$, $u = (p_f - p_{W^+})^2$. The factor N_c is 3 for quarks and 1 for leptons.

The analogous cross-section for $q_i \bar{q}_j \rightarrow W^\pm Z^0$ is

$$\begin{aligned} \frac{d\sigma}{dt} &= \frac{\pi\alpha^2 |V_{ij}|^2}{6s^2 x_W^2} \left\{ \left(\frac{1}{s-m_W^2} \right)^2 \left[\left(\frac{9-8x_W}{4} \right) (ut - m_W^2 m_Z^2) \right. \right. \\ &+ (8x_W - 6) s (m_W^2 + m_Z^2) \left. \right] \\ &+ \left[\frac{ut - m_W^2 m_Z^2 - s(m_W^2 + m_Z^2)}{s - m_W^2} \right] \left[\frac{\ell_j}{t} - \frac{\ell_i}{u} \right] \\ &\left. + \frac{ut - m_W^2 m_Z^2}{4(1-x_W)} \left[\frac{\ell_j^2}{t^2} + \frac{\ell_i^2}{u^2} \right] + \frac{s(m_W^2 + m_Z^2)}{2(1-x_W)} \frac{\ell_i \ell_j}{tu} \right\}, \end{aligned} \quad (39.21)$$

where ℓ_i and ℓ_j are the couplings of the left-handed q_i and q_j as defined above. The CKM matrix element between q_i and q_j is V_{ij} .

The cross section for $q_i \bar{q}_i \rightarrow Z^0 Z^0$ is

$$\frac{d\sigma}{dt} = \frac{\pi\alpha^2}{96} \frac{\ell_i^4 + r_i^4}{x_W^2 (1-x_W^2) s^2} \left[\frac{t}{u} + \frac{u}{t} + \frac{4m_Z^2 s}{tu} - m_Z^4 \left(\frac{1}{t^2} + \frac{1}{u^2} \right) \right]. \quad (39.22)$$

39.5. Production of Higgs Bosons

39.5.1. Resonant Production :

The Higgs boson of the Standard Model can be produced resonantly in the collisions of quarks, leptons, W or Z bosons, gluons, or photons. The production cross section is thus controlled by the partial width of the Higgs boson into the entrance channel and its total width. The branching fractions for the Standard Model Higgs boson are shown in Fig. 1 of the ‘‘Searches for Higgs bosons’’ review in the Particle Listings section, as a function of the Higgs boson mass. The partial widths are given by the relations

$$\Gamma(H \rightarrow f\bar{f}) = \frac{G_F m_f^2 m_H N_c}{4\pi\sqrt{2}} \left(1 - 4m_f^2/m_H^2 \right)^{3/2}, \quad (39.23)$$

$$\Gamma(H \rightarrow W^+W^-) = \frac{G_F m_H^3 \beta_W}{32\pi\sqrt{2}} (4 - 4a_W + 3a_W^2), \quad (39.24)$$

$$\Gamma(H \rightarrow ZZ) = \frac{G_F m_H^3 \beta_Z}{64\pi\sqrt{2}} (4 - 4a_Z + 3a_Z^2), \quad (39.25)$$

where N_c is 3 for quarks and 1 for leptons and where $a_W = 1 - \beta_W^2 = 4m_W^2/m_H^2$ and $a_Z = 1 - \beta_Z^2 = 4m_Z^2/m_H^2$. The decay to two gluons proceeds through quark loops, with the t quark dominating [2]. Explicitly,

$$\Gamma(H \rightarrow gg) = \frac{\alpha_s^2 G_F m_H^3}{36\pi^3 \sqrt{2}} \left| \sum_q I(m_q^2/m_H^2) \right|^2, \quad (39.26)$$

where $I(z)$ is complex for $z < 1/4$. For $z < 2 \times 10^{-3}$, $|I(z)|$ is small so the light quarks contribute negligibly. For $m_H < 2m_t$, $z > 1/4$ and

$$I(z) = 3 \left[2z + 2z(1-4z) \left(\sin^{-1} \frac{1}{2\sqrt{z}} \right)^2 \right], \quad (39.27)$$

which has the limit $I(z) \rightarrow 1$ as $z \rightarrow \infty$.

39.5.2. Higgs Boson Production in W^* and Z^* decay :

The Standard Model Higgs boson can be produced in the decay of a virtual W or Z (‘‘Higgstrahlung’’) [3,4]: In particular, if k is the c.m. momentum of the Higgs boson,

$$\sigma(q_i \bar{q}_j \rightarrow WH) = \frac{\pi\alpha^2 |V_{ij}|^2}{36 \sin^4\theta_W} \frac{2k}{\sqrt{s}} \frac{k^2 + 3m_W^2}{(s - m_W^2)^2} \quad (39.28)$$

$$\sigma(f\bar{f} \rightarrow ZH) = \frac{2\pi\alpha^2 (\ell_f^2 + r_f^2)}{48N_c \sin^4\theta_W \cos^4\theta_W} \frac{2k}{\sqrt{s}} \frac{k^2 + 3m_Z^2}{(s - m_Z^2)^2}, \quad (39.29)$$

where ℓ and r are defined as above.

39.5.3. W and Z Fusion :

Just as high-energy electrons can be regarded as sources of virtual photon beams, at very high energies they are sources of virtual W and Z beams. For Higgs boson production, it is the longitudinal components of the W s and Z s that are important [5]. The distribution of longitudinal W s carrying a fraction y of the electron's energy is [6]

$$f(y) = \frac{g^2}{16\pi^2} \frac{1-y}{y}, \quad (39.30)$$

where $g = e/\sin\theta_W$. In the limit $s \gg m_H \gg m_W$, the partial decay rate is $\Gamma(H \rightarrow W_L W_L) = (g^2/64\pi)(m_H^3/m_W^2)$ and in the equivalent W approximation [7]

$$\begin{aligned} \sigma(e^+e^- \rightarrow \bar{\nu}_e \nu_e H) &= \frac{1}{16m_W^2} \left(\frac{\alpha}{\sin^2\theta_W} \right)^3 \\ &\times \left[\left(1 + \frac{m_H^2}{s} \right) \log \frac{s}{m_H^2} - 2 + 2\frac{m_H^2}{s} \right]. \end{aligned} \quad (39.31)$$

There are significant corrections to this relation when m_H is not large compared to m_W [8]. For $m_H = 150$ GeV, the estimate is too high by 51% for $\sqrt{s} = 1000$ GeV, 32% too high at $\sqrt{s} = 2000$ GeV, and 22% too high at $\sqrt{s} = 4000$ GeV. Fusion of ZZ to make a Higgs boson can be treated similarly. Identical formulae apply for Higgs production in the collisions of quarks whose charges permit the emission of a W^+ and a W^- , except that QCD corrections and CKM matrix elements are required. Even in the absence of QCD corrections, the fine-structure constant ought to be evaluated at the scale of the collision, say m_W . All quarks contribute to the ZZ fusion process.

39.6. Inclusive hadronic reactions

One-particle inclusive cross sections $E d^3\sigma/d^3p$ for the production of a particle of momentum p are conveniently expressed in terms of rapidity y (see above) and the momentum p_T transverse to the beam direction (in the c.m.):

$$E \frac{d^3\sigma}{d^3p} = \frac{d^3\sigma}{d\phi dy p_T dp_T^2}. \quad (39.32)$$

In appropriate circumstances, the cross section may be decomposed as a partonic cross section multiplied by the probabilities of finding partons of the prescribed momenta:

$$\sigma_{\text{hadronic}} = \sum_{ij} \int dx_1 dx_2 f_i(x_1) f_j(x_2) d\hat{\sigma}_{\text{partonic}}, \quad (39.33)$$

The probability that a parton of type i carries a fraction of the incident particle's that lies between x_1 and $x_1 + dx_1$ is $f_i(x_1)dx_1$ and similarly for partons in the other incident particle. The partonic collision is specified by its c.m. energy squared $\hat{s} = x_1x_2s$ and the momentum transfer squared \hat{t} . The final hadronic state is more conveniently specified by the rapidities y_1, y_2 of the two jets resulting from the collision and the transverse momentum p_T . The connection between the differentials is

$$dx_1 dx_2 d\hat{t} = dy_1 dy_2 \frac{\hat{s}}{s} dp_T^2, \quad (39.34)$$

so that

$$\frac{d^3\sigma}{dy_1 dy_2 dp_T^2} = \frac{\hat{s}}{s} \left[f_i(x_1) f_j(x_2) \frac{d\hat{\sigma}}{d\hat{t}}(\hat{s}, \hat{t}, \hat{u}) + f_i(x_2) f_j(x_1) \frac{d\hat{\sigma}}{d\hat{t}}(\hat{s}, \hat{u}, \hat{t}) \right], \quad (39.35)$$

where we have taken into account the possibility that the incident parton types might arise from either incident particle. The second term should be dropped if the types are identical: $i = j$.

39.7. Two-photon processes

In the Weizsäcker-Williams picture, a high-energy electron beam is accompanied by a spectrum of virtual photons of energies ω and invariant-mass squared $q^2 = -Q^2$, for which the photon number density is

$$dn = \frac{\alpha}{\pi} \left[1 - \frac{\omega}{E} + \frac{\omega^2}{E^2} - \frac{m_e^2 \omega^2}{Q^2 E^2} \right] \frac{d\omega}{\omega} \frac{dQ^2}{Q^2}, \quad (39.36)$$

where E is the energy of the electron beam. The cross section for $e^+e^- \rightarrow e^+e^-X$ is then [9]

$$d\sigma_{e^+e^- \rightarrow e^+e^-X}(s) = dn_1 dn_2 d\sigma_{\gamma\gamma \rightarrow X}(W^2), \quad (39.37)$$

where $W^2 = m_X^2$. Integrating from the lower limit $Q^2 = m_e^2 \frac{\omega_i^2}{E_i(E_i - \omega_i)}$ to a maximum Q^2 gives

$$\sigma_{e^+e^- \rightarrow e^+e^-X}(s) = \frac{\alpha^2}{\pi^2} \int_{z_{\text{th}}}^1 \frac{dz}{z} \times \left[\left(\ln \frac{Q_{\text{max}}^2}{zm_e^2} - 1 \right)^2 f(z) + \frac{1}{3} (\ln z)^3 \right] \sigma_{\gamma\gamma \rightarrow X}(zs), \quad (39.38)$$

where

$$f(z) = \left(1 + \frac{1}{2}z \right)^2 \ln(1/z) - \frac{1}{2}(1-z)(3+z). \quad (39.39)$$

The appropriate value of Q_{max}^2 depends on the properties of the produced system X . For production of hadronic systems, $Q_{\text{max}}^2 \approx m_\rho^2$, while for lepton-pair production, $Q^2 \approx W^2$. For production of a resonance with spin $J \neq 1$, we have

$$\sigma_{e^+e^- \rightarrow e^+e^-R}(s) = (2J+1) \frac{8\alpha^2 \Gamma_{R \rightarrow \gamma\gamma}}{m_R^3} \times \left[f(m_R^2/s) \left(\ln \frac{m_V^2 s}{m_e^2 m_R^2} - 1 \right)^2 - \frac{1}{3} \left(\ln \frac{s}{M_R^2} \right)^3 \right], \quad (39.40)$$

where m_V is the mass that enters into the form factor for the $\gamma\gamma \rightarrow R$ transition, typically m_ρ .

PART II: PROCESSES BEYOND THE STANDARD MODEL

39.8. Production of supersymmetric particles

In supersymmetric (SUSY) theories (see Supersymmetric Particle Searches in this *Review*), every boson has a fermionic superpartner, and every fermion has a bosonic superpartner. The minimal supersymmetric Standard Model (MSSM) is a direct supersymmetrization of the Standard Model (SM), although a second Higgs doublet is needed to avoid triangle anomalies [10]. Under *soft* SUSY breaking, superpartner masses are lifted above the SM particle masses. In weak scale SUSY, the superpartners are invoked to stabilize the weak scale under radiative corrections, so the superpartners are expected to have masses of order the TeV scale.

39.8.1. Gluino and squark production :

The superpartners of gluons are the color octet, spin- $\frac{1}{2}$ gluinos (\tilde{g}), while each helicity component of quark flavor has a spin-0 *squark* partner, e.g. \tilde{q}_L and \tilde{q}_R . Third generation left- and right- squarks are expected to have large mixing, resulting in mass eigenstates \tilde{q}_1 and \tilde{q}_2 , with $m_{\tilde{q}_1} < m_{\tilde{q}_2}$ (here, q denotes any of the SM flavors of quarks and \tilde{q}_i the corresponding flavor and type ($i = L, R$ or 1, 2) of squark). Gluino pair production ($\tilde{g}\tilde{g}$) takes place via either glue-gluon or quark-antiquark annihilation [11].

The subprocess cross sections are usually presented as differential distributions in the Mandelstam variables s , t and u . Note that for a $2 \rightarrow 2$ scattering subprocess $ab \rightarrow cd$, the Mandelstam variable $s = (p_a + p_b)^2 = (p_c + p_d)^2$, where p_a is the 4-momentum of particle a , and so forth. The variable $t = (p_c - p_a)^2$, where c and a are taken conventionally to be the most similar particles in the subprocess. The variable u would then be equal to $(p_d - p_a)^2$. Note that since s , t and u are squares of 4-vectors, they are invariants in any inertial reference frame.

Gluino pair production at hadron colliders is described by:

$$\frac{d\sigma}{dt}(gg \rightarrow \tilde{g}\tilde{g}) = \frac{9\pi\alpha_s^2}{4s^2} \left\{ \frac{2(m_{\tilde{g}}^2 - t)(m_{\tilde{g}}^2 - u)}{s^2} + \frac{(m_{\tilde{g}}^2 - t)(m_{\tilde{g}}^2 - u) - 2m_{\tilde{g}}^2(m_{\tilde{g}}^2 + t)}{(m_{\tilde{g}}^2 - t)^2} + \frac{(m_{\tilde{g}}^2 - t)(m_{\tilde{g}}^2 - u) - 2m_{\tilde{g}}^2(m_{\tilde{g}}^2 + u)}{(m_{\tilde{g}}^2 - u)^2} + \frac{m_{\tilde{g}}^2(s - 4m_{\tilde{g}}^2)}{(m_{\tilde{g}}^2 - t)(m_{\tilde{g}}^2 - u)} - \frac{(m_{\tilde{g}}^2 - t)(m_{\tilde{g}}^2 - u) + m_{\tilde{g}}^2(u - t)}{s(m_{\tilde{g}}^2 - t)} - \frac{(m_{\tilde{g}}^2 - t)(m_{\tilde{g}}^2 - u) + m_{\tilde{g}}^2(t - u)}{s(m_{\tilde{g}}^2 - u)} \right\}, \quad (39.41)$$

where α_s is the strong fine structure constant. Also,

$$\begin{aligned} \frac{d\sigma}{dt}(q\bar{q} \rightarrow \tilde{g}\tilde{g}) &= \frac{8\pi\alpha_s^2}{9s^2} \left\{ \frac{4}{3} \left(\frac{m_g^2 - t}{m_q^2 - t} \right)^2 + \frac{4}{3} \left(\frac{m_g^2 - u}{m_q^2 - u} \right)^2 \right. \\ &+ \frac{3}{s^2} \left[(m_g^2 - t)^2 + (m_g^2 - u)^2 + 2m_g^2 s \right] - 3 \frac{[(m_g^2 - t)^2 + m_g^2 s]}{s(m_q^2 - t)} \\ &\left. - 3 \frac{[(m_g^2 - u)^2 + m_g^2 s]}{s(m_q^2 - u)} + \frac{1}{3} \frac{m_g^2 s}{(m_q^2 - t)(m_q^2 - u)} \right\}. \end{aligned} \quad (39.42)$$

Glueinos can also be produced in association with squarks: $\tilde{g}\tilde{q}_i$ production, where \tilde{q}_i represents any of the various types (left-, right- or mixed) and flavors of squarks. The subprocess cross section is independent of whether the squark is the right-, left- or mixed type:

$$\begin{aligned} \frac{d\sigma}{dt}(gq \rightarrow \tilde{g}\tilde{q}_i) &= \frac{\pi\alpha_s^2}{24s^2} \frac{\left[\frac{16}{3}(s^2 + (m_{\tilde{q}_i}^2 - u)^2) + \frac{4}{3}s(m_{\tilde{q}_i}^2 - u) \right]}{s(m_g^2 - t)(m_{\tilde{q}_i}^2 - u)^2} \\ &\times \left((m_g^2 - u)^2 + (m_{\tilde{q}_i}^2 - m_g^2)^2 + \frac{2sm_g^2(m_{\tilde{q}_i}^2 - m_g^2)}{(m_g^2 - t)} \right). \end{aligned} \quad (39.43)$$

There are many different subprocesses for production of squark pairs. Since left- and right- squarks generally have different masses and different decay patterns, we present the differential cross section for each subprocess of \tilde{q}_i ($i = L, R$ or 1, 2) separately. (In early literature, the following formulae were often combined into a single equation which didn't differentiate the various squark types.) The result for $gg \rightarrow \tilde{q}_i\tilde{q}_i$ is:

$$\begin{aligned} \frac{d\sigma}{dt}(gg \rightarrow \tilde{q}_i\tilde{q}_i) &= \frac{\pi\alpha_s^2}{4s^2} \left\{ \frac{1}{3} \left(\frac{m_q^2 + t}{m_q^2 - t} \right)^2 + \frac{1}{3} \left(\frac{m_q^2 + u}{m_q^2 - u} \right)^2 \right. \\ &+ \frac{3}{32s^2} (8s(4m_q^2 - s) + 4(u - t)^2) + \frac{7}{12} \\ &- \frac{1}{48} \frac{(4m_q^2 - s)^2}{(m_q^2 - t)(m_q^2 - u)} \\ &+ \frac{3}{32} \frac{[(t - u)(4m_q^2 + 4t - s) - 2(m_q^2 - u)(6m_q^2 + 2t - s)]}{s(m_q^2 - t)} \\ &+ \frac{3}{32} \frac{[(u - t)(4m_q^2 + 4u - s) - 2(m_q^2 - t)(6m_q^2 + 2u - s)]}{s(m_q^2 - u)} \\ &\left. + \frac{7}{96} \frac{[4m_q^2 + 4t - s]}{m_q^2 - t} + \frac{7}{96} \frac{[4m_q^2 + 4u - s]}{m_q^2 - u} \right\}, \end{aligned} \quad (39.44)$$

which has an obvious $u \leftrightarrow t$ symmetry.

For $q\bar{q} \rightarrow \tilde{q}_i\tilde{q}_i$ with the same initial and final state flavors, we have

$$\begin{aligned} \frac{d\sigma}{dt}(q\bar{q} \rightarrow \tilde{q}_i\tilde{q}_i) &= \frac{2\pi\alpha_s^2}{9s^2} \left\{ \frac{1}{(t - m_g^2)^2} + \frac{2}{s^2} - \frac{2/3}{s(t - m_g^2)} \right\} \\ &\times [-st - (t - m_{\tilde{q}_i}^2)^2], \end{aligned} \quad (39.45)$$

while if initial and final state flavors are different ($q\bar{q} \rightarrow \tilde{q}_i\tilde{q}_j$) we instead have

$$\frac{d\sigma}{dt}(q\bar{q} \rightarrow \tilde{q}_i\tilde{q}_j) = \frac{4\pi\alpha_s^2}{9s^4} [-st - (t - m_{\tilde{q}_i}^2)^2]. \quad (39.46)$$

If the two initial state quarks are of different flavors, then we have

$$\frac{d\sigma}{dt}(q\bar{q}' \rightarrow \tilde{q}_i\tilde{q}_j) = \frac{2\pi\alpha_s^2}{9s^2} \frac{-st - (t - m_{\tilde{q}_i}^2)^2}{(t - m_g^2)^2}. \quad (39.47)$$

If the initial quarks are of different flavor and final state squarks are of different type ($i \neq j$) then

$$\frac{d\sigma}{dt}(q\bar{q}' \rightarrow \tilde{q}_i\tilde{q}_j) = \frac{2\pi\alpha_s^2}{9s^2} \frac{m_g^2 s}{(t - m_g^2)^2}. \quad (39.48)$$

For same-flavor initial state quarks, but final state unlike-type squarks, we also have

$$\frac{d\sigma}{dt}(q\bar{q} \rightarrow \tilde{q}_i\tilde{q}_j) = \frac{2\pi\alpha_s^2}{9s^2} \frac{m_g^2 s}{(t - m_g^2)^2}. \quad (39.49)$$

There also exist cross sections for quark-quark annihilation to squark pairs. For same flavor quark-quark annihilation to same flavor/same type final state squarks,

$$\begin{aligned} \frac{d\sigma}{dt}(qq \rightarrow \tilde{q}_i\tilde{q}_i) &= \\ &= \frac{\pi\alpha_s^2}{9s^2} m_g^2 s \left\{ \frac{1}{(t - m_g^2)^2} + \frac{1}{(u - m_g^2)^2} - \frac{2/3}{(t - m_g^2)(u - m_g^2)} \right\}, \end{aligned} \quad (39.50)$$

while if the final type squarks are different ($i \neq j$), we have

$$\begin{aligned} \frac{d\sigma}{dt}(qq \rightarrow \tilde{q}_i\tilde{q}_j) &= \\ &= \frac{2\pi\alpha_s^2}{9s^2} \left\{ \frac{[-st - (t - m_{\tilde{q}_i}^2)(t - m_{\tilde{q}_j}^2)]}{(t - m_g^2)} + \frac{[-su - (u - m_{\tilde{q}_i}^2)(u - m_{\tilde{q}_j}^2)]}{(u - m_g^2)} \right\}. \end{aligned} \quad (39.51)$$

If initial/final state flavors are different, but final state squark types are the same, then

$$\frac{d\sigma}{dt}(q\bar{q}' \rightarrow \tilde{q}_i\tilde{q}_i) = \frac{2\pi\alpha_s^2}{9s^2} \frac{m_g^2 s}{(t - m_g^2)^2}. \quad (39.52)$$

If initial quark flavors are different and final squark types are different, then

$$\frac{d\sigma}{dt}(q\bar{q}' \rightarrow \tilde{q}_i\tilde{q}_j) = \frac{2\pi\alpha_s^2}{9s^2} \frac{-st - (t - m_{\tilde{q}_i}^2)(t - m_{\tilde{q}_j}^2)}{(t - m_g^2)^2}. \quad (39.53)$$

39.8.2. Gluino and squark associated production :

In the MSSM, the charged spin- $\frac{1}{2}$ winos and higgsinos mix to make chargino states $\chi_{1,2}^{\pm}$ and χ_3^0 , with $m_{\chi_1^{\pm}} < m_{\chi_2^{\pm}}$. The spin- $\frac{1}{2}$ neutral bino, wino and higgsino fields mix to give four neutralino mass eigenstates $\chi_{1,2,3,4}^0$ ordered according to mass. We sometimes denote the charginos and neutralinos collectively as -inos for notational simplicity

For gluino and squark production in association with charginos and neutralinos [12], the quark-squark-neutralino couplings* are defined by the interaction Lagrangian terms $\mathcal{L}_{ff\tilde{\chi}_i^0} =$

$$\left[iA_{\tilde{\chi}_i^0}^f \tilde{f}_L^{\dagger} \tilde{\chi}_i^0 P_L f + iB_{\tilde{\chi}_i^0}^f \tilde{f}_R^{\dagger} \tilde{\chi}_i^0 P_R f + \text{h.c.} \right],$$

where $A_{\tilde{\chi}_i^0}^f$ and $B_{\tilde{\chi}_i^0}^f$ are coupling constants involving gauge couplings, neutralino mixing elements and in the case of third generation fermions, Yukawa couplings. Their form depends on the conventions used for setting up the MSSM Lagrangian, and can be found in various reviews [13] and textbooks [14,15]. P_L and P_R are the usual left- and right-spinor projection operators and f denotes any of the SM fermions u, d, e, ν_e, \dots . The fermion-sfermion- chargino couplings have the form $\mathcal{L} = \left[iA_{\tilde{\chi}_i^{\pm}}^d \tilde{u}_L^{\dagger} \tilde{\chi}_i^{\pm} P_L d + iA_{\tilde{\chi}_i^{\pm}}^u \tilde{d}_L^{\dagger} \tilde{\chi}_i^{\pm} P_L u + \text{h.c.} \right]$ for u and d

* The couplings $A_{\tilde{\chi}_i^0}^f$ and $B_{\tilde{\chi}_i^0}^f$ are given explicitly in Ref. 15 in Eq. (8.87). Also, the couplings $A_{\tilde{\chi}_i^{\pm}}^d$ and $A_{\tilde{\chi}_i^{\pm}}^u$ are given in Eq. (8.93). The couplings X_i^j and Y_i^j are given by Eq. (8.103), while the x_i and y_i couplings are given in Eq. (8.100). Finally, the couplings W_{ij} are given in Eq. (8.101).

Table 39.1: The constants α_f and β_f that appear in in the SM neutral current Lagrangian. Here $t \equiv \tan \theta_W$ and $c \equiv \cot \theta_W$.

f	q_f	α_f	β_f
ℓ	-1	$\frac{1}{4}(3t - c)$	$\frac{1}{4}(t + c)$
ν_ℓ	0	$\frac{1}{4}(t + c)$	$-\frac{1}{4}(t + c)$
u	$\frac{2}{3}$	$-\frac{5}{12}t + \frac{1}{4}c$	$-\frac{1}{4}(t + c)$
d	$-\frac{1}{3}$	$\frac{1}{12}t - \frac{1}{4}c$	$\frac{1}{4}(t + c)$

quarks, where the $A_{\tilde{\chi}_i^-}^d$ and $A_{\tilde{\chi}_i^-}^u$ couplings are again convention-dependent, and can be found in textbooks. The superscript c denotes ‘‘charge conjugate spinor’’, defined by $\psi^c \equiv C\bar{\psi}^T$.

The subprocess cross sections for chargino-squark associated production occur via squark exchange and are given by

$$\frac{d\sigma}{dt}(\bar{u}g \rightarrow \tilde{\chi}_i^- \bar{d}_L) = \frac{\alpha_s}{24s^2} |A_{\tilde{\chi}_i^-}^u|^2 \psi(m_{\tilde{d}_L}, m_{\tilde{\chi}_i^-}, t), \quad (39.54)$$

$$\frac{d\sigma}{dt}(dg \rightarrow \tilde{\chi}_i^- \bar{u}_L) = \frac{\alpha_s}{24s^2} |A_{\tilde{\chi}_i^-}^d|^2 \psi(m_{\tilde{u}_L}, m_{\tilde{\chi}_i^-}, t), \quad (39.55)$$

while neutralino-squark production is given by

$$\frac{d\sigma}{dt}(q\bar{q} \rightarrow \tilde{\chi}_i^0 \bar{q}) = \frac{\alpha_s}{24s^2} \left(|A_{\tilde{\chi}_i^0}^q|^2 + |B_{\tilde{\chi}_i^0}^q|^2 \right) \psi(m_{\tilde{q}}, m_{\tilde{\chi}_i^0}, t), \quad (39.56)$$

where

$$\psi(m_1, m_2, t) = \frac{s + t - m_1^2}{2s} - \frac{m_1^2(m_2^2 - t)}{(m_1^2 - t)^2} + \frac{t(m_2^2 - m_1^2) + m_2^2(s - m_2^2 + m_1^2)}{s(m_1^2 - t)}. \quad (39.57)$$

Here, the variable t is given by the square of ‘‘squark-minus-quark’’ four-momentum. The neutralino-gluino associated production cross section also occurs via squark exchange and is given by

$$\frac{d\sigma}{dt}(q\bar{q} \rightarrow \tilde{\chi}_i^0 \bar{g}) = \frac{\alpha_s}{18s^2} \left(|A_{\tilde{\chi}_i^0}^q|^2 + |B_{\tilde{\chi}_i^0}^q|^2 \right) \left[\frac{(m_{\tilde{\chi}_i^0}^2 - t)(m_g^2 - t)}{(m_{\tilde{q}}^2 - t)^2} + \frac{(m_{\tilde{\chi}_i^0}^2 - u)(m_g^2 - u)}{(m_{\tilde{q}}^2 - u)^2} - \frac{2\eta_i \eta_g m_{\tilde{g}} m_{\tilde{\chi}_i^0} s}{(m_{\tilde{q}}^2 - t)(m_{\tilde{q}}^2 - u)} \right], \quad (39.58)$$

where η_i is the sign of the neutralino mass eigenvalue and η_g is the sign of the gluino mass eigenvalue. We also have chargino-gluino associated production:

$$\frac{d\sigma}{dt}(\bar{u}d \rightarrow \tilde{\chi}_i^- \bar{g}) = \frac{\alpha_s}{18s^2} \left[|A_{\tilde{\chi}_i^-}^u|^2 \frac{(m_{\tilde{\chi}_i^-}^2 - t)(m_g^2 - t)}{(m_{\tilde{d}_L}^2 - t)^2} + |A_{\tilde{\chi}_i^-}^d|^2 \frac{(m_{\tilde{\chi}_i^-}^2 - u)(m_g^2 - u)}{(m_{\tilde{u}_L}^2 - u)^2} + \frac{2\eta_{\tilde{g}} \text{Re}(A_{\tilde{\chi}_i^-}^u A_{\tilde{\chi}_i^-}^d)}{(m_{\tilde{d}_L}^2 - t)(m_{\tilde{u}_L}^2 - u)} \right], \quad (39.59)$$

where $\hat{t} = (\hat{g} - d)^2$ and in the third term one must take the real part of the in general complex coupling constant product.

39.8.3. Slepton and sneutrino production :

The subprocess cross section for $\tilde{\ell}_L \tilde{\nu}_{\ell L}$ production ($\ell = e$ or μ) occurs via s -channel W exchange and is given by

$$\frac{d\sigma}{dt}(d\bar{u} \rightarrow \tilde{\ell}_L \tilde{\nu}_{\ell L}) = \frac{g^4 |D_W(s)|^2}{192\pi s^2} (tu - m_{\tilde{\ell}_L}^2 m_{\tilde{\nu}_{\ell L}}^2), \quad (39.60)$$

where $D_W(s) = 1/(s - M_W^2 + iM_W\Gamma_W)$ is the W -boson propagator denominator. The production of $\tilde{\tau}_1 \tilde{\nu}_\tau$ is given as above, but replacing $m_{\tilde{\ell}_L} \rightarrow m_{\tilde{\tau}_1}$, $m_{\tilde{\nu}_{\ell L}} \rightarrow m_{\tilde{\nu}_\tau}$ and multiplying by an overall factor of $\cos^2 \theta_\tau$ (where θ_τ is the tau-slepton mixing angle). Similar substitutions hold for $\tilde{\tau}_2 \tilde{\nu}_\tau$ production, except the overall factor is $\sin^2 \theta_\tau$.

The subprocess cross section for $\tilde{\ell}_L \tilde{\bar{\ell}}_L$ production occurs via s -channel γ and Z exchange, and depends on the neutral current interaction, with fermion couplings to γ and Z^0 given by $\mathcal{L}_{\text{neutral}} = -eq_f \bar{f} \gamma^\mu f A_\mu + e \bar{f} \gamma^\mu (\alpha_f + \beta_f \gamma_5) f Z_\mu$ (with values of q_f , α_f , and β_f given in Table 39.1).

The subprocess cross section is given by

$$\frac{d\sigma}{dt}(q\bar{q} \rightarrow \tilde{\ell}_L \tilde{\bar{\ell}}_L) = \frac{e^4}{24\pi s^2} (tu - m_{\tilde{\ell}_L}^4) \times \left\{ \frac{q_\ell^2 q_q^2}{s^2} + (\alpha_\ell - \beta_\ell)^2 (\alpha_q^2 + \beta_q^2) |D_Z(s)|^2 + \frac{2q_\ell q_q \alpha_q (\alpha_\ell - \beta_\ell) (s - M_Z^2)}{s} |D_Z(s)|^2 \right\}, \quad (39.61)$$

where $D_Z(s) = 1/(s - M_Z^2 + iM_Z\Gamma_Z)$. The cross section for sneutrino production is given by the same formula, but with α_ℓ , β_ℓ , q_ℓ and $m_{\tilde{\ell}_L}$ replaced by α_ν , β_ν , 0 and $m_{\tilde{\nu}_L}$, respectively. The cross section for $\tilde{\tau}_1 \tilde{\nu}_\tau$ production is obtained by replacing $m_{\tilde{\ell}_L} \rightarrow m_{\tilde{\tau}_1}$ and $\beta_\ell \rightarrow \beta_\ell \cos 2\theta_\tau$.

The cross section for $\tilde{\ell}_R \tilde{\bar{\ell}}_R$ production is given by substituting $\alpha_\ell - \beta_\ell \rightarrow \alpha_\ell + \beta_\ell$ and $m_{\tilde{\ell}_L} \rightarrow m_{\tilde{\ell}_R}$ in the equation above. The cross section for $\tilde{\tau}_2 \tilde{\nu}_\tau$ production is obtained from the formula for $\tilde{\ell}_R \tilde{\bar{\ell}}_R$ production by replacing $m_{\tilde{\ell}_R} \rightarrow m_{\tilde{\tau}_2}$ and $\beta_\ell \rightarrow \beta_\ell \cos 2\theta_\tau$.

Finally, the cross section for $\tilde{\tau}_1 \tilde{\nu}_\tau$ production occurs only via Z exchange, and is given by

$$\frac{d\sigma}{dt}(q\bar{q} \rightarrow \tilde{\tau}_1 \tilde{\nu}_\tau) = \frac{d\sigma}{dt}(q\bar{q} \rightarrow \tilde{\tau}_1 \tilde{\tau}_2) = \frac{e^4}{24\pi s^2} (\alpha_q^2 + \beta_q^2) \beta_\ell^2 \sin^2 2\theta_\tau |D_Z(s)|^2 (ut - m_{\tilde{\tau}_1}^2 m_{\tilde{\tau}_2}^2). \quad (39.62)$$

39.8.4. Chargino and neutralino pair production :

39.8.4.1. $\tilde{\chi}_i^- \tilde{\chi}_j^0$ production:

The subprocess cross section for $d\bar{u} \rightarrow \tilde{\chi}_i^- \tilde{\chi}_j^0$ depends on Lagrangian couplings $\mathcal{L}_{W\bar{u}d} = -\frac{g}{\sqrt{2}} \bar{u} \gamma_\mu P_L d W^{+\mu} + \text{h.c.}$, $\mathcal{L}_{W\tilde{\chi}_i^- \tilde{\chi}_j^0} = -g(-i)^{\theta_j} \bar{\tilde{\chi}}_i^- [X_i^j + Y_i^j \gamma_5] \gamma_\mu \tilde{\chi}_j^0 W^{-\mu} + \text{h.c.}$, $\mathcal{L}_{q\bar{q}\tilde{\chi}_i^-} = iA_{\tilde{\chi}_i^-}^d \bar{u}_L \tilde{\chi}_i^- P_L d + iA_{\tilde{\chi}_i^-}^u \bar{d}_L \tilde{\chi}_i^- P_L u + \text{h.c.}$ and $\mathcal{L}_{q\bar{q}\tilde{\chi}_j^0} = iA_{\tilde{\chi}_j^0}^q \bar{q}_L \tilde{\chi}_j^0 P_L q + \text{h.c.}$. Contributing diagrams include W exchange and also \tilde{d}_L and \tilde{u}_L squark exchange. The X_i^j and Y_i^j couplings are new, and again convention-dependent: the cross section formulae works if the interaction Lagrangian is written in the above form, so that the couplings can be suitably extracted. The term $\theta_j = 0$ (1) if $m_{\tilde{\chi}_j^0} > 0$ (< 0); it comes about because the neutralino field must be re-defined by a $-i\gamma_5$ transformation if its mass eigenvalue is negative [15]. The subprocess cross section is given in terms of dot products of four momenta, where particle labels are used to denote their four-momenta; note that all mass terms in the cross section formulae are positive definite, so that the signs of mass eigenstates have been absorbed into the Lagrangian couplings, as for instance in Ref. [15]. We then have

$$\frac{d\sigma}{dt}(d\bar{u} \rightarrow \tilde{\chi}_i^- \tilde{\chi}_j^0) = \frac{1}{192\pi s^2}$$

$$\left[T_W + T_{\tilde{d}_L} + T_{\tilde{u}_L} + T_{W\tilde{d}_L} + T_{W\tilde{u}_L} + T_{\tilde{d}_L \tilde{u}_L} \right] \quad (39.63)$$

where

$$T_W = 8g^4 |D_W(s)|^2 \left\{ [X_i^j]^2 + [Y_i^j]^2 (\tilde{\chi}_j^0 \cdot d\tilde{\chi}_i^- \cdot \bar{u} + \tilde{\chi}_j^0 \cdot \bar{u}\tilde{\chi}_i^- \cdot d) + 2(X_i^j Y_i^j) (\tilde{\chi}_j^0 \cdot d\tilde{\chi}_i^- \cdot \bar{u} - \tilde{\chi}_j^0 \cdot \bar{u}\tilde{\chi}_i^- \cdot d) + [X_i^j]^2 - [Y_i^j]^2 m_{\tilde{\chi}_i^-} m_{\tilde{\chi}_j^0} d \cdot \bar{u} \right\}, \quad (39.64)$$

$$T_{\tilde{d}_L} = \frac{4|A_{\tilde{\chi}_i^-}^u|^2|A_{\tilde{\chi}_j^0}^d|^2}{[(\tilde{\chi}_i^- - \bar{u})^2 - m_{\tilde{d}_L}^2]^2} d \cdot \tilde{\chi}_j^0 \tilde{\chi}_i^- \cdot \bar{u}, \quad (39.65)$$

$$T_{\tilde{u}_L} = \frac{4|A_{\tilde{\chi}_i^-}^d|^2|A_{\tilde{\chi}_j^0}^u|^2}{[(\tilde{\chi}_j^0 - \bar{u})^2 - m_{\tilde{u}_L}^2]^2} \bar{u} \cdot \tilde{\chi}_j^0 \tilde{\chi}_i^- \cdot d \quad (39.66)$$

$$T_{W\tilde{d}_L} = \frac{-\sqrt{2}g^2 \text{Re}[A_{\tilde{\chi}_j^0}^{d*} A_{\tilde{\chi}_i^-}^u (-i)^{\theta_j}](s - M_W^2)|D_W(s)|^2}{(\tilde{\chi}_i^- - \bar{u})^2 - m_{\tilde{d}_L}^2} \times \left\{ 8(X_i^j + Y_i^j)\tilde{\chi}_j^0 \cdot \bar{d}\bar{u} \cdot \tilde{\chi}_i^- + 4(X_i^j - Y_i^j)m_{\tilde{\chi}_i^-} m_{\tilde{\chi}_j^0} d \cdot \bar{u} \right\} \quad (39.67)$$

$$T_{W\tilde{u}_L} = \frac{\sqrt{2}g^2 \text{Re}[A_{\tilde{\chi}_i^-}^{d*} A_{\tilde{\chi}_j^0}^u (-i)^{\theta_j}](s - M_W^2)|D_W(s)|^2}{(\tilde{\chi}_j^0 - \bar{u})^2 - m_{\tilde{u}_L}^2} \times \left\{ 8(X_i^j - Y_i^j)\tilde{\chi}_j^0 \cdot \bar{u}\bar{d} \cdot \tilde{\chi}_i^- + 4(X_i^j + Y_i^j)m_{\tilde{\chi}_i^-} m_{\tilde{\chi}_j^0} d \cdot \bar{u} \right\} \quad (39.68)$$

and

$$T_{\tilde{d}_L\tilde{u}_L} = -\frac{4\text{Re}[A_{\tilde{\chi}_j^0}^d A_{\tilde{\chi}_i^-}^{u*} A_{\tilde{\chi}_i^-}^{d*} A_{\tilde{\chi}_j^0}^u]m_{\tilde{\chi}_i^-} m_{\tilde{\chi}_j^0} d \cdot \bar{u}}{[(\tilde{\chi}_i^- - \bar{u})^2 - m_{\tilde{d}_L}^2][(\tilde{\chi}_j^0 - \bar{u})^2 - m_{\tilde{u}_L}^2]}. \quad (39.69)$$

39.8.4.2. Chargino pair production:

The subprocess cross section for $d\bar{d} \rightarrow \tilde{\chi}_i^- \tilde{\chi}_i^+$ ($i = 1, 2$) depends on Lagrangian couplings $\mathcal{L} = e\tilde{\chi}_i^- \gamma_\mu \tilde{\chi}_i^+ A^\mu - e \cot \theta_W \tilde{\chi}_i^- \gamma_\mu (x_i - y_i \gamma_5) \tilde{\chi}_i^+ Z^\mu$ and also $\mathcal{L} \ni iA_{\tilde{\chi}_i^-}^d \tilde{u}_L^\dagger \tilde{\chi}_i^- P_L d + iA_{\tilde{\chi}_i^-}^u \tilde{d}_L^\dagger \tilde{\chi}_i^- P_L u + \text{h.c.}$. Contributing diagrams include s -channel γ , Z^0 exchange and t -channel \tilde{u}_L exchange [16,17]. The couplings x_i and y_i are again new and as usual convention-dependent.

The subprocess cross section is given by

$$\frac{d\sigma}{dt}(d\bar{d} \rightarrow \tilde{\chi}_i^- \tilde{\chi}_i^+) = \frac{1}{192\pi s^2} [T_\gamma + T_Z + T_{\tilde{u}_L} + T_{\gamma Z} + T_{\gamma\tilde{u}_L} + T_{Z\tilde{u}_L}] \quad (39.70)$$

where

$$T_\gamma = \frac{32e^4 q_d^2}{s^2} \left[d \cdot \tilde{\chi}_i^+ \bar{d} \cdot \tilde{\chi}_i^- + d \cdot \tilde{\chi}_i^- \bar{d} \cdot \tilde{\chi}_i^+ + m_{\tilde{\chi}_i^-}^2 d \cdot \bar{d} \right] \quad (39.71)$$

$$T_Z = 32e^4 \cot^2 \theta_W |D_Z(s)|^2$$

$$\left\{ (\alpha_d^2 + \beta_d^2)(x_i^2 + y_i^2) \left[d \cdot \tilde{\chi}_i^+ \bar{d} \cdot \tilde{\chi}_i^- + d \cdot \tilde{\chi}_i^- \bar{d} \cdot \tilde{\chi}_i^+ + m_{\tilde{\chi}_i^-}^2 d \cdot \bar{d} \right] \right. \\ \left. \mp 4\alpha_d \beta_d x_i y_i \left[d \cdot \tilde{\chi}_i^+ \bar{d} \cdot \tilde{\chi}_i^- - d \cdot \tilde{\chi}_i^- \bar{d} \cdot \tilde{\chi}_i^+ \right] - 2y_i^2 (\alpha_d^2 + \beta_d^2) m_{\tilde{\chi}_i^-}^2 d \cdot \bar{d} \right\}, \quad (39.72)$$

$$T_{\tilde{u}_L} = \frac{4|A_{\tilde{\chi}_i^-}^d|^4}{[(d - \tilde{\chi}_i^-)^2 - m_{\tilde{u}_L}^2]^2} d \cdot \tilde{\chi}_i^- \bar{d} \cdot \tilde{\chi}_i^+ \quad (39.73)$$

$$T_{\gamma Z} = \frac{64e^4 \cot \theta_W q_d (s - M_Z^2)|D_Z(s)|^2}{s} \times \left\{ \alpha_d x_i \left(d \cdot \tilde{\chi}_i^+ \bar{d} \cdot \tilde{\chi}_i^- + d \cdot \tilde{\chi}_i^- \bar{d} \cdot \tilde{\chi}_i^+ + m_{\tilde{\chi}_i^-}^2 d \cdot \bar{d} \right) \right. \\ \left. \pm \beta_d y_i \left(d \cdot \tilde{\chi}_i^- \bar{d} \cdot \tilde{\chi}_i^+ - d \cdot \tilde{\chi}_i^+ \bar{d} \cdot \tilde{\chi}_i^- \right) \right\} \quad (39.74)$$

$$T_{\tilde{u}_L} = \mp \frac{8e^2 q_d}{s} \frac{|A_{\tilde{\chi}_i^-}^d|^2}{[(d - \tilde{\chi}_i^-)^2 - m_{\tilde{u}_L}^2]} \left\{ 2\bar{d} \cdot \tilde{\chi}_i^+ d \cdot \tilde{\chi}_i^- + m_{\tilde{\chi}_i^-}^2 d \cdot \bar{d} \right\} \quad (39.75)$$

and

$$T_{Z\tilde{u}_L} = \mp 8e^2 \cot \theta_W |D_Z(s)|^2 \frac{|A_{\tilde{\chi}_i^-}^d|^2 (s - M_Z^2)}{[(d - \tilde{\chi}_i^-)^2 - m_{\tilde{u}_L}^2]} (\alpha_d - \beta_d) \times \left\{ 2(x_i \mp y_i) d \cdot \tilde{\chi}_i^- \bar{d} \cdot \tilde{\chi}_i^+ + m_{\tilde{\chi}_i^-}^2 (x_i \pm y_i) d \cdot \bar{d} \right\} \quad (39.76)$$

using the upper of the sign choices.

The cross section for $u\bar{u} \rightarrow \tilde{\chi}_i^+ \tilde{\chi}_i^-$ can be obtained from the above by replacing $\alpha_d \rightarrow \alpha_u$, $\beta_d \rightarrow \beta_u$, $q_d \rightarrow q_u$, $\tilde{u}_L \rightarrow \tilde{d}_L$, $A_{\tilde{\chi}_i^-}^d \rightarrow A_{\tilde{\chi}_i^-}^u$, $d \rightarrow \bar{u}$, $\bar{d} \rightarrow u$ and adopting the lower of the sign choices everywhere.

The cross section for $q\bar{q} \rightarrow \tilde{\chi}_1^- \tilde{\chi}_2^+$, $\tilde{\chi}_1^+ \tilde{\chi}_2^-$ can occur via Z and \tilde{q}_L exchange. It is usually much smaller than $\tilde{\chi}_{1,2}^- \tilde{\chi}_{1,2}^+$ production, so the cross section will not be presented here. It can be found in Appendix A of Ref. 15.

39.8.4.3. Neutralino pair production:

Neutralino pair production via $q\bar{q}$ fusion takes place via s -channel Z exchange plus t - and u -channel left- and right- squark exchange (5 diagrams) [17,18]. The Lagrangian couplings (see previous footnote*) needed include terms given above plus terms of the form $\mathcal{L} = W_{ij} \tilde{\chi}_i^0 \gamma_\mu (\gamma_5)^{\theta_i + \theta_j + 1} \tilde{\chi}_j^0 Z^\mu$. The couplings W_{ij} depend only on the *higgsino* components of the neutralinos i and j . The subprocess cross section is given by:

$$\frac{d\sigma}{dt}(q\bar{q} \rightarrow \tilde{\chi}_i^0 \tilde{\chi}_j^0) = \frac{1}{192\pi s^2} [T_Z + T_{\tilde{q}_L} + T_{\tilde{q}_R} + T_{Z\tilde{q}_L} + T_{Z\tilde{q}_R}] \quad (39.77)$$

where

$$T_Z = 128e^2 |W_{ij}|^2 (\alpha_q^2 + \beta_q^2) |D_Z(s)|^2$$

$$\left[q \cdot \tilde{\chi}_i^0 \bar{q} \cdot \tilde{\chi}_j^0 + q \cdot \tilde{\chi}_j^0 \bar{q} \cdot \tilde{\chi}_i^0 - \eta_i \eta_j m_{\tilde{\chi}_i^0} m_{\tilde{\chi}_j^0} q \cdot \bar{q} \right], \quad (39.78)$$

$$T_{\tilde{q}_L} = 4|A_{\tilde{\chi}_i^0}^q|^2 |A_{\tilde{\chi}_j^0}^q|^2 \left\{ \frac{q \cdot \tilde{\chi}_i^0 \bar{q} \cdot \tilde{\chi}_j^0}{[(\tilde{\chi}_i^0 - q)^2 - m_{\tilde{q}_L}^2]^2} + \frac{q \cdot \tilde{\chi}_j^0 \bar{q} \cdot \tilde{\chi}_i^0}{[(\tilde{\chi}_j^0 - q)^2 - m_{\tilde{q}_L}^2]^2} \right. \\ \left. - \eta_i \eta_j \frac{m_{\tilde{\chi}_i^0} m_{\tilde{\chi}_j^0} q \cdot \bar{q}}{[(\tilde{\chi}_i^0 - q)^2 - m_{\tilde{q}_L}^2][(\tilde{\chi}_j^0 - q)^2 - m_{\tilde{q}_L}^2]} \right\} \quad (39.79)$$

$$T_{\tilde{q}_R} = 4|B_{\tilde{\chi}_i^0}^q|^2 |B_{\tilde{\chi}_j^0}^q|^2 \left\{ \frac{q \cdot \tilde{\chi}_i^0 \bar{q} \cdot \tilde{\chi}_j^0}{[(\tilde{\chi}_i^0 - q)^2 - m_{\tilde{q}_R}^2]^2} + \frac{q \cdot \tilde{\chi}_j^0 \bar{q} \cdot \tilde{\chi}_i^0}{[(\tilde{\chi}_j^0 - q)^2 - m_{\tilde{q}_R}^2]^2} \right. \\ \left. - \eta_i \eta_j \frac{m_{\tilde{\chi}_i^0} m_{\tilde{\chi}_j^0} q \cdot \bar{q}}{[(\tilde{\chi}_i^0 - q)^2 - m_{\tilde{q}_R}^2][(\tilde{\chi}_j^0 - q)^2 - m_{\tilde{q}_R}^2]} \right\} \quad (39.80)$$

$$T_{Z\tilde{q}_L} = 16e(\alpha_q - \beta_q)(s - M_Z^2)|D_Z(s)|^2 \left\{ \frac{\text{Re}(W_{ij} A_{\tilde{\chi}_i^0}^{q*} A_{\tilde{\chi}_j^0}^q)}{[(\tilde{\chi}_i^0 - q)^2 - m_{\tilde{q}_L}^2]} \left[2q \cdot \tilde{\chi}_i^0 \bar{q} \cdot \tilde{\chi}_j^0 - \eta_i \eta_j m_{\tilde{\chi}_i^0} m_{\tilde{\chi}_j^0} q \cdot \bar{q} \right] \right. \\ \left. + \eta_i \eta_j \frac{\text{Re}(W_{ij} A_{\tilde{\chi}_i^0}^q A_{\tilde{\chi}_j^0}^{q*})}{[(\tilde{\chi}_j^0 - q)^2 - m_{\tilde{q}_L}^2]} \left[2q \cdot \tilde{\chi}_j^0 \bar{q} \cdot \tilde{\chi}_i^0 - \eta_i \eta_j m_{\tilde{\chi}_i^0} m_{\tilde{\chi}_j^0} q \cdot \bar{q} \right] \right\} \quad (39.81)$$

$$T_{Z\tilde{q}_R} = 16e(\alpha_q + \beta_q)(s - M_Z^2)|D_Z(s)|^2 \left\{ \frac{\text{Re}(W_{ij} B_{\tilde{\chi}_i^0}^{q*} B_{\tilde{\chi}_j^0}^q)}{[(\tilde{\chi}_i^0 - q)^2 - m_{\tilde{q}_R}^2]} \left[2q \cdot \tilde{\chi}_i^0 \bar{q} \cdot \tilde{\chi}_j^0 - \eta_i \eta_j m_{\tilde{\chi}_i^0} m_{\tilde{\chi}_j^0} q \cdot \bar{q} \right] \right. \\ \left. - \frac{\text{Re}(W_{ij} B_{\tilde{\chi}_i^0}^q B_{\tilde{\chi}_j^0}^{q*})}{[(\tilde{\chi}_j^0 - q)^2 - m_{\tilde{q}_R}^2]} \left[2q \cdot \tilde{\chi}_j^0 \bar{q} \cdot \tilde{\chi}_i^0 - \eta_i \eta_j m_{\tilde{\chi}_i^0} m_{\tilde{\chi}_j^0} q \cdot \bar{q} \right] \right\}. \quad (39.82)$$

As before, $\eta_i = \pm 1$ corresponding to whether the neutralino mass eigenvalue is positive or negative. When $i = j$ in the above formula, one must remember to integrate over just 2π steradians of solid angle to avoid double counting in the total cross section.

39.9. Universal extra dimensions

In the Universal Extra Dimension (UED) model of Ref. [19] (see Ref. [20] for a review of models with extra spacetime dimensions), the Standard Model is embedded in a five dimensional theory, where the fifth dimension is compactified on an S_1/Z_2 orbifold. Each SM chirality state is then the zero mode of an infinite tower of Kaluza-Klein excitations labelled by $n = 0 - \infty$. A KK parity is usually assumed to hold, where each state is assigned KK-parity $P = (-1)^n$. If the compactification scale is around a TeV, then the $n = 1$ (or even higher) KK modes may be accessible to collider searches.

Of interest for hadron colliders are the production of massive $n \geq 1$ quark or gluon pairs. These production cross sections have been calculated in Ref. [21,22]. We list here results for the $n = 1$ case only with $M_1 = 1/R$ (R is the compactification radius) and s , t and u are the usual Mandelstam variables; more general formulae can be found in Ref. [22]. The superscript $*$ stands for any KK excited state, while \bullet stands for left chirality states and \circ stands for right chirality states.

$$\frac{d\sigma}{dt} = \frac{1}{16\pi s^2} T \quad (39.83)$$

where

$$T(q\bar{q} \rightarrow g^* g^*) = \frac{2g_s^4}{27} \left[M_1^2 \left(-\frac{4s^3}{t'^2 u'^2} + \frac{57s}{t'u'} - \frac{108}{s} \right) + \frac{20s^2}{t'u'} - 93 + \frac{108t'u'}{s^2} \right] \quad (39.84)$$

and

$$T(gg \rightarrow g^* g^*) = \frac{9g_s^4}{27} \left[3M_1^4 \frac{s^2 + t'^2 + u'^2}{t'^2 u'^2} - 3M_1^2 \frac{s^2 + t'^2 + u'^2}{st'u'} + 1 + \frac{(s^2 + t'^2 + u'^2)^3}{4s^2 t'^2 u'^2} - \frac{t'u'}{s^2} \right] \quad (39.85)$$

where $t' = t - M_1^2$ and $u' = u - M_1^2$.

Also,

$$T(q\bar{q} \rightarrow q_1^* \bar{q}_1^*) = \frac{4g_s^4}{9} \left[\frac{2M_1^2}{s} + \frac{t'^2 + u'^2}{s^2} \right],$$

$$T(q\bar{q} \rightarrow q_1^* \bar{q}_1^*) = \frac{g_s^4}{9} \left[2M_1^2 \left(\frac{4}{s} + \frac{s}{t'^2} - \frac{1}{t'} \right) \right.$$

$$\left. + \frac{23}{6} + \frac{2s^2}{t'^2} + \frac{8s}{3t'} + \frac{6t'}{s} + \frac{8t'^2}{s^2} \right],$$

$$T(qq \rightarrow q_1^* \bar{q}_1^*) = \frac{g_s^4}{27} \left[M_1^2 \left(6\frac{t'}{u'^2} + 6\frac{u'}{t'^2} - \frac{s}{t'u'} \right) \right.$$

$$\left. + 2 \left(3\frac{t'^2}{u'^2} + 3\frac{u'^2}{t'^2} + 4\frac{s^2}{t'u'} - 5 \right) \right],$$

$$T(gg \rightarrow q_1^* \bar{q}_1^*) = g_s^4 \left[M_1^4 \frac{-4}{t'u'} \left(\frac{s^2}{6t'u'} - \frac{3}{8} \right) \right.$$

$$\left. + M_1^2 \frac{4}{s} \left(\frac{s^2}{6t'u'} - \frac{3}{8} \right) + \frac{s^2}{6t'u'} - \frac{17}{24} + \frac{3t'u'}{4s^2} \right],$$

$$T(gg \rightarrow g^* q_1^*) = \frac{-g_s^4}{3} \left[\frac{5s^2}{12t'^2} + \frac{s^3}{t'^2 u'} + \frac{11su'}{6t'^2} + \frac{5u'^2}{12t'^2} + \frac{u'^3}{st'^2} \right],$$

$$T(q\bar{q}' \rightarrow q_1^* \bar{q}_1^*) = \frac{g_s^4}{18} \left[4M_1^4 \frac{s}{t'^2} + 5 + 4\frac{s^2}{t'^2} + 8\frac{s}{t'} \right],$$

$$T(qq' \rightarrow q_1^* \bar{q}_1^*) = \frac{2g_s^4}{9} \left[-M_1^2 \frac{s}{t'^2} + \frac{1}{4} + \frac{s^2}{t'^2} \right],$$

$$T(qq \rightarrow q_1 \bullet q_1^\circ) = \frac{g_s^4}{9} \left[M_1^2 \left(\frac{2s^3}{t'^2 u'^2} - \frac{4s}{t'u'} \right) + 2\frac{s^4}{t'^2 u'^2} - 8\frac{s^2}{t'u'} + 5 \right],$$

$$T(qq' \rightarrow q_1 \bullet \bar{q}_1^\circ) = \frac{g_s^4}{9} \left[2M_1^2 \left(\frac{1}{t'} + \frac{u'}{t'^2} \right) + \frac{5}{2} + \frac{4u'}{t'} + \frac{2u'^2}{t'^2} \right],$$

and

$$T(qq' \rightarrow q_1 \bullet q_1^\circ) = \frac{g_s^4}{9} \left[-2M_1^2 \left(\frac{1}{t'} + \frac{u'}{t'^2} \right) + \frac{1}{2} + \frac{2u'^2}{t'^2} \right].$$

39.10. Large extra dimensions

In the ADD theory [23] with large extra dimensions (LED), the SM particles are confined to a 3-brane, while gravity propagates in the bulk. It is assumed that the n extra dimensions are compactified on an n -dimensional torus of volume $(2\pi r)^n$, so that the fundamental $4+n$ dimensional Planck scale M_* is related to the usual 4-dimensional Planck scale M_{Pl} by $M_{Pl}^2 = M_*^{n+2} (2\pi r)^n$. If $M_* \sim 1$ TeV, then the $M_W - M_{Pl}$ hierarchy problem is just due to gravity propagating in the large extra dimensions.

In these theories, the KK-excited graviton states $G_{\mu\nu}^n$ for $n = 1 - \infty$ can be produced at collider experiments. The graviton couplings to matter are suppressed by $1/M_{Pl}$, so that graviton emission cross sections $d\sigma/dt \sim 1/M_{Pl}^2$. However, the mass splittings between the excited graviton states can be tiny, so the graviton eigenstates are usually approximated by a continuum distribution. A summation (integration) over all allowed graviton emissions ends up cancelling the $1/M_{Pl}^2$ factor, so that observable cross section rates can be attained. Some of the fundamental production formulae for a KK graviton (denoted G) of mass m at hadron colliders include the subprocesses

$$\frac{d\sigma_m}{dt}(f\bar{f} \rightarrow \gamma G) = \frac{\alpha Q_f^2}{16N_f s M_{Pl}^2} F_1\left(\frac{t}{s}, \frac{m^2}{s}\right), \quad (39.86)$$

where Q_f is the charge of fermion f and N_f is the number of QCD colors of f . Also,

$$\frac{d\sigma_m}{dt}(q\bar{q} \rightarrow gG) = \frac{\alpha_s}{36 s M_{Pl}^2} F_1\left(\frac{t}{s}, \frac{m^2}{s}\right), \quad (39.87)$$

$$\frac{d\sigma_m}{dt}(qq \rightarrow qG) = \frac{\alpha_s}{96 s M_{Pl}^2} F_2\left(\frac{t}{s}, \frac{m^2}{s}\right), \quad (39.88)$$

$$\frac{d\sigma_m}{dt}(gg \rightarrow gG) = \frac{3\alpha_s}{16 s M_{Pl}^2} F_3\left(\frac{t}{s}, \frac{m^2}{s}\right), \quad (39.89)$$

where

$$F_1(x, y) = \frac{1}{x(y-1-x)} \left[-4x(1+x)(1+2x+2x^2) + y(1+6x+18x^2+16x^3) - 6y^2x(1+2x) + y^3(1+4x) \right] \quad (39.90)$$

$$F_2(x, y) = -(y-1-x)F_1\left(\frac{x}{y-1-x}, \frac{y}{y-1-x}\right) \quad (39.91)$$

and

$$F_3(x, y) = \frac{1}{x(y-1-x)} \left[1 + 2x + 3x^2 + 2x^3 + x^4 - 2y(1+x^3) + 3y^2(1+x^2) - 2y^3(1+x) + y^4 \right]. \quad (39.92)$$

These formulae must then be multiplied by the graviton density of states formula $dN = S_{n-1} \frac{M_{Pl}^2}{M_*^{n+2}} m^{n-1} dm$ to gain the cross section

$$\frac{d^2\sigma}{dt dm} = S_{n-1} \frac{M_{Pl}^2}{M_*^{n+2}} m^{n-1} \frac{d\sigma_m}{dt} \quad (39.93)$$

where $S_n = \frac{(2\pi)^{n/2}}{\Gamma(n/2)}$ is the surface area of an n -dimensional sphere of unit radius.

Virtual graviton processes can also be searched for at colliders. For instance, in Ref. [24] the cross section for Drell-Yan production of lepton pairs via gluon fusion was calculated, where it is found that, in the center-of-mass system

$$\frac{d\sigma}{dz}(gg \rightarrow \ell^+ \ell^-) = \frac{\lambda^2 s^3}{64\pi M_*^8} (1-z^2)(1+z^2) \quad (39.94)$$

where $z = \cos \theta$ and λ is a model-dependent coupling constant ~ 1 . Formulae for Drell-Yan production via $q\bar{q}$ fusion can also be found in Ref. [24,25].

39.11. Warped extra dimensions

In the Randall-Sundrum model [26] of warped extra dimensions, the arena for physics is a 5-d anti-deSitter (AdS_5) spacetime, for which a non-factorizable metric exists with a metric warp factor $e^{-2\sigma(\phi)}$. It is assumed that two opposite tension 3-branes exist within AdS_5 at the two ends of an S_1/Z_2 orbifold parametrized by co-ordinate ϕ which runs from $0 - \pi$. The 4-D solution of the Einstein equations yields $\sigma(\phi) = kr_c|\phi|$, where r_c is the compactification radius of the extra dimension and $k \sim M_{Pl}$. The 4-D effective action allows one to identify $\overline{M}_{Pl}^2 = \frac{M^3}{k}(1 - e^{-2kr_c\pi})$, where M is the 5-D Planck scale. Physical particles on the TeV scale (SM) brane have mass $m = e^{-kr_c\pi} m_0$, where m_0 is a fundamental mass of order the Planck scale. Thus, the weak scale-Planck scale hierarchy occurs due to the existence of the exponential warp factor if $kr_c \sim 12$.

In the simplest versions of the RS model, the TeV-scale brane contains only SM particles plus a tower of KK gravitons. The RS gravitons have mass $m_n = kx_n e^{-kr_c\pi}$, where the x_i are roots of Bessel functions $J_1(x_n) = 0$, with $x_1 \simeq 3.83$, $x_2 \simeq 7.02$ etc. While the RS zero-mode graviton couplings suppressed by $1/\overline{M}_{Pl}$ and are thus inconsequential for collider searches, the $n = 1$ and higher modes have couplings suppressed instead by $A_\pi = e^{-kr_c\pi} \overline{M}_{Pl} \sim TeV$. The $n = 1$ RS graviton should have width $\Gamma_1 = \rho m_1 x_1^2 (k/\overline{M}_{Pl})^2$, where ρ is a constant depending on how many decay modes are open. The formulae for dilepton production via virtual RS graviton exchange can be gained from the above formulae for the ADD scenario via the replacement [27]

$$\frac{\lambda}{M_*^4} \rightarrow \frac{i^2}{8A_\pi^2} \sum_{n=1}^{\infty} \frac{1}{s - m_n^2 + im_n \Gamma_n}. \quad (39.95)$$

References:

1. J.F. Owens *et al.*, Phys. Rev. **D18**, 1501 (1978). Note that cross section given in previous editions of RPP for $gg \rightarrow q\bar{q}$ lacked a factor of π .
2. F. Wilczek, Phys. Rev. Lett. **39**, 1304 (1977).
3. B.L. Ioffe and V.Khoze, Leningrad Report 274, 1976; Sov. J. Nucl. Phys. **9**, 50 (1978).
4. J. Ellis *et al.*, Nucl. Phys. **B106**, 292 (1976).
5. R.N. Cahn and S. Dawson, Phys. Lett. **B136**, 196 (1984), erratum, Phys. Lett. **B138**, 464 (1984).
6. S. Dawson, Nucl. Phys. **B249**, 42 (1985).
7. M.S. Chanowitz and M.K. Gaillard, Phys. Lett. **B142**, 85 (1984).
8. R.N. Cahn, Nucl. Phys. **B255**, 341 (1985).
9. For an exhaustive treatment, see V.M. Budnev *et al.*, Phys. Reports **15C**, 181(1975).
10. See *e.g.* H. Haber, *Supersymmetry, Part I (Theory)*, this review.
11. P. R. Harrison and C. H. Llewellyn Smith, Nucl. Phys. **B213**, 223 (1983), Erratum-*ibid.*, **B223**, 542 (1983); S. Dawson, E. Eichten, and C. Quigg, Phys. Rev. **D31**, 1581 (1985); V. Barger *et al.*, Phys. Rev. **D31**, 528 (1985); H. Baer and X. Tata, Phys. Lett. **B160**, 159 (1985).
12. H. Baer, D. Karatas, and X. Tata, Phys. Rev. **D42**, 2259 (1990).
13. H. Haber and G. Kane, Phys. Rept. **117**, 75 (1985).
14. Theory and Phenomenology of Sparticles, M. Drees, R. Godbole, and P. Roy (World Scientific) 2005.
15. Weak Scale Supersymmetry: From Superfields to Scattering Events, H. Baer and X. Tata (Cambridge University Press) 2006.
16. A. Bartl, H. Fraas, and W. Majerotto, Z. Phys. **C30**, 441 (1986).
17. H. Baer *et al.*, Int. J. Mod. Phys. **A4**, 4111 (1989).
18. A. Bartl, H. Fraas and W. Majerotto, Nucl. Phys. **B278**, 1 (1986).
19. T. Appelquist, H.C. Cheng, and B. Dobrescu, Phys. Rev. **D64**, 035002 (2001).
20. For a review of models with extra spacetime dimensions, see G. Giudice and J. Wells, *Extra Dimensions*, this review.
21. J.M. Smillie and B.R. Webber, JHEP **0510**, 069 (2005).
22. C. Macesanu, C.D. McMullen, and S. Nandi, Phys. Rev. **D66**, 015009 (2002).
23. N. Arkani-Hamed, S. Dimopoulos, and G. Dvali, Phys. Lett. **B429**, 263 (1998) and Phys. Rev. **D59**, 086004 (1999).
24. J. L. Hewett, Phys. Rev. Lett. **82**, 4765 (1999).
25. G. Giudice, R. Rattazzi, and J. Wells, Nucl. Phys. **B544**, 3 (1999); E.A. Mirabelli, M. Perelstein, and M.E. Peskin, Phys. Rev. Lett. **82**, 2236 (1999); T. Han, J. Lykken, and R. Zhang, Phys. Rev. **D59**, 105006 (1999).
26. L. Randall and R.S. Sundrum, Phys. Rev. Lett. **83**, 3370 (1999).
27. H. Davoudiasl, J.L. Hewett, and T.G. Rizzo, Phys. Rev. Lett. **84**, 2080 (2000).

40. PLOTS OF CROSS SECTIONS AND RELATED QUANTITIES

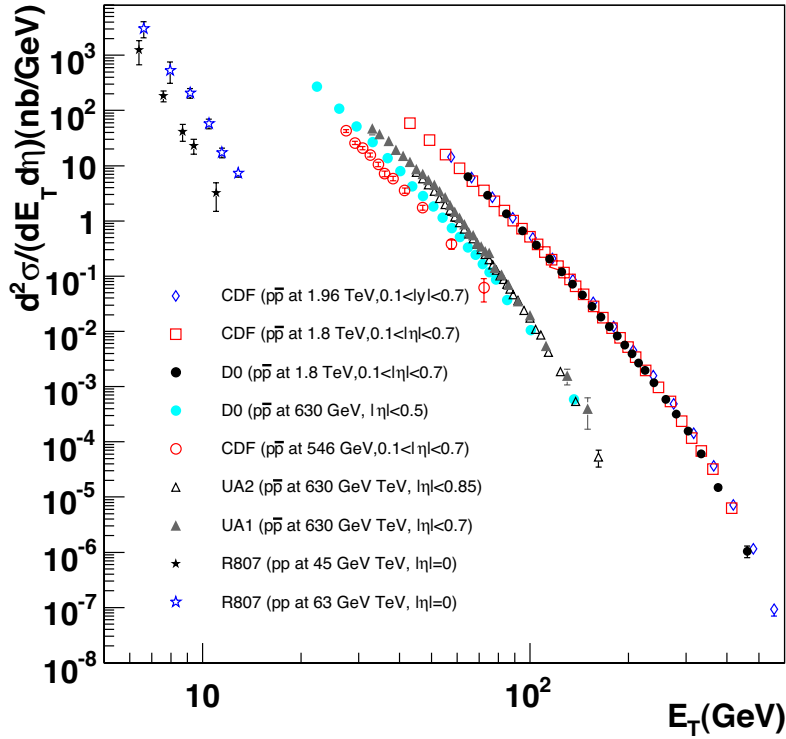
Jet Production in pp and $\bar{p}p$ Interactions

Figure 40.1: Inclusive differential jet cross sections plotted as a function of the jet transverse energy. The CDF and D0 measurements use a cone algorithm of radius 0.7 for all results shown except for the CDF measurement at 1.96 TeV which uses a k_T algorithm with a D parameter of 0.7. The cone/ k_T results should be similar if $R_{cone} = D$. UA1 (UA2) uses a non-iterative cone algorithm with a radius of 1.0 (1.3). Recent NLO QCD predictions (such as CTEQ6M) provide a good description of the CDF and D0 jet cross sections, Rept. on Prog. in Phys. **70**, 89 (2007). Comparisons with the older cross sections are more difficult due to the nature of the jet algorithms used. **CDF**: Phys. Rev. **D75**, 092006 (2007), Phys. Rev. **D64**, 032001 (2001), Phys. Rev. Lett. **70**, 1376 (1993); **D0**: Phys. Rev. **D64**, 032003 (2001); **UA2**: Phys. Lett. **B257**, 232 (1991); **UA1**: Phys. Lett. **B172**, 461 (1986); **R807**: Phys. Lett. **B123**, 133 (1983). (Courtesy of J. Huston, Michigan State University, 2007) Color version at end of book.

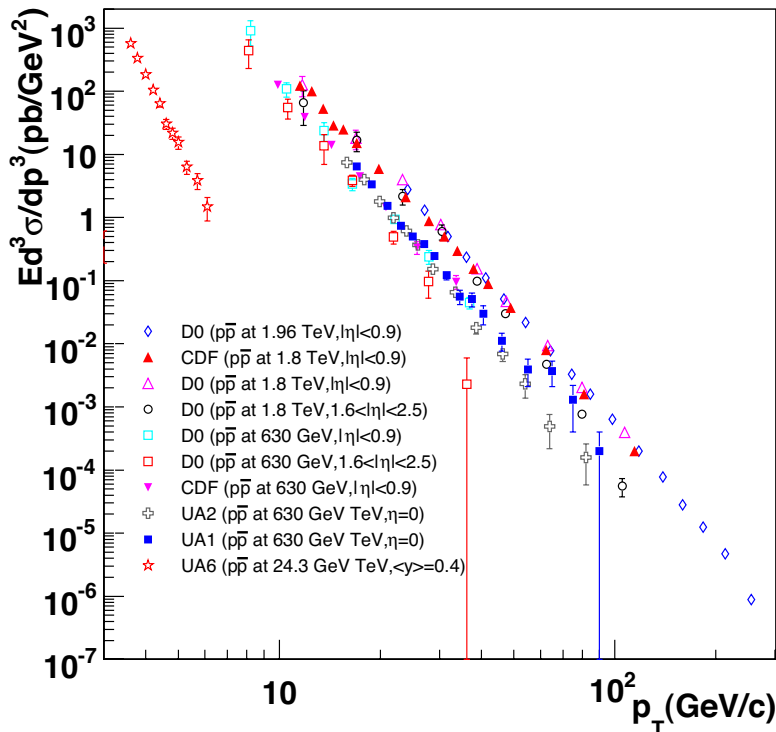
Direct γ Production in $\bar{p}p$ Interactions

Figure 40.2: Isolated photon cross sections plotted as a function of the photon transverse momentum. The errors are either statistical only (CDF, D0 (1.96 TeV), UA1, UA2, UA6) or uncorrelated (D0 1.8 TeV, 630 GeV). The data are generally in good agreement with NLO QCD predictions, albeit with a tendency for the data to be above (below) the theory for lower (large) transverse momenta, Phys. Rev. **D59**, 074007 (1999). **D0**: Phys. Lett. **B639**, 151 (2006), Phys. Rev. Lett. **87**, 251805 (2001); **CDF**: Phys. Rev. **D65**, 112003 (2002); **UA6**: Phys. Lett. **B206**, 163 (1988); **UA1**: Phys. Lett. **B209**, 385 (1988); **UA2**: Phys. Lett. **B288**, 386 (1992). (Courtesy of J. Huston, Michigan State University, 2007) Color version at end of book.

Differential Cross Section for W and Z Boson Production

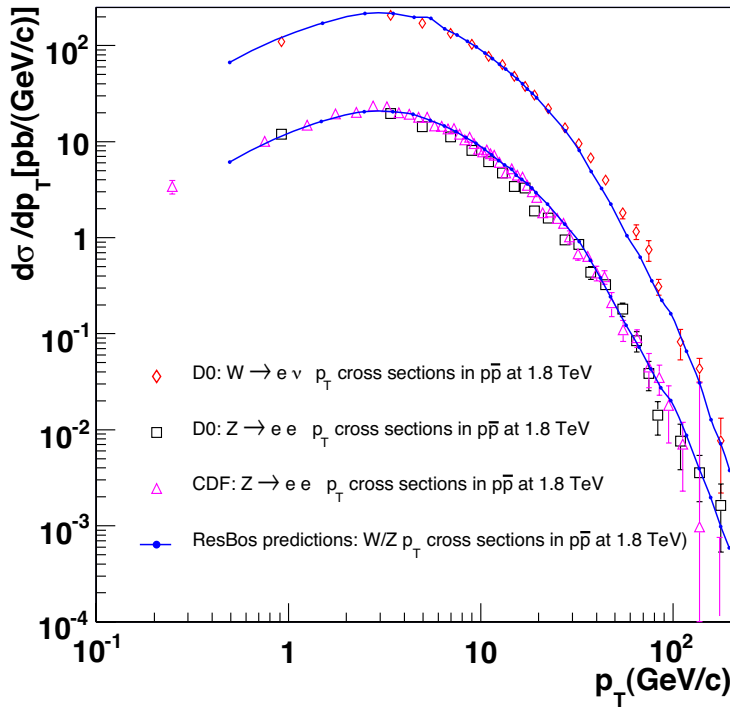


Figure 40.3: Differential cross sections for W and Z production shown as a function of the boson transverse momentum. The D0 results include only the statistical error while the CDF results include all errors except for the 3.9% integrated luminosity error. The results are in good agreement with theoretical predictions that include both the effects of NLO corrections and of q_T resummation, such as the ResBos (Phys. Rev. **D67**, 073016 (2003)) predictions indicated on the plot. **D0:** Phys. Lett. **B513**, 292 (2001), Phys. Rev. Lett. **84**, 2792 (2000). **CDF:** Phys. Rev. Lett. **84**, 845 (2000). (Courtesy of J. Huston, Michigan State University, 2007)

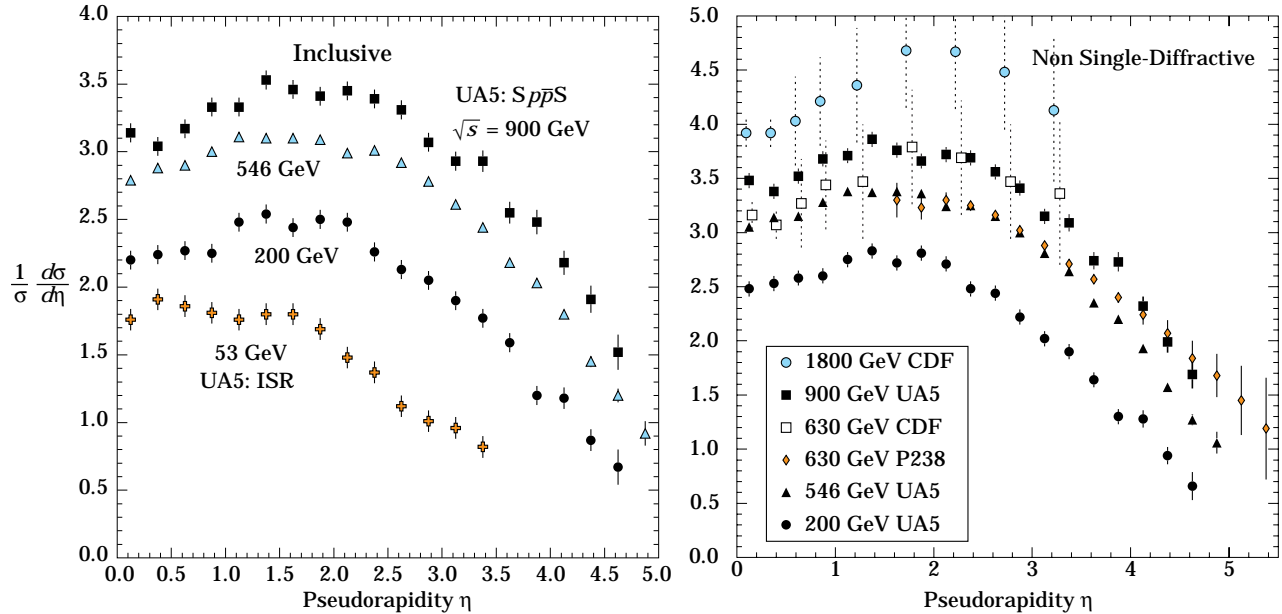
Pseudorapidity Distributions in $\bar{p}p$ Interactions

Figure 40.4: Charged particle pseudorapidity distributions in $\bar{p}p$ collisions for $53 \text{ GeV} \leq \sqrt{s} \leq 1800 \text{ GeV}$. UA5 data from the $S\bar{p}pS$ are taken from G.J. Alner *et al.*, Z. Phys. **C33**, 1 (1986), and from the ISR from K. Alpgöard *et al.*, Phys. Lett. **112B**, 193 (1982). The UA5 data are shown for both the full inelastic cross section and with singly diffractive events excluded. Additional non single-diffractive measurements are available from CDF at the Tevatron, F. Abe *et al.*, Phys. Rev. **D41**, 2330 (1990) and Experiment P238 at the $S\bar{p}pS$, R. Harr *et al.*, Phys. Lett. **B401**, 176 (1997). (Courtesy of D.R. Ward, Cambridge Univ., 1999)

Average Hadron Multiplicities in Hadronic e^+e^- Annihilation Events

Table 40.1: Average hadron multiplicities per hadronic e^+e^- annihilation event at $\sqrt{s} \approx 10, 29\text{--}35, 91$, and $130\text{--}200$ GeV. The rates given include decay products from resonances with $c\tau < 10$ cm, and include the corresponding anti-particle state. Correlations of the systematic uncertainties were considered for the calculation of the averages. (Updated August 2007 by O. Biebel, LMU, Munich)

Particle	$\sqrt{s} \approx 10$ GeV	$\sqrt{s} = 29\text{--}35$ GeV	$\sqrt{s} = 91$ GeV	$\sqrt{s} = 130\text{--}200$ GeV
Pseudoscalar mesons:				
π^+	6.6 ± 0.2	10.3 ± 0.4	17.02 ± 0.19	21.24 ± 0.39
π^0	3.2 ± 0.3	5.83 ± 0.28	9.42 ± 0.32	
K^+	0.90 ± 0.04	1.48 ± 0.09	2.228 ± 0.059	2.82 ± 0.19
K^0	0.91 ± 0.05	1.48 ± 0.07	2.049 ± 0.026	2.10 ± 0.12
η	0.20 ± 0.04	0.61 ± 0.07	1.049 ± 0.080	
$\eta(958)$	0.03 ± 0.01	0.26 ± 0.10	0.152 ± 0.020	
D^+	$0.194 \pm 0.019^{(k)}$	0.17 ± 0.03	0.175 ± 0.016	
D^0	$0.446 \pm 0.032^{(k)}$	0.45 ± 0.07	0.454 ± 0.030	
D_s^+	$0.063 \pm 0.014^{(k)}$	$0.45 \pm 0.20^{(a)}$	0.131 ± 0.021	
B^+, B_d^0	—	—	$0.165 \pm 0.026^{(b)}$	
B_u^+	—	—	$0.178 \pm 0.006^{(b)}$	
B_s^0	—	—	$0.057 \pm 0.013^{(b)}$	
Scalar mesons:				
$f_0(980)$	0.024 ± 0.006	$0.05 \pm 0.02^{(c)}$	0.146 ± 0.012	
$a_0(980)^\pm$	—	—	$0.27 \pm 0.11^{(d)}$	
Vector mesons:				
$\rho(770)^0$	0.35 ± 0.04	0.81 ± 0.08	1.231 ± 0.098	
$\rho(770)^\pm$	—	—	$2.40 \pm 0.43^{(d)}$	
$\omega(782)$	0.30 ± 0.08	—	1.016 ± 0.065	
$K^*(892)^+$	0.27 ± 0.03	0.64 ± 0.05	0.715 ± 0.059	
$K^*(892)^0$	0.29 ± 0.03	0.56 ± 0.06	0.738 ± 0.024	
$\phi(1020)$	0.044 ± 0.003	0.085 ± 0.011	0.0963 ± 0.0032	
$D^*(2010)^+$	$0.177 \pm 0.022^{(k)}$	0.43 ± 0.07	$0.1937 \pm 0.0057^{(j)}$	
$D^*(2007)^0$	$0.168 \pm 0.019^{(k)}$	0.27 ± 0.11	—	
$D_s^*(2112)^+$	$0.048 \pm 0.014^{(k)}$	—	$0.101 \pm 0.048^{(g)}$	
B^* ^(e)	—	—	0.288 ± 0.026	
$J/\psi(1S)$	$0.00050 \pm 0.00005^{(k)}$	—	$0.0052 \pm 0.0004^{(f)}$	
$\psi(2S)$	—	—	$0.0023 \pm 0.0004^{(f)}$	
$\Upsilon(1S)$	—	—	$0.00014 \pm 0.00007^{(f)}$	
Pseudovector mesons:				
$f_1(1285)$	—	—	0.165 ± 0.051	
$f_1(1420)$	—	—	0.056 ± 0.012	
$\chi_{c1}(3510)$	—	—	$0.0041 \pm 0.0011^{(f)}$	
Tensor mesons:				
$f_2(1270)$	0.09 ± 0.02	0.14 ± 0.04	0.166 ± 0.020	
$f_2'(1525)$	—	—	0.012 ± 0.006	
$K_2^*(1430)^+$	—	0.09 ± 0.03	—	
$K_2^*(1430)^0$	—	0.12 ± 0.06	0.084 ± 0.022	
B^{**} ⁽ⁱ⁾	—	—	0.118 ± 0.024	
D_{s1}^\pm	—	—	$0.0052 \pm 0.0011^{(l)}$	
$D_{s2}^{*\pm}$	—	—	$0.0083 \pm 0.0031^{(l)}$	
Baryons:				
p	0.253 ± 0.016	0.640 ± 0.050	1.050 ± 0.032	1.41 ± 0.18
Λ	0.080 ± 0.007	0.205 ± 0.010	0.3915 ± 0.0065	0.39 ± 0.03
Σ^0	0.023 ± 0.008	—	0.076 ± 0.011	
Σ^-	—	—	0.081 ± 0.010	
Σ^+	—	—	0.107 ± 0.011	
Σ^\pm	—	—	0.174 ± 0.009	
Ξ^-	0.0059 ± 0.0007	0.0176 ± 0.0027	0.0258 ± 0.0010	
$\Delta(1232)^{++}$	0.040 ± 0.010	—	0.085 ± 0.014	
$\Sigma(1385)^-$	0.006 ± 0.002	0.017 ± 0.004	0.0240 ± 0.0017	
$\Sigma(1385)^+$	0.005 ± 0.001	0.017 ± 0.004	0.0239 ± 0.0015	
$\Sigma(1385)^\pm$	0.0106 ± 0.0020	0.033 ± 0.008	0.0462 ± 0.0028	
$\Xi(1530)^0$	0.0015 ± 0.0006	—	0.0068 ± 0.0006	
Ω^-	0.0007 ± 0.0004	0.014 ± 0.007	0.0016 ± 0.0003	
Λ_c^+	$0.074 \pm 0.031^{(i)}$	0.110 ± 0.050	0.078 ± 0.017	
Λ_b^0	—	—	0.031 ± 0.016	
$\Sigma_c^{++}, \Sigma_c^0$	0.014 ± 0.007	—	—	
$\Lambda(1520)$	0.008 ± 0.002	—	0.0222 ± 0.0027	

Notes for Table 40.1:

- (a) $B(D_s \rightarrow \eta\pi, \eta'\pi)$ was used (RPP 1994).
- (b) The Standard Model $B(Z \rightarrow b\bar{b}) = 0.217$ was used.
- (c) $x_p = p/p_{\text{beam}} > 0.1$ only.
- (d) Both charge states.
- (e) Any charge state (*i.e.*, B_d^* , B_u^* , or B_s^*).
- (f) $B(Z \rightarrow \text{hadrons}) = 0.699$ was used (RPP 1994).
- (g) $B(D_s^* \rightarrow D_S^+ \gamma)$, $B(D_s^+ \rightarrow \phi\pi^+)$, $B(\phi \rightarrow K^+K^-)$ have been used (RPP 1998).
- (h) Any charge state (*i.e.*, B_d^{**} , B_u^{**} , or B_s^{**}).
- (i) The value was derived from the cross section of $A_c^+ \rightarrow p\pi K$ using (k) and assuming the branching fraction to be $(5.0 \pm 1.3)\%$ (RPP 2004).
- (j) $B(D^*(2010)^+ \rightarrow D^0\pi^+) \times B(D^0 \rightarrow K^-\pi^+)$ has been used (RPP 2000).
- (k) $\sigma_{\text{had}} = 3.33 \pm 0.05 \pm 0.21$ nb (CLEO: Phys. Rev. **D29**, 1254 (1984)) has been used in converting the measured cross sections to average hadron multiplicities.
- (l) Assumes $B(D_{s1}^+ \rightarrow D^{*+}K^0 + D^{*0}K^+) = 100\%$ and $B(D_{s2}^+ \rightarrow D^0K^+) = 45\%$.

References for Table 40.1:

- RPP 1992:** Phys. Rev. **D45** (1992) and references therein.
- RPP 1994:** Phys. Rev. **D50**, 1173 (1994) and references therein.
- RPP 1996:** Phys. Rev. **D54**, 1 (1996) and references therein.
- RPP 1998:** Eur. Phys. J. **C3**, 1 (1998) and references therein.
- RPP 2000:** Eur. Phys. J. **C15**, 1 (2000) and references therein.
- RPP 2002:** Phys. Rev. **D66**, 010001 (2002) and references therein.
- RPP 2004:** Phys. Lett. **B592**, 1 (2004) and references therein.
- RPP 2006:** J. Phys. **G33**, 1 (2006) and references therein.
- R. Marshall, Rept. on Prog. in Phys. **52**, 1329 (1989). A. De Angelis, J. Phys. **G19**, 1233 (1993) and references therein.
- ALEPH:** D. Buskulic *et al.*: Phys. Lett. **B295**, 396 (1992); Z. Phys. **C64**, 361 (1994); **C69**, 15 (1996); **C69**, 379 (1996); **C73**, 409 (1997); and R. Barate *et al.*: Z. Phys. **C74**, 451 (1997); Phys. Reports **294**, 1 (1998); Eur. Phys. J. **C5**, 205 (1998); **C16**, 597 (2000); **C16**, 613 (2000); and A. Heister *et al.*: Phys. Lett. **B526**, 34 (2002); **B528**, 19 (2002).
- ARGUS:** H. Albrecht *et al.*: Phys. Lett. **230B**, 169 (1989); Z. Phys. **C44**, 547 (1989); **C46**, 15 (1990); **C54**, 1 (1992); **C58**, 199 (1993); **C61**, 1 (1994); Phys. Rep. **276**, 223 (1996).
- BaBar:** B. Aubert *et al.*: Phys. Rev. Lett. **87**, 162002 (2001); Phys. Rev. **D65**, 091104 (2002).
- Belle:** K. Abe *et al.*, Phys. Rev. Lett. **88**, 052001 (2002); and R. Seuster *et al.*, Phys. Rev. **D73**, 032002 (2006).
- CELLO:** H.J. Behrend *et al.*: Z. Phys. **C46**, 397 (1990); **C47**, 1 (1990).
- CLEO:** D. Bortoletto *et al.*, Phys. Rev. **D37**, 1719 (1988); erratum *ibid.* **D39**, 1471 (1989); and M. Artuso *et al.*, Phys. Rev. **D70**, 112001 (2004).
- Crystal Ball:** Ch. Bieler *et al.*, Z. Phys. **C49**, 225 (1991).
- DELPHI:** P. Abreu *et al.*: Z. Phys. **C57**, 181 (1993); **C59**, 533 (1993); **C61**, 407 (1994); **C65**, 587 (1995); **C67**, 543 (1995); **C68**, 353 (1995); **C73**, 61 (1996); Nucl. Phys. **B444**, 3 (1995); Phys. Lett. **B341**, 109 (1994); **B345**, 598 (1995); **B361**, 207 (1995); **B372**, 172 (1996); **B379**, 309 (1996); **B416**, 233 (1998); **B449**, 364 (1999); **B475**, 429 (2000); Eur. Phys. J. **C6**, 19 (1999); **C5**, 585 (1998); **C18**, 203 (2000); and J. Abdallah *et al.*, Phys. Lett. **B569**, 129 (2003); Phys. Lett. **B576**, 29 (2003); Eur. Phys. J. **C44**, 299 (2005); and W. Adam *et al.*: Z. Phys. **C69**, 561 (1996); **C70**, 371 (1996).
- HRS:** S. Abachi *et al.*, Phys. Rev. Lett. **57**, 1990 (1986); and M. Derrick *et al.*, Phys. Rev. **D35**, 2639 (1987).
- L3:** M. Acciarri *et al.*: Phys. Lett. **B328**, 223 (1994); **B345**, 589 (1995); **B371**, 126 (1996); **B371**, 137 (1996); **B393**, 465 (1997); **B404**, 390 (1997); **B407**, 351 (1997); **B407**, 389 (1997), erratum *ibid.* **B427**, 409 (1998); **B453**, 94 (1999); **B479**, 79 (2000).
- MARK II:** H. Schellman *et al.*, Phys. Rev. **D31**, 3013 (1985); and G. Wormser *et al.*, Phys. Rev. Lett. **61**, 1057 (1988).
- JADE:** W. Bartel *et al.*, Z. Phys. **C20**, 187 (1983); and D.D. Pietzl *et al.*, Z. Phys. **C46**, 1 (1990).
- OPAL:** R. Akers *et al.*: Z. Phys. **C63**, 181 (1994); **C66**, 555 (1995); **C67**, 389 (1995); **C68**, 1 (1995); and G. Alexander *et al.*: Phys. Lett. **B358**, 162 (1995); Z. Phys. **C70**, 197 (1996); **C72**, 1 (1996); **C72**, 191 (1996); **C73**, 569 (1997); **C73**, 587 (1997); Phys. Lett. **B370**, 185 (1996); and K. Ackerstaff *et al.*: Z. Phys. **C75**, 192 (1997); Phys. Lett. **B412**, 210 (1997); Eur. Phys. J. **C1**, 439 (1998); **C4**, 19 (1998); **C5**, 1 (1998); **C5**, 411 (1998); and G. Abbiendi *et al.*: Eur. Phys. J. **C16**, 185 (2000); **C17**, 373 (2000).
- PLUTO:** Ch. Berger *et al.*, Phys. Lett. **104B**, 79 (1981).
- SLD:** K. Abe, Phys. Rev. **D59**, 052001 (1999); Phys. Rev. **D69**, 072003 (2004).
- TASSO:** H. Aihara *et al.*, Z. Phys. **C27**, 27 (1985).
- TPC:** H. Aihara *et al.*, Phys. Rev. Lett. **53**, 2378 (1984).

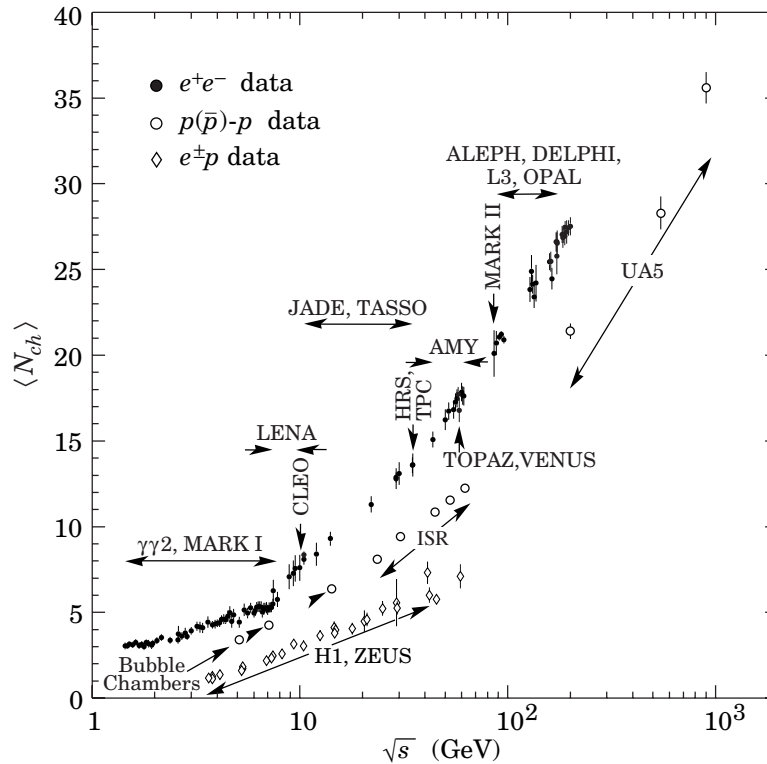
Average e^+e^- , pp , and $p\bar{p}$ Multiplicity

Figure 40.5: Average multiplicity as a function of \sqrt{s} for e^+e^- and $p\bar{p}$ annihilations, and pp and ep collisions. The indicated errors are statistical and systematic errors added in quadrature, except when no systematic errors are given. Files of the data shown in this figure are given in <http://pdg.lbl.gov/current/avg-multiplicity/>.

e^+e^- : Most e^+e^- measurements include contributions from K_S^0 and Λ decays. The $\gamma\gamma 2$ and MARK I measurements contain a systematic 5% error. Points at identical energies have been spread horizontally for clarity:

ALEPH: D. Buskulic *et al.*, Z. Phys. **C69**, 15 (1995); and Z. Phys. **C73**, 409 (1997);
A. Heister *et al.*, Eur. Phys. J. **C35**, 457 (2004).

ARGUS: H. Albrecht *et al.*, Z. Phys. **C54**, 13 (1992).

DELPHI: P. Abreu *et al.*, Eur. Phys. J. **C6**, 19 (1999); Phys. Lett. **B372**, 172 (1996); Phys. Lett. **B416**, 233 (1998); and Eur. Phys. J. **C18**, 203 (2000).

L3: M. Acciarri *et al.*, Phys. Lett. **B371**, 137 (1996); Phys. Lett. **B404**, 390 (1997); and Phys. Lett. **B444**, 569 (1998);
P. Achard *et al.*, Phys. Reports **339**, 71 (2004).

OPAL: G. Abbiendi *et al.*, Eur. Phys. J. **C16**, 185 (2000); and Eur. Phys. J. **C37**, 25 (2004);
K. Ackerstaff *et al.*, Z. Phys. **C75**, 193 (1997);
P.D. Acton *et al.*, Z. Phys. **C53**, 539 (1992) and references therein;
R. Akers *et al.*, Z. Phys. **C68**, 203 (1995).

TOPAZ: K. Nakabayashi *et al.*, Phys. Lett. **B413**, 447 (1997).

VENUS: K. Okabe *et al.*, Phys. Lett. **B423**, 407 (1998).

$e^\pm p$: Multiplicities have been measured in the current fragmentation region of the Breit frame:

H1: C. Adloff *et al.*, Nucl. Phys. **B504**, 3 (1997).

ZEUS: J. Breitweg *et al.*, Eur. Phys. J. **C11**, 251 (1999);
S. Chekanov *et al.*, Phys. Lett. **B510**, 36 (2001).

$p(\bar{p})$: The errors of the $p(\bar{p})$ measurements are the quadratically added statistical and systematic errors, except for the bubble chamber measurements for which only statistical errors are given in the references. The values measured by UA5 exclude single diffractive dissociation:
bubble chamber: J. Benecke *et al.*, Nucl. Phys. **B76**, 29 (1976); W.M. Morse *et al.*, Phys. Rev. **D15**, 66 (1977).

ISR: A. Breakstone *et al.*, Phys. Rev. **D30**, 528 (1984).

UA5: G.J. Alner *et al.*, Phys. Lett. **167B**, 476 (1986);
R.E. Ansorge *et al.*, Z. Phys. **C43**, 357 (1989).

(Courtesy of O. Biebel, LMU, Munich, 2005)

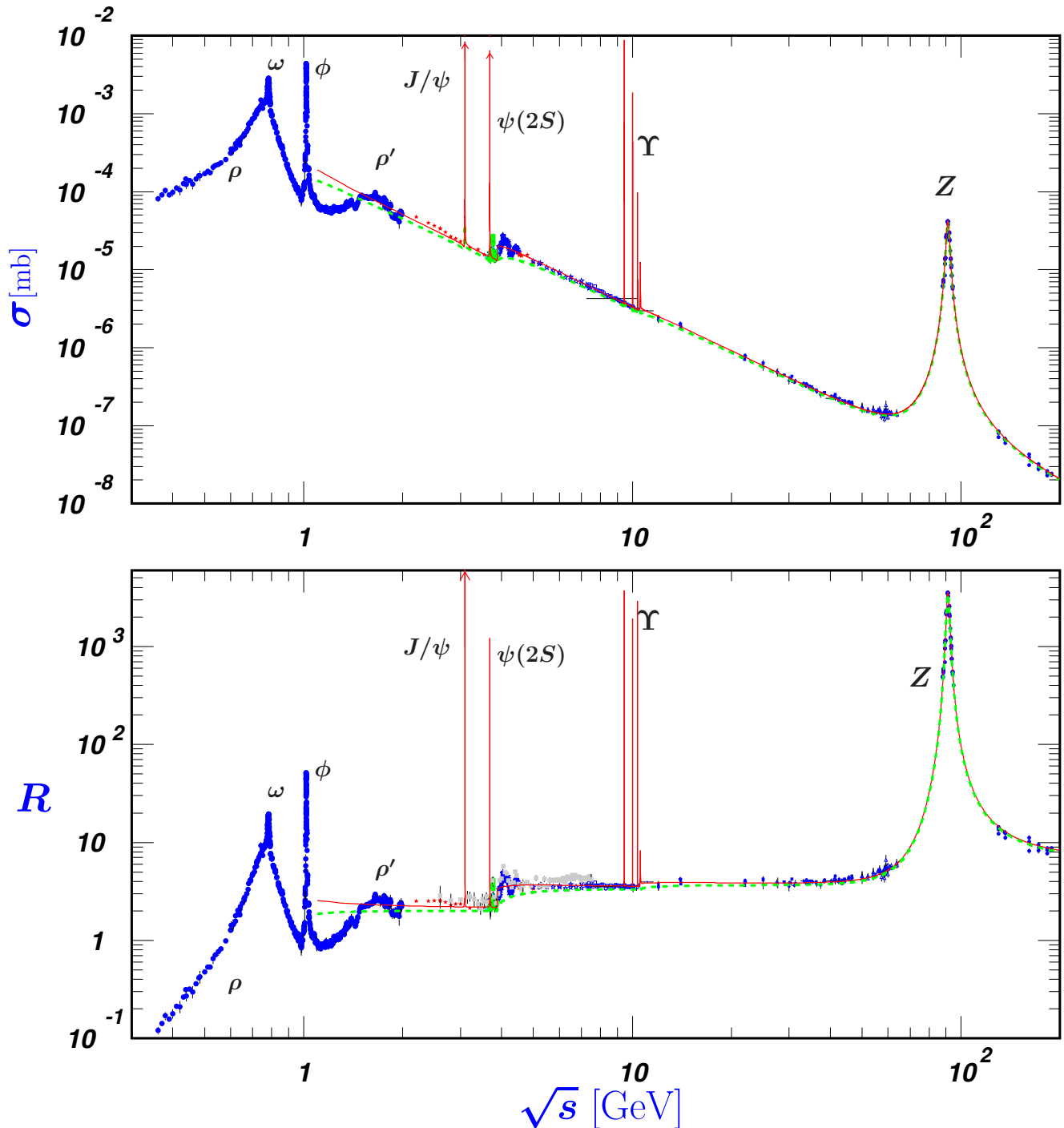
σ and R in e^+e^- Collisions

Figure 40.6: World data on the total cross section of $e^+e^- \rightarrow \text{hadrons}$ and the ratio $R(s) = \sigma(e^+e^- \rightarrow \text{hadrons}, s) / \sigma(e^+e^- \rightarrow \mu^+\mu^-, s)$. $\sigma(e^+e^- \rightarrow \text{hadrons}, s)$ is the experimental cross section corrected for initial state radiation and electron-positron vertex loops, $\sigma(e^+e^- \rightarrow \mu^+\mu^-, s) = 4\pi\alpha^2(s)/3s$. Data errors are total below 2 GeV and statistical above 2 GeV. The curves are an educative guide: the broken one (green) is a naive quark-parton model prediction, and the solid one (red) is 3-loop pQCD prediction (see “Quantum Chromodynamics” section of this Review, Eq. (9.12) or, for more details, K. G. Chetyrkin *et al.*, Nucl. Phys. **B586**, 56 (2000) (Erratum *ibid.* **B634**, 413 (2002))). Breit-Wigner parameterizations of J/ψ , $\psi(2S)$, and $\Upsilon(nS)$, $n = 1, 2, 3, 4$ are also shown. The full list of references to the original data and the details of the R ratio extraction from them can be found in [arXiv:hep-ph/0312114]. Corresponding computer-readable data files are available at <http://pdg.lbl.gov/current/xsect/>. (Courtesy of the COMPAS (Protvino) and HEPDATA (Durham) Groups, August 2007. Corrections by P. Janot (CERN) and M. Schmitt (Northwestern U.)) Color version at end of book.

R in Light-Flavor, Charm, and Beauty Threshold Regions

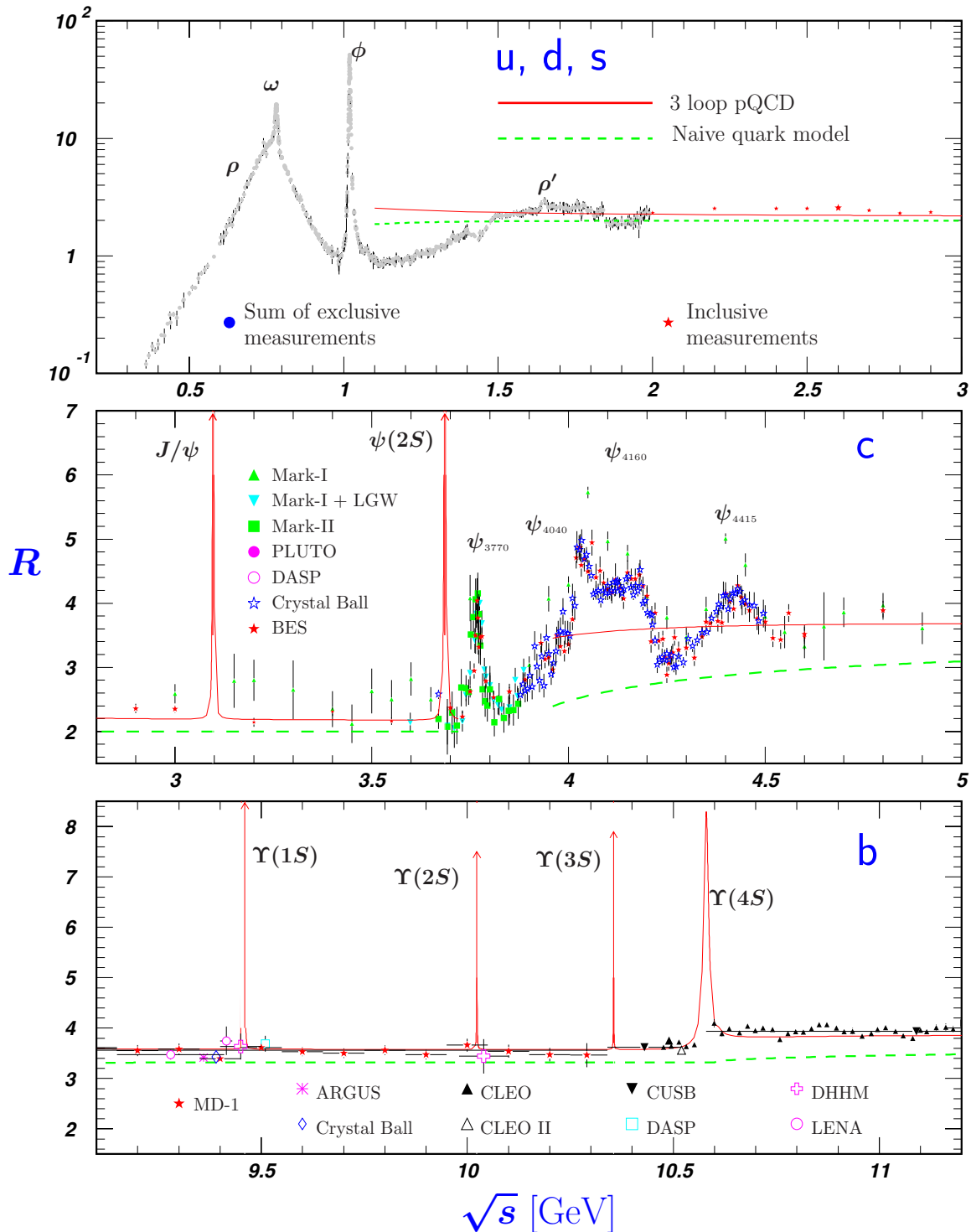


Figure 40.7: R in the light-flavor, charm, and beauty threshold regions. Data errors are total below 2 GeV and statistical above 2 GeV. The curves are the same as in Fig. 40.6. **Note:** CLEO data above $\Upsilon(4S)$ were not fully corrected for radiative effects, and we retain them on the plot only for illustrative purposes with a normalization factor of 0.8. The full list of references to the original data and the details of the R ratio extraction from them can be found in [arXiv:hep-ph/0312114]. The computer-readable data are available at <http://pdg.lbl.gov/current/xsect/>. (Courtesy of the COMPAS (Protvino) and HEPDATA (Durham) Groups, August 2007) Color version at end of book.

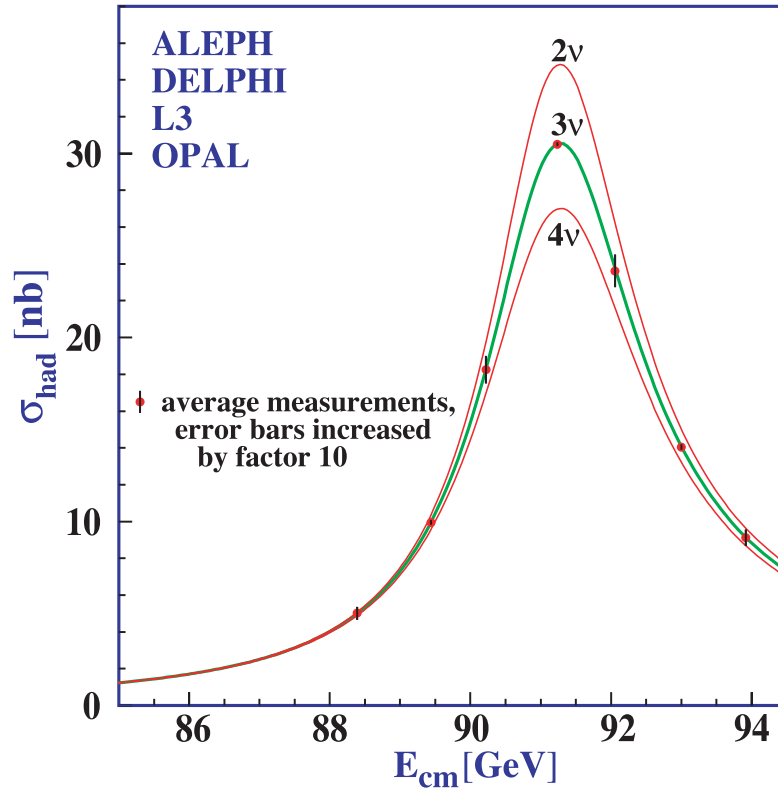
Annihilation Cross Section Near M_Z 

Figure 40.8: Combined data from the ALEPH, DELPHI, L3, and OPAL Collaborations for the cross section in e^+e^- annihilation into hadronic final states as a function of the center-of-mass energy near the Z pole. The curves show the predictions of the Standard Model with two, three, and four species of light neutrinos. The asymmetry of the curve is produced by initial-state radiation. Note that the error bars have been increased by a factor ten for display purposes. References:

ALEPH: R. Barate *et al.*, Eur. Phys. J. **C14**, 1 (2000).

DELPHI: P. Abreu *et al.*, Eur. Phys. J. **C16**, 371 (2000).

L3: M. Acciarri *et al.*, Eur. Phys. J. **C16**, 1 (2000).

OPAL: G. Abbiendi *et al.*, Eur. Phys. J. **C19**, 587 (2001).

Combination: The ALEPH, DELPHI, L3, OPAL, SLD Collaborations, the LEP Electroweak Working Group, and the SLD Electroweak and Heavy Flavor Groups, Phys. Rept. **427**, 257 (2006) [[arXiv:hep-ex/0509008](https://arxiv.org/abs/hep-ex/0509008)].

(Courtesy of M. Grünewald and the LEP Electroweak Working Group, 2007)

Muon Neutrino and Anti-Neutrino Charged-Current Total Cross Section

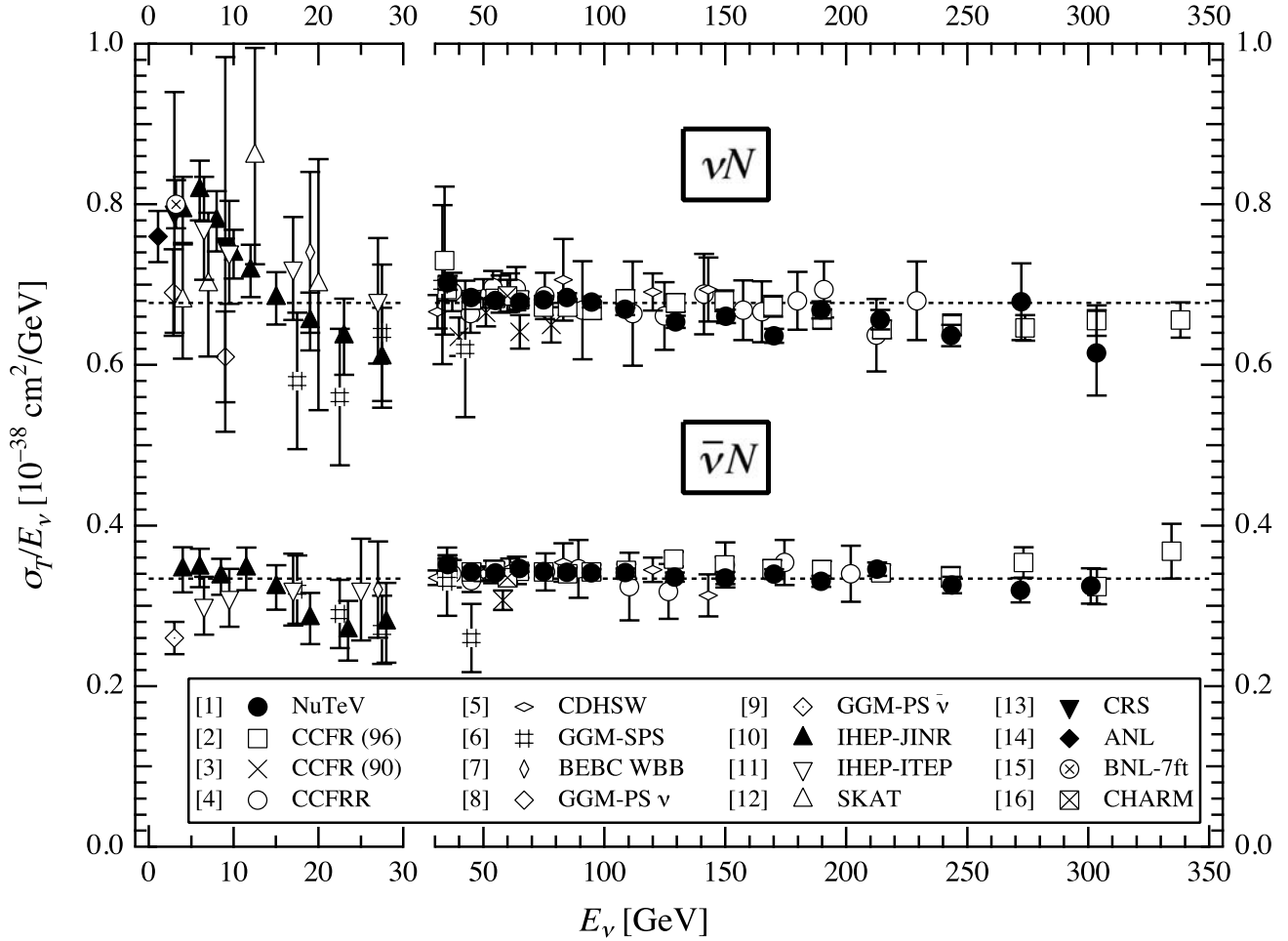


Figure 40.9: σ_T/E_ν for the muon neutrino and anti-neutrino charged-current total cross section as a function of neutrino energy. The error bars include both statistical and systematic errors. The straight lines are the isoscalar-corrected total cross-section values averaged over 30-200 GeV as measured by the experiments in Refs. [3–5]: $\sigma^{\nu Iso}/E_\nu = (0.677 \pm 0.014) \times 10^{-38} \text{cm}^2/\text{GeV}$; $\sigma^{\bar{\nu} Iso}/E_{\bar{\nu}} = (0.334 \pm 0.008) \times 10^{-38} \text{cm}^2/\text{GeV}$. The average ratio of the anti-neutrino to neutrino cross section in the energy range 30-200 GeV is $\sigma^{\bar{\nu} Iso}/\sigma^{\nu Iso} = 0.504 \pm 0.003$ as measured by Refs. [1–5]. Note the change in the energy scale at 30 GeV. (Courtesy W. Seligman and M.H. Shaevitz, Columbia University, 2007)

- [1] M. Tzanov *et al.*, Phys. Rev. **D74**, 012008 (2006);
- [2] W. Seligman, Ph.D. Thesis, Nevis Report 292 (1996);
- [3] P.S. Auchincloss *et al.*, Z. Phys. **C48**, 411 (1990);
- [4] D.B. MacFarlane *et al.*, Z. Phys. **C26**, 1 (1984);
- [5] P. Berge *et al.*, Z. Phys. **C35**, 443 (1987);
- [6] J. Morfin *et al.*, Phys. Lett. **104B**, 235 (1981);
- [7] D.C. Colley *et al.*, Z. Phys. **C2**, 187 (1979);
- [8] S. Campolillo *et al.*, Phys. Lett. **84B**, 281 (1979);

- [9] O. Erriquez *et al.*, Phys. Lett. **80B**, 309 (1979);
- [10] V.B. Anikeev *et al.*, Z. Phys. **C70**, 39 (1996);
- [11] A.S. Vovenko *et al.*, Sov. J. Nucl. Phys. **30**, 527 (1979);
- [12] D.S. Baranov *et al.*, Phys. Lett. **81B**, 255 (1979);
- [13] C. Baltay *et al.*, Phys. Rev. Lett. **44**, 916 (1980);
- [14] S.J. Barish *et al.*, Phys. Rev. **D19**, 2521 (1979);
- [15] N.J. Baker *et al.*, Phys. Rev. **D25**, 617 (1982);
- [15] J.V. Allaby *et al.*, Z. Phys. **C38**, 403 (1988).

Table 40.2: Total hadronic cross section. Analytic S -matrix and Regge theory suggest a variety of parameterizations of total cross sections at high energies with different areas of applicability and fits quality.

A ranking procedure, based on measures of different aspects of the quality of the fits to the current evaluated experimental database, allows one to single out the following parameterization of highest rank[1]

$$\sigma^{ab} = Z^{ab} + B \log^2(s/s_0) + Y_1^{ab}(s_1/s)^{\eta_1} - Y_2^{ab}(s_1/s)^{\eta_2}, \quad \sigma^{\bar{a}b} = Z^{ab} + B \log^2(s/s_0) + Y_1^{ab}(s_1/s)^{\eta_1} + Y_2^{ab}(s_1/s)^{\eta_2},$$

where Z^{ab}, B, Y_i^{ab} are in mb, and $s, s_1,$ and s_0 are in GeV^2 . The scales $s_0, s_1,$ the rate of universal rise of the cross sections $B,$ and exponents η_1 and η_2 are independent of the colliding particles. The scale s_1 is fixed at 1 GeV^2 . Terms $Z^{ab} + B \log^2(s/s_0)$ represent the pomerons. The exponents η_1 and η_2 represent lower-lying C -even and C -odd exchanges, respectively. Requiring $\eta_1 = \eta_2$ results in somewhat poorer fits. In addition to total cross sections $\sigma,$ the measured ratios of the real-to-imaginary parts of the forward scattering amplitudes $\rho = \text{Re}(T)/\text{Im}(T)$ were included in the fits by using s to u crossing symmetry. Global fits were made to the 2005-updated data for $\bar{p}(p)p, \Sigma^-p, \pi^\pm p, K^\pm p, \gamma p,$ and $\gamma\gamma$ collisions.

Exact factorization hypothesis in the form $(Z^{\gamma p}, B^{\gamma p}) = \delta \cdot (Z^{pp}, B), (Z^{\gamma\gamma}, B^{\gamma\gamma}) = \delta^2 \cdot (Z^{pp}, B)$ was used to extend the universal rise of the total hadronic cross sections to the $\gamma p \rightarrow \text{hadrons}$ and $\gamma\gamma \rightarrow \text{hadrons}$ collisions. This resulted in reducing the number of adjusted parameters from 21 used for the 2002 edition to 19, and in the higher quality rank of the parameterization. The asymptotic parameters thus obtained were then fixed and used as inputs to a fit to a larger data sample that included cross sections on deuterons (d) and neutrons (n). All fits included data above $\sqrt{s_{\text{min}}} = 5 \text{ GeV}$.

Fits to $\bar{p}(p)p, \Sigma^-p, \pi^\pm p, K^\pm p, \gamma p, \gamma\gamma$			Beam/ Target	Fits to groups				χ^2/dof by groups
Z	Y_1	Y_2		Z	Y_1	Y_2	B	
35.45(48)	42.53(1.35)	33.34(1.04)	$\bar{p}(p)/p$	35.45(48)	42.53(23)	33.34(33)	0.308(10)	1.029
			$\bar{p}(p)/n$	35.80(16)	40.15(1.59)	30.00(96)	0.308(10)	
35.20(1.46)	-199(102)	-264(126)	Σ^-/p	35.20(1.41)	-199(86)	-264(112)	0.308(10)	0.565
20.86(40)	19.24(1.22)	6.03(19)	π^\pm/p	20.86(3)	19.24(18)	6.03(9)	0.308(10)	0.955
17.91(36)	7.1(1.5)	13.45(40)	K^\pm/p	17.91(3)	7.14(25)	13.45(13)	0.308(10)	0.669
			K^\pm/n	17.87(6)	5.17(50)	7.23(28)	0.308(10)	
	0.0317(6)		γ/p		0.0320(40)		0.308(10)	0.766
	-0.61(62)E-3		γ/γ		-0.58(61)E-3		0.308(10)	
$\chi^2/dof = 0.971,$	$B = 0.308(10) \text{ mb},$		$\bar{p}(p)/d$	64.35(38)	130(3)	85.5(1.3)	0.537(31)	1.432
$\eta_1 = 0.458(17),$	$\eta_2 = 0.545(7)$		π^\pm/d	38.62(21)	59.62(1.53)	1.60(41)	0.461(14)	0.735
$\delta = 0.00308(2),$	$\sqrt{s_0} = 5.38(50) \text{ GeV}$		K^\pm/d	33.41(20)	23.66(1.45)	28.70(37)	0.449(14)	0.814

The fitted functions are shown in the following figures, along with one-standard-deviation error bands. When the reduced χ^2 is greater than one, a scale factor has been included to evaluate the parameter values, and to draw the error bands. Where appropriate, statistical and systematic errors were combined quadratically in constructing weights for all fits. On the plots, only statistical error bars are shown. Vertical arrows indicate lower limits on the p_{lab} or E_{cm} range used in the fits.

One can find the details of the global fits and ranking procedure, in the paper [1]. Database is practically the same as for the 2004 edition (it was slightly changed in the low energy regions not used in the fits).

Recently, the statement in [1] that the models with $\log^2(s/s_0)$ asymptotic terms work much better than the models with $\log(s/s_0)$ or $(s/s_0)^\epsilon$ terms was confirmed in [2] and [3], based on matching traditional asymptotic parameterizations with low energy data in different ways. Both these references, however, questioned the statement in [1] on the universality of the coefficient of the $\log^2(s/s_0)$ term for all processes with nucleon and gamma targets. The two references give different predictions at superhigh energies: $\sigma_{\pi N}^{as} > \sigma_{NN}^{as}$ [2] and $\sigma_{\pi N}^{as} \sim 2/3 \sigma_{NN}^{as}$ [3]. A broader universality of σ_{tot}^{as} has been recently advocated in [4] for hadron-nucleus collisions. It should be noted that asymptotic rate universality in hadron-deuteron collisions has not been established at available energies (see Table).

Computer-readable data files are available at <http://pdg.lbl.gov/current/xsect/>. (Courtesy of the COMPAS group, IHEP, Protvino, August 2005)

On-line ‘‘Predictor’’ to calculate σ and ρ for any energy from five high rank models is also available at <http://nuclth02.phys.ulg.ac.be/compete/predictor.html>.

References:

1. J.R. Cudell *et al.* (COMPETE Collab.), Phys. Rev. **D65**, 074024 (2002).
2. K. Igi and M. Ishida, Phys. Rev. **D66**, 034023 (2002), Phys. Lett. **B622**, 286 (2005).
3. M. M. Block and F. Halzen, Phys. Rev. **D70**, 091901 (2004), Phys. Rev. **D72**, 036006 (2005).
4. L. Frankfurt, M. Strikman, and M. Zhalov, Phys. Lett. **B616**, 59 (2005).

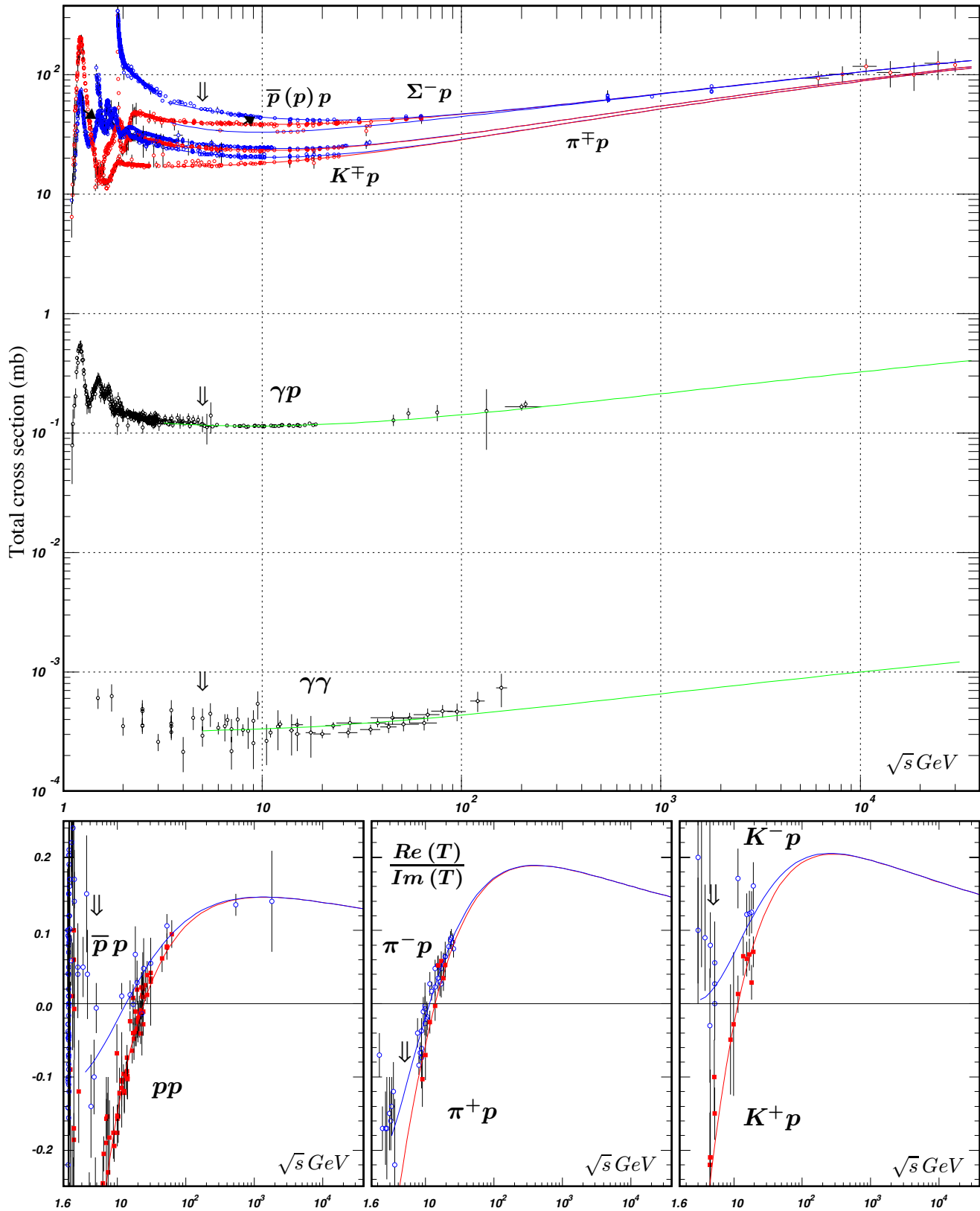


Figure 40.10: Summary of hadronic, γp , and $\gamma\gamma$ total cross sections, and ratio of the real to imaginary parts of the forward hadronic amplitudes. Corresponding computer-readable data files may be found at <http://pdg.lbl.gov/current/xsect/>. (Courtesy of the COMPAS group, IHEP, Protvino, August 2005) Color version at end of book.

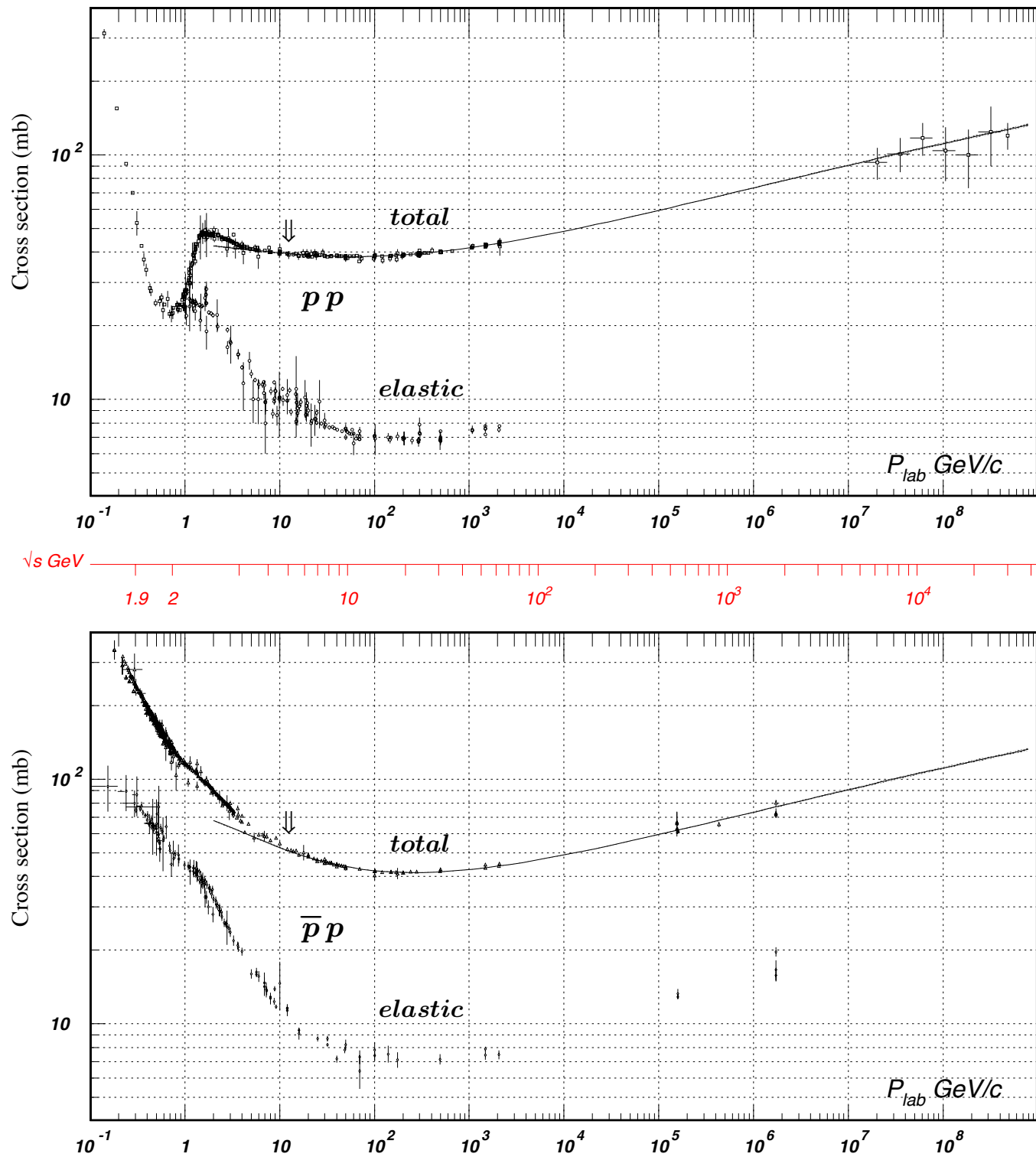


Figure 40.11: Total and elastic cross sections for pp and $\bar{p}p$ collisions as a function of laboratory beam momentum and total center-of-mass energy. Corresponding computer-readable data files may be found at <http://pdg.lbl.gov/current/xsect/>. (Courtesy of the COMPAS group, IHEP, Protvino, August 2005)

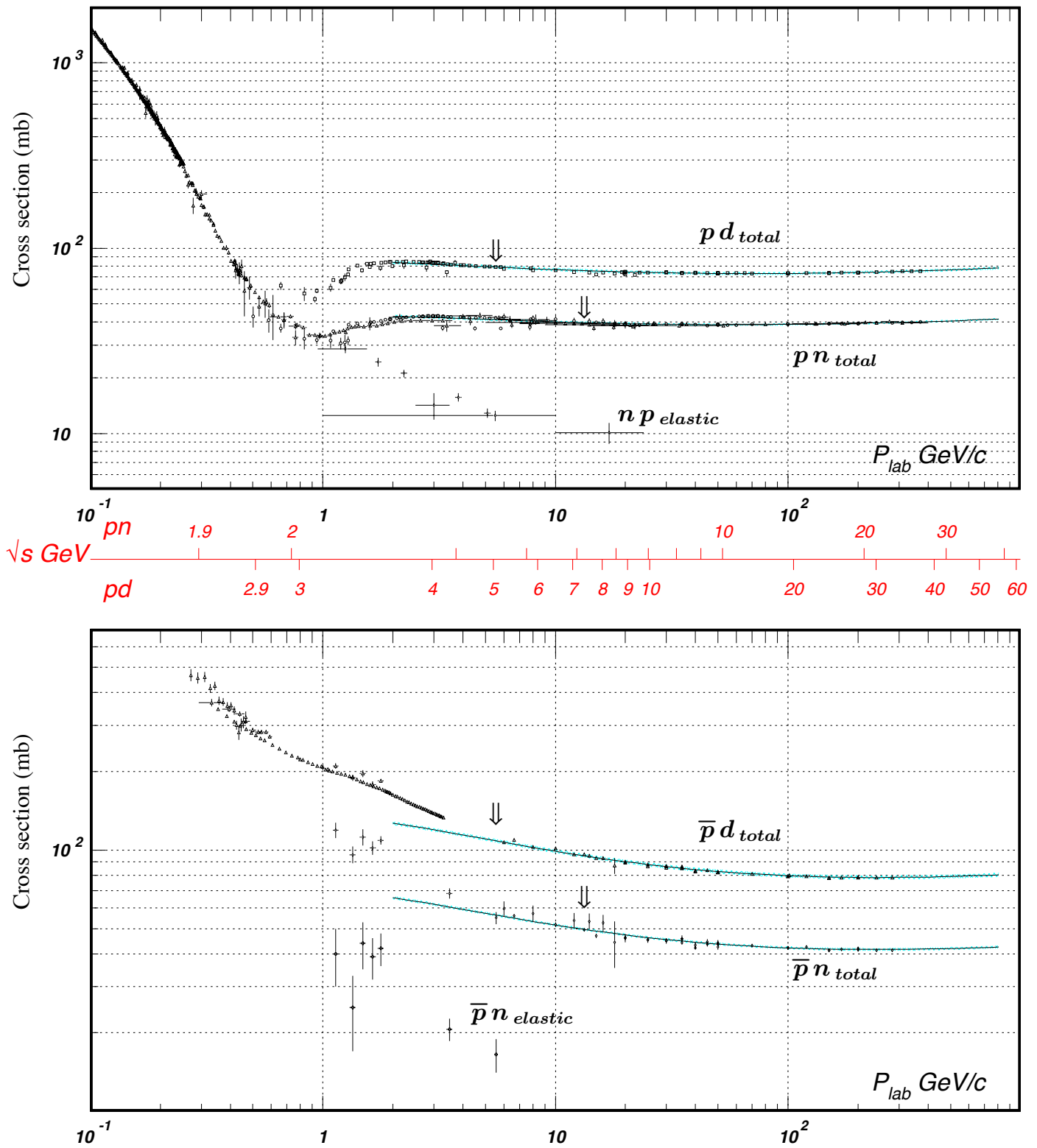


Figure 40.12: Total and elastic cross sections for pd (total only), np , $\bar{p}d$ (total only), and $\bar{p}n$ collisions as a function of laboratory beam momentum and total center-of-mass energy. Corresponding computer-readable data files may be found at <http://pdg.lbl.gov/current/xsect/>. (Courtesy of the COMPAS Group, IHEP, Protvino, August 2005)

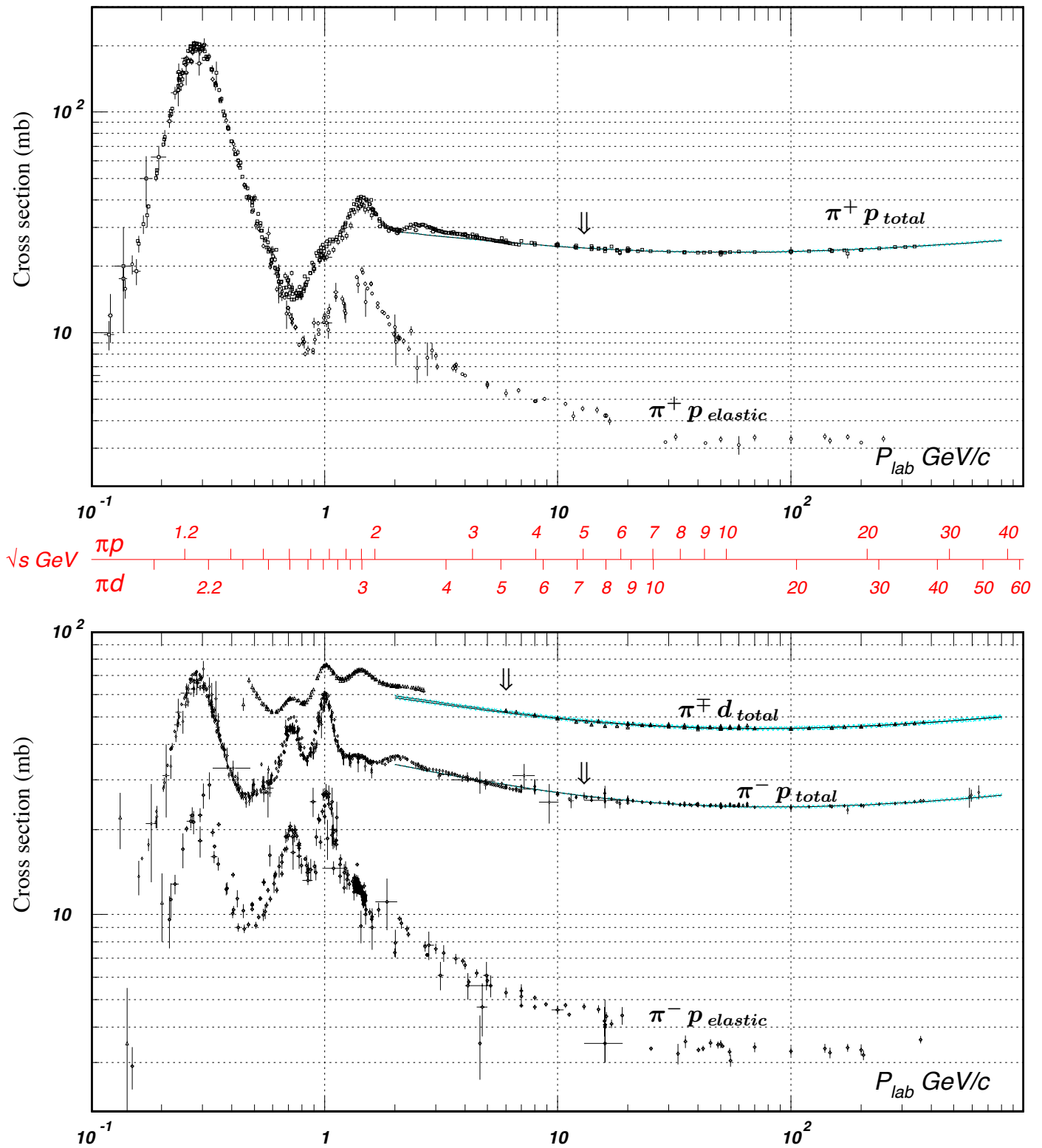


Figure 40.13: Total and elastic cross sections for $\pi^\pm p$ and $\pi^\pm d$ (total only) collisions as a function of laboratory beam momentum and total center-of-mass energy. Corresponding computer-readable data files may be found at <http://pdg.lbl.gov/current/xsect/>. (Courtesy of the COMPAS Group, IHEP, Protvino, August 2005)

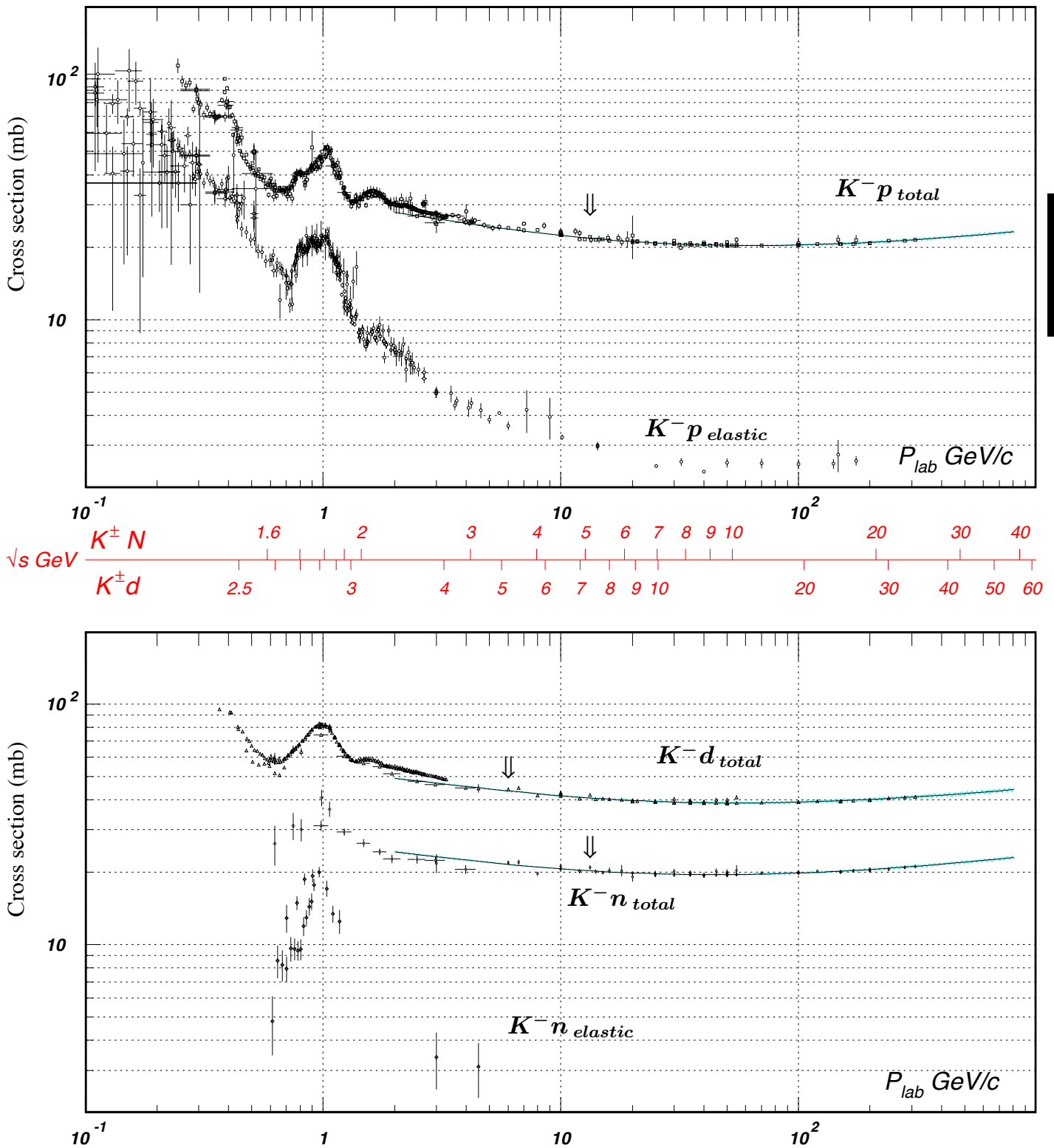


Figure 40.14: Total and elastic cross sections for K^-p and K^-d (total only), and K^-n collisions as a function of laboratory beam momentum and total center-of-mass energy. Corresponding computer-readable data files may be found at <http://pdg.lbl.gov/current/xsect/>. (Courtesy of the COMPAS Group, IHEP, Protvino, August 2005)

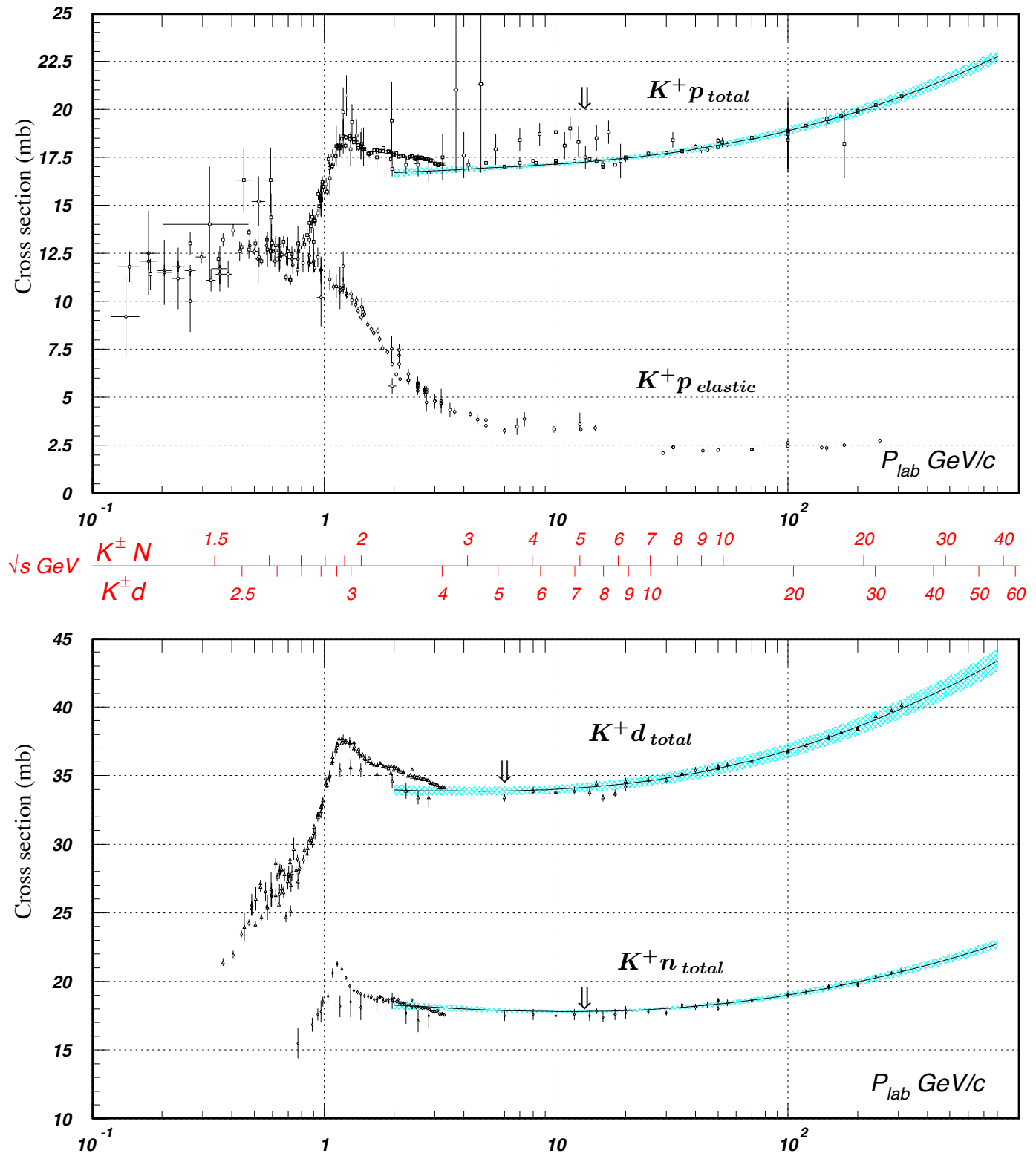


Figure 40.15: Total and elastic cross sections for K^+p and total cross sections for K^+d and K^+n collisions as a function of laboratory beam momentum and total center-of-mass energy. Corresponding computer-readable data files may be found at <http://pdg.lbl.gov/current/xsect/>. (Courtesy of the COMPAS Group, IHEP, Protvino, August 2005)

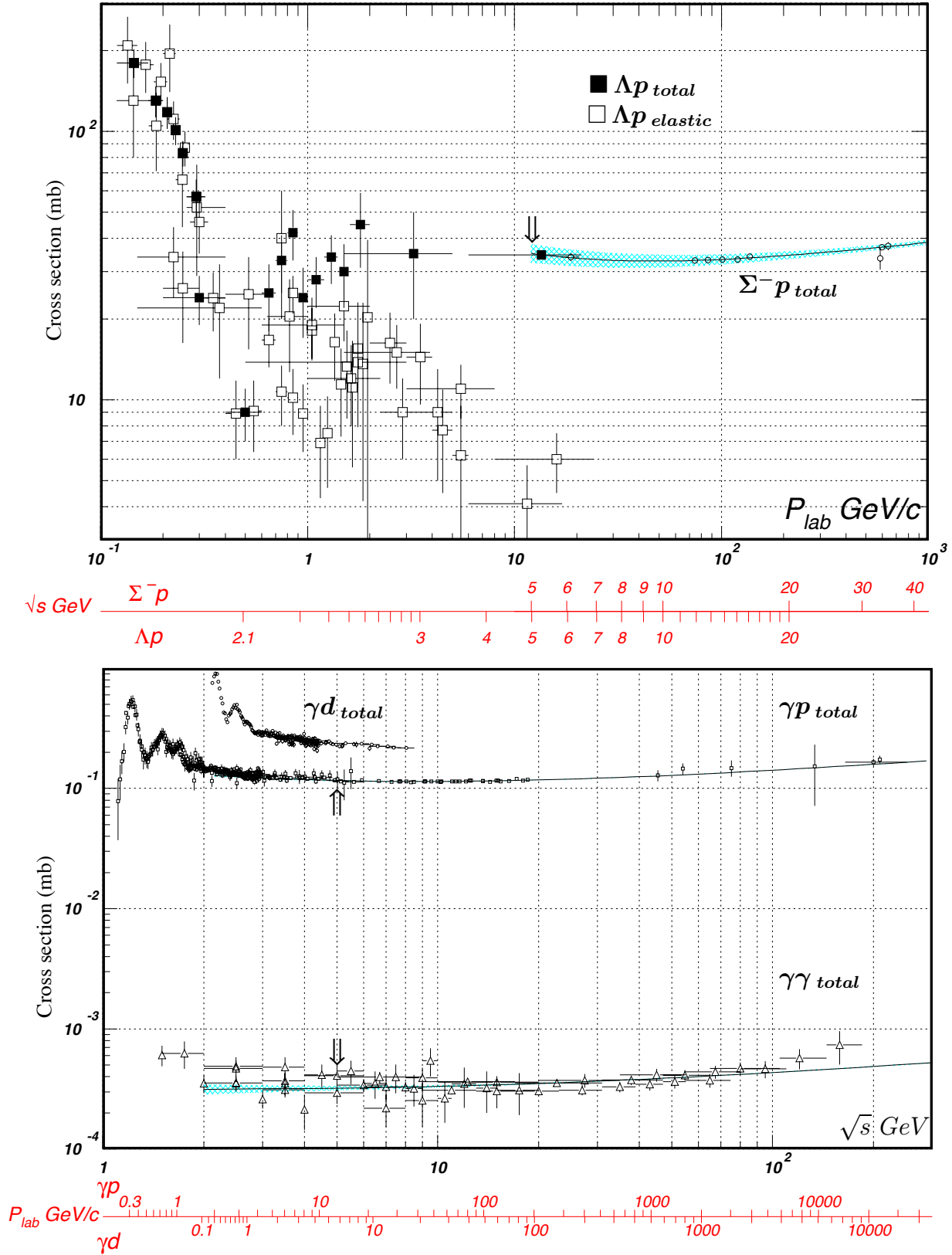


Figure 40.16: Total and elastic cross sections for Λp , total cross section for $\Sigma^- p$, and total hadronic cross sections for γd , γp , and $\gamma\gamma$ collisions as a function of laboratory beam momentum and the total center-of-mass energy. Corresponding computer-readable data files may be found at <http://pdg.lbl.gov/current/xsect/>. (Courtesy of the COMPAS group, IHEP, Protvino, August 2005)

INTRODUCTION TO THE PARTICLE LISTINGS

Illustrative key	373
Abbreviations	374





Illustrative Key to the Particle Listings

Name of particle. "Old" name used before 1986 renaming scheme also given if different. See the section "Naming Scheme for Hadrons" for details.

$a_0(1200)$

$$I^G(J^{PC}) = 1^-(0^+)$$

Particle quantum numbers (where known).

OMITTED FROM SUMMARY TABLE
Evidence not compelling, may be a kinematic effect.

Indicates particle omitted from Particle Physics Summary Table, implying particle's existence is not confirmed.

Quantity tabulated below.

$a_0(1200)$ MASS

Top line gives our best value (and error) of quantity tabulated here, based on weighted average of measurements used. Could also be from fit, best limit, estimate, or other evaluation. See next page for details.

VALUE (MeV)	EVTS	DOCUMENT ID	TECN	CHG	COMMENT
1206 ± 7 OUR AVERAGE					
1210 ± 8 ± 9	3000	FENNER 87	MMS	-	3.5 $\pi^- p$
1198 ± 10		PIERCE 83	ASPK	+	2.1 $K^- p$
1216 ± 11 ± 9	1500	MERRILL 81	HBC	0	3.2 $K^- p$
• • • We do not use the following data for averages, fits, limits, etc. • • •					
1192 ± 16		LYNCH 81	HBC	±	2.7 $\pi^- p$
1 Systematic error was added quadratically by us in our 1986 edition.					

General comments on particle.

Footnote number linking measurement to text of footnote.

$a_0(1200)$ WIDTH

Number of events above background.

Measured value used in averages, fits, limits, etc.

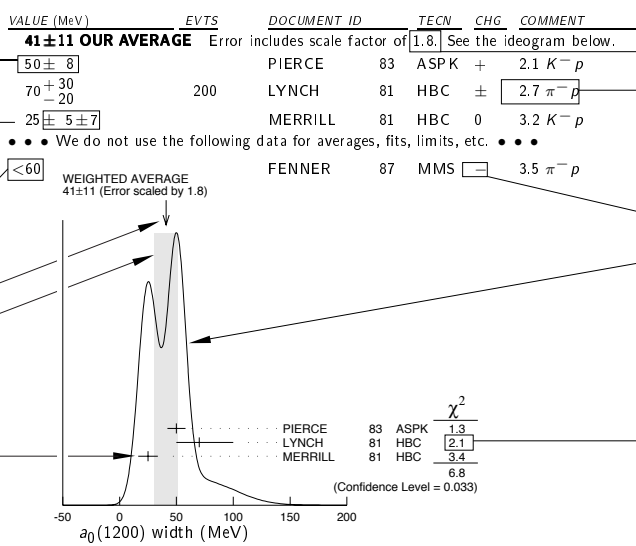
Error in measured value (often statistical only; followed by systematic if separately known; the two are combined in quadrature for averaging and fitting.)

Measured value *not* used in averages, fits, limits, etc. See the Introductory Text for explanations.

Arrow points to weighted average.

Shaded pattern extends $\pm 1\sigma$ (scaled by "scale factor" S) from weighted average.

Value and error for each experiment.



"Document id" for this result; full reference given below.

Measurement technique. (See abbreviations on next page.)

Scale factor > 1 indicates possibly inconsistent data.

Reaction producing particle, or general comments.

"Change bar" indicates result added or changed since previous edition.

Charge(s) of particle(s) detected.

Ideogram to display possibly inconsistent data. Curve is sum of Gaussians, one for each experiment (area of Gaussian = 1/error; width of Gaussian = \pm error). See Introductory Text for discussion.

Contribution of experiment to χ^2 (if no entry present, experiment not used in calculating χ^2 or scale factor because of very large error).

$a_0(1200)$ DECAY MODES

Partial decay mode (labeled by Γ_i).

Mode	Fraction (Γ_i/Γ)	Scale factor/ Confidence level
Γ_1 3π	(65.2 ± 1.3) %	S=1.7
Γ_2 $K\bar{K}$	(34.8 ± 1.3) %	S=1.7
Γ_3 $\eta\pi^\pm$	< 4.9 × 10 ⁻⁴	CL=95%

Our best value for branching fraction as determined from data averaging, fitting, evaluating, limit selection, etc. This list is basically a compact summary of results in the Branching Ratio section below.

$a_0(1200)$ BRANCHING RATIOS

Branching ratio.

Our best value (and error) of quantity tabulated, as determined from constrained fit (using *all significant* measured branching ratios for this particle).

Weighted average of measurements of this ratio only.

Footnote (referring to LYNCH 81).

VALUE	DOCUMENT ID	TECN	CHG	COMMENT
$\Gamma(3\pi)/\Gamma_{total}$				
0.652 ± 0.013 OUR FIT				Error includes scale factor of 1.7.
0.643 ± 0.010 OUR AVERAGE				
0.64 ± 0.01	PIERCE 83	ASPK	+	2.1 $K^- p$
0.74 ± 0.06	MERRILL 81	HBC	0	3.2 $K^- p$
• • • We do not use the following data for averages, fits, limits, etc. • • •				
0.48 ± 0.15	² LYNCH 81	HBC	±	2.7 $\pi^- p$
² Data has questionable background subtraction.				
$\Gamma(K\bar{K})/\Gamma_{total}$				
0.348 ± 0.013 OUR FIT				Error includes scale factor of 1.7.
0.35 ± 0.05	PIERCE 83	ASPK	+	2.1 $K^- p$
$\Gamma(K\bar{K})/\Gamma(3\pi)$				
0.535 ± 0.030 OUR FIT				Error includes scale factor of 1.7.
0.50 ± 0.03	MERRILL 81	HBC	0	3.2 $K^- p$
$\Gamma(\eta(\text{neutral decay})\pi^\pm)/\Gamma_{total}$				
<3.5	PIERCE 83	ASPK	+	2.1 $K^- p$

Confidence level for measured upper limit.

References, ordered inversely by year, then author.

"Document id" used on data entries above.

Journal, report, preprint, etc. (See abbreviations on next page.)

$a_0(1200)$ REFERENCES

FENNER 87	PRL 55 14	H. Fenner et al.	(SLAC)
PIERCE 83	PL 123B 230	J.H. Pierce	(FNAL) JUP
LYNCH 81	PR D24 610	G.R. Lynch et al.	(CLEO Collab.)
MERRILL 81	PRL 47 143	D.W. Merrill et al.	(SACL, CERN)

Partial list of author(s) in addition to first author.

Quantum number determinations in this reference.

Institution(s) of author(s). (See abbreviations on next page.)

Abbreviations Used in the Particle Listings

Indicator of Procedure Used to Obtain Our Result

OUR AVERAGE	From a weighted average of selected data.
OUR FIT	From a constrained or overdetermined multiparameter fit of selected data.
OUR EVALUATION	Not from a direct measurement, but evaluated from measurements of other quantities.
OUR ESTIMATE	Based on the observed range of the data. Not from a formal statistical procedure.
OUR LIMIT	For special cases where the limit is evaluated by us from measured ratios or other data. Not from a direct measurement.

Measurement Techniques

(i.e., Detectors and Methods of Analysis)

ACCM	ACCMOR Collaboration
AEMS	Argonne effective mass spectrometer
ALEP	ALEPH – CERN LEP detector
AMND	AMANDA South Pole neutrino detector
AMY	AMY detector at KEK-TRISTAN
APEX	FNAL APEX Collab.
ARG	ARGUS detector at DORIS
ARGD	Fit to semicircular amplitude path on Argand diagram
ASP	Anomalous single-photon detector
ASPK	Automatic spark chambers
ASTE	ASTERIX detector at LEAR
ASTR	Astronomy
B787	BNL experiment 787 detector
B791	BNL experiment 791 detector
B845	BNL experiment 845 detector
B852	BNL E-852
B865	BNL E865 detector
B871	BNL experiment 871 detector
B949	BNL E949 detector at AGS
BABR	BaBar Collab.
BAKS	Baksan underground scintillation telescope
BC	Bubble chamber
BDMP	Beam dump
BEAT	CERN BEATRICE Collab.
BEBC	Big European bubble chamber at CERN
BELL	Belle Collab.
BES	BES Beijing Spectrometer at Beijing Electron-Positron Collider
BES2	BES Beijing Spectrometer at Beijing Electron-Positron Collider
BIS2	BIS-2 spectrometer at Serpukhov
BKEI	BENKEI spectrometer system at KEK Proton Synchrotron
BOLO	Bolometer, a cryogenic thermal detector
BONA	Bonanza nonmagnetic detector at DORIS
BORX	BOREXINO
BPWA	Barrelet-zero partial-wave analysis
CALO	Calorimeter
CAST	CAST experiment at CERN
CBAL	Crystal Ball detector at SLAC-SPEAR or DORIS
CBAR	Crystal Barrel detector at CERN-LEAR
CBOX	Crystal Box at LAMPF
CC	Cloud chamber
CCFR	Columbia-Chicago-Fermilab-Rochester detector
CDF	Collider detector at Fermilab
CDF2	CDF-II Collab.
CDHS	CDHS neutrino detector at CERN
CDMS	CDMS Collab.
CELL	CELLO detector at DESY
CHER	Cherenkov detector
CHM2	CHARM-II neutrino detector (glass) at CERN
CHOZ	Nuclear Power Station near Chooz, France
CHRM	CHARM neutrino detector (marble) at CERN
CHRS	CHORUS Collaboration – CERN SPS
CIB	Cosmic Infrared Background
CIBS	CERN-IHEP boson spectrometer
CLAS	Jefferson CLAS Collab.
CLE2	CLEO II detector at CESR
CLE3	CLEO III detector at CESR
CLEO	Cornell magnetic detector at CESR
CMB	Cosmic Microwave Background
CMD	Cryogenic magnetic detector at VEPP-2M, Novosibirsk
CMD2	Cryogenic magnetic detector 2 at VEPP-2M, Novosibirsk
CNTR	Counters
COSM	Cosmology and astrophysics
COSY	COSY-TOF Collaboration
CPLR	CLEAR Collaboration

CRES	CRESST cryogenic detector
CRYB	Crystal Ball at BNL
CSB2	Columbia U. - Stony Brook BGO calorimeter inserted in NaI array
CSME	COSME Collaboration
CUOR	CUORICINO experiment at Gran Sasso Laboratory.
CUSB	Columbia U. - Stony Brook segmented NaI detector at CESR
D0	D0 detector at Fermilab Tevatron Collider
DAMA	DAMA, dark matter detector at Gran Sasso National Lab.
DASP	DESY double-arm spectrometer
DBC	Deuterium bubble chamber
DLCO	DELCO detector at SLAC-SPEAR or SLAC-PEP
DLPH	DELPHI detector at LEP
DM1	Magnetic detector no. 1 at Orsay DCI collider
DM2	Magnetic detector no. 2 at Orsay DCI collider
DONU	DONUT Collab.
DPWA	Energy-dependent partial-wave analysis
E621	Fermilab E621 detector
E653	Fermilab E653 detector
E665	Fermilab E665 detector
E687	Fermilab E687 detector
E691	Fermilab E691 detector
E705	Fermilab E705 Spectrometer-Calorimeter
E731	Fermilab E731 Spectrometer-Calorimeter
E756	Fermilab E756 detector
E760	Fermilab E760 detector
E761	Fermilab E761 detector
E771	Fermilab E771 detector
E773	Fermilab E773 Spectrometer-Calorimeter
E789	Fermilab E789 detector
E791	Fermilab E791 detector
E799	Fermilab E799 Spectrometer-Calorimeter
E835	Fermilab E835 detector
EDEL	EDELWEISS dark matter search Collaboration
EHS	Four-pi detector at CERN
ELEC	Electronic combination
EMC	European muon collaboration detector at CERN
EMUL	Emulsions
FBC	Freon bubble chamber
FENI	FENICE (at the ADONE collider of Frascati)
FIT	Fit to previously existing data
FMPS	Fermilab Multiparticle Spectrometer
FOCS	FNAL E831 FOCUS Collab.
FRAB	ADONE $B\bar{B}$ group detector
FRAG	ADONE $\gamma\gamma$ group detector
FRAM	ADONE MEA group detector
FREJ	FREJUS Collaboration – modular flash chamber detector (calorimeter)
GA24	Hodoscope Cherenkov γ calorimeter (IHEP GAMS-2000) (CERN GAMS-4000)
GALX	GALLEX solar neutrino detector in the Gran Sasso Underground Lab.
GAM2	IHEP hodoscope Cherenkov γ calorimeter GAMS-2000
GAM4	CERN hodoscope Cherenkov γ calorimeter GAMS-4000
GAMS	IHEP hodoscope Cherenkov γ calorimeter GAMS-4 π
GNO	Gallium Neutrino Observatory in the Gran Sasso Underground Lab.
GOLI	CERN Goliath spectrometer
H1	H1 detector at DESY/HERA
HBC	Hydrogen bubble chamber
HDBC	Hydrogen and deuterium bubble chambers
HDMO	Heidelberg-Moscow Experiment
HDMS	Heidelberg Dark Matter Search Experiment
HEBC	Helium bubble chamber
HEPT	Helium proportional tubes
HERB	HERA-B detector at DESY/HERA
HERM	HERMES detector at DESY/HERA
HLBC	Heavy-liquid bubble chamber
HOME	Homestake underground scintillation detector
HPW	Harvard-Pennsylvania-Wisconsin detector
HRS	SLAC high-resolution spectrometer
HYBR	Hybrid: bubble chamber + electronics
HYCP	HyperCP Collab. (FNAL E-871)
ICAR	ICARUS experiment at Gran Sasso Laboratory.
IGEX	IGEX Collab.
IMB	Irvine-Michigan-Brookhaven underground Cherenkov detector
IMB3	Irvine-Michigan-Brookhaven underground Cherenkov detector
INDU	Magnetic induction

Abbreviations Used in the Particle Listings

IPWA	Energy-independent partial-wave analysis	RVUE	Review of previous data
ISTR	IHEP ISTR+ spectrometer-calorimeter	SAGE	US - Russian Gallium Experiment
JADE	JADE detector at DESY	SELX	FNAL SELEX Collab.
K246	KEK E246 detector with polarimeter	SFM	CERN split-field magnet
K2K	KEK to Super-Kamiokande	SHF	SLAC Hybrid Facility Photon Collaboration
K391	KEK E391a detector	SIGM	Serpukhov CERN-IHEP magnetic spectrometer (SIGMA)
K470	KEK-E470 Stopping K detector	SILI	Silicon detector
KAM2	KAMIOKANDE-II underground Cherenkov detector	SIMP	SIMPLE, dark matter detector at Laboratori Nazionali del Sud
KAMI	KAMIOKANDE underground Cherenkov detector	SKAM	Super-Kamiokande Collab.
KAR2	KARMEN2 calorimeter at the ISIS neutron spallation source at Rutherford	SLAX	Solar Axion Experiment in Canfranc Underground Laboratory
KARM	KARMEN calorimeter at the ISIS neutron spallation source at Rutherford	SLD	SLC Large Detector for e^+e^- colliding beams at SLAC
KEDR	detector operating at VEPP-4M collider (Novosibirsk)	SMPL	SIMPLE superheated droplet detector.
KIMS	Korea Invisible Mass Search experiment at YangYang, Korea	SND	Novosibirsk Spherical neutral detector at VEPP-2M
KLND	KamLand Collab. (Japan)	SNDR	SINDRUM spectrometer at PSI
KLOE	KLOE detector at DAFNE (the Frascati e+e- collider Italy)	SNO	SNO Collaboration (Sudbury Neutrino Observatory)
KOLR	Kolar Gold Field underground detector	SOU2	Soudan 2 underground detector
KTEV	KTeV Collaboration	SOUND	Soudan underground detector
L3	L3 detector at LEP	SPEC	Spectrometer
LASS	Large-angle superconducting solenoid spectrometer at SLAC	SPED	From maximum of speed plot or resonant amplitude
LATT	Lattice calculations	SPHR	Bonn SAPHIR Collab.
LEBC	Little European bubble chamber at CERN	SPNX	SPHINX spectrometer at IHEP accelerator
LEGS	BNL LEGS Collab.	SPRK	Spark chamber
LENA	Nonmagnetic lead-glass NaI detector at DORIS	SQID	SQUID device
LEP	From combination of all 4 LEP experiments: ALEPH, DELPHI, L3, OPAL	STRC	Streamer chamber
LEPS	Low-Energy Pion Spectrometer at the Paul Scherrer Institute	SVD2	SVD-2 experiment at IHEP, Protvino
LGW	Lead Glass Wall collaboration at SPEAR/SLAC	TASS	DESY TASSO detector
LSD	Mont Blanc liquid scintillator detector	TEVA	Combined analysis of CDF and DØ experiments
LSND	Liquid Scintillator Neutrino Detector	THEO	Theoretical or heavily model-dependent result
MAC	MAC detector at PEP/SLAC	TNF	TNF-IHEP facility at 70 GeV IHEP accelerator
MBOO	Fermilab MiniBooNE neutrino experiment	TOF	Time-of-flight
MBR	Molecular beam resonance technique	TOPZ	TOPAZ detector at KEK-TRISTAN
MCRO	MACRO detector in Gran Sasso	TPC	TPC detector at PEP/SLAC
MD1	Magnetic detector at VEPP-4, Novosibirsk	TPS	Tagged photon spectrometer at Fermilab
MDRP	Millikan drop measurement	TRAP	Penning trap
MICA	Underground mica deposits	TWST	TWIST spectrometer at TRIUMF
MINS	Fermilab MINOS experiment	UA1	UA1 detector at CERN
MIRA	MIRABELLE Liquid-hydrogen bubble chamber	UA2	UA2 detector at CERN
MLEV	Magnetic levitation	UA5	UA5 detector at CERN
MMS	Missing mass spectrometer	UKDM	UK Dark Matter Collab.
MPS	Multiparticle spectrometer at BNL	VES	Vertex Spectrometer Facility at 70 GeV IHEP accelerator
MPS2	Multiparticle spectrometer upgrade at BNL	VNS	VENUS detector at KEK-TRISTAN
MPSF	Multiparticle spectrometer at Fermilab	WA75	CERN WA75 experiment
MPWA	Model-dependent partial-wave analysis	WA82	CERN WA82 experiment
MRK1	SLAC Mark-I detector	WA89	CERN WA89 experiment
MRK2	SLAC Mark-II detector	WASA	WASA detector at CELSIUS, Uppsala and at COSY, Juelich
MRK3	SLAC Mark-III detector	WIRE	Wire chamber
MRKJ	Mark-J detector at DESY	XE10	XENON10 experiment at Gran Sasso National Laboratory
MRS	Magnetic resonance spectrometer	XEBC	Xenon bubble chamber
MUG2	MUON(g-2)	ZEP2	ZEPLIN-II dark matter detector
MWPC	Multi-Wire Proportional Chamber	ZEPL	ZEPLIN-I galactic dark matter detector
NA14	CERN NA14	ZEUS	ZEUS detector at DESY/HERA
NA31	CERN NA31 Spectrometer-Calorimeter		
NA32	CERN NA32 Spectrometer		
NA48	CERN NA48 Collaboration		
NA49	CERN NA49		
NAIA	NAIAD (NaI Advanced Detector) dark matter search experiment		
ND	NaI detector at VEPP-2M, Novosibirsk		
NICE	Serpukhov nonmagnetic precision spectrometer		
NMR	Nuclear magnetic resonance		
NOMD	NOMAD Collaboration, CERN SPS		
NTEV	NuTeV Collab. at Fermilab		
NUSX	Mont Blanc NUSEX underground detector		
OBLX	OBELIX detector at LEAR		
OLYA	Detector at VEPP-2M and VEPP-4, Novosibirsk		
OMEG	CERN OMEGA spectrometer		
OPAL	OPAL detector at LEP		
OSPK	Optical spark chamber		
PIBE	The PIBETA detector at the Paul Scherrer Institute (PSI), Switzerland.		
PICA	PICASSO dark matter search experiment		
PLAS	Plastic detector		
PLUT	DESY PLUTO detector		
PWA	Partial-wave analysis		
REDE	Resonance depolarization		

Conferences

Conferences are generally referred to by the location at which they were held (e.g., HAMBURG, TORONTO, CORNELL, BRIGHTON, etc.).

Journals

AA	Astronomy and Astrophysics
ADVP	Advances in Physics
AFIS	Anales de Fisica
AJP	American Journal of Physics
ANP	Annals of Physics
ANPL	Annals of Physics (Leipzig)
ANYAS	Annals of the New York Academy of Sciences
AP	Atomic Physics
APAH	Acta Physica Academiae Scientiarum Hungaricae
APJ	Astrophysical Journal
APJS	Astrophysical Journal Suppl.
APP	Acta Physica Polonica
APS	Acta Physica Slovaca
ARNPS	Annual Review of Nuclear and Particle Science
ARNS	Annual Review of Nuclear Science
ASP	Astroparticle Physics
BAPS	Bulletin of the American Physical Society
BASUP	Bulletin of the Academy of Science, USSR (Physics)
CJNP	Chinese Journal of Nuclear Physics

Abbreviations Used in the Particle Listings

CJP	Canadian Journal of Physics	
CNPP	Comments on Nuclear and Particle Physics	
CTP	Communications in Theoretical Physics	
CZJP	Czechoslovak Journal of Physics	
DANS	Doklady Akademii nauk SSSR	
EPJ	The European Physical Journal	
EPL	Europhysics Letters	
FECAY	Fizika Elementarnykh Chastits i Atomnogo Yadra	
HADJ	Hadronic Journal	
IJMP	International Journal of Modern Physics	
JAP	Journal of Applied Physics	
JCAP	Journal of Cosmology and Astroparticle Physics	
JETP	English Translation of Soviet Physics ZETF	
JETPL	English Translation of Soviet Physics ZETF Letters	
JHEP	Journal of High Energy Physics	
JINR	Joint Inst. for Nuclear Research	
JINRRC	JINR Rapid Communications	
JPA	Journal of Physics, A	
JPB	Journal of Physics, B	
JPCRD	Journal of Physical and Chemical Reference Data	
JPG	Journal of Physics, G	
JPSJ	Journal of the Physical Society of Japan	
LNC	Lettere Nuovo Cimento	
MNRAS	Monthly Notices of the Royal Astronomical Society	
MPL	Modern Physics Letters	
NAT	Nature	
NC	Nuovo Cimento	
NIM	Nuclear Instruments and Methods	
NJP	New Journal of Physics	
NP	Nuclear Physics	
NPBPS	Nuclear Physics B Proceedings Supplement	
PAN	Physics of Atomic Nuclei (formerly SJNP)	
PD	Physics Doklady (Magazine)	
PDAT	Physik Daten	
PL	Physics Letters	
PN	Particles and Nuclei	
PPCF	Plasma Physics Control Fusion	
PPN	Physics of Particles and Nuclei (formerly SJPN)	
PPNL	Physics of Particles and Nuclei Letters	
PPNP	Progress in Particles and Nuclear Physics	
PPSL	Proc. of the Physical Society of London	
PR	Physical Review	
PRAM	Pramana	
PRL	Physical Review Letters	
PRPL	Physics Reports (Physics Letters C)	
PRSE	Proc. of the Royal Society of Edinburgh	
PRSL	Proc. of the Royal Society of London, Section A	
PS	Physica Scripta	
PTP	Progress of Theoretical Physics	
PTPS	Progress of Theoretical Physics Supplement	
PTRSL	Phil. Trans. Royal Society of London	
RA	Radiochimica Acta	
RMP	Reviews of Modern Physics	
RNC	La Rivista del Nuovo Cimento	
RPP	Reports on Progress in Physics	
RRP	Revue Roumaine de Physique	
SCI	Science	
SJNP	Soviet Journal of Nuclear Physics	
SJPN	Soviet Journal of Particles and Nuclei	
SPD	Soviet Physics Doklady (Magazine)	
SPU	Soviet Physics - Uspekhi	
UFN	Usp. Fiz. Nauk - Russian version of SPU	
YAF	Yadernaya Fizika	
ZETF	Zhurnal Eksperimental'noi i Teoreticheskoi Fiziki	
ZETFp	Zhurnal Eksperimental'noi i Teoreticheskoi Fiziki, Pis'ma v Redakts	
ZNAT	Zeitschrift fur Naturforschung	
ZPHY	Zeitschrift fur Physik	
Institutions		
AACH	Phys. Inst. der Techn. Hochschule Aachen (Historical, use for general Inst. der Techn. Hochschule)	Aachen, Germany
AACH1	I Phys. Inst. RWTH Aachen Ib	Aachen, Germany
AACH3	III Phys. Inst. der Techn. Hochschule Aachen	Aachen, Germany
AACHT	Institut für Theoretische Physik E, RWTH Aachen	Aachen , Germany
AARH	Univ. of Aarhus	Aarhus C, Denmark
ABO	Åbo Akademi; Accelerator Lab., Porthankatu 3; Dept. of Physics, Porthansgatan 3	Turku (Åbo), Finland
ADEL	Adelphi Univ.	Garden City, NY, USA
ADLD	The Univ. of Adelaide ; Dept. of Physics; Centre for Subatomic Structure of Matter (CSSM)	Adelaide, SA, Australia
AERE	Atomic Energy Research Establishment.	Didcot, United Kingdom
AFRR	Armed Forces Radiobiology Res. Inst.	Bethesda, MD, USA
AHMED	Physical Research Lab.	Ahmedabad , Gujarat, India
AICH	Aichi Univ. of Education	Aichi, Japan
AKIT	Akita Univ.	Akita, Japan
ALAH	Univ. of Alabama (Huntsville)	Huntsville, AL, USA
ALAT	Univ. of Alabama (Tuscaloosa)	Tuscaloosa, AL, USA
ALBA	SUNY at Albany	Albany, NY, USA
ALBE	Univ. of Alberta	Edmonton, AB, Canada
AMES	Ames Lab.	Ames, IA, USA
AMHT	Amherst College	Amherst, MA, USA
AMST	Univ. van Amsterdam	Amsterdam, The Netherlands
ANIK	NIKHEF	Amsterdam , The Netherlands
ANKA	Middle East Technical Univ.; Dept. of Physics; Experimental HEP Lab	Ankara, Turkey
ANL	Argonne National Lab.; High Energy Physics Division, Bldg. 362; Physics Division, Bldg. 203	Argonne, IL, USA
ANSM	St. Anselm Coll.	Manchester, NH, USA
ARCBO	Arecibo Observatory	Arecibo, PR, USA
ARIZ	Univ. of Arizona	Tucson, AZ, USA
ARZS	Arizona State Univ.	Tempe, AZ, USA
ASCI	Russian Academy of Sciences	Moscow , Russian Federation
AST	Inst. of Phys.	Nankang, Taipei, The Republic of China (Taiwan)
ATEN	NCSR " Demokritos "	Aghia Paraskevi, Greece
ATHU	Univ. of Athens	Athens, Greece
AUCK	Univ. of Auckland	Auckland, New Zealand
BAKU	Natl. Azerbaijan Academy of Sciences , Inst. of Physics	Baku , Azerbaijan
BANGB	Bangabasi College	Calcutta, India
BARC	Univ. Autònoma de Barcelona	Bellaterra (Barcelona), Spain
BARI	Univ. di Bari	Bari, Italy
BART	Univ. of Delaware ; Bartol Research Inst.	Newark, DE, USA
BASL	Inst. für Physik der Univ. Basel	Basel, Switzerland
BAYR	Univ. Bayreuth	Bayreuth, Germany
BCEN	Centre d'Etudes Nucleaires de Bordeaux-Gradignan	Gradignan, France
BCIP	Natl. Inst. for Physics & Nuclear Eng. "Horia Hulubei" (IFIN-HH)	Bucharest -Magurele, Romania
BELJ	Beijing Univ.	Beijing, The People's Republic of China
BELJT	Inst. of Theoretical Physics	Beijing , The People's Republic of China
BELG	Inter-University Inst. for High Energies (ULB-VUB)	Brussel , Belgium
BELL	AT & T Bell Labs	Murray Hill, NJ, USA
BERG	Univ. of Bergen	Bergen, Norway
BERL	DESY	Zurich , Germany
BERN	Univ. of Berne	Berne, Switzerland
BGNA	Univ. di Bologna , & INFN, Sezione di Bologna; Viale C. Berti Pichat, n. 6/2; Via Irnerio, 46, I-40126 Bologna	Bologna, Italy
BHAB	Bhabha Atomic Research Center	Trombay, Bombay, India

Abbreviations Used in the Particle Listings

BHEP	Inst. of High Energy Physics	Beijing , The People's Republic of China	CINV	CINVESTAV-IPN, Centro de Investigacion y de Estudios Avanzados del IPN	México , DF, Mexico
BIEL	Univ. Bielefeld	Bielefeld, Germany	CIT	California Inst. of Tech.	Pasadena, CA, USA
BING	SUNY at Binghamton	Binghamton, NY, USA	CLER	Univ. de Clermont-Ferrand	Aubière, France
BIRK	Birkbeck College, Univ. of London	London, United Kingdom	CLEV	Cleveland State Univ.	Cleveland, OH, USA
BIRM	Univ. of Birmingham	Edgbaston, Birmingham, United Kingdom	CMNS	Comenius Univ. (FMFI UK)	Bratislava , Slovakia
BLSU	Bloomsburg Univ.	Bloomsburg, PA, USA	CMU	Carnegie Mellon Univ.	Pittsburgh, PA, USA
BNL	Brookhaven National Lab.	Upton, NY, USA	CNEA	Comisión Nacional de Energía Atómica	Buenos Aires, Argentina
BOCH	Ruhr Univ. Bochum	Bochum, Germany	CNRC	Centre for Research in Particle Physics	Ottawa, ON, Canada
BOHR	Niels Bohr Inst.	Copenhagen Ø, Denmark	COLO	Univ. of Colorado	Boulder, CO, USA
BOIS	Boise State Univ.	Boise, ID, USA	COLU	Columbia Univ.	New York, NY, USA
BOMB	Univ. of Bombay	Bombay, India	CONC	Concordia University	Montreal, PQ, Canada
BONN	Rheinische Friedrich-Wilhelms-Univ. Bonn	Bonn, Germany	CORN	Cornell Univ.	Ithaca, NY, USA
BORD	Univ. de Bordeaux I	Gradignan, France	COSU	Colorado State Univ.	Fort Collins, CO, USA
BOSE	S.N. Bose National Centre for Basis Sciences	Calcutta, India	CPPM	Centre National de la Recherche Scientifique, Luminy	Marseille , France
BOSK	"Rudjer Bošković" Inst.	Zagreb, Croatia	CRAC	Henryk Niewodnicza'nski Inst. of Nuclear Physics	Kraków , Poland
BOST	Boston Univ.	Boston, MA, USA	CRNL	Chalk River Labs.	Chalk River, ON, Canada
BRAN	Brandeis Univ.	Waltham, MA, USA	CSOK	Oklahoma Central State Univ.	Edmond, OK, USA
BRCO	Univ. of British Columbia	Vancouver, BC, Canada	CST	Univ. of Science and Technology of China	Hefei , Anhui 230026, The People's Republic of China
BRIS	Univ. of Bristol	Bristol, United Kingdom	CSULB	California State Univ.	Long Beach, CA, USA
BROW	Brown Univ.	Providence, RI, USA	CUNY	City College of New York	New York, NY, USA
BRUN	Brunel Univ.	Uxbridge, Middlesex, United Kingdom	CURCP	Univ. Pierre et Marie Curie (Paris VI), LCP	Paris, France
BRUX	Univ. Libre de Bruxelles ; Service de Physique des Particules Élémentaires	Bruxelles, Belgium	CURIN	Univ. Pierre et Marie Curie (Paris VI), LPNHE	Paris, France
BRUXT	Univ. Libre de Bruxelles ; Physique Théorique	Bruxelles, Belgium	CURIT	Univ. Pierre et Marie Curie (Paris VI), LPTHE	Paris, France
BUCH	Univ. of Bucharest	Bucharest-Magurele, Romania	DALH	Dalhousie Univ.	Halifax, NS, Canada
BUDA	KFKI Research Inst. for Particle & Nuclear Physics	Budapest , Hungary	DARE	Daresbury Lab	Cheshire, United Kingdom
BUFF	SUNY at Buffalo	Buffalo, NY, USA	DARM	Tech. Hochschule Darmstadt	Darmstadt, Germany
BURE	Inst. des Hautes Etudes Scientifiques	Bures-sur-Yvette , France	DELA	Univ. of Delaware ; Dept. of Physics & Astronomy; Bartol Research Inst.	Newark, DE, USA
CAEN	Lab. de Physique Corpusculaire, ENSICAEN	Caen , France	DELH	Univ. of Delhi	Delhi, India
CAGL	Univ. degli Studi di Cagliari	Monserrato (CA), Italy	DESY	DESY , Deutsches Elektronen-Synchrotron	Hamburg , Germany
CAIR	Cairo University	Orman, Giza, Cairo, Egypt	DFAB	Escuela de Ingenieros	Bilbao , Spain
CAIW	Carnegie Inst. of Washington	Washington, DC, USA	DOE	Department of Energy	Washington, DC, USA
CALC	Univ. of Calcutta	Calcutta, India	DORT	Univ. Dortmund	Dortmund, Germany
CAMB	DAMTP	Cambridge, United Kingdom	DUKE	Duke Univ.	Durham, NC, USA
CAMP	Univ. Estadual de Campinas (UNICAMP)	Campinas , SP, Brasil	DURH	Univ. of Durham	Durham, United Kingdom
CANB	Australian National Univ.	Canberra, ACT, Australia	DUUC	University College Dublin	Dublin, Ireland
CAPE	University of Cape Town	Rondebosch, Cape Town, South Africa	EDIN	Univ. of Edinburgh	Edinburgh, United Kingdom
CARA	Univ. Central de Venezuela	Caracas, Venezuela	EFI	Enrico Fermi Inst.	Chicago , IL, USA
CARL	Carleton Univ.	Ottawa, ON, Canada	ELMT	Elmhurst College	Elmhurst, IL, USA
CARLC	Carleton College	Northfield, MN, USA	ENSP	l'Ecole Normale Supérieure	Paris , France
CASE	Case Western Reserve Univ.	Cleveland, OH, USA	EOTV	Eötvös University	Budapest, Hungary
CAST	China Center of Advanced Science and Technology	Beijing, The People's Republic of China	EPOL	École Polytechnique	Palaiseau , France
CATA	Univ. di Catania	Catania, Italy	ERLA	Univ. Erlangen-Nurnberg	Erlangen, Germany
CATH	Catholic Univ. of America	Washington, DC, USA	ETH	Univ. Zürich	Zürich, Switzerland
CAVE	Cavendish Lab.	Cambridge, United Kingdom	FERR	Univ. di Ferrara	Ferrara, Italy
CBNM	CBNM	Geel , Belgium	FIRZ	Univ. degli Studi di Firenze	Sesto Fiorentino, Italy
CCAC	Allegheny College	Meadville, PA, USA	FISK	Fisk Univ.	Nashville, TN, USA
CDEF	Univ. Paris VII, Denis Diderot	Paris, France	FLOR	Univ. of Florida	Gainesville, FL, USA
CEA	Cambridge Electron Accelerator (Historical in <i>Review</i>)	Cambridge, MA , USA	FNAL	Fermilab	Batavia, IL, USA
CEBAF	Jefferson Lab—Thomas Jefferson National Accelerator Facility	Newport News, VA, USA	FOM	FOM , Stichting voor Fundamenteel Onderzoek der Materie	JP Utrecht , The Netherlands
CENG	Centre d'Etudes Nucleaires	Grenoble , France	FRAN	Frankfurt Inst. for Advanced Studies (FIAS)	Frankfurt am Main, Germany
CERN	CERN , European Organization for Nuclear Research	Genève, Switzerland	FRAS	Lab. Nazionali di Frascati dell'INFN	Frascati (Roma), Italy
CFPA	Univ. of California, (Berkeley)	Berkeley, CA, USA	FREIB	Albert-Ludwigs Univ.	Freiburg , Germany
CHIC	Univ. of Chicago	Chicago, IL, USA	FREIE	Freie Univ. Berlin	Berlin, Germany
CIAE	China Institute of Atomic Energy	Beijing , The People's Republic of China	FRIB	Univ. de Fribourg	Fribourg, Switzerland
CINC	Univ. of Cincinnati	Cincinnati, OH, USA	FSU	Florida State Univ.; High Energy Physics	Tallahassee, FL, USA

Abbreviations Used in the Particle Listings

FSUSC	Florida State Univ. ; SCS (School of Computational Science)	Tallahassee, FL, USA	INEL	E G and G Idaho , Inc.	Idaho Falls, ID, USA
FUKI	Fukui Univ.	Fukui, Japan	INFN	Ist. Nazionale di Fisica Nucleare (Generic INFN, unknown location)	Various places, Italy
FUKU	Fukushima Univ.	Fukushima, Japan	INNS	Univ. of Innsbruck	Innsbruck , Austria
GENO	Univ. di Genova	Genova, Italy	INPK	Inst. of Nuclear Physics	Kraków , Poland
GEOR	Georgian Academy of Sciences	Tbilisi, Republic of Georgia	INRM	INR , Inst. for Nucl. Research	Moscow , Russian Federation
GESC	General Electric Co.	Schenectady, NY, USA	INUS	KEK , High Energy Accelerator Research Organization	Tokyo, Japan
GEVA	Univ. de Genève	Genève, Switzerland	IOAN	Univ. of Ioannina	Ioannina, Greece
GIES	Univ. Giessen	Giessen, Germany	IOFF	A.F. Ioffe Phys. Tech. Inst.	St. Petersburg , Russian Federation
GIFU	Gifu Univ.	Gifu, Japan	IOWA	Univ. of Iowa	Iowa City, IA, USA
GLAS	Univ. of Glasgow	Glasgow, United Kingdom	IPN	IPN , Inst. de Phys. Nucl.	Orsay , France
GMAS	George Mason Univ.	Fairfax, VA, USA	IPNP	Univ. Pierre et Marie Curie (Paris VI)	Paris, France
GOET	Univ. Göttingen	Göttingen, Germany	IRAD	Inst. du Radium (Historical)	Paris , France
GRAN	Univ. de Granada	Granada, Spain	ISNG	Lab. de Physique Subatomique et de Cosmologie (LPSC)	Grenoble , France
GRAZ	Univ. Graz	Graz, Austria	ISU	Iowa State Univ.	Ames, IA, USA
GRON	Univ. of Groningen	Groningen, The Netherlands	ITEP	ITEP , Inst. of Theor. and Exp. Physics	Moscow , Russian Federation
GSCO	Geological Survey of Canada	Ottawa, ON, Canada	ITHA	Ithaca College	Ithaca, NY, USA
GSI	Darmstadt Gesellschaft für Schwerionenforschung (GSI)	Darmstadt, Germany	IUPU	Indiana Univ., Purdue Univ. Indianapolis	Indianapolis, IN, USA
GUAN	Univ. de Guanajuato	León, Gto., Mexico	JADA	Jadavpur Univ.	Calcutta, India
GUEL	Univ. of Guelph	Guelph, ON, Canada	JAGL	Jagiellonian Univ.	Kraków, Poland
GWU	George Washington Univ.	Washington, DC, USA	JHU	Johns Hopkins Univ.	Baltimore, MD, USA
HAHN	Hahn-Meitner Inst. Berlin GmbH	Berlin, Germany	JINR	JINR , Joint Inst. for Nucl. Research	Dubna , Russian Federation
HAIF	Technion – Israel Inst. of Tech.	Technion, Haifa, Israel	JULI	Forschungszentrum Jülich	Jülich, Germany
HAMB	Univ. Hamburg	Hamburg, Germany	JYV	Univ. of Jyväskylä	Jyväskylä, Finland
HANN	Univ. Hannover	Hannover, Germany	KAGO	Univ. of Kagoshima	Kagoshima-shi, Japan
HARC	Houston Advanced Research Ctr.	The Woodlands, TX, USA	KANS	Univ. of Kansas	Lawrence, KS, USA
HARV	Harvard Univ.	Cambridge, MA, USA	KARL	Univ. Karlsruhe ; (unspecified division) (Historical in <i>Review</i>)	Karlsruhe, Germany
HAWA	Univ. of Hawai'i	Honolulu, HI, USA	KARLE	Univ. Karlsruhe ; Inst. für Experimentelle Kernphysik	Karlsruhe, Germany
HEBR	Hebrew Univ.	Jerusalem, Israel	KARLK	Forschungszentrum Karlsruhe	Karlsruhe, Germany
HEID	Univ. Heidelberg ; (unspecified division) (Historical in <i>Review</i>)	Heidelberg, Germany	KARLT	Univ. Karlsruhe ; Inst. für Theoretische Teilchenphysik	Karlsruhe, Germany
HEIDH	Ruprecht-Karls Univ. Heidelberg	Heidelberg, Germany	KAZA	Kazakh Inst. of High Energy Physics	Alma Ata, Kazakhstan
HEIDP	Univ. Heidelberg ; Physikalisches Inst.	Heidelberg, Germany	KEK	KEK , High Energy Accelerator Research Organization	Ibaraki-ken, Japan
HEIDT	Univ. Heidelberg ; Inst. für Theoretische Physik	Heidelberg, Germany	KENT	Univ. of Kent	Canterbury, United Kingdom
HELH	Univ. of Helsinki ; Dept. of Phys. Sci., High Energy Phys. Div. (SEFO); Dept. of Phys. Sci., Theor. Phys. Div. (TFO); Helsinki Institute of Physics (HIP)	University of Helsinki, Finland	KEYN	Open Univ.	Milton Keynes, United Kingdom
HIRO	Hiroshima Univ.	Higashi-Hiroshima, Japan	KFTI	Kharkov Inst. of Physics and Tech. (KFTI)	Kharkov, Ukraine
HOUS	Univ. of Houston	Houston, TX, USA	KIAE	The Russian Research Center, Kurchatov Inst.	Moscow , Russian Federation
HPC	Hewlett-Packard Corp.	Cupertino, CA, USA	KIAM	Keldysh Inst. of Applied Math., Acad. Sci., Russia	Moscow, Russian Federation
HSCA	Harvard-Smithsonian Center for Astrophysics	Cambridge, MA, USA	KIDR	Vinča Inst. of Nuclear Sciences	Belgrade, Serbia and Montenegro
IAS	Inst. for Advanced Study	Princeton, NJ, USA	KIEV	Institute for Nuclear Research	Kyiv , Ukraine
IASD	Dublin Inst. for Advanced Studies	Dublin, Ireland	KINK	Kinki Univ.	Osaka, Japan
IBAR	Ibaraki Univ.	Ibaraki, Japan	KNTY	Univ. of Kentucky	Lexington, KY, USA
IBM	IBM Corp.	Palo Alto, CA, USA	KOBE	Kobe Univ.	Kobe, Japan
IBMY	IBM	Yorktown Heights, NY, USA	KOMAB	Univ. of Tokyo, Komaba	Tokyo, Japan
IBS	Inst. for Boson Studies	Pasadena, CA, USA	KONAN	Konan Univ.	Kobe, Japan
ICEPP	Univ. of Tokyo ; Int. Center for Elementary Particle Physics (ICEPP)	Tokyo, Japan	KOSI	Inst. of Experimental Physics SAS	Košice , Slovakia
ICRR	Univ. of Tokyo	Chiba, Japan	KYOT	Kyoto Univ. ; Dept. of Physics, Graduate School of Science	Kyoto, Japan
ICTP	Abdus Salam International Centre for Theoretical Physics	Trieste , Italy	KYOTU	Kyoto Univ. ; Yukawa Inst. for Theor. Physics	Kyoto, Japan
IFIC	IFIC (Instituto de Física Corpuscular)	Valencia , Spain	KYUN	Kyungpook National Univ.	Daegu, Republic of Korea
IFRJ	Univ. Federal do Rio de Janeiro	Rio de Janeiro, RJ, Brasil	KYUSH	Kyushu Univ.	Fukuoka, Japan
IIT	Illinois Inst. of Tech.	Chicago, IL, USA	LALO	LAL , Laboratoire de l'Accélérateur Linéaire	Orsay , France
ILL	Univ. of Illinois at Urbana-Champaign	Urbana, IL, USA	LANC	Lancaster Univ.	Lancaster, United Kingdom
ILLC	Univ. of Illinois at Chicago	Chicago, IL, USA	LANL	Los Alamos National Lab. (LANL)	Los Alamos, NM, USA
ILLG	Inst. Laue-Langevin	Grenoble, France			
IND	Indiana Univ.	Bloomington, IN, USA			

Abbreviations Used in the Particle Listings

LAPP	LAPP , Lab. d'Annecy-le-Vieux de Phys. des Particules	Annecy-le-Vieux , France	MIYA	Miyazaki Univ.	Miyazaki-shi, Japan
LASL	U.C. Los Alamos Scientific Lab. (Old name for LANL)	Los Alamos, NM, USA	MONP	Univ. de Montpellier II	Montpellier, France
LATV	Latvian State Univ.	Riga, Latvia	MONS	Univ. de Mons-Hainaut	Mons, Belgium
LAUS	EPFL Lausanne	Lausanne, Switzerland	MONT	Univ. de Montréal ; Pavillon René-J.-A.-Lévesque	Montréal, PQ, Canada
LAVL	Univ. Laval	Quebec, QC, Canada	MONTC	Univ. de Montréal ; Centre de recherches mathématiques	Montréal, PQ, Canada
LBL	Lawrence Berkeley National Lab.	Berkeley, CA, USA	MOSU	Skobeltsyn Inst. of Nuclear Physics, Lomonosov Moscow State Univ.; Experimental HEP Division; Theoretical HEP Division	Moscow , Russian Federation
LCGT	Univ. di Torino	Turin, Italy	MPCM	Max Planck Inst. fur Chemie	Mainz , Germany
LEBD	Lebedev Physical Inst.	Moscow , Russian Federation	MPEI	Moscow Physical Engineering Inst.	Moscow, Russian Federation
LECE	Univ. di Lecce	Lecce, Italy	MPIA	Max-Planck-Institute für Astrophysik	Garching, Germany
LEED	Univ. of Leeds	Leeds, United Kingdom	MPIH	Max-Planck-Inst. für Kernphysik	Heidelberg , Germany
LEHI	Lehigh Univ.	Bethlehem, PA, USA	MPIM	Max-Planck-Inst. für Physik	München , Germany
LEHM	Lehman College of CUNY	Bronx, NY, USA	MSU	Michigan State Univ.	East Lansing, MI, USA
LEID	Univ. Leiden	Leiden, The Netherlands	MTHO	Mount Holyoke College	South Hadley, MA, USA
LEMO	Le Moyne Coll.	Syracuse, NY, USA	MULH	Centre Univ. du Haut-Rhin	Mulhouse, France
LEUV	Katholieke Univ. Leuven	Leuven, Belgium	MUNI	Ludwig-Maximilians-Univ. München	Garching, Germany
LINZ	Univ. Linz	Linz, Austria	MUNT	Tech. Univ. München	Garching, Germany
LISB	Inst. Nacional de Investigacion Cientifica	Lisboa CODEX, Portugal	MURA	Midwestern Univ. Research Assoc. (Historical in <i>Review</i>)	Stroughton, WI, USA
LISBT	Univ. Técnica de Lisboa, Inst. Superior Técnico	Lisboa , Portugal	NAAS	North American Aviation Science Center (Historical in <i>Review</i>)	Thousand Oaks, CA, USA
LIVP	Univ. of Liverpool	Liverpool, United Kingdom	NAGO	Nagoya Univ.	Nagoya, Japan
LLL	Lawrence Livermore Lab. (Old name for LLNL)	Livermore, CA, USA	NAPL	Univ. di Napoli "Federico II"	Napoli, Italy
LLNL	Lawrence Livermore National Lab.	Livermore, CA, USA	NASA	NASA	Greenbelt, MD, USA
LOCK	Lockheed Palo Alto Res. Lab	Palo Alto, CA, USA	NBS	U.S. National Bureau of Standards (Old name for NIST)	Gaithersburg, MD, USA
LOIC	Imperial College of Science Tech. & Medicine	London, United Kingdom	NBSB	National Inst. Standards Tech.	Boulder, CO, USA
LOQM	Queen Mary, Univ. of London	London, United Kingdom	NCAR	National Center for Atmospheric Research	Boulder, CO, USA
LOUC	University College London	London, United Kingdom	NCARO	North Carolina State Univ.	Raleigh , NC, USA
LOUV	Univ. Catholique de Louvain	Louvain-la-Neuve, Belgium	NDAM	Univ. of Notre Dame	Notre Dame, IN, USA
LOWC	Westfield College (Historical, see LOQM (Queen Mary and Westfield joined))	London, United Kingdom	NEAS	Northeastern Univ.	Boston, MA, USA
LRL	U.C. Lawrence Radiation Lab. (Old name for LBL)	Berkeley , CA, USA	NEUC	Univ. de Neuchâtel	Neuchâtel, Switzerland
LSU	Louisiana State Univ.	Baton Rouge, LA, USA	NICEA	Univ. de Nice	Nice, France
LUND	Fysiska Institutionen	Lund , Sweden	NICEO	Observatoire de Nice	Nice, France
LUND	Lund Univ.	Lund, Sweden	NIHO	Nihon Univ.	Tokyo, Japan
LYON	Institute de Physique Nucléaire de Lyon (IPN)	Villeurbanne, France	NIIG	Niigata Univ.	Niigata, Japan
MADE	UAM/CSIC , Inst. de Física Teórica	Madrid , Cantoblanco, Spain	NIJM	Radboud Univ. Nijmegen	ED Nijmegen , The Netherlands
MADR	C.I.E.M.A.T	Madrid , Spain	NIRS	Nat. Inst. Radiological Sciences	Chiba , Japan
MADU	Univ. Autónoma de Madrid	Cantoblanco, Madrid, Spain	NIST	National Institute of Standards & Technology	Gaithersburg, MD, USA
MANI	Univ. of Manitoba	Winnipeg, MB, Canada	NIU	Northern Illinois Univ.	De Kalb, IL, USA
MANZ	Johannes-Gutenberg-Univ.	Mainz , Germany	NMSU	New Mexico State Univ.; Dept. of Physics, MSC 3D; Part. & Nucl. Phys. Group, Box 30001/Dept.	Las Cruces, NM, USA
MARB	Univ. Marburg	Marburg, Germany	NORD	Nordita	Stockholm, Sweden
MARS	Centre de Physique des Particules de Marseille	Marseille, France	NOTT	Univ. of Nottingham	Nottingham, United Kingdom
MASA	Univ. of Massachusetts Amherst	Amherst , MA, USA	NOVM	Inst. of Mathematics	Novosibirsk , Russian Federation
MASB	Univ. of Massachusetts Boston	Boston , MA, USA	NOVO	BINP, Budker Inst. of Nuclear Physics	Novosibirsk , Russian Federation
MASD	Univ. of Massachusetts Dartmouth	N. Dartmouth , MA, USA	NPOL	Polytechnic of North London	London, United Kingdom
MCGI	McGill Univ.	Montreal, QC, Canada	NRL	Naval Research Lab	Washington, DC, USA
MCHS	Univ. of Manchester	Manchester, United Kingdom	NSF	National Science Foundation	Arlington, VA, USA
MCMS	McMaster Univ.	Hamilton, ON, Canada	NTHU	National Tsing Hua Univ.	Hsinchu, The Republic of China (Taiwan)
MEHTA	Harish-Chandra Research Inst.	Allahabad, India	NTUA	National Tech. Univ. of Athens	Athens, Greece
MEIS	Meisei Univ.	Tokyo, Japan	NWES	Northwestern Univ.	Evanston, IL, USA
MELB	Univ. of Melbourne	Victoria, Australia	NYU	New York Univ.	New York, NY, USA
MEUD	Observatoire de Meudon	Meudon, France	OBER	Oberlin College	Oberlin, OH, USA
MICH	Univ. of Michigan	Ann Arbor, MI, USA	OCH	Ochanomizu Univ.	Tokyo, Japan
MILA	Univ. di Milano	Milano, Italy			
MILAI	INFN, Sez. di Milano	Milano, Italy			
MINN	Univ. of Minnesota	Minneapolis, MN, USA			
MISS	Univ. of Mississippi	University, MS, USA			
MISSR	Univ. of Missouri	Rolla, MO, USA			
MIT	MIT Massachusetts Inst. of Technology	Cambridge, MA, USA			
MIU	Maharishi International Univ.	Fairfield, IA, USA			

Abbreviations Used in the Particle Listings

OHIO	Ohio Univ.	Athens, OH, USA	ROSE	Rose-Hulman Inst. of Technology	Terre Haute IN, USA
OKAY	Okayama Univ.	Okayama, Japan	RPI	Rensselaer Polytechnic Inst.	Troy, NY, USA
OKLA	Univ. of Oklahoma	Norman, OK, USA	RUTG	Rutgers , the State Univ. of New Jersey	Piscataway, NJ, USA
OKSU	Oklahoma State Univ.	Stillwater, OK, USA	SACL	CEA Saclay , DAP-NIA; Service d'Etude des Accélérateurs, de Cryogénie et de Magnétisme	Gif-sur-Yvette, France
OREG	Univ. of Oregon ; Inst. of Theor. Science; U.O. Center for High Energy Physics	Eugene, OR, USA	SACLD	CEA Saclay , DAPNIA; Direction	Gif-sur-Yvette, France
ORNL	Oak Ridge National Laboratory	Oak Ridge, TN, USA	SAGA	Saga Univ.	Saga-shi, Japan
ORSAY	Univ. de Paris Sud	Orsay CEDEX, France	SAHA	Saha Inst. of Nuclear Physics	Bidhannagar, Calcutta, India
ORST	Oregon State Univ.	Corvallis, OR, USA	SANG	Kyoto Sangyo Univ.	Kyoto-shi, Japan
OSAK	Osaka Univ.	Osaka, Japan	SANI	Physics Lab., Ist. Superiore di Sanità	Roma , Italy
OSKC	Osaka City Univ.	Osaka-shi, Japan	SASK	Univ. of Saskatchewan	Saskatoon, SK, Canada
OSLO	Univ. of Oslo	Oslo, Norway	SASSO	Lab. Naz. Gran Sasso dell'INFN	Assergi (AQ), Italy
OSU	Ohio State Univ.	Columbus, OH, USA	SAVO	Univ. de Savoie	Chambery, France
OTTA	Univ. of Ottawa	Ottawa, ON, Canada	SBER	California State Univ.	San Bernardino , CA, USA
OXF	University of Oxford	Oxford, United Kingdom	SCHAF	W.J. Schafer Assoc.	Livermore, DA, USA
OXFTP	Univ. of Oxford	Oxford, United Kingdom	SCIT	Science Univ. of Tokyo	Tokyo, Japan
PADO	Univ. degli Studi di Padova	Padova, Italy	SCOT	Scottish Univ. Research and Reactor Ctr.	Glasgow, United Kingdom
PARIN	Univ. Paris VI et Paris VII , IN ² P ³ /CNRS	Paris, France	SCUC	Univ. of South Carolina	Columbia, SC, USA
PARIS	Univ. de Paris (Historical)	Paris , France	SEAT	Seattle Pacific Coll.	Seattle, WA, USA
PARIT	Univ. Paris VII , LPTHE	Paris, France	SEIB	Austrian Research Center, Seibersdorf LTD.	Seibersdorf, Austria
PARM	Gruppo Collegato INFN	Parma, Italy	SEOU	Korea Univ.; Dept. of Physics; HEP Group	Seoul, Republic of Korea
PAST	Institut Pasteur	Paris , France	SEOUL	Seoul National Univ.; Dept. of Physics & Astronomy, Coll. of Natural Sciences; Center for Theoretical Physics	Seoul, Republic of Korea
PATR	Univ. of Patras	Patras, Greece	SERP	IHEP , Inst. for High Energy Physics	Protvino, Russian Federation
PAVI	Univ. di Pavia	Pavia, Italy	SETO	Seton Hall Univ.	South Orange, NJ, USA
PENN	Univ. of Pennsylvania	Philadelphia, PA, USA	SFLA	Univ. of South Florida	Tampa, FL, USA
PGIA	INFN, Sezione di Perugia	Perugia, Italy	SFRA	Simon Fraser University	Burnaby, BC, Canada
PISA	Univ. di Pisa	Pisa, Italy	SFSU	California State Univ.	San Francisco , CA, USA
PISAI	INFN, Sez. di Pisa	Pisa, Italy	SHAMS	Ain Shams University	Abbassia, Cairo, Egypt
PITT	Univ. of Pittsburgh	Pittsburgh, PA, USA	SHEF	Univ. of Sheffield	Sheffield, United Kingdom
PLAT	SUNY at Plattsburgh	Plattsburgh, NY, USA	SHMP	Univ. of Southampton	Southampton, United Kingdom
PLRM	Univ. di Palermo	Palermo, Italy	SIEG	Univ. Siegen	Siegen, Germany
PNL	Battelle Memorial Inst.	Richland, WA, USA	SILES	Univ. of Silesia	Katowice, Poland
PNPI	Petersburg Nuclear Physics Inst. of Russian Academy of Sciences	Gatchina, Russian Federation	SIN	Swiss Inst. of Nuclear Research (Old name for VILL)	Villigen , Switzerland
PPA	Princeton-Penn. Proton Accelerator (Historical in <i>Review</i>)	Princeton, NJ, USA	SING	National Univ. of Singapore	Kent Ridge, Singapore
PRAG	Inst. of Physics, ASCR	Prague , Czech Republic	SISSA	Scuola Internazionale Superiore di Studi Avanzati	Trieste , Italy
PRIN	Princeton Univ.	Princeton, NJ, USA	SLAC	Stanford Linear Accelerator Center	Menlo Park, CA, USA
PSI	Paul Scherrer Inst.	Villigen PSI, Switzerland	SLOV	Inst. of Physics, Slovak Acad. of Sciences	Bratislava , Slovakia
PSLL	Physical Science Lab	Las Cruces, NM, USA	SMU	Southern Methodist Univ.	Dallas, TX, USA
PSU	Penn State Univ.	University Park, PA, USA	SNSP	Scuola Normale Superiore	Pisa , Italy
PUCB	Pontificia Univ. Católica do Rio de Janeiro	Rio de Janeiro, RJ, Brasil	SOFI	Inst. for Nuclear Research and Nuclear Energy	Sofia , Bulgaria
PUEB	Univ. Autonoma de Puebla	Puebla , Pue, Mexico	SOFU	Univ. of Sofia "St. Kliment Ohridski"	Sofia, Bulgaria
PURD	Purdue Univ.	West Lafayette, IN, USA	SPAUL	Univ. de São Paulo	São Paulo, SP, Brasil
QUKI	Queen's Univ.	Kingston, ON, Canada	SPIFT	Inst. de Física Teórica (IFT)	São Paulo , SP, Brasil
RAL	Rutherford Appleton Lab.	Didcot, Oxfordshire, United Kingdom	SSL	Univ. of California (Berkeley)	Berkeley, CA, USA
REGE	Univ. Regensburg	Regensburg, Germany	STAN	Stanford Univ.	Stanford, CA, USA
REHO	Weizmann Inst. of Science	Rehovot, Israel	STEV	Stevens Inst. of Tech.	Hoboken, NJ, USA
RHBL	Royal Holloway, Univ. of London	Egham, Surrey, United Kingdom	STLO	St. Louis Univ.	St. Louis, MO, USA
RHEL	Rutherford High Energy Lab (Old name for RAL)	Chilton, Didcot, Oxon., United Kingdom	STOH	Stockholm Univ.	Stockholm, Sweden
RICE	Rice Univ.	Houston, TX, USA	STON	SUNY at Stony Brook	Stony Brook, NY, USA
RIKEN	Riken Accelerator Research Facility (RARF), Cyclotron Lab	Saitama, Japan	STRB	Inst. Pluridisciplinaire Hubert Curien (CNRS)	Strasbourg , France
RIKK	Rikkyo Univ.	Tokyo, Japan	STUT	Univ. Stuttgart	Stuttgart, Germany
RIS	Rowland Inst. for Science	Cambridge, MA, USA	STUTM	Max-Planck-Inst.	Stuttgart , Germany
RISC	Rockwell International	Thousand Oaks, CA, USA	SUGI	Sugiyama Jogakuen Univ.	Aichi, Japan
RISL	Universities Research Reactor	Risley , Warrington, United Kingdom	SURR	Univ. of Surrey	Guildford, Surrey, United Kingdom
RISO	Riso National Laboratory	Roskilde, Denmark	SUSS	Univ. of Sussex	Brighton, United Kingdom
RL	Rutherford High Energy Lab (Old name for RAL)	Chilton, Didcot, Oxon., United Kingdom			
RMCS	Royal Military Coll. of Science	Swindon, Wilts., United Kingdom			
ROCH	Univ. of Rochester	Rochester, NY, USA			
ROCK	Rockefeller Univ.	New York, NY, USA			
ROMA	Univ. di Roma (Historical)	Roma , Italy			
ROMA2	Univ. di Roma , "Tor Vergata"	Roma, Italy			
ROMAI	INFN, Sez. di Roma	Roma, Italy			

Abbreviations Used in the Particle Listings

SVR	Savannah River Labs.	Aiken, SC, USA	UNCCH	Univ. of North Carolina at Chapel Hill	Chapel Hill, NC, USA
SYDN	Univ. of Sydney	Sydney, NSW, Australia	UNCS	Union College	Schenectady, NY, USA
SYRA	Syracuse Univ.	Syracuse, NY, USA	UNH	Univ. of New Hampshire	Durham, NH, USA
TAJK	Acad. Sci., Tadjhik SSR	Dushanbe , Tadjzhikstan	UNM	Univ. of New Mexico	Albuquerque, NM, USA
TAMU	Texas A&M Univ.	College Station, TX, USA	UOEH	Univ. of Occupational and Environmental Health	Kitakyushu , Japan
TATA	Tata Inst. of Fundamental Research	Bombay, India	UPNJ	Uppsala College	East Orange, NJ, USA
TBIL	Tbilisi State University	Tbilisi, Republic of Georgia	UPPS	Uppsala Univ.	Uppsala , Sweden
TELA	Tel-Aviv Univ.	Tel Aviv, Israel	UPR	Univ. of Puerto Rico	Rio Piedras , PR, USA
TELE	Teledyne Brown Engineering	Huntsville, AL, USA	URI	Univ. of Rhode Island	Kingston, RI, USA
TEMP	Temple Univ.	Philadelphia, PA, USA	USC	Univ. of Southern California	Los Angeles, CA, USA
TENN	Univ. of Tennessee	Knoxville, TN, USA	USF	Univ. of San Francisco	San Francisco, CA, USA
TEXA	Univ. of Texas at Austin	Austin, TX, USA	UTAH	Univ. of Utah ; Dept. of Physics; High-Energy Astrophysics Inst.	Salt Lake City, UT, USA
TGAK	Tokyo Gakugei Univ.	Tokyo, Japan	UTRE	Univ. of Utrecht	Utrecht, The Netherlands
TGU	Tohoku Gakuin Univ.	Miyagi, Japan	UTRO	Norwegian Univ. of Science & Technology	Trondheim, Norway
THES	Aristotle Univ. of Thessaloniki (AUPh)	Thessaloniki, Greece	UZINR	Acad. Sci., Ukrainian SSR	Uzhgorod , Ukraine
TINT	Tokyo Inst. of Technology	Tokyo, Japan	VALE	Univ. de Valencia	Burjassot, Valencia , Spain
TISA	Sagamihara Inst. of Space & Astronautical Sci.	Kanagawa, Japan	VALP	Valparaiso Univ.	Valparaiso, IN, USA
TMSK	Nuclear Physics Institute	Tomsk , Russian Federation	VAND	Vanderbilt Univ.	Nashville, TN, USA
TMTC	Tokyo Metropolitan Coll. Tech.	Tokyo, Japan	VASS	Vassar College	Poughkeepsie, NY, USA
TMU	Tokyo Metropolitan Univ.	Tokyo, Japan	VICT	Univ. of Victoria	Victoria, BC, Canada
TNTO	Univ. of Toronto	Toronto, ON, Canada	VIEN	Inst. für Hochenergiephysik (HEPHY)	Vienna , Austria
TOHO	Toho Univ.	Chiba, Japan	VILL	Inst. for Particle Physics of ETH Zürich	Zürich , Switzerland
TOHOK	Tohoku Univ.	Sendai, Japan	VRG	Univ. of Virginia	Charlottesville, VA, USA
TOKA	Tokai Univ.	Shimizu, Japan	VPI	Virginia Tech.	Blacksburg, VA, USA
TOKAH	Tokai Univ.	Hiratsuka, Japan	VRIJ	Vrije Univ.	HV Amsterdam , The Netherlands
TOKMS	Univ. of Tokyo ; Meson Science Laboratory	Tokyo, Japan	WABRN	Eidgenössisches Amt für Messwesen	Waber , Switzerland
TOKU	Univ. of Tokushima	Tokushima-shi, Japan	WARS	Warsaw Univ.	Warsaw, Poland
TOKY	Univ. of Tokyo ; High-Energy Physics Theory Group	Tokyo, Japan	WASCR	Waseda Univ.; Cosmic Ray Division	Tokyo, Japan
TOKYC	Univ. of Tokyo ; Dept. of Chemistry	Tokyo, Japan	WASH	Univ. of Washington ; Elem. Particle Experiment (EPE); Particle Astrophysics (PA)	Seattle, WA, USA
TORI	Univ. degli Studi di Torino	Torino, Italy	WASU	Waseda Univ.; Dept. of Physics, High Energy Physics Group	Tokyo, Japan
TPTI	Uzbek Academy of Sciences	Tashkent , Republic of Uzbekistan	WAYN	Wayne State Univ.	Detroit, MI, USA
TRIN	Trinity College Dublin	Dublin, Ireland	WESL	Wesleyan Univ.	Middletown, CT, USA
TRIU	TRIUMF	Vancouver, BC, Canada	WIEN	Univ. Wien	Vienna, Austria
TRST	Univ. di Trieste	Trieste, Italy	WILL	Coll. of William and Mary	Williamsburg, VA, USA
TRSTI	INFN, Sez. di Trieste	Trieste, Italy	WINR	Andrzej Soltan Inst. for Nuclear Studies	Warsaw , Poland
TRSTT	Univ. degli Studi di Trieste	Trieste , Italy	WISC	Univ. of Wisconsin	Madison, WI, USA
TSUK	Univ. of Tsukuba	Ibaraki-ken, Japan	WITW	Univ. of the Witwatersrand	Wits, South Africa
TTAM	Tamagawa Univ.	Tokyo, Japan	WMIU	Western Michigan Univ.	Kalamazoo, MI, USA
TUAT	Tokyo Univ. of Agriculture Tech.	Tokyo, Japan	WONT	The Univ. of Western Ontario	London, ON, Canada
TUBIN	Univ. Tübingen	Tübingen, Germany	WOOD	Woodstock College (No longer in existence)	Woodstock, MD, USA
TUFTS	Tufts Univ.	Medford, MA, USA	WUPP	Bergische Univ. Wuppertal	Wuppertal , Germany
TUW	Technische Univ. Wien	Vienna, Austria	WURZ	Univ. Würzburg	Würzburg, Germany
TUZL	Tuzla Univ.	Tuzla, Argentina	WUSL	Washington Univ.	St. Louis, MO, USA
UCB	Univ. of California (Berkeley)	Berkeley, CA, USA	WYOM	Univ. of Wyoming	Laramie, WY, USA
UCD	Univ. of California (Davis)	Davis, CA, USA	YALE	Yale Univ.	New Haven, CT, USA
UCI	Univ. of California (Irvine)	Irvine, CA, USA	YARO	Yaroslavl State Univ.	Yaroslavl, Russian Federation
UCLA	Univ. of California (Los Angeles)	Los Angeles, CA, USA	YCC	Yokohama Coll. of Commerce	Yokohama, Japan
UCND	Union Carbide Corp.	Oak Ridge, TN, USA	YERE	Yerevan Physics Inst.	Yerevan, Armenia
UCR	Univ. of California (Riverside)	Riverside, CA, USA	YOKO	Yokohama National Univ.	Yokohama-shi, Japan
UCSB	Univ. of California (Santa Barbara) ; Physics Dept.	Santa Barbara, CA, USA	YORKC	York Univ.	Toronto, Canada
UCSBT	Univ. of California (Santa Barbara) ; Kavli Inst. for Theoretical Physics	Santa Barbara, CA, USA	ZAGR	Zagreb Univ.	Zagreb, Croatia
UCSC	Univ. of California (Santa Cruz)	Santa Cruz, CA, USA	ZARA	Univ. de Zaragoza	Zaragoza, Spain
UCSD	Univ. of California (San Diego)	La Jolla, CA, USA	ZEEM	Univ. van Amsterdam	TV Amsterdam, The Netherlands
UMD	Univ. of Maryland	College Park, MD, USA	ZURI	Univ. Zürich	Zürich, Switzerland
UNC	Univ. of North Carolina	Greensboro, NC, USA			



GAUGE AND HIGGS BOSONS

γ	385
g (gluon)	385
graviton	385
W	386
Z	393
Higgs Bosons — H^0 and H^\pm	414
Heavy Bosons Other than Higgs Bosons	443
Axions (A^0) and Other Very Light Bosons	459

Notes in the Gauge and Higgs Boson Listings

The Mass of the W Boson (rev.)	386
Triple Gauge Couplings	389
Anomalous W/Z Quartic Couplings	392
The Z Boson (rev.)	393
Anomalous $ZZ\gamma$, $Z\gamma\gamma$, and ZZV Couplings	411
Anomalous W/Z Quartic Couplings	412
Searches for Higgs Bosons (rev.)	414
The W' Searches (rev.)	443
The Z' Searches (rev.)	446
Leptoquark Quantum Numbers (new)	452
Axions and Other Very Light Bosons (new)	459





GAUGE AND HIGGS BOSONS

 γ

$$I(J^PC) = 0,1(1^{-})$$

 γ MASS

For a review of the photon mass, see BYRNE 77.

VALUE (eV)	CL%	DOCUMENT ID	TECN	COMMENT
< 1	$\times 10^{-18}$	1 RYUTOV 07		MHD of solar wind
••• We do not use the following data for averages, fits, limits, etc. •••				
< 1	$\times 10^{-26}$	2 ADELBERGER 07A		Galactic field existence if Higgs mass
< 1.4	$\times 10^{-7}$	ACCIOLY 04		Dispersion of GHz radio waves by sun
< 2	$\times 10^{-16}$	FULLEKRUG 04		Speed of 5-50 Hz radiation in atmosphere
< 7	$\times 10^{-19}$	3 LUO 03		Modulation torsion balance
< 1	$\times 10^{-17}$	4 LAKES 98		Torque on toroid balance
< 6	$\times 10^{-17}$	5 RYUTOV 97		MHD of solar wind
< 9	$\times 10^{-16}$	90 6 FISCHBACH 94		Earth magnetic field
<(4.73±0.45) $\times 10^{-12}$		7 CHERNIKOV 92	SQID	Ampere-law null test
<(9.0 ± 8.1) $\times 10^{-10}$		8 RYAN 85		Coulomb-law null test
< 3	$\times 10^{-27}$	9 CHIBISOV 76		Galactic magnetic field
< 6	$\times 10^{-16}$	99.7 DAVIS 75		Jupiter magnetic field
< 7.3	$\times 10^{-16}$	HOLLWEG 74		Alfven waves
< 6	$\times 10^{-17}$	10 FRANKEN 71		Low freq. res. cir.
< 1	$\times 10^{-14}$	WILLIAMS 71	CNTR	Tests Gauss law
< 2.3	$\times 10^{-15}$	GOLDHABER 68		Satellite data
< 6	$\times 10^{-15}$	10 PATEL 65		Satellite data
< 6	$\times 10^{-15}$	GINTSBURG 64		Satellite data

- 1 RYUTOV 07 extends the method of RYUTOV 67 to the radius of Pluto's orbit.
- 2 When trying to measure m one must distinguish between measurements performed on large and small scales. If the photon acquires mass by the Higgs mechanism, the large-scale behavior of the photon might be effectively Maxwellian. If, on the other hand, one postulates the Proca regime for all scales, the very existence of the galactic field implies $m < 10^{-26}$ eV, as correctly calculated by YAMAGUCHI 59 and CHIBISOV 76.
- 3 LUO 03 determine a limit on $\mu^2 A < 1.1 \times 10^{-11}$ T m/m² (with μ^{-1} =characteristic length for photon mass; A=ambient vector potential) — similar to the LAKES 98 technique. Unlike LAKES 98 who used static, the authors used dynamic torsion balance. Assuming A to be 10^{12} T m, they obtain $\mu < 1.2 \times 10^{-51}$ g, equivalent to 6.7×10^{-19} eV. The rotating modified Cavendish balance removes dependence on the direction of A . GOLDHABER 03 argue that because plasma current effects are neglected, the LUO 03 limit does not provide the best available limit on $\mu^2 A$ nor a reliable limit at all on μ . The reason is that the A associated with cluster magnetic fields could become arbitrarily small in plasma voids, whose existence would be compatible with present knowledge. LUO 03 reply that fields of distant clusters are not accurately mapped, but assert that a zero A is unlikely given what we know about the magnetic field in our galaxy.
- 4 LAKES 98 reports limits on torque on a toroid Cavendish balance, obtaining a limit on $\mu^2 A < 2 \times 10^{-9}$ Tm/m² via the Maxwell-Proca equations, where μ^{-1} is the characteristic length associated with the photon mass and A is the ambient vector potential in the Lorentz gauge. Assuming $A \approx 1 \times 10^{12}$ Tm due to cluster fields he obtains $\mu^{-1} > 2 \times 10^{10}$ m, corresponding to $\mu < 1 \times 10^{-17}$ eV. A more conservative limit, using $A \approx (1 \mu\text{G}) \times (600 \text{ pc})$ based on the galactic field, is $\mu^{-1} > 1 \times 10^9$ m or $\mu < 2 \times 10^{-16}$ eV.
- 5 RYUTOV 97 uses a magnetohydrodynamics argument concerning survival of the Sun's field to the radius of the Earth's orbit. "To reconcile observations to theory, one has to reduce [the photon mass] by approximately an order of magnitude compared with" DAVIS 75.
- 6 FISCHBACH 94 report $< 8 \times 10^{-16}$ with unknown CL. We report Bayesian CL used elsewhere in these Listings and described in the Statistics section.
- 7 CHERNIKOV 92 measures the photon mass at 1.24 K, following a theoretical suggestion that electromagnetic gauge invariance might break down at some low critical temperature. See the erratum for a correction, included here, to the published result.
- 8 RYAN 85 measures the photon mass at 1.36 K (see the footnote to CHERNIKOV 92).
- 9 CHIBISOV 76 depends in critical way on assumptions such as applicability of virial theorem. Some of the arguments given only in unpublished references.
- 10 See criticism questioning the validity of these results in GOLDHABER 71, PARK 71 and KROLL 71. See also review GOLDHABER 71b.

 γ CHARGE

VALUE (e)	DOCUMENT ID	TECN	COMMENT
< 5 $\times 10^{-30}$	11 RAFFELT 94	TOF	Pulsar $f_1 - f_2$
••• We do not use the following data for averages, fits, limits, etc. •••			
< 8.5 $\times 10^{-17}$	12 SEMERTZIDIS 03		Laser light deflection in B-field
< 2 $\times 10^{-28}$	13 COCCONI 92		VLBA radio telescope resolution
< 2 $\times 10^{-32}$	COCCONI 88	TOF	Pulsar $f_1 - f_2$ TOF
11 RAFFELT 94 notes that COCCONI 88 neglects the fact that the time delay due to dispersion by free electrons in the interstellar medium has the same photon energy dependence as that due to bending of a charged photon in the magnetic field. His limit is based on the assumption that the entire observed dispersion is due to photon charge. It is a factor of 200 less stringent than the COCCONI 88 limit.			
12 SEMERTZIDIS 03 reports the first laboratory limit on the photon charge in the last 30 years. Straightforward improvements in the apparatus could attain a sensitivity of 10^{-20} e.			
13 See COCCONI 92 for less stringent limits in other frequency ranges. Also see RAFFELT 94 note.			

 γ REFERENCES

ADELBERGER 07A	PRL 98 010402	E. Adelberger, G. Dvali, A. Gruzinov (WASH, NYU)
RYUTOV 07	PPCF 49 B429	D.D. Ryutov (LLNL)
ACCIOLY 04	PR D69 107501	A. Accioly, R. Paszko
FULLEKRUG 04	PRL 93 043901	M. Fullekrug
GOLDHABER 03	PRL 91 149101	A.S. Goldhaber, M.M. Nieto
LUO 03	PRL 90 081801	J. Luo et al.
LUO 03B	PRL 91 149102	J. Luo et al.
SEMERTZIDIS 03	PR D67 017701	Y.K. Semertzidis, G.T. Danby, D.M. Lazarus
LAKES 98	PRL 80 1826	R. Lakes (WIS C)
RYUTOV 97	PPCF 39 A73	D.D. Ryutov (LLNL)
FISCHBACH 94	PRL 73 514	E. Fischbach et al. (PURD, JHU+)
RAFFELT 94	PR D50 7729	G. Raffelt (MFM)
CHERNIKOV 92	PRL 68 3383	M.A. Chernikov et al. (ETH)
Also	PRL 69 2999 (erratum)	M.A. Chernikov et al. (ETH)
COCCONI 92	AJP 60 750	G. Cocconi (CERN)
COCCONI 88	PL B206 705	G. Cocconi (CERN)
RYAN 85	PR D32 802	J.J. Ryan, F. Accetta, R.H. Austin (PRIN)
BYRNE 77	Ast.Sp.Sci. 46 115	J. Byrne (LOIC)
CHIBISOV 76	SPU 19 624	G.V. Chibisov (LEBD)
DAVIS 75	PRL 35 1402	L. Davis, A.S. Goldhaber, M.M. Nieto (CIT, STON+)
HOLLWEG 74	PRL 32 961	J.V. Hollweg (NCAR)
FRANKEN 71	PRL 26 115	P.A. Franken, G.W. Ampulski (MICH)
GOLDHABER 71	PRL 26 1390	A.S. Goldhaber, M.M. Nieto (STON, BOHR, UCSB)
GOLDHABER 71B	RMP 43 277	A.S. Goldhaber, M.M. Nieto (STON, BOHR, UCSB)
KROLL 71	PRL 26 1395	N.M. Kroll (SLAC)
PARK 71	PRL 26 1393	D. Park, E.R. Williams (WILC)
WILLIAMS 71	PRL 26 721	E.R. Williams, J.E. Faller, H.A. Hill (WESL)
GOLDHABER 68	PRL 21 567	A.S. Goldhaber, M.M. Nieto (STON)
PATEL 65	PL 14 105	V.L. Patel (DUKE)
GINTSBURG 64	Sov. Astr. AJ7 536	M.A. Gintsburg (ASCI)
YAMAGUCHI 59	PTPS 11 37	Y. Yamaguchi

 g
or gluon

$$I(J^P) = 0(1^{-})$$

SU(3) color octet

Mass $m = 0$. Theoretical value. A mass as large as a few MeV may not be precluded, see YNDURAIN 95.

VALUE	DOCUMENT ID	TECN	COMMENT
••• We do not use the following data for averages, fits, limits, etc. •••			
	ABREU 92E	DLPH	Spin 1, not 0
	ALEXANDER 91H	OPAL	Spin 1, not 0
	BEHREND 82D	CELL	Spin 1, not 0
	BERGER 80D	PLUT	Spin 1, not 0
	BRANDELIK 80C	TASS	Spin 1, not 0

gluon REFERENCES

YNDURAIN 95	PL B345 524	F.J. Yndurain (MADU)
ABREU 92E	PL B274 498	P. Abreu et al. (DELPHI Collab.)
ALEXANDER 91H	ZPHY C52 543	G. Alexander et al. (OPAL Collab.)
BEHREND 82D	PL B110 329	H.J. Behrend et al. (CELLO Collab.)
BERGER 80D	PL B97 459	C. Berger et al. (PLUTO Collab.)
BRANDELIK 80C	PL B97 453	R. Brandelik et al. (TASSO Collab.)

graviton

$$J = 2$$

OMITTED FROM SUMMARY TABLE

graviton MASS

All of the following limits are obtained assuming Yukawa potential in weak field limit. VANDAM 70 argue that a massive field cannot approach general relativity in the zero-mass limit; however, see GOLDHABER 74 and references therein. h_0 is the Hubble constant in units of $100 \text{ km s}^{-1} \text{ Mpc}^{-1}$.

VALUE (eV)	DOCUMENT ID	COMMENT
••• We do not use the following data for averages, fits, limits, etc. •••		
< 7 $\times 10^{-32}$	1 CHOUDHURY 04	Weak gravitational lensing
< 7.6 $\times 10^{-20}$	2 FINN 02	Binary Pulsars
	3 DAMOUR 91	Binary pulsar PSR 1913+16
< 2 $\times 10^{-29} h_0^{-1}$	GOLDHABER 74	Rich clusters
< 7 $\times 10^{-28}$	HARE 73	Galaxy
< 8 $\times 10^4$	HARE 73	2 γ decay

- 1 CHOUDHURY 04 sets limits based on nonobservation of a distortion in the measured values of the variance of the power spectrum.
- 2 FINN 02 analyze the orbital decay rates of PSR B1913+16 and PSR B1534+12 with a possible graviton mass as a parameter. The combined frequentist mass limit is at 90% CL.
- 3 DAMOUR 91 is an analysis of the orbital period change in binary pulsar PSR 1913+16, and confirms the general relativity prediction to 0.8%. "The theoretical importance of the [rate of orbital period decay] measurement has long been recognized as a direct confirmation that the gravitational interaction propagates with velocity c (which is the immediate cause of the appearance of a damping force in the binary pulsar system) and thereby as a test of the existence of gravitational radiation and of its quadrupolar nature." TAYLOR 93 adds that orbital parameter studies now agree with general relativity to 0.5%, and set limits on the level of scalar contribution in the context of a family of tensor [spin 2]-biscalar theories.

Gauge & Higgs Boson Particle Listings

graviton, W

graviton REFERENCES

CHOUDHURY	04	ASP 21 559	S.R. Choudhury <i>et al.</i>	(DELPH, MELB)
FINN	02	PR D65 044022	L.S. Finn, P.J. Sutton	
TAYLOR	93	NAT 355 132	J.N. Taylor <i>et al.</i>	(PRIN, ARCEO, BURE+)
DAMOUR	91	APJ 366 501	T. Damour, J.H. Taylor	(BURE, MEUD, PRIN)
GOLDBABER	74	PR D9 1119	A.S. Goldhaber, M.M. Nieto	(LANL, STON)
HARE	73	CJP 51 431	M.G. Hare	(SASK)
VANDAM	70	NP B22 397	H. van Dam, M. Veltman	(UTRE)

W

$J = 1$

THE MASS AND WIDTH OF THE W BOSON

Revised March 2008 by C. Caso (University of Genova), M. W. Grünewald (University College Dublin and University Ghent), and A. Gurtu (Tata Institute).

The W mass and width definition used here corresponds to a Breit-Wigner with mass-dependent width.

Until 1995, the production and study of the W boson was the exclusive domain of the $\bar{p}p$ colliders at CERN and Fermilab. W production at hadron colliders is tagged by a high p_T lepton from W decay. Owing to unknown parton-parton effective energy and missing energy in the longitudinal direction, the experiments reconstruct only the transverse mass of the W , and derive the W mass from comparing the transverse mass distribution with Monte Carlo predictions as a function of M_W . These analyses use the electron and muon decay modes.

Beginning in 1996, the energy of the LEP accelerator increased to above 161 GeV, the threshold for W -pair production. A precise knowledge of the e^+e^- center-of-mass energy enables one to reconstruct the W mass, even if one of them decays leptonically. At LEP two methods have been used to obtain the W mass. In the first method the measured W -pair production cross sections, $\sigma(e^+e^- \rightarrow W^+W^-)$, have been used to determine the W mass using the predicted dependence of this cross section on M_W . At 161 GeV, which is just above the W -pair production threshold, this dependence is a much more sensitive function of the W mass than at the higher energies (172 to 209 GeV) at which LEP ran during 1996–2000. In the second method, which is used at the higher energies, the W mass has been determined by directly reconstructing the W and its invariant mass from its decay products.

Each LEP experiment has combined their own mass values properly taking into account the common systematic errors. In order to compute the LEP average W mass, each experiment has provided its measured W mass for the $q\bar{q}q\bar{q}$ and $q\bar{q}\ell\bar{\nu}_\ell$, $\ell = e, \mu, \tau$ channels at each center-of-mass energy, along with a detailed break-up of errors (statistical and uncorrelated, partially correlated and fully correlated systematics [1]). These have been properly combined to obtain a LEP W mass of $M_W = 80.376 \pm 0.033$ GeV, which includes W mass determination from W -pair production cross section variation at threshold. Errors due to uncertainties in LEP energy (9 MeV), and possible effect of color reconnection (CR) and Bose-Einstein correlations (BEC) between quarks from different W 's (8 MeV) are included. The mass difference between $q\bar{q}q\bar{q}$ and $q\bar{q}\ell\bar{\nu}_\ell$ final states (due to possible CR and BEC effects) is -12 ± 45 MeV.

In a similar manner, the width results obtained at LEP have been combined, resulting in $\Gamma_W = 2.196 \pm 0.083$ GeV [1].

The two Tevatron experiments have also carried out the exercise of identifying common systematic errors and obtain an average W mass of $M_W = 80.430 \pm 0.040$ GeV and a preliminary W width of $\Gamma_W = 2.049 \pm 0.058$ GeV [2].

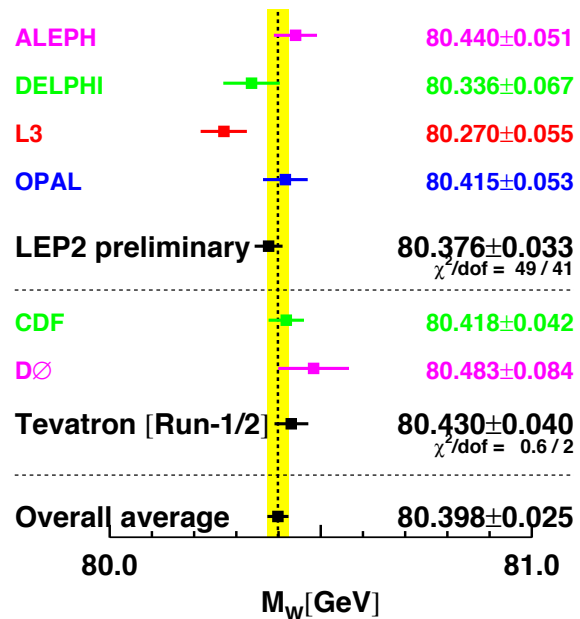


Figure 1: Measurements of the W -boson mass by the LEP and Tevatron experiments. Color version at end of book.

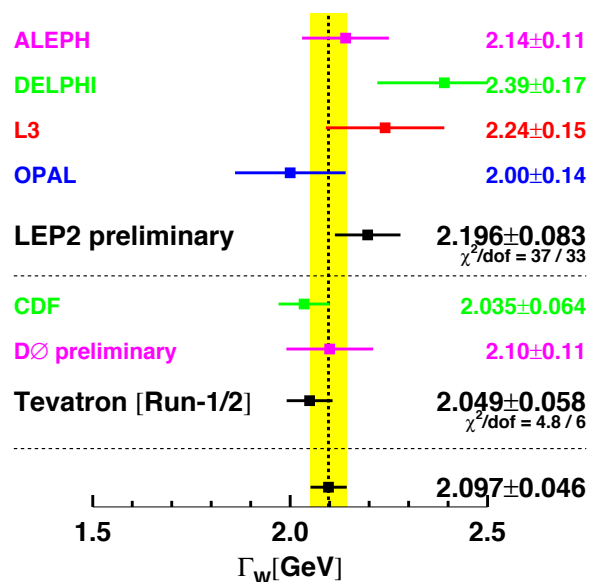


Figure 2: Measurements of the W -boson width by the LEP and Tevatron experiments. Color version at end of book.

The LEP and Tevatron results on mass and width, which are based on all published and preliminary results available, are compared in Fig. 1 and Fig. 2. Combining these results, assuming no common systematics between the LEP and Tevatron measurements, yields an average W mass of $M_W = 80.398 \pm 0.025$ GeV and a preliminary W width of $\Gamma_W = 2.097 \pm 0.046$ GeV.

The Standard Model prediction from the electroweak fit, using Z -pole data plus m_{top} measurement, gives a W -boson mass of $M_W = 80.360 \pm 0.020$ GeV and a W -boson width of $\Gamma_W = 2.091 \pm 0.002$ GeV [3].

OUR FIT in the listing below is obtained by combining only published LEP and Tevatron results using the same procedure as above.

References

1. The LEP Collaborations: ALEPH, DELPHI, L3, OPAL, the LEP Electroweak Working Group, CERN-PH-EP/2006-042, hep-ex/0612034 (14 December 2006).
2. The Tevatron Electroweak Working Group, for the CDF and DØ Collaborations: *Combination of CDF and DØ Results on the W Boson Mass and Width*, March 2008 (unpublished).
3. The LEP Collaborations: ALEPH, DELPHI, L3, OPAL, the LEP Electroweak Working Group, CERN-PH-EP/2007-039, arXiv:0712.0929 [hep-ex] (6 December 2007).

W MASS

The W -mass listed here corresponds to the mass parameter in a Breit-Wigner distribution with mass-dependent width. To obtain the world average, common systematics between experiments are properly taken into account. The LEP average W mass based on published results is 80.376 ± 0.030 GeV [CERN-PH-EP/2006-042]. The combined Tevatron data yields an average W mass of 80.430 ± 0.040 GeV.

OUR FIT uses these average LEP and Tevatron mass values.

VALUE (GeV)	EVTS	DOCUMENT ID	TECN	COMMENT
80.398 ± 0.025 OUR FIT				
80.336 ± 0.055 ± 0.039	10.3k	1 ABDALLAH	08A DLPH	$E_{\text{cm}}^{\text{e}^{\pm}e^{\pm}} = 161\text{--}209$ GeV
80.413 ± 0.034 ± 0.034	115k	2 AALTONEN	07F CDF	$E_{\text{cm}}^{\text{p}\bar{\text{p}}} = 1.96$ TeV
80.415 ± 0.042 ± 0.031	11830	3 ABBIENDI	06 OPAL	$E_{\text{cm}}^{\text{e}^{\pm}e^{\pm}} = 170\text{--}209$ GeV
80.270 ± 0.046 ± 0.031	9909	4 ACHARD	06 L3	$E_{\text{cm}}^{\text{e}^{\pm}e^{\pm}} = 161\text{--}209$ GeV
80.440 ± 0.043 ± 0.027	8692	5 SCHAEEL	06 ALEP	$E_{\text{cm}}^{\text{e}^{\pm}e^{\pm}} = 161\text{--}209$ GeV
80.483 ± 0.084	49247	6 ABAZOV	02D D0	$E_{\text{cm}}^{\text{p}\bar{\text{p}}} = 1.8$ TeV
80.433 ± 0.079	53841	7 AFFOLDER	01E CDF	$E_{\text{cm}}^{\text{p}\bar{\text{p}}} = 1.8$ TeV
• • • We do not use the following data for averages, fits, limits, etc. • • •				
82.87 ± 1.82 $\begin{smallmatrix} +0.30 \\ -0.16 \end{smallmatrix}$	1500	8 AKTAS	06 H1	$e^{\pm}p \rightarrow \bar{\nu}_e(\nu_e)X$, $\sqrt{s} \approx 300$ GeV
80.3 ± 2.1 ± 1.2 ± 1.0	645	9 CHEKANOV	02C ZEUS	$e^-p \rightarrow \nu_e X$, $\sqrt{s} = 318$ GeV
81.4 $\begin{smallmatrix} +2.7 \\ -2.6 \end{smallmatrix}$ ± 2.0 $\begin{smallmatrix} +3.3 \\ -3.0 \end{smallmatrix}$	1086	10 BREITWEG	00D ZEUS	$e^+p \rightarrow \bar{\nu}_e X$, $\sqrt{s} \approx 300$ GeV
80.84 ± 0.22 ± 0.83	2065	11 ALITTI	92B UA2	See W/Z ratio below
80.79 ± 0.31 ± 0.84		12 ALITTI	90B UA2	$E_{\text{cm}}^{\text{p}\bar{\text{p}}} = 546,630$ GeV
80.0 ± 3.3 ± 2.4	22	13 ABE	89I CDF	$E_{\text{cm}}^{\text{p}\bar{\text{p}}} = 1.8$ TeV
82.7 ± 1.0 ± 2.7	149	14 ALBAJAR	89 UA1	$E_{\text{cm}}^{\text{p}\bar{\text{p}}} = 546,630$ GeV
81.8 $\begin{smallmatrix} +6.0 \\ -5.3 \end{smallmatrix}$ ± 2.6	46	15 ALBAJAR	89 UA1	$E_{\text{cm}}^{\text{p}\bar{\text{p}}} = 546,630$ GeV
89 ± 3 ± 6	32	16 ALBAJAR	89 UA1	$E_{\text{cm}}^{\text{p}\bar{\text{p}}} = 546,630$ GeV
81. ± 5.	6	ARNISON	83 UA1	$E_{\text{cm}}^{\text{e}^{\pm}e^{\pm}} = 546$ GeV
80. $\begin{smallmatrix} +10. \\ -6. \end{smallmatrix}$	4	BANNER	83B UA2	Repl. by ALITTI 90B

¹ ABDALLAH 08A use direct reconstruction of the kinematics of $W^+W^- \rightarrow q\bar{q}\ell\nu$ and $W^+W^- \rightarrow q\bar{q}q\bar{q}$ events for energies 172 GeV and above. The W mass was also extracted from the dependence of the WW cross section close to the production threshold and combined appropriately to obtain the final result. The systematic error includes ± 0.025 GeV due to final state interactions and ± 0.009 GeV due to LEP energy uncertainty.

- 2 AALTONEN 07F obtain high purity $W \rightarrow e\nu_e$ and $W \rightarrow \mu\nu_\mu$ candidate samples totaling 63,964 and 51,128 events respectively. The W mass value quoted above is derived by simultaneously fitting the transverse mass and the lepton, and neutrino p_T distributions.
- 3 ABBIENDI 06 use direct reconstruction of the kinematics of $W^+W^- \rightarrow q\bar{q}\ell\nu_\ell$ and $W^+W^- \rightarrow q\bar{q}q\bar{q}$ events. The result quoted here is obtained combining this mass value with the results using $W^+W^- \rightarrow \ell\nu_\ell\ell'\nu_{\ell'}$ events in the energy range 183–207 GeV (ABBIENDI 03c) and the dependence of the WW production cross-section on m_W at threshold. The systematic error includes ± 0.009 GeV due to the uncertainty on the LEP beam energy.
- 4 ACHARD 06 use direct reconstruction of the kinematics of $W^+W^- \rightarrow q\bar{q}\ell\nu_\ell$ and $W^+W^- \rightarrow q\bar{q}q\bar{q}$ events in the C.M. energy range 189–209 GeV. The result quoted here is obtained combining this mass value with the results obtained from a direct W mass reconstruction at 172 and 183 GeV and with those from the dependence of the WW production cross-section on m_W at 161 and 172 GeV (ACCIARRI 99).
- 5 SCHAEEL 06 use direct reconstruction of the kinematics of $W^+W^- \rightarrow q\bar{q}\ell\nu_\ell$ and $W^+W^- \rightarrow q\bar{q}q\bar{q}$ events in the C.M. energy range 183–209 GeV. The result quoted here is obtained combining this mass value with those obtained from the dependence of the W pair production cross-section on m_W at 161 and 172 GeV (BARATE 97 and BARATE 97s respectively). The systematic error includes ± 0.009 GeV due to possible effects of final state interactions in the $q\bar{q}q\bar{q}$ channel and ± 0.009 GeV due to the uncertainty on the LEP beam energy.
- 6 ABAZOV 02D improve the measurement of the W -boson mass including $W \rightarrow e\nu_e$ events in which the electron is close to a boundary of a central electromagnetic calorimeter module. Properly combining the results obtained by fitting $m_T(W)$, $p_T(e)$, and $p_T(\nu)$, this sample provides a mass value of 80.574 ± 0.405 GeV. The value reported here is a combination of this measurement with all previous DØ W -boson mass measurements.
- 7 AFFOLDER 01E fit the transverse mass spectrum of 30115 $W \rightarrow e\nu_e$ events ($M_W = 80.473 \pm 0.065 \pm 0.092$ GeV) and of 14740 $W \rightarrow \mu\nu_\mu$ events ($M_W = 80.465 \pm 0.100 \pm 0.103$ GeV) obtained in the run IB (1994–95). Combining the electron and muon results, accounting for correlated uncertainties, yields $M_W = 80.470 \pm 0.089$ GeV. They combine this value with their measurement of ABE 95P reported in run IA (1992–93) to obtain the quoted value.
- 8 AKTAS 06 fit the Q^2 dependence ($300 < Q^2 < 30,000$ GeV²) of the charged-current differential cross section with a propagator mass. The first error is experimental and the second corresponds to uncertainties due to input parameters and model assumptions.
- 9 CHEKANOV 02c fit the Q^2 dependence ($200 < Q^2 < 60,000$ GeV²) of the charged-current differential cross sections with a propagator mass fit. The last error is due to the uncertainty on the probability density functions.
- 10 BREITWEG 00D fit the Q^2 dependence ($200 < Q^2 < 225,000$ GeV²) of the charged-current differential cross sections with a propagator mass fit. The last error is due to the uncertainty on the probability density functions.
- 11 ALITTI 92B result has two contributions to the systematic error (± 0.83); one (± 0.81) cancels in m_W/m_Z and one (± 0.17) is noncancelling. These were added in quadrature. We choose the ALITTI 92B value without using the LEP m_Z value, because we perform our own combined fit.
- 12 There are two contributions to the systematic error (± 0.84): one (± 0.81) which cancels in m_W/m_Z and one (± 0.21) which is non-cancelling. These were added in quadrature.
- 13 ABE 89I systematic error dominated by the uncertainty in the absolute energy scale.
- 14 ALBAJAR 89 result is from a total sample of 299 $W \rightarrow e\nu_e$ events.
- 15 ALBAJAR 89 result is from a total sample of 67 $W \rightarrow \mu\nu$ events.
- 16 ALBAJAR 89 result is from $W \rightarrow \tau\nu$ events.

W/Z MASS RATIO

VALUE	EVTS	DOCUMENT ID	TECN	COMMENT
0.8819 ± 0.0012 OUR AVERAGE				
0.8821 ± 0.0011 ± 0.0008	28323	17 ABBOTT	98N D0	$E_{\text{cm}}^{\text{p}\bar{\text{p}}} = 1.8$ TeV
0.88114 ± 0.00154 ± 0.00252	5982	18 ABBOTT	98P D0	$E_{\text{cm}}^{\text{p}\bar{\text{p}}} = 1.8$ TeV
0.8813 ± 0.0036 ± 0.0019	156	19 ALITTI	92B UA2	$E_{\text{cm}}^{\text{p}\bar{\text{p}}} = 630$ GeV
17 ABBOTT 98N obtain this from a study of 28323 $W \rightarrow e\nu_e$ and 3294 $Z \rightarrow e^+e^-$ decays. Of this latter sample, 2179 events are used to calibrate the electron energy scale.				
18 ABBOTT 98P obtain this from a study of 5982 $W \rightarrow e\nu_e$ events. The systematic error includes an uncertainty of ± 0.00175 due to the electron energy scale.				
19 Scale error cancels in this ratio.				
$m_Z - m_W$				
VALUE (GeV)	DOCUMENT ID	TECN	COMMENT	
10.4 ± 1.4 ± 0.8	ALBAJAR	89 UA1	$E_{\text{cm}}^{\text{p}\bar{\text{p}}} = 546,630$ GeV	
• • • We do not use the following data for averages, fits, limits, etc. • • •				
11.3 ± 1.3 ± 0.9	ANSARI	87 UA2	$E_{\text{cm}}^{\text{p}\bar{\text{p}}} = 546,630$ GeV	
$m_{W^+} - m_{W^-}$				
Test of CPT invariance.				
VALUE (GeV)	EVTS	DOCUMENT ID	TECN	COMMENT
-0.19 ± 0.58	1722	ABE	90G CDF	$E_{\text{cm}}^{\text{p}\bar{\text{p}}} = 1.8$ TeV

Gauge & Higgs Boson Particle Listings

W

W WIDTH

To obtain OUR FIT, the correlation between systematics within LEP experiments and within Tevatron experiments is properly taken into account as given in the LEP note, CERN-PH-EP/2006-042, and in the CDF paper, AALTONEN 08B. The respective average values are 2.196 ± 0.083 GeV from LEP and 2.056 ± 0.062 GeV from Tevatron.

The extracted W width determined by $p\bar{p}$ collider experiments agrees with the directly determined value.

VALUE (GeV)	EVTS	DOCUMENT ID	TECN	COMMENT
2.141 ± 0.041 OUR FIT				
2.032 ± 0.045 ± 0.057	6055	20 AALTONEN	08B CDF	$E_{cm}^{pp} = 1.96$ TeV
2.404 ± 0.140 ± 0.101	10.3k	21 ABDALLAH	08A DLPH	$E_{cm}^{ee} = 183-209$ GeV
1.996 ± 0.096 ± 0.102	10729	22 ABBIENDI	06 OPAL	$E_{cm}^{ee} = 170-209$ GeV
2.18 ± 0.11 ± 0.09	9795	23 ACHARD	06 L3	$E_{cm}^{ee} = 172-209$ GeV
2.14 ± 0.09 ± 0.06	8717	24 SCHAEEL	06 ALEP	$E_{cm}^{ee} = 183-209$ GeV
2.23 $^{+0.15}_{-0.14}$ ± 0.10	294	25 ABAZOV	02E D0	Direct meas.
2.05 ± 0.10 ± 0.08	662	26 AFFOLDER	00M CDF	Direct meas.
• • • We do not use the following data for averages, fits, limits, etc. • • •				
2.152 ± 0.066	79176	27 ABBOTT	00B D0	Extracted value
2.064 ± 0.060 ± 0.059		28 ABE	95W CDF	Extracted value
2.10 $^{+0.14}_{-0.13}$ ± 0.09	3559	29 ALITTI	92 UA2	Extracted value
2.18 $^{+0.26}_{-0.24}$ ± 0.04		30 ALBAJAR	91 UA1	Extracted value

- 20 AALTONEN 08B obtain this result fitting the high-end tail (90–200 GeV) of the transverse mass spectrum in semileptonic $W \rightarrow e\nu_e$ and $W \rightarrow \mu\nu_\mu$ decays.
- 21 ABDALLAH 08A use direct reconstruction of the kinematics of $W^+W^- \rightarrow q\bar{q}\ell\nu$ and $W^+W^- \rightarrow q\bar{q}q\bar{q}$ events. The systematic error includes ± 0.065 GeV due to final state interactions.
- 22 ABBIENDI 06 use direct reconstruction of the kinematics of $W^+W^- \rightarrow q\bar{q}\ell\nu_\ell$ and $W^+W^- \rightarrow q\bar{q}q\bar{q}$ events. The systematic error includes ± 0.003 GeV due to the uncertainty on the LEP beam energy.
- 23 ACHARD 06 use direct reconstruction of the kinematics of $W^+W^- \rightarrow q\bar{q}\ell\nu_\ell$ and $W^+W^- \rightarrow q\bar{q}q\bar{q}$ events in the C.M. energy range 189–209 GeV. The result quoted here is obtained combining this value of the width with the result obtained from a direct W mass reconstruction at 172 and 183 GeV (ACCIARRI 99).
- 24 SCHAEEL 06 use direct reconstruction of the kinematics of $W^+W^- \rightarrow q\bar{q}\ell\nu_\ell$ and $W^+W^- \rightarrow q\bar{q}q\bar{q}$ events. The systematic error includes ± 0.05 GeV due to possible effects of final state interactions in the $q\bar{q}q\bar{q}$ channel and ± 0.01 GeV due to the uncertainty on the LEP beam energy.
- 25 ABAZOV 02E obtain this result fitting the high-end tail (90–200 GeV) of the transverse-mass spectrum in semileptonic $W \rightarrow e\nu_e$ decays.
- 26 AFFOLDER 00M fit the high transverse mass (100–200 GeV) $W \rightarrow e\nu_e$ and $W \rightarrow \mu\nu_\mu$ events to obtain $\Gamma(W) = 2.04 \pm 0.11(\text{stat}) \pm 0.09(\text{syst})$ GeV. This is combined with the earlier CDF measurement (ABE 95C) to obtain the quoted result.
- 27 ABBOTT 00B measure $R = 10.43 \pm 0.27$ for the $W \rightarrow e\nu_e$ decay channel. They use the SM theoretical predictions for $\sigma(W)/\sigma(Z)$ and $\Gamma(W \rightarrow e\nu_e)$ and the world average for $B(Z \rightarrow e\bar{e})$. The value quoted here is obtained combining this result (2.169 ± 0.070 GeV) with that of ABBOTT 99H.
- 28 ABE 95W measured $R = 10.90 \pm 0.32 \pm 0.29$. They use $m_W = 80.23 \pm 0.18$ GeV, $\sigma(W)/\sigma(Z) = 3.35 \pm 0.03$, $\Gamma(W \rightarrow e\nu) = 225.9 \pm 0.9$ MeV, $\Gamma(Z \rightarrow e^+e^-) = 83.98 \pm 0.18$ MeV, and $\Gamma(Z) = 2.4969 \pm 0.0038$ GeV.
- 29 ALITTI 92 measured $R = 10.4 \pm 0.7 \pm 0.3$. The values of $\sigma(Z)$ and $\sigma(W)$ come from $O(\alpha_s^2)$ calculations using $m_W = 80.14 \pm 0.27$ GeV, and $m_Z = 91.175 \pm 0.021$ GeV along with the corresponding value of $\sin^2\theta_W = 0.2274$. They use $\sigma(W)/\sigma(Z) = 3.26 \pm 0.07 \pm 0.05$ and $\Gamma(Z) = 2.487 \pm 0.010$ GeV.
- 30 ALBAJAR 91 measured $R = 9.5 \pm 1.1$ (stat. + syst.). $\sigma(W)/\sigma(Z)$ is calculated in QCD at the parton level using $m_W = 80.18 \pm 0.28$ GeV and $m_Z = 91.172 \pm 0.031$ GeV along with $\sin^2\theta_W = 0.2322 \pm 0.0014$. They use $\sigma(W)/\sigma(Z) = 3.23 \pm 0.05$ and $\Gamma(Z) = 2.498 \pm 0.020$ GeV. This measurement is obtained combining both the electron and muon channels.

W⁺ DECAY MODES

W^- modes are charge conjugates of the modes below.

Mode	Fraction (Γ_i/Γ)	Confidence level
Γ_1 $\ell^+\nu$	[a] $(10.80 \pm 0.09)\%$	
Γ_2 $e^+\nu$	$(10.75 \pm 0.13)\%$	
Γ_3 $\mu^+\nu$	$(10.57 \pm 0.15)\%$	
Γ_4 $\tau^+\nu$	$(11.25 \pm 0.20)\%$	
Γ_5 hadrons	$(67.60 \pm 0.27)\%$	
Γ_6 $\pi^+\gamma$	< 8	$\times 10^{-5}$ 95%
Γ_7 $D_s^+\gamma$	< 1.3	$\times 10^{-3}$ 95%
Γ_8 $c\bar{X}$	$(33.4 \pm 2.6)\%$	
Γ_9 $c\bar{s}$	(31 ± 13)	(-11) %
Γ_{10} invisible	[b] $(1.4 \pm 2.8)\%$	

[a] ℓ indicates each type of lepton (e , μ , and τ), not sum over them.

[b] This represents the width for the decay of the W boson into a charged particle with momentum below detectability, $p < 200$ MeV.

W PARTIAL WIDTHS

 $\Gamma(\text{invisible})$ Γ_{10}

This represents the width for the decay of the W boson into a charged particle with momentum below detectability, $p < 200$ MeV.

VALUE (MeV)	DOCUMENT ID	TECN	COMMENT
30 $^{+52}_{-48} \pm 33$	31 BARATE	99I ALEP	$E_{cm}^{ee} = 161+172+183$ GeV
• • • We do not use the following data for averages, fits, limits, etc. • • •			
	32 BARATE	99L ALEP	$E_{cm}^{ee} = 161+172+183$ GeV

31 BARATE 99I measure this quantity using the dependence of the total cross section σ_{WW} upon a change in the total width. The fit is performed to the WW measured cross sections at 161, 172, and 183 GeV. This partial width is < 139 MeV at 95%CL.

32 BARATE 99L use W -pair production to search for effectively invisible W decays, tagging with the decay of the other W boson to Standard Model particles. The partial width for effectively invisible decay is < 27 MeV at 95%CL.

W BRANCHING RATIOS

Overall fits are performed to determine the branching ratios of the W . LEP averages on $W \rightarrow e\nu_e$, $W \rightarrow \mu\nu_\mu$, and $W \rightarrow \tau\nu_\tau$, and their correlations are first obtained by combining results from the four experiments taking properly into account the common systematics. The procedure is described in the note LEPEWWG/XSEC/2001-02, 30 March 2001, at <http://lepewwg.web.cern.ch/LEPEWWG/lepww/4f/PDG01>. The LEP average values so obtained, using published data, are given in the note LEPEWWG/XSEC/2005-01 accessible at <http://lepewwg.web.cern.ch/LEPEWWG/lepww/4f/PDG05/>. These results, together with results from the $p\bar{p}$ colliders are then used in fits to obtain the world average W branching ratios. A first fit determines three individual leptonic branching ratios, $B(W \rightarrow e\nu_e)$, $B(W \rightarrow \mu\nu_\mu)$, and $B(W \rightarrow \tau\nu_\tau)$. This fit has a $\chi^2 = 4.7$ for 10 degrees of freedom. A second fit assumes lepton universality and determines the leptonic branching ratio $B(W \rightarrow \ell\nu_\ell)$ and the hadronic branching ratio is derived as $B(W \rightarrow \text{hadrons}) = 1-3B(W \rightarrow \ell\nu)$. This fit has a $\chi^2=11.3$ for 12 degrees of freedom.

The LEP $W \rightarrow \ell\nu$ data are obtained by the Collaborations using individual leptonic channels and are, therefore, not included in the overall fits to avoid double counting.

Note: The LEP combination including the new OPAL results, ABBIENDI 07A, could not be performed in time for this Review. Thus, the OUR FIT values quoted below use the previous OPAL results as in ABBIENDI, G 00.

 $\Gamma(\ell^+\nu)/\Gamma_{\text{total}}$ Γ_1/Γ

ℓ indicates average over e , μ , and τ modes, not sum over modes.

VALUE (units 10^{-2})	EVTS	DOCUMENT ID	TECN	COMMENT
10.80 ± 0.09 OUR FIT				
10.86 ± 0.12 ± 0.08	16438	ABBIENDI	07A OPAL	$E_{cm}^{ee} = 161-209$ GeV
10.85 ± 0.14 ± 0.08	13600	ABDALLAH	04G DLPH	$E_{cm}^{ee} = 161-209$ GeV
10.83 ± 0.14 ± 0.10	11246	ACHARD	04J L3	$E_{cm}^{ee} = 161-209$ GeV
10.96 ± 0.12 ± 0.05	16116	SCHAEEL	04A ALEP	$E_{cm}^{ee} = 183-209$ GeV
11.02 ± 0.52	11858	33 ABBOTT	99H D0	$E_{cm}^{pp} = 1.8$ TeV
10.4 ± 0.8	3642	34 ABE	92I CDF	$E_{cm}^{pp} = 1.8$ TeV
33 ABBOTT 99H measure $R \equiv [\sigma_W B(W \rightarrow \ell\nu_\ell)]/[\sigma_Z B(Z \rightarrow \ell\ell)] = 10.90 \pm 0.52$ combining electron and muon channels. They use $M_W = 80.39 \pm 0.06$ GeV and the SM theoretical predictions for $\sigma(W)/\sigma(Z)$ and $B(Z \rightarrow \ell\ell)$.				
34 $1216 \pm 38 \pm 27$ $W \rightarrow \mu\nu$ events from ABE 92I and $2426 W \rightarrow e\nu$ events of ABE 91C. ABE 92I give the inverse quantity as 9.6 ± 0.7 and we have inverted.				

 $\Gamma(e^+\nu)/\Gamma_{\text{total}}$ Γ_2/Γ

VALUE (units 10^{-2})	EVTS	DOCUMENT ID	TECN	COMMENT
10.75 ± 0.13 OUR FIT				
10.71 ± 0.25 ± 0.11	2374	ABBIENDI	07A OPAL	$E_{cm}^{ee} = 161-209$ GeV
10.55 ± 0.31 ± 0.14	1804	ABDALLAH	04G DLPH	$E_{cm}^{ee} = 161-209$ GeV
10.78 ± 0.29 ± 0.13	1576	ACHARD	04J L3	$E_{cm}^{ee} = 161-209$ GeV
10.78 ± 0.27 ± 0.10	2142	SCHAEEL	04A ALEP	$E_{cm}^{ee} = 183-209$ GeV
• • • We do not use the following data for averages, fits, limits, etc. • • •				
10.61 ± 0.28		35 ABAZOV	04D TEVA	$E_{cm}^{pp} = 1.8$ TeV

35 ABAZOV 04D take into account all correlations to properly combine the CDF (ABE 95W) and DØ (ABBOTT 00B) measurements of the ratio R in the electron channel. The ratio R is defined as $[\sigma_W \cdot B(W \rightarrow e\nu_e)] / [\sigma_Z \cdot B(Z \rightarrow e\bar{e})]$. The combination gives $R^{\text{Tevatron}} = 10.59 \pm 0.23$. σ_W/σ_Z is calculated at next-to-next-to-leading order (3.360 ± 0.051). The branching fraction $B(Z \rightarrow e\bar{e})$ is taken from this Review as (3.363 ± 0.004)%.

 $\Gamma(\mu^+\nu)/\Gamma_{\text{total}}$ Γ_3/Γ

VALUE (units 10^{-2})	EVTS	DOCUMENT ID	TECN	COMMENT
10.57 ± 0.15 OUR FIT				
10.78 ± 0.24 ± 0.10	2397	ABBIENDI	07A OPAL	$E_{cm}^{ee} = 161-209$ GeV
10.65 ± 0.26 ± 0.08	1998	ABDALLAH	04G DLPH	$E_{cm}^{ee} = 161-209$ GeV
10.03 ± 0.29 ± 0.12	1423	ACHARD	04J L3	$E_{cm}^{ee} = 161-209$ GeV
10.87 ± 0.25 ± 0.08	2216	SCHAEEL	04A ALEP	$E_{cm}^{ee} = 183-209$ GeV

See key on page 373

Gauge & Higgs Boson Particle Listings

W

$\Gamma(\tau^+\nu)/\Gamma_{\text{total}}$					Γ_4/Γ
VALUE (units 10^{-2})	EVTS	DOCUMENT ID	TECN	COMMENT	
11.25 ± 0.20 OUR FIT					
11.14 ± 0.31 ± 0.17	2177	ABBIENDI	07A OPAL	$E_{\text{cm}}^{\text{ee}} = 161\text{--}209$ GeV	
11.46 ± 0.39 ± 0.19	2034	ABDALLAH	04G DLPH	$E_{\text{cm}}^{\text{ee}} = 161\text{--}209$ GeV	
11.89 ± 0.40 ± 0.20	1375	ACHARD	04J L3	$E_{\text{cm}}^{\text{ee}} = 161\text{--}209$ GeV	
11.25 ± 0.32 ± 0.20	2070	SCHAEEL	04A ALEP	$E_{\text{cm}}^{\text{ee}} = 183\text{--}209$ GeV	

$\Gamma(\text{hadrons})/\Gamma_{\text{total}}$					Γ_5/Γ
OUR FIT value is obtained by a fit to the lepton branching ratio data assuming lepton universality.					
VALUE (units 10^{-2})	EVTS	DOCUMENT ID	TECN	COMMENT	
67.60 ± 0.27 OUR FIT					
67.41 ± 0.37 ± 0.23	16438	ABBIENDI	07A OPAL	$E_{\text{cm}}^{\text{ee}} = 161\text{--}209$ GeV	
67.45 ± 0.41 ± 0.24	13600	ABDALLAH	04G DLPH	$E_{\text{cm}}^{\text{ee}} = 161\text{--}209$ GeV	
67.50 ± 0.42 ± 0.30	11246	ACHARD	04J L3	$E_{\text{cm}}^{\text{ee}} = 161\text{--}209$ GeV	
67.13 ± 0.37 ± 0.15	16116	SCHAEEL	04A ALEP	$E_{\text{cm}}^{\text{ee}} = 183\text{--}209$ GeV	

$\Gamma(\mu^+\nu)/\Gamma(e^+\nu)$					Γ_3/Γ_2
VALUE	EVTS	DOCUMENT ID	TECN	COMMENT	
0.983 ± 0.018 OUR FIT					
0.89 ± 0.10	13k	36 ABACHI	95D D0	$E_{\text{cm}}^{\text{pp}} = 1.8$ TeV	
1.02 ± 0.08	1216	37 ABE	92I CDF	$E_{\text{cm}}^{\text{pp}} = 1.8$ TeV	
1.00 ± 0.14 ± 0.08	67	ALBAJAR	89 UA1	$E_{\text{cm}}^{\text{pp}} = 546,630$ GeV	

$\Gamma(\tau^+\nu)/\Gamma(e^+\nu)$					Γ_4/Γ_2
VALUE	EVTS	DOCUMENT ID	TECN	COMMENT	
1.046 ± 0.023 OUR FIT					
0.961 ± 0.061	980	38 ABBOTT	00D D0	$E_{\text{cm}}^{\text{pp}} = 1.8$ TeV	
0.94 ± 0.14	179	39 ABE	92E CDF	$E_{\text{cm}}^{\text{pp}} = 1.8$ TeV	
1.04 ± 0.08 ± 0.08	754	40 ALITTI	92F UA2	$E_{\text{cm}}^{\text{pp}} = 630$ GeV	
1.02 ± 0.20 ± 0.12	32	ALBAJAR	89 UA1	$E_{\text{cm}}^{\text{pp}} = 546,630$ GeV	

• • • We do not use the following data for averages, fits, limits, etc. • • •

1.24 $^{+0.6}_{-0.4}$ 14 ARNISON 84D UA1 Repl. by ALBAJAR 89

36 ABACHI 95D obtain this result from the measured $\sigma_{\text{WB}}(W \rightarrow \mu\nu) = 2.09 \pm 0.23 \pm 0.11$ nb and $\sigma_{\text{WB}}(W \rightarrow e\nu) = 2.36 \pm 0.07 \pm 0.13$ nb in which the first error is the combined statistical and systematic uncertainty, the second reflects the uncertainty in the luminosity.

37 ABE 92I obtain $\sigma_{\text{WB}}(W \rightarrow \mu\nu) = 2.21 \pm 0.07 \pm 0.21$ and combine with ABE 91C $\sigma_{\text{WB}}(W \rightarrow e\nu)$ to give a ratio of the couplings from which we derive this measurement.

$\Gamma(\tau^+\nu)/\Gamma(e^+\nu)$					Γ_4/Γ_2
VALUE	EVTS	DOCUMENT ID	TECN	COMMENT	
1.046 ± 0.023 OUR FIT					
0.961 ± 0.061	980	38 ABBOTT	00D D0	$E_{\text{cm}}^{\text{pp}} = 1.8$ TeV	
0.94 ± 0.14	179	39 ABE	92E CDF	$E_{\text{cm}}^{\text{pp}} = 1.8$ TeV	
1.04 ± 0.08 ± 0.08	754	40 ALITTI	92F UA2	$E_{\text{cm}}^{\text{pp}} = 630$ GeV	
1.02 ± 0.20 ± 0.12	32	ALBAJAR	89 UA1	$E_{\text{cm}}^{\text{pp}} = 546,630$ GeV	

• • • We do not use the following data for averages, fits, limits, etc. • • •

0.995 ± 0.112 ± 0.083 198 ALITTI 91C UA2 Repl. by ALITTI 92F

1.02 ± 0.20 ± 0.10 32 ALBAJAR 87 UA1 Repl. by ALBAJAR 89

38 ABBOTT 00D measure $\sigma_{\text{WB}}(W \rightarrow \tau\nu_\tau) = 2.22 \pm 0.09 \pm 0.10 \pm 0.10$ nb. Using the ABBOTT 00B result $\sigma_{\text{WB}}(W \rightarrow e\nu_e) = 2.31 \pm 0.01 \pm 0.05 \pm 0.10$ nb, they quote the ratio of the couplings from which we derive this measurement.

39 ABE 92E use two procedures for selecting $W \rightarrow \tau\nu_\tau$ events. The missing E_T trigger leads to $132 \pm 14 \pm 8$ events and the τ trigger to $47 \pm 9 \pm 4$ events. Proper statistical and systematic correlations are taken into account to arrive at $\sigma_B(W \rightarrow \tau\nu) = 2.05 \pm 0.27$ nb. Combined with ABE 91C result on $\sigma_B(W \rightarrow e\nu)$, ABE 92E quote a ratio of the couplings from which we derive this measurement.

40 This measurement is derived by us from the ratio of the couplings of ALITTI 92F.

$\Gamma(\pi^+\gamma)/\Gamma(e^+\nu)$					Γ_6/Γ_2
VALUE	CL%	DOCUMENT ID	TECN	COMMENT	
< 7 × 10⁻⁴	95	ABE	98H CDF	$E_{\text{cm}}^{\text{pp}} = 1.8$ TeV	
< 4.9 × 10 ⁻³	95	41 ALITTI	92D UA2	$E_{\text{cm}}^{\text{pp}} = 630$ GeV	
< 58 × 10 ⁻³	95	42 ALBAJAR	90 UA1	$E_{\text{cm}}^{\text{pp}} = 546, 630$ GeV	

41 ALITTI 92D limit is 3.8×10^{-3} at 90% CL.

42 ALBAJAR 90 obtain < 0.048 at 90% CL.

$\Gamma(D_s^+\gamma)/\Gamma(e^+\nu)$					Γ_7/Γ_2
VALUE	CL%	DOCUMENT ID	TECN	COMMENT	
< 1.2 × 10⁻²	95	ABE	98P CDF	$E_{\text{cm}}^{\text{pp}} = 1.8$ TeV	

$\Gamma(cX)/\Gamma(\text{hadrons})$					Γ_8/Γ_5
VALUE	EVTS	DOCUMENT ID	TECN	COMMENT	
0.49 ± 0.04 OUR AVERAGE					
0.481 ± 0.042 ± 0.032	3005	43 ABBIENDI	00V OPAL	$E_{\text{cm}}^{\text{ee}} = 183 + 189$ GeV	
0.51 ± 0.05 ± 0.03	746	44 BARATE	99M ALEP	$E_{\text{cm}}^{\text{ee}} = 172 + 183$ GeV	

43 ABBIENDI 00V tag $W \rightarrow cX$ decays using measured jet properties, lifetime information, and leptons produced in charm decays. From this result, and using the additional measurements of $\Gamma(W)$ and $B(W \rightarrow \text{hadrons})$, $|V_{cs}|$ is determined to be $0.969 \pm 0.045 \pm 0.036$.

44 BARATE 99M tag c jets using a neural network algorithm. From this measurement $|V_{cs}|$ is determined to be $1.00 \pm 0.11 \pm 0.07$.

$R_{c,s} = \Gamma(c\bar{s})/\Gamma(\text{hadrons})$					Γ_9/Γ_5
VALUE	DOCUMENT ID	TECN	COMMENT		
0.46 $^{+0.18}_{-0.14} \pm 0.07$	45 ABREU	98N DLPH	$E_{\text{cm}}^{\text{ee}} = 161+172$ GeV		

45 ABREU 98N tag c and s jets by identifying a charged kaon as the highest momentum particle in a hadronic jet. They also use a lifetime tag to independently identify a c jet, based on the impact parameter distribution of charged particles in a jet. From this measurement $|V_{cs}|$ is determined to be $0.94^{+0.32}_{-0.26} \pm 0.13$.

AVERAGE PARTICLE MULTIPLICITIES IN HADRONIC W DECAY

Summed over particle and antiparticle, when appropriate.

$\langle N_{\pi^\pm} \rangle$				
VALUE	DOCUMENT ID	TECN	COMMENT	
15.70 ± 0.35	46 ABREU,P	00F DLPH	$E_{\text{cm}}^{\text{ee}} = 189$ GeV	

46 ABREU,P 00F measure $\langle N_{\pi^\pm} \rangle = 31.65 \pm 0.48 \pm 0.76$ and $15.51 \pm 0.38 \pm 0.40$ in the fully hadronic and semileptonic final states respectively. The value quoted is a weighted average without assuming any correlations.

$\langle N_{K^\pm} \rangle$				
VALUE	DOCUMENT ID	TECN	COMMENT	
2.20 ± 0.19	47 ABREU,P	00F DLPH	$E_{\text{cm}}^{\text{ee}} = 189$ GeV	

47 ABREU,P 00F measure $\langle N_{K^\pm} \rangle = 4.38 \pm 0.42 \pm 0.12$ and $2.23 \pm 0.32 \pm 0.17$ in the fully hadronic and semileptonic final states respectively. The value quoted is a weighted average without assuming any correlations.

$\langle N_p \rangle$				
VALUE	DOCUMENT ID	TECN	COMMENT	
0.92 ± 0.14	48 ABREU,P	00F DLPH	$E_{\text{cm}}^{\text{ee}} = 189$ GeV	

48 ABREU,P 00F measure $\langle N_p \rangle = 1.82 \pm 0.29 \pm 0.16$ and $0.94 \pm 0.23 \pm 0.06$ in the fully hadronic and semileptonic final states respectively. The value quoted is a weighted average without assuming any correlations.

$\langle N_{\text{charged}} \rangle$				
VALUE	DOCUMENT ID	TECN	COMMENT	
19.39 ± 0.08 OUR AVERAGE				
19.38 ± 0.05 ± 0.08	49 ABBIENDI	06A OPAL	$E_{\text{cm}}^{\text{ee}} = 189\text{--}209$ GeV	
19.44 ± 0.17	50 ABREU,P	00F DLPH	$E_{\text{cm}}^{\text{ee}} = 183+189$ GeV	
19.3 ± 0.3 ± 0.3	51 ABBIENDI	99N OPAL	$E_{\text{cm}}^{\text{ee}} = 183$ GeV	
19.23 ± 0.74	52 ABREU	98C DLPH	$E_{\text{cm}}^{\text{ee}} = 172$ GeV	

49 ABBIENDI 06A measure $\langle N_{\text{charged}} \rangle = 38.74 \pm 0.12 \pm 0.26$ when both W bosons decay hadronically and $\langle N_{\text{charged}} \rangle = 19.39 \pm 0.11 \pm 0.09$ when one W boson decays semileptonically. The value quoted here is obtained under the assumption that there is no color reconnection between W bosons; the value is a weighted average taking into account correlations in the systematic uncertainties.

50 ABREU,P 00F measure $\langle N_{\text{charged}} \rangle = 39.12 \pm 0.33 \pm 0.36$ and $38.11 \pm 0.57 \pm 0.44$ in the fully hadronic final states at 189 and 183 GeV respectively, and $\langle N_{\text{charged}} \rangle = 19.49 \pm 0.31 \pm 0.27$ and $19.78 \pm 0.49 \pm 0.43$ in the semileptonic final states. The value quoted is a weighted average without assuming any correlations.

51 ABBIENDI 99N use the final states $W^+W^- \rightarrow q\bar{q}l\bar{l}$ to derive this value.

52 ABREU 98C combine results from both the fully hadronic as well semileptonic WW final states after demonstrating that the W decay charged multiplicity is independent of the topology within errors.

TRIPLE GAUGE COUPLINGS (TGC'S)

Revised March 2006 by C. Caso (University of Genova) and A. Gurtu (Tata Institute).

Fourteen independent couplings, 7 each for ZWW and γWW , completely describe the VWW vertices within the most general framework of the electroweak Standard Model (SM) consistent with Lorentz invariance and U(1) gauge invariance. Of each of the 7 TGC's, 3 conserve C and P individually, 3 violate CP , and one TGC violates C and P individually while conserving CP . Assumption of C and P conservation and electromagnetic gauge invariance reduces the independent VWW couplings to five: one common set [1,2] is $(\kappa_\gamma, \kappa_Z, \lambda_\gamma, \lambda_Z, g_1^Z)$, where $\kappa_\gamma = \kappa_Z = g_1^Z = 1$ and $\lambda_\gamma = \lambda_Z = 0$ in the Standard Model at the tree level. The parameters κ_Z and λ_Z are related to the other three due to constraints of gauge invariance as follows: $\kappa_Z = g_1^Z - (\kappa_\gamma - 1)\tan^2\theta_W$ and $\lambda_Z = \lambda_\gamma$, where θ_W is the weak mixing angle. The W magnetic dipole moment, μ_W , and the W electric quadrupole

Gauge & Higgs Boson Particle Listings

W

moment, q_W , are expressed as $\mu_W = e(1 + \kappa_\gamma + \lambda_\gamma)/2M_W$ and $q_W = -e(\kappa_\gamma - \lambda_\gamma)/M_W^2$.

Precision measurements of suitable observables at LEP1 has already led to an exploration of much of the TGC parameter space. At LEP2 the VWW coupling arises in W -pair production via s -channel exchange or in single W production via the radiation of a virtual photon off the incident e^+ or e^- . At the TEVATRON hard photon bremsstrahlung off a produced W or Z signals the presence of a triple gauge vertex. In order to extract the value of one TGC the others are generally kept fixed to their SM values.

References

1. K. Hagiwara *et al.*, Nucl. Phys. **B282**, 253 (1987).
2. G. Gounaris *et al.*, CERN 96-01 p. 525.

 g_1^Z

OUR FIT below is obtained by combining the measurements taking into account properly the common systematic errors (see LEPEWWG/TGC/2005-01 at <http://lepewwg.web.cern.ch/LEPEWWG/lepww/tgc/>).

VALUE	EVTS	DOCUMENT ID	TECN	COMMENT
$0.984^{+0.022}_{-0.019}$ OUR FIT				
$1.001 \pm 0.027 \pm 0.013$	9310	53 SCHAEL	05A ALEP	$E_{cm}^{ee} = 183-209$ GeV
$0.987^{+0.034}_{-0.033}$	9800	54 ABBIENDI	04D OPAL	$E_{cm}^{ee} = 183-209$ GeV
$0.966^{+0.034}_{-0.032} \pm 0.015$	8325	55 ACHARD	04D L3	$E_{cm}^{ee} = 161-209$ GeV
• • • We do not use the following data for averages, fits, limits, etc. • • •				
	13	56 ABAZOV	07Z D0	$E_{cm}^{pp} = 1.96$ TeV
	2.3	57 ABAZOV	05S D0	$E_{cm}^{pp} = 1.96$ TeV
$0.98 \pm 0.07 \pm 0.01$	2114	58 ABREU	01I DLPH	$E_{cm}^{ee} = 183+189$ GeV
	331	59 ABBOTT	99I D0	$E_{cm}^{pp} = 1.8$ TeV

53 SCHAEL 05A study single-photon, single- W , and WW -pair production from 183 to 209 GeV. The result quoted here is derived from the WW -pair production sample. Each parameter is determined from a single-parameter fit in which the other parameters assume their Standard Model values.

54 ABBIENDI 04D combine results from W^+W^- in all decay channels. Only CP -conserving couplings are considered and each parameter is determined from a single-parameter fit in which the other parameters assume their Standard Model values. The 95% confidence interval is $0.923 < g_1^Z < 1.054$.

55 ACHARD 04D study WW -pair production, single- W production and single-photon production with missing energy from 189 to 209 GeV. The result quoted here is obtained from the WW -pair production sample including data from 161 to 183 GeV, ACCIARRI 99Q. Each parameter is determined from a single-parameter fit in which the other parameters assume their Standard Model values.

56 ABAZOV 07Z set limits on anomalous TGCs using the measured cross section and $p_T(Z)$ distribution in WZ production with both the W and the Z decaying leptonically into electrons and muons. Setting other couplings to their standard model values, the 95% C.L. limits for a form factor scale $\Lambda = 1.5$ TeV are $-0.15 < \Delta g_1^Z < 0.35$, and for $\Lambda = 2$ TeV are $-0.14 < \Delta g_1^Z < 0.34$.

57 ABAZOV 05S study $\bar{p}p \rightarrow WZ$ production with a subsequent trilepton decay to $\ell\nu\ell'\bar{\ell}'$ (ℓ and $\ell' = e$ or μ). Three events (estimated background 0.71 ± 0.08 events) with WZ decay characteristics are observed from which they derive limits on the anomalous WWZ couplings. The 95% CL limit for a form factor scale $\Lambda = 1.5$ TeV is $0.51 < g_1^Z < 1.66$, fixing λ_Z and κ_Z to their Standard Model values.

58 ABREU 01I combine results from e^+e^- interactions at 189 GeV leading to W^+W^- and $W\nu_e$ final states with results from ABREU 99L at 183 GeV. The 95% confidence interval is $0.84 < g_1^Z < 1.13$.

59 ABBOTT 99I perform a simultaneous fit to the $W\gamma$, $WW \rightarrow$ dilepton, $WW/WZ \rightarrow e\nu jj$, $WW/WZ \rightarrow \mu\nu jj$, and $WZ \rightarrow$ trilepton data samples. For $\Lambda = 2.0$ TeV, the 95%CL limits are $0.63 < g_1^Z < 1.57$, fixing λ_Z and κ_Z to their Standard Model values, and assuming Standard Model values for the $WW\gamma$ couplings.

 κ_γ

OUR FIT below is obtained by combining the measurements taking into account properly the common systematic errors (see LEPEWWG/TGC/2005-01 at <http://lepewwg.web.cern.ch/LEPEWWG/lepww/tgc/>).

VALUE	EVTS	DOCUMENT ID	TECN	COMMENT
$0.973^{+0.044}_{-0.045}$ OUR FIT				
$0.971 \pm 0.055 \pm 0.030$	10689	60 SCHAEL	05A ALEP	$E_{cm}^{ee} = 183-209$ GeV
$0.88^{+0.09}_{-0.08}$	9800	61 ABBIENDI	04D OPAL	$E_{cm}^{ee} = 183-209$ GeV
$1.013^{+0.067}_{-0.064} \pm 0.026$	10575	62 ACHARD	04D L3	$E_{cm}^{ee} = 161-209$ GeV

• • • We do not use the following data for averages, fits, limits, etc. • • •

	1617	63 AALTONEN	07L CDF	$E_{cm}^{pp} = 1.96$ GeV
	17	64 ABAZOV	06H D0	$E_{cm}^{pp} = 1.96$ TeV
	141	65 ABAZOV	05J D0	$E_{cm}^{pp} = 1.96$ TeV
$1.25^{+0.21}_{-0.20} \pm 0.06$	2298	66 ABREU	01I DLPH	$E_{cm}^{ee} = 183+189$ GeV
		67 BREITWEG	00 ZEUS	$e^+p \rightarrow e^+W^\pm X$, $\sqrt{s} \approx 300$ GeV
0.92 ± 0.34	331	68 ABBOTT	99I D0	$E_{cm}^{pp} = 1.8$ TeV

60 SCHAEL 05A study single-photon, single- W , and WW -pair production from 183 to 209 GeV. Each parameter is determined from a single-parameter fit in which the other parameters assume their Standard Model values.

61 ABBIENDI 04D combine results from W^+W^- in all decay channels. Only CP -conserving couplings are considered and each parameter is determined from a single-parameter fit in which the other parameters assume their Standard Model values. The 95% confidence interval is $0.73 < \kappa_\gamma < 1.07$.

62 ACHARD 04D study WW -pair production, single- W production and single-photon production with missing energy from 189 to 209 GeV. The result quoted here is obtained including data from 161 to 183 GeV, ACCIARRI 99Q. Each parameter is determined from a single-parameter fit in which the other parameters assume their Standard Model values.

63 AALTONEN 07L set limits on anomalous TGCs using the $p_T(W)$ distribution in WW and WZ production with the W decaying to an electron or muon and the Z to 2 jets. Setting other couplings to their standard model value, the 95% C.L. limits are $0.54 < \kappa_\gamma < 1.39$ for a form factor scale $\Lambda = 1.5$ TeV.

64 ABAZOV 06H study $\bar{p}p \rightarrow WW$ production with a subsequent decay $WW \rightarrow e^+\nu_e e^-\bar{\nu}_e$, $WW \rightarrow e^\pm\nu_e\mu^\mp\nu_\mu$ or $WW \rightarrow \mu^\pm\nu_\mu\mu^\mp\nu_\mu$. The 95% C.L. limit for a form factor scale $\Lambda = 1$ TeV is $-0.05 < \kappa_\gamma < 2.29$, fixing $\lambda_\gamma = 0$. With the assumption that the $WW\gamma$ and WWZ couplings are equal the 95% C.L. one-dimensional limit ($\Lambda = 2$ TeV) is $0.68 < \kappa < 1.45$.

65 ABAZOV 05J perform a likelihood fit to the photon E_T spectrum of $W\gamma + X$ events, where the W decays to an electron or muon which is required to be well separated from the photon. For $\Lambda = 2.0$ TeV the 95% CL limits are $0.12 < \kappa_\gamma < 1.96$. In the fit λ_γ is kept fixed to its Standard Model value.

66 ABREU 01I combine results from e^+e^- interactions at 189 GeV leading to W^+W^- , $W\nu_e$, and $\nu\bar{\nu}\gamma$ final states with results from ABREU 99L at 183 GeV. The 95% confidence interval is $0.87 < \kappa_\gamma < 1.68$.

67 BREITWEG 00 search for W production in events with large hadronic p_T . For $p_T > 20$ GeV, the upper limit on the cross section gives the 95%CL limit $-3.7 < \kappa_\gamma < 2.5$ (for $\lambda_\gamma = 0$).

68 ABBOTT 99I perform a simultaneous fit to the $W\gamma$, $WW \rightarrow$ dilepton, $WW/WZ \rightarrow e\nu jj$, $WW/WZ \rightarrow \mu\nu jj$, and $WZ \rightarrow$ trilepton data samples. For $\Lambda = 2.0$ TeV, the 95%CL limits are $0.75 < \kappa_\gamma < 1.39$.

 λ_γ

OUR FIT below is obtained by combining the measurements taking into account properly the common systematic errors (see LEPEWWG/TGC/2005-01 at <http://lepewwg.web.cern.ch/LEPEWWG/lepww/tgc/>).

VALUE	EVTS	DOCUMENT ID	TECN	COMMENT
$-0.028^{+0.020}_{-0.021}$ OUR FIT				
$-0.012 \pm 0.027 \pm 0.011$	10689	69 SCHAEL	05A ALEP	$E_{cm}^{ee} = 183-209$ GeV
$-0.060^{+0.034}_{-0.033}$	9800	70 ABBIENDI	04D OPAL	$E_{cm}^{ee} = 183-209$ GeV
$-0.021^{+0.035}_{-0.034} \pm 0.017$	10575	71 ACHARD	04D L3	$E_{cm}^{ee} = 161-209$ GeV

• • • We do not use the following data for averages, fits, limits, etc. • • •

	1617	72 AALTONEN	07L CDF	$E_{cm}^{pp} = 1.96$ GeV
	17	73 ABAZOV	06H D0	$E_{cm}^{pp} = 1.96$ TeV
	141	74 ABAZOV	05J D0	$E_{cm}^{pp} = 1.96$ TeV
$0.05 \pm 0.09 \pm 0.01$	2298	75 ABREU	01I DLPH	$E_{cm}^{ee} = 183+189$ GeV
		76 BREITWEG	00 ZEUS	$e^+p \rightarrow e^+W^\pm X$, $\sqrt{s} \approx 300$ GeV
$0.00^{+0.10}_{-0.09}$	331	77 ABBOTT	99I D0	$E_{cm}^{pp} = 1.8$ TeV

69 SCHAEL 05A study single-photon, single- W , and WW -pair production from 183 to 209 GeV. Each parameter is determined from a single-parameter fit in which the other parameters assume their Standard Model values.

70 ABBIENDI 04D combine results from W^+W^- in all decay channels. Only CP -conserving couplings are considered and each parameter is determined from a single-parameter fit in which the other parameters assume their Standard Model values. The 95% confidence interval is $-0.13 < \lambda_\gamma < 0.01$.

71 ACHARD 04D study WW -pair production, single- W production and single-photon production with missing energy from 189 to 209 GeV. The result quoted here is obtained including data from 161 to 183 GeV, ACCIARRI 99Q. Each parameter is determined from a single-parameter fit in which the other parameters assume their Standard Model values.

72 AALTONEN 07L set limits on anomalous TGCs using the $p_T(W)$ distribution in WW and WZ production with the W decaying to an electron or muon and the Z to 2 jets. Setting other couplings to their standard model value, the 95% C.L. limits are $-0.18 < \lambda_\gamma < 0.17$ for a form factor scale $\Lambda = 1.5$ TeV.

73 ABAZOV 06H study $\bar{p}p \rightarrow WW$ production with a subsequent decay $WW \rightarrow e^+\nu_e e^-\bar{\nu}_e$, $WW \rightarrow e^\pm\nu_e\mu^\mp\nu_\mu$ or $WW \rightarrow \mu^\pm\nu_\mu\mu^\mp\nu_\mu$. The 95% C.L. limit for a form factor scale $\Lambda = 1$ TeV is $-0.97 < \lambda_\gamma < 1.04$, fixing $\kappa_\gamma = 1$. With the assumption that the $WW\gamma$ and WWZ couplings are equal the 95% C.L. one-dimensional limit ($\Lambda = 2$ TeV) is $-0.29 < \lambda < 0.30$.

74 ABAZOV 05J perform a likelihood fit to the photon E_T spectrum of $W\gamma + X$ events, where the W decays to an electron or muon which is required to be well separated from

the photon. For $\Lambda = 2.0$ TeV the 95% CL limits are $-0.20 < \lambda_\gamma < 0.20$. In the fit κ_γ is kept fixed to its Standard Model value.

⁷⁵ ABREU 01i combine results from e^+e^- interactions at 189 GeV leading to W^+W^- , $W\nu_e$, and $\nu\bar{\nu}\gamma$ final states with results from ABREU 99L at 183 GeV. The 95% confidence interval is $-0.11 < \lambda_\gamma < 0.23$.

⁷⁶ BREITWEG 00 search for W production in events with large hadronic p_T . For $p_T > 20$ GeV, the upper limit on the cross section gives the 95%CL limit $-3.2 < \lambda_\gamma < 3.2$ for κ_γ fixed to its Standard Model value.

⁷⁷ ABBOTT 99i perform a simultaneous fit to the $W\gamma$, $WW \rightarrow$ dilepton, $WW/WZ \rightarrow e\nu jj$, $WW/WZ \rightarrow \mu\nu jj$, and $WZ \rightarrow$ trilepton data samples. For $\Lambda = 2.0$ TeV, the 95%CL limits are $-0.18 < \lambda_\gamma < 0.19$.

 κ_Z

This coupling is CP-conserving (C- and P- separately conserving).

VALUE	EVTS	DOCUMENT ID	TECN	COMMENT
$0.924^{+0.059}_{-0.056} \pm 0.024$	7171	⁷⁸ ACHARD	04D L3	$E_{cm}^{ee} = 189\text{--}209$ GeV
• • •				We do not use the following data for averages, fits, limits, etc. • • •
	17	⁷⁹ ABAZOV	06H D0	$E_{cm}^{pp} = 1.96$ TeV
	2.3	⁸⁰ ABAZOV	05s D0	$E_{cm}^{pp} = 1.96$ TeV

⁷⁸ ACHARD 04d study WW -pair production, single- W production and single-photon production with missing energy from 189 to 209 GeV. The result quoted here is obtained using the WW -pair production sample. Each parameter is determined from a single-parameter fit in which the other parameters assume their Standard Model values.

⁷⁹ ABAZOV 06H study $\bar{p}p \rightarrow WW$ production with a subsequent decay $WW \rightarrow e^+\nu_e e^-\bar{\nu}_e$, $WW \rightarrow e^\pm\nu_e\mu^\mp\nu_\mu$ or $WW \rightarrow \mu^\pm\nu_\mu\mu^\mp\nu_\mu$. The 95% C.L. limit for a form factor scale $\Lambda = 2$ TeV is $0.55 < \kappa_Z < 1.55$, fixing $\lambda_Z = 0$. With the assumption that the $WW\gamma$ and WWZ couplings are equal the 95% C.L. one-dimensional limit ($\Lambda = 2$ TeV) is $0.68 < \kappa < 1.45$.

⁸⁰ ABAZOV 05s study $\bar{p}p \rightarrow WZ$ production with a subsequent trilepton decay to $e\nu\ell\bar{\nu}$ (ℓ and $\ell' = e$ or μ). Three events (estimated background 0.71 ± 0.08 events) with WZ decay characteristics are observed from which they derive limits on the anomalous WWZ couplings. The 95% CL limit for a form factor scale $\Lambda = 1$ TeV is $-1.0 < \kappa_Z < 3.4$, fixing λ_Z and g_1^Z to their Standard Model values.

 λ_Z

This coupling is CP-conserving (C- and P- separately conserving).

VALUE	EVTS	DOCUMENT ID	TECN	COMMENT
$-0.088^{+0.060}_{-0.057} \pm 0.023$	7171	⁸¹ ACHARD	04D L3	$E_{cm}^{ee} = 189\text{--}209$ GeV
• • •				We do not use the following data for averages, fits, limits, etc. • • •
	13	⁸² ABAZOV	07z D0	$E_{cm}^{pp} = 1.96$ TeV
	17	⁸³ ABAZOV	06H D0	$E_{cm}^{pp} = 1.96$ TeV
	2.3	⁸⁴ ABAZOV	05s D0	$E_{cm}^{pp} = 1.96$ TeV

⁸¹ ACHARD 04d study WW -pair production, single- W production and single-photon production with missing energy from 189 to 209 GeV. The result quoted here is obtained using the WW -pair production sample. Each parameter is determined from a single-parameter fit in which the other parameters assume their Standard Model values.

⁸² ABAZOV 07z set limits on anomalous TGCs using the measured cross section and $p_T(Z)$ distribution in WZ production with both the W and the Z decaying leptonically into electrons and muons. Setting other couplings to their standard model values, the 95% C.L. limits for a form factor scale $\Lambda = 1.5$ TeV are $-0.18 < \lambda_Z < 0.22$, and for $\Lambda = 2$ TeV are $-0.17 < \lambda_Z < 0.21$.

⁸³ ABAZOV 06H study $\bar{p}p \rightarrow WW$ production with a subsequent decay $WW \rightarrow e^+\nu_e e^-\bar{\nu}_e$, $WW \rightarrow e^\pm\nu_e\mu^\mp\nu_\mu$ or $WW \rightarrow \mu^\pm\nu_\mu\mu^\mp\nu_\mu$. The 95% C.L. limit for a form factor scale $\Lambda = 2$ TeV is $-0.39 < \lambda_Z < 0.39$, fixing $\kappa_Z = 1$. With the assumption that the $WW\gamma$ and WWZ couplings are equal the 95% C.L. one-dimensional limit ($\Lambda = 2$ TeV) is $-0.29 < \lambda < 0.30$.

⁸⁴ ABAZOV 05s study $\bar{p}p \rightarrow WZ$ production with a subsequent trilepton decay to $e\nu\ell\bar{\nu}$ (ℓ and $\ell' = e$ or μ). Three events (estimated background 0.71 ± 0.08 events) with WZ decay characteristics are observed from which they derive limits on the anomalous WWZ couplings. The 95% CL limit for a form factor scale $\Lambda = 1.5$ TeV is $-0.48 < \lambda_Z < 0.48$, fixing g_1^Z and κ_Z to their Standard Model values.

 g_5^Z

This coupling is CP-conserving but C- and P-violating.

VALUE	EVTS	DOCUMENT ID	TECN	COMMENT
0.93 ± 0.09 OUR AVERAGE				Error includes scale factor of 1.1.
$0.96^{+0.13}_{-0.12}$	9800	⁸⁵ ABBIENDI	04D OPAL	$E_{cm}^{ee} = 183\text{--}209$ GeV
$1.00 \pm 0.13 \pm 0.05$	7171	⁸⁶ ACHARD	04D L3	$E_{cm}^{ee} = 189\text{--}209$ GeV
$0.56^{+0.23}_{-0.22} \pm 0.12$	1154	⁸⁷ ACCIARRI	99Q L3	$E_{cm}^{ee} = 161+172+ 183$ GeV
• • •				We do not use the following data for averages, fits, limits, etc. • • •
0.84 ± 0.23		⁸⁸ EBOLI	00 THEO LEP1, SLC+ Tevatron	

⁸⁵ ABBIENDI 04d combine results from W^+W^- in all decay channels. Only CP-conserving couplings are considered and each parameter is determined from a single-parameter fit in which the other parameters assume their Standard Model values. The 95% confidence interval is $0.72 < g_5^Z < 1.21$.

⁸⁶ ACHARD 04d study WW -pair production, single- W production and single-photon production with missing energy from 189 to 209 GeV. The result quoted here is obtained using the WW -pair production sample. Each parameter is determined from a single-parameter fit in which the other parameters assume their Standard Model values.

⁸⁷ ACCIARRI 99Q study W -pair, single- W , and single photon events.

⁸⁸ EBOLI 00 extract this indirect value of the coupling studying the non-universal one-loop contributions to the experimental value of the $Z \rightarrow b\bar{b}$ width ($\Lambda = 1$ TeV is assumed).

 g_4^Z

This coupling is CP-violating (C-violating and P-conserving).

VALUE	EVTS	DOCUMENT ID	TECN	COMMENT
$-0.02^{+0.32}_{-0.33}$	1065	⁸⁹ ABBIENDI	01H OPAL	$E_{cm}^{ee} = 189$ GeV

⁸⁹ ABBIENDI 01H study W -pair events, with one leptonically and one hadronically decaying W . The coupling is extracted using information from the W production angle together with decay angles from the leptonically decaying W .

 $\tilde{\kappa}_Z$

This coupling is CP-violating (C-conserving and P-violating).

VALUE	EVTS	DOCUMENT ID	TECN	COMMENT
$-0.20^{+0.10}_{-0.07}$	1065	⁹⁰ ABBIENDI	01H OPAL	$E_{cm}^{ee} = 189$ GeV

⁹⁰ ABBIENDI 01H study W -pair events, with one leptonically and one hadronically decaying W . The coupling is extracted using information from the W production angle together with decay angles from the leptonically decaying W .

 $\tilde{\lambda}_Z$

This coupling is CP-violating (C-conserving and P-violating).

VALUE	EVTS	DOCUMENT ID	TECN	COMMENT
$-0.18^{+0.24}_{-0.16}$	1065	⁹¹ ABBIENDI	01H OPAL	$E_{cm}^{ee} = 189$ GeV

⁹¹ ABBIENDI 01H study W -pair events, with one leptonically and one hadronically decaying W . The coupling is extracted using information from the W production angle together with decay angles from the leptonically decaying W .

W ANOMALOUS MAGNETIC MOMENT

The full magnetic moment is given by $\mu_W = e(1 + \kappa + \lambda)/2m_W$. In the Standard Model, at tree level, $\kappa = 1$ and $\lambda = 0$. Some papers have defined $\Delta\kappa = 1 - \kappa$ and assume that $\lambda = 0$. Note that the electric quadrupole moment is given by $-e(\kappa - \lambda)/m_W^2$. A description of the parameterization of these moments and additional references can be found in HAGIWARA 87 and BAUR 88. The parameter Λ appearing in the theoretical limits below is a regularization cutoff which roughly corresponds to the energy scale where the structure of the W boson becomes manifest.

VALUE ($e/2m_W$)	EVTS	DOCUMENT ID	TECN	COMMENT
$2.22^{+0.20}_{-0.19}$	2298	⁹² ABREU	01i DLPH	$E_{cm}^{ee} = 183+189$ GeV

• • • We do not use the following data for averages, fits, limits, etc. • • •

⁹³ ABE	95G	CDF
⁹⁴ ALITTI	92c	UA2
⁹⁵ SAMUEL	92	THEO
⁹⁶ SAMUEL	91	THEO
⁹⁷ GRIFOLS	88	THEO
⁹⁸ GROTCHE	87	THEO
⁹⁹ VANDERBIJ	87	THEO
¹⁰⁰ GRAU	85	THEO
¹⁰¹ SUZUKI	85	THEO
¹⁰² HERZOG	84	THEO

⁹² ABREU 01i combine results from e^+e^- interactions at 189 GeV leading to W^+W^- , $W\nu_e$, and $\nu\bar{\nu}\gamma$ final states with results from ABREU 99L at 183 GeV to determine Δg_1^Z , $\Delta\kappa_\gamma$, and λ_γ . $\Delta\kappa_\gamma$ and λ_γ are simultaneously floated in the fit to determine μ_W .

⁹³ ABE 95G report $-1.3 < \kappa < 3.2$ for $\lambda = 0$ and $-0.7 < \lambda < 0.7$ for $\kappa = 1$ in $p\bar{p} \rightarrow e\nu_e\gamma X$ and $\mu\nu_\mu\gamma X$ at $\sqrt{s} = 1.8$ TeV.

⁹⁴ ALITTI 92c measure $\kappa = 1 + \frac{2.6}{-2.2}$ and $\lambda = \frac{0+1.7}{-1.8}$ in $p\bar{p} \rightarrow e\nu\gamma + X$ at $\sqrt{s} = 630$ GeV. At 95%CL they report $-3.5 < \kappa < 5.9$ and $-3.6 < \lambda < 3.5$.

⁹⁵ SAMUEL 92 use preliminary CDF and UA2 data and find $-2.4 < \kappa < 3.7$ at 96%CL and $-3.1 < \kappa < 4.2$ at 95%CL respectively. They use data for $W\gamma$ production and radiative W decay.

⁹⁶ SAMUEL 91 use preliminary CDF data for $p\bar{p} \rightarrow W\gamma X$ to obtain $-11.3 \leq \Delta\kappa \leq 10.9$. Note that their $\kappa = 1 - \Delta\kappa$.

⁹⁷ GRIFOLS 88 uses deviation from ρ parameter to set limit $\Delta\kappa \lesssim 65 (M_W^2/\Lambda^2)$.

⁹⁸ GROTCHE 87 finds the limit $-37 < \Delta\kappa < 73.5$ (90% CL) from the experimental limits on $e^+e^- \rightarrow \nu\bar{\nu}\gamma$ assuming three neutrino generations and $-19.5 < \Delta\kappa < 56$ for four generations. Note their $\Delta\kappa$ has the opposite sign as our definition.

⁹⁹ VANDERBIJ 87 uses existing limits to the photon structure to obtain $|\Delta\kappa| < 33 (m_W/\Lambda)$. In addition VANDERBIJ 87 discusses problems with using the ρ parameter of the Standard Model to determine $\Delta\kappa$.

¹⁰⁰ GRAU 85 uses the muon anomaly to derive a coupled limit on the anomalous magnetic dipole and electric quadrupole (λ) moments $1.05 > \Delta\kappa \ln(\Lambda/m_W) + \lambda/2 > -2.77$. In the Standard Model $\lambda = 0$.

¹⁰¹ SUZUKI 85 uses partial-wave unitarity at high energies to obtain $|\Delta\kappa| \lesssim 190 (m_W/\Lambda)^2$. From the anomalous magnetic moment of the muon, SUZUKI 85 obtains $|\Delta\kappa| \lesssim 2.2/\ln(\Lambda/m_W)$. Finally SUZUKI 85 uses deviations from the ρ parameter and obtains a very qualitative, order-of-magnitude limit $|\Delta\kappa| \lesssim 150 (m_W/\Lambda)^4$ if $|\Delta\kappa| \ll 1$.

¹⁰² HERZOG 84 consider the contribution of W -boson to muon magnetic moment including anomalous coupling of $W W\gamma$. Obtain a limit $-1 < \Delta\kappa < 3$ for $\Lambda \gtrsim 1$ TeV.

Gauge & Higgs Boson Particle Listings

W

ANOMALOUS W/Z QUARTIC COUPLINGS

Revised March 2006 by C. Caso (University of Genova) and A. Gurtu (Tata Institute).

The Standard Model predictions for $WWWW$, $WWZZ$, $WWZ\gamma$, $WW\gamma\gamma$, and $ZZ\gamma\gamma$ couplings are small at LEP, but expected to become important at a TeV Linear Collider. Outside the Standard Model framework such possible couplings, a_0, a_c, a_n , are expressed in terms of the following dimension-6 operators [1,2];

$$L_6^0 = -\frac{e^2}{16\Lambda^2} a_0 F^{\mu\nu} F_{\mu\nu} \vec{W}^\alpha \cdot \vec{W}_\alpha$$

$$L_6^c = -\frac{e^2}{16\Lambda^2} a_c F^{\mu\alpha} F_{\mu\beta} \vec{W}^\beta \cdot \vec{W}_\alpha$$

$$L_6^n = -i\frac{e^2}{16\Lambda^2} a_n \epsilon_{ijk} W_{\mu\alpha}^{(i)} W_{\nu}^{(j)} W^{(k)\alpha} F^{\mu\nu}$$

$$\tilde{L}_6^0 = -\frac{e^2}{16\Lambda^2} \tilde{a}_0 F^{\mu\nu} \tilde{F}_{\mu\nu} \vec{W}^\alpha \cdot \vec{W}_\alpha$$

$$\tilde{L}_6^n = -i\frac{e^2}{16\Lambda^2} \tilde{a}_n \epsilon_{ijk} W_{\mu\alpha}^{(i)} W_{\nu}^{(j)} W^{(k)\alpha} \tilde{F}^{\mu\nu}$$

where F, W are photon and W fields, L_6^0 and L_6^c conserve C, P separately (\tilde{L}_6^0 conserves only C) and generate anomalous $W^+W^-\gamma\gamma$ and $ZZ\gamma\gamma$ couplings, L_6^n violates CP (\tilde{L}_6^n violates both C and P) and generates an anomalous $W^+W^-Z\gamma$ coupling, and Λ is an energy scale for new physics. For the $ZZ\gamma\gamma$ coupling the CP -violating term represented by L_6^n does not contribute. These couplings are assumed to be real and to vanish at tree level in the Standard Model.

Within the same framework as above, a more recent description of the quartic couplings [3] treats the anomalous parts of the $WW\gamma\gamma$ and $ZZ\gamma\gamma$ couplings separately leading to two sets parameterized as a_0^V/Λ^2 and a_c^V/Λ^2 , where $V = W$ or Z .

At LEP the processes studied in search of these quartic couplings are $e^+e^- \rightarrow WW\gamma$, $e^+e^- \rightarrow \gamma\gamma\nu\bar{\nu}$, and $e^+e^- \rightarrow Z\gamma\gamma$ and limits are set on the quantities $a_0^W/\Lambda^2, a_c^W/\Lambda^2, a_n/\Lambda^2$. The characteristics of the first process depend on all the three couplings whereas those of the latter two depend only on the two CP -conserving couplings. The sensitive measured variables are the cross sections for these processes as well as the energy and angular distributions of the photon and recoil mass to the photon pair.

References

- G. Belanger and F. Boudjema, Phys. Lett. **B288**, 201 (1992).
- J.W. Stirling and A. Werthenbach, Eur. Phys. J. **C14**, 103 (2000);
J.W. Stirling and A. Werthenbach, Phys. Lett. **B466**, 369 (1999);
A. Denner *et al.*, Eur. Phys. J. **C20**, 201 (2001);
G. Montagna *et al.*, Phys. Lett. **B515**, 197 (2001).
- G. Belanger *et al.*, Eur. Phys. J. **C13**, 103 (2000).

$a_0/\Lambda^2, a_c/\Lambda^2, a_n/\Lambda^2$

Using the $WW\gamma$ final state, the LEP combined 95% CL limits on the anomalous contributions to the $WW\gamma\gamma$ and $WWZ\gamma$ vertices (as of summer 2003) are given below:

(See P. Wells, "Experimental Tests of the Standard Model," Int. Europhysics Conference on High-Energy Physics, Aachen, Germany, 17–23 July 2003)

$$-0.02 < a_0^W/\Lambda^2 < 0.02 \text{ GeV}^{-2},$$

$$-0.05 < a_c^W/\Lambda^2 < 0.03 \text{ GeV}^{-2},$$

$$-0.15 < a_n/\Lambda^2 < 0.15 \text{ GeV}^{-2}.$$

VALUE DOCUMENT ID TECN

••• We do not use the following data for averages, fits, limits, etc. •••

103	ABBIENDI	04B	OPAL
104	ABBIENDI	04L	OPAL
105	HEISTER	04A	ALEP
106	ABDALLAH	03I	DLPH
107	ACHARD	02F	L3
103	ABBIENDI	04B	select 187 $e^+e^- \rightarrow W^+W^-\gamma$ events in the C.M. energy range 180–209 GeV, where $E_\gamma > 2.5$ GeV, the photon has a polar angle $ \cos\theta_\gamma < 0.975$ and is well isolated from the nearest jet and charged lepton, and the effective masses of both fermion-antifermion systems agree with the W mass within $3\Gamma_W$. The measured differential cross section as a function of the photon energy and photon polar angle is used to extract the 95% CL limits: $-0.020 \text{ GeV}^{-2} < a_0^W/\Lambda^2 < 0.020 \text{ GeV}^{-2}$, $-0.053 \text{ GeV}^{-2} < a_c^W/\Lambda^2 < 0.037 \text{ GeV}^{-2}$ and $-0.16 \text{ GeV}^{-2} < a_n/\Lambda^2 < 0.15 \text{ GeV}^{-2}$.
104	ABBIENDI	04L	select 20 $e^+e^- \rightarrow \nu\bar{\nu}\gamma\gamma$ acoplanar events in the energy range 180–209 GeV and 176 $e^+e^- \rightarrow q\bar{q}\gamma\gamma$ events in the energy range 130–209 GeV. These samples are used to constrain possible anomalous $W^+W^-\gamma\gamma$ and $ZZ\gamma\gamma$ quartic couplings. Further combining with the $W^+W^-\gamma$ sample of ABBIENDI 04B the following one-parameter 95% CL limits are obtained: $-0.007 < a_0^W/\Lambda^2 < 0.023 \text{ GeV}^{-2}$, $-0.029 < a_c^W/\Lambda^2 < 0.029 \text{ GeV}^{-2}$, $-0.020 < a_0^Z/\Lambda^2 < 0.020 \text{ GeV}^{-2}$, $-0.052 < a_c^Z/\Lambda^2 < 0.037 \text{ GeV}^{-2}$.
105	HEISTER	04A	In the CM energy range 183 to 209 GeV HEISTER 04A select 30 $e^+e^- \rightarrow \nu\bar{\nu}\gamma\gamma$ events with two acoplanar, high energy and high transverse momentum photons. The photon-photon acoplanarity is required to be $> 5^\circ$, $E_\gamma/\sqrt{s} > 0.025$ (the more energetic photon having energy $> 0.2\sqrt{s}$), $p_{T,\gamma}/E_{\text{beam}} > 0.05$ and $ \cos\theta_\gamma < 0.94$. A likelihood fit to the photon energy and recoil missing mass yields the following one-parameter 95% CL limits: $-0.012 < a_0^Z/\Lambda^2 < 0.019 \text{ GeV}^{-2}$, $-0.041 < a_c^Z/\Lambda^2 < 0.044 \text{ GeV}^{-2}$, $-0.060 < a_0^W/\Lambda^2 < 0.055 \text{ GeV}^{-2}$, $-0.099 < a_c^W/\Lambda^2 < 0.093 \text{ GeV}^{-2}$.
106	ABDALLAH	03I	select 122 $e^+e^- \rightarrow W^+W^-\gamma$ events in the C.M. energy range 189–209 GeV, where $E_\gamma > 5$ GeV, the photon has a polar angle $ \cos\theta_\gamma < 0.95$ and is well isolated from the nearest charged fermion. A fit to the photon energy spectra yields $a_c/\Lambda^2 = 0.000 \pm 0.019 \text{ GeV}^{-2}$, $a_0/\Lambda^2 = -0.004 \pm 0.018 \text{ GeV}^{-2}$, $\tilde{a}_0/\Lambda^2 = -0.007 \pm 0.019 \text{ GeV}^{-2}$, $a_n/\Lambda^2 = -0.09 \pm 0.16 \text{ GeV}^{-2}$, and $\tilde{a}_n/\Lambda^2 = +0.05 \pm 0.15 \text{ GeV}^{-2}$, keeping the other parameters fixed to their Standard Model values (0). The 95% CL limits are: $-0.063 \text{ GeV}^{-2} < a_c/\Lambda^2 < +0.032 \text{ GeV}^{-2}$, $-0.020 \text{ GeV}^{-2} < a_0/\Lambda^2 < +0.020 \text{ GeV}^{-2}$, $-0.020 \text{ GeV}^{-2} < \tilde{a}_0/\Lambda^2 < +0.020 \text{ GeV}^{-2}$, $-0.18 \text{ GeV}^{-2} < a_n/\Lambda^2 < +0.14 \text{ GeV}^{-2}$, $-0.16 \text{ GeV}^{-2} < \tilde{a}_n/\Lambda^2 < +0.17 \text{ GeV}^{-2}$.
107	ACHARD	02F	select 86 $e^+e^- \rightarrow W^+W^-\gamma$ events at 192–207 GeV, where $E_\gamma > 5$ GeV and the photon is well isolated. They also select 43 acoplanar $e^+e^- \rightarrow \nu\bar{\nu}\gamma\gamma$ events in this energy range, where the photon energies are > 5 GeV and > 1 GeV and the photon polar angles are between 14° and 166° . All these 43 events are in the recoil mass region corresponding to the Z (75–110 GeV). Using the shape and normalization of the photon spectra in the $W^+W^-\gamma$ events, and combining with the 42 event sample from 189 GeV data (ACCIARRI 00T), they obtain: $a_0/\Lambda^2 = 0.000 \pm 0.010 \text{ GeV}^{-2}$, $a_c/\Lambda^2 = -0.013 \pm 0.023 \text{ GeV}^{-2}$, and $a_n/\Lambda^2 = -0.002 \pm 0.076 \text{ GeV}^{-2}$. Further combining the analyses of $W^+W^-\gamma$ events with the low recoil mass region of $\nu\bar{\nu}\gamma\gamma$ events (including samples collected at 183 + 189 GeV), they obtain the following one-parameter 95% CL limits: $-0.015 \text{ GeV}^{-2} < a_0/\Lambda^2 < 0.015 \text{ GeV}^{-2}$, $-0.048 \text{ GeV}^{-2} < a_c/\Lambda^2 < 0.026 \text{ GeV}^{-2}$, and $-0.14 \text{ GeV}^{-2} < a_n/\Lambda^2 < 0.13 \text{ GeV}^{-2}$.

W REFERENCES

AALTONEN	08B	PRL 100 071801	T. Aaltonen <i>et al.</i>	(CDF Collab.)
ABDALLAH	08A	EPJ C55 1	J. Abdallah <i>et al.</i>	(DELPHI Collab.)
AALTONEN	07F	PRL 99 151801	T. Aaltonen <i>et al.</i>	(CDF Collab.)
AALTONEN	07L	PR D76 111103R	T. Aaltonen <i>et al.</i>	(CDF Collab.)
ABAZOV	07Z	PR D76 111104R	V.M. Abazov <i>et al.</i>	(DO Collab.)
ABBIENDI	07A	EPJ C52 767	G. Abbiendi <i>et al.</i>	(OPAL Collab.)
ABAZOV	06H	PR D74 057101	V.M. Abazov <i>et al.</i>	(DO Collab.)
Also		PR D74 059904 (erratum)	V.M. Abazov <i>et al.</i>	(DO Collab.)
ABBIENDI	06	EPJ C45 307	G. Abbiendi <i>et al.</i>	(OPAL Collab.)
ABBIENDI	06A	EPJ C45 291	G. Abbiendi <i>et al.</i>	(OPAL Collab.)
ACHARD	06	EPJ C45 569	P. Achard <i>et al.</i>	(L3 Collab.)
AKTAS	06	PL B632 35	A. Aktas <i>et al.</i>	(HI Collab.)
SCHAEEL	06	EPJ C47 309	S. Schaeel <i>et al.</i>	(ALEPH Collab.)
ABAZOV	05J	PR D71 091108R	V.M. Abazov <i>et al.</i>	(DO Collab.)
ABAZOV	05S	PRL 95 141802	V.M. Abazov <i>et al.</i>	(DO Collab.)
SCHAEEL	05A	PL B614 7	S. Schaeel <i>et al.</i>	(ALEPH Collab.)
ABAZOV	04D	PR D70 092008	V.M. Abazov <i>et al.</i>	(CDF, DO Collab.)
ABBIENDI	04B	PL B580 17	G. Abbiendi <i>et al.</i>	(OPAL Collab.)
ABBIENDI	04D	EPJ C33 463	G. Abbiendi <i>et al.</i>	(OPAL Collab.)
ABBIENDI	04L	PR D70 032005	G. Abbiendi <i>et al.</i>	(OPAL Collab.)
ABDALLAH	04G	EPJ C34 1277	J. Abdallah <i>et al.</i>	(DELPHI Collab.)
ACHARD	04D	PL B586 151	P. Achard <i>et al.</i>	(L3 Collab.)
ACHARD	04J	PL B600 22	P. Achard <i>et al.</i>	(L3 Collab.)
HEISTER	04A	PL B602 31	A. Heister <i>et al.</i>	(ALEPH Collab.)
SCHAEEL	04A	EPJ C38 147	S. Schaeel <i>et al.</i>	(ALEPH Collab.)
ABBIENDI	03C	EPJ C26 321	G. Abbiendi <i>et al.</i>	(OPAL Collab.)
ABDALLAH	03I	EPJ C31 139	J. Abdallah <i>et al.</i>	(DELPHI Collab.)
ABAZOV	02D	PR D66 012001	V.M. Abazov <i>et al.</i>	(DO Collab.)
ABAZOV	02E	PR D66 032008	V.M. Abazov <i>et al.</i>	(DO Collab.)
ACHARD	02F	PL B527 29	P. Achard <i>et al.</i>	(L3 Collab.)
CHEKANOV	02C	PL B539 197	S. Chekanov <i>et al.</i>	(ZEUS Collab.)
ABBIENDI	01H	EPJ C19 229	G. Abbiendi <i>et al.</i>	(OPAL Collab.)
ABREU	01I	PL B502 9	P. Abreu <i>et al.</i>	(DELPHI Collab.)
AFFOLDER	01E	PR D64 052001	T. Affolder <i>et al.</i>	(CDF Collab.)
ABBIENDI	00V	PL B490 71	G. Abbiendi <i>et al.</i>	(OPAL Collab.)
ABBIENDI,G	00	PL B493 249	G. Abbiendi <i>et al.</i>	(OPAL Collab.)
ABBOTT	00B	PR D61 072001	B. Abbott <i>et al.</i>	(DO Collab.)
ABBOTT	00D	PRL 84 5710	B. Abbott <i>et al.</i>	(DO Collab.)
ABREU,P	00F	EPJ C18 203	P. Abreu <i>et al.</i>	(DELPHI Collab.)
Also		EPJ C25 493 (erratum)	P. Abreu <i>et al.</i>	(DELPHI Collab.)
ACCIARRI	00T	PL B490 187	M. Acciarri <i>et al.</i>	(L3 Collab.)
AFFOLDER	00M	PRL 85 3347	T. Affolder <i>et al.</i>	(CDF Collab.)
BREITWEG	00	PL B471 411	J. Breitweg <i>et al.</i>	(ZEUS Collab.)
BREITWEG	00D	EPJ C12 411	J. Breitweg <i>et al.</i>	(ZEUS Collab.)

EBOLI	00	MPL A15 1	O. Eboli, M. Gonzalez-Garcia, S. Novaes
ABBIENDI	99N	PL B453 153	G. Abbiendi <i>et al.</i>
ABBOTT	99H	PR D60 052003	B. Abbott <i>et al.</i> (OPAL Collab.)
ABBOTT	99I	PR D60 072002	B. Abbott <i>et al.</i> (DO Collab.)
ABREU	99L	PL B459 382	P. Abreu <i>et al.</i> (DELPHI Collab.)
ACCIARRI	99	PL B454 386	M. Acciari <i>et al.</i> (L3 Collab.)
ACCIARRI	99Q	PL B467 171	M. Acciari <i>et al.</i> (L3 Collab.)
BARATE	99I	PL B453 107	R. Barate <i>et al.</i> (ALEPH Collab.)
BARATE	99L	PL B462 389	R. Barate <i>et al.</i> (ALEPH Collab.)
BARATE	99M	PL B465 349	R. Barate <i>et al.</i> (ALEPH Collab.)
ABBOTT	98N	PR D58 092003	B. Abbott <i>et al.</i> (DO Collab.)
ABBOTT	98P	PR D58 012002	B. Abbott <i>et al.</i> (DO Collab.)
ABE	98H	PR D58 031101	F. Abe <i>et al.</i> (CDF Collab.)
ABE	98P	PR D58 091101	F. Abe <i>et al.</i> (CDF Collab.)
ABREU	98C	PL B416 233	P. Abreu <i>et al.</i> (DELPHI Collab.)
ABREU	98N	PL B439 209	P. Abreu <i>et al.</i> (DELPHI Collab.)
BARATE	97	PL B401 347	R. Barate <i>et al.</i> (ALEPH Collab.)
BARATE	97S	PL B415 435	R. Barate <i>et al.</i> (ALEPH Collab.)
ABACHI	95D	PRL 75 1456	S. Abachi <i>et al.</i> (DO Collab.)
ABE	95C	PRL 74 341	F. Abe <i>et al.</i> (CDF Collab.)
ABE	95G	PRL 74 1936	F. Abe <i>et al.</i> (CDF Collab.)
ABE	95P	PRL 75 11	F. Abe <i>et al.</i> (CDF Collab.)
Also		PR D52 4784	F. Abe <i>et al.</i> (CDF Collab.)
ABE	95W	PR D52 2624	F. Abe <i>et al.</i> (CDF Collab.)
Also		PRL 73 220	F. Abe <i>et al.</i> (CDF Collab.)
ABE	92E	PRL 68 3398	F. Abe <i>et al.</i> (CDF Collab.)
ABE	92I	PRL 69 28	F. Abe <i>et al.</i> (CDF Collab.)
ALITTI	92	PL B276 365	J. Alitti <i>et al.</i> (UA2 Collab.)
ALITTI	92B	PL B276 354	J. Alitti <i>et al.</i> (UA2 Collab.)
ALITTI	92C	PL B277 194	J. Alitti <i>et al.</i> (UA2 Collab.)
ALITTI	92D	PL B277 203	J. Alitti <i>et al.</i> (UA2 Collab.)
ALITTI	92F	PL B280 137	J. Alitti <i>et al.</i> (UA2 Collab.)
SAMUEL	92	PL B280 124	M.A. Samuel <i>et al.</i> (OKSU, CARL)
ABE	91C	PR D44 29	F. Abe <i>et al.</i> (CDF Collab.)
ALBAJAR	91	PL B253 503	C. Albajar <i>et al.</i> (UA1 Collab.)
ALITTI	91C	ZPHY C52 209	J. Alitti <i>et al.</i> (UA2 Collab.)
SAMUEL	91	PRL 67 9	M.A. Samuel <i>et al.</i> (OKSU, CARL)
Also		PRL 67 2920 (erratum)	M.A. Samuel <i>et al.</i>
ABE	90G	PRL 65 2243	F. Abe <i>et al.</i> (CDF Collab.)
Also		PR D43 2070	F. Abe <i>et al.</i> (CDF Collab.)
ALBAJAR	90	PL B241 283	C. Albajar <i>et al.</i> (UA1 Collab.)
ALITTI	90B	PL B241 150	J. Alitti <i>et al.</i> (UA2 Collab.)
ABE	89I	PRL 62 1005	F. Abe <i>et al.</i> (CDF Collab.)
ALBAJAR	89	ZPHY C44 15	C. Albajar <i>et al.</i> (UA1 Collab.)
BAUR	88	NP B308 127	U. Baur, D. Zeppenfeld
GRIFOLS	88	IJMP A3 225	J.A. Grifols, S. Peris, J. Sola
Also		PL B197 437	J.A. Grifols, S. Peris, J. Sola
ALBAJAR	87	PL B185 233	C. Albajar <i>et al.</i> (UA1 Collab.)
ANSARI	87	PL B186 440	R. Ansari <i>et al.</i> (UA2 Collab.)
GROTH	87	PR D36 2153	H. Groth, R.W. Robinett
HAGIWARA	87	NP B282 253	K. Hagiwara <i>et al.</i> (KEK, UCLA, FSU)
VANDERBIJ	87	PR D35 1088	J.J. van der Bij
GRAU	85	PL B348 283	A. Grau, J.A. Grifols
SUZUKI	85	PL B348 289	M. Suzuki
ARNISON	84D	PL B348 469	G.T.J. Aronson <i>et al.</i> (UA1 Collab.)
HERZOG	84	PL B348 355	F. Herzog
Also		PL B348 468 (erratum)	F. Herzog
ARNISON	83	PL B348 103	G.T.J. Aronson <i>et al.</i> (UA1 Collab.)
BANNER	83B	PL B348 476	M. Banner <i>et al.</i> (UA2 Collab.)



$$J = 1$$

THE Z BOSON

Revised March 2008 by C. Caso (U. of Genova), M. Grünewald (U. College Dublin and U. Ghent), and A. Gurtu (Tata Inst.).

Precision measurements at the Z -boson resonance using electron–positron colliding beams began in 1989 at the SLC and at LEP. During 1989–95, the four LEP experiments (ALEPH, DELPHI, L3, OPAL) made high-statistics studies of the production and decay properties of the Z . Although the SLD experiment at the SLC collected much lower statistics, it was able to match the precision of LEP experiments in determining the effective electroweak mixing angle $\sin^2\theta_W$ and the rates of Z decay to b - and c -quarks, owing to availability of polarized electron beams, small beam size, and stable beam spot.

The Z -boson properties reported in this section may broadly be categorized as:

- The standard ‘lineshape’ parameters of the Z consisting of its mass, M_Z , its total width, Γ_Z , and its partial decay widths, $\Gamma(\text{hadrons})$, and $\Gamma(\ell\bar{\ell})$ where $\ell = e, \mu, \tau, \nu$;
- Z asymmetries in leptonic decays and extraction of Z couplings to charged and neutral leptons;
- The b - and c -quark-related partial widths and charge asymmetries which require special techniques;

- Determination of Z decay modes and the search for modes that violate known conservation laws;
- Average particle multiplicities in hadronic Z decay;
- Z anomalous couplings.

Details on Z -parameter and asymmetries determination and the study of $Z \rightarrow b\bar{b}, c\bar{c}$ at LEP, and SLC are given in this note.

The standard ‘lineshape’ parameters of the Z are determined from an analysis of the production cross sections of these final states in e^+e^- collisions. The $Z \rightarrow \nu\bar{\nu}(\gamma)$ state is identified directly by detecting single photon production and indirectly by subtracting the visible partial widths from the total width. Inclusion in this analysis of the forward-backward asymmetry of charged leptons, $A_{FB}^{(0,\ell)}$, of the τ polarization, $P(\tau)$, and its forward-backward asymmetry, $P(\tau)^{fb}$, enables the separate determination of the effective vector (\bar{g}_V) and axial vector (\bar{g}_A) couplings of the Z to these leptons and the ratio (\bar{g}_V/\bar{g}_A), which is related to the effective electroweak mixing angle $\sin^2\theta_W$ (see the ‘Electroweak Model and Constraints on New Physics’ Review).

Determination of the b - and c -quark-related partial widths and charge asymmetries involves tagging the b and c quarks for which various methods are employed: requiring the presence of a high momentum prompt lepton in the event with high transverse momentum with respect to the accompanying jet; impact parameter and lifetime tagging using precision vertex measurement with high-resolution detectors; application of neural-network techniques to classify events as b or non- b on a statistical basis using event–shape variables; and using the presence of a charmed meson (D/D^*) or a kaon as a tag.

Z -parameter determination

LEP was run at energy points on and around the Z mass (88–94 GeV) constituting an energy ‘scan.’ The shape of the cross-section variation around the Z peak can be described by a Breit-Wigner *ansatz* with an energy-dependent total width [1–3]. The **three** main properties of this distribution, viz., the **position** of the peak, the **width** of the distribution, and the **height** of the peak, determine respectively the values of M_Z , Γ_Z , and $\Gamma(e^+e^-) \times \Gamma(f\bar{f})$, where $\Gamma(e^+e^-)$ and $\Gamma(f\bar{f})$ are the electron and fermion partial widths of the Z . The quantitative determination of these parameters is done by writing analytic expressions for these cross sections in terms of the parameters, and fitting the calculated cross sections to the measured ones by varying these parameters, taking properly into account all the errors. Single-photon exchange (σ_γ^0) and γ - Z interference ($\sigma_{\gamma Z}^0$) are included, and the large ($\sim 25\%$) initial-state radiation (ISR) effects are taken into account by convoluting the analytic expressions over a ‘Radiator Function’ [1–5] $H(s, s')$. Thus for the process $e^+e^- \rightarrow f\bar{f}$:

$$\sigma_f(s) = \int H(s, s') \sigma_f^0(s') ds' \quad (1)$$

$$\sigma_f^0(s) = \sigma_Z^0 + \sigma_\gamma^0 + \sigma_{\gamma Z}^0 \quad (2)$$

Gauge & Higgs Boson Particle Listings

Z

$$\sigma_Z^0 = \frac{12\pi}{M_Z^2} \frac{\Gamma(e^+e^-)\Gamma(f\bar{f})}{\Gamma_Z^2} \frac{s\Gamma_Z^2}{(s-M_Z^2)^2 + s^2\Gamma_Z^2/M_Z^2} \quad (3)$$

$$\sigma_\gamma^0 = \frac{4\pi\alpha^2(s)}{3s} Q_f^2 N_c^f \quad (4)$$

$$\sigma_{\gamma Z}^0 = -\frac{2\sqrt{2}\alpha(s)}{3} (Q_f G_F N_c^f \mathcal{G}_V^e \mathcal{G}_V^f) \times \frac{(s-M_Z^2)M_Z^2}{(s-M_Z^2)^2 + s^2\Gamma_Z^2/M_Z^2} \quad (5)$$

where Q_f is the charge of the fermion, $N_c^f = 3$ for quarks and 1 for leptons, and \mathcal{G}_V^f is the vector coupling of the Z to the fermion-antifermion pair $f\bar{f}$.

Since $\sigma_{\gamma Z}^0$ is expected to be much less than σ_Z^0 , the LEP Collaborations have generally calculated the interference term in the framework of the Standard Model. This fixing of $\sigma_{\gamma Z}^0$ leads to a tighter constraint on M_Z , and consequently a smaller error on its fitted value. It is possible to relax this constraint and carry out the fit within the S-matrix framework, which is briefly described in the next section.

In the above framework, the QED radiative corrections have been explicitly taken into account by convoluting over the ISR and allowing the electromagnetic coupling constant to run [6]: $\alpha(s) = \alpha/(1 - \Delta\alpha)$. On the other hand, weak radiative corrections that depend upon the assumptions of the electroweak theory and on the values of M_{top} and M_{Higgs} are accounted for by **absorbing them into the couplings**, which are then called the *effective* couplings \mathcal{G}_V and \mathcal{G}_A (or alternatively the effective parameters of the \star scheme of Kennedy and Lynn [7].)

\mathcal{G}_V^f and \mathcal{G}_A^f are complex numbers with small imaginary parts. As experimental data does not allow simultaneous extraction of both real and imaginary parts of the effective couplings, the convention $g_A^f = \text{Re}(\mathcal{G}_A^f)$ and $g_V^f = \text{Re}(\mathcal{G}_V^f)$ is used and the imaginary parts are added in the fitting code [4].

Defining

$$A_f = 2 \frac{g_V^f \cdot g_A^f}{(g_V^f)^2 + (g_A^f)^2} \quad (6)$$

the lowest-order expressions for the various lepton-related asymmetries on the Z pole are [8–10] $A_{FB}^{(0,\ell)} = (3/4)A_e A_f$, $P(\tau) = -A_\tau$, $P(\tau)^{fb} = -(3/4)A_e$, $A_{LR} = A_e$. The full analysis takes into account the energy dependence of the asymmetries. Experimentally A_{LR} is defined as $(\sigma_L - \sigma_R)/(\sigma_L + \sigma_R)$, where $\sigma_{L(R)}$ are the $e^+e^- \rightarrow Z$ production cross sections with left(right)-handed electrons.

The definition of the partial decay width of the Z to $f\bar{f}$ includes the effects of QED and QCD final state corrections, as well as the contribution due to the imaginary parts of the couplings:

$$\Gamma(f\bar{f}) = \frac{G_F M_Z^3}{6\sqrt{2}\pi} N_c^f (|\mathcal{G}_A^f|^2 R_A^f + |\mathcal{G}_V^f|^2 R_V^f) + \Delta_{ew/QCD} \quad (7)$$

where R_V^f and R_A^f are radiator factors to account for final state QED and QCD corrections, as well as effects due to nonzero

fermion masses, and $\Delta_{ew/QCD}$ represents the non-factorizable electroweak/QCD corrections.

S-matrix approach to the Z

While most experimental analyses of LEP/SLC data have followed the ‘Breit-Wigner’ approach, an alternative S-matrix-based analysis is also possible. The Z , like all unstable particles, is associated with a complex pole in the S matrix. The pole position is process-independent and gauge-invariant. The mass, \overline{M}_Z , and width, $\overline{\Gamma}_Z$, can be defined in terms of the pole in the energy plane via [11–14]

$$\overline{s} = \overline{M}_Z^2 - i\overline{M}_Z\overline{\Gamma}_Z \quad (8)$$

leading to the relations

$$\begin{aligned} \overline{M}_Z &= M_Z / \sqrt{1 + \Gamma_Z^2/M_Z^2} \\ &\approx M_Z - 34.1 \text{ MeV} \end{aligned} \quad (9)$$

$$\begin{aligned} \overline{\Gamma}_Z &= \Gamma_Z / \sqrt{1 + \Gamma_Z^2/M_Z^2} \\ &\approx \Gamma_Z - 0.9 \text{ MeV} . \end{aligned} \quad (10)$$

The L3 and OPAL Collaborations at LEP (ACCIARRI 00Q and ABBIENDI 04G) have analyzed their data using the S-matrix approach as defined in Eq. (8), in addition to the conventional one. They observe a downward shift in the Z mass as expected.

Handling the large-angle e^+e^- final state

Unlike other $f\bar{f}$ decay final states of the Z , the e^+e^- final state has a contribution not only from the s -channel but also from the t -channel and s - t interference. The full amplitude is not amenable to fast calculation, which is essential if one has to carry out minimization fits within reasonable computer time. The usual procedure is to calculate the non- s channel part of the cross section separately using the Standard Model programs ALIBABA [15] or TOPAZO [16], with the measured value of M_{top} , and $M_{\text{Higgs}} = 150$ GeV, and add it to the s -channel cross section calculated as for other channels. This leads to two additional sources of error in the analysis: firstly, the theoretical calculation in ALIBABA itself is known to be accurate to $\sim 0.5\%$, and secondly, there is uncertainty due to the error on M_{top} and the unknown value of M_{Higgs} (100–1000 GeV). These errors are propagated into the analysis by including them in the systematic error on the e^+e^- final state. As these errors are common to the four LEP experiments, this is taken into account when performing the LEP average.

Errors due to uncertainty in LEP energy determination [17–22]

The systematic errors related to the LEP energy measurement can be classified as:

- The absolute energy scale error;
- Energy-point-to-energy-point errors due to the non-linear response of the magnets to the exciting currents;
- Energy-point-to-energy-point errors due to possible higher-order effects in the relationship between the dipole field and beam energy;
- Energy reproducibility errors due to various unknown uncertainties in temperatures, tidal effects, corrector settings, RF status, *etc.*

Precise energy calibration was done outside normal data taking using the resonant depolarization technique. Run-time energies were determined every 10 minutes by measuring the relevant machine parameters and using a model which takes into account all the known effects, including leakage currents produced by trains in the Geneva area and the tidal effects due to gravitational forces of the Sun and the Moon. The LEP Energy Working Group has provided a covariance matrix from the determination of LEP energies for the different running periods during 1993–1995 [17].

Choice of fit parameters

The LEP Collaborations have chosen the following primary set of parameters for fitting: M_Z , Γ_Z , σ_{hadron}^0 , $R(\text{lepton})$, $A_{FB}^{(0,\ell)}$, where $R(\text{lepton}) = \Gamma(\text{hadrons})/\Gamma(\text{lepton})$, $\sigma_{\text{hadron}}^0 = 12\pi\Gamma(e^+e^-)\Gamma(\text{hadrons})/M_Z^2\Gamma_Z^2$. With a knowledge of these fitted parameters and their covariance matrix, any other parameter can be derived. The main advantage of these parameters is that they form a physics motivated set of parameters with much reduced correlations.

Thus, the most general fit carried out to cross section and asymmetry data determines the **nine parameters**: M_Z , Γ_Z , σ_{hadron}^0 , $R(e)$, $R(\mu)$, $R(\tau)$, $A_{FB}^{(0,e)}$, $A_{FB}^{(0,\mu)}$, $A_{FB}^{(0,\tau)}$. Assumption of lepton universality leads to a **five-parameter fit** determining M_Z , Γ_Z , σ_{hadron}^0 , $R(\text{lepton})$, $A_{FB}^{(0,\ell)}$.

Combining results from LEP and SLC experiments

With a steady increase in statistics over the years and improved understanding of the common systematic errors between LEP experiments, the procedures for combining results have evolved continuously [23]. The Line Shape Sub-group of the LEP Electroweak Working Group investigated the effects of these common errors, and devised a combination procedure for the precise determination of the Z parameters from LEP experiments. Using these procedures, this note also gives the results after combining the final parameter sets from the four experiments, and these are the results quoted as the fit results in the Z listings below. Transformation of variables leads to values of derived parameters like partial decay widths and branching ratios to hadrons and leptons. Finally, transforming the LEP combined nine parameter set to $(M_Z, \Gamma_Z, \sigma_{\text{hadron}}^0, g_V^f, g_V^f, f = e, \mu, \tau)$ using the average values of lepton asymmetry parameters (A_e, A_μ, A_τ) as constraints, leads to the best fitted values of the vector and axial-vector couplings (g_V, g_A) of the charged leptons to the Z .

Brief remarks on the handling of common errors and their magnitudes are given below. The identified common errors are those coming from

(a) LEP energy calibration uncertainties, and

(b) the theoretical uncertainties in (i) the luminosity determination using small angle Bhabha scattering, (ii) estimating the non-s channel contribution to large angle Bhabha scattering, (iii) the calculation of QED radiative effects, and (iv) the parametrization of the cross section in terms of the parameter set used.

Common LEP energy errors

All the collaborations incorporate in their fit the full LEP energy error matrix as provided by the LEP energy group for their intersection region [17]. The effect of these errors is separated out from that of other errors by carrying out fits with energy errors scaled up and down by $\sim 10\%$ and redoing the fits. From the observed changes in the overall error matrix, the covariance matrix of the common energy errors is determined. Common LEP energy errors lead to uncertainties on M_Z , Γ_Z , and σ_{hadron}^0 of 1.7, 1.2 MeV, and 0.011 nb, respectively.

Common luminosity errors

BHLUMI 4.04 [24] is used by all LEP collaborations for small-angle Bhabha scattering leading to a common uncertainty in their measured cross sections of 0.061% [25]. BHLUMI does not include a correction for production of light fermion pairs. OPAL explicitly corrects for this effect and reduces their luminosity uncertainty to 0.054%, which is taken fully correlated with the other experiments. The other three experiments among themselves have a common uncertainty of 0.061%.

Common non-s channel uncertainties

The same standard model programs ALIBABA [15] and TOPAZ0 [16] are used to calculate the non-s channel contribution to the large angle Bhabha scattering [26]. As this contribution is a function of the Z mass, which itself is a variable in the fit, it is parametrized as a function of M_Z by each collaboration to properly track this contribution as M_Z varies in the fit. The common errors on R_e and $A_{FB}^{(0,e)}$ are 0.024 and 0.0014 respectively, and are correlated between them.

Common theoretical uncertainties: QED

There are large initial-state photon and fermion pair radiation effects near the Z resonance, for which the best currently available evaluations include contributions up to $\mathcal{O}(\alpha^3)$. To estimate the remaining uncertainties, different schemes are incorporated in the standard model programs ZFITTER [5], TOPAZ0 [16], and MIZA [27]. Comparing the different options leads to error estimates of 0.3 and 0.2 MeV on M_Z and Γ_Z respectively, and of 0.02% on σ_{hadron}^0 .

Common theoretical uncertainties: parametrization of lineshape and asymmetries

To estimate uncertainties arising from ambiguities in the model-independent parametrization of the differential cross-section near the Z resonance, results from TOPAZ0 and ZFITTER were compared by using ZFITTER to fit the cross sections

Gauge & Higgs Boson Particle Listings

Z

and asymmetries calculated using TOPAZ0. The resulting uncertainties on M_Z , Γ_Z , σ_{hadron}^0 , $R(\text{lepton})$, and $A_{FB}^{(0,\ell)}$ are 0.1 MeV, 0.1 MeV, 0.001 nb, 0.004, and 0.0001 respectively.

Thus, the overall theoretical errors on M_Z , Γ_Z , σ_{hadron}^0 are 0.3 MeV, 0.2 MeV, and 0.008 nb respectively; on each $R(\text{lepton})$ is 0.004 and on each $A_{FB}^{(0,\ell)}$ is 0.0001. Within the set of three $R(\text{lepton})$'s and the set of three $A_{FB}^{(0,\ell)}$'s, the respective errors are fully correlated.

All the theory-related errors mentioned above utilize Standard Model programs which need the Higgs mass and running electromagnetic coupling constant as inputs; uncertainties on these inputs will also lead to common errors. All LEP collaborations used the same set of inputs for Standard Model calculations: $M_Z = 91.187$ GeV, the Fermi constant $G_F = (1.16637 \pm 0.00001) \times 10^{-5}$ GeV $^{-2}$ [28], $\alpha^{(5)}(M_Z) = 1/128.877 \pm 0.090$ [29], $\alpha_s(M_Z) = 0.119$ [30], $M_{\text{top}} = 174.3 \pm 5.1$ GeV [30] and $M_{\text{Higgs}} = 150$ GeV. The only observable effect, on M_Z , is due to the variation of M_{Higgs} between 100–1000 GeV (due to the variation of the γ/Z interference term which is taken from the Standard Model): M_Z changes by +0.23 MeV per unit change in $\log_{10} M_{\text{Higgs}}/\text{GeV}$, which is not an error but a correction to be applied once M_{Higgs} is determined. The effect is much smaller than the error on M_Z (± 2.1 MeV).

Methodology of combining the LEP experimental results

The LEP experimental results actually used for combination are slightly modified from those published by the experiments (which are given in the Listings below). This has been done in order to facilitate the procedure by making the inputs more consistent. These modified results are given explicitly in [23]. The main differences compared to the published results are (a) consistent use of ZFITTER 6.23 and TOPAZ0. The published ALEPH results used ZFITTER 6.10; (b) use of the combined energy-error matrix, which makes a difference of 0.1 MeV on the M_Z and Γ_Z for L3 only as at that intersection the RF modeling uncertainties are the largest.

Thus, nine-parameter sets from all four experiments with their covariance matrices are used together with all the common errors correlations. A grand covariance matrix, V , is constructed and a combined nine-parameter set is obtained by minimizing $\chi^2 = \Delta^T V^{-1} \Delta$, where Δ is the vector of residuals of the combined parameter set to the results of individual experiments. Imposing lepton universality in the combination results in the combined five parameter set.

Study of $Z \rightarrow b\bar{b}$ and $Z \rightarrow c\bar{c}$

In the sector of c - and b -physics, the LEP experiments have measured the ratios of partial widths $R_b = \Gamma(Z \rightarrow b\bar{b})/\Gamma(Z \rightarrow \text{hadrons})$, and $R_c = \Gamma(Z \rightarrow c\bar{c})/\Gamma(Z \rightarrow \text{hadrons})$, and the forward-backward (charge) asymmetries $A_{FB}^{b\bar{b}}$ and $A_{FB}^{c\bar{c}}$. The SLD experiment at SLC has measured the ratios R_c and R_b and, utilizing the polarization of the electron beam, was able to obtain the final state coupling parameters A_b and A_c from a measurement of the left-right forward-backward asymmetry of

b - and c -quarks. The high precision measurement of R_c at SLD was made possible owing to the small beam size and very stable beam spot at SLC, coupled with a highly precise CCD pixel detector. Several of the analyses have also determined other quantities, in particular the semileptonic branching ratios, $B(b \rightarrow \ell^-)$, $B(b \rightarrow c \rightarrow \ell^+)$, and $B(c \rightarrow \ell^+)$, the average time-integrated $B^0\bar{B}^0$ mixing parameter $\bar{\chi}$ and the probabilities for a c -quark to fragment into a D^+ , a D_s , a D^{*+} , or a charmed baryon. The latter measurements do not concern properties of the Z boson, and hence they do not appear in the Listing below. However, for completeness, we will report at the end of this minireview their values as obtained fitting the data contained in the Z section. All these quantities are correlated with the electroweak parameters, and since the mixture of b hadrons is different from the one at the $\Upsilon(4S)$, their values might differ from those measured at the $\Upsilon(4S)$.

All the above quantities are correlated to each other since:

- Several analyses (for example the lepton fits) determine more than one parameter simultaneously;
- Some of the electroweak parameters depend explicitly on the values of other parameters (for example R_b depends on R_c);
- Common tagging and analysis techniques produce common systematic uncertainties.

The LEP Electroweak Heavy Flavour Working Group has developed [31] a procedure for combining the measurements taking into account known sources of correlation. The combining procedure determines fourteen parameters: the six parameters of interest in the electroweak sector, R_b , R_c , $A_{FB}^{b\bar{b}}$, $A_{FB}^{c\bar{c}}$, A_b and A_c and, in addition, $B(b \rightarrow \ell^-)$, $B(b \rightarrow c \rightarrow \ell^+)$, $B(c \rightarrow \ell^+)$, $\bar{\chi}$, $f(D^+)$, $f(D_s)$, $f(c_{\text{baryon}})$ and $P(c \rightarrow D^{*+}) \times B(D^{*+} \rightarrow \pi^+ D^0)$, to take into account their correlations with the electroweak parameters. Before the fit both the peak and off-peak asymmetries are translated to the common energy $\sqrt{s} = 91.26$ GeV using the predicted energy dependence from ZFITTER [5].

Summary of the measurements and of the various kinds of analysis

The measurements of R_b and R_c fall into two classes. In the first, named single-tag measurement, a method for selecting b and c events is applied and the number of tagged events is counted. A second technique, named double-tag measurement, has the advantage that the tagging efficiency is directly derived from the data thereby reducing the systematic error on the measurement.

The measurements in the b - and c -sector can be essentially grouped in the following categories:

- Lifetime (and lepton) double-tagging measurements of R_b . These are the most precise measurements of R_b and obviously dominate the combined result. The main sources of systematics come from the charm contamination and from estimating the hemisphere b -tagging efficiency correlation;
- Analyses with $D/D^{*\pm}$ to measure R_c . These measurements make use of several different tagging techniques (inclusive/exclusive double tag, exclusive double tag, reconstruction of all weakly decaying charmed states) and no assumptions are made on the energy dependence of charm fragmentation;
- A measurement of R_c using single leptons and assuming $B(b \rightarrow c \rightarrow \ell^+)$;
- Lepton fits which use hadronic events with one or more leptons in the final state to measure the asymmetries $A_{FB}^{b\bar{b}}$ and $A_{FB}^{c\bar{c}}$. Each analysis usually gives several other electroweak parameters. The dominant sources of systematics are due to lepton identification, to other semileptonic branching ratios and to the modeling of the semileptonic decay;
- Measurements of $A_{FB}^{b\bar{b}}$ using lifetime tagged events with a hemisphere charge measurement. These measurements dominate the combined result;
- Analyses with $D/D^{*\pm}$ to measure $A_{FB}^{c\bar{c}}$ or simultaneously $A_{FB}^{b\bar{b}}$ and $A_{FB}^{c\bar{c}}$;
- Measurements of A_b and A_c from SLD, using several tagging methods (lepton, kaon, D/D^* , and vertex mass). These quantities are directly extracted from a measurement of the left–right forward–backward asymmetry in $c\bar{c}$ and $b\bar{b}$ production using a polarized electron beam.

Averaging procedure

All the measurements are provided by the LEP and SLD Collaborations in the form of tables with a detailed breakdown of the systematic errors of each measurement and its dependence on other electroweak parameters.

The averaging proceeds via the following steps:

- Define and propagate a consistent set of external inputs such as branching ratios, hadron lifetimes, fragmentation models *etc.* All the measurements are checked to ensure that all use a common set of assumptions (for instance, since the QCD corrections for the forward–backward asymmetries are strongly dependent on the experimental conditions, the data are corrected before combining);
- Form the full (statistical and systematic) covariance matrix of the measurements. The systematic correlations between different analyses are calculated from the detailed error breakdown in the measurement tables. The correlations relating several measurements made by the same analysis are also used;
- Take into account any explicit dependence of a measurement on the other electroweak parameters. As an example of this dependence, we illustrate the case of the double-tag measurement of R_b , where c -quarks constitute the main background. The normalization of the charm contribution is not usually fixed by the data and the measurement of R_b depends on the assumed value of R_c , which can be written as:

$$R_b = R_b^{\text{meas}} + a(R_c) \frac{(R_c - R_c^{\text{used}})}{R_c}, \quad (11)$$
 where R_b^{meas} is the result of the analysis which assumed a value of $R_c = R_c^{\text{used}}$ and $a(R_c)$ is the constant which gives the dependence on R_c ;
- Perform a χ^2 minimization with respect to the combined electroweak parameters.

After the fit the average peak asymmetries $A_{FB}^{c\bar{c}}$ and $A_{FB}^{b\bar{b}}$ are corrected for the energy shift from 91.26 GeV to M_Z and for QED (initial state radiation), γ exchange, and γZ interference effects, to obtain the corresponding pole asymmetries $A_{FB}^{0,c}$ and $A_{FB}^{0,b}$.

This averaging procedure, using the fourteen parameters described above, and applied to the data contained in the Z particle listing below, gives the following results (where the last 8 parameters do not depend directly on the Z):

$$R_b^0 = 0.21629 \pm 0.00066$$

$$R_c^0 = 0.1721 \pm 0.0030$$

$$A_{FB}^{0,b} = 0.0992 \pm 0.0016$$

$$A_{FB}^{0,c} = 0.0707 \pm 0.0035$$

$$A_b = 0.923 \pm 0.020$$

$$A_c = 0.670 \pm 0.027$$

$$B(b \rightarrow \ell^-) = 0.1071 \pm 0.0022$$

$$B(b \rightarrow c \rightarrow \ell^+) = 0.0801 \pm 0.0018$$

$$B(c \rightarrow \ell^+) = 0.0969 \pm 0.0031$$

$$\bar{\chi} = 0.1250 \pm 0.0039$$

$$f(D^+) = 0.235 \pm 0.016$$

$$f(D_s) = 0.126 \pm 0.026$$

$$f(c_{\text{baryon}}) = 0.093 \pm 0.022$$

$$P(c \rightarrow D^{*+}) \times B(D^{*+} \rightarrow \pi^+ D^0) = 0.1622 \pm 0.0048$$

Among the non–electroweak observables, the B semileptonic branching fraction $B(b \rightarrow \ell^-)$ is of special interest, since the dominant error source on this quantity is the dependence on

Gauge & Higgs Boson Particle Listings

Z

the semileptonic decay model for $b \rightarrow \ell^-$, with $\Delta B(b \rightarrow \ell^-)_{b \rightarrow \ell^- \text{ model}} = 0.0012$. Extensive studies have been made to understand the size of this error. Among the electroweak quantities, the quark asymmetries with leptons depend also on the semileptonic decay model, while the asymmetries using other methods usually do not. The fit implicitly requires that the different methods give consistent results and this effectively constrains the decay model, and thus reduces in principle the error from this source in the fit result.

To obtain a conservative estimate of the modelling error, the above fit has been repeated removing all asymmetry measurements. The results of the fit on B-decay related observables are [23]: $B(b \rightarrow \ell^-) = 0.1069 \pm 0.0022$, with $\Delta B(b \rightarrow \ell^-)_{b \rightarrow \ell^- \text{ model}} = 0.0013$, $B(b \rightarrow c \rightarrow \ell^+) = 0.0802 \pm 0.0019$ and $\bar{\chi} = 0.1259 \pm 0.0042$.

References

1. R.N. Cahn, Phys. Rev. **D36**, 2666 (1987).
2. F.A. Berends *et al.*, "Z Physics at LEP 1," CERN Report 89-08 (1989), Vol. 1, eds. G. Altarelli, R. Kleiss, and C. Verzegnassi, p. 89.
3. A. Borrelli *et al.*, Nucl. Phys. **B333**, 357 (1990).
4. D. Bardin and G. Passarino, "Upgrading of Precision Calculations for Electroweak Observables," hep-ph/9803425; D. Bardin, G. Passarino, and M. Grunewald, "Precision Calculation Project Report," hep-ph/9902452.
5. D. Bardin *et al.*, Z. Phys. **C44**, 493 (1989); Comp. Phys. Comm. **59**, 303 (1990); D. Bardin *et al.*, Nucl. Phys. **B351**, 1 (1991); Phys. Lett. **B255**, 290 (1991), and CERN-TH/6443/92 (1992); Comp. Phys. Comm. **133**, 229 (2001).
6. G. Burgers *et al.*, "Z Physics at LEP 1," CERN Report 89-08 (1989), Vol. 1, eds. G. Altarelli, R. Kleiss, and C. Verzegnassi, p. 55.
7. D.C. Kennedy and B.W. Lynn, Nucl. Phys. **B322**, 1 (1989).
8. M. Consoli *et al.*, "Z Physics at LEP 1," CERN Report 89-08 (1989), Vol. 1, eds. G. Altarelli, R. Kleiss, and C. Verzegnassi, p. 7.
9. M. Bohm *et al.*, *ibid.*, p. 203.
10. S. Jadach *et al.*, *ibid.*, p. 235.
11. R. Stuart, Phys. Lett. **B262**, 113 (1991).
12. A. Sirlin, Phys. Rev. Lett. **67**, 2127 (1991).
13. A. Leike, T. Riemann, and J. Rose, Phys. Lett. **B273**, 513 (1991).
14. See also D. Bardin *et al.*, Phys. Lett. **B206**, 539 (1988).
15. W. Beenakker, F.A. Berends, and S.C. van der Marck, Nucl. Phys. **B349**, 323 (1991).
16. G. Montagna *et al.*, Nucl. Phys. **B401**, 3 (1993); Comp. Phys. Comm. **76**, 328 (1993); Comp. Phys. Comm. **93**, 120 (1996); G. Montagna *et al.*, Comp. Phys. Comm. **117**, 278 (1999).
17. R. Assmann *et al.*, (Working Group on LEP Energy), Eur. Phys. J. **C6**, 187 (1999).
18. R. Assmann *et al.*, (Working Group on LEP Energy), Z. Phys. **C66**, 567 (1995).
19. L. Arnaudon *et al.*, (Working Group on LEP Energy and LEP Collaborations), Phys. Lett. **B307**, 187 (1993).
20. L. Arnaudon *et al.*, (Working Group on LEP Energy), CERN-PPE/92-125 (1992).
21. L. Arnaudon *et al.*, Phys. Lett. **B284**, 431 (1992).
22. R. Bailey *et al.*, 'LEP Energy Calibration' CERN-SL-90-95-AP, Proceedings of the "2nd European Particle Accelerator Conference," Nice, France, 12-16 June 1990, pp. 1765-1767.
23. The LEP Collaborations: ALEPH, DELPHI, L3, OPAL, and the LEP Electroweak Working Group: CERN-PH-EP/2007-039 (2007); CERN-PH-EP/2006-042 (2006). The LEP Collaborations: ALEPH, DELPHI, L3, OPAL, the LEP Electroweak Working Group, and the SLD Heavy Flavour Group: Phys. Reports **427**, 257 (2006); CERN-PH-EP/2005-051 (2005); CERN-PH-EP/2004-069 (2004); CERN-EP/2003-091 (2003); CERN-EP/2002-091 (2002); CERN-EP/2001-098 (2001); CERN-EP/2001-021 (2001); CERN-EP/2000-016 (1999); CERN-EP/99-15 (1998); CERN-PPE/97-154 (1997); CERN-PPE/96-183 (1996); CERN-PPE/95-172 (1995); CERN-PPE/94-187 (1994); CERN-PPE/93-157 (1993).
24. S. Jadach *et al.*, BHLUMI 4.04, Comp. Phys. Comm. **102**, 229 (1997); S. Jadach and O. Nicosini, Event generators for Bhabha scattering, in Physics at LEP2, CERN-96-01 Vol. 2, February 1996.
25. B.F.L. Ward *et al.*, Phys. Lett. **B450**, 262 (1999).
26. W. Beenakker and G. Passarino, Phys. Lett. **B425**, 199 (1998).
27. M. Martinez *et al.*, Z. Phys. **C49**, 645 (1991); M. Martinez and F. Teubert, Z. Phys. **C65**, 267 (1995), updated with results summarized in S. Jadach, B. Pietrzyk, and M. Skrzypek, Phys. Lett. **B456**, 77 (1999) and Reports of the working group on precision calculations for the Z resonance, CERN 95-03, ed. D. Bardin, W. Hollik, and G. Passarino, and references therein.
28. T. van Ritbergen and R. Stuart, Phys. Lett. **B437**, 201 (1998); Phys. Rev. Lett. **82**, 488 (1999).
29. S. Eidelman and F. Jegerlehner, Z. Phys. **C67**, 585 (1995); M. Steinhäuser, Phys. Lett. **B429**, 158 (1998).
30. Particle Data Group (D.E. Groom *et al.*), Eur. Phys. J. **C15**, 1 (2000).
31. The LEP Experiments: ALEPH, DELPHI, L3, and OPAL Nucl. Instrum. Methods **A378**, 101 (1996).

Z MASS

OUR FIT is obtained using the fit procedure and correlations as determined by the LEP Electroweak Working Group (see the note "The Z boson" and ref. LEP-SLC 06). The fit is performed using the Z mass and width, the Z hadronic pole cross section, the ratios of hadronic to leptonic partial widths, and the Z pole forward-backward lepton asymmetries. This set is believed to be most free of correlations.

The Z-boson mass listed here corresponds to the mass parameter in a Breit-Wigner distribution with mass dependent width. The value is 34 MeV greater than the real part of the position of the pole (in the energy-squared plane) in the Z-boson propagator. Also the LEP experiments have generally assumed a fixed value of the $\gamma - Z$ interferences term based on the standard model. Keeping this term as free parameter leads to a somewhat larger error on the fitted Z mass. See ACCIARRI 00q and ABBIENDI 04g for a detailed investigation of both these issues.

VALUE (GeV)	EVTs	DOCUMENT ID	TECN	COMMENT
91.1876 ± 0.0021 OUR FIT				
91.1852 ± 0.0030	4.57M	¹ ABBIENDI	01A OPAL	$E_{\text{cm}}^{\text{ec}}$ = 88-94 GeV
91.1863 ± 0.0028	4.08M	² ABREU	00F DLPH	$E_{\text{cm}}^{\text{ec}}$ = 88-94 GeV

See key on page 373

Gauge & Higgs Boson Particle Listings

Z

91.1898 ± 0.0031	3.96M	³ ACCIARRI	00c L3	$E_{cm}^{ee} = 88-94$ GeV
91.1885 ± 0.0031	4.57M	⁴ BARATE	00c ALEP	$E_{cm}^{ee} = 88-94$ GeV
• • • We do not use the following data for averages, fits, limits, etc. • • •				
91.1872 ± 0.0033		⁵ ABBIENDI	04c OPAL	$E_{cm}^{ee} = \text{LEP1} + 130-209$ GeV
91.272 ± 0.032 ± 0.033		⁶ ACHARD	04c L3	$E_{cm}^{ee} = 183-209$ GeV
91.1875 ± 0.0039	3.97M	⁷ ACCIARRI	00q L3	$E_{cm}^{ee} = \text{LEP1} + 130-189$ GeV
91.151 ± 0.008		⁸ MIYABAYASHI	95 TOPZ	$E_{cm}^{ee} = 57.8$ GeV
91.74 ± 0.28 ± 0.93	156	⁹ ALITTI	92b UA2	$E_{cm}^{pp} = 630$ GeV
90.9 ± 0.3 ± 0.2	188	¹⁰ ABE	89c CDF	$E_{cm}^{pp} = 1.8$ TeV
91.14 ± 0.12	480	¹¹ ABRAMS	89b MRK2	$E_{cm}^{ee} = 89-93$ GeV
93.1 ± 1.0 ± 3.0	24	¹² ALBAJAR	89 UA1	$E_{cm}^{pp} = 546,630$ GeV

¹ ABBIENDI 01A error includes approximately 2.3 MeV due to statistics and 1.8 MeV due to LEP energy uncertainty.

² The error includes 1.6 MeV due to LEP energy uncertainty.

³ The error includes 1.8 MeV due to LEP energy uncertainty.

⁴ BARATE 00c error includes approximately 2.4 MeV due to statistics, 0.2 MeV due to experimental systematics, and 1.7 MeV due to LEP energy uncertainty.

⁵ ABBIENDI 04c obtain this result using the S-matrix formalism for a combined fit to their cross section and asymmetry data at the Z peak and their data at 130–209 GeV. The authors have corrected the measurement for the 34 MeV shift with respect to the Breit-Wigner fits.

⁶ ACHARD 04c select $e^+e^- \rightarrow Z\gamma$ events with hard initial-state radiation. Z decays to $q\bar{q}$ and muon pairs are considered. The fit results obtained in the two samples are found consistent to each other and combined considering the uncertainty due to ISR modelling as fully correlated.

⁷ ACCIARRI 00q interpret the s-dependence of the cross sections and lepton forward-backward asymmetries in the framework of the S-matrix formalism. They fit to their cross section and asymmetry data at high energies, using the results of S-matrix fits to Z-peak data (ACCIARRI 00c) as constraints. The 130–189 GeV data constrains the γ/Z interference term. The authors have corrected the measurement for the 34.1 MeV shift with respect to the Breit-Wigner fits. The error contains a contribution of ± 2.3 MeV due to the uncertainty on the γ/Z interference.

⁸ MIYABAYASHI 95 combine their low energy total hadronic cross-section measurement with the ACTON 93D data and perform a fit using an S-matrix formalism. As expected, this result is below the mass values obtained with the standard Breit-Wigner parametrization.

⁹ Enters fit through W/Z mass ratio given in the W Particle Listings. The ALITTI 92b systematic error (± 0.93) has two contributions: one (± 0.92) cancels in m_W/m_Z and one (± 0.12) is noncancelling. These were added in quadrature.

¹⁰ First error of ABE 89 is combination of statistical and systematic contributions; second is mass scale uncertainty.

¹¹ ABRAMS 89B uncertainty includes 35 MeV due to the absolute energy measurement.

¹² ALBAJAR 89 result is from a total sample of $33 Z \rightarrow e^+e^-$ events.

Z WIDTH

OUR FIT is obtained using the fit procedure and correlations as determined by the LEP Electroweak Working Group (see the note "The Z boson" and ref. LEP-SLC 06).

VALUE (GeV)	EVTS	DOCUMENT ID	TECN	COMMENT
2.4952 ± 0.0023 OUR FIT				
2.4948 ± 0.0041	4.57M	¹³ ABBIENDI	01A OPAL	$E_{cm}^{ee} = 88-94$ GeV
2.4876 ± 0.0041	4.08M	¹⁴ ABREU	00F DLPH	$E_{cm}^{ee} = 88-94$ GeV
2.5024 ± 0.0042	3.96M	¹⁵ ACCIARRI	00c L3	$E_{cm}^{ee} = 88-94$ GeV
2.4951 ± 0.0043	4.57M	¹⁶ BARATE	00c ALEP	$E_{cm}^{ee} = 88-94$ GeV
• • • We do not use the following data for averages, fits, limits, etc. • • •				
2.4943 ± 0.0041		¹⁷ ABBIENDI	04g OPAL	$E_{cm}^{ee} = \text{LEP1} + 130-209$ GeV
2.5025 ± 0.0041	3.97M	¹⁸ ACCIARRI	00q L3	$E_{cm}^{ee} = \text{LEP1} + 130-189$ GeV
2.50 ± 0.21 ± 0.06		¹⁹ ABREU	96R DLPH	$E_{cm}^{ee} = 91.2$ GeV
3.8 ± 0.8 ± 1.0	188	ABE	89c CDF	$E_{cm}^{pp} = 1.8$ TeV
2.42 + 0.45 - 0.35	480	²⁰ ABRAMS	89b MRK2	$E_{cm}^{ee} = 89-93$ GeV
2.7 + 1.2 - 1.0 ± 1.3	24	²¹ ALBAJAR	89 UA1	$E_{cm}^{pp} = 546,630$ GeV
2.7 ± 2.0 ± 1.0	25	²² ANSARI	87 UA2	$E_{cm}^{pp} = 546,630$ GeV

¹³ ABBIENDI 01A error includes approximately 3.6 MeV due to statistics, 1 MeV due to event selection systematics, and 1.3 MeV due to LEP energy uncertainty.

¹⁴ The error includes 1.2 MeV due to LEP energy uncertainty.

¹⁵ The error includes 1.3 MeV due to LEP energy uncertainty.

¹⁶ BARATE 00c error includes approximately 3.8 MeV due to statistics, 0.9 MeV due to experimental systematics, and 1.3 MeV due to LEP energy uncertainty.

¹⁷ ABBIENDI 04g obtain this result using the S-matrix formalism for a combined fit to their cross section and asymmetry data at the Z peak and their data at 130–209 GeV. The authors have corrected the measurement for the 1 MeV shift with respect to the Breit-Wigner fits.

¹⁸ ACCIARRI 00q interpret the s-dependence of the cross sections and lepton forward-backward asymmetries in the framework of the S-matrix formalism. They fit to their cross section and asymmetry data at high energies, using the results of S-matrix fits to Z-peak data (ACCIARRI 00c) as constraints. The 130–189 GeV data constrains the γ/Z interference term. The authors have corrected the measurement for the 0.9 MeV shift with respect to the Breit-Wigner fits.

¹⁹ ABREU 96R obtain this value from a study of the interference between initial and final state radiation in the process $e^+e^- \rightarrow Z \rightarrow \mu^+\mu^-$.

²⁰ ABRAMS 89B uncertainty includes 50 MeV due to the miniSAM background subtraction error.

²¹ ALBAJAR 89 result is from a total sample of $33 Z \rightarrow e^+e^-$ events.

²² Quoted values of ANSARI 87 are from direct fit. Ratio of Z and W production gives either $\Gamma(Z) < (1.09 \pm 0.07) \times \Gamma(W)$, CL = 90% or $\Gamma(Z) = (0.82^{+0.19}_{-0.14} \pm 0.06) \times \Gamma(W)$. Assuming Standard-Model value $\Gamma(W) = 2.65$ GeV then gives $\Gamma(Z) < 2.89 \pm 0.19$ or $= 2.17^{+0.50}_{-0.37} \pm 0.16$.

Z DECAY MODES

Mode	Fraction (Γ_i/Γ)	Scale factor/ Confidence level
Γ_1 e^+e^-	(3.363 ± 0.004) %	
Γ_2 $\mu^+\mu^-$	(3.366 ± 0.007) %	
Γ_3 $\tau^+\tau^-$	(3.370 ± 0.008) %	
Γ_4 $\ell^+\ell^-$	[a] (3.3658 ± 0.0023) %	
Γ_5 invisible	(20.00 ± 0.06) %	
Γ_6 hadrons	(69.91 ± 0.06) %	
Γ_7 $(u\bar{u} + c\bar{c})/2$	(11.6 ± 0.6) %	
Γ_8 $(d\bar{d} + s\bar{s} + b\bar{b})/3$	(15.6 ± 0.4) %	
Γ_9 $c\bar{c}$	(12.03 ± 0.21) %	
Γ_{10} $b\bar{b}$	(15.12 ± 0.05) %	
Γ_{11} $b\bar{b}b\bar{b}$	(3.6 ± 1.3) × 10 ⁻⁴	
Γ_{12} $g\bar{g}$	< 1.1	CL=95%
Γ_{13} $\pi^0\gamma$	< 5.2	× 10 ⁻⁵ CL=95%
Γ_{14} $\eta\gamma$	< 5.1	× 10 ⁻⁵ CL=95%
Γ_{15} $\omega\gamma$	< 6.5	× 10 ⁻⁴ CL=95%
Γ_{16} $\eta'(958)\gamma$	< 4.2	× 10 ⁻⁵ CL=95%
Γ_{17} $\gamma\gamma$	< 5.2	× 10 ⁻⁵ CL=95%
Γ_{18} $\gamma\gamma\gamma$	< 1.0	× 10 ⁻⁵ CL=95%
Γ_{19} $\pi^\pm W^\mp$	[b] < 7	× 10 ⁻⁵ CL=95%
Γ_{20} $\rho^\pm W^\mp$	[b] < 8.3	× 10 ⁻⁵ CL=95%
Γ_{21} $J/\psi(1S)X$	(3.51 $^{+0.23}_{-0.25}$) × 10 ⁻³	S=1.1
Γ_{22} $\psi(2S)X$	(1.60 ± 0.29) × 10 ⁻³	
Γ_{23} $\chi_{c1}(1P)X$	(2.9 ± 0.7) × 10 ⁻³	
Γ_{24} $\chi_{c2}(1P)X$	< 3.2	× 10 ⁻³ CL=90%
Γ_{25} $\Upsilon(1S)X + \Upsilon(2S)X + \Upsilon(3S)X$	(1.0 ± 0.5) × 10 ⁻⁴	
Γ_{26} $\Upsilon(1S)X$	< 4.4	× 10 ⁻⁵ CL=95%
Γ_{27} $\Upsilon(2S)X$	< 1.39	× 10 ⁻⁴ CL=95%
Γ_{28} $\Upsilon(3S)X$	< 9.4	× 10 ⁻⁵ CL=95%
Γ_{29} $(D^0/\bar{D}^0)X$	(20.7 ± 2.0) %	
Γ_{30} $D^\pm X$	(12.2 ± 1.7) %	
Γ_{31} $D^*(2010)^\pm X$	[b] (11.4 ± 1.3) %	
Γ_{32} $D_{s1}(2536)^\pm X$	(3.6 ± 0.8) × 10 ⁻³	
Γ_{33} $D_{sJ}(2573)^\pm X$	(5.8 ± 2.2) × 10 ⁻³	
Γ_{34} $D^{*'}(2629)^\pm X$	searched for	
Γ_{35} BX		
Γ_{36} B^*X		
Γ_{37} B^+X	(6.10 ± 0.14) %	
Γ_{38} B_s^0X	(1.56 ± 0.13) %	
Γ_{39} $B_s^\pm X$	searched for	
Γ_{40} $A_c^\pm X$	(1.54 ± 0.33) %	
Γ_{41} $\Xi_c^\pm X$	seen	
Γ_{42} $\Xi_b^\pm X$	seen	
Γ_{43} b -baryon X	(1.38 ± 0.22) %	
Γ_{44} anomalous γ + hadrons	[c] < 3.2	× 10 ⁻³ CL=95%
Γ_{45} $e^+e^- \gamma$	[c] < 5.2	× 10 ⁻⁴ CL=95%
Γ_{46} $\mu^+\mu^- \gamma$	[c] < 5.6	× 10 ⁻⁴ CL=95%
Γ_{47} $\tau^+\tau^- \gamma$	[c] < 7.3	× 10 ⁻⁴ CL=95%
Γ_{48} $\ell^+\ell^- \gamma\gamma$	[d] < 6.8	× 10 ⁻⁶ CL=95%
Γ_{49} $q\bar{q}\gamma\gamma$	[d] < 5.5	× 10 ⁻⁶ CL=95%
Γ_{50} $\nu\bar{\nu}\gamma\gamma$	[d] < 3.1	× 10 ⁻⁶ CL=95%
Γ_{51} $e^\pm \mu^\mp$	LF [b] < 1.7	× 10 ⁻⁶ CL=95%
Γ_{52} $e^\pm \tau^\mp$	LF [b] < 9.8	× 10 ⁻⁶ CL=95%
Γ_{53} $\mu^\pm \tau^\mp$	LF [b] < 1.2	× 10 ⁻⁵ CL=95%
Γ_{54} $p\bar{e}$	L,B < 1.8	× 10 ⁻⁶ CL=95%
Γ_{55} $p\mu$	L,B < 1.8	× 10 ⁻⁶ CL=95%

[a] ℓ indicates each type of lepton (e , μ , and τ), not sum over them.

[b] The value is for the sum of the charge states or particle/antiparticle states indicated.

[c] See the Particle Listings below for the γ energy range used in this measurement.

[d] For $m_{\gamma\gamma} = (60 \pm 5)$ GeV.

Gauge & Higgs Boson Particle Listings

Z

Z PARTIAL WIDTHS

 $\Gamma(e^+e^-)$ Γ_1

For the LEP experiments, this parameter is not directly used in the overall fit but is derived using the fit results; see the note "The Z boson" and ref. LEP-SLC 06.

VALUE (MeV)	EVTs	DOCUMENT ID	TECN	COMMENT
83.91 ± 0.12 OUR FIT				
83.66 ± 0.20	137.0K	ABBIENDI	01A OPAL	$E_{cm}^{ee} = 88-94$ GeV
83.54 ± 0.27	117.8k	ABREU	00F DLPH	$E_{cm}^{ee} = 88-94$ GeV
84.16 ± 0.22	124.4k	ACCIARRI	00c L3	$E_{cm}^{ee} = 88-94$ GeV
83.88 ± 0.19		BARATE	00c ALEP	$E_{cm}^{ee} = 88-94$ GeV
82.89 ± 1.20 ± 0.89		²³ ABE	95J SLD	$E_{cm}^{ee} = 91.31$ GeV

²³ ABE 95J obtain this measurement from Bhabha events in a restricted fiducial region to improve systematics. They use the values 91.187 and 2.489 GeV for the Z mass and total decay width to extract this partial width.

 $\Gamma(\mu^+\mu^-)$ Γ_2

This parameter is not directly used in the overall fit but is derived using the fit results; see the note "The Z boson" and ref. LEP-SLC 06.

VALUE (MeV)	EVTs	DOCUMENT ID	TECN	COMMENT
83.99 ± 0.18 OUR FIT				
84.03 ± 0.30	182.8K	ABBIENDI	01A OPAL	$E_{cm}^{ee} = 88-94$ GeV
84.48 ± 0.40	157.6k	ABREU	00F DLPH	$E_{cm}^{ee} = 88-94$ GeV
83.95 ± 0.44	113.4k	ACCIARRI	00c L3	$E_{cm}^{ee} = 88-94$ GeV
84.02 ± 0.28		BARATE	00c ALEP	$E_{cm}^{ee} = 88-94$ GeV

 $\Gamma(\tau^+\tau^-)$ Γ_3

This parameter is not directly used in the overall fit but is derived using the fit results; see the note "The Z boson" and ref. LEP-SLC 06.

VALUE (MeV)	EVTs	DOCUMENT ID	TECN	COMMENT
84.08 ± 0.22 OUR FIT				
83.94 ± 0.41	151.5K	ABBIENDI	01A OPAL	$E_{cm}^{ee} = 88-94$ GeV
83.71 ± 0.58	104.0k	ABREU	00F DLPH	$E_{cm}^{ee} = 88-94$ GeV
84.23 ± 0.58	103.0k	ACCIARRI	00c L3	$E_{cm}^{ee} = 88-94$ GeV
84.38 ± 0.31		BARATE	00c ALEP	$E_{cm}^{ee} = 88-94$ GeV

 $\Gamma(\ell^+\ell^-)$ Γ_4

In our fit $\Gamma(\ell^+\ell^-)$ is defined as the partial Z width for the decay into a pair of massless charged leptons. This parameter is not directly used in the 5-parameter fit assuming lepton universality but is derived using the fit results. See the note "The Z boson" and ref. LEP-SLC 06.

VALUE (MeV)	EVTs	DOCUMENT ID	TECN	COMMENT
83.984 ± 0.086 OUR FIT				
83.82 ± 0.15	471.3K	ABBIENDI	01A OPAL	$E_{cm}^{ee} = 88-94$ GeV
83.85 ± 0.17	379.4k	ABREU	00F DLPH	$E_{cm}^{ee} = 88-94$ GeV
84.14 ± 0.17	340.8k	ACCIARRI	00c L3	$E_{cm}^{ee} = 88-94$ GeV
84.02 ± 0.15	500k	BARATE	00c ALEP	$E_{cm}^{ee} = 88-94$ GeV

 $\Gamma(\text{invisible})$ Γ_5

We use only direct measurements of the invisible partial width using the single photon channel to obtain the average value quoted below. OUR FIT value is obtained as a difference between the total and the observed partial widths assuming lepton universality.

VALUE (MeV)	EVTs	DOCUMENT ID	TECN	COMMENT
499.0 ± 1.5 OUR FIT				
503 ± 16 OUR AVERAGE	Error includes scale factor of 1.2.			
498 ± 12 ± 12	1791	ACCIARRI	98G L3	$E_{cm}^{ee} = 88-94$ GeV
539 ± 26 ± 17	410	AKERS	95c OPAL	$E_{cm}^{ee} = 88-94$ GeV
450 ± 34 ± 34	258	BUSKULIC	93L ALEP	$E_{cm}^{ee} = 88-94$ GeV
540 ± 80 ± 40	52	ADEVA	92 L3	$E_{cm}^{ee} = 88-94$ GeV
• • • We do not use the following data for averages, fits, limits, etc. • • •				
498.1 ± 2.6		²⁴ ABBIENDI	01A OPAL	$E_{cm}^{ee} = 88-94$ GeV
498.1 ± 3.2		²⁴ ABREU	00F DLPH	$E_{cm}^{ee} = 88-94$ GeV
499.1 ± 2.9		²⁴ ACCIARRI	00c L3	$E_{cm}^{ee} = 88-94$ GeV
499.1 ± 2.5		²⁴ BARATE	00c ALEP	$E_{cm}^{ee} = 88-94$ GeV

²⁴ This is an indirect determination of $\Gamma(\text{invisible})$ from a fit to the visible Z decay modes.

 $\Gamma(\text{hadrons})$ Γ_6

This parameter is not directly used in the 5-parameter fit assuming lepton universality, but is derived using the fit results. See the note "The Z boson" and ref. LEP-SLC 06.

VALUE (MeV)	EVTs	DOCUMENT ID	TECN	COMMENT
1744.4 ± 2.0 OUR FIT				
1745.4 ± 3.5	4.10M	ABBIENDI	01A OPAL	$E_{cm}^{ee} = 88-94$ GeV
1738.1 ± 4.0	3.70M	ABREU	00F DLPH	$E_{cm}^{ee} = 88-94$ GeV
1751.1 ± 3.8	3.54M	ACCIARRI	00c L3	$E_{cm}^{ee} = 88-94$ GeV
1744.0 ± 3.4	4.07M	BARATE	00c ALEP	$E_{cm}^{ee} = 88-94$ GeV

Z BRANCHING RATIOS

OUR FIT is obtained using the fit procedure and correlations as determined by the LEP Electroweak Working Group (see the note "The Z boson" and ref. LEP-SLC 06).

 $\Gamma(\text{hadrons})/\Gamma(e^+e^-)$ Γ_6/Γ_1

VALUE	EVTs	DOCUMENT ID	TECN	COMMENT
20.804 ± 0.050 OUR FIT				
20.902 ± 0.084	137.0K	²⁵ ABBIENDI	01A OPAL	$E_{cm}^{ee} = 88-94$ GeV
20.88 ± 0.12	117.8k	ABREU	00F DLPH	$E_{cm}^{ee} = 88-94$ GeV
20.816 ± 0.089	124.4k	ACCIARRI	00c L3	$E_{cm}^{ee} = 88-94$ GeV
20.677 ± 0.075		²⁶ BARATE	00c ALEP	$E_{cm}^{ee} = 88-94$ GeV
• • • We do not use the following data for averages, fits, limits, etc. • • •				
27.0 +11.7 -8.8	12	²⁷ ABRAMS	89D MRK2	$E_{cm}^{ee} = 89-93$ GeV

²⁵ ABBIENDI 01A error includes approximately 0.067 due to statistics, 0.040 due to event selection systematics, 0.027 due to the theoretical uncertainty in t -channel prediction, and 0.014 due to LEP energy uncertainty.

²⁶ BARATE 00c error includes approximately 0.062 due to statistics, 0.033 due to experimental systematics, and 0.026 due to the theoretical uncertainty in t -channel prediction.

²⁷ ABRAMS 89D have included both statistical and systematic uncertainties in their quoted errors.

 $\Gamma(\text{hadrons})/\Gamma(\mu^+\mu^-)$ Γ_6/Γ_2

OUR FIT is obtained using the fit procedure and correlations as determined by the LEP Electroweak Working Group (see the note "The Z boson" and ref. LEP-SLC 06).

VALUE	EVTs	DOCUMENT ID	TECN	COMMENT
20.785 ± 0.033 OUR FIT				
20.811 ± 0.058	182.8K	²⁸ ABBIENDI	01A OPAL	$E_{cm}^{ee} = 88-94$ GeV
20.65 ± 0.08	157.6k	ABREU	00F DLPH	$E_{cm}^{ee} = 88-94$ GeV
20.861 ± 0.097	113.4k	ACCIARRI	00c L3	$E_{cm}^{ee} = 88-94$ GeV
20.799 ± 0.056		²⁹ BARATE	00c ALEP	$E_{cm}^{ee} = 88-94$ GeV
• • • We do not use the following data for averages, fits, limits, etc. • • •				
18.9 +7.1 -5.3	13	³⁰ ABRAMS	89D MRK2	$E_{cm}^{ee} = 89-93$ GeV

²⁸ ABBIENDI 01A error includes approximately 0.050 due to statistics and 0.027 due to event selection systematics.

²⁹ BARATE 00c error includes approximately 0.053 due to statistics and 0.021 due to experimental systematics.

³⁰ ABRAMS 89D have included both statistical and systematic uncertainties in their quoted errors.

 $\Gamma(\text{hadrons})/\Gamma(\tau^+\tau^-)$ Γ_6/Γ_3

OUR FIT is obtained using the fit procedure and correlations as determined by the LEP Electroweak Working Group (see the note "The Z boson" and ref. LEP-SLC 06).

VALUE	EVTs	DOCUMENT ID	TECN	COMMENT
20.764 ± 0.045 OUR FIT				
20.832 ± 0.091	151.5K	³¹ ABBIENDI	01A OPAL	$E_{cm}^{ee} = 88-94$ GeV
20.84 ± 0.13	104.0k	ABREU	00F DLPH	$E_{cm}^{ee} = 88-94$ GeV
20.792 ± 0.133	103.0k	ACCIARRI	00c L3	$E_{cm}^{ee} = 88-94$ GeV
20.707 ± 0.062		³² BARATE	00c ALEP	$E_{cm}^{ee} = 88-94$ GeV
• • • We do not use the following data for averages, fits, limits, etc. • • •				
15.2 +4.8 -3.9	21	³³ ABRAMS	89D MRK2	$E_{cm}^{ee} = 89-93$ GeV

³¹ ABBIENDI 01A error includes approximately 0.055 due to statistics and 0.071 due to event selection systematics.

³² BARATE 00c error includes approximately 0.054 due to statistics and 0.033 due to experimental systematics.

³³ ABRAMS 89D have included both statistical and systematic uncertainties in their quoted errors.

 $\Gamma(\text{hadrons})/\Gamma(\ell^+\ell^-)$ Γ_6/Γ_4

ℓ indicates each type of lepton (e , μ , and τ), not sum over them.

Our fit result is obtained requiring lepton universality.

VALUE	EVTs	DOCUMENT ID	TECN	COMMENT
20.767 ± 0.025 OUR FIT				
20.823 ± 0.044	471.3K	³⁴ ABBIENDI	01A OPAL	$E_{cm}^{ee} = 88-94$ GeV
20.730 ± 0.060	379.4k	ABREU	00F DLPH	$E_{cm}^{ee} = 88-94$ GeV
20.810 ± 0.060	340.8k	ACCIARRI	00c L3	$E_{cm}^{ee} = 88-94$ GeV
20.725 ± 0.039	500k	³⁵ BARATE	00c ALEP	$E_{cm}^{ee} = 88-94$ GeV
• • • We do not use the following data for averages, fits, limits, etc. • • •				
18.9 +3.6 -3.2	46	ABRAMS	89B MRK2	$E_{cm}^{ee} = 89-93$ GeV

³⁴ ABBIENDI 01A error includes approximately 0.034 due to statistics and 0.027 due to event selection systematics.

³⁵ BARATE 00c error includes approximately 0.033 due to statistics, 0.020 due to experimental systematics, and 0.005 due to the theoretical uncertainty in t -channel prediction.

 $\Gamma(\text{hadrons})/\Gamma_{\text{total}}$ Γ_6/Γ

This parameter is not directly used in the overall fit but is derived using the fit results; see the note "The Z boson" and ref. LEP-SLC 06.

VALUE (%)	DOCUMENT ID
69.911 ± 0.056 OUR FIT	

See key on page 373

Gauge & Higgs Boson Particle Listings

Z

 $\Gamma(e^+e^-)/\Gamma_{\text{total}}$ Γ_1/Γ

This parameter is not directly used in the overall fit but is derived using the fit results; see the note "The Z boson" and ref. LEP-SLC 06.

VALUE (%) DOCUMENT ID
3.3632 ± 0.0042 OUR FIT

 $\Gamma(\mu^+\mu^-)/\Gamma_{\text{total}}$ Γ_2/Γ

This parameter is not directly used in the overall fit but is derived using the fit results; see the note "The Z boson" and ref. LEP-SLC 06.

VALUE (%) DOCUMENT ID
3.3662 ± 0.0066 OUR FIT

 $\Gamma(\mu^+\mu^-)/\Gamma(e^+e^-)$ Γ_2/Γ_1

This parameter is not directly used in the overall fit but is derived using the fit results; see the note "The Z boson" and ref. LEP-SLC 06.

VALUE (%) DOCUMENT ID
1.0009 ± 0.0028 OUR FIT

 $\Gamma(\tau^+\tau^-)/\Gamma_{\text{total}}$ Γ_3/Γ

This parameter is not directly used in the overall fit but is derived using the fit results; see the note "The Z boson" and ref. LEP-SLC 06.

VALUE (%) DOCUMENT ID
3.3696 ± 0.0083 OUR FIT

 $\Gamma(\tau^+\tau^-)/\Gamma(e^+e^-)$ Γ_3/Γ_1

This parameter is not directly used in the overall fit but is derived using the fit results; see the note "The Z boson" and ref. LEP-SLC 06.

VALUE (%) DOCUMENT ID
1.0019 ± 0.0032 OUR FIT

 $\Gamma(\ell^+\ell^-)/\Gamma_{\text{total}}$ Γ_4/Γ

ℓ indicates each type of lepton (e , μ , and τ), not sum over them.

Our fit result assumes lepton universality.

This parameter is not directly used in the overall fit but is derived using the fit results; see the note "The Z boson" and ref. LEP-SLC 06.

VALUE (%) DOCUMENT ID
3.3658 ± 0.0023 OUR FIT

 $\Gamma(\text{invisible})/\Gamma_{\text{total}}$ Γ_5/Γ

See the data, the note, and the fit result for the partial width, Γ_5 , above.

VALUE (%) DOCUMENT ID
20.000 ± 0.055 OUR FIT

 $\Gamma((u\bar{u} + c\bar{c})/2)/\Gamma(\text{hadrons})$ Γ_7/Γ_6

This quantity is the branching ratio of $Z \rightarrow$ "up-type" quarks to $Z \rightarrow$ hadrons. Except ACKERSTAFF 97T the values of $Z \rightarrow$ "up-type" and $Z \rightarrow$ "down-type" branchings are extracted from measurements of $\Gamma(\text{hadrons})$, and $\Gamma(Z \rightarrow \gamma + \text{jets})$ where γ is a high-energy (>5 or 7 GeV) isolated photon. As the experiments use different procedures and slightly different values of M_Z , $\Gamma(\text{hadrons})$ and α_s in their extraction procedures, our average has to be taken with caution.

VALUE (%) DOCUMENT ID TECN COMMENT
0.166 ± 0.009 OUR AVERAGE

0.172 ± 0.011 -0.010	36	ABBIENDI	04E	OPAL	$E_{\text{cm}}^{\text{ee}} = 91.2$ GeV
$0.160 \pm 0.019 \pm 0.019$	37	ACKERSTAFF	97T	OPAL	$E_{\text{cm}}^{\text{ee}} = 88-94$ GeV
0.137 ± 0.038 -0.054	38	ABREU	95X	DLPH	$E_{\text{cm}}^{\text{ee}} = 88-94$ GeV
0.137 ± 0.033	39	ADRIANI	93	L3	$E_{\text{cm}}^{\text{ee}} = 91.2$ GeV

36 ABBIENDI 04E select photons with energy > 7 GeV and use $\Gamma(\text{hadrons}) = 1744.4 \pm 2.0$ MeV and $\alpha_s = 0.1172 \pm 0.002$ to obtain $\Gamma_u = 300 \pm 19$ MeV.

37 ACKERSTAFF 97T measure $\Gamma_{u\bar{u}}/(\Gamma_{d\bar{d}} + \Gamma_{u\bar{u}} + \Gamma_{s\bar{s}}) = 0.258 \pm 0.031 \pm 0.032$. To obtain this branching ratio authors use $R_c + R_b = 0.380 \pm 0.010$. This measurement is fully negatively correlated with the measurement of $\Gamma_{d\bar{d},s\bar{s}}/(\Gamma_{d\bar{d}} + \Gamma_{u\bar{u}} + \Gamma_{s\bar{s}})$ given in the next data block.

38 ABREU 95X use $M_Z = 91.187 \pm 0.009$ GeV, $\Gamma(\text{hadrons}) = 1725 \pm 12$ MeV and $\alpha_s = 0.123 \pm 0.005$. To obtain this branching ratio we divide their value of $C_{2/3} = 0.91 \pm 0.25$ by their value of $(3C_{1/3} + 2C_{2/3}) = 6.66 \pm 0.05$.

39 ADRIANI 93 use $M_Z = 91.181 \pm 0.022$ GeV, $\Gamma(\text{hadrons}) = 1742 \pm 19$ MeV and $\alpha_s = 0.125 \pm 0.009$. To obtain this branching ratio we divide their value of $C_{2/3} = 0.92 \pm 0.22$ by their value of $(3C_{1/3} + 2C_{2/3}) = 6.720 \pm 0.076$.

 $\Gamma((d\bar{d} + s\bar{s} + b\bar{b})/3)/\Gamma(\text{hadrons})$ Γ_8/Γ_6

This quantity is the branching ratio of $Z \rightarrow$ "down-type" quarks to $Z \rightarrow$ hadrons. Except ACKERSTAFF 97T the values of $Z \rightarrow$ "up-type" and $Z \rightarrow$ "down-type" branchings are extracted from measurements of $\Gamma(\text{hadrons})$, and $\Gamma(Z \rightarrow \gamma + \text{jets})$ where γ is a high-energy (>5 or 7 GeV) isolated photon. As the experiments use different procedures and slightly different values of M_Z , $\Gamma(\text{hadrons})$ and α_s in their extraction procedures, our average has to be taken with caution.

VALUE (%) DOCUMENT ID TECN COMMENT
0.223 ± 0.006 OUR AVERAGE

0.218 ± 0.007	40	ABBIENDI	04E	OPAL	$E_{\text{cm}}^{\text{ee}} = 91.2$ GeV
$0.230 \pm 0.010 \pm 0.010$	41	ACKERSTAFF	97T	OPAL	$E_{\text{cm}}^{\text{ee}} = 88-94$ GeV
0.243 ± 0.036 -0.026	42	ABREU	95X	DLPH	$E_{\text{cm}}^{\text{ee}} = 88-94$ GeV
0.243 ± 0.022	43	ADRIANI	93	L3	$E_{\text{cm}}^{\text{ee}} = 91.2$ GeV

40 ABBIENDI 04E select photons with energy > 7 GeV and use $\Gamma(\text{hadrons}) = 1744.4 \pm 2.0$ MeV and $\alpha_s = 0.1172 \pm 0.002$ to obtain $\Gamma_d = 381 \pm 12$ MeV.

41 ACKERSTAFF 97T measure $\Gamma_{d\bar{d},s\bar{s}}/(\Gamma_{d\bar{d}} + \Gamma_{u\bar{u}} + \Gamma_{s\bar{s}}) = 0.371 \pm 0.016 \pm 0.016$. To obtain this branching ratio authors use $R_c + R_b = 0.380 \pm 0.010$. This measurement is fully negatively correlated with the measurement of $\Gamma_{u\bar{u}}/(\Gamma_{d\bar{d}} + \Gamma_{u\bar{u}} + \Gamma_{s\bar{s}})$ presented in the previous data block.

42 ABREU 95X use $M_Z = 91.187 \pm 0.009$ GeV, $\Gamma(\text{hadrons}) = 1725 \pm 12$ MeV and $\alpha_s = 0.123 \pm 0.005$. To obtain this branching ratio we divide their value of $C_{1/3} = 1.62 \pm 0.24$ by their value of $(3C_{1/3} + 2C_{2/3}) = 6.66 \pm 0.05$.

43 ADRIANI 93 use $M_Z = 91.181 \pm 0.022$ GeV, $\Gamma(\text{hadrons}) = 1742 \pm 19$ MeV and $\alpha_s = 0.125 \pm 0.009$. To obtain this branching ratio we divide their value of $C_{1/3} = 1.63 \pm 0.15$ by their value of $(3C_{1/3} + 2C_{2/3}) = 6.720 \pm 0.076$.

 $R_c = \Gamma(c\bar{c})/\Gamma(\text{hadrons})$ Γ_9/Γ_6

OUR FIT is obtained by a simultaneous fit to several c - and b -quark measurements as explained in the note "The Z boson" and ref. LEP-SLC 06.

The Standard Model predicts $R_c = 0.1723$ for $m_t = 174.3$ GeV and $M_H = 150$ GeV.

VALUE (%) DOCUMENT ID TECN COMMENT
0.1721 ± 0.0030 OUR FIT

$0.1744 \pm 0.0031 \pm 0.0021$	44	ABE	05F	SLD	$E_{\text{cm}}^{\text{ee}} = 91.28$ GeV
$0.1665 \pm 0.0051 \pm 0.0081$	45	ABREU	00	DLPH	$E_{\text{cm}}^{\text{ee}} = 88-94$ GeV
0.1698 ± 0.0069	46	BARATE	00B	ALEP	$E_{\text{cm}}^{\text{ee}} = 88-94$ GeV
$0.180 \pm 0.011 \pm 0.013$	47	ACKERSTAFF	98E	OPAL	$E_{\text{cm}}^{\text{ee}} = 88-94$ GeV
$0.167 \pm 0.011 \pm 0.012$	48	ALEXANDER	96R	OPAL	$E_{\text{cm}}^{\text{ee}} = 88-94$ GeV

• • • We do not use the following data for averages, fits, limits, etc. • • •

0.1623 ± 0.0085 ± 0.0209 49 ABREU 95D DLPH $E_{\text{cm}}^{\text{ee}} = 88-94$ GeV

44 ABE 05F use hadronic Z decays collected during 1996-98 to obtain an enriched sample of $c\bar{c}$ events using a double tag method. The single c -tag is obtained with a neural network trained to perform flavor discrimination using as input several signatures (corrected secondary vertex mass, vertex decay length, multiplicity and total momentum of the hemisphere). A multitag approach is used, defining 4 regions of the output value of the neural network and R_c is extracted from a simultaneous fit to the count rates of the 4 different tags. The quoted systematic error includes an uncertainty of ± 0.0006 due to the uncertainty on R_b .

45 ABREU 00 obtain this result properly combining the measurement from the D^{*+} production rate ($R_c = 0.1610 \pm 0.0104 \pm 0.0077 \pm 0.0043$ (BR)) with that from the overall charm counting ($R_c = 0.1692 \pm 0.0047 \pm 0.0063 \pm 0.0074$ (BR)) in $c\bar{c}$ events. The systematic error includes an uncertainty of ± 0.0054 due to the uncertainty on the charmed hadron branching fractions.

46 BARATE 00B use exclusive decay modes to independently determine the quantities $R_c \times f(c \rightarrow X)$, $X = D^0, D^+, D_s^+, \text{ and } \Lambda_c$. Estimating $R_c \times f(c \rightarrow \Xi_c / \Omega_c) = 0.0034$, they simply sum over all the charm decays to obtain $R_c = 0.1738 \pm 0.0047 \pm 0.0088 \pm 0.0075$ (BR). This is combined with all previous ALEPH measurements (BARATE 98T and BUSKULIC 94G, $R_c = 0.1681 \pm 0.0054 \pm 0.0062$) to obtain the quoted value.

47 ACKERSTAFF 98E use an inclusive/exclusive double tag. In one jet $D^{*\pm}$ mesons are exclusively reconstructed in several decay channels and in the opposite jet a slow pion (opposite charge inclusive $D^{*\pm}$) tag is used. The b content of this sample is measured by the simultaneous detection of a lepton in one jet and an inclusively reconstructed $D^{*\pm}$ meson in the opposite jet. The systematic error includes an uncertainty of ± 0.006 due to the external branching ratios.

48 ALEXANDER 96R obtain this value via direct charm counting, summing the partial contributions from $D^0, D^+, D_s^+, \text{ and } \Lambda_c^+$, and assuming that strange-charmed baryons account for the 15% of the Λ_c^+ production. An uncertainty of ± 0.005 due to the uncertainties in the charm hadron branching ratios is included in the overall systematics.

49 ABREU 95D perform a maximum likelihood fit to the combined p and p_T distributions of single and dilepton samples. The second error includes an uncertainty of ± 0.0124 due to models and branching ratios.

 $R_b = \Gamma(b\bar{b})/\Gamma(\text{hadrons})$ Γ_{10}/Γ_6

OUR FIT is obtained by a simultaneous fit to several c - and b -quark measurements as explained in the note "The Z boson" and ref. LEP-SLC 06.

The Standard Model predicts $R_b = 0.21581$ for $m_t = 174.3$ GeV and $M_H = 150$ GeV.

VALUE (%) DOCUMENT ID TECN COMMENT
0.21629 ± 0.00066 OUR FIT

$0.21594 \pm 0.00094 \pm 0.00075$	50	ABE	05F	SLD	$E_{\text{cm}}^{\text{ee}} = 91.28$ GeV
$0.2174 \pm 0.0015 \pm 0.0028$	51	ACCIARRI	00	L3	$E_{\text{cm}}^{\text{ee}} = 89-93$ GeV
$0.2178 \pm 0.0011 \pm 0.0013$	52	ABBIENDI	99B	OPAL	$E_{\text{cm}}^{\text{ee}} = 88-94$ GeV
$0.21634 \pm 0.00067 \pm 0.00060$	53	ABREU	99B	DLPH	$E_{\text{cm}}^{\text{ee}} = 88-94$ GeV
$0.2159 \pm 0.0009 \pm 0.0011$	54	BARATE	97F	ALEP	$E_{\text{cm}}^{\text{ee}} = 88-94$ GeV

• • • We do not use the following data for averages, fits, limits, etc. • • •

$0.2145 \pm 0.0089 \pm 0.0067$	55	ABREU	95D	DLPH	$E_{\text{cm}}^{\text{ee}} = 88-94$ GeV
$0.219 \pm 0.006 \pm 0.005$	56	BUSKULIC	94G	ALEP	$E_{\text{cm}}^{\text{ee}} = 88-94$ GeV
$0.251 \pm 0.049 \pm 0.030$	57	JACOBSEN	91	MRK2	$E_{\text{cm}}^{\text{ee}} = 91$ GeV

50 ABE 05F use hadronic Z decays collected during 1996-98 to obtain an enriched sample of $b\bar{b}$ events using a double tag method. The single b -tag is obtained with a neural network trained to perform flavor discrimination using as input several signatures (corrected secondary vertex mass, vertex decay length, multiplicity and total momentum of the hemisphere; the key tag is obtained requiring the secondary vertex corrected mass to be above the D -meson mass). ABE 05F obtain $R_b = 0.21604 \pm 0.00098 \pm 0.00074$ where the systematic error includes an uncertainty of ± 0.00012 due to the uncertainty on R_c . The value reported here is obtained properly combining with ABE 98D. The quoted systematic error includes an uncertainty of ± 0.00012 due to the uncertainty on R_c .

51 ACCIARRI 00 obtain this result using a double-tagging technique, with a high p_T lepton tag and an impact parameter tag in opposite hemispheres.

Gauge & Higgs Boson Particle Listings

Z

⁵² ABBIENDI 99b tag $Z \rightarrow b\bar{b}$ decays using leptons and/or separated decay vertices. The b -tagging efficiency is measured directly from the data using a double-tagging technique.

⁵³ ABREU 99b obtain this result combining in a multivariate analysis several tagging methods (impact parameter and secondary vertex reconstruction, complemented by event shape variables). For R_C different from its Standard Model value of 0.172, R_b varies as $-0.024 \times (R_C - 0.172)$.

⁵⁴ BARATE 97f combine the lifetime-mass hemisphere tag (BARATE 97E) with event shape information and lepton tag to identify $Z \rightarrow b\bar{b}$ candidates. They further use c - and ud -selection tags to identify the background. For R_C different from its Standard Model value of 0.172, R_b varies as $-0.019 \times (R_C - 0.172)$.

⁵⁵ ABREU 95d perform a maximum likelihood fit to the combined p and p_T distributions of single and dilepton samples. The second error includes an uncertainty of ± 0.0023 due to models and branching ratios.

⁵⁶ BUSKULIC 94g perform a simultaneous fit to the p and p_T spectra of both single and dilepton events.

⁵⁷ JACOBSEN 91 tagged $b\bar{b}$ events by requiring coincidence of ≥ 3 tracks with significant impact parameters using vertex detector. Systematic error includes lifetime and decay uncertainties (± 0.014).

$\Gamma(b\bar{b}b\bar{b})/\Gamma(\text{hadrons})$ Γ_{11}/Γ_6

VALUE (units 10^{-4})	CL%	DOCUMENT ID	TECN	COMMENT
5.2 ± 1.9 OUR AVERAGE				

$3.6 \pm 1.7 \pm 2.7$		⁵⁸ ABBIENDI	01G	OPAL $E_{\text{cm}}^{\text{ee}} = 88-94$ GeV
$6.0 \pm 1.9 \pm 1.4$		⁵⁹ ABREU	99U	DLPH $E_{\text{cm}}^{\text{ee}} = 88-94$ GeV

⁵⁸ ABBIENDI 01G use a sample of four-jet events from hadronic Z decays. To enhance the $b\bar{b}b\bar{b}$ signal, at least three of the four jets are required to have a significantly detached secondary vertex.

⁵⁹ ABREU 99U force hadronic Z decays into 3jets to use all the available phase space and require a b tag for every jet. This decay mode includes primary and secondary 4b production, e.g. from gluon splitting to $b\bar{b}$.

$\Gamma(ggg)/\Gamma(\text{hadrons})$ Γ_{12}/Γ_6

VALUE	CL%	DOCUMENT ID	TECN	COMMENT
$<1.6 \times 10^{-2}$	95	⁶⁰ ABREU	96S	DLPH $E_{\text{cm}}^{\text{ee}} = 88-94$ GeV

⁶⁰ This branching ratio is slightly dependent on the jet-finder algorithm. The value we quote is obtained using the JADE algorithm, while using the DURHAM algorithm ABREU 96S obtain an upper limit of 1.5×10^{-2} .

$\Gamma(\pi^0\gamma)/\Gamma_{\text{total}}$ Γ_{13}/Γ

VALUE	CL%	DOCUMENT ID	TECN	COMMENT
$<5.2 \times 10^{-5}$	95	⁶¹ ACCIARRI	95G	L3 $E_{\text{cm}}^{\text{ee}} = 88-94$ GeV
$<5.5 \times 10^{-5}$	95	ABREU	94B	DLPH $E_{\text{cm}}^{\text{ee}} = 88-94$ GeV
$<2.1 \times 10^{-4}$	95	DECAMP	92	ALEP $E_{\text{cm}}^{\text{ee}} = 88-94$ GeV
$<1.4 \times 10^{-4}$	95	AKRAWY	91F	OPAL $E_{\text{cm}}^{\text{ee}} = 88-94$ GeV

⁶¹ This limit is for both decay modes $Z \rightarrow \pi^0\gamma/\gamma\gamma$ which are indistinguishable in ACCIARRI 95G.

$\Gamma(\eta\gamma)/\Gamma_{\text{total}}$ Γ_{14}/Γ

VALUE	CL%	DOCUMENT ID	TECN	COMMENT
$<7.6 \times 10^{-5}$	95	ACCIARRI	95G	L3 $E_{\text{cm}}^{\text{ee}} = 88-94$ GeV
$<8.0 \times 10^{-5}$	95	ABREU	94B	DLPH $E_{\text{cm}}^{\text{ee}} = 88-94$ GeV
$<5.1 \times 10^{-5}$	95	DECAMP	92	ALEP $E_{\text{cm}}^{\text{ee}} = 88-94$ GeV
$<2.0 \times 10^{-4}$	95	AKRAWY	91F	OPAL $E_{\text{cm}}^{\text{ee}} = 88-94$ GeV

$\Gamma(\omega\gamma)/\Gamma_{\text{total}}$ Γ_{15}/Γ

VALUE	CL%	DOCUMENT ID	TECN	COMMENT
$<6.5 \times 10^{-4}$	95	ABREU	94B	DLPH $E_{\text{cm}}^{\text{ee}} = 88-94$ GeV

$\Gamma(\eta'(958)\gamma)/\Gamma_{\text{total}}$ Γ_{16}/Γ

VALUE	CL%	DOCUMENT ID	TECN	COMMENT
$<4.2 \times 10^{-5}$	95	DECAMP	92	ALEP $E_{\text{cm}}^{\text{ee}} = 88-94$ GeV

$\Gamma(\gamma\gamma)/\Gamma_{\text{total}}$ Γ_{17}/Γ

This decay would violate the Landau-Yang theorem.

VALUE	CL%	DOCUMENT ID	TECN	COMMENT
$<5.2 \times 10^{-5}$	95	⁶² ACCIARRI	95G	L3 $E_{\text{cm}}^{\text{ee}} = 88-94$ GeV
$<5.5 \times 10^{-5}$	95	ABREU	94B	DLPH $E_{\text{cm}}^{\text{ee}} = 88-94$ GeV
$<1.4 \times 10^{-4}$	95	AKRAWY	91F	OPAL $E_{\text{cm}}^{\text{ee}} = 88-94$ GeV

⁶² This limit is for both decay modes $Z \rightarrow \pi^0\gamma/\gamma\gamma$ which are indistinguishable in ACCIARRI 95G.

$\Gamma(\gamma\gamma\gamma)/\Gamma_{\text{total}}$ Γ_{18}/Γ

VALUE	CL%	DOCUMENT ID	TECN	COMMENT
$<1.0 \times 10^{-5}$	95	⁶³ ACCIARRI	95C	L3 $E_{\text{cm}}^{\text{ee}} = 88-94$ GeV
$<1.7 \times 10^{-5}$	95	⁶³ ABREU	94B	DLPH $E_{\text{cm}}^{\text{ee}} = 88-94$ GeV
$<6.6 \times 10^{-5}$	95	AKRAWY	91F	OPAL $E_{\text{cm}}^{\text{ee}} = 88-94$ GeV

⁶³ Limit derived in the context of composite Z model.

$\Gamma(\pi^\pm W^\mp)/\Gamma_{\text{total}}$ Γ_{19}/Γ

The value is for the sum of the charge states indicated.

VALUE	CL%	DOCUMENT ID	TECN	COMMENT
$<7 \times 10^{-5}$	95	DECAMP	92	ALEP $E_{\text{cm}}^{\text{ee}} = 88-94$ GeV

$\Gamma(\rho^\pm W^\mp)/\Gamma_{\text{total}}$ Γ_{20}/Γ

The value is for the sum of the charge states indicated.

VALUE	CL%	DOCUMENT ID	TECN	COMMENT
$<8.3 \times 10^{-5}$	95	DECAMP	92	ALEP $E_{\text{cm}}^{\text{ee}} = 88-94$ GeV

$\Gamma(J/\psi(1S)X)/\Gamma_{\text{total}}$ Γ_{21}/Γ

VALUE (units 10^{-3})	EVTS	DOCUMENT ID	TECN	COMMENT
--------------------------	------	-------------	------	---------

$3.51^{+0.23}_{-0.25}$ OUR AVERAGE Error includes scale factor of 1.1.

$3.21 \pm 0.21 \pm 0.19$	553	⁶⁴ ACCIARRI	99F	L3 $E_{\text{cm}}^{\text{ee}} = 88-94$ GeV
$3.9 \pm 0.2 \pm 0.3$	511	⁶⁵ ALEXANDER	96B	OPAL $E_{\text{cm}}^{\text{ee}} = 88-94$ GeV
$3.73 \pm 0.39 \pm 0.36$	153	⁶⁶ ABREU	94P	DLPH $E_{\text{cm}}^{\text{ee}} = 88-94$ GeV

⁶⁴ ACCIARRI 99F combine $\mu^+\mu^-$ and $e^+e^- J/\psi(1S)$ decay channels. The branching ratio for prompt $J/\psi(1S)$ production is measured to be $(2.1 \pm 0.6 \pm 0.4^{+0.4}_{-0.2}(\text{theor.})) \times 10^{-4}$.

⁶⁵ ALEXANDER 96B identify $J/\psi(1S)$ from the decays into lepton pairs. $(4.8 \pm 2.4)\%$ of this branching ratio is due to prompt $J/\psi(1S)$ production (ALEXANDER 96N).

⁶⁶ Combining $\mu^+\mu^-$ and e^+e^- channels and taking into account the common systematic errors. $(7.7^{+6.3}_{-5.4})\%$ of this branching ratio is due to prompt $J/\psi(1S)$ production.

$\Gamma(\psi(2S)X)/\Gamma_{\text{total}}$ Γ_{22}/Γ

VALUE (units 10^{-3})	EVTS	DOCUMENT ID	TECN	COMMENT
--------------------------	------	-------------	------	---------

1.60 ± 0.29 OUR AVERAGE

$1.6 \pm 0.5 \pm 0.3$	39	⁶⁷ ACCIARRI	97J	L3 $E_{\text{cm}}^{\text{ee}} = 88-94$ GeV
$1.6 \pm 0.3 \pm 0.2$	46.9	⁶⁸ ALEXANDER	96B	OPAL $E_{\text{cm}}^{\text{ee}} = 88-94$ GeV
$1.60 \pm 0.73 \pm 0.33$	5.4	⁶⁹ ABREU	94P	DLPH $E_{\text{cm}}^{\text{ee}} = 88-94$ GeV

⁶⁷ ACCIARRI 97J measure this branching ratio via the decay channel $\psi(2S) \rightarrow \ell^+\ell^-$ ($\ell = \mu, e$).

⁶⁸ ALEXANDER 96B measure this branching ratio via the decay channel $\psi(2S) \rightarrow J/\psi\pi^+\pi^-$, with $J/\psi \rightarrow \ell^+\ell^-$.

⁶⁹ ABREU 94P measure this branching ratio via decay channel $\psi(2S) \rightarrow J/\psi\pi^+\pi^-$, with $J/\psi \rightarrow \mu^+\mu^-$.

$\Gamma(\chi_{c1}(1P)X)/\Gamma_{\text{total}}$ Γ_{23}/Γ

VALUE (units 10^{-3})	EVTS	DOCUMENT ID	TECN	COMMENT
--------------------------	------	-------------	------	---------

2.9 ± 0.7 OUR AVERAGE

$2.7 \pm 0.6 \pm 0.5$	33	⁷⁰ ACCIARRI	97J	L3 $E_{\text{cm}}^{\text{ee}} = 88-94$ GeV
$5.0 \pm 2.1^{+1.5}_{-0.9}$	6.4	⁷¹ ABREU	94P	DLPH $E_{\text{cm}}^{\text{ee}} = 88-94$ GeV

⁷⁰ ACCIARRI 97J measure this branching ratio via the decay channel $\chi_{c1} \rightarrow J/\psi + \gamma$, with $J/\psi \rightarrow \ell^+\ell^-$ ($\ell = \mu, e$). The $M(\ell^+\ell^-) - M(\ell^+\ell^-)$ mass difference spectrum is fitted with two gaussian shapes for χ_{c1} and χ_{c2} .

⁷¹ This branching ratio is measured via the decay channel $\chi_{c1} \rightarrow J/\psi + \gamma$, with $J/\psi \rightarrow \mu^+\mu^-$.

$\Gamma(\chi_{c2}(1P)X)/\Gamma_{\text{total}}$ Γ_{24}/Γ

VALUE	CL%	DOCUMENT ID	TECN	COMMENT
-------	-----	-------------	------	---------

$<3.2 \times 10^{-3}$

$<3.2 \times 10^{-3}$	90	⁷² ACCIARRI	97J	L3 $E_{\text{cm}}^{\text{ee}} = 88-94$ GeV
-----------------------	----	------------------------	-----	--

⁷² ACCIARRI 97J derive this limit via the decay channel $\chi_{c2} \rightarrow J/\psi + \gamma$, with $J/\psi \rightarrow \ell^+\ell^-$ ($\ell = \mu, e$). The $M(\ell^+\ell^-) - M(\ell^+\ell^-)$ mass difference spectrum is fitted with two gaussian shapes for χ_{c1} and χ_{c2} .

$\Gamma(\mathcal{T}(1S)X + \mathcal{T}(2S)X + \mathcal{T}(3S)X)/\Gamma_{\text{total}}$ $\Gamma_{25}/\Gamma = (\Gamma_{26} + \Gamma_{27} + \Gamma_{28})/\Gamma$

VALUE (units 10^{-4})	EVTS	DOCUMENT ID	TECN	COMMENT
--------------------------	------	-------------	------	---------

$1.0 \pm 0.4 \pm 0.22$

$1.0 \pm 0.4 \pm 0.22$	6.4	⁷³ ALEXANDER	96F	OPAL $E_{\text{cm}}^{\text{ee}} = 88-94$ GeV
------------------------	-----	-------------------------	-----	--

⁷³ ALEXANDER 96F identify the \mathcal{T} (which refers to any of the three lowest bound states) through its decay into e^+e^- and $\mu^+\mu^-$. The systematic error includes an uncertainty of ± 0.2 due to the production mechanism.

$\Gamma(\mathcal{T}(1S)X)/\Gamma_{\text{total}}$ Γ_{26}/Γ

VALUE	CL%	DOCUMENT ID	TECN	COMMENT
-------	-----	-------------	------	---------

$<4.4 \times 10^{-5}$

$<4.4 \times 10^{-5}$	95	⁷⁴ ACCIARRI	99F	L3 $E_{\text{cm}}^{\text{ee}} = 88-94$ GeV
-----------------------	----	------------------------	-----	--

⁷⁴ ACCIARRI 99F search for $\mathcal{T}(1S)$ through its decay into $\ell^+\ell^-$ ($\ell = e$ or μ).

$\Gamma(\mathcal{T}(2S)X)/\Gamma_{\text{total}}$ Γ_{27}/Γ

VALUE	CL%	DOCUMENT ID	TECN	COMMENT
-------	-----	-------------	------	---------

$<13.9 \times 10^{-5}$

$<13.9 \times 10^{-5}$	95	⁷⁵ ACCIARRI	97R	L3 $E_{\text{cm}}^{\text{ee}} = 88-94$ GeV
------------------------	----	------------------------	-----	--

⁷⁵ ACCIARRI 97R search for $\mathcal{T}(2S)$ through its decay into $\ell^+\ell^-$ ($\ell = e$ or μ).

$\Gamma(\mathcal{T}(3S)X)/\Gamma_{\text{total}}$ Γ_{28}/Γ

VALUE	CL%	DOCUMENT ID	TECN	COMMENT
-------	-----	-------------	------	---------

$<9.4 \times 10^{-5}$

$<9.4 \times 10^{-5}$	95	⁷⁶ ACCIARRI	97R	L3 $E_{\text{cm}}^{\text{ee}} = 88-94$ GeV
-----------------------	----	------------------------	-----	--

⁷⁶ ACCIARRI 97R search for $\mathcal{T}(3S)$ through its decay into $\ell^+\ell^-$ ($\ell = e$ or μ).

$\Gamma((D^0/\bar{D}^0)X)/\Gamma(\text{hadrons})$ Γ_{29}/Γ_6

VALUE	EVTS	DOCUMENT ID	TECN	COMMENT
-------	------	-------------	------	---------

$0.296 \pm 0.019 \pm 0.021$

$0.296 \pm 0.019 \pm 0.021$	369	⁷⁷ ABREU	93I	DLPH $E_{\text{cm}}^{\text{ee}} = 88-94$ GeV
-----------------------------	-----	---------------------	-----	--

⁷⁷ The (D^0/\bar{D}^0) states in ABREU 93I are detected by the $K\pi$ decay mode. This is a corrected result (see the erratum of ABREU 93I).

$\Gamma(D^{\pm X})/\Gamma(\text{hadrons})$ Γ_{30}/Γ_6

VALUE	EVTS	DOCUMENT ID	TECN	COMMENT
0.174 ± 0.016 ± 0.018	539	⁷⁸ ABREU	93i	DLPH $E_{\text{cm}}^{\text{e}} = 88\text{--}94$ GeV

⁷⁸ The D^{\pm} states in ABREU 93i are detected by the $K\pi\pi$ decay mode. This is a corrected result (see the erratum of ABREU 93i).

 $\Gamma(D^*(2010)^{\pm X})/\Gamma(\text{hadrons})$ Γ_{31}/Γ_6

The value is for the sum of the charge states indicated.

VALUE	EVTS	DOCUMENT ID	TECN	COMMENT
0.163 ± 0.019 OUR AVERAGE				Error includes scale factor of 1.3.
0.155 ± 0.010 ± 0.013	358	⁷⁹ ABREU	93i	DLPH $E_{\text{cm}}^{\text{e}} = 88\text{--}94$ GeV
0.21 ± 0.04	362	⁸⁰ DECAMP	91j	ALEP $E_{\text{cm}}^{\text{e}} = 88\text{--}94$ GeV

⁷⁹ $D^*(2010)^{\pm}$ in ABREU 93i are reconstructed from $D^0\pi^{\pm}$, with $D^0 \rightarrow K^-\pi^+$. The new CLEO II measurement of $B(D^{*\pm} \rightarrow D^0\pi^{\pm}) = (68.1 \pm 1.6)\%$ is used. This is a corrected result (see the erratum of ABREU 93i).

⁸⁰ DECAMP 91j report $B(D^*(2010)^+ \rightarrow D^0\pi^+) B(D^0 \rightarrow K^-\pi^+) \Gamma(D^*(2010)^{\pm X}) / \Gamma(\text{hadrons}) = (5.11 \pm 0.34) \times 10^{-3}$. They obtained the above number assuming $B(D^0 \rightarrow K^-\pi^+) = (3.62 \pm 0.34 \pm 0.44)\%$ and $B(D^*(2010)^+ \rightarrow D^0\pi^+) = (55 \pm 4)\%$. We have rescaled their original result of 0.26 ± 0.05 taking into account the new CLEO II branching ratio $B(D^*(2010)^+ \rightarrow D^0\pi^+) = (68.1 \pm 1.6)\%$.

 $\Gamma(D_{s1}(2536)^{\pm X})/\Gamma(\text{hadrons})$ Γ_{32}/Γ_6

$D_{s1}(2536)^{\pm}$ is an expected orbitally-excited state of the D_s meson.

VALUE (%)	EVTS	DOCUMENT ID	TECN	COMMENT
0.52 ± 0.09 ± 0.06	92	⁸¹ HEISTER	02b	ALEP $E_{\text{cm}}^{\text{e}} = 88\text{--}94$ GeV

⁸¹ HEISTER 02b reconstruct this meson in the decay modes $D_{s1}(2536)^{\pm} \rightarrow D^{*\pm} K^0$ and $D_{s1}(2536)^{\pm} \rightarrow D^{*0} K^{\pm}$. The quoted branching ratio assumes that the decay width of the $D_{s1}(2536)$ is saturated by the two measured decay modes.

 $\Gamma(D_{sJ}(2573)^{\pm X})/\Gamma(\text{hadrons})$ Γ_{33}/Γ_6

$D_{sJ}(2573)^{\pm}$ is an expected orbitally-excited state of the D_s meson.

VALUE (%)	EVTS	DOCUMENT ID	TECN	COMMENT
0.83 ± 0.29 ± 0.07 ± 0.13	64	⁸² HEISTER	02b	ALEP $E_{\text{cm}}^{\text{e}} = 88\text{--}94$ GeV

⁸² HEISTER 02b reconstruct this meson in the decay mode $D_{sJ}(2573)^{\pm} \rightarrow D^0 K^{\pm}$. The quoted branching ratio assumes that the detected decay mode represents 45% of the full decay width.

 $\Gamma(D^{*}(2629)^{\pm X})/\Gamma(\text{hadrons})$ Γ_{34}/Γ_6

$D^{*}(2629)^{\pm}$ is a predicted radial excitation of the $D^*(2010)^{\pm}$ meson.

VALUE	DOCUMENT ID	TECN	COMMENT
searched for	⁸³ ABBIENDI	01N	OPAL $E_{\text{cm}}^{\text{e}} = 88\text{--}94$ GeV

⁸³ ABBIENDI 01N searched for the decay mode $D^{*}(2629)^{\pm} \rightarrow D^{*\pm}\pi^+\pi^-$ with $D^{*+} \rightarrow D^0\pi^+$, and $D^0 \rightarrow K^-\pi^+$. They quote a 95% CL limit for $Z \rightarrow D^{*}(2629)^{\pm} \times B(D^{*}(2629)^+ \rightarrow D^{*+}\pi^+\pi^-) < 3.1 \times 10^{-3}$.

 $\Gamma(B^* X)/[\Gamma(BX) + \Gamma(B^* X)]$ $\Gamma_{36}/(\Gamma_{35} + \Gamma_{36})$

As the experiments assume different values of the b -baryon contribution, our average should be taken with caution.

VALUE	EVTS	DOCUMENT ID	TECN	COMMENT
0.75 ± 0.04 OUR AVERAGE				
0.760 ± 0.036 ± 0.083		⁸⁴ ACKERSTAFF	97M	OPAL $E_{\text{cm}}^{\text{e}} = 88\text{--}94$ GeV
0.771 ± 0.026 ± 0.070		⁸⁵ BUSKULIC	96D	ALEP $E_{\text{cm}}^{\text{e}} = 88\text{--}94$ GeV
0.72 ± 0.03 ± 0.06		⁸⁶ ABREU	95R	DLPH $E_{\text{cm}}^{\text{e}} = 88\text{--}94$ GeV
0.76 ± 0.08 ± 0.06	1378	⁸⁷ ACCIARRI	95B	L3 $E_{\text{cm}}^{\text{e}} = 88\text{--}94$ GeV

⁸⁴ ACKERSTAFF 97M use an inclusive B reconstruction method and assume a (13.2 ± 4.1)% b -baryon contribution. The value refers to a b -flavored meson mixture of B_u , B_d , and B_s .

⁸⁵ BUSKULIC 96D use an inclusive reconstruction of B hadrons and assume a (12.2 ± 4.3)% b -baryon contribution. The value refers to a b -flavored mixture of B_u , B_d , and B_s .

⁸⁶ ABREU 95R use an inclusive B -reconstruction method and assume a (10 ± 4)% b -baryon contribution. The value refers to a b -flavored meson mixture of B_u , B_d , and B_s .

⁸⁷ ACCIARRI 95B assume a 9.4% b -baryon contribution. The value refers to a b -flavored mixture of B_u , B_d , and B_s .

 $\Gamma(B^+ X)/\Gamma(\text{hadrons})$ Γ_{37}/Γ_6

"OUR EVALUATION" is obtained using our current values for $f(\bar{b} \rightarrow B^+)$ and $R_b = \Gamma(b\bar{b})/\Gamma(\text{hadrons})$. We calculate $\Gamma(B^+ X)/\Gamma(\text{hadrons}) = R_b \times f(\bar{b} \rightarrow B^+)$.

VALUE	DOCUMENT ID	TECN	COMMENT
0.0872 ± 0.0020 OUR EVALUATION			
0.0887 ± 0.0030	⁸⁸ ABDALLAH	03k	DLPH $E_{\text{cm}}^{\text{e}} = 88\text{--}94$ GeV

⁸⁸ ABDALLAH 03k measure the production fraction of B^+ mesons in hadronic Z decays $f(B^+) = (40.99 \pm 0.82 \pm 1.11)\%$. The value quoted here is obtained multiplying this production fraction by our value of $R_b = \Gamma(b\bar{b})/\Gamma(\text{hadrons})$.

 $\Gamma(B_s^0 X)/\Gamma(\text{hadrons})$ Γ_{38}/Γ_6

"OUR EVALUATION" is obtained using our current values for $f(\bar{b} \rightarrow B_s^0)$ and $R_b = \Gamma(b\bar{b})/\Gamma(\text{hadrons})$. We calculate $\Gamma(B_s^0 X)/\Gamma(\text{hadrons}) = R_b \times f(\bar{b} \rightarrow B_s^0)$.

VALUE	DOCUMENT ID	TECN	COMMENT
0.0223 ± 0.0019 OUR EVALUATION			
seen	⁸⁹ ABREU	92M	DLPH $E_{\text{cm}}^{\text{e}} = 88\text{--}94$ GeV
seen	⁹⁰ ACTON	92N	OPAL $E_{\text{cm}}^{\text{e}} = 88\text{--}94$ GeV
seen	⁹¹ BUSKULIC	92E	ALEP $E_{\text{cm}}^{\text{e}} = 88\text{--}94$ GeV

⁸⁹ ABREU 92M reported value is $\Gamma(B_s^0 X) \times B(B_s^0 \rightarrow D_s \mu \nu_\mu X) \times B(D_s \rightarrow \phi \pi)/\Gamma(\text{hadrons}) = (18 \pm 8) \times 10^{-5}$.

⁹⁰ ACTON 92N find evidence for B_s^0 production using $D_s\text{-}\ell$ correlations, with $D_s^+ \rightarrow \phi \pi^+$ and $K^*(892) K^+$. Assuming R_b from the Standard Model and averaging over the e and μ channels, authors measure the product branching fraction to be $f(\bar{b} \rightarrow B_s^0) \times B(B_s^0 \rightarrow D_s^- \ell^+ \nu_\ell X) \times B(D_s^- \rightarrow \phi \pi^-) = (3.9 \pm 1.1 \pm 0.8) \times 10^{-4}$.

⁹¹ BUSKULIC 92E find evidence for B_s^0 production using $D_s\text{-}\ell$ correlations, with $D_s^+ \rightarrow \phi \pi^+$ and $K^*(892) K^+$. Using $B(D_s^+ \rightarrow \phi \pi^+) = (2.7 \pm 0.7)\%$ and summing up the e and μ channels, the weighted average product branching fraction is measured to be $B(\bar{b} \rightarrow B_s^0) \times B(B_s^0 \rightarrow D_s^- \ell^+ \nu_\ell X) = 0.040 \pm 0.011^{+0.010}_{-0.012}$.

 $\Gamma(B_c^+ X)/\Gamma(\text{hadrons})$ Γ_{39}/Γ_6

VALUE	DOCUMENT ID	TECN	COMMENT
searched for	⁹² ACKERSTAFF	98o	OPAL $E_{\text{cm}}^{\text{e}} = 88\text{--}94$ GeV
searched for	⁹³ ABREU	97E	DLPH $E_{\text{cm}}^{\text{e}} = 88\text{--}94$ GeV
searched for	⁹⁴ BARATE	97H	ALEP $E_{\text{cm}}^{\text{e}} = 88\text{--}94$ GeV

⁹² ACKERSTAFF 98o searched for the decay modes $B_c \rightarrow J/\psi \pi^+$, $J/\psi \pi^+$, and $J/\psi \ell^+ \nu_\ell$, with $J/\psi \rightarrow \ell^+ \ell^-$, $\ell = e, \mu$. The number of candidates (background) for the three decay modes is 2 (0.63 ± 0.2), 0 (1.10 ± 0.22), and 1 (0.82 ± 0.19) respectively. Interpreting the 2 $B_c \rightarrow J/\psi \pi^+$ candidates as signal, they report $\Gamma(B_c^+ X) \times B(B_c \rightarrow J/\psi \pi^+)/\Gamma(\text{hadrons}) = (3.8^{+5.0}_{-2.4} \pm 0.5) \times 10^{-5}$. Interpreted as background, the 90% CL bounds are $\Gamma(B_c^+ X) \times B(B_c \rightarrow J/\psi \pi^+)/\Gamma(\text{hadrons}) < 1.06 \times 10^{-4}$, $\Gamma(B_c^+ X) \times B(B_c \rightarrow J/\psi \pi^+)/\Gamma(\text{hadrons}) < 5.29 \times 10^{-4}$, $\Gamma(B_c^+ X) \times B(B_c \rightarrow J/\psi \ell^+ \nu_\ell)/\Gamma(\text{hadrons}) < 6.96 \times 10^{-5}$.

⁹³ ABREU 97E searched for the decay modes $B_c \rightarrow J/\psi \pi^+$, $J/\psi \ell^+ \nu_\ell$, and $J/\psi(3\pi)^+$, with $J/\psi \rightarrow \ell^+ \ell^-$, $\ell = e, \mu$. The number of candidates (background) for the three decay modes is 1 (1.7), 0 (0.3), and 1 (2.3) respectively. They report the following 90% CL limits: $\Gamma(B_c^+ X) \times B(B_c \rightarrow J/\psi \pi^+)/\Gamma(\text{hadrons}) < (1.05\text{--}0.84) \times 10^{-4}$, $\Gamma(B_c^+ X) \times B(B_c \rightarrow J/\psi \ell^+ \nu_\ell)/\Gamma(\text{hadrons}) < (5.8\text{--}5.0) \times 10^{-5}$, $\Gamma(B_c^+ X) \times B(B_c \rightarrow J/\psi(3\pi)^+)/\Gamma(\text{hadrons}) < 1.75 \times 10^{-4}$, where the ranges are due to the predicted B_c lifetime (0.4–1.4) ps.

⁹⁴ BARATE 97H searched for the decay modes $B_c \rightarrow J/\psi \pi^+$ and $J/\psi \ell^+ \nu_\ell$ with $J/\psi \rightarrow \ell^+ \ell^-$, $\ell = e, \mu$. The number of candidates (background) for the two decay modes is 0 (0.44) and 2 (0.81) respectively. They report the following 90% CL limits: $\Gamma(B_c^+ X) \times B(B_c \rightarrow J/\psi \pi^+)/\Gamma(\text{hadrons}) < 3.6 \times 10^{-5}$ and $\Gamma(B_c^+ X) \times B(B_c \rightarrow J/\psi \ell^+ \nu_\ell)/\Gamma(\text{hadrons}) < 5.2 \times 10^{-5}$.

 $\Gamma(\Lambda_c^+ X)/\Gamma(\text{hadrons})$ Γ_{40}/Γ_6

VALUE	DOCUMENT ID	TECN	COMMENT
0.022 ± 0.005 OUR AVERAGE			
0.024 ± 0.005 ± 0.006	⁹⁵ ALEXANDER	96R	OPAL $E_{\text{cm}}^{\text{e}} = 88\text{--}94$ GeV
0.021 ± 0.003 ± 0.005	⁹⁶ BUSKULIC	96Y	ALEP $E_{\text{cm}}^{\text{e}} = 88\text{--}94$ GeV

⁹⁵ ALEXANDER 96R measure $R_b \times f(b \rightarrow \Lambda_c^+ X) \times B(\Lambda_c^+ \rightarrow p K^- \pi^+) = (0.122 \pm 0.023 \pm 0.010)\%$ in hadronic Z decays; the value quoted here is obtained using our best value $B(\Lambda_c^+ \rightarrow p K^- \pi^+) = (5.0 \pm 1.3)\%$. The first error is the total experiment's error and the second error is the systematic error due to the branching fraction uncertainty.

⁹⁶ BUSKULIC 96Y obtain the production fraction of Λ_c^+ baryons in hadronic Z decays $f(b \rightarrow \Lambda_c^+ X) = 0.110 \pm 0.014 \pm 0.006$ using $B(\Lambda_c^+ \rightarrow p K^- \pi^+) = (4.4 \pm 0.6)\%$; we have rescaled using our best value $B(\Lambda_c^+ \rightarrow p K^- \pi^+) = (5.0 \pm 1.3)\%$ obtaining $f(b \rightarrow \Lambda_c^+ X) = 0.097 \pm 0.013 \pm 0.025$ where the first error is their total experiment's error and the second error is the systematic error due to the branching fraction uncertainty. The value quoted here is obtained multiplying this production fraction by our value of $R_b = \Gamma(b\bar{b})/\Gamma(\text{hadrons})$.

 $\Gamma(\Xi_b^0 X)/\Gamma(\text{hadrons})$ Γ_{41}/Γ_6

VALUE	DOCUMENT ID	TECN	COMMENT
• • • We do not use the following data for averages, fits, limits, etc. • • •			
seen	⁹⁷ ABDALLAH	05c	DLPH $E_{\text{cm}}^{\text{e}} = 88\text{--}94$ GeV

⁹⁷ ABDALLAH 05c searched for the charmed strange baryon Ξ_b^0 in the decay channel $\Xi_b^0 \rightarrow \Xi^- \pi^+$ ($\Xi^- \rightarrow \Lambda \pi^-$). The production rate is measured to be $f_{\Xi_b^0} \times B(\Xi_b^0 \rightarrow \Xi^- \pi^+) = (4.7 \pm 1.4 \pm 1.1) \times 10^{-4}$ per hadronic Z decay.

 $\Gamma(\Xi_b^- X)/\Gamma(\text{hadrons})$ Γ_{42}/Γ_6

Here Ξ_b^- is used as a notation for the strange b -baryon states Ξ_b^- and Ξ_b^0 .

VALUE	DOCUMENT ID	TECN	COMMENT
• • • We do not use the following data for averages, fits, limits, etc. • • •			
seen	⁹⁸ ABDALLAH	05c	DLPH $E_{\text{cm}}^{\text{e}} = 88\text{--}94$ GeV
seen	⁹⁹ BUSKULIC	96T	ALEP $E_{\text{cm}}^{\text{e}} = 88\text{--}94$ GeV
seen	¹⁰⁰ ABREU	95v	DLPH $E_{\text{cm}}^{\text{e}} = 88\text{--}94$ GeV

Gauge & Higgs Boson Particle Listings

Z

⁹⁸ ABDALLAH 05c searched for the beauty strange baryon Ξ_b in the inclusive semileptonic decay channel $\Xi_b \rightarrow \Xi^- \ell^- \bar{\nu}_\ell X$. Evidence for the Ξ_b production is seen from the observation of Ξ^\mp production accompanied by a lepton of the same sign. From the excess of "right-sign" pairs $\Xi^\mp \ell^\mp$ compared to "wrong-sign" pairs $\Xi^\mp \ell^\pm$ the production rate is measured to be $B(b \rightarrow \Xi_b) \times B(\Xi_b \rightarrow \Xi^- \ell^- X) = (3.0 \pm 1.0 \pm 0.3) \times 10^{-4}$ per lepton species, averaged over electrons and muons.

⁹⁹ BUSKULIC 96r investigate Ξ -lepton correlations and find a significant excess of "right-sign" pairs $\Xi^\mp \ell^\mp$ compared to "wrong-sign" pairs $\Xi^\mp \ell^\pm$. This excess is interpreted as evidence for Ξ_b semileptonic decay. The measured product branching ratio is $B(b \rightarrow \Xi_b) \times B(\Xi_b \rightarrow X_C X \ell^- \bar{\nu}_\ell) \times B(X_C \rightarrow \Xi^- X') = (5.4 \pm 1.1 \pm 0.8) \times 10^{-4}$ per lepton species, averaged over electrons and muons, with X_C a charmed baryon.

¹⁰⁰ ABREU 95v observe an excess of "right-sign" pairs $\Xi^\mp \ell^\mp$ compared to "wrong-sign" pairs $\Xi^\mp \ell^\pm$ in jets: this excess is interpreted as evidence for the beauty strange baryon Ξ_b production, with $\Xi_b \rightarrow \Xi^- \ell^- \bar{\nu}_\ell X$. They find that the probability for this signal to come from non b -baryon decays is less than 5×10^{-4} and that Λ_b decays can account for less than 10% of these events. The Ξ_b production rate is then measured to be $B(b \rightarrow \Xi_b) \times B(\Xi_b \rightarrow \Xi^- \ell^- X) = (5.9 \pm 2.1 \pm 1.0) \times 10^{-4}$ per lepton species, averaged over electrons and muons.

$\Gamma(b\text{-baryon } X)/\Gamma(\text{hadrons})$ **Γ_{43}/Γ_6**
 "OUR EVALUATION" is obtained using our current values for $f(b \rightarrow b\text{-baryon})$ and $R_b = \Gamma(b\bar{b})/\Gamma(\text{hadrons})$. We calculate $\Gamma(b\text{-baryon } X)/\Gamma(\text{hadrons}) = R_b \times f(b \rightarrow b\text{-baryon})$.

VALUE	CL%	DOCUMENT ID	TECN	COMMENT
0.0197 ± 0.0032 OUR EVALUATION				
0.0221 ± 0.0015 ± 0.0058		101 BARATE	98v ALEP	$E_{cm}^{ee} = 88\text{--}94$ GeV

¹⁰¹ BARATE 98v use the overall number of identified protons in b -hadron decays to measure $f(b \rightarrow b\text{-baryon}) = 0.102 \pm 0.007 \pm 0.027$. They assume $BR(b\text{-baryon} \rightarrow pX) = (58 \pm 6)\%$ and $BR(B_s^0 \rightarrow pX) = (8.0 \pm 4.0)\%$. The value quoted here is obtained multiplying this production fraction by our value of $R_b = \Gamma(b\bar{b})/\Gamma(\text{hadrons})$.

$\Gamma(\text{anomalous } \gamma + \text{hadrons})/\Gamma_{\text{total}}$ **Γ_{44}/Γ**
 Limits on additional sources of prompt photons beyond expectations for final-state bremsstrahlung.

VALUE	CL%	DOCUMENT ID	TECN	COMMENT
<3.2 × 10⁻³	95	102 AKRAWY	90j OPAL	$E_{cm}^{ee} = 88\text{--}94$ GeV

¹⁰² AKRAWY 90j report $\Gamma(\gamma X) < 8.2$ MeV at 95%CL. They assume a three-body $\gamma q\bar{q}$ distribution and use $E(\gamma) > 10$ GeV.

$\Gamma(e^+ e^- \gamma)/\Gamma_{\text{total}}$ **Γ_{45}/Γ**

VALUE	CL%	DOCUMENT ID	TECN	COMMENT
<5.2 × 10⁻⁴	95	103 ACTON	91B OPAL	$E_{cm}^{ee} = 91.2$ GeV

¹⁰³ ACTON 91B looked for isolated photons with $E > 2\%$ of beam energy (> 0.9 GeV).

$\Gamma(\mu^+ \mu^- \gamma)/\Gamma_{\text{total}}$ **Γ_{46}/Γ**

VALUE	CL%	DOCUMENT ID	TECN	COMMENT
<5.6 × 10⁻⁴	95	104 ACTON	91B OPAL	$E_{cm}^{ee} = 91.2$ GeV

¹⁰⁴ ACTON 91B looked for isolated photons with $E > 2\%$ of beam energy (> 0.9 GeV).

$\Gamma(\tau^+ \tau^- \gamma)/\Gamma_{\text{total}}$ **Γ_{47}/Γ**

VALUE	CL%	DOCUMENT ID	TECN	COMMENT
<7.3 × 10⁻⁴	95	105 ACTON	91B OPAL	$E_{cm}^{ee} = 91.2$ GeV

¹⁰⁵ ACTON 91B looked for isolated photons with $E > 2\%$ of beam energy (> 0.9 GeV).

$\Gamma(\ell^+ \ell^- \gamma\gamma)/\Gamma_{\text{total}}$ **Γ_{48}/Γ**
 The value is the sum over $\ell = e, \mu, \tau$.

VALUE	CL%	DOCUMENT ID	TECN	COMMENT
<6.8 × 10⁻⁶	95	106 ACTON	93E OPAL	$E_{cm}^{ee} = 88\text{--}94$ GeV

¹⁰⁶ For $m_{\gamma\gamma} = 60 \pm 5$ GeV.

$\Gamma(q\bar{q}\gamma\gamma)/\Gamma_{\text{total}}$ **Γ_{49}/Γ**

VALUE	CL%	DOCUMENT ID	TECN	COMMENT
<5.5 × 10⁻⁶	95	107 ACTON	93E OPAL	$E_{cm}^{ee} = 88\text{--}94$ GeV

¹⁰⁷ For $m_{\gamma\gamma} = 60 \pm 5$ GeV.

$\Gamma(\nu\bar{\nu}\gamma\gamma)/\Gamma_{\text{total}}$ **Γ_{50}/Γ**

VALUE	CL%	DOCUMENT ID	TECN	COMMENT
<3.1 × 10⁻⁶	95	108 ACTON	93E OPAL	$E_{cm}^{ee} = 88\text{--}94$ GeV

¹⁰⁸ For $m_{\gamma\gamma} = 60 \pm 5$ GeV.

$\Gamma(e^\pm \mu^\mp)/\Gamma_{\text{total}}$ **Γ_{51}/Γ**
 Test of lepton family number conservation. The value is for the sum of the charge states indicated.

VALUE	CL%	DOCUMENT ID	TECN	COMMENT
<2.5 × 10 ⁻⁶	95	ABREU	97c DLPH	$E_{cm}^{ee} = 88\text{--}94$ GeV
<1.7 × 10⁻⁶	95	AKERS	95w OPAL	$E_{cm}^{ee} = 88\text{--}94$ GeV
<0.6 × 10 ⁻⁵	95	ADRIANI	93i L3	$E_{cm}^{ee} = 88\text{--}94$ GeV
<2.6 × 10 ⁻⁵	95	DECAMP	92 ALEP	$E_{cm}^{ee} = 88\text{--}94$ GeV

$\Gamma(e^\pm \mu^\mp)/\Gamma(e^+ e^-)$ **Γ_{51}/Γ_1**
 Test of lepton family number conservation. The value is for the sum of the charge states indicated.

VALUE	CL%	DOCUMENT ID	TECN	COMMENT
<0.07	90	ALBAJAR	89 UA1	$E_{cm}^{pp} = 546,630$ GeV

$\Gamma(e^\pm \tau^\mp)/\Gamma_{\text{total}}$ **Γ_{52}/Γ**
 Test of lepton family number conservation. The value is for the sum of the charge states indicated.

VALUE	CL%	DOCUMENT ID	TECN	COMMENT
<2.2 × 10 ⁻⁵	95	ABREU	97c DLPH	$E_{cm}^{ee} = 88\text{--}94$ GeV
<9.8 × 10⁻⁶	95	AKERS	95w OPAL	$E_{cm}^{ee} = 88\text{--}94$ GeV
<1.3 × 10 ⁻⁵	95	ADRIANI	93i L3	$E_{cm}^{ee} = 88\text{--}94$ GeV
<1.2 × 10 ⁻⁴	95	DECAMP	92 ALEP	$E_{cm}^{ee} = 88\text{--}94$ GeV

$\Gamma(\mu^\pm \tau^\mp)/\Gamma_{\text{total}}$ **Γ_{53}/Γ**
 Test of lepton family number conservation. The value is for the sum of the charge states indicated.

VALUE	CL%	DOCUMENT ID	TECN	COMMENT
<1.2 × 10⁻⁵	95	ABREU	97c DLPH	$E_{cm}^{ee} = 88\text{--}94$ GeV
<1.7 × 10 ⁻⁵	95	AKERS	95w OPAL	$E_{cm}^{ee} = 88\text{--}94$ GeV
<1.9 × 10 ⁻⁵	95	ADRIANI	93i L3	$E_{cm}^{ee} = 88\text{--}94$ GeV
<1.0 × 10 ⁻⁴	95	DECAMP	92 ALEP	$E_{cm}^{ee} = 88\text{--}94$ GeV

$\Gamma(\rho e)/\Gamma_{\text{total}}$ **Γ_{54}/Γ**
 Test of baryon number and lepton number conservations. Charge conjugate states are implied.

VALUE	CL%	DOCUMENT ID	TECN	COMMENT
<1.8 × 10⁻⁶	95	109 ABBIENDI	99i OPAL	$E_{cm}^{ee} = 88\text{--}94$ GeV

¹⁰⁹ ABBIENDI 99i give the 95%CL limit on the partial width $\Gamma(Z^0 \rightarrow \rho e) < 4.6$ KeV and we have transformed it into a branching ratio.

$\Gamma(\rho\mu)/\Gamma_{\text{total}}$ **Γ_{55}/Γ**
 Test of baryon number and lepton number conservations. Charge conjugate states are implied.

VALUE	CL%	DOCUMENT ID	TECN	COMMENT
<1.8 × 10⁻⁶	95	110 ABBIENDI	99i OPAL	$E_{cm}^{ee} = 88\text{--}94$ GeV

¹¹⁰ ABBIENDI 99i give the 95%CL limit on the partial width $\Gamma(Z^0 \rightarrow \rho\mu) < 4.4$ KeV and we have transformed it into a branching ratio.

AVERAGE PARTICLE MULTIPLICITIES IN HADRONIC Z DECAY

Summed over particle and antiparticle, when appropriate.

$\langle N_\gamma \rangle$

VALUE	DOCUMENT ID	TECN	COMMENT
20.97 ± 0.02 ± 1.15	ACKERSTAFF 98A	OPAL	$E_{cm}^{ee} = 91.2$ GeV

$\langle N_{\pi^\pm} \rangle$

VALUE	DOCUMENT ID	TECN	COMMENT
17.03 ± 0.16 OUR AVERAGE			
17.007 ± 0.209	ABE	04c SLD	$E_{cm}^{ee} = 91.2$ GeV
17.26 ± 0.10 ± 0.88	ABREU	98l DLPH	$E_{cm}^{ee} = 91.2$ GeV
17.04 ± 0.31	BARATE	98v ALEP	$E_{cm}^{ee} = 91.2$ GeV
17.05 ± 0.43	AKERS	94p OPAL	$E_{cm}^{ee} = 91.2$ GeV

$\langle N_{p^0} \rangle$

VALUE	DOCUMENT ID	TECN	COMMENT
9.76 ± 0.26 OUR AVERAGE			
9.55 ± 0.06 ± 0.75	ACKERSTAFF 98A	OPAL	$E_{cm}^{ee} = 91.2$ GeV
9.63 ± 0.13 ± 0.63	BARATE	97j ALEP	$E_{cm}^{ee} = 91.2$ GeV
9.90 ± 0.02 ± 0.33	ACCIARRI	96 L3	$E_{cm}^{ee} = 91.2$ GeV
9.2 ± 0.2 ± 1.0	ADAM	96 DLPH	$E_{cm}^{ee} = 91.2$ GeV

$\langle N_\eta \rangle$

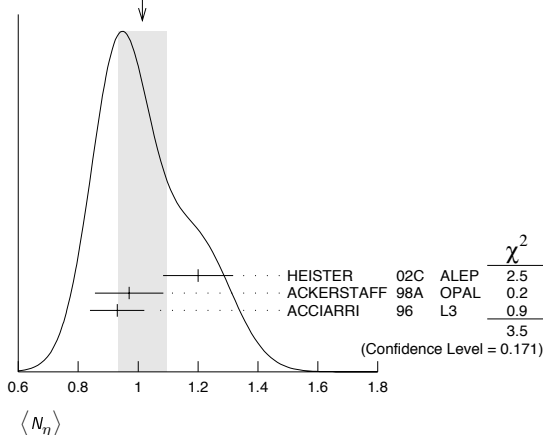
VALUE	DOCUMENT ID	TECN	COMMENT
1.01 ± 0.08 OUR AVERAGE			Error includes scale factor of 1.3. See the ideogram below.
1.20 ± 0.04 ± 0.11	HEISTER	02c ALEP	$E_{cm}^{ee} = 91.2$ GeV
0.97 ± 0.03 ± 0.11	ACKERSTAFF 98A	OPAL	$E_{cm}^{ee} = 91.2$ GeV
0.93 ± 0.01 ± 0.09	ACCIARRI	96 L3	$E_{cm}^{ee} = 91.2$ GeV

See key on page 373

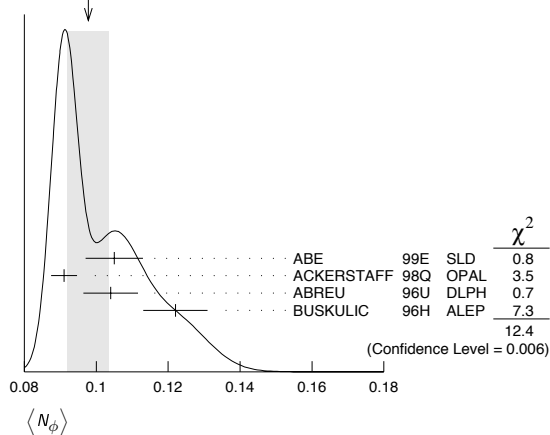
Gauge & Higgs Boson Particle Listings

Z

WEIGHTED AVERAGE
1.01±0.08 (Error scaled by 1.3)



WEIGHTED AVERAGE
0.098±0.006 (Error scaled by 2.0)



$\langle N_{\rho^\pm} \rangle$

VALUE	DOCUMENT ID	TECN	COMMENT
2.40±0.06±0.43	ACKERSTAFF 98A	OPAL	$E_{cm}^{ee} = 91.2$ GeV

$\langle N_{\rho^0} \rangle$

VALUE	DOCUMENT ID	TECN	COMMENT
1.24±0.10 OUR AVERAGE	Error includes scale factor of 1.1.		
1.19±0.10	ABREU 99J	DLPH	$E_{cm}^{ee} = 91.2$ GeV
1.45±0.06±0.20	BUSKULIC 96H	ALEP	$E_{cm}^{ee} = 91.2$ GeV

$\langle N_\omega \rangle$

VALUE	DOCUMENT ID	TECN	COMMENT
1.02±0.06 OUR AVERAGE			
1.00±0.03±0.06	HEISTER 02C	ALEP	$E_{cm}^{ee} = 91.2$ GeV
1.04±0.04±0.14	ACKERSTAFF 98A	OPAL	$E_{cm}^{ee} = 91.2$ GeV
1.17±0.09±0.15	ACCIARRI 97D	L3	$E_{cm}^{ee} = 91.2$ GeV

$\langle N_{\eta'} \rangle$

VALUE	DOCUMENT ID	TECN	COMMENT
0.17 ±0.05 OUR AVERAGE	Error includes scale factor of 2.4.		
0.14 ±0.01 ±0.02	ACKERSTAFF 98A	OPAL	$E_{cm}^{ee} = 91.2$ GeV
0.25 ±0.04	111 ACCIARRI 97D	L3	$E_{cm}^{ee} = 91.2$ GeV
0.068±0.018±0.016	112 BUSKULIC 92D	ALEP	$E_{cm}^{ee} = 91.2$ GeV

• • • We do not use the following data for averages, fits, limits, etc. • • •
 111 ACCIARRI 97D obtain this value averaging over the two decay channels $\eta' \rightarrow \pi^+ \pi^- \eta$ and $\eta' \rightarrow \rho^0 \gamma$.
 112 BUSKULIC 92D obtain this value for $x > 0.1$.

$\langle N_{\eta(980)} \rangle$

VALUE	DOCUMENT ID	TECN	COMMENT
0.147±0.011 OUR AVERAGE			
0.164±0.021	ABREU 99J	DLPH	$E_{cm}^{ee} = 91.2$ GeV
0.141±0.007±0.011	ACKERSTAFF 98Q	OPAL	$E_{cm}^{ee} = 91.2$ GeV

$\langle N_{\eta(980)^\pm} \rangle$

VALUE	DOCUMENT ID	TECN	COMMENT
0.27±0.04±0.10	ACKERSTAFF 98A	OPAL	$E_{cm}^{ee} = 91.2$ GeV

$\langle N_\phi \rangle$

VALUE	DOCUMENT ID	TECN	COMMENT
0.098±0.006 OUR AVERAGE	Error includes scale factor of 2.0. See the ideogram below.		
0.105±0.008	ABE 99E	SLD	$E_{cm}^{ee} = 91.2$ GeV
0.091±0.002±0.003	ACKERSTAFF 98Q	OPAL	$E_{cm}^{ee} = 91.2$ GeV
0.104±0.003±0.007	ABREU 96U	DLPH	$E_{cm}^{ee} = 91.2$ GeV
0.122±0.004±0.008	BUSKULIC 96H	ALEP	$E_{cm}^{ee} = 91.2$ GeV

$\langle N_{f_1(1270)} \rangle$

VALUE	DOCUMENT ID	TECN	COMMENT
0.169±0.025 OUR AVERAGE	Error includes scale factor of 1.4.		
0.214±0.038	ABREU 99J	DLPH	$E_{cm}^{ee} = 91.2$ GeV
0.155±0.011±0.018	ACKERSTAFF 98Q	OPAL	$E_{cm}^{ee} = 91.2$ GeV

$\langle N_{f_1(1285)} \rangle$

VALUE	DOCUMENT ID	TECN	COMMENT
0.165 ±0.051	113 ABDALLAH 03H	DLPH	$E_{cm}^{ee} = 91.2$ GeV
113 ABDALLAH 03H assume a $K \bar{K} \pi$ branching ratio of $(9.0 \pm 0.4)\%$.			

$\langle N_{f_1(1420)} \rangle$

VALUE	DOCUMENT ID	TECN	COMMENT
0.056 ±0.012	114 ABDALLAH 03H	DLPH	$E_{cm}^{ee} = 91.2$ GeV
114 ABDALLAH 03H assume a $K \bar{K} \pi$ branching ratio of 100%.			

$\langle N_{f_2'(1525)} \rangle$

VALUE	DOCUMENT ID	TECN	COMMENT
0.012 ±0.006	ABREU 99J	DLPH	$E_{cm}^{ee} = 91.2$ GeV

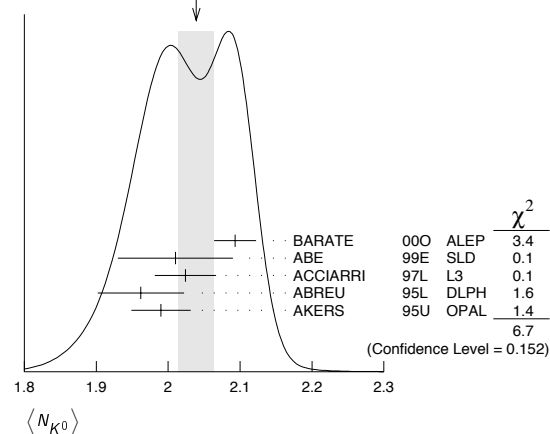
$\langle N_{K^\pm} \rangle$

VALUE	DOCUMENT ID	TECN	COMMENT
2.24 ±0.04 OUR AVERAGE			
2.203±0.071	ABE 04C	SLD	$E_{cm}^{ee} = 91.2$ GeV
2.21 ±0.05 ±0.05	ABREU 98L	DLPH	$E_{cm}^{ee} = 91.2$ GeV
2.26 ±0.12	BARATE 98V	ALEP	$E_{cm}^{ee} = 91.2$ GeV
2.42 ±0.13	AKERS 94P	OPAL	$E_{cm}^{ee} = 91.2$ GeV

$\langle N_{K^0} \rangle$

VALUE	DOCUMENT ID	TECN	COMMENT
2.039±0.025 OUR AVERAGE	Error includes scale factor of 1.3. See the ideogram below.		
2.093±0.004±0.029	BARATE 00O	ALEP	$E_{cm}^{ee} = 91.2$ GeV
2.01 ±0.08	ABE 99E	SLD	$E_{cm}^{ee} = 91.2$ GeV
2.024±0.006±0.042	ACCIARRI 97L	L3	$E_{cm}^{ee} = 91.2$ GeV
1.962±0.022±0.056	ABREU 95L	DLPH	$E_{cm}^{ee} = 91.2$ GeV
1.99 ±0.01 ±0.04	AKERS 95U	OPAL	$E_{cm}^{ee} = 91.2$ GeV

WEIGHTED AVERAGE
2.039±0.025 (Error scaled by 1.3)



Gauge & Higgs Boson Particle Listings

Z

$\langle N_{K^*(892)^\pm} \rangle$

VALUE	DOCUMENT ID	TECN	COMMENT
0.72 ± 0.05 OUR AVERAGE			
0.712 ± 0.031 ± 0.059	ABREU	95L	DLPH $E_{cm}^{ee} = 91.2$ GeV
0.72 ± 0.02 ± 0.08	ACTON	93	OPAL $E_{cm}^{ee} = 91.2$ GeV

$\langle N_{K^*(892)^0} \rangle$

VALUE	DOCUMENT ID	TECN	COMMENT
0.739 ± 0.022 OUR AVERAGE			
0.707 ± 0.041	ABE	99E	SLD $E_{cm}^{ee} = 91.2$ GeV
0.74 ± 0.02 ± 0.02	ACKERSTAFF	97S	OPAL $E_{cm}^{ee} = 91.2$ GeV
0.77 ± 0.02 ± 0.07	ABREU	96U	DLPH $E_{cm}^{ee} = 91.2$ GeV
0.83 ± 0.01 ± 0.09	BUSKULIC	96H	ALEP $E_{cm}^{ee} = 91.2$ GeV
0.97 ± 0.18 ± 0.31	ABREU	93	DLPH $E_{cm}^{ee} = 91.2$ GeV

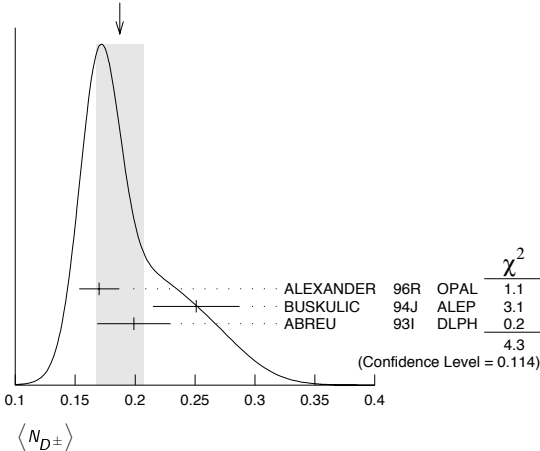
$\langle N_{K_2^*(1430)} \rangle$

VALUE	DOCUMENT ID	TECN	COMMENT
0.073 ± 0.023	ABREU	99J	DLPH $E_{cm}^{ee} = 91.2$ GeV
• • • We do not use the following data for averages, fits, limits, etc. • • •			
0.19 ± 0.04 ± 0.06	115 AKERS	95X	OPAL $E_{cm}^{ee} = 91.2$ GeV
115 AKERS 95X obtain this value for $x < 0.3$.			

$\langle N_{D^\pm} \rangle$

VALUE	DOCUMENT ID	TECN	COMMENT
0.187 ± 0.020 OUR AVERAGE	Error includes scale factor of 1.5. See the ideogram below.		
0.170 ± 0.009 ± 0.014	ALEXANDER	96R	OPAL $E_{cm}^{ee} = 91.2$ GeV
0.251 ± 0.026 ± 0.025	BUSKULIC	94J	ALEP $E_{cm}^{ee} = 91.2$ GeV
0.199 ± 0.019 ± 0.024	116 ABREU	93I	DLPH $E_{cm}^{ee} = 91.2$ GeV
116 See ABREU 95 (erratum).			

WEIGHTED AVERAGE
0.187 ± 0.020 (Error scaled by 1.5)



$\langle N_{D^0} \rangle$

VALUE	DOCUMENT ID	TECN	COMMENT
0.462 ± 0.026 OUR AVERAGE			
0.465 ± 0.017 ± 0.027	ALEXANDER	96R	OPAL $E_{cm}^{ee} = 91.2$ GeV
0.518 ± 0.052 ± 0.035	BUSKULIC	94J	ALEP $E_{cm}^{ee} = 91.2$ GeV
0.403 ± 0.038 ± 0.044	117 ABREU	93I	DLPH $E_{cm}^{ee} = 91.2$ GeV
117 See ABREU 95 (erratum).			

$\langle N_{D_s^\pm} \rangle$

VALUE	DOCUMENT ID	TECN	COMMENT
0.131 ± 0.010 ± 0.018	ALEXANDER	96R	OPAL $E_{cm}^{ee} = 91.2$ GeV

$\langle N_{D^*(2010)^\pm} \rangle$

VALUE	DOCUMENT ID	TECN	COMMENT
0.183 ± 0.008 OUR AVERAGE			
0.1854 ± 0.0041 ± 0.0091	118 ACKERSTAFF	98E	OPAL $E_{cm}^{ee} = 91.2$ GeV
0.187 ± 0.015 ± 0.013	BUSKULIC	94J	ALEP $E_{cm}^{ee} = 91.2$ GeV
0.171 ± 0.012 ± 0.016	119 ABREU	93I	DLPH $E_{cm}^{ee} = 91.2$ GeV
118 ACKERSTAFF 98E systematic error includes an uncertainty of ± 0.0069 due to the branching ratios $B(D^{*+} \rightarrow D^0 \pi^+) = 0.683 \pm 0.014$ and $B(D^0 \rightarrow K^- \pi^+) = 0.0383 \pm 0.0012$.			
119 See ABREU 95 (erratum).			

$\langle N_{D_{s1}(2536)^+} \rangle$

VALUE (units 10^{-3})	DOCUMENT ID	TECN	COMMENT
0.28 ± 0.01 ± 0.03			
2.9 ^{+0.7} _{-0.6} ± 0.2	120 ACKERSTAFF	97W	OPAL $E_{cm}^{ee} = 91.2$ GeV
120 ACKERSTAFF 97W obtain this value for $x > 0.6$ and with the assumption that its decay width is saturated by the $D^* K$ final states.			

$\langle N_{B^*} \rangle$

VALUE	DOCUMENT ID	TECN	COMMENT
0.28 ± 0.01 ± 0.03	121 ABREU	95R	DLPH $E_{cm}^{ee} = 91.2$ GeV
121 ABREU 95R quote this value for a flavor-averaged excited state.			

$\langle N_{J/\psi(1S)} \rangle$

VALUE	DOCUMENT ID	TECN	COMMENT
0.0056 ± 0.0003 ± 0.0004	122 ALEXANDER	96B	OPAL $E_{cm}^{ee} = 91.2$ GeV
122 ALEXANDER 96B identify $J/\psi(1S)$ from the decays into lepton pairs.			

$\langle N_{\psi(2S)} \rangle$

VALUE	DOCUMENT ID	TECN	COMMENT
0.0023 ± 0.0004 ± 0.0003	ALEXANDER	96B	OPAL $E_{cm}^{ee} = 91.2$ GeV

$\langle N_p \rangle$

VALUE	DOCUMENT ID	TECN	COMMENT
1.046 ± 0.026 OUR AVERAGE			
1.054 ± 0.035	ABE	04C	SLD $E_{cm}^{ee} = 91.2$ GeV
1.08 ± 0.04 ± 0.03	ABREU	98L	DLPH $E_{cm}^{ee} = 91.2$ GeV
1.00 ± 0.07	BARATE	98V	ALEP $E_{cm}^{ee} = 91.2$ GeV
0.92 ± 0.11	AKERS	94P	OPAL $E_{cm}^{ee} = 91.2$ GeV

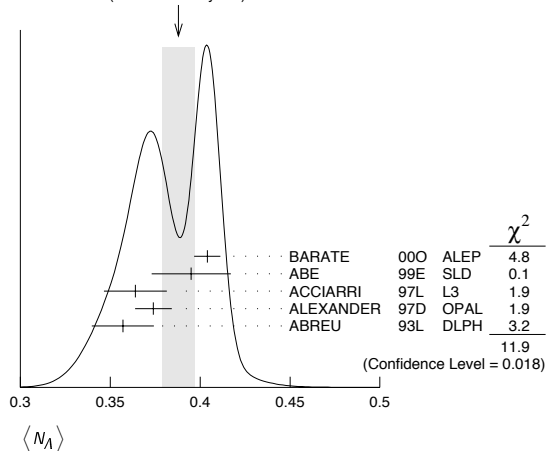
$\langle N_{\Delta(1232)^{++}} \rangle$

VALUE	DOCUMENT ID	TECN	COMMENT
0.087 ± 0.033 OUR AVERAGE	Error includes scale factor of 2.4.		
0.079 ± 0.009 ± 0.011	ABREU	95W	DLPH $E_{cm}^{ee} = 91.2$ GeV
0.22 ± 0.04 ± 0.04	ALEXANDER	95D	OPAL $E_{cm}^{ee} = 91.2$ GeV

$\langle N_\Lambda \rangle$

VALUE	DOCUMENT ID	TECN	COMMENT
0.388 ± 0.009 OUR AVERAGE	Error includes scale factor of 1.7. See the ideogram below.		
0.404 ± 0.002 ± 0.007	BARATE	00O	ALEP $E_{cm}^{ee} = 91.2$ GeV
0.395 ± 0.022	ABE	99E	SLD $E_{cm}^{ee} = 91.2$ GeV
0.364 ± 0.004 ± 0.017	ACCIARRI	97L	L3 $E_{cm}^{ee} = 91.2$ GeV
0.374 ± 0.002 ± 0.010	ALEXANDER	97D	OPAL $E_{cm}^{ee} = 91.2$ GeV
0.357 ± 0.003 ± 0.017	ABREU	93L	DLPH $E_{cm}^{ee} = 91.2$ GeV

WEIGHTED AVERAGE
0.388 ± 0.009 (Error scaled by 1.7)



$\langle N_{\Lambda(1520)} \rangle$

VALUE	DOCUMENT ID	TECN	COMMENT
0.0224 ± 0.0027 OUR AVERAGE			
0.029 ± 0.005 ± 0.005	ABREU	00P	DLPH $E_{cm}^{ee} = 91.2$ GeV
0.0213 ± 0.0021 ± 0.0019	ALEXANDER	97D	OPAL $E_{cm}^{ee} = 91.2$ GeV

$\langle N_{\Sigma^+} \rangle$

VALUE	DOCUMENT ID	TECN	COMMENT
0.107 ± 0.010 OUR AVERAGE			
0.114 ± 0.011 ± 0.009	ACCIARRI	00J	L3 $E_{cm}^{ee} = 91.2$ GeV
0.099 ± 0.008 ± 0.013	ALEXANDER	97E	OPAL $E_{cm}^{ee} = 91.2$ GeV

See key on page 373

Gauge & Higgs Boson Particle Listings

Z

$\langle N_{\Sigma^-} \rangle$

VALUE	DOCUMENT ID	TECN	COMMENT
0.082 ± 0.007 OUR AVERAGE			
0.081 ± 0.002 ± 0.010	ABREU 00P	DLPH	$E_{cm}^{ee} = 91.2$ GeV
0.083 ± 0.006 ± 0.009	ALEXANDER 97E	OPAL	$E_{cm}^{ee} = 91.2$ GeV

$\langle N_{\Sigma^+ + \Sigma^-} \rangle$

VALUE	DOCUMENT ID	TECN	COMMENT
0.181 ± 0.018 OUR AVERAGE			
0.182 ± 0.010 ± 0.016	123 ALEXANDER 97E	OPAL	$E_{cm}^{ee} = 91.2$ GeV
0.170 ± 0.014 ± 0.061	ABREU 95O	DLPH	$E_{cm}^{ee} = 91.2$ GeV

123 We have combined the values of $\langle N_{\Sigma^+} \rangle$ and $\langle N_{\Sigma^-} \rangle$ from ALEXANDER 97E adding the statistical and systematic errors of the two final states separately in quadrature. If isospin symmetry is assumed this value becomes 0.174 ± 0.010 ± 0.015.

$\langle N_{\Sigma^0} \rangle$

VALUE	DOCUMENT ID	TECN	COMMENT
0.076 ± 0.010 OUR AVERAGE			
0.095 ± 0.015 ± 0.013	ACCIARRI 00J	L3	$E_{cm}^{ee} = 91.2$ GeV
0.071 ± 0.012 ± 0.013	ALEXANDER 97E	OPAL	$E_{cm}^{ee} = 91.2$ GeV
0.070 ± 0.010 ± 0.010	ADAM 96B	DLPH	$E_{cm}^{ee} = 91.2$ GeV

$\langle N_{(\Sigma^+ + \Sigma^- + \Sigma^0)/3} \rangle$

VALUE	DOCUMENT ID	TECN	COMMENT
0.084 ± 0.005 ± 0.008	ALEXANDER 97E	OPAL	$E_{cm}^{ee} = 91.2$ GeV

$\langle N_{\Sigma(1385)^+} \rangle$

VALUE	DOCUMENT ID	TECN	COMMENT
0.0239 ± 0.0009 ± 0.0012	ALEXANDER 97D	OPAL	$E_{cm}^{ee} = 91.2$ GeV

$\langle N_{\Sigma(1385)^-} \rangle$

VALUE	DOCUMENT ID	TECN	COMMENT
0.0240 ± 0.0010 ± 0.0014	ALEXANDER 97D	OPAL	$E_{cm}^{ee} = 91.2$ GeV

$\langle N_{\Sigma(1385)^+ + \Sigma(1385)^-} \rangle$

VALUE	DOCUMENT ID	TECN	COMMENT
0.046 ± 0.004 OUR AVERAGE			
0.0479 ± 0.0013 ± 0.0026	ALEXANDER 97D	OPAL	$E_{cm}^{ee} = 91.2$ GeV
0.0382 ± 0.0028 ± 0.0045	ABREU 95O	DLPH	$E_{cm}^{ee} = 91.2$ GeV

Error includes scale factor of 1.6.

$\langle N_{\Xi^-} \rangle$

VALUE	DOCUMENT ID	TECN	COMMENT
0.0258 ± 0.0009 OUR AVERAGE			
0.0247 ± 0.0009 ± 0.0025	ABDALLAH 06E	DLPH	$E_{cm}^{ee} = 91.2$ GeV
0.0259 ± 0.0004 ± 0.0009	ALEXANDER 97D	OPAL	$E_{cm}^{ee} = 91.2$ GeV

$\langle N_{\Xi(1530)^0} \rangle$

VALUE	DOCUMENT ID	TECN	COMMENT
0.0059 ± 0.0011 OUR AVERAGE			
0.0045 ± 0.0005 ± 0.0006	ABDALLAH 05C	DLPH	$E_{cm}^{ee} = 91.2$ GeV
0.0068 ± 0.0005 ± 0.0004	ALEXANDER 97D	OPAL	$E_{cm}^{ee} = 91.2$ GeV

Error includes scale factor of 2.3.

$\langle N_{\Omega^-} \rangle$

VALUE	DOCUMENT ID	TECN	COMMENT
0.00164 ± 0.00028 OUR AVERAGE			
0.0018 ± 0.0003 ± 0.0002	ALEXANDER 97D	OPAL	$E_{cm}^{ee} = 91.2$ GeV
0.0014 ± 0.0002 ± 0.0004	ADAM 96B	DLPH	$E_{cm}^{ee} = 91.2$ GeV

$\langle N_{\Lambda_b^+} \rangle$

VALUE	DOCUMENT ID	TECN	COMMENT
0.078 ± 0.012 ± 0.012	ALEXANDER 96R	OPAL	$E_{cm}^{ee} = 91.2$ GeV

$\langle N_{\mathcal{D}} \rangle$

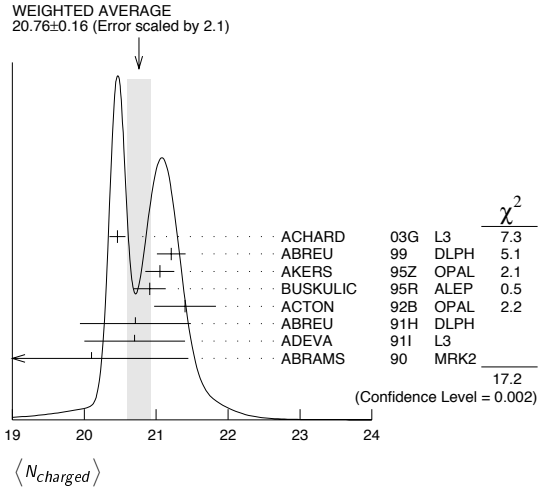
VALUE (units 10 ⁻⁶)	DOCUMENT ID	TECN	COMMENT
0.03817 ± 0.00047 OUR FIT			
5.9 ± 1.8 ± 0.5	124 SCHAEEL 06A	ALEP	$E_{cm}^{ee} = 91.2$ GeV

124 SCHAEEL 06A obtain this anti-deuteron production rate per hadronic Z decay in the anti-deuteron momentum range from 0.62 to 1.03 GeV/c.

$\langle N_{charged} \rangle$

VALUE	DOCUMENT ID	TECN	COMMENT
20.76 ± 0.16 OUR AVERAGE			
20.46 ± 0.01 ± 0.11	ACHARD 03G	L3	$E_{cm}^{ee} = 91.2$ GeV
21.21 ± 0.01 ± 0.20	ABREU 99	DLPH	$E_{cm}^{ee} = 91.2$ GeV
21.05 ± 0.20	AKERS 95Z	OPAL	$E_{cm}^{ee} = 91.2$ GeV
20.91 ± 0.03 ± 0.22	BUSKULIC 95R	ALEP	$E_{cm}^{ee} = 91.2$ GeV
21.40 ± 0.43	ACTON 92B	OPAL	$E_{cm}^{ee} = 91.2$ GeV
20.71 ± 0.04 ± 0.77	ABREU 91H	DLPH	$E_{cm}^{ee} = 91.2$ GeV
20.7 ± 0.7	ADEVA 91I	L3	$E_{cm}^{ee} = 91.2$ GeV
20.1 ± 1.0 ± 0.9	ABRAMS 90	MRK2	$E_{cm}^{ee} = 91.1$ GeV

Error includes scale factor of 2.1. See the ideogram below.



Z HADRONIC POLE CROSS SECTION

OUR FIT is obtained using the fit procedure and correlations as determined by the LEP Electroweak Working Group (see the note "The Z boson" and ref. LEP-SLC 06). This quantity is defined as

$$\sigma_h^0 = \frac{12\pi}{M_Z^2} \frac{\Gamma(e^+e^-) \Gamma(\text{hadrons})}{\Gamma_Z^2}$$

It is one of the parameters used in the Z lineshape fit.

VALUE (nb)	EVTS	DOCUMENT ID	TECN	COMMENT
41.541 ± 0.037 OUR FIT				
41.501 ± 0.055	4.10M	125 ABBIENDI 01A	OPAL	$E_{cm}^{ee} = 88-94$ GeV
41.578 ± 0.069	3.70M	ABREU 00F	DLPH	$E_{cm}^{ee} = 88-94$ GeV
41.535 ± 0.055	3.54M	ACCIARRI 00C	L3	$E_{cm}^{ee} = 88-94$ GeV
41.559 ± 0.058	4.07M	126 BARATE 00C	ALEP	$E_{cm}^{ee} = 88-94$ GeV

• • • We do not use the following data for averages, fits, limits, etc. • • •

VALUE	EVTS	DOCUMENT ID	TECN	COMMENT
42 ± 4	450	ABRAMS 89B	MRK2	$E_{cm}^{ee} = 89.2-93.0$ GeV

125 ABBIENDI 01A error includes approximately 0.031 due to statistics, 0.033 due to event selection systematics, 0.029 due to uncertainty in luminosity measurement, and 0.011 due to LEP energy uncertainty.

126 BARATE 00C error includes approximately 0.030 due to statistics, 0.026 due to experimental systematics, and 0.025 due to uncertainty in luminosity measurement.

Z VECTOR COUPLINGS TO CHARGED LEPTONS

These quantities are the effective vector couplings of the Z to charged leptons. Their magnitude is derived from a measurement of the Z lineshape and the forward-backward lepton asymmetries as a function of energy around the Z mass. The relative sign among the vector to axial-vector couplings is obtained from a measurement of the Z asymmetry parameters, A_e , A_μ , and A_τ . By convention the sign of g_A^e is fixed to be negative (and opposite to that of g_V^e obtained using ν_e scattering measurements). The fit values quoted below correspond to global nine- or five-parameter fits to lineshape, lepton forward-backward asymmetry, and A_e , A_μ , and A_τ measurements. See the note "The Z boson" and ref. LEP-SLC 06 for details. Where $p\bar{p}$ data is quoted, OUR FIT value corresponds to a weighted average of this with the LEP/SLD fit result.

VALUE	EVTS	DOCUMENT ID	TECN	COMMENT
-0.03817 ± 0.00047 OUR FIT				
-0.058 ± 0.016 ± 0.007	5026	127 ACOSTA 05M	CDF	$E_{cm}^{p\bar{p}} = 1.96$ TeV
-0.0346 ± 0.0023	137.0K	128 ABBIENDI 01O	OPAL	$E_{cm}^{ee} = 88-94$ GeV
-0.0412 ± 0.0027	124.4k	129 ACCIARRI 00C	L3	$E_{cm}^{ee} = 88-94$ GeV
-0.0400 ± 0.0037		BARATE 00C	ALEP	$E_{cm}^{ee} = 88-94$ GeV
-0.0414 ± 0.0020	130	ABE 95J	SLD	$E_{cm}^{ee} = 91.31$ GeV

127 ACOSTA 05M determine the forward-backward asymmetry of e^+e^- pairs produced via $q\bar{q} \rightarrow Z/\gamma^* \rightarrow e^+e^-$ in 15 M(e^+e^-) effective mass bins ranging from 40 GeV to 600 GeV. These results are used to obtain the vector and axial-vector couplings of the Z to e^+e^- , assuming the quark couplings are as predicted by the standard model. Higher order radiative corrections have not been taken into account.

128 ABBIENDI 01O use their measurement of the τ polarization in addition to the lineshape and forward-backward lepton asymmetries.

129 ACCIARRI 00C use their measurement of the τ polarization in addition to forward-backward lepton asymmetries.

130 ABE 95J obtain this result combining polarized Bhabha results with the A_{LR} measurement of ABE 94c. The Bhabha results alone give $-0.0507 \pm 0.0096 \pm 0.0020$.

Gauge & Higgs Boson Particle Listings

Z

 g_V^{μ}

VALUE	EVTS	DOCUMENT ID	TECN	COMMENT
-0.0367 ± 0.0023 OUR FIT				
-0.0388 ^{+0.0060} _{-0.0064}	182.8K	131 ABBIENDI	01o OPAL	$E_{cm}^{ee} = 88-94$ GeV
-0.0386 ± 0.0073	113.4k	132 ACCIARRI	00c L3	$E_{cm}^{ee} = 88-94$ GeV
-0.0362 ± 0.0061		BARATE	00c ALEP	$E_{cm}^{ee} = 88-94$ GeV
••• We do not use the following data for averages, fits, limits, etc. •••				
-0.0413 ± 0.0060	66143	133 ABBIENDI	01k OPAL	$E_{cm}^{ee} = 89-93$ GeV

- 131 ABBIENDI 01o use their measurement of the τ polarization in addition to the lineshape and forward-backward lepton asymmetries.
- 132 ACCIARRI 00c use their measurement of the τ polarization in addition to forward-backward lepton asymmetries.
- 133 ABBIENDI 01k obtain this from an angular analysis of the muon pair asymmetry which takes into account effects of initial state radiation on an event by event basis and of initial-final state interference.

 g_V^{τ}

VALUE	EVTS	DOCUMENT ID	TECN	COMMENT
-0.0366 ± 0.0010 OUR FIT				
-0.0365 ± 0.0023	151.5K	134 ABBIENDI	01o OPAL	$E_{cm}^{ee} = 88-94$ GeV
-0.0384 ± 0.0026	103.0k	135 ACCIARRI	00c L3	$E_{cm}^{ee} = 88-94$ GeV
-0.0361 ± 0.0068		BARATE	00c ALEP	$E_{cm}^{ee} = 88-94$ GeV

- 134 ABBIENDI 01o use their measurement of the τ polarization in addition to the lineshape and forward-backward lepton asymmetries.
- 135 ACCIARRI 00c use their measurement of the τ polarization in addition to forward-backward lepton asymmetries.

 g_V^e

VALUE	EVTS	DOCUMENT ID	TECN	COMMENT
-0.03783 ± 0.00041 OUR FIT				
-0.0358 ± 0.0014	471.3K	136 ABBIENDI	01o OPAL	$E_{cm}^{ee} = 88-94$ GeV
-0.0397 ± 0.0020	379.4k	137 ABREU	00f DLPH	$E_{cm}^{ee} = 88-94$ GeV
-0.0397 ± 0.0017	340.8k	138 ACCIARRI	00c L3	$E_{cm}^{ee} = 88-94$ GeV
-0.0383 ± 0.0018	500k	BARATE	00c ALEP	$E_{cm}^{ee} = 88-94$ GeV

- 136 ABBIENDI 01o use their measurement of the τ polarization in addition to the lineshape and forward-backward lepton asymmetries.
- 137 Using forward-backward lepton asymmetries.
- 138 ACCIARRI 00c use their measurement of the τ polarization in addition to forward-backward lepton asymmetries.

Z AXIAL-VECTOR COUPLINGS TO CHARGED LEPTONS

These quantities are the effective axial-vector couplings of the Z to charged leptons. Their magnitude is derived from a measurement of the Z lineshape and the forward-backward lepton asymmetries as a function of energy around the Z mass. The relative sign among the vector to axial-vector couplings is obtained from a measurement of the Z asymmetry parameters, A_e , A_μ , and A_τ . By convention the sign of g_A^e is fixed to be negative (and opposite to that of $g^{V\mu}$ obtained using ν_e scattering measurements). The fit values quoted below correspond to global nine- or five-parameter fits to lineshape, lepton forward-backward asymmetry, and A_e , A_μ , and A_τ measurements. See the note "The Z boson" and ref. LEP-SLC 06 for details. Where $p\bar{p}$ data is quoted, OUR FIT value corresponds to a weighted average of this with the LEP/SLD fit result.

 g_A^e

VALUE	EVTS	DOCUMENT ID	TECN	COMMENT
-0.50111 ± 0.00035 OUR FIT				
-0.528 ± 0.123 ± 0.059	5026	139 ACOSTA	05M CDF	$E_{cm}^{p\bar{p}} = 1.96$ TeV
-0.50062 ± 0.00062	137.0K	140 ABBIENDI	01o OPAL	$E_{cm}^{ee} = 88-94$ GeV
-0.5015 ± 0.0007	124.4k	141 ACCIARRI	00c L3	$E_{cm}^{ee} = 88-94$ GeV
-0.50166 ± 0.00057		BARATE	00c ALEP	$E_{cm}^{ee} = 88-94$ GeV
-0.4977 ± 0.0045	142 ABE	95J SLD	95J SLD	$E_{cm}^{ee} = 91.31$ GeV

- 139 ACOSTA 05M determine the forward-backward asymmetry of e^+e^- pairs produced via $q\bar{q} \rightarrow Z/\gamma^* \rightarrow e^+e^-$ in 15 M(e^+e^-) effective mass bins ranging from 40 GeV to 600 GeV. These results are used to obtain the vector and axial-vector couplings of the Z to e^+e^- , assuming the quark couplings are as predicted by the standard model. Higher order radiative corrections have not been taken into account.

- 140 ABBIENDI 01o use their measurement of the τ polarization in addition to the lineshape and forward-backward lepton asymmetries.
- 141 ACCIARRI 00c use their measurement of the τ polarization in addition to forward-backward lepton asymmetries.
- 142 ABE 95J obtain this result combining polarized Bhabha results with the A_{LR} measurement of ABE 94c. The Bhabha results alone give $-0.4968 \pm 0.0039 \pm 0.0027$.

 g_A^{μ}

VALUE	EVTS	DOCUMENT ID	TECN	COMMENT
-0.50120 ± 0.00054 OUR FIT				
-0.50117 ± 0.00099	182.8K	143 ABBIENDI	01o OPAL	$E_{cm}^{ee} = 88-94$ GeV
-0.5009 ± 0.0014	113.4k	144 ACCIARRI	00c L3	$E_{cm}^{ee} = 88-94$ GeV
-0.50046 ± 0.00093		BARATE	00c ALEP	$E_{cm}^{ee} = 88-94$ GeV
••• We do not use the following data for averages, fits, limits, etc. •••				
-0.520 ± 0.015	66143	145 ABBIENDI	01k OPAL	$E_{cm}^{ee} = 89-93$ GeV

- 143 ABBIENDI 01o use their measurement of the τ polarization in addition to the lineshape and forward-backward lepton asymmetries.
- 144 ACCIARRI 00c use their measurement of the τ polarization in addition to forward-backward lepton asymmetries.
- 145 ABBIENDI 01k obtain this from an angular analysis of the muon pair asymmetry which takes into account effects of initial state radiation on an event by event basis and of initial-final state interference.

 g_A^{τ}

VALUE	EVTS	DOCUMENT ID	TECN	COMMENT
-0.50204 ± 0.00064 OUR FIT				
-0.50165 ± 0.00124	151.5K	146 ABBIENDI	01o OPAL	$E_{cm}^{ee} = 88-94$ GeV
-0.5023 ± 0.0017	103.0k	147 ACCIARRI	00c L3	$E_{cm}^{ee} = 88-94$ GeV
-0.50216 ± 0.00100		BARATE	00c ALEP	$E_{cm}^{ee} = 88-94$ GeV

- 146 ABBIENDI 01o use their measurement of the τ polarization in addition to the lineshape and forward-backward lepton asymmetries.
- 147 ACCIARRI 00c use their measurement of the τ polarization in addition to forward-backward lepton asymmetries.

 g_A^e

VALUE	EVTS	DOCUMENT ID	TECN	COMMENT
-0.50123 ± 0.00026 OUR FIT				
-0.50089 ± 0.00045	471.3K	148 ABBIENDI	01o OPAL	$E_{cm}^{ee} = 88-94$ GeV
-0.5007 ± 0.0005	379.4k	ABREU	00f DLPH	$E_{cm}^{ee} = 88-94$ GeV
-0.50153 ± 0.00053	340.8k	149 ACCIARRI	00c L3	$E_{cm}^{ee} = 88-94$ GeV
-0.50150 ± 0.00046	500k	BARATE	00c ALEP	$E_{cm}^{ee} = 88-94$ GeV

- 148 ABBIENDI 01o use their measurement of the τ polarization in addition to the lineshape and forward-backward lepton asymmetries.
- 149 ACCIARRI 00c use their measurement of the τ polarization in addition to forward-backward lepton asymmetries.

Z COUPLINGS TO NEUTRAL LEPTONS

Averaging over neutrino species, the invisible Z decay width determines the effective neutrino coupling $g^{V\nu}$. For $g^{V\nu}$ and $g^{V\mu}$, $\nu_e e$ and $\nu_\mu e$ scattering results are combined with g_A^e and g_V^e measurements at the Z mass to obtain $g^{V\nu}$ and $g^{V\mu}$ following NOVIKOV 93c.

 $g^{V\nu}$

VALUE	DOCUMENT ID	TECN	COMMENT
0.50076 ± 0.00076	150 LEP-SLC	06	$E_{cm}^{ee} = 88-94$ GeV

- 150 From invisible Z-decay width.

 $g^{V\mu}$

VALUE	DOCUMENT ID	TECN	COMMENT
0.528 ± 0.085	151 VILAIN	94	CHM2 From $\nu_\mu e$ and $\nu_e e$ scattering

- 151 VILAIN 94 derive this value from their value of $g^{V\mu}$ and their ratio $g^{V\nu}/g^{V\mu} = 1.05^{+0.15}_{-0.18}$.

 $g^{V\mu}$

VALUE	DOCUMENT ID	TECN	COMMENT
0.502 ± 0.017	152 VILAIN	94	CHM2 From $\nu_\mu e$ scattering

- 152 VILAIN 94 derive this value from their measurement of the couplings $g_A^{e\nu\mu} = -0.503 \pm 0.017$ and $g_V^{e\nu\mu} = -0.035 \pm 0.017$ obtained from $\nu_\mu e$ scattering. We have re-evaluated this value using the current PDG values for g_A^e and g_V^e .

Z ASYMMETRY PARAMETERS

For each fermion-antifermion pair coupling to the Z these quantities are defined as

$$A_f = \frac{2g_V^f g_A^f}{(g_V^f)^2 + (g_A^f)^2}$$

where g_V^f and g_A^f are the effective vector and axial-vector couplings. For their relation to the various lepton asymmetries see the note "The Z boson" and ref. LEP-SLC 06.

 A_e

Using polarized beams, this quantity can also be measured as $(\sigma_L - \sigma_R)/(\sigma_L + \sigma_R)$, where σ_L and σ_R are the e^+e^- production cross sections for Z bosons produced with left-handed and right-handed electrons respectively.

VALUE	EVTS	DOCUMENT ID	TECN	COMMENT
0.1515 ± 0.0019 OUR AVERAGE				
0.1454 ± 0.0108 ± 0.0036	144810	153 ABBIENDI	01o OPAL	$E_{cm}^{ee} = 88-94$ GeV
0.1516 ± 0.0021	559000	154 ABE	01B SLD	$E_{cm}^{ee} = 91.24$ GeV
0.1504 ± 0.0068 ± 0.0008	155	HEISTER	01 ALEP	$E_{cm}^{ee} = 88-94$ GeV
0.1382 ± 0.0116 ± 0.0005	105000	156 ABREU	00E DLPH	$E_{cm}^{ee} = 88-94$ GeV
0.1678 ± 0.0127 ± 0.0030	137092	157 ACCIARRI	98H L3	$E_{cm}^{ee} = 88-94$ GeV
0.162 ± 0.041 ± 0.014	89838	158 ABE	97 SLD	$E_{cm}^{ee} = 91.27$ GeV
0.202 ± 0.038 ± 0.008	159	ABE	95J SLD	$E_{cm}^{ee} = 91.31$ GeV

- 153 ABBIENDI 01o fit for A_e and A_τ from measurements of the τ polarization at varying τ production angles. The correlation between A_e and A_τ is less than 0.03.
- 154 ABE 01b use the left-right production and left-right forward-backward decay asymmetries in leptonic Z decays to obtain a value of 0.1544 ± 0.0060 . This is combined with left-right production asymmetry measurement using hadronic Z decays (ABE 00b) to obtain the quoted value.
- 155 HEISTER 01 obtain this result fitting the τ polarization as a function of the polar production angle of the τ .
- 156 ABREU 00e obtain this result fitting the τ polarization as a function of the polar τ production angle. This measurement is a combination of different analyses (exclusive τ decay modes, inclusive hadronic 1-prong reconstruction, and a neural network analysis).
- 157 Derived from the measurement of forward-backward τ polarization asymmetry.
- 158 ABE 97 obtain this result from a measurement of the observed left-right charge asymmetry, $A_Q^{\text{obs}} = 0.225 \pm 0.056 \pm 0.019$, in hadronic Z decays. If they combine this value of A_Q^{obs} with their earlier measurement of A_{LR}^{obs} they determine A_e to be $0.1574 \pm 0.0197 \pm 0.0067$ independent of the beam polarization.
- 159 ABE 95j obtain this result from polarized Bhabha scattering.

 A_μ

This quantity is directly extracted from a measurement of the left-right forward-backward asymmetry in $\mu^+\mu^-$ production at SLC using a polarized electron beam. This double asymmetry eliminates the dependence on the Z-e-e coupling parameter A_e .

VALUE	EVTS	DOCUMENT ID	TECN	COMMENT
0.142 ± 0.015	16844	160 ABE	01b SLD	$E_{\text{cm}}^e = 91.24$ GeV

- 160 ABE 01b obtain this direct measurement using the left-right production and left-right forward-backward polar angle asymmetries in $\mu^+\mu^-$ decays of the Z boson obtained with a polarized electron beam.

 A_τ

The LEP Collaborations derive this quantity from the measurement of the τ polarization in $Z \rightarrow \tau^+\tau^-$. The SLD Collaboration directly extracts this quantity from its measured left-right forward-backward asymmetry in $Z \rightarrow \tau^+\tau^-$ produced using a polarized e^- beam. This double asymmetry eliminates the dependence on the Z-e-e coupling parameter A_e .

VALUE	EVTS	DOCUMENT ID	TECN	COMMENT
0.143 ± 0.004 OUR AVERAGE				
0.1456 ± 0.0076 ± 0.0057	144810	161 ABBIENDI	01o OPAL	$E_{\text{cm}}^e = 88-94$ GeV
0.136 ± 0.015	16083	162 ABE	01b SLD	$E_{\text{cm}}^e = 91.24$ GeV
0.1451 ± 0.0052 ± 0.0029		163 HEISTER	01 ALEP	$E_{\text{cm}}^e = 88-94$ GeV
0.1359 ± 0.0079 ± 0.0055	105000	164 ABREU	00e DLPH	$E_{\text{cm}}^e = 88-94$ GeV
0.1476 ± 0.0088 ± 0.0062	137092	ACCIARRI	98h L3	$E_{\text{cm}}^e = 88-94$ GeV

- 161 ABBIENDI 01o fit for A_e and A_τ from measurements of the τ polarization at varying τ production angles. The correlation between A_e and A_τ is less than 0.03.
- 162 ABE 01b obtain this direct measurement using the left-right production and left-right forward-backward polar angle asymmetries in $\tau^+\tau^-$ decays of the Z boson obtained with a polarized electron beam.
- 163 HEISTER 01 obtain this result fitting the τ polarization as a function of the polar production angle of the τ .
- 164 ABREU 00e obtain this result fitting the τ polarization as a function of the polar τ production angle. This measurement is a combination of different analyses (exclusive τ decay modes, inclusive hadronic 1-prong reconstruction, and a neural network analysis).

 A_S

The SLD Collaboration directly extracts this quantity by a simultaneous fit to four measured s-quark polar angle distributions corresponding to two states of e^- polarization (positive and negative) and to the K^+K^- and $K^\pm K_S^0$ strange particle tagging modes in the hadronic final states.

VALUE	EVTS	DOCUMENT ID	TECN	COMMENT
0.895 ± 0.066 ± 0.062	2870	165 ABE	00d SLD	$E_{\text{cm}}^e = 91.2$ GeV

- 165 ABE 00d tag $Z \rightarrow s\bar{s}$ events by an absence of B or D hadrons and the presence in each hemisphere of a high momentum K^\pm or K_S^0 .

 A_C

This quantity is directly extracted from a measurement of the left-right forward-backward asymmetry in $c\bar{c}$ production at SLC using polarized electron beam. This double asymmetry eliminates the dependence on the Z-e-e coupling parameter A_e . OUR FIT is obtained by a simultaneous fit to several c- and b-quark measurements as explained in the note "The Z boson" and ref. LEP-SLC 06.

VALUE	DOCUMENT ID	TECN	COMMENT
0.670 ± 0.027 OUR FIT			
0.6712 ± 0.0224 ± 0.0157	166 ABE	05 SLD	$E_{\text{cm}}^e = 91.24$ GeV

- • • We do not use the following data for averages, fits, limits, etc. • • •
- 0.583 ± 0.055 ± 0.055
 167 ABE | 02g SLD | $E_{\text{cm}}^e = 91.24$ GeV |

0.688 ± 0.041
 168 ABE | 01c SLD | $E_{\text{cm}}^e = 91.25$ GeV |

166 ABE 05 use hadronic Z decays collected during 1996-98 to obtain an enriched sample of $c\bar{c}$ events tagging on the invariant mass of reconstructed secondary decay vertices. The charge of the underlying c-quark is obtained with an algorithm that takes into account the net charge of the vertex as well as the charge of tracks emanating from the vertex and identified as kaons. This yields (9970 events) $A_C = 0.6747 \pm 0.0290 \pm 0.0233$. Taking into account all correlations with earlier results reported in ABE 02g and ABE 01c, they obtain the quoted overall SLD result.

167 ABE 02g tag b and c quarks through their semileptonic decays into electrons and muons. A maximum likelihood fit is performed to extract simultaneously A_b and A_C .

168 ABE 01c tag $Z \rightarrow c\bar{c}$ events using two techniques: exclusive reconstruction of D^{*+} , D^+ and D^0 mesons and the soft pion tag for $D^{*+} \rightarrow D^0\pi^+$. The large background from D mesons produced in $b\bar{b}$ events is separated efficiently from the signal using precision vertex information. When combining the A_C values from these two samples, care is taken to avoid double counting of events common to the two samples, and common systematic errors are properly taken into account.

 A_b

This quantity is directly extracted from a measurement of the left-right forward-backward asymmetry in $b\bar{b}$ production at SLC using polarized electron beam. This double asymmetry eliminates the dependence on the Z-e-e coupling parameter A_e . OUR FIT is obtained by a simultaneous fit to several c- and b-quark measurements as explained in the note "The Z boson" and ref. LEP-SLC 06.

VALUE	EVTS	DOCUMENT ID	TECN	COMMENT
0.923 ± 0.020 OUR FIT				
0.9170 ± 0.0147 ± 0.0145	169 ABE	05 SLD	$E_{\text{cm}}^e = 91.24$ GeV	• • • We do not use the following data for averages, fits, limits, etc. • • •
0.907 ± 0.020 ± 0.024	48028	170 ABE	03f SLD	$E_{\text{cm}}^e = 91.24$ GeV
0.919 ± 0.030 ± 0.024		171 ABE	02g SLD	$E_{\text{cm}}^e = 91.24$ GeV
0.855 ± 0.088 ± 0.102	7473	172 ABE	99L SLD	$E_{\text{cm}}^e = 91.27$ GeV

- 169 ABE 05 use hadronic Z decays collected during 1996-98 to obtain an enriched sample of $b\bar{b}$ events tagging on the invariant mass of reconstructed secondary decay vertices. The charge of the underlying b-quark is obtained with an algorithm that takes into account the net charge of the vertex as well as the charge of tracks emanating from the vertex and identified as kaons. This yields (25917 events) $A_b = 0.9173 \pm 0.0184 \pm 0.0173$. Taking into account all correlations with earlier results reported in ABE 03f, ABE 02g and ABE 99L, they obtain the quoted overall SLD result.
- 170 ABE 03f obtain an enriched sample of $b\bar{b}$ events tagging on the invariant mass of a 3-dimensional topologically reconstructed secondary decay. The charge of the underlying b quark is obtained using a self-calibrating track-charge method. For the 1996-1998 data sample they measure $A_b = 0.906 \pm 0.022 \pm 0.023$. The value quoted here is obtained combining the above with the result of ABE 98l (1993-1995 data sample).
- 171 ABE 02g tag b and c quarks through their semileptonic decays into electrons and muons. A maximum likelihood fit is performed to extract simultaneously A_b and A_C .
- 172 ABE 99L obtain an enriched sample of $b\bar{b}$ events tagging with an inclusive vertex mass cut. For distinguishing b and \bar{b} quarks they use the charge of identified K^\pm .

TRANSVERSE SPIN CORRELATIONS IN $Z \rightarrow \tau^+\tau^-$

The correlations between the transverse spin components of $\tau^+\tau^-$ produced in Z decays may be expressed in terms of the vector and axial-vector couplings:

$$C_{TT} = \frac{|g_V^\tau|^2 - |g_A^\tau|^2}{|g_V^\tau|^2 + |g_A^\tau|^2}$$

$$C_{TN} = -2 \frac{|g_V^\tau||g_A^\tau|}{|g_V^\tau|^2 + |g_A^\tau|^2} \sin(\phi_{g_V^\tau} - \phi_{g_A^\tau})$$

C_{TT} refers to the transverse-transverse (within the collision plane) spin correlation and C_{TN} refers to the transverse-normal (to the collision plane) spin correlation.

The longitudinal τ polarization $P_\tau (= -A_\tau)$ is given by:

$$P_\tau = -2 \frac{|g_V^\tau||g_A^\tau|}{|g_V^\tau|^2 + |g_A^\tau|^2} \cos(\phi_{g_V^\tau} - \phi_{g_A^\tau})$$

Here Φ is the phase and the phase difference $\phi_{g_V^\tau} - \phi_{g_A^\tau}$ can be obtained using both the measurements of C_{TN} and P_τ .

 C_{TT}

VALUE	EVTS	DOCUMENT ID	TECN	COMMENT
1.01 ± 0.12 OUR AVERAGE				
0.87 ± 0.20 ^{+0.10} _{-0.12}	9.1k	ABREU	97g DLPH	$E_{\text{cm}}^e = 91.2$ GeV
1.06 ± 0.13 ± 0.05	120k	BARATE	97d ALEP	$E_{\text{cm}}^e = 91.2$ GeV

 C_{TN}

VALUE	EVTS	DOCUMENT ID	TECN	COMMENT
0.08 ± 0.13 ± 0.04	120k	173 BARATE	97d ALEP	$E_{\text{cm}}^e = 91.2$ GeV

- 173 BARATE 97d combine their value of C_{TN} with the world average $P_\tau = -0.140 \pm 0.007$ to obtain $\tan(\phi_{g_V^\tau} - \phi_{g_A^\tau}) = -0.57 \pm 0.97$.

FORWARD-BACKWARD $e^+e^- \rightarrow f\bar{f}$ CHARGE ASYMMETRIES

These asymmetries are experimentally determined by tagging the respective lepton or quark flavor in e^+e^- interactions. Details of heavy flavor (c- or b-quark) tagging at LEP are described in the note on "The Z boson" and ref. LEP-SLC 06. The Standard Model predictions for LEP data have been (re)computed using the ZFITTER package (version 6.36) with input parameters $M_Z = 91.187$ GeV, $M_{\text{top}} = 174.3$ GeV, $M_{\text{Higgs}} = 150$ GeV, $\alpha_S = 0.119$, $\alpha^{(5)}$ (M_Z) = $1/128.877$ and the Fermi constant $G_F = 1.16637 \times 10^{-5}$ GeV⁻² (see the note on "The Z boson" for references). For non-LEP data the Standard Model predictions are as given by the authors of the respective publications.

 $A_{FB}^{(0,e)}$ CHARGE ASYMMETRY IN $e^+e^- \rightarrow e^+e^-$

OUR FIT is obtained using the fit procedure and correlations as determined by the LEP Electroweak Working Group (see the note "The Z boson" and ref. LEP-SLC 06). For the Z peak, we report the pole asymmetry defined

Gauge & Higgs Boson Particle Listings

Z

by $(3/4)A_0^2$ as determined by the nine-parameter fit to cross-section and lepton forward-backward asymmetry data.

ASYMMETRY (%)	STD. MODEL	\sqrt{s} (GeV)	DOCUMENT ID	TECN
1.45 ± 0.25 OUR FIT				
0.89 ± 0.44	1.57	91.2	174 ABBIENDI 01A	OPAL
1.71 ± 0.49	1.57	91.2	ABREU 00F	DLPH
1.06 ± 0.58	1.57	91.2	ACCIARRI 00C	L3
1.88 ± 0.34	1.57	91.2	175 BARATE 00C	ALEP

174 ABBIENDI 01A error includes approximately 0.38 due to statistics, 0.16 due to event selection systematics, and 0.18 due to the theoretical uncertainty in t -channel prediction.
175 BARATE 00C error includes approximately 0.31 due to statistics, 0.06 due to experimental systematics, and 0.13 due to the theoretical uncertainty in t -channel prediction.

$A_{FB}^{(0,\mu)}$ CHARGE ASYMMETRY IN $e^+e^- \rightarrow \mu^+\mu^-$

OUR FIT is obtained using the fit procedure and correlations as determined by the LEP Electroweak Working Group (see the note "The Z boson" and ref. LEP-SLC 06). For the Z peak, we report the pole asymmetry defined by $(3/4)A_0A_\mu$ as determined by the nine-parameter fit to cross-section and lepton forward-backward asymmetry data.

ASYMMETRY (%)	STD. MODEL	\sqrt{s} (GeV)	DOCUMENT ID	TECN
1.69 ± 0.13 OUR FIT				
1.59 ± 0.23	1.57	91.2	176 ABBIENDI 01A	OPAL
1.65 ± 0.25	1.57	91.2	ABREU 00F	DLPH
1.88 ± 0.33	1.57	91.2	ACCIARRI 00C	L3
1.71 ± 0.24	1.57	91.2	177 BARATE 00C	ALEP

• • • We do not use the following data for averages, fits, limits, etc. • • •

9 ± 30	-1.3	20	178 ABREU 95M	DLPH
7 ± 26	-8.3	40	178 ABREU 95M	DLPH
-11 ± 33	-24.1	57	178 ABREU 95M	DLPH
-62 ± 17	-44.6	69	178 ABREU 95M	DLPH
-56 ± 10	-63.5	79	178 ABREU 95M	DLPH
-13 ± 5	-34.4	87.5	178 ABREU 95M	DLPH
-29.0 ± 5.0 ± 0.5	-32.1	56.9	179 ABE 90I	VNS
-9.9 ± 1.5 ± 0.5	-9.2	35	HEGNER 90	JADE
0.05 ± 0.22	0.026	91.14	180 ABRAMS 89D	MRK2
-43.4 ± 17.0	-24.9	52.0	181 BACALA 89	AMY
-11.0 ± 16.5	-29.4	55.0	181 BACALA 89	AMY
-30.0 ± 12.4	-31.2	56.0	181 BACALA 89	AMY
-46.2 ± 14.9	-33.0	57.0	181 BACALA 89	AMY
-29 ± 13	-25.9	53.3	ADACHI 88C	TOPZ
+ 5.3 ± 5.0 ± 0.5	-1.2	14.0	ADEVA 88	MRKJ
-10.4 ± 1.3 ± 0.5	-8.6	34.8	ADEVA 88	MRKJ
-12.3 ± 5.3 ± 0.5	-10.7	38.3	ADEVA 88	MRKJ
-15.6 ± 3.0 ± 0.5	-14.9	43.8	ADEVA 88	MRKJ
-1.0 ± 6.0	-1.2	13.9	BRAUNSCH... 88D	TASS
-9.1 ± 2.3 ± 0.5	-8.6	34.5	BRAUNSCH... 88D	TASS
-10.6 ± 2.2 ± 0.5	-8.9	35.0	BRAUNSCH... 88D	TASS
-17.6 ± 4.4 ± 0.5	-15.2	43.6	BRAUNSCH... 88D	TASS
-4.8 ± 6.5 ± 1.0	-11.5	39	BEHREND 87C	CELL
-18.8 ± 4.5 ± 1.0	-15.5	44	BEHREND 87C	CELL
+ 2.7 ± 4.9	-1.2	13.9	BARTEL 86C	JADE
-11.1 ± 1.8 ± 1.0	-8.6	34.4	BARTEL 86C	JADE
-17.3 ± 4.8 ± 1.0	-13.7	41.5	BARTEL 86C	JADE
-22.8 ± 5.1 ± 1.0	-16.6	44.8	BARTEL 86C	JADE
-6.3 ± 0.8 ± 0.2	-6.3	29	ASH 85	MAC
-4.9 ± 1.5 ± 0.5	-5.9	29	DERRICK 85	HRS
-7.1 ± 1.7	-5.7	29	LEVI 83	MRK2
-16.1 ± 3.2	-9.2	34.2	BRANDELIK 82C	TASS

176 ABBIENDI 01A error is almost entirely on account of statistics.

177 BARATE 00C error is almost entirely on account of statistics.

178 ABREU 95M perform this measurement using radiative muon-pair events associated with high-energy isolated photons.

179 ABE 90I measurements in the range $50 \leq \sqrt{s} \leq 60.8$ GeV.

180 ABRAMS 89D asymmetry includes both $9 \mu^+\mu^-$ and $15 \tau^+\tau^-$ events.

181 BACALA 89 systematic error is about 5%.

$A_{FB}^{(0,\tau)}$ CHARGE ASYMMETRY IN $e^+e^- \rightarrow \tau^+\tau^-$

OUR FIT is obtained using the fit procedure and correlations as determined by the LEP Electroweak Working Group (see the note "The Z boson" and ref. LEP-SLC 06). For the Z peak, we report the pole asymmetry defined by $(3/4)A_0A_\tau$ as determined by the nine-parameter fit to cross-section and lepton forward-backward asymmetry data.

ASYMMETRY (%)	STD. MODEL	\sqrt{s} (GeV)	DOCUMENT ID	TECN
1.88 ± 0.17 OUR FIT				
1.45 ± 0.30	1.57	91.2	182 ABBIENDI 01A	OPAL
2.41 ± 0.37	1.57	91.2	ABREU 00F	DLPH
2.60 ± 0.47	1.57	91.2	ACCIARRI 00C	L3
1.70 ± 0.28	1.57	91.2	183 BARATE 00C	ALEP

• • • We do not use the following data for averages, fits, limits, etc. • • •

-32.8 ± 6.4 ± 1.5	-32.1	56.9	184 ABE 90I	VNS
-8.1 ± 2.0 ± 0.6	-9.2	35	HEGNER 90	JADE
-18.4 ± 19.2	-24.9	52.0	185 BACALA 89	AMY
-17.7 ± 26.1	-29.4	55.0	185 BACALA 89	AMY
-45.9 ± 16.6	-31.2	56.0	185 BACALA 89	AMY
-49.5 ± 18.0	-33.0	57.0	185 BACALA 89	AMY
-20 ± 14	-25.9	53.3	ADACHI 88C	TOPZ
-10.6 ± 3.1 ± 1.5	-8.5	34.7	ADEVA 88	MRKJ
-8.5 ± 6.6 ± 1.5	-15.4	43.8	ADEVA 88	MRKJ
-6.0 ± 2.5 ± 1.0	8.8	34.6	BARTEL 85F	JADE
-11.8 ± 4.6 ± 1.0	14.8	43.0	BARTEL 85F	JADE
-5.5 ± 1.2 ± 0.5	-0.063	29.0	FERNANDEZ 85	MAC
-4.2 ± 2.0	0.057	29	LEVI 83	MRK2
-10.3 ± 5.2	-9.2	34.2	BEHREND 82	CELL
-0.4 ± 6.6	-9.1	34.2	BRANDELIK 82C	TASS

182 ABBIENDI 01A error includes approximately 0.26 due to statistics and 0.14 due to event selection systematics.

183 BARATE 00C error includes approximately 0.26 due to statistics and 0.11 due to experimental systematics.

184 ABE 90I measurements in the range $50 \leq \sqrt{s} \leq 60.8$ GeV.

185 BACALA 89 systematic error is about 5%.

$A_{FB}^{(0,\ell)}$ CHARGE ASYMMETRY IN $e^+e^- \rightarrow \ell^+\ell^-$

For the Z peak, we report the pole asymmetry defined by $(3/4)A_0^2$ as determined by the five-parameter fit to cross-section and lepton forward-backward asymmetry data assuming lepton universality. For details see the note "The Z boson" and ref. LEP-SLC 06.

ASYMMETRY (%)	STD. MODEL	\sqrt{s} (GeV)	DOCUMENT ID	TECN
1.71 ± 0.10 OUR FIT				
1.45 ± 0.17	1.57	91.2	186 ABBIENDI 01A	OPAL
1.87 ± 0.19	1.57	91.2	ABREU 00F	DLPH
1.92 ± 0.24	1.57	91.2	ACCIARRI 00C	L3
1.73 ± 0.16	1.57	91.2	187 BARATE 00C	ALEP

186 ABBIENDI 01A error includes approximately 0.15 due to statistics, 0.06 due to event selection systematics, and 0.03 due to the theoretical uncertainty in t -channel prediction.

187 BARATE 00C error includes approximately 0.15 due to statistics, 0.04 due to experimental systematics, and 0.02 due to the theoretical uncertainty in t -channel prediction.

$A_{FB}^{(0,u)}$ CHARGE ASYMMETRY IN $e^+e^- \rightarrow u\bar{u}$

ASYMMETRY (%)	STD. MODEL	\sqrt{s} (GeV)	DOCUMENT ID	TECN
4.0 ± 6.7 ± 2.8	7.2	91.2	188 ACKERSTAFF 97T	OPAL

188 ACKERSTAFF 97T measure the forward-backward asymmetry of various fast hadrons made of light quarks. Then using SU(2) isospin symmetry and flavor independence for down and strange quarks authors solve for the different quark types.

$A_{FB}^{(0,s)}$ CHARGE ASYMMETRY IN $e^+e^- \rightarrow s\bar{s}$

The s -quark asymmetry is derived from measurements of the forward-backward asymmetry of fast hadrons containing an s quark.

ASYMMETRY (%)	STD. MODEL	\sqrt{s} (GeV)	DOCUMENT ID	TECN
9.8 ± 1.1 OUR AVERAGE				
10.08 ± 1.13 ± 0.40	10.1	91.2	189 ABREU 00B	DLPH
6.8 ± 3.5 ± 1.1	10.1	91.2	190 ACKERSTAFF 97T	OPAL

189 ABREU 00B tag the presence of an s quark requiring a high-momentum-identified charged kaon. The s -quark pole asymmetry is extracted from the charged-kaon asymmetry taking the expected d - and u -quark asymmetries from the Standard Model and using the measured values for the c - and b -quark asymmetries.

190 ACKERSTAFF 97T measure the forward-backward asymmetry of various fast hadrons made of light quarks. Then using SU(2) isospin symmetry and flavor independence for down and strange quarks authors solve for the different quark types. The value reported here corresponds then to the forward-backward asymmetry for "down-type" quarks.

$A_{FB}^{(0,c)}$ CHARGE ASYMMETRY IN $e^+e^- \rightarrow c\bar{c}$

OUR FIT, which is obtained by a simultaneous fit to several c - and b -quark measurements as explained in the note "The Z boson" and ref. LEP-SLC 06, refers to the **Z pole** asymmetry. The experimental values, on the other hand, correspond to the measurements carried out at the respective energies.

ASYMMETRY (%)	STD. MODEL	\sqrt{s} (GeV)	DOCUMENT ID	TECN
7.07 ± 0.35 OUR FIT				
6.31 ± 0.93 ± 0.65	6.35	91.26	191 ABDALLAH 04F	DLPH
5.68 ± 0.54 ± 0.39	6.3	91.25	192 ABBIENDI 03P	OPAL
6.45 ± 0.57 ± 0.37	6.10	91.21	193 HEISTER 02H	ALEP
6.59 ± 0.94 ± 0.35	6.2	91.235	194 ABREU 99Y	DLPH
6.3 ± 0.9 ± 0.3	6.1	91.22	195 BARATE 98C	ALEP
6.3 ± 1.2 ± 0.6	6.1	91.22	196 ALEXANDER 97C	OPAL
8.3 ± 3.8 ± 2.7	6.2	91.24	197 ADRIANI 92D	L3

• • • We do not use the following data for averages, fits, limits, etc. • • •

3.1 ± 3.5 ± 0.5	-3.5	89.43	191	ABDALLAH	04F	DLPH
11.0 ± 2.8 ± 0.7	12.3	92.99	191	ABDALLAH	04F	DLPH
-6.8 ± 2.5 ± 0.9	-3.0	89.51	192	ABBIENDI	03P	OPAL
14.6 ± 2.0 ± 0.8	12.2	92.95	192	ABBIENDI	03P	OPAL
-12.4 ± 15.9 ± 2.0	-9.6	88.38	193	HEISTER	02H	ALEP
-2.3 ± 2.6 ± 0.2	-3.8	89.38	193	HEISTER	02H	ALEP
-0.3 ± 8.3 ± 0.6	0.9	90.21	193	HEISTER	02H	ALEP
10.6 ± 7.7 ± 0.7	9.6	92.05	193	HEISTER	02H	ALEP
11.9 ± 2.1 ± 0.6	12.2	92.94	193	HEISTER	02H	ALEP
12.1 ± 11.0 ± 1.0	14.2	93.90	193	HEISTER	02H	ALEP
-4.96 ± 3.68 ± 0.53	-3.5	89.434	194	ABREU	99Y	DLPH
11.80 ± 3.18 ± 0.62	12.3	92.990	194	ABREU	99Y	DLPH
-1.0 ± 4.3 ± 1.0	-3.9	89.37	195	BARATE	98O	ALEP
11.0 ± 3.3 ± 0.8	12.3	92.96	195	BARATE	98O	ALEP
3.9 ± 5.1 ± 0.9	-3.4	89.45	196	ALEXANDER	97C	OPAL
15.8 ± 4.1 ± 1.1	12.4	93.00	196	ALEXANDER	97C	OPAL
-12.9 ± 7.8 ± 5.5	-13.6	35	BEHREND	90D	CELL	
7.7 ± 13.4 ± 5.0	-22.1	43	BEHREND	90D	CELL	
-12.8 ± 4.4 ± 4.1	-13.6	35	ELSEN	90	JADE	
-10.9 ± 12.9 ± 4.6	-23.2	44	ELSEN	90	JADE	
-14.9 ± 6.7	-13.3	35	OULD-SAADA	89	JADE	

191 ABDALLAH 04F tag b^- and c^- quarks using semileptonic decays combined with charge flow information from the hemisphere opposite to the lepton. Enriched samples of $c\bar{c}$ and $b\bar{b}$ events are obtained using lifetime information.

192 ABBIENDI 03P tag heavy flavors using events with one or two identified leptons. This allows the simultaneous fitting of the b and c quark forward-backward asymmetries as well as the average B^0 - \bar{B}^0 mixing.

193 HEISTER 02H measure simultaneously b and c quark forward-backward asymmetries using their semileptonic decays to tag the quark charge. The flavor separation is obtained with a discriminating multivariate analysis.

194 ABREU 99Y tag $Z \rightarrow b\bar{b}$ and $Z \rightarrow c\bar{c}$ events by an exclusive reconstruction of several D meson decay modes (D^{*+} , D^0 , and D^+ with their charge-conjugate states).

195 BARATE 98O tag $Z \rightarrow c\bar{c}$ events requiring the presence of high-momentum reconstructed D^{*+} , D^+ , or D^0 mesons.

196 ALEXANDER 97C identify the b and c events using a D/D^* tag.

197 ADRIANI 92D use both electron and muon semileptonic decays.

$A_{FB}^{(0,b)}$ CHARGE ASYMMETRY IN $e^+e^- \rightarrow b\bar{b}$

OUR FIT, which is obtained by a simultaneous fit to several c^- and b^- quark measurements as explained in the note "The Z boson" and ref. LEP-SLC 06, refers to the **Z pole** asymmetry. The experimental values, on the other hand, correspond to the measurements carried out at the respective energies.

ASYMMETRY (%)	STD. MODEL	\sqrt{s} (GeV)	DOCUMENT ID	TECN
9.92 ± 0.16 OUR FIT				
9.58 ± 0.32 ± 0.14	9.68	91.231	198 ABDALLAH	05 DLPH
10.04 ± 0.56 ± 0.25	9.69	91.26	199 ABDALLAH	04F DLPH
9.72 ± 0.42 ± 0.15	9.67	91.25	200 ABBIENDI	03P OPAL
9.77 ± 0.36 ± 0.18	9.69	91.26	201 ABBIENDI	02I OPAL
9.52 ± 0.41 ± 0.17	9.59	91.21	202 HEISTER	02H ALEP
10.00 ± 0.27 ± 0.11	9.63	91.232	203 HEISTER	01D ALEP
7.62 ± 1.94 ± 0.85	9.64	91.235	204 ABREU	99Y DLPH
9.60 ± 0.66 ± 0.33	9.69	91.26	205 ACCIARRI	99D L3
9.31 ± 1.01 ± 0.55	9.65	91.24	206 ACCIARRI	98U L3
9.4 ± 2.7 ± 2.2	9.61	91.22	207 ALEXANDER	97C OPAL
• • • We do not use the following data for averages, fits, limits, etc. • • •				
6.37 ± 1.43 ± 0.17	5.8	89.449	198 ABDALLAH	05 DLPH
10.41 ± 1.15 ± 0.24	12.1	92.990	198 ABDALLAH	05 DLPH
6.7 ± 2.2 ± 0.2	5.7	89.43	199 ABDALLAH	04F DLPH
11.2 ± 1.8 ± 0.2	12.1	92.99	199 ABDALLAH	04F DLPH
4.7 ± 1.8 ± 0.1	5.9	89.51	200 ABBIENDI	03P OPAL
10.3 ± 1.5 ± 0.2	12.0	92.95	200 ABBIENDI	03P OPAL
5.82 ± 1.53 ± 0.12	5.9	89.50	201 ABBIENDI	02I OPAL
12.21 ± 1.23 ± 0.25	12.0	92.91	201 ABBIENDI	02I OPAL
-13.1 ± 13.5 ± 1.0	3.2	88.38	202 HEISTER	02H ALEP
5.5 ± 1.9 ± 0.1	5.6	89.38	202 HEISTER	02H ALEP
-0.4 ± 6.7 ± 0.8	7.5	90.21	202 HEISTER	02H ALEP
11.1 ± 6.4 ± 0.5	11.0	92.05	202 HEISTER	02H ALEP
10.4 ± 1.5 ± 0.3	12.0	92.94	202 HEISTER	02H ALEP
13.8 ± 9.3 ± 1.1	12.9	93.90	202 HEISTER	02H ALEP
4.36 ± 1.19 ± 0.11	5.8	89.472	203 HEISTER	01D ALEP
11.72 ± 0.97 ± 0.11	12.0	92.950	203 HEISTER	01D ALEP
5.67 ± 7.56 ± 1.17	5.7	89.434	204 ABREU	99Y DLPH
8.82 ± 6.33 ± 1.22	12.1	92.990	204 ABREU	99Y DLPH
6.11 ± 2.93 ± 0.43	5.9	89.50	205 ACCIARRI	99D L3
13.71 ± 2.40 ± 0.44	12.2	93.10	205 ACCIARRI	99D L3
4.95 ± 5.23 ± 0.40	5.8	89.45	206 ACCIARRI	98U L3
11.37 ± 3.99 ± 0.65	12.1	92.99	206 ACCIARRI	98U L3
-8.6 ± 10.8 ± 2.9	5.8	89.45	207 ALEXANDER	97C OPAL
-2.1 ± 9.0 ± 2.6	12.1	93.00	207 ALEXANDER	97C OPAL
-71 ± 34 ± 7	-58	58.3	SHIMONAKA	91 TOPZ
-22.2 ± 7.7 ± 3.5	-26.0	35	BEHREND	90D CELL

-49.1 ± 16.0 ± 5.0	-39.7	43	BEHREND	90D	CELL
-28 ± 11	-23	35	BRAUNSCH...	90	TASS
-16.6 ± 7.7 ± 4.8	-24.3	35	ELSEN	90	JADE
-33.6 ± 22.2 ± 5.2	-39.9	44	ELSEN	90	JADE
3.4 ± 7.0 ± 3.5	-16.0	29.0	BAND	89	MAC
-72 ± 28 ± 13	-56	55.2	SAGAWA	89	AMY

198 ABDALLAH 05 obtain an enriched samples of $b\bar{b}$ events using lifetime information. The quark (or antiquark) charge is determined with a neural network using the secondary vertex charge, the jet charge and particle identification.

199 ABDALLAH 04F tag b^- and c^- quarks using semileptonic decays combined with charge flow information from the hemisphere opposite to the lepton. Enriched samples of $c\bar{c}$ and $b\bar{b}$ events are obtained using lifetime information.

200 ABBIENDI 03P tag heavy flavors using events with one or two identified leptons. This allows the simultaneous fitting of the b and c quark forward-backward asymmetries as well as the average B^0 - \bar{B}^0 mixing.

201 ABBIENDI 02I tag $Z^0 \rightarrow b\bar{b}$ decays using a combination of secondary vertex and lepton tags. The sign of the b -quark charge is determined using an inclusive tag based on jet, vertex, and kaon charges.

202 HEISTER 02H measure simultaneously b and c quark forward-backward asymmetries using their semileptonic decays to tag the quark charge. The flavor separation is obtained with a discriminating multivariate analysis.

203 HEISTER 01D tag $Z \rightarrow b\bar{b}$ events using the impact parameters of charged tracks complemented with information from displaced vertices, event shape variables, and lepton identification. The b -quark direction and charge is determined using the hemisphere charge method along with information from fast kaon tagging and charge estimators of primary and secondary vertices. The change in the quoted value due to variation of $A_{FB}^{(0,b)}$ and R_b is given as $+0.103(A_{FB}^{(0,b)} - 0.0651) - 0.440(R_b - 0.21585)$.

204 ABREU 99Y tag $Z \rightarrow b\bar{b}$ and $Z \rightarrow c\bar{c}$ events by an exclusive reconstruction of several D meson decay modes (D^{*+} , D^0 , and D^+ with their charge-conjugate states).

205 ACCIARRI 99D tag $Z \rightarrow b\bar{b}$ events using high p and p_T leptons. The analysis determines simultaneously a mixing parameter $\chi_b = 0.1192 \pm 0.0068 \pm 0.0051$ which is used to correct the observed asymmetry.

206 ACCIARRI 98U tag $Z \rightarrow b\bar{b}$ events using lifetime and measure the jet charge using the hemisphere charge.

207 ALEXANDER 97C identify the b and c events using a D/D^* tag.

CHARGE ASYMMETRY IN $e^+e^- \rightarrow q\bar{q}$

Summed over five lighter flavors.

Experimental and Standard Model values are somewhat event-selection dependent. Standard Model expectations contain some assumptions on B^0 - \bar{B}^0 mixing and on other electroweak parameters.

ASYMMETRY (%)	STD. MODEL	\sqrt{s} (GeV)	DOCUMENT ID	TECN
• • • We do not use the following data for averages, fits, limits, etc. • • •				
-0.76 ± 0.12 ± 0.15		91.2	208 ABREU	92I DLPH
4.0 ± 0.4 ± 0.63	4.0	91.3	209 ACTON	92L OPAL
9.1 ± 1.4 ± 1.6	9.0	57.9	ADACHI	91 TOPZ
-0.84 ± 0.15 ± 0.04		91	DECAMP	91B ALEP
8.3 ± 2.9 ± 1.9	8.7	56.6	STUART	90 AMY
11.4 ± 2.2 ± 2.1	8.7	57.6	ABE	89L VNS
6.0 ± 1.3	5.0	34.8	GREENSHAW	89 JADE
8.2 ± 2.9	8.5	43.6	GREENSHAW	89 JADE

208 ABREU 92I has 0.14 systematic error due to uncertainty of quark fragmentation.

209 ACTON 92L use the weight function method on 259k selected $Z \rightarrow$ hadrons events. The systematic error includes a contribution of 0.2 due to B^0 - \bar{B}^0 mixing effect, 0.4 due to Monte Carlo (MC) fragmentation uncertainties and 0.3 due to MC statistics. ACTON 92L derive a value of $\sin^2\theta_W^{\text{eff}}$ to be $0.2321 \pm 0.0017 \pm 0.0028$.

CHARGE ASYMMETRY IN $p\bar{p} \rightarrow Z \rightarrow e^+e^-$

ASYMMETRY (%)	STD. MODEL	\sqrt{s} (GeV)	DOCUMENT ID	TECN
• • • We do not use the following data for averages, fits, limits, etc. • • •				
5.2 ± 5.9 ± 0.4		91	ABE	91E CDF

ANOMALOUS $Z\gamma$, $Z\gamma\gamma$, AND ZZV COUPLINGS

Revised March 2006 by C. Caso (University of Genova) and A. Gurtu (Tata Institute).

In the reaction $e^+e^- \rightarrow Z\gamma$, deviations from the Standard Model for the $Z\gamma\gamma^*$ and $Z\gamma Z^*$ couplings may be described in terms of 8 parameters, h_i^V ($i = 1, 4$; $V = \gamma, Z$) [1]. The parameters h_i^Z describe the $Z\gamma\gamma^*$ couplings and the parameters h_i^Z the $Z\gamma Z^*$ couplings. In this formalism h_1^V and h_2^V lead to CP -violating and h_3^V and h_4^V to CP -conserving effects. All these anomalous contributions to the cross section increase rapidly with center-of-mass energy. In order to ensure unitarity,

Gauge & Higgs Boson Particle Listings

Z

these parameters are usually described by a form-factor representation, $h_i^V(s) = h_{i0}^V/(1 + s/\Lambda^2)^n$, where Λ is the energy scale for the manifestation of a new phenomenon and n is a sufficiently large power. By convention one uses $n = 3$ for $h_{1,3}^V$ and $n = 4$ for $h_{2,4}^V$. Usually limits on h_i^V 's are put assuming some value of Λ (sometimes ∞).

Above the $e^+e^- \rightarrow ZZ$ threshold, deviations from the Standard Model for the $ZZ\gamma^*$ and ZZZ^* couplings may be described by means of four anomalous couplings f_i^V ($i = 4, 5; V = \gamma, Z$) [2]. As above, the parameters f_i^γ describe the $Z\gamma\gamma^*$ couplings and the parameters f_i^Z the ZZZ^* couplings. The anomalous couplings f_3^V lead to violation of C and P symmetries while f_4^V introduces CP violation.

All these couplings h_i^V and f_i^V are zero at tree level in the Standard Model.

References

1. U. Baur and E.L. Berger Phys. Rev. **D47**, 4889 (1993).
2. K. Hagiwara *et al.*, Nucl. Phys. **B282**, 253 (1987).

h_i^V

Combining the LEP results properly taking into account the correlations the following 95% CL limits are derived (CERN-PH-EP/2005-051 or hep-ex/0511027):

$$\begin{aligned} -0.13 < h_1^Z < +0.13, & \quad -0.078 < h_2^Z < +0.071, \\ -0.20 < h_3^Z < +0.07, & \quad -0.05 < h_4^Z < +0.12, \\ -0.056 < h_1^\gamma < +0.055, & \quad -0.045 < h_2^\gamma < +0.025, \\ -0.049 < h_3^\gamma < -0.008, & \quad -0.002 < h_4^\gamma < +0.034. \end{aligned}$$

VALUE	DOCUMENT ID	TECN	COMMENT
• • • We do not use the following data for averages, fits, limits, etc. • • •			
	210	ABAZOV	07M D0
	211	ABDALLAH	07c DLPH $E_{\text{cm}}^e = 183\text{--}208$ GeV
	212	ACHARD	04H L3
	213	ABBIENDI,G	00c OPAL
	214	ABBOTT	98M D0
	215	ABREU	98K DLPH

210 ABAZOV 07M use 968 $p\bar{p} \rightarrow e^+e^-/\mu^+\mu^- \gamma X$ candidates, at 1.96 TeV center of mass energy, to tag $p\bar{p} \rightarrow Z\gamma$ events by requiring $E_T(\gamma) > 7$ GeV, lepton-gamma separation $\Delta R_{\ell\gamma} > 0.7$, and di-lepton invariant mass > 30 GeV. The cross section is in agreement with the SM prediction. Using these $Z\gamma$ events they obtain 95% C.L. limits on each h_i^V , keeping all others fixed at their SM values. They report: $-0.083 < h_{30}^Z < 0.082$, $-0.0053 < h_{40}^Z < 0.0054$, $-0.085 < h_{30}^\gamma < 0.084$, $-0.0053 < h_{40}^\gamma < 0.0054$, for the form factor scale $\Lambda = 1.2$ TeV.

211 Using data collected at $\sqrt{s} = 183\text{--}208$, ABDALLAH 07c select 1,877 $e^+e^- \rightarrow Z\gamma$ events with $Z \rightarrow q\bar{q}$ or $\nu\bar{\nu}$, 171 $e^+e^- \rightarrow ZZ$ events with $Z \rightarrow q\bar{q}$ or lepton pair (except an explicit τ pair), and 74 $e^+e^- \rightarrow Z\gamma^*$ events with a $q\bar{q}\mu^+\mu^-$ or $q\bar{q}e^+e^-$ signature, to derive 95% CL limits on h_i^V . Each limit is derived with other parameters set to zero. They report: $-0.23 < h_1^Z < 0.23$, $-0.30 < h_3^Z < 0.16$, $-0.14 < h_1^\gamma < 0.14$, $-0.049 < h_3^\gamma < 0.044$.

212 ACHARD 04H select 3515 $e^+e^- \rightarrow Z\gamma$ events with $Z \rightarrow q\bar{q}$ or $\nu\bar{\nu}$ at $\sqrt{s} = 189\text{--}209$ GeV to derive 95% CL limits on h_i^V . For deriving each limit the other parameters are fixed at zero. They report: $-0.153 < h_1^Z < 0.141$, $-0.087 < h_2^Z < 0.079$, $-0.220 < h_3^Z < 0.112$, $-0.068 < h_4^Z < 0.148$, $-0.057 < h_1^\gamma < 0.057$, $-0.050 < h_2^\gamma < 0.023$, $-0.059 < h_3^\gamma < 0.004$, $-0.004 < h_4^\gamma < 0.042$.

213 ABBIENDI,G 00c study $e^+e^- \rightarrow Z\gamma$ events (with $Z \rightarrow q\bar{q}$ and $Z \rightarrow \nu\bar{\nu}$) at 189 GeV to obtain the central values (and 95% CL limits) of these couplings: $h_1^Z = 0.000 \pm 0.100$ ($-0.190, 0.190$), $h_2^Z = 0.000 \pm 0.068$ ($-0.128, 0.128$), $h_3^Z = -0.074 \pm 0.102$ ($-0.269, 0.119$), $h_4^Z = 0.046 \pm 0.068$ ($-0.084, 0.175$), $h_1^\gamma = 0.000 \pm 0.061$ ($-0.115, 0.115$), $h_2^\gamma = 0.000 \pm 0.041$ ($-0.077, 0.077$), $h_3^\gamma = -0.080 \pm 0.039$ ($-0.164, -0.006$), $h_4^\gamma = 0.064 \pm 0.033$ ($+0.007, +0.134$). The results are derived assuming that only one coupling at a time is different from zero.

214 ABBOTT 98M study $p\bar{p} \rightarrow Z\gamma + X$, with $Z \rightarrow e^+e^-, \mu^+\mu^-, \nu\bar{\nu}$ at 1.8 TeV, to obtain 95% CL limits at $\Lambda = 750$ GeV: $|h_{30}^Z| < 0.36$, $|h_{40}^Z| < 0.05$ (keeping $h_1^\gamma = 0$), and $|h_{30}^\gamma| < 0.37$, $|h_{40}^\gamma| < 0.05$ (keeping $h_2^\gamma = 0$). Limits on the CP -violating couplings are $|h_{10}^Z| < 0.36$, $|h_{20}^Z| < 0.05$ (keeping $h_1^\gamma = 0$), and $|h_{10}^\gamma| < 0.37$, $|h_{20}^\gamma| < 0.05$ (keeping $h_2^\gamma = 0$).

215 ABREU 98K determine a 95% CL upper limit on $\sigma(e^+e^- \rightarrow \gamma + \text{invisible particles}) < 2.5$ pb using 161 and 172 GeV data. This is used to set 95% CL limits on $|h_{30}^\gamma| < 0.8$ and $|h_{30}^Z| < 1.3$, derived at a scale $\Lambda = 1$ TeV and with $n=3$ in the form factor representation.

f_i^V

Combining the LEP results properly taking into account the correlations the following 95% CL limits are derived (CERN-PH-EP/2005-051 or hep-ex/0511027):

$$\begin{aligned} -0.30 < f_4^Z < +0.30, & \quad -0.34 < f_5^Z < +0.38, \\ -0.17 < f_4^\gamma < +0.19, & \quad -0.32 < f_5^\gamma < +0.36. \end{aligned}$$

VALUE	DOCUMENT ID	TECN	COMMENT
• • • We do not use the following data for averages, fits, limits, etc. • • •			
	216	ABDALLAH	07c DLPH $E_{\text{cm}}^e = 183\text{--}208$ GeV
	217	ABBIENDI	04c OPAL
	218	ACHARD	03D L3

216 Using data collected at $\sqrt{s} = 183\text{--}208$, ABDALLAH 07c select 171 $e^+e^- \rightarrow ZZ$ events with $Z \rightarrow q\bar{q}$ or lepton pair (except an explicit τ pair), and 74 $e^+e^- \rightarrow Z\gamma^*$ events with a $q\bar{q}\mu^+\mu^-$ or $q\bar{q}e^+e^-$ signature, to derive 95% CL limits on f_i^V . Each limit is derived with other parameters set to zero. They report: $-0.40 < f_4^Z < 0.42$, $-0.38 < f_5^Z < 0.62$, $-0.23 < f_4^\gamma < 0.25$, $-0.52 < f_5^\gamma < 0.48$.

217 ABBIENDI 04c study ZZ production in e^+e^- collisions in the C.M. energy range 190–209 GeV. They select 340 events with an expected background of 180 events. Including the ABBIENDI 00N data at 183 and 189 GeV (118 events with an expected background of 65 events) they report the following 95% CL limits: $-0.45 < f_4^Z < 0.58$, $-0.94 < f_5^Z < 0.25$, $-0.32 < f_4^\gamma < 0.33$, and $-0.71 < f_5^\gamma < 0.59$.

218 ACHARD 03D study Z -boson pair production in e^+e^- collisions in the C.M. energy range 200–209 GeV. They select 549 events with an expected background of 432 events. Including the ACCIARRI 99G and ACCIARRI 99O data (183 and 189 GeV respectively, 286 events with an expected background of 241 events) and the 192–202 GeV ACCIARRI 01I results (656 events, expected background of 512 events), they report the following 95% CL limits: $-0.48 \leq f_4^Z \leq 0.46$, $-0.36 \leq f_5^Z \leq 1.03$, $-0.28 \leq f_4^\gamma \leq 0.28$, and $-0.40 \leq f_5^\gamma \leq 0.47$.

ANOMALOUS W/Z QUARTIC COUPLINGS

Revised March 2006 by C. Caso (University of Genova) and A. Gurtu (Tata Institute).

The Standard Model predictions for $WWWW$, $WWZZ$, $WWZ\gamma$, $WW\gamma\gamma$, and $ZZ\gamma\gamma$ couplings are small at LEP, but expected to become important at a TeV Linear Collider. Outside the Standard Model framework such possible couplings, a_0, a_c, a_n , are expressed in terms of the following dimension-6 operators [1,2];

$$\begin{aligned} L_6^0 &= -\frac{e^2}{16\Lambda^2} a_0 F^{\mu\nu} F_{\mu\nu} \vec{W}^\alpha \cdot \vec{W}_\alpha \\ L_6^c &= -\frac{e^2}{16\Lambda^2} a_c F^{\mu\alpha} F_{\mu\beta} \vec{W}^\beta \cdot \vec{W}_\alpha \\ L_6^n &= -i\frac{e^2}{16\Lambda^2} a_n \epsilon_{ijk} W_{\mu\alpha}^{(i)} W_{\nu}^{(j)} W^{(k)\alpha} F^{\mu\nu} \\ \tilde{L}_6^0 &= -\frac{e^2}{16\Lambda^2} \tilde{a}_0 F^{\mu\nu} \tilde{F}_{\mu\nu} \vec{W}^\alpha \cdot \vec{W}_\alpha \\ \tilde{L}_6^n &= -i\frac{e^2}{16\Lambda^2} \tilde{a}_n \epsilon_{ijk} W_{\mu\alpha}^{(i)} W_{\nu}^{(j)} W^{(k)\alpha} \tilde{F}^{\mu\nu} \end{aligned}$$

where F, W are photon and W fields, L_6^0 and L_6^c conserve C , P separately (\tilde{L}_6^0 conserves only C) and generate anomalous $W^+W^-\gamma\gamma$ and $ZZ\gamma\gamma$ couplings, L_6^n violates CP (\tilde{L}_6^n violates both C and P) and generates an anomalous $W^+W^-Z\gamma$ coupling, and Λ is an energy scale for new physics. For the $ZZ\gamma\gamma$ coupling the CP -violating term represented by L_6^n does not contribute. These couplings are assumed to be real and to vanish at tree level in the Standard Model.

Within the same framework as above, a more recent description of the quartic couplings [3] treats the anomalous parts of the $WW\gamma\gamma$ and $ZZ\gamma\gamma$ couplings separately leading to two sets parameterized as a_0^V/Λ^2 and a_c^V/Λ^2 , where $V = W$ or Z .

At LEP the processes studied in search of these quartic couplings are $e^+e^- \rightarrow WW\gamma$, $e^+e^- \rightarrow \gamma\gamma\nu\bar{\nu}$, and $e^+e^- \rightarrow Z\gamma\gamma$ and limits are set on the quantities a_0^W/Λ^2 , a_c^W/Λ^2 , a_n/Λ^2 . The characteristics of the first process depend on all the three couplings whereas those of the latter two depend only on the two CP -conserving couplings. The sensitive measured variables

are the cross sections for these processes as well as the energy and angular distributions of the photon and recoil mass to the photon pair.

References

1. G. Belanger and F. Boudjema, Phys. Lett. **B288**, 201 (1992).
2. J.W. Stirling and A. Werthenbach, Eur. Phys. J. **C14**, 103 (2000);
J.W. Stirling and A. Werthenbach, Phys. Lett. **B466**, 369 (1999);
A. Denner *et al.*, Eur. Phys. J. **C20**, 201 (2001);
G. Montagna *et al.*, Phys. Lett. **B515**, 197 (2001).
3. G. Belanger *et al.*, Eur. Phys. J. **C13**, 103 (2000).

$a_0/\Lambda^2, a_c/\Lambda^2$

Combining published and unpublished preliminary LEP results the following 95% CL intervals for the QGCs associated with the $Z\bar{Z}\gamma\gamma$ vertex are derived (CERN-PH-EP/2005-051 or hep-ex/0511027):

$$-0.008 < a_0^Z/\Lambda^2 < +0.021$$

$$-0.029 < a_c^Z/\Lambda^2 < +0.039$$

VALUE DOCUMENT ID TECN

- • • We do not use the following data for averages, fits, limits, etc. • • •
- | VALUE | DOCUMENT ID | TECN |
|-------|-------------|----------|
| 219 | ABBIENDI | 04L OPAL |
| 220 | HEISTER | 04A ALEP |
| 221 | ACHARD | 02G L3 |
- 219 ABBIENDI 04L select $20 e^+e^- \rightarrow \nu\bar{\nu}\gamma\gamma$ acoplanar events in the energy range 180–209 GeV and $176 e^+e^- \rightarrow q\bar{q}\gamma\gamma$ events in the energy range 130–209 GeV. These samples are used to constrain possible anomalous $W^+W^-\gamma\gamma$ and $ZZ\gamma\gamma$ quartic couplings. Further combining with the $W^+W^-\gamma$ sample of ABBIENDI 04B the following one-parameter 95% CL limits are obtained: $-0.007 < a_0^Z/\Lambda^2 < 0.023 \text{ GeV}^{-2}$, $-0.029 < a_c^Z/\Lambda^2 < 0.029 \text{ GeV}^{-2}$, $-0.020 < a_0^W/\Lambda^2 < 0.020 \text{ GeV}^{-2}$, $-0.052 < a_c^W/\Lambda^2 < 0.037 \text{ GeV}^{-2}$.
- 220 In the CM energy range 183 to 209 GeV HEISTER 04A select $30 e^+e^- \rightarrow \nu\bar{\nu}\gamma\gamma$ events with two acoplanar, high energy and high transverse momentum photons. The photon-photon acoplanarity is required to be $> 5^\circ$, $E_\gamma/\sqrt{s} > 0.025$ (the more energetic photon having energy $> 0.2\sqrt{s}$), $p_{T,\gamma}/E_{\text{beam}} > 0.05$ and $|\cos\theta_\gamma| < 0.94$. A likelihood fit to the photon energy and recoil missing mass yields the following one-parameter 95% CL limits: $-0.012 < a_0^Z/\Lambda^2 < 0.019 \text{ GeV}^{-2}$, $-0.041 < a_c^Z/\Lambda^2 < 0.044 \text{ GeV}^{-2}$, $-0.060 < a_0^W/\Lambda^2 < 0.055 \text{ GeV}^{-2}$, $-0.099 < a_c^W/\Lambda^2 < 0.093 \text{ GeV}^{-2}$.
- 221 ACHARD 02G study $e^+e^- \rightarrow Z\gamma\gamma \rightarrow q\bar{q}\gamma\gamma$ events using data at center-of-mass energies from 200 to 209 GeV. The photons are required to be isolated, each with energy $> 5 \text{ GeV}$ and $|\cos\theta| < 0.97$, and the di-jet invariant mass to be compatible with that of the Z boson (74–111 GeV). Cuts on Z velocity ($\beta < 0.73$) and on the energy of the most energetic photon reduce the backgrounds due to non-resonant production of the $q\bar{q}\gamma\gamma$ state and due to ISR respectively, yielding a total of 40 candidate events of which 8.6 are expected to be due to background. The energy spectra of the least energetic photon are fitted for all ten center-of-mass energy values from 130 GeV to 209 GeV (as obtained adding to the present analysis 130–202 GeV data of ACCIARRI 01E, for a total of 137 events with an expected background of 34.1 events) to obtain the fitted values $a_0/\Lambda^2 = 0.00 \pm 0.02 \text{ GeV}^{-2}$ and $a_c/\Lambda^2 = 0.03 \pm 0.01 \text{ GeV}^{-2}$, where the other parameter is kept fixed to its Standard Model value (0). A simultaneous fit to both parameters yields the 95% CL limits $-0.02 \text{ GeV}^{-2} < a_0/\Lambda^2 < 0.03 \text{ GeV}^{-2}$ and $-0.07 \text{ GeV}^{-2} < a_c/\Lambda^2 < 0.05 \text{ GeV}^{-2}$.

Z REFERENCES

ABAZOV	07M	PL B653 378	V.M. Abazov <i>et al.</i>	(DO Collab.)
ABDALLAH	07C	EPJ C51 525	J. Abdallah <i>et al.</i>	(DELPHI Collab.)
ABDALLAH	06E	PL B639 179	J. Abdallah <i>et al.</i>	(DELPHI Collab.)
LEP-SLC	06	PRPL 427 257	ALEPH, DELPHI, L3, OPAL, SLD and working groups	
SCHAEF	06A	PL B639 192	S. Schaeff <i>et al.</i>	(ALEPH Collab.)
ABDALLAH	05	EPJ C40 1	J. Abdallah <i>et al.</i>	(DELPHI Collab.)
ABDALLAH	05C	EPJ C44 299	J. Abdallah <i>et al.</i>	(DELPHI Collab.)
ABE	05	PRL 94 091801	K. Abe <i>et al.</i>	(SLD Collab.)
ABE	05F	PR D71 112004	K. Abe <i>et al.</i>	(SLD Collab.)
ACOSTA	05M	PR D71 052002	D. Acosta <i>et al.</i>	(CDF Collab.)
ABBIENDI	04B	PL B580 17	G. Abbiendi <i>et al.</i>	(OPAL Collab.)
ABBIENDI	04C	EPJ C32 303	G. Abbiendi <i>et al.</i>	(OPAL Collab.)
ABBIENDI	04E	PL B586 167	G. Abbiendi <i>et al.</i>	(OPAL Collab.)
ABBIENDI	04G	EPJ C33 173	G. Abbiendi <i>et al.</i>	(OPAL Collab.)
ABDALLAH	04F	PR D70 032005	G. Abbiendi <i>et al.</i>	(OPAL Collab.)
ABDALLAH	04F	EPJ C34 109	J. Abdallah <i>et al.</i>	(DELPHI Collab.)
ABE	04C	PR D69 072003	K. Abe <i>et al.</i>	(SLD Collab.)
ACHARD	04C	PL B585 42	P. Achard <i>et al.</i>	(L3 Collab.)
ACHARD	04H	PL B597 119	P. Achard <i>et al.</i>	(L3 Collab.)
HEISTER	04A	PL B602 31	A. Heister <i>et al.</i>	(ALEPH Collab.)
ABBIENDI	03P	PL B577 18	G. Abbiendi <i>et al.</i>	(OPAL Collab.)
ABDALLAH	03H	PL B569 129	J. Abdallah <i>et al.</i>	(DELPHI Collab.)
ABDALLAH	03K	PL B576 29	J. Abdallah <i>et al.</i>	(DELPHI Collab.)
ABE	03F	PRL 90 141804	K. Abe <i>et al.</i>	(SLD Collab.)
ACHARD	03D	PL B572 133	P. Achard <i>et al.</i>	(L3 Collab.)
ACHARD	03G	PL B577 109	P. Achard <i>et al.</i>	(L3 Collab.)
ABBIENDI	02I	PL B546 29	G. Abbiendi <i>et al.</i>	(OPAL Collab.)
ABE	02G	PRL 88 151801	K. Abe <i>et al.</i>	(SLD Collab.)
ACHARD	02G	PL B540 43	P. Achard <i>et al.</i>	(L3 Collab.)
HEISTER	02B	PL B526 34	A. Heister <i>et al.</i>	(ALEPH Collab.)
HEISTER	02C	PL B528 19	A. Heister <i>et al.</i>	(ALEPH Collab.)
HEISTER	02H	EPJ C24 177	A. Heister <i>et al.</i>	(ALEPH Collab.)
ABBIENDI	01A	EPJ C19 587	G. Abbiendi <i>et al.</i>	(OPAL Collab.)
ABBIENDI	01G	EPJ C18 447	G. Abbiendi <i>et al.</i>	(OPAL Collab.)
ABBIENDI	01K	PL B516 1	G. Abbiendi <i>et al.</i>	(OPAL Collab.)
ABBIENDI	01N	EPJ C20 445	G. Abbiendi <i>et al.</i>	(OPAL Collab.)
ABBIENDI	01O	EPJ C21 1	G. Abbiendi <i>et al.</i>	(OPAL Collab.)
ABE	01B	PRL 86 1162	K. Abe <i>et al.</i>	(SLD Collab.)
ABE	01C	PR D63 032005	K. Abe <i>et al.</i>	(SLD Collab.)
ACCIARRI	01E	PL B505 47	M. Acciari <i>et al.</i>	(L3 Collab.)
ACCIARRI	01I	PL B497 23	M. Acciari <i>et al.</i>	(L3 Collab.)
HEISTER	01I	EPJ C20 401	A. Heister <i>et al.</i>	(ALEPH Collab.)
HEISTER	01D	EPJ C22 201	A. Heister <i>et al.</i>	(ALEPH Collab.)
ABBIENDI	00N	PL B476 256	G. Abbiendi <i>et al.</i>	(OPAL Collab.)
ABBIENDI,G	00C	EPJ C17 553	G. Abbiendi <i>et al.</i>	(OPAL Collab.)
ABE	00B	PRL 84 5945	K. Abe <i>et al.</i>	(SLD Collab.)
ABE	00D	PRL 85 3059	K. Abe <i>et al.</i>	(SLD Collab.)
ABREU	00	EPJ C12 225	P. Abreu <i>et al.</i>	(DELPHI Collab.)
ABREU	00B	EPJ C14 613	P. Abreu <i>et al.</i>	(DELPHI Collab.)
ABREU	00E	EPJ C14 585	P. Abreu <i>et al.</i>	(DELPHI Collab.)
ABREU	00F	EPJ C16 371	P. Abreu <i>et al.</i>	(DELPHI Collab.)
ABREU	00P	PL B475 429	P. Abreu <i>et al.</i>	(DELPHI Collab.)
ACCIARRI	00	EPJ C13 47	M. Acciari <i>et al.</i>	(L3 Collab.)
ACCIARRI	00C	EPJ C16 1	M. Acciari <i>et al.</i>	(L3 Collab.)
ACCIARRI	00J	PL B479 79	M. Acciari <i>et al.</i>	(L3 Collab.)
ACCIARRI	00K	PL B489 93	M. Acciari <i>et al.</i>	(L3 Collab.)
BARATE	00B	EPJ C16 597	R. Barate <i>et al.</i>	(ALEPH Collab.)
BARATE	00C	EPJ C14 1	R. Barate <i>et al.</i>	(ALEPH Collab.)
BARATE	00O	EPJ C16 613	R. Barate <i>et al.</i>	(ALEPH Collab.)
ABBIENDI	99B	EPJ C8 217	G. Abbiendi <i>et al.</i>	(OPAL Collab.)
ABBIENDI	99I	PL B447 157	G. Abbiendi <i>et al.</i>	(OPAL Collab.)
ABE	99E	PR D59 052001	K. Abe <i>et al.</i>	(SLD Collab.)
ABE	99L	PRL 83 1902	K. Abe <i>et al.</i>	(SLD Collab.)
ABREU	99	EPJ C6 19	P. Abreu <i>et al.</i>	(DELPHI Collab.)
ABREU	99B	EPJ C10 415	P. Abreu <i>et al.</i>	(DELPHI Collab.)
ABREU	99J	PL B449 364	P. Abreu <i>et al.</i>	(DELPHI Collab.)
ABREU	99Y	PL B462 425	P. Abreu <i>et al.</i>	(DELPHI Collab.)
ABREU	99Y	EPJ C10 219	P. Abreu <i>et al.</i>	(DELPHI Collab.)
ACCIARRI	99D	PL B448 152	M. Acciari <i>et al.</i>	(L3 Collab.)
ACCIARRI	99F	PL B459 94	M. Acciari <i>et al.</i>	(L3 Collab.)
ACCIARRI	99G	PL B450 281	M. Acciari <i>et al.</i>	(L3 Collab.)
ACCIARRI	99O	PL B465 363	M. Acciari <i>et al.</i>	(L3 Collab.)
ABBOTT	98M	PR D57 R3817	B. Abbott <i>et al.</i>	(D0 Collab.)
ABE	98D	PRL 80 660	K. Abe <i>et al.</i>	(SLD Collab.)
ABE	98I	PRL 81 942	K. Abe <i>et al.</i>	(SLD Collab.)
ABREU	98K	PL B423 194	P. Abreu <i>et al.</i>	(DELPHI Collab.)
ABREU	98L	EPJ C5 585	P. Abreu <i>et al.</i>	(DELPHI Collab.)
ACCIARRI	98H	PL B431 199	M. Acciari <i>et al.</i>	(L3 Collab.)
ACCIARRI	98G	PL B429 387	M. Acciari <i>et al.</i>	(L3 Collab.)
ACCIARRI	98J	PL B439 225	M. Acciari <i>et al.</i>	(L3 Collab.)
ACKERSTAFF	98A	EPJ C5 111	K. Ackerstaff <i>et al.</i>	(OPAL Collab.)
ACKERSTAFF	98E	EPJ C1 439	K. Ackerstaff <i>et al.</i>	(OPAL Collab.)
ACKERSTAFF	98O	PL B420 157	K. Ackerstaff <i>et al.</i>	(OPAL Collab.)
ACKERSTAFF	98Q	EPJ C4 19	K. Ackerstaff <i>et al.</i>	(OPAL Collab.)
BARATE	98O	PL B434 415	R. Barate <i>et al.</i>	(ALEPH Collab.)
BARATE	98T	EPJ C4 557	R. Barate <i>et al.</i>	(ALEPH Collab.)
BARATE	98V	EPJ C5 205	R. Barate <i>et al.</i>	(ALEPH Collab.)
ABE	97	PRL 78 17	K. Abe <i>et al.</i>	(SLD Collab.)
ABREU	97C	ZPHY C73 243	P. Abreu <i>et al.</i>	(DELPHI Collab.)
ABREU	97E	PL B398 207	P. Abreu <i>et al.</i>	(DELPHI Collab.)
ABREU	97G	PL B404 194	P. Abreu <i>et al.</i>	(DELPHI Collab.)
ACCIARRI	97D	PL B393 465	M. Acciari <i>et al.</i>	(L3 Collab.)
ACCIARRI	97J	PL B407 351	M. Acciari <i>et al.</i>	(L3 Collab.)
ACCIARRI	97L	PL B407 389	M. Acciari <i>et al.</i>	(L3 Collab.)
ACCIARRI	97R	PL B413 167	M. Acciari <i>et al.</i>	(L3 Collab.)
ACKERSTAFF	97M	ZPHY C74 413	K. Ackerstaff <i>et al.</i>	(OPAL Collab.)
ACKERSTAFF	97S	PL B412 210	K. Ackerstaff <i>et al.</i>	(OPAL Collab.)
ACKERSTAFF	97T	ZPHY C76 387	K. Ackerstaff <i>et al.</i>	(OPAL Collab.)
ACKERSTAFF	97W	ZPHY C76 425	K. Ackerstaff <i>et al.</i>	(OPAL Collab.)
ALEXANDER	97C	ZPHY C73 379	G. Alexander <i>et al.</i>	(OPAL Collab.)
ALEXANDER	97D	ZPHY C73 569	G. Alexander <i>et al.</i>	(OPAL Collab.)
ALEXANDER	97E	ZPHY C73 587	G. Alexander <i>et al.</i>	(OPAL Collab.)
BARATE	97D	PL B401 191	R. Barate <i>et al.</i>	(ALEPH Collab.)
BARATE	97E	PL B401 150	R. Barate <i>et al.</i>	(ALEPH Collab.)
BARATE	97F	PL B401 163	R. Barate <i>et al.</i>	(ALEPH Collab.)
BARATE	97H	PL B402 213	R. Barate <i>et al.</i>	(ALEPH Collab.)
BARATE	97J	ZPHY C74 451	R. Barate <i>et al.</i>	(ALEPH Collab.)
ABREU	96R	ZPHY C72 31	P. Abreu <i>et al.</i>	(DELPHI Collab.)
ABREU	96S	PL B389 405	P. Abreu <i>et al.</i>	(DELPHI Collab.)
ABREU	96U	ZPHY C73 61	P. Abreu <i>et al.</i>	(DELPHI Collab.)
ACCIARRI	96	PL B371 126	M. Acciari <i>et al.</i>	(L3 Collab.)
ADAM	96	ZPHY C69 561	W. Adam <i>et al.</i>	(DELPHI Collab.)
ADAM	96B	ZPHY C70 371	W. Adam <i>et al.</i>	(DELPHI Collab.)
ALEXANDER	96L	ZPHY C65 197	G. Alexander <i>et al.</i>	(OPAL Collab.)
ALEXANDER	96F	PL B370 185	G. Alexander <i>et al.</i>	(OPAL Collab.)
ALEXANDER	96N	PL B384 343	G. Alexander <i>et al.</i>	(OPAL Collab.)
ALEXANDER	96R	ZPHY C72 1	G. Alexander <i>et al.</i>	(OPAL Collab.)
BUSKULIC	96D	ZPHY C69 393	D. Buskulic <i>et al.</i>	(ALEPH Collab.)
BUSKULIC	96H	ZPHY C69 379	D. Buskulic <i>et al.</i>	(ALEPH Collab.)
BUSKULIC	96T	PL B384 449	D. Buskulic <i>et al.</i>	(ALEPH Collab.)
BUSKULIC	96Y	PL B388 648	D. Buskulic <i>et al.</i>	(ALEPH Collab.)
ABE	95J	PRL 74 2880	K. Abe <i>et al.</i>	(SLD Collab.)
ABREU	95	ZPHY C65 709 (erratum)	P. Abreu <i>et al.</i>	(DELPHI Collab.)
ABREU	95D	ZPHY C66 323	P. Abreu <i>et al.</i>	(DELPHI Collab.)
ABREU	95L	ZPHY C65 587	P. Abreu <i>et al.</i>	(DELPHI Collab.)
ABREU	95M	ZPHY C65 603	P. Abreu <i>et al.</i>	(DELPHI Collab.)
ABREU	95O	ZPHY C67 543	P. Abreu <i>et al.</i>	(DELPHI Collab.)
ABREU	95R	ZPHY C68 353	P. Abreu <i>et al.</i>	(DELPHI Collab.)
ABREU	95V	ZPHY C68 541	P. Abreu <i>et al.</i>	(DELPHI Collab.)
ABREU	95W	PL B361 207	P. Abreu <i>et al.</i>	(DELPHI Collab.)
ABREU	95X	ZPHY C69 1	P. Abreu <i>et al.</i>	(DELPHI Collab.)
ACCIARRI	95B	PL B345 589	M. Acciari <i>et al.</i>	(L3 Collab.)
ACCIARRI	95C	PL B345 609	M. Acciari <i>et al.</i>	(L3 Collab.)
ACCIARRI	95G	PL B353 136	M. Acciari <i>et al.</i>	(L3 Collab.)
AKERS	95C	ZPHY C65 47	R. Akers <i>et al.</i>	(OPAL Collab.)
AKERS	95U	ZPHY C67 389	R. Akers <i>et al.</i>	(OPAL Collab.)
AKERS	95W	ZPHY C67 555	R. Akers <i>et al.</i>	(OPAL Collab.)
AKERS	95Z	ZPHY C68 1	R. Akers <i>et al.</i>	(OPAL Collab.)
AKERS	95X	ZPHY C68 203	R. Akers <i>et al.</i>	(OPAL Collab.)
ALEXANDER	95D	PL B358 162	G. Alexander <i>et al.</i>	(OPAL Collab.)
BUSKULIC	95R	ZPHY C69 15	D. Buskulic <i>et al.</i>	(ALEPH Collab.)
MIYABAYASHI	95	PL B347 171	K. Miyabayashi <i>et al.</i>	(TOPAZ Collab.)
ABE	94C	PRL 73 25	K. Abe <i>et al.</i>	(SLD Collab.)
ABREU	94B	PL B327 386	P. Abreu <i>et al.</i>	(DELPHI Collab.)
ABREU	94P	PL B341 109	P. Abreu <i>et al.</i>	(DELPHI Collab.)
AKERS	94P	ZPHY C63 181	R. Akers <i>et al.</i>	(OPAL Collab.)
BUSKULIC	94G	ZPHY C62 179	D. Buskulic <i>et al.</i>	(ALEPH Collab.)
BUSKULIC	94J	ZPHY C62 1	D. Buskulic <i>et al.</i>	(ALEPH Collab.)
VILAIN	94	PL B320 203	P. Vilain <i>et al.</i>	(CHARM II Collab.)
ABREU	93	PL B298 236	P. Abreu	

Gauge & Higgs Boson Particle Listings

 Z , Higgs Bosons — H^0 and H^\pm

ABREU	93I	ZPHY C59 533	P. Abreu <i>et al.</i>	(DELPHI Collab.)
Also		ZPHY C65 709 (erratum)	P. Abreu <i>et al.</i>	(DELPHI Collab.)
ABREU	93L	PL B318 249	P. Abreu <i>et al.</i>	(DELPHI Collab.)
ACTON	93	PL B305 407	P.D. Acton <i>et al.</i>	(OPAL Collab.)
ACTON	93D	ZPHY C58 219	P.D. Acton <i>et al.</i>	(OPAL Collab.)
ACTON	93E	PL B311 391	P.D. Acton <i>et al.</i>	(OPAL Collab.)
ADRIANI	93	PL B301 136	O. Adriani <i>et al.</i>	(L3 Collab.)
ADRIANI	93I	PL B316 427	O. Adriani <i>et al.</i>	(L3 Collab.)
BUSKULIC	93L	PL B313 520	D. Buskulle <i>et al.</i>	(ALEPH Collab.)
NOVIKOV	93C	PL B298 453	V.A. Novikov, L.B. Okun, M.I. Vysotsky	(ITEP)
ABREU	92I	PL B277 371	P. Abreu <i>et al.</i>	(DELPHI Collab.)
ABREU	92M	PL B289 199	P. Abreu <i>et al.</i>	(DELPHI Collab.)
ACTON	92B	ZPHY C53 539	D.P. Acton <i>et al.</i>	(OPAL Collab.)
ACTON	92L	PL B294 436	P.D. Acton <i>et al.</i>	(OPAL Collab.)
ACTON	92N	PL B295 357	P.D. Acton <i>et al.</i>	(OPAL Collab.)
ADEVA	92	PL B275 209	B. Adeva <i>et al.</i>	(L3 Collab.)
ADRIANI	92D	PL B292 454	O. Adriani <i>et al.</i>	(L3 Collab.)
ALITTI	92B	PL B276 354	J. Alitti <i>et al.</i>	(UA2 Collab.)
BUSKULIC	92D	PL B292 210	D. Buskulle <i>et al.</i>	(ALEPH Collab.)
BUSKULIC	92E	PL B294 145	D. Buskulle <i>et al.</i>	(ALEPH Collab.)
DECAMP	92	PRPL 216 253	D. Decamp <i>et al.</i>	(ALEPH Collab.)
ABE	91E	PRL 67 1502	F. Abe <i>et al.</i>	(CDF Collab.)
ABREU	91H	ZPHY C50 185	P. Abreu <i>et al.</i>	(DELPHI Collab.)
ACTON	91B	PL B273 338	D.P. Acton <i>et al.</i>	(OPAL Collab.)
ADACHI	91	PL B255 613	I. Adachi <i>et al.</i>	(TOPAZ Collab.)
ADEVA	91I	PL B259 199	B. Adeva <i>et al.</i>	(L3 Collab.)
AKRAWY	91F	PL B257 531	M.Z. Akrawy <i>et al.</i>	(OPAL Collab.)
DECAMP	91B	PL B259 377	D. Decamp <i>et al.</i>	(ALEPH Collab.)
DECAMP	91J	PL B266 218	D. Decamp <i>et al.</i>	(ALEPH Collab.)
JACOBSEN	91	PRL 67 3347	R.G. Jacobsen <i>et al.</i>	(Mark II Collab.)
SHIMONAKA	91	PL B268 457	A. Shimonaka <i>et al.</i>	(TOPAZ Collab.)
ABE	90I	ZPHY C48 13	K. Abe <i>et al.</i>	(VENUS Collab.)
ABRAMS	90	PRL 64 1334	G.S. Abrams <i>et al.</i>	(Mark II Collab.)
AKRAWY	90J	PL B246 285	M.Z. Akrawy <i>et al.</i>	(OPAL Collab.)
BEHREND	90D	ZPHY C47 333	H.J. Behrend <i>et al.</i>	(CELLO Collab.)
BRAUNSCH...	90	ZPHY C48 433	W. Braunschweig <i>et al.</i>	(TASSO Collab.)
ELSEN	90	ZPHY C46 349	E. Elsen <i>et al.</i>	(JADE Collab.)
HEGNER	90	ZPHY C46 547	S. Hegner <i>et al.</i>	(JADE Collab.)
STUART	90	PRL 64 983	D. Stuart <i>et al.</i>	(AMY Collab.)
ABE	89	PRL 62 613	F. Abe <i>et al.</i>	(CDF Collab.)
ABE	89C	PRL 63 720	F. Abe <i>et al.</i>	(CDF Collab.)
ABE	89L	PL B232 425	K. Abe <i>et al.</i>	(VENUS Collab.)
ABRAMS	89B	PRL 63 2173	G.S. Abrams <i>et al.</i>	(Mark II Collab.)
ABRAMS	89D	PRL 63 2780	G.S. Abrams <i>et al.</i>	(Mark II Collab.)
ALBAJAR	89	ZPHY C44 15	C. Albajar <i>et al.</i>	(UA1 Collab.)
BACALA	89	PL B218 112	A. Bacala <i>et al.</i>	(AMY Collab.)
BAND	89	PL B218 369	H.R. Band <i>et al.</i>	(MAC Collab.)
GREENSHAW	89	ZPHY C42 1	T. Greenshaw <i>et al.</i>	(JADE Collab.)
OULD-SAAD	89	ZPHY C44 567	F. Ould-Saada <i>et al.</i>	(JADE Collab.)
SAGAWA	89	PRL 63 2341	H. Sagawa <i>et al.</i>	(AMY Collab.)
ADACHI	88C	PL B208 319	I. Adachi <i>et al.</i>	(TOPAZ Collab.)
ADEVA	88	PR D38 2665	B. Adeva <i>et al.</i>	(Mark-J Collab.)
BRAUNSCH...	88D	ZPHY C40 163	W. Braunschweig <i>et al.</i>	(TASSO Collab.)
ANSARI	87	PL B186 440	R. Ansari <i>et al.</i>	(UA2 Collab.)
BEHREND	87C	PL B191 209	H.J. Behrend <i>et al.</i>	(CELLO Collab.)
BARTEL	86C	ZPHY C30 371	W. Bartel <i>et al.</i>	(JADE Collab.)
Also		ZPHY C26 507	W. Bartel <i>et al.</i>	(JADE Collab.)
Also		PL 108B 140	W. Bartel <i>et al.</i>	(JADE Collab.)
ASH	85	PRL 55 1831	W.W. Ash <i>et al.</i>	(MAC Collab.)
BARTEL	85F	PL 161B 188	W. Bartel <i>et al.</i>	(JADE Collab.)
DERRICK	85	PR D31 2352	M. Derrick <i>et al.</i>	(HRS Collab.)
FERNANDEZ	85	PRL 54 1624	E. Fernandez <i>et al.</i>	(MAC Collab.)
LEVI	83	PRL 51 1941	M.E. Levi <i>et al.</i>	(Mark II Collab.)
BEHREND	82	PL 114B 282	H.J. Behrend <i>et al.</i>	(CELLO Collab.)
BRANDELIC	82C	PL 110B 173	R. Brandelik <i>et al.</i>	(TASSO Collab.)

Higgs Bosons — H^0 and H^\pm , Searches for

HIGGS BOSONS: THEORY AND SEARCHES

Written November 2007 by G. Bernardi (LPNHE, CNRS/IN2P3, U. of Paris VI & VII), M. Carena (FNAL), and T. Junk (FNAL).

I. Introduction

Understanding the mechanism that breaks electroweak symmetry and generates the mass of all known elementary particles is one of the most fundamental problems in particle physics. The Higgs mechanism [1] provides a general framework to explain the observed masses of the W^\pm and Z gauge bosons by means of charged and neutral Goldstone bosons that end up as the longitudinal components of the gauge bosons. These Goldstone bosons are generated by the underlying dynamics of electroweak symmetry breaking (EWSB). However, the fundamental dynamics of the electroweak symmetry breaking are unknown, and there are two main classes of theories proposed in the literature, those with weakly coupled dynamics - such as in the Standard Model (SM) [2] - and those with strongly coupled dynamics.

In the SM, the electroweak interactions are described by a gauge field theory based on the $SU(2)_L \times U(1)_Y$ symmetry group.

The Higgs mechanism posits a self-interacting complex doublet of scalar fields, and renormalizable interactions are arranged such that the neutral component of the scalar doublet acquires a vacuum expectation value $v = 246$ GeV which sets the scale of EWSB. Three massless Goldstone bosons are generated, which are absorbed to give masses to the W^\pm and Z gauge bosons. The remaining component of the complex doublet becomes the Higgs boson - a new fundamental scalar particle. The masses of all fermions are also a consequence of EWSB since the Higgs doublet is postulated to couple to the fermions through Yukawa interactions. If the Higgs mass m_H is below 180 GeV, all fields remain weakly interacting up to the Planck scale, M_{Pl} .

The validity of the SM as an effective theory describing physics up to the Planck scale is questionable, however, because of the following “naturalness” argument. All fermion masses and dimensionless couplings are logarithmically sensitive to the scale Λ at which new physics becomes relevant. In contrast, scalar squared masses are quadratically sensitive to Λ . Thus, the observable SM Higgs mass has the following form:

$$m_H^2 = (m_H^2)_0 + \frac{kg^2\Lambda^2}{16\pi^2},$$

where the first term, $(m_H)_0$, is a fundamental parameter of the theory. The second term is a one-loop correction in which g is an electroweak coupling and k is a constant, presumably of $\mathcal{O}(1)$, that is calculable within the low-energy effective theory. The two contributions arise from independent sources and one would not expect that the observable Higgs mass is significantly smaller than either of the two terms. Hence, if the scale of new physics Λ is much larger than the electroweak scale, unnatural cancellations must occur to remove the quadratic dependence of the Higgs mass on this large energy scale and to give a Higgs mass of order of the electroweak scale, as required from unitarity constraints [3,4], and as preferred by precision measurements of electroweak observables [5]. Thus, the SM is expected to be embedded in a more fundamental theory which will stabilize the hierarchy between the electroweak scale and the Planck scale in a natural way. A theory of that type would usually predict the onset of new physics at scales of the order of, or just above, the electroweak scale. This prediction is somewhat in tension with the fact that precision electroweak measurements strongly constrain contributions of new physics below the TeV scale. Theorists strive to construct models of new physics that keep the successful features of the SM while curing its shortcomings, including the absence of a dark matter candidate or an electroweak scale explanation of the observed baryon asymmetry of the universe.

In the weakly-coupled approach to electroweak symmetry breaking, supersymmetric (SUSY) extensions of the SM provide a possible explanation for the stability of the electroweak energy scale in the presence of quantum corrections [6]. These theories predict a spectrum of Higgs scalars [7]. The properties of the lightest Higgs scalar often resemble those of the SM Higgs boson, with a mass that is predicted to be less than 135 GeV

See key on page 373

Gauge & Higgs Boson Particle Listings

Higgs Bosons — H^0 and H^\pm

in the simplest supersymmetric model. Additional neutral and charged Higgs bosons with masses of order of the weak scale are also predicted. Moreover, low-energy supersymmetry with a supersymmetry breaking scale of order 1 TeV allows for grand unification of the electromagnetic, weak and strong gauge interactions in a consistent way, strongly supported by the prediction of the electroweak mixing angle at low energy scales, with an accuracy at the percent level [8,9].

Alternatively, new strong interactions near the TeV scale can induce strong breaking of the electroweak symmetry [10]. Recently, the so-called “Little Higgs” models have been proposed in which the scale of the new strong interactions is pushed up above 10 TeV [11], and the lightest Higgs scalar resembles the weakly-coupled SM Higgs boson.

In a more speculative direction, a new approach to electroweak symmetry breaking has been explored in which extra space dimensions beyond the usual 3+1 dimensional space-time are introduced [12] with characteristic sizes of order $(1 \text{ TeV})^{-1}$. In such scenarios, the mechanisms for electroweak symmetry breaking are inherently extra-dimensional and the resulting Higgs phenomenology can depart significantly from the SM paradigm [13].

Prior to 1989, when the e^+e^- collider LEP at CERN came into operation, searches for Higgs bosons were sensitive only to Higgs bosons with masses below a few GeV [14]. In the LEP1 phase, the collider operated at center-of-mass energies close to M_Z . During the LEP2 phase, the energy was increased in steps, reaching 209 GeV in the year 2000 before the final shutdown. The combined data of the four LEP experiments, ALEPH, DELPHI, L3, and OPAL, was sensitive to neutral Higgs bosons with masses up to about 115 GeV and to charged Higgs bosons with masses up to about 90 GeV [15,16].

The search for the Higgs boson continues at the Tevatron $p\bar{p}$ collider, operating at a center-of-mass energy of 1.96 TeV. The sensitivity of the two experiments, CDF and $D\bar{O}$, is improving, and with the full Tevatron integrated luminosity, should be high enough to probe SM Higgs boson masses beyond the LEP reach [17]. Other neutral and charged Higgs particles postulated in most theories beyond the SM are also actively sought at the Tevatron. The searches for Higgs bosons will continue with significantly higher sensitivities in the coming years at the LHC pp collider, and is expected to cover masses up to about 1 TeV for the SM Higgs boson [18,19]. Once evidence for the dynamics of electroweak symmetry breaking is obtained, a more complete understanding of the mechanism will require measurements at future e^+e^- [20] and perhaps $\mu^+\mu^-$ colliders [21].

In order to keep this review up to date, some unpublished results are quoted. LEP results are marked with (*) in the reference list and can be accessed conveniently from the public web page <http://lephiggs.web.cern.ch/LEPHIGGS/pdg2008/>. Preliminary results from the CDF collaboration are marked with (**) and can be obtained from the public web page

<http://www-cdf.fnal.gov/physics/physics.html>;
those from $D\bar{O}$ are marked with (***) and can be obtained at <http://www-d0.fnal.gov/Run2Physics/WWW/results.htm>.

II. The Standard Model Higgs Boson

In the SM, the Higgs boson mass is given by $m_H = \sqrt{\lambda/2} v$, where λ is the Higgs self-coupling parameter and v is the vacuum expectation value of the Higgs field, $v = (\sqrt{2}G_F)^{-1/2} = 246 \text{ GeV}$, fixed by the Fermi coupling G_F . Since λ is presently unknown, the value of the SM Higgs boson mass m_H cannot be predicted. However, besides the upper bound on the Higgs mass from unitarity constraints [3,4], additional theoretical arguments place approximate upper and lower bounds on m_H [22]. There is an upper bound based on the perturbativity of the theory up to the scale Λ at which the SM breaks down, and a lower bound derived from the stability of the Higgs potential. If m_H is too large, then the Higgs self-coupling diverges at some scale Λ below the Planck scale. If m_H is too small, then the Higgs potential develops a second (global) minimum at a large value of the scalar field of order Λ . New physics must enter at a scale Λ or below, so that the global minimum of the theory corresponds to the observed $SU(2)_L \times U(1)_Y$ broken vacuum with $v = 246 \text{ GeV}$. Given a value of Λ , one can compute the minimum and maximum allowed Higgs boson mass. Conversely, the value of m_H itself can provide an important constraint on the scale up to which the SM remains successful as an effective theory. In particular, a Higgs boson with mass in the range $130 \text{ GeV} \lesssim m_H \lesssim 180 \text{ GeV}$ is consistent with an effective SM description that survives all the way to the Planck scale, although the hierarchy problem between the electroweak scale and $\Lambda = M_{\text{Pl}}$ still persists. The lower bound on m_H can be reduced to about 115 GeV [23], if one allows for the electroweak vacuum to be metastable, with a lifetime greater than the age of the universe.

The SM Higgs couplings to fundamental fermions are proportional to the fermion masses, and the couplings to bosons are proportional to the squares of the boson masses. In particular, the SM Higgs boson is a CP -even scalar, and its couplings to gauge bosons, Higgs bosons and fermions are given by:

$$g_{Hf\bar{f}} = \frac{m_f}{v}, \quad g_{HVV} = \frac{2m_V^2}{v}, \quad g_{HHVV} = \frac{2m_V^2}{v^2}$$

$$g_{HHH} = \frac{3m_H^2}{v}, \quad g_{HHHH} = \frac{3m_H^2}{v^2}$$

where $V = W^\pm$ or Z . In Higgs boson production and decay processes, the dominant mechanisms involve the coupling of the H to the W^\pm , Z and/or the third generation quarks and leptons. The Higgs boson’s coupling to gluons, Hgg , is induced by a one-loop graph in which the H couples to a virtual $t\bar{t}$ pair. Likewise, the Higgs boson’s coupling to photons, $H\gamma\gamma$, is also generated via loops, although in this case the one-loop graph with a virtual W^+W^- pair provides the dominant contribution [7]. Reviews of the SM Higgs boson’s properties

Gauge & Higgs Boson Particle Listings

Higgs Bosons — H^0 and H^\pm

and its phenomenology, with an emphasis on the impact of loop corrections to the Higgs decay rates and cross sections, can be found in Refs. [24,25].

The cross sections for the production of SM Higgs bosons are summarized in Fig. 1 for $p\bar{p}$ collisions at the Tevatron, and in Fig. 2 for pp collisions at the LHC [26]. The cross section for the $gg \rightarrow H + X$ process is known at next-to-next-to-leading order (NNLO) QCD, in the large top-mass limit, and at NLO in QCD for arbitrary top mass [27]. The NLO QCD corrections approximately double the leading-order prediction, and the NNLO corrections add approximately 50% to the NLO prediction. NLO electroweak corrections are also available for Higgs boson masses below $2M_W$, and range between 5% and 8% of the LO term. The electroweak corrections are not included in the figures. The residual uncertainty for this process is $\sim 10\%$. The cross sections for the associated production processes $q\bar{q} \rightarrow W^\pm H + X$ and $q\bar{q} \rightarrow ZH + X$ are known at NNLO for the QCD corrections and at NLO for the electroweak corrections [28,29]. The residual uncertainty is rather small, less than 5%. For the vector boson fusion processes $qq \rightarrow qqH + X$, corrections to the production cross section are known at NLO in QCD and the remaining theoretical uncertainties are less than 10% [30]. The cross section for the associated production process $t\bar{t}H$ has been calculated at NLO in QCD [31], while the bottom fusion Higgs boson production cross section is known at NNLO in the case of five quark flavors [28,32,33].

The branching ratios for the most relevant decay modes of the SM Higgs boson are shown in Fig. 3 as functions of m_H , and the total decay width is shown in Fig. 4, also as function of m_H [34]. For masses below 135 GeV, decays to fermion pairs dominate, of which the decay $H \rightarrow b\bar{b}$ has the largest branching ratio. Decays to $\tau^+\tau^-$, $c\bar{c}$ and gluon pairs together contribute less than 15%. For such low masses, the total decay width is less than 10 MeV. For Higgs boson masses above 135 GeV, the W^+W^- decay dominates (below the W^+W^- threshold, one of the W bosons is virtual) with an important contribution from $H \rightarrow ZZ$, and the decay width rises rapidly, reaching about 1 GeV at $m_H = 200$ GeV and 100 GeV at $m_H = 500$ GeV. Above the $t\bar{t}$ threshold, the branching ratio into top-quark pairs increases rapidly as a function of the Higgs boson mass, reaching a maximum of about 20% at $m_H \sim 450$ GeV.

Searches for the SM Higgs Boson at LEP

The principal mechanism for producing the SM Higgs boson in e^+e^- collisions at LEP energies is Higgs-strahlung in the s -channel, $e^+e^- \rightarrow HZ$ [35]. The Z boson in the final state is either virtual (LEP1), or on mass shell (LEP2). The SM Higgs boson can also be produced by W^+W^- and ZZ fusion in the t -channel [36], but at LEP these processes have small cross sections. The sensitivity of the LEP searches to the Higgs boson is primarily a function of the center-of-mass energy, E_{CM} . For $m_H < E_{CM} - M_Z$, the cross section is quite large, of order

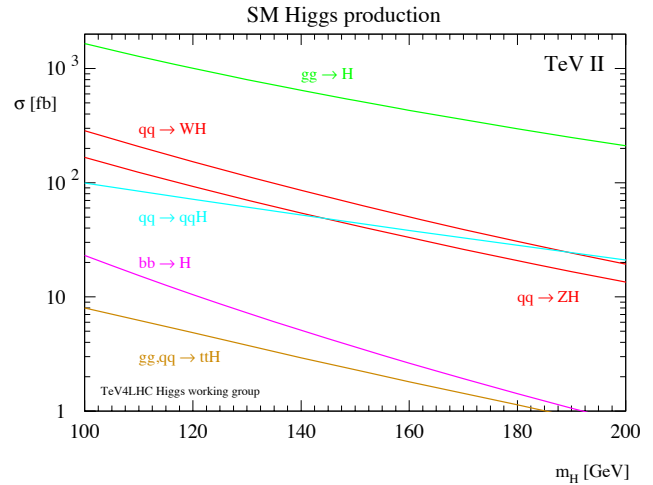


Figure 1: SM Higgs production cross sections for $p\bar{p}$ collisions at 1.96 TeV [26]. Color version at end of book.

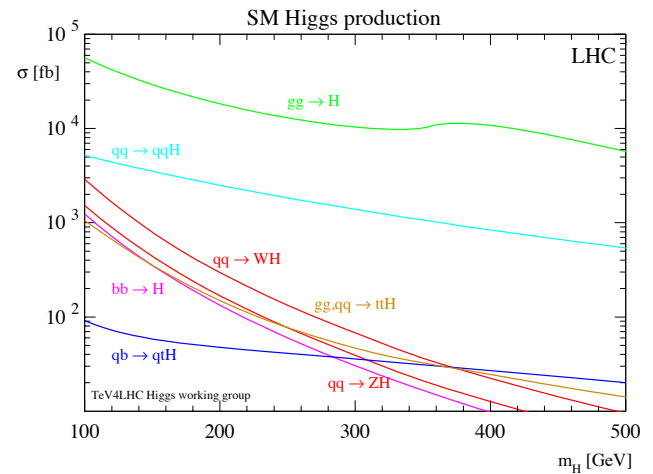


Figure 2: SM Higgs production cross sections for pp collisions at 14 TeV [26]. Color version at end of book.

1 pb or more, while for $m_H > E_{CM} - M_Z$, the cross section is smaller by an order of magnitude or more.

During the LEP1 phase, the ALEPH, DELPHI, L3 and OPAL collaborations analyzed over 17 million Z decays and set lower bounds of approximately 65 GeV on the mass of the SM Higgs boson [37]. At LEP2, substantial data samples were collected at center-of-mass energies up to 209 GeV.

Each production and decay mode was analyzed separately. Data recorded at each center-of-mass energy were studied independently and the results from the four LEP experiments were then combined. Distributions of neural network discriminants which are functions of reconstructed event quantities such as invariant masses and b -tagging discriminants were assembled for the data, and also for the signal and background predictions. The CL_s method [38] was used to compute the observed

Gauge & Higgs Boson Particle Listings

Higgs Bosons — H^0 and H^\pm

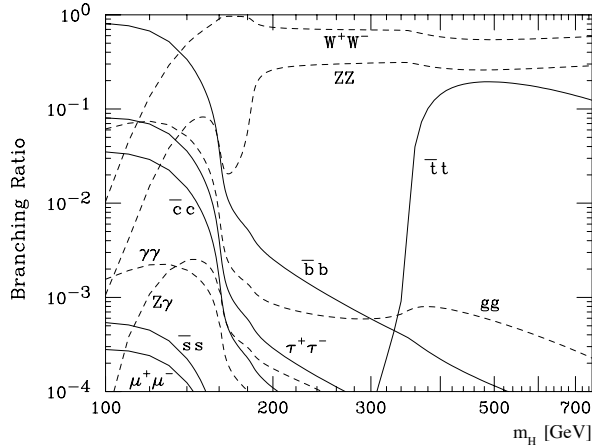


Figure 3: Branching ratios for the main decays of the SM Higgs boson [34].

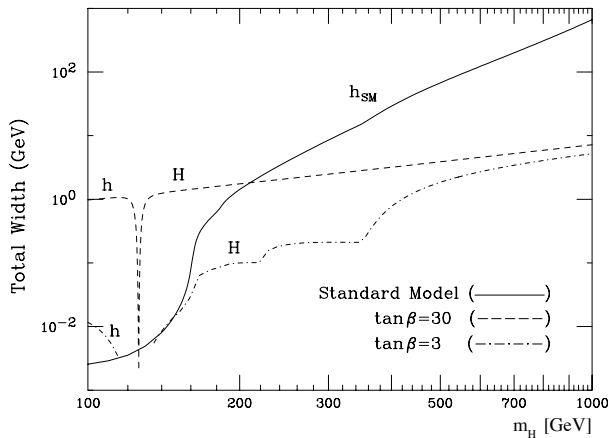


Figure 4: The total decay width of the SM Higgs boson, shown as a function of m_H [34]. Also shown are the decay widths for the CP-even neutral Higgs bosons, h and H , for two choices of $\tan\beta$, in the MSSM benchmark scenario m_{h^-} -max, described in Section III.

and expected limits on the Higgs boson production cross section as functions of the Higgs boson mass sought, and from that, a lower bound on m_H was derived. The p -value for the background-only hypothesis, which is the probability for the background model to produce a fluctuation as signal-like as that seen in the data or more, was also computed.

Higgs bosons were sought in four final state topologies: The four-jet topology in which $H \rightarrow b\bar{b}$ and $Z \rightarrow q\bar{q}$; the final states with tau leptons produced in the processes $H \rightarrow \tau^+\tau^-$ where $Z \rightarrow q\bar{q}$, together with the mode $H \rightarrow b\bar{b}$ with $Z \rightarrow \tau^+\tau^-$; the missing energy topology produced mainly in the process $H \rightarrow b\bar{b}$ with $Z \rightarrow \nu\bar{\nu}$, and finally the leptonic states $H \rightarrow b\bar{b}$ with $Z \rightarrow e^+e^-, \mu^+\mu^-$. At LEP1, only the modes with $Z \rightarrow \ell^+\ell^-$ and $Z \rightarrow \nu\bar{\nu}$ were used because the backgrounds in the other channels were prohibitive. For the data collected at LEP2, all decay modes were used.

For very light Higgs bosons, with $m_H < 2m_\tau$, the decay modes exploited above are not kinematically allowed, and decays to jets, muons, pion pairs and lighter particles dominate, depending sensitively on m_H . For very low masses, OPAL's decay-mode independent search [39] for the Bjorken process $e^+e^- \rightarrow S^0 Z$, where S^0 denotes a generic neutral, scalar particle, provides sensitivity. This search is based on studies of the recoil mass spectrum in events with $Z \rightarrow e^+e^-$ and $Z \rightarrow \mu^+\mu^-$ decays, and on the final states $Z \rightarrow \nu\bar{\nu}$ and $S^0 \rightarrow e^+e^-$ or photons. Upper bounds on the cross section are produced for scalar masses between 1 KeV and 100 GeV.

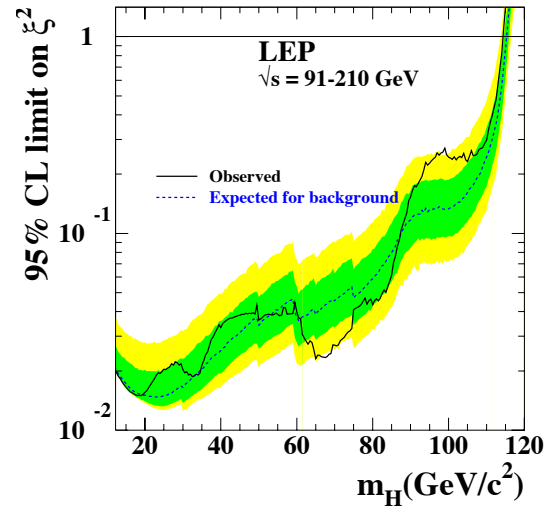


Figure 5: The 95% confidence level upper bound on the ratio $\xi^2 = (g_{HZZ}/g_{HZZ}^{SM})^2$ [15]. The solid line indicates the observed limit, and the dashed line indicates the median limit expected in the absence of a Higgs boson signal. The dark and light shaded bands around the expected limit line correspond to the 68% and 95% probability bands, indicating the range of statistical fluctuations of the expected outcomes. The horizontal line corresponds to the Standard Model coupling. Standard Model Higgs boson decay branching fractions are assumed. Color version at end of book.

The LEP searches did not show any conclusive evidence for the production of a SM Higgs boson. However, in the LEP2 data, ALEPH reported an excess of about three standard deviations, suggesting the production of a SM Higgs boson with mass ~ 115 GeV [40]. Analyses of the data from DELPHI [41], L3 [42], and OPAL [43] did not show evidence for such an excess, but could not, however, exclude a 115 GeV Higgs boson at the 95% C.L. When the data of the four experiments are combined, the overall significance of a possible signal at $m_H = 115$ GeV is low, as given by the background-only p -value of 0.09 [15]. The same combination of the LEP data yields a 95% C.L. lower bound of 114.4 GeV for the mass of the SM

Gauge & Higgs Boson Particle Listings

Higgs Bosons — H^0 and H^\pm

Higgs boson. The median limit one would expect to obtain in a large ensemble of identical experiments with no signal present is 115.3 GeV. Fig. 5 shows the observed production cross section limits, relative to the SM Higgs boson production rate (including vector-boson fusion), assuming SM Higgs boson branching ratios.

Indirect Constraints on the SM Higgs Boson

Indirect experimental bounds for the SM Higgs boson mass are obtained from fits to precision measurements of electroweak observables. The Higgs boson contributes to the W^\pm and Z vacuum polarization through loop effects, leading to a logarithmic sensitivity of the ratio of the W^\pm and Z gauge boson masses on the Higgs boson mass. A global fit to precision electroweak data, accumulated in the last decade at LEP, SLC, Tevatron and elsewhere [5], gives $m_H = 76^{+33}_{-24}$ GeV, or $m_H < 144$ GeV at 95% C.L. [5]. The top quark contributes to the W^\pm boson vacuum polarization through loop effects that depend quadratically on the top mass, which plays an important role in the global fit. A top quark mass of 170.9 ± 1.8 GeV [44] and a W^\pm boson mass of 80.398 ± 0.025 GeV [45] were used. If the direct LEP search limit of $m_H > 114.4$ GeV is taken into account, an upper limit of $m_H < 182$ GeV at 95% C.L. is obtained.

Searches for the SM Higgs Boson at the Tevatron

At the Tevatron, the most important SM Higgs boson production processes are gluon fusion ($gg \rightarrow H$) and Higgs boson production in association with a vector boson ($W^\pm H$ or ZH) [46]. For masses less than about 135 GeV, the most promising discovery channels are $W^\pm H$ and ZH with $H \rightarrow b\bar{b}$. The contribution of $H \rightarrow W^*W$ is dominant at higher masses, $m_H > 135$ GeV. Using this decay mode, both the direct ($gg \rightarrow H$) and the associated production ($p\bar{p} \rightarrow W^\pm H$ or ZH) channels are explored, and the results of both Tevatron experiments are combined to maximize the sensitivity to the Higgs boson.

The signal-to-background ratio is much smaller in the Tevatron searches than in the LEP analyses, and the systematic uncertainties on the estimated background rates are typically larger than the signal rates. In order to estimate the background rates in the selected samples more accurately, auxiliary measurements are made in data samples which are expected to be depleted in Higgs boson signal. These auxiliary samples are chosen to maximize the sensitivity to each specific background in turn. Then, Monte Carlo simulations are used to extrapolate these measurements into the Higgs signal regions. The dominant physics backgrounds such as top-pair, diboson, $W^\pm b\bar{b}$ and single-top production are estimated by Monte Carlo simulations in this way, i.e. after having been tuned or verified by corresponding measurements in dedicated analyses, thereby reducing the uncertainty on the total background estimate. The uncertainties on the background rates diminish with increasing integrated luminosity because increasingly larger data samples are used to constrain them, and thus these uncertainties are not expected to be limiting factors in the sensitivity of the searches.

At masses below about 135 GeV, the searches for associated production, $p\bar{p} \rightarrow W^\pm H, ZH$ are performed in different channels:

a) $p\bar{p} \rightarrow W^\pm H$, where the W^\pm decays leptonically and $H \rightarrow b\bar{b}$; such searches have been published by the CDF and DØ collaborations on ~ 0.3 fb $^{-1}$ of data [47,48] and are regularly updated with larger data samples [49,50]. The latest updates (August 2007) are based on 1.7 fb $^{-1}$ of data [51,52]; the Higgs boson production cross section limits obtained by both collaborations are about ten times higher than the SM expectation in this channel. These updates use advanced analysis techniques such as neural networks to separate a potential signal from the background processes, and also to separate correctly identified b -jets from jets originating from gluons or from u, d, s or c quarks, mistakenly identified as b -jets.

b) $p\bar{p} \rightarrow ZH$, where the Z decays into $\nu\bar{\nu}$, is also a sensitive channel, but, since the final state is characterized by missing transverse energy and two b -jets, multijet backgrounds without Z bosons require special care. The sensitivity of this search is enhanced by $W^\pm H$ events in which the charged lepton from the W^\pm decay escapes detection; these events have the same experimental signature as the $ZH \rightarrow \nu\bar{\nu}$ signal. The DØ Collaboration has published a result in this channel with 0.3 fb $^{-1}$ of data [53]. Updates with 0.9 fb $^{-1}$ (DØ [54]) and 1.7 fb $^{-1}$ (CDF [55]) have been released in 2007 using multivariate techniques and enhanced event reconstruction and selection, which increase the signal acceptance. The sensitivity is comparable to that obtained in the $W^\pm H$ channel.

c) $p\bar{p} \rightarrow ZH$, where the Z decays into charged leptons (e or μ), suffers from a smaller Z branching fraction, but has lower background, so its sensitivity is not much lower than that of the previous two channels. The DØ Collaboration has published a result based on 0.45 fb $^{-1}$ of data [56], and updates with ~ 1 fb $^{-1}$ of data are available from both CDF and DØ [57,58].

When combining the three low-mass channels of the two collaborations, the expected (observed) limit is 4.3 (6.2) times higher than the expected SM production cross section for $m_H = 115$ GeV, as can be seen in Fig. 6 [59]. With the projected improvements in analysis sensitivity, and the accumulation of more integrated luminosity (up to 7 to 8 fb $^{-1}$), the low-mass Higgs boson is expected to be probed at the Tevatron.

Around $m_H = 135$ GeV, where all branching fractions are below 50%, no channel is dominant and the overall sensitivity is weaker. At these masses, the $WH \rightarrow WWW^*$ channel ¹The star indicates that below the $H \rightarrow W^+W^-$ threshold, one of the W^\pm bosons is virtual. brings further sensitivity [60–62] beyond the $b\bar{b}$ channel alone.

To probe masses above 135 GeV, the dominant $H \rightarrow WW^*$ decay mode is best exploited in direct $gg \rightarrow H$ production, using the leptonic decays of the W^\pm which provide a clean, distinct final state. The WW pair issued from a Higgs boson decay has a spin correlation which is different from that of the dominant background, electroweak WW production.

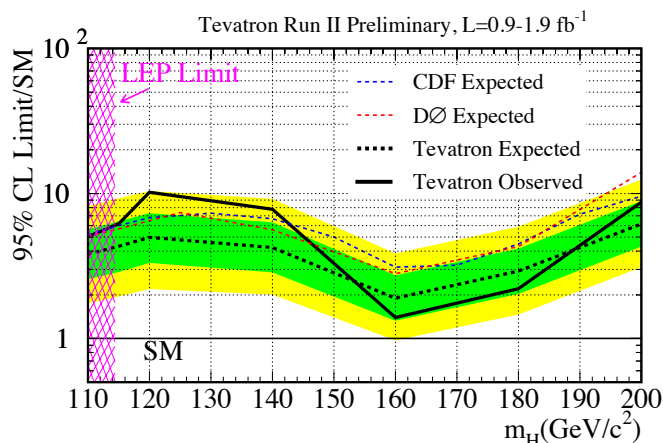


Figure 6: Upper bound on the SM Higgs boson cross section obtained by combining CDF and $D\bar{0}$ search results, as a function of the mass of the Higgs boson sought. The limits are shown as a multiple of the SM cross section. The ratios of different production and decay modes are assumed to be as predicted by the SM. The solid curve shows the observed upper bound, the dashed black curve shows the median expected upper bound assuming no signal is present, and the colored bands show the 68% and 95% probability bands around the expected upper bound. The CDF and $D\bar{0}$ combined expected limits are also shown separately. See Ref. 59 for details and status of these results. Color version at end of book.

These spin correlations are transmitted to the distributions of observed leptons, providing a handle to separate the signal from the background. The invariant mass of the Higgs boson decay products cannot be reconstructed due to the undetected neutrinos, but the sensitivity is nevertheless significant. Results were published with 0.4 fb^{-1} [63,64]. The current updates with $\sim 2 \text{ fb}^{-1}$ of data [65,66] allow to set a combined expected (observed) upper limit on the $gg \rightarrow H$ cross section 1.9 (1.4) times higher than the SM prediction at $m_H = 160 \text{ GeV}$ [59].

Overall, the combined CDF and $D\bar{0}$ analyses are expected to test, at the 95% C.L. or better, the SM Higgs boson predictions for masses between the LEP limit and about 185 GeV before the end of Run II (see Fig. 6). The channels used at the Tevatron for Higgs masses below 130 GeV are different from those dominantly used at the LHC, hence with the full Run II luminosity, they are expected to provide complementary information if a low mass Higgs boson exists.

Studies to assess the sensitivity to diffractive Higgs production at the Tevatron and the LHC are being actively pursued [67]. Three different diffractive production mechanisms can be considered: exclusive production, $p\bar{p}, pp \rightarrow p + H + \bar{p}, p$; inclusive production, $p\bar{p}, pp \rightarrow X + H + Y$; and central inelastic

production, $p\bar{p}, pp \rightarrow p + (HX) + \bar{p}, p$, where a plus sign indicates the presence of a rapidity gap. Tests of the different production mechanisms using appropriate final states in the Tevatron data are important for improving predictions for diffractive Higgs production at the LHC.

Prospects for SM Higgs Boson Searches at the LHC

At the LHC, the main production processes will be gluon fusion ($gg \rightarrow H$), Higgs boson production in association with a vector boson ($W^\pm H$ or ZH) or with a top-quark pair ($t\bar{t}H$), and the vector boson fusion process (qqH or $q\bar{q}H$) [46]. This array of production and decay modes, together with a large integrated luminosity, allows for a variety of search channels. Search strategies have been explored in many analyses over the last years [18,19]. The searches in the inclusive channels $H \rightarrow \gamma\gamma$ (for low mass) and $H \rightarrow ZZ^* \rightarrow 4\ell$ (for high mass) will be complemented with more exclusive searches in order to strengthen the discovery potential, particularly at low mass. Vector boson fusion processes, making use of forward jet tagging and the decay modes $H \rightarrow \tau^+\tau^-$, $H \rightarrow \gamma\gamma$ as well as $H \rightarrow W^+W^-$ [68] will provide additional sensitivity. Other analyses, expected to be relevant at higher integrated luminosities, select Higgs boson decays to $b\bar{b}$ or $\gamma\gamma$ in association with a lepton from the decay of an associated W^\pm boson, Z boson, or top quark.

The projections of the ATLAS and CMS collaborations show that, with an integrated luminosity of 10 - 30 fb^{-1} , the SM Higgs boson is expected to be discovered if it exists and has a mass below 1 TeV. With a lower integrated luminosity, the discovery of a Higgs boson with a mass below 130 GeV is challenging. If the Higgs boson's mass is in this range, a few years of running may be needed to discover it. However, the combination of the results in all channels of the two experiments could allow for a 5σ discovery with about 5 fb^{-1} of data, once the detectors and the composition of the selected event samples are understood [69].

If a SM Higgs boson is discovered, its properties could be studied at the LHC. Its mass could be measured by each experiment with a precision of $\sim 0.1\%$ in the 100–400 GeV mass range [19,70]. This projection is based on the invariant mass reconstruction from electromagnetic calorimeter objects, using the decays $H \rightarrow \gamma\gamma$ or $H \rightarrow ZZ^* \rightarrow 4\ell$. The precision would be degraded at higher masses because of the larger decay width, but even at $m_H \sim 700 \text{ GeV}$ a precision of 1% on m_H is expected to be achievable. The width of the SM Higgs boson would be too narrow to be measured directly for $m_H < 200 \text{ GeV}$; nonetheless, it could be constrained indirectly using partial width measurements [71,72]. For $300 < m_H < 700 \text{ GeV}$, a direct measurement of the decay width could be performed with a precision of about 6%. The possibilities for measuring other properties of the Higgs boson, such as its spin, its CP -eigenvalue, its couplings to bosons and fermions, and its self-coupling, have been investigated in

Gauge & Higgs Boson Particle Listings

Higgs Bosons — H^0 and H^\pm

numerous studies [70,73]. Given a sufficiently high integrated luminosity (300 fb^{-1}), most of these properties are expected to be accessible to analysis for some specific mass ranges. The measurement of Higgs self-couplings, however, appears to be impossible at the LHC, although a luminosity upgrade, the so-called Super-LHC, could allow for such a measurement. The results of these measurements could either firmly establish the Higgs mechanism, or point the way to new physics.

III. Higgs Bosons in the MSSM

Electroweak symmetry breaking driven by a weakly-coupled elementary scalar sector requires a mechanism to explain the smallness of the electroweak symmetry breaking scale compared with the Planck scale [74]. Within supersymmetric extensions of the SM, supersymmetry-breaking effects, whose origins may lie at energy scales much larger than 1 TeV, can induce a radiative breaking of the electroweak symmetry due to the effects of the large Higgs-top quark Yukawa coupling [75]. In this way, the electroweak symmetry breaking scale is intimately tied to the mechanism of supersymmetry breaking. Thus, supersymmetry provides an explanation for the stability of the hierarchy of scales, provided that supersymmetry-breaking masses are of $\mathcal{O}(1 \text{ TeV})$ or less [74].

A fundamental theory of supersymmetry breaking is unknown at this time. Nevertheless, one can parameterize the low-energy theory in terms of the most general set of soft supersymmetry-breaking renormalizable operators [76]. The Minimal Supersymmetric extension of the Standard Model (MSSM) [77] associates a supersymmetric partner to each gauge boson and chiral fermion of the SM, and provides a realistic model of physics at the weak scale. However, even in this minimal model with the most general set of soft supersymmetry-breaking terms, more than 100 new parameters are introduced [78]. Fortunately, only a small number of these parameters impact the Higgs phenomenology through tree level and quantum effects.

The MSSM contains the particle spectrum of a two-Higgs-doublet model (2HDM) extension of the SM and the corresponding supersymmetric partners. Two Higgs doublets, H_u and H_d , are required to ensure an anomaly-free SUSY extension of the SM and to generate mass for both “up”-type and “down”-type quarks and charged leptons [7]. After the spontaneous breaking of the electroweak symmetry, five physical Higgs particles are left in the spectrum: one charged Higgs pair, H^\pm , one CP -odd scalar, A , and two CP -even states, H and h .

The supersymmetric structure of the theory imposes constraints on the Higgs sector of the model. In particular, the parameters of the Higgs self-interaction are not independent of the gauge coupling constants. As a result, all Higgs sector parameters at tree level are determined by only two free parameters: the ratio of the H_u and H_d vacuum expectation values,

$$\tan \beta = v_u/v_d,$$

with $v_u^2 + v_d^2 = (246 \text{ GeV})^2$; and one Higgs mass, conventionally chosen to be m_A . The other tree-level Higgs masses are then given in terms of these parameters

$$m_{H^\pm}^2 = m_A^2 + M_W^2$$

$$m_{H,h}^2 = \frac{1}{2} \left[m_A^2 + M_Z^2 \pm \sqrt{(m_A^2 + M_Z^2)^2 - 4(M_Z m_A \cos 2\beta)^2} \right]$$

and α is the angle that diagonalizes the CP -even Higgs squared-mass matrix.

An important consequence of these mass formulae is that the mass of the lightest CP -even Higgs boson is bounded from above:

$$m_h \leq M_Z |\cos 2\beta|.$$

This contrasts sharply with the SM, in which this Higgs mass is only constrained by perturbativity and unitarity bounds. In the large m_A limit, also called the decoupling limit [79], one finds $m_h^2 \simeq (M_Z \cos 2\beta)^2$ and $m_A \simeq m_H \simeq m_{H^\pm}$, up to corrections of $\mathcal{O}(M_Z^2/m_A)$. Below the scale m_A , the effective Higgs sector consists only of h , which behaves very similarly to the SM Higgs boson.

The phenomenology of the Higgs sector depends on the couplings of the Higgs bosons to gauge bosons and fermions. The couplings of the two CP -even Higgs bosons to W^\pm and Z bosons are given in terms of the angles α and β by

$$g_{hVV} = g_V m_V \sin(\beta - \alpha) \quad g_{HVV} = g_V m_V \cos(\beta - \alpha),$$

where $g_V \equiv 2m_V/v$. There are no tree-level couplings of A or H^\pm to VV . The couplings of the Z boson to two neutral Higgs bosons, which must have opposite CP -quantum numbers, are given by

$$g_{hAZ} = g_Z \cos(\beta - \alpha)/2$$

$$g_{HAZ} = -g_Z \sin(\beta - \alpha)/2.$$

Charged Higgs- W boson couplings to neutral Higgs bosons and four-point couplings of vector bosons and Higgs bosons can be found in Ref. 7.

The tree-level Higgs couplings to fermions obey the following property: the neutral components of one Higgs doublet couples exclusively to down-type fermion pairs while the neutral components of the other couples exclusively to up-type fermion pairs [7,80]. This pattern of Higgs-fermion couplings defines the Type-II (2HDM) ² In the Type-I 2HDM, one field couples to all fermions while the other field is decoupled from them.. Fermion masses are generated when the neutral Higgs components acquire vacuum expectation values. The relations between Yukawa couplings and fermion masses are (in third-generation notation)

$$h_b = \sqrt{2} m_b/v_d = \sqrt{2} m_b/(v \cos \beta)$$

$$h_t = \sqrt{2} m_t/v_u = \sqrt{2} m_t/(v \sin \beta).$$

Similarly, one can define the Yukawa coupling of the Higgs boson to τ -leptons (the latter is a down-type fermion).

See key on page 373

Gauge & Higgs Boson Particle Listings

Higgs Bosons — H^0 and H^\pm

The couplings of the neutral Higgs bosons to $f\bar{f}$ relative to the SM value, $gm_f/2M_W$, are given by

$$\begin{aligned} h\bar{b}b &: & -\sin\alpha/\cos\beta = \sin(\beta - \alpha) - \tan\beta\cos(\beta - \alpha), \\ ht\bar{t} &: & \cos\alpha/\sin\beta = \sin(\beta - \alpha) + \cot\beta\cos(\beta - \alpha), \\ H\bar{b}b &: & \cos\alpha/\cos\beta = \cos(\beta - \alpha) + \tan\beta\sin(\beta - \alpha), \\ Ht\bar{t} &: & \sin\alpha/\sin\beta = \cos(\beta - \alpha) - \cot\beta\sin(\beta - \alpha), \\ Abb &: & \gamma_5\tan\beta, \quad Att &: & \gamma_5\cot\beta, \end{aligned}$$

where the γ_5 indicates a pseudoscalar coupling. In each relation above, the factor listed for $b\bar{b}$ also pertains to $\tau^+\tau^-$. The charged Higgs boson couplings to fermion pairs are given by

$$g_{H^-t\bar{b}} = \frac{g}{\sqrt{2}M_W} [m_t \cot\beta P_R + m_b \tan\beta P_L],$$

$$g_{H^-\tau^+\nu} = \frac{g}{\sqrt{2}M_W} [m_\tau \tan\beta P_L],$$

with $P_{L,R} = (1 \mp \gamma_5)/2$.

The Higgs couplings to down-type fermions can be significantly enhanced at large $\tan\beta$ in the following two cases: (i) If $m_A \gg M_Z$, then $|\cos(\beta - \alpha)| \ll 1$, $m_H \simeq m_A$, and the $b\bar{b}H$ and $b\bar{b}A$ couplings have equal strength and are significantly enhanced by a factor of $\tan\beta$ relative to the SM $b\bar{b}H$ coupling, whereas the VVH coupling is negligibly small. The values of the VVh and $b\bar{b}h$ couplings are equal to the corresponding couplings of the SM Higgs boson. (ii) If $m_A < M_Z$ and $\tan\beta \gg 1$, then $|\cos(\beta - \alpha)| \approx 1$ and $m_h \simeq m_A$. In this case, the $b\bar{b}h$ and $b\bar{b}A$ couplings have equal strength and are significantly enhanced by a factor of $\tan\beta$ relative to the SM $b\bar{b}H$ coupling, while the VVh coupling is negligibly small. In addition, the VVH coupling is equal in strength to the SM VVH coupling and one can refer to H as a SM-like Higgs boson, although the value of the $b\bar{b}H$ coupling can differ from the corresponding SM $b\bar{b}H$ coupling. Note that in both cases (i) and (ii) above, only two of the three neutral Higgs bosons have enhanced couplings to $b\bar{b}$.

Radiative Corrections to MSSM Higgs Masses and Couplings

Radiative corrections can have a significant impact on the values of Higgs masses and couplings in the MSSM. Important contributions come from loops of SM particles as well as their supersymmetric partners. The dominant effects arise from the incomplete cancellation between top and scalar-top (stop) loops. For large $\tan\beta$, effects from the bottom-sbottom sector are also relevant. The stop and sbottom masses and mixing angles depend on the supersymmetric Higgsino mass parameter μ and on the soft-supersymmetry-breaking parameters [77]: M_Q, M_U, M_D, A_t and A_b , where the first three are the left-chiral and the two right-chiral top and bottom scalar quark mass parameters, respectively, and the last two are the trilinear parameters that enter the off-diagonal squark mixing elements: $X_t \equiv A_t - \mu \cot\beta$ and $X_b \equiv A_b - \mu \tan\beta$. The corrections affecting the Higgs boson masses, production,

and decay properties depend on all of these parameters. For simplicity, we shall initially assume that A_t, A_b and μ are real parameters. The impact of complex phases on MSSM parameters, which will induce CP -violation in the Higgs sector, is addressed below.

The radiative corrections to the Higgs masses have been computed using a number of techniques, with a variety of approximations [81–91]. They depend strongly on the top quark mass ($\sim m_t^4$) and the stop mixing parameter X_t , and there is also a logarithmic dependence on the stop masses. One of the most striking effects is the increase of the upper bound of the light CP -even Higgs mass, as first noted in [81,82]. The value of m_h is maximized for large $m_A \gg M_Z$, when all other MSSM parameters are fixed. Moreover, $\tan\beta \gg 1$ also maximizes m_h , when all other parameters are held fixed. Taking m_A large (the decoupling limit) and $\tan\beta \gg 1$, the value of m_h can be further maximized at one-loop level for $X_t \simeq \sqrt{6}M_{\text{SUSY}}$, where $M_{\text{SUSY}} \simeq M_Q \simeq M_U \simeq M_D$ is an assumed common value of the soft SUSY-breaking squark mass parameters. This choice of X_t is called the “maximal-mixing scenario” which will be indicated by m_h -max. Instead, for $X_t = 0$, which is called the “no-mixing scenario,” the value of m_h has its lowest possible value, for fixed m_A and all other MSSM parameters. The value of m_h also depends on the specific value of M_{SUSY} and μ and more weakly on the electroweak gaugino mass as well as the gluino mass at two-loop level. For example, raising M_{SUSY} from 1 TeV to 2 TeV can increase m_h by 2–5 GeV. Variation of the value of m_t by 1 GeV changes the value of m_h by about the same amount. For any given scenario defined by a full set of MSSM parameters, we will denote the maximum value of m_h by $m_h^{\text{max}}(\tan\beta)$, for each value of $\tan\beta$. Allowing for the experimental uncertainty on m_t and for the uncertainty inherent in the theoretical analysis, one finds for $M_{\text{SUSY}} \lesssim 2$ TeV, large m_A and $\tan\beta \gg 1$, $m_h^{\text{max}} = 135$ GeV in the m_h -max scenario, and $m_h^{\text{max}} = 122$ GeV in the no-mixing scenario. In practice, parameter values leading to maximal mixing are not obtained in most models of supersymmetry breaking, so typical upper limits on m_h will lie between these two extremes. The relatively small mass of the lightest neutral scalar boson is a prediction for both the CP -conserving (CPC) and CP -violating (CPV) scenarios [92,93], which emphasizes the importance of the searches at currently available and future accelerators.

Radiative corrections also modify significantly the values of the Higgs boson couplings to fermion pairs and to vector boson pairs. The tree-level Higgs couplings depend strongly on the value of $\cos(\beta - \alpha)$. In a first approximation, when radiative corrections of the Higgs squared-mass matrix are computed, the diagonalizing angle α is shifted from its tree-level value, and hence one may compute a “radiatively-corrected” value for $\cos(\beta - \alpha)$. This shift provides one important source of the radiative corrections to the Higgs couplings. In particular, depending on the sign of μX_t and the magnitude of

Gauge & Higgs Boson Particle Listings

Higgs Bosons — H^0 and H^\pm

X_t/M_{SUSY} , modifications of α can lead to important variations of the SM-like Higgs boson coupling to bottom quarks and tau leptons [90]. Additional contributions from the one-loop vertex corrections to tree-level Higgs couplings must also be considered [86,94–100]. These contributions alter significantly the Higgs-fermion Yukawa couplings at large $\tan\beta$, both in the neutral and charged Higgs sector. Moreover, these radiative corrections can modify the basic relationship $g_{h,H,A\bar{b}b}/g_{h,H,A\tau^+\tau^-} \propto m_b/m_\tau$, and change the main features of MSSM Higgs phenomenology.

Decay Properties of MSSM Higgs Bosons

In the MSSM, neglecting CP -violating effects, one must consider the decay properties of three neutral Higgs bosons and one charged Higgs pair. In the region of parameter space where $m_A \gg m_Z$ and the masses of supersymmetric particles are large, the decoupling limit applies, and the decay rates of h into SM particles are nearly indistinguishable from those of the SM Higgs boson. Hence, the h boson will decay mainly to fermion pairs, since the mass, less than about 135 GeV, is far below the W^+W^- threshold. The SM-like branching ratios of h are modified if decays into supersymmetric particles are kinematically allowed [101]. In addition, if light superpartners exist that can couple to photons and/or gluons, then the decay rates to gg and $\gamma\gamma$ could deviate from the corresponding SM rates. In the decoupling limit, the heavier Higgs states, H , A and H^\pm , are roughly mass degenerate, and their decay branching ratios strongly depend on $\tan\beta$ as shown below. For values of $m_A \sim \mathcal{O}(M_Z)$, all Higgs boson states lie below 200 GeV in mass. In this parameter regime, there is a significant area of the parameter space in which none of the neutral Higgs boson decay properties approximates that of the SM Higgs boson. For $\tan\beta \gg 1$, the resulting Higgs phenomenology shows marked differences from that of the SM Higgs boson [102] and significant modifications to the $b\bar{b}$ and/or the $\tau^+\tau^-$ decay rates may occur via radiative effects.

After incorporating the leading radiative corrections to Higgs couplings from both QCD and supersymmetry, the following decay features are relevant in the MSSM. The decay modes $h, H, A \rightarrow b\bar{b}$, $\tau^+\tau^-$ dominate the neutral Higgs boson decay modes when $\tan\beta$ is large for all values of the Higgs masses. For small $\tan\beta$, these modes are significant for neutral Higgs boson masses below $2m_t$ (although there are other competing modes in this mass range), whereas the $t\bar{t}$ decay mode dominates above its kinematic threshold. In contrast to the SM Higgs boson, the vector boson decay modes of H are strongly suppressed at large m_H due to the suppressed HVV couplings in the decoupling limit. For the charged Higgs boson, $H^\pm \rightarrow \tau^+\nu_\tau$ dominates below $t\bar{b}$ threshold, while $H^\pm \rightarrow t\bar{b}$ dominates for large values of m_{H^\pm} . For low values of $\tan\beta$ ($\lesssim 1$) and low values of the charged Higgs mass ($\lesssim 120$ GeV), the decay mode $H^\pm \rightarrow c\bar{s}$ becomes relevant.

In addition to the decay modes of the neutral Higgs bosons into fermion and gauge boson final states, additional decay channels may be allowed which involve scalars of the extended Higgs sector, *e.g.*, $h \rightarrow AA$. Supersymmetric final states from Higgs boson decays into charginos, neutralinos and third-generation squarks and sleptons can be important if they are kinematically allowed [103]. One interesting possibility is a significant branching ratio for the decay of a neutral Higgs boson to the invisible mode $\tilde{\chi}_1^0\tilde{\chi}_1^0$ (where the lightest neutralino $\tilde{\chi}_1^0$ is the lightest supersymmetric particle) [104], which poses a significant challenge at hadron colliders.

Searches for Neutral Higgs Bosons (CPC Scenario)

Most of the experimental investigations carried out at LEP and the Tevatron assume CP -conservation (CPC) in the MSSM Higgs sector. In many cases the search results are interpreted in a number of specific benchmark models where a representative set of the relevant SUSY breaking parameters are specified [92]. Some of these parameter choices illustrate scenarios in which the detection of Higgs bosons at LEP or in hadron collisions is experimentally challenging due to the limited phase space or the suppression of the main discovery channels. For instance, the m_h -max scenario defined above maximizes the allowed values of m_h , for a given $\tan\beta$, M_{SUSY} , and m_t , leading to relatively conservative exclusion limits.

Searches for Neutral MSSM Higgs Bosons at LEP

In e^+e^- collisions at LEP energies, the main production mechanisms of the neutral MSSM Higgs bosons are the Higgs-strahlung processes $e^+e^- \rightarrow hZ$, HZ and the pair production processes $e^+e^- \rightarrow hA$, HA , while the fusion processes play a marginal role. The cross sections can be expressed in terms of the SM cross section and the parameters α and β introduced above. For the light CP -even Higgs boson h the following expressions hold, in good approximation,

$$\sigma_{hZ} = \sin^2(\beta - \alpha)\sigma_{hZ}^{\text{SM}}, \quad \sigma_{hA} = \cos^2(\beta - \alpha)\bar{\lambda}\sigma_{hZ}^{\text{SM}}$$

where σ_{hZ}^{SM} stands for a SM cross section with a SM Higgs boson of mass equal to m_h . The phase space functions are

$$\bar{\lambda} = \lambda_{Ah}^{3/2} / \left[\lambda_{Zh}^{1/2} (12M_Z^2/s + \lambda_{Zh}) \right]$$

and $\lambda_{ij} = [1 - (m_i + m_j)^2/s][1 - (m_i - m_j)^2/s]$, where s is the square of the e^+e^- collision energy. These Higgs-strahlung and pair production cross sections are complementary since $\sin^2(\beta - \alpha) + \cos^2(\beta - \alpha) = 1$. The cross sections for the heavy scalar boson H are obtained by interchanging $\sin^2(\beta - \alpha)$ and $\cos^2(\beta - \alpha)$ and replacing the index h by H in the above expressions, and by defining σ_{HZ}^{SM} similarly to σ_{hZ}^{SM} . The Higgs-strahlung process $e^+e^- \rightarrow hZ$ is relevant for large $m_A > m_h^{\text{max}}(\tan\beta)$ or low $m_A < m_h^{\text{max}}(\tan\beta)$ and low $\tan\beta$; while the pair-production process $e^+e^- \rightarrow hA$ is relevant for low $m_A < m_h^{\text{max}}(\tan\beta)$. The heavy CP -even H boson contributes when kinematically allowed via

See key on page 373

Gauge & Higgs Boson Particle Listings

Higgs Bosons — H^0 and H^\pm

the Higgs-strahlung process for low $m_A < m_h^{\max}(\tan\beta)$, or for large $m_A > m_h^{\max}(\tan\beta)$ via the pair production process $e^+e^- \rightarrow HA$.

The searches at LEP exploit the complementarity between the Higgs-strahlung process $e^+e^- \rightarrow hZ$, and the pair-production process $e^+e^- \rightarrow hA$. In addition, when $m_A < m_h^{\max}(\tan\beta)$, the H boson has SM-like couplings to the Z boson, so if kinematically allowed, $e^+e^- \rightarrow HZ$ is also considered. For Higgs-strahlung, the searches for the SM Higgs boson are re-interpreted, taking into account the MSSM reduction factor $\sin^2(\beta - \alpha)$ for h ($\cos^2(\beta - \alpha)$ for H). For pair production, dedicated searches are performed for the $(b\bar{b})(b\bar{b})$ and $(\tau^+\tau^-)(q\bar{q})$ final states.

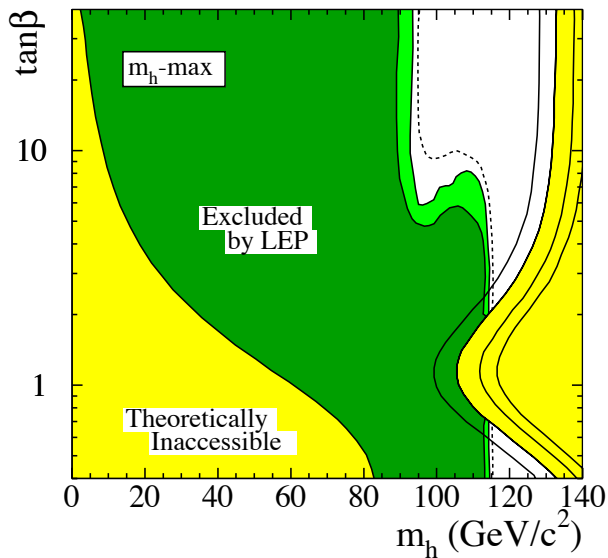


Figure 7: The MSSM exclusion contours, at 95% C.L. (light-green) and 99.7% CL (dark-green), obtained by LEP for the CP m_h -max benchmark scenario, with $m_t = 174.3$ GeV. The figure shows the excluded and theoretically inaccessible regions in the $(m_h, \tan\beta)$ projection. The upper edge of the theoretically allowed region is sensitive to the top quark mass; it is indicated, from left to right, for $m_t = 169.3$, 174.3, 179.3 and 183.0 GeV. The dashed lines indicate the boundaries of the regions which are expected to be excluded on the basis of Monte Carlo simulations with no signal (from Ref. 16). Color version at end of book.

The limits from the four LEP experiments are described in Refs. [40,41,105,106]. The combined LEP data did not reveal any excess of events which would indicate the production of Higgs bosons, and combined limits were derived [16]. These limits are shown in Fig. 7 for the m_h -max scenario, in the $(m_h, \tan\beta)$ parameter plane (see Ref. 16 for other projections and other benchmark models). For values of $\tan\beta$ below ~ 5 , the limit on m_h is nearly that of the SM searches, as $\sin^2(\beta - \alpha) \approx 1$. For higher values of $\tan\beta$, the $e^+e^- \rightarrow hA$ searches become the

most important, and they do not set as stringent a limit on m_h . In this scenario, the 95% C.L. mass bounds are $m_h > 92.8$ GeV and $m_A > 93.4$ GeV, and values of $\tan\beta$ from 0.7 to 2.0 are excluded taking $m_t = 174.3$ GeV. This excluded $\tan\beta$ range depends on M_{SUSY} and m_t ; larger values of either of these masses increase the Higgs mass, and reduce the excluded range of $\tan\beta$. Furthermore, the uncertainty on the SM-like Higgs mass from higher-order corrections, which were not included in the current analysis, is about 3 GeV [107].

The neutral Higgs bosons may also be produced by Yukawa processes $e^+e^- \rightarrow f\bar{f}\phi$, where the Higgs particle $\phi \equiv h, H, A$, is radiated off a massive fermion ($f \equiv b$ or τ^\pm). These processes can be dominant at low masses, and whenever the $e^+e^- \rightarrow hZ$ and hA processes are suppressed. The corresponding ratios of the $f\bar{f}h$ and $f\bar{f}A$ couplings to the SM coupling are $\sin\alpha/\cos\beta$ and $\tan\beta$, respectively. The LEP data have been used to search for $b\bar{b}b\bar{b}$, $b\bar{b}\tau^+\tau^-$, and $\tau^+\tau^-\tau^+\tau^-$ final states [108,109]. Regions of low mass and high enhancement factors are excluded by these searches.

Searches for Neutral MSSM Higgs Bosons at Hadron Colliders

The production mechanisms for the SM Higgs boson at hadron colliders can also be relevant for the production of the MSSM neutral Higgs bosons. However, one must take into account the possibility of enhanced or suppressed couplings with respect to those of the Standard Model, since these can significantly modify the production cross-sections of neutral Higgs bosons. The supersymmetric-QCD corrections due to the exchange of virtual squarks and gluinos may modify the cross sections depending on the values of these supersymmetric particle masses. The MSSM neutral Higgs production cross sections at hadron colliders have been computed in Refs. [90,100,110].

Over a large fraction of the MSSM parameter space, one of the CP -even neutral Higgs bosons (h or H) couples to the vector bosons with SM-like strength and has a mass below 135 GeV. As shown in the SM Higgs section above (Fig. 6), the current searches for SM-like Higgs bosons at the Tevatron are not yet able to cover that mass range. However, if the expected improvements in sensitivity are achieved, the regions of MSSM parameter space in which one of these two scalars behaves like the SM Higgs will also be probed [111].

Scenarios with enhanced Higgs boson production cross sections are studied at the Tevatron. The best sensitivity is in the regime with low to moderate m_A and with large $\tan\beta$ which enhances the couplings of the Higgs bosons to down-type fermions. The corresponding limits on the Higgs production cross section times the branching ratio of the Higgs boson into down-type fermions can be interpreted in MSSM benchmark scenarios [112]. If $\phi = A, H$ for $m_A > m_h^{\max}$, and $\phi = A, h$ for $m_A < m_h^{\max}$, the most promising channels at the Tevatron are $b\bar{b}\phi$, $\phi \rightarrow b\bar{b}$ or $\phi \rightarrow \tau^+\tau^-$, with three tagged b -jets or $b\tau\tau$ in the final state, respectively, and the inclusive $p\bar{p} \rightarrow \phi \rightarrow \tau^+\tau^-$

Gauge & Higgs Boson Particle Listings

Higgs Bosons — H^0 and H^\pm

process, with contributions from both $gg \rightarrow \phi$ and $b\bar{b}\phi$ production. Although Higgs boson production via gluon fusion has a higher cross section than via associated production, it cannot be used to study the $\phi \rightarrow b\bar{b}$ decay mode since the signal is overwhelmed by QCD background.

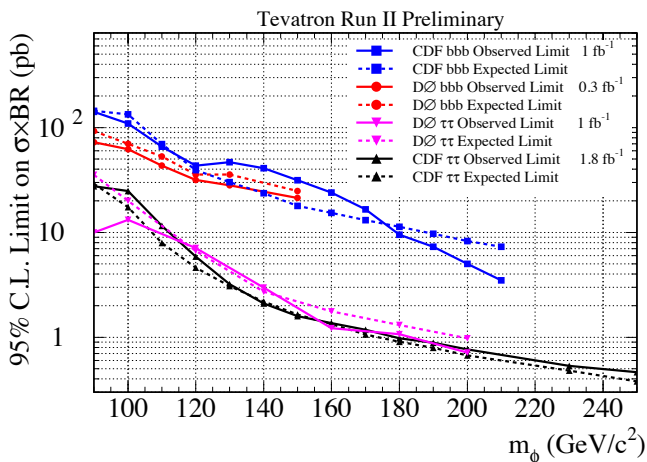


Figure 8: The 95% C.L. limits on the production cross section times the relevant decay branching ratios for the Tevatron searches for $\phi \rightarrow b\bar{b}$ and $\phi \rightarrow \tau^+\tau^-$. The observed limits are indicated with solid lines, and the expected limits are indicated with dashed lines. The limits are to be compared with the sum of signal predictions for Higgs boson with similar masses. The decay widths of the Higgs bosons are assumed to be much smaller than the experimental resolution. Color version at end of book.

The CDF and D0 collaborations have searched for neutral Higgs bosons produced in association with bottom quarks and which decay into $b\bar{b}$ [113,114], or into $\tau^+\tau^-$ [115]. The most recent searches in the $b\bar{b}\phi$ channel with $\phi \rightarrow b\bar{b}$ analyze approximately 1 fb^{-1} of data. Dedicated triggers are used to collect the data samples, but the multijet QCD background remains very large. These triggers require the presence of at least three jets, and also require tracks reconstructed with large impact parameters which point near calorimeter energy deposits. The data are analyzed by requiring three well-separated jets with reconstructed secondary vertices indicating the presence of B hadrons. The invariant mass of the two leading jets would be more sharply peaked for the Higgs boson signal than for the background. The QCD background rates and shapes are inferred from data control samples, in particular, the sample with two b tagged jets and a third, untagged jet. Monte Carlo models are used to estimate the biases on the shapes of the background predictions due to the requirement of a third b tag. Separate signal hypotheses are tested and limits are placed on $\sigma(p\bar{p} \rightarrow b\bar{b}\phi) \times \text{BR}(\phi \rightarrow b\bar{b})$. Fig. 8 shows the upper limits from

CDF and D0 assuming that the decay widths of the Higgs bosons are small compared with the experimental resolution.

CDF and D0 have also performed searches for inclusive production of Higgs bosons with subsequent decays to $\tau^+\tau^-$ using dedicated triggers designed for these searches [116–119]. Tau leptons are more difficult to identify than jets containing B -hadrons, as only some of the possible τ lepton decays are sufficiently distinct from the jet backgrounds. Both CDF and D0 search for pairs of isolated tau leptons; one of the tau leptons is required to decay leptonically (either to an electron and two neutrinos, or a muon and two neutrinos), while the other tau may decay either leptonically or hadronically. Requirements placed on the energies and angles of the visible tau decay products help to reduce the background from W +jets processes, where a jet is falsely reconstructed as a tau lepton. The dominant remaining background process is $Z \rightarrow \tau^+\tau^-$, which can be separated from a Higgs boson signal by using the invariant mass of the observed decay products of the tau leptons. Fig. 8 shows the limits on $\sigma(p\bar{p} \rightarrow \phi + X) \times \text{BR}(\phi \rightarrow \tau^+\tau^-)$ for the CDF and D0 searches, which use 1.0 and 1.8 fb^{-1} of data, respectively. The decay widths of the Higgs bosons are assumed to be small compared with the experimental resolution, which is much broader in the tau channels than in the $bbb(b)$ search, due to the presence of energetic neutrinos in the tau decay products.

In order to interpret the experimental data in terms of MSSM benchmark scenarios, it is necessary to consider carefully the effect of radiative corrections on the production and decay processes. The bounds from the $b\bar{b}\phi, \phi \rightarrow b\bar{b}$ channel depend strongly on the radiative corrections affecting the relation between the bottom quark mass and the bottom Yukawa coupling. In the channels with $\tau^+\tau^-$ final states, however, compensations occur between large corrections in the Higgs boson production and decay. The total production rate of bottom quarks and τ pairs mediated by the production of a CP -odd Higgs boson in the large $\tan\beta$ regime is approximately given by

$$\sigma(b\bar{b}A) \times \text{BR}(A \rightarrow b\bar{b}) \simeq \sigma(b\bar{b}A)_{\text{SM}} \frac{\tan^2\beta}{(1 + \Delta_b)^2} \frac{9}{(1 + \Delta_b)^2 + 9},$$

and

$$\sigma(gg \rightarrow A, b\bar{b}A) \times \text{BR}(A \rightarrow \tau^+\tau^-) \simeq \sigma(gg \rightarrow A, b\bar{b}A)_{\text{SM}} \frac{\tan^2\beta}{(1 + \Delta_b)^2 + 9},$$

where $\sigma(b\bar{b}A)_{\text{SM}}$ and $\sigma(gg \rightarrow A, b\bar{b}A)_{\text{SM}}$ denote the values of the corresponding SM Higgs boson cross sections for a SM Higgs boson mass equal to m_A . The function Δ_b includes the dominant effects of SUSY radiative corrections for large $\tan\beta$ [98,99]. The main radiative contributions in Δ_b depend strongly on $\tan\beta$ and on the SUSY mass parameters [90]. The $b\bar{b}A$ channel is more sensitive to the value of Δ_b through the factor $1/(1 + \Delta_b)^2$ than the inclusive $\tau^+\tau^-$ channel, for which this leading dependence on Δ_b cancels out. As a consequence,

See key on page 373

Gauge & Higgs Boson Particle Listings

Higgs Bosons — H^0 and H^\pm

the limits derived from the inclusive $\tau^+\tau^-$ channel depend less on the precise MSSM scenario chosen than those of the $b\bar{b}A$ channel.

The production and decay rates of the CP -even Higgs bosons with $\tan\beta$ -enhanced couplings to down-type fermions — H (or h) for m_A larger (or smaller) than m_h^{\max} , respectively — are governed by formulae similar to the ones presented above. At high $\tan\beta$, one of the CP -even and the CP -odd Higgs bosons are nearly degenerate in mass enhancing the signal cross section by roughly a factor of two, without complicating the experimental signature except in a small mass region in which the three neutral MSSM Higgs boson masses are close together and each boson contributes to the total production rate. A detailed discussion of the impact of radiative corrections in these search modes is presented in Ref. 112.

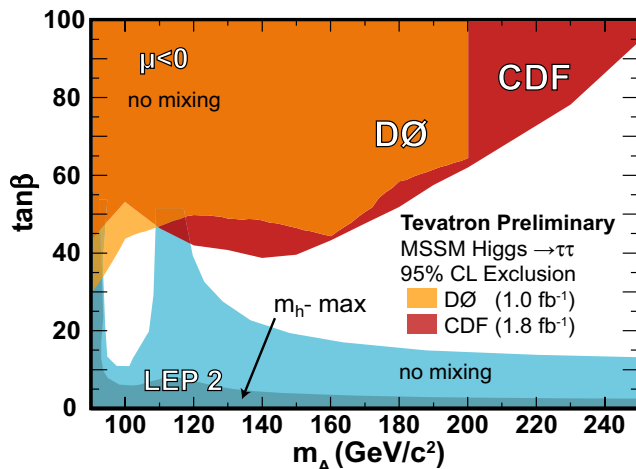


Figure 9: The 95% C.L. MSSM exclusion contours obtained by CDF and DØ in the $H \rightarrow \tau^+\tau^-$ searches in the *no-mixing* benchmark scenario with $\mu = -200$ GeV, projected onto the $(m_A, \tan\beta)$ plane [118,119]. The Tevatron limits for the m_h -max scenario are nearly the same as in the *no-mixing* scenario. Also shown are the regions excluded by LEP searches [16], separately for the m_h -max scenario (darker shading) and the *no-mixing* scenario, (lighter shading). The LEP limits are shown for a top quark mass of 174.3 GeV (the Tevatron results are not sensitive to the precise value of the top mass). Color version at end of book.

The excluded domains for the inclusive $\phi \rightarrow \tau^+\tau^-$ channels are shown in Fig. 9, in the $(m_A, \tan\beta)$ projection, considering the contribution of both the CP -odd and CP -even neutral Higgs bosons with enhanced couplings to bottom quarks. Also shown in the figure are the LEP limits, for the *no-mixing* and the m_h -max scenarios. The limits from the Tevatron are shown only for the *no-mixing* scenario, but, as discussed above, due to the tiny dependence of this channel under variations of the SUSY parameter space, the Tevatron limits are nearly

identical in the m_h -max scenario. Even though $\text{BR}(\phi \rightarrow b\bar{b})$ exceeds $\text{BR}(\phi \rightarrow \tau^+\tau^-)$ by an order of magnitude for the models considered, the $bbb(b)$ channel limits are weaker due to the much larger background, and the $\tau^+\tau^-$ channels exclude the domain tested by the $bbb(b)$ channels. The interpretation of the $bbb(b)$ data includes treatment of the Higgs boson decay widths [114], further reducing the sensitivity of this channel.

The sensitivity of the Tevatron searches will improve with the continuously growing data samples and with the combination of all channels of both experiments. The small backgrounds in the $\tau^+\tau^-$ channels, and the fact that better exclusions in the $bbb(b)$ channel imply narrower Higgs decay widths, which feeds back to improve the sensitivity of the searches, mean that the limits on the cross sections are expected to improve faster than $1/\sqrt{\mathcal{L}}$, where \mathcal{L} is the integrated luminosity. Eventually, $\tan\beta$ down to about 20 should be tested for values of m_A up to a few hundred GeV. The projected sensitivity by the end of Run II for the associated production of a SM Higgs boson in $W^\pm H$ and ZH should have a strong impact on the excluded domains in Fig. 9. In the *no-mixing* benchmark scenario, the LEP limits have been obtained assuming $m_t = 174.3$ GeV. For a lower top mass, as presently measured, the excluded LEP region becomes larger towards higher $\tan\beta$, and for $M_{\text{SUSY}} \simeq 1$ TeV, this scenario would be strongly constrained. The combination of the LEP and Tevatron searches is expected to probe vast regions of the $\tan\beta$ - m_A plane.

Searches for charged Higgs bosons at the Tevatron are presented in Section IV, in the more general framework of the 2HDM.

Prospects for discovering the MSSM Higgs bosons at the LHC have been explored in detail, see Refs. [70,73] for reviews of these studies. They predict that the reach of the LHC experiments would be sufficient to discover MSSM Higgs bosons in many different channels. The main channels for the SM-like Higgs boson are expected to be $q\bar{q}\phi \rightarrow q\bar{q}\tau^+\tau^-$ and inclusive $\phi \rightarrow \gamma\gamma$, where $\phi = h$ or H , depending on m_A . The discovery of a light SM-like Higgs boson with $m_h < 130$ GeV would require a few years of running. With an integrated luminosity larger than 30 fb^{-1} , the $t\bar{t}\phi$ production process may become effective. For non-SM-like MSSM Higgs bosons, the most relevant channels are expected to be $pp \rightarrow H/A + X$, with $H/A \rightarrow \tau^+\tau^-$ and $pp \rightarrow tH^\pm + X$ with $H^\pm \rightarrow \tau\nu_\tau$ [111]. After the inclusion of supersymmetric radiative corrections to the production cross sections and decay widths [112,120], the prospective discovery reach in these channels is robust, with mild dependence on the specific MSSM parameters.

Effects of CP Violation on the MSSM Higgs Spectrum

In the Standard Model, CP -violation (CPV) is induced by phases in the Yukawa couplings of the quarks to the Higgs field, which results in one non-trivial phase in the CKM mixing matrix. SUSY scenarios with new CPV phases are theoretically appealing, since additional CPV beyond that observed in the

Gauge & Higgs Boson Particle Listings

Higgs Bosons — H^0 and H^\pm

K and B meson systems is required to explain the observed cosmic matter-antimatter asymmetry [121,122]. In the MSSM, there are additional sources of CPV from phases in the various supersymmetric mass parameters. In particular, the gaugino mass parameters (M_i , $i = 1, 2, 3$), the Higgsino mass parameter, μ , the bilinear Higgs squared-mass parameter, m_{12}^2 , and the trilinear couplings of the squark and slepton fields (\tilde{f}) to the Higgs fields, A_f , may carry non-trivial phases. The two parameter combinations $\arg[\mu A_f(m_{12}^2)^*]$ and $\arg[\mu M_i(m_{12}^2)^*]$ are invariant under phase redefinitions of the MSSM fields [123,124]. Therefore, if one of these quantities is non-zero, there would be new sources of CP -violation, which affects the MSSM Higgs sector through radiative corrections [93,125–129]. The mixing of the neutral CP -odd and CP -even Higgs boson states is no longer forbidden. Hence, m_A is no longer a physical parameter. However, the charged Higgs mass m_{H^\pm} is still physical and can be used as an input for the computation of the neutral Higgs spectrum of the theory.

For large values of m_{H^\pm} , corresponding to the decoupling limit, the properties of the lightest neutral Higgs boson state approach those of the SM Higgs boson. That is, for $m_{H^\pm} \gg M_W$, the lightest neutral Higgs boson is approximately a CP -even state, with CPV couplings that are suppressed by terms of $\mathcal{O}(m_W^2/m_{H^\pm}^2)$. In particular, the upper bound on the lightest neutral Higgs boson mass, takes the same value as in the CP -conserving case [124]. Nevertheless, there still can be significant mixing between the two heavier neutral mass eigenstates. For a detailed study of the Higgs mass spectrum and parametric dependence of the Higgs mass radiative corrections, see [125,128].

Major variations to the MSSM Higgs phenomenology occur in the presence of explicit CPV phases. In the CPV case, vector boson pairs couple to all three neutral Higgs mass eigenstates, H_i ($i = 1, 2, 3$), with couplings

$$g_{H_i VV} = \cos \beta \mathcal{O}_{1i} + \sin \beta \mathcal{O}_{2i}$$

$$g_{H_i H_j Z} = \mathcal{O}_{3i}(\cos \beta \mathcal{O}_{2j} - \sin \beta \mathcal{O}_{1j}) - \mathcal{O}_{3j}(\cos \beta \mathcal{O}_{2i} - \sin \beta \mathcal{O}_{1i})$$

where the $g_{H_i VV}$ couplings are normalized to the analogous SM coupling and the $g_{H_i H_j Z}$ have been normalized to $g_z/2$. \mathcal{O}_{ij} is the orthogonal matrix relating the weak eigenstates to the mass eigenstates. It has non-zero off-diagonal entries mixing the CP -even and CP -odd components of the weak eigenstates. The above couplings obey the relations

$$\sum_{i=1}^3 g_{H_i Z Z}^2 = 1 \quad \text{and} \quad g_{H_k Z Z} = \varepsilon_{ijk} g_{H_i H_j Z}$$

where ε_{ijk} is the usual Levi-Civita symbol.

Another consequence of CPV effects in the scalar sector is that all neutral Higgs bosons can couple to both scalar and pseudoscalar fermion bilinear densities. The couplings of the mass eigenstates H_i to fermions depend on the loop-corrected fermion Yukawa couplings (similarly to the CPC case), on $\tan \beta$ and on the \mathcal{O}_{ji} . The resulting expressions for the scalar and

pseudoscalar components of the neutral Higgs mass eigenstates to fermions and the charged Higgs boson to fermions are given in Refs. [125,130].

Regarding their decay properties, the lightest mass eigenstate, H_1 , predominantly decays to $b\bar{b}$ if kinematically allowed, with a smaller fraction decaying to $\tau^+\tau^-$, similar to the CPC case. If kinematically allowed, a SM-like neutral Higgs boson, H_2 or H_3 will decay predominantly to $H_1 H_1$; otherwise it will decay preferentially to $b\bar{b}$.

Searches for Neutral Higgs Bosons in CPV Scenarios

In CPV MSSM scenarios, the three neutral Higgs eigenstates H_i do not have well-defined CP quantum numbers; they all could be produced by Higgs-strahlung, $e^+e^- \rightarrow H_i Z$, and in pairs, $e^+e^- \rightarrow H_i H_j$ ($i \neq j$), with rates which depend on the details of the CPV scenario. Possible cascade decays such as H_2 or $H_3 \rightarrow H_1 H_1$ can lead to interesting experimental signatures in the Higgs-strahlung processes, $e^+e^- \rightarrow H_2 Z$ or $H_3 Z$. For wide ranges of the model parameters, the lightest neutral Higgs boson H_1 has a predicted mass that would be accessible at LEP, if it would couple to the Z boson with SM-like strength. The second- and third-lightest Higgs bosons H_2 and H_3 may have been either out of reach, or may have had small cross sections. Altogether, the searches in the CPV MSSM scenario are experimentally more difficult, and hence have a weaker sensitivity.

The cross section for the Higgs-strahlung and pair production processes are given by [93,124,125,129]

$$\sigma_{H_i Z} = g_{H_i Z Z}^2 \sigma_{H_i Z}^{\text{SM}} \quad \sigma_{H_i H_j} = g_{H_i H_j Z}^2 \bar{\lambda} \sigma_{H_i Z}^{\text{SM}}$$

In the expression of $\bar{\lambda}$, defined for the CPC case, the indices h and A are to be replaced by H_i and H_j , respectively, $\sigma_{H_i Z}^{\text{SM}}$ stands for the SM cross section for a SM Higgs boson with a mass equal to m_{H_i} , and the couplings are defined above in term of the orthogonal matrix relating the weak eigenstates to the mass eigenstates.

The Higgs boson searches at LEP were interpreted [16] in a CPV benchmark scenario [93] for which the parameters were chosen so as to maximize the phenomenological differences with respect to the CPC scenario. Fig. 10 shows the exclusion limits of LEP in the $(m_{H_1}, \tan \beta)$ plane for $m_t = 174.3$ GeV. Values of $\tan \beta$ less than about 3 are excluded in this scenario. However, no absolute lower bound can be set for the mass of the lightest neutral Higgs boson H_1 , for an updated study see Ref. 131. Similar exclusion plots, for other choices of model parameters, can be found in Ref. 16. No direct CPV searches have yet been completed at hadron colliders.

Indirect Constraints from Electroweak and B -physics Observables and Dark Matter Searches

Indirect bounds from a global fit to precision measurements of electroweak observables can be derived in terms of MSSM parameters [132] in a way similar to what was done in the SM. The minimum χ^2 for the MSSM fit is slightly lower than

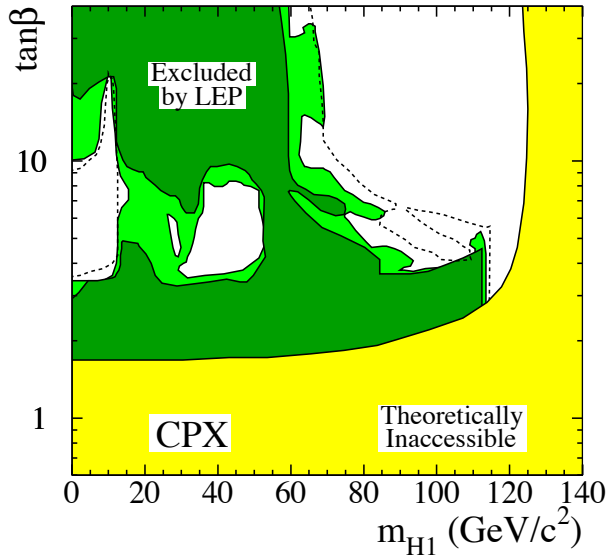


Figure 10: The MSSM exclusion contours, at 95% C.L. (light-green) and 99.7% CL (dark-green), obtained by LEP for a CPV scenario, called CPX, specified by $|A_t| = |A_b| = 1000$ GeV, $\phi_A = \phi_{m_{\tilde{g}}} = \pi/2$, $\mu = 2$ TeV, $M_{\text{SUSY}} = 500$ GeV [16]. Here, $m_t = 174.3$ GeV. The figure shows the excluded and theoretically inaccessible regions in the $(m_{H_1}, \tan\beta)$ projection. The dashed lines indicate the boundaries of the regions which are expected to be excluded on the basis of simulations with no signal. Color version at end of book.

what is obtained for the SM, and the fit accommodates a low value of the lightest Higgs boson mass which is a prediction of the MSSM. Given the MSSM and SM predictions for M_W as a function of m_t , and varying the Higgs mass and the SUSY spectrum, one finds that the MSSM overlaps with the SM when SUSY masses are large, of $\mathcal{O}(2$ TeV), and the light SM-like Higgs boson has a mass close to the experimental bound of 114.4 GeV. The MSSM Higgs mass expectations are compatible with the constraints provided by the measurements of m_t and M_W .

Recent improvements in our understanding of B -physics observables put indirect constraints on MSSM scenarios in regions in which Higgs boson searches at the Tevatron and the LHC are sensitive. In particular, $\text{BR}(B_s \rightarrow \mu^+\mu^-)$, $\text{BR}(b \rightarrow s\gamma)$ and $\text{BR}(B_u \rightarrow \tau\nu)$ play an important role within minimal flavor-violating (MFV) models [133], in which flavor effects are induced by loop factors proportional to the CKM matrix elements, as in the SM. For recent studies, see Refs. [111,134–136]. The supersymmetric contributions to these observables come both at the tree- and loop-level, and have a different parametric dependence, but share the property that they become significant for large values of $\tan\beta$, which is also the regime in which

searches for non-standard MSSM Higgs bosons at hadron colliders become relevant. The recent measurement of ΔM_s by the CDF and D0 collaborations [137] could also have implications for MSSM Higgs physics, but within minimal flavor-violating models, the ΔM_s constraints are automatically satisfied once the upper limit on $\text{BR}(B_s \rightarrow \mu^+\mu^-)$ from the Tevatron [138] is imposed. However, ΔM_s may be relevant within more general flavor models [139].

In the SM, the relevant contributions to the rare decay $B_s \rightarrow \mu^+\mu^-$ come through the Z -penguin and the W^\pm -box diagrams [140]. In supersymmetry with large $\tan\beta$, there are also significant contributions from Higgs-mediated neutral currents [141–143], which grow with the sixth power of $\tan\beta$ and decrease with the fourth power of the CP -odd Higgs boson mass m_A . Therefore, the upper limits from the Tevatron [138] put strong restrictions on possible flavor-changing neutral currents (FCNC) in the MSSM at large $\tan\beta$.

Further constraints are obtained from the rare decay $b \rightarrow s\gamma$. The SM rate is known up to NNLO corrections [144] and is in good agreement with measurements [145,146]. In the minimal flavor-violating MSSM, there are new contributions from charged Higgs and chargino-stops diagrams. The charged Higgs contribution is enhanced for small values of the charged Higgs mass and can be partially canceled by the chargino contribution or by higher-order $\tan\beta$ -enhanced loop effects.

The branching ratio $B_u \rightarrow \tau\nu$, measured by the Belle [147] and BaBar [148] collaborations, also constrains the MSSM. The SM expectation is in good agreement with the experimental value [149]. In the MSSM, there is an extra tree-level contribution from the charged Higgs which interferes destructively with the SM contribution, and which increases for small values of the charged Higgs mass and large values of $\tan\beta$ [150].

Several studies [111,134–136] have shown that, in extended regions of parameter space, the combined B -physics measurements impose strong constraints on the MSSM models to which Higgs boson searches at the Tevatron are sensitive. Consequently, the observation of a non-SM Higgs boson at the Tevatron would point to a rather narrow, well-defined region of MSSM parameter space [111,151] or to something beyond the minimal flavor violation framework.

Another indirect constraint on the Higgs sector comes from the search for dark matter. If dark matter particles are weakly-interacting and massive, then particle physics can provide models which predict the correct relic density of the universe. In particular, the lightest supersymmetric particle, typically the lightest neutralino, is an excellent dark matter particle candidate [152]. Within the MSSM, the measured relic density places constraints in the parameter space, which in turn have implications for Higgs searches at colliders, and also for experiments looking for direct evidence of dark matter particles in elastic scattering with atomic nuclei. Large values of $\tan\beta$ and small m_A are relevant for the $b\bar{b}A/H$ and $A/H \rightarrow \tau^+\tau^-$ searches at the Tevatron, and also provide a significant contribution from the CP -even Higgs H exchange

Gauge & Higgs Boson Particle Listings

Higgs Bosons — H^0 and H^\pm

to the spin-independent cross-sections for direct detection experiments such as CDMS. Consequently, a positive signal at the Tevatron would raise prospects for a signal at CDMS, and vice-versa [151,153–155]. However, theoretical uncertainties in the calculation of dark matter scattering cross-sections, and in the precise value of the local dark matter density, render these considerations rather qualitative.

IV. Charged Higgs Bosons

Charged Higgs bosons are predicted by models with an extended Higgs sector, for example, models with two Higgs field doublets (2HDM). The MSSM is a special Type-II 2HDM in which the mass of the charged Higgs boson is strongly correlated with the other Higgs boson masses. The charged Higgs boson mass in the MSSM is restricted at tree level by $m_{H^\pm} > M_W$. This restriction does not hold for some regions of parameter space after including radiative corrections. Due to the correlations among Higgs boson masses in the MSSM, the results of searches for charged Higgs bosons from LEP and the Tevatron do not significantly constrain the MSSM parameter space beyond what is already obtained from the searches for neutral Higgs bosons.

In e^+e^- collisions, charged Higgs bosons would be pair-produced via s -channel exchange of a photon or a Z boson [156]. In the 2HDM framework, the couplings are specified by the electric charge and the weak mixing angle θ_W , and the cross section at tree level depends only on the mass m_{H^\pm} . Charged Higgs bosons decay preferentially to heavy particles, but the branching ratios are model-dependent. In the Type-II 2HDM and for masses which are accessible at LEP energies, the decays $H^\pm \rightarrow c\bar{s}$ and $\tau^+\nu$ dominate. The final states $H^+H^- \rightarrow (c\bar{s})(\bar{c}s)$, $(\tau^+\nu_\tau)(\tau^-\bar{\nu}_\tau)$, and $(c\bar{s})(\tau^-\bar{\nu}_\tau) + (\bar{c}s)(\tau^+\nu_\tau)$ were considered, and the search results are usually presented as a function of $\text{BR}(H^+ \rightarrow \tau^+\nu)$. The sensitivity of the LEP searches was limited to $m_{H^\pm} < 90$ GeV, due to the background from $e^+e^- \rightarrow W^+W^-$ [157], and the kinematic limitation on the production cross-section. The combined LEP data constrain $m_{H^\pm} > 78.6$ GeV independently of $\text{BR}(H^+ \rightarrow \tau^+\nu)$ [158]. The excluded limits, translated to the $(\tan\beta, m_{H^\pm})$ plane using tree level calculations of Type-II 2HDM, are shown in Fig. 11.

In the Type-I 2HDM, and if the CP -odd neutral Higgs boson A is light (which is not excluded in the general 2HDM case), the decay $H^\pm \rightarrow W^\pm A$ may be dominant for masses accessible at LEP [159], a possibility that was investigated by the DELPHI collaboration [160].

At hadron colliders, charged Higgs bosons can be produced in different modes. If $m_{H^\pm} < m_t - m_b$, the charged Higgs can be produced in the decays of the top quark via the decay $t \rightarrow bH^+$, which would compete with the SM process $t \rightarrow bW^+$. Relevant QCD and SUSY-QCD corrections to $\text{BR}(t \rightarrow H^+b)$ have been computed [161–164]. For $m_{H^\pm} < m_t - m_b$, the total cross-section for charged Higgs production (in the narrow-width approximation) is given by

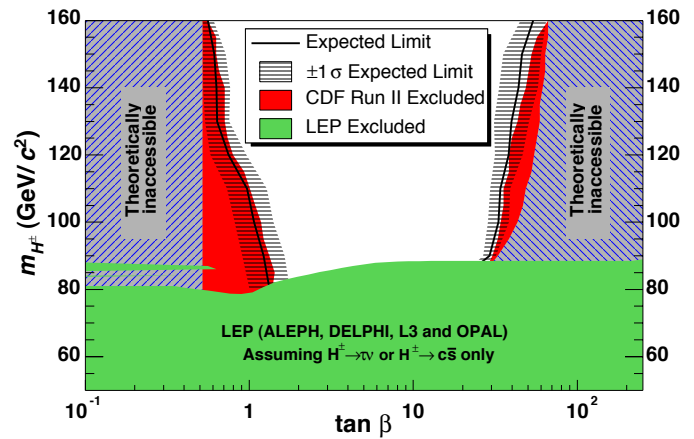


Figure 11: Summary of the 95% C.L. exclusions in the $(m_{H^\pm}, \tan\beta)$ plane obtained by LEP [158] and CDF [177]. The benchmark scenario parameters used to interpret the CDF results are very close to those of the m_h^{max} scenario, and m_t is assumed to be 175 GeV. The full lines indicate the median limits expected in the absence of a H^\pm signal, and the horizontal hatching represents the $\pm 1\sigma$ bands about this expectation. Color version at end of book.

³For values of m_{H^\pm} near m_t , the width effects are important. In addition, the full $2 \rightarrow 3$ processes $p\bar{p} \rightarrow H^+t\bar{b} + X$ and $p\bar{p} \rightarrow H^-t\bar{b} + X$ must be considered.

$$\sigma(p\bar{p} \rightarrow H^\pm + X) = (1 - [\text{BR}(t \rightarrow bW^+)]^2) \sigma(p\bar{p} \rightarrow t\bar{t} + X).$$

In general, in the Type-II 2HDM, the H^+ may be observed in the decay $t \rightarrow bH^+$ at the Tevatron or at the LHC for $\tan\beta \lesssim 1$ or $\tan\beta \gg 1$.

If $m_{H^\pm} > m_t - m_b$, then charged Higgs boson production occurs mainly through radiation off a third generation quark. Single charged Higgs associated production proceeds via the $2 \rightarrow 3$ partonic processes $gq, q\bar{q} \rightarrow t\bar{b}H^-$ (and the charge conjugate final state). For charged Higgs production cross sections at the Tevatron and the LHC, see [77,165–171].

Charged Higgs bosons can also be produced via associated production with W^\pm bosons through $b\bar{b}$ annihilation and gg -fusion [172]. They can also be produced in pairs via $q\bar{q}$ annihilation [173]. The inclusive H^+H^- cross-section is less than the cross-section for single charged Higgs associated production [173–175].

At the Tevatron, earlier searches by the DØ and CDF collaborations are reported in [176], and a more recent search by CDF is presented in [177]. The search is based on $t\bar{t}$ cross section measurements in four non-overlapping data samples corresponding to the dilepton, lepton+jets (1 and ≥ 2 b -tags) and lepton+ τ +jets topologies (here leptons are e or μ). The samples are very pure in $t\bar{t}$ decays, and the expected event count in each sample depends on $\text{BR}(t \rightarrow bH^+)$ as well as the decay branching ratios of the H^+ . The decays considered

See key on page 373

Gauge & Higgs Boson Particle Listings

Higgs Bosons — H^0 and H^\pm

are $H^+ \rightarrow \tau^+ \nu_\tau, c\bar{s}, t^*\bar{b}$, and $H^+ \rightarrow W^+ \phi$ with $\phi \rightarrow b\bar{b}$. The ϕ may be any of the possible neutral Higgs boson states. The selection efficiencies in each data sample for each decay mode are computed, taking into account the decays of both top quarks in each event. The predictions of the SM and of those of models including $t \rightarrow bH^+$ are compared with the four data measurements, and exclusion regions in the $(\tan\beta, m_{H^\pm})$ plane are derived for specific models. Fig. 11 shows the regions excluded by the CDF search, along with the charged Higgs LEP excluded regions, for a choice of MSSM parameters which is almost identical to the m_h -max benchmark scenario adopted by the LEP collaborations in their search for neutral MSSM Higgs bosons.

Indirect limits in the $(m_{H^\pm}, \tan\beta)$ plane have been obtained by comparing the measured rate of $b \rightarrow s\gamma$ to the SM prediction. In the Type-II 2HDM and in the absence of other sources of new physics at the electroweak scale, a bound $m_{H^\pm} > 295$ GeV has been derived [144]. Although this indirect bound appears much stronger than the results from direct searches, it can be invalidated by new physics contributions, such as those which can be present in the MSSM.

Doubly-Charged Higgs Bosons

Higgs bosons with double electric charge are predicted, for example, by models with additional triplet scalar fields or left-right symmetric models [178]. It has been emphasized that the see-saw mechanism could lead to doubly-charged Higgs bosons with masses which are accessible to current and future colliders [179]. Searches were performed at LEP for the pair-production process $e^+e^- \rightarrow H^{++}H^{--}$ with four prompt leptons in the final state [180–182]. Lower mass bounds between 95 GeV and 100 GeV were obtained for left-right symmetric models (the exact limits depend on the lepton flavors). Doubly-charged Higgs bosons were also searched for in single production [183]. Furthermore, such particles would modify the Bhabha scattering cross section and forward-backward asymmetry via t -channel exchange. The absence of a significant deviation from the SM prediction puts constraints on the Yukawa coupling of $H^{\pm\pm}$ to electrons for Higgs masses which reach into the TeV range [182,183].

Searches have also been carried out at the Tevatron for the pair production process $p\bar{p} \rightarrow H^{++}H^{--}$. The DØ search is performed in the $\mu^+\mu^+\mu^-\mu^-$ final state [184], while CDF also considers $e^+e^+e^-e^-$ and $e^+\mu^+e^-\mu^-$, and final states with τ leptons [185]. Lower bounds are obtained for left- and right-handed $H^{\pm\pm}$ bosons. For example, assuming 100% branching ratio for $H^{\pm\pm} \rightarrow \mu^\pm\mu^\pm$, the DØ (CDF) data exclude a left- and a right-chiral doubly-charged Higgs boson with mass larger than 150 (136) GeV and 127 (113) GeV, respectively, at 95% C.L. A search of CDF for a long-lived $H^{\pm\pm}$ boson, which would decay outside the detector, is described in [186]. The current status of the mass and coupling limits, from direct searches at LEP and at the Tevatron, is summarized in Fig. 12.

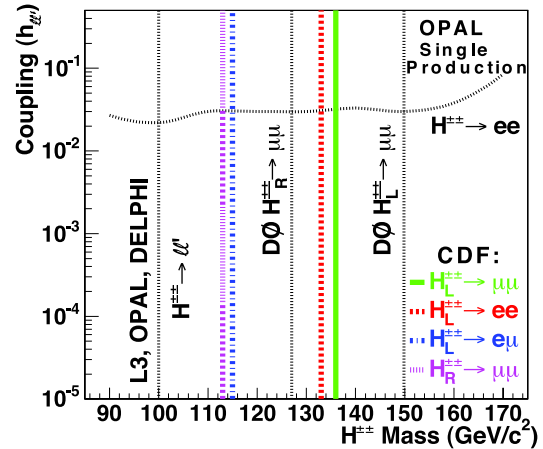


Figure 12: The 95% C.L. exclusion limits on the masses and couplings to leptons of right- and left-handed doubly-charged Higgs bosons, obtained by LEP and Tevatron experiments (from Ref. 185). Color version at end of book.

V. Other Model Extensions

There are many ways to extend the minimal Higgs sector of the Standard Model. In the preceding sections we have considered the phenomenology of the MSSM Higgs sector, which at tree-level is a constrained Type-II 2HDM (with restrictions on the Higgs boson masses and couplings), and also more general 2HDMs of Types I and II. Other extensions of the Higgs sector can include multiple copies of $SU(2)_L$ doublets, additional Higgs singlets, triplets or more complicated combinations of Higgs multiplets. It is also possible to enlarge the gauge symmetry beyond $SU(2)_L \times U(1)_Y$ along with the necessary Higgs structure to generate gauge boson and fermion masses. There are two main experimental constraints that govern these extensions: (i) precision measurements, which constrain $\rho = m_W^2 / (m_Z^2 \cos^2 \theta_W)$ to be very close to 1. In electroweak models based on the SM gauge group, the tree-level value of ρ is determined by the Higgs multiplet structure. By suitable choices for the hypercharges, and in some cases the mass splitting between the charged and neutral Higgs sector or the vacuum expectation values of the Higgs fields, it is possible to obtain a richer combination of singlets, doublets, triplets and higher multiplets compatible with precision measurements [187]; (ii) the second important constraint comes from flavor changing neutral current (FCNC) effects. In the presence of multiple Higgs doublets, the Glashow-Weinberg theorem [188] states that tree-level FCNC's mediated by neutral Higgs bosons will be absent if all fermions of a given electric charge couple to no more than one Higgs doublet. The Higgs doublet models Type-I and Type-II are two different ways of satisfying this theorem. The coupling pattern of these two types can be arranged by imposing either a discrete symmetry or, in the case of Type-II, supersymmetry. The resulting phenomenology of

Gauge & Higgs Boson Particle Listings

Higgs Bosons — H^0 and H^\pm

extended Higgs sectors can differ significantly from that of the SM Higgs boson.

The most studied extension of the MSSM has a scalar singlet and its supersymmetric partner [189,190]. These models have an extended Higgs sector with two additional neutral scalar states (one CP -even and one CP -odd), beyond those present in the MSSM. In these models, the tree-level bound on the lightest Higgs boson, considering arguments of perturbativity of the theory up to the GUT scale, is about 100 GeV. The radiative corrections to the masses are similar to those in the MSSM, and yield an upper bound of about 145 GeV for the mass of the lightest neutral CP -even scalar [191,192]. The precise LEP II bounds on the Higgs masses depend on the couplings of the Higgs bosons to the gauge bosons and such couplings tend to be weakened somewhat from mixing with the singlet. The DELPHI Collaboration places a constraint on such models [193].

Another extension of the MSSM which can raise the value of the lightest Higgs mass to a few hundred GeV is based on gauge extensions of the MSSM [194,195]. The addition of asymptotically-free gauge interactions naturally yields extra contributions to the quartic Higgs couplings. These extended gauge sector models can be combined with the presence of extra singlets or replace the singlet with a pair of triplets [196]. In some of these models, a rich and distinctive phenomenology can be expected.

Many non-SUSY solutions to the problem of electroweak symmetry breaking and the hierarchy problem are being developed. For example, the so-called “Little Higgs” models propose additional sets of heavy vector-like quarks, gauge bosons, and scalar particles, with masses in the 100 GeV to a few TeV range. The couplings of the new particles are tuned in such a way that the quadratic divergences induced in the SM by the top, gauge-boson and Higgs loops are canceled at the one-loop level. If the Little Higgs mechanism successfully resolves the hierarchy problem, it should be possible to detect some of these new states at the LHC. For reviews of models and phenomenology, and a more complete list of references, see Refs. [197,198].

In Little Higgs models the production and decays of the Higgs boson are modified. For example, when the dominant production mode of the Higgs is through gluon fusion, the contribution of new fermions in the loop diagrams involved in the effective ϕgg vertex can reduce the production rate. The rate is generally suppressed relative to the SM rate due to the symmetries which protect the Higgs mass from quadratic divergences at the one-loop level. However, the branching ratio of the Higgs to photon pairs can be enhanced in these models [199]. By design, Little Higgs models are valid only up to a scale $\Lambda \sim 5$ -10 TeV. The new physics which would enter above Λ remains unspecified, and will impact the Higgs sector. In general, it can modify Higgs couplings to third-generation fermions and gauge bosons, though these modifications are suppressed by $1/\Lambda$ [200].

Distinctive features in the Higgs phenomenology of Little Higgs models may also stem from the fact that loop-level electroweak precision bounds on models with a tree-level custodial symmetry allows for a Higgs boson heavier than the one permitted by precision electroweak fits in the SM. This looser bound follows from a cancelation of the effects on the ρ parameter of a higher mass Higgs boson and the heavy partner of the top quark. The Higgs can have a mass as high as 800-1000 GeV in some Little Higgs models and still be consistent with electroweak precision data [201]. Lastly, the scalar content of a Little Higgs structure is model dependent. There could be two, or even more scalar doublets in a little Higgs model, or even different representations of the electroweak gauge group [202].

Models of extra space dimensions present an alternative way of avoiding the scale hierarchy problem [12]. New states, known as Kaluza-Klein (KK) excitations, can appear at the TeV scale, where gravity-mediated interactions may become relevant. They share the quantum numbers of the graviton and/or SM particles. In a particular realization of these models, based on warped extra dimensions, a light Higgs-like particle, the radion, may appear in the spectrum [203]. The mass of the radion, as well as its possible mixing with the light Higgs boson, depends strongly on the mechanism that stabilizes the extra dimension, and on the curvature-Higgs mixing.

The radion couples to the trace of the energy-momentum tensor of the SM particles, leading to effective interactions with quarks, leptons and weak gauge bosons which are similar to the ones of the Higgs boson, although they are suppressed by the ratio of the weak scale to the characteristic mass of the new excitations. An important characteristic of the radion is its enhanced couplings to gluons. Therefore, if it is light and mixes with the Higgs boson, it may modify the standard Higgs phenomenology at lepton and hadron colliders. A search for the radion in LEP data, conducted by OPAL using both b -tagged and flavor-independent searches, gave negative results [204]. Radion masses below 58 GeV are excluded for the mass eigenstate which becomes the Higgs boson in the no-mixing limit, for all parameters of the Randall-Sundrum model.

In models of warped extra dimensions in which the SM particles propagate in the extra dimensions, the KK excitations of the vector-like fermions may be pair-produced at colliders and decay into combinations of two Higgs bosons and jets, or one Higgs boson, a gauge boson, and jets. KK excitations may also be singly-produced. Some of these interesting possible new signatures for SM-like Higgs bosons in association with top or bottom quarks have been studied [13].

If Higgs bosons are not discovered at the Tevatron or the LHC, other studies might be able to test alternative theories of dynamical electroweak symmetry breaking which do not involve a fundamental Higgs scalar [205].

VI. Other Searches for Higgs Bosons Beyond the SM

Decays of Higgs bosons into invisible (weakly-interacting and neutral) particles may occur in many models. For example, in the MSSM the Higgs can decay into pairs of neutralinos. In a different context, Higgs bosons might also decay into pairs of Goldstone bosons or Majorons [206]. In the process $e^+e^- \rightarrow hZ$, the mass of the invisible Higgs boson can be inferred from the kinematics of the reconstructed Z boson by using the beam energy constraint. Results from the LEP experiments can be found in Refs. [40,207]. A preliminary combination of LEP data yields a 95% C.L. lower bound of 114.4 GeV for the mass of a Higgs boson, if it is produced with SM production rate, and if it decays exclusively into invisible final states [208].

Most of the searches for the processes $e^+e^- \rightarrow hZ$ and hA , which have been discussed in the context of the *CPC*-MSSM, rely on the assumption that the Higgs bosons have a sizable branching ratio to $b\bar{b}$. However, for specific parameters of the MSSM [209], the general 2HDM case, or composite models [90,92,210], decays to non- $b\bar{b}$ final states may be significantly enhanced. Some flavor-independent searches have been reported at LEP which do not require the experimental signature of a b -jet [211], and a preliminary combination of LEP data has been performed [16,212]. If Higgs bosons are produced at the SM rate and decay only to jets of hadrons, then the 95% C.L. lower limit on the mass of the Higgs boson is 112.9 GeV, independent of the fractions of gluons and b , c , s , u and d -quarks in Higgs boson decay. In conjunction with b -flavor sensitive searches, large domains of the general Type-II 2HDM parameter space have been excluded [213].

Photonic final states from the processes $e^+e^- \rightarrow Z/\gamma^* \rightarrow H\gamma$ and from $H \rightarrow \gamma\gamma$, do not occur in the SM at tree level, but may have a low rate due to W^\pm and top quark loops [214]. Additional loops from SUSY particles would modify the rates only slightly [215], but models with anomalous couplings predict enhancements by orders of magnitude. Searches for the processes $e^+e^- \rightarrow (H \rightarrow b\bar{b})\gamma$, $(H \rightarrow \gamma\gamma)q\bar{q}$, and $(H \rightarrow \gamma\gamma)\gamma$ have been used to set limits on such anomalous couplings. Furthermore, they constrain the so-called Type-I “fermiophobic” 2HDM [216], which also predicts an enhanced $h \rightarrow \gamma\gamma$ rate. The LEP searches are described in [217,218]. In a preliminary combination of LEP data [220], a fermiophobic Higgs boson with mass less than 108.2 GeV (95% C.L.) has been excluded. Limits of about 80 GeV have been obtained at the Tevatron in Run I [221]. Run II preliminary results on 1.1 fb^{-1} of DØ data extend the exclusion to 92 GeV [222], and other production of fermiophobic Higgs bosons, leading to a 3-photons final state, have also been searched for [223]. The Type-I 2HDM also predicts an enhanced rate for the decays $h \rightarrow W^*W$ and Z^*Z , a possibility that has been addressed by L3 [218] and ALEPH [219].

The DELPHI collaboration has used the LEP 1 and LEP 2 data to search for Higgs bosons produced in pairs, in association

with Z bosons, and in association with b quarks, τ leptons. The decays considered are $\phi \rightarrow b\bar{b}, \tau^+\tau^-$, and to pairs of Higgs bosons, yielding four- b , four- b +jets, six- b and four- τ final states. No evidence for a Higgs boson was found [109], and DELPHI set mass-dependent limits on a variety of processes, which apply to a large class of models. The limits on the cross sections of Yukawa production of Higgs bosons are typically more than 100 times larger than the SM predictions, while Higgs-strahlung limits for b and τ decays extend up to the kinematic limits of approximately 114 GeV. Limits on pair-produced Higgs bosons extend up to approximately $m_h + m_A = 140$ GeV for full-strength production, assuming $b\bar{b}$ and $\tau^+\tau^-$ decays.

OPAL’s decay-mode independent search for $e^+e^- \rightarrow S^0Z$ [39] provides sensitivity to arbitrarily-decaying scalar particles, as only the recoiling Z boson is required to be reconstructed. The energy and momentum constraints provided by the e^+e^- collisions allow the S^0 ’s four-vector to be reconstructed and limits placed on its production independent of its decay characteristics, allowing sensitivity for very light scalar masses. The limits obtained in this search are less than one-tenth of the SM Higgs-strahlung production rate for $1 \text{ keV} < m_{S^0} < 19 \text{ GeV}$, and less than the SM Higgs-strahlung rate for $m_{S^0} < 81 \text{ GeV}$.

VII. Outlook

At the Tevatron, Higgs searches performed in several channels with 1 to 2 fb^{-1} are close to achieving the sensitivity needed to probe the SM Higgs boson sector beyond the LEP bound. With an anticipated improvement in analysis sensitivity, the expected increase of luminosity up to about $7\text{-}8 \text{ fb}^{-1}$, and the combination of results from both experiments, the Tevatron should be able to exclude most of the SM Higgs mass range up to 185 GeV (at 95% C.L.), and could produce 3σ evidence for a Higgs boson with a mass close to 115 GeV or 160 GeV. The Tevatron searches are also sensitive to the neutral Higgs bosons of the MSSM in large domains of parameter space.

The LHC is expected to deliver proton-proton collisions at 14 TeV in 2008. The ATLAS and CMS detectors have been optimized for Higgs boson searches. The discovery of a SM Higgs boson is expected to be possible over the mass range between 100 GeV and 1 TeV, given sufficient integrated luminosity. This broad range is covered by a variety of searches based on several production and decay processes. The LHC experiments are expected to provide full coverage of the MSSM parameter space by direct searches for the h , H , A , and H^\pm bosons, and by searching for h bosons in cascade decays of SUSY particles. The simultaneous discovery of several of the Higgs bosons is expected to be possible over extended domains of the MSSM parameter space.

A high-energy e^+e^- linear collider may start operation around the year 2020. According to present planning, it would run initially at a center-of-mass energy of 500 GeV, and an upgrade would allow running at 1 TeV later [20]. One of the primary goals is to extend precision measurements, which are typical of e^+e^- colliders, to the Higgs sector. According

Gauge & Higgs Boson Particle Listings

Higgs Bosons — H^0 and H^\pm

to several studies, the Higgs couplings to fermions and vector bosons could be measured with a precision of a few percent, and the parameters of the MSSM could be studied in great detail. At the highest collider energies and luminosities, the self-coupling of the Higgs fields could be measured directly through final states with two Higgs bosons [224].

Higgs production in the s -channel might be possible at a future $\mu^+\mu^-$ collider [21]. Mass measurements with a precision of a few MeV would be possible, and the total width could be obtained directly from Breit-Wigner scans. The heavy CP -even and CP -odd bosons, H and A , degenerate over most of the MSSM parameter space, could be directly disentangled from the line shape.

Higgs bosons enter calculations of electroweak observables through loop effects, so it has been possible to constrain the SM Higgs sector using a global fit to precision electroweak measurements. The fit favors Higgs bosons that are not very heavy, a fact which is compatible with the predictions of the MSSM. B -physics observables explored at CLEO, BaBar, Belle and the Tevatron independently constrain the MSSM parameter space available for Higgs searches. These indirect limits derive in part from the specific effects on flavor physics of the supersymmetry-breaking mechanism. The combined information of direct and indirect SUSY Higgs searches together with the results from direct search for dark matter, could provide unique information about supersymmetry.

In the theoretical landscape, several models are emerging with novel approaches to the problem of electroweak symmetry breaking. Many of them incorporate a Higgs sector with features distinctly different from the SM, and their phenomenology could be studied at the LHC.

There is uncertainty on the mass range for the scale of new physics. It arises from one side by the attempt to explain the hierarchy between the electroweak scale and the Planck scale in a natural way, which demands new physics at or below the TeV scale, and on the other side by the strong bounds at that same scale, of order of a TeV or larger, that come from the precise measurements delivered by the experiments in the last two decades. Supersymmetry remains one suggestive candidate for new physics. Models with no fundamental Higgs bosons are harder to accommodate with precision data, but the LHC and a future lepton collider will have the final word on the mechanism of electroweak symmetry breaking.

References

1. P.W. Higgs, Phys. Rev. Lett. **12**, 132 (1964); *idem.*, Phys. Rev. **145**, 1156 (1966); F. Englert and R. Brout, Phys. Rev. Lett. **13**, 321 (1964); G.S. Guralnik, C.R. Hagen, and T.W. Kibble, Phys. Rev. Lett. **13**, 585 (1964).
2. S.L. Glashow, Nucl. Phys. **20**, 579 (1961); S. Weinberg, Phys. Rev. Lett. **19**, 1264 (1967); A. Salam, *Elementary Particle Theory*, eds.: Svartholm, Almquist, and Wiksell, Stockholm, 1968; S. Glashow, J. Iliopoulos, and L. Maiani, Phys. Rev. **D2**, 1285 (1970).
3. J.M. Cornwall, D.N. Levin, and G. Tiktopoulos, Phys. Rev. Lett. **30**, 1286 (1973); Phys. Rev. **D10**, 1145 (1974).; C.H. Llewellyn Smith, Phys. Lett. **B46**, 233 (1973).
4. B.W. Lee, C. Quigg and H.B. Thacker, Phys. Rev. **D16**, 1519 (1977).
5. LEP Electroweak Working Group, status of September 2007, <http://lepewwg.web.cern.ch/LEPEWWG/>; M. Grunewald, arXiv:0709.3744v1(2007); J. Erler and P. Langacker, *Electroweak Model and Constraints on New Physics*, in this volume.
6. J. Wess and B. Zumino, Nucl. Phys. **B70**, 39 (1974); *idem.*, Phys. Lett. **49B**, 52 (1974); H.P. Nilles, Phys. Rev. **C110**, 1984 (1); H.E. Haber and G.L. Kane, Phys. Rev. **C117**, 75 (1985); S.P. Martin, hep-ph/9709356; P. Fayet, Phys. Lett. **B69**, 489 (1977); *ibid.*, **B84**, 421 (1979); *ibid.*, **B86**, 272 (1979); *idem.*, Nucl. Phys. **B101**, 81 (2001).
7. J.F. Gunion *et al.*, *The Higgs Hunter's Guide* (Addison-Wesley) 1990; A. Djouadi, arXiv:hep-ph/0503172, hep-ph/0503173.
8. L.E. Ibáñez and G.G. Ross, Phys. Lett. **B105**, 439 (1981); S. Dimopoulos, S. Raby, and F. Wilczek, Phys. Rev. **D24**, 1681 (1981); M.B. Einhorn and D.R.T. Jones, Nucl. Phys. **B196**, 475 (1982); W.J. Marciano and G. Senjanovic, Phys. Rev. **D25**, 3092 (1982).
9. J. Ellis, S. Kelley, and D.V. Nanopoulos, Phys. Lett. **B249**, 441 (1990); P. Langacker and M. Luo, Phys. Rev. **D44**, 817 (1991); U. Amaldi, W. de Boer, and H. Fürstenau, Phys. Lett. **B260**, 447 (1991); P. Langacker and N. Polonsky, Phys. Rev. **D52**, 3081 (1995); S. Pokorski, Act. Phys. Pol., **B30**, 1759 (1999); For a recent review, see: R.N. Mohapatra, in *Particle Physics 1999, Proceedings of the ICTP Summer School in Particle Physics*, Trieste, Italy, 21 June–9 July, 1999, edited by G. Senjanovic and A.Yu. Smirnov. (World Scientific, Singapore, 2000) pp. 336–394.
10. S. Weinberg, Phys. Rev. **D13**, 974 (1979); Phys. Rev. **D19**, 1277 (1979); L. Susskind, Phys. Rev. **D20**, 2619 (1979); E. Farhi and L. Susskind, Phys. Rev. **74**, 277 (1981); R.K. Kaul, Rev. Mod. Phys. **55**, 449 (1983); C.T. Hill and E.H. Simmons, Phys. Reports **381**, 235 (2003) [E: *ibid.*, **390**, 553 (2004)].
11. N. Arkani-Hamed, A.G. Cohen, and H. Georgi, Phys. Lett. **B513**, 232 (2001); N. Arkani-Hamed *et al.*, JHEP **0207**, 034 (2002); N. Arkani-Hamed *et al.*, JHEP **0208**, 020 (2002); N. Arkani-Hamed *et al.*, JHEP **0208**, 021 (2002); I. Low, W. Skiba, and D. Smith, Phys. Rev. **D66**, 072001 (2002).
12. I. Antoniadis, Phys. Lett. **B246**, 377 (1990); N. Arkani-Hamed, S. Dimopoulos, and G.R. Dvali, Phys. Lett. **B429**, 263 (1998); L. Randall and R. Sundrum, Phys. Rev. Lett. **83**, 3370 (1999) *idem.*, **84**, 4690 (1999);

- G.F. Giudice *et al.*, Nucl. Phys. **B544**, 3 (1999);
C. Csáki *et al.*, Phys. Rev. **D63**, 065002 (2001).
13. J. A. Aguilar-Saavedra, JHEP **0612**, 033 (2006);
M. Carena *et al.*, Phys. Rev. **D76**, 035006 (2007);
A. D. Medina, N. R. Shah, and C. E. M. Wagner,
arXiv:0706.1281;
A. Djouadi and G. Moreau, arXiv:0707.3800;
H. Davoudiasl, B. Lillie, and T. G. Rizzo, JHEP **0608**,
042 (2006);
A. Falkowski, arXiv:0711.0828.
 14. P.J. Franzini and P. Taxil, in *Z physics at LEP 1*, CERN
89-08 (1989).
 15. ALEPH, DELPHI, L3, and OPAL Collaborations, The
LEP Working Group for Higgs Boson Searches, Phys.
Lett. **B565**, 61 (2003).
 16. ALEPH, DELPHI, L3, and OPAL Collaborations, The
LEP Working Group for Higgs Boson Searches, Eur.
Phys. J. **C47**, 547 (2006).
 17. CDF and $D\bar{O}$ Collaborations, *Results of the Tevatron
Higgs Sensitivity Study*, FERMILAB-PUB-03/320-E (2003).
 18. ATLAS TDR on Physics performance, Vol. II, Chap.
19, *Higgs Bosons* (1999);
S. Asai, *et al.*, SN-ATLAS-2003-024;
L. Carminati, ATLAS-PHYS-CONF-2006-018; ATLAS-COM-
PHYS-2006-076.
 19. CMS Collab., CERN-LHCC-2006-001,
CERN-LHCC-2006-021; CMS Note 2003/033.
 20. E. Accomando *et al.*, Physics Reports **299**, 1–78 (1998);
TESLA Technical Design Report, Part 3: *Physics at an
 e^+e^- Linear Collider*, hep-ph/0106315;
ACFA Linear Collider Working Group, *Particle Physics
Experiments at JLC*, hep-ph/0109166;
A. Djouadi *et al.*, *ILC Global Design Effort and World
Wide Study*, arXiv:0709.1893 [hep-ph];
E. Accomando *et al.*, *CLIC Physics Working Group*,
hep-ph/0412251.
 21. B. Autin *et al.*, (eds.), CERN 99-02;
C.M. Ankenbrandt *et al.*, Phys. Rev. ST Acc. Beams **2**,
081001 (1999);
C. Blochinger *et al.*, *Physics Opportunities at $\mu^+\mu^-$ Higgs
Factories*, hep-ph/0202199.
 22. N. Cabibbo *et al.*, Nucl. Phys. **B158**, 295 (1979);
See, *e.g.*, G. Altarelli and G. Isidori, Phys. Lett. **B337**,
141 (1994);
J.A. Casas, J.R. Espinosa, and M. Quirós, Phys. Lett.
B342, 171 (1995) *idem.*, Phys. Lett. **B382**, 374 (1996);
T. Hambye and K. Riesselmann, Phys. Rev. **D55**, 7255
(1997).
 23. J. R. Espinosa and M. Quiros, Phys. Lett. **B353**, 257
(1995);
G. Isidori *et al.*, Nucl. Phys. **B609**, 387 (2001).
 24. B.A. Kniehl, Phys. Rept. **240**, 211 (1994).
 25. E. Gross *et al.*, Z. Phys. **C63**, 417 (1994); [E: *ibid.*, **C66**,
32 (1995)];
E. Braaten and J.P. Leveille, Phys. Rev. **D22**, 715
(1980);
N. Sakai, Phys. Rev. **D22**, 2220 (1980);
T. Inami and T. Kubota, Nucl. Phys. **B179**, 171 (1981);
S.G. Gorishniĭ, A.L. Kataev, and S.A. Larin, Sov. J.
Nucl. Phys. **40**, 329 (1984) [Yad. Fiz. **40** (1984) 517];
M. Drees and K. Hikasa, Phys. Lett. **B240**, 455 (1990)
[E: **B262** (1991) 497];
 - A. Djouadi, M. Spira, and P.M. Zerwas, Z. Phys. **C70**,
675 (1996);
A. Djouadi, J. Kalinowski, and M. Spira, Comput. Phys.
Commun. **108**, 56 (1998);
B.A. Kniehl, Nucl. Phys. **B376**, 3 (1992);
A.L. Kataev, Sov. Phys. JETP Lett. **66**, 327 (1997)
[Pis'ma Zh. Éksp. Teor. Fiz. **66** (1997) 308].
 26. For a compilation of the most accurate theoretical results
for SM and MSSM Higgs cross sections at the Tevatron
and the LHC see:
<http://maltoni.home.cern.ch/maltoni/TeV4LHC/>.
 27. D. Graudenz, M. Spira, and P.M. Zerwas, Phys. Rev.
Lett. **70**, 1372 (1993);
S. Catani *et al.*, JHEP **0307**, 028 (2003);
R.V. Harlander and W.B. Kilgore, Phys. Rev. Lett. **88**,
201801 (2002);
C. Anastasiou, K. Melnikov, Nucl. Phys. **B646**, 220
(2002);
C. Anastasiou, K. Melnikov, and F. Petriello, Phys. Rev.
Lett. **93**, 262002 (2004);
U. Aglietti *et al.*, Phys. Lett. **B595**, 432 (2004);
G. Degrossi and F. Maltoni, Phys. Lett. **B600**, 255
(2004).
 28. K.A. Assamagan *et al.*, arXiv:hep-ph/0406152.
 29. O. Brein, A. Djouadi, and R. Harlander, Phys. Lett.
B579, 149 (2004);
M.L. Ciccolini, S. Dittmaier, and M. Krämer, Phys. Rev.
D68, 073003 (2003).
 30. T. Han, G. Valencia, and S. Willenbrock, Phys. Rev.
Lett. **69**, 3274 (1992);
E.L. Berger and J. Campbell, Phys. Rev. **D70**, 073011
(2004);
T. Figy, C. Oleari, and D. Zeppenfeld, Phys. Rev. **D68**,
073005 (2003).
 31. W. Beenakker *et al.*, Phys. Rev. Lett. **87**, 201805 (2001);
L. Reina and S. Dawson, Phys. Rev. Lett. **87**, 201804
(2001);
S. Dawson *et al.*, Phys. Rev. **D67**, 071503 (2003).
 32. R.V. Harlander and W.B. Kilgore, Phys. Rev. **D68**,
013001 (2003);
J. Campbell *et al.*, Phys. Rev. **D67**, 095002 (2003);
S. Dawson *et al.*, Phys. Rev. Lett. **94**, 031802 (2005);
S. Dittmaier, M. Krämer, and M. Spira, Phys. Rev. **D70**,
074010 (2004);
S. Dawson *et al.*, Phys. Rev. **D69**, 074027 (2004).
 33. W.J. Stirling and D.J. Summers, Phys. Lett. **B283**, 411
(1992);
F. Maltoni *et al.*, Phys. Rev. **D64**, 094023 (2001).
 34. M. Carena and H.E. Haber, Prog. in Part. Nucl. Phys. **50**,
152 (2003).
 35. J. Ellis *et al.*, Nucl. Phys. **B106**, 292 (1976);
B.L. Ioffe and V.A. Khoze, Sov. J. Nucl. Phys. **9**, 50
(1978).
 36. D.R.T. Jones and S.T. Petcov, Phys. Lett. **84B**, 440
(1979);
R.N. Cahn and S. Dawson, Phys. Lett. **136B**, 96 (1984);
ibid., **138B**, 464 (1984);
W. Kilian *et al.*, Phys. Lett. **B373**, 135 (1996).
 37. P. Janot, “Searching for Higgs Bosons at LEP 1 and
LEP 2,” in *Perspectives in Higgs Physics II*, World
Scientific, ed. G.L. Kane (1998).
 38. K. Hagiwara *et al.*, Phys. Rev. **D66**, 010001-1 (2002),
Review No. 31 on *Statistics*, p. 229.

Gauge & Higgs Boson Particle Listings

Higgs Bosons — H^0 and H^\pm

39. OPAL Collab., Eur. Phys. J. **C27**, 311 (2003).
40. ALEPH Collab., Phys. Lett. **B526**, 191 (2002).
41. DELPHI Collab., Eur. Phys. J. **C32**, 145 (2004).
42. L3 Collab., Phys. Lett. **B517**, 319 (2001).
43. OPAL Collab., Eur. Phys. J. **C26**, 479 (2003).
44. The CDF and DØ Collaborations, and the Tevatron Electroweak Working Group, *Combination of the CDF and DØ Results on the Top-Quark Mass*, hep-ex/0703034.
45. CDF Collab., Phys. Rev. Lett. **99**, 151801 (2007).
46. S.L. Glashow, D.V. Nanopoulos, and A. Yildiz, Phys. Rev. **D18**, 1724 (1978); A. Stange, W. Marciano, and S. Willenbrock, Phys. Rev. **D49**, 1354 (1994); *ibid.*, **D50**, 4491 (1994).
47. CDF Collab., Phys. Rev. Lett. **96**, 081803 (2006).
48. DØ Collab., Phys. Rev. Lett. **94**, 091802 (2005).
49. CDF Collab., “Search for Standard Model Higgs Bosons Produced in Association with W Bosons,” FERMILAB-PUB-07-567, arXiv:0710.4363 subm. to Phys. Rev. Lett.
50. DØ Collab., “A Combined Search for the Standard Model Higgs Boson at $\sqrt{s} = 1.96$ TeV,” to be submitted to Phys. Lett. B.
51. (**) CDF Collab., CDF Note 8957, “Search for Standard Model Higgs Boson Production in Association with W^\pm Boson at CDF with 1.7 fb^{-1} ” (2007).
52. (***) DØ Collab., DØ Note 5472-CONF, “Search for WH Production using a Neural Network approach in $p\bar{p}$ Collisions at $\sqrt{s} = 1.96$ TeV with 1.7 fb^{-1} of Data” (2007).
53. DØ Collab., Phys. Rev. Lett. **97**, 161803 (2006).
54. (***) DØ Collab., DØ Note 5506-CONF, “A Search for the Standard Model Higgs Boson in the Channel $ZH \rightarrow \nu\bar{\nu}b\bar{b}$ at $\sqrt{s} = 1.96$ TeV” (2007).
55. (**) CDF Collab., CDF Note 8973, “Search for the Standard Model Higgs Boson in the \cancel{E}_T and b-jet Signature in $p\bar{p}$ Collisions at $\sqrt{s} = 1.96$ TeV” (2007).
56. DØ Collab., Phys. Lett. **B655**, 209 (2007).
57. (**) CDF Collab., CDF Note 8742, “Search for $ZH \rightarrow \ell^+\ell^-b\bar{b}$ in 1 fb^{-1} of CDF Run 2 Data” (2007).
58. (***) DØ Collab., DØ Note 5482-CONF, “Search for $ZH(\rightarrow \ell^+\ell^-b\bar{b})$ in $p\bar{p}$ collisions at $\sqrt{s} = 1.96$ TeV” (2007).
59. (**,**) The Tevatron NP-Higgs Working Group for the CDF and DØ Collab., CDF Note 8941 and DØ Note 5536, “Combined CDF and DØ Upper Limits on Standard Model Higgs-Boson Production.” Results not to be quoted before CDF and DØ Collab. approval. To be released as a public note at the beginning of December 2007, see CDF and DØ web-pages for latest updates (2007).
60. DØ Collab., Phys. Rev. Lett. **97**, 151804 (2006).
61. (**) CDF Collab., CDF Note 7307, “Search for the WH Production Using High- p_T Isolated Like-Sign Dilepton Events in Run II” (2004).
62. (***) DØ Collab., DØ Note 5485-CONF, “Search for the Associated Higgs Boson Production $p\bar{p} \rightarrow WH \rightarrow WWW^* \rightarrow \ell^\pm\nu\ell^\pm\nu' + X$ at $\sqrt{s} = 1.96\text{TeV}$ ” (2007).
63. CDF Collab., Phys. Rev. Lett. **97**, 081802 (2006).
64. DØ Collab. Phys. Rev. Lett. **96**, 011801 (2006).
65. (**) CDF Collab., CDF Note 8958, “Search for $H \rightarrow WW^*$ Production with Matrix Element Methods at Tevatron Using 1.9 fb^{-1} Data” (2007).
66. (***) DØ Collab., DØ Note 5502-CONF, “Search for the Higgs boson in $H \rightarrow WW^* \rightarrow ee$ decays with 0.63 fb^{-1} at DØ in Run IIB” (2007); (***) DØ Collab., DØ Note 5489-CONF, “Search for the Higgs boson in $H \rightarrow WW^* \rightarrow e\mu$ decays at DØ in Run IIB” (2007); (***) DØ Collab., DØ Note 5538-CONF, “Search for the Higgs boson in $H \rightarrow WW^*$ decays with 1.7 fb^{-1} of data at DØ in Run IIB” (2007); (***) DØ Collab., DØ Note 5332-CONF, “Search for the Higgs boson in events with $H \rightarrow WW^* \rightarrow \mu + \tau_{had}$ signature with 1 fb^{-1} at DØ in Run II” (2007); (***) DØ Collab., DØ Note 5194-CONF, “Search for the Higgs boson in $H \rightarrow WW^* \rightarrow \mu\mu$ decays with 930 pb^{-1} at DØ in Run II” (2006); (***) DØ Collab., DØ Note 5063-CONF, “Search for the Higgs boson in $H \rightarrow WW^* \rightarrow \ell\ell'(\ell, \ell' = e, \mu)$ decays with 950 pb^{-1} at DØ in Run II” (2006).
67. A. Schafer, O. Nachtmann, and R. Schopf, Phys. Lett. **B249**, 331 (1990).; A. Bialas and P. V. Landshoff, Phys. Lett. **B256**, 540 (1991); M. Heyssler, Z. Kunszt, and W. J. Stirling Phys. Lett. **B406**, 95 (1997); R. Enberg *et al.*, Phys. Rev. Lett. **89**, 081801 (2002); V. A. Khoze, A. D. Martin, and M. G. Ryskin, Phys. Lett. **B401**, 330 (1997); Eur. Phys. J. **C14**, 525 (2000); Eur. Phys. J. **C25**, 391 (2002); Eur. Phys. J. **C26**, 229 (2002); A. B. Kaidalov *et al.*, Eur. Phys. J. **C33**, 261 (2004); C. Royon, Mod. Phys. Lett. **A18**, 2169 (2003).
68. E. Yazgan *et al.*, CMS-NOTE-2007-011 and arXiv:0706.1898 [hep-ex].
69. J.-J. Blaising *et al.*, “Potential LHC contributions to Europe’s future Strategy at the high energy frontier”, input number 54 to the CERN Council Strategy Group <http://council-strategygroup.web.cern.ch/council-strategygroup/>.
70. V. Buescher and K. Jakobs, Int. J. Mod. Phys. **A20**, 2523 (2005).
71. D. Zeppenfeld *et al.*, Phys. Rev. **D62**, 013009 (2000); D. Zeppenfeld, “Higgs Couplings at the LHC,” in *Proceedings of the APS/DPF/DPB Summer Study on the Future of Particle Physics* (Snowmass 2001), edited by R. Davidson and C. Quigg, SNOWMASS-2001-P123 arXiv:hep-ph/0203123.
72. M. Dührssen *et al.*, Phys. Rev. **D70**, 113009 (2004).
73. CMS Collab., J. Phys. **G34**, 995 (2007).
74. E. Witten, Nucl. Phys. **B188**, 513 (1981); R.K. Kaul, Phys. Lett. **109B**, 19 (1982); *Pramana* **19**, 183 (1982); L. Susskind, Phys. Rev. **104**, 181 (1984).
75. L.E. Ibáñez and G.G. Ross, Phys. Lett. **B110**, 215 (1982); L.E. Ibáñez, Phys. Lett. **B118**, 73 (1982); J. Ellis, D.V. Nanopoulos, and K. Tamvakis, Phys. Lett. **B121**, 123 (1983); L. Alvarez-Gaumé, J. Polchinski, and M.B. Wise, Nucl. Phys. **B221**, 495 (1983).

See key on page 373

Gauge & Higgs Boson Particle Listings

Higgs Bosons — H^0 and H^\pm

76. S. Dimopoulos and H. Georgi, Nucl. Phys. **B193**, 150 (1981);
K. Harada and N. Sakai, Prog. Theor. Phys. **67**, 1877 (1982);
K. Inoue *et al.*, Prog. Theor. Phys. **67**, 1889 (1982);
L. Girardello and M.T. Grisaru, Nucl. Phys. **B194**, 65 (1982);
L.J. Hall and L. Randall, Phys. Rev. Lett. **65**, 2939 (1990);
I. Jack and D.R.T. Jones, Phys. Lett. **B457**, 101 (1999).
77. H.E. Haber and G.L. Kane, Phys. Rev. **C117**, 75 (1985);
H.E. Haber, *Supersymmetry*, in this volume.
78. S. Dimopoulos and D.W. Sutter, Nucl. Phys. **B452**, 496 (1995);
D.W. Sutter, Stanford Ph. D. thesis, hep-ph/9704390;
H.E. Haber, Nucl. Phys. B (Proc. Suppl.) **62A-C**, 469 (1998).
79. H. E. Haber and Y. Nir, Nucl. Phys. **B335**, 363 (1990);
A. Dobado, M. J. Herrero, and S. Penaranda, Eur. Phys. J. **C17**, 487 (2000);
J. F. Gunion and H. E. Haber, Phys. Rev. **D67**, 075019 (2003).
80. L.J. Hall and M.B. Wise, Nucl. Phys. **B187**, 397 (1981).
81. Y. Okada, M. Yamaguchi, and T. Yanagida, Prog. Theor. Phys. **85**, 1 (1991);
J. Ellis, G. Ridolfi, and F. Zwirner, Phys. Lett. **B257**, 83 (1991).
82. H.E. Haber and R. Hempfling, Phys. Rev. Lett. **66**, 1815 (1991).
83. S.P. Li and M. Sher, Phys. Lett. **B140**, 339 (1984);
R. Barbieri and M. Frigeni, Phys. Lett. **B258**, 395 (1991);
M. Drees and M.M. Nojiri, Phys. Rev. **D45**, 2482 (1992);
J.A. Casas *et al.*, Nucl. Phys. **B436**, 3 (1995) [E: **B439** (1995) 466];
J. Ellis, G. Ridolfi, and F. Zwirner, Phys. Lett. **B262**, 477 (1991);
A. Brignole *et al.*, Phys. Lett. **B271**, 123 (1991) [E: **B273** (1991) 550].
84. R.-J. Zhang, Phys. Lett. **B447**, 89 (1999);
J.R. Espinosa and R.-J. Zhang, JHEP **0003**, 026 (2000);
J.R. Espinosa and R.-J. Zhang, Nucl. Phys. **B586**, 3 (2000);
A. Brignole *et al.*, Nucl. Phys. **B631**, 195 (2002), Nucl. Phys. **B643**, 79 (2002).
85. H.E. Haber and R. Hempfling, Phys. Rev. Lett. **66**, 1815 (1991);
J.F. Gunion and A. Turski, Phys. Rev. **D39**, 2701 (1989), Phys. Rev. **D40**, 2333 (1989);
M.S. Berger, Phys. Rev. **D41**, 225 (1990);
A. Brignole, Phys. Lett. **B277**, 313 (1992) Phys. Lett. **B281**, 284 (1992);
M.A. Díaz and H.E. Haber, Phys. Rev. **D45**, 4246 (1992);
P.H. Chankowski, S. Pokorski, and J. Rosiek, Phys. Lett. **B274**, 191 (1992), Nucl. Phys. **B423**, 437 (1994);
A. Yamada, Phys. Lett. **B263**, 233 (1991), Z. Phys. **C61**, 247 (1994);
A. Dabelstein, Z. Phys. **C67**, 496 (1995);
R. Hempfling and A.H. Hoang, Phys. Lett. **B331**, 99 (1994);
S. Heinemeyer, W. Hollik, and G. Weiglein, Phys. Rev. **D58**, 091701 (1998), Phys. Lett. **B440**, 296 (1998), Eur. Phys. J. **C9**, 343 (1999).
86. D.M. Pierce *et al.*, Nucl. Phys. **B491**, 3 (1997).
87. R. Barbieri, M. Frigeni, and F. Caravaglios, Phys. Lett. **B258**, 167 (1991);
Y. Okada, M. Yamaguchi, and T. Yanagida, Phys. Lett. **B262**, 45 (1991);
J.R. Espinosa and M. Quirós, Phys. Lett. **B266**, 389 (1991);
D.M. Pierce, A. Papadopoulos, and S. Johnson, Phys. Rev. Lett. **68**, 3678 (1992);
K. Sasaki, M. Carena, and C.E.M. Wagner, Nucl. Phys. **B381**, 66 (1992);
R. Hempfling, in *Phenomenological Aspects of Supersymmetry*, edited by W. Hollik, R. Rückl, and J. Wess (Springer-Verlag, Berlin, 1992) pp. 260–279;
J. Kodaira, Y. Yasui, and K. Sasaki, Phys. Rev. **D50**, 7035 (1994);
H.E. Haber and R. Hempfling, Phys. Rev. **D48**, 4280 (1993);
M. Carena *et al.*, Phys. Lett. **B355**, 209 (1995);
M. Carena, M. Quirós, and C.E.M. Wagner, Nucl. Phys. **B461**, 407 (1996).
88. H.E. Haber, R. Hempfling, and A.H. Hoang, Z. Phys. **C75**, 539 (1997);
M. Carena *et al.*, Nucl. Phys. **B580**, 29 (2000).
89. S. Martin, Phys. Rev. **D67**, 095012 (2003); Phys. Rev. **D71**, 016012 (2005); Phys. Rev. **D75**, 055005 (2007).
90. M. Carena, S. Mrenna, and C.E.M. Wagner, Phys. Rev. **D60**, 075010 (1999);
ibid., Phys. Rev. **D62**, 055008 (2000).
91. S. Heinemeyer, W. Hollik, and G. Weiglein, Phys. Lett. **B455**, 179 (1999);
J.R. Espinosa and I. Navarro, Nucl. Phys. **B615**, 82 (2001);
G. Degrassi, P. Slavich, and F. Zwirner, Nucl. Phys. **B611**, 403 (2001).
92. M. Carena *et al.*, hep-ph/9912223; *idem.*, Eur. Phys. J. **C26**, 601 (2003).
93. M. Carena *et al.*, Phys. Lett. **B495**, 155 (2000);
M. Carena *et al.*, Nucl. Phys. **B625**, 345 (2002).
94. A. Dabelstein, Nucl. Phys. **B456**, 25 (1995);
F. Borzumati *et al.*, Nucl. Phys. **B555**, 53 (1999);
H. Eberl *et al.*, Phys. Rev. **D62**, 055006 (2000).
95. J.A. Coarasa, R.A. Jiménez, and J. Solà, Phys. Lett. **B389**, 312 (1996);
R.A. Jiménez and J. Solà, Phys. Lett. **B389**, 53 (1996);
A. Bartl *et al.*, Phys. Lett. **B378**, 167 (1996).
96. S. Heinemeyer, W. Hollik, and G. Weiglein, Eur. Phys. J. **C16**, 139 (2000).
97. H.E. Haber *et al.*, and D. Temes, Phys. Rev. **D63**, 055004 (2001).
98. L. Hall, R. Rattazzi, and U. Sarid, Phys. Rev. **D50**, 7048 (1994);
R. Hempfling, Phys. Rev. **D49**, 6168 (1994).
99. M. Carena *et al.*, Nucl. Phys. **B426**, 269 (1994).
100. M. Carena *et al.*, Phys. Lett. **B499**, 141 (2001).
101. E. Berger *et al.*, Phys. Rev. **D66**, 095001 (2002).
102. E. Boos *et al.*, Phys. Rev. **D66**, 055004 (2002).
103. A. Djouadi, J. Kalinowski, and P.M. Zerwas, Z. Phys. **C57**, 569 (1993);

Gauge & Higgs Boson Particle Listings

Higgs Bosons — H^0 and H^\pm

- H. Baer *et al.*, Phys. Rev. **D47**, 1062 (1993);
A. Djouadi *et al.*, Phys. Lett. **B376**, 220 (1996);
A. Djouadi *et al.*, Z. Phys. **C74**, 93 (1997);
S. Heinemeyer and W. Hollik, Nucl. Phys. **B474**, 32 (1996).
104. J.F. Gunion, Phys. Rev. Lett. **72**, 199 (1994);
D. Choudhury and D.P. Roy, Phys. Lett. **B322**, 368 (1994);
O.J. Eboli and D. Zeppenfeld, Phys. Lett. **B495**, 147 (2000);
B.P. Kersevan, M. Malawski, and E. Richter-Was, Eur. Phys. J. **C29**, 541 (2003).
105. OPAL Collab., Eur. Phys. J. **C37**, 49 (2004).
106. L3 Collab., Phys. Lett. **B545**, 30 (2002).
107. G. Degross *et al.*, Eur. Phys. J. **C28**, 133 (2003).
108. OPAL Collab., Eur. Phys. J. **C23**, 397 (2002).
109. DELPHI Collab., Eur. Phys. J. **C38**, 1 (2004).
110. J.F. Gunion and H.E. Haber, Nucl. Phys. **B278**, 449 (1986) [E: **B402**, 567 (1993)];
S. Dawson, A. Djouadi, and M. Spira, Phys. Rev. Lett. **77**, 16 (1996);
A. Djouadi, Phys. Lett. **B435**, 101 (1998);
A. Djouadi *et al.*, Phys. Lett. **B318**, 347 (1993);
R.V. Harlander and W.B. Kilgore, JHEP **0210**, 017 (2002);
C. Anastasiou and K. Melnikov, Phys. Rev. **D67**, 037501 (2003);
J. Guasch, P. Hafliger, and M. Spira, Phys. Rev. **D68**, 115001 (2003);
R.V. Harlander and M. Steinhauser, JHEP **0409**, 066 (2004);
S. Dawson *et al.*, Mod. Phys. Lett. **A21**, 89 (2006);
A. Djouadi and M. Spira, Phys. Rev. **D62**, 014004 (2000);
M. Muhlleitner and M. Spira, Nucl. Phys. **B790**, 1 (2008).
111. M. Carena, A. Menon, and C. E. M. Wagner, Phys. Rev. **D76**, 035004 (2007).
112. M. Carena *et al.*, Eur. Phys. J. **C45**, 797 (2006).
113. DØ Collab., Phys. Rev. Lett. **95**, 151801 (2005).
114. (**) CDF Collab., CDF Note 8954, "Search for Higgs Bosons Produced in Association with b-Quarks" (2007).
115. (***) DØ Collab., DØ Note 5246-CONF, "Search for Neutral Higgs Bosons at high $\tan\beta$ in the $b(h/H/A) \rightarrow b\tau\tau$ Channel" (2007).
116. CDF Collab., Phys. Rev. Lett. **96**, 011802 (2006).
117. DØ Collab., Phys. Rev. Lett. **97**, 121802 (2006).
118. (**) CDF Collab., CDF Note 9071, "Search for Neutral MSSM Higgs Bosons Decaying to Tau Pairs with 1.8 fb⁻¹ of Data" (2007).
119. (***) DØ Collab., DØ Note 5331-CONF, "Search for Neutral Higgs Boson Production in the Decay $h \rightarrow \tau_\mu\tau$ with the DØ Detector at $\sqrt{s}=1.96$ TeV" (2007).
120. S. Gennai *et al.*, Eur. Phys. J. **C52**, 383 (2007).
121. A. D. Sakharov, JETP Lett. **5**, 24 (1967).
122. M. Carena *et al.*, Nucl. Phys. **B599**, 158 (2001).
123. S. Dimopoulos and S. Thomas, Nucl. Phys. **B465**, 23, (1996);
S. Thomas, Int. J. Mod. Phys. **A13**, 2307 (1998).
124. A. Pilaftsis and C.E.M. Wagner, Nucl. Phys. **B553**, 3 (1999).
125. M. Carena *et al.*, Nucl. Phys. **B586**, 92 (2000).
126. A. Pilaftsis, Phys. Rev. **D58**, 096010 (1998); Phys. Lett. **B435**, 88 (1998);
K.S. Babu *et al.*, Phys. Rev. **D59**, 016004 (1999).
127. G.L. Kane and L.-T. Wang, Phys. Lett. **B488**, 383 (2000);
S.Y. Choi, M. Drees, and J.S. Lee, Phys. Lett. **B481**, 57 (2000);
S.Y. Choi and J.S. Lee, Phys. Rev. **D61**, 015003 (2000);
S.Y. Choi, K. Hagiwara, and J.S. Lee, Phys. Rev. **D64**, 032004 (2001); Phys. Lett. **B529**, 212 (2002);
T. Ibrahim and P. Nath, Phys. Rev. **D63**, 035009 (2001);
T. Ibrahim, Phys. Rev. **D64**, 035009 (2001);
S. Heinemeyer, Eur. Phys. J. **C22**, 521 (2001);
S.W. Ham *et al.*, Phys. Rev. **D68**, 055003 (2003).
128. M. Frank *et al.*, JHEP **0702**, 047 (2007);
S. Heinemeyer *et al.*, Phys. Lett. **B652**, 300 (2007);
T. Hahn *et al.*, arXiv:0710.4891.
129. D.A. Demir, Phys. Rev. **D60**, 055006 (1999);
S. Y. Choi *et al.*, Phys. Lett. **B481**, 57 (2000).
130. E. Christova *et al.*, Nucl. Phys. **B639**, 263 (2002) [E: Nucl. Phys. **B647**, 359 (2002)].
131. K. E. Williams and G. Weiglein, arXiv:0710.5320.
132. W. de Boer and C. Sander, Phys. Lett. **B585**, 276 (2004);
S. Heinemeyer *et al.*, JHEP **0608**, 052 (2006);
A. Djouadi *et al.*, Phys. Rev. Lett. **78**, 3626 (1997); Phys. Rev. **D57**, 4179 (1998);
S. Heinemeyer and G. Weiglein, JHEP **10** (2002) 072.;
J. Haestier *et al.*, JHEP **0512**, 027, (2005);
S. Heinemeyer, W. Hollik, and G. Weiglein, Phys. Rept. **425**, 265 (2006);
S. Heinemeyer *et al.*, arXiv:0710.2972.
133. G. D'Ambrosio *et al.*, Nucl. Phys. **B645**, 155 (2002).
134. J. R. Ellis *et al.*, JHEP **0708**, 083 (2007).
135. E. Lunghi, W. Porod, and O. Vives, Phys. Rev. **D74**, 075003 (2006).
136. M. Carena *et al.*, Phys. Rev. **D74**, 015009 (2006).
137. DØ Collab., Phys. Rev. Lett. **97**, 021802 (2006);
CDF Collab., Phys. Rev. Lett. **97**, 062003 (2006); *idem.*, Phys. Rev. Lett. **97**, 242004 (3006).
138. CDF Collab., Phys. Rev. Lett. **95**, 221805 (2005);
DØ Collab., Phys. Rev. **D** 74,031107(2006);
(**) CDF Collab., CDF Note 8956, "Search for $B_s^0 \rightarrow \mu^+\mu^-$ and $B_d^0 \rightarrow \mu^+\mu^-$ Decays in 2 fb⁻¹ of $p\bar{p}$ Collisions with CDF II" (2007);
(***) DØ Collab., DØ Note 5344-CONF, "A new upper limit for the rare decay $B_s \rightarrow \mu^+\mu^-$ " (2007).
139. J. Foster, K. i. Okumura, and L. Roszkowski, JHEP **0508**, 094 (2005);
L. Roszkowski *et al.*, JHEP **0707**, 075 (2007), Phys. Lett. **B641**, 452 (2006).
140. G. Buchalla, A. J. Buras, and M. E. Lautenbacher, Rev. Mod. Phys. **68**, 1125 (1996).
141. A. Dedes and A. Pilaftsis, Phys. Rev. **D67**, 015012 (2003).
142. A. J. Buras *et al.*, Phys. Lett. **B546**, 96 (2002).
143. A. J. Buras *et al.*, Nucl. Phys. **B659**, 2 (2003).
144. M. Misiak *et al.*, Phys. Rev. Lett. **98**, 022002 (2007), and Refs. therein.

See key on page 373

Gauge & Higgs Boson Particle Listings
Higgs Bosons — H^0 and H^\pm

145. Heavy Flavor Averaging Group (HFAG), arXiv:hep-ex/0603003.
146. T. Becher and M. Neubert, Phys. Rev. Lett. **98**, 022003 (2007).
147. BELLE Collab., Phys. Rev. Lett. **97**, 251802 (2006).
148. BABAR Collab., Phys. Rev. **D76**, 052002 (2007).
149. M. Bona *et al.*, [UTfit Collab.], JHEP **0610**, 081 (2006).
150. G. Isidori and P. Paradisi, Phys. Lett. **B639**, 499 (2006).
151. J. Ellis *et al.*, Phys. Lett. **B653**, 292 (2007).
152. N. Cabibbo, G. R. Farrar, and L. Maiani, Phys. Lett. **B105**, 155 (1981); H. Goldberg, Phys. Rev. Lett. **50**, 1419 (1983); J. R. Ellis *et al.*, Nucl. Phys. **B238**, 453 (1984); G. Bertone, D. Hooper, and J. Silk, Phys. Reports **405**, 279 (2005).
153. M. Carena, D. Hooper, and A. Vallinotto, Phys. Rev. **D75**, 055010 (2007); M. Carena, D. Hooper, and P. Skands, Phys. Rev. Lett. **97**, 051801 (2006).
154. A. Djouadi and Y. Mambrini, JHEP **0612**, 001 (2006).
155. J. Ellis, K. A. Olive, and Y. Santoso, Phys. Rev. **D71**, 095007 (2005).
156. A. Djouadi, M. Spira, and P.M. Zerwas, Z. Phys. **C70**, 675 (1996).
157. ALEPH Collab., Phys. Lett. **B543**, 1 (2002); DELPHI Collab., Phys. Lett. **B525**, 17 (2002); L3 Collab., Phys. Lett. **B575**, 208 (2003); OPAL Collab., Eur. Phys. J. **C7**, 407 (1999).
158. (*) ALEPH, DELPHI, L3 and OPAL Collaborations, The LEP Working Group for Higgs Boson Searches, *Search for Charged Higgs Bosons: Preliminary ...*, LHWG-Note/2001-05.
159. A. G. Akeroyd *et al.*, Eur. Phys. J. **C20**, 51 (2001).
160. DELPHI Collab., Eur. Phys. J. **C34**, 399 (2004).
161. J.A. Coarasa *et al.*, Eur. Phys. J. **C2**, 373 (1998).
162. C.S. Li and T.C. Yuan, Phys. Rev. **D42**, 3088 (1990); [E: Phys. Rev. **D47**, 2156 (1993); A. Czarnecki and S. Davidson, Phys. Rev. **D47**, 3063 (1993); C.S. Li, Y.-S. Wei, and J.-M. Yang, Phys. Lett. **B285**, 137 (1992).
163. J. Guasch, R.A. Jiménez, and J. Solà, Phys. Lett. **B360**, 47 (1995).
164. M. Carena *et al.*, Nucl. Phys. **B577**, 88 (2000).
165. M. Guchait and S. Moretti, JHEP **0201**, 001 (2002).
166. R.M. Barnett, H.E. Haber, and D.E. Soper, Nucl. Phys. **B306**, 697 (1988).
167. F. Olness and W.-K. Tung, Nucl. Phys. **B308**, 813 (1988).
168. F. Borzumati, J.-L. Kneur, and N. Polonsky, Phys. Rev. **D60**, 115011 (1999).
169. A. Belyaev *et al.*, JHEP **0206**, 059 (2002).
170. L.G. Jin *et al.*, Eur. Phys. J. **C14**, 91 (2000); Phys. Rev. **D62**, 053008 (2000); A. Belyaev *et al.*, Phys. Rev. **D65**, 031701 (2002); G. Gao *et al.*, Phys. Rev. **D66**, 015007 (2002).
171. S.-H. Zhu, Phys. Rev. **D67**, 075006 (2005); T. Plehn, Phys. Rev. **D67**, 014018 (2003).
172. A.A. Barrientos BendeZú and B.A. Kniehl, Phys. Rev. **D59**, 015009 (1999); Phys. Rev. **D61**, 015009 (2000); Phys. Rev. **D63**, 015009 (2001).
173. A.A. Barrientos BendeZú and B.A. Kniehl, Nucl. Phys. **B568**, 305 (2000).
174. A. Krause *et al.*, Nucl. Phys. **B519**, 85 (1998).
175. O. Brein and W. Hollik, Eur. Phys. J. **C13**, 175 (2000).
176. DØ Collab., Phys. Rev. Lett. **82**, 4975 (1999); *idem.*, **88**, 151803 (2002); CDF Collab., Phys. Rev. **D62**, 012004 (2000); *idem.*, Phys. Rev. Lett. **79**, 357 (1997).
177. CDF Collab., Phys. Rev. Lett. **96**, 042003 (2006).
178. G.B. Gelmini and M. Roncadelli, Phys. Lett. **B99**, 411 (1981); R.N. Mohapatra and J.D. Vergados, Phys. Rev. Lett. **47**, 1713 (1981); V. Barger *et al.*, Phys. Rev. **D26**, 218 (1982).
179. B. Dutta and R.N. Mohapatra, Phys. Rev. **D59**, 015018-1 (1999); C. S. Aulakh *et al.*, Phys. Rev. **D58**, 115007 (1998); C. S. Aulakh, A. Melfo, and G. Senjanovic, Phys. Rev. **D57**, 4174 (1998).
180. DELPHI Collab., Phys. Lett. **B552**, 127 (2003).
181. OPAL Collab., Phys. Lett. **B295**, 347 (1992); *idem.*, **B526**, 221 (2002).
182. L3 Collab., Phys. Lett. **B576**, 18 (2003).
183. OPAL Collab., Phys. Lett. **B577**, 93 (2003).
184. DØ Collab., Phys. Rev. Lett. **93**, 141801 (2004); (***) DØ Collab., DØ Note 5458-CONF, “Search for Pair Production of Doubly-charged Higgs Bosons in the $H^{++}H^{--}$ to 4 muons final state”.
185. CDF Collab., Phys. Rev. Lett. **93**, 221802 (2004); (***) CDF Collab., CDF Note 8624, “Search for Doubly-Charged Higgs Bosons with Lepton-Flavor-Violating Decays involving Tau Leptons,” submitted to Phys. Rev. Lett. (2007).
186. CDF Collab., Phys. Rev. Lett. **95**, 071801 (2005).
187. H.E. Haber, *Proceedings of the 1990 Theoretical Advanced Study Institute in Elementary Particle Physics*, edited by M. Cvetič and Paul Langacker (World Scientific, Singapore, 1991) pp. 340–475, and References therein.
188. S. Glashow and S. Weinberg, Phys. Rev. **D15**, 1958 (1977).
189. P. Fayet, Phys. Lett. **B90**, 104 (1975); H.-P. Nilles, M. Srednicki, and D. Wyler, Phys. Lett. **B120**, 346 (1983); J.-M. Frere, D.R.T. Jones, and S. Raby, Nucl. Phys. **B222**, 11 (1983); J.-P. Derendinger and C.A. Savoy, Nucl. Phys. **B237**, 307 (1984); B.R. Greene and P.J. Miron, Phys. Lett. **B168**, 226 (1986); J. Ellis *et al.*, Phys. Lett. **B176**, 403 (1986); L. Durand and J.L. Lopez, Phys. Lett. **B217**, 463 (1989); M. Drees, Int. J. Mod. Phys. **A4**, 3635 (1989); U. Ellwanger, Phys. Lett. **B303**, 271 (1993); U. Ellwanger, M. Rausch de Taubenberg, and C.A. Savoy, Phys. Lett. **B315**, 331 (1993); Z. Phys. **C67**, 665 (1995); Phys. Lett. **B492**, 21 (1997); P.N. Pandita, Phys. Lett. **B318**, 338 (1993); Z. Phys. **C59**, 575 (1993); T. Elliott, S.F. King, and P.L. White, Phys. Lett. **B305**,

Gauge & Higgs Boson Particle Listings

Higgs Bosons — H^0 and H^\pm

- 71 (1993); Phys. Lett. **B314**, 56 (1993); Phys. Rev. **D49**, 2435 (1994); Phys. Lett. **B351**, 213 (1995); K.S. Babu and S.M. Barr, Phys. Rev. **D49**, R2156 (1994); S.F. King and P.L. White, Phys. Rev. **D52**, 4183 (1995); N. Haba, M. Matsuda, and M. Tanimoto, Phys. Rev. **D54**, 6928 (1996); F. Franke and H. Fraas, Int. J. Mod. Phys. **A12**, 479 (1997); S.W. Ham, S.K. Oh, and H.S. Song, Phys. Rev. **D61**, 055010 (2000); D.A. Demir, E. Ma, and U. Sarkar, J. Phys. **G26**, L117, (2000); R. B. Nevzorov and M. A. Trusov, Phys. Atom. Nucl. **64**, 1299 (2001); U. Ellwanger and C. Hugonie, Eur. Phys. J. **C25**, 297 (2002); U. Ellwanger *et al.*, arXiv:hep-ph/0305109; D. J. Miller and S. Moretti, arXiv:hep-ph/0403137.
190. A. Dedes *et al.*, Phys. Rev. **D63**, 055009 (2001); A. Menon, D. Morrissey, and C.E.M. Wagner, Phys. Rev. **D70**, 035005 (2004).
191. J. R. Espinosa and M. Quiros, Phys. Lett. **B279**, 92 (1992).
192. U. Ellwanger and C. Hugonie, Mod. Phys. Lett. **A22**, 1581 (2007).
193. (*) DELPHI Collab., *Interpretation of the searches for Higgs bosons in the MSSM with an additional scalar singlet*, DELPHI 1999-97 CONF 284.
194. P. Batra *et al.*, JHEP **0402**, 043 (2004); P. Batra *et al.*, JHEP **0406**, 032 (2004).
195. M. Dine, N. Seiberg, and S. Thomas, Phys. Rev. **D76**, 095004 (2007) and Refs. therein.
196. J. R. Espinosa and M. Quiros, Phys. Rev. Lett. **81**, 516 (1998).
197. M. Perelstein, Prog. Part. Nucl. Phys. **58**, 247 (2007).
198. M. Schmaltz and D. Tucker-Smith, Ann. Rev. Nucl. Part. Sci. **55**, 229 (2005).
199. C. R. Chen, K. Tobe, and C. P. Yuan, Phys. Lett. **B640**, 263 (2006).
200. G. F. Giudice *et al.*, JHEP **0706**, 045 (2007).
201. J. Hubisz *et al.*, JHEP **0601**, 135 (2006).
202. I. Low, W. Skiba, and D. Smith, Phys. Rev. **D66**, 072001 (2002).
203. G. F. Giudice, R. Rattazzi, and J. D. Wells, Nucl. Phys. **B595**, 250 (2001); M. Chaichian *et al.*, Phys. Lett. **B524**, 161 (2002); D. Dominici *et al.*, Acta Phys. Polon. **B33**, 2507 (2002); J. L. Hewett and T. G. Rizzo, JHEP **0308**, 028 (2003).
204. OPAL Collab., Phys. Lett. **B609**, 20 (2005).
205. S. Chivukula *et al.*, *Dynamical Electroweak Symmetry Breaking*, in this volume.
206. Y. Chikashige *et al.*, Phys. Lett. **98B**, 265 (1981); A.S. Joshipura and S.D. Rindani, Phys. Rev. Lett. **69**, 3269 (1992); F. de Campos *et al.*, Phys. Rev. **D55**, 1316 (1997).
207. DELPHI Collab., Eur. Phys. J. **C32**, 475 (2004); L3 Collab., Phys. Lett. **B609**, 35 (2005); OPAL Collab., Phys. Lett. **B377**, 273 (1996).
208. (*) ALEPH, DELPHI, L3 and OPAL Collaborations, The LEP Working Group for Higgs Boson Searches, *Search for Invisible Higgs Bosons: Preliminary ...*, LHWG-Note/2001-06.
209. E. L. Berger *et al.*, Phys. Rev. **D66**, 095001 (2002).
210. W. Loinaz and J. Wells, Phys. Lett. **B445**, 178 (1998); X. Calmet and H. Fritzsch, Phys. Lett. **B496**, 190 (2000).
211. ALEPH Collab., Phys. Lett. **B544**, 25 (2002); DELPHI Collab., Eur. Phys. J. **C44**, 147 (2005); L3 Collab., Phys. Lett. **B583**, 14 (2004); OPAL Collab., Eur. Phys. J. **C18**, 425 (2001).
212. (*) The LEP Working Group for Higgs Boson Searches, *Flavour Independent Search for Hadronically Decaying Neutral Higgs Bosons at LEP*, LHWG Note 2001-07.
213. OPAL Collab., Eur. Phys. J. **C18**, 425 (2001); DELPHI Collab., Eur. Phys. J. **C38**, 1 (2004).
214. J. Ellis *et al.*, Nucl. Phys. **B106**, 292 (1976); A. Abbasabadi *et al.*, Phys. Rev. **D52**, 3919 (1995); R.N. Cahn *et al.*, Phys. Lett. **B82**, 113 (1997).
215. G. Gamberini *et al.*, Nucl. Phys. **B292**, 237 (1987); R. Bates *et al.*, Phys. Rev. **D34**, 172 (1986); K. Hagiwara *et al.*, Phys. Lett. **B318**, 155 (1993); O.J.P. Éboli *et al.*, Phys. Lett. **B434**, 340 (1998).
216. A. G. Akeroyd, Phys. Lett. **B368**, 89 (1996); H. Haber *et al.*, Nucl. Phys. **B161**, 493 (1979).
217. ALEPH Collab., Phys. Lett. **B544**, 16 (2002); DELPHI Collab., Eur. Phys. J. **C35**, 313 (2004); OPAL Collab., Phys. Lett. **B544**, 44 (2002).
218. L3 Collab., Phys. Lett. **B534**, 28 (2002).
219. ALEPH Collab., Eur. Phys. J. **C49**, 439 (2007).
220. (*) ALEPH, DELPHI, L3 and OPAL Collaborations, The LEP Working Group for Higgs Boson Searches, *Search for Higgs Bosons Decaying into Photons: Combined ...*, LHWG Note/2002-02.
221. DØ Collab., Phys. Rev. Lett. **82**, 2244 (1999); CDF Collab., Phys. Rev. **D64**, 092002 (2001).
222. (***) DØ Collab., DØ Note 5426-CONF, “Search for Light Higgs Boson in $\gamma\gamma + X$ Final State with the DØ Detector at $\sqrt{s} = 1.96$ TeV” (2007).
223. (***) DØ Collab., DØ Note 5067-CONF, “Search for Fermiophobic Higgs Boson in $3\gamma + X$ Events” (2007).
224. G.J. Gounaris *et al.*, Phys. Lett. **B83**, 191 (1979); V. Barger *et al.*, Phys. Rev. **D38**, 2766 (1988); F. Boudjema and E. Chopin, Z. Phys. **C37**, 85 (1996); A. Djouadi *et al.*, Eur. Phys. J. **C10**, 27 (1999).

STANDARD MODEL H^0 (Higgs Boson) MASS LIMITS

These limits apply to the Higgs boson of the three-generation Standard Model with the minimal Higgs sector. For a review and a bibliography, see the Note above on “Searches for Higgs Bosons.”

Limits from Coupling to Z/W^\pm

Limits on the Standard Model Higgs obtained from the study of Z^0 decays rule out conclusively its existence in the whole mass region $m_{H^0} \lesssim 60$ GeV. These limits, as well as stronger limits obtained from e^+e^- collisions at LEP at energies up to 202 GeV, and weaker limits obtained from other sources, have been superseded by the more recent data of LEP. They have been removed from this compilation, and are documented in previous editions of this Review of Particle Physics.

In this Section, unless otherwise stated, limits from the four LEP experiments (ALEPH, DELPHI, L3, and OPAL) are obtained from the study of the $e^+e^- \rightarrow H^0 Z$ process, at center-of-mass energies reported in the comment lines.

VALUE (GeV)	CL%	DOCUMENT ID	TECN	COMMENT
>114.1	95	¹ ABDALLAH	04 DLFH	$E_{\text{cm}} \leq 209$ GeV
>112.7	95	¹ ABBIENDI	03B OPAL	$E_{\text{cm}} \leq 209$ GeV
> 114.4	95	^{1,2} HEISTER	03D LEP	$E_{\text{cm}} \leq 209$ GeV
>111.5	95	^{1,3} HEISTER	02 ALEP	$E_{\text{cm}} \leq 209$ GeV
>112.0	95	¹ ACHARD	01c L3	$E_{\text{cm}} \leq 209$ GeV

See key on page 373

Gauge & Higgs Boson Particle Listings

Higgs Bosons — H^0 and H^\pm

• • • We do not use the following data for averages, fits, limits, etc. • • •

4	ABAZOV	07X	D0	$p\bar{p} \rightarrow H^0 Z X$
5	ABAZOV	06	D0	$p\bar{p} \rightarrow H^0 X, H^0 \rightarrow WW^*$
6	ABAZOV	06Q	D0	$p\bar{p} \rightarrow H^0 WX, H^0 \rightarrow WW^*$
7	ABAZOV	06Q	D0	$p\bar{p} \rightarrow H^0 Z X$
8	ABAZOV	06Q	D0	$p\bar{p} \rightarrow H^0 WX$
9	ABULENCIA	06H	CDF	$p\bar{p} \rightarrow H^0 WX$
10	ABULENCIA	06A	CDF	$p\bar{p} \rightarrow H^0 X, H^0 \rightarrow WW^*$
11	ABAZOV	05F	D0	$p\bar{p} \rightarrow H^0 WX$
12	ACOSTA	05K	CDF	$p\bar{p} \rightarrow H^0 Z X$
13	ABE	98T	CDF	$p\bar{p} \rightarrow H^0 WX, H^0 Z X$

¹ Search for $e^+e^- \rightarrow H^0 Z$ in the final states $H^0 \rightarrow b\bar{b}$ with $Z \rightarrow \ell\bar{\ell}, \nu\bar{\nu}, q\bar{q}, \tau^+\tau^-$ and $H^0 \rightarrow \tau^+\tau^-$ with $Z \rightarrow q\bar{q}$.

² Combination of the results of all LEP experiments.

³ A 3σ excess of candidate events compatible with m_{H^0} near 114 GeV is observed in the combined channels $q\bar{q}q\bar{q}, q\bar{q}\ell\bar{\ell}, q\bar{q}\tau^+\tau^-$.

⁴ ABAZOV 07X search for associated $H^0 Z$ production in $p\bar{p}$ collisions at $E_{cm} = 1.96$ TeV in the final state $Z \rightarrow e^+e^-$ or $\mu^+\mu^-$; $H^0 \rightarrow b\bar{b}$. A limit $\sigma(ZH^0) \cdot B(H^0 \rightarrow b\bar{b}) < (4.4-3.1)$ pb (95%CL) is given for $m_{H^0} = 105-145$ GeV, which is more than 40 times larger than the expected Standard Model cross section.

⁵ ABAZOV 06 search for Higgs boson production in $p\bar{p}$ collisions at $E_{cm} = 1.96$ TeV with the decay chain $H^0 \rightarrow WW^* \rightarrow \ell^\pm \nu \ell^\mp \bar{\nu}$. A limit $\sigma(H^0) \cdot B(H^0 \rightarrow WW^*) < (5.6-3.2)$ pb (95%CL) is given for $m_{H^0} = 120-200$ GeV, which far exceeds the expected Standard Model cross section.

⁶ ABAZOV 06Q search for associated $H^0 W$ production in $p\bar{p}$ collisions at $E_{cm} = 1.96$ TeV with the decay $H^0 \rightarrow WW^* \rightarrow \ell^\pm \ell'^\mp \nu \nu' X$ where $\ell = e, \mu$. A limit $\sigma(H^0 W) \cdot B(H^0 \rightarrow WW^*) < (3.2-2.8)$ pb (95%CL) is given for $m_{H^0} = 115-175$ GeV, which far exceeds the expected Standard Model cross section.

⁷ ABAZOV 06Q search for associated $H^0 Z$ production in $p\bar{p}$ collisions at $E_{cm} = 1.96$ TeV with $Z \rightarrow \nu\bar{\nu}$ and $H^0 \rightarrow b\bar{b}$. A limit $\sigma(H^0 Z) \cdot B(H^0 \rightarrow b\bar{b}) < (3.4-2.5)$ pb (95%CL) for $m_{H^0} = 105-135$ GeV is derived, which is more than one order of magnitude larger than the expected Standard Model cross section.

⁸ ABAZOV 06Q search for associated $H^0 W$ production in $p\bar{p}$ collisions at $E_{cm} = 1.96$ TeV with $W \rightarrow \ell\nu$ (ℓ missing) and $H^0 \rightarrow b\bar{b}$. A limit $\sigma(H^0 W) \cdot B(H^0 \rightarrow b\bar{b}) < (8.3-6.3)$ pb (95%CL) for $m_{H^0} = 105-135$ GeV is derived, which is more than one order of magnitude larger than the expected Standard Model cross section.

⁹ ABULENCIA 06H search for associated $H^0 W$ production in $p\bar{p}$ collisions at $E_{cm} = 1.96$ TeV in the final state $W \rightarrow e\nu, \mu\nu$; $H^0 \rightarrow b\bar{b}$. A limit $\sigma(WH^0) \cdot B(H^0 \rightarrow b\bar{b}) < (10-3)$ pb (95%CL) is given for $m_{H^0} = 110-150$ GeV, which is more than 50 times larger than the expected Standard Model cross section.

¹⁰ ABULENCIA, A 06A search for Higgs boson production in $p\bar{p}$ collisions at $E_{cm} = 1.96$ TeV with the decay chain $H^0 \rightarrow WW^* \rightarrow e^+e^- \nu\bar{\nu}, e^\pm \mu^\mp \nu\bar{\nu}, \mu^+\mu^- \nu\bar{\nu}$. A limit $\sigma(H^0) \cdot B(H^0 \rightarrow WW^*) < (3.2-5.2)$ pb (95%CL) is given for $m_{H^0} = 120-200$ GeV, which far exceeds the expected Standard Model cross section.

¹¹ ABAZOV 05F search for associated $H^0 W$ production in $p\bar{p}$ collisions at $E_{cm} = 1.96$ TeV in the final state $W \rightarrow e\nu, H^0 \rightarrow b\bar{b}$. A limit $\sigma(WH^0) \cdot B(H^0 \rightarrow b\bar{b}) < [9.0, 9.1, 12.2]$ pb (95%CL) is given for $m_{H^0} = [115, 125, 135]$ GeV, which far exceeds the expected Standard Model cross section.

¹² ACOSTA 05K search for associated $H^0 Z$ production in $p\bar{p}$ collisions at $E_{cm} = 1.8$ TeV with $Z \rightarrow \ell\bar{\ell}, \nu\bar{\nu}$ and $H^0 \rightarrow b\bar{b}$. Combined with ABE 98T, a limit $\sigma(H^0 + W/Z) \cdot B(H^0 \rightarrow b\bar{b}) < (7.8-6.6)$ pb (95%CL) for $m_{H^0} = 90-130$ GeV is derived, which is more than one order of magnitude larger than the expected Standard Model cross section.

¹³ ABE 98T search for associated $H^0 W$ and $H^0 Z$ production in $p\bar{p}$ collisions at $\sqrt{s} = 1.8$ TeV with $W(Z) \rightarrow q\bar{q}(\ell)$, $H^0 \rightarrow b\bar{b}$. The results are combined with the search in ABE 97W, resulting in the cross-section limit $\sigma(H^0 + W/Z) \cdot B(H^0 \rightarrow b\bar{b}) < (23-17)$ pb (95%CL) for $m_{H^0} = 70-140$ GeV. This limit is one to two orders of magnitude larger than the expected cross section in the Standard Model.

H^0 Indirect Mass Limits from Electroweak Analysis

For limits obtained before the direct measurement of the top quark mass, see the 1996 (Physical Review **D54** 1 (1996)) Edition of this Review. Other studies based on data available prior to 1996 can be found in the 1998 Edition (The European Physical Journal **C3** 1 (1998)) of this Review. For indirect limits obtained from other considerations of theoretical nature, see the Note on "Searches for Higgs Bosons."

VALUE (GeV)	DOCUMENT ID	TECN
129^{+74}_{-49}	14 LEP-SLC	06 RVUE

¹⁴ LEP-SLC 06 make Standard Model fits to Z parameters from LEP/SCL and m_t, m_W , and Γ_W measurements available in 2005 with $\Delta\alpha_{had}^{(5)}(m_Z) = 0.02758 \pm 0.00035$. The 95% CL limit is 285 GeV.

MASS LIMITS FOR NEUTRAL HIGGS BOSONS IN SUPERSYMMETRIC MODELS

The minimal supersymmetric model has two complex doublets of Higgs bosons. The resulting physical states are two scalars [H_1^0 and H_2^0], where we define $m_{H_1^0} < m_{H_2^0}$, a pseudoscalar (A^0), and a charged Higgs pair

(H^\pm). H_1^0 and H_2^0 are also called h and H in the literature. There are two free parameters in the theory which can be chosen to be m_{A^0} and $\tan\beta = v_2/v_1$, the ratio of vacuum expectation values of the two Higgs doublets. Tree-level Higgs masses are constrained by the model to be $m_{H_1^0} \leq$

$m_Z, m_{H_2^0} \geq m_Z, m_{A^0} \geq m_{H_1^0}$, and $m_{H^\pm} \geq m_W$. However, as described in the review on "Searches for Higgs Bosons" in this Volume these relations are violated by radiative corrections.

Unless otherwise noted, the experiments in e^+e^- collisions search for the processes $e^+e^- \rightarrow H_1^0 Z^0$ in the channels used for the Standard Model Higgs searches and $e^+e^- \rightarrow H_1^0 A^0$ in the final states $b\bar{b}b\bar{b}$ and $b\bar{b}\tau^+\tau^-$. Limits on the A^0 mass arise from these direct searches, as well as from the relations valid in the minimal supersymmetric model between m_{A^0} and $m_{H_1^0}$. As discussed in the review on "Searches for Higgs Bosons" in this Volume, these relations depend, via potentially large radiative corrections, on the mass of the t quark and on the supersymmetric parameters, in particular those of the stop sector. The limits are weaker for larger t and \bar{t} masses. To include the radiative corrections to the Higgs masses, unless otherwise stated, the listed papers use the two-loop results with $m_t = 175$ GeV, the universal scalar mass of 1 TeV, SU(2) gaugino mass of 200 GeV, and the Higgsino mass parameter $\mu = +200$ GeV or $\mu = -200$ GeV, and examine the two scenarios of no scalar top mixing and the m_h^{\max} benchmark scenario (which gives rise to the most conservative upper bound on the mass of H_1^0 for given values of m_{A^0} and $\tan\beta$), see CARENA 99B and CARENA 03.

Limits in the low-mass region of H_1^0 , as well as other by now obsolete limits from different techniques, have been removed from this compilation, and can be found in earlier editions of this Review. Unless otherwise stated, the following results assume no invisible H_1^0 or A^0 decays.

H_1^0 (Higgs Boson) MASS LIMITS in Supersymmetric Models

VALUE (GeV)	CL%	DOCUMENT ID	TECN	COMMENT
> 92.8	95	15 SCHAEEL	06B LEP	
> 84.5	95	16,17 ABBIENDI	04M OPAL	$E_{cm} \leq 209$ GeV
> 89.7	95	16,18 ABDALLAH	04 DLPH	$E_{cm} \leq 209$ GeV, $\tan\beta > 0.4$
> 86.0	95	16,19 ACHARD	02H L3	$E_{cm} \leq 209$ GeV, $\tan\beta > 0.4$
> 100	95	20 AFFOLDER	01D CDF	$p\bar{p} \rightarrow b\bar{b}H_1^0, \tan\beta \gtrsim 55$

• • • We do not use the following data for averages, fits, limits, etc. • • •

21 ABBIENDI 03G OPAL $H_1^0 \rightarrow A^0 A^0$

22 HEISTER 02 ALEP $E_{cm} \leq 209$ GeV, $\tan\beta > 0.5$

¹⁵ SCHAEEL 06B make a combined analysis of the LEP data. The quoted limit is for the m_h^{\max} scenario with $m_t = 174.3$ GeV. In the CP-violating CPX scenario no lower bound on $m_{H_1^0}$ can be set at 95% CL. See paper for excluded regions in various scenarios. See Figs. 2-6 and Tabs. 14-21 for limits on $\sigma(ZH^0) \cdot B(H^0 \rightarrow b\bar{b}, \tau^+\tau^-)$ and $\sigma(H_1^0 H_2^0) \cdot B(H_1^0 H_2^0 \rightarrow b\bar{b}, \tau^+\tau^-)$.

¹⁶ Search for $e^+e^- \rightarrow H_1^0 A^0$ in the final states $b\bar{b}b\bar{b}$ and $b\bar{b}\tau^+\tau^-$, and $e^+e^- \rightarrow H_1^0 Z$. Universal scalar mass of 1 TeV, SU(2) gaugino mass of 200 GeV, and $\mu = -200$ GeV are assumed, and two-loop radiative corrections incorporated. The limits hold for $m_t = 175$ GeV, and for the m_h^{\max} scenario.

¹⁷ ABBIENDI 04M exclude $0.7 < \tan\beta < 1.9$, assuming $m_t = 174.3$ GeV. Limits for other MSSM benchmark scenarios, as well as for CP violating cases, are also given.

¹⁸ This limit applies also in the no-mixing scenario. Furthermore, ABDALLAH 04 excludes the range $0.54 < \tan\beta < 2.36$. The limit improves in the region $\tan\beta < 6$ (see Fig. 28). Limits for $\mu = 1$ TeV are given in Fig. 30.

¹⁹ ACHARD 02H also search for the final state $H_1^0 Z \rightarrow 2A^0 q\bar{q}, A^0 \rightarrow q\bar{q}$. In addition, the MSSM parameter set in the "large- μ " and "no-mixing" scenarios are examined.

²⁰ AFFOLDER 01D search for final states with 3 or more b -tagged jets. See Figs. 2 and 3 for Higgs mass limits as a function of $\tan\beta$, and for different stop mixing scenarios. Stronger limits are obtained at larger $\tan\beta$ values.

²¹ ABBIENDI 03G search for $e^+e^- \rightarrow H_1^0 Z$ followed by $H_1^0 \rightarrow A^0 A^0, A^0 \rightarrow c\bar{c}, gg$, or $\tau^+\tau^-$. In the no-mixing scenario, the region $m_{H_1^0} = 45-85$ GeV and $m_{A^0} = 2-9.5$ GeV is excluded at 95% CL.

²² HEISTER 02 excludes the range $0.7 < \tan\beta < 2.3$. A wider range is excluded with different stop mixing assumptions. Updates BARATE 01C.

A^0 (Pseudoscalar Higgs Boson) MASS LIMITS in Supersymmetric Models

VALUE (GeV)	CL%	DOCUMENT ID	TECN	COMMENT
> 93.4	95	23 SCHAEEL	06B LEP	
> 85.0	95	24,25 ABBIENDI	04M OPAL	$E_{cm} \leq 209$ GeV
> 90.4	95	24,26 ABDALLAH	04 DLPH	$E_{cm} \leq 209$ GeV, $\tan\beta > 0.4$
> 86.5	95	24,27 ACHARD	02H L3	$E_{cm} \leq 209$ GeV, $\tan\beta > 0.4$
> 90.1	95	24,28 HEISTER	02 ALEP	$E_{cm} \leq 209$ GeV, $\tan\beta > 0.5$
> 100	95	29 AFFOLDER	01D CDF	$p\bar{p} \rightarrow b\bar{b}A^0, \tan\beta \gtrsim 55$

• • • We do not use the following data for averages, fits, limits, etc. • • •

30 ABAZOV 06J D0 $p\bar{p} \rightarrow H^0 X, H^0 \rightarrow \tau^+\tau^-$

31 ABULENCIA 06 CDF $p\bar{p} \rightarrow H_{1,2}^0/A^0 + X$

32 ABAZOV 05T D0 $p\bar{p} \rightarrow b\bar{b}H_{1,2}^0/A^0 + X$

33 ACOSTA 05Q CDF $p\bar{p} \rightarrow H_{1,2}^0/A^0 + X$

34 ABBIENDI 03G OPAL $H_1^0 \rightarrow A^0 A^0$

35 AKEROYD 02 RVUE

Gauge & Higgs Boson Particle Listings

Higgs Bosons — H^0 and H^\pm

- 23 SCHAEEL 06b make a combined analysis of the LEP data. The quoted limit is for the m_h^{\max} scenario with $m_t = 174.3$ GeV. In the CP -violating CPX scenario no lower bound on $m_{H_1^0}$ can be set at 95% CL. See paper for excluded regions in various scenarios. See Figs. 2-6 and Tabs. 14-21 for limits on $\sigma(ZH^0) \cdot B(H^0 \rightarrow b\bar{b}, \tau^+\tau^-)$ and $\sigma(H_1^0 H_2^0) \cdot B(H_1^0 H_2^0 \rightarrow b\bar{b}, \tau^+\tau^-)$.
- 24 Search for $e^+e^- \rightarrow H_1^0 A^0$ in the final states $b\bar{b}b\bar{b}$ and $b\bar{b}\tau^+\tau^-$, and $e^+e^- \rightarrow H_1^0 Z$. Universal scalar mass of 1 TeV, SU(2) gaugino mass of 200 GeV, and $\mu = -200$ GeV are assumed, and two-loop radiative corrections incorporated. The limits hold for $m_t=175$ GeV, and for the m_h^{\max} scenario.
- 25 ABBIENDI 04M exclude $0.7 < \tan\beta < 1.9$, assuming $m_t = 174.3$ GeV. Limits for other MSSM benchmark scenarios, as well as for CP violating cases, are also given.
- 26 This limit applies also in the no-mixing scenario. Furthermore, ABDALLAH 04 excludes the range $0.54 < \tan\beta < 2.36$. The limit improves in the region $\tan\beta < 6$ (see Fig. 28). Limits for $\mu = 1$ TeV are given in Fig. 30.
- 27 ACHARD 02H also search for the final state $H_1^0 Z \rightarrow 2A^0 q\bar{q}, A^0 \rightarrow q\bar{q}$. In addition, the MSSM parameter set in the "large- μ " and "no-mixing" scenarios are examined.
- 28 HEISTER 02 excludes the range $0.7 < \tan\beta < 2.3$. A wider range is excluded with different stop mixing assumptions. Updates BARATE 01c.
- 29 AFFOLDER 01D search for final states with 3 or more b -tagged jets. See Figs. 2 and 3 for Higgs mass limits as a function of $\tan\beta$, and for different stop mixing scenarios. Stronger limits are obtained at larger $\tan\beta$ values.
- 30 ABAZOV 06a search for Higgs boson production in $p\bar{p}$ collisions at $E_{cm} = 1.96$ TeV with the decay $H_{1,2}^0, A^0 \rightarrow \tau^+\tau^-$. See their Fig. 3 for the region in the MSSM parameter space excluded by this analysis and the results or ABAZOV 05T.
- 31 ABULENCIA 06 search for $H_{1,2}^0/A^0$ production in $p\bar{p}$ collisions at $E_{cm} = 1.96$ TeV with $H_{1,2}^0/A^0 \rightarrow \tau^+\tau^-$. A region with $\tan\beta > 40$ (100) is excluded for $m_{A^0} = 90$ (170) GeV.
- 32 ABAZOV 05T search for $H_{1,2}^0/A^0$ production in association with bottom quarks in $p\bar{p}$ collisions at $E_{cm} = 1.96$ TeV, with the $b\bar{b}$ decay mode. See their Fig. 5 for the excluded parameter regions in the m_h^{\max} and no-mixing scenarios for $\mu = -200$ GeV.
- 33 ACOSTA 05q search for $H_{1,2}^0/A^0$ production in $p\bar{p}$ collisions at $E_{cm} = 1.8$ TeV with $H_{1,2}^0/A^0 \rightarrow \tau^+\tau^-$. At $m_{A^0} = 100$ GeV, the obtained cross section upper limit is above theoretical expectation.
- 34 ABBIENDI 03g search for $e^+e^- \rightarrow H_1^0 Z$ followed by $H_1^0 \rightarrow A^0 A^0, A^0 \rightarrow c\bar{c}, gg$, or $\tau^+\tau^-$. In the no-mixing scenario, the region $m_{H_1^0} = 45-85$ GeV and $m_{A^0} = 2-9.5$ GeV is excluded at 95% CL.
- 35 AKEROYD 02 examine the possibility of a light A^0 with $\tan\beta < 1$. Electroweak measurements are found to be inconsistent with such a scenario.

 H^0 (Higgs Boson) MASS LIMITS in Extended Higgs Models

This Section covers models which do not fit into either the Standard Model or its simplest minimal Supersymmetric extension (MSSM), leading to anomalous production rates, or nonstandard final states and branching ratios. In particular, this Section covers limits which may apply to generic two-Higgs-doublet models (2HDM), or to special regions of the MSSM parameter space where decays to invisible particles or to photon pairs are dominant (see the Note on 'Searches for Higgs Bosons' at the beginning of this Chapter). See the footnotes or the comment lines for details on the nature of the models to which the limits apply.

VALUE (GeV)	CL%	DOCUMENT ID	TECN	COMMENT
• • •		We do not use the following data for averages, fits, limits, etc. • • •		
>105.8	95	36 ABBIENDI 07 OPAL 37 SCHAEEL 07 ALEP		invisible H^0 , large width $e^+e^- \rightarrow H^0 Z, H^0 \rightarrow W W^*$
none 1-55	95	38 ABBIENDI 05A OPAL		H_1^0 , Type II model
none 3-63	95	38 ABBIENDI 05A OPAL		A^0 , Type II model
>110.6	95	39 ABDALLAH 05D DLPH		$H^0 \rightarrow 2$ jets
>112.3	95	40 ACHARD 05 L3		invisible H^0
>104	95	41 ABBIENDI 04K OPAL		$H^0 \rightarrow 2$ jets
>112.1	95	42 ABDALLAH 04 DLPH		$H^0 V V$ couplings
>104.1	95	40 ABDALLAH 04B DLPH 43,44 ABDALLAH 04L DLPH		Invisible H^0 $e^+e^- \rightarrow H^0 Z, H^0 \rightarrow \gamma\gamma$
>110.3	95	45 ABDALLAH 04o DLPH 46 ABDALLAH 04o DLPH		$Z \rightarrow f\bar{f}H^0$ $e^+e^- \rightarrow H^0 Z, H^0 A^0$
>107	95	47 ACHARD 04B L3 48 ACHARD 04F L3		$H^0 \rightarrow 2$ jets Anomalous coupling
>105.5	95	49 ABBIENDI 03F OPAL		$e^+e^- \rightarrow H^0 Z, H^0 \rightarrow$ any
>105.4	95	50 ABBIENDI 03G OPAL		$H^0 \rightarrow A^0 A^0$
>114.1	95	51 ACHARD 03C L3		$H^0 \rightarrow W W^*, Z Z^*, \gamma\gamma$
>105.4	95	52 ABBIENDI 02D OPAL		$e^+e^- \rightarrow b\bar{b}H$
>109.1	95	43,53 ABBIENDI 02F OPAL		$H^0 \rightarrow \gamma\gamma$
>109.1	95	54 ACHARD 02C L3		$H_1^0 \rightarrow \gamma\gamma$
>109.1	95	40 HEISTER 02 ALEP		Invisible $H^0, E_{cm} \leq 209$ GeV
>109.1	95	43,55 HEISTER 02L ALEP		$H_1^0 \rightarrow \gamma\gamma$
none 1-44	95	56 HEISTER 02M ALEP		$H^0 \rightarrow 2$ jets or $\tau^+\tau^-$
none 12-56	95	57 ABBIENDI 01E OPAL		H_1^0 , Type-II model
> 98	95	57 ABBIENDI 01E OPAL		A^0 , Type-II model
>106.4	95	58 AFFOLDER 01H CDF		$p\bar{p} \rightarrow H^0 W/Z, H^0 \rightarrow \gamma\gamma$
> 89.2	95	40 BARATE 01c ALEP 59 ACCIARRI 00M L3		Invisible $H^0, E_{cm} \leq 202$ GeV Invisible H^0

60 ACCIARRI 00R L3		$e^+e^- \rightarrow H^0 \gamma$ and/or $H^0 \rightarrow \gamma\gamma$
61 ACCIARRI 00R L3		$e^+e^- \rightarrow e^+e^- H^0$
> 94.9	95	62 ACCIARRI 00s L3 $e^+e^- \rightarrow H^0 Z, H^0 \rightarrow \gamma\gamma$
>100.7	95	63 BARATE 00L ALEP $e^+e^- \rightarrow H^0 Z, H^0 \rightarrow \gamma\gamma$
> 68.0	95	64 ABBIENDI 99E OPAL $\tan\beta > 1$
> 96.2	95	65 ABBIENDI 99o OPAL $e^+e^- \rightarrow H^0 Z, H^0 \rightarrow \gamma\gamma$
> 78.5	95	66 ABBOTT 99B D0 $p\bar{p} \rightarrow H^0 W/Z, H^0 \rightarrow \gamma\gamma$
		67 ABREU 99P DLPH $e^+e^- \rightarrow H^0 \gamma$ and/or $H^0 \rightarrow \gamma\gamma$
		68 GONZALEZ-G. 98B RVUE Anomalous coupling
		69 KRAWCZYK 97 RVUE $(g-2)_\mu$
		70 ALEXANDER 96H OPAL $Z \rightarrow H^0 \gamma$
		71 ABREU 95H DLPH $Z \rightarrow H^0 Z^*, H^0 A^0$
		72 PICH 92 RVUE Very light Higgs
36 ABBIENDI 07 search for $e^+e^- \rightarrow H^0 Z$ with $Z \rightarrow q\bar{q}$ and H^0 decaying to invisible final states. The H^0 width is varied between 1 GeV and 3 TeV. A limit $\sigma \cdot B(H^0 \rightarrow \text{invisible}) < (0.07-0.57)$ pb (95%CL) is obtained at $E_{cm} = 206$ GeV for $m_{H^0} = 60-114$ GeV.		
37 SCHAEEL 07 search for Higgs bosons in association with a fermion pair and decaying to $W W^*$. The limit is from this search and HEISTER 02L for a H^0 with SM production cross section and $B(H^0 \rightarrow f\bar{f}) = 0$ for all fermions f .		
38 ABBIENDI 05A search for $e^+e^- \rightarrow H_1^0 A^0$ in general Type-II two-doublet models, with decays $H_1^0, A^0 \rightarrow q\bar{q}, gg, \tau^+\tau^-$, and $H_1^0 \rightarrow A^0 A^0$.		
39 ABDALLAH 05D search for $e^+e^- \rightarrow H^0 Z$ and $H^0 A^0$ with H^0, A^0 decaying to two jets of any flavor including gg . The limit is for SM $H^0 Z$ production cross section with $B(H^0 \rightarrow jj) = 1$.		
40 Search for $e^+e^- \rightarrow H^0 Z$ with H^0 decaying invisibly. The limit assumes SM production cross section and $B(H^0 \rightarrow \text{invisible}) = 1$.		
41 ABBIENDI 04K search for $e^+e^- \rightarrow H^0 Z$ with H^0 decaying to two jets of any flavor including gg . The limit is for SM production cross section with $B(H^0 \rightarrow jj) = 1$.		
42 ABDALLAH 04 consider the full combined LEP and LEP2 datasets to set limits on the Higgs coupling to W or Z bosons, assuming SM decays of the Higgs. Results in Fig. 26.		
43 Search for associated production of a $\gamma\gamma$ resonance with a Z boson, followed by $Z \rightarrow q\bar{q}, \ell^+\ell^-,$ or $\nu\bar{\nu}$, at $E_{cm} \leq 209$ GeV. The limit is for a H^0 with SM production cross section and $B(H^0 \rightarrow f\bar{f})=0$ for all fermions f .		
44 Updates ABREU 01F.		
45 ABDALLAH 04o search for $Z \rightarrow b\bar{b}H^0, b\bar{b}A^0, \tau^+\tau^-H^0$ and $\tau^+\tau^-A^0$ in the final states $4b, b\bar{b}\tau^+\tau^-$, and 4τ . See paper for limits on Yukawa couplings.		
46 ABDALLAH 04o search for $e^+e^- \rightarrow H^0 Z$ and $H^0 A^0$ with H^0, A^0 decaying to $b\bar{b}, \tau^+\tau^-$, or $H^0 \rightarrow A^0 A^0$ at $E_{cm} = 189-208$ GeV. See paper for limits on couplings.		
47 ACHARD 04B search for $e^+e^- \rightarrow H^0 Z$ with H^0 decaying to $b\bar{b}, c\bar{c}$, or gg . The limit is for SM production cross section with $B(H^0 \rightarrow jj) = 1$.		
48 ACHARD 04F search for H^0 with anomalous coupling to gauge boson pairs in the processes $e^+e^- \rightarrow H^0 \gamma, e^+e^- H^0, H^0 Z$ with decays $H^0 \rightarrow f\bar{f}, \gamma\gamma, Z\gamma$, and $W^* W$ at $E_{cm} = 189-209$ GeV. See paper for limits.		
49 ABBIENDI 03F search for $H^0 \rightarrow$ anything in $e^+e^- \rightarrow H^0 Z$, using the recoil mass spectrum of $Z \rightarrow e^+e^-$ or $\mu^+\mu^-$. In addition, it searched for $Z \rightarrow \nu\bar{\nu}$ and $H^0 \rightarrow e^+e^-$ or photons. Scenarios with large width or continuum H^0 mass distribution are considered. See their Figs. 11-14 for the results.		
50 ABBIENDI 03G search for $e^+e^- \rightarrow H_1^0 Z$ followed by $H_1^0 \rightarrow A^0 A^0, A^0 \rightarrow c\bar{c}, gg$, or $\tau^+\tau^-$ in the region $m_{H_1^0} = 45-86$ GeV and $m_{A^0} = 2-11$ GeV. See their Fig. 7 for the limits.		
51 ACHARD 03c search for $e^+e^- \rightarrow ZH^0$ followed by $H^0 \rightarrow W W^*$ or $Z Z^*$ at $E_{cm} = 200-209$ GeV and combine with the ACHARD 02c result. The limit is for a H^0 with SM production cross section and $B(H^0 \rightarrow f\bar{f}) = 0$ for all f . For $B(H^0 \rightarrow W W^*) + B(H^0 \rightarrow Z Z^*) = 1, m_{H^0} > 108.1$ GeV is obtained. See fig. 6 for the limits under different BR assumptions.		
52 ABBIENDI 02D search for $Z \rightarrow b\bar{b}H_1^0$ and $b\bar{b}A^0$ with $H_1^0/A^0 \rightarrow \tau^+\tau^-$, in the range $4 < m_H < 12$ GeV. See their Fig. 8 for limits on the Yukawa coupling.		
53 For $B(H^0 \rightarrow \gamma\gamma)=1, m_{H^0} > 117$ GeV is obtained.		
54 ACHARD 02c search for associated production of a $\gamma\gamma$ resonance with a Z boson, followed by $Z \rightarrow q\bar{q}, \ell^+\ell^-,$ or $\nu\bar{\nu}$, at $E_{cm} \leq 209$ GeV. The limit is for a H^0 with SM production cross section and $B(H^0 \rightarrow f\bar{f})=0$ for all fermions f . For $B(H^0 \rightarrow \gamma\gamma)=1, m_{H^0} > 114$ GeV is obtained.		
55 For $B(H^0 \rightarrow \gamma\gamma)=1, m_{H^0} > 113.1$ GeV is obtained.		
56 HEISTER 02M search for $e^+e^- \rightarrow H^0 Z$, assuming that H^0 decays to $q\bar{q}, gg$, or $\tau^+\tau^-$ only. The limit assumes SM production cross section.		
57 ABBIENDI 01E search for neutral Higgs bosons in general Type-II two-doublet models, at $E_{cm} \leq 189$ GeV. In addition to usual final states, the decays $H_1^0, A^0 \rightarrow q\bar{q}, gg$ are searched for. See their Figs. 15,16 for excluded regions.		
58 AFFOLDER 01H search for associated production of a $\gamma\gamma$ resonance and a W or Z (tagged by two jets, an isolated lepton, or missing E_T). The limit assumes Standard Model values for the production cross section and for the couplings of the H^0 to W and Z bosons. See their Fig. 11 for limits with $B(H^0 \rightarrow \gamma\gamma) < 1$.		
59 ACCIARRI 00M search for $e^+e^- \rightarrow ZH^0$ with H^0 decaying invisibly at $E_{cm}=183-189$ GeV. The limit assumes SM production cross section and $B(H^0 \rightarrow \text{invisible})=1$. See their Fig. 6 for limits for smaller branching ratios.		
60 ACCIARRI 00R search for $e^+e^- \rightarrow H^0 \gamma$ with $H^0 \rightarrow b\bar{b}, Z\gamma$, or $\gamma\gamma$. See their Fig. 3 for limits on $\sigma \cdot B$. Explicit limits within an effective interaction framework are also given, for which the Standard Model Higgs search results are used in addition.		
61 ACCIARRI 00R search for the two-photon type processes $e^+e^- \rightarrow e^+e^- H^0$ with $H^0 \rightarrow b\bar{b}$ or $\gamma\gamma$. See their Fig. 4 for limits on $\Gamma(H^0 \rightarrow \gamma\gamma) \cdot B(H^0 \rightarrow \gamma\gamma \text{ or } b\bar{b})$ for $m_{H^0}=70-170$ GeV.		

- ⁶² ACCIARRI 00s search for associated production of a $\gamma\gamma$ resonance with a $q\bar{q}, \nu\bar{\nu}$, or $\ell^+\ell^-$ pair in e^+e^- collisions at $E_{\text{cm}} = 189$ GeV. The limit is for a H^0 with SM production cross section and $B(H^0 \rightarrow f\bar{f})=0$ for all fermions f . For $B(H^0 \rightarrow \gamma\gamma)=1$, $m_{H^0} > 98$ GeV is obtained. See their Fig. 5 for limits on $B(H \rightarrow \gamma\gamma)\sigma(e^+e^- \rightarrow Hf\bar{f})/\sigma(e^+e^- \rightarrow Hf\bar{f})$ (SM).
- ⁶³ BARATE 00L search for associated production of a $\gamma\gamma$ resonance with a $q\bar{q}, \nu\bar{\nu}$, or $\ell^+\ell^-$ pair in e^+e^- collisions at $E_{\text{cm}} = 88\text{--}202$ GeV. The limit is for a H^0 with SM production cross section and $B(H^0 \rightarrow f\bar{f})=0$ for all fermions f . For $B(H^0 \rightarrow \gamma\gamma)=1$, $m_{H^0} > 109$ GeV is obtained. See their Fig. 3 for limits on $B(H \rightarrow \gamma\gamma)\sigma(e^+e^- \rightarrow Hf\bar{f})/\sigma(e^+e^- \rightarrow Hf\bar{f})$ (SM).
- ⁶⁴ ABBIENDI 99E search for $e^+e^- \rightarrow H^0 A^0$ and $H^0 Z$ at $E_{\text{cm}} = 183$ GeV. The limit is with $m_H = m_A$ in general two Higgs-doublet models. See their Fig. 18 for the exclusion limit in the $m_H\text{--}m_A$ plane. Updates the results of ACKERSTAFF 98s.
- ⁶⁵ ABBIENDI 99b search for associated production of a $\gamma\gamma$ resonance with a $q\bar{q}, \nu\bar{\nu}$, or $\ell^+\ell^-$ pair in e^+e^- collisions at 189 GeV. The limit is for a H^0 with SM production cross section and $B(H^0 \rightarrow f\bar{f})=0$, for all fermions f . See their Fig. 4 for limits on $\sigma(e^+e^- \rightarrow H^0 Z^0) \times B(H^0 \rightarrow \gamma\gamma) \times B(\chi^0 \rightarrow f\bar{f})$ for various masses. Updates the results of ACKERSTAFF 98y.
- ⁶⁶ ABBOTT 99b search for associated production of a $\gamma\gamma$ resonance and a dijet pair. The limit assumes Standard Model values for the production cross section and for the couplings of the H^0 to W and Z bosons. Limits in the range of $\sigma(H^0 + Z/W) \times B(H^0 \rightarrow \gamma\gamma) = 0.80\text{--}0.34$ pb are obtained in the mass range $m_{H^0} = 65\text{--}150$ GeV.
- ⁶⁷ ABREU 99p search for $e^+e^- \rightarrow H^0\gamma$ with $H^0 \rightarrow b\bar{b}$ or $\gamma\gamma$, and $e^+e^- \rightarrow H^0 q\bar{q}$ with $H^0 \rightarrow \gamma\gamma$. See their Fig. 4 for limits on $\sigma \times B$. Explicit limits within an effective interaction framework are also given.
- ⁶⁸ GONZALEZ-GARCIA 98b use $D\bar{D}$ limit for $\gamma\gamma$ events with missing E_T in $p\bar{p}$ collisions (ABBOTT 98) to constrain possible ZH or WH production followed by unconventional $H \rightarrow \gamma\gamma$ decay which is induced by higher-dimensional operators. See their Figs. 1 and 2 for limits on the anomalous couplings.
- ⁶⁹ KRAWCZYK 97 analyse the muon anomalous magnetic moment in a two-doublet Higgs model (with type II Yukawa couplings) assuming no $H^0 Z Z$ coupling and obtain $m_{H^0} \gtrsim 5$ GeV or $m_{A^0} \gtrsim 5$ GeV for $\tan\beta > 50$. Other Higgs bosons are assumed to be much heavier.
- ⁷⁰ ALEXANDER 96H give $B(Z \rightarrow H^0\gamma) \times B(H^0 \rightarrow q\bar{q}) < 1.4 \times 10^{-5}$ (95%CL) and $B(Z \rightarrow H^0\gamma) \times B(H^0 \rightarrow b\bar{b}) < 0.7\text{--}2 \times 10^{-5}$ (95%CL) in the range $20 < m_{H^0} < 80$ GeV.
- ⁷¹ See Fig. 4 of ABREU 95H for the excluded region in the $m_{H^0} - m_{A^0}$ plane for general two-doublet models. For $\tan\beta > 1$, the region $m_{H^0} + m_{A^0} \lesssim 87$ GeV, $m_{H^0} < 47$ GeV is excluded at 95% CL.
- ⁷² PICH 92 analyse H^0 with $m_{H^0} < 2m_\mu$ in general two-doublet models. Excluded regions in the space of mass-mixing angles from LEP, beam dump, and π^\pm, η rare decays are shown in Figs. 3,4. The considered mass region is not totally excluded.

H^\pm (Charged Higgs) MASS LIMITS

Unless otherwise stated, the limits below assume $B(H^\pm \rightarrow \tau^\pm \nu_\tau) + B(H^\pm \rightarrow c\bar{s}) = 1$, and hold for all values of $B(H^\pm \rightarrow \tau^\pm \nu_\tau)$, and assume H^\pm weak isospin of $T_3 = \pm 1/2$. In the following, $\tan\beta$ is the ratio of the two vacuum expectation values in two-doublet models (2HDM).

The limits are also applicable to point-like technipions. For a discussion of techniparticles, see the Review of Dynamical Electroweak Symmetry Breaking in this Review.

For limits obtained in hadronic collisions before the observation of the top quark, and based on the top mass values inconsistent with the current measurements, see the 1996 (Physical Review **D54** 1 (1996)) Edition of this Review.

Searches in e^+e^- collisions at and above the Z pole have conclusively ruled out the existence of a charged Higgs in the region $m_{H^\pm} \lesssim 45$ GeV, and are now superseded by the most recent searches in higher energy e^+e^- collisions at LEP. Results by now obsolete are therefore not included in this compilation, and can be found in the previous Edition (The European Physical Journal **C15** 1 (2000)) of this Review.

In the following, and unless otherwise stated, results from the LEP experiments (ALEPH, DELPHI, L3, and OPAL) are assumed to derive from the study of the $e^+e^- \rightarrow H^\pm H^\mp$ process. Limits from $b \rightarrow s\gamma$ decays are usually stronger in generic 2HDM models than in Supersymmetric models.

VALUE (GeV)	CL%	DOCUMENT ID	TECN	COMMENT
> 74.4	95	ABDALLAH 04i	DLPH	$E_{\text{cm}} \leq 209$ GeV
> 76.5	95	ACHARD 03E	L3	$E_{\text{cm}} \leq 209$ GeV
> 79.3	95	HEISTER 02p	ALEP	$E_{\text{cm}} \leq 209$ GeV

••• We do not use the following data for averages, fits, limits, etc. •••

> 92.0	95	73 ABULENCIA 06E	CDF	$t \rightarrow bH^\pm$
> 76.7	95	74 ABDALLAH 04i	OPAL	$B(\tau\nu) = 1$
		74 ABDALLAH 04i	DLPH	Type I
		75 ABBIENDI 03	OPAL	$\tau \rightarrow \mu\nu_\mu, e\bar{\nu}_e$
		76 ABAZOV 02b	D0	$t \rightarrow bH^\pm, H \rightarrow \tau\nu$
		77 BORZUMATI 02	RVUE	
		78 ABBIENDI 01Q	OPAL	$B \rightarrow \tau\nu_\tau X$
		79 BARATE 01E	ALEP	$B \rightarrow \tau\nu_\tau$
> 315	99	80 GAMBINO 01	RVUE	$b \rightarrow s\gamma$
		81 AFFOLDER 00i	CDF	$t \rightarrow bH^\pm, H \rightarrow \tau\nu$
> 59.5	95	ABBIENDI 99E	OPAL	$E_{\text{cm}} \leq 183$ GeV
		82 ABBOTT 99E	D0	$t \rightarrow bH^\pm$

		83 ACKERSTAFF 99D	OPAL	$\tau \rightarrow e\nu\nu, \mu\nu\nu$
		84 ACCIARRI 97F	L3	$B \rightarrow \tau\nu_\tau$
		85 AMMAR 97B	CLEO	$\tau \rightarrow \mu\nu\nu$
		86 COARASA 97	RVUE	$B \rightarrow \tau\nu_\tau X$
		87 GUCHAIT 97	RVUE	$t \rightarrow bH^\pm, H \rightarrow \tau\nu$
		88 MANGANO 97	RVUE	$B_{U(C)} \rightarrow \tau\nu_\tau$
		89 STAHL 97	RVUE	$\tau \rightarrow \mu\nu\nu$
> 244	95	90 ALAM 95	CLE2	$b \rightarrow s\gamma$
		91 BUSKULIC 95	ALEP	$b \rightarrow \tau\nu_\tau X$

- ⁷³ ABULENCIA 06E search for associated $H^0 W$ production in $p\bar{p}$ collisions at $E_{\text{cm}} = 1.96$ TeV. A fit is made for $t\bar{t}$ production processes in dilepton, lepton + jets, and lepton + τ final states, with the decays $t \rightarrow W^+ b$ and $t \rightarrow H^+ b$ followed by $H^\pm \rightarrow \tau^\pm \nu, c\bar{s}, t^* \bar{b},$ or $W^+ H^0$. Within the MSSM the search is sensitive to the region $\tan\beta < 1$ or > 30 in the mass range $m_{H^\pm} = 80\text{--}160$ GeV. See Fig. 2 for the excluded region in a certain MSSM scenario.
- ⁷⁴ ABDALLAH 04i search for $e^+e^- \rightarrow H^\pm H^\mp$ with H^\pm decaying to $\tau\nu, c\bar{s}$, or $W^* A^0$ in Type-I two-Higgs-doublet models.
- ⁷⁵ ABBIENDI 03 give a limit $m_{H^\pm} > 1.28 \tan\beta$ GeV (95%CL) in Type II two-doublet models.
- ⁷⁶ ABAZOV 02b search for a charged Higgs boson in top decays with $H^\pm \rightarrow \tau^\pm \nu$ at $E_{\text{cm}} = 1.8$ TeV. For $m_{H^\pm} = 75$ GeV, the region $\tan\beta > 32.0$ is excluded at 95%CL. The excluded mass region extends to over 140 GeV for $\tan\beta$ values above 100.
- ⁷⁷ BORZUMATI 02 point out that the decay modes such as $b\bar{b}W, A^0 W,$ and supersymmetric ones can have substantial branching fractions in the mass range explored at LEP II and Tevatron.
- ⁷⁸ ABBIENDI 01Q give a limit $\tan\beta/m_{H^\pm} < 0.53$ GeV $^{-1}$ (95%CL) in Type II two-doublet models.
- ⁷⁹ BARATE 01E give a limit $\tan\beta/m_{H^\pm} < 0.40$ GeV $^{-1}$ (90% CL) in Type II two-doublet models. An independent measurement of $B \rightarrow \tau\nu_\tau X$ gives $\tan\beta/m_{H^\pm} < 0.49$ GeV $^{-1}$ (90% CL).
- ⁸⁰ GAMBINO 01 use the world average data in the summer of 2001 $B(b \rightarrow s\gamma) = (3.23 \pm 0.42) \times 10^{-4}$. The limit applies for Type-II two-doublet models.
- ⁸¹ AFFOLDER 00i search for a charged Higgs boson in top decays with $H^\pm \rightarrow \tau^\pm \nu$ in $p\bar{p}$ collisions at $E_{\text{cm}} = 1.8$ TeV. The excluded mass region extends to over 120 GeV for $\tan\beta$ values above 100 and $B(\tau\nu) = 1$. If $B(t \rightarrow bH^\pm) \gtrsim 0.6$, m_{H^\pm} up to 160 GeV is excluded. Updates ABE 97L.
- ⁸² ABBOTT 99e search for a charged Higgs boson in top decays in $p\bar{p}$ collisions at $E_{\text{cm}} = 1.8$ TeV, by comparing the observed $t\bar{t}$ cross section (extracted from the data assuming the dominant decay $t \rightarrow bW^+$) with theoretical expectation. The search is sensitive to regions of the domains $\tan\beta \lesssim 1, 50 < m_{H^\pm} < 120$ and $\tan\beta \gtrsim 40, 50 < m_{H^\pm} < 160$. See Fig. 3 for the details of the excluded region.
- ⁸³ ACKERSTAFF 99D measure the Michel parameters $\rho, \xi, \eta,$ and $\xi\delta$ in leptonic τ decays from $Z \rightarrow \tau\tau$. Assuming $e\text{--}\mu$ universality, the limit $m_{H^\pm} > 0.97 \tan\beta$ GeV (95%CL) is obtained for two-doublet models in which only one doublet couples to leptons.
- ⁸⁴ ACCIARRI 97F give a limit $m_{H^\pm} > 2.6 \tan\beta$ GeV (90% CL) from their limit on the exclusive $B \rightarrow \tau\nu_\tau$ branching ratio.
- ⁸⁵ AMMAR 97b measure the Michel parameter ρ from $\tau \rightarrow e\nu\nu$ decays and assumes e/μ universality to extract the Michel η parameter from $\tau \rightarrow \mu\nu\nu$ decays. The measurement is translated to a lower limit on m_{H^\pm} in a two-doublet model $m_{H^\pm} > 0.97 \tan\beta$ GeV (90% CL).
- ⁸⁶ COARASA 97 reanalyzed the constraint on the $(m_{H^\pm}, \tan\beta)$ plane derived from the inclusive $B \rightarrow \tau\nu_\tau X$ branching ratio in GROSSMAN 95b and BUSKULIC 95. They show that the constraint is quite sensitive to supersymmetric one-loop effects.
- ⁸⁷ GUCHAIT 97 studies the constraints on m_{H^\pm} set by Tevatron data on $\ell\tau$ final states in $t\bar{t} \rightarrow (Wb)(Hb), W \rightarrow \ell\nu, H \rightarrow \tau\nu_\tau$. See Fig. 2 for the excluded region.
- ⁸⁸ MANGANO 97 reconsiders the limit in ACCIARRI 97F including the effect of the potentially large $B_c \rightarrow \tau\nu_\tau$ background to $B_U \rightarrow \tau\nu_\tau$ decays. Stronger limits are obtained.
- ⁸⁹ STAHL 97 fit τ lifetime, leptonic branching ratios, and the Michel parameters and derive limit $m_{H^\pm} > 1.5 \tan\beta$ GeV (90% CL) for a two-doublet model. See also STAHL 94.
- ⁹⁰ ALAM 95 measure the inclusive $b \rightarrow s\gamma$ branching ratio at $T(45)$ and give $B(b \rightarrow s\gamma) < 4.2 \times 10^{-4}$ (95% CL), which translates to the limit $m_{H^\pm} > [244 + 63/(\tan\beta)]^{1.3}$ GeV in the Type II two-doublet model. Light supersymmetric particles can invalidate this bound.
- ⁹¹ BUSKULIC 95 give a limit $m_{H^\pm} > 1.9 \tan\beta$ GeV (90% CL) for Type-II models from $b \rightarrow \tau\nu_\tau X$ branching ratio, as proposed in GROSSMAN 94.

MASS LIMITS for $H^{\pm\pm}$ (doubly-charged Higgs boson)

This section covers searches for a doubly-charged Higgs boson with couplings to lepton pairs. Its weak isospin T_3 is thus restricted to two possibilities depending on lepton chiralities: $T_3(H^{\pm\pm}) = \pm 1$, with the coupling $g_{\ell\ell}$ to $\ell_L^+ \ell_L^-$ and $\ell_R^+ \ell_R^+$ ("left-handed") and $T_3(H^{\pm\pm}) = 0$, with the coupling to $\ell_R^+ \ell_R^-$ and $\ell_L^+ \ell_L^+$ ("right-handed"). These Higgs bosons appear in some left-right symmetric models based on the gauge group $SU(2)_L \times SU(2)_R \times U(1)$. These two cases are listed separately in the following. Unless noted, one of the lepton flavor combinations is assumed to be dominant in the decay.

LIMITS for $H^{\pm\pm}$ with $T_3 = \pm 1$

VALUE	CL%	DOCUMENT ID	TECN	COMMENT
> 118.4	95	92 ABAZOV 04E	D0	$\mu\mu$
> 136	95	93 ACOSTA 04G	CDF	$\mu\mu$
> 98.1	95	94 ABDALLAH 03	DLPH	$\tau\tau$
> 99.0	95	95 ABBIENDI 02C	OPAL	$\tau\tau$

Gauge & Higgs Boson Particle Listings

Higgs Bosons — H^0 and H^\pm

• • • We do not use the following data for averages, fits, limits, etc. • • •

>133	95	96 AKTAS	06A	H1	single $H^{\pm\pm}$
		97 ACOSTA	05L	CDF	stable
		98 ABBIENDI	03Q	OPAL	$E_{\text{cm}} \leq 209$ GeV, single $H^{\pm\pm}$
		99 GORDEEV	97	SPEC	muonium conversion
		100 ASAKA	95	THEO	
> 45.6	95	101 ACTON	92M	OPAL	
> 30.4	95	102 ACTON	92M	OPAL	
none 6.5–36.6	95	103 SWARTZ	90	MRK2	

92 ABAZOV 04E search for $H^{++}H^{--}$ pair production in $H^{\pm\pm} \rightarrow \mu^\pm\mu^\pm$. The limit is valid for $g_{\mu\mu} \gtrsim 10^{-7}$.

93 ACOSTA 04G search for $H^{++}H^{--}$ pair production in $p\bar{p}$ collisions with muon and electron final states. The limit holds for $\mu\mu$. For $e\mu$ and $e\mu$ modes, the limits are 133 and 115 GeV, respectively. The limits are valid for $g_{\ell\ell} \gtrsim 10^{-5}$.

94 ABDALLAH 03 search for $H^{++}H^{--}$ pair production either followed by $H^{++} \rightarrow \tau^+\tau^+$, or decaying outside the detector.

95 ABBIENDI 02c searches for pair production of $H^{++}H^{--}$, with $H^{\pm\pm} \rightarrow \ell^\pm\ell^\pm$ ($\ell, \ell' = e, \mu, \tau$). The limit holds for $\ell = \ell' = \tau$, and becomes stronger for other combinations of leptonic final states. To ensure the decay within the detector, the limit only applies for $g(H\ell\ell) \gtrsim 10^{-7}$.

96 AKTAS 06A search for single $H^{\pm\pm}$ production in ep collisions at HERA. Assuming that H^{++} only couples to $e^+\mu^+$ with $g_{e\mu} = 0.3$ (electromagnetic strength), a limit $m_{H^{++}} > 141$ GeV (95% CL) is derived. For the case where H^{++} couples to $e\tau$ only the limit is 112 GeV.

97 ACOSTA 05L search for $H^{++}H^{--}$ pair production in $p\bar{p}$ collisions. The limit is valid for $g_{\ell\ell} < 10^{-8}$ so that the Higgs decays outside the detector.

98 ABBIENDI 03Q searches for single $H^{\pm\pm}$ via direct production in $e^+e^- \rightarrow e^\mp e^\mp H^{\pm\pm}$, and via t -channel exchange in $e^+e^- \rightarrow e^+e^-$. In the direct case, and assuming $B(H^{\pm\pm} \rightarrow \ell^\pm\ell^\pm) = 1$, a 95% CL limit on $h_{ee} < 0.071$ is set for $m_{H^{\pm\pm}} < 160$ GeV (see Fig. 6). In the second case, indirect limits on h_{ee} are set for $m_{H^{\pm\pm}} < 2$ TeV (see Fig. 8).

99 GORDEEV 97 search for muonium-antimuonium conversion and find $G_{M\bar{M}}/G_F < 0.14$ (90% CL), where $G_{M\bar{M}}$ is the lepton-flavor violating effective four-fermion coupling. This limit may be converted to $m_{H^{++}} > 210$ GeV if the Yukawa couplings of H^{++} to ee and $\mu\mu$ are as large as the weak gauge coupling. For similar limits on muonium-antimuonium conversion, see the muon Particle Listings.

100 ASAKA 95 point out that H^{++} decays dominantly to four fermions in a large region of parameter space where the limit of ACTON 92M from the search of dilepton modes does not apply.

101 ACTON 92M limit assumes $H^{\pm\pm} \rightarrow \ell^\pm\ell^\pm$ or $H^{\pm\pm}$ does not decay in the detector. Thus the region $g_{\ell\ell} \approx 10^{-7}$ is not excluded.

102 ACTON 92M from $\Delta\Gamma_Z < 40$ MeV.

103 SWARTZ 90 assume $H^{\pm\pm} \rightarrow \ell^\pm\ell^\pm$ (any flavor). The limits are valid for the Higgs-lepton coupling $g(H\ell\ell) \gtrsim 7.4 \times 10^{-7}/[m_H/\text{GeV}]^{1/2}$. The limits improve somewhat for ee and $\mu\mu$ decay modes.

LIMITS for $H^{\pm\pm}$ with $T_3 = 0$

VALUE	CL%	DOCUMENT ID	TECN	COMMENT
> 98.2	95	104 ABAZOV	04E D0	$\mu\mu$
>113	95	105 ACOSTA	04G CDF	$\mu\mu$
> 97.3	95	106 ABDALLAH	03 DLPH	$\tau\tau$
> 97.3	95	107 ACHARD	03F L3	$\tau\tau$
> 98.5	95	108 ABBIENDI	02C OPAL	$\tau\tau$

• • • We do not use the following data for averages, fits, limits, etc. • • •

>109	95	109 AKTAS	06A	H1	single $H^{\pm\pm}$
		110 ACOSTA	05L	CDF	stable
		111 ABBIENDI	03Q	OPAL	$E_{\text{cm}} \leq 209$ GeV, single $H^{\pm\pm}$
		112 GORDEEV	97	SPEC	muonium conversion
> 45.6	95	113 ACTON	92M	OPAL	
> 25.5	95	114 ACTON	92M	OPAL	
none 7.3–34.3	95	115 SWARTZ	90	MRK2	

104 ABAZOV 04E search for $H^{++}H^{--}$ pair production in $H^{\pm\pm} \rightarrow \mu^\pm\mu^\pm$. The limit is valid for $g_{\mu\mu} \gtrsim 10^{-7}$.

105 ACOSTA 04G search for $H^{++}H^{--}$ pair production in $p\bar{p}$ collisions with muon and electron final states. The limit holds for $\mu\mu$.

106 ABDALLAH 03 search for $H^{++}H^{--}$ pair production either followed by $H^{++} \rightarrow \tau^+\tau^+$, or decaying outside the detector.

107 ACHARD 03F search for $e^+e^- \rightarrow H^{++}H^{--}$ with $H^{\pm\pm} \rightarrow \ell^\pm\ell^\pm$. The limit holds for $\ell = \ell' = \tau$, and slightly different limits apply for other flavor combinations. The limit is valid for $g_{\ell\ell} \gtrsim 10^{-7}$.

108 ABBIENDI 02c searches for pair production of $H^{++}H^{--}$, with $H^{\pm\pm} \rightarrow \ell^\pm\ell^\pm$ ($\ell, \ell' = e, \mu, \tau$). The limit holds for $\ell = \ell' = \tau$, and becomes stronger for other combinations of leptonic final states. To ensure the decay within the detector, the limit only applies for $g(H\ell\ell) \gtrsim 10^{-7}$.

109 AKTAS 06A search for single $H^{\pm\pm}$ production in ep collisions at HERA. Assuming that H^{++} only couples to $e^+\mu^+$ with $g_{e\mu} = 0.3$ (electromagnetic strength), a limit $m_{H^{++}} > 141$ GeV (95% CL) is derived. For the case where H^{++} couples to $e\tau$ only the limit is 112 GeV.

110 ACOSTA 05L search for $H^{++}H^{--}$ pair production in $p\bar{p}$ collisions. The limit is valid for $g_{\ell\ell} < 10^{-8}$ so that the Higgs decays outside the detector.

111 ABBIENDI 03Q searches for single $H^{\pm\pm}$ via direct production in $e^+e^- \rightarrow e^\mp e^\mp H^{\pm\pm}$, and via t -channel exchange in $e^+e^- \rightarrow e^+e^-$. In the direct case, and assuming $B(H^{\pm\pm} \rightarrow \ell^\pm\ell^\pm) = 1$, a 95% CL limit on $h_{ee} < 0.071$ is set for $m_{H^{\pm\pm}} < 160$ GeV

(see Fig. 6). In the second case, indirect limits on h_{ee} are set for $m_{H^{\pm\pm}} < 2$ TeV (see Fig. 8).

112 GORDEEV 97 search for muonium-antimuonium conversion and find $G_{M\bar{M}}/G_F < 0.14$ (90% CL), where $G_{M\bar{M}}$ is the lepton-flavor violating effective four-fermion coupling.

This limit may be converted to $m_{H^{++}} > 210$ GeV if the Yukawa couplings of H^{++} to ee and $\mu\mu$ are as large as the weak gauge coupling. For similar limits on muonium-antimuonium conversion, see the muon Particle Listings.

113 ACTON 92M limit assumes $H^{\pm\pm} \rightarrow \ell^\pm\ell^\pm$ or $H^{\pm\pm}$ does not decay in the detector. Thus the region $g_{\ell\ell} \approx 10^{-7}$ is not excluded.

114 ACTON 92M from $\Delta\Gamma_Z < 40$ MeV.

115 SWARTZ 90 assume $H^{\pm\pm} \rightarrow \ell^\pm\ell^\pm$ (any flavor). The limits are valid for the Higgs-lepton coupling $g(H\ell\ell) \gtrsim 7.4 \times 10^{-7}/[m_H/\text{GeV}]^{1/2}$. The limits improve somewhat for ee and $\mu\mu$ decay modes.

H^0 and H^\pm REFERENCES

ABAZOV	07X	PL B655 209	V.M. Abazov et al.	(D0 Collab.)
ABBIENDI	07	EPJ C49 457	G. Abbiendi et al.	(OPAL Collab.)
SCHAEEL	07	EPJ C49 439	S. Schaeel et al.	(ALEPH Collab.)
ABAZOV	06	PRL 96 011801	V.M. Abazov et al.	(D0 Collab.)
ABAZOV	06J	PRL 97 121802	V.M. Abazov et al.	(D0 Collab.)
ABAZOV	06O	PRL 97 151804	V.M. Abazov et al.	(D0 Collab.)
ABAZOV	06Q	PRL 97 161803	V.M. Abazov et al.	(D0 Collab.)
ABULENCIA	06	PRL 96 011802	A. Abulencia et al.	(CDF Collab.)
ABULENCIA	06E	PRL 96 042003	A. Abulencia et al.	(CDF Collab.)
ABULENCIA	06H	PRL 96 081803	A. Abulencia et al.	(CDF Collab.)
ABULENCIA	06A	PRL 97 081802	A. Abulencia et al.	(CDF Collab.)
AKTAS	06A	PL B638 432	A. Aktas et al.	(H1 Collab.)
LEP-SLC	06	PRPL 427 257	ALEPH, DELPHI, L3, OPAL, SLD and working groups	(LEP Collab.)
SCHAEEL	06B	EPJ C47 547	S. Schaeel et al.	(D0 Collab.)
ABAZOV	05F	PRL 94 091802	V.M. Abazov et al.	(D0 Collab.)
ABAZOV	05T	PRL 95 151801	V.M. Abazov et al.	(D0 Collab.)
ABBIENDI	05A	EPJ C40 317	G. Abbiendi et al.	(OPAL Collab.)
ABDALLAH	05D	EPJ C44 147	J. Abdallah et al.	(DELPHI Collab.)
ACHARD	05	PL B609 35	P. Achard et al.	(L3 Collab.)
ACOSTA	05K	PRL 95 051801	D. Acosta et al.	(CDF Collab.)
ACOSTA	05L	PRL 95 071801	D. Acosta et al.	(CDF Collab.)
ACOSTA	05Q	PR D72 072004	D. Acosta et al.	(CDF Collab.)
ABAZOV	04E	PRL 93 141801	V.M. Abazov et al.	(D0 Collab.)
ABBIENDI	04	EPJ C32 453	G. Abbiendi et al.	(OPAL Collab.)
ABBIENDI	04M	PL B597 11	G. Abbiendi et al.	(OPAL Collab.)
ABBIENDI	04K	EPJ C37 49	G. Abbiendi et al.	(OPAL Collab.)
ABDALLAH	04	EPJ C32 145	J. Abdallah et al.	(DELPHI Collab.)
ABDALLAH	04B	EPJ C32 475	J. Abdallah et al.	(DELPHI Collab.)
ABDALLAH	04I	EPJ C34 399	J. Abdallah et al.	(DELPHI Collab.)
ABDALLAH	04J	EPJ C35 313	J. Abdallah et al.	(DELPHI Collab.)
ABDALLAH	04O	EPJ C38 1	J. Abdallah et al.	(DELPHI Collab.)
ACHARD	04B	PL B583 34	P. Achard et al.	(L3 Collab.)
AORZUMATI	04F	PL B589 89	M.S. Carena et al.	(L3 Collab.)
ACOSTA	04G	PRL 93 221802	D. Acosta et al.	(CDF Collab.)
ABBIENDI	03	PL B551 35	G. Abbiendi et al.	(OPAL Collab.)
ABBIENDI	03B	EPJ C26 479	G. Abbiendi et al.	(OPAL Collab.)
ABBIENDI	03F	EPJ C27 311	G. Abbiendi et al.	(OPAL Collab.)
ABBIENDI	03G	EPJ C27 483	G. Abbiendi et al.	(OPAL Collab.)
ABBIENDI	03Q	PL B577 93	G. Abbiendi et al.	(OPAL Collab.)
ABDALLAH	03	PL B552 127	J. Abdallah et al.	(DELPHI Collab.)
ACHARD	03C	PL B568 191	P. Achard et al.	(L3 Collab.)
ACHARD	03E	PL B575 208	P. Achard et al.	(L3 Collab.)
ACHARD	03F	PL B576 18	P. Achard et al.	(L3 Collab.)
CARENA	03	EPJ C26 601	M.S. Carena et al.	(L3 Collab.)
HEISTER	03D	PL B565 61	A. Heister et al.	(ALEPH, DELPHI, L3 +)
ALEPH, DELPHI, L3, OPAL, LEP Higgs Working Group				
ABAZOV	02B	PRL 88 151803	V.M. Abazov et al.	(D0 Collab.)
ABBIENDI	02C	PL B526 221	G. Abbiendi et al.	(OPAL Collab.)
ABBIENDI	02D	EPJ C23 397	G. Abbiendi et al.	(OPAL Collab.)
ABBIENDI	02F	PL B544 44	G. Abbiendi et al.	(OPAL Collab.)
ACHARD	02C	PL B534 28	P. Achard et al.	(L3 Collab.)
ACHARD	02H	PL B545 30	P. Achard et al.	(L3 Collab.)
AKEROYD	02	PR D56 037702	A.G. Akeroyd et al.	(L3 Collab.)
BORZUMATI	02	PL B549 170	F.M. Borzumati, A. Djouadi	(L3 Collab.)
HEISTER	02	PL B526 191	A. Heister et al.	(ALEPH Collab.)
HEISTER	02L	PL B544 16	A. Heister et al.	(ALEPH Collab.)
HEISTER	02M	PL B544 25	A. Heister et al.	(ALEPH Collab.)
HEISTER	02P	PL B543 1	A. Heister et al.	(ALEPH Collab.)
ABBIENDI	01E	EPJ C18 425	G. Abbiendi et al.	(OPAL Collab.)
ABBIENDI	01Q	PL B520 1	G. Abbiendi et al.	(OPAL Collab.)
ABREU	01F	PL B507 89	P. Abreu et al.	(DELPHI Collab.)
ACHARD	01C	PL B517 319	P. Achard et al.	(L3 Collab.)
AFFOLDER	01D	PRL 86 4472	T. Affolder et al.	(CDF Collab.)
AFFOLDER	01H	PR D64 092002	T. Affolder et al.	(CDF Collab.)
BARATE	01C	PL B499 53	R. Barate et al.	(ALEPH Collab.)
BARATE	01E	EPJ C19 213	R. Barate et al.	(ALEPH Collab.)
GAMBINO	01	NP B611 338	P. Gambino, M. Misiak	(L3 Collab.)
ACCIARRI	00M	PL B485 85	M. Acciari et al.	(L3 Collab.)
ACCIARRI	00R	PL B489 102	M. Acciari et al.	(L3 Collab.)
ACCIARRI	00S	PL B489 115	M. Acciari et al.	(L3 Collab.)
AFFOLDER	00I	PR D62 012004	T. Affolder et al.	(CDF Collab.)
BARATE	00L	PL B487 241	R. Barate et al.	(ALEPH Collab.)
PDG	00	EPJ C15 1	D.E. Groom et al.	(OPAL Collab.)
ABBIENDI	99E	EPJ C7 407	G. Abbiendi et al.	(OPAL Collab.)
ABBIENDI	99O	PL B464 311	G. Abbiendi et al.	(OPAL Collab.)
ABBOTT	99B	PRL 82 2244	B. Abbott et al.	(D0 Collab.)
ABBOTT	99E	PRL 82 4975	B. Abbott et al.	(D0 Collab.)
ABREU	99P	PL B458 431	P. Abreu et al.	(DELPHI Collab.)
ACKERSTAFF	99D	EPJ C8 3	K. Ackerstaff et al.	(OPAL Collab.)
CARENA	99B	hep-ph/9912223	M.S. Carena et al.	(OPAL Collab.)
CERN-TH/99-374				
ABBOTT	98	PRL 80 442	B. Abbott et al.	(D0 Collab.)
ABE	98T	PRL 81 5748	F. Abe et al.	(CDF Collab.)
ACKERSTAFF	98S	EPJ C5 19	K. Ackerstaff et al.	(OPAL Collab.)
ACKERSTAFF	98Y	PL B437 218	K. Ackerstaff et al.	(OPAL Collab.)
GONZALEZ-G.	98B	PR D57 7045	M.C. Gonzalez-Garcia, S.M. Lietti, S.F. Novas	(CDF Collab.)
PDG	98	EPJ C3	C. Caso et al.	(CDF Collab.)
ABE	97L	PRL 79 357	F. Abe et al.	(CDF Collab.)
ABE	97W	PRL 79 3819	F. Abe et al.	(CDF Collab.)
ACCIARRI	97F	PL B396 327	M. Acciari et al.	(L3 Collab.)
AMMAR	97B	PRL 78 4686	R. Ammar et al.	(CLEO Collab.)
COARASA	97	PL B406 337	J.A. Coarasa, R.A. Jimenez, J. Sola	(OPAL Collab.)
GORDEEV	97	PAN 60 1164	V.A. Gordeev et al.	(PNPI)

Translated from YAF 60 1291.

See key on page 373

Gauge & Higgs Boson Particle Listings

Higgs Bosons — H^0 and H^\pm , Heavy Bosons Other than Higgs Bosons

GUCHAIT	97	PR D55 7263	M. Guchait, D.P. Roy	(TATA)
KRAWCZYK	97	PR D55 6968	M. Krawczyk, J. Zochowski	(WARSA)
MANGANO	97	PL B410 299	M. Mangano, S. Slabospitsky	
STAHL	97	ZPHY C74 73	A. Stahl, H. Voss	(BONN)
ALEXANDER	96H	ZPHY C71 1	G. Alexander et al.	(OPAL Collab.)
PDG	96	PR D54 1	R. M. Barnett et al.	
ABREU	95H	ZPHY C67 69	P. Abreu et al.	(DELPHI Collab.)
ALAM	95	PRL 74 2085	M.S. Alam et al.	(CLEO Collab.)
ASAKA	95	PL B345 36	T. Asaka, K.I. Hikasa	(TOHOK)
BUSKULIC	95	PL B343 444	D. Buskulić et al.	(ALEPH Collab.)
GROSSMAN	95B	PL B357 630	Y. Grossman, H. Haber, Y. Nir	
GROSSMAN	94	PL B332 373	Y. Grossman, Z. Ligeti	
STAHL	94	PL B324 121	A. Stahl	(BONN)
ACTON	92M	PL B295 347	P.D. Acton et al.	(OPAL Collab.)
PICH	92	NP B388 31	A. Pich, J. Prades, P. Yepes	(CERN, CPPM)
SWARTZ	90	PRL 64 2877	M.L. Swartz et al.	(Mark II Collab.)

Heavy Bosons Other Than Higgs Bosons, Searches for

We list here various limits on charged and neutral heavy vector bosons (other than W 's and Z 's), heavy scalar bosons (other than Higgs bosons), vector or scalar leptoquarks, and axiguons.

W' -BOSON SEARCHES

Written November 2007 by M.-C. Chen (UC Irvine) and B.A. Dobrescu (Fermilab).

The W' boson is a hypothetical massive particle of electric charge ± 1 and spin 1, which is predicted in various extensions of the standard model.

W' couplings to quarks and leptons. The Lagrangian terms describing couplings of a W' boson to fermions are given by

$$W'_\mu \left[\bar{u}_i \left(C_{qij}^R P_R + C_{qij}^L P_L \right) \gamma^\mu d_j + \bar{\nu}_i \left(C_{lij}^R P_R + C_{lij}^L P_L \right) \gamma^\mu e_j \right] + \text{h.c.} \quad (1)$$

Here u, d, ν and e are the standard model fermions in the mass eigenstate basis, $i, j = 1, 2, 3$ label the fermion generation, and $P_{R,L} = (1 \pm \gamma_5)/2$. The coefficients $C_{qij}^L, C_{qij}^R, C_{lij}^L, C_{lij}^R$ are complex dimensionless parameters. If $C_{lij}^R \neq 0$, then the i th generation includes a right-handed neutrino. It is often assumed that there are correlations between the left- and right-handed couplings [1]. Although this is true in some of the original models that include a W' [2], there exist theories where all the left- and right-handed couplings are free parameters.

Unitarity considerations imply that the W' is a gauge boson associated with a spontaneously broken gauge symmetry. This is true even when it is a composite particle (*e.g.*, the charged techni- ρ in technicolor theories [3]) or a Kaluza-Klein mode in theories where the W boson propagates in extra dimensions [4]. The simplest extension of the electroweak gauge group that includes a W' is $SU(2)_1 \times SU(2)_2 \times U(1)$, but larger groups are also encountered in some theories. A generic property of all these gauge theories is that besides a W' they contain at least a Z' boson, whose mass is typically comparable or smaller than $M_{W'}$. Despite the severe limits on Z' bosons [5], theories where the properties of the new gauge bosons would allow the W' to be discovered before the Z' are quite common (for example, a leptophobic W' decaying to $t\bar{b}$ may be observed easier than a Z' in the $t\bar{t}$ final state which has higher backgrounds).

The renormalizable photon- W' coupling is completely fixed by electromagnetic gauge invariance. By contrast, the renormalizable $W'WZ$ and $W'W'Z$ couplings are model dependent, and the same is true for the W' couplings to Z' or Higgs bosons.

Depending on the symmetry breaking sector, a tree-level mass mixing may be induced between the electrically-charged gauge bosons. Upon diagonalization of their mass matrix, the $W - Z$ mass ratio and the couplings of the observed W are shifted from the standard model values. Given that these are well measured, the mixing angle between the two gauge bosons must be smaller than about 10^{-2} . Similarly, a $Z - Z'$ mixing is induced in generic theories, leading to even tighter constraints. There are, however, theories in which these mixings are negligible even when the W' and Z' masses are below the electroweak scale (for example, this is a consequence of a new parity, as in [7]).

A popular model [2] is based on the “left-right symmetric” gauge group, $SU(2)_L \times SU(2)_R \times U(1)_{B-L}$, with the standard model fermions that couple to W transforming as doublets under $SU(2)_L$ and the other ones transforming as doublets under $SU(2)_R$. In this model the W' couples primarily to the right-handed fermions, and its coupling to left-handed fermions arises solely due to $W-W'$ mixing. As a result, C_q^L is proportional to the CKM matrix, and its elements are much smaller than the diagonal elements of C_q^R .

There are many other models based on the $SU(2)_1 \times SU(2)_2 \times U(1)$ gauge symmetry. In the “alternate left-right” model [8], all the couplings shown in Eq. (1) vanish, but there are some new fermions such that the W' couples to pairs involving a standard model fermion and a new fermion. In the “unified standard model” [9], the left-handed quarks are doublets under one $SU(2)$ and the left-handed leptons are doublets under a different $SU(2)$, leading to a mostly leptophobic W' : $C_{lij}^L \ll C_{qij}^L$ and $C_{qij}^R = C_{lij}^R = 0$. Fermions of different generations may also transform as doublets under different $SU(2)$ gauge groups [10]. In particular, the couplings to third generation quarks may be enhanced [11].

The W' couplings to standard model fermions may be highly suppressed if the quarks and leptons are singlets under one $SU(2)$ [12], or if there are some vectorlike fermions that mix with the standard model ones [13,14]. Gauge groups that embed the electroweak symmetry, such as $SU(3)_W \times U(1)$ or $SU(4)_W \times U(1)$, also include one or more W' bosons [15].

Collider searches. At LEP-II, W' bosons could have been produced in pairs via their photon and Z couplings. The production cross section depends only on the W' mass, and is large enough for $M_{W'} \leq \sqrt{s}/2 \approx 105$ GeV so that W' bosons are ruled out for essentially any pattern of decay modes.

Searches for W' bosons in the Run II at the Tevatron have been performed so far by the DØ and CDF Collaborations for W' decays into $e\nu$ [16,17] or $t\bar{b}$ [18,19]. Assuming that the W' boson has a narrow width, the contribution of the s -channel W' exchange to the total rate for $p\bar{p} \rightarrow f\bar{f}'X$, where f and f' are fermions and X is any final state of charge ± 1 , may be

Gauge & Higgs Boson Particle Listings

Heavy Bosons Other than Higgs Bosons

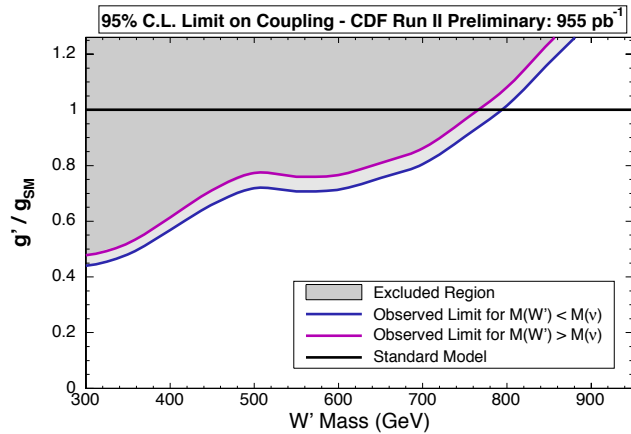


Figure 1: 95% CL exclusion limit from CDF [19] in the gauge coupling versus $M_{W'}$ plane, using the $t\bar{b}$ and $t\bar{b}$ final states.

approximated by the branching fraction $B(W' \rightarrow f\bar{f}')$ times the production cross section

$$\sigma(p\bar{p} \rightarrow W'X) \approx \frac{\pi}{48s} \sum_{i,j} \left[(C_{qij}^L)^2 + (C_{qij}^R)^2 \right] w_{ij}(s, M_{W'}^2), \quad (2)$$

where the i, j indices label the fermion generations. The functions w_{ij} include the information about proton structure, and are given to leading order in α_s by

$$w_{ij}(z) = \int_z^1 \frac{dx}{x} [u_i(x) d_j(z/x) + \bar{u}_i(x) \bar{d}_j(z/x)], \quad (3)$$

where $u_i(x)$ and $d_i(x)$ are the parton distributions inside the proton for the up- and down-type quark of the i th generation, respectively. QCD corrections to W' production are sizable, but preserve the above factorization of couplings at next-to-leading order [20].

Similar considerations apply at the LHC, except that the $q\bar{q}$ initial state involves a sea parton in pp collisions. Nevertheless, the energy and luminosity will be substantially higher than at the Tevatron, so that W' bosons with masses in the several TeV range will be probed [21]. If a W' boson will be discovered and the final state fermions have left-handed helicity, then the effects of $W - W'$ interference could be observed at the LHC [22] (and perhaps at the Tevatron [23]), providing useful information about the W' couplings.

In the $e\nu$ channel, the signal consists of a high-energy electron and a large missing transverse energy, with the invariant mass distribution forming a peak at $M_{W'}$. The best upper limit to date on the production cross-section $\sigma(p\bar{p} \rightarrow W'X)$ times the branching fraction $B(W' \rightarrow e\nu)$ has been set by DØ at around 200 fb for $M_{W'}$ in the 0.5 – 1 TeV range [17]. This preliminary limit at 95% CL, based on 900 pb⁻¹ of data, applies only if the right-handed neutrino of the first generation is light compared to $M_{W'}/2$ and escapes the detector. In the particular case $C_q^R = gV_{CKM}$, $C_l^R = g$, $C_q^L = C_l^L = 0$, the limit corresponds to $M_{W'} > 965$ GeV.

In the $t\bar{b}$ channel, the signal consists of a W decaying leptonically and two b -jets. The current best upper limit on the W' coupling to quarks (C_{q11}^R normalized to the standard model W coupling) set by CDF with 955 pb⁻¹ [19], is shown in Fig. 1.

In some theories (*e.g.*, [7]) the W' couplings to standard model fermions are suppressed due to a discrete symmetry. The W' bosons may then be produced in pairs via their couplings to the photon and Z . The decay modes are model dependent and often involve other particles beyond the standard model. The ensuing collider signals arise from cascade decays and typically include missing transverse energy.

Low-energy constraints. The properties of the W' are also constrained by measurements of processes at energies much below $M_{W'}$. The bounds on the tree-level $W - W'$ mixing [6] are mostly due to the change in the properties of the W boson compared to the standard model. Limits on the deviation in the ZWW coupling provide a leading constraint for fermiophobic W' bosons [13].

Constraints arising from low-energy effects of W' exchange are strongly model dependent. If the W' couplings to quarks are not suppressed, then box diagrams involving a W and a W' contribute to neutral meson mixing. In the case of W' couplings to right-handed quarks as in the left-right symmetric model, the limit from $K_L - K_s$ mixing is severe: $M_{W'} > 2.5$ TeV [24]. However, if no correlation between C_{qij}^R and C_{lij}^R is assumed, then the limit on $M_{W'}$ may be significantly relaxed [1]. There are also contributions of W' to the neutron electric dipole moment, muon decays and other processes.

If right-handed neutrinos have Majorana masses, then there are tree-level contributions to neutrinoless double-beta decay, and a limit on $M_{W'}$ versus the ν_R mass may be derived [25]. For ν_R masses below a few GeV, W' contributes to leptonic and semileptonic B meson decays, so that limits may be placed on various combinations of W' parameters [1]. For right-handed neutrino masses below ~ 30 MeV, most stringent constraints on $M_{W'}$ are due to the limits on ν_R emission from supernova.

References

1. P. Langacker, S.U. Sankar, Phys. Rev. D **40**, 1569 (1989).
2. R.N. Mohapatra and J.C. Pati, Phys. Rev. D **11**, 566 (1975); G. Senjanovic and R.N. Mohapatra, Phys. Rev. D **12**, 1502 (1975).
3. M. Bando, T. Kugo, and K. Yamawaki, Phys. Rept. **164**, 217 (1988).
4. H.C. Cheng *et al*, Phys. Rev. D **64**, 065007 (2001).
5. See the Section on “ Z' searches” in this *Review*.
6. See the particle listings for W' in this *Review*.
7. H.C. Cheng and I. Low, JHEP **0309**, 051 (2003).
8. K.S. Babu, X.G. He, and E. Ma, Phys. Rev. D **36**, 878 (1987).
9. H. Georgi, E.E. Jenkins, and E.H. Simmons, Nucl. Phys. B **331**, 541 (1990).
10. See, *e.g.*, X.-y. Li and E. Ma, J. Phys. G **19**, 1265 (1993).

See key on page 373

Gauge & Higgs Boson Particle Listings

Heavy Bosons Other than Higgs Bosons

11. D.J. Muller and S. Nandi, Phys. Lett. B **383**, 345 (1996)
E. Malkawi, T. Tait and, C.P. Yuan, Phys. Lett. B **385**, 304 (1996).
12. A. Donini *et al*, Nucl. Phys. B **507**, 51 (1997).
13. R.S. Chivukula *et al*, Phys. Rev. D **74**, 075011 (2006).
14. H.J. He, T. Tait and C.P. Yuan, Phys. Rev. D **62**, 011702 (2000).
15. F. Pisano and V. Pleitez, Phys. Rev. D **46**, 410 (1992);
Phys. Rev. D **51**, 3865 (1995).
16. A. Abulencia *et al*. [CDF Collaboration], Phys. Rev. D **75**, 091101 (2007).
17. DØ Collaboration, note 5191-Conf (2006).
18. V.M. Abazov *et al*. [DØ Collaboration], Phys. Lett. B **641**, 423 (2006).
19. CDF Collaboration, note 8747 (2007).
20. Z. Sullivan, Phys. Rev. D **66**, 075011 (2002).
21. See *e.g.*, V. Buescher *et al*, hep-ph/0608322; Z. Sullivan,
hep-ph/0306266.
22. T.G. Rizzo, JHEP **0705**, 037 (2007).
23. E. Boos *et al*, hep-ph/0610080.
24. Y. Zhang *et al*, hep-ph/0704.1662.
25. See Fig. 5 of G. Prezeau, M. Ramsey-Musolf, and P. Vogel,
Phys. Rev. D **68**, 034016 (2003).

MASS LIMITS for W' (Heavy Charged Vector Boson Other Than W) in Hadron Collider Experiments

Couplings of W' to quarks and leptons are taken to be identical with those of W . The following limits are obtained from $p\bar{p} \rightarrow W'X$ with W' decaying to the mode indicated in the comments. New decay channels (*e.g.*, $W' \rightarrow WZ$) are assumed to be suppressed. UA1 and UA2 experiments assume that the $t\bar{b}$ channel is not open.

VALUE (GeV)	CL%	DOCUMENT ID	TECN	COMMENT
>1000	95	ABAZOV	08C D0	$W' \rightarrow e\nu$
••• We do not use the following data for averages, fits, limits, etc. •••				
> 788	95	ABULENCIA	07k CDF	$W' \rightarrow e\nu$
none 200–610	95	1 ABAZOV	06N D0	$W' \rightarrow t\bar{b}$
> 800	95	ABAZOV	04C D0	$W' \rightarrow q\bar{q}$
225–536	95	2 ACOSTA	03B CDF	$W' \rightarrow t\bar{b}$
none 200–480	95	3 AFFOLDER	02c CDF	$W' \rightarrow WZ$
> 786	95	4 AFFOLDER	01i CDF	$W' \rightarrow e\nu, \mu\nu$
> 660	95	5 ABE	00 CDF	$W' \rightarrow \mu\nu$
none 300–420	95	6 ABE	97G CDF	$W' \rightarrow q\bar{q}$
> 720	95	7 ABACHI	96C D0	$W' \rightarrow e\nu$
> 610	95	8 ABACHI	95E D0	$W' \rightarrow e\nu, \tau\nu$
> 652	95	9 ABE	95M CDF	$W' \rightarrow e\nu$
> 251	90	10 ALITTI	93 UA2	$W' \rightarrow q\bar{q}$
none 260–600	95	11 RIZZO	93 RVUE	$W' \rightarrow q\bar{q}$
> 220	90	12 ALBAJAR	89 UA1	$W' \rightarrow e\nu$
> 209	90	13 ANSARI	87D UA2	$W' \rightarrow e\nu$

¹ The ABAZOV 06N quoted limit is for W' with SM-like coupling which interferes with the SM W boson. For W' with right-handed coupling, $M_{W'}$ between 200 and 630 (670) GeV is excluded for $M_{\nu_R} \ll M_{W'}$ ($M_{\nu_R} > M_{W'}$).

² The ACOSTA 03B quoted limit is for $M_{W'} \gg M_{\nu_R}$. For $M_{W'} < M_{\nu_R}$, $M_{W'}$ between 225 and 566 GeV is excluded.

³ The quoted limit is obtained assuming $W'WZ$ coupling strength is the same as the ordinary WWZ coupling strength in the Standard Model. See their Fig. 2 for the limits on the production cross sections as a function of the W' width.

⁴ AFFOLDER 01i combine a new bound on $W' \rightarrow e\nu$ of 754 GeV with the bound of ABE 00 on $W' \rightarrow \mu\nu$ to obtain quoted bound.

⁵ ABE 00 assume that the neutrino from W' decay is stable and has a mass significantly less than $m_{W'}$.

⁶ ABE 97G search for new particle decaying to dijets.

⁷ For bounds on W_R with nonzero right-handed mass, see Fig. 5 from ABACHI 96C.

⁸ ABACHI 95E assume that the decay $W' \rightarrow WZ$ is suppressed and that the neutrino from W' decay is stable and has a mass significantly less $m_{W'}$.

⁹ ABE 95M assume that the decay $W' \rightarrow WZ$ is suppressed and the (right-handed) neutrino is light, noninteracting, and stable. If $m_{\nu} = 60$ GeV, for example, the effect on the mass limit is negligible.

¹⁰ ALITTI 93 search for resonances in the two-jet invariant mass. The limit assumes $\Gamma(W')/m_{W'} = \Gamma(W)/m_W$ and $B(W' \rightarrow jj) = 2/3$. This corresponds to W_R with $m_{\nu_R} > m_{W'}$ (no leptonic decay) and $W_R \rightarrow t\bar{b}$ allowed. See their Fig. 4 for limits in the $m_{W'} - B(q\bar{q})$ plane.

¹¹ RIZZO 93 analyses CDF limit on possible two-jet resonances. The limit is sensitive to the inclusion of the assumed K factor.

¹² ALBAJAR 89 cross section limit at 630 GeV is $\sigma(W') B(e\nu) < 4.1$ pb (90% CL).

¹³ See Fig. 5 of ANSARI 87D for the excluded region in the $m_{W'} - [(g_{W'q})^2 B(W' \rightarrow e\bar{\nu})]$ plane. Note that the quantity $(g_{W'q})^2 B(W' \rightarrow e\bar{\nu})$ is normalized to unity for the standard W couplings.

W_R (Right-Handed W Boson) MASS LIMITS

Assuming a light right-handed neutrino, except for BEALL 82, LANGACKER 89b, and COLANGELO 91. $g_R = g_L$ assumed. [Limits in the section MASS LIMITS for W' below are also valid for W_R if $m_{\nu_R} \ll m_{W_R}$.] Some limits assume manifest left-right symmetry, *i.e.*, the equality of left- and right Cabibbo-Kobayashi-Maskawa matrices. For a comprehensive review, see LANGACKER 89b. Limits on the $W_L - W_R$ mixing angle ζ are found in the next section. Values in brackets are from cosmological and astrophysical considerations and assume a light right-handed neutrino.

VALUE (GeV)	CL%	DOCUMENT ID	TECN	COMMENT
> 715	90	14 CZAKON	99 RVUE	Electroweak
••• We do not use the following data for averages, fits, limits, etc. •••				
> 180	90	15 MELCONIAN	07 CNTR	^{37}K β^+ decay
> 290.7	90	16 SCHUMANN	07 CNTR	Polarized neutron decay
[> 3300]	95	17 CYBURT	05 COSM	Nucleosynthesis; light ν_R
> 310	90	18 THOMAS	01 CNTR	β^+ decay
> 137	95	19 ACKERSTAFF	99D OPAL	τ decay
>1400	68	20 BARENBOIM	98 RVUE	Electroweak, Z-Z' mixing
> 549	68	21 BARENBOIM	97 RVUE	μ decay
> 220	95	22 STAHL	97 RVUE	τ decay
> 220	90	23 ALLET	96 CNTR	β^+ decay
> 281	90	24 KUZNETSOV	95 CNTR	Polarized neutron decay
> 282	90	25 KUZNETSOV	94B CNTR	Polarized neutron decay
> 439	90	26 BHATTACH...	93 RVUE	Z-Z' mixing
> 250	90	27 SEVERIJNS	93 CNTR	β^+ decay
		28 IMAZATO	92 CNTR	K^+ decay
> 475	90	29 POLAK	92B RVUE	μ decay
> 240	90	30 AQUINO	91 RVUE	Neutron decay
> 496	90	30 AQUINO	91 RVUE	Neutron and muon decay
> 700		31 COLANGELO	91 THEO	$m_{K_L^0} - m_{K_S^0}$
> 477	90	32 POLAK	91 RVUE	μ decay
[none 540–23000]		33 BARBIERI	89B ASTR	SN 1987A; light ν_R
> 300	90	34 LANGACKER	89B RVUE	General
> 160	90	35 BALKE	88 CNTR	$\mu \rightarrow e\nu\bar{\nu}$
> 406	90	36 JODIDIO	86 ELEC	Any ζ
> 482	90	36 JODIDIO	86 ELEC	$\zeta = 0$
> 800		MOHAPATRA	86 RVUE	$SU(2)_L \times SU(2)_R \times U(1)$
> 400	95	37 STOKER	85 ELEC	Any ζ
> 475	95	37 STOKER	85 ELEC	$\zeta < 0.041$
		38 BERGSMA	83 CHRM	$\nu_\mu e \rightarrow \mu\nu_e$
> 380	90	39 CARR	83 ELEC	μ^+ decay
>1600		40 BEALL	82 THEO	$m_{K_L^0} - m_{K_S^0}$

¹⁴ CZAKON 99 perform a simultaneous fit to charged and neutral sectors.

¹⁵ MELCONIAN 07 measure the neutrino angular asymmetry in β^+ -decays of polarized ^{37}K , stored in a magneto-optical trap. Result is consistent with SM prediction and does not constrain the $W_L - W_R$ mixing angle appreciably.

¹⁶ SCHUMANN 07 limit is from measurements of the asymmetry $\langle \bar{\beta}_\nu \cdot \sigma_n \rangle$ in the β decay of polarized neutrons. Zero mixing is assumed.

¹⁷ CYBURT 05 limit follows by requiring that three light ν_R 's decouple when $T_{dec} > 140$ MeV. For different T_{dec} , the bound becomes $M_{W_R} > 3.3 \text{ TeV} (T_{dec} / 140 \text{ MeV})^{3/4}$.

¹⁸ THOMAS 01 limit is from measurement of β^+ polarization in decay of polarized ^{12}N . The listed limit assumes no mixing.

¹⁹ ACKERSTAFF 99D limit is from τ decay parameters. Limit increase to 145 GeV for zero mixing.

²⁰ BARENBOIM 98 assumes minimal left-right model with Higgs of $SU(2)_R$ in $SU(2)_L$ doublet. For Higgs in $SU(2)_L$ triplet, $m_{W_R} > 1100$ GeV. Bound calculated from effect of corresponding Z_{LR} on electroweak data through Z- Z_{LR} mixing.

²¹ The quoted limit is from μ decay parameters. BARENBOIM 97 also evaluate limit from $K_L - K_S$ mass difference.

²² STAHL 97 limit is from fit to τ -decay parameters.

²³ ALLET 96 measured polarization-asymmetry correlation in ^{12}N β^+ decay. The listed limit assumes zero $L-R$ mixing.

²⁴ KUZNETSOV 95 limit is from measurements of the asymmetry $\langle \bar{\beta}_\nu \cdot \sigma_n \rangle$ in the β decay of polarized neutrons. Zero mixing assumed. See also KUZNETSOV 94B.

²⁵ KUZNETSOV 94B limit is from measurements of the asymmetry $\langle \bar{\beta}_\nu \cdot \sigma_n \rangle$ in the β decay of polarized neutrons. Zero mixing assumed.

²⁶ BHATTACHARYYA 93 uses Z-Z' mixing limit from LEP '90 data, assuming a specific Higgs sector of $SU(2)_L \times SU(2)_R \times U(1)$ gauge model. The limit is for $m_t = 200$ GeV and slightly improves for smaller m_t .

²⁷ SEVERIJNS 93 measured polarization-asymmetry correlation in ^{107}In β^+ decay. The listed limit assumes zero $L-R$ mixing. Value quoted here is from SEVERIJNS 94 erratum.

²⁸ IMAZATO 92 measure positron asymmetry in $K^+ \rightarrow \mu^+ \nu_\mu$ decay and obtain $\epsilon_{P_{us}}^R > 0.990$ (90% CL). If W_R couples to $u\bar{s}$ with full weak strength ($V_{us}^R = 1$), the result corresponds to $m_{W_R} > 653$ GeV. See their Fig. 4 for m_{W_R} limits for general $|V_{us}^R|^2 = 1 - |V_{ud}^R|^2$.

²⁹ POLAK 92B limit is from fit to muon decay parameters and is essentially determined by JODIDIO 86 data assuming $\zeta = 0$. Supersedes POLAK 91.

³⁰ AQUINO 91 limits obtained from neutron lifetime and asymmetries together with unitarity of the CKM matrix. Manifest left-right symmetry assumed. Stronger of the two limits also includes muon decay results.

Gauge & Higgs Boson Particle Listings

Heavy Bosons Other than Higgs Bosons

- ³¹ COLANGELO 91 limit uses hadronic matrix elements evaluated by QCD sum rule and is less restrictive than BEALL 82 limit which uses vacuum saturation approximation. Manifest left-right symmetry assumed.
- ³² POLAK 91 limit is from fit to muon decay parameters and is essentially determined by JODIDIO 86 data assuming $\zeta=0$. Superseded by POLAK 92B.
- ³³ BARBIERI 89b limit holds for $m_{\nu_R} \leq 10$ MeV.
- ³⁴ LANGACKER 89b limit is for any ν_R mass (either Dirac or Majorana) and for a general class of right-handed quark mixing matrices.
- ³⁵ BALKE 88 limit is for $m_{\nu_{eR}} = 0$ and $m_{\nu_{\mu R}} \leq 50$ MeV. Limits come from precise measurements of the muon decay asymmetry as a function of the positron energy.
- ³⁶ JODIDIO 86 is the same TRIUMF experiment as STOKER 85 (and CARR 83); however, it uses a different technique. The results given here are combined results of the two techniques. The technique here involves precise measurement of the end-point e^+ spectrum in the decay of the highly polarized μ^+ .
- ³⁷ STOKER 85 is same TRIUMF experiment as CARR 83. Here they measure the decay e^+ spectrum asymmetry above 46 MeV/c using a muon-spin-rotation technique. Assumed a light right-handed neutrino. Quoted limits are from combining with CARR 83.
- ³⁸ BERGSMAN 83 set limit $m_{W_2}/m_{W_1} > 1.9$ at CL = 90%.
- ³⁹ CARR 83 is TRIUMF experiment with a highly polarized μ^+ beam. Looked for deviation from $V-A$ at the high momentum end of the decay e^+ energy spectrum. Limit from previous world-average muon polarization parameter is $m_{W_R} > 240$ GeV. Assumes a light right-handed neutrino.
- ⁴⁰ BEALL 82 limit is obtained assuming that W_R contribution to $K_L^0 - K_S^0$ mass difference is smaller than the standard one, neglecting the top quark contributions. Manifest left-right symmetry assumed.

Limit on W_L - W_R Mixing Angle ζ

Lighter mass eigenstate $W_1 = W_L \cos \zeta - W_R \sin \zeta$. Light ν_R assumed unless noted. Values in brackets are from cosmological and astrophysical considerations.

VALUE	CL%	DOCUMENT ID	TECN	COMMENT
< 0.12	95	41 ACKERSTAFF 99D	OPAL	τ decay
< 0.013	90	42 CZAKON 99	RVUE	Electroweak
< 0.0333		43 BARENBOIM 97	RVUE	μ decay
< 0.04	90	44 MISHRA 92	CCFR	νN scattering
-0.006 to 0.0028	90	45 AQUINO 91	RVUE	
[none 0.00001-0.02]		46 BARBIERI 89b	ASTR	SN 1987A
< 0.040	90	47 JODIDIO 86	ELEC	μ decay
-0.056 to 0.040	90	47 JODIDIO 86	ELEC	μ decay

- • • We do not use the following data for averages, fits, limits, etc. • • •
- ⁴¹ ACKERSTAFF 99D limit is from τ decay parameters.
- ⁴² CZAKON 99 perform a simultaneous fit to charged and neutral sectors.
- ⁴³ The quoted limit is from μ decay parameters. BARENBOIM 97 also evaluate limit from $K_L - K_S$ mass difference.
- ⁴⁴ MISHRA 92 limit is from the absence of extra large- x , large- y $\bar{\nu}_\mu N \rightarrow \bar{\nu}_\mu X$ events at Tevatron, assuming left-handed ν and right-handed $\bar{\nu}$ in the neutrino beam. The result gives $\zeta^2(1-2m_{W_1}^2/m_{W_2}^2) < 0.0015$. The limit is independent of ν_R mass.
- ⁴⁵ AQUINO 91 limits obtained from neutron lifetime and asymmetries together with unitarity of the CKM matrix. Manifest left-right asymmetry is assumed.
- ⁴⁶ BARBIERI 89b limit holds for $m_{\nu_R} \leq 10$ MeV.
- ⁴⁷ First JODIDIO 86 result assumes $m_{W_R} = \infty$, second is for unconstrained m_{W_R} .

Z' -BOSON SEARCHES

Written November 2007 by M.-C. Chen (UC Irvine) and B.A. Dobrescu (Fermilab).

The Z' boson is a hypothetical massive, electrically-neutral and color-singlet particle of spin 1. This particle is predicted in many extensions of the standard model, and has been the object of extensive phenomenological studies [1].

Z' couplings to quarks and leptons. The couplings of a Z' boson to the first-generation fermions are given by

$$Z'_\mu (g_u^L \bar{u}_L \gamma^\mu u_L + g_d^L \bar{d}_L \gamma^\mu d_L + g_u^R \bar{u}_R \gamma^\mu u_R + g_d^R \bar{d}_R \gamma^\mu d_R + g_\nu^L \bar{\nu}_L \gamma^\mu \nu_L + g_e^L \bar{e}_L \gamma^\mu e_L + g_e^R \bar{e}_R \gamma^\mu e_R) , \quad (1)$$

where u, d, ν and e are the quark and lepton fields in the mass eigenstate basis, and the coefficients $g_u^L, g_d^L, g_u^R, g_d^R, g_\nu^L, g_e^L, g_e^R$ are real dimensionless parameters. If the Z' couplings to quarks and leptons are generation-independent, then these seven parameters describe the couplings of the Z' to all standard-model fermions. More generally, however, the Z' couplings to fermions are generation-dependent, in which case Eq. (1) may

be written with some generation indices $i, j = 1, 2, 3$ labelling the quark and lepton fields, and with the seven coefficients promoted to 3×3 Hermitian matrices.

These parameters describing the Z' interactions with quarks and leptons are subject to some theoretical constraints. Quantum field theories that include a heavy spin-1 particle are well behaved at high energies only if that particle is a gauge boson associated with a spontaneously broken gauge symmetry. Quantum effects preserve the gauge symmetry only if the couplings of the gauge boson to fermions satisfy a certain set of equations called anomaly cancellation conditions. Furthermore, the charges of quarks and leptons under the new gauge symmetry are constrained by the requirement that the quarks and leptons get masses from gauge-invariant interactions with Higgs doublets or whatever else breaks the electroweak symmetry.

The relation between the couplings displayed in Eq. (1) and the gauge charges z_f^L and z_f^R of the fermions $f = u, d, \nu, e$ involves the unitary 3×3 matrices V_f^L and V_f^R that transform the gauge eigenstate fermions f_L and f_R , respectively, into the mass eigenstate ones. In addition, the Z' couplings are modified if the new gauge boson \tilde{Z}'_μ (in the gauge eigenstate basis) has a kinetic mixing $(-\chi/2)B^{\mu\nu}\tilde{Z}'_{\mu\nu}$ with the hypercharge gauge boson B^μ , or a mass mixing $\delta M^2 \tilde{Z}'^\mu \tilde{Z}'_\mu$ with the linear combination (\tilde{Z}_μ) of neutral bosons which has same couplings as the Z^0 in the standard model [2]. Both the kinetic and mass mixings shift the mass and couplings of the Z boson, such that the electroweak measurements impose upper limits on χ and $\delta M^2/(M_{Z'}^2 - M_Z^2)$ of the order of 10^{-3} [3]. Keeping only linear terms in these two small quantities, the couplings of the mass-eigenstate Z' boson are given by

$$g_f^L = g_z V_f^L z_f^L (V_f^L)^\dagger + \frac{e}{c_W} \left(\frac{s_W \chi M_{Z'}^2 + \delta M^2}{2s_W (M_{Z'}^2 - M_Z^2)} \sigma_f^3 - \epsilon Q_f \right) ,$$

$$g_f^R = g_z V_f^R z_f^R (V_f^R)^\dagger - \frac{e}{c_W} \epsilon Q_f , \quad (2)$$

where g_z is the new gauge coupling, Q_f is the electric charge of f , e is the electromagnetic gauge coupling, s_W and c_W are the sine and cosine of the weak mixing angle, $\sigma_f^3 = +1$ for $f = u, \nu$ and $\sigma_f^3 = -1$ for $f = d, e$, and

$$\epsilon = \frac{\chi (M_{Z'}^2 - c_W^2 M_Z^2) + s_W \delta M^2}{M_{Z'}^2 - M_Z^2} . \quad (3)$$

$U(1)$ gauge groups. A simple origin of a Z' is a new $U(1)'$ gauge symmetry. In that case, the matrixial equalities $z_u^L = z_d^L$ and $z_\nu^L = z_e^L$ are required by the $SU(2)_W$ gauge symmetry. Given that the $U(1)'$ interaction is not asymptotically free, the theory may be well-behaved at high energies (for example, by embedding $U(1)'$ in a non-Abelian gauge group) only if the Z' couplings are commensurate numbers, *i.e.*, any ratio of couplings is a rational number. Satisfying the anomaly cancellation conditions (which include an equation cubic in charges) with rational numbers is highly nontrivial, and in general new fermions charged under $U(1)'$ are necessary. Even then, one

See key on page 373

Gauge & Higgs Boson Particle Listings

Heavy Bosons Other than Higgs Bosons

should make sure that some anomaly-free set of fermions exists before assuming specific couplings of the Z' to quarks and leptons.

Table 1: Examples of generation-independent $U(1)'$ charges for quarks and leptons. The parameter x is an arbitrary rational number. Anomaly cancellation requires certain new fermions [4].

fermion	$U(1)_{B-xL}$	$U(1)_{10+x\bar{5}}$	$U(1)_{d-xu}$	$U(1)_{q+xu}$
(u_L, d_L)	1/3	1/3	0	1/3
u_R	1/3	-1/3	$-x/3$	$x/3$
d_R	1/3	$-x/3$	1/3	$(2-x)/3$
(ν_L, e_L)	$-x$	$x/3$	$(-1+x)/3$	-1
e_R	$-x$	-1/3	$x/3$	$-(2+x)/3$

Consider first the case where the couplings are generation-independent (the V_f matrices then disappear from Eq. (2)), so that there are five commensurate couplings: $g_q^r, g_u^r, g_d^r, g_l^r, g_e^r$. Four sets of charges are displayed in Table 1, each of them spanned by one free parameter, x [4]. The first set, labelled $B-xL$, has charges proportional to the baryon number minus x times the lepton number. These charges allow all standard model Yukawa couplings to a Higgs doublet which is neutral under $U(1)_{B-xL}$, so that there is no tree-level $\tilde{Z}-\tilde{Z}'$ mixing. For $x=1$ one recovers the $U(1)_{B-L}$ group, which is non-anomalous in the presence of one “right-handed neutrino” (a chiral fermion that is a singlet under the standard model gauge group) per generation. For $x \neq 1$, it is necessary to include some fermions that are vectorlike (*i.e.*, their mass terms are gauge invariant) with respect to the electroweak gauge group and chiral with respect to $U(1)_{B-xL}$. In the particular cases $x=0$ or $x \gg 1$ the Z' is leptophobic or quark-phobic, respectively.

The second set, $U(1)_{10+x\bar{5}}$, has charges that commute with the representations of the $SU(5)$ grand unified group. Here x is related to the mixing angle between the two $U(1)$ bosons encountered in the $E_6 \rightarrow SU(5) \times U(1) \times U(1)$ symmetry breaking patterns of grand unified theories [1,5]. This set leads to $\tilde{Z}-\tilde{Z}'$ mass mixing at tree level, such that for a Z' mass close to the electroweak scale, the measurements at the Z -pole require some fine tuning between the charges and VEVs of two Higgs doublets. Vectorlike fermions charged under the electroweak gauge group and also carrying color are required (except for $x=-3$) to make this set anomaly free. The particular cases $x=-3, 1, -1/2$ are usually labelled $U(1)_\chi, U(1)_\psi$, and $U(1)_\eta$, respectively. Under the third set, $U(1)_{d-xu}$, the weak-doublet quarks are neutral, and the ratio of u_R and d_R charges is $-x$. For $x=1$ this is the “right-handed” group $U(1)_R$. For $x=0$, the charges are those of the E_6 -inspired $U(1)_I$ group, which requires new quarks and leptons.

Table 2: Lepton-flavor dependent charges under various $U(1)$ gauge groups. No new fermions other than right-handed neutrinos are required.

fermion	$B-xL_e-yL_\mu$	2+1 leptocratic
q_{1L}, q_{2L}, q_{3L}	1/3	1/3
u_R, c_R, t_R	1/3	$x/3$
d_R, s_R, b_R	1/3	$(2-x)/3$
(ν_L^e, e_L)	$-x$	$-1-2y$
(ν_L^μ, μ_L)	$-y$	$-1+y$
(ν_L^τ, τ_L)	$x+y-3$	$-1+y$
e_R	$-x$	$-(2+x)/3-2y$
μ_R	$-y$	$-(2+x)/3+y$
τ_R	$x+y-3$	$-(2+x)/3+y$

In the absence of new fermions charged under the standard model group, the most general generation-independent charge assignment is $U(1)_{q+xu}$, which is a linear combination of hypercharge and $B-L$. Many other anomaly-free solutions exist if generation-dependent charges are allowed. Table 2 shows such solutions that depend on two free parameters, x and y , with generation dependence only in the lepton sector, which includes one right-handed neutrino per generation. The charged-lepton masses may be generated by Yukawa couplings to a single Higgs doublet. These are forced to be flavor diagonal by the generation-dependent $U(1)'$ charges, so that there are no tree-level flavor-changing neutral current (FCNC) processes involving electrically-charged leptons. For the “leptocratic” set, neutrino masses are induced by operators of high dimensionality that may explain their smallness [6].

If the $SU(2)_W$ -doublet quarks have generation-dependent $U(1)'$ charges, then the mass eigenstate quarks have flavor off-diagonal couplings to the Z' (see Eq. (1), and note that $V_u^L (V_d^L)^\dagger$ is the CKM matrix). These are severely constrained by measurements of FCNC processes, which in this case are mediated at tree-level by Z' exchange [7]. The constraints are relaxed if the first and second generation charges are the same, although they are increasingly tightened by the measurements of B meson properties. If only the $SU(2)_W$ -singlet quarks have generation-dependent $U(1)'$ charges, there is more freedom in adjusting the flavor off-diagonal couplings because the $V_{u,d}^R$ matrices are not observable in the standard model.

The anomaly cancellation conditions for $U(1)'$ could be relaxed only if at scales above $\sim 4\pi M_{Z'}/g_z$ there is an axion which has certain dimension-5 couplings to the gauge bosons. However, such a scenario violates unitarity unless the quantum field theory description breaks down at a scale near $M_{Z'}$.

Other models. Z' bosons may also arise from larger gauge groups. These may be orthogonal to the electroweak group, as in $SU(2)_W \times U(1)_Y \times SU(2)'$, or may embed the electroweak group, as in $SU(3)_W \times U(1)$. If the larger group is spontaneously broken down to $SU(2)_W \times U(1)_Y \times U(1)'$ at a scale v' larger than

Gauge & Higgs Boson Particle Listings

Heavy Bosons Other than Higgs Bosons

the electroweak scale v , then the above discussion applies up to corrections of order $(v/v')^2$. In some cases, though, the larger gauge group may break together with the electroweak symmetry directly to the electromagnetic $U(1)_{\text{em}}$. Consequently, the left-handed fermion charges are no longer correlated, *i.e.*, $z_u^L \neq z_d^L$ and $z_\nu^L \neq z_e^L$. Furthermore, additional gauge bosons are present at the electroweak scale, including at least a W' boson [8], and the Z' couples to a pair of W bosons.

If the electroweak gauge bosons propagate in extra dimensions, then their Kaluza-Klein excitations include a series of Z' boson pairs. Each of these pairs can be associated with a different $SU(2) \times U(1)$ gauge group in four dimensions. The properties of the Kaluza-Klein particles depend strongly on the extra-dimensional theory [9]. For example, in universal extra dimensions there is a parity that forces all couplings of Eq. (1) to vanish in the case of the lightest Kaluza-Klein bosons, while allowing couplings to pairs of fermions involving a standard model one and a heavy vectorlike fermion. There are also 4-dimensional gauge theories (*e.g.*, little Higgs with T parity) with Z' bosons exhibiting similar properties. By contrast, in a warped extra dimension, the couplings of Eq. (1) may be sizable even when standard model fields propagate along the extra dimension.

Z' bosons may also be composite particles. For example, in technicolor theories, the techni- ρ is a spin-1 boson that may be interpreted as arising from a spontaneously broken gauge symmetry [10].

Resonances versus cascade decays. In the presence of the couplings shown in Eq. (1), the Z' boson may be produced in the s -channel at hadron or lepton colliders, and would decay to pairs of fermions. The decay width into a pair of electrons is given by

$$\Gamma(Z' \rightarrow e^+e^-) \approx \left[(g_e^L)^2 + (g_e^R)^2 \right] \frac{M_{Z'}}{24\pi}, \quad (4)$$

where small corrections from electroweak loops are not included. The decay width into $q\bar{q}$ is similar, except for an additional color factor of 3, QCD radiative corrections, and fermion mass corrections. Thus, one may compute the Z' branching fractions in terms of the couplings of Eq. (1). However, other decay channels, such as WW or a pair of new particles, could have large widths and need to be added to the total decay width.

As mentioned above, there are interesting theories in which the Z' couplings are controlled by a discrete symmetry which does not allow its decay into a pair of standard model particles. Typically, such theories involve several new particles, which may be produced only in pairs and undergo cascade decays through Z' 's, leading to signals involving some missing transverse energy. Given that the cascade decays depend on the properties of new particles other than Z' , this case is not discussed further here.

LEP-II limits. The Z' contribution to the cross sections for $e^+e^- \rightarrow f\bar{f}$ proceeds through an s -channel Z' exchange (when $f = e$, there are also t - and u -channel exchanges). For

$M_{Z'} < \sqrt{s}$, the Z' appears as an $f\bar{f}$ resonance in the radiative return process where photon emission tunes the effective center-of-mass energy to $M_{Z'}$. The agreement between the LEP-II measurements and the standard model predictions implies that either the Z' couplings are smaller than or of order 10^{-2} , or else $M_{Z'}$ is above 209 GeV, the maximum energy of LEP-II. In the latter case, the Z' effects may be approximated up to corrections of order $s/M_{Z'}^2$ by the contact interactions

$$\frac{g_z^2}{M_{Z'}^2 - s} [\bar{e}\gamma_\mu (z_e^L P_L + z_e^R P_R) e] [\bar{f}\gamma^\mu (z_f^L P_L + z_f^R P_R) f], \quad (5)$$

where $P_{L,R}$ are chirality projection operators, and the relation between Z' couplings and charges (see Eq. (2) in the limit where the mass and kinetic mixings are neglected) was used assuming generation-independent charges. The four LEP collaborations have set limits on the coefficients of such operators for all possible chiral structures and for various combinations of fermions [11]. Thus, one may derive bounds on $(M_{Z'}/g_z)|z_e^L z_f^L|^{-1/2}$ and the analogous combinations of LR , RL and RR charges, which are typically on the order of a few TeV. Fig. 1 shows the LEP-II limits derived in [4] on the four sets of charges shown in Table 1.

Somewhat stronger bounds could be set on $M_{Z'}/g_z$ for specific sets of Z' couplings if the combined effects of several operators from Eq. (5) are taken into account. Even better limits on Z' bosons having various couplings could be set by dedicated analyses by the LEP collaborations. Such analyses have so far been performed only for fixed values of the gauge coupling (see section 3.5.2 of [11]).

Tevatron searches. At hadron colliders, Z' bosons with couplings to quarks (see Eq. (1)) may be produced in the s channel, and would show up as resonances in the invariant mass distribution of the decay products. Searches for Z' bosons in the Run II at the Tevatron have been performed by the CDF and D0 Collaborations in e^+e^- [12,13], $\mu^+\mu^-$ [14], $e\mu$ [15], $\tau^+\tau^-$ [16] and $t\bar{t}$ [17] final states. In addition to the invariant mass distribution for each of these pairs, the angular distribution can be used to set limits on (or measure, after discovery) several combinations of Z' parameters.

The Z' decay into e^+e^- is interesting due to relatively good mass resolution and large acceptance. Fig. 1 shows the limits on the sets of $U(1)$ charges from Table 1 obtained by CDF with 450 pb^{-1} in the e^+e^- final state [14]. The Z' decay into $\mu^+\mu^-$, $e\mu$ and $\tau^+\tau^-$, along with $t\bar{t}$ which suffers from larger backgrounds, are also important as they probe various combinations of couplings. Furthermore, these channels are sensitive to Z' bosons with suppressed couplings to the electrons (see Table 2), which are not constrained by the LEP searches.

Gauge & Higgs Boson Particle Listings

Heavy Bosons Other than Higgs Bosons

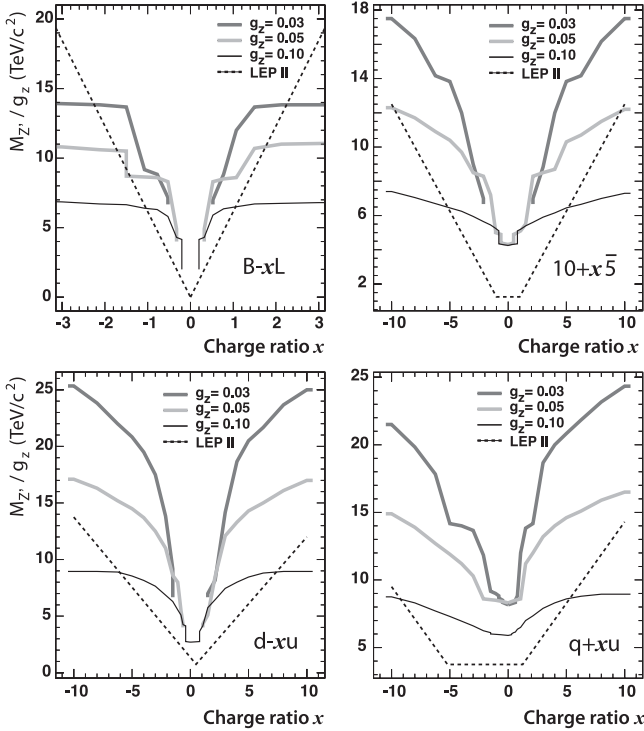


Figure 1: Exclusion limits on the sets of $U(1)$ charges shown in Table 1, from CDF (for different values of the gauge coupling g_z) and the LEP-II experiments (adapted from [13]). The CDF analysis combined the invariant mass and angular distributions of the e^+e^- final state.

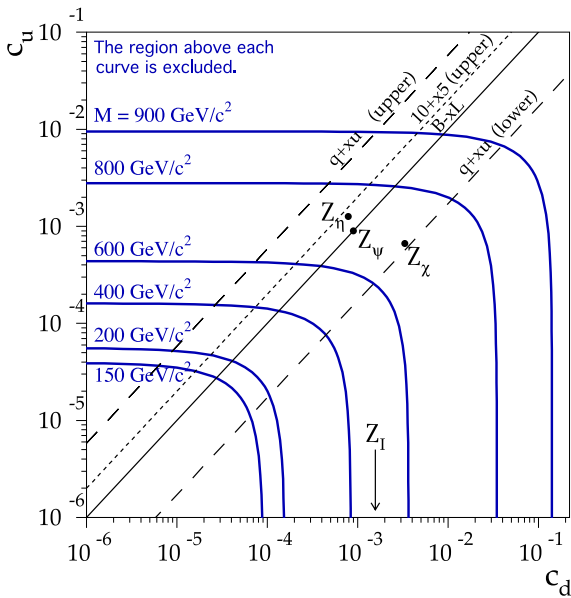


Figure 2: Exclusion region in the $c_u - c_d$ plane (see Eq. (7)) for given $M_{Z'}$. Figure adapted from [14].

The total cross section is typically the most sensitive observable to a Z' . For a narrow s -channel resonance, the interference of Z' with the Z or photon may be neglected, and the total cross section in the dilepton channel takes the form

$$\sigma(p\bar{p} \rightarrow Z'X \rightarrow \ell^+\ell^-X) = \frac{\pi}{48s} \sum_q c_q w_q(s, M_{Z'}^2) \quad (6)$$

for flavor-diagonal couplings to quarks. The coefficients

$$c_q = \left[(g_q^L)^2 + (g_q^R)^2 \right] B(Z' \rightarrow \ell^+\ell^-) \quad (7)$$

contain all the dependence on the couplings of quarks and leptons to the Z' , while the functions w_q include all the information about parton distributions and QCD corrections [4]. This factorization holds exactly to NLO, and the deviations from it induced at NNLO are very small. Note that only the w_u and w_d functions are likely to be sizable.

The results are often presented as an exclusion limit in the $\sigma(p\bar{p} \rightarrow Z'X \rightarrow \ell^+\ell^-X)$ versus $M_{Z'}$ plane (the current limit for the e^+e^- channel, based on 1.3 fb^{-1} of data, is 20 fb for $M_{Z'} \approx 300 \text{ GeV}$, decreasing to 6 fb for $M_{Z'} > 600 \text{ GeV}$ [12]). An alternative is to plot exclusion curves for fixed $M_{Z'}$ values in the $c_u - c_d$ plane. Fig. 2 shows the 95% limits set by CDF with 200 pb^{-1} by combining the e^+e^- and $\mu^+\mu^-$ final states, assuming generation-independent $M_{Z'}$ couplings. The diagonal lines indicate the regions allowed for the sets of $U(1)$ charges shown in Table 1. The $B - xL$ set implies $c_u = c_d$, for $10 + x\bar{5}$ all values $c_u \leq 2c_d$ are allowed, while the $q + xu$ set is restricted between the two dashed lines. The points marked Z_χ , Z_ψ , Z_η and Z_I correspond to the E_6 -inspired $U(1)'$ couplings with the gauge coupling g_z fixed by some unification condition [1,5].

LHC discovery potential. Z' bosons may be discovered at the LHC through their decays into e^+e^- , $\mu^+\mu^-$ and other fermion pairs. The factorization given in Eq. (6) is also applicable to the LHC, with different w_q functions, which now depend on the PDF's for the two incoming protons. Assuming that the couplings to fermions are of order 0.1 or larger, the ATLAS and CMS experiments will probe Z' masses up to 5 TeV with 100 fb^{-1} of data [18]. A 1% accuracy in the total cross sections at the LHC may be obtained by measuring the ratio of the Z' and Z productions. Even though the original quark direction in a pp collider is unknown, the leptonic forward-backward asymmetry A_{FB}^ℓ can be extracted from the kinematics of the dilepton system. These measurements, combined with a fit to the Z' rapidity distribution and other observables have the potential to distinguish the Z' couplings to fermions arising from different models. The ATLAS and CMS experiments may also be sensitive to the effects of the Z' interference with the Z and photon contributions to the dilepton signal.

Low-energy constraints. Z' properties are also constrained by a variety of low-energy experiments [19]. Polarized electron-nucleon scattering and atomic parity violation are sensitive to electron-quark contact interactions, which get contributions

Gauge & Higgs Boson Particle Listings

Heavy Bosons Other than Higgs Bosons

from Z' exchange that can be expressed in terms of the couplings introduced in Eq. (1) and M'_{ZZ} . Further corrections to the electron-quark contact interactions are induced in the presence of $\tilde{Z} - Z'$ mixing because of the shifts in the Z couplings to quarks and leptons [2]. Deep-inelastic neutrino-nucleon scattering is similarly affected by Z' bosons. Other low-energy observables are discussed in [3].

Although the LEP and Tevatron data are most constraining for many Z' models, one should be careful in assessing the relative reach of various experiments given the freedom in Z' couplings. For example, a Z' associated with the $U(1)_{B-xL_e-yL_\mu}$ model (see Table 2) for $x = 0$ and $y \gg 1$ couples only to leptons of the second and third generations, with implications for the muon $g - 2$, neutrino oscillations or τ decays, and would be hard to see in processes involving first-generation fermions.

References

- For reviews, see J. Hewett and T. Rizzo, Phys. Rept. **183**, 193 (1989); A. Leike, Phys. Rept. **317**, 143 (1999).
- K.S. Babu, C. Kolda, and J. March-Russell, Phys. Rev. **D57**, 6788 (1998); B. Holdom, Phys. Lett. **B259**, 329 (1991).
- J. Erler and P. Langacker, "Electroweak model and constraints on new physics" in this *Review*.
- M.S. Carena *et al.*, Phys. Rev. D **70**, 093009 (2004).
- See, *e.g.*, F. Del Aguila, M. Cvetič, and P. Langacker, Phys. Rev. D **52**, 37 (1995).
- M.-C. Chen, A. de Gouvêa, and B.A. Dobrescu, Phys. Rev. D **75**, 055009 (2007).
- P. Langacker and M. Plumacher, Phys. Rev. D **62**, 013006 (2000); R.S. Chivukula and E.H. Simmons, Phys. Rev. D **66**, 015006 (2002).
- See the Section on " W' searches" in this *Review*.
- G.F. Giudice and J.D. Wells, "Extra dimensions" in this *Review*.
- M. Bando, T. Kugo, and K. Yamawaki, Phys. Rept. **164**, 217 (1988).
- J. Alcaraz *et al.* [ALEPH, DELPHI, L3, OPAL Collaborations, LEP Electroweak Working Group], hep-ex/0612034.
- T. Aaltonen *et al.* [CDF Collaboration], hep-ex/0707.2524; DØ Collaboration, note 4375-Conf (2004).
- A. Abulencia *et al.* [CDF Collaboration], Phys. Rev. Lett. **96**, 211801 (2006).
- A. Abulencia *et al.* [CDF Collaboration], Phys. Rev. Lett. **95**, 252001 (2005); DØ Collaboration, note 4577-Conf (2004).
- A. Abulencia *et al.* [CDF Collaboration], Phys. Rev. Lett. **96**, 211802 (2006).
- D. Acosta *et al.* [CDF Collaboration], Phys. Rev. Lett. **95**, 131801 (2005).
- T. Aaltonen *et al.* [CDF Collaboration], hep-ex/0709.0705; CDF Collaboration, note 8675 (2007); DØ Collaboration, notes 5443-Conf and 5393-Conf (2007).
- See, *e.g.*, M. Dittmar, A.S. Nicollerat, and A. Djouadi, Phys. Lett. B **583**, 111 (2004).

- See, *e.g.*, V.D. Barger *et al.*, Phys. Rev. D **57**, 391 (1998).

MASS LIMITS for Z' (Heavy Neutral Vector Boson Other Than Z)

Limits for Z'_{SM}

Z'_{SM} is assumed to have couplings with quarks and leptons which are identical to those of Z , and decays only to known fermions.

VALUE (GeV)	CL%	DOCUMENT ID	TECN	COMMENT
> 923	95	48 AALTONEN 07H	CDF	$p\bar{p}; Z'_{SM} \rightarrow e^+e^-$
>1305	95	49 ABDALLAH 06C	DLPH	e^+e^-
>1500	95	50 CHEUNG 01B	RVUE	Electroweak
••• We do not use the following data for averages, fits, limits, etc. •••				
> 850		51 ABULENCIA 06L	CDF	Repl. by AALTONEN 07H
> 825	95	52 ABULENCIA 05A	CDF	$p\bar{p}; Z'_{SM} \rightarrow e^+e^-, \mu^+\mu^-$
> 399	95	53 ACOSTA 05R	CDF	$p\bar{p}; Z'_{SM} \rightarrow \tau^+\tau^-$
none 400-640	95	ABAZOV 04C	D0	$p\bar{p}; Z'_{SM} \rightarrow q\bar{q}$
>1018	95	54 ABBIENDI 04G	OPAL	e^+e^-
> 670	95	55 ABAZOV 01B	D0	$p\bar{p}; Z'_{SM} \rightarrow e^+e^-$
> 710	95	56 ABREU 00s	DLPH	e^+e^-
> 898	95	57 BARATE 00i	ALEP	e^+e^-
> 809	95	58 ERLER 99	RVUE	Electroweak
> 690	95	59 ABE 97s	CDF	$p\bar{p}; Z'_{SM} \rightarrow e^+e^-, \mu^+\mu^-$
> 490	95	ABACHI 96D	D0	$p\bar{p}; Z'_{SM} \rightarrow e^+e^-$
> 398	95	60 VILAIN 94B	CHM2	$\nu_\mu e \rightarrow \nu_\mu e$ and $\bar{\nu}_\mu e \rightarrow \bar{\nu}_\mu e$
> 237	90	61 ALITTI 93	UA2	$p\bar{p}; Z'_{SM} \rightarrow q\bar{q}$
none 260-600	95	62 RIZZO 93	RVUE	$p\bar{p}; Z'_{SM} \rightarrow q\bar{q}$
> 426	90	63 ABE 90F	VNS	e^+e^-

48 AALTONEN 07H search for resonances decaying to e^+e^- in $p\bar{p}$ collisions at $\sqrt{s} = 1.96$ TeV.

49 ABDALLAH 06C use data $\sqrt{s} = 130-207$ GeV.

50 CHEUNG 01B limit is derived from bounds on contact interactions in a global electroweak analysis.

51 ABULENCIA 06L search for resonances decaying to e^+e^- in $p\bar{p}$ collisions at $\sqrt{s} = 1.96$ TeV.

52 ABULENCIA 05A search for resonances decaying to electron or muon pairs in $p\bar{p}$ collisions at $\sqrt{s} = 1.96$ TeV.

53 ACOSTA 05R search for resonances decaying to tau lepton pairs in $p\bar{p}$ collisions at $\sqrt{s} = 1.96$ TeV.

54 ABBIENDI 04G give 95% CL limit on $Z-Z'$ mixing $-0.00422 < \theta < 0.00091$. $\sqrt{s} = 91$ to 207 GeV.

55 ABAZOV 01B search for resonances in $p\bar{p} \rightarrow e^+e^-$ at $\sqrt{s}=1.8$ TeV. They find $\sigma \cdot B(Z' \rightarrow ee) < 0.06$ pb for $M_{Z'} > 500$ GeV.

56 ABREU 00s uses LEP data at $\sqrt{s}=90$ to 189 GeV.

57 BARATE 00i search for deviations in cross section and asymmetries in $e^+e^- \rightarrow$ fermions at $\sqrt{s}=90$ to 183 GeV. Assume $\theta=0$. Bounds in the mass-mixing plane are shown in their Figure 18.

58 ERLER 99 give 90%CL limit on the $Z-Z'$ mixing $-0.0041 < \theta < 0.0003$. $\rho_0=1$ is assumed.

59 ABE 97s find $\sigma(Z') \times B(e^+e^-, \mu^+\mu^-) < 40$ fb for $m_{Z'} > 600$ GeV at $\sqrt{s}=1.8$ TeV.

60 VILAIN 94B assume $m_t = 150$ GeV.

61 ALITTI 93 search for resonances in the two-jet invariant mass. The limit assumes $B(Z' \rightarrow q\bar{q})=0.7$. See their Fig. 5 for limits in the $m_{Z'}-B(q\bar{q})$ plane.

62 RIZZO 93 analyses CDF limit on possible two-jet resonances.

63 ABE 90F use data for $R, R_{\ell\ell}$, and $A_{\ell\ell}$. They fix $m_W = 80.49 \pm 0.43 \pm 0.24$ GeV and $m_Z = 91.13 \pm 0.03$ GeV.

Limits for Z'_{LR}

Z'_{LR} is the extra neutral boson in left-right symmetric models. $g_L = g_R$ is assumed unless noted. Values in parentheses assume stronger constraint on the Higgs sector, usually motivated by specific left-right symmetric models (see the Note on the W'). Values in brackets are from cosmological and astrophysical considerations and assume a light right-handed neutrino. Direct search bounds assume decays to Standard Model fermions only, unless noted.

VALUE (GeV)	CL%	DOCUMENT ID	TECN	COMMENT
>600	95	SCHAEEL 07A	ALEP	e^+e^-
>860	95	64 CHEUNG 01B	RVUE	Electroweak
>630	95	65 ABE 97s	CDF	$p\bar{p}; Z'_{LR} \rightarrow e^+e^-, \mu^+\mu^-$
••• We do not use the following data for averages, fits, limits, etc. •••				
>455	95	66 ABDALLAH 06C	DLPH	e^+e^-
>518	95	67 ABBIENDI 04G	OPAL	e^+e^-
>380	95	68 ABREU 00s	DLPH	e^+e^-
>436	95	69 BARATE 00i	ALEP	Repl. by SCHAEEL 07A
>550	95	70 CHAY 00	RVUE	Electroweak
		71 ERLER 00	RVUE	Cs
		72 CASALBUONI 99	RVUE	Cs
(> 1205)	90	73 CZAKON 99	RVUE	Electroweak
>564	95	74 ERLER 99	RVUE	Electroweak
(> 1673)	95	75 ERLER 99	RVUE	Electroweak
(> 1700)	68	76 BARENBOIM 98	RVUE	Electroweak
>244	95	77 CONRAD 98	RVUE	$\nu_\mu N$ scattering
>253	95	78 VILAIN 94B	CHM2	$\nu_\mu e \rightarrow \nu_\mu e$ and $\bar{\nu}_\mu e \rightarrow \bar{\nu}_\mu e$
none 200-600	95	79 RIZZO 93	RVUE	$p\bar{p}; Z'_{LR} \rightarrow q\bar{q}$
[> 2000]		WALKER 91	COSM	Nucleosynthesis; light ν_R
none 200-500		80 GRIFOLS 90	ASTR	SN 1987A; light ν_R
none 350-2400		81 BARBIERI 89B	ASTR	SN 1987A; light ν_R

Gauge & Higgs Boson Particle Listings

Heavy Bosons Other than Higgs Bosons

- ⁶⁴ CHEUNG 01B limit is derived from bounds on contact interactions in a global electroweak analysis.
- ⁶⁵ ABE 97s find $\sigma(Z') \times B(e^+ e^-, \mu^+ \mu^-) < 40$ fb for $m_{Z'} > 600$ GeV at $\sqrt{s} = 1.8$ TeV.
- ⁶⁶ ABDALLAH 06c give 95% CL limit $|\theta| < 0.0028$. See their Fig. 14 for limit contours in the mass-mixing plane.
- ⁶⁷ ABBIENDI 04G give 95% CL limit on Z-Z' mixing $-0.0098 < \theta < 0.00190$. See their Fig. 20 for the limit contour in the mass-mixing plane. $\sqrt{s} = 91$ to 207 GeV.
- ⁶⁸ ABREU 00s give 95% CL limit on Z-Z' mixing $|\theta| < 0.0018$. See their Fig. 6 for the limit contour in the mass-mixing plane. $\sqrt{s} = 90$ to 189 GeV.
- ⁶⁹ BARATE 00i search for deviations in cross section and asymmetries in $e^+ e^- \rightarrow$ fermions at $\sqrt{s} = 90$ to 183 GeV. Assume $\theta = 0$. Bounds in the mass-mixing plane are shown in their Figure 18.
- ⁷⁰ CHAY 00 also find $-0.0003 < \theta < 0.0019$. For g_R free, $m_{Z'} > 430$ GeV.
- ⁷¹ ERLER 00 discuss the possibility that a discrepancy between the observed and predicted values of $Q_W(Cs)$ is due to the exchange of Z'. The data are better described in a certain class of the Z' models including Z_{LR} and Z_χ .
- ⁷² CASALBUONI 99 discuss the discrepancy between the observed and predicted values of $Q_W(Cs)$. It is shown that the data are better described in a class of models including the Z_{LR} model.
- ⁷³ CZAKON 99 perform a simultaneous fit to charged and neutral sectors. Assumes manifest left-right symmetric model. Finds $|\theta| < 0.0042$.
- ⁷⁴ ERLER 99 give 90% CL limit on the Z-Z' mixing $-0.0009 < \theta < 0.0017$.
- ⁷⁵ ERLER 99 assumes 2 Higgs doublets, transforming as 10 of SO(10), embedded in E_6 .
- ⁷⁶ BARENBOIM 98 also gives 68% CL limits on the Z-Z' mixing $-0.0005 < \theta < 0.0033$. Assumes Higgs sector of minimal left-right model.
- ⁷⁷ CONRAD 98 limit is from measurements at CCFR, assuming no Z-Z' mixing.
- ⁷⁸ VILAIN 94B assume $m_t = 150$ GeV and $\theta = 0$. See Fig. 2 for limit contours in the mass-mixing plane.
- ⁷⁹ RIZZO 93 analyses CDF limit on possible two-jet resonances.
- ⁸⁰ GRIFOLS 90 limit holds for $m_{\nu_R} \lesssim 1$ MeV. A specific Higgs sector is assumed. See also GRIFOLS 90b, RIZZO 91.
- ⁸¹ BARBIERI 89b limit holds for $m_{\nu_R} \leq 10$ MeV. Bounds depend on assumed supernova core temperature.

Limits for Z_χ

Z_χ is the extra neutral boson in $SO(10) \rightarrow SU(5) \times U(1)_\chi$. $g_\chi = e/\cos\theta_W$ is assumed unless otherwise stated. We list limits with the assumption $\rho = 1$ but with no further constraints on the Higgs sector. Values in parentheses assume stronger constraint on the Higgs sector motivated by superstring models. Values in brackets are from cosmological and astrophysical considerations and assume a light right-handed neutrino.

VALUE (GeV)	CL%	DOCUMENT ID	TECN	COMMENT
> 822	95	82 AALTONEN	07H CDF	$p\bar{p}, Z'_\chi \rightarrow e^+ e^-$
> 781	95	83 ABBIENDI	04G OPAL	$e^+ e^-$
• • • We do not use the following data for averages, fits, limits, etc. • • •				
> 680	95	SCHAEEL	07A ALEP	$e^+ e^-$
> 545	95	84 ABDALLAH	06c DLPH	$e^+ e^-$
> 740		85 ABULENCIA	06L CDF	Repl. by AALTONEN 07H
> 690	95	86 ABULENCIA	05A CDF	$p\bar{p}, Z'_\chi \rightarrow e^+ e^-, \mu^+ \mu^-$
> 2100		87 BARGER	03B COSM	Nucleosynthesis; light ν_R
> 680	95	88 CHEUNG	01B RVUE	Electroweak
> 440	95	89 ABREU	00s DLPH	$e^+ e^-$
> 533	95	90 BARATE	00i ALEP	Repl. by SCHAEEL 07A
> 554	95	91 CHO	00 RVUE	Electroweak
		92 ERLER	00 RVUE	Cs
		93 ROSNER	00 RVUE	Cs
> 545	95	94 ERLER	99 RVUE	Electroweak
(> 1368)	95	95 ERLER	99 RVUE	Electroweak
> 215	95	96 CONRAD	98 RVUE	$\nu_\mu N$ scattering
> 595	95	97 ABE	97s CDF	$p\bar{p}, Z'_\chi \rightarrow e^+ e^-, \mu^+ \mu^-$
> 190	95	98 ARIMA	97 VNS	Bhabha scattering
> 262	95	99 VILAIN	94B CHM2	$\nu_\mu e \rightarrow \nu_\mu e; \bar{\nu}_\mu e \rightarrow \bar{\nu}_\mu e$
> 1470]		100 FARAGGI	91 COSM	Nucleosynthesis; light ν_R
> 231	90	101 ABE	90f VNS	$e^+ e^-$
> 1140]		102 GONZALEZ-G.	90b COSM	Nucleosynthesis; light ν_R
> 2100]		103 GRIFOLS	90 ASTR	SN 1987A; light ν_R

- ⁸² AALTONEN 07H search for resonances decaying to $e^+ e^-$ in $p\bar{p}$ collisions at $\sqrt{s} = 1.96$ TeV.
- ⁸³ ABBIENDI 04G give 95% CL limit on Z-Z' mixing $-0.0099 < \theta < 0.00194$. See their Fig. 20 for the limit contour in the mass-mixing plane. $\sqrt{s} = 91$ to 207 GeV.
- ⁸⁴ ABDALLAH 06c give 95% CL limit $|\theta| < 0.0031$. See their Fig. 14 for limit contours in the mass-mixing plane.
- ⁸⁵ ABULENCIA 06L search for resonances decaying to $e^+ e^-$ in $p\bar{p}$ collisions at $\sqrt{s} = 1.96$ TeV.
- ⁸⁶ ABULENCIA 05A search for resonances decaying to electron or muon pairs in $p\bar{p}$ collisions at $\sqrt{s} = 1.96$ TeV.
- ⁸⁷ BARGER 03B limit is from the nucleosynthesis bound on the effective number of light neutrino $\delta N_\nu < 1$. The quark-hadron transition temperature $T_C = 150$ MeV is assumed. The limit with $T_C = 400$ MeV is > 4300 GeV.
- ⁸⁸ CHEUNG 01B limit is derived from bounds on contact interactions in a global electroweak analysis.
- ⁸⁹ ABREU 00s give 95% CL limit on Z-Z' mixing $|\theta| < 0.0017$. See their Fig. 6 for the limit contour in the mass-mixing plane. $\sqrt{s} = 90$ to 189 GeV.
- ⁹⁰ BARATE 00i search for deviations in cross section and asymmetries in $e^+ e^- \rightarrow$ fermions at $\sqrt{s} = 90$ to 183 GeV. Assume $\theta = 0$. Bounds in the mass-mixing plane are shown in their Figure 18.

- ⁹¹ CHO 00 use various electroweak data to constrain Z' models assuming $m_H = 100$ GeV. See Fig. 3 for limits in the mass-mixing plane.
- ⁹² ERLER 00 discuss the possibility that a discrepancy between the observed and predicted values of $Q_W(Cs)$ is due to the exchange of Z'. The data are better described in a certain class of the Z' models including Z_{LR} and Z_χ .
- ⁹³ ROSNER 00 discusses the possibility that a discrepancy between the observed and predicted values of $Q_W(Cs)$ is due to the exchange of Z'. The data are better described in a certain class of the Z' models including Z_χ .
- ⁹⁴ ERLER 99 give 90% CL limit on the Z-Z' mixing $-0.0020 < \theta < 0.0015$.
- ⁹⁵ ERLER 99 assumes 2 Higgs doublets, transforming as 10 of SO(10), embedded in E_6 .
- ⁹⁶ CONRAD 98 limit is from measurements at CCFR, assuming no Z-Z' mixing.
- ⁹⁷ ABE 97s find $\sigma(Z') \times B(e^+ e^-, \mu^+ \mu^-) < 40$ fb for $m_{Z'} > 600$ GeV at $\sqrt{s} = 1.8$ TeV.
- ⁹⁸ Z-Z' mixing is assumed to be zero. $\sqrt{s} = 57.77$ GeV.
- ⁹⁹ VILAIN 94B assume $m_t = 150$ GeV and $\theta = 0$. See Fig. 2 for limit contours in the mass-mixing plane.
- ¹⁰⁰ FARAGGI 91 limit assumes the nucleosynthesis bound on the effective number of neutrinos $\Delta N_\nu < 0.5$ and is valid for $m_{\nu_R} < 1$ MeV.
- ¹⁰¹ ABE 90f use data for $R, R_{\ell\ell}$, and $A_{\ell\ell}$. ABE 90f fix $m_W = 80.49 \pm 0.43 \pm 0.24$ GeV and $m_Z = 91.13 \pm 0.03$ GeV.
- ¹⁰² Assumes the nucleosynthesis bound on the effective number of light neutrinos ($\delta N_\nu < 1$) and that ν_R is light ($\lesssim 1$ MeV).
- ¹⁰³ GRIFOLS 90 limit holds for $m_{\nu_R} \lesssim 1$ MeV. See also GRIFOLS 90b, RIZZO 91.

Limits for Z_ψ

Z_ψ is the extra neutral boson in $E_6 \rightarrow SO(10) \times U(1)_\psi$. $g_\psi = e/\cos\theta_W$ is assumed unless otherwise stated. We list limits with the assumption $\rho = 1$ but with no further constraints on the Higgs sector. Values in brackets are from cosmological and astrophysical considerations and assume a light right-handed neutrino.

VALUE (GeV)	CL%	DOCUMENT ID	TECN	COMMENT
> 822	95	104 AALTONEN	07H CDF	$p\bar{p}, Z'_\psi \rightarrow e^+ e^-$
> 475	95	105 ABDALLAH	06c DLPH	$e^+ e^-$
• • • We do not use the following data for averages, fits, limits, etc. • • •				
> 410	95	SCHAEEL	07A ALEP	$e^+ e^-$
> 725		106 ABULENCIA	06L CDF	Repl. by AALTONEN 07H
> 675	95	107 ABULENCIA	05A CDF	$p\bar{p}, Z'_\psi \rightarrow e^+ e^-, \mu^+ \mu^-$
> 366	95	108 ABBIENDI	04G OPAL	$e^+ e^-$
> 600		109 BARGER	03B COSM	Nucleosynthesis; light ν_R
> 350	95	110 ABREU	00s DLPH	$e^+ e^-$
> 294	95	111 BARATE	00i ALEP	Repl. by SCHAEEL 07A
> 137	95	112 CHO	00 RVUE	Electroweak
> 146	95	113 ERLER	99 RVUE	Electroweak
> 54	95	114 CONRAD	98 RVUE	$\nu_\mu N$ scattering
> 590	95	115 ABE	97s CDF	$p\bar{p}, Z'_\psi \rightarrow e^+ e^-, \mu^+ \mu^-$
> 135	95	116 VILAIN	94B CHM2	$\nu_\mu e \rightarrow \nu_\mu e; \bar{\nu}_\mu e \rightarrow \bar{\nu}_\mu e$
> 105	90	117 ABE	90f VNS	$e^+ e^-$
> 160]		118 GONZALEZ-G.	90b COSM	Nucleosynthesis; light ν_R
> 2000]		119 GRIFOLS	90d ASTR	SN 1987A; light ν_R

- ¹⁰⁴ AALTONEN 07H search for resonances decaying to $e^+ e^-$ in $p\bar{p}$ collisions at $\sqrt{s} = 1.96$ TeV.
- ¹⁰⁵ ABDALLAH 06c give 95% CL limit $|\theta| < 0.0027$. See their Fig. 14 for limit contours in the mass-mixing plane.
- ¹⁰⁶ ABULENCIA 06L search for resonances decaying to $e^+ e^-$ in $p\bar{p}$ collisions at $\sqrt{s} = 1.96$ TeV.
- ¹⁰⁷ ABULENCIA 05A search for resonances decaying to electron or muon pairs in $p\bar{p}$ collisions at $\sqrt{s} = 1.96$ TeV.
- ¹⁰⁸ ABBIENDI 04G give 95% CL limit on Z-Z' mixing $-0.00129 < \theta < 0.00258$. See their Fig. 20 for the limit contour in the mass-mixing plane. $\sqrt{s} = 91$ to 207 GeV.
- ¹⁰⁹ BARGER 03B limit is from the nucleosynthesis bound on the effective number of light neutrino $\delta N_\nu < 1$. The quark-hadron transition temperature $T_C = 150$ MeV is assumed. The limit with $T_C = 400$ MeV is > 1100 GeV.
- ¹¹⁰ ABREU 00s give 95% CL limit on Z-Z' mixing $|\theta| < 0.0018$. See their Fig. 6 for the limit contour in the mass-mixing plane. $\sqrt{s} = 90$ to 189 GeV.
- ¹¹¹ BARATE 00i search for deviations in cross section and asymmetries in $e^+ e^- \rightarrow$ fermions at $\sqrt{s} = 90$ to 183 GeV. Assume $\theta = 0$. Bounds in the mass-mixing plane are shown in their Figure 18.
- ¹¹² CHO 00 use various electroweak data to constrain Z' models assuming $m_H = 100$ GeV. See Fig. 3 for limits in the mass-mixing plane.
- ¹¹³ ERLER 99 give 90% CL limit on the Z-Z' mixing $-0.0013 < \theta < 0.0024$.
- ¹¹⁴ CONRAD 98 limit is from measurements at CCFR, assuming no Z-Z' mixing.
- ¹¹⁵ ABE 97s find $\sigma(Z') \times B(e^+ e^-, \mu^+ \mu^-) < 40$ fb for $m_{Z'} > 600$ GeV at $\sqrt{s} = 1.8$ TeV.
- ¹¹⁶ VILAIN 94B assume $m_t = 150$ GeV and $\theta = 0$. See Fig. 2 for limit contours in the mass-mixing plane.
- ¹¹⁷ ABE 90f use data for $R, R_{\ell\ell}$, and $A_{\ell\ell}$. ABE 90f fix $m_W = 80.49 \pm 0.43 \pm 0.24$ GeV and $m_Z = 91.13 \pm 0.03$ GeV.
- ¹¹⁸ Assumes the nucleosynthesis bound on the effective number of light neutrinos ($\delta N_\nu < 1$) and that ν_R is light ($\lesssim 1$ MeV).
- ¹¹⁹ GRIFOLS 90d limit holds for $m_{\nu_R} \lesssim 1$ MeV. See also RIZZO 91.

Gauge & Higgs Boson Particle Listings

Heavy Bosons Other than Higgs Bosons

Limits for Z_η

Z_η is the extra neutral boson in E_6 models, corresponding to $Q_\eta = \sqrt{3/8} Q_\chi - \sqrt{5/8} Q_\psi$. $g_\eta = e/\cos\theta_{WW}$ is assumed unless otherwise stated. We list limits with the assumption $\rho=1$ but with no further constraints on the Higgs sector. Values in parentheses assume stronger constraint on the Higgs sector motivated by superstring models. Values in brackets are from cosmological and astrophysical considerations and assume a light right-handed neutrino.

VALUE (GeV)	CL%	DOCUMENT ID	TECN	COMMENT
> 891	95	120 AALTONEN	07H CDF	$p\bar{p}, Z'_\eta \rightarrow e^+e^-$
> 515	95	121 ABBIENDI	04G OPAL	e^+e^-
> 619	95	122 CHO	00 RVUE	Electroweak
••• We do not use the following data for averages, fits, limits, etc. •••				
> 350	95	123 SCHAEEL	07A ALEP	e^+e^-
> 360	95	123 ABDALLAH	06C DLPH	e^+e^-
> 745		124 ABULENCIA	06L CDF	Repl. by AALTONEN 07H
> 720	95	125 ABULENCIA	05A CDF	$p\bar{p}, Z'_\eta \rightarrow e^+e^-, \mu^+\mu^-$
>1600		126 BARGER	03B COSM	Nucleosynthesis; light ν_R
> 310	95	127 ABREU	00s DLPH	e^+e^-
> 329	95	128 BARATE	00i ALEP	Repl. by SCHAEEL 07A
> 365	95	129 ERLER	99 RVUE	Electroweak
> 87	95	130 CONRAD	98 RVUE	$\nu_\mu N$ scattering
> 620	95	131 ABE	97s CDF	$p\bar{p}, Z'_\eta \rightarrow e^+e^-, \mu^+\mu^-$
> 100	95	132 VILAIN	94B CHM2	$\nu_\mu e \rightarrow \nu_\mu e; \bar{\nu}_\mu e \rightarrow \bar{\nu}_\mu e$
> 125	90	133 ABE	90F VNS	e^+e^-
[> 820]		134 GONZALEZ-G.	90D COSM	Nucleosynthesis; light ν_R
[> 3300]		135 GRIFOLS	90 ASTR	SN 1987A; light ν_R
[> 1040]		134 LOPEZ	90 COSM	Nucleosynthesis; light ν_R

- 120 AALTONEN 07H search for resonances decaying to e^+e^- in $p\bar{p}$ collisions at $\sqrt{s} = 1.96$ TeV.
- 121 ABBIENDI 04G give 95% CL limit on Z - Z' mixing $-0.00447 < \theta < 0.00331$. See their Fig. 20 for the limit contour in the mass-mixing plane. $\sqrt{s} = 91$ to 207 GeV.
- 122 CHO 00 use various electroweak data to constrain Z' models assuming $m_H=100$ GeV. See Fig. 3 for limits in the mass-mixing plane.
- 123 ABDALLAH 06C give 95% CL limit $|\theta| < 0.0092$. See their Fig. 14 for limit contours in the mass-mixing plane.
- 124 ABULENCIA 06L search for resonances decaying to e^+e^- in $p\bar{p}$ collisions at $\sqrt{s} = 1.96$ TeV.
- 125 ABULENCIA 05A search for resonances decaying to electron or muon pairs in $p\bar{p}$ collisions at $\sqrt{s} = 1.96$ TeV.
- 126 BARGER 03B limit is from the nucleosynthesis bound on the effective number of light neutrino $\delta N_\nu < 1$. The quark-hadron transition temperature $T_C=150$ MeV is assumed. The limit with $T_C=400$ MeV is >3300 GeV.
- 127 ABREU 00s give 95% CL limit on Z - Z' mixing $|\theta| < 0.0024$. See their Fig. 6 for the limit contour in the mass-mixing plane. $\sqrt{s}=90$ to 189 GeV.
- 128 BARATE 00i search for deviations in cross section and asymmetries in $e^+e^- \rightarrow$ fermions at $\sqrt{s}=90$ to 183 GeV. Assume $\theta=0$. Bounds in the mass-mixing plane are shown in their Figure 18.
- 129 ERLER 99 give 90% CL limit on the Z - Z' mixing $-0.0062 < \theta < 0.0011$.
- 130 CONRAD 98 limit is from measurements at CCFR, assuming no Z - Z' mixing.
- 131 ABE 97s find $\sigma(Z') \times B(e^+e^-, \mu^+\mu^-) < 40$ fb for $m_{Z'} > 600$ GeV at $\sqrt{s} = 1.8$ TeV.
- 132 VILAIN 94B assume $m_t = 150$ GeV and $\theta=0$. See Fig. 2 for limit contours in the mass-mixing plane.
- 133 ABE 90F use data for $R, R_{\ell\ell}$, and $A_{\ell\ell}$. ABE 90F fix $m_W = 80.49 \pm 0.43 \pm 0.24$ GeV and $m_Z = 91.13 \pm 0.03$ GeV.
- 134 These authors claim that the nucleosynthesis bound on the effective number of light neutrinos ($\delta N_\nu < 1$) constrains Z' masses if ν_R is light ($\lesssim 1$ MeV).
- 135 GRIFOLS 90 limit holds for $m_{\nu_R} \lesssim 1$ MeV. See also GRIFOLS 90D, RIZZO 91.

Limits for other Z'

VALUE (GeV)	DOCUMENT ID	TECN	COMMENT
••• We do not use the following data for averages, fits, limits, etc. •••			
	136 ABULENCIA	06M CDF	$Z' \rightarrow e\mu$
	137 ABAZOV	04A D0	$Z' \rightarrow t\bar{t}$
	138 BARGER	03B COSM	Nucleosynthesis; light ν_R
	139 CHO	00 RVUE	E_6 -motivated
	140 CHO	98 RVUE	E_6 -motivated
	141 ABE	97G CDF	$Z' \rightarrow \bar{q}q$

- 136 ABULENCIA 06M search for new particle with lepton flavor violating decay at $\sqrt{s} = 1.96$ TeV. See their Fig. 4 for an exclusion plot on a mass-coupling plane.
- 137 Search for narrow resonance decaying to $t\bar{t}$. See their Fig. 2 for limit on σB .
- 138 BARGER 03B use the nucleosynthesis bound on the effective number of light neutrino δN_ν . See their Figs. 4-5 for limits in general E_6 motivated models.
- 139 CHO 00 use various electroweak data to constrain Z' models assuming $m_H=100$ GeV. See Fig. 2 for limits in general E_6 -motivated models.
- 140 CHO 98 study constraints on four-Fermi contact interactions obtained from low-energy electroweak experiments, assuming no Z - Z' mixing.
- 141 Search for Z' decaying to dijets at $\sqrt{s}=1.8$ TeV. For Z' with electromagnetic strength coupling, no bound is obtained.

Indirect Constraints on Kaluza-Klein Gauge Bosons

Bounds on a Kaluza-Klein excitation of the Z boson or photon in $d=1$ extra dimension. These bounds can also be interpreted as a lower bound on $1/R$, the size of the extra dimension. Unless otherwise stated, bounds assume all fermions live on a single brane and all gauge fields occupy the $4+d$ -dimensional bulk. See also the section on "Extra Dimensions" in the "Searches" Listings in this Review.

VALUE (TeV)	CL%	DOCUMENT ID	TECN	COMMENT
••• We do not use the following data for averages, fits, limits, etc. •••				
> 4.7		142 MUECK	02 RVUE	Electroweak
> 3.3	95	143 CORNET	00 RVUE	$e\nu q q'$
>5000		144 DELGADO	00 RVUE	e_K
> 2.6	95	145 DELGADO	00 RVUE	Electroweak
> 3.3	95	146 RIZZO	00 RVUE	Electroweak
> 2.9	95	147 MARCIANO	99 RVUE	Electroweak
> 2.5	95	148 MASIP	99 RVUE	Electroweak
> 1.6	90	149 NATH	99 RVUE	Electroweak
> 3.4	95	150 STRUMIA	99 RVUE	Electroweak

- 142 MUECK 02 limit is 2σ and is from global electroweak fit ignoring correlations among observables. Higgs is assumed to be confined on the brane and its mass is fixed. For scenarios of bulk Higgs, of brane-SU(2) $_L$, bulk-U(1) $_\gamma$, and of bulk-SU(2) $_L$, brane-U(1) $_\gamma$, the corresponding limits are > 4.6 TeV, > 4.3 TeV and > 3.0 TeV, respectively.
- 143 Bound is derived from limits on $e\nu q q'$ contact interaction, using data from HERA and the Tevatron.
- 144 Bound holds only if first two generations of quarks lives on separate branes. If quark mixing is not complex, then bound lowers to 400 TeV from Δm_K .
- 145 See Figs. 1 and 2 of DELGADO 00 for several model variations. Special boundary conditions can be found which permit KK states down to 950 GeV and that agree with the measurement of $Q_W(Cs)$. Quoted bound assumes all Higgs bosons confined to brane; placing one Higgs doublet in the bulk lowers bound to 2.3 TeV.
- 146 Bound is derived from global electroweak analysis assuming the Higgs field is trapped on the matter brane. If the Higgs propagates in the bulk, the bound increases to 3.8 TeV.
- 147 Bound is derived from global electroweak analysis but considering only presence of the KK W bosons.
- 148 Global electroweak analysis used to obtain bound independent of position of Higgs on brane or in bulk.
- 149 Bounds from effect of KK states on $G_F, \alpha, M_W,$ and M_Z . Hard cutoff at string scale determined using gauge coupling unification. Limits for $d=2,3,4$ rise to 3.5, 5.7, and 7.8 TeV.
- 150 Bound obtained for Higgs confined to the matter brane with $m_H=500$ GeV. For Higgs in the bulk, the bound increases to 3.5 TeV.

LEPTOQUARKS

Written November 2007 by S. Rolli (Tufts U.) and M. Tanabashi (Nagoya U.)

Leptoquarks are hypothetical particles carrying both baryon number (B) and lepton number (L). The possible quantum numbers of leptoquark states can be restricted by assuming that their direct interactions with the ordinary SM fermions are dimensionless and invariant under the standard model (SM) gauge group. Table 1 shows the list of all possible quantum numbers with this assumption [1]. The columns of $SU(3)_C$, $SU(2)_W$, and $U(1)_Y$ in Table 1 indicate the QCD representation, the weak isospin representation, and the weak hypercharge, respectively. The spin of a leptoquark state is taken to be 1 (vector leptoquark) or 0 (scalar leptoquark).

Table 1: Possible leptoquarks and their quantum numbers.

Spin	$3B+L$	$SU(3)_c$	$SU(2)_W$	$U(1)_Y$	Allowed coupling
0	-2	$\bar{3}$	1	1/3	$\bar{q}_L^\ell e_R$ or $\bar{u}_R^\ell e_R$
0	-2	$\bar{3}$	1	4/3	$\bar{d}_R^\ell e_R$
0	-2	$\bar{3}$	3	1/3	$\bar{q}_L^\ell \ell_L$
1	-2	$\bar{3}$	2	5/6	$\bar{q}_L^\ell \gamma^\mu e_R$ or $\bar{d}_R^\ell \gamma^\mu \ell_L$
1	-2	$\bar{3}$	2	-1/6	$\bar{u}_R^\ell \gamma^\mu \ell_L$
0	0	3	2	7/6	$\bar{q}_L e_R$ or $\bar{u}_R \ell_L$
0	0	3	2	1/6	$\bar{d}_R \ell_L$
1	0	3	1	2/3	$\bar{q}_L \gamma^\mu \ell_L$ or $\bar{d}_R \gamma^\mu e_R$
1	0	3	1	5/3	$\bar{u}_R \gamma^\mu e_R$
1	0	3	3	2/3	$\bar{q}_L \gamma^\mu \ell_L$

See key on page 373

Gauge & Higgs Boson Particle Listings

Heavy Bosons Other than Higgs Bosons

If we do not require leptoquark states to couple directly with SM fermions, different assignments of quantum numbers become possible [2,3].

Leptoquark states are expected to exist in various extensions of SM. The Pati-Salam model [4] is an example predicting the existence of a leptoquark state. Vector leptoquark states also exist in grand unification theories based on $SU(5)$ [5], $SO(10)$ [6], which includes Pati-Salam color $SU(4)$, and larger gauge groups. Scalar quarks in supersymmetric models with R-parity violation may also have leptoquark-type Yukawa couplings. The bounds on the leptoquark states can therefore be applied to constraining R-parity-violating supersymmetric models. Scalar leptoquarks are expected to exist at TeV scale in extended technicolor models [7,8] where leptoquark states appear as the bound states of techni-fermions. Compositeness of quarks and leptons also provides examples of models which may have light leptoquark states [9].

Bounds on leptoquark states are obtained both directly and indirectly. Direct limits are from their production cross sections at colliders, while indirect limits are calculated from the bounds on the leptoquark-induced four-fermion interactions, which are obtained from low-energy experiments, or from collider experiments below threshold.

If a leptoquark couples to fermions more than a single generation in the mass eigenbasis of the SM fermions, it can induce four-fermion interactions causing flavor-changing neutral currents and lepton-family-number violations. The quantum number assignment of Table 1 allows several leptoquark states to couple to both left- and right-handed quarks simultaneously. Such leptoquark states are called non-chiral and may cause four-fermion interactions affecting the $(\pi \rightarrow e\nu)/(\pi \rightarrow \mu\nu)$ ratio [10]. Non-chiral scalar leptoquarks also contribute to the muon anomalous magnetic moment [11,12]. Indirect limits provide stringent constraints on these leptoquarks.

It is therefore often assumed that a leptoquark state couples only to a single generation in a chiral interaction, where indirect limits become much weaker. This assumption gives strong constraints on concrete models of leptoquarks, however. Leptoquark states which couple only to left- or right-handed quarks are called chiral leptoquarks. Leptoquark states which couple only to the first (second, third) generation are referred as the first- (second-, third-) generation leptoquarks. Refs. [13,14] give extensive lists of the bounds on the leptoquark-induced four-fermion interactions. For the isoscalar and vector leptoquarks S_0 and V_0 , for example, which couple with the first- (second-) generation left-handed quark, and the first-generation left-handed lepton, the bounds of Ref. 13 read $\lambda^2 < 0.03 \times (M_{LQ}/300 \text{ GeV})^2$ for S_0 , and $\lambda^2 < 0.02 \times (M_{LQ}/300 \text{ GeV})^2$ for V_0 ($\lambda^2 < 5 \times (M_{LQ}/300 \text{ GeV})^2$ for S_0 , and $\lambda^2 < 3 \times (M_{LQ}/300 \text{ GeV})^2$ for V_0) with λ being the leptoquark coupling strength. The e^+e^- experiments are sensitive to the indirect effects coming from t - and u -channel exchanges of leptoquarks in the $e^+e^- \rightarrow q\bar{q}$ process. The HERA experiments give bounds on the leptoquark-induced

four-fermion interaction. For detailed bounds obtained in this way, see the Boson Particle Listings for ‘‘Indirect Limits for Leptoquarks’’ and its references.

Collider experiments provide direct limits on the leptoquark states through limits on the pair- and single-production cross sections. The leading-order cross sections of the parton processes

$$\begin{aligned} q + \bar{q} &\rightarrow LQ + \overline{LQ} \\ g + g &\rightarrow LQ + \overline{LQ} \\ e + q &\rightarrow LQ \end{aligned} \quad (1)$$

may be written as [15]

$$\begin{aligned} \hat{\sigma}_{\text{LO}} [q\bar{q} \rightarrow LQ + \overline{LQ}] &= \frac{2\alpha_s^2\pi}{27\hat{s}}\beta^3, \\ \hat{\sigma}_{\text{LO}} [gg \rightarrow LQ + \overline{LQ}] &= \frac{\alpha_s^2\pi}{96\hat{s}} \\ &\times \left[\beta(41 - 31\beta^2) + (18\beta^2 - \beta^4 - 17) \log \frac{1+\beta}{1-\beta} \right], \\ \hat{\sigma}_{\text{LO}} [eq \rightarrow LQ] &= \frac{\pi\lambda^2}{4}\delta(\hat{s} - M_{LQ}^2) \end{aligned} \quad (2)$$

for a scalar leptoquark. Here $\sqrt{\hat{s}}$ is the invariant energy of the parton subprocess, and $\beta \equiv \sqrt{1 - 4M_{LQ}^2/\hat{s}}$. The leptoquark Yukawa coupling is given by λ . Leptoquarks are also produced singly at hadron colliders through $g + q \rightarrow LQ + \ell$ [16], which allows extending the collider reach in the leptoquark search [17], depending on the leptoquark Yukawa coupling.

The Tevatron and LEP experiments search for pair production of the leptoquark states, which arises from the leptoquark gauge interaction. The gauge couplings of a scalar leptoquark are determined uniquely according to its quantum numbers in Table 1. Since all of the leptoquark states belong to color-triplet representation, the scalar leptoquark pair-production cross section at Tevatron can be determined solely as a function of the leptoquark mass without making further assumptions. This is in contrast to the indirect or single-production limits, which give constraints in the leptoquark mass-coupling plane. For the first- and second-generation scalar leptoquark states with decaying branching fraction $B(eq) = 1$ and $B(\mu q) = 1$, the CDF and D0 experiments obtain the lower bounds on the leptoquark mass $> 236 \text{ GeV}$ (first generation, CDF) [18], $> 256 \text{ GeV}$ (first generation, D0) [19], $> 226 \text{ GeV}$ (second generation, CDF) [20], and $> 251 \text{ GeV}$ (second generation, D0) [21] at 95% CL. On the other hand, the magnetic-dipole-type and the electric-quadrupole-type interactions of a vector leptoquark are not determined even if we fix its gauge quantum numbers as listed in the Table [22]. The production of vector leptoquarks depends in general on additional assumptions that the leptoquark couplings and their pair-production cross sections are enhanced relative to the scalar leptoquark contributions. At the Tevatron for instance, since the acceptance for vector and scalar leptoquark detection is similar, limits on the vector leptoquark

Gauge & Higgs Boson Particle Listings

Heavy Bosons Other than Higgs Bosons

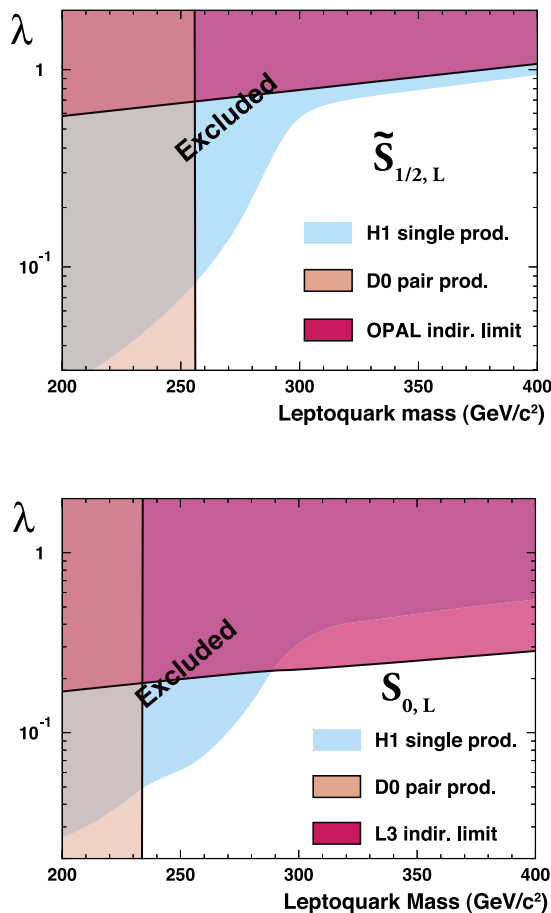


Figure 1: Limits on two typical first-generation scalar leptoquark states in the mass-coupling plane. The upper figure is for a weak-isodoublet, weak-hypercharge $7/6$, $3B + L = 0$ leptoquark state, while the lower figure is for a weak-isosinglet, weak-hypercharge $-1/3$, $3B + L = 2$ state. Color version at end of book.

mass will be more stringent. The leptoquark pair-production cross sections in e^+e^- collisions depend on the leptoquark $SU(2) \times U(1)$ quantum numbers and Yukawa coupling with electron [23]. The OPAL experiment gives mass bounds on various leptoquark states from the pair-production cross sections [24]. For a second-generation weak-isosinglet weak-hypercharge $-4/3$ scalar-leptoquark state, for example, the OPAL pair-production bound is $M_{LQ} > 100$ GeV at 95% CL.

The searches for the leptoquark single production are performed by the HERA experiments. Since the leptoquark single-production cross section depends on the leptoquark Yukawa coupling, the leptoquark limits from HERA are usually displayed in the mass-coupling plane. For leptoquark Yukawa coupling $\lambda = 0.1$, the ZEUS bounds on the first-generation leptoquarks range from 248 to 290 GeV, depending on the leptoquark species [25]. Similar bounds are obtained by H1 [26].

The LEP experiments also search for the single production of the leptoquark states from the process $e\gamma \rightarrow LQ + q$.

Fig. 1 summarizes D0, LEP, and H1 limits on two typical first-generation scalar-leptoquark states in the mass-coupling plane [26].

The search for LQ will be continued soon at the CERN LHC. Preliminary feasibility studies by the LHC experiments ATLAS [27] and CMS [28] indicate that clear signals can be established for masses up to about $M(LQ)$ 1.3 to 1.4 TeV for first- and second-generation scalar LQ, with a final reach of presumably 1.5 TeV.

Reference

1. W. Buchmüller, R. Rückl, and D. Wyler, Phys. Lett. **B191**, 442 (1987).
2. K. S. Babu, C. F. Kolda, and J. March-Russell, Phys. Lett. **B408**, 261 (1997).
3. J. L. Hewett and T. G. Rizzo, Phys. Rev. **D58**, 055005 (1998).
4. J.C. Pati and A. Salam, Phys. Rev. **D10**, 275 (1974).
5. H. Georgi and S.L. Glashow, Phys. Rev. Lett. **32**, 438 (1974).
6. H. Georgi, AIP Conf. Proc. **23**, 575 (1975); H. Fritzsch and P. Minkowski, Ann. Phys. **93**, 193 (1975).
7. For a review, see, E. Farhi and L. Susskind, Phys. Reports **74**, 277 (1981).
8. K. Lane and M. Ramana, Phys. Rev. **D44**, 2678 (1991).
9. See, for example, B. Schrepf and F. Schrepf, Phys. Lett. **153B**, 101 (1985).
10. O. Shanker, Nucl. Phys. **B204**, 375, (1982).
11. U. Mahanta, Eur. Phys. J. **C21**, 171 (2001) [Phys. Lett. **B515**, 111 (2001)].
12. K. Cheung, Phys. Rev. **D64**, 033001 (2001).
13. S. Davidson, D.C. Bailey, and B.A. Campbell, Z. Phys. **C61**, 613 (1994).
14. M. Leurer, Phys. Rev. **D49**, 333 (1994); Phys. Rev. **D50**, 536 (1994).
15. T. Plehn *et al.*, Z. Phys. **C74**, 611 (1997); M. Kramer *et al.*, Phys. Rev. Lett. **79**, 341 (1997); and references therein.
16. J.L. Hewett and S. Pakvasa, Phys. Rev. **D37**, 3165 (1988); O.J.P. Eboli and A.V. Olinto, Phys. Rev. **D38**, 3461 (1988); A. Dobado, M.J. Herrero, and C. Munoz, Phys. Lett. **207B**, 97 (1988); V.D. Barger *et al.*, Phys. Lett. **B220**, 464 (1989); M. De Montigny and L. Marleau, Phys. Rev. **D40**, 2869 (1989) [Erratum-*ibid.* **D56**, 3156 (1997)].
17. A. Belyaev *et al.*, JHEP **0509**, 005 (2005).
18. D. Acosta *et al.*, [CDF Collaboration], Phys. Rev. **D72**, 051107 (2005).
19. V.M. Abazov *et al.*, [D0 Collaboration], Phys. Rev. **D71**, 071104 (2005).
20. A. Abulencia *et al.*, [CDF Collaboration], Phys. Rev. **D73**, 051102 (2006).
21. V.M. Abazov *et al.*, [D0 Collaboration], Phys. Lett. **B636**, 183 (2006).

22. J. Blümlein, E. Boos, and A. Kryukov, *Z. Phys.* **C76**, 137 (1997).
23. J. Blümlein and R. Ruckl, *Phys. Lett.* **B304**, 337 (1993).
24. G. Abbiendi *et al.*, [OPAL Collaboration], *Eur. Phys. J.* **C31**, 281 (2003).
25. S. Chekanov *et al.*, [ZEUS Collaboration], *Phys. Rev.* **D68**, 052004 (2003).
26. A. Aktas *et al.*, [H1 Collaboration], *Phys. Lett.* **B629**, 9 (2005).
27. V.A. Mitsou *et al.*, *hep-ph/0411189*.
28. S. Abdulin and F. Charles, *Phys. Lett.* **B464**, 223 (1999).

MASS LIMITS for Leptoquarks from Pair Production

These limits rely only on the color or electroweak charge of the leptoquark.

VALUE (GeV)	CL%	DOCUMENT ID	TECN	COMMENT
>229	95	151 ABAZOV	07J D0	Third generation
>251	95	152 ABAZOV	06A D0	Second generation
>226	95	153 ABULENCIA	06T CDF	Second generation
>256	95	154 ABAZOV	05H D0	First generation
>236	95	155 ACOSTA	05P CDF	First generation
• • •				We do not use the following data for averages, fits, limits, etc. • • •
>136	95	156 ABAZOV	06L D0	All generations
>117	95	157 ACOSTA	05I CDF	First generation
>99	95	158 ABBIENDI	03R OPAL	First generation
>100	95	158 ABBIENDI	03R OPAL	Second generation
>98	95	158 ABBIENDI	03R OPAL	Third generation
>98	95	159 ABAZOV	02 D0	All generations
>225	95	160 ABAZOV	01D D0	First generation
>85.8	95	161 ABBIENDI	00M OPAL	Superseded by ABBIENDI 03R
>85.5	95	161 ABBIENDI	00M OPAL	Superseded by ABBIENDI 03R
>82.7	95	161 ABBIENDI	00M OPAL	Superseded by ABBIENDI 03R
>200	95	162 ABBOTT	00C D0	Second generation
>123	95	163 AFFOLDER	00K CDF	Second generation
>148	95	164 AFFOLDER	00K CDF	Third generation
>160	95	165 ABBOTT	99J D0	Second generation
>225	95	166 ABBOTT	98E D0	First generation
>94	95	167 ABBOTT	98J D0	Third generation
>202	95	168 ABE	98S CDF	Second generation
>242	95	169 GROSS-PILCH.	98 First generation	
>99	95	170 ABE	97F CDF	Third generation
>213	95	171 ABE	97X CDF	First generation
>45.5	95	172,173 ABREU	93J DLPH	First + second generation
>44.4	95	174 ADRIANI	93M L3	First generation
>44.5	95	174 ADRIANI	93M L3	Second generation
>45	95	174 DECAMP	92 ALEP	Third generation
none 8.9–22.6	95	175 KIM	90 AMY	First generation
none 10.2–23.2	95	175 KIM	90 AMY	Second generation
none 5–20.8	95	176 BARTEL	87B JADE	
none 7–20.5	95	177 BEHREND	86B CELL	

- 151 ABAZOV 07J search for pair productions of scalar leptoquark state decaying to νb in $p\bar{p}$ collisions at $E_{cm} = 1.96$ TeV. The limit above assumes $B(\nu b) = 1$.
- 152 ABAZOV 06A search for scalar leptoquarks using $\mu\mu jj$ events in $p\bar{p}$ collisions at $E_{cm} = 1.8$ TeV and at 1.96 TeV. The limit above assumes $B(\mu q) = 1$. For $B(\mu q) = 0.5$, the limit becomes 204 GeV.
- 153 ABULENCIA 06T search for scalar leptoquarks using $\mu\mu jj$, $\nu\nu jj$, and $\nu\nu jj$ events in $p\bar{p}$ collisions at $E_{cm} = 1.96$ TeV. The quoted limit assumes $B(\mu q) = 1$. For $B(\mu q) = 0.5$ or 0.1, the bound becomes 208 GeV or 143 GeV, respectively. See their Fig. 4 for the exclusion limit as a function of $B(\mu q)$.
- 154 ABAZOV 05H search for scalar leptoquarks using $e\bar{e}jj$ and $e\nu jj$ events in $\bar{p}p$ collisions at $E_{cm} = 1.8$ TeV and 1.96 TeV. The limit above assumes $B(eq) = 1$. For $B(eq) = 0.5$ the bound becomes 234 GeV.
- 155 ACOSTA 05P search for scalar leptoquarks using $e\bar{e}jj$, $e\nu jj$ events in $\bar{p}p$ collisions at $E_{cm} = 1.96$ TeV. The limit above assumes $B(eq) = 1$. For $B(eq) = 0.5$ and 0.1, the bound becomes 205 GeV and 145 GeV, respectively.
- 156 ABAZOV 06I search for scalar leptoquarks using $\nu\nu jj$ events in $p\bar{p}$ collisions at $E_{cm} = 1.8$ TeV and at 1.96 TeV. The limit above assumes $B(\nu q) = 1$.
- 157 ACOSTA 05I search for scalar leptoquarks using $\nu\nu jj$ events in $\bar{p}p$ collisions at $E_{cm} = 1.96$ TeV. The limit above assumes $B(\nu q) = 1$.
- 158 ABBIENDI 03R search for scalar/vector leptoquarks in e^+e^- collisions at $\sqrt{s} = 189-209$ GeV. The quoted limits are for charge $-4/3$ isospin 0 scalar-leptoquark with $B(\ell q) = 1$. See their table 12 for other cases.
- 159 ABAZOV 02 search for scalar leptoquarks using $\nu\nu jj$ events in $\bar{p}p$ collisions at $E_{cm} = 1.8$ TeV. The bound holds for all leptoquark generations. Vector leptoquarks are likewise constrained to lie above 200 GeV.
- 160 ABAZOV 01D search for scalar leptoquarks using $e\nu jj$, $e\bar{e}jj$, and $\nu\nu jj$ events in $p\bar{p}$ collisions at $E_{cm} = 1.8$ TeV. The limit above assumes $B(eq) = 1$. For $B(eq) = 0.5$ and 0, the bound becomes 204 and 79 GeV, respectively. Bounds for vector leptoquarks are also given. Supersedes ABBOTT 98E.
- 161 ABBIENDI 00M search for scalar/vector leptoquarks in e^+e^- collisions at $\sqrt{s} = 183$ GeV. The quoted limits are for charge $-4/3$ isospin 0 scalar-leptoquarks with $B(\ell q) = 1$. See their Table 8 and Figs. 6–9 for other cases.
- 162 ABBOTT 00C search for scalar leptoquarks using $\mu\mu jj$, $\nu\nu jj$, and $\nu\nu jj$ events in $p\bar{p}$ collisions at $E_{cm} = 1.8$ TeV. The limit above assumes $B(\mu q) = 1$. For $B(\mu q) = 0.5$ and 0, the bound becomes 180 and 79 GeV respectively. Bounds for vector leptoquarks are also given.

- 163 AFFOLDER 00K search for scalar leptoquark using $\nu\nu cc$ events in $p\bar{p}$ collisions at $E_{cm} = 1.8$ TeV. The quoted limit assumes $B(\nu c) = 1$. Bounds for vector leptoquarks are also given.
- 164 AFFOLDER 00K search for scalar leptoquark using $\nu\nu bb$ events in $p\bar{p}$ collisions at $E_{cm} = 1.8$ TeV. The quoted limit assumes $B(\nu b) = 1$. Bounds for vector leptoquarks are also given.
- 165 ABBOTT 99J search for leptoquarks using $\mu\nu jj$ events in $p\bar{p}$ collisions at $E_{cm} = 1.8$ TeV. The quoted limit is for a scalar leptoquark with $B(\mu q) = B(\nu q) = 0.5$. Limits on vector leptoquarks range from 240 to 290 GeV.
- 166 ABBOTT 98E search for scalar leptoquarks using $e\nu jj$, $e\bar{e}jj$, and $\nu\nu jj$ events in $p\bar{p}$ collisions at $E_{cm} = 1.8$ TeV. The limit above assumes $B(eq) = 1$. For $B(eq) = 0.5$ and 0, the bound becomes 204 and 79 GeV, respectively.
- 167 ABBOTT 98J search for charge $-1/3$ third generation scalar and vector leptoquarks in $p\bar{p}$ collisions at $E_{cm} = 1.8$ TeV. The quoted limit is for scalar leptoquark with $B(\nu b) = 1$.
- 168 ABE 98S search for scalar leptoquarks using $\mu\mu jj$ events in $p\bar{p}$ collisions at $E_{cm} = 1.8$ TeV. The limit is for $B(\mu q) = 1$. For $B(\mu q) = B(\nu q) = 0.5$, the limit is > 160 GeV.
- 169 GROSS-PILCHER 98 is the combined limit of the CDF and DØ Collaborations as determined by a joint CDF/DØ working group and reported in this FNAL Technical Memo. Original data published in ABE 97X and ABBOTT 98E.
- 170 ABE 97F search for third generation scalar and vector leptoquarks in $p\bar{p}$ collisions at $E_{cm} = 1.8$ TeV. The quoted limit is for scalar leptoquark with $B(\tau b) = 1$.
- 171 ABE 97X search for scalar leptoquarks using $e\bar{e}jj$ events in $p\bar{p}$ collisions at $E_{cm} = 1.8$ TeV. The limit is for $B(eq) = 1$.
- 172 Limit is for charge $-1/3$ isospin-0 leptoquark with $B(\ell q) = 2/3$.
- 173 First and second generation leptoquarks are assumed to be degenerate. The limit is slightly lower for each generation.
- 174 Limits are for charge $-1/3$, isospin-0 scalar leptoquarks decaying to $\ell^- q$ or νq with any branching ratio. See paper for limits for other charge-isospin assignments of leptoquarks.
- 175 KIM 90 assume pair production of charge $2/3$ scalar-leptoquark via photon exchange. The decay of the first (second) generation leptoquark is assumed to be any mixture of $d\bar{e}^+$ and $u\bar{\nu}$ ($s\mu^+$ and $c\bar{\nu}$). See paper for limits for specific branching ratios.
- 176 BARTEL 87B limit is valid when a pair of charge $2/3$ spinless leptoquarks X is produced with point coupling, and when they decay under the constraint $B(X \rightarrow c\bar{\nu}_\mu) + B(X \rightarrow s\mu^+) = 1$.
- 177 BEHREND 86B assumed that a charge $2/3$ spinless leptoquark, χ , decays either into $s\mu^+$ or $c\bar{\nu}$: $B(\chi \rightarrow s\mu^+) + B(\chi \rightarrow c\bar{\nu}) = 1$.

MASS LIMITS for Leptoquarks from Single Production

These limits depend on the q - ℓ -leptoquark coupling g_{LQ} . It is often assumed that $g_{LQ}^2/4\pi = 1/137$. Limits shown are for a scalar, weak isoscalar, charge $-1/3$ leptoquark.

VALUE (GeV)	CL%	DOCUMENT ID	TECN	COMMENT
>298	95	178 CHEKANOV	03B ZEUS	First generation
>73	95	179 ABREU	93J DLPH	Second generation
• • •				We do not use the following data for averages, fits, limits, etc. • • •
>295	95	180 ABAZOV	07E D0	Second generation
		181 AKTAS	05B H1	First generation
		182 CHEKANOV	05A ZEUS	Lepton-flavor violation
>197	95	183 ABBIENDI	02B OPAL	First generation
		184 CHEKANOV	02C ZEUS	Repl. by CHEKANOV 05A
>290	95	185 ADLOFF	01C H1	First generation
>204	95	186 BREITWEG	01 ZEUS	First generation
		187 BREITWEG	00E ZEUS	First generation
>161	95	188 ABREU	99G DLPH	First generation
>200	95	189 ADLOFF	99 H1	First generation
		190 DERRICK	97 ZEUS	Lepton-flavor violation
>168	95	191 DERRICK	93 ZEUS	First generation

- 178 CHEKANOV 03B limit is for a scalar, weak isoscalar, charge $-1/3$ leptoquark coupled with e_τ . See their Figs. 11–12 and Table 5 for limits on states with different quantum numbers.
- 179 Limit from single production in Z decay. The limit is for a leptoquark coupling of electromagnetic strength and assumes $B(\ell q) = 2/3$. The limit is 77 GeV if first and second leptoquarks are degenerate.
- 180 ABAZOV 07E search for leptoquark single production through qg fusion process in $p\bar{p}$ collisions. See their Fig. 4 for exclusion plot in mass-coupling plane.
- 181 AKTAS 05B limit is for a scalar, weak isoscalar, charge $-1/3$ leptoquark coupled with e_τ . See their Fig. 3 for limits on states with different quantum numbers.
- 182 CHEKANOV 05 search for various leptoquarks with lepton-flavor violating couplings. See their Figs. 6–10 and Tables 1–8 for detailed limits.
- 183 For limits on states with different quantum numbers and the limits in the mass-coupling plane, see their Fig. 4 and Fig. 5.
- 184 CHEKANOV 02 search for various leptoquarks with lepton-flavor violating couplings. See their Figs. 6–7 and Tables 5–6 for detailed limits.
- 185 For limits on states with different quantum numbers and the limits in the mass-coupling plane, see their Fig. 3.
- 186 See their Fig. 14 for limits in the mass-coupling plane.
- 187 BREITWEG 00E search for $F=0$ leptoquarks in e^+p collisions. For limits in mass-coupling plane, see their Fig. 11.
- 188 ABREU 99G limit obtained from process $e\gamma \rightarrow LQ+q$. For limits on vector and scalar states with different quantum numbers and the limits in the coupling-mass plane, see their Fig. 4 and Table 2.
- 189 For limits on states with different quantum numbers and the limits in the mass-coupling plane, see their Fig. 13 and Fig. 14. ADLOFF 99 also search for leptoquarks with lepton-flavor violating couplings. ADLOFF 99 supersedes AID 96B.
- 190 DERRICK 97 search for various leptoquarks with lepton-flavor violating couplings. See their Figs. 5–8 and Table 1 for detailed limits.
- 191 DERRICK 93 search for single leptoquark production in $e p$ collisions with the decay $e q$ and νq . The limit is for leptoquark coupling of electromagnetic strength and assumes

Gauge & Higgs Boson Particle Listings

Heavy Bosons Other than Higgs Bosons

$B(eq) = B(\nu q) = 1/2$. The limit for $B(eq) = 1$ is 176 GeV. For limits on states with different quantum numbers, see their Table 3.

Indirect Limits for Leptoquarks

VALUE (TeV)	CL%	DOCUMENT ID	TECN	COMMENT
• • • We do not use the following data for averages, fits, limits, etc. • • •				
>	0.49	192 AKTAS	07A H1	Lepton-flavor violation
>		193 SCHAEEL	07A ALEP	$e^+e^- \rightarrow q\bar{q}$
>		194 SMIRNOV	07 RVUE	$K \rightarrow e\mu, B \rightarrow e\tau$
>	1.7	195 CHEKANOV	05A ZEUS	Lepton-flavor violation
>	46	196 ADLOFF	03 H1	First generation
>		197 CHANG	03 BELL	Pati-Salam type
>		198 CHEKANOV	02 ZEUS	Repl. by CHEKANOV 05A
>	1.7	199 CHEUNG	01B RVUE	First generation
>	0.39	200 ACCIARRI	00P L3	$e^+e^- \rightarrow qq$
>	1.5	201 ADLOFF	00 H1	First generation
>	0.2	202 BARATE	00 ALEP	Repl. by SCHAEEL 07A
>		203 BARGER	00 RVUE	Cs
>		204 GABRIELLI	00 RVUE	Lepton flavor violation
>	0.74	205 ZARNECKI	00 RVUE	S_1 leptoquark
>		206 ABBIENDI	99 OPAL	
>	19.3	207 ABE	98V CDF	$B_s \rightarrow e^\pm \mu^\mp$, Pati-Salam type
>		208 ACCIARRI	98J L3	$e^+e^- \rightarrow q\bar{q}$
>		209 ACKERSTAFF	98V OPAL	$e^+e^- \rightarrow q\bar{q}, e^+e^- \rightarrow b\bar{b}$
>	0.76	210 DEANDREA	97 RVUE	\tilde{R}_2 leptoquark
>		211 DERRICK	97 ZEUS	Lepton-flavor violation
>		212 GROSSMAN	97 RVUE	$B \rightarrow \tau^+\tau^-(X)$
>		213 JADACH	97 RVUE	$e^+e^- \rightarrow q\bar{q}$
>	>1200	214 KUZNETSOV	95B RVUE	Pati-Salam type
>		215 MIZUKOSHI	95 RVUE	Third generation scalar leptoquark
>	0.3	216 BHATTACH...	94 RVUE	Spin-0 leptoquark coupled to $\bar{\nu}_R t_L$
>		217 DAVIDSON	94 RVUE	
>	18	218 KUZNETSOV	94 RVUE	Pati-Salam type
>	0.43	219 LEURER	94 RVUE	First generation spin-1 leptoquark
>	0.44	219 LEURER	94B RVUE	First generation spin-0 leptoquark
>		220 MAHANTA	94 RVUE	P and T violation
>	1	221 SHANKER	82 RVUE	Nonchiral spin-0 leptoquark
>	125	221 SHANKER	82 RVUE	Nonchiral spin-1 leptoquark

- 192 AKTAS 07A search for lepton-flavor violation in ep collision. See their Tables 4–7 for limits on lepton-flavor violating four-fermion interactions induced by various leptoquarks.
- 193 SCHAEEL 07A limit is for the weak-isoscalar spin-0 left-handed leptoquark with the coupling of electromagnetic strength. For the limits of leptoquarks with different quantum numbers, see their Table 35.
- 194 SMIRNOV 07 obtains mass limits for the vector and scalar chiral leptoquark states from $K \rightarrow e\mu, B \rightarrow e\tau$ decays.
- 195 CHEKANOV 05 search for various leptoquarks with lepton-flavor violating couplings. See their Figs. 6–10 and Tables 1–8 for detailed limits.
- 196 ADLOFF 03 limit is for the weak isotriplet spin-0 leptoquark at strong coupling $\lambda = \sqrt{4\pi}$. For the limits of leptoquarks with different quantum numbers, see their Table 3. Limits are derived from bounds on $e^\pm q$ contact interactions.
- 197 The bound is derived from $B(B^0 \rightarrow e^\pm \mu^\mp) < 1.7 \times 10^{-7}$.
- 198 CHEKANOV 02 search for lepton-flavor violation in ep collisions. See their Tables 1–4 for limits on lepton-flavor violating and four-fermion interactions induced by various leptoquarks.
- 199 CHEUNG 01B quoted limit is for a scalar, weak isoscalar, charge $-1/3$ leptoquark with a coupling of electromagnetic strength. The limit is derived from bounds on contact interactions in a global electroweak analysis. For the limits of leptoquarks with different quantum numbers, see Table 5.
- 200 ACCIARRI 00P limit is for the weak isoscalar spin-0 leptoquark with the coupling of electromagnetic strength. For the limits of leptoquarks with different quantum numbers, see their Table 4.
- 201 ADLOFF 00 limit is for the weak isotriplet spin-0 leptoquark at strong coupling, $\lambda = \sqrt{4\pi}$. For the limits of leptoquarks with different quantum numbers, see their Table 2.
- ADLOFF 00 limits are from the Q^2 spectrum measurement of $e^+p \rightarrow e^+X$.
- 202 BARATE 00i search for deviations in cross section and jet-charge asymmetry in $e^+e^- \rightarrow \bar{q}q$ due to t -channel exchange of a leptoquark at $\sqrt{s}=130$ to 183 GeV. Limits for other scalar and vector leptoquarks are also given in their Table 22.
- 203 BARGER 00 explain the deviation of atomic parity violation in cesium atoms from prediction is explained by scalar leptoquark exchange.
- 204 GABRIELLI 00 calculate various process with lepton flavor violation in leptoquark models.
- 205 ZARNECKI 00 limit is derived from data of HERA, LEP, and Tevatron and from various low-energy data including atomic parity violation. Leptoquark coupling with electromagnetic strength is assumed.
- 206 ABBIENDI 99 limits are from $e^+e^- \rightarrow q\bar{q}$ cross section at 130–136, 161–172, 183 GeV. See their Fig. 8 and Fig. 9 for limits in mass-coupling plane.
- 207 ABE 98V quoted limit is from $B(B_s \rightarrow e^\pm \mu^\mp) < 8.2 \times 10^{-6}$. ABE 98V also obtain a similar limit on $M_{LQ} > 20.4$ TeV from $B(B_d \rightarrow e^\pm \mu^\mp) < 4.5 \times 10^{-6}$. Both bounds assume the non-canonical association of the b quark with electrons or muons under $SU(4)$.
- 208 ACCIARRI 98J limit is from $e^+e^- \rightarrow q\bar{q}$ cross section at $\sqrt{s}=130$ –172 GeV which can be affected by the t - and u -channel exchanges of leptoquarks. See their Fig. 4 and Fig. 5 for limits in the mass-coupling plane.
- 209 ACKERSTAFF 98V limits are from $e^+e^- \rightarrow q\bar{q}$ and $e^+e^- \rightarrow b\bar{b}$ cross sections at $\sqrt{s}=130$ –172 GeV, which can be affected by the t - and u -channel exchanges of leptoquarks. See their Fig. 21 and Fig. 22 for limits of leptoquarks in mass-coupling plane.
- 210 DEANDREA 97 limit is for \tilde{R}_2 leptoquark obtained from atomic parity violation (APV). The coupling of leptoquark is assumed to be electromagnetic strength. See Table 2 for limits of the four-fermion interactions induced by various scalar leptoquark exchange. DEANDREA 97 combines APV limit and limits from Tevatron and HERA. See Fig. 1–4 for combined limits of leptoquark in mass-coupling plane.

- 211 DERRICK 97 search for lepton-flavor violation in ep collision. See their Tables 2–5 for limits on lepton-flavor violating four-fermion interactions induced by various leptoquarks.
- 212 GROSSMAN 97 estimate the upper bounds on the branching fraction $B \rightarrow \tau^+\tau^-(X)$ from the absence of the B decay with large missing energy. These bounds can be used to constrain leptoquark induced four-fermion interactions.
- 213 JADACH 97 limit is from $e^+e^- \rightarrow q\bar{q}$ cross section at $\sqrt{s}=172.3$ GeV which can be affected by the t - and u -channel exchanges of leptoquarks. See their Fig. 1 for limits on vector leptoquarks in mass-coupling plane.
- 214 KUZNETSOV 95B use π, K, B, τ decays and μe conversion and give a list of bounds on the leptoquark mass and the fermion mixing matrix in the Pati-Salam model. The quoted limit is from $K_L \rightarrow \mu e$ decay assuming zero mixing.
- 215 MIZUKOSHI 95 calculate the one-loop radiative correction to the Z -physics parameters in various scalar leptoquark models. See their Fig. 4 for the exclusion plot of third generation leptoquark models in mass-coupling plane.
- 216 BHATTACHARYYA 94 limit is from one-loop radiative correction to the leptonic decay width of the Z . $m_H=250$ GeV, $\alpha_s(m_Z)=0.12$, $m_t=180$ GeV, and the electroweak strength of leptoquark coupling are assumed. For leptoquark coupled to $\bar{\nu}_L t_R, \bar{\nu} t$, and $\bar{\nu} \tau$, see Fig. 2 in BHATTACHARYYA 94b erratum and Fig. 3.
- 217 DAVIDSON 94 gives an extensive list of the bounds on leptoquark-induced four-fermion interactions from π, K, D, B, μ, τ decays and meson mixings, etc. See Table 15 of DAVIDSON 94 for detail.
- 218 KUZNETSOV 94 gives mixing independent bound of the Pati-Salam leptoquark from the cosmological limit on $\pi^0 \rightarrow \bar{\nu}\nu$.
- 219 LEURER 94, LEURER 94B limits are obtained from atomic parity violation and apply to any chiral leptoquark which couples to the first generation with electromagnetic strength. For a nonchiral leptoquark, universality in π_{e2} decay provides a much more stringent bound.
- 220 MAHANTA 94 gives bounds of P - and T -violating scalar-leptoquark couplings from atomic and molecular experiments.
- 221 From $(\pi \rightarrow e\nu)/(\pi \rightarrow \mu\nu)$ ratio. SHANKER 82 assumes the leptoquark induced four-fermion coupling $4g^2/M^2 (\bar{\nu}_{eL} u_R) (\bar{\nu}_{eL} e_R)$ with $g=0.004$ for spin-0 leptoquark and $g^2/M^2 (\bar{\nu}_{eL} \gamma^\mu u_L) (\bar{\nu}_{eL} \gamma^\mu e_R)$ with $g=0.6$ for spin-1 leptoquark.

MASS LIMITS for Diquarks

VALUE (GeV)	CL%	DOCUMENT ID	TECN	COMMENT
• • • We do not use the following data for averages, fits, limits, etc. • • •				
none 290–420	95	222 ABE	97G CDF	E_6 diquark
none 15–31.7	95	223 ABREU	94O DLPH	SUSY E_6 diquark
222 ABE 97G search for new particle decaying to dijets.				
223 ABREU 94O limit is from $e^+e^- \rightarrow \bar{c}cs$. Range extends up to 43 GeV if diquarks are degenerate in mass.				

MASS LIMITS for g_A (axigluon)

Axigluons are massive color-octet gauge bosons in chiral color models and have axial-vector coupling to quarks with the same coupling strength as gluons.

VALUE (GeV)	CL%	DOCUMENT ID	TECN	COMMENT
• • • We do not use the following data for averages, fits, limits, etc. • • •				
>910	95	224 CHOUDHURY	07 RVUE	$p\bar{p} \rightarrow t\bar{t}X$
>365	95	225 DONCHESKI	98 RVUE	$\Gamma(Z \rightarrow \text{hadron})$
none 200–980	95	226 ABE	97G CDF	$p\bar{p} \rightarrow g_A X, g_A \rightarrow 2$ jets
none 200–870	95	227 ABE	95N CDF	$p\bar{p} \rightarrow g_A X, g_A \rightarrow q\bar{q}$
none 240–640	95	228 ABE	93G CDF	$p\bar{p} \rightarrow g_A X, g_A \rightarrow 2$ jets
> 50	95	229 CUYPERS	91 RVUE	$\sigma(e^+e^- \rightarrow \text{hadrons})$
none 120–210	95	230 ABE	90H CDF	$p\bar{p} \rightarrow g_A X, g_A \rightarrow 2$ jets
> 29		231 ROBINETT	89 THEO	Partial-wave unitarity
none 150–310	95	232 ALBAJAR	88B UA1	$p\bar{p} \rightarrow g_A X, g_A \rightarrow 2$ jets
> 20		BERGSTROM	88 RVUE	$p\bar{p} \rightarrow TX$ via $g_A g$
> 9		233 CUYPERS	88 RVUE	T decay
> 25		234 DONCHESKI	88B RVUE	T decay
224 CHOUDHURY 07 limit is from the $t\bar{t}$ production cross section measured at CDF.				
225 DONCHESKI 98 compare α_s derived from low-energy data and that from $\Gamma(Z \rightarrow \text{hadrons})/\Gamma(Z \rightarrow \text{leptons})$.				
226 ABE 97G search for new particle decaying to dijets.				
227 ABE 95N assume axigluons decaying to quarks in the Standard Model only.				
228 ABE 93G assume $\Gamma(g_A) = N\alpha_s m_{g_A}/6$ with $N = 10$.				
229 CUYPERS 91 compare α_s measured in T decay and that from R at PEP/PETRA energies.				
230 ABE 90H assumes $\Gamma(g_A) = N\alpha_s m_{g_A}/6$ with $N = 5$ ($\Gamma(g_A) = 0.09 m_{g_A}$). For $N = 10$, the excluded region is reduced to 120–150 GeV.				
231 ROBINETT 89 result demands partial-wave unitarity of $J = 0$ $t\bar{t} \rightarrow t\bar{t}$ scattering amplitude and derives a limit $m_{g_A} > 0.5 m_t$. Assumes $m_t > 56$ GeV.				
232 ALBAJAR 88B result is from the nonobservation of a peak in two-jet invariant mass distribution. $\Gamma(g_A) < 0.4 m_{g_A}$ assumed. See also BAGGER 88.				
233 CUYPERS 88 requires $\Gamma(T \rightarrow g g_A) < \Gamma(T \rightarrow g g g)$. A similar result is obtained by DONCHESKI 88.				
234 DONCHESKI 88B requires $\Gamma(T \rightarrow g q\bar{q})/\Gamma(T \rightarrow g g g) < 0.25$, where the former decay proceeds via axigluon exchange. A more conservative estimate of < 0.5 leads to $m_{g_A} > 21$ GeV.				

X^0 (Heavy Boson) Searches in Z Decays

Searches for radiative transition of Z to a lighter spin-0 state X^0 decaying to hadrons, a lepton pair, a photon pair, or invisible particles as shown in the comments. The limits are for the product of branching ratios.

VALUE	CL%	DOCUMENT ID	TECN	COMMENT
• • • We do not use the following data for averages, fits, limits, etc. • • •				

See key on page 373

Gauge & Higgs Boson Particle Listings

Heavy Bosons Other than Higgs Bosons

	235	BARATE	98U	ALEP	$X^0 \rightarrow \ell\bar{\ell}, q\bar{q}, gg, \gamma\gamma, \nu\bar{\nu}$
	236	ACCIARRI	97Q	L3	$X^0 \rightarrow$ invisible particle(s)
	237	ACTON	93E	OPAL	$X^0 \rightarrow \gamma\gamma$
	238	ABREU	92D	DLPH	$X^0 \rightarrow$ hadrons
	239	ADRIANI	92F	L3	$X^0 \rightarrow$ hadrons
	240	ACTON	91	OPAL	$X^0 \rightarrow$ anything
$<1.1 \times 10^{-4}$	95	241	ACTON	91B	OPAL $X^0 \rightarrow e^+e^-$
$<9 \times 10^{-5}$	95	241	ACTON	91B	OPAL $X^0 \rightarrow \mu^+\mu^-$
$<1.1 \times 10^{-4}$	95	241	ACTON	91B	OPAL $X^0 \rightarrow \tau^+\tau^-$
$<2.8 \times 10^{-4}$	95	242	ADEVA	91D	L3 $X^0 \rightarrow e^+e^-$
$<2.3 \times 10^{-4}$	95	242	ADEVA	91D	L3 $X^0 \rightarrow \mu^+\mu^-$
$<4.7 \times 10^{-4}$	95	243	ADEVA	91D	L3 $X^0 \rightarrow$ hadrons
$<8 \times 10^{-4}$	95	244	AKRAWY	90J	OPAL $X^0 \rightarrow$ hadrons

235 BARATE 98U obtain limits on $B(Z \rightarrow \gamma X^0)B(X^0 \rightarrow \ell\bar{\ell}, q\bar{q}, gg, \gamma\gamma, \nu\bar{\nu})$. See their Fig. 17.

236 See Fig. 4 of ACCIARRI 97Q for the upper limit on $B(Z \rightarrow \gamma X^0; E_{\gamma} > E_{\min})$ as a function of E_{\min} .

237 ACTON 93E give $\sigma(e^+e^- \rightarrow X^0\gamma) \cdot B(X^0 \rightarrow \gamma\gamma) < 0.4$ pb (95%CL) for $m_{X^0} = 60 \pm 2.5$ GeV. If the process occurs via s -channel γ exchange, the limit translates to $\Gamma(X^0) \cdot B(X^0 \rightarrow \gamma\gamma)^2 < 20$ MeV for $m_{X^0} = 60 \pm 1$ GeV.

238 ABREU 92D give $\sigma_Z \cdot B(Z \rightarrow \gamma X^0) \cdot B(X^0 \rightarrow \text{hadrons}) < (3-10)$ pb for $m_{X^0} = 10-78$ GeV. A very similar limit is obtained for spin-1 X^0 .

239 ADRIANI 92F search for isolated γ in hadronic Z decays. The limit $\sigma_Z \cdot B(Z \rightarrow \gamma X^0) \cdot B(X^0 \rightarrow \text{hadrons}) < (2-10)$ pb (95%CL) is given for $m_{X^0} = 25-85$ GeV.

240 ACTON 91 searches for $Z \rightarrow Z^* X^0, Z^* \rightarrow e^+e^-, \mu^+\mu^-,$ or $\nu\bar{\nu}$. Excludes any new scalar X^0 with $m_{X^0} < 9.5$ GeV/c if it has the same coupling to ZZ^* as the MSM Higgs boson.

241 ACTON 91B limits are for $m_{X^0} = 60-85$ GeV.

242 ADEVA 91D limits are for $m_{X^0} = 30-89$ GeV.

243 ADEVA 91D limits are for $m_{X^0} = 30-86$ GeV.

244 AKRAWY 90J give $\Gamma(Z \rightarrow \gamma X^0) \cdot B(X^0 \rightarrow \text{hadrons}) < 1.9$ MeV (95%CL) for $m_{X^0} = 32-80$ GeV. We divide by $\Gamma(Z) = 2.5$ GeV to get product of branching ratios. For nonresonant transitions, the limit is $B(Z \rightarrow \gamma q\bar{q}) < 8.2$ MeV assuming three-body phase space distribution.

MASS LIMITS for a Heavy Neutral Boson Coupling to e^+e^-

VALUE (GeV)	CL%	DOCUMENT ID	TECN	COMMENT
none 55-61		245 ODAKA	89 VNS	$\Gamma(X^0 \rightarrow e^+e^-) \cdot B(X^0 \rightarrow \text{had.}) \gtrsim 0.2$ MeV
>45	95	246 DERRICK	86 HRS	$\Gamma(X^0 \rightarrow e^+e^-) = 6$ MeV
>46.6	95	247 ADEVA	85 MRKJ	$\Gamma(X^0 \rightarrow e^+e^-) = 10$ keV
>48	95	247 ADEVA	85 MRKJ	$\Gamma(X^0 \rightarrow e^+e^-) = 4$ MeV
		248 BERGER	85B PLUT	
none 39.8-45.5		249 ADEVA	84 MRKJ	$\Gamma(X^0 \rightarrow e^+e^-) = 10$ keV
>47.8	95	249 ADEVA	84 MRKJ	$\Gamma(X^0 \rightarrow e^+e^-) = 4$ MeV
none 39.8-45.2		249 BEHREND	84C CELL	
>47	95	249 BEHREND	84C CELL	$\Gamma(X^0 \rightarrow e^+e^-) = 4$ MeV
245		ODAKA 89		looked for a narrow or wide scalar resonance in $e^+e^- \rightarrow$ hadrons at $E_{\text{cm}} = 55.0-60.8$ GeV.
246		DERRICK 86		found no deviation from the Standard Model Bhabha scattering at $E_{\text{cm}} = 29$ GeV and set limits on the possible scalar boson e^+e^- coupling. See their figure 4 for excluded region in the $\Gamma(X^0 \rightarrow e^+e^-) \cdot m_{X^0}$ plane. Electronic chiral invariance requires a parity doublet of X^0 , in which case the limit applies for $\Gamma(X^0 \rightarrow e^+e^-) = 3$ MeV.
247		ADEVA 85		first limit is from $2\gamma, \mu^+\mu^-,$ hadrons assuming X^0 is a scalar. Second limit is from e^+e^- channel. $E_{\text{cm}} = 40-47$ GeV. Supersedes ADEVA 84.
248		BERGER 85B		looked for effect of spin-0 boson exchange in $e^+e^- \rightarrow e^+e^-$ and $\mu^+\mu^-$ at $E_{\text{cm}} = 34.7$ GeV. See Fig. 5 for excluded region in the $m_{X^0} - \Gamma(X^0)$ plane.
249		ADEVA 84 and BEHREND 84C		have $E_{\text{cm}} = 39.8-45.5$ GeV. MARK-J searched X^0 in $e^+e^- \rightarrow$ hadrons, $2\gamma, \mu^+\mu^-, e^+e^-$ and CELLO in the same channels plus τ pair. No narrow or broad X^0 is found in the energy range. They also searched for the effect of X^0 with $m_X > E_{\text{cm}}$. The second limits are from Bhabha data and for spin-0 singlet. The same limits apply for $\Gamma(X^0 \rightarrow e^+e^-) = 2$ MeV if X^0 is a spin-0 doublet. The second limit of BEHREND 84C was read off from their figure 2. The original papers also list limits in other channels.

Search for X^0 Resonance in e^+e^- Collisions

The limit is for $\Gamma(X^0 \rightarrow e^+e^-) \cdot B(X^0 \rightarrow f)$, where f is the specified final state. Spin 0 is assumed for X^0 .

VALUE (keV)	CL%	DOCUMENT ID	TECN	COMMENT
$<10^3$	95	250 ABE	93C VNS	$\Gamma(ee)$
$<(0.4-10)$	95	251 ABE	93C VNS	$f = \gamma\gamma$
$<(0.3-5)$	95	252,253 ABE	93D TOPZ	$f = \gamma\gamma$
$<(2-12)$	95	252,253 ABE	93D TOPZ	$f = \text{hadrons}$
$<(4-200)$	95	253,254 ABE	93D TOPZ	$f = ee$
$<(0.1-6)$	95	253,254 ABE	93D TOPZ	$f = \mu\mu$
$<(0.5-8)$	90	255 STERNER	93 AMY	$f = \gamma\gamma$

• • • We do not use the following data for averages, fits, limits, etc. • • •

250 Limit is for $\Gamma(X^0 \rightarrow e^+e^-) m_{X^0} = 56-63.5$ GeV for $\Gamma(X^0) = 0.5$ GeV.

251 Limit is for $m_{X^0} = 56-61.5$ GeV and is valid for $\Gamma(X^0) \ll 100$ MeV. See their Fig. 5 for limits for $\Gamma = 1, 2$ GeV.

252 Limit is for $m_{X^0} = 57.2-60$ GeV.

253 Limit is for $\Gamma(X^0) \ll 100$ MeV. See paper for limits for $\Gamma = 1$ GeV and those for $J = 2$ resonances.

254 Limit is for $m_{X^0} = 56.6-60$ GeV.

255 STERNER 93 limit is for $m_{X^0} = 57-59.6$ GeV and is valid for $\Gamma(X^0) < 100$ MeV. See their Fig. 2 for limits for $\Gamma = 1, 3$ GeV.

Search for X^0 Resonance in ep Collisions

VALUE	CL%	DOCUMENT ID	TECN	COMMENT
• • •				We do not use the following data for averages, fits, limits, etc. • • •
		256 CHEKANOV 02B	ZEUS	$X \rightarrow jj$
256		CHEKANOV 02B		search for photoproduction of X decaying into dijets in ep collisions. See their Fig. 5 for the limit on the photoproduction cross section.

Search for X^0 Resonance in Two-Photon Process

The limit is for $\Gamma(X^0) \cdot B(X^0 \rightarrow \gamma\gamma)^2$. Spin 0 is assumed for X^0 .

VALUE (MeV)	CL%	DOCUMENT ID	TECN	COMMENT
• • •				We do not use the following data for averages, fits, limits, etc. • • •
<2.6	95	257 ACTON	93E OPAL	$m_{X^0} = 60 \pm 1$ GeV
<2.9	95	BUSKULIC	93F ALEP	$m_{X^0} \sim 60$ GeV
257		ACTON 93E		limit for a $J = 2$ resonance is 0.8 MeV.

Search for X^0 Resonance in $e^+e^- \rightarrow X^0\gamma$

VALUE (GeV)	CL%	DOCUMENT ID	TECN	COMMENT
• • •				We do not use the following data for averages, fits, limits, etc. • • •
		258 ABBIENDI 03D	OPAL	$X^0 \rightarrow \gamma\gamma$
		259 ABREU 00Z	DLPH	X^0 decaying invisibly
		260 ADAM 96C	DLPH	X^0 decaying invisibly
258		ABBIENDI 03D		measure the $e^+e^- \rightarrow \gamma\gamma\gamma$ cross section at $\sqrt{s}=181-209$ GeV. The upper bound on the production cross section, $\sigma(e^+e^- \rightarrow X^0\gamma)$ times the branching ratio for $X^0 \rightarrow \gamma\gamma$, is less than 0.03 pb at 95%CL for X^0 masses between 20 and 180 GeV. See their Fig. 9b for the limits in the mass-cross section plane.
259		ABREU 00Z		is from the single photon cross section at $\sqrt{s}=183, 189$ GeV. The production cross section upper limit is less than 0.3 pb for X^0 mass between 40 and 160 GeV. See their Fig. 4 for the limit in mass-cross section plane.
260		ADAM 96C		is from the single photon production cross at $\sqrt{s}=130, 136$ GeV. The upper bound is less than 3 pb for X^0 masses between 60 and 130 GeV. See their Fig. 5 for the exact bound on the cross section $\sigma(e^+e^- \rightarrow \gamma X^0)$.

Search for X^0 Resonance in $Z \rightarrow f\bar{f}X^0$

The limit is for $B(Z \rightarrow f\bar{f}X^0) \cdot B(X^0 \rightarrow F)$ where f is a fermion and F is the specified final state. Spin 0 is assumed for X^0 .

VALUE	CL%	DOCUMENT ID	TECN	COMMENT
• • •				We do not use the following data for averages, fits, limits, etc. • • •
$<3.7 \times 10^{-6}$	95	261 ABREU 96T	DLPH	$f=e,\mu,\tau; F=\gamma\gamma$
		262 ABREU 96T	DLPH	$f=\nu; F=\gamma\gamma$
		263 ABREU 96T	DLPH	$f=q; F=\gamma\gamma$
$<6.8 \times 10^{-6}$	95	262 ACTON 93E	OPAL	$f=e,\mu,\tau; F=\gamma\gamma$
$<5.5 \times 10^{-6}$	95	262 ACTON 93E	OPAL	$f=q; F=\gamma\gamma$
$<3.1 \times 10^{-6}$	95	262 ACTON 93E	OPAL	$f=\nu; F=\gamma\gamma$
$<6.5 \times 10^{-6}$	95	262 ACTON 93E	OPAL	$f=e,\mu; F=\ell\bar{\ell}, q\bar{q}, \nu\bar{\nu}$
$<7.1 \times 10^{-6}$	95	262 BUSKULIC 93F	ALEP	$f=e,\mu; F=\ell\bar{\ell}, q\bar{q}, \nu\bar{\nu}$
		264 ADRIANI 92F	L3	$f=q; F=\gamma\gamma$
261		ABREU 96T		obtain limit as a function of m_{X^0} . See their Fig. 6.
262				Limit is for m_{X^0} around 60 GeV.
263		ABREU 96T		obtain limit as a function of m_{X^0} . See their Fig. 15.
264		ADRIANI 92F		give $\sigma_Z \cdot B(Z \rightarrow q\bar{q}X^0) \cdot B(X^0 \rightarrow \gamma\gamma) < (0.75-1.5)$ pb (95%CL) for $m_{X^0} = 10-70$ GeV. The limit is 1 pb at 60 GeV.

Search for X^0 Resonance in $p\bar{p} \rightarrow W X^0$

VALUE (MeV)	CL%	DOCUMENT ID	TECN	COMMENT
• • •				We do not use the following data for averages, fits, limits, etc. • • •
		265 ABE 97W	CDF	$X^0 \rightarrow b\bar{b}$
265		ABE 97W		search for X^0 production associated with W in $p\bar{p}$ collisions at $E_{\text{cm}}=1.8$ TeV. The 95%CL upper limit on the production cross section times the branching ratio for $X^0 \rightarrow b\bar{b}$ ranges from 14 to 19 pb for X^0 mass between 70 and 120 GeV. See their Fig. 3 for upper limits of the production cross section as a function of m_{X^0} .

Heavy Particle Production in Quarkonium Decays

Limits are for branching ratios to modes shown.

VALUE	CL%	DOCUMENT ID	TECN	COMMENT
• • •				We do not use the following data for averages, fits, limits, etc. • • •

Gauge & Higgs Boson Particle Listings

Heavy Bosons Other than Higgs Bosons

$< 1.5 \times 10^{-5}$	90	266	BALEST	95	CLE2	$\Upsilon(1S) \rightarrow X^0 \gamma$ $m_{X^0} < 5 \text{ GeV}$
$< 3 \times 10^{-5} - 6 \times 10^{-3}$	90	267	BALEST	95	CLE2	$\Upsilon(1S) \rightarrow X^0 \bar{X}^0 \gamma$ $m_{X^0} < 3.9 \text{ GeV}$
$< 5.6 \times 10^{-5}$	90	268	ANTREASIAN	90c	CBAL	$\Upsilon(1S) \rightarrow X^0 \gamma$ $m_{X^0} < 7.2 \text{ GeV}$
		269	ALBRECHT	89	ARG	

266 BALEST 95 two-body limit is for pseudoscalar X^0 . The limit becomes $< 10^{-4}$ for $m_{X^0} < 7.7 \text{ GeV}$.

267 BALEST 95 three-body limit is for phase-space photon energy distribution and angular distribution same as for $\Upsilon \rightarrow g g \gamma$.

268 ANTREASIAN 90c assume that X^0 does not decay in the detector.

269 ALBRECHT 89 give limits for $B(\Upsilon(1S), \Upsilon(2S) \rightarrow X^0 \gamma) \cdot B(X^0 \rightarrow \pi^+ \pi^-, K^+ K^-, p \bar{p})$ for $m_{X^0} < 3.5 \text{ GeV}$.

REFERENCES FOR Searches for Heavy Bosons Other Than Higgs Bosons

ABAZOV 06C	PRL 100 031804	V. M. Abazov et al.	(DO Collab.)
ABALTONEN 07H	PRL 99 171802	T. Aaltonen et al.	(CDF Collab.)
ABAZOV 07E	PL B647 74	V. M. Abazov et al.	(DO Collab.)
ABAZOV 07J	PRL 99 061801	V. M. Abazov et al.	(DO Collab.)
ABULENCIA 07K	PR D75 091101R	A. Abulencia et al.	(CDF Collab.)
AKTAS 07A	EPJ C52 833	A. Aktas et al.	(H1 Collab.)
CHOUDHURY 07	PL B657 69	D. Choudhury et al.	
MELCONIAN 07	PL B649 370	D. Melconian et al.	
SCHAEF 07A	EPJ C49 411	S. Schaefer et al.	(TRIUMF)
SCHUMANN 07	PRL 99 191803	M. Schumann et al.	(HEID, ILLG, KARL+)
SMIRNOV 07	MPL A22 2353	A. D. Smirnov	(DO Collab.)
ABAZOV 06A	PL B636 183	V. M. Abazov et al.	(DO Collab.)
ABAZOV 06L	PL B640 230	V. M. Abazov et al.	(DO Collab.)
ABAZOV 06N	PL B641 423	V. M. Abazov et al.	(DO Collab.)
ABDALLAH 06C	EPJ C54 589	J. Abdallah et al.	(DELPHI Collab.)
ABULENCIA 06L	PRL 96 211801	A. Abulencia et al.	(CDF Collab.)
ABULENCIA 06M	PRL 96 211802	A. Abulencia et al.	(CDF Collab.)
ABULENCIA 06T	PR D73 051102R	A. Abulencia et al.	(CDF Collab.)
ABAZOV 05H	PR D71 071104R	V. M. Abazov et al.	(DO Collab.)
ABULENCIA 05A	PRL 95 252001	A. Abulencia et al.	(CDF Collab.)
ACOSTA 05I	PR D71 112001	D. Acosta et al.	(CDF Collab.)
ACOSTA 05P	PR D72 051107R	D. Acosta et al.	(CDF Collab.)
ACOSTA 05R	PRL 95 131801	D. Acosta et al.	(CDF Collab.)
AKTAS 05B	PL B629 9	A. Aktas et al.	(H1 Collab.)
CHEKANOV 05	PL B610 212	S. Chekanov et al.	(HERA ZEUS Collab.)
CHEKANOV 05A	EPJ C44 463	S. Chekanov et al.	
CYBURT 05	ASP 23 313	R.H. Cyburt et al.	
ABAZOV 04A	PRL 92 221801	V. M. Abazov et al.	(DO Collab.)
ABAZOV 04C	PR D69 111101R	V. M. Abazov et al.	(DO Collab.)
ABBIENDI 04G	EPJ C33 173	G. Abbiendi et al.	(OPAL Collab.)
ABBIENDI 03D	EPJ C26 331	G. Abbiendi et al.	(OPAL Collab.)
ABBIENDI 03R	EPJ C31 281	G. Abbiendi et al.	(OPAL Collab.)
ACOSTA 03B	PRL 90 081802	D. Acosta et al.	(CDF Collab.)
ADLOFF 03	PL B568 35	C. Adloff et al.	(H1 Collab.)
BARGER 03B	PR D67 075009	V. Barger, P. Langacker, H. Lee	
CHANG 03	PR D68 111101R	M.-C. Chang et al.	(BELLE Collab.)
CHEKANOV 03B	PR D68 052004	S. Chekanov et al.	(ZEUS Collab.)
ABAZOV 02	PRL 88 191801	V. M. Abazov et al.	(DO Collab.)
ABBIENDI 02B	PL B526 233	G. Abbiendi et al.	(OPAL Collab.)
AFFOLDER 02C	PRL 88 071806	T. Affolder et al.	(CDF Collab.)
CHEKANOV 02	PR D65 092004	S. Chekanov et al.	(ZEUS Collab.)
CHEKANOV 02B	PL B531 9	S. Chekanov et al.	(ZEUS Collab.)
MUECK 02	PR D65 085037	A. Mueck, A. Pilaftsis, R. Rueckl	
ABAZOV 01B	PRL 87 061802	V. M. Abazov et al.	(DO Collab.)
ABAZOV 01D	PR D64 092004	V. M. Abazov et al.	(DO Collab.)
ADLOFF 01C	PL B593 234	C. Adloff et al.	(H1 Collab.)
AFFOLDER 01I	PRL 87 231803	T. Affolder et al.	(CDF Collab.)
BREITWEG 01	PR D63 052002	J. Breitweg et al.	(ZEUS Collab.)
CHEUNG 01B	PL B517 167	K. Cheung	
THOMAS 01	NP A694 559	E. Thomas et al.	
ABBIENDI 00M	EPJ C13 15	G. Abbiendi et al.	(OPAL Collab.)
ABBOTT 00C	PRL 84 2088	B. Abbott et al.	(DO Collab.)
ABE 00	PRL 84 5716	F. Abe et al.	(CDF Collab.)
ABREU 00S	PL B485 45	P. Abreu et al.	(DELPHI Collab.)
ABREU 00Z	EPJ C17 53	P. Abreu et al.	(DELPHI Collab.)
ACCIARRI 00P	PL B409 81	M. Acciari et al.	(L3 Collab.)
ADLOFF 00	PL B479 358	C. Adloff et al.	(H1 Collab.)
AFFOLDER 00K	PRL 85 2056	T. Affolder et al.	(CDF Collab.)
BARATE 00I	EPJ C12 183	R. Barate et al.	(ALEPH Collab.)
BARGER 00	PL B480 149	V. Barger, K. Cheung	
BREITWEG 00E	EPJ C16 253	J. Breitweg et al.	(ZEUS Collab.)
CHAY 00	PR D61 035002	J. Chay, K.Y. Lee, S. Nam	
CHO 00	MPL A15 311	G. Cho	
CORNET 00	PR D61 037701	F. Cornet, M. Relano, J. Rico	
DELGADO 00	JHEP 0001 030	A. Delgado, A. Pomarol, M. Quiros	
ERLER 00	PRL 84 212	J. Erler, P. Langacker	
GABRIELLI 00	PR D62 055009	E. Gabrielli	
RIZZO 00	PR D61 015007	T. G. Rizzo, J.D. Wells	
ROSENBERG 00	PR D61 016006	J.L. Rosenberg	
ZARNECKI 00	EPJ C17 695	A. Zarnecki	
ABBIENDI 99	EPJ C6 1	G. Abbiendi et al.	(OPAL Collab.)
ABBOTT 99J	PRL 83 2896	B. Abbott et al.	(DO Collab.)
ABREU 99G	PL B446 62	P. Abreu et al.	(DELPHI Collab.)
ACKERSTAFF 99D	EPJ C8 3	K. Ackerstaff et al.	(OPAL Collab.)
ADLOFF 99	EPJ C11 447	C. Adloff et al.	(H1 Collab.)
Also	EPJ C14 553 (erratum)	C. Adloff et al.	(H1 Collab.)
CASALBUONI 99	PL B460 135	R. Casalbuoni et al.	
ERLER 99	PL B458 355	M. Czakon, J. Gluza, M. Zralek	
ERLER 99	PL B456 68	J. Erler, P. Langacker	
MARCIANO 99	PR D60 093006	W. Marciano	
MASIP 99	PR D60 096005	M. Masip, A. Pomarol	
NATH 99	PR D60 116004	P. Nath, M. Yamaguchi	
STRUMIA 99	PL B466 107	A. Strumia	
ABBOTT 98E	PRL 80 2051	B. Abbott et al.	(DO Collab.)
ABBOTT 98J	PRL 81 38	B. Abbott et al.	(DO Collab.)
ABE 98S	PRL 81 4806	F. Abe et al.	(CDF Collab.)
ABE 98V	PRL 81 5742	F. Abe et al.	(CDF Collab.)
ACCIARRI 98J	PL B433 163	M. Acciari et al.	(L3 Collab.)
ACKERSTAFF 98V	EPJ C2 441	K. Ackerstaff et al.	(OPAL Collab.)
BARATE 98U	EPJ C4 571	R. Barate et al.	(ALEPH Collab.)
BARENBOIM 98	EPJ C1 319	G. Barenboim	
CHO 98	EPJ C5 155	G. Cho, K. Hagiwara, S. Matsumoto	
CONRAD 98	RMP 70 1341	J.M. Conrad, M.H. Shaevitz, T. Bolton	
DONCHESKI 98	PR D58 097702	M.A. Doncheski, R.W. Robinett	
GROSS-PILCHER 98	hep-ex/9810015	C. Grosso-Pilcher, G. Landsberg, M. Paterno	
ABE 97F	PRL 78 2906	F. Abe et al.	(CDF Collab.)
ABE 97G	PR D55 R5263	F. Abe et al.	(CDF Collab.)

ABE 97S	PRL 79 2192	F. Abe et al.	(CDF Collab.)
ABE 97W	PRL 79 3819	F. Abe et al.	(CDF Collab.)
ABE 97X	PRL 79 4327	F. Abe et al.	(CDF Collab.)
ACCIARRI 97Q	PL B412 201	M. Acciari et al.	(L3 Collab.)
ARIMA 97	PR D55 19	T. Arima et al.	(VENUS Collab.)
BARENBOIM 97	PR D55 4213	G. Barenboim et al.	(VALE, IFIC)
DEANDREA 97	PL B409 277	A. Deandrea	(MARS)
DERRICK 97	ZPHY C73 613	M. Derrick et al.	(ZEUS Collab.)
GROSSMAN 97	PR D55 2768	V. Grossman, Z. Ligeti, E. Nardi	(REHO, CIT)
JADACH 97	PL B408 281	S. Jadach, B.F.L. Ward, Z. Was	(CERN, INPK+)
STAHL 97	ZPHY C74 73	A. Stahl, H. Voss	(BONN)
ABACHI 96C	PRL 76 3271	S. Abachi et al.	(DO Collab.)
ABACHI 96D	PL B385 471	S. Abachi et al.	(DO Collab.)
ABREU 96T	ZPHY C72 179	P. Abreu et al.	(DELPHI Collab.)
ADAM 96C	PL B380 471	W. Adam et al.	(DELPHI Collab.)
AID 96B	PL B369 173	S. Aid et al.	(H1 Collab.)
ALLET 96	PL B383 139	M. Allet et al.	(VILL, LEUV, LOUV, WIS C)
ABACHI 95E	PL B358 405	S. Abachi et al.	(DO Collab.)
ABE 95M	PRL 74 2900	F. Abe et al.	(CDF Collab.)
ABE 95N	PRL 74 3538	F. Abe et al.	(CDF Collab.)
BALEST 95	PR D51 2053	R. Balest et al.	(CLEO Collab.)
KUZNETSOV 95	PRL 75 794	I.A. Kuznetsov et al.	(PNPI, KIAE, HARV+)
KUZNETSOV 95B	PAN 58 2113	A.V. Kuznetsov, N.V. Mikheev	(YARO)
Also	Translated from YAF 58 2228.		
MIZUKOSHI 95	NP B443 20	J.K. Mizukoshi, O.J.P. Ebofi, M.C. Gonzalez-Garcia	
ABREU 94O	ZPHY C64 183	P. Abreu et al.	(DELPHI Collab.)
BHATTACH... 94	PL B336 100	G. Bhattacharyya, J. Ellis, K. Sridhar	(CERN)
Also	PL B338 522 (erratum)	G. Bhattacharyya, J. Ellis, K. Sridhar	(CERN)
BHATTACH... 94B	PL B338 522 (erratum)	G. Bhattacharyya, J. Ellis, K. Sridhar	(CERN)
DAVIDSON 94	ZPHY C61 613	S. Davidson, D. Bailey, B.A. Campbell	(CFPA+)
KUZNETSOV 94B	PL B329 295	A.V. Kuznetsov, N.V. Mikheev	(YARO)
KUZNETSOV 94B	JETPL 60 315	I.A. Kuznetsov et al.	(PNPI, KIAE, HARV+)
Also	Translated from ZETFP 60 311.		
LEURER 94	PR D50 536	M. Leurer	(REHO)
LEURER 94B	PR D49 333	M. Leurer	(REHO)
Also	PRL 71 1324	M. Leurer	(REHO)
MAHANTA 94	PL B337 128	U. Mahanta	(MEHTA)
SEVERIJNS 94	PRL 73 611 (erratum)	N. Severijns et al.	(LOUV, WISC, LEUV+)
VILAIN 94B	PL B332 465	P. Vilain et al.	(CHARM II Collab.)
ABE 93C	PL B302 119	K. Abe et al.	(VENUS Collab.)
ABE 93D	PL B304 373	T. Abe et al.	(TOPAZ Collab.)
ABE 93G	PRL 71 2542	F. Abe et al.	(CDF Collab.)
ABREU 93J	PL B316 620	P. Abreu et al.	(DELPHI Collab.)
ACTON 93M	PL B311 391	P.D. Acton et al.	(OPAL Collab.)
ADRIANI 93E	PR D47 R3693	O. Adriani et al.	(L3 Collab.)
ALITTI 93	NP B400 3	J. Alitti et al.	(UA2 Collab.)
BHATTACH... 93	PR D47 R3693	G. Bhattacharyya et al.	(CALC, JADA, ICTF+)
BUSKULIC 93F	PL B308 425	D. Buskulic et al.	(ALEPH Collab.)
DERRICK 93	PL B306 173	M. Derrick et al.	(ZEUS Collab.)
RIZZO 93	PR D48 4470	T.G. Rizzo	(ANL)
SEVERIJNS 93	PRL 70 4047	N. Severijns et al.	(LOUV, WISC, LEUV+)
Also	PRL 73 611 (erratum)	N. Severijns et al.	(LOUV, WISC, LEUV+)
STERNER 93	PL B303 385	K.L. Sterner et al.	(AMY Collab.)
ABREU 92D	ZPHY C53 555	P. Abreu et al.	(DELPHI Collab.)
ADRIANI 92F	PL B292 472	O. Adriani et al.	(L3 Collab.)
DECAMP 92	PR D47 R3693	D. Decamp et al.	(ALEPH Collab.)
IMAZATO 92	PRL 69 877	J. Imazato et al.	(KEK, INUS, TOKY+)
MISHRA 92	PRL 68 3499	S.R. Mishra et al.	(COLU, CHIC, FNAL+)
POLAK 92B	PR D46 3871	J. Polak, M. Zralek	(SILES)
ACTON 91	PL B268 122	D.P. Acton et al.	(OPAL Collab.)
ACTON 91B	PL B273 338	D.P. Acton et al.	(OPAL Collab.)
ADEVA 91D	PL B262 155	B. Adeva et al.	(L3 Collab.)
AQUINO 91	PL B261 280	M. Aquino, A. Fernandez, A. Garcia	(CINV, PUEB)
COLANGELO 91	PL B253 154	P. Colangelo, G. Nardulli	(BARI)
CUYPERS 91	PL B259 173	F. Cuypers, A.F. Falk, P.H. Frampton	(DURH, HARV+)
FARAGGI 91	MPL A6 61	A.E. Faraggi, D.V. Nanopoulos	(TAMU)
POLAK 91	NP B363 385	J. Polak, M. Zralek	(SILES)
RIZZO 91	PR D44 202	T.G. Rizzo	(WISC, IU)
WALKER 91	APJ 376 51	T.P. Walker et al.	(HSCA, OSU, CHIC+)
ABE 90F	PL B246 297	K. Abe et al.	(VENUS Collab.)
ABE 90H	PR D41 1722	F. Abe et al.	(CDF Collab.)
AKRAWY 90J	PL B246 285	M.J. Akrawy et al.	(OPAL Collab.)
ANTREASIAN 90C	PL B251 204	D. Antreasian et al.	(Crystal Ball Collab.)
GONZALEZ-G... 90D	PL B240 163	M.C. Gonzalez-Garcia, J.W.F. Valle	(VALE)
GRIFOLS 90	NP B331 244	J.A. Grifols, E. Maso	(BARC)
GRIFOLS 90D	PR D42 3293	J.A. Grifols, E. Maso, T.G. Rizzo	(BARC, CERN+)
KIM 90	PL B240 243	G.N. Kim et al.	(AMY Collab.)
LOPEZ 90	PL B241 392	J.L. Lopez, D.V. Nanopoulos	(TAMU)
ALBAJAR 89	ZPHY C44 15	C. Albjajar et al.	(UA1 Collab.)
ALBRECHT 89	ZPHY C42 349	H. Albrecht et al.	(ARGUS Collab.)
BARBIERI 89B	PR D39 1229	R. Barbieri, R.N. Mohapatra	(PISA, UMD)
LANGACKER 89	PR D40 1569	P. Langacker, S. Uma Sankar	(FNIN)
ODAKA 89	JPS J58 3037	S. Odaoka et al.	(VENUS Collab.)
ROBINETT 89	PR D39 834	R.W. Robinett	(PSU)
ALBAJAR 88B	PL B209 127	C. Albjajar et al.	(UA1 Collab.)
BAGGER 88	PR D37 1188	J. Bagger, C. Schmidt, S. King	(HARV, BOST)
BALKE 88	PR D37 587	B. Balke et al.	(LBL, UC, COLO, NWES+)
BERGSTROM 88	PL B212 386	L. Bergstrom	(STOH)
CUYPERS 88	PRL 60 1237	F. Cuypers, P.H. Frampton	(UNCCB)
DONCHESKI 88	PL B206 137	M.A. Doncheski, H. Grotch, R. Robinett	(PSU)
DONCHESKI 88B	PR D38 412	M.A. Doncheski, H. Grotch, R.W. Robinett	(PSU)
ANSARI 87D	PL B195 613	R. Ansari et al.	(UA2 Collab.)
BARTEL 87B	ZPHY C36 15	W. Bartel et al.	(JADE Collab.)
BEHREND 86B	PL B178 452	H.J. Behrend et al.	(CELLO Collab.)
DERRICK 86	PL B168 463	M. Derrick et al.	(HRS Collab.)
Also	PR D34 3286	M. Derrick et al.	(HRS Collab.)
JODIDIO 86	PR D34 1967	A. Jodidio et al.	(LBL, NWES, TRIU)
Also	PR D37 237 (erratum)	A. Jodidio et al.	(LBL, NWES, TRIU)
MOHAPATRA 86	PR D34 909	R.N. Mohapatra	(UMD)
ADEVA 85	PL B52B 439	B. Adeva et al.	(Mark-J Collab.)
BERGER 85B	ZPHY C27 341	C. Berger et al.	(PLUTO Collab.)
STOKER 85	PRL 54 1887	D.P. Stoker et al.	(LBL, NWES, TRIU)
ADEVA 84C	PRL 53 134	B. Adeva et al.	(Mark-J Collab.)
BEHREND 84	PL B40B 130	H.J. Behrend et al.	(CELLO Collab.)
BERG			

Axions (A^0) and Other Very Light Bosons, Searches for

AXIONS

Written in August 2007 by C. Hagmann (LLNL), H. Murayama (UC Berkeley), G.G. Raffelt (MPI Physics), L.J. Rosenberg (U. of Washington), and K. van Bibber (LLNL).

Introduction: In this section, we list mass and coupling-strength limits for very light neutral scalar or pseudoscalar bosons that couple weakly to normal matter and radiation. Such bosons may arise from a global spontaneously broken U(1) symmetry, resulting in a massless Nambu-Goldstone (NG) boson. If there is a small explicit symmetry breaking, either already in the Lagrangian or due to quantum-mechanical effects such as anomalies, the boson acquires a mass and is called a pseudo-NG boson. Typical examples are axions (A^0) [1,2], familons [3] and Majorons [4], associated, respectively, with a spontaneously broken Peccei-Quinn, family and lepton-number symmetry.

A common characteristic among these light bosons ϕ is that their coupling to Standard-Model particles is suppressed by the energy scale that characterizes the symmetry breaking, *i.e.*, the decay constant f . The interaction Lagrangian is

$$\mathcal{L} = f^{-1} J^\mu \partial_\mu \phi, \quad (1)$$

where J^μ is the Noether current of the spontaneously broken global symmetry. If f is very large, these new particles interact very weakly. Conversely, detecting them would provide a window to physics far beyond what can be probed at accelerators.

The interest in global symmetries and the associated NG bosons has somewhat waned except for the case of axions where it has held steady since they were proposed 30 years ago. This is because the Peccei-Quinn (PQ) mechanism remains perhaps the most credible scheme to preserve CP in QCD; axions are a plausible candidate for the cold dark matter of the universe and they are searched for in experiments with a realistic chance of discovery. Originally it was assumed that the PQ scale f_A was related to the electroweak symmetry-breaking scale $v_{\text{weak}} = (\sqrt{2}G_F)^{-1/2} = 247$ GeV. However, the associated “standard” and “variant” axions were quickly excluded, leaving “invisible axions” with $f_A \gg v_{\text{weak}}$ as the main possibility. We refer to the Listings for limits on standard and variant axions, whereas here we focus primarily on very low-mass, very weakly-interacting axions and axion-like particles.

I. THEORY

I.1 Peccei-Quinn mechanism and axions: QCD includes a CP -violating Lagrangian $\mathcal{L}_\Theta = \bar{\Theta} (\alpha_s/8\pi) G^{\mu\nu a} \tilde{G}_{\mu\nu}^a$, where $-\pi \leq \bar{\Theta} \leq +\pi$ is the effective Θ parameter after diagonalization of the quark masses, G is the color field strength tensor, and \tilde{G} its dual. Experimental limits on the neutron electric dipole moment [5] imply $|\bar{\Theta}| \lesssim 10^{-10}$ even though $\bar{\Theta} = \mathcal{O}(1)$ is otherwise completely satisfactory. The spontaneously broken

global Peccei-Quinn symmetry U(1)_{PQ} was introduced to solve this “strong CP problem” [1], and an axion is the pseudo-NG boson of U(1)_{PQ} [2]. This symmetry is exact on the classical level, but is broken quantum mechanically due to the axion’s anomalous triangle coupling to gluons,

$$\mathcal{L} = \left(\bar{\Theta} - \frac{\phi_A}{f_A} \right) \frac{\alpha_s}{8\pi} G^{\mu\nu a} \tilde{G}_{\mu\nu}^a, \quad (2)$$

where ϕ_A is the axion field and f_A the axion decay constant. Color anomaly factors have been absorbed in the normalization of f_A which is defined by this Lagrangian. Thus normalized, f_A is the quantity that enters all low-energy phenomena [6]. Non-perturbative effects induce a potential for ϕ_A whose minimum is at $\phi_A = \bar{\Theta} f_A$, thereby canceling the $\bar{\Theta}$ term in the QCD Lagrangian, and thus restoring the CP symmetry.

The resulting axion mass is given by $m_A f_A \approx m_\pi f_\pi$ where $m_\pi = 135$ MeV and $f_\pi \approx 92$ MeV is the pion decay constant. In more detail one finds

$$m_A = \frac{z^{1/2}}{1+z} \frac{f_\pi m_\pi}{f_A} = \frac{0.60 \text{ meV}}{f_A/10^{10} \text{ GeV}}, \quad (3)$$

where $z = m_u/m_d$ is the up/down quark-mass ratio. For this numerical estimate we used a canonical value of $z = 0.56$ [7], but it could vary in the range $z = 0.3\text{--}0.6$ [8].

In the original axion model, $f_A \sim v_{\text{weak}}$ [1,2]. Tree-level flavor conservation fixes the axion mass and its couplings in terms of a single parameter $\tan\beta$, the ratio of the vacuum expectation values of the two Higgs fields that appear as a minimal ingredient. This “standard axion” is excluded after extensive experimental searches [9]. A reported observation of a narrow-peak structure in positron spectra from heavy ion collisions [10] suggested an axion-like particle of mass 1.8 MeV that decays into e^+e^- , but extensive searches for the $A^0(1.8 \text{ MeV})$ ended negative. “Variant axion models” were proposed which keep $f_A \sim v_{\text{weak}}$ while dropping the constraint of tree-level flavor conservation [11], but these models are also excluded [12].

Axions with $f_A \gg v_{\text{weak}}$ evade all existing experimental limits. Two classes of models are often discussed in the literature. In “hadronic axion models,” one introduces new heavy quarks carrying the U(1)_{PQ} charge, leaving the usual quarks and leptons without any tree-level axion couplings. The prototype is the KSVZ model [13], which has the additional property that the heavy quarks are electrically neutral. Another model class simply requires a minimum of two Higgs doublets with the usual quarks and leptons carrying PQ charges, the prototype being the DFSZ model [14]. All of these models contain at least one electroweak singlet scalar boson, which acquires a vacuum expectation value and thereby breaks the PQ symmetry. The KSVZ and DFSZ models are frequently used as generic examples, but other models exist where both heavy quarks and Higgs doublets carry PQ charges. In one recent example, the PQ charges of all fields were derived within a superstring model [15].

Gauge & Higgs Boson Particle Listings

Axions (A^0) and Other Very Light Bosons

I.2 Model-dependent axion couplings: Although the generic axion interactions scale approximately with f_π/f_A from the corresponding π^0 couplings, there are non-negligible model-dependent factors and uncertainties. The axion's two-photon interaction plays a key role for many searches,

$$\mathcal{L}_{A\gamma\gamma} = \frac{G_{A\gamma\gamma}}{4} F_{\mu\nu} \tilde{F}^{\mu\nu} \phi_A = -G_{A\gamma\gamma} \mathbf{E} \cdot \mathbf{B} \phi_A. \quad (4)$$

Here, F is the electromagnetic field-strength tensor, \tilde{F} its dual, and \mathbf{E} and \mathbf{B} the electric and magnetic fields, respectively. The coupling constant is

$$\begin{aligned} G_{A\gamma\gamma} &= \frac{\alpha}{2\pi f_A} \left(\frac{E}{N} - \frac{2}{3} \frac{4+z}{1+z} \right) \\ &= \frac{\alpha}{2\pi} \left(\frac{E}{N} - \frac{2}{3} \frac{4+z}{1+z} \right) \frac{1+z}{z^{1/2}} \frac{m_A}{m_\pi f_\pi}, \end{aligned} \quad (5)$$

where E and N , respectively, are the electromagnetic and color anomalies of the axial current associated with the axion. In grand unified models, and notably in the DFSZ case [14], we have $E/N = 8/3$, whereas $E/N = 0$ for KSVZ [13] if the electric charge of the new heavy quark is taken to vanish. However, in general, E/N is not known so that for fixed f_A , a broad range of $G_{A\gamma\gamma}$ values is possible [16].

Axions or axion-like particles with a two-photon vertex decay with a rate

$$\begin{aligned} \Gamma_{A \rightarrow \gamma\gamma} &= \frac{G_{A\gamma\gamma}^2 m_A^3}{64\pi} \\ &= \frac{\alpha^2}{256\pi^3} \left(\frac{E}{N} - \frac{2}{3} \frac{4+z}{1+z} \right)^2 \frac{(1+z)^2}{z} \frac{m_A^5}{m_\pi^2 f_\pi^2} \\ &= 1.1 \times 10^{-24} \text{ s}^{-1} \left(\frac{m_A}{\text{eV}} \right)^5, \end{aligned} \quad (6)$$

where the first expression is for general pseudoscalars, the second for axions, and the third assumes $z = 0.56$ and $E/N = 0$. Axions decay faster than the age of the universe if $m_A \gtrsim 20$ eV.

The interaction with fermions f has a derivative structure so that it is invariant under a constant shift $\phi_A \rightarrow \phi_A + \phi_0$ as behooves a NG boson,

$$\mathcal{L}_{Aff} = \frac{C_f}{2f_A} \bar{\Psi}_f \gamma^\mu \gamma_5 \Psi_f \partial_\mu \phi_A \quad \text{or} \quad -i \frac{C_f m_f}{f_A} \bar{\Psi}_f \gamma_5 \Psi_f \phi_A. \quad (7)$$

Here, Ψ_f is the fermion field, m_f its mass, and C_f a model-dependent numerical coefficient. The dimensionless combination $g_{Aff} \equiv C_f m_f / f_A$ plays the role of a Yukawa coupling and $\alpha_{Aff} \equiv g_{Aff}^2 / 4\pi$ of a ‘‘fine-structure constant.’’ The pseudoscalar form is usually equivalent to the derivative structure, but one has to be careful in processes where two NG bosons are attached to one fermion line, for example in the context of axion emission by nucleon bremsstrahlung [17].

Hadronic axions do not couple to ordinary quarks and leptons at tree level. In the DFSZ model [14], the coupling coefficient to electrons is

$$C_e = \frac{\cos^2 \beta}{3}, \quad (8)$$

where $\tan \beta$ is the ratio of two Higgs vacuum expectation values that are generic to this and similar models.

The nucleon couplings $C_{n,p}$ are related to nucleon axial-vector current matrix elements by generalized Goldberger-Treiman relations,

$$\begin{aligned} C_p &= (C_u - \eta) \Delta u + (C_d - \eta z) \Delta d + (C_s - \eta w) \Delta s, \\ C_n &= (C_u - \eta) \Delta d + (C_d - \eta z) \Delta u + (C_s - \eta w) \Delta s. \end{aligned} \quad (9)$$

Here, $\eta = (1+z+w)^{-1}$ with $z = m_u/m_d$ and $w = m_u/m_s \ll z$. Δq represents the axial-vector current couplings to the proton by $\Delta q S_\mu = \langle p | \bar{q} \gamma_\mu \gamma_5 q | p \rangle$, where S_μ is the proton spin.

Neutron beta decay and strong isospin symmetry considerations imply $\Delta u - \Delta d = F + D = 1.267 \pm 0.0035$, whereas hyperon decays and flavor SU(3) symmetry imply $\Delta u + \Delta d - 2\Delta s = 3F - D = 0.585 \pm 0.025$. The strange-quark contribution is $\Delta s = -0.08 \pm 0.01_{\text{stat}} \pm 0.05_{\text{sys}}$ from the COMPASS experiment [18], and $\Delta s = -0.085 \pm 0.008_{\text{exp}} \pm 0.013_{\text{theor}} \pm 0.009_{\text{evol}}$ from HERMES [19], in agreement with each other and with an early estimate of $\Delta s = -0.11 \pm 0.03$ [20]. We thus adopt

$$\begin{aligned} \Delta u &= +0.841 \pm 0.020, \\ \Delta d &= -0.426 \pm 0.020, \\ \Delta s &= -0.085 \pm 0.015, \end{aligned} \quad (10)$$

which are very similar to what was used in the axion literature.

The uncertainty of the axion-nucleon couplings is dominated by the uncertainty $z = 0.3-0.6$ that we mentioned earlier. For hadronic axions $C_{u,d,s} = 0$, so that $C_p = -0.55$ and $C_n = +0.14$, if $z = 0.3$ and $C_p = -0.37$ and $C_n = -0.05$ if $z = 0.6$. While it is well possible that $C_n = 0$, C_p does not vanish within the plausible z range. In the DFSZ model, $C_u = \frac{1}{3} \sin^2 \beta$ and $C_d = \frac{1}{3} \cos^2 \beta$. Even with the large z -uncertainty, C_n and C_p never vanish simultaneously. An extreme case is $\cos^2 \beta = 0$, where $C_p = 0$ for $z = 0.3$, but in this case $C_n = -0.27$.

The axion-pion interaction is given by the Lagrangian [21]

$$\mathcal{L}_{A\pi} = \frac{C_{A\pi}}{f_\pi f_A} (\pi^0 \pi^+ \partial_\mu \pi^- + \pi^0 \pi^- \partial_\mu \pi^+ - 2\pi^+ \pi^- \partial_\mu \pi^0) \partial_\mu \phi_A. \quad (11)$$

In hadronic axion models, the coupling constant is

$$C_{A\pi} = \frac{1-z}{3(1+z)}. \quad (12)$$

In general the chiral symmetry-breaking Lagrangian contributes an additional piece to $\mathcal{L}_{A\pi}$ proportional to $(m_\pi^2 / f_\pi f_A) (\pi^0 \pi^0 + 2\pi^- \pi^+) \pi^0 \phi_A$. For hadronic axions, this term vanishes identically, in contrast, for example, to the DFSZ model (Roberto Peccei, private communication).

II. LABORATORY SEARCHES

II.1 Photon regeneration: Searching for ‘‘invisible axions’’ in laboratory experiments is extremely challenging. The most promising approaches use the axion-two-photon vertex, allowing axions and photons to convert into each other in the presence of external electric or magnetic fields [22]. When the external field is the Coulomb field of a charged particle, the conversion is best viewed as an ordinary scattering process, $\gamma + Ze \leftrightarrow Ze + A$,

See key on page 373

Gauge & Higgs Boson Particle Listings Axions (A^0) and Other Very Light Bosons

called Primakoff effect in analogy to the corresponding π^0 process [23]. In the other extreme of a macroscopic field, usually a large-scale B -field, the momentum transfer is small, the interaction coherent over a large distance, and the conversion is best viewed as an axion-photon oscillation phenomenon in analogy to neutrino-flavor oscillations [24]. The search for solar axions with the “helioscope technique” [22], or for dark-matter axions with the “haloscope technique” [22], are based on this concept and will be discussed in the sections on stellar and cosmological axions below, whereas here we concentrate on pure laboratory experiments that do not require astrophysical sources.

Photons propagating through a transverse magnetic field, with incident \mathbf{E} and magnet \mathbf{B} parallel, may convert into axions. For light axions with $m_A^2 L/2\omega \ll 2\pi$, where L is the length of the magnetic field conversion region and ω the photon energy, the resultant axion beam is collinear and coherent with the incident photon beam, and the conversion probability Π is given by $\Pi \sim (1/4)(G_{A\gamma\gamma}BL)^2$. A practical realization of this concept is a laser beam propagating down the bore of a long superconducting dipole magnet (like the bending magnets in high-energy accelerators). If another such dipole magnet is in line with the first, with an optical barrier separating the two, then photons may be regenerated and detected in the second magnet from the pure axion beam [25]. The overall probability $P(\gamma \rightarrow A \rightarrow \gamma) = \Pi^2$.

Such an experiment has been carried out, utilizing two magnets of length $L = 4.4$ m and $B = 3.7$ T. For $m_A < 1$ meV, the coupling was found to be constrained by $G_{A\gamma\gamma} < 6.7 \times 10^{-7}$ GeV $^{-1}$ at 95% CL [26]. More recently, the Light Pseudo Scalar Search project (LIPSS) collaboration has taken data at the Jefferson Laboratory free-electron infrared laser facility. The claimed sensitivity of their detector is $G_{A\gamma\gamma} = 1.7 \times 10^{-6}$ GeV $^{-1}$ [27]. Another recent experiment uses a pulsed laser with similar sensitivity [28]. Most recently, the GammeV Particle Search Experiment experiment at FNAL has reported a 3σ constraint of $G_{A\gamma\gamma} < 3.2 \times 10^{-7}$ GeV $^{-1}$ in the limit $m_A = 0$ [29]. Other experiments that are planned or under construction include the Axion-Like Particle Search experiment (ALPS) at DESY, and the Optical Search for QED vacuum magnetic birefringence experiment at CERN.

A new concept has been proposed, resonantly-enhanced photon regeneration, which may enable searches into unexplored regions of axion-photon couplings [30]. In this scheme, both the production and detection magnets are within Fabry-Perot optical cavities and actively locked in frequency. The enhancement is $P^{\text{res}}(\gamma \rightarrow a \rightarrow \gamma) = (2\mathcal{F}\mathcal{F}'/\pi^2) \times P^{\text{non-res}}$, where \mathcal{F} and \mathcal{F}' are the finesse of the two optical cavities. Feasibly, the resonant enhancement could be of order $10^{(10-12)}$, leading to improvements in sensitivity in $G_{A\gamma\gamma}$ of $10^{(2.5-3)}$.

II.2 Photon polarization: An alternative to regenerating the lost photons is to use the beam itself to detect the B -field-induced photon-axion conversion: the polarization of light

propagating through a transverse magnetic field suffers dichroism and birefringence [31]. Dichroism: The E_{\parallel} component, but not the E_{\perp} component, will be depleted by the production of axions, and thus there will be in general a small rotation of the polarization vector of linearly-polarized light. The effect will be constant for all sufficiently light axions, such that the oscillation length is much longer than the magnet $m_A^2 L/2\omega \ll 2\pi$. For heavier axions, the effect oscillates and diminishes as m_A increases, and vanishes for $m_A > \omega$. Birefringence: This rotation occurs because there is mixing of virtual axions in the E_{\parallel} state, but not for the E_{\perp} state. Hence, initially linearly polarized light will become elliptically polarized. Higher-order QED also induces vacuum birefringence. A search for these effects was performed on the same dipole magnets in the early experiment above [32]. Any effect increases linearly when the beam passes through an optical cavity within the magnet. The dichroic rotation gave a stronger limit than the ellipticity rotation: $G_{A\gamma\gamma} < 3.6 \times 10^{-7}$ GeV $^{-1}$ at 95% CL for $m_A < 5 \times 10^{-4}$ eV. The ellipticity rotation limits are better at higher masses, as they fall off smoothly and do not terminate at m_A .

In 2006, a publication by the PVLAS collaboration reported a signature of magnetically induced vacuum dichroism, which could have been interpreted as evidence for a light pseudoscalar with a mass of 1–1.5 meV and a photon coupling of $(1.6-5) \times 10^{-6}$ GeV $^{-1}$ [33]. This result was problematic from several points of view, not the least of which was the difficulty in reconciling the magnitude of the signal with the much more restrictive limits on $G_{A\gamma\gamma}$ from the Sun, horizontal branch stars, and CAST (see below). Furthermore, the PVLAS data themselves evidenced large systematic errors of unknown origin. More recently, the PVLAS collaboration issued a report retracting their earlier findings. They conclude the effects were instrumental artifacts, with no evidence for new physics [34].

II.3 Long-range forces: New bosons would mediate long-range forces, which are severely constrained by “fifth force” experiments [35]. These experiments, notably those looking for new mass-spin couplings, provide significant constraints on axion-like particles [36,37]. The limits on the product of couplings at the mass- and spin-coupled interaction vertices (Figure 1) may be related to limits on the DFSZ model [36].

In summary, pure laboratory searches for invisible axions have not yet provided useful limits on plausible models. Photon propagation or long-range force experiments are only sensitive for small m_A , so that the corresponding coupling strengths that scale with $f_A^{-1} \approx m_A/m_{\pi}f_{\pi}$ are too small to be detected. However, these efforts provide constraints on general low-mass bosons, and have searched for axions of non-standard masses and couplings.

Gauge & Higgs Boson Particle Listings

Axions (A^0) and Other Very Light Bosons

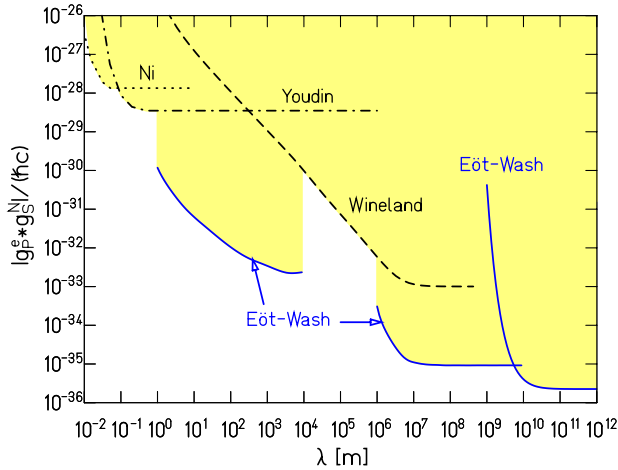


Figure 1: Short-distance gravity upper limits [37] on the product of mass- and spin-vertex couplings as a function of the interaction range λ ; the shaded region is excluded at 95% confidence. Figure courtesy E. Adelberger.

III. AXIONS FROM ASTROPHYSICAL SOURCES

III.1 Stellar energy-loss limits: Low-mass weakly-interacting particles (neutrinos, gravitons, axions, baryonic or leptonic gauge bosons, *etc.*) are produced in hot astrophysical plasmas, and can thus transport energy out of stars. The coupling strength of the particles with normal matter and radiation is bounded by the constraint that stellar-evolution lifetimes or energy-loss rates not conflict with observation [38–40].

We begin with our Sun and concentrate on hadronic axion models. The dominant production is by the Primakoff process $\gamma + Ze \rightarrow Ze + A$, where photons convert into axions in the electric fields of the charged particles in the plasma. Integrating over a standard solar model, one finds an axion luminosity [53]

$$L_A = G_{10}^2 1.85 \times 10^{-3} L_\odot, \quad (13)$$

where $G_{10} = G_{A\gamma\gamma} \times 10^{10}$ GeV. The maximum of the spectrum is at 3.0 keV, the average at 4.2 keV, and the number flux at Earth is $G_{10}^2 3.75 \times 10^{11}$ cm $^{-2}$ s $^{-1}$.

The axion losses lead to an enhanced consumption of nuclear fuel. The standard Sun is halfway through its hydrogen-burning phase so that the solar axion luminosity cannot significantly exceed its photon luminosity L_\odot . For a more refined constraint, we note that a model of the present-day Sun, with the integrated effect of axion losses taken into account, differs from a standard solar model for sufficiently large values of the coupling constant. The modified sound-speed profile can be diagnosed by helioseismology, providing a conservative limit $G_{10} \lesssim 10$, corresponding to $L_A \lesssim 0.20 L_\odot$ [41]. More recent determinations of the solar metal abundances have spoiled the almost perfect agreement between standard solar models

and helioseismology [42], a problem that is not yet resolved. However, the axion limit probably remains unaffected.

The energy loss by solar axion emission requires enhanced nuclear burning, and thus an increased temperature. Self-consistent solar models with axion losses reveal that $G_{10} = 4.5$ causes a 20% increase of the solar ^8B neutrino flux [41]. The measured all-flavor ^8B solar neutrino flux is 4.94×10^6 cm $^{-2}$ s $^{-1}$ with an uncertainty of about 8.8% [43]. The old standard solar model predictions were 5.7–5.9 in the same units, whereas the new metal abundances imply 4.5–4.6, each time with a 16% “theoretical 1σ error” [42]. Therefore, the measured neutrino fluxes imply a limit $G_{10} \lesssim 5$, corresponding to $L_A \lesssim 0.04 L_\odot$.

A more restrictive limit on $G_{A\gamma\gamma}$ arises from globular-cluster (GC) stars. A GC is a gravitationally bound system of a homogeneous population of low-mass stars, allowing for detailed tests of stellar-evolution theory. The stars on the horizontal branch (HB) in the color-magnitude diagram have reached helium burning, where their core (mass $\sim 0.5 M_\odot$, density $\sim 10^4$ g cm $^{-3}$, temperature $\sim 10^8$ K) generates energy by fusing helium to carbon and oxygen with a core-averaged energy release of about 80 erg g $^{-1}$ s $^{-1}$. The core-averaged Primakoff axion loss rate is about $G_{10}^2 30$ erg g $^{-1}$ s $^{-1}$. The main effect is accelerated consumption of helium, and thus a reduction of the HB lifetime by about $80/(80 + 30 G_{10}^2)$. The HB lifetime is measured relative to the red-giant branch (RGB) evolutionary time scale by comparing the number of HB stars with the number of RGB stars. This number ratio agrees with expectations within 20–40% in any one of 15 studied GCs [44]. Compounding the results of all 15 GCs, the agreement is within about 10% [39]. A reasonably conservative limit is

$$G_{A\gamma\gamma} \lesssim 1 \times 10^{-10} \text{ GeV}^{-1}, \quad (14)$$

although an objective error budget is not available.

We translate this nominal constraint on the axion-photon interaction strength to $f_A > 2.3 \times 10^7$ GeV (and thus $m_A < 0.3$ eV), using $z = 0.56$ and $E/N = 0$ as in the KSVZ model, and show the excluded range in Figure 2. For the DFSZ model with $E/N = 8/3$, the corresponding limits are slightly less restrictive, $f_A > 0.8 \times 10^7$ GeV (and thus $m_A < 0.7$ eV). The exact high-mass end of the exclusion range has not been determined. We note that the relevant temperature is around 10 keV, and the average photon energy is therefore around 30 keV. The excluded m_A range thus certainly extends beyond the shown 100 keV.

In models where axions couple directly to electrons, processes of the form $\gamma + e^- \rightarrow e^- + a$ and $e^- + Ze \rightarrow Ze + e^- + a$ are more efficient than the Primakoff process. Moreover, bremsstrahlung is efficient in degenerate stars such as white dwarfs, where the Primakoff and Compton processes are suppressed by the large photon plasma frequency. One limit comes from GC stars where the enhanced energy losses would delay helium ignition so that the tip of the RGB would be brighter than observed [45], implying $\alpha_{Aee} \lesssim 0.5 \times 10^{-26}$. Axion emission would also enhance white-dwarf cooling, leading to a similar

See key on page 373

Gauge & Higgs Boson Particle Listings Axions (A^0) and Other Very Light Bosons

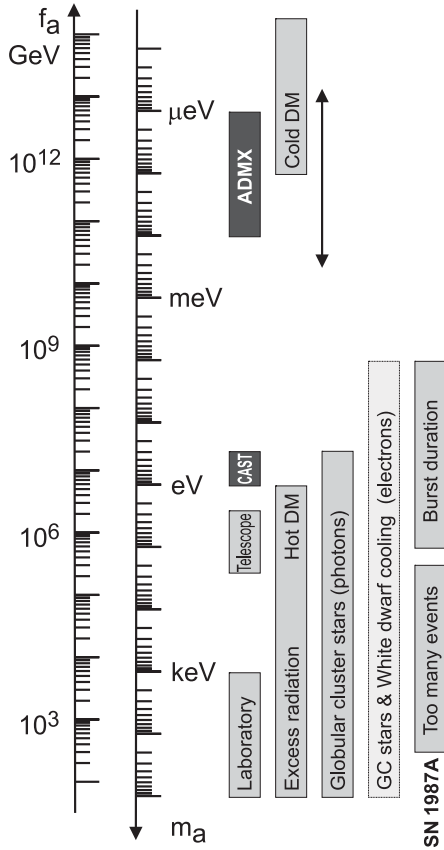


Figure 2: Exclusion and experimental search ranges as described in the text. Limits on coupling strengths are translated into limits on m_A and f_A using $z = 0.56$ and the KSVZ values for the coupling strengths. The “Laboratory” bar is a rough representation of the exclusion range for standard or variant axions. The “GC stars and white-dwarf cooling” range uses the DFSZ model with an axion-electron coupling corresponding to $\cos^2 \beta = 1/2$. The Cold Dark Matter exclusion range is particularly uncertain. We show the benchmark case from the misalignment mechanism.

limit $\alpha_{Aee} \lesssim 1 \times 10^{-26}$ from the white-dwarf luminosity function [46]. For pulsationally unstable white dwarfs (ZZ Ceti stars), the period decrease \dot{P}/P is a measure of the cooling speed. A well-studied case is the star G117–B15A, where \dot{P}/P has been measured, implying [47]

$$\alpha_{Aee} < 1.3 \times 10^{-27} \quad (15)$$

at a statistical 95% CL. (We have corrected the published limit for an apparent misprint.) This result is equivalent to $g_{Aee} < 1.3 \times 10^{-13}$ or in the DFSZ model to $f_A > 1.3 \times 10^9 \text{ GeV} \cos^2 \beta$ and $m_A < 4.5 \text{ meV}/\cos^2 \beta$. We show these constraints in Figure 2 for $\cos^2 \beta = 1/2$.

Similar constraints are provided by the neutrino signal of the supernova SN 1987A. Several detectors registered together about two dozen events spread over about 10 s, showing

that the burst duration was not significantly shortened by a new energy-loss channel. Numerical simulations for a variety of cases, including axions and Kaluza-Klein gravitons, reveal that the energy-loss rate of a nuclear medium at the density $3 \times 10^{14} \text{ g cm}^{-3}$ and temperature 30 MeV should not exceed about $1 \times 10^{19} \text{ erg g}^{-1} \text{ s}^{-1}$ [39]. Translating this nominal criterion into a limit on the axion-nucleon coupling depends on a calculation of bremsstrahlung emission $N + N \rightarrow N + N + a$ in a nuclear medium. The energy loss rate per unit mass is found to be $(C_N/2f_A)^2 (T^4/\pi^2 m_N) F$. Here F is a numerical factor that represents an integral over the dynamical spin-density structure function, because axions couple to the nucleon spin and thus are essentially emitted by the fluctuating nuclear spins of the dense medium. In a dilute medium, F would have the interpretation of $\Gamma/2T$ with Γ a typical nucleon spin fluctuation rate. For realistic conditions, even after considerable effort, one is limited to a heuristic estimate leading to $F \approx 1$ [40].

The SN 1987A limits are of particular interest for hadronic axions where the bounds on α_{Aee} are moot. Therefore, we use $C_p = -0.4$ and $C_n = 0$. We use an initial proton fraction of 0.3 to scale the emission rate to the proton density. With $F = 1$ and $T = 30 \text{ MeV}$ we find [40]

$$f_A \gtrsim 4 \times 10^8 \text{ GeV} \quad \text{and} \quad m_A \lesssim 16 \text{ meV}. \quad (16)$$

If axions interact sufficiently strongly they are trapped, like neutrinos, so that only about three orders of magnitude in g_{ANN} or m_A are excluded by the burst duration. We show the excluded range somewhat schematically in Figure 2. For even larger couplings, the axion flux would have been negligible, yet it would have triggered additional events in the detectors, excluding a further range of couplings [48]. A possible gap between the exclusion ranges of these two SN 1987A arguments was discussed as the “hadronic axion window” under the assumption that $G_{A\gamma\gamma}$ was anomalously small [49]. This range is now excluded by the cosmic structure-formation arguments to be discussed in the section on cosmological axions.

III.2 Searches for solar axions: Instead of using stellar energy losses to derive limits on axion parameters, one can also search directly for these fluxes in the laboratory, notably those from our Sun. The main experimental focus has been on axion-like particles with a two-photon vertex. They are produced by the Primakoff process with a flux given by Equation 13, and can be detected at Earth with the reverse process in a macroscopic B -field (“axion helioscope”) [22]. Viewing this re-conversion as a particle oscillation process, we note that the average energy of solar axions is 4.2 keV, implying a photon-axion oscillation length in vacuum of $2\pi(2\omega/m_A^2) \sim \mathcal{O}(1 \text{ mm})$, precluding the vacuum mixing from achieving its theoretical maximum in any practical magnet. However, one can endow the photon with an effective mass in a gas, $m_\gamma = \omega_{\text{plas}}$, thus matching the axion and photon dispersion relations [50].

Gauge & Higgs Boson Particle Listings

Axions (A^0) and Other Very Light Bosons

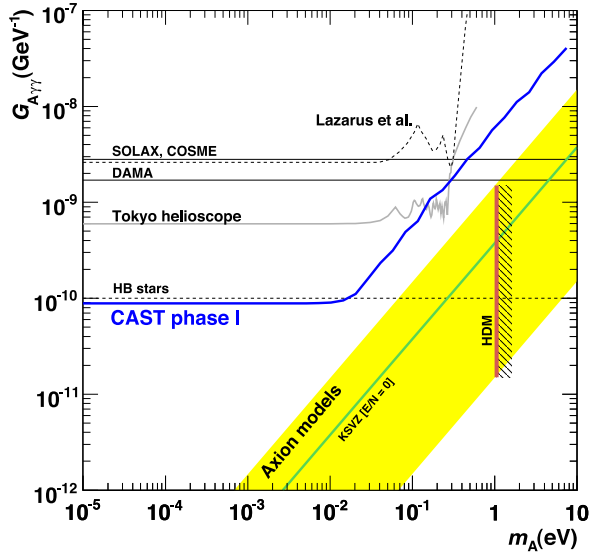


Figure 3: Solar-axion exclusion plot in the $G_{A\gamma\gamma}$ - m_A -plane for axion-like particles [53]. For small masses, the most restrictive limit is from CAST-I [53], and is shown with previous helioscopes Lazarus *et al.* [51] and the Tokyo helioscope [52]. Also shown are constraints from experiments using the Bragg technique SOLAX [55], COSME [56], and DAMA [57]. The vertical red line (HDM) is the hot dark-matter limit [64]. The yellow band represents models with $|E/N - 1.92|$ in the range 0.07–7, while the green solid line corresponds to the KSVZ case.

An early implementation of these ideas was carried out using a conventional dipole magnet, with a conversion volume of variable-pressure gas with a xenon proportional chamber as x-ray detector [51]. The conversion magnet was fixed in orientation and collected data for about 1000 s/day. Axions were excluded for $G_{A\gamma\gamma} < 3.6 \times 10^{-9} \text{ GeV}^{-1}$ for $m_A < 0.03 \text{ eV}$, and $G_{A\gamma\gamma} < 7.7 \times 10^{-9} \text{ GeV}^{-1}$ for $0.03 < m_A < 0.11 \text{ eV}$ at 95% CL. Later, the Tokyo axion helioscope used a superconducting magnet on a tracking mount, viewing the Sun continuously. They reported $G_{A\gamma\gamma} < 6 \times 10^{-10} \text{ GeV}^{-1}$ for $m_A < 0.3 \text{ eV}$ [52]. The exclusion ranges are shown in Figure 3.

The most recent helioscope CAST (CERN Axion Solar Telescope) uses a decommissioned LHC dipole magnet on a tracking mount and is actively taking data. The hardware includes grazing-incidence x-ray optics with solid-state x-ray detectors, as well as a novel x-ray Micromegas position-sensitive gaseous detector. CAST has established a 95% CL limit $G_{A\gamma\gamma} < 8.8 \times 10^{-11} \text{ GeV}^{-1}$ for $m_a < 0.02 \text{ eV}$ [53]. To cover larger masses and to “cross the axion line,” the conversion region in the magnet bores is filled with a gas at varying pressure. The runs with ^4He gas are complete and cover masses up to about 0.4 eV, but exact limits on $G_{A\gamma\gamma}$ in this range have

not yet been established [54]. Forthcoming runs with ^3He gas will explore axion masses up to 1.16 eV within about 3 years.

Other Primakoff searches for solar axions have been carried out using crystal detectors, exploiting the coherent conversion of axions into photons when the axion angle of incidence satisfies a Bragg condition with a crystalline plane. Limits from SOLAX [55], COSME [56], and DAMA [57] are summarized in Figure 4.

Another idea is to look at the Sun with an x-ray satellite when the Earth is in between. Solar axions would be converted in the Earth magnetic field on the far side relative to the Sun into x-rays, and could be picked up by the detector [58]. The sensitivity to $G_{A\gamma\gamma}$ could be comparable to CAST, but only for much smaller m_A .

III.3 Conversion of astrophysical photon fluxes: Large-scale magnetic fields exist in astrophysics that can induce axion-photon oscillations. In practical cases, B is much smaller than the laboratory fields used, for example, in helioscopes, whereas the conversion region L is much larger. Therefore, while the product BL can be large, any realistic sensitivity is usually restricted to very low-mass particles, far away from the “axion line” in a plot like Figure 3.

One example is SN 1987A, which would have emitted a burst of axion-like particles due to the Primakoff production in its core. They would have partially converted into γ -rays in the galactic B -field. The absence of a γ -ray burst in coincidence with the SN 1987A neutrino burst provides a limit $G_{A\gamma\gamma} \lesssim 1 \times 10^{-11} \text{ GeV}^{-1}$ for $m_A \lesssim 10^{-9} \text{ eV}$ [59]. This is the most restrictive limit for very small m_A .

Axion-like particles from other stars could be converted to photons in astrophysical B -fields, but no tangible new limits or signatures seem to have appeared.

Conversely, photons from distant sources could be converted to axion-like particles, depleting the original flux, thereby dimming the sources. This mechanism was proposed as an alternative explanation to cosmic acceleration for the apparent dimming of distant SNe of type Ia [60]. However, this dimming would apply to all distant sources, including quasars and the cosmic microwave background radiation, and would depend on energy. All things considered, this mechanism can only play a subdominant role [61].

High-energy γ -rays are typically produced in magnetized environments where cosmic rays are accelerated. The conversion into axion-like particles can then, in principle, imprint observable features on the spectrum for a range of coupling constants not excluded by other arguments [62].

IV. COSMIC AXIONS

IV.1 Cosmic axion populations: In the early universe, axions are produced by processes involving their couplings to quarks and gluons [63]. After the QCD confinement transition, the dominant thermalization process is $\pi + \pi \leftrightarrow \pi + a$ [21]. The resulting cosmic axion population would contribute a hot

See key on page 373

Gauge & Higgs Boson Particle Listings Axions (A^0) and Other Very Light Bosons

dark-matter fraction in analogy to massive neutrinos. Cosmological precision data provide restrictive constraints on a possible hot dark-matter fraction that translate into $m_A < 0.4\text{--}1.2$ eV at the 95% statistical CL [64]. The spread of the published limits reflects the use of different cosmological data. Including Lyman- α data leads to more restrictive limits that are, however, vulnerable to poorly controlled systematic uncertainties.

For $m_A \gtrsim 20$ eV, axions decay into photons faster than a cosmic time scale, removing the axion population while injecting radiation. This excess radiation provides additional limits up to very large axion masses [65]. An anomalously small $G_{A\gamma\gamma}$ provides no loophole because suppressing decays leads to thermal axions overdominating the mass density of the universe.

The main cosmological interest in axions derives from their possible role as cold dark matter (CDM). In addition to thermal processes, axions are abundantly produced by the “misalignment mechanism” [66]. After the spontaneous breakdown of the PQ symmetry at high energies, the axion field relaxes somewhere in the “bottom of the wine bottle” potential. Near the QCD epoch, instanton effects explicitly break the PQ symmetry, the very effect that causes the dynamical PQ symmetry restoration. This “tilting of the wine bottle bottom” causes the axion field to roll toward the CP -conserving minimum, thereby exciting coherent oscillations of the axion field that ultimately represent a “condensate” of CDM. The cosmic mass density in this homogeneous field mode is [67]

$$\Omega_A h^2 \approx 0.7 \left(\frac{f_A}{10^{12} \text{ GeV}} \right)^{7/6} \left(\frac{\bar{\Theta}_i}{\pi} \right)^2, \quad (17)$$

where h is the present-day Hubble expansion parameter in units of $100 \text{ km s}^{-1} \text{ Mpc}^{-1}$, and $-\pi \leq \bar{\Theta}_i \leq \pi$ is the initial “misalignment angle” relative to the CP -conserving position. If the PQ symmetry breakdown takes place after inflation, $\bar{\Theta}_i$ will take on different values in different patches of the universe. The average contribution is [67]

$$\Omega_A h^2 \approx 0.3 \left(\frac{f_A}{10^{12} \text{ GeV}} \right)^{7/6}. \quad (18)$$

Comparing with the measured CDM density of $\Omega_{\text{CDM}} h^2 \approx 0.13$ implies that axions with $m_A \approx 10 \mu\text{eV}$ provide the dark matter, whereas smaller masses are excluded (Figure 2).

This density sets only a crude scale of the expected m_A . Apart from the overall particle physics uncertainties, the cosmological sequence of events plays a crucial role. Assuming axions make up CDM, significantly smaller masses are possible if inflation took place after the PQ transition and the initial value $\bar{\Theta}_i$ was small. Conversely, if the PQ transition took place after inflation, there are additional sources for nonthermal axions, notably the formation and decay of cosmic strings and domain walls. However, these populations are comparable to the misalignment contribution [67]. Still, the mass of CDM axions could be significantly smaller or larger than $10 \mu\text{eV}$ [67].

If the reheat temperature after inflation is too small to restore the PQ symmetry, the axion field is present during inflation, and subject to quantum mechanical fluctuations that lead to isocurvature fluctuations that are severely constrained by precision cosmological data [67,68]. One consequence is that the cosmic axion population cannot be arbitrarily small, even for a very small initial $\bar{\Theta}_i$.

In the opposite case without inflation after the PQ transition, the spatial axion density variation is large at the QCD transition. These density variations are not erased by free streaming. When matter begins to dominate the universe, gravitationally bound “axion mini clusters” form promptly [69]. A significant fraction of CDM axions can reside in these objects.

The hot and cold cosmic axion populations are not entirely independent. Most cold axions are produced shortly before the QCD phase transition. For $f_A \lesssim 10^8$ GeV, axions reach thermal equilibrium after this epoch, thermalizing the axion field, thereby erasing the cold populations.

IV.2 Telescope searches: The two-photon decay rate of cosmic axions is extremely slow for axions with masses in the CDM regime, but could be detectable for eV-mass axions. The signature would be a quasi-monochromatic emission line from galaxies and galaxy clusters. This line, corrected for the host Doppler shift, would appear at half the axion mass, and its width would be similar to the virial width of objects in the host. The expected optical line intensity for DFSZ axions is similar to the continuum night emission. An early search in three rich Abell clusters [70], and a recent search in two rich Abell clusters [71], exclude the “Telescope” range in Figure 2 unless the axion–photon coupling is strongly suppressed. Of course, axions in this mass range would also provide an excessive hot DM contribution.

Very low-mass axions in halos produce a weak quasi-monochromatic spectral line in the radio. Virial velocities in undisrupted dwarf galaxies are very low, and the axion emission line would therefore be extremely narrow. A search with the Haystack radio telescope on three nearby dwarf galaxies provided a limit $G_{A\gamma\gamma} < 1.0 \times 10^{-9} \text{ GeV}^{-1}$ at 96% CL for $298 < m_A < 363 \mu\text{eV}$ [72]. However, this combination of m_A and $G_{A\gamma\gamma}$ does not yet include plausible axion models.

IV.3 Microwave cavity experiments: The astrophysical and cosmological limits of Figure 2 suggest that axions, if they exist, provide a significant fraction or all of the cosmic CDM. In a broad range of the plausible m_A range for CDM axions, galactic halo axions may be detected by their resonant conversion into a quasi-monochromatic microwave signal in a high-Q electromagnetic cavity permeated by a strong static magnetic field [22,73]. The cavity frequency is tunable, and the signal is maximized when the frequency is the total axion energy, rest mass plus kinetic energy, of $\nu = (m_A/2\pi) [1 + \mathcal{O}(10^{-6})]$, the width above the rest mass representing the virial axion distribution in the galactic gravitational potential. The frequency spectrum width may also have finer structure from axions more

Gauge & Higgs Boson Particle Listings

Axions (A^0) and Other Very Light Bosons

recently fallen into the galactic potential and not yet completely virialized [74].

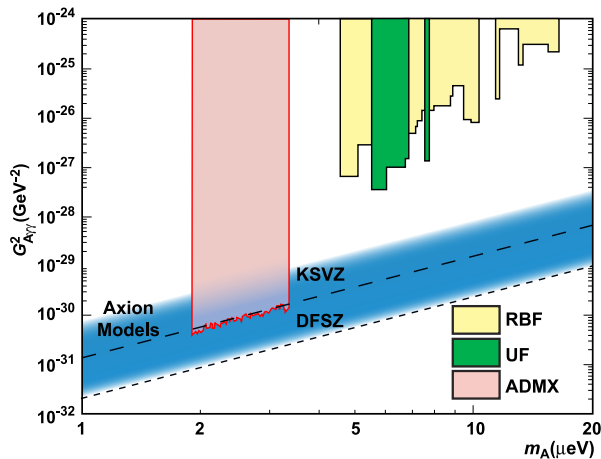


Figure 4: Exclusion region reported from the microwave cavity experiments RBF and UF [75] and ADMX [76]. A local dark-matter density of 450 MeV cm^{-3} is assumed. Color version at end of book.

The feasibility of this technique was established in early experiments of relatively small sensitive volume, $\mathcal{O}(1 \text{ liter})$ [75], with HFET-based amplifiers, setting limits in the range $4.5 < m_A < 16.3 \mu\text{eV}$, but lacking by 2–3 orders of magnitude the sensitivity required to detect realistic axions. ADMX, a later experiment ($B \sim 8 \text{ T}$, $V \sim 200 \text{ liters}$) has achieved sensitivity to KSVZ axions, assuming they saturate the local dark matter halo and are well virialized, over the mass range $1.9\text{--}3.3 \mu\text{eV}$ [76]. Should halo axions have a component not yet virialized, ADMX is sensitive to DFSZ axions [77]. The corresponding 90% CL exclusion regions shown in Figure 4 are normalized to an assumed local CDM density of $7.5 \times 10^{-25} \text{ g cm}^{-3}$ (450 MeV cm^{-3}) [78]. The ADMX experiment is currently undergoing commissioning of an upgrade that replaces the microwave HFET amplifiers by near quantum-limited low-noise dc SQUID amplifiers [79], allowing a significant improvement in the experiment sensitivity. A Rydberg atom single-photon detector [80] can in principle evade the standard quantum limit [81] for coherent detection, thus achieving very good sensitivity. Efforts are underway to incorporate Rydberg atom systems in RF cavity axion searches [82].

Conclusions: Experimental, astrophysical, and cosmological limits have been refined and indicate that axions, if they exist, are likely very light, $m_A \lesssim 10 \text{ meV}$, suggesting that axions are a non-negligible fraction of the cosmic CDM. The upgraded versions of the ADMX experiment will ultimately cover the range $1\text{--}100 \mu\text{eV}$ with a sensitivity allowing one to detect axions, unless the local DM density is unexpectedly small or the axion–photon coupling anomalously weak. Other experimental techniques remain of interest to search for general

axion-like particles, although at present no method besides the DM search is known that could detect realistic axions obeying the astrophysical and cosmological limits, and fulfilling the QCD-implied relationship between mass and coupling strength.

References

1. R.D. Peccei and H. Quinn, Phys. Rev. Lett. **38**, 1440 (1977), Phys. Rev. **D16**, 1791 (1977).
2. S. Weinberg, Phys. Rev. Lett. **40**, 223 (1978); F. Wilczek, Phys. Rev. Lett. **40**, 279 (1978).
3. F. Wilczek, Phys. Rev. Lett. **49**, 1549 (1982).
4. Y. Chikashige, R.N. Mohapatra, and R.D. Peccei, Phys. Lett. **98B**, 265 (1981); G.B. Gelmini and M. Roncadelli, Phys. Lett. **99B**, 411 (1981).
5. C.A. Baker *et al.*, Phys. Rev. Lett. **97**, 131801 (2006).
6. H. Georgi, D.B. Kaplan, and L. Randall, Phys. Lett. **B169**, 73 (1986).
7. H. Leutwyler, Phys. Lett. **B378**, 313 (1996).
8. W.M. Yao *et al.*, (Particle Data Group), J. Phys. G: Nucl. Part. Phys. **33**, 1 (2006).
9. T.W. Donnelly *et al.*, Phys. Rev. **D18**, 1607 (1978); S. Barshay *et al.*, Phys. Rev. Lett. **46**, 1361 (1981); A. Barroso and N.C. Mukhopadhyay, Phys. Lett. **B106**, 91 (1981); R.D. Peccei, in *Proceedings of Neutrino '81*, Honolulu, Hawaii, Vol. 1, p. 149 (1981); L.M. Krauss and F. Wilczek, Phys. Lett. **B173**, 189 (1986).
10. J. Schweppe *et al.*, Phys. Rev. Lett. **51**, 2261 (1983); T. Cowan *et al.*, Phys. Rev. Lett. **54**, 1761 (1985).
11. R.D. Peccei, T.T. Wu, and T. Yanagida, Phys. Lett. **B172**, 435 (1986).
12. W.A. Bardeen, R.D. Peccei, and T. Yanagida, Nucl. Phys. **B279**, 401 (1987).
13. J.E. Kim, Phys. Rev. Lett. **43**, 103 (1979); M.A. Shifman, A.I. Vainshtein, and V.I. Zakharov, Nucl. Phys. **B166**, 493 (1980).
14. M. Dine, W. Fischler, and M. Srednicki, Phys. Lett. **B104**, 199 (1981); A.R. Zhitnitsky, Sov. J. Nucl. Phys. **31**, 260 (1980).
15. K.S. Choi, I.W. Kim, and J.E. Kim, JHEP **0703**, 116 (2007).
16. S.L. Cheng, C.Q. Geng, and W.T. Ni, Phys. Rev. **D52**, 3132 (1995).
17. G. Raffelt and D. Seckel, Phys. Rev. Lett. **60**, 1793 (1988); M. Carena and R.D. Peccei, Phys. Rev. **D40**, 652 (1989); K. Choi, K. Kang, and J.E. Kim, Phys. Rev. Lett. **62**, 849 (1989).
18. V.Y. Alexakhin *et al.*, (COMPASS Collaboration), Phys. Lett. **B647**, 8 (2007).
19. A. Airapetian *et al.*, (HERMES Collaboration), Phys. Rev. **D75**, 012007 (2007) and Erratum *ibid.*, **D76**, 039901 (2007).
20. J.R. Ellis and M. Karliner, in: *The spin structure of the nucleon: International school of nucleon structure* (3–10 August 1995, Erice, Italy), ed. by B. Frois, V.W. Hughes, and N. De Groot (World Scientific, Singapore, 1997) [hep-ph/9601280].
21. S. Chang and K. Choi, Phys. Lett. **B316**, 51 (1993).

See key on page 373

Gauge & Higgs Boson Particle Listings Axions (A^0) and Other Very Light Bosons

22. P. Sikivie, Phys. Rev. Lett. **51**, 1415 (1983) and Erratum *ibid.*, **52**, 695 (1984).
23. D.A. Dicus *et al.*, Phys. Rev. **D18**, 1829 (1978).
24. G. Raffelt and L. Stodolsky, Phys. Rev. **D37**, 1237 (1988).
25. K. van Bibber *et al.*, Phys. Rev. Lett. **59**, 759 (1987).
26. G. Ruoso *et al.*, Z. Phys. **C56**, 505 (1992);
R. Cameron *et al.*, Phys. Rev. **D47**, 3707 (1993).
27. A. Afanasev *et al.*, arXiv:hep-ph/0605250.
28. C. Robilliard *et al.*, Phys. Rev. Lett. **99**, 190403 (2007).
29. A.S. Chou *et al.* (GammeV Collab.), Phys. Rev. Lett. **100**, 080402 (2008).
30. P. Sikivie, D. Tanner, and K. van Bibber, Phys. Rev. Lett. **98**, 172002 (2007).
31. L. Maiani *et al.*, Phys. Lett. **B175**, 359 (1986).
32. Y. Semertzidis *et al.*, Phys. Rev. Lett. **64**, 2988 (1990).
33. E. Zavattini *et al.*, (PVLAS Collab.), Phys. Rev. Lett. **96**, 110406 (2006).
34. E. Zavattini *et al.*, (PVLAS Collab.), Phys. Rev. **D77**, 032006 (2008).
35. E. Fischbach and C. Talmadge, Nature **356**, 207 (1992).
36. J.E. Moody and F. Wilczek, Phys. Rev. D **30**, 130(1984).
37. A.N. Youdin *et al.*, Phys. Rev. Lett. **77**, 2170 (1996);
Wei-Tou Ni *et al.*, Phys. Rev. Lett. **82**, 2439 (1999);
D.F. Phillips *et al.*, Phys. Rev. **D63**, 111101 (R)(2001);
B.R. Heckel *et al.*, (Eöt-Wash Collaboration), Phys. Rev. Lett. **97**, 021603 (2006).
38. M.S. Turner, Phys. Reports **197**, 67 (1990);
G.G. Raffelt, Phys. Reports **198**, 1 (1990).
39. G.G. Raffelt, *Stars as Laboratories for Fundamental Physics*, (Univ. of Chicago Press, Chicago, 1996).
40. G.G. Raffelt, Lect. Notes Phys. **741**, 51 (2008) (Springer Verlag).
41. H. Schlattl, A. Weiss, and G. Raffelt, Astropart. Phys. **10**, 353 (1999).
42. J.N. Bahcall, A.M. Serenelli, and S. Basu, Astrophys. J. **21**, L85 (2005).
43. Q.R. Ahmad *et al.*, (SNO Collaboration), Phys. Rev. Lett. **89**, 011301 (2002);
B. Aharmim *et al.*, (SNO Collaboration), Phys. Rev. **C72**, 055502 (2005).
44. A. Buzzoni *et al.*, Astron. Astrophys. **128**, 94 (1983).
45. G. Raffelt and A. Weiss, Phys. Rev. **D51**, 1495 (1995);
M. Catelan, J.A. de Freitas Pacheco, and J.E. Horvath, Astrophys. J. **461**, 231 (1996).
46. G.G. Raffelt, Phys. Lett. **B166**, 402 (1986);
S.I. Blinnikov and N.V. Dunina-Barkovskaya, Mon. Not. R. Astron. Soc. **266**, 289 (1994).
47. A.H. Córscico *et al.*, New Astron. **6**, 197 (2001);
J. Isern and E. García-Berro, Nucl. Phys. B Proc. Suppl. **114**, 107 (2003).
48. J. Engel, D. Seckel, and A.C. Hayes, Phys. Rev. Lett. **65**, 960 (1990).
49. T. Moroi and H. Murayama, Phys. Lett. **B440**, 69 (1998).
50. K. van Bibber *et al.*, Phys. Rev. **D39**, 2089 (1989).
51. D. Lazarus *et al.*, Phys. Rev. Lett. **69**, 2333 (1992).
52. S. Moriyama *et al.*, Phys. Lett. **B434**, 147 (1998);
Y. Inoue *et al.*, Phys. Lett. **B536**, 18 (2002).
53. K. Zioutas *et al.*, (CAST Collaboration), Phys. Rev. Lett. **94**, 121301 (2005);
S. Andriamonje *et al.*, (CAST Collaboration), JCAP **0704**, 010 (2007).
54. K. Zioutas *et al.*, (CAST Collaboration), “Status Report of the CAST experiment and request to run beyond 2007,” CERN-SPSC-2007-013 (5 April 2007), see <http://doc.cern.ch/archive/electronic/cern/preprints/spsc/public/spsc-2007-013.pdf>.
55. F.T. Avignone III *et al.*, Phys. Rev. Lett. **81**, 5068 (1998).
56. A. Morales *et al.*, (COSME Collaboration), Astropart. Phys. **16**, 325 (2002).
57. R. Bernabei *et al.*, Phys. Lett. **B515**, 6 (2001).
58. H. Davoudiasl and P. Huber, Phys. Rev. Lett. **97**, 141302 (2006).
59. J.W. Brockway, E.D. Carlson, and G.G. Raffelt, Phys. Lett. **B383**, 439 (1996);
J.A. Grifols, E. Massó, and R. Toldrà, Phys. Rev. Lett. **77**, 2372 (1996).
60. C. Csaki, N. Kaloper, and J. Terning, Phys. Rev. Lett. **88**, 161302 (2002).
61. A. Mirizzi, G.G. Raffelt, and P.D. Serpico, Lect. Notes Phys. **741**, 115 (2008).
62. D. Hooper and P.D. Serpico, Phys. Rev. Lett. **99**, 231102 (2007);
K.A. Hochmuth and G. Sigl, Phys. Rev. **D76**, 123011 (2007).
63. M.S. Turner, Phys. Rev. Lett. **59**, 2489 (1987) and Erratum *ibid.*, **60**, 1101 (1988);
E. Massó, F. Rota, and G. Zsembinski, Phys. Rev. **D66**, 023004 (2002).
64. S. Hannestad, A. Mirizzi, and G. Raffelt, JCAP **0507**, 002 (2005);
A. Melchiorri, O. Mena, and A. Slosar, Phys. Rev. **D76**, 041303 (2007);
S. Hannestad *et al.*, JCAP **0708**, 015 (2007).
65. E. Massó and R. Toldrà, Phys. Rev. **D55**, 7967 (1997).
66. J. Preskill, M.B. Wise, and F. Wilczek, Phys. Lett. **B120**, 127 (1983);
L.F. Abbott and P. Sikivie, Phys. Lett. **B120**, 133 (1983);
M. Dine and W. Fischler, Phys. Lett. **B120**, 137 (1983).
67. P. Sikivie, Lect. Notes Phys. **741**, 19 (2008).
68. M. Beltrán, J. García-Bellido, and J. Lesgourgues, Phys. Rev. **D75**, 103507 (2007).
69. E.W. Kolb and I.I. Tkachev, Phys. Rev. Lett. **71**, 3051 (1993);
E.W. Kolb and I.I. Tkachev, Astrophys. J. **460**, L25 (1996).
70. M. Bershadsky *et al.*, Phys. Rev. Lett. **66**, 1398 (1991);
M. Ressel, Phys. Rev. **D44**, 3001 (1991).
71. D. Grin *et al.*, Phys. Rev. **D5**, 105018 (2007).
72. B.D. Blout *et al.*, Astrophys. J. **546**, 825 (2001).
73. P. Sikivie, Phys. Rev. **D32**, 2988 (1985);
L. Krauss *et al.*, Phys. Rev. Lett. **55**, 1797 (1985);
R. Bradley *et al.*, Rev. Mod. Phys. **75**, 777 (2003).
74. P. Sikivie and J. Ipser, Phys. Lett. **B291**, 288 (1992);
P. Sikivie *et al.*, Phys. Rev. Lett. **75**, 2911 (1995).
75. S. DePaenfilis *et al.*, Phys. Rev. Lett. **59**, 839 (1987);
W. Wuensch *et al.*, Phys. Rev. **D40**, 3153 (1989);
C. Hagmann *et al.*, Phys. Rev. **D42**, 1297 (1990).
76. S. Asztalos *et al.*, Phys. Rev. **D69**, 011101 (2004).
77. L. Duffy *et al.*, Phys. Rev. Lett. **95**, 091304 (2005).

Gauge & Higgs Boson Particle Listings

Axions (A^0) and Other Very Light Bosons

78. E. Gates *et al.*, *Astrophys. J.* **449**, 123 (1995).
 79. M. Mück, J.B. Kycia, and J. Clarke, *Appl. Phys. Lett.* **78**, 967 (2001).
 80. I. Ogawa, S. Matsuki, and K. Yamamoto, *Phys. Rev.* **D53**, 1740 (1996).
 81. V. Braginsky and F. Khalili in: *Quantum Measurement*, ed. by K. Thorne (Cambridge University Press, Cambridge) 1992.
 82. S. Matsuki *et al.*, *Nucl. Phys. B (Proc. Suppl.)* **51**, 213 (1996);
 Y. Kishimoto *et al.*, *Phys. Lett.* **A303**, 279 (2002);
 M. Tada *et al.*, *Phys. Lett.* **A303**, 285 (2002).

A^0 (Axion) MASS LIMITS FROM Astrophysics and Cosmology

These bounds depend on model-dependent assumptions (i.e. — on a combination of axion parameters).

VALUE (MeV)	DOCUMENT ID	TECN	COMMENT
••• We do not use the following data for averages, fits, limits, etc. •••			
>0.2	1 BARROSO 82	ASTR	Standard Axion
>0.25	1 RAFFELT 82	ASTR	Standard Axion
>0.2	2 DICUS 78c	ASTR	Standard Axion
	MIKAEKIAN 78	ASTR	Stellar emission
>0.3	2 SATO 78	ASTR	Standard Axion
>0.2	VYSOTSKII 78	ASTR	Standard Axion
1 Lower bound from 5.5 MeV γ -ray line from the sun. 2 Lower bound from requiring the red giants' stellar evolution not be disrupted by axion emission.			

A^0 (Axion) and Other Light Boson (X^0) Searches in Hadron Decays

Limits are for branching ratios.

VALUE	CL%	DOCUMENT ID	TECN	COMMENT
••• We do not use the following data for averages, fits, limits, etc. •••				
<7 $\times 10^{-10}$	90	3 PARK 05	HYCP	$\Sigma^+ \rightarrow pA^0, A^0 \rightarrow \mu^+ \mu^-$
<7.3 $\times 10^{-11}$	90	4 ADLER 04	B787	$K^+ \rightarrow \pi^+ X^0$
<4.5 $\times 10^{-11}$	90	5 ANISIMOVSK.04	B949	$K^+ \rightarrow \pi^+ X^0$
<4 $\times 10^{-5}$	90	6 ADLER 02c	B787	$K^+ \rightarrow \pi^+ X^0$
<4.9 $\times 10^{-5}$	90	7 ADLER 01	B787	$K^+ \rightarrow \pi^+ \pi^0 A^0$
<5.3 $\times 10^{-5}$	90	AMMAR 01b	CLEO	$B^\pm \rightarrow \pi^\pm (K^\pm) X^0$
<3.3 $\times 10^{-5}$	90	AMMAR 01b	CLEO	$B^0 \rightarrow K_S^0 X^0$
<5.0 $\times 10^{-8}$	90	8 ALTEGOER 98	NOMD	$\pi^0 \rightarrow \gamma X^0, m_{X^0} < 120$ MeV
<5.2 $\times 10^{-10}$	90	9 KITCHING 97	B787	$K^+ \rightarrow \pi^+ X^0 (X^0 \rightarrow \gamma\gamma)$
<2.8 $\times 10^{-4}$	90	10 ADLER 96	B787	$K^+ \rightarrow \pi^+ X^0$
<3 $\times 10^{-4}$	90	11 AMSLER 96b	CBAR	$\pi^0 \rightarrow \gamma X^0, m_{X^0} < 65$ MeV
<4 $\times 10^{-5}$	90	11 AMSLER 96b	CBAR	$\eta \rightarrow \gamma X^0, m_{X^0} = 50-200$ MeV
<6 $\times 10^{-5}$	90	11 AMSLER 96b	CBAR	$\eta' \rightarrow \gamma X^0, m_{X^0} = 50-925$ MeV
<6 $\times 10^{-5}$	90	11 AMSLER 94b	CBAR	$\pi^0 \rightarrow \gamma X^0, m_{X^0} = 65-125$ MeV
<6 $\times 10^{-5}$	90	11 AMSLER 94b	CBAR	$\eta \rightarrow \gamma X^0, m_{X^0} = 200-525$ MeV
<7 $\times 10^{-3}$	90	12 MEIJERDREES 94	CNTR	$\pi^0 \rightarrow \gamma X^0, m_{X^0} = 25$ MeV
<2 $\times 10^{-7}$	90	12 MEIJERDREES 94	CNTR	$\pi^0 \rightarrow \gamma X^0, m_{X^0} = 100$ MeV
<3 $\times 10^{-13}$	90	13 ATIYA 93b	B787	Sup. by ADLER 04
<1.1 $\times 10^{-8}$	90	14 NG 93	COSM	$\pi^0 \rightarrow \gamma X^0$
<5 $\times 10^{-4}$	90	15 ALLIEGRO 92	SPEC	$K^+ \rightarrow \pi^+ X^0 (X^0 \rightarrow e^+ e^-)$
<4 $\times 10^{-6}$	90	16 ATIYA 92	B787	$\pi^0 \rightarrow \gamma X^0$
	90	17 MEIJERDREES 92	SPEC	$\pi^0 \rightarrow \gamma X^0, X^0 \rightarrow e^+ e^-, m_{X^0} = 100$ MeV
<1 $\times 10^{-7}$	90	18 ATIYA 90b	B787	Sup. by KITCHING 97
<1.3 $\times 10^{-8}$	90	19 KORENCHENKO...	87	SPEC $\pi^+ \rightarrow e^+ \nu A^0 (A^0 \rightarrow e^+ e^-)$
<1 $\times 10^{-9}$	90	20 EICHLER 86	SPEC	Stopped $\pi^+ \rightarrow e^+ \nu A^0$
<2 $\times 10^{-5}$	90	21 YAMAZAKI 84	SPEC	For $160 < m < 260$ MeV
<(1.5-4) $\times 10^{-6}$	90	21 YAMAZAKI 84	SPEC	K decay, $m_{X^0} \ll 100$ MeV
	90	22 ASANO 82	CNTR	Stopped $K^+ \rightarrow \pi^+ X^0$
	90	23 ASANO 81b	CNTR	Stopped $K^+ \rightarrow \pi^+ X^0$
	90	24 ZHITNITSKII 79		Heavy axion

3 PARK 05 found three candidate events for $\Sigma^+ \rightarrow p\mu^+\mu^-$ in the HyperCP experiment. Due to a narrow spread in dimuon mass, they hypothesize the events as a possible signal of a new boson. It can be interpreted as an axion-like particle with $m_{A^0} = 214.3 \pm 0.5$ MeV and the branching fraction $B(\Sigma^+ \rightarrow pA^0) \times B(A^0 \rightarrow \mu^+\mu^-) = (3.1^{+2.4}_{-1.9} \pm 1.5) \times 10^{-8}$.

4 This limit applies for a mass near 180 MeV. For other masses in the range $m_{X^0} = 150-250$ MeV the limit is less restrictive, but still improves ADLER 02c and ATIYA 93b.

5 ANISIMOVSKY 04 bound is for $m_{X^0} = 0$.

6 ADLER 02c bound is for $m_{X^0} < 60$ MeV. See Fig. 2 for limits at higher masses.

7 The quoted limit is for $m_{X^0} = 0-80$ MeV. See their Fig. 5 for the limit at higher mass. The branching fraction limit assumes pure phase space decay distributions.

8 ALTEGOER 98 looked for X^0 from π^0 decay which penetrate the shielding and convert to π^0 in the external Coulomb field of a nucleus.

9 KITCHING 97 limit is for $B(K^+ \rightarrow \pi^+ X^0) \cdot B(X^0 \rightarrow \gamma\gamma)$ and applies for $m_{X^0} \approx 50$ MeV, $\tau_{X^0} < 10^{-10}$ s. Limits are provided for $0 < m_{X^0} < 100$ MeV, $\tau_{X^0} < 10^{-8}$ s.

10 ADLER 96 looked for a peak in missing-mass distribution. This work is an update of ATIYA 93. The limit is for massless stable X^0 particles and extends to $m_{X^0} = 80$ MeV at the same level. See paper for dependence on finite lifetime.

11 AMSLER 94b and AMSLER 96b looked for a peak in missing-mass distribution.

12 The MEIJERDREES 94 limit is based on inclusive photon spectrum and is independent of X^0 decay modes. It applies to $\tau(X^0) > 10^{-23}$ sec.

13 ATIYA 93b looked for a peak in missing mass distribution. The bound applies for stable X^0 of $m_{X^0} = 150-250$ MeV, and the limit becomes stronger (10^{-8}) for $m_{X^0} = 180-240$ MeV.

14 NG 93 studied the production of X^0 via $\gamma\gamma \rightarrow \pi^0 \rightarrow \gamma X^0$ in the early universe at $T \approx 1$ MeV. The bound on extra neutrinos from nucleosynthesis $\Delta N_\nu < 0.3$ (WALKER 91) is employed. It applies to $m_{X^0} \ll 1$ MeV in order to be relativistic down to nucleosynthesis temperature. See paper for heavier X^0 .

15 ALLIEGRO 92 limit applies for $m_{X^0} = 150-340$ MeV and is the branching ratio times the decay probability. Limit is $< 1.5 \times 10^{-8}$ at 99% CL.

16 ATIYA 92 looked for a peak in missing mass distribution. The limit applies to $m_{X^0} = 0-130$ MeV in the narrow resonance limit. See paper for the dependence on lifetime. Covariance requires X^0 to be a vector particle.

17 MEIJERDREES 92 limit applies for $\tau_{X^0} = 10^{-23}-10^{-11}$ sec. Limits between 2×10^{-4} and 4×10^{-6} are obtained for $m_{X^0} = 25-120$ MeV. Angular momentum conservation requires that X^0 has spin ≥ 1 .

18 ATIYA 90b limit is for $B(K^+ \rightarrow \pi^+ X^0) \cdot B(X^0 \rightarrow \gamma\gamma)$ and applies for $m_{X^0} = 50$ MeV, $\tau_{X^0} < 10^{-10}$ s. Limits are also provided for $0 < m_{X^0} < 100$ MeV, $\tau_{X^0} < 10^{-8}$ s.

19 KORENCHENKO 87 limit assumes $m_{A^0} = 1.7$ MeV, $\tau_{A^0} \lesssim 10^{-12}$ s, and $B(A^0 \rightarrow e^+ e^-) = 1$.

20 EICHLER 86 looked for $\pi^+ \rightarrow e^+ \nu A^0$ followed by $A^0 \rightarrow e^+ e^-$. Limits on the branching fraction depend on the mass and lifetime of A^0 . The quoted limits are valid when $\tau(A^0) \gtrsim 3 \times 10^{-10}$ s if the decays are kinematically allowed.

21 YAMAZAKI 84 looked for a discrete line in $K^+ \rightarrow \pi^+ X$. Sensitive to wide mass range (5-300 MeV), independent of whether X decays promptly or not.

22 ASANO 82 at KEK set limits for $B(K^+ \rightarrow \pi^+ X^0)$ for $m_{X^0} < 100$ MeV as $BR < 4 \times 10^{-8}$ for $\tau(X^0 \rightarrow n\gamma's) > 1 \times 10^{-9}$ s, $BR < 1.4 \times 10^{-6}$ for $\tau < 1 \times 10^{-9}$ s.

23 ASANO 81b is KEK experiment. Set $B(K^+ \rightarrow \pi^+ X^0) < 3.8 \times 10^{-8}$ at CL = 90%.

24 ZHITNITSKII 79 argue that a heavy axion predicted by YANG 78 ($3 < m < 40$ MeV) contradicts experimental muon anomalous magnetic moments.

A^0 (Axion) Searches in Quarkonium Decays

Decay or transition of quarkonium. Limits are for branching ratio.

VALUE	CL%	DOCUMENT ID	TECN	COMMENT
••• We do not use the following data for averages, fits, limits, etc. •••				
<1.3 $\times 10^{-5}$	90	25 BALEST 95	CLEO	$\Upsilon(1S) \rightarrow A^0 \gamma$
<4.0 $\times 10^{-5}$	90	25 ANTREASNYAN 90c	CBAL	$\Upsilon(1S) \rightarrow A^0 \gamma$
		26 ANTREASNYAN 90c	RVUE	
<5 $\times 10^{-5}$	90	27 DRUZHININ 87	ND	$\phi \rightarrow A^0 \gamma (A^0 \rightarrow e^+ e^-)$
<2 $\times 10^{-3}$	90	28 DRUZHININ 87	ND	$\phi \rightarrow A^0 \gamma (A^0 \rightarrow \gamma\gamma)$
<7 $\times 10^{-6}$	90	29 DRUZHININ 87	ND	$\phi \rightarrow A^0 \gamma (A^0 \rightarrow \text{missing})$
<3.1 $\times 10^{-4}$	90	30 ALBRECHT 86d	ARG	$\Upsilon(1S) \rightarrow A^0 \gamma (A^0 \rightarrow e^+ e^-)$
<4 $\times 10^{-4}$	90	30 ALBRECHT 86d	ARG	$\Upsilon(1S) \rightarrow A^0 \gamma (A^0 \rightarrow \mu^+ \mu^-, \pi^+ \pi^-, K^+ K^-)$
<8 $\times 10^{-4}$	90	31 ALBRECHT 86d	ARG	$\Upsilon(1S) \rightarrow A^0 \gamma$
<1.3 $\times 10^{-3}$	90	32 ALBRECHT 86d	ARG	$\Upsilon(1S) \rightarrow A^0 \gamma (A^0 \rightarrow e^+ e^-, \gamma\gamma)$
<2 $\times 10^{-3}$	90	33 BOWCOCK 86	CLEO	$\Upsilon(2S) \rightarrow \Upsilon(1S) \rightarrow A^0$
<5 $\times 10^{-3}$	90	34 MAGERAS 86	CUSB	$\Upsilon(1S) \rightarrow A^0 \gamma$
<3 $\times 10^{-4}$	90	35 ALAM 83	CLEO	$\Upsilon(1S) \rightarrow A^0 \gamma$
<9.1 $\times 10^{-4}$	90	36 NICZYPORUK 83	LENA	$\Upsilon(1S) \rightarrow A^0 \gamma$
<1.4 $\times 10^{-5}$	90	37 EDWARDS 82	CBAL	$J/\psi \rightarrow A^0 \gamma$
<3.5 $\times 10^{-4}$	90	38 SIVERTZ 82	CUSB	$\Upsilon(1S) \rightarrow A^0 \gamma$
<1.2 $\times 10^{-4}$	90	38 SIVERTZ 82	CUSB	$\Upsilon(3S) \rightarrow A^0 \gamma$

25 BALEST 95 looked for a monochromatic γ from $\Upsilon(1S)$ decay. The bound is for $m_{A^0} < 5.0$ GeV. See Fig. 7 in the paper for bounds for heavier m_{A^0} . They also quote a bound on branching ratios $10^{-3}-10^{-5}$ of three-body decay $\gamma X \bar{X}$ for $0 < m_X < 3.1$ GeV.

26 The combined limit of ANTREASNYAN 90c and EDWARDS 82 excludes standard axion with $m_{A^0} < 2m_e$ at 90% CL as long as $C_T C_{J/\psi} > 0.09$, where $C_V (V = \Upsilon, J/\psi)$ is the reduction factor for $\Gamma(V \rightarrow A^0 \gamma)$ due to QCD and/or relativistic corrections. The same data excludes $0.02 < x < 260$ (90% CL) if $C_T = C_{J/\psi} = 0.5$, and further combining with ALBRECHT 86d result excludes $5 \times 10^{-5} < x < 260$. x is the ratio of the vacuum expectation values of the two Higgs fields. These limits use conventional assumption $\Gamma(A^0 \rightarrow ee) \propto x^{-2}$. The alternative assumption $\Gamma(A^0 \rightarrow ee) \propto x^2$ gives a somewhat different excluded region $0.00075 < x < 44$.

27 The first DRUZHININ 87 limit is valid when $\tau_{A^0}/m_{A^0} < 3 \times 10^{-13}$ s/MeV and $m_{A^0} < 20$ MeV.

28 The second DRUZHININ 87 limit is valid when $\tau_{A^0}/m_{A^0} < 5 \times 10^{-13}$ s/MeV and $m_{A^0} < 20$ MeV.

29 The third DRUZHININ 87 limit is valid when $\tau_{A^0}/m_{A^0} > 7 \times 10^{-12}$ s/MeV and $m_{A^0} < 200$ MeV.

See key on page 373

Gauge & Higgs Boson Particle Listings
Axions (A^0) and Other Very Light Bosons

- ³⁰ $\tau_{A^0} < 1 \times 10^{-13}$ s and $m_{A^0} < 1.5$ GeV. Applies for $A^0 \rightarrow \gamma\gamma$ when $m_{A^0} < 100$ MeV.
- ³¹ $\tau_{A^0} > 1 \times 10^{-7}$ s.
- ³² Independent of τ_{A^0} .
- ³³ BOWCOCK 86 looked for A^0 that decays into e^+e^- in the cascade decay $\Upsilon(2S) \rightarrow \Upsilon(1S)\pi^+\pi^-$ followed by $\Upsilon(1S) \rightarrow A^0\gamma$. The limit for $B(\Upsilon(1S) \rightarrow A^0\gamma)B(A^0 \rightarrow e^+e^-)$ depends on m_{A^0} and τ_{A^0} . The quoted limit for $m_{A^0}=1.8$ MeV is at $\tau_{A^0} \sim 2 \times 10^{-12}$ s, where the limit is the worst. The same limit 2×10^{-3} applies for all lifetimes for masses $2m_e < m_{A^0} < 2m_\mu$ when the results of this experiment are combined with the results of ALAM 83.
- ³⁴ MAGERAS 86 looked for $\Upsilon(1S) \rightarrow \gamma A^0$ ($A^0 \rightarrow e^+e^-$). The quoted branching fraction limit is for $m_{A^0} = 1.7$ MeV, at $\tau(A^0) \sim 4 \times 10^{-13}$ s where the limit is the worst.
- ³⁵ ALAM 83 is at CESR. This limit combined with limit for $B(J/\psi \rightarrow A^0\gamma)$ (EDWARDS 82) excludes standard axion.
- ³⁶ NICZYPOKUK 83 is DESY-DORIS experiment. This limit together with lower limit 9.2×10^{-4} of $B(\Upsilon \rightarrow A^0\gamma)$ derived from $B(J/\psi(1S) \rightarrow A^0\gamma)$ limit (EDWARDS 82) excludes standard axion.
- ³⁷ EDWARDS 82 looked for $J/\psi \rightarrow \gamma A^0$ decays by looking for events with a single γ [of energy $\sim 1/2$ the $J/\psi(1S)$ mass], plus nothing else in the detector. The limit is inconsistent with the axion interpretation of the FAISSNER 81B result.
- ³⁸ SIVERTZ 82 is CESR experiment. Looked for $\Upsilon \rightarrow \gamma A^0$, A^0 undetected. Limit for 1S (3S) is valid for $m_{A^0} < 7$ GeV (4 GeV).

 A^0 (Axion) Searches in Positronium Decays

Decay or transition of positronium. Limits are for branching ratio.

VALUE	CL%	DOCUMENT ID	TECN	COMMENT
••• We do not use the following data for averages, fits, limits, etc. •••				
$< 4.4 \times 10^{-5}$	90	³⁹ BADERT... 02	CNTR	α -Ps $\rightarrow \gamma X_1 X_2$, $m_{X_1} + m_{X_2} \leq 900$ keV
$< 2 \times 10^{-4}$	90	MAENO 95	CNTR	α -Ps $\rightarrow A^0\gamma$ $m_{A^0} = 850-1013$ keV
$< 3.0 \times 10^{-3}$	90	⁴⁰ ASAI 94	CNTR	α -Ps $\rightarrow A^0\gamma$ $m_{A^0} = 30-500$ keV
$< 2.8 \times 10^{-5}$	90	⁴¹ AKOPYAN 91	CNTR	α -Ps $\rightarrow A^0\gamma$ ($A^0 \rightarrow \gamma\gamma$), $m_{A^0} < 30$ keV
$< 1.1 \times 10^{-6}$	90	⁴² ASAI 91	CNTR	α -Ps $\rightarrow A^0\gamma$, $m_{A^0} < 800$ keV
$< 3.8 \times 10^{-4}$	90	GNINENKO 90	CNTR	α -Ps $\rightarrow A^0\gamma$, $m_{A^0} < 30$ keV
$< (1-5) \times 10^{-4}$	95	⁴³ TSUCHIAKI 90	CNTR	α -Ps $\rightarrow A^0\gamma$, $m_{A^0} = 300-900$ keV
$< 6.4 \times 10^{-5}$	90	⁴⁴ ORITO 89	CNTR	α -Ps $\rightarrow A^0\gamma$, $m_{A^0} < 30$ keV
		⁴⁵ AMALDI 85	CNTR	Ortho-positronium
		⁴⁶ CARBONI 83	CNTR	Ortho-positronium
³⁹ BADERTSCHER 02 looked for a three-body decay of ortho-positronium into a photon and two penetrating (neutral or milli-charged) particles.				
⁴⁰ The ASAI 94 limit is based on inclusive photon spectrum and is independent of A^0 decay modes.				
⁴¹ The AKOPYAN 91 limit applies for a short-lived A^0 with $\tau_{A^0} < 10^{-13}$ m_{A^0} [keV]s.				
⁴² ASAI 91 limit translates to $g_{A^0 e e}^2 / 4\pi < 1.1 \times 10^{-11}$ (90% CL) for $m_{A^0} < 800$ keV.				
⁴³ The TSUCHIAKI 90 limit is based on inclusive photon spectrum and is independent of A^0 decay modes.				
⁴⁴ ORITO 89 limit translates to $g_{A^0 e e}^2 / 4\pi < 6.2 \times 10^{-10}$. Somewhat more sensitive limits are obtained for larger m_{A^0} : $B < 7.6 \times 10^{-6}$ at 100 keV.				
⁴⁵ AMALDI 85 set limits $B(A^0\gamma) / B(\gamma\gamma\gamma) < (1-5) \times 10^{-6}$ for $m_{A^0} = 900-100$ keV which are about 1/10 of the CARBONI 83 limits.				
⁴⁶ CARBONI 83 looked for ortho-positronium $\rightarrow A^0\gamma$. Set limit for A^0 electron coupling squared, $g(eeA^0)^2 / (4\pi) < 6 \times 10^{-10} - 7 \times 10^{-9}$ for m_{A^0} from 150-900 keV (CL = 99.7%). This is about 1/10 of the bound from $g-2$ experiments.				

 A^0 (Axion) Search in Photoproduction

VALUE	CL%	DOCUMENT ID	COMMENT
••• We do not use the following data for averages, fits, limits, etc. •••			
		⁴⁷ BASSOMPIE... 95	$m_{A^0} = 1.8 \pm 0.2$ MeV
⁴⁷ BASSOMPIERRE 95 is an extension of BASSOMPIERRE 93. They looked for a peak in the invariant mass of e^+e^- pairs in the region $m_{e^+e^-} = 1.8 \pm 0.2$ MeV. They obtained bounds on the production rate A^0 for $\tau(A^0) = 10^{-18}-10^{-9}$ sec. They also found an excess of events in the range $m_{e^+e^-} = 2.1-3.5$ MeV.			

 A^0 (Axion) Production in Hadron CollisionsLimits are for $\sigma(A^0) / \sigma(\pi^0)$.

VALUE	CL%	EVTS	DOCUMENT ID	TECN	COMMENT
••• We do not use the following data for averages, fits, limits, etc. •••					
			⁴⁸ JAIN 07	CNTR	$A^0 \rightarrow e^+e^-$
			⁴⁹ AHMAD 97	SPEC	e^+ production
			⁵⁰ LEINBERGER 97	SPEC	$A^0 \rightarrow e^+e^-$
			⁵¹ GANZ 96	SPEC	$A^0 \rightarrow e^+e^-$
			⁵² KAMEL 96	EMUL	$32S$ emulsion, $A^0 \rightarrow e^+e^-$
			⁵³ BLUEMLEIN 92	BDMP	$A^0 N_Z \rightarrow \ell^+ \ell^- N_Z$
			⁵⁴ MEIJERDRES 92	SPEC	$\pi^- p \rightarrow n A^0$, $A^0 \rightarrow e^+e^-$
			⁵⁵ BLUEMLEIN 91	BDMP	$A^0 \rightarrow e^+e^-, 2\gamma$

			⁵⁶ FAISSNER 89	OSPK	Beam dump, $A^0 \rightarrow e^+e^-$
			⁵⁷ DEBOER 88	RVUE	$A^0 \rightarrow e^+e^-$
			⁵⁸ EL-NADI 88	EMUL	$A^0 \rightarrow e^+e^-$
			⁵⁹ FAISSNER 88	OSPK	Beam dump, $A^0 \rightarrow 2\gamma$
			⁶⁰ BADIER 86	BDMP	$A^0 \rightarrow e^+e^-$
			⁶¹ BERGSMA 85	CHRM	CERN beam dump
			⁶¹ BERGSMA 85	CHRM	CERN beam dump
			⁶² FAISSNER 83	OSPK	Beam dump, $A^0 \rightarrow 2\gamma$
			⁶³ FAISSNER 83B	RVUE	LAMPF beam dump
			⁶⁴ FRANK 83B	RVUE	LAMPF beam dump
			⁶⁵ HOFFMAN 83	CNTR	$\pi p \rightarrow n A^0$ ($A^0 \rightarrow e^+e^-$)
			⁶⁶ FETSCHER 82	RVUE	See FAISSNER 81B
			⁶⁷ FAISSNER 81	OSPK	CERN PS ν wideband
			⁶⁸ FAISSNER 81B	OSPK	Beam dump, $A^0 \rightarrow 2\gamma$
			⁶⁹ KIM 81	OSPK	26 GeV $pN \rightarrow A^0 X$
			⁷⁰ FAISSNER 80	OSPK	Beam dump, $A^0 \rightarrow e^+e^-$
			⁷¹ JACQUES 80	HLBC	28 GeV protons
			⁷¹ JACQUES 80	HLBC	Beam dump
			⁷² SOUKAS 80	CALO	28 GeV p beam dump
			⁷³ BECHIS 79	CNTR	
			⁷⁴ COTEUS 79	OSPK	Beam dump
			⁷⁵ DISHAW 79	CALO	400 GeV pp
			⁷⁶ ALIBRAN 78	HYBR	Beam dump
			⁷⁶ ASRATYAN 78B	CALO	Beam dump
			⁷⁶ BELLOTTI 78	HLBC	Beam dump
			⁷⁶ BELLOTTI 78	HLBC	$m_{A^0} = 1.5$ MeV
			⁷⁶ BELLOTTI 78	HLBC	$m_{A^0} = 1$ MeV
			⁷⁷ BOSETTI 78B	HYBR	Beam dump
			⁷⁸ DONNELLY 78		
			⁷⁹ HANSL 78D	WIRE	Beam dump
			⁷⁹ MICELMAC... 78		
			⁸⁰ VYSOTSKI 78		

- ⁴⁸ JAIN 07 claims evidence for $A^0 \rightarrow e^+e^-$ produced in ^{207}Pb collision on nuclear emulsion (Ag/Br) for $m(A^0) = 7 \pm 1$ or 19 ± 1 MeV and $\tau(A^0) \leq 10^{-13}$ s.
- ⁴⁹ AHMAD 97 reports a result of APEX Collaboration which studied positron production in $^{238}\text{U} + ^{232}\text{Th}$ and $^{238}\text{U} + ^{181}\text{Ta}$ collisions, without requiring a coincident electron. No narrow lines were found for $250 < E_{e^+} < 750$ keV.
- ⁵⁰ LEINBERGER 97 (ORANGE Collaboration) at GSI looked for a narrow sum-energy e^+e^- line at ~ 635 keV in $^{238}\text{U} + ^{181}\text{Ta}$ collision. Limits on the production probability for a narrow sum-energy e^+e^- line are set. See their Table 2.
- ⁵¹ GANZ 96 (EPOS II Collaboration) has placed upper bounds on the production cross section of e^+e^- pairs from $^{238}\text{U} + ^{181}\text{Ta}$ and $^{238}\text{U} + ^{232}\text{Th}$ collisions at GSI. See Table 2 for limits both for back-to-back and isotropic configurations of e^+e^- pairs. These limits rule out the existence of peaks in the e^+e^- sum-energy distribution, reported by an earlier version of this experiment.
- ⁵² KAMEL 96 looked for e^+e^- pairs from the collision of ^{32}S (200 GeV/nucleon) and emulsion. No evidence of mass peaks is found in the region of sensitivity $m_{ee} > 2$ MeV.
- ⁵³ BLUEMLEIN 92 is a proton beam dump experiment at Serpukhov with a secondary target to induce Bethe-Heitler production of e^+e^- or $\mu^+\mu^-$ from the produce A^0 . See Fig. 5 for the excluded region in m_{A^0} - x plane. For the standard axion, $0.3 < x < 25$ is excluded at 95% CL. If combined with BLUEMLEIN 91, $0.008 < x < 32$ is excluded.
- ⁵⁴ MEIJERDRES 92 give $\Gamma(\pi^- p \rightarrow n A^0) / B(A^0 \rightarrow e^+e^-) / \Gamma(\pi^- p \rightarrow \text{all}) < 10^{-5}$ (90% CL) for $m_{A^0} = 100$ MeV, $\tau_{A^0} = 10^{-11}-10^{-23}$ sec. Limits ranging from 2.5×10^{-3} to 10^{-7} are given for $m_{A^0} = 25-136$ MeV.
- ⁵⁵ BLUEMLEIN 91 is a proton beam dump experiment at Serpukhov. No candidate event for $A^0 \rightarrow e^+e^-, 2\gamma$ are found. Fig. 6 gives the excluded region in m_{A^0} - x plane ($x = \tan\beta = v_2/v_1$). Standard axion is excluded for $0.2 < m_{A^0} < 3.2$ MeV for most $x > 1$, $0.2-11$ MeV for most $x < 1$.
- ⁵⁶ FAISSNER 89 searched for $A^0 \rightarrow e^+e^-$ in a proton beam dump experiment at SIN. No excess of events was observed over the background. A standard axion with mass $2m_e-20$ MeV is excluded. Lower limit on f_{A^0} of $\approx 10^4$ GeV is given for $m_{A^0} = 2m_e-20$ MeV.
- ⁵⁷ DEBOER 88 reanalyze EL-NADI 88 data and claim evidence for three distinct states with mass $\sim 1.1, \sim 2.1$, and ~ 9 MeV, lifetimes $10^{-16}-10^{-15}$ s decaying to e^+e^- and note the similarity of the data with those of a cosmic-ray experiment by Bristol group (B. M. Anand, Proc. of the Royal Society of London, Section A **A22** 183 (1953)). For a criticism see PERKINS 89, who suggests that the events are compatible with π^0 Dalitz decay. DEBOER 89B is a reply which contests the criticism.
- ⁵⁸ EL-NADI 88 claim the existence of a neutral particle decaying into e^+e^- with mass 1.60 ± 0.59 MeV, lifetime $(0.15 \pm 0.01) \times 10^{-14}$ s, which is produced in heavy ion interactions with emulsion nuclei at ~ 4 GeV/c/nucleon.
- ⁵⁹ FAISSNER 88 is a proton beam dump experiment at SIN. They found no candidate event for $A^0 \rightarrow \gamma\gamma$. A standard axion decaying to 2γ is excluded except for a region $x \approx 1$. Lower limit on f_{A^0} of 10^2-10^3 GeV is given for $m_{A^0} = 0.1-1$ MeV.
- ⁶⁰ BADIER 86 did not find long-lived A^0 in 300 GeV π^- Beam Dump Experiment that decays into e^+e^- in the mass range $m_{A^0} = (20-200)$ MeV, which excludes the A^0 decay constant $f(A^0)$ in the interval (60-600) GeV. See their figure 6 for excluded region on $f(A^0)-m_{A^0}$ plane.
- ⁶¹ BERGSMA 85 look for $A^0 \rightarrow 2\gamma, e^+e^-, \mu^+\mu^-$. First limit above is for $m_{A^0} = 1$ MeV; second is for 200 MeV. See their figure 4 for excluded region on $f_{A^0}-m_{A^0}$ plane, where f_{A^0} is A^0 decay constant. For Pececi-Quinn PECCCI 77 A^0 , $m_{A^0} < 180$ keV and $\tau > 0.037$ s. (CL = 90%). For the axion of FAISSNER 81B at 250 keV, BERGSMA 85 expect 15 events but observe zero.

Gauge & Higgs Boson Particle Listings

Axions (A^0) and Other Very Light Bosons

- ⁶² FAISSNER 83 observed 19 $1\text{-}\gamma$ and 12 $2\text{-}\gamma$ events where a background of 4.8 and 2.3 respectively is expected. A small-angle peak is observed even if iron wall is set in front of the decay region.
- ⁶³ FAISSNER 83B extrapolate SIN γ signal to LAMPF ν experimental condition. Resulting 370 γ 's are not at variance with LAMPF upper limit of 450 γ 's. Derived from LAMPF limit that $[d\sigma(A^0)/d\omega \text{ at } 90^\circ] m_{A^0}/\tau_{A^0} < 14 \times 10^{-35} \text{ cm}^2 \text{ sr}^{-1} \text{ MeV ms}^{-1}$. See comment on FRANK 83B.
- ⁶⁴ FRANK 83B stress the importance of LAMPF data bins with negative net signal. By statistical analysis say that LAMPF and SIN-A0 are at variance when extrapolation by phase-space model is done. They find LAMPF upper limit is 248 not 450 γ 's. See comment on FAISSNER 83B.
- ⁶⁵ HOFFMAN 83 set CL = 90% limit $d\sigma/dt B(e^+e^-) < 3.5 \times 10^{-32} \text{ cm}^2/\text{GeV}^2$ for 140 $< m_{A^0} < 160$ MeV. Limit assumes $\tau(A^0) < 10^{-9}$ s.
- ⁶⁶ FETSCHER 82 reanalyzes SIN beam-dump data of FAISSNER 81. Claims no evidence for axion since $2\text{-}\gamma$ peak rate remarkably decreases if iron wall is set in front of the decay region.
- ⁶⁷ FAISSNER 81 see excess μe events. Suggest axion interactions.
- ⁶⁸ FAISSNER 81B is SIN 590 MeV proton beam dump. Observed 14.5 ± 5.0 events of $2\text{-}\gamma$ decay of long-lived neutral penetrating particle with $m_{2\gamma} \lesssim 1$ MeV. Axion interpretation with $\eta\text{-}A^0$ mixing gives $m_{A^0} = 250 \pm 25$ keV, $\tau(2\gamma) = (7.3 \pm 3.7) \times 10^{-3}$ s from above rate. See critical remarks below in comments of FETSCHER 82, FAISSNER 83, FAISSNER 83B, FRANK 83B, and BERGSMAN 85. Also see in the next subsection ALEKSEEV 82B, CAVAINAC 83, and ANANEV 85.
- ⁶⁹ KIM 81 analyzed 8 candidates for $A^0 \rightarrow 2\gamma$ obtained by Aachen-Padova experiment at CERN with 26 GeV protons on Be. Estimated axion mass is about 300 keV and lifetime is $(0.86\text{--}5.6) \times 10^{-3}$ s depending on models. Faisner (private communication), says axion production underestimated and mass overestimated. Correct value around 200 keV.
- ⁷⁰ FAISSNER 80 is SIN beam dump experiment with 590 MeV protons looking for $A^0 \rightarrow e^+e^-$ decay. Assuming $A^0/\pi^0 = 5.5 \times 10^{-7}$, obtained decay rate limit $20/(A^0 \text{ mass}) \text{ MeV/s}$ (CL = 90%), which is about 10^{-7} below theory and interpreted as upper limit to $m_{A^0} < 2m_{e^-}$.
- ⁷¹ JACQUES 80 is a BNL beam dump experiment. First limit above comes from nonobservation of excess neutral-current-type events $[\sigma(\text{production})\sigma(\text{interaction}) < 7. \times 10^{-68} \text{ cm}^4]$, CL = 90%. Second limit is from nonobservation of axion decays into 2γ 's or e^+e^- , and for axion mass a few MeV.
- ⁷² SOUKAS 80 at BNL observed no excess of neutral-current-type events in beam dump.
- ⁷³ BECHIS 79 looked for the axion production in low energy electron Bremsstrahlung and the subsequent decay into either 2γ or e^+e^- . No signal found. CL = 90% limits for model parameter(s) are given.
- ⁷⁴ COTEUS 79 is a beam dump experiment at BNL.
- ⁷⁵ DISHAW 79 is a calorimetric experiment and looks for low energy tail of energy distributions due to energy lost to weakly interacting particles.
- ⁷⁶ BELLOTTI 78 first value comes from search for $A^0 \rightarrow e^+e^-$. Second value comes from search for $A^0 \rightarrow 2\gamma$, assuming mass $< 2m_{e^-}$. For any mass satisfying this, limit is above value $\times (\text{mass}^{-4})$. Third value uses data of PL 60B 401 and quotes $\sigma(\text{production})\sigma(\text{interaction}) < 10^{-67} \text{ cm}^4$.
- ⁷⁷ BOSETTI 78B quotes $\sigma(\text{production})\sigma(\text{interaction}) < 2. \times 10^{-67} \text{ cm}^4$.
- ⁷⁸ DONNELLY 78 examines data from reactor neutrino experiments of REINES 76 and GURR 74 as well as SLAC beam dump experiment. Evidence is negative.
- ⁷⁹ MICELMACHER 78 finds no evidence of axion existence in reactor experiments of REINES 76 and GURR 74. (See reference on DONNELLY 78 below).
- ⁸⁰ VYSOTSKI 78 derived lower limit for the axion mass 25 keV from luminosity of the sun and 200 keV from red supergiants.

A^0 (Axion) Searches in Reactor Experiments

VALUE	DOCUMENT ID	TECN	COMMENT
• • • We do not use the following data for averages, fits, limits, etc. • • •			
	81 CHANG 07		Primakoff or Compton
	82 ALTMANN 95	CNTR	Reactor; $A^0 \rightarrow e^+e^-$
	83 KETOV 86	SPEC	Reactor; $A^0 \rightarrow \gamma\gamma$
	84 KOCH 86	SPEC	Reactor; $A^0 \rightarrow \gamma\gamma$
	85 DATAR 82	CNTR	Light water reactor
	86 VUILLEUMIER 81	CNTR	Reactor; $A^0 \rightarrow 2\gamma$
• • • We do not use the following data for averages, fits, limits, etc. • • •			
	81 CHANG 07		looked for monochromatic photons from Primakoff or Compton conversion of axions from the Kuo-Sheng reactor due to axion coupling to photon or electron, respectively. The search places model-independent limits on the products $G_{A\gamma\gamma}G_{ANN}$ and $G_{Aee}G_{ANN}$ for $m(A^0)$ less than the MeV range.
	82 ALTMANN 95		looked for A^0 decaying into e^+e^- from the Bugey5 nuclear reactor. They obtain an upper limit on the A^0 production rate of $\omega(A^0)/\omega(\gamma) \times B(A^0 \rightarrow e^+e^-) < 10^{-16}$ for $m_{A^0} = 1.5$ MeV at 90% CL. The limit is weaker for heavier A^0 . In the case of a standard axion, this limit excludes a mass in the range $2m_e < m_{A^0} < 4.8$ MeV at 90% CL. See Fig. 5 of their paper for exclusion limits of axion-like resonances Z^0 in the (m_{X^0}, f_{X^0}) plane.
	83 KETOV 86		searched for A^0 at the Rovno nuclear power plant. They found an upper limit on the A^0 production probability of $0.8 [100 \text{ keV}/m_{A^0}]^6 \times 10^{-6}$ per fission. In the standard axion model, this corresponds to $m_{A^0} > 150$ keV. Not valid for $m_{A^0} \gtrsim 1$ MeV.
	84 KOCH 86		searched for $A^0 \rightarrow \gamma\gamma$ at nuclear power reactor Biblis A. They found an upper limit on the A^0 production rate of $\omega(A^0)/\omega(\gamma(M1)) < 1.5 \times 10^{-10}$ (CL=95%). Standard axion with $m_{A^0} = 250$ keV gives 10^{-5} for the ratio. Not valid for $m_{A^0} > 1022$ keV.
	85 DATAR 82		looked for $A^0 \rightarrow 2\gamma$ in neutron capture ($np \rightarrow dA^0$) at Tarapur 500 MW reactor. Sensitive to sum of $l = 0$ and $l = 1$ amplitudes. With ZEHNDER 81 ($l = 0$) - ($l = 1$) result, assert nonexistence of standard A^0 .

⁸⁶ VUILLEUMIER 81 is at Grenoble reactor. Set limit $m_{A^0} < 280$ keV.

A^0 (Axion) and Other Light Boson (X^0) Searches in Nuclear Transitions

Limits are for branching ratio.

VALUE	CL%	DOCUMENT ID	TECN	COMMENT
• • • We do not use the following data for averages, fits, limits, etc. • • •				
$< 8.5 \times 10^{-6}$	90	87 DERBIN 02	CNTR	^{125m}Te decay
		88 DEBOER 97C	RVUE	M1 transitions
$< 5.5 \times 10^{-10}$	95	89 TSUNODA 95	CNTR	^{252}Cf fission, $A^0 \rightarrow ee$
$< 1.2 \times 10^{-6}$	95	90 MINOWA 93	CNTR	$^{139}\text{La}^* \rightarrow ^{139}\text{La}A^0$
$< 2 \times 10^{-4}$	90	91 HICKS 92	CNTR	^{35}S decay, $A^0 \rightarrow \gamma\gamma$
$< 1.5 \times 10^{-9}$	95	92 ASANUMA 90	CNTR	^{241}Am decay
$< (0.4\text{--}10) \times 10^{-3}$	95	93 DEBOER 90	CNTR	$^8\text{Be}^* \rightarrow ^8\text{Be}A^0$
$< (0.2\text{--}1) \times 10^{-3}$	90	94 BINI 89	CNTR	$^{16}\text{O}^* \rightarrow ^{16}\text{O}X^0$, $X^0 \rightarrow e^+e^-$
		95 AVIGNONE 88	CNTR	$\text{Cu}^* \rightarrow \text{Cu}A^0 (A^0 \rightarrow 2\gamma, A^0 e^+ \rightarrow \gamma e, A^0 Z \rightarrow \gamma Z)$
$< 1.5 \times 10^{-4}$	90	96 DATAR 88	CNTR	$^{12}\text{C}^* \rightarrow ^{12}\text{C}A^0$
$< 5 \times 10^{-3}$	90	97 DEBOER 88C	CNTR	$^{16}\text{O}^* \rightarrow ^{16}\text{O}X^0$, $X^0 \rightarrow e^+e^-$
$< 3.4 \times 10^{-5}$	95	98 DOEHNER 88	SPEC	$^2\text{H}^*, A^0 \rightarrow e^+e^-$
$< 4 \times 10^{-4}$	95	99 SAVAGE 88	CNTR	Nuclear decay (isovector)
$< 3 \times 10^{-3}$	95	99 SAVAGE 88	CNTR	Nuclear decay (isoscalar)
$< 10.6 \times 10^{-2}$	90	100 HALLIN 86	SPEC	^6Li isovector decay
< 10.8	90	100 HALLIN 86	SPEC	^{10}B isoscalar decays
< 2.2	90	100 HALLIN 86	SPEC	^{14}N isoscalar decays
$< 4 \times 10^{-4}$	90	101 SAVAGE 86B	CNTR	$^{14}\text{N}^*$
		102 ANANEV 85	CNTR	$\text{Li}^*, \text{deut}^* A^0 \rightarrow 2\gamma$
		103 CAVAINAC 83	CNTR	$^{97}\text{Nb}^*, \text{deut}^* \text{ transition } A^0 \rightarrow 2\gamma$
		104 ALEKSEEV 82B	CNTR	$\text{Li}^*, \text{deut}^* \text{ transition } A^0 \rightarrow 2\gamma$
		105 LEHMANN 82	CNTR	$\text{Cu}^* \rightarrow \text{Cu}A^0 (A^0 \rightarrow 2\gamma)$
		106 ZEHNDER 82	CNTR	$\text{Li}^*, \text{Nb}^* \text{ decay, } n\text{-capt.}$
		107 ZEHNDER 81	CNTR	$\text{Ba}^* \rightarrow \text{Ba}A^0 (A^0 \rightarrow 2\gamma)$
		108 CALAPRICE 79		Carbon
		87 DERBIN 02		looked for the axion emission in an M1 transition in ^{125m}Te decay. They looked for a possible presence of a shifted energy spectrum in gamma rays due to the undetected axion.
		88 DEBOER 97C		reanalyzed the existent data on Nuclear M1 transitions and find that a 9 MeV boson decaying into e^+e^- would explain the excess of events with large opening angles. See also DEBOER 01 for follow-up experiments.
		89 TSUNODA 95		looked for axion emission when ^{252}Cf undergoes a spontaneous fission, with the axion decaying into e^+e^- . The bound is for $m_{A^0} = 40$ MeV. It improves to 2.5×10^{-5} for $m_{A^0} = 200$ MeV.
		90 MINOWA 93		studied chain process, $^{139}\text{Ce} \rightarrow ^{139}\text{La}^*$ by electron capture and M1 transition of $^{139}\text{La}^*$ to the ground state. It does not assume decay modes of A^0 . The bound applies for $m_{A^0} < 166$ keV.
		91 HICKS 92		bound is applicable for $\tau_{X^0} < 4 \times 10^{-11}$ sec.
		92 The BINI 89		limit is for the branching fraction of X^0 emission per ^{241}Am α decay and valid for $\tau_{X^0} < 3 \times 10^{-11}$ s.
		93 The DEBOER 90		limit is for the branching ratio $^8\text{Be}^* (18.15 \text{ MeV}, 1^+) \rightarrow ^8\text{Be}A^0, A^0 \rightarrow e^+e^-$ for the mass range $m_{A^0} = 4\text{--}15$ MeV.
		94 The BINI 89		limit is for the branching fraction of $^{16}\text{O}^* (6.05 \text{ MeV}, 0^+) \rightarrow ^{16}\text{O}X^0, X^0 \rightarrow e^+e^-$ for $m_{X^0} = 1.5\text{--}3.1$ MeV. $\tau_{X^0} \lesssim 10^{-11}$ s is assumed. The spin-parity of X is restricted to $0^+ \text{ or } 1^-$.
		95 AVIGNONE 88		looked for the 1115 keV transition $\text{C}^* \rightarrow \text{Cu}A^0$, either from $A^0 \rightarrow 2\gamma$ in-flight decay or from the secondary A^0 interactions by Compton and by Primakoff processes. Limits for axion parameters are obtained for $m_{A^0} < 1.1$ MeV.
		96 DATAR 88		rule out light pseudoscalar particle emission through its decay $A^0 \rightarrow e^+e^-$ in the mass range $1.02\text{--}2.5$ MeV and lifetime range $10^{-13}\text{--}10^{-8}$ s. The above limit is for $\tau = 5 \times 10^{-13}$ s and $m = 1.7$ MeV; see the paper for the $\tau\text{-}m$ dependence of the limit.
		97 The limit is for the branching fraction of $^{16}\text{O}^* (6.05 \text{ MeV}, 0^+) \rightarrow ^{16}\text{O}X^0, X^0 \rightarrow e^+e^-$ against internal pair conversion for $m_{X^0} = 1.7$ MeV and $\tau_{X^0} < 10^{-11}$ s. Similar limits are obtained for $m_{X^0} = 1.3\text{--}3.2$ MeV. The spin parity of X^0 must be either $0^+ \text{ or } 1^-$. The limit at 1.7 MeV is translated into a limit for the X^0 -nucleon coupling constant: $g_{X^0 NN}^2/4\pi < 2.3 \times 10^{-9}$.		
		98 The DOEHNER 88		limit is for $m_{A^0} = 1.7$ MeV, $\tau(A^0) < 10^{-10}$ s. Limits less than 10^{-4} are obtained for $m_{A^0} = 1.2\text{--}2.2$ MeV.
		99 SAVAGE 88		looked for A^0 that decays into e^+e^- in the decay of the 9.17 MeV $J^P = 2^+$ state in ^{14}N , 17.64 MeV state $J^P = 1^+$ in ^8Be , and the 18.15 MeV state $J^P = 1^+$ in ^8Be . This experiment constrains the isovector coupling of A^0 to hadrons, if $m_{A^0} = (1.1 \rightarrow 2.2)$ MeV and the isoscalar coupling of A^0 to hadrons, if $m_{A^0} = (1.1 \rightarrow 2.6)$ MeV. Both limits are valid only if $\tau(A^0) \lesssim 1 \times 10^{-11}$ s.
		100 Limits are for $\Gamma(A^0(1.8 \text{ MeV}))/\Gamma(\pi M1)$; i.e., for 1.8 MeV axion emission normalized to the rate for internal emission of e^+e^- pairs. Valid for $\tau_{A^0} < 2 \times 10^{-11}$ s. ^6Li isovector decay data strongly disfavor PECCCI 86 model I, whereas the ^{10}B and ^{14}N isoscalar decay data strongly reject PECCCI 86 model II and III.		

See key on page 373

Gauge & Higgs Boson Particle Listings

Axions (A^0) and Other Very Light Bosons

- 101 SAVAGE 86B looked for A^0 that decays into e^+e^- in the decay of the 9.17 MeV $J^P = 2^+$ state in ^{14}N . Limit on the branching fraction is valid if $\tau_{A^0} \lesssim 1. \times 10^{-11}\text{s}$ for $m_{A^0} = (1.1-1.7)$ MeV. This experiment constrains the iso-vector coupling of A^0 to hadrons.
- 102 ANANEV 85 with IBR-2 pulsed reactor exclude standard A^0 at CL = 95% masses below 470 keV (Li^* decay) and below $2m_e$ for deuteron* decay.
- 103 CAVIGNAC 83 at Bugey reactor exclude axion at any $m_{97\text{Nb}^*}\text{decay}$ and axion with m_{A^0} between 275 and 288 keV (deuteron* decay).
- 104 ALEKSEEV 82 with IBR-2 pulsed reactor exclude standard A^0 at CL = 95% mass-ranges $m_{A^0} < 400$ keV (Li^* decay) and 330 keV $< m_{A^0} < 2.2$ MeV. (deuteron* decay).
- 105 LEHMANN 82 obtained $A^0 \rightarrow 2\gamma$ rate $< 6.2 \times 10^{-5}/\text{s}$ (CL = 95%) excluding m_{A^0} between 100 and 1000 keV.
- 106 ZEHNDER 82 used Gosgen 2.8GW light-water reactor to check A^0 production. No 2γ peak in Li^* , Nb^* decay (both single p transition) nor in n capture (combined with previous Ba^* negative result) rules out standard A^0 . Set limit $m_{A^0} < 60$ keV for any A^0 .
- 107 ZEHNDER 81 looked for $\text{Ba}^* \rightarrow A^0\text{Ba}$ transition with $A^0 \rightarrow 2\gamma$. Obtained 2γ coincidence rate $< 2.2 \times 10^{-5}/\text{s}$ (CL = 95%) excluding $m_{A^0} > 160$ keV (or 200 keV depending on Higgs mixing). However, see BARROSO 81.
- 108 CALAPRICE 79 saw no axion emission from excited states of carbon. Sensitive to axion mass between 1 and 15 MeV.

- < 31 95 LORENZ 88 CNTR $m_{A^0} = 1.646$ MeV
- < 94 95 LORENZ 88 CNTR $m_{A^0} = 1.726$ MeV
- < 23 95 LORENZ 88 CNTR $m_{A^0} = 1.782$ MeV
- < 19 95 LORENZ 88 CNTR $m_{A^0} = 1.837$ MeV
- < 3.8 97 123 TSERTOS 88 CNTR $m_{A^0} = 1.832$ MeV
- 124 VANKLINKEN 88 CNTR
- 125 MAIER 87 CNTR
- <2500 90 MILLS 87 CNTR $m_{A^0} = 1.8$ MeV
- 126 VONWIMMER.87 CNTR
- 117 HALLIN 92 quote limits on lifetime, $8 \times 10^{-14} - 5 \times 10^{-13}$ sec depending on mass, assuming $B(A^0 \rightarrow e^+e^-) = 100\%$. They say that TSERTOS 91 overstated their sensitivity by a factor of 3.
- 118 HENDERSON 92c exclude axion with lifetime $\tau_{A^0} = 1.4 \times 10^{-12} - 4.0 \times 10^{-10}$ s, assuming $B(A^0 \rightarrow e^+e^-) = 100\%$. HENDERSON 92c also exclude a vector boson with $\tau = 1.4 \times 10^{-12} - 6.0 \times 10^{-10}$ s.
- 119 WU 92 quote limits on lifetime $> 3.3 \times 10^{-13}$ s assuming $B(A^0 \rightarrow e^+e^-) = 100\%$. They say that TSERTOS 89 overestimate the limit by a factor of $\pi/2$. WU 92 also quote a bound for vector boson, $\tau > 8.2 \times 10^{-13}$ s.
- 120 WIDMANN 91 bound applies exclusively to the case $B(A^0 \rightarrow e^+e^-) = 1$, since the detection efficiency varies substantially as $\Gamma(A^0)_{\text{total}}$ changes. See their Fig. 6.
- 121 JUDGE 90 excludes an elastic pseudoscalar e^+e^- resonance for $4.5 \times 10^{-13} \text{ s} < \tau(A^0) < 7.5 \times 10^{-12} \text{ s}$ (95% CL) at $m_{A^0} = 1.832$ MeV. Comparable limits can be set for $m_{A^0} = 1.776-1.856$ MeV.
- 122 See also TSERTOS 88B in references.
- 123 The upper limit listed in TSERTOS 88 is too large by a factor of 4. See TSERTOS 88B, footnote 3.
- 124 VANKLINKEN 88 looked for relatively long-lived resonance ($\tau = 10^{-10}-10^{-12}$ s). The sensitivity is not sufficient to exclude such a narrow resonance.
- 125 MAIER 87 obtained limits $R\Gamma \lesssim 60$ eV (100 eV) at $m_{A^0} \simeq 1.64$ MeV (1.83 MeV) for energy resolution $\Delta E_{\text{cm}} \simeq 3$ keV, where R is the resonance cross section normalized to that of Bhabha scattering, and $\Gamma = \Gamma_{e^+e^-}^2/\Gamma_{\text{total}}$. For a discussion implying that $\Delta E_{\text{cm}} \simeq 10$ keV, see TSERTOS 89.
- 126 VONWIMMERSPERG 87 measured Bhabha scattering for $E_{\text{cm}} = 1.37-1.86$ MeV and found a possible peak at 1.73 with $\int \sigma dE_{\text{cm}} = 14.5 \pm 6.8$ keV.b. For a comment and a reply, see VANKLINKEN 88B and VONWIMMERSPERG 88. Also see CONNELL 88.

A^0 (Axion) Limits from Its Electron Coupling

Limits are for $\tau(A^0 \rightarrow e^+e^-)$.

VALUE (s)	CL%	DOCUMENT ID	TECN	COMMENT
none $4 \times 10^{-16}-4.5 \times 10^{-12}$	90	109 BROSS	91	BDMP $eN \rightarrow eA^0N$ ($A^0 \rightarrow ee$)
		110 GUO	90	BDMP $eN \rightarrow eA^0N$ ($A^0 \rightarrow ee$)
		111 BJORKEN	88	CALO $A \rightarrow e^+e^-$ or 2γ
		112 BLINOV	88	MD1 $ee \rightarrow eeA^0$ ($A^0 \rightarrow ee$)
none $1 \times 10^{-14}-1 \times 10^{-10}$	90	113 RIORDAN	87	BDMP $eN \rightarrow eA^0N$ ($A^0 \rightarrow ee$)
none $1 \times 10^{-14}-1 \times 10^{-11}$	90	114 BROWN	86	BDMP $eN \rightarrow eA^0N$ ($A^0 \rightarrow ee$)
none $6 \times 10^{-14}-9 \times 10^{-11}$	95	115 DAVIER	86	BDMP $eN \rightarrow eA^0N$ ($A^0 \rightarrow ee$)
none $3 \times 10^{-13}-1 \times 10^{-7}$	90	116 KONAKA	86	BDMP $eN \rightarrow eA^0N$ ($A^0 \rightarrow ee$)

- 109 The listed BROSS 91 limit is for $m_{A^0} = 1.14$ MeV. $B(A^0 \rightarrow e^+e^-) = 1$ assumed. Excluded domain in the $\tau_{A^0}-m_{A^0}$ plane extends up to $m_{A^0} \approx 7$ MeV (see Fig. 5). Combining with electron $g-2$ constraint, axions coupling only to e^+e^- ruled out for $m_{A^0} < 4.8$ MeV (90% CL).
- 110 GUO 90 use the same apparatus as BROWN 86 and improve the previous limit in the shorter lifetime region. Combined with $g-2$ constraint, axions coupling only to e^+e^- are ruled out for $m_{A^0} < 2.7$ MeV (90% CL).
- 111 BJORKEN 88 reports limits on axion parameters (f_A, m_A, τ_A) for $m_{A^0} < 200$ MeV from electron beam-dump experiment with production via Primakoff photoproduction, bremsstrahlung from electrons, and resonant annihilation of positrons on atomic electrons.
- 112 BLINOV 88 assume zero spin, $m = 1.8$ MeV and lifetime $< 5 \times 10^{-12}$ s and find $\Gamma(A^0 \rightarrow \gamma\gamma)B(A^0 \rightarrow e^+e^-) < 2$ eV (CL=90%).
- 113 Assumes $A^0\gamma\gamma$ coupling is small and hence Primakoff production is small. Their figure 2 shows limits on axions for $m_{A^0} < 15$ MeV.
- 114 Uses electrons in hadronic showers from an incident 800 GeV proton beam. Limits for $m_{A^0} < 15$ MeV are shown in their figure 3.
- 115 $m_{A^0} = 1.8$ MeV assumed. The excluded domain in the $\tau_{A^0}-m_{A^0}$ plane extends up to $m_{A^0} \approx 14$ MeV, see their figure 4.
- 116 The limits are obtained from their figure 3. Also given is the limit on the $A^0\gamma\gamma-A^0e^+e^-$ coupling plane by assuming Primakoff production.

Search for A^0 (Axion) Resonance in Bhabha Scattering

The limit is for $\Gamma(A^0)|B(A^0 \rightarrow e^+e^-)|^2$.

VALUE (10^{-3} eV)	CL%	DOCUMENT ID	TECN	COMMENT
< 1.3	97	117 HALLIN	92	CNTR $m_{A^0} = 1.75-1.88$ MeV
none 0.0016-0.47	90	118 HENDERSON	92c	CNTR $m_{A^0} = 1.5-1.86$ MeV
< 2.0	90	119 WU	92	CNTR $m_{A^0} = 1.56-1.86$ MeV
< 0.013	95	TSERTOS	91	CNTR $m_{A^0} = 1.832$ MeV
none 0.19-3.3	95	120 WIDMANN	91	CNTR $m_{A^0} = 1.78-1.92$ MeV
< 5	97	BAUER	90	CNTR $m_{A^0} = 1.832$ MeV
none 0.09-1.5	95	121 JUDGE	90	CNTR $m_{A^0} = 1.832$ MeV, elastic
< 1.9	97	122 TSERTOS	89	CNTR $m_{A^0} = 1.82$ MeV
<(10-40)	97	122 TSERTOS	89	CNTR $m_{A^0} = 1.51-1.65$ MeV
<(1-2.5)	97	122 TSERTOS	89	CNTR $m_{A^0} = 1.80-1.86$ MeV

Search for A^0 (Axion) Resonance in $e^+e^- \rightarrow \gamma\gamma$

The limit is for $\Gamma(A^0 \rightarrow e^+e^-)\Gamma(A^0 \rightarrow \gamma\gamma)/\Gamma_{\text{total}}$

VALUE (10^{-3} eV)	CL%	DOCUMENT ID	TECN	COMMENT
< 0.18	95	VO	94	CNTR $m_{A^0} = 1.1$ MeV
< 1.5	95	VO	94	CNTR $m_{A^0} = 1.4$ MeV
< 12	95	VO	94	CNTR $m_{A^0} = 1.7$ MeV
< 6.6	95	127 TRZASKA	91	CNTR $m_{A^0} = 1.8$ MeV
< 4.4	95	WIDMANN	91	CNTR $m_{A^0} = 1.78-1.92$ MeV
		128 FOX	89	CNTR
< 0.11	95	129 MINOWA	89	CNTR $m_{A^0} = 1.062$ MeV
< 33	97	CONNELL	88	CNTR $m_{A^0} = 1.580$ MeV
< 42	97	CONNELL	88	CNTR $m_{A^0} = 1.642$ MeV
< 73	97	CONNELL	88	CNTR $m_{A^0} = 1.782$ MeV
< 79	97	CONNELL	88	CNTR $m_{A^0} = 1.832$ MeV

- 127 TRZASKA 91 also give limits in the range $(6.6-30) \times 10^{-3}$ eV (95%CL) for $m_{A^0} = 1.6-2.0$ MeV.
- 128 FOX 89 measured positron annihilation with an electron in the source material into two photons and found no signal at 1.062 MeV ($< 9 \times 10^{-5}$ of two-photon annihilation at rest).
- 129 Similar limits are obtained for $m_{A^0} = 1.045-1.085$ MeV.

Search for X^0 (Light Boson) Resonance in $e^+e^- \rightarrow \gamma\gamma\gamma$

The limit is for $\Gamma(X^0 \rightarrow e^+e^-)\Gamma(X^0 \rightarrow \gamma\gamma\gamma)/\Gamma_{\text{total}}$. C invariance forbids spin-0 X^0 coupling to both e^+e^- and $\gamma\gamma\gamma$.

VALUE (10^{-3} eV)	CL%	DOCUMENT ID	TECN	COMMENT
< 0.2	95	130 VO	94	CNTR $m_{X^0} = 1.1-1.9$ MeV
< 1.0	95	131 VO	94	CNTR $m_{X^0} = 1.1$ MeV
< 2.5	95	131 VO	94	CNTR $m_{X^0} = 1.4$ MeV
< 120	95	131 VO	94	CNTR $m_{X^0} = 1.7$ MeV
< 3.8	95	132 SKALSEY	92	CNTR $m_{X^0} = 1.5$ MeV

- 130 VO 94 looked for $X^0 \rightarrow \gamma\gamma\gamma$ decaying at rest. The precise limits depend on m_{X^0} . See Fig. 2(b) in paper.
- 131 VO 94 looked for $X^0 \rightarrow \gamma\gamma\gamma$ decaying in flight.
- 132 SKALSEY 92 also give limits 4.3 for $m_{X^0} = 1.54$ and 7.5 for 1.64 MeV. The spin of X^0 is assumed to be one.

Light Boson (X^0) Search in Nonresonant e^+e^- Annihilation at Rest

Limits are for the ratio of $n\gamma + X^0$ production relative to $\gamma\gamma$.

VALUE (units 10^{-6})	CL%	DOCUMENT ID	TECN	COMMENT
< 1.3	97	117 HALLIN	92	CNTR $m_{A^0} = 1.75-1.88$ MeV

- • • We do not use the following data for averages, fits, limits, etc. • • •

Gauge & Higgs Boson Particle Listings

Axions (A^0) and Other Very Light Bosons

< 4.2	90	133	MITSUI	96	CNTR	γX^0
< 4	68	134	SKALSEY	95	CNTR	γX^0
< 40	68	135	SKALSEY	95	RVUE	γX^0
< 0.18	90	136	ADACHI	94	CNTR	$\gamma\gamma X^0, X^0 \rightarrow \gamma\gamma$
< 0.26	90	137	ADACHI	94	CNTR	$\gamma\gamma X^0, X^0 \rightarrow \gamma\gamma$
< 0.33	90	138	ADACHI	94	CNTR	$\gamma X^0, X^0 \rightarrow \gamma\gamma\gamma$

133 MITSUI 96 looked for a monochromatic γ . The bound applies for a vector X^0 with $C = -1$ and $m_{X^0} < 200$ keV. They derive an upper bound on $e e X^0$ coupling and hence on the branching ratio $B(\rho\text{-Ps} \rightarrow \gamma\gamma X^0) < 6.2 \times 10^{-6}$. The bounds weaken for heavier X^0 .

134 SKALSEY 95 looked for a monochromatic γ without an accompanying γ in e^+e^- annihilation. The bound applies for scalar and vector X^0 with $C = -1$ and $m_{X^0} = 100\text{--}1000$ keV.

135 SKALSEY 95 reinterpreted the bound on γA^0 decay of ρ -Ps by ASA1 91 where 3% of delayed annihilations are not from 3S_1 states. The bound applies for scalar and vector X^0 with $C = -1$ and $m_{X^0} = 0\text{--}800$ keV.

136 ADACHI 94 looked for a peak in the $\gamma\gamma$ invariant mass distribution in $\gamma\gamma\gamma\gamma$ production from e^+e^- annihilation. The bound applies for $m_{X^0} = 70\text{--}800$ keV.

137 ADACHI 94 looked for a peak in the missing-mass mass distribution in $\gamma\gamma$ channel, using $\gamma\gamma\gamma\gamma$ production from e^+e^- annihilation. The bound applies for $m_{X^0} < 800$ keV.

138 ADACHI 94 looked for a peak in the missing mass distribution in $\gamma\gamma\gamma$ channel, using $\gamma\gamma\gamma\gamma$ production from e^+e^- annihilation. The bound applies for $m_{X^0} = 200\text{--}900$ keV.

Searches for Goldstone Bosons (X^0)

(Including Horizontal Bosons and Majorons.) Limits are for branching ratios.

VALUE	CL%	DOCUMENT ID	TECN	COMMENT
••• We do not use the following data for averages, fits, limits, etc. •••				
		139	LESSA	07 RVUE Meson, ℓ decays to Majoron
		140	DIAZ	98 THEO $H^0 \rightarrow X^0 X^0, A^0 \rightarrow X^0 X^0 X^0$, Majoron
		141	BOBRAKOV	91 Electron quasi-magnetic interaction
$< 3.3 \times 10^{-2}$	95	142	ALBRECHT	90E ARG $\tau \rightarrow \mu X^0$, Familon
$< 1.8 \times 10^{-2}$	95	142	ALBRECHT	90E ARG $\tau \rightarrow e X^0$, Familon
$< 6.4 \times 10^{-9}$	90	143	ATIYA	90 B787 $K^+ \rightarrow \pi^+ X^0$, Familon
$< 1.1 \times 10^{-9}$	90	144	BOLTON	88 CBOX $\mu^+ \rightarrow e^+ X^0$, Familon
		145	CHANDA	88 ASTR Sun, Majoron
		146	CHOI	88 ASTR Majoron, SN 1987A
$< 5 \times 10^{-6}$	90	147	PICCIOTTO	88 CNTR $\pi \rightarrow e\nu X^0$, Majoron
$< 1.3 \times 10^{-9}$	90	148	GOLDMAN	87 CNTR $\mu \rightarrow e\gamma X^0$, Familon
$< 3 \times 10^{-4}$	90	149	BRYMAN	86BV RVUE $\mu \rightarrow e X^0$, Familon
$< 1 \times 10^{-10}$	90	150	EICHLER	86 SPEC $\mu^+ \rightarrow e^+ X^0$, Familon
$< 2.6 \times 10^{-6}$	90	151	JODIDIO	86 SPEC $\mu^+ \rightarrow e^+ X^0$, Familon
		152	BALTRUSAITIS	.85 MRK3 $\tau \rightarrow \ell X^0$, Familon
		153	DICUS	83 COSM $\nu(\text{h}\nu) \rightarrow \nu(\text{light}) X^0$

- 139 LESSA 07 consider decays of the form Meson $\rightarrow \ell\nu$ Majoron and $\ell \rightarrow \ell'\nu\bar{\nu}$ Majoron and use existing data to derive limits on the neutrino-Majoron Yukawa couplings $g_{\alpha\beta}$ ($\alpha, \beta = e, \mu, \tau$). Their best limits are $|g_{e\alpha}|^2 < 5.5 \times 10^{-6}$, $|g_{\mu\alpha}|^2 < 4.5 \times 10^{-5}$, $|g_{\tau\alpha}|^2 < 5.5 \times 10^{-2}$ at CL = 90%.
- 140 DIAZ 98 studied models of spontaneously broken lepton number with both singlet and triplet Higgses. They obtain limits on the parameter space from invisible decay $Z \rightarrow H^0 A^0 \rightarrow X^0 X^0 X^0 X^0$ and $e^+e^- \rightarrow Z H^0$ with $H^0 \rightarrow X^0 X^0$.
- 141 BOBRAKOV 91 searched for anomalous magnetic interactions between polarized electrons expected from the exchange of a massless pseudoscalar boson (arion). A limit $x_e^2 < 2 \times 10^{-4}$ (95%CL) is found for the effective anomalous magneton parametrized as $x_e(G_F/8\pi\sqrt{2})^{1/2}$.
- 142 ALBRECHT 90E limits are for $B(\tau \rightarrow \ell X^0)/B(\tau \rightarrow \ell\nu\bar{\nu})$. Valid for $m_{X^0} < 100$ MeV. The limits rise to 7.1% (for μ), 5.0% (for e) for $m_{X^0} = 500$ MeV.
- 143 ATIYA 90 limit is for $m_{X^0} = 0$. The limit $B < 1 \times 10^{-8}$ holds for $m_{X^0} < 95$ MeV. For the reduction of the limit due to finite lifetime of X^0 , see their Fig. 3.
- 144 BOLTON 88 limit corresponds to $F > 3.1 \times 10^9$ GeV, which does not depend on the chirality property of the coupling.
- 145 CHANDA 88 find $v_T < 10$ MeV for the weak-triplet Higgs vacuum expectation value in Gelmini-Roncadelli model, and $v_S > 5.8 \times 10^6$ GeV in the singlet Majoron model.
- 146 CHOI 88 used the observed neutrino flux from the supernova SN1987A to exclude the neutrino Majoron Yukawa coupling h in the range $2 \times 10^{-5} < h < 3 \times 10^{-4}$ for the interaction $L_{\text{int}} = \frac{1}{2} i h \bar{\nu}_\nu \gamma_5 \psi_\nu \phi_X$. For several families of neutrinos, the limit applies for $(\Sigma h_i^4)^{1/4}$.
- 147 PICCIOTTO 88 limit applies when $m_{X^0} < 55$ MeV and $\tau_{X^0} > 2$ ns, and it decreases to 4×10^{-7} at $m_{X^0} = 125$ MeV, beyond which no limit is obtained.
- 148 GOLDMAN 87 limit corresponds to $F > 2.9 \times 10^9$ GeV for the family symmetry breaking scale from the Lagrangian $L_{\text{int}} = (1/F) \bar{\psi} \gamma^\mu (\alpha + b\gamma_5) \psi_e \theta_{\mu\phi} X^0$ with $a^2 + b^2 = 1$. This is not as sensitive as the limit $F > 9.9 \times 10^9$ GeV derived from the search for $\mu^+ \rightarrow e^+ X^0$ by JODIDIO 86, but does not depend on the chirality property of the coupling.
- 149 Limits are for $\Gamma(\mu \rightarrow e X^0)/\Gamma(\mu \rightarrow e\nu\bar{\nu})$. Valid when $m_{X^0} = 0\text{--}93.4, 98.1\text{--}103.5$ MeV.
- 150 EICHLER 86 looked for $\mu^+ \rightarrow e^+ X^0$ followed by $X^0 \rightarrow e^+e^-$. Limits on the branching fraction depend on the mass and lifetime of X^0 . The quoted limits are valid when $\tau_{X^0} \lesssim 3 \times 10^{-10}$ s if the decays are kinematically allowed.

- 151 JODIDIO 86 corresponds to $F > 9.9 \times 10^9$ GeV for the family symmetry breaking scale with the parity-conserving effective Lagrangian $L_{\text{int}} = (1/F) \bar{\psi} \gamma^\mu \psi_e \theta_{\mu\phi} X^0$.
- 152 BALTRUSAITIS 85 search for light Goldstone boson (X^0) of broken U(1). CL = 95% limits are $B(\tau \rightarrow \mu^+ X^0)/B(\tau \rightarrow \mu^+ \nu\bar{\nu}) < 0.125$ and $B(\tau \rightarrow e^+ X^0)/B(\tau \rightarrow e^+ \nu\bar{\nu}) < 0.04$. Inferred limit for the symmetry breaking scale is $m > 3000$ TeV.
- 153 The primordial heavy neutrino must decay into ν and familon, f_A , early so that the red-shifted decay products are below critical density, see their table. In addition, $K \rightarrow \pi f_A$ and $\mu \rightarrow e f_A$ are unseen. Combining these excludes $m_{\text{heavy}\nu}$ between 5×10^{-5} and 5×10^{-4} MeV (μ decay) and $m_{\text{heavy}\nu}$ between 5×10^{-5} and 0.1 MeV (K -decay).

Majoron Searches in Neutrinoless Double β Decay

Limits are for the half-life of neutrinoless $\beta\beta$ decay with a Majoron emission.

No experiment currently claims any such evidence. Only the best or comparable limits for each isotope are reported. Also see the reviews ZUBER 98 and FAESSLER 98b.

$t_{1/2}(10^{21}$ yr)	CL%	ISOTOPE	TRANSITION	METHOD	DOCUMENT ID
> 7200		90 128Te	CNTR		154 BERNATOW... 92
••• We do not use the following data for averages, fits, limits, etc. •••					
> 27	90	100Mo	$0\nu 1\chi$	NEMO-3	155 ARNOLD 06
> 15	90	82Se	$0\nu 1\chi$	NEMO-3	156 ARNOLD 06
> 14	90	100Mo	$0\nu 1\chi$	NEMO-3	157 ARNOLD 04
> 12	90	82Se	$0\nu 1\chi$	NEMO-3	158 ARNOLD 04
> 2.2	90	130Te	$0\nu 1\chi$	Cryog. det.	159 ARNABOLDI 03
> 0.9	90	130Te	$0\nu 2\chi$	Cryog. det.	160 ARNABOLDI 03
> 8	90	116Cd	$0\nu 1\chi$	CdWO ₄ scint.	161 DANEVICH 03
> 0.8	90	116Cd	$0\nu 2\chi$	CdWO ₄ scint.	162 DANEVICH 03
> 500	90	136Xe	$0\nu\chi$	Liquid Xe Scint.	163 BERNABEI 02b
> 5.8	90	100Mo	$0\nu\chi$	ELEGANT V	164 FUSHIMI 02
> 0.32	90	100Mo	$0\nu\chi$	Liq. Ar ioniz.	165 ASHITKOV 01
> 0.0035	90	160Gd	$0\nu\chi$	¹⁶⁰ Gd ₂ SiO ₅ :Ce	166 DANEVICH 01
> 0.013	90	160Gd	$0\nu 2\chi$	¹⁶⁰ Gd ₂ SiO ₅ :Ce	167 DANEVICH 01
> 2.3	90	82Se	$0\nu\chi$	NEMO 2	168 ARNOLD 00
> 0.31	90	96Zr	$0\nu\chi$	NEMO 2	169 ARNOLD 00
> 0.63	90	82Se	$0\nu 2\chi$	NEMO 2	170 ARNOLD 00
> 0.063	90	96Zr	$0\nu 2\chi$	NEMO 2	170 ARNOLD 00
> 0.16	90	100Mo	$0\nu 2\chi$	NEMO 2	170 ARNOLD 00
> 2.4	90	82Se	$0\nu\chi$	NEMO 2	171 ARNOLD 98
> 7.2	90	136Xe	$0\nu 2\chi$	TPC	172 LUESCHER 98
> 7.91	90	76Ge		SPEC	173 GUENTHER 96
> 17	90	76Ge		CNTR	BECK 93

- 154 BERNATOWICZ 92 studied double- β decays of ¹²⁸Te and ¹³⁰Te, and found the ratio $\tau(^{130}\text{Te})/\tau(^{128}\text{Te}) = (3.52 \pm 0.11) \times 10^{-4}$ in agreement with relatively stable theoretical predictions. The bound is based on the requirement that Majoron-emitting decay cannot be larger than the observed double-beta rate of ¹²⁸Te of $(7.7 \pm 0.4) \times 10^{24}$ year. We calculated 90% CL limit as $(7.7\text{--}1.28 \times 0.4 = 7.2) \times 10^{24}$.
- 155 ARNOLD 06 use ¹⁰⁰Mo data taken with the NEMO-3 tracking detector. The reported limit corresponds to $\langle g_{\nu\chi} \rangle < (0.4\text{--}1.8) \times 10^{-4}$ using a range of matrix element calculations. Supersedes ARNOLD 04.
- 156 NEMO-3 tracking calorimeter is used in ARNOLD 06. Reported half-life limit for ⁸²Se corresponds to $\langle g_{\nu\chi} \rangle < (0.66\text{--}1.9) \times 10^{-4}$ using a range of matrix element calculations. Supersedes ARNOLD 04.
- 157 ARNOLD 04 use the NEMO-3 tracking detector. The limit corresponds to $\langle g_{\nu\chi} \rangle < (0.5\text{--}0.9) \times 10^{-4}$ using the matrix elements of SIMKOVIC 99, STOICA 01 and CIVITARESE 03.
- 158 ARNOLD 04 use the NEMO-3 tracking detector. The limit corresponds to $\langle g_{\nu\chi} \rangle < (0.7\text{--}1.6) \times 10^{-4}$ using the matrix elements of SIMKOVIC 99, STOICA 01 and CIVITARESE 03.
- 159 Supersedes ALESSANDRELLO 00. Array of TeO₂ crystals in high resolution cryogenic calorimeter. Some enriched in ¹³⁰Te. Derive $\langle g_{\nu\chi} \rangle < 17\text{--}33 \times 10^{-5}$ depending on matrix element.
- 160 Supersedes ALESSANDRELLO 00. Cryogenic calorimeter search.
- 161 Limit for the $0\nu\chi$ decay with Majoron emission of ¹¹⁶Cd using enriched CdWO₄ scintillators. $\langle g_{\nu\chi} \rangle < 4.6\text{--}8.1 \times 10^{-5}$ depending on the matrix element. Supersedes DANEVICH 00.
- 162 Limit for the $0\nu 2\chi$ decay of ¹¹⁶Cd. Supersedes DANEVICH 00.
- 163 BERNABEI 02b obtain limit for $0\nu\chi$ decay with Majoron emission of ¹³⁶Xe using liquid Xe scintillation detector. They derive $\langle g_{\nu\chi} \rangle < 2.0\text{--}3.0 \times 10^{-5}$ with several nuclear matrix elements.
- 164 Replaces TANAKA 93. FUSHIMI 02 derive half-life limit for the $0\nu\chi$ decay by means of tracking calorimeter ELEGANT V. Considering various matrix element calculations, a range of limits for the Majoron-neutrino coupling is given: $\langle g_{\nu\chi} \rangle < (6.3\text{--}360) \times 10^{-5}$.
- 165 ASHITKOV 01 result for $0\nu\chi$ of ¹⁰⁰Mo is less stringent than ARNOLD 00.
- 166 DANEVICH 01 obtain limit for the $0\nu\chi$ decay with Majoron emission of ¹⁶⁰Gd using Gd₂SiO₅:Ce crystal scintillators.
- 167 DANEVICH 01 obtain limit for the $0\nu 2\chi$ decay with 2 Majoron emission of ¹⁶⁰Gd.
- 168 ARNOLD 00 reports limit for the $0\nu\chi$ decay with Majoron emission derived from tracking calorimeter NEMO 2. Using ⁸²Se source: $\langle g_{\nu\chi} \rangle < 1.6 \times 10^{-4}$. Matrix element from GUENTHER 96.
- 169 Using ⁹⁶Zr source: $\langle g_{\nu\chi} \rangle < 2.6 \times 10^{-4}$. Matrix element from ARNOLD 99.
- 170 ARNOLD 00 reports limit for the $0\nu 2\chi$ decay with two Majoron emission derived from tracking calorimeter NEMO 2.
- 171 ARNOLD 98 determine the limit for $0\nu\chi$ decay with Majoron emission of ⁸²Se using the NEMO-2 tracking detector. They derive $\langle g_{\nu\chi} \rangle < 2.3\text{--}4.3 \times 10^{-4}$ with several nuclear matrix elements.

See key on page 373

Gauge & Higgs Boson Particle Listings Axions (A^0) and Other Very Light Bosons

- 172 LUESCHER 98 report a limit for the 0ν decay with Majoron emission of ^{136}Xe using Xe TPC. This result is more stringent than BARABASH 89. Using the matrix elements of ENGEL 88, they obtain a limit on $\langle g_{\nu\chi} \rangle$ of 2.0×10^{-4} .
- 173 See Table 1 in GUENTHER 96 for limits on the Majoron coupling in different models.

Invisible A^0 (Axion) MASS LIMITS from Astrophysics and Cosmology

$v_1 = v_2$ is usually assumed ($v_i =$ vacuum expectation values). For a review of these limits, see RAFFELT 91 and TURNER 90. In the comment lines below, D and K refer to DFSZ and KSVZ axion types, discussed in the above minireview.

VALUE (eV)	CL%	DOCUMENT ID	TECN	COMMENT
< 1.02	95	174 HANNESTAD 08	COSM	K, hot dark matter
< 1.2	95	175 HANNESTAD 07	COSM	K, hot dark matter
< 0.42	95	176 MELCHIORRI 07A	COSM	K, hot dark matter
< 1.05	95	177 HANNESTAD 05A	COSM	K, hot dark matter
3 to 20		178 MOROI 98	COSM	K, hot dark matter
< 0.007		179 BORISOV 97	ASTR	D, neutron star
< 4		180 KACHELRIESS 97	ASTR	D, neutron star cooling
$< (0.5-6) \times 10^{-3}$		181 KEIL 97	ASTR	SN 1987A
< 0.018		182 RAFFELT 95	ASTR	D, red giant
< 0.010		183 ALTHERR 94	ASTR	D, red giants, white dwarfs
< 0.01		184 CHANG 93	ASTR	K, SN 1987A
< 0.03		WANG 92	ASTR	D, white dwarf
none 3-8		WANG 92c	ASTR	D, C-O burning
		185 BERSHADY 91	ASTR	D, K, intergalactic light
< 10		186 KIM 91c	COSM	D, K, mass density of the universe, super-symmetry
< 1	$\times 10^{-3}$	187 RAFFELT 91B	ASTR	D, K, SN 1987A
none 10^{-3-3}		188 RESSELL 91	ASTR	K, intergalactic light
		BURROWS 90	ASTR	D, K, SN 1987A
< 0.02		189 ENGEL 90	ASTR	D, K, SN 1987A
< 1	$\times 10^{-3}$	190 RAFFELT 90D	ASTR	D, red giant
< (1.4-10) $\times 10^{-3}$		191 BURROWS 89	ASTR	D, K, SN 1987A
< 3.6	$\times 10^{-4}$	192 ERICSON 89	ASTR	D, K, SN 1987A
< 12		193 MAYLE 89	ASTR	D, K, SN 1987A
< 1	$\times 10^{-3}$	CHANDA 88	ASTR	D, Sun
		RAFFELT 88B	ASTR	red giant
< 0.07		194 RAFFELT 88B	ASTR	red giant
< 0.7		FRIEMAN 87	ASTR	D, red giant
< 2-5		195 RAFFELT 87	ASTR	K, red giant
< 0.01		TURNER 87	COSM	K, thermal production
< 0.06		196 DEARBORN 86	ASTR	D, red giant
< 0.7		RAFFELT 86	ASTR	D, red giant
< 0.03		197 RAFFELT 86B	ASTR	D, white dwarf
< 1		RAFFELT 86B	ASTR	D, white dwarf
< 0.003-0.02		198 KAPLAN 85	ASTR	K, red giant
> 1	$\times 10^{-5}$	IWAMOTO 84	ASTR	D, K, neutron star
> 1	$\times 10^{-5}$	ABBOTT 83	COSM	D, K, mass density of the universe
> 1	$\times 10^{-5}$	DINE 83	COSM	D, K, mass density of the universe
< 0.04		ELLIS 83B	ASTR	D, red giant
> 1	$\times 10^{-5}$	PRESKILL 83	COSM	D, K, mass density of the universe
< 0.1		BARROSO 82	ASTR	D, red giant
< 1		199 FUKUGITA 82	ASTR	D, stellar cooling
< 0.07		FUKUGITA 82B	ASTR	D, red giant

- 174 This is an update of HANNESTAD 07 including 5 years of WMAP data.
- 175 This is an update of HANNESTAD 05A with new cosmological data, notably WMAP (3 years) and baryon acoustic oscillations (BAO). Lyman- α data are left out, in contrast to HANNESTAD 05A and MELCHIORRI 07A, because it is argued that systematic errors are large. It uses Bayesian statistics and marginalizes over a possible neutrino hot dark matter component.
- 176 MELCHIORRI 07A is analogous to HANNESTAD 05A, with updated cosmological data, notably WMAP (3 years). Uses Bayesian statistics and marginalizes over a possible neutrino hot dark matter component. Leaving out Lyman- α data, a conservative limit is 1.4 eV.
- 177 HANNESTAD 05A puts an upper limit on the mass of hadronic axion because in this mass range it would have been thermalized and contribute to the hot dark matter component of the universe. The limit is based on the CMB anisotropy from WMAP, SDSS large scale structure, Lyman α , and the prior Hubble parameter from HST Key Project. A χ^2 statistic is used. Neutrinos are assumed not to contribute to hot dark matter.
- 178 MOROI 98 points out that a KSVZ axion of this mass range (see CHANG 93) can be a viable hot dark matter of Universe, as long as the model-dependent $G_{A\gamma\gamma}$ is accidentally small enough as originally emphasized by KAPLAN 85; see Fig. 1.
- 179 BORISOV 97 bound is on the axion-electron coupling $g_{ae} < 1 \times 10^{-13}$ from the photo-production of axions off of magnetic fields in the outer layers of neutron stars.
- 180 KACHELRIESS 97 bound is on the axion-electron coupling $g_{ae} < 1 \times 10^{-10}$ from the production of axions in strongly magnetized neutron stars. The authors also quote a stronger limit, $g_{ae} < 9 \times 10^{-13}$ which is strongly dependent on the strength of the magnetic field in white dwarfs.
- 181 KEIL 97 uses new measurements of the axial-vector coupling strength of nucleons, as well as a reanalysis of many-body effects and pion-emission processes in the core of the neutron star, to update limits on the invisible-axion mass.
- 182 RAFFELT 95 reexamined the constraints on axion emission from red giants due to the axion-electron coupling. They improve on DEARBORN 86 by taking into proper account degeneracy effects in the bremsstrahlung rate. The limit comes from requiring the red

- giant core mass at helium ignition not to exceed its standard value by more than 5% (0.025 solar masses).
- 183 ALTHERR 94 bound is on the axion-electron coupling $g_{ae} < 1.5 \times 10^{-13}$, from energy loss via axion emission.
- 184 CHANG 93 updates ENGEL 90 bound with the Kaplan-Manohar ambiguity in $z=m_u/m_d$ (see the Note on the Quark Masses in the Quark Particle Listings). It leaves the window $f_A=3 \times 10^5-3 \times 10^6$ GeV open. The constraint from Big-Bang Nucleosynthesis is satisfied in this window as well.
- 185 BERSHADY 91 searched for a line at wave length from 3100-8300 Å expected from 2- γ decays of relic thermal axions in intergalactic light of three rich clusters of galaxies.
- 186 KIM 91c argues that the bound from the mass density of the universe will change drastically for the supersymmetric models due to the entropy production of saxion (scalar component in the axionic chiral multiplet) decay. Note that it is an upperbound rather than a lowerbound.
- 187 RAFFELT 91B argue that previous SN 1987A bounds must be relaxed due to corrections to nucleon bremsstrahlung processes.
- 188 RESSELL 91 uses absence of any intracluster line emission to set limit.
- 189 ENGEL 90 rule out $10^{-10} \lesssim g_{AN} \lesssim 10^{-3}$, which for a hadronic axion with EMC motivated axion-nucleon couplings corresponds to $2.5 \times 10^{-3} \text{ eV} \lesssim m_{A^0} \lesssim 2.5 \times 10^4 \text{ eV}$. The constraint is loose in the middle of the range, i.e. for $g_{AN} \sim 10^{-6}$.
- 190 RAFFELT 90D is a re-analysis of DEARBORN 86.
- 191 The region $m_{A^0} \gtrsim 2 \text{ eV}$ is also allowed.
- 192 ERICSON 89 considered various nuclear corrections to axion emission in a supernova core, and found a reduction of the previous limit (MAYLE 88) by a large factor.
- 193 MAYLE 89 limit based on naive quark model couplings of axion to nucleons. Limit based on couplings motivated by EMC measurements is 2-4 times weaker. The limit from axion-electron coupling is weak: see HATSUDA 88B.
- 194 RAFFELT 88B derives a limit for the energy generation rate by exotic processes in helium-burning stars $\epsilon < 100 \text{ erg g}^{-1} \text{ s}^{-1}$, which gives a firmer basis for the axion limits based on red giant cooling.
- 195 RAFFELT 87 also gives a limit $g_{A\gamma} < 1 \times 10^{-10} \text{ GeV}^{-1}$.
- 196 DEARBORN 86 also gives a limit $g_{A\gamma} < 1.4 \times 10^{-11} \text{ GeV}^{-1}$.
- 197 RAFFELT 86 gives a limit $g_{A\gamma} < 1.1 \times 10^{-10} \text{ GeV}^{-1}$ from red giants and $< 2.4 \times 10^{-9} \text{ GeV}^{-1}$ from the sun.
- 198 KAPLAN 85 says $m_{A^0} < 23 \text{ eV}$ is allowed for a special choice of model parameters.
- 199 FUKUGITA 82 gives a limit $g_{A\gamma} < 2.3 \times 10^{-10} \text{ GeV}^{-1}$.

Search for Relic Invisible Axions

Limits are for $[G_{A\gamma\gamma}/m_{A^0}]^2 \rho_A$ where $G_{A\gamma\gamma}$ denotes the axion two-photon coupling,

$$L_{\text{int}} = \frac{G_{A\gamma\gamma}}{4} \phi_A F_{\mu\nu} \tilde{F}^{\mu\nu} = G_{A\gamma\gamma} \phi_A \mathbf{E} \cdot \mathbf{B}, \text{ and } \rho_A \text{ is the axion energy density near the earth.}$$

VALUE	CL%	DOCUMENT ID	TECN	COMMENT
< 1.9 $\times 10^{-43}$	97.7	200 DUFFY 06	CNTR	$m_{A^0} = 1.98-2.17 \times 10^{-6} \text{ eV}$
< 5.5 $\times 10^{-43}$	90	201 ASZTALOS 04	CNTR	$m_{A^0} = 1.9-3.3 \times 10^{-6} \text{ eV}$
		202 KIM 98	THEO	
< 2		203 HAGMANN 90	CNTR	$m_{A^0} = (5.4-5.9) 10^{-6} \text{ eV}$
< 1.3 $\times 10^{-42}$	95	204 WUENSCH 89	CNTR	$m_{A^0} = (4.5-10.2) 10^{-6} \text{ eV}$
< 2		204 WUENSCH 89	CNTR	$m_{A^0} = (11.3-16.3) 10^{-6} \text{ eV}$
200 DUFFY 06				used the upgraded detector of ASZTALOS 04, while assuming a smaller velocity dispersion than the isothermal model as in Eq. (8) of their paper. See Fig. 10 of their paper on the axion mass dependence of the limit.
201 ASZTALOS 04				looked for a conversion of halo axions to microwave photons in magnetic field. At 90% CL, the KSVZ axion cannot have a local halo density more than 0.45 GeV/cm^3 in the quoted mass range. See Fig. 7 of their paper on the axion mass dependence of the limit.
202 KIM 98				calculated the axion-to-photon couplings for various axion models and compared them to the HAGMANN 90 bounds. This analysis demonstrates a strong model dependence of $G_{A\gamma\gamma}$ and hence the bound from relic axion search.
203 HAGMANN 90				experiment is based on the proposal of SIKIVIE 83.
204 WUENSCH 89				looks for condensed axions near the earth that could be converted to photons in the presence of an intense electromagnetic field via the Primakoff effect, following the proposal of SIKIVIE 83. The theoretical prediction with $[G_{A\gamma\gamma}/m_{A^0}]^2 = 2 \times 10^{-14} \text{ MeV}^{-4}$ (the three generation DFSZ model) and $\rho_A = 300 \text{ MeV}/\text{cm}^3$ that makes up galactic halos gives $(G_{A\gamma\gamma}/m_{A^0})^2 \rho_A = 4 \times 10^{-44}$. Note that our definition of $G_{A\gamma\gamma}$ is $(1/4\pi)$ smaller than that of WUENSCH 89.

Invisible A^0 (Axion) Limits from Photon Coupling

Limits are for the axion-two-photon coupling $G_{A\gamma\gamma}$ defined by $L = G_{A\gamma\gamma} \phi_A \mathbf{E} \cdot \mathbf{B}$.

Related limits from astrophysics can be found in the "Invisible A^0 (Axion) Mass Limits from Astrophysics and Cosmology" section.

VALUE (GeV^{-1})	CL%	DOCUMENT ID	TECN	COMMENT
< 3.5 $\times 10^{-7}$	99.7	205 CHOU 08		$m_{A^0} < 0.5 \text{ MeV}$
< 5		206 ZAVATTINI 08		$m_{A^0} < 1 \text{ MeV}$
< 8.8 $\times 10^{-11}$	95	207 ANDRIAMON...07	CAST	$m_{A^0} < 0.02 \text{ eV}$
< 1.25 $\times 10^{-6}$	95	208 ROBILLIARD 07		$m_{A^0} < 1 \text{ MeV}$

• • • We do not use the following data for averages, fits, limits, etc. • • •

Gauge & Higgs Boson Particle Listings

Axions (A^0) and Other Very Light Bosons

2.5×10^{-6}	209	ZAVATTINI	06	$m_{A^0} = 1-1.5$ meV	
$<1.1 \times 10^{-9}$	95	210	INOUE	02	$m_{A^0} = 0.05-0.27$ eV
$<2.78 \times 10^{-9}$	95	211	MORALES	02B	$m_{A^0} < 1$ keV
$<1.7 \times 10^{-9}$	90	212	BERNABEI	01B	$m_{A^0} < 100$ eV
$<1.5 \times 10^{-4}$	90	213	ASTIER	00B	NOMD $m_{A^0} < 40$ eV
		214	MASSO	00	THEO induced γ coupling
$<2.7 \times 10^{-9}$	95	215	AVIGNONE	98	SLAX $m_{A^0} < 1$ keV
$<6.0 \times 10^{-10}$	95	216	MORIYAMA	98	$m_{A^0} < 0.03$ eV
$<3.6 \times 10^{-7}$	95	217	CAMERON	93	$m_{A^0} < 10^{-3}$ eV, optical rotation
$<6.7 \times 10^{-7}$	95	218	CAMERON	93	$m_{A^0} < 10^{-3}$ eV, photon regeneration
$<3.6 \times 10^{-9}$	99.7	219	LAZARUS	92	$m_{A^0} = 0.03-0.11$ eV
$<7.7 \times 10^{-9}$	99.7	219	LAZARUS	92	$m_{A^0} = 0.03-0.11$ eV
$<7.7 \times 10^{-7}$	99	220	RUOSO	92	$m_{A^0} < 10^{-3}$ eV
$<2.5 \times 10^{-6}$		221	SEMERTZIDIS	90	$m_{A^0} < 7 \times 10^{-4}$ eV

205 CHOU 08 perform a variable-baseline photon regeneration experiment. See their Fig. 3 for mass-dependent limits. Excludes the PVLAS result of ZAVATTINI 06.

206 ZAVATTINI 08 is an upgrade of ZAVATTINI 06, see their Fig. 8 for mass-dependent limits. They now exclude the parameter range where ZAVATTINI 06 had seen a positive signature.

207 ANDRIAMONJE 07 looked for Primakoff conversion of solar axions in 9T superconducting magnet into X-rays. Supersedes ZIOUTAS 05.

208 ROBILLIARD 07 perform a photon regeneration experiment with a pulsed laser and pulsed magnetic field. See their Fig. 4 for mass-dependent limits. Excludes the PVLAS result of ZAVATTINI 06 with a CL exceeding 99.9%.

209 ZAVATTINI 06 propagate a laser beam in a magnetic field and observe dichroism and birefringence effects that could be attributed to an axion-like particle. This result is now excluded by ROBILLIARD 07, ZAVATTINI 08, and CHOU 08.

210 INOUE 02 looked for Primakoff conversion of solar axions in 4T superconducting magnet into X ray.

211 MORALES 02B looked for the coherent conversion of solar axions to photons via the Primakoff effect in Germanium detector.

212 BERNABEI 01B looked for Primakoff coherent conversion of solar axions into photons via Bragg scattering in NaI crystal in DAMA dark matter detector.

213 ASTIER 00B looked for production of axions from the interaction of high-energy photons with the horn magnetic field and their subsequent re-conversion to photons via the interaction with the NOMAD dipole magnetic field.

214 MASSO 00 studied limits on axion-proton coupling using the induced axion-photon coupling through the proton loop and CAMERON 93 bound on the axion-photon coupling using optical rotation. They obtained the bound $g_{p\gamma}^2/4\pi < 1.7 \times 10^{-9}$ for the coupling $g_{p\gamma}^2 P^{\phi A}$.

215 AVIGNONE 98 result is based on the coherent conversion of solar axions to photons via the Primakoff effect in a single crystal germanium detector.

216 Based on the conversion of solar axions to X-rays in a strong laboratory magnetic field.

217 Experiment based on proposal by MAIANI 86.

218 Experiment based on proposal by VANBIBBER 87.

219 LAZARUS 92 experiment is based on proposal found in VANBIBBER 89.

220 RUOSO 92 experiment is based on the proposal by VANBIBBER 87.

221 SEMERTZIDIS 90 experiment is based on the proposal of MAIANI 86. The limit is obtained by taking the noise amplitude as the upper limit. Limits extend to $m_{A^0} = 4 \times 10^{-3}$ where $G_{A\gamma\gamma} < 1 \times 10^{-4}$ GeV $^{-1}$.

Limit on Invisible A^0 (Axion) Electron Coupling

The limit is for $G_{Aee} \partial_\mu \phi_A \bar{e} \gamma^\mu \gamma_5 e$ in GeV $^{-1}$, or equivalently, the dipole-dipole potential $\frac{G_{Aee}^2}{4\pi} ((\sigma_1 \cdot \sigma_2) - 3(\sigma_1 \cdot \mathbf{n})(\sigma_2 \cdot \mathbf{n}))/r^3$ where $\mathbf{n} = \mathbf{r}/r$.

The limits below apply to invisible axion of $m_A \leq 10^{-6}$ eV.

VALUE (GeV $^{-1}$)	CL%	DOCUMENT ID	TECN	COMMENT	
• • • We do not use the following data for averages, fits, limits, etc. • • •					
$<5.3 \times 10^{-5}$	66	222	NI	94	Induced magnetism
$<6.7 \times 10^{-5}$	66	222	CHUI	93	Induced magnetism
$<3.6 \times 10^{-4}$	66	223	PAN	92	Torsion pendulum
$<2.7 \times 10^{-5}$	95	222	BOBRAKOV	91	Induced magnetism
$<1.9 \times 10^{-3}$	66	224	WINELAND	91	NMR
$<8.9 \times 10^{-4}$	66	223	RITTER	90	Torsion pendulum
$<6.6 \times 10^{-5}$	95	222	VOROBYOV	88	Induced magnetism
222 These experiments measured induced magnetization of a bulk material by the spin-dependent potential generated from other bulk material with aligned electron spins, where the magnetic field is shielded with superconductor.					
223 These experiments used a torsion pendulum to measure the potential between two bulk matter objects where the spins are polarized but without a net magnetic field in either of them.					
224 WINELAND 91 looked for an effect of bulk matter with aligned electron spins on atomic hyperfine splitting using nuclear magnetic resonance.					

Invisible A^0 (Axion) Limits from Nucleon Coupling

Limits are for the axion mass in eV.

VALUE (eV)	CL%	DOCUMENT ID	TECN	COMMENT	
• • • We do not use the following data for averages, fits, limits, etc. • • •					
		225	BELLINI	08	CNTR Solar axion
		226	ADELBERGER	07	Test of Newton's law

<360	90	227	DERBIN	07	CNTR Solar axion
<216	95	228	NAMBA	07	CNTR Solar axion
$< 1.6 \times 10^4$	90	229	DERBIN	05	CNTR Solar axion
<400	95	230	LJUBICIC	04	CNTR Solar axion
$< 3.2 \times 10^4$	95	231	KRCMAR	01	CNTR Solar axion
<745	95	232	KRCMAR	98	CNTR Solar axion

225 BELLINI 08 consider solar axions emitted in the M1 transition of ${}^7\text{Li}^*$ (478 keV) and look for a peak at 478 keV in the energy spectra of the Counting Test Facility (CTF), a Borexino prototype. For $m_{A^0} < 450$ keV they find mass-dependent limits on products of axion couplings to photons, electrons, and nucleons.

226 ADELBERGER 07 use precision tests of Newton's law to constrain a force contribution from the exchange of two pseudoscalars. See their Fig. 5 for limits on the pseudoscalar coupling to nucleons, relevant for m_{A^0} below about 1 meV.

227 DERBIN 07 is analogous to KRCMAR 98.

228 NAMBA 07 is analogous to KRCMAR 98.

229 DERBIN 05 bound is based on the same principle as KRCMAR 01.

230 LJUBICIC 04 looked for ejection of K-shell electrons by the axioelectric effect of 14.4 keV solar axions in a Germanium detector. The limit assumes the hadronic axion model and the same solar axion flux as in KRCMAR 98 and KRCMAR 01.

231 KRCMAR 01 looked for solar axions emitted by the M1 transition of ${}^7\text{Li}$ after the electron capture by ${}^7\text{Be}$ and the emission of 384 keV line neutrino, using their resonant capture on ${}^7\text{Li}$ in the laboratory. The mass bound assumes $m_u/m_d = 0.56$ and the flavor-singlet axial-vector matrix element $S=0.4$.

232 KRCMAR 98 looked for solar axions emitted by the M1 transition of thermally excited ${}^{57}\text{Fe}$ nuclei in the Sun, using their possible resonant capture on ${}^{57}\text{Fe}$ in the laboratory, following MORIYAMA 95b. The mass bound assumes $m_u/m_d = 0.56$ and the flavor-singlet axial-vector matrix element $S=3F-D=0.5$.

Axion Limits from T -violating Medium-Range Forces

The limit is for the coupling g in a T -violating potential between nucleons or nucleon and electron of the form $V = \frac{g\hbar^2}{8\pi m_\rho} (\sigma \cdot \hat{r}) \left(\frac{1}{r^2} + \frac{m_A c}{\hbar r} \right) e^{-m_A r/\hbar}$

VALUE	DOCUMENT ID	TECN	COMMENT	
• • • We do not use the following data for averages, fits, limits, etc. • • •				
	233	BAESSLER	07	ultracold neutrons
	234	HECKEL	06	torsion pendulum
	235	NI	99	paramagnetic Tb F ₃
	236	POPELOV	98	THEO neutron EDM
	237	YOUNDIN	96	
	238	RITTER	93	torsion pendulum
	239	VENEMA	92	nuclear spin-precession frequencies
	240	WINELAND	91	NMR
233 BAESSLER 07 use the observation of quantum states of ultracold neutrons in the Earth's gravitational field to constrain g for an interaction range 1 μm –a few mm. See their Fig. 3 for results.				
234 HECKEL 06 studied the influence of unpolarized bulk matter, including the laboratory's surroundings or the Sun, on a torsion pendulum containing about 9×10^{22} polarized electrons. See their Fig. 4 for limits on g as a function of interaction range.				
235 NI 99 searched for a T -violating medium-range force acting on paramagnetic Tb F ₃ salt. See their Fig. 1 for the result.				
236 POPELOV 98 studied the possible contribution of T -violating Medium-Range Force to the neutron electric dipole moment, which is possible when axion interactions violate CP. The size of the force among nucleons must be smaller than gravity by a factor of 2×10^{-10} (1 cm/ λ_A), where $\lambda_A = \hbar/m_A c$.				
237 YOUNDIN 96 compared the precession frequencies of atomic ${}^{199}\text{Hg}$ and Cs when a large mass is positioned near the cells, relative to an applied magnetic field. See Fig. 3 for their limits.				
238 RITTER 93 studied the influence of bulk mass with polarized electrons on an unpolarized torsion pendulum, providing limits in the interaction range from 1 to 100 cm.				
239 VENEMA 92 looked for an effect of Earth's gravity on nuclear spin-precession frequencies of ${}^{199}\text{Hg}$ and ${}^{201}\text{Hg}$ atoms.				
240 WINELAND 91 looked for an effect of bulk matter with aligned electron spins on atomic hyperfine resonances in stored ${}^9\text{Be}^+$ ions using nuclear magnetic resonance.				

REFERENCES FOR Searches for Axions (A^0) and Other Very Light Bosons

BELLINI	08	EPJ C54 61	G. Bellini et al.	(Borexino Collab.)
CHOU	08	PRL 100 080402	A.S. Chou et al.	(GammeV Collab.)
HANNENSTAD	08	JCAP 0804 019	S. Hannenstad et al.	
ZAVATTINI	08	PR D77 032006	E. Zavattini et al.	(PVLAS Collab.)
ADELBERGER	07	PRL 98 131104	E.G. Adelberger et al.	
ANDRIAMONJE	07	JCAP 0704 010	S. Andriamonje et al.	(CAST Collab.)
BAESSLER	07	PR D75 075006	S. Baessler et al.	
CHANG	07	PR D75 052004	H.M. Chang et al.	(TEXONO Collab.)
DERBIN	07	JETPL 85 12	A.V. Derbin et al.	
HANNENSTAD	07	JCAP 0708 015	S. Hannenstad et al.	
JAIN	07	JPG 34 129	P.L. Jain, G. Singh	
LESSA	07	PR D75 094001	A.P. Lessa, O.L.G. Peres	
MELCHIORRI	07A	PR D76 041303R	A. Melchiorri, O. Mena, A. Slosar	
NAMBA	07	PL B645 398	T. Namba	
ROBILLIARD	07	PRL 99 190403	C. Robilliard et al.	
ARNOLD	06	NP A765 483	R. Arnold et al.	(NEMO-3 Collab.)
DUFFY	06	PR D74 012006	L.D. Duffy et al.	
HECKEL	06	PRL 97 021603	B.R. Heckel et al.	
ZAVATTINI	06	PRL 96 110406	E. Zavattini et al.	(PVLAS Collab.)
DERBIN	06	JETPL 81 365	A.V. Derbin et al.	
Translated from ZETFP 81 453.				
HANNENSTAD	05A	JCAP 0507 002	S. Hannenstad, A. Mirizzi, G. Raffelt	
PARK	05	PRL 94 021801	H.K. Park et al.	(FNAL HyperCP Collab.)
ZIOUTAS	05	PRL 94 121301	K. Zioutas et al.	(CAST Collab.)
ADLER	04	PR D70 037102	S. Adler et al.	(BNL E787 Collab.)
ANISIMOVSK...	04	PRL 93 031801	V.V. Anisimovskiy et al.	(BNL E949 Collab.)
ARNOLD	04	JETPL 80 377	R. Arnold et al.	(NEMO3 Detector Collab.)
Translated from ZETFP 80 429.				

Gauge & Higgs Boson Particle Listings

Axions (A^0) and Other Very Light Bosons

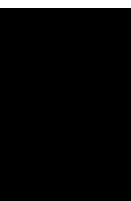
ASANO	82	PL 113B 195	Y. Asano <i>et al.</i>	(KEK, TOKY, INUS, OSAK)	ALIBRAN	78	PL 74B 134	P. Alibrán <i>et al.</i>	(Gargamelle Collab.)
BARROS O	82	PL 116B 247	A. Barroso, G.C. Branco	(LISB)	ASRATYAN	78B	PL 79B 497	A.E. Asratyan <i>et al.</i>	(ITEP, SERP)
DATAR	82	PL 114B 63	V.M. Datar <i>et al.</i>	(BHAB)	BELLOTTI	78	PL 76B 223	E. Bellotti, E. Fiorini, L. Zanotti	(MILA)
EDWARDS	82	PRL 48 903	C. Edwards <i>et al.</i>	(Crystal Ball Collab.)	BOSETTI	78B	PL 74B 143	P.C. Bosetti <i>et al.</i>	(BECB Collab.)
FETSCHER	82	JPG 8 L147	W. Fetscher	(ETH)	DICUS	78C	PR D18 1829	D.A. Dicus <i>et al.</i>	(TEXA, VPI, STAN)
FUKUGITA	82	PRL 48 1522	M. Fukugita, S. Watamura, M. Yoshimura	(KEK)	DONNELLY	78	PR D18 1607	T.W. Donnelly <i>et al.</i>	(STAN)
FUKUGITA	82B	PR D26 1840	M. Fukugita, S. Watamura, M. Yoshimura	(KEK)	Also		PRL 37 315	F. Reines, H.S. Gurr, H.W. Sobel	(UCI)
LEHMANN	82	PL 115B 270	P. Lehmann <i>et al.</i>	(SACL)	Also		PRL 33 179	H.S. Gurr, F. Reines, H.W. Sobel	(UCI)
RAFFELT	82	PL 119B 323	G. Raffelt, L. Stodolsky	(MPIM)	HANSL	78D	PL 74B 139	T. Hansl <i>et al.</i>	(CDHS Collab.)
SIVERTZ	82	PR D26 717	J.M. Sivertz <i>et al.</i>	(CUSB Collab.)	MICELMAC...	78	LNC 21 441	G.V. Mitselmakher, B. Pontecorvo	(JINR)
ZEHNDER	82	PL 110B 419	A. Zehnder, K. Gabathuler, J.L. Vuilleumier	(ETH+)	MIKAELIAN	78	PR D18 3605	K.O. Mikaelian	(FNAL, NWES)
ASANO	81B	PL 107B 159	Y. Asano <i>et al.</i>	(KEK, TOKY, INUS, OSAK)	SATO	78	PTP 60 1942	K. Sato	(KYOT)
BARROS O	81	PL 106B 91	A. Barroso, N.C. Mukhopadhyay	(SIN)	VYSOTSKII	78	JETPL 27 502	M.I. Vysotsky <i>et al.</i>	(ASCI)
FAISSNER	81	ZPHY C10 95	H. Faissner <i>et al.</i>	(AACH3)	Also		Translated from ZETFP 27 533.		
FAISSNER	81B	PL 103B 234	H. Faissner <i>et al.</i>	(AACH3)	YANG	78	PRL 41 523	T.C. Yang	(MASA)
KIM	81	PL 105B 55	B.R. Kim, C. Stamm	(AACH3)	PECCEI	77	PR D16 1791	R.D. Peccei, H.R. Quinn	(STAN, SLAC)
VUILLEUMIER	81	PL 101B 341	J.L. Vuilleumier <i>et al.</i>	(CIT, MUNI)	Also		PRL 38 1440	R.D. Peccei, H.R. Quinn	(STAN, SLAC)
ZEHNDER	81	PL 104B 494	A. Zehnder	(ETH)	REINES	76	PRL 37 315	F. Reines, H.S. Gurr, H.W. Sobel	(UCI)
FAISSNER	80	PL 96B 201	H. Faissner <i>et al.</i>	(AACH3)	GURR	74	PRL 33 179	H.S. Gurr, F. Reines, H.W. Sobel	(UCI)
JACQUES	80	PR D21 1206	P.F. Jacques <i>et al.</i>	(RUTG, STEV, COLU)	ANAND	53	PRSL A22 183	B.M. Anand	
SOUKAS	80	PRL 44 564	A. Soukas <i>et al.</i>	(BNL, HARV, ORNL, PENN)					
BECHIS	79	PRL 42 1511	D.J. Bechis <i>et al.</i>	(UMD, COLU, AFRR)					
CALAPRICE	79	PR D20 2708	F.P. Calaprice <i>et al.</i>	(PRIN)					
COTEUS	79	PRL 42 1438	P. Coteus <i>et al.</i>	(COLU, ILL, BNL)					
DISHAW	79	PL 85B 142	J.P. Dishaw <i>et al.</i>	(SLAC, CIT)					
ZHITNITSKII	79	SJNP 29 517	A.R. Zhitnitsky, Y.I. Skovpen	(NOVO)					
Translated from YAF 29 1001.									
					OTHER RELATED PAPERS				
SREDNICKI	85	NP B260 689	M. Srednicki	(UCSB)					
BARDEEN	78	PL 74B 229	W.A. Bardeen, S.-H.H. Tye	(FNAL)					

LEPTONS

e	479
μ	480
τ	489
Heavy Charged Lepton Searches	516
Neutrino Properties	517
Number of Neutrino Types	523
Double- β Decay	525
Neutrino Mixing	530
Heavy Neutral Leptons, Searches for	545

Notes in the Lepton Listings

Muon Anomalous Magnetic Moment (rev.)	481
Muon Decay Parameters (rev.)	485
τ Branching Fractions (rev.)	493
τ -Lepton Decay Parameters (rev.)	511
Introduction to the Neutrino Properties Listings (rev.)	517
Number of Light Neutrino Types from Collider Experiments (rev.)	523
Neutrinoless Double- β Decay (rev.)	525
Solar Neutrinos Review (rev.)	531
Introduction to Three-Neutrino Mixing Parameters Listings (rev.)	540





LEPTONS

e

$$J = \frac{1}{2}$$

e MASS (atomic mass units u)

The primary determination of an electron's mass comes from measuring the ratio of the mass to that of a nucleus, so that the result is obtained in u (atomic mass units). The conversion factor to MeV is more uncertain than the mass of the electron in u ; indeed, the recent improvements in the mass determination are not evident when the result is given in MeV. In this datablock we give the result in u , and in the following datablock in MeV.

VALUE ($10^{-6} u$)	DOCUMENT ID	TECN	COMMENT
548.5799043 ± 0.0000023	MOHR	08	RVUE 2006 CODATA value
• • • We do not use the following data for averages, fits, limits, etc. • • •			
548.5799045 ± 0.0000024	MOHR	05	RVUE 2002 CODATA value
548.5799092 ± 0.0000004	1 BEIER	02	CNTR Penning trap
548.5799110 ± 0.0000012	MOHR	99	RVUE 1998 CODATA value
548.5799111 ± 0.0000012	2 FARNHAM	95	CNTR Penning trap
548.579903 ± 0.000013	COHEN	87	RVUE 1986 CODATA value

¹ BEIER 02 compares Larmor frequency of the electron bound in a $^{12}\text{C}^{5+}$ ion with the cyclotron frequency of a single trapped $^{12}\text{C}^{5+}$ ion.

² FARNHAM 95 compares cyclotron frequency of trapped electrons with that of a single trapped $^{12}\text{C}^{6+}$ ion.

e MASS

2006 CODATA (MOHR 08) gives the conversion factor from u (atomic mass units, see the above datablock) to MeV as 931.494 028 (23). Earlier values use the then-current conversion factor. The conversion error dominates the uncertainty of the masses given below.

VALUE (MeV)	DOCUMENT ID	TECN	COMMENT
0.510998910 ± 0.00000013	MOHR	08	RVUE 2006 CODATA value
• • • We do not use the following data for averages, fits, limits, etc. • • •			
0.510998918 ± 0.000000044	MOHR	05	RVUE 2002 CODATA value
0.510998901 ± 0.000000020	3,4 BEIER	02	CNTR Penning trap
0.510998902 ± 0.000000021	MOHR	99	RVUE 1998 CODATA value
0.510998903 ± 0.000000020	3,5 FARNHAM	95	CNTR Penning trap
0.510998895 ± 0.000000024	3 COHEN	87	RVUE 1986 CODATA value
0.51100034 ± 0.0000014	COHEN	73	RVUE 1973 CODATA value

³ Converted to MeV using the 1998 CODATA value of the conversion constant, 931.494013 ± 0.000037 MeV/ u .

⁴ BEIER 02 compares Larmor frequency of the electron bound in a $^{12}\text{C}^{5+}$ ion with the cyclotron frequency of a single trapped $^{12}\text{C}^{5+}$ ion.

⁵ FARNHAM 95 compares cyclotron frequency of trapped electrons with that of a single trapped $^{12}\text{C}^{6+}$ ion.

$$(m_{e^+} - m_{e^-}) / m_{\text{average}}$$

A test of CPT invariance.

VALUE	CL%	DOCUMENT ID	TECN	COMMENT
< 8 × 10⁻⁹	90	6 FEE	93	CNTR Positronium spectroscopy
• • • We do not use the following data for averages, fits, limits, etc. • • •				
< 4 × 10 ⁻⁸	90	CHU	84	CNTR Positronium spectroscopy

⁶ FEE 93 value is obtained under the assumption that the positronium Rydberg constant is exactly half the hydrogen one.

$$|q_{e^+} + q_{e^-}|/e$$

A test of CPT invariance. See also similar tests involving the proton.

VALUE	DOCUMENT ID	TECN	COMMENT
< 4 × 10⁻⁸	7 HUGHES	92	RVUE
• • • We do not use the following data for averages, fits, limits, etc. • • •			
< 2 × 10 ⁻¹⁸	8 SCHAEFER	95	THEO Vacuum polarization
< 1 × 10 ⁻¹⁸	9 MUELLER	92	THEO Vacuum polarization

⁷ HUGHES 92 uses recent measurements of Rydberg-energy and cyclotron-frequency ratios.

⁸ SCHAEFER 95 removes model dependency of MUELLER 92.

⁹ MUELLER 92 argues that an inequality of the charge magnitudes would, through higher-order vacuum polarization, contribute to the net charge of atoms.

e MAGNETIC MOMENT ANOMALY

$$\mu_e/\mu_B - 1 = (g-2)/2$$

The CODATA value assumes the $g/2$ values for e^+ and e^- are equal, as required by CPT .

VALUE (units 10^{-6})	DOCUMENT ID	TECN	CHG	COMMENT
1159.65218111 ± 0.00000074	MOHR	08	RVUE	2006 CODATA value
• • • We do not use the following data for averages, fits, limits, etc. • • •				
1159.65218085 ± 0.00000076	ODOM	06	MRS	single electron
1159.6521859 ± 0.00000038	MOHR	05	RVUE	2002 CODATA value
1159.6521869 ± 0.00000041	MOHR	99	RVUE	1998 CODATA value
1159.652193 ± 0.000010	COHEN	87	RVUE	1986 CODATA value
1159.6521884 ± 0.00000043	VANDYCK	87	MRS	Single electron
1159.6521879 ± 0.00000043	VANDYCK	87	MRS	Single positron

$$(g_{e^+} - g_{e^-}) / g_{\text{average}}$$

A test of CPT invariance.

VALUE (units 10^{-12})	CL%	DOCUMENT ID	TECN	COMMENT
- 0.5 ± 2.1	10	VANDYCK	87	MRS Penning trap
• • • We do not use the following data for averages, fits, limits, etc. • • •				
< 12	95	11 VASSERMAN	87	CNTR Assumes $m_{e^+} = m_{e^-}$
22 ± 64		SCHWINBERG	81	MRS Penning trap

¹⁰ VANDYCK 87 measured $(g_-/g_+) - 1$ and we converted it.

¹¹ VASSERMAN 87 measured $(g_+ - g_-)/(g-2)$. We multiplied by $(g-2)/g = 1.2 \times 10^{-3}$.

e ELECTRIC DIPOLE MOMENT (d)

A nonzero value is forbidden by both T invariance and P invariance.

VALUE (10^{-26} ecm)	CL%	DOCUMENT ID	TECN	COMMENT
0.069 ± 0.074		REGAN	02	MRS ²⁰⁵ Tl beams
• • • We do not use the following data for averages, fits, limits, etc. • • •				
0.18 ± 0.12 ± 0.10	12	COMMINS	94	MRS ²⁰⁵ Tl beams
- 0.27 ± 0.83	12	ABDULLAH	90	MRS ²⁰⁵ Tl beams
- 14 ± 24		CHO	89	NMR Tl F molecules
- 1.5 ± 5.5 ± 1.5		MURTHY	89	Cesium, no B field
- 50 ± 110		LAMOREAUX	87	NMR ¹⁹⁹ Hg
190 ± 340	90	SANDARS	75	MRS Thallium
70 ± 220	90	PLAYER	70	MRS Xenon
< 300	90	WEISSKOPF	68	MRS Cesium

¹² ABDULLAH 90, COMMINS 94, and REGAN 02 use the relativistic enhancement of a valence electron's electric dipole moment in a high- Z atom.

e⁻ MEAN LIFE / BRANCHING FRACTION

A test of charge conservation. See the "Note on Testing Charge Conservation and the Pauli Exclusion Principle" following this section in our 1992 edition (Physical Review **D45** S1 (1992), p. VI.10).

Most of these experiments are one of three kinds: Attempts to observe (a) the 255.5 keV gamma ray produced in $e^- \rightarrow \nu_e \gamma$, (b) the (K) shell x ray produced when an electron decays without additional energy deposit, e.g., $e^- \rightarrow \nu_e \bar{\nu}_e \nu_e$ ("disappearance" experiments), and (c) nuclear de-excitation gamma rays after the electron disappears from an atomic shell and the nucleus is left in an excited state. The last can include both weak boson and photon mediating processes. We use the best $e^- \rightarrow \nu_e \gamma$ limit for the Summary Tables.

Note that we use the mean life rather than the half life, which is often reported.

e → $\nu_e \gamma$ and astrophysical limits

VALUE (yr)	CL%	DOCUMENT ID	TECN	COMMENT
> 4.6 × 10²⁶	90	BACK	02	BORX $e^- \rightarrow \nu \gamma$
• • • We do not use the following data for averages, fits, limits, etc. • • •				
> 1.22 × 10 ²⁶	68	13 KLAPDOR-K...	07	CNTR $e^- \rightarrow \nu \gamma$
> 3.4 × 10 ²⁶	68	BELLI	00B	DAMA $e^- \rightarrow \nu \gamma$, liquid Xe
> 3.7 × 10 ²⁵	68	AHARONOV	95B	CNTR $e^- \rightarrow \nu \gamma$
> 2.35 × 10 ²⁵	68	BALYSH	93	CNTR $e^- \rightarrow \nu \gamma$, ⁷⁶ Ge detector
> 1.5 × 10 ²⁵	68	AVIGNONE	86	CNTR $e^- \rightarrow \nu \gamma$
> 1 × 10 ³⁹		14 ORITO	85	ASTR Astrophysical argument
> 3 × 10 ²³	68	BELLOTTI	83B	CNTR $e^- \rightarrow \nu \gamma$

¹³ The authors of A. Derbin et al, arXiv:0704.2047v1 argue that this limit is overestimated by at least a factor of 5.

¹⁴ ORITO 85 assumes that electromagnetic forces extend out to large enough distances and that the age of our galaxy is 10^{10} years.

Lepton Particle Listings

e, μ

Disappearance and nuclear-de-excitation experiments

VALUE (yr)	CL%	DOCUMENT ID	TECN	COMMENT
$>6.4 \times 10^{24}$	68	15 BELLI	99B DAMA	De-excitation of ^{129}Xe
••• We do not use the following data for averages, fits, limits, etc. •••				
$>4.2 \times 10^{24}$	68	BELLI	99 DAMA	Iodine L-shell disappearance
$>2.4 \times 10^{23}$	90	16 BELLI	99D DAMA	De-excitation of ^{127}I (in NaI)
$>4.3 \times 10^{23}$	68	AHARONOV	95B CNTR	Ge K-shell disappearance
$>2.7 \times 10^{23}$	68	REUSSER	91 CNTR	Ge K-shell disappearance
$>2 \times 10^{22}$	68	BELLOTTI	83B CNTR	Ge K-shell disappearance
15 BELLI 99B limit on charge nonconserving e^- capture involving excitation of the 236.1 keV nuclear state of ^{129}Xe ; the 90% CL limit is 3.7×10^{24} yr. Less stringent limits for other states are also given.				
16 BELLI 99D limit on charge nonconserving e^- capture involving excitation of the 57.6 keV nuclear state of ^{127}I . Less stringent limits for the other states and for the state of ^{23}Na are also given.				

LIMITS ON LEPTON-FLAVOR VIOLATION IN PRODUCTION

Forbidden by lepton family number conservation.

This section was added for the 2008 edition of this Review and is not complete. For a list of further measurements see references in the papers listed below.

$\sigma(e^+e^- \rightarrow e^\pm\tau^\mp) / \sigma(e^+e^- \rightarrow \mu^+\mu^-)$

VALUE	CL%	DOCUMENT ID	TECN	COMMENT
$<8.9 \times 10^{-6}$	95	AUBERT	07P BABR	e^+e^- at $E_{cm} = 10.58$ GeV
••• We do not use the following data for averages, fits, limits, etc. •••				
$<1.8 \times 10^{-3}$	95	GOMEZ-CAD...	91 MRK2	e^+e^- at $E_{cm} = 29$ GeV

$\sigma(e^+e^- \rightarrow \mu^\pm\tau^\mp) / \sigma(e^+e^- \rightarrow \mu^+\mu^-)$

VALUE	CL%	DOCUMENT ID	TECN	COMMENT
$<4.0 \times 10^{-6}$	95	AUBERT	07P BABR	e^+e^- at $E_{cm} = 10.58$ GeV
••• We do not use the following data for averages, fits, limits, etc. •••				
$<6.1 \times 10^{-3}$	95	GOMEZ-CAD...	91 MRK2	e^+e^- at $E_{cm} = 29$ GeV

e REFERENCES

MOHR 08 arXiv:0801.0028[atom-ph] P.J. Mohr, B.N. Taylor, D.B. Newell (NIST) to appear in RMP and JPCRD

AUBERT 07P PR D75 031103R B. Aubert et al. (BABAR Collab.)

KLAPDOR-K... 07 PL B644 109 H.V. Klapdor-Kleingrothaus, I.V. Krivosheina, I.V. Titkova

ODOM 06 PRL 97 030801 B. Odom et al. (HARV)

MOHR 05 RMP 77 1 P.J. Mohr, B.N. Taylor (NIST)

BACK 02 PL B525 29 H.O. Back et al. (BOREXINO/SASSO Collab.)

BEIER 02 PRL 88 011603 T. Beier et al.

REGAN 02 PRL 88 071805 B.C. Regan et al.

BELLI 00B PR D61 117301 P. Belli et al. (DAMA Collab.)

BELLI 99 PL B460 236 P. Belli et al. (DAMA Collab.)

BELLI 99B PL B465 315 P. Belli et al. (DAMA Collab.)

BELLI 99D PR C60 065501 P. Belli et al. (DAMA Collab.)

MOHR 99 JPCRD 28 1713 P.J. Mohr, B.N. Taylor (NIST)

Also RMP 72 351 P.J. Mohr, B.N. Taylor (NIST)

AHARONOV 95B PR D52 3785 Y. Aharonov et al. (SCUC, PNL, ZARA+)

Also PL B353 168 Y. Aharonov et al. (SCUC, PNL, ZARA+)

FARNHAM 95 PRL 75 3598 D.L. Farnham, R.S. van Dyck, P.B. Schwinberg (WASH)

SCHAEFER 95 PR A51 838 A. Schaefer, J. Reinhardt (FRAN)

COMMINS 94 PR A50 2960 E.D. Commins et al.

BALYSH 93 PL B298 278 A. Balysh et al. (KIAE, MPH, SASSO)

FEE 93 PR A48 192 M.S. Fee et al.

HUGHES 92 PRL 69 578 R.J. Hughes, B.I. Deutch (LANL, AARH)

MUELLER 92 PRL 69 3432 B. Muller, M.H. Thoma (DUKE)

PDG 92 PR D45 51 K. Hikasa et al. (KEK, LBL, BOST+)

GOMEZ-CAD... 91 PRL 66 1007 J.J. Gomez-Cadenas et al. (SLAC, MARK-2 Collab.)

REUSSER 91 PL B255 143 D. Reusser et al. (NEUC, CIT, PSI)

ABDULLAH 90 PRL 65 2347 K. Abdullah et al. (LBL, UCB)

CHO 89 PRL 63 2559 D. Cho, K. Sangster, E.A. Hinds (YALE)

MURTHY 89 PRL 63 965 S.A. Murthy et al. (AMHT)

COHEN 87 RMP 59 1121 E.R. Cohen, B.N. Taylor (RIS, C, NBS)

LAMOREAUX 87 PRL 59 2275 S.K. Lamoreaux et al. (WASH)

VANDYCK 87 PRL 59 26 R.S. van Dyck, P.B. Schwinberg, H.G. Dehmelt (WASH)

VASSERMAN 87 PL B198 302 I.B. Vasserman et al. (NOVO)

Also PL B187 172 I.B. Vasserman et al. (NOVO)

AVIGNONE 86 PR D34 97 F.T. Avignone et al. (PNL, SCUC)

ORITO 85 PRL 54 2457 S. Orito, M. Yoshimura (TOKY, KEK)

CHU 84 PRL 52 1689 S. Chu, A.P. Mills, J.L. Hall (BELL, NBS, COLO)

BELLOTTI 83B PL 124B 435 E. Bellotti et al. (MILA)

SCHWINBERG 81 PRL 47 1679 P.B. Schwinberg, R.S. van Dyck, H.G. Dehmelt (WASH)

SANDARS 75 PR A11 473 P.G.H. Sandars, D.M. Sternheimer (OXF, BNL)

COHEN 73 JPCRD 2 664 E.R. Cohen, B.N. Taylor (RIS, C, NBS)

PLAYER 70 JPB 3 1620 M.A. Player, P.G.H. Sandars (OXF)

WEISSKOPF 68 PRL 21 1645 M.C. Weisskopf et al. (BRAN)



$$J = \frac{1}{2}$$

μ MASS (atomic mass units u)

The muon's mass is obtained from the muon-electron mass ratio as determined from the measurement of Zeeman transition frequencies in muonium (μ^+e^- atom). Since the electron's mass is most accurately known in u, the muon's mass is also most accurately known in u. The conversion factor to MeV has approximately the same relative uncertainty as the mass of the muon in u. In this datablock we give the result in u, and in the following datablock in MeV.

VALUE (u)	DOCUMENT ID	TECN	COMMENT
0.1134289256 ± 0.0000000029	MOHR	08 RVUE	2006 CODATA value
••• We do not use the following data for averages, fits, limits, etc. •••			
0.1134289264 ± 0.0000000030	MOHR	05 RVUE	2002 CODATA value
0.1134289168 ± 0.0000000034	¹ MOHR	99 RVUE	1998 CODATA value
0.113428913 ± 0.000000017	² COHEN	87 RVUE	1986 CODATA value

¹ MOHR 99 make use of other 1998 CODATA entries below.
² COHEN 87 make use of other 1986 CODATA entries below.

μ MASS

2006 CODATA (MOHR 08) gives the conversion factor from u (atomic mass units, see the above datablock) to MeV as 931.494 028 (23). Earlier values use the then-current conversion factor. The conversion error contributes significantly to the uncertainty of the masses given below.

VALUE (MeV)	DOCUMENT ID	TECN	CHG	COMMENT
105.6583668 ± 0.00000038	MOHR	08 RVUE		2006 CODATA value
••• We do not use the following data for averages, fits, limits, etc. •••				
105.6583692 ± 0.00000094	MOHR	05 RVUE		2002 CODATA value
105.6583568 ± 0.00000052	MOHR	99 RVUE		1998 CODATA value
105.658353 ± 0.0000016	³ COHEN	87 RVUE		1986 CODATA value
105.658386 ± 0.0000044	⁴ MARIAM	82 CNTR	+	
105.65836 ± 0.000026	⁵ CROWE	72 CNTR		
105.65865 ± 0.000044	⁶ CRANE	71 CNTR		

³ Converted to MeV using the 1998 CODATA value of the conversion constant, 931.494013 ± 0.000037 MeV/u.

⁴ MARIAM 82 give $m_\mu/m_e = 206.768259(62)$.

⁵ CROWE 72 give $m_\mu/m_e = 206.7682(5)$.

⁶ CRANE 71 give $m_\mu/m_e = 206.76878(85)$.

μ MEAN LIFE τ

Measurements with an error $> 0.001 \times 10^{-6}$ s have been omitted.

VALUE (10^{-6} s)	DOCUMENT ID	TECN	CHG	COMMENT
2.197019 ± 0.000021 OUR AVERAGE	Error includes scale factor of 1.1.			
2.197013 ± 0.000021 ± 0.000011	CHITWOOD	07 CNTR	+	Surface μ^+ at PSI
2.197078 ± 0.000073	BARDIN	84 CNTR	+	
2.197025 ± 0.000155	BARDIN	84 CNTR	-	
2.19695 ± 0.000006	GIOVANETTI	84 CNTR	+	
2.19711 ± 0.000008	BALANDIN	74 CNTR	+	
2.1973 ± 0.0003	DUCLOS	73 CNTR	+	

$\tau_{\mu^+}/\tau_{\mu^-}$ MEAN LIFE RATIO

A test of CPT invariance.

VALUE	DOCUMENT ID	TECN	COMMENT
1.000024 ± 0.000078	BARDIN	84 CNTR	
••• We do not use the following data for averages, fits, limits, etc. •••			
1.0008 ± 0.0010	BAILEY	79 CNTR	Storage ring
1.000 ± 0.001	MEYER	63 CNTR	Mean life μ^+/μ^-

$(\tau_{\mu^+} - \tau_{\mu^-}) / \tau_{\text{average}}$

A test of CPT invariance. Calculated from the mean-life ratio, above.

VALUE	DOCUMENT ID
$(2 \pm 8) \times 10^{-5}$ OUR EVALUATION	

μ/p MAGNETIC MOMENT RATIO

This ratio is used to obtain a precise value of the muon mass and to reduce experimental muon Larmor frequency measurements to the muon magnetic moment anomaly. Measurements with an error > 0.00001 have been omitted. By convention, the minus sign on this ratio is omitted. CODATA values were fitted using their selection of data, plus other data from multiparameter fits.

VALUE	DOCUMENT ID	TECN	CHG	COMMENT
3.183345137 ± 0.000000085	MOHR	08	RVUE	2006 CODATA value
• • • We do not use the following data for averages, fits, limits, etc. • • •				
3.183345118 ± 0.000000089	MOHR	05	RVUE	2002 CODATA value
3.18334513 ± 0.000000039	LIU	99	CNTR +	HFS in muonium
3.18334539 ± 0.000000010	MOHR	99	RVUE	1998 CODATA value
3.18334547 ± 0.000000047	COHEN	87	RVUE	1986 CODATA value
3.1833441 ± 0.000000017	KLEMPPT	82	CNTR +	Precession strob
3.1833461 ± 0.000000011	MARIAM	82	CNTR +	HFS splitting
3.1833448 ± 0.000000029	CAMANI	78	CNTR +	See KLEMPPT 82
3.1833403 ± 0.000000044	CASPERSON	77	CNTR +	HFS splitting
3.1833402 ± 0.000000072	COHEN	73	RVUE	1973 CODATA value
3.1833467 ± 0.000000082	CROWE	72	CNTR +	Precession phase

THE MUON ANOMALOUS MAGNETIC MOMENT

Updated July 2007 by A. Höcker (CERN) and W.J. Marciano (BNL)

The Dirac equation predicts a muon magnetic moment, $\vec{M} = g_\mu \frac{e}{2m_\mu} \vec{S}$, with gyromagnetic ratio $g_\mu = 2$. Quantum loop effects lead to a small calculable deviation from $g_\mu = 2$, parameterized by the anomalous magnetic moment

$$a_\mu \equiv \frac{g_\mu - 2}{2}. \quad (1)$$

That quantity can be accurately measured and, within the Standard Model (SM) framework, precisely predicted. Hence, comparison of experiment and theory tests the SM at its quantum loop level. A deviation in a_μ^{exp} from the SM expectation would signal effects of new physics, with current sensitivity reaching up to mass scales of $\mathcal{O}(\text{TeV})$ [1,2]. For a recent and very thorough muon $g - 2$ review, see Ref. 3.

The E821 experiment at Brookhaven National Lab (BNL) studied the precession of μ^+ and μ^- in a constant external magnetic field as they circulated in a confining storage ring. It found [4]

$$\begin{aligned} a_{\mu^+}^{\text{exp}} &= 11\,659\,203(6)(5) \times 10^{-10}, \\ a_{\mu^-}^{\text{exp}} &= 11\,659\,214(8)(3) \times 10^{-10}, \end{aligned} \quad (2)$$

where the first errors are statistical and the second systematic. Assuming CPT invariance and taking into account correlations between systematic errors, one finds for their average [4]

$$a_\mu^{\text{exp}} = 11\,659\,208.0(5.4)(3.3) \times 10^{-10}. \quad (3)$$

These results represent about a factor of 14 improvement over the classic CERN experiments of the 1970's [5].

The SM prediction for a_μ^{SM} is generally divided into three parts (see Fig. 1 for representative Feynman diagrams)

$$a_\mu^{\text{SM}} = a_\mu^{\text{QED}} + a_\mu^{\text{EW}} + a_\mu^{\text{Had}}. \quad (4)$$

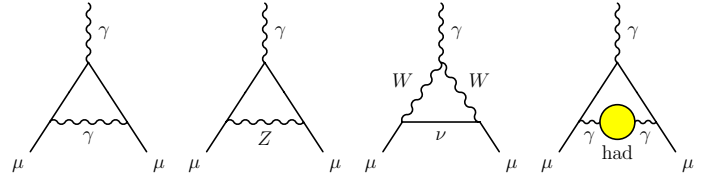


Figure 1: Representative diagrams contributing to a_μ^{SM} . From left to right: first order QED (Schwinger term), lowest-order weak, lowest-order hadronic.

The QED part includes all photonic and leptonic (e, μ, τ) loops starting with the classic $\alpha/2\pi$ Schwinger contribution. It has been computed through 4 loops and estimated at the 5-loop level [6]

$$\begin{aligned} a_\mu^{\text{QED}} &= \frac{\alpha}{2\pi} + 0.765857410(27) \left(\frac{\alpha}{\pi}\right)^2 + 24.05050964(87) \left(\frac{\alpha}{\pi}\right)^3 \\ &\quad + 130.8055(80) \left(\frac{\alpha}{\pi}\right)^4 + 663(20) \left(\frac{\alpha}{\pi}\right)^5 + \dots \end{aligned} \quad (5)$$

Employing $\alpha^{-1} = 137.035999070(98)$, determined [6,7] from the electron a_e measurement, leads to

$$a_\mu^{\text{QED}} = 116\,584\,718.10(0.16) \times 10^{-11}, \quad (6)$$

where the error results from uncertainties in the coefficients of Eq. (5) and in α .

Loop contributions involving heavy W^\pm, Z or Higgs particles are collectively labeled as a_μ^{EW} . They are suppressed by at least a factor of $\frac{\alpha}{\pi} \frac{m_\mu^2}{m_W^2} \simeq 4 \times 10^{-9}$. At 1-loop order [8]

$$\begin{aligned} a_\mu^{\text{EW}}[1\text{-loop}] &= \frac{G_\mu m_\mu^2}{8\sqrt{2}\pi^2} \left[\frac{5}{3} + \frac{1}{3} (1 - 4\sin^2\theta_W)^2 \right. \\ &\quad \left. + \mathcal{O}\left(\frac{m_\mu^2}{M_W^2}\right) + \mathcal{O}\left(\frac{m_\mu^2}{m_H^2}\right) \right], \\ &= 194.8 \times 10^{-11}, \end{aligned} \quad (7)$$

for $\sin^2\theta_W \equiv 1 - M_W^2/M_Z^2 \simeq 0.223$, and where $G_\mu \simeq 1.166 \times 10^{-5} \text{ GeV}^{-2}$ is the Fermi coupling constant. Two-loop corrections are relatively large and negative [9]

$$a_\mu^{\text{EW}}[2\text{-loop}] = -40.7(1.0)(1.8) \times 10^{-11}, \quad (8)$$

where the errors stem from quark triangle loops and the assumed Higgs mass range between 100 and 500 GeV. The 3-loop leading logarithms are negligible [9,10], $\mathcal{O}(10^{-12})$, implying in total

$$a_\mu^{\text{EW}} = 154(1)(2) \times 10^{-11}. \quad (9)$$

Hadronic (quark and gluon) loop contributions to a_μ^{SM} give rise to its main theoretical uncertainties. At present, those effects are not calculable from first principles, but such an approach, at least partially, may become possible as lattice QCD matures. Instead, one currently relies on a dispersion relation approach to evaluate the lowest-order (*i.e.*, $\mathcal{O}(\alpha^2)$) hadronic vacuum

Lepton Particle Listings

μ

polarization contribution $a_\mu^{\text{Had}}[\text{LO}]$ from corresponding cross section measurements [11]

$$a_\mu^{\text{Had}}[\text{LO}] = \frac{1}{3} \left(\frac{\alpha}{\pi} \right)^2 \int ds \frac{K(s)}{s} R^{(0)}(s), \quad (10)$$

where $K(s)$ is a QED kernel function [12], and where $R^{(0)}(s)$ denotes the ratio of the bare¹ cross section for e^+e^- annihilation into hadrons to the pointlike muon-pair cross section at center-of-mass energy \sqrt{s} . The function $K(s) \sim 1/s$ in Eq. (10) gives a strong weight to the low-energy part of the integral. Hence, $a_\mu^{\text{Had}}[\text{LO}]$ is dominated by the $\rho(770)$ resonance.

Currently, the available $\sigma(e^+e^- \rightarrow \text{hadrons})$ data give a leading-order hadronic vacuum polarization (representative) contribution of [13]

$$a_\mu^{\text{Had}}[\text{LO}] = 6894(42)(18) \times 10^{-11}, \quad (11)$$

where the first error is experimental (dominated by systematic uncertainties), and the second due to QED radiative corrections to the data.

Alternatively, one can use precise vector spectral functions from $\tau \rightarrow \nu_\tau + \text{hadrons}$ decays [14] that can be related to isovector $e^+e^- \rightarrow \text{hadrons}$ cross sections by isospin rotation. When isospin-violating corrections (from QED and $m_d - m_u \neq 0$) are applied, one finds [15,16]

$$a_\mu^{\text{Had}}[\text{LO}] = 7103(50)(7)(28) \times 10^{-11} (\tau), \quad (12)$$

where the errors are statistical and systematic, and where the last error is an estimate for the uncertainty in the isospin-breaking corrections. The discrepancy between the e^+e^- and τ -based determinations of $a_\mu^{\text{Had}}[\text{LO}]$ is currently unexplained. It may be indicative of problems with one or both data sets. It may also suggest the need for additional isospin-violating corrections to the τ data. Forthcoming low-energy e^+e^- and τ data may help to resolve this discrepancy and should reduce the hadronic uncertainty.

Higher order, $\mathcal{O}(\alpha^3)$, hadronic contributions are obtained from dispersion relations using the same $e^+e^- \rightarrow \text{hadrons}$ data [13,14,17], giving $a_\mu^{\text{Had,Disp}}[\text{NLO}] = (-98 \pm 1) \times 10^{-11}$, along with model-dependent estimates of the hadronic light-by-light scattering contribution, $a_\mu^{\text{Had,LBL}}[\text{NLO}]$, motivated by large- N_C QCD [18–23].² Following [2], one finds for the sum of the two terms

$$a_\mu^{\text{Had}}[\text{NLO}] = 22(35) \times 10^{-11}, \quad (13)$$

¹ The bare cross section is defined as the measured cross section corrected for initial-state radiation, electron-vertex loop contributions and vacuum-polarization effects in the photon propagator. However, QED effects in the hadron vertex and final state, such as photon radiation, are included.

² Some representative recent estimates of the hadronic light-by-light scattering contribution, $a_\mu^{\text{Had,LBL}}[\text{NLO}]$, that followed after the sign correction of [20], are: $120(35) \times 10^{-11}$ [2], $110(40) \times 10^{-11}$ [18], $136(25) \times 10^{-11}$ [19], $100(39) \times 10^{-11}$ [24].

where the error is dominated by hadronic light-by-light uncertainties.

Adding Eqs. (6), (9), (11) and (13) gives the representative e^+e^- data-based SM prediction

$$a_\mu^{\text{SM}} = 116\,591\,788(2)(46)(35) \times 10^{-11}, \quad (14)$$

where the errors are due to the electroweak, lowest-order hadronic, and higher-order hadronic contributions, respectively. The difference between experiment and theory

$$\Delta a_\mu = a_\mu^{\text{exp}} - a_\mu^{\text{SM}} = 292(63)(58) \times 10^{-11}, \quad (15)$$

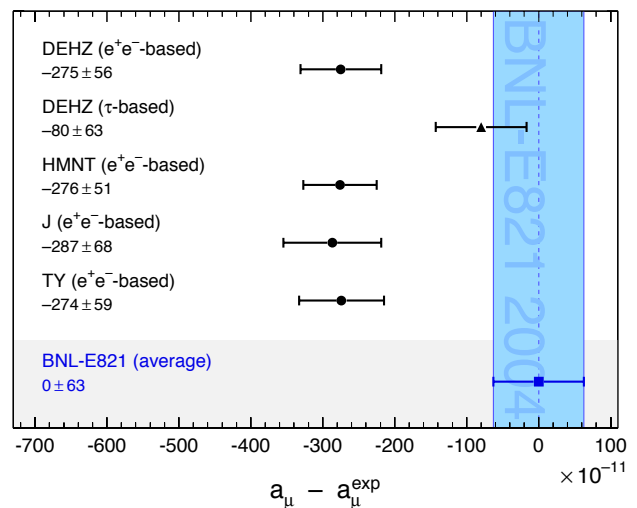


Figure 2: Compilation of recently published results for a_μ (in units of 10^{-11}), subtracted by the central value of the experimental average (3). The shaded band indicates the experimental error. The SM predictions are taken from: DEHZ [15,16], TY [25], HMNT [13], J [24]. Note that the quoted errors do not include the uncertainty on the subtracted experimental value. To obtain for each theory calculation a result equivalent to Eq. (15), the errors from theory and experiment must be added in quadrature.

(with all errors combined in quadrature) represents an interesting but not yet conclusive discrepancy of 3.4 times the estimated 1σ error. All the recent estimates for the hadronic contribution compiled in Fig. 2 exhibit similar discrepancies. Switching to τ data reduces the discrepancy to 0.9σ , assuming the isospin-violating corrections are under control within the estimated uncertainties.

An alternate interpretation is that Δa_μ may be a new physics signal with supersymmetric particle loops as the leading candidate explanation. Such a scenario is quite natural, since generically, supersymmetric models predict [1] an additional contribution to a_μ^{SM}

$$a_\mu^{\text{SUSY}} \simeq \pm 130 \times 10^{-11} \cdot \left(\frac{100 \text{ GeV}}{m_{\text{SUSY}}} \right)^2 \tan\beta, \quad (16)$$

where m_{SUSY} is a representative supersymmetric mass scale, and $\tan\beta \simeq 3\text{--}40$ is a potential enhancement factor. Supersymmetric particles in the mass range 100–500 GeV could be the source of the deviation Δa_μ . If so, those particles could be directly observed at the next generation of high energy colliders. New physics effects [1] other than supersymmetry could also explain a non-vanishing Δa_μ .

References

- A. Czarnecki and W.J. Marciano, Phys. Rev. **D64**, 013014 (2001).
- M. Davier and W.J. Marciano, Ann. Rev. Nucl. and Part. Sci. **54**, 115 (2004).
- J. Miller, E. de Rafael, and B. Lee Roberts, Rep. Progress Phys. **70**, 75 (2007).
- G.W. Bennett *et al.*, Phys. Rev. Lett. **89**, 101804 (2002); Erratum *ibid.* Phys. Rev. Lett. **89**, 129903 (2002); G.W. Bennett *et al.*, Phys. Rev. Lett. **92**, 161802 (2004); G.W. Bennett *et al.*, Phys. Rev. **D73**, 072003 (2006).
- J. Bailey *et al.*, Nucl. Phys. **B150**, 1 (1979).
- T. Kinoshita and M. Nio, Phys. Rev. **D73**, 013003 (2006); T. Aoyama *et al.*, Phys. Rev. Lett. **99**, 110406 (2007); T. Kinoshita and M. Nio, Phys. Rev. **D70**, 113001 (2004); T. Kinoshita, Nucl. Phys. **B144**, 206 (2005)(Proc. Supp.); T. Kinoshita and M. Nio, Phys. Rev. **D73**, 053007 (2006); A.L. Kataev, arXiv:hep-ph/0602098; M. Passera, J. Phys. **G31**, 75 (2005).
- G. Gabrielse *et al.*, Phys. Rev. Lett. **97**, 030802 (2006); Erratum *ibid.* Phys. Rev. Lett. **99**, 039902 (2007).
- R. Jackiw and S. Weinberg, Phys. Rev. **D5**, 2396 (1972); G. Altarelli *et al.*, Phys. Lett. **B40**, 415 (1972); I. Bars and M. Yoshimura, Phys. Rev. **D6**, 374 (1972).
- A. Czarnecki *et al.*, Phys. Rev. **D67**, 073006 (2003); S. Heinemeyer, D. Stockinger, and G. Weiglein, Nucl. Phys. **B699**, 103 (2004); T. Gribouk and A. Czarnecki, Phys. Rev. **D72**, 053016 (2005).
- G. Degrossi and G.F. Giudice, Phys. Rev. **D58**, 053007 (1998).
- C. Bouchiat and L. Michel, J. Phys. Radium **22**, 121 (1961); M. Gourdin and E. de Rafael, Nucl. Phys. **B10**, 667 (1969).
- S.J. Brodsky and E. de Rafael, Phys. Rev. **168**, 1620 (1968).
- K. Hagiwara *et al.*, Phys. Lett. **B649**, 173 (2007).
- R. Alemany *et al.*, Eur. Phys. J. **C2**, 123 (1998).
- M. Davier, Nucl. Phys. (Proc. Suppl.), **B169**, 288 (2007).
- M. Davier *et al.*, Eur. Phys. J. **C31**, 503 (2003); M. Davier *et al.*, Eur. Phys. J. **C27**, 497 (2003).
- B.Krause, Phys. Lett. **B390**, 392 (1997).
- J. Bijnens and J. Prades, Mod. Phys. Lett. **A22**, 767 (2007).
- K. Melnikov and A. Vainshtein, Phys. Rev. **D70**, 113006 (2004).
- M. Knecht and A. Nyffeler, Phys. Rev. **D65**, 073034 (2002); M. Knecht *et al.*, Phys. Rev. Lett. **88**, 071802 (2002).
- J. Bijnens *et al.*, Nucl. Phys. **B626**, 410 (2002).
- J. Hayakawa and T. Kinoshita, Erratum Phys. Rev. **D66**, 019902 (2002).
- E. de Rafael, Phys. Lett. **B322**, 239 (1994).
- F. Jegerlehner, arXiv:hep-ph/0703125 (2007).
- J.F. de Trocóniz and F.J. Ynduráin, Phys. Rev. **D71**, 073008 (2005).

μ MAGNETIC MOMENT ANOMALY

The parity-violating decay of muons in a storage ring is observed. The difference frequency ω_a between the muon spin precession and the orbital angular frequency ($e/m_\mu c \langle B \rangle$) is measured, as is the free proton NMR frequency ω_p , thus determining the ratio $R = \omega_a / \omega_p$. Given the magnetic moment ratio $\lambda = \mu_\mu / \mu_p$ (from hyperfine structure in muonium), $(g-2)/2 = R/(\lambda-R)$.

$$\mu_\mu / (e\hbar/2m_\mu) - 1 = (g_\mu - 2)/2$$

VALUE (units 10^{-10})	DOCUMENT ID	TECN	CHG	COMMENT
11659208.0 ± 5.4 ± 3.3	BENNETT	06	MUG2	Average μ^+ and μ^-
••• We do not use the following data for averages, fits, limits, etc. •••				
11659208 ± 6	BENNETT	04	MUG2	Average μ^+ and μ^-
11659214 ± 8 ± 3	BENNETT	04	MUG2	Storage ring
11659203 ± 6 ± 5	BENNETT	04	MUG2	Storage ring
11659204 ± 7 ± 5	BENNETT	02	MUG2	Storage ring
11659202 ± 14 ± 6	BROWN	01	MUG2	Storage ring
11659191 ± 59	BROWN	00	MUG2	Storage ring
11659100 ± 110	⁷ BAILEY	79	CNTR	Storage ring
11659360 ± 120	⁷ BAILEY	79	CNTR	Storage ring
11659230 ± 85	⁷ BAILEY	79	CNTR	Storage ring
11620000 ± 5000	CHARPAK	62	CNTR	

⁷BAILEY 79 values recalculated by HUGHES 99 using the COHEN 87 μ/p magnetic moment. The improved MOHR 99 value does not change the result.

$$(g_{\mu^+} - g_{\mu^-}) / g_{\text{average}}$$

A test of CPT invariance.

VALUE (units 10^{-8})	DOCUMENT ID	TECN
-0.11 ± 0.12	BENNETT	04 MUG2
••• We do not use the following data for averages, fits, limits, etc. •••		
-2.6 ± 1.6	BAILEY	79 CNTR

μ ELECTRIC DIPOLE MOMENT (d)

A nonzero value is forbidden by both T invariance and P invariance.

VALUE (10^{-19} ecm)	DOCUMENT ID	TECN	CHG	COMMENT
3.7 ± 3.4	⁸ BAILEY	78	CNTR	Storage ring
••• We do not use the following data for averages, fits, limits, etc. •••				
8.6 ± 4.5	BAILEY	78	CNTR	Storage rings
0.8 ± 4.3	BAILEY	78	CNTR	Storage rings

⁸This is the combination of the two BAILEY 78 results given below.

MUON-ELECTRON CHARGE RATIO ANOMALY $q_{\mu^+}/q_{e^-} + 1$

VALUE	DOCUMENT ID	TECN	CHG	COMMENT
(1.1 ± 2.1) × 10⁻⁹	⁹ MEYER	00	CNTR	1s-2s muonium interval

⁹MEYER 00 measure the 1s-2s muonium interval, and then interpret the result in terms of muon-electron charge ratio q_{μ^+}/q_{e^-} .

μ^- DECAY MODES

μ^+ modes are charge conjugates of the modes below.

Mode	Fraction (Γ_i/Γ)	Confidence level
Γ_1 $e^- \bar{\nu}_e \bar{\nu}_\mu$	$\approx 100\%$	
Γ_2 $e^- \bar{\nu}_e \nu_\mu \gamma$	[a] (1.4 ± 0.4) %	
Γ_3 $e^- \bar{\nu}_e \nu_\mu e^+ e^-$	[b] (3.4 ± 0.4) × 10 ⁻⁵	

Lepton Family number (LF) violating modes

Mode	LF	[c] < 1.2 %	90%
Γ_4 $e^- \nu_e \bar{\nu}_\mu$	LF	< 1.2	× 10 ⁻¹¹
Γ_5 $e^- \gamma$	LF	< 1.0	× 10 ⁻¹²
Γ_6 $e^- e^+ e^-$	LF	< 7.2	× 10 ⁻¹¹
Γ_7 $e^- 2\gamma$	LF	< 7.2	× 10 ⁻¹¹

Lepton Particle Listings

 μ

[a] This only includes events with the γ energy > 10 MeV. Since the $e^- \bar{\nu}_e \nu_\mu$ and $e^- \bar{\nu}_e \nu_\mu \gamma$ modes cannot be clearly separated, we regard the latter mode as a subset of the former.

[b] See the Particle Listings below for the energy limits used in this measurement.

[c] A test of additive vs. multiplicative lepton family number conservation.

 μ^- BRANCHING RATIOS
 $\Gamma(e^- \bar{\nu}_e \nu_\mu \gamma) / \Gamma_{\text{total}}$ Γ_2 / Γ

VALUE	EVTS	DOCUMENT ID	TECN	CHG	COMMENT
0.014 ± 0.004		CRITTENDEN 61	CNTR		γ KE > 10 MeV
••• We do not use the following data for averages, fits, limits, etc. •••					
	862	BOGART 67	CNTR		γ KE > 14.5 MeV
0.0033 ± 0.0013		CRITTENDEN 61	CNTR		γ KE > 20 MeV
	27	ASHKIN 59	CNTR		

 $\Gamma(e^- \bar{\nu}_e \nu_\mu e^+ e^-) / \Gamma_{\text{total}}$ Γ_3 / Γ

VALUE (units 10^{-5})	EVTS	DOCUMENT ID	TECN	CHG	COMMENT
3.4 ± 0.2 ± 0.3	7443	10 BERTL 85	SPEC	+	SINDRUM
••• We do not use the following data for averages, fits, limits, etc. •••					
2.2 ± 1.5	7	11 CRITTENDEN 61	HLBC	+	$E(e^+ e^-) > 10$ MeV
2	1	12 GUREVICH 60	EMUL	+	
1.5 ± 1.0	3	13 LEE 59	HBC	+	

¹⁰BERTL 85 has transverse momentum cut $p_T > 17$ MeV/c. Systematic error was increased by us.

¹¹CRITTENDEN 61 count only those decays where total energy of either (e^+ , e^-) combination is > 10 MeV.

¹²GUREVICH 60 interpret their event as either virtual or real photon conversion. e^+ and e^- energies not measured.

¹³In the three LEE 59 events, the sum of energies $E(e^+) + E(e^-) + E(e^+)$ was 51 MeV, 55 MeV, and 33 MeV.

 $\Gamma(e^- \nu_e \bar{\nu}_\mu) / \Gamma_{\text{total}}$ Γ_4 / Γ

Forbidden by the additive conservation law for lepton family number. A multiplicative law predicts this branching ratio to be 1/2. For a review see NEMETHY 81.

VALUE	CL%	DOCUMENT ID	TECN	CHG	COMMENT
< 0.012	90	14 FREEDMAN 93	CNTR	+	ν oscillation search
••• We do not use the following data for averages, fits, limits, etc. •••					
< 0.018	90	KRAKAUER 91B	CALO	+	
< 0.05	90	15 BERGSMA 83	CALO		$\bar{\nu}_\mu e \rightarrow \mu^- \bar{\nu}_e$
< 0.09	90	JONKER 80	CALO		See BERGSMA 83
-0.001 ± 0.061		WILLIS 80	CNTR	+	
0.13 ± 0.15		BLIETSCHAU 78	HLBC	±	Avg. of 4 values
< 0.25	90	EICHTEIN 73	HLBC	+	

¹⁴FREEDMAN 93 limit on $\bar{\nu}_e$ observation is here interpreted as a limit on lepton family number violation.

¹⁵BERGSMA 83 gives a limit on the inverse muon decay cross-section ratio $\sigma(\bar{\nu}_\mu e^- \rightarrow \mu^- \bar{\nu}_e) / \sigma(\nu_\mu e^- \rightarrow \mu^- \nu_e)$, which is essentially equivalent to $\Gamma(e^- \nu_e \bar{\nu}_\mu) / \Gamma_{\text{total}}$ for small values like that quoted.

 $\Gamma(e^- \gamma) / \Gamma_{\text{total}}$ Γ_5 / Γ

Forbidden by lepton family number conservation.

VALUE (units 10^{-11})	CL%	DOCUMENT ID	TECN	CHG	COMMENT
< 1.2	90	BROOKS 99	SPEC	+	LAMPF
••• We do not use the following data for averages, fits, limits, etc. •••					
< 1.2	90	AHMED 02	SPEC	+	MEGA
< 4.9	90	BOLTON 88	CBOX	+	LAMPF
< 100	90	AZUELOS 83	CNTR	+	TRIUMF
< 17	90	KINNISON 82	SPEC	+	LAMPF
< 100	90	SCHAAF 80	ELEC	+	SIN

 $\Gamma(e^- e^+ e^-) / \Gamma_{\text{total}}$ Γ_6 / Γ

Forbidden by lepton family number conservation.

VALUE (units 10^{-12})	CL%	DOCUMENT ID	TECN	CHG	COMMENT
< 1.0	90	16 BELLGARDT 88	SPEC	+	SINDRUM
••• We do not use the following data for averages, fits, limits, etc. •••					
< 36	90	BARA NOV 91	SPEC	+	ARES
< 35	90	BOLTON 88	CBOX	+	LAMPF
< 2.4	90	16 BERTL 85	SPEC	+	SINDRUM
< 160	90	16 BERTL 84	SPEC	+	SINDRUM
< 130	90	16 BOLTON 84	CNTR		LAMPF

¹⁶These experiments assume a constant matrix element.

 $\Gamma(e^- 2\gamma) / \Gamma_{\text{total}}$ Γ_7 / Γ

Forbidden by lepton family number conservation.

VALUE (units 10^{-11})	CL%	DOCUMENT ID	TECN	CHG	COMMENT
< 7.2	90	BOLTON 88	CBOX	+	LAMPF
••• We do not use the following data for averages, fits, limits, etc. •••					
< 840	90	17 AZUELOS 83	CNTR	+	TRIUMF
< 5000	90	18 BOWMAN 78	CNTR		DEPOMMIER 77 data

¹⁷AZUELOS 83 uses the phase space distribution of BOWMAN 78.

¹⁸BOWMAN 78 assumes an interaction Lagrangian local on the scale of the inverse μ mass.

LIMIT ON $\mu^- \rightarrow e^-$ CONVERSION

Forbidden by lepton family number conservation.

 $\sigma(\mu^- 32S \rightarrow e^- 32S) / \sigma(\mu^- 32S \rightarrow \nu_\mu 32P^*)$

VALUE	CL%	DOCUMENT ID	TECN	COMMENT
< 7 × 10⁻¹¹	90	BADERT...	80	STRC SIN
••• We do not use the following data for averages, fits, limits, etc. •••				
< 4 × 10 ⁻¹⁰	90	BADERT...	77	STRC SIN

 $\sigma(\mu^- Cu \rightarrow e^- Cu) / \sigma(\mu^- Cu \rightarrow \text{capture})$

VALUE	CL%	DOCUMENT ID	TECN	COMMENT
••• We do not use the following data for averages, fits, limits, etc. •••				
< 1.6 × 10 ⁻⁸	90	BRYMAN 72	SPEC	

 $\sigma(\mu^- Ti \rightarrow e^- Ti) / \sigma(\mu^- Ti \rightarrow \text{capture})$

VALUE	CL%	DOCUMENT ID	TECN	COMMENT
< 4.3 × 10⁻¹²	90	19 DOHMEN 93	SPEC	SINDRUM II
••• We do not use the following data for averages, fits, limits, etc. •••				
< 4.6 × 10 ⁻¹²	90	AHMAD 88	TPC	TRIUMF
< 1.6 × 10 ⁻¹¹	90	BRYMAN 85	TPC	TRIUMF

¹⁹DOHMEN 93 assumes $\mu^- \rightarrow e^-$ conversion leaves the nucleus in its ground state, a process enhanced by coherence and expected to dominate.

 $\sigma(\mu^- Pb \rightarrow e^- Pb) / \sigma(\mu^- Pb \rightarrow \text{capture})$

VALUE	CL%	DOCUMENT ID	TECN	COMMENT
< 4.6 × 10⁻¹¹	90	HONECKER 96	SPEC	SINDRUM II
••• We do not use the following data for averages, fits, limits, etc. •••				
< 4.9 × 10 ⁻¹⁰	90	AHMAD 88	TPC	TRIUMF

 $\sigma(\mu^- Au \rightarrow e^- Au) / \sigma(\mu^- Au \rightarrow \text{capture})$

VALUE	CL%	DOCUMENT ID	TECN	CHG	COMMENT
< 7 × 10⁻¹³	90	BERTL 06	SPEC	-	SINDRUM II

LIMIT ON $\mu^- \rightarrow e^+$ CONVERSION

Forbidden by total lepton number conservation.

 $\sigma(\mu^- 32S \rightarrow e^+ 32Si^*) / \sigma(\mu^- 32S \rightarrow \nu_\mu 32P^*)$

VALUE	CL%	DOCUMENT ID	TECN	COMMENT
< 9 × 10⁻¹⁰	90	BADERT...	80	STRC SIN
••• We do not use the following data for averages, fits, limits, etc. •••				
< 1.5 × 10 ⁻⁹	90	BADERT...	78	STRC SIN

 $\sigma(\mu^- 127I \rightarrow e^+ 127Sb^*) / \sigma(\mu^- 127I \rightarrow \text{anything})$

VALUE	CL%	DOCUMENT ID	TECN	COMMENT
< 3 × 10⁻¹⁰	90	20 ABELA 80	CNTR	Radiochemical tech.

²⁰ABELA 80 is upper limit for $\mu^- e^+$ conversion leading to particle-stable states of ¹²⁷Sb. Limit for total conversion rate is higher by a factor less than 4 (G. Backenstoss, private communication).

 $\sigma(\mu^- Cu \rightarrow e^+ Co) / \sigma(\mu^- Cu \rightarrow \nu_\mu Ni)$

VALUE	CL%	DOCUMENT ID	TECN	COMMENT
••• We do not use the following data for averages, fits, limits, etc. •••				
< 2.6 × 10 ⁻⁸	90	BRYMAN 72	SPEC	
< 2.2 × 10 ⁻⁷	90	CONFORTO 62	OSP K	

 $\sigma(\mu^- Ti \rightarrow e^+ Ca) / \sigma(\mu^- Ti \rightarrow \text{capture})$

VALUE	CL%	EVTS	DOCUMENT ID	TECN	CHG	COMMENT
< 3.6 × 10⁻¹¹	90	1, 21, 22	KAULARD 98	SPEC	-	SINDRUM II
••• We do not use the following data for averages, fits, limits, etc. •••						
< 1.7 × 10 ⁻¹²	90	1, 22, 23	KAULARD 98	SPEC	-	SINDRUM II
< 4.3 × 10 ⁻¹²	90	23	DOHMEN 93	SPEC		SINDRUM II
< 8.9 × 10 ⁻¹¹	90	21	DOHMEN 93	SPEC		SINDRUM II
< 1.7 × 10 ⁻¹⁰	90	24	AHMAD 88	TPC		TRIUMF

²¹This limit assumes a giant resonance excitation of the daughter Ca nucleus (mean energy and width both 20 MeV).

²²KAULARD 98 obtained these same limits using the unified classical analysis of FELDMAN 98.

²³This limit assumes the daughter Ca nucleus is left in the ground state. However, the probability of this is unknown.

²⁴Assuming a giant-resonance-excitation model.

LIMIT ON MUONIUM \rightarrow ANTIMUONIUM CONVERSION

Forbidden by lepton family number conservation.

$$R_g = G_C / G_F$$

The effective Lagrangian for the $\mu^+ e^- \rightarrow \mu^- e^+$ conversion is assumed to be

$$\mathcal{L} = 2^{-1/2} G_C [\bar{\psi}_\mu \gamma_\lambda (1 - \gamma_5) \psi_e] [\bar{\psi}_\mu \gamma_\lambda (1 - \gamma_5) \psi_e] + \text{h.c.}$$

The experimental result is then an upper limit on G_C/G_F , where G_F is the Fermi coupling constant.

VALUE	CL%	EVS	DOCUMENT ID	TECN	CHG	COMMENT
< 0.0030	90	1	25 WILLMANN	99	SPEC +	μ^+ at 26 GeV/c
••• We do not use the following data for averages, fits, limits, etc. •••						
< 0.14	90	1	26 GORDEEV	97	SPEC +	JINR phasotron
< 0.018	90	0	27 ABELA	96	SPEC +	μ^+ at 24 MeV
< 6.9	90		NI	93	CBOX	LAMPF
< 0.16	90		MATTHIAS	91	SPEC	LAMPF
< 0.29	90		HUBER	90b	CNTR	TRIUMF
< 20	95		BEER	86	CNTR	TRIUMF
< 42	95		MARSHALL	82	CNTR	
25 WILLMANN 99 quote both probability $P_{MM} < 8.3 \times 10^{-11}$ at 90% CL in a 0.1 T field and $R_g = G_C/G_F$.						
26 GORDEEV 97 quote limits on both $f = G_{MM}/G_F$ and the probability $W_{MM} < 4.7 \times 10^{-7}$ (90% CL).						
27 ABELA 96 quote both probability $P_{MM} < 8 \times 10^{-9}$ at 90% CL and $R_g = G_C/G_F$.						

MUON DECAY PARAMETERS

Revised June 2007 by W. Fetscher and H.-J. Gerber (ETH Zürich).

Introduction: All measurements in direct muon decay, $\mu^- \rightarrow e^- + 2$ neutrals, and its inverse, $\nu_\mu + e^- \rightarrow \mu^- +$ neutral, are successfully described by the “V-A interaction,” which is a particular case of a local, derivative-free, lepton-number-conserving, four-fermion interaction [1]. As shown below, within this framework, the Standard Model assumptions, such as the V-A form and the nature of the neutrals (ν_μ and $\bar{\nu}_e$), and hence the doublet assignments ($\nu_e e^-$)_L and ($\nu_\mu \mu^-$)_L, have been determined from experiments [2,3]. All considerations on muon decay are valid for the leptonic tau decays $\tau \rightarrow \ell + \nu_\tau + \bar{\nu}_e$ with the replacements $m_\mu \rightarrow m_\tau$, $m_e \rightarrow m_\ell$.

Parameters: The differential decay probability to obtain an e^\pm with (reduced) energy between x and $x + dx$, emitted in the direction $\hat{\mathbf{x}}_3$ at an angle between ϑ and $\vartheta + d\vartheta$ with respect to the muon polarization vector \mathbf{P}_μ , and with its spin parallel to the arbitrary direction $\hat{\boldsymbol{\zeta}}$, neglecting radiative corrections, is given by

$$\frac{d^2\Gamma}{dx d\cos\vartheta} = \frac{m_\mu}{4\pi^3} W_{e\mu}^4 G_F^2 \sqrt{x^2 - x_0^2} \times (F_{\text{IS}}(x) \pm P_\mu \cos\vartheta F_{\text{AS}}(x)) \times [1 + \hat{\boldsymbol{\zeta}} \cdot \mathbf{P}_e(x, \vartheta)] \quad (1)$$

Here, $W_{e\mu} = \max(E_e) = (m_\mu^2 + m_e^2)/2m_\mu$ is the maximum e^\pm energy, $x = E_e/W_{e\mu}$ is the reduced energy, $x_0 = m_e/W_{e\mu} = 9.67 \times 10^{-3}$, and $P_\mu = |\mathbf{P}_\mu|$ is the degree of muon polarization. $\hat{\boldsymbol{\zeta}}$ is the direction in which a perfect polarization-sensitive electron detector is most sensitive. The isotropic part of the spectrum, $F_{\text{IS}}(x)$, the anisotropic part $F_{\text{AS}}(x)$, and the electron polarization, $\mathbf{P}_e(x, \vartheta)$, may be parametrized by the Michel parameter ρ [1], by η [4], by ξ and δ [5,6], etc. These are bilinear combinations of the coupling constants $g_{\mu e}^2$, which occur in the matrix element (given below).

If the masses of the neutrinos as well as x_0^2 are neglected, the energy and angular distribution of the electron in the rest frame of a muon (μ^\pm) measured by a polarization insensitive detector, is given by

$$\frac{d^2\Gamma}{dx d\cos\vartheta} \sim x^2 \cdot \left\{ 3(1-x) + \frac{2\rho}{3}(4x-3) + 3\eta x_0(1-x)/x \pm P_\mu \cdot \xi \cdot \cos\vartheta \left[1-x + \frac{2\delta}{3}(4x-3) \right] \right\} \quad (2)$$

Here, ϑ is the angle between the electron momentum and the muon spin, and $x \equiv 2E_e/m_\mu$. For the Standard Model coupling, we obtain $\rho = \xi\delta = 3/4$, $\xi = 1$, $\eta = 0$ and the differential decay rate is

$$\frac{d^2\Gamma}{dx d\cos\vartheta} = \frac{G_F^2 m_\mu^5}{192\pi^3} [3 - 2x \pm P_\mu \cos\vartheta(2x-1)] x^2 \quad (3)$$

The coefficient in front of the square bracket is the total decay rate.

If only the neutrino masses are neglected, and if the e^\pm polarization is detected, then the functions in Eq. (1) become

$$\begin{aligned} F_{\text{IS}}(x) &= x(1-x) + \frac{2}{9} \rho(4x^2 - 3x - x_0^2) + \eta \cdot x_0(1-x) \\ F_{\text{AS}}(x) &= \frac{1}{3} \xi \sqrt{x^2 - x_0^2} \\ &\quad \times [1 - x + \frac{2}{3} \delta(4x - 3) + (\sqrt{1 - x_0^2} - 1)] \\ \mathbf{P}_e(x, \vartheta) &= P_{T_1} \cdot \hat{\mathbf{x}}_1 + P_{T_2} \cdot \hat{\mathbf{x}}_2 + P_L \cdot \hat{\mathbf{x}}_3 \end{aligned} \quad (4)$$

Here $\hat{\mathbf{x}}_1$, $\hat{\mathbf{x}}_2$, and $\hat{\mathbf{x}}_3$ are orthogonal unit vectors defined as follows:

$$\begin{aligned} \hat{\mathbf{x}}_3 &\text{ is along the } e \text{ momentum } \mathbf{p}_e \\ \frac{\hat{\mathbf{x}}_3 \times \mathbf{P}_\mu}{|\hat{\mathbf{x}}_3 \times \mathbf{P}_\mu|} &= \hat{\mathbf{x}}_2 \text{ is transverse to } \mathbf{p}_e \text{ and perpendicular to the “decay plane”} \\ \hat{\mathbf{x}}_2 \times \hat{\mathbf{x}}_3 &= \hat{\mathbf{x}}_1 \text{ is transverse to the } \mathbf{p}_e \text{ and in the “decay plane.”} \end{aligned}$$

The components of \mathbf{P}_e then are given by

$$\begin{aligned} P_{T_1}(x, \vartheta) &= P_\mu \sin\vartheta \cdot F_{T_1}(x) / (F_{\text{IS}}(x) \pm P_\mu \cos\vartheta \cdot F_{\text{AS}}(x)) \\ P_{T_2}(x, \vartheta) &= P_\mu \sin\vartheta \cdot F_{T_2}(x) / (F_{\text{IS}}(x) \pm P_\mu \cos\vartheta \cdot F_{\text{AS}}(x)) \\ P_L(x, \vartheta) &= \left(\pm F_{\text{IP}}(x) + P_\mu \cos\vartheta \right. \\ &\quad \left. \times F_{\text{AP}}(x) \right) / (F_{\text{IS}}(x) \pm P_\mu \cos\vartheta \cdot F_{\text{AS}}(x)) \end{aligned} \quad ,$$

where

$$\begin{aligned} F_{T_1}(x) &= \frac{1}{12} \left\{ -2 \left[\xi'' + 12(\rho - \frac{3}{4}) \right] (1-x)x_0 \right. \\ &\quad \left. - 3\eta(x^2 - x_0^2) + \eta''(-3x^2 + 4x - x_0^2) \right\} \\ F_{T_2}(x) &= \frac{1}{3} \sqrt{x^2 - x_0^2} \left\{ 3 \frac{\alpha'}{A} (1-x) + 2 \frac{\beta'}{A} \sqrt{1-x_0^2} \right\} \\ F_{\text{IP}}(x) &= \frac{1}{54} \sqrt{x^2 - x_0^2} \left\{ 9\xi' \left(-2x + 2 + \sqrt{1-x_0^2} \right) \right. \\ &\quad \left. + 4\xi(\delta - \frac{3}{4})(4x - 4 + \sqrt{1-x_0^2}) \right\} \\ F_{\text{AP}}(x) &= \frac{1}{6} \left\{ \xi''(2x^2 - x - x_0^2) + 4(\rho - \frac{3}{4})(4x^2 - 3x - x_0^2) \right. \\ &\quad \left. + 2\eta''(1-x)x_0 \right\} \end{aligned} \quad (5)$$

Lepton Particle Listings

μ

For the experimental values of the parameters ρ , ξ , ξ' , ξ'' , δ , η , η'' , α/A , β/A , α'/A , β'/A , which are not all independent, see the Data Listings below. Experiments in the past have also been analyzed using the parameters a , b , c , a' , b' , c' , α/A , β/A , α'/A , β'/A (and $\eta = (\alpha - 2\beta)/2A$), as defined by Kinoshita and Sirlin [5,6]. They serve as a model-independent summary of all possible measurements on the decay electron (see Listings below). The relations between the two sets of parameters are

$$\begin{aligned}\rho - \frac{3}{4} &= \frac{3}{4}(-a + 2c)/A, \\ \eta &= (\alpha - 2\beta)/A, \\ \eta'' &= (3\alpha + 2\beta)/A, \\ \delta - \frac{3}{4} &= \frac{9}{4} \cdot \frac{(a' - 2c')/A}{1 - [a + 3a' + 4(b + b') + 6c - 14c']/A}, \\ 1 - \xi \frac{\delta}{\rho} &= 4 \frac{[(b + b') + 2(c - c')]/A}{1 - (a - 2c)/A}, \\ 1 - \xi' &= [(a + a') + 4(b + b') + 6(c + c')]/A, \\ 1 - \xi'' &= (-2a + 20c)/A,\end{aligned}$$

where

$$A = a + 4b + 6c. \quad (6)$$

The differential decay probability to obtain a *left-handed* ν_e with (reduced) energy between y and $y + dy$, neglecting radiative corrections as well as the masses of the electron and of the neutrinos, is given by [7]

$$\frac{d\Gamma}{dy} = \frac{m_\mu^5 G_F^2}{16\pi^3} \cdot Q_L^{\nu_e} \cdot y^2 \left\{ (1 - y) - \omega_L \cdot (y - \frac{3}{4}) \right\}. \quad (7)$$

Here, $y = 2 E_{\nu_e}/m_\mu$. $Q_L^{\nu_e}$ and ω_L are parameters. ω_L is the neutrino analog of the spectral shape parameter ρ of Michel. Since in the Standard Model, $Q_L^{\nu_e} = 1$, $\omega_L = 0$, the measurement of $d\Gamma/dy$ has allowed a null-test of the Standard Model (see Listings below).

Matrix element: All results in direct muon decay (energy spectra of the electron and of the neutrinos, polarizations, and angular distributions), and in inverse muon decay (the reaction cross section) at energies well below $m_W c^2$, may be parametrized in terms of amplitudes $g_{\varepsilon\mu}^\gamma$ and the Fermi coupling constant G_F , using the matrix element

$$\frac{4G_F}{\sqrt{2}} \sum_{\substack{\gamma=S,V,T \\ \varepsilon,\mu=R,L}} g_{\varepsilon\mu}^\gamma \langle \bar{e}_\varepsilon | \Gamma^\gamma | (\nu_e)_n \rangle \langle (\bar{\nu}_\mu)_m | \Gamma_\gamma | \mu_\mu \rangle. \quad (8)$$

We use the notation of Fetscher *et al.* [2], who in turn use the sign conventions and definitions of Scheck [8]. Here, $\gamma = S, V, T$ indicates a scalar, vector, or tensor interaction; and $\varepsilon, \mu = R, L$ indicate a right- or left-handed chirality of the electron or muon. The chiralities n and m of the ν_e and $\bar{\nu}_\mu$ are then determined by the values of γ, ε , and μ . The particles are represented by fields of definite chirality [9].

As shown by Langacker and London [10], explicit lepton-number nonconservation still leads to a matrix element equivalent to Eq. (8). They conclude that it is not possible, even in

principle, to test lepton-number conservation in (leptonic) muon decay if the final neutrinos are massless and are not observed.

The ten complex amplitudes $g_{\varepsilon\mu}^\gamma$ (g_{RR}^T and g_{LL}^T are identically zero) and G_F constitute 19 independent (real) parameters to be determined by experiment. The Standard Model interaction corresponds to one single amplitude g_{LL}^V being unity and all the others being zero.

The (direct) muon decay experiments are compatible with an arbitrary mix of the scalar and vector amplitudes g_{LL}^S and g_{LL}^V – in the extreme even with purely scalar $g_{LL}^S = 2$, $g_{LL}^V = 0$. The decision in favour of the Standard Model comes from the quantitative observation of inverse muon decay, which would be forbidden for pure g_{LL}^S [2].

Experimental determination of V–A: In order to determine the amplitudes $g_{\varepsilon\mu}^\gamma$ uniquely from experiment, the following set of equations, where the left-hand sides represent experimental results, has to be solved.

$$\begin{aligned}a &= 16(|g_{RL}^V|^2 + |g_{LR}^V|^2) + |g_{RL}^S + 6g_{RL}^T|^2 + |g_{LR}^S + 6g_{LR}^T|^2 \\ a' &= 16(|g_{RL}^V|^2 - |g_{LR}^V|^2) + |g_{RL}^S + 6g_{RL}^T|^2 - |g_{LR}^S + 6g_{LR}^T|^2 \\ \alpha &= 8\text{Re} \left\{ g_{RL}^V (g_{LR}^{S*} + 6g_{LR}^{T*}) + g_{LR}^V (g_{RL}^{S*} + 6g_{RL}^{T*}) \right\} \\ \alpha' &= 8\text{Im} \left\{ g_{LR}^V (g_{RL}^{S*} + 6g_{RL}^{T*}) - g_{RL}^V (g_{LR}^{S*} + 6g_{LR}^{T*}) \right\} \\ b &= 4(|g_{RR}^V|^2 + |g_{LL}^V|^2) + |g_{RR}^S|^2 + |g_{LL}^S|^2 \\ b' &= 4(|g_{RR}^V|^2 - |g_{LL}^V|^2) + |g_{RR}^S|^2 - |g_{LL}^S|^2 \\ \beta &= -4\text{Re} \left\{ g_{RR}^V g_{LL}^{S*} + g_{LL}^V g_{RR}^{S*} \right\} \\ \beta' &= 4\text{Im} \left\{ g_{RR}^V g_{LL}^{S*} - g_{LL}^V g_{RR}^{S*} \right\} \\ c &= \frac{1}{2} \left\{ |g_{RL}^S - 2g_{RL}^T|^2 + |g_{LR}^S - 2g_{LR}^T|^2 \right\} \\ c' &= \frac{1}{2} \left\{ |g_{RL}^S - 2g_{RL}^T|^2 - |g_{LR}^S - 2g_{LR}^T|^2 \right\}\end{aligned}$$

and

$$\begin{aligned}Q_L^{\nu_e} &= 1 - \left\{ \frac{1}{4}|g_{LR}^S|^2 + \frac{1}{4}|g_{LL}^S|^2 + |g_{RR}^V|^2 + |g_{RL}^V|^2 + 3|g_{LR}^T|^2 \right\} \\ \omega_L &= \frac{3}{4} \frac{\{|g_{RR}^S|^2 + 4|g_{LR}^V|^2 + |g_{RL}^S + 2g_{RL}^T|^2\}}{|g_{RL}^S|^2 + |g_{RR}^S|^2 + 4|g_{LL}^V|^2 + 4|g_{LR}^V|^2 + 12|g_{RL}^T|^2}.\end{aligned}$$

It has been noted earlier by C. Jarlskog [11], that certain experiments observing the decay electron are especially informative if they yield the *V–A* values. The complete solution is now found as follows. Fetscher *et al.* [2] introduced four probabilities $Q_{\varepsilon\mu}(\varepsilon, \mu = R, L)$ for the decay of a μ -handed muon into an ε -handed electron, and showed that there exist upper bounds on Q_{RR} , Q_{LR} , and Q_{RL} , and a lower bound on Q_{LL} . These probabilities are given in terms of the $g_{\varepsilon\mu}^\gamma$'s by

$$Q_{\varepsilon\mu} = \frac{1}{4}|g_{\varepsilon\mu}^S|^2 + |g_{\varepsilon\mu}^V|^2 + 3(1 - \delta_{\varepsilon\mu})|g_{\varepsilon\mu}^T|^2, \quad (9)$$

where $\delta_{\varepsilon\mu} = 1$ for $\varepsilon = \mu$, and $\delta_{\varepsilon\mu} = 0$ for $\varepsilon \neq \mu$. They are related to the parameters a , b , c , a' , b' , and c' by

$$\begin{aligned}
Q_{RR} &= 2(b + b')/A, \\
Q_{LR} &= [(a - a') + 6(c - c')]/2A, \\
Q_{RL} &= [(a + a') + 6(c + c')]/2A, \\
Q_{LL} &= 2(b - b')/A,
\end{aligned} \tag{10}$$

with $A = 16$. In the Standard Model, $Q_{LL} = 1$ and the others are zero.

Since the upper bounds on Q_{RR} , Q_{LR} , and Q_{RL} are found to be small, and since the helicity of the ν_μ in pion decay is known from experiment [12,13] to very high precision to be -1 [14], the cross section S of *inverse* muon decay, normalized to the V - A value, yields [2]

$$|g_{LL}^S|^2 \leq 4(1 - S) \tag{11}$$

and

$$|g_{LL}^V|^2 = S. \tag{12}$$

Thus the Standard Model assumption of a pure V - A leptonic charged weak interaction of e and μ is derived (within errors) from experiments at energies far below mass of the W^\pm : Eq. (12) gives a lower limit for V - A , and Eqs. (9) and (11) give upper limits for the other four-fermion interactions. The existence of such upper limits may also be seen from $Q_{RR} + Q_{RL} = (1 - \xi')/2$ and $Q_{RR} + Q_{LR} = \frac{1}{2}(1 + \xi/3 - 16 \xi\delta/9)$. Table 1 gives the current experimental limits on the magnitudes of the $g_{e\mu}^2$'s. More stringent limits on the six coupling constants g_{LR}^S , g_{LR}^V , g_{LR}^T , g_{RL}^S , g_{RL}^V , and g_{RL}^T have been derived from upper limits on the neutrino mass [17]. Limits on the ‘‘charge retention’’ coordinates, as used in the older literature (*e.g.*, Ref. 18), are given by Burkard *et al.* [19].

Table 1. Coupling constants $g_{e\mu}^2$. Ninety-percent confidence level experimental limits. The limits on $|g_{LL}^S|$ and $|g_{LL}^V|$ are from Ref. 15, and the others from a general analysis of muon decay measurements [16]. The experimental uncertainty on the muon polarization in pion decay is included. Note that, by definition, $|g_{e\mu}^S| \leq 2$, $|g_{e\mu}^V| \leq 1$ and $|g_{e\mu}^T| \leq 1/\sqrt{3}$.

$ g_{RR}^S < 0.067$	$ g_{RR}^V < 0.034$	$ g_{RR}^T \equiv 0$
$ g_{LR}^S < 0.088$	$ g_{LR}^V < 0.036$	$ g_{LR}^T < 0.025$
$ g_{RL}^S < 0.417$	$ g_{RL}^V < 0.104$	$ g_{RL}^T < 0.104$
$ g_{LL}^S < 0.550$	$ g_{LL}^V > 0.960$	$ g_{LL}^T \equiv 0$
$ g_{LR}^S + 6g_{LR}^T < 0.143$	$ g_{RL}^S + 6g_{RL}^T < 0.418$	
$ g_{LR}^S + 2g_{LR}^T < 0.108$	$ g_{RL}^S + 2g_{RL}^T < 0.417$	
$ g_{LR}^S - 2g_{LR}^T < 0.070$	$ g_{RL}^S - 2g_{RL}^T < 0.418$	

References

- L. Michel, Proc. Phys. Soc. **A63**, 514 (1950).
- W. Fetscher, H.-J. Gerber, and K.F. Johnson, Phys. Lett. **B173**, 102 (1986).
- P. Langacker, Comm. Nucl. Part. Phys. **19**, 1 (1989).
- C. Bouchiat and L. Michel, Phys. Rev. **106**, 170 (1957).
- T. Kinoshita and A. Sirlin, Phys. Rev. **107**, 593 (1957).
- T. Kinoshita and A. Sirlin, Phys. Rev. **108**, 844 (1957).
- W. Fetscher, Phys. Rev. **D49**, 5945 (1994).
- F. Scheck, in *Electroweak and Strong Interactions* (Springer Verlag, 1996).
- K. Mursula and F. Scheck, Nucl. Phys. **B253**, 189 (1985).
- P. Langacker and D. London, Phys. Rev. **D39**, 266 (1989).
- C. Jarlskog, Nucl. Phys. **75**, 659 (1966).
- A. Jodidio *et al.*, Phys. Rev. **D34**, 1967 (1986); A. Jodidio *et al.*, Phys. Rev. **D37**, 237 (1988).
- L.Ph. Roesch *et al.*, Helv. Phys. Acta **55**, 74 (1982).
- W. Fetscher, Phys. Lett. **140B**, 117 (1984).
- S.R. Mishra *et al.*, Phys. Lett. **B252**, 170 (1990); S.R. Mishra, private communication; See also P. Vilain *et al.*, Phys. Lett. **B364**, 121 (1995).
- C.A. Gagliardi, R.E. Tribble, and N.J. Williams, Phys. Rev. **D72**, 073002 (2005).
- Gary Prézeau and Andriy Kurylov, Phys. Rev. Lett. **95**, 101802 (2005).
- S.E. Derenzo, Phys. Rev. **181**, 1854 (1969).
- H. Burkard *et al.*, Phys. Lett. **160B**, 343 (1985).

μ DECAY PARAMETERS

ρ PARAMETER

(V - A) theory predicts $\rho = 0.75$.

VALUE	EVTs	DOCUMENT ID	TECN	CHG	COMMENT	
0.7509 ± 0.0010 OUR AVERAGE						
0.75080 ± 0.00032 ± 0.00100	6G	²⁸ MUSSER	05	SPEC	+	surface μ^+ at TRIUMF
0.7518 ± 0.0026		DERENZO	69	RVUE		
• • • We do not use the following data for averages, fits, limits, etc. • • •						
0.72 ± 0.06 ± 0.08		AMORUSO	04	ICAR		Liquid Ar TPC
0.762 ± 0.008	170k	²⁹ FRYBERGER	68	ASPK	+	25-53 MeV e^+
0.760 ± 0.009	280k	²⁹ SHERWOOD	67	ASPK	+	25-53 MeV e^+
0.7503 ± 0.0026	800k	²⁹ PEOPLES	66	ASPK	+	20-53 MeV e^+

²⁸The quoted systematic error includes a contribution of 0.00023 (added in quadrature) from the dependence on the Michel parameter η .

²⁹ η constrained = 0. These values incorporated into a two parameter fit to ρ and η by DERENZO 69.

η PARAMETER

(V - A) theory predicts $\eta = 0$.

VALUE	EVTs	DOCUMENT ID	TECN	CHG	COMMENT	
0.001 ± 0.024 OUR AVERAGE						
0.071 ± 0.037 ± 0.005	30M	DANNEBERG	05	CNTR	+	7-53 MeV e^+
-0.007 ± 0.013	5.3M	³⁰ BURKARD	85B	FIT	+	9-53 MeV e^+
-0.12 ± 0.21	6346	DERENZO	69	HBC	+	1.6-6.8 MeV e^+
• • • We do not use the following data for averages, fits, limits, etc. • • •						
-0.0021 ± 0.0070 ± 0.0010	30M	³¹ DANNEBERG	05	CNTR	+	7-53 MeV e^+
-0.012 ± 0.015 ± 0.003	5.3M	³¹ BURKARD	85B	CNTR	+	9-53 MeV e^+
0.011 ± 0.081 ± 0.026	5.3M	BURKARD	85B	CNTR	+	9-53 MeV e^+
-0.7 ± 0.5	170k	³² FRYBERGER	68	ASPK	+	25-53 MeV e^+
-0.7 ± 0.6	280k	³² SHERWOOD	67	ASPK	+	25-53 MeV e^+
0.05 ± 0.5	800k	³² PEOPLES	66	ASPK	+	20-53 MeV e^+
-2.0 ± 0.9	9213	³³ PLANO	60	HBC	+	Whole spectrum e^+

³⁰Global fit to all measured parameters. Correlation coefficients are given in BURKARD 85B.

³¹ $\alpha = \alpha' = 0$ assumed.

³² ρ constrained = 0.75.

³³Two parameter fit to ρ and η ; PLANO 60 discounts value for η .

δ PARAMETER

(V - A) theory predicts $\delta = 0.75$.

VALUE	EVTs	DOCUMENT ID	TECN	CHG	COMMENT	
0.7495 ± 0.0012 OUR AVERAGE						
0.74964 ± 0.00066 ± 0.00112	6G	GAPONENKO	05	SPEC	+	surface μ^+ at TRIUMF
0.7486 ± 0.0026 ± 0.0028		³⁴ BALKE	88	SPEC	+	Surface μ^+ 's

Lepton Particle Listings

 μ

••• We do not use the following data for averages, fits, limits, etc. •••

VALUE	EVTS	DOCUMENT ID	TECN	CHG	COMMENT
0.752 ± 0.009	490k	35 VOSSLER 69	FRYBERGER 68	ASPK +	25–53 MeV e^+
0.782 ± 0.031		KRUGER 61			
0.78 ± 0.05	8354	PLANO 60	HBC +		Whole spectrum

³⁴ BALKE 88 uses $\rho = 0.752 \pm 0.003$.

³⁵ VOSSLER 69 has measured the asymmetry below 10 MeV. See comments about radiative corrections in VOSSLER 69.

[(ξ PARAMETER) × (μ LONGITUDINAL POLARIZATION)]

($V-A$) theory predicts $\xi = 1$, longitudinal polarization = 1.

VALUE	EVTS	DOCUMENT ID	TECN	CHG	COMMENT
1.0007 ± 0.0035 OUR AVERAGE					
1.0003 ± 0.0006 ± 0.0038		JAMIESON 06	TWST +		surface μ^+ beam
1.0027 ± 0.0079 ± 0.0030		BELTRAMI 87	CNTR		SIN, π decay in flight

••• We do not use the following data for averages, fits, limits, etc. •••

1.0013 ± 0.0030 ± 0.0053		36 IMAZATO 92	SPEC +		$K^+ \rightarrow \mu^+ \nu_\mu$
0.975 ± 0.015		AKHMANOV 68	EMUL		140 kG
0.975 ± 0.030	66k	GUREVICH 64	EMUL		See AKHMANOV 68
0.903 ± 0.027		37 ALI-ZADE 61	EMUL +		27 kG
0.93 ± 0.06	8354	PLANO 60	HBC +		8.8 kG
0.97 ± 0.05	9k	BARDON 59	CNTR		Bromoform target

³⁶ The corresponding 90% confidence limit from IMAZATO 92 is $|\xi P_\mu| > 0.990$. This measurement is of K^+ decay, not π^+ decay, so we do not include it in an average, nor do we yet set up a separate data block for K results.

³⁷ Depolarization by medium not known sufficiently well.

$\xi \times (\mu$ LONGITUDINAL POLARIZATION) $\times \delta / \rho$

VALUE	CL%	DOCUMENT ID	TECN	CHG	COMMENT
> 0.99682	90	38 JODIDIO 86	SPEC +		TRIUMF

••• We do not use the following data for averages, fits, limits, etc. •••

> 0.9966	90	39 STOKER 85	SPEC +		μ -spin rotation
> 0.9959	90	CARR 83	SPEC +		11 kG

³⁸ JODIDIO 86 includes data from CARR 83 and STOKER 85. The value here is from the erratum.

³⁹ STOKER 85 find $(\xi P_\mu \delta / \rho) > 0.9955$ and > 0.9966 , where the first limit is from new μ spin-rotation data and the second is from combination with CARR 83 data. In $V-A$ theory, $(\delta / \rho) = 1.0$.

$\xi' =$ LONGITUDINAL POLARIZATION OF e^+

($V-A$) theory predicts the longitudinal polarization = ± 1 for e^\pm , respectively. We have flipped the sign for e^- so our programs can average.

VALUE	EVTS	DOCUMENT ID	TECN	CHG	COMMENT
1.00 ± 0.04 OUR AVERAGE					
0.998 ± 0.045	1M	BURKARD 85	CNTR +		Bhabha + annihilation
0.89 ± 0.28	29k	SCHWARTZ 67	OSPK -		Moller scattering
1.04 ± 0.38		BLOOM 64	CNTR +		Brems. transmiss.
1.04 ± 0.18		DUCLOS 64	CNTR +		Bhabha scattering
1.05 ± 0.30		BUHLER 63	CNTR +		Annihilation

ξ'' PARAMETER

VALUE	EVTS	DOCUMENT ID	TECN	CHG	COMMENT
0.65 ± 0.36	326k	40 BURKARD 85	CNTR +		Bhabha + annihilation

⁴⁰ BURKARD 85 measure $(\xi'' - \xi \xi') / \xi$ and ξ' and set $\xi = 1$.

TRANSVERSE e^+ POLARIZATION IN PLANE OF μ SPIN, e^+ MOMENTUM

VALUE (units 10^{-3})	EVTS	DOCUMENT ID	TECN	CHG	COMMENT
7 ± 8 OUR AVERAGE					
6.3 ± 7.7 ± 3.4	30M	DANNEBERG 05	CNTR +		7–53 MeV e^+
16 ± 21 ± 10	5.3M	BURKARD 85B	CNTR +		Annihil 9–53 MeV

TRANSVERSE e^+ POLARIZATION NORMAL TO PLANE OF μ SPIN, e^+ MOMENTUM

Zero if T invariance holds.

VALUE (units 10^{-3})	EVTS	DOCUMENT ID	TECN	CHG	COMMENT
-2 ± 8 OUR AVERAGE					
-3.7 ± 7.7 ± 3.4	30M	DANNEBERG 05	CNTR +		7–53 MeV e^+
7 ± 22 ± 7	5.3M	BURKARD 85B	CNTR +		Annihil 9–53 MeV

α/A

VALUE (units 10^{-3})	EVTS	DOCUMENT ID	TECN	CHG	COMMENT
0.4 ± 4.3		41 BURKARD 85B	FIT		

••• We do not use the following data for averages, fits, limits, etc. •••

15 ± 50 ± 14	5.3M	BURKARD 85B	CNTR +		9–53 MeV e^+
--------------	------	-------------	--------	--	----------------

⁴¹ Global fit to all measured parameters. Correlation coefficients are given in BURKARD 85B.

α'/A

Zero if T invariance holds.

VALUE (units 10^{-3})	EVTS	DOCUMENT ID	TECN	CHG	COMMENT
0 ± 4 OUR AVERAGE					
-3.4 ± 21.3 ± 4.9	30M	DANNEBERG 05	CNTR +		7–53 MeV e^+
-0.2 ± 4.3		42 BURKARD 85B	FIT		

••• We do not use the following data for averages, fits, limits, etc. •••

-47 ± 50 ± 14	5.3M	43 BURKARD 85B	CNTR +		9–53 MeV e^+
---------------	------	----------------	--------	--	----------------

⁴² Global fit to all measured parameters. Correlation coefficients are given in BURKARD 85B.

⁴³ BURKARD 85B measure e^+ polarizations P_{T_1} and P_{T_2} versus e^+ energy.

β/A

VALUE (units 10^{-3})	EVTS	DOCUMENT ID	TECN	CHG	COMMENT
3.9 ± 6.2		44 BURKARD 85B	FIT		

••• We do not use the following data for averages, fits, limits, etc. •••

2 ± 17 ± 6	5.3M	BURKARD 85B	CNTR +		9–53 MeV e^+
------------	------	-------------	--------	--	----------------

⁴⁴ Global fit to all measured parameters. Correlation coefficients are given in BURKARD 85B.

β'/A

Zero if T invariance holds.

VALUE (units 10^{-3})	EVTS	DOCUMENT ID	TECN	CHG	COMMENT
1 ± 5 OUR AVERAGE					
-0.5 ± 7.8 ± 1.8	30M	DANNEBERG 05	CNTR +		7–53 MeV e^+
1.5 ± 6.3		45 BURKARD 85B	FIT		

••• We do not use the following data for averages, fits, limits, etc. •••

-1.3 ± 3.5 ± 0.6	30M	46 DANNEBERG 05	CNTR +		7–53 MeV e^+
17 ± 17 ± 6	5.3M	47 BURKARD 85B	CNTR +		9–53 MeV e^+

⁴⁵ Global fit to all measured parameters. Correlation coefficients are given in BURKARD 85B.

⁴⁶ $\alpha = \alpha' = 0$ assumed.

⁴⁷ BURKARD 85B measure e^+ polarizations P_{T_1} and P_{T_2} versus e^+ energy.

a/A

This comes from an alternative parameterization to that used in the Summary Table (see the "Note on Muon Decay Parameters" above).

VALUE (units 10^{-3})	CL%	DOCUMENT ID	TECN	CHG	COMMENT
< 15.9	90	48 BURKARD 85B	FIT		

••• We do not use the following data for averages, fits, limits, etc. •••

⁴⁸ Global fit to all measured parameters. Correlation coefficients are given in BURKARD 85B.

a'/A

This comes from an alternative parameterization to that used in the Summary Table (see the "Note on Muon Decay Parameters" above).

VALUE (units 10^{-3})	DOCUMENT ID	TECN	CHG	COMMENT
5.3 ± 4.1	49 BURKARD 85B	FIT		

••• We do not use the following data for averages, fits, limits, etc. •••

⁴⁹ Global fit to all measured parameters. Correlation coefficients are given in BURKARD 85B.

$(b'+b)/A$

This comes from an alternative parameterization to that used in the Summary Table (see the "Note on Muon Decay Parameters" above).

VALUE (units 10^{-3})	CL%	DOCUMENT ID	TECN	CHG	COMMENT
< 1.04	90	50 BURKARD 85B	FIT		

••• We do not use the following data for averages, fits, limits, etc. •••

⁵⁰ Global fit to all measured parameters. Correlation coefficients are given in BURKARD 85B.

c/A

This comes from an alternative parameterization to that used in the Summary Table (see the "Note on Muon Decay Parameters" above).

VALUE (units 10^{-3})	CL%	DOCUMENT ID	TECN	CHG	COMMENT
< 6.4	90	51 BURKARD 85B	FIT		

••• We do not use the following data for averages, fits, limits, etc. •••

⁵¹ Global fit to all measured parameters. Correlation coefficients are given in BURKARD 85B.

c'/A

This comes from an alternative parameterization to that used in the Summary Table (see the "Note on Muon Decay Parameters" above).

VALUE (units 10^{-3})	DOCUMENT ID	TECN	CHG	COMMENT
3.5 ± 2.0	52 BURKARD 85B	FIT		

••• We do not use the following data for averages, fits, limits, etc. •••

⁵² Global fit to all measured parameters. Correlation coefficients are given in BURKARD 85B.

τ PARAMETER(V-A) theory predicts $\overline{\tau} = 0$. $\overline{\tau}$ affects spectrum of radiative muon decay.

VALUE	DOCUMENT ID	TECN	CHG	COMMENT
0.02 ± 0.08 OUR AVERAGE				
-0.014 ± 0.090	EICHENBER... 84	ELEC	+	ρ free
+0.09 ± 0.14	BOGART 67	CNTR	+	
• • • We do not use the following data for averages, fits, limits, etc. • • •				
-0.035 ± 0.098	EICHENBER... 84	ELEC	+	$\rho=0.75$ assumed

 μ REFERENCES

MOHR 06	arXiv:0801.0028[atomp-ph]	P.J. Mohr, B.N. Taylor, D.B. Newell	(NIST)
to appear in RMP and JPCRD			
CHITWOOD 07	PRL 99 032001	D.B. Chitwood et al.	(MULAN Collab.)
BENNETT 06	PR D73 072003	G.W. Bennett et al.	(MUG-2 Collab.)
BERTL 06	EPJ C47 337	W. Bertl et al.	(SINDRUM II Collab.)
JAMIESON 06	PR D74 072007	B. Jamieson et al.	(TWIST Collab.)
DANNEBERG 05	PRL 94 021802	N. Danneberg et al.	(ETH, JAGL, PSI+)
GAPONENKO 05	PR D71 071101R	A. Gaponenko et al.	(TWIST Collab.)
MOHR 05	RMP 77 1	P.J. Mohr, B.N. Taylor	(NIST)
MUSSER 05	PRL 94 101805	J.R. Musser et al.	(TWIST Collab.)
AMORUSSO 04	EPJ C33 233	S. Amoruso et al.	(ICARUS Collab.)
BENNETT 04	PRL 92 161802	G.W. Bennett et al.	(Muon(g-2) Collab.)
AHMED 02	PR D65 112002	M. Ahmed et al.	(MEGA Collab.)
BENNETT 02	PRL 89 101804	G.W. Bennett et al.	(Muon(g-2) Collab.)
BROWN 01	PRL 86 2227	H.N. Brown et al.	(Muon(g-2) Collab.)
BROWN 00	PR D62 091101R	H.N. Brown et al.	(BNL/G-2 Collab.)
MEYER 00	PRL 84 1136	V. Meyer et al.	
BROOKS 99	PRL 83 1521	M.L. Brooks et al.	(MEGA/LAMPF Collab.)
HUGHES 99	RMP 71 5133	V.W. Hughes, T. Kinoshita	
LIU 99	PRL 82 711	W. Liu et al.	(LAMPF Collab.)
MOHR 99	JPCRD 28 1713	P.J. Mohr, B.N. Taylor	(NIST)
Also RMP 72 351		P.J. Mohr, B.N. Taylor	(NIST)
WILLMANN 99	PRL 82 49	L. Willmann et al.	
FELDMAN 98	PR D57 3873	G.J. Feldman, R.D. Cousins	
KAULARD 98	PL B422 334	J. Kaulard et al.	(SINDRUM-II Collab.)
GORDEEV 97	PAN 60 1164	V.A. Gordeev et al.	(PNPI)
Translated from YAF 60 1291.			
ABELA 96	PRL 77 1950	R. Abela et al.	(PSI, ZURI, HEIDH, TBIL+)
HONECKER 96	PRL 76 200	W. Honecker et al.	(SINDRUM II Collab.)
DOHMEN 93	PL B317 631	C. Dolmen et al.	(PSI SINDRUM-II Collab.)
FREEDMAN 93	PR D47 811	S.J. Freedman et al.	(LAMPF E645 Collab.)
NI 93	PR D48 1976	B. Ni et al.	(LAMPF CrystalBox Collab.)
IMAZATO 92	PRL 69 877	J. Imaizato et al.	(KEK, INUS, TOKY+)
BARANOV 91	SJNP 53 802	V.A. Baranov et al.	(JINR)
Translated from YAF 53 1302.			
KRAKAUER 91B	PL B263 534	D.A. Krakauer et al.	(UMD, UCI, LANL)
MATTHIAS 91	PRL 66 2716	B.E. Matthias et al.	(YALE, HEIDP, WILL+)
Also PRL 67 932 (erratum)		B.E. Matthias et al.	(YALE, HEIDP, WILL+)
HUBER 90B	PR D41 2709	T.M. Huber et al.	(WYOM, VICT, ARIZ+)
AHMAD 88	PR D38 2102	S. Ahmad et al.	(TRIU, VICT, VPI, BRCO+)
Also PR 59 970		S. Ahmad et al.	(TRIU, VPI, VICT, BRCO+)
BALKE 88	PR D37 587	B. Balke et al.	(LBL, UCB, COLO, NWES+)
BELLGARDT 88	NP B299 1	U. Bellgardt et al.	(SINDRUM Collab.)
BOLTON 88	PR D38 2077	R.D. Bolton et al.	(LANL, STAN, CHIC+)
Also PRL 56 2461		R.D. Bolton et al.	(LANL, STAN, CHIC+)
Also PRL 57 3241		D. Grosnick et al.	(CHIC, LANL, STAN+)
BELTRAMI 87	PL B194 326	I. Beltrami et al.	(ETH, SIN, MANZ)
COHEN 87	RMP 59 1121	E.R. Cohen, B.N. Taylor	(RIS, NBS)
BEER 86	PRL 57 671	G.A. Beer et al.	(VICT, TRIU, WYOM)
JODIDIO 86	PR D34 1967	A. Jodidio et al.	(LBL, NWES, TRIU)
Also PR D37 237 (erratum)		A. Jodidio et al.	(LBL, NWES, TRIU)
BERTL 85	NP B290 1	W. Bertl et al.	(SINDRUM Collab.)
BRYMAN 85	PL 55 465	D.A. Bryman et al.	(TRIU, CNRC, BRCO+)
BURKARD 85	PL 150B 242	H. Burkhardt et al.	(ETH, SIN, MANZ)
BURKARD 85B	PL 160B 343	H. Burkhardt et al.	(ETH, SIN, MANZ)
Also PR D24 2004		F. Corvieu et al.	(ETH, SIN, MANZ)
Also PL 129B 260		F. Corvieu et al.	(ETH, SIN, MANZ)
STOKER 85	PRL 54 1887	D.P. Stoker et al.	(LBL, NWES, TRIU)
BARDIN 84	PL 137B 135	G. Bardin et al.	(SACL, CERN, BGNA, FIRZ)
BERTL 84	PL 140B 299	W. Bertl et al.	(SINDRUM Collab.)
BOLTON 84	PRL 53 1415	R.D. Bolton et al.	(LANL, CHIC, STAN+)
EICHENBER... 84	NP A412 523	W. Eichenberger, R. Engfer, A. van der Schaff	(WILL)
GIOVANNETTI 84	PR D29 343	K.L. Giovannetti et al.	(MONT, TRIU, BRCO)
AZUELOS 83	PRL 51 164	G. Azuelos et al.	(MONT, BRCO, TRIU+)
Also PRL 39 1113		P. Depommier et al.	(CHARM Collab.)
BERGSMAN 83	PL 122B 465	F. Bergsma et al.	(LBL, NWES, TRIU)
CARR 83	PRL 51 627	J. Carr et al.	(ETH, STAN, LANL)
KINNISSON 82	PR D25 2846	W.W. Kinnison et al.	(EFI, STAN, LANL)
Also PRL 42 556		J.D. Bowman et al.	(LASL, EFI, STAN)
KLEMPIT 82	PR D25 652	E. Klempit et al.	(MANZ, ETH)
MARIAM 82	PRL 49 993	F.G. Mariani et al.	(YALE, HEIDH, BERN)
MARSHALL 82	PR D25 1174	G.M. Marshall et al.	(BRCO)
NEMETHY 81	CNPP 10 147	P. Nemethy, V.W. Hughes	(LBL, YALE)
ABELA 80	PL 95B 318	R. Abela et al.	(BASL, KARLK, KARLE)
BADERT... 80	LNC 28 401	A. Badertscher et al.	(BERN)
Also NP A377 406		A. Badertscher et al.	(BERN)
JONKER 80	PL 93B 203	M. Jonker et al.	(CHARM Collab.)
SCHAAF 80	NP A340 249	A. van der Schaaf et al.	(ZURI, ETH+)
Also PL 72B 183		H.P. Povel et al.	(ZURI, ETH, SIN)
WILLIS 80	PRL 44 522	S.E. Willis et al.	(YALE, LBL, LASL+)
Also PRL 45 1370		S.E. Willis et al.	(YALE, LBL, LASL+)
BAILEY 79	NP B150 1	J.M. Bailey	(CERN, DARE, MANZ)
BADERT... 78	PL 79B 371	A. Badertscher et al.	(BERN)
BAILEY 78	JPG 4 345	J.M. Bailey (DARE, BERN, SHEF, MANZ, RMCS+)	
Also NP B150 1		J.M. Bailey (DARE, BERN, SHEF, MANZ, RMCS+)	
BLIETS CHAU 78	NP B133 205	J. Blietschau et al.	(Gargamelle Collab.)
BOWMAN 78	PRL 41 442	J.D. Bowman et al.	(LASL, IAS, CMU+)
CAMANI 78	PL 77B 326	M. Camani et al.	(ETH, MANZ)
BADERT... 77	PRL 39 1385	A. Badertscher et al.	(BERN)
CASPERSON 77	PRL 38 956	D.E. Casperson et al.	(BERN, HEIDH, LASL+)
DEPOMMIER 77	PRL 39 1113	P. Depommier et al.	(MONT, BRCO, TRIU+)
BALANDIN 74	JETP 40 811	M.P. Balandin et al.	(JINR)
Translated from ZETF 67 1631.			
COHEN 73	JPCRD 2 664	E.R. Cohen, B.N. Taylor	(RIS, NBS)
DUCLOS 73	PL 47B 491	J. Duclos, A. Magnon, J. Picard	(SACL)
EICHEN 73	PL 46B 281	T. Eichten et al.	(Gargamelle Collab.)
BRYMAN 72	PRL 28 1469	D.A. Bryman et al.	(VPI)
CROWE 72	PR D5 2145	K.M. Crowe et al.	(LBL, WASH)
CRANE 71	PRL 27 474	T. Crane et al.	(YALE)
DERENZO 69	PR 181 1854	S.E. Derenzo	(EFI)
VOSSLER 69	NC 63A 423	C. Vossler	(EFI)
AKHMANOV 68	SJNP 6 230	V.V. Akhmanov et al.	(KIAE)
Translated from YAF 6 316.			

FRYBERGER 68	PR 166 1379	D. Fryberger	(EFI)
BOGART 67	PR 156 1405	E. Bogart et al.	(COLU)
SCHWARTZ 67	PR 162 1306	D.M. Schwartz	(EFI)
SHERWOOD 67	PR 156 1475	B.A. Sherwood	(EFI)
PEOPLES 66	Nevis 147 unpub.	J. Peoples	(COLU)
BLOOM 64	PL 8 87	S. Bloom et al.	(CERN)
DUCLOS 64	PL 9 62	J. Duclos et al.	(CERN)
GUREVICH 64	PL 11 185	I.I. Gurevich et al.	(KIAE)
BUHLER 63	PL 7 368	A. Buhler-Broglin et al.	(CERN)
MEYER 63	PR 132 2693	S.L. Meyer et al.	(COLU)
CHARPAK 62	PL 1 16	G. Charpak et al.	(CERN)
CONFORTO 62	NC 26 261	G. Conforto et al.	(INFN, ROMA, CERN)
ALI-ZADE 61	JETP 13 313	S.A. Ali-Zade, I.I. Gurevich, B.A. Nikolsky	
Translated from ZETF 40 452.			
CRITTENDEN 61	PR 121 1823	R.R. Crittenden, W.D. Walker, J. Ballam	(WIS C+)
KRUGER 61	UCRL 9322 unpub.	H. Kruger	(LRL)
GUREVICH 60	JETP 10 225	I.I. Gurevich, B.A. Nikolsky, L.V. Surkova	(ITEP)
Translated from ZETF 37 318.			
PLANO 60	PR 119 1400	R.J. Plano	(COLU)
ASHKIN 59	NC 14 1266	J. Ashkin et al.	(CERN)
BARDON 59	PRL 2 56	M. Bardon, D. Berley, L.M. Lederman	(COLU)
LEE 59	PRL 3 55	J. Lee, N.P. Samios	(COLU)

 τ

$$J = \frac{1}{2}$$

τ discovery paper was PERL 75. $e^+e^- \rightarrow \tau^+\tau^-$ cross-section threshold behavior and magnitude are consistent with pointlike spin-1/2 Dirac particle. BRANDELIK 78 ruled out pointlike spin-0 or spin-1 particle. FELDMAN 78 ruled out $J = 3/2$. KIRKBY 79 also ruled out $J = \text{integer}$, $J = 3/2$.

 τ MASS

VALUE (MeV)	EVTS	DOCUMENT ID	TECN	COMMENT
1776.84 ± 0.17 OUR AVERAGE				
1776.81 ^{+0.25} _{-0.23} ± 0.15	81	ANASHIN 07	KEDR	6.7 pb ⁻¹ , $E_{cm}^{ee} = 3.54\text{--}3.78$ GeV
1776.61 ± 0.13 ± 0.35		¹ BELOUSI 07	BELL	414 fb ⁻¹ , $E_{cm}^{ee} = 10.6$ GeV
1775.1 ± 1.6 ± 1.0	13.3k	² ABBIENDI 00A	OPAL	1990-1995 LEP runs
1778.2 ± 0.8 ± 1.2		ANASTASSOV 97	CLEO	$E_{cm}^{ee} = 10.6$ GeV
1776.96 ^{+0.18+0.25} _{-0.21-0.17}	65	³ BAI 96	BES	$E_{cm}^{ee} = 3.54\text{--}3.57$ GeV
1776.3 ± 2.4 ± 1.4	11k	⁴ ALBRECHT 92M	ARG	$E_{cm}^{ee} = 9.4\text{--}10.6$ GeV
1783 ⁺⁴ ₋₃	692	⁵ BACINO 78B	DLCO	$E_{cm}^{ee} = 3.1\text{--}7.4$ GeV
• • • We do not use the following data for averages, fits, limits, etc. • • •				
1777.8 ± 0.7 ± 1.7	35k	⁶ BALEST 93	CLEO	Repl. by ANASTASSOV 97
1776.9 ^{+0.4} _{-0.5} ± 0.2	14	⁷ BAI 92	BES	Repl. by BAI 96

- ¹BELOUSI 07 fit τ pseudomass spectrum in $\tau \rightarrow \pi\pi^+\pi^-\nu_\tau$ decays. Result assumes $m_{\nu_\tau} = 0$.
- ²ABBIENDI 00A fit τ pseudomass spectrum in $\tau \rightarrow \pi^\pm \leq 2\pi^0\nu_\tau$ and $\tau \rightarrow \pi^\pm\pi^+\pi^- \leq 1\pi^0\nu_\tau$ decays. Result assumes $m_{\nu_\tau} = 0$.
- ³BAI 96 fit $\sigma(e^+e^- \rightarrow \tau^+\tau^-)$ at different energies near threshold.
- ⁴ALBRECHT 92M fit τ pseudomass spectrum in $\tau^- \rightarrow 2\pi^-\pi^+\nu_\tau$ decays. Result assumes $m_{\nu_\tau} = 0$.
- ⁵BACINO 78B value comes from $e^\pm X^\mp$ threshold. Published mass 1782 MeV increased by 1 MeV using the high precision $\psi(2S)$ mass measurement of ZHOLENTZ 80 to eliminate the absolute SPEAR energy calibration uncertainty.
- ⁶BALEST 93 fit spectra of minimum kinematically allowed τ mass in events of the type $e^+e^- \rightarrow \tau^+\tau^- \rightarrow (\pi^+n\pi^0\nu_\tau)(\pi^-m\pi^0\nu_\tau)$, $n \leq 2$, $1 \leq m \leq 3$. If $m_{\nu_\tau} \neq 0$, result increases by $(m_{\nu_\tau}^2/1100 \text{ MeV})$.
- ⁷BAI 92 fit $\sigma(e^+e^- \rightarrow \tau^+\tau^-)$ near threshold using $e\mu$ events.

$$(m_{\tau^+} - m_{\tau^-})/m_{\text{average}}$$

A test of CPT invariance.

VALUE	CL%	DOCUMENT ID	TECN	COMMENT
<2.8 × 10⁻⁴	90	BELOUSI 07	BELL	414 fb ⁻¹ , $E_{cm}^{ee} = 10.6$ GeV
• • • We do not use the following data for averages, fits, limits, etc. • • •				
<3.0 × 10 ⁻³	90	ABBIENDI 00A	OPAL	1990-1995 LEP runs

 τ MEAN LIFE

VALUE (10 ⁻¹⁵ s)	EVTS	DOCUMENT ID	TECN	COMMENT
290.6 ± 1.0 OUR AVERAGE				
290.9 ± 1.4 ± 1.0		ABDALLAH 04T	DLPH	1991-1995 LEP runs
293.2 ± 2.0 ± 1.5		ACCIARRI 00B	L3	1991-1995 LEP runs
291.0 ± 1.5 ± 1.1		BARATE 97R	ALEP	1989-1994 LEP runs
289.2 ± 1.7 ± 1.2		ALEXANDER 96E	OPAL	1990-1994 LEP runs
289.0 ± 2.8 ± 4.0	57.4k	BALEST 96	CLEO	$E_{cm}^{ee} = 10.6$ GeV

Lepton Particle Listings

τ

• • • We do not use the following data for averages, fits, limits, etc. • • •

291.2 ± 2.0 ± 1.2		BARATE	97i	ALEP	Repl. by BARATE 97R
291.4 ± 3.0		ABREU	96B	DLPH	Repl. by ABDAL-LAH 04T
290.1 ± 4.0	34k	ACCIARRI	96k	L3	Repl. by ACCIARRI 00B
297 ± 9 ± 5	1671	ABE	95Y	SLD	1992-1993 SLC runs
304 ± 14 ± 7	4100	BATTLE	92	CLEO	$E_{cm}^{ee} = 10.6$ GeV
301 ± 29	3780	KLEINWORT	89	JADE	$E_{cm}^{ee} = 35-46$ GeV
288 ± 16 ± 17	807	AMIDEI	88	MRK2	$E_{cm}^{ee} = 29$ GeV
306 ± 20 ± 14	695	BRAUNSCH...	88c	TASS	$E_{cm}^{ee} = 36$ GeV
299 ± 15 ± 10	1311	ABACHI	87c	HRS	$E_{cm}^{ee} = 29$ GeV
295 ± 14 ± 11	5696	ALBRECHT	87P	ARG	$E_{cm}^{ee} = 9.3-10.6$ GeV
309 ± 17 ± 7	3788	BAND	87B	MAC	$E_{cm}^{ee} = 29$ GeV
325 ± 14 ± 18	8470	BEBEK	87C	CLEO	$E_{cm}^{ee} = 10.5$ GeV
460 ± 190	102	FELDMAN	82	MRK2	$E_{cm}^{ee} = 29$ GeV

τ MAGNETIC MOMENT ANOMALY

The q^2 dependence is expected to be small providing no thresholds are nearby.

$$\mu_\tau / (e\hbar/2m_\tau) - 1 = (g_\tau - 2)/2$$

For a theoretical calculation $[(g_\tau - 2)/2 = 117 721(5) \times 10^{-8}]$, see EIDELMAN 07.

VALUE	CL%	DOCUMENT ID	TECN	COMMENT
> -0.052 and < 0.013 (CL = 95%) OUR LIMIT				
> -0.052 and < 0.013	95	¹ ABDALLAH	04k	DLPH $e^+e^- \rightarrow e^+e^-\tau^+\tau^-$ at LEP2
< 0.107	95	² ACHARD	04g	L3 $e^+e^- \rightarrow e^+e^-\tau^+\tau^-$ at LEP2
> -0.007 and < 0.005	95	³ GONZALEZ-S.	00	RVUE $e^+e^- \rightarrow \tau^+\tau^-$ and $W \rightarrow \tau\nu_\tau$
> -0.052 and < 0.058	95	⁴ ACCIARRI	98e	L3 1991-1995 LEP runs
> -0.068 and < 0.065	95	⁵ ACKERSTAFF	98N	OPAL 1990-1995 LEP runs
> -0.004 and < 0.006	95	⁶ ESCRIBANO	97	RVUE $Z \rightarrow \tau^+\tau^-$ at LEP
< 0.01	95	⁷ ESCRIBANO	93	RVUE $Z \rightarrow \tau^+\tau^-$ at LEP
< 0.12	90	GRIFOLS	91	RVUE $Z \rightarrow \tau\tau\gamma$ at LEP
< 0.023	95	⁸ SILVERMAN	83	RVUE $e^+e^- \rightarrow \tau^+\tau^-$ at PETRA

- ¹ ABDALLAH 04k limit is derived from $e^+e^- \rightarrow e^+e^-\tau^+\tau^-$ total cross-section measurements at \sqrt{s} between 183 and 208 GeV. In addition to the limits, the authors also quote a value of -0.018 ± 0.017 .
- ² ACHARD 04g limit is derived from $e^+e^- \rightarrow e^+e^-\tau^+\tau^-$ total cross-section measurements at \sqrt{s} between 189 and 206 GeV, and is on the absolute value of the magnetic moment anomaly.
- ³ GONZALEZ-SPRINBERG 00 use data on tau lepton production at LEP1, SLC, and LEP2, and data from colliders and LEP2 to determine limits. Assume imaginary component is zero.
- ⁴ ACCIARRI 98e use $Z \rightarrow \tau^+\tau^-\gamma$ events. In addition to the limits, the authors also quote a value of $0.004 \pm 0.027 \pm 0.023$.
- ⁵ ACKERSTAFF 98N use $Z \rightarrow \tau^+\tau^-\gamma$ events. The limit applies to an average of the form factor for off-shell τ 's having p^2 ranging from m_τ^2 to $(M_Z - m_\tau)^2$.
- ⁶ ESCRIBANO 97 use preliminary experimental results.
- ⁷ ESCRIBANO 93 limit derived from $\Gamma(Z \rightarrow \tau^+\tau^-)$, and is on the absolute value of the magnetic moment anomaly.
- ⁸ SILVERMAN 83 limit is derived from $e^+e^- \rightarrow \tau^+\tau^-$ total cross-section measurements for q^2 up to $(37 \text{ GeV})^2$.

τ ELECTRIC DIPOLE MOMENT (d_τ)

A nonzero value is forbidden by both T invariance and P invariance.

The q^2 dependence is expected to be small providing no thresholds are nearby.

Re(d_τ)

VALUE (10^{-16} ecm)	CL%	DOCUMENT ID	TECN	COMMENT
- 0.22 to 0.45	95	¹ INAMI	03	BELL $E_{cm}^{ee} = 10.6$ GeV
< 3.7	95	² ABDALLAH	04k	DLPH $e^+e^- \rightarrow e^+e^-\tau^+\tau^-$ at LEP2
< 11.4	95	³ ACHARD	04g	L3 $e^+e^- \rightarrow e^+e^-\tau^+\tau^-$ at LEP2
< 4.6	95	⁴ ALBRECHT	00	ARG $E_{cm}^{ee} = 10.4$ GeV
> -3.1 and < 3.1	95	ACCIARRI	98e	L3 1991-1995 LEP runs
> -3.8 and < 3.6	95	⁵ ACKERSTAFF	98N	OPAL 1990-1995 LEP runs
< 0.11	95	^{6,7} ESCRIBANO	97	RVUE $Z \rightarrow \tau^+\tau^-$ at LEP
< 0.5	95	⁸ ESCRIBANO	93	RVUE $Z \rightarrow \tau^+\tau^-$ at LEP
< 7	90	GRIFOLS	91	RVUE $Z \rightarrow \tau\tau\gamma$ at LEP
< 1.6	90	DELAGUILA	90	RVUE $e^+e^- \rightarrow \tau^+\tau^-$ $E_{cm}^{ee} = 35$ GeV

- • • We do not use the following data for averages, fits, limits, etc. • • •
- < 3.7
- < 11.4
- < 4.6
- > -3.1 and < 3.1
- > -3.8 and < 3.6
- < 0.11
- < 0.5
- < 7
- < 1.6

- ¹ INAMI 03 use $e^+e^- \rightarrow \tau^+\tau^-$ events.
- ² ABDALLAH 04k limit is derived from $e^+e^- \rightarrow e^+e^-\tau^+\tau^-$ total cross-section measurements at \sqrt{s} between 183 and 208 GeV and is on the absolute value of d_τ .
- ³ ACHARD 04g limit is derived from $e^+e^- \rightarrow e^+e^-\tau^+\tau^-$ total cross-section measurements at \sqrt{s} between 189 and 206 GeV, and is on the absolute value of d_τ .
- ⁴ ALBRECHT 00 use $e^+e^- \rightarrow \tau^+\tau^-$ events. Limit is on the absolute value of $\text{Re}(d_\tau)$.
- ⁵ ACKERSTAFF 98N use $Z \rightarrow \tau^+\tau^-\gamma$ events. The limit applies to an average of the form factor for off-shell τ 's having p^2 ranging from m_τ^2 to $(M_Z - m_\tau)^2$.
- ⁶ ESCRIBANO 97 derive the relationship $|d_\tau| = \cot \theta_W |d_\tau^W|$ using effective Lagrangian methods, and use a conference result $|d_\tau^W| < 5.8 \times 10^{-18} \text{ ecm}$ at 95% CL (L. Silvestris, ICHEP96) to obtain this result.
- ⁷ ESCRIBANO 97 use preliminary experimental results.
- ⁸ ESCRIBANO 93 limit derived from $\Gamma(Z \rightarrow \tau^+\tau^-)$, and is on the absolute value of the electric dipole moment.

Im(d_τ)

VALUE (10^{-16} ecm)	CL%	DOCUMENT ID	TECN	COMMENT
- 0.25 to 0.008	95	¹ INAMI	03	BELL $E_{cm}^{ee} = 10.6$ GeV
< 1.8	95	² ALBRECHT	00	ARG $E_{cm}^{ee} = 10.4$ GeV

- • • We do not use the following data for averages, fits, limits, etc. • • •
- < 1.8
- ¹ INAMI 03 use $e^+e^- \rightarrow \tau^+\tau^-$ events.
- ² ALBRECHT 00 use $e^+e^- \rightarrow \tau^+\tau^-$ events. Limit is on the absolute value of $\text{Im}(d_\tau)$.

τ WEAK DIPOLE MOMENT (d_τ^W)

A nonzero value is forbidden by CP invariance.

The q^2 dependence is expected to be small providing no thresholds are nearby.

Re(d_τ^W)

VALUE (10^{-17} ecm)	CL%	DOCUMENT ID	TECN	COMMENT
< 0.50	95	¹ HEISTER	03F	ALEP 1990-1995 LEP runs
< 3.0	90	¹ ACCIARRI	98c	L3 1991-1995 LEP runs
< 0.56	95	ACKERSTAFF	97L	OPAL 1991-1995 LEP runs
< 0.78	95	² AKERS	95F	OPAL Repl. by ACKERSTAFF 97L
< 1.5	95	² BUSKULIC	95c	ALEP Repl. by HEISTER 03F
< 7.0	95	² ACTON	92F	OPAL $Z \rightarrow \tau^+\tau^-$ at LEP
< 3.7	95	² BUSKULIC	92J	ALEP Repl. by BUSKULIC 95c

- • • We do not use the following data for averages, fits, limits, etc. • • •
- < 3.0
- < 0.56
- < 0.78
- < 1.5
- < 7.0
- < 3.7
- ¹ Limit is on the absolute value of the real part of the weak dipole moment.
- ² Limit is on the absolute value of the real part of the weak dipole moment, and applies for $q^2 = m_Z^2$.

Im(d_τ^W)

VALUE (10^{-17} ecm)	CL%	DOCUMENT ID	TECN	COMMENT
< 1.1	95	¹ HEISTER	03F	ALEP 1990-1995 LEP runs
< 1.5	95	ACKERSTAFF	97L	OPAL 1991-1995 LEP runs
< 4.5	95	² AKERS	95F	OPAL Repl. by ACKERSTAFF 97L

- • • We do not use the following data for averages, fits, limits, etc. • • •
- < 1.5
- < 4.5
- ¹ HEISTER 03F limit is on the absolute value of the imaginary part of the weak dipole moment.
- ² Limit is on the absolute value of the imaginary part of the weak dipole moment, and applies for $q^2 = m_Z^2$.

τ WEAK ANOMALOUS MAGNETIC DIPOLE MOMENT (α_τ^W)

Electroweak radiative corrections are expected to contribute at the 10^{-6} level. See BERNABEU 95.

The q^2 dependence is expected to be small providing no thresholds are nearby.

Re(α_τ^W)

VALUE	CL%	DOCUMENT ID	TECN	COMMENT
< 1.1×10^{-3}	95	¹ HEISTER	03F	ALEP 1990-1995 LEP runs
> -0.0024 and < 0.0025	95	² GONZALEZ-S.	00	RVUE $e^+e^- \rightarrow \tau^+\tau^-$ and $W \rightarrow \tau\nu_\tau$
< 4.5×10^{-3}	90	¹ ACCIARRI	98c	L3 1991-1995 LEP runs

- • • We do not use the following data for averages, fits, limits, etc. • • •
- > -0.0024 and < 0.0025
- < 4.5×10^{-3}
- ¹ Limit is on the absolute value of the real part of the weak anomalous magnetic dipole moment.
- ² GONZALEZ-SPRINBERG 00 use data on tau lepton production at LEP1, SLC, and LEP2, and data from colliders and LEP2 to determine limits. Assume imaginary component is zero.

Im(α_τ^W)

VALUE	CL%	DOCUMENT ID	TECN	COMMENT
< 2.7×10^{-3}	95	¹ HEISTER	03F	ALEP 1990-1995 LEP runs
< 9.9×10^{-3}	90	¹ ACCIARRI	98c	L3 1991-1995 LEP runs

- • • We do not use the following data for averages, fits, limits, etc. • • •
- < 9.9×10^{-3}
- ¹ Limit is on the absolute value of the imaginary part of the weak anomalous magnetic dipole moment.

τ^- DECAY MODES

τ^+ modes are charge conjugates of the modes below. " h^\pm " stands for π^\pm or K^\pm . " e " stands for e or μ . "Neutrals" stands for γ 's and/or π^0 's.

Mode	Fraction (Γ_i/Γ)	Scale factor/ Confidence level
Modes with one charged particle		
Γ_1 particle $^- \geq 0$ neutrals $\geq 0K^0 \nu_\tau$ ("1-prong")	(85.36±0.08) %	S=1.3
Γ_2 particle $^- \geq 0$ neutrals $\geq 0K_L^0 \nu_\tau$	(84.73±0.08) %	S=1.4
Γ_3 $\mu^- \bar{\nu}_\mu \nu_\tau$	[a] (17.36±0.05) %	
Γ_4 $\mu^- \bar{\nu}_\mu \nu_\tau \gamma$	[b] (3.6 ± 0.4) × 10 ⁻³	
Γ_5 $e^- \bar{\nu}_e \nu_\tau$	[a] (17.85±0.05) %	
Γ_6 $e^- \bar{\nu}_e \nu_\tau \gamma$	[b] (1.75 ± 0.18) %	
Γ_7 $h^- \geq 0K_L^0 \nu_\tau$	(12.13±0.07) %	S=1.1
Γ_8 $h^- \nu_\tau$	(11.60±0.06) %	S=1.1
Γ_9 $\pi^- \nu_\tau$	[a] (10.91±0.07) %	S=1.1
Γ_{10} $K^- \nu_\tau$	[a] (6.95 ± 0.23) × 10 ⁻³	S=1.1
Γ_{11} $h^- \geq 1$ neutrals ν_τ	(37.08±0.11) %	S=1.2
Γ_{12} $h^- \geq 1\pi^0 \nu_\tau$ (ex. K^0)	(36.54±0.11) %	S=1.2
Γ_{13} $h^- \pi^0 \nu_\tau$	(25.95±0.10) %	S=1.1
Γ_{14} $\pi^- \pi^0 \nu_\tau$	[a] (25.52±0.10) %	S=1.1
Γ_{15} $\pi^- \pi^0$ non- $\rho(770) \nu_\tau$	(3.0 ± 3.2) × 10 ⁻³	
Γ_{16} $K^- \pi^0 \nu_\tau$	[a] (4.28 ± 0.15) × 10 ⁻³	
Γ_{17} $h^- \geq 2\pi^0 \nu_\tau$	(10.84±0.12) %	S=1.3
Γ_{18} $h^- 2\pi^0 \nu_\tau$	(9.49 ± 0.11) %	S=1.2
Γ_{19} $h^- 2\pi^0 \nu_\tau$ (ex. K^0)	(9.33 ± 0.12) %	S=1.2
Γ_{20} $\pi^- 2\pi^0 \nu_\tau$ (ex. K^0)	[a] (9.27 ± 0.12) %	S=1.2
Γ_{21} $\pi^- 2\pi^0 \nu_\tau$ (ex. K^0), scalar	< 9 × 10 ⁻³	CL=95%
Γ_{22} $\pi^- 2\pi^0 \nu_\tau$ (ex. K^0), vector	< 7 × 10 ⁻³	CL=95%
Γ_{23} $K^- 2\pi^0 \nu_\tau$ (ex. K^0)	[a] (6.3 ± 2.3) × 10 ⁻⁴	
Γ_{24} $h^- \geq 3\pi^0 \nu_\tau$	(1.35 ± 0.07) %	S=1.1
Γ_{25} $h^- \geq 3\pi^0 \nu_\tau$ (ex. K^0)	(1.26 ± 0.07) %	S=1.1
Γ_{26} $h^- 3\pi^0 \nu_\tau$	(1.18 ± 0.08) %	
Γ_{27} $\pi^- 3\pi^0 \nu_\tau$ (ex. K^0)	[a] (1.04 ± 0.07) %	
Γ_{28} $K^- 3\pi^0 \nu_\tau$ (ex. K^0, η)	[a] (4.7 ± 2.1) × 10 ⁻⁴	
Γ_{29} $h^- 4\pi^0 \nu_\tau$ (ex. K^0)	(1.6 ± 0.4) × 10 ⁻³	
Γ_{30} $h^- 4\pi^0 \nu_\tau$ (ex. K^0, η)	[a] (1.0 ± 0.4) × 10 ⁻³	
Γ_{31} $K^- \geq 0\pi^0 \geq 0K^0 \geq 0\gamma \nu_\tau$	(1.57 ± 0.04) %	S=1.1
Γ_{32} $K^- \geq 1$ (π^0 or K^0 or γ) ν_τ	(8.74 ± 0.32) × 10 ⁻³	
Modes with K^0's		
Γ_{33} K_S^0 (particles) $^- \nu_\tau$	(9.2 ± 0.4) × 10 ⁻³	S=1.4
Γ_{34} $h^- \bar{K}^0 \nu_\tau$	(10.0 ± 0.5) × 10 ⁻³	S=1.8
Γ_{35} $\pi^- \bar{K}^0 \nu_\tau$	[a] (8.4 ± 0.4) × 10 ⁻³	S=2.0
Γ_{36} $\pi^- \bar{K}^0$ (non- $K^*(892)^-$) ν_τ	(5.4 ± 2.1) × 10 ⁻⁴	
Γ_{37} $K^- K^0 \nu_\tau$	[a] (1.58 ± 0.16) × 10 ⁻³	
Γ_{38} $K^- K^0 \geq 0\pi^0 \nu_\tau$	(3.16 ± 0.23) × 10 ⁻³	
Γ_{39} $h^- \bar{K}^0 \pi^0 \nu_\tau$	(5.5 ± 0.4) × 10 ⁻³	
Γ_{40} $\pi^- \bar{K}^0 \pi^0 \nu_\tau$	[a] (3.9 ± 0.4) × 10 ⁻³	
Γ_{41} $\bar{K}^0 \rho^- \nu_\tau$	(2.2 ± 0.5) × 10 ⁻³	
Γ_{42} $K^- K^0 \pi^0 \nu_\tau$	[a] (1.58 ± 0.20) × 10 ⁻³	
Γ_{43} $\pi^- \bar{K}^0 \geq 1\pi^0 \nu_\tau$	(3.2 ± 1.0) × 10 ⁻³	
Γ_{44} $\pi^- \bar{K}^0 \pi^0 \pi^0 \nu_\tau$	(2.6 ± 2.4) × 10 ⁻⁴	
Γ_{45} $K^- K^0 \pi^0 \pi^0 \nu_\tau$	< 1.6 × 10 ⁻⁴	CL=95%
Γ_{46} $\pi^- K^0 \bar{K}^0 \nu_\tau$	(1.7 ± 0.4) × 10 ⁻³	S=1.6
Γ_{47} $\pi^- K_S^0 K_S^0 \nu_\tau$	[a] (2.4 ± 0.5) × 10 ⁻⁴	
Γ_{48} $\pi^- K_S^0 K_L^0 \nu_\tau$	[a] (1.2 ± 0.4) × 10 ⁻³	S=1.7
Γ_{49} $\pi^- K^0 \bar{K}^0 \pi^0 \nu_\tau$	(3.1 ± 2.3) × 10 ⁻⁴	
Γ_{50} $\pi^- K_S^0 K_S^0 \pi^0 \nu_\tau$	< 2.0 × 10 ⁻⁴	CL=95%
Γ_{51} $\pi^- K_S^0 K_L^0 \pi^0 \nu_\tau$	(3.1 ± 1.2) × 10 ⁻⁴	
Γ_{52} $K^0 h^+ h^- h^- \geq 0$ neutrals ν_τ	< 1.7 × 10 ⁻³	CL=95%
Γ_{53} $K^0 h^+ h^- h^- \nu_\tau$	(2.3 ± 2.0) × 10 ⁻⁴	
Modes with three charged particles		
Γ_{54} $h^- h^- h^+ \geq 0$ neutrals $\geq 0K_L^0 \nu_\tau$	(15.18±0.08) %	S=1.4
Γ_{55} $h^- h^- h^+ \geq 0$ neutrals ν_τ (ex. $K_S^0 \rightarrow \pi^+ \pi^-$) ("3-prong")	(14.56±0.08) %	S=1.3
Γ_{56} $h^- h^- h^+ \nu_\tau$	(9.80 ± 0.08) %	S=1.4
Γ_{57} $h^- h^- h^+ \nu_\tau$ (ex. K^0)	(9.45 ± 0.07) %	S=1.3
Γ_{58} $h^- h^- h^+ \nu_\tau$ (ex. K^0, ω)	(9.42 ± 0.07) %	S=1.3
Γ_{59} $\pi^- \pi^+ \pi^- \nu_\tau$	(9.32 ± 0.07) %	S=1.2
Γ_{60} $\pi^- \pi^+ \pi^- \nu_\tau$ (ex. K^0)	(9.03 ± 0.06) %	S=1.2

Γ_{61} $\pi^- \pi^+ \pi^- \nu_\tau$ (ex. K^0), non-axial vector	< 2.4 %	CL=95%
Γ_{62} $\pi^- \pi^+ \pi^- \nu_\tau$ (ex. K^0, ω)	[a] (8.99 ± 0.06) %	S=1.2
Γ_{63} $h^- h^- h^+ \geq 1$ neutrals ν_τ	(5.38 ± 0.07) %	S=1.2
Γ_{64} $h^- h^- h^+ \geq 1\pi^0 \nu_\tau$ (ex. K^0)	(5.08 ± 0.06) %	S=1.1
Γ_{65} $h^- h^- h^+ \pi^0 \nu_\tau$	(4.75 ± 0.06) %	S=1.2
Γ_{66} $h^- h^- h^+ \pi^0 \nu_\tau$ (ex. K^0)	(4.56 ± 0.06) %	S=1.2
Γ_{67} $h^- h^- h^+ \pi^0 \nu_\tau$ (ex. K^0, ω)	(2.79 ± 0.08) %	S=1.2
Γ_{68} $\pi^- \pi^+ \pi^- \pi^0 \nu_\tau$	(4.61 ± 0.06) %	S=1.1
Γ_{69} $\pi^- \pi^+ \pi^- \pi^0 \nu_\tau$ (ex. K^0)	(4.48 ± 0.06) %	S=1.1
Γ_{70} $\pi^- \pi^+ \pi^- \pi^0 \nu_\tau$ (ex. K^0, ω)	[a] (2.70 ± 0.08) %	S=1.2
Γ_{71} $h^- \rho \pi^0 \nu_\tau$		
Γ_{72} $h^- \rho^+ h^- \nu_\tau$		
Γ_{73} $h^- \rho^- h^+ \nu_\tau$		
Γ_{74} $h^- h^- h^+ \geq 2\pi^0 \nu_\tau$ (ex. K^0)	(5.16 ± 0.33) × 10 ⁻³	
Γ_{75} $h^- h^- h^+ 2\pi^0 \nu_\tau$	(5.04 ± 0.32) × 10 ⁻³	
Γ_{76} $h^- h^- h^+ 2\pi^0 \nu_\tau$ (ex. K^0)	(4.94 ± 0.32) × 10 ⁻³	
Γ_{77} $h^- h^- h^+ 2\pi^0 \nu_\tau$ (ex. K^0, ω, η)	[a] (9 ± 4) × 10 ⁻⁴	
Γ_{78} $h^- h^- h^+ 3\pi^0 \nu_\tau$	[a] (2.3 ± 0.6) × 10 ⁻⁴	S=1.2
Γ_{79} $K^- h^+ h^- \geq 0$ neutrals ν_τ	(6.24 ± 0.24) × 10 ⁻³	S=1.5
Γ_{80} $K^- h^+ \pi^- \nu_\tau$ (ex. K^0)	(4.27 ± 0.19) × 10 ⁻³	S=2.4
Γ_{81} $K^- h^+ \pi^- \pi^0 \nu_\tau$ (ex. K^0)	(8.7 ± 1.2) × 10 ⁻⁴	S=1.1
Γ_{82} $K^- \pi^+ \pi^- \geq 0$ neutrals ν_τ	(4.78 ± 0.21) × 10 ⁻³	S=1.3
Γ_{83} $K^- \pi^+ \pi^- \geq 0\pi^0 \nu_\tau$ (ex. K^0)	(3.68 ± 0.19) × 10 ⁻³	S=1.4
Γ_{84} $K^- \pi^+ \pi^- \nu_\tau$	(3.41 ± 0.16) × 10 ⁻³	S=1.8
Γ_{85} $K^- \pi^+ \pi^- \nu_\tau$ (ex. K^0)	[a] (2.87 ± 0.16) × 10 ⁻³	S=2.1
Γ_{86} $K^- \rho^0 \nu_\tau \rightarrow$ $K^- \pi^+ \pi^- \nu_\tau$	(1.4 ± 0.5) × 10 ⁻³	
Γ_{87} $K^- \pi^+ \pi^- \pi^0 \nu_\tau$	(1.35 ± 0.14) × 10 ⁻³	
Γ_{88} $K^- \pi^+ \pi^- \pi^0 \nu_\tau$ (ex. K^0)	(8.1 ± 1.2) × 10 ⁻⁴	
Γ_{89} $K^- \pi^+ \pi^- \pi^0 \nu_\tau$ (ex. K^0, η)	[a] (7.5 ± 1.2) × 10 ⁻⁴	
Γ_{90} $K^- \pi^+ \pi^- \pi^0 \nu_\tau$ (ex. K^0, ω)	(3.7 ± 0.9) × 10 ⁻⁴	
Γ_{91} $K^- \pi^+ K^- \geq 0$ neut. ν_τ	< 9 × 10 ⁻⁴	CL=95%
Γ_{92} $K^- K^+ \pi^- \geq 0$ neut. ν_τ	(1.46 ± 0.06) × 10 ⁻³	S=1.6
Γ_{93} $K^- K^+ \pi^- \nu_\tau$	[a] (1.40 ± 0.05) × 10 ⁻³	S=1.7
Γ_{94} $K^- K^+ \pi^- \pi^0 \nu_\tau$	[a] (6.1 ± 2.5) × 10 ⁻⁵	S=1.4
Γ_{95} $K^- K^+ K^- \geq 0$ neut. ν_τ	< 2.1 × 10 ⁻³	CL=95%
Γ_{96} $K^- K^+ K^- \nu_\tau$	(1.58 ± 0.18) × 10 ⁻⁵	
Γ_{97} $K^- K^+ K^- \nu_\tau$ (ex. ϕ)	< 2.5 × 10 ⁻⁶	CL=90%
Γ_{98} $K^- K^+ K^- \pi^0 \nu_\tau$	< 4.8 × 10 ⁻⁶	CL=90%
Γ_{99} $\pi^- K^+ \pi^- \geq 0$ neut. ν_τ	< 2.5 × 10 ⁻³	CL=95%
Γ_{100} $e^- e^- e^+ \bar{\nu}_e \nu_\tau$	(2.8 ± 1.5) × 10 ⁻⁵	
Γ_{101} $\mu^- e^- e^+ \bar{\nu}_\mu \nu_\tau$	< 3.6 × 10 ⁻⁵	CL=90%
Modes with five charged particles		
Γ_{102} $3h^- 2h^+ \geq 0$ neutrals ν_τ (ex. $K_S^0 \rightarrow \pi^- \pi^+$) ("5-prong")	(1.02 ± 0.04) × 10 ⁻³	S=1.1
Γ_{103} $3h^- 2h^+ \nu_\tau$ (ex. K^0)	[a] (8.39 ± 0.35) × 10 ⁻⁴	S=1.1
Γ_{104} $3h^- 2h^+ \pi^0 \nu_\tau$ (ex. K^0)	[a] (1.78 ± 0.27) × 10 ⁻⁴	
Γ_{105} $3h^- 2h^+ 2\pi^0 \nu_\tau$	< 3.4 × 10 ⁻⁶	CL=90%
Miscellaneous other allowed modes		
Γ_{106} $(5\pi)^- \nu_\tau$	(7.6 ± 0.5) × 10 ⁻³	
Γ_{107} $4h^- 3h^+ \geq 0$ neutrals ν_τ ("7-prong")	< 3.0 × 10 ⁻⁷	CL=90%
Γ_{108} $4h^- 3h^+ \nu_\tau$	< 4.3 × 10 ⁻⁷	CL=90%
Γ_{109} $4h^- 3h^+ \pi^0 \nu_\tau$	< 2.5 × 10 ⁻⁷	CL=90%
Γ_{110} X^- ($S=-1$) ν_τ	(2.85 ± 0.07) %	S=1.3
Γ_{111} $K^*(892)^- \geq 0$ neutrals \geq $0K_L^0 \nu_\tau$	(1.42 ± 0.18) %	S=1.4
Γ_{112} $K^*(892)^- \nu_\tau$	(1.20 ± 0.07) %	S=1.8
Γ_{113} $K^*(892)^- \nu_\tau \rightarrow \pi^- \bar{K}^0 \nu_\tau$	(7.8 ± 0.5) × 10 ⁻³	
Γ_{114} $K^*(892)^0 K^- \geq 0$ neutrals ν_τ	(3.2 ± 1.4) × 10 ⁻³	
Γ_{115} $K^*(892)^0 K^- \nu_\tau$	(2.1 ± 0.4) × 10 ⁻³	
Γ_{116} $\bar{K}^*(892)^0 \pi^- \geq 0$ neutrals ν_τ	(3.8 ± 1.7) × 10 ⁻³	
Γ_{117} $\bar{K}^*(892)^0 \pi^- \nu_\tau$	(2.2 ± 0.5) × 10 ⁻³	
Γ_{118} $(\bar{K}^*(892) \pi)^- \nu_\tau \rightarrow$ $\pi^- \bar{K}^0 \pi^0 \nu_\tau$	(1.0 ± 0.4) × 10 ⁻³	
Γ_{119} $K_1(1270)^- \nu_\tau$	(4.7 ± 1.1) × 10 ⁻³	
Γ_{120} $K_1(1400)^- \nu_\tau$	(1.7 ± 2.6) × 10 ⁻³	S=1.7
Γ_{121} $K^*(1410)^- \nu_\tau$	(1.5 ± 1.4) × 10 ⁻³	
Γ_{122} $K_0^*(1430)^- \nu_\tau$	< 5 × 10 ⁻⁴	CL=95%
Γ_{123} $K_2^*(1430)^- \nu_\tau$	< 3 × 10 ⁻³	CL=95%
Γ_{124} $a_0(980)^- \geq 0$ neutrals ν_τ		

x_{35}	-1									
x_{37}	0	-3								
x_{40}	0	-10	0							
x_{42}	0	-2	-17	-19						
x_{47}	0	-2	-1	-2	0					
x_{48}	-1	-22	-6	-17	-5	-4				
x_{62}	-9	0	0	1	0	0	0			
x_{70}	3	3	1	3	0	0	2	-14		
x_{77}	4	-2	0	-1	0	0	-1	-4	-7	
x_{78}	-1	0	0	0	0	0	0	0	-1	-1
x_{85}	-5	-1	0	-1	0	0	-1	37	-8	-2
x_{89}	-1	-1	0	-1	0	0	-1	-2	-7	-1
x_{93}	-4	-1	0	-1	0	0	-1	35	-7	-2
x_{94}	0	0	0	0	0	0	0	0	-1	0
x_{103}	0	-2	0	-2	0	0	-2	-4	-1	1
x_{104}	-1	0	0	0	0	0	0	-2	0	1
x_{126}	-7	-2	0	-1	0	0	-1	0	1	-16
x_{128}	0	0	-2	0	-2	0	0	0	0	0
x_{146}	1	0	0	0	0	0	0	-8	-69	-4
x_{148}	3	-3	0	-3	0	0	-2	-5	-9	-60
	x_{30}	x_{35}	x_{37}	x_{40}	x_{42}	x_{47}	x_{48}	x_{62}	x_{70}	x_{77}
x_{85}	0									
x_{89}	-1	-2								
x_{93}	0	69	-2							
x_{94}	0	0	-3	0						
x_{103}	0	-3	-1	-3	0					
x_{104}	0	-1	0	-1	0	-5				
x_{126}	0	-1	0	0	0	-1	0			
x_{128}	0	0	-12	0	0	0	0	0		
x_{146}	-1	-4	3	-3	0	-1	0	0	0	
x_{148}	-2	-3	-2	-3	0	1	1	-2	0	-5
	x_{78}	x_{85}	x_{89}	x_{93}	x_{94}	x_{103}	x_{104}	x_{126}	x_{128}	x_{146}

 τ BRANCHING FRACTIONS

Revised April 2008 by K.G. Hayes (Hillsdale College).

The B factories continue to dominate experimental publications on the τ . Since the previous edition of this *Review*, there have been 15 published papers that have contributed measurements to the τ Listings, including 6 from the BaBar Collaboration and 8 from the Belle Collaboration. Seven of these papers have provided new upper limits on the branching fractions for neutrinoless τ -decay modes. Of the 57 neutrinoless τ -decay modes in the τ Listings, 2 are new and 25 have had improved limits set. The upper limits have been reduced by factors that range between 1.1 and 127, and the average reduction factor is 29.

There are now 13 measurements and 6 upper limits from Belle and BaBar on branching fractions of conventional τ decay modes, up from 1 measurement and 3 upper limits in the 2006 edition of this *Review*. For those branching fractions where older non- B -factory measurements existed, the new B -factory measurements have on average about fifty times the number of events as the most precise earlier measurements, and the statistical uncertainties on the B -factory measurements are on average about seven times smaller. However, the systematic uncertainties now greatly exceed the statistical uncertainties on nearly all B -factory branching fraction measurements, except those with the smallest measured branching fractions. For example, the average ratio of systematic to statistical uncertainty of the B -factory measurements of branching fractions larger

than 10^{-4} is about 6.5, while the average ratio for branching fractions smaller than 10^{-4} is about 1.0. Thus, the total uncertainty on the branching fraction measurements from B factories is on average only about 3 times smaller than the previous most precise non- B -factory measurements.

The constrained fit to τ branching fractions: The Lepton Summary Table and the List of τ -Decay Modes contain branching fractions for 119 conventional τ -decay modes and upper limits on the branching fractions for 28 other conventional τ -decay modes. Of the 119 modes with branching fractions, 82 are derived from a constrained fit to τ branching fraction data. The goal of the constrained fit is to make optimal use of the experimental data to determine τ branching fractions. For example, the branching fractions for the decay mode $\tau^- \rightarrow \pi^- \pi^+ \pi^- \pi^0 \nu_\tau$ is determined mostly from experimental measurements of the branching fraction for $\tau^- \rightarrow h^- h^- h^+ \pi^0 \nu_\tau$ and measurements of exclusive branching fractions for 3-prong modes containing charged kaons and 1 π^0 .

Branching fractions from the constrained fit are derived from a set of basis modes. The basis modes form an exclusive set whose branching fractions are constrained to sum exactly to one. The set of selected basis modes expands as branching fraction measurements for new τ -decay modes are published. The number of basis modes has expanded from 12 in the year 1994 fit to 31 in the 2002 through 2008 fits. The 31 basis modes selected for the 2008 fit are listed in Table 1. See the 1996 edition of this *Review* [1] for a complete description of our notation for naming τ -decay modes and the selection of the basis modes. For each edition since the 1996 edition, the changes in the selected basis modes from the previous edition are described in the τ Branching Fractions Review. Figure 1 illustrates the basis mode branching fractions from the 2008 fit.

Table 1: Basis modes for the 2008 fit to τ branching fraction data.

$e^- \bar{\nu}_e \nu_\tau$	$K^- K^0 \pi^0 \nu_\tau$
$\mu^- \bar{\nu}_\mu \nu_\tau$	$\pi^- \pi^+ \pi^- \nu_\tau$ (ex. K^0, ω)
$\pi^- \nu_\tau$	$\pi^- \pi^+ \pi^- \pi^0 \nu_\tau$ (ex. K^0, ω)
$\pi^- \pi^0 \nu_\tau$	$K^- \pi^+ \pi^- \nu_\tau$ (ex. K^0)
$\pi^- 2\pi^0 \nu_\tau$ (ex. K^0)	$K^- \pi^+ \pi^- \pi^0 \nu_\tau$ (ex. K^0, η)
$\pi^- 3\pi^0 \nu_\tau$ (ex. K^0)	$K^- K^+ \pi^- \nu_\tau$
$h^- 4\pi^0 \nu_\tau$ (ex. K^0, η)	$K^- K^+ \pi^- \pi^0 \nu_\tau$
$K^- \nu_\tau$	$h^- h^- h^+ 2\pi^0 \nu_\tau$ (ex. K^0, ω, η)
$K^- \pi^0 \nu_\tau$	$h^- h^- h^+ 3\pi^0 \nu_\tau$
$K^- 2\pi^0 \nu_\tau$ (ex. K^0)	$3h^- 2h^+ \nu_\tau$ (ex. K^0)
$K^- 3\pi^0 \nu_\tau$ (ex. K^0, η)	$3h^- 2h^+ \pi^0 \nu_\tau$ (ex. K^0)
$\pi^- \bar{K}^0 \nu_\tau$	$h^- \omega \nu_\tau$
$\pi^- \bar{K}^0 \pi^0 \nu_\tau$	$h^- \omega \pi^0 \nu_\tau$
$\pi^- K_S^0 K_S^0 \nu_\tau$	$\eta \pi^- \pi^0 \nu_\tau$
$\pi^- K_S^0 K_L^0 \nu_\tau$	$\eta K^- \nu_\tau$
$K^- K^0 \nu_\tau$	

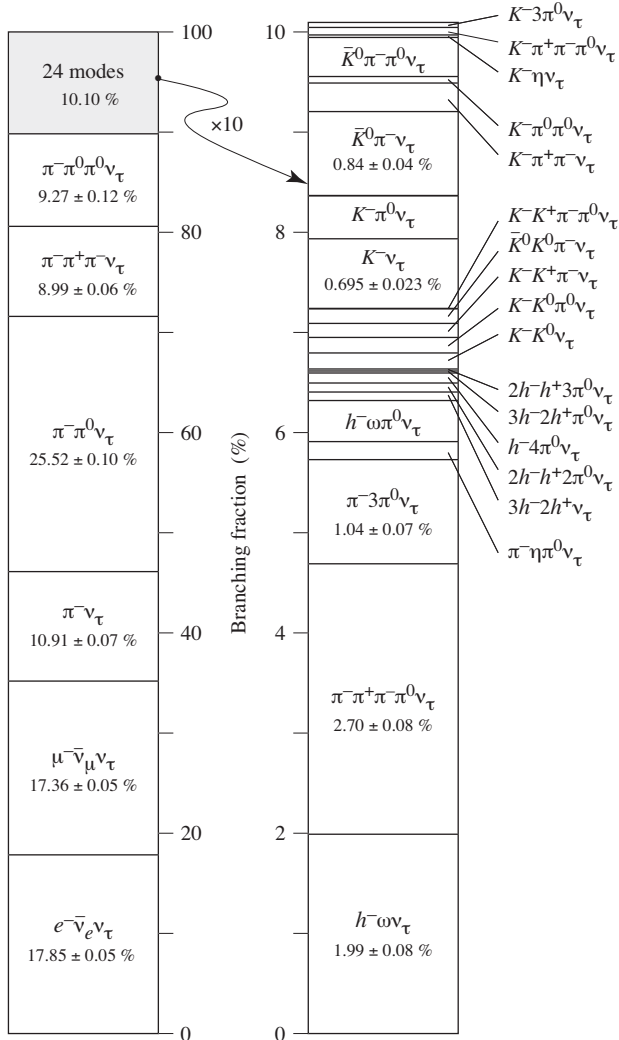


Figure 1: Basis mode branching fractions of the τ . Six modes account for 90% of the decays, 25 modes account for the last 10%. The list of excluded intermediate states for each basis mode has been suppressed.

In selecting the basis modes, assumptions and choices must be made. For example, we assume the decays $\tau^- \rightarrow \pi^- K^+ \pi^- \geq 0\pi^0 \nu_\tau$ and $\tau^- \rightarrow \pi^+ K^- K^- \geq 0\pi^0 \nu_\tau$ have negligible branching fractions. This is consistent with standard model predictions for τ decay, although the experimental limits for these branching fractions are not very stringent. The 95% confidence level upper limits for these branching fractions in the current Listings are $B(\tau^- \rightarrow \pi^- K^+ \pi^- \geq 0\pi^0 \nu_\tau) < 0.25\%$ and $B(\tau^- \rightarrow \pi^+ K^- K^- \geq 0\pi^0 \nu_\tau) < 0.09\%$, values not so different from measured branching fractions for allowed 3-prong modes containing charged kaons. Although our usual goal is to impose as few theoretical constraints as possible so that the world averages and fit results can be used to test the theoretical constraints (*i.e.*, we do not make use of the theoretical constraint from lepton universality on the ratio of the τ -leptonic branching

fractions $B(\tau^- \rightarrow \mu^- \bar{\nu}_\mu \nu_\tau) / B(\tau^- \rightarrow e^- \bar{\nu}_e \nu_\tau) = 0.9726$), the experimental challenge to identify charged prongs in 3-prong τ decays is sufficiently difficult that experimenters have been forced to make these assumptions when measuring the branching fractions of the allowed decays. We are constrained by the assumptions made by the experimenters.

There are several τ -decay modes with small but well-measured (> 2.5 sigma from zero) branching fractions [2] which cannot be expressed in terms of the selected basis modes and are therefore left out of the fit:

$$\begin{aligned} B(\tau^- \rightarrow \pi^- K_S^0 K_L^0 \pi^0 \nu_\tau) &= (3.1 \pm 1.2) \times 10^{-4} \\ B(\tau^- \rightarrow 2K^- K^+ \nu_\tau) &= (0.158 \pm 0.018) \times 10^{-4} \\ B(\tau^- \rightarrow \eta \bar{K}^0 \pi^- \nu_\tau) &= (2.2 \pm 0.7) \times 10^{-4} \end{aligned}$$

Certain components of other small but well-measured τ -decay modes cannot be expressed in terms of the selected basis modes and therefore are also left out of the fit:

$$\begin{aligned} B(\tau^- \rightarrow \eta \pi^- \pi^0 \pi^0 \nu_\tau) \times \\ B(\eta \rightarrow \gamma\gamma \text{ or } \eta \rightarrow \pi^+ \pi^- \gamma \text{ or } \eta \rightarrow 3\pi^0) &= (1.1 \pm 0.4) \times 10^{-4}, \\ B(\tau^- \rightarrow \eta \pi^- \pi^+ \pi^- \nu_\tau) \times \\ B(\eta \rightarrow \gamma\gamma \text{ or } \eta \rightarrow \pi^+ \pi^- \gamma) &= (1.0 \pm 0.2) \times 10^{-4}, \\ B(\tau^- \rightarrow \phi K^- \nu_\tau) \times \\ B(\phi \rightarrow K_S^0 K_L^0 \text{ or } \phi \rightarrow \eta\gamma) &= (0.13 \pm 0.01) \times 10^{-4}, \\ B(\tau^- \rightarrow f_1(1285) \pi^- \nu_\tau) B(f_1(1285) \rightarrow \rho^0 \gamma) &= (0.27 \pm 0.07) \times 10^{-4}, \\ B(\tau^- \rightarrow h^- \omega \pi^0 \pi^0 \nu_\tau) B(\omega \rightarrow \pi^0 \gamma) &= (0.12 \pm 0.04) \times 10^{-4}, \\ B(\tau^- \rightarrow 2h^- h^+ \omega \nu_\tau) B(\omega \rightarrow \pi^0 \gamma) &= (0.10 \pm 0.02) \times 10^{-4}. \end{aligned}$$

The sum of these excluded branching fractions is $(0.08 \pm 0.01)\%$. This is near our goal of 0.1% for the internal consistency of the τ Listings for this edition, and thus for simplicity we do not include these small branching fraction decay modes in the basis set.

Beginning with the 2002 edition, the fit algorithm has been improved to allow for correlations between branching fraction measurements used in the fit. If only a few measurements are correlated, the correlation coefficients are listed in the footnote for each measurement. If a large number of measurements are correlated, then the full correlation matrix is listed in the footnote to the measurement that first appears in the τ Listings. Footnotes to the other measurements refer to the first measurement. For example, the large correlation matrices for the branching fraction measurements contained in Refs. [3,4] are listed in Footnotes to the $\Gamma(e^- \bar{\nu}_e \nu_\tau) / \Gamma_{\text{total}}$ and $\Gamma(h^- \nu_\tau) / \Gamma_{\text{total}}$ measurements respectively. Sometimes experimental papers contain correlation coefficients between measurements using only statistical errors without including systematic errors. We usually cannot make use of these correlation coefficients.

The 2008 constrained fit has a χ^2 of 95.7 for 100 degrees of freedom up from 77.5 for 95 degrees of freedom in the 2006 fit. No basis-mode branching fractions changed by more than 1.5σ from their 2006 values. However, some of the new precise B -factory branching-fraction measurements are somewhat inconsistent with earlier less precise measurements.

For example, seven decay modes used in the 2008 fit had fit scale factors larger than 1.6, while there were no modes in the 2006 fit with scale factors this large. Most of the large scale factors can be traced to the inclusion of three new measurements: the Belle Collaboration [5] measurement of $B(\pi^- \bar{K}^0 \nu_\tau)$, and the BaBar Collaboration [6] measurements of $B(K^- \pi^+ \pi^- \nu_\tau (\text{ex. } K^0))$ and $B(K^- K^+ \pi^- \nu_\tau)$.

Overconsistency of Leptonic Branching Fraction Measurements: To minimize the effects of older experiments which often have larger systematic errors and sometimes make assumptions that have later been shown to be invalid, we exclude old measurements in decay modes which contain at least several newer data of much higher precision. As a rule, we exclude those experiments with large errors which together would contribute no more than 5% of the weight in the average. This procedure leaves five measurements for $B_e \equiv B(\tau^- \rightarrow e^- \bar{\nu}_e \nu_\tau)$ and five measurements for $B_\mu \equiv B(\tau^- \rightarrow \mu^- \bar{\nu}_\mu \nu_\tau)$. For both B_e and B_μ , the selected measurements are considerably more consistent with each other than should be expected from the quoted errors on the individual measurements. The χ^2 from the calculation of the average of the selected measurements is 0.34 for B_e and 0.08 for B_μ . Assuming normal errors, the probability of a smaller χ^2 is 1.3% for B_e and 0.08% for B_μ .

References

1. R.M. Barnett *et al.* (Particle Data Group), *Review of Particle Physics*, Phys. Rev. **D54**, 1 (1996).
2. See the τ Listings for references.
3. S. Schael *et al.* (Aleph Collab.), Phys. Rep. **421**, 191 (2005).
4. J. Abdallah *et al.* (Delphi Collab.), Eur. Phys. J. **C46**, 1 (2006).
5. D. Epifanov *et al.* (Belle Collab.), Phys. Lett. **B654**, 65 (2007).
6. B. Aubert *et al.* (BaBar Collab.), Phys. Rev. Lett. **100**, 011801 (2008).

τ^- BRANCHING RATIOS

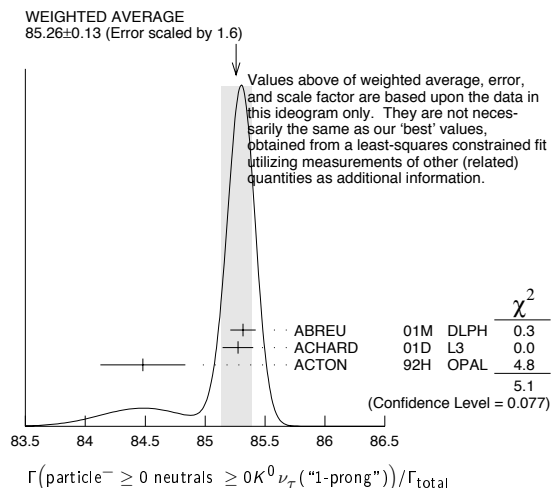
$$\Gamma(\text{particle}^- \geq 0 \text{ neutrals} \geq 0 K^0 \nu_\tau (\text{"1-prong"})) / \Gamma_{\text{total}} \quad \Gamma_1 / \Gamma$$

$$\Gamma_1 / \Gamma = (\Gamma_3 + \Gamma_5 + \Gamma_9 + \Gamma_{10} + \Gamma_{14} + \Gamma_{16} + \Gamma_{20} + \Gamma_{23} + \Gamma_{27} + \Gamma_{28} + \Gamma_{30} + \Gamma_{35} + \Gamma_{37} + \Gamma_{40} + \Gamma_{42} + 2\Gamma_{47} + \Gamma_{48} + 0.708\Gamma_{126} + 0.715\Gamma_{128} + 0.09\Gamma_{146} + 0.09\Gamma_{148}) / \Gamma$$

The charged particle here can be e , μ , or hadron. In many analyses, the sum of the topological branching fractions (1, 3, and 5 prongs) is constrained to be unity. Since the 5-prong fraction is very small, the measured 1-prong and 3-prong fractions are highly correlated and cannot be treated as independent quantities in our overall fit. We arbitrarily choose to use the 3-prong fraction in our fit, and leave the 1-prong fraction out. We do, however, use these 1-prong measurements in our average below. The measurements used only for the average are marked "avg," whereas "f&a" marks a result used for the fit and the average.

VALUE (%)	EVTS	DOCUMENT ID	TECN	COMMENT
85.36 ± 0.08 OUR FIT	Error includes scale factor of 1.3.			
85.26 ± 0.13 OUR AVERAGE	Error includes scale factor of 1.6. See the ideogram below.			
85.316 ± 0.093 ± 0.049	avg 78k	¹ ABREU	01M DLPH	1992-1995 LEP runs
85.274 ± 0.105 ± 0.073	avg	² ACHARD	01D L3	1992-1995 LEP runs
84.48 ± 0.27 ± 0.23	avg	ACTON	92H OPAL	1990-1991 LEP runs
• • • We do not use the following data for averages, fits, limits, etc. • • •				
85.45 ± 0.69 / -0.73 ± 0.65		DECAMP	92c ALEP	Repl. by SCHAELE 05c

- ¹ The correlation coefficients between this measurement and the ABREU 01M measurements of $B(\tau^- \rightarrow 3\text{-prong})$ and $B(\tau^- \rightarrow 5\text{-prong})$ are -0.98 and -0.08 respectively.
- ² The correlation coefficients between this measurement and the ACHARD 01D measurements of $B(\tau^- \rightarrow "3\text{-prong}")$ and $B(\tau^- \rightarrow "5\text{-prong}")$ are -0.978 and -0.082 respectively.



$$\Gamma(\text{particle}^- \geq 0 \text{ neutrals} \geq 0 K^0 \nu_\tau) / \Gamma_{\text{total}} \quad \Gamma_2 / \Gamma$$

$$\Gamma_2 / \Gamma = (\Gamma_3 + \Gamma_5 + \Gamma_9 + \Gamma_{10} + \Gamma_{14} + \Gamma_{16} + \Gamma_{20} + \Gamma_{23} + \Gamma_{27} + \Gamma_{28} + \Gamma_{30} + 0.6569\Gamma_{35} + 0.6569\Gamma_{37} + 0.6569\Gamma_{40} + 0.6569\Gamma_{42} + 1.0985\Gamma_{47} + 0.3139\Gamma_{48} + 0.708\Gamma_{126} + 0.715\Gamma_{128} + 0.09\Gamma_{146} + 0.09\Gamma_{148}) / \Gamma$$

VALUE (%)	EVTS	DOCUMENT ID	TECN	COMMENT
84.73 ± 0.08 OUR FIT	Error includes scale factor of 1.4.			
85.1 ± 0.4 OUR AVERAGE				
85.6 ± 0.6 ± 0.3	avg 3300	¹ ADEVA	91F L3	$E_{\text{cm}}^{\text{ee}} = 88.3\text{--}94.3$ GeV
84.9 ± 0.4 ± 0.3	avg	BEHREND	89B CELL	$E_{\text{cm}}^{\text{ee}} = 14\text{--}47$ GeV
84.7 ± 0.8 ± 0.6	avg	² AIHARA	87B TPC	$E_{\text{cm}}^{\text{ee}} = 29$ GeV
• • • We do not use the following data for averages, fits, limits, etc. • • •				
86.4 ± 0.3 ± 0.3		ABACHI	89B HRS	$E_{\text{cm}}^{\text{ee}} = 29$ GeV
87.1 ± 1.0 ± 0.7		³ BURCHAT	87 MRK2	$E_{\text{cm}}^{\text{ee}} = 29$ GeV
87.2 ± 0.5 ± 0.8		SCHMIDKE	86 MRK2	$E_{\text{cm}}^{\text{ee}} = 29$ GeV
84.7 ± 1.1 ± 1.6 / -1.3	169	⁴ ALTHOFF	85 TASS	$E_{\text{cm}}^{\text{ee}} = 34.5$ GeV
86.1 ± 0.5 ± 0.9		BARTELE	85F JADE	$E_{\text{cm}}^{\text{ee}} = 34.6$ GeV
87.8 ± 1.3 ± 3.9		⁵ BERGER	85 PLUT	$E_{\text{cm}}^{\text{ee}} = 34.6$ GeV
86.7 ± 0.3 ± 0.6		FERNANDEZ	85 MAC	$E_{\text{cm}}^{\text{ee}} = 29$ GeV

- ¹ Not independent of ADEVA 91F $\Gamma(h^- h^- h^+ \geq 0 \text{ neutrals} \geq 0 K_L^0 \nu_\tau) / \Gamma_{\text{total}}$ value.
- ² Not independent of AIHARA 87B $\Gamma(\mu^- \bar{\nu}_\mu \nu_\tau) / \Gamma_{\text{total}}$, $\Gamma(e^- \bar{\nu}_e \nu_\tau) / \Gamma_{\text{total}}$, and $\Gamma(h^- h^- h^+ \geq 0 \text{ neutrals} \geq 0 K_L^0 \nu_\tau) / \Gamma_{\text{total}}$ values.
- ³ Not independent of SCHMIDKE 86 value (also not independent of BURCHAT 87 value for $\Gamma(h^- h^- h^+ \geq 0 \text{ neutrals} \geq 0 K_L^0 \nu_\tau) / \Gamma_{\text{total}}$).
- ⁴ Not independent of ALTHOFF 85 $\Gamma(\mu^- \bar{\nu}_\mu \nu_\tau) / \Gamma_{\text{total}}$, $\Gamma(e^- \bar{\nu}_e \nu_\tau) / \Gamma_{\text{total}}$, $\Gamma(h^- \geq 0 \text{ neutrals} \geq 0 K_L^0 \nu_\tau) / \Gamma_{\text{total}}$, and $\Gamma(h^- h^- h^+ \geq 0 \text{ neutrals} \geq 0 K_L^0 \nu_\tau) / \Gamma_{\text{total}}$ values.
- ⁵ Not independent of (1-prong + $0\pi^0$) and (1-prong + $\geq 1\pi^0$) values.

$\Gamma(\mu^- \bar{\nu}_\mu \nu_\tau) / \Gamma_{\text{total}} \quad \Gamma_3 / \Gamma$
Data marked "avg" are highly correlated with data appearing elsewhere in the Listings, and are therefore used for the average given below but not in the overall fits. "f&a" marks results used for the fit and the average.

To minimize the effect of experiments with large systematic errors, we exclude experiments which together would contribute 5% of the weight in the average.

VALUE (%)	EVTS	DOCUMENT ID	TECN	COMMENT
17.36 ± 0.05 OUR FIT				
17.33 ± 0.05 OUR AVERAGE				
17.319 ± 0.070 ± 0.032 f&a	54k	¹ SCHAELE	05c ALEP	1991-1995 LEP runs
17.34 ± 0.09 ± 0.06 f&a	31.4k	ABBIENDI	03 OPAL	1990-1995 LEP runs
17.342 ± 0.110 ± 0.067 f&a	21.5k	² ACCIARRI	01F L3	1991-1995 LEP runs
17.325 ± 0.095 ± 0.077 f&a	27.7k	ABREU	99X DLPH	1991-1995 LEP runs
17.37 ± 0.08 ± 0.18 avg		³ ANASTASSOV	97 CLEO	$E_{\text{cm}}^{\text{ee}} = 10.6$ GeV
• • • We do not use the following data for averages, fits, limits, etc. • • •				
17.31 ± 0.11 ± 0.05	20.7k	BUSKULIC	96c ALEP	Repl. by SCHAELE 05c
17.02 ± 0.19 ± 0.24	6586	ABREU	95T DLPH	Repl. by ABREU 99X
17.36 ± 0.27	7941	AKERS	95I OPAL	Repl. by ABBIENDI 03
17.6 ± 0.4 ± 0.4	2148	ADRIANI	93M L3	Repl. by ACCIARRI 01F
17.4 ± 0.3 ± 0.5		⁴ ALBRECHT	93G ARG	$E_{\text{cm}}^{\text{ee}} = 9.4\text{--}10.6$ GeV
17.35 ± 0.41 ± 0.37		DECAMP	92c ALEP	1989-1990 LEP runs
17.7 ± 0.8 ± 0.4	568	BEHREND	90 CELL	$E_{\text{cm}}^{\text{ee}} = 35$ GeV
17.4 ± 1.0	2197	ADEVA	88 MRKJ	$E_{\text{cm}}^{\text{ee}} = 14\text{--}16$ GeV

Lepton Particle Listings

τ

17.7	± 1.2	± 0.7	AIHARA	87B	TPC	$E_{cm}^{ee} = 29$ GeV
18.3	± 0.9	± 0.8	BURCHAT	87	MRK2	$E_{cm}^{ee} = 29$ GeV
18.6	± 0.8	± 0.7	558	5	BARTEL	86D JADE $E_{cm}^{ee} = 34.6$ GeV
12.9	± 1.7	$\begin{smallmatrix} +0.7 \\ -0.5 \end{smallmatrix}$	ALTHOFF	85	TASS	$E_{cm}^{ee} = 34.5$ GeV
18.0	± 0.9	± 0.5	473	5	ASH	85B MAC $E_{cm}^{ee} = 29$ GeV
18.0	± 1.0	± 0.6		6	BALTRUSAITIS	85 MRK3 $E_{cm}^{ee} = 3.77$ GeV
19.4	± 1.6	± 1.7	153	BERGER	85	PLUT $E_{cm}^{ee} = 34.6$ GeV
17.6	± 2.6	± 2.1	47	BEHREND	83C	CELL $E_{cm}^{ee} = 34$ GeV
17.8	± 2.0	± 1.8		BERGER	81B	PLUT $E_{cm}^{ee} = 9-32$ GeV

- (9) $\Gamma(\tau^- \rightarrow \pi^- \pi^+ \pi^- \pi^0 \nu_\tau (\text{ex. } K^0)) / \Gamma_{\text{total}}$
- (10) $\Gamma(\tau^- \rightarrow h^- h^- h^+ 2\pi^0 \nu_\tau (\text{ex. } K^0)) / \Gamma_{\text{total}}$
- (11) $\Gamma(\tau^- \rightarrow h^- h^- h^+ 3\pi^0 \nu_\tau) / \Gamma_{\text{total}}$
- (12) $\Gamma(\tau^- \rightarrow 3h^- 2h^+ \nu_\tau (\text{ex. } K^0)) / \Gamma_{\text{total}}$
- (13) $\Gamma(\tau^- \rightarrow 3h^- 2h^+ \pi^0 \nu_\tau (\text{ex. } K^0)) / \Gamma_{\text{total}}$

(1)	(2)	(3)	(4)	(5)	(6)	(7)	(8)	(9)	(10)	(11)	(12)
(2)	-20										
(3)	-9	-6									
(4)	-16	-12	2								
(5)	-5	-5	-17	-37							
(6)	0	-4	-15	2	-27						
(7)	-2	-4	-24	-15	20	-47					
(8)	-14	-9	15	-5	-17	-14	-8				
(9)	-13	-12	-25	-30	4	-2	16	-15			
(10)	0	-2	-23	-14	4	10	13	-6	-17		
(11)	1	0	-5	1	4	6	0	-9	-2	-11	
(12)	0	1	9	4	-8	-4	-6	9	-5	-4	-2
(13)	1	-4	-3	-5	3	2	-4	-3	-1	4	1

¹ See footnote to SCHAEEL 05c $\Gamma(\tau^- \rightarrow e^- \bar{\nu}_e \nu_\tau) / \Gamma_{\text{total}}$ measurement for correlations with other measurements.
² The correlation coefficient between this measurement and the ACCIARRI 01F measurement of $B(\tau^- \rightarrow e^- \bar{\nu}_e \nu_\tau)$ is 0.08.
³ The correlation coefficients between this measurement and the ANASTASSOV 97 measurements of $B(e \bar{\nu}_e \nu_\tau)$, $B(\mu \bar{\nu}_\mu \nu_\tau) / B(e \bar{\nu}_e \nu_\tau)$, $B(h^- \nu_\tau)$, and $B(h^- \nu_\tau) / B(e \bar{\nu}_e \nu_\tau)$ are 0.50, 0.58, 0.50, and 0.08 respectively.
⁴ Not independent of ALBRECHT 92D $\Gamma(\mu^- \bar{\nu}_\mu \nu_\tau) / \Gamma(e^- \bar{\nu}_e \nu_\tau)$ and ALBRECHT 93G $\Gamma(\mu^- \bar{\nu}_\mu \nu_\tau) \times \Gamma(e^- \bar{\nu}_e \nu_\tau) / \Gamma_{\text{total}}^2$ values.
⁵ Modified using $B(e^- \bar{\nu}_e \nu_\tau) / B(\text{"1 prong"})$ and $B(\text{"1 prong"}) = 0.855$.
⁶ Error correlated with BALTRUSAITIS 85 $e \nu \bar{\nu}$ value.

$\Gamma(\mu^- \bar{\nu}_\mu \nu_\tau \gamma) / \Gamma_{\text{total}}$		Γ_4 / Γ	
VALUE (%)	EVTS	DOCUMENT ID	TECN COMMENT
0.361 ± 0.016 ± 0.035		¹ BERGFELD 00	CLEO $E_{cm}^{ee} = 10.6$ GeV
• • • We do not use the following data for averages, fits, limits, etc. • • •			
0.30 ± 0.04 ± 0.05	116	² ALEXANDER 96S	OPAL 1991-1994 LEP runs
0.23 ± 0.10	10	³ WU 90	MRK2 $E_{cm}^{ee} = 29$ GeV

¹ BERGFELD 00 impose requirements on detected γ 's corresponding to a τ -rest-frame energy cutoff $E_\gamma^* > 10$ MeV. For $E_\gamma^* > 20$ MeV, they quote $(3.04 \pm 0.14 \pm 0.30) \times 10^{-3}$.
² ALEXANDER 96S impose requirements on detected γ 's corresponding to a τ -rest-frame energy cutoff $E_\gamma > 20$ MeV.
³ WU 90 reports $\Gamma(\mu^- \bar{\nu}_\mu \nu_\tau \gamma) / \Gamma(\mu^- \bar{\nu}_\mu \nu_\tau) = 0.013 \pm 0.006$, which is converted to $\Gamma(\mu^- \bar{\nu}_\mu \nu_\tau \gamma) / \Gamma_{\text{total}}$ using $\Gamma(\mu^- \bar{\nu}_\mu \nu_\tau \gamma) / \Gamma_{\text{total}} = 17.35\%$. Requirements on detected γ 's correspond to a τ rest frame energy cutoff $E_\gamma > 37$ MeV.

$\Gamma(e^- \bar{\nu}_e \nu_\tau) / \Gamma_{\text{total}}$		Γ_5 / Γ	
VALUE (%)	EVTS	DOCUMENT ID	TECN COMMENT
17.85 ± 0.05 OUR FIT			
17.82 ± 0.05 OUR AVERAGE			

To minimize the effect of experiments with large systematic errors, we exclude experiments which together would contribute 5% of the weight in the average.

17.837 ± 0.072 ± 0.036	56k	¹ SCHAEEL 05c	ALEP 1991-1995 LEP runs
17.806 ± 0.104 ± 0.076	24.7k	² ACCIARRI 01F	L3 1991-1995 LEP runs
17.81 ± 0.09 ± 0.06	33.1k	ABBIENDI 99X	OPAL 1991-1995 LEP runs
17.877 ± 0.109 ± 0.110	23.3k	ABREU 99X	DLPH 1991-1995 LEP runs
17.76 ± 0.06 ± 0.17		³ ANASTASSOV 97	CLEO $E_{cm}^{ee} = 10.6$ GeV
• • • We do not use the following data for averages, fits, limits, etc. • • •			
17.78 ± 0.10 ± 0.09	25.3k	ALEXANDER 96D	OPAL Repl. by ABBI-ENDDI 99H
17.79 ± 0.12 ± 0.06	20.6k	BUSKULIC 96c	ALEP Repl. by SCHAEEL 05c
17.51 ± 0.23 ± 0.31	5059	ABREU 95T	DLPH Repl. by ABREU 99X
17.9 ± 0.4 ± 0.4	2892	ADRIANI 93M	L3 Repl. by ACCIARRI 01F
17.5 ± 0.3 ± 0.5		⁴ ALBRECHT 93G	ARG $E_{cm}^{ee} = 9.4-10.6$ GeV
17.97 ± 0.14 ± 0.23	3970	AKERIB 92	CLEO Repl. by ANASTASSOV 97
19.1 ± 0.4 ± 0.6	2960	⁵ AMMAR 92	CLEO $E_{cm}^{ee} = 10.5-10.9$ GeV
18.09 ± 0.45 ± 0.45		DECAMP 92c	ALEP Repl. by SCHAEEL 05c
17.0 ± 0.5 ± 0.6	1.7k	ABACHI 90	HRS $E_{cm}^{ee} = 29$ GeV
18.4 ± 0.8 ± 0.4	644	BEHREND 90	CELL $E_{cm}^{ee} = 35$ GeV
16.3 ± 0.3 ± 3.2		JANSSEN 89	CBAL $E_{cm}^{ee} = 9.4-10.6$ GeV
18.4 ± 1.2 ± 1.0		AIHARA 87B	TPC $E_{cm}^{ee} = 29$ GeV
19.1 ± 0.8 ± 1.1		BURCHAT 87	MRK2 $E_{cm}^{ee} = 29$ GeV
16.8 ± 0.7 ± 0.9	515	⁵ BARTEL 86D	JADE $E_{cm}^{ee} = 34.6$ GeV
20.4 ± 3.0 $\begin{smallmatrix} +1.4 \\ -0.9 \end{smallmatrix}$		ALTHOFF 85	TASS $E_{cm}^{ee} = 34.5$ GeV
17.8 ± 0.9 ± 0.6	390	⁵ ASH 85B	MAC $E_{cm}^{ee} = 29$ GeV
18.2 ± 0.7 ± 0.5		⁶ BALTRUSAITIS 85	MRK3 $E_{cm}^{ee} = 3.77$ GeV
13.0 ± 1.9 ± 2.9		BERGER 85	PLUT $E_{cm}^{ee} = 34.6$ GeV
18.3 ± 2.4 ± 1.9	60	BEHREND 83C	CELL $E_{cm}^{ee} = 34$ GeV
16.0 ± 1.3	459	⁷ BACINO 78B	DLCO $E_{cm}^{ee} = 3.1-7.4$ GeV

¹ Correlation matrix for SCHAEEL 05c branching fractions, in percent:
 (1) $\Gamma(\tau^- \rightarrow e^- \bar{\nu}_e \nu_\tau) / \Gamma_{\text{total}}$
 (2) $\Gamma(\tau^- \rightarrow \mu^- \bar{\nu}_\mu \nu_\tau) / \Gamma_{\text{total}}$
 (3) $\Gamma(\tau^- \rightarrow \pi^- \nu_\tau) / \Gamma_{\text{total}}$
 (4) $\Gamma(\tau^- \rightarrow \pi^- \pi^0 \nu_\tau) / \Gamma_{\text{total}}$
 (5) $\Gamma(\tau^- \rightarrow \pi^- 2\pi^0 \nu_\tau (\text{ex. } K^0)) / \Gamma_{\text{total}}$
 (6) $\Gamma(\tau^- \rightarrow \pi^- 3\pi^0 \nu_\tau (\text{ex. } K^0)) / \Gamma_{\text{total}}$
 (7) $\Gamma(\tau^- \rightarrow h^- 4\pi^0 \nu_\tau (\text{ex. } K^0, \eta)) / \Gamma_{\text{total}}$
 (8) $\Gamma(\tau^- \rightarrow \pi^- \pi^+ \pi^- \nu_\tau (\text{ex. } K^0, \omega)) / \Gamma_{\text{total}}$

(1) (2) (3) (4) (5) (6) (7) (8) (9) (10) (11) (12)
 (2) -20
 (3) -9 -6
 (4) -16 -12 2
 (5) -5 -5 -17 -37
 (6) 0 -4 -15 2 -27
 (7) -2 -4 -24 -15 20 -47
 (8) -14 -9 15 -5 -17 -14 -8
 (9) -13 -12 -25 -30 4 -2 16 -15
 (10) 0 -2 -23 -14 4 10 13 -6 -17
 (11) 1 0 -5 1 4 6 0 -9 -2 -11
 (12) 0 1 9 4 -8 -4 -6 9 -5 -4 -2
 (13) 1 -4 -3 -5 3 2 -4 -3 -1 4 1 -24

² The correlation coefficient between this measurement and the ACCIARRI 01F measurement of $B(\tau^- \rightarrow \mu^- \bar{\nu}_\mu \nu_\tau)$ is 0.08.
³ The correlation coefficients between this measurement and the ANASTASSOV 97 measurements of $B(\mu \bar{\nu}_\mu \nu_\tau)$, $B(\mu \bar{\nu}_\mu \nu_\tau) / B(e \bar{\nu}_e \nu_\tau)$, $B(h^- \nu_\tau)$, and $B(h^- \nu_\tau) / B(e \bar{\nu}_e \nu_\tau)$ are 0.50, -0.42, 0.48, and -0.39 respectively.
⁴ Not independent of ALBRECHT 92D $\Gamma(\mu^- \bar{\nu}_\mu \nu_\tau) / \Gamma(e^- \bar{\nu}_e \nu_\tau)$ and ALBRECHT 93G $\Gamma(\mu^- \bar{\nu}_\mu \nu_\tau) \times \Gamma(e^- \bar{\nu}_e \nu_\tau) / \Gamma_{\text{total}}^2$ values.
⁵ Modified using $B(e^- \bar{\nu}_e \nu_\tau) / B(\text{"1 prong"})$ and $B(\text{"1 prong"}) = 0.855$.
⁶ Error correlated with BALTRUSAITIS 85 $\Gamma(\mu^- \bar{\nu}_\mu \nu_\tau) / \Gamma_{\text{total}}$.
⁷ BACINO 78B value comes from fit to events with e^\pm and one other nonelectron charged prong.

$\Gamma(\mu^- \bar{\nu}_\mu \nu_\tau) / \Gamma(e^- \bar{\nu}_e \nu_\tau)$		Γ_3 / Γ_5	
VALUE	DOCUMENT ID	TECN	COMMENT
0.973 ± 0.004 OUR FIT			
0.978 ± 0.011 OUR AVERAGE			

Standard Model prediction including mass effects is 0.9726.
 Data marked "avg" are highly correlated with data appearing elsewhere in the Listings, and are therefore used for the average given below but not in the overall fits. "f&a" marks results used for the fit and the average.

0.9777 ± 0.0063 ± 0.0087	f&a	¹ ANASTASSOV 97	CLEO $E_{cm}^{ee} = 10.6$ GeV
0.997 ± 0.035 ± 0.040	f&a	ALBRECHT 92D	ARG $E_{cm}^{ee} = 9.4-10.6$ GeV

¹ The correlation coefficients between this measurement and the ANASTASSOV 97 measurements of $B(\mu \bar{\nu}_\mu \nu_\tau)$, $B(e \bar{\nu}_e \nu_\tau)$, $B(h^- \nu_\tau)$, and $B(h^- \nu_\tau) / B(e \bar{\nu}_e \nu_\tau)$ are 0.58, -0.42, 0.07, and 0.45 respectively.

$\Gamma(e^- \bar{\nu}_e \nu_\tau \gamma) / \Gamma_{\text{total}}$		Γ_6 / Γ	
VALUE (%)	DOCUMENT ID	TECN	COMMENT
1.75 ± 0.06 ± 0.17		¹ BERGFELD 00	CLEO $E_{cm}^{ee} = 10.6$ GeV

¹ BERGFELD 00 impose requirements on detected γ 's corresponding to a τ -rest-frame energy cutoff $E_\gamma^* > 10$ MeV.

$\Gamma(h^- \geq 0 K_L^0 \nu_\tau) / \Gamma_{\text{total}}$		Γ_7 / Γ	
VALUE (%)	EVTS	DOCUMENT ID	TECN COMMENT
12.13 ± 0.07 OUR FIT			
12.2 ± 0.4 OUR AVERAGE			

$\Gamma_7 / \Gamma = (\Gamma_9 + \Gamma_{10} + \frac{1}{2} \Gamma_{35} + \frac{1}{2} \Gamma_{37} + \Gamma_{47}) / \Gamma$
 Data marked "avg" are highly correlated with data appearing elsewhere in the Listings, and are therefore used for the average given below but not in the overall fits. "f&a" marks results used for the fit and the average.

12.47 ± 0.26 ± 0.43	f&a 2967	¹ ACCIARRI 95	L3 1992 LEP run
12.4 ± 0.7 ± 0.7	f&a 283	² ABREU 92N	DLPH 1990 LEP run
12.1 ± 0.7 ± 0.5	f&a 309	ALEXANDER 91D	OPAL 1990 LEP run
11.3 ± 0.5 ± 0.8	avg 798	³ FORD 87	MAC $E_{cm}^{ee} = 29$ GeV
• • • We do not use the following data for averages, fits, limits, etc. • • •			
12.44 ± 0.11 ± 0.11	15k	⁴ BUSKULIC 96	ALEP Repl. by SCHAEEL 05c
11.7 ± 0.6 ± 0.8		⁵ ALBRECHT 92D	ARG $E_{cm}^{ee} = 9.4-10.6$ GeV
12.98 ± 0.44 ± 0.33		⁶ DECAMP 92c	ALEP Repl. by SCHAEEL 05c
12.3 ± 0.9 ± 0.5	1338	BEHREND 90	CELL $E_{cm}^{ee} = 35$ GeV
11.1 ± 1.1 ± 1.4		⁷ BURCHAT 87	MRK2 $E_{cm}^{ee} = 29$ GeV
12.3 ± 0.6 ± 1.1	328	⁸ BARTEL 86D	JADE $E_{cm}^{ee} = 34.6$ GeV
13.0 ± 2.0 ± 4.0		BERGER 85	PLUT $E_{cm}^{ee} = 34.6$ GeV
11.2 ± 1.7 ± 1.2	34	⁹ BEHREND 83C	CELL $E_{cm}^{ee} = 34$ GeV

¹ ACCIARRI 95 with 0.65% added to remove their correction for $\pi^- K_L^0$ backgrounds.
² ABREU 92N with 0.5% added to remove their correction for $K^*(892)^-$ backgrounds.
³ FORD 87 result for $B(\pi^- \nu_\tau)$ with 0.67% added to remove their K^- correction and adjusted for 1992 B("1 prong").
⁴ BUSKULIC 96 quote $11.78 \pm 0.11 \pm 0.13$ We add 0.66 to undo their correction for unseen K_L^0 and modify the systematic error accordingly.
⁵ Not independent of ALBRECHT 92D $\Gamma(\mu^- \bar{\nu}_\mu \nu_\tau) / \Gamma(e^- \bar{\nu}_e \nu_\tau)$, $\Gamma(\mu^- \bar{\nu}_\mu \nu_\tau) \times \Gamma(e^- \bar{\nu}_e \nu_\tau)$, and $\Gamma(h^- \geq 0 K_L^0 \nu_\tau) / \Gamma(e^- \bar{\nu}_e \nu_\tau)$ values.

⁶ DECAMP 92c quote $B(h^- \geq 0 K_L^0 \geq 0 (K_S^0 \rightarrow \pi^+ \pi^-) \nu_\tau) = 13.32 \pm 0.44 \pm 0.33$. We subtract 0.35 to correct for their inclusion of the K_S^0 decays.

⁷ BURCHAT 87 with 1.1% added to remove their correction for K^- and $K^*(892)^-$ backgrounds.

⁸ BARTEL 86D result for $B(\pi^- \nu_\tau)$ with 0.59% added to remove their K^- correction and adjusted for 1992 B("1 prong").

⁹ BEHREND 83c quote $B(\pi^- \nu_\tau) = 9.9 \pm 1.7 \pm 1.3$ after subtracting 1.3 ± 0.5 to correct for $B(K^- \nu_\tau)$.

$\Gamma(h^- \nu_\tau)/\Gamma_{\text{total}}$ **$\Gamma_8/\Gamma = (\Gamma_9 + \Gamma_{10})/\Gamma$**
 Data marked "avg" are highly correlated with data appearing elsewhere in the Listings, and are therefore used for the average given below but not in the overall fits. "f&a" marks results used for the fit and the average.

VALUE (%)	EVTS	DOCUMENT ID	TECN	COMMENT
11.60 ± 0.06 OUR FIT				Error includes scale factor of 1.1.
11.63 ± 0.12 OUR AVERAGE				Error includes scale factor of 1.4. See the ideogram below.
11.571 ± 0.120 ± 0.114	f&a 19k	¹ ABDALLAH 06A	DLPH	1992-1995 LEP runs
11.98 ± 0.13 ± 0.16	f&a	ACKERSTAFF 98M	OPAL	1991-1995 LEP runs
11.52 ± 0.05 ± 0.12	f&a	² ANASTASSOV 97	CLEO	$E_{\text{cm}}^{\text{ee}} = 10.6$ GeV

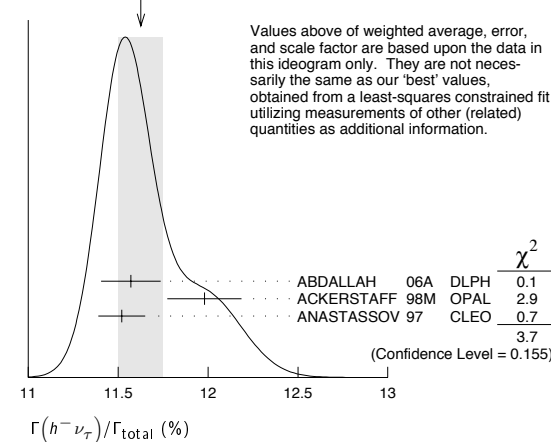
¹ Correlation matrix for ABDALLAH 06A branching fractions, in percent:

- (1) $\Gamma(\tau^- \rightarrow h^- \nu_\tau)/\Gamma_{\text{total}}$
- (2) $\Gamma(\tau^- \rightarrow h^- \pi^0 \nu_\tau)/\Gamma_{\text{total}}$
- (3) $\Gamma(\tau^- \rightarrow h^- \geq 1 \pi^0 \nu_\tau (\text{ex. } K^0))/\Gamma_{\text{total}}$
- (4) $\Gamma(\tau^- \rightarrow h^- 2 \pi^0 \nu_\tau (\text{ex. } K^0))/\Gamma_{\text{total}}$
- (5) $\Gamma(\tau^- \rightarrow h^- \geq 3 \pi^0 \nu_\tau (\text{ex. } K^0))/\Gamma_{\text{total}}$
- (6) $\Gamma(\tau^- \rightarrow h^- h^- h^+ \nu_\tau (\text{ex. } K^0))/\Gamma_{\text{total}}$
- (7) $\Gamma(\tau^- \rightarrow h^- h^- h^+ \pi^0 \nu_\tau (\text{ex. } K^0))/\Gamma_{\text{total}}$
- (8) $\Gamma(\tau^- \rightarrow h^- h^- h^+ \geq 1 \pi^0 \nu_\tau (\text{ex. } K^0))/\Gamma_{\text{total}}$
- (9) $\Gamma(\tau^- \rightarrow h^- h^- h^+ \geq 2 \pi^0 \nu_\tau (\text{ex. } K^0))/\Gamma_{\text{total}}$
- (10) $\Gamma(\tau^- \rightarrow 3h^- 2h^+ \nu_\tau (\text{ex. } K^0))/\Gamma_{\text{total}}$
- (11) $\Gamma(\tau^- \rightarrow 3h^- 2h^+ \pi^0 \nu_\tau (\text{ex. } K^0))/\Gamma_{\text{total}}$

	(1)	(2)	(3)	(4)	(5)	(6)	(7)	(8)	(9)	(10)
(1)	-34									
(2)	-47	56								
(3)	6	-66	15							
(4)	-6	38	11	-86						
(5)	-7	-8	15	0	-2					
(6)	-2	-1	-5	-3	3	-53				
(7)	-4	-4	-13	-4	-2	-56	75			
(8)	-1	-1	-4	3	-6	26	-78	-16		
(9)	-1	-1	1	0	0	-2	-3	-1	3	
(10)	0	0	0	0	0	1	0	-5	5	-57
(11)										

² The correlation coefficients between this measurement and the ANASTASSOV 97 measurements of $B(\mu \bar{\nu}_\mu \nu_\tau)$, $B(e \bar{\nu}_e \nu_\tau)$, $B(\mu \bar{\nu}_\mu \nu_\tau)/B(e \bar{\nu}_e \nu_\tau)$, and $B(h^- \nu_\tau)/B(e \bar{\nu}_e \nu_\tau)$ are 0.50, 0.48, 0.07, and 0.63 respectively.

WEIGHTED AVERAGE
 11.63±0.12 (Error scaled by 1.4)



$\Gamma(h^- \nu_\tau)/\Gamma(e^- \bar{\nu}_e \nu_\tau)$ **$\Gamma_8/\Gamma_5 = (\Gamma_9 + \Gamma_{10})/\Gamma_5$**

Data marked "avg" are highly correlated with data appearing elsewhere in the Listings, and are therefore used for the average given below but not in the overall fits. "f&a" marks results used for the fit and the average.

VALUE	DOCUMENT ID	TECN	COMMENT
0.650 ± 0.004 OUR FIT			Error includes scale factor of 1.1.
0.6484 ± 0.0041 ± 0.0060 avg	¹ ANASTASSOV 97	CLEO	$E_{\text{cm}}^{\text{ee}} = 10.6$ GeV

¹ The correlation coefficients between this measurement and the ANASTASSOV 97 measurements of $B(\mu \bar{\nu}_\mu \nu_\tau)$, $B(e \bar{\nu}_e \nu_\tau)$, $B(\mu \bar{\nu}_\mu \nu_\tau)/B(e \bar{\nu}_e \nu_\tau)$, and $B(h^- \nu_\tau)$ are 0.08, -0.39, 0.45, and 0.63 respectively.

$\Gamma(\pi^- \nu_\tau)/\Gamma_{\text{total}}$ **Γ_9/Γ**
 Data marked "avg" are highly correlated with data appearing elsewhere in the Listings, and are therefore used for the average given below but not in the overall fits. "f&a" marks results used for the fit and the average.

VALUE (%)	EVTS	DOCUMENT ID	TECN	COMMENT
10.91 ± 0.07 OUR FIT				Error includes scale factor of 1.1.
10.828 ± 0.070 ± 0.078 f&a	38k	¹ SCHAEEL 05c	ALEP	1991-1995 LEP runs
• • •				We do not use the following data for averages, fits, limits, etc. • • •
11.06 ± 0.11 ± 0.14		² BUSKULIC 96	ALEP	Repl. by SCHAEEL 05c
11.7 ± 0.4 ± 1.8	1138	BLOCKER 82D	MRK2	$E_{\text{cm}}^{\text{ee}} = 3.5-6.7$ GeV

¹ See footnote to SCHAEEL 05c $\Gamma(\tau^- \rightarrow e^- \bar{\nu}_e \nu_\tau)/\Gamma_{\text{total}}$ measurement for correlations with other measurements.

² Not independent of BUSKULIC 96 $B(h^- \nu_\tau)$ and $B(K^- \nu_\tau)$ values.

$\Gamma(K^- \nu_\tau)/\Gamma_{\text{total}}$ **Γ_{10}/Γ**

VALUE (%)	EVTS	DOCUMENT ID	TECN	COMMENT
0.695 ± 0.023 OUR FIT				Error includes scale factor of 1.1.
0.685 ± 0.023 OUR AVERAGE				
0.658 ± 0.027 ± 0.029		¹ ABBIENDI 01J	OPAL	1990-1995 LEP runs
0.696 ± 0.025 ± 0.014	2032	BARATE 99k	ALEP	1991-1995 LEP runs
0.85 ± 0.18	27	ABREU 94k	DLPH	LEP 1992 Z data
0.66 ± 0.07 ± 0.09	99	BATTLE 94	CLEO	$E_{\text{cm}}^{\text{ee}} \approx 10.6$ GeV
• • •				We do not use the following data for averages, fits, limits, etc. • • •
0.72 ± 0.04 ± 0.04	728	BUSKULIC 96	ALEP	Repl. by BARATE 99k
0.59 ± 0.18	16	MILLS 84	DLCO	$E_{\text{cm}}^{\text{ee}} = 29$ GeV
1.3 ± 0.5	15	BLOCKER 82B	MRK2	$E_{\text{cm}}^{\text{ee}} = 3.9-6.7$ GeV

¹ The correlation coefficient between this measurement and the ABBIENDI 01J $B(\tau^- \rightarrow K^- \geq 0 \pi^0 \geq 0 K^0 \geq 0 \gamma \nu_\tau)$ is 0.60.

$\Gamma(h^- \geq 1 \text{ neutrals } \nu_\tau)/\Gamma_{\text{total}}$ **Γ_{11}/Γ**

$$\Gamma_{11}/\Gamma = (\Gamma_{14} + \Gamma_{16} + \Gamma_{20} + \Gamma_{23} + \Gamma_{27} + \Gamma_{28} + \Gamma_{30} + 0.157\Gamma_{35} + 0.157\Gamma_{37} + 0.157\Gamma_{40} + 0.157\Gamma_{42} + 0.0985\Gamma_{47} + 0.708\Gamma_{126} + 0.715\Gamma_{128} + 0.09\Gamma_{146} + 0.09\Gamma_{148})/\Gamma$$

VALUE (%)	DOCUMENT ID	TECN	COMMENT
37.08 ± 0.11 OUR FIT			Error includes scale factor of 1.2.
• • •			We do not use the following data for averages, fits, limits, etc. • • •
36.14 ± 0.33 ± 0.58	¹ AKERS 94E	OPAL	1991-1992 LEP runs
38.4 ± 1.2 ± 1.0	² BURCHAT 87	MRK2	$E_{\text{cm}}^{\text{ee}} = 29$ GeV
42.7 ± 2.0 ± 2.9	BERGER 85	PLUT	$E_{\text{cm}}^{\text{ee}} = 34.6$ GeV

¹ Not independent of ACKERSTAFF 98M $B(h^- \pi^0 \nu_\tau)$ and $B(h^- \geq 2 \pi^0 \nu_\tau)$ values.

² BURCHAT 87 quote for $B(\pi^\pm \geq 1 \text{ neutral } \nu_\tau) = 0.378 \pm 0.012 \pm 0.010$. We add 0.006 to account for contribution from $(K^* \nu_\tau)$ which they fixed at BR = 0.013.

$\Gamma(h^- \geq 1 \pi^0 \nu_\tau (\text{ex. } K^0))/\Gamma_{\text{total}}$ **$\Gamma_{12}/\Gamma = (\Gamma_{14} + \Gamma_{16} + \Gamma_{20} + \Gamma_{23} + \Gamma_{27} + \Gamma_{28} + \Gamma_{30} + 0.325\Gamma_{126} + 0.325\Gamma_{128})/\Gamma$**

VALUE (%)	EVTS	DOCUMENT ID	TECN	COMMENT
36.54 ± 0.11 OUR FIT				Error includes scale factor of 1.2.
36.641 ± 0.155 ± 0.127 avg	45k	¹ ABDALLAH 06A	DLPH	1992-1995 LEP runs

¹ See footnote to ABDALLAH 06A $\Gamma(\tau^- \rightarrow h^- \nu_\tau)/\Gamma_{\text{total}}$ measurement for correlations with other measurements.

$\Gamma(h^- \pi^0 \nu_\tau)/\Gamma_{\text{total}}$ **$\Gamma_{13}/\Gamma = (\Gamma_{14} + \Gamma_{16})/\Gamma$**

VALUE (%)	EVTS	DOCUMENT ID	TECN	COMMENT
25.95 ± 0.10 OUR FIT				Error includes scale factor of 1.1.
25.74 ± 0.17 OUR AVERAGE				
25.740 ± 0.201 ± 0.138	35k	¹ ABDALLAH 06A	DLPH	1992-1995 LEP runs
25.89 ± 0.17 ± 0.29		ACKERSTAFF 98M	OPAL	1991-1995 LEP runs
25.05 ± 0.35 ± 0.50	6613	ACCIARRI 95	L3	1992 LEP run
25.87 ± 0.12 ± 0.42	51k	² ARTUSO 94	CLEO	$E_{\text{cm}}^{\text{ee}} = 10.6$ GeV
• • •				We do not use the following data for averages, fits, limits, etc. • • •
25.76 ± 0.15 ± 0.13	31k	BUSKULIC 96	ALEP	Repl. by SCHAEEL 05c
25.98 ± 0.36 ± 0.52		³ AKERS 94E	OPAL	Repl. by ACKERSTAFF 98M
22.9 ± 0.8 ± 1.3	283	⁴ ABREU 92N	DLPH	$E_{\text{cm}}^{\text{ee}} = 88.2-94.2$ GeV
23.1 ± 0.4 ± 0.9	1249	⁵ ALBRECHT 92c	ARG	$E_{\text{cm}}^{\text{ee}} = 10$ GeV
25.02 ± 0.64 ± 0.88	1849	DECAMP 92Q	ALEP	1989-1990 LEP runs
22.0 ± 0.8 ± 1.9	779	ANTREASYAN 91	CBAL	$E_{\text{cm}}^{\text{ee}} = 9.4-10.6$ GeV
22.6 ± 1.5 ± 0.7	1101	BEHREND 90	CELL	$E_{\text{cm}}^{\text{ee}} = 35$ GeV
23.1 ± 1.9 ± 1.6		BEHREND 84	CELL	$E_{\text{cm}}^{\text{ee}} = 14, 22$ GeV

¹ See footnote to ABDALLAH 06A $\Gamma(\tau^- \rightarrow h^- \nu_\tau)/\Gamma_{\text{total}}$ measurement for correlations with other measurements.

² ARTUSO 94 reports the combined result from three independent methods, one of which (23% of the $\tau^- \rightarrow h^- \pi^0 \nu_\tau$) is normalized to the inclusive one-prong branching fraction, taken as 0.854 ± 0.004 . Renormalization to the present value causes negligible change.

³ AKERS 94E quote $(26.25 \pm 0.36 \pm 0.52) \times 10^{-2}$; we subtract 0.27% from their number to correct for $\tau^- \rightarrow h^- K_L^0 \nu_\tau$.

⁴ ABREU 92N with 0.5% added to remove their correction for $K^*(892)^-$ backgrounds.

⁵ ALBRECHT 92Q with 0.5% added to remove their correction for $\tau^- \rightarrow K^*(892)^- \nu_\tau$ background.

Lepton Particle Listings

 τ $\Gamma(\pi^- \pi^0 \nu_\tau)/\Gamma_{\text{total}}$ Γ_{14}/Γ

Data marked "avg" are highly correlated with data appearing elsewhere in the Listings, and are therefore used for the average given below but not in the overall fits. "f&a" marks results used for the fit and the average.

VALUE (%)	EVTS	DOCUMENT ID	TECN	COMMENT
25.52 ± 0.10 OUR FIT				Error includes scale factor of 1.1.
25.46 ± 0.12 OUR AVERAGE				
25.471 ± 0.097 ± 0.085 f&a	81k	¹ SCHAEEL	05c ALEP	1991-1995 LEP runs
25.36 ± 0.44 avg		² ARTUSO	94 CLEO	$E_{\text{cm}}^{\text{ee}} = 10.6$ GeV
••• We do not use the following data for averages, fits, limits, etc. •••				
25.30 ± 0.15 ± 0.13		³ BUSKULIC	96 ALEP	Repl. by SCHAEEL 05c
21.5 ± 0.4 ± 1.9	4400	^{4,5} ALBRECHT	88L ARG	$E_{\text{cm}}^{\text{ee}} = 10$ GeV
23.0 ± 1.3 ± 1.7	582	ADLER	87B MRK3	$E_{\text{cm}}^{\text{ee}} = 3.77$ GeV
25.8 ± 1.7 ± 2.5		⁶ BURCHAT	87 MRK2	$E_{\text{cm}}^{\text{ee}} = 29$ GeV
22.3 ± 0.6 ± 1.4	629	⁵ YELTON	86 MRK2	$E_{\text{cm}}^{\text{ee}} = 29$ GeV

- See footnote to SCHAEEL 05c $\Gamma(\tau^- \rightarrow e^- \bar{\nu}_e \nu_\tau)/\Gamma_{\text{total}}$ measurement for correlations with other measurements.
- Not independent of ARTUSO 94 $B(h^- \pi^0 \nu_\tau)$ and BATTLE 94 $B(K^- \pi^0 \nu_\tau)$ values.
- Not independent of BUSKULIC 96 $B(h^- \pi^0 \nu_\tau)$ and $B(K^- \pi^0 \nu_\tau)$ values.
- The authors divide by $(\Gamma_3 + \Gamma_5 + \Gamma_9 + \Gamma_{10})/\Gamma = 0.467$ to obtain this result.
- Experiment had no hadron identification. Kaon corrections were made, but insufficient information is given to permit their removal.
- BURCHAT 87 value is not independent of YELTON 86 value. Nonresonant decays included.

 $\Gamma(\pi^- \pi^0 \text{non-}\rho(770)\nu_\tau)/\Gamma_{\text{total}}$ Γ_{15}/Γ

VALUE (%)	DOCUMENT ID	TECN	COMMENT
0.3 ± 0.1 ± 0.3	¹ BEHREND 84	CELL	$E_{\text{cm}}^{\text{ee}} = 14,22$ GeV

- BEHREND 84 assume a flat nonresonant mass distribution down to the $\rho(770)$ mass, using events with mass above 1300 to set the level.

 $\Gamma(K^- \pi^0 \nu_\tau)/\Gamma_{\text{total}}$ Γ_{16}/Γ

VALUE (%)	EVTS	DOCUMENT ID	TECN	COMMENT
0.428 ± 0.015 OUR FIT				Error includes scale factor of 1.1.
0.426 ± 0.016 OUR AVERAGE				
0.416 ± 0.003 ± 0.018	78k	AUBERT	07AP BABR	230 fb^{-1} $E_{\text{cm}}^{\text{ee}} = 10.6$ GeV
0.471 ± 0.059 ± 0.023	360	ABBIENDI	04J OPAL	1991-1995 LEP runs
0.444 ± 0.026 ± 0.024	923	BARATE	99K ALEP	1991-1995 LEP runs
0.51 ± 0.10 ± 0.07	37	BATTLE	94 CLEO	$E_{\text{cm}}^{\text{ee}} \approx 10.6$ GeV
••• We do not use the following data for averages, fits, limits, etc. •••				
0.52 ± 0.04 ± 0.05	395	BUSKULIC	96 ALEP	Repl. by BARATE 99k

 $\Gamma(h^- \geq 2\pi^0 \nu_\tau)/\Gamma_{\text{total}}$ Γ_{17}/Γ

$$\Gamma_{17}/\Gamma = (\Gamma_{20} + \Gamma_{23} + \Gamma_{27} + \Gamma_{28} + \Gamma_{30} + 0.157\Gamma_{35} + 0.157\Gamma_{37} + 0.157\Gamma_{40} + 0.157\Gamma_{42} + 0.0985\Gamma_{47} + 0.319\Gamma_{126} + 0.322\Gamma_{128})/\Gamma$$

Data marked "avg" are highly correlated with data appearing elsewhere in the Listings, and are therefore used for the average given below but not in the overall fits. "f&a" marks results used for the fit and the average.

VALUE (%)	EVTS	DOCUMENT ID	TECN	COMMENT
10.84 ± 0.12 OUR FIT				Error includes scale factor of 1.3.
9.91 ± 0.31 ± 0.27 f&a		ACKERSTAFF 98M	OPAL	1991-1995 LEP runs
••• We do not use the following data for averages, fits, limits, etc. •••				
9.89 ± 0.34 ± 0.55		¹ AKERS	94E OPAL	Repl. by ACKER-STAFF 98M
14.0 ± 1.2 ± 0.6	938	² BEHREND	90 CELL	$E_{\text{cm}}^{\text{ee}} = 35$ GeV
12.0 ± 1.4 ± 2.5		³ BURCHAT	87 MRK2	$E_{\text{cm}}^{\text{ee}} = 29$ GeV
13.9 ± 2.0 ± 1.9 -2.2		⁴ AIHARA	86E TPC	$E_{\text{cm}}^{\text{ee}} = 29$ GeV

- AKERS 94E not independent of AKERS 94E $B(h^- \geq 1\pi^0 \nu_\tau)$ and $B(h^- \pi^0 \nu_\tau)$ measurements.
- No independent of BEHREND 90 $\Gamma(h^- 2\pi^0 \nu_\tau \text{ (exp. } K^0))$ and $\Gamma(h^- \geq 3\pi^0 \nu_\tau)$.
- Error correlated with BURCHAT 87 $\Gamma(\rho^- \nu_e)/\Gamma(\text{total})$ value.
- AIHARA 86E (TPC) quote $B(2\pi^0 \pi^- \nu_\tau) + 1.6B(3\pi^0 \pi^- \nu_\tau) + 1.1B(\pi^0 \eta \pi^- \nu_\tau)$.

 $\Gamma(h^- 2\pi^0 \nu_\tau)/\Gamma_{\text{total}}$ Γ_{18}/Γ

$$\Gamma_{18}/\Gamma = (\Gamma_{20} + \Gamma_{23} + 0.157\Gamma_{35} + 0.157\Gamma_{37})/\Gamma$$

VALUE (%)	EVTS	DOCUMENT ID	TECN	COMMENT
9.49 ± 0.11 OUR FIT				Error includes scale factor of 1.2.
••• We do not use the following data for averages, fits, limits, etc. •••				
9.48 ± 0.13 ± 0.10	12k	¹ BUSKULIC	96 ALEP	Repl. by SCHAEEL 05c
¹ BUSKULIC 96 quote $9.29 \pm 0.13 \pm 0.10$. We add 0.19 to undo their correction for $\tau^- \rightarrow h^- K^0 \nu_\tau$.				

 $\Gamma(h^- 2\pi^0 \nu_\tau \text{ (ex. } K^0))/\Gamma_{\text{total}}$ Γ_{19}/Γ

Data marked "avg" are highly correlated with data appearing elsewhere in the Listings, and are therefore used for the average given below but not in the overall fits. f&a marks results used for the fit and the average.

VALUE (%)	EVTS	DOCUMENT ID	TECN	COMMENT
9.33 ± 0.12 OUR FIT				Error includes scale factor of 1.2.
9.17 ± 0.27 OUR AVERAGE				
9.498 ± 0.320 ± 0.275 f&a	9.5k	¹ ABDALLAH 06A	DLPH	1992-1995 LEP runs
8.88 ± 0.37 ± 0.42 f&a	1060	ACCIARRI	95 L3	1992 LEP run
8.96 ± 0.16 ± 0.44 avg		² PROCARIO	93 CLEO	$E_{\text{cm}}^{\text{ee}} \approx 10.6$ GeV

••• We do not use the following data for averages, fits, limits, etc. •••

10.38 ± 0.66 ± 0.82	809	³ DECAMP	92c ALEP	Repl. by SCHAEEL 05c
5.7 ± 0.5 ± 1.7 -1.0	133	⁴ ANTREASIAN	91 CBAL	$E_{\text{cm}}^{\text{ee}} = 9.4-10.6$ GeV
10.0 ± 1.5 ± 1.1	333	⁵ BEHREND	90 CELL	$E_{\text{cm}}^{\text{ee}} = 35$ GeV
8.7 ± 0.4 ± 1.1	815	⁶ BAND	87 MAC	$E_{\text{cm}}^{\text{ee}} = 29$ GeV
6.2 ± 0.6 ± 1.2		⁷ GAN	87 MRK2	$E_{\text{cm}}^{\text{ee}} = 29$ GeV
6.0 ± 3.0 ± 1.8		BEHREND	84 CELL	$E_{\text{cm}}^{\text{ee}} = 14,22$ GeV

- See footnote to ABDALLAH 06A $\Gamma(\tau^- \rightarrow h^- \nu_\tau)/\Gamma_{\text{total}}$ measurement for correlations with other measurements.
- PROCARIO 93 entry is obtained from $B(h^- 2\pi^0 \nu_\tau)/B(h^- \pi^0 \nu_\tau)$ using ARTUSO 94 result for $B(h^- \pi^0 \nu_\tau)$.
- We subtract 0.0015 to account for $\tau^- \rightarrow K^*(892)^- \nu_\tau$ contribution.
- ANTREASIAN 91 subtract 0.001 to account for the $\tau^- \rightarrow K^*(892)^- \nu_\tau$ contribution.
- BEHREND 90 subtract 0.002 to account for the $\tau^- \rightarrow K^*(892)^- \nu_\tau$ contribution.
- BAND 87 assume $B(\pi^- 3\pi^0 \nu_\tau) = 0.01$ and $B(\pi^- \pi^0 \eta \nu_\tau) = 0.005$.
- GAN 87 analysis use photon multiplicity distribution.

 $\Gamma(h^- 2\pi^0 \nu_\tau \text{ (ex. } K^0))/\Gamma(h^- \pi^0 \nu_\tau)$ Γ_{19}/Γ_{13}

$$\Gamma_{19}/\Gamma_{13} = (\Gamma_{20} + \Gamma_{23})/(\Gamma_{14} + \Gamma_{16})$$

VALUE	DOCUMENT ID	TECN	COMMENT
0.360 ± 0.005 OUR FIT			Error includes scale factor of 1.2.
0.342 ± 0.006 ± 0.016	¹ PROCARIO 93	CLEO	$E_{\text{cm}}^{\text{ee}} \approx 10.6$ GeV

- PROCARIO 93 quote $0.345 \pm 0.006 \pm 0.016$ after correction for 2 kaon backgrounds assuming $B(K^* \nu_\tau) = 1.42 \pm 0.18\%$ and $B(h^- K^0 \pi^0 \nu_\tau) = 0.48 \pm 0.48\%$. We multiply by 0.990 ± 0.010 to remove these corrections to $B(h^- \pi^0 \nu_\tau)$.

 $\Gamma(\pi^- 2\pi^0 \nu_\tau \text{ (ex. } K^0))/\Gamma_{\text{total}}$ Γ_{20}/Γ

Data marked "avg" are highly correlated with data appearing elsewhere in the Listings, and are therefore used for the average given below but not in the overall fits. "f&a" marks results used for the fit and the average.

VALUE (%)	EVTS	DOCUMENT ID	TECN	COMMENT
9.27 ± 0.12 OUR FIT				Error includes scale factor of 1.2.
9.239 ± 0.086 ± 0.090 f&a	31k	¹ SCHAEEL	05c ALEP	1991-1995 LEP runs
••• We do not use the following data for averages, fits, limits, etc. •••				
9.21 ± 0.13 ± 0.11		² BUSKULIC	96 ALEP	Repl. by SCHAEEL 05c

- See footnote to SCHAEEL 05c $\Gamma(\tau^- \rightarrow e^- \bar{\nu}_e \nu_\tau)/\Gamma_{\text{total}}$ measurement for correlations with other measurements.
- Not independent of BUSKULIC 96 $B(h^- 2\pi^0 \nu_\tau \text{ (ex. } K^0))$ and $B(K^- 2\pi^0 \nu_\tau \text{ (ex. } K^0))$ values.

 $\Gamma(\pi^- 2\pi^0 \nu_\tau \text{ (ex. } K^0), \text{ scalar})/\Gamma(\pi^- 2\pi^0 \nu_\tau \text{ (ex. } K^0))$ Γ_{21}/Γ_{20}

VALUE	CL%	DOCUMENT ID	TECN	COMMENT
<0.094	95	¹ BROWDER	00 CLEO	4.7 fb^{-1} $E_{\text{cm}}^{\text{ee}} = 10.6$ GeV

- Model-independent limit from structure function analysis on contribution to $B(\tau^- \rightarrow \pi^- 2\pi^0 \nu_\tau \text{ (ex. } K^0))$ from scalars.

 $\Gamma(\pi^- 2\pi^0 \nu_\tau \text{ (ex. } K^0), \text{ vector})/\Gamma(\pi^- 2\pi^0 \nu_\tau \text{ (ex. } K^0))$ Γ_{22}/Γ_{20}

VALUE	CL%	DOCUMENT ID	TECN	COMMENT
<0.073	95	¹ BROWDER	00 CLEO	4.7 fb^{-1} $E_{\text{cm}}^{\text{ee}} = 10.6$ GeV

- Model-independent limit from structure function analysis on contribution to $B(\tau^- \rightarrow \pi^- 2\pi^0 \nu_\tau \text{ (ex. } K^0))$ from vectors.

 $\Gamma(K^- 2\pi^0 \nu_\tau \text{ (ex. } K^0))/\Gamma_{\text{total}}$ Γ_{23}/Γ

VALUE (units 10^{-4})	EVTS	DOCUMENT ID	TECN	COMMENT
6.3 ± 2.3 OUR FIT				Error includes scale factor of 1.1.
5.8 ± 2.4 OUR AVERAGE				
5.6 ± 2.0 ± 1.5	131	BARATE	99k ALEP	1991-1995 LEP runs
9 ± 10 ± 3	3	¹ BATTLE	94 CLEO	$E_{\text{cm}}^{\text{ee}} \approx 10.6$ GeV

••• We do not use the following data for averages, fits, limits, etc. •••

- BATTLE 94 quote $(14 \pm 10 \pm 3) \times 10^{-4}$ or $< 30 \times 10^{-4}$ at 90% CL. We subtract $(5 \pm 2) \times 10^{-4}$ to account for $\tau^- \rightarrow K^-(K^0 \rightarrow \pi^0 \pi^0) \nu_\tau$ background.

 $\Gamma(h^- \geq 3\pi^0 \nu_\tau)/\Gamma_{\text{total}}$ Γ_{24}/Γ

$$\Gamma_{24}/\Gamma = (\Gamma_{27} + \Gamma_{28} + \Gamma_{30} + 0.157\Gamma_{40} + 0.157\Gamma_{42} + 0.0985\Gamma_{47} + 0.319\Gamma_{126} + 0.322\Gamma_{128})/\Gamma$$

VALUE (%)	EVTS	DOCUMENT ID	TECN	COMMENT
1.35 ± 0.07 OUR FIT				Error includes scale factor of 1.1.
••• We do not use the following data for averages, fits, limits, etc. •••				
1.53 ± 0.40 ± 0.46	186	DECAMP	92c ALEP	Repl. by SCHAEEL 05c
3.2 ± 1.0 ± 1.0		BEHREND	90 CELL	$E_{\text{cm}}^{\text{ee}} = 35$ GeV

 $\Gamma(h^- \geq 3\pi^0 \nu_\tau \text{ (ex. } K^0))/\Gamma_{\text{total}}$ Γ_{25}/Γ

$$\Gamma_{25}/\Gamma = (\Gamma_{27} + \Gamma_{28} + \Gamma_{30} + 0.325\Gamma_{126} + 0.325\Gamma_{128})/\Gamma$$

VALUE (%)	EVTS	DOCUMENT ID	TECN	COMMENT
1.26 ± 0.07 OUR FIT				Error includes scale factor of 1.1.
1.403 ± 0.214 ± 0.224	1.1k	¹ ABDALLAH 06A	DLPH	1992-1995 LEP runs

- See footnote to ABDALLAH 06A $\Gamma(\tau^- \rightarrow h^- \nu_\tau)/\Gamma_{\text{total}}$ measurement for correlations with other measurements.

$$\Gamma(h^- 3\pi^0 \nu_\tau)/\Gamma_{\text{total}} \quad \Gamma_{26}/\Gamma$$

$$\Gamma_{26}/\Gamma = (\Gamma_{27} + \Gamma_{28} + 0.157\Gamma_{40} + 0.157\Gamma_{42} + 0.322\Gamma_{128})/\Gamma$$

Data marked "avg" are highly correlated with data appearing elsewhere in the Listings, and are therefore used for the average given below but not in the overall fits. "f&a" marks results used for the fit and the average.

VALUE (%)	EVTS	DOCUMENT ID	TECN	COMMENT
-----------	------	-------------	------	---------

1.18 ± 0.08 OUR FIT

1.21 ± 0.17 OUR AVERAGE Error includes scale factor of 1.2.

1.70 ± 0.24 ± 0.38	f&a	293	ACCIARRI	95 L3	1992 LEP run
1.15 ± 0.08 ± 0.13	avg	1	PROCARIO	93 CLEO	$E_{\text{cm}}^{\text{ee}} \approx 10.6$ GeV

• • • We do not use the following data for averages, fits, limits, etc. • • •

1.24 ± 0.09 ± 0.11	2.3k	2	BUSKULIC	96 ALEP	Repl. by SCHAEF 05c
0.0	+1.4 -0.1	+1.1 -0.1	3	GAN	87 MRK2 $E_{\text{cm}}^{\text{ee}} = 29$ GeV

¹ PROCARIO 93 entry is obtained from $B(h^- 3\pi^0 \nu_\tau)/B(h^- \pi^0 \nu_\tau)$ using ARTUSO 94 result for $B(h^- \pi^0 \nu_\tau)$.

² BUSKULIC 96 quote $B(h^- 3\pi^0 \nu_\tau(\text{ex. } K^0)) = 1.17 \pm 0.09 \pm 0.11$. We add 0.07 to remove their correction for K^0 backgrounds.

³ Highly correlated with GAN 87 $\Gamma(\eta\pi^0 \nu_\tau)/\Gamma_{\text{total}}$ value. Authors quote $B(\pi^\pm 3\pi^0 \nu_\tau) + 0.67B(\pi^\pm \eta\pi^0 \nu_\tau) = 0.047 \pm 0.010 \pm 0.011$.

$$\Gamma(h^- 3\pi^0 \nu_\tau)/\Gamma(h^- \pi^0 \nu_\tau) \quad \Gamma_{26}/\Gamma_{13}$$

$$\Gamma_{26}/\Gamma_{13} = (\Gamma_{27} + \Gamma_{28} + 0.157\Gamma_{40} + 0.157\Gamma_{42} + 0.322\Gamma_{128})/(\Gamma_{14} + \Gamma_{16})$$

VALUE (%)	DOCUMENT ID	TECN	COMMENT
-----------	-------------	------	---------

0.0456 ± 0.0029 OUR FIT

0.044 ± 0.003 ± 0.005 ¹ PROCARIO 93 CLEO $E_{\text{cm}}^{\text{ee}} \approx 10.6$ GeV

¹ PROCARIO 93 quote $0.041 \pm 0.003 \pm 0.005$ after correction for 2 kaon backgrounds assuming $B(K^* \nu_\tau) = 1.42 \pm 0.18\%$ and $B(h^- K^0 \pi^0 \nu_\tau) = 0.48 \pm 0.48\%$. We add 0.003 ± 0.003 and multiply the sum by 0.990 ± 0.010 to remove these corrections.

$$\Gamma(\pi^- 3\pi^0 \nu_\tau(\text{ex. } K^0))/\Gamma_{\text{total}} \quad \Gamma_{27}/\Gamma$$

VALUE (%)	EVTS	DOCUMENT ID	TECN	COMMENT
-----------	------	-------------	------	---------

1.04 ± 0.07 OUR FIT

0.977 ± 0.069 ± 0.058 6.1k ¹ SCHAEF 05c ALEP 1991-1995 LEP runs

¹ See footnote to SCHAEF 05c $\Gamma(\tau^- \rightarrow e^- \bar{\nu}_e \nu_\tau)/\Gamma_{\text{total}}$ measurement for correlations with other measurements.

$$\Gamma(K^- 3\pi^0 \nu_\tau(\text{ex. } K^0, \eta))/\Gamma_{\text{total}} \quad \Gamma_{28}/\Gamma$$

VALUE (units 10^{-4})	EVTS	DOCUMENT ID	TECN	COMMENT
--------------------------	------	-------------	------	---------

4.7 ± 2.1 OUR FIT

3.7 ± 2.1 ± 1.1 22 BARATE 99k ALEP 1991-1995 LEP runs

• • • We do not use the following data for averages, fits, limits, etc. • • •

5 ± 13 ¹ BUSKULIC 94E ALEP Repl. by BARATE 99k

¹ BUSKULIC 94E quote $B(K^- \geq 0\pi^0 \geq 0K^0 \nu_\tau) - [B(K^- \nu_\tau) + B(K^- \pi^0 \nu_\tau) + B(K^- K^0 \nu_\tau) + B(K^- \pi^0 \pi^0 \nu_\tau) + B(K^- \pi^0 K^0 \nu_\tau)] = (5 \pm 13) \times 10^{-4}$ accounting for common systematic errors in BUSKULIC 94E and BUSKULIC 94F measurements of these modes. We assume $B(K^- \geq 2K^0 \nu_\tau)$ and $B(K^- \geq 4\pi^0 \nu_\tau)$ are negligible.

$$\Gamma(h^- 4\pi^0 \nu_\tau(\text{ex. } K^0))/\Gamma_{\text{total}} \quad \Gamma_{29}/\Gamma$$

VALUE (%)	EVTS	DOCUMENT ID	TECN	COMMENT
-----------	------	-------------	------	---------

0.16 ± 0.04 OUR FIT

0.16 ± 0.05 ± 0.05 ¹ PROCARIO 93 CLEO $E_{\text{cm}}^{\text{ee}} \approx 10.6$ GeV

• • • We do not use the following data for averages, fits, limits, etc. • • •

0.16 ± 0.04 ± 0.09 232 ² BUSKULIC 96 ALEP Repl. by SCHAEF 05c

¹ PROCARIO 93 quotes $B(h^- 4\pi^0 \nu_\tau)/B(h^- \pi^0 \nu_\tau) = 0.006 \pm 0.002 \pm 0.002$. We multiply by the ARTUSO 94 result for $B(h^- \pi^0 \nu_\tau)$ to obtain $B(h^- 4\pi^0 \nu_\tau)$. PROCARIO 93 assume $B(h^- \geq 5\pi^0 \nu_\tau)$ is small and do not correct for it.

² BUSKULIC 96 quote result for $\tau^- \rightarrow h^- \geq 4\pi^0 \nu_\tau$. We assume $B(h^- \geq 5\pi^0 \nu_\tau)$ is negligible.

$$\Gamma(h^- 4\pi^0 \nu_\tau(\text{ex. } K^0, \eta))/\Gamma_{\text{total}} \quad \Gamma_{30}/\Gamma$$

VALUE (%)	EVTS	DOCUMENT ID	TECN	COMMENT
-----------	------	-------------	------	---------

0.10 ± 0.04 OUR FIT

0.112 ± 0.037 ± 0.035 957 ¹ SCHAEF 05c ALEP 1991-1995 LEP runs

¹ See footnote to SCHAEF 05c $\Gamma(\tau^- \rightarrow e^- \bar{\nu}_e \nu_\tau)/\Gamma_{\text{total}}$ measurement for correlations with other measurements.

$$\Gamma(K^- \geq 0\pi^0 \geq 0K^0 \geq 0\gamma \nu_\tau)/\Gamma_{\text{total}} \quad \Gamma_{31}/\Gamma$$

VALUE (%)	EVTS	DOCUMENT ID	TECN	COMMENT
-----------	------	-------------	------	---------

1.57 ± 0.04 OUR FIT

1.53 ± 0.04 OUR AVERAGE Error includes scale factor of 1.1.

1.528 ± 0.039 ± 0.040	f&a	1	ABBIENDI	01J OPAL	1990-1995 LEP runs
1.520 ± 0.040 ± 0.041	avg	4006	2	BARATE	99k ALEP 1991-1995 LEP runs
1.54 ± 0.24	f&a		ABREU	94k DLPH	LEP 1992 Z data
1.70 ± 0.12 ± 0.19	f&a	202	3	BATTLE	94 CLEO $E_{\text{cm}}^{\text{ee}} \approx 10.6$ GeV

• • • We do not use the following data for averages, fits, limits, etc. • • •

1.70 ± 0.05 ± 0.06	1610	4	BUSKULIC	96 ALEP	Repl. by BARATE 99k
1.6 ± 0.4 ± 0.2	35		AIHARA	87b TPC	$E_{\text{cm}}^{\text{ee}} = 29$ GeV
1.71 ± 0.29	53		MILLS	84 DLCO	$E_{\text{cm}}^{\text{ee}} = 29$ GeV

¹ The correlation coefficient between this measurement and the ABBIENDI 01J $B(\tau^- \rightarrow K^- \nu_\tau)$ is 0.60.

² Not independent of BARATE 99k $B(K^- \nu_\tau)$, $B(K^- \pi^0 \nu_\tau)$, $B(K^- 2\pi^0 \nu_\tau(\text{ex. } K^0))$, $B(K^- 3\pi^0 \nu_\tau(\text{ex. } K^0))$, $B(K^- K^0 \nu_\tau)$, and $B(K^- K^0 \pi^0 \nu_\tau)$ values.

³ BATTLE 94 quote $1.60 \pm 0.12 \pm 0.19$. We add 0.10 ± 0.02 to correct for their rejection of $K_S^0 \rightarrow \pi^+ \pi^-$ decays.

⁴ Not independent of BUSKULIC 96 $B(K^- \nu_\tau)$, $B(K^- \pi^0 \nu_\tau)$, $B(K^- 2\pi^0 \nu_\tau)$, $B(K^- K^0 \nu_\tau)$, and $B(K^- K^0 \pi^0 \nu_\tau)$ values.

$$\Gamma(K^- \geq 1(\pi^0 \text{ or } K^0 \text{ or } \gamma) \nu_\tau)/\Gamma_{\text{total}} \quad \Gamma_{32}/\Gamma$$

$$\Gamma_{32}/\Gamma = (\Gamma_{16} + \Gamma_{23} + \Gamma_{28} + \Gamma_{37} + \Gamma_{42} + 0.715\Gamma_{128})/\Gamma$$

Data marked "avg" are highly correlated with data appearing elsewhere in the Listings, and are therefore used for the average given below but not in the overall fits. "f&a" marks results used for the fit and the average.

VALUE (%)	EVTS	DOCUMENT ID	TECN	COMMENT
-----------	------	-------------	------	---------

0.874 ± 0.032 OUR FIT

0.86 ± 0.05 OUR AVERAGE

0.869 ± 0.031 ± 0.034	avg	1	ABBIENDI	01J OPAL	1990-1995 LEP runs
0.69 ± 0.25	avg	2	ABREU	94k DLPH	LEP 1992 Z data

• • • We do not use the following data for averages, fits, limits, etc. • • •

1.2 ± 0.5	+0.2 -0.4	9	AIHARA	87b TPC	$E_{\text{cm}}^{\text{ee}} = 29$ GeV
-----------	-----------	---	--------	---------	--------------------------------------

¹ Not independent of ABBIENDI 01J $B(\tau^- \rightarrow K^- \nu_\tau)$ and $B(\tau^- \rightarrow K^- \geq 0\pi^0 \geq 0K^0 \geq 0\gamma \nu_\tau)$ values.

² Not independent of ABREU 94k $B(K^- \nu_\tau)$ and $B(K^- \geq 0$ neutrals $\nu_\tau)$ measurements.

$$\Gamma(K_S^0(\text{particles})^- \nu_\tau)/\Gamma_{\text{total}} \quad \Gamma_{33}/\Gamma$$

VALUE (%)	EVTS	DOCUMENT ID	TECN	COMMENT
-----------	------	-------------	------	---------

0.92 ± 0.04 OUR FIT

0.97 ± 0.07 OUR AVERAGE

0.970 ± 0.058 ± 0.062	929	BARATE	98E ALEP	1991-1995 LEP runs
0.97 ± 0.09 ± 0.06	141	AKERS	94G OPAL	$E_{\text{cm}}^{\text{ee}} = 88-94$ GeV

$\Gamma_{33}/\Gamma = (\frac{1}{2}\Gamma_{35} + \frac{1}{2}\Gamma_{37} + \frac{1}{2}\Gamma_{40} + \frac{1}{2}\Gamma_{42} + \Gamma_{47} + \Gamma_{48})/\Gamma$

Error includes scale factor of 1.4.

• • • We do not use the following data for averages, fits, limits, etc. • • •

1.2 ± 0.5 ± 0.4 9 AIHARA 87b TPC $E_{\text{cm}}^{\text{ee}} = 29$ GeV

¹ Not independent of ABBIENDI 01J $B(\tau^- \rightarrow K^- \nu_\tau)$ and $B(\tau^- \rightarrow K^- \geq 0\pi^0 \geq 0K^0 \geq 0\gamma \nu_\tau)$ values.

² Not independent of ABREU 94k $B(K^- \nu_\tau)$ and $B(K^- \geq 0$ neutrals $\nu_\tau)$ measurements.

$$\Gamma(h^- \bar{K}^0 \nu_\tau)/\Gamma_{\text{total}} \quad \Gamma_{34}/\Gamma = (\Gamma_{35} + \Gamma_{37})/\Gamma$$

Data marked "avg" are highly correlated with data appearing elsewhere in the Listings, and are therefore used for the average given below but not in the overall fits. "f&a" marks results used for the fit and the average.

VALUE (%)	EVTS	DOCUMENT ID	TECN	COMMENT
-----------	------	-------------	------	---------

1.00 ± 0.05 OUR FIT

0.90 ± 0.11 OUR AVERAGE

1.01 ± 0.07 ± 0.07	avg	555	1	BARATE	98E ALEP 1991-1995 LEP runs
0.855 ± 0.036 ± 0.073	f&a	1242	COAN	96 CLEO	$E_{\text{cm}}^{\text{ee}} \approx 10.6$ GeV

• • • We do not use the following data for averages, fits, limits, etc. • • •

¹ Not independent of BARATE 98E $B(\tau^- \rightarrow \pi^- \bar{K}^0 \nu_\tau)$ and $B(\tau^- \rightarrow K^- K^0 \nu_\tau)$ values.

$$\Gamma(\pi^- \bar{K}^0 \nu_\tau)/\Gamma_{\text{total}} \quad \Gamma_{35}/\Gamma$$

Data marked "avg" are highly correlated with data appearing elsewhere in the Listings, and are therefore used for the average given below but not in the overall fits. "f&a" marks results used for the fit and the average.

VALUE (%)	EVTS	DOCUMENT ID	TECN	COMMENT
-----------	------	-------------	------	---------

0.84 ± 0.04 OUR FIT

0.831 ± 0.030 OUR AVERAGE

0.808 ± 0.004 ± 0.026	f&a	53k	EPIFANOV	07 BELL	351 fb ⁻¹ $E_{\text{cm}}^{\text{ee}} = 10.6$ GeV
0.933 ± 0.068 ± 0.049	f&a	377	ABBIENDI	00c OPAL	1991-1995 LEP runs
0.928 ± 0.045 ± 0.034	f&a	937	1	BARATE	99k ALEP 1991-1995 LEP runs
0.855 ± 0.117 ± 0.066	avg	509	2	BARATE	98E ALEP 1991-1995 LEP runs
0.704 ± 0.041 ± 0.072	avg		3	COAN	96 CLEO $E_{\text{cm}}^{\text{ee}} \approx 10.6$ GeV
0.95 ± 0.15 ± 0.06	f&a		4	ACCIARRI	95F L3 1991-1993 LEP runs

• • • We do not use the following data for averages, fits, limits, etc. • • •

0.79 ± 0.10 ± 0.09 98 ⁵ BUSKULIC 96 ALEP Repl. by BARATE 99k

¹ BARATE 99k measure K_S^0 's by detecting K_L^0 's in their hadron calorimeter.

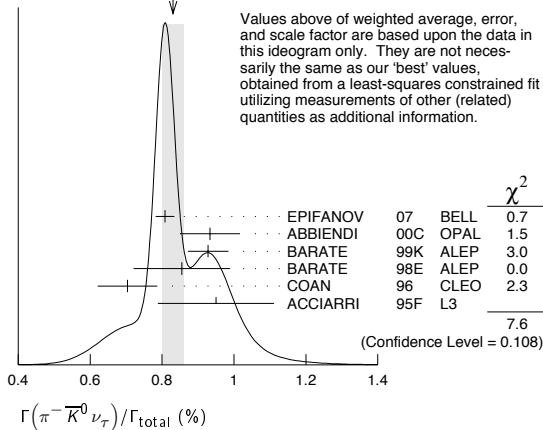
² BARATE 98E reconstruct K_S^0 's using $K_S^0 \rightarrow \pi^+ \pi^-$ decays. Not independent of BARATE 98E $B(K^0 \text{ particles}^- \nu_\tau)$ value.

³ Not independent of COAN 96 $B(h^- K^0 \nu_\tau)$ and $B(K^- K^0 \nu_\tau)$ measurements.

⁴ ACCIARRI 95F do not identify π^-/K^- and assume $B(K^- K^0 \nu_\tau) = (0.29 \pm 0.12)\%$.

⁵ BUSKULIC 96 measure K_S^0 's by detecting K_L^0 's in their hadron calorimeter.

Lepton Particle Listings

 τ WEIGHTED AVERAGE
0.831±0.030 (Error scaled by 1.4) $\Gamma(\pi^- \bar{K}^0 \nu_\tau) / \Gamma_{\text{total}}$ Γ_{36} / Γ

VALUE (units 10^{-4})	CL%	DOCUMENT ID	TECN	COMMENT
5.4 ± 2.1		¹ EPIFANOV 07 BELL	351 fb ⁻¹ $E_{\text{cm}}^{\text{ee}} = 10.6$ GeV	
• • • We do not use the following data for averages, fits, limits, etc. • • •				
<17	95	ACCIARRI 95F L3	1991-1993 LEP runs	
¹ EPIFANOV 07 quote $B(\tau^- \rightarrow K^*(892)^- \nu_\tau) B(K^*(892)^- \rightarrow K_S^0 \pi^-) / B(\tau^- \rightarrow K_S^0 \pi^- \nu_\tau) = 0.933 \pm 0.027$. We multiply their $B(\tau^- \rightarrow \bar{K}^0 \pi^- \nu_\tau)$ by $[1 - (0.933 \pm 0.027)]$ to obtain this result.				

 $\Gamma(K^- K^0 \nu_\tau) / \Gamma_{\text{total}}$ Γ_{37} / Γ

VALUE (%)	EVTS	DOCUMENT ID	TECN	COMMENT
0.158 ± 0.016 OUR FIT				
0.158 ± 0.017 OUR AVERAGE				
0.162 ± 0.021 ± 0.011	150	¹ BARATE 99K ALEP	1991-1995 LEP runs	
0.158 ± 0.042 ± 0.017	46	² BARATE 98E ALEP	1991-1995 LEP runs	
0.151 ± 0.021 ± 0.022	111	COAN 96 CLEO	$E_{\text{cm}}^{\text{ee}} \approx 10.6$ GeV	
• • • We do not use the following data for averages, fits, limits, etc. • • •				
0.26 ± 0.09 ± 0.02	13	³ BUSKULIC 96 ALEP	Repl. by BARATE 99K	
¹ BARATE 99K measure K^0 's by detecting K_L^0 's in their hadron calorimeter.				
² BARATE 98E reconstruct K^0 's using $K_S^0 \rightarrow \pi^+ \pi^-$ decays.				
³ BUSKULIC 96 measure K^0 's by detecting K_L^0 's in their hadron calorimeter.				

 $\Gamma(K^- K^0 \geq 0\pi^0 \nu_\tau) / \Gamma_{\text{total}}$ $\Gamma_{38} / \Gamma = (\Gamma_{37} + \Gamma_{42}) / \Gamma$

VALUE (%)	EVTS	DOCUMENT ID	TECN	COMMENT
0.316 ± 0.023 OUR FIT				
0.330 ± 0.055 ± 0.039	124	ABBIENDI 00c OPAL	1991-1995 LEP runs	

 $\Gamma(h^- \bar{K}^0 \pi^0 \nu_\tau) / \Gamma_{\text{total}}$ $\Gamma_{39} / \Gamma = (\Gamma_{40} + \Gamma_{42}) / \Gamma$

Data marked "avg" are highly correlated with data appearing elsewhere in the Listings, and are therefore used for the average given below but not in the overall fits. "f&a" marks results used for the fit and the average.

VALUE (%)	EVTS	DOCUMENT ID	TECN	COMMENT
0.55 ± 0.04 OUR FIT				
0.50 ± 0.06 OUR AVERAGE				Error includes scale factor of 1.2.
0.446 ± 0.052 ± 0.046	avg 157	¹ BARATE 98E ALEP	1991-1995 LEP runs	
0.562 ± 0.050 ± 0.048	f&a 264	COAN 96 CLEO	$E_{\text{cm}}^{\text{ee}} \approx 10.6$ GeV	

¹ Not independent of BARATE 98E $B(\tau^- \rightarrow \pi^- \bar{K}^0 \pi^0 \nu_\tau)$ and $B(\tau^- \rightarrow K^- K^0 \pi^0 \nu_\tau)$ values. $\Gamma(\pi^- \bar{K}^0 \pi^0 \nu_\tau) / \Gamma_{\text{total}}$ Γ_{40} / Γ

Data marked "avg" are highly correlated with data appearing elsewhere in the Listings, and are therefore used for the average given below but not in the overall fits. "f&a" marks results used for the fit and the average.

VALUE (%)	EVTS	DOCUMENT ID	TECN	COMMENT
0.39 ± 0.04 OUR FIT				
0.36 ± 0.04 OUR AVERAGE				
0.347 ± 0.053 ± 0.037	f&a 299	¹ BARATE 99K ALEP	1991-1995 LEP runs	
0.294 ± 0.073 ± 0.037	f&a 142	² BARATE 98E ALEP	1991-1995 LEP runs	
0.417 ± 0.058 ± 0.044	avg	³ COAN 96 CLEO	$E_{\text{cm}}^{\text{ee}} \approx 10.6$ GeV	
0.41 ± 0.12 ± 0.03	f&a	⁴ ACCIARRI 95F L3	1991-1993 LEP runs	

• • • We do not use the following data for averages, fits, limits, etc. • • •

0.32 ± 0.11 ± 0.05 23 ⁵ BUSKULIC 96 ALEP Repl. by BARATE 99K¹ BARATE 99K measure K^0 's by detecting K_L^0 's in their hadron calorimeter.² BARATE 98E reconstruct K^0 's using $K_S^0 \rightarrow \pi^+ \pi^-$ decays.³ Not independent of COAN 96 $B(h^- \bar{K}^0 \pi^0 \nu_\tau)$ and $B(K^- K^0 \pi^0 \nu_\tau)$ measurements.⁴ ACCIARRI 95F do not identify π^- / K^- and assume $B(K^- K^0 \pi^0 \nu_\tau) = (0.05 \pm 0.05)\%$.⁵ BUSKULIC 96 measure K^0 's by detecting K_L^0 's in their hadron calorimeter. $\Gamma(\bar{K}^0 \rho^- \nu_\tau) / \Gamma_{\text{total}}$ Γ_{41} / Γ

VALUE (%)	DOCUMENT ID	TECN	COMMENT
0.22 ± 0.05 OUR AVERAGE			
0.250 ± 0.057 ± 0.044	¹ BARATE 99K ALEP	1991-1995 LEP runs	
0.188 ± 0.054 ± 0.038	² BARATE 98E ALEP	1991-1995 LEP runs	

¹ BARATE 99K measure K^0 's by detecting K_L^0 's in hadron calorimeter. They determine the $\bar{K}^0 \rho^-$ fraction in $\tau^- \rightarrow \pi^- \bar{K}^0 \pi^0 \nu_\tau$ decays to be $(0.72 \pm 0.12 \pm 0.10)$ and multiply their $B(\pi^- \bar{K}^0 \pi^0 \nu_\tau)$ measurement by this fraction to obtain the quoted result.² BARATE 98E reconstruct K^0 's using $K_S^0 \rightarrow \pi^+ \pi^-$ decays. They determine the $\bar{K}^0 \rho^-$ fraction in $\tau^- \rightarrow \pi^- \bar{K}^0 \pi^0 \nu_\tau$ decays to be $(0.64 \pm 0.09 \pm 0.10)$ and multiply their $B(\pi^- \bar{K}^0 \pi^0 \nu_\tau)$ measurement by this fraction to obtain the quoted result. $\Gamma(K^- K^0 \pi^0 \nu_\tau) / \Gamma_{\text{total}}$ Γ_{42} / Γ

VALUE (%)	EVTS	DOCUMENT ID	TECN	COMMENT
0.158 ± 0.020 OUR FIT				
0.144 ± 0.023 OUR AVERAGE				
0.143 ± 0.025 ± 0.015	78	¹ BARATE 99K ALEP	1991-1995 LEP runs	
0.152 ± 0.076 ± 0.021	15	² BARATE 98E ALEP	1991-1995 LEP runs	
0.145 ± 0.036 ± 0.020	32	COAN 96 CLEO	$E_{\text{cm}}^{\text{ee}} \approx 10.6$ GeV	

• • • We do not use the following data for averages, fits, limits, etc. • • •

0.10 ± 0.05 ± 0.03 5 ³ BUSKULIC 96 ALEP Repl. by BARATE 99K¹ BARATE 99K measure K^0 's by detecting K_L^0 's in their hadron calorimeter.² BARATE 98E reconstruct K^0 's using $K_S^0 \rightarrow \pi^+ \pi^-$ decays.³ BUSKULIC 96 measure K^0 's by detecting K_L^0 's in their hadron calorimeter. $\Gamma(\pi^- \bar{K}^0 \geq 1\pi^0 \nu_\tau) / \Gamma_{\text{total}}$ $\Gamma_{43} / \Gamma = (\Gamma_{40} + \Gamma_{44}) / \Gamma$

VALUE (%)	EVTS	DOCUMENT ID	TECN	COMMENT
0.324 ± 0.074 ± 0.066	148	ABBIENDI 00c OPAL	1991-1995 LEP runs	

 $\Gamma(\pi^- \bar{K}^0 \pi^0 \pi^0 \nu_\tau) / \Gamma_{\text{total}}$ Γ_{44} / Γ

VALUE (units 10^{-3})	CL%	EVTS	DOCUMENT ID	TECN	COMMENT
0.26 ± 0.24					
• • • We do not use the following data for averages, fits, limits, etc. • • •					
<0.66	95	17	² BARATE 99K ALEP	1991-1995 LEP runs	
0.58 ± 0.33 ± 0.14	5		³ BARATE 98E ALEP	1991-1995 LEP runs	

¹ BARATE 99K combine the BARATE 98E and BARATE 99K measurements to obtain this value.² BARATE 99K measure K^0 's by detecting K_L^0 's in their hadron calorimeter.³ BARATE 98E reconstruct K^0 's using $K_S^0 \rightarrow \pi^+ \pi^-$ decays. $\Gamma(K^- K^0 \pi^0 \nu_\tau) / \Gamma_{\text{total}}$ Γ_{45} / Γ

VALUE	CL%	DOCUMENT ID	TECN	COMMENT
<0.16 × 10⁻³				
<0.18 × 10 ⁻³	95	² BARATE 99K ALEP	1991-1995 LEP runs	
<0.39 × 10 ⁻³	95	³ BARATE 98E ALEP	1991-1995 LEP runs	

¹ BARATE 99K combine the BARATE 98E and BARATE 99K bounds to obtain this value.² BARATE 99K measure K^0 's by detecting K_L^0 's in hadron calorimeter.³ BARATE 98E reconstruct K^0 's by using $K_S^0 \rightarrow \pi^+ \pi^-$ decays. $\Gamma(\pi^- K^0 \bar{K}^0 \nu_\tau) / \Gamma_{\text{total}}$ $\Gamma_{46} / \Gamma = (2\Gamma_{47} + \Gamma_{48}) / \Gamma$

Data marked "avg" are highly correlated with data appearing elsewhere in the Listings, and are therefore used for the average given below but not in the overall fits. "f&a" marks results used for the fit and the average.

VALUE (%)	EVTS	DOCUMENT ID	TECN	COMMENT
0.17 ± 0.04 OUR FIT				Error includes scale factor of 1.6.
0.153 ± 0.030 ± 0.016 avg	74	¹ BARATE 98E ALEP	1991-1995 LEP runs	
• • • We do not use the following data for averages, fits, limits, etc. • • •				
0.31 ± 0.12 ± 0.04		² ACCIARRI 95F L3	1991-1993 LEP runs	

¹ BARATE 98E obtain this value by adding twice their $B(\pi^- K_S^0 K_S^0 \nu_\tau)$ value to their $B(\pi^- K_L^0 K_L^0 \nu_\tau)$ value.² ACCIARRI 95F assume $B(\pi^- K_S^0 K_S^0 \nu) = B(\pi^- K_S^0 K_L^0 \nu) = 1/2 B(\pi^- K_S^0 K_L^0 \nu)$. $\Gamma(\pi^- K_S^0 K_S^0 \nu_\tau) / \Gamma_{\text{total}}$ Γ_{47} / Γ

VALUE (units 10^{-4})	EVTS	DOCUMENT ID	TECN	COMMENT
2.4 ± 0.5 OUR FIT				
2.4 ± 0.5 OUR AVERAGE				
2.6 ± 1.0 ± 0.5	6	BARATE 98E ALEP	1991-1995 LEP runs	
2.3 ± 0.5 ± 0.3	42	COAN 96 CLEO	$E_{\text{cm}}^{\text{ee}} \approx 10.6$ GeV	

 $\Gamma(\pi^- K_S^0 K_L^0 \nu_\tau) / \Gamma_{\text{total}}$ Γ_{48} / Γ

VALUE (units 10^{-4})	EVTS	DOCUMENT ID	TECN	COMMENT
12 ± 4 OUR FIT				Error includes scale factor of 1.7.
10.1 ± 2.3 ± 1.3	68	BARATE 98E ALEP	1991-1995 LEP runs	

 $\Gamma(\pi^- K^0 \bar{K}^0 \pi^0 \nu_\tau) / \Gamma_{\text{total}}$ Γ_{49} / Γ

VALUE	DOCUMENT ID	TECN	COMMENT
(0.31 ± 0.23) × 10⁻³	¹ BARATE 99K ALEP	1991-1995 LEP runs	
• • • We do not use the following data for averages, fits, limits, etc. • • •			
¹ BARATE 99K combine $\Gamma(\pi^- K_S^0 K_S^0 \pi^0 \nu_\tau) / \Gamma_{\text{total}}$ and $\Gamma(\pi^- K_S^0 K_L^0 \pi^0 \nu_\tau) / \Gamma_{\text{total}}$ measurements to obtain this value.			

$\Gamma(\pi^- K_S^0 K_S^0 \pi^0 \nu_\tau)/\Gamma_{\text{total}}$		Γ_{50}/Γ		
VALUE (units 10^{-4})	CL%	DOCUMENT ID	TECN	COMMENT
<2.0	95	BARATE	98E ALEP	1991-1995 LEP runs

$\Gamma(\pi^- K_S^0 K_L^0 \pi^0 \nu_\tau)/\Gamma_{\text{total}}$		Γ_{51}/Γ		
VALUE (units 10^{-4})	EVTS	DOCUMENT ID	TECN	COMMENT
3.1 ± 1.1 ± 0.5	11	BARATE	98E ALEP	1991-1995 LEP runs

$\Gamma(K^0 h^+ h^- h^- \geq 0 \text{ neutrals } \nu_\tau)/\Gamma_{\text{total}}$		Γ_{52}/Γ		
VALUE (%)	CL%	DOCUMENT ID	TECN	COMMENT
<0.17	95	TSCHIRHART	88 HRS	$E_{\text{cm}}^{ee} = 29 \text{ GeV}$
• • • We do not use the following data for averages, fits, limits, etc. • • •				
<0.27	90	BELTRAMI	85 HRS	$E_{\text{cm}}^{ee} = 29 \text{ GeV}$

$\Gamma(K^0 h^+ h^- h^- \nu_\tau)/\Gamma_{\text{total}}$		Γ_{53}/Γ		
VALUE (units 10^{-4})	EVTS	DOCUMENT ID	TECN	COMMENT
2.3 ± 1.9 ± 0.7	6	¹ BARATE	98E ALEP	1991-1995 LEP runs
¹ BARATE 98E reconstruct K^0 's using $K_S^0 \rightarrow \pi^+ \pi^-$ decays.				

$\Gamma(h^- h^- h^+ \geq 0 \text{ neutrals } \geq 0 K_L^0 \nu_\tau)/\Gamma_{\text{total}}$		Γ_{54}/Γ		
$\Gamma_{54}/\Gamma = (0.3431\Gamma_{35} + 0.3431\Gamma_{37} + 0.3431\Gamma_{40} + 0.3431\Gamma_{42} + 0.4307\Gamma_{47} + 0.6861\Gamma_{48} + \Gamma_{62} + \Gamma_{70} + \Gamma_{77} + \Gamma_{78} + \Gamma_{85} + \Gamma_{89} + \Gamma_{93} + \Gamma_{94} + 0.285\Gamma_{126} + 0.285\Gamma_{128} + 0.9101\Gamma_{146} + 0.9101\Gamma_{148})/\Gamma$				

VALUE (%)	EVTS	DOCUMENT ID	TECN	COMMENT
15.18 ± 0.08 OUR FIT	Error includes scale factor of 1.4.			
14.8 ± 0.4 OUR AVERAGE				
14.4 ± 0.6 ± 0.3		ADEVA	91F L3	$E_{\text{cm}}^{ee} = 88.3-94.3 \text{ GeV}$
15.0 ± 0.4 ± 0.3		BEHREND	89B CELL	$E_{\text{cm}}^{ee} = 14-47 \text{ GeV}$
15.1 ± 0.8 ± 0.6		AIHARA	87B TPC	$E_{\text{cm}}^{ee} = 29 \text{ GeV}$
• • • We do not use the following data for averages, fits, limits, etc. • • •				
13.5 ± 0.3 ± 0.3		ABACHI	89B HRS	$E_{\text{cm}}^{ee} = 29 \text{ GeV}$
12.8 ± 1.0 ± 0.7		¹ BURCHAT	87 MRK2	$E_{\text{cm}}^{ee} = 29 \text{ GeV}$
12.1 ± 0.5 ± 1.2		RUCKSTUHL	86 DLCO	$E_{\text{cm}}^{ee} = 29 \text{ GeV}$
12.8 ± 0.5 ± 0.8	1420	SCHMIDKE	86 MRK2	$E_{\text{cm}}^{ee} = 29 \text{ GeV}$
15.3 ± 1.1 $\pm_{-1.6}^{+1.3}$	367	ALTHOFF	85 TASS	$E_{\text{cm}}^{ee} = 34.5 \text{ GeV}$
13.6 ± 0.5 ± 0.8		BARTEL	85F JADE	$E_{\text{cm}}^{ee} = 34.6 \text{ GeV}$
12.2 ± 1.3 ± 3.9		² BERGER	85 PLUT	$E_{\text{cm}}^{ee} = 34.6 \text{ GeV}$
13.3 ± 0.3 ± 0.6		FERNANDEZ	85 MAC	$E_{\text{cm}}^{ee} = 29 \text{ GeV}$
24 ± 6	35	BRANDELIK	80 TASS	$E_{\text{cm}}^{ee} = 30 \text{ GeV}$
32 ± 5	692	³ BACINO	78B DLCO	$E_{\text{cm}}^{ee} = 3.1-7.4 \text{ GeV}$
35 ± 11		³ BRANDELIK	78 DASP	Assumes $V-A$ decay
18 ± 6.5	33	³ JAROS	78 LGW	$E_{\text{cm}}^{ee} > 6 \text{ GeV}$

- ¹ BURCHAT 87 value is not independent of SCHMIDKE 86 value.
- ² Not independent of BERGER 85 $\Gamma(\mu^- \bar{\nu}_\mu \nu_\tau)/\Gamma_{\text{total}}$, $\Gamma(e^- \bar{\nu}_e \nu_\tau)/\Gamma_{\text{total}}$, $\Gamma(h^- \geq 1 \text{ neutrals } \nu_\tau)/\Gamma_{\text{total}}$, and $\Gamma(h^- \geq 0 K_L^0 \nu_\tau)/\Gamma_{\text{total}}$, and therefore not used in the fit.
- ³ Low energy experiments are not in average or fit because the systematic errors in background subtraction are judged to be large.

$\Gamma(h^- h^- h^+ \geq 0 \text{ neutrals } \nu_\tau \text{ (ex. } K_S^0 \rightarrow \pi^+ \pi^- \text{)})/\Gamma_{\text{total}}$		Γ_{55}/Γ		
$\Gamma_{55}/\Gamma = (\Gamma_{62} + \Gamma_{70} + \Gamma_{77} + \Gamma_{78} + \Gamma_{85} + \Gamma_{89} + \Gamma_{93} + \Gamma_{94} + 0.285\Gamma_{126} + 0.285\Gamma_{128} + 0.9101\Gamma_{146} + 0.9101\Gamma_{148})/\Gamma$				

Data marked "avg" are highly correlated with data appearing elsewhere in the Listings, and are therefore used for the average given below but not in the overall fits. "f&a" marks results used for the fit and the average.

VALUE (%)	EVTS	DOCUMENT ID	TECN	COMMENT
14.56 ± 0.08 OUR FIT	Error includes scale factor of 1.3.			
14.61 ± 0.06 OUR AVERAGE				
14.652 ± 0.067 ± 0.086	avg	SCHAEEL	05c ALEP	1991-1995 LEP runs
14.569 ± 0.093 ± 0.048	avg	¹ ABREU	01M DLPH	1992-1995 LEP runs
14.556 ± 0.105 ± 0.076	f&a	² ACHARD	01d L3	1992-1995 LEP runs
14.96 ± 0.09 ± 0.22	f&a	AKERS	95Y OPAL	1991-1994 LEP runs
14.22 ± 0.10 ± 0.37	avg	³ BALEST	95c CLEO	$E_{\text{cm}}^{ee} \approx 10.6 \text{ GeV}$
• • • We do not use the following data for averages, fits, limits, etc. • • •				
15.26 ± 0.26 ± 0.22		ACTON	92H OPAL	Repl. by AKERS 95Y
13.3 ± 0.3 ± 0.8		⁴ ALBRECHT	92D ARG	$E_{\text{cm}}^{ee} = 9.4-10.6 \text{ GeV}$
14.35 $\pm_{-0.45}^{+0.40}$ ± 0.24		DECAMP	92c ALEP	1989-1990 LEP runs

- ¹ The correlation coefficients between this measurement and the ABREU 01M measurements of $B(\tau \rightarrow 1\text{-prong})$ and $B(\tau \rightarrow 5\text{-prong})$ are -0.98 and -0.08 respectively.
- ² The correlation coefficients between this measurement and the ACHARD 01D measurements of $B(\tau \rightarrow 1\text{-prong})$ and $B(\tau \rightarrow 5\text{-prong})$ are -0.978 and -0.19 respectively.
- ³ Not independent of BALEST 95c $B(h^- h^- h^+ \geq 0 \text{ neutrals } \nu_\tau)$ and $B(h^- h^- h^+ \pi^0 \nu_\tau)$ values, and BORTOLETTO 93 $B(h^- h^- h^+ \pi^0 \nu_\tau)/B(h^- h^- h^+ \geq 0 \text{ neutrals } \nu_\tau)$ value.
- ⁴ This ALBRECHT 92D value is not independent of their $\Gamma(\mu^- \bar{\nu}_\mu \nu_\tau)\Gamma(e^- \bar{\nu}_e \nu_\tau)/\Gamma_{\text{total}}^2$ value.

$\Gamma(h^- h^- h^+ \nu_\tau)/\Gamma_{\text{total}}$		Γ_{56}/Γ		
$\Gamma_{56}/\Gamma = (0.3431\Gamma_{35} + 0.3431\Gamma_{37} + \Gamma_{62} + \Gamma_{85} + \Gamma_{93} + 0.017\Gamma_{146})/\Gamma$				

Data marked "avg" are highly correlated with data appearing elsewhere in the Listings, and are therefore used for the average given below but not in the overall fits. "f&a" marks results used for the fit and the average.

VALUE (%)	EVTS	DOCUMENT ID	TECN	COMMENT
9.80 ± 0.08 OUR FIT	Error includes scale factor of 1.4.			
7.6 ± 0.1 ± 0.5 avg	7.5k	¹ ALBRECHT	96E ARG	$E_{\text{cm}}^{ee} = 9.4-10.6 \text{ GeV}$
• • • We do not use the following data for averages, fits, limits, etc. • • •				
9.92 ± 0.10 ± 0.09	11.2k	² BUSKULIC	96 ALEP	Repl. by SCHAEEL 05c
9.49 ± 0.36 ± 0.63		DECAMP	92c ALEP	Repl. by SCHAEEL 05c
8.7 ± 0.7 ± 0.3	694	³ BEHREND	90 CELL	$E_{\text{cm}}^{ee} = 35 \text{ GeV}$
7.0 ± 0.3 ± 0.7	1566	⁴ BAND	87 MAC	$E_{\text{cm}}^{ee} = 29 \text{ GeV}$
6.7 ± 0.8 ± 0.9		⁵ BURCHAT	87 MRK2	$E_{\text{cm}}^{ee} = 29 \text{ GeV}$
6.4 ± 0.4 ± 0.9		⁶ RUCKSTUHL	86 DLCO	$E_{\text{cm}}^{ee} = 29 \text{ GeV}$
7.8 ± 0.5 ± 0.8	890	SCHMIDKE	86 MRK2	$E_{\text{cm}}^{ee} = 29 \text{ GeV}$
8.4 ± 0.4 ± 0.7	1255	⁶ FERNANDEZ	85 MAC	$E_{\text{cm}}^{ee} = 29 \text{ GeV}$
9.7 ± 2.0 ± 1.3		BEHREND	84 CELL	$E_{\text{cm}}^{ee} = 14.22 \text{ GeV}$

- ¹ ALBRECHT 96E not independent of ALBRECHT 93c $\Gamma(h^- h^- h^+ \nu_\tau \text{ (ex. } K^0)) \times \Gamma(\text{particle}^- \geq 0 \text{ neutrals } \geq 0 K_L^0 \nu_\tau)/\Gamma_{\text{total}}^2$ value.
- ² BUSKULIC 96 quote $B(h^- h^- h^+ \nu_\tau \text{ (ex. } K^0)) = 9.50 \pm 0.10 \pm 0.11$. We add 0.42 to remove their K^0 correction and reduce the systematic error accordingly.
- ³ BEHREND 90 subtract 0.3% to account for the $\tau^- \rightarrow K^*(892)^- \nu_\tau$ contribution to measured events.
- ⁴ BAND 87 subtract for charged kaon modes; not independent of FERNANDEZ 85 value.
- ⁵ BURCHAT 87 value is not independent of SCHMIDKE 86 value.
- ⁶ Value obtained by multiplying paper's $R = B(h^- h^- h^+ \nu_\tau)/B(3\text{-prong})$ by $B(3\text{-prong}) = 0.143$ and subtracting 0.3% for $K^*(892)$ background.

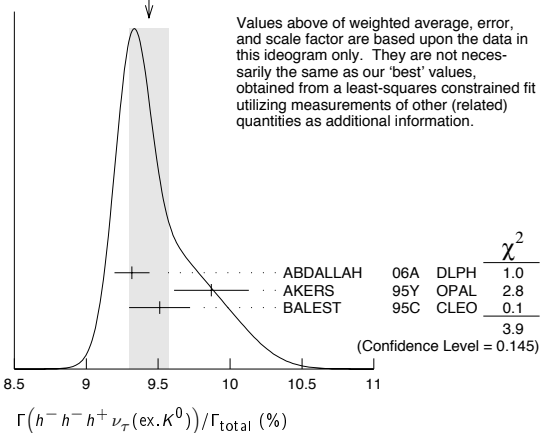
$\Gamma(h^- h^- h^+ \nu_\tau \text{ (ex. } K^0))/\Gamma_{\text{total}}$		Γ_{57}/Γ		
$\Gamma_{57}/\Gamma = (\Gamma_{62} + \Gamma_{85} + \Gamma_{93} + 0.017\Gamma_{146})/\Gamma$				

Data marked "avg" are highly correlated with data appearing elsewhere in the Listings, and are therefore used for the average given below but not in the overall fits. "f&a" marks results used for the fit and the average.

VALUE (%)	EVTS	DOCUMENT ID	TECN	COMMENT
9.45 ± 0.07 OUR FIT	Error includes scale factor of 1.3.			
9.44 ± 0.14 OUR AVERAGE	Error includes scale factor of 1.4. See the ideogram below.			
9.317 ± 0.090 ± 0.082	f&a	12.2k	¹ ABDALLAH	06A DLPH 1992-1995 LEP runs
9.87 ± 0.10 ± 0.24	avg		² AKERS	95Y OPAL 1991-1994 LEP runs
9.51 ± 0.07 ± 0.20	f&a	37.7k	BALEST	95c CLEO $E_{\text{cm}}^{ee} \approx 10.6 \text{ GeV}$
• • • We do not use the following data for averages, fits, limits, etc. • • •				
9.50 ± 0.10 ± 0.11	11.2k	³ BUSKULIC	96 ALEP	Repl. by SCHAEEL 05c

- ¹ See footnote to ABDALLAH 06A $\Gamma(\tau^- \rightarrow h^- \nu_\tau)/\Gamma_{\text{total}}$ measurement for correlations with other measurements.
- ² Not independent of AKERS 95Y $B(h^- h^- h^+ \geq 0 \text{ neutrals } \nu_\tau \text{ (ex. } K_S^0 \rightarrow \pi^+ \pi^-))$ and $B(h^- h^- h^+ \nu_\tau \text{ (ex. } K^0))/B(h^- h^- h^+ \geq 0 \text{ neutrals } \nu_\tau \text{ (ex. } K_S^0 \rightarrow \pi^+ \pi^-))$ values.
- ³ Not independent of BUSKULIC 96 $B(h^- h^- h^+ \nu_\tau)$ value.

WEIGHTED AVERAGE
9.44 ± 0.14 (Error scaled by 1.4)



$\Gamma(h^- h^- h^+ \nu_\tau \text{ (ex. } K^0))/\Gamma_{\text{total}}$		Γ_{57}/Γ_{55}		
$\Gamma_{57}/\Gamma_{55} = (\Gamma_{62} + \Gamma_{85} + \Gamma_{93} + 0.017\Gamma_{146})/(\Gamma_{62} + \Gamma_{70} + \Gamma_{77} + \Gamma_{78} + \Gamma_{85} + \Gamma_{89} + \Gamma_{93} + \Gamma_{94} + 0.285\Gamma_{126} + 0.285\Gamma_{128} + 0.9101\Gamma_{146} + 0.9101\Gamma_{148})$				

VALUE (%)	DOCUMENT ID	TECN	COMMENT
0.649 ± 0.004 OUR FIT	Error includes scale factor of 1.2.		
0.660 ± 0.004 ± 0.014	AKERS	95Y OPAL	1991-1994 LEP runs

Lepton Particle Listings

 τ

$\Gamma(h^- h^- h^+ \nu_\tau (\text{ex. } K^0, \omega))/\Gamma_{\text{total}}$		$\Gamma_{58}/\Gamma = (\Gamma_{62} + \Gamma_{85} + \Gamma_{93})/\Gamma$	
VALUE (%)	DOCUMENT ID		
9.42 ± 0.07 OUR FIT		Error includes scale factor of 1.3.	

$\Gamma(\pi^- \pi^+ \pi^- \nu_\tau)/\Gamma_{\text{total}}$		$\Gamma_{59}/\Gamma = (0.3431\Gamma_{35} + \Gamma_{62} + 0.017\Gamma_{146})/\Gamma$	
VALUE (%)	DOCUMENT ID		
9.32 ± 0.07 OUR FIT		Error includes scale factor of 1.2.	

$\Gamma(\pi^- \pi^+ \pi^- \nu_\tau (\text{ex. } K^0))/\Gamma_{\text{total}}$		$\Gamma_{60}/\Gamma = (\Gamma_{62} + 0.017\Gamma_{146})/\Gamma$	
VALUE (%)	EVTS	DOCUMENT ID	TECN COMMENT
9.03 ± 0.06 OUR FIT		Error includes scale factor of 1.2.	
8.85 ± 0.13 OUR AVERAGE			
8.83 ± 0.01 ± 0.13	1.6M	¹ AUBERT	08 BABR 342 fb ⁻¹ $E_{\text{cm}}^{\text{ex}} = 10.6$ GeV
9.13 ± 0.05 ± 0.46	43k	² BRIERE	03 CLE3 $E_{\text{cm}}^{\text{ex}} = 10.6$ GeV

¹ Correlation matrix for AUBERT 08 branching fractions:

- (1) $\Gamma(\tau^- \rightarrow \pi^- \pi^+ \pi^- \nu_\tau (\text{ex. } K^0))/\Gamma_{\text{total}}$
- (2) $\Gamma(\tau^- \rightarrow K^- \pi^+ \pi^- \nu_\tau (\text{ex. } K^0))/\Gamma_{\text{total}}$
- (3) $\Gamma(\tau^- \rightarrow K^- K^+ \pi^- \nu_\tau)/\Gamma_{\text{total}}$
- (4) $\Gamma(\tau^- \rightarrow K^- K^+ K^- \nu_\tau)/\Gamma_{\text{total}}$

	(1)	(2)	(3)
(2)	0.544		
(3)	0.390	0.177	
(4)	0.031	0.093	0.087

² 47% correlated with BRIERE 03 $\tau^- \rightarrow K^- \pi^+ \pi^- \nu_\tau$ and 71% correlated with $\tau^- \rightarrow K^- K^+ \pi^- \nu_\tau$ because of a common 5% normalization error.

$\Gamma(\pi^- \pi^+ \pi^- \nu_\tau (\text{ex. } K^0), \text{non-axial vector})/\Gamma(\pi^- \pi^+ \pi^- \nu_\tau (\text{ex. } K^0))$		$\Gamma_{61}/\Gamma_{60} = \Gamma_{61}/(\Gamma_{62} + 0.017\Gamma_{146})$	
VALUE	CL%	DOCUMENT ID	TECN COMMENT
<0.261	95	¹ ACKERSTAFF	97R OPAL 1992-1994 LEP runs

¹ Model-independent limit from structure function analysis on contribution to $B(\tau^- \rightarrow \pi^- \pi^+ \pi^- \nu_\tau (\text{ex. } K^0))$ from non-axial vectors.

$\Gamma(\pi^- \pi^+ \pi^- \nu_\tau (\text{ex. } K^0, \omega))/\Gamma_{\text{total}}$		Γ_{62}/Γ	
VALUE (%)	EVTS	DOCUMENT ID	TECN COMMENT
8.99 ± 0.06 OUR FIT		Error includes scale factor of 1.2.	
9.041 ± 0.060 ± 0.076	29k	¹ SCHAEEL	05c ALEP 1991-1995 LEP runs

¹ See footnote to SCHAEEL 05c $\Gamma(\tau^- \rightarrow e^- \bar{\nu}_e \nu_\tau)/\Gamma_{\text{total}}$ measurement for correlations with other measurements.

$\Gamma(h^- h^- h^+ \geq 1 \text{ neutrals } \nu_\tau)/\Gamma_{\text{total}}$		Γ_{63}/Γ	
VALUE (%)	EVTS	DOCUMENT ID	TECN COMMENT
5.39 ± 0.07 OUR FIT		Error includes scale factor of 1.2.	

VALUE (%)	EVTS	DOCUMENT ID	TECN COMMENT
5.39 ± 0.07 OUR FIT		Error includes scale factor of 1.2.	
• • •		We do not use the following data for averages, fits, limits, etc. • • •	
5.6 ± 0.7 ± 0.3	352	¹ BEHREND	90 CELL $E_{\text{cm}}^{\text{ex}} = 35$ GeV
4.2 ± 0.5 ± 0.9	203	² ALBRECHT	87L ARG $E_{\text{cm}}^{\text{ex}} = 10$ GeV
6.1 ± 0.8 ± 0.9		³ BURCHAT	87 MRK2 $E_{\text{cm}}^{\text{ex}} = 29$ GeV
7.6 ± 0.4 ± 0.9		^{4,5} RUCKSTUHL	86 DLCO $E_{\text{cm}}^{\text{ex}} = 29$ GeV
4.7 ± 0.5 ± 0.8	530	⁶ SCHMIDKE	86 MRK2 $E_{\text{cm}}^{\text{ex}} = 29$ GeV
5.6 ± 0.4 ± 0.7		⁵ FERNANDEZ	85 MAC $E_{\text{cm}}^{\text{ex}} = 29$ GeV
6.2 ± 2.3 ± 1.7		BEHREND	84 CELL $E_{\text{cm}}^{\text{ex}} = 14, 22$ GeV

¹ BEHREND 90 value is not independent of BEHREND 90 $B(3h^- h^+ \geq 1 \text{ neutrals}) + B(5\text{-prong})$.

² ALBRECHT 87L measure the product of branching ratios $B(3\pi^\pm \pi^0 \nu_\tau) B(e\bar{\nu}_e \mu\bar{\nu}_\mu \text{ or } \pi\text{ or } K \text{ or } \rho) \nu_\tau = 0.029$ and use the PDG 86 values for the second branching ratio which sum to 0.69 ± 0.03 to get the quoted value.

³ BURCHAT 87 value is not independent of SCHMIDKE 86 value.

⁴ Contributions from kaons and from $>1\pi^0$ are subtracted. Not independent of (3-prong + $0\pi^0$) and (3-prong + $\geq 0\pi^0$) values.

⁵ Value obtained using paper's $R = B(h^- h^- h^+ \nu_\tau)/B(3\text{-prong})$ and current $B(3\text{-prong}) = 0.143$.

⁶ Not independent of SCHMIDKE 86 $h^- h^- h^+ \nu_\tau$ and $h^- h^- h^+ (\geq 0\pi^0) \nu_\tau$ values.

$\Gamma(h^- h^- h^+ \geq 1 \pi^0 \nu_\tau (\text{ex. } K^0))/\Gamma_{\text{total}}$		Γ_{64}/Γ	
VALUE (%)	EVTS	DOCUMENT ID	TECN COMMENT
5.10 ± 0.12 OUR AVERAGE			
5.106 ± 0.083 ± 0.103	avg 10.1k	¹ ABDALLAH	06A DLPH 1992-1995 LEP runs
5.09 ± 0.10 ± 0.23	avg	² AKERS	95Y OPAL 1991-1994 LEP runs

Data marked "avg" are highly correlated with data appearing elsewhere in the Listings, and are therefore used for the average given below but not in the overall fits. "f&a" marks results used for the fit and the average.

VALUE (%)	EVTS	DOCUMENT ID	TECN COMMENT
5.08 ± 0.06 OUR FIT		Error includes scale factor of 1.1.	
5.10 ± 0.12 OUR AVERAGE			
5.106 ± 0.083 ± 0.103	avg 10.1k	¹ ABDALLAH	06A DLPH 1992-1995 LEP runs
5.09 ± 0.10 ± 0.23	avg	² AKERS	95Y OPAL 1991-1994 LEP runs

• • • We do not use the following data for averages, fits, limits, etc. • • •

4.95 ± 0.29 ± 0.65 570 DECAMP 92c ALEP Repl. by SCHAEEL 05c

¹ See footnote to ABDALLAH 06A $\Gamma(\tau^- \rightarrow h^- \nu_\tau)/\Gamma_{\text{total}}$ measurement for correlations with other measurements.

² Not independent of AKERS 95Y $B(h^- h^- h^+ \geq 0 \text{ neutrals } \nu_\tau (\text{ex. } K_S^0 \rightarrow \pi^+ \pi^-))$ and $B(h^- h^- h^+ \geq 0 \text{ neutrals } \nu_\tau (\text{ex. } K_S^0 \rightarrow \pi^+ \pi^-))$ values.

$\Gamma(h^- h^- h^+ \pi^0 \nu_\tau)/\Gamma_{\text{total}}$		Γ_{65}/Γ	
VALUE (%)	EVTS	DOCUMENT ID	TECN COMMENT
4.75 ± 0.06 OUR FIT		Error includes scale factor of 1.2.	

• • • We do not use the following data for averages, fits, limits, etc. • • •

4.45 ± 0.09 ± 0.07 6.1k ¹BUSKULIC 96 ALEP Repl. by SCHAEEL 05c

¹ BUSKULIC 96 quote $B(h^- h^- h^+ \pi^0 \nu_\tau (\text{ex. } K^0)) = 4.30 \pm 0.09 \pm 0.09$. We add 0.15 to remove their K^0 correction and reduce the systematic error accordingly.

$\Gamma(h^- h^- h^+ \pi^0 \nu_\tau (\text{ex. } K^0))/\Gamma_{\text{total}}$		Γ_{66}/Γ	
VALUE (%)	EVTS	DOCUMENT ID	TECN COMMENT
4.56 ± 0.06 OUR FIT		Error includes scale factor of 1.2.	
4.45 ± 0.14 OUR AVERAGE		Error includes scale factor of 1.2.	
4.545 ± 0.106 ± 0.103	8.9k	¹ ABDALLAH	06A DLPH 1992-1995 LEP runs
4.23 ± 0.06 ± 0.22	7.2k	BALEST	95c CLEO $E_{\text{cm}}^{\text{ex}} \approx 10.6$ GeV

¹ See footnote to ABDALLAH 06A $\Gamma(\tau^- \rightarrow h^- \nu_\tau)/\Gamma_{\text{total}}$ measurement for correlations with other measurements.

$\Gamma(h^- h^- h^+ \pi^0 \nu_\tau (\text{ex. } K^0, \omega))/\Gamma_{\text{total}}$		$\Gamma_{67}/\Gamma = (\Gamma_{70} + \Gamma_{89} + \Gamma_{94} + 0.226\Gamma_{128})/\Gamma$	
VALUE (%)	EVTS	DOCUMENT ID	TECN COMMENT
2.79 ± 0.08 OUR FIT		Error includes scale factor of 1.2.	

$\Gamma(\pi^- \pi^+ \pi^- \pi^0 \nu_\tau)/\Gamma_{\text{total}}$		$\Gamma_{68}/\Gamma = (0.3431\Gamma_{40} + \Gamma_{70} + 0.888\Gamma_{146} + 0.017\Gamma_{148})/\Gamma$	
VALUE (%)	EVTS	DOCUMENT ID	TECN COMMENT
4.61 ± 0.06 OUR FIT		Error includes scale factor of 1.1.	

$\Gamma(\pi^- \pi^+ \pi^- \pi^0 \nu_\tau (\text{ex. } K^0))/\Gamma_{\text{total}}$		$\Gamma_{69}/\Gamma = (\Gamma_{70} + 0.888\Gamma_{146} + 0.017\Gamma_{148})/\Gamma$	
VALUE (%)	EVTS	DOCUMENT ID	TECN COMMENT
4.48 ± 0.06 OUR FIT		Error includes scale factor of 1.1.	
4.55 ± 0.13 OUR AVERAGE		Error includes scale factor of 1.6.	
4.598 ± 0.057 ± 0.064	16k	¹ SCHAEEL	05c ALEP 1991-1995 LEP runs
4.19 ± 0.10 ± 0.21		² EDWARDS	00A CLEO 4.7 fb ⁻¹ $E_{\text{cm}}^{\text{ex}} = 10.6$ GeV

¹ SCHAEEL 05c quote $(4.590 \pm 0.057 \pm 0.064)\%$. We add 0.008% to remove their correction for $\tau^- \rightarrow \pi^- \pi^0 \omega \nu_\tau \rightarrow \pi^- \pi^0 \pi^+ \pi^- \nu_\tau$ decays. See footnote to SCHAEEL 05c $\Gamma(\tau^- \rightarrow e^- \bar{\nu}_e \nu_\tau)/\Gamma_{\text{total}}$ measurement for correlations with other measurements.

² EDWARDS 00A quote $(4.19 \pm 0.10) \times 10^{-2}$ with a 5% systematic error.

$\Gamma(\pi^- \pi^+ \pi^- \pi^0 \nu_\tau (\text{ex. } K^0, \omega))/\Gamma_{\text{total}}$		Γ_{70}/Γ	
VALUE (%)	EVTS	DOCUMENT ID	TECN COMMENT
2.70 ± 0.08 OUR FIT		Error includes scale factor of 1.2.	

$\Gamma(h^- \rho \pi^0 \nu_\tau)/\Gamma(h^- h^- h^+ \pi^0 \nu_\tau)$		Γ_{71}/Γ_{65}	
VALUE	EVTS	DOCUMENT ID	TECN COMMENT
0.30 ± 0.04 ± 0.02	393	ALBRECHT	91D ARG $E_{\text{cm}}^{\text{ex}} = 9.4\text{-}10.6$ GeV

$\Gamma(h^- \rho^+ h^- \nu_\tau)/\Gamma(h^- h^- h^+ \pi^0 \nu_\tau)$		Γ_{72}/Γ_{65}	
VALUE	EVTS	DOCUMENT ID	TECN COMMENT
0.10 ± 0.03 ± 0.04	142	ALBRECHT	91D ARG $E_{\text{cm}}^{\text{ex}} = 9.4\text{-}10.6$ GeV

$\Gamma(h^- \rho^- h^+ \nu_\tau)/\Gamma(h^- h^- h^+ \pi^0 \nu_\tau)$		Γ_{73}/Γ_{65}	
VALUE	EVTS	DOCUMENT ID	TECN COMMENT
0.26 ± 0.05 ± 0.01	370	ALBRECHT	91D ARG $E_{\text{cm}}^{\text{ex}} = 9.4\text{-}10.6$ GeV

$\Gamma(h^- h^- h^+ \geq 2\pi^0 \nu_\tau (\text{ex. } K^0))/\Gamma_{\text{total}}$		$\Gamma_{74}/\Gamma = (\Gamma_{77} + \Gamma_{78} + 0.226\Gamma_{126} + 0.888\Gamma_{148})/\Gamma$	
VALUE (%)	EVTS	DOCUMENT ID	TECN COMMENT
0.516 ± 0.033 OUR FIT			
0.561 ± 0.068 ± 0.095	1.3k	¹ ABDALLAH	06A DLPH 1992-1995 LEP runs

¹ See footnote to ABDALLAH 06A $\Gamma(\tau^- \rightarrow h^- \nu_\tau)/\Gamma_{\text{total}}$ measurement for correlations with other measurements.

$\Gamma(h^- h^- h^+ 2\pi^0 \nu_\tau)/\Gamma_{\text{total}}$		Γ_{75}/Γ	
VALUE (%)	EVTS	DOCUMENT ID	TECN COMMENT
0.504 ± 0.032 OUR FIT			

$\Gamma(h^- h^- h^+ 2\pi^0 \nu_\tau (\text{ex. } K^0))/\Gamma_{\text{total}}$		Γ_{76}/Γ	
VALUE (%)	EVTS	DOCUMENT ID	TECN COMMENT
0.494 ± 0.032 OUR FIT			
0.435 ± 0.030 ± 0.035	2.6k	¹ SCHAEEL	05c ALEP 1991-1995 LEP runs

• • • We do not use the following data for averages, fits, limits, etc. • • •

0.50 ± 0.07 ± 0.07 1.8k BUSKULIC 96 ALEP Repl. by SCHAEEL 05c

¹ SCHAEEL 05c quote $(0.392 \pm 0.030 \pm 0.035)\%$. We add 0.043% to remove their correction for $\tau^- \rightarrow \pi^- \eta \pi^0 \nu_\tau \rightarrow \pi^- \pi^+ \pi^- 2\pi^0 \nu_\tau$ and $\tau^- \rightarrow K^*(892) \eta \nu_\tau \rightarrow K^- \pi^+ \pi^- 2\pi^0 \nu_\tau$ decays. See footnote to SCHAEEL 05c $\Gamma(\tau^- \rightarrow e^- \bar{\nu}_e \nu_\tau)/\Gamma_{\text{total}}$ measurement for correlations with other measurements.

$$\Gamma(h^- h^- h^+ 2\pi^0 \nu_\tau(\text{ex. } K^0)) / \Gamma(h^- h^- h^+ \geq 0 \text{ neutrals } \geq 0 K^0 \nu_\tau) \quad \Gamma_{76} / \Gamma_{54}$$

$$\Gamma_{76} / \Gamma_{54} = (\Gamma_{77} + 0.226\Gamma_{126} + 0.888\Gamma_{148}) / (0.3431\Gamma_{35} + 0.3431\Gamma_{37} + 0.3431\Gamma_{40} + 0.3431\Gamma_{42} + 0.4307\Gamma_{47} + 0.6861\Gamma_{48} + \Gamma_{62} + \Gamma_{70} + \Gamma_{77} + \Gamma_{78} + \Gamma_{85} + \Gamma_{89} + \Gamma_{93} + \Gamma_{94} + 0.285\Gamma_{126} + 0.285\Gamma_{128} + 0.9101\Gamma_{146} + 0.9101\Gamma_{148})$$

VALUE	EVTS	DOCUMENT ID	TECN	COMMENT
0.0325 ± 0.0021 OUR FIT				Error includes scale factor of 1.1.
0.034 ± 0.002 ± 0.003	668	BORTOLETTO93	CLEO	$E_{cm}^{ee} \approx 10.6$ GeV

$$\Gamma(h^- h^- h^+ 2\pi^0 \nu_\tau(\text{ex. } K^0, \omega, \eta)) / \Gamma_{\text{total}} \quad \Gamma_{77} / \Gamma$$

VALUE (units 10^{-4})	DOCUMENT ID
9 ± 4 OUR FIT	

$$\Gamma(h^- h^- h^+ 3\pi^0 \nu_\tau) / \Gamma_{\text{total}} \quad \Gamma_{78} / \Gamma$$

VALUE (units 10^{-4})	CL%	DOCUMENT ID	TECN	COMMENT
2.3 ± 0.6 OUR FIT				Error includes scale factor of 1.2.
2.2 ± 0.3 ± 0.4	139	ANASTASSOV 01	CLEO	$E_{cm}^{ee} = 10.6$ GeV

• • • We do not use the following data for averages, fits, limits, etc. • • •

< 4.9	95	SCHAEEL	05c	ALEP	1991-1995 LEP runs
2.85 ± 0.56 ± 0.51	57	ANDERSON	97	CLEO	Repl. by ANASTASSOV 01
11 ± 4 ± 5	440	¹ BUSKULIC	96	ALEP	Repl. by SCHAEEL 05c

¹BUSKULIC 96 state their measurement is for $B(h^- h^- h^+ \geq 3\pi^0 \nu_\tau)$. We assume that $B(h^- h^- h^+ \geq 4\pi^0 \nu_\tau)$ is very small.

$$\Gamma(K^- h^+ h^- \geq 0 \text{ neutrals } \nu_\tau) / \Gamma_{\text{total}} \quad \Gamma_{79} / \Gamma = (0.3431\Gamma_{37} + 0.3431\Gamma_{42} + \Gamma_{85} + \Gamma_{89} + \Gamma_{93} + \Gamma_{94} + 0.285\Gamma_{128}) / \Gamma$$

VALUE (%)	CL%	DOCUMENT ID	TECN	COMMENT
0.624 ± 0.024 OUR FIT				Error includes scale factor of 1.5.
< 0.6	90	AIHARA	84c	TPC $E_{cm}^{ee} = 29$ GeV

$$\Gamma(K^- h^+ \pi^- \nu_\tau(\text{ex. } K^0)) / \Gamma_{\text{total}} \quad \Gamma_{80} / \Gamma = (\Gamma_{85} + \Gamma_{93}) / \Gamma$$

VALUE (%)	DOCUMENT ID
0.427 ± 0.019 OUR FIT	

$$\Gamma(K^- h^+ \pi^- \nu_\tau(\text{ex. } K^0)) / \Gamma(\pi^- \pi^+ \pi^- \nu_\tau(\text{ex. } K^0)) \quad \Gamma_{80} / \Gamma_{60} = (\Gamma_{85} + \Gamma_{93}) / (\Gamma_{62} + 0.017\Gamma_{146})$$

VALUE (%)	EVTS	DOCUMENT ID	TECN	COMMENT
4.73 ± 0.21 OUR FIT				Error includes scale factor of 2.4.
5.44 ± 0.21 ± 0.53	7.9k	RICHICHI	99	CLEO $E_{cm}^{ee} = 10.6$ GeV

$$\Gamma(K^- h^+ \pi^- \pi^0 \nu_\tau(\text{ex. } K^0)) / \Gamma_{\text{total}} \quad \Gamma_{81} / \Gamma = (\Gamma_{89} + \Gamma_{94} + 0.226\Gamma_{128}) / \Gamma$$

VALUE (units 10^{-4})	DOCUMENT ID
8.7 ± 1.2 OUR FIT	

$$\Gamma(K^- h^+ \pi^- \pi^0 \nu_\tau(\text{ex. } K^0)) / \Gamma(\pi^- \pi^+ \pi^- \pi^0 \nu_\tau(\text{ex. } K^0)) \quad \Gamma_{81} / \Gamma_{69} = (\Gamma_{89} + \Gamma_{94} + 0.226\Gamma_{128}) / (\Gamma_{70} + 0.888\Gamma_{146} + 0.017\Gamma_{148})$$

VALUE (%)	EVTS	DOCUMENT ID	TECN	COMMENT
1.94 ± 0.27 OUR FIT				
2.61 ± 0.45 ± 0.42	719	RICHICHI	99	CLEO $E_{cm}^{ee} = 10.6$ GeV

$$\Gamma(K^- \pi^+ \pi^- \geq 0 \text{ neutrals } \nu_\tau) / \Gamma_{\text{total}} \quad \Gamma_{82} / \Gamma = (0.3431\Gamma_{37} + 0.3431\Gamma_{42} + \Gamma_{85} + \Gamma_{89} + 0.285\Gamma_{128}) / \Gamma$$

VALUE (%)	EVTS	DOCUMENT ID	TECN	COMMENT
0.478 ± 0.021 OUR FIT				Error includes scale factor of 1.3.
0.58 ^{+0.15} _{-0.13} ± 0.12	20	¹ BAUER	94	TPC $E_{cm}^{ee} = 29$ GeV

• • • We do not use the following data for averages, fits, limits, etc. • • •

0.22 ^{+0.16} _{-0.13} ± 0.05	9	² MILLS	85	DLCO $E_{cm}^{ee} = 29$ GeV
---	---	--------------------	----	-----------------------------

¹We multiply 0.58% by 0.20, the relative systematic error quoted by BAUER 94, to obtain the systematic error.

²Error correlated with MILLS 85 ($K K \pi \nu$) value. We multiply 0.22% by 0.23, the relative systematic error quoted by MILLS 85, to obtain the systematic error.

$$\Gamma(K^- \pi^+ \pi^- \geq 0 \pi^0 \nu_\tau(\text{ex. } K^0)) / \Gamma_{\text{total}} \quad \Gamma_{83} / \Gamma = (\Gamma_{85} + \Gamma_{89} + 0.226\Gamma_{128}) / \Gamma$$

Data marked "avg" are highly correlated with data appearing elsewhere in the Listings, and are therefore used for the average given below but not in the overall fits. "f&a" marks results used for the fit and the average.

VALUE (%)	DOCUMENT ID	TECN	COMMENT
0.368 ± 0.019 OUR FIT			Error includes scale factor of 1.4.
0.30 ± 0.05 OUR AVERAGE			
0.343 ± 0.073 ± 0.031	avg	ABBIENDI	00D OPAL 1990-1995 LEP runs
0.275 ± 0.064	avg	¹ BARATE	98 ALEP 1991-1995 LEP runs

¹Not independent of BARATE 98 $\Gamma(\tau^- \rightarrow K^- \pi^+ \pi^- \nu_\tau) / \Gamma_{\text{total}}$ and $\Gamma(\tau^- \rightarrow K^- \pi^+ \pi^- \pi^0 \nu_\tau) / \Gamma_{\text{total}}$ values.

$$\Gamma(K^- \pi^+ \pi^- \nu_\tau) / \Gamma_{\text{total}} \quad \Gamma_{84} / \Gamma = (0.3431\Gamma_{37} + \Gamma_{85}) / \Gamma$$

VALUE (%)	DOCUMENT ID
0.341 ± 0.016 OUR FIT	

Error includes scale factor of 1.8.

$$\Gamma(K^- \pi^+ \pi^- \nu_\tau(\text{ex. } K^0)) / \Gamma_{\text{total}} \quad \Gamma_{85} / \Gamma$$

Data marked "avg" are highly correlated with data appearing elsewhere in the Listings, and are therefore used for the average given below but not in the overall fits. "f&a" marks results used for the fit and the average.

VALUE (%)	EVTS	DOCUMENT ID	TECN	COMMENT
0.287 ± 0.016 OUR FIT				Error includes scale factor of 2.1.
0.280 ± 0.019 OUR AVERAGE				Error includes scale factor of 2.1. See the ideogram below.

0.273 ± 0.002 ± 0.009 f&a	70k	¹ AUBERT	08	BABR	342 fb ⁻¹ $E_{cm}^{ee} = 10.6$ GeV
0.415 ± 0.053 ± 0.040 f&a	269	ABBIENDI	04J	OPAL	1991-1995 LEP runs
0.384 ± 0.014 ± 0.038 f&a	3.5k	² BRIERE	03	CLE3	$E_{cm}^{ee} = 10.6$ GeV
0.346 ± 0.023 ± 0.056 avg	158	³ RICHICHI	99	CLEO	$E_{cm}^{ee} = 10.6$ GeV
0.214 ± 0.037 ± 0.029 f&a		BARATE	98	ALEP	1991-1995 LEP runs

• • • We do not use the following data for averages, fits, limits, etc. • • •

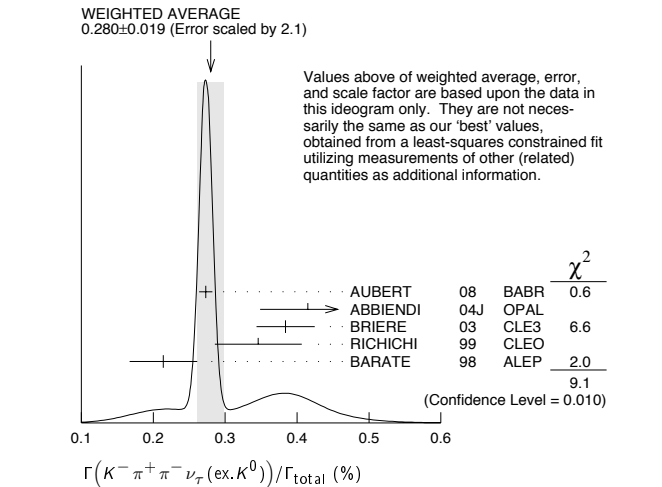
0.360 ± 0.082 ± 0.048		ABBIENDI	00D	OPAL	1990-1995 LEP runs
-----------------------	--	----------	-----	------	--------------------

¹See footnote to AUBERT 08 $\Gamma(\tau^- \rightarrow \pi^- \pi^+ \pi^- \nu_\tau(\text{ex. } K^0)) / \Gamma_{\text{total}}$ measurement for correlations with other measurements.

²47% correlated with BRIERE 03 $\tau^- \rightarrow \pi^- \pi^+ \pi^- \nu_\tau$ and 34% correlated with $\tau^- \rightarrow K^- K^+ \pi^- \nu_\tau$ because of a common 5% normalization error.

³Not independent of RICHICHI 99

$\Gamma(\tau^- \rightarrow K^- h^+ \pi^- \nu_\tau(\text{ex. } K^0)) / \Gamma(\tau^- \rightarrow \pi^- \pi^+ \pi^- \nu_\tau(\text{ex. } K^0))$, $\Gamma(\tau^- \rightarrow K^- K^+ \pi^- \nu_\tau) / \Gamma(\tau^- \rightarrow \pi^- \pi^+ \pi^- \nu_\tau(\text{ex. } K^0))$ and BALEST 95c $\Gamma(\tau^- \rightarrow h^- h^- h^+ \nu_\tau(\text{ex. } K^0)) / \Gamma_{\text{total}}$ values.



$$\Gamma(K^- \pi^0 \nu_\tau \rightarrow K^- \pi^+ \pi^- \nu_\tau) / \Gamma(K^- \pi^+ \pi^- \nu_\tau(\text{ex. } K^0)) \quad \Gamma_{86} / \Gamma_{85}$$

VALUE	DOCUMENT ID	TECN	COMMENT
0.48 ± 0.14 ± 0.10			
0.39 ± 0.14			

• • • We do not use the following data for averages, fits, limits, etc. • • •

0.39 ± 0.14	² BARATE	99R	ALEP 1991-1995 LEP runs
-------------	---------------------	-----	-------------------------

¹ASNER 00b assume $\tau^- \rightarrow K^- \pi^+ \pi^- \nu_\tau(\text{ex. } K^0)$ decays proceed only through $K \rho$ and $K^* \pi$ intermediate states. They assume the resonance structure of $\tau^- \rightarrow K^- \pi^+ \pi^- \nu_\tau(\text{ex. } K^0)$ decays is dominated by $K_1(1270)^-$ and $K_1(1400)^-$ resonances, and assume $B(K_1(1270) \rightarrow K^*(892)\pi) = (16 \pm 5)\%$, $B(K_1(1270) \rightarrow K\rho) = (42 \pm 6)\%$, and $B(K_1(1400) \rightarrow K\rho) = 0$.

²BARATE 99R assume $\tau^- \rightarrow K^- \pi^+ \pi^- \nu_\tau(\text{ex. } K^0)$ decays proceed only through $K \rho$ and $K^* \pi$ intermediate states. The quoted error is statistical only.

$$\Gamma(K^- \pi^+ \pi^- \pi^0 \nu_\tau) / \Gamma_{\text{total}} \quad \Gamma_{87} / \Gamma = (0.3431\Gamma_{42} + \Gamma_{89} + 0.226\Gamma_{128}) / \Gamma$$

VALUE (units 10^{-4})	DOCUMENT ID
13.5 ± 1.4 OUR FIT	

$$\Gamma(K^- \pi^+ \pi^- \pi^0 \nu_\tau(\text{ex. } K^0)) / \Gamma_{\text{total}} \quad \Gamma_{88} / \Gamma = (\Gamma_{89} + 0.226\Gamma_{128}) / \Gamma$$

Data marked "avg" are highly correlated with data appearing elsewhere in the Listings, and are therefore used for the average given below but not in the overall fits. "f&a" marks results used for the fit and the average.

VALUE (units 10^{-4})	CL%	DOCUMENT ID	TECN	COMMENT
8.1 ± 1.2 OUR FIT				
7.3 ± 1.2 OUR AVERAGE				

7.4 ± 0.8 ± 1.1	f&a	¹ ARMS	05	CLE3	7.6 fb ⁻¹ , $E_{cm}^{ee} = 10.6$ GeV
7.5 ± 2.6 ± 1.8	avg	² RICHICHI	99	CLEO	$E_{cm}^{ee} = 10.6$ GeV
6.1 ± 3.9 ± 1.8	f&a	BARATE	98	ALEP	1991-1995 LEP runs

• • • We do not use the following data for averages, fits, limits, etc. • • •

< 17	95	ABBIENDI	00D	OPAL	1990-1995 LEP runs
------	----	----------	-----	------	--------------------

¹Not independent of ARMS 05 $\Gamma(\tau^- \rightarrow K^- \pi^+ \pi^- \pi^0 \nu_\tau(\text{ex. } K^0, \omega)) / \Gamma_{\text{total}}$ and $\Gamma(\tau^- \rightarrow K^- \omega \nu_\tau) / \Gamma_{\text{total}}$ values.

²Not independent of RICHICHI 99

$\Gamma(\tau^- \rightarrow K^- h^+ \pi^- \nu_\tau(\text{ex. } K^0)) / \Gamma(\tau^- \rightarrow \pi^- \pi^+ \pi^- \nu_\tau(\text{ex. } K^0))$, $\Gamma(\tau^- \rightarrow K^- K^+ \pi^- \nu_\tau) / \Gamma(\tau^- \rightarrow \pi^- \pi^+ \pi^- \nu_\tau(\text{ex. } K^0))$ and BALEST 95c $\Gamma(\tau^- \rightarrow h^- h^- h^+ \nu_\tau(\text{ex. } K^0)) / \Gamma_{\text{total}}$ values.

Lepton Particle Listings

 τ

$\Gamma(K^- \pi^+ \pi^- \pi^0 \nu_\tau (\text{ex. } K^0, \eta))/\Gamma_{\text{total}}$		Γ_{89}/Γ
VALUE (units 10^{-4})	DOCUMENT ID	
7.5 ± 1.2 OUR FIT		

$\Gamma(K^- \pi^+ \pi^- \pi^0 \nu_\tau (\text{ex. } K^0, \omega))/\Gamma_{\text{total}}$		Γ_{90}/Γ		
VALUE (units 10^{-4})	EVTs	DOCUMENT ID	TECN	COMMENT
3.7 ± 0.5 ± 0.8	833	ARMS	05	CLE3 7.6 fb ⁻¹ , $E_{\text{cm}}^{\text{ee}} = 10.6$ GeV

$\Gamma(K^- \pi^+ K^- \geq 0 \text{ neut. } \nu_\tau)/\Gamma_{\text{total}}$		Γ_{91}/Γ		
VALUE (%)	CL%	DOCUMENT ID	TECN	COMMENT
< 0.09	95	BAUER	94	TPC $E_{\text{cm}}^{\text{ee}} = 29$ GeV

$\Gamma(K^- K^+ \pi^- \geq 0 \text{ neut. } \nu_\tau)/\Gamma_{\text{total}}$		$\Gamma_{92}/\Gamma = (\Gamma_{93} + \Gamma_{94})/\Gamma$		
VALUE (%)	EVTs	DOCUMENT ID	TECN	COMMENT
0.146 ± 0.006 OUR FIT				Error includes scale factor of 1.6.
0.203 ± 0.031 OUR AVERAGE				
0.159 ± 0.053 ± 0.020	f&a	1	ABBIENDI 00D	OPAL 1990-1995 LEP runs
0.238 ± 0.042	avg	1	BARATE	98 ALEP 1991-1995 LEP runs
0.15 ± 0.09 ± 0.03	f&a	4	2	BAUER 94 TPC $E_{\text{cm}}^{\text{ee}} = 29$ GeV

Data marked "avg" are highly correlated with data appearing elsewhere in the Listings, and are therefore used for the average given below but not in the overall fits. "f&a" marks results used for the fit and the average.

¹ Not independent of BARATE 98 $\Gamma(\tau^- \rightarrow K^- K^+ \pi^- \nu_\tau)/\Gamma_{\text{total}}$ and $\Gamma(\tau^- \rightarrow K^- K^+ \pi^- \pi^0 \nu_\tau)/\Gamma_{\text{total}}$ values.

² We multiply 0.15% by 0.20, the relative systematic error quoted by BAUER 94, to obtain the systematic error.

$\Gamma(K^- K^+ \pi^- \nu_\tau)/\Gamma_{\text{total}}$		Γ_{93}/Γ		
VALUE (%)	EVTs	DOCUMENT ID	TECN	COMMENT
1.40 ± 0.05 OUR FIT				Error includes scale factor of 1.7.
1.37 ± 0.06 OUR AVERAGE				Error includes scale factor of 1.8.
1.346 ± 0.010 ± 0.036	f&a	18k	1	AUBERT 08 BABR 342 fb ⁻¹ $E_{\text{cm}}^{\text{ee}} = 10.6$ GeV
1.55 ± 0.06 ± 0.09	f&a	932	2	BRIERE 03 CLE3 $E_{\text{cm}}^{\text{ee}} = 10.6$ GeV
0.87 ± 0.56 ± 0.40	avg			ABBIENDI 00D OPAL 1990-1995 LEP runs
1.45 ± 0.13 ± 0.28	avg	2.3k	3	RICHICHI 99 CLEO $E_{\text{cm}}^{\text{ee}} = 10.6$ GeV
1.63 ± 0.21 ± 0.17	f&a			BARATE 98 ALEP 1991-1995 LEP runs

Data marked "avg" are highly correlated with data appearing elsewhere in the Listings, and are therefore used for the average given below but not in the overall fits. "f&a" marks results used for the fit and the average.

¹ See footnote to AUBERT 08 $\Gamma(\tau^- \rightarrow \pi^- \pi^+ \pi^- \nu_\tau (\text{ex. } K^0))/\Gamma_{\text{total}}$ measurement for correlations with other measurements.

² 71% correlated with BRIERE 03 $\tau^- \rightarrow \pi^- \pi^+ \pi^- \nu_\tau$ and 34% correlated with $\tau^- \rightarrow K^- \pi^+ \pi^- \nu_\tau$ because of a common 5% normalization error.

³ Not independent of RICHICHI 99 $\Gamma(\tau^- \rightarrow K^- K^+ \pi^- \nu_\tau)/\Gamma_{\text{total}}$ and BALEST 95c $\Gamma(\tau^- \rightarrow h^- h^+ h^+ \nu_\tau (\text{ex. } K^0))/\Gamma_{\text{total}}$ values.

⁴ Error correlated with MILLS 85 ($K\pi\pi^0\nu$) value. We multiply 0.22% by 0.23, the relative systematic error quoted by MILLS 85, to obtain the systematic error.

$\Gamma(K^- K^+ \pi^- \nu_\tau)/\Gamma(\pi^- \pi^+ \pi^- \nu_\tau (\text{ex. } K^0))$		$\Gamma_{93}/\Gamma_{60} = \Gamma_{93}/(\Gamma_{62} + 0.017\Gamma_{146})$		
VALUE (%)	EVTs	DOCUMENT ID	TECN	COMMENT
1.55 ± 0.06 OUR FIT				Error includes scale factor of 1.6.
1.60 ± 0.15 ± 0.30	2.3k	RICHICHI	99	CLEO $E_{\text{cm}}^{\text{ee}} = 10.6$ GeV

$\Gamma(K^- K^+ \pi^- \nu_\tau)/\Gamma_{\text{total}}$		Γ_{94}/Γ		
VALUE (%)	EVTs	DOCUMENT ID	TECN	COMMENT
0.61 ± 0.25 OUR FIT				Error includes scale factor of 1.4.
0.60 ± 0.18 OUR AVERAGE				
0.55 ± 0.14 ± 0.12	f&a	48	ARMS	05 CLE3 7.6 fb ⁻¹ , $E_{\text{cm}}^{\text{ee}} = 10.6$ GeV
3.3 ± 1.8 ± 0.7	avg	158	1	RICHICHI 99 CLEO $E_{\text{cm}}^{\text{ee}} = 10.6$ GeV
7.5 ± 2.9 ± 1.5	f&a			BARATE 98 ALEP 1991-1995 LEP runs

Data marked "avg" are highly correlated with data appearing elsewhere in the Listings, and are therefore used for the average given below but not in the overall fits. "f&a" marks results used for the fit and the average.

¹ Not independent of RICHICHI 99 $\Gamma(\tau^- \rightarrow K^- K^+ \pi^- \nu_\tau)/\Gamma_{\text{total}}$ and BALEST 95c $\Gamma(\tau^- \rightarrow h^- h^+ h^+ \nu_\tau (\text{ex. } K^0))/\Gamma_{\text{total}}$ values.

$\Gamma(K^- K^+ \pi^- \nu_\tau)/\Gamma(\pi^- \pi^+ \pi^- \nu_\tau (\text{ex. } K^0))$		$\Gamma_{94}/\Gamma_{69} = \Gamma_{94}/(\Gamma_{70} + 0.888\Gamma_{146} + 0.017\Gamma_{146})$		
VALUE (%)	EVTs	DOCUMENT ID	TECN	COMMENT
0.14 ± 0.05 OUR FIT				Error includes scale factor of 1.3.
0.79 ± 0.44 ± 0.16	158	1	RICHICHI 99	CLEO $E_{\text{cm}}^{\text{ee}} = 10.6$ GeV

¹ RICHICHI 99 also quote a 95%CL upper limit of 0.0157 for this measurement.

$\Gamma(K^- K^+ K^- \geq 0 \text{ neut. } \nu_\tau)/\Gamma_{\text{total}}$		Γ_{95}/Γ		
VALUE (%)	CL%	DOCUMENT ID	TECN	COMMENT
< 0.21	95	BAUER	94	TPC $E_{\text{cm}}^{\text{ee}} = 29$ GeV

$\Gamma(K^- K^+ K^- \nu_\tau)/\Gamma_{\text{total}}$		Γ_{96}/Γ			
VALUE (units 10^{-5})	CL%	EVTs	DOCUMENT ID	TECN	COMMENT
1.58 ± 0.13 ± 0.12		275	1	AUBERT 08 BABR 342 fb ⁻¹	$E_{\text{cm}}^{\text{ee}} = 10.6$ GeV

• • • We do not use the following data for averages, fits, limits, etc. • • •

< 3.7 90 BRIERE 03 CLE3 $E_{\text{cm}}^{\text{ee}} = 10.6$ GeV

< 19 90 BARATE 98 ALEP 1991-1995 LEP runs

¹ See footnote to AUBERT 08 $\Gamma(\tau^- \rightarrow \pi^- \pi^+ \pi^- \nu_\tau (\text{ex. } K^0))/\Gamma_{\text{total}}$ measurement for correlations with other measurements.

$\Gamma(K^- K^+ K^- \nu_\tau (\text{ex. } \phi))/\Gamma_{\text{total}}$		Γ_{97}/Γ		
VALUE	CL%	DOCUMENT ID	TECN	COMMENT
< 2.5 × 10⁻⁶	90	AUBERT	08	BABR 342 fb ⁻¹ $E_{\text{cm}}^{\text{ee}} = 10.6$ GeV

$\Gamma(K^- K^+ K^- \pi^0 \nu_\tau)/\Gamma_{\text{total}}$		Γ_{98}/Γ		
VALUE	CL%	DOCUMENT ID	TECN	COMMENT
< 4.8 × 10⁻⁶	90	ARMS	05	CLE3 7.6 fb ⁻¹ , $E_{\text{cm}}^{\text{ee}} = 10.6$ GeV

$\Gamma(\pi^- K^+ \pi^- \geq 0 \text{ neut. } \nu_\tau)/\Gamma_{\text{total}}$		Γ_{99}/Γ		
VALUE (%)	CL%	DOCUMENT ID	TECN	COMMENT
< 0.25	95	BAUER	94	TPC $E_{\text{cm}}^{\text{ee}} = 29$ GeV

$\Gamma(e^- e^- e^+ \bar{\nu}_e \nu_\tau)/\Gamma_{\text{total}}$		Γ_{100}/Γ		
VALUE (units 10^{-5})	EVTs	DOCUMENT ID	TECN	COMMENT
2.8 ± 1.4 ± 0.4	5	ALAM	96	CLEO $E_{\text{cm}}^{\text{ee}} = 10.6$ GeV

$\Gamma(e^- e^- e^+ \bar{\nu}_\mu \nu_\tau)/\Gamma_{\text{total}}$		Γ_{101}/Γ		
VALUE (units 10^{-5})	CL%	DOCUMENT ID	TECN	COMMENT
< 3.6		ALAM	96	CLEO $E_{\text{cm}}^{\text{ee}} = 10.6$ GeV

$\Gamma(3h^- 2h^+ \geq 0 \text{ neutrals } \nu_\tau (\text{ex. } K_S^0 \rightarrow \pi^- \pi^+))(\text{"5-prong"})/\Gamma_{\text{total}}$		Γ_{102}/Γ		
VALUE (%)	EVTs	DOCUMENT ID	TECN	COMMENT
0.102 ± 0.004 OUR FIT				Error includes scale factor of 1.1.
0.107 ± 0.007 OUR AVERAGE				Error includes scale factor of 1.1.
0.093 ± 0.009 ± 0.012	avg			SCHAEEL 05c ALEP 1991-1995 LEP runs
0.115 ± 0.013 ± 0.006	avg	112	1	ABREU 01M DLPH 1992-1995 LEP runs
0.170 ± 0.022 ± 0.026	f&a			2 ACHARD 01D L3 1992-1995 LEP runs
0.119 ± 0.013 ± 0.008	avg	119	3	ACKERSTAFF 99E OPAL 1991-1995 LEP runs
0.097 ± 0.005 ± 0.011	f&a	419		GIBAUT 94B CLEO $E_{\text{cm}}^{\text{ee}} = 10.6$ GeV
0.102 ± 0.029	f&a	13		BYLSMA 87 HRS $E_{\text{cm}}^{\text{ee}} = 29$ GeV

• • • We do not use the following data for averages, fits, limits, etc. • • •

0.26 ± 0.06 ± 0.05 ACTON 92H OPAL $E_{\text{cm}}^{\text{ee}} = 88.2-94.2$ GeV

0.10 ± 0.05 ± 0.03 DECA MP 92c ALEP 1989-1990 LEP runs

0.16 ± 0.13 ± 0.04 BEHREND 89B CELL $E_{\text{cm}}^{\text{ee}} = 14-47$ GeV

0.3 ± 0.1 ± 0.2 BARTEL 85F JADE $E_{\text{cm}}^{\text{ee}} = 34.6$ GeV

0.13 ± 0.04 10 BELTRAMI 85 HRS Repl. by BYLSMA 87

0.16 ± 0.08 ± 0.04 4 BURCHAT 85 MRK2 $E_{\text{cm}}^{\text{ee}} = 29$ GeV

1.0 ± 0.4 10 BEHREND 82 CELL Repl. by BEHREND 89b

¹ The correlation coefficients between this measurement and the ABREU 01M measurements of $B(\tau^- \rightarrow 1\text{-prong})$ and $B(\tau^- \rightarrow 3\text{-prong})$ are -0.08 and -0.08 respectively.

² The correlation coefficients between this measurement and the ACHARD 01D measurements of $B(\tau^- \rightarrow "1\text{-prong}")$ and $B(\tau^- \rightarrow "3\text{-prong}")$ are -0.082 and -0.19 respectively.

³ Not independent of ACKERSTAFF 99E $B(\tau^- \rightarrow 3h^- 2h^+ \nu_\tau (\text{ex. } K^0))$ and $B(\tau^- \rightarrow 3h^- 2h^+ \pi^0 \nu_\tau (\text{ex. } K^0))$ measurements.

$\Gamma(3h^- 2h^+ \nu_\tau (\text{ex. } K^0))/\Gamma_{\text{total}}$		Γ_{103}/Γ		
VALUE (units 10^{-4})	EVTs	DOCUMENT ID	TECN	COMMENT
8.39 ± 0.35 OUR FIT				Error includes scale factor of 1.1.
8.32 ± 0.35 OUR AVERAGE				
9.7 ± 1.5 ± 0.5	96	1	ABDALLAH 06A	DLPH 1992-1995 LEP runs
8.56 ± 0.05 ± 0.42	34k			AUBERT,B 05w BABR 232 fb ⁻¹ , $E_{\text{cm}}^{\text{ee}} = 10.6$ GeV
7.2 ± 0.9 ± 1.2	165	2	SCHAEEL 05c	ALEP 1991-1995 LEP runs
9.1 ± 1.4 ± 0.6	97			ACKERSTAFF 99E OPAL 1991-1995 LEP runs
7.7 ± 0.5 ± 0.9	295			GIBAUT 94B CLEO $E_{\text{cm}}^{\text{ee}} = 10.6$ GeV
6.4 ± 2.3 ± 1.0	12			ALBRECHT 88B ARG $E_{\text{cm}}^{\text{ee}} = 10$ GeV
5.1 ± 2.0	7			BYLSMA 87 HRS $E_{\text{cm}}^{\text{ee}} = 29$ GeV

• • • We do not use the following data for averages, fits, limits, etc. • • •

8.0 ± 1.1 ± 1.3 58 BUSKULIC 96 ALEP Repl. by SCHAEEL 05c

6.7 ± 3.0 5 3 BELTRAMI 85 HRS Repl. by BYLSMA 87

¹ See footnote to ABDALLAH 06A $\Gamma(\tau^- \rightarrow h^- \nu_\tau)/\Gamma_{\text{total}}$ measurement for correlations with other measurements.

² See footnote to SCHAEEL 05c $\Gamma(\tau^- \rightarrow e^- \bar{\nu}_e \nu_\tau)/\Gamma_{\text{total}}$ measurement for correlations with other measurements.

³ The error quoted is statistical only.

$\Gamma(3h-2h^+\pi^0\nu_\tau(\text{ex.}K^0))/\Gamma_{\text{total}}$ Γ_{104}/Γ

VALUE (units 10^{-4})	EVTS	DOCUMENT ID	TECN	COMMENT
1.78 ± 0.27 OUR FIT				
1.74 ± 0.27 OUR AVERAGE				
1.6 ± 1.2 ± 0.6	13	¹ ABDALLAH 06A	DLPH	1992-1995 LEP runs
2.1 ± 0.7 ± 0.9	95	² SCHAEEL 05c	ALEP	1991-1995 LEP runs
1.7 ± 0.2 ± 0.2	231	ANASTASSOV 01	CLEO	$E_{\text{cm}}^{\text{ee}} = 10.6$ GeV
2.7 ± 1.8 ± 0.9	23	ACKERSTAFF 99E	OPAL	1991-1995 LEP runs
• • • We do not use the following data for averages, fits, limits, etc. • • •				
1.8 ± 0.7 ± 1.2	18	BUSKULIC 96	ALEP	Repl. by SCHAEEL 05c
1.9 ± 0.4 ± 0.4	31	GIBAUT 94B	CLEO	Repl. by ANASTASSOV 01
5.1 ± 2.2	6	BYLSMA 87	HRS	$E_{\text{cm}}^{\text{ee}} = 29$ GeV
6.7 ± 3.0	5	³ BELTRAMI 85	HRS	Repl. by BYLSMA 87

¹ See footnote to ABDALLAH 06A $\Gamma(\tau^- \rightarrow h^- \nu_\tau)/\Gamma_{\text{total}}$ measurement for correlations with other measurements.
² SCHAEEL 05c quote $(1.4 \pm 0.7 \pm 0.9) \times 10^{-4}$. We add 0.7×10^{-4} to remove their correction for $\tau^- \rightarrow \eta\pi^-\pi^+\pi^-\nu_\tau \rightarrow 3\pi^-2\pi^+\pi^0\nu_\tau$ and $\tau^- \rightarrow K^*(892)^-\eta\nu_\tau \rightarrow 3\pi^-2\pi^+\pi^0\nu_\tau$ decays. See footnote to SCHAEEL 05c $\Gamma(\tau^- \rightarrow e^-\bar{\nu}_e\nu_\tau)/\Gamma_{\text{total}}$ measurement for correlations with other measurements.
³ The error quoted is statistical only.

$\Gamma(3h-2h^+2\pi^0\nu_\tau)/\Gamma_{\text{total}}$ Γ_{105}/Γ

VALUE	CL%	DOCUMENT ID	TECN	COMMENT
<3.4 × 10⁻⁶	90	AUBERT,B 06	BABR	232 fb ⁻¹ $E_{\text{cm}}^{\text{ee}} = 10.6$ GeV
• • • We do not use the following data for averages, fits, limits, etc. • • •				
<1.1 × 10 ⁻⁴	90	GIBAUT 94B	CLEO	$E_{\text{cm}}^{\text{ee}} = 10.6$ GeV

$\Gamma((5\pi^-)\nu_\tau)/\Gamma_{\text{total}}$ Γ_{106}/Γ

$\Gamma_{106}/\Gamma = (\Gamma_{30} + \Gamma_{47} + \Gamma_{77} + \Gamma_{103} + 0.553\Gamma_{126} + 0.888\Gamma_{148})/\Gamma$
 Data marked "avg" are highly correlated with data appearing elsewhere in the Listings, and are therefore used for the average given below but not in the overall fits. "f&a" marks results used for the fit and the average.

VALUE (%)	DOCUMENT ID	TECN	COMMENT
0.76 ± 0.05 OUR FIT			
0.61 ± 0.06 ± 0.08 avg	¹ GIBAUT 94B	CLEO	$E_{\text{cm}}^{\text{ee}} = 10.6$ GeV

¹ Not independent of GIBAUT 94B $B(3h-2h^+\nu_\tau)$, PROCARIO 93 $B(h^-4\pi^0\nu_\tau)$, and BORTOLETTO 93 $B(2h^-h^+2\pi^0\nu_\tau)/B(\text{"3prong"})$ measurements. Result is corrected for η contributions.

$\Gamma(4h-3h^+ \geq 0 \text{ neutrals } \nu_\tau(\text{"7-prong"}))/\Gamma_{\text{total}}$ Γ_{107}/Γ

VALUE	CL%	DOCUMENT ID	TECN	COMMENT
<3.0 × 10⁻⁷	90	AUBERT,B 05F	BABR	232 fb ⁻¹ , $E_{\text{cm}}^{\text{ee}} = 10.6$ GeV
• • • We do not use the following data for averages, fits, limits, etc. • • •				
<1.8 × 10 ⁻⁵	95	ACKERSTAFF 97J	OPAL	1990-1995 LEP runs
<2.4 × 10 ⁻⁶	90	EDWARDS 97B	CLEO	$E_{\text{cm}}^{\text{ee}} = 10.6$ GeV
<2.9 × 10 ⁻⁴	90	BYLSMA 87	HRS	$E_{\text{cm}}^{\text{ee}} = 29$ GeV

$\Gamma(4h-3h^+\nu_\tau)/\Gamma_{\text{total}}$ Γ_{108}/Γ

VALUE	CL%	DOCUMENT ID	TECN	COMMENT
<4.3 × 10⁻⁷	90	AUBERT,B 05F	BABR	232 fb ⁻¹ , $E_{\text{cm}}^{\text{ee}} = 10.6$ GeV

$\Gamma(4h-3h^+\pi^0\nu_\tau)/\Gamma_{\text{total}}$ Γ_{109}/Γ

VALUE	CL%	DOCUMENT ID	TECN	COMMENT
<2.5 × 10⁻⁷	90	AUBERT,B 05F	BABR	232 fb ⁻¹ , $E_{\text{cm}}^{\text{ee}} = 10.6$ GeV

$\Gamma(X^-(S=-1)\nu_\tau)/\Gamma_{\text{total}}$ $\Gamma_{110}/\Gamma = (\Gamma_{10} + \Gamma_{16} + \Gamma_{23} + \Gamma_{28} + \Gamma_{35} + \Gamma_{40} + \Gamma_{85} + \Gamma_{89} + \Gamma_{128})/\Gamma$

Data marked "avg" are highly correlated with data appearing elsewhere in the Listings, and are therefore used for the average given below but not in the overall fits. "f&a" marks results used for the fit and the average.

VALUE (%)	DOCUMENT ID	TECN	COMMENT
2.85 ± 0.07 OUR FIT			
2.87 ± 0.12 avg	¹ BARATE 99R	ALEP	1991-1995 LEP runs

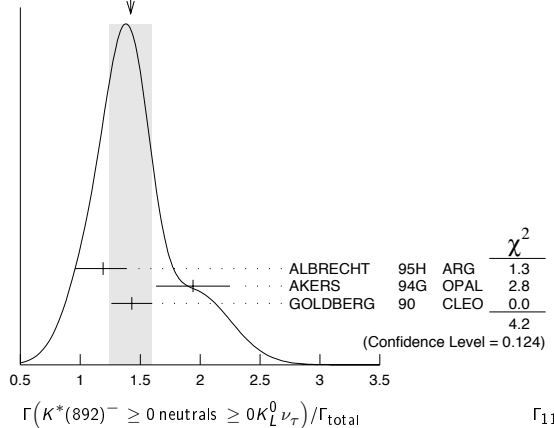
¹ BARATE 99R perform a combined analysis of all ALEPH LEP 1 data on τ branching fraction measurements for decay modes having total strangeness equal to -1.

$\Gamma(K^*(892)^- \geq 0 \text{ neutrals } \geq 0K_L^0\nu_\tau)/\Gamma_{\text{total}}$ Γ_{111}/Γ

VALUE (%)	EVTS	DOCUMENT ID	TECN	COMMENT
1.42 ± 0.18 OUR AVERAGE				Error includes scale factor of 1.4. See the ideogram below.
1.19 ± 0.15 ± 0.13	104	ALBRECHT 95H	ARG	$E_{\text{cm}}^{\text{ee}} = 9.4-10.6$ GeV
1.94 ± 0.27 ± 0.15	74	¹ AKERS 94G	OPAL	$E_{\text{cm}}^{\text{ee}} = 88-94$ GeV
1.43 ± 0.11 ± 0.13	475	² GOLDBERG 90	CLEO	$E_{\text{cm}}^{\text{ee}} = 9.4-10.9$ GeV

¹ AKERS 94G reject events in which a K_S^0 accompanies the $K^*(892)^-$. We do not correct for them.
² GOLDBERG 90 estimates that 10% of observed $K^*(892)$ are accompanied by a π^0 .

WEIGHTED AVERAGE
1.42±0.18 (Error scaled by 1.4)

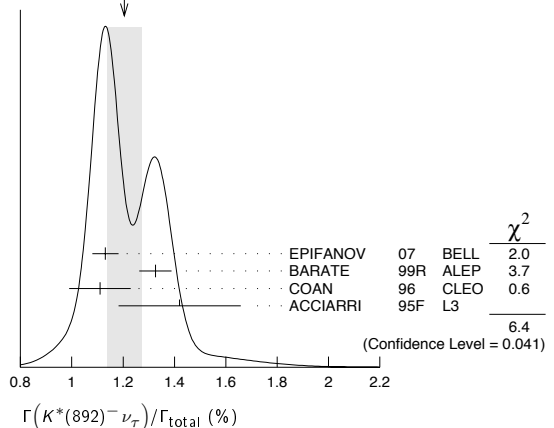


$\Gamma(K^*(892)^-\nu_\tau)/\Gamma_{\text{total}}$ Γ_{112}/Γ

VALUE (%)	EVTS	DOCUMENT ID	TECN	COMMENT
1.20 ± 0.07 OUR AVERAGE				Error includes scale factor of 1.8. See the ideogram below.
1.131 ± 0.006 ± 0.051	49k	¹ EPIFANOV 07	BELL	351 fb ⁻¹ $E_{\text{cm}}^{\text{ee}} = 10.6$ GeV
1.326 ± 0.063		BARATE 99R	ALEP	1991-1995 LEP runs
1.11 ± 0.12		² COAN 96	CLEO	$E_{\text{cm}}^{\text{ee}} \approx 10.6$ GeV
1.42 ± 0.22 ± 0.09		³ ACCIARRI 95F	L3	1991-1993 LEP runs
• • • We do not use the following data for averages, fits, limits, etc. • • •				
1.39 ± 0.09 ± 0.10		⁴ BUSKULIC 96	ALEP	Repl. by BARATE 99R
1.45 ± 0.13 ± 0.11	273	⁵ BUSKULIC 94F	ALEP	Repl. by BUSKULIC 96
1.23 ± 0.21 ± 0.11	54	⁶ ALBRECHT 88L	ARG	$E_{\text{cm}}^{\text{ee}} = 10$ GeV
1.9 ± 0.3 ± 0.4	44	⁷ TSCHIRHART 88C	HRS	$E_{\text{cm}}^{\text{ee}} = 29$ GeV
1.5 ± 0.4 ± 0.4	15	⁸ AIHARA 87C	TPC	$E_{\text{cm}}^{\text{ee}} = 29$ GeV
1.3 ± 0.3 ± 0.3	31	YELTON 86	MRK2	$E_{\text{cm}}^{\text{ee}} = 29$ GeV
1.7 ± 0.7	11	DORFAN 81	MRK2	$E_{\text{cm}}^{\text{ee}} = 4.2-6.7$ GeV

¹ EPIFANOV 07 quote $B(\tau^- \rightarrow K^*(892)^-\nu_\tau) B(K^*(892)^- \rightarrow K_S^0\pi^-) = (3.77 \pm 0.02(\text{stat}) \pm 0.12(\text{sys}) \pm 0.12(\text{mod})) \times 10^{-3}$. We add the systematic and model uncertainties in quadrature and divide by $B(K^*(892)^- \rightarrow K_S^0\pi^-) = 0.3333$.
² Not independent of COAN 96 $B(\pi^-\bar{K}^0\nu_\tau)$ and BATTLE 94 $B(K^-\pi^0\nu_\tau)$ measurements. K final states are consistent with and assumed to originate from $K^*(892)^-$ production.
³ This result is obtained from their $B(\pi^-\bar{K}^0\nu_\tau)$ assuming all those decays originate in $K^*(892)^-$ decays.
⁴ Not independent of BUSKULIC 96 $B(\pi^-\bar{K}^0\nu_\tau)$ and $B(K^-\pi^0\nu_\tau)$ measurements.
⁵ BUSKULIC 94F obtain this result from BUSKULIC 94F $B(\bar{K}^0\pi^-\nu_\tau)$ and BUSKULIC 94E $B(K^-\pi^0\nu_\tau)$ assuming all of those decays originate in $K^*(892)^-$ decays.
⁶ The authors divide by $\Gamma_2/\Gamma = 0.865$ to obtain this result.
⁷ Not independent of TSCHIRHART 88 $\Gamma(\tau^- \rightarrow h^-\bar{K}^0 \geq 0 \text{ neutrals } \geq 0K_L^0\nu_\tau) / \Gamma$.
⁸ Decay π^- identified in this experiment, is assumed in the others.

WEIGHTED AVERAGE
1.20±0.07 (Error scaled by 1.8)



$\Gamma(K^*(892)^-\nu_\tau)/\Gamma(\pi^-\pi^0\nu_\tau)$ Γ_{112}/Γ_{14}

VALUE	DOCUMENT ID	TECN	COMMENT
0.075 ± 0.027	¹ ABREU 94K	DLPH	LEP 1992 Z data
0.025 ± 0.009			We divide by $B(K^*(892)^- \rightarrow K^-\pi^0)/B(\tau^- \rightarrow \rho^-\nu_\tau) = 0.333$ to obtain this result.

Lepton Particle Listings

 τ

$\Gamma(K^*(892)^-\nu_\tau \rightarrow \pi^-\bar{K}^0\nu_\tau)/\Gamma(\pi^-\bar{K}^0\nu_\tau)$					Γ_{113}/Γ_{35}
VALUE	EVTS	DOCUMENT ID	TECN	COMMENT	
0.933 ± 0.027	49k	EPIFANOV	07 BELL	$E_{cm}^{ee} = 10.6$ GeV	

$\Gamma(K^*(892)^0 K^- \geq 0 \text{ neutrals } \nu_\tau)/\Gamma_{total}$					Γ_{114}/Γ
VALUE (%)	EVTS	DOCUMENT ID	TECN	COMMENT	
0.32 ± 0.08 ± 0.12	119	GOLDBERG	90 CLEO	$E_{cm}^{ee} = 9.4\text{--}10.9$ GeV	

$\Gamma(K^*(892)^0 K^-\nu_\tau)/\Gamma_{total}$					Γ_{115}/Γ
VALUE (%)	EVTS	DOCUMENT ID	TECN	COMMENT	
0.21 ± 0.04 OUR AVERAGE					
0.213 ± 0.048					
0.20 ± 0.05 ± 0.04	47	1 BARATE	98 ALEP	1991–1995 LEP runs	
		ALBRECHT	95H ARG	$E_{cm}^{ee} = 9.4\text{--}10.6$ GeV	

¹ BARATE 98 measure the $K^-(\rho^0 \rightarrow \pi^+\pi^-)$ fraction in $\tau^- \rightarrow K^-\pi^+\pi^-\nu_\tau$ decays to be $(35 \pm 11)\%$ and derive this result from their measurement of $\Gamma(\tau^- \rightarrow K^-\pi^+\pi^-\nu_\tau)/\Gamma_{total}$ assuming the intermediate states are all $K^-\rho$ and $K^*K^*(892)^0$.

$\Gamma(\bar{K}^*(892)^0 \pi^- \geq 0 \text{ neutrals } \nu_\tau)/\Gamma_{total}$					Γ_{116}/Γ
VALUE (%)	EVTS	DOCUMENT ID	TECN	COMMENT	
0.38 ± 0.11 ± 0.13	105	GOLDBERG	90 CLEO	$E_{cm}^{ee} = 9.4\text{--}10.9$ GeV	

$\Gamma(\bar{K}^*(892)^0 \pi^-\nu_\tau)/\Gamma_{total}$					Γ_{117}/Γ
VALUE (%)	EVTS	DOCUMENT ID	TECN	COMMENT	
0.22 ± 0.05 OUR AVERAGE					
0.209 ± 0.058					
0.25 ± 0.10 ± 0.05	27	1 BARATE	98 ALEP	1991–1995 LEP runs	
		ALBRECHT	95H ARG	$E_{cm}^{ee} = 9.4\text{--}10.6$ GeV	

¹ BARATE 98 measure the $K^*K^*(892)^0$ fraction in $\tau^- \rightarrow K^*K^+\pi^-\nu_\tau$ decays to be $(87 \pm 13)\%$ and derive this result from their measurement of $\Gamma(\tau^- \rightarrow K^*K^+\pi^-\nu_\tau)/\Gamma_{total}$.

$\Gamma(\bar{K}^*(892)^0 \pi^-\nu_\tau \rightarrow \pi^-\bar{K}^0\nu_\tau)/\Gamma_{total}$					Γ_{118}/Γ
VALUE (%)	EVTS	DOCUMENT ID	TECN	COMMENT	
0.10 ± 0.04 OUR AVERAGE					
0.097 ± 0.044 ± 0.036		1 BARATE	99k ALEP	1991–1995 LEP runs	
0.106 ± 0.037 ± 0.032		2 BARATE	98E ALEP	1991–1995 LEP runs	

¹ BARATE 99k measure K^0 's by detecting K^0_S 's in their hadron calorimeter. They determine the $\bar{K}^0\rho^-$ fraction in $\tau^- \rightarrow \pi^-\bar{K}^0\nu_\tau$ decays to be $(0.72 \pm 0.12 \pm 0.10)$ and multiply their $B(\pi^-\bar{K}^0\nu_\tau)$ measurement by one minus this fraction to obtain the quoted result.

² BARATE 98E reconstruct K^0 's using $K^0_S \rightarrow \pi^+\pi^-$ decays. They determine the $\bar{K}^0\rho^-$ fraction in $\tau^- \rightarrow \pi^-\bar{K}^0\nu_\tau$ decays to be $(0.64 \pm 0.09 \pm 0.10)$ and multiply their $B(\pi^-\bar{K}^0\nu_\tau)$ measurement by one minus this fraction to obtain the quoted result.

$\Gamma(K_1(1270)^-\nu_\tau)/\Gamma_{total}$					Γ_{119}/Γ
VALUE (%)	EVTS	DOCUMENT ID	TECN	COMMENT	
0.47 ± 0.11 OUR AVERAGE					
0.48 ± 0.11		BARATE	99R ALEP	1991–1995 LEP runs	
0.41 ^{+0.41} _{-0.35} ± 0.10	5	1 BAUER	94 TPC	$E_{cm}^{ee} = 29$ GeV	

¹ We multiply 0.41% by 0.25, the relative systematic error quoted by BAUER 94, to obtain the systematic error.

$\Gamma(K_1(1400)^-\nu_\tau)/\Gamma_{total}$					Γ_{120}/Γ
VALUE (%)	EVTS	DOCUMENT ID	TECN	COMMENT	
0.17 ± 0.26 OUR AVERAGE					
0.05 ± 0.17		BARATE	99R ALEP	1991–1995 LEP runs	Error includes scale factor of 1.7.
0.76 ^{+0.40} _{-0.33} ± 0.20	11	1 BAUER	94 TPC	$E_{cm}^{ee} = 29$ GeV	

¹ We multiply 0.76% by 0.25, the relative systematic error quoted by BAUER 94, to obtain the systematic error.

$[\Gamma(K_1(1270)^-\nu_\tau) + \Gamma(K_1(1400)^-\nu_\tau)]/\Gamma_{total}$					$(\Gamma_{119} + \Gamma_{120})/\Gamma$
VALUE (%)	EVTS	DOCUMENT ID	TECN	COMMENT	
1.17^{+0.41}_{-0.37} ± 0.29	16	1 BAUER	94 TPC	$E_{cm}^{ee} = 29$ GeV	

¹ We multiply 1.17% by 0.25, the relative systematic error quoted by BAUER 94, to obtain the systematic error. Not independent of BAUER 94 $B(K_1(1270)^-\nu_\tau)$ and BAUER 94 $B(K_1(1400)^-\nu_\tau)$ measurements.

$\Gamma(K_1(1270)^-\nu_\tau)/[\Gamma(K_1(1270)^-\nu_\tau) + \Gamma(K_1(1400)^-\nu_\tau)]$					$\Gamma_{119}/(\Gamma_{119} + \Gamma_{120})$
VALUE	DOCUMENT ID	TECN	COMMENT		
0.69 ± 0.15 OUR AVERAGE					
0.71 ± 0.16 ± 0.11	1 ABBIENDI	00D OPAL	1990–1995 LEP runs		
0.66 ± 0.19 ± 0.13	2 ASNER	00B CLEO	$E_{cm}^{ee} = 10.6$ GeV		

¹ ABBIENDI 00D assume the resonance structure of $\tau^- \rightarrow K^-\pi^+\pi^-\nu_\tau$ decays is dominated by the $K_1(1270)^-$ and $K_1(1400)^-$ resonances.

² ASNER 00B assume the resonance structure of $\tau^- \rightarrow K^-\pi^+\pi^-\nu_\tau$ (ex. K^0) decays is dominated by $K_1(1270)^-$ and $K_1(1400)^-$ resonances.

$\Gamma(K^*(1410)^-\nu_\tau)/\Gamma_{total}$					Γ_{121}/Γ
VALUE (units 10^{-3})	DOCUMENT ID	TECN	COMMENT		
1.5 ± 1.4	BARATE	99R ALEP	1991–1995 LEP runs		

$\Gamma(K_0^*(1430)^-\nu_\tau)/\Gamma_{total}$					Γ_{122}/Γ
VALUE (units 10^{-3})	CL%	DOCUMENT ID	TECN	COMMENT	
< 0.5	95	BARATE	99R ALEP	1991–1995 LEP runs	

$\Gamma(K_2^*(1430)^-\nu_\tau)/\Gamma_{total}$					Γ_{123}/Γ
VALUE (%)	CL%	EVTS	DOCUMENT ID	TECN	COMMENT
< 0.3	95		TSCHIRHART	88 HRS	$E_{cm}^{ee} = 29$ GeV

• • • We do not use the following data for averages, fits, limits, etc. • • •
 < 0.33 95 ¹ ACCIARRI 95F L3 1991–1993 LEP runs
 < 0.9 95 0 DORFAN 81 MRK2 $E_{cm}^{ee} = 4.2\text{--}6.7$ GeV
¹ ACCIARRI 95F quote $B(\tau^- \rightarrow K^*(1430)^- \rightarrow \pi^-\bar{K}^0\nu_\tau) < 0.11\%$. We divide by $B(K^*(1430)^- \rightarrow \pi^-\bar{K}^0) = 0.33$ to obtain the limit shown.

$\Gamma(a_0(980)^- \geq 0 \text{ neutrals } \nu_\tau)/\Gamma_{total} \times B(a_0(980)^- \rightarrow K^0 K^-)$					$\Gamma_{124}/\Gamma \times B$
VALUE (units 10^{-4})	CL%	DOCUMENT ID	TECN	COMMENT	
< 2.8	90	GOLDBERG	90 CLEO	$E_{cm}^{ee} = 9.4\text{--}10.9$ GeV	

$\Gamma(\eta\pi^-\nu_\tau)/\Gamma_{total}$					Γ_{125}/Γ
VALUE (units 10^{-4})	CL%	EVTS	DOCUMENT ID	TECN	COMMENT
< 1.4	95	0	BARTELT	96 CLEO	$E_{cm}^{ee} \approx 10.6$ GeV

• • • We do not use the following data for averages, fits, limits, etc. • • •
 < 6.2 95 BUSKULIC 97C ALEP 1991–1994 LEP runs
 < 3.4 95 ARTUSO 92 CLEO $E_{cm}^{ee} \approx 10.6$ GeV
 < 90 95 ALBRECHT 88M ARG $E_{cm}^{ee} \approx 10$ GeV
 < 140 90 BEHREND 88 CELL $E_{cm}^{ee} = 14\text{--}46.8$ GeV
 < 180 95 BARINGER 87 CLEO $E_{cm}^{ee} = 10.5$ GeV
 < 250 90 0 COFFMAN 87 MRK3 $E_{cm}^{ee} = 3.77$ GeV
 510 ± 100 ± 120 65 DERRICK 87 HRS $E_{cm}^{ee} = 29$ GeV
 < 100 95 GAN 87B MRK2 $E_{cm}^{ee} = 29$ GeV

$\Gamma(\eta\pi^-\pi^0\nu_\tau)/\Gamma_{total}$					Γ_{126}/Γ
VALUE (%)	CL%	EVTS	DOCUMENT ID	TECN	COMMENT
0.181 ± 0.024 OUR FIT					
0.173 ± 0.024 OUR AVERAGE					
0.18 ± 0.04 ± 0.02			BUSKULIC	97C ALEP	1991–1994 LEP runs
0.17 ± 0.02 ± 0.02	125		ARTUSO	92 CLEO	$E_{cm}^{ee} \approx 10.6$ GeV

• • • We do not use the following data for averages, fits, limits, etc. • • •
 < 1.10 95 ALBRECHT 88M ARG $E_{cm}^{ee} \approx 10$ GeV
 < 2.10 95 BARINGER 87 CLEO $E_{cm}^{ee} = 10.5$ GeV
 4.20^{+0.70}_{-1.20} ± 1.60 ¹ GAN 87 MRK2 $E_{cm}^{ee} = 29$ GeV

¹ Highly correlated with GAN 87 $\Gamma(\pi^- 3\pi^0\nu_\tau)/\Gamma_{total}$ value.

$\Gamma(\eta\pi^-\pi^0\nu_\tau)/\Gamma_{total}$					Γ_{127}/Γ
VALUE (units 10^{-4})	CL%	EVTS	DOCUMENT ID	TECN	COMMENT
1.5 ± 0.5	30		1 ANASTASSOV	01 CLEO	$E_{cm}^{ee} = 10.6$ GeV

• • • We do not use the following data for averages, fits, limits, etc. • • •
 1.4 ± 0.6 ± 0.3 15 ² BERGFELD 97 CLEO Repl. by ANASTASSOV 01
 < 4.3 95 ARTUSO 92 CLEO $E_{cm}^{ee} \approx 10.6$ GeV
 < 120 95 ALBRECHT 88M ARG $E_{cm}^{ee} \approx 10$ GeV

¹ Weighted average of BERGFELD 97 and ANASTASSOV 01 value of $(1.5 \pm 0.6 \pm 0.3) \times 10^{-4}$ obtained using η 's reconstructed from $\eta \rightarrow \pi^+\pi^-\pi^0$ decays.

² BERGFELD 97 reconstruct η 's using $\eta \rightarrow \gamma\gamma$ decays.

$\Gamma(\eta K^-\nu_\tau)/\Gamma_{total}$					Γ_{128}/Γ
VALUE (units 10^{-4})	CL%	EVTS	DOCUMENT ID	TECN	COMMENT
2.7 ± 0.6 OUR FIT					
2.7 ± 0.6 OUR AVERAGE					
2.9 ^{+1.3} _{-1.2} ± 0.7			BUSKULIC	97C ALEP	1991–1994 LEP runs
2.6 ± 0.5 ± 0.5	85		BARTELT	96 CLEO	$E_{cm}^{ee} \approx 10.6$ GeV

• • • We do not use the following data for averages, fits, limits, etc. • • •
 < 4.7 95 ARTUSO 92 CLEO $E_{cm}^{ee} \approx 10.6$ GeV

$\Gamma(\eta K^*(892)^-\nu_\tau)/\Gamma_{total}$					Γ_{129}/Γ
VALUE (units 10^{-4})	EVTS	DOCUMENT ID	TECN	COMMENT	
2.90 ± 0.80 ± 0.42	25	BISHAI	99 CLEO	$E_{cm}^{ee} = 10.6$ GeV	

$\Gamma(\eta K^-\pi^0\nu_\tau)/\Gamma_{total}$					Γ_{130}/Γ
VALUE (units 10^{-4})	EVTS	DOCUMENT ID	TECN	COMMENT	
1.77 ± 0.56 ± 0.71	36	BISHAI	99 CLEO	$E_{cm}^{ee} = 10.6$ GeV	

$\Gamma(\eta\bar{K}^0\pi^-\nu_\tau)/\Gamma_{total}$					Γ_{131}/Γ
VALUE (units 10^{-4})	EVTS	DOCUMENT ID	TECN	COMMENT	
2.20 ± 0.70 ± 0.22	15	1 BISHAI	99 CLEO	$E_{cm}^{ee} = 10.6$ GeV	

¹ We multiply the BISHAI 99 measurement $B(\tau^- \rightarrow \eta K_S^0 \pi^-\nu_\tau) = (1.10 \pm 0.35 \pm 0.11) \times 10^{-4}$ by 2 to obtain the listed value.

$\Gamma(\eta\pi^+\pi^-\pi^0 \geq 0 \text{ neutrals } \nu_\tau)/\Gamma_{\text{total}}$					Γ_{132}/Γ
VALUE (%)	CL%	DOCUMENT ID	TECN	COMMENT	
<0.3	90	ABACHI	87b HRS	$E_{\text{cm}}^{\text{ee}} = 29 \text{ GeV}$	

$\Gamma(\eta\pi^-\pi^+\pi^-\nu_\tau)/\Gamma_{\text{total}}$					Γ_{133}/Γ
VALUE (units 10^{-4})	EVTS	DOCUMENT ID	TECN	COMMENT	
2.3 ± 0.5	170	¹ ANASTASSOV 01	CLEO	$E_{\text{cm}}^{\text{ee}} = 10.6 \text{ GeV}$	
••• We do not use the following data for averages, fits, limits, etc. •••					
$3.4_{-0.5}^{+0.6} \pm 0.6$	89	² BERGFELD 97	CLEO	Repl. by ANASTASSOV 01	

¹Weighted average of BERGFELD 97 and ANASTASSOV 01 measurements using η^{\pm} reconstructed from $\eta \rightarrow \pi^+\pi^-\pi^0$ and $\eta \rightarrow 3\pi^0$ decays.
²BERGFELD 97 reconstruct η^{\pm} using $\eta \rightarrow \gamma\gamma$ and $\eta \rightarrow 3\pi^0$ decays.

$\Gamma(\eta a_1(1260)^-\nu_\tau \rightarrow \eta\pi^-\rho^0\nu_\tau)/\Gamma_{\text{total}}$					Γ_{134}/Γ
VALUE	CL%	DOCUMENT ID	TECN	COMMENT	
< 3.9×10^{-4}	90	BERGFELD 97	CLEO	$E_{\text{cm}}^{\text{ee}} = 10.6 \text{ GeV}$	

$\Gamma(\eta\eta\pi^-\nu_\tau)/\Gamma_{\text{total}}$					Γ_{135}/Γ
VALUE (units 10^{-4})	CL%	DOCUMENT ID	TECN	COMMENT	
< 1.1	95	ARTUSO 92	CLEO	$E_{\text{cm}}^{\text{ee}} \approx 10.6 \text{ GeV}$	
••• We do not use the following data for averages, fits, limits, etc. •••					
<83	95	ALBRECHT 88M	ARG	$E_{\text{cm}}^{\text{ee}} \approx 10 \text{ GeV}$	

$\Gamma(\eta\eta\pi^-\pi^0\nu_\tau)/\Gamma_{\text{total}}$					Γ_{136}/Γ
VALUE (units 10^{-4})	CL%	DOCUMENT ID	TECN	COMMENT	
< 2.0	95	ARTUSO 92	CLEO	$E_{\text{cm}}^{\text{ee}} \approx 10.6 \text{ GeV}$	
••• We do not use the following data for averages, fits, limits, etc. •••					
<90	95	ALBRECHT 88M	ARG	$E_{\text{cm}}^{\text{ee}} \approx 10 \text{ GeV}$	

$\Gamma(\eta'(958)\pi^-\nu_\tau)/\Gamma_{\text{total}}$					Γ_{137}/Γ
VALUE	CL%	DOCUMENT ID	TECN	COMMENT	
< 7.4×10^{-5}	90	BERGFELD 97	CLEO	$E_{\text{cm}}^{\text{ee}} = 10.6 \text{ GeV}$	

$\Gamma(\eta'(958)\pi^-\pi^0\nu_\tau)/\Gamma_{\text{total}}$					Γ_{138}/Γ
VALUE	CL%	DOCUMENT ID	TECN	COMMENT	
< 8.0×10^{-5}	90	BERGFELD 97	CLEO	$E_{\text{cm}}^{\text{ee}} = 10.6 \text{ GeV}$	

$\Gamma(\phi\pi^-\nu_\tau)/\Gamma_{\text{total}}$					Γ_{139}/Γ
VALUE (units 10^{-5})	CL%	EVTS	DOCUMENT ID	TECN	COMMENT
$3.42 \pm 0.55 \pm 0.25$		344	AUBERT 08	BABR	342 fb^{-1} $E_{\text{cm}}^{\text{ee}} = 10.6 \text{ GeV}$
••• We do not use the following data for averages, fits, limits, etc. •••					
< 20	90		¹ AVERY 97	CLEO	$E_{\text{cm}}^{\text{ee}} = 10.6 \text{ GeV}$
< 35	90		ALBRECHT 95H	ARG	$E_{\text{cm}}^{\text{ee}} = 9.4\text{--}10.6 \text{ GeV}$
¹ AVERY 97 limit varies from $(1.2\text{--}2.0) \times 10^{-4}$ depending on decay model assumptions.					

$\Gamma(\phi K^-\nu_\tau)/\Gamma_{\text{total}}$					Γ_{140}/Γ
VALUE (units 10^{-5})	CL%	EVTS	DOCUMENT ID	TECN	COMMENT
3.70 ± 0.33 OUR AVERAGE			Error includes scale factor of 1.3.		
$3.39 \pm 0.20 \pm 0.28$		274	AUBERT 08	BABR	342 fb^{-1} $E_{\text{cm}}^{\text{ee}} = 10.6 \text{ GeV}$
$4.05 \pm 0.25 \pm 0.26$		551	INAMI 06	BELL	401 fb^{-1} $E_{\text{cm}}^{\text{ee}} = 10.6 \text{ GeV}$
••• We do not use the following data for averages, fits, limits, etc. •••					
<6.7	90		¹ AVERY 97	CLEO	$E_{\text{cm}}^{\text{ee}} = 10.6 \text{ GeV}$
¹ AVERY 97 limit varies from $(5.4\text{--}6.7) \times 10^{-5}$ depending on decay model assumptions.					

$\Gamma(f_1(1285)\pi^-\nu_\tau)/\Gamma_{\text{total}}$					Γ_{141}/Γ
VALUE (units 10^{-4})	EVTS	DOCUMENT ID	TECN	COMMENT	
4.1 ± 0.8 OUR AVERAGE					
$3.9 \pm 0.7 \pm 0.5$	1.4k	¹ AUBERT,B 05w	BABR	232 fb^{-1} , $E_{\text{cm}}^{\text{ee}} = 10.6 \text{ GeV}$	
$5.8_{-1.3}^{+1.4} \pm 1.8$	54	² BERGFELD 97	CLEO	$E_{\text{cm}}^{\text{ee}} = 10.6 \text{ GeV}$	
¹ AUBERT,B 05w use the $f_1(1285) \rightarrow 2\pi^+\pi^-$ decay mode.					
² BERGFELD 97 use the $f_1(1285) \rightarrow \eta\pi^+\pi^-$ decay mode.					

$\Gamma(f_1(1285)\pi^-\nu_\tau \rightarrow \eta\pi^-\pi^+\pi^-\nu_\tau)/\Gamma(\eta\pi^-\pi^+\pi^-\nu_\tau)$					$\Gamma_{142}/\Gamma_{133}$
VALUE	DOCUMENT ID	TECN	COMMENT		
0.55 ± 0.14	BERGFELD 97	CLEO	$E_{\text{cm}}^{\text{ee}} = 10.6 \text{ GeV}$		

$\Gamma(\pi(1300)^-\nu_\tau \rightarrow (\rho\pi)^-\nu_\tau \rightarrow (3\pi)^-\nu_\tau)/\Gamma_{\text{total}}$					Γ_{143}/Γ
VALUE	CL%	DOCUMENT ID	TECN	COMMENT	
< 1.0×10^{-4}	90	ASNER 00	CLEO	$E_{\text{cm}}^{\text{ee}} = 10.6 \text{ GeV}$	

$\Gamma(\pi(1300)^-\nu_\tau \rightarrow ((\pi\pi)_S\text{-wave } \pi)^-\nu_\tau \rightarrow (3\pi)^-\nu_\tau)/\Gamma_{\text{total}}$					Γ_{144}/Γ
VALUE	CL%	DOCUMENT ID	TECN	COMMENT	
< 1.9×10^{-4}	90	ASNER 00	CLEO	$E_{\text{cm}}^{\text{ee}} = 10.6 \text{ GeV}$	

$\Gamma(h^-\omega \geq 0 \text{ neutrals } \nu_\tau)/\Gamma_{\text{total}}$					Γ_{145}/Γ
VALUE (%)	EVTS	DOCUMENT ID	TECN	COMMENT	
1.99 ± 0.07 OUR FIT		Error includes scale factor of 1.2.			
$1.65 \pm 0.3 \pm 0.2$ avg	1513	ALBRECHT 88M	ARG	$E_{\text{cm}}^{\text{ee}} \approx 10 \text{ GeV}$	

Data marked "avg" are highly correlated with data appearing elsewhere in the Listings, and are therefore used for the average given below but not in the overall fits. "f&a" marks results used for the fit and the average.

$\Gamma(h^-\omega\nu_\tau)/\Gamma_{\text{total}}$					Γ_{146}/Γ
VALUE (%)	EVTS	DOCUMENT ID	TECN	COMMENT	
1.99 ± 0.08 OUR FIT		Error includes scale factor of 1.3.			
1.92 ± 0.07 OUR AVERAGE					
$1.91 \pm 0.07 \pm 0.06$	f&a 5803	BUSKULIC 97c	ALEP	1991–1994 LEP runs	
$1.95 \pm 0.07 \pm 0.11$	avg 2223	¹ BALEST 95c	CLEO	$E_{\text{cm}}^{\text{ee}} \approx 10.6 \text{ GeV}$	
$1.60 \pm 0.27 \pm 0.41$	f&a 139	BARINGER 87	CLEO	$E_{\text{cm}}^{\text{ee}} = 10.5 \text{ GeV}$	
¹ Not independent of BALEST 95c $B(\tau^- \rightarrow h^-\omega\nu_\tau)/B(\tau^- \rightarrow h^-\pi^+\pi^0\nu_\tau)$ value.					

$\Gamma(h^-\omega\nu_\tau)/\Gamma(h^-\pi^+\pi^0\nu_\tau \text{ (ex. } K^0))$					Γ_{146}/Γ_{66}
VALUE	EVTS	DOCUMENT ID	TECN	COMMENT	
0.437 ± 0.017 OUR FIT		Error includes scale factor of 1.2.			
0.453 ± 0.019 OUR AVERAGE					
0.431 ± 0.033	2350	¹ BUSKULIC 96	ALEP	LEP 1991–1993 data	
$0.464 \pm 0.016 \pm 0.017$	2223	² BALEST 95c	CLEO	$E_{\text{cm}}^{\text{ee}} \approx 10.6 \text{ GeV}$	
••• We do not use the following data for averages, fits, limits, etc. •••					
$0.37 \pm 0.05 \pm 0.02$	458	³ ALBRECHT 91D	ARG	$E_{\text{cm}}^{\text{ee}} = 9.4\text{--}10.6 \text{ GeV}$	
¹ BUSKULIC 96 quote the fraction of $\tau \rightarrow h^-\pi^+\pi^0\nu_\tau$ (ex. K^0) decays which originate in a $h^-\omega$ final state = 0.383 ± 0.029 . We divide this by the $\omega(782) \rightarrow \pi^+\pi^-\pi^0$ branching fraction (0.888).					
² BALEST 95c quote the fraction of $\tau^- \rightarrow h^-\pi^+\pi^0\nu_\tau$ (ex. K^0) decays which originate in a $h^-\omega$ final state equals $0.412 \pm 0.014 \pm 0.015$. We divide this by the $\omega(782) \rightarrow \pi^+\pi^-\pi^0$ branching fraction (0.888).					
³ ALBRECHT 91D quote the fraction of $\tau^- \rightarrow h^-\pi^+\pi^0\nu_\tau$ decays which originate in a $\pi^-\omega$ final state equals $0.33 \pm 0.04 \pm 0.02$. We divide this by the $\omega(782) \rightarrow \pi^+\pi^-\pi^0$ branching fraction (0.888).					

$\Gamma(K^-\omega\nu_\tau)/\Gamma_{\text{total}}$					Γ_{147}/Γ
VALUE (units 10^{-4})	EVTS	DOCUMENT ID	TECN	COMMENT	
$4.1 \pm 0.6 \pm 0.7$	500	ARMS 05	CLE3	7.6 fb^{-1} , $E_{\text{cm}}^{\text{ee}} = 10.6 \text{ GeV}$	

$\Gamma(h^-\omega\pi^0\nu_\tau)/\Gamma_{\text{total}}$					Γ_{148}/Γ
VALUE (%)	EVTS	DOCUMENT ID	TECN	COMMENT	
0.41 ± 0.04 OUR FIT					
$0.43 \pm 0.06 \pm 0.05$	7283	BUSKULIC 97c	ALEP	1991–1994 LEP runs	

$\Gamma(h^-\omega\pi^0\nu_\tau)/\Gamma(h^-\pi^+\pi^0\nu_\tau \geq 0 \text{ neutrals } \geq 0 K^0\nu_\tau)$					Γ_{148}/Γ_{54}
VALUE	EVTS	DOCUMENT ID	TECN	COMMENT	
0.269 ± 0.0028 OUR FIT					
$0.028 \pm 0.003 \pm 0.003$ avg	430	¹ BORTOLETTO93	CLEO	$E_{\text{cm}}^{\text{ee}} \approx 10.6 \text{ GeV}$	
¹ Not independent of BORTOLETTO 93 $\Gamma(\tau^- \rightarrow h^-\omega\pi^0\nu_\tau)/\Gamma(\tau^- \rightarrow h^-\pi^+\pi^0\nu_\tau \text{ (ex. } K^0))$ value.					

$\Gamma(h^-\omega\pi^0\nu_\tau)/\Gamma(h^-\pi^+\pi^0\nu_\tau \text{ (ex. } K^0))$					Γ_{148}/Γ_{76}
VALUE	EVTS	DOCUMENT ID	TECN	COMMENT	
0.83 ± 0.08 OUR FIT					
$0.81 \pm 0.06 \pm 0.06$		BORTOLETTO93	CLEO	$E_{\text{cm}}^{\text{ee}} \approx 10.6 \text{ GeV}$	

$\Gamma(h^-\omega 2\pi^0\nu_\tau)/\Gamma_{\text{total}}$					Γ_{149}/Γ
VALUE (units 10^{-4})	EVTS	DOCUMENT ID	TECN	COMMENT	
$1.4 \pm 0.4 \pm 0.3$	53	ANASTASSOV 01	CLEO	$E_{\text{cm}}^{\text{ee}} = 10.6 \text{ GeV}$	
••• We do not use the following data for averages, fits, limits, etc. •••					
$1.89_{-0.67}^{+0.74} \pm 0.40$	19	ANDERSON 97	CLEO	Repl. by ANASTASSOV 01	

$\Gamma(h^-\omega 2\pi^0\nu_\tau)/\Gamma(h^-\pi^+\pi^0\nu_\tau \text{ (ex. } K^0))$					Γ_{148}/Γ_{76}
VALUE	EVTS	DOCUMENT ID	TECN	COMMENT	
0.83 ± 0.08 OUR FIT					
$0.81 \pm 0.06 \pm 0.06$		BORTOLETTO93	CLEO	$E_{\text{cm}}^{\text{ee}} \approx 10.6 \text{ GeV}$	

$\Gamma(h^-\omega 2\pi^0\nu_\tau)/\Gamma_{\text{total}}$					Γ_{149}/Γ
VALUE (units 10^{-4})	EVTS	DOCUMENT ID	TECN	COMMENT	
$1.4 \pm 0.4 \pm 0.3$	53	ANASTASSOV 01	CLEO	$E_{\text{cm}}^{\text{ee}} = 10.6 \text{ GeV}$	
••• We do not use the following data for averages, fits, limits, etc. •••					
$1.89_{-0.67}^{+0.74} \pm 0.40$	19	ANDERSON 97	CLEO	Repl. by ANASTASSOV 01	

$\Gamma(h^-\omega 2\pi^0\nu_\tau)/\Gamma(h^-\pi^+\pi^0\nu_\tau \text{ (ex. } K^0))$					Γ_{148}/Γ_{76}
VALUE	EVTS	DOCUMENT ID	TECN	COMMENT	
0.83 ± 0.08 OUR FIT					
$0.81 \pm 0.06 \pm 0.06$		BORTOLETTO93	CLEO	$E_{\text{cm}}^{\text{ee}} \approx 10.6 \text{ GeV}$	

$\Gamma(h^-\omega 2\pi^0\nu_\tau)/\Gamma_{\text{total}}$					Γ_{149}/Γ
VALUE (units 10^{-4})	EVTS	DOCUMENT ID	TECN	COMMENT	
$1.4 \pm 0.4 \pm 0.3$	53	ANASTASSOV 01	CLEO	$E_{\text{cm}}^{\text{ee}} = 10.6 \text{ GeV}$	
••• We do not use the following data for averages, fits, limits, etc. •••					
$1.89_{-0.67}^{+0.74} \pm 0.40$	19	ANDERSON 97	CLEO	Repl. by ANASTASSOV 01	

$\Gamma(h^-\omega 2\pi^0\nu_\tau)/\Gamma_{\text{total}}$					Γ_{150}/Γ
VALUE	CL%	DOCUMENT ID	TECN	COMMENT	
< 5.4×10^{-7}	90	AUBERT,B 06	BABR	232 fb^{-1} $E_{\text{cm}}^{\text{ee}} = 10.6 \text{ GeV}$	

$\Gamma(2h^-\pi^+\omega\nu_\tau)/\Gamma_{\text{total}}$					Γ_{151}/Γ
VALUE (units 10^{-4})	EVTS	DOCUMENT ID	TECN	COMMENT	
$1.2 \pm 0.2 \pm 0.1$	110	ANASTASSOV 01	CLEO	$E_{\text{cm}}^{\text{ee}} = 10.6 \text{ GeV}$	

$\Gamma(\mu^- \pi^0 \eta)/\Gamma_{\text{total}}$					Γ_{199}/Γ
Test of lepton family number conservation.					
VALUE	CL%	DOCUMENT ID	TECN	COMMENT	
$<22 \times 10^{-6}$	90	BONVICINI	97	CLEO $E_{\text{cm}}^{\text{e}e} = 10.6 \text{ GeV}$	

$\Gamma(\bar{p}\gamma)/\Gamma_{\text{total}}$					Γ_{200}/Γ
Test of lepton number and baryon number conservation.					
VALUE	CL%	DOCUMENT ID	TECN	COMMENT	
$<3.5 \times 10^{-6}$	90	GODANG	99	CLEO $E_{\text{cm}}^{\text{e}e} = 10.6 \text{ GeV}$	
• • • We do not use the following data for averages, fits, limits, etc. • • •					
$<29 \times 10^{-5}$	90	ALBRECHT	92k	ARG $E_{\text{cm}}^{\text{e}e} = 10 \text{ GeV}$	

$\Gamma(\bar{p}\pi^0)/\Gamma_{\text{total}}$					Γ_{201}/Γ
Test of lepton number and baryon number conservation.					
VALUE	CL%	DOCUMENT ID	TECN	COMMENT	
$<15 \times 10^{-6}$	90	GODANG	99	CLEO $E_{\text{cm}}^{\text{e}e} = 10.6 \text{ GeV}$	
• • • We do not use the following data for averages, fits, limits, etc. • • •					
$<66 \times 10^{-5}$	90	ALBRECHT	92k	ARG $E_{\text{cm}}^{\text{e}e} = 10 \text{ GeV}$	

$\Gamma(\bar{p}2\pi^0)/\Gamma_{\text{total}}$					Γ_{202}/Γ
Test of lepton number and baryon number conservation.					
VALUE	CL%	DOCUMENT ID	TECN	COMMENT	
$<33 \times 10^{-6}$	90	GODANG	99	CLEO $E_{\text{cm}}^{\text{e}e} = 10.6 \text{ GeV}$	

$\Gamma(\bar{p}\eta)/\Gamma_{\text{total}}$					Γ_{203}/Γ
Test of lepton number and baryon number conservation.					
VALUE	CL%	DOCUMENT ID	TECN	COMMENT	
$<8.9 \times 10^{-6}$	90	GODANG	99	CLEO $E_{\text{cm}}^{\text{e}e} = 10.6 \text{ GeV}$	
• • • We do not use the following data for averages, fits, limits, etc. • • •					
$<130 \times 10^{-5}$	90	ALBRECHT	92k	ARG $E_{\text{cm}}^{\text{e}e} = 10 \text{ GeV}$	

$\Gamma(\bar{p}\pi^0\eta)/\Gamma_{\text{total}}$					Γ_{204}/Γ
Test of lepton number and baryon number conservation.					
VALUE	CL%	DOCUMENT ID	TECN	COMMENT	
$<27 \times 10^{-6}$	90	GODANG	99	CLEO $E_{\text{cm}}^{\text{e}e} = 10.6 \text{ GeV}$	

$\Gamma(\Lambda\pi^-)/\Gamma_{\text{total}}$					Γ_{205}/Γ
Test of lepton number and baryon number conservation.					
VALUE	CL%	DOCUMENT ID	TECN	COMMENT	
$<0.72 \times 10^{-7}$	90	MIYAZAKI	06	BELL 154 fb^{-1} , $E_{\text{cm}}^{\text{e}e} = 10.6 \text{ GeV}$	

$\Gamma(\bar{\Lambda}\pi^-)/\Gamma_{\text{total}}$					Γ_{206}/Γ
Test of lepton number and baryon number conservation.					
VALUE	CL%	DOCUMENT ID	TECN	COMMENT	
$<1.4 \times 10^{-7}$	90	MIYAZAKI	06	BELL 154 fb^{-1} , $E_{\text{cm}}^{\text{e}e} = 10.6 \text{ GeV}$	

$\Gamma(e^- \text{light boson})/\Gamma(e^- \bar{\nu}_e \nu_\tau)$					Γ_{207}/Γ_5
Test of lepton family number conservation.					
VALUE	CL%	DOCUMENT ID	TECN	COMMENT	
<0.015	95	1 ALBRECHT	95G	ARG $E_{\text{cm}}^{\text{e}e} = 9.4\text{--}10.6 \text{ GeV}$	
• • • We do not use the following data for averages, fits, limits, etc. • • •					
<0.018	95	2 ALBRECHT	90E	ARG $E_{\text{cm}}^{\text{e}e} = 9.4\text{--}10.6 \text{ GeV}$	
<0.040	95	3 BALTRUSAITIS	85	MRK3 $E_{\text{cm}}^{\text{e}e} = 3.77 \text{ GeV}$	

- ¹ ALBRECHT 95G limit holds for bosons with mass $< 0.4 \text{ GeV}$. The limit rises to 0.036 for a mass of 1.0 GeV, then falls to 0.006 at the upper mass limit of 1.6 GeV.
² ALBRECHT 90E limit applies for spinless boson with mass $< 100 \text{ MeV}$, and rises to 0.050 for mass = 500 MeV.
³ BALTRUSAITIS 85 limit applies for spinless boson with mass $< 100 \text{ MeV}$.

$\Gamma(\mu^- \text{light boson})/\Gamma(e^- \bar{\nu}_e \nu_\tau)$					Γ_{208}/Γ_5
Test of lepton family number conservation.					
VALUE	CL%	DOCUMENT ID	TECN	COMMENT	
<0.026	95	1 ALBRECHT	95G	ARG $E_{\text{cm}}^{\text{e}e} = 9.4\text{--}10.6 \text{ GeV}$	
• • • We do not use the following data for averages, fits, limits, etc. • • •					
<0.033	95	2 ALBRECHT	90E	ARG $E_{\text{cm}}^{\text{e}e} = 9.4\text{--}10.6 \text{ GeV}$	
<0.125	95	3 BALTRUSAITIS	85	MRK3 $E_{\text{cm}}^{\text{e}e} = 3.77 \text{ GeV}$	

- ¹ ALBRECHT 95G limit holds for bosons with mass $< 1.3 \text{ GeV}$. The limit rises to 0.034 for a mass of 1.4 GeV, then falls to 0.003 at the upper mass limit of 1.6 GeV.
² ALBRECHT 90E limit applies for spinless boson with mass $< 100 \text{ MeV}$, and rises to 0.071 for mass = 500 MeV.
³ BALTRUSAITIS 85 limit applies for spinless boson with mass $< 100 \text{ MeV}$.

 τ -DECAY PARAMETERS **τ -LEPTON DECAY PARAMETERS**

Updated July 2007 by A. Stahl (RWTH Aachen).

The purpose of the measurements of the decay parameters (*i.e.*, Michel parameters) of the τ is to determine the structure (spin and chirality) of the current mediating its decays.

Leptonic Decays: The Michel parameters are extracted from the energy spectrum of the charged daughter lepton $\ell = e, \mu$ in the decays $\tau \rightarrow \ell \nu_\ell \nu_\tau$. Ignoring radiative corrections, neglecting terms of order $(m_\ell/m_\tau)^2$ and $(m_\tau/\sqrt{s})^2$, and setting the neutrino masses to zero, the spectrum in the laboratory frame reads

$$\frac{d\Gamma}{dx} = \frac{G_{\tau\ell}^2 m_\tau^5}{192 \pi^3} \times \left\{ f_0(x) + \rho f_1(x) + \eta \frac{m_\ell}{m_\tau} f_2(x) - P_\tau [\xi g_1(x) + \delta g_2(x)] \right\}, \quad (1)$$

with

$$\begin{aligned} f_0(x) &= 2 - 6x^2 + 4x^3 \\ f_1(x) &= -\frac{4}{9} + 4x^2 - \frac{32}{9}x^3 & g_1(x) &= -\frac{2}{3} + 4x - 6x^2 + \frac{8}{3}x^3 \\ f_2(x) &= 12(1-x)^2 & g_2(x) &= \frac{4}{9} - \frac{16}{3}x + 12x^2 - \frac{64}{9}x^3. \end{aligned}$$

The quantity x is the fractional energy of the daughter lepton ℓ , *i.e.*, $x = E_\ell/E_{\ell,\text{max}} \approx E_\ell/(\sqrt{s}/2)$ and P_τ is the polarization of the tau leptons. The integrated decay width is given by

$$\Gamma = \frac{G_{\tau\ell}^2 m_\tau^5}{192 \pi^3} \left(1 + 4\eta \frac{m_\ell}{m_\tau} \right). \quad (2)$$

The situation is similar to muon decays $\mu \rightarrow e \nu_e \nu_\mu$. The generalized matrix element with the couplings $g_{\tau\mu}^\gamma$ and their relations to the Michel parameters ρ, η, ξ , and δ have been described in the “Note on Muon Decay Parameters.” The Standard Model expectations are 3/4, 0, 1, and 3/4, respectively. For more details, see Ref. 1.

Hadronic Decays: In the case of hadronic decays $\tau \rightarrow h \nu_\tau$, with $h = \pi, \rho$, or a_1 , the ansatz is restricted to purely vectorial currents. The matrix element is

$$\frac{G_{\tau h}}{\sqrt{2}} \sum_{\lambda=R,L} g_\lambda \langle \bar{\Psi}_\omega(\nu_\tau) | \gamma^\mu | \Psi_\lambda(\tau) \rangle J_\mu^h \quad (3)$$

with the hadronic current J_μ^h . The neutrino chirality ω is uniquely determined from λ . The spectrum depends only on a single parameter ξ_h

$$\frac{d^n \Gamma}{dx_1 dx_2 \dots dx_n} = f(\vec{x}) + \xi_h P_\tau g(\vec{x}), \quad (4)$$

with f and g being channel-dependent functions of the n observables $\vec{x} = (x_1, x_2, \dots, x_n)$ (see Ref. 2). The parameter ξ_h is related to the couplings through

$$\xi_h = |g_L|^2 - |g_R|^2. \quad (5)$$

ξ_h is the negative of the chirality of the τ neutrino in these decays. In the Standard Model, $\xi_h = 1$. Also included in the

Lepton Particle Listings

τ

Data Listings for ξ_h are measurements of the neutrino helicity which coincide with ξ_h , if the neutrino is massless (ASNER 00, ACKERSTAFF 97R, AKERS 95P, ALBRECHT 93C, and ALBRECHT 90I).

Combination of Measurements: The individual measurements are combined, taking into account the correlations between the parameters. In a first fit, universality between the two leptonic decays, and between all hadronic decays, is assumed. A second fit is made without these assumptions. The results of the two fits are provided as OUR FIT in the Data Listings below in the tables whose title includes “(e or mu)” or “(all hadronic modes),” and “(e),” “(mu)” *etc.*, respectively. The measurements show good agreement with the Standard Model. The χ^2 values with respect to the Standard model predictions are 24.1 for 41 degrees of freedom and 26.8 for 56 degrees of freedom, respectively. The correlations are reduced through this combination to less than 20%, with the exception of ρ and η which are correlated by +23%, for the fit with universality and by +70% for $\tau \rightarrow \mu\nu_\mu\nu_\tau$.

Model-independent Analysis: From the Michel parameters, limits can be derived on the couplings $g_{e\lambda}^\kappa$ without further module assumptions. In the Standard model $g_{LL}^V = 1$ (leptonic decays), and $g_L = 1$ (hadronic decays) and all other couplings vanish. First, the partial decay widths have to be compared to the Standard Model predictions to derive limits on the normalization of the couplings $A_x = G_{\tau x}^2/G_F^2$ with Fermi's constant G_F :

$$\begin{aligned} A_e &= 1.0012 \pm 0.0053, \\ A_\mu &= 0.981 \pm 0.018, \\ A_\pi &= 1.018 \pm 0.012. \end{aligned} \quad (6)$$

Then limits on the couplings (95% CL) can be extracted (see Ref. 3 and Ref. 4). Without the assumption of universality, the limits given in Table 1 are derived.

Model-dependent Interpretation: More stringent limits can be derived assuming specific models. For example, in the framework of a two Higgs doublet model, the measurements correspond to a limit of $m_{H^\pm} > 1.9 \text{ GeV} \times \tan\beta$ on the mass of the charged Higgs boson, or a limit of 253 GeV on the mass of the second W boson in left-right symmetric models for arbitrary mixing (both 95% CL). See Ref. 4 and Ref. 5.

Footnotes and References

1. F. Scheck, Phys. Reports **44**, 187 (1978);
W. Fetscher and H.J. Gerber in *Precision Tests of the Standard Model*, edited by P. Langacker, World Scientific, 1993;
A. Stahl, *Physics with τ Leptons*, Springer Tracts in Modern Physics.
2. M. Davier *et al.*, Phys. Lett. **B306**, 411 (1993).
3. OPAL Collab., K. Ackerstaff *et al.*, Eur. Phys. J. **C8**, 3 (1999).
4. A. Stahl, Nucl. Phys. (Proc. Supp.) **B76**, 173 (1999).

Table 1: Coupling constants $g_{e\mu}^\gamma$. 95% confidence level experimental limits. The limits include the quoted values of A_e , A_μ , and A_π and assume $A_\rho = A_{a_1} = 1$.

$\tau \rightarrow e\nu_e\nu_\tau$		
$ g_{RR}^S < 0.70$	$ g_{RR}^V < 0.17$	$ g_{RR}^T \equiv 0$
$ g_{LR}^S < 0.99$	$ g_{LR}^V < 0.13$	$ g_{LR}^T < 0.082$
$ g_{RL}^S < 2.01$	$ g_{RL}^V < 0.52$	$ g_{RL}^T < 0.51$
$ g_{LL}^S < 2.01$	$ g_{LL}^V < 1.005$	$ g_{LL}^T \equiv 0$
$\tau \rightarrow \mu\nu_\mu\nu_\tau$		
$ g_{RR}^S < 0.72$	$ g_{RR}^V < 0.18$	$ g_{RR}^T \equiv 0$
$ g_{LR}^S < 0.95$	$ g_{LR}^V < 0.12$	$ g_{LR}^T < 0.079$
$ g_{RL}^S < 2.01$	$ g_{RL}^V < 0.52$	$ g_{RL}^T < 0.51$
$ g_{LL}^S < 2.01$	$ g_{LL}^V < 1.005$	$ g_{LL}^T \equiv 0$
$\tau \rightarrow \pi\nu_\tau$		
$ g_R^V < 0.15$	$ g_L^V > 0.992$	
$\tau \rightarrow \rho\nu_\tau$		
$ g_R^V < 0.10$	$ g_L^V > 0.995$	
$\tau \rightarrow a_1\nu_\tau$		
$ g_R^V < 0.16$	$ g_L^V > 0.987$	

5. M.-T. Dova *et al.*, Phys. Rev. **D58**, 015005 (1998);
T. Hebbeker and W. Lohmann, Z. Phys. **C74**, 399 (1997);
A. Pich and J.P. Silva, Phys. Rev. **D52**, 4006 (1995).

$\rho(e \text{ or } \mu)$ PARAMETER

($V-A$) theory predicts $\rho = 0.75$.

VALUE	EVTs	DOCUMENT ID	TECN	COMMENT
0.745 ± 0.008 OUR FIT				
0.749 ± 0.008 OUR AVERAGE				
0.742 ± 0.014 ± 0.006	81k	HEISTER	01E ALEP	1991-1995 LEP runs
0.775 ± 0.023 ± 0.020	36k	ABREU	00L DLPH	1992-1995 runs
0.781 ± 0.028 ± 0.018	46k	ACKERSTAFF	99D OPAL	1990-1995 LEP runs
0.762 ± 0.035	54k	ACCIARRI	98R L3	1991-1995 LEP runs
0.731 ± 0.031		¹ ALBRECHT	98 ARG	$E_{cm}^{ee} = 9.5-10.6 \text{ GeV}$
0.72 ± 0.09 ± 0.03		² ABE	97O SLD	1993-1995 SLC runs
0.747 ± 0.010 ± 0.006	55k	ALEXANDER	97F CLEO	$E_{cm}^{ee} = 10.6 \text{ GeV}$
0.79 ± 0.10 ± 0.10	3732	FORD	87B MAC	$E_{cm}^{ee} = 29 \text{ GeV}$
0.71 ± 0.09 ± 0.03	1426	BEHRENDTS	85 CLEO	e^+e^- near $\Upsilon(4S)$
• • • We do not use the following data for averages, fits, limits, etc. • • •				
0.735 ± 0.013 ± 0.008	31k	AMMAR	97B ALEP	Repl. by ALEXANDER 97F
0.794 ± 0.039 ± 0.031	18k	ACCIARRI	96H L3	Repl. by ACCIARRI 98R
0.732 ± 0.034 ± 0.020	8.2k	³ ALBRECHT	95 ARG	$E_{cm}^{ee} = 9.5-10.6 \text{ GeV}$
0.738 ± 0.038		⁴ ALBRECHT	95C ARG	Repl. by ALBRECHT 98
0.751 ± 0.039 ± 0.022		BUSKULIC	95D ALEP	Repl. by HEISTER 01E
0.742 ± 0.035 ± 0.020	8000	ALBRECHT	90E ARG	$E_{cm}^{ee} = 9.4-10.6 \text{ GeV}$

¹ Combined fit to ARGUS tau decay parameter measurements in ALBRECHT 98, ALBRECHT 95C, ALBRECHT 93G, and ALBRECHT 94E. ALBRECHT 98 use tau pair events of the type $\tau^-\tau^+ \rightarrow (\ell^-\bar{\nu}_\ell\nu_\tau)(\pi^+\pi^0\bar{\nu}_\tau)$, and their charged conjugates.

² ABE 97O assume $\eta = 0$ in their fit. Letting η vary in the fit gives a ρ value of $0.69 \pm 0.13 \pm 0.05$.

³ Value is from a simultaneous fit for the ρ and η decay parameters to the lepton energy spectrum. Not independent of ALBRECHT 90E $\rho(e \text{ or } \mu)$ value which assumes $\eta = 0$. Result is strongly correlated with ALBRECHT 95C.

⁴ Combined fit to ARGUS tau decay parameter measurements in ALBRECHT 95C, ALBRECHT 93G, and ALBRECHT 94E.

$\rho(e)$ PARAMETER $(V-A)$ theory predicts $\rho = 0.75$.

VALUE	EVTS	DOCUMENT ID	TECN	COMMENT
0.747±0.010 OUR FIT				
0.744±0.010 OUR AVERAGE				
0.747±0.019±0.014	44k	HEISTER	01E ALEP	1991–1995 LEP runs
0.744±0.036±0.037	17k	ABREU	00L DLPH	1992–1995 runs
0.779±0.047±0.029	25k	ACKERSTAFF	99D OPAL	1990–1995 LEP runs
0.68 ±0.04 ±0.07		¹ ALBRECHT	98 ARG	$E_{cm}^{ee} = 9.5\text{--}10.6$ GeV
0.71 ±0.14 ±0.05		ABE	97O SLD	1993–1995 SLC runs
0.747±0.012±0.004	34k	ALEXANDER	97F CLEO	$E_{cm}^{ee} = 10.6$ GeV
0.735±0.036±0.020	4.7k	² ALBRECHT	95 ARG	$E_{cm}^{ee} = 9.5\text{--}10.6$ GeV
0.79 ±0.08 ±0.06	3230	³ ALBRECHT	93G ARG	$E_{cm}^{ee} = 9.4\text{--}10.6$ GeV
0.64 ±0.06 ±0.07	2753	JANSSEN	89 CBAL	$E_{cm}^{ee} = 9.4\text{--}10.6$ GeV
0.62 ±0.17 ±0.14	1823	FORD	87B MAC	$E_{cm}^{ee} = 29$ GeV
0.60 ±0.13	699	BEHRENDIS	85 CLEO	e^+e^- near $\Upsilon(4S)$
0.72 ±0.10 ±0.11	594	BACINO	79B DLCO	$E_{cm}^{ee} = 3.5\text{--}7.4$ GeV

• • • We do not use the following data for averages, fits, limits, etc. • • •

0.732±0.014±0.009	19k	AMMAR	97B CLEO	Repl. by ALEXANDER 97F
0.793±0.050±0.025		BUSKULIC	95D ALEP	Repl. by HEISTER 01E
0.747±0.045±0.028	5106	ALBRECHT	90E ARG	Repl. by ALBRECHT 95

¹ ALBRECHT 98 use tau pair events of the type $\tau^-\tau^+ \rightarrow (\ell^-\bar{\nu}_\ell\nu_\tau)(\pi^+\pi^0\bar{\nu}_\tau)$, and their charged conjugates.

² ALBRECHT 95 use tau pair events of the type $\tau^-\tau^+ \rightarrow (\ell^-\bar{\nu}_\ell\nu_\tau)(h^+h^-\pi^0\bar{\nu}_\tau)$ and their charged conjugates.

³ ALBRECHT 93G use tau pair events of the type $\tau^-\tau^+ \rightarrow (\mu^-\bar{\nu}_\mu\nu_\tau)(e^+\nu_e\bar{\nu}_\tau)$ and their charged conjugates.

 $\rho(\mu)$ PARAMETER $(V-A)$ theory predicts $\rho = 0.75$.

VALUE	EVTS	DOCUMENT ID	TECN	COMMENT
0.763±0.020 OUR FIT				
0.770±0.022 OUR AVERAGE				
0.776±0.045±0.019	46k	HEISTER	01E ALEP	1991–1995 LEP runs
0.999±0.098±0.045	22k	ABREU	00L DLPH	1992–1995 runs
0.777±0.044±0.016	27k	ACKERSTAFF	99D OPAL	1990–1995 LEP runs
0.69 ±0.06 ±0.06		¹ ALBRECHT	98 ARG	$E_{cm}^{ee} = 9.5\text{--}10.6$ GeV
0.54 ±0.28 ±0.14		ABE	97O SLD	1993–1995 SLC runs
0.750±0.017±0.045	22k	ALEXANDER	97F CLEO	$E_{cm}^{ee} = 10.6$ GeV
0.76 ±0.07 ±0.08	3230	ALBRECHT	93G ARG	$E_{cm}^{ee} = 9.4\text{--}10.6$ GeV
0.734±0.055±0.027	3041	ALBRECHT	90E ARG	$E_{cm}^{ee} = 9.4\text{--}10.6$ GeV
0.89 ±0.14 ±0.08	1909	FORD	87B MAC	$E_{cm}^{ee} = 29$ GeV
0.81 ±0.13	727	BEHRENDIS	85 CLEO	e^+e^- near $\Upsilon(4S)$

• • • We do not use the following data for averages, fits, limits, etc. • • •

0.747±0.048±0.044	13k	AMMAR	97B CLEO	Repl. by ALEXANDER 97F
0.693±0.057±0.028		BUSKULIC	95D ALEP	Repl. by HEISTER 01E

¹ ALBRECHT 98 use tau pair events of the type $\tau^-\tau^+ \rightarrow (\ell^-\bar{\nu}_\ell\nu_\tau)(\pi^+\pi^0\bar{\nu}_\tau)$, and their charged conjugates.

 $\xi(e$ or $\mu)$ PARAMETER $(V-A)$ theory predicts $\xi = 1$.

VALUE	EVTS	DOCUMENT ID	TECN	COMMENT
0.985±0.030 OUR FIT				
0.981±0.031 OUR AVERAGE				
0.986±0.068±0.031	81k	HEISTER	01E ALEP	1991–1995 LEP runs
0.929±0.070±0.030	36k	ABREU	00L DLPH	1992–1995 runs
0.98 ±0.22 ±0.10	46k	ACKERSTAFF	99D OPAL	1990–1995 LEP runs
0.70 ±0.16	54k	ACCIARRI	98R L3	1991–1995 LEP runs
1.03 ±0.11		¹ ALBRECHT	98 ARG	$E_{cm}^{ee} = 9.5\text{--}10.6$ GeV
1.05 ±0.35 ±0.04		² ABE	97O SLD	1993–1995 SLC runs
1.007±0.040±0.015	55k	ALEXANDER	97F CLEO	$E_{cm}^{ee} = 10.6$ GeV

• • • We do not use the following data for averages, fits, limits, etc. • • •

0.94 ±0.21 ±0.07	18k	ACCIARRI	96H L3	Repl. by ACCIARRI 98R
0.97 ±0.14		³ ALBRECHT	95C ARG	Repl. by ALBRECHT 98
1.18 ±0.15 ±0.16		BUSKULIC	95D ALEP	Repl. by HEISTER 01E
0.90 ±0.15 ±0.10	3230	⁴ ALBRECHT	93G ARG	$E_{cm}^{ee} = 9.4\text{--}10.6$ GeV

¹ Combined fit to ARGUS tau decay parameter measurements in ALBRECHT 98, ALBRECHT 95C, ALBRECHT 93G, and ALBRECHT 94E. ALBRECHT 98 use tau pair events of the type $\tau^-\tau^+ \rightarrow (\ell^-\bar{\nu}_\ell\nu_\tau)(\pi^+\pi^0\bar{\nu}_\tau)$, and their charged conjugates.

² ABE 97O assume $\eta = 0$ in their fit. Letting η vary in the fit gives a ξ value of $1.02 \pm 0.36 \pm 0.05$.

³ Combined fit to ARGUS tau decay parameter measurements in ALBRECHT 95C, ALBRECHT 93G, and ALBRECHT 94E. ALBRECHT 95C uses events of the type $\tau^-\tau^+ \rightarrow (\ell^-\bar{\nu}_\ell\nu_\tau)(h^+h^-\pi^0\bar{\nu}_\tau)$ and their charged conjugates.

⁴ ALBRECHT 93G measurement determines $|\xi|$ for the case $\xi(e) = \xi(\mu)$, but the authors point out that other LEP experiments determine the sign to be positive.

 $\xi(e)$ PARAMETER $(V-A)$ theory predicts $\xi = 1$.

VALUE	EVTS	DOCUMENT ID	TECN	COMMENT
0.994±0.040 OUR FIT				
1.00 ±0.04 OUR AVERAGE				
1.011±0.094±0.038	44k	HEISTER	01E ALEP	1991–1995 LEP runs
1.01 ±0.12 ±0.05	17k	ABREU	00L DLPH	1992–1995 runs
1.13 ±0.39 ±0.14	25k	ACKERSTAFF	99D OPAL	1990–1995 LEP runs
1.11 ±0.20 ±0.08		¹ ALBRECHT	98 ARG	$E_{cm}^{ee} = 9.5\text{--}10.6$ GeV
1.16 ±0.52 ±0.06		ABE	97O SLD	1993–1995 SLC runs
0.979±0.048±0.016	34k	ALEXANDER	97F CLEO	$E_{cm}^{ee} = 10.6$ GeV

• • • We do not use the following data for averages, fits, limits, etc. • • •

1.03 ±0.23 ±0.09 BUSKULIC 95D ALEP Repl. by HEISTER 01E

¹ ALBRECHT 98 use tau pair events of the type $\tau^-\tau^+ \rightarrow (\ell^-\bar{\nu}_\ell\nu_\tau)(\pi^+\pi^0\bar{\nu}_\tau)$, and their charged conjugates.

 $\xi(\mu)$ PARAMETER $(V-A)$ theory predicts $\xi = 1$.

VALUE	EVTS	DOCUMENT ID	TECN	COMMENT
1.030±0.059 OUR FIT				
1.06 ±0.06 OUR AVERAGE				
1.030±0.120±0.050	46k	HEISTER	01E ALEP	1991–1995 LEP runs
1.16 ±0.19 ±0.06	22k	ABREU	00L DLPH	1992–1995 runs
0.79 ±0.41 ±0.09	27k	ACKERSTAFF	99D OPAL	1990–1995 LEP runs
1.26 ±0.27 ±0.14		¹ ALBRECHT	98 ARG	$E_{cm}^{ee} = 9.5\text{--}10.6$ GeV
0.75 ±0.50 ±0.14		ABE	97O SLD	1993–1995 SLC runs
1.054±0.069±0.047	22k	ALEXANDER	97F CLEO	$E_{cm}^{ee} = 10.6$ GeV

• • • We do not use the following data for averages, fits, limits, etc. • • •

1.23 ±0.22 ±0.10 BUSKULIC 95D ALEP Repl. by HEISTER 01E

¹ ALBRECHT 98 use tau pair events of the type $\tau^-\tau^+ \rightarrow (\ell^-\bar{\nu}_\ell\nu_\tau)(\pi^+\pi^0\bar{\nu}_\tau)$, and their charged conjugates.

 $\eta(e$ or $\mu)$ PARAMETER $(V-A)$ theory predicts $\eta = 0$.

VALUE	EVTS	DOCUMENT ID	TECN	COMMENT
0.013±0.020 OUR FIT				
0.015 ±0.021 OUR AVERAGE				
0.012±0.026±0.004	81k	HEISTER	01E ALEP	1991–1995 LEP runs
−0.005±0.036±0.037		ABREU	00L DLPH	1992–1995 runs
0.027±0.055±0.005	46k	ACKERSTAFF	99D OPAL	1990–1995 LEP runs
0.27 ±0.14	54k	ACCIARRI	98R L3	1991–1995 LEP runs
−0.13 ±0.47 ±0.15		ABE	97O SLD	1993–1995 SLC runs
−0.015±0.061±0.062	31k	AMMAR	97B CLEO	$E_{cm}^{ee} = 10.6$ GeV
−0.03 ±0.18 ±0.12	8.2k	ALBRECHT	95 ARG	$E_{cm}^{ee} = 9.5\text{--}10.6$ GeV

• • • We do not use the following data for averages, fits, limits, etc. • • •

0.25 ±0.17 ±0.11 18k ACCIARRI 96H L3 Repl. by ACCIARRI 98R

−0.04 ±0.15 ±0.11 BUSKULIC 95D ALEP Repl. by HEISTER 01E

 $\eta(\mu)$ PARAMETER $(V-A)$ theory predicts $\eta = 0$.

VALUE	EVTS	DOCUMENT ID	TECN	COMMENT
0.094±0.073 OUR FIT				
0.17 ±0.15 OUR AVERAGE				
0.160±0.150±0.060	46k	HEISTER	01E ALEP	1991–1995 LEP runs
0.72 ±0.32 ±0.15		ABREU	00L DLPH	1992–1995 runs
−0.59 ±0.82 ±0.45		¹ ABE	97O SLD	1993–1995 SLC runs
0.010±0.149±0.171	13k	² AMMAR	97B CLEO	$E_{cm}^{ee} = 10.6$ GeV

• • • We do not use the following data for averages, fits, limits, etc. • • •

0.010±0.065±0.001 27k ³ ACKERSTAFF 99D OPAL 1990–1995 LEP runs

−0.24 ±0.23 ±0.18 BUSKULIC 95D ALEP Repl. by HEISTER 01E

¹ Highly correlated (corr. = 0.92) with ABE 97O $\rho(\mu)$ measurement.

² Highly correlated (corr. = 0.949) with AMMAR 97B $\rho(\mu)$ value.

³ ACKERSTAFF 99D result is dominated by a constraint on η from the OPAL measurements of the τ lifetime and $B(\tau^- \rightarrow \mu^-\bar{\nu}_\mu\nu_\tau)$ assuming lepton universality for the total coupling strength.

 $(\delta\xi)(e$ or $\mu)$ PARAMETER $(V-A)$ theory predicts $(\delta\xi) = 0.75$.

VALUE	EVTS	DOCUMENT ID	TECN	COMMENT
0.746±0.021 OUR FIT				
0.744±0.022 OUR AVERAGE				
0.776±0.045±0.024	81k	HEISTER	01E ALEP	1991–1995 LEP runs
0.779±0.070±0.028	36k	ABREU	00L DLPH	1992–1995 runs
0.65 ±0.14 ±0.07	46k	ACKERSTAFF	99D OPAL	1990–1995 LEP runs
0.70 ±0.11	54k	ACCIARRI	98R L3	1991–1995 LEP runs
0.63 ±0.09		¹ ALBRECHT	98 ARG	$E_{cm}^{ee} = 9.5\text{--}10.6$ GeV
0.88 ±0.27 ±0.04		² ABE	97O SLD	1993–1995 SLC runs
0.745±0.026±0.009	55k	ALEXANDER	97F CLEO	$E_{cm}^{ee} = 10.6$ GeV

• • • We do not use the following data for averages, fits, limits, etc. • • •

0.81 ±0.14 ±0.06 18k ACCIARRI 96H L3 Repl. by ACCIARRI 98R

0.65 ±0.12 ³ ALBRECHT 95C ARG Repl. by ALBRECHT 98

0.88 ±0.11 ±0.07 BUSKULIC 95D ALEP Repl. by HEISTER 01E

Lepton Particle Listings

 τ

¹ Combined fit to ARGUS tau decay parameter measurements in ALBRECHT 98, ALBRECHT 95c, ALBRECHT 93g, and ALBRECHT 94e. ALBRECHT 98 use tau pair events of the type $\tau^- \tau^+ \rightarrow (\ell^- \bar{\nu}_\ell \nu_\tau)(\pi^+ \pi^0 \bar{\nu}_\tau)$, and their charged conjugates.

² ABE 97o assume $\eta = 0$ in their fit. Letting η vary in the fit gives a $(\delta\xi)$ value of $0.87 \pm 0.27 \pm 0.04$.

³ Combined fit to ARGUS tau decay parameter measurements in ALBRECHT 95c, ALBRECHT 93g, and ALBRECHT 94e. ALBRECHT 95c uses events of the type $\tau^- \tau^+ \rightarrow (\ell^- \bar{\nu}_\ell \nu_\tau)(h^+ h^- h^+ \bar{\nu}_\tau)$ and their charged conjugates.

 $(\delta\xi)(e)$ PARAMETER

($V-A$) theory predicts $(\delta\xi) = 0.75$.

VALUE	EVTS	DOCUMENT ID	TECN	COMMENT
0.734 ± 0.028 OUR FIT				
0.731 ± 0.029 OUR AVERAGE				
0.778 ± 0.066 ± 0.024	44k	HEISTER	01E ALEP	1991–1995 LEP runs
0.85 ± 0.12 ± 0.04	17k	ABREU	00L DLPH	1992–1995 runs
0.72 ± 0.31 ± 0.14	25k	ACKERSTAFF	99D OPAL	1990–1995 LEP runs
0.56 ± 0.14 ± 0.06		¹ ALBRECHT	98 ARG	$E_{\text{cm}}^e = 9.5\text{--}10.6$ GeV
0.85 ± 0.43 ± 0.08		ABE	97o SLD	1993–1995 SLC runs
0.720 ± 0.032 ± 0.010	34k	ALEXANDER	97F CLEO	$E_{\text{cm}}^e = 10.6$ GeV

• • • We do not use the following data for averages, fits, limits, etc. • • •

1.11 ± 0.17 ± 0.07 BUSKULIC 95D ALEP Repl. by HEISTER 01E

¹ ALBRECHT 98 use tau pair events of the type $\tau^- \tau^+ \rightarrow (\ell^- \bar{\nu}_\ell \nu_\tau)(\pi^+ \pi^0 \bar{\nu}_\tau)$, and their charged conjugates.

 $(\delta\xi)(\mu)$ PARAMETER

($V-A$) theory predicts $(\delta\xi) = 0.75$.

VALUE	EVTS	DOCUMENT ID	TECN	COMMENT
0.778 ± 0.037 OUR FIT				
0.79 ± 0.04 OUR AVERAGE				
0.786 ± 0.066 ± 0.028	46k	HEISTER	01E ALEP	1991–1995 LEP runs
0.86 ± 0.13 ± 0.04	22k	ABREU	00L DLPH	1992–1995 runs
0.63 ± 0.23 ± 0.05	27k	ACKERSTAFF	99D OPAL	1990–1995 LEP runs
0.73 ± 0.18 ± 0.10		¹ ALBRECHT	98 ARG	$E_{\text{cm}}^e = 9.5\text{--}10.6$ GeV
0.82 ± 0.32 ± 0.07		ABE	97o SLD	1993–1995 SLC runs
0.786 ± 0.041 ± 0.032	22k	ALEXANDER	97F CLEO	$E_{\text{cm}}^e = 10.6$ GeV

• • • We do not use the following data for averages, fits, limits, etc. • • •

0.71 ± 0.14 ± 0.06 BUSKULIC 95D ALEP Repl. by HEISTER 01E

¹ ALBRECHT 98 use tau pair events of the type $\tau^- \tau^+ \rightarrow (\ell^- \bar{\nu}_\ell \nu_\tau)(\pi^+ \pi^0 \bar{\nu}_\tau)$, and their charged conjugates.

 $\xi(\pi)$ PARAMETER

($V-A$) theory predicts $\xi(\pi) = 1$.

VALUE	EVTS	DOCUMENT ID	TECN	COMMENT
0.993 ± 0.022 OUR FIT				
0.994 ± 0.023 OUR AVERAGE				
0.994 ± 0.020 ± 0.014	27k	HEISTER	01E ALEP	1991–1995 LEP runs
0.81 ± 0.17 ± 0.02		ABE	97o SLD	1993–1995 SLC runs
1.03 ± 0.06 ± 0.04	2.0k	COAN	97 CLEO	$E_{\text{cm}}^e = 10.6$ GeV

• • • We do not use the following data for averages, fits, limits, etc. • • •

0.987 ± 0.057 ± 0.027 BUSKULIC 95D ALEP Repl. by HEISTER 01E

0.95 ± 0.11 ± 0.05 ¹ BUSKULIC 94D ALEP 1990+1991 LEP run

¹ Superseded by BUSKULIC 95D.

 $\xi(\rho)$ PARAMETER

($V-A$) theory predicts $\xi(\rho) = 1$.

VALUE	EVTS	DOCUMENT ID	TECN	COMMENT
0.994 ± 0.008 OUR FIT				
0.994 ± 0.009 OUR AVERAGE				
0.987 ± 0.012 ± 0.011	59k	HEISTER	01E ALEP	1991–1995 LEP runs
0.99 ± 0.12 ± 0.04		ABE	97o SLD	1993–1995 SLC runs
0.995 ± 0.010 ± 0.003	66k	ALEXANDER	97F CLEO	$E_{\text{cm}}^e = 10.6$ GeV
1.022 ± 0.028 ± 0.030	1.7k	¹ ALBRECHT	94E ARG	$E_{\text{cm}}^e = 9.4\text{--}10.6$ GeV

• • • We do not use the following data for averages, fits, limits, etc. • • •

1.045 ± 0.058 ± 0.032 BUSKULIC 95D ALEP Repl. by HEISTER 01E

1.03 ± 0.11 ± 0.05 ² BUSKULIC 94D ALEP 1990+1991 LEP run

¹ ALBRECHT 94E measure the square of this quantity and use the sign determined by ALBRECHT 90I to obtain the quoted result.

² Superseded by BUSKULIC 95D.

 $\xi(a_1)$ PARAMETER

($V-A$) theory predicts $\xi(a_1) = 1$.

VALUE	EVTS	DOCUMENT ID	TECN	COMMENT
1.001 ± 0.027 OUR FIT				
1.002 ± 0.028 OUR AVERAGE				
1.000 ± 0.016 ± 0.024	35k	¹ HEISTER	01E ALEP	1991–1995 LEP runs
1.02 ± 0.13 ± 0.03	17.2k	ASNER	00 CLEO	$E_{\text{cm}}^e = 10.6$ GeV
1.29 ± 0.26 ± 0.11	7.4k	² ACKERSTAFF	97R OPAL	1992–1994 LEP runs
0.85 ± 0.15 ± 0.05		ALBRECHT	95C ARG	$E_{\text{cm}}^e = 9.5\text{--}10.6$ GeV
1.25 ± 0.23 ± 0.15 ± 0.08	7.5k	ALBRECHT	93C ARG	$E_{\text{cm}}^e = 9.4\text{--}10.6$ GeV

• • • We do not use the following data for averages, fits, limits, etc. • • •

1.08 ± 0.46 ± 0.14 ± 0.41 ± 0.25 2.6k ³ AKERS 95P OPAL Repl. by ACKERSTAFF 97R

0.937 ± 0.116 ± 0.064 BUSKULIC 95D ALEP Repl. by HEISTER 01E

¹ HEISTER 01E quote $1.000 \pm 0.016 \pm 0.013 \pm 0.020$ where the errors are statistical, systematic, and an uncertainty due to the final state model. We combine the systematic error and model uncertainty.

² ACKERSTAFF 97R obtain this result with a model independent fit to the hadronic structure functions. Fitting with the model of Kuhn and Santamaria (ZPHY C48, 445 (1990)) gives $0.87 \pm 0.16 \pm 0.04$, and with the model of Isgur *et al.* (PR D39,1357 (1989)) they obtain $1.20 \pm 0.21 \pm 0.14$.

³ AKERS 95P obtain this result with a model independent fit to the hadronic structure functions. Fitting with the model of Kuhn and Santamaria (ZPHY C48, 445 (1990)) gives $0.87 \pm 0.27 \pm 0.05$, and with the model of Isgur *et al.* (PR D39,1357 (1989)) they obtain $1.10 \pm 0.31 \pm 0.13 \pm 0.14$.

 $\xi(\text{all hadronic modes})$ PARAMETER

($V-A$) theory predicts $\xi = 1$.

VALUE	EVTS	DOCUMENT ID	TECN	COMMENT
0.995 ± 0.007 OUR FIT				
0.997 ± 0.007 OUR AVERAGE				
0.992 ± 0.007 ± 0.008	102k	¹ HEISTER	01E ALEP	1991–1995 LEP runs
0.997 ± 0.027 ± 0.011	39k	² ABREU	00L DLPH	1992–1995 runs
1.02 ± 0.13 ± 0.03	17.2k	³ ASNER	00 CLEO	$E_{\text{cm}}^e = 10.6$ GeV
1.032 ± 0.031	37k	⁴ ACCIARRI	98R L3	1991–1995 LEP runs
0.93 ± 0.10 ± 0.04		ABE	97o SLD	1993–1995 SLC runs
1.29 ± 0.26 ± 0.11	7.4k	⁵ ACKERSTAFF	97R OPAL	1992–1994 LEP runs
0.995 ± 0.010 ± 0.003	66k	⁶ ALEXANDER	97F CLEO	$E_{\text{cm}}^e = 10.6$ GeV
1.03 ± 0.06 ± 0.04	2.0k	⁷ COAN	97 CLEO	$E_{\text{cm}}^e = 10.6$ GeV
1.017 ± 0.039		⁸ ALBRECHT	95C ARG	$E_{\text{cm}}^e = 9.5\text{--}10.6$ GeV
1.25 ± 0.23 ± 0.15 ± 0.08	7.5k	⁹ ALBRECHT	93C ARG	$E_{\text{cm}}^e = 9.4\text{--}10.6$ GeV

• • • We do not use the following data for averages, fits, limits, etc. • • •

0.970 ± 0.053 ± 0.011 14k ¹⁰ ACCIARRI 96H L3 Repl. by ACCIARRI 98R

1.08 ± 0.46 ± 0.14 ± 0.41 ± 0.25 2.6k ¹¹ AKERS 95P OPAL Repl. by ACKERSTAFF 97R

1.006 ± 0.032 ± 0.019 ¹² BUSKULIC 95D ALEP Repl. by HEISTER 01E

1.022 ± 0.028 ± 0.030 1.7k ¹³ ALBRECHT 94E ARG $E_{\text{cm}}^e = 9.4\text{--}10.6$ GeV

0.99 ± 0.07 ± 0.04 ¹⁴ BUSKULIC 94D ALEP 1990+1991 LEP run

¹ HEISTER 01E quote $0.992 \pm 0.007 \pm 0.006 \pm 0.005$ where the errors are statistical, systematic, and an uncertainty due to the final state model. We combine the systematic error and model uncertainty. They use $\tau \rightarrow \pi \nu_\tau$, $\tau \rightarrow K \nu_\tau$, $\tau \rightarrow \rho \nu_\tau$, and $\tau \rightarrow a_1 \nu_\tau$ decays.

² ABREU 00L use $\tau^- \rightarrow h^- \geq 0\pi^0 \nu_\tau$ decays.

³ ASNER 00 use $\tau^- \rightarrow \pi^- 2\pi^0 \nu_\tau$ decays.

⁴ ACCIARRI 98R use $\tau \rightarrow \pi \nu_\tau$, $\tau \rightarrow K \nu_\tau$, and $\tau \rightarrow \rho \nu_\tau$ decays.

⁵ ACKERSTAFF 97R use $\tau \rightarrow a_1 \nu_\tau$ decays.

⁶ ALEXANDER 97F use $\tau \rightarrow \rho \nu_\tau$ decays.

⁷ COAN 97 use $h^+ h^-$ energy correlations.

⁸ Combined fit to ARGUS tau decay parameter measurements in ALBRECHT 95c, ALBRECHT 93g, and ALBRECHT 94e.

⁹ Uses $\tau \rightarrow a_1 \nu_\tau$ decays. Replaced by ALBRECHT 95c.

¹⁰ ACCIARRI 96H use $\tau \rightarrow \pi \nu_\tau$, $\tau \rightarrow K \nu_\tau$, and $\tau \rightarrow \rho \nu_\tau$ decays.

¹¹ AKERS 95P use $\tau \rightarrow a_1 \nu_\tau$ decays.

¹² BUSKULIC 95D use $\tau \rightarrow \pi \nu_\tau$, $\tau \rightarrow \rho \nu_\tau$, and $\tau \rightarrow a_1 \nu_\tau$ decays.

¹³ ALBRECHT 94E measure the square of this quantity and use the sign determined by ALBRECHT 90I to obtain the quoted result. Uses $\tau \rightarrow a_1 \nu_\tau$ decays. Replaced by ALBRECHT 95c.

¹⁴ BUSKULIC 94D use $\tau \rightarrow \pi \nu_\tau$ and $\tau \rightarrow \rho \nu_\tau$ decays. Superseded by BUSKULIC 95D.

 τ REFERENCES

AUBERT	08	PRL 100 011801	B. Aubert <i>et al.</i>	(BABAR Collab.)
AUBERT	08K	PRL 100 071802	B. Aubert <i>et al.</i>	(BABAR Collab.)
MIYAZAKI	08	PL B660 154	Y. Miyazaki <i>et al.</i>	(BELLE Collab.)
NISHIO	08	PL B664 35	Y. Nishio <i>et al.</i>	(BELLE Collab.)
ANASHIN	07	JETPL 85 347	V.V. Anashin <i>et al.</i>	(KEDR Collab.)
Translated from ZETFF 85 429.				
AUBERT	07AP	PR D76 05104R	B. Aubert <i>et al.</i>	(BABAR Collab.)
AUBERT	07BK	PRL 99 251803	B. Aubert <i>et al.</i>	(BABAR Collab.)
AUBERT	07I	PRL 98 061803	B. Aubert <i>et al.</i>	(BABAR Collab.)
BELOUS	07	PRL 99 011801	K. Belous <i>et al.</i>	(BELLE Collab.)
EIDELMAN	07	MPL A22 159	S. Eidelman, M. Passera	(NOVO, PADO)
EPIFANOV	07	PL B654 65	D. Epifanov <i>et al.</i>	(BELLE Collab.)
MIYAZAKI	07	PL B648 341	Y. Miyazaki <i>et al.</i>	(BELLE Collab.)
ABDALLAH	06A	EPJ C46 1	J. Abdallah <i>et al.</i>	(DELPHI Collab.)
AUBERT	06C	PRL 96 041801	B. Aubert <i>et al.</i>	(BABAR Collab.)
AUBERT	06	PR D73 112003	B. Aubert <i>et al.</i>	(BABAR Collab.)
INAMI	06	PL B643 5	K. Inami <i>et al.</i>	(BELLE Collab.)
MIYAZAKI	06	PL B632 51	Y. Miyazaki <i>et al.</i>	(BELLE Collab.)
MIYAZAKI	06A	PL B639 159	Y. Miyazaki <i>et al.</i>	(BELLE Collab.)
YUSA	06	PL B640 138	Y. Yusa <i>et al.</i>	(BELLE Collab.)
ARMS	05	PRL 94 241802	K. Arms <i>et al.</i>	(CLEO Collab.)
AUBERT	05A	PRL 95 041802	B. Aubert <i>et al.</i>	(BABAR Collab.)
AUBERT	05F	PR D72 012003	B. Aubert <i>et al.</i>	(BABAR Collab.)
AUBERT	05W	PR D72 072001	B. Aubert <i>et al.</i>	(BABAR Collab.)
AUBERT	05D	PRL 95 191801	B. Aubert <i>et al.</i>	(BABAR Collab.)
ENARI	05	PL B622 218	Y. Enari <i>et al.</i>	(BELLE Collab.)
HAYASAKA	05	PL B613 20	K. Hayasaka <i>et al.</i>	(BELLE Collab.)
SCHAEL	05C	PRPL 421 191	S. Schael <i>et al.</i>	(ALEPH Collab.)
ABBIENDI	04J	EPJ C35 437	G. Abbiendi <i>et al.</i>	(OPAL Collab.)
ABDALLAH	04K	EPJ C35 159	J. Abdallah <i>et al.</i>	(DELPHI Collab.)
ABDALLAH	04T	EPJ C36 283	J. Abdallah <i>et al.</i>	(DELPHI Collab.)
ABE	04B	PRL 92 171802	K. Abe <i>et al.</i>	(BELLE Collab.)
ACHARD	04G	PL B585 53	P. Achard <i>et al.</i>	(L3 Collab.)
AUBERT	04J	PRL 92 121801	B. Aubert <i>et al.</i>	(BABAR Collab.)
ENARI	04	PRL 93 081803	Y. Enari <i>et al.</i>	(BELLE Collab.)
YUSA	04	PL B589 103	Y. Yusa <i>et al.</i>	(BELLE Collab.)
ABBIENDI	03	PL B551 35	G. Abbiendi <i>et al.</i>	(OPAL Collab.)
BRIERE	03	PRL 90 181802	R. A. Briere <i>et al.</i>	(CLEO Collab.)
HEISTER	03F	EPJ C30 291	A. Heister <i>et al.</i>	(ALEPH Collab.)
INAMI	03	PL B551 16	K. Inami <i>et al.</i>	(BELLE Collab.)
CHEN	02C	PR D66 071101R	S. Chen <i>et al.</i>	(CLEO Collab.)

ABBIENDI	01J	EPJ C19 653	G. Abbiendi et al.	(OPAL Collab.)	DECAMP	92C	ZPHY C54 211	D. Decamp et al.	(ALEPH Collab.)
ABREU	01M	EPJ C20 617	P. Abreu et al.	(DELPHI Collab.)	ADEVA	91F	PL B265 451	B. Adeva et al.	(L3 Collab.)
ACCIARRI	01F	PL B507 47	M. Acciari et al.	(L3 Collab.)	ALBRECHT	91D	PL B260 259	H. Albrecht et al.	(ARGUS Collab.)
ACHARD	01D	PL B519 189	P. Achard et al.	(L3 Collab.)	ALEXANDER	91D	PL B266 201	G. Alexander et al.	(OPAL Collab.)
ANASTASSOV	01	PRL 86 4667	A. Anastassov et al.	(CLEO Collab.)	ANTREASYAN	91	PL B259 216	D. Antreasyan et al.	(Crystal Ball Collab.)
HEISTER	01E	EPJ C22 217	A. Heister et al.	(ALEPH Collab.)	GRIFOLS	91	PL B255 611	J.A. Grifols, A. Mendez	(BARC)
ABBIENDI	00A	PL B492 23	G. Abbiendi et al.	(OPAL Collab.)	ABACHI	90	PR D41 1414	S. Abachi et al.	(HRS Collab.)
ABBIENDI	00C	EPJ C13 213	G. Abbiendi et al.	(OPAL Collab.)	ALBRECHT	90E	PL B246 278	H. Albrecht et al.	(ARGUS Collab.)
ABBIENDI	00D	EPJ C13 197	G. Abbiendi et al.	(OPAL Collab.)	ALBRECHT	90E	PL B250 164	H. Albrecht et al.	(ARGUS Collab.)
ABREU	00L	EPJ C16 229	P. Abreu et al.	(DELPHI Collab.)	BEHREND	90	ZPHY C46 537	H.J. Behrend et al.	(CELLO Collab.)
ACCIARRI	00B	PL B479 67	M. Acciari et al.	(L3 Collab.)	BOWCOCK	90	PR D41 805	T.J.V. Bowcock et al.	(CLEO Collab.)
AHMED	00	PR D61 071101R	S. Ahmed et al.	(CLEO Collab.)	DELAGUILA	90	PL B252 116	F. del Aguila, M. Sher	(BARC, WILL)
ALBRECHT	00	PL B485 37	H. Albrecht et al.	(ARGUS Collab.)	GOLDBERG	90	PL B251 223	M. Goldberg et al.	(CLEO Collab.)
ASNER	00	PR D61 012002	D.M. Asner et al.	(CLEO Collab.)	WU	90	PR D41 2339	D.Y. Wu et al.	(Mark II Collab.)
ASNER	00B	PR D62 072006	D.M. Asner et al.	(CLEO Collab.)	ABACHI	89B	PR D40 902	S. Abachi et al.	(HRS Collab.)
BERGFELD	00	PRL 84 830	T. Bergfeld et al.	(CLEO Collab.)	BEHREND	89B	PL B222 163	H.J. Behrend et al.	(CELLO Collab.)
BROWDER	00	PR D61 052004	T.E. Browder et al.	(CLEO Collab.)	JANSEN	89	PL B228 273	H. Jansen et al.	(Crystal Ball Collab.)
EDWARDS	00A	PR D61 072003	K.W. Edwards et al.	(CLEO Collab.)	KLEINWORT	89	ZPHY C42 7	C. Kleinwort et al.	(JADE Collab.)
GONZALEZ-S.	00	NP B582 3	G. Gonzalez-Sprinberg et al.	(CLEO Collab.)	ADEVA	88	PR D38 2665	B. Adeva et al.	(Mark-J Collab.)
ABBIENDI	99X	PL B447 134	G. Abbiendi et al.	(OPAL Collab.)	ALBRECHT	88B	PL B202 149	H. Albrecht et al.	(ARGUS Collab.)
ABREU	99X	EPJ C10 201	P. Abreu et al.	(DELPHI Collab.)	ALBRECHT	88B	ZPHY C41 1	H. Albrecht et al.	(ARGUS Collab.)
ACKERSTAFF	99D	EPJ C8 3	K. Ackerstaff et al.	(OPAL Collab.)	ALBRECHT	88M	ZPHY C41 405	H. Albrecht et al.	(ARGUS Collab.)
ACKERSTAFF	99E	EPJ C8 183	K. Ackerstaff et al.	(OPAL Collab.)	AMIDEI	88	PR D37 1750	D. Amidei et al.	(Mark II Collab.)
BARATE	99K	EPJ C10 1	R. Barate et al.	(ALEPH Collab.)	BEHREND	88	PL B200 226	H.J. Behrend et al.	(CELLO Collab.)
BARATE	99R	EPJ C11 599	R. Barate et al.	(ALEPH Collab.)	BRAUNSCHEIDT	88C	ZPHY C39 331	W. Braunschweig et al.	(TASSO Collab.)
BISHAI	99	PRL 82 281	M. Bishai et al.	(CLEO Collab.)	KEH	88	PL B212 123	S. Keh et al.	(Crystal Ball Collab.)
GODANG	99	PR D59 091303	R. Godang et al.	(CLEO Collab.)	TSCHIRHART	88	PL B205 407	R. Tschirhart et al.	(HRS Collab.)
RICHICHI	99	PR D60 112002	S.J. Richichi et al.	(CLEO Collab.)	ABACHI	87B	PL B197 291	S. Abachi et al.	(HRS Collab.)
ACCIARRI	98C	PL B426 207	M. Acciari et al.	(L3 Collab.)	ABACHI	87C	PRL 59 2519	S. Abachi et al.	(HRS Collab.)
ACCIARRI	98E	PL B434 169	M. Acciari et al.	(L3 Collab.)	ADLER	87B	PRL 59 1527	J. Adler et al.	(Mark III Collab.)
ACCIARRI	98R	PL B438 405	M. Acciari et al.	(L3 Collab.)	AHARA	87B	PR D35 1553	H. Ahara et al.	(TPC Collab.)
ACKERSTAFF	98M	EPJ C4 193	K. Ackerstaff et al.	(OPAL Collab.)	AHARA	87C	PRL 59 751	H. Ahara et al.	(TPC Collab.)
ACKERSTAFF	98N	PL B431 188	K. Ackerstaff et al.	(OPAL Collab.)	ALBRECHT	87L	PL B185 223	H. Albrecht et al.	(ARGUS Collab.)
ALBRECHT	98	PL B431 179	H. Albrecht et al.	(ARGUS Collab.)	ALBRECHT	87P	PL B199 580	H. Albrecht et al.	(ARGUS Collab.)
BARATE	98	EPJ C1 65	R. Barate et al.	(ALEPH Collab.)	BAND	87	PL B198 297	H.R. Band et al.	(MAC Collab.)
BARATE	98E	EPJ C4 29	R. Barate et al.	(ALEPH Collab.)	BAND	87B	PRL 59 415	H.R. Band et al.	(MAC Collab.)
BLISS	98	PR D57 5903	D.W. Bliss et al.	(CLEO Collab.)	BARINGER	87	PRL 59 1993	P. Baringer et al.	(CLEO Collab.)
ABE	97O	PRL 78 4691	K. Abe et al.	(SLD Collab.)	BEBEK	87C	PR D36 690	C. Bebek et al.	(CLEO Collab.)
ACKERSTAFF	97J	PL B404 213	K. Ackerstaff et al.	(OPAL Collab.)	BURCHAT	87	PR D35 27	P.R. Burchat et al.	(Mark II Collab.)
ACKERSTAFF	97L	ZPHY C74 403	K. Ackerstaff et al.	(OPAL Collab.)	BYLSMA	87	PR D35 2269	B.C. Bylsma et al.	(HRS Collab.)
ACKERSTAFF	97R	ZPHY C75 593	K. Ackerstaff et al.	(OPAL Collab.)	COFFMAN	87	PR D36 2185	D.M. Coffman et al.	(Mark III Collab.)
ALEXANDER	97F	PR D56 5329	J.P. Alexander et al.	(CLEO Collab.)	DERRICK	87	PL B189 260	M. Derrick et al.	(HRS Collab.)
AMMAR	97B	PRL 78 4686	R. Ammar et al.	(CLEO Collab.)	FORD	87	PR D35 408	W.T. Ford et al.	(MAC Collab.)
ANASTASSOV	97	PR D55 2559	A. Anastassov et al.	(CLEO Collab.)	FORD	87B	PR D36 1971	W.T. Ford et al.	(MAC Collab.)
Also		PR D58 119903 (erratum)	A. Anastassov et al.	(CLEO Collab.)	GAN	87	PRL 59 411	K.K. Gan et al.	(Mark II Collab.)
ANDERSON	97	PRL 79 3814	S. Anderson et al.	(CLEO Collab.)	GAN	87B	PL B197 561	K.K. Gan et al.	(Mark II Collab.)
AVERY	97	PR D55 R1119	P. Avery et al.	(CLEO Collab.)	AHARA	86E	PRL 57 1836	H. Ahara et al.	(TPC Collab.)
BARATE	97I	ZPHY C74 387	R. Barate et al.	(ALEPH Collab.)	BARTEL	86D	PL B182 216	W. Bartel et al.	(JADE Collab.)
BARATE	97R	PL B414 362	R. Barate et al.	(ALEPH Collab.)	PDG	86	PL 170B 1	M. Aguilar-Benitez et al.	(CERN, CIT+)
BERGFELD	97	PRL 79 2406	T. Bergfeld et al.	(CLEO Collab.)	RUCKSTUHL	86	PRL 56 2132	W. Ruckstuhl et al.	(DELCO Collab.)
BONVICINI	97	PRL 79 1221	G. Bonvicini et al.	(CLEO Collab.)	SCHMIDKE	86	PRL 57 527	W.B. Schmidke et al.	(Mark II Collab.)
BUSKULIC	97C	ZPHY C74 263	D. Buskulić et al.	(ALEPH Collab.)	YELTON	86	PL 56 812	J.M. Yelton et al.	(Mark II Collab.)
COAN	97	PR D55 7291	T.E. Coan et al.	(CLEO Collab.)	ALTHOFF	85	ZPHY C25 521	M. Althoff et al.	(TASSO Collab.)
EDWARDS	97	PR D55 R3919	K.W. Edwards et al.	(CLEO Collab.)	ASH	85B	PRL 55 2118	W.W. Ash et al.	(MAC Collab.)
EDWARDS	97B	PR D56 R5297	K.W. Edwards et al.	(CLEO Collab.)	BALTRUSAITIS	85	PRL 55 1842	R.M. Baltrusaitis et al.	(Mark III Collab.)
ESCRIBANO	97	PL B395 369	R. Escrivano, E. Masso	(BARC, PARIT)	BARTEL	85F	PL 161B 188	W. Bartel et al.	(JADE Collab.)
ABREU	96B	PL B365 448	P. Abreu et al.	(DELPHI Collab.)	BEHREND	85	PR D32 2468	S. Behrend et al.	(CLEO Collab.)
ACCIARRI	96H	PL B377 313	M. Acciari et al.	(L3 Collab.)	BELTRAMI	85	PRL 54 1775	I. Beltrami et al.	(HRS Collab.)
ACCIARRI	96K	PL B389 187	M. Acciari et al.	(L3 Collab.)	BERGER	85	ZPHY C28 1	C. Berger et al.	(PLUTO Collab.)
ALAM	96	PRL 76 2637	M.S. Alam et al.	(CLEO Collab.)	BURCHAT	85	PRL 54 2489	P.R. Burchat et al.	(Mark II Collab.)
ALBRECHT	96E	PRPL 276 223	H. Albrecht et al.	(ARGUS Collab.)	FERNANDEZ	85	PRL 54 1624	E. Fernandez et al.	(MAC Collab.)
ALEXANDER	96D	PL B369 163	G. Alexander et al.	(OPAL Collab.)	MILLS	85	PRL 54 624	G.B. Mills et al.	(DELCO Collab.)
ALEXANDER	96E	PL B374 341	G. Alexander et al.	(OPAL Collab.)	AHARA	84C	PR D30 2436	H. Ahara et al.	(TPC Collab.)
ALEXANDER	96F	PL B388 407	G. Alexander et al.	(OPAL Collab.)	BEHREND	84	ZPHY C23 103	H.J. Behrend et al.	(CELLO Collab.)
BAI	96	PR D53 20	J.Z. Bai et al.	(BES Collab.)	MILLS	84	PRL 52 1944	G.B. Mills et al.	(DELCO Collab.)
BALEST	96	PL B388 402	R. Balest et al.	(CLEO Collab.)	BEHREND	83C	PL 127B 270	H.J. Behrend et al.	(CELLO Collab.)
BARTELT	96	PRL 76 4119	J.E. Bartelt et al.	(CLEO Collab.)	SILVERMAN	83C	PR D27 1196	D.J. Silverman, G.L. Shaw	(UCI)
BUSKULIC	96	ZPHY C70 579	D. Buskulić et al.	(ALEPH Collab.)	BEHREND	82	PL 114B 282	H.J. Behrend et al.	(CELLO Collab.)
BUSKULIC	96C	ZPHY C70 561	D. Buskulić et al.	(ALEPH Collab.)	BLOCKER	82B	PRL 48 1586	C.A. Blocker et al.	(Mark II Collab.)
COAN	96	PR D53 6037	T.E. Coan et al.	(CLEO Collab.)	BLOCKER	82D	PL 109B 119	C.A. Blocker et al.	(Mark II Collab.)
ABE	95Y	PR D52 4828	K. Abe et al.	(SLD Collab.)	FELDMAN	82	PRL 48 66	G.J. Feldman et al.	(Mark II Collab.)
ABREU	95T	PL B357 715	P. Abreu et al.	(DELPHI Collab.)	HAYES	82	PR D25 2869	K.G. Hayes et al.	(Mark II Collab.)
ABREU	95U	PL B359 411	P. Abreu et al.	(DELPHI Collab.)	BERGER	81B	PL 98B 489	C. Berger et al.	(PLUTO Collab.)
ACCIARRI	95	PL B345 93	M. Acciari et al.	(L3 Collab.)	DORFAN	81	PRL 46 215	J.M. Dorfán et al.	(Mark II Collab.)
ACCIARRI	95F	PL B359 487	M. Acciari et al.	(L3 Collab.)	BRANDELIK	80	PL 92B 199	R. Brandelik et al.	(TASSO Collab.)
AKERS	95F	ZPHY C66 31	R. Akers et al.	(OPAL Collab.)	ZHOLENTZ	80	PL 96B 214	A.A. Zholents et al.	(NOVO)
AKERS	95I	ZPHY C66 543	R. Akers et al.	(OPAL Collab.)	Also		SJNP 34 814	A.A. Zholents et al.	(NOVO)
AKERS	95P	ZPHY C67 45	R. Akers et al.	(OPAL Collab.)	BACINO	79B	PRL 42 749	W.J. Bacino et al.	(DELCO Collab.)
AKERS	95Y	ZPHY C68 555	R. Akers et al.	(OPAL Collab.)	KIRKBY	79	SLAC-PUB-2419	J. Kirkby	(SLAC)
ALBRECHT	95	PL B341 441	H. Albrecht et al.	(ARGUS Collab.)	Also		Translated from YAF 34 1471		
ALBRECHT	95C	PL B349 576	H. Albrecht et al.	(ARGUS Collab.)	BACINO	78B	PRL 41 13	W.J. Bacino et al.	(DELCO Collab.)
ALBRECHT	95G	ZPHY C68 25	H. Albrecht et al.	(ARGUS Collab.)	Also		Tokyo Conf. 249	J. Kirz	(ST ON)
ALBRECHT	95H	ZPHY C68 215	H. Albrecht et al.	(ARGUS Collab.)	BRANDELIK	78	PL 73B 109	R. Brandelik et al.	(NOVO)
BALEST	95C	PRL 75 3809	R. Balest et al.	(CLEO Collab.)	FELDMAN	78	Tokyo Conf. 777	G.J. Feldman	(SLAC)
BERNABEU	95	NP B436 474	J. Bernabeu et al.	(ALEPH Collab.)	JAROS	78	PRL 40 1120	J. Jaros et al.	(LGW Collab.)
BUSKULIC	95C	PL B346 371	D. Buskulić et al.	(ALEPH Collab.)	PERL	75	PRL 35 1489	M.L. Perl et al.	(LBL, SLAC)
BUSKULIC	95D	PL B346 379	D. Buskulić et al.	(ALEPH Collab.)					
Also		PL B363 265 (erratum)	D. Buskulić et al.	(ALEPH Collab.)					
ABREU	94K	PL B334 435	P. Abreu et al.	(DELPHI Collab.)					
AKERS	94E	PL B328 207	R. Akers et al.	(OPAL Collab.)					
AKERS	94G	PL B339 278	R. Akers et al.	(OPAL Collab.)					
ALBRECHT	94E	PL B337 383	H. Albrecht et al.	(ARGUS Collab.)					
ARTUSO	94	PRL 72 3762	M. Artuso et al.	(CLEO Collab.)					
BARTELT	94	PRL 73 1890	J.E. Bartelt et al.	(CLEO Collab.)					
BATTLE	94	PRL 73 1079	M. Battle et al.	(CLEO Collab.)					
BAUER	94	PR D50 R13	D.A. Bauer et al.	(TPC/2em ma Collab.)					
BUSKULIC	94D	PL B321 168	D. Buskulić et al.	(ALEPH Collab.)					
BUSKULIC	94E	PL B332 209	D. Buskulić et al.	(ALEPH Collab.)					
BUSKULIC	94F	PL B332 219	D. Buskulić et al.	(ALEPH Collab.)					
GIBAUT	94B	PRL 73 934	D. Gibaut et al.	(CLEO Collab.)					
ADRIANI	93M	PRPL 236 1	O. Adriani et al.	(L3 Collab.)					
ALBRECHT	93C	ZPHY C58 61	H. Albrecht et al.	(ARGUS Collab.)					
ALBRECHT	93G	PL B316 608	H. Albrecht et al.	(ARGUS Collab.)					
BALEST	93	PR D47 R3671	R. Balest et al.	(CLEO Collab.)					
BEAN	93	PRL 70 138	A. Bean et al.	(CLEO Collab.)					
BORTOLETTO	93	PRL 71 1791	D. Bortoletto et al.	(CLEO Collab.)					
ESCRIBANO	93	PL B301 419	R. Escrivano, E. Masso	(BARC)					
PROCARIO	93	PRL 70 1207	M. Procaro et al.	(CLEO Collab.)					
ABREU	92N	ZPHY C55 555	P. Abreu et al.	(DELPHI Collab.)					
ACTON	92F	PL B281 405	D.P. Acton et al.	(OPAL Collab.)					
ACTON	92H	PL B288 373	P.D. Acton et al.	(OPAL Collab.)					
AKERIB	92	PRL 69 3610	D.S. Akerib et al.						

Lepton Particle Listings

Heavy Charged Lepton Searches

Heavy Charged Lepton Searches

Charged Heavy Lepton MASS LIMITS

Sequential Charged Heavy Lepton (L^\pm) MASS LIMITS

These experiments assumed that a fourth generation L^\pm decayed to a fourth generation ν_L (or L^0) where ν_L was stable, or that L^\pm decays to a light ν_ℓ via mixing.

See the "Quark and Lepton Compositeness, Searches for" Listings for limits on radiatively decaying excited leptons, i.e. $\ell^* \rightarrow \ell\gamma$. See the "WIMPs and other Particle Searches" section for heavy charged particle search limits in which the charged particle could be a lepton.

VALUE (GeV)	CL%	DOCUMENT ID	TECN	COMMENT
>100.8	95	ACHARD 01B	L3	Decay to νW
>101.9	95	ACHARD 01B	L3	$m_L - m_{L^0} > 15$ GeV
• • • We do not use the following data for averages, fits, limits, etc. • • •				
> 81.5	95	ACKERSTAFF 98c	OPAL	Assumed $m_{L^\pm} - m_{L^0} > 8.4$ GeV
> 80.2	95	ACKERSTAFF 98c	OPAL	$m_{L^0} > m_{L^\pm}$ and $L^\pm \rightarrow \nu W$
< 48 or > 61	95	1 ACCIARRI 96G	L3	
> 63.9	95	ALEXANDER 96P	OPAL	Decay to massless ν 's
> 63.5	95	BUSKULIC 96S	ALEP	$m_L - m_{L^0} > 7$ GeV
> 65	95	BUSKULIC 96S	ALEP	Decay to massless ν 's
none 10–225		2 AHMED 94	CNTR	H1 Collab. at HERA
none 12.6–29.6	95	KIM 91B	AMY	Massless ν assumed
> 44.3	95	AKRAWY 90G	OPAL	
none 0.5–10	95	3 RILES 90	MRK2	For $(m_{L^0} - m_{L^+}) > 0.25-0.4$ GeV
> 8		4 STOKER 89	MRK2	For $(m_{L^+} - m_{L^0}) = 0.4$ GeV
> 12		4 STOKER 89	MRK2	For $m_{L^0} = 0.9$ GeV
none 18.4–27.6	95	5 ABE 88	VNS	
> 25.5	95	6 ADACHI 88B	TOPZ	
none 1.5–22.0	95	BEHREND 88c	CELL	
> 41	90	7 ALBAJAR 87B	UA1	
> 22.5	95	8 ADEVA 85	MRKJ	
> 18.0	95	9 BARTEL 83	JADE	
none 4–14.5	95	10 BERGER 81B	PLUT	
> 15.5	95	11 BRANDELIK 81	TASS	
> 13.		12 AZIMOV 80		
> 16.	95	13 BARBER 80B	CNTR	
> 0.490		14 ROTHE 69	RVUE	

- 1 ACCIARRI 96G assumes LEP result that the associated neutral heavy lepton mass > 40 GeV.
- 2 The AHMED 94 limits are from a search for neutral and charged sequential heavy leptons at HERA via the decay channels $L^- \rightarrow e\gamma$, $L^- \rightarrow \nu W^-$, $L^- \rightarrow eZ$; and $L^0 \rightarrow \nu\gamma$, $L^0 \rightarrow e^- W^+$, $L^- \rightarrow \nu Z$, where the W decays to $\ell\nu_\ell$, or to jets, and Z decays to $\ell^+ \ell^-$ or jets.
- 3 RILES 90 limits were the result of a special analysis of the data in the case where the mass difference $m_{L^\pm} - m_{L^0}$ was allowed to be quite small, where L^0 denotes the neutrino into which the sequential charged lepton decays. With a slightly reduced m_{L^\pm} range, the mass difference extends to about 4 GeV.
- 4 STOKER 89 (Mark II at PEP) gives bounds on charged heavy lepton (L^+) mass for the generalized case in which the corresponding neutral heavy lepton (L^0) in the SU(2) doublet is not of negligible mass.
- 5 ABE 88 search for L^+ and $L^- \rightarrow$ hadrons looking for acoplanar jets. The bound is valid for $m_\nu < 10$ GeV.
- 6 ADACHI 88B search for hadronic decays giving acoplanar events with large missing energy. $E_{cm}^{ee} = 52$ GeV.
- 7 Assumes associated neutrino is approximately massless.
- 8 ADEVA 85 analyze one-isolated-muon data and sensitive to $\tau < 10$ nanosec. Assume $B(\text{lepton}) = 0.30$. $E_{cm} = 40-47$ GeV.
- 9 BARTEL 83 limit is from PETRA $e^+ e^-$ experiment with average $E_{cm} = 34.2$ GeV.
- 10 BERGER 81B is DESY DORIS and PETRA experiment. Looking for $e^+ e^- \rightarrow L^+ L^-$.
- 11 BRANDELIK 81 is DESY-PETRA experiment. Looking for $e^+ e^- \rightarrow L^+ L^-$.
- 12 AZIMOV 80 estimated probabilities for $M^+ N$ type events in $e^+ e^- \rightarrow L^+ L^-$ deducing semi-hadronic decay multiplicities of L from $e^+ e^-$ annihilation data at $E_{cm} = (2/3)m_L$. Obtained above limit comparing these with $e^+ e^-$ data (BRANDELIK 80).
- 13 BARBER 80B looked for $e^+ e^- \rightarrow L^+ L^-$, $L \rightarrow \nu_L^+ X$ with MARK-J at DESY-PETRA.
- 14 ROTHE 69 examines previous data on μ pair production and π and K decays.

Stable Charged Heavy Lepton (L^\pm) MASS LIMITS

VALUE (GeV)	CL%	DOCUMENT ID	TECN	
>102.6	95	ACHARD 01B	L3	
• • • We do not use the following data for averages, fits, limits, etc. • • •				
> 28.2	95	15 ADACHI 90c	TOPZ	
none 18.5–42.8	95	AKRAWY 90o	OPAL	
> 26.5	95	DECAMP 90F	ALEP	
none $m_\mu - 36.3$	95	SODERSTROM90	MRK2	

- 15 ADACHI 90c put lower limits on the mass of stable charged particles with electric charge Q satisfying $2/3 < Q/e < 4/3$ and with spin 0 or 1/2. We list here the special case for a stable charged heavy lepton.

Charged Long-Lived Heavy Lepton MASS LIMITS

VALUE (GeV)	CL%	EVTs	DOCUMENT ID	TECN	CHG	COMMENT
>102.0	95		ABBIENDI 03L	OPAL		pair produced in $e^+ e^-$
> 0.1		0	16 ANSORGE 73B	HBC	—	Long-lived
none 0.55–4.5			17 BUSHNIN 73	CNTR	—	Long-lived
none 0.2–0.92			18 BARNA 68	CNTR	—	Long-lived
none 0.97–1.03			18 BARNA 68	CNTR	—	Long-lived

- 16 ANSORGE 73B looks for electron pair production and electron-like Bremsstrahlung.
 17 BUSHNIN 73 is SERPUKHOV 70 GeV p experiment. Masses assume mean life above 7×10^{-10} and 3×10^{-8} respectively. Calculated from cross section (see "Charged Quasi-Stable Lepton Production Differential Cross Section" below) and 30 GeV muon pair production data.
 18 BARNA 68 is SLAC photoproduction experiment.

Doubly-Charged Heavy Lepton MASS LIMITS

VALUE (GeV)	CL%	DOCUMENT ID	TECN	CHG
none 1–9 GeV	90	19 CLARK 81	SPEC	++

- • • We do not use the following data for averages, fits, limits, etc. • • •
 19 CLARK 81 is FNAL experiment with 209 GeV muons. Bounds apply to $\mu\mu$ which couples with full weak strength to muon. See also section on "Doubly-Charged Lepton Production Cross Section."

Doubly-Charged Lepton Production Cross Section (μN Scattering)

VALUE (cm ²)	EVTs	DOCUMENT ID	TECN	CHG
< 6×10^{-38}	0	20 CLARK 81	SPEC	++

- • • We do not use the following data for averages, fits, limits, etc. • • •
 20 CLARK 81 is FNAL experiment with 209 GeV muon. Looked for μ^+ nucleon $\rightarrow \bar{\mu}_P^0 X$, $\bar{\mu}_P^0 \rightarrow \mu^+ \mu^- \bar{\nu}_\mu$ and $\mu^+ n \rightarrow \mu_P^+ X$, $\mu_P^+ \rightarrow 2\mu^+ \nu_\mu$. Above limits are for $\sigma \times BR$ taken from their mass-dependence plot figure 2.

REFERENCES FOR HEAVY CHARGED LEPTON SEARCHES

ABBIENDI 03L	PL B572 8	G. Abbiendi <i>et al.</i>	(OPAL Collab.)
ACHARD 01B	PL B517 75	P. Achard <i>et al.</i>	(L3 Collab.)
ACKERSTAFF 98C	EPJ C1 45	K. Ackerstaff <i>et al.</i>	(OPAL Collab.)
ACCIARRI 96G	PL B377 304	M. Acciari <i>et al.</i>	(L3 Collab.)
ALEXANDER 96P	PL B385 433	G. Alexander <i>et al.</i>	(OPAL Collab.)
BUSKULIC 96S	PL B384 439	D. Buskulic <i>et al.</i>	(ALEPH Collab.)
AHMED 94	PL B340 205	T. Ahmed <i>et al.</i>	(HI Collab.)
KIM 91B	IJMP A6 2583	G.N. Kim <i>et al.</i>	(AMY Collab.)
ADACHI 90C	PL B244 352	I. Adachi <i>et al.</i>	(TOPAZ Collab.)
AKRAWY 90G	PL B240 250	M.Z. Akrawy <i>et al.</i>	(OPAL Collab.)
AKRAWY 90O	PL B252 290	M.Z. Akrawy <i>et al.</i>	(OPAL Collab.)
DECAMP 90F	PL B236 511	D. Decamp <i>et al.</i>	(ALEPH Collab.)
RILES 90	PR D42 1	K. Riles <i>et al.</i>	(Mark II Collab.)
SODERSTROM 90	PRL 64 2980	E. Soderstrom <i>et al.</i>	(Mark II Collab.)
STOKER 89	PR D39 1811	D.P. Stoker <i>et al.</i>	(Mark II Collab.)
ABE 88	PRL 61 915	K. ABE <i>et al.</i>	(VENUS Collab.)
ADACHI 88B	PR D37 1339	I. Adachi <i>et al.</i>	(TOPAZ Collab.)
BEHREND 88C	ZPHY C41 7	H.J. Behrend <i>et al.</i>	(CELLO Collab.)
ALBAJAR 87B	PL B185 241	C. Albajar <i>et al.</i>	(UA1 Collab.)
ADEVA 85	PL 152B 439	B. Adeva <i>et al.</i>	(Mark-J Collab.)
Also	PRPL 109 131	B. Adeva <i>et al.</i>	(Mark-J Collab.)
BARTEL 83	PL 123B 353	W. Bartel <i>et al.</i>	(JADE Collab.)
BERGER 81B	PL 99B 489	C. Berger <i>et al.</i>	(PLUTO Collab.)
BRANDELIK 80C	PL 99B 163	R. Brandelik <i>et al.</i>	(TASSO Collab.)
CLARK 81	PRL 46 239	A.R. Clark <i>et al.</i>	(UCB, LBL, FNAL+)
Also	PR D25 2762	W.H. Smith <i>et al.</i>	(LBL, FNAL, PRIN)
AZIMOV 80	JETPL 32 664	Y.I. Azimov, V.A. Khoze	(PNPI)
Also	Translated from ZETFP 32 677.		
BARBER 80B	PRL 45 1904	D.P. Barber <i>et al.</i>	(Mark-J Collab.)
BRANDELIK 80	PL 92B 199	R. Brandelik <i>et al.</i>	(TASSO Collab.)
ANSORGE 73B	PR D7 26	R.E. Ansonge <i>et al.</i>	(CAVE)
BUSHNIN 73	NP B58 476	Y.B. Bushnin <i>et al.</i>	(SERP)
Also	PL 42B 136	S.V. Golovkin <i>et al.</i>	(SERP)
ROTHE 69	NP B10 241	K.W. Rothe, A.M. Wolsky	(PENN)
BARNA 68	PR 173 1391	A. Barna <i>et al.</i>	(SLAC, STAN)

OTHER RELATED PAPERS

PERL 81	SLAC-PUB-2752	M.L. Perl	(SLAC)
Physics in Collision Conference.			

See key on page 373

Neutrino Properties**INTRODUCTION TO THE NEUTRINO PROPERTIES LISTINGS**

Revised August 2007 by P. Vogel (Caltech) and A. Piepke (University of Alabama).

The following Listings concern measurements of various properties of neutrinos. Nearly all of the measurements, all of which so far are upper limits, actually concern superpositions of the mass eigenstates ν_i , which are in turn related to the weak eigenstates ν_ℓ , via the neutrino mixing matrix

$$|\nu_\ell\rangle = \sum_i U_{\ell i} |\nu_i\rangle.$$

In the analogous case of quark mixing via the CKM matrix, the smallness of the off-diagonal terms (small mixing angles) permits a “dominant eigenstate” approximation. Previous editions of this *Review* had assumed that the dominant eigenstate paradigm applied to neutrinos as well. However, the present results of neutrino oscillation searches show that the mixing matrix contains two large mixing angles. We cannot, therefore, associate any particular state $|\nu_i\rangle$ with any particular lepton label e, μ or τ . Nevertheless, neutrinos are produced in weak decays with a definite lepton flavor, and are typically detected by the charged current weak interaction again associated with a specific lepton flavor. The Listings for the neutrino mass that follow are separated into the three associated charged-lepton categories. Other properties (mean lifetime, magnetic moment, charge, and charge radius) are no longer separated this way. If needed, the associated lepton flavor is reported in the footnotes.

Measured quantities (mass-squared, magnetic moments, mean lifetimes, *etc.*) all depend upon the mixing parameters $|U_{\ell i}|^2$, but to some extent also on experimental conditions (*e.g.*, on energy resolution). Most of these observables, in particular mass-squared, cannot distinguish between Dirac and Majorana neutrinos, and are unaffected by *CP* phases.

Direct neutrino mass measurements are usually based on the analysis of the kinematics of charged particles (leptons, pions) emitted together with neutrinos (flavor states) in various weak decays. The most sensitive neutrino mass measurement to date, involving electron type neutrinos, is based on fitting the shape of the beta spectrum. The quantity $\langle m_\beta^2 \rangle = \sum_i |U_{ei}|^2 m_{\nu_i}^2$ is determined or constrained, where the sum is over all mass eigenvalues m_{ν_i} that are too close together to be resolved experimentally. If the energy resolution is better than $\Delta m_{ij}^2 \equiv m_{\nu_i}^2 - m_{\nu_j}^2$, the corresponding heavier m_{ν_i} and mixing parameter could be determined by fitting the resulting spectral anomaly (step or kink).

A limit on $\langle m_\beta^2 \rangle$ implies an *upper* limit on the *minimum* value m_{\min}^2 of $m_{\nu_i}^2$, independent of the mixing parameters U_{ei} : $m_{\min}^2 \leq \langle m_\beta^2 \rangle$. However, if and when the value of $\langle m_\beta^2 \rangle$ is determined and the study of neutrino oscillations provides us

with the values of *all* neutrino mass-squared differences Δm_{ij}^2 and the mixing parameters $|U_{ei}|^2$, then the individual neutrino mass squares $m_{\nu_j}^2 = \langle m_\beta^2 \rangle - \sum_i |U_{ei}|^2 \Delta m_{ij}^2$ can be determined.

All confirmed neutrino oscillation experiments using solar, reactor, atmospheric and accelerator neutrinos can be described using three active neutrino flavors, *i.e.*, two mass splittings and three mixing angles. Combined three neutrino analyses determine the squared mass differences and two of the mixing angles to within reasonable accuracy. For given $|\Delta m_{ij}^2|$, a limit on $\langle m_\beta^2 \rangle$ from beta decay defines an *upper* limit on the *maximum* value m_{\max} of m_{ν_i} : $m_{\max}^2 \leq \langle m_\beta^2 \rangle + \sum_{i < j} |\Delta m_{ij}^2|$. The analysis of the low energy beta decay of tritium, combined with the oscillation results, thus limits *all* active neutrino masses. Traditionally experimental neutrino mass limits obtained from pion decay $\pi^+ \rightarrow \mu^+ + \nu_\mu$, or the shape of the spectrum of decay products of the τ lepton, did not distinguish between flavor and mass eigenstates. These results are reported as limits of the μ and τ based neutrino mass. After the determination of the $|\Delta m_{ij}^2|$'s, the corresponding neutrino mass limits are no longer competitive with those derived from low energy beta decays, with the proviso, however, that the oscillation searches, reported below, can be regarded as a reliable source of *all* $|\Delta m_{ij}^2|$ values.

The spread of arrival times of the neutrinos from SN1987A, coupled with the measured neutrino energies, provided a time-of-flight limit on a quantity similar to $\langle m_\beta \rangle \equiv \sqrt{\langle m_\beta^2 \rangle}$. This statement, clothed in various degrees of sophistication, has been the basis for a very large number of papers. The resulting limits, however, are no longer comparable with the limits from tritium beta decay.

Constraint on the sum of the neutrino masses can be obtained from the analysis of the cosmic microwave background anisotropy, combined with the galaxy redshift surveys and other data. These limits are reported in a separate table (Sum of Neutrino Masses, m_{tot}). Discussion concerning the model dependence of this limit is continuing.

 $\bar{\nu}$ MASS (electron based)

Those limits given below are for the square root of $m_{\nu_e}^{2(\text{eff})} \equiv \sum_i |U_{ei}|^2 m_{\nu_i}^2$. Limits that come from the kinematics of ${}^3\text{H}\beta^-$ decay are the square roots of the limits for $m_{\nu_e}^{2(\text{eff})}$. Obtained from the measurements reported in the Listings for “ $\bar{\nu}$ Mass Squared,” below.

VALUE (eV)	CL%	DOCUMENT ID	TECN	COMMENT
< 2 OUR EVALUATION				
< 2.3	95	1 KRAUS	05 SPEC	${}^3\text{H}$ β decay
< 2.5	95	2 LOBASHEV	99 SPEC	${}^3\text{H}$ β decay
• • • We do not use the following data for averages, fits, limits, etc. • • •				
<21.7	90	3 ARNABOLDI	03A BOLO	187 Re β -decay
< 5.7	95	4 LOREDO	02 ASTR	SN1987A
< 2.8	95	5 WEINHEIMER	99 SPEC	${}^3\text{H}$ β decay
< 4.35	95	6 BELESEV	95 SPEC	${}^3\text{H}$ β decay
<12.4	95	7 CHING	95 SPEC	${}^3\text{H}$ β decay
<92	95	8 HIDDEMANN	95 SPEC	${}^3\text{H}$ β decay
15 $^{+32}_{-15}$		HIDDEMANN	95 SPEC	${}^3\text{H}$ β decay
<19.6	95	9 KERNAN	95 ASTR	SN 1987A
< 7.0	95	9 STOEFFL	95 SPEC	${}^3\text{H}$ β decay

Lepton Particle Listings

Neutrino Properties

< 7.2	95	10 WEINHEIMER 93	SPEC	^3H β decay
<11.7	95	11 HOLZSCHUH 92b	SPEC	^3H β decay
<13.1	95	12 KAWAKAMI 91	SPEC	^3H β decay
< 9.3	95	13 ROBERTSON 91	SPEC	^3H β decay
<14	95	AVIGNONE 90	ASTR	SN 1987A
<16		SPERGEL 88	ASTR	SN 1987A
17 to 40		14 BORIS 87	SPEC	^3H β decay

¹ KRAUS 05 is a continuation of the work reported in WEINHEIMER 99. This result represents the final analysis of data taken from 1997 to 2001. Various sources of systematic uncertainties have been identified and quantified. The background has been reduced compared to the initial running period. A spectral anomaly at the endpoint, reported in LOBASHEV 99, was not observed.

² LOBASHEV 99 report a new measurement which continues the work reported in BELESEV 95. This limit depends on phenomenological fit parameters used to derive their best fit to m_ν^2 , making an unambiguous interpretation difficult. See the footnote under " \overline{m} Mass Squared."

³ ARNABOLDI 03A *et al.* report kinematical neutrino mass limit using β -decay of ^{187}Re . Bolometric AgReO₄ micro-calorimeters are used. Mass bound is substantially weaker than those derived from tritium β -decays but has different systematic uncertainties.

⁴ LOREDO 02 updates LOREDO 89.

⁵ WEINHEIMER 99 presents two analyses which exclude the spectral anomaly and result in an acceptable m_ν^2 . We report the most conservative limit, but the other is nearly the same. See the footnote under " \overline{m} Mass Squared."

⁶ BELESEV 95 (Moscow) use an integral electrostatic spectrometer with adiabatic magnetic collimation and a gaseous tritium sources. A fit to a normal Kurie plot above 18300–18350 eV (to avoid a low-energy anomaly) plus a monochromatic line 7–15 eV below the endpoint yields $m_\nu^2 = -4.1 \pm 10.9 \text{ eV}^2$, leading to this Bayesian limit.

⁷ CHING 95 quotes results previously given by SUN 93; no experimental details are given. A possible explanation for consistently negative values of m_ν^2 is given.

⁸ HIDDEMANN 95 (Munich) experiment uses atomic tritium embedded in a metal-dioxide lattice. Bayesian limit calculated from the weighted mean $m_\nu^2 = 221 \pm 4244 \text{ eV}^2$ from the two runs listed below.

⁹ STOEFFL 95 (LLNL) result is the Bayesian limit obtained from the m_ν^2 errors given below but with m_ν^2 set equal to 0. The anomalous endpoint accumulation leads to a value of m_ν^2 which is negative by more than 5 standard deviations.

¹⁰ WEINHEIMER 93 (Mainz) is a measurement of the endpoint of the tritium β spectrum using an electrostatic spectrometer with a magnetic guiding field. The source is molecular tritium frozen onto an aluminum substrate.

¹¹ HOLZSCHUH 92b (Zurich) result is obtained from the measurement $m_\nu^2 = -24 \pm 48 \pm 61$ (1 σ errors), in eV², using the PDG prescription for conversion to a limit in m_ν .

¹² KAWAKAMI 91 (Tokyo) experiment uses tritium-labeled arachidic acid. This result is the Bayesian limit obtained from the m_ν^2 limit with the errors combined in quadrature. This was also done in ROBERTSON 91, although the authors report a different procedure.

¹³ ROBERTSON 91 (LANL) experiment uses gaseous molecular tritium. The result is in strong disagreement with the earlier claims by the ITP group [LUBIMOV 80, BORIS 87 (+ BORIS 88 erratum)] that m_ν lies between 17 and 40 eV. However, the probability of a positive m_ν^2 is only 3% if statistical and systematic error are combined in quadrature.

¹⁴ See also comment in BORIS 87b and erratum in BORIS 88.

\overline{m} MASS SQUARED (electron based)

Given troubling systematics which result in improbably negative estimators of $m_{\nu_e}^{2(\text{eff})} \equiv \sum_i |U_{ei}|^2 m_{\nu_i}^2$, in many experiments, we use only KRAUS 05 and LOBASHEV 99 for our average.

VALUE (eV ²)	CL%	DOCUMENT ID	TECN	COMMENT
– 1.1 ± 2.4	OUR AVERAGE			
– 0.6 ± 2.2 ± 2.1		15 KRAUS 05	SPEC	^3H β decay
– 1.9 ± 3.4 ± 2.2		16 LOBASHEV 99	SPEC	^3H β decay
••• We do not use the following data for averages, fits, limits, etc. •••				
– 3.7 ± 5.3 ± 2.1		17 WEINHEIMER 99	SPEC	^3H β decay
– 22 ± 4.8		18 BELESEV 95	SPEC	^3H β decay
129 ± 6010		19 HIDDEMANN 95	SPEC	^3H β decay
313 ± 5994		19 HIDDEMANN 95	SPEC	^3H β decay
–130 ± 20 ± 15	95	20 STOEFFL 95	SPEC	^3H β decay
– 31 ± 75 ± 48		21 SUN 93	SPEC	^3H β decay
– 39 ± 34 ± 15		22 WEINHEIMER 93	SPEC	^3H β decay
– 24 ± 48 ± 61		23 HOLZSCHUH 92b	SPEC	^3H β decay
– 65 ± 85 ± 65		24 KAWAKAMI 91	SPEC	^3H β decay
–147 ± 68 ± 41		25 ROBERTSON 91	SPEC	^3H β decay

¹⁵ KRAUS 05 is a continuation of the work reported in WEINHEIMER 99. This result represents the final analysis of data taken from 1997 to 2001. Problems with significantly negative squared neutrino masses, observed in some earlier experiments, have been resolved in this work.

¹⁶ LOBASHEV 99 report a new measurement which continues the work reported in BELESEV 95. The data were corrected for electron trapping effects in the source, eliminating the dependence of the fitted neutrino mass on the fit interval. The analysis assuming a pure beta spectrum yields significantly negative fitted $m_\nu^2 \approx -(20-10) \text{ eV}^2$. This problem is attributed to a discrete spectral anomaly of about 6×10^{-11} intensity with a time-dependent energy of 5–15 eV below the endpoint. The data analysis accounts

for this anomaly by introducing two extra phenomenological fit parameters resulting in a best fit of $m_\nu^2 = -1.9 \pm 3.4 \pm 2.2 \text{ eV}^2$ which is used to derive a neutrino mass limit. However, the introduction of phenomenological fit parameters which are correlated with the derived m_ν^2 limit makes unambiguous interpretation of this result difficult.

¹⁷ WEINHEIMER 99 is a continuation of the work reported in WEINHEIMER 93. Using a lower temperature of the frozen tritium source eliminated the dewetting of the T_2 film, which introduced a dependence of the fitted neutrino mass on the fit interval in the earlier work. An indication for a spectral anomaly reported in LOBASHEV 99 has been seen, but its time dependence does not agree with LOBASHEV 99. Two analyses, which exclude the spectral anomaly either by choice of the analysis interval or by using a particular data set which does not exhibit the anomaly, result in acceptable m_ν^2 fits and are used to derive the neutrino mass limit published by the authors. We list the most conservative of the two.

¹⁸ BELESEV 95 (Moscow) use an integral electrostatic spectrometer with adiabatic magnetic collimation and a gaseous tritium sources. This value comes from a fit to a normal Kurie plot above 18300–18350 eV (to avoid a low-energy anomaly), including the effects of an apparent peak 7–15 eV below the endpoint.

¹⁹ HIDDEMANN 95 (Munich) experiment uses atomic tritium embedded in a metal-dioxide lattice. They quote measurements from two data sets.

²⁰ STOEFFL 95 (LLNL) uses a gaseous source of molecular tritium. An anomalous pileup of events at the endpoint leads to the negative value for m_ν^2 . The authors acknowledge that "the negative value for the best fit of m_ν^2 has no physical meaning" and discuss possible explanations for this effect.

²¹ SUN 93 uses a tritiated hydrocarbon source. See also CHING 95.

²² WEINHEIMER 93 (Mainz) is a measurement of the endpoint of the tritium β spectrum using an electrostatic spectrometer with a magnetic guiding field. The source is molecular tritium frozen onto an aluminum substrate.

²³ HOLZSCHUH 92b (Zurich) source is a monolayer of tritiated hydrocarbon.

²⁴ KAWAKAMI 91 (Tokyo) experiment uses tritium-labeled arachidic acid.

²⁵ ROBERTSON 91 (LANL) experiment uses gaseous molecular tritium. The result is in strong disagreement with the earlier claims by the ITP group [LUBIMOV 80, BORIS 87 (+ BORIS 88 erratum)] that m_ν lies between 17 and 40 eV. However, the probability of a positive m_ν^2 is only 3% if statistical and systematic error are combined in quadrature.

ν MASS (electron based)

These are measurement of m_ν (in contrast to $m_{\overline{\nu}}$ given above). The masses can be different for a Dirac neutrino in the absence of CPT invariance. The possible distinction between ν and $\overline{\nu}$ properties is usually ignored elsewhere in these Listings.

VALUE (eV)	CL%	DOCUMENT ID	TECN	COMMENT
<460	68	YASUMI 94	CNTR	^{163}Ho decay
<225	95	SPRINGER 87	CNTR	^{163}Ho decay

ν MASS (muon based)

Limits given below are for the square root of $m_{\nu_\mu}^{2(\text{eff})} \equiv \sum_i |U_{\mu i}|^2 m_{\nu_i}^2$.

In some of the COSM papers listed below, the authors did not distinguish between weak and mass eigenstates.

OUR EVALUATION is based on OUR AVERAGE for the π^\pm mass and the ASSAMAGAN 96 value for the muon momentum for the π^\pm decay at rest. The limit is calculated using the unified classical analysis of FELDMAN 98 for a Gaussian distribution near a physical boundary. WARNING: since $m_{\nu_\mu}^{2(\text{eff})}$ is calculated from the differences of large numbers, it and the corresponding limits are extraordinarily sensitive to small changes in the pion mass, the decay muon momentum, and their errors. For example, the limits obtained using JECKELMANN 94, LENZ 98, and the weighted averages are 0.15, 0.29, and 0.19 MeV, respectively.

VALUE (MeV)	CL%	DOCUMENT ID	TECN	COMMENT
<0.19 (CL = 90%) OUR EVALUATION				
<0.17	90	²⁶ ASSAMAGAN 96	SPEC	$m_\nu^2 = -0.016 \pm 0.023$
••• We do not use the following data for averages, fits, limits, etc. •••				
<0.15		²⁷ DOLGOV 95	COSM	Nucleosynthesis
<0.48		²⁸ ENQVIST 93	COSM	Nucleosynthesis
<0.3		²⁹ FULLER 91	COSM	Nucleosynthesis
<0.42		²⁹ LAM 91	COSM	Nucleosynthesis
<0.50	90	³⁰ ANDERHUB 82	SPEC	$m_\nu^2 = -0.14 \pm 0.20$
<0.65	90	CLARK 74	ASPK	$K_{\mu 3}$ decay

²⁶ ASSAMAGAN 96 measurement of p_μ from $\pi^+ \rightarrow \mu^+ \nu$ at rest combined with JECKELMANN 94 Solution B pion mass yields $m_\nu^2 = -0.016 \pm 0.023$ with corresponding Bayesian limit listed above. If Solution A is used, $m_\nu^2 = -0.143 \pm 0.024 \text{ MeV}^2$. Replaces ASSAMAGAN 94.

²⁷ DOLGOV 95 removes earlier assumptions (DOLGOV 93) about thermal equilibrium below T_{QCD} for wrong-helicity Dirac neutrinos (ENQVIST 93, FULLER 91) to set more stringent limits.

²⁸ ENQVIST 93 bases limit on the fact that thermalized wrong-helicity Dirac neutrinos would speed up expansion of early universe, thus reducing the primordial abundance.

FULLER 91 exploits the same mechanism but in the older calculation obtains a larger production rate for these states, and hence a lower limit. Neutrino lifetime assumed to exceed nucleosynthesis time, ~ 1 s.

²⁹ Assumes neutrino lifetime >1 s. For Dirac neutrinos only. See also ENQVIST 93.

³⁰ ANDERHUB 82 kinematics is insensitive to the pion mass.

ν MASS (tau based)

The limits given below are the square roots of limits for $m_{\nu_\tau}^{2(\text{eff})} \equiv \sum_i |U_{\tau i}|^2 m_{\nu_i}^2$.

In some of the ASTR and COSM papers listed below, the authors did not distinguish between weak and mass eigenstates.

VALUE (MeV)	CL%	EVTs	DOCUMENT ID	TECN	COMMENT
< 18.2	95		31 BARATE	98F ALEP	1991-1995 LEP runs
< 28	95		32 ATHANAS	00 CLEO	$E_{\text{cm}}^{\text{ee}} = 10.6$ GeV
< 27.6	95		33 ACKERSTAFF	98T OPAL	1990-1995 LEP runs
< 30	95	473	34 AMMAR	98 CLEO	$E_{\text{cm}}^{\text{ee}} = 10.6$ GeV
< 60	95		35 ANASTASSOV	97 CLEO	$E_{\text{cm}}^{\text{ee}} = 10.6$ GeV
< 0.37 or > 22	95		36 FIELDS	97 COSM	Nucleosynthesis
< 68	95		37 SWAIN	97 THEO	m_τ, τ_τ, τ partial widths
< 29.9	95		38 ALEXANDER	96M OPAL	1990-1994 LEP runs
< 149	95		39 BOTTINO	96 THEO	π, μ, τ leptonic decays
< 1 or > 25	95		40 HANNESTAD	96C COSM	Nucleosynthesis
< 71	95		41 SOBIE	96 THEO	$m_\tau, \tau_\tau, B(\tau^- \rightarrow e^- \bar{\nu}_e \nu_\tau)$
< 24	95	25	42 BUSKULIC	95H ALEP	1991-1993 LEP runs
< 0.19	95		43 DOLGOV	95 COSM	Nucleosynthesis
< 3	95		44 SIGL	95 ASTR	SN 1987A
< 0.4 or > 30	95		45 DODELSON	94 COSM	Nucleosynthesis
< 0.1 or > 50	95		46 KAWASAKI	94 COSM	Nucleosynthesis
155-225	95	113	47 PERES	94 THEO	π, K, μ, τ weak decays
< 32.6	95		48 CINABRO	93 CLEO	$E_{\text{cm}}^{\text{ee}} \approx 10.6$ GeV
< 0.3 or > 35	95		49 DOLGOV	93 COSM	Nucleosynthesis
< 0.74	95		50 ENQVIST	93 COSM	Nucleosynthesis
< 31	95	19	51 ALBRECHT	92M ARG	$E_{\text{cm}}^{\text{ee}} = 9.4-10.6$ GeV
< 0.3	95		52 FULLER	91 COSM	Nucleosynthesis
< 0.5 or > 25	95		53 KOLB	91 COSM	Nucleosynthesis
< 0.42	95		52 LAM	91 COSM	Nucleosynthesis

³¹ BARATE 98F result based on kinematics of 2939 $\tau^- \rightarrow 2\pi^- \pi^+ \nu_\tau$ and 52 $\tau^- \rightarrow 3\pi^- 2\pi^+ (\pi^0) \nu_\tau$ decays. If possible 2.5% excited a_1 decay is included in 3-prong sample analysis, limit increases to 19.2 MeV.

³² ATHANAS 00 bound comes from analysis of $\tau^- \rightarrow \pi^- \pi^+ \pi^- \pi^0 \nu_\tau$ decays.

³³ ACKERSTAFF 98T use $\tau \rightarrow 5\pi^\pm \nu_\tau$ decays to obtain a limit of 43.2 MeV (95%CL). They combine this with ALEXANDER 96M value using $\tau \rightarrow 3h^\pm \nu_\tau$ decays to obtain quoted limit.

³⁴ AMMAR 98 limit comes from analysis of $\tau^- \rightarrow 3\pi^- 2\pi^+ \nu_\tau$ and $\tau^- \rightarrow 2\pi^- \pi^+ 2\pi^0 \nu_\tau$ decay modes.

³⁵ ANASTASSOV 97 derive limit by comparing their m_τ measurement (which depends on m_{ν_τ}) to BAI 96 m_τ threshold measurement.

³⁶ FIELDS 97 limit for a Dirac neutrino. For a Majorana neutrino the mass region < 0.93 or > 31 MeV is excluded. These bounds assume $N_\nu < 4$ from nucleosynthesis; a wider excluded region occurs with a smaller N_ν upper limit.

³⁷ SWAIN 97 derive their limit from the Standard Model relationships between the tau mass, lifetime, branching fractions for $\tau^- \rightarrow e^- \bar{\nu}_e \nu_\tau, \tau^- \rightarrow \mu^- \bar{\nu}_\mu \nu_\tau, \tau^- \rightarrow \pi^- \nu_\tau$, and $\tau^- \rightarrow K^- \nu_\tau$, and the muon mass and lifetime by assuming lepton universality and using world average values. Limit is reduced to 48 MeV when the CLEO τ mass measurement (BALEST 93) is included; see CLEO's more recent m_{ν_τ} limit (ANASTASSOV 97). Consideration of mixing with a fourth generation heavy neutrino yields $\sin^2 \theta_L < 0.016$ (95%CL).

³⁸ ALEXANDER 96M bound comes from analyses of $\tau^- \rightarrow 3\pi^- 2\pi^+ \nu_\tau$ and $\tau^- \rightarrow h^- h^- h^+ \nu_\tau$ decays.

³⁹ BOTTINO 96 assumes three generations of neutrinos with mixing, finds consistency with massless neutrinos with no mixing based on 1995 data for masses, lifetimes, and leptonic partial widths.

⁴⁰ HANNESTAD 96C limit is on the mass of a Majorana neutrino. This bound assumes $N_\nu < 4$ from nucleosynthesis. A wider excluded region occurs with a smaller N_ν upper limit. This paper is the corrected version of HANNESTAD 96; see the erratum: HANNESTAD 96B.

⁴¹ SOBIE 96 derive their limit from the Standard Model relationship between the tau mass, lifetime, and leptonic branching fraction, and the muon mass and lifetime, by assuming lepton universality and using world average values.

⁴² BUSKULIC 95H bound comes from a two-dimensional fit of the visible energy and invariant mass distribution of $\tau \rightarrow 5\pi(\pi^0) \nu_\tau$ decays. Replaced by BARATE 98F.

⁴³ DOLGOV 95 removes earlier assumptions (DOLGOV 93) about thermal equilibrium below T_{QCD} for wrong-helicity Dirac neutrinos (ENQVIST 93, FULLER 91) to set more stringent limits. DOLGOV 96 argues that a possible window near 20 MeV is excluded.

⁴⁴ SIGL 95 exclude massive Dirac or Majorana neutrinos with lifetimes between 10^{-3} and 10^8 seconds if the decay products are predominantly γ or $e^+ e^-$.

⁴⁵ DODELSON 94 calculate constraints on ν_τ mass and lifetime from nucleosynthesis for 4 generic decay modes. Limits depend strongly on decay mode. Quoted limit is valid for all decay modes of Majorana neutrinos with lifetime greater than about 300 s. For Dirac neutrinos limits change to < 0.3 or > 33 .

⁴⁶ KAWASAKI 94 excluded region is for Majorana neutrino with lifetime > 1000 s. Other limits are given as a function of ν_τ lifetime for decays of the type $\nu_\tau \rightarrow \nu_\mu \phi$ where ϕ is a Nambu-Goldstone boson.

⁴⁷ PERES 94 used PDG 92 values for parameters to obtain a value consistent with mixing. Reexamination by BOTTINO 96 which included radiative corrections and 1995 PDG parameters resulted in two allowed regions, $m_3 < 70$ MeV and 140 MeV $m_3 < 149$ MeV.

⁴⁸ CINABRO 93 bound comes from analysis of $\tau^- \rightarrow 3\pi^- 2\pi^+ \nu_\tau$ and $\tau^- \rightarrow 2\pi^- \pi^+ 2\pi^0 \nu_\tau$ decay modes.

⁴⁹ DOLGOV 93 assumes neutrino lifetime > 100 s. For Majorana neutrinos, the low mass limit is 0.5 MeV. KAWANO 92 points out that these bounds can be overcome for a Dirac neutrino if it possesses a magnetic moment. See also DOLGOV 96.

⁵⁰ ENQVIST 93 bases limit on the fact that thermalized wrong-helicity Dirac neutrinos would speed up expansion of early universe, thus reducing the primordial abundance. FULLER 91 exploits the same mechanism but in the older calculation obtains a larger production rate for these states, and hence a lower limit. Neutrino lifetime assumed to exceed nucleosynthesis time, ~ 1 s.

⁵¹ ALBRECHT 92M reports measurement of a slightly lower τ mass, which has the effect of reducing the ν_τ mass reported in ALBRECHT 88B. Bound is from analysis of $\tau^- \rightarrow 3\pi^- 2\pi^+ \nu_\tau$ mode.

⁵² Assumes neutrino lifetime > 1 s. For Dirac neutrinos. See also ENQVIST 93.

⁵³ KOLB 91 exclusion region is for Dirac neutrino with lifetime > 1 s; other limits are given.

Revised April 1998 by K.A. Olive (University of Minnesota).

The limits on low mass ($m_\nu \lesssim 1$ MeV) neutrinos apply to m_{tot} given by

$$m_{\text{tot}} = \sum_\nu (g_\nu/2) m_\nu,$$

where g_ν is the number of spin degrees of freedom for ν plus $\bar{\nu}$: $g_\nu = 4$ for neutrinos with Dirac masses; $g_\nu = 2$ for Majorana neutrinos. Stable neutrinos in this mass range make a contribution to the total energy density of the Universe which is given by

$$\rho_\nu = m_{\text{tot}} n_\nu = m_{\text{tot}} (3/11) n_\gamma,$$

where the factor 3/11 is the ratio of (light) neutrinos to photons. Writing $\Omega_\nu = \rho_\nu / \rho_c$, where ρ_c is the critical energy density of the Universe, and using $n_\gamma = 412 \text{ cm}^{-3}$, we have

$$\Omega_\nu h^2 = m_{\text{tot}} / (94 \text{ eV}).$$

Therefore, a limit on $\Omega_\nu h^2$ such as $\Omega_\nu h^2 < 0.25$ gives the limit

$$m_{\text{tot}} < 24 \text{ eV}.$$

The limits on high mass ($m_\nu > 1$ MeV) neutrinos apply separately to each neutrino type.

SUM OF THE NEUTRINO MASSES, m_{tot}

(Defined in the above note), of effectively stable neutrinos (i.e., those with mean lives greater than or equal to the age of the universe). These papers assumed Dirac neutrinos. When necessary, we have generalized the results reported so they apply to m_{tot} . For other limits, see SZALAY 76, VYSOTSKY 77, BERNSTEIN 81, FREESE 84, SCHRAMM 84, and COWSIK 85.

VALUE (eV)	CL%	DOCUMENT ID	TECN	COMMENT
------------	-----	-------------	------	---------

• • • We do not use the following data for averages, fits, limits, etc. • • •

< 0.17-2.3		54 FOGLI	07	COSM
< 0.66		55 SPERGEL	07	COSM
< 0.63-2.2		56 ZUNCKEL	07	COSM
< 0.24	95	57 CIRELLI	06	COSM
< 0.62	95	58 HANNESTAD	06	COSM
< 0.52	95	59 KRISTIANSEN	06	COSM

Lepton Particle Listings

Neutrino Properties

< 1.2	60	SANCHEZ	06	COSM
< 0.17	95	57 SELJAK	06	COSM
< 2.0	95	61 ICHIKAWA	05	COSM
< 0.75		62 BARGER	04	COSM
< 1.0		63 CROTTY	04	COSM
< 0.7		64 SPERGEL	03	COSM WMAP
< 0.9		65 LEWIS	02	COSM
< 4.2		66 WANG	02	COSM CMB
< 2.7		67 FUKUGITA	00	COSM
< 5.5		68 CROFT	99	ASTR Ly α power spec
<180		SZALAY	74	COSM
<132		COWSIK	72	COSM
<280		MARX	72	COSM
<400		GERSHTEIN	66	COSM

- 54 Constrains the total mass of neutrinos from neutrino oscillation experiments and cosmological data. The most conservative limit uses only WMAP three-year data, while the most stringent limit includes CMB, large-scale structure, supernova, and Lyman-alpha forest data.
- 55 Constrains the total mass of neutrinos from three-year WMAP data combined with other CMB, large-scale structure and supernova data.
- 56 Constrains the total mass of neutrinos from the CMB and the large scale structure data. The most conservative limit is obtained when generic initial conditions are allowed.
- 57 Constrains the total mass of neutrinos from recent CMB, large scale structure, Lyman-alpha forest, and SNIa data.
- 58 Constrains the total mass of neutrinos from recent CMB and large scale structure data. See also GOOBAR 06.
- 59 Constrains the total mass of neutrinos from recent CMB, large scale structure, SNIa, HST, BBN, and baryon acoustic oscillation data. The limit relaxes to 1.66 when WMAP data alone is used.
- 60 Constrains the total mass of neutrinos from the CMB and the final 2dF Galaxy Redshift Survey.
- 61 Constrains the total mass of neutrinos from the CMB experiments alone, assuming Λ CDM Universe. FUKUGITA 06 show that this result is unchanged by the 3-year WMAP data.
- 62 Constrains the total mass of neutrinos from the power spectrum of fluctuations derived from the Sloan Digital Sky Survey and the 2dF galaxy redshift survey, WMAP and 27 other CMB experiments and measurements by the HST Key project.
- 63 Constrains the total mass of neutrinos from the power spectrum of fluctuations derived from the Sloan Digital Sky Survey, the 2dF galaxy redshift survey, WMAP and ACBAR. The limit is strengthened to 0.6 eV when measurements by the HST Key project and supernovae data are included.
- 64 Constrains the fractional contribution of neutrinos to the total matter density in the Universe from WMAP data combined with other CMB measurements, the 2dFGRS data, and Lyman α data. The limit does not noticeably change if the Lyman α data are not used.
- 65 LEWIS 02 constrains the total mass of neutrinos from the power spectrum of fluctuations derived from the CMB, HST Key project, 2dF galaxy redshift survey, supernovae type Ia, and BBN.
- 66 WANG 02 constrains the total mass of neutrinos from the power spectrum of fluctuations derived from the CMB and other cosmological data sets such as galaxy clustering and the Lyman α forest.
- 67 FUKUGITA 00 is a limit on neutrino masses from structure formation. The constraint is based on the clustering scale σ_8 and the COBE normalization and leads to a conservative limit of 0.9 eV assuming 3 nearly degenerate neutrinos. The quoted limit is on the sum of the light neutrino masses.
- 68 CROFT 99 result based on the power spectrum of the Ly α forest. If $\Omega_{\text{matter}} < 0.5$, the limit is improved to $m_\nu < 2.4 (\Omega_{\text{matter}}/0.17-1)$ eV.

Limits on MASSES of Light Stable Right-Handed ν (with necessarily suppressed interaction strengths)

VALUE	DOCUMENT ID	TECN	COMMENT
<100-200	69 OLIVE	82	COSM Dirac ν
<200-2000	69 OLIVE	82	COSM Majorana ν

69 Depending on interaction strength G_R where $G_R < G_F$.

Limits on MASSES of Heavy Stable Right-Handed ν (with necessarily suppressed interaction strengths)

VALUE	DOCUMENT ID	TECN	COMMENT
> 10	70 OLIVE	82	COSM $G_R/G_F < 0.1$
>100	70 OLIVE	82	COSM $G_R/G_F < 0.01$

70 These results apply to heavy Majorana neutrinos and are summarized by the equation: $m_\nu > 1.2 \text{ GeV} (G_F/G_R)$. The bound saturates, and if G_R is too small no mass range is allowed.

ν CHARGE

VALUE (units: electron charge)	CL%	DOCUMENT ID	TECN	COMMENT
<3.7 $\times 10^{-12}$	90	71 GNINENKO	07	RVUE Nuclear reactor
<2 $\times 10^{-14}$		72 RAFFELT	99	ASTR Red giant luminosity
<6 $\times 10^{-14}$		73 RAFFELT	99	ASTR Solar cooling
<4 $\times 10^{-4}$		74 BABU	94	RVUE BEBC beam dump

<3 $\times 10^{-4}$	75	DAVIDSON	91	RVUE SLAC e^- beam dump
<2 $\times 10^{-15}$	76	BARBIELLINI	87	ASTR SN 1987A
<1 $\times 10^{-13}$	77	BERNSTEIN	63	ASTR Solar energy losses

- 71 GNINENKO 07 use limit on $\overline{\nu}_e$ magnetic moment from LI 03b to derive this result. The limit is considerably weaker than the limits on the charge of ν_e and $\overline{\nu}_e$ from various astrophysics considerations.
- 72 This RAFFELT 99 limit applies to all neutrino flavors which are light enough (<5 keV) to be emitted from globular-cluster red giants.
- 73 This RAFFELT 99 limit is derived from the helioseismological limit on a new energy-loss channel of the Sun, and applies to all neutrino flavors which are light enough (<1 keV) to be emitted from the sun.
- 74 BABU 94 use COOPER-SARKAR 92 limit on ν magnetic moment to derive quoted result. It applies to ν_τ .
- 75 DAVIDSON 91 use data from early SLAC electron beam dump experiment to derive charge limit as a function of neutrino mass. It applies to ν_τ .
- 76 Exact BARBIELLINI 87 limit depends on assumptions about the intergalactic or galactic magnetic fields and about the direct distance and time through the field. It applies to ν_e .
- 77 The limit applies to all flavors.

ν (MEAN LIFE) / MASS

Measures $[\sum |U_{\ell j}|^2 \Gamma_j m_j]^{-1}$, where the sum is over mass eigenstates which cannot be resolved experimentally. Some of the limits constrain the radiative decay and are based on the limit of the corresponding photon flux. Other apply to the decay of a heavier neutrino into the lighter one and a Majoron or other invisible particle. Many of these limits apply to any ν within the indicated mass range.

Limits on the radiative decay are either directly based on the limits of the corresponding photon flux, or are derived from the limits on the neutrino magnetic moments. In the later case the transition rate for $\nu_i \rightarrow \nu_j + \gamma$ is constrained by $\Gamma_{ij} = \frac{1}{\tau_{ij}} = \frac{(m_i^2 - m_j^2)^3}{m_i^2} \mu_{ij}^2$ where μ_{ij} is the neutrino transition moment in the mass eigenstates basis. Typically, the limits on lifetime based on the magnetic moments are many orders of magnitude more restrictive than limits based on the nonobservation of photons.

VALUE (s/eV)	CL%	DOCUMENT ID	TECN	COMMENT
> 15.4	90	78 KRAKAUER	91	CNTR $\nu_\mu, \overline{\nu}_\mu$ at LAMPF
> 7 $\times 10^9$		79 RAFFELT	85	ASTR
> 300	90	80 REINES	74	CNTR $\overline{\nu}_e$
•••				We do not use the following data for averages, fits, limits, etc. •••
	90	81 MIRIZZI	07	CMB radiative decay
	90	82 MIRIZZI	07	CIB radiative decay
		83 WONG	07	CNTR Reactor $\overline{\nu}_e$
> 0.11	90	84 XIN	05	CNTR Reactor ν_e
		85 XIN	05	CNTR Reactor ν_e
> 0.004	90	86 AHARMIM	04	SNO quasidegen. ν masses
> 4.4 $\times 10^{-5}$	90	86 AHARMIM	04	SNO hierarchical ν masses
$\gtrsim 100$	95	87 CECCHINI	04	ASTR Radiative decay for ν mass > 0.01 eV
> 0.067	90	88 EGUCHI	04	KLND quasidegen. ν masses
> 1.1 $\times 10^{-3}$	90	88 EGUCHI	04	KLND hierarchical ν masses
> 8.7 $\times 10^{-5}$	99	89 BANDYOPA...	03	FIT nonradiative decay
≥ 4200	90	90 DERBIN	02B	CNTR Solar pp and Be ν
> 2.8 $\times 10^{-5}$	99	91 JOSHIPURA	02B	FIT nonradiative decay
		92 DOLGOV	99	COSM
		93 BILLER	98	ASTR $m_\nu = 0.05-1$ eV
> 2.8 $\times 10^{15}$	94,95	94 BLUDMAN	92	ASTR $m_\nu < 50$ eV
none $10^{-12} - 5 \times 10^4$		96 DODELSON	92	ASTR $m_\nu = 1-300$ keV
< 10^{-12} or $> 5 \times 10^4$		96 DODELSON	92	ASTR $m_\nu = 1-300$ keV
		97 GRANEK	91	COSM Decaying L^0
> 6.4	90	98 KRAKAUER	91	CNTR ν_e at LAMPF
> 1.1 $\times 10^{15}$		99 WALKER	90	ASTR $m_\nu = 0.03 - \sim 2$ MeV
> 6.3 $\times 10^{15}$	95,100	100 CHUPP	89	ASTR $m_\nu < 20$ eV
> 1.7 $\times 10^{15}$		95 KOLB	89	ASTR $m_\nu < 20$ eV
		101 RAFFELT	89	RVUE $\overline{\nu}$ (Dirac, Majorana)
		102 RAFFELT	89B	ASTR
> 8.3 $\times 10^{14}$		103 VONFEILIT...	88	ASTR
> 22	68	104 OBERAUER	87	$\overline{\nu}_R$ (Dirac)
> 38	68	104 OBERAUER	87	$\overline{\nu}$ (Majorana)
> 59	68	104 OBERAUER	87	$\overline{\nu}_L$ (Dirac)
> 30	68	KETOV	86	CNTR $\overline{\nu}$ (Dirac)
> 20	68	KETOV	86	CNTR $\overline{\nu}$ (Majorana)
		105 BINETRUY	84	COSM $m_\nu \sim 1$ MeV
> 0.11	90	106 FRANK	81	CNTR $\nu \overline{\nu}$ LAMPF
> 2 $\times 10^{21}$		107 STECKER	80	ASTR $m_\nu = 10-100$ eV
> 1.0 $\times 10^{-2}$	90	106 BLIETSCHAU	78	HLBC ν_μ , CERN GGM
> 1.7 $\times 10^{-2}$	90	106 BLIETSCHAU	78	HLBC $\overline{\nu}_\mu$, CERN GGM
< 3 $\times 10^{-11}$		108 FALK	78	ASTR $m_\nu < 10$ MeV
> 2.2 $\times 10^{-3}$	90	106 BARNES	77	DBC ν , ANL 12-ft
		109 COWSIK	77	ASTR

> 3. $\times 10^{-3}$ 90 106 BELLOTTI 76 HLBC ν , CERN GGM
> 1.3 $\times 10^{-2}$ 90 106 BELLOTTI 76 HLBC $\bar{\nu}$, CERN GGM

78 KRAKAUER 91 quotes the limit $\tau/m_{\nu_1} > (0.75a^2 + 21.65a + 26.3) \text{ s/eV}$, where a is a parameter describing the asymmetry in the neutrino decay defined as $dN_\gamma/d\cos\theta = (1/2)(1 + a\cos\theta)$. The parameter $a=0$ for a Majorana neutrino, but can vary from -1 to 1 for a Dirac neutrino. The bound given by the authors is the most conservative (which applies for $a = -1$).

79 RAFFELT 85 limit on the radiative decay is from solar x - and γ -ray fluxes. Limit depends on ν flux from pp , now established from GALLEX and SAGE to be > 0.5 of expectation.

80 REINES 74 looked for ν of nonzero mass decaying radiatively to a neutral of lesser mass $+\gamma$. Used liquid scintillator detector near fission reactor. Finds lab lifetime 6×10^7 s or more. Above value of (mean life)/mass assumes average effective neutrino energy of 0.2 MeV. To obtain the limit 6×10^7 s REINES 74 assumed that the full $\bar{\nu}_e$ reactor flux could be responsible for yielding decays with photon energies in the interval 0.1 MeV $- 0.5$ MeV. This represents some overestimate so their lower limit is an over-estimate of the lab lifetime (VOGEL 84). If so, OBERAUER 87 may be comparable or better.

81 MIRIZZI 07 determine a limit on the neutrino radiative decay from analysis of the maximum allowed distortion of the CMB spectrum as measured by the COBE/FIRAS. For the decay $\nu_2 \rightarrow \nu_1$ the lifetime limit is $\lesssim 4 \times 10^{20}$ s for $m_{\min} \lesssim 0.14$ eV. For transition with the $|\Delta m_{31}|$ mass difference the lifetime limit is $\sim 2 \times 10^{19}$ s for $m_{\min} \lesssim 0.14$ eV and $\sim 5 \times 10^{20}$ s for $m_{\min} \gtrsim 0.14$ eV.

82 MIRIZZI 07 determine a limit on the neutrino radiative decay from analysis of the cosmic infrared background (CIB) using the Spitzer Observatory data. For transition with the $|\Delta m_{31}|$ mass difference they obtain the lifetime limit $\sim 10^{20}$ s for $m_{\min} \lesssim 0.14$ eV.

83 WONG 07 use their limit on the neutrino magnetic moment together with the assumed experimental value of $\Delta m_{13}^2 \sim 2 \times 10^{-3} \text{ eV}^2$ to obtain $\tau_{13}/m_1^2 > 3.2 \times 10^{27} \text{ s/eV}^3$ for the radiative decay in the case of the inverted mass hierarchy. Similarly to RAFFELT 89 this limit can be violated if electric and magnetic moments are equal to each other. Analogous, but numerically somewhat different limits are obtained for τ_{23} and τ_{21} .

84 XIN 05 search for the γ from radiative decay of ν_e produced by the electron capture on ^{51}Cr . No events were seen and the limit on τ/m_ν was derived. This is a weaker limit on the decay of ν_e than KRAKAUER 91.

85 XIN 05 use their limit on the neutrino magnetic moment of ν_e together with the assumed experimental value of $\Delta m_{13}^2 \sim 2 \times 10^{-3} \text{ eV}^2$ to obtain $\tau_{13}/m_1^2 > 1 \times 10^{23} \text{ s/eV}^3$ for the radiative decay in the case of the inverted mass hierarchy. Similarly to RAFFELT 89 this limit can be violated if electric and magnetic moments are equal to each other. Analogous, but numerically somewhat different limits are obtained for τ_{23} and τ_{21} . Again, this limit is specific for ν_e .

86 AHARMIM 04 obtained these results from the solar $\bar{\nu}_e$ flux limit set by the SNO measurement assuming ν_2 decay through nonradiative process $\nu_2 \rightarrow \bar{\nu}_1 X$, where X is a Majoron or other invisible particle. Limits are given for the cases of quasidegenerate and hierarchical neutrino masses.

87 CECCHINI 04 obtained this bound through the observations performed on the occasion of the 21 June 2001 total solar eclipse, looking for visible photons from radiative decays of solar neutrinos. Limit is a τ/m_{ν_2} in $\nu_2 \rightarrow \nu_1 \gamma$. Limit ranges from ~ 100 to 10^7 s/eV for $0.01 < m_{\nu_1} < 0.1$ eV.

88 EGUCHI 04 obtained these results from the solar $\bar{\nu}_e$ flux limit set by the KamLAND measurement assuming ν_2 decay through nonradiative process $\nu_2 \rightarrow \bar{\nu}_1 X$, where X is a Majoron or other invisible particle. Limits are given for the cases of quasidegenerate and hierarchical neutrino masses.

89 The ratio of the lifetime over the mass derived by BANDYOPADHYAY 03 is for ν_2 . They obtained this result using the following solar-neutrino data: total rates measured in Cl and Ga experiments, the Super-Kamiokande's zenith-angle spectra, and SNO's day and night spectra. They assumed that ν_1 is the lowest mass, stable or nearly stable neutrino state and ν_2 decays through nonradiative Majoron emission process, $\nu_2 \rightarrow \bar{\nu}_1 + J$, or through nonradiative process with all the final state particles being sterile. The best fit is obtained in the region of the LMA solution.

90 DERBIN 02b (also BACK 03b) obtained this bound for the radiative decay from the results of background measurements with Counting Test Facility (the prototype of theorexino detector). The laboratory gamma spectrum is given as $dN_\gamma/d\cos\theta = (1/2)(1 + \alpha\cos\theta)$ with $\alpha=0$ for a Majorana neutrino, and α varying to -1 to 1 for a Dirac neutrino. The listed bound is for the case of $\alpha=0$. The most conservative bound $1.5 \times 10^3 \text{ s eV}^{-1}$ is obtained for the case of $\alpha=-1$.

91 The ratio of the lifetime over the mass derived by JOSHIPURA 02b is for ν_2 . They obtained this result from the total rates measured in all solar neutrino experiments. They assumed that ν_1 is the lowest mass, stable or nearly stable neutrino state and ν_2 decays through nonradiative process like Majoron emission decay, $\nu_2 \rightarrow \nu'_1 + J$ where ν'_1 state is sterile. The exact limit depends on the specific solution of the solar neutrino problem. The quoted limit is for the LMA solution.

92 DOLGOV 99 places limits in the (Majorana) τ -associated ν mass-lifetime plane based on nucleosynthesis. Results would be considerably modified if neutrino oscillations exist.

93 BILLER 98 use the observed TeV γ -ray spectra to set limits on the mean life of any radiatively decaying neutrino between 0.05 and 1 eV. Curve shows $\tau_\nu/B_\gamma > 0.15 \times 10^{21} \text{ s}$ at 0.05 eV, $> 1.2 \times 10^{21} \text{ s}$ at 0.17 eV, $> 3 \times 10^{21} \text{ s}$ at 1 eV, where B_γ is the branching ratio to photons.

94 BLUDMAN 92 sets additional limits by this method for higher mass ranges. Cosmological limits are also obtained.

95 Limit on the radiative decay based on nonobservation of γ 's in coincidence with ν 's from SN 1987A.

96 DODELSON 92 range is for wrong-helicity keV mass Dirac ν 's from the core of neutron star in SN 1987A decaying to ν 's that would have interacted in KAM2 or IMB detectors.

97 GRANEK 91 considers heavy neutrino decays to $\gamma\nu_L$ and $3\nu_L$, where $m_{\nu_L} < 100$ keV. Lifetime is calculated as a function of heavy neutrino mass, branching ratio into $\gamma\nu_L$, and m_{ν_L} .

98 KRAKAUER 91 quotes the limit for $\nu_e, \tau/m_\nu > (0.3a^2 + 9.8a + 15.9) \text{ s/eV}$, where a is a parameter describing the asymmetry in the radiative neutrino decay defined as $dN_\gamma/d\cos\theta = (1/2)(1 + a\cos\theta)$ $a=0$ for a Majorana neutrino, but can vary from -1 to 1 for a Dirac neutrino. The bound given by the authors is the most conservative (which applies for $a = -1$).

99 WALKER 90 uses SN 1987A γ flux limits after 289 days.

100 CHUPP 89 should be multiplied by a branching ratio (about 1) and a detection efficiency (about 1/4), and pertains to radiative decay of any neutrino to a lighter or sterile neutrino.

101 RAFFELT 89 uses KYULDJIEV 84 to obtain $\tau m^3 > 3 \times 10^{18} \text{ s eV}^3$ (based on $\bar{\nu}_e e^-$ cross sections). The bound for the radiative decay is not valid if electric and magnetic transition moments are equal for Dirac neutrinos.

102 RAFFELT 89b analyze stellar evolution and exclude the region $3 \times 10^{12} < \tau m^3 < 3 \times 10^{21} \text{ s eV}^3$.

103 Model-dependent theoretical analysis of SN 1987A neutrinos. Quoted limit is for $[\sum_j |U_{ej}|^2 \Gamma_j m_j]^{-1}$, where $\ell = \mu, \tau$. Limit is $3.3 \times 10^{14} \text{ s/eV}$ for $\ell = e$.

104 OBERAUER 87 looks for photons and e^+e^- pairs from radiative decays of reactor neutrinos.

105 BINETRUY 84 finds $\tau < 10^8 \text{ s}$ for neutrinos in a radiation-dominated universe.

106 These experiments look for $\nu_k \rightarrow \nu_j \gamma$ or $\bar{\nu}_k \rightarrow \bar{\nu}_j \gamma$.

107 STECKER 80 limit based on UV background; result given is $\tau > 4 \times 10^{22} \text{ s}$ at $m_\nu = 20$ eV.

108 FALK 78 finds lifetime constraints based on supernova energetics.

109 COWSIK 77 considers variety of scenarios. For neutrinos produced in the big bang, present limits on optical photon flux require $\tau > 10^{23} \text{ s}$ for $m_\nu \sim 1$ eV. See also COWSIK 79 and GOLDMAN 79.

ν MAGNETIC MOMENT

The coupling of neutrinos to an electromagnetic field is characterized by a 3×3 matrix λ of the magnetic (μ) and electric (d) dipole moments ($\lambda = \mu - id$). For Majorana neutrinos the matrix λ is antisymmetric and only transition moments are allowed, while for Dirac neutrinos λ is a general 3×3 matrix. In the standard electroweak theory extended to include neutrino masses (see FUJIKAWA 80) $\mu_\nu = 3eG_F m_\nu / (8\pi^2 \sqrt{2}) = 3.2 \times 10^{-19} (m_\nu/\text{eV}) \mu_B$, i.e. it is unobservably small given the known small neutrino masses. In more general models there is no longer a proportionality between neutrino mass and its magnetic moment, even though only massive neutrinos have nonvanishing magnetic moments without fine tuning.

Laboratory bounds on λ are obtained via elastic ν - e scattering, where the scattered neutrino is not observed. The combinations of matrix elements of λ that are constrained by various experiments depend on the initial neutrino flavor and on its propagation between source and detector (e.g., solar ν_e and reactor $\bar{\nu}_e$ do not constrain the same combinations). The listings below therefore identify the initial neutrino flavor.

Other limits, e.g. from various stellar cooling processes, apply to all neutrino flavors. Analogous flavor independent, but weaker, limits are obtained from the analysis of $e^+e^- \rightarrow \nu\bar{\nu}$ collider experiments.

VALUE ($10^{-10} \mu_B$)	CL%	DOCUMENT ID	TECN	COMMENT
< 0.74	(CL = 90%)	OUR LIMIT		
< 0.74	90	110 WONG	07 CNTR	Reactor $\bar{\nu}_e$
< 6.8	90	111 AUERBACH	01 LSND	$\nu_{ee}, \nu_{\mu e}$ scattering
< 3900	90	112 SCHWIENHO...	01 DONU	$\nu_\tau e^- \rightarrow \nu_\tau e^-$
• • •		We do not use the following data for averages, fits, limits, etc. • • •		
< 0.9	90	113 DARAKTCH...	05	Reactor $\bar{\nu}_e$
< 130	90	114 XIN	05 CNTR	Reactor ν_e
< 37	95	115 GRIFOLS	04 FIT	Solar $^8\text{B } \nu$ (SNO NC)
< 3.6	90	116 LIU	04 SKAM	Solar ν spectrum shape
< 1.1	90	117 LIU	04 SKAM	Solar ν spectrum shape (LMA region)
< 5.5	90	118 BACK	03B CNTR	Solar pp and Be ν
< 1.0	90	119 DARAKTCH...	03	Reactor $\bar{\nu}_e$
< 1.3	90	120 LI	03B CNTR	Reactor $\bar{\nu}_e$
< 2	90	121 GRIMUS	02 FIT	solar + reactor (Majorana ν)
< 80000	90	122 TANIMOTO	00 RVUE	$e^+e^- \rightarrow \nu\bar{\nu}\gamma$
< 0.01-0.04		123 AYALA	99 ASTR	$\nu_L \rightarrow \nu_R$ in SN 1987A
< 1.5	90	124 BEACOM	99 SKAM	ν spectrum shape
< 0.03		125 RAFFELT	99 ASTR	Red giant luminosity
< 4		126 RAFFELT	99 ASTR	Solar cooling
< 44000	90	ABREU	97J DLPH	$e^+e^- \rightarrow \nu\bar{\nu}\gamma$ at LEP
< 33000	90	127 ACCIARRI	97Q L3	$e^+e^- \rightarrow \nu\bar{\nu}\gamma$ at LEP
< 0.62		128 ELMFORS	97 COSM	Depolarization in early universe plasma
< 27000	95	129 ESCRIBANO	97 RVUE	$\Gamma(Z \rightarrow \nu\nu)$ at LEP
< 30	90	VILAIN	95B CHM2	$\nu_\mu e \rightarrow \nu_\mu e$
< 55000	90	GOULD	94 RVUE	$e^+e^- \rightarrow \nu\bar{\nu}\gamma$ at LEP
< 1.9	95	130 DERBIN	93 CNTR	Reactor $\bar{\nu}_e \rightarrow \bar{\nu}_e$
< 5400	90	131 COOPER...	92 BEBC	$\nu_\tau e^- \rightarrow \nu_\tau e^-$
< 2.4	90	132 VIDYAKIN	92 CNTR	Reactor $\bar{\nu}_e \rightarrow \bar{\nu}_e$
< 56000	90	DESHPANDE	91 RVUE	$e^+e^- \rightarrow \nu\bar{\nu}\gamma$

Lepton Particle Listings

Neutrino Properties

< 100	95	133	DORENBOS...	91	CHRM	$\nu_\mu e \rightarrow \nu_\mu e$
< 8.5	90		AHRENS	90	CNTR	$\nu_\mu e \rightarrow \nu_\mu e$
< 10.8	90	134	KRAKAUER	90	CNTR	LAMPF $\nu e \rightarrow \nu e$
< 7.4	90	134	KRAKAUER	90	CNTR	LAMPF ($\nu_\mu, \bar{\nu}_\mu$) e elast.
< 0.02		135	RAFFELT	90	ASTR	Red giant luminosity
< 0.1		136	RAFFELT	89B	ASTR	Cooling helium stars
		137	FUKUGITA	88	COSM	Primordial magn. fields
< 40000	90	138	GROTCH	88	RVUE	$e^+ e^- \rightarrow \nu \bar{\nu} \gamma$
< .3		136	RAFFELT	88B	ASTR	He burning stars
< 0.11		136	FUKUGITA	87	ASTR	Cooling helium stars
< 0.0006		139	NUSSINOV	87	ASTR	Cosmic EM back-grounds
< 0.1-0.2			MORGAN	81	COSM	^4He abundance
< 0.85			BEG	78	ASTR	Stellar plasmons
< 0.6		140	SUTHERLAND	76	ASTR	Red giants + degenerate dwarfs
< 81		141	KIM	74	RVUE	$\bar{\nu}_\mu e \rightarrow \bar{\nu}_\mu e$
< 1			BERNSTEIN	63	ASTR	Solar cooling
< 14			COWAN	57	CNTR	Reactor $\bar{\nu}$

110 WONG 07 performed search for non-standard $\bar{\nu}_e$ - e scattering at the Kuo-Sheng nuclear reactor. Ge detector equipped with active anti-Compton shield is used. Most stringent laboratory limit on magnetic moment of reactor $\bar{\nu}_e$. Supersedes LI 03B.

111 AUERBACH 01 limit is based on the LSND ν_e and ν_μ electron scattering measurements. The limit is slightly more stringent than KRAKAUER 90.

112 SCHWIENHORST 01 quote an experimental sensitivity of 4.9×10^{-7} .

113 DARAKTCHIEVA 05 present the final analysis of the search for non-standard $\bar{\nu}_e$ - e scattering component at Bugey nuclear reactor. Full kinematical event reconstruction of both the kinetic energy above 700 keV and scattering angle of the recoil electron, by use of TPC. Most stringent laboratory limit on magnetic moment. Supersedes DARAKTCHIEVA 03.

114 XIN 05 evaluated the ν_e flux at the Kuo-Sheng nuclear reactor and searched for non-standard ν_e - e scattering. Ge detector equipped with active anti-Compton shield was used. This laboratory limit on magnetic moment is considerably less stringent than the limits for reactor $\bar{\nu}_e$, but is specific to ν_e .

115 GRIFOLS 04 obtained this bound using the SNO data of the solar ^8B neutrino flux measured with deuteron breakup. This bound applies to $\mu_{\text{eff}} = (\mu_{21}^2 + \mu_{22}^2 + \mu_{23}^2)^{1/2}$.

116 LIU 04 obtained this limit using the shape of the recoil electron energy spectrum from the Super-Kamiokande-I 1496 days of solar neutrino data. Neutrinos are assumed to have only diagonal magnetic moments, $\mu_{\nu 1} = \mu_{\nu 2}$. This limit corresponds to the oscillation parameters in the vacuum oscillation region.

117 LIU 04 obtained this limit using the shape of the recoil electron energy spectrum from the Super-Kamiokande-I 1496 live-day solar neutrino data, by limiting the oscillation parameter region in the LMA region allowed by solar neutrino experiments plus KamLAND. $\mu_{\nu 1} = \mu_{\nu 2}$ is assumed. In the LMA region, the same limit would be obtained even if neutrinos have off-diagonal magnetic moments.

118 BACK 03B obtained this bound from the results of background measurements with Counting Test Facility (the prototype of the Borexino detector). Standard Solar Model flux was assumed. This μ_ν can be different from the reactor μ_ν in certain oscillation scenarios (see BEACOM 99).

119 DARAKTCHIEVA 03 searched for non-standard $\bar{\nu}_e$ - e scattering component at Bugey nuclear reactor. Full kinematical event reconstruction by use of TPC. Superseded by DARAKTCHIEVA 05.

120 LI 03B used Ge detector in active shield near nuclear reactor to test for nonstandard $\bar{\nu}_e$ - e scattering.

121 GRIMUS 02 obtain stringent bounds on all Majorana neutrino transition moments from a simultaneous fit of LMA-MSW oscillation parameters and transition moments to global solar neutrino data + reactor data. Using only solar neutrino data, a 90% CL bound of $6.3 \times 10^{-10} \mu_B$ is obtained.

122 TANIMOTO 00 combined $e^+ e^- \rightarrow \nu \bar{\nu} \gamma$ data from VENUS, TOPAZ, and AMY.

123 AYALA 99 improves the limit of BARBIERI 88.

124 BEACOM 99 obtain the limit using the shape, but not the absolute magnitude which is affected by oscillations, of the solar neutrino spectrum obtained by Superkamiokande (825 days). This μ_ν can be different from the reactor μ_ν in certain oscillation scenarios.

125 RAFFELT 99 is an update of RAFFELT 90. This limit applies to all neutrino flavors which are light enough (< 5 keV) to be emitted from globular-cluster red giants. This limit pertains equally to electric dipole moments and magnetic transition moments, and it applies to both Dirac and Majorana neutrinos.

126 RAFFELT 99 is essentially an update of BERNSTEIN 63, but is derived from the helioseismological limit on a new energy-loss channel of the Sun. This limit applies to all neutrino flavors which are light enough (< 1 keV) to be emitted from the Sun. This limit pertains equally to electric dipole and magnetic transition moments, and it applies to both Dirac and Majorana neutrinos.

127 ACCIARRI 97Q result applies to both direct and transition magnetic moments and for $q^2=0$.

128 ELMFORS 97 calculate the rate of depolarization in a plasma for neutrinos with a magnetic moment and use the constraints from a big-bang nucleosynthesis on additional degrees of freedom.

129 Applies to absolute value of magnetic moment.

130 DERBIN 93 determine the cross section for 0.6-2.0 MeV electron energy as $(1.28 \pm 0.63) \times \sigma_{\text{weak}}$. However, the (reactor on - reactor off)/(reactor off) is only $\sim 1/100$.

131 COOPER-SARKAR 92 assume $f_{D_s}/f_\pi = 2$ and D_s, \bar{D}_s production cross section = $2.6 \mu\text{b}$ to calculate ν flux.

132 VIDYAKIN 92 limit is from a $e\bar{\nu}_e$ elastic scattering experiment. No experimental details are given except for the cross section from which this limit is derived. Signal/noise was 1/10. The limit uses $\sin^2\theta_W = 0.23$ as input.

133 DORENBOSCH 91 corrects an incorrect statement in DORENBOSCH 89 that the ν magnetic moment is $< 1 \times 10^{-9}$ at the 95%CL. DORENBOSCH 89 measures both $\nu_\mu e$ and $\bar{\nu} e$ elastic scattering and assume $\mu(\nu) = \mu(\bar{\nu})$.

134 KRAKAUER 90 experiment fully reported in ALLEN 93.

135 RAFFELT 90 limit applies for a diagonal magnetic moment of a Dirac neutrino, or for a transition magnetic moment of a Majorana neutrino. In the latter case, the same analysis gives $< 1.4 \times 10^{-12}$. Limit at 95%CL obtained from δM_C .

136 Significant dependence on details of stellar models.

137 FUKUGITA 88 find magnetic dipole moments of any two neutrino species are bounded by $\mu < 10^{-16} [10^{-9} G/B_0]$ where B_0 is the present-day intergalactic field strength.

138 GROTCH 88 combined data from MAC, ASP, CELLO, and Mark J.

139 For $m_\nu = 8-200$ eV. NUSSINOV 87 examines transition magnetic moments for $\nu_\mu \rightarrow \nu_e$ and obtain $< 3 \times 10^{-15}$ for $m_\nu > 16$ eV and $< 6 \times 10^{-14}$ for $m_\nu > 4$ eV.

140 We obtain above limit from SUTHERLAND 76 using their limit $f < 1/3$.

141 KIM 74 is a theoretical analysis of $\bar{\nu}_\mu$ reaction data.

NEUTRINO CHARGE RADIUS SQUARED

We report limits on the so-called neutrino charge radius squared. While the straight-forward definition of a neutrino charge radius has been proven to be gauge-dependent and, hence, unphysical (LEE 77c), there have been recent attempts to define a physically observable neutrino charge radius (BERNABEU 00, BERNABEU 02). The issue is still controversial (FUJIKAWA 03, BERNABEU 03). A more general interpretation of the experimental results is that they are limits on certain nonstandard contributions to neutrino scattering.

VALUE (10^{-32}cm^2)	CL%	DOCUMENT ID	TECN	COMMENT
-2.97 to 4.14	90	142 AUERBACH	01 LSND	$\nu_e e \rightarrow \nu_e e$
< 0.68, > -0.53	90	143 HIRSCH	03	$\nu_\mu e$ scat.
< 9.9 and > -8.2	90	144 HIRSCH	03	anomalous $e^+ e^- \rightarrow \nu \bar{\nu} \gamma$
< 0.6	90	VILAIN	95B CHM2	$\nu_\mu e$ elastic scat.
0.9 \pm 2.7		ALLEN	93 CNTR	LAMPF $\nu e \rightarrow \nu e$
< 2.3	95	MOURAO	92 ASTR	HOME/KAM2 ν rates
< 7.3	90	145 VIDYAKIN	92 CNTR	Reactor $\bar{\nu} e \rightarrow \bar{\nu} e$
1.1 \pm 2.3		ALLEN	91 CNTR	Repl. by ALLEN 93
-1.1 \pm 1.0		146 AHRENS	90 CNTR	$\nu_\mu e$ elastic scat.
-0.3 \pm 1.5		146 DORENBOS...	89 CHRM	$\nu_\mu e$ elastic scat.
		147 GRIFOLS	89B ASTR	SN 1987A

• • • We do not use the following data for averages, fits, limits, etc. • • •

142 AUERBACH 01 measure $\nu_e e$ elastic scattering with LSND detector. The cross section agrees with the Standard Model expectation, including the charge and neutral current interference. The 90% CL applies to the range shown.

143 Based on analysis of CCFR 98 results. Limit is on $\langle r_{\nu}^2 \rangle + \langle r_A^2 \rangle$. The CHARM II and E734 at BNL results are reanalyzed, and weaker bounds on the charge radius squared than previously published are obtained. The NuTeV result is discussed; when tentatively interpreted as ν_μ charge radius it implies $\langle r_{\nu}^2 \rangle + \langle r_A^2 \rangle = (4.20 \pm 1.64) \times 10^{-33} \text{cm}^2$.

144 Results of LEP-2 are interpreted as limits on the axial-vector charge radius squared of a Majorana ν_τ . Slightly weaker limits for both vector and axial-vector charge radius squared are obtained for the Dirac case, and somewhat weaker limits are obtained from the analysis of lower energy data (LEP-1.5 and TRISTAN).

145 VIDYAKIN 92 limit is from a $e\bar{\nu}$ elastic scattering experiment. No experimental details are given except for the cross section from which this limit is derived. Signal/noise was 1/10. The limit uses $\sin^2\theta_W = 0.23$ as input.

146 Result is obtained from reanalysis given in ALLEN 91, followed by our reduction to obtain 1 σ errors.

147 GRIFOLS 89B sets a limit of $\langle r^2 \rangle < 0.2 \times 10^{-32} \text{cm}^2$ for right-handed neutrinos.

REFERENCES FOR Neutrino Properties

FOGLI	07	PR D75 053001	G.L. Fogli <i>et al.</i>
GNINENKO	07	PR D75 075014	S.N. Gninenko, N.V. Krasnikov, A. Rubbia
MIRIZZI	07	PR D76 053007	A. Mirizzi, D. Montanino, P.D. Serpico
SPERGEL	07	APJS 170 377	D.M. Spergel <i>et al.</i>
WONG	07	PR D75 012001	H.T. Wong <i>et al.</i>
ZUNCKEL	07	JCAP 0708 004	C. Zunckel, P. Ferreira
CIRELLI	06	JCAP 0612 013	M. Cirelli <i>et al.</i>
FUKUGITA	06	PR D74 027302	M. Fukugita <i>et al.</i>
GOOBAR	06	JCAP 0606 019	A. Goobar <i>et al.</i>
HANNESSTAD	06	JCAP 0611 016	S. Hannestad, G. Raffelt
KRISTIANSEN	06	PR D74 123005	J. Kristiansen, O. Elgarøy, H. Eriksson
SANCHEZ	06	MNRAS 366 189	A.G. Sanchez <i>et al.</i>
SELJAK	06	JCAP 0610 014	U. Seljak, A. Slosar, P. McDonald
DARAKTCHIEVA	05	PL B615 153	Z. Daraktchieva <i>et al.</i>
ICHIKAWA	05	PR D71 043001	K. Ichikawa, M. Fukugita, M. Kawasaki
KRAUS	05	EPL C40 447	Ch. Kraus <i>et al.</i>
XIN	05	PR D72 012006	B. Xin <i>et al.</i>
AHARIMIM	04	PR D70 093014	B. Aharimim <i>et al.</i>
BARGER	04	PL B595 55	V. Barger, D. Marfatia, A. Tregre
CECCHINI	04	ASP 21 183	S. Cecchini <i>et al.</i>
CROTTY	04	PR D69 123007	P. Crotty, J. Lesgourgues, S. Pastor
EGUCHI	04	PRL 92 071301	K. Eguchi <i>et al.</i>
GRIFOLS	04	PL B587 184	J.A. Grifols, E. Masso, S. Mohanty

(TEXONO Collab.)

(MUNU Collab.)

(ICRR)

(TEXONO Collab.)

(SNO Collab.)

(BGN +)

(KamLAND Collab.)

(BARC, AHMED)

See key on page 373

Lepton Particle Listings

Neutrino Properties, Number of Neutrino Types

LIU	04	PRL 93 021802	D.W. Liu et al. (Super-Kamiokande Collab.)	VONFEILITZ...	88	PL B200 580	F. von Feilitzsch, L. Oberauer (MUNT)
ARNABOLDI	03A	PRL 91 161802	C. Arnaboldi et al. (Borexino Collab.)	BARBIELLINI	87	NAT 329 21	G. Barbiellini, G. Cocconi (CERN)
BACK	02B	PL B563 35	H.O. Back et al. (Borexino Collab.)	BORIS	87	PRL 58 2019	S.D. Boris et al. (ITEP, ASCI)
BANDYOPA...	03	PL B555 33	A. Bandyopadhyay, S. Choubey, S. Goswami (SAHA+)	Also		PRL 61 245 (erratum)	S.D. Boris et al. (ITEP, ASCI)
BERNABEU	03	hep-ph/0303202	J. Bernabeu, J. Papavassiliou, J. Vidal	BORIS	87B	JETPL 45 333	S.D. Boris et al. (ITEP)
DARAKTCH...	03	PL B564 190	Z. Darakchieva et al. (MUNU Collab.)			Translated from ZETFP 45 267.	
FUJIKAWA	03	hep-ph/0303188	K. Fujikawa, R. Shrock	FUKUGITA	87	PR D36 3817	M. Fukugita, S. Yazaki (KYOTU, TOKYO)
HIRSCH	03	PR D67 033005	M. Hirsch et al. (TEXONO Collab.)	NUSSINOV	87	PR D36 2278	S. Nussinov, Y. Rephaeli (TELA)
LI	03B	PRL 90 131802	H.B. et al.	OBERAUER	87	PL B198 113	L.F. Oberauer, F. von Feilitzsch, R.L. Mossbauer
SPERGEL	03	APJS 148 175	D.N. Spergel et al.	SPRINGER	87	PR A35 679	P.T. Springer et al. (LLNL)
BERNABEU	02	PRL 89 101802	J. Bernabeu, J. Papavassiliou, J. Vidal	KETOV	86	JETPL 44 146	S.N. Ketov et al. (KITAE)
Also		PRL 89 229902 (erratum)	J. Bernabeu, J. Papavassiliou, J. Vidal			Translated from ZETFP 44 114.	
DERBIN	02B	JETPL 76 409	A.V. Derbin, O.Ju. Smirnov	COWSIK	85	PL 151B 62	R. Cowzik (TATA)
		Translated from ZETFP 76 483.		RAFFELT	85	PR D31 3002	G.G. Raffelt (MPIM)
GRIMUS	02	NP B648 376	W. Grimus et al.	BINETRUY	84	PL 134B 174	P. Binetruy, G. Girardi, P. Salati (LAPP)
JOSHIPURA	02B	PR D66 113008	A.S. Joshipura, E. Masso, S. Mohanty	FRESE	84	NP B233 167	K. Freese, D.N. Schramm (CHIC, FNAL)
LEWIS	02	PR D66 103511	A. Lewis, S. Bridle	KYULDJIEV	84	NP B243 387	A.V. Kyuldjiev (SOFI)
LOREDO	02	PR D65 063002	T.J. Loredo, D.Q. Lamb	SCHRAMM	84	PL 141B 337	D.N. Schramm, G. Steigman (FNAL, BOST)
WANG	02	PR D65 123001	X. Wang, M. Tegmark, M. Zaldarriaga	VOGEL	84	PR D30 1505	P. Vogel (ETH, SIN)
AUERBACH	01	PR D63 112001	L.B. Auerbach et al. (LSND Collab.)	ANDERHUB	82	PL 114B 76	H.B. Auerbach et al. (CHIC, UCSB)
SCHWIENHO...	01	PL B513 23	R. Schwenhorst et al. (OSQAR Collab.)	OLIVE	82	PR D25 213	K.A. Olive, M.S. Turner (STEVE, COLU)
ATHANAS	00	PR D61 052002	M. Athanas et al. (CLEO Collab.)	BERNSTEIN	81	PL 101B 39	J. Bernstein, G. Feinberg (LASL, YALE, MIT+)
BERNABEU	00	PR D62 113012	J. Bernabeu et al.	FRANK	81	PR D24 2001	J.A. Frank et al. (SUSS)
FUKUGITA	00	PRL 84 1082	M. Fukugita, G.C. Liu, N. Sugiyama	MORGAN	81	PL 102B 247	K. Fujikawa, R. Shrock (STON)
TANIMOTO	00	PL B478 1	N. Tanimoto et al.	FUJIKAWA	80	PRL 45 963	K. Fujikawa, R. Shrock (NASA)
AYALA	99	PR D59 111901	A. Ayala, J.C. D'Olivo, M. Torres	LUBIMOV	80	PL 94B 266	V.A. Lyubimov et al. (ITEP)
BEACOM	99	PRL 83 5222	J.F. Beacom, P. Vogel	STECKER	80	PRL 45 1460	F.W. Stecker (NASA)
CROFT	99	PRL 83 1092	R.A.C. Croft, W. Hu, R. Dave	COWSIK	79	PR D19 2219	R. Cowzik (TATA)
DOLGOV	99	NP B548 385	A.D. Dolgov et al.	GOLDMAN	79	PR D19 2215	T. Goldman, G.J. Stephenson (LASL)
LOBASHEV	99	PR B460 227	V.M. Lobashev et al.	BEG	78	PR D17 1395	M.A.B. Beg, W.J. Marciano, M. Ruderman (ROCK+)
RAFFELT	99	PRPL 320 319	G.G. Raffelt	BLIETSCHAU	78	NP B133 205	J. Blietschau et al. (Gargamelle Collab.)
WEINHEIMER	99	PR B460 219	Ch. Weinheimer et al. (OPAL Collab.)	FALK	78	PL 79B 511	S.W. Falk, D.N. Schramm (CHIC)
ACKERSTAFF	98T	EPL C5 229	K. Akerstaff et al. (CLEO Collab.)	BARNES	77	PRL 38 1049	V.E. Barnes et al. (PURD, ANL)
AMMAR	98	PR B431 209	R. Ammar et al. (OPAL Collab.)	COWSIK	77	PRL 39 784	R. Cowzik (MPIM, TATA)
BARATE	98F	EPL C2 395	R. Barate et al. (ALEPH Collab.)	LEE	77C	PR D16 1444	B.W. Lee, R.E. Shrock (STON)
BILLER	98	PRL 80 2992	S.D. Biller et al. (WHIPPLe Collab.)	VYSOTSKY	77	JETPL 26 188	M.I. Vyssotsky, A.D. Dolgov, Y.B. Zeldovich (ITEP)
FELDMAN	98	PR D57 3873	G.J. Feldman, R.D. Cousins			Translated from ZETFP 26 200.	
LENZ	98	PL B416 50	S. Lenz et al. (DELPHI Collab.)	BELLOTTI	76	LNC 17 553	E. Bellotti et al. (MILA)
ABREU	97J	ZPHY C74 577	P. Abreu et al. (L3 Collab.)	SUTHERLAND	76	PR D13 2700	P. Sutherland et al. (PENN, COLU, NYU)
ACCIARRI	97Q	PL B412 201	M. Acciari et al. (CLEO Collab.)	SZALAY	76	AA 49 437	A.S. Szalay, G. Marx (EOTV)
ANASTASSOV	97	PR D55 2559	A. Anastassov et al. (CLEO Collab.)	CLARK	74	PR D9 533	A.R. Clark et al. (LBL)
Also		PR D58 119903 (erratum)	A. Anastassov et al. (CLEO Collab.)	KIM	74	PR D9 3050	J.E. Kim, V.S. Mathur, S. Okubo (ROCH)
ELMFORS	97	NP B503 3	P. Elmfors et al. (BARC, PARIT)	REINES	74	PR D32 180	F. Reines, H.W. Sobel, H.S. Gurr (UCI)
ESCRIBANO	97	PR B395 369	R. Escrivano, E. Masso (BARC, PARIT)	SZALAY	74	APAH 35 8	A.S. Szalay, G. Marx (EOTV)
FIELDS	97	ASP 6 169	B.D. Fields, K. Kainulainen, K.A. Olive (NDAM+)	COWSIK	72	PRL 29 669	R. Cowzik, J. McClelland (UCB)
SWAIN	97	PR D55 R11	J. Swain, L. Taylor (NEAS)	MARX	72	Nu Conf. Budapest	G. Marx, A.S. Szalay (EOTV)
ALEXANDER	96M	ZPHY C72 231	G. Alexander et al. (OPAL Collab.)	GERSHTEIN	66	JETPL 4 120	S.S. Gershtein, Y.B. Zeldovich (KIAM)
ASSAMAGAN	96	PR D53 6065	K.A. Assamagan et al. (PSI, ZURI, VILL+)			Translated from ZETFP 4 189.	
BAI	96	PR D53 20	J.Z. Bai et al. (BES Collab.)	BERNSTEIN	63	PR 132 1227	J. Bernstein, M. Ruderman, G. Feinberg (NYU+)
BOTTINO	96	PR D53 6361	A. Bottino et al. (IFIC, VALE)	COWAN	57	PR 107 528	C.L. Cowan, F. Reines (LANL)
DOLGOV	96	PL B383 193	A.D. Dolgov, S. Pastor, J.W.F. Valle (IFIC, VALE)				
HANNES TAD	96	PR L76 2848	S. Hannestad, J. Madsen (AARH)				
HANNES TAD	96B	PRL 77 5148 (erratum)	S. Hannestad, J. Madsen (AARH)				
HANNES TAD	96C	PR D54 7894	S. Hannestad, J. Madsen (AARH)				
SOBIE	96	ZPHY C70 383	S. Sobie, R.K. Keeler, I. Lawson (VICT)				
BELESSEV	95	PL B350 263	A.I. Belessev et al. (INRM, KIAE)				
BUSKULIC	95H	PL B349 585	D. Buskulić et al. (ALEPH Collab.)				
CHING	95	JMP A10 2841	C.R. Ching et al. (CST, BEJT, CIAE)				
DOLGOV	95	PR D51 4129	A.D. Dolgov, K. Kainulainen, I.Z. Rothstein (MICH+)				
HIDDEMANN	95	JPG 21 639	K.H. Hidemann, H. Daniel, O. Schwentker (MUNT)				
KERNAN	95	NP B437 243	P.J. Kernan, L.M. Krauss (CASE)				
SIGL	95	PR D51 1499	G. Sigl, M.S. Turner (FNAL, EFI)				
STOEFL	95	PRL 75 3237	W. Stoefl, D.J. Decman (LLNL)				
VILAIN	95B	PL B345 115	P. Vilain et al. (CHARM II Collab.)				
ASSAMAGAN	94	PL B335 231	K.A. Assamagan et al. (PSI, ZURI, VILL+)				
BABU	94	PL B21 180	K.S. Babu, T.M. Gould, I.Z. Rothstein (BART+)				
DODELSON	94	PR D49 5068	S. Dodelson, G. Gyuk, M.S. Turner (FNAL, CHIC+)				
GOULD	94	PL B333 545	T.M. Gould, I.Z. Rothstein (JHU, MICH)				
JECKELMANN	94	PL B335 326	B. Jäckelmann, P.F.A. Gondsmitt, H.J. Leisi (WABRN+)				
KAWASAKI	94	NP B419 105	M. Kawasaki et al. (OSU)				
PERES	94	PR D50 513	O.L.G. Peres, V. Pleitez, R. Zukanovich Funchal				
YASUMI	94	PL B334 229	S. Yasumi et al. (KEK, TSUK, KYOT+)				
ALLEN	93	PR D47 11	R.C. Allen et al. (UCI, LANL, ANL+)				
BALEST	93	PR D47 R3671	R. Balest et al. (CLEO Collab.)				
CINABRO	93	PRL 70 3700	D. Cinabro et al. (CLEO Collab.)				
DERBIN	93	JETPL 57 768	A.V. Derbin et al. (PNPI)				
		Translated from ZETFP 57 755.					
DOLGOV	93	PRL 71 476	A.D. Dolgov, I.Z. Rothstein (MICH)				
ENQVIST	93	PL B301 376	K. Enqvist, H. Ullbo (ROBPD)				
SUN	93	CMP 19 241	H. Sun et al. (CIAE, CST, BEJT)				
WEINHEIMER	93	PL B300 210	C. Weinheimer et al. (MANZ)				
ALBRECHT	92M	PL B292 221	H. Albrecht et al. (ARGUS Collab.)				
BLUDMAN	92	PR D45 4720	S.A. Bludman (CFPA)				
COOPER...	92	PL B280 153	A.M. Cooper-Sarkar et al. (BEBC WA66 Collab.)				
DODELSON	92	PRL 68 2572	S. Dodelson, J.A. Frieman, M.S. Turner (FNAL+)				
HOLZSCHUH	92B	PL B287 381	E. Holzschuh, M. Fritsch, W. Kundig (ZURI)				
KAWANO	92	PL B275 487	L.H. Kawano et al. (CIT, UCSD, LLL+)				
MOURAO	92	PL B285 364	A.M. Mourao, J. Pulido, J.P. Ralston (LISB, LISBT+)				
PDG	92	PR D45 S1	K. Hikasa et al. (KEK, LBL, BOST+)				
VIDYAKIN	92	JETPL 55 206	G.S. Vidyakin et al. (KIAE)				
		Translated from ZETFP 55 212.					
ALLEN	91	PR D43 R1	R.C. Allen et al. (UCI, LANL, UMD)				
DAVIDSON	91	PR D43 2314	S. Davidson, B.A. Campbell, D. Bailey (ALBE+)				
DESHPANDE	91	PR D43 943	N.G. Deshpande, K.V.L. Sarna (OREG, TATA)				
DORENBOS...	91	ZPHY C51 142 (erratum)	J. Dorenbosch et al. (CHARM Collab.)				
FULLER	91	PR D43 3136	G.M. Fuller, R.A. Malaney (UCSD)				
GRANEK	91	JMP A6 2387	H. GraneK, B.H.J. McKellar (MELB)				
KAWAKAMI	91	PL B256 105	H. Kawakami et al. (INUS, TOHOK, TINT+)				
KOLB	91	PRL 67 533	E.W. Kolb et al. (FNAL, CHIC)				
KRAKAUER	91	PR D44 R6	D.A. Krakauer et al. (LAMPF E225 Collab.)				
LAM	91	PR D44 3345	W.P. Lam, K.W. Ng (AST)				
ROBERTSON	91	PRL 67 957	R.G.H. Robertson et al. (LASL, LLL)				
AHRENS	90	PR D41 3297	L.A. Ahrens et al. (BNL, BROW, HIRO+)				
AVIGNONE	90	PR D41 682	F.T. Avignone, J.I. Collar (CGUC)				
KRAKAUER	90	PL B252 177	D.A. Krakauer et al. (LAMPF E225 Collab.)				
RAFFELT	90	PRL 64 2856	G.G. Raffelt (MPIM)				
WALKER	90	PR D41 689	T.P. Walker (HARV)				
CHUPP	89	PRL 62 505	E.L. Chupp, W.T. Vestrand, C. Reppin (UNH, MPIM)				
DORENBOS...	89	ZPHY C41 567	J. Dorenbosch et al. (CHARM Collab.)				
GRIFOLS	89B	PR D40 3819	J.A. Grifols, E. Masso (BARC)				
KOLB	89	PRL 62 509	E.W. Kolb, M.S. Turner (CHIC, FNAL)				
LOREDO	89	ANYAS 571 601	T.J. Loredo, D.Q. Lamb (CHIC)				
RAFFELT	89	PR D39 2066	G.G. Raffelt (PRIN, UCB)				
RAFFELT	89B	APJ 336 61	G. Raffelt, D. Dearborn, J. Silk (UCB, LLL)				
ALBRECHT	88B	PL B202 149	H. Albrecht et al. (ARGUS Collab.)				
BARBIERI	88	PRL 61 27	R. Barbieri, R.N. Mohapatra (PISA, UMD)				
BORIS	88	PRL 61 245 (erratum)	S.D. Boris et al. (ITEP, ASCI)				
FUKUGITA	88	PRL 60 879	M. Fukugita et al. (KYOTU, MPIM, UCB)				
GROTCHE	88	ZPHY C39 553	H. Grotch, R.W. Robinett (PSU)				
RAFFELT	88B	PR D37 549	G.G. Raffelt, D.S.P. Dearborn (UCB, LLL)				
SPERGEL	88	PL B200 366	D.N. Spergel, J.N. Bahcall (LASL)				

Number of Neutrino Types

The neutrinos referred to in this section are those of the Standard $SU(2) \times U(1)$ Electroweak Model possibly extended to allow nonzero neutrino masses. Light neutrinos are those with $m < m_Z/2$. The limits are on the number of neutrino mass eigenstates, including ν_1 , ν_2 , and ν_3 .

THE NUMBER OF LIGHT NEUTRINO TYPES FROM COLLIDER EXPERIMENTS

Revised March 2008 by D. Karlen (University of Victoria and TRIUMF).

The most precise measurements of the number of light neutrino types, N_ν , come from studies of Z production in e^+e^- collisions. The invisible partial width, Γ_{inv} , is determined by subtracting the measured visible partial widths, corresponding to Z decays into quarks and charged leptons, from the total Z width. The invisible width is assumed to be due to N_ν light neutrino species each contributing the neutrino partial width Γ_ν as given by the Standard Model. In order to reduce the model dependence, the Standard Model value for the ratio of the neutrino to charged leptonic partial widths, $(\Gamma_\nu/\Gamma_\ell)_{\text{SM}} = 1.991 \pm 0.001$, is used instead of $(\Gamma_\nu)_{\text{SM}}$ to determine the number of light neutrino types:

$$N_\nu = \frac{\Gamma_{\text{inv}}}{\Gamma_\ell} \left(\frac{\Gamma_\ell}{\Gamma_\nu} \right)_{\text{SM}} \quad (1)$$

The combined result from the four LEP experiments is $N_\nu = 2.984 \pm 0.008$ [1].

In the past, when only small samples of Z decays had been recorded by the LEP experiments and by the Mark II at SLC, the uncertainty in N_ν was reduced by using Standard Model

Lepton Particle Listings

Number of Neutrino Types

fits to the measured hadronic cross sections at several center-of-mass energies near the Z resonance. Since this method is much more dependent on the Standard Model, the approach described above is favored.

Before the advent of the SLC and LEP, limits on the number of neutrino generations were placed by experiments at lower-energy e^+e^- colliders by measuring the cross section of the process $e^+e^- \rightarrow \nu\bar{\nu}\gamma$. The ASP, CELLO, MAC, MARK J, and VENUS experiments observed a total of 3.9 events above background [2], leading to a 95% CL limit of $N_\nu < 4.8$. This process has a much larger cross section at center-of-mass energies near the Z mass and has been measured at LEP by the ALEPH, DELPHI, L3, and OPAL experiments [3]. These experiments have observed several thousand such events, and the combined result is $N_\nu = 3.00 \pm 0.08$. The same process has also been measured by the LEP experiments at much higher center-of-mass energies, between 130 and 208 GeV, in searches for new physics [4]. Combined with the lower energy data, the result is $N_\nu = 2.92 \pm 0.05$.

Experiments at $p\bar{p}$ colliders also placed limits on N_ν by determining the total Z width from the observed ratio of $W^\pm \rightarrow \ell^\pm\nu$ to $Z \rightarrow \ell^+\ell^-$ events [5]. This involved a calculation that assumed Standard Model values for the total W width and the ratio of W and Z leptonic partial widths, and used an estimate of the ratio of Z to W production cross sections. Now that the Z width is very precisely known from the LEP experiments, the approach is now one of those used to determine the W width.

References

1. ALEPH, DELPHI, L3, OPAL, and SLD Collaborations, and LEP Electroweak Working Group, and SLD Electroweak Group, and SLD Heavy Flavour Group, Phys. Reports **427**, 257 (2006).
2. VENUS: K. Abe *et al.*, Phys. Lett. **B232**, 431 (1989); ASP: C. Hearty *et al.*, Phys. Rev. **D39**, 3207 (1989); CELLO: H.J. Behrend *et al.*, Phys. Lett. **B215**, 186 (1988); MAC: W.T. Ford *et al.*, Phys. Rev. **D33**, 3472 (1986); MARK J: H. Wu, Ph.D. Thesis, Univ. Hamburg (1986).
3. L3: M. Acciarri *et al.*, Phys. Lett. **B431**, 199 (1998); DELPHI: P. Abreu *et al.*, Z. Phys. **C74**, 577 (1997); OPAL: R. Akers *et al.*, Z. Phys. **C65**, 47 (1995); ALEPH: D. Buskulic *et al.*, Phys. Lett. **B313**, 520 (1993).
4. DELPHI: J. Abdallah *et al.*, Eur. Phys. J. **C38**, 395 (2005); L3: P. Achard *et al.*, Phys. Lett. **B587**, 16 (2004); ALEPH: A. Heister *et al.*, Eur. Phys. J. **C28**, 1 (2003); OPAL: G. Abbiendi *et al.*, Eur. Phys. J. **C18**, 253 (2000).
5. UA1: C. Albajar *et al.*, Phys. Lett. **B198**, 271 (1987); UA2: R. Ansari *et al.*, Phys. Lett. **B186**, 440 (1987).

Number from e^+e^- Colliders

Number of Light ν Types

VALUE	DOCUMENT ID	TECN
2.9840 ± 0.0082	¹ LEP-SLC	06 RVUE

• • • We do not use the following data for averages, fits, limits, etc. • • •

3.00 ± 0.05	² LEP	92 RVUE
-------------	------------------	---------

¹ Combined fit from ALEPH, DELPHI, L3 and OPAL Experiments.

² Simultaneous fits to all measured cross section data from all four LEP experiments.

Number of Light ν Types from Direct Measurement of Invisible Z Width

In the following, the invisible Z width is obtained from studies of single-photon events from the reaction $e^+e^- \rightarrow \nu\bar{\nu}\gamma$. All are obtained from LEP runs in the $E_{\text{cm}}^{\text{eff}}$ range 88–209 GeV.

VALUE	DOCUMENT ID	TECN	COMMENT
2.92 ± 0.05 OUR AVERAGE	Error includes scale factor of 1.2.		
2.84 ± 0.10 ± 0.14	ABDALLAH 05B	DLPH	$\sqrt{s} = 180\text{--}209$ GeV
2.98 ± 0.05 ± 0.04	ACHARD 04E	L3	1990–2000 LEP runs
2.86 ± 0.09	HEISTER 03C	ALEP	$\sqrt{s} = 189\text{--}209$ GeV
2.69 ± 0.13 ± 0.11	ABBIENDI,G 00D	OPAL	1998 LEP run
2.89 ± 0.32 ± 0.19	ABREU 97J	DLPH	1993–1994 LEP runs
3.23 ± 0.16 ± 0.10	AKERS 95C	OPAL	1990–1992 LEP runs
2.68 ± 0.20 ± 0.20	BUSKULIC 93L	ALEP	1990–1991 LEP runs
• • • We do not use the following data for averages, fits, limits, etc. • • •			
2.84 ± 0.15 ± 0.14	ABREU 00Z	DLPH	1997–1998 LEP runs
3.01 ± 0.08	ACCIARRI 99R	L3	1991–1998 LEP runs
3.1 ± 0.6 ± 0.1	ADAM 96C	DLPH	$\sqrt{s} = 130, 136$ GeV

Limits from Astrophysics and Cosmology

Number of Light ν Types

("light" means $<$ about 1 MeV). See also OLIVE 81. For a review of limits based on Nucleosynthesis, Supernovae, and also on terrestrial experiments, see DENEGR1 90. Also see "Big-Bang Nucleosynthesis" in this Review.

VALUE	CL%	DOCUMENT ID	TECN	COMMENT
• • • We do not use the following data for averages, fits, limits, etc. • • •				
0.9 < N_ν < 8.2		³ ICHIKAWA 07	COSM	
3 < N_ν < 7	95	⁴ CIRELLI 06	COSM	
2.7 < N_ν < 4.6	95	⁵ HANNESTAD 06	COSM	
3.6 < N_ν < 7.4	95	⁴ SELJAK 06	COSM	
< 4.4		⁶ CYBURT 05	COSM	
< 3.3		⁷ BARGER 03C	COSM	
1.4 < N_ν < 6.8		⁸ CROTTY 03	COSM	
1.9 < N_ν < 6.6		⁸ PIERPAOLI 03	COSM	
2 < N_ν < 4		LISI 99	BBN	
< 4.3		OLIVE 99	BBN	
< 4.9		COPI 97	Cosmology	
< 3.6		HATA 97B	High D/H quasar abs.	
< 4.0		OLIVE 97	BBN; high ⁴ He and ⁷ Li	
< 4.7		CARDALL 96B	COSM High D/H quasar abs.	
< 3.9		FIELDS 96	COSM BBN; high ⁴ He and ⁷ Li	
< 4.5		KERNAN 96	COSM High D/H quasar abs.	
< 3.6		OLIVE 95	BBN; ≥ 3 massless ν	
< 3.3		WALKER 91	Cosmology	
< 3.4		OLIVE 90	Cosmology	
< 4		YANG 84	Cosmology	
< 4		YANG 79	Cosmology	
< 7		STEIGMAN 77	Cosmology	
		PEEBLES 71	Cosmology	
< 16		⁹ SHVARTSMAN 69	Cosmology	
		HOYLE 64	Cosmology	

³ Constrains the number of neutrino types from recent CMB and large scale structure data. No priors on other cosmological parameters are used.

⁴ Constrains the number of neutrino types from recent CMB, large scale structure, Lyman-alpha forest, and SN1a data. The slight preference for $N_\nu > 3$ comes mostly from the Lyman-alpha forest data.

⁵ Constrains the number of neutrino types from recent CMB and large scale structure data. See also HAMANN 07.

⁶ Limit on the number of neutrino types based on ⁴He and D/H abundance assuming a baryon density fixed to the WMAP data. Limit relaxes to 4.6 if D/H is not used or to 5.8 if only D/H and the CMB are used. See also CYBURT 01 and CYBURT 03.

⁷ Limit on the number of neutrino types based on combination of WMAP data and big-bang nucleosynthesis. The limit from WMAP data alone is 8.3. See also KNELLER 01. $N_\nu \geq 3$ is assumed to compute the limit.

⁸ 95% confidence level range on the number of neutrino flavors from WMAP data combined with other CMB measurements, the 2dFGRS data, and HST data.

⁹ SHVARTSMAN 69 limit inferred from his equations.

Number Coupling with Less Than Full Weak Strength

VALUE	DOCUMENT ID	TECN
• • • We do not use the following data for averages, fits, limits, etc. • • •		
< 20	¹⁰ OLIVE 81C	COSM
< 20	¹⁰ STEIGMAN 79	COSM

¹⁰ Limit varies with strength of coupling. See also WALKER 91.

REFERENCES FOR Limits on Number of Neutrino Types

HAMANN	07	JCAP 0708 021	J. Hamann et al.	
ICHIKAWA	07	JCAP 0705 007	K. Ichikawa, M. Kawasaki, F. Takahashi	
CIRELLI	06	JCAP 0612 013	M. Cirelli et al.	
HANNESTAD	06	JCAP 0611 016	S. Hannestad, G. Raffelt	
LEP-SLC	06	PRPL 427 257	ALEPH, DELPHI, L3, OPAL, SLD and working groups	
SELJAK	06	JCAP 0610 014	U. Seljak, A. Slosar, P. McDonald	
ABDALLAH	05B	EPJ C38 395	J. Abdallah et al.	(DELPHI Collab.)
CYBURT	05	ASP 23 313	R.H. Cyburt et al.	
ACHARD	04E	PL B587 16	P. Achard et al.	(L3 Collab.)
BARGER	03C	PL B566 9	V. Barger et al.	
CROTTY	03	PR D67 123005	P. Crotty, J. Lesgourgues, S. Pastor	
CYBURT	03	PL B567 227	R.H. Cyburt, B.D. Fields, K.A. Olive	
HEISTER	03C	EPJ C28 1	A. Heister et al.	(ALEPH Collab.)
PIERPAOLI	03	MNRAS 342 L63	E. Pierpaoli	
CYBURT	01	ASP 17 87	R.H. Cyburt, B.D. Fields, K.A. Olive	
KNELLER	01	PR D64 123506	J.P. Kneller et al.	
ABBIENDI,G	00D	EPJ C18 253	G. Abbiendi et al.	(OPAL Collab.)
ABREU	00Z	EPJ C17 53	P. Abreu et al.	(DELPHI Collab.)
ACCIARRI	99R	PL B470 268	M. Acciarri et al.	(L3 Collab.)
LSI	99	PR D59 123520	E. Lisi, S. Sarkar, F.L. Villante	
OLIVE	99	ASP 11 403	K.A. Olive, D. Thomas	(DELPHI Collab.)
ABREU	97J	ZPHY C74 577	P. Abreu et al.	(CHIC)
COP1	97	PR D55 3389	C.J. Coppi, D.N. Schramm, M.S. Turner	(OSU, PENN)
HATA	97B	PR D55 540	N. Hata et al.	(MINN, FLOR)
OLIVE	97	ASP 7 27	K.A. Olive, D. Thomas	(DELPHI Collab.)
ADAM	96C	PL B380 471	W. Adam et al.	(UCSD)
CARDALL	96B	APJ 472 435	C.Y. Cardall, G.M. Fuller	(NDAM, CERN, MINN+)
FIELDS	96	New Ast 1 77	B.D. Fields et al.	(CASE, OXFTP)
KERNAN	96	PR D54 3681	P.S. Kernan, S. Sarkar	(OPAL Collab.)
AKERS	95C	ZPHY C65 47	R. Akers et al.	(MINN, OSU)
OLIVE	95	PL B354 357	K.A. Olive, G. Steigman	(ALEPH Collab.)
BUSKULIC	93L	PL B313 520	D. Buskulić et al.	(LEP, ALEPH, DELPHI, L3, OPAL)
LEP	92	PL B276 247	LEP Collab.	(HSCA, OSU, CHIC+)
WALKER	91	APJ 376 51	T.P. Walker et al.	(CERN, UCB+)
DENEGRI	90	RMP 62 1	D. Denegri, B. Sadoulet, M. Spiro	(MINN, CHIC, OSU+)
OLIVE	90	PL B236 454	K.A. Olive et al.	(CHIC, BART)
YANG	84	APJ 281 493	J. Yang et al.	(CHIC, BART)
OLIVE	81	APJ 246 557	K.A. Olive et al.	(EFI+)
OLIVE	81C	NP B180 497	K.A. Olive, D.N. Schramm, G. Steigman	(BART+)
STEIGMAN	79	PRL 43 239	G. Steigman, K.A. Olive, D.N. Schramm	(CHIC, YALE, VIRG)
YANG	79	APJ 227 697	J. Yang et al.	(CHIC, YALE, CHIC+)
STEIGMAN	77	PL 66B 202	G. Steigman, D.N. Schramm, J.E. Gunn	(PRIN)
PEEBLES	71	Physical Cosmology	P.Z. Peebles	
SHWARTSMAN	69	Princeton Univ. Press (1971) JETPL 9 184	V.F. Shwartzman	(MOSU)
HOYLE	64	Translated from ZETFP 9 315. NAT 203 1108	F. Hoyle, R.J. Tayler	(CAMB)

Double- β Decay

OMITTED FROM SUMMARY TABLE

NEUTRINOLESS DOUBLE- β DECAY

Revised November 2007 by P. Vogel (Caltech) and A. Piepke (University of Alabama).

Neutrinoless double-beta ($0\nu\beta\beta$) decay would signal violation of total lepton number conservation. The process can be mediated by an exchange of a light Majorana neutrino, or by an exchange of other particles. However, the existence of $0\nu\beta\beta$ decay requires Majorana neutrino mass, no matter what the actual mechanism is. As long as only a limit on the lifetime is available, limits on the effective Majorana neutrino mass, on the lepton-number violating right-handed current or other possible mechanisms mediating $0\nu\beta\beta$ decay, can be obtained, independently of the actual mechanism. These limits are listed in the next three tables, together with a claimed $0\nu\beta\beta$ decay signal reported by part of the Heidelberg-Moscow collaboration. A 4σ excess of counts at the decay energy is used for a determination of the Majorana neutrino mass. This signal has not yet been independently confirmed. In the following we assume that the exchange of light Majorana neutrinos ($m_{\nu_i} \leq 10$ MeV) contributes dominantly to the decay rate.

Besides a dependence on the phase space ($G^{0\nu}$) and the nuclear matrix element ($M^{0\nu}$), the observable $0\nu\beta\beta$ decay rate is proportional to the square of the effective Majorana mass $\langle m_{\beta\beta} \rangle$, $(T_{1/2}^{0\nu})^{-1} = G^{0\nu} \cdot |M^{0\nu}|^2 \cdot \langle m_{\beta\beta} \rangle^2$, with $\langle m_{\beta\beta} \rangle^2 = |\sum_i U_{ei}^2 m_{\nu_i}|^2$. The sum contains, in general, complex CP -phases in U_{ei}^2 , *i.e.*, cancellations may occur. For three neutrino flavors, there are three physical phases for Majorana neutrinos and one for Dirac

neutrinos. The two additional Majorana phase differences affect only processes to which lepton-number-changing amplitudes contribute. Given the general 3×3 mixing matrix for Majorana neutrinos, one can construct other analogous lepton number violating quantities, $\langle m_{\ell\ell'} \rangle = \sum_i U_{\ell i} U_{\ell' i} m_{\nu_i}$. However, these are currently much less constrained than $\langle m_{\beta\beta} \rangle$.

Nuclear structure calculations are needed to deduce $\langle m_{\beta\beta} \rangle$ from the decay rate. While $G^{0\nu}$ can be calculated reliably, the computation of $M^{0\nu}$ is subject to uncertainty. Indiscriminate averaging over all published matrix element values would result, for any given nuclide, in a factor of ~ 3 uncertainty in the derived $\langle m_{\beta\beta} \rangle$ values. More recent evaluations, insisting that the known $2\nu\beta\beta$ rate is correctly reproduced, result in a considerable reduction in the spread of the $M^{0\nu}$ values. *E.g.* in [1] the spread appears to be as low as $\pm 30\%$. The particle physics quantities to be determined are thus nuclear model-dependent, so the half-life measurements are listed first. Where possible, we reference the nuclear matrix elements used in the subsequent analysis. Since rates for the more conventional $2\nu\beta\beta$ decay serve to calibrate the nuclear theory, results for this process are also given.

Oscillation experiments utilizing atmospheric-, accelerator-, solar-, and reactor-produced neutrinos and anti-neutrinos yield strong evidence that at least some neutrinos are massive. However, these findings shed no light on the mass hierarchy (*i.e.*, on the sign of Δm_{atm}^2), the absolute neutrino mass values, or the properties of neutrinos under CPT -conjugation (Dirac or Majorana).

All confirmed oscillation experiments can be consistently described using three interacting neutrino species with two mass splittings and three mixing angles. Full three flavor analyses such as *e.g.* [2] yield: $\Delta m_{atm}^2 = (2.6 \pm 0.4) \times 10^{-3}$ eV² and $\sin^2 \theta_{atm} = 0.45^{+0.16}_{-0.09}$ for the parameters observed in atmospheric and accelerator experiments. Oscillations of solar ν_e and reactor $\bar{\nu}_e$ lead to $\Delta m_{\odot}^2 = (7.92 \pm 0.71) \times 10^{-5}$ eV² and $\sin^2 \theta_{\odot} = 0.314^{+0.057}_{-0.047}$. (All errors correspond to 95% CL.) The investigation of reactor $\bar{\nu}_e$ at ~ 1 km baseline, combined with solar neutrino and long baseline reactor experiments, indicates that electron type neutrinos couple only weakly to the third mass eigenstate with $\sin^2 \theta_{13} < 0.031$.

Based on the 3-neutrino analysis: $\langle m_{\beta\beta} \rangle^2 \approx |\cos^2 \theta_{\odot} m_1 + e^{i\Delta\alpha_{21}} \sin^2 \theta_{\odot} m_2 + e^{i\Delta\alpha_{31}} \sin^2 \theta_{13} m_3|^2$, with $\Delta\alpha_{21}, \Delta\alpha_{31}$ denoting the physically relevant Majorana CP -phase differences (possible Dirac phase δ is absorbed in these $\Delta\alpha$). Given the present knowledge of the neutrino oscillation parameters one can derive the relation between the effective Majorana mass and the mass of the lightest neutrino, as illustrated in the left panel of Fig. 1. The three mass hierarchies allowed by the oscillation data: normal ($m_1 < m_2 < m_3$), inverted ($m_3 < m_1 < m_2$), and degenerate ($m_1 \approx m_2 \approx m_3$), result in different projections. The width of the innermost hatched bands reflects the uncertainty introduced by the unknown Majorana phases. If the experimental errors of the oscillation parameters are taken into

Lepton Particle Listings

Double- β Decay

account, then the allowed areas are widened as shown by the outer bands of Fig. 1. Because of the overlap of the different mass scenarios, a measurement of $\langle m_{\beta\beta} \rangle$ in the degenerate or inversely hierarchical ranges would not determine the hierarchy. The middle panel of Fig. 1 depicts the relation of $\langle m_{\beta\beta} \rangle$ with the summed neutrino mass $M = m_1 + m_2 + m_3$, constrained by observational cosmology. The oscillation data thus allow a test of whether observed values of $\langle m_{\beta\beta} \rangle$ and M are consistent within the 3 neutrino framework. The right hand panel of Fig. 1, finally, shows $\langle m_{\beta\beta} \rangle$ as a function of the average mass $\langle m_{\beta} \rangle = [\sum |U_{ei}|^2 m_{\nu_i}^2]^{1/2}$ determined through the analysis of low energy beta decays. The rather large intrinsic width of the $\beta\beta$ decay constraint essentially does not allow one to positively identify the inverted hierarchy, and thus the sign of Δm_{atm}^2 , even in combination with these other observables. Naturally, if the value of $\langle m_{\beta\beta} \rangle \leq 0.01$ eV is ever established, then normal hierarchy becomes the only possible scenario.

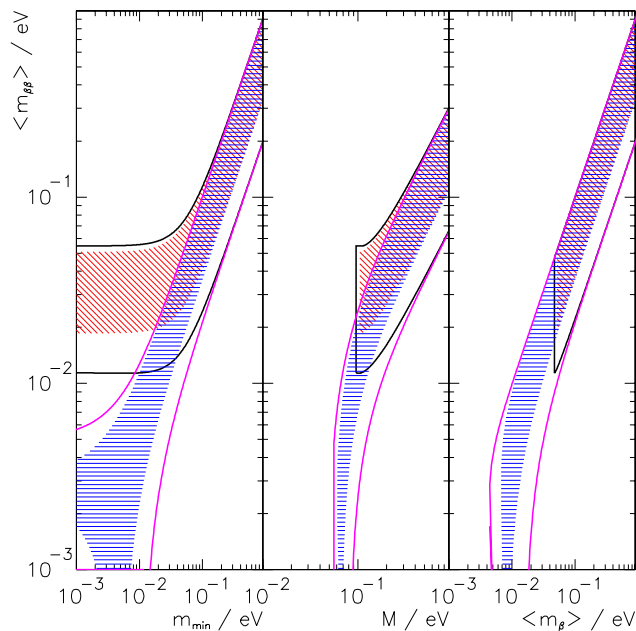


Figure 1: The left panel shows the dependence of $\langle m_{\beta\beta} \rangle$ on the absolute mass of the lightest neutrino m_{min} . The middle panel shows $\langle m_{\beta\beta} \rangle$ as a function of the summed neutrino mass M , while the right panel depicts $\langle m_{\beta\beta} \rangle$ as a function of the mass $\langle m_{\beta} \rangle$. In all panels, the width of the hatched areas is due to the unknown Majorana phases and thus irreducible. The allowed areas given by the solid lines are obtained by taking into account the errors of the oscillation parameters. The two sets of solid lines correspond to the normal and inverted hierarchies. These sets merge into each other for $\langle m_{\beta\beta} \rangle \geq 0.1$ eV, which corresponds to the degenerate mass pattern.

It should be noted that systematic uncertainties of the nuclear matrix elements are not folded into the mass limits reported by $\beta\beta$ decay experiments. Taking this additional uncertainty into account would further widen the projections. The uncertainties in oscillation parameters affect the width of the allowed bands in an asymmetric manner, as shown in Fig. 1. For example, for the degenerate mass pattern ($\langle m_{\beta\beta} \rangle \geq 0.1$ eV), the upper edge is simply $\langle m_{\beta\beta} \rangle \sim m$, where m is the common mass of the degenerate multiplet, independent of the oscillation parameters, while the lower edge is $m \cos(2\theta_{\odot})$. Similar arguments explain the other features of Fig. 1.

If the neutrinoless double-beta decay is observed, it will be possible to fix a *range* of absolute values of the masses m_{ν_i} . Unlike the direct neutrino mass measurements, however, a limit on $\langle m_{\beta\beta} \rangle$ does not allow one to constrain the individual mass values m_{ν_i} even when the mass differences Δm^2 are known.

Neutrino oscillation data imply, for the first time, the existence of a *lower limit* ~ 0.012 eV for the Majorana neutrino mass for the inverted hierarchy mass pattern while $\langle m_{\beta\beta} \rangle$ could, by fine tuning, vanish in the case of the normal mass hierarchy. Several new double-beta searches have been proposed to probe the interesting $\langle m_{\beta\beta} \rangle$ mass range.

If lepton-number-violating right-handed current weak interactions exist, their strength can be characterized by the phenomenological coupling constants η and λ (η describes the coupling between the right-handed lepton current and left-handed quark current while λ describes the coupling when both currents are right-handed). The $0\nu\beta\beta$ decay rate then depends on $\langle \eta \rangle = \eta \sum_i U_{ei} V_{ei}$ and $\langle \lambda \rangle = \lambda \sum_i U_{ei} V_{ei}$ that vanish for massless or unmixed neutrinos ($V_{\ell j}$ is a matrix analogous to $U_{\ell j}$ but describing the mixing with the hypothetical right-handed neutrinos). This mechanism of the $0\nu\beta\beta$ decay could be, in principle, distinguished from the light Majorana neutrino exchange by the observation of the single electron spectra. The limits on $\langle \eta \rangle$ and $\langle \lambda \rangle$ are listed in a separate table. The reader is cautioned that a number of earlier experiments did not distinguish between η and λ . In addition, see the section on majoron searches for additional limits set by these experiments.

References

1. V.A. Rodin *et al.*, Phys. Rev. **C68**, 044302 (2003); V.A. Rodin *et al.*, Nucl. Phys. **A766**, 107 (2006); erratum, Nucl. Phys. **A793**, 213 (2007).
2. G.L. Fogli *et al.*, Phys. Rev. **D75**, 053001 (2007).

Half-life Measurements and Limits for Double- β Decay

In most cases the transitions $(Z,A) \rightarrow (Z-2,A) + 2e^- + (0 \text{ or } 2) \bar{\nu}_e$ to the 0^+ ground state of the final nucleus are listed. However, we also list transitions that increase the nuclear charge ($2e^+$, e^+ /EC and ECEC) and transitions to excited states of the final nuclei (0_i^+ , 2^+ , and 2_i^+). In the following Listings, only best or comparable limits or lifetimes for each isotope are reported. For 2ν decay, which is well established, only measured half-lives are reported.

$t_{1/2}(10^{21} \text{ yr})$	CL% ISOTOPE	TRANSITION	METHOD	DOCUMENT ID
•••	We do not use the following data for averages, fits, limits, etc. •••			
> 0.004	90 ^{64}Zn 0ν	2K	ZnWO ₄ scint.	¹ BELLI 08
> 0.22	90 ^{64}Zn 0ν		ZnWO ₄ scint.	² BELLI 08

See key on page 373

Lepton Particle Listings
Double- β Decay

$0.57^{+0.13}_{-0.09} \pm 0.08$	68	^{100}Mo	2ν	$0^+ \rightarrow 0^+_1$	NEMO-3	3	ARNOLD	07	> 27	68	^{82}Se	0ν	$0^+ \rightarrow 0^+$	TPC	ELLIOTT	92	
									$0.108^{+0.026}_{-0.006}$		^{82}Se	2ν	$0^+ \rightarrow 0^+$	TPC	ELLIOTT	92	
> 89	90	^{100}Mo	0ν	$0^+ \rightarrow 0^+_1$	NEMO-3	4	ARNOLD	07	2.0 ± 0.6		^{238}U	$0\nu+2\nu$		Radiochem	67	TURKEVICH	91
> 1.1	90	^{100}Mo	2ν	$0^+ \rightarrow 2^+$	NEMO-3	5	ARNOLD	07	> 9.5	76	^{48}Ca	0ν		CaF ₂ scint.		YOU	91
> 160	90	^{100}Mo	0ν	$0^+ \rightarrow 2^+$	NEMO-3	6	ARNOLD	07	$0.12 \pm 0.01 \pm 0.04$	68	^{82}Se	$0\nu+2\nu$		Geochem.	68	LIN	88
> 0.0019	90	^{74}Se	$0\nu+2\nu$		γ in Ge det.	7	BARABASH	07	$0.75 \pm 0.03 \pm 0.23$	68	^{130}Te	$0\nu+2\nu$		Geochem.	69	LIN	88
> 0.0055	90	^{74}Se	$0\nu+2\nu$	$0^+ \rightarrow 2^+_2$	γ in Ge det.	8	BARABASH	07	1800 ± 700	68	^{128}Te	$0\nu+2\nu$		Geochem.	70	LIN	88B
$> (1.9-6.0) \cdot 10^{-4}$	90	^{120}Te	0ν		γ in Ge det.	9	BARABASH	07B	2.60 ± 0.28		^{130}Te	$0\nu+2\nu$		Geochem	71	KIRSTEN	83
$> 1.9 \times 10^{-4}$	90	^{120}Te	$0\nu+2\nu$		γ in Ge det.	10	BARABASH	07B									
$> 7.5 \times 10^{-4}$	90	^{120}Te	$0\nu+2\nu$	$0^+ \rightarrow 2^+$	γ in Ge det.	11	BARABASH	07B									
$> 1.19 \times 10^{-4}$	90	^{64}Zn	0ν		CdZnTe calorim.	12	BLOXHAM	07									
$> 1.21 \times 10^{-4}$	90	^{120}Te	0ν		CdZnTe calorim.	13	BLOXHAM	07									
$> 2.68 \times 10^{-6}$	90	^{120}Te	0ν		CdZnTe calorim.	14	BLOXHAM	07									
$> 9.72 \times 10^{-6}$	90	^{120}Te	0ν	$0^+ \rightarrow 2^+_1$	CdZnTe calorim.	15	BLOXHAM	07									
22300^{+4400}_{-3100}	68	^{76}Ge	0ν		Enriched HPGe	16	KLAPDOR-K...	06A									
> 1800	90	^{130}Te	0ν		Cryog. det.	17	ARNABOLDI	05									
> 460	90	^{100}Mo	0ν		NEMO-3	18	ARNOLD	05A									
> 100	90	^{82}Se	0ν		NEMO-3	19	ARNOLD	05A									
$(7.11 \pm 0.02 \pm 0.54)\text{E-3}$	^{100}Mo	2ν			NEMO-3	20	ARNOLD	05A									
$(9.6 \pm 0.3 \pm 1.0)\text{E-2}$	^{82}Se	2ν			NEMO-3	21	ARNOLD	05A									
> 550	90	^{130}Te	0ν		Cryog. det.	22	ARNABOLDI	04									
> 310	90	^{100}Mo	0ν		NEMO-3	23	ARNOLD	04									
> 140	90	^{82}Se	0ν		NEMO-3	24	ARNOLD	04									
$(7.68 \pm 0.02 \pm 0.54)\text{E-3}$	^{100}Mo	2ν			NEMO-3	25	ARNOLD	04									
$(10.3 \pm 0.3 \pm 0.7)\text{E-2}$	^{82}Se	2ν			NEMO-3	26	ARNOLD	04									
$0.14^{+0.04}_{-0.02} \pm 0.03$	68	^{150}Nd	$0\nu+2\nu$	$0^+ \rightarrow 0^+_1$	γ in Ge det.	27	BARABASH	04									
11900^{+29900}_{-5000}	99.7	^{76}Ge	0ν		Enriched HPGe	28	KLAPDOR-K...	04A									
> 14	90	^{48}Ca	0ν		CaF ₂ scint.	29	OGAWA	04									
> 210	90	^{130}Te	0ν		Cryog. det.	30	ARNABOLDI	03									
> 31	90	^{130}Te	0ν	$0^+ \rightarrow 2^+$	Cryog. det.	31	ARNABOLDI	03									
$0.61 \pm 0.14^{+0.29}_{-0.35}$	90	^{130}Te	2ν		Cryog. det.	32	ARNABOLDI	03									
> 110	90	^{128}Te	0ν		Cryog. det.	33	ARNABOLDI	03									
$(0.029^{+0.004}_{-0.003})$		^{116}Cd	2ν		$^{116}\text{CdWO}_4$ scint.	34	DANEVICH	03									
> 170	90	^{116}Cd	0ν		$^{116}\text{CdWO}_4$ scint.	35	DANEVICH	03									
> 29	90	^{116}Cd	0ν	$0^+ \rightarrow 2^+$	$^{116}\text{CdWO}_4$ scint.	36	DANEVICH	03									
> 14	90	^{116}Cd	0ν	$0^+ \rightarrow 0^+_1$	$^{116}\text{CdWO}_4$ scint.	37	DANEVICH	03									
> 6	90	^{116}Cd	0ν	$0^+ \rightarrow 0^+_2$	$^{116}\text{CdWO}_4$ scint.	38	DANEVICH	03									
$1.74 \pm 0.01^{+0.18}_{-0.16}$		^{76}Ge	2ν		Enriched HPGe	39	DOERR	03									
> 15700	90	^{76}Ge	0ν		Enriched HPGe	40	AALSETH	02B									
> 58	90	^{134}Xe	0ν		Liquid Xe Scint.	41	BERNABEI	02D									
> 1200	90	^{136}Xe	0ν		Liquid Xe Scint.	42	BERNABEI	02D									
$15000^{+168000}_{-7500}$		^{76}Ge	0ν		Enriched HPGe	43	KLAPDOR-K...	02D									
$(7.2 \pm 0.9 \pm 1.8)\text{E-3}$		^{100}Mo	2ν		Liq. Ar ioniz.	44	ASHITKOV	01									
> 4.9	90	^{100}Mo	0ν		Liq. Ar ioniz.	45	ASHITKOV	01									
> 1.3	90	^{160}Gd	0ν		Gd ₂ SiO ₅ :Ce	46	DANEVICH	01									
> 1.3	90	^{160}Gd	0ν	$0^+ \rightarrow 2^+$	Gd ₂ SiO ₅ :Ce	47	DANEVICH	01									
$0.59^{+0.17}_{-0.11} \pm 0.06$		^{100}Mo	$0\nu+2\nu$	$0^+ \rightarrow 0^+_1$	Ge coinc.	48	DEBRAECKEL	01									
> 55	90	^{100}Mo	$0\nu, \langle m_\nu \rangle$		ELEGANT V	49	EJIRI	01									
> 42	90	^{100}Mo	$0\nu, \langle \lambda \rangle$		ELEGANT V	49	EJIRI	01									
> 49	90	^{100}Mo	$0\nu, \langle \eta \rangle$		ELEGANT V	49	EJIRI	01									
> 19000	90	^{76}Ge	0ν		Enriched HPGe	50	KLAPDOR-K...	01									
$1.55 \pm 0.001^{+0.19}_{-0.15}$	90	^{76}Ge	2ν		Enriched HPGe	51	KLAPDOR-K...	01									
$(9.4 \pm 3.2)\text{E-3}$	90	^{96}Zr	$0\nu+2\nu$		Geochem	52	WIESER	01									
$0.042^{+0.033}_{-0.013}$		^{48}Ca	2ν		Ge spectrometer	53	BRUDANIN	00									
$0.021^{+0.008}_{-0.004} \pm 0.002$		^{96}Zr	2ν		NEMO-2	54	ARNOLD	99									
> 1.0	90	^{96}Zr	0ν		NEMO-2	54	ARNOLD	99									
$(8.3 \pm 1.0 \pm 0.7)\text{E-2}$		^{82}Se	2ν		NEMO-2	55	ARNOLD	98									
> 9.5	90	^{82}Se	0ν		NEMO-2	56	ARNOLD	98									
> 2.8	90	^{82}Se	0ν	$0^+ \rightarrow 2^+$	NEMO-2	57	ARNOLD	98									
$(7.6^{+2.2}_{-1.4})\text{E-3}$		^{100}Mo	2ν		Si(Li)	58	ALSTON...	97									
$(6.82^{+0.38}_{-0.53} \pm 0.68)\text{E-3}$		^{100}Mo	2ν		TPC	59	DESILVA	97									
$(6.75^{+0.37}_{-0.42} \pm 0.68)\text{E-3}$		^{150}Nd	2ν		TPC	60	DESILVA	97									
> 1.2	90	^{150}Nd	0ν		TPC	61	DESILVA	97									
$(3.75 \pm 0.35 \pm 0.21)\text{E-2}$		^{116}Cd	2ν	$0^+ \rightarrow 0^+$	NEMO 2	62	ARNOLD	96									
$0.043^{+0.024}_{-0.011} \pm 0.014$		^{48}Ca	2ν		TPC	63	BALYSH	96									
0.79 ± 0.10		^{130}Te	$0\nu+2\nu$		Geochem	64	TAKAOKA	96									
$0.61^{+0.18}_{-0.11}$		^{100}Mo	$0\nu+2\nu$	$0^+ \rightarrow 0^+_1$	γ in HPGe	65	BARABASH	95									
$(9.5 \pm 0.4 \pm 0.9)\text{E-3}$		^{100}Mo	2ν		NEMO 2		DASSIE	95									
> 0.6	90	^{100}Mo	0ν	$0^+ \rightarrow 0^+_1$	NEMO 2		DASSIE	95									
$0.026^{+0.009}_{-0.005}$		^{116}Cd	2ν	$0^+ \rightarrow 0^+$	ELEGANT IV		EJIRI	95									
$0.017^{+0.010}_{-0.005} \pm 0.0035$		^{150}Nd	2ν	$0^+ \rightarrow 0^+$	TPC		ARTEMEV	93									
0.039 ± 0.009		^{96}Zr	$0\nu+2\nu$		Geochem		KAWASHIMA	93									
2.7 ± 0.1		^{130}Te	$0\nu+2\nu$		Geochem		BERNATOW...	92									
7200 ± 400		^{128}Te	$0\nu+2\nu$		Geochem		BERNATOW...	92									

Lepton Particle Listings

Double- β Decay

- leads to a 4.2 σ evidence for observation of $0\nu\beta\beta$ -decay and a finite Majorana neutrino mass. Stated error is purely statistical. No systematic errors are mentioned in the paper. More details can be found in KLAPDOR-KLEINGROTHAUS 04c.
- 29 CaF_2 scintillation calorimeter ELEGANT VI used to set limit on $0\nu\beta\beta$ -decay rate of ^{48}Ca . The stated half-life limit benefits from a downward fluctuation on the number of background events. The experimental sensitivity is 5.9×10^{21} yr. at 90 % CL. Replaces YOU 91 as the most stringent experiment using ^{48}Ca .
- 30 Supersedes ALESSANDRELLO 00. Array of TeO_2 crystals in high resolution cryogenic calorimeter. Some enriched in ^{130}Te . Ground state to ground state decay.
- 31 Decay into first excited state of daughter nucleus.
- 32 Two neutrino decay into ground state. Relatively large error mainly due to uncertainties in background determination. Reported value is shorter than the geochemical measurements of KIRSTEN 83 and BERNATOWICZ 92 but in agreement with LIN 88 and TAKAOKA 96.
- 33 Supersedes ALESSANDRELLO 00. Array of TeO_2 crystals in high resolution cryogenic calorimeter. Some enriched in ^{128}Te . Ground state to ground state decay.
- 34 Calorimetric measurement of 2ν ground state decay of ^{116}Cd using enriched CdWO_4 scintillators. Agrees with EJIRI 95 and ARNOLD 96. Supersedes DANEVICH 00.
- 35 Limit on 0ν decay of ^{116}Cd using enriched CdWO_4 scintillators. Supersedes DANEVICH 00.
- 36 Limit on 0ν decay of ^{116}Cd into first excited 2^+ state of daughter nucleus using enriched CdWO_4 scintillators. Supersedes DANEVICH 00.
- 37 Limit on 0ν decay of ^{116}Cd into first excited 0^+ state of daughter nucleus using enriched CdWO_4 scintillators. Supersedes DANEVICH 00.
- 38 Limit on 0ν decay of ^{116}Cd into second excited 0^+ state of daughter nucleus using enriched CdWO_4 scintillators. Supersedes DANEVICH 00.
- 39 Results of the Heidelberg-Moscow experiment (KLAPDOR-KLEINGROTHAUS 01 and GUENTHER 97) are reanalyzed using a new simulation of the complete background spectrum. The $\beta\beta 2\nu$ -decay rate is deduced from a 41.57 kg-y exposure. The result is in agreement and supersedes the above referenced halflives with similar statistical and systematic errors.
- 40 AALSETH 02b limit is based on 117 mol-yr of data using enriched Ge detectors. Background reduction by means of pulse shape analysis is applied to part of the data set. Reported limit is slightly less restrictive than that in KLAPDOR-KLEINGROTHAUS 01. However, it excludes part of the allowed half-life range reported in KLAPDOR-KLEINGROTHAUS 01b for the same nuclide. The analysis has been criticized in KLAPDOR-KLEINGROTHAUS 04b. The criticism was addressed and disputed in AALSETH 04.
- 41 BERNABEI 02b report a limit for the $0\nu, 0^+ \rightarrow 0^+$ decay of ^{134}Xe , present in the source at 17%, by considering the maximum number of events for this mode compatible with the fitted smooth background.
- 42 BERNABEI 02d report a limit for the $0\nu, 0^+ \rightarrow 0^+$ decay of ^{136}Xe , by considering the maximum number of events for this mode compatible with the fitted smooth background. The quoted sensitivity is 450×10^{21} yr. The Feldman and Cousins method is used to obtain the quoted limit.
- 43 KLAPDOR-KLEINGROTHAUS 02d is an expanded version of KLAPDOR-KLEINGROTHAUS 01b. The authors re-evaluate the data collected by the Heidelberg-Moscow experiment (KLAPDOR-KLEINGROTHAUS 01) and present a more detailed description of their analysis of an excess of counts at the energy expected for neutrinoless double-beta decay. They interpret this excess, which has a significance of 2.2 to 3.1 σ depending on the data analysis, as evidence for the observation of Lepton Number violation and violation of Baryon minus Lepton Number. The analysis has been criticized by AALSETH 02 and others. The criticisms have been addressed in KLAPDOR-KLEINGROTHAUS 02. See also KLAPDOR-KLEINGROTHAUS 02b. GROMOV 06 analysis of the background supports the assignment of the weak γ transitions near 2040 keV to the decay of ^{214}Bi as claimed in KLAPDOR-KLEINGROTHAUS 04a and KLAPDOR-KLEINGROTHAUS 04c, and in earlier works.
- 44 ASHITKOV 01 result for 2ν of ^{100}Mo is in agreement with other determinations of that half-life.
- 45 ASHITKOV 01 result for 0ν of ^{100}Mo is less stringent than EJIRI 01.
- 46 DANEVICH 01 place limit on 0ν decay of ^{160}Gd using $\text{Gd}_2\text{SiO}_5:\text{Ce}$ crystal scintillators. The limit is more stringent than KOBAYASHI 95.
- 47 DANEVICH 01 place limits on 0ν decay of ^{160}Gd into excited 2^+ state of daughter nucleus using $\text{Gd}_2\text{SiO}_5:\text{Ce}$ crystal scintillators.
- 48 DEBRAECKELEER 01 performed an inclusive measurement of the $\beta\beta$ decay into the second excited state of the daughter nucleus. A novel coincidence technique counting the de-excitation photons is employed. The result agrees with BARABASH 95.
- 49 EJIRI 01 uses tracking calorimeter and isotopically enriched passive source. Efficiencies were calculated assuming $\langle m_\nu \rangle$, $\langle \lambda \rangle$, or $\langle \eta \rangle$ driven decay. This is a continuation of EJIRI 96 which it supersedes.
- 50 KLAPDOR-KLEINGROTHAUS 01 is a continuation of the work published in BAUDIS 99. Isotopically enriched Ge detectors are used in calorimetric measurement. The most stringent bound is derived from the data set in which pulse-shape analysis has been used to reduce background. Exposure time is 35.5 kg y. Supersedes BAUDIS 99 as most stringent result.
- 51 KLAPDOR-KLEINGROTHAUS 01 is a measurement of the $\beta\beta 2\nu$ -decay rate with higher statistics than GUENTHER 97. The reported value has a larger systematic error than their previous result.
- 52 WIESER 01 reports an inclusive geochemical measurement of ^{96}Zr $\beta\beta$ half life. Their result agrees within 2σ with ARNOLD 99 but only marginally, within 3σ , with KAWASHIMA 93.
- 53 BRUDANIN 00 determine the 2ν half-life of ^{48}Ca . Their value is less accurate than BALLYSH 96.
- 54 ARNOLD 99 measure directly the 2ν decay of Zr for the first time, using the NEMO-2 tracking detector and an isotopically enriched source. The lifetime is more accurate than the geochemical result of KAWASHIMA 93.
- 55 ARNOLD 98 measure the 2ν decay of ^{82}Se by comparing the spectra in an enriched and natural selenium source using the NEMO-2 tracking detector. The measured half-life is in agreement, perhaps slightly shorter, than ELLIOTT 92.
- 56 ARNOLD 98 determine the limit for 0ν decay to the ground state of ^{82}Se using the NEMO-2 tracking detector. The half-life limit is in agreement, but less stringent, than ELLIOTT 92.
- 57 ARNOLD 98 determine the limit for 0ν decay to the excited 2^+ state of ^{82}Se using the NEMO-2 tracking detector.
- 58 ALSTON-GARNJOST 97 report evidence for 2ν decay of ^{100}Mo . This decay has been also observed by EJIRI 91, DASSIE 95, and DESILVA 97.
- 59 DESILVA 97 result for 2ν decay of ^{100}Mo is in agreement with ALSTON-GARNJOST 97 and DASSIE 95. This measurement has the smallest errors.
- 60 DESILVA 97 result for 2ν decay of ^{150}Nd is in marginal agreement with ARTEMEV 93. It has smaller errors.
- 61 DESILVA 97 do not explain whether their efficiency for 0ν decay of ^{150}Nd was calculated under the assumption of a $\langle m_\nu \rangle$, $\langle \lambda \rangle$, or $\langle \eta \rangle$ driven decay.
- 62 ARNOLD 96 measure the 2ν decay of ^{116}Cd . This result is in agreement with EJIRI 95, but has smaller errors. Supersedes ARNOLD 95.
- 63 BALLYSH 96 measure the 2ν decay of ^{48}Ca , using a passive source of enriched ^{48}Ca in a TPC.
- 64 TAKAOKA 96 measure the geochemical half-life of ^{130}Te . Their value is in disagreement with the quoted values of BERNATOWICZ 92 and KIRSTEN 83; but agrees with several other unquoted determinations, e.g., MANUEL 91.
- 65 BARABASH 95 cannot distinguish 0ν and 2ν , but it is inferred indirectly that the 0ν mode accounts for less than 0.026% of their event sample. They also note that their result disagrees with the previous experiment by the NEMO group (BLUM 92).
- 66 BERNATOWICZ 92 finds $^{128}\text{Te}/^{130}\text{Te}$ activity ratio from slope of $^{128}\text{Xe}/^{132}\text{Xe}$ vs $^{130}\text{Xe}/^{132}\text{Xe}$ ratios during extraction, and normalizes to lead-dated ages for the ^{130}Te lifetime. The authors state that their results imply that "(a) the double beta decay of ^{128}Te has been firmly established and its half-life has been determined ... without any ambiguity due to trapped Xe interferences ... (b) Theoretical calculations ... underestimate the [long half-lives of ^{128}Te ^{130}Te] by 1 or 2 orders of magnitude, pointing to a real suppression in the 2ν decay rate of these isotopes. (c) Despite [this], most $\beta\beta$ -models predict a ratio of 2ν decay widths ... in fair agreement with observation." Further details of the experiment are given in BERNATOWICZ 93. Our listed half-life has been revised downward from the published value by the authors, on the basis of reevaluated cosmic-ray ^{128}Xe production corrections.
- 67 TURKEVICH 91 observes activity in old U sample. The authors compare their results with theoretical calculations. They state "Using the phase-space factors of Boehm and Vogel (BOEHM 87) leads to matrix element values for the ^{238}U transition in the same range as deduced for ^{130}Te and ^{76}Ge . On the other hand, the latest theoretical estimates (STAUDT 90) give an upper limit that is 10 times lower. This large discrepancy implies either a defect in the calculations or the presence of a faster path than the standard two-neutrino mode in this case." See BOEHM 87 and STAUDT 90.
- 68 Result agrees with direct determination of ELLIOTT 92.
- 69 Inclusive half life inferred from mass spectroscopic determination of abundance of $\beta\beta$ -decay product ^{130}Te in mineral kilaite (NiTeSe). Systematic uncertainty reflects variations in U-Xe gas-retention-age derived from different uranite samples. Agrees with geochemical determination of TAKAOKA 96 and direct measurement of ARNABOLDI 03. Inconsistent with results of KIRSTEN 83 and BERNATOWICZ 92.
- 70 Ratio of inclusive double beta half lives of ^{128}Te and ^{130}Te determined from minerals melonite (NiTe_2) and altaite (PbTe) by means of mass spectroscopic measurement of abundance of $\beta\beta$ -decay products. As gas-retention-age could not be determined the authors use half life of ^{130}Te (LIN 88) to infer the half life of ^{128}Te . No estimate of the systematic uncertainty of this method is given. The directly determined half life ratio agrees with BERNATOWICZ 92. However, the inferred ^{128}Te half life disagrees with KIRSTEN 83 and BERNATOWICZ 92.
- 71 KIRSTEN 83 reports " 2σ " error. References are given to earlier determinations of the ^{130}Te lifetime.

$\langle m_\nu \rangle$, The Effective Weighted Sum of Majorana Neutrino Masses Contributing to Neutrinoless Double- β Decay

$\langle m_\nu \rangle = |\sum U_{ej}^2 m_{\nu_j}|$, where the sum goes from 1 to n and where n = number of neutrino generations, and ν_j is a Majorana neutrino. Note that U_{ej}^2 , not $|U_{ej}|^2$, occurs in the sum. The possibility of cancellations has been stressed. In the following Listings, only best or comparable limits or lifetimes for each isotope are reported.

VALUE (eV)	CL% ISOTOPE	TRANSITION	METHOD	DOCUMENT ID
• • • We do not use the following data for averages, fits, limits, etc. • • •				
< 9.3-60	90 ^{100}Mo	$0^+ \rightarrow 0^+_1$	NEMO-3	72 ARNOLD 07
< 6500	90 ^{100}Mo	$0^+ \rightarrow 2^+$	NEMO-3	73 ARNOLD 07
0.32 ± 0.03	68 ^{76}Ge	0ν	Enriched HP Ge	74 KLAPDOR-K...06A
< 0.2-1.1	90 ^{130}Te		Cryog. det.	75 ARNABOLDI 05
< 0.7-2.8	90 ^{100}Mo	0ν	NEMO-3	76 ARNOLD 05A
< 1.7-4.9	90 ^{82}Se	0ν	NEMO-3	77 ARNOLD 05A
< 0.37-1.9	90 ^{130}Te		Cryog. det.	78 ARNABOLDI 04
< 0.8-1.2	90 ^{100}Mo	0ν	NEMO-3	79 ARNOLD 04
< 1.5-3.1	90 ^{82}Se	0ν	NEMO-3	79 ARNOLD 04
0.1-0.9	99.7 ^{76}Ge		Enriched HP Ge	80 KLAPDOR-K...04A
< 7.2-44.7	90 ^{48}Ca		CaF_2 scint.	81 OGAWA 04
< 1.1-2.6	90 ^{130}Te		Cryog. det.	82 ARNABOLDI 03
< 1.5-1.7	90 ^{116}Cd	0ν	$^{116}\text{CdWO}_4$ scint.	83 DANEVICH 03

< 0.33–1.35	90		Enriched HP Ge	⁸⁴ AALSETH	02B
< 2.9	90	¹³⁶ Xe	Liquid Xe Scint.	⁸⁵ BERNABEI	02D
$0.39^{+0.17}_{-0.28}$	76	Ge	Enriched HP Ge	⁸⁶ KLAPDOR-K...	02D
< 2.1–4.8	90	¹⁰⁰ Mo	ELEGANT V	⁸⁷ EJIRI	01
< 0.35	90	⁷⁶ Ge	Enriched HP Ge	⁸⁸ KLAPDOR-K...	01
< 23	90	⁹⁶ Zr	NEMO-2	⁸⁹ ARNOLD	99
< 1.1–1.5		¹²⁸ Te	Geochem	⁹⁰ BERNATOW...	92
< 5	68	⁸² Se	TPC	⁹¹ ELLIOTT	92
< 8.3	76	⁴⁸ Ca	CaF ₂ scint.	YOU	91

⁷²ARNOLD 07 use NEMO-3 half life limit for 0ν -decay of ¹⁰⁰Mo to the first excited 0^+_{1-} state of daughter nucleus to obtain neutrino mass limit. The spread reflects the choice of two different nuclear matrix elements. This limit is not competitive when compared to the decay to the ground state.

⁷³ARNOLD 07 use NEMO-3 half life limit for 0ν -decay of ¹⁰⁰Mo to the first excited 2^+_{1-} state of daughter nucleus to obtain neutrino mass limit. This limit is not competitive when compared to the decay to the ground state.

⁷⁴Re-analysis of data originally published in KLAPDOR-KLEINGROTHAUS 04A. Modified pulse shape analysis leads the authors to claim 6σ statistical evidence for observation of 0ν -decay. Authors use matrix element of STAUDT 90. Uncertainty of nuclear matrix element is not reflected in stated error. Supersedes KLAPDOR-KLEINGROTHAUS 04A.

⁷⁵Supersedes ARNABOLDI 04. Reported range of limits due to use of different nuclear matrix calculations.

⁷⁶Mass limits reported in ARNOLD 05A are derived from ¹⁰⁰Mo data, obtained by the NEMO-3 collaboration. The range reflects the spread of matrix element calculations considered in this work. Supersedes ARNOLD 04.

⁷⁷Neutrino mass limits based on ⁸²Se data utilizing the NEMO-3 detector. The range reported in ARNOLD 05A reflects the spread of matrix element calculations considered in this work. Supersedes ARNOLD 04.

⁷⁸Supersedes ARNABOLDI 03. Reported range of limits due to use of different nuclear matrix element calculations.

⁷⁹ARNOLD 04 limit is based on the nuclear matrix elements of SIMKOVIC 99, STOICA 01 and CIVITARESE 03.

⁸⁰Supersedes KLAPDOR-KLEINGROTHAUS 02D. Event excess at $\beta\beta$ -decay energy is used to derive Majorana neutrino mass using the nuclear matrix elements of STAUDT 90. The mass range shown is based on the authors evaluation of the uncertainties of the STAUDT 90 matrix element calculation. If this uncertainty is neglected, and only statistical errors are considered, the range in $\langle m_{\nu} \rangle$ becomes (0.2–0.6) eV at the 3σ level.

⁸¹Calorimetric CaF₂ scintillator. Range of limits reflects authors' estimate of the uncertainty of the nuclear matrix elements. Replaces YOU 91 as the most stringent limit based on ⁴⁸Ca.

⁸²Supersedes ALESSANDRELLO 00. Cryogenic calorimeter search. Reported a range reflecting uncertainty in nuclear matrix element calculations.

⁸³Limit for $\langle m_{\nu} \rangle$ is based on the nuclear matrix elements of STAUDT 90 and ARNOLD 96. Supersedes DANEVICH 00.

⁸⁴AALSETH 02B reported range of limits on $\langle m_{\nu} \rangle$ reflects the spread of theoretical nuclear matrix elements. Excludes part of allowed mass range reported in KLAPDOR-KLEINGROTHAUS 01B.

⁸⁵BERNABEI 02D limit is based on the matrix elements of SIMKOVIC 02. The range of neutrino masses based on a variety of matrix elements is 1.1–2.9 eV.

⁸⁶KLAPDOR-KLEINGROTHAUS 02D is a detailed description of the analysis of the data collected by the Heidelberg-Moscow experiment, previously presented in KLAPDOR-KLEINGROTHAUS 01B. Matrix elements in STAUDT 90 have been used. See the footnote in the preceding table for further details. See also KLAPDOR-KLEINGROTHAUS 02B.

⁸⁷The range of the reported $\langle m_{\nu} \rangle$ values reflects the spread of the nuclear matrix elements. On axis value assuming $\langle \lambda \rangle = \langle \eta \rangle = 0$.

⁸⁸KLAPDOR-KLEINGROTHAUS 01 uses the calculation by STAUDT 90. Using several other models in the literature could worsen the limit up to 1.2 eV. This is the most stringent experimental bound on m_{ν} . It supersedes BAUDIS 99B.

⁸⁹ARNOLD 99 limit based on the nuclear matrix elements of STAUDT 90.

⁹⁰BERNATOWICZ 92 finds these majorana neutrino mass limits assuming that the measured geochemical decay width is a limit on the 0ν decay width. The range is the range found using matrix elements from HAXTON 84, TOMODA 87, and SUHONEN 91. Further details of the experiment are given in BERNATOWICZ 93.

⁹¹ELLIOTT 92 uses the matrix elements of HAXTON 84.

Limits on Lepton-Number Violating ($V+A$) Current Admixture

For reasons given in the discussion at the beginning of this section, we list only results from 1989 and later. $\langle \lambda \rangle = \lambda \sum U_{ej} V_{ej}$ and $\langle \eta \rangle = \eta \sum U_{ej} V_{ej}$, where the sum is over the number of neutrino generations. This sum vanishes for massless or unmixed neutrinos. In the following Listings, only best or comparable limits or lifetimes for each isotope are reported.

$\langle \lambda \rangle$ (10^{-6})	CL%	$\langle \eta \rangle$ (10^{-8})	CL%	ISOTOPE	METHOD	DOCUMENT ID
< 120	90			¹⁰⁰ Mo	$0^+ \rightarrow 2^+$	⁹² ARNOLD 07
$0.692^{+0.058}_{-0.056}$	68	$0.305^{+0.026}_{-0.025}$	68	⁷⁶ Ge	Enriched HP Ge	⁹³ KLAPDOR-K...06A
< 2.5	90			¹⁰⁰ Mo	0ν , NEMO-3	⁹⁴ ARNOLD 05A
< 3.8	90			⁸² Se	0ν , NEMO-3	⁹⁵ ARNOLD 05A
< 1.5–2.0	90			¹⁰⁰ Mo	0ν , NEMO-3	⁹⁶ ARNOLD 04
< 3.2–3.8	90			⁸² Se	0ν , NEMO-3	⁹⁷ ARNOLD 04

• • • We do not use the following data for averages, fits, limits, etc. • • •

< 1.6–2.4	90	< 0.9–5.3	90	¹³⁰ Te	Cryog. det.	⁹⁸ ARNABOLDI	03
< 2.2	90	< 2.5	90	¹¹⁶ Cd	¹¹⁶ CdWO ₄ scint.	⁹⁹ DANEVICH	03
< 3.2–4.7	90	< 2.4–2.7	90	¹⁰⁰ Mo	ELEGANT V	¹⁰⁰ EJIRI	01
< 1.1	90	< 0.64	90	⁷⁶ Ge	Enriched HP Ge	¹⁰¹ GUENTHER	97
< 4.4	90	< 2.3	90	¹³⁶ Xe	TPC	¹⁰² VUILLEUMIER	93
		< 5.3		¹²⁸ Te	Geochem	¹⁰³ BERNATOW...	92

⁹²ARNOLD 07 use NEMO-3 half life limit for 0ν -decay of ¹⁰⁰Mo to the first excited 2^+_{1-} state of daughter nucleus to limit the right-right handed admixture of weak currents $\langle \lambda \rangle$. This limit is not competitive when compared to the decay to the ground state.

⁹³Re-analysis of data originally published in KLAPDOR-KLEINGROTHAUS 04A. Modified pulse shape analysis leads the authors to claim 6σ statistical evidence for observation of 0ν -decay. Authors use matrix element of STAUDT 90 to determine $\langle \lambda \rangle$ and $\langle \eta \rangle$. Uncertainty of nuclear matrix element is not reflected in stated errors.

⁹⁴ARNOLD 05A derive limit for $\langle \lambda \rangle$ based on ¹⁰⁰Mo data collected with NEMO-3 detector. No limit for $\langle \eta \rangle$ is given. Supersedes ARNOLD 04.

⁹⁵ARNOLD 05A derive limit for $\langle \lambda \rangle$ based on ⁸²Se data collected with NEMO-3 detector. No limit for $\langle \eta \rangle$ is given. Supersedes ARNOLD 04.

⁹⁶ARNOLD 04 use the matrix elements of SUHONEN 94 to obtain a limit for $\langle \lambda \rangle$, no limit for $\langle \eta \rangle$ is given. This limit is more stringent than the limit in EJIRI 01 for the same nucleus.

⁹⁷ARNOLD 04 use the matrix elements of TOMODA 91 and SUHONEN 91 to obtain a limit for $\langle \lambda \rangle$, no limit for $\langle \eta \rangle$ is given.

⁹⁸Supersedes ALESSANDRELLO 00. Cryogenic calorimeter search. Reported a range reflecting uncertainty in nuclear matrix element calculations.

⁹⁹Limits for $\langle \lambda \rangle$ and $\langle \eta \rangle$ are based on nuclear matrix elements of STAUDT 90. Supersedes DANEVICH 00.

¹⁰⁰The range of the reported $\langle \lambda \rangle$ and $\langle \eta \rangle$ values reflects the spread of the nuclear matrix elements. On axis value assuming $\langle m_{\nu} \rangle = 0$ and $\langle \lambda \rangle = \langle \eta \rangle = 0$, respectively.

¹⁰¹GUENTHER 97 limits use the matrix elements of STAUDT 90. Supersedes BALYSH 95 and BALYSH 92.

¹⁰²VUILLEUMIER 93 uses the matrix elements of MUTO 89. Based on a half-life limit 2.6×10^{23} y at 90%CL.

¹⁰³BERNATOWICZ 92 takes the measured geochemical decay width as a limit on the 0ν width, and uses the SUHONEN 91 coefficients to obtain the least restrictive limit on η . Further details of the experiment are given in BERNATOWICZ 93.

Double- β Decay REFERENCES

BELLI	08	PL B658 193	P. Belli et al.	(INFN Gran Sasso)
ARNOLD	07	NP A781 209	R. Arnold et al.	(NEMO-3 Collab.)
BARABASH	07	NP A785 371	A.S. Barabash et al.	
BARABASH	07B	JPG 34 1721	A.S. Barabash et al.	
BLOXHAM	07	PR C76 025501	T. Bloxham et al.	(COBRA Collab.)
GROMOV	06	PNPL 3 157	K. Gromov et al.	
KLAPDOR-K...	06A	MPL A21 1547	H.V. Klapdor-Kleingrothaus, I.V. Krivosheina	
ARNABOLDI	05A	PRL 95 142501	C. Arnaboldi et al.	(CUORICINO Collab.)
ARNOLD	05A	PRL 95 162302	R. Arnold et al.	(NEMO-3 Collab.)
AALSETH	04	PR D70 078302	C.E. Aalseth et al.	
ARNABOLDI	04	PL B584 260	C. Arnaboldi et al.	
ARNOLD	04	JETPL 80 377	R. Arnold et al.	(NEMO3 Detector Collab.)
Translated from ZETFP 80 429.				
BARABASH	04	JETPL 79 110	A.S. Barabash et al.	
KLAPDOR-K...	04A	PL B586 198	H.V. Klapdor-Kleingrothaus et al.	
KLAPDOR-K...	04B	PR D70 078301	H.V. Klapdor-Kleingrothaus, A. Dietz, I.V. Krivosheina	
KLAPDOR-K...	04C	NIM A522 371	H.V. Klapdor-Kleingrothaus et al.	
OGAWA	04	NP A730 215	I. Ogawa et al.	
ARNABOLDI	03	PL B557 167	C. Arnaboldi et al.	
CIVITARESE	03	NP A729 867	O. Civitarese, J. Suhonen	
DANEVICH	03	PR C68 035501	F.A. Danevich et al.	
DOERR	03	NIM A513 596	C. Doerr, H.V. Klapdor-Kleingrothaus	
AALSETH	02	MPL A17 1475	C.E. Aalseth et al.	
AALSETH	02B	NP A694 269	C.E. Aalseth et al.	(IGEX Collab.)
BERNABEI	02D	PL B546 23	R. Bernabei et al.	(DAMA Collab.)
KLAPDOR-K...	02	hep-ph/0205228	H.V. Klapdor-Kleingrothaus	
KLAPDOR-K...	02B	PNPL 110 57	H.V. Klapdor-Kleingrothaus, A. Dietz, I.V. Krivosheina	
KLAPDOR-K...	02D	FP 32 1181	H.V. Klapdor-Kleingrothaus, A. Dietz, I.V. Krivosheina	
SIMKOVIC	02	hep-ph/0204278	F. Simkovic, P. Domin, A. Faessler	
ASHITKOV	01	JETPL 74 529	V.D. Ashitkov et al.	
Translated from ZETFP 74 601.				
DANEVICH	01	NP A694 375	F.A. Danevich et al.	
DEBRAECKEL...	01	PRL 86 3510	L. De Braeckeleer et al.	
EJIRI	01	PR C63 065501	H. Ejiri et al.	
KLAPDOR-K...	01	EPJ A12 147	H.V. Klapdor-Kleingrothaus et al.	
KLAPDOR-K...	01B	MPL A16 2409	H.V. Klapdor-Kleingrothaus et al.	
STOICA	01	NP A694 269	S. Stoica, H.V. Klapdor-Kleingrothaus	
WIESSER	01	PR C64 024308	M.E. Wieser, J.R. De Laeter	
ALESSAND...	00	PL B486 13	A. Alessandrello et al.	
BRUDANIN	00	PL B495 63	V.B. Brudanin et al.	
DANEVICH	00	PR C62 045501	F.A. Danevich et al.	
ARNOLD	99	NP A658 299	R. Arnold et al.	(NEMO Collab.)
BAUDIS	99	PR D59 022001	L. Baudis et al.	(Heidelberg-Moscow Collab.)
BAUDIS	99B	PRL 83 41	L. Baudis et al.	(Heidelberg-Moscow Collab.)
SIMKOVIC	99	PR C60 055502	F. Simkovic et al.	
ARNOLD	98	NP A636 209	R. Arnold et al.	(NEMO-2 Collab.)
ALSTON...	97	PR C55 474	M. Alston-Garnjost et al.	(LBL, ITHO-)
DESILVA	97	PR C56 2451	A. de Silva et al.	(UCI)
GUENTHER	97	PR D55 54	M. Gunther et al.	(Heidelberg-Moscow Collab.)
ARNOLD	96	ZPHY C72 239	R. Arnold et al.	(BCEAN, CAEN, JINR+)
BALYSH	96	PRL 77 5186	A. Balysh et al.	(KIAE, UCI, CIT)
EJIRI	96	NP A611 85	H. Ejiri et al.	(OSAK)
TAKAOKA	96	PR C53 1557	N. Takaoka, Y. Motomura, K. Nagao	(KYUSHU, OKAY)
ARNOLD	95	JETPL 61 170	R.G. Arnold et al.	(NEMO Collab.)
Translated from ZETFP 61 168.				
BALYSH	95	PL B356 450	A. Balysh et al.	(Heidelberg-Moscow Collab.)
BARABASH	95	PL B345 408	A.S. Barabash et al.	(ITEP, SCUC, PNL+)
DASSIE	95	PR D51 2090	D. Dassié et al.	(NEMO Collab.)
EJIRI	95	PSJ J 64 339	H. Ejiri et al.	(OSAK, KIEV)
KOBAYASHI	95	NP A586 457	M. Kobayashi, M. Kobayashi	(KEK, SAGA)
SUHONEN	94	PR C49 3055	J. Suhonen, O. Civitarese	
ARTEMEV	93	JETPL 58 262	V.A. Artemiev et al.	(ITEP, INRM)
Translated from ZETFP 58 256.				

Lepton Particle Listings

Double- β Decay, Neutrino Mixing

BERNATOW...	93	PR C47 806	T. Bernatowicz <i>et al.</i>	(WUSL, TATA)
KAWASHIMA	93	PR C47 R2452	A. Kawashima, K. Takahashi, A. Masuda	(TOKYU C+)
VUILLEUMIER	93	PR D48 1009	J.C. Vuilleumier <i>et al.</i>	(NEUC, CIT, VILL)
BALYSH	92	PL B283 32	A. Balysh <i>et al.</i>	(MPIH, KIAE, SASSO)
BERNATOW...	92	PRL 69 2341	T. Bernatowicz <i>et al.</i>	(WUSL, TATA)
BLUM	92	PL B275 506	D. Blum <i>et al.</i>	(NEMO Collab.)
ELLIOTT	92	PR C46 1535	S.R. Elliott <i>et al.</i>	(UCI)
EJRI	91	PL B250 17	H. Ejri <i>et al.</i>	(OSAK)
MANUEL	91	JPG 17 5221	O.K. Manuel	(MISSR)
SUHONEN	91	NP A535 509	J. Suhonen, S.B. Khadkikar, A. Faessler	(WUSL, TATA)
TOMODA	91	RPP 54 53	T. Tomoda	(JYV+)
TURKEVICH	91	PRL 67 3211	A. Turkevich, T.E. Economou, G.A. Cowan	(CHIC+)
YOU	91	PL B265 53	K. You <i>et al.</i>	(BHEP, CAST+)
STAUDT	90	EPL 13 31	A. Staudt, K. Muto, H.V. Klapdor-Kleingrothaus	
MUTO	89	ZPHY A334 187	K. Muto, E. Bender, H.V. Klapdor	(TINT, MPIH)
LIN	88	NP A481 477	W.J. Lin <i>et al.</i>	
LIN	88B	NP A481 484	W.J. Lin <i>et al.</i>	
BOEHM	87	Massive Neutrinos	F. Bohm, P. Vogel	(CIT)
Cambridge Univ. Press, Cambridge				
TOMODA	87	PL B199 475	T. Tomoda, A. Faessler	(TUBIN)
HAXTON	84	PPNP 12 409	W.C. Haxton, G.J. Stevenson	
KIRSTEN	83	PRL 50 474	T. Kirsten, H. Richter, E. Jessberger	(MPIH)

Neutrino Mixing

With the exception of the LSND anomaly, current neutrino data can be described within the framework of a 3×3 mixing matrix between the flavor eigenstates ν_e , ν_μ , and ν_τ and the mass eigenstates ν_1 , ν_2 , and ν_3 . (See Eq. (13.30) of the Review "Neutrino Mass, Mixing and Flavor Change" by B. Kayser.) The Listings are divided into the following sections:

(A) Neutrino fluxes and event ratios: shows measurements which correspond to various oscillation tests for Accelerator, Reactor, Atmospheric, and Solar neutrino experiments. Typically ratios involve a measurement in a realm sensitive to oscillations compared to one for which no oscillation effect is expected.

(B) Three neutrino mixing parameters: shows measurements of $\sin^2(2\theta_{12})$, $\sin^2(2\theta_{23})$, Δm_{21}^2 , Δm_{32}^2 , and limits for $\sin^2(2\theta_{13})$ which are all interpretations of data based on the three neutrino mixing scheme described in the review "Neutrino Mass, Mixing and Flavor Change."

(C) Other neutrino mixing results: shows measurements and limits for the probability of oscillation for experiments which might be relevant to the LSND oscillation claim. Included are experiments which are sensitive to $\nu_\mu \rightarrow \nu_e$, $\bar{\nu}_\mu \rightarrow \bar{\nu}_e$, sterile neutrinos, and CPT tests.

(A) Neutrino fluxes and event ratios

Events (observed/expected) from accelerator ν_μ experiments.

Some neutrino oscillation experiments compare the flux in two or more detectors. This is usually quoted as the ratio of the event rate in the far detector to the expected rate based on an extrapolation from the near detector in the absence of oscillations.

VALUE	DOCUMENT ID	TECN	COMMENT
0.71 ± 0.08	1 AHN	06A K2K	K2K to Super-K
0.64 ± 0.05	2 MICHAEL	06 MINS	All charged current events
0.71 $^{+0.08}_{-0.09}$	3 ALIU	05 K2K	KEK to Super-K
0.70 $^{+0.10}_{-0.11}$	4 AHN	03 K2K	KEK to Super-K

¹ Based on the observation of 112 events when $158.1^{+9.2}_{-8.6}$ were expected without oscillations. Including not only the number of events but also the shape of the energy distribution, the evidence for oscillation is at the level of about 4.3σ . Supersedes ALIU 05.

² This ratio is based on the observation of 215 events compared to an expectation of 336 ± 14 without oscillations.

³ This ratio is based on the observation of 107 events at the far detector 250 km away from KEK, and an expectation of 151^{+12}_{-10} .

⁴ This ratio is based on the observation of 56 events with an expectation of $80.1^{+6.2}_{-5.4}$.

Events (observed/expected) from reactor $\bar{\nu}_e$ experiments.

The quoted values are the ratios of the measured reactor $\bar{\nu}_e$ event rate at the quoted distances, and the rate expected without oscillations. The expected rate is based on the experimental data for the most significant reactor fuels (^{235}U , ^{239}Pu , ^{241}Pu) and on calculations for ^{238}U .

VALUE	DOCUMENT ID	TECN	COMMENT
0.658 ± 0.044 ± 0.047	⁵ ARAKI	05 KLND	Japanese react. ~ 180 km
0.611 ± 0.085 ± 0.041	⁶ EGUCHI	03 KLND	Japanese react. ~ 180 km
1.01 ± 0.024 ± 0.053	⁷ BOEHM	01	Palo Verde react. 0.75–0.89 km
1.01 ± 0.028 ± 0.027	⁸ APOLLONIO	99 CHOZ	Chooz reactors 1 km
0.987 ± 0.006 ± 0.037	⁹ GREENWOOD	96	Savannah River, 18.2 m
0.988 ± 0.004 ± 0.05	ACHKAR	95 CNTR	Bugey reactor, 15 m
0.994 ± 0.010 ± 0.05	ACHKAR	95 CNTR	Bugey reactor, 40 m
0.915 ± 0.132 ± 0.05	ACHKAR	95 CNTR	Bugey reactor, 95 m
0.987 ± 0.014 ± 0.027	¹⁰ DECLAIS	94 CNTR	Bugey reactor, 15 m
0.985 ± 0.018 ± 0.034	KUVSHINN...	91 CNTR	Rovno reactor
1.05 ± 0.02 ± 0.05	VUILLEUMIER	82	Gösgen reactor
0.955 ± 0.035 ± 0.110	¹¹ KWON	81	$\bar{\nu}_e p \rightarrow e^+ n$
0.89 ± 0.15	¹¹ BOEHM	80	$\bar{\nu}_e p \rightarrow e^+ n$

⁵ Updated result of KamLAND, including the data used in EGUCHI 03. Note that the survival probabilities for different periods are not directly comparable because the effective baseline varies with power output of the reactor sources involved, and there were large variations in the reactor power production in Japan in 2003.

⁶ EGUCHI 03 observe reactor neutrino disappearance at ~ 180 km baseline to various Japanese nuclear power reactors.

⁷ BOEHM 01 search for neutrino oscillations at 0.75 and 0.89 km distance from the Palo Verde reactors.

⁸ APOLLONIO 99, APOLLONIO 98 search for neutrino oscillations at 1.1 km fixed distance from Chooz reactors. They use $\bar{\nu}_e p \rightarrow e^+ n$ in Gd-loaded scintillator target. APOLLONIO 99 supersedes APOLLONIO 98. See also APOLLONIO 03 for detailed description.

⁹ GREENWOOD 96 search for neutrino oscillations at 18 m and 24 m from the reactor at Savannah River.

¹⁰ DECLAIS 94 result based on integral measurement of neutrons only. Result is ratio of measured cross section to that expected in standard V-A theory. Replaced by ACHKAR 95.

¹¹ KWON 81 represents an analysis of a larger set of data from the same experiment as BOEHM 80.

Atmospheric neutrinos

Neutrinos and antineutrinos produced in the atmosphere induce μ -like and e -like events in underground detectors. The ratio of the numbers of the two kinds of events is defined as μ/e . It has the advantage that systematic effects, such as flux uncertainty, tend to cancel, for both experimental and theoretical values of the ratio. The "ratio of the ratios" of experimental to theoretical μ/e , $R(\mu/e)$, or that of experimental to theoretical μ/total , $R(\mu/\text{total})$ with $\text{total} = \mu + e$, is reported below. If the actual value is not unity, the value obtained in a given experiment may depend on the experimental conditions. In addition, the measured "up-down asymmetry" for μ ($N_{up}(\mu)/N_{down}(\mu)$) or e ($N_{up}(e)/N_{down}(e)$) is reported. The expected "up-down asymmetry" is nearly unity if there is no neutrino oscillation.

$R(\mu/e) = (\text{Measured Ratio } \mu/e) / (\text{Expected Ratio } \mu/e)$

VALUE	DOCUMENT ID	TECN	COMMENT
0.658 ± 0.016 ± 0.035	¹² ASHIE	05 SKAM	sub-GeV
0.702 $^{+0.032}_{-0.030}$ ± 0.101	¹³ ASHIE	05 SKAM	multi-GeV
0.69 ± 0.10 ± 0.06	¹⁴ SANCHEZ	03 SOU2	Calorimeter raw data
1.00 ± 0.15 ± 0.08	¹⁵ FUKUDA	96B KAMI	Water Cherenkov
0.60 $^{+0.06}_{-0.05}$ ± 0.05	¹⁶ DAUM	95 FREJ	Calorimeter
0.60 $^{+0.06}_{-0.05}$ ± 0.05	¹⁷ FUKUDA	94 KAMI	sub-GeV
0.57 $^{+0.08}_{-0.07}$ ± 0.07	¹⁸ FUKUDA	94 KAMI	multi-GeV
	¹⁹ BECKER-SZ...	92B IMB	Water Cherenkov

¹² ASHIE 05 results are based on an exposure of 92 kton yr during the complete Super-Kamiokande I running period. The analyzed data sample consists of fully-contained single-ring e -like events with $0.1 \text{ GeV}/c < p_e$ and μ -like events $0.2 \text{ GeV}/c < p_\mu$, both having a visible energy $< 1.33 \text{ GeV}$. These criteria match the definition used by FUKUDA 94.

¹³ ASHIE 05 results are based on an exposure of 92 kton yr during the complete Super-Kamiokande I running period. The analyzed data sample consists of fully-contained single-ring events with visible energy $> 1.33 \text{ GeV}$ and partially-contained events. All partially-contained events are classified as μ -like.

¹⁴ SANCHEZ 03 result is based on an exposure of 5.9 kton yr, and updates ALLISON 99 result. The analyzed data sample consists of fully-contained e -flavor and μ -flavor events having lepton momentum $> 0.3 \text{ GeV}/c$.

¹⁵ FUKUDA 96b studied neutron background in the atmospheric neutrino sample observed in the Kamiokande detector. No evidence for the background contamination was found.

¹⁶ DAUM 95 results are based on an exposure of 2.0 kton yr which includes the data used by BERGER 90b. This ratio is for the contained and semicontained events. DAUM 95

also report $R(\mu/e) = 0.99 \pm 0.13 \pm 0.08$ for the total neutrino induced data sample which includes upward going stopping muons and horizontal muons in addition to the contained and semicontained events.

17 FUKUDA 94 result is based on an exposure of 7.7 kton yr and updates the HIRATA 92 result. The analyzed data sample consists of fully-contained e -like events with $0.1 < p_e < 1.33$ GeV/c and fully-contained μ -like events with $0.2 < p_\mu < 1.5$ GeV/c.

18 FUKUDA 94 analyzed the data sample consisting of fully contained events with visible energy > 1.33 GeV and partially contained μ -like events.

19 BECKER-SZENDY 92B reports the fraction of nonshowering events (mostly muons from atmospheric neutrinos) as $0.36 \pm 0.02 \pm 0.02$, as compared with expected fraction $0.51 \pm 0.01 \pm 0.05$. After cutting the energy range to the Kamiokande limits, BEIER 92 finds $R(\mu/e)$ very close to the Kamiokande value.

$R(\nu_\mu) = (\text{Measured Flux of } \nu_\mu) / (\text{Expected Flux of } \nu_\mu)$

VALUE	DOCUMENT ID	TECN	COMMENT
• • • We do not use the following data for averages, fits, limits, etc. • • •			
0.84 ± 0.12	20 ADAMSON	06 MINS	MINOS atmospheric
$0.72 \pm 0.026 \pm 0.13$	21 AMBROSIO	01 MCRO	upward through-going
$0.57 \pm 0.05 \pm 0.15$	22 AMBROSIO	00 MCRO	upgoing partially contained
$0.71 \pm 0.05 \pm 0.19$	23 AMBROSIO	00 MCRO	downgoing partially contained + upgoing stopping
$0.74 \pm 0.036 \pm 0.046$	24 AMBROSIO	98 MCRO	Streamer tubes
	25 CASPER	91 IMB	Water Cherenkov
	26 AGLIETTA	89 NUSX	
0.95 ± 0.22	27 BOLIEV	81	Baksan
0.62 ± 0.17	CROUCH	78	Case Western /UCI

20 ADAMSON 06 uses a measurement of 107 total neutrinos compared to an expected rate of 127 \pm 13 without oscillations.

21 AMBROSIO 01 result is based on the upward through-going muon tracks with $E_\mu > 1$ GeV. The data came from three different detector configurations, but the statistics is largely dominated by the full detector run, from May 1994 to December 2000. The total live time, normalized to the full detector configuration, is 6.17 years. The first error is the statistical error, the second is the systematic error, dominated by the theoretical error in the predicted flux.

22 AMBROSIO 00 result is based on the upgoing partially contained event sample. It came from 4.1 live years of data taking with the full detector, from April 1994 to February 1999. The average energy of atmospheric muon neutrinos corresponding to this sample is 4 GeV. The first error is statistical, the second is the systematic error, dominated by the 25% theoretical error in the rate (20% in the flux and 15% in the cross section, added in quadrature). Within statistics, the observed deficit is uniform over the zenith angle.

23 AMBROSIO 00 result is based on the combined samples of downgoing partially contained events and upgoing stopping events. These two subsamples could not be distinguished due to the lack of timing information. The result came from 4.1 live years of data taking with the full detector, from April 1994 to February 1999. The average energy of atmospheric muon neutrinos corresponding to this sample is 4 GeV. The first error is statistical, the second is the systematic error, dominated by the 25% theoretical error in the rate (20% in the flux and 15% in the cross section, added in quadrature). Within statistics, the observed deficit is uniform over the zenith angle.

24 AMBROSIO 98 result is for all nadir angles and updates AHLEN 95 result. The lower cutoff on the muon energy is 1 GeV. In addition to the statistical and systematic errors, there is a Monte Carlo flux error (theoretical error) of ± 0.13 . With a neutrino oscillation hypothesis, the fit either to the flux or zenith distribution independently yields $\sin^2 2\theta = 1.0$ and $\Delta(m^2) \sim$ a few times 10^{-3} eV². However, the fit to the observed zenith distribution gives a maximum probability for χ^2 of only 5% for the best oscillation hypothesis.

25 CASPER 91 correlates showering/nonshowering signature of single-ring events with parent atmospheric-neutrino flavor. They find nonshowering ($\approx \nu_\mu$ induced) fraction is $0.41 \pm 0.03 \pm 0.02$, as compared with expected 0.51 ± 0.05 (syst).

26 AGLIETTA 89 finds no evidence for any anomaly in the neutrino flux. They define $\rho = (\text{measured number of } \nu_e) / (\text{measured number of } \nu_\mu)$. They report $\rho(\text{measured}) = \rho(\text{expected}) = 0.96 \pm 0.32$.

27 From this data BOLIEV 81 obtain the limit $\Delta(m^2) \leq 6 \times 10^{-3}$ eV² for maximal mixing, $\nu_\mu \leftrightarrow \nu_\mu$ type oscillation.

$R(\mu/\text{total}) = (\text{Measured Ratio } \mu/\text{total}) / (\text{Expected Ratio } \mu/\text{total})$

VALUE	DOCUMENT ID	TECN	COMMENT
• • • We do not use the following data for averages, fits, limits, etc. • • •			
$1.1 \pm 0.07 \pm 0.11$	28 CLARK	97 IMB	multi-GeV

28 CLARK 97 obtained this result by an analysis of fully contained and partially contained events in the IMB water-Cherenkov detector with visible energy > 0.95 GeV.

$N_{\text{up}}(\mu) / N_{\text{down}}(\mu)$

VALUE	DOCUMENT ID	TECN	COMMENT
• • • We do not use the following data for averages, fits, limits, etc. • • •			
$0.551 \pm 0.035 \pm 0.004$	29 ASHIE	05 SKAM	multi-GeV

29 ASHIE 05 results are based on an exposure of 92 kton yr during the complete Super-Kamiokande I running period. The analyzed data sample consists of fully-contained single-ring μ -like events with visible energy > 1.33 GeV and partially-contained events. All partially-contained events are classified as μ -like. Upward-going events are those with $-1 < \cos(\text{zenith angle}) < -0.2$ and downward-going events are those with $0.2 < \cos(\text{zenith angle}) < 1$. The μ -like up-down ratio for the multi-GeV data deviates from 1 (the expectation for no atmospheric ν_μ oscillations) by more than 12 standard deviations.

$N_{\text{up}}(e) / N_{\text{down}}(e)$

VALUE	DOCUMENT ID	TECN	COMMENT
• • • We do not use the following data for averages, fits, limits, etc. • • •			
$0.961 \pm 0.086 \pm 0.016$	30 ASHIE	05 SKAM	multi-GeV

30 ASHIE 05 results are based on an exposure of 92 kton yr during the complete Super-Kamiokande I running period. The analyzed data sample consists of fully-contained single-ring e -like events with visible energy > 1.33 GeV. Upward-going events are those with $-1 < \cos(\text{zenith angle}) < -0.2$ and downward-going events are those with $0.2 < \cos(\text{zenith angle}) < 1$. The e -like up-down ratio for the multi-GeV data is consistent with 1 (the expectation for no atmospheric ν_e oscillations).

$R(\text{up/down}; \mu) = (\text{Measured up/down}; \mu) / (\text{Expected up/down}; \mu)$

VALUE	DOCUMENT ID	TECN	COMMENT
• • • We do not use the following data for averages, fits, limits, etc. • • •			
$0.62 \pm 0.19 \pm 0.02$	31 ADAMSON	06 MINS	atmospheric ν with far detector

31 ADAMSON 06 result is obtained with the MINOS far detector with an exposure of 4.54 kton yr. The expected ratio is calculated with no neutrino oscillation.

$R(\mu^+ / \mu^-) = (\text{Measured } N(\mu^+) / N(\mu^-)) / (\text{Expected } N(\mu^+) / N(\mu^-))$

VALUE	DOCUMENT ID	TECN	COMMENT
• • • We do not use the following data for averages, fits, limits, etc. • • •			
$1.39 \pm 0.35 \pm 0.08$	32 ADAMSON	07 MINS	Upward and horizontal μ with far detector
$0.96 \pm 0.38 \pm 0.15$	33 ADAMSON	06 MINS	atmospheric ν with far detector

32 ADAMSON 07 result is obtained with the MINOS far detector in 854.24 live days, based on neutrino-induced upward-going and horizontal muons. This result is consistent with CPT conservation.

33 ADAMSON 06 result is obtained with the MINOS far detector with an exposure of 4.54 kton yr, based on contained events. The expected ratio is calculated by assuming the same oscillation parameters for neutrinos and antineutrinos.

Solar neutrinos

Solar neutrinos are produced by thermonuclear fusion reactions in the Sun. Radiochemical experiments measure particular combinations of fluxes from various neutrino-producing reactions, whereas water-Cherenkov experiments mainly measure a flux of neutrinos from decay of ⁸B. Solar neutrino fluxes are composed of all active neutrino species, ν_e , ν_μ , and ν_τ . In addition, some other mechanisms may cause antineutrino components in solar neutrino fluxes. Each measurement method is sensitive to a particular component or a combination of components of solar neutrino fluxes. For details, see the following minireview.

SOLAR NEUTRINOS REVIEW

Revised December 2007 by K. Nakamura (KEK, High Energy Accelerator Research Organization, Japan).

1. Introduction

The Sun is a main-sequence star at a stage of stable hydrogen burning. It produces an intense flux of electron neutrinos as a consequence of nuclear fusion reactions whose combined effect is

$$4p \rightarrow {}^4\text{He} + 2e^+ + 2\nu_e. \quad (1)$$

Positrons annihilate with electrons. Therefore, when considering the solar thermal energy generation, a relevant expression is

$$4p + 2e^- \rightarrow {}^4\text{He} + 2\nu_e + 26.73 \text{ MeV} - E_\nu, \quad (2)$$

where E_ν represents the energy taken away by neutrinos, with an average value being $\langle E_\nu \rangle \sim 0.6$ MeV. The neutrino-producing reactions which are at work inside the Sun are enumerated in the first column in Table 1. The second column in Table 1 shows abbreviation of these reactions. The energy spectrum of each reaction is shown in Fig. 1.

Observation of solar neutrinos directly addresses the theory of stellar structure and evolution, which is the basis of the

Lepton Particle Listings

Neutrino Mixing

standard solar model (SSM). The Sun as a well-defined neutrino source also provides extremely important opportunities to investigate nontrivial neutrino properties such as nonzero mass and mixing, because of the wide range of matter density and the great distance from the Sun to the Earth.

A pioneering solar neutrino experiment by Davis and collaborators using ^{37}Cl started in the late 1960's. From the very beginning of the solar-neutrino observation [1], it was recognized that the observed flux was significantly smaller than the SSM prediction, provided nothing happens to the electron neutrinos after they are created in the solar interior. This deficit has been called "the solar-neutrino problem."

In spite of the challenges by the chlorine and gallium radiochemical experiments (GALLEX, SAGE, and GNO) and water-Cherenkov experiments (Kamiokande and Super-Kamiokande), the solar-neutrino problem had persisted for more than 30 years. However, there have been remarkable developments in the past seven years. Thanks to the achievements of a heavy water Cherenkov experiment SNO and a reactor long baseline neutrino oscillation experiment KamLAND, the solar-neutrino problem has been finally solved.

In 2001, the initial result from SNO [2] on the solar-neutrino flux measured via charged-current (CC) reaction, $\nu_e d \rightarrow e^- pp$, combined with the Super-Kamiokande's high-statistics flux measurement via νe elastic scattering [3], provided direct evidence for flavor conversion of solar neutrinos [2]. Later in 2002, SNO's measurement of the neutral-current (NC) rate, $\nu d \rightarrow \nu pn$, and the updated CC result further strengthened this conclusion [4].

The most probable explanation which can also solve the solar-neutrino problem is neutrino oscillation. At this stage, the LMA (large mixing angle) solution was the most promising. However, at 3σ confidence level (CL), LOW (low probability or low mass) and/or VAC (vacuum) solutions were allowed depending on the method of analysis [5]. LMA and LOW are solutions of neutrino oscillation in matter [6,7] and VAC is a solution of neutrino oscillation in vacuum. Typical parameter values [5] corresponding to these solutions are

- LMA: $\Delta m^2 = 5.0 \times 10^{-5} \text{ eV}^2$, $\tan^2 \theta = 0.42$
- LOW: $\Delta m^2 = 7.9 \times 10^{-8} \text{ eV}^2$, $\tan^2 \theta = 0.61$
- VAC: $\Delta m^2 = 4.6 \times 10^{-10} \text{ eV}^2$, $\tan^2 \theta = 1.8$.

It should be noted that all these solutions have large mixing angles. SMA (small mixing angle) solution (typical parameter values [5] are $\Delta m^2 = 5.0 \times 10^{-6} \text{ eV}^2$ and $\tan^2 \theta = 1.5 \times 10^{-3}$) was once favored, but after SNO it was excluded at $> 3\sigma$ [5].

In December 2002, KamLAND observed clear evidence of neutrino oscillation with the allowed parameter region overlapping with the parameter region of the LMA solution [8]. Assuming CPT invariance, this result directly implies that the true solution of the solar ν_e oscillation has been determined to be LMA. A combined analysis of all the solar-neutrino data and KamLAND data significantly constrained the allowed parameter region. Inside the LMA region, the allowed region splits into

two bands with lower Δm^2 ($\sim 7 \times 10^{-5} \text{ eV}^2$, called LMA I) and higher Δm^2 ($\sim 2 \times 10^{-4} \text{ eV}^2$, called LMA II).

In September, 2003, SNO reported [9] salt-phase results on solar-neutrino fluxes observed with NaCl added in heavy water: this improved the sensitivity for the detection of the NC reaction. A global analysis of all the solar neutrino data combined with the KamLAND data restricted the allowed parameter region to the LMA I region at greater than 99% CL.

Later, further results from KamLAND [10] significantly more constrained the allowed Δm^2 region. SNO also reported results from the complete salt phase [11]. A combined two-neutrino oscillation analysis [11] using the data from all solar-neutrino experiments and from KamLAND yields $\Delta m^2 = (8.0^{+0.6}_{-0.4}) \times 10^{-5} \text{ eV}^2$ and $\tan^2 \theta = 0.45^{+0.09}_{-0.07}$ ($\theta = 33.9^{+2.4}_{-2.2}$ degrees).

Recently, a new solar neutrino experiment Borexino reported [12] the first realtime measurement of sub-MeV solar neutrinos with a low-background liquid scintillator detector. It is expected that Borexino as well as other low-energy solar neutrino experiments will further study properties of neutrinos and their interactions with matter on the one hand and the SSM on the other hand.

2. Solar Model Predictions

A standard solar model is based on the standard theory of stellar evolution. A variety of input information is needed in the evolutionary calculations. The most elaborate SSM calculations have been developed by Bahcall and his collaborators, who define their SSM as the solar model which is constructed with the best available physics and input data. Though they used no helioseismological constraints in defining the SSM, favorable models show an excellent agreement between the calculated and the helioseismologically-determined sound speeds to a precision of 0.1% rms throughout essentially the entire Sun. This greatly strengthens the confidence in the solar model. The currently preferred SSM is BS05(OP) developed by Bahcall and Serenelli [13,14]. This model uses newly calculated radiative opacities from the Opacity Project (OP) and previously standard heavy-element abundances (instead of the recently determined lower heavy-element abundances). However, BS05 (OP) [13] adopted conservative theoretical uncertainties in the solar-neutrino fluxes in order to account for the differences between these two heavy-element abundance values. The BS05(OP) prediction [13] for the fluxes from neutrino-producing reactions is given in Table 1. The solar-neutrino spectra calculated with this model [13], is shown in Fig. 1. The event rates in chlorine and gallium solar-neutrino experiments are calculated by scaling the BP2000 SSM results [15] (see Table 1 in p. 460 of 2004 edition of Review of Particle Physics [16]) to the BS05(OP) fluxes, and are shown in Table 2. It should be noted, however, that Basu et al. have found [17] that models constructed with lower heavy-element abundances are incompatible with the observations of low-degree acoustic solar oscillation modes that probe the solar

core. They therefore claim that the uncertainties in BS05(OP) predictions on the solar-neutrino fluxes (shown in Table 1) can be lowered.

Other recent solar-model prediction for solar-neutrino fluxes is given by Turck-Chièze *et al.* [18]. Their model, called a seismic model [19], is based on the standard theory of stellar evolution where the best physics available is adopted, but some fundamental inputs such as the pp reaction rate and the heavy-element abundances in the Sun are seismically adjusted within the commonly estimated errors aiming at reducing the residual differences between the helioseismologically-determined and the model-calculated sound speeds. Their prediction for the event rates in chlorine and gallium solar-neutrino experiments as well as ${}^8\text{B}$ solar-neutrino flux is shown in the last line in Table 2.

Table 1: Neutrino-producing reactions in the Sun (first column) and their abbreviations (second column). The neutrino fluxes predicted by the BS05(OP) model [13] are listed in the third column. The theoretical errors of the neutrino fluxes are taken from “Historical (conservative)” errors given in Table 8 of Ref. [14].

Reaction	Abbr.	Flux ($\text{cm}^{-2} \text{s}^{-1}$)
$pp \rightarrow d e^+ \nu$	pp	$5.99(1.00 \pm 0.01) \times 10^{10}$
$pe^+p \rightarrow d \nu$	pep	$1.42(1.00 \pm 0.02) \times 10^8$
${}^3\text{He} p \rightarrow {}^4\text{He} e^+ \nu$	hep	$7.93(1.00 \pm 0.16) \times 10^3$
${}^7\text{Be} e^- \rightarrow {}^7\text{Li} \nu + (\gamma)$	${}^7\text{Be}$	$4.84(1.00 \pm 0.11) \times 10^9$
${}^8\text{B} \rightarrow {}^8\text{Be}^* e^+ \nu$	${}^8\text{B}$	$5.69(1.00 \pm 0.16) \times 10^6$
${}^{13}\text{N} \rightarrow {}^{13}\text{C} e^+ \nu$	${}^{13}\text{N}$	$3.07(1.00^{+0.31}_{-0.28}) \times 10^8$
${}^{15}\text{O} \rightarrow {}^{15}\text{N} e^+ \nu$	${}^{15}\text{O}$	$2.33(1.00^{+0.33}_{-0.29}) \times 10^8$
${}^{17}\text{F} \rightarrow {}^{17}\text{O} e^+ \nu$	${}^{17}\text{F}$	$5.84(1.00 \pm 0.52) \times 10^6$

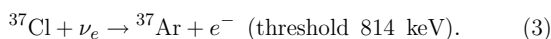
3. Solar Neutrino Experiments

So far, seven solar-neutrino experiments have published results. The most recent published results on the average event rates or flux from these experiments are listed in Table 2 and compared to the two recent solar-model predictions.

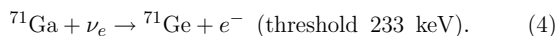
3.1. Radiochemical Experiments

Radiochemical experiments exploit electron neutrino absorption on nuclei followed by their decay through orbital electron capture. Produced Auger electrons are counted.

The Homestake chlorine experiment in USA uses the reaction



Three gallium experiments (GALLEX and GNO at Gran Sasso in Italy and SAGE at Baksan in Russia) use the reaction



The produced ${}^{37}\text{Ar}$ and ${}^{71}\text{Ge}$ atoms are both radioactive, with half lives ($\tau_{1/2}$) of 34.8 days and 11.43 days, respectively. After an exposure of the detector for two to three times $\tau_{1/2}$, the reaction products are chemically extracted and introduced into

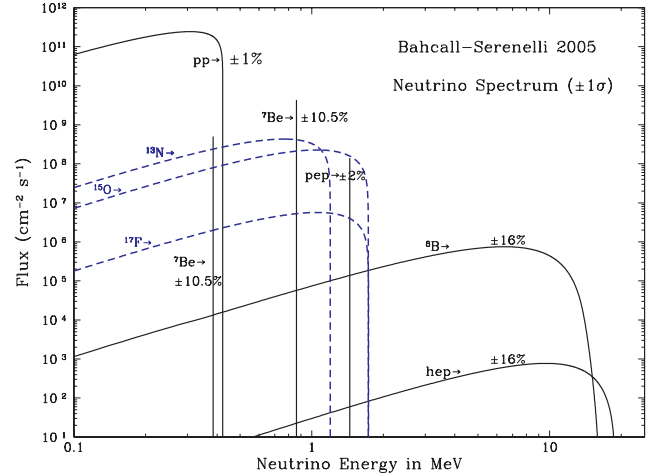


Figure 1: The solar neutrino spectrum predicted by the BS05(OP) standard solar model [13]. The neutrino fluxes from continuum sources are given in units of number $\text{cm}^{-2}\text{s}^{-1}\text{MeV}^{-1}$ at one astronomical unit, and the line fluxes are given in number $\text{cm}^{-2}\text{s}^{-1}$.

a low-background proportional counter, where they are counted for a sufficiently long period to determine the exponentially decaying signal and a constant background.

Solar-model calculations predict that the dominant contribution in the chlorine experiment comes from ${}^8\text{B}$ neutrinos, but ${}^7\text{Be}$, pep , ${}^{13}\text{N}$, and ${}^{15}\text{O}$ neutrinos also contribute. At present, the most abundant pp neutrinos can be detected only in gallium experiments. Even so, according to the solar-model calculations, almost half of the capture rate in the gallium experiments is due to other solar neutrinos.

The Homestake chlorine experiment was the first to attempt the observation of solar neutrinos. Initial results obtained in 1968 showed no events above background with upper limit for the solar-neutrino flux of 3 SNU [1]. After introduction of an improved electronics system which discriminates signal from background by measuring the rise time of the pulses from proportional counters, a finite solar-neutrino flux has been observed since 1970. The solar-neutrino capture rate shown in Table 2 is a combined result of 108 runs between 1970 and 1994 [20]. It is only about 1/3 of the solar-model predictions [13, 18].

GALLEX presented the first evidence of pp solar-neutrino observation in 1992 [26]. Here also, the observed capture rate is significantly less than the SSM prediction. SAGE initially reported very low capture rate, $20^{+15}_{-20} \pm 32$ SNU, with a 90% confidence-level upper limit of 79 SNU [27]. Later, SAGE [28] observed similar capture rate to that of GALLEX. Both GALLEX and SAGE groups tested the overall detector response with intense man-made ${}^{51}\text{Cr}$ neutrino sources, and observed good agreement between the measured ${}^{71}\text{Ge}$ production

Lepton Particle Listings

Neutrino Mixing

Table 2: Results from the seven solar-neutrino experiments. Recent solar model calculations are also presented. The first and the second errors in the experimental results are the statistical and systematic errors, respectively. SNU (Solar Neutrino Unit) is defined as 10^{-36} neutrino captures per atom per second.

	$^{37}\text{Cl} \rightarrow ^{37}\text{Ar}$ (SNU)	$^{71}\text{Ga} \rightarrow ^{71}\text{Ge}$ (SNU)	$^8\text{B } \nu$ flux ($10^6 \text{cm}^{-2} \text{s}^{-1}$)
Homestake (CLEVELAND 98)[20]	$2.56 \pm 0.16 \pm 0.16$	—	—
GALLEX (HAMPEL 99)[21]	—	$77.5 \pm 6.2^{+4.3}_{-4.7}$	—
GNO (ALTMANN 05)[22]	—	$62.9^{+5.5}_{-5.3} \pm 2.5$	—
GNO+GALLEX (ALTMANN 05)[22]	—	$69.3 \pm 4.1 \pm 3.6$	—
SAGE (ABDURASHI...02)[23]	—	$70.8^{+5.3+3.7}_{-5.2-3.2}$	—
Kamiokande (FUKUDA 96)[24]	—	—	$2.80 \pm 0.19 \pm 0.33^\dagger$
Super-Kamiokande (HOSAKA 05)[25]	—	—	$2.35 \pm 0.02 \pm 0.08^\dagger$
SNO (pure D_2O) (AHMAD 02)[4]	—	—	$1.76^{+0.06}_{-0.05} \pm 0.09^\ddagger$
	—	—	$2.39^{+0.24}_{-0.23} \pm 0.12^\dagger$
	—	—	$5.09^{+0.44+0.46*}_{-0.43-0.43}$
SNO (NaCl in D_2O) (AHARMIM 05)[11]	—	—	$1.68 \pm 0.06^{+0.08}_{-0.09}^\ddagger$
	—	—	$2.35 \pm 0.22 \pm 0.15^\dagger$
	—	—	$4.94 \pm 0.21^{+0.38*}_{-0.34}$
BS05(OP) SSM [13]	8.1 ± 1.3	126 ± 10	$5.69(1.00 \pm 0.16)$
Seismic model [18]	7.64 ± 1.1	123.4 ± 8.2	5.31 ± 0.6

* Flux measured via the neutral-current reaction.

† Flux measured via νe elastic scattering.

‡ Flux measured via the charged-current reaction.

rate and that predicted from the source activity, demonstrating the reliability of these experiments. The GALLEX Collaboration formally finished observations in early 1997. Since April, 1998, a newly defined collaboration, GNO (Gallium Neutrino Observatory) continued the observations until April 2003. The complete GNO results are published in Ref. [22]. The GNO + GALLEX joint analysis results are also presented [22] (see Table 2).

3.2 Kamiokande and Super-Kamiokande

Kamiokande and Super-Kamiokande in Japan are real-time experiments utilizing νe scattering

$$\nu_x + e^- \rightarrow \nu_x + e^- \quad (5)$$

in a large water-Cherenkov detector. It should be noted that the reaction Eq. (5) is sensitive to all active neutrinos, $x = e, \mu,$ and τ . However, the sensitivity to ν_μ and ν_τ is much smaller

than the sensitivity to ν_e , $\sigma(\nu_{\mu,\tau}e) \approx 0.16 \sigma(\nu_e e)$. The solar-neutrino flux measured via νe scattering is deduced assuming no neutrino oscillations.

These experiments take advantage of the directional correlation between the incoming neutrino and the recoil electron. This feature greatly helps the clear separation of the solar-neutrino signal from the background. Due to the high thresholds (7 MeV in Kamiokande and 5 MeV at present in Super-Kamiokande) the experiments observe pure ^8B solar neutrinos because *hep* neutrinos contribute negligibly according to the SSM.

The Kamiokande-II Collaboration started observing ^8B solar neutrinos at the beginning of 1987. Because of the strong directional correlation of νe scattering, this result gave the first direct evidence that the Sun emits neutrinos [29] (no directional information is available in radiochemical solar-neutrino experiments). The observed solar-neutrino flux was also significantly less than the SSM prediction. In addition, Kamiokande-II obtained the energy spectrum of recoil electrons and the fluxes separately measured in the daytime and nighttime. The Kamiokande-II experiment came to an end at the beginning of 1995.

Super-Kamiokande is a 50-kton second-generation solar-neutrino detector, which is characterized by a significantly larger counting rate than the first-generation experiments. This experiment started observation in April 1996. In November 2001, Super-Kamiokande suffered from an accident in which substantial number of photomultiplier tubes were lost. The detector was rebuilt within a year with about half of the original number of photomultiplier tubes. The experiment with the detector before the accident is called Super-Kamiokande-I, and that after the accident is called Super-Kamiokande-II. The complete Super-Kamiokande-I solar-neutrino results are reported in Ref. [25]. The solar-neutrino flux is measured as a function of zenith angle and recoil-electron energy. The average solar-neutrino flux is given in Table 2. The observed day-night asymmetry is $A_{\text{DN}} = \frac{\text{Day} - \text{Night}}{0.5(\text{Day} + \text{Night})} = -0.021 \pm 0.020^{+0.013}_{-0.012}$. No indication of spectral distortion is observed.

3.3 SNO

In 1999, a new real time solar-neutrino experiment, SNO, in Canada started observation. This experiment uses 1000 tons of ultra-pure heavy water (D_2O) contained in a spherical acrylic vessel, surrounded by an ultra-pure H_2O shield. SNO measures ^8B solar neutrinos via the reactions

$$\nu_e + d \rightarrow e^- + p + p \quad (6)$$

and

$$\nu_x + d \rightarrow \nu_x + p + n, \quad (7)$$

as well as νe scattering, Eq. (5). The CC reaction, Eq. (6), is sensitive only to electron neutrinos, while the NC reaction, Eq. (7), is sensitive to all active neutrinos.

The Q -value of the CC reaction is -1.4 MeV and the electron energy is strongly correlated with the neutrino energy. Thus, the CC reaction provides an accurate measure of the shape of the ${}^8\text{B}$ solar-neutrino spectrum. The contributions from the CC reaction and νe scattering can be distinguished by using different $\cos\theta_\odot$ distributions where θ_\odot is the angle of the electron momentum with respect to the direction from the Sun to the Earth. While the νe scattering events have a strong forward peak, CC events have an approximate angular distribution of $1 - 1/3 \cos\theta_\odot$.

The threshold of the NC reaction is 2.2 MeV. In the pure D_2O , the signal of the NC reaction is neutron capture in deuterium, producing a 6.25-MeV γ -ray. In this case, the capture efficiency is low and the deposited energy is close to the detection threshold of 5 MeV. In order to enhance both the capture efficiency and the total γ -ray energy (8.6 MeV), 2 tons of NaCl were added to the heavy water in the second phase of the experiment. In addition, discrete ${}^3\text{He}$ neutron counters were installed and the NC measurement with them are being made as the third phase of the SNO experiment.

In 2001, SNO published the initial results on the measurement of the ${}^8\text{B}$ solar-neutrino flux via CC reaction [2]. The electron energy spectrum and the $\cos\theta_\odot$ distribution were also measured. The spectral shape of the electron energy was consistent with the expectations for an undistorted ${}^8\text{B}$ solar-neutrino spectrum.

SNO also measured the ${}^8\text{B}$ solar-neutrino flux via νe scattering [2]. Though the latter result had poor statistics, it was consistent with the high-statistics Super-Kamiokande result. Thus, the SNO group compared their CC result with Super-Kamiokande's νe scattering result, and obtained evidence of an active non- ν_e component in the solar-neutrino flux [2], as further described in Sec. 3.5.

Later, in April, 2002, SNO reported the first result on the ${}^8\text{B}$ solar-neutrino flux measurement via NC reaction [4]. The total flux measured via NC reaction was consistent with the solar-model predictions (see Table 2). Also, the SNO's CC and νe scattering results were updated [4]. These results were consistent with the earlier results [2].

The SNO Collaboration made a global analysis (see Sect. 3.6) of the SNO's day and night energy spectra together with the data from other solar-neutrino experiments. The results strongly favored the LMA solution, with the LOW solution allowed at 99.5% CL [30]. (In most of the similar global analyses, the VAC solution was also allowed at 99.9 ~ 99.73% CL [5]).

In September, 2003, SNO has released the first results of solar-neutrino flux measurements with dissolved NaCl in the heavy water [9]. The complete salt phase results are also reported recently [11]. Using the salt phase results, the SNO Collaboration made a global solar-neutrino analysis and a global solar + KamLAND analysis. Implications of these analyses are described in Sect. 5.

SNO also studied the energy spectrum and day-night flux asymmetries for both pure D_2O [30] and salt phases [11]. The energy spectrum deduced from the CC reaction is consistent with the spectrum expected from an undistorted ${}^8\text{B}$ spectral shape. No significant day-night flux asymmetries are observed within uncertainties. These observations are consistent with the best-fit LMA solution from the global solar + KamLAND analysis.

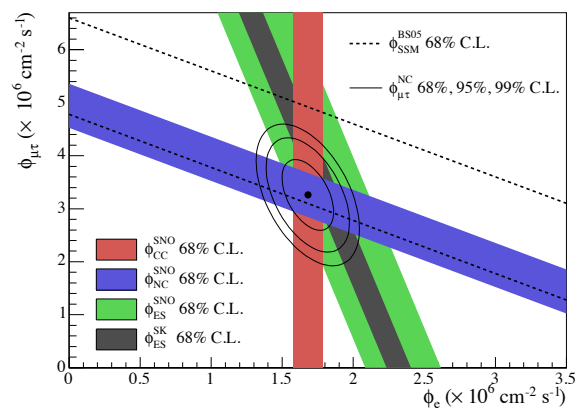


Figure 2: Fluxes of ${}^8\text{B}$ solar neutrinos, $\phi(\nu_e)$, and $\phi(\nu_\mu \text{ or } \tau)$, deduced from the SNO's charged-current (CC), ν_e elastic scattering (ES), and neutral-current (NC) results for the salt phase measurement [11]. The Super-Kamiokande ES flux is from Ref. [36]. The BS05(OP) standard solar model prediction [13] is also shown. The bands represent the 1σ error. The contours show the 68%, 95%, and 99% joint probability for $\phi(\nu_e)$ and $\phi(\nu_\mu \text{ or } \tau)$. This figure is taken from Ref. [11]. Color version at end of book.

3.4 Comparison of Experimental Results with Solar-Model Predictions

It is clearly seen from Table 2 that the results from all the solar-neutrino experiments, except the SNO's NC result, indicate significantly less flux than expected from the solar-model predictions [13, 18].

There has been a consensus that a consistent explanation of all the results of solar-neutrino observations is unlikely within the framework of astrophysics using the solar-neutrino spectra given by the standard electroweak model. Many authors made solar model-independent analyses constrained by the observed solar luminosity [31–35], where they attempted to fit the measured solar-neutrino capture rates and ${}^8\text{B}$ flux with normalization-free, undistorted energy spectra. All these attempts only obtained solutions with very low probabilities.

The data therefore suggest that the solution to the solar-neutrino problem requires nontrivial neutrino properties.

Lepton Particle Listings

Neutrino Mixing

3.5 Evidence for Solar Neutrino Oscillations

Denoting the ^8B solar-neutrino flux obtained by the SNO's CC measurement as $\phi_{\text{SNO}}^{\text{CC}}(\nu_e)$ and that obtained by the Super-Kamiokande ν_e scattering as $\phi_{\text{SK}}^{\text{ES}}(\nu_x)$, $\phi_{\text{SNO}}^{\text{CC}}(\nu_e) = \phi_{\text{SK}}^{\text{ES}}(\nu_x)$ is expected for the standard neutrino physics. However, SNO's initial data [2] indicated

$$\phi_{\text{SK}}^{\text{ES}}(\nu_x) - \phi_{\text{SNO}}^{\text{CC}}(\nu_e) = (0.57 \pm 0.17) \times 10^6 \text{ cm}^{-2}\text{s}^{-1}. \quad (8)$$

The significance of the difference was $> 3\sigma$, implying direct evidence for the existence of a non- ν_e active neutrino flavor component in the solar-neutrino flux. A natural and most probable explanation of neutrino flavor conversion is neutrino oscillation. Note that both the SNO [2] and Super-Kamiokande [3] flux results were obtained by assuming the standard ^8B neutrino spectrum shape. This assumption was justified by the measured energy spectra in both experiments.

The SNO's results for the pure D_2O phase, reported in 2002 [4], provided stronger evidence for neutrino oscillation than Eq. (8). The fluxes measured with CC, ES, and NC events were deduced. Here, the spectral distributions of the CC and ES events were constrained to an undistorted ^8B shape. The results are

$$\phi_{\text{SNO}}^{\text{CC}}(\nu_e) = (1.76_{-0.05}^{+0.06} \pm 0.09) \times 10^6 \text{ cm}^{-2}\text{s}^{-1}, \quad (9)$$

$$\phi_{\text{SNO}}^{\text{ES}}(\nu_x) = (2.39_{-0.23}^{+0.24} \pm 0.12) \times 10^6 \text{ cm}^{-2}\text{s}^{-1}, \quad (10)$$

$$\phi_{\text{SNO}}^{\text{NC}}(\nu_x) = (5.09_{-0.43}^{+0.44+0.46}) \times 10^6 \text{ cm}^{-2}\text{s}^{-1}. \quad (11)$$

Eq. (11) is a mixing-independent result and therefore tests solar models. It shows good agreement with the ^8B solar-neutrino flux predicted by the solar models [13, 18]. The flux of non- ν_e active neutrinos, $\phi(\nu_\mu \text{ or } \tau)$, can be deduced from these results. It is

$$\phi(\nu_\mu \text{ or } \tau) = (3.41_{-0.64}^{+0.66}) \times 10^6 \text{ cm}^{-2}\text{s}^{-1} \quad (12)$$

where the statistical and systematic errors are added in quadrature. This $\phi(\nu_\mu \text{ or } \tau)$ is 5.3σ above 0. The non-zero $\phi(\nu_\mu \text{ or } \tau)$ is strong evidence for neutrino flavor transformation.

From the salt phase measurement [11], the fluxes measured with CC and ES events were deduced with no constraint of the ^8B energy spectrum. The results are

$$\phi_{\text{SNO}}^{\text{CC}}(\nu_e) = (1.68 \pm 0.06_{-0.09}^{+0.08}) \times 10^6 \text{ cm}^{-2}\text{s}^{-1}, \quad (13)$$

$$\phi_{\text{SNO}}^{\text{ES}}(\nu_x) = (2.35 \pm 0.22 \pm 0.15) \times 10^6 \text{ cm}^{-2}\text{s}^{-1}, \quad (14)$$

$$\phi_{\text{SNO}}^{\text{NC}}(\nu_x) = (4.94 \pm 0.21_{-0.34}^{+0.38}) \times 10^6 \text{ cm}^{-2}\text{s}^{-1}. \quad (15)$$

These results are consistent with the results from the pure D_2O phase. Fig. 2 shows the salt phase result of $\phi(\nu_\mu \text{ or } \tau)$ versus the flux of electron neutrinos $\phi(\nu_e)$ with the 68%, 95%, and 99% joint probability contours.

4. KamLAND Reactor Neutrino Oscillation Experiment

KamLAND is a 1-kton ultra-pure liquid scintillator detector located at the old Kamiokande's site in Japan. Although the

ultimate goal of KamLAND is observation of ^7Be solar neutrinos with much lower energy threshold, the initial phase of the experiment is a long baseline (flux-weighted average distance of ~ 180 km) neutrino oscillation experiment using $\bar{\nu}_e$'s emitted from power reactors. The reaction $\bar{\nu}_e + p \rightarrow e^+ + n$ is used to detect reactor $\bar{\nu}_e$'s and delayed coincidence with 2.2 MeV γ -ray from neutron capture on a proton is used to reduce the backgrounds.

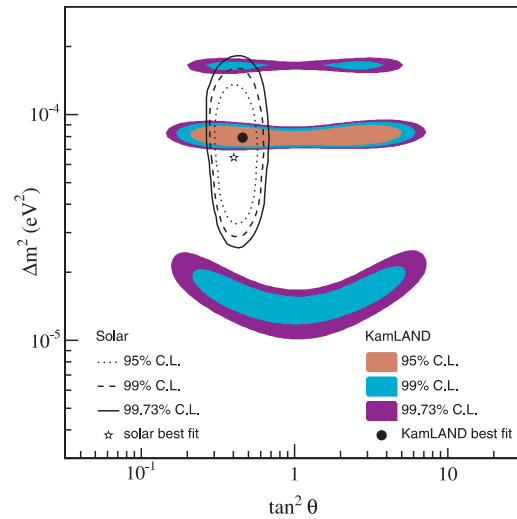


Figure 3: Allowed regions of neutrino-oscillation parameters from the KamLAND 766 ton-yr exposure $\bar{\nu}_e$ data [10]. The LMA region from solar-neutrino experiments [9] is also shown. This figure is taken from Ref. [10]. Color version at end of book.

With the reactor $\bar{\nu}_e$'s energy spectrum (< 8 MeV) and a prompt-energy analysis threshold of 2.6 MeV, this experiment has a sensitive Δm^2 range down to $\sim 10^{-5}$ eV^2 . Therefore, if the LMA solution is the real solution of the solar neutrino problem, KamLAND should observe reactor $\bar{\nu}_e$ disappearance, assuming CPT invariance.

The first KamLAND results [8] with 162 ton-yr exposure were reported in December 2002. The ratio of observed to expected (assuming no neutrino oscillation) number of events was

$$\frac{N_{\text{obs}} - N_{\text{BG}}}{N_{\text{NoOsc}}} = 0.611 \pm 0.085 \pm 0.041. \quad (16)$$

with obvious notation. This result shows clear evidence of event deficit expected from neutrino oscillation. The 95% CL allowed regions are obtained from the oscillation analysis with the observed event rates and positron spectrum shape. There are two bands of regions allowed by both solar and KamLAND data in the region. The LOW and VAC solutions are excluded by the KamLAND results. A combined global solar + KamLAND

See key on page 373

analysis showed that the LMA is a unique solution to the solar neutrino problem with $> 5\sigma$ CL [37].

In June 2004, KamLAND released the results from 766 ton-yr exposure [10]. In addition to the deficit of events, the observed positron spectrum showed the distortion expected from neutrino oscillation. Fig. 3 shows the allowed regions in the neutrino-oscillation parameter space. The best-fit point lies in the region called LMA I. The LMA II region is disfavored at the 98% CL.

5. Global Neutrino Oscillation Analysis

The SNO Collaboration updated [11] a global two-neutrino oscillation analysis of the solar-neutrino data including the SNO's complete salt phase data, and global solar + KamLAND 766 ton-yr data [10]. The resulting neutrino oscillation contours are shown in Fig. 4. The best fit parameters for the global solar analysis are $\Delta m^2 = 6.5^{+4.4}_{-2.3} \times 10^{-5} \text{ eV}^2$ and $\tan^2\theta = 0.45^{+0.09}_{-0.08}$. The inclusion of the KamLAND data significantly constrains the allowed Δm^2 region, but shifts the best-fit Δm^2 value. The best-fit parameters for the global solar + KamLAND analysis are $\Delta m^2 = 8.0^{+0.6}_{-0.4} \times 10^{-5} \text{ eV}^2$ and $\tan^2\theta = 0.45^{+0.09}_{-0.07}$ ($\theta = 33.9^{+2.4}_{-2.2}$).

A number of authors [38 - 40] also made combined global neutrino oscillation analysis of solar + KamLAND data in mostly three-neutrino oscillation framework using the SNO complete salt phase data [11] and the KamLAND 766 ton-yr data [10]. These give consistent results with the SNO's two-neutrino oscillation analysis [11].

6. Recent Progress and Future Prospects

Now that the solar-neutrino problem has been essentially solved, what are the future prospects of the solar-neutrino experiments?

From the particle-physics point of view, precise determination of the oscillation parameters and search for non-standard physics such as a small admixture of a sterile component in the solar-neutrino flux will be still of interest. More precise NC measurements by SNO will contribute in reducing the uncertainty of the mixing angle [41]. Measurements of the pp flux to an accuracy comparable to the quoted accuracy ($\pm 1\%$) of the SSM calculation will significantly improve the precision of the mixing angle [42,43].

An important task of the future solar neutrino experiments is further tests of the SSM by measuring monochromatic ${}^7\text{Be}$ neutrinos and fundamental pp neutrinos. The ${}^7\text{Be}$ neutrino flux will be measured by a new experiment, Borexino, at Gran Sasso via νe scattering in 300 tons of ultra-pure liquid scintillator with a detection threshold as low as 250 keV. KamLAND will also observe ${}^7\text{Be}$ neutrinos if the detection threshold can be lowered to a level similar to that of Borexino.

Borexino has recently reported the first realtime observation of monochromatic 0.862 MeV ${}^7\text{Be}$ solar neutrinos [12]. With 47.4 live days, the observed rate, $47 \pm 7 \pm 12$ counts/(100

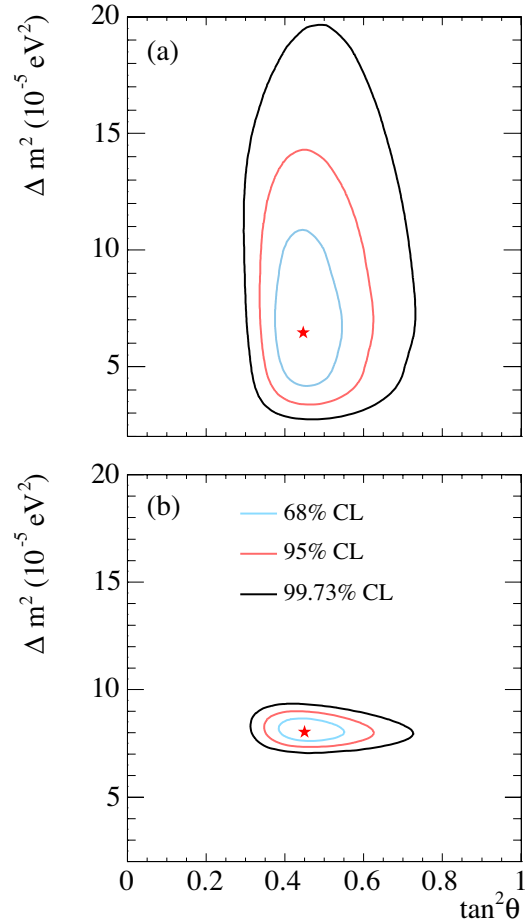


Figure 4: Update of the global neutrino oscillation contours given by the SNO Collaboration assuming that the ${}^8\text{B}$ neutrino flux is free and the ${}^{\text{hep}}$ neutrino flux is fixed. (a) Solar global analysis. (b) Solar global + KamLAND. This figure is taken from Ref. [11].

ton-day), is consistent with the rate calculated with SSM and neutrino oscillations, 49 ± 4 counts/(100 ton-day). For comparison, the expected rate with no neutrino oscillations is 75 ± 4 counts/(100 ton-day).

For the detection of pp neutrinos, various ideas for the detection scheme have been presented. However, no experiments have been approved yet, and extensive R&D efforts are still needed for any of these ideas to prove its feasibility.

References

1. D. Davis, Jr., D.S. Harmer, and K.C. Hoffman, Phys. Rev. Lett. **20**, 1205 (1968).
2. Q.R. Ahmad *et al.*, Phys. Rev. Lett. **87**, 071301 (2001).
3. Y. Fukuda *et al.*, Phys. Rev. Lett. **86**, 5651 (2001).
4. Q.R. Ahmad *et al.*, Phys. Rev. Lett. **89**, 011301 (2002).

Lepton Particle Listings

Neutrino Mixing

5. See, for example, J.N. Bahcall, C.M. Gonzalez-Garcia, and C. Peña-Garay, JHEP 0207, 054 (2002).
6. L. Wolfenstein, Phys. Rev. **D17**, 2369 (1978).
7. S.P. Mikheyev and A. Yu. Smirnov, Sov. J. Nucl. Phys. **42**, 913 (1985).
8. K. Eguchi *et al.*, Phys. Rev. Lett. **90**, 021802 (2003).
9. S.N. Ahmed *et al.*, Phys. Rev. Lett. **92**, 181301 (2004).
10. T. Araki *et al.*, Phys. Rev. Lett. **94**, 081801 (2005).
11. B. Aharmim *et al.*, Phys. Rev. **C72**, 055502 (2005).
12. C. Arpesella *et al.*, Phys. Lett. **B658**, 101 (2008).
13. J.N. Bahcall, A.M. Serenelli, and S. Basu, Astrophys. J. **621**, L85 (2005).
14. J.N. Bahcall and A.M. Serenelli Astrophys. J. **626**, 530 (2005).
15. J.N. Bahcall, M.H. Pinsonneault, and S. Basu, Astrophys. J. **555**, 990 (2001).
16. S. Eidelman *et al.*, Phys. Lett. **B592**, 1 (2004).
17. S. Basu *et al.*, Astrophys. J. **655**, 660 (2007).
18. S. Turck-Chièze *et al.*, Phys. Rev. Lett. **93**, 211102 (2004).
19. S. Couvidat, S. Turck-Chièze, and A.G. Kosovichev, Astrophys. J. **599**, 1434 (2003).
20. B.T. Cleveland *et al.*, Ap. J. **496**, 505 (1998).
21. W. Hampel *et al.*, Phys. Lett. **B447**, 127 (1999).
22. M. Altmann *et al.*, Phys. Lett. **B616**, 174 (2005).
23. J.N. Abdurashitov *et al.*, Sov. Phys. JETP **95**, 181 (2002).
24. Y. Fukuda *et al.*, Phys. Rev. Lett. **77**, 1683 (1996).
25. J. Hosaka *et al.*, Phys. Rev. **D73**, 112001 (2006).
26. P. Anselmann *et al.*, Phys. Lett. **B285**, 376 (1992).
27. A.I. Abazov *et al.*, Phys. Rev. Lett. **67**, 3332 (1991).
28. J.N. Abdurashitov *et al.*, Phys. Lett. **B328**, 234 (1994).
29. K.S. Hirata *et al.*, Phys. Rev. Lett. **63**, 16 (1989).
30. Q.R. Ahmad *et al.*, Phys. Rev. Lett. **89**, 011302 (2002).
31. N. Hata, S. Bludman, and P. Langacker, Phys. Rev. **D49**, 3622 (1994).
32. N. Hata and P. Langacker, Phys. Rev. **D52**, 420 (1995).
33. N. Hata and P. Langacker, Phys. Rev. **D56**, 6107 (1997).
34. S. Parke, Phys. Rev. Lett. **74**, 839 (1995).
35. K.M. Heeger and R.G.H. Robertson, Phys. Rev. Lett. **77**, 3720 (1996).
36. Y. Fukuda *et al.*, Phys. Lett. **B539**, 179 (2002).
37. See, for example, J.N. Bahcall, M.C. Gonzalez-Garcia, and C. Peña-Garay, JHEP 0302, 009 (2003).
38. A.B. Balantekin *et al.*, Phys. Lett. **B613**, 61 (2005).
39. A. Strumia and F. Vissani, Nucl. Phys. **B726**, 294 (2005).
40. G.L. Fogli *et al.*, Prog. Part. Nucl. Phys. **57**, 742 (2006).
41. A. Bandyopadhyay *et al.*, Phys. Lett. **B608**, 115 (2005).
42. J.N. Bahcall and C. Peña-Garay, JHEP 0311, 004 (2003).
43. A. Bandyopadhyay *et al.*, Phys. Rev. **D72**, 033013 (2005).

 ν_e Capture Rates from Radiochemical Experiments

1 SNU (Solar Neutrino Unit) = 10^{-36} captures per atom per second.

VALUE (SNU)	DOCUMENT ID	TECN	COMMENT
$62.9^{+5.5}_{-5.3} \pm 2.5$	³⁴ ALTMANN 05	GNO	⁷¹ Ga → ⁷¹ Ge
$69.3 \pm 4.1 \pm 3.6$	³⁵ ALTMANN 05	GNO	GNO + GALX combined
$70.8^{+5.3}_{-5.2} \pm 3.7$	³⁶ ABDURASHI... 02	SAGE	⁷¹ Ga → ⁷¹ Ge
$77.5 \pm 6.2^{+4.3}_{-4.7}$	³⁷ HAMPEL 99	GALX	⁷¹ Ga → ⁷¹ Ge
$2.56 \pm 0.16 \pm 0.16$	³⁸ CLEVELAND 98	HOME	³⁷ Cl → ³⁷ Ar

• • • We do not use the following data for averages, fits, limits, etc. • • •

- ³⁴ALTMANN 05 reports the complete result from the GNO solar neutrino experiment (GNO I+II+III), which is the successor project of GALLEX. Experimental technique of GNO is essentially the same as that of GALLEX. The run data cover the period 20 May 1998 through 9 April 2003.
- ³⁵Combined result of GALLEX I+II+III+IV (HAMPEL 99) and GNO I+II+III.
- ³⁶ABDURASHITOV 02 report a combined analysis of 92 runs of the SAGE solar-neutrino experiment during the period January 1990 through December 2001, and updates the ABDURASHITOV 99B result. A total of 406.4 ⁷¹Ge events were observed. No evidence was found for temporal variations of the neutrino capture rate over the entire observation period.
- ³⁷HAMPEL 99 report the combined result for GALLEX I+II+III+IV (65 runs in total), which update the HAMPEL 96 result. The GALLEX IV result (12 runs) is $118.4 \pm 17.8 \pm 6.6$ SNU. (HAMPEL 99 discuss the consistency of partial results with the mean.) The GALLEX experimental program has been completed with these runs. The total run data cover the period 14 May 1991 through 23 January 1997. A total of 300 ⁷¹Ge events were observed.
- ³⁸CLEVELAND 98 is a detailed report of the ³⁷Cl experiment at the Homestake Mine. The average solar neutrino-induced ³⁷Ar production rate from 108 runs between 1970 and 1994 updates the DAVIS 89 result.

 Φ_{ES} (⁸B)

⁸B solar-neutrino flux measured via νe elastic scattering. This process is sensitive to all active neutrino flavors, but with reduced sensitivity to ν_μ, ν_τ due to the cross-section difference, $\sigma(\nu_{\mu,\tau} e) \sim 0.16\sigma(\nu_e e)$. If the ⁸B solar-neutrino flux involves nonelectron flavor active neutrinos, their contribution to the flux is ~ 0.16 times of ν_e .

VALUE ($10^6 \text{ cm}^{-2} \text{ s}^{-1}$)	DOCUMENT ID	TECN	COMMENT
$2.35 \pm 0.02 \pm 0.08$	³⁹ HOSAKA	06	SKAM average flux
$2.35 \pm 0.22 \pm 0.15$	⁴⁰ AHARMIM	05A	SNO Salty D ₂ O; ⁸ B shape not constrained
$2.34 \pm 0.23^{+0.15}_{-0.14}$	⁴⁰ AHARMIM	05A	SNO Salty D ₂ O; ⁸ B shape constrained
$2.39^{+0.24}_{-0.23} \pm 0.12$	⁴¹ AHMAD	02	SNO average flux
$2.39 \pm 0.34^{+0.16}_{-0.14}$	⁴² AHMAD	01	SNO average flux
$2.80 \pm 0.19 \pm 0.33$	⁴³ FUKUDA	96	KAMI average flux
2.70 ± 0.27	⁴³ FUKUDA	96	KAMI day flux
$2.87^{+0.27}_{-0.26}$	⁴³ FUKUDA	96	KAMI night flux

• • • We do not use the following data for averages, fits, limits, etc. • • •

- ³⁹HOSAKA 06 reports the final results for 1496 live days with Super-Kamiokande-I between May 31, 1996 and July 15, 2001, and replace FUKUDA 02 results. The analysis threshold is 5 MeV except for the first 280 live days (6.5 MeV).
- ⁴⁰AHARMIM 05A measurements were made with dissolved NaCl (0.195% by weight) in heavy water over the period between July 26, 2001 and August 28, 2003, corresponding to 391.4 live days, and update AHMED 04A. The CC, ES, and NC events were statistically separated. In one method, the ⁸B energy spectrum was not constrained. In the other method, the constraint of an undistorted ⁸B energy spectrum was added for comparison with AHMAD 02 results.
- ⁴¹AHMAD 02 reports the ⁸B solar-neutrino flux measured via νe elastic scattering above the kinetic energy threshold of 5 MeV. The data correspond to 306.4 live days with SNO between November 2, 1999 and May 28, 2001, and updates AHMAD 01 results.
- ⁴²AHMAD 01 reports the ⁸B solar-neutrino flux measured via νe elastic scattering above the kinetic energy threshold of 6.75 MeV. The data correspond to 241 live days with SNO between November 2, 1999 and January 15, 2001.
- ⁴³FUKUDA 96 results are for a total of 2079 live days with Kamiokande II and III from January 1987 through February 1995, covering the entire solar cycle 22, with threshold $E_e > 9.3$ MeV (first 449 days), > 7.5 MeV (middle 794 days), and > 7.0 MeV (last 836 days). These results update the HIRATA 90 result for the average ⁸B solar-neutrino flux and HIRATA 91 result for the day-night variation in the ⁸B solar-neutrino flux. The total data sample was also analyzed for short-term variations: within experimental errors, no strong correlation of the solar-neutrino flux with the sunspot numbers was found.

 Φ_{CC} (⁸B)

⁸B solar-neutrino flux measured with charged-current reaction which is sensitive exclusively to ν_e .

VALUE ($10^6 \text{ cm}^{-2} \text{ s}^{-1}$)	DOCUMENT ID	TECN	COMMENT
$1.68 \pm 0.06^{+0.08}_{-0.09}$	⁴⁴ AHARMIM	05A	SNO Salty D ₂ O; ⁸ B shape not const.
$1.72 \pm 0.05 \pm 0.11$	⁴⁴ AHARMIM	05A	SNO Salty D ₂ O; ⁸ B shape constrained
$1.76^{+0.06}_{-0.05} \pm 0.09$	⁴⁵ AHMAD	02	SNO average flux
$1.75 \pm 0.07^{+0.12}_{-0.11} \pm 0.05$	⁴⁶ AHMAD	01	SNO average flux

• • • We do not use the following data for averages, fits, limits, etc. • • •

- ⁴⁴AHARMIM 05A measurements were made with dissolved NaCl (0.195% by weight) in heavy water over the period between July 26, 2001 and August 28, 2003, corresponding to 391.4 live days, and update AHMED 04A. The CC, ES, and NC events were statistically separated. In one method, the ⁸B energy spectrum was not constrained. In the other method, the constraint of an undistorted ⁸B energy spectrum was added for comparison with AHMAD 02 results.

See key on page 373

Lepton Particle Listings
Neutrino Mixing

⁴⁵AHMAD 02 reports the SNO result of the ⁸B solar-neutrino flux measured with charged-current reaction on deuterium, $\nu_e d \rightarrow pp e^-$, above the kinetic energy threshold of 5 MeV. The data correspond to 306.4 live days with SNO between November 2, 1999 and May 28, 2001, and updates AHMAD 01 results. The complete description of the SNO Phase I data set is given in AHARMIM 07.

⁴⁶AHMAD 01 reports the first SNO result of the ⁸B solar-neutrino flux measured with the charged-current reaction on deuterium, $\nu_e d \rightarrow pp e^-$, above the kinetic energy threshold of 6.75 MeV. The data correspond to 241 live days with SNO between November 2, 1999 and January 15, 2001.

 ϕ_{NC} (⁸B)

⁸B solar neutrino flux measured with neutral-current reaction, which is equally sensitive to ν_e , ν_μ , and ν_τ .

VALUE ($10^6 \text{ cm}^{-2}\text{s}^{-1}$)	DOCUMENT ID	TECN	COMMENT
$4.94 \pm 0.21 +0.38 -0.34$	47 AHARMIM	05A SNO	Salty D ₂ O; ⁸ B shape not const.
$4.81 \pm 0.19 +0.28 -0.27$	47 AHARMIM	05A SNO	Salty D ₂ O; ⁸ B shape constrained
$5.09 \pm 0.44 +0.46 -0.43$	48 AHMAD	02 SNO	average flux; ⁸ B shape const.
$6.42 \pm 1.57 +0.55 -0.58$	48 AHMAD	02 SNO	average flux; ⁸ B shape not const.

• • • We do not use the following data for averages, fits, limits, etc. • • •

⁴⁷AHARMIM 05A measurements were made with dissolved NaCl (0.195% by weight) in heavy water over the period between July 26, 2001 and August 28, 2003, corresponding to 391.4 live days, and update AHMED 04A. The CC, ES, and NC events were statistically separated. In one method, the ⁸B energy spectrum was not constrained. In the other method, the constraint of an undistorted ⁸B energy spectrum was added for comparison with AHMAD 02 results.

⁴⁸AHMAD 02 reports the first SNO result of the ⁸B solar-neutrino flux measured with the neutral-current reaction on deuterium, $\nu_e d \rightarrow np \nu_e$, above the neutral-current reaction threshold of 2.2 MeV. The data correspond to 306.4 live days with SNO between November 2, 1999 and May 28, 2001. The complete description of the SNO Phase I data set is given in AHARMIM 07.

 $\phi_{\nu_\mu+\nu_\tau}$ (⁸B)

Nonelectron-flavor active neutrino component (ν_μ and ν_τ) in the ⁸B solar-neutrino flux.

VALUE ($10^6 \text{ cm}^{-2}\text{s}^{-1}$)	DOCUMENT ID	TECN	COMMENT
$3.26 \pm 0.25 +0.40 -0.35$	49 AHARMIM	05A SNO	From ϕ_{NC} , ϕ_{CC} , and ϕ_{ES} ; ⁸ B shape not const.
$3.09 \pm 0.22 +0.30 -0.27$	49 AHARMIM	05A SNO	From ϕ_{NC} , ϕ_{CC} , and ϕ_{ES} ; ⁸ B shape constrained
$3.41 \pm 0.45 +0.48 -0.45$	50 AHMAD	02 SNO	From ϕ_{NC} , ϕ_{CC} , and ϕ_{ES}
3.69 ± 1.13	51 AHMAD	01	Derived from SNO+SuperKam, water Cherenkov

• • • We do not use the following data for averages, fits, limits, etc. • • •

⁴⁹AHARMIM 05A measurements were made with dissolved NaCl (0.195% by weight) in heavy water over the period between July 26, 2001 and August 28, 2003, corresponding to 391.4 live days, and update AHMED 04A. The CC, ES, and NC events were statistically separated. In one method, the ⁸B energy spectrum was not constrained. In the other method, the constraint of an undistorted ⁸B energy spectrum was added for comparison with AHMAD 02 results.

⁵⁰AHMAD 02 deduced the nonelectron-flavor active neutrino component (ν_μ and ν_τ) in the ⁸B solar-neutrino flux, by combining the charged-current result, the ν_e elastic-scattering result and the neutral-current result. The complete description of the SNO Phase I data set is given in AHARMIM 07.

⁵¹AHMAD 01 deduced the nonelectron-flavor active neutrino component (ν_μ and ν_τ) in the ⁸B solar-neutrino flux, by combining the SNO charged-current result (AHMAD 01) and the Super-Kamiokande ν_e elastic-scattering result (FUKUDA 01).

Total Flux of Active ⁸B Solar Neutrinos

Total flux of active neutrinos (ν_e , ν_μ , and ν_τ).

VALUE ($10^6 \text{ cm}^{-2}\text{s}^{-1}$)	DOCUMENT ID	TECN	COMMENT
$4.94 \pm 0.21 +0.38 -0.34$	52 AHARMIM	05A SNO	From ϕ_{NC} ; ⁸ B shape not const.
$4.81 \pm 0.19 +0.28 -0.27$	52 AHARMIM	05A SNO	From ϕ_{NC} ; ⁸ B shape constrained
$5.09 \pm 0.44 +0.46 -0.43$	53 AHMAD	02 SNO	Direct measurement from ϕ_{NC}
5.44 ± 0.99	54 AHMAD	01	Derived from SNO+SuperKam, water Cherenkov

• • • We do not use the following data for averages, fits, limits, etc. • • •

⁵²AHARMIM 05A measurements were made with dissolved NaCl (0.195% by weight) in heavy water over the period between July 26, 2001 and August 28, 2003, corresponding to 391.4 live days, and update AHMED 04A. The CC, ES, and NC events were statistically separated. In one method, the ⁸B energy spectrum was not constrained. In the other method, the constraint of an undistorted ⁸B energy spectrum was added for comparison with AHMAD 02 results.

⁵³AHMAD 02 determined the total flux of active ⁸B solar neutrinos by directly measuring the neutral-current reaction, $\nu_e d \rightarrow np \nu_e$, which is equally sensitive to ν_e , ν_μ , and ν_τ . The complete description of the SNO Phase I data set is given in AHARMIM 07.

⁵⁴AHMAD 01 deduced the total flux of active ⁸B solar neutrinos by combining the SNO charged-current result (AHMAD 01) and the Super-Kamiokande ν_e elastic-scattering result (FUKUDA 01).

Day-Night Asymmetry (⁸B)

$$A = (\phi_{\text{night}} - \phi_{\text{day}}) / \phi_{\text{average}}$$

VALUE	DOCUMENT ID	TECN	COMMENT
$0.021 \pm 0.020 +0.012 -0.013$	55 HOSAKA	06 SKAM	Based on ϕ_{ES}
$0.017 \pm 0.016 +0.012 -0.013$	56 HOSAKA	06 SKAM	Fitted in the LMA region
$-0.056 \pm 0.074 \pm 0.053$	57 AHARMIM	05A SNO	From salty SNO ϕ_{CC}
$-0.037 \pm 0.063 \pm 0.032$	57 AHARMIM	05A SNO	From salty SNO ϕ_{CC} ; const. of no ϕ_{NC} asymmetry
$0.14 \pm 0.063 +0.015 -0.014$	58 AHMAD	02B SNO	Derived from SNO ϕ_{CC}
$0.07 \pm 0.049 +0.013 -0.012$	59 AHMAD	02B SNO	Const. of no ϕ_{NC} asymmetry

• • • We do not use the following data for averages, fits, limits, etc. • • •

⁵⁵HOSAKA 06 reports the final results for 1496 live days with Super-Kamiokande-I between May 31, 1996 and July 15, 2001, and replace FUKUDA 02 results. The analysis threshold is 5 MeV except for the first 280 live days (6.5 MeV).

⁵⁶This result with reduced statistical uncertainty is obtained by assuming two-neutrino oscillations within the LMA (large mixing angle) region and by fitting the time variation of the solar neutrino flux measured via ν_e elastic scattering to the variations expected from neutrino oscillations. For details, see SMY 04. There is an additional small systematic error of ± 0.0004 coming from uncertainty of oscillation parameters.

⁵⁷AHARMIM 05A measurements were made with dissolved NaCl (0.195% by weight) in heavy water over the period between July 26, 2001 and August 28, 2003, with 176.5 days of the live time recorded during the day and 214.9 days during the night. This result is obtained with the spectral distribution of the CC events not constrained to the ⁸B shape.

⁵⁸AHMAD 02B results are based on the charged-current interactions recorded between November 2, 1999 and May 28, 2001, with the day and night live times of 128.5 and 177.9 days, respectively. The complete description of the SNO Phase I data set is given in AHARMIM 07.

⁵⁹AHMAD 02B results are derived from the charged-current interactions, neutral-current interactions, and ν_e elastic scattering, with the total flux of active neutrinos constrained to have no asymmetry. The data were recorded between November 2, 1999 and May 28, 2001, with the day and night live times of 128.5 and 177.9 days, respectively. The complete description of the SNO Phase I data set is given in AHARMIM 07.

 ϕ_{ES} (hep)

hep solar-neutrino flux measured via ν_e elastic scattering. This process is sensitive to all active neutrino flavors, but with reduced sensitivity to ν_μ , ν_τ due to the cross-section difference, $\sigma(\nu_{\mu,\tau} e) \sim 0.16\sigma(\nu_e e)$. If the hep solar-neutrino flux involves nonelectron flavor active neutrinos, their contribution to the flux is ~ 0.16 times of ν_e .

VALUE ($10^3 \text{ cm}^{-2}\text{s}^{-1}$)	CL%	DOCUMENT ID	TECN
<73	90	60 HOSAKA	06 SKAM

• • • We do not use the following data for averages, fits, limits, etc. • • •

⁶⁰HOSAKA 06 result is obtained from the recoil electron energy window of 18–21 MeV, and updates FUKUDA 01 result.

 ϕ_{ν_e} (⁸B)

Searches are made for electron antineutrino flux from the Sun. Flux limits listed here are derived relative to the BS05(OP) Standard Solar Model ⁸B solar neutrino flux, with an assumption that solar $\bar{\nu}_e$ s follow an unoscillated ⁸B neutrino spectrum.

VALUE (%)	CL%	DOCUMENT ID	TECN	COMMENT
<1.9	90	61 BALATA	06 CNTR	$1.8 < E_{\bar{\nu}_e} < 20.0$ MeV
<0.72	90	AHARMIM	04 SNO	$4.0 < E_{\bar{\nu}_e} < 14.8$ MeV
<0.025	90	EGUCHI	04 KLND	$8.3 < E_{\bar{\nu}_e} < 14.8$ MeV
<0.7	90	GANDO	03 SKAM	$8.0 < E_{\bar{\nu}_e} < 20.0$ MeV
<1.7	90	AGLIETTA	96 LSD	$7 < E_{\bar{\nu}_e} < 17$ MeV

• • • We do not use the following data for averages, fits, limits, etc. • • •

⁶¹BALATA 06 obtained this result from the search for $\bar{\nu}_e$ interactions with Counting Test Facility (the prototype of the Borexino detector).

Lepton Particle Listings

Neutrino Mixing

(B) Three-neutrino mixing parameters

INTRODUCTION TO THREE-NEUTRINO MIXING PARAMETERS LISTINGS

Updated October 2007 by M. Goodman (ANL).

Introduction and Notation: With the exception of the LSND anomaly, current accelerator, reactor, solar and atmospheric neutrino data can be described within the framework of a 3×3 mixing matrix between the flavor eigenstates ν_e , ν_μ , and ν_τ and mass eigenstates ν_1 , ν_2 and ν_3 . (See Eq. (13.30) of the Review “Neutrino Mass, Mixing, and Flavor Change,” by B. Kayser.) Whether or not this is the ultimately correct framework, it is currently widely used to parameterize neutrino mixing data and to plan new experiments.

The mass differences are called Δm_{21}^2 and Δm_{32}^2 following Eq. (13.29) in the review. In these Listings, we assume that $\Delta m_{32}^2 \sim \Delta m_{31}^2$, although in the future, experiments may be precise enough to measure these separately. The angles, as specified in Eq. (13.30) of the review, are labeled θ_{12} , θ_{23} , and θ_{13} . The CP violating phase is called δ , but that does not yet appear in the Listings. The familiar two-neutrino form for oscillations is given in Eqs. (13.19) and (13.20). Despite the fact that the mixing angles have been measured to be much larger than in the quark sector, the two-neutrino form is often a very good approximation and is used in many situations.

The angles appear in the equations below in many forms. They most often appear as $\sin^2(2\theta)$. The Listings currently use this convention.

Accelerator neutrino experiments: Ignoring the small Δm_{21}^2 scale, CP violation, and matter effects, the equations for the probability of appearance in an accelerator oscillation experiment are:

$$P(\nu_\mu \rightarrow \nu_\tau) = \sin^2(2\theta_{23}) \cos^4(\theta_{13}) \sin^2(\Delta m_{32}^2 L/4E) \quad (1)$$

$$P(\nu_\mu \rightarrow \nu_e) = \sin^2(2\theta_{13}) \sin^2(\theta_{23}) \sin^2(\Delta m_{32}^2 L/4E) \quad (2)$$

$$P(\nu_e \rightarrow \nu_\mu) = \sin^2(2\theta_{13}) \sin^2(\theta_{23}) \sin^2(\Delta m_{32}^2 L/4E) \quad (3)$$

$$P(\nu_e \rightarrow \nu_\tau) = \sin^2(2\theta_{13}) \cos^2(\theta_{23}) \sin^2(\Delta m_{32}^2 L/4E) \quad (4)$$

For the case of negligible θ_{13} , these probabilities vanish except for $P(\nu_\mu \rightarrow \nu_\tau)$, which then takes the familiar two-neutrino form.

New long-baseline experiments are being planned to search for non-zero θ_{13} through $P(\nu_\mu \rightarrow \nu_e)$. Including the CP violating terms and low mass scale, the equation for neutrino oscillation in vacuum is:

$$\begin{aligned} P(\nu_\mu \rightarrow \nu_e) &= P1 + P2 + P3 + P4 \\ P1 &= \sin^2(\theta_{23}) \sin^2(2\theta_{13}) \sin^2(\Delta m_{32}^2 L/4E) \\ P2 &= \cos^2(\theta_{23}) \sin^2(2\theta_{13}) \sin^2(\Delta m_{21}^2 L/4E) \\ P3 &= -/ + J \sin(\delta) \sin(\Delta m_{32}^2 L/4E) \\ P4 &= J \cos(\delta) \cos(\Delta m_{32}^2 L/4E) \end{aligned} \quad (5)$$

where

$$J = \cos(\theta_{13}) \sin(2\theta_{12}) \sin(2\theta_{13}) \sin(2\theta_{23}) \times \sin(\Delta m_{32}^2 L/4E) \sin(\Delta m_{21}^2 L/4E) \quad (6)$$

and the sign in P3 is negative for neutrinos and positive for anti-neutrinos. For most new proposed long-baseline accelerator experiments, P2 can safely be neglected, but depending on the values of θ_{13} and δ , the other three terms could be comparable. Also, depending on the distance and the mass hierarchy, matter effects will need to be included.

Reactor neutrino experiments: Nuclear reactors are prolific sources of $\bar{\nu}_e$ with an energy near 4 MeV. The oscillation probability can be expressed

$$P(\bar{\nu}_e \rightarrow \bar{\nu}_e) = 1 - \cos^4(\theta_{13}) \sin^2(2\theta_{12}) \sin^2(\Delta m_{21}^2 L/4E) - \sin^2(2\theta_{13}) \sin^2(\Delta m_{32}^2 L/4E) \quad (7)$$

For short distances ($L < 5$ km), it is a good approximation to ignore the second term on the right, and this takes the familiar two-neutrino form with θ_{13} and Δm_{32}^2 . For long distances and small θ_{13} , the second term oscillates rapidly and averages to zero for an experiment with finite energy resolution, leading to the familiar two-neutrino form with θ_{12} and Δm_{21}^2 .

Solar and Atmospheric neutrino experiments: Solar neutrino experiments are sensitive to ν_e disappearance and have allowed the measurement of θ_{12} and Δm_{21}^2 . They are also sensitive to θ_{13} . In the discussion after Eq. (13.22) in “Neutrino Mass Mixing and Flavor Change” in this *Review*, we identify $\Delta m_{\odot}^2 = \Delta m_{21}^2$ and $\theta_{\odot} = \theta_{12}$.

Atmospheric neutrino experiments are primarily sensitive to ν_μ disappearance through $\nu_\mu \rightarrow \nu_\tau$ oscillations, and have allowed the measurement of θ_{23} and Δm_{32}^2 . In Fig. (13.1) in “Neutrino Mass Mixing and Flavor Change” in this *Review*, we identify $\Delta m_{atm}^2 = \Delta m_{32}^2$ and $\theta_{atm} = \theta_{23}$. Despite the large ν_e component of the atmospheric neutrino flux, it is difficult to measure Δm_{21}^2 effects. This is because of a cancellation between $\nu_\mu \rightarrow \nu_e$ and $\nu_e \rightarrow \nu_\mu$, together with the fact that the ratio of ν_μ and ν_e atmospheric fluxes, which arise from sequential π and μ decay, is near 2.

 $\sin^2(2\theta_{12})$

VALUE	DOCUMENT ID	TECN	COMMENT
$0.86^{+0.03}_{-0.04}$	62 AHARMIM	05A	FIT KamLAND + global solar
• • • We do not use the following data for averages, fits, limits, etc. • • •			
$0.85^{+0.04}_{-0.06}$	63 HOSAKA	06	FIT KamLAND + global solar
$0.85^{+0.06}_{-0.05}$	64 HOSAKA	06	FIT SKAM+SNO+KamLAND
$0.86^{+0.05}_{-0.07}$	65 HOSAKA	06	FIT SKAM+SNO
$0.75-0.95$	66 AHARMIM	05A	FIT global solar
0.82 ± 0.05	67 ARAKI	05	FIT KamLAND + global solar
0.82 ± 0.04	68 AHMED	04A	FIT KamLAND + global solar
$0.71-0.93$	69 AHMED	04A	FIT global solar
$0.85^{+0.05}_{-0.07}$	70 SMY	04	FIT KamLAND + global solar
$0.83^{+0.06}_{-0.08}$	71 SMY	04	FIT global solar
$0.87^{+0.07}_{-0.08}$	72 SMY	04	FIT SKAM + SNO
$0.62-0.88$	73 AHMAD	02B	FIT global solar
$0.62-0.95$	74 FUKUDA	02	FIT global solar

See key on page 373

Lepton Particle Listings
Neutrino Mixing

- ⁶²The result given by AHARMIM 05A is $\theta = (33.9 \pm 1.6)^\circ$. This result is obtained by a two-neutrino oscillation analysis using SNO pure deuterium and salt phase data, SK ν_e data, CI and Ga CC data, and KamLAND data (ARAKI 05). *CPT* invariance is assumed. AHARMIM 05A also quotes $\theta = (33.9^{+2.4}_{-2.2})^\circ$ as the error enveloping the 68% CL two-dimensional region. This translates into $\sin^2 2\theta = 0.86^{+0.05}_{-0.06}$.
- ⁶³HOSAKA 06 obtained this result by a two-neutrino oscillation analysis using SK ν_e data, CC data from other solar neutrino experiments, and KamLAND data (ARAKI 05). *CPT* invariance is assumed.
- ⁶⁴HOSAKA 06 obtained this result by a two-neutrino oscillation analysis using the data from Super-Kamiokande, SNO (AHMAD 02 and AHMAD 02B), and KamLAND (ARAKI 05) experiments. *CPT* invariance is assumed.
- ⁶⁵HOSAKA 06 obtained this result by a two-neutrino oscillation analysis using the Super-Kamiokande and SNO (AHMAD 02 and AHMAD 02B) solar neutrino data.
- ⁶⁶AHARMIM 05A obtained this result by a two-neutrino oscillation analysis using the data from all solar neutrino experiments. The listed range of the parameter envelops the 95% CL two-dimensional region shown in figure 35a of AHARMIM 05A. AHARMIM 05A also quotes $\tan^2 \theta = 0.45^{+0.09}_{-0.08}$ as the error enveloping the 68% CL two-dimensional region. This translates into $\sin^2 2\theta = 0.86^{+0.05}_{-0.07}$.
- ⁶⁷ARAKI 05 obtained this result by a two-neutrino oscillation analysis using KamLAND and solar neutrino data. *CPT* invariance is assumed. The 1σ error shown here is translated from the number provided by the KamLAND collaboration, $\tan^2 \theta = 0.40^{+0.07}_{-0.05}$. The corresponding number quoted in ARAKI 05 is $\tan^2 \theta = 0.40^{+0.10}_{-0.07}$ ($\sin^2 2\theta = 0.82 \pm 0.07$), which envelops the 68% CL two-dimensional region.
- ⁶⁸The result given by AHMED 04A is $\theta = (32.5^{+1.7}_{-1.6})^\circ$. This result is obtained by a two-neutrino oscillation analysis using solar neutrino and KamLAND data (EGUCHI 03). *CPT* invariance is assumed. AHMED 04A also quotes $\theta = (32.5^{+2.4}_{-2.3})^\circ$ as the error enveloping the 68% CL two-dimensional region. This translates into $\sin^2 2\theta = 0.82 \pm 0.06$.
- ⁶⁹AHMED 04A obtained this result by a two-neutrino oscillation analysis using the data from all solar neutrino experiments. The listed range of the parameter envelops the 95% CL two-dimensional region shown in Fig. 5(a) of AHMED 04A. The best-fit point is $\Delta(m^2) = 6.5 \times 10^{-5} \text{ eV}^2$, $\tan^2 \theta = 0.40$ ($\sin^2 2\theta = 0.82$).
- ⁷⁰The result given by SMY 04 is $\tan^2 \theta = 0.44 \pm 0.08$. This result is obtained by a two-neutrino oscillation analysis using solar neutrino and KamLAND data (IANNI 03). *CPT* invariance is assumed.
- ⁷¹SMY 04 obtained this result by a two-neutrino oscillation analysis using the data from all solar neutrino experiments. The 1σ errors are read from Fig. 6(a) of SMY 04.
- ⁷²SMY 04 obtained this result by a two-neutrino oscillation analysis using the Super-Kamiokande and SNO (AHMAD 02 and AHMAD 02B) solar neutrino data. The 1σ errors are read from Fig. 6(a) of SMY 04.
- ⁷³AHMAD 02B obtained this result by a two-neutrino oscillation analysis using the data from all solar neutrino experiments. The listed range of the parameter envelops the 95% CL two-dimensional region shown in Fig. 4(b) of AHMAD 02B. The best fit point is $\Delta(m^2) = 5.0 \times 10^{-5} \text{ eV}^2$ and $\tan \theta = 0.34$ ($\sin^2 2\theta = 0.76$).
- ⁷⁴FUKUDA 02 obtained this result by a two-neutrino oscillation analysis using the data from all solar neutrino experiments. The listed range of the parameter envelops the 95% CL two-dimensional region shown in Fig. 4 of FUKUDA 02. The best fit point is $\Delta(m^2) = 6.9 \times 10^{-5} \text{ eV}^2$ and $\tan^2 \theta = 0.38$ ($\sin^2 2\theta = 0.80$).

 Δm_{21}^2

VALUE (10^{-5} eV^2)	DOCUMENT ID	TECN	COMMENT
8.0 ± 0.3	⁷⁵ HOSAKA	06	FIT KamLAND + global solar
8.0 ± 0.3	⁷⁶ HOSAKA	06	FIT SKAM+SNO+KamLAND
$6.3^{+3.7}_{-1.5}$	⁷⁷ HOSAKA	06	FIT SKAM+SNO
5–12	⁷⁸ HOSAKA	06	FIT SKAM day/night in the LMA region
$8.0^{+0.4}_{-0.3}$	⁷⁹ AHARMIM	05A	FIT KamLAND + global solar LMA
3.3–14.4	⁸⁰ AHARMIM	05A	FIT global solar
$7.9^{+0.4}_{-0.3}$	⁸¹ ARAKI	05	FIT KamLAND + global solar
$7.1^{+1.0}_{-0.3}$	⁸² AHMED	04A	FIT KamLAND + global solar
3.2–13.7	⁸³ AHMED	04A	FIT global solar
$7.1^{+0.6}_{-0.5}$	⁸⁴ SMY	04	FIT KamLAND + global solar
$6.0^{+1.7}_{-1.6}$	⁸⁵ SMY	04	FIT global solar
$6.0^{+2.5}_{-1.6}$	⁸⁶ SMY	04	FIT SKAM + SNO
2.8–12.0	⁸⁷ AHMAD	02B	FIT global solar
3.2–19.1	⁸⁸ FUKUDA	02	FIT global solar

- $\bullet \bullet \bullet$ We do not use the following data for averages, fits, limits, etc. $\bullet \bullet \bullet$
- ⁷⁵HOSAKA 06 obtained this result by a two-neutrino oscillation analysis using solar neutrino and KamLAND data (ARAKI 05). *CPT* invariance is assumed.
- ⁷⁶HOSAKA 06 obtained this result by a two-neutrino oscillation analysis using the data from Super-Kamiokande, SNO (AHMAD 02 and AHMAD 02B), and KamLAND (ARAKI 05) experiments. *CPT* invariance is assumed.
- ⁷⁷HOSAKA 06 obtained this result by a two-neutrino oscillation analysis using the Super-Kamiokande and SNO (AHMAD 02 and AHMAD 02B) solar neutrino data.
- ⁷⁸HOSAKA 06 obtained this result from the consistency between the observed and expected day-night flux asymmetry amplitude. The listed 68% CL range is derived from the 1σ boundary of the amplitude fit to the data. Oscillation parameters are constrained to be in the LMA region. The mixing angle is fixed at $\tan^2 \theta = 0.44$ because the fit depends only very weakly on it.

- ⁷⁹AHARMIM 05A obtained this result by a two-neutrino oscillation analysis using solar neutrino and KamLAND data (ARAKI 05). *CPT* invariance is assumed. AHARMIM 05A also quotes $\Delta(m^2) = (8.0^{+0.6}_{-0.4}) \times 10^{-5} \text{ eV}^2$ as the error enveloping the 68% CL two-dimensional region.
- ⁸⁰AHARMIM 05A obtained this result by a two-neutrino oscillation analysis using the data from all solar neutrino experiments. The listed range of the parameter envelops the 95% CL two-dimensional region shown in figure 35a of AHARMIM 05A. AHARMIM 05A also quotes $\Delta(m^2) = (6.5^{+4.4}_{-2.3}) \times 10^{-5} \text{ eV}^2$ as the error enveloping the 68% CL two-dimensional region.
- ⁸¹ARAKI 05 obtained this result by a two-neutrino oscillation analysis using KamLAND and solar neutrino data. *CPT* invariance is assumed. The 1σ error shown here is provided by the KamLAND collaboration. The error quoted in ARAKI 05, $\Delta(m^2) = (7.9^{+0.6}_{-0.5}) \times 10^{-5}$, envelops the 68% CL two-dimensional region.
- ⁸²AHMED 04A obtained this result by a two-neutrino oscillation analysis using solar neutrino and KamLAND data (EGUCHI 03). *CPT* invariance is assumed. AHMED 04A also quotes $\Delta(m^2) = (7.1^{+1.2}_{-0.6}) \times 10^{-5} \text{ eV}^2$ as the error enveloping the 68% CL two-dimensional region.
- ⁸³AHMED 04A obtained this result by a two-neutrino oscillation analysis using the data from all solar neutrino experiments. The listed range of the parameter envelops the 95% CL two-dimensional region shown in Fig. 5(a) of AHMED 04A. The best-fit point is $\Delta(m^2) = 6.5 \times 10^{-5} \text{ eV}^2$, $\tan^2 \theta = 0.40$ ($\sin^2 2\theta = 0.82$).
- ⁸⁴SMY 04 obtained this result by a two-neutrino oscillation analysis using solar neutrino and KamLAND data (IANNI 03). *CPT* invariance is assumed.
- ⁸⁵SMY 04 obtained this result by a two-neutrino oscillation analysis using the data from all solar neutrino experiments. The 1σ errors are read from Fig. 6(a) of SMY 04.
- ⁸⁶SMY 04 obtained this result by a two-neutrino oscillation analysis using the Super-Kamiokande and SNO (AHMAD 02 and AHMAD 02B) solar neutrino data. The 1σ errors are read from Fig. 6(a) of SMY 04.
- ⁸⁷AHMAD 02B obtained this result by a two-neutrino oscillation analysis using the data from all solar neutrino experiments. The listed range of the parameter envelops the 95% CL two-dimensional region shown in Fig. 4(b) of AHMAD 02B. The best fit point is $\Delta(m^2) = 5.0 \times 10^{-5} \text{ eV}^2$ and $\tan \theta = 0.34$ ($\sin^2 2\theta = 0.76$).
- ⁸⁸FUKUDA 02 obtained this result by a two-neutrino oscillation analysis using the data from all solar neutrino experiments. The listed range of the parameter envelops the 95% CL two-dimensional region shown in Fig. 4 of FUKUDA 02. The best fit point is $\Delta(m^2) = 6.9 \times 10^{-5} \text{ eV}^2$ and $\tan^2 \theta = 0.38$ ($\sin^2 2\theta = 0.80$).

 $\sin^2(2\theta_{23})$

The ranges below correspond to the projection onto the $\sin^2(2\theta_{23}) - \Delta m_{32}^2$ plane presented by the authors.

VALUE	DOCUMENT ID	TECN	COMMENT
>0.92	⁸⁹ ASHIE	05	SKAM Super-Kamiokande
>0.2	⁹⁰ ADAMSON	06	MINS atmospheric ν with far detector
>0.59	⁹¹ AHN	06A	K2K KEK to Super-K
>0.91	⁹² HOSAKA	06A	SKAM 3ν oscillation; normal mass hierarchy
>0.86	⁹³ HOSAKA	06A	SKAM 3ν oscillation; inverted mass hierarchy
>0.7	⁹⁴ MICHAEL	06	MINS MINOS
>0.58	⁹⁵ ALIU	05	K2K KEK to Super-K
>0.6	⁹⁶ ALLISON	05	SOU2
>0.80	⁹⁷ AMBROSIO	04	MCRO MACRO
>0.90	⁹⁸ ASHIE	04	SKAM L/E distribution
>0.30	⁹⁹ AHN	03	K2K KEK to Super-K
>0.45	¹⁰⁰ AMBROSIO	03	MCRO MACRO
>0.77	¹⁰¹ AMBROSIO	03	MCRO MACRO
>0.50	¹⁰² SANCHEZ	03	SOU2 Soudan-2 Atmospheric
>0.80	¹⁰³ AMBROSIO	01	MCRO upward μ
>0.82	¹⁰⁴ AMBROSIO	01	MCRO upward μ
>0.45	¹⁰⁵ FUKUDA	99C	SKAM upward μ
>0.70	¹⁰⁶ FUKUDA	99D	SKAM upward μ
>0.30	¹⁰⁷ FUKUDA	99D	SKAM stop μ / through
>0.82	¹⁰⁸ FUKUDA	98C	SKAM Super-Kamiokande
>0.30	¹⁰⁹ HATAKEYAMA	98	KAMI Kamiokande
>0.73	¹¹⁰ HATAKEYAMA	98	KAMI Kamiokande
>0.65	¹¹¹ FUKUDA	94	KAMI Kamiokande

- $\bullet \bullet \bullet$ We do not use the following data for averages, fits, limits, etc. $\bullet \bullet \bullet$
- ⁸⁹ASHIE 05 obtained this result by a two-neutrino oscillation analysis using 92 kton yr atmospheric neutrino data from the complete Super-Kamiokande I running period.
- ⁹⁰ADAMSON 06 obtained this result by a two-neutrino oscillation analysis of the L/E distribution using 4.54 kton yr atmospheric neutrino data with the MINOS far detector.
- ⁹¹Supercedes ALIU 05.
- ⁹²HOSAKA 06A obtained this result ($\sin^2 \theta_{23} = 0.37\text{--}0.65$) by a three-neutrino oscillation analysis with one mass scale dominance ($\Delta m_{21}^2 = 0$) using the Super-Kamiokande-I atmospheric neutrino data. The normal mass hierarchy is assumed.
- ⁹³HOSAKA 06A obtained this result ($\sin^2 \theta_{23} = 0.37\text{--}0.69$) by a three-neutrino oscillation analysis with one mass scale dominance ($\Delta m_{21}^2 = 0$) using the Super-Kamiokande-I atmospheric neutrino data. The inverted mass hierarchy is assumed.
- ⁹⁴MICHAEL 06 best fit is for maximal mixing.
- ⁹⁵The best fit is for maximal mixing.
- ⁹⁶ALLISON 05 result is based upon atmospheric neutrino interactions including upward-stopping muons, with an exposure of 5.9 kton yr. From a two-flavor oscillation analysis the best-fit point is $\Delta m^2 = 0.0017 \text{ eV}^2$ and $\sin^2(2\theta) = 0.97$.

Lepton Particle Listings

Neutrino Mixing

- ⁹⁷ AMBROSIO 04 obtained this result, without using the absolute normalization of the neutrino flux, by combining the angular distribution of upward through-going muon tracks with $E_\mu > 1$ GeV, N_{low} and N_{high} , and the numbers of InDown + UpStop and InUp events. Here, N_{low} and N_{high} are the number of events with reconstructed neutrino energies < 30 GeV and > 130 GeV, respectively. InDown and InUp represent events with downward and upward-going tracks starting inside the detector due to neutrino interactions, while UpStop represents entering upward-going tracks which stop in the detector. The best fit is for maximal mixing.
- ⁹⁸ ASHIE 04 obtained this result from the $L(\text{flight length})/E(\text{estimated neutrino energy})$ distribution of ν_μ disappearance probability, using the Super-Kamiokande-I 1489 live-day atmospheric neutrino data.
- ⁹⁹ There are several islands of allowed region from this K2K analysis, extending to high values of Δm^2 . We only include the one that overlaps atmospheric neutrino analyses. The best fit is for maximal mixing.
- ¹⁰⁰ AMBROSIO 03 obtained this result on the basis of the ratio $R = N_{low}/N_{high}$, where N_{low} and N_{high} are the number of upward through-going muon events with reconstructed neutrino energy < 30 GeV and > 130 GeV, respectively. The data came from the full detector run started in 1994. The method of FELDMAN 98 is used to obtain the limits.
- ¹⁰¹ AMBROSIO 03 obtained this result by using the ratio R and the angular distribution of the upward through-going muons. R is given in the previous note and the angular distribution is reported in AMBROSIO 01. The method of FELDMAN 98 is used to obtain the limits. The best fit is to maximal mixing.
- ¹⁰² SANCHEZ 03 is based on an exposure of 5.9 kton yr. The result is obtained using a likelihood analysis of the neutrino L/E distribution for a selection μ flavor sample while the e -flavor sample provides flux normalization. The method of FELDMAN 98 is used to obtain the allowed region. The best fit is $\sin^2(2\theta) = 0.97$.
- ¹⁰³ AMBROSIO 01 result is based on the angular distribution of upward through-going muon tracks with $E_\mu > 1$ GeV. The data came from three different detector configurations, but the statistics is largely dominated by the full detector run, from May 1994 to December 2000. The total live time, normalized to the full detector configuration is 6.17 years. The best fit is obtained outside the physical region. The method of FELDMAN 98 is used to obtain the limits. The best fit is for maximal mixing.
- ¹⁰⁴ AMBROSIO 01 result is based on the angular distribution and normalization of upward through-going muon tracks with $E_\mu > 1$ GeV. See the previous footnote.
- ¹⁰⁵ FUKUDA 99c obtained this result from a total of 537 live days of upward through-going muon data in Super-Kamiokande between April 1996 to January 1998. With a threshold of $E_\mu > 1.6$ GeV, the observed flux is $(1.74 \pm 0.07 \pm 0.02) \times 10^{-13} \text{ cm}^{-2}\text{s}^{-1}\text{sr}^{-1}$. The best fit is $\sin^2(2\theta) = 0.95$.
- ¹⁰⁶ FUKUDA 99d obtained this result from a simultaneous fitting to zenith angle distributions of upward-stopping and through-going muons. The flux of upward-stopping muons of minimum energy of 1.6 GeV measured between April 1996 and January 1998 is $(0.39 \pm 0.04 \pm 0.02) \times 10^{-13} \text{ cm}^{-2}\text{s}^{-1}\text{sr}^{-1}$. This is compared to the expected flux of $(0.73 \pm 0.16 \text{ (theoretical error)}) \times 10^{-13} \text{ cm}^{-2}\text{s}^{-1}\text{sr}^{-1}$. The best fit is to maximal mixing.
- ¹⁰⁷ FUKUDA 99d obtained this result from the zenith dependence of the upward-stopping/through-going flux ratio. The best fit is to maximal mixing.
- ¹⁰⁸ FUKUDA 98c obtained this result by an analysis of 33.0 kton yr atmospheric neutrino data. The best fit is for maximal mixing.
- ¹⁰⁹ HATAKEYAMA 98 obtained this result from a total of 2456 live days of upward-going muon data in Kamiokande between December 1985 and May 1995. With a threshold of $E_\mu > 1.6$ GeV, the observed flux of upward through-going muons is $(1.94 \pm 0.10^{+0.07}_{-0.06}) \times 10^{-13} \text{ cm}^{-2}\text{s}^{-1}\text{sr}^{-1}$. This is compared to the expected flux of $(2.46 \pm 0.54 \text{ (theoretical error)}) \times 10^{-13} \text{ cm}^{-2}\text{s}^{-1}\text{sr}^{-1}$. The best fit is for maximal mixing.
- ¹¹⁰ HATAKEYAMA 98 obtained this result from a combined analysis of Kamiokande contained events (FUKUDA 94) and upward going muon events. The best fit is $\sin^2(2\theta) = 0.95$.
- ¹¹¹ FUKUDA 94 obtained the result by a combined analysis of sub- and multi-GeV atmospheric neutrino events in Kamiokande. The best fit is for maximal mixing.

 Δm_{32}^2

The sign of Δm_{32}^2 is not known at this time. Only the absolute value is quoted below. The ranges below correspond to the projection onto the Δm_{32}^2 axis of the 90% CL contours in the $\sin^2(2\theta_{23}) - \Delta m_{32}^2$ plane presented by the authors.

VALUE (10^{-3} eV^2)	DOCUMENT ID	TECN	COMMENT
1.9 to 3.0	112 ASHIE	04 SKAM	L/E distribution
0.07–5.0	113 ADAMSON	06 MINS	atmospheric ν with far detector
1.9–4.0	114,115 AHN	06A K2K	KEK to Super-K
1.8–3.1	116 HOSAKA	06A SKAM	3ν oscillation; normal mass hierarchy
1.8–3.7	117 HOSAKA	06A SKAM	3ν oscillation; inverted mass hierarchy
2.2–3.8	118 MICHAEL	06 MINS	MINOS
1.9–3.6	114 ALIU	05 K2K	KEK to Super-K
0.3–12	119 ALLISON	05 SOU2	
1.5–3.4	120 ASHIE	05 SKAM	atmospheric neutrino
0.6–8.0	121 AMBROSIO	04 MCRO	MACRO
1.5–3.9	122 AHN	03 K2K	KEK to Super-K
0.25–9.0	123 AMBROSIO	03 MCRO	MACRO
0.6–7.0	124 AMBROSIO	03 MCRO	MACRO
0.15–15	125 SANCHEZ	03 SOU2	Soudan-2 Atmospheric
0.6–15	126 AMBROSIO	01 MCRO	upward μ

• • • We do not use the following data for averages, fits, limits, etc. • • •

- 1.0–6.0 ¹²⁷ AMBROSIO 01 MCRO upward μ
- 1.0–50 ¹²⁸ FUKUDA 99c SKAM upward μ
- 1.5–15.0 ¹²⁹ FUKUDA 99d SKAM upward μ
- 0.7–18 ¹³⁰ FUKUDA 99d SKAM stop μ / through
- 0.5–6.0 ¹³¹ FUKUDA 98c SKAM Super-Kamiokande
- 0.55–5.0 ¹³² HATAKEYAMA 98 KAMI Kamiokande
- 4–23 ¹³³ HATAKEYAMA 98 KAMI Kamiokande
- 5–25 ¹³⁴ FUKUDA 94 KAMI Kamiokande
- ¹¹² ASHIE 04 obtained this result from the $L(\text{flight length})/E(\text{estimated neutrino energy})$ distribution of ν_μ disappearance probability, using the Super-Kamiokande-I 1489 live-day atmospheric neutrino data. The best fit is for $\Delta m^2 = 2.4 \times 10^{-3} \text{ eV}^2$.
- ¹¹³ ADAMSON 06 obtained this result by a two-neutrino oscillation analysis of the L/E distribution using 4.54 kton yr atmospheric neutrino data with the MINOS far detector.
- ¹¹⁴ The best fit in the physical region is for $\Delta m^2 = 2.8 \times 10^{-3} \text{ eV}^2$.
- ¹¹⁵ Supercedes ALIU 05.
- ¹¹⁶ HOSAKA 06a obtained this result by a three-neutrino oscillation analysis with one mass scale dominance ($\Delta m_{21}^2 = 0$) using the Super-Kamiokande-I atmospheric neutrino data. The normal mass hierarchy is assumed.
- ¹¹⁷ HOSAKA 06a obtained this result by a three-neutrino oscillation analysis with one mass scale dominance ($\Delta m_{21}^2 = 0$) using the Super-Kamiokande-I atmospheric neutrino data. The inverted mass hierarchy is assumed.
- ¹¹⁸ MICHAEL 06 best fit is $2.74 \times 10^{-3} \text{ eV}^2$.
- ¹¹⁹ ALLISON 05 result is based on an atmospheric neutrino observation with an exposure of 5.9 kton yr. From a two-flavor oscillation analysis the best-fit point is $\Delta m^2 = 0.0017 \text{ eV}^2$ and $\sin^2 2\theta = 0.97$.
- ¹²⁰ ASHIE 05 obtained this result by a two-neutrino oscillation analysis using 92 kton yr atmospheric neutrino data from the complete Super-Kamiokande I running period. The best fit is for $\Delta m^2 = 2.1 \times 10^{-3} \text{ eV}^2$.
- ¹²¹ AMBROSIO 04 obtained this result, without using the absolute normalization of the neutrino flux, by combining the angular distribution of upward through-going muon tracks with $E_\mu > 1$ GeV, N_{low} and N_{high} , and the numbers of InDown + UpStop and InUp events. Here, N_{low} and N_{high} are the number of events with reconstructed neutrino energies < 30 GeV and > 130 GeV, respectively. InDown and InUp represent events with downward and upward-going tracks starting inside the detector due to neutrino interactions, while UpStop represents entering upward-going tracks which stop in the detector. The best fit is for $\Delta m^2 = 2.3 \times 10^{-3} \text{ eV}^2$.
- ¹²² There are several islands of allowed region from this K2K analysis, extending to high values of Δm^2 . We only include the one that overlaps atmospheric neutrino analyses. The best fit is for $\Delta m^2 = 2.8 \times 10^{-3} \text{ eV}^2$.
- ¹²³ AMBROSIO 03 obtained this result on the basis of the ratio $R = N_{low}/N_{high}$, where N_{low} and N_{high} are the number of upward through-going muon events with reconstructed neutrino energy < 30 GeV and > 130 GeV, respectively. The data came from the full detector run started in 1994. The method of FELDMAN 98 is used to obtain the limits. The best fit is for $\Delta m^2 = 2.5 \times 10^{-3} \text{ eV}^2$.
- ¹²⁴ AMBROSIO 03 obtained this result by using the ratio R and the angular distribution of the upward through-going muons. R is given in the previous note and the angular distribution is reported in AMBROSIO 01. The method of FELDMAN 98 is used to obtain the limits. The best fit is for $\Delta m^2 = 2.5 \times 10^{-3} \text{ eV}^2$.
- ¹²⁵ SANCHEZ 03 is based on an exposure of 5.9 kton yr. The result is obtained using a likelihood analysis of the neutrino L/E distribution for a selection μ flavor sample while the e -flavor sample provides flux normalization. The method of FELDMAN 98 is used to obtain the allowed region. The best fit is for $\Delta m^2 = 5.2 \times 10^{-3} \text{ eV}^2$.
- ¹²⁶ AMBROSIO 01 result is based on the angular distribution of upward through-going muon tracks with $E_\mu > 1$ GeV. The data came from three different detector configurations, but the statistics is largely dominated by the full detector run, from May 1994 to December 2000. The total live time, normalized to the full detector configuration is 6.17 years. The best fit is obtained outside the physical region. The method of FELDMAN 98 is used to obtain the limits.
- ¹²⁷ AMBROSIO 01 result is based on the angular distribution and normalization of upward through-going muon tracks with $E_\mu > 1$ GeV. See the previous footnote.
- ¹²⁸ FUKUDA 99c obtained this result from a total of 537 live days of upward through-going muon data in Super-Kamiokande between April 1996 to January 1998. With a threshold of $E_\mu > 1.6$ GeV, the observed flux is $(1.74 \pm 0.07 \pm 0.02) \times 10^{-13} \text{ cm}^{-2}\text{s}^{-1}\text{sr}^{-1}$. The best fit is for $\Delta m^2 = 5.9 \times 10^{-3} \text{ eV}^2$.
- ¹²⁹ FUKUDA 99d obtained this result from a simultaneous fitting to zenith angle distributions of upward-stopping and through-going muons. The flux of upward-stopping muons of minimum energy of 1.6 GeV measured between April 1996 and January 1998 is $(0.39 \pm 0.04 \pm 0.02) \times 10^{-13} \text{ cm}^{-2}\text{s}^{-1}\text{sr}^{-1}$. This is compared to the expected flux of $(0.73 \pm 0.16 \text{ (theoretical error)}) \times 10^{-13} \text{ cm}^{-2}\text{s}^{-1}\text{sr}^{-1}$. The best fit is for $\Delta m^2 = 3.9 \times 10^{-3} \text{ eV}^2$.
- ¹³⁰ FUKUDA 99d obtained this result from the zenith dependence of the upward-stopping/through-going flux ratio. The best fit is for $\Delta m^2 = 3.1 \times 10^{-3} \text{ eV}^2$.
- ¹³¹ FUKUDA 98c obtained this result by an analysis of 33.0 kton yr atmospheric neutrino data. The best fit is for $\Delta m^2 = 2.2 \times 10^{-3} \text{ eV}^2$.
- ¹³² HATAKEYAMA 98 obtained this result from a total of 2456 live days of upward-going muon data in Kamiokande between December 1985 and May 1995. With a threshold of $E_\mu > 1.6$ GeV, the observed flux of upward through-going muons is $(1.94 \pm 0.10^{+0.07}_{-0.06}) \times 10^{-13} \text{ cm}^{-2}\text{s}^{-1}\text{sr}^{-1}$. This is compared to the expected flux of $(2.46 \pm 0.54 \text{ (theoretical error)}) \times 10^{-13} \text{ cm}^{-2}\text{s}^{-1}\text{sr}^{-1}$. The best fit is for $\Delta m^2 = 2.2 \times 10^{-3} \text{ eV}^2$.
- ¹³³ HATAKEYAMA 98 obtained this result from a combined analysis of Kamiokande contained events (FUKUDA 94) and upward going muon events. The best fit is for $\Delta m^2 = 13 \times 10^{-3} \text{ eV}^2$.
- ¹³⁴ FUKUDA 94 obtained the result by a combined analysis of sub- and multi-GeV atmospheric neutrino events in Kamiokande. The best fit is for $\Delta m^2 = 16 \times 10^{-3} \text{ eV}^2$.

$\sin^2(2\theta_{13})$

At present time, limits of $\sin^2(2\theta_{13})$ are derived from the search for the reactor $\bar{\nu}_e$ disappearance at distances corresponding to the Δm_{23}^2 value, i.e. $L \sim 1$ km. Alternatively, somewhat weaker limits can be obtained from the analysis of the solar neutrino data.

VALUE	CL%	DOCUMENT ID	TECN	COMMENT
<0.19	90	135 APOLLONIO	99	CHOZ Reactor Experiment

• • • We do not use the following data for averages, fits, limits, etc. • • •

<0.48	90	136 HOSAKA	06A	SKAM 3ν oscillation; normal mass hierarchy
<0.79	90	137 HOSAKA	06A	SKAM 3ν oscillation; inverted mass hierarchy
<0.36	138	YAMAMOTO	06	K2K Accelerator experiment
<0.48	90	139 AHN	04	K2K Accelerator experiment
<0.36	90	140 BOEHM	01	Palo Verde react.
<0.45	90	141 BOEHM	00	Palo Verde react.

135 The quoted limit is for $\Delta m_{32}^2 = 1.9 \times 10^{-3} \text{ eV}^2$. That value of Δm_{32}^2 is the 1- σ low value for ALIU 05. For the ALIU 05 best fit value of $2.8 \times 10^{-3} \text{ eV}^2$, the $\sin^2 2\theta_{13}$ limit is < 0.13. See also APOLLONIO 03 for a detailed description of the experiment.

136 HOSAKA 06A obtained this result by a three-neutrino oscillation analysis with one mass scale dominance ($\Delta m_{21}^2 = 0$) using the Super-Kamiokande-I atmospheric neutrino data. The normal mass hierarchy is assumed.

137 HOSAKA 06A obtained this result by a three-neutrino oscillation analysis with one mass scale dominance ($\Delta m_{21}^2 = 0$) using the Super-Kamiokande-I atmospheric neutrino data. The inverted mass hierarchy is assumed.

138 YAMAMOTO 06 searched for $\nu_\mu \rightarrow \nu_e$ appearance. Assumes $2 \sin^2(2\theta_{\mu e}) = \sin^2(2\theta_{13})$. The quoted limit is for $\Delta m_{32}^2 = 1.9 \times 10^{-3} \text{ eV}^2$. That value of Δm_{32}^2 is the one- σ low value for AHN 06A. For the AHN 06A best fit value of $2.8 \times 10^{-3} \text{ eV}^2$, the $\sin^2(2\theta_{13})$ limit is < 0.26. Supersedes AHN 04.

139 AHN 04 searched for $\nu_\mu \rightarrow \nu_e$ appearance. Assuming $2 \sin^2(2\theta_{\mu e}) = \sin^2(2\theta_{13})$, a limit on $\sin^2(2\theta_{\mu e})$ is converted to a limit on $\sin^2(2\theta_{13})$. The quoted limit is for $\Delta m_{32}^2 = 1.9 \times 10^{-3} \text{ eV}^2$. That value of Δm_{32}^2 is the one- σ low value for ALIU 05. For the ALIU 05 best fit value of $2.8 \times 10^{-3} \text{ eV}^2$, the $\sin^2(2\theta_{13})$ limit is < 0.30.

140 The quoted limit is for $\Delta m_{32}^2 = 1.9 \times 10^{-3} \text{ eV}^2$. That value of Δm_{32}^2 is the 1- σ low value for ALIU 05. For the ALIU 05 best fit value of $2.8 \times 10^{-3} \text{ eV}^2$, the $\sin^2 2\theta_{13}$ limit is < 0.19. In this range, the θ_{13} limit is larger for lower values of Δm_{32}^2 , and smaller for higher values of Δm_{32}^2 .

141 The quoted limit is for $\Delta m_{32}^2 = 1.9 \times 10^{-3} \text{ eV}^2$. That value of Δm_{32}^2 is the 1- σ low value for ALIU 05. For the ALIU 05 best fit value of $2.8 \times 10^{-3} \text{ eV}^2$, the $\sin^2 2\theta_{13}$ limit is < 0.23.

(C) Other neutrino mixing results

The LSND collaboration reported in AGUILAR 01 a signal which is consistent with $\bar{\nu}_\mu \rightarrow \bar{\nu}_e$ oscillations. In a three neutrino framework, this would be a measurement of θ_{12} and Δm_{21}^2 . This does not appear to be consistent with the interpretation of other neutrino data. The MiniBooNE experiment, reported in AGUILAR-AREVALO 07, does a two-neutrino analysis which, assuming *CPT* conservation, rules out AGUILAR 01. The following listings include results which might be relevant towards understanding these observations. They include searches for $\nu_\mu \rightarrow \nu_e$, $\bar{\nu}_\mu \rightarrow \bar{\nu}_e$, sterile neutrino oscillations, and *CPT* violation.

 $\Delta(m^2)$ for $\sin^2(2\theta) = 1$ ($\nu_\mu \rightarrow \nu_e$)

VALUE (eV ²)	CL%	DOCUMENT ID	TECN	COMMENT
--------------------------	-----	-------------	------	---------

• • • We do not use the following data for averages, fits, limits, etc. • • •

<0.034	90	AGUILAR-AR...07	MBOO	MiniBooNE
<0.0008	90	AHN	04	K2K Water Cherenkov
<0.4	90	ASTIER	03	NOMD CERN SPS
<2.4	90	AVVAKUMOV	02	NTEV NUTEV FNAL
		142 AGUILAR	01	LSND $\nu_\mu \rightarrow \nu_e$ osc.prob.
0.03 to 0.3	95	143 ATHANASSO...98	LSND	$\nu_\mu \rightarrow \nu_e$
<2.3	90	144 LOVERRE	96	CHARM/CDHS
<0.9	90	VILAIN	94c	CHM2 CERN SPS
<0.09	90	ANGELINI	86	HLBC BEBC CERN P5

142 AGUILAR 01 is the final analysis of the LSND full data set. Search is made for the $\nu_\mu \rightarrow \nu_e$ oscillations using ν_μ from π^+ decay in flight by observing beam-on electron events from $\nu_e C \rightarrow e^- X$. Present analysis results in $8.1 \pm 12.2 \pm 1.7$ excess events in the $60 < E_e < 200$ MeV energy range, corresponding to oscillation probability of $0.10 \pm 0.16 \pm 0.04\%$. This is consistent, though less significant, with the previous result of ATHANASSOPOULOS 98, which it supersedes. The present analysis uses selection criteria developed for the decay at rest region, and is less effective in removing the background above 60 MeV than ATHANASSOPOULOS 98.

143 ATHANASSOPOULOS 98 is a search for the $\nu_\mu \rightarrow \nu_e$ oscillations using ν_μ from π^+ decay in flight. The 40 observed beam-on electron events are consistent with $\nu_e C \rightarrow e^- X$; the expected background is 21.9 ± 2.1 . Authors interpret this excess as evidence for an oscillation signal corresponding to oscillations with probability $(0.26 \pm 0.10 \pm 0.05)\%$. Although the significance is only 2.3σ , this measurement is an important and consistent

cross check of ATHANASSOPOULOS 96 who reported evidence for $\bar{\nu}_\mu \rightarrow \bar{\nu}_e$ oscillations from μ^+ decay at rest. See also ATHANASSOPOULOS 98b.

144 LOVERRE 96 uses the charged-current to neutral-current ratio from the combined CHARM (ALLABY 86) and CDHS (ABRAMOWICZ 86) data from 1986.

 $\sin^2(2\theta)$ for "Large" $\Delta(m^2)$ ($\nu_\mu \rightarrow \nu_e$)

VALUE (units 10^{-3})	CL%	DOCUMENT ID	TECN	COMMENT
--------------------------	-----	-------------	------	---------

• • • We do not use the following data for averages, fits, limits, etc. • • •

< 1.8	90	145 AGUILAR-AR...07	MBOO	MiniBooNE
<110	90	146 AHN	04	K2K Water Cherenkov
< 1.4	90	ASTIER	03	NOMD CERN SPS
< 1.6	90	AVVAKUMOV	02	NTEV NUTEV FNAL
		147 AGUILAR	01	LSND $\nu_\mu \rightarrow \nu_e$ osc.prob.
0.5 to 30	95	148 ATHANASSO...98	LSND	$\nu_\mu \rightarrow \nu_e$
< 3.0	90	149 LOVERRE	96	CHARM/CDHS
< 9.4	90	VILAIN	94c	CHM2 CERN SPS
< 5.6	90	150 VILAIN	94c	CHM2 CERN SPS

145 The limit is $\sin^2 2\theta < 0.9 \times 10^{-3}$ at $\Delta m^2 = 2 \text{ eV}^2$. That value of Δm^2 corresponds to the smallest mixing angle consistent with the reported signal from LSND in AGUILAR 01.

146 The limit becomes $\sin^2 2\theta < 0.15$ at $\Delta m^2 = 2.8 \times 10^{-3} \text{ eV}^2$, the best-fit value of the ν_μ disappearance analysis in K2K.

147 AGUILAR 01 is the final analysis of the LSND full data set of the search for the $\nu_\mu \rightarrow \nu_e$ oscillations. See footnote in preceding table for further details.

148 ATHANASSOPOULOS 98 report $(0.26 \pm 0.10 \pm 0.05)\%$ for the oscillation probability; the value of $\sin^2 2\theta$ for large Δm^2 is deduced from this probability. See footnote in preceding table for further details, and see the paper for a plot showing allowed regions. If effect is due to oscillation, it is most likely to be intermediate $\sin^2 2\theta$ and Δm^2 . See also ATHANASSOPOULOS 98b.

149 LOVERRE 96 uses the charged-current to neutral-current ratio from the combined CHARM (ALLABY 86) and CDHS (ABRAMOWICZ 86) data from 1986.

150 VILAIN 94c limit derived by combining the ν_μ and $\bar{\nu}_\mu$ data assuming *CP* conservation.

 $\Delta(m^2)$ for $\sin^2(2\theta) = 1$ ($\bar{\nu}_\mu \rightarrow \bar{\nu}_e$)

VALUE (eV ²)	CL%	DOCUMENT ID	TECN	COMMENT
--------------------------	-----	-------------	------	---------

• • • We do not use the following data for averages, fits, limits, etc. • • •

<0.055	90	151 ARMBRUSTER02	KAR2	Liquid Sci. calor.
<2.6	90	AVVAKUMOV	02	NTEV NUTEV FNAL
0.03-0.05		152 AGUILAR	01	LSND LAMPF
0.05-0.08	90	153 ATHANASSO...96	LSND	LAMPF
0.048-0.090	80	154 ATHANASSO...95		
<0.07	90	155 HILL		
<0.9	90	VILAIN	94c	CHM2 CERN SPS
<0.14	90	156 FREEDMAN	93	CNTR LAMPF

151 ARMBRUSTER 02 is the final analysis of the KARMEN 2 data for 17.7 m distance from the ISIS stopped pion and muon neutrino source. It is a search for $\bar{\nu}_e$ detected by the inverse β -decay reaction on protons and ^{12}C . 15 candidate events are observed, and 15.8 \pm 0.5 background events are expected, hence no oscillation signal is detected. The results exclude large regions of the parameter area favored by the LSND experiment.

152 AGUILAR 01 is the final analysis of the LSND full data set. It is a search for $\bar{\nu}_e$ 30 m from LAMPF beam stop. Neutrinos originate mainly from π^+ decay at rest. $\bar{\nu}_e$ are detected through $\bar{\nu}_e p \rightarrow e^+ n$ ($20 < E_{e^+} < 60$ MeV) in delayed coincidence with $np \rightarrow d \gamma$. Authors observe $87.9 \pm 22.4 \pm 6.0$ total excess events. The observation is attributed to $\bar{\nu}_\mu \rightarrow \bar{\nu}_e$ oscillations with the oscillation probability of $0.264 \pm 0.067 \pm 0.045\%$, consistent with the previously published result. Taking into account all constraints, the most favored allowed region of oscillation parameters is a band of $\Delta(m^2)$ from 0.2-2.0 eV². Supersedes ATHANASSOPOULOS 95, ATHANASSOPOULOS 96, and ATHANASSOPOULOS 98.

153 ATHANASSOPOULOS 96 is a search for $\bar{\nu}_e$ 30 m from LAMPF beam stop. Neutrinos originate mainly from π^+ decay at rest. $\bar{\nu}_e$ could come from either $\bar{\nu}_\mu \rightarrow \bar{\nu}_e$ or $\nu_e \rightarrow \bar{\nu}_e$; our entry assumes the first interpretation. They are detected through $\bar{\nu}_e p \rightarrow e^+ n$ ($20 \text{ MeV} < E_{e^+} < 60 \text{ MeV}$) in delayed coincidence with $np \rightarrow d \gamma$. Authors observe $51 \pm 20 \pm 8$ total excess events over an estimated background 12.5 ± 2.9 . ATHANASSOPOULOS 96b is a shorter version of this paper.

154 ATHANASSOPOULOS 95 error corresponds to the 1.6 σ band in the plot. The expected background is 2.7 ± 0.4 events. Corresponds to an oscillation probability of $(0.34 \pm 0.20 \pm 0.18 \pm 0.07)\%$. For a different interpretation, see HILL 95. Replaced by ATHANASSOPOULOS 96.

155 HILL 95 is a report by one member of the LSND Collaboration, reporting a different conclusion from the analysis of the data of this experiment (see ATHANASSOPOULOS 95). Contrary to the rest of the LSND Collaboration, Hill finds no evidence for the neutrino oscillation $\bar{\nu}_\mu \rightarrow \bar{\nu}_e$ and obtains only upper limits.

156 FREEDMAN 93 is a search at LAMPF for $\bar{\nu}_e$ generated from any of the three neutrino types ν_μ , $\bar{\nu}_\mu$, and ν_e which come from the beam stop. The $\bar{\nu}_e$'s would be detected by the reaction $\bar{\nu}_e p \rightarrow e^+ n$. FREEDMAN 93 replaces DURKIN 88.

 $\sin^2(2\theta)$ for "Large" $\Delta(m^2)$ ($\bar{\nu}_\mu \rightarrow \bar{\nu}_e$)

VALUE (units 10^{-3})	CL%	DOCUMENT ID	TECN	COMMENT
--------------------------	-----	-------------	------	---------

• • • We do not use the following data for averages, fits, limits, etc. • • •

Lepton Particle Listings

Neutrino Mixing

<1.7	90	157	ARMBRUSTER02	KAR2	Liquid Sci. calor.
<1.1	90		AVVAKUMOV 02	NTEV	NUTEV FNAL
5.3 ± 1.3 ± 9.0		158	AGUILAR 01	LSND	LAMPF
6.2 ± 2.4 ± 1.0		159	ATHANASSO...96	LSND	LAMPF
3-12	80	160	ATHANASSO...95		
<6	90	161	HILL 95		

157 ARMBRUSTER 02 is the final analysis of the KARMEN 2 data. See footnote in the preceding table for further details, and the paper for the exclusion plot.

158 AGUILAR 01 is the final analysis of the LSND full data set. The deduced oscillation probability is $0.264 \pm 0.067 \pm 0.045\%$; the value of $\sin^2 2\theta$ for large $\Delta(m^2)$ is twice this probability (although these values are excluded by other constraints). See footnote in preceding table for further details, and the paper for a plot showing allowed regions. Supersedes ATHANASSOPOULOS 95, ATHANASSOPOULOS 96, and ATHANASSOPOULOS 98.

159 ATHANASSOPOULOS 96 reports $(0.31 \pm 0.12 \pm 0.05)\%$ for the oscillation probability; the value of $\sin^2 2\theta$ for large $\Delta(m^2)$ should be twice this probability. See footnote in preceding table for further details, and see the paper for a plot showing allowed regions.

160 ATHANASSOPOULOS 95 error corresponds to the 1.6σ band in the plot. The expected background is 2.7 ± 0.4 events. Corresponds to an oscillation probability of $(0.34 \pm 0.20 \pm 0.18 \pm 0.07)\%$. For a different interpretation, see HILL 95. Replaced by ATHANASSOPOULOS 96.

161 HILL 95 is a report by one member of the LSND Collaboration, reporting a different conclusion from the analysis of the data of this experiment (see ATHANASSOPOULOS 95). Contrary to the rest of the LSND Collaboration, Hill finds no evidence for the neutrino oscillation $\bar{\nu}_\mu \rightarrow \bar{\nu}_e$ and obtains only upper limits.

$\Delta(m^2)$ for $\sin^2(2\theta) = 1$ ($\nu_\mu(\bar{\nu}_\mu) \rightarrow \nu_e(\bar{\nu}_e)$)

VALUE (eV ²)	CL%	DOCUMENT ID	TECN	COMMENT
<0.075	90	BORODOV... 92	CNTR	BNL E776

• • • We do not use the following data for averages, fits, limits, etc. • • •

<1.6	90	162	ROMOSAN 97	CCFR	FNAL
------	----	-----	------------	------	------

162 ROMOSAN 97 uses wideband beam with a 0.5 km decay region.

$\sin^2(2\theta)$ for "Large" $\Delta(m^2)$ ($\nu_\mu(\bar{\nu}_\mu) \rightarrow \nu_e(\bar{\nu}_e)$)

VALUE (units 10 ⁻³)	CL%	DOCUMENT ID	TECN	COMMENT	
<1.8	90	163	ROMOSAN 97	CCFR	FNAL

• • • We do not use the following data for averages, fits, limits, etc. • • •

<3.8	90	164	MCFARLAND 95	CCFR	FNAL
------	----	-----	--------------	------	------

<3	90		BORODOV... 92	CNTR	BNL E776
----	----	--	---------------	------	----------

163 ROMOSAN 97 uses wideband beam with a 0.5 km decay region.

164 MCFARLAND 95 state that "This result is the most stringent to date for $250 < \Delta(m^2) < 450$ eV² and also excludes at 90%CL much of the high $\Delta(m^2)$ region favored by the recent LSND observation." See ATHANASSOPOULOS 95 and ATHANASSOPOULOS 96.

$\Delta(m^2)$ for $\sin^2(2\theta) = 1$ ($\bar{\nu}_e \not\rightarrow \bar{\nu}_e$)

VALUE (eV ²)	CL%	DOCUMENT ID	TECN	COMMENT	
<0.01	90	165	ACHKAR 95	CNTR	Bugey reactor

• • • We do not use the following data for averages, fits, limits, etc. • • •

165 ACHKAR 95 bound is for $L=15, 40,$ and 95 m.

$\sin^2(2\theta)$ for "Large" $\Delta(m^2)$ ($\bar{\nu}_e \not\rightarrow \bar{\nu}_e$)

VALUE	CL%	DOCUMENT ID	TECN	COMMENT	
<0.02	90	166	ACHKAR 95	CNTR	For $\Delta(m^2) = 0.6$ eV ²

• • • We do not use the following data for averages, fits, limits, etc. • • •

166 ACHKAR 95 bound is from data for $L=15, 40,$ and 95 m distance from the Bugey reactor.

Sterile neutrino limits from atmospheric neutrino studies

$\Delta(m^2)$ for $\sin^2(2\theta) = 1$ ($\nu_\mu \rightarrow \nu_s$)

ν_s means ν_τ or any sterile (noninteracting) ν .

VALUE (10 ⁻⁵ eV ²)	CL%	DOCUMENT ID	TECN	COMMENT
<3000 (or <550)	90	167	OYAMA 89	KAMI Water Cherenkov
< 4.2 or > 54.	90	IMB	IMB	Flux has $\nu_\mu, \bar{\nu}_\mu, \nu_e,$ and $\bar{\nu}_e$

• • • We do not use the following data for averages, fits, limits, etc. • • •

167 OYAMA 89 gives a range of limits, depending on assumptions in their analysis. They argue that the region $\Delta(m^2) = (100-1000) \times 10^{-5}$ eV² is not ruled out by any data for large mixing.

Search for $\nu_\mu \rightarrow \nu_s$

VALUE	DOCUMENT ID	TECN	COMMENT
<3000 (or <550)	167	OYAMA 89	KAMI Water Cherenkov
< 4.2 or > 54.	90	IMB	IMB Flux has $\nu_\mu, \bar{\nu}_\mu, \nu_e,$ and $\bar{\nu}_e$

• • • We do not use the following data for averages, fits, limits, etc. • • •

168	AMBROSIO 01	MCRO	matter effects
169	FUKUDA 00	SKAM	neutral currents + matter effects

168 AMBROSIO 01 tested the pure 2-flavor $\nu_\mu \rightarrow \nu_s$ hypothesis using matter effects which change the shape of the zenith-angle distribution of upward through-going muons. With maximum mixing and $\Delta(m^2)$ around 0.0024 eV², the $\nu_\mu \rightarrow \nu_s$ oscillation is disfavored with 99% confidence level with respect to the $\nu_\mu \rightarrow \nu_\tau$ hypothesis.

169 FUKUDA 00 tested the pure 2-flavor $\nu_\mu \rightarrow \nu_s$ hypothesis using three complementary atmospheric-neutrino data samples. With this hypothesis, zenith-angle distributions are expected to show characteristic behavior due to neutral currents and matter effects. In the $\Delta(m^2)$ and $\sin^2 2\theta$ region preferred by the Super-Kamiokande data, the $\nu_\mu \rightarrow \nu_s$ hypothesis is rejected at the 99% confidence level, while the $\nu_\mu \rightarrow \nu_\tau$ hypothesis consistently fits all of the data sample.

CPT tests

$\langle \Delta m_{21}^2 - \Delta m_{21}^2 \rangle$

VALUE (10 ⁻⁴ eV ²)	CL%	DOCUMENT ID	TECN	COMMENT
---	-----	-------------	------	---------

• • • We do not use the following data for averages, fits, limits, etc. • • •

<1.1	99.7	170	DEGOUVEA 05	FIT	solar vs. reactor
------	------	-----	-------------	-----	-------------------

170 DEGOUVEA 05 obtained this bound at the 3σ CL from the KamLAND (ARAKI 05) and solar neutrino data.

REFERENCES FOR Neutrino Mixing

ADAMSON 07	PR D75 092003	P. Adamson <i>et al.</i>	(MINOS Collab.)
AGUILAR-AR... 07	PRL 98 231801	A.A. Aguilar-Arevalo <i>et al.</i>	(MiniBooNE Collab.)
AHARMIM 07	PR C75 045502	B. Aharmim <i>et al.</i>	(SNO Collab.)
ADAMSON 06	PR D73 072002	P. Adamson <i>et al.</i>	(MINOS Collab.)
AHN 06A	PR D74 072003	M.H. Ahn <i>et al.</i>	(K2K Collab.)
BALATA 06	EPJ C47 21	M. Balata <i>et al.</i>	(Borexino Collab.)
HOSAKA 06	PR D73 112001	J. Hosaka <i>et al.</i>	(Super-Kamiokande Collab.)
HOSAKA 06A	PR D74 032002	J. Hosaka <i>et al.</i>	(Super-Kamiokande Collab.)
MICHAEL 06	PRL 97 191801	D. Michael <i>et al.</i>	(MINOS Collab.)
YAMAMOTO 06	PRL 96 181801	S. Yamamoto <i>et al.</i>	(K2K Collab.)
AHARMIM 05A	PR C72 055502	B. Aharmim <i>et al.</i>	(SNO Collab.)
ALIU 05	PRL 94 081802	E. Aliu <i>et al.</i>	(K2K Collab.)
ALLISON 05	PR D72 052005	W.W.M. Allison <i>et al.</i>	(SOUDAN-2 Collab.)
ALTMANN 05	PL B616 174	M. Altmann <i>et al.</i>	(GNO Collab.)
ARAKI 05	PRL 94 081801	T. Araki <i>et al.</i>	(KamLAND Collab.)
ASHIE 05	PR D71 112005	Y. Ashie <i>et al.</i>	(SuperK Collab.)
DEGOUVEA 05	PR D71 093002	A. de Gouvea, C. Pena-Garay	(SuperK Collab.)
AHARMIM 04	PR D70 093014	B. Aharmim <i>et al.</i>	(SNO Collab.)
AHMED 04A	PRL 92 181301	S.N. Ahmed <i>et al.</i>	(SNO Collab.)
AHN 04	PRL 93 051801	M.H. Ahn <i>et al.</i>	(K2K Collab.)
AMBROSIO 04	EPJ C36 323	M. Ambrosio <i>et al.</i>	(MACRO Collab.)
ASHIE 04	PRL 93 101801	Y. Ashie <i>et al.</i>	(Super-Kamiokande Collab.)
EGUCHI 04	PRL 92 071301	K. Eguchi <i>et al.</i>	(KamLAND Collab.)
SMY 04	PR D69 011104R	M.B. Smy <i>et al.</i>	(Super-Kamiokande Collab.)
AHN 03	PRL 90 041801	M.H. Ahn <i>et al.</i>	(K2K Collab.)
AMBROSIO 03	PL B566 35	M. Ambrosio <i>et al.</i>	(MACRO Collab.)
APOLLONIO 03	EPJ C27 331	M. Apollonio <i>et al.</i>	(CHOOZ Collab.)
ASTIER 03	PL B570 19	P. Astier <i>et al.</i>	(NOMAD Collab.)
EGUCHI 03	PRL 90 021802	K. Eguchi <i>et al.</i>	(KamLAND Collab.)
GANDO 03	PRL 90 171302	Y. Gando <i>et al.</i>	(Super-Kamiokande Collab.)
IANNI 03	JPG 29 2107	A. Ianni	(INFN Gran Sasso)
SANCHEZ 03	PR D68 113004	M. Sanchez <i>et al.</i>	(Soudan 2 Collab.)
ABDURASH... 02	JETP 95 181	J.N. Abdurashitov <i>et al.</i>	(SAGE Collab.)
Translated from ZETF 122 211.			
AHMAD 02	PRL 89 011301	Q.R. Ahmad <i>et al.</i>	(SNO Collab.)
AHMAD 02B	PRL 89 011302	Q.R. Ahmad <i>et al.</i>	(SNO Collab.)
ARMBRUSTER 02	PR D65 112001	B. Armbuster <i>et al.</i>	(KARMEN 2 Collab.)
AVVAKUMOV 02	PRL 89 011804	S. Avvakumov <i>et al.</i>	(NuTeV Collab.)
FUKUDA 02	PL B539 179	S. Fukuda <i>et al.</i>	(Super-Kamiokande Collab.)
AGUILAR 01	PRL 84 112007	A. Aguilar <i>et al.</i>	(LSND Collab.)
AHMAD 01	PRL 87 071301	Q.R. Ahmad <i>et al.</i>	(SNO Collab.)
AMBROSIO 01	PL B517 59	M. Ambrosio <i>et al.</i>	(MACRO Collab.)
BOEHM 01	PR D64 112001	F. Boehm <i>et al.</i>	(Super-Kamiokande Collab.)
FUKUDA 01	PRL 86 5651	S. Fukuda <i>et al.</i>	(Super-Kamiokande Collab.)
AMBROSIO 00	PL B478 5	M. Ambrosio <i>et al.</i>	(MACRO Collab.)
BOEHM 00	PRL 84 3764	F. Boehm <i>et al.</i>	(Super-Kamiokande Collab.)
FUKUDA 00	PRL 85 3999	S. Fukuda <i>et al.</i>	(Super-Kamiokande Collab.)
ABDURASH... 99B	PR C60 055801	J.N. Abdurashitov <i>et al.</i>	(SAGE Collab.)
ALLISON 99	PL B449 137	W.W.M. Allison <i>et al.</i>	(Soudan 2 Collab.)
APOLLONIO 99	PL B466 415	M. Apollonio <i>et al.</i>	(CHOOZ Collab.)
Also	PL B472 434 (erratum)	M. Apollonio <i>et al.</i>	(CHOOZ Collab.)
FUKUDA 99C	PRL 82 2644	Y. Fukuda <i>et al.</i>	(Super-Kamiokande Collab.)
FUKUDA 99D	PL B467 185	Y. Fukuda <i>et al.</i>	(Super-Kamiokande Collab.)
HAMPEL 99	PL B447 127	W. Hampel <i>et al.</i>	(GALLEX Collab.)
AMBROSIO 98	PL B434 451	M. Ambrosio <i>et al.</i>	(MACRO Collab.)
APOLLONIO 98	PL B420 397	M. Apollonio <i>et al.</i>	(CHOOZ Collab.)
ATHANASSO... 98	PRL 81 1774	C. Athanassopoulos <i>et al.</i>	(LSND Collab.)
ATHANASSO... 98B	PR C58 2489	C. Athanassopoulos <i>et al.</i>	(LSND Collab.)
CLEVELAND 98	APJ 496 505	B.T. Cleveland <i>et al.</i>	(Homestake Collab.)
FELDMAN 98	PR D57 3873	G.J. Feldman, R.D. Cousins	(Super-Kamiokande Collab.)
FUKUDA 98C	PRL 81 1562	Y. Fukuda <i>et al.</i>	(Super-Kamiokande Collab.)
HATAKEYAMA 98	PRL 81 2016	S. Hatakeyama <i>et al.</i>	(Kamikoande Collab.)
CLARK 95	PRL 75 2950	R. Clark <i>et al.</i>	(PRL 75 2950)
ROMOSAN 97	PRL 78 2912	A. Romosan <i>et al.</i>	(CCFR Collab.)
AGLIETTA 96	JETPL 63 791	M. Aglietta <i>et al.</i>	(LSD Collab.)
Translated from ZETFP 63 763.			
ATHANASSO... 96	PR C54 2685	C. Athanassopoulos <i>et al.</i>	(LSND Collab.)
ATHANASSO... 96B	PRL 77 3082	C. Athanassopoulos <i>et al.</i>	(LSND Collab.)
FUKUDA 96	PRL 77 1683	Y. Fukuda <i>et al.</i>	(Kamikoande Collab.)
FUKUDA 96B	PL B388 397	Y. Fukuda <i>et al.</i>	(Kamikoande Collab.)
GREENWOOD 96	PR D53 6054	Z.D. Greenwood <i>et al.</i>	(UCI, SVR, SUCU)
HAMPEL 96	PL B388 384	W. Hampel <i>et al.</i>	(GALLEX Collab.)
LOVERRE 96	PL B370 156	P.F. Loverre	(SING, SAACL, CPPM, CDEF+)
ACHKAR 95	NP B434 503	B. Achkar <i>et al.</i>	(MACRO Collab.)
AHLEN 95	PRL B357 481	S.P. Ahlen <i>et al.</i>	(MACRO Collab.)
ATHANASSO... 95	PRL 75 2950	C. Athanassopoulos <i>et al.</i>	(LSND Collab.)
DAUM 95	ZPHY C65 417	K. Daum <i>et al.</i>	(FREJUS Collab.)
HILL 95	PRL 75 2654	J.E. Hill	(PENN)
MCFARLAND 95	PRL 75 3993	K.S. McFarland <i>et al.</i>	(CCFR Collab.)
DECLAIS 94	PL B338 383	Y. Declais <i>et al.</i>	(Kamikoande Collab.)
FUKUDA 94	PL B335 237	Y. Fukuda <i>et al.</i>	(Kamikoande Collab.)
VILAIN 94C	ZPHY C64 539	P. Vilain <i>et al.</i>	(CHARM II Collab.)
FREEDMAN 93	PR D47 811	S.J. Freedman <i>et al.</i>	(LAMPF E645 Collab.)
BECKER-SZ... 92B	PR D46 3720	R.A. Becker-Szendy <i>et al.</i>	(IMB Collab.)
BEIER 92	PL B283 446	E.W. Beier <i>et al.</i>	(KAM2 Collab.)
Also	PTRSL A346 63	E.W. Beier, E.D. Frank	(PENN)

Lepton Particle Listings

Neutrino Mixing, Heavy Neutral Leptons, Searches for

BORODOV...	92	PRL 68 274	L. Borodovsky et al.	(COLU, JHU, ILL)
HIRATA	92	PL B280 146	K.S. Hirata et al.	(Kamiokande II Collab.)
CASPER	91	PRL 66 2561	D. Casper et al.	(IMB Collab.)
HIRATA	91	PRL 66 9	K.S. Hirata et al.	(Kamiokande II Collab.)
KUVSHINN...	91	JETPL 54 253	A.A. Kuvshinnikov et al.	(KIAE)
BERGER	90B	PL B245 305	C. Berger et al.	(FREJUS Collab.)
HIRATA	90	PRL 65 1297	K.S. Hirata et al.	(Kamiokande II Collab.)
AGLIETTA	89	EPL 8 611	M. Aglietta et al.	(FREJUS Collab.)
DAVIS	89	ARIP 39 467	R. Davis, A.K. Mann, L. Wolfenstein	(BNL, PENN+)
OYAMA	89	PR D39 1481	Y. Oyama et al.	(Kamiokande II Collab.)
BIONTA	88	PR D38 768	R.M. Bionta et al.	(IMB Collab.)
DURKIN	88	PRL 61 1811	L.S. Durkin et al.	(OSU, ANL, CIT+)
ABRAMOWICZ	86	PRL 57 298	H. Abramowicz et al.	(CDHS Collab.)
ALLABY	86	PL B177 446	J.V. Allaby et al.	(CHARM Collab.)
ANGELINI	86	PL B179 307	C. Angelini et al.	(PISA, ATHU, PADO+)
VUILLEUMIER	82	PL 114B 298	J.L. Vuilleumier et al.	(CIT, SIN, MUNI)
BOLIEV	81	SJNP 34 787	M.M. Boliev et al.	(INRM)
Translated from YAF 34 1418.				
KWON	81	PR D24 1097	H. Kwon et al.	(CIT, ISNG, MUNI)
BOEHM	80	PL 97B 310	F. Boehm et al.	(ILLG, CIT, ISNG, MUNI)
CROUCH	78	PR D18 2239	M.F. Crouch et al.	(CASE, UCI, WITW)

none 10–2400	90	⁹ REUSSER	91	CNTR	HPGe search
none 3–100	90	SATO	91	KAM2	Kamiokande II
		¹⁰ ENQVIST	89	COSM	
none 12–1400		⁶ CALDWELL	88	COSM	Dirac ν
none 4–16	90	^{6,7} OLIVE	88	COSM	Dirac ν
none 4–35	90	OLIVE	88	COSM	Majorana ν
>4.2 to 4.7		SREDNICKI	88	COSM	Dirac ν
>5.3 to 7.4		SREDNICKI	88	COSM	Majorana ν
none 20–1000	95	⁶ AHLEN	87	COSM	Dirac ν
>4.1		GRIEST	87	COSM	Dirac ν

⁵ FARGION 95 bound is sensitive to assumed ν concentration in the Galaxy. See also KONOPLICH 94.

⁶ These results assume that neutrinos make up dark matter in the galactic halo.

⁷ Limits based on annihilations in the sun and are due to an absence of high energy neutrinos detected in underground experiments.

⁸ MORI 92B results assume that neutrinos make up dark matter in the galactic halo. Limits based on annihilations in earth are also given.

⁹ REUSSER 91 uses existing $\beta\beta$ detector (see FISHER 89) to search for CDM Dirac neutrinos.

¹⁰ ENQVIST 89 argue that there is no cosmological upper bound on heavy neutrinos.

Heavy Neutral Leptons, Searches for

(A) Heavy Neutral Leptons

Stable Neutral Heavy Lepton MASS LIMITS

Note that LEP results in combination with REUSSER 91 exclude a fourth stable neutrino with $m < 2400$ GeV.

VALUE (GeV)	CL%	DOCUMENT ID	TECN	COMMENT
>45.0	95	ABREU 92B	DLPH	Dirac
>39.5	95	ABREU 92B	DLPH	Majorana
>44.1	95	ALEXANDER 91F	OPAL	Dirac
>37.2	95	ALEXANDER 91F	OPAL	Majorana
none 3–100	90	SATO 91	KAM2	Kamiokande II
>42.8	95	¹ ADEVA 90S	L3	Dirac
>34.8	95	¹ ADEVA 90S	L3	Majorana
>42.7	95	DECAMP 90F	ALEP	Dirac

¹ ADEVA 90S limits for the heavy neutrino apply if the mixing with the charged leptons satisfies $|U_{1j}|^2 + |U_{2j}|^2 + |U_{3j}|^2 > 6.2 \times 10^{-8}$ at $m_{L0} = 20$ GeV and $> 5.1 \times 10^{-10}$ for $m_{L0} = 40$ GeV.

Heavy Neutral Lepton MASS LIMITS

Limits apply only to heavy lepton type given in comment at right of data Listings.

See the "Quark and Lepton Compositeness, Searches for" Listings for limits on radiatively decaying excited neutral leptons, i.e. $\nu^* \rightarrow \nu\gamma$.

VALUE (GeV)	CL%	DOCUMENT ID	TECN	COMMENT
>101.3	95	ACHARD 01B	L3	Dirac coupling to e
>101.5	95	ACHARD 01B	L3	Dirac coupling to μ
> 90.3	95	ACHARD 01B	L3	Dirac coupling to τ
> 89.5	95	ACHARD 01B	L3	Majorana coupling to e
> 90.7	95	ACHARD 01B	L3	Majorana coupling to μ
> 80.5	95	ACHARD 01B	L3	Majorana coupling to τ

••• We do not use the following data for averages, fits, limits, etc. •••

> 76.0	95	ABBIENDI 00I	OPAL	Majorana, coupling to e
> 88.0	95	ABBIENDI 00I	OPAL	Dirac, coupling to e
> 76.0	95	ABBIENDI 00I	OPAL	Majorana, coupling to μ
> 88.1	95	ABBIENDI 00I	OPAL	Dirac, coupling to μ
> 53.8	95	ABBIENDI 00I	OPAL	Majorana, coupling to τ
> 71.1	95	ABBIENDI 00I	OPAL	Dirac, coupling to τ
> 76.5	95	ABREU 990	DLPH	Dirac coupling to e
> 79.5	95	ABREU 990	DLPH	Dirac coupling to μ
> 60.5	95	ABREU 990	DLPH	Dirac coupling to τ
> 63	95	^{2,3} BUSKULIC 96S	ALEP	Dirac
> 54.3	95	^{2,4} BUSKULIC 96S	ALEP	Majorana

² BUSKULIC 96S requires the decay length of the heavy lepton to be < 1 cm, limiting the square of the mixing angle $|U_{Ej}|^2$ to 10^{-10} .

³ BUSKULIC 96S limit for mixing with τ . Mass is > 63.6 GeV for mixing with e or μ .

⁴ BUSKULIC 96S limit for mixing with τ . Mass is > 55.2 GeV for mixing with e or μ .

Astrophysical Limits on Neutrino MASS for $m_\nu > 1$ GeV

VALUE (GeV)	CL%	DOCUMENT ID	TECN	COMMENT
none 60–115		⁵ FARGION 95	ASTR	Dirac
none 9.2–2000		⁶ GARCIA 95	COSM	Nucleosynthesis
none 26–4700		⁶ BECK 94	COSM	Dirac
none 6 – hundreds		^{7,8} MORI 92B	KAM2	Dirac neutrino
none 24 – hundreds		^{7,8} MORI 92B	KAM2	Majorana neutrino

••• We do not use the following data for averages, fits, limits, etc. •••

(B) Other Bounds from Nuclear and Particle Decays

Limits on $|U_{eX}|^2$ as Function of m_{ν_X}

Peak and kink search tests

Limits on $|U_{eX}|^2$ as function of m_{ν_X}

VALUE	CL%	DOCUMENT ID	TECN	COMMENT
$< 1 \times 10^{-7}$	90	¹¹ BRITTON 92B	CNTR	50 MeV $< m_{\nu_X} < 130$ MeV
••• We do not use the following data for averages, fits, limits, etc. •••				
$< 5 \times 10^{-6}$	90	DELEENER... 91		$m_{\nu_X} = 20$ MeV
$< 5 \times 10^{-7}$	90	DELEENER... 91		$m_{\nu_X} = 40$ MeV
$< 3 \times 10^{-7}$	90	DELEENER... 91		$m_{\nu_X} = 60$ MeV
$< 1 \times 10^{-6}$	90	DELEENER... 91		$m_{\nu_X} = 80$ MeV
$< 1 \times 10^{-6}$	90	DELEENER... 91		$m_{\nu_X} = 100$ MeV
$< 5 \times 10^{-7}$	90	AZUELOS 86	CNTR	$m_{\nu_X} = 60$ MeV
$< 2 \times 10^{-7}$	90	AZUELOS 86	CNTR	$m_{\nu_X} = 80$ MeV
$< 3 \times 10^{-7}$	90	AZUELOS 86	CNTR	$m_{\nu_X} = 100$ MeV
$< 1 \times 10^{-6}$	90	AZUELOS 86	CNTR	$m_{\nu_X} = 120$ MeV
$< 2 \times 10^{-7}$	90	AZUELOS 86	CNTR	$m_{\nu_X} = 130$ MeV
$< 1 \times 10^{-4}$	90	¹² BRYMAN 83B	CNTR	$m_{\nu_X} = 5$ MeV
$< 1.5 \times 10^{-6}$	90	BRYMAN 83B	CNTR	$m_{\nu_X} = 53$ MeV
$< 1 \times 10^{-5}$	90	BRYMAN 83B	CNTR	$m_{\nu_X} = 70$ MeV
$< 1 \times 10^{-4}$	90	BRYMAN 83B	CNTR	$m_{\nu_X} = 130$ MeV
$< 1 \times 10^{-4}$	68	¹³ SHROCK 81	THEO	$m_{\nu_X} = 10$ MeV
$< 5 \times 10^{-6}$	68	¹³ SHROCK 81	THEO	$m_{\nu_X} = 60$ MeV
$< 1 \times 10^{-5}$	68	¹⁴ SHROCK 80	THEO	$m_{\nu_X} = 80$ MeV
$< 3 \times 10^{-6}$	68	¹⁴ SHROCK 80	THEO	$m_{\nu_X} = 160$ MeV

¹¹ BRITTON 92B is from a search for additional peaks in the e^+ spectrum from $\pi^+ \rightarrow e^+ \nu_e$ decay at TRIUMF. See also BRITTON 92.

¹² BRYMAN 83B obtain upper limits from both direct peak search and analysis of $B(\pi \rightarrow e\nu)/B(\pi \rightarrow \mu\nu)$. Latter limits are not listed, except for this entry (i.e. — we list the most stringent limits for given mass).

¹³ Analysis of $(\pi^+ \rightarrow e^+ \nu_e)/(\pi^+ \rightarrow \mu^+ \nu_\mu)$ and $(K^+ \rightarrow e^+ \nu_e)/(K^+ \rightarrow \mu^+ \nu_\mu)$ decay ratios.

¹⁴ Analysis of $(K^+ \rightarrow e^+ \nu_e)$ spectrum.

Kink search in nuclear β decay

High-sensitivity follow-up experiments show that indications for a neutrino with mass 17 keV (Simpson, Hime, and others) were not valid. Accordingly, we no longer list the experiments by these authors and some others which made positive claims of 17 keV neutrino emission. Complete listings are given in the 1994 edition (Physical Review D50 1173 (1994)) and in the 1998 edition (The European Physical Journal C3 1 (1998)). We list below only the best limits on $|U_{eX}|^2$ for each m_{ν_X} . See WIETFELDT 96 for a comprehensive review.

VALUE (units 10^{-3})	CL%	m_{ν_X} (keV)	ISOTOPE	METHOD	DOCUMENT ID
••• We do not use the following data for averages, fits, limits, etc. •••					
$< 4-20$	90	700–3500	^{38m} K	Trap	15 TRINCZEK 03
$< 9-116$	95	1–0.1	¹⁸⁷ Re	cryog.	16 GALEAZZI 01
< 1	95	10–90	³⁵ S	Mag spect	17 HOLZSCHUH 00
< 4	95	14–17	²⁴¹ Pu	Electrostatic spec	18 DRAGON 99
< 1	95	4–30	⁶³ Ni	Mag spect	19 HOLZSCHUH 99
$< 10-40$	90	370–640	³⁷ Ar	EC ion recoil	20 HINDI 98
< 10	95	1	³ H	SPEC	21 HIDDEMANN 95

Lepton Particle Listings

Heavy Neutral Leptons, Searches for

< 6	95	2	³ H	SPEC	21	HIDDEMANN	95
< 2	95	3	³ H	SPEC	21	HIDDEMANN	95
< 0.7	99	16.3-16.6	³ H	Prop chamber	22	KALBFLEISCH	93
< 2	95	13-40	³⁵ S		23	MORTARA	93
< 0.73	95	17	⁶³ Ni	Mag spect		OHSHIMA	93
< 1.0	95	10-24	⁶³ Ni	Mag spect		KAWAKAMI	92
< 0.9-2.5	90	1200-6800	²⁰ F	beta spectrum	24	DEUTSCH	90
< 8	90	80	³⁵ S	Mag spect	25	APALIKOV	85
< 1.5	90	60	³⁵ S	Mag spect		APALIKOV	85
< 3.0	90	5-50		Mag spect		MARKEY	85
< 0.62	90	48	³⁵ S	Si(Li)		OHI	85
< 0.90	90	30	³⁵ S	Si(Li)		OHI	85
< 4	90	140	⁶⁴ Cu	Mag spect	26	SCHRECK...	83
< 8	90	440	⁶⁴ Cu	Mag spect	26	SCHRECK...	83
<100	90	0.1-3000		THEO	27	SHROCK	80
< 0.1	68	80		THEO	28	SHROCK	80

- 15 TRINCZEK 03 is a search for admixture of heavy neutrino ν_e , in contrast to $\bar{\nu}_e$ used in many other searches. Full kinematic reconstruction of the neutrino momentum by use of a magneto optical trap.
- 16 GALEAZZI 01 use an cryogenic microcalorimeter to search for mass 50-1000 eV neutrino admixtures using the ¹⁸⁷Re beta spectrum with 2.4 keV endpoint. They derive limits for the admixture of heavy neutrinos, ranging from 9×10^{-3} for mass 1 keV to 0.116 for mass 100 eV. This is a significant improvement with respect to HIDDEMANN 95, especially for masses below ~ 500 MeV, where the limit is about a factor of ~ 2 higher.
- 17 HOLZSCHUH 00 use an iron-free β spectrometer to measure the ³⁵S β decay spectrum. An analysis of the spectrum in the energy range 56-173 keV is used to derive limits for the admixture of heavy neutrinos. This extends the range of neutrino masses explored in HOLZSCHUH 99.
- 18 DRAGON 99 analyze the β decay spectrum of ²⁴¹Pu in the energy range 0.2-9.2 keV to derive limits for the admixture of heavy neutrinos. It is not competitive with HOLZSCHUH 99.
- 19 HOLZSCHUH 99 use an iron-free β spectrometer to measure the ⁶³Ni β decay spectrum. An analysis of the spectrum in the energy range 33-67.8 keV is used to derive limits for the admixture of heavy neutrinos.
- 20 HINDI 98 obtain a limit on heavy neutrino admixture from EC decay of ³⁷Ar by measuring the time-of-flight distribution of the recoiling ions in coincidence with x-rays or Auger electrons. The authors report upper limit for $|U_{ex}|^2$ of $\approx 3\%$ for $m_{\nu_x} = 500$ keV, 1% for $m_{\nu_x} = 550$ keV, 2% for $m_{\nu_x} = 600$ keV, and 4% for $m_{\nu_x} = 650$ keV. Their reported limits for $m_{\nu_x} \leq 450$ keV are inferior to the limits of SCHRECKENBACH 83.
- 21 In the beta spectrum from tritium β decay nonvanishing or mixed m_{ν_1} state in the mass region 0.01-4 keV. For $m_{\nu_x} < 1$ keV, their upper limit on $|U_{ex}|^2$ becomes less
- 22 KALBFLEISCH 93 extends the 17 keV neutrino search of BAHRAN 92, using an improved proportional chamber to which a small amount of ³H is added. Systematics are significantly reduced, allowing for an improved upper limit. The authors give a 99% confidence limit on $|U_{ex}|^2$ as a function of m_{ν_x} in the range from 13.5 keV to 17.5 keV. See also the related papers BAHRAN 93, BAHRAN 93b, and BAHRAN 95 on theoretical aspects of beta spectra and fitting methods for heavy neutrinos.
- 23 MORTARA 93 limit is from study using a high-resolution solid-state detector with a superconducting solenoid. The authors note that "The sensitivity to neutrino mass is verified by measurement with a mixed source of ³⁵S and ¹⁴C, which artificially produces a distortion in the beta spectrum similar to that expected from the massive neutrino."
- 24 DEUTSCH 90 search for emission of heavy $\bar{\nu}_e$ in super-allowed beta decay of ²⁰F by spectral analysis of the electrons.
- 25 This limit was taken from the figure 3 of APALIKOV 85; the text gives a more restrictive limit of 1.7×10^{-3} at CL = 90%.
- 26 SCHRECKENBACH 83 is a combined measurement of the β^+ and β^- spectrum.
- 27 SHROCK 80 was a retroactive analysis of data on several superallowed β decays to search for kinks in the Kurie plot.
- 28 Application of test to search for kinks in β decay Kurie plots.

Searches for Decays of Massive ν

Limits on $|U_{ex}|^2$ as function of m_{ν_x}

VALUE	CL%	DOCUMENT ID	TECN	COMMENT
•••	•••	•••	•••	•••
<1.6 × 10 ⁻⁴	90	29 BACK 03A	CNTR	$m_{\nu_x} = 4$ MeV
<4.5 × 10 ⁻⁵	90	29 BACK 03A	CNTR	$m_{\nu_x} = 7$ MeV
<3.8 × 10 ⁻⁵	90	29 BACK 03A	CNTR	$m_{\nu_x} = 10$ MeV
<1.5 × 10 ⁻³	95	ACHARD 01	L3	$m_{\nu_x} = 80$ GeV
<2 × 10 ⁻²	95	ACHARD 01	L3	$m_{\nu_x} = 175$ GeV
<0.3	95	ACHARD 01	L3	$m_{\nu_x} = 200$ GeV
<4 × 10 ⁻³	95	ACCIARRI 99K	L3	$m_{\nu_x} = 80$ GeV
<5 × 10 ⁻²	95	ACCIARRI 99K	L3	$m_{\nu_x} = 175$ GeV
<2 × 10 ⁻⁵	95	30 ABREU 97I	DLPH	$m_{\nu_x} = 6$ GeV
<3 × 10 ⁻⁵	95	30 ABREU 97I	DLPH	$m_{\nu_x} = 50$ GeV
<1.8 × 10 ⁻³	90	31 HAGNER 95	MWPC	$m_{\nu_h} = 1.5$ MeV
<2.5 × 10 ⁻⁴	90	31 HAGNER 95	MWPC	$m_{\nu_h} = 4$ MeV
<4.2 × 10 ⁻³	90	31 HAGNER 95	MWPC	$m_{\nu_h} = 9$ MeV
<1 × 10 ⁻⁵	90	32 BARANOV 93		$m_{\nu_x} = 100$ MeV

<1 × 10 ⁻⁶	90	32 BARANOV 93		$m_{\nu_x} = 200$ MeV
<3 × 10 ⁻⁷	90	32 BARANOV 93		$m_{\nu_x} = 300$ MeV
<2 × 10 ⁻⁷	90	32 BARANOV 93		$m_{\nu_x} = 400$ MeV
<6.2 × 10 ⁻⁸	95	ADEVA 90S	L3	$m_{\nu_x} = 20$ GeV
<5.1 × 10 ⁻¹⁰	95	ADEVA 90S	L3	$m_{\nu_x} = 40$ GeV
all values ruled out	95	33 BURCHAT 90	MRK2	$m_{\nu_x} < 19.6$ GeV
<1 × 10 ⁻¹⁰	95	33 BURCHAT 90	MRK2	$m_{\nu_x} = 22$ GeV
<1 × 10 ⁻¹¹	95	33 BURCHAT 90	MRK2	$m_{\nu_x} = 41$ GeV
all values ruled out	95	DECAMP 90F	ALEP	$m_{\nu_x} = 25.0-42.7$ GeV
<1 × 10 ⁻¹³	95	DECAMP 90F	ALEP	$m_{\nu_x} = 42.7-45.7$ GeV
<5 × 10 ⁻³	90	AKERLOF 88	HRS	$m_{\nu_x} = 1.8$ GeV
<2 × 10 ⁻⁵	90	AKERLOF 88	HRS	$m_{\nu_x} = 4$ GeV
<3 × 10 ⁻⁶	90	AKERLOF 88	HRS	$m_{\nu_x} = 6$ GeV
<1.2 × 10 ⁻⁷	90	BERNARDI 88	CNTR	$m_{\nu_x} = 100$ MeV
<1 × 10 ⁻⁸	90	BERNARDI 88	CNTR	$m_{\nu_x} = 200$ MeV
<2.4 × 10 ⁻⁹	90	BERNARDI 88	CNTR	$m_{\nu_x} = 300$ MeV
<2.1 × 10 ⁻⁹	90	BERNARDI 88	CNTR	$m_{\nu_x} = 400$ MeV
<2 × 10 ⁻²	68	34 OBERAUER 87		$m_{\nu_x} = 1.5$ MeV
<8 × 10 ⁻⁴	68	34 OBERAUER 87		$m_{\nu_x} = 4.0$ MeV
<8 × 10 ⁻³	90	BADIER 86	CNTR	$m_{\nu_x} = 400$ MeV
<8 × 10 ⁻⁵	90	BADIER 86	CNTR	$m_{\nu_x} = 1.7$ GeV
<8 × 10 ⁻⁸	90	BERNARDI 86	CNTR	$m_{\nu_x} = 100$ MeV
<4 × 10 ⁻⁸	90	BERNARDI 86	CNTR	$m_{\nu_x} = 200$ MeV
<6 × 10 ⁻⁹	90	BERNARDI 86	CNTR	$m_{\nu_x} = 400$ MeV
<3 × 10 ⁻⁵	90	DORENBOS... 86	CNTR	$m_{\nu_x} = 150$ MeV
<1 × 10 ⁻⁶	90	DORENBOS... 86	CNTR	$m_{\nu_x} = 500$ MeV
<1 × 10 ⁻⁷	90	DORENBOS... 86	CNTR	$m_{\nu_x} = 1.6$ GeV
<7 × 10 ⁻⁷	90	35 COOPER... 85	HLBC	$m_{\nu_x} = 0.4$ GeV
<8 × 10 ⁻⁸	90	35 COOPER... 85	HLBC	$m_{\nu_x} = 1.5$ GeV
<1 × 10 ⁻²	90	36 BERGSMA 83B	CNTR	$m_{\nu_x} = 10$ MeV
<1 × 10 ⁻⁵	90	36 BERGSMA 83B	CNTR	$m_{\nu_x} = 110$ MeV
<6 × 10 ⁻⁷	90	36 BERGSMA 83B	CNTR	$m_{\nu_x} = 410$ MeV
<1 × 10 ⁻⁵	90	GRONAU 83		$m_{\nu_x} = 160$ MeV
<1 × 10 ⁻⁶	90	GRONAU 83		$m_{\nu_x} = 480$ MeV

- 29 BACK 03A searched for heavy neutrinos emitted from ⁸B decay in the Sun using the decay $\nu_h \rightarrow \nu_e e^+ e^-$ in the Counting Test Facility (the prototype of the Borexino detector) and obtained limits on heavy neutrino admixture for the ν_h mass range 1.1-12 MeV.
- 30 ABREU 97I long-lived ν_x analysis. Short-lived analysis extends limit to lower masses with decreasing sensitivity except at 3.5 GeV, where the limit is the same as at 6 GeV.
- 31 HAGNER 95 obtain limits on heavy neutrino admixture from the decay $\nu_h \rightarrow \nu_e e^+ e^-$ at a nuclear reactor for the ν_h mass range 2-9 MeV.
- 32 BARANOV 93 is a search for neutrino decays into $e^+ e^- \nu_e$ using a beam dump experiment at the 70 GeV Serpukhov proton synchrotron. The limits are not as good as those achieved earlier by BERGSMA 83 and BERNARDI 86, BERNARDI 88.
- 33 BURCHAT 90 includes the analyses reported in JUNG 90, ABRAMS 89c, and WENDT 87.
- 34 OBERAUER 87 bounds from search for $\nu \rightarrow \nu' e e$ decay mode using reactor (anti)neutrinos.
- 35 COOPER-SARKAR 85 also give limits based on model-dependent assumptions for ν_τ flux. We do not list these. Note that for this bound to be nontrivial, x is not equal to 3, i.e. ν_x cannot be the dominant mass eigenstate in ν_τ since $m_{\nu_3} < 70$ MeV (ALBRECHT 85i). Also, of course, x is not equal to 1 or 2, so a fourth generation would be required for this bound to be nontrivial.
- 36 BERGSMA 83B also quote limits on $|U_{e3}|^2$ where the index 3 refers to the mass eigenstate dominantly coupled to the τ . Those limits were based on assumptions about the D_S mass and $D_S \rightarrow \tau \nu_\tau$ branching ratio which are no longer valid. See COOPER-SARKAR 85.

Limits on Coupling of μ to ν_x as Function of m_{ν_x}

Peak search test

Limits on $B(\pi \text{ (or } K) \rightarrow \mu \nu_x)$.

VALUE	CL%	DOCUMENT ID	TECN	COMMENT
•••	•••	•••	•••	•••
<6.0 × 10 ⁻¹⁰	95	37 ASTIER 02	NOMD	$\pi \rightarrow \mu X$ for $m_X = 33.9$ MeV
		38 DAUM 00	CNTR	$\pi \rightarrow \mu X$ for $m_X = 33.9$ MeV
		39 FORMAGGIO 00	CNTR	$\pi \rightarrow \mu X$ for $m_X = 33.9$ MeV
<0.22	90	40 ASSAMAGAN 98	SILI	$m_{\nu_x} = 0.53$ MeV
<0.029	90	40 ASSAMAGAN 98	SILI	$m_{\nu_x} = 0.75$ MeV
<0.016	90	40 ASSAMAGAN 98	SILI	$m_{\nu_x} = 1.0$ MeV
<4-6 × 10 ⁻⁵		41 BRYMAN 96	CNTR	$m_{\nu_x} = 30-33.91$ MeV
$\sim 1 \times 10^{-16}$		42 ARMBRUSTER 95	KARM	$m_{\nu_x} = 33.9$ MeV
<4 × 10 ⁻⁷	95	43 BILGER 95	LEPS	$m_{\nu_x} = 33.9$ MeV

<7	$\times 10^{-8}$	95	43 BILGER	95	LEPS	$m_{\nu_x} = 33.9$ MeV
<2.6	$\times 10^{-8}$	95	43 DAUM	95b	TOF	$m_{\nu_x} = 33.9$ MeV
<2	$\times 10^{-2}$	90	DAUM	87		$m_{\nu_x} = 1$ MeV
<1	$\times 10^{-3}$	90	DAUM	87		$m_{\nu_x} = 2$ MeV
<6	$\times 10^{-5}$	90	DAUM	87		$3 \text{ MeV} < m_{\nu_x} < 19.5$ MeV
<3	$\times 10^{-2}$	90	44 MINEHART	84		$m_{\nu_x} = 2$ MeV
<1	$\times 10^{-3}$	90	44 MINEHART	84		$m_{\nu_x} = 4$ MeV
<3	$\times 10^{-4}$	90	44 MINEHART	84		$m_{\nu_x} = 10$ GeV
<5	$\times 10^{-6}$	90	45 HAYANO	82		$m_{\nu_x} = 330$ MeV
<1	$\times 10^{-4}$	90	45 HAYANO	82		$m_{\nu_x} = 70$ MeV
<9	$\times 10^{-7}$	90	45 HAYANO	82		$m_{\nu_x} = 250$ MeV
<1	$\times 10^{-1}$	90	44 ABELA	81		$m_{\nu_x} = 4$ MeV
<7	$\times 10^{-5}$	90	44 ABELA	81		$m_{\nu_x} = 10.5$ MeV
<2	$\times 10^{-4}$	90	44 ABELA	81		$m_{\nu_x} = 11.5$ MeV
<2	$\times 10^{-5}$	90	44 ABELA	81		$m_{\nu_x} = 16\text{--}30$ MeV

37 ASTIER 02 search for anomalous pion decay into a 33.9 MeV neutral particle. No evidence was found and the sensitivity to the branching ratio $B(\pi \rightarrow \mu X) \cdot B(X \rightarrow \nu e^+ e^-)$ is as low as 3.7×10^{-15} , depending on the X lifetime.

38 DAUM 00 search for anomalous pion decay into a 33.9 MeV neutral particle that might be responsible for the time-distribution anomaly observed by the KARMEN Collaboration.

39 FORMAGGIO 00 search for anomalous pion decay into a 33.9 MeV neutral particle Q^0 that might be responsible for the time-distribution anomaly observed by the KARMEN Collaboration. In the E815 (NuTeV) experiment at Fermilab no evidence was found, with sensitivity for the pion branching ratio $B(\pi \rightarrow \mu Q^0) \cdot B(Q^0 \rightarrow \text{visible})$ as low as 10^{-13} .

40 ASSAMAGAN 98 obtain a limit on heavy neutrino admixture from π^+ decay essentially at rest, by measuring with good resolution the momentum distribution of the muons. However, the search uses an ad hoc shape correction. The authors report upper limit for $|U_{\mu x}|^2$ of 0.22 for $m_\nu = 0.53$ MeV, 0.029 for $m_\nu = 0.75$ MeV, and 0.016 for $m_\nu = 1.0$ MeV at 90%CL.

41 BRYMAN 96 search for massive unconventional neutrinos of mass m_{ν_x} in π^+ decay.

42 ARMBRUSTER 95 study the reactions $^{12}\text{C}(\nu_e, e^-)^{12}\text{N}$ and $^{12}\text{C}(\nu, \nu')^{12}\text{C}^*$ induced by neutrinos from π^+ and μ^+ decay at the ISIS neutron spallation source at the Rutherford-Appleton laboratory. An anomaly in the time distribution can be interpreted as the decay $\pi^+ \rightarrow \mu^+ \nu_x$, where ν_x is a neutral weakly interacting particle with mass ≈ 33.9 MeV and spin 1/2. The lower limit to the branching ratio is a function of the lifetime of the new massive neutral particle, and reaches a minimum of a few $\times 10^{-16}$ for $\tau_x \sim 5$ s.

43 From experiments of π^+ and π^- decay in flight at PSI, to check the claim of the KARMEN Collaboration quoted above (ARMBRUSTER 95).

44 $\pi^+ \rightarrow \mu^+ \nu_\mu$ peak search experiment.

45 $K^+ \rightarrow \mu^+ \nu_\mu$ peak search experiment.

Peak search test

Limits on $|U_{\mu x}|^2$ as function of m_{ν_x}

VALUE	CL%	DOCUMENT ID	TECN	COMMENT
-------	-----	-------------	------	---------

• • • We do not use the following data for averages, fits, limits, etc. • • •

<1-10	$\times 10^{-4}$	46 BRYMAN	96	CNTR	$m_{\nu_x} = 30\text{--}33.91$ MeV
<2	$\times 10^{-5}$	47 ASANO	81		$m_{\nu_x} = 70$ MeV
<3	$\times 10^{-6}$	47 ASANO	81		$m_{\nu_x} = 210$ MeV
<3	$\times 10^{-6}$	47 ASANO	81		$m_{\nu_x} = 230$ MeV
<6	$\times 10^{-6}$	48 ASANO	81		$m_{\nu_x} = 240$ MeV
<5	$\times 10^{-7}$	48 ASANO	81		$m_{\nu_x} = 280$ MeV
<6	$\times 10^{-6}$	48 ASANO	81		$m_{\nu_x} = 300$ MeV
<1	$\times 10^{-2}$	95 CALAPRICE	81		$m_{\nu_x} = 7$ MeV
<3	$\times 10^{-3}$	95 CALAPRICE	81		$m_{\nu_x} = 33$ MeV
<1	$\times 10^{-4}$	68 50 SHROCK	81	THEO	$m_{\nu_x} = 13$ MeV
<3	$\times 10^{-5}$	68 50 SHROCK	81	THEO	$m_{\nu_x} = 33$ MeV
<6	$\times 10^{-3}$	68 51 SHROCK	81	THEO	$m_{\nu_x} = 80$ MeV
<5	$\times 10^{-3}$	68 51 SHROCK	81	THEO	$m_{\nu_x} = 120$ MeV

46 BRYMAN 96 search for massive unconventional neutrinos of mass m_{ν_x} in π^+ decay. They interpret the result as an upper limit for the admixture of a heavy sterile or otherwise

47 $K^+ \rightarrow \mu^+ \nu_\mu$ peak search experiment.

48 Analysis of experiment on $K^+ \rightarrow \mu^+ \nu_\mu \nu_x \bar{\nu}_x$ decay.

49 $\pi^+ \rightarrow \mu^+ \nu_\mu$ peak search experiment.

50 Analysis of magnetic spectrometer experiment, bubble chamber experiment, and emulsion experiment on $\pi^+ \rightarrow \mu^+ \nu_\mu$ decay.

51 Analysis of magnetic spectrometer experiment on $K \rightarrow \mu, \nu_\mu$ decay.

Peak Search in Muon Capture

Limits on $|U_{\mu x}|^2$ as function of m_{ν_x}

VALUE	DOCUMENT ID	TECN	COMMENT
-------	-------------	------	---------

• • • We do not use the following data for averages, fits, limits, etc. • • •

<1	$\times 10^{-1}$	DEUTSCH	83	$m_{\nu_x} = 45$ MeV
<7	$\times 10^{-3}$	DEUTSCH	83	$m_{\nu_x} = 70$ MeV
<1	$\times 10^{-1}$	DEUTSCH	83	$m_{\nu_x} = 85$ MeV

Searches for Decays of Massive ν

Limits on $|U_{\mu x}|^2$ as function of m_{ν_x}

VALUE	CL%	DOCUMENT ID	TECN	COMMENT
-------	-----	-------------	------	---------

• • • We do not use the following data for averages, fits, limits, etc. • • •

<5	$\times 10^{-7}$	90 52 VAITAITIS	99	CCFR	$m_{\nu_x} = 0.28$ GeV
<8	$\times 10^{-8}$	90 52 VAITAITIS	99	CCFR	$m_{\nu_x} = 0.37$ GeV
<5	$\times 10^{-7}$	90 52 VAITAITIS	99	CCFR	$m_{\nu_x} = 0.50$ GeV
<6	$\times 10^{-8}$	90 52 VAITAITIS	99	CCFR	$m_{\nu_x} = 1.50$ GeV
<2	$\times 10^{-5}$	95 53 ABREU	97i	DLPH	$m_{\nu_x} = 6$ GeV
<3	$\times 10^{-5}$	95 53 ABREU	97i	DLPH	$m_{\nu_x} = 50$ GeV
<3	$\times 10^{-6}$	90 GALLAS	95	CNTR	$m_{\nu_x} = 1$ GeV
<3	$\times 10^{-5}$	90 54 VILAIN	95c	CHM2	$m_{\nu_x} = 2$ GeV
<6.2	$\times 10^{-8}$	95 ADEVA	90s	L3	$m_{\nu_x} = 20$ GeV
<5.1	$\times 10^{-10}$	95 ADEVA	90s	L3	$m_{\nu_x} = 40$ GeV
all values ruled out		95 55 BURCHAT	90	MRK2	$m_{\nu_x} < 19.6$ GeV
<1	$\times 10^{-10}$	95 55 BURCHAT	90	MRK2	$m_{\nu_x} = 22$ GeV
<1	$\times 10^{-11}$	95 55 BURCHAT	90	MRK2	$m_{\nu_x} = 41$ GeV
all values ruled out		95 DECAMP	90f	ALEP	$m_{\nu_x} = 25.0\text{--}42.7$ GeV
<1	$\times 10^{-13}$	95 DECAMP	90f	ALEP	$m_{\nu_x} = 42.7\text{--}45.7$ GeV
<5	$\times 10^{-3}$	90 AKERLOF	88	HRS	$m_{\nu_x} = 1.8$ GeV
<2	$\times 10^{-5}$	90 AKERLOF	88	HRS	$m_{\nu_x} = 4$ GeV
<3	$\times 10^{-6}$	90 AKERLOF	88	HRS	$m_{\nu_x} = 6$ GeV
<1	$\times 10^{-7}$	90 BERNARDI	88	CNTR	$m_{\nu_x} = 200$ MeV
<3	$\times 10^{-9}$	90 BERNARDI	88	CNTR	$m_{\nu_x} = 300$ MeV
<4	$\times 10^{-4}$	90 56 MISHRA	87	CNTR	$m_{\nu_x} = 1.5$ GeV
<4	$\times 10^{-3}$	90 56 MISHRA	87	CNTR	$m_{\nu_x} = 2.5$ GeV
<0.9	$\times 10^{-2}$	90 56 MISHRA	87	CNTR	$m_{\nu_x} = 5$ GeV
<0.1		90 56 MISHRA	87	CNTR	$m_{\nu_x} = 10$ GeV
<8	$\times 10^{-4}$	90 BADIÉ	86	CNTR	$m_{\nu_x} = 600$ MeV
<1.2	$\times 10^{-5}$	90 BADIÉ	86	CNTR	$m_{\nu_x} = 1.7$ GeV
<3	$\times 10^{-8}$	90 BERNARDI	86	CNTR	$m_{\nu_x} = 200$ MeV
<6	$\times 10^{-9}$	90 BERNARDI	86	CNTR	$m_{\nu_x} = 350$ MeV
<1	$\times 10^{-6}$	90 DORENBOS...	86	CNTR	$m_{\nu_x} = 500$ MeV
<1	$\times 10^{-7}$	90 DORENBOS...	86	CNTR	$m_{\nu_x} = 1600$ MeV
<0.8	$\times 10^{-5}$	90 57 COOPER...	85	HLBC	$m_{\nu_x} = 0.4$ GeV
<1.0	$\times 10^{-7}$	90 57 COOPER...	85	HLBC	$m_{\nu_x} = 1.5$ GeV

52 VAITAITIS 99 search for $L_\mu^0 \rightarrow \mu X$. See paper for rather complicated limit as function of m_{ν_x} .

53 ABREU 97i long-lived ν_x analysis. Short-lived analysis extends limit to lower masses with decreasing sensitivity except at 3.5 GeV, where the limit is the same as at 6 GeV.

54 VILAIN 95c is a search for the decays of heavy isosinglet neutrinos produced by neutral current neutrino interactions. Limits were quoted for masses in the range from 0.3 to 24 GeV. The best limit is listed above.

55 BURCHAT 90 includes the analyses reported in JUNG 90, ABRAMS 89c, and WENDT 87.

56 See also limits on $|U_{3x}|$ from WENDT 87.

57 COOPER-SARKAR 85 also give limits based on model-dependent assumptions for ν_τ flux. We do not list these. Note that for this bound to be nontrivial, x is not equal to 3, i.e. ν_x cannot be the dominant mass eigenstate in ν_τ since $m_{\nu_3} < 70$ MeV (ALBRECHT 85i). Also, of course, x is not equal to 1 or 2, so a fourth generation would be required for this bound to be nontrivial.

Limits on $|U_{\tau x}|^2$ as a Function of m_{ν_x}

VALUE	CL%	DOCUMENT ID	TECN	COMMENT
-------	-----	-------------	------	---------

• • • We do not use the following data for averages, fits, limits, etc. • • •

<1	$\times 10^{-2}$	90 58 ORLOFF	02	CHRM	$m_{\nu_x} = 45$ MeV
<1.4	$\times 10^{-4}$	90 58 ORLOFF	02	CHRM	$m_{\nu_x} = 180$ MeV
<0.025		90 ASTIER	01		$m_{\nu_x} = 45$ MeV
<0.002		90 ASTIER	01		$m_{\nu_x} = 140$ MeV
<2	$\times 10^{-5}$	95 59 ABREU	97i	DLPH	$m_{\nu_x} = 6$ GeV
<3	$\times 10^{-5}$	95 59 ABREU	97i	DLPH	$m_{\nu_x} = 50$ GeV
<6.2	$\times 10^{-8}$	95 ADEVA	90s	L3	$m_{\nu_x} = 20$ GeV
<5.1	$\times 10^{-10}$	95 ADEVA	90s	L3	$m_{\nu_x} = 40$ GeV

Lepton Particle Listings

Heavy Neutral Leptons, Searches for

all values ruled out	95	60	BURCHAT	90	MRK2	$m_{\nu_x} < 19.6$ GeV
$<1 \times 10^{-10}$	95	60	BURCHAT	90	MRK2	$m_{\nu_x} = 22$ GeV
$<1 \times 10^{-11}$	95	60	BURCHAT	90	MRK2	$m_{\nu_x} = 41$ GeV
all values ruled out	95	DECAMP	90F	ALEP	$m_{\nu_x} = 25.0-42.7$ GeV	
$<1 \times 10^{-13}$	95	DECAMP	90F	ALEP	$m_{\nu_x} = 42.7-45.7$ GeV	
$<5 \times 10^{-2}$	80	AKERLOF	88	HRS	$m_{\nu_x} = 2.5$ GeV	
$<9 \times 10^{-5}$	80	AKERLOF	88	HRS	$m_{\nu_x} = 4.5$ GeV	

⁵⁸ORLOFF 02 use the negative result of a search for neutral particles decaying into two electrons performed by CHARM to get these limits for a mostly isosinglet heavy neutrino.

⁵⁹ABREU 97i long-lived ν_x analysis. Short-lived analysis extends limit to lower masses with decreasing sensitivity.

⁶⁰BURCHAT 90 includes the analyses reported in JUNG 90, ABRAMS 89c, and WENDT 87.

Limits on $|U_{ax}|^2$

Where $a = e, \mu$ from ρ parameter in μ decay.

VALUE	CL%	DOCUMENT ID	TECN	COMMENT
$<1 \times 10^{-2}$	68	SHROCK 81B	THEO	$m_{\nu_x} = 10$ GeV
$<2 \times 10^{-3}$	68	SHROCK 81B	THEO	$m_{\nu_x} = 40$ MeV
$<4 \times 10^{-2}$	68	SHROCK 81B	THEO	$m_{\nu_x} = 70$ MeV

Limits on $|U_{1j} \times U_{2j}|$ as Function of m_{ν_j}

VALUE	CL%	DOCUMENT ID	TECN	COMMENT
$<3 \times 10^{-5}$	90	61 BARANOV 93		$m_{\nu_j} = 80$ MeV
$<3 \times 10^{-6}$	90	61 BARANOV 93		$m_{\nu_j} = 160$ MeV
$<6 \times 10^{-7}$	90	61 BARANOV 93		$m_{\nu_j} = 240$ MeV
$<2 \times 10^{-7}$	90	61 BARANOV 93		$m_{\nu_j} = 320$ MeV
$<9 \times 10^{-5}$	90	BERNARDI 86	CNTR	$m_{\nu_j} = 25$ MeV
$<3.6 \times 10^{-7}$	90	BERNARDI 86	CNTR	$m_{\nu_j} = 100$ MeV
$<3 \times 10^{-8}$	90	BERNARDI 86	CNTR	$m_{\nu_j} = 200$ MeV
$<6 \times 10^{-9}$	90	BERNARDI 86	CNTR	$m_{\nu_j} = 350$ MeV
$<1 \times 10^{-2}$	90	BERGSMA 83B	CNTR	$m_{\nu_j} = 10$ MeV
$<1 \times 10^{-5}$	90	BERGSMA 83B	CNTR	$m_{\nu_j} = 140$ MeV
$<7 \times 10^{-7}$	90	BERGSMA 83B	CNTR	$m_{\nu_j} = 370$ MeV

⁶¹BARANOV 93 is a search for neutrino decays into $e^+ e^- \nu_e$ using a beam dump experiment at the 70 GeV Serpukhov proton synchrotron.

DRAGOUN 99	JPG 25 1839	O. Dragoun <i>et al.</i>	
HOLZSCHUH 99	PL B451 247	E. Holzschuh <i>et al.</i>	
VAITAITIS 99	PRL 83 4943	A. Vaitaitis <i>et al.</i>	(CCFR Collab.)
ASSAMAGAN 98	PL B434 158	K. Assamagan <i>et al.</i>	
HINDI 98	PR C58 2512	M.M. Hindi <i>et al.</i>	
PDG 98	EPJ C3 1	C. Caso <i>et al.</i>	
ABREU 97i	ZPHY C74 57	P. Abreu <i>et al.</i>	(DELPHI Collab.)
Also	ZPHY C75 580 (erratum)	P. Abreu <i>et al.</i>	(DELPHI Collab.)
BRYMAN 96	PR D53 558	D.A. Bryman, T. Numao	(TRIUMF)
BUSKULIC 96S	PL B384 439	D. Buskulic <i>et al.</i>	(ALEPH Collab.)
WIETFIELDT 96	PRPL 273 149	F.E. Wietfeldt, E.B. Norman	(LBL)
ARMBRUSTER 95	PL B348 19	B. Armbruster <i>et al.</i>	(KARMEN Collab.)
BAHRAN 95	PL B354 481	M.Y. Bahrán, G.R. Kalbfleisch	(OKLA)
BILGER 95	PL B363 41	R. Bilger <i>et al.</i>	(TUBIN, KARLE, PSI)
DAUM 95B	PL B361 179	M. Daum <i>et al.</i>	(PSI, VIRG)
FARGION 95	PR D52 1828	D. Fargion <i>et al.</i>	(ROMA, KIAM, MPEI)
GALLAS 95	PR D52 6	E. Gallas <i>et al.</i>	(MSU, FNAL, MIT, FLOR)
GARCIA 95	PR D51 1458	E. Garcia <i>et al.</i>	(ZARA, SCUC, PNL)
HAGNER 95	PR D52 1343	C. Hagner <i>et al.</i>	(MUNT, LAPP, CPM)
HIDDEMANN 95	JPG 21 639	K.H. Hiddeemann, H. Daniel, O. Schwesinger	(MUNT)
VILAIN 95C	PL B351 387	P. Vilain <i>et al.</i>	(CHARM II Collab.)
Also	PL B343 453	P. Vilain <i>et al.</i>	(CHARM II Collab.)
BECK 94	PL B336 141	M. Beck <i>et al.</i>	(MPH, KIAE, SASSO)
KONOPLICH 94	PAN 57 425	R.V. Konoplich, M.Y. Khlopov	(MPEI)
PDG 94	PR D50 1173	L. Montanet <i>et al.</i>	(CERN, LBL, BOST+)
BAHRAN 93B	PR D47 R754	M. Bahrán, G.R. Kalbfleisch	(OKLA)
BAHRAN 93B	PR D47 R759	M. Bahrán, G.R. Kalbfleisch	(OKLA)
BARANOV 93	PL B302 336	S.A. Baranov <i>et al.</i>	(JINR, SERP, BUDA)
KALBFLEISCH 93	PL B303 355	G.R. Kalbfleisch, M.Y. Bahrán	(OKLA)
MORTARA 93	PRL 70 394	J.L. Mortara <i>et al.</i>	(ANL, LBL, UCB)
OSHIMA 93	PR D47 4840	T. Oshima <i>et al.</i>	(KEK, THUAT, RIKEN+)
ABREU 92B	PL B274 230	P. Abreu <i>et al.</i>	(DELPHI Collab.)
BAHRAN 92	PL B291 336	M.Y. Bahrán, G.R. Kalbfleisch	(OKLA)
BRITTON 92	PRL 68 3000	D.I. Britton <i>et al.</i>	(TRIUMF, CARL)
Also	PR D49 28	D.I. Britton <i>et al.</i>	(TRIUMF, CARL)
BRITTON 92B	PR D46 R885	D.I. Britton <i>et al.</i>	(TRIUMF, CARL)
KAWAKAMI 92	PL B287 45	H. Kawakami <i>et al.</i>	(INUS, KEK, SCUC+)
MORI 92B	PL B289 463	M. Mori <i>et al.</i>	(KAM2 Collab.)
ALEXANDER 91F	ZPHY C52 175	G. Alexander <i>et al.</i>	(OPAL Collab.)
DELEENER... 91	PR D43 3611	N. de Leener-Rosier <i>et al.</i>	(LOUV, ZURI+)
REUSSER 91	PL B255 143	D. Reusser <i>et al.</i>	(NEUC, CIT, PSI)
SATO 91	PR D44 2220	N. Sato <i>et al.</i>	(Kamikande Collab.)
ADEVA 90S	PL B251 321	B. Adeva <i>et al.</i>	(LS Collab.)
BURCHAT 90	PR D41 3542	P.R. Burchat <i>et al.</i>	(Mark II Collab.)
DECAMP 90F	PL B236 511	D. Decamp <i>et al.</i>	(ALEPH Collab.)
DEUTSCH 90	NP A518 149	J. Deutsch, M. Lebrun, R. Prieels	
JUNG 90	PRL 64 1091	C. Jung <i>et al.</i>	(Mark II Collab.)
ABRAMS 89C	PRL 63 2447	G.S. Abrams <i>et al.</i>	(Mark II Collab.)
ENQVIST 89	NP B317 647	K. Enqvist, K. Kainulainen, J. Maalampi	(HELS)
FISHER 89	PL B218 257	P.H. Fisher <i>et al.</i>	(CIT, NEUC, PSI)
AKERLOF 88	PR D37 577	C.W. Akerlof <i>et al.</i>	(HRS Collab.)
BERNARDI 88	PL B203 332	G. Bernardi <i>et al.</i>	(PARIN, CERN, INFN+)
CALDWELL 88	PRL 61 510	D.O. Caldwell <i>et al.</i>	(UCSB, UCB, LBL)
OLIVE 88	PL B205 553	K.A. Olive, M. Srednicki	(MINN, UCSB)
SREDNICKI 88	NP B310 693	M. Srednicki, R. Watkins, K.A. Olive	(MINN, UCSB)
AHLEN 87	PL B195 603	S.P. Ahlen <i>et al.</i>	(BOST, SCUC, HARV+)
DAUM 87	PR D36 2624	M. Daum <i>et al.</i>	(SIN, VIRG)
GRIEST 87	NP B283 681	K. Griest, D. Seckel	(UCSC, CERN)
Also	NP B296 1034 (erratum)	K. Griest, D. Seckel	(UCSC, CERN)
MISHRA 87	PRL 59 1397	S.R. Mishra <i>et al.</i>	(COLU, CIT, FNAL+)
OBERAUER 87	PL B198 113	L.F. Oberauer, F. von Feilitzsch, R.L. Mossbauer	
WENDT 87	PRL 58 1810	C. Wendt <i>et al.</i>	(Mark II Collab.)
AZUELOS 86	PRL 56 2241	G. Azuelos <i>et al.</i>	(TRIUMF, CNRC)
BADIER 86	ZPHY C31 21	J. Badier <i>et al.</i>	(NAS Collab.)
BERNARDI 86	PL 166B 479	G. Bernardi <i>et al.</i>	(CURIN, INFN, CDF+)
DORENBOSCH... 86	PL 166B 473	J. Dorenbosch <i>et al.</i>	(CHARM Collab.)
ALBRECHT 85I	PL 163B 404	H. Albrecht <i>et al.</i>	(ARGUS Collab.)
APALIKOV 85	JETPL 42 289	A.M. Apalikhov <i>et al.</i>	(ITEP)
COOPER... 85	PL 160B 207	A.M. Cooper-Sarkar <i>et al.</i>	(CERN, LOIC+)
MARKEY 85	PR C32 2215	J. Markey, F. Boehm	(CIT)
OHI 85	PL 160B 322	T. Ohi <i>et al.</i>	(TOKY, INUS, KEK)
MINEHART 84	PRL 52 804	R.C. Minehart <i>et al.</i>	(VIRG, SIN)
BERGSMA 83B	PL 122B 465	F. Bergsma <i>et al.</i>	(CHARM Collab.)
BERGSMA 83B	PL 128B 361	F. Bergsma <i>et al.</i>	(CHARM Collab.)
BRYMAN 83B	PRL 50 1546	D.A. Bryman <i>et al.</i>	(TRIUMF, CNRC)
DEUTSCH 83	PR D27 1644	J.P. Deutsch, M. Lebrun, R. Prieels	(LOUV)
GRONAU 83	PR D28 2762	M. Gronau	(HAIF)
SCHRECK... 83	PL 129B 265	K. Schreckenbach <i>et al.</i>	(ISNG, ILLG)
HAYANO 82	PRL 49 1305	R.S. Hayano <i>et al.</i>	(TOKY, KEK, TSUK)
ABELA 81	PL 105B 263	R. Abela <i>et al.</i>	(SIN)
ASANO 81	PL 104B 84	Y. Asano <i>et al.</i>	(KEK, TOKY, INUS, OSAK)
CALAPRICE 81	PL 106B 175	F.P. Calaprice <i>et al.</i>	(PRIN, IND)
SHROCK 81	PR D24 1232	R.E. Shrock	(STON)
SHROCK 81B	PR D24 1275	R.E. Shrock	(STON)
SHROCK 80	PL 96B 159	R.E. Shrock	(STON)

REFERENCES FOR Heavy Neutral Leptons, Searches for

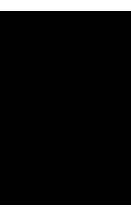
BACK 03A	JETPL 78 261	H.O. Back <i>et al.</i>	(Borexino Collab.)
TRINCEK 03	Translated from ZETFP 78 707	M. Trinczek <i>et al.</i>	
ASTIER 02	PRL 90 012501	P. Astier <i>et al.</i>	(NOMAD Collab.)
ORLOFF 02	PL B527 23	J. Orloff <i>et al.</i>	
ACHARD 01	PL B517 67	P. Achard <i>et al.</i>	(L3 Collab.)
ACHARD 01B	PL B517 75	P. Achard <i>et al.</i>	(L3 Collab.)
ASTIER 01	PL B506 27	P. Astier <i>et al.</i>	(NOMAD Collab.)
GALEAZZI 01	PRL 86 1978	M. Galeazzi <i>et al.</i>	
ABBIENDI 00I	EPJ C14 73	G. Abbiendi <i>et al.</i>	(OPAL Collab.)
DAUM 00	PRL 85 1815	M. Daum <i>et al.</i>	
FORMAGGIO 00	PRL 84 4043	J.A. Formaggio <i>et al.</i>	
HOLZSCHUH 00	PL B482 1	E. Holzschuh <i>et al.</i>	
ABREU 99O	EPJ C8 41	P. Abreu <i>et al.</i>	(DELPHI Collab.)
ACCIARRI 99K	PL B461 397	M. Acciarri <i>et al.</i>	(L3 Collab.)

QUARKS

<i>u</i>	557
<i>d</i>	558
<i>s</i>	558
<i>c</i>	561
<i>b</i>	562
<i>t</i>	563
<i>b'</i> (Fourth Generation) Quark	576
<i>t'</i> (Fourth Generation) Quark	577
Free Quark Searches	577

Notes in the Quark Listings

Quark Masses (rev.)	551
The Top Quark (rev.)	563
Free Quark Searches	577





QUARKS

QUARK MASSES

Updated February 2008 by A.V. Manohar (University of California, San Diego) and C.T. Sachrajda (University of Southampton)

A. Introduction

This note discusses some of the theoretical issues relevant for the determination of quark masses, which are fundamental parameters of the Standard Model of particle physics. Unlike the leptons, quarks are confined inside hadrons and are not observed as physical particles. Quark masses therefore cannot be measured directly, but must be determined indirectly through their influence on hadronic properties. Although one often speaks loosely of quark masses as one would of the mass of the electron or muon, any quantitative statement about the value of a quark mass must make careful reference to the particular theoretical framework that is used to define it. It is important to keep this *scheme dependence* in mind when using the quark mass values tabulated in the data listings.

Historically, the first determinations of quark masses were performed using quark models. The resulting masses only make sense in the limited context of a particular quark model, and cannot be related to the quark mass parameters of the Standard Model. In order to discuss quark masses at a fundamental level, definitions based on quantum field theory be used, and the purpose of this note is to discuss these definitions and the corresponding determinations of the values of the masses.

B. Mass parameters and the QCD Lagrangian

The QCD [1] Lagrangian for N_F quark flavors is

$$\mathcal{L} = \sum_{k=1}^{N_F} \bar{q}_k (i\mathcal{D} - m_k) q_k - \frac{1}{4} G_{\mu\nu} G^{\mu\nu}, \quad (1)$$

where $\mathcal{D} = (\partial_\mu - igA_\mu) \gamma^\mu$ is the gauge covariant derivative, A_μ is the gluon field, $G_{\mu\nu}$ is the gluon field strength, m_k is the mass parameter of the k^{th} quark, and q_k is the quark Dirac field. After renormalization, the QCD Lagrangian Eq. (1) gives finite values for physical quantities, such as scattering amplitudes. Renormalization is a procedure that invokes a subtraction scheme to render the amplitudes finite, and requires the introduction of a dimensionful scale parameter μ . The mass parameters in the QCD Lagrangian Eq. (1) depend on the renormalization scheme used to define the theory, and also on the scale parameter μ . The most commonly used renormalization scheme for QCD perturbation theory is the $\overline{\text{MS}}$ scheme.

The QCD Lagrangian has a chiral symmetry in the limit that the quark masses vanish. This symmetry is spontaneously broken by dynamical chiral symmetry breaking, and explicitly broken by the quark masses. The nonperturbative scale of dynamical chiral symmetry breaking, Λ_χ , is around 1 GeV [2]. It is conventional to call quarks heavy if $m > \Lambda_\chi$, so that explicit

chiral symmetry breaking dominates (c , b , and t quarks are heavy), and light if $m < \Lambda_\chi$, so that spontaneous chiral symmetry breaking dominates (u , d and s quarks are light). The determination of light- and heavy-quark masses is considered separately in sections D and E below.

At high energies or short distances, nonperturbative effects, such as chiral symmetry breaking, become small and one can, in principle, determine quark masses by analyzing mass-dependent effects using QCD perturbation theory. Such computations are conventionally performed using the $\overline{\text{MS}}$ scheme at a scale $\mu \gg \Lambda_\chi$, and give the $\overline{\text{MS}}$ “running” mass $\overline{m}(\mu)$. We use the $\overline{\text{MS}}$ scheme when reporting quark masses; one can readily convert these values into other schemes using perturbation theory.

The μ dependence of $\overline{m}(\mu)$ at short distances can be calculated using the renormalization group equation,

$$\mu^2 \frac{d\overline{m}(\mu)}{d\mu^2} = -\gamma(\overline{\alpha}_s(\mu)) \overline{m}(\mu), \quad (2)$$

where γ is the anomalous dimension which is now known to four-loop order in perturbation theory [3,4]. $\overline{\alpha}_s$ is the coupling constant in the $\overline{\text{MS}}$ scheme. Defining the expansion coefficients γ_r by

$$\gamma(\overline{\alpha}_s) \equiv \sum_{r=1}^{\infty} \gamma_r \left(\frac{\overline{\alpha}_s}{4\pi} \right)^r,$$

the first four coefficients are given by

$$\begin{aligned} \gamma_1 &= 4, \\ \gamma_2 &= \frac{202}{3} - \frac{20N_L}{9}, \\ \gamma_3 &= 1249 + \left(-\frac{2216}{27} - \frac{160}{3}\zeta(3) \right) N_L - \frac{140}{81} N_L^2, \\ \gamma_4 &= \frac{4603055}{162} + \frac{135680}{27}\zeta(3) - 8800\zeta(5) \\ &\quad + \left(-\frac{91723}{27} - \frac{34192}{9}\zeta(3) + 880\zeta(4) + \frac{18400}{9}\zeta(5) \right) N_L \\ &\quad + \left(\frac{5242}{243} + \frac{800}{9}\zeta(3) - \frac{160}{3}\zeta(4) \right) N_L^2 \\ &\quad + \left(-\frac{332}{243} + \frac{64}{27}\zeta(3) \right) N_L^3, \end{aligned}$$

where N_L is the number of active light quark flavors at the scale μ , i.e. flavors with masses $< \mu$, and ζ is the Riemann zeta function ($\zeta(3) \simeq 1.2020569$, $\zeta(4) \simeq 1.0823232$, and $\zeta(5) \simeq 1.0369278$). In addition, as the renormalization scale crosses quark mass thresholds one needs to match the scale dependence of m below and above the threshold. There are finite threshold corrections; the necessary formulae can be found in Ref. [5].

C. Lattice Gauge Theory

The use of the lattice simulations for *ab initio* determinations of the fundamental parameters of QCD, including the coupling constant and quark masses (except for the top-quark

Quark Particle Listings

Quarks

mass) is a very active area of research, with the current emphasis being on the reduction and control of the systematic uncertainties. We now briefly review some of the features of lattice QCD. In this approach space-time is approximated by a finite, discrete *lattice* of points and multi-local correlation functions are computed by the numerical evaluation of the corresponding functional integrals. To determine quark masses, one computes a convenient and appropriate set of physical quantities (frequently chosen to be a set of hadronic masses) using lattice QCD for a variety of input values of the quark masses. The true (physical) values of the quark masses are those which correctly reproduce the set of physical quantities being used for calibration.

The values of the quark masses obtained directly in lattice simulations are bare quark masses, with the lattice spacing a (i.e. the distance between neighboring points of the lattice) as the ultraviolet cut-off. In order for the lattice results to be useful in phenomenology, it is therefore necessary to relate the bare quark masses in a lattice formulation of QCD to renormalized masses in some standard renormalization scheme such as $\overline{\text{MS}}$. Provided that both the ultraviolet cut-off a^{-1} and the renormalization scale are much greater than Λ_{QCD} , the bare and renormalized masses can, in principle, be related in perturbation theory (this is frequently facilitated by the use of chiral Ward identities). However, the coefficients in lattice perturbation theory are often found to be large, and our ignorance of higher order terms is generally a significant source of systematic uncertainty. Increasingly, non-perturbative renormalization is used to calculate the relation between the bare and renormalized masses, circumventing the need for lattice perturbation theory.

The precision with which quark masses can be determined in lattice simulations is limited by the available computing resources. There are a number of sources of systematic uncertainty and there continues to be considerable progress in reducing these. In general, the main source of uncertainty arises from the difficulty of performing simulations with three flavors of sea quarks, with u and d quarks sufficiently light for chiral perturbation theory (see section D) to be valid. In the past the computations were performed without including sea quarks at all (this is the so-called *quenched approximation*). Current simulations are generally unquenched, but m_u and m_d are larger than their physical values and the results are extrapolated, using chiral perturbation theory where possible, to the physical point. Reducing the uncertainty in this *chiral extrapolation* is the principal challenge in improving the precision in the determination of physical quantities from lattice simulations.

In addition one has to consider the uncertainties due to the fact that the lattice spacing is non-zero (lattice artefacts) and that the volume is not infinite. The former are studied by observing the stability of the results as a is varied or by using "improved" formulations of lattice QCD. By varying the

volume of the lattice one checks that finite-volume effects are indeed small.

D. Light quarks

For light quarks, one can use the techniques of chiral perturbation theory [6,7,8] to extract quark mass ratios. The mass term for light quarks in the QCD Lagrangian is

$$\overline{\Psi}M\Psi = \overline{\Psi}_L M \Psi_R + \overline{\Psi}_R M^\dagger \Psi_L, \quad (3)$$

where M is the light quark mass matrix M ,

$$M = \begin{pmatrix} m_u & 0 & 0 \\ 0 & m_d & 0 \\ 0 & 0 & m_s \end{pmatrix}, \quad (4)$$

and $\Psi = (u, d, s)$. The mass term is the only term in the QCD Lagrangian that mixes left- and right-handed quarks. In the limit $M \rightarrow 0$, there is an independent $SU(3) \times U(1)$ flavor symmetry for the left- and right-handed quarks. The vector $U(1)$ symmetry is baryon number; the axial $U(1)$ symmetry of the classical theory is broken in the quantum theory due to the anomaly. The remaining $G_\chi = SU(3)_L \times SU(3)_R$ chiral symmetry of the QCD Lagrangian is spontaneously broken to $SU(3)_V$, which, in the limit $M \rightarrow 0$, leads to eight massless Goldstone bosons, the π 's, K 's, and η .

The symmetry G_χ is only an approximate symmetry, since it is explicitly broken by the quark mass matrix M . The Goldstone bosons acquire masses which can be computed in a systematic expansion in M , in terms of low-energy constants, which are unknown nonperturbative parameters of the theory, and are not fixed by the symmetries. One treats the quark mass matrix M as an external field that transforms under G_χ as $M \rightarrow LMR^\dagger$, where $\Psi_L \rightarrow L\Psi_L$ and $\Psi_R \rightarrow R\Psi_R$ are the $SU(3)_L$ and $SU(3)_R$ transformations, and writes down the most general Lagrangian invariant under G_χ . Then one sets M to its given constant value Eq. (4), which implements the symmetry breaking. To first order in M one finds that [9]

$$\begin{aligned} m_{\pi^0}^2 &= B(m_u + m_d), \\ m_{\pi^\pm}^2 &= B(m_u + m_d) + \Delta_{\text{em}}, \\ m_{K^0}^2 &= m_{K^\pm}^2 = B(m_d + m_s), \\ m_{K^\pm}^2 &= B(m_u + m_s) + \Delta_{\text{em}}, \\ m_\eta^2 &= \frac{1}{3}B(m_u + m_d + 4m_s), \end{aligned} \quad (5)$$

with two unknown constants B and Δ_{em} , the electromagnetic mass difference. From Eq. (5), one can determine the quark mass ratios [9]

$$\begin{aligned} \frac{m_u}{m_d} &= \frac{2m_{\pi^0}^2 - m_{\pi^\pm}^2 + m_{K^\pm}^2 - m_{K^0}^2}{m_{K^0}^2 - m_{K^\pm}^2 + m_{\pi^\pm}^2} = 0.56, \\ \frac{m_s}{m_d} &= \frac{m_{K^0}^2 + m_{K^\pm}^2 - m_{\pi^\pm}^2}{m_{K^0}^2 + m_{\pi^\pm}^2 - m_{K^\pm}^2} = 20.1, \end{aligned} \quad (6)$$

to lowest order in chiral perturbation theory, with an error which will be estimated below. Since the mass ratios extracted using

chiral perturbation theory use the symmetry transformation property of M under the chiral symmetry G_χ , it is important to use a renormalization scheme for QCD that does not change this transformation law. Any mass independent subtraction scheme such as $\overline{\text{MS}}$ is suitable. The ratios of quark masses are scale independent in such a scheme, and Eq. (6) can be taken to be the ratio of $\overline{\text{MS}}$ masses. Chiral perturbation theory cannot determine the overall scale of the quark masses, since it uses only the symmetry properties of M , and any multiple of M has the same G_χ transformation law as M .

Chiral perturbation theory is a systematic expansion in powers of the light quark masses. The typical expansion parameter is $m_K^2/\Lambda_\chi^2 \sim 0.25$ if one uses $SU(3)$ chiral symmetry, and $m_\pi^2/\Lambda_\chi^2 \sim 0.02$ if one uses $SU(2)$ chiral symmetry. Electromagnetic effects at the few percent level also break $SU(2)$ and $SU(3)$ symmetry. The mass formulæ Eq. (5) were derived using $SU(3)$ chiral symmetry, and are expected to have a 25% uncertainty due to second order corrections.

There is a subtlety which arises when one tries to determine quark mass ratios at second order in chiral perturbation theory. The second order quark mass term [10]

$$\left(M^\dagger\right)^{-1} \det M^\dagger \quad (7)$$

(which can be generated by instantons) transforms in the same way under G_χ as M . Chiral perturbation theory cannot distinguish between M and $\left(M^\dagger\right)^{-1} \det M^\dagger$; one can make the replacement $M \rightarrow M(\lambda) = M + \lambda M \left(M^\dagger M\right)^{-1} \det M^\dagger$ in the chiral Lagrangian,

$$\begin{aligned} M(\lambda) &= \text{diag}(m_u(\lambda), m_d(\lambda), m_s(\lambda)) \\ &= \text{diag}(m_u + \lambda m_d m_s, m_d + \lambda m_u m_s, m_s + \lambda m_u m_d), \end{aligned} \quad (8)$$

and leave all observables unchanged.

The combination

$$\left(\frac{m_u}{m_d}\right)^2 + \frac{1}{Q^2} \left(\frac{m_s}{m_d}\right)^2 = 1 \quad (9)$$

where

$$Q^2 = \frac{m_s^2 - \hat{m}^2}{m_d^2 - m_u^2}, \quad \hat{m} = \frac{1}{2}(m_u + m_d),$$

is insensitive to the transformation in Eq. (8). Eq. (9) gives an ellipse in the $m_u/m_d - m_s/m_d$ plane. The ellipse is well-determined by chiral perturbation theory, but the exact location on the ellipse, and the absolute normalization of the quark masses, has larger uncertainties. Q is determined to be in the range 21–25 from $\eta \rightarrow 3\pi$ decay and the electromagnetic contribution to the $K^+ - K^0$ and $\pi^+ - \pi^0$ mass differences [11].

It is particularly important to determine the quark mass ratio m_u/m_d , since there is no strong CP problem if $m_u = 0$. The chiral symmetry G_χ of the QCD Lagrangian is not enhanced even if $m_u = 0$. [The possible additional axial u -quark number symmetry is anomalous. The only additional symmetry when $m_u = 0$ is CP .] As a result $m_u = 0$ is not a special value for chiral perturbation theory.

The absolute normalization of the quark masses can be determined by using methods that go beyond chiral perturbation theory, such as spectral function sum rules [12,13] for hadronic correlation functions or lattice simulations.

Sum Rules: Sum rule methods have been extensively used to determine quark masses and for illustration we briefly discuss here their application to hadronic τ decays [14]. Other applications involve very similar techniques.

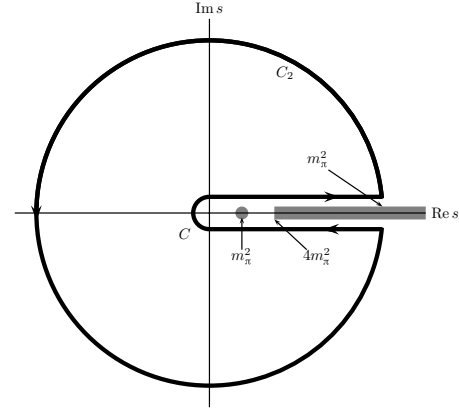


Figure 1: The analytic structure of $\Pi(s)$ in the complex s -plane. The contours C_1 and C_2 are the integration contours discussed in the text.

The experimentally measured quantity is R_τ ,

$$\frac{dR_\tau}{ds} = \frac{d\Gamma/ds(\tau^- \rightarrow \text{hadrons} + \nu_\tau(\gamma))}{\Gamma(\tau^- \rightarrow e^- \bar{\nu}_e \nu_\tau(\gamma))} \quad (10)$$

the hadronic invariant mass spectrum in semihadronic τ decay, normalized to the leptonic τ decay rate. It is useful to define q as the total momentum of the hadronic final state, so $s = q^2$ is the hadronic invariant mass. The total hadronic τ decay rate R_τ is then given by integrating dR_τ/ds over the kinematically allowed range $0 \leq s \leq M_\tau^2$.

R_τ can be written as

$$\begin{aligned} R_\tau &= 12\pi \int_0^{M_\tau^2} \frac{ds}{M_\tau^2} \left(1 - \frac{s}{M_\tau^2}\right)^2 \\ &\quad \times \left[\left(1 + 2\frac{s}{M_\tau^2}\right) \text{Im} \Pi^T(s) + \text{Im} \Pi^L(s) \right] \end{aligned} \quad (11)$$

where $s = q^2$, and the hadronic spectral functions $\Pi^{L,T}$ are defined from the time-ordered correlation function of two weak currents is the time-ordered correlator of the weak interaction current ($j^\mu(x)$ and $j^\nu(0)$) by

$$\Pi^{\mu\nu}(q) = i \int d^4x e^{iq \cdot x} \langle 0 | T \left(j^\mu(x) j^\nu(0)^\dagger \right) | 0 \rangle, \quad (12)$$

$$\Pi^{\mu\nu}(q) = (-g^{\mu\nu} + q^\mu q^\nu) \Pi^T(s) + q^\mu q^\nu \Pi^L(s), \quad (13)$$

and the decomposition Eq. (13) is the most general possible structure consistent with Lorentz invariance.

Quark Particle Listings

Quarks

By the optical theorem, the imaginary part of $\Pi^{\mu\nu}$ is proportional to the total cross-section for the current to produce all possible states. A detailed analysis including the phase space factors leads to Eq. (11). The spectral functions $\Pi^{L,T}(s)$ are analytic in the complex s plane, with singularities along the real axis. There is an isolated pole at $s = m_\pi^2$, and single- and multi-particle singularities for $s \geq 4m_\pi^2$, the two-particle threshold. The discontinuity along the real axis is $\Pi^{L,T}(s + i0^+) - \Pi^{L,T}(s - i0^+) = 2i\text{Im} \Pi^{L,T}(s)$. As a result, Eq. (11) can be rewritten with the replacement $\text{Im} \Pi^{L,T}(s) \rightarrow -i\Pi^{L,T}(s)/2$, and the integration being over the contour C_1 . Finally, the contour C_1 can be deformed to C_2 without crossing any singularities, and so leaving the integral unchanged. One can derive a series of sum rules analogous to Eq. (11) by weighting the differential τ hadronic decay rate by different powers of the hadronic invariant mass,

$$R_\tau^{kl} = \int_0^{M_\tau^2} ds \left(1 - \frac{s}{M_\tau^2}\right)^k \left(\frac{s}{M_\tau^2}\right)^l \frac{dR_\tau}{ds} \quad (14)$$

where dR_τ/ds is the hadronic invariant mass distribution in τ decay normalized to the leptonic decay rate. This leads to the final form of the sum rule(s),

$$R_\tau^{kl} = -6\pi i \int_{C_2} \frac{ds}{M_\tau^2} \left(1 - \frac{s}{M_\tau^2}\right)^{2+k} \left(\frac{s}{M_\tau^2}\right)^l \times \left[\left(1 + 2\frac{s}{M_\tau^2}\right) \Pi^T(s) + \Pi^L(s) \right]. \quad (15)$$

The manipulations so far are completely rigorous and exact, relying only on the general analytic structure of quantum field theory. The left-hand side of the sum rule Eq. (15) is obtained from experiment. The right hand-side can be computed for s far away from any physical cuts using the operator product expansion (OPE) for the time-ordered product of currents in Eq. (12), and QCD perturbation theory. The OPE is an expansion for the time-ordered product Eq. (12) in a series of local operators, and is an expansion about the $q \rightarrow \infty$ limit. It gives $\Pi(s)$ as an expansion in powers of $\alpha_s(s)$ and Λ_{QCD}^2/s , and is valid when s is far (in units of Λ_{QCD}^2) from any singularities in the complex s -plane.

The OPE gives $\Pi(s)$ as a series in α_s , quark masses, and various non-perturbative vacuum matrix element. By computing $\Pi(s)$ theoretically, and comparing with the experimental values of R_τ^{kl} , one determines various parameters such as α_s and the quark masses. The theoretical uncertainties in using Eq. (15) arise from neglected higher order corrections (both perturbative and non-perturbative), and because the OPE is no longer valid near the real axis, where Π has singularities. The contribution of neglected higher order corrections can be estimated as for any other perturbative computation. The error due to the failure of the OPE is more difficult to estimate. In Eq. (15), the OPE fails on the endpoints of C_2 that touch the real axis at $s = M_\tau^2$. The weight factor $(1 - s/M_\tau^2)$ in Eq. (15) vanishes at this point, so the importance of the endpoint can be reduced by choosing larger values of k .

Lattice Gauge Theory: Lattice simulations allow for detailed studies of the behaviour of hadronic masses and matrix elements as functions of the quark masses. Moreover, the quark masses do not have to take their physical values, but can be varied freely and chiral perturbation theory applies also for unphysical masses, provided that they are sufficiently light. From such recent studies of pseudoscalar masses and decay constants, the relevant higher-order couplings in the chiral Lagrangian have been estimated, strongly suggesting that $m_u \neq 0$ [15,16,17]. In order to make this evidence conclusive, the lattice systematic errors must be reduced; in particular the range of light quark masses should be increased and the validity of chiral perturbation theory for this range established.

In recent years there have been a number of unquenched determinations of the masses of the light quarks using a variety of formulations of lattice QCD (see, for example, the set of results in refs. [18,19,20,21,22,23,24,25]). Some of the simulations have been performed with two flavors of sea quarks and some with three flavors. The lattice systematic uncertainties in these determinations are different (e.g. due to the different lattice formulations of QCD, the use of perturbative and non-perturbative renormalization and the different chiral and continuum extrapolations). Taking these into consideration, we give below our current estimates for the quark masses determined from lattice simulations.

In current lattice simulations it is the combination $(m_u + m_d)/2$ which can be determined. In the evaluation of m_s one gets a result which is about 20–25% larger if the ϕ -meson is used as input rather than the K -meson. This is evidence that the errors due to quenching are significant. It is reassuring that this difference is eliminated or reduced significantly in the cited unquenched studies.

The quark masses for light quarks discussed so far are often referred to as current quark masses. Nonrelativistic quark models use constituent quark masses, which are of order 350 MeV for the u and d quarks. Constituent quark masses model the effects of dynamical chiral symmetry breaking, and are not related to the quark mass parameters m_k of the QCD Lagrangian Eq. (1). Constituent masses are only defined in the context of a particular hadronic model.

E. Heavy quarks

The masses and decay rates of hadrons containing a single heavy quark, such as the B and D mesons can be determined using the heavy quark effective theory (HQET) [26]. The theoretical calculations involve radiative corrections computed in perturbation theory with an expansion in $\alpha_s(m_Q)$ and non-perturbative corrections with an expansion in powers of Λ_{QCD}/m_Q . Due to the asymptotic nature of the QCD perturbation series, the two kinds of corrections are intimately related; an example of this are renormalon effects in the perturbative expansion which are associated with non-perturbative corrections.

Systems containing two heavy quarks such as the Υ or J/Ψ are treated using NRQCD [27]. The typical momentum

and energy transfers in these systems are $\alpha_s m_Q$, and $\alpha_s^2 m_Q$, respectively, so these bound states are sensitive to scales much smaller than m_Q . However, smeared observables, such as the cross-section for $e^+e^- \rightarrow \bar{b}b$ averaged over some range of s that includes several bound state energy levels, are better behaved and only sensitive to scales near m_Q . For this reason, most determinations of the b quark mass using perturbative calculations compare smeared observables with experiment [28,29,30].

Lattice simulations of QCD requires the quark mass to be much smaller than a^{-1} , where a is the lattice spacing, in order to avoid large errors due to the granularity of the lattice. Since computing resources limit a^{-1} in current simulations to be typically in the range 1.5–2.5 GeV, this is not possible for the b -quark and is marginal for the c -quark. For this reason, particularly for the b -quark, simulations are performed using effective theories, including HQET and NRQCD. Using effective theories, m_b is obtained from what is essentially a computation of the difference of $M_{H_b} - m_b$, where M_{H_b} is the mass of a hadron H_b containing a b -quark. The relative error on m_b is therefore much smaller than that for $M_{H_b} - m_b$, and this is the reason for the small errors quoted in section F. The principal systematic errors are the matching of the effective theories to QCD and the presence of power divergences in a^{-1} in the $1/m_b$ corrections which have to be subtracted numerically. The use of HQET or NRQCD is less precise for the charm quark, and in this case *improved* formulations of QCD, in which the errors to the finite lattice spacing are formally reduced are being used (see in particular refs. [31,32]).

For an observable particle such as the electron, the position of the pole in the propagator is the definition of the particle mass. In QCD this definition of the quark mass is known as the pole mass. It is known that the on-shell quark propagator has no infrared divergences in perturbation theory [33,34], so this provides a perturbative definition of the quark mass. The pole mass cannot be used to arbitrarily high accuracy because of nonperturbative infrared effects in QCD. The full quark propagator has no pole because the quarks are confined, so that the pole mass cannot be defined outside of perturbation theory. The relation between the pole mass m_Q and the $\overline{\text{MS}}$ mass \overline{m}_Q is known to three loops [35,36,37,38]

$$m_Q = \overline{m}_Q(\overline{m}_Q) \left\{ 1 + \frac{4\overline{\alpha}_s(\overline{m}_Q)}{3\pi} + \left[-1.0414 \sum_k \left(1 - \frac{4\overline{m}_{Q_k}}{3\overline{m}_Q} \right) + 13.4434 \right] \left[\frac{\overline{\alpha}_s(\overline{m}_Q)}{\pi} \right]^2 + [0.6527N_L^2 - 26.655N_L + 190.595] \left[\frac{\overline{\alpha}_s(\overline{m}_Q)}{\pi} \right]^3 \right\}, \quad (16)$$

where $\overline{\alpha}_s(\mu)$ is the strong interaction coupling constants in the $\overline{\text{MS}}$ scheme, and the sum over k extends over the N_L flavors Q_k lighter than Q . The complete mass dependence of the α_s^2 term can be found in [35]; the mass dependence of the α_s^3 term is not known. For the b -quark, Eq. (16) reads

$$m_b = \overline{m}_b(\overline{m}_b) [1 + 0.09 + 0.05 + 0.03], \quad (17)$$

where the contributions from the different orders in α_s are shown explicitly. The two and three loop corrections are comparable in size and have the same sign as the one loop term. This is a signal of the asymptotic nature of the perturbation series [there is a renormalon in the pole mass]. Such a badly behaved perturbation expansion can be avoided by directly extracting the $\overline{\text{MS}}$ mass from data without extracting the pole mass as an intermediate step.

F. Numerical values and caveats

The quark masses in the particle data listings have been obtained by using a wide variety of methods. Each method involves its own set of approximations and errors. In most cases, the errors are a best guess at the size of neglected higher-order corrections or other uncertainties. The expansion parameters for some of the approximations are not very small (for example, they are $m_K^2/\Lambda_\chi^2 \sim 0.25$ for the chiral expansion and $\Lambda_{\text{QCD}}/m_b \sim 0.1$ for the heavy-quark expansion), so an unexpectedly large coefficient in a neglected higher-order term could significantly alter the results. It is also important to note that the quark mass values can be significantly different in the different schemes.

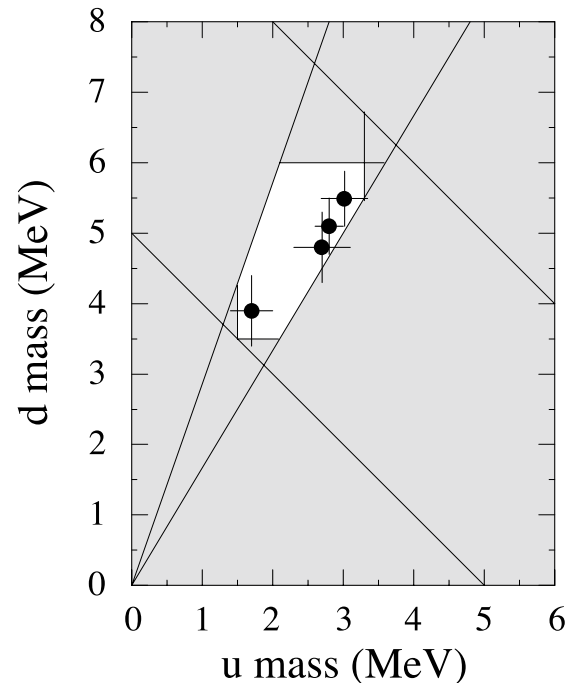


Figure 2: The allowed region (shown in white) for up quark and down quark masses. This region was determined in part from papers reporting values for m_u and m_d (data points shown) and in part from analysis of the allowed ranges of other mass parameters (see Fig. 3). The parameter $(m_u + m_d)/2$ yields the two downward-sloping lines, while m_u/m_d yields the two rising lines originating at $(0,0)$. The grey point is from a paper giving no error bars.

Quark Particle Listings

Quarks

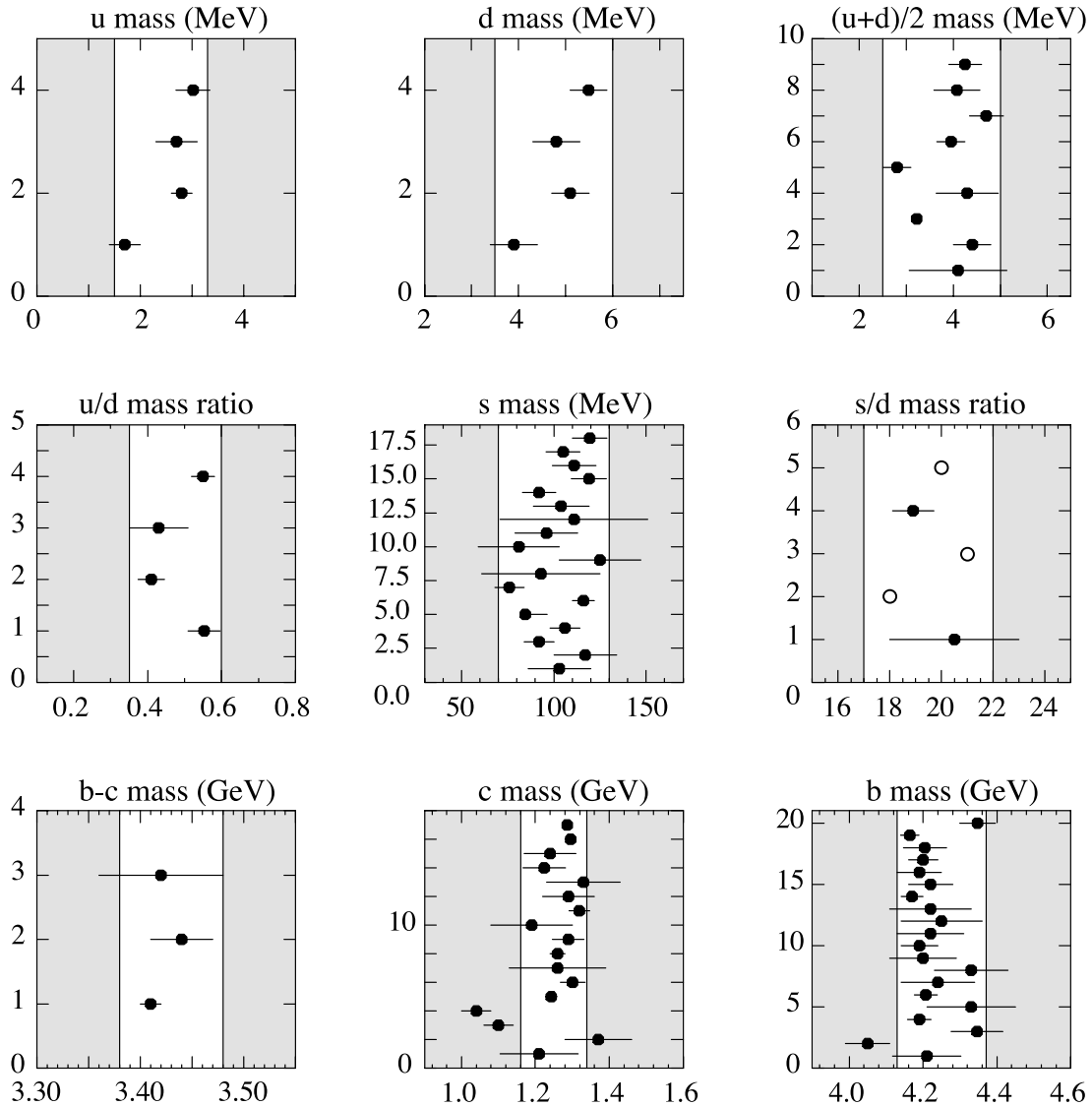


Figure 3. The values of each quark mass parameter taken from the Data Listings. Points from papers reporting no error bars are shown as open circles. Arrows indicate limits reported. The grey regions indicate values excluded by our evaluations; some regions were determined in part though examination of Fig. 2.

See key on page 373

The heavy quark masses obtained using HQET, QCD sum rules, or lattice gauge theory are consistent with each other if they are all converted into the same scheme and scale. We have specified all masses in the $\overline{\text{MS}}$ scheme. For light quarks, the renormalization scale has been chosen to be $\mu = 2 \text{ GeV}$. The light quark masses at 1 GeV are significantly different from those at 2 GeV, $\overline{m}(1 \text{ GeV})/\overline{m}(2 \text{ GeV}) \sim 1.35$. It is conventional to choose the renormalization scale equal to the quark mass for a heavy quark, so we have quoted $\overline{m}_Q(\mu)$ at $\mu = \overline{m}_Q$ for the c and b quarks.

Recent analyses of inclusive B meson decays have shown that recently proposed mass definitions lead to a better behaved perturbation series than for the $\overline{\text{MS}}$ mass, and hence to more accurate mass values. We have chosen to also give values for one of these, the b quark mass in the 1S-scheme [39,40]. Other schemes that have been proposed are the PS-scheme [41] and the kinetic scheme [42].

These schemes have been reviewed in [43]. One can convert a mass from one scheme to another using equations analogous to the conversion formula between the MS-bar and pole masses in Eq. (16). The conversion formulae can be found in [43].

If necessary, we have converted values in the original papers to our chosen scheme using two-loop formulae. It is important to realize that our conversions introduce significant additional errors. In converting to the $\overline{\text{MS}}$ b -quark mass, for example, the three-loop conversions from the 1S and pole masses give values about 40 MeV and 135 MeV lower than the two-loop conversions. The uncertainty in $\alpha_s(M_Z) = 0.1187(20)$ gives an uncertainty of ± 20 MeV and ± 35 MeV respectively in the same conversions. We have not added these additional errors when we do our conversions.

References

1. See the review of QCD in this volume.
2. A.V. Manohar and H. Georgi, Nucl. Phys. **B234**, 189 (1984).
3. K.G. Chetyrkin, Phys. Lett. **B404**, 161 (1997).
4. J.A.M. Vermaseren, S.A. Larin, and T. van Ritbergen, Phys. Lett. **B405**, 327 (1997).
5. K.G. Chetyrkin, B.A. Kniehl, and M. Steinhauser, Nucl. Phys. **B510**, 61 (1998).
6. S. Weinberg, Physica **96A**, 327 (1979).
7. J. Gasser and H. Leutwyler, Ann. Phys. **158**, 142 (184).
8. For a review, see A. Pich, Rept. Prog. Phys. **58**, 563 (1995).
9. S. Weinberg, Trans. N.Y. Acad. Sci. **38**, 185 (1977).
10. D.B. Kaplan and A.V. Manohar, Phys. Rev. Lett. **56**, 2004 (1986).
11. H. Leutwyler, Phys. Lett. **B374**, 163 (1996).
12. S. Weinberg, Phys. Rev. Lett. **18**, 507 (1967).
13. M.A. Shifman, A.I. Vainshtein, and V.I. Zakharov, Nucl. Phys. **B147**, 385 (1979).
14. E. Braaten, S. Narison, and A. Pich, Nucl. Phys. **B373**, 581 (1992).
15. J. Heitger *et al.* (Alpha Collab.), Nucl. Phys. **B588**, 377 (2000).
16. A.C. Irving *et al.* (UKQCD Collab.), hep-lat/0107023 (2001).
17. D.R. Nelson, G.T. Fleming, and G.W. Kilcup, hep-lat/0112029 (2001).
18. C. Aubin *et al.* (HPQCD Collab.), Phys. Rev. **D70**, 031504 (2004).
19. C. Aubin *et al.* (MILC Collab.), Phys. Rev. **D70**, 114501 (2004).
20. T. Ishikawa *et al.* (CP-PACS Collab.), Nucl. Phys. (Proc. Supp.) **B140**, 225 (2005).
21. D. Becirevic *et al.* (SPQcdR Collab.), Nucl. Phys. (Proc. Supp.) **B140**, 246 (2005).
22. M. Gockeler *et al.* (QCDSF Collab.), hep-ph/0409312.
23. M. Della Morte *et al.* (ALPHA Collab.), hep-lat/0507035.
24. S. Aoki *et al.* (JLQCD Collab.), Phys. Rev. **D68**, 054502 (2003).
25. A. Ali Khan *et al.* (CP-PACS Collab.), Phys. Rev. **D65**, 054505 (2002); Erratum *ibid.*, **D67**, 059901 (2003).
26. N. Isgur and M.B. Wise, Phys. Lett. **B232**, 113 (1989), *ibid.*, **B237**, 527 (1990).
27. G.T. Bodwin, E. Braaten, and G.P. Lepage, Phys. Rev. **D51**, 1125 (1995).
28. A.H. Hoang, Phys. Rev. **D61**, 034005 (2000).
29. K. Melnikov and A. Yelkhovsky, Phys. Rev. **D59**, 114009 (1999).
30. M. Beneke and A. Signer, Phys. Lett. **B471**, 233 (1999).
31. A.X. El-Khadra, A.S. Kronfeld, and P.B. Mackenzie, Phys. Rev. **D55**, 3933 (1997).
32. S. Aoki, Y. Kuramashi, and S.I. Tominaga, Prog. Theor. Phys. **109**, 383 (2003).
33. R. Tarrach, Nucl. Phys. **B183**, 384 (1981).
34. A. Kronfeld, Phys. Rev. **D58**, 051501 (1998).
35. N. Gray *et al.*, Z. Phys. **C48**, 673 (1990).
36. D.J. Broadhurst, N. Gray, and K. Schilcher, Z. Phys. **C52**, 111 (1991).
37. K.G. Chetyrkin and M. Steinhauser, Phys. Rev. Lett. **83**, 4001 (1999).
38. K. Melnikov and T. van Ritbergen, Phys. Lett. **B482**, 99 (2000).
39. A.H. Hoang, Z. Ligeti, and A.V. Manohar, Phys. Rev. Lett. **82**, 277 (1999).
40. A.H. Hoang, Z. Ligeti, and A.V. Manohar, Phys. Rev. **D59**, 074017 (1999).
41. M. Beneke, Phys. Lett. **B434**, 115 (1998).
42. P. Gambino and N. Uraltsev, Eur. Phys. J. **C34**, 181 (2004).
43. A.X. El-Khadra and M. Luke, Ann. Rev. Nucl. and Part. Sci. **52**, 201 (2002).

u

$$I(J^P) = \frac{1}{2}(\frac{1}{2}^+)$$

$$\text{Mass } m = 1.5 \text{ to } 3.0 \text{ MeV} \quad \text{Charge} = \frac{2}{3} e \quad I_z = +\frac{1}{2}$$

$$m_u/m_d = 0.3 \text{ to } 0.6$$

Quark Particle Listings

d, s, Light Quarks (u, d, s)

d

$I(J^P) = \frac{1}{2}(\frac{1}{2}^+)$

Mass $m = 3$ to 7 MeV Charge = $-\frac{1}{3} e$ $I_z = -\frac{1}{2}$
 $m_s/m_d = 17$ to 22
 $\bar{m} = (m_u + m_d)/2 = 2.5$ to 5.5 MeV

s

$I(J^P) = 0(\frac{1}{2}^+)$

Mass $m = 95 \pm 25$ MeV Charge = $-\frac{1}{3} e$ Strangeness = -1
 $(m_s - (m_u + m_d)/2)/(m_d - m_u) = 30$ to 50

LIGHT QUARKS (*u, d, s*)

OMITTED FROM SUMMARY TABLE

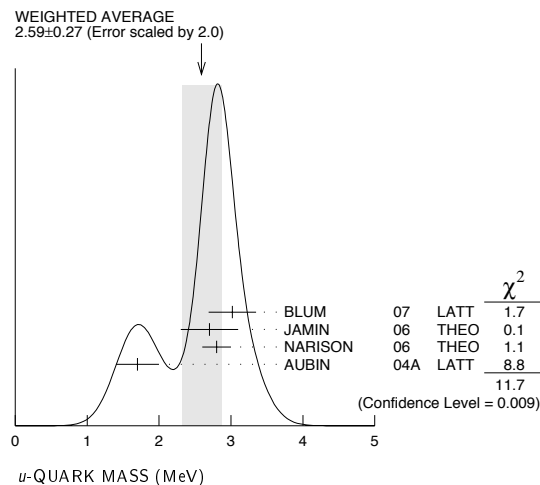
u-QUARK MASS

The *u*-, *d*-, and *s*-quark masses are estimates of so-called “current-quark masses,” in a mass-independent subtraction scheme such as \overline{MS} . The ratios m_u/m_d and m_s/m_d are extracted from pion and kaon masses using chiral symmetry. The estimates of *d* and *u* masses are not without controversy and remain under active investigation. Within the literature there are even suggestions that the *u* quark could be essentially massless. The *s*-quark mass is estimated from SU(3) splittings in hadron masses.

We have normalized the \overline{MS} masses at a renormalization scale of $\mu = 2$ GeV. Results quoted in the literature at $\mu = 1$ GeV have been rescaled by dividing by 1.35. The values of “Our Evaluation” were determined in part via Figures 1 and 2.

VALUE (MeV)	DOCUMENT ID	TECN	COMMENT
$2.55^{+0.75}_{-1.05}$ (1.5–3.3) OUR EVALUATION	See the ideogram below.		
3.02 ± 0.33	1 BLUM	07 LATT	\overline{MS} scheme
2.7 ± 0.4	2 JAMIN	06 THEO	\overline{MS} scheme
2.8 ± 0.2	3 NARISON	06 THEO	\overline{MS} scheme
1.7 ± 0.3	4 AUBIN	04A LATT	\overline{MS} scheme
• • • We do not use the following data for averages, fits, limits, etc. • • •			
2.9 ± 0.6	5 JAMIN	02 THEO	\overline{MS} scheme
2.3 ± 0.4	6 NARISON	99 THEO	\overline{MS} scheme
3.9 ± 1.1	7 JAMIN	95 THEO	\overline{MS} scheme
3.0 ± 0.7	8 NARISON	95c THEO	\overline{MS} scheme

- 1 BLUM 07 determine quark mass using a QED plus QCD lattice computation with two dynamical flavors of the pseudoscalar meson masses.
- 2 JAMIN 06 determine $m_u(2 \text{ GeV})$ by combining the value of m_s obtained from the spectral function for the scalar $K\pi$ form factor with other determinations of the quark mass ratios.
- 3 NARISON 06 uses sum rules for $e^+e^- \rightarrow$ hadrons to order α_s^3 to determine m_s combined with other determinations of the quark mass ratios.
- 4 AUBIN 04A employ a partially quenched lattice calculation of the pseudoscalar meson masses.
- 5 JAMIN 02 first calculates the strange quark mass from QCD sum rules using the scalar channel, and then combines with the quark mass ratios obtained from chiral perturbation theory to obtain m_u .
- 6 NARISON 99 uses sum rules to order α_s^3 for ϕ meson decays to get m_s , and finds m_u by combining with sum rule estimates of m_u+m_d and Dashen's formula.
- 7 JAMIN 95 uses QCD sum rules at next-to-leading order. We have rescaled $m_u(1 \text{ GeV}) = 5.3 \pm 1.5$ to $\mu = 2$ GeV.
- 8 For NARISON 95c, we have rescaled $m_u(1 \text{ GeV}) = 4 \pm 1$ to $\mu = 2$ GeV.



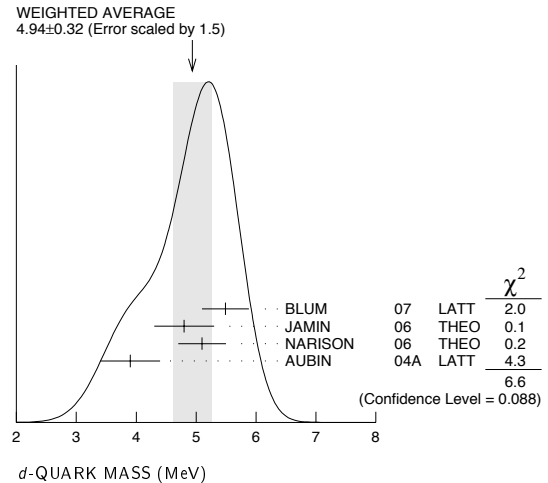
d-QUARK MASS

See the comment for the *u* quark above.

We have normalized the \overline{MS} masses at a renormalization scale of $\mu = 2$ GeV. Results quoted in the literature at $\mu = 1$ GeV have been rescaled by dividing by 1.35. The values of “Our Evaluation” were determined in part via Figures 1 and 2.

VALUE (MeV)	DOCUMENT ID	TECN	COMMENT
$5.04^{+0.96}_{-1.54}$ (3.5–6.0) OUR EVALUATION	See the ideogram below.		
5.49 ± 0.39	9 BLUM	07 LATT	\overline{MS} scheme
4.8 ± 0.5	10 JAMIN	06 THEO	\overline{MS} scheme
5.1 ± 0.4	11 NARISON	06 THEO	\overline{MS} scheme
3.9 ± 0.5	12 AUBIN	04A LATT	\overline{MS} scheme
• • • We do not use the following data for averages, fits, limits, etc. • • •			
5.2 ± 0.9	13 JAMIN	02 THEO	\overline{MS} scheme
6.4 ± 1.1	14 NARISON	99 THEO	\overline{MS} scheme
7.0 ± 1.1	15 JAMIN	95 THEO	\overline{MS} scheme
7.4 ± 0.7	16 NARISON	95c THEO	\overline{MS} scheme

- 9 BLUM 07 determine quark mass using a QED plus QCD lattice computation with two dynamical flavors of the pseudoscalar meson masses.
- 10 JAMIN 06 determine $m_d(2 \text{ GeV})$ by combining the value of m_s obtained from the spectral function for the scalar $K\pi$ form factor with other determinations of the quark mass ratios.
- 11 NARISON 06 uses sum rules for $e^+e^- \rightarrow$ hadrons to order α_s^3 to determine m_s combined with other determinations of the quark mass ratios.
- 12 AUBIN 04A perform three flavor dynamical lattice calculation of pseudoscalar meson masses, with continuum estimate of electromagnetic effects in the kaon masses, and one-loop perturbative renormalization constant.
- 13 JAMIN 02 first calculates the strange quark mass from QCD sum rules using the scalar channel, and then combines with the quark mass ratios obtained from chiral perturbation theory to obtain m_d .
- 14 NARISON 99 uses sum rules to order α_s^3 for ϕ meson decays to get m_s , and finds m_d by combining with sum rule estimates of m_u+m_d and Dashen's formula.
- 15 JAMIN 95 uses QCD sum rules at next-to-leading order. We have rescaled $m_d(1 \text{ GeV}) = 9.4 \pm 1.5$ to $\mu = 2$ GeV.
- 16 For NARISON 95c, we have rescaled $m_d(1 \text{ GeV}) = 10 \pm 1$ to $\mu = 2$ GeV.



$$\bar{m} = (m_u + m_d)/2$$

See the comments for the *u* quark above.

We have normalized the \overline{MS} masses at a renormalization scale of $\mu = 2$ GeV. Results quoted in the literature at $\mu = 1$ GeV have been rescaled by dividing by 1.35. The values of “Our Evaluation” were determined in part via Figures 1 and 2.

VALUE (MeV)	DOCUMENT ID	TECN	COMMENT
$3.79^{+1.21}_{-1.29}$ (2.5–5.0) OUR EVALUATION	See the ideogram below.		
4.25 ± 0.35	17 BLUM	07 LATT	\overline{MS} scheme
$4.08 \pm 0.25 \pm 0.42$	18 GOCKELER	06 LATT	\overline{MS} scheme
$4.7 \pm 0.2 \pm 0.3$	19 GOCKELER	06A LATT	\overline{MS} scheme
3.95 ± 0.3	20 NARISON	06 THEO	\overline{MS} scheme
2.8 ± 0.3	21 AUBIN	04 LATT	\overline{MS} scheme
$4.29 \pm 0.14 \pm 0.65$	22 AOKI	03 LATT	\overline{MS} scheme
3.223 ± 0.3	23 AOKI	03B LATT	\overline{MS} scheme
$4.4 \pm 0.1 \pm 0.4$	24 BECIREVIC	03 LATT	\overline{MS} scheme
$4.1 \pm 0.3 \pm 1.0$	25 CHIU	03 LATT	\overline{MS} scheme

See key on page 373

Quark Particle Listings

Light Quarks (u, d, s)

• • • We do not use the following data for averages, fits, limits, etc. • • •

3.45 \pm 0.14 -0.20	26 ALIKHAN	02	LATT	\overline{MS} scheme
5.3 \pm 0.3	27 CHIU	02	LATT	\overline{MS} scheme
3.9 \pm 0.6	28 MALTMAN	02	THEO	\overline{MS} scheme
3.9 \pm 0.6	29 MALTMAN	01	THEO	\overline{MS} scheme
4.57 \pm 0.18	30 AOKI	00	LATT	\overline{MS} scheme
4.4 \pm 2	31 GOCKELER	00	LATT	\overline{MS} scheme
4.23 \pm 0.29	32 AOKI	99	LATT	\overline{MS} scheme
\geq 2.1	33 STEELE	99	THEO	\overline{MS} scheme
4.5 \pm 0.4	34 BECIREVIC	98	LATT	\overline{MS} scheme
4.6 \pm 1.2	35 DOSCH	98	THEO	\overline{MS} scheme
4.7 \pm 0.9	36 PRADES	98	THEO	\overline{MS} scheme
2.7 \pm 0.2	37 EICKER	97	LATT	\overline{MS} scheme
3.6 \pm 0.6	38 GOUGH	97	LATT	\overline{MS} scheme
3.4 \pm 0.4 \pm 0.3	39 GUPTA	97	LATT	\overline{MS} scheme
$>$ 3.8	40 LELLOUCH	97	THEO	\overline{MS} scheme
4.5 \pm 1.0	41 BIJNENS	95	THEO	\overline{MS} scheme

17 BLUM 07 determine quark mass using a QED plus QCD lattice computation with two dynamical flavors of the pseudoscalar meson masses.

18 GOCKELER 06 use an unquenched lattice computation of the axial Ward Identity with $N_f = 2$ dynamical light quark flavors, and non-perturbative renormalization, to obtain $\overline{m}(2 \text{ GeV}) = 4.08 \pm 0.25 \pm 0.19 \pm 0.23 \text{ MeV}$, where the first error is statistical, the second and third are systematic due to the fit range and force scale uncertainties, respectively. We have combined the systematic errors linearly.

19 GOCKELER 06A use an unquenched lattice computation of the pseudoscalar meson masses with $N_f = 2$ dynamical light quark flavors, and non-perturbative renormalization.

20 NARISON 06 uses sum rules for $e^+e^- \rightarrow$ hadrons to order α_s^3 to determine m_s combined with other determinations of the quark mass ratios.

21 AUBIN 04 perform three flavor dynamical lattice calculation of pseudoscalar meson masses, with one-loop perturbative renormalization constant.

22 AOKI 03 uses quenched lattice simulation of the meson and baryon masses with degenerate light quarks. The extrapolations are done using quenched chiral perturbation theory.

23 The errors given in AOKI 03B were ± 0.046 and -0.069 . We changed them to ± 0.3 for calculating the overall best values. AOKI 03B uses lattice simulation of the meson and baryon masses with two dynamical light quarks. Simulations are performed using the $\mathcal{O}(a)$ improved Wilson action.

24 BECIREVIC 03 perform quenched lattice computation using the vector and axial Ward identities. Uses $\mathcal{O}(a)$ improved Wilson action and nonperturbative renormalization.

25 CHIU 03 determines quark masses from the pion and kaon masses using a lattice simulation with a chiral fermion action in quenched approximation.

26 ALIKHAN 02 uses lattice simulation of the meson and baryon masses with two dynamical flavors and degenerate light quarks.

27 CHIU 02 extracts the average light quark mass from quenched lattice simulations using quenched chiral perturbation theory.

28 MALTMAN 02 uses finite energy sum rules in the ud and us pseudoscalar channels. Other mass values are also obtained by similar methods.

29 MALTMAN 01 uses Borel transformed and finite energy sum rules.

30 AOKI 00 obtain the light quark masses from a quenched lattice simulation of the meson and baryon spectrum with the Wilson quark action.

31 GOCKELER 00 obtained from a quenched lattice computation of the pseudoscalar meson masses using $\mathcal{O}(a)$ improved Wilson fermions and nonperturbative renormalization.

32 AOKI 99 obtain the light quark masses from a quenched lattice simulation of the meson spectrum with the staggered quark action employing the regularization independent scheme.

33 STEELE 99 obtain a bound on the light quark masses by applying the Holder inequality to a sum rule. We have converted their bound of $(m_u+m_d)/2 \geq 3 \text{ MeV}$ at $\mu=1 \text{ GeV}$ to $\mu=2 \text{ GeV}$.

34 BECIREVIC 98 compute the quark mass using the Alpha action in the quenched approximation. The conversion from the regularization independent scheme to the \overline{MS} scheme is at NNLO.

35 DOSCH 98 use sum rule determinations of the quark condensate and chiral perturbation theory to obtain $9.4 \leq (m_u+m_d)(1 \text{ GeV}) \leq 15.7 \text{ MeV}$. We have converted to result to $\mu=2 \text{ GeV}$.

36 PRADES 98 uses finite energy sum rules for the axial current correlator.

37 EICKER 97 use lattice gauge computations with two dynamical light flavors.

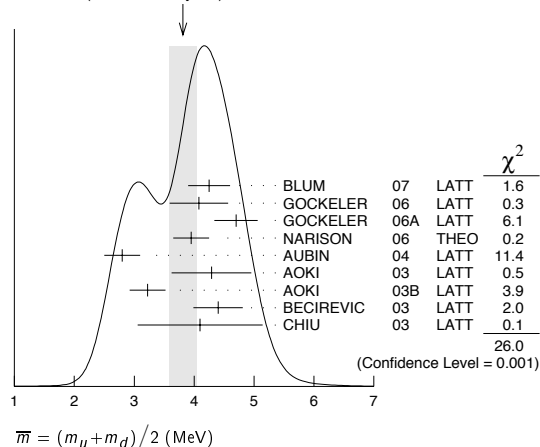
38 GOUGH 97 use lattice gauge computations in the quenched approximation. Correcting for quenching gives $2.1 < \overline{m} < 3.5 \text{ MeV}$ at $\mu=2 \text{ GeV}$.

39 GUPTA 97 use Lattice Monte Carlo computations in the quenched approximation. The value for two light dynamic flavors at $\mu = 2 \text{ GeV}$ is $2.7 \pm 0.3 \pm 0.3 \text{ MeV}$.

40 LELLOUCH 97 obtain lower bounds on quark masses using hadronic spectral functions.

41 BIJNENS 95 determines $m_u+m_d(1 \text{ GeV}) = 12 \pm 2.5 \text{ MeV}$ using finite energy sum rules. We have rescaled this to 2 GeV .

WEIGHTED AVERAGE
3.81 \pm 0.23 (Error scaled by 1.8)



m_u/m_d MASS RATIO

VALUE	DOCUMENT ID	TECN	COMMENT
0.506 \pm 0.094 -0.156	(0.35-0.60) OUR EVALUATION		See the ideogram below.
0.550 \pm 0.031	42 BLUM	07	LATT \overline{MS} scheme
0.43 \pm 0.08	43 AUBIN	04A	LATT \overline{MS} scheme
0.410 \pm 0.036	44 NELSON	03	LATT \overline{MS} scheme
0.553 \pm 0.043	45 LEUTWYLER	96	THEO Compilation
• • • We do not use the following data for averages, fits, limits, etc. • • •			
0.44	46 GAO	97	THEO \overline{MS} scheme
$<$ 0.3	47 CHOI	92	THEO
0.26	48 DONOGHUE	92	THEO
0.30 \pm 0.07	49 DONOGHUE	92B	THEO
0.66	50 GERARD	90	THEO
0.4 to 0.65	51 LEUTWYLER	90B	THEO
0.05 to 0.78	52 MALTMAN	90	THEO

42 BLUM 07 determine quark mass using a QED plus QCD lattice computation with two dynamical flavors of the pseudoscalar meson masses.

43 AUBIN 04A perform three flavor dynamical lattice calculation of pseudoscalar meson masses, with continuum estimate of electromagnetic effects in the kaon masses.

44 NELSON 03 computes coefficients in the order p^4 chiral Lagrangian using a lattice calculation with three dynamical flavors. The ratio m_u/m_d is obtained by combining this with the chiral perturbation theory computation of the meson masses to order p^4 .

45 LEUTWYLER 96 uses a combined fit to $\eta \rightarrow 3\pi$ and $\psi' \rightarrow J/\psi(\pi,\eta)$ decay rates, and the electromagnetic mass differences of the π and K .

46 GAO 97 uses electromagnetic mass splittings of light mesons.

47 CHOI 92 result obtained from the decays $\psi(2S) \rightarrow J/\psi(1S)\pi$ and $\psi(2S) \rightarrow J/\psi(1S)\eta$, and a dilute instanton gas estimate of some unknown matrix elements.

48 DONOGHUE 92 result is from a combined analysis of meson masses, $\eta \rightarrow 3\pi$ using second-order chiral perturbation theory including nonanalytic terms, and $(\psi(2S) \rightarrow J/\psi(1S)\pi)/(\psi(2S) \rightarrow J/\psi(1S)\eta)$.

49 DONOGHUE 92B computes quark mass ratios using $(\psi(2S) \rightarrow J/\psi(1S)\pi)/(\psi(2S) \rightarrow J/\psi(1S)\eta)$, and an estimate of L_{14} using Weinberg sum rules.

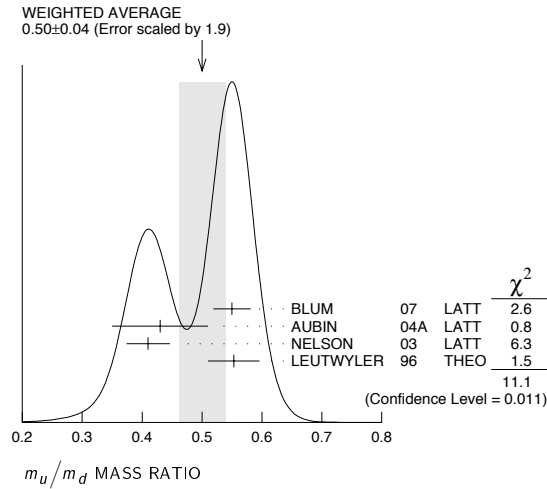
50 GERARD 90 uses large N and η - η' mixing.

51 LEUTWYLER 90B determines quark mass ratios using second-order chiral perturbation theory for the meson and baryon masses, including nonanalytic corrections. Also uses Weinberg sum rules to determine L_7 .

52 MALTMAN 90 uses second-order chiral perturbation theory including nonanalytic terms for the meson masses. Uses a criterion of "maximum reasonableness" that certain coefficients which are expected to be of order one are ≤ 3 .

Quark Particle Listings

Light Quarks (u, d, s)



s-QUARK MASS

See the comment for the u quark above.

We have normalized the \overline{MS} masses at a renormalization scale of $\mu = 2$ GeV. Results quoted in the literature at $\mu = 1$ GeV have been rescaled by dividing by 1.35.

VALUE (MeV)	DOCUMENT ID	TECN	COMMENT
104⁺²⁶₋₃₄ (70-130) OUR EVALUATION	See the ideogram below.		
119.5 ± 9.3	53 BLUM	07 LATT	\overline{MS} scheme
105 ± 6 ± 7	54 CHETYRKIN	06 THEO	\overline{MS} scheme
111 ± 6 ± 10	55 GOCKELER	06 LATT	\overline{MS} scheme
119 ± 5 ± 8	56 GOCKELER	06A LATT	\overline{MS} scheme
92 ± 9	57 JAMIN	06 THEO	\overline{MS} scheme
104 ± 15	58 NARISON	06 THEO	\overline{MS} scheme
≥ 71 ± 4, ≤ 151 ± 14	59 NARISON	06 THEO	\overline{MS} scheme
96 ⁺⁵ ₋₃ ⁺¹⁶ ₋₁₈	60 BAIKOV	05 THEO	\overline{MS} scheme
81 ± 22	61 GAMIZ	05 THEO	\overline{MS} scheme
125 ± 28	62 GORBUNOV	05 THEO	\overline{MS} scheme
93 ± 32	63 NARISON	05 THEO	\overline{MS} scheme
76 ± 8	64 AUBIN	04 LATT	\overline{MS} scheme
116 ± 6 ± 0.65	65 AOKI	03 LATT	\overline{MS} scheme
84.5 ⁺¹² _{-1.7}	66 AOKI	03B LATT	\overline{MS} scheme
106 ± 2 ± 8	67 BECIREVIC	03 LATT	\overline{MS} scheme
92 ± 9 ± 16	68 CHIU	03 LATT	\overline{MS} scheme
117 ± 17	69 GAMIZ	03 THEO	\overline{MS} scheme
103 ± 17	70 GAMIZ	03 THEO	\overline{MS} scheme
• • • We do not use the following data for averages, fits, limits, etc. • • •			
88 ⁺³ ₋₆	71 ALIKHAN	02 LATT	\overline{MS} scheme
115 ± 8	72 CHIU	02 LATT	\overline{MS} scheme
99 ± 16	73 JAMIN	02 THEO	\overline{MS} scheme
100 ± 12	74 MALTMAN	02 THEO	\overline{MS} scheme
116 ⁺²⁰ ₋₂₅	75 CHEN	01B THEO	\overline{MS} scheme
125 ± 27	76 KOERNER	01 THEO	\overline{MS} scheme
130 ± 15	77 AOKI	00 LATT	\overline{MS} scheme
97 ± 4	78 GARDEN	00 LATT	\overline{MS} scheme
105 ± 4	79 GOCKELER	00 LATT	\overline{MS} scheme
118 ± 14	80 AOKI	99 LATT	\overline{MS} scheme
170 ⁺⁴⁴ ₋₅₅	81 BARATE	99R ALEP	\overline{MS} scheme
115 ± 8	82 MALTMAN	99 THEO	\overline{MS} scheme
129 ± 24	83 NARISON	99 THEO	\overline{MS} scheme
114 ± 23	84 PICH	99 THEO	\overline{MS} scheme
111 ± 12	85 BECIREVIC	98 LATT	\overline{MS} scheme
148 ± 48	86 CHETYRKIN	98 THEO	\overline{MS} scheme
103 ± 10	87 CUCCHIERI	98 LATT	\overline{MS} scheme
115 ± 19	88 DOMINGUEZ	98 THEO	\overline{MS} scheme
152.4 ± 14.1	89 CHETYRKIN	97 THEO	\overline{MS} scheme
≥ 89	90 COLANGELO	97 THEO	\overline{MS} scheme
140 ± 20	91 EICKER	97 LATT	\overline{MS} scheme
95 ± 16	92 GOUGH	97 LATT	\overline{MS} scheme
100 ± 21 ± 10	93 GUPTA	97 LATT	\overline{MS} scheme
> 100	94 LELLOUCH	97 THEO	\overline{MS} scheme
140 ± 24	95 JAMIN	95 THEO	\overline{MS} scheme

- 53 BLUM 07 determine quark mass using a QED plus QCD lattice computation with two dynamical flavors of the pseudoscalar meson masses.
- 54 CHETYRKIN 06 use QCD sum rules in the pseudoscalar channel to order α_s^4 .
- 55 GOCKELER 06 use an unquenched lattice computation of the axial Ward Identity with $N_f = 2$ dynamical light quark flavors, and non-perturbative renormalization, to obtain $\overline{m}_s(2 \text{ GeV}) = 111 \pm 6 \pm 4 \pm 6 \text{ MeV}$, where the first error is statistical, the second and third are systematic due to the fit range and force scale uncertainties, respectively. We have combined the systematic errors linearly.
- 56 GOCKELER 06A use an unquenched lattice computation of the pseudoscalar meson masses with $N_f = 2$ dynamical light quark flavors, and non-perturbative renormalization.
- 57 JAMIN 06 determine $\overline{m}_s(2 \text{ GeV})$ from the spectral function for the scalar $K\pi$ form factor.
- 58 NARISON 06 uses sum rules for $e^+e^- \rightarrow$ hadrons to order α_s^3 .
- 59 NARISON 06 obtains the quoted range from positivity of the spectral functions.
- 60 BAIKOV 05 determines $\overline{m}_s(M_\tau) = 100^{+5}_{-3} + 17_{-19}$ from sum rules using the strange spectral function in τ decay. The computations were done to order α_s^3 , with an estimate of the α_s^4 terms. We have converted the result to $\mu = 2 \text{ GeV}$.
- 61 GAMIZ 05 determines $\overline{m}_s(2 \text{ GeV})$ from sum rules using the strange spectral function in τ decay. The computations were done to order α_s^2 , with an estimate of the α_s^3 terms.
- 62 GORBUNOV 05 use hadronic tau decays to $N^3\text{LO}$, including power corrections.
- 63 NARISON 05 determines $\overline{m}_s(2 \text{ GeV})$ from sum rules using the strange spectral function in τ decay. The computations were done to order α_s^3 .
- 64 AUBIN 04 perform three flavor dynamical lattice calculation of pseudoscalar meson masses, with one-loop perturbative renormalization constant.
- 65 AOKI 03 uses quenched lattice simulation of the meson and baryon masses with degenerate light quarks. The extrapolations are done using quenched chiral perturbation theory. Determines $m_s = 113.8 \pm 2.3^{+5.8}_{-2.9}$ using K mass as input and $m_s = 142.3 \pm 5.8^{+22}_{-0}$ using ϕ mass as input. We have performed a weighted average of these values.
- 66 AOKI 03B uses lattice simulation of the meson and baryon masses with two dynamical light quarks. Simulations are performed using the $\mathcal{O}(a)$ improved Wilson action.
- 67 BECIREVIC 03 perform quenched lattice computation using the vector and axial Ward identities. Uses $\mathcal{O}(a)$ improved Wilson action and nonperturbative renormalization. They also quote $\overline{m}/m_s = 24.3 \pm 0.2 \pm 0.6$.
- 68 CHIU 03 determines quark masses from the pion and kaon masses using a lattice simulation with a chiral fermion action in quenched approximation.
- 69 GAMIZ 03 determines m_s from SU(3) breaking in the τ hadronic width. The value of V_{us} is chosen to satisfy CKM unitarity.
- 70 GAMIZ 03 determines m_s from SU(3) breaking in the τ hadronic width. The value of V_{us} is taken from the PDG.
- 71 ALIKHAN 02 uses lattice simulation of the meson and baryon masses with two dynamical flavors and degenerate light quarks. The above value uses the K -meson mass to determine m_s . If the ϕ meson is used, the number changes to 90^{+5}_{-10} .
- 72 CHIU 02 extracts the strange quark mass from quenched lattice simulations using quenched chiral perturbation theory.
- 73 JAMIN 02 calculates the strange quark mass from QCD sum rules using the scalar channel.
- 74 MALTMAN 02 uses finite energy sum rules in the ud and us pseudoscalar channels. Other mass values are also obtained by similar methods.
- 75 CHEN 01B uses an analysis of the hadronic spectral function in τ decay.
- 76 KOERNER 01 obtain the s quark mass of $m_s(m_\tau) = 130 \pm 27(\text{exp}) \pm 9(\text{thy}) \text{ MeV}$ from an analysis of Cabibbo suppressed τ decays. We have converted this to $\mu = 2 \text{ GeV}$.
- 77 AOKI 00 obtain the light quark masses from a quenched lattice simulation of the meson and baryon spectrum with the Wilson quark action. We have averaged their results of $m_s = 115.6 \pm 2.3$ and $m_s = 143.7 \pm 5.8$ obtained using m_K and m_ϕ , respectively, to normalize the spectrum.
- 78 GARDEN 00 use a quenched lattice computation of the hadron spectrum.
- 79 GOCKELER 00 obtained from a quenched lattice computation of the pseudoscalar meson masses using $\mathcal{O}(a)$ improved Wilson fermions and nonperturbative renormalization.
- 80 AOKI 99 obtain the light quark masses from a quenched lattice simulation of the meson spectrum with the Staggered quark action employing the regularization independent scheme. We have averaged their results of $m_s = 106.0 \pm 7.1$ and $m_s = 129 \pm 12$ obtained using m_K and m_ϕ , respectively, to normalize the spectrum.
- 81 BARATE 99R obtain the strange quark mass from an analysis of the observed mass spectra in τ decay. We have converted their value of $m_s(m_\tau) = 176^{+46}_{-57} \text{ MeV}$ to $\mu = 2 \text{ GeV}$.
- 82 MALTMAN 99 determines the strange quark mass using finite energy sum rules.
- 83 NARISON 99 uses sum rules to order α_s^3 for ϕ meson decays.
- 84 PICH 99 obtain the s -quark mass from an analysis of the moments of the invariant mass distribution in τ decays.
- 85 BECIREVIC 98 compute the quark mass using the Alpha action in the quenched approximation. The conversion from the regularization independent scheme to the \overline{MS} scheme is at NNLO.
- 86 CHETYRKIN 98 uses spectral moments of hadronic τ decays to determine $m_s(1 \text{ GeV}) = 200 \pm 70 \text{ MeV}$. We have rescaled the result to $\mu = 2 \text{ GeV}$.
- 87 CUCCHIERI 98 obtains the quark mass using a quenched lattice computation of the hadronic spectrum.
- 88 DOMINGUEZ 98 uses hadronic spectral function sum rules (to four loops, and including dimension six operators) to determine $m_s(1 \text{ GeV}) < 155 \pm 25 \text{ MeV}$. We have rescaled the result to $\mu = 2 \text{ GeV}$.
- 89 CHETYRKIN 97 obtains $205.5 \pm 19.1 \text{ MeV}$ at $\mu = 1 \text{ GeV}$ from QCD sum rules including fourth-order QCD corrections. We have rescaled the result to 2 GeV .
- 90 COLANGELO 97 is QCD sum rule computation. We have rescaled $m_s(1 \text{ GeV}) > 120$ to $\mu = 2 \text{ GeV}$.
- 91 EICKER 97 use lattice gauge computations with two dynamical light flavors.
- 92 GOUGH 97 use lattice gauge computations in the quenched approximation. Correcting for quenching gives $54 < m_s < 92 \text{ MeV}$ at $\mu = 2 \text{ GeV}$.
- 93 GUPTA 97 use Lattice Monte Carlo computations in the quenched approximation. The value for two light dynamical flavors at $\mu = 2 \text{ GeV}$ is $68 \pm 12 \pm 7 \text{ MeV}$.
- 94 LELLOUCH 97 obtain lower bounds on quark masses using hadronic spectral functions.

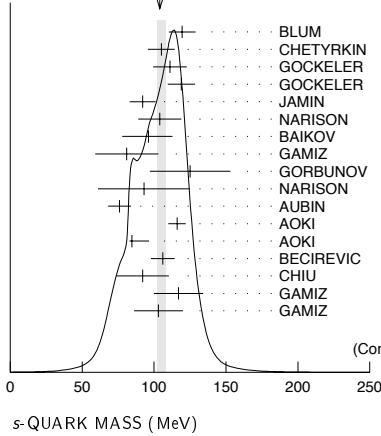
See key on page 373

Quark Particle Listings

Light Quarks (*u, d, s, c*)

⁹⁵ JAMIN 95 uses QCD sum rules at next-to-leading order. We have rescaled $m_s(1 \text{ GeV}) = 189 \pm 32$ to $\mu = 2 \text{ GeV}$.

WEIGHTED AVERAGE
104.0+3.6-2.0 (Error scaled by 1.4)



Author	Year	Method	χ^2
BLUM	07	LATT	2.8
CHETYRKIN	06	THEO	0.0
GOCKELER	06	LATT	0.4
GOCKELER 06A	06A	LATT	2.5
JAMIN	06	THEO	1.8
NARISON	06	THEO	0.0
BAIKOV	05	THEO	0.2
GAMIZ	05	THEO	1.1
GORBUNOV	05	THEO	0.6
NARISON	05	THEO	0.1
AUBIN	04	LATT	12.2
AOKI	03	LATT	4.0
AOKI 03B	03B	LATT	2.6
BECIREVIC	03	LATT	0.1
CHIU	03	LATT	0.4
GAMIZ	03	THEO	0.6
GAMIZ	03	THEO	0.0
			29.4
			(Confidence Level = 0.022)

MALTMAN	02	PR D65 074013	K. Maltman, J. Kambor
CHEN	01B	EPJ C22 31	S. Chen et al.
KOERNER	01	EPJ C20 259	J.G. Koerner, F. Krajewski, A.A. Pivovarov
MALTMAN	01	PL B517 332	K. Maltman, J. Kambor
AOKI	00	PRL 84 238	S. Aoki et al. (CP-PACS Collab.)
GARDEN	00	NP B571 237	J. Garden et al. (ALPHA, UKQCD Collabs)
GOCKELER	00	PR D62 054504	M. Gockeler et al.
AOKI	99	PRL 82 4392	S. Aoki et al. (JLQCD Collab.)
BARATE	99	EPJ C11 539	R. Barate et al. (ALEPH Collab.)
MALTMAN	99	PL B462 135	K. Maltman
NARISON	99	PL B466 345	S. Narison
PICH	99	JHEP 9910 004	A. Pich, J. Prades
STEELE	99	PL B451 201	T.G. Steele, K. Kostuik, J. Kwan
BECIREVIC	98	PL B444 401	D. Becirevic et al.
CHETYRKIN	98	NP B533 473	K.G. Chetyrkin, J.H. Kuehn, A.A. Pivovarov
CUCCHIERI	98	PL B422 212	A. Chuchieri et al.
DOMINGUEZ	98	PL B425 193	C.A. Dominguez, L. Pirovano, K. Schilcher
DOSCH	98	PL B417 173	H.G. Dosch, S. Narison
PRADES	98	NPBPS 64 253	J. Prades
CHETYRKIN	97	PL B404 337	K.G. Chetyrkin, D. Pirjol, K. Schilcher
COLANGELO	97	PL B408 340	P. Colangelo et al.
EICKER	97	PL B407 290	N. Eicker et al. (SESAM Collab.)
GAO	97	PR D56 4115	D.-N. Gao, B.A. Li, M.-L. Yan
GOUGH	97	PRL 79 1622	B. Gough et al.
GUPTA	97	PR D55 7203	R. Gupta, T. Bhattacharya
LELLOUCH	97	PL B414 195	L. Lellouch, E. de Rafael, J. Taron
ANISOVICH	96	PL B375 335	A.V. Anisovich, H. Leutwyler
LEUTWYLER	96	PL B378 313	H. Leutwyler
BIJNENS	95	PL B348 226	J. Bijnens, J. Prades, E. de Rafael (NORD, BOHR+)
JAMIN	95	ZPHY C66 633	M. Jamin, M. Munz (HEIDT, MUNT)
NARISON	95C	PL B358 113	S. Narison (MONP)
CHOI	92	PL B292 159	K.W. Choi (UCSD)
DONOGHUE	92	PRL 69 3444	J.F. Donoghue, B.R. Holstein, D. Wyler (MASA+)
DONOGHUE	92B	PR D45 892	J.F. Donoghue, D. Wyler (MASA, ZURI, UCSBT)
GERARD	90	MPL A5 391	J.M. Gerard (MFIM)
LEUTWYLER	90B	NP B337 108	H. Leutwyler (BERN)
MALTMAN	90	PL B234 158	K. Maltman, T. Goldman, Stephenson Jr. (YORKC+)

OTHER LIGHT QUARK MASS RATIOS

m_s/m_d MASS RATIO

VALUE	DOCUMENT ID	TECN	COMMENT
17 to 22 OUR EVALUATION			
• • •	We do not use the following data for averages, fits, limits, etc. • • •		
20.0	⁹⁶ GAO	97	THEO \overline{MS} scheme
18.9 ± 0.8	⁹⁷ LEUTWYLER	96	THEO Compilation
21	⁹⁸ DONOGHUE	92	THEO
18	⁹⁹ GERARD	90	THEO
18 to 23	¹⁰⁰ LEUTWYLER	90B	THEO

⁹⁶ GAO 97 uses electromagnetic mass splittings of light mesons.
⁹⁷ LEUTWYLER 96 uses a combined fit to $\eta \rightarrow 3\pi$ and $\psi' \rightarrow J/\psi(\pi, \eta)$ decay rates, and the electromagnetic mass differences of the π and K .
⁹⁸ DONOGHUE 92 result is from a combined analysis of meson masses, $\eta \rightarrow 3\pi$ using second-order chiral perturbation theory including nonanalytic terms, and $(\psi(2S) \rightarrow J/\psi(1S)\pi)/(\psi(2S) \rightarrow J/\psi(1S)\eta)$.
⁹⁹ GERARD 90 uses large N and η - η' mixing.
¹⁰⁰ LEUTWYLER 90B determines quark mass ratios using second-order chiral perturbation theory for the meson and baryon masses, including nonanalytic corrections. Also uses Weinberg sum rules to determine L_7 .

m_s/\overline{m} MASS RATIO

VALUE	DOCUMENT ID	TECN	
25 to 30 OUR EVALUATION			
• • •	We do not use the following data for averages, fits, limits, etc. • • •		
27.4 ± 0.4	¹⁰¹ AUBIN	04	LATT

¹⁰¹ Three flavor dynamical lattice calculation of pseudoscalar meson masses.

Q MASS RATIO

$Q \equiv \sqrt{(m^2_s - \overline{m}^2)/(m^2_d - \overline{m}^2)}$; $\overline{m} \equiv (m_u + m_d)/2$

VALUE	DOCUMENT ID	TECN	
• • •	We do not use the following data for averages, fits, limits, etc. • • •		
22.8 ± 0.4	¹⁰² MARTEMYAN.05	THEO	
22.7 ± 0.8	¹⁰³ ANISOVICH	96	THEO

¹⁰² MARTEMYANOV 05 determine Q from $\eta \rightarrow 3\pi$ decay.
¹⁰³ ANISOVICH 96 find Q from $\eta \rightarrow \pi^+ \pi^- \pi^0$ decay using dispersion relations and chiral perturbation theory.

LIGHT QUARKS (*u, d, s*) REFERENCES

BLUM	07	PR D76 114508	T. Blum et al. (RBC Collab.)
CHETYRKIN	06	EPJ C46 721	K.G. Chetyrkin, A. Khodjamirian (QCDSF, UKQCD Collabs)
GOCKELER	06	PR D73 054508	M. Gockeler et al. (QCDSF, UKQCD Collabs)
GOCKELER 06A	06A	PL B639 307	M. Gockeler et al. (QCDSF, UKQCD Collabs)
JAMIN	06	PR D74 074009	M. Jamin, J.A. Oller, A. Pich
NARISON	06	PR D74 034013	S. Narison
BAIKOV	05	PRL 95 012003	P.A. Baikov, K.G. Chetyrkin, J.H. Kuhn
GAMIZ	05	PRL 94 011803	E. Gamiz et al.
GORBUNOV	05	PR D71 013002	D.S. Gorbunov, A.A. Pivovarov
MARTEMYAN.05	05	PR D71 017501	B.V. Martemyanov, V.S. Sopoov
NARISON	05	PL B626 101	S. Narison
AUBIN	04	PR D70 031504R	C. Aubin et al. (HPQCD, MILC, UKQCD Collabs.)
AUBIN	04A	PR D70 114501	C. Aubin et al. (MILC Collab.)
AOKI	03	PR D67 034503	S. Aoki et al. (CP-PACS Collab.)
AOKI 03B	03B	PR D68 054502	S. Aoki et al. (CP-PACS Collab.)
BECIREVIC	03	PL B558 69	D. Becirevic, V. Lubicz, C. Tarantino
CHIU	03	NP B673 217	T.-W. Chiu, T.-H. Hsieh
GAMIZ	03	JHEP 0301 060	E. Gamiz et al.
NELSON	03	PRL 90 021601	D. Nelson, G.T. Fleming, G.W. Kilcup
ALIKHAN	02	PR D65 054505	A. Ali Khan et al. (CP-PACS Collab.)
Also		PR D67 059901 (erratum)	A. Ali Khan et al. (CP-PACS Collab.)
CHIU	02	PL B538 298	T.-W. Chiu, T.-H. Hsieh
JAMIN	02	EPJ C24 237	M. Jamin, J.A. Oller, A. Pich



$$I(J^P) = 0(\frac{1}{2}^+)$$

Charge = $\frac{2}{3} e$ Charm = +1

c-QUARK MASS

The c -quark mass corresponds to the "running" mass $m_c(\mu = m_c)$ in the \overline{MS} scheme. We have converted masses in other schemes to the \overline{MS} scheme using two-loop QCD perturbation theory with $\alpha_s(\mu = m_c) = 0.39$. The range 1.0–1.4 GeV for the \overline{MS} mass corresponds to 1.47–1.83 GeV for the pole mass (see the "Note on Quark Masses").

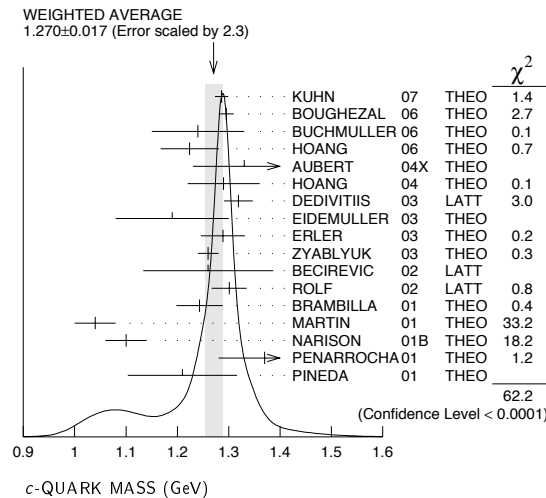
VALUE (GeV)	DOCUMENT ID	TECN	COMMENT
1.27 \pm 0.07 \pm 0.11 OUR EVALUATION			
1.286 ± 0.013	¹ KUHN	07	THEO \overline{MS} scheme
1.295 ± 0.015	² BOUGHEZAL	06	THEO \overline{MS} scheme
1.24 ± 0.09	³ BUCHMULLER	06	THEO \overline{MS} scheme
1.224 ± 0.017 ± 0.054	⁴ HOANG	06	THEO \overline{MS} scheme
1.33 ± 0.10	⁵ AUBERT	04x	THEO \overline{MS} scheme
1.29 ± 0.07	⁶ HOANG	04	THEO \overline{MS} scheme
1.319 ± 0.028	⁷ DEDIVITIIS	03	LATT \overline{MS} scheme
1.19 ± 0.11	⁸ EIDEMULLER	03	THEO \overline{MS} scheme
1.289 ± 0.043	⁹ ERLER	03	THEO \overline{MS} scheme
1.26 ± 0.02	¹⁰ ZYABLYUK	03	THEO \overline{MS} scheme
1.26 ± 0.04 ± 0.12	¹¹ BECIREVIC	02	LATT \overline{MS} scheme
1.301 ± 0.034	¹² ROLF	02	LATT \overline{MS} scheme
1.243 ± 0.045	¹³ BRAMBILLA	01	THEO \overline{MS} scheme
1.04 ± 0.04	¹⁴ MARTIN	01	THEO \overline{MS} scheme
1.1 ± 0.04	¹⁵ NARISON	01B	THEO \overline{MS} scheme
1.37 ± 0.09	¹⁶ PENARROCHA	01	THEO \overline{MS} scheme
1.210 ± 0.070 ± 0.080	¹⁷ PINEDA	01	THEO \overline{MS} scheme
• • •	We do not use the following data for averages, fits, limits, etc. • • •		
1.23 ± 0.09	¹⁸ EIDEMULLER	01	THEO \overline{MS} scheme
1.304 ± 0.027	¹⁹ KUHN	01	THEO \overline{MS} scheme
1.3 ± 0.3 ± 0.3	²⁰ ASTIER	00D	NOMD
1.79 ± 0.38	²¹ VILAIN	99	THEO \overline{MS} scheme

¹ KUHN 07 determine $\overline{m}_c(\mu = 3 \text{ GeV}) = 0.986 \pm 0.013 \text{ GeV}$ and $\overline{m}_c(\overline{m}_c)$ from a four-loop sum-rule computation of the cross-section for $e^+e^- \rightarrow$ hadrons in the charm threshold region.
² BOUGHEZAL 06 result comes from the first moment of the hadronic production cross-section to order α_s^3 .
³ BUCHMULLER 06 determine m_b and m_c by a global fit to inclusive B decay spectra.
⁴ HOANG 06 determines $\overline{m}_c(\overline{m}_c)$ from a global fit to inclusive B decay data. The B decay distributions were computed to order $\alpha_s^2 g_0$, and the conversion between different m_c mass schemes to order α_s^3 .
⁵ AUBERT 04x obtain m_c from a fit to the hadron mass and lepton energy distributions in semileptonic B decay. The paper quotes values in the kinetic scheme. The \overline{MS} value has been provided by the BABAR collaboration.
⁶ HOANG 04 determines $\overline{m}_c(\overline{m}_c)$ from moments at order α_s^2 of the charm production cross-section in e^+e^- annihilation.
⁷ DEDIVITIIS 03 use a quenched lattice computation of heavy-heavy and heavy-light meson masses.
⁸ EIDEMULLER 03 determines m_b and m_c using QCD sum rules.
⁹ ERLER 03 determines m_b and m_c using QCD sum rules. Includes recent BES data.
¹⁰ ZYABLYUK 03 determines m_c by using QCD sum rules in the pseudoscalar channel and comparing with the η_c mass.

Quark Particle Listings

c, b

- ¹¹ BECIREVIC 02 uses Monte-Carlo calculations of lattice Ward identities and the D_S mass. The authors estimate an error of about 5% for use of the quenched approximation, not included in systematic error of 0.12.
- ¹² ROLF 02 determines m_c from a quenched lattice calculation of the D_S mass. The error estimate is for all systematics except the quenched approximation, including lattice spacing effects, finite volume effects, excited states contamination, rounding errors, and the scale uncertainty. The authors estimate the uncertainty due to the quenched approximation may be about 3%.
- ¹³ BRAMBILLA 01 determine $\overline{m}_c(\overline{m}_c)$ from a computation of the J/ψ mass.
- ¹⁴ MARTIN 01 obtain a pole mass of 1.33–1.4 GeV from an analysis of R , the rate for $e^+e^- \rightarrow$ hadrons. We have converted this to the \overline{MS} scheme using the two-loop formula.
- ¹⁵ NARISON 01B uses pseudoscalar sum rules in the B and D meson channels.
- ¹⁶ PENARROCHA 01 result is from an analysis of the BES-II e^+e^- data using finite energy sum rules.
- ¹⁷ PINEDA 01 uses the $\mathcal{T}(1S)$ system and the B - D mass difference to determine m_c . The errors are due to theory, and the uncertainty in λ_1 and m_b .
- ¹⁸ EIDEMULLER 01 result is QCD sum rule analysis of charmonium using NRQCD at next-to-next-to-leading order.
- ¹⁹ KUHN 01 uses an analysis of the e^+e^- total cross section to hadrons.
- ²⁰ Study of opposite sign dimuon events.
- ²¹ VILAIN 99 obtain the charm quark mass from an analysis of charm production in neutrino scattering.

 $m_b - m_c$ QUARK MASS DIFFERENCE

VALUE (GeV) DOCUMENT ID TECN

3.38 to 3.48 OUR EVALUATION

••• We do not use the following data for averages, fits, limits, etc. •••

3.42±0.06	²² ABDALLAH	06B	DLPH
3.44±0.03	²³ AUBERT	04X	BABR
3.41±0.01	²³ BAUER	04	THEO

²² ABDALLAH 06B determine $m_b - m_c$ from moments of the hadron invariant mass and lepton energy spectra in semileptonic inclusive B decays.

²³ Determine $m_b - m_c$ from a global fit to inclusive B decay spectra.

c-QUARK REFERENCES

KUHN	07	NP B778 192	J.H. Kuhn, M. Steinhauser, C. Sturm (DELPHI Collab.)
ABDALLAH	06B	EPJ C45 35	J. Abdallah et al.
BOUGHEZAL	06	PR D74 074006	R. Boughezal, M. Czakon, T. Schutzmeier
BUCHMULLER	06	PR D73 073008	O.L. Buchmuller, H.U. Flaecher
HOANG	06	PL B633 526	A.H. Hoang, A.V. Manohar
AUBERT	04X	PRL 93 011803	B. Aubert et al. (BABAR Collab.)
BAUER	04	PR D70 094017	C. Bauer et al.
HOANG	04	PL B594 127	A.H. Hoang, M. Jamin
DEDIVITIIS	03	NP B675 309	G.M. de Divitiis et al.
EIDEMULLER	03	PR D67 113002	M. Eidemuller
ERLER	03	PL B558 125	J. Erler, M. Luo
ZYABLYUK	03	JHEP 0301 081	K.N. Zybalyuk (ITEP)
BECIREVIC	02	PL B524 115	D. Becirevic, V. Lubicz, G. Martinelli
ROLF	02	JHEP 0212 007	J. Rolf, S. Sint
BRAMBILLA	01	PL B513 381	N. Brambilla, Y. Sumino, A. Vairo
EIDEMULLER	01	PL B498 203	M. Eidemuller, M. Jamin
KUHN	01	NP B619 588	J.H. Kuhn, M. Steinhauser
MARTIN	01	EPJ C19 681	A.D. Martin, J. Outhwaite, M.G. Ryskin
NARISON	01B	PL B520 115	S. Narison
PENARROCHA	01	PL B515 291	J. Penarrocha, K. Schilcher
PINEDA	01	JHEP 0106 022	A. Pineda
ASTIER	00D	PL B486 35	P. Astier et al. (CERN NOMAD Collab.)
VILAIN	99	EPJ C11 19	P. Vilain et al. (CHARM II Collab.)

b

$$I(J^P) = 0(\frac{1}{2}^+)$$

Charge = $-\frac{1}{3}e$ Bottom = -1

b-QUARK MASS

The first value is the “running mass” $\overline{m}_b(\mu = \overline{m}_b)$ in the \overline{MS} scheme, and the second value is the 1S mass, which is half the mass of the $\mathcal{T}(1S)$ in perturbation theory. For a review of different quark mass definitions and their properties, see EL-KHADRA 02. The 1S mass is better suited for use in analyzing B decays than the \overline{MS} mass because it gives a stable perturbative expansion. We have converted masses in other schemes to the \overline{MS} mass and 1S mass using two-loop QCD perturbation theory with $\alpha_s(\mu = \overline{m}_b) = 0.22$. The values $4.20^{+0.17}_{-0.07}$ GeV for the \overline{MS} mass and $4.68^{+0.17}_{-0.07}$ GeV for the 1S mass correspond to $4.79^{+0.19}_{-0.08}$ GeV for the pole mass, using the two-loop conversion formula. A discussion of masses in different schemes can be found in the “Note on Quark Masses.”

 \overline{MS} MASS (GeV) 1S MASS (GeV) DOCUMENT ID TECN4.20 $^{+0.17}_{-0.07}$ OUR EVALUATION of \overline{MS} Mass. See the ideogram below.4.68 $^{+0.17}_{-0.07}$ OUR EVALUATION of 1S Mass. See the ideogram below.

4.347±0.048	4.838 ± 0.053	¹ DELLA-MOR...	07	LATT
4.164±0.025	4.635 ± 0.028	² KUHN	07	THEO
4.205±0.058	4.68 ± 0.06	³ BOUGHEZAL	06	THEO
4.20 ± 0.04	4.67 ± 0.04	⁴ BUCHMULLER	06	THEO
4.19 ± 0.06	4.66 ± 0.07	⁵ PINEDA	06	THEO
4.4 ± 0.3	4.9 ± 0.3	^{6,7} GRAY	05	LATT
4.22 ± 0.06	4.72 ± 0.07	⁸ AUBERT	04X	THEO
4.17 ± 0.03	4.68 ± 0.03	⁹ BAUER	04	THEO
4.22 ± 0.11	4.72 ± 0.12	^{7,10} HOANG	04	THEO
4.25 ± 0.11	4.76 ± 0.12	^{7,11} MCNEILE	04	LATT
4.22 ± 0.09	4.74 ± 0.10	¹² BAUER	03	THEO
4.19 ± 0.05	4.66 ± 0.05	¹³ BORDES	03	THEO
4.20 ± 0.09	4.67 ± 0.10	¹⁴ CORCELLA	03	THEO
4.33 ± 0.10	4.84 ± 0.11	^{7,15} DEDIVITIIS	03	LATT
4.24 ± 0.10	4.72 ± 0.11	¹⁶ EIDEMULLER	03	THEO
4.207±0.031	4.682 ± 0.035	¹⁷ ERLER	03	THEO
4.33 ± 0.06 ± 0.10	4.82 ± 0.07 ± 0.11	¹⁸ MAHMOOD	03	THEO
4.190±0.032	4.663 ± 0.036	¹⁹ BRAMBILLA	02	THEO
4.346±0.070	4.837 ± 0.078	²⁰ PENIN	02	THEO
4.05 ± 0.06	4.51 ± 0.07	²¹ NARISON	01B	THEO
4.210±0.090±0.025	4.69 ± 0.100 ± 0.028	²² PINEDA	01	THEO

••• We do not use the following data for averages, fits, limits, etc. •••

4.19 ± 0.40	4.66 ± 0.45	²³ ABDALLAH	06D	DLPH
3.95 ± 0.57	4.40 ± 0.63	²⁴ ABBIENDI	01S	OPAL
4.203±0.026	4.678 ± 0.029	²⁵ BRAMBILLA	01	THEO
4.21 ± 0.05	4.69 ± 0.06	²⁶ KUHN	01	THEO
4.7 ± 0.74	5.23 ± 0.82	²⁷ BARATE	00v	ALEP
4.20 ± 0.06	4.71 ± 0.03	²⁸ HOANG	00	THEO
4.437+0.045 -0.029	4.938+0.050 -0.032	²⁹ LUCHA	00	THEO
4.454+0.045 -0.029	4.957+0.050 -0.032	²⁹ PINEDA	00	THEO
4.25 ± 0.08	4.73 ± 0.09	³⁰ BENEKE	99	THEO
3.8 $^{+0.77}_{-2.0}$	4.23 $^{+0.86}_{-2.0}$	³¹ BRANDENB...	99	
4.25 ± 0.09	4.73 ± 0.10	³² HOANG	99	THEO
4.2 ± 0.1	4.67 ± 0.11	³³ MELNIKOV	99	THEO
4.21 ± 0.11	4.69 ± 0.12	³⁴ PENIN	99	THEO
3.91 ± 0.67	4.35 ± 0.75	³⁵ ABREU	98I	DLPH
4.14 ± 0.04	4.61 ± 0.05	³⁶ KUEHN	98	THEO
4.15 ± 0.05 ± 0.20	4.62 ± 0.06 ± 0.22	³⁷ GIMENEZ	97	LATT
4.19 ± 0.06	4.66 ± 0.07	³⁸ JAMIN	97	THEO
4.16 ± 0.32 ± 0.60	4.63 ± 0.36 ± 0.67	³⁹ RODRIGO	97	THEO

¹ DELLA-MORTE 07 determine $\overline{m}_b(\overline{m}_b)$ from a computation of the spin-averaged B meson mass using quenched lattice HQET at order $1/m$.

² KUHN 07 determine $\overline{m}_b(\mu = 10 \text{ GeV}) = 3.609 \pm 0.025 \text{ GeV}$ and $\overline{m}_b(\overline{m}_b)$ from a four-loop sum-rule computation of the cross-section for $e^+e^- \rightarrow$ hadrons in the bottom threshold region. We have converted this to the 1S scheme.

³ BOUGHEZAL 06 \overline{MS} scheme result comes from the first moment of the hadronic production cross-section to order α_s^3 . We have converted it to the 1S scheme.

⁴ BUCHMULLER 06 determine m_b and m_c by a global fit to inclusive B decay spectra. We have converted this to the 1S scheme.

⁵ PINEDA 06 \overline{MS} scheme result comes from a partial NNLL evaluation (complete at NNLO) of sum rules of the bottom production cross-section in e^+e^- annihilation. We have converted it to the 1S scheme.

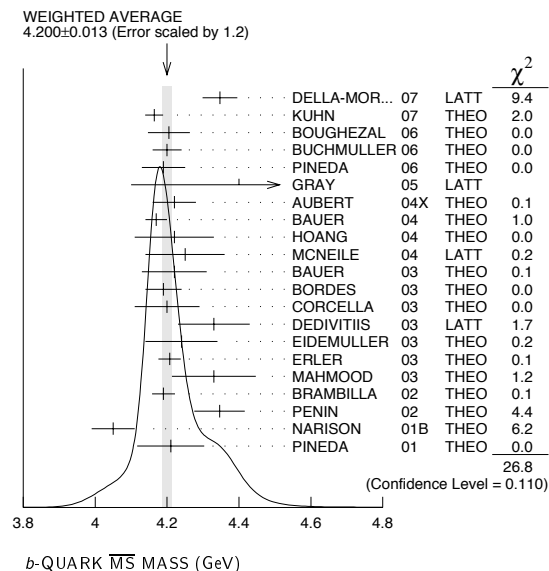
⁶ GRAY 05 determines $\overline{m}_b(\overline{m}_b)$ from a lattice computation of the \mathcal{T} spectrum. The simulations have 2+1 dynamical light flavors. The b quark is implemented using NRQCD. We have converted m_b to the 1S scheme.

⁸ AUBERT 04X obtain m_b from a fit to the hadron mass and lepton energy distributions in semileptonic B decay. The paper quotes values in the kinetic scheme. The \overline{MS} value has been provided by the BABAR collaboration, and we have converted this to the 1S scheme.

⁹ BAUER 04 determine m_b , m_c and $m_b - m_c$ by a global fit to inclusive B decay spectra.

¹⁰ HOANG 04 determines $m_b(\overline{m}_b)$ from moments at order α_s^2 of the bottom production cross-section in e^+e^- annihilation.

- 11 MCNEILE 04 use lattice QCD with dynamical light quarks and a static heavy quark to compute the masses of heavy-light mesons.
- 12 BAUER 03 determine the b quark mass by a global fit to B decay observables. The experimental data includes lepton energy and hadron invariant mass moments in semileptonic $B \rightarrow X_c \ell \nu_\ell$ decay, and the inclusive photon spectrum in $B \rightarrow X_s \gamma$ decay. The theoretical expressions used are of order $1/m^3$, and $\alpha_s^2 \beta_0$.
- 13 BORDES 03 determines m_b using QCD finite energy sum rules to order α_s^2 .
- 14 CORCELLA 03 determines \overline{m}_b using sum rules computed to order α_s^2 . Includes charm quark mass effects.
- 15 DEDIVITIIS 03 use a quenched lattice computation of heavy-heavy and heavy-light meson masses.
- 16 EIDEMULLER 03 determines \overline{m}_b and \overline{m}_c using QCD sum rules.
- 17 ERLER 03 determines \overline{m}_b and \overline{m}_c using QCD sum rules. Includes recent BES data.
- 18 MAHMOOD 03 determines m_b^{1S} by a fit to the lepton energy moments in $B \rightarrow X_c \ell \nu_\ell$ decay. The theoretical expressions used are of order $1/m^3$ and $\alpha_s^2 \beta_0$. We have converted their result to the \overline{MS} scheme.
- 19 BRAMBILLA 02 determine $\overline{m}_b(\overline{m}_b)$ from a computation of the $\Upsilon(1S)$ mass to order α_s^4 , including finite m_c corrections. We have converted this to the 1S scheme.
- 20 PENIN 02 determines \overline{m}_b from the spectrum of the Υ system.
- 21 NARISON 01B uses pseudoscalar sum rules in the B and D meson channels.
- 22 PINEDA 01 uses the $\Upsilon(1S)$ system to determine the quark mass. The errors are due to theory, and the uncertainty in α_s .
- 23 ABDALLAH 06D determine $m_b(M_Z) = 2.85 \pm 0.32$ GeV from Z-decay three-jet events containing a b-quark. We have converted this to $\overline{m}_b(\overline{m}_b)$ and m_b^{1S} .
- 24 ABBIENDI 01s find $\overline{m}_b(M_Z) = 2.67 \pm 0.4$ GeV from an analysis of $Z \rightarrow b$ decays.
- 25 BRAMBILLA 01 determine $\overline{m}_b(\overline{m}_b)$ from a computation of the J/ψ mass. We have converted this to the 1S scheme.
- 26 KUHN 01 uses an analysis of the e^+e^- total cross section to hadrons.
- 27 BARATE 00v obtain the b quark mass $\overline{m}_b(M_Z) = 3.27 \pm 0.22(\text{stat}) \pm 0.22(\text{exp}) \pm 0.38(\text{had}) \pm 0.16(\text{thy})$ from an analysis of event shape variables in Z decays. We have converted this to $\mu = \overline{m}_b$.
- 28 HOANG 00 uses a NNLO calculation of the vacuum polarization function to determine spectral moments of the masses and electronic decay widths of the Υ mesons.
- 29 LUCHA 00, PINEDA 00 obtain the b-quark mass from a perturbative calculation of the Υ spectrum and decay widths to order α_s^4 .
- 30 BENEKE 99 uses a calculation of the $b\overline{b}$ production cross section and the mass of the Υ meson at NNLO.
- 31 BRANDENBURG 99 obtain a b-quark mass of $\overline{m}_b(M_Z) = 2.56 \pm 0.27^{+0.28+0.49}_{-0.38-1.48}$ from a study of three-jet events at the Z. We have converted this to $\mu = \overline{m}_b$.
- 32 HOANG 99 uses a NNLO calculation of the vacuum polarization function to determine spectral moments of the masses and electronic decay widths of the Υ mesons.
- 33 MELNIKOV 99 compute the quark mass using Υ sum rules at NNLO.
- 34 PENIN 99 compute the quark mass using Υ sum rules at NNLO.
- 35 ABREU 98i determines the \overline{MS} mass $\overline{m}_b = 2.67 \pm 0.25 \pm 0.34 \pm 0.27$ GeV at $\mu = M_Z$ from three jet heavy quark production at LEP. ABREU 98i have rescaled the result to $\mu = \overline{m}_b$ using $\alpha_s = 0.118 \pm 0.003$.
- 36 KUEHN 98 uses a calculation of the vacuum polarization function, including resumming threshold effects, to determine spectral moments of the masses of the Υ mesons. We have converted their extracted value of 4.75 ± 0.04 for the pole mass to the \overline{MS} scheme.
- 37 GIMENEZ 97 uses lattice computations of the B-meson propagator and the B-meson binding energy $\overline{\Lambda}$ in the HQET. Their systematic (second) error for the \overline{MS} mass is an estimate of the effects of higher-order corrections in the matching of the HQET operators (renormalon effects).
- 38 JAMIN 97 apply the QCD moment method to the Υ system. They also find a pole mass of 4.60 ± 0.02 .
- 39 RODRIGO 97 determines the \overline{MS} mass $\overline{m}_b = 2.85 \pm 0.22 \pm 0.20 \pm 0.36$ GeV at $\mu = M_Z$ from three jet heavy quark production at LEP. We have rescaled the result.



b-QUARK REFERENCES

DELLA-MOR...	07	JHEP 0701 007	M. Della Morte et al.
KUHN	07	NP B778 192	J.H. Kuhn, M. Steinhauser, C. Sturm
ABDALLAH	06D	EPJ C46 569	J. Abdallah et al. (DELPHI Collab.)
BOUGHEZAL	06	PR D74 074006	R. Boughezal, M. Czakon, T. Schutzmeier
BUCHMULLER	06	PR D73 073008	O.L. Buchmuller, H.U. Flacher
PINEDA	06	PR D73 111501R	A. Pineda, A. Signer
GRAY	05	PR D72 094507	A. Gray et al. (HPQCD, UKQCD Collab.)
AUBERT	04X	PRL 93 011803	B. Aubert et al. (BABAR Collab.)
BAUER	04	PR D70 094017	C. Bauer et al.
HOANG	04	PL B594 127	A.H. Hoang, M. Jamin
MCNEILE	04	PL B600 77	C. McNeile, C. Michael, G. Thompson (UKQCD Collab.)
BAUER	03	PR D67 054012	C.W. Bauer et al.
BORDES	03	PL B562 81	J. Bordes, J. Penarrocha, K. Schilcher
CORCELLA	03	PL B554 133	G. Corcella, A.H. Hoang
DEDIVITIIS	03	NP B675 309	G.M. de Divitiis et al.
EIDEMULLER	03	PR D67 113002	M. Eidemuller
ERLER	03	PL B558 125	J. Erler, M. Luo
MAHMOOD	03	PR D67 072001	A.H. Mahmood et al. (CLEO Collab.)
BRAMBILLA	02	PR D65 034001	N. Brambilla, Y. Sumino, A. Vairo
EL-KHADRA	02	ARNPS 52 201	A.X. El-Khadra, M. Luke
PENIN	02	PL B538 335	A. Penin, M. Steinhauser
ABBIENDI	01S	EPJ C21 411	G. Abbiendi et al. (OPAL Collab.)
BRAMBILLA	01	PL B513 381	N. Brambilla, Y. Sumino, A. Vairo
KUHN	01	NP B619 588	J.H. Kuhn, M. Steinhauser
NARISON	01B	PL B520 115	S. Narison
PINEDA	01	JHEP 0106 022	A. Pineda
BARATE	00V	EPJ C18 1	R. Barate et al. (ALEPH Collab.)
HOANG	00	PR D61 034005	A.H. Hoang
LUCHA	00	PR D62 097501	W. Lucha, F.F. Schoeberl
PINEDA	00	PR D61 077505	A. Pineda, F.J. Yndurain
BENEKE	99	PL B471 233	M. Beneke, A. Signer
BRANDENBURG	99	PL B468 168	A. Brandenburg et al.
HOANG	99	PR D59 014039	A.H. Hoang
MELNIKOV	99	PR D59 114009	K. Melnikov, A. Yelkhovskiy
PENIN	99	NP B549 217	A.A. Penin, A.A. Pivovarov
ABREU	98I	PL B418 430	P. Abreu et al. (DELPHI Collab.)
KUEHN	98	NP B534 356	J.H. Kuehn, A.A. Penin, A.A. Pivovarov
GIMENEZ	97	PL B393 124	V. Gimenez, G. Martinelli, C.T. Sachrajda
JAMIN	97	NP B507 334	M. Jamin, A. Pich
RODRIGO	97	PRL 79 193	G. Rodrigo, A. Santamaría, M.S. Bilenky

t

$$I(J^P) = 0(\frac{1}{2}^+)$$

$$\text{Charge} = \frac{2}{3} e \quad \text{Top} = +1$$

THE TOP QUARK

Updated March 2008 by T. M. Liss (Illinois) and A. Quadt (Göttingen).

A. Introduction: The top quark is the $Q = 2/3$, $T_3 = +1/2$ member of the weak-isospin doublet containing the bottom quark (see the review on the “Standard Model of Electroweak Interactions” for more information). This note summarizes the properties of the top quark (mass, production cross section, decay branching ratios, etc.), and provides a discussion of the experimental and theoretical issues involved in their determination.

B. Top quark production at the Tevatron: All direct measurements of production and decay of the top quark have been made by the CDF and DØ experiments in $p\overline{p}$ collisions at the Fermilab Tevatron collider. The first studies were performed during Run I, at $\sqrt{s} = 1.8$ TeV, which was completed in 1996. The most recent, and highest-statistics, measurements are from Run II, which started in 2001 at $\sqrt{s} = 1.96$ TeV. This note will discuss primarily results from Run II.

In hadron collisions, top quarks are produced dominantly in pairs through the QCD processes $q\overline{q} \rightarrow t\overline{t}$ and $gg \rightarrow t\overline{t}$. At 1.96 TeV (1.8 TeV), the production cross section in these channels is expected to be approximately 7 pb (5 pb) for $m_t = 175$ GeV/ c^2 , with a contribution of 85% (90%) from $q\overline{q}$ annihilation [1]. Somewhat smaller cross sections are expected from electroweak single-top production mechanisms, namely from $q\overline{q}' \rightarrow t\overline{b}$ [2] and $qb \rightarrow q't$ [3], mediated by virtual s-channel and t-channel W bosons, respectively. The combined rate for the single-top processes at 1.96 TeV is approximately 3 pb for $m_t = 175$ GeV/ c^2 [4]. The identification of top quarks

Quark Particle Listings

t

in the electroweak single-top channel is much more difficult than in the QCD $t\bar{t}$ channel, due to a less distinctive signature and significantly larger backgrounds.

In top decay, the Ws and Wd final states are expected to be suppressed relative to Wb by the square of the CKM matrix elements V_{ts} and V_{td} . Assuming unitarity of the three-generation CKM matrix, these matrix element values can be estimated to be less than 0.043 and 0.014, respectively (see the review “The CKM Quark-Mixing Matrix” for more information). With a mass above the Wb threshold, and V_{tb} close to unity, the decay width of the top quark is expected to be dominated by the two-body channel $t \rightarrow Wb$. Neglecting terms of order m_b^2/m_t^2 , α_s^2 , and $(\alpha_s/\pi)M_W^2/m_t^2$, the width predicted in the Standard Model (SM) at next-to-leading-order is [5]:

$$\Gamma_t = \frac{G_F m_t^3}{8\pi\sqrt{2}} \left(1 - \frac{M_W^2}{m_t^2}\right)^2 \left(1 + 2\frac{M_W^2}{m_t^2}\right) \left[1 - \frac{2\alpha_s}{3\pi} \left(\frac{2\pi^2}{3} - 5\right)\right], \quad (1)$$

where m_t refers to the top quark pole mass. The width increases with mass, changing, for example, from 1.02 GeV/ c^2 for $m_t = 160$ GeV/ c^2 to 1.56 GeV/ c^2 for $m_t = 180$ GeV/ c^2 (we use $\alpha_s(M_Z) = 0.118$). With its correspondingly short lifetime of $\approx 0.5 \times 10^{-24}$ s, the top quark is expected to decay before top-flavored hadrons or $t\bar{t}$ -quarkonium-bound states can form [6]. The order α_s^2 QCD corrections to Γ_t are also available [7], thereby improving the overall theoretical accuracy to better than 1%.

The final states for the leading pair-production process can be divided into three classes:

- A. $t\bar{t} \rightarrow W^+ b W^- \bar{b} \rightarrow q\bar{q}' b q''\bar{q}'''\bar{b}$, (46.2%)
- B. $t\bar{t} \rightarrow W^+ b W^- \bar{b} \rightarrow q\bar{q}' b \ell \bar{\nu}_\ell \bar{b} + \bar{\ell} \nu_\ell b q \bar{q}' \bar{b}$, (43.5%)
- C. $t\bar{t} \rightarrow W^+ b W^- \bar{b} \rightarrow \bar{\ell} \nu_\ell b \ell' \bar{\nu}_{\ell'} \bar{b}$. (10.3%)

The quarks in the final state evolve into jets of hadrons. A, B, and C are referred to as the all-jets, lepton+jets (ℓ +jets), and dilepton ($\ell\ell$) channels, respectively. Their relative contributions, including hadronic corrections, are given in parentheses. While ℓ in the above processes refers to e , μ , or τ , most of the results to date rely on the e and μ channels. Therefore, in what follows, we will use ℓ to refer to e or μ , unless noted otherwise.

The initial and final-state quarks can radiate gluons that can be detected as additional jets. The number of jets reconstructed in the detectors depends on the decay kinematics, as well as on the algorithm for reconstructing jets used by the analysis. The transverse momenta of neutrinos are reconstructed from the imbalance in transverse momentum measured in each event (missing p_T , which is here also missing E_T).

The observation of $t\bar{t}$ pairs has been reported in all of the above decay classes. As discussed below, the production and decay properties of the top quark extracted from the three-decay classes are consistent within their experimental uncertainty. In particular, the $t \rightarrow Wb$ decay mode is supported through the reconstruction of the $W \rightarrow jj$ invariant mass in events with two identified b -jets in the $\ell\nu_\ell b\bar{b}jj$ final state [8,9]. Also the CDF and $D\bar{O}$ measurements of the top quark mass in lepton+jets

events, where the jet energy scale is calibrated *in situ* using the invariant mass of the hadronically decaying W boson [10,11], support this decay mode.

The extraction of top-quark properties from Tevatron data relies on good understanding of the production and decay mechanisms of the top quark, as well as of the background processes. For the background, the jets are expected to have a steeply falling E_T spectrum, to have an angular distribution peaked at small angles with respect to the beam, and to contain b - and c -quarks at the few-percent level. On the contrary, for the top signal, the fraction of events containing b jets is expected to be $\approx 100\%$, and the jets to be rather energetic, since they come from the decay of a massive object. It is therefore possible to improve the S/B ratio by requiring the presence of a b quark, or by selecting very energetic and central kinematic configurations, or both.

Background estimates can be checked using control samples with fewer jets, where there is little top contamination (0 or 1 jet for dilepton channels, 1 or 2 jets for lepton+jets channels, and ≤ 4 jets or multijets, ignoring b -tagging for the all-jets channel).

Electroweak s - and t -channel production of single top quarks is expected to occur at the Tevatron at a rate of 0.88 ± 0.11 pb for the s -channel, and 1.98 ± 0.25 pb for the t -channel [4], a little less than half of the $t\bar{t}$ production rate. However, significant challenges in signal and background separation have slowed the observation of this important production channel. The cross sections for these processes are proportional to $|V_{tb}|^2$, and no assumption is needed on the number of families or on the unitarity of the CKM matrix in extracting $|V_{tb}|$. Separate measurements of the s - and t -channel processes provide sensitivity to physics beyond the SM [12].

Next-to-leading-order Monte-Carlo programs have recently become available for both signal and background processes [13], but for the backgrounds, the jet multiplicities required in $t\bar{t}$ analyses are not yet available. Theoretical estimates of the background processes (W or Z bosons+jets and dibosons+jets) using LO calculations have large uncertainties. While this limitation affects estimates of the overall production rates, it is believed that the LO determination of event kinematics, and of the fraction of W +multi-jet events that contain b - or c -quarks, are relatively accurate [14]. Comparison to CDF and $D\bar{O}$ data, however, indicates the b - and c -quark fractions to be underestimated by the LO generators.

C. Measured top properties: Current measurements of top properties are based on Run-II data with integrated luminosities up to 2 fb $^{-1}$ for both CDF and $D\bar{O}$.

C.1 $t\bar{t}$ Production Cross Section: Both experiments determine the $t\bar{t}$ -production cross section, $\sigma_{t\bar{t}}$, from the number of observed top candidates, estimated background, $t\bar{t}$ acceptance, and integrated luminosity. The cross section has been measured in the dilepton, lepton+jets, and all-jets decay modes. To separate signal from background, the experiments use identification

of jets likely to contain b -quarks (“ b -tagging”) and/or discriminating kinematic observables. Techniques used for b -tagging include identification of a secondary vertex (“vtx b -tag”), a probability that a jet contains a secondary vertex based on the measured impact parameter of tracks (“jet probability”), or identification of a muon from a semileptonic b decay (“soft μ b -tag”). CDF and DØ also use artificial neural network-based b -tagging algorithms that combine the properties of displaced tracks and secondary vertex information.

Due to the lepton identification (ID) requirements in the ℓ +jets and $\ell\ell$ modes, in particular the p_T requirement, the sensitivity is primarily to e and μ decays of the W , with only a small contribution from $W \rightarrow \tau\nu$ due to secondary $\tau \rightarrow (e, \mu)\nu X$ decays. In the $\ell\ell$ mode, when only one lepton is required to satisfy lepton ID criteria (ℓ +track), there is greater sensitivity to $W \rightarrow \tau\nu$. CDF uses a missing- E_T +jets selection in the ℓ +jets mode that does not require specific lepton-ID, and therefore has significant acceptance to $W \rightarrow \tau\nu$ decays, including hadronic τ decays, in addition to $W \rightarrow e\nu, \mu\nu$ decays. In a direct search for the tau decay mode of $t\bar{t}$ pairs in the lepton+hadronic tau channel, the ratio $r_\tau \equiv B(t \rightarrow b\tau\nu)/B_{SM}(t \rightarrow b\tau\nu)$ is found to be $r_\tau < 5.2$ at 95% C.L. [15]. DØ finds the production cross section (and visible cross section $\sigma \cdot Br$) to be consistent with Standard Model expectations in the lepton+hadronic tau channel [16] as well as in the tau+jets channel [17]. Table 1 shows the measured cross sections from DØ and CDF. These should be compared to the theoretical calculations that yield 5.8 – 7.4 pb for a top mass of 175 GeV/ c^2 [1] (see Listings).

Next-to-leading-order calculations predict forward-backward asymmetries of 5-10% in $t\bar{t}$ production [18]. The CDF measurement in 1.9 fb $^{-1}$ yields $17 \pm 8\%$ [19], while the DØ measurement of this asymmetry yields $12 \pm 8\%$ at the detector level [20] using 0.9 fb $^{-1}$. Both results are presently consistent with the NLO prediction.

The theory calculations at next-to-leading-order, including soft-gluon resummation [1], are in good agreement with all the measurements. The increased precision of combined measurements from larger Run-II samples can serve to constrain, or probe, exotic production mechanisms or decay channels that are predicted by some models [21–24]. Such non-SM effects would yield discrepancies between theory and data. New sources of top could also modify kinematic distributions, such as the invariant mass of the $t\bar{t}$ pair or the transverse momentum (p_T) of the top quark. Run-I studies of the $t\bar{t}$ invariant mass by CDF and DØ [25,26], and of p_T distributions by CDF [27], show no deviation from expected behavior. DØ [28] also found these kinematic distributions to be consistent with expectations of the SM in Run I. In Run II, distributions of primary kinematic variables such as the lepton p_T , missing E_T , and angular variables have been investigated [29–42] and found to be consistent with the SM. Recently, CDF has measured the differential production cross section $d\sigma/dM_{t\bar{t}}$ in 2 fb $^{-1}$ [43]. Comparing the shape to the SM expectation, they find a p -value of 0.45. Also,

Table 1: Cross section for $t\bar{t}$ production in $p\bar{p}$ collisions at $\sqrt{s} = 1.96$ TeV from CDF and DØ ($m_t = 175$ GeV/ c^2). Only preliminary results (not yet submitted for publication as of March 2008) are shown; for published results see the Listings. Uncertainties given are the quadrature sum of statistical and systematic uncertainties of each measurement.

$\sigma_{t\bar{t}}(\text{pb})$	Source	$\int \mathcal{L} dt$ (pb $^{-1}$)	Ref.	Method
7.3 ± 2.0	DØ	430	[30]	ℓ + jets/soft μ b -tag
5.1 ± 4.4	DØ	350	[17]	τ + jets
6.2 ± 1.2	DØ	1050	[31]	$\ell\ell$ + ℓ +track/vtx b -tag
8.3 ± 2.3	DØ	1000	[16]	$\ell\tau$ /vtx b -tag
12.1 ± 6.7	DØ	360	[9]	all-jets/vtx b -tags
$7.1^{+1.9}_{-1.7}$	DØ	220-240	[32]	combined
8.2 ± 1.1	CDF	1120	[33]	ℓ + jets/vtx b -tag
7.8 ± 2.0	CDF	760	[34]	ℓ + jets/soft μ b -tag
6.0 ± 1.1	CDF	760	[35]	ℓ + jets/kinematics
6.2 ± 1.4	CDF	1200	[36]	$\ell\ell$
8.3 ± 1.6	CDF	1100	[37]	ℓ +track
10.1 ± 2.2	CDF	1000	[38]	ℓ +track+ b -tag
$8.3^{+2.3}_{-1.9}$	CDF	1020	[39]	all-jets/kin+vtx b -tags
7.3 ± 0.9	CDF	760	[40]	combined

the $t\bar{t}$ invariant mass distributions have been studied [44,45]. These tests are presently statistics-limited, and will be more incisive with larger data sets in Run II.

C.2 Electroweak Single-Top Quark Production: DØ has reported first evidence for single-top production, applying a multivariate analysis to 900 pb $^{-1}$ of Run-II data [46]. Using a decision tree (DT) technique, they measure a cross section of $\sigma(p\bar{p} \rightarrow tb + X, tqb + X) = 4.9 \pm 1.4$ pb. The probability for such a measurement in the absence of a signal is 0.035%, corresponding to a 3.4 standard deviation significance. A more recent DØ analysis on the same data set [47], combining the DT analysis with two independent analyses based on the matrix element method and a bayesian neural network technique, yields $\sigma(p\bar{p} \rightarrow tb + X, tqb + X) = 4.7 \pm 1.3$ pb, corresponding to a probability of 0.014, or 3.6 standard deviation significance. With 2.2 fb $^{-1}$, CDF has recently reported evidence [48] with three techniques: a likelihood based on expected kinematic distributions, an event-probability-density based on matrix elements, and a neural-network approach. Combining these three approaches in a single analysis yields a cross section of $\sigma(p\bar{p} \rightarrow tb + X, tqb + X) = 2.2 \pm 0.7$ pb. The probability for this measurement in the absence of a signal is 0.0094%, corresponding to 3.7 standard deviation significance. These measurements are also used to directly determine the CKM-matrix element $|V_{tb}|$. DØ measures $|V_{tb}| = 1.3 \pm 0.2$, while the CDF measurement is $|V_{tb}| = 0.88 \pm 0.16$.

C.3 Top Quark Mass Measurements: The top mass has been measured in the lepton+jets, dilepton, and the all-jets channel by both CDF and DØ. At present, the most precise measurements come from the lepton+jets channel containing

Quark Particle Listings

t

four or more jets, and large missing E_T . The samples for the mass measurement are selected using topological (topo) or b -tagging methods. In this channel, four basic techniques are employed to extract the top mass. In the first, the so-called “template method” (TM) [49], an over-constrained (2C) kinematic fit is performed to the hypothesis $t\bar{t} \rightarrow W^+ b W^- \bar{b} \rightarrow \ell \bar{\nu}_\ell b q \bar{q}' \bar{b}$ for each event, assuming that the four jets of highest E_T originate from the four quarks in $t\bar{t}$ decay. There are 24 possible solutions, reflecting the allowed assignment of the final-state quarks to jets, and the two possible solutions for the longitudinal momentum, p_z , of the neutrino when the W -mass constraint is imposed on the leptonic W decay. The number of solutions is reduced to 12 when a jet is b -tagged and assigned as one of the b quarks, and to 4 when the event has two such b -tags. A χ^2 variable describes the agreement of the measurements with each possible solution under the $t\bar{t}$ hypothesis given jet-energy resolutions. The solution with the lowest χ^2 is defined as the best choice, resulting in one value for the reconstructed top quark mass per event. The distribution of reconstructed top-quark mass from the data events is then compared to templates modeled from a combination of signal and background distributions for a series of assumed top masses. The best fit value for the top quark mass and its uncertainty are obtained from a maximum-likelihood fit. In the second method, the “Matrix Element/Dynamic Likelihood Method” (ME/DLM), similar to that originally suggested by Kondo *et al.* [50] and Dalitz and Goldstein [51], a probability for each event is calculated as a function of the top mass, using an LO matrix element for the production and decay of $t\bar{t}$ pairs. All possible assignments of reconstructed jets to final-state quarks are used, each weighted by a probability determined from the matrix element. The correspondence between measured four-vectors and parton-level four-vectors is taken into account using probabilistic transfer functions. In a third method, the “Ideogram Method” [52,53], which combines some of the features of the above two techniques, each event is compared to the signal and background mass spectrum, weighted by the χ^2 probability of the kinematic fit for all 24 jet-quark combinations and an event probability. The latter is determined from the signal fraction in the sample and the event-by-event purity, as determined from a topological discriminant in Monte Carlo events. An additional variation on these techniques is the “Multivariate Likelihood” (ML) technique, where an integral over the matrix element is performed for each permutation, and then summed with weights determined by the b -tagging information on each jet. Backgrounds are handled in the ML technique by “deweighting” events according to a background probability calculated using variables based on the topology of the event.

With at least four jets in the final state, the dominant systematic uncertainty on the top quark mass is from the uncertainty on the jet-energy scale. CDF (TM, ME, ML) and DØ (ME) have reduced the jet-energy scale uncertainty by performing a simultaneous, *in situ*, fit to the $W \rightarrow jj$ hypothesis.

The fourth technique [54] relies solely on tracking, and thus avoids the jet-energy scale uncertainty. This method exploits the fact that, in the rest frame of the top quark, the boost given to the bottom quark has a Lorentz factor $\gamma_b \approx 0.4 m_t/m_b$. The measurement of the transverse decay length L_{xy} of the b -hadrons from the top quark decay is therefore sensitive to the mass of the top quark.

Additional determinations of the top mass come from the dilepton channel with two or more jets and large missing E_T , and from the all-jets channel. The dilepton channel, with two unmeasured neutrinos, is under-constrained by one measurement. It is not possible to extract a value for the top-quark mass from direct reconstruction without adding additional information. Assuming a value for m_t , the $t\bar{t}$ system can be reconstructed up to an eight-fold ambiguity from the choice of associating leptons and quarks to jets, and due to the two solutions for the p_z of each neutrino. Recently, an analytic solution to the problem has been proposed [55]. At the Tevatron, two basic techniques are employed: one based on templates, and one using matrix elements. The first class of techniques incorporates additional information to render the kinematic system solvable. In this class, there are two techniques that assign a weight as a function of top mass for each event based on solving for either the azimuth, ϕ , of each neutrino given an assumed pseudorapidity, η , ($\eta(\nu)$) [56,57], or for η of each neutrino given an assumed ϕ , ($\phi(\nu)$) [58]. An alternative approach, (MWT) [56], solves for η of each neutrino requiring the sum of the neutrino \vec{p}_T 's to equal the measured missing \vec{E}_T vector. In another technique, ($p_z(t\bar{t})$) [58], the kinematic system is rendered solvable by the addition of the requirement that the p_z of the $t\bar{t}$ system, equal to the sum of the p_z of the t and \bar{t} , be zero within a Gaussian uncertainty of 180 GeV/c. In a variation of the $p_z(t\bar{t})$ technique, the theoretical relation between the top mass and its production cross section is used as an additional constraint. In most of the techniques in this class, a single mass per event is extracted and a top-mass value found using a Monte Carlo template fit to the single-event masses, in a manner similar to that employed in the lepton+jets TM technique. The DØ ($\eta(\nu)$) analysis uses the shape of the weight distribution as a function of m_t in the template fit. The second class, ME/DLM, uses weights based on the LO matrix element for an assumed mass, given the measured four-vectors (and integrating over the unknowns) to form a joint likelihood as a function of the top mass for the ensemble of fitted events.

The P_T spectrum of the leptons in the dilepton channel has also been used to extract a top mass measurement [59]. The resulting statistical uncertainty of the measurement is large, but as with the L_{xy} technique, it is free of the systematic uncertainty due to the jet-energy scale.

In the most recent set of CDF results, a measurement has been done using the lepton+jets and dilepton channels simultaneously. In the lepton+jets channel, the TM is used together with an *in situ* $W \rightarrow jj$ fit. In the dilepton channel,

Table 2: Measurements of top-quark mass from CDF and DØ. $\int \mathcal{L}dt$ is given in pb^{-1} . Only preliminary results (not yet submitted for publication as of March 2008) are shown; for published results see the Listings. Statistical uncertainties are listed first, followed by systematic uncertainties.

m_t (GeV/ c^2)	Source	$\int \mathcal{L}dt$	Ref.	Method
$169.9 \pm 5.8^{+7.8}_{-7.1}$	DØ Run II	230	[68]	ℓ +jets/topo, TM
$170.6 \pm 4.2 \pm 6.0$	DØ Run II	230	[68]	ℓ +jets/ b -tag, TM
$172.2 \pm 1.1 \pm 1.6$	DØ Run II	2100	[69]	ℓ +jets/ b -tag, ME($W \rightarrow jj$)
$176.6 \pm 11.2 \pm 3.8$	DØ Run II	370	[70]	$\ell\ell$ / b -tag, \mathcal{MWT}
$173.7 \pm 5.4 \pm 3.4$	DØ Run II	1000	[72]	$\ell\ell$, $\eta(\nu)$ + \mathcal{MWT}
$166.1 \pm 5.7 \pm 5.8(th)DØ$	Run II	1000	[60]	$\sigma_{t\bar{t}}^{\ell+jets}$
$174.1 \pm 9.1 \pm 5.1(th)DØ$	Run II	1000	[60]	$\sigma_{t\bar{t}}^{\ell\ell}$
$172.1 \pm 1.5 \pm 1.9$	DØ Run I+II	1000	[65]	DØ combined
$172.7 \pm 1.8 \pm 1.2$	CDF Run II	1900	[76]	ℓ +jets/ b -tag, ML($W \rightarrow jj$)
$171.8 \pm 1.9 \pm 1.0$	CDF Run II	1900	[77]	ℓ +jets/ b -tag, TM($W \rightarrow jj$)
$171.9 \pm 1.7 \pm 1.0$	CDF Run II	1900	[77]	ℓ +jets TM($W \rightarrow jj$) & $\ell\ell$ $\eta(\nu)+H_T$
$171.2 \pm 2.7 \pm 2.9$	CDF Run II	1900	[78]	$\ell\ell$, ME
$171.6^{+3.4}_{-3.2} \pm 3.8$	CDF Run II	1900	[77]	$\ell\ell$, $\eta(\nu)+H_T$
$167.7^{+4.2}_{-4.0} \pm 3.1$	CDF Run II	1900	[79]	$\ell\ell$, $\eta(\nu)$
$156 \pm 20 \pm 4.6$	CDF Run II	1800	[59]	$\ell\ell$, $P_T(\ell)$
$177.0 \pm 3.7 \pm 1.6$	CDF Run II	1900	[80]	all jets, TM($W \rightarrow jj$)
$171.1 \pm 3.7 \pm 2.1$	CDF Run II	943	[81]	all jets, TM+ME($W \rightarrow jj$)
$172.9 \pm 1.2 \pm 1.5$	CDF Run I+II	110-2000	[82]	CDF Combined
$171.2 \pm 1.2 \pm 1.8^*$	CDF,DØ (I+II)	110-1000		publ. results, PDG best
$172.6 \pm 0.8 \pm 1.1^{**}$	CDF,DØ (I+II)	110-2100	[61]	publ. or prelim. results

* PDG uses this TevEWWG result as its best value. It is a combination of published Run I + II measurements, yielding a χ^2 of 10.6 for 10 deg. of freedom.

**The TevEWWG world average is a combination of published Run-I and preliminary or published Run-II measurements, yielding a χ^2 of 6.9 for 11 deg. of freedom.

$\eta(\nu)$ is used plus a fit to the scalar sum of transverse energies (H_T), which is sensitive to the top mass.

In the all-jets channel, there is no unknown neutrino momentum to deal with, but the S/B is the poorest. Both CDF and DØ use events with 6 or more jets, of which at least one is b -tagged. In addition, both experiments have employed a neural network selection, based on an array of kinematic variables to improve the S/B. At DØ, a top-quark mass is reconstructed from the jet-quark combination that best fits the hadronic W -mass constraint and the equal-mass constraint for the two top quarks. At CDF, the top-quark mass for each event was reconstructed applying the same fitting technique used in the ℓ +jets mode. In the most recent analysis, the *in situ* jet-energy scale calibration from the $W \rightarrow jj$ fit is also used. At both CDF and DØ, the resulting mass distribution is compared to Monte Carlo templates for various top-quark masses and the background distribution, and a maximum likelihood technique is used to extract the final measured value of m_t and its uncertainty.

DØ also measures the top-quark mass via comparison of the $t\bar{t}$ production cross section with the Standard Model expectation [60]. This method has the advantage that it is very simple and sensitive to the top quark pole mass, which is a very well defined concept. The fully-inclusive cross-section calculation, used for comparison, contains current best theoretical knowledge with reduced-scheme or scale-dependence.

Recent results are shown in Table 2. See the Top Quark Listings for a complete set of published results. The systematic uncertainty (second uncertainty shown) is comparable to the statistical uncertainty, and is primarily due to uncertainties in the jet-energy scale and in the Monte Carlo modeling. In the Run-II analyses, CDF and DØ have controlled the jet-energy scale uncertainty via *in situ* $W \rightarrow jj$ calibration using the same $t\bar{t}$ events, as mentioned above.

The Tevatron Electroweak Working Group (TevEWWG), responsible for the combined CDF/DØ average top mass in Table 2, took account of correlations between systematic uncertainties in the different measurements in a sophisticated

Quark Particle Listings

t

manner [61]. The Particle Data Group (PDG) uses their combination of published Run-I and Run-II top-mass measurements, $m_t = 171.2 \pm 2.1 \text{ GeV}/c^2$ (statistical and systematic uncertainties combined in quadrature), as the PDG best value. The latest TevEWWG world average [61], also including published and some preliminary Run-II results, yields $m_t = 172.6 \pm 1.4 \text{ GeV}/c^2$ (statistical and systematic uncertainties combined in quadrature).

Given the experimental technique used to extract the top mass, these mass values should be taken as representing the top *pole mass* (see the review “Note on Quark Masses” in this *Review* for more information). The top pole mass, like any quark mass, is defined up to an intrinsic ambiguity of order $\Lambda_{QCD} \sim 200 \text{ MeV}$ [62]. Ultimately, the precision of the mass measurements will be limited by the theoretical understanding of the relation between the observables and the theoretical definition of the mass.

Current global fits performed within the SM or its minimal supersymmetric extension, in which the top-mass measurements play a crucial role, provide indications for a relatively light Higgs (see “ H^0 Indirect Mass Limits” in the Particle Listings of this *Review* for more information). Such fits, including Z -pole data [63] and direct measurements of the mass and width of the W -boson, yield $m_t = 179_{-9}^{+12} \text{ GeV}/c^2$ [64]. A fit including additional electroweak precision data (see the review “Electroweak Model and Constraints on New Physics” in this *Review*) yields $m_t = 174.7_{-7.8}^{+10.0} \text{ GeV}/c^2$ (OUR EVALUATION). Both indirect evaluations are in good agreement with the direct top-quark mass measurements.

C.4 Top Quark Electric Charge: The top quark is the only quark whose electric charge has not been measured through production at threshold in e^+e^- collisions. Since the CDF and DØ analyses on top quark production do not associate the b , \bar{b} , and W^\pm uniquely to the top or antitop, decays such as $t \rightarrow W^+\bar{b}, \bar{t} \rightarrow W^-b$ are not excluded. A charge $4/3$ quark of this kind would be consistent with current electroweak precision data. The $Z \rightarrow \ell^+\ell^-$ and $Z \rightarrow b\bar{b}$ data can be fitted with a top quark of mass $m_t = 270 \text{ GeV}/c^2$, provided that the right-handed b quark mixes with the isospin $+1/2$ component of an exotic doublet of charge $-1/3$ and $-4/3$ quarks, $(Q_1, Q_4)_R$ [24,85]. CDF and DØ study the top quark charge in double-tagged lepton+jets events and (CDF) single-tagged dilepton events. Assuming the top and antitop quarks have equal but opposite electric charge, then reconstructing the charge of the b -quark through jet charge discrimination techniques, the $|Q_{top}| = 4/3$ and $|Q_{top}| = 2/3$ scenarios can be differentiated. For the exotic model of Chang [85] with a top-quark charge $|Q_{top}| = 4/3$, DØ yields a p -value, corresponding to the probability of consistency with the exotic model, of 7.8% [86]. CDF excludes the model at 87% C.L. [87]. While these two results are not directly comparable, they both indicate that the top quark is indeed consistent with being a Standard Model $|Q_{top}| = 2/3$ quark.

C.5 Top Branching Ratio & $|V_{tb}|$: CDF and DØ report direct measurements of the $t \rightarrow Wb$ branching ratio [88–89]. Comparing the number of events with 0, 1 and 2 tagged b jets in the lepton+jets channel, and for CDF also in the dilepton channel, and using the known b -tagging efficiency, the ratio $R = B(t \rightarrow Wb) / \sum_{q=d,s,b} B(t \rightarrow Wq)$ can be extracted. DØ performs a simultaneous fit for the number of $t\bar{t}$ events and the ratio R . A deviation of R from unity would imply either non-SM top decay, a non-SM background to $t\bar{t}$ production, or a fourth generation of quarks. Assuming that all top decays have a W boson in the final state, that only three generations of fermions exist, and that the CKM matrix is unitary, CDF and DØ also extract the CKM matrix-element $|V_{tb}|$. The results of recent measurements are summarized in Table 3.

Table 3: Measurements and 95% C.L. lower limits of $R = B(t \rightarrow Wb)/B(t \rightarrow Wq)$ and indirect $|V_{tb}|$ from CDF and DØ. The direct measurements of $|V_{tb}|$ from the single-top analyses are shown in the bottom of the table. A complete set of published results can be found in the Listings.

R or $ V_{tb} $	Source	$\int \mathcal{L} dt$ (pb $^{-1}$)	Ref.
$R = 0.97_{-0.08}^{+0.09}$	DØ Run II	900	[29]
$R > 0.79$	DØ Run II	900	[29]
$ V_{tb} > 0.89$	DØ Run II	900	[29]
$ V_{tb} = 0.88 \pm 0.16$	CDF Run II	2200	[48]
$ V_{tb} = 1.3 \pm 0.2$	DØ Run II	900	[46]

C.6 W -Boson Helicity: Studies of decay angular distributions provide a direct check of the $V-A$ nature of the Wtb coupling and information on the relative coupling of longitudinal and transverse W bosons to the top quark. In the SM, the fraction of decays to longitudinally polarized W bosons is expected to be [90] $\mathcal{F}_0^{\text{SM}} = x/(1+x)$, $x = m_t^2/2M_W^2$ ($\mathcal{F}_0^{\text{SM}} \sim 70\%$ for $m_t = 175 \text{ GeV}/c^2$). Fractions of left- or right-handed W bosons are denoted as \mathcal{F}_- and \mathcal{F}_+ , respectively. In the SM, \mathcal{F}_- is expected to be $\approx 30\%$ and $\mathcal{F}_+ \approx 0\%$. CDF and DØ use various techniques to measure the helicity of the W boson in top quark decays, in both the lepton+jets events and dilepton channels. The first method uses a kinematic fit, similar to that used in the lepton+jets mass analyses, but with the top quark mass constrained to $175 \text{ GeV}/c^2$, to improve the reconstruction of final-state observables, and render the under-constrained dilepton channel solvable. The distribution of the helicity angle ($\cos\theta^*$) between the lepton and the b quark in the W rest frame provides the most direct measure of the W helicity. The second method (p_T^ℓ) uses the different lepton p_T spectra from longitudinally or transversely polarized W -decays to determine the relative contributions. A third method uses the invariant mass of the lepton and the b -quark in top decays ($M_{\ell b}^2$) as an observable, which is directly related to $\cos\theta^*$. Finally, the Matrix Element method (ME) has also been used, in which a likelihood

is formed from a product of event probabilities calculated from the ME for a given set of measured kinematic variables and assumed W -helicity fractions. The results of recent CDF and $D\bar{O}$ analyses are summarized in Table 4; a complete set of published results can be found in the Listings. All results are in agreement with the SM expectation.

Table 4: Measurement and 95% C.L. upper limits of the W helicity in top quark decays. Published results are given in the Listings. Results listed are preliminary and not yet submitted for publication, as of March 2008.

W Helicity	Source	$\int \mathcal{L} dt$ (pb^{-1})	Ref.	Method
$\mathcal{F}_0 = 0.66 \pm 0.12$	CDF Run II	1900	[91]	$\cos \theta^*$
$\mathcal{F}_0 = 0.64 \pm 0.11$	CDF Run II	1900	[92]	ME
$\mathcal{F}_+ < 0.07 @ 95\% \text{ C.L.}$	CDF Run II	1900	[93]	$\cos \theta^*$

C.7 $t\bar{t}$ Spin Correlations & Top Width: $D\bar{O}$ has searched for evidence of spin correlation of $t\bar{t}$ pairs [94]. The t and \bar{t} are expected to be unpolarized, but to be correlated in their spins. Since top quarks decay before hadronizing, their spins at production are transmitted to their decay-daughter particles. Spin correlation is studied by analyzing the joint decay angular distribution of one t daughter and one \bar{t} daughter. The sensitivity to top spin is greatest when the daughters are down-type fermions (charged leptons or d -type quarks), in which case, the joint distribution is [95–97]

$$\frac{1}{\sigma} \frac{d^2\sigma}{d(\cos\theta_+)d(\cos\theta_-)} = \frac{1 + \kappa \cdot \cos\theta_+ \cdot \cos\theta_-}{4}, \quad (2)$$

where θ_+ and θ_- are the angles of the daughters in the top rest frames with respect to a particular spin quantization axis, the optimal choice being the off-diagonal basis [95]. In this basis, the SM predicts maximum correlation with $\kappa = 0.88$ at the Tevatron. In Run I, $D\bar{O}$ analyzed six dilepton events, and obtained a likelihood as a function of κ , which weakly favored the SM ($\kappa = 0.88$) over no correlation ($\kappa = 0$) or anticorrelation ($\kappa = -1$, as would be expected for $t\bar{t}$ produced via an intermediate scalar). $D\bar{O}$ quotes a limit $\kappa > -0.25$ at 68% C.L.

Related to the measurement of top-spin correlations, which require a top lifetime less than the hadronization timescale, is the measurement of the top width. The top width is expected to be of order 1 GeV/c^2 (Eq. 1). The sensitivity of current experiments does not approach this level, but CDF has made the first direct measurement of the top width using the mass fitting template method in lepton+jets events, fixing the top mass at 175 GeV/c^2 and varying the top width in constructing the Monte Carlo templates. The top width is found to be less than 12.7 GeV/c^2 at the 95% C.L. [98].

C.8 Non-SM $t\bar{t}$ Production: Motivated by the large mass of the top quark, several models suggest that the top quark plays a role in the dynamics of electroweak symmetry breaking. One example is topcolor [21], where a large top quark mass can be generated through the formation of a dynamic $t\bar{t}$ condensate, X , which is formed by a new strong gauge force coupling preferentially to the third generation. Another example is topcolor-assisted technicolor [22], predicting a heavy Z' boson that couples preferentially to the third generation of quarks with cross sections expected to be visible at the Tevatron. CDF and $D\bar{O}$ have searched for $t\bar{t}$ production via intermediate, narrow-width, heavy-vector bosons X in the lepton+jets channels. The possible $t\bar{t}$ production via an intermediate resonance X is sought for as a peak in the spectrum of the invariant $t\bar{t}$ mass. CDF and $D\bar{O}$ exclude narrow-width heavy-vector bosons X in the top-assisted technicolor model [99], with mass $M_X < 480 \text{ GeV}/c^2$ and $M_X < 560 \text{ GeV}/c^2$, respectively, in Run I [25,26], and $M_X < 725 \text{ GeV}/c^2$ and $M_X < 760 \text{ GeV}/c^2$ in Run II [44,45]. With 955 pb^{-1} of Run-II data, CDF has produced a less model-dependent limit for a narrow-width Z' , ruling out at the 95% C.L. a contribution greater than 0.7 pb for a Z' heavier than 700 GeV/c^2 decaying to $t\bar{t}$ [100]; $D\bar{O}$ excludes at the 95% C.L. that the $t\bar{t}$ signal is entirely produced through a Z' resonance for $550 < m_{Z'} < 1000 \text{ GeV}/c^2$ [20]. A recent CDF analysis has placed limits on the coupling strength of a massive gluon to $t\bar{t}$ [101]. In 1 fb^{-1} , $D\bar{O}$ has set limits on scalar top-quark pair production, with subsequent decays to top quarks in the lepton+jets channel [42].

C.9 Non-SM Top Decays: Both CDF and $D\bar{O}$ have searched for non-SM top decays [102–105], particularly those expected in supersymmetric models, such as $t \rightarrow H^+b$, followed by $H^+ \rightarrow \tau^+\bar{\nu}$ or $c\bar{s}$. The $t \rightarrow H^+b$ branching ratio has a minimum at $\tan\beta = \sqrt{m_t/m_b} \simeq 6$, and is large in the region of either $\tan\beta \ll 6$ or $\tan\beta \gg 6$. In the former range, $H^+ \rightarrow c\bar{s}$ is dominant, while $H^+ \rightarrow \tau^+\bar{\nu}$ dominates in the latter range. These studies are based either on direct searches for these final states, or on top “disappearance.” In the standard lepton+jets or dilepton cross-section analyses, any charged-Higgs decays are not detected as efficiently as $t \rightarrow W^\pm b$, primarily because the selection criteria are optimized for the standard decays, and because of the absence of energetic isolated leptons in Higgs decays. A significant $t \rightarrow H^+b$ contribution would give rise to measured $t\bar{t}$ cross sections that would be lower than the prediction from the SM (assuming that non-SM contributions to $t\bar{t}$ production are negligible), and the measured cross-section ratio $\sigma_{t\bar{t}}^{\ell^+ \text{jets}} / \sigma_{t\bar{t}}^{\ell\ell}$ would differ from unity.

In Run II, CDF has searched for charged-Higgs production in dilepton, lepton+jets, and lepton+hadronic tau final states, considering possible H^+ decays to $c\bar{s}$, $\tau\bar{\nu}$, t^*b , or W^+h^0 , in addition to the Standard Model decay $t \rightarrow W^+b$ [104]. Depending on the top and Higgs-decay branching ratios, which are scanned in a particular 2-Higgs doublet benchmark model, the number of expected events in these decay channels can show an

Quark Particle Listings

t

excess or deficit when compared to SM expectations. A model-independent interpretation yields a limit of $B(t \rightarrow H^\pm b) < 0.91$ at 95% C.L. for $m_{H^\pm} \approx 100$ GeV, and $B(t \rightarrow H^\pm b) < 0.4$ in the tauonic model with $B(H^\pm \rightarrow \tau\nu) = 100\%$ [104]. The DØ collaboration interprets their measured cross-section ratio $\sigma_{t\bar{t}}^{\ell+jets}/\sigma_{t\bar{t}}^{\ell\ell} = 1.21_{-0.26}^{+0.27}$ using 1 fb^{-1} in a model with a charged Higgs boson of mass $80 \text{ GeV}/c^2$ and the exclusive decay $H^+ \rightarrow c\bar{s}$, finding a limit of $B(t \rightarrow H^\pm b) < 0.35$ at 95% C.L. [105].

More details, and the results of these studies for the exclusion in the $m_{H^\pm}, \tan\beta$ plane, can be found in the review ‘‘Search for Higgs bosons’’ and in the ‘‘ H^+ Mass Limits’’ section of the Higgs Particle Listings of the current edition.

In the Standard Model, the top-quark lifetime is expected to be about $0.5 \times 10^{-24} \text{ s}$ ($c\tau_t \approx 3 \times 10^{-10} \mu\text{m}$), while additional quark generations, non-standard top-quark decays, or other extensions of the Standard Model could yield long-lived top quarks in the data. CDF has studied the top-quark lifetime by measuring the distance between the initial $p\bar{p}$ scattering and the leptonic W^\pm decay vertex in lepton+jets events [106]. The measured lifetime is consistent with zero, and an upper limit $c\tau_t < 52.5 \mu\text{m}$ is found at 95% C.L.

In 230 pb^{-1} of Run-II data, DØ uses their single-top analysis to place limits on anomalous single-top quark production via the flavor-changing neutral-current (FCNC) coupling of a gluon to the top quark and a charm (tcg) or up quark (tug) [107], or via the decay of a heavy W' boson to a top quark and a bottom quark in 900 pb^{-1} [108]. The observed limits are at 95% C.L.: $\kappa_g^c/A < 0.15 \text{ TeV}^{-1}$ and $\kappa_g^u/A < 0.037 \text{ TeV}^{-1}$. DØ excludes the production of W' bosons with masses below 731 GeV for a W' boson with standard-model-like couplings, below 739 GeV for a W' boson with right-handed couplings that is allowed to decay to both leptons and quarks, and below 768 GeV for a W' boson with right-handed couplings that is only allowed to decay to quarks. CDF has recently released W' limits also using the single-top analysis [109]. In 1900 pb^{-1} of Run-II data, a W' with Standard-Model couplings is searched for in the $t\bar{b}$ decay mode. Masses below 800 GeV are excluded, assuming that any right-handed neutrino is lighter than the W' , and below 825 GeV if the right-handed neutrino is heavier than the W' .

CDF reported a search for flavor-changing neutral-current (FCNC) decays of the top quark $t \rightarrow q\gamma$ and $t \rightarrow qZ$ in the Run-I data [110], and recently with enhanced sensitivity in Run II [111]. The SM predicts such small rates that any observation would be a sign of new physics. CDF assumes that one top decays via FCNC, while the other decays via Wb . The Run-I analysis included a $t \rightarrow q\gamma$ search in which two signatures are examined, depending on whether the W decays leptonically or hadronically. For leptonic W decay, the signature is $\gamma\ell$ and missing E_T and two or more jets, while for hadronic W decay, it is $\gamma+$ ≥ 4 jets. In either case, one of the jets must have a secondary vertex b tag. One event is observed ($\mu\gamma$) with an expected background of less than half an event, giving an upper limit on the top branching ratio of $B(t \rightarrow q\gamma) < 3.2\%$ at 95%

C.L. In the search for $t \rightarrow qZ$, CDF considers $Z \rightarrow \mu\mu$ or ee and $W \rightarrow qq'$, giving a $Z +$ four jets signature. A Run-II dataset of 1900 pb^{-1} is found consistent with background expectations and a 95% C.L. on the $t \rightarrow qZ$ branching fraction of $< 3.7\%$ (for $M_{\text{top}}=175 \text{ GeV}/c^2$) is set.

Constraints on FCNC couplings of the top quark can also be obtained from searches for anomalous single-top production in e^+e^- collisions, via the process $e^+e^- \rightarrow \gamma, Z^* \rightarrow t\bar{q}$ and its charge-conjugate ($q = u, c$), or in $e^\pm p$ collisions, via the process $e^\pm u \rightarrow e^\pm t$. For a leptonic W decay, the topology is at least a high- p_T lepton, a high- p_T jet and missing E_T , while for a hadronic W -decay, the topology is three high- p_T jets. Limits on the cross section for this reaction have been obtained by the LEP collaborations [112] in e^+e^- collisions, and by H1 [113] and ZEUS [114] in $e^\pm p$ collisions. When interpreted in terms of branching ratios in top decay [115,116], the LEP limits lead to typical 95% C.L. upper bounds of $B(t \rightarrow qZ) < 0.137$, which are stronger than the direct CDF limit. Assuming no coupling to the Z boson, the 95% C.L. limits on the anomalous FCNC coupling $\kappa_\gamma < 0.17$ and < 0.27 by ZEUS and H1, respectively, are stronger than the CDF limit of $\kappa_\gamma < 0.42$, and improve over LEP sensitivity in that domain. The H1 limit is slightly weaker than the ZEUS limit due to an observed excess of five-candidates events over an expected background of 1.31 ± 0.22 . If this excess is attributed to FCNC top-quark production, this leads to a total cross section of $\sigma(ep \rightarrow e + t + X, \sqrt{s} = 319 \text{ GeV}) = 0.29_{-0.14}^{+0.15} \text{ pb}$ [113,117].

Appendix. Expected Sensitivity at the LHC:

The top pair-production cross section at the LHC is predicted at NLO to be about 800 pb [118]. There will be 8 million $t\bar{t}$ pairs produced per year at a luminosity of $10^{33} \text{ cm}^{-2} \text{ s}^{-1}$. Such large event samples will permit precision measurements of the top-quark parameters. The statistical uncertainties on m_t will become negligible, and systematic uncertainties better than $\pm 2 \text{ GeV}/c^2$ per channel are anticipated [119–121].

Precision measurements of the top pair-production cross section are expected to be limited by the estimated 3-10% accuracy on the luminosity determination [119,120], but far more accurate measurements would be available from the ratio of the $t\bar{t}$ production to inclusive W or Z production.

Single-top production will also be of keen interest at the LHC, where a $|V_{tb}|$ measurement at the 5% level per experiment is projected with 10 fb^{-1} [119,120].

Tests of the $V-A$ nature of the tWb vertex through a measurement of the W helicity will be extended from the Tevatron to the LHC. Current estimates are that the longitudinal fraction can be measured with a precision of about 5% [120] with 10 fb^{-1} of data.

Top-antitop spin correlations should be relatively easy to observe and measure at the LHC, where the preferred dilepton mode will have large event samples, despite the small branching fraction. At the LHC, where $t\bar{t}$ is dominantly produced through gluon fusion, the correlation is such that the top quarks are

See key on page 373

mainly either both left- or both right-handed. The CMS collaboration [120] estimates that the relative asymmetry (defined as the difference in the fraction of like-handed and the fraction of oppositely-handed $t\bar{t}$ pairs) can be measured to about 17% accuracy with 10 fb^{-1} of data.

In addition to these SM measurements, the large-event samples will allow sensitive searches for new physics. The search for heavy resonances that decay to $t\bar{t}$, already begun at the Tevatron, will acquire enhanced reach both in mass and $\sigma \cdot B$. The ATLAS collaboration [119] has studied the reach for a 5σ discovery of a narrow resonance decaying to $t\bar{t}$. With 30 fb^{-1} , it is estimated that a resonance can be discovered at $4 \text{ TeV}/c^2$ for $\sigma \cdot B = 10 \text{ fb}$, and at $1 \text{ TeV}/c^2$ for $\sigma \cdot B = 1000 \text{ fb}$. FCNC decays, $t \rightarrow Zq, \gamma q, gq$, can take place in the SM, or in the MSSM, but at rates too small to be observed even at the LHC. As such, searches for these decay modes can provide sensitive tests of other extensions of the SM [119,120].

References

CDF note references can be retrieved from www-cdf.fnal.gov/physics/new/top/top.html, and DØ note references from www-d0.fnal.gov/Run2Physics/WWW/documents/Run2Results.htm.

1. M. Cacciari *et al.*, JHEP **04**, 68 (2004); N. Kidonakis and R. Vogt, Phys. Rev. **D68**, 114014 (2003).
2. S. Cortese and R. Petronzio, Phys. Lett. **B253**, 494 (1991).
3. S. Willenbrock and D. Dicus, Phys. Rev. **D34**, 155 (1986).
4. B.W. Harris *et al.*, Phys. Rev. **D66**, 054024 (2002); Z. Sullivan, Phys. Rev. **D70**, 114012 (2004); N. Kidonakis Phys. Rev. **D74**, 114012 (2006).
5. M. Jeżabek and J.H. Kühn, Nucl. Phys. **B314**, 1 (1989).
6. I.I.Y. Bigi *et al.*, Phys. Lett. **B181**, 157 (1986).
7. A. Czarnecki and K. Melnikov, Nucl. Phys. **B544**, 520 (1999); K.G. Chetyrkin *et al.*, Phys. Rev. **D60**, 114015 (1999).
8. F. Abe *et al.* (CDF Collab.), Phys. Rev. Lett. **80**, 5720 (1998).
9. V.M. Abazov *et al.* (DØ Collab.), DØ conference note 5057 (2006).
10. A. Abulencia *et al.* (CDF Collab.), Phys. Rev. Lett. **96**, 022004 (2006); Phys. Rev. **D73**, 032003 (2006); Phys. Rev. **D73**, 092002 (2006).
11. V.M. Abazov *et al.* (DØ Collab.), Phys. Rev. **D79**, 092005 (2006); V.M. Abazov *et al.* (DØ Collab.), Phys. Rev. **D79**, 092001 (2007).
12. T. Tait and C.-P. Yuan, Phys. Rev. **D63**, 014018 (2001).
13. S. Frixione and B. Webber, hep-ph/0402116; S. Frixione and B. Webber, JHEP **06**, 029 (2002); S. Frixione, P. Nason and B. Webber, JHEP **08**, 007 (2003); S. Frixione, P. Nason and G. Ridolfi, hep-ph/07073088.
14. J.M. Campbell and R.K. Ellis, Phys. Rev. **D62**, 114012 (2000), Phys. Rev. **D65**, 113007 (2002); J.M. Campbell and J. Huston, Phys. Rev. **D70**, 094021 (2004).
15. A. Abulencia *et al.* (CDF Collab.), Phys. Lett. **B639**, 172 (2006).
16. DØ Collab., DØ conference note 5451 (2007).
17. DØ Collab., DØ conference note 5234 (2006).
18. J.H. Kühn and G. Rodrigo, Phys. Rev. Lett. **81**, 49 (1998); M.T. Bowen *et al.*, hep-ph/0509267; S. Dittmaier *et al.*, hep-ph/0703120.
19. CDF Collab., CDF conference notes 9156 & 9169 (2007).
20. V.M. Abazov *et al.* (DØ Collab.), hep-ex/0712.0851, Submitted to Phys. Rev. Lett.
21. C.T. Hill, Phys. Lett. **B266**, 419 (1991).
22. C.T. Hill, Phys. Lett. **B345**, 483 (1995).
23. C.T. Hill and S.J. Park, Phys. Rev. **D49**, 4454 (1994); H.P. Nilles, Phys. Reports **110**, 1 (1984); H.E. Haber and G.L. Kane, Phys. Reports **117**, 75 (1985); E.H. Simmons, Thinking About Top: Looking Outside The Standard Model, hep-ph/9908511, and references therein; E.H. Simmons, The Top Quark: Experimental Roots and Branches of Theory, hep-ph/0211335, and references therein.
24. D. Choudhury, T.M.P. Tait, and C.E.M. Wagner, Phys. Rev. **D65**, 053002 (2002).
25. T. Affolder *et al.* (CDF Collab.), Phys. Rev. Lett. **85**, 2062 (2000).
26. V.M. Abazov *et al.* (DØ Collab.), Phys. Rev. Lett. **92**, 221801 (2004).
27. T. Affolder *et al.* (CDF Collab.), Phys. Rev. Lett. **87**, 102001 (2001).
28. B. Abbott *et al.* (DØ Collab.), Phys. Rev. **D58**, 052001 (1998); S. Abachi *et al.* (DØ Collab.), Phys. Rev. Lett. **79**, 1197 (1997).
29. V.M. Abazov *et al.* (DØ Collab.), hep-ex/0801.1326, Submitted to Phys. Rev. Lett.
30. DØ Collab., DØ conference note 5257 (2006).
31. DØ Collab., DØ conference note 5477 (2007).
32. DØ Collab., DØ conference note 4906 (2005).
33. CDF Collab., CDF conference note 8795 (2007).
34. CDF Collab., CDF conference note 8565 (2006).
35. CDF Collab., CDF conference note 8092 (2006).
36. CDF Collab., CDF conference note 8802 (2007).
37. CDF Collab., CDF conference note 8770 (2007).
38. CDF Collab., CDF conference note 8912 (2007).
39. CDF Collab., CDF conference note 8402 (2007).
40. CDF Collab., CDF conference note 8148 (2006).
41. D. Acosta *et al.* (CDF Collab.), Phys. Rev. Lett. **95**, 022001 (2005).
42. DØ Collab., DØ conference note 5438 (2007).
43. CDF Collab., CDF conference note 9157 (2007).
44. CDF Collab., CDF conference note 8087 (2006).
45. DØ Collab., DØ conference note 5600 (2008).
46. V.M. Abazov *et al.* (DØ Collab.), Phys. Rev. Lett. **98**, 181802 (2007).
47. V.M. Abazov *et al.* (DØ Collab.), hep-ex/0803.0739, Submitted to Phys. Rev. D.
48. CDF Collab., conference note 9251 (2008).
49. F. Abe *et al.* (CDF Collab.), Phys. Rev. **D50**, 2966 (1994); F. Abe *et al.* (DØ Collab.), Phys. Rev. Lett. **74**, 2626 (1995); S. Abachi *et al.* (DØ Collab.), Phys. Rev. Lett. **74**, 2632 (1995).
50. K. Kondo *et al.*, J. Phys. Soc. Jpn. **G62**, 1177 (1993).

Quark Particle Listings

t

51. R.H. Dalitz and G.R. Goldstein, Phys. Rev. **D45**, 1531 (1992); Phys. Lett. **B287**, 225 (1992); Proc. Royal Soc. London **A445**, 2803 (1999).
52. P. Abreu *et al.* (DELPHI Collab.), Eur. Phys. J. **C2**, 581 (1998).
53. V.M. Abazov *et al.* (DØ Collab.), Phys. Rev. **D75**, 092001 (2007).
54. A. Abulencia *et al.* (CDF Collab.), Phys. Rev. **D75**, 071102 (2007).
55. L. Sonnenschein, Phys. Rev. D 73.054015(2006).
56. B. Abbott *et al.* (DØ Collab.), Phys. Rev. Lett. **80**, 2063 (1998); B. Abbott *et al.* (DØ Collab.), Phys. Rev. **D60**, 052001 (1999).
57. F. Abe *et al.* (CDF Collab.), Phys. Rev. Lett. **82**, 271 (1999).
58. A. Abulencia *et al.* (CDF Collab.), Phys. Rev. **D73**, 112006 (2006).
59. CDF Collab., CDF conference note 8959 (2007).
60. DØ Collab., DØ conference note 5459 (2007).
61. The Tevatron Electroweak Working Group, For the CDF and DØ Collaborations, [arXiv:0803.1683](https://arxiv.org/abs/0803.1683).
62. M. Smith and S. Willenbrock, Phys. Rev. Lett. **79**, 3825 (1997).
63. ALEPH, DELPHI, L3, OPAL, SLD and Working Groups, Phys. Reports **427**, 257 (2006).
64. The LEP Collaborations: ALEPH, DELPHI, L3, OPAL Collaborations, and the LEP Electroweak Working Group, [hep-ex/07120929](https://arxiv.org/abs/hep-ex/07120929).
65. DØ Collab., DØ conference note 5498 (2007).
66. B. Abbott *et al.* (DØ Collab.), Phys. Rev. **D60**, 052001 (1999); B. Abbott *et al.* (DØ Collab.), Phys. Rev. Lett. **80**, 2063 (1998).
67. V.M. Abazov *et al.* (DØ Collab.), Phys. Lett. **B606**, 25 (2005).
68. DØ Collab., DØ conference note 4728 (2005).
69. DØ Collab., DØ conference note 5610 (2008).
70. DØ Collab., DØ conference note 5032 (2005).
71. DØ Collab., DØ conference note 5200 (2006).
72. DØ Collab., DØ conference note 5460 (2007).
73. F. Abe *et al.* (CDF Collab.), Phys. Rev. Lett. **80**, 2767 (1998).
74. T. Affolder *et al.* (CDF Collab.), Phys. Rev. **D63**, 032003 (2001).
75. F. Abe *et al.* (CDF Collab.), Phys. Rev. Lett. **79**, 1992 (1997).
76. CDF Collab., CDF conference note 9196 (2008).
77. CDF Collab., CDF conference note 9206 (2008).
78. CDF Collab., CDF conference note 9130 (2007).
79. CDF Collab., CDF conference note 9048 (2007).
80. CDF Collab., CDF conference note 9165 (2007).
81. CDF Collab., CDF conference note 8709 (2007).
82. CDF Collab., CDF conference note 9214 (2008).
83. CDF Collab., CDF conference note 8090 (2006).
84. CDF Collab., CDF conference note 8118 (2006).
85. D. Chang, W.F. Chang, and E. Ma, Phys. Rev. **D59**, 091503 (1999), Phys. Rev. **D61**, 037301 (2000).
86. V.M. Abazov *et al.* (DØ Collab.), Phys. Rev. Lett. **98**, 04181 (2007).
87. CDF Collab., CDF conference note 8967 (2007).
88. T. Affolder *et al.* (CDF Collab.), Phys. Rev. Lett. **86**, 3233 (2001).
89. V.M. Abazov *et al.* (DØ Collab.), Phys. Lett. **B639**, 616 (2006).
90. G.L. Kane, G.A. Ladinsky, and C.P. Yuan, Phys. Rev. **D45**, 124 (1992).
91. CDF Collab., CDF conference note 9114 (2007).
92. CDF Collab., CDF conference note 9144 (2007).
93. CDF Collab., CDF conference note 9215 (2008).
94. B. Abbott *et al.* (DØ Collab.), Phys. Rev. Lett. **85**, 256 (2000).
95. G. Mahlon and S. Parke, Phys. Rev. **D53**, 4886 (1996); G. Mahlon and S. Parke, Phys. Lett. **B411**, 173 (1997).
96. G.R. Goldstein, in *Spin 96: Proceedings of the 12th International Symposium on High Energy Spin Physics*, Amsterdam, 1996, ed. C.W. Jager (World Scientific, Singapore, 1997), p. 328.
97. T. Stelzer and S. Willenbrock, Phys. Lett. **B374**, 169 (1996).
98. CDF Collab., CDF conference note 8953 (2007).
99. R.M. Harris, C.T. Hill, and S.J. Parke, [hep-ph/9911288](https://arxiv.org/abs/hep-ph/9911288) (1995).
100. CDF Collab., CDF conference note 8675 (2007).
101. CDF collab., CDF conference note 9164 (2007).
102. F. Abe *et al.* (CDF Collab.), Phys. Rev. Lett. **79**, 357 (1997); T. Affolder *et al.* (CDF Collab.), Phys. Rev. **D62**, 012004 (2000).
103. B. Abbott *et al.* (DØ Collab.), Phys. Rev. Lett. **82**, 4975 (1999); V.M. Abazov *et al.* (DØ Collab.), Phys. Rev. Lett. **88**, 151803 (2002).
104. A. Abulencia *et al.* (CDF Collab.), Phys. Rev. Lett. **96**, 042003 (2006).
105. DØ Collab., DØ conference note 5466 (2007).
106. CDF Collab., CDF conference note 8104 (2006).
107. V.M. Abazov *et al.* (DØ Collab.), Phys. Rev. Lett. **99**, 191802 (2007).
108. V.M. Abazov *et al.* (DØ Collab.), [hep-ex/0803.3256](https://arxiv.org/abs/hep-ex/0803.3256), Submitted to Phys. Rev. Lett.
109. CDF Collab., CDF conference note 9150 (2008).
110. F. Abe *et al.* (CDF Collab.), Phys. Rev. Lett. **80**, 2525 (1998).
111. CDF Collab., CDF conference note 9202 (2008).
112. A. Heister *et al.* (ALEPH Collab.), Phys. Lett. **B543**, 173 (2002); J. Abdallah *et al.* (DELPHI Collab.), Phys. Lett. **B590**, 21 (2004); P. Achard *et al.* (L3 Collab.), Phys. Lett. **B549**, 290 (2002); G. Abbiendi *et al.* (OPAL Collab.), Phys. Lett. **B521**, 181 (2001).
113. A. Aktas *et al.* (H1 Collab.), Eur. Phys. J. **C33**, 9 (2004).
114. S. Chekanov *et al.* (ZEUS Collab.), Phys. Lett. **B559**, 153 (2003).
115. M. Beneke, *et al.*, [hep-ph/0003033](https://arxiv.org/abs/hep-ph/0003033), in *Proceedings of 1999 CERN Workshop on Standard Model Physics (and more) at the LHC*, G. Altarelli and M.L. Mangano eds.

116. V.F. Obraztsov, S.R. Slabospitsky, and O.P. Yushchenko, Phys. Lett. **B426**, 393 (1998).
117. T. Carli, D. Dannheim, and L. Bellagamba, Mod. Phys. Lett. **A19**, 1881 (2004).
118. R. Bonciani *et al.*, Nucl. Phys. **B529** 424 (1998).
119. The ATLAS Collaboration, *ATLAS Detector and Physics Performance TDR, Volume II*, CERN/LHCC 99-14/15.
120. The CMS Collaboration, *CMS Detector and Physics Performance TDR, Volume II*, CERN/LHCC 2006/021.
121. I. Borjanovic *et al.*, Eur. Phys. J. **C39S2**, 63 (2005).

t-Quark Mass in $p\bar{p}$ Collisions

OUR EVALUATION of $171.2 \pm 1.2 \pm 1.8$ GeV (TEVEWWG 08a) is an average of top mass measurements from Tevatron Run-I (1992–1996) and Run-II (2001–present) that were published at the time of preparing this Review. This average was provided by the Tevatron Electroweak Working Group (TEVEWWG). It takes correlated uncertainties properly into account and has a χ^2 of 10.6 for 10 degrees of freedom. Including the most recent unpublished top mass measurements from Run-II, the TEVEWWG reports an average top mass of $172.6 \pm 0.8 \pm 1.1$ GeV (TEVEWWG 08). See the note “The Top Quark” in these Quark Particle Listings.

For earlier search limits see PDG 96, Physical Review **D54** 1 (1996). We no longer include a compilation of indirect top mass determinations from Standard Model Electroweak fits in the Listings (our last compilation can be found in the Listings of the 2007 partial update). For a discussion of current results see the reviews “The Top Quark” and “Electroweak Model and Constraints on New Physics.”

VALUE (GeV)	DOCUMENT ID	TECN	COMMENT
171.2 ± 2.1 OUR EVALUATION	See comments in the header above.		
174.0 ± 2.2 ± 4.8	¹ AALTONEN	07D CDF	≥ 6 jets, vtx <i>b</i> -tag
170.8 ± 2.2 ± 1.4	^{2,3} AALTONEN	07I CDF	lepton + jets (<i>b</i> -tag)
176.2 ± 9.2 ± 3.9	⁴ ABAZOV	07W D0	dilepton (MWT)
179.5 ± 7.4 ± 5.6	⁴ ABAZOV	07W D0	dilepton (μ WT)
164.5 ± 3.9 ± 3.9	^{3,5} ABULENCIA	07D CDF	dilepton
180.7 ^{+15.5} _{-13.4} ± 8.6	⁶ ABULENCIA	07I CDF	lepton + jets
170.3 ^{+4.1} _{-4.5} ± 1.2	^{3,7} ABAZOV	06U D0	lepton + jets (<i>b</i> -tag)
180.1 ± 3.6 ± 3.9	^{8,9} ABAZOV	04G D0	lepton + jets
176.1 ± 5.1 ± 5.3	¹⁰ AFFOLDER	01 CDF	lepton + jets
167.4 ± 10.3 ± 4.8	^{11,12} ABE	99B CDF	dilepton
168.4 ± 12.3 ± 3.6	⁹ ABBOTT	98D D0	dilepton
186 ± 10 ± 5.7	^{11,13} ABE	97R CDF	6 or more jets
• • • We do not use the following data for averages, fits, limits, etc. • • •			
170.7 ^{+4.2} _{-3.9} ± 3.5	^{14,15} AALTONEN	08C CDF	dilepton, $\sigma_{t\bar{t}}$ constrained
177.1 ± 4.9 ± 4.7	^{16,17} AALTONEN	07 CDF	6 jets with ≥ 1 <i>b</i> vtx
172.3 ^{+10.8} _{-9.6} ± 10.8	¹⁸ AALTONEN	07B CDF	≥ 4 jets (<i>b</i> -tag)
173.7 ± 4.4 ^{+2.1} _{-2.0} ± 3.2	^{17,19} ABAZOV	07F D0	lepton + jets
173.2 ^{+2.6} _{-2.4} ± 3.2	^{20,21} ABULENCIA	06D CDF	lepton + jets
173.5 ^{+3.7} _{-3.6} ± 1.3	^{15,20} ABULENCIA	06D CDF	lepton + jets
165.2 ± 6.1 ± 3.4	^{3,22} ABULENCIA	06G CDF	dilepton
170.1 ± 6.0 ± 4.1	^{15,23} ABULENCIA	06V CDF	dilepton
178.5 ± 13.7 ± 7.7	^{24,25} ABAZOV	05 D0	6 or more jets
176.1 ± 6.6	²⁶ AFFOLDER	01 CDF	dilepton, lepton+jets, all-jets
172.1 ± 5.2 ± 4.9	²⁷ ABBOTT	99G D0	di-lepton, lepton+jets
176.0 ± 6.5	^{12,28} ABE	99B CDF	dilepton, lepton+jets, all-jets
173.3 ± 5.6 ± 5.5	^{9,29} ABBOTT	98F D0	lepton + jets
175.9 ± 4.8 ± 5.3	^{11,30} ABE	98E CDF	lepton + jets
161 ± 17 ± 10	¹¹ ABE	98F CDF	dilepton
172.1 ± 5.2 ± 4.9	³¹ BHAT	98B RVUE	dilepton and lepton+jets
173.8 ± 5.0	³² BHAT	98B RVUE	dilepton, lepton+jets, all-jets
173.3 ± 5.6 ± 6.2	⁹ ABACHI	97E D0	lepton + jets
199 ⁺¹⁹ ₋₂₁ ± 22	ABACHI	95 D0	lepton + jets
176 ± 8 ± 10	ABE	95F CDF	lepton + <i>b</i> -jet
174 ± 10 ± 13 ₋₁₂	ABE	94E CDF	lepton + <i>b</i> -jet

¹ Based on 1.02 fb^{-1} of data at $\sqrt{s} = 1.96$ TeV.

² Based on 955 pb^{-1} of data at $\sqrt{s} = 1.96$ TeV. m_t and JES (Jet Energy Scale) are fitted simultaneously, and the first error contains the JES contribution of 1.5 GeV.

³ Matrix element method.

⁴ Based on 370 pb^{-1} of data at $\sqrt{s} = 1.96$ TeV. Combined result of MWT (Matrix-element Weighting Technique) and μ WT (μ Weighting Technique) analyses is $178.1 \pm 6.7 \pm 4.8$ GeV.

⁵ Based on 1.0 fb^{-1} of data at $\sqrt{s} = 1.96$ TeV. ABULENCIA 07D improves the matrix element description by including the effects of initial-state radiation.

⁶ Based on 695 pb^{-1} of data at $\sqrt{s} = 1.96$ TeV. The transverse decay length of the *b* hadron is used to determine m_t , and the result is free from the JES (jet energy scale) uncertainty.

⁷ Based on $\sim 400 \text{ pb}^{-1}$ of data at $\sqrt{s} = 1.96$ TeV. The first error includes statistical and systematic jet energy scale uncertainties, the second error is from the other systematics. The result is obtained with the *b*-tagging information. The result without *b*-tagging is $169.2^{+5.0+1.5}_{-7.4-1.4}$ GeV.

⁸ Obtained by re-analysis of the lepton + jets candidate events that led to ABBOTT 98F. It is based upon the maximum likelihood method which makes use of the leading order matrix elements.

⁹ Based on $125 \pm 7 \text{ pb}^{-1}$ of data at $\sqrt{s} = 1.8$ TeV.

¹⁰ Based on $\sim 106 \text{ pb}^{-1}$ of data at $\sqrt{s} = 1.8$ TeV.

¹¹ Based on $109 \pm 7 \text{ pb}^{-1}$ of data at $\sqrt{s} = 1.8$ TeV.

¹² See AFFOLDER 01 for details of systematic error re-evaluation.

¹³ Based on the first observation of all hadronic decays of $t\bar{t}$ pairs. Single *b*-quark tagging with jet-shape variable constraints was used to select signal enriched multi-jet events. The updated systematic error is listed. See AFFOLDER 01, appendix C.

¹⁴ Reports measurement of $170.7^{+4.2}_{-3.9} \pm 2.6 \pm 2.4$ GeV based on 1.2 fb^{-1} of data at $\sqrt{s} = 1.96$ TeV. The last error is due to the theoretical uncertainty on $\sigma_{t\bar{t}}$. Without the cross-section constraint a top mass of $169.7^{+5.2}_{-4.9} \pm 3.1$ GeV is obtained.

¹⁵ Template method.

¹⁶ Based on 310 pb^{-1} of data at $\sqrt{s} = 1.96$ TeV.

¹⁷ Ideogram method.

¹⁸ Based on 311 pb^{-1} of data at $\sqrt{s} = 1.96$ TeV. Events with 4 or more jets with $E_T > 15$ GeV, significant missing E_T , and secondary vertex *b*-tag are used in the fit. About 44% of the signal acceptance is from $\tau\nu + 4$ jets. Events with identified *e* or μ are vetoed to provide a statistically independent measurement.

¹⁹ Based on 425 pb^{-1} of data at $\sqrt{s} = 1.96$ TeV. The first error is a combination of statistics and JES (Jet Energy Scale) uncertainty, which has been measured simultaneously to give $JES = 0.989 \pm 0.029(\text{stat})$.

²⁰ Based on 318 pb^{-1} of data at $\sqrt{s} = 1.96$ TeV.

²¹ Dynamical likelihood method.

²² Based on 340 pb^{-1} of data at $\sqrt{s} = 1.96$ TeV.

²³ Based on 360 pb^{-1} of data at $\sqrt{s} = 1.96$ TeV.

²⁴ Based on $110.2 \pm 5.8 \text{ pb}^{-1}$ at $\sqrt{s} = 1.8$ TeV.

²⁵ Based on the all hadronic decays of $t\bar{t}$ pairs. Single *b*-quark tagging via the decay chain $b \rightarrow c \rightarrow \mu$ was used to select signal enriched multi-jet events. The result was obtained by the maximum likelihood method after bias correction.

²⁶ Obtained by combining the measurements in the lepton + jets [AFFOLDER 01], all-jets [ABE 97R, ABE 99B], and dilepton [ABE 99B] decay topologies.

²⁷ Obtained by combining the D0 result m_t (GeV) = $168.4 \pm 12.3 \pm 3.6$ from 6 di-lepton events (see also ABBOTT 98D) and m_t (GeV) = $173.3 \pm 5.6 \pm 5.5$ from lepton+jets events (ABBOTT 98F).

²⁸ Obtained by combining the CDF results of m_t (GeV) = $167.4 \pm 10.3 \pm 4.8$ from 8 dilepton events, m_t (GeV) = $175.9 \pm 4.8 \pm 5.3$ from lepton+jets events (ABE 98E), and m_t (GeV) = $186.0 \pm 10.0 \pm 5.7$ from all-jet events (ABE 97R). The systematic errors in the latter two measurements are changed in this paper.

²⁹ See ABAZOV 04G.

³⁰ The updated systematic error is listed. See AFFOLDER 01, appendix C.

³¹ Obtained by combining the D0 results of m_t (GeV) = $168.4 \pm 12.3 \pm 3.6$ from 6 dilepton events and m_t (GeV) = $173.3 \pm 5.6 \pm 5.5$ from 77 lepton+jets events.

³² Obtained by combining the D0 results from dilepton and lepton+jets events, and the CDF results (ABE 99B) from dilepton, lepton+jets events, and all-jet events.

t DECAY MODES

Mode	Fraction (Γ_i/Γ)	Confidence level
Γ_1 Wq ($q = b, s, d$)		
Γ_2 Wb		
Γ_3 $\ell\nu_\ell$ anything	[a,b] (9.4 ± 2.4) %	
Γ_4 $\tau\nu_\tau b$		
Γ_5 γq ($q = u, c$)	[c] < 5.9	95%

$\Delta T = 1$ weak neutral current (T_1) modes

Γ_6 Zq ($q = u, c$)	T_1 [d] < 13.7	95%
--------------------------------	------------------	-----

[a] ℓ means *e* or μ decay mode, not the sum over them.

[b] Assumes lepton universality and *W*-decay acceptance.

[c] This limit is for $\Gamma(t \rightarrow \gamma q)/\Gamma(t \rightarrow Wb)$.

[d] This limit is for $\Gamma(t \rightarrow Zq)/\Gamma(t \rightarrow Wb)$.

t BRANCHING RATIOS

$\Gamma(Wb)/\Gamma(Wq$ ($q = b, s, d$))	DOCUMENT ID	TECN	Γ_2/Γ_1
---	-------------	------	---------------------

1.06^{+0.16}_{-0.14} OUR AVERAGE

1.03^{+0.19}_{-0.17} ¹ABAZOV 06K D0

1.12^{+0.21+0.17}_{-0.19-0.13} ²ACOSTA 05A CDF

• • • We do not use the following data for averages, fits, limits, etc. • • •

0.94^{+0.26+0.17}_{-0.21-0.12} ³AFFOLDER 01C CDF

Quark Particle Listings

t

- ¹ ABAZOV 06k result is from the analysis of $t\bar{t} \rightarrow \ell\nu + \geq 3$ jets with 230 pb⁻¹ of data at $\sqrt{s} = 1.96$ TeV. It gives $R > 0.61$ and $|V_{tb}| > 0.78$ at 95% CL.
- ² ACOSTA 05A result is from the analysis of lepton + jets and di-lepton + jets final states of $t\bar{t}$ candidate events with ~ 162 pb⁻¹ of data at $\sqrt{s} = 1.96$ TeV. The first error is statistical and the second systematic. It gives $R > 0.61$, or $|V_{tb}| > 0.78$ at 95% CL.
- ³ AFFOLDER 01c measures the top-quark decay width ratio $R = \Gamma(Wb)/\Gamma(Wq)$, where q is a d , s , or b quark, by using the number of events with multiple b tags. The first error is statistical and the second systematic. A numerical integration of the likelihood function gives $R > 0.61$ (0.56) at 90% (95%) CL. By assuming three generation unitarity, $|V_{tb}| = 0.97^{+0.16}_{-0.12}$ or $|V_{tb}| > 0.78$ (0.75) at 90% (95%) CL is obtained. The result is based on 109 pb⁻¹ of data at $\sqrt{s} = 1.8$ TeV.

$\Gamma(\ell\nu_{\tau} \text{ anything})/\Gamma_{\text{total}}$		Γ_3/Γ	
VALUE	DOCUMENT ID	TECN	COMMENT
0.094 ± 0.024	¹ ABE	98x	CDF

¹ ℓ means e or μ decay mode, not the sum. Assumes lepton universality and W -decay acceptance.

$\Gamma(\tau\nu_{\tau} b)/\Gamma_{\text{total}}$		Γ_4/Γ	
VALUE	DOCUMENT ID	TECN	COMMENT

• • • We do not use the following data for averages, fits, limits, etc. • • •

	¹ ABULENCIA	06R	CDF	$\ell\tau + \text{jets}$
	² ABE	97V	CDF	$\ell\tau + \text{jets}$

- ¹ ABULENCIA 06R looked for $t\bar{t} \rightarrow (\ell\nu_{\tau})(\tau\nu_{\tau})b\bar{b}$ events in 194 pb⁻¹ of $p\bar{p}$ collisions at $\sqrt{s} = 1.96$ TeV. 2 events are found where 1.00 ± 0.17 signal and 1.29 ± 0.25 background events are expected, giving a 95% CL upper bound for the partial width ratio $\Gamma(t \rightarrow \tau\nu)/\Gamma_{\text{SM}}(t \rightarrow \tau\nu q) < 5.2$.
- ² ABE 97V searched for $t\bar{t} \rightarrow (\ell\nu_{\tau})(\tau\nu_{\tau})b\bar{b}$ events in 109 pb⁻¹ of $p\bar{p}$ collisions at $\sqrt{s} = 1.8$ TeV. They observed 4 candidate events where one expects ~ 1 signal and ~ 2 background events. Three of the four observed events have jets identified as b candidates.

$\Gamma(\gamma q (q=u,c))/\Gamma_{\text{total}}$		Γ_5/Γ	
VALUE	CL%	DOCUMENT ID	TECN COMMENT

<0.0132 95 ¹ AKTAS 04 H1 $B(t \rightarrow \gamma u)$

<**0.0059** 95 ² CHEKANOV 03 ZEUS $B(t \rightarrow \gamma u)$

• • • We do not use the following data for averages, fits, limits, etc. • • •

<0.0465	95	³ ABDALLAH	04c	DLPH $B(\gamma c \text{ or } \gamma u)$
<0.041	95	⁴ ACHARD	02j	L3 $B(t \rightarrow \gamma c \text{ or } \gamma u)$
<0.032	95	⁵ ABE	98g	CDF $t\bar{t} \rightarrow (Wb)(\gamma c \text{ or } \gamma u)$

- ¹ AKTAS 04 looked for single top production via FCNC in e^{\pm} collisions at HERA with 118.3 pb⁻¹, and found 5 events in the e or μ channels. By assuming that they are due to statistical fluctuation, the upper bound on the $t u \gamma$ coupling $\kappa_{t u \gamma} < 0.27$ (95% CL) is obtained. The conversion to the partial width limit, when $B(\gamma c) = B(Z u) = B(Z c) = 0$, is from private communication, E. Perez, May 2005.

- ² CHEKANOV 03 looked for single top production via FCNC in the reaction $e^{\pm} p \rightarrow e^{\pm}(t \text{ or } \bar{t}) X$ in 130.1 pb⁻¹ of data at $\sqrt{s} = 300\text{--}318$ GeV. No evidence for top production and its decay into bW was found. The result is obtained for $m_t = 175$ GeV when $B(\gamma c) = B(Z q) = 0$, where q is a u or c quark. Bounds on the effective $t\text{--}u\text{--}\gamma$ and $t\text{--}u\text{--}Z$ couplings are found in their Fig. 4. The conversion to the constraint listed is from private communication, E. Gallo, January 2004.

- ³ ABDALLAH 04c looked for single top production via FCNC in the reaction $e^{\pm} e^{\mp} \rightarrow \bar{t}c$ or $\bar{t}u$ in 541 pb⁻¹ of data at $\sqrt{s} = 189\text{--}208$ GeV. No deviation from the SM is found, which leads to the bound on $B(t \rightarrow \gamma q)$, where q is a u or a c quark, for $m_t = 175$ GeV when $B(t \rightarrow Zq) = 0$ is assumed. The conversion to the listed bound is from private communication, O. Yushchenko, April 2005. The bounds on the effective $t\text{--}q\text{--}\gamma$ and $t\text{--}q\text{--}Z$ couplings are given in their Fig. 7 and Table 4, for $m_t = 170\text{--}180$ GeV, where most conservative bounds are found by choosing the chiral couplings to maximize the negative interference between the virtual γ and Z exchange amplitudes.

- ⁴ ACHARD 02j looked for single top production via FCNC in the reaction $e^+ e^- \rightarrow \bar{t}c$ or $\bar{t}u$ in 634 pb⁻¹ of data at $\sqrt{s} = 189\text{--}209$ GeV. No deviation from the SM is found, which leads to a bound on the top-quark decay branching fraction $B(\gamma q)$, where q is a u or c quark. The bound assumes $B(Z q) = 0$ and is for $m_t = 175$ GeV; bounds for $m_t = 170$ GeV and 180 GeV and $B(Z q) \neq 0$ are given in Fig. 5 and Table 7.

- ⁵ ABE 98g looked for $t\bar{t}$ events where one t decays into $q\gamma$ while the other decays into bW . The quoted bound is for $\Gamma(\gamma q)/\Gamma(Wb)$.

$\Gamma(Z q (q=u,c))/\Gamma_{\text{total}}$		Γ_6/Γ	
---	--	-------------------	--

Test for $\Delta T = 1$ weak neutral current. Allowed by higher-order electroweak interaction.

<0.159	95	¹ ABDALLAH	04c	DLPH $e^+ e^- \rightarrow \bar{t}c$ or $\bar{t}u$
<0.137	95	² ACHARD	02j	L3 $e^+ e^- \rightarrow \bar{t}c$ or $\bar{t}u$
<0.14	95	³ HEISTER	02q	ALEP $e^+ e^- \rightarrow \bar{t}c$ or $\bar{t}u$
< 0.137	95	⁴ ABBIENDI	01T	OPAL $e^+ e^- \rightarrow \bar{t}c$ or $\bar{t}u$

• • • We do not use the following data for averages, fits, limits, etc. • • •

<0.17	95	⁵ BARATE	00s	ALEP $e^+ e^- \rightarrow \bar{t}c$ or $\bar{t}u$
<0.33	95	⁶ ABE	98g	CDF $t\bar{t} \rightarrow (Wb)(Zc \text{ or } Z u)$

- ¹ ABDALLAH 04c looked for single top production via FCNC in the reaction $e^+ e^- \rightarrow \bar{t}c$ or $\bar{t}u$ in 541 pb⁻¹ of data at $\sqrt{s} = 189\text{--}208$ GeV. No deviation from the SM is found, which leads to the bound on $B(t \rightarrow Zq)$, where q is a u or a c quark, for $m_t = 175$ GeV when $B(t \rightarrow \gamma q) = 0$ is assumed. The conversion to the listed bound is from private communication, O. Yushchenko, April 2005. The bounds on the effective $t\text{--}q\text{--}\gamma$ and $t\text{--}q\text{--}Z$ couplings are given in their Fig. 7 and Table 4, for $m_t = 170\text{--}180$ GeV, where most conservative bounds are found by choosing the chiral couplings to maximize the negative interference between the virtual γ and Z exchange amplitudes.

- ² ACHARD 02j looked for single top production via FCNC in the reaction $e^+ e^- \rightarrow \bar{t}c$ or $\bar{t}u$ in 634 pb⁻¹ of data at $\sqrt{s} = 189\text{--}209$ GeV. No deviation from the SM is found, which leads to a bound on the top-quark decay branching fraction $B(Z q)$, where q is a u or c quark. The bound assumes $B(\gamma q) = 0$ and is for $m_t = 175$ GeV; bounds for

- $m_t = 170$ GeV and 180 GeV and $B(\gamma q) \neq 0$ are given in Fig. 5 and Table 7. Table 6 gives constraints on $t\text{--}c\text{--}e\text{--}e$ four-fermi contact interactions.

- ³ HEISTER 02q looked for single top production via FCNC in the reaction $e^+ e^- \rightarrow \bar{t}c$ or $\bar{t}u$ in 214 pb⁻¹ of data at $\sqrt{s} = 204\text{--}209$ GeV. No deviation from the SM is found, which leads to a bound on the branching fraction $B(Z q)$, where q is a u or c quark. The bound assumes $B(\gamma q) = 0$ and is for $m_t = 174$ GeV. Bounds on the effective $t\text{--}(c \text{ or } u)\text{--}\gamma$ and $t\text{--}(c \text{ or } u)\text{--}Z$ couplings are given in their Fig. 2.

- ⁴ ABBIENDI 01T looked for single top production via FCNC in the reaction $e^+ e^- \rightarrow \bar{t}c$ or $\bar{t}u$ in 600 pb⁻¹ of data at $\sqrt{s} = 189\text{--}209$ GeV. No deviation from the SM is found, which leads to bounds on the branching fractions $B(Z q)$ and $B(\gamma q)$, where q is a u or c quark. The result is obtained for $m_t = 174$ GeV. The upper bound becomes 9.7% (20.6%) for $m_t = 169$ (179) GeV. Bounds on the effective $t\text{--}(c \text{ or } u)\text{--}\gamma$ and $t\text{--}(c \text{ or } u)\text{--}Z$ couplings are given in their Fig. 4.

- ⁵ BARATE 00s looked for single top production via FCNC in the reaction $e^+ e^- \rightarrow \bar{t}c$ or $\bar{t}u$ in 411 pb⁻¹ of data at c.m. energies between 189 and 202 GeV. No deviation from the SM is found, which leads to a bound on the branching fraction. The bound assumes $B(\gamma q) = 0$. Bounds on the effective $t\text{--}(c \text{ or } u)\text{--}\gamma$ and $t\text{--}(c \text{ or } u)\text{--}Z$ couplings are given in their Fig. 4.

- ⁶ ABE 98g looked for $t\bar{t}$ events where one t decays into three jets and the other decays into qZ with $Z \rightarrow \ell\ell$. The quoted bound is for $\Gamma(Z q)/\Gamma(Wb)$.

t Decay Vertices in $p\bar{p}$ Collisions

W helicity fractions in top decays. F_0 is the fraction of longitudinal and F_{\pm} the fraction of right-handed W bosons. F_{V+A} is the fraction of $V+A$ current in top decays.

VALUE	CL%	DOCUMENT ID	TECN COMMENT
-------	-----	-------------	--------------

• • • We do not use the following data for averages, fits, limits, etc. • • •

0.425 ± 0.166 ± 0.102		¹ ABAZOV	08B D0	$F_0 = B(t \rightarrow W_0 b)$
0.119 ± 0.090 ± 0.053		¹ ABAZOV	08B D0	$F_{\pm} = B(t \rightarrow W_{\pm} b)$
0.056 ± 0.080 ± 0.057		² ABAZOV	07D D0	$F_{\pm} = B(t \rightarrow W_{\pm} b)$
-0.06 ± 0.22 ± 0.12		³ ABULENCIA	07G CDF	$F_{V+A} = B(t \rightarrow W b_R)$
< 0.29	95	³ ABULENCIA	07G CDF	$F_{V+A} = B(t \rightarrow W b_R)$
0.85 ^{+0.15} _{-0.22} ± 0.06		⁴ ABULENCIA	07I CDF	$F_0 = B(t \rightarrow W_0 b)$
0.05 ^{+0.11} _{-0.05} ± 0.03		⁴ ABULENCIA	07I CDF	$F_{\pm} = B(t \rightarrow W_{\pm} b)$
< 0.26	95	⁴ ABULENCIA	07I CDF	$F_{\pm} = B(t \rightarrow W_{\pm} b)$
0.74 ^{+0.22} _{-0.34}		⁵ ABULENCIA	06U CDF	$F_0 = B(t \rightarrow W_0 b)$
< 0.27	95	⁵ ABULENCIA	06U CDF	$F_{\pm} = B(t \rightarrow W_{\pm} b)$
0.56 ± 0.31		⁶ ABAZOV	05G D0	$F_0 = B(t \rightarrow W_0 b)$
0.00 ± 0.13 ± 0.07		⁷ ABAZOV	05L D0	$F_{\pm} = B(t \rightarrow W_{\pm} b)$
< 0.25	95	⁷ ABAZOV	05L D0	$F_{\pm} = B(t \rightarrow W_{\pm} b)$
< 0.80	95	⁸ ACOSTA	05D CDF	$F_{V+A} = B(t \rightarrow W b_R)$
< 0.24	95	⁸ ACOSTA	05D CDF	$F_{\pm} = B(t \rightarrow W_{\pm} b)$
0.91 ± 0.37 ± 0.13		⁹ AFFOLDER	00B CDF	$F_0 = B(t \rightarrow W_0 b)$
0.11 ± 0.15		⁹ AFFOLDER	00B CDF	$F_{\pm} = B(t \rightarrow W_{\pm} b)$

- ¹ Based on 1 fb⁻¹ at $\sqrt{s} = 1.96$ TeV.

- ² Based on 370 pb⁻¹ of data at $\sqrt{s} = 1.96$ TeV, using the $\ell + \text{jets}$ and dilepton decay channels. The result assumes $F_0 = 0.70$, and it gives $F_{\pm} < 0.23$ at 95% CL.

- ³ Based on 700 pb⁻¹ of data at $\sqrt{s} = 1.96$ TeV.

- ⁴ Based on 318 pb⁻¹ of data at $\sqrt{s} = 1.96$ TeV.

- ⁵ Based on 200 pb⁻¹ of data at $\sqrt{s} = 1.96$ TeV. $t \rightarrow Wb \rightarrow \ell\nu b$ ($\ell = e$ or μ). The errors are stat + syst.

- ⁶ ABAZOV 05G studied the angular distribution of leptonic decays of W bosons in $t\bar{t}$ candidate events with lepton + jets final states, and obtained the fraction of longitudinally polarized W under the constraint of no right-handed current, $F_{\pm} = 0$. Based on 125 pb⁻¹ of data at $\sqrt{s} = 1.8$ TeV.

- ⁷ ABAZOV 05L studied the angular distribution of leptonic decays of W bosons in $t\bar{t}$ events, where one of the W 's from t or \bar{t} decays into e or μ and the other decays hadronically. The fraction of the "+" helicity W boson is obtained by assuming $F_0 = 0.7$, which is the generic prediction for any linear combination of V and A currents. Based on 230 ± 15 pb⁻¹ of data at $\sqrt{s} = 1.96$ TeV.

- ⁸ ACOSTA 05d measures the $m_{\ell^+ b}^2$ distribution in $t\bar{t}$ production events where one or both W 's decay leptonically to $\ell = e$ or μ , and finds a bound on the $V+A$ coupling of the $t b W$ vertex. By assuming the SM value of the longitudinal W fraction $F_0 = B(t \rightarrow W_0 b) = 0.70$, the bound on F_{\pm} is obtained. If the results are combined with those of AFFOLDER 00B, the bounds become $F_{V+A} < 0.61$ (95% CL) and $F_{\pm} < 0.18$ (95% CL), respectively. Based on 109 ± 7 pb⁻¹ of data at $\sqrt{s} = 1.8$ TeV (run I).

- ⁹ AFFOLDER 00B studied the angular distribution of leptonic decays of W bosons in $t \rightarrow Wb$ events. The ratio F_0 is the fraction of the helicity zero (longitudinal) W bosons in the decaying top quark rest frame. $B(t \rightarrow W_{\pm} b)$ is the fraction of positive helicity (right-handed) positive charge W bosons in the top quark decays. It is obtained by assuming the Standard Model value of F_0 .

t-quark FCNC couplings $\kappa_{t u g}^{u g}/\Lambda$ and $\kappa_{t g}^{c g}/\Lambda$

VALUE (TeV ⁻¹)	CL%	DOCUMENT ID	TECN COMMENT
----------------------------	-----	-------------	--------------

• • • We do not use the following data for averages, fits, limits, etc. • • •

<0.037	95	¹ ABAZOV	07V D0	$\kappa_{t u g}^{u g}/\Lambda$
<0.15	95	¹ ABAZOV	07V D0	$\kappa_{t g}^{c g}/\Lambda$

- ¹ Result is based on 230 pb⁻¹ of data at $\sqrt{s} = 1.96$ TeV. Absence of single top quark production events via FCNC $t\text{--}u\text{--}g$ and $t\text{--}c\text{--}g$ couplings lead to the upper bounds on the dimensionful couplings, $\kappa_{t u g}^{u g}/\Lambda$ and $\kappa_{t g}^{c g}/\Lambda$, respectively.

Single t-Quark Production Cross Section in $p\bar{p}$ Collisions at $\sqrt{s} = 1.8$ TeVDirect probes of the $t\bar{b}W$ coupling and possible new physics at $\sqrt{s} = 1.8$ TeV.

VALUE (pb)	CL%	DOCUMENT ID	TECN	COMMENT
<24	95	¹ ACOSTA 04H	CDF	$p\bar{p} \rightarrow t\bar{b} + X, tqb + X$
<18	95	² ACOSTA 02	CDF	$p\bar{p} \rightarrow t\bar{b} + X$
<13	95	³ ACOSTA 02	CDF	$p\bar{p} \rightarrow tqb + X$

¹ ACOSTA 04H bounds single top-quark production from the s -channel W -exchange process, $q'\bar{q} \rightarrow t\bar{b}$, and the t -channel W -exchange process, $q'g \rightarrow qt\bar{b}$. Based on ~ 106 pb⁻¹ of data.

² ACOSTA 02 bounds the cross section for single top-quark production via the s -channel W -exchange process, $q'\bar{q} \rightarrow t\bar{b}$. Based on ~ 106 pb⁻¹ of data.

³ ACOSTA 02 bounds the cross section for single top-quark production via the t -channel W -exchange process, $q'g \rightarrow qt\bar{b}$. Based on ~ 106 pb⁻¹ of data.

Single t-Quark Production Cross Section in $p\bar{p}$ Collisions at $\sqrt{s} = 1.96$ TeVDirect probes of the $t\bar{b}W$ coupling and possible new physics at $\sqrt{s} = 1.96$ TeV.

VALUE (pb)	CL%	DOCUMENT ID	TECN	COMMENT
4.9 ± 1.4		¹ ABAZOV 07H	D0	s -channel + t -channel
< 6.4	95	² ABAZOV 05P	D0	$p\bar{p} \rightarrow t\bar{b} + X$
< 5.0	95	² ABAZOV 05P	D0	$p\bar{p} \rightarrow tqb + X$
< 10.1	95	³ ACOSTA 05N	CDF	$p\bar{p} \rightarrow tqb + X$
< 13.6	95	³ ACOSTA 05N	CDF	$p\bar{p} \rightarrow t\bar{b} + X$
< 17.8	95	³ ACOSTA 05N	CDF	$p\bar{p} \rightarrow t\bar{b} + X, tqb + X$

¹ Result is based on 0.9 fb⁻¹ of data. This result constrains V_{tb} to $0.68 < |V_{tb}| \leq 1$ at 95% CL.

² ABAZOV 05P bounds single top-quark production from either the s -channel W -exchange process, $q'\bar{q} \rightarrow t\bar{b}$, or the t -channel W -exchange process, $q'g \rightarrow qt\bar{b}$, based on ~ 230 pb⁻¹ of data.

³ ACOSTA 05N bounds single top-quark production from the t -channel W -exchange process ($q'g \rightarrow qt\bar{b}$), the s -channel W -exchange process ($q'\bar{q} \rightarrow t\bar{b}$), and from the combined cross section of t - and s -channel. Based on ~ 162 pb⁻¹ of data.

Single t-Quark Production Cross Section in $e\bar{p}$ Collisions

VALUE (pb)	CL%	DOCUMENT ID	TECN	COMMENT
0.55	95	¹ AKTAS 04	H1	$e^{\pm}p \rightarrow e^{\pm}tX$

¹ AKTAS 04 looked for single top production via FCNC in e^{\pm} collisions at HERA with 118.3 pb⁻¹, and found 5 events in the e or μ channels while 1.31 ± 0.22 events are expected from the Standard Model background. No excess was found for the hadronic channel. The observed cross section of $\sigma(e\bar{p} \rightarrow e\bar{t}X) = 0.29^{+0.15}_{-0.14}$ pb at $\sqrt{s} = 319$ GeV gives the quoted upper bound if the observed events are due to statistical fluctuation.

 $t\bar{t}$ production cross section in $p\bar{p}$ collisions at $\sqrt{s} = 1.8$ TeVOnly the final combined $t\bar{t}$ production cross sections obtained from Tevatron Run I by the CDF and D0 experiments are quoted below.

VALUE (pb)	DOCUMENT ID	TECN	COMMENT
6.59 ± 1.21 ± 1.04	¹ ABAZOV 03A	D0	Combined Run I data
6.5 ^{+1.7} _{-1.4}	² AFFOLDER 01A	CDF	Combined Run I data

¹ Combined result from 110 pb⁻¹ of Tevatron Run I data. Assume $m_t = 172.1$ GeV.

² Combined result from 105 pb⁻¹ of Tevatron Run I data. Assume $m_t = 175$ GeV.

 $t\bar{t}$ production cross section in $p\bar{p}$ collisions at $\sqrt{s} = 1.96$ TeV

VALUE (pb)	DOCUMENT ID	TECN	COMMENT
------------	-------------	------	---------

• • • We do not use the following data for averages, fits, limits, etc. • • •

8.3 ± 1.0 ^{+2.0} _{-1.5} ± 0.5	¹ AALTONEN 07b	CDF	≥ 6 jets, vtx b -tag
7.4 ± 1.4 ± 1.0	² ABAZOV 07b	D0	$\ell\ell$ + jets, vtx b -tag
4.5 ^{+2.0} _{-1.9} ± 1.4 ± 0.3	³ ABAZOV 07P	D0	≥ 6 jets, vtx b -tag
6.4 ^{+1.3} _{-1.2} ± 0.7 ± 0.4	⁴ ABAZOV 07R	D0	ℓ + ≥ 4 jets
6.6 ± 0.9 ± 0.4	⁵ ABAZOV 06X	D0	ℓ + jets, vtx b -tag
8.7 ± 0.9 ^{+1.1} _{-0.9}	⁶ ABULENCIA 06Z	CDF	ℓ + jets, vtx b -tag
5.8 ± 1.2 ^{+0.9} _{-0.7}	⁷ ABULENCIA,A 06C	CDF	missing E_T + jets, vtx b -tag
7.5 ± 2.1 ^{+3.3} _{-2.2} ± 0.5	⁸ ABULENCIA,A 06E	CDF	6–8 jets, b -tag
8.9 ± 1.0 ^{+1.1} _{-1.0}	⁹ ABULENCIA,A 06F	CDF	ℓ + ≥ 3 jets, b -tag
8.6 ^{+1.6} _{-1.5} ± 0.6	¹⁰ ABAZOV 05Q	D0	ℓ + n jets
8.6 ^{+3.2} _{-2.7} ± 1.1 ± 0.6	¹¹ ABAZOV 05R	D0	di-lepton + n jets
6.7 ^{+1.4} _{-1.3} ± 1.6 ± 0.4	¹² ABAZOV 05X	D0	ℓ + jets / kinematics
5.3 ± 3.3 ^{+1.3} _{-1.0}	¹³ ACOSTA 05S	CDF	ℓ + jets / soft μ b -tag
6.6 ± 1.1 ± 1.5	¹⁴ ACOSTA 05T	CDF	ℓ + jets / kinematics
6.0 ^{+1.5} _{-1.6} ± 1.2	¹⁵ ACOSTA 05U	CDF	ℓ + jets / kinematics + vtx b -tag
5.6 ^{+1.2} _{-1.1} ± 0.9	¹⁶ ACOSTA 05V	CDF	ℓ + n jets
7.0 ^{+2.4} _{-2.1} ± 1.6 ± 0.4	¹⁷ ACOSTA 04I	CDF	di-lepton + jets + missing ET

¹ Based on 1.02 fb⁻¹ of data. Result is for $m_t = 175$ GeV. The last error is for luminosity. Secondary vertex b -tag and neural network selections are used to achieve a signal-to-background ratio of about 1/2.

² Based on 425 pb⁻¹ of data. Result is for $m_t = 175$ GeV. For $m_t = 170.9$ GeV, 7.8 ± 1.8(stat + syst) pb is obtained.

³ Based on 405 ± 25 pb⁻¹ of data. Result is for $m_t = 175$ GeV. The last error is for luminosity. Secondary vertex b -tag and neural network are used to separate the signal events from the background.

⁴ Based on 425 pb⁻¹ of data. Assumes $m_t = 175$ GeV. The last error is for luminosity.

⁵ Based on ~ 425 pb⁻¹. Assuming $m_t = 175$ GeV. The first error is combined statistical and systematic, the second one is luminosity.

⁶ Based on ~ 318 pb⁻¹. Assuming $m_t = 178$ GeV. The cross section changes by ±0.08 pb for each ±1 GeV change in the assumed m_t . Result is for at least one b -tag. For at least two b -tagged jets, $t\bar{t}$ signal of significance greater than 5 σ is found, and the cross section is 10.1 ^{+1.6} _{-1.4} ± 2.0 ± 1.3 pb for $m_t = 178$ GeV.

⁷ Based on ~ 311 pb⁻¹. Assuming $m_t = 178$ GeV. The first error is statistical and the second systematic. For $m_t = 175$ GeV, the result is 6.0 ± 1.2 ^{+0.9} _{-0.7}. This is the first CDF measurement without lepton identification, and hence it has sensitivity to the $W \rightarrow \tau\nu$ mode.

⁸ ABULENCIA,A 06E measures the $t\bar{t}$ production cross section in the all hadronic decay mode by selecting events with 6 to 8 jets and at least one b -jet. $S/B = 1/5$ has been achieved. Based on 311 pb⁻¹. Assuming $m_t = 178$ GeV. The first error is statistical, the second is systematic, and the third one is luminosity.

⁹ Based on ~ 318 pb⁻¹. Assuming $m_t = 178$ GeV. Result is for at least one b -tag. For at least two b -tagged jets, the cross section is 11.1 ^{+2.3} _{-1.9} ± 2.5 ± 1.9 pb.

¹⁰ ABAZOV 05Q measures the top-quark pair production cross section with ~ 230 pb⁻¹ of data, based on the analysis of W plus n -jet events where W decays into e or μ plus neutrino, and at least one of the jets is b -jet like. The first error is statistical and systematic, and the second accounts for the luminosity uncertainty. The result assumes $m_t = 175$ GeV; the mean value changes by $(175 - m_t(\text{GeV})) \times 0.06$ pb in the mass range 160 to 190 GeV.

¹¹ ABAZOV 05R measures the top-quark pair production cross section with 224–243 pb⁻¹ of data, based on the analysis of events with two charged leptons in the final state. The first error is statistical, the second one is systematic, and the last one gives the luminosity uncertainty. The result assumes $m_t = 175$ GeV; the mean value changes by $(175 - m_t(\text{GeV})) \times 0.08$ pb in the mass range 160 to 190 GeV.

¹² Based on 230 pb⁻¹. Assuming $m_t = 175$ GeV. The last error accounts for the luminosity uncertainty.

¹³ Based on 194 pb⁻¹. Assuming $m_t = 175$ GeV.

¹⁴ Based on 194 ± 11 pb⁻¹. Assuming $m_t = 175$ GeV.

¹⁵ Based on 162 ± 10 pb⁻¹. Assuming $m_t = 175$ GeV.

¹⁶ ACOSTA 05V measures the top-quark pair production cross section with ~ 162 pb⁻¹ data, based on the analysis of W plus n -jet events where W decays into e or μ plus neutrino, and at least one of the jets is b -jet like. Assumes $m_t = 175$ GeV. The first error is statistical and the latter is systematic, which include the luminosity uncertainty.

¹⁷ ACOSTA 04I measures the top-quark pair production cross section with 197 ± 12 pb⁻¹ data, based on the analysis of events with two charged leptons in the final state. Assumes $m_t = 175$ GeV. The first error is statistical, the second one is systematic, and the last one gives the luminosity uncertainty.

t-Quark Electric Charge

VALUE	DOCUMENT ID	TECN	COMMENT
• • • We do not use the following data for averages, fits, limits, etc. • • •			
	¹ ABAZOV 07c	D0	fraction of $ q = 4e/3$ pair

¹ ABAZOV 07c reports an upper limit $\rho < 0.80$ (90% CL) on the fraction ρ of exotic quark pairs $Q\bar{Q}$ with electric charge $|q| = 4e/3$ in $t\bar{t}$ candidate events with high p_T lepton, missing E_T and ≥ 4 jets. The result is obtained by measuring the fraction of events in which the quark pair decays into $W^- + b$ and $W^+ + \bar{b}$, where b and \bar{b} jets are discriminated by using the charge and momenta of tracks within the jet cones. The maximum CL at which the model of CHANG 99 can be excluded is 92%. Based on 370 pb⁻¹ of data at $\sqrt{s} = 1.96$ TeV.

t-Quark REFERENCES

AALTONEN 08C	PRL 100 062005	T. Aaltonen et al.	(CDF Collab.)
ABAZOV 08B	PRL 100 062004	V.M. Abazov et al.	(D0 Collab.)
TEVEWVG 08	arXiv:0803.1683v1[hep-ex]	CDF, D0 Collab., Tevatron Electroweak Working Group	(D0 Collab.)
TEVEWVG 08A	Private communication	CDF, D0 Collab., Tevatron Electroweak Working Group	(D0 Collab.)
AALTONEN 07F	PRL 98 142001	T. Aaltonen et al.	(CDF Collab.)
AALTONEN 07B	PR D75 111103R	T. Aaltonen et al.	(CDF Collab.)
AALTONEN 07D	PR D76 072009	T. Aaltonen et al.	(CDF Collab.)
AALTONEN 07E	PRL 99 182002	T. Aaltonen et al.	(CDF Collab.)
ABAZOV 07C	PRL 98 041801	V.M. Abazov et al.	(D0 Collab.)
ABAZOV 07D	PR D75 031102R	V.M. Abazov et al.	(D0 Collab.)
ABAZOV 07F	PR D75 092001	V.M. Abazov et al.	(D0 Collab.)
ABAZOV 07H	PRL 98 181802	V.M. Abazov et al.	(D0 Collab.)
ABAZOV 07O	PR D76 052006	V.M. Abazov et al.	(D0 Collab.)
ABAZOV 07P	PR D76 072007	V.M. Abazov et al.	(D0 Collab.)
ABAZOV 07R	PR D76 092007	V.M. Abazov et al.	(D0 Collab.)
ABAZOV 07V	PRL 99 191802	V.M. Abazov et al.	(D0 Collab.)
ABAZOV 07W	PL B655 7	V.M. Abazov et al.	(D0 Collab.)
ABULENCIA 07D	PR D75 031105R	A. Abulencia et al.	(CDF Collab.)
ABULENCIA 07G	PRL 98 072001	A. Abulencia et al.	(CDF Collab.)
ABULENCIA 07I	PR D75 052001	A. Abulencia et al.	(CDF Collab.)
ABULENCIA 07J	PR D75 071102R	A. Abulencia et al.	(CDF Collab.)
ABAZOV 06K	PL B639 616	V.M. Abazov et al.	(D0 Collab.)
ABAZOV 06U	PR D74 092005	V.M. Abazov et al.	(D0 Collab.)
ABAZOV 06X	PR D74 112004	V.M. Abazov et al.	(D0 Collab.)
ABULENCIA 06D	PRL 96 022004	A. Abulencia et al.	(CDF Collab.)
Also	PR D73 032003	A. Abulencia et al.	(CDF Collab.)
Also	PR D73 092002	A. Abulencia et al.	(CDF Collab.)
ABULENCIA 06G	PRL 96 152002	A. Abulencia et al.	(CDF Collab.)
Also	PR D74 032009	A. Abulencia et al.	(CDF Collab.)
ABULENCIA 06R	PL B639 172	A. Abulencia et al.	(CDF Collab.)
ABULENCIA 06U	PR D73 111103R	A. Abulencia et al.	(CDF Collab.)
ABULENCIA 06V	PR D73 112006	A. Abulencia et al.	(CDF Collab.)
ABULENCIA 06Z	PRL 97 082004	A. Abulencia et al.	(CDF Collab.)
ABULENCIA,A 06C	PRL 96 202002	A. Abulencia et al.	(CDF Collab.)

Quark Particle Listings

t, *b'* (Fourth Generation) Quark

ABULENCIA,A	06E	PR D74 072005	A. Abulencia et al.	(CDF Collab.)
ABULENCIA,A	06F	PR D74 072006	A. Abulencia et al.	(CDF Collab.)
ABAZOV	05	PL B606 25	V.M. Abazov et al.	(D0 Collab.)
ABAZOV	05G	PL B617 1	V.M. Abazov et al.	(D0 Collab.)
ABAZOV	05L	PR D72 011104R	V.M. Abazov et al.	(D0 Collab.)
ABAZOV	05P	PL B622 265	V.M. Abazov et al.	(D0 Collab.)
Also		PL B517 282	V.M. Abazov et al.	(D0 Collab.)
Also		PR D63 031101	B. Abbott et al.	(D0 Collab.)
Also		PR D75 092007	V.M. Abazov et al.	(D0 Collab.)
ABAZOV	05Q	PL B626 35	V.M. Abazov et al.	(D0 Collab.)
ABAZOV	05R	PL B626 55	V.M. Abazov et al.	(D0 Collab.)
ABAZOV	05X	PL B626 45	V.M. Abazov et al.	(D0 Collab.)
ACOSTA	05A	PRL 95 102002	D. Acosta et al.	(CDF Collab.)
ACOSTA	05D	PR D71 031101R	D. Acosta et al.	(CDF Collab.)
ACOSTA	05N	PR D71 012005	D. Acosta et al.	(CDF Collab.)
ACOSTA	05S	PR D72 032002	D. Acosta et al.	(CDF Collab.)
ACOSTA	05T	PR D72 052003	D. Acosta et al.	(CDF Collab.)
ACOSTA	05U	PR D71 072005	D. Acosta et al.	(CDF Collab.)
ACOSTA	05V	PR D71 052003	D. Acosta et al.	(CDF Collab.)
ABAZOV	04G	NAT 429 638	V.M. Abazov et al.	(D0 Collab.)
ABDALLAH	04C	PL B590 21	J. Abdallah et al.	(DELPHI Collab.)
ACOSTA	04H	PR D69 052003	D. Acosta et al.	(CDF Collab.)
ACOSTA	04I	PRL 93 142001	D. Acosta et al.	(CDF Collab.)
AKTAS	04	EPJ C33 9	A. Aktas et al.	(H1 Collab.)
ABAZOV	03A	PR D67 012004	V.M. Abazov et al.	(D0 Collab.)
CHEKANOV	03	PL B559 153	S. Chekanov et al.	(ZEUS Collab.)
ACHARD	02J	PL B549 290	P. Achard et al.	(L3 Collab.)
ACOSTA	02	PR D65 091102	D. Acosta et al.	(CDF Collab.)
HEISTER	02Q	PL B543 173	A. Heister et al.	(ALEPH Collab.)
ABBIENDI	01T	PL B521 181	G. Abbiendi et al.	(OPAL Collab.)
AFFOLDER	01	PR D63 032003	T. Affolder et al.	(CDF Collab.)
AFFOLDER	01A	PR D64 032002	T. Affolder et al.	(CDF Collab.)
AFFOLDER	01C	PRL 86 3233	T. Affolder et al.	(CDF Collab.)
AFFOLDER	00B	PRL 84 216	T. Affolder et al.	(CDF Collab.)
BARATE	00S	PL B494 33	S. Barate et al.	(ALEPH Collab.)
ABBOTT	99G	PR D60 052001	B. Abbott et al.	(D0 Collab.)
ABE	99B	PRL 82 271	F. Abe et al.	(CDF Collab.)
Also		PRL 82 2808 (erratum)	F. Abe et al.	(CDF Collab.)
CHANG	99	PR D59 091503	D. Chang, W. Chang, E. Ma	(D0 Collab.)
ABBOTT	98D	PRL 80 2063	B. Abbott et al.	(D0 Collab.)
ABBOTT	98F	PR D58 052001	B. Abbott et al.	(D0 Collab.)
ABE	98E	PRL 80 2767	F. Abe et al.	(CDF Collab.)
ABE	98F	PRL 80 2779	F. Abe et al.	(CDF Collab.)
ABE	98G	PRL 80 2525	F. Abe et al.	(CDF Collab.)
ABE	98X	PRL 80 2773	F. Abe et al.	(CDF Collab.)
BHAT	98B	JUMP A13 5113	P.C. Bhat, H.B. Prosper, S.S. Snyder	(D0 Collab.)
ABACHI	97E	PRL 79 1197	S. Abachi et al.	(D0 Collab.)
ABE	97R	PRL 79 1992	F. Abe et al.	(CDF Collab.)
ABE	97V	PRL 79 3585	F. Abe et al.	(CDF Collab.)
PDG	96	PR D54 1	R. M. Barnett et al.	(D0 Collab.)
ABACHI	95	PRL 74 2632	S. Abachi et al.	(D0 Collab.)
ABE	95F	PRL 74 2626	F. Abe et al.	(CDF Collab.)
ABE	94E	PR D50 2966	F. Abe et al.	(CDF Collab.)
Also		PRL 73 225	F. Abe et al.	(CDF Collab.)

- 8 ABE 92 dilepton analysis limit of >85 GeV at CL=95% also applies to *b'* quarks, as discussed in ABE 90B.
- 9 ABE 90b exclude the region 28–72 GeV.
- 10 AKESSON 90 searched for events having an electron with $p_T > 12$ GeV, missing momentum > 15 GeV, and a jet with $E_T > 10$ GeV, $|\eta| < 2.2$, and excluded $m_{b'}$ between 30 and 69 GeV.
- 11 For the reduction of the limit due to non-charged-current decay modes, see Fig. 19 of ALBAJAR 90B.
- 12 ALBAJAR 88 study events at $E_{cm} = 546$ and 630 GeV with a muon or isolated electron, accompanied by one or more jets and find agreement with Monte Carlo predictions for the production of charm and bottom, without the need for a new quark. The lower mass limit is obtained by using a conservative estimate for the $b'\bar{b}'$ production cross section and by assuming that it cannot be produced in W decays. The value quoted here is revised using the full $O(\alpha_S^3)$ cross section of ALTARELLI 88.

MASS LIMITS for *b'* (4th Generation) Quark or Hadron in e^+e^- Collisions

Search for hadrons containing a fourth-generation $-1/3$ quark denoted *b'*.

The last column specifies the assumption for the decay mode (*CC* denotes the conventional charged-current decay) and the event signature which is looked for.

VALUE (GeV)	CL%	DOCUMENT ID	TECN	COMMENT
>46.0	95	13 DECAMP	90F ALEP	any decay
•••				We do not use the following data for averages, fits, limits, etc. •••
none 96–103	95	14 ABDALLAH	07 DLPH	$b' \rightarrow bZ, cW$
		15 ADRIANI	93G L3	Quarkonium
>44.7	95	ADRIANI	93M L3	$\Gamma(Z)$
>45	95	ABREU	91F DLPH	$\Gamma(Z)$
none 19.4–28.2	95	ABE	90D VNS	Any decay; event shape
>45.0	95	ABREU	90D DLPH	$B(C C) = 1$; event shape
>44.5	95	16 ABREU	90D DLPH	$b' \rightarrow cH^-, H^- \rightarrow \bar{c}s, \tau^- \nu$
>40.5	95	17 ABREU	90D DLPH	$\Gamma(Z \rightarrow \text{hadrons})$
>28.3	95	ADACHI	90 TOPZ	$B(\text{FCNC})=100\%$; isol. γ or 4 jets
>41.4	95	18 AKRAWY	90B OPAL	Any decay; acoplanarity
>45.2	95	18 AKRAWY	90B OPAL	$B(C C) = 1$; acoplanarity
>46	95	19 AKRAWY	90I OPAL	$b' \rightarrow \gamma + \text{any}$
>27.5	95	20 ABE	89E VNS	$B(C C) = 1$; μ, e
none 11.4–27.3	95	21 ABE	89G VNS	$B(b' \rightarrow b\gamma) > 10\%$; isolated γ
>44.7	95	22 ABRAMS	89C MRK2	$B(C C) = 100\%$; isol. track
>42.7	95	22 ABRAMS	89C MRK2	$B(bg) = 100\%$; event shape
>42.0	95	22 ABRAMS	89C MRK2	Any decay; event shape
>28.4	95	23,24 ADACHI	89C TOPZ	$B(C C) = 1$; μ
>28.8	95	25 ENO	89 AMY	$B(C C) \gtrsim 90\%$; μ, e
>27.2	95	25,26 ENO	89 AMY	any decay; event shape
>29.0	95	25 ENO	89 AMY	$B(b' \rightarrow bg) \gtrsim 85\%$; event shape
>24.4	95	27 IGARASHI	88 AMY	μ, e
>23.8	95	28 SAGAWA	88 AMY	event shape
>22.7	95	29 ADEVA	86 MRKJ	μ
>21	95	30 ALTHOFF	84C TASS	R, event shape
>19	95	31 ALTHOFF	84I TASS	Aplanarity

- 13 DECAMP 90F looked for isolated charged particles, for isolated photons, and for four-jet final states. The modes $b' \rightarrow bg$ for $B(b' \rightarrow bg) > 65\%$ $b' \rightarrow b\gamma$ for $B(b' \rightarrow b\gamma) > 5\%$ are excluded. Charged Higgs decay were not discussed.
- 14 ABDALLAH 07 searched for *b'* pair production at $E_{cm}=196\text{--}209$ GeV, with 420 pb⁻¹. No signal leads to the 95% CL upper limits on $B(b' \rightarrow bZ)$ and $B(b' \rightarrow cW)$ for $m_{b'} = 96$ to 103 GeV.
- 15 ADRIANI 93g search for vector quarkonium states near Z and give limit on quarkonium-Z mixing parameter $\delta m^2 < (10\text{--}30)$ GeV² (95%CL) for the mass 88–94.5 GeV. Using Richardson potential, a 1S (*b'* \bar{b}') state is excluded for the mass range 87.7–94.7 GeV. This range depends on the potential choice.
- 16 ABREU 90D assumed $m_{H^-} < m_{b'} - 3$ GeV.
- 17 Superseded by ABREU 91F.
- 18 AKRAWY 90b search was restricted to data near the Z peak at $E_{cm} = 91.26$ GeV at LEP. The excluded region is between 23.6 and 41.4 GeV if no H^\pm decays exist. For charged Higgs decays the excluded regions are between $(m_{H^\pm} + 1.5 \text{ GeV})$ and 45.5 GeV.
- 19 AKRAWY 90j search for isolated photons in hadronic Z decay and derive $B(Z \rightarrow b'\bar{b}') \cdot B(b' \rightarrow \gamma X) / B(Z \rightarrow \text{hadrons}) < 2.2 \times 10^{-3}$. Mass limit assumes $B(b' \rightarrow \gamma X) > 10\%$.
- 20 ABE 89e search at $E_{cm} = 56\text{--}57$ GeV at TRISTAN for multihadron events with a spherical shape (using thrust and acoplanarity) or containing isolated leptons.
- 21 ABE 89g search was at $E_{cm} = 55\text{--}60.8$ GeV at TRISTAN.
- 22 If the photonic decay mode is large ($B(b' \rightarrow b\gamma) > 25\%$), the ABRAMS 89c limit is 45.4 GeV. The limit for for Higgs decay ($b' \rightarrow cH^-, H^- \rightarrow \bar{c}s$) is 45.2 GeV.
- 23 ADACHI 89c search was at $E_{cm} = 56.5\text{--}60.8$ GeV at TRISTAN using multi-hadron events accompanying muons.
- 24 ADACHI 89c also gives limits for any mixture of CC and bg decays.
- 25 ENO 89 search at $E_{cm} = 50\text{--}60.8$ at TRISTAN.
- 26 ENO 89 considers arbitrary mixture of the charged current, bg, and $b\gamma$ decays.
- 27 IGARASHI 88 searches for leptons in low-thrust events and gives $\Delta R(b') < 0.26$ (95% CL) assuming charged current decay, which translates to $m_{b'} > 24.4$ GeV.

b' (4th Generation) Quark, Searches for

MASS LIMITS for *b'* (4th Generation) Quark or Hadron in $p\bar{p}$ Collisions

VALUE (GeV)	CL%	DOCUMENT ID	TECN	COMMENT
>268	95	1 AALTONEN	07c CDF	$B(b' \rightarrow bZ) = 1$ assumed
>190	95	2 ACOSTA	03 CDF	quasi-stable <i>b'</i>
>128	95	3 ABACHI	95F D0	$\ell\ell + \text{jets}, \ell + \text{jets}$
•••				We do not use the following data for averages, fits, limits, etc. •••
>199	95	4 AFFOLDER	00 CDF	NC: $b' \rightarrow bZ$
>148	95	5 ABE	98N CDF	NC: $b' \rightarrow bZ + \text{decay vertex}$
> 96	95	6 ABACHI	97D D0	NC: $b' \rightarrow b\gamma$
> 75	95	7 MUKHOPAD...	93 RVUE	NC: $b' \rightarrow b\ell\ell$
> 85	95	8 ABE	92 CDF	CC: $\ell\ell$
> 72	95	9 ABE	90B CDF	CC: $e + \mu$
> 54	95	10 AKESSON	90 UA2	CC: $e + \text{jets} + \text{missing } E_T$
> 43	95	11 ALBAJAR	90B UA1	CC: $\mu + \text{jets}$
> 34	95	12 ALBAJAR	88 UA1	CC: e or $\mu + \text{jets}$

- 1 Result is based on 1.06 fb^{-1} of data. No excess from the SM $Z + \text{jets}$ events is found when Z decays into e^+e^- or $\mu^+\mu^-$. The $m_{b'}$ bound is found by comparing the resulting upper bound on $\sigma(b'\bar{b}') [1 - (1 - B(b' \rightarrow bZ))^2]$ and the LO estimate of the *b'* pair production cross section shown in Fig. 38 of the article.
- 2 ACOSTA 03 looked for long-lived fourth generation quarks in the data sample of 90 pb⁻¹ of $\sqrt{s}=1.8$ TeV $p\bar{p}$ collisions by using the muon-like penetration and anomalously high ionization energy loss signature. The corresponding lower mass bound for the charge $(2/3)e$ quark (*t'*) is 220 GeV. The *t'* bound is higher than the *b'* bound because *t'* is more likely to produce charged hadrons than *b'*. The 95% CL upper bounds for the production cross sections are given in their Fig. 3.
- 3 ABACHI 95F bound on the top-quark also applies to *b'* and *t'* quarks that decay predominantly into W . See FROGGATT 97.
- 4 AFFOLDER 00 looked for *b'* that decays in to $b+Z$. The signal searched for is $bbZZ$ events where one Z decays into e^+e^- or $\mu^+\mu^-$ and the other Z decays hadronically. The bound assumes $B(b' \rightarrow bZ) = 100\%$. Between 100 GeV and 199 GeV, the 95%CL upper bound on $\sigma(b' \rightarrow \bar{b}') \times B^2(b' \rightarrow bZ)$ is also given (see their Fig. 2).
- 5 ABE 98n looked for $Z \rightarrow e^+e^-$ decays with displaced vertices. Quoted limit assumes $B(b' \rightarrow bZ) = 1$ and $c\tau_{b'} = 1 \text{ cm}$. The limit is lower than $m_Z + m_{b'}$ (~ 96 GeV) if $c\tau > 22 \text{ cm}$ or $c\tau < 0.009 \text{ cm}$. See their Fig. 4.
- 6 ABACHI 97D searched for *b'* that decays mainly via FCNC. They obtained 95%CL upper bounds on $B(b'\bar{b}' \rightarrow \gamma + 3 \text{ jets})$ and $B(b'\bar{b}' \rightarrow 2\gamma + 2 \text{ jets})$, which can be interpreted as the lower mass bound $m_{b'} > m_Z + m_b$.
- 7 MUKHOPADHYAYA 93 analyze CDF dilepton data of ABE 92G in terms of a new quark decaying via flavor-changing neutral current. The above limit assumes $B(b' \rightarrow b\ell^+\ell^-) = 1\%$. For an exotic quark decaying only via virtual Z [$B(b\ell^+\ell^-) = 3\%$], the limit is 85 GeV.

See key on page 373

Quark Particle Listings

 b' (Fourth Generation) Quark, t' (Fourth Generation) Quark, Free Quark Searches

- ²⁸ SAGAWA 88 set limit $\sigma(\text{top}) < 6.1$ pb at CL=95% for top-flavored hadron production from event shape analyses at $E_{\text{cm}} = 52$ GeV. By using the quark parton model cross-section formula near threshold, the above limit leads to lower mass bounds of 23.8 GeV for charge $-1/3$ quarks.
- ²⁹ ADEVA 86 give 95%CL upper bound on an excess of the normalized cross section, ΔR , as a function of the minimum c.m. energy (see their figure 3). Production of a pair of $1/3$ charge quarks is excluded up to $E_{\text{cm}} = 45.4$ GeV.
- ³⁰ ALTHOFF 84c narrow state search sets limit $\Gamma(e^+e^-)B(\text{hadrons}) < 2.4$ keV CL = 95% and heavy charge $1/3$ quark pair production $m > 21$ GeV, CL = 95%.
- ³¹ ALTHOFF 84i exclude heavy quark pair production for $7 < m < 19$ GeV ($1/3$ charge) using aplanarity distributions (CL = 95%).

REFERENCES FOR Searches for (Fourth Generation) b' Quark

Author	Year	Pub	CL%	Doc ID	TECN	Comment
AALTONEN	07C	PR D76 072006				(CDF Collab.)
ABDALLAH	07	EPL C50 507				(DELPHI Collab.)
ACOSTA	03	PRL 90 131801				(CDF Collab.)
AFFOLDER	00	PRL 84 835				(CDF Collab.)
ABE	98N	PR D58 051102				(CDF Collab.)
ABACHI	97D	PRL 78 3818				(DO Collab.)
FROGGATT	97	ZPHY C73 333				(GLAS+)
ABACHI	95F	PR D52 4877				(DO Collab.)
ADRIANI	93G	PL B313 326				(L3 Collab.)
ADRIANI	93M	PRPL 236 1				(L3 Collab.)
MUKHOPAD...	93	PR D48 2105				(TATA)
ABE	92	PRL 68 447				(CDF Collab.)
Also		PR D45 3921				(CDF Collab.)
ABE	92G	PR D45 3921				(CDF Collab.)
ABREU	91F	NP B367 511				(DELPHI Collab.)
ABE	90B	PRL 64 147				(CDF Collab.)
ABE	90D	PL B234 382				(VENUS Collab.)
ABREU	90D	PL B242 536				(DELPHI Collab.)
ADACHI	90	PL B234 197				(TOPAZ Collab.)
AKESSON	90	ZPHY C46 179				(UA2 Collab.)
AKRAWY	90B	PL B236 364				(OPAL Collab.)
AKRAWY	90J	PL B246 285				(OPAL Collab.)
ALBAJAR	90B	ZPHY C48 1				(UA1 Collab.)
DECAMP	90F	PL B236 511				(ALEPH Collab.)
ABE	89E	PR D39 3524				(VENUS Collab.)
ABE	89G	PRL 63 1776				(VENUS Collab.)
ABRAMS	89C	PRL 63 2447				(Mark II Collab.)
ADACHI	89C	PL B229 427				(TOPAZ Collab.)
ENO	89	PRL 63 1910				(AMY Collab.)
ALBAJAR	88	ZPHY C37 505				(UA1 Collab.)
ALTARELLI	88	NP B308 724				(CERN, ROMA, ETH)
IGARASHI	88	PRL 60 2359				(AMY Collab.)
SAGAWA	88	PRL 60 93				(AMY Collab.)
ADEVA	86	PR D34 681				(Mark-J Collab.)
ALTHOFF	84C	PL 138B 441				(TASSO Collab.)
ALTHOFF	84I	ZPHY C22 307				(TASSO Collab.)

 t' (4th Generation) Quark, Searches forMASS LIMITS for t' (4th Generation) Quark or Hadron in $p\bar{p}$ Collisions

VALUE (GeV)	CL%	DOCUMENT ID	TECN	COMMENT
>256	95	¹ AALTONEN 08H CDF	$p\bar{p}$	at 1.96 GeV

- ¹ Searches for pair production of a new heavy top-like quark t' decaying to a W boson and another quark by fitting the observed spectrum of total transverse energy and reconstructed t' mass in the lepton + jets events.

REFERENCES FOR Searches for (Fourth Generation) t' Quark

AALTONEN	08H	PRL 100 161803	T. Aaltonene et al.	(CDF Collab.)
----------	-----	----------------	---------------------	---------------

Free Quark Searches

FREE QUARK SEARCHES

The basis for much of the theory of particle scattering and hadron spectroscopy is the construction of the hadrons from a set of fractionally charged constituents (quarks). A central but unproven hypothesis of this theory, Quantum Chromodynamics, is that quarks cannot be observed as free particles but are confined to mesons and baryons.

Experiments show that it is at best difficult to “unglue” quarks. Accelerator searches at increasing energies have produced no evidence for free quarks, while only a few cosmic-ray and matter searches have produced uncorroborated events.

This compilation is only a guide to the literature, since the quoted experimental limits are often only indicative. Reviews can be found in Refs. 1–4.

References

- M.L. Perl, E.R. Lee, and D. Lomba, Mod. Phys. Lett. **A19**, 2595 (2004).
- P.F. Smith, Ann. Rev. Nucl. and Part. Sci. **39**, 73 (1989).
- L. Lyons, Phys. Reports **129**, 225 (1985).
- M. Marinelli and G. Morigio, Phys. Reports **85**, 161 (1982).

Quark Production Cross Section — Accelerator Searches

X-SECT (cm ²)	CHG (e/3)	MASS (GeV)	ENERGY (GeV)	BEAM	EVTS	DOCUMENT ID	TECN
<1.3E-36	±2	45-84	130-172	e^+e^-	0	ABREU	97D DLPH
<2.E-35	+2	250	1800	$p\bar{p}$	0	¹ ABE	92J CDF
<1.E-35	+4	250	1800	$p\bar{p}$	0	¹ ABE	92J CDF
<3.8E-28			14.5A	²⁸ Si-Pb	0	² HE	91 PLAS
<3.2E-28			14.5A	²⁸ Si-Cu	0	² HE	91 PLAS
<1.E-40	±1,2	<10		$p,\nu,\bar{\nu}$	0	BERGSM	84B CHRM
<1.E-36	±1,2	<9	200	μ	0	AUBERT	83C SPEC
<2.E-10	±2,4	1-3	200	p	0	³ BUSSIERE	80 CNTR
<5.E-38	+1,2	>5	300	p	0	^{4,5} STEVENSON	79 CNTR
<1.E-33	±1	<20	52	pp	0	BASILE	78 SPEC
<9.E-39	±1,2	<6	400	p	0	⁴ ANTREASNYAN	77 SPEC
<8.E-35	+1,2	<20	52	pp	0	⁶ FABJAN	75 CNTR
<5.E-38	-1,2	4-9	200	p	0	NASH	74 CNTR
<1.E-32	+2,4	4-24	52	pp	0	ALPER	73 SPEC
<5.E-31	+1,2,4	<12	300	p	0	LEIPUNER	73 CNTR
<6.E-34	±1,2	<13	52	pp	0	BOTT	72 CNTR
<1.E-36	-4	4	70	p	0	ANTIPOV	71 CNTR
<1.E-35	±1,2	2	28	p	0	⁷ ALLABY	69B CNTR
<4.E-37	-2	<5	70	p	0	³ ANTIPOV	69 CNTR
<3.E-37	-1,2	2-5	70	p	0	⁷ ANTIPOV	69B CNTR
<1.E-35	+1,2	<7	30	p	0	DORFAN	65 CNTR
<2.E-35	-2	<2.5-5	30	p	0	⁸ FRANZINI	65B CNTR
<5.E-35	+1,2	<2.2	21	p	0	BINGHAM	64 HLBC
<1.E-32	+1,2	<4.0	28	p	0	BLUM	64 HBC
<1.E-35	+1,2	<2.5	31	p	0	⁸ HAGOPIAN	64 HBC
<1.E-34	+1	<2	28	p	0	LEIPUNER	64 CNTR
<1.E-33	+1,2	<2.4	24	p	0	MORRISON	64 HBC

¹ ABE 92J flux limits decrease as the mass increases from 50 to 500 GeV.

² HE 91 limits are for charges of the form $N\pm 1/3$ from 23/3 to 38/3.

³ Hadronic or leptonic quarks.

⁴ Cross section cm²/GeV².

⁵ 3×10^{-5} <lifetime < 1×10^{-3} s.

⁶ Includes BOTT 72 results.

⁷ Assumes isotropic cm production.

⁸ Cross section inferred from flux.

Quark Differential Production Cross Section — Accelerator Searches

X-SECT (cm ² sr ⁻¹ GeV ⁻¹)	CHG (e/3)	MASS (GeV)	ENERGY (GeV)	BEAM	EVTS	DOCUMENT ID	TECN
<4.E-36	-2,4	1.5-6	70	p	0	BALDIN	76 CNTR
<2.E-33	±4	5-20	52	pp	0	ALBROW	75 SPEC
<5.E-34	<7	7-15	44	pp	0	JOVANOV...	75 CNTR
<5.E-35			20	γ	0	⁹ GALIK	74 CNTR
<9.E-35	-1,2		200	p	0	NASH	74 CNTR
<4.E-36	-4	2.3-2.7	70	p	0	ANTIPOV	71 CNTR
<3.E-35	±1,2	<2.7	27	p	0	ALLABY	69B CNTR
<7.E-38	-1,2	<2.5	70	p	0	ANTIPOV	69B CNTR

⁹ Cross section in cm²/sr/equivalent quanta.

Quark Flux — Accelerator Searches

The definition of FLUX depends on the experiment

- is the ratio of measured free quarks to predicted free quarks if there is no “confinement.”
- is the probability of fractional charge on nuclear fragments. Energy is in GeV/nucleon.
- is the 90%CL upper limit on fractionally-charged particles produced per interaction.
- is quarks per collision.
- is inclusive quark-production cross-section ratio to $\sigma(e^+e^- \rightarrow \mu^+\mu^-)$.
- is quark flux per charged particle.
- is the flux per ν -event.
- is quark yield per π^- yield.
- is 2-body exclusive quark-production cross-section ratio to $\sigma(e^+e^- \rightarrow \mu^+\mu^-)$.

FLUX	CHG (e/3)	MASS (GeV)	ENERGY (GeV)	BEAM	EVTS	DOCUMENT ID	TECN	
<1.6E-3	b	see note	200	³² S-Pb	0	¹⁰ HUENTRUP	96 PLAS	
<6.2E-4	b	see note	10.6	³² S-Pb	0	¹⁰ HUENTRUP	96 PLAS	
<0.94E-4	e	±2	2-30	88-94	e^+e^-	0	AKERS	95R OPAL
<1.7E-4	e	±2	30-40	88-94	e^+e^-	0	AKERS	95R OPAL

Quark Particle Listings

Free Quark Searches

<3.6E-4	e	±4	5-30	88-94	e ⁺ e ⁻	0	AKERS	95R	OPAL
<1.9E-4	e	±4	30-45	88-94	e ⁺ e ⁻	0	AKERS	95R	OPAL
<2.E-3	e	+1	5-40	88-94	e ⁺ e ⁻	0	11 BUSKULIC	93C	ALEP
<6.E-4	e	+2	5-30	88-94	e ⁺ e ⁻	0	11 BUSKULIC	93C	ALEP
<1.2E-3	e	+4	15-40	88-94	e ⁺ e ⁻	0	11 BUSKULIC	93C	ALEP
<3.6E-4	i	+4	5.0-10.2	88-94	e ⁺ e ⁻	0	BUSKULIC	93C	ALEP
<3.6E-4	i	+4	16.5-26.0	88-94	e ⁺ e ⁻	0	BUSKULIC	93C	ALEP
<6.9E-4	i	+4	26.0-33.3	88-94	e ⁺ e ⁻	0	BUSKULIC	93C	ALEP
<9.1E-4	i	+4	33.3-38.6	88-94	e ⁺ e ⁻	0	BUSKULIC	93C	ALEP
<1.1E-3	i	+4	38.6-44.9	88-94	e ⁺ e ⁻	0	BUSKULIC	93C	ALEP
<1.6E-4	b	see note	see note			0	12 CECCHINI	93	PLAS
	b	4,5,7,8	2.1A	16 O	0,2,0,6		13 GHOSH	92	EMUL
<6.4E-5	g	1			$\nu, \bar{\nu}$	1	14 BASILE	91	CNTR
<3.7E-5	g	2			$\nu, \bar{\nu}$	0	14 BASILE	91	CNTR
<3.9E-5	g	1			$\nu, \bar{\nu}$	1	15 BASILE	91	CNTR
<2.8E-5	g	2			$\nu, \bar{\nu}$	0	15 BASILE	91	CNTR
<1.9E-4	c		14.5A	28 Si-Pb	0		16 HE	91	PLAS
<3.9E-4	c		14.5A	28 Si-Cu	0		16 HE	91	PLAS
<1.E-9	c	±1,2,4	14.5A	16 O-Ar	0		MATIS	91	MDRP
<5.1E-10	c	±1,2,4	14.5A	16 O-Hg	0		MATIS	91	MDRP
<8.1E-9	c	±1,2,4	14.5A	Si-Hg	0		MATIS	91	MDRP
<1.7E-6	c	±1,2,4	60A	16 O-Hg	0		MATIS	91	MDRP
<3.5E-7	c	±1,2,4	200A	16 O-Hg	0		MATIS	91	MDRP
<1.3E-6	c	±1,2,4	200A	5-Hg	0		MATIS	91	MDRP
<5E-2	e	2	19-27	52-60	e ⁺ e ⁻	0	ADACHI	90C	TOPZ
<5E-2	e	4	<24	52-60	e ⁺ e ⁻	0	ADACHI	90C	TOPZ
<1.E-4	e	+2	<3.5	10	e ⁺ e ⁻	0	BOWCOCK	89B	CLEO
<1.E-6	d	±1,2	60	16 O-Hg	0		CALLOWAY	89	MDRP
<3.5E-7	d	±1,2	200	16 O-Hg	0		CALLOWAY	89	MDRP
<1.3E-6	d	±1,2	200	5-Hg	0		CALLOWAY	89	MDRP
<1.2E-10	d	±1	1	800	p-Hg	0	MATIS	89	MDRP
<1.1E-10	d	±2	1	800	p-Hg	0	MATIS	89	MDRP
<1.2E-10	d	±1	1	800	p-N ₂	0	MATIS	89	MDRP
<7.7E-11	d	±2	1	800	p-N ₂	0	MATIS	89	MDRP
<6.E-9	h	-5	0.9-2.3	12	p	0	NAKAMURA	89	SPEC
<5.E-5	g	1,2	<0.5		$\nu, \bar{\nu}d$	0	ALLASIA	88	BEBC
<3.E-4	b	See note	14.5	16 O-Pb	0		17 HOFFMANN	88	PLAS
<2.E-4	b	See note	200	16 O-Pb	0		18 HOFFMANN	88	PLAS
<8E-5	b	19,20,22,23	200A				GERBIER	87	PLAS
<2.E-4	a	±1,2	<300	320	$\bar{p}p$	0	LYONS	87	MLEV
<1.E-9	c	±1,2,4,5	14.5	16 O-Hg	0		SHAW	87	MDRP
<3.E-3	d	-1,2,3,4,6	<5	2	Si-Si	0	19 ABACHI	86C	CNTR
<1.E-4	e	±1,2,4	<4	10	e ⁺ e ⁻	0	ALBRECHT	85G	ARG
<6.E-5	e	±1,2	1	540	$p\bar{p}$	0	BANNER	85	UA2
<5.E-3	e	-4	1-8	29	e ⁺ e ⁻	0	AIHARA	84	TPC
<1.E-2	e	±1,2	1-13	29	e ⁺ e ⁻	0	AIHARA	84B	TPC
<2.E-4	b	±1	72	40 Ar	0		20 BARWICK	84	CNTR
<1.E-4	e	±2	<0.4	1.4	e ⁺ e ⁻	0	BONDAR	84	OLYA
<5.E-1	e	±1,2	<13	29	e ⁺ e ⁻	0	GURYN	84	CNTR
<3.E-3	b	±1,2	<2	540	$p\bar{p}$	0	BANNER	83	CNTR
<1.E-4	b	±1,2	106	56 Fe	0		LINDGREN	83	CNTR
<3.E-3	b	> ±0.1	74	40 Ar	0		20 PRICE	83	PLAS
<1.E-2	e	±1,2	<14	29	e ⁺ e ⁻	0	MARINI	82B	CNTR
<8.E-2	e	±1,2	<12	29	e ⁺ e ⁻	0	ROSS	82	CNTR
<3.E-4	e	±2	1.8-2	7	e ⁺ e ⁻	0	WEISS	81	MRK2
<5.E-2	e	+1,2,4,5	2-12	27	e ⁺ e ⁻	0	BARTEL	80	JADE
<2.E-5	g	1,2			ν	0	14,15 BASILE	80	CNTR
<3.E-10	f	±2,4	1-3	200	p	0	21 BOZZOLI	79	CNTR
<6.E-11	f	±1	<21	52	$p\bar{p}$	0	BASILE	78	SPEC
<5.E-3	g				ν_μ	0	BASILE	78B	CNTR
<2.E-9	f	±1	<26	62	$p\bar{p}$	0	BASILE	77	SPEC
<7.E-10	f	+1,2	<20	52	p	0	22 FABJAN	75	CNTR
		+1,2	>4.5		γ	0	14,15 GALIK	74	CNTR
		+1,2	>1.5	12	e ⁻	0	14,15 BELLAMY	68	CNTR
		+1,2	>0.9		γ	0	15 BATHOW	67	CNTR
		+1,2	>0.9	6	γ	0	15 FOSS	67	CNTR

10 HUENTRUP 96 quote 95% CL limits for production of fragments with charge differing by as much as ±1/3 (in units of e) for charge 6 ≤ Z ≤ 10.
 11 BUSKULIC 93C limits for inclusive quark production are more conservative if the ALEPH hadronic fragmentation function is assumed.
 12 CECCHINI 93 limit at 90%CL for 23/3 ≤ Z ≤ 40/3, for 16A GeV O, 14.5A Si, and 200A S incident on Cu target. Other limits are 2.3 × 10⁻⁴ for 17/3 ≤ Z ≤ 20/3 and 1.2 × 10⁻⁴ for 20/3 ≤ Z ≤ 23/3.
 13 GHOSH 92 reports measurement of spallation fragment charge based on ionization in emulsion. Out of 650 measured tracks, 2 were consistent with charge 5e/3, and 4 with 7e/3.
 14 Hadronic quark.
 15 Leptonic quark.
 16 HE 91 limits are for charges of the form N±1/3 from 23/3 to 38/3, and correspond to cross-section limits of 380μb (Pb) and 320μb (Cu).
 17 The limits apply to projectile fragment charges of 17, 19, 20, 22, 23 in units of e/3.
 18 The limits apply to projectile fragment charges of 16, 17, 19, 20, 22, 23 in units of e/3.
 19 Flux limits and mass range depend on charge.
 20 Bound to nuclei.
 21 Quark lifetimes > 1 × 10⁻⁸ s.

22 One candidate m < 0.17 GeV.

Quark Flux — Cosmic Ray Searches

Shielding values followed with an asterisk indicate altitude in km. Shielding values not followed with an asterisk indicate sea level in kg/cm².

FLUX (cm ⁻² sr ⁻¹ s ⁻¹)	CHG (e/3)	MASS (GeV)	SHIELDING	EVTS	DOCUMENT ID	TECN
< 9.2E-15	±1		3800	0	23 AMBROSIO	00C MCRO
< 2.1E-15	±1			0	MORI	91 KAM2
< 2.3E-15	±2			0	MORI	91 KAM2
< 2.E-10	±1,2		0.3	0	WADA	88 CNTR
			0.3	12	24 WADA	88 CNTR
			0.3	9	25 WADA	86 CNTR
< 1.E-12	±2,3/2		-70.	0	26 KAWAGOE	84B PLAS
< 9.E-10	±1,2		0.3	0	WADA	84B CNTR
< 4.E-9	±4		0.3	7	WADA	84B CNTR
< 2.E-12	±1,2,3		-0.3*	0	MASHIMO	83 CNTR
< 3.E-10	±1,2		0.3	0	MARINI	82 CNTR
< 2.E-11	±1,2			0	MASHIMO	82 CNTR
< 8.E-10	±1,2		0.3	0	26 NAPOLITANO	82 CNTR
				3	27 YOCK	78 CNTR
< 1.E-9				0	28 BRIATORE	76 ELEC
< 2.E-11	+1			0	29 HAZEN	75 CC
< 2.E-10	+1,2			0	KRISOR	75 CNTR
< 1.E-7	+1,2			0	29,30 CLARK	74B CC
< 3.E-10	+1	>20		0	KIFUNE	74 CNTR
< 8.E-11	+1			0	29 ASHTON	73 CNTR
< 2.E-8	+1,2			0	HICKS	73B CNTR
< 5.E-10	+4		2.8*	0	BEAUCHAMP	72 CNTR
< 1.E-10	+1,2			0	29 BOHM	72B CNTR
< 1.E-10	+1,2		2.8*	0	COX	72 ELEC
< 3.E-10	+2			0	CROUCH	72 CNTR
< 3.E-8			7	0	28 DARDO	72 CNTR
< 4.E-9	+1			0	29 EVANS	72 CC
< 2.E-9		>10		0	28 TONWAR	72 CNTR
< 2.E-10	+1		2.8*	0	CHIN	71 CNTR
< 3.E-10	+1,2			0	29 CLARK	71B CC
< 1.E-10	+1,2			0	29 HAZEN	71 CC
< 5.E-10	+1,2	3.5*		0	BOSIA	70 CNTR
	+1,2	<6.5		1	29 CHU	70 HLBC
< 2.E-9	+1			0	FAISSNER	70B CNTR
< 2.E-10	+1,2		0.8*	0	KRIDER	70 CNTR
< 5.E-11	+2			4	CAIRNS	69 CC
< 8.E-10	+1,2	<10		1	29,31 FUKUSHIMA	69 CNTR
	+2			1	29,31 MCCUSKER	69 CC
< 1.E-10		>5	1.7,3.6	0	28 BJORNBOE	68 CNTR
< 1.E-8	±1,2,4		6.3, 2*	0	26 BRIATORE	68 CNTR
< 3.E-8		>2		0	FRANZINI	68 CNTR
< 9.E-11	±1,2			0	GARMIRE	68 CNTR
< 4.E-10	±1			0	HANAYAMA	68 CNTR
< 3.E-8		>15		0	KASHA	68 OSPK
< 2.E-10	+2			0	KASHA	68B CNTR
< 2.E-10	+4			0	KASHA	68C CNTR
< 2.E-10	+2		6	0	BARTON	67 CNTR
< 2.E-7	+4	0.008, 0.5*		0	BUHLER	67 CNTR
< 5.E-10	1,2	0.008, 0.5*		0	BUHLER	67B CNTR
< 4.E-10	+1,2			0	GOMEZ	67 CNTR
< 2.E-9	+2			0	KASHA	67 CNTR
< 2.E-10	+2		220	0	BARTON	66 CNTR
< 2.E-9	+1,2	0.5*		0	BUHLER	66 CNTR
< 3.E-9	+1,2			0	KASHA	66 CNTR
< 2.E-9	+1,2			0	LAMB	66 CNTR
< 2.E-8	+1,2	>7	2.8*	0	DELISE	65 CNTR
< 5.E-8	+2	>2.5	0.5*	0	MASSAM	65 CNTR
< 2.E-8	+1		2.5*	0	BOWEN	64 CNTR
< 2.E-7	+1		0.8	0	SUNYAR	64 CNTR

23 AMBROSIO 00C limit is below 11 × 10⁻¹⁵ for 0.25 < q/e < 0.5, and is changing rapidly near q/e=2/3, where it is 2 × 10⁻¹⁴.
 24 Distribution in celestial sphere was described as anisotropic.
 25 With telescope axis at zenith angle 40° to the south.
 26 Leptonic quarks.
 27 Lifetime > 10⁻⁸ s; charge ±0.70, 0.68, 0.42; and mass >4.4, 4.8, and 20 GeV, respectively.
 28 Time delayed air shower search.
 29 Prompt air shower search.
 30 Also e/4 and e/6 charges.
 31 No events in subsequent experiments.

Quark Density — Matter Searches

QUARKS/NUCLEON	CHG (e/3)	MASS (GeV)	MATERIAL/METHOD	EVTS	DOCUMENT ID	
< 1.17E-22			silicone oil drops	0	32 LEE	02
< 4.71E-22			silicone oil drops	1	33 HALYO	00
< 4.7E-21	±1,2		silicone oil drops	0	MAR	96
< 8.E-22	+2		Si/infrared photoionization	0	PERERA	93
< 5.E-27	±1,2		sea water/levitation	0	HOMER	92
< 4.E-20	±1,2		meteorites/mag. levitation	0	JONES	89

Quark Particle Listings

Free Quark Searches

See key on page 373

<1.E-19	±1,2	various/spectrometer	0	MILNER	87	BONDAR	84	JETPL 40 1265	A.E. Bondar et al.	(NOVO)
<5.E-22	±1,2	W/levitation	0	SMITH	87	GURYN	84	Translated from ZETFP 40 440.	W. Guryn et al.	(FRAS, LBL, NWES, STAN+)
<3.E-20	+1,2	org liq/droplet tower	0	VANPOLEN	87	KAWAGOE	84B	LNC 41 604	K. Kawagoe et al.	(TOKY)
<6.E-20	-1,2	org liq/droplet tower	0	VANPOLEN	87	KUTSCHERA	84	PR D29 791	W. Kutschera et al.	(ANL, FNAL)
<3.E-21	±1	Hg drops-untreated	0	SAVAGE	86	MARINELLI	84	PL 137B 439	M. Marinelli, G. Morpurgo	(GENO)
<3.E-22	±1,2	levitated niobium	0	SMITH	86	WADA	84B	LNC 40 329	T. Wada, Y. Yamashita, I. Yamamoto	(OKAY)
<2.E-26	±1,2	⁴ He/levitation	0	SMITH	86B	AUBERT	83C	PL 133B 461	J.J. Aubert et al.	(EMC Collab.)
<2.E-20	>±1	0.2-250 niobium+tungs/ion	0	MILNER	85	BANNER	83	PL 121B 187	M. Banner et al.	(UA2 Collab.)
<1.E-21	±1	levitated niobium	0	SMITH	85	JOYCE	83	PRL 51 731	D.C. Joyce et al.	(FSU)
	+1,2	<100 niobium/mass spec	0	KUTSCHERA	84	LIEBOWITZ	83	PRL 50 1640	D. Liebowitz, M. Binder, K.O.H. Zlock	(VIRG)
<5.E-22		levitated steel	0	MARINELLI	84	LINDGREN	83	PRL 51 1621	M.A. Lindgren et al.	(FSU, UCR, UCI+)
<9.E-20	±<13	water/oil drop	0	JOYCE	83	MASHIMO	83	PL 128B 327	T. Mashimo et al.	(ICEPP)
<2.E-21	> ±1/2	levitated steel	0	LIEBOWITZ	83	PRICE	83	PRL 50 566	P.B. Price et al.	(UCB)
<1.E-19	±1,2	photo ion spec	0	VANDESTEEG	83	VANDESTEEG	83	PRL 50 1234	M.J.H. van de Steeg, H.W.H.M. Jongbloets, P. Wyder	
<2.E-20		mercury/oil drop	0	HODGES	81	MARINI	82	PR D26 1777	A. Marini et al.	(FRAS, LBL, NWES, STAN+)
1.E-20	+1	levitated niobium	4	LARUE	81	MARINI	82B	PL 48 1649	A. Marini et al.	(FRAS, LBL, NWES, STAN+)
1.E-20	-1	levitated niobium	4	LARUE	81	MASHIMO	82	JPS J 51 3067	T. Mashimo, K. Kawagoe, M. Koshida	(INUS)
<1.E-21		levitated steel	0	MARINELLI	80B	NAPOLITANO	82	PR D25 2837	J. Napolitano et al.	(STAN, FRAS, LBL+)
<6.E-16		helium/mass spec	0	BOYD	79	ROSS	82	PL 118B 199	M.C. Ross et al.	(FRAS, LBL, NWES, STAN+)
1.E-20	+1	levitated niobium	2	LARUE	79	HODGES	81	PRL 47 1651	C.L. Hodges et al.	(UCR, FSU)
<4.E-28		earth+/ion beam	0	OGOROD...	79	LARUE	81	PRL 46 967	G.S. Larue, J.D. Phillips, W.M. Fairbank	(STAN)
<5.E-15	+1	tungs./mass spec	0	BOYD	78	WEISS	81	PL 101B 439	J.M. Weiss et al.	(SLAC, LBL, UCB)
<5.E-16	+3	<1.7 hydrogen/mass spec	0	BOYD	78B	BARTEL	80	ZPHY C6 295	W. Bartel et al.	(JADE Collab.)
<1.E-21	±2,4	water/ion beam	0	LUND	78	BASILE	80	LNC 29 251	M. Basile et al.	(BGNA, CERN, FRAS, ROMA+)
<6.E-15	>1/2	levitated tungsten	0	PUTT	78	BUSSIERE	80	NP B174 1	A. Bussiere et al.	(BGNA, SACL, LAPP)
<1.E-22		metals/mass spec	0	SCHIFFER	78	MARINELLI	80B	PL 94B 433	M. Marinelli, G. Morpurgo	(GENO)
<5.E-15		levitated tungsten ox	0	BLAND	77	BOYD	79	PL 94B 427	M. Marinelli, G. Morpurgo	(GENO)
<3.E-21		levitated iron	0	GALLINARO	77	BOYD	79	PL 43 1208	R.N. Boyd et al.	(ROCH)
2.E-21	-1	levitated niobium	1	LARUE	77	LUND	78	RA 25 75	T. Lund, R. Brandt, Y. Fares	(MARB)
4.E-21	+1	levitated niobium	2	LARUE	77	PUTT	78	PR D17 1466	G.D. Putt, P.C.M. Yock	(AUCK)
<1.E-13	+3	<7.7 hydrogen/mass spec	0	MULLER	77	SCHIFFER	78	PR D17 2241	J.P. Schiffer et al.	(CHIC, ANL)
<5.E-27		water+/ion beam	0	OGOROD...	77	YOCK	78	PR D18 641	P.C.M. Yock	(AUCK)
<1.E-21		lunar+/ion spec	0	STEVENS	76	ANTREASAYAN	77	PRL 39 513	D. Antreasayan et al.	(EFI, PRIN)
<1.E-15	+1	<60 oxygen+/ion spec	0	ELBERT	70	BASILE	77	NC 40A 41	M. Basile et al.	(CERN, BGNA)
<5.E-19		levitated graphite	0	MORPURGO	70	BLAND	77	PRL 39 369	R.W. Bland et al.	(FSU)
<5.E-23		water+/atom beam	0	COOK	69	GALLINARO	77	PRL 38 1255	G. Gallinaro, M. Marinelli, G. Morpurgo	(GENO)
<1.E-17	±1,2	levitated graphite	0	BRAGINSK	68	JONES	77B	RMI 149 717	L.W. Jones	
<1.E-17		water+/uv spec	0	RANK	67	LARUE	77	PL 38 1011	G.S. Larue, W.M. Fairbank, A.F. Hebard	(STAN)
<3.E-19	±1	levitated iron	0	STOVER	67	MULLER	77	SCI 195 821	R. Muller et al.	(LBL)
<1.E-10		sun/uv spec	0	BENNETT	66	OGOROD...	77	JETP 45 857	D.D. Ogorodnikov, I.M. Samoilov, A.M. Solntsev	
<1.E-17	+1,2	meteorites+/ion beam	0	CHUPKA	66	BALDIN	76	SJNP 22 264	B.Y. Baldin et al.	(JINR)
<1.E-16	±1	levitated graphite	0	GALLINARO	66	BRIATORE	76	NC 31A 553	L. Briatore et al.	(LCGT, FRAS, FREIB)
<1.E-22	-2	argon/electrometer	0	HILLAS	59	STEVENS	76	PR D14 716	C.M. Stevens, J.P. Schiffer, W. Chupka	(ANL)
		levitated oil	0	MILLIKAN	10	ALBROW	75	NP B97 189	M.G. Albrow et al.	(CERN, DARE, FOM)

32 95% CL limit for fractional charge particles with $0.18e \leq |Q_{residual}| \leq 0.82e$ in total of 70.1 mg of silicone oil.

33 95% CL limit for particles with fractional charge $|Q_{residual}| > 0.16e$ in total of 17.4 mg of silicone oil.

34 Also set limits for $Q = \pm e/6$.

35 Note that in PHILLIPS 88 these authors report a subtle magnetic effect which could account for the apparent fractional charges.

36 Limit inferred by JONES 77b.

REFERENCES FOR Free Quark Searches

LEE	02	PR D66 012002	I.T. Lee et al.	
AMBROSIO	00C	PR D62 052003	M. Ambrosio et al.	(MACRO Collab.)
HALYO	00	PRL 84 2576	V. Halayo et al.	
ABREU	97D	PL B396 315	P. Abreu et al.	(DELPHI Collab.)
HUENTRUP	96	PR C53 358	G. Huentrup et al.	(SIEG)
MAR	96	PR D53 6017	N.M. Mar et al.	(SLAC, SCHAFF, LANL, UCI)
AKERS	95R	ZPHY C67 203	R. Akers et al.	(OPAL Collab.)
BUSKULIC	93C	PL B303 198	D. Buskulic et al.	(ALEPH Collab.)
CECCHINI	93	ASP 1 369	S. Cecchini et al.	(PITT)
FERERA	93	PRL 70 1053	A.G.U. Ferera et al.	(CDF Collab.)
ABE	92J	PR D46 R1889	F. ABE et al.	(JADA, BANGB)
GHOSH	92	NC 105A 99	D. Ghosh et al.	(RAL, SHMP, LOQM)
HOMER	92	ZPHY C55 549	G.J. Homer et al.	(BGNA, INFN, CERN, PLRM+)
BASILE	91	NC 104A 405	M. Basile et al.	(UCB)
HE	91	PR C44 1672	Y.B. He, P.B. Price	
MATIS	91	NP A525 513c	H.S. Matis et al.	(LBL, FSU, UCI+)
MORI	91	PR D43 2843	M. Mori et al.	(Kamioke II Collab.)
ADACHI	90C	PL B244 352	I. Adachi et al.	(TOPAZ Collab.)
BOWCOCK	89B	PR D40 263	T.J.V. Bowcock et al.	(CLEO Collab.)
CALLOWAY	89	PL B232 549	D. Calloway et al.	(FSU, UCI, LBL+)
JONES	89	ZPHY C43 349	W.G. Jones et al.	(LOIC, RAL)
MATIS	89	PR D39 1851	H.S. Matis et al.	(LBL, FSU, UCI+)
NAKAMURA	89	PR D39 1261	T.T. Nakamura et al.	(KYOT, TMTCC)
ALLASIA	88	PR D37 219	D. Allasia et al.	(WIASZ Collab.)
HOFFMANN	88	PL B200 583	A. Hoffmann et al.	(SIEG, USF)
PHILLIPS	88	NIM A264 125	J.D. Phillips, W.M. Fairbank, J. Navarro	(STAN)
WADA	88	NC 11C 229	T. Wada, Y. Yamashita, I. Yamamoto	(OKAY)
GERBIER	87	PRL 59 2535	G. Gerbier et al.	(UCB, CERN)
LYONS	87	ZPHY C36 363	L. Lyons et al.	(OXF, RAL, LOIC)
MILNER	87	PR D36 37	R.E. Milner et al.	(CIT)
SHAW	87	PR D36 3533	G.L. Shaw et al.	(UCI, LBL, LANL, FSU)
SMITH	87	PL B197 447	P.F. Smith et al.	(RAL, LOIC)
VANPOLEN	87	PR D36 1983	F. van Polen, R.T. Hagstrom, G. Hirsch	(ANL+)
ABACHI	86C	PR D33 2733	S. Abachi et al.	(UCLA, LBL, UCSD)
SAVAGE	86	PL 167B 481	M.L. Savage et al.	(FSU)
SMITH	86	PL B171 129	P.F. Smith et al.	(RAL, LOIC)
SMITH	86B	PL B181 407	P.F. Smith et al.	(RAL, LOIC)
WADA	86	NC 9C 358	T. Wada	(OKAY)
ALBRECHT	85G	PL 156B 134	H. Albrecht et al.	(ARGUS Collab.)
BANNER	85	PL 156B 129	M. Banner et al.	(UA2 Collab.)
MILNER	85	PRL 54 1472	R.E. Milner et al.	(CIT)
SMITH	85	PL 153B 188	P.F. Smith et al.	(RAL, LOIC)
AIHARA	84	PRL 52 168	H. Aihara et al.	(TPC Collab.)
AIHARA	84B	PRL 52 2332	H. Aihara et al.	(TPC Collab.)
BARWICK	84	PR D30 691	S.W. Barwick, J.A. Musser, J.D. Stevenson	(UCB)
BERGSMAS	84B	ZPHY C24 217	F. Bergsmas et al.	(CHARM Collab.)
BONDAR	84	JETPL 40 1265	A.E. Bondar et al.	(NOVO)
KAWAGOE	84B	LNC 41 604	K. Kawagoe et al.	(TOKY)
KUTSCHERA	84	PR D29 791	W. Kutschera et al.	(ANL, FNAL)
MARINELLI	84	PL 137B 439	M. Marinelli, G. Morpurgo	(GENO)
WADA	84B	LNC 40 329	T. Wada, Y. Yamashita, I. Yamamoto	(OKAY)
AUBERT	83C	PL 133B 461	J.J. Aubert et al.	(EMC Collab.)
BANNER	83	PL 121B 187	M. Banner et al.	(UA2 Collab.)
JOYCE	83	PRL 51 731	D.C. Joyce et al.	(FSU)
LIEBOWITZ	83	PRL 50 1640	D. Liebowitz, M. Binder, K.O.H. Zlock	(VIRG)
LINDGREN	83	PRL 51 1621	M.A. Lindgren et al.	(FSU, UCR, UCI+)
MASHIMO	83	PL 128B 327	T. Mashimo et al.	(ICEPP)
PRICE	83	PRL 50 566	P.B. Price et al.	(UCB)
VANDESTEEG	83	PRL 50 1234	M.J.H. van de Steeg, H.W.H.M. Jongbloets, P. Wyder	
MARINI	82	PR D26 1777	A. Marini et al.	(FRAS, LBL, NWES, STAN+)
MARINI	82B	PL 48 1649	A. Marini et al.	(FRAS, LBL, NWES, STAN+)
MASHIMO	82	JPS J 51 3067	T. Mashimo, K. Kawagoe, M. Koshida	(INUS)
NAPOLITANO	82	PR D25 2837	J. Napolitano et al.	(STAN, FRAS, LBL+)
ROSS	82	PL 118B 199	M.C. Ross et al.	(FRAS, LBL, NWES, STAN+)
HODGES	81	PRL 47 1651	C.L. Hodges et al.	(UCR, FSU)
LARUE	81	PRL 46 967	G.S. Larue, J.D. Phillips, W.M. Fairbank	(STAN)
WEISS	81	PL 101B 439	J.M. Weiss et al.	(SLAC, LBL, UCB)
BARTEL	80	ZPHY C6 295	W. Bartel et al.	(JADE Collab.)
BASILE	80	LNC 29 251	M. Basile et al.	(BGNA, CERN, FRAS, ROMA+)
BUSSIERE	80	NP B174 1	A. Bussiere et al.	(BGNA, SACL, LAPP)
MARINELLI	80B	PL 94B 433	M. Marinelli, G. Morpurgo	(GENO)
BOYD	79	PL 94B 427	M. Marinelli, G. Morpurgo	(GENO)
BOYD	79	PL 43 1208	R.N. Boyd et al.	(ROCH)
BOZZOLI	79	NP B159 363	W. Bozzoli et al.	(BGNA, LAPP, SACL+)
LARUE	79	PRL 42 142	G.S. Larue, W.M. Fairbank, J.D. Phillips	(STAN)
OGOROD...	79	JETP 49 953	D.D. Ogorodnikov, I.M. Samoilov, A.M. Solntsev	
STEVENSON	79	PR D20 82	M.L. Stevenson	
BASILE	78	NC 45A 171	M. Basile et al.	(CERN, BGNA)
BASILE	78B	NC 45A 281	M. Basile et al.	(CERN, BGNA)
BOYD	78	PL 72B 484	R.N. Boyd et al.	(ROCH)
LUND	78	RA 25 75	T. Lund, R. Brandt, Y. Fares	(MARB)
PUTT	78	PR D17 1466	G.D. Putt, P.C.M. Yock	(AUCK)
SCHIFFER	78	PR D17 2241	J.P. Schiffer et al.	(CHIC, ANL)
YOCK	78	PR D18 641	P.C.M. Yock	(AUCK)
ANTREASAYAN	77	PRL 39 513	D. Antreasayan et al.	(EFI, PRIN)
BASILE	77	NC 40A 41	M. Basile et al.	(CERN, BGNA)
BLAND	77	PRL 39 369	R.W. Bland et al.	(FSU)
GALLINARO	77	PRL 38 1255	G. Gallinaro, M. Marinelli, G. Morpurgo	(GENO)
JONES	77B	RMI 149 717	L.W. Jones	
LARUE	77	PL 38 1011	G.S. Larue, W.M. Fairbank, A.F. Hebard	(STAN)
MULLER	77	SCI 195 821	R. Muller et al.	(LBL)
OGOROD...	77	JETP 45 857	D.D. Ogorodnikov, I.M. Samoilov, A.M. Solntsev	
BALDIN	76	SJNP 22 264	B.Y. Baldin et al.	(JINR)
BRIATORE	76	NC 31A 553	L. Briatore et al.	(LCGT, FRAS, FREIB)
STEVENS	76	PR D14 716	C.M. Stevens, J.P. Schiffer, W. Chupka	(ANL)
ALBROW	75	NP B97 189	M.G. Albrow et al.	(CERN, DARE, FOM)
FABJAN	75	NP B101 349	C.W. Fabjan et al.	(CERN, MPIM)
HAZEN	75	NP B95 189	W.E. Hazen et al.	(MICH, LEED)
JOVANOVICH	75	PL 56B 105	J.V. Jovanovich et al.	(MANI, AACH, CERN+)
KRISOR	75	NC 27A 132	K. Krisor	(AACH3)
CLARK	74B	PR D10 2721	A.F. Clark et al.	(LLL)
GALIK	74	PR D9 1856	R.S. Galik et al.	(SLAC, FNAL)
KIFUNE	74	JPS J 36 629	T. Kifune et al.	(TOKY, KEK)
NASH	74	PRL 32 858	T. Nash et al.	(FNAL, CORN, NYU)
ALPER	73	PL 46B 265	B. Alper et al.	(CERN, LVP, LUND, BOHR+)
ASHTON	73	JPA 6 577	F. Ashton et al.	(DURH)
HICKS	73B	NC 14A 65	R.B. Hicks, R.W. Flint, S	

Quark Particle Listings

Free Quark Searches

DELISE	65	PR 140B 458	D.A. de Lise, T. Bowen	(ARIZ)
DORFAN	65	PRL 14 999	D.E. Dorfán <i>et al.</i>	(COLU)
FRANZINI	65B	PRL 14 196	P. Franzini <i>et al.</i>	(BNL, COLU)
MASSAM	65	NC 40A 589	T. Massam, T. Müller, A. Zichichi	(CERN)
BINGHAM	64	PL 9 201	H.H. Bingham <i>et al.</i>	(CERN, EPOL)
BLUM	64	PRL 13 353A	W. Blum <i>et al.</i>	(CERN)
BOWEN	64	PRL 13 728	T. Bowen <i>et al.</i>	(ARIZ)
HAGOPIAN	64	PRL 13 280	V. Hagopian <i>et al.</i>	(PENN, BNL)
LEIPUNER	64	PRL 12 423	L.B. Leipuner <i>et al.</i>	(BNL, YALE)
MORRISON	64	PL 9 199	D.R.O. Morrison	(CERN)
SUNYAR	64	PR 136 B1157	A.W. Sunyar, A.Z. Schwarzschild, P.I. Connors	(BNL)
HILLAS	59	NAT 184 B92	A.M. Hillas, T.E. Cranshaw	(AERE)
MILLIKAN	10	Phil Mag 19 209	R.A. Millikan	(CHIC)

OTHER RELATED PAPERS

LYONS	85	PRPL C129 225	L. Lyons	(OXF)
Review				
MARINELLI	82	PRPL 85 161	M. Marinelli, G. Morpurgo	(GENO)
Review				

LIGHT UNFLAVORED MESONS ($S = C = B = 0$)

- π^\pm 583
- π^0 587
- η 589
- $f_0(600)$ 594
- $\rho(770)$ 599
- $\omega(782)$ 605
- $\eta'(958)$ 610
- $f_0(980)$ 613
- $a_0(980)$ 615
- $\phi(1020)$ 618
- $h_1(1170)$ 623
- $b_1(1235)$ 624
- $a_1(1260)$ 625
- $f_2(1270)$ 627
- $f_1(1285)$ 630
- $\eta(1295)$ 632
- $\pi(1300)$ 633
- $a_2(1320)$ 634
- $f_0(1370)$ 637
- $h_1(1380)$ 640
- $\pi_1(1400)$ 640
- $\eta(1405)$ 641
- $f_1(1420)$ 645
- $\omega(1420)$ 647
- $f_2(1430)$ 648
- $a_0(1450)$ 648
- $\rho(1450)$ 649
- $\eta(1475)$ 651
- $f_0(1500)$ 652
- $f_1(1510)$ 655
- $f_2'(1525)$ 655
- $f_2(1565)$ 658
- $\rho(1570)$ 659
- $h_1(1595)$ 660
- $\pi_1(1600)$ 660
- $a_1(1640)$ 661
- $f_2(1640)$ 661
- $\eta_2(1645)$ 662
- $\omega(1650)$ 662
- $\omega_3(1670)$ 663
- $\pi_2(1670)$ 664
- $\phi(1680)$ 666
- $\rho_3(1690)$ 667
- $\rho(1700)$ 670
- $a_2(1700)$ 674
- $f_0(1710)$ 675
- $\eta(1760)$ 678
- $\pi(1800)$ 678
- $f_2(1810)$ 679
- $X(1835)$ 680
- $\phi_3(1850)$ 681
- $\eta_2(1870)$ 681
- $\pi_2(1880)$ 681
- $\rho(1900)$ 682
- $f_2(1910)$ 682
- $f_2(1950)$ 683

- $\rho_3(1990)$ 684
- $f_2(2010)$ 685
- $f_0(2020)$ 685
- $a_4(2040)$ 685
- $f_4(2050)$ 686
- $\pi_2(2100)$ 688
- $f_0(2100)$ 688
- $f_2(2150)$ 688
- $\rho(2150)$ 690
- $\phi(2170)$ 691
- $f_0(2200)$ 691
- $f_J(2220)$ 692
- $\eta(2225)$ 693
- $\rho_3(2250)$ 693
- $f_2(2300)$ 694
- $f_4(2300)$ 694
- $f_0(2330)$ 695
- $f_2(2340)$ 695
- $\rho_5(2350)$ 696
- $a_6(2450)$ 696
- $f_6(2510)$ 697

OTHER LIGHT UNFLAVORED ($S = C = B = 0$)

- Further States 698

STRANGE MESONS ($S = \pm 1, C = B = 0$)

- K^\pm 704
- K^0 721
- K_S^0 725
- K_L^0 728
- $K_0^*(800)$ 749
- $K^*(892)$ 750
- $K_1(1270)$ 752
- $K_1(1400)$ 754
- $K^*(1410)$ 755
- $K_0^*(1430)$ 755
- $K_2^*(1430)$ 756
- $K(1460)$ 758
- $K_2(1580)$ 758
- $K(1630)$ 759
- $K_1(1650)$ 759
- $K^*(1680)$ 759
- $K_2(1770)$ 760
- $K_3^*(1780)$ 760
- $K_2(1820)$ 762
- $K(1830)$ 762
- $K_0^*(1950)$ 762
- $K_2^*(1980)$ 763
- $K_4^*(2045)$ 763
- $K_2(2250)$ 764
- $K_3(2320)$ 764
- $K_5^*(2380)$ 764
- $K_4(2500)$ 764
- $K(3100)$ 765

• Indicates the particle is in the Meson Summary Table

(continued on the next page)

CHARMED MESONS ($C = \pm 1$)

• D^\pm	766
• D^0	783
• $D^*(2007)^0$	810
• $D^*(2010)^\pm$	811
• $D_0^*(2400)^0$	812
• $D_0^*(2400)^\pm$	812
• $D_1(2420)^0$	812
• $D_1(2420)^\pm$	813
• $D_1(2430)^0$	813
• $D_2^*(2460)^0$	814
• $D_2^*(2460)^\pm$	815
• $D^*(2640)^\pm$	815

CHARMED, STRANGE MESONS ($C = S = \pm 1$)

• D_s^\pm	816
• $D_s^{*\pm}$	827
• $D_{s0}^*(2317)^\pm$	827
• $D_{s1}(2460)^\pm$	828
• $D_{s1}(2536)^\pm$	830
• $D_{s2}(2573)^\pm$	831
• $D_{s1}(2700)^\pm$	832

BOTTOM MESONS ($B = \pm 1$)

• B -particle organization	833
• B^\pm	842
• B^0	878
• B^\pm/B^0 ADMIXTURE	932
• $B^\pm/B^0/B_s^0/b$ -baryon ADMIXTURE	945
• V_{cb} and V_{ub} CKM Matrix Elements	951
• B^*	966
• $B_1(5721)^0$	966
• $B_J^*(5732)$	966
• $B_2^*(5747)^0$	967

BOTTOM, STRANGE MESONS ($B = \pm 1, S = \mp 1$)

• B_s^0	968
• B_s^*	974
• $B_{s1}(5830)^0$	974
• $B_{s2}^*(5840)^0$	974
• $B_{sJ}^*(5850)$	975

BOTTOM, CHARMED MESONS ($B = C = \pm 1$)

• B_c^\pm	976
-------------	-----

$c\bar{c}$ MESONS

• Charmonium system	977
• $\eta_c(1S)$	977
• $J/\psi(1S)$	981
• $\chi_{c0}(1P)$	999
• $\chi_{c1}(1P)$	1005
• $h_c(1P)$	1008
• $\chi_{c2}(1P)$	1008
• $\eta_c(2S)$	1013
• $\psi(2S)$	1014
• $\psi(3770)$	1026

• $X(3872)$	1035
• $\chi_{c2}(2P)$	1037
• $X(3940)$	1037
• $X(3945)$	1037
• $\psi(4040)$	1038
• $\psi(4160)$	1039
• $X(4260)$	1039
• $X(4360)$	1040
• $\psi(4415)$	1041

$b\bar{b}$ MESONS

• Bottomonium system	1042
• $\eta_b(1S)$	1043
• $\Upsilon(1S)$	1043
• $\chi_{b0}(1P)$	1046
• $\chi_{b1}(1P)$	1047
• $\chi_{b2}(1P)$	1047
• $\Upsilon(2S)$	1047
• $\Upsilon(1D)$	1049
• $\chi_{b0}(2P)$	1049
• $\chi_{b1}(2P)$	1050
• $\chi_{b2}(2P)$	1051
• $\Upsilon(3S)$	1051
• $\Upsilon(4S)$	1054
• $\Upsilon(10860)$	1055
• $\Upsilon(11020)$	1056

NON- $q\bar{q}$ CANDIDATES

• Non- $q\bar{q}$ Candidates	1057
------------------------------	------

Notes in the Meson Listings

• Form Factors for Radiative Pion & Kaon Decays	584
• Note on Scalar Mesons (rev.)	594
• The $\rho(770)$ (rev.)	599
• The $\eta(1405)$, $\eta(1475)$, $f_1(1420)$, and $f_1(1510)$ (rev.)	641
• The $\rho(1450)$ and the $\rho(1700)$ (rev.)	670
• The Charged Kaon Mass	704
• Rare Kaon Decays (rev.)	706
• Dalitz Plot Parameters for $K \rightarrow 3\pi$ Decays	715
• $K_{\ell 3}^\pm$ and $K_{\ell 3}^0$ Form Factors (rev.)	717
• CPT Invariance Tests in Neutral Kaon Decay (new)	721
• CP Violation in $K_S \rightarrow 3\pi$	727
• V_{ud} , V_{us} , Cabibbo Angle, and CKM Unitarity (rev.)	733
• CP -Violation in K_L Decays (rev.)	741
• Dalitz-Plot Analysis Formalism	771
• Review of Charm Dalitz-Plot Analyses (rev.)	774
• $D^0-\bar{D}^0$ Mixing (rev.)	783
• Decay Constant of Charged Pseudoscalar Mesons (new)	818
• Production and Decay of b -flavored Hadrons (rev.)	833
• A note on HFAG Activities (rev.)	842
• Polarization in B Decays (rev.)	910
• $B^0-\bar{B}^0$ Mixing (rev.)	914
• Determination of V_{cb} and V_{ub} (rev.)	951
• Branching Ratios of $\psi(2S)$ and $\chi_{c0,1,2}$ (rev.)	997
• New Charmonium-like States (new)	1029
• Width Determinations of the Υ States	1042

• Indicates the particle is in the Meson Summary Table

LIGHT UNFLAVORED MESONS ($S = C = B = 0$)

For $l = 1$ (π, b, ρ, a): $u\bar{d}, (u\bar{u}-d\bar{d})/\sqrt{2}, d\bar{u}$;
for $l = 0$ ($\eta, \eta', h, h', \omega, \phi, f, f'$): $c_1(u\bar{u} + d\bar{d}) + c_2(s\bar{s})$

 π^\pm

$$I^G(J^P) = 1^-(0^-)$$

We have omitted some results that have been superseded by later experiments. The omitted results may be found in our 1988 edition Physics Letters **B204** 1 (1988).

π^\pm MASS

The most accurate charged pion mass measurements are based upon x-ray wavelength measurements for transitions in π^- -mesonic atoms. The observed line is the blend of three components, corresponding to different K-shell occupancies. JECKELMANN 94 revisits the occupancy question, with the conclusion that two sets of occupancy ratios, resulting in two different pion masses (Solutions A and B), are equally probable. We choose the higher Solution B since only this solution is consistent with a positive mass-squared for the muon neutrino, given the precise muon momentum measurements now available (DAUM 91, ASSAMAGAN 94, and ASSAMAGAN 96) for the decay of pions at rest. Earlier mass determinations with π^- -mesonic atoms may have used incorrect K-shell screening corrections.

Measurements with an error of > 0.005 MeV have been omitted from this Listing.

VALUE (MeV)	DOCUMENT ID	TECN	CHG	COMMENT
139.57018 ± 0.00035 OUR FIT	Error includes scale factor of 1.2.			
139.57018 ± 0.00035 OUR AVERAGE	Error includes scale factor of 1.2.			
139.57071 ± 0.00053	¹ LENZ	98	CNTR	— pionic N2-atoms gas target
139.56995 ± 0.00035	² JECKELMANN 94	CNTR	—	π^- atom, Soln. B
• • • We do not use the following data for averages, fits, limits, etc. • • •				
139.57022 ± 0.00014	³ ASSAMAGAN 96	SPEC	+	$\pi^+ \rightarrow \mu^+ \nu_\mu$
139.56782 ± 0.00037	⁴ JECKELMANN 94	CNTR	—	π^- atom, Soln. A
139.56996 ± 0.00067	⁵ DAUM 91	SPEC	+	$\pi^+ \rightarrow \mu^+ \nu$
139.56752 ± 0.00037	⁶ JECKELMANN 86b	CNTR	—	Mesonic atoms
139.5704 ± 0.0011	⁵ ABELA 84	SPEC	+	See DAUM 91
139.5664 ± 0.0009	⁷ LU 80	CNTR	—	Mesonic atoms
139.5686 ± 0.0020	CARTER 76	CNTR	—	Mesonic atoms
139.5660 ± 0.0024	^{7,8} MARUSHEN... 76	CNTR	—	Mesonic atoms

¹ LENZ 98 result does not suffer K-electron configuration uncertainties as does JECKELMANN 94.

² JECKELMANN 94 Solution B (dominant 2-electron K-shell occupancy), chosen for consistency with positive $m_{\nu_\mu}^2$.

³ ASSAMAGAN 96 measures the μ^+ momentum p_μ in $\pi^+ \rightarrow \mu^+ \nu_\mu$ decay at rest to be 29.79200 ± 0.00011 MeV/c. Combined with the μ^+ mass and the assumption $m_{\nu_\mu} = 0$, this gives the π^+ mass above; if $m_{\nu_\mu} > 0$, m_{π^+} given above is a lower limit. Combined instead with m_μ and (assuming CPT) the π^- mass of JECKELMANN 94, p_μ gives an upper limit on m_{ν_μ} (see the ν_μ).

⁴ JECKELMANN 94 Solution A (small 2-electron K-shell occupancy) in combination with either the DAUM 91 or ASSAMAGAN 94 pion decay muon momentum measurement yields a significantly negative $m_{\nu_\mu}^2$. It is accordingly not used in our fits.

⁵ The DAUM 91 value includes the ABELA 84 result. The value is based on a measurement of the μ^+ momentum for π^+ decay at rest, $p_\mu = 29.79179 \pm 0.00053$ MeV, uses $m_\mu = 105.658389 \pm 0.000034$ MeV, and assumes that $m_{\nu_\mu} = 0$. The last assumption means that in fact the value is a lower limit.

⁶ JECKELMANN 86b gives $m_\pi/m_e = 273.12677(71)$. We use $m_e = 0.51099906(15)$ MeV from COHEN 87. The authors note that two solutions for the probability distribution of K-shell occupancy fit equally well, and use other data to choose the lower of the two possible π^\pm masses.

⁷ These values are scaled with a new wavelength-energy conversion factor $\lambda = 1.23984244(37) \times 10^{-6}$ eV m from COHEN 87. The LU 80 screening correction relies upon a theoretical calculation of inner-shell refilling rates.

⁸ This MARUSHENKO 76 value used at the authors' request to use the accepted set of calibration γ energies. Error increased from 0.0017 MeV to include QED calculation error of 0.0017 MeV (12 ppm).

$$m_{\pi^+} - m_{\mu^+}$$

Measurements with an error > 0.05 MeV have been omitted from this Listing.

VALUE (MeV)	EVTS	DOCUMENT ID	TECN	CHG	COMMENT
• • • We do not use the following data for averages, fits, limits, etc. • • •					
33.91157 ± 0.00067	⁹ DAUM	91	SPEC	+	$\pi^+ \rightarrow \mu^+ \nu$
33.9111 ± 0.0011	ABELA	84	SPEC	—	See DAUM 91
33.925 ± 0.025	BOOTH	70	CNTR	+	Magnetic spect.
33.881 ± 0.035	145 HYMAN	67	HEBC	+	K^- He

⁹ The DAUM 91 value assumes that $m_{\nu_\mu} = 0$ and uses our $m_\mu = 105.658389 \pm 0.000034$ MeV.

$$(m_{\pi^+} - m_{\pi^-}) / m_{\text{average}}$$

A test of CPT invariance.

VALUE (units 10^{-4})	DOCUMENT ID	TECN
2 ± 5	AYRES	71 CNTR

π^\pm MEAN LIFE

Measurements with an error $> 0.02 \times 10^{-8}$ s have been omitted.

VALUE (10^{-8} s)	DOCUMENT ID	TECN	CHG	COMMENT	
2.6033 ± 0.0005 OUR AVERAGE	Error includes scale factor of 1.2.				
2.60361 ± 0.00052	¹⁰ KOPTEV	95	SPEC	+	Surface μ^+ 's
2.60231 ± 0.00050 ± 0.00084	NUMAO	95	SPEC	+	Surface μ^+ 's
2.609 ± 0.008	DUNAITSEV	73	CNTR	+	
2.602 ± 0.004	AYRES	71	CNTR	±	
2.604 ± 0.005	NORDBERG	67	CNTR	+	
2.602 ± 0.004	ECKHAUSE	65	CNTR	+	
• • • We do not use the following data for averages, fits, limits, etc. • • •					
2.640 ± 0.008	¹¹ KINSEY	66	CNTR	+	

¹⁰ KOPTEV 95 combines the statistical and systematic errors; the statistical error dominates.

¹¹ Systematic errors in the calibration of this experiment are discussed by NORDBERG 67.

$$(\tau_{\pi^+} - \tau_{\pi^-}) / \tau_{\text{average}}$$

A test of CPT invariance.

VALUE (units 10^{-4})	DOCUMENT ID	TECN
5.5 ± 7.1	AYRES	71 CNTR
• • • We do not use the following data for averages, fits, limits, etc. • • •		
-14 ± 29	PETRUKHIN	68 CNTR
40 ± 70	BARDON	66 CNTR
23 ± 40	¹² LOBKOWICZ	66 CNTR

¹² This is the most conservative value given by LOBKOWICZ 66.

π^+ DECAY MODES

π^- modes are charge conjugates of the modes below.

For decay limits to particles which are not established, see the appropriate Search sections (Massive Neutrino Peak Search Test, A^0 (axion), and Other Light Boson (X^0) Searches, etc.).

Mode	Fraction (Γ_i/Γ)	Confidence level
Γ_1 $\mu^+ \nu_\mu$	[a] (99.98770 ± 0.00004) %	
Γ_2 $\mu^+ \nu_\mu \gamma$	[b] (2.00 ± 0.25) × 10 ⁻⁴	
Γ_3 $e^+ \nu_e$	[a] (1.230 ± 0.004) × 10 ⁻⁴	
Γ_4 $e^+ \nu_e \gamma$	[b] (1.61 ± 0.23) × 10 ⁻⁷	
Γ_5 $e^+ \nu_e \pi^0$	(1.036 ± 0.006) × 10 ⁻⁸	
Γ_6 $e^+ \nu_e e^+ e^-$	(3.2 ± 0.5) × 10 ⁻⁹	
Γ_7 $e^+ \nu_e \nu \bar{\nu}$	< 5 × 10 ⁻⁶	90%
Lepton Family number (LF) or Lepton number (L) violating modes		
Γ_8 $\mu^+ \bar{\nu}_e$	L [c] < 1.5 × 10 ⁻³	90%
Γ_9 $\mu^+ \nu_e$	LF [c] < 8.0 × 10 ⁻³	90%
Γ_{10} $\mu^- e^+ e^+ \nu$	LF < 1.6 × 10 ⁻⁶	90%

[a] Measurements of $\Gamma(e^+ \nu_e)/\Gamma(\mu^+ \nu_\mu)$ always include decays with γ 's, and measurements of $\Gamma(e^+ \nu_e \gamma)$ and $\Gamma(\mu^+ \nu_\mu \gamma)$ never include low-energy γ 's. Therefore, since no clean separation is possible, we consider the modes with γ 's to be subreactions of the modes without them, and let $[\Gamma(e^+ \nu_e) + \Gamma(\mu^+ \nu_\mu \gamma)]/\Gamma_{\text{total}} = 100\%$.

[b] See the Particle Listings below for the energy limits used in this measurement; low-energy γ 's are not included.

[c] Derived from an analysis of neutrino-oscillation experiments.

π^+ BRANCHING RATIOS

$$\Gamma(e^+ \nu_e)/\Gamma_{\text{total}}$$

See note [a] in the list of π^+ decay modes just above, and see also the next block of data. See also the note on "Decay Constants of Charged Pseudoscalar Mesons" in the D_s^\pm Listings.

$$\Gamma_3/\Gamma$$

VALUE (units 10^{-4})	DOCUMENT ID
1.230 ± 0.004 OUR EVALUATION	

Meson Particle Listings

 π^\pm

$$\frac{\Gamma(e^+\nu_e) + \Gamma(e^+\nu_e\gamma)}{\Gamma(\mu^+\nu_\mu) + \Gamma(\mu^+\nu_\mu\gamma)} \quad (\Gamma_3 + \Gamma_4) / (\Gamma_1 + \Gamma_2)$$

See note [a] in the list of π^\pm decay modes above. See NUMAO 92 for a discussion of $e\text{-}\mu$ universality. See also the note on "Decay Constants of Charged Pseudoscalar Mesons" in the D_s^\pm Listings.

VALUE (units 10^{-4})	EVTS	DOCUMENT ID	TECN	COMMENT
1.230 ± 0.004 OUR AVERAGE				
1.2346 ± 0.0035 ± 0.0036	120k	CZAPEK 93	CALO	Stopping π^+
1.2265 ± 0.0034 ± 0.0044	190k	BRITTON 92	CNTR	Stopping π^+
1.218 ± 0.014	32k	BRYMAN 86	CNTR	Stopping π^+
••• We do not use the following data for averages, fits, limits, etc. •••				
1.273 ± 0.028	11k	¹³ DICAPUA 64	CNTR	
1.21 ± 0.07		ANDERSON 60	SPEC	
¹³ DICAPUA 64 has been updated using the current mean life.				

$$\Gamma(\mu^+\nu_\mu\gamma) / \Gamma_{\text{total}} \quad \Gamma_2 / \Gamma$$

Note that measurements here do not cover the full kinematic range.

VALUE (units 10^{-4})	EVTS	DOCUMENT ID	TECN	CHG	COMMENT
2.0 ± 0.24 ± 0.08		14 BRESSI 98	CALO	+	Stopping π^+
••• We do not use the following data for averages, fits, limits, etc. •••					
1.24 ± 0.25	26	CASTAGNOLI 58	EMUL		$KE_\mu < 3.38$ MeV

¹⁴BRESSI 98 result is given for $E_\gamma > 1$ MeV only. Result agrees with QED expectation, 2.283×10^{-4} and does not confirm discrepancy of earlier experiment CASTAGNOLI 58.

$$\Gamma(e^+\nu_e\gamma) / \Gamma_{\text{total}} \quad \Gamma_4 / \Gamma$$

Note that measurements here do not cover the full kinematic range.

VALUE (units 10^{-8})	EVTS	DOCUMENT ID	TECN	CHG	COMMENT
16.1 ± 2.3		15 BOLOTOV 90B	SPEC	17 GeV	$\pi^- \rightarrow e^- \bar{\nu}_e \gamma$
••• We do not use the following data for averages, fits, limits, etc. •••					
5.6 ± 0.7	226	¹⁶ STETZ 78	SPEC		$P_e > 56$ MeV/c
3.0	143	DEPOMMIER 63B	CNTR	(KE)	$e^+\gamma > 48$ MeV

¹⁵BOLOTOV 90B is for $E_\gamma > 21$ MeV, $E_e > 70 - 0.8E_\gamma$.

¹⁶STETZ 78 is for an $e^- \gamma$ opening angle $> 132^\circ$. Obtains 3.7 when using same cutoffs as DEPOMMIER 63B.

$$\Gamma(e^+\nu_e\pi^0) / \Gamma_{\text{total}} \quad \Gamma_5 / \Gamma$$

VALUE (units 10^{-8})	EVTS	DOCUMENT ID	TECN	CHG	COMMENT
1.036 ± 0.006 OUR AVERAGE					
1.036 ± 0.006	17,18	POCANIC 04	PIBE	+	π decay at rest
1.026 ± 0.039	1224	¹⁹ MCFARLANE 85	CNTR	+	Decay in flight
1.00 + 0.08 - 0.10	332	DEPOMMIER 68	CNTR	+	
1.07 ± 0.21	38	²⁰ BACASTOW 65	OSPK	+	
1.10 ± 0.26		²⁰ BERTRAM 65	OSPK	+	
1.1 ± 0.2	43	²⁰ DUNAITSEV 65	CNTR	+	
0.97 ± 0.20	36	²⁰ BARTLETT 64	OSPK	+	
••• We do not use the following data for averages, fits, limits, etc. •••					
1.15 ± 0.22	52	²⁰ DEPOMMIER 63	CNTR	+	See DEPOMMIER 68

¹⁷POCANIC 04 normalizes to $e^+\nu_e$ decays, using the PDG 2004 value $B(\pi^+ \rightarrow e^+\nu_e) = (1.230 \pm 0.004) \times 10^{-4}$. We add their statistical (0.004×10^{-8}) , systematic (0.004×10^{-8}) and systematic error due to the uncertainty of $B(\pi^+ \rightarrow e^+\nu_e)$ (0.003×10^{-8}) in quadrature.

¹⁸This result can be used to calculate V_{ud} from pion beta decay: $V_{ud}^{PIBETA} = 0.9728 \pm 0.0030$.

¹⁹MCFARLANE 85 combines a measured rate $(0.394 \pm 0.015)/s$ with 1982 PDG mean life.

²⁰DEPOMMIER 68 says the result of DEPOMMIER 63 is at least 10% too large because of a systematic error in the π^0 detection efficiency, and that this may be true of all the previous measurements (also V. Soergel, private communication, 1972).

$$\Gamma(e^+\nu_e e^+) / \Gamma(\mu^+\nu_\mu) \quad \Gamma_6 / \Gamma_1$$

VALUE (units 10^{-3})	CL%	EVTS	DOCUMENT ID	TECN	COMMENT
3.2 ± 0.5 ± 0.2		98	EGLI 89	SPEC	Uses $R_{PCAC} = 0.068 \pm 0.004$
••• We do not use the following data for averages, fits, limits, etc. •••					
0.46 ± 0.16 ± 0.07	7	²¹ BARANOV 92	SPEC		Stopped π^+
< 4.8	90	KORENCHE... 76B	SPEC		
< 34	90	KORENCHE... 71	OSPK		

²¹This measurement by BARANOV 92 is of the structure-dependent part of the decay. The value depends on values assumed for ratios of form factors.

$$\Gamma(e^+\nu_e\nu\bar{\nu}) / \Gamma_{\text{total}} \quad \Gamma_7 / \Gamma$$

VALUE (units 10^{-6})	CL%	DOCUMENT ID	TECN	COMMENT
< 5	90	PICCIOTTO 88	SPEC	

$$\Gamma(\mu^+\bar{\nu}_e) / \Gamma_{\text{total}} \quad \Gamma_8 / \Gamma$$

Forbidden by total lepton number conservation. See the note on "Decay Constants of Charged Pseudoscalar Mesons" in the D_s^\pm Listings.

VALUE (units 10^{-3})	CL%	DOCUMENT ID	TECN	COMMENT
< 1.5	90	²² COOPER 82	HLBC	Wideband ν beam

²²COOPER 82 limit on $\bar{\nu}_e$ observation is here interpreted as a limit on lepton number violation.

$$\Gamma(\mu^+\nu_e) / \Gamma_{\text{total}} \quad \Gamma_9 / \Gamma$$

Forbidden by lepton family number conservation.

VALUE (units 10^{-3})	CL%	DOCUMENT ID	TECN	COMMENT
< 8.0	90	²³ COOPER 82	HLBC	Wideband ν beam
²³ COOPER 82 limit on ν_e observation is here interpreted as a limit on lepton family number violation.				

$$\Gamma(\mu^- e^+ e^+ \nu) / \Gamma_{\text{total}} \quad \Gamma_{10} / \Gamma$$

Forbidden by lepton family number conservation.

VALUE (units 10^{-6})	CL%	DOCUMENT ID	TECN	CHG
< 1.6	90	BARANOV 91B	SPEC	+
••• We do not use the following data for averages, fits, limits, etc. •••				
< 7.7	90	KORENCHE... 87	SPEC	+

 π^+ — POLARIZATION OF EMITTED μ^+ $\pi^+ \rightarrow \mu^+ \nu$

Tests the Lorentz structure of leptonic charged weak interactions.

VALUE	CL%	DOCUMENT ID	TECN	CHG	COMMENT
••• We do not use the following data for averages, fits, limits, etc. •••					
< (-0.9959)	90	²⁴ FETSCHER 84	RVUE	+	
-0.99 ± 0.16		²⁵ ABELA 83	SPEC	-	μ X-rays
²⁴ FETSCHER 84 uses only the measurement of CARR 83.					
²⁵ Sign of measurement reversed in ABELA 83 to compare with μ^+ measurements.					

FORM FACTORS FOR RADIATIVE PION AND KAON DECAYS

Written December 2007 by W. Bertl (Paul Scherrer Inst.)

The radiative decays, $\pi^\pm \rightarrow l^\pm \nu \gamma$ and $K^\pm \rightarrow l^\pm \nu \gamma$, with l standing for an e or a μ , and γ for a real or virtual photon (e^+e^- pair), represent a powerful tool to investigate the hadronic structure of pions and kaons. The structure-dependent part SD_i of the amplitude describes the emission of photons from virtual hadronic states, and is parametrized in terms of form factors F_i , with $i = V, A$ (vector, axial vector), in the standard description [1,2]. Exotic, non-standard contributions like $i = T, S$ (tensor, scalar) have also been considered, and we shall discuss them below. Apart from the SD terms, the decay amplitude depends also on Inner Bremsstrahlung IB from the weak decay $\pi^\pm(K^\pm) \rightarrow l^\pm \nu$ accompanied by the photon radiated from the external charged particles. Naturally, experiments try to optimize their kinematics so as to minimize the "trivial" IB part of the amplitude.

The SD amplitude in its standard form is given as

$$M(SD_V) = \frac{-eG_F V_{qq'}}{\sqrt{2}m_P} \epsilon^\mu \ell^\nu F_V^P \epsilon_{\mu\nu\sigma\tau} k^\sigma q^\tau \quad (1)$$

$$M(SD_A) = \frac{-ieG_F V_{qq'}}{\sqrt{2}m_P} \epsilon^\mu \ell^\nu \{F_A^P [(qk - k^2)g_{\mu\nu} - q_\mu k_\nu] + R^P k^2 g_{\mu\nu}\} \quad (2)$$

which contains an additional axial form factor R^P which only can be accessed if the photon remains virtual. $V_{qq'}$ is the Cabibbo-Kobayashi-Maskawa mixing-matrix element; ϵ^μ is the polarization vector of the photon (or the effective vertex, $\epsilon^\mu = (e/k^2)\bar{u}(p_-)\gamma^\mu v(p_+)$, of the e^+e^- pair); $\ell^\nu = \bar{u}(p_\nu)\gamma^\nu(1 - \gamma_5)v(p_e)$ is the lepton-neutrino current; q and k are the meson and photon four-momenta ($k = p_+ + p_-$ for virtual photons); and P stands for π or K .

The pion vector form factor, F_V^π , is related via CVC (Conserved Vector Current) to the $\pi^0 \rightarrow \gamma\gamma$ decay width,

$|F_V^\pi| = (1/\alpha)\sqrt{2\Gamma_{\pi^0\rightarrow\gamma\gamma}/\pi m_{\pi^0}}$ [3]. The resulting value of $F_V^\pi(0) = 0.0259(9)$ has been confirmed by calculations based on chiral perturbation theory (χPT) [4], and by two experiments given in the Listings below. A very recent experiment by the PIBETA collaboration [5] reported a new measurement of F_V which is in excellent agreement with the CVC hypothesis and, for the first time, has also determined the slope parameter of the pion vector form factor $a = 0.095 \pm 0.058$, given by $F_V^\pi(s) = F_V^\pi(0)(1 + a \cdot s)$ with $s = (1 - 2E_\gamma/m_\pi)$ in the meson's rest frame. A functional dependence on s is expected for all form factors. While for pion decays it becomes non-negligible in the case of $F_V^\pi(s)$ when a wide range of photon momenta is recorded, proper treatment in the analysis of K decays is mandatory.

The form factor, R^P , can be related to the electromagnetic radius, r_P , of the meson [2], $R^P = \frac{1}{3}m_P f_P \langle r_P^2 \rangle$ using PCAC (Partial Conserved Axial vector Current; f_P is the meson decay constant). In lowest order χPT , the ratio $\gamma = F_A/F_V$ is related to the pion electric polarizability $\alpha_E = [\alpha/(8\pi^2 m_\pi f_\pi^2)] \times F_A/F_V$ [6]. The calculation of the other form factors, F_A^π, F_V^K , and F_A^K , is model-dependent [1,2,4].

For decay processes where the photon is real, the partial decay width can be written in analytical form as a sum of IB, SD and IB/SD interference terms INT [1,4]:

$$\begin{aligned} \frac{d^2\Gamma_{P\rightarrow\ell\nu\gamma}}{dxdy} &= \frac{d^2(\Gamma_{\text{IB}} + \Gamma_{\text{SD}} + \Gamma_{\text{INT}})}{dxdy} \\ &= \frac{\alpha}{2\pi}\Gamma_{P\rightarrow\ell\nu}\frac{1}{(1-r)^2}\left\{\text{IB}(x,y)\right. \\ &+ \frac{1}{r}\left(\frac{m_P}{2f_P}\right)^2\left[(F_V + F_A)^2\text{SD}^+(x,y) + (F_V - F_A)^2\text{SD}^-(x,y)\right] \\ &+ \left.\frac{m_P}{f_P}\left[(F_V + F_A)\text{S}_{\text{INT}}^+(x,y) + (F_V - F_A)\text{S}_{\text{INT}}^-(x,y)\right]\right\}. \quad (3) \end{aligned}$$

Here

$$\begin{aligned} \text{IB}(x,y) &= \left[\frac{1-y+r}{x^2(x+y-1-r)}\right] \\ &\quad \left[x^2 + 2(1-x)(1-r) - \frac{2xr(1-r)}{x+y-1-r}\right] \\ \text{SD}^+(x,y) &= (x+y-1-r)\left[(x+y-1)(1-x) - r\right] \\ \text{SD}^-(x,y) &= (1-y+r)\left[(1-x)(1-y) + r\right] \\ \text{S}_{\text{INT}}^+(x,y) &= \left[\frac{1-y+r}{x(x+y-1-r)}\right]\left[(1-x)(1-x-y) + r\right] \\ \text{S}_{\text{INT}}^-(x,y) &= \left[\frac{1-y+r}{x(x+y-1-r)}\right]\left[x^2 - (1-x)(1-x-y) - r\right] \end{aligned} \quad (4)$$

where $x = 2E_\gamma/m_P$, $y = 2E_\ell/m_P$, and $r = (m_\ell/m_P)^2$. Recently, formulas (3) and (4) have been extended to describe polarized distributions in radiative meson and muon decays [7].

The ‘‘helicity’’ factor r is responsible for the enhancement of the SD over the IB amplitude in the decays $\pi^\pm \rightarrow e^\pm\nu\gamma$, while $\pi^\pm \rightarrow \mu^\pm\nu\gamma$ is dominated by IB. Interference terms are important for the decay $K^\pm \rightarrow \mu^\pm\nu\gamma$ [8], but contribute only a few percent correction to pion decays. However, they provide the basis for determining the signs of F_V and F_A . Radiative corrections to the decay $\pi^+ \rightarrow e^+\nu\gamma$ have to be taken into account in the analysis of the precision experiments. They make up to 4% corrections in the total decay rate [9]. In $\pi^\pm \rightarrow e^\pm\nu e^+e^-$ and $K^\pm \rightarrow \ell^\pm\nu e^+e^-$ decays, all three form factors, F_V^P, F_A^P , and R^P , can be determined [10,11].

We give the experimental π^\pm form factors F_V^π, F_A^π , and R^π in the Listings below. In the K^\pm Listings, we give the extracted sum $F_A^K + F_V^K$ and difference $F_A^K - F_V^K$, as well as F_V^K, F_A^K and R^K .

Several searches for the exotic form factors F_T^π, F_T^K (tensor), and F_S^K (scalar) have been pursued in the past, some of them claiming non-zero results [12,13]. In particular, F_T^π has been brought into focus by experimental as well as theoretical work. It was shown that a tensor contribution could destructively interfere with the inner bremsstrahlung amplitude, leading to a substantial reduction of the branching ratio as compared with standard V–A calculations [14]. In addition, a tensor contribution as large as $F_T = -(5.6 \pm 1.7) \times 10^{-3}$ could not be completely ruled out by constraints from other measurements [15]. New high statistic data from the PIBETA collaboration have been re-analyzed together with an additional data set optimized for low backgrounds in the radiative pion decay. In particular, lower beam rates have been used in order to reduce the accidental background, thereby making the treatment of systematic uncertainties easier and more reliable. The PIBETA analysis now restricts the existence of a tensor form factor within $-5.2 \times 10^{-4} < F_T < 4.0 \times 10^{-4}$ at a 90% confidence limit [5]. This result is in excellent agreement with the most recent theoretical work [4].

Precision measurements of radiative pion and kaon decays are effective tools to study QCD in the non-perturbative region. The structure-dependent form factors have direct relations to (renormalized) coupling constants of chiral perturbation theories. Therefore, they are of interest beyond the scope of radiative decays. On the other hand, the interest in searching for new physics manifesting in exotic form factors F_T or F_S has weakened over the last years mainly for two reasons: (i) On the experimental side, the lack of results confirming the non-zero findings, and, (ii) on the theoretical side, numerical uncertainties are still too large to allow a clear distinction of exotic and standard contributions at the currently required level. Likely this will change in the future, but meanwhile other processes like, *e.g.*, $\pi^+ \rightarrow e^+\nu$, seem to be better suited to search for new physics at the precision frontier, because of the very accurate and reliable theoretical predictions and the more straightforward experimental analysis.

Meson Particle Listings

 π^\pm

References

- D.A. Bryman *et al.*, Phys. Reports **88**, 151 (1982). See also our note on "Pseudoscalar-Meson Decay Constants," above;
S.G. Brown and S.A. Bludman, Phys. Rev. **136**, B1160 (1964);
P. DeBaenst and J. Pestieau, Nuovo Cim. **A53**, 137 (1968).
- W.T. Chu *et al.*, Phys. Rev. **166**, 1577 (1968);
D.Yu. Bardin and E.A. Ivanov, Sov. J. Part. Nucl. **7**, 286 (1976);
A. Kersch and F. Scheck, Nucl. Phys. **B263**, 475 (1986).
- V.G. Vaks and B.L. Ioffe, Nuovo Cim. **10**, 342 (1958);
V.F. Muller, Z. Phys. **173**, 438 (1963).
- C.Q. Geng, I-Lin Ho, and T.H. Wu, Nucl. Phys. **B684**, 281 (2004);
J. Bijnens and P. Talavera, Nucl. Phys. **B489**, 387 (1997);
V. Mateu and J. Portoles, Eur. Phys. J. **C52**, 325 (2007);
R. Unterdorfer and H. Pichl, hep-ph 0801.2482v1.
- D. Počanić *et al.*, Phys. Rev. Lett. **93**, 181803 (2004);
E. Frlež *et al.*, Phys. Rev. Lett. **93**, 181804 (2004);
M. Bychkov *et al.*, arXiv:0804.1815 [hep-ex].
- J.F. Donoghue and B.R. Holstein, Phys. Rev. **D40**, 2378 (1989).
- E. Gabrielli and L. Trentadue, Nucl. Phys. **B792**, 48 (2008).
- S. Adler *et al.*, Phys. Rev. Lett. **85**, 2256 (2000).
- Yu.M. Bystritsky, E.A. Kuraev, and E.P. Velicheva, Phys. Rev. **D69**, 114004 (2004);
R. Unterdorfer and H. Pichl have treated radiative corrections of the structure terms to lowest order within χPT for the first time. See the reference under [4].
- S. Egli *et al.*, Phys. Lett. **B175**, 97 (1986).
- A.A. Poblaguev *et al.*, Phys. Rev. Lett. **89**, 061803 (2002).
- V.N. Bolotov *et al.*, Phys. Lett. **B243**, 308 (1990).
- S.A. Akimenko *et al.*, Phys. Lett. **B259**, 225 (1991).
- A.A. Poblaguev, Phys. Lett. **B238**, 108 (1990);
V.M. Belyaev and I.I. Kogan, Phys. Lett. **B280**, 238 (1992);
A.V. Chernyshev *et al.*, Mod. Phys. Lett. **A12**, 1669 (1997);
A.A. Poblaguev, Phys. Rev. **D68**, 054020 (2003);
M.V. Chizhov, Phys. Part. Nucl. Lett. **2**, 193 (2005).
- P. Herzceg, Phys. Rev. **D49**, 247 (1994).

 π^\pm FORM FACTORS F_V VECTOR FORM FACTOR

VALUE	EVTS	DOCUMENT ID	TECN	COMMENT
0.017±0.008 OUR AVERAGE				
0.014±0.009	26	BOLOTOV	90B	SPEC 17 GeV $\pi^- \rightarrow e^- \bar{\nu}_e \gamma$
0.023 $^{+0.015}_{-0.013}$	98	EGLI	89	SPEC $\pi^+ \rightarrow e^+ \nu_e e^+ e^-$

²⁶BOLOTOV 90B only determines the absolute value.

 F_A AXIAL-VECTOR FORM FACTOR

VALUE	EVTS	DOCUMENT ID	TECN	CHG	COMMENT
0.0115±0.0005 OUR AVERAGE					Error includes scale factor of 1.2.
0.0115±0.0004	27,28	FRLEZ	04	PIBE	+ $\pi^+ \rightarrow e^+ \nu \gamma$ at rest
0.0106±0.0060	27,29	BOLOTOV	90B	SPEC	17 GeV $\pi^- \rightarrow e^- \bar{\nu}_e \gamma$
0.0135±0.0016	27,29	BAY	86	SPEC	$\pi^+ \rightarrow e^+ \nu \gamma$
0.006±0.003	27,29	PILLONEN	86	SPEC	$\pi^+ \rightarrow e^+ \nu \gamma$
0.011±0.003	27,29,30	STETZ	78	SPEC	$\pi^+ \rightarrow e^+ \nu \gamma$
0.021 $^{+0.011}_{-0.013}$	98	EGLI	89	SPEC	$\pi^+ \rightarrow e^+ \nu_e e^+ e^-$

••• We do not use the following data for averages, fits, limits, etc. •••

²⁷Using the vector form factor from CVC prediction, $F_V = 0.0259 \pm 0.0005$.

²⁸The sign of $\gamma = F_A / F_V$ is determined to be positive.

²⁹Only the absolute value of F_A is determined.

³⁰The result of STETZ 78 has a two-fold ambiguity. We take the solution compatible with later determinations.

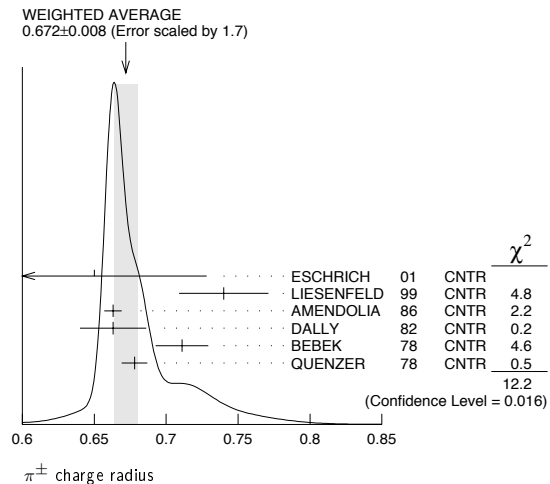
R, SECOND AXIAL-VECTOR FORM FACTOR

VALUE	EVTS	DOCUMENT ID	TECN	COMMENT
0.059$^{+0.009}_{-0.008}$ OUR AVERAGE	98	EGLI	89	SPEC $\pi^+ \rightarrow e^+ \nu_e e^+ e^-$

 π^\pm CHARGE RADIUS

VALUE (fm)	DOCUMENT ID	TECN	COMMENT
0.672±0.008 OUR AVERAGE	Error includes scale factor of 1.7. See the ideogram below.		
0.65 ± 0.05 ± 0.06	ESCHRICH	01	CNTR $\pi e \rightarrow \pi e$
0.740±0.031	LIESENFELD	99	CNTR $e p \rightarrow e \pi^+ n$
0.663±0.006	AMENDOLIA	86	CNTR $\pi e \rightarrow \pi e$
0.663±0.023	DALLY	82	CNTR $\pi e \rightarrow \pi e$
0.711±0.009±0.016	BEBEK	78	CNTR $e N \rightarrow e \pi N$
0.678±0.004±0.008	QUENZER	78	CNTR $e^+ e^- \rightarrow \pi^+ \pi^-$
0.661±0.012	³¹ BIJNENS	98	CNTR χPT extraction
0.660±0.024	AMENDOLIA	84	CNTR $\pi e \rightarrow \pi e$
0.78 $^{+0.09}_{-0.10}$	ADYLOV	77	CNTR $\pi e \rightarrow \pi e$
0.74 $^{+0.11}_{-0.13}$	BARDIN	77	CNTR $e p \rightarrow e \pi^+ n$
0.56 ± 0.04	DALLY	77	CNTR $\pi e \rightarrow \pi e$

³¹BIJNENS 98 fits existing data.

 π^\pm REFERENCES

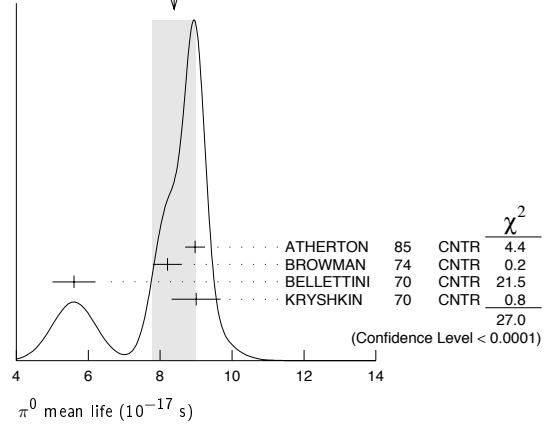
We have omitted some papers that have been superseded by later experiments. The omitted papers may be found in our 1988 edition Physics Letters **B204** 1 (1988).

FRLEZ	04	PRL 93 181804	E. Frlež <i>et al.</i>	(PIBETA Collab.)
POCANIC	04	PRL 93 181803	D. Pocanic <i>et al.</i>	(PIBETA Collab.)
ESCHRICH	01	PL B522 233	I. Eschrich <i>et al.</i>	(FNAL SELEX Collab.)
LIESENFELD	99	PL B468 20	A. Liesenfeld <i>et al.</i>	
BIJNENS	98	JHEP 9805 014	J. Bijnens <i>et al.</i>	
BRESSI	98	NP B513 955	G. Bressi <i>et al.</i>	
LENZ	98	PL B416 50	S. Lenz <i>et al.</i>	
ASSAMAGAN	96	PR D53 6065	K.A. Assamagan <i>et al.</i>	(PSI, ZURI, VILL+)
KOPEV	95	JETPL 61 877	V.P. Koptev <i>et al.</i>	(PNPI)
			Translated from ZETFP 61 865.	
NUMAO	95	PR D52 4855	T. Numao <i>et al.</i>	(TRIU, BRCO)
ASSAMAGAN	94	PL B335 231	K.A. Assamagan <i>et al.</i>	(PSI, ZURI, VILL+)
JECKELMANN	94	PL B335 326	B. Jeckelmann, P.F.A. Goudsmit, H.J. Leisi	(WABRN+)
CZAPEK	93	PRL 70 17	G. Czapek <i>et al.</i>	(BERN, JINR)
BARANOV	92	SJNP 55 1644	V.A. Baranov <i>et al.</i>	(JINR)
			Translated from YAF 55 2940.	
BRITTON	92	PRL 68 3000	D.I. Britton <i>et al.</i>	(TRIU, CARL)
			Also PR D49 28	(TRIU, CARL)
NUMAO	92	MPL A7 3357	T. Numao	(TRIU)
BARANOV	91B	SJNP 54 790	V.A. Baranov <i>et al.</i>	(JINR)
			Translated from YAF 54 1298.	
DAUM	91	PL B265 425	M. Daum <i>et al.</i>	(VILL)
BOLOTOV	90B	PL B243 308	V.N. Bolotov <i>et al.</i>	(INRM)
EGLI	89B	PL B222 533	S. Egli <i>et al.</i>	(SINDRUM Collab.)
			Also PL B175 97	(AACH3, ETH, SIN, ZURI)
PDG	88	PL B204 1	G.P. Yost <i>et al.</i>	(LBL+)
PICCIOTTO	88	PR D37 1131	C.E. Picciotto <i>et al.</i>	(TRIU, CNRC)
COHEN	87	RMP 59 1121	E.R. Cohen, B.N. Taylor	(RIS C, NBS)
KORENCHEN...	87	SJNP 46 192	S.M. Korenchenko <i>et al.</i>	(JINR)
			Translated from YAF 46 313.	

AMENDOLIA 86	NP B277 168	S.R. Amendolia et al.	(CERN NA7 Collab.)
BAY 86	PL B174 445	A. Bay et al.	(LAUS, ZURI)
BRYMAN 86	PR D33 1211	D.A. Bryman et al.	(TRIU, CNRC)
Also	PRL 50 7	D.A. Bryman et al.	(TRIU, CNRC)
JECKELMANN 86B	NP A457 709	B. Jeckelmann et al.	(ETH, FRIB)
Also	PRL 56 1444	B. Jeckelmann et al.	(ETH, FRIB)
PIILONEN 86	PRL 57 1402	L.E. Piilonen et al.	(LANL, TEMP, CHIC)
MCFARLANE 85	PR D32 547	W.K. McFarlane et al.	(TEMP, LANL)
ABELA 84	PL 146B 431	R. Abela et al.	(SIN)
Also	PL 74B 126	M. Daum et al.	(SIN)
Also	PR D20 2692	M. Daum et al.	(SIN)
AMENDOLIA 84	PL 146B 116	S.R. Amendolia et al.	(CERN NA7 Collab.)
FETSCHER 84	PL 140B 117	W. Fetscher	(ETH)
ABELA 83	NP A395 413	R. Abela et al.	(BASL, KARLK, KARLE)
CARR 83	PRL 51 627	J. Carr et al.	(LBL, NWES, TRIU)
COOPER 82	PL 112B 97	A.M. Cooper et al.	(RL)
DALLY 82	PRL 48 375	E.B. Dally et al.	(YALE, COLU, JHU)
LU 80	PRL 45 1066	D.C. Lu et al.	(YALE, COLU, JHU)
BEBEK 78	PR D17 1693	C.J. Bebek et al.	(LALO)
QUENZER 78	PL 76B 512	A. Quenzler et al.	(LALO)
STETZ 78	NP B138 285	A.W. Stetz et al.	(LBL, UCLA)
ADYLOV 77	NP B128 461	G.T. Adylov et al.	(LRL, UCSB)
BARDIN 77	NP B120 45	G. Bardin et al.	(LRL, UCSB)
DALLY 77	PRL 39 1176	E.B. Dally et al.	(LRL, UCSB)
CARTER 76	PRL 37 1380	A.L. Carter et al.	(CARL, CNRC, CHIC+)
KORENCHENKO... 76B	JETP 44 35	S.M. Korenchenko et al.	(JINR)
Translated from ZETP 71 61			
MARUSHENKO... 76	JETPL 23 72	V.I. Marushenko et al.	(PNPI)
Also	Private Comm.	R.E. Shafer	(FNAL)
Also	Private Comm.	A. Smirnov	(PNPI)
DUNAITSEV 73	SJNP 16 292	A.F. Dunaitsev et al.	(SERP)
Translated from YAF 16 524			
AYRES 71	PR D3 1051	D.S. Ayres et al.	(LRL, UCSB)
Also	PR 157 1208	D.S. Ayres et al.	(LRL)
Also	PRL 21 261	D.S. Ayres et al.	(LRL, UCSB)
Also	Thesis UCLR 18369	D.S. Ayres	(LRL)
Also	PRL 23 1267	A.J. Greenberg et al.	(LRL, UCSB)
KORENCHENKO... 71	SJNP 13 189	S.M. Korenchenko et al.	(JINR)
Translated from YAF 13 339			
BOOTH 70	PL 32B 723	P.S.L. Booth et al.	(LIVP)
DEPOMMIER 68	NP B4 189	P. Depommier et al.	(CERN)
PETRUKHIN 68	JINR P1 3862	V.I. Petrukhin et al.	(JINR)
HYMAN 67	PL 25B 376	L.G. Hyman et al.	(ANL, CMU, NWES)
NORDBERG 67	PL 24B 594	M.E. Nordberg, F. Lobkowicz, R.L. Burman	(ROCH)
BARDON 66	PRL 16 775	M. Bardon et al.	(COLU)
KINSEY 66	PR 144 1132	K.F. Kinsey, F. Lobkowicz, M.E. Nordberg	(ROCH)
LOBKOWICZ 66	PRL 17 548	F. Lobkowicz et al.	(ROCH, BNL)
BACASTOW 65	PR 139 B407	R.B. Bacastow et al.	(LRL, SLAC)
BERTRAM 65	PR 139 B617	W.K. Bertram et al.	(MICH, CMU)
DUNAITSEV 65	JETP 20 58	A.F. Dunaitsev et al.	(JINR)
Translated from ZETF 47 84			
ECKHAUSE 65	PL 19 348	M. Eckhause et al.	(WILL)
BARTLETT 64	PR 136 B1452	D. Bartlett et al.	(COLU)
DICAPUA 64	PR 133 B1333	M. DiCapua et al.	(COLU)
Also	Private Comm.	L. Pondrom	(WISC)
DEPOMMIER 63	PL 5 61	P. Depommier et al.	(CERN)
DEPOMMIER 63B	PL 7 285	P. Depommier et al.	(CERN)
ANDERSON 60	PR 119 2050	H.L. Anderson et al.	(EFI)
CASTAGNOLI 58	PR 112 1779	C. Castagnoli, M. Muchnik	(ROMA)

¹ BROWMAN 74 gives a π^0 width $\Gamma = 8.02 \pm 0.42$ eV. The mean life is \hbar/Γ .
² WILLIAMS 88 gives $\Gamma(\gamma\gamma) = 7.7 \pm 0.5 \pm 0.5$ eV. We give here $\tau = \hbar/\Gamma(\text{total})$.

WEIGHTED AVERAGE
 8.4 ± 0.6 (Error scaled by 3.0)



π^0 DECAY MODES

For decay limits to particles which are not established, see the appropriate Search sections (A^0 (axion) and Other Light Boson (X^0) Searches, etc.).

Mode	Fraction (Γ_i/Γ)	Scale factor / Confidence level
Γ_1 2γ	$(98.798 \pm 0.032) \%$	S=1.1
Γ_2 $e^+e^-\gamma$	$(1.198 \pm 0.032) \%$	S=1.1
Γ_3 γ positronium	$(1.82 \pm 0.29) \times 10^{-9}$	
Γ_4 $e^+e^+e^-e^-$	$(3.14 \pm 0.30) \times 10^{-5}$	
Γ_5 e^+e^-	$(6.46 \pm 0.33) \times 10^{-8}$	
Γ_6 4γ	< 2	CL=90%
Γ_7 $\nu\bar{\nu}$	$[a] < 2.7$	CL=90%
Γ_8 $\nu_e\bar{\nu}_e$	< 1.7	CL=90%
Γ_9 $\nu_\mu\bar{\nu}_\mu$	< 1.6	CL=90%
Γ_{10} $\nu_\tau\bar{\nu}_\tau$	< 2.1	CL=90%
Γ_{11} $\gamma\nu\bar{\nu}$	< 6	CL=90%

Charge conjugation (C) or Lepton Family number (LF) violating modes

Γ_{12} 3γ	C	< 3.1	$\times 10^{-8}$	CL=90%
Γ_{13} μ^+e^-	LF	< 3.8	$\times 10^{-10}$	CL=90%
Γ_{14} μ^-e^+	LF	< 3.4	$\times 10^{-9}$	CL=90%
Γ_{15} $\mu^+e^- + \mu^-e^+$	LF	< 1.72	$\times 10^{-8}$	CL=90%

[a] Astrophysical and cosmological arguments give limits of order 10^{-13} ; see the Particle Listings below.

CONSTRAINED FIT INFORMATION

An overall fit to 2 branching ratios uses 4 measurements and one constraint to determine 3 parameters. The overall fit has a $\chi^2 = 1.9$ for 2 degrees of freedom.

The following off-diagonal array elements are the correlation coefficients $\langle \delta x_i \delta x_j \rangle / (\delta x_i \delta x_j)$, in percent, from the fit to the branching fractions, $x_i \equiv \Gamma_i / \Gamma_{\text{total}}$. The fit constrains the x_i whose labels appear in this array to sum to one.

$$\begin{matrix} x_2 & \begin{matrix} -100 \\ -1 \end{matrix} \\ x_4 & \begin{matrix} -1 & 0 \\ x_1 & x_2 \end{matrix} \end{matrix}$$

π^0 BRANCHING RATIOS

$\Gamma(e^+e^-\gamma)/\Gamma(2\gamma)$	VALUE (%)	EVTS	DOCUMENT ID	TECN	COMMENT	Γ_2/Γ_1
1.213 ± 0.033 OUR FIT					Error includes scale factor of 1.1.	
1.213 ± 0.030 OUR AVERAGE						
	1.25 ± 0.04		SCHARDT 81	SPEC	$\pi^-p \rightarrow n\pi^0$	
	1.166 ± 0.047	3071	³ SAMIOS 61	HBC	$\pi^-p \rightarrow n\pi^0$	
	1.17 ± 0.15	27	BUDAGOV 60	HBC		
	1.196		JOSEPH 60	THEO	QED calculation	

• • • We do not use the following data for averages, fits, limits, etc. • • •
³ SAMIOS 61 value uses a Panofsky ratio = 1.62.

π^0

$I^G(J^{PC}) = 1^-(0^{-+})$

We have omitted some results that have been superseded by later experiments. The omitted results may be found in our 1988 edition Physics Letters B204 1 (1988).

π^0 MASS

The value is calculated from m_{π^\pm} and $(m_{\pi^\pm} - m_{\pi^0})$. See notes under the π^\pm Mass Listings concerning recent revision of the charged pion mass.

VALUE (MeV)	DOCUMENT ID
134.9766 ± 0.0006 OUR FIT	Error includes scale factor of 1.1.

$m_{\pi^\pm} - m_{\pi^0}$

Measurements with an error > 0.01 MeV have been omitted.

VALUE (MeV)	DOCUMENT ID	TECN	COMMENT
4.5936 ± 0.0005 OUR FIT			
4.5936 ± 0.0005 OUR AVERAGE			
4.59364 ± 0.00048	CRAWFORD 91	CNTR	$\pi^-p \rightarrow \pi^0 n, n$ TOF
4.5930 ± 0.0013	CRAWFORD 86	CNTR	$\pi^-p \rightarrow \pi^0 n, n$ TOF
• • • We do not use the following data for averages, fits, limits, etc. • • •			
4.59366 ± 0.00048	CRAWFORD 88B	CNTR	See CRAWFORD 91
4.6034 ± 0.0052	VASILEVSKY 66	CNTR	
4.6056 ± 0.0055	CZIRR 63	CNTR	

π^0 MEAN LIFE

Measurements with an error > 1×10^{-17} s have been omitted.

VALUE (10^{-17} s)	EVTS	DOCUMENT ID	TECN	COMMENT
8.4 ± 0.6 OUR AVERAGE				Error includes scale factor of 3.0. See the ideogram below.
8.97 ± 0.22 ± 0.17		ATHERTON 85	CNTR	
8.2 ± 0.4		¹ BROWMAN 74	CNTR	Primakoff effect
5.6 ± 0.6		BELLETTINI 70	CNTR	Primakoff effect
9 ± 0.68		KRYSHKIN 70	CNTR	Primakoff effect
• • • We do not use the following data for averages, fits, limits, etc. • • •				
8.4 ± 0.5 ± 0.5	1182	² WILLIAMS 88	CBAL	$e^+e^- \rightarrow e^+e^-\pi^0$

Meson Particle Listings

 π^0

$\Gamma(\gamma\text{positronium})/\Gamma(2\gamma)$		Γ_3/Γ_1	
VALUE (units 10^{-9})	EVTS	DOCUMENT ID	TECN COMMENT
1.84 ± 0.29	277	AFANASYEV 90	CNTR pC 70 GeV

$\Gamma(e^+e^-e^-)/\Gamma(2\gamma)$		Γ_4/Γ_1	
VALUE (units 10^{-5})	EVTS	DOCUMENT ID	TECN
3.18 ± 0.30 OUR FIT			
3.18 ± 0.30	146	⁴ SAMIOS 62B	HBC

⁴ SAMIOS 62B value uses a Panofsky ratio = 1.62.

$\Gamma(e^+e^-)/\Gamma_{\text{total}}$		Γ_5/Γ	
Experimental results are listed; branching ratios corrected for radiative effects are given in the footnotes. BERMAN 60 found $B(\pi^0 \rightarrow e^+e^-) \geq 4.69 \times 10^{-8}$ via an exact QED calculation.			

VALUE (units 10^{-8})	EVTS	DOCUMENT ID	TECN	CHG	COMMENT
6.46 ± 0.33 OUR AVERAGE					
6.44 ± 0.25 ± 0.22	794	⁵ ABOUZAID 07	KTEV		$K_L^0 \rightarrow 3\pi^0$ in flight
6.9 ± 2.3 ± 0.6	21	⁶ DESHPANDE 93	SPEC		$K^+ \rightarrow \pi^+\pi^0$
7.6 $\begin{smallmatrix} +2.9 \\ -2.8 \end{smallmatrix}$ ± 0.5	8	⁷ MCFARLAND 93	SPEC		$K_L^0 \rightarrow 3\pi^0$ in flight

• • • We do not use the following data for averages, fits, limits, etc. • • •

6.09 ± 0.40 ± 0.24 275 ⁸ ALAVI-HARATI 99c SPEC 0 Repl. by ABOUZAID 07

⁵ ABOUZAID 07 result is for $m_{e^+e^-}/m_{\pi^0} > 0.95$. With radiative corrections the result becomes $(7.48 \pm 0.29 \pm 0.25) \times 10^{-8}$.

⁶ The DESHPANDE 93 result with bremsstrahlung radiative corrections is $(8.0 \pm 2.6 \pm 0.6) \times 10^{-8}$.

⁷ The MCFARLAND 93 result is for $B[\pi^0 \rightarrow e^+e^-, (m_{e^+e^-}/m_{\pi^0})^2 > 0.95]$. With radiative corrections it becomes $(8.8^{+4.5}_{-3.2} \pm 0.6) \times 10^{-8}$.

⁸ ALAVI-HARATI 99c quote result for $B[\pi^0 \rightarrow e^+e^-, (m_{e^+e^-}/m_{\pi^0})^2 > 0.95]$ to minimize radiative contributions from $\pi^0 \rightarrow e^+e^-\gamma$. After radiative corrections they obtain $(7.04 \pm 0.46 \pm 0.28) \times 10^{-8}$.

$\Gamma(e^+e^-)/\Gamma(2\gamma)$		Γ_5/Γ_1	
VALUE (units 10^{-7})	CL% EVTS	DOCUMENT ID	TECN COMMENT
• • • We do not use the following data for averages, fits, limits, etc. • • •			
<1.3	90	NIEBUHR 89	SPEC $\pi^-p \rightarrow \pi^0 n$ at rest
<5.3	90	ZEPHAT 87	SPEC $\pi^-p \rightarrow \pi^0 n$ 0.3 GeV/c
1.7 ± 0.6 ± 0.3	59	FRANK 83	SPEC $\pi^-p \rightarrow n\pi^0$
1.8 ± 0.6	58	MISCHKE 82	SPEC See FRANK 83
2.23 $\begin{smallmatrix} +2.40 \\ -1.10 \end{smallmatrix}$	90	8 FISCHER 78B	SPRK $K^+ \rightarrow \pi^+\pi^0$

$\Gamma(4\gamma)/\Gamma_{\text{total}}$		Γ_6/Γ	
VALUE (units 10^{-8})	CL% EVTS	DOCUMENT ID	TECN COMMENT
< 2	90	MCDONOUGH 88	CBOX π^-p at rest
• • • We do not use the following data for averages, fits, limits, etc. • • •			
<160	90	BOLOTOV 86c	CALO
<440	90	0 AUERBACH 80	CNTR

$\Gamma(\nu\bar{\nu})/\Gamma_{\text{total}}$		Γ_7/Γ	
The astrophysical and cosmological limits are many orders of magnitude lower, but we use the best laboratory limit for the Summary Tables.			

VALUE (units 10^{-6})	CL% EVTS	DOCUMENT ID	TECN	COMMENT
< 0.27	90	⁹ ARTAMONOV 05A	B949	$K^+ \rightarrow \pi^+\pi^0$
• • • We do not use the following data for averages, fits, limits, etc. • • •				
< 0.83	90	⁹ ATIYA 91	B787	$K^+ \rightarrow \pi^+\nu\nu'$
< 2.9 × 10 ⁻⁷		¹⁰ LAM 91		Cosmological limit
< 3.2 × 10 ⁻⁷		¹¹ NATALE 91	SN 1987A	
< 6.5	90	DORENBOS... 88	CHRM	Beam dump, prompt ν
<24	90	0 ⁹ HERCZEG 81	RVUE	$K^+ \rightarrow \pi^+\nu\nu'$

⁹ This limit applies to all possible $\nu\nu'$ states as well as to other massless, weakly interacting states.

¹⁰ LAM 91 considers the production of right-handed neutrinos produced from the cosmic thermal background at the temperature of about the pion mass through the reaction $\gamma\gamma \rightarrow \pi^0 \rightarrow \nu\bar{\nu}$.

¹¹ NATALE 91 considers the excess energy-loss rate from SN1987A if the process $\gamma\gamma \rightarrow \pi^0 \rightarrow \nu\bar{\nu}$ occurs, permitted if the neutrinos have a right-handed component. As pointed out in LAM 91 (and confirmed by Natale), there is a factor 4 error in the NATALE 91 published result (0.8×10^{-7}) .

$\Gamma(\nu_e\bar{\nu}_e)/\Gamma_{\text{total}}$		Γ_8/Γ	
VALUE (units 10^{-6})	CL%	DOCUMENT ID	TECN COMMENT
<1.7	90	DORENBOS... 88	CHRM Beam dump, prompt ν
• • • We do not use the following data for averages, fits, limits, etc. • • •			
<3.1	90	¹² HOFFMAN 88	RVUE Beam dump, prompt ν

¹² HOFFMAN 88 analyzes data from a 400-GeV BEBC beam-dump experiment.

$\Gamma(\nu_\mu\bar{\nu}_\mu)/\Gamma_{\text{total}}$		Γ_9/Γ	
VALUE (units 10^{-6})	CL% EVTS	DOCUMENT ID	TECN COMMENT
<1.6	90	8.7 AUERBACH 04	LSND 800 MeV p on Cu
<3.1	90	¹³ HOFFMAN 88	RVUE Beam dump, prompt ν
• • • We do not use the following data for averages, fits, limits, etc. • • •			
<7.8	90	DORENBOS... 88	CHRM Beam dump, prompt ν
¹³ HOFFMAN 88 analyzes data from a 400-GeV BEBC beam-dump experiment.			

$\Gamma(\nu_\tau\bar{\nu}_\tau)/\Gamma_{\text{total}}$		Γ_{10}/Γ	
VALUE (units 10^{-6})	CL%	DOCUMENT ID	TECN COMMENT
<2.1	90	¹⁴ HOFFMAN 88	RVUE Beam dump, prompt ν
• • • We do not use the following data for averages, fits, limits, etc. • • •			
<4.1	90	DORENBOS... 88	CHRM Beam dump, prompt ν
¹⁴ HOFFMAN 88 analyzes data from a 400-GeV BEBC beam-dump experiment.			

$\Gamma(\gamma\nu\bar{\nu})/\Gamma_{\text{total}}$		Γ_{11}/Γ	
Standard Model prediction is 6×10^{-18} .			
VALUE	CL%	DOCUMENT ID	TECN COMMENT
<6 × 10⁻⁴	90	ATIYA 92	CNTR $K^+ \rightarrow \gamma\nu\bar{\nu}\pi^+$

$\Gamma(3\gamma)/\Gamma_{\text{total}}$		Γ_{12}/Γ	
Forbidden by C invariance.			
VALUE (units 10^{-8})	CL% EVTS	DOCUMENT ID	TECN COMMENT
< 3.1	90	MCDONOUGH 88	CBOX π^-p at rest
• • • We do not use the following data for averages, fits, limits, etc. • • •			
< 38	90	0 HIGHLAND 80	CNTR
<150	90	0 AUERBACH 78	CNTR
<490	90	0 ¹⁵ DUCLOS 65	CNTR
<490	90	¹⁵ KUTIN 65	CNTR
¹⁵ These experiments give $B(3\gamma/2\gamma) < 5.0 \times 10^{-6}$.			

$\Gamma(\mu^+e^-)/\Gamma_{\text{total}}$		Γ_{13}/Γ	
Forbidden by lepton family number conservation.			
VALUE (units 10^{-9})	CL% EVTS	DOCUMENT ID	TECN COMMENT
< 0.38	90	0 APPEL 00	SPEC $K^+ \rightarrow \pi^+\mu^+e^-$
• • • We do not use the following data for averages, fits, limits, etc. • • •			
<16	90	LEE 90	SPEC $K^+ \rightarrow \pi^+\mu^+e^-$
<78	90	CAMPAGNARI 88	SPEC See LEE 90

$\Gamma(\mu^-e^+)/\Gamma_{\text{total}}$		Γ_{14}/Γ	
Forbidden by lepton family number conservation.			
VALUE (units 10^{-9})	CL% EVTS	DOCUMENT ID	TECN COMMENT
<3.4	90	0 APPEL 00B	B865 0 $K^+ \rightarrow \pi^+e^+\mu^-$

$[\Gamma(\mu^+e^-) + \Gamma(\mu^-e^+)]/\Gamma_{\text{total}}$		Γ_{15}/Γ	
Forbidden by lepton family number conservation.			
VALUE (units 10^{-9})	CL%	DOCUMENT ID	TECN COMMENT
< 17.2	90	KROLAK 94	E799 $\ln K_L^0 \rightarrow 3\pi^0$
• • • We do not use the following data for averages, fits, limits, etc. • • •			
<140		HERCZEG 84	RVUE $K^+ \rightarrow \pi^+\mu e$
< 2 × 10 ⁻⁶		HERCZEG 84	THEO $\mu^- \rightarrow e^-$ conversion
< 70	90	BRYMAN 82	RVUE $K^+ \rightarrow \pi^+\mu e$

 π^0 ELECTROMAGNETIC FORM FACTOR

The amplitude for the process $\pi^0 \rightarrow e^+e^- \gamma$ contains a form factor $F(x)$ at the $\pi^0\gamma\gamma$ vertex, where $x = [m_{e^+e^-}/m_{\pi^0}]^2$. The parameter a in the linear expansion $F(x) = 1 + ax$ is listed below.

All the measurements except that of BEHREND 91 are in the time-like region of momentum transfer.

LINEAR COEFFICIENT OF π^0 ELECTROMAGNETIC FORM FACTOR

VALUE	CL%	EVTS	DOCUMENT ID	TECN	COMMENT
0.032 ± 0.004 OUR AVERAGE					
+0.026 ± 0.024 ± 0.048		7548	FARZANPAY 92	SPEC	$\pi^-p \rightarrow \pi^0 n$ at rest
+0.025 ± 0.014 ± 0.026		54k	MEIJERDREES 92B	SPEC	$\pi^-p \rightarrow \pi^0 n$ at rest
+0.0326 ± 0.0026 ± 0.0026		127	¹⁶ BEHREND 91	CELL	$e^+e^- \rightarrow \pi^0$
-0.11 ± 0.03 ± 0.08		32k	FONVIEILLE 89	SPEC	Radiation corr.
• • • We do not use the following data for averages, fits, limits, etc. • • •					
0.12 $\begin{smallmatrix} +0.05 \\ -0.04 \end{smallmatrix}$			¹⁷ TUPPER 83	THEO	FISCHER 78 data
+0.10 ± 0.03		31k	¹⁸ FISCHER 78	SPEC	Radiation corr.
+0.01 ± 0.11		2200	DEVONS 69	OSP K	No radiation corr.
-0.15 ± 0.10		7676	KOBRAK 61	HBC	No radiation corr.
-0.24 ± 0.16		3071	SAMIOS 61	HBC	No radiation corr.

¹⁶ BEHREND 91 estimates that their systematic error is of the same order of magnitude as their statistical error, and so we have included a systematic error of this magnitude. The value of a is obtained by extrapolation from the region of large space-like momentum transfer assuming vector dominance.

¹⁷ TUPPER 83 is a theoretical analysis of FISCHER 78 including 2-photon exchange in the corrections.

¹⁸ The FISCHER 78 error is statistical only. The result without radiation corrections is $+0.05 \pm 0.03$.

Meson Particle Listings

 η

Γ_4	$\pi^0 2\gamma$	(5.7 \pm 2.0) $\times 10^{-4}$	1.9
Γ_9	$\pi^+ \pi^- \pi^0$	0.295 \pm 0.016	
Γ_{10}	$\pi^+ \pi^- \gamma$	0.060 \pm 0.004	1.2
Γ_{11}	$e^+ e^- \gamma$	0.0089 \pm 0.0011	1.5
Γ_{12}	$\mu^+ \mu^- \gamma$	(4.0 \pm 0.6) $\times 10^{-4}$	
Γ_{16}	$\pi^+ \pi^- e^+ e^-$	(5.5 \pm 1.5) $\times 10^{-4}$	

 η DECAY RATES

$\Gamma(2\gamma)$ Γ_2
 See the table immediately above giving the fitted decay rates. Following the advice of NEFKENS 02, we have removed the Primakoff-effect measurement from the average. See also the "Note on the Decay Width $\Gamma(\eta \rightarrow \gamma\gamma)$," in our 1994 edition, Phys. Rev. D50, 1 August 1994, Part 1, p. 1451, for a discussion of the various measurements.

VALUE (keV)	EVTS	DOCUMENT ID	TECN	COMMENT
0.510 \pm 0.026 OUR FIT				
0.510 \pm 0.026 OUR AVERAGE				
0.51 \pm 0.12 \pm 0.05	36	BARU	90 MD1	$e^+ e^- \rightarrow e^+ e^- \eta$
0.490 \pm 0.010 \pm 0.048	2287	ROE	90 ASP	$e^+ e^- \rightarrow e^+ e^- \eta$
0.514 \pm 0.017 \pm 0.035	1295	WILLIAMS	88 CBAL	$e^+ e^- \rightarrow e^+ e^- \eta$
0.53 \pm 0.04 \pm 0.04		BARTEL	85E JADE	$e^+ e^- \rightarrow e^+ e^- \eta$
• • • We do not use the following data for averages, fits, limits, etc. • • •				
0.64 \pm 0.14 \pm 0.13		AIHARA	86 TPC	$e^+ e^- \rightarrow e^+ e^- \eta$
0.56 \pm 0.16	56	WEINSTEIN	83 CBAL	$e^+ e^- \rightarrow e^+ e^- \eta$
0.324 \pm 0.046		BROWMAN	74B CNTR	Primakoff effect
1.00 \pm 0.22		² BEMPORAD	67 CNTR	Primakoff effect

² BEMPORAD 67 gives $\Gamma(2\gamma) = 1.21 \pm 0.26$ keV assuming $\Gamma(2\gamma)/\Gamma(\text{total}) = 0.314$.

Bemporad private communication gives $\Gamma(2\gamma)^2/\Gamma(\text{total}) = 0.380 \pm 0.083$. We evaluate this using $\Gamma(2\gamma)/\Gamma(\text{total}) = 0.38 \pm 0.01$. Not included in average because the uncertainty resulting from the separation of the coulomb and nuclear amplitudes has apparently been underestimated.

 η BRANCHING RATIOS

Neutral modes

$\Gamma(\text{neutral modes})/\Gamma_{\text{total}}$	$\Gamma_1/\Gamma = (\Gamma_2 + \Gamma_3 + \Gamma_4)/\Gamma$			
VALUE	EVTS	DOCUMENT ID	TECN	COMMENT
0.7191 \pm 0.0034 OUR FIT				Error includes scale factor of 1.2.
0.705 \pm 0.008	16k	BASILE	71D CNTR	MM spectrometer
• • • We do not use the following data for averages, fits, limits, etc. • • •				
0.79 \pm 0.08		BUNIATOV	67 OSPK	

$\Gamma(2\gamma)/\Gamma_{\text{total}}$	Γ_2/Γ			
VALUE (units 10^{-2})	EVTS	DOCUMENT ID	TECN	COMMENT
39.31 \pm 0.20 OUR FIT				Error includes scale factor of 1.1.
39.49 \pm 0.17 \pm 0.30	65k	ABEGG	96 SPEC	$p d \rightarrow {}^3\text{He} \eta$
• • • We do not use the following data for averages, fits, limits, etc. • • •				
38.45 \pm 0.40 \pm 0.36	14k	³ LOPEZ	07 CLEO	$\psi(2S) \rightarrow J/\psi \eta$

³ Not independent of other results listed for LOPEZ 07. Assuming decays of $\eta \rightarrow \gamma\gamma$, $3\pi^0$, $\pi^+ \pi^- \pi^0$, $\pi^+ \pi^- \gamma$, and $e^+ e^- \gamma$ account for all η decays within a contribution of 0.3% to the systematic error.

$\Gamma(2\gamma)/\Gamma(\text{neutral modes})$	$\Gamma_2/\Gamma_1 = \Gamma_2/(\Gamma_2 + \Gamma_3 + \Gamma_4)$			
VALUE	EVTS	DOCUMENT ID	TECN	COMMENT
0.5466 \pm 0.0019 OUR FIT				
0.548 \pm 0.023 OUR AVERAGE				Error includes scale factor of 1.5.
0.535 \pm 0.018		BUTTRAM	70 OSPK	
0.59 \pm 0.033		BUNIATOV	67 OSPK	
• • • We do not use the following data for averages, fits, limits, etc. • • •				
0.52 \pm 0.09	88	ABROSIMOV	80 HLBC	
0.60 \pm 0.14	113	KENDALL	74 OSPK	
0.57 \pm 0.09		STRUGALSKI	71 HLBC	
0.579 \pm 0.052		FELDMAN	67 OSPK	
0.416 \pm 0.044		DIGIUGNO	66 CNTR	Error doubled
0.44 \pm 0.07		GRUNHAUS	66 OSPK	
0.39 \pm 0.06		⁴ JONES	66 CNTR	

⁴ This result from combining cross sections from two different experiments.

$\Gamma(3\pi^0)/\Gamma_{\text{total}}$	Γ_3/Γ			
VALUE (units 10^{-2})	EVTS	DOCUMENT ID	TECN	COMMENT
32.56 \pm 0.23 OUR FIT				Error includes scale factor of 1.1.
• • • We do not use the following data for averages, fits, limits, etc. • • •				
34.03 \pm 0.56 \pm 0.49	1821	⁵ LOPEZ	07 CLEO	$\psi(2S) \rightarrow J/\psi \eta$

⁵ Not independent of other results listed for LOPEZ 07. Assuming decays of $\eta \rightarrow \gamma\gamma$, $3\pi^0$, $\pi^+ \pi^- \pi^0$, $\pi^+ \pi^- \gamma$, and $e^+ e^- \gamma$ account for all η decays within a contribution of 0.3% to the systematic error.

$\Gamma(3\pi^0)/\Gamma(\text{neutral modes})$	$\Gamma_3/\Gamma_1 = \Gamma_3/(\Gamma_2 + \Gamma_3 + \Gamma_4)$			
VALUE	EVTS	DOCUMENT ID	TECN	COMMENT
0.4528 \pm 0.0019 OUR FIT				
0.439 \pm 0.024		BUTTRAM	70 OSPK	
• • • We do not use the following data for averages, fits, limits, etc. • • •				
0.44 \pm 0.08	75	ABROSIMOV	80 HLBC	
0.32 \pm 0.09		STRUGALSKI	71 HLBC	
0.41 \pm 0.033		BUNIATOV	67 OSPK	Not indep. of $\Gamma(2\gamma)/\Gamma(\text{neutral modes})$
0.177 \pm 0.035		FELDMAN	67 OSPK	
0.209 \pm 0.054		DIGIUGNO	66 CNTR	Error doubled
0.29 \pm 0.10		GRUNHAUS	66 OSPK	

$\Gamma(3\pi^0)/\Gamma(2\gamma)$	Γ_3/Γ_2			
VALUE	EVTS	DOCUMENT ID	TECN	COMMENT
0.828 \pm 0.006 OUR FIT				
0.829 \pm 0.007 OUR AVERAGE				
0.884 \pm 0.022 \pm 0.019	1821	LOPEZ	07 CLEO	$\psi(2S) \rightarrow J/\psi \eta$
0.817 \pm 0.012 \pm 0.032	17.4k	⁶ AKHMETSHIN	05 CMD2	$e^+ e^- \rightarrow \phi \rightarrow \eta\gamma$
0.826 \pm 0.024		ACHASOV	00D SND	$e^+ e^- \rightarrow \phi \rightarrow \eta\gamma$
0.832 \pm 0.005 \pm 0.012		KRUSCHE	95D SPEC	$\gamma p \rightarrow \eta p$, threshold
0.841 \pm 0.034		AMSLER	93 CBAR	$\bar{p} p \rightarrow \pi^+ \pi^- \eta$ at rest
0.822 \pm 0.009		ALDE	84 GAM2	
• • • We do not use the following data for averages, fits, limits, etc. • • •				
0.796 \pm 0.016 \pm 0.016		ACHASOV	00 SND	See ACHASOV 00D
0.91 \pm 0.14		COX	70B HBC	
0.75 \pm 0.09		DEVONS	70 OSPK	
0.88 \pm 0.16		BALTAY	67D DBC	
1.1 \pm 0.2		CENCE	67 OSPK	
1.25 \pm 0.39		BACCI	63 CNTR	Inverse BR reported

⁶ Uses result from AKHMETSHIN 01b.

$\Gamma(\pi^0 2\gamma)/\Gamma_{\text{total}}$	Γ_4/Γ				
VALUE (units 10^{-4})	CL%	EVTS	DOCUMENT ID	TECN	COMMENT
4.4 \pm 1.5 OUR FIT					Error includes scale factor of 2.0.
3.5 \pm 0.7 \pm 0.6	1.6k	^{7,8} PRAKHOV	05 CRYB	$p(720 \text{ MeV}/c) \pi^- \rightarrow n\eta$	

• • • We do not use the following data for averages, fits, limits, etc. • • •

<8.4 90 7 ACHASOV 01D SND $e^+ e^- \rightarrow \phi \rightarrow \eta\gamma$

<30 90 0 DAVYDOV 81 GAM2 $\pi^- p \rightarrow \eta n$

⁷ Normalized using $\Gamma(\eta \rightarrow 2\gamma)/\Gamma = 0.3943 \pm 0.0026$.

⁸ This measurement and the independent analysis of the same data by KNECHT 04 both imply a lower value of $\Gamma(\pi^0 2\gamma)$ than the one obtained by ALDE 84 from $\Gamma(\pi^0 2\gamma)/\Gamma(2\gamma)$.

$\Gamma(\pi^0 2\gamma)/\Gamma(2\gamma)$	Γ_4/Γ_2				
VALUE (units 10^{-3})	EVTS	DOCUMENT ID	TECN	CHG	COMMENT
1.1 \pm 0.4 OUR FIT					Error includes scale factor of 1.9.
1.8 \pm 0.4		ALDE	84 GAM2	0	
• • • We do not use the following data for averages, fits, limits, etc. • • •					
2.5 \pm 0.6	70	BINON	82 GAM2		See ALDE 84

$\Gamma(\pi^0 2\gamma)/\Gamma(3\pi^0)$	Γ_4/Γ_3			
VALUE (units 10^{-4})	EVTS	DOCUMENT ID	TECN	COMMENT
14 \pm 5 OUR FIT				Error includes scale factor of 1.9.
• • • We do not use the following data for averages, fits, limits, etc. • • •				
8.3 \pm 2.8 \pm 1.4		⁹ KNECHT	04 CRYB	$\pi^- p \rightarrow n\eta$

⁹ Independent analysis of same data as PRAKHOV 05.

$\Gamma(\pi^0 \pi^0 \gamma\gamma)/\Gamma_{\text{total}}$	Γ_5/Γ				
VALUE	CL%	EVTS	DOCUMENT ID	TECN	COMMENT
<1.2 $\times 10^{-3}$	90	¹⁰ NEFKENS	05A CRYB	$p(720 \text{ MeV}/c) \pi^- \rightarrow n\eta$	
• • • We do not use the following data for averages, fits, limits, etc. • • •					
<4.0 $\times 10^{-3}$	90	BLIK	07 GAM4	$\pi^- p \rightarrow \eta n$	

¹⁰ Measurement is done in limited $\gamma\gamma$ energy range.

$\Gamma(4\gamma)/\Gamma_{\text{total}}$	Γ_6/Γ			
VALUE	CL%	DOCUMENT ID	TECN	COMMENT
<2.8 $\times 10^{-4}$	90	BLIK	07 GAM4	$\pi^- p \rightarrow \eta n$

$\Gamma(\text{invisible})/\Gamma(2\gamma)$	Γ_7/Γ_2			
VALUE	CL%	DOCUMENT ID	TECN	COMMENT
<1.65 $\times 10^{-3}$	90	¹¹ ABLIKIM	06Q BES2	$J/\psi \rightarrow \phi\eta$

¹¹ Based on 58M J/ψ decays.

Charged modes

$\Gamma(\pi^+ \pi^- \pi^0)/\Gamma_{\text{total}}$	Γ_9/Γ			
VALUE (units 10^{-2})	EVTS	DOCUMENT ID	TECN	COMMENT
22.73 \pm 0.28 OUR FIT				Error includes scale factor of 1.2.
• • • We do not use the following data for averages, fits, limits, etc. • • •				
22.60 \pm 0.35 \pm 0.29	3915	¹² LOPEZ	07 CLEO	$\psi(2S) \rightarrow J/\psi \eta$

¹² Not independent of other results listed for LOPEZ 07. Assuming decays of $\eta \rightarrow \gamma\gamma$, $3\pi^0$, $\pi^+ \pi^- \pi^0$, $\pi^+ \pi^- \gamma$, and $e^+ e^- \gamma$ account for all η decays within a contribution of 0.3% to the systematic error.

$\Gamma(\text{neutral modes})/\Gamma(\pi^+\pi^-\pi^0)$ $\Gamma_1/\Gamma_9 = (\Gamma_2+\Gamma_3+\Gamma_4)/\Gamma_9$

VALUE	EVTS	DOCUMENT ID	TECN
3.16 ± 0.05 OUR FIT			
Error includes scale factor of 1.2.			
3.26 ± 0.30 OUR AVERAGE			
2.54 ± 1.89	74	KENDALL	74 OSPK
3.4 ± 1.1	29	AGUILAR...	72B HBC
2.83 ± 0.80	70	BLOODW...	72B HBC
3.6 ± 0.6	244	FLATTE	67B HBC
2.89 ± 0.56		ALFF...	66 HBC
3.6 ± 0.8	50	KRAEMER	64 DBC
3.8 ± 1.1		PAULI	64 DBC

¹³ Error increased from published value 0.5 by Bloodworth (private communication).

$\Gamma(2\gamma)/\Gamma(\pi^+\pi^-\pi^0)$ Γ_2/Γ_9

VALUE	EVTS	DOCUMENT ID	TECN	COMMENT
1.729 ± 0.028 OUR FIT				
Error includes scale factor of 1.2.				
1.70 ± 0.04 OUR AVERAGE				
1.704 ± 0.032 ± 0.026	3915	¹⁴ LOPEZ	07 CLEO	$\psi(2S) \rightarrow J/\psi\eta$
1.61 ± 0.14		ABLIKIM	06E BES2	$e^+e^- \rightarrow J/\psi \rightarrow \eta\gamma$
1.78 ± 0.10 ± 0.13	1077	AMSLER	95 CBAR	$\bar{p}p \rightarrow \pi^+\pi^-\eta$ at rest
1.72 ± 0.25	401	BAGLIN	69 HLBC	
1.61 ± 0.39		FOSTER	65 HBC	

¹⁴ LOPEZ 07 reports $\Gamma(\eta \rightarrow \pi^+\pi^-\pi^0) / \Gamma(\eta \rightarrow 2\gamma) = \Gamma_9/\Gamma_2 = 0.587 \pm 0.011 \pm 0.009$.

$\Gamma(3\pi^0)/\Gamma(\pi^+\pi^-\pi^0)$ Γ_3/Γ_9

VALUE	EVTS	DOCUMENT ID	TECN	COMMENT
1.432 ± 0.026 OUR FIT				
Error includes scale factor of 1.2.				
1.48 ± 0.05 OUR AVERAGE				
1.46 ± 0.03 ± 0.09		ACHASOV	06A SND	$e^+e^- \rightarrow \eta\gamma$
1.52 ± 0.04 ± 0.08	23k	¹⁵ AKHMETSHIN	01B CMD2	$e^+e^- \rightarrow \phi \rightarrow \eta\gamma$
1.44 ± 0.09 ± 0.10	1627	AMSLER	95 CBAR	$\bar{p}p \rightarrow \pi^+\pi^-\eta$ at rest
1.50 ^{+0.15} _{-0.29}	199	BAGLIN	69 HLBC	
1.47 ^{+0.20} _{-0.17}		BULLOCK	68 HLBC	

• • • We do not use the following data for averages, fits, limits, etc. • • •

1.3 ± 0.4		BAGLIN	67B HLBC
0.90 ± 0.24		FOSTER	65 HBC
2.0 ± 1.0		FOELSCH	64 HBC
0.83 ± 0.32		CRAWFORD	63 HBC

¹⁵ AKHMETSHIN 01B uses results from AKHMETSHIN 99F.

$\Gamma(\pi^+\pi^-\pi^0)/[\Gamma(2\gamma) + \Gamma(3\pi^0)]$ $\Gamma_9/(\Gamma_2+\Gamma_3)$

VALUE	EVTS	DOCUMENT ID	TECN	COMMENT
0.316 ± 0.005 OUR FIT				
Error includes scale factor of 1.2.				
0.304 ± 0.012				
		ACHASOV	00D SND	$e^+e^- \rightarrow \phi \rightarrow \eta\gamma$
• • • We do not use the following data for averages, fits, limits, etc. • • •				
0.3141 ± 0.0081 ± 0.0058		ACHASOV	00B SND	See ACHASOV 00D

$\Gamma(\pi^+\pi^-\gamma)/\Gamma_{\text{total}}$ Γ_{10}/Γ

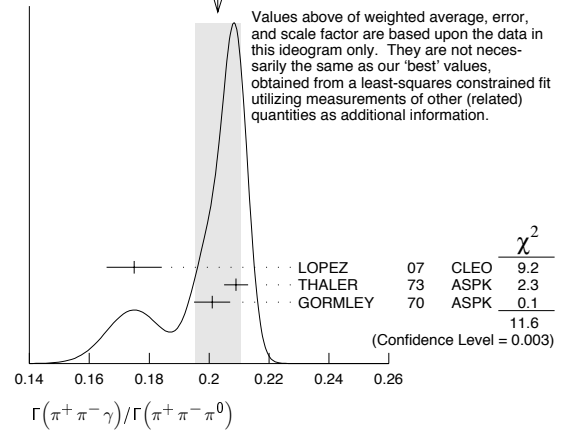
VALUE (units 10 ⁻²)	EVTS	DOCUMENT ID	TECN	COMMENT
4.60 ± 0.16 OUR FIT				
Error includes scale factor of 2.1.				
• • • We do not use the following data for averages, fits, limits, etc. • • •				
3.96 ± 0.14 ± 0.14	859	¹⁶ LOPEZ	07 CLEO	$\psi(2S) \rightarrow J/\psi\eta$

¹⁶ Not independent of other results listed for LOPEZ 07. Assuming decays of $\eta \rightarrow \gamma\gamma$, $3\pi^0$, $\pi^+\pi^-\pi^0$, $\pi^+\pi^-\gamma$, and $e^+e^-\gamma$ account for all η decays within a contribution of 0.3% to the systematic error.

$\Gamma(\pi^+\pi^-\gamma)/\Gamma(\pi^+\pi^-\pi^0)$ Γ_{10}/Γ_9

VALUE	EVTS	DOCUMENT ID	TECN	COMMENT
0.202 ± 0.007 OUR FIT				
Error includes scale factor of 2.4.				
0.203 ± 0.008 OUR AVERAGE				
Error includes scale factor of 2.4. See the ideogram below.				
0.175 ± 0.007 ± 0.006	859	LOPEZ	07 CLEO	$\psi(2S) \rightarrow J/\psi\eta$
0.209 ± 0.004	18k	THALER	73 ASPK	
0.201 ± 0.006	7250	GORMLEY	70 ASPK	
• • • We do not use the following data for averages, fits, limits, etc. • • •				
0.28 ± 0.04		BALTAY	67B DBC	
0.25 ± 0.035		LITCHFIELD	67 DBC	
0.30 ± 0.06		CRAWFORD	66 HBC	
0.196 ± 0.041		FOSTER	65c HBC	

WEIGHTED AVERAGE
0.203 ± 0.008 (Error scaled by 2.4)



$\Gamma(e^+e^-\gamma)/\Gamma_{\text{total}}$ Γ_{11}/Γ

VALUE (units 10 ⁻³)	EVTS	DOCUMENT ID	TECN	COMMENT
6.8 ± 0.8 OUR FIT				
Error includes scale factor of 1.7.				
6.3 ± 1.0 OUR AVERAGE				
Error includes scale factor of 1.6.				
5.15 ± 0.62 ± 0.74	283	ACHASOV	01B SND	$e^+e^- \rightarrow \phi \rightarrow \eta\gamma$
7.10 ± 0.64 ± 0.46	323	AKHMETSHIN	01 CMD2	$e^+e^- \rightarrow \phi \rightarrow \eta\gamma$
• • • We do not use the following data for averages, fits, limits, etc. • • •				
9.4 ± 0.7 ± 0.5	172	¹⁷ LOPEZ	07 CLEO	$\psi(2S) \rightarrow J/\psi\eta$

¹⁷ Not independent of other results listed for LOPEZ 07. Assuming decays of $\eta \rightarrow \gamma\gamma$, $3\pi^0$, $\pi^+\pi^-\pi^0$, $\pi^+\pi^-\gamma$, and $e^+e^-\gamma$ account for all η decays within a contribution of 0.3% to the systematic error.

$\Gamma(e^+e^-\gamma)/\Gamma(\pi^+\pi^-\gamma)$ Γ_{11}/Γ_{10}

VALUE	EVTS	DOCUMENT ID	TECN	COMMENT
0.149 ± 0.019 OUR FIT				
Error includes scale factor of 1.7.				
0.237 ± 0.021 ± 0.015	172	LOPEZ	07 CLEO	$\psi(2S) \rightarrow J/\psi\eta$

$\Gamma(e^+e^-\gamma)/\Gamma(\pi^+\pi^-\pi^0)$ Γ_{11}/Γ_9

VALUE (units 10 ⁻²)	EVTS	DOCUMENT ID	TECN	COMMENT
3.0 ± 0.4 OUR FIT				
Error includes scale factor of 1.7.				
2.1 ± 0.5	80	JANE	75B OSPK	See the erratum

$\Gamma(\text{neutral modes})/[\Gamma(\pi^+\pi^-\pi^0) + \Gamma(\pi^+\pi^-\gamma) + \Gamma(e^+e^-\gamma)]$
 $\Gamma_1/(\Gamma_9+\Gamma_{10}+\Gamma_{11}) = (\Gamma_2+\Gamma_3+\Gamma_4)/(\Gamma_9+\Gamma_{10}+\Gamma_{11})$

VALUE	EVTS	DOCUMENT ID	TECN	COMMENT
2.57 ± 0.04 OUR FIT				
Error includes scale factor of 1.2.				
2.64 ± 0.23				
		BALTAY	67B DBC	
• • • We do not use the following data for averages, fits, limits, etc. • • •				
4.5 ± 1.0	280	¹⁸ JAMES	66 HBC	
3.20 ± 1.26	53	¹⁸ BASTIEN	62 HBC	
2.5 ± 1.0	10	¹⁸ PICKUP	62 HBC	

¹⁸ These experiments are not used in the averages as they do not separate clearly $\eta \rightarrow \pi^+\pi^-\pi^0$ and $\eta \rightarrow \pi^+\pi^-\gamma$ from each other. The reported values thus probably contain some unknown fraction of $\eta \rightarrow \pi^+\pi^-\gamma$.

$\Gamma(2\gamma)/[\Gamma(\pi^+\pi^-\pi^0) + \Gamma(\pi^+\pi^-\gamma) + \Gamma(e^+e^-\gamma)]$ $\Gamma_2/(\Gamma_9+\Gamma_{10}+\Gamma_{11})$

VALUE	EVTS	DOCUMENT ID	TECN	COMMENT
1.403 ± 0.023 OUR FIT				
Error includes scale factor of 1.2.				
1.1 ± 0.4 OUR AVERAGE				
1.51 ± 0.93	75	KENDALL	74 OSPK	
0.99 ± 0.48		CRAWFORD	63 HBC	

$\Gamma(\mu^+\mu^-\gamma)/\Gamma_{\text{total}}$ Γ_{12}/Γ

VALUE (units 10 ⁻⁴)	EVTS	DOCUMENT ID	TECN	COMMENT
3.1 ± 0.4 OUR FIT				
Error includes scale factor of 1.2.				
3.1 ± 0.4	600	DZHELADIN	80 SPEC	$\pi^-p \rightarrow \eta n$
• • • We do not use the following data for averages, fits, limits, etc. • • •				
1.5 ± 0.75	100	BUSHNIN	78 SPEC	See DZHELADIN 80

$\Gamma(e^+e^-)/\Gamma_{\text{total}}$ Γ_{13}/Γ

VALUE	CL%	DOCUMENT ID	TECN	COMMENT
< 0.77 × 10⁻⁴	90	BROWDER	97B CLE2	$e^+e^- \simeq 10.5$ GeV
• • • We do not use the following data for averages, fits, limits, etc. • • •				
< 2 × 10 ⁻⁴	90	WHITE	96 SPEC	$p d \rightarrow \eta^3\text{He}$
< 3 × 10 ⁻⁴	90	DAVIES	74 RVUE	Uses ESTEN 67

Meson Particle Listings

 η $\Gamma(\mu^+ \mu^-)/\Gamma_{\text{total}}$ Γ_{14}/Γ

VALUE (units 10^{-6})	CL%	EVTS	DOCUMENT ID	TECN	COMMENT
5.8 ± 0.8 OUR AVERAGE					

5.7 ± 0.7 ± 0.5	114	ABEGG	94	SPEC	$pd \rightarrow \eta^3 \text{He}$
6.5 ± 2.1	27	DZHELADIN	80B	SPEC	$\pi^- p \rightarrow \eta n$

• • • We do not use the following data for averages, fits, limits, etc. • • •

5.6 ± 0.6 ± 0.5	100	KESSLER	93	SPEC	See ABEGG 94
< 20	95	0	WEHMANN	68	OSPK

 $\Gamma(\mu^+ \mu^-)/\Gamma(2\gamma)$ Γ_{14}/Γ_2

VALUE (units 10^{-9})	DOCUMENT ID	TECN	
5.9 ± 2.2	HYAMS	69	OSPK

• • • We do not use the following data for averages, fits, limits, etc. • • •

 $\Gamma(e^+ e^- e^+ e^-)/\Gamma_{\text{total}}$ Γ_{15}/Γ

VALUE	CL%	DOCUMENT ID	TECN	COMMENT
< 6.9 × 10⁻⁵	90	AKHMETSHIN 01	CMD2	$e^+ e^- \rightarrow \phi \rightarrow \eta \gamma$

 $\Gamma(\pi^+ \pi^- e^+ e^-)/\Gamma_{\text{total}}$ Γ_{16}/Γ

VALUE (units 10^{-4})	EVTS	DOCUMENT ID	TECN	CHG	COMMENT
4.2 ± 1.2 OUR FIT					

4.3 ± 1.3 ± 0.4	16	BARGHOLTZ	07	CNTR	0	$pd \rightarrow {}^3\text{He} \eta$
3.7 ± 2.5 ± 0.3	4	AKHMETSHIN 01	CMD2			$e^+ e^- \rightarrow \phi \rightarrow \eta \gamma$

 $\Gamma(\pi^+ \pi^- e^+ e^-)/\Gamma(\pi^+ \pi^- \gamma)$ Γ_{16}/Γ_{10}

VALUE (units 10^{-2})	EVTS	DOCUMENT ID	TECN
0.92 ± 0.25 OUR FIT			

2.6 ± 2.6	1	GROSSMAN	66	HBC
-----------	---	----------	----	-----

 $\Gamma(\pi^+ \pi^- 2\gamma)/\Gamma(\pi^+ \pi^- \pi^0)$ Γ_{17}/Γ_9

VALUE	CL%	DOCUMENT ID	TECN	
< 9 × 10⁻³		PRICE	67	HBC

< 16 × 10 ⁻³	95	BALTAY	67B	DBC
-------------------------	----	--------	-----	-----

• • • We do not use the following data for averages, fits, limits, etc. • • •

 $\Gamma(\pi^+ \pi^- \pi^0 \gamma)/\Gamma(\pi^+ \pi^- \pi^0)$ Γ_{18}/Γ_9

VALUE	CL%	EVTS	DOCUMENT ID	TECN	
< 0.24 × 10⁻²	90	0	THALER	73	ASPK

< 1.7 × 10 ⁻²	90	ARNOLD	68	HLBC
< 1.6 × 10 ⁻²	95	BALTAY	67B	DBC
< 7.0 × 10 ⁻²		FLATTE	67	HBC
< 0.9 × 10 ⁻²		PRICE	67	HBC

• • • We do not use the following data for averages, fits, limits, etc. • • •

 $\Gamma(\pi^0 \mu^+ \mu^- \gamma)/\Gamma_{\text{total}}$ Γ_{19}/Γ

VALUE	CL%	DOCUMENT ID	TECN	COMMENT
< 3 × 10⁻⁶	90	DZHELADIN 81	SPEC	$\pi^- p \rightarrow \eta n$

Forbidden modes $\Gamma(\pi^0 \gamma)/\Gamma_{\text{total}}$ Γ_{20}/Γ

Forbidden by angular momentum conservation.

VALUE	CL%	DOCUMENT ID	TECN	COMMENT
< 9 × 10⁻⁵	90	NEFKENS	05A	CRYB p(720 MeV/c) $\pi^- \rightarrow n \eta$

 $\Gamma(\pi^+ \pi^-)/\Gamma_{\text{total}}$ Γ_{21}/Γ

Forbidden by P and CP invariance.

VALUE	CL%	EVTS	DOCUMENT ID	TECN	COMMENT
< 0.13 × 10⁻⁴	90	16M	AMBROSINO 05A	KLOE	$e^+ e^- \rightarrow \phi \rightarrow \eta \gamma$

< 3.3 × 10 ⁻⁴	90	AKHMETSHIN 99B	CMD2	$e^+ e^- \rightarrow \phi \rightarrow \eta \gamma$
< 9 × 10 ⁻⁴	90	AKHMETSHIN 97C	CMD2	See AKHMETSHIN 99B
< 15 × 10 ⁻⁴	0	THALER	73	ASPK

 $\Gamma(\pi^0 \pi^0)/\Gamma_{\text{total}}$ Γ_{22}/Γ

Forbidden by P and CP invariance.

VALUE	CL%	DOCUMENT ID	TECN	COMMENT
< 3.5 × 10⁻⁴	90	BLIK	07	GAM4 $\pi^- p \rightarrow \eta n$

< 4.3 × 10 ⁻⁴	90	AKHMETSHIN 99C	CMD2	$e^+ e^- \rightarrow \phi \rightarrow \eta \gamma$
< 6 × 10 ⁻⁴	90	19	ACHASOV 98	SND $e^+ e^- \rightarrow \phi \rightarrow \eta \gamma$

¹⁹ACHASOV 98 observes one event in a $\pm 3\sigma$ region around the η mass, while a Monte Carlo calculation gives 10 ± 5 events. The limit here is the Poisson upper limit for one observed event and no background.

 $\Gamma(\pi^0 \pi^0 \gamma)/\Gamma_{\text{total}}$ Γ_{23}/Γ

Forbidden by C invariance.

VALUE	CL%	DOCUMENT ID	TECN	CHG	COMMENT
< 5 × 10⁻⁴	90	NEFKENS	05	CRYB	0 p(720 MeV/c) $\pi^- \rightarrow n \eta$

< 17 × 10 ⁻⁴	90	BLIK	07	GAM4	$\pi^- p \rightarrow \eta n$
-------------------------	----	------	----	------	------------------------------

 $\Gamma(\pi^0 \pi^0 \pi^0 \gamma)/\Gamma_{\text{total}}$ Γ_{24}/Γ

Forbidden by C invariance.

VALUE	CL%	DOCUMENT ID	TECN	CHG	COMMENT
< 6 × 10⁻⁵	90	NEFKENS	05	CRYB	0 p(720 MeV/c) $\pi^- \rightarrow n \eta$

< 24 × 10 ⁻⁵	90	BLIK	07	GAM4	$\pi^- p \rightarrow \eta n$
-------------------------	----	------	----	------	------------------------------

• • • We do not use the following data for averages, fits, limits, etc. • • •

 $\Gamma(3\gamma)/\Gamma_{\text{total}}$ Γ_{25}/Γ

Forbidden by C invariance.

VALUE	CL%	DOCUMENT ID	TECN	COMMENT
< 16 × 10 ⁻⁵	90	BLIK	07	GAM4 $\pi^- p \rightarrow \eta n$
< 4 × 10 ⁻⁵	90	NEFKENS	05A	CRYB p(720 MeV/c) $\pi^- \rightarrow n \eta$

 $\Gamma(3\gamma)/\Gamma(2\gamma)$ Γ_{25}/Γ_2

VALUE	CL%	DOCUMENT ID	TECN	CHG	
< 1.2 × 10 ⁻³	95	ALDE	84	GAM2	0

 $\Gamma(3\gamma)/\Gamma(3\pi^0)$ Γ_{25}/Γ_3

VALUE	CL%	DOCUMENT ID	TECN	COMMENT
< 4.9 × 10⁻⁵	90	ALOISIO	04	KLOE $\phi \rightarrow \eta \gamma$

 $\Gamma(4\pi^0)/\Gamma_{\text{total}}$ Γ_{26}/Γ

Forbidden by P and CP invariance.

VALUE	CL%	DOCUMENT ID	TECN	COMMENT
< 6.9 × 10⁻⁷	90	PRAKHOV	00	CRYB $\pi^- p \rightarrow n \eta$, 720 MeV/c

< 200 × 10 ⁻⁷	90	BLIK	07	GAM4 $\pi^- p \rightarrow \eta n$
--------------------------	----	------	----	-----------------------------------

• • • We do not use the following data for averages, fits, limits, etc. • • •

 $\Gamma(\pi^0 e^+ e^-)/\Gamma_{\text{total}}$ Γ_{27}/Γ

C parity forbids this to occur as a single-photon process.

VALUE	CL%	DOCUMENT ID	TECN	
< 1.6 × 10 ⁻⁴	90	MARTYNOV	76	HLBC
< 8.4 × 10 ⁻⁴	90	BAZIN	68	DBC
< 70 × 10 ⁻⁴		RITTENBERG	65	HBC

 $\Gamma(\pi^0 e^+ e^-)/\Gamma(\pi^+ \pi^- \pi^0)$ Γ_{27}/Γ_9

C parity forbids this to occur as a single-photon process.

VALUE	CL%	EVTS	DOCUMENT ID	TECN	
< 1.9 × 10⁻⁴	90		JANE	75	OSPK

< 42 × 10 ⁻⁴	90	BAGLIN	67	HLBC	
< 16 × 10 ⁻⁴	90	0	BILLING	67	HLBC
< 77 × 10 ⁻⁴	0	FOSTER	65B	HBC	
< 110 × 10 ⁻⁴		PRICE	65	HBC	

• • • We do not use the following data for averages, fits, limits, etc. • • •

 $\Gamma(\pi^0 \mu^+ \mu^-)/\Gamma_{\text{total}}$ Γ_{28}/Γ

C parity forbids this to occur as a single-photon process.

VALUE	CL%	DOCUMENT ID	TECN	COMMENT
< 5 × 10⁻⁶	90	DZHELADIN 81	SPEC	$\pi^- p \rightarrow \eta n$

< 500 × 10 ⁻⁶		WEHMANN	68	OSPK
--------------------------	--	---------	----	------

• • • We do not use the following data for averages, fits, limits, etc. • • •

 $[\Gamma(\mu^+ e^-) + \Gamma(\mu^- e^+)]/\Gamma_{\text{total}}$ Γ_{29}/Γ

Forbidden by lepton family number conservation.

VALUE	CL%	DOCUMENT ID	TECN	COMMENT
< 6 × 10⁻⁶	90	WHITE	96	SPEC $pd \rightarrow \eta^3 \text{He}$

 η C-NONCONSERVING DECAY PARAMETERS $\pi^+ \pi^- \pi^0$ LEFT-RIGHT ASYMMETRY PARAMETER

Measurements with an error $> 1.0 \times 10^{-2}$ have been omitted.

VALUE (units 10^{-2})	EVTS	DOCUMENT ID	TECN
0.09 ± 0.17 OUR AVERAGE			

0.28 ± 0.26	165k	JANE	74	OSPK
-0.05 ± 0.22	220k	LAYTER	72	ASPK

1.5 ± 0.5	37k	20	GORMLEY	68c	ASPK
-----------	-----	----	---------	-----	------

²⁰The GORMLEY 68c asymmetry is probably due to unmeasured ($\mathbf{E} \times \mathbf{B}$) spark chamber effects. New experiments with ($\mathbf{E} \times \mathbf{B}$) controls don't observe an asymmetry.

 $\pi^+ \pi^- \pi^0$ SEXTANT ASYMMETRY PARAMETER

Measurements with an error $> 2.0 \times 10^{-2}$ have been omitted.

VALUE (units 10^{-2})	EVTS	DOCUMENT ID	TECN
0.18 ± 0.16 OUR AVERAGE			

0.20 ± 0.25	165k	JANE	74	OSPK
0.10 ± 0.22	220k	LAYTER	72	ASPK
0.5 ± 0.5	37k	GORMLEY	68c	WIRE

 $\pi^+ \pi^- \pi^0$ QUADRANT ASYMMETRY PARAMETER

VALUE (units 10^{-2})	EVTS	DOCUMENT ID	TECN
-0.17 ± 0.17 OUR AVERAGE			

-0.30 ± 0.25	165k	JANE	74	OSPK
-0.07 ± 0.22	220k	LAYTER	72	ASPK

$\pi^+\pi^-\gamma$ LEFT-RIGHT ASYMMETRY PARAMETERMeasurements with an error $> 2.0 \times 10^{-2}$ have been omitted.

VALUE (units 10^{-2})	EVTS	DOCUMENT ID	TECN
0.9 ± 0.4 OUR AVERAGE			
1.2 ± 0.6	35k	JANE 74B	OSPK
0.5 ± 0.6	36k	THALER 72	ASPK
1.22 ± 1.56	7257	GORMLEY 70	ASPK

 $\pi^+\pi^-\gamma$ PARAMETER β (D -wave)Sensitive to a D -wave contribution: $dN/d\cos\theta = \sin^2\theta (1 + \beta \cos^2\theta)$.

VALUE	EVTS	DOCUMENT ID	TECN
-0.02 ± 0.07 OUR AVERAGE			
-0.11 ± 0.11	35k	JANE 74B	OSPK
-0.060 ± 0.065	7250	GORMLEY 70	WIRE

• • • We do not use the following data for averages, fits, limits, etc. • • •

0.12 ± 0.06	21	THALER 72	ASPK
-------------	----	-----------	------

²¹The authors don't believe this indicates D -wave because the dependence of β on the γ energy is inconsistent with the theoretical prediction. A $\cos^2\theta$ dependence can also come from P - and F -wave interference.

ENERGY DEPENDENCE OF $\eta \rightarrow 3\pi$ DALITZ PLOTSPARAMETERS FOR $\eta \rightarrow \pi^+\pi^-\pi^0$ See the "Note on η Decay Parameters" in our 1994 edition, Phys. Rev. **D50**, 1 August 1994, Part I, p. 1454. The following experiments fit to one or more of the coefficients a, b, c, d, e for $|\text{matrix element}|^2 = 1 + ay + by^2 + cx + dx^2 + exy$.

VALUE	EVTS	DOCUMENT ID	TECN	COMMENT
• • • We do not use the following data for averages, fits, limits, etc. • • •				
3230	²²	ABELE 98D	CBAR	$\bar{p}p \rightarrow \pi^0\pi^0\eta$ at rest
1077	²³	AMSLER 95	CBAR	$\bar{p}p \rightarrow \pi^+\pi^-\eta$ at rest
81k		LAYTER 73	ASPK	
220k		LAYTER 72	ASPK	
1138		CARPENTER 70	HBC	
349		DANBURG 70	DBC	
7250		GORMLEY 70	WIRE	
526		BAGLIN 69	HLBC	
7170		CNOP5 68	OSPK	
37k		GORMLEY 68C	WIRE	
1300		CLPWY 66	HBC	
705		LARRIBE 66	HBC	

²²ABELE 98D obtains $a = -1.22 \pm 0.07$ and $b = 0.22 \pm 0.11$ when c (our d) is fixed at 0.06.

²³AMSLER 95 fits to $(1+ay+by^2)$ and obtains $a = -0.94 \pm 0.15$ and $b = 0.11 \pm 0.27$.

 α PARAMETER FOR $\eta \rightarrow 3\pi^0$ See the "Note on η Decay Parameters" in our 1994 edition, Phys. Rev. **D50**, 1 August 1994, Part I, p. 1454. The value here is of α in $|\text{matrix element}|^2 = 1 + 2\alpha z$.

VALUE	EVTS	DOCUMENT ID	TECN	COMMENT
-0.031 ± 0.004 OUR AVERAGE				
-0.026 ± 0.010 ± 0.010	75k	BASHKANOV 07	WASA	$pp \rightarrow pp\eta$
-0.010 ± 0.021 ± 0.010	12k	ACHASOV 01C	SND	$e^+e^- \rightarrow \phi \rightarrow \eta\gamma$
-0.031 ± 0.004	1M	TIPPENS 01	CRYB	$\pi^-\pi^+ \rightarrow \eta\eta, 720 \text{ MeV}$
-0.052 ± 0.017 ± 0.010	98k	ABELE 98C	CBAR	$\bar{p}p \rightarrow 5\pi^0$
-0.022 ± 0.023	50k	ALDE 84	GAM2	
• • • We do not use the following data for averages, fits, limits, etc. • • •				
-0.32 ± 0.37	192	BAGLIN 70	HLBC	

 η REFERENCES

AMBROSINO 07B	JHEP 0712 073	F. Ambrosino et al.	(KLOE Collab.)
BARGHOLTZ 07	PL B644 299	Chr. Bargholtz et al.	(CELSIUS/WASA Collab.)
BASHKANOV 07	PR C76 048201	M. Bashkanov et al.	(CELSIUS/WASA Collab.)
BLIK 07	PAN 70 693	A.M. Blik et al.	(GAMS Collab.)
	Translated from YAF 70 724.		
LOPEZ 07	PRL 99 122001	A. Lopez et al.	(CLEO Collab.)
MILLER 07	PRL 99 122002	D.H. Miller et al.	(CLEO Collab.)
ABLIKIM 06E	PR D73 052008	M. Ablikim et al.	(BES Collab.)
ABLIKIM 06Q	PRL 97 202002	M. Ablikim et al.	(BES Collab.)
ACHASOV 06A	PR D74 014016	M.N. Achasov et al.	(SND Collab.)
ABDEL-BARY 05	PL B619 281	M. Abdel-Bary et al.	(GEM Collab.)
AKHMETSHIN 05	PL B605 26	R.R. Akhmetshin et al.	(Novosibirsk CMD-2 Collab.)
AMBROSINO 05A	PL B606 276	F. Ambrosino et al.	(KLOE Collab.)
NEFKENS 05	PRL 94 041601	B.M.K. Nefkens et al.	(BNL Crystal Ball Collab.)
NEFKENS 05A	PR C72 035212	B.M.K. Nefkens et al.	(BNL Crystal Ball Collab.)
PRAKHOV 05	PR C72 025201	S. Prakhov et al.	(BNL Crystal Ball Collab.)
ALOISIO 04	PL B591 49	A. Aloisio et al.	(KLOE Collab.)
KNECHT 04	PL B589 14	N. Knecht et al.	(KLOE Collab.)
LAI 02	PL B533 196	A. Lai et al.	(CERN NA48 Collab.)
NEFKENS 02	PS T99 114	B.M.K. Nefkens, J.W. Price	(UCLA)
ACHASOV 01B	PL B504 275	M.N. Achasov et al.	(Novosibirsk SND Collab.)
ACHASOV 01C	JETPL 73 451	M.N. Achasov et al.	(Novosibirsk SND Collab.)
	Translated from ZETFP 73 511		
ACHASOV 01D	NP B600 3	M.N. Achasov et al.	(Novosibirsk SND Collab.)
AKHMETSHIN 01	PL B501 191	R.R. Akhmetshin et al.	(Novosibirsk CMD-2 Collab.)
AKHMETSHIN 01B	PL B509 217	R.R. Akhmetshin et al.	(Novosibirsk CMD-2 Collab.)
TIPPENS 01	PRL 87 192001	W.B. Tippens et al.	(BNL Crystal Ball Collab.)
ACHASOV 00	EPJ C12 25	M.N. Achasov et al.	(Novosibirsk SND Collab.)
ACHASOV 00B	JETP 90 17	M.N. Achasov et al.	(Novosibirsk SND Collab.)
	Translated from ZETP 117 22		
ACHASOV 00D	JETPL 72 282	M.N. Achasov et al.	(Novosibirsk SND Collab.)
	Translated from ZETFP 72 411.		

PRAKHOV 00	PRL 84 4802	S. Prakhov et al.	(BNL Crystal Ball Collab.)
AKHMETSHIN 99B	PL B462 371	R.R. Akhmetshin et al.	(Novosibirsk CMD-2 Collab.)
AKHMETSHIN 99C	PL B462 380	R.R. Akhmetshin et al.	(Novosibirsk CMD-2 Collab.)
AKHMETSHIN 99F	PL B460 242	R.R. Akhmetshin et al.	(Novosibirsk CMD-2 Collab.)
ABELE 98E	PL B417 193	A. Abele et al.	(Crystal Barrel Collab.)
ABELE 98D	PL B417 197	A. Abele et al.	(Crystal Barrel Collab.)
ACHASOV 98	PL B425 388	M.N. Achasov et al.	(Novosibirsk SND Collab.)
AKHMETSHIN 97C	PL B415 452	R.R. Akhmetshin et al.	(Novosibirsk CMD-2 Collab.)
BROWDER 97B	PR D56 5359	T.E. Browder et al.	(CLEO Collab.)
ABEGG 96	PR D53 11	R. Abegg et al.	(Saturne SPES2 Collab.)
WHITE 96	PR D53 6658	D.B. White et al.	(Saturne SPES2 Collab.)
AMSLER 95	PL B346 203	C. Amisler et al.	(Crystal Barrel Collab.)
KRUSCHE 95D	ZPHY A351 237	B. Krusche et al.	(TAPS + A2 Collab.)
ABEGG 94	PR D50 92	R. Abegg et al.	(Saturne SPES2 Collab.)
AMSLER 93	ZPHY C58 175	C. Amisler et al.	(Crystal Barrel Collab.)
KESSLER 93	PRL 70 892	R.S. Kessler et al.	(Saturne SPES2 Collab.)
PLOUIN 92	PL B276 526	F. Plouin et al.	(Saturne SPES4 Collab.)
BARU 90	ZPHY C48 581	S.E. Baru et al.	(MD-1 Collab.)
ROE 90	PR D41 17	N.A. Roe et al.	(ASP Collab.)
WILLIAMS 88	PR D38 1365	D.A. Williams et al.	(Crystal Ball Collab.)
AIHARA 86	PR D33 844	H. Aihara et al.	(TPC-2 γ Collab.)
BARTEL 85E	PL 160B 421	W. Bartel et al.	(JADE Collab.)
LANDSBERG 85C	PRPL 128 301	L.G. Landsberg	(SERP)
ALDE 84	ZPHY C25 225	D.M. Alde et al.	(SERP, BELG, LAPP)
	SJNP 40 918	D.M. Alde et al.	(SERP, BELG, LAPP)
	Translated from YAF 40 1447.		
WEINSTEIN 83	PR D28 2896	A.J. Weinstein et al.	(Crystal Ball Collab.)
BINON 82	SJNP 36 391	F.G. Binon et al.	(SERP, BELG, LAPP+)
	Translated from YAF 36 670.		
	NC 71A 497	F.G. Binon et al.	(SERP, BELG, LAPP+)
DAVYDOV 81	LNC 32 45	V.A. Davydov et al.	(SERP, BELG, LAPP+)
	SJNP 33 825	V.A. Davydov et al.	(SERP, BELG, LAPP+)
	Translated from YAF 33 1534.		
DZHELJADIN 81	PL 105B 239	R.I. Dzhelezadine et al.	(SERP)
	SJNP 33 822	R.I. Dzhelezadine et al.	(SERP)
	Translated from YAF 33 1529.		
ABROSIMOV 80	SJNP 31 195	A.T. Abrosimov et al.	(JINR)
	Translated from YAF 31 371.		
DZHELJADIN 80	PL 94B 548	R.I. Dzhelezadine et al.	(SERP)
	SJNP 32 516	R.I. Dzhelezadine et al.	(SERP)
	Translated from YAF 32 998.		
DZHELJADIN 80B	PL 97B 471	R.I. Dzhelezadine et al.	(SERP)
	SJNP 32 518	R.I. Dzhelezadine et al.	(SERP)
	Translated from YAF 32 1002.		
BUSHNIN 78	PL 79B 147	Y.B. Bushnin et al.	(SERP)
	SJNP 28 775	Y.B. Bushnin et al.	(SERP)
	Translated from YAF 28 1507.		
MARTYNOV 76	SJNP 23 48	A.S. Martynov et al.	(JINR)
	Translated from YAF 23 93.		
JANE 75	PL 59B 99	M.R. Jane et al.	(RHEL, LOWC)
JANE 75B	PL 59B 103	M.R. Jane et al.	(RHEL, LOWC)
	PL 73B 503	M.R. Jane	
	Erratum in private communication.		
BROWMAN 74B	PRL 32 1067	A. Browman et al.	(CORN, BING)
DAVIES 74	NC 24A 324	J.D. Davies, J.G. Guy, R.K.P. Zia	(BIRM, RHEL+)
DUANE 74	PRL 32 425	A. Duane et al.	(LOIC, SHMP)
JANE 74	PL 48B 260	M.R. Jane et al.	(RHEL, LOWC, SUSS)
JANE 74B	PL 48B 265	M.R. Jane et al.	(RHEL, LOWC, SUSS)
KENDALL 74	NC 21B 287	B.N. Kendall et al.	(BROW, BARI, MIT)
LAYTER 73	PR D7 2565	J.G. Layter et al.	(COLU)
THALER 73	PR D7 2569	J.J. Thaler et al.	(COLU)
AGUILAR... 72B	PR D6 29	M. Aguilar-Benitez et al.	(BNL)
BLOODW... 72B	NP B39 525	I.J. Bloodworth et al.	(TNTO)
LAYTER 72	PRL 29 316	J.G. Layter et al.	(COLU)
THALER 72	PRL 29 313	J.J. Thaler et al.	(COLU, STRB)
BASILE 71D	NC 3A 796	M. Basile et al.	(CERN, BGNA, STRB)
STRUGALSKI 71	NP B27 429	Z.S. Strugalski et al.	(JINR)
BAGLIN 70	NP B22 66	C. Baglin et al.	(EPOL, MADR, STRB)
BUTTRAM 70	PRL 25 1358	M.T. Buttram, M.N. Kreisler, R.E. Mischke	(PRIN)
CARPENTER 70	PR D1 1303	D.W. Carpenter et al.	(DUKE)
COX 70B	PRL 24 534	B. Cox, L. Fortney, J.P. Gosson	(DUKE)
DANBURG 70	PR D2 2564	J.S. Danburg et al.	(LRL)
DEVONS 70	PR D1 1936	S. Devons et al.	(COLU, SYRA)
GORMLEY 70	PR D2 501	M. Gormley et al.	(COLU, BNL)
BAGLIN 69	PL 29B 445	C. Baglin et al.	(EPOL, UCB, MADR, STRB)
	NP B22 66	C. Baglin et al.	(EPOL, MADR, STRB)
HYAMS 69	PL 29B 128	B.D. Hyams et al.	(CERN, MPIM)
ARNOLD 68	PL 27B 466	R.G. Arnold et al.	(STRB, MADR, EPOL+)
BAZIN 68	PRL 20 935	M.J. Bazin et al.	(PRIN, UKND)
BULLOCK 68	PRL 27 402	F.W. Bullock et al.	(LOU)
CNOP5 68	PRL 21 1609	A.M. Cnop5 et al.	(BNL, ORNL, UCSD+)
GORMLEY 68C	PRL 21 402	M. Gormley et al.	(COLU, BNL)
WEHMANN 68	PRL 20 748	A.W. Wehmann et al.	(HARV, CASE, SLAC+)
BAGLIN 67	PL 24B 637	C. Baglin et al.	(EPOL, UCB)
BAGLIN 67B	BAPS 12 567	C. Baglin et al.	(EPOL, UCB)
BALTAY 67B	PRL 19 1498	C. Baltay et al.	(COLU, STON)
BALTAY 67D	PRL 19 1495	C. Baltay et al.	(COLU, BRAN)
BEMPORAD 67	PL 25B 380	C. Bemporad et al.	(PIA, BONN)
	Also Private Comm.		
BILLING 67	PL 25B 435	K.D. Billing et al.	(LOUC, OXF)
BUNJATOV 67	PL 25B 560	S.A. Bunyatov et al.	(CERN, KARL)
CENCE 67	PRL 19 1393	R.J. Cence et al.	(HAWA, LRL)
ESTEN 67	PL 24B 115	M.J. Esten et al.	(LOUC, OXF)
FELDMAN 67	PRL 18 868	M. Feldman et al.	(PEN)
FLATTE 67	PRL 18 976	S.M. Flatte	(LRL)
FLATTE 67B	PR 163 1441	S.M. Flatte, C.G. Wohl	(LRL)
LITFIELD 67	PL 24B 486	P.J. Litfield et al.	(RHEL, SACL)
PRICE 67	PRL 18 1207	L.R. Price, F.S. Crawford	(LRL)
ALFF... 66	PR 145 1072	C. Alff-Steinberger et al.	(COLU, RUTG)
CLPWY 66	PR 149 1044	C. Balay et al.	(SCUC, LRL, PURD, WISC, YALE)
CRAWFORD 66	PRL 16 333	F.S. Crawford, L.R. Price	(LRL)
DIGUGNO 66	PRL 16 767	G. di Gugno et al.	(LRL)
GROSSMAN 66	PR 146 993	R.A. Grossman, L.R. Price, F.S. Crawford	(MAPL, TRST, FRAS)
GRUNHAUS 66	Thesis	J. Grunhaus	(COLU)
JAMES 66	PR 142 896	F.E. James, H.L. Kraybill	(YALE, BNL)
JONES 66	PL 23 597	W.G. Jones et al.	(LOIC, RHEL)
LARRIBE 66	PL 23 600	A. Larribe et al.	(SACL, RHE)
FOSTER 65	PR 138 B652	M. Foster et al.	(WIS C, PURD)
FOSTER 65B	Athens Conf.	M. Foster, M. Good, M. Meier	(WIS C)
FOSTER 65C	Thesis	M. Foster	(WIS C)
PRICE 65	PRL 15 123	L.R. Price, F.S. Crawford	(LRL)
RITTENBERG 65	PRL 15 556	A. Rittenberg, G.R. Kalbfleisch	(LRL, BNL)
FOELSCH 64	PR 134 B1138	H.W.J. Foelsche, H.L. Kraybill	(YALE)
KRAEMER 64	PR 136 B496	R.W. Kraemer et al.	(JHU, NWES, WOOD)
PAULI 64	PL 13 351	E. Pauli, A. Muller	(SACL)
BACCI 63	PRL 11 37	C. Bacci et al.	(ROMA, FRAS)
CRAWFORD 63	PRL 10 546	F.S. Crawford, L.J. Lloyd, E.C. Fowler	(LRL+)
	Also PRL 16 907	F.S. Crawford, L.J. Lloyd, E.C. Fowler	(LRL+)
ALFF... 62	PRL 9 322	C. Alff-Steinberger et al.	(COLU, RUTG)
BASTIEN 62	PRL 8 114	P.L. Bastien et al.	(LRL)
PICKUP 62	PRL 8 329	E. Pickup, D.K. Robinson, E.O. Salant	(CNR C+)

Meson Particle Listings

 $f_0(600)$

$f_0(600)$ or σ

$$I^G(J^{PC}) = 0^+(0^{++})$$

NOTE ON SCALAR MESONS

Revised January 2008 by S. Spanier (University of Tennessee), N.A. Törnqvist (University of Helsinki), and C. Amsler (University of Zurich).

I. Introduction:

The scalar mesons are especially important to understand because they have the same quantum numbers as the vacuum ($J^{PC} = 0^{++}$). Therefore they can condense into the vacuum and break a symmetry like a global chiral $U(N_f) \times U(N_f)$. The details of how this symmetry breaking is implemented in Nature is one of the most profound problems in particle physics.

In contrast to the vector and tensor mesons, the identification of the scalar mesons is a long-standing puzzle. Scalar resonances are difficult to resolve because of their large decay widths which cause a strong overlap between resonances and background, and also because several decay channels open up within a short mass interval. In addition, the $K\bar{K}$ and $\eta\eta$ thresholds produce sharp cusps in the energy dependence of the resonant amplitude. Furthermore, one expects non- $q\bar{q}$ scalar objects, like glueballs and multi-quark states in the mass range below 1800 MeV. For some recent reviews see AMSLER 04, BUGG 04C, CLOSE 02B, and KLEMP 07.

Scalars are produced, for example, in πN scattering on polarized/unpolarized targets, $p\bar{p}$ annihilation, central hadronic production, J/Ψ , B^- , D^- and K^- -meson decays, $\gamma\gamma$ formation, and ϕ radiative decays. Experiments are accompanied by the development of theoretical models for the reaction amplitudes, which are based on common fundamental principles of two-body unitarity, analyticity, Lorentz invariance, and chiral- and flavor-symmetry using different techniques (K -matrix formalism, N/D -method, Dalitz Tuan ansatz, unitarized quark models with coupled channels, effective chiral field theories like the linear sigma model, *etc.*). Dynamics near the lowest two-body thresholds in some analyses is described by crossed channel (t , u) meson exchange or with an effective range parameterization instead of or in addition to resonant features in the s -channel, only. Furthermore, elastic S -wave scattering amplitudes involving soft pions have zeros close to threshold (ADLER 65, 65A), which may be shifted or removed in associated production processes.

The mass and width of a resonance are found from the position of the nearest pole in the process amplitude (T -matrix or S -matrix) at an unphysical sheet of the complex energy plane: $(E - i\Gamma/2)$. It is important to notice that only in the case of narrow well-separated resonances, far away from the opening of decay channels, does the naive Breit-Wigner parameterization (or K -matrix pole parameterization) agree with this pole position.

In this note, we discuss all light scalars organized in the listings under the entries ($I = 1/2$) $K_0^*(800)$ (or κ), $K_0^*(1430)$,

($I = 1$) $a_0(980)$, $a_0(1450)$, and ($I = 0$) $f_0(600)$ (or σ), $f_0(980)$, $f_0(1370)$, and $f_0(1500)$. This list is minimal and does not necessarily exhaust the list of actual resonances. The ($I = 2$) $\pi\pi$ and ($I = 3/2$) $K\pi$ phase shifts do not exhibit any resonant behavior. See also our notes in previous issues for further comments on *e.g.*, scattering lengths and older papers.

II. The $I = 1/2$ States: The $K_0^*(1430)$ (ASTON 88) is perhaps the least controversial of the light scalar mesons. The $K\pi$ S -wave scattering has two possible isospin channels, $I = 1/2$ and $I = 3/2$. The $I = 3/2$ wave is elastic and repulsive up to 1.7 GeV (ESTABROOKS 78) and contains no known resonances. The $I = 1/2$ $K\pi$ phase shift, measured from about 100 MeV above threshold in Kp production, rises smoothly, passes 90° at 1350 MeV, and continues to rise to about 170° at 1600 MeV. The first important inelastic threshold is $K\eta'(958)$. In the inelastic region the continuation of the amplitude is uncertain since the partial-wave decomposition has several solutions. The data are extrapolated towards the $K\pi$ threshold using effective range type formulas (ASTON 88, ABELE 98) or chiral perturbation predictions (BERNARD 91, JAMIN 00, CHERRY 01). In analyses using unitarized amplitudes there is agreement on the presence of a resonance pole around 1410 MeV having a width of about 300 MeV. With reduced model dependence (LINK 07) finds a larger width of 500 MeV.

In recent years there has been controversy about the existence of a light and very broad “ κ ” meson in the 700-900 MeV region. Hadronic D -meson decays provide additional data points in the vicinity of the $K\pi$ threshold - experimental results from E791 (*e.g.* AITALA 02, 06), FOCUS (LINK 02, 07), CLEO (CAWLFIELD 06A), and BaBar (AUBERT 07T) are discussed in the *Review of Charm Dalitz Plot Analyses*. Precision information from semileptonic D decays avoiding theoretically ambiguous three-body final state interactions is not available. BES II finds a κ like structure in J/ψ decays to $\bar{K}^{*0}(892)K^+\pi^-$ where κ recoils against the $K^*(892)$ (ABLIKIM 06C, re-analyzed by (GUO 06)). Also clean with respect to final state interaction is the decay $\tau^- \rightarrow K_S^0\pi^-\nu_\tau$ studied by Belle (EPIFANOV 07), with $K^*(800)$ parameters fixed to (ABLIKIM 06C).

Some authors find a κ pole in their phenomenological analysis (see *e.g.* ANISOVICH 97C, DELBOURGO 98, OLLER 99, 99C, JAMIN 00, SHAKIN 01, SCADRON 03, BLACK 01,03, BUGG 03, ISHIDA 03, ZHENG 04, PALAEZ 04A, ZHOU 06, CAWLFIELD 06A, LINK 07B), while others do not (*e.g.* AUBERT 07T, LINK 02E, 05I, CHERRY 01, KOPP 01). Since it appears to be a very wide object ($\Gamma \approx 500$ MeV) near the $K\pi$ threshold, its presence and properties have been difficult to establish.

Recently a pole position for the κ was found in a theoretical analysis by DESCOTES-GENON 06 in the $K\pi \rightarrow K\pi$ amplitude on the second sheet. Their analysis involves the Mandelstam representation, which includes unitarity, analyticity and crossing symmetry. The precise position of the pole

should be confirmed by independent analyses and different experiments.

III. The $I = 1$ States: Two isovector states are known, the established $a_0(980)$ and the $a_0(1450)$. Independent of any model, the $K\bar{K}$ component in the $a_0(980)$ wave function must be large: it lies just below the opening of the $K\bar{K}$ channel to which it strongly couples. This generates an important cusp-like behavior in the resonant amplitude. Hence, its mass and width parameters are strongly distorted. To reveal its true coupling constants, a coupled channel model with energy-dependent widths and mass shift contributions is necessary. In all measurements in our listings, the mass position agrees on a value near 984 MeV, but the width takes values between 50 and 100 MeV, mostly due to the different models. For example, the analysis of the $p\bar{p}$ -annihilation data (ABELE 98) using an unitary K -matrix description finds a width as determined from the T -matrix pole of 92 ± 8 MeV, while the observed width of the peak in the $\pi\eta$ mass spectrum is about 45 MeV.

The relative coupling $K\bar{K}/\pi\eta$ is determined indirectly from $f_1(1285)$ (BARBERIS 98C, CORDEN 78, DEFOIX 72) or $\eta(1410)$ decays (BAI 90C, BOLTON 92B, AMSLER 95C), from the line shape observed in the $\pi\eta$ decay mode (FLATTE 76, AMSLER 94D, BUGG 94, JANSSEN 95), or from the coupled-channel analysis of $\pi\pi\eta$ and $K\bar{K}\pi$ final states of $p\bar{p}$ annihilation at rest (ABELE 98).

The $a_0(1450)$ is seen in $p\bar{p}$ annihilation experiments with stopped and higher momenta \bar{p} , with a mass of about 1450 MeV or close to the $a_2(1320)$ meson which is typically a dominant feature. The broad structure at about 1300 MeV observed in $\pi N \rightarrow K\bar{K}N$ reactions (MARTIN 79) needs further confirmation in its existence and isospin assignment.

IV. The $I = 0$ States: The $I = 0 J^{PC} = 0^{++}$ sector is the most complex one, both experimentally and theoretically. The data have been obtained from $\pi\pi$, $K\bar{K}$, $\eta\eta$, 4π , and $\eta\eta'(958)$ systems produced in S -wave. Analyses based on several different production processes conclude that probably four poles are needed in the mass range from $\pi\pi$ threshold to about 1600 MeV. The claimed isoscalar resonances are found under separate entries σ or $f_0(600)$, $f_0(980)$, $f_0(1370)$, and $f_0(1500)$.

For discussions of the $\pi\pi$ S wave below the $K\bar{K}$ threshold and on the long history of the $\sigma(600)$, which was suggested in linear sigma models about 50 years ago, see our reviews in previous editions and the conference proceedings KYOTO 00.

Information on the $\pi\pi$ S -wave phase shift $\delta_J^I = \delta_0^0$ was already extracted 30 years ago from the πN scattering (GRAYER 74, BECKER 79), and near threshold from the K_{e4} -decay (ROSSELET 77). The reported $\pi\pi \rightarrow K\bar{K}$ cross sections (WETZEL 76, POLYCHRONAKOS 79, COHEN 80, and ETKIN 82B) have large uncertainties. Recently, the πN data have been analyzed in combination with high-statistics data (see entries labeled as RVUE for re-analyses of the data). The $2\pi^0$ invariant mass spectra of the $p\bar{p}$ annihilation at rest (AMSLER 95D, ABELE 96) and the central collision (ALDE 97) do not show a distinct resonance structure below 900 MeV,

but these data are consistently described with the standard solution for πN data (GRAYER 74, KAMINSKI 97), which allows for the existence of the broad σ . An enhancement is observed in the $\pi^+\pi^-$ invariant mass near threshold in the decays $D^+ \rightarrow \pi^+\pi^-\pi^+$ (AITALA 01B, LINK 04, BONVICINI 07) and $J/\psi \rightarrow \omega\pi^+\pi^-$ (AUGUSTIN 89, ABLIKIM 04A), and in $\psi(2S) \rightarrow J/\psi\pi^+\pi^-$ with very limited phase space (GALLEGOS 04, ABLIKIM 07A).

The precise σ pole is difficult to establish because of its large width, and because it can certainly not be modelled by a naive Breit-Wigner resonance. It is distorted by background as required by chiral symmetry, and from crossed channel exchanges, the $f_0(1370)$, and other dynamical features. However, most of the analyzes under $f_0(600)$ listed in our previous issues agree on a pole position near $(500 - i250)$ MeV.

The existence of the light and very broad σ resonance in the 500 MeV region has been proposed by many authors for over 10 years. In particular, data analyses that included unitarity, $\pi\pi$ threshold behavior and the chiral symmetry constraints from Adler zeroes and scattering lengths needed the light and broad σ in the $\pi\pi$ data.

A precise pole position with an uncertainty of less than 20 MeV (see our table for T -matrix pole) is derived by CAPRINI 06 using unitarized chiral perturbation theory. An important ingredient is the use of Roy-Steiner equations derived from crossing symmetry, analyticity and unitarity. With these constraints CAPRINI 06 find that their position of the σ pole depends, almost exclusively, only on the value of the isosinglet S -wave phase shift at 800 MeV and the S -wave scattering lengths a_0^0 and a_0^2 . Using analyticity and unitarity only to describe data from $K_{2\pi}$ and K_{14} decays GARCIA-MARTIN 07 find comparable pole position and scattering length a_0^0 .

PENNINGTON 06, 07 found that the data for $\sigma \rightarrow \gamma\gamma$ are consistent with what is expected for a two step process of $\gamma\gamma \rightarrow \pi^+\pi^-$ via pion exchange in the t - and u -channel, followed by a final state interaction $\pi^+\pi^- \rightarrow \pi^0\pi^0$. Therefore it may be difficult to learn anything new about the nature of the σ from its $\gamma\gamma$ coupling. There are theoretical indications (*e.g.* PELAEZ 06, CHEN 07A, GIACOSA 07, MAIANI 07) that the σ pole behaves differently from a $q\bar{q}$ -state.

The $f_0(980)$ overlaps strongly with the σ and background represented by a very slow varying phase extending to higher masses and/or the $f_0(1370)$. This can lead to a dip in the $\pi\pi$ spectrum at the $K\bar{K}$ threshold. It changes from a dip into a peak structure in the $\pi^0\pi^0$ invariant mass spectrum of the reaction $\pi^-p \rightarrow \pi^0\pi^0n$ (ACHASOV 98E), with increasing four-momentum transfer to the $\pi^0\pi^0$ system, which means increasing the a_1 -exchange contribution in the amplitude, while the π -exchange decreases. The σ , and the $f_0(980)$, are also observed in radiative decays ($\phi \rightarrow f_0\gamma$) in SND data (ACHASOV 00F, ACHASOV 00H), CMD2 (AKHMETSHIN 99B), and in KLOE data (ALOISIO 02C, AMBROSINO 07). Analyses of $\gamma\gamma \rightarrow \pi\pi$ data (BOGLIONE 99, MORI 07) underline the importance of the $K\bar{K}$ coupling of $f_0(980)$.

Meson Particle Listings

$f_0(600)$

The f_0 's above 1 GeV. A meson resonance that is very well studied experimentally, is the $f_0(1500)$ seen by the Crystal Barrel experiment in five decay modes: $\pi\pi$, $K\bar{K}$, $\eta\eta$, $\eta\eta'(958)$, and 4π (AMSLER 95D, ABELE 96, and ABELE 98). Due to its interference with the $f_0(1370)$ (and $f_0(1710)$), the peak attributed to $f_0(1500)$ can appear shifted in invariant mass spectra. Therefore, the application of simple Breit-Wigner forms arrive at slightly different resonance masses for $f_0(1500)$. Analyses of central-production data of the likewise five decay modes (BARBERIS 99D, BARBERIS 00E) agree on the description of the S -wave with the one above. The $p\bar{p}$, $p\bar{n}/n\bar{p}$ (GASPERO 93, ADAMO 93, AMSLER 94, ABELE 96) show a single enhancement at 1400 MeV in the invariant 4π mass spectra, which is resolved into $f_0(1370)$ and $f_0(1500)$ (ABELE 01, ABELE01B). The data on 4π from central production (BARBERIS 00C) require both resonances, too, but disagree on the relative content of $\rho\rho$ and $\sigma\sigma$ in 4π . All investigations agree, that the 4π decay mode represents about half of the $f_0(1500)$ decay width and is dominant for $f_0(1370)$.

The determination of the $\pi\pi$ coupling of $f_0(1370)$ is aggravated by the strong overlap with the broad $f_0(600)$ and $f_0(1500)$. Since it does not show up prominently in the 2π spectra, its mass and width are difficult to determine. Multi-channel analyses of hadronically produced two- and three-body final states agree on a mass between 1300 MeV and 1400 MeV and a narrow $f_0(1500)$, but arrive at a somewhat smaller width for $f_0(1370)$.

Both Belle and BaBar have observed strong indications of scalars in B meson decays. They observe a broad structure between 1 and 1.6 GeV in K^+K^- and $\pi^+\pi^-$ decays (GARMASH 02, 06, 07, AUBERT 06O, 07BB). It could be a result of interference of several resonances in this mass range, but lack of statistics prevent from an unambiguous identification of this effect.

V. Interpretation of the scalars below 1 GeV: In the literature, many suggestions are discussed such as conventional $q\bar{q}$ mesons, $q\bar{q}q\bar{q}$ or meson-meson bound states mixed with a scalar glueball. In reality, they can be superpositions of these components, and one depends on models to determine the dominant one. Although we have seen progress in recent years, this question remains open. Here, we mention some of the present conclusions.

If one uses the naive quark model it is natural to assume the $f_0(1370)$, $a_0(1450)$, and the $K_0^*(1430)$ are in the same SU(3) flavor nonet being the $(u\bar{u} + d\bar{d})$, $u\bar{d}$ and $u\bar{s}$ state, respectively. In this picture, the choice of the ninth member of the nonet is ambiguous. The controversially discussed candidates are $f_0(1500)$ and $f_0(1700)$. Compared to the above states, the $f_0(1500)$ is very narrow. Thus, it is unlikely to be their isoscalar partner. It is also too light to be the first radial excitation.

The $f_0(980)$ and $a_0(980)$ are often interpreted as multi-quark states (JAFFE 77, ALFORD 00, MAIANI 04A) or $K\bar{K}$ bound states (WEINSTEIN 90). The insight into their internal

structure using two-photon widths (BARNES 85, LI 91, DELBOURGO 99, LUCIO 99, ACHASOV 00H) is not conclusive. The $f_0(980)$ appears as a peak structure in $J/\psi \rightarrow \phi\pi^+\pi^-$ and in D_s decays without $f_0(600)$ background. Based on that observation it is suggested that $f_0(980)$ has a large $s\bar{s}$ component, which according to (DEANDREA 01) is surrounded by a virtual $K\bar{K}$ cloud. Data on radiative decays ($\phi \rightarrow f_0\gamma$ and $\phi \rightarrow a_0\gamma$) from SND, CMD2, and KLOE (see above) favor a 4-quark picture of the $f_0(980)$ and $a_0(980)$. The underlying model for this conclusion (BOGLIONE 03, OLLER 03B) however may be oversimplified. But it remains quite possible that the states $f_0(980)$ and $a_0(980)$, together with the $f_0(600)$ and the $K_0^*(800)$, form a new low-mass state nonet of predominantly four-quark states, where at larger distances the quarks recombine into a pair of pseudoscalar mesons forming by a meson cloud.

Attempts have been made to start directly from chiral Lagrangians (SCADRON 99, OLLER 99, ISHIDA 99, TORNQVIST 99, OLLER 03B, NAPSUCIALE 04, 04A) which predict the existence of the σ meson near 500 MeV. Hence, *e.g.*, in the chiral linear sigma model with 3 flavors, the σ , $a_0(980)$, $f_0(980)$, and κ (or $K_0^*(1430)$) would form a nonet (not necessarily $q\bar{q}$), while the lightest pseudoscalars would be their chiral partners.

In such models inspired by the linear sigma model the light $\sigma(600)$ is often referred to as the "Higgs boson of strong interactions", since the σ plays a role similar to the Higgs particle in electro-weak symmetry breaking. It is important for chiral symmetry breaking which generates most of the proton and η' mass, and what is referred to as the constituent quark mass.

In the approach of (OLLER 99) the above resonances are generated starting from chiral perturbation theory predictions near the first open channel, and then by extending the predictions to the resonance regions using unitarity.

In the unitarized quark model with coupled $q\bar{q}$ and meson-meson channels, the light scalars can be understood as additional manifestations of bare $q\bar{q}$ confinement states, strongly mass shifted from the 1.3 - 1.5 GeV region and very distorted due to the strong 3P_0 coupling to S -wave two-meson decay channels (TORNQVIST 95, 96, BEVEREN 86, 99, 01B). Thus, the light scalar nonet comprising the $f_0(600)$, $f_0(980)$, $K_0^*(800)$, and $a_0(980)$, as well as the regular nonet consisting of the $f_0(1370)$, $f_0(1500)$ (or $f_0(1700)$), $K_0^*(1430)$, and $a_0(1450)$, respectively, are two manifestations of the same bare input states (see also BOGLIONE 02).

Other models with different groupings of the observed resonances exist and may *e.g.* be found in earlier versions of this review and papers listed as other related papers below.

VI. Interpretation of the f_0 's above 1 GeV: The $f_0(1370)$ and $f_0(1500)$ decay mostly into pions (2π and 4π) while the $f_0(1710)$ decays mainly into $K\bar{K}$ final states. The $K\bar{K}$ decay branching ratio of the $f_0(1500)$ is small (ABELE 96B,98, BARBERIS 99D). Naively, this suggests a $n\bar{n}$ ($= u\bar{u} + d\bar{d}$) structure for the $f_0(1370)$ and $f_0(1500)$, and $s\bar{s}$ for the $f_0(1710)$. The

See key on page 373

Meson Particle Listings

$f_0(600)$

latter is not observed in $p\bar{p}$ annihilation (AMSLER 02), as expected from the OZI suppression for an $s\bar{s}$ state.

However, in $\gamma\gamma$ collisions leading to $K_S^0 K_S^0$ (ACCIA-
RRI 01H) and $K^+ K^-$ (ABE 04), a spin 0 signal is observed
at the $f_0(1710)$ mass (together with a dominant spin 2
component), while the $f_0(1500)$ is not observed in $\gamma\gamma \rightarrow K\bar{K}$ nor
 $\pi^+ \pi^-$ (BARATE 00E). The upper limit from $\pi^+ \pi^-$ excludes a
large $n\bar{n}$ content, and hence would point to a mainly $s\bar{s}$
content for the $f_0(1500)$ (AMSLER 02B). This appears to
contradict the small $K\bar{K}$ decay branching ratio of the
 $f_0(1500)$ and makes a $q\bar{q}$ assignment difficult for this
state. Hence the $f_0(1500)$ could be mainly glue due to
its absence of 2γ -coupling, while the $f_0(1710)$ coupling
to 2γ would be compatible with an $s\bar{s}$ state. However,
the 2γ -couplings are sensitive to glue mixing with $q\bar{q}$
(CLOSE 05).

The narrow width of $f_0(1500)$, and its enhanced produc-
tion at low transverse momentum transfer in central collisions
(CLOSE 97,98B, KIRK 00) also favor $f_0(1500)$ to be non- $q\bar{q}$.
In the mixing scheme of CLOSE 05, which uses central produc-
tion data from WA102 and the recent hadronic J/ψ decay data
from BES (ABLIKIM 04E, 05), glue is shared between $f_0(1370)$,
 $f_0(1500)$ and $f_0(1710)$. The $f_0(1370)$ is mainly $n\bar{n}$, the
 $f_0(1500)$ mainly glue and the $f_0(1710)$ dominantly $s\bar{s}$. This
agrees with previous analyses (AMSLER 96, CLOSE 01B), but
alternative schemes have been proposed (e.g. LEE 00, MINKOWSKI 99;
for a review see e.g. AMSLER 04). In particular, for a scalar
glueball, the two-gluon coupling to $n\bar{n}$ appears to be suppressed
by chiral symmetry (CHANOWITZ 05) and therefore the $K\bar{K}$
decay could be enhanced.

Whether the $f_0(1500)$ is observed in 'gluon rich' radiative
 J/ψ decays is debatable (ABLIKIM 06V) because of the limited
amount of data - more data for this and the $\gamma\gamma$ mode are needed.

References

References can be found at the end of the $f_0(600)$ listing.

$f_0(600)$ T-MATRIX POLE \sqrt{s}

Note that $\Gamma \approx 2 \text{Im}(\sqrt{s_{\text{pole}}})$.

VALUE (MeV)	DOCUMENT ID	TECN	COMMENT
(400-1200) OUR ESTIMATE			
• • • We do not use the following data for averages, fits, limits, etc. • • •			
$(552 \pm 84) - i(232 \pm 81)$	1	ABLIKIM 07A	BES2 $\psi(2S) \rightarrow \pi^+ \pi^- J/\psi$
$(466 \pm 18) - i(223 \pm 28)$	2	BONVICINI 07	CLEO $D^+ \rightarrow \pi^- \pi^+ \pi^+$
$(484 \pm 17) - i(255 \pm 10)$		GARCIA-MAR...07	RVUE $K e 4$
$(441 \pm 16) - i(272 \pm 9)$	3	CAPRINI 06	RVUE $\pi\pi \rightarrow \pi\pi$
$(470 \pm 50) - i(285 \pm 25)$	4	ZHOU 05	RVUE
$(541 \pm 39) - i(252 \pm 42)$	5	ABLIKIM 04A	BES2 $J/\psi \rightarrow \omega \pi^+ \pi^-$
$(528 \pm 32) - i(207 \pm 23)$	6	GALLEGOS 04	RVUE Compilation
$(440 \pm 8) - i(212 \pm 15)$	7	PELAEZ 04A	RVUE $\pi\pi \rightarrow \pi\pi$
$(533 \pm 25) - i(247 \pm 25)$	8	BUGG 03	RVUE
$532 - i272$		BLACK 01	RVUE $\pi^0 \pi^0 \rightarrow \pi^0 \pi^0$
$(470 \pm 30) - i(295 \pm 20)$	3	COLANGELO 01	RVUE $\pi\pi \rightarrow \pi\pi$
$(535 \pm 48) - i(155 \pm 76)$	9	ISHIDA 01	$\Upsilon(3S) \rightarrow \Upsilon \pi\pi$
$610 \pm 14 - i620 \pm 26$	10	SUROVTSEV 01	RVUE $\pi\pi \rightarrow \pi\pi, K\bar{K}$
$(558 \pm 34) - i(196 \pm 32)$		ISHIDA 00B	$p\bar{p} \rightarrow \pi^0 \pi^0 \pi^0$
$445 - i235$		HANNAH 99	RVUE π scalar form factor
$(523 \pm 12) - i(259 \pm 7)$		KAMINSKI 99	RVUE $\pi\pi \rightarrow \pi\pi, K\bar{K}, \sigma\sigma$
$442 - i 227$		OLLER 99	RVUE $\pi\pi \rightarrow \pi\pi, K\bar{K}$
$469 - i203$		OLLER 99B	RVUE $\pi\pi \rightarrow \pi\pi, K\bar{K}$
$445 - i221$		OLLER 99C	RVUE $\pi\pi \rightarrow \pi\pi, K\bar{K}, \eta\eta$
$(1530 \pm 90) - i(560 \pm 40)$		ANISOVICH 98B	RVUE Compilation

$420 - i 212$		LOCHER 98	RVUE $\pi\pi \rightarrow \pi\pi, K\bar{K}$
$(602 \pm 26) - i(196 \pm 27)$	11	ISHIDA 97	$\pi\pi \rightarrow \pi\pi$
$(537 \pm 20) - i(250 \pm 17)$	12	KAMINSKI 97B	RVUE $\pi\pi \rightarrow \pi\pi, K\bar{K}, 4\pi$
$470 - i250$	13,14	TORNQVIST 96	RVUE $\pi\pi \rightarrow \pi\pi, K\bar{K}, K\pi,$ $\eta\pi$
$\sim (1100 - i300)$		AMSLER 95B	CBAR $\bar{p}p \rightarrow 3\pi^0$
$400 - i500$	14,15	AMSLER 95D	CBAR $\bar{p}p \rightarrow 3\pi^0$
$1100 - i137$	14,16	AMSLER 95D	CBAR $\bar{p}p \rightarrow 3\pi^0$
$387 - i305$	14,17	JANSEN 95	RVUE $\pi\pi \rightarrow \pi\pi, K\bar{K}$
$525 - i269$	18	ACHASOV 94	RVUE $\pi\pi \rightarrow \pi\pi$
$(506 \pm 10) - i(247 \pm 3)$		KAMINSKI 94	RVUE $\pi\pi \rightarrow \pi\pi, K\bar{K}$
$370 - i356$	19	ZOU 94B	RVUE $\pi\pi \rightarrow \pi\pi, K\bar{K}$
$408 - i342$	14,19	ZOU 93	RVUE $\pi\pi \rightarrow \pi\pi, K\bar{K}$
$870 - i370$	14,20	AU 87	RVUE $\pi\pi \rightarrow \pi\pi, K\bar{K}$
$470 - i208$	21	VANBEVEREN 86	RVUE $\pi\pi \rightarrow \pi\pi, K\bar{K}, \eta\eta,$ \dots
$(750 \pm 50) - i(450 \pm 50)$	22	ESTABROOKS 79	RVUE $\pi\pi \rightarrow \pi\pi, K\bar{K}$
$(660 \pm 100) - i(320 \pm 70)$		PROTOPOESCU... 73	HBC $\pi\pi \rightarrow \pi\pi, K\bar{K}$
$650 - i370$	23	BASDEVANT 72	RVUE $\pi\pi \rightarrow \pi\pi$

1 From a mean of three different $f_0(600)$ parameterizations. Uses 40k events.

2 From an isobar model using 2.6k events.

3 From the solution of the Roy equation (ROY 71) for the isoscalar S-wave and using a phase-shift analysis of HYAMS 73 and PROTOPOESCU 73 data.

4 Reanalysis of the data from PROTOPOESCU 73, ESTABROOKS 74, GRAYER 74, ROSSELET 77, PISLAK 03, and AKHMETSHIN 04.

5 From a mean of six different analyses and $f_0(600)$ parameterizations.

6 Using data on $\psi(2S) \rightarrow J/\psi \pi\pi$ from BAI 00E and on $\Upsilon(nS) \rightarrow \Upsilon(mS) \pi\pi$ from BUTLER 94B and ALEXANDER 98.

7 Reanalysis of data from PROTOPOESCU 73, ESTABROOKS 74, GRAYER 74, and COHEN 80 in the unitarized ChPT model.

8 From a combined analysis of HYAMS 73, AUGUSTIN 89, AITALA 01B, and PISLAK 01.

9 A similar analysis (KOMADA 01) finds $(580 \pm 79) - i(190 \pm 107)$ MeV.

10 Coupled channel reanalysis of BATON 70, BENSINGER 71, BAILLON 72, HYAMS 73, HYAMS 75, ROSSELET 77, COHEN 80, and ET KIN 82B using the uniformizing variable.

11 Reanalysis of data from HYAMS 73, GRAYER 74, SRINIVASAN 75, and ROSSELET 77 using the interfering amplitude method.

12 Average and spread of 4 variants ("up" and "down") of KAMINSKI 97B 3-channel model.

13 Uses data from BEIER 72B, OCHS 73, HYAMS 73, GRAYER 74, ROSSELET 77, CASON 83, ASTON 88, and ARMSTRONG 91B. Coupled channel analysis with flavor symmetry and all light two-pseudoscalars systems.

14 Demonstrates explicitly that $f_0(600)$ and $f_0(1370)$ are two different poles.

15 Coupled channel analysis of $\bar{p}p \rightarrow 3\pi^0, \pi^0 \eta\eta$ and $\pi^0 \pi^0 \eta$ on sheet II.

16 Coupled channel analysis of $\bar{p}p \rightarrow 3\pi^0, \pi^0 \eta\eta$ and $\pi^0 \pi^0 \eta$ on sheet III.

17 Analysis of data from FALVARD 88.

18 Analysis of data from OCHS 73, ESTABROOKS 75, ROSSELET 77, and MUKHIN 80.

19 Analysis of data from OCHS 73, GRAYER 74, and ROSSELET 77.

20 Analysis of data from OCHS 73, GRAYER 74, BECKER 79, and CASON 83.

21 Coupled-channel analysis using data from PROTOPOESCU 73, HYAMS 73, HYAMS 75, GRAYER 74, ESTABROOKS 74, ESTABROOKS 75, FROGGATT 77, CORDEN 79, BISWAS 81.

22 Analysis of data from APEL 73, GRAYER 74, CHASON 76, PAWLICKI 77. Includes spread and errors of 4 solutions.

23 Analysis of data from BATON 70, BENSINGER 71, COLTON 71, BAILLON 72, PROTOPOESCU 73, and WALKER 67.

$f_0(600)$ BREIT-WIGNER MASS OR K-MATRIX POLE PARAMETERS

VALUE (MeV)	DOCUMENT ID	TECN	COMMENT
(400-1200) OUR ESTIMATE			
513 ± 32	24	MURAMATSU 02	CLEO $e^+ e^- \approx 10 \text{ GeV}$
• • • We do not use the following data for averages, fits, limits, etc. • • •			
$478 \pm 24 \pm 17$		AITALA 01B	E791 $D^+ \rightarrow \pi^- \pi^+ \pi^+$
$563 \pm 58 - 29$	25	ISHIDA 01	$\Upsilon(3S) \rightarrow \Upsilon \pi\pi$
555	26	ASNER 00	CLE2 $\tau^- \rightarrow \pi^- \pi^0 \pi^0 \nu_\tau$
540 ± 36		ISHIDA 00B	$p\bar{p} \rightarrow \pi^0 \pi^0 \pi^0$
750 ± 4		ALEKSEEV 99	SPEC $1.78 \pi^- p_{\text{polar}} \rightarrow \pi^- \pi^+ n$
744 ± 5		ALEKSEEV 98	SPEC $1.78 \pi^- p_{\text{polar}} \rightarrow \pi^- \pi^+ n$
759 ± 5	27	TROYAN 98	$5.2 n p \rightarrow n p \pi^+ \pi^-$
780 ± 30		ALDE 97	GAM2 $450 p p \rightarrow p p \pi^0 \pi^0$
585 ± 20	28	ISHIDA 97	$\pi\pi \rightarrow \pi\pi$
761 ± 12	29	SVEC 96	RVUE $6-17 \pi N_{\text{polar}} \rightarrow \pi^+ \pi^- N$
~ 860	30,31	TORNQVIST 96	RVUE $\pi\pi \rightarrow \pi\pi, K\bar{K}, K\pi, \eta\pi$
1165 ± 50	32,33	ANISOVICH 95	RVUE $\pi^- p \rightarrow \pi^0 \pi^0 n,$ $\bar{p}p \rightarrow \pi^0 \pi^0 \pi^0, \pi^0 \pi^0 \eta,$ $\pi^0 \eta\eta$
~ 1000	34	ACHASOV 94	RVUE $\pi\pi \rightarrow \pi\pi$
414 ± 20	29	AUGUSTIN 89	DM2

24 Statistical uncertainty only.

25 A similar analysis (KOMADA 01) finds 526 ± 48 MeV.

26 From the best fit of the Dalitz plot.

27 6σ effect, no PWA.

28 Reanalysis of data from HYAMS 73, GRAYER 74, SRINIVASAN 75, and ROSSELET 77 using the interfering amplitude method.

29 Breit-Wigner fit to S-wave intensity measured in $\pi N \rightarrow \pi^- \pi^+ N$ on polarized targets. The fit does not include $f_0(980)$.

Meson Particle Listings

 $f_0(600)$

- ³⁰ Uses data from ASTON 88, OCHS 73, HYAMS 73, ARMSTRONG 91b, GRAYER 74, CASON 83, ROSSELET 77, and BEIER 72b. Coupled channel analysis with flavor symmetry and all light two-pseudoscalars systems.
- ³¹ Also observed by ASNER 00 in $\tau^- \rightarrow \pi^- \pi^0 \pi^0 \nu_\tau$ decays.
- ³² Uses $\pi^0 \pi^0$ data from ANISOVICH 94, AMSLER 94d, and ALDE 95b, $\pi^+ \pi^-$ data from OCHS 73, GRAYER 74 and ROSSELET 77, and $\eta\eta$ data from ANISOVICH 94.
- ³³ The pole is on Sheet III. Demonstrates explicitly that $f_0(600)$ and $f_0(1370)$ are two different poles.
- ³⁴ Analysis of data from OCHS 73, ESTABROOKS 75, ROSSELET 77, and MUKHIN 80.

 $f_0(600)$ BREIT-WIGNER WIDTH

VALUE (MeV)	DOCUMENT ID	TECN	COMMENT
(600-1000) OUR ESTIMATE			
335 ± 67	³⁵ MURAMATSU 02	CLEO	$e^+ e^- \approx 10 \text{ GeV}$
• • • We do not use the following data for averages, fits, limits, etc. • • •			
$324^{+42}_{-40} \pm 21$	AITALA	01B E791	$D^+ \rightarrow \pi^- \pi^+ \pi^+$
372^{+229}_{-95}	³⁶ ISHIDA	01	$\Upsilon(3S) \rightarrow \Upsilon \pi \pi$
540	³⁷ ASNER	00 CLE2	$\tau^- \rightarrow \pi^- \pi^0 \pi^0 \nu_\tau$
372 ± 80	ISHIDA	00B	$p\bar{p} \rightarrow \pi^0 \pi^0 \pi^0$
119 ± 13	ALEKSEEV	99 SPEC	$1.78 \pi^- p_{\text{polar}} \rightarrow \pi^- \pi^+ n$
77 ± 22	ALEKSEEV	98 SPEC	$1.78 \pi^- p_{\text{polar}} \rightarrow \pi^- \pi^+ n$
35 ± 12	³⁸ TROYAN	98	$5.2 n p \rightarrow n p \pi^+ \pi^-$
780 ± 60	ALDE	97 GAM2	$450 p p \rightarrow p p \pi^0 \pi^0$
385 ± 70	³⁹ ISHIDA	97	$\pi \pi \rightarrow \pi \pi$
290 ± 54	⁴⁰ SVEC	96 RVUE	$6-17 \pi N_{\text{polar}} \rightarrow \pi^+ \pi^- N$
~ 880	^{41,42} TORNVQVIST	96 RVUE	$\pi \pi \rightarrow \pi \pi, K\bar{K}, K \pi, \eta \pi$
460 ± 40	^{43,44} ANISOVICH	95 RVUE	$\pi^- p \rightarrow \pi^0 \pi^0 n, \pi^0 \pi^0 \eta, \pi^0 \eta \eta$
~ 3200	⁴⁵ ACHASOV	94 RVUE	$\pi \pi \rightarrow \pi \pi$
494 ± 58	⁴⁰ AUGUSTIN	89 DM2	

³⁵ Statistical uncertainty only.

³⁶ A similar analysis (KOMADA 01) finds 301^{+145}_{-100} MeV.

³⁷ From the best fit of the Dalitz plot.

³⁸ 6σ effect, no PWA.

³⁹ Reanalysis of data from HYAMS 73, GRAYER 74, SRINIVASAN 75, and ROSSELET 77 using the interfering amplitude method.

⁴⁰ Breit-Wigner fit to S-wave intensity measured in $\pi N \rightarrow \pi^- \pi^+ N$ on polarized targets. The fit does not include $f_0(980)$.

⁴¹ Uses data from ASTON 88, OCHS 73, HYAMS 73, ARMSTRONG 91b, GRAYER 74, CASON 83, ROSSELET 77, and BEIER 72b. Coupled channel analysis with flavor symmetry and all light two-pseudoscalars systems.

⁴² Also observed by ASNER 00 in $\tau^- \rightarrow \pi^- \pi^0 \pi^0 \nu_\tau$ decays.

⁴³ Uses $\pi^0 \pi^0$ data from ANISOVICH 94, AMSLER 94d, and ALDE 95b, $\pi^+ \pi^-$ data from OCHS 73, GRAYER 74 and ROSSELET 77, and $\eta\eta$ data from ANISOVICH 94.

⁴⁴ The pole is on Sheet III. Demonstrates explicitly that $f_0(600)$ and $f_0(1370)$ are two different poles.

⁴⁵ Analysis of data from OCHS 73, ESTABROOKS 75, ROSSELET 77, and MUKHIN 80.

 $f_0(600)$ DECAY MODES

Mode	Fraction (Γ_i/Γ)
Γ_1 $\pi \pi$	dominant
Γ_2 $\gamma \gamma$	seen

 $f_0(600)$ PARTIAL WIDTHS

$\Gamma(\gamma\gamma)$	DOCUMENT ID	TECN	COMMENT
4.1 ± 0.3	⁴⁶ PENNINGTON 06	RVUE	$\gamma\gamma \rightarrow \pi^0 \pi^0$
3.8 ± 1.5	^{47,48} BOGLIONE 99	RVUE	$\gamma\gamma \rightarrow \pi^+ \pi^-, \pi^0 \pi^0$
5.4 ± 2.3	⁴⁷ MORGAN 90	RVUE	$\gamma\gamma \rightarrow \pi^+ \pi^-, \pi^0 \pi^0$
10 ± 6	COURAU 86	DM1	$e^+ e^- \rightarrow \pi^+ \pi^- e^+ e^-$

• • • We do not use the following data for averages, fits, limits, etc. • • •

4.1 ± 0.3	⁴⁶ PENNINGTON 06	RVUE	$\gamma\gamma \rightarrow \pi^0 \pi^0$
3.8 ± 1.5	^{47,48} BOGLIONE 99	RVUE	$\gamma\gamma \rightarrow \pi^+ \pi^-, \pi^0 \pi^0$
5.4 ± 2.3	⁴⁷ MORGAN 90	RVUE	$\gamma\gamma \rightarrow \pi^+ \pi^-, \pi^0 \pi^0$
10 ± 6	COURAU 86	DM1	$e^+ e^- \rightarrow \pi^+ \pi^- e^+ e^-$

⁴⁶ Using unitarity and the σ pole position from CAPRINI 06.

⁴⁷ This width could equally well be assigned to the $f_0(1370)$. The authors analyse data from BOYER 90 and MARSISKE 90 and report strong correlation with $\gamma\gamma$ width of $f_2(1270)$.

⁴⁸ Supersedes MORGAN 90.

 $f_0(600)$ REFERENCES

ABLIKIM 07A	PL B645 19	M. Ablikim et al.	(BES Collab.)
BONVICINI 07	PR D76 012001	G. Bonvicini et al.	(CLEO Collab.)
GARCIA-MAR... 07	PR D76 074034	R. Garcia-Martin, J.R. Pelaez, F.J. Yndurain	(BCIP+)
CAPRINI 06	PRL 96 132001	I. Caprini, G. Colangelo, H. Leutwyler	(BCIP+)
PENNINGTON 06	PRL 97 011601	M.R. Pennington	
ZHOU 05	JHEP 0502 043	Z.Y. Zhou et al.	
ABLIKIM 04A	PL B598 149	M. Ablikim et al.	(BES Collab.)
AKHMETSHIN 04	PL B578 285	R.R. Akhmetshin et al.	(Novosibirsk CMD-2 Collab.)
GALLEGOS 04	PR D69 074033	A. Gallegos et al.	
PELAEZ 04A	MPL A19 2879	J.R. Pelaez	
BUGG 03	PL B572 1	D.V. Bugg	
PISLAK 03	PR D67 072004	S. Pislak et al.	(BNL E865 Collab.)
MURAMATSU 02	PRL 89 251802	H. Muramatsu et al.	(CLEO Collab.)
Also	PRL 90 059901 (erratum)	H. Muramatsu et al.	(CLEO Collab.)
AITALA 01B	PRL 86 770	E.M. Aitala et al.	(FNAL E791 Collab.)

BLACK 01	PR D64 014031	D. Black et al.	
COLANGELO 01	NP B603 125	G. Colangelo, J. Gasser, H. Leutwyler	
ISHIDA 01	PL B518 47	M. Ishida et al.	
KOMADA 01	PL B508 31	T. Komada et al.	
PISLAK 01	PRL 87 221801	S. Pislak et al.	(BNL E865 Collab.)
Also	PR D67 072004	S. Pislak et al.	(BNL E865 Collab.)
SUROVITSEV 01	PR D63 054024	Y.S. Surouvtsev, D. Krupa, M. Nagy	
ASNER 00	PR D61 012002	D.M. Asner et al.	(CLEO Collab.)
BAI 00E	PR D62 032002	J. Bai et al.	(BES Collab.)
ISHIDA 00B	PTP 104 203	M. Ishida et al.	
ALEKSEEV 99	NP B541 3	I.G. Alekseev et al.	
BOGLIONE 99	EPJ C9 11	M. Boglione, M.R. Pennington	
HANNAH 99	PR D60 017502	T. Hannah	
KAMINSKI 99	EPJ C9 141	R. Kaminski, L. Lesniak, B. Loiseau	(CRAC, PARIN)
OLLER 99	PR D60 099906 (erratum)	J.A. Oller et al.	
OLLER 99B	NP A652 407 (erratum)	J.A. Oller, E. Oset	
OLLER 99C	PR D60 074023	J.A. Oller, E. Oset	
ALEKSEEV 98	PAN 61 174	I.G. Alekseev et al.	
ALEXANDER 98	PR D58 052004	J.P. Alexander et al.	(CLEO Collab.)
ANISOVICH 98B	SPU 41 419	V.V. Anisovich et al.	
Also	Translated from UFN 168 481	V.V. Anisovich et al.	
LOCHER 98	EPJ C4 317	M.P. Locher et al.	(PSI)
TROYAN 98	JINRRC 5-91 33	Yu. Troyan et al.	
ALDE 97	PL B397 350	D.M. Alde et al.	(GAMS Collab.)
ISHIDA 97	PTP 98 1005	S. Ishida et al.	(TOKY, MIYA, KEK)
KAMINSKI 97B	PL B413 130	R. Kaminski, L. Lesniak, B. Loiseau	(CRAC, IPN)
Also	PTP 95 745	S. Ishida et al.	(TOKY, MIYA, KEK)
SVEC 96	PR D53 2343	M. Svec	(MCGI)
TORNVQVIST 96	PRL 76 1575	N.A. Tornqvist, M. Roos	(HELS)
ALDE 95B	ZPHY C66 375	D.M. Alde et al.	(GAMS Collab.)
AMSLER 95B	PL B342 433	C. Amisler et al.	(Crystal Barrel Collab.)
AMSLER 95D	PL B355 425	C. Amisler et al.	(Crystal Barrel Collab.)
ANISOVICH 95	PL B355 363	V.V. Anisovich et al.	(PNPI, SERP)
JANSSEN 95	PR D52 2690	G. Janssen et al.	(STON, ADD, JULI)
ACHASOV 94	PR D49 5779	N.N. Achasov, G.N. Shestakov	(NOVM)
AMSLER 94D	PL B333 277	C. Amisler et al.	(Crystal Barrel Collab.)
ANISOVICH 94	PL B323 233	V.V. Anisovich et al.	(Crystal Barrel Collab.)
BUTLER 94B	PR D49 40	F. Butler et al.	(CLEO Collab.)
KAMINSKI 94	PR D50 3145	R. Kaminski, L. Lesniak, J.P. Maillet	(CRA C+)
ZOU 94B	PR D50 591	B.S. Zou, D.V. Bugg	(LOQM)
ZOU 94	PRL 73 13949	B.S. Zou, D.V. Bugg	(LOQM)
ARMSTRONG 91B	ZPHY C52 389	T.A. Armstrong et al.	(ATHU, BARI, BIRN+)
BOYER 90	PR D42 1350	J. Boyer et al.	(Mark II Collab.)
MARSISKE 90	PR D41 3324	H. Marsiske et al.	(Crystal Ball Collab.)
MORGAN 90	ZPHY C48 623	D. Morgan, M.R. Pennington	(RAL, DURH)
AUGUSTIN 89	NP B320 1	J.E. Augustin, G. Cosme	(DM2 Collab.)
ASTON 88	NP B296 493	D. Aston et al.	(SLAC, NAGO, CINC, INUS)
FALVARD 88	PR D38 2706	A. Falvard et al.	(CLER, FRAS, LALO+)
AU 87	PR D35 1633	K.L. Au, D. Morgan, M.R. Pennington	(DURH, RAL)
COURAU 86	NP B271 1	A. Courau et al.	(CLER, BIEL)
VANBEVEREN 86	ZPHY C30 615	E. van Beveren et al.	(NIJM, LALO)
CASON 82	PR D28 1556	N.M. Cason et al.	(NDAM, ANL)
ETKIN 82B	PR D25 1786	A. Etkin et al.	(BNL, CUNY, TUFTS, YANU)
BISWAS 81	PRL 47 1378	N.N. Biswas et al.	(NDAM, ANL)
COHEN 80	PR D22 2595	D. Cohen et al.	(KIAE)
MUKHIN 80	JETPL 32 601	K.N. Mukhin et al.	(KIAE)
Also	Translated from ZETFP 32 616.	K.N. Mukhin et al.	
BECKER 79	NP B151 46	H. Becker et al.	(MPIM, CERN, ZEEM, CRAC)
CORDEN 79	NP B157 250	M.J. Corden et al.	(BIRM, RHEL, TELA+ JP)
ESTABROOKS 79	PR D19 2678	P. Estabrooks	(CARL)
FROGGATT 77	NP B129 89	C.D. Froggatt, J.L. Petersen	(GLAS, NORD)
PAWLIKCI 77	PR D15 3196	A.J. Pawlikci et al.	(ANL) IJ
ROSSELET 77	PR D15 574	L. Rosselet et al.	(GEVA, SAEL)
CASON 76	PRL 36 1485	N.M. Cason et al.	(NDAM, ANL) IJ
ESTABROOKS 75	NP B95 322	P.G. Estabrooks, A.D. Martin	(DURH)
HYAMS 75	NP B100 205	B.D. Hyams et al.	(CERN, MPIM)
SRINIVASAN 75	PR D12 681	V. Srinivasan et al.	(NDAM, ANL)
ESTABROOKS 74	NP B79 301	P.G. Estabrooks, A.D. Martin	(DURH)
GRAYER 74	NP B75 189	G. Graye et al.	(CERN, MPIM)
APEL 73	PL 41B 542	W.D. Apel et al.	(KARL, PISA)
HYAMS 73	NP B64 134	B.D. Hyams et al.	(CERN, MPIM)
OCHS 73	Thisis	W. Ochs	(MPIM, MIUNI)
PROTOPOP... 73	PR D7 1279	S.D. Protopopescu et al.	(LBL)
BAILLON 72	PL 38B 555	P.H. Baillon et al.	(SLAC)
BASDEVANT 72	PL 41B 178	J.L. Basdevant, C.D. Froggatt, J.L. Petersen	(CERN)
BEIER 72B	PRL 29 511	E.W. Beier et al.	(PENN)
BENSINGER 71	PL 36B 134	J.R. Bensingier et al.	(WIS C)
COLTON 71	PR D3 2028	E.P. Colton et al.	(LBL, FNAL, UCLA+)
ROY 71	PL 36B 353	S.M. Roy	
BATON 70	PL 33B 528	J.P. Baton, G. Laurens, J. Reigner	(SAEL)
WALKER 67	RMP 39 695	W.D. Walker	(WIS C)

OTHER RELATED PAPERS

GIACOSA 08	PR D77 034007	F. Giacosa, T. Gutsche, V.E. Lyubovitskij	
LIU 08B	PR D77 034025	Y.-H. Liu et al.	
ACHASOV 07	PRL 99 072001	N.N. Achasov, G.N. Shestakov	
AMBROSINO 07	EPJ C49 473	F. Ambrosino et al.	(KLOE Collab.)
AUBERT 07AX	PRL 99 161802	B. Aubert et al.	(BABAR Collab.)
AUBERT 07BB	PRL 99 221801	B. Aubert et al.	(BABAR Collab.)
AUBERT 07T	PR D76 011102R	B. Aubert et al.	(BABAR Collab.)
CHEW 07E	PR D76 094025	H.-Y. Cheng, A. Hosaka, S.L. Zhu	
GIACOSA 07	PR D75 054007	F. Giacosa	
GIACOSA 07A	PR C76 065204	F. Giacosa, G. Pagliara	
KLEMPPT 07	PRPL 454 1	E. Klemp, A. Zaitsev	
MAIANI 07	EPJ C50 609	L. Maiani et al.	
MATHEUS 07A	PR D76 056005	R.D. Matheus	
MATHUR 07	PR D76 114505	N. Mathur	
PENNINGTON 07	MPL A22 1439	M.R. Pennington	
SU 07	NP A792 288	M.X. Su et al.	
WADA 07	PR B652 250	H. Wada et al.	
XIAO 07	JMP A22 4603	L.Y. Xiao, Z.-H. Guo, H.Q. Zheng	
ABLIKIM 06B	EPJ C45 337	M. Ablikim et al.	(BES Collab.)
ABLIKIM 06C	PL B633 681	M. Ablikim et al.	(BES Collab.)
ABLIKIM 06V	PL B642 441	M. Ablikim et al.	(BES Collab.)
AITALA 06	PR D73 032004	E.M. Aitala et al.	(FNAL E791 Collab.)
Also	PR D74 059901 (erratum)	E.M. Aitala et al.	(FNAL E791 Collab.)
ANISOVICH 06	JMP A21 3615	V.V. Anisovich	
BEDIAGA 06	PL B633 167	I. Bediaga, J.M. de Miranda	
CHENG 06	PR D73 014017	H.-Y. Cheng, C.-K. Chua, K.-C. Yang	
CHENG 06A	PR D74 094005	H.-Y. Cheng, C.-K. Chua, K.-F. Liu	
DESCOTES-G... 06	EPJ C48 553	S. Descotes-Genon, B. Moussallam	
FARBORZ 06	PR D74 054030	A.H. Farboorz	
GIACOSA 06	PR D74 014028	F. Giacosa	
KAMANO 06	PR C73 055203	H. Kamano, M. Arima	
LEE 06	EPJ A30 423	H.-J. Lee	
PELAEZ 06	PRL 97 242002	J.R. Pelaez, G. Rios	
SCHUMACHER 06	EPJ A30 413	M. Schumacher	
VANBEVEREN 06	PL B641 265	E. van Beveren et al.	
VANBEVEREN 06A	PR D74 037501	E. van Beveren et al.	
VANBEVEREN 06B	PRL 97 202001	E. van Beveren, G. Rupp	

See key on page 373

Meson Particle Listings

 $f_0(600), \rho(770)$

VENTO	06	PR D73 054006	V. Vento	
ABLUKIM	05	PL B607 243	M. Ablukim et al.	(BES Collab.)
ABLUKIM	05Q	PR D72 092002	M. Ablukim et al.	(BES Collab.)
AUBERT,B	05G	PR D72 052002	B. Aubert et al.	(BABAR Collab.)
BRITO	05	PL B608 69	T.V. Brito et al.	
CHANOWITZ	05	PRL 95 172001	M. Chanowitz	
CLOSE	05	PR D71 094022	F.E. Close, Q. Zhao	
CRONIN-HEN.	05	PR D72 031102R	D. Cronin-Hennessy et al.	(CLEO Collab.)
GIACOSA	05	PR C71 025202	F. Giacosa et al.	
JAFFE	05	PRPL 409 1	R.L. Jaffe	
LI	05B	EPJ A25 263	D.-M. Li, K.-W. Wei, H. Yu	
LINK	05I	PL B621 72	J.M. Link et al.	(FNAL FOCUS Collab.)
RODRIGUEZ	05	PR D71 074008	S. Rodriguez, M. Napsuciale	
VJANDE	05	PR D72 034025	J. Vijande, A. Valcaro, F. Fernandez	
ABE	04	EPJ C32 323	K. Abe et al.	(BELLE Collab.)
ABLUKIM	04E	PL B603 138	M. Ablukim et al.	(BES Collab.)
AKHMETSHIN	04B	PL B580 119	R.R. Akhmetshin et al.	(Novosibirsk CMD-2 Collab.)
AMSLER	04	PRPL 389 61	C. Amisler, N.A. Tornqvist	
AUBERT,B	04O	PR D70 091103R	B. Aubert et al.	(BABAR Collab.)
AUBERT,B	04P	PR D70 092001	B. Aubert et al.	(BABAR Collab.)
BUGG	04C	PRPL 397 257	D.V. Bugg	
BUGG	04D	EPJ C37 433	D.V. Bugg	
FARIBORZ	04	IJMP A19 2095	A.H. Fariborz	
KALOSHIN	04	EPJ A20 475	A.E. Kaloshin et al.	
LINK	04	PL B585 200	J.M. Link et al.	(FNAL FOCUS Collab.)
MAIANI	04A	PRL 93 212002	L. Maiani et al.	
NAPSUCIALE	04	PL B603 195	M. Napsuciale, S. Rodriguez	(GUAN)
NAPSUCIALE	04A	PR D70 094043	N.N. Napsuciale, S. Rodriguez	
PELAEZ	04	PRL 92 102001	J.R. Pelaez	
PRAKHOV	04	PR C69 042202R	S. Prakhov et al.	(BNL Crystal Ball Collab.)
PRAKHOV	04A	PR C69 045202	S. Prakhov et al.	
PRAKHOV	04B	PR C70 034605	S. Prakhov et al.	
TESHIMA	04	JPG 30 663	T. Teshima et al.	
VANBEVEREN	04	MPL A19 1949	E. van Beveren, G. Rupp	
ZHENG	04	NP A733 235	H.Q. Zheng et al.	
ABDEL-REHIM	03	PR D67 054001	A. Abdel-Rehim et al.	
ABDEL-REHIM	03B	PR D68 013008	A. Abdel-Rehim et al.	
BOGLIONE	03	EPJ C30 503	M. Boglione, M.R. Pennington	
ISHIDA	03	PTPS 149 190	M. Ishida	
KAMINSKI	03	PL B551 241	R. Kaminski, L. Lesniak, B. Loiseau	
OLLER	03B	NP A714 161	J.A. Oller et al.	
SCADRON	03	NP A724 391	M.D. Scadron et al.	
SEMENOV	03	PAN 66 526	S.V. Semenov	
		Translated from YAF 66 553		
ACHASOV	02F	PL B537 201	M.N. Achasov et al.	(Novosibirsk SND Collab.)
AITALA	02	PRL 89 121801	E.M. Aitala et al.	(FNAL E791 Collab.)
ALOISIO	02C	PL B536 209	A. Aloisio et al.	(KLOE Collab.)
ALOISIO	02D	PL B537 21	A. Aloisio et al.	(KLOE Collab.)
AMSLER	02	EPJ C23 29	C. Amisler et al.	
AMSLER	02B	PL B541 22	C. Amisler	
BLACK	02	PRL 88 181603	D. Black, M. Harada, J. Schechter	
BOGLIONE	02	PR D65 114010	M. Boglione, M.R. Pennington	
BRAMON	02	EPJ C26 293	A. Bramon et al.	
CLOSE	02B	JPG 28 R249	F.E. Close, N. Tornqvist	(BELLE Collab.)
GARMASH	02	PR D65 092005	A. Garmash et al.	
HE	02	PL B536 59	J. He, Z.G. Xiao, H.Q. Zheng	
HERNANDEZ	02	PR C66 065201	E. Hernandez, E. Oset, M.J. Vicente Vacas	
ISHIDA	02	PL B539 249	S. Ishida, M. Ishida	
KAMINSKI	02	EPJ Direct C4 1	R. Kaminski, L. Lesniak, K. Rybicki	
LINK	02	PL B525 205	J.M. Link et al.	(FNAL FOCUS Collab.)
LINK	02E	PL B535 43	J.M. Link et al.	(FNAL FOCUS Collab.)
TESHIMA	02	JPG 28 1391	T. Teshima, I. Kitamura, N. Morisita	
VANBEVEREN	02	MPL A17 1673	E. van Beveren et al.	
ABELE	01B	EPJ C21 261	A. Abele et al.	(Crystal Barrel Collab.)
ABELE	01	EPJ C21 261	A. Abele et al.	(Crystal Barrel Collab.)
ACCIARRI	01H	PL B501 173	M. Acciarri et al.	(L3 Collab.)
CHERRY	01	NP A688 823	S.N. Cherry, M.R. Pennington	
CLOSE	01B	EPJ C21 531	F.E. Close, A. Kirk	
DEANDREA	01	PL B502 79	A. Deandrea et al.	
FAZIO	01	PL B521 15	F. De Fazio, M.R. Pennington	
GOKALP	01	PR D64 053017	A. Gokalp, O. Yilmaz	
KOPP	01	PR D63 092001	S. Kopp et al.	(CLEO Collab.)
LI	01	JPG 27 807	D.-M. Li, H. Yu, Q.-X. Shen	
NARISON	01C	NPBPS 96 244	S. Narison	
SHAKIN	01	PR D63 014019	C.M. Shakin, H. Wang	
VANBEVEREN	01B	EPJ C22 493	E. van Beveren	
XIAO	01	NP A695 273	Z. Xiao, H. Zheng	
ACHASOV	00F	PL B479 53	M.N. Achasov et al.	(Novosibirsk SND Collab.)
ACHASOV	00H	PL B485 349	M.N. Achasov et al.	(Novosibirsk SND Collab.)
ALFORD	00	NP B578 367	M. Alford, R.L. Jaffe	
BARATE	00E	PL B472 189	R. Barate et al.	(ALEPH Collab.)
BARBERIS	00C	PL B471 440	D. Barberis et al.	(WA 102 Collab.)
BARBERIS	00E	PL B479 59	D. Barberis et al.	(WA 102 Collab.)
BLACK	00B	PR D61 074030	D. Black, A. Fariborz, J. Schechter	
FANG	00	NP A671 416	Fang Shi et al.	
JAMIN	00	NP B587 331	M. Jamin et al.	
KAMINSKI	00	APP B31 895	R. Kaminski, L. Lesniak, K. Rybicki	
KIRK	00	PL B489 29	A. Kirk	
KYOTO	00	KEK-Proceedings 2000-4	S. Ishida (ed.) et al.	
LEE	00	PR D61 014015	W. Lee, D. Weingarten	
MONTANET	00	NPBPS 86 381	L. Montanet	
ABREU	99J	PL B449 364	P. Abreu et al.	(DELPHI Collab.)
AKHMETSHIN	99B	PL B462 371	R.R. Akhmetshin et al.	(Novosibirsk CMD-2 Collab.)
BARBERIS	99D	PL B462 462	D. Barberis et al.	(Omega Expt.)
BLACK	99	PR D59 074026	D. Black et al.	
DELBOROUGH	99	PL B446 332	R. Delbourgo, D. Liu, M. Scadron	
IGI	99	PR D59 034005	K. Igi, K. Hikasa	
ISHIDA	99	PTP 101 661	M. Ishida	
LUCIO	99	PL B454 365	J.L. Lucio, M. Napsuciale	
MINKOWSKI	99	EPJ C9 283	P. Minkowski, W. Ochs	
SCADRON	99	EPJ C6 141	M. Scadron	
TAKAMATSU	99	PAN 62 435	K. Takamatsu	
TORNQVIST	99	EPJ C11 359	N. Tornqvist	
VANBEVEREN	99	EPJ C10 469	E. van Beveren, G. Rupp	
ABELE	98	PR D57 3860	A. Abele et al.	(Crystal Barrel Collab.)
ACHASOV	98E	PR D58 054011	M.N. Achasov, G.N. Shestakov	
ACKERSTAFF	98A	EPJ C5 411	K. Ackerstaff et al.	(OPAL Collab.)
ANISOVICH	98	PL B437 209	V.V. Anisovich et al.	
BARBERIS	98C	PL B440 225	D. Barberis et al.	(WA 102 Collab.)
CLOSE	98B	PL B419 387	F.E. Close	
DELBOROUGH	98	IJMP A13 657	R. Delbourgo et al.	
OLLER	98	PRL 80 3452	J.A. Oller et al.	
ANISOVICH	97	PL B395 123	A.V. Anisovich, A.V. Sarantsev	(PNPI)
ANISOVICH	97C	PL B413 137	A.V. Anisovich, A.V. Sarantsev	
ANISOVICH	97D	ZPHY A359 173	A.V. Anisovich, V.V. Anisovich, A.V. Sarantsev	(RAL, BIRM)
CLOSE	97	PL B397 333	F. Close et al.	
HARADA	97	PRL 78 1603	M. Harada, F. Sannino, J. Schechter	
ISHIDA	97B	PTP 98 621	S. Ishida et al.	
KAMINSKI	97	ZPHY C74 79	R. Kaminski, L. Lesniak, K. Rybicki	(CRAC)
MALTMAN	97	PL B393 19	K. Maltman, C.E. Wolfe	(YORKC)
OLLER	97	NP A620 438	J.A. Oller et al.	(VALE)
SVEC	97	PR D55 4355	M. Svec	(MCGI)
SVEC	97B	PR D55 5727	M. Svec	(MCGI)
ABELE	96	PL B380 453	A. Abele et al.	(Crystal Barrel Collab.)
ABELE	96B	PL B385 425	A. Abele et al.	(Crystal Barrel Collab.)
AMSLER	96	PR D53 295	C. Amisler, F.E. Close	(ZURI, RAL)
BIJNENS	96	PL B374 210	J. Bijnens et al.	(NORD, BERN, WIEN+)
BONUTTI	96	PRL 77 603	F. Bonutti et al.	(TRSTI, TRSTT, TRIU)
BUGG	96	NP B471 59	D.V. Bugg, A.V. Sarantsev, B.S. Zou	(LOQM, FNPI)
HARADA	96	PR D54 1991	M. Harada et al.	(SYRA)
ISHIDA	96	PTP 95 745	S. Ishida et al.	(TOKY, MINA, KEK)
AMSLER	95C	PL B353 571	C. Amisler et al.	(Crystal Barrel Collab.)
ANTINORI	95	PL B353 589	F. Antinori et al.	(ATHU, BARI, BIRM+)
GASPERO	95	NP A588 861	M. Gaspero	(ROMA)
TORNQVIST	95	ZPHY C68 647	N.A. Tornqvist	(HELS)
AMSLER	94	PL B322 431	C. Amisler et al.	(Crystal Barrel Collab.)
BUGG	94	PR D50 4412	D.V. Bugg et al.	(LOQM)
ZOU	94	PL B329 519	Y. Zou et al.	(RUTG, MINN, MICH)
ADAMO	93	NP A558 13C	A. Adamo et al.	(OBELIX Collab.)
GASPERO	93	NP A562 407	M. Gaspero	(ROMA)
MORGAN	93	PR D48 1185	D. Morgan, M.R. Pennington	(RAL, DURH)
		Also NC A Conf. Suppl.	D. Morgan	(RAL)
BOLTON	92B	PRL 69 1328	T. Bolton et al.	(Mark III Collab.)
SVEC	92	PR D45 55	M. Svec, A. de Lesquen, L. van Rossum	(MCGI+)
SVEC	92B	PR D45 1518	M. Svec, A. de Lesquen, L. van Rossum	(MCGI+)
SVEC	92C	PR D46 949	M. Svec, A. de Lesquen, L. van Rossum	(MCGI+)
BERNARD	91	PR D43 2757	V. Bernard, N. Kaiser, U.G. Meissner	
LI	91	PR D43 2161	Z.P. Li et al.	(TENN)
RIGGENBACH	91	PR D43 127	C. Riggenbach et al.	(BERN, CERN, MASS)
BAI	90C	PRL 65 2507	Z. Bai et al.	(Mark III Collab.)
LOHSE	90	PL B234 235	D. Lohse et al.	
WEINSTEIN	90	PR D41 2236	J. Weinstein, N. Isgur	(TNTO)
ASTON	89D	NP B301 525	D. Aston et al.	(SLAC, NAGO, CIN, INUS)
BARNES	85	PL B165 434	T. Barnes	
ACHASOV	84	ZPHY C22 53	N.N. Achasov, S.A. Devyanin, G.N. Shestakov	(NOVM)
GASSER	84	ANP 158 142	J. Gasser, H. Leutwyler	
TORNQVIST	82	PRL 49 624	N.A. Tornqvist	(HELS)
COSTA	80	NP B175 402	G. Costa et al.	(BARI, BONN, CERN, GLAS+)
BECKER	79B	NP B150 301	H. Becker et al.	(MPI, CERN, ZEEM, CRAC)
MARTIN	79	NP B158 520	A.D. Martin, E.N. Ozmutlu	(DURH) IJP
NAGELS	79	PR D20 1633	M.M. Nagels, T.A. Rijken, J.J. de Swart	(NIJM)
POLYCHRO...	79	PR D19 1317	V.A. Polychronakos et al.	(NDAM, ANL) IJP
CORDEN	78	NP B144 253	M.J. Corden et al.	(BIRM, RHEL, TEL+)
ESTABROOKS	78	NP B133 490	P.G. Estabrooks et al.	(MCGI, CARL, DURH+)
JAFFE	77	PL D15 267,281	R. Jaffe	(MIT)
FLATTE	76	PL B38 224	S.M. Flatte	(CERN)
WETZEL	76	NP B115 208	W. Wetzel et al.	(ETH, CERN, LOIC)
DEFOIX	72	NP B44 125	C. Defoix et al.	(CDEF, CERN)
ADLER	65	PR 137 B1022	S.L. Adler	
ADLER	65A	PR 139 B1638	S.L. Adler	

 $\rho(770)$

$$I^G(J^{PC}) = 1^+(1^-)$$

THE $\rho(770)$

Updated April 2008 by S. Eidelman (Novosibirsk).

The determination of the parameters of the $\rho(770)$ is beset with many difficulties because of its large width. In physical region fits, the line shape does not correspond to a relativistic Breit-Wigner function with a P -wave width, but requires some additional shape parameter. This dependence on parameterization was demonstrated long ago by PISUT 68. Bose-Einstein correlations are another source of shifts in the $\rho(770)$ line shape, particularly in multiparticle final state systems (LAFFERTY 93).

The same model-dependence afflicts any other source of resonance parameters, such as the energy-dependence of the phase shift δ_1^+ , or the pole position. It is, therefore, not surprising that a study of $\rho(770)$ dominance in the decays of the η and η' reveals the need for specific dynamical effects, in addition to the $\rho(770)$ pole (ABELE 97B, BENAYOUN 03B).

The cleanest determination of the $\rho(770)$ mass and width comes from the e^+e^- annihilation and τ -lepton decays. BARATE 97M showed that the charged $\rho(770)$ parameters measured from τ -lepton decays are consistent with those of the neutral one determined from e^+e^- data of BARKOV 85. This conclusion is qualitatively supported by the high statistics study of ANDERSON 00A. However, model-independent comparison of the two-pion mass spectrum in τ decays, and the $e^+e^- \rightarrow \pi^+\pi^-$ cross section, gave indications of discrepancies between the overall normalization: τ data are about 3% higher than e^+e^- data (ANDERSON 00A, EIDELMAN 99). A detailed analysis using such two-pion mass spectra from τ decays measured by OPAL

Meson Particle Listings

$\rho(770)$

(ACKERSTAFF 99F), CLEO (ANDERSON 00A), and ALEPH (DAVIER 03A, SCHAEEL 05C) as well as recent pion form factor measurements in e^+e^- annihilation by CMD-2 (AKHMETSHIN 02, AKHMETSHIN 04), showed that the discrepancy can be as high as 10% above the ρ meson (DAVIER 03, DAVIER 03B). This discrepancy remains after recent measurements of the two-pion cross section in e^+e^- annihilation at KLOE (ALOISIO 05) and SND (ACHASOV 05A, ACHASOV 06). This effect is not accounted for by isospin-breaking (ALEMANY 98, CZYZ 01, CIRIGLIANO 01, CIRIGLIANO 02), but the accuracy of its calculation may be overestimated (MALTMAN 06). GHOZZI 04 suggested that this effect can be explained if the charged ρ mass were higher than that of the neutral one by a few MeV. Existing theoretical models of the possible mass difference predict either a much smaller value (BIJNENS 96), or a heavier neutral ρ meson (ACHASOV 99F). Experimental accuracy is not yet sufficient for unambiguous conclusions. The size of the effect is also sensitive to the possible width difference (SANCHEZ 07, FLOREZ-BAEZ 07). Recently BENAYOUN 08 performed a detailed analysis of the whole set of the ρ , ω , and ϕ decays, consistently taking into account mixing effects in the hidden local symmetry model, and claimed that in this approach, τ decays to two pions can be naturally accounted for.

$\rho(770)$ MASS

We no longer list S-wave Breit-Wigner fits, or data with high combinatorial background.

NEUTRAL ONLY, e^+e^-

VALUE (MeV)	EVTS	DOCUMENT ID	TECN	CHG	COMMENT
775.49 ± 0.34 OUR AVERAGE					
775.97 ± 0.46 ± 0.70	900k	1 AKHMETSHIN 07			$e^+e^- \rightarrow \pi^+\pi^-$
774.6 ± 0.4 ± 0.5	800k	2,3 ACHASOV 06	SND		$e^+e^- \rightarrow \pi^+\pi^-$
775.65 ± 0.64 ± 0.50	114k	4,5 AKHMETSHIN 04	CMD2		$e^+e^- \rightarrow \pi^+\pi^-$
775.9 ± 0.5 ± 0.5	1.98M	6 ALOISIO 03	KLOE		$1.02 e^+e^- \rightarrow \pi^+\pi^-$
775.8 ± 0.9 ± 2.0	500k	6 ACHASOV 02	SND		$1.02 e^+e^- \rightarrow \pi^+\pi^-$
775.9 ± 1.1		7 BARKOV 85	OLYA		$e^+e^- \rightarrow \pi^+\pi^-$
••• We do not use the following data for averages, fits, limits, etc. •••					
775.8 ± 0.5 ± 0.3	1.98M	8 ALOISIO 03	KLOE		$1.02 e^+e^- \rightarrow \pi^+\pi^-$
775.9 ± 0.6 ± 0.5	1.98M	9 ALOISIO 03	KLOE		$1.02 e^+e^- \rightarrow \pi^+\pi^-$
775.0 ± 0.6 ± 1.1	500k	10 ACHASOV 02	SND		$1.02 e^+e^- \rightarrow \pi^+\pi^-$
775.1 ± 0.7 ± 5.3		11 BENAYOUN 98	RVUE		$e^+e^- \rightarrow \pi^+\pi^-$, $\mu^+\mu^-$
770.5 ± 1.9 ± 5.1		12 GARDNER 98	RVUE		$0.28-0.92 e^+e^- \rightarrow \pi^+\pi^-$
764.1 ± 0.7		13 O'CONNELL 97	RVUE		$e^+e^- \rightarrow \pi^+\pi^-$
757.5 ± 1.5		14 BERNICHA 94	RVUE		$e^+e^- \rightarrow \pi^+\pi^-$
768 ± 1		15 GESHKEN... 89	RVUE		$e^+e^- \rightarrow \pi^+\pi^-$

CHARGED ONLY, τ DECAYS and e^+e^-

VALUE (MeV)	EVTS	DOCUMENT ID	TECN	CHG	COMMENT
775.4 ± 0.4 OUR AVERAGE					
775.5 ± 0.7		16 SCHAEEL 05c	ALEP		$\tau^- \rightarrow \pi^- \pi^0 \nu_\tau$
775.5 ± 0.5 ± 0.4	1.98M	6 ALOISIO 03	KLOE		$1.02 e^+e^- \rightarrow \pi^+\pi^-$
775.1 ± 1.1 ± 0.5	87k	17,18 ANDERSON 00A	CLE2		$\tau^- \rightarrow \pi^- \pi^0 \nu_\tau$
••• We do not use the following data for averages, fits, limits, etc. •••					
774.8 ± 0.6 ± 0.4	1.98M	9 ALOISIO 03	KLOE	-	$1.02 e^+e^- \rightarrow \pi^+\pi^- \pi^0$
776.3 ± 0.6 ± 0.7	1.98M	9 ALOISIO 03	KLOE	+	$1.02 e^+e^- \rightarrow \pi^+\pi^- \pi^0$
773.9 ± 2.0 ± 0.3		19 SANZ-CILLERO03	RVUE		$\tau^- \rightarrow \pi^- \pi^0 \nu_\tau$
774.5 ± 0.7 ± 1.5	500k	6 ACHASOV 02	SND	±	$1.02 e^+e^- \rightarrow \pi^+\pi^- \pi^0$
775.1 ± 0.5		20 PICH 01	RVUE		$\tau^- \rightarrow \pi^- \pi^0 \nu_\tau$

MIXED CHARGES, OTHER REACTIONS

VALUE (MeV)	EVTS	DOCUMENT ID	TECN	CHG	COMMENT
763.0 ± 0.3 ± 1.2	600k	21 ABELE 99E	CBAR	0±	$0.0 \bar{p}p \rightarrow \pi^+\pi^-\pi^0$

CHARGED ONLY, HADROPRODUCED

VALUE (MeV)	EVTS	DOCUMENT ID	TECN	CHG	COMMENT
766.5 ± 1.1 OUR AVERAGE					
763.7 ± 3.2		ABELE 97	CBAR		$\bar{p}n \rightarrow \pi^- \pi^0 \pi^0$
768 ± 9		AGUILAR... 91	EHS		400 pp
767 ± 3	2935	22 CAPRARO 87	SPEC	-	$200 \pi^- \pi^0 \text{Cu} \rightarrow \pi^- \pi^0 \text{Cu}$
761 ± 5	967	22 CAPRARO 87	SPEC	-	$200 \pi^- \pi^0 \text{Pb} \rightarrow \pi^- \pi^0 \text{Pb}$
771 ± 4		HUSTON 86	SPEC	+	$202 \pi^+ \pi^0 \text{A} \rightarrow \pi^+ \pi^0 \text{A}$
766 ± 7	6500	23 BYERLY 73	OSPK	-	$5 \pi^- p$
766.8 ± 1.5	9650	24 PISUT 68	RVUE	-	$1.7-3.2 \pi^- p, t < 10$
767 ± 6	900	22 EISNER 67	HBC	-	$4.2 \pi^- p, t < 10$

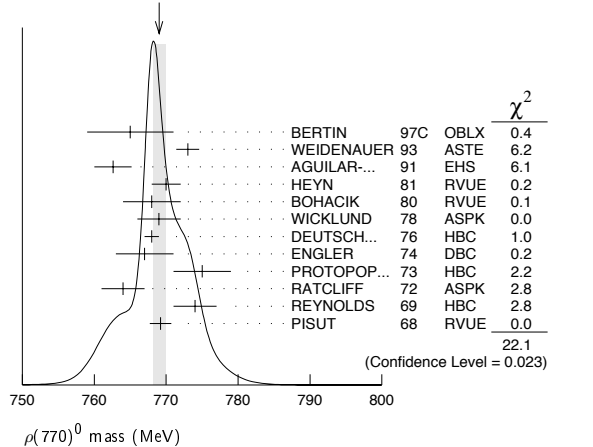
NEUTRAL ONLY, PHOTOPRODUCED

VALUE (MeV)	EVTS	DOCUMENT ID	TECN	CHG	COMMENT
768.5 ± 1.1 OUR AVERAGE					
770 ± 2 ± 1	79k	25 BREITWEG 98B	ZEUS	0	50-100 γp
767.6 ± 2.7		BARTALUCCI 78	CNTR	0	$\gamma p \rightarrow e^+e^- p$
775 ± 5		GLADDING 73	CNTR	0	2.9-4.7 γp
767 ± 4	1930	BALLAM 72	HBC	0	2.8 γp
770 ± 4	2430	BALLAM 72	HBC	0	4.7 γp
765 ± 10		ALVENSLEB... 70	CNTR	0	$\gamma A, t < 0.01$
767.7 ± 1.9	140k	BIGGS 70	CNTR	0	$< 4.1 \gamma C \rightarrow \pi^+ \pi^- C$
765 ± 5	4000	ASBURY 67B	CNTR	0	$\gamma + \text{Pb}$
••• We do not use the following data for averages, fits, limits, etc. •••					
771 ± 2	79k	26 BREITWEG 98B	ZEUS	0	50-100 γp

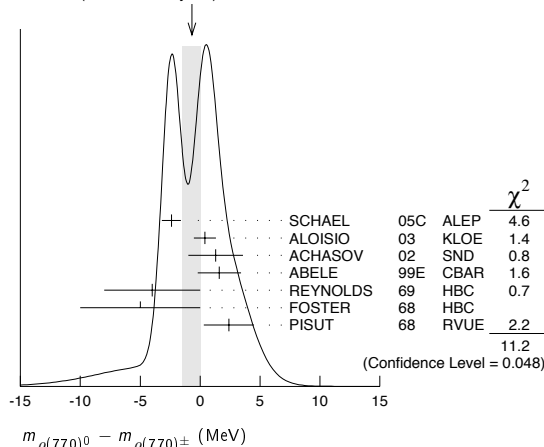
NEUTRAL ONLY, OTHER REACTIONS

VALUE (MeV)	EVTS	DOCUMENT ID	TECN	CHG	COMMENT
769.0 ± 0.9 OUR AVERAGE					Error includes scale factor of 1.4. See the ideogram below.
765 ± 6		BERTIN 97c	OBLX		$0.0 \bar{p}p \rightarrow \pi^+\pi^-\pi^0$
773 ± 1.6		WEIDENAUER 93	ASTE		$\bar{p}p \rightarrow \pi^+\pi^-\omega$
762.6 ± 2.6		AGUILAR... 91	EHS		400 pp
770 ± 2		27 HEYN 81	RVUE		Pion form factor
768 ± 4	28,29	BOHACIK 80	RVUE	0	
769 ± 3	23	WICKLUND 78	ASPK	0	$3,4,6 \pi^\pm N$
768 ± 1	76000	DEUTSCH... 76	HBC	0	$16 \pi^+ p$
767 ± 4	4100	ENGLER 74	DBC	0	$6 \pi^+ n \rightarrow \pi^+\pi^- p$
775 ± 4	32000	28 PROTOPOP... 73	HBC	0	$7.1 \pi^+ p, t < 0.4$
764 ± 3	6800	RATCLIFF 72	ASPK	0	$15 \pi^- p, t < 0.3$
774 ± 3	1700	REYNOLDS 69	HBC	0	$2.26 \pi^- p$
769.2 ± 1.5	13300	30 PISUT 68	RVUE	0	$1.7-3.2 \pi^- p, t < 10$
••• We do not use the following data for averages, fits, limits, etc. •••					
773.5 ± 2.5		31 COLANGELO 01	RVUE		$\pi\pi \rightarrow \pi\pi$
762.3 ± 0.5 ± 1.2	600k	32 ABELE 99E	CBAR	0	$0.0 \bar{p}p \rightarrow \pi^+\pi^-\pi^0$
777 ± 2	4943	33 ADAMS 97	E665		$470 \mu p \rightarrow \mu X B$
770 ± 2		34 BOGOLYUB... 97	MIRA		$32 \bar{p}p \rightarrow \pi^+\pi^- X$
768 ± 8		34 BOGOLYUB... 97	MIRA		$32 pp \rightarrow \pi^+\pi^- X$
761.1 ± 2.9		DUBNICKA 89	RVUE		π form factor
777.4 ± 2.0		35 CHABAUD 83	ASPK	0	$17 \pi^- p$ polarized
769.5 ± 0.7	28,29	LANG 79	RVUE	0	
770 ± 9		29 ESTABROOKS 74	RVUE	0	$17 \pi^- p \rightarrow \pi^+\pi^- n$
773.5 ± 1.7	11200	22 JACOBS 72	HBC	0	$2.8 \pi^- p$
775 ± 3	2250	HYAMS 68	OSPK	0	$11.2 \pi^- p$

WEIGHTED AVERAGE
769.0 ± 0.9 (Error scaled by 1.4)



- 1 A combined fit of AKHMETSHIN 07, AULCHENKO 06, and AULCHENKO 05.
 2 Supersedes ACHASOV 05A.
 3 A fit of the SND data from 400 to 1000 MeV using parameters of the $\rho(1450)$ and $\rho(1700)$ from a fit of the data of BARKOV 85, BISELLO 89 and ANDERSON 00A.
 4 Using the GOUNARIS 68 parametrization with the complex phase of the ρ - ω interference.
 5 Update of AKHMETSHIN 02.
 6 Assuming $m_{\rho^+} = m_{\rho^-}$, $\Gamma_{\rho^+} = \Gamma_{\rho^-}$.
 7 From the GOUNARIS 68 parametrization of the pion form factor.
 8 Assuming $m_{\rho^+} = m_{\rho^-} = m_{\rho^0}$, $\Gamma_{\rho^+} = \Gamma_{\rho^-} = \Gamma_{\rho^0}$.
 9 Without limitations on masses and widths.
 10 Assuming $m_{\rho^0} = m_{\rho^\pm}$, $g_{\rho^0\pi\pi} = g_{\rho^\pm\pi\pi}$.
 11 Using the data of BARKOV 85 in the hidden local symmetry model.
 12 From the fit to $e^+e^- \rightarrow \pi^+\pi^-$ data from the compilations of HEYN 81 and BARKOV 85, including the GOUNARIS 68 parametrization of the pion form factor.
 13 A fit of BARKOV 85 data assuming the direct $\omega\pi\pi$ coupling.
 14 Applying the S-matrix formalism to the BARKOV 85 data.
 15 Includes BARKOV 85 data. Model-dependent width definition.
 16 From the GOUNARIS 68 parametrization of the pion form factor. The error combines statistical and systematic uncertainties. Supersedes BARATE 97M.
 17 $\rho(1700)$ mass and width fixed at 1700 MeV and 235 MeV respectively.
 18 From the GOUNARIS 68 parametrization of the pion form factor. The second error is a model error taking into account different parametrizations of the pion form factor.
 19 Using the data of BARATE 97M and the effective chiral Lagrangian.
 20 From a fit of the model-independent parametrization of the pion form factor to the data of BARATE 97M.
 21 Assuming the equality of ρ^+ and ρ^- masses and widths.
 22 Mass errors enlarged by us to Γ/\sqrt{N} ; see the note with the $K^*(892)$ mass.
 23 Phase shift analysis. Systematic errors added corresponding to spread of different fits.
 24 From fit of 3-parameter relativistic P-wave Breit-Wigner to total mass distribution. Includes BATON 68, MILLER 67B, ALFF-STEINBERGER 66, HAGOPIAN 66, HAGOPIAN 66B, JACOBS 66B, JAMES 66, WEST 66, BLIEDEN 65 and CARMONY 64.
 25 From the parametrization according to SOEDING 66.
 26 From the parametrization according to ROSS 66.
 27 HEYN 81 includes all spacelike and timelike F_π values until 1978.
 28 From pole extrapolation.
 29 From phase shift analysis of GRAYER 74 data.
 30 Includes MALAMUD 69, ARMENISE 68, BACON 67, HUWE 67, MILLER 67B, ALFF-STEINBERGER 66, HAGOPIAN 66, HAGOPIAN 66B, JACOBS 66B, JAMES 66, WEST 66, GOLDHABER 64, ABOLINS 63.
 31 Breit-Wigner mass from a phase-shift analysis of HYAMS 73 and PROTOPODESCU 73 data.
 32 Using relativistic Breit-Wigner and taking into account ρ - ω interference.
 33 Systematic errors not evaluated.
 34 Systematic effects not studied.
 35 From fit of 3-parameter relativistic Breit-Wigner to helicity-zero part of P-wave intensity. CHABAUD 83 includes data of GRAYER 74.

WEIGHTED AVERAGE
-0.7±0.8 (Error scaled by 1.5) $m_{\rho(770)^+} - m_{\rho(770)^-}$

VALUE (MeV)	EVTS	DOCUMENT ID	TECN	COMMENT
••• We do not use the following data for averages, fits, limits, etc. •••				
1.5±0.8±0.7	1.98M	40 ALOISIO	03	KLOE 1.02 $e^+e^- \rightarrow \pi^+\pi^-\pi^0$

40 Without limitations on masses and widths.

 $\rho(770)$ RANGE PARAMETER

The range parameter R enters an energy-dependent correction to the width, of the form $(1 + q^2 R^2) / (1 + q^2 R^2)$, where q is the momentum of one of the pions in the $\pi\pi$ rest system. At resonance, $q = q_r$.

VALUE (GeV ⁻¹)	DOCUMENT ID	TECN	CHG	COMMENT
5.3 ^{+0.9} _{-0.7}	CHABAUD	83	ASPK 0	17 $\pi^-\pi^0$ polarized

 $\rho(770)$ WIDTH

We no longer list S-wave Breit-Wigner fits, or data with high combinatorial background.

 $m_{\rho(770)^0} - m_{\rho(770)^\pm}$

VALUE (MeV)	EVTS	DOCUMENT ID	TECN	CHG	COMMENT
-0.7±0.8 OUR AVERAGE	Error includes scale factor of 1.5. See the ideogram below.				
-2.4±0.8	36	SCHAEEL	05C	ALEP	$\tau^- \rightarrow \pi^-\pi^0\nu_\tau$
0.4±0.7±0.6	1.98M	37 ALOISIO	03	KLOE	1.02 $e^+e^- \rightarrow \pi^+\pi^-\pi^0$
1.3±1.1±2.0	500k	37 ACHASOV	02	SND	1.02 $e^+e^- \rightarrow \pi^+\pi^-\pi^0$
1.6±0.6±1.7	600k	ABELE	99E	CBAR 0±	0.0 $\bar{p}p \rightarrow \pi^+\pi^-\pi^0$
-4 ±4	3000	38 REYNOLDS	69	HBC -0	2.26 $\pi^-\rho$
-5 ±5	3600	38 FOSTER	68	HBC ±0	0.0 $\bar{p}p$
2.4±2.1	22950	39 PISUT	68	RVUE	$\pi N \rightarrow \rho N$

36 From the combined fit of the τ^- data from ANDERSON 00A and SCHAEEL 05c and e^+e^- data from the compilation of BARKOV 85, AKHMETSHIN 04, and ALOISIO 05. Supersedes BARATE 97M.

37 Assuming $m_{\rho^+} = m_{\rho^-}$, $\Gamma_{\rho^+} = \Gamma_{\rho^-}$.

38 From quoted masses of charged and neutral modes.

39 Includes MALAMUD 69, ARMENISE 68, BATON 68, BACON 67, HUWE 67, MILLER 67B, ALFF-STEINBERGER 66, HAGOPIAN 66, HAGOPIAN 66B, JACOBS 66B, JAMES 66, WEST 66, BLIEDEN 65, CARMONY 64, GOLDHABER 64, ABOLINS 63.

NEUTRAL ONLY, e^+e^-

VALUE (MeV)	EVTS	DOCUMENT ID	TECN	CHG	COMMENT
146.2 ± 0.7 OUR AVERAGE	Error includes scale factor of 1.1.				
145.98±0.75±0.50	900k	41 AKHMETSHIN	07		$e^+e^- \rightarrow \pi^+\pi^-$
146.1 ± 0.8 ± 1.5	800k	42,43 ACHASOV	06	SND	$e^+e^- \rightarrow \pi^+\pi^-$
143.85 ± 1.33 ± 0.80	114k	44,45 AKHMETSHIN	04	CMD2	$e^+e^- \rightarrow \pi^+\pi^-$
147.3 ± 1.5 ± 0.7	1.98M	46 ALOISIO	03	KLOE	1.02 $e^+e^- \rightarrow \pi^+\pi^-\pi^0$
151.1 ± 2.6 ± 3.0	500k	46 ACHASOV	02	SND 0	1.02 $e^+e^- \rightarrow \pi^+\pi^-\pi^0$
150.5 ± 3.0		47 BARKOV	85	OLYA 0	$e^+e^- \rightarrow \pi^+\pi^-$
••• We do not use the following data for averages, fits, limits, etc. •••					
143.9 ± 1.3 ± 1.1	1.98M	48 ALOISIO	03	KLOE	1.02 $e^+e^- \rightarrow \pi^+\pi^-\pi^0$
147.4 ± 1.5 ± 0.7	1.98M	49 ALOISIO	03	KLOE	1.02 $e^+e^- \rightarrow \pi^+\pi^-\pi^0$
149.8 ± 2.2 ± 2.0	500k	50 ACHASOV	02	SND	1.02 $e^+e^- \rightarrow \pi^+\pi^-\pi^0$
147.9 ± 1.5 ± 7.5		51 BENAYOUN	98	RVUE	$e^+e^- \rightarrow \pi^+\pi^-, \mu^+\mu^-$
153.5 ± 1.3 ± 4.6		52 GARDNER	98	RVUE	0.28-0.92 $e^+e^- \rightarrow \pi^+\pi^-$
145.0 ± 1.7		53 O'CONNELL	97	RVUE	$e^+e^- \rightarrow \pi^+\pi^-$
142.5 ± 3.5		54 BERNICHA	94	RVUE	$e^+e^- \rightarrow \pi^+\pi^-$
138 ± 1		55 GESKEN...	89	RVUE	$e^+e^- \rightarrow \pi^+\pi^-$

CHARGED ONLY, τ DECAYS and e^+e^-

VALUE (MeV)	EVTS	DOCUMENT ID	TECN	CHG	COMMENT
149.4 ± 1.0 OUR FIT					
149.4 ± 1.0 OUR AVERAGE					
149.0 ± 1.2	56	SCHAEEL	05C	ALEP	$\tau^- \rightarrow \pi^-\pi^0\nu_\tau$
149.9 ± 2.3 ± 2.0	500k	46 ACHASOV	02	SND ±	1.02 $e^+e^- \rightarrow \pi^+\pi^-\pi^0$
150.4 ± 1.4 ± 1.4	87k	57,58 ANDERSON	00A	CLE2	$\tau^- \rightarrow \pi^-\pi^0\nu_\tau$
••• We do not use the following data for averages, fits, limits, etc. •••					
143.7 ± 1.3 ± 1.2	1.98M	46 ALOISIO	03	KLOE ±	1.02 $e^+e^- \rightarrow \pi^+\pi^-\pi^0$
142.9 ± 1.3 ± 1.4	1.98M	49 ALOISIO	03	KLOE -	1.02 $e^+e^- \rightarrow \pi^+\pi^-\pi^0$
144.7 ± 1.4 ± 1.2	1.98M	49 ALOISIO	03	KLOE +	1.02 $e^+e^- \rightarrow \pi^+\pi^-\pi^0$
150.2 ± 2.0 ^{+0.7} _{-1.6}		59 SANZ-CILLERO	03	RVUE	$\tau^- \rightarrow \pi^-\pi^0\nu_\tau$
150.9 ± 2.2 ± 2.0	500k	50 ACHASOV	02	SND	1.02 $e^+e^- \rightarrow \pi^+\pi^-\pi^0$

CONSTRAINED FIT INFORMATION

An overall fit to the total width, a partial width, and 7 branching ratios uses 20 measurements and one constraint to determine 9 parameters. The overall fit has a $\chi^2 = 5.5$ for 12 degrees of freedom.

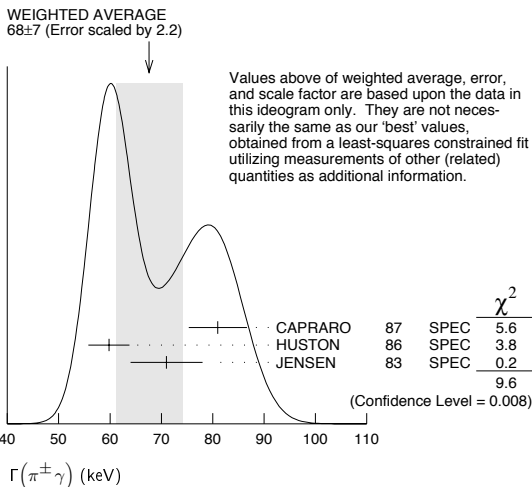
The following *off-diagonal* array elements are the correlation coefficients $\langle \delta p_i \delta p_j \rangle / (\delta p_i \delta p_j)$, in percent, from the fit to parameters p_i , including the branching fractions, $x_i \equiv \Gamma_i / \Gamma_{\text{total}}$. The fit constrains the x_i whose labels appear in this array to sum to one.

x_7	-100																				
x_8	-5	0																			
x_9	-1	0	1																		
x_{10}	-1	0	0	0																	
x_{11}	2	-3	0	0	0																
x_{12}	1	0	-8	-10	0	0															
x_{14}	-1	0	0	0	0	0	0														
Γ	0	0	5	6	0	0	-59	0													
		x_6	x_7	x_8	x_9	x_{10}	x_{11}	x_{12}	x_{14}												

Mode	Rate (MeV)
Γ_6 $\pi^+ \pi^-$	147.8 ± 1.0
Γ_7 $\pi^+ \pi^- \gamma$	1.48 ± 0.24
Γ_8 $\pi^0 \gamma$	0.090 ± 0.012
Γ_9 $\eta \gamma$	0.0449 ± 0.0031
Γ_{10} $\pi^0 \pi^0 \gamma$	0.0067 ± 0.0012
Γ_{11} $\mu^+ \mu^-$	[a] 0.0068 ± 0.0004
Γ_{12} $e^+ e^-$	[a] 0.00704 ± 0.00006
Γ_{14} $\pi^+ \pi^- \pi^+ \pi^-$	0.0027 ± 0.0014

$\rho(770)$ PARTIAL WIDTHS

$\Gamma(\pi^\pm \gamma)$	VALUE (keV)	DOCUMENT ID	TECN	CHG	COMMENT
68 ± 7 OUR FIT					Error includes scale factor of 2.3.
68 ± 7 OUR AVERAGE					Error includes scale factor of 2.2. See the ideogram below.
81 ± 4 ± 4		CAPRARO	87	SPEC	- 200 $\pi^- A \rightarrow \pi^- \pi^0 A$
59.8 ± 4.0		HUSTON	86	SPEC	+ 202 $\pi^+ A \rightarrow \pi^+ \pi^0 A$
71 ± 7		JENSEN	83	SPEC	- 156-260 $\pi^- A \rightarrow \pi^- \pi^0 A$



$\Gamma(e^+ e^-)$	VALUE (keV)	EVTS	DOCUMENT ID	TECN	COMMENT
7.04 ± 0.06 OUR FIT					
7.04 ± 0.06 OUR AVERAGE					
7.048 ± 0.057 ± 0.050		900k	41 AKHMETSHIN 07		$e^+ e^- \rightarrow \pi^+ \pi^-$
7.06 ± 0.11 ± 0.05		114k	74,75 AKHMETSHIN 04	CMD2	$e^+ e^- \rightarrow \pi^+ \pi^-$
6.77 ± 0.10 ± 0.30			BARKOV 85	OLYA	$e^+ e^- \rightarrow \pi^+ \pi^-$
• • • We do not use the following data for averages, fits, limits, etc. • • •					
7.12 ± 0.02 ± 0.11		800k	76 ACHASOV 06	SND	$e^+ e^- \rightarrow \pi^+ \pi^-$
6.3 ± 0.1			77 BENAYOUN 98	RVUE	$e^+ e^- \rightarrow \pi^+ \pi^-$, $\mu^+ \mu^-$

$\Gamma(\pi^0 \gamma)$	VALUE (keV)	EVTS	DOCUMENT ID	TECN	COMMENT
• • • We do not use the following data for averages, fits, limits, etc. • • •					
77 ± 17 ± 11		36500	78 ACHASOV 03	SND	0.60-0.97 $e^+ e^- \rightarrow \pi^0 \gamma$
121 ± 31			DOLINSKY 89	ND	$e^+ e^- \rightarrow \pi^0 \gamma$

$\Gamma(\eta \gamma)$	VALUE (keV)	DOCUMENT ID	TECN	COMMENT
• • • We do not use the following data for averages, fits, limits, etc. • • •				
62 ± 17		79 DOLINSKY 89	ND	$e^+ e^- \rightarrow \eta \gamma$

$\Gamma(\pi^+ \pi^- \pi^+ \pi^-)$	VALUE (keV)	EVTS	DOCUMENT ID	TECN	COMMENT
• • • We do not use the following data for averages, fits, limits, etc. • • •					
2.8 ± 1.4 ± 0.5		153	AKHMETSHIN 00	CMD2	0.6-0.97 $e^+ e^- \rightarrow \pi^+ \pi^- \pi^+ \pi^-$
74					Using the GOUNARIS 68 parametrization with the complex phase of the ρ - ω interference.
75					From a fit in the energy range 0.61 to 0.96 GeV. Update of AKHMETSHIN 02.
76					Supersedes ACHASOV 05A.
77					Using the data of BARKOV 85 in the hidden local symmetry model.
78					Using $\Gamma_{\text{total}} = 147.9 \pm 1.3$ MeV and $B(\rho \rightarrow \pi^0 \gamma)$ from ACHASOV 03.
79					Solution corresponding to constructive ω - ρ interference.

$\rho(770) \Gamma(e^+ e^-) \Gamma(i) / \Gamma^2(\text{total})$

$\Gamma(e^+ e^-) \times \Gamma(\pi^+ \pi^-) / \Gamma_{\text{total}}^2$	VALUE (units 10^{-5})	EVTS	DOCUMENT ID	TECN	COMMENT
4.876 ± 0.023 ± 0.064		800k	80,81 ACHASOV 06	SND	$e^+ e^- \rightarrow \pi^+ \pi^-$
80					Supersedes ACHASOV 05A.
81					A fit of the SND data from 400 to 1000 MeV using parameters of the $\rho(1450)$ and $\rho(1700)$ from a fit of the data of BARKOV 85, BISELLO 89 and ANDERSON 00A.

$\Gamma(e^+ e^-) \times \Gamma(\eta \gamma) / \Gamma_{\text{total}}^2$	VALUE (units 10^{-8})	EVTS	DOCUMENT ID	TECN	COMMENT
1.42 ± 0.10 OUR FIT					
1.45 ± 0.12 OUR AVERAGE					
1.32 ± 0.14 ± 0.08		33k	84 ACHASOV 07B	SND	0.6-1.38 $e^+ e^- \rightarrow \eta \gamma$
1.50 ± 0.65 ± 0.09		17.4k	85 AKHMETSHIN 05	CMD2	0.60-1.38 $e^+ e^- \rightarrow \eta \gamma$
1.61 ± 0.20 ± 0.11		23k	86,87 AKHMETSHIN 01B	CMD2	$e^+ e^- \rightarrow \eta \gamma$
1.85 ± 0.49			88 DOLINSKY 89	ND	$e^+ e^- \rightarrow \eta \gamma$

$\Gamma(e^+ e^-) \times \Gamma(\pi^0 \gamma) / \Gamma_{\text{total}}^2$	VALUE (units 10^{-8})	EVTS	DOCUMENT ID	TECN	COMMENT
2.8 ± 0.4 OUR FIT					
2.8 ± 0.4 OUR AVERAGE					
2.90 ± 0.60 ± 0.18		18680	AKHMETSHIN 05	CMD2	0.60-1.38 $e^+ e^- \rightarrow \pi^0 \gamma$
2.37 ± 0.53 ± 0.33		36500	82 ACHASOV 03	SND	0.60-0.97 $e^+ e^- \rightarrow \pi^0 \gamma$
3.61 ± 0.74 ± 0.49		10625	88 DOLINSKY 89	ND	$e^+ e^- \rightarrow \pi^0 \gamma$
82					Using $\sigma_{\phi \rightarrow \pi^0 \gamma}$ from ACHASOV 00 and $m_\rho = 775.97$ MeV in the model with the energy-independent phase of ρ - ω interference equal to $(-10.2 \pm 7.0)^\circ$.

$\Gamma(e^+ e^-) \times \Gamma(\pi^+ \pi^- \pi^0) / \Gamma_{\text{total}}^2$	VALUE (units 10^{-9})	EVTS	DOCUMENT ID	TECN	COMMENT
• • • We do not use the following data for averages, fits, limits, etc. • • •					
4.58 ± 2.46 ± 1.56		1.2M	83 ACHASOV 03D	RVUE	0.44-2.00 $e^+ e^- \rightarrow \pi^+ \pi^- \pi^0$
83					Statistical significance in less than 3 σ .
84					From a combined fit of $\sigma(e^+ e^- \rightarrow \eta \gamma)$ with $\eta \rightarrow 3\pi^0$ and $\eta \rightarrow \pi^+ \pi^- \pi^0$, and fixing $B(\eta \rightarrow 3\pi^0) / B(\eta \rightarrow \pi^+ \pi^- \pi^0) = 1.44 \pm 0.04$. Recalculated by us from the cross section at the peak. Supersedes ACHASOV 00D and ACHASOV 06A.
85					From the $\eta \rightarrow 2\gamma$ decay and using $B(\eta \rightarrow \gamma \gamma) = 39.43 \pm 0.26\%$.
86					From the $\eta \rightarrow 3\pi^0$ decay and using $B(\eta \rightarrow 3\pi^0) = (32.24 \pm 0.29) \times 10^{-2}$.
87					The combined fit from 600 to 1380 MeV taking into account $\rho(770)$, $\omega(782)$, $\phi(1020)$, and $\rho(1450)$ (mass and width fixed at 1450 MeV and 310 MeV respectively).
88					Recalculated by us from the cross section in the peak.

$\rho(770)$ BRANCHING RATIOS

$\Gamma(\pi^\pm \eta) / \Gamma(\pi \pi)$	VALUE (units 10^{-4})	CL%	DOCUMENT ID	TECN	CHG	COMMENT
<60		84	FERBEL 66	HBC	±	$\pi^\pm p$ above 2.5
$\Gamma(\pi^\pm \pi^+ \pi^- \pi^0) / \Gamma(\pi \pi)$	VALUE (units 10^{-4})	CL%	DOCUMENT ID	TECN	CHG	COMMENT
<20		84	FERBEL 66	HBC	±	$\pi^\pm p$ above 2.5
• • • We do not use the following data for averages, fits, limits, etc. • • •						
35 ± 40			JAMES 66	HBC	+	2.1 $\pi^+ p$

Meson Particle Listings

 $\rho(770)$ $\Gamma(\mu^+\mu^-)/\Gamma(\pi^+\pi^-)$ Γ_{11}/Γ_6

VALUE (units 10^{-5})	DOCUMENT ID	TECN	COMMENT
4.60 ± 0.28 OUR FIT			
4.6 ± 0.2 ± 0.2	ANTIPOV	89	SIGM $\pi^- \text{Cu} \rightarrow \mu^+ \mu^- \pi^- \text{Cu}$
• • • We do not use the following data for averages, fits, limits, etc. • • •			
8.2 $^{+1.6}_{-3.6}$	89 ROTHWELL	69	CNTR Photoproduction
5.6 ± 1.5	90 WEHMANN	69	OSPK 12 $\pi^- \text{C, Fe}$
9.7 $^{+3.1}_{-3.3}$	91 HYAMS	67	OSPK 11 $\pi^- \text{Li, H}$

 $\Gamma(e^+e^-)/\Gamma(\pi\pi)$ Γ_{12}/Γ_1

VALUE (units 10^{-4})	DOCUMENT ID	TECN	COMMENT
• • • We do not use the following data for averages, fits, limits, etc. • • •			
0.40 ± 0.05	92 BENAKSAS	72	OSPK $e^+e^- \rightarrow \pi^+\pi^-$

 $\Gamma(\eta\gamma)/\Gamma_{\text{total}}$ Γ_9/Γ

VALUE (units 10^{-4})	EVTS	DOCUMENT ID	TECN	CHG	COMMENT
3.00 ± 0.21 OUR FIT					
2.90 ± 0.32 OUR AVERAGE					
2.80 ± 0.34 ± 0.03	33k	93 ACHASOV	07b	SND	0.6–1.38 $e^+e^- \rightarrow \eta\gamma$
3.6 ± 0.9		94 ANDREWS	77	CNTR	0 6.7–10 γCu
• • • We do not use the following data for averages, fits, limits, etc. • • •					
3.21 ± 1.39 ± 0.20	17.4k	95,96 AKHMETSHIN	05	CMD2	0.60–1.38 $e^+e^- \rightarrow \eta\gamma$
3.39 ± 0.42 ± 0.23	94,97,98	AKHMETSHIN	01b	CMD2	$e^+e^- \rightarrow \eta\gamma$
1.9 $^{+0.6}_{-0.8}$		99 BENAYOUN	96	RVUE	0.54–1.04 $e^+e^- \rightarrow \eta\gamma$
4.0 ± 1.1	94,96	DOLINSKY	89	ND	$e^+e^- \rightarrow \eta\gamma$

 $\Gamma(\pi^+\pi^-\pi^+\pi^-)/\Gamma_{\text{total}}$ Γ_{14}/Γ

VALUE (units 10^{-5})	CL%	EVTS	DOCUMENT ID	TECN	COMMENT
1.8 ± 0.9 OUR FIT					
1.8 ± 0.9 ± 0.3		153	AKHMETSHIN	00	CMD2 0.6–0.97 $e^+e^- \rightarrow \pi^+\pi^-\pi^+\pi^-$
• • • We do not use the following data for averages, fits, limits, etc. • • •					
<20	90	KURDADZE	88	OLYA	$e^+e^- \rightarrow \pi^+\pi^-\pi^+\pi^-$

 $\Gamma(\pi^+\pi^-\pi^+\pi^-)/\Gamma(\pi\pi)$ Γ_{14}/Γ_1

VALUE (units 10^{-4})	CL%	DOCUMENT ID	TECN	CHG	COMMENT
• • • We do not use the following data for averages, fits, limits, etc. • • •					
<15	90	ERBE	69	HBC	0 2.5–5.8 γp
<20		CHUNG	68	HBC	0 3.2, 4.2 $\pi^- p$
<20	90	HUSON	68	HLBC	0 16.0 $\pi^- p$
<80		JAMES	66	HBC	0 2.1 $\pi^+ p$

 $\Gamma(\pi^+\pi^-\pi^0)/\Gamma_{\text{total}}$ Γ_{13}/Γ

VALUE (units 10^{-4})	CL%	EVTS	DOCUMENT ID	TECN	COMMENT
• • • We do not use the following data for averages, fits, limits, etc. • • •					
1.01 $^{+0.54}_{-0.36} \pm 0.34$		1.2M	100 ACHASOV	03b	RVUE 0.44–2.00 $e^+e^- \rightarrow \pi^+\pi^-\pi^0$
<1.2	90	VASSERMAN	88b	ND	$e^+e^- \rightarrow \pi^+\pi^-\pi^0$

 $\Gamma(\pi^+\pi^-\pi^0)/\Gamma(\pi\pi)$ Γ_{13}/Γ_1

VALUE	CL%	DOCUMENT ID	TECN	CHG	COMMENT
• • • We do not use the following data for averages, fits, limits, etc. • • •					
~ 0.01		BRAMON	86	RVUE	0 $J/\psi \rightarrow \omega\pi^0$
<0.01	84	101 ABRAMS	71	HBC	0 3.7 $\pi^+ p$

 $\Gamma(\pi^+\pi^-\pi^0\pi^0)/\Gamma_{\text{total}}$ Γ_{15}/Γ

VALUE (units 10^{-4})	CL%	DOCUMENT ID	TECN	CHG	COMMENT
<0.4	90	AULCHENKO	87c	ND	0 $e^+e^- \rightarrow \pi^+\pi^-\pi^0\pi^0$
• • • We do not use the following data for averages, fits, limits, etc. • • •					
<2	90	KURDADZE	86	OLYA	0 $e^+e^- \rightarrow \pi^+\pi^-\pi^0\pi^0$

 $\Gamma(\pi^+\pi^-\gamma)/\Gamma_{\text{total}}$ Γ_7/Γ

VALUE	CL%	DOCUMENT ID	TECN	COMMENT
0.0099 ± 0.0016 OUR FIT				
0.0099 ± 0.0016		102 DOLINSKY	91	ND $e^+e^- \rightarrow \pi^+\pi^-\gamma$
• • • We do not use the following data for averages, fits, limits, etc. • • •				
0.0111 ± 0.0014		103 VASSERMAN	88	ND $e^+e^- \rightarrow \pi^+\pi^-\gamma$
<0.005	90	104 VASSERMAN	88	ND $e^+e^- \rightarrow \pi^+\pi^-\gamma$

 $\Gamma(\pi^0\gamma)/\Gamma_{\text{total}}$ Γ_8/Γ

VALUE (units 10^{-4})	EVTS	DOCUMENT ID	TECN	COMMENT
• • • We do not use the following data for averages, fits, limits, etc. • • •				
6.21 $^{+1.28}_{-1.18} \pm 0.39$	18680	105,106 AKHMETSHIN	05	CMD2 0.60–1.38 $e^+e^- \rightarrow \pi^0\gamma$
5.22 ± 1.17 ± 0.75	36500	106,107 ACHASOV	03	SND 0.60–0.97 $e^+e^- \rightarrow \pi^0\gamma$
6.8 ± 1.7	108	BENAYOUN	96	RVUE 0.54–1.04 $e^+e^- \rightarrow \pi^0\gamma$
7.9 ± 2.0	106	DOLINSKY	89	ND $e^+e^- \rightarrow \pi^0\gamma$

 $\Gamma(\pi^0e^+e^-)/\Gamma_{\text{total}}$ Γ_{16}/Γ

VALUE (units 10^{-5})	DOCUMENT ID	TECN	COMMENT
• • • We do not use the following data for averages, fits, limits, etc. • • •			
<1.6	AKHMETSHIN 05A	CMD2	0.72–0.84 e^+e^-

 $\Gamma(\eta e^+e^-)/\Gamma_{\text{total}}$ Γ_{17}/Γ

VALUE (units 10^{-5})	DOCUMENT ID	TECN	COMMENT
• • • We do not use the following data for averages, fits, limits, etc. • • •			
<0.7	AKHMETSHIN 05A	CMD2	0.72–0.84 e^+e^-

 $\Gamma(\pi^0\pi^0\gamma)/\Gamma_{\text{total}}$ Γ_{10}/Γ

VALUE (units 10^{-5})	EVTS	DOCUMENT ID	TECN	COMMENT
4.5 ± 0.8 OUR FIT				
4.5 ± 0.9 OUR AVERAGE				
5.2 $^{+1.5}_{-1.3} \pm 0.6$	190	109 AKHMETSHIN	04b	CMD2 0.6–0.97 $e^+e^- \rightarrow \pi^0\pi^0\gamma$
4.1 $^{+1.0}_{-0.9} \pm 0.3$	295	110 ACHASOV	02f	SND 0.36–0.97 $e^+e^- \rightarrow \pi^0\pi^0\gamma$
• • • We do not use the following data for averages, fits, limits, etc. • • •				
4.8 $^{+3.4}_{-1.8} \pm 0.5$	63	111 ACHASOV	00g	SND $e^+e^- \rightarrow \pi^0\pi^0\gamma$

- 89 Possibly large ρ - ω interference leads us to increase the minus error.
- 90 Result contains $11 \pm 11\%$ correction using SU(3) for central value. The error on the correction takes account of possible ρ - ω interference and the upper limit agrees with the upper limit of $\omega \rightarrow \mu^+\mu^-$ from this experiment.
- 91 HYAMS 67's mass resolution is 20 MeV. The ω region was excluded.
- 92 The ρ' contribution is not taken into account.
- 93 ACHASOV 07b reports $[B(\rho(770) \rightarrow \eta\gamma)] \times [B(\rho(770) \rightarrow e^+e^-)] = (1.32 \pm 0.14 \pm 0.08) \times 10^{-8}$. We divide by our best value $B(\rho(770) \rightarrow e^+e^-) = (4.71 \pm 0.05) \times 10^{-5}$. Our first error is their experiment's error and our second error is the systematic error from using our best value. Supersedes ACHASOV 00d and ACHASOV 06a.
- 94 Structure corresponding to constructive ω - ρ interference.
- 95 Using $B(\rho \rightarrow e^+e^-) = (4.67 \pm 0.09) \times 10^{-5}$ and $B(\eta \rightarrow \gamma\gamma) = 39.43 \pm 0.26\%$.
- 96 Not independent of the corresponding $\Gamma(e^+e^-) \times \Gamma(\eta\gamma)/\Gamma_{\text{total}}^2$.
- 97 The combined fit from 600 to 1380 MeV taking into account $\rho(770)$, $\omega(782)$, $\phi(1020)$, and $\rho(1450)$ (mass and width fixed at 1450 MeV and 310 MeV respectively).
- 98 Using $B(\rho \rightarrow e^+e^-) = (4.75 \pm 0.10) \times 10^{-5}$ from AKHMETSHIN 02 and $B(\eta \rightarrow 3\pi^0) = (32.24 \pm 0.29) \times 10^{-2}$.
- 99 Reanalysis of DRUZHININ 84, DOLINSKY 89, and DOLINSKY 91 taking into account a triangle anomaly contribution. Constructive ρ - ω interference solution.
- 100 Statistical significance is less than 3 σ .
- 101 Model dependent, assumes $l = 1, 2, \text{ or } 3$ for the 3π system.
- 102 Bremsstrahlung from a decay pion and for photon energy above 50 MeV.
- 103 Superseded by DOLINSKY 91.
- 104 Structure radiation due to quark rearrangement in the decay.
- 105 Using $B(\rho \rightarrow e^+e^-) = (4.67 \pm 0.09) \times 10^{-5}$.
- 106 Not independent of the corresponding $\Gamma(e^+e^-) \times \Gamma(\pi^0\gamma)/\Gamma_{\text{total}}^2$.
- 107 Using $B(\rho \rightarrow e^+e^-) = (4.54 \pm 0.10) \times 10^{-5}$.
- 108 Reanalysis of DRUZHININ 84, DOLINSKY 89, and DOLINSKY 91 taking into account a triangle anomaly contribution.
- 109 This branching ratio includes the conventional VMD mechanism $\rho \rightarrow \omega\pi^0$, $\omega \rightarrow \pi^0\gamma$, and the new decay mode $\rho \rightarrow f_0(600)\gamma$, $f_0(600) \rightarrow \pi^0\pi^0$ with a branching ratio $(2.0 \pm 1.1 \pm 0.3) \times 10^{-5}$ differing from zero by 2.0 standard deviations.
- 110 This branching ratio includes the conventional VMD mechanism $\rho \rightarrow \omega\pi^0$, $\omega \rightarrow \pi^0\gamma$ and the new decay mode $\rho \rightarrow f_0(600)\gamma$, $f_0(600) \rightarrow \pi^0\pi^0$ with a branching ratio $(1.9 \pm 0.9 \pm 0.4) \times 10^{-5}$ differing from zero by 2.4 standard deviations. Supersedes ACHASOV 00g.
- 111 Superseded by ACHASOV 02f.

 $\rho(770)$ REFERENCES

ACHASOV	07b	PR D76 077101	M.N. Achasov et al.	(SND Collab.)
AKHMETSHIN	07	PL B648 28	R. Akhmetshin et al.	(Novosibirsk CMD-2 Collab.)
ACHASOV	06	JETP 103 380	M.N. Achasov et al.	(Novosibirsk SND Collab.)
		Translated from ZETF 130 437.		
ACHASOV	06a	PR D74 014016	M.N. Achasov et al.	(SND Collab.)
AULCHENKO	06	JETPL 84 413	V.M. Aulchenko et al.	(Novosibirsk CMD-2 Collab.)
		Translated from ZETFP 84 491.		
ACHASOV	05a	JETP 101 1053	M.N. Achasov et al.	(Novosibirsk SND Collab.)
		Translated from ZETF 128 1201.		
AKHMETSHIN	05	PL B605 26	R.R. Akhmetshin et al.	(Novosibirsk CMD-2 Collab.)
AKHMETSHIN	05a	PL B613 29	R.R. Akhmetshin et al.	(Novosibirsk CMD-2 Collab.)
ALOISIO	05	PL B606 12	A. Aloisio et al.	(KLOE Collab.)
AULCHENKO	05	JETPL 82 743	V.M. Aulchenko et al.	(Novosibirsk CMD-2 Collab.)
		Translated from ZETFP 82 841.		

Meson Particle Listings

 $\rho(770)$, $\omega(782)$

See key on page 373

SCHAEEL	05C	PRPL 421 191	S. Schaeel et al.	(ALEPH Collab.)	DAVIER	06	RMP 78 1043	M. Davier, A. Hocker, Z. Zhang	(LALO, PARIN+)
AKHMETS SHIN	04	PL B578 285	R.R. Akhmetshin et al.	(Novosibirsk CMD-2 Collab.)	MALTMAN	06	PR D73 013004	K. Maltman, C.E. Wolfe	
AKHMETS SHIN	04B	PL B580 119	R.R. Akhmetshin et al.	(Novosibirsk CMD-2 Collab.)	AULCHENKO	05	JETPL 82 743	V.M. Aulchenko et al.	(Novosibirsk CMD-2 Collab.)
ACHASOV	03	PL B559 171	M.N. Achasov et al.	(Novosibirsk SND Collab.)			Translated from ZETFP 82 841.		
ACHASOV	03D	PR D68 052006	M.N. Achasov et al.	(Novosibirsk SND Collab.)	GHOZZI	04	PL B583 222	S. Ghozzi, F. Jegerlehner	
ALOISIO	03	PL B561 55	A. Aloisio et al.	(KLOE Collab.)	ACHASOV	03C	JETP 96 789	M.N. Achasov et al.	(Novosibirsk SND Collab.)
SANZ-CILLERO	03	EPJ C27 587	J.J. Sanz-Cillero, A. Pich				Translated from ZETF 123 899.		
ACHASOV	02	PR D65 032002	M.N. Achasov et al.	(Novosibirsk SND Collab.)	AZIMOV	03	EPJ A16 209	Yal. Azimov	
ACHASOV	02F	PL B537 201	M.N. Achasov et al.	(Novosibirsk SND Collab.)	BENAYOUN	03	EPJ C29 397	M. Benayoun et al.	
AKHMETS SHIN	02	PL B527 161	R.R. Akhmetshin et al.	(Novosibirsk CMD-2 Collab.)	BENAYOUN	03B	EPJ C31 525	M. Benayoun et al.	
AKHMETS SHIN	01B	PL B509 217	R.R. Akhmetshin et al.	(Novosibirsk CMD-2 Collab.)	DAVIER	03	EPJ C27 497	M. Davier et al.	
COLANGELO	01	NP B603 125	G. Colangelo, J. Gasser, H. Leutwyler		DAVIER	03A	NPBPS 123 47	M. Davier et al.	
PICH	01	PR D63 093005	A. Pich, J. Portales		DAVIER	03B	EPJ C31 503	M. Davier et al.	
ACHASOV	00	EPJ C12 25	M.N. Achasov et al.	(Novosibirsk SND Collab.)	CIRIGLIANO	02	EPJ C23 121	V. Cirigliano et al.	(VIEN, VALE, MARS)
ACHASOV	00D	JETPL 72 282	M.N. Achasov et al.	(Novosibirsk SND Collab.)	BENAYOUN	01	EPJ C22 503	M. Benayoun, H.B. O'Connell	
		Translated from ZETFP 72 411.			CIRIGLIANO	01	PL B513 361	V. Cirigliano, G. Ecker, H. Neufeld	
ACHASOV	00G	JETPL 71 355	M.N. Achasov et al.	(Novosibirsk SND Collab.)	CZYZ	01	EPJ C18 497	H. Czyz, J.J. Kuhn	
		Translated from ZETFP 71 519.			EIDELMAN	01	NPBPS 98 201	S. Eidelman	
AKHMETS SHIN	00	PL B475 199	R.R. Akhmetshin et al.	(Novosibirsk CMD-2 Collab.)	FEUILLAT	01	PL B501 37	M. Feuillat, J.L. Lucio, M.J. Pestleau	
ANDERSON	00A	PR D61 112002	S. Anderson et al.	(CLEO Collab.)	GOKALP	01B	EPJ C22 327	A. Gokalp, Y. Sarac, O. Yilmaz	
ABELE	99E	PL B469 270	A. Abele et al.	(Crystal Barrel Collab.)	MELNIKOV	01	IJMP A16 4591	K. Melnikov	
BENAYOUN	98	EPJ C2 269	M. Benayoun et al.	(IPNP, NOVO, ADL+)	ADLOFF	00F	EPJ C13 371	C. Adloff et al.	(H1 Collab.)
BREITWEG	98B	EPJ C2 247	J. Breitweg et al.	(ZEUS Collab.)	ACHASOV	99F	JETPL 69 7	M.N. Achasov, N.N. Achasov	
GARDNER	98	PR D57 2716	S. Gardner, H.B. O'Connell		ACKERSTAFF	99F	EPJ C7 571	K. Ackerstaff et al.	
		Also PR D62 019903 (erratum)	S. Gardner, H.B. O'Connell		BENAYOUN	99	PR D59 074020	M. Benayoun et al.	
ABELE	97	PL B391 191	A. Abele et al.	(Crystal Barrel Collab.)	EIDELMAN	99	NPBPS 76 319	S. Eidelman, V. Ivanchenko	
ADAMS	97	ZPHY C74 237	M.R. Adams et al.	(E665 Collab.)	MARCO	99	PL B470 20	E. Marco et al.	
BARATE	97M	ZPHY C76 15	R. Barate et al.	(ALEPH Collab.)	ROOS	99	APS 49 142 vii	M. Roos	
BERTIN	97C	PL B408 476	A. Bertin et al.	(OBELIX Collab.)	ALEMANY	98	EPJ C2 123	R. Alemany et al.	
BOGOLYUB...	97	PAN 60 46	M.Y. Bogolyubsky et al.	(MOSU, SERP)	ABELE	97B	PL B402 195	A. Abele et al.	(Crystal Barrel Collab.)
		Translated from YAF 60 53.			ABELE	97F	PL B411 354	A. Abele et al.	(Crystal Barrel Collab.)
O'CONNELL	97	NP A623 559	H.B. O'Connell et al.	(ADLD)	BIJNENS	96	PL B374 210	J. Bijmens et al.	(NORD, BERN, WIEN+)
BENAYOUN	96	ZPHY C72 221	M. Benayoun et al.	(IPNP, NOVO)	BENAYOUN	93	ZPHY C58 31	M. Benayoun et al.	(CDFE, CERN, BARI)
BERNICHIA	94	PR D50 4454	A. Bernicha, G. Lopez Castro, J. Pesticau	(LOU+)	LAFFERTY	93	ZPHY C60 659	G.D. Lafferty	(MCHS)
WEIDENAUER	93	ZPHY C59 387	P. Weidenauer et al.	(LEBEX Collab.)	KAMAL	92	PL B284 421	A.N. Kamal, Q.P. Xu	(ALBE)
AGUILAR...	91	ZPHY C50 405	M. Aguilar-Benitez et al.	(ASTER-Collab.)	KUHN	90	ZPHY C48 445	J.H. Kuhn et al.	(MPIM)
DOLINSKY	91	PRPL 202 99	S.I. Dolinsky et al.	(NOVO)	ERKAL	85	ZPHY C29 485	C. Erkal, M.G. Olsson	(WIS C)
ANTIPOV	89	ZPHY C42 185	Y.M. Antipov et al.	(SERP, JINR, BGNA+)	RYBICKI	85	ZPHY C28 65	K. Rybicki, I. Sakrejda	(CRAC)
BISELO	89	PL B220 321	D. Bisello et al.	(DM2 Collab.)	KURDADZE	83	JETPL 37 733	L.M. Kurdadze et al.	(NOVO)
DOLINSKY	89	ZPHY C42 511	S.I. Dolinsky et al.	(NOVO)			Translated from ZETFP 37 613.		
DUBNICKA	89	JPG 15 1349	S. Dubnicka et al.	(JINR, SLOV)	ALEKSEEV	82	JETP 55 531	E.A. Alekseeva et al.	(KIAE)
GESHKEN...	89	ZPHY C45 351	B.V. Geshkenbein	(ITEP)			Translated from ZETF 82 1007.		
KURDADZE	88	JETPL 47 512	L.M. Kurdadze et al.	(NOVO)	KENNEY	62	PR 126 736	V.P. Kenney, W.D. Shephard, C.D. Gall	(KNTY)
		Translated from ZETFP 47 432.			SAMIOS	62	PRL 9 139	N.P. Samios et al.	(BNL, CUNY, COLU+)
VASSERMAN	88	SJNP 47 1035	I.B. Vasserman et al.	(NOVO)	XUONG	62	PR 128 1849	H. Nguyen Ngoc, G.R. Lynch	(LRL)
		Translated from YAF 47 1638.			ANDERSON	61	PRL 6 365	J.A. Anderson et al.	(LRL)
VASSERMAN	88B	SJNP 48 489	I.B. Vasserman et al.	(NOVO)	ERWIN	61	PRL 6 628	A.R. Erwin et al.	(WIS C)
		Translated from YAF 48 753.							
AULCHENKO	87C	IYF 87-90 Preprint	V.M. Aulchenko et al.	(NOVO)					
CAPRARO	87	NP B288 659	L. Capraro et al.	(CLER, FRAS, MILA+)					
BRAMON	86	PL B173 97	A. Bramon, J. Casulleras	(BARC)					
HUSTON	86	PR D33 3199	J. Huston et al.	(ROCH, FNAL, MINN)					
KURDADZE	86	JETPL 43 643	L.M. Kurdadze et al.	(NOVO)					
		Translated from ZETFP 43 497.							
BARKOV	85	NP B256 365	L.M. Barkov et al.	(NOVO)					
DRUZHININ	84	PL 144B 136	V.P. Druzhinin et al.	(NOVO)					
CHABAUD	83	NP B223 1	V. Chabaud et al.	(CERN, CRAC, MPIM)					
JENSEN	83	PR D27 26	T. Jensen et al.	(ROCH, FNAL, MINN)					
HEYN	81	ZPHY C7 169	M.F. Heyn, C.B. Lang	(GRAZ)					
BOHACIK	80	PR D21 1342	J. Bohacik, H. Kuhnelt	(SLOV, WIEN)					
LANG	79	PR D19 956	C.B. Lang, A. Mahne-Parareda	(GRAZ)					
BARTALUCCI	78	NC 44A 587	S. Bartalucci et al.	(DESY, FRAS)					
WICKLUND	78	PR D17 1197	A.B. Wicklund et al.	(ANL)					
ANDREWS	77	PL 38 1198	D.E. Andrews et al.	(ROCH)					
DEUTSCH...	76	NP B103 426	M. Deutschnann et al.	(AACH3, BERL, BONN+)					
ENGLER	74	PR D10 2070	A. Engler et al.	(CMU, CASE)					
ESTABROOKS	74	NP B79 301	P.G. Estabrooks, A.D. Martin	(DURH)					
GRAYER	74	NP B75 189	G. Grayer et al.	(CERN, MPIM)					
BYERLY	73	PR D7 637	W.L. Byerly et al.	(MICH)					
GLADDING	73	PR D8 3721	G.E. Gladding et al.	(HARV)					
HYAMS	73	NP B64 134	B.D. Hyams et al.	(CERN, MPIM)					
PROTOPOP...	73	PR D7 1279	S.D. Protopopescu et al.	(LBL)					
BALLAM	72	PR D5 545	J. Ballam et al.	(SLAC, LBL, TUFTS)					
BENAKASS	72	PL 39B 289	D. Benakass et al.	(ORSAY)					
JACOBS	72	PR D4 1241	L.D. Jacobs et al.	(SACL)					
RATCLIFF	72	PL 38B 345	B.N. Ratcliff et al.	(SLAC)					
ABRAMS	71	PR D4 653	G.S. Abrams et al.	(LBL)					
ALVENSEN...	70	PRL 24 786	H. Alvensen et al.	(DESY)					
BIGGS	70	PRL 24 1197	P.J. Biggs et al.	(DARE)					
ERBE	69	PR 188 2060	R. Erbe et al.	(German Bubble Chamber Collab.)					
MALAMUD	69	Argonne Conf. 93	E.I. Malamud, P.E. Schlein	(UCLA)					
REYNOLDS	69	PR 184 1424	B.G. Reynolds et al.	(FSU)					
ROTHWELL	69	PRL 23 1521	P.L. Rothwell et al.	(NEAS)					
WEHMANN	69	PR 178 2095	A.A. Wehmann et al.	(HARV, CASE, SLAC+)					
ARMENISE	68	NC 54A 999	N. Armenise et al.	(BARI, BGNA, FIRZ+)					
BATON	68	PR 176 1574	J.P. Baton, G. Laurens	(SACL)					
CHUNG	68	PR 165 1491	S.U. Chung et al.	(LRL)					
FOSTER	68	NP B6 107	M. Foster et al.	(CERN, CDFE)					
GOUNARIS	68	PRL 21 244	G.J. Gounaris, J.J. Sakurai						
HUSON	68	PL 28B 208	R. Huson et al.	(ORSAY, MILA, UCLA)					
HYAMS	68	NP B7 1	B.D. Hyams et al.	(CERN, MPIM)					
LANZEROTTI	68	PR 166 1365	L.J. Lanzerotti et al.	(HARV)					
PISUT	68	NP B6 325	J. Pisut, M. Roos	(CERN)					
ASBURY	67B	PRL 19 865	J.G. Asbury et al.	(DESY, COLU)					
BACON	67	PR 157 1263	T.C. Bacon et al.	(BNL)					
EISNER	67	PR 164 1699	R.L. Eisner et al.	(PURD)					
HUWE	67	PL 24B 232	D.O. Huwe et al.	(COLU)					
HYAMS	67	PL 24B 634	B.D. Hyams et al.	(CERN, MPIM)					
MILLER	67B	PR 153 1423	D.H. Miller et al.	(PURD)					
ALFF...	66	PR 145 1072	C. Alff-Steinberger et al.	(COLU, RUTG)					
FERBEL	66	PL 21 111	T. Ferbel	(ROCH)					
HAGOPIAN	66	PR 145 1128	V. Hagopian et al.	(PENN, SACL)					
HAGOPIAN	66B	PR 152 1183	V. Hagopian, Y.L. Pan	(PENN, LRL)					
JACOBS	66B	UCRL 16877	L.D. Jacobs	(LRL)					
JAMES	66	PR 142 896	F.E. James, H.L. Kravbill	(YALE, BNL)					
ROSS	66	PR 149 1172	M. Ross, L. Stodolsky						
SOEDING	66	PL B19 702	P. Soeding						
WEST	66	PR 149 1089	E. West et al.	(WIS C)					
BLIEDEN	65	PL 19 444	H.R. Blieden et al.						
CARMONY	64	PRL 12 254	D.D. Carmony et al.	(UCB)					
GOLDBERGER	64	PRL 12 336	G. Goldhaber et al.	(LRL, UCB)					
ABOLINS	63	PRL 11 381	M.A. Abolins et al.	(UCSD)					

OTHER RELATED PAPERS

BENAYOUN	08	EPJ C55 199	M. Benayoun et al.	
FLOREZ-BAEZ	07	PR D76 096010	F.V. Florez-Baez et al.	
SAN CHEZ	07	PR D76 033001	G. Toledo Sanchez, J.L. Garcia-Luna, V. Gonzalez-Enciso	
AULCHENKO	06	JETPL 84 413	V.M. Aulchenko et al.	(Novosibirsk CMD-2 Collab.)
		Translated from ZETFP 84 491.		

 $\omega(782)$

$$I^G(J^{PC}) = 0^-(1^--)$$

 $\omega(782)$ MASS

VALUE (MeV)	EVTS	DOCUMENT ID	TECN	COMMENT
782.65 ± 0.12 OUR AVERAGE		Error includes scale factor of 1.9. See the ideogram below.		
783.20 ± 0.13 ± 0.16	18680	AKHMETS SHIN 05	CMD2	0.60-1.38 e ⁺ e ⁻ → π ⁰ γ
782.68 ± 0.09 ± 0.04	11200	1 AKHMETS SHIN 04	CMD2	e ⁺ e ⁻ → π ⁺ π ⁻ π ⁰
782.79 ± 0.08 ± 0.09	1.2M	2 ACHASOV 03D	RVUE	0.44-2.00 e ⁺ e ⁻ → π ⁺ π ⁻ π ⁰
782.7 ± 0.1 ± 1.5	19500	WURZINGER 95	SPEC	1.33 p d → ³ Heω
781.96 ± 0.17 ± 0.80	11k	3 AMSLER 94C	CBAR	0.0 p p → ωηπ ⁰
782.08 ± 0.36 ± 0.82	3463	4 AMSLER 94C	CBAR	0.0 p p → ωηπ ⁰
781.96 ± 0.13 ± 0.17	15k	AMSLER 93B	CBAR	

$\Gamma(e^+e^-) \times \Gamma(\pi^+\pi^-)/\Gamma_{total}^2$					Γ_9/Γ_2^2
VALUE (units 10^{-6})	EVTS	DOCUMENT ID	TECN	COMMENT	
1.225 ± 0.058 ± 0.041	800k	23 ACHASOV	06	SND	$e^+e^- \rightarrow \pi^+\pi^-$
23 Supersedes ACHASOV 05A.					

$\Gamma(e^+e^-) \times \Gamma(\eta\gamma)/\Gamma_{total}^2$					$\Gamma_9/\Gamma_5/\Gamma_2^2$
VALUE (units 10^{-8})	EVTS	DOCUMENT ID	TECN	COMMENT	
3.31 ± 0.28 OUR FIT	Error includes scale factor of 1.1.				
3.18 ± 0.28 OUR AVERAGE					
3.10 ± 0.31 ± 0.11	33k	24 ACHASOV	07B	SND	0.6-1.38 $e^+e^- \rightarrow \eta\gamma$
3.17 ^{+1.85} _{-1.31} ± 0.21	17.4k	25 AKHMETSHIN	05	CMD2	0.60-1.38 $e^+e^- \rightarrow \eta\gamma$
3.41 ± 0.52 ± 0.21	23k	26,27 AKHMETSHIN	01B	CMD2	$e^+e^- \rightarrow \eta\gamma$

24 From a combined fit of $\sigma(e^+e^- \rightarrow \eta\gamma)$ with $\eta \rightarrow 3\pi^0$ and $\eta \rightarrow \pi^+\pi^-\pi^0$, and fixing $B(\eta \rightarrow 3\pi^0) / B(\eta \rightarrow \pi^+\pi^-\pi^0) = 1.44 \pm 0.04$. Recalculated by us from the cross section at the peak. Supersedes ACHASOV 00D and ACHASOV 06A.

25 From the $\eta \rightarrow 2\gamma$ decay and using $B(\eta \rightarrow \gamma\gamma) = 39.43 \pm 0.26\%$.

26 From the $\eta \rightarrow 3\pi^0$ decay and using $B(\eta \rightarrow 3\pi^0) = (32.24 \pm 0.29) \times 10^{-2}$.

27 The combined fit from 600 to 1380 MeV taking into account $\rho(770)$, $\omega(782)$, $\phi(1020)$, and $\rho(1450)$ (mass and width fixed at 1450 MeV and 310 MeV respectively).

$\omega(782)$ BRANCHING RATIOS

$\Gamma(\pi^+\pi^-\pi^0)/\Gamma_{total}$					Γ_1/Γ
VALUE	EVTS	DOCUMENT ID	TECN	COMMENT	
••• We do not use the following data for averages, fits, limits, etc. •••					
0.8965 ± 0.0016 ± 0.0048	1.2M	28,29 ACHASOV	03D	RVUE	0.44-2.00 $e^+e^- \rightarrow \pi^+\pi^-\pi^0$
0.880 ± 0.020 ± 0.032	11200	29,30 AKHMETSHIN	00C	CMD2	$e^+e^- \rightarrow \pi^+\pi^-\pi^0$
0.8942 ± 0.0062		29 DOLINSKY	89	ND	$e^+e^- \rightarrow \pi^+\pi^-\pi^0$
28 Using ACHASOV 03, ACHASOV 03D and $B(\omega \rightarrow \pi^+\pi^-) = (1.70 \pm 0.28)\%$.					
29 Not independent of the corresponding $\Gamma(e^+e^-) \times \Gamma(\pi^+\pi^-\pi^0)/\Gamma_{total}^2$.					
30 Using $\Gamma(e^+e^-) = 0.60 \pm 0.02$ keV.					

$\Gamma(\pi^0\gamma)/\Gamma_{total}$					Γ_2/Γ
VALUE (units 10^{-2})	EVTS	DOCUMENT ID	TECN	COMMENT	
••• We do not use the following data for averages, fits, limits, etc. •••					
9.06 ± 0.20 ± 0.57	18680	31,32 AKHMETSHIN	05	CMD2	0.60-1.38 $e^+e^- \rightarrow \pi^0\gamma$
9.34 ± 0.15 ± 0.31	36500	32 ACHASOV	03	SND	0.60-0.97 $e^+e^- \rightarrow \pi^0\gamma$
8.65 ± 0.16 ± 0.42	1.2M	33,34 ACHASOV	03D	RVUE	0.44-2.00 $e^+e^- \rightarrow \pi^0\gamma$
8.39 ± 0.24	9975	35 BENAYOUN	96	RVUE	$e^+e^- \rightarrow \pi^0\gamma$
8.88 ± 0.62	10625	32 DOLINSKY	89	ND	$e^+e^- \rightarrow \pi^0\gamma$
31 Using $B(\omega \rightarrow e^+e^-) = (7.14 \pm 0.13) \times 10^{-5}$.					
32 Not independent of the corresponding $\Gamma(e^+e^-) \times \Gamma(\pi^0\gamma)/\Gamma_{total}^2$.					
33 Using ACHASOV 03, ACHASOV 03D and $B(\omega \rightarrow \pi^+\pi^-) = (1.70 \pm 0.28)\%$.					
34 Not independent of the corresponding $\Gamma(e^+e^-) \times \Gamma(\pi^+\pi^-\pi^0)/\Gamma_{total}^2$.					
35 Reanalysis of DRUZHININ 84, DOLINSKY 89, DOLINSKY 91 taking into account the triangle anomaly contributions.					

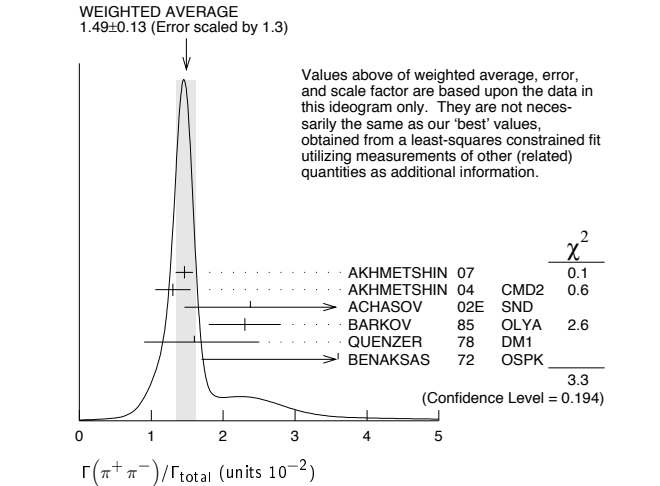
$\Gamma(\pi^0\gamma)/\Gamma(\pi^+\pi^-\pi^0)$					Γ_2/Γ_1
VALUE (units 10^{-2})	DOCUMENT ID	TECN	COMMENT		
9.99 ± 0.26 OUR FIT	Error includes scale factor of 1.1.				
9.7 ± 0.5 OUR AVERAGE					
9.94 ± 0.36 ± 0.38	36 AULCHENKO	00A	SND	$e^+e^- \rightarrow \pi^+\pi^-\pi^0\pi^0, \pi^0\pi^0\gamma$	
8.4 ± 1.3	KEYNE	76	CNTR	$\pi^-\rho \rightarrow \omega\eta$	
10.9 ± 2.5	BENAKSAS	72C	OSPK	$e^+e^- \rightarrow \pi^0\gamma$	
8.1 ± 2.0	BALDIN	71	HLBC	2.9 $\pi^+\rho$	
13 ± 4	JACQUET	69B	HLBC	2.05 $\pi^+\rho \rightarrow \pi^+\rho\omega$	
••• We do not use the following data for averages, fits, limits, etc. •••					
9.7 ± 0.2 ± 0.5	37,38 ACHASOV	03D	RVUE	0.44-2.00 $e^+e^- \rightarrow \pi^+\pi^-\pi^0$	
9.9 ± 0.7	37 DOLINSKY	89	ND	$e^+e^- \rightarrow \pi^0\gamma$	
36 From $\sigma_0^{\omega\pi^0} \rightarrow \pi^0\pi^0\gamma(m_\phi)/\sigma_0^{\omega\pi^0} \rightarrow \pi^+\pi^-\pi^0\pi^0(m_\phi)$ with a phase-space correction factor of 1/1.023.					
37 Not independent of the corresponding $\Gamma(e^+e^-) \times \Gamma(\pi^0\gamma)/\Gamma_{total}^2$.					
38 Using ACHASOV 03. Based on 1.2M events.					

$\Gamma(\pi^+\pi^-)/\Gamma_{total}$					Γ_3/Γ
VALUE (units 10^{-2})	EVTS	DOCUMENT ID	TECN	COMMENT	
1.53 ± 0.11 ± 0.13 OUR FIT	Error includes scale factor of 1.2.				
1.49 ± 0.13 OUR AVERAGE	Error includes scale factor of 1.3. See the ideogram below.				
1.46 ± 0.12 ± 0.02	900k	39 AKHMETSHIN	07		$e^+e^- \rightarrow \pi^+\pi^-$
1.30 ± 0.24 ± 0.05	11.2k	40 AKHMETSHIN	04	CMD2	$e^+e^- \rightarrow \pi^+\pi^-$
2.38 ^{+1.77} _{-0.90} ± 0.18	5.4k	41 ACHASOV	02E	SND	1.1-1.38 $e^+e^- \rightarrow \pi^+\pi^-$
2.3 ± 0.5		BARKOV	85	OLYA	$e^+e^- \rightarrow \pi^+\pi^-$
1.6 ^{+0.9} _{-0.7}		QUENZER	78	DM1	$e^+e^- \rightarrow \pi^+\pi^-$
3.6 ± 1.9		BENAKSAS	72	OSPK	$e^+e^- \rightarrow \pi^+\pi^-$

••• We do not use the following data for averages, fits, limits, etc. •••

1.75 ± 0.11	4.5M	42 ACHASOV	05A	SND	$e^+e^- \rightarrow \pi^+\pi^-$
2.01 ± 0.29		43 BENAYOUN	03	RVUE	$e^+e^- \rightarrow \pi^+\pi^-$
1.9 ± 0.3		44 GARDNER	99	RVUE	$e^+e^- \rightarrow \pi^+\pi^-$
2.3 ± 0.4		45 BENAYOUN	98	RVUE	$e^+e^- \rightarrow \pi^+\pi^-, \mu^+\mu^-$
1.0 ± 0.11		46 WICKLUND	78	ASPK	3,4,6 $\pi^\pm N$
1.22 ± 0.30		ALVENSLEB...	71c	CNTR	Photoproduction
1.3 ^{+1.2} _{-0.9}		MOFFEIT	71	HBC	2,8,4,7 $\gamma\rho$
0.80 ^{+0.28} _{-0.20}		47 BIGGS	70B	CNTR	4.2 $\gamma C \rightarrow \pi^+\pi^- C$

39 A combined fit of AKHMETSHIN 07, AULCHENKO 06, and AULCHENKO 05.
 40 Update of AKHMETSHIN 02.
 41 From the $m_{\pi^+\pi^-}$ spectrum taking into account the interference of the $\rho\pi$ and $\omega\pi$ amplitudes.
 42 Using $\Gamma(\omega \rightarrow e^+e^-)$ from the 2004 Edition of this Review (PDG 04).
 43 Using the data of AKHMETSHIN 02 in the hidden local symmetry model.
 44 Using the data of BARKOV 85.
 45 Using the data of BARKOV 85 in the hidden local symmetry model.
 46 From a model-dependent analysis assuming complete coherence.
 47 Re-evaluated under $\Gamma(\pi^+\pi^-)/\Gamma(\pi^+\pi^-\pi^0)$ by BEHREND 71 using more accurate $\omega \rightarrow \rho$ photoproduction cross-section ratio.



$\Gamma(\pi^+\pi^-)/\Gamma(\pi^+\pi^-\pi^0)$					Γ_3/Γ_1
VALUE	EVTS	DOCUMENT ID	TECN	COMMENT	
0.0172 ± 0.0014 OUR FIT	Error includes scale factor of 1.2.				
0.026 ± 0.005 OUR AVERAGE					
0.021 ^{+0.028} _{-0.009}	48,49	RATCLIFF	72	ASPK	15 $\pi^-\rho \rightarrow n2\pi$
0.028 ± 0.006		48 BEHREND	71	ASPK	Photoproduction
0.022 ^{+0.009} _{-0.01}		50 ROOS	70	RVUE	

48 The fitted width of these data is 160 MeV in agreement with present average, thus the ω contribution is overestimated. Assuming ρ width 145 MeV.
 49 Significant interference effect observed. NB of $\omega \rightarrow 3\pi$ comes from an extrapolation.
 50 ROOS 70 combines ABRAMOVICH 70 and BIZZARRI 70.

$\Gamma(\pi^+\pi^-)/\Gamma(\pi^0\gamma)$					Γ_3/Γ_2
VALUE	EVTS	DOCUMENT ID	TECN	COMMENT	
0.20 ± 0.04	1.98M	51 ALOISIO	03	KLOE	1.02 $e^+e^- \rightarrow \pi^+\pi^-\pi^0$
51 Using the data of ALOISIO 02D.					

$\Gamma(\text{neutrals})/\Gamma_{total}$					$(\Gamma_2+\Gamma_4)/\Gamma$
VALUE	EVTS	DOCUMENT ID	TECN	COMMENT	
0.091 ± 0.006 OUR FIT	Error includes scale factor of 1.3. See the ideogram below.				
0.081 ± 0.011 OUR AVERAGE					
0.075 ± 0.025		BIZZARRI	71	HBC	0.0 $\rho\bar{\rho}$
0.079 ± 0.019		DEINET	69B	OSPK	1.5 $\pi^-\rho$
0.084 ± 0.015		BOLLINI	68C	CNTR	2.1 $\pi^-\rho$
••• We do not use the following data for averages, fits, limits, etc. •••					
0.073 ± 0.018		42 BASILE	72B	CNTR	1.67 $\pi^-\rho$

Meson Particle Listings

 $\omega(782)$

$\Gamma(\text{neutrals})/\Gamma(\pi^+\pi^-\pi^0)$		$(\Gamma_2+\Gamma_4)/\Gamma_1$			
VALUE	EVTS	DOCUMENT ID	TECN	COMMENT	
0.102±0.008 OUR FIT					
0.103±0.011 OUR AVERAGE					
0.15 ± 0.04	46	AGUILAR-...	72B	HBC	3.9,4.6 K^-p
0.10 ± 0.03	19	BARASH	67B	HBC	0.0 $\bar{p}p$
0.134±0.026	850	DIGIUGNO	66B	CNTR	1.4 π^-p
0.097±0.016	348	FLATTE	66	HBC	1.4 - 1.7 $K^-p \rightarrow \Lambda MM$
0.06 +0.05 -0.02		JAMES	66	HBC	2.1 π^+p
0.08 ± 0.03	35	KRAEMER	64	DBC	1.2 π^+d
• • • We do not use the following data for averages, fits, limits, etc. • • •					
0.11 ± 0.02	20	BUSCHBECK	63	HBC	1.5 K^-p

$\Gamma(\pi^0\gamma)/\Gamma(\text{neutrals})$		$\Gamma_2/(\Gamma_2+\Gamma_4)$			
VALUE	CL%	DOCUMENT ID	TECN	COMMENT	
• • • We do not use the following data for averages, fits, limits, etc. • • •					
0.78 ± 0.07		52 DAKIN	72	OSPK	1.4 $\pi^-p \rightarrow nMM$
>0.81	90	DEINET	69B	OSPK	
52 Error statistical only. Authors obtain good fit also assuming $\pi^0\gamma$ as the only neutral decay.					

$\Gamma(\text{neutrals})/\Gamma(\text{charged particles})$		$(\Gamma_2+\Gamma_4)/(\Gamma_1+\Gamma_3)$			
VALUE		DOCUMENT ID	TECN	COMMENT	
0.100±0.008 OUR FIT					
0.124±0.021					
		FELDMAN	67C	OSPK	1.2 π^-p

$\Gamma(\eta\gamma)/\Gamma_{\text{total}}$		Γ_5/Γ			
VALUE (units 10^{-4})	EVTS	DOCUMENT ID	TECN	COMMENT	
4.6 ± 0.4 OUR FIT Error includes scale factor of 1.1.					
6.3 ± 1.3 OUR AVERAGE Error includes scale factor of 1.2.					
6.6 ± 1.7		53 ABELE	97E	CBAR	0.0 $\bar{p}p \rightarrow 5\gamma$
8.3 ± 2.1		ALDE	93	GAM2	38 $\pi^-p \rightarrow \omega n$
3.0 +2.5 -1.8		54 ANDREWS	77	CNTR	6.7-10 γCu
• • • We do not use the following data for averages, fits, limits, etc. • • •					
4.3 ± 0.5 ± 0.1	33k	55 ACHASOV	07B	SND	0.6-1.38 $e^+e^- \rightarrow \eta\gamma$
4.44 +2.59 -1.83 ± 0.28	17.4k	56,57 AKHMETSHIN	05	CMD2	0.60-1.38 $e^+e^- \rightarrow \eta\gamma$
5.10 ± 0.72 ± 0.34	23k	58 AKHMETSHIN	01B	CMD2	$e^+e^- \rightarrow \eta\gamma$
0.7 ± 0.5		59 CASE	00	CBAR	0.0 $p\bar{p} \rightarrow \eta\eta\gamma$
6.56 +2.41 -2.55	3525	54,60 BENAYOUN	96	RVUE	$e^+e^- \rightarrow \eta\gamma$
7.3 ± 2.9		54,56 DOLINSKY	89	ND	$e^+e^- \rightarrow \eta\gamma$

53 No flat $\eta\eta\gamma$ background assumed.
54 Solution corresponding to constructive $\omega\rho$ interference.
55 ACHASOV 07B reports $[B(\omega(782) \rightarrow \eta\gamma)] \times [B(\omega(782) \rightarrow e^+e^-)] = (3.10 \pm 0.31 \pm 0.11) \times 10^{-8}$. We divide by our best value $B(\omega(782) \rightarrow e^+e^-) = (7.16 \pm 0.12) \times 10^{-5}$. Our first error is their experiment's error and our second error is the systematic error from using our best value. Supersedes ACHASOV 00D and ACHASOV 06A.
56 Not independent of the corresponding $\Gamma(e^+e^-) \times \Gamma(\eta\gamma)/\Gamma_{\text{total}}^2$.
57 Using $B(\omega \rightarrow e^+e^-) = (7.14 \pm 0.13) \times 10^{-5}$ and $B(\eta \rightarrow \gamma\gamma) = 39.43 \pm 0.26\%$.
58 Using $B(\omega \rightarrow e^+e^-) = (7.07 \pm 0.19) \times 10^{-5}$ and using $B(\eta \rightarrow 3\pi^0) = (32.24 \pm 0.29) \times 10^{-2}$. Solution corresponding to constructive $\omega\rho$ interference. The combined fit from 600 to 1380 MeV taking into account $\rho(770)$, $\omega(782)$, $\phi(1020)$, and $\rho(1450)$ (mass and width fixed at 1450 MeV and 310 MeV respectively). Not independent of the corresponding $\Gamma(e^+e^-) \times \Gamma(\eta\gamma)/\Gamma_{\text{total}}^2$.
59 Depending on the degree of coherence with the flat $\eta\eta\gamma$ background and using $B(\omega \rightarrow \pi^0\gamma) = (8.5 \pm 0.5) \times 10^{-2}$.
60 Reanalysis of DRUZHININ 84, DOLINSKY 89, DOLINSKY 91 taking into account the triangle anomaly contributions.

$\Gamma(\eta\gamma)/\Gamma(\pi^0\gamma)$		Γ_5/Γ_2			
VALUE		DOCUMENT ID	TECN	COMMENT	
• • • We do not use the following data for averages, fits, limits, etc. • • •					
0.0098 ± 0.0024		61 ALDE	93	GAM2	38 $\pi^-p \rightarrow \omega n$
0.0082 ± 0.0033		62 DOLINSKY	89	ND	$e^+e^- \rightarrow \eta\gamma$
0.010 ± 0.045		APEL	72B	OSPK	4-8 $\pi^-p \rightarrow n3\gamma$
61 Model independent determination. 62 Solution corresponding to constructive $\omega\rho$ interference.					

$\Gamma(\pi^0 e^+ e^-)/\Gamma_{\text{total}}$		Γ_6/Γ			
VALUE (units 10^{-4})	EVTS	DOCUMENT ID	TECN	COMMENT	
7.7 ± 0.9 OUR FIT Error includes scale factor of 1.1.					
7.7 ± 0.9 OUR AVERAGE Error includes scale factor of 1.1.					
8.19 ± 0.71 ± 0.62		AKHMETSHIN	05A	CMD2	0.72-0.84 e^+e^-
5.9 ± 1.9	43	DOLINSKY	88	ND	$e^+e^- \rightarrow \pi^0 e^+e^-$

$\Gamma(\pi^0 \mu^+ \mu^-)/\Gamma_{\text{total}}$		Γ_7/Γ			
VALUE (units 10^{-4})		DOCUMENT ID	TECN	COMMENT	
0.96 ± 0.23 OUR FIT					
0.96 ± 0.23					
		DZHELADIN	81B	CNTR	25-33 $\pi^-p \rightarrow \omega n$

$\Gamma(\eta e^+ e^-)/\Gamma_{\text{total}}$		Γ_8/Γ			
VALUE (units 10^{-5})		DOCUMENT ID	TECN	COMMENT	
• • • We do not use the following data for averages, fits, limits, etc. • • •					
<1.1		AKHMETSHIN	05A	CMD2	0.72-0.84 e^+e^-

$\Gamma(e^+ e^-)/\Gamma_{\text{total}}$		Γ_9/Γ			
VALUE (units 10^{-4})	EVTS	DOCUMENT ID	TECN	COMMENT	
0.716 ± 0.012 OUR FIT Error includes scale factor of 1.1.					
• • • We do not use the following data for averages, fits, limits, etc. • • •					
0.700 ± 0.016	11200	63,64 AKHMETSHIN	04	CMD2	$e^+e^- \rightarrow \pi^+\pi^-\pi^0$
0.752 ± 0.004 ± 0.024	1.2M	64,65 ACHASOV	03D	RVUE	0.44-2.00 $e^+e^- \rightarrow \pi^+\pi^-\pi^0$
0.714 ± 0.036		64 DOLINSKY	89	ND	$e^+e^- \rightarrow \pi^+\pi^-\pi^0$
0.72 ± 0.03		64 BARKOV	87	CMD	$e^+e^- \rightarrow \pi^+\pi^-\pi^0$
0.64 ± 0.04	1488	64 KURDADZE	83B	OLYA	$e^+e^- \rightarrow \pi^+\pi^-\pi^0$
0.675 ± 0.069	433	64 CORDIER	80	DM1	$e^+e^- \rightarrow \pi^+\pi^-\pi^0$
0.83 ± 0.10	451	64 BENAKSAS	72B	OSPK	$e^+e^- \rightarrow \pi^+\pi^-\pi^0$
0.77 ± 0.06		66 AUGUSTIN	69D	OSPK	$e^+e^- \rightarrow \pi^+\pi^-\pi^0$
0.65 ± 0.13	33	67 ASTVACAT...	68	OSPK	Assume SU(3)+mixing

63 Using $B(\omega \rightarrow \pi^+\pi^-\pi^0) = 0.891 \pm 0.007$. Update of AKHMETSHIN 00c.
64 Not independent of the corresponding $\Gamma(e^+e^-) \times \Gamma(\pi^+\pi^-\pi^0)/\Gamma_{\text{total}}^2$.
65 Using ACHASOV 03, ACHASOV 03D and $B(\omega \rightarrow \pi^+\pi^-) = (1.70 \pm 0.28)\%$.
66 Rescaled by us to correspond to ω width 8.4 MeV. Systematic errors underestimated.
67 Not resolved from ρ decay. Error statistical only.

$\Gamma(\pi^+\pi^-\pi^0\pi^0)/\Gamma_{\text{total}}$		Γ_{10}/Γ			
VALUE (units 10^{-2})	CL%	DOCUMENT ID	TECN	COMMENT	
<2					
	90	KURDADZE	86	OLYA	$e^+e^- \rightarrow \pi^+\pi^-\pi^0\pi^0$

$\Gamma(\pi^+\pi^-\gamma)/\Gamma_{\text{total}}$		Γ_{11}/Γ			
VALUE	CL%	DOCUMENT ID	TECN	COMMENT	
<0.0036					
	95	WEIDENAUER	90	ASTE	$p\bar{p} \rightarrow \pi^+\pi^-\pi^+\pi^-\gamma$
• • • We do not use the following data for averages, fits, limits, etc. • • •					
<0.004	95	BITYUKOV	88B	SPEC	32 $\pi^-p \rightarrow \pi^+\pi^-\gamma X$

$\Gamma(\pi^+\pi^-\gamma)/\Gamma(\pi^+\pi^-\pi^0)$		Γ_{11}/Γ_1			
VALUE	CL%	DOCUMENT ID	TECN	COMMENT	
• • • We do not use the following data for averages, fits, limits, etc. • • •					
<0.066	90	KALBFLEISCH	75	HBC	2.18 $K^-p \rightarrow \Lambda\pi^+\pi^-\gamma$
<0.05	90	FLATTE	66	HBC	1.2 - 1.7 $K^-p \rightarrow \Lambda\pi^+\pi^-\gamma$

$\Gamma(\pi^+\pi^-\pi^+\pi^-)/\Gamma_{\text{total}}$		Γ_{12}/Γ			
VALUE	CL%	DOCUMENT ID	TECN	COMMENT	
<1 × 10⁻³					
	90	KURDADZE	88	OLYA	$e^+e^- \rightarrow \pi^+\pi^-\pi^+\pi^-$

$\Gamma(\pi^0\pi^0\gamma)/\Gamma_{\text{total}}$		Γ_{13}/Γ			
VALUE (units 10^{-5})	EVTS	DOCUMENT ID	TECN	COMMENT	
6.7 ± 1.1 OUR FIT					
6.5 ± 1.2 OUR AVERAGE					
6.4 +2.4 -2.0 ± 0.8	190	68 AKHMETSHIN	04B	CMD2	0.6-0.97 $e^+e^- \rightarrow \pi^0\pi^0\gamma$
6.6 +1.4 -1.3 ± 0.6	295	ACHASOV	02F	SND	0.36-0.97 $e^+e^- \rightarrow \pi^0\pi^0\gamma$
• • • We do not use the following data for averages, fits, limits, etc. • • •					
11.8 +2.1 -1.9 ± 1.4	190	69 AKHMETSHIN	04B	CMD2	0.6-0.97 $e^+e^- \rightarrow \pi^0\pi^0\gamma$
7.8 ± 2.7 ± 2.0	63	68,70 ACHASOV	00G	SND	$e^+e^- \rightarrow \pi^0\pi^0\gamma$
12.7 ± 2.3 ± 2.5	63	69,70 ACHASOV	00G	SND	$e^+e^- \rightarrow \pi^0\pi^0\gamma$
68 In the model assuming the $\rho \rightarrow \pi^0\pi^0\gamma$ decay via the $\omega\pi$ and $f_0(600)\gamma$ mechanisms. 69 In the model assuming the $\rho \rightarrow \pi^0\pi^0\gamma$ decay via the $\omega\pi$ mechanism only. 70 Superseded by ACHASOV 02F.					

$\Gamma(\pi^0\pi^0\gamma)/\Gamma(\pi^+\pi^-\pi^0)$		Γ_{13}/Γ_1			
VALUE	CL%	DOCUMENT ID	TECN	COMMENT	
<0.00045					
	90	DOLINSKY	89	ND	$e^+e^- \rightarrow \pi^0\pi^0\gamma$
• • • We do not use the following data for averages, fits, limits, etc. • • •					
<0.08	95	JACQUET	69B	HLBC	2.05 $\pi^+p \rightarrow \pi^+\rho$

$\Gamma(\pi^0\pi^0\gamma)/\Gamma(\pi^0\gamma)$		Γ_{13}/Γ_2			
VALUE (units 10^{-4})	CL%	EVTS	DOCUMENT ID	TECN	COMMENT
7.6 ± 1.3 OUR FIT					
8.5 ± 2.9					
		40 ± 14	ALDE	94B	GAM2 38 $\pi^-p \rightarrow \pi^0\pi^0\gamma n$
• • • We do not use the following data for averages, fits, limits, etc. • • •					
< 50	90		DOLINSKY	89	ND $e^+e^- \rightarrow \pi^0\pi^0\gamma$
<1800	95		KEYNE	76	CNTR $\pi^-p \rightarrow \omega n$
<1500	90		BENAKSAS	72C	OSPK e^+e^-
<1400			BALDIN	71	HLBC 2.9 π^+p
<1000	90		BARMIN	64	HLBC 1.3-2.8 π^-p

$\Gamma(\pi^0\pi^0\gamma)/\Gamma(\text{neutrals})$ $\Gamma_{13}/(\Gamma_2+\Gamma_4)$

VALUE	CL%	DOCUMENT ID	TECN	COMMENT
0.22±0.07		71 DAKIN	72 OSPK	1.4 $\pi^- p \rightarrow nMM$
<0.19	90	DEINET	69B OSPK	

71 See $\Gamma(\pi^0\gamma)/\Gamma(\text{neutrals})$. $\Gamma(\eta\pi^0\gamma)/\Gamma_{\text{total}}$ Γ_{14}/Γ

VALUE (units 10^{-5})	CL%	DOCUMENT ID	TECN	COMMENT
<3.3	90	AKHMETSHIN 04B	CMD2	$0.6-0.97 e^+ e^- \rightarrow \eta\pi^0\gamma$

 $\Gamma(\mu^+\mu^-)/\Gamma_{\text{total}}$ Γ_{15}/Γ

VALUE (units 10^{-9})	EVTS	DOCUMENT ID	TECN	COMMENT
9.0±3.1. OUR FIT				
9.0±2.9±1.1	18	HEISTER	02c ALEP	$Z \rightarrow \mu^+\mu^- + X$

 $\Gamma(\mu^+\mu^-)/\Gamma(\pi^+\pi^-\pi^0)$ Γ_{15}/Γ_1

VALUE (units 10^{-3})	CL%	DOCUMENT ID	TECN	COMMENT
<0.2	90	WILSON	69 OSPK	12 $\pi^- C \rightarrow Fe$
<1.7	74	FLATTE	66 HBC	$1.2 - 1.7 K^- p \rightarrow \Lambda\mu^+\mu^-$
<1.2		BARBARO...	65 HBC	$2.7 K^- p$

 $\Gamma(\pi^0\mu^+\mu^-)/\Gamma(\mu^+\mu^-)$ Γ_7/Γ_{15}

VALUE	EVTS	DOCUMENT ID	TECN	COMMENT
1.2±0.6	30	72 DZHELYADIN 79	CNTR	25-33 $\pi^- p$

72 Superseded by DZHELYADIN 81b result above.

 $\Gamma(3\gamma)/\Gamma_{\text{total}}$ Γ_{16}/Γ

VALUE (units 10^{-4})	CL%	DOCUMENT ID	TECN	COMMENT
<1.9	95	73 ABELE 97E	CBAR	$0.0 \bar{p} p \rightarrow 5\gamma$
<2	90	73 PROKOSHKIN 95	GAM2	$38 \pi^- p \rightarrow 3\gamma n$

73 From direct 3γ decay search. $\Gamma(\eta\pi^0)/\Gamma_{\text{total}}$ Γ_{17}/Γ

VALUE	CL%	DOCUMENT ID	TECN	COMMENT
<0.001	90	ALDE	94B GAM2	$38 \pi^- p \rightarrow \eta\pi^0 n$

Violates C conservation.

 $[\Gamma(\eta\gamma) + \Gamma(\eta\pi^0)]/\Gamma(\pi^+\pi^-\pi^0)$ $(\Gamma_5 + \Gamma_{17})/\Gamma_1$

VALUE	CL%	DOCUMENT ID	TECN	COMMENT
<0.016	90	74 FLATTE 66	HBC	$1.2 - 1.7 K^- p \rightarrow \Lambda\pi^+\pi^- MM$
<0.045	95	JACQUET 69B	HLBC	$2.05 \pi^+ p \rightarrow \pi^+ p \omega$

74 Restated by us using $B(\eta \rightarrow \text{charged modes}) = 29.2\%$. $\Gamma(3\pi^0)/\Gamma_{\text{total}}$ Γ_{18}/Γ

VALUE	CL%	DOCUMENT ID	TECN	COMMENT
<0.0003	90	PROKOSHKIN 95	GAM2	$38 \pi^- p \rightarrow 3\pi^0 n$

Violates C conservation.

 $\Gamma(3\pi^0)/\Gamma(\pi^+\pi^-\pi^0)$ Γ_{18}/Γ_1

VALUE	CL%	DOCUMENT ID	COMMENT
<0.009	90	BARBERIS 01	$450 pp \rightarrow p_f 3\pi^0 p_s$

 $\omega(782)$ REFERENCES

ACHASOV 07B	PR D76 077101	M.N. Achasov et al.	(SND Collab.)
AKHMETSHIN 07	PL B648 28	R. Akhmetshin et al.	(Novosibirsk CMD-2 Collab.)
ACHASOV 06	JETP 103 380	M.N. Achasov et al.	(Novosibirsk SND Collab.)
	Translated from ZETF 130 437.		
ACHASOV 06A	PR D74 014016	M.N. Achasov et al.	(SND Collab.)
AULCHENKO 06	JETPL 84 413	V.M. Aulchenko et al.	(Novosibirsk CMD-2 Collab.)
	Translated from ZETFP 84 491.		
ACHASOV 05A	JETP 101 1059	M.N. Achasov et al.	(Novosibirsk SND Collab.)
	Translated from ZETF 128 1201.		
AKHMETSHIN 05	PL B605 26	R.R. Akhmetshin et al.	(Novosibirsk CMD-2 Collab.)
AKHMETSHIN 05A	PL B613 29	R.R. Akhmetshin et al.	(Novosibirsk CMD-2 Collab.)
AULCHENKO 05	JETPL 82 743	V.M. Aulchenko et al.	(Novosibirsk CMD-2 Collab.)
	Translated from ZETFP 82 841.		
AKHMETSHIN 04	PL B578 285	R.R. Akhmetshin et al.	(Novosibirsk CMD-2 Collab.)
AKHMETSHIN 04B	PL B580 119	R.R. Akhmetshin et al.	(Novosibirsk CMD-2 Collab.)
AUBERT B 04N	PR D70 072004	B. Aubert et al.	(BABAR Collab.)
PDG 04	PL B592 1	S. Eidelman et al.	
ACHASOV 03	PL B559 171	M.N. Achasov et al.	(Novosibirsk SND Collab.)
ACHASOV 03D	PR D68 052006	M.N. Achasov et al.	(Novosibirsk SND Collab.)
ALOISIO 03	PL B561 55	A. Aloisio et al.	(KLOE Collab.)
BENAYOUN 03	EPJ C29 397	M. Benayoun et al.	
ACHASOV 02E	PR D66 032001	M.N. Achasov et al.	(Novosibirsk SND Collab.)
ACHASOV 02F	PL B537 201	M.N. Achasov et al.	(Novosibirsk SND Collab.)
AKHMETSHIN 02	PL B527 161	R.R. Akhmetshin et al.	(Novosibirsk CMD-2 Collab.)
ALOISIO 02D	PL B537 21	A. Aloisio et al.	(KLOE Collab.)
HEISTER 02C	PL B528 19	A. Heister et al.	(ALEPH Collab.)
ACHASOV 01E	PR D63 072002	M.N. Achasov et al.	(Novosibirsk SND Collab.)
AKHMETSHIN 01B	PL B509 217	R.R. Akhmetshin et al.	(Novosibirsk CMD-2 Collab.)
BARBERIS 01	PL B507 14	D. Barberis et al.	
ACHASOV 00	EPJ C12 25	M.N. Achasov et al.	(Novosibirsk SND Collab.)
ACHASOV 00D	JETPL 72 282	M.N. Achasov et al.	(Novosibirsk SND Collab.)
	Translated from ZETFP 72 411.		

ACHASOV 00G	JETPL 71 355	M.N. Achasov et al.	(Novosibirsk SND Collab.)
	Translated from ZETFP 71 519.		
AKHMETSHIN 00C	PL B476 33	R.R. Akhmetshin et al.	(Novosibirsk CMD-2 Collab.)
AULCHENKO 00A	JETP 90 927	V.M. Aulchenko et al.	(Novosibirsk SND Collab.)
	Translated from ZETF 117 1067.		
CASE 00	PR D61 032002	T. Case et al.	(Crystal Barrel Collab.)
ACHASOV 99E	PL B462 365	M.N. Achasov et al.	(Novosibirsk SND Collab.)
GARDNER 99	PR D59 076002	S. Gardner, H.B. O'Connell	
BENAYOUN 98	EPJ C2 269	M. Benayoun et al.	(IPNP, NOVO, ADLO+)
ABELE 97E	PL B411 361	A. Abele et al.	(Crystal Barrel Collab.)
BENAYOUN 96	ZPHY C72 221	M. Benayoun et al.	(IPNP, NOVO)
PROKOSHKIN 95	SPD 40 273	Y.D. Prokoshkin, V.D. Samoilenko	(SERP)
	Translated from DANS 342 610.		
WURZINGER 95	PR C51 443	R. Wurzinger et al.	(BONN, ORSAY, SACL+)
ALDE 94B	PL B340 122	D.M. Alde et al.	(SERP, BELG, LANL, LAPP+)
AMSLER 94C	PL B327 425	C. Amstler et al.	(Crystal Barrel Collab.)
ALDE 93	PAN 56 1229	D.M. Alde et al.	(SERP, LAPP, LANL, BELG+)
	Translated from YAF 56 137.		
	Also		
ZPHY C61 35		D.M. Alde et al.	(SERP, LAPP, LANL, BELG+)
AMSLER 93B	PL B311 362	C. Amstler et al.	(Crystal Barrel Collab.)
WEIDENAUER 93	ZPHY C59 387	P. Weidenauer et al.	(ASTERIX Collab.)
ANTONELLI 92	ZPHY C56 15	A. Antonelli et al.	(DMZ Collab.)
DOLINSKY 91	PRPL 202 99	S.I. Dolinsky et al.	(NOVO)
WEIDENAUER 90	ZPHY C47 353	P. Weidenauer et al.	(ASTERIX Collab.)
DOLINSKY 89	ZPHY C42 511	S.I. Dolinsky et al.	(NOVO)
BITYUKOV 88B	SJNP 47 800	S.I. Bityukov et al.	(SERP)
	Translated from YAF 47 1258.		
DOLINSKY 88	SJNP 48 277	S.I. Dolinsky et al.	(NOVO)
	Translated from YAF 48 442.		
KURDADZE 88	JETPL 47 512	L.M. Kurdadze et al.	(NOVO)
	Translated from ZETFP 47 432.		
AULCHENKO 87	PL B186 432	V.M. Aulchenko et al.	(NOVO)
BARKOV 87	JETPL 46 164	L.M. Barkov et al.	(NOVO)
	Translated from ZETFP 46 132.		
KURDADZE 86	JETPL 43 643	L.M. Kurdadze et al.	(NOVO)
	Translated from ZETFP 43 497.		
BARKOV 85	NP B256 365	L.M. Barkov et al.	(NOVO)
DRUZHININ 84	PL 3448 136	V.P. Druzhinin et al.	(NOVO)
KURDADZE 83B	JETPL 36 274	A.M. Kurdadze et al.	(NOVO)
	Translated from ZETFP 36 221.		
DZHELYADIN 81B	PL 102B 296	R.I. Dzhelyadin et al.	(SERP)
CORDIER 80	NP B172 13	A. Cordier et al.	(LAL)
ROOS 80	LNC 27 321	M. Roos, A. Pellinen	(HELS)
BENKHEIRI 79	NP B150 268	P. Benkheiri et al.	(EPOL, CERN, CDF+)
DZHELYADIN 79	PL 84B 143	R.I. Dzhelyadin et al.	(SERP)
COOPER 78B	NP B146 1	A.M. Cooper et al.	(TATA, CERN, CDF+)
QUENZER 78	PL 76B 512	A. Quenzer et al.	(LAL)
VANAP... 78	NP B133 245	S.V. van Apeldoorn et al.	(ZEM)
WICKLUND 78	PR D17 1197	A.B. Wicklund et al.	(ANL)
ANDREWS 77	PRL 38 198	D.E. Andrews et al.	(ROCH)
GESSAROLI 77	NP B126 382	R. Gessaroli et al.	(BGNA, FIRZ, GENO+)
KEYNE 76	PR D14 28	J. Keyne et al.	(LOIC, SHMP)
	Also		
PR D8 2789		D.M. Binnie et al.	(LOIC, SHMP)
KALBFLEISCH 75B	PR D11 987	G.R. Kalbfleisch, R.C. Strand, J.W. Chapman	(BNL+)
AGUILAR... 72B	PR D6 29	M. Aguilar-Benitez et al.	(BNL)
APEL 72B	PL 41B 234	W.D. Apel et al.	(KARLK, KARLE, PISA)
BASILE 72B	Phil. Conf. 153	M. Basile et al.	(CERN)
BENAKSAS 72	PL 39B 209	D. Benaksas et al.	(ORSAY)
BENAKSAS 72B	PL 42B 507	D. Benaksas et al.	(ORSAY)
BENAKSAS 72C	PL 42B 511	D. Benaksas et al.	(ORSAY)
BORNSTEIN 72	PR D5 1559	S.R. Bornstein et al.	(BNL, MICH)
BROWN 72	PL 42B 117	R.M. Brown et al.	(ILL, ILLC)
DAKIN 72	PR D6 2321	J.T. Dakin et al.	(PRIN)
RATCLIFF 72	PL 38B 345	B.N. Ratcliff et al.	(SLAC)
ALVENSEL... 71C	PRL 27 888	H. Alvensleben et al.	(DESY)
BALDIN 71	SJNP 13 758	A.B. Baldin et al.	(ITEP)
	Translated from YAF 13 1318.		
BEHREND 71	PR 27 61	H.J. Behrend et al.	(ROCH, CORN, FNAL)
BIZZARRI 71	NP B27 140	R. Bizzarri et al.	(CERN, CDF)
COYNE 71	NP B32 333	D.G. Coyne et al.	(LRL)
MOFFEIT 71	NP B29 349	K.C. Moffeit et al.	(LRL, UC, SLAC+)
ABRAMOV... 70	NP B20 209	M. Abramovich et al.	(CERN)
BIGGS 70B	PRL 24 1201	P.J. Biggs et al.	(DARE)
BIZZARRI 70	PRL 25 1385	R. Bizzarri et al.	(ROMA, SYRA)
ROOS 70	DNPL/R7 173	M. Roos	(CERN)
	Proc. Daresbury Study Weekend No. 1.		
AUGUSTIN 69D	PL 28B 513	J.E. Augustin et al.	(ORSAY)
BIZZARRI 69	NP B14 169	R. Bizzarri et al.	(CERN, CDF)
DEINET 69B	PL 30B 426	W. Deinet et al.	(KARL, CERN)
JACQUET 69B	NC 63A 743	F. Jacquet et al.	(EPOL, BERG)
WILSON 69	Private Comm.	R. Wilson	(HARV)
	Also		
PR 178 2095		A.A. Wehmman et al.	(HARV, CASE, SLAC+)
ASTVACAT... 68C	PL 27B 45	R.G. Astvatsaturov et al.	(JINR, MOSU)
BOLLINI 68C	NC 56A 531	D. Bollini et al.	(CERN, BGNA, STRB)
BARASH 67B	PR 156 1399	N. Barash et al.	(COLU)
FELDMAN 67C	PR 159 1219	M. Feldman et al.	(PENN)
DIGIUGNO 66B	NC 44A 1272	G. Di Giugno et al.	(NAPL, FRAS, TRST)
FLATTE 66	PR 145 1050	S.M. Flatte et al.	(LRL)
JAMES 66	PR 142 896	F.E. James, H.L. Kraybill	(YALE, BNL)
BARBARO... 65	PRL 14 279	A. Barbaro-Galhier, R.D. Tripp	(LRL)
BARMIN 64	JETP 18 1289	V.V. Barmin et al.	(ITEP)
	Translated from ZETF 45 1879.		
KRAEMER 64	PR 136 B496	R.W. Kraemer et al.	(JHU, NWES, WOOD)
BUSCHBECK 63	Siena Conf. 1 166	B. Buschbeck et al.	(VIEN, CERN, ANIK)

OTHER RELATED PAPERS

AZIMOV 03	EPJ A16 209	Ya.I. Aximov	
BENAYOUN 01	EPJ C22 503	M. Benayoun, H.B. O'Connell	
GOKALP 01B	EPJ C22 327	A. Gokalp, Y. Sarac, O. Yilmaz	
DELBOURGO 99B	PR D59 113006	R. Delbourgo et al.	
GARDNER 98	PR D57 2716	S. Gardner, H.B. O'Connell	
	Also		
PR D62 019903 (erratum)		S. Gardner, H.B. O'Connell	
ABELE 97F	PL B411 354	A. Abele et al.	(Crystal Barrel Collab.)
DOLINSKY 87C	PL B174 453	S.I. Dolinsky et al.	(NOVO)
KURDADZE 83B	JETPL 37 733	L.M. Kurdadze et al.	(NOVO)
	Translated from ZETFP 37 613.		
ALFF... 82B	PRL 9 325	C. Alf-Steinberger et al.	(COLU, RUTG)
STEVENSON 62	PR 125 687	M.L. Stevenson et al.	(LRL)
MAGLICH 61	PRL 7 178	B.C. Maglich et al.	(LRL)
PEVNER 61	PRL 7 421	A. Pevner et al.	(JHU)
XUONG 61	PRL 7 327	H. Nguyen Ngoc, G.R. Lynch	(LRL)

Meson Particle Listings

 $\eta'(958)$ $\eta'(958)$

$$J^{G(J^{PC})} = 0^+(0^{-+})$$

 $\eta'(958)$ MASS

VALUE (MeV)	EVTS	DOCUMENT ID	TECN	COMMENT
957.66 ± 0.24 OUR AVERAGE				
957.9 ± 0.2 ± 0.6	4800	WURZINGER 96	SPEC	1.68 $p d \rightarrow {}^3\text{He} \eta'$
957.46 ± 0.33		DUA NE 74	MMS	$\pi^- p \rightarrow n \text{MM}$
958.2 ± 0.5	1414	DANBURG 73	HBC	2.2 $K^- p \rightarrow \Lambda \eta'$
958 ± 1	400	JACOBS 73	HBC	2.9 $K^- p \rightarrow \Lambda \eta'$
956.1 ± 1.1	3415	¹ BASILE 71	CNTR	1.6 $\pi^- p \rightarrow n \eta'$
• • • We do not use the following data for averages, fits, limits, etc. • • •				
957.5 ± 0.2		BAI 04J	BES2	$J/\psi \rightarrow \gamma \gamma \pi^+ \pi^-$
959 ± 1	630	² BELADIDZE 92c	VES	36 $\pi^- \text{Be} \rightarrow \pi^- \eta' \eta \text{Be}$
958 ± 1	340	² ARMSTRONG 91B	OMEG	300 $p p \rightarrow p p \eta \pi^+ \pi^-$
958.2 ± 0.4	622	² AUGUSTIN 90	DM2	$J/\psi \rightarrow \gamma \eta \pi^+ \pi^-$
957.8 ± 0.2	2420	² AUGUSTIN 90	DM2	$J/\psi \rightarrow \gamma \gamma \pi^+ \pi^-$
956.3 ± 1.0	143	² GIDAL 87	MRK2	$e^+ e^- \rightarrow e^+ e^- \eta \pi^+ \pi^-$
957.4 ± 1.4	535	³ BASILE 71	CNTR	1.6 $\pi^- p \rightarrow n \eta'$
957 ± 1		RITTENBERG 69	HBC	1.7–2.7 $K^- p$

¹ Using all η' decays.² Systematic uncertainty not estimated.³ Using η' decays into neutrals. Not independent of the other listed BASILE 71 η' mass measurement. $\eta'(958)$ WIDTH

VALUE (MeV)	EVTS	DOCUMENT ID	TECN	CHG	COMMENT
0.205 ± 0.015 OUR FIT					Error includes scale factor of 1.2.
0.30 ± 0.09 OUR AVERAGE					
0.40 ± 0.22	4800	WURZINGER 96	SPEC		1.68 $p d \rightarrow {}^3\text{He} \eta'$
0.28 ± 0.10	1000	BINNIE 79	MMS	0	$\pi^- p \rightarrow n \text{MM}$
• • • We do not use the following data for averages, fits, limits, etc. • • •					
0.20 ± 0.04		BAI 04J	BES2		$J/\psi \rightarrow \gamma \gamma \pi^+ \pi^-$

 $\eta'(958)$ DECAY MODES

Mode	Fraction (Γ_i/Γ)	Scale factor/ Confidence level
Γ_1 $\pi^+ \pi^- \eta$	(44.6 ± 1.4) %	S=1.2
Γ_2 $\rho^0 \gamma$ (including non-resonant $\pi^+ \pi^- \gamma$)	(29.4 ± 0.9) %	S=1.1
Γ_3 $\pi^0 \pi^0 \eta$	(20.7 ± 1.2) %	S=1.2
Γ_4 $\omega \gamma$	(3.02 ± 0.31) %	
Γ_5 $\gamma \gamma$	(2.10 ± 0.12) %	S=1.2
Γ_6 $3\pi^0$	(1.54 ± 0.26) × 10 ⁻³	
Γ_7 $\mu^+ \mu^- \gamma$	(1.03 ± 0.26) × 10 ⁻⁴	
Γ_8 $\pi^+ \pi^- \pi^0$	< 5 %	CL=90%
Γ_9 $\pi^0 \rho^0$	< 4 %	CL=90%
Γ_{10} $\pi^+ \pi^+ \pi^- \pi^-$	< 1 %	CL=90%
Γ_{11} $\pi^+ \pi^+ \pi^- \pi^-$ neutrals	< 1 %	CL=95%
Γ_{12} $\pi^+ \pi^+ \pi^- \pi^- \pi^0$	< 1 %	CL=90%
Γ_{13} 6π	< 1 %	CL=90%
Γ_{14} $\pi^+ \pi^- e^+ e^-$	< 6 × 10 ⁻³	CL=90%
Γ_{15} $\gamma e^+ e^-$	< 9 × 10 ⁻⁴	CL=90%
Γ_{16} $\pi^0 \gamma \gamma$	< 8 × 10 ⁻⁴	CL=90%
Γ_{17} $4\pi^0$	< 5 × 10 ⁻⁴	CL=90%
Γ_{18} $e^+ e^-$	< 2.1 × 10 ⁻⁷	CL=90%
Γ_{19} invisible	< 1.4 × 10 ⁻³	CL=90%

Charge conjugation (C), Parity (P),
Lepton family number (LF) violating modes

Γ_{20} $\pi^+ \pi^-$	P, CP	< 2.9	× 10 ⁻³	CL=90%
Γ_{21} $\pi^0 \pi^0$	P, CP	< 9	× 10 ⁻⁴	CL=90%
Γ_{22} $\pi^0 e^+ e^-$	C	[a] < 1.4	× 10 ⁻³	CL=90%
Γ_{23} $\eta e^+ e^-$	C	[a] < 2.4	× 10 ⁻³	CL=90%
Γ_{24} 3γ	C	< 1.0	× 10 ⁻⁴	CL=90%
Γ_{25} $\mu^+ \mu^- \pi^0$	C	[a] < 6.0	× 10 ⁻⁵	CL=90%
Γ_{26} $\mu^+ \mu^- \eta$	C	[a] < 1.5	× 10 ⁻⁵	CL=90%
Γ_{27} $e \mu$	LF	< 4.7	× 10 ⁻⁴	CL=90%

[a] C parity forbids this to occur as a single-photon process.

CONSTRAINED FIT INFORMATION

An overall fit to the total width, a partial width, 2 combinations of partial widths obtained from integrated cross section, and 16 branching ratios uses 50 measurements and one constraint to determine 7 parameters. The overall fit has a $\chi^2 = 36.9$ for 44 degrees of freedom.

The following *off-diagonal* array elements are the correlation coefficients $\langle \delta p_i \delta p_j \rangle / (\delta p_i \delta p_j)$, in percent, from the fit to parameters p_i , including the branching fractions, $x_i \equiv \Gamma_i / \Gamma_{\text{total}}$. The fit constrains the x_i whose labels appear in this array to sum to one.

x_2	-35					
x_3	-77	-28				
x_4	-35	-24	33			
x_5	-23	-10	23	7		
x_6	-28	-11	35	11	8	
Γ	29	-5	-21	-4	-85	-7
	x_1	x_2	x_3	x_4	x_5	x_6

Mode	Rate (MeV)	Scale factor
Γ_1 $\pi^+ \pi^- \eta$	0.091 ± 0.008	1.1
Γ_2 $\rho^0 \gamma$ (including non-resonant $\pi^+ \pi^- \gamma$)	0.060 ± 0.005	1.2
Γ_3 $\pi^0 \pi^0 \eta$	0.042 ± 0.004	1.5
Γ_4 $\omega \gamma$	0.0062 ± 0.0008	1.2
Γ_5 $\gamma \gamma$	0.00430 ± 0.00015	1.1
Γ_6 $3\pi^0$	(3.2 ± 0.6) × 10 ⁻⁴	1.1

 $\eta'(958)$ PARTIAL WIDTHS

VALUE (keV)	EVTS	DOCUMENT ID	TECN	COMMENT	Γ_5
4.30 ± 0.15 OUR FIT				Error includes scale factor of 1.1.	
4.28 ± 0.19 OUR AVERAGE					
4.17 ± 0.10 ± 0.27	2000	⁴ ACCIARRI 98Q	L3	$e^+ e^- \rightarrow e^+ e^- \pi^+ \pi^- \gamma$	
4.53 ± 0.29 ± 0.51	266	KARCH 92	CBAL	$e^+ e^- \rightarrow e^+ e^- \eta \pi^0 \pi^0$	
3.61 ± 0.13 ± 0.48		⁵ BEHREND 91	CELL	$e^+ e^- \rightarrow e^+ e^- \eta'(958)$	
4.6 ± 1.1 ± 0.6	23	BARU 90	MD1	$e^+ e^- \rightarrow e^+ e^- \pi^+ \pi^- \gamma$	
4.57 ± 0.25 ± 0.44		BUTLER 90	MRK2	$e^+ e^- \rightarrow e^+ e^- \eta'(958)$	
5.08 ± 0.24 ± 0.71	547	⁶ ROE 90	ASP	$e^+ e^- \rightarrow e^+ e^- 2\gamma$	
3.8 ± 0.7 ± 0.6	34	AIHARA 88c	TPC	$e^+ e^- \rightarrow e^+ e^- \eta \pi^+ \pi^-$	
4.9 ± 0.5 ± 0.5	136	⁷ WILLIAMS 88	CBAL	$e^+ e^- \rightarrow e^+ e^- 2\gamma$	
• • • We do not use the following data for averages, fits, limits, etc. • • •					
4.7 ± 0.6 ± 0.9	143	⁸ GIDAL 87	MRK2	$e^+ e^- \rightarrow e^+ e^- \eta \pi^+ \pi^-$	
4.0 ± 0.9		⁹ BARTEL 85E	JADE	$e^+ e^- \rightarrow e^+ e^- 2\gamma$	
⁴ No non-resonant $\pi^+ \pi^-$ contribution found.					
⁵ Reevaluated by us using $B(\eta' \rightarrow \rho(770) \gamma) = (30.2 \pm 1.3)\%$.					
⁶ Reevaluated by us using $B(\eta' \rightarrow \gamma \gamma) = (2.11 \pm 0.13)\%$.					
⁷ Reevaluated by us using $B(\eta' \rightarrow \gamma \gamma) = (2.11 \pm 0.13)\%$.					
⁸ Superseded by BUTLER 90.					
⁹ Systematic error not evaluated.					

 $\eta'(958)$ $\Gamma(i)\Gamma(\gamma\gamma)/\Gamma(\text{total})$

This combination of a partial width with the partial width into $\gamma\gamma$ and with the total width is obtained from the integrated cross section into channel(i) in the $\gamma\gamma$ annihilation.

VALUE (keV)	EVTS	DOCUMENT ID	TECN	COMMENT	$\Gamma_5 \Gamma_2 / \Gamma$
1.26 ± 0.05 OUR FIT				Error includes scale factor of 1.1.	
1.26 ± 0.07 OUR AVERAGE				Error includes scale factor of 1.2.	
1.09 ± 0.04 ± 0.13		BEHREND 91	CELL	$e^+ e^- \rightarrow e^+ e^- \rho(770)^0 \gamma$	
1.35 ± 0.09 ± 0.21		AIHARA 87	TPC	$e^+ e^- \rightarrow e^+ e^- \rho \gamma$	
1.13 ± 0.04 ± 0.13	867	ALBRECHT 87B	ARG	$e^+ e^- \rightarrow e^+ e^- \rho \gamma$	
1.53 ± 0.09 ± 0.21		ALTHOFF 84E	TASS	$e^+ e^- \rightarrow e^+ e^- \rho \gamma$	
1.14 ± 0.08 ± 0.11	243	BERGER 84B	PLUT	$e^+ e^- \rightarrow e^+ e^- \rho \gamma$	
1.73 ± 0.34 ± 0.35	95	JENNI 83	MRK2	$e^+ e^- \rightarrow e^+ e^- \rho \gamma$	
1.49 ± 0.13 ± 0.027	213	BARTEL 82B	JADE	$e^+ e^- \rightarrow e^+ e^- \rho \gamma$	
• • • We do not use the following data for averages, fits, limits, etc. • • •					
1.85 ± 0.31 ± 0.24	43	BEHREND 83B	CELL	$e^+ e^- \rightarrow e^+ e^- \rho \gamma$	

 $\Gamma(\gamma\gamma) \times \Gamma(\pi^0 \pi^0 \eta) / \Gamma(\text{total})$ $\Gamma_5 \Gamma_3 / \Gamma$

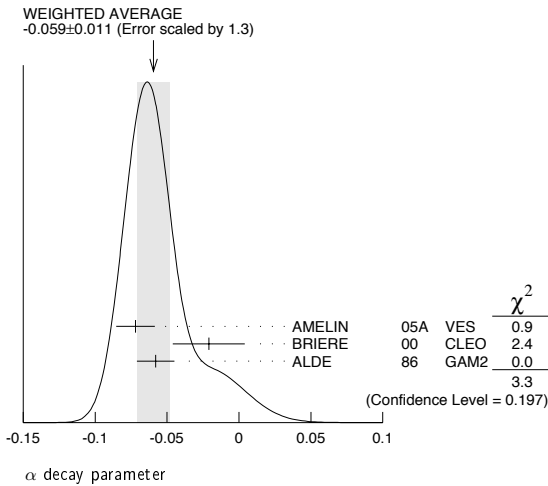
VALUE (keV)	DOCUMENT ID	TECN	COMMENT	$\Gamma_5 \Gamma_3 / \Gamma$
0.89 ± 0.06 OUR FIT			Error includes scale factor of 1.2.	
0.92 ± 0.06 ± 0.11				
0.95 ± 0.05 ± 0.08	¹⁰ KARCH 92	CBAL	$e^+ e^- \rightarrow e^+ e^- \eta \pi^0 \pi^0$	
• • • We do not use the following data for averages, fits, limits, etc. • • •				
1.09 ± 0.08 ± 0.10	¹¹ KARCH 90	CBAL	$e^+ e^- \rightarrow e^+ e^- \eta \pi^0 \pi^0$	
1.00 ± 0.08 ± 0.10	^{11,12} ANTREASNYAN 87	CBAL	$e^+ e^- \rightarrow e^+ e^- \eta \pi^0 \pi^0$	

¹⁰Reevaluated by us using $B(\eta \rightarrow \gamma\gamma) = (39.21 \pm 0.34)\%$. Supersedes ANTREASYAN 87 and KARCH 90.
¹¹Superseded by KARCH 92.
¹²Using $BR(\eta \rightarrow 2\gamma) = (38.9 \pm 0.5)\%$.

$\eta'(958)$ DECAY PARAMETERS
|MATRIX ELEMENT|² = |1 + αy |² + $c x$ + $d x^2$

α decay parameter

VALUE	EVTS	DOCUMENT ID	TECN	COMMENT
-0.059 ± 0.011 OUR AVERAGE				Error includes scale factor of 1.3. See the ideogram below.
-0.072 ± 0.012 ± 0.006	7k	¹³ AMELIN	05A VES	28 $\pi^- A \rightarrow \eta' \pi^- A^*$
-0.021 ± 0.025	6.7k	¹⁴ BRIERE	00 CLEO	10.6 $e^+ e^- \rightarrow$ hadrons
-0.058 ± 0.013		^{15,16} ALDE	86 GAM2	38 $\pi^- p \rightarrow n \eta 2\pi^0$
• • • We do not use the following data for averages, fits, limits, etc. • • •				
-0.08 ± 0.03		^{15,16} KALBFLEISCH	74 RVUE	$\eta' \rightarrow \eta \pi^+ \pi^-$
¹³ This is a real part of α while $\text{Im}(\alpha) = 0.0 \pm 0.1 \pm 0.0$.				
¹⁴ Assuming $\text{Im}(\alpha) = 0$, $c = 0$, and $d = 0$.				
¹⁵ May not necessarily be the same for $\eta' \rightarrow \eta \pi^+ \pi^-$ and $\eta' \rightarrow \eta \pi^0 \pi^0$.				
¹⁶ Assuming $\text{Im}(\alpha) = 0$, $c = 0$.				



c C-violating decay parameter

VALUE	EVTS	DOCUMENT ID	TECN	COMMENT
0.015 ± 0.011 ± 0.014	20k	¹⁷ DOROFEEV	07 VES	27 $\pi^- p \rightarrow \eta' n$ and $\pi^- A \rightarrow \eta' \pi^- A^*$
• • • We do not use the following data for averages, fits, limits, etc. • • •				
0.020 ± 0.018 ± 0.004	7k	AMELIN	05A VES	Sup. by DOROFEEV 07
¹⁷ Using the more general parameterization $ M ^2 = 1 + aY + bY^2 + cX + dX^2$.				

$\eta'(958)$ β PARAMETER
|MATRIX ELEMENT|² = (1 + 2 βZ)

See the "Note on η Decay Parameters" in our 1994 edition Physical Review D50 1173 (1994), p. 1454.

β decay parameter

VALUE	DOCUMENT ID	TECN	COMMENT
-0.1 ± 0.3	ALDE	87B GAM2	38 $\pi^- p \rightarrow n 3\pi^0$

$\eta'(958)$ BRANCHING RATIOS

$\Gamma(\pi^+ \pi^- \eta(\text{charged decay}))/\Gamma_{\text{total}}$					0.286Γ_1/Γ
VALUE	EVTS	DOCUMENT ID	TECN	COMMENT	
0.127 ± 0.004 OUR FIT				Error includes scale factor of 1.2.	
0.116 ± 0.013 OUR AVERAGE					
0.123 ± 0.014	107	RITTENBERG	69 HBC	1.7-2.7 $K^- p$	
0.10 ± 0.04	10	LONDON	66 HBC	2.24 $K^- p \rightarrow \Lambda \pi^+ \pi^- \pi^0$	
0.07 ± 0.04	7	BADIER	65B HBC	3 $K^- p$	
$\Gamma(\pi^+ \pi^- \eta(\text{neutral decay}))/\Gamma_{\text{total}}$					0.714Γ_1/Γ
VALUE	EVTS	DOCUMENT ID	TECN	COMMENT	
0.318 ± 0.010 OUR FIT				Error includes scale factor of 1.2.	
0.314 ± 0.026	281	RITTENBERG	69 HBC	1.7-2.7 $K^- p$	

$\Gamma(\rho^0 \gamma(\text{including non-resonant } \pi^+ \pi^- \gamma))/\Gamma_{\text{total}}$					Γ_2/Γ
VALUE	EVTS	DOCUMENT ID	TECN	COMMENT	
0.294 ± 0.009 OUR FIT				Error includes scale factor of 1.1.	
0.319 ± 0.030 OUR AVERAGE					
0.329 ± 0.033	298	RITTENBERG	69 HBC	1.7-2.7 $K^- p$	
0.2 ± 0.1	20	LONDON	66 HBC	2.24 $K^- p \rightarrow \Lambda \pi^+ \pi^- \gamma$	
0.34 ± 0.09	35	BADIER	65B HBC	3 $K^- p$	

$\Gamma(\pi^+ \pi^- \eta)/\Gamma(\rho^0 \gamma(\text{including non-resonant } \pi^+ \pi^- \gamma))$					Γ_1/Γ_2
VALUE	DOCUMENT ID	TECN	COMMENT		
1.45 ± 0.07	ABLIKIM	06E BES2	$J/\psi \rightarrow \eta' \gamma$		

$\Gamma(\rho^0 \gamma(\text{including non-resonant } \pi^+ \pi^- \gamma))/\Gamma(\pi^+ \pi^- \eta(\text{neutral decay}))$					$\Gamma_2/0.714\Gamma_1$
VALUE	EVTS	DOCUMENT ID	TECN	COMMENT	
0.92 ± 0.05 OUR FIT				Error includes scale factor of 1.1.	
0.97 ± 0.09 OUR AVERAGE					
0.70 ± 0.22		AMSLER	04B CBAR	0 $\bar{p} p \rightarrow \pi^+ \pi^- \eta$	
1.07 ± 0.17		BELADIDZE	92c VES	36 $\pi^- \text{Be} \rightarrow \pi^- \eta' \eta \text{Be}$	
0.92 ± 0.14	473	DANBURG	73 HBC	2.2 $K^- p \rightarrow \Lambda X^0$	
1.11 ± 0.18	192	JACOBS	73 HBC	2.9 $K^- p \rightarrow \Lambda X^0$	

$\Gamma(\pi^0 \pi^0 \eta(3\pi^0 \text{ decay}))/\Gamma_{\text{total}}$					0.321Γ_3/Γ
VALUE	EVTS	DOCUMENT ID	TECN	COMMENT	
0.067 ± 0.004 OUR FIT				Error includes scale factor of 1.2.	
0.11 ± 0.06	4	BENSINGER	70 DBC	2.2 $\pi^+ d$	

$\Gamma(\rho^0 \gamma(\text{including non-resonant } \pi^+ \pi^- \gamma))/\Gamma(\pi\pi\eta)$					$\Gamma_2/(\Gamma_1 + \Gamma_3)$
VALUE	DOCUMENT ID	TECN	COMMENT		
0.450 ± 0.020 OUR FIT			Error includes scale factor of 1.1.		
0.426 ± 0.028 OUR AVERAGE					
0.43 ± 0.02 ± 0.02		BARBERIS	98c OMEG	450 $p p \rightarrow p_f \eta' p_s$	
0.31 ± 0.15		DAVIS	68 HBC	5.5 $K^- p$	

$\Gamma(\omega \gamma)/\Gamma(\pi^+ \pi^- \eta)$					Γ_4/Γ_1
VALUE	EVTS	DOCUMENT ID	TECN	COMMENT	
0.068 ± 0.008 OUR FIT				Error includes scale factor of 1.1.	
0.068 ± 0.013	68	ZANFINO	77 ASPK	8.4 $\pi^- p$	

$\Gamma(\omega \gamma)/\Gamma(\pi^0 \pi^0 \eta)$					Γ_4/Γ_3
VALUE	DOCUMENT ID	TECN	COMMENT		
0.146 ± 0.014 OUR FIT					
0.147 ± 0.016	ALDE	87B GAM2	38 $\pi^- p \rightarrow n 4\gamma$		

$\Gamma(\rho^0 \gamma(\text{including non-resonant } \pi^+ \pi^- \gamma))/[\Gamma(\pi^+ \pi^- \eta) + \Gamma(\pi^0 \pi^0 \eta) + \Gamma(\omega \gamma)]$					$\Gamma_2/(\Gamma_1 + \Gamma_3 + \Gamma_4)$
VALUE	DOCUMENT ID	TECN	COMMENT		
0.430 ± 0.019 OUR FIT			Error includes scale factor of 1.1.		
0.25 ± 0.14	DAUBER	64 HBC	1.95 $K^- p$		

$[\Gamma(\pi^0 \pi^0 \eta(\text{charged decay})) + \Gamma(\omega(\text{charged decay}))]/\Gamma_{\text{total}}$					(0.286$\Gamma_3 + 0.89\Gamma_4)/\Gamma$
VALUE	EVTS	DOCUMENT ID	TECN	COMMENT	
0.086 ± 0.005 OUR FIT				Error includes scale factor of 1.2.	
0.045 ± 0.029	42	RITTENBERG	69 HBC	1.7-2.7 $K^- p$	

$\Gamma(\pi^+ \pi^- \text{ neutrals})/\Gamma_{\text{total}}$					(0.714$\Gamma_1 + 0.286\Gamma_3 + 0.89\Gamma_4)/\Gamma$
VALUE	EVTS	DOCUMENT ID	TECN	COMMENT	
0.404 ± 0.007 OUR FIT				Error includes scale factor of 1.1.	
0.36 ± 0.05 OUR AVERAGE					
0.4 ± 0.1	39	LONDON	66 HBC	2.24 $K^- p \rightarrow \Lambda \pi^+ \pi^- \text{ neutrals}$	
0.35 ± 0.06	33	BADIER	65B HBC	3 $K^- p$	

$\Gamma(\gamma \gamma)/\Gamma_{\text{total}}$					Γ_5/Γ
VALUE (units 10^{-2})	EVTS	DOCUMENT ID	TECN	COMMENT	
2.10 ± 0.12 OUR FIT				Error includes scale factor of 1.2.	
1.97 ± 0.13 OUR AVERAGE					
1.99 ^{+0.31} _{-0.27} ± 0.07	114	¹⁸ WICHT	08 BELL	$B^\pm \rightarrow K^\pm \gamma \gamma$	
2.00 ± 0.18		¹⁹ STANTON	80 SPEC	8.45 $\pi^- p \rightarrow n \pi^+ \pi^- 2\gamma$	
2.5 ± 0.7		DUANE	74 MMS	$\pi^- p \rightarrow n \text{MM}$	
1.71 ± 0.33	68	DALPIAZ	72 CNTR	1.6 $\pi^- p \rightarrow n X^0$	
2.0 ^{+0.8} _{-0.6}	31	HARVEY	71 OSPK	3.65 $\pi^- p \rightarrow n X^0$	
• • • We do not use the following data for averages, fits, limits, etc. • • •					
1.8 ± 0.2	6000	²⁰ APEL	79 NICE	15-40 $\pi^- p \rightarrow n 2\gamma$	

¹⁸WICHT 08 reports $[B(\eta'(958) \rightarrow \gamma\gamma)] \times [B(B^+ \rightarrow \eta' K^+)] = (1.40^{+0.16+0.15}_{-0.15-0.12}) \times 10^{-6}$. We divide by our best value $B(B^+ \rightarrow \eta' K^+) = (7.02 \pm 0.25) \times 10^{-5}$. Our first error is their experiment's error and our second error is the systematic error from using our best value.
¹⁹Includes APEL 79 result.
²⁰Data is included in STANTON 80 evaluation.

$\Gamma(\gamma \gamma)/\Gamma(\rho^0 \gamma(\text{including non-resonant } \pi^+ \pi^- \gamma))$					Γ_5/Γ_2
VALUE	DOCUMENT ID	TECN	COMMENT		
0.080 ± 0.008	ABLIKIM	06E BES2	$J/\psi \rightarrow \eta' \gamma$		

Meson Particle Listings

 $\eta'(958)$ $\Gamma(\gamma\gamma)/\Gamma(\pi^0\pi^0\eta)$ Γ_5/Γ_3

VALUE	DOCUMENT ID	TECN	COMMENT
0.101 ± 0.007 OUR FIT			Error includes scale factor of 1.5.
0.105 ± 0.010 OUR AVERAGE			Error includes scale factor of 1.9.
0.091 ± 0.009	AMSLER 93	CBAR	0.0 $\bar{p}p$
0.112 ± 0.002 ± 0.006	ALDE 87B	GAM2	38 $\pi^- p \rightarrow n2\gamma$

 $\Gamma(\gamma\gamma)/\Gamma(\pi^0\pi^0\eta(\text{neutral decay}))$ $\Gamma_5/0.714\Gamma_3$

VALUE	EVTS	DOCUMENT ID	TECN	COMMENT
0.142 ± 0.010 OUR FIT				Error includes scale factor of 1.5.
0.188 ± 0.058	16	APEL 72	OSPK	3.8 $\pi^- p \rightarrow nX^0$

 $\Gamma(\text{neutrals})/\Gamma_{\text{total}}$ $(0.714\Gamma_3 + 0.09\Gamma_4 + \Gamma_5)/\Gamma$

VALUE	EVTS	DOCUMENT ID	TECN	COMMENT
0.172 ± 0.009 OUR FIT				Error includes scale factor of 1.2.
0.187 ± 0.017 OUR AVERAGE				
0.185 ± 0.022	535	BASILE 71	CNTR	1.6 $\pi^- p \rightarrow nX^0$
0.189 ± 0.026	123	RITTENBERG 69	HBC	1.7–2.7 $K^- p$

 $\Gamma(3\pi^0)/\Gamma(\pi^0\pi^0\eta)$ Γ_6/Γ_3

VALUE (units 10^{-4})	DOCUMENT ID	TECN	COMMENT
74 ± 12 OUR FIT			
74 ± 12 OUR AVERAGE			
74 ± 15	ALDE 87B	GAM2	38 $\pi^- p \rightarrow n6\gamma$
75 ± 18	BINON 84	GAM2	30–40 $\pi^- p \rightarrow n6\gamma$

 $\Gamma(\mu^+\mu^-\gamma)/\Gamma(\gamma\gamma)$ Γ_7/Γ_5

VALUE (units 10^{-3})	EVTS	DOCUMENT ID	TECN	COMMENT
4.9 ± 1.2	33	VIKTOROV 80	CNTR	25,33 $\pi^- p \rightarrow 2\mu\gamma$

 $\Gamma(\pi^+\pi^-\pi^0)/\Gamma_{\text{total}}$ Γ_8/Γ

VALUE	CL%	DOCUMENT ID	TECN	COMMENT
<0.05	90	RITTENBERG 69	HBC	1.7–2.7 $K^- p$
••• We do not use the following data for averages, fits, limits, etc. •••				
<0.09	95	DANBURG 73	HBC	2.2 $K^- p \rightarrow \Lambda X^0$

 $\Gamma(\pi^0\rho^0)/\Gamma_{\text{total}}$ Γ_9/Γ

VALUE	CL%	DOCUMENT ID	TECN	COMMENT
<0.04	90	RITTENBERG 65	HBC	2.7 $K^- p$

 $\Gamma(\pi^+\pi^+\pi^-\pi^-)/\Gamma_{\text{total}}$ Γ_{10}/Γ

VALUE	CL%	DOCUMENT ID	TECN	COMMENT
<0.01	90	RITTENBERG 69	HBC	1.7–2.7 $K^- p$

 $\Gamma(\pi^+\pi^+\pi^-\pi^- \text{ neutrals})/\Gamma_{\text{total}}$ Γ_{11}/Γ

VALUE	CL%	DOCUMENT ID	TECN	COMMENT
<0.01	95	DANBURG 73	HBC	2.2 $K^- p \rightarrow \Lambda X^0$
••• We do not use the following data for averages, fits, limits, etc. •••				
<0.01	90	RITTENBERG 69	HBC	1.7–2.7 $K^- p$

 $\Gamma(\pi^+\pi^+\pi^-\pi^-\pi^0)/\Gamma_{\text{total}}$ Γ_{12}/Γ

VALUE	CL%	DOCUMENT ID	TECN	COMMENT
<0.01	90	RITTENBERG 69	HBC	1.7–2.7 $K^- p$

 $\Gamma(6\pi)/\Gamma_{\text{total}}$ Γ_{13}/Γ

VALUE	CL%	DOCUMENT ID	TECN	COMMENT
<0.01	90	LONDON 66	HBC	Compilation

 $\Gamma(\pi^+\pi^-\pi^+\pi^-)/\Gamma_{\text{total}}$ Γ_{14}/Γ

VALUE	CL%	DOCUMENT ID	TECN	COMMENT
<0.006	90	RITTENBERG 65	HBC	2.7 $K^- p$

 $\Gamma(\gamma e^+e^-)/\Gamma_{\text{total}}$ Γ_{15}/Γ

VALUE (units 10^{-3})	CL%	DOCUMENT ID	TECN	COMMENT
<0.9	90	BRIERE 00	CLEO	10.6 e^+e^-

 $\Gamma(\pi^0\gamma\gamma)/\Gamma(\pi^0\pi^0\eta)$ Γ_{16}/Γ_3

VALUE (units 10^{-4})	CL%	DOCUMENT ID	TECN	COMMENT
<37	90	ALDE 87B	GAM2	38 $\pi^- p \rightarrow n4\gamma$

 $\Gamma(4\pi^0)/\Gamma(\pi^0\pi^0\eta)$ Γ_{17}/Γ_3

VALUE (units 10^{-4})	CL%	DOCUMENT ID	TECN	COMMENT
<23	90	ALDE 87B	GAM2	38 $\pi^- p \rightarrow n8\gamma$

 $\Gamma(e^+e^-)/\Gamma_{\text{total}}$ Γ_{18}/Γ

VALUE (units 10^{-7})	CL%	DOCUMENT ID	TECN	COMMENT
<2.1	90	VOROBYEV 88	ND	$e^+e^- \rightarrow \pi^+\pi^-\eta$

 $\Gamma(\text{invisible})/\Gamma(\gamma\gamma)$ Γ_{19}/Γ_5

VALUE (units 10^{-2})	CL%	DOCUMENT ID	TECN	COMMENT
<6.69	90	ABLIKIM 06Q	BES	$J/\psi \rightarrow \phi\eta'$

 $\Gamma(\pi^+\pi^-)/\Gamma_{\text{total}}$ Γ_{20}/Γ

VALUE (units 10^{-4})	CL%	DOCUMENT ID	TECN	COMMENT
< 29	90	21 MORI 07A	BELL	$\gamma\gamma \rightarrow \pi^+\pi^-$
••• We do not use the following data for averages, fits, limits, etc. •••				
< 3.3	90	22 MORI 07A	BELL	$\gamma\gamma \rightarrow \pi^+\pi^-$
<800	95	DANBURG 73	HBC	2.2 $K^- p \rightarrow \Lambda X^0$
<200	90	RITTENBERG 69	HBC	1.7–2.7 $K^- p$

21 Taking into account interference with the $\gamma\gamma \rightarrow \pi^+\pi^-$ continuum.
22 Without interference with the $\gamma\gamma \rightarrow \pi^+\pi^-$ continuum.

 $\Gamma(\pi^0\pi^0)/\Gamma(\pi^0\pi^0\eta)$ Γ_{21}/Γ_3

VALUE (units 10^{-4})	CL%	DOCUMENT ID	TECN	COMMENT
<45	90	ALDE 87B	GAM2	38 $\pi^- p \rightarrow n4\gamma$

 $\Gamma(\pi^0 e^+ e^-)/\Gamma_{\text{total}}$ Γ_{22}/Γ

VALUE (units 10^{-3})	CL%	DOCUMENT ID	TECN	COMMENT
< 1.4	90	BRIERE 00	CLEO	10.6 e^+e^-
••• We do not use the following data for averages, fits, limits, etc. •••				
<13	90	RITTENBERG 65	HBC	2.7 $K^- p$

 $\Gamma(\eta e^+ e^-)/\Gamma_{\text{total}}$ Γ_{23}/Γ

VALUE (units 10^{-3})	CL%	DOCUMENT ID	TECN	COMMENT
< 2.4	90	BRIERE 00	CLEO	10.6 e^+e^-
••• We do not use the following data for averages, fits, limits, etc. •••				
<11	90	RITTENBERG 65	HBC	2.7 $K^- p$

 $\Gamma(3\gamma)/\Gamma(\pi^0\pi^0\eta)$ Γ_{24}/Γ_3

VALUE (units 10^{-4})	CL%	DOCUMENT ID	TECN	COMMENT
<4.6	90	ALDE 87B	GAM2	38 $\pi^- p \rightarrow n3\gamma$

 $\Gamma(\mu^+\mu^-\pi^0)/\Gamma_{\text{total}}$ Γ_{25}/Γ

VALUE (units 10^{-5})	CL%	DOCUMENT ID	TECN	COMMENT
<6.0	90	DZHELADIN 81	CNTR	30 $\pi^- p \rightarrow \eta' n$

 $\Gamma(\mu^+\mu^-\eta)/\Gamma_{\text{total}}$ Γ_{26}/Γ

VALUE (units 10^{-5})	CL%	DOCUMENT ID	TECN	COMMENT
<1.5	90	DZHELADIN 81	CNTR	30 $\pi^- p \rightarrow \eta' n$

 $\Gamma(e\mu)/\Gamma_{\text{total}}$ Γ_{27}/Γ

VALUE (units 10^{-4})	CL%	DOCUMENT ID	TECN	COMMENT
<4.7	90	BRIERE 00	CLEO	10.6 e^+e^-

 $\eta'(958)$ C-NONCONSERVING DECAY PARAMETER

See the note on η decay parameters in the Stable Particle Particle Listings for definition of this parameter.

DECAY ASYMMETRY PARAMETER FOR $\pi^+\pi^-\gamma$

VALUE	EVTS	DOCUMENT ID	TECN	COMMENT
-0.01 ± 0.04 OUR AVERAGE				
-0.019 ± 0.056		AIHARA 87	TPC	$2\gamma \rightarrow \pi^+\pi^-\gamma$
-0.069 ± 0.078	295	GRIGORIAN 75	STRC	2.1 $\pi^- p$
0.00 ± 0.10	103	KALBFLEISCH 75	HBC	2.18 $K^- p \rightarrow \Lambda\pi^+\pi^-\gamma$
0.07 ± 0.08	152	RITTENBERG 65	HBC	2.1–2.7 $K^- p$

 $\eta'(958)$ REFERENCES

WICHT 08	PL B662 323	J. Wicht et al.	(BELLE Collab.)
DOROFEEV 07	PL B651 22	V. Dorofeev et al.	(VES Collab.)
MORI 07A	JPSJ 76 074102	T. Mori et al.	(BELLE Collab.)
ABLIKIM 06E	PR D73 052008	M. Ablikim et al.	(BES Collab.)
ABLIKIM 06Q	PRL 97 202002	M. Ablikim et al.	(BES Collab.)
AMELIN 05A	PAN 68 372	D.V. Amelin et al.	(VES Collab.)
Translated from YAF 68 401.			
AMSLER 04B	EPJ C33 23	C. Amisler et al.	(Crystal Barrel Collab.)
BAI 04J	PL B594 47	J.Z. Bai et al.	(BES Collab.)
BRIERE 00	PRL 84 26	R. Briere et al.	(CLEO Collab.)
ACCIARRI 98Q	PL B418 399	M. Acciarri et al.	(L3 Collab.)
BARBERIS 98C	PL B440 225	D. Barberis et al.	(WA 102 Collab.)
WURZINGER 96	PL B374 283	R. Wurzinger et al.	(BONN, ORSAY, SACL+)
PDG 94	PR D50 1173	L. Montanet et al.	(CERN, LBL, BOST+)
AMSLER 93	ZPHY C58 175	C. Amisler et al.	(Crystal Barrel Collab.)
BELADIDZE 92C	SJNP 55 1535	G.M. Beladidze, S.I. Bityukov, G.V. Borisov	(SERP+)
Translated from YAF 55 2748.			
KARCH 92	ZPHY C54 33	K. Karch et al.	(Crystal Ball Collab.)
ARMSTRONG 91B	ZPHY C52 389	T.A. Armstrong et al.	(ATHU, BARI, BIRU+)
BEHREND 91	ZPHY C49 401	H.J. Behrend et al.	(CLEO Collab.)
AUGUSTIN 90	PR D42 10	J.E. Augustin et al.	(DM2 Collab.)
BARU 90	ZPHY C48 581	S.E. Baru et al.	(MD-1 Collab.)
BUTLER 90	PR D42 1368	F. Butler et al.	(Mark II Collab.)
KARCH 90	PL B249 353	K. Karch et al.	(Crystal Ball Collab.)
ROE 90	PR D41 17	N.A. Roe et al.	(ASP Collab.)
AIHARA 88C	PR D38 1	H. Aihara et al.	(TPC-2 γ Collab.)
VOROBYEV 88	SJNP 48 273	P.V. Vorobiev et al.	(NOVO)
Translated from YAF 48 436.			

See key on page 373

Meson Particle Listings

 $\eta'(958)$, $f_0(980)$

WILLIAMS	88	PR D38 1365	D.A. Williams <i>et al.</i>	(Crystal Ball Collab.)	975 ± 4 ± 6	17	AKHMETSHIN	99c	CMD2	$e^+e^- \rightarrow \pi^+\pi^-\gamma$,	
AIHARA	87	PR D35 2650	H. Aihara <i>et al.</i>	(TPC-C2γ Collab.) JP			BARBERIS	99	OMEG	$450 \rho\rho \rightarrow \pi^0\pi^0\gamma$	
ALBRECHT	87B	PL B199 457	H. Albrecht <i>et al.</i>	(ARGUS Collab.)	985 ± 10		BARBERIS	99B	OMEG	$450 \rho\rho \rightarrow \rho_S \rho_f K^+K^-$	
ALDE	87B	ZPHY C36 603	D.M. Alde <i>et al.</i>	(LANL, BELG, SERP, LAPP)			BARBERIS	99C	OMEG	$450 \rho\rho \rightarrow \rho_S \rho_f \pi^+\pi^-$	
ANTREASIAN	87	PR D36 2633	D. Antreasian <i>et al.</i>	(Crystal Ball Collab.)			BARBERIS	99D	OMEG	$450 \rho\rho \rightarrow K^+K^-\pi^+\pi^-$	
GIDAL	87	PRL 59 2012	G. Gidal <i>et al.</i>	(LBL, SLAC, HARV)	982 ± 3		BELLAZZINI	99	GAM4	$450 \rho\rho \rightarrow \rho\rho\pi^0\pi^0$	
ALDE	86	PL B177 115	M. Alde <i>et al.</i>	(SERP, BELG, LANL, LAPP)	982 ± 3		19	KAMINSKI	99	RVUE	$\pi\pi \rightarrow \pi\pi, K\bar{K}, \sigma\sigma$
BARTEL	85E	PL 160B 421	W. Bartel <i>et al.</i>	(JADE Collab.)	987 ± 6 ± 6		19	OLLER	99	RVUE	$\pi\pi \rightarrow \pi\pi, K\bar{K}$
ALTHOFF	84E	PL 147B 487	M. Althoff <i>et al.</i>	(TASSO Collab.)			19	OLLER	99B	RVUE	$\pi\pi \rightarrow \pi\pi, K\bar{K}$
BERGER	84B	PL 142B 125	C. Berger	(PLUTO Collab.)	989 ± 15		19	OLLER	99C	RVUE	$\pi\pi \rightarrow \pi\pi, K\bar{K}, \eta\eta$
BINON	84	PL 140B 264	F.G. Binon <i>et al.</i>	(SERP, BELG, LAPP+)	991 ± 3		20	ACKERSTAFF	98Q	OPAL	$Z \rightarrow f_0 X$
BEHREND	83B	PL 125B 518 (erratum)	H.J. Behrend <i>et al.</i>	(CELLO Collab.)	~ 980		ALDE	98	GAM4		
Also		PL 114B 378	H.J. Behrend <i>et al.</i>	(CELLO Collab.)	~ 993.5		19	ANISOVICH	98B	RVUE	Compilation
JENNI	83	PR D27 1031	P. Jenni <i>et al.</i>	(SLAC, LBL)	~ 987		21	LOCHER	98	RVUE	$\pi\pi \rightarrow \pi\pi, K\bar{K}$
BARTEL	82B	PL 113B 190	W. Bartel <i>et al.</i>	(JADE Collab.)	957 ± 6		20	ALDE	97	GAM2	$450 \rho\rho \rightarrow \rho\rho\pi^0\pi^0$
DZHELJADIN	81	PL 105B 239	R.I. Dzhelezhadine <i>et al.</i>	(SERP)	1015 ± 15		22	BERTIN	97C	OBLX	$0.0 \bar{p}p \rightarrow \pi^+\pi^-\pi^0$
STANTON	80	PL B92 353	N.R. Stanton <i>et al.</i>	(OSU, CARL, MCGI+)	955 ± 10		23	ISHIDA	96	RVUE	$\pi\pi \rightarrow \pi\pi, K\bar{K}$
VIKTOROV	80	SJNP 32 520	V.A. Viktorov <i>et al.</i>	(SERP)	994 ± 9		23	TORNQVIST	96	RVUE	$\pi\pi \rightarrow \pi\pi, K\bar{K}, K\pi$
Translated from YAF 32	1005				993.2 ± 6.5 ± 6.9		24	ALDE	95B	GAM2	$38 \pi^-p \rightarrow \pi^0\pi^0 n$
APEL	79	PL 83B 131	W.D. Apel, K.H. Augenstein, E. Bertolucci	(KARLK+)	1006		25	ALDE	95B	GAM2	$38 \pi^-p \rightarrow \pi^0\pi^0 n$
BINNIE	79	PL 83B 141	D.M. Binnie <i>et al.</i>	(LOIC)	997 ± 5	3k	25	AMSLER	95B	CBAR	$0.0 \bar{p}p \rightarrow 3\pi^0$
ZANFINO	77	PRL 38 930	C. Zanfino <i>et al.</i>	(CARL, MCGI, OHIO+)	960 ± 10	10k	26	AMSLER	95D	CBAR	$0.0 \bar{p}p \rightarrow \pi^0\pi^0\eta, \pi^0\pi^0\eta$
GRIGORIAN	75	NP B91 232	A. Grigorian <i>et al.</i>	(+)	994 ± 5		27	ANISOVICH	95	RVUE	$\pi\pi \rightarrow \pi\pi, K\bar{K}$
KALBFLEISCH	75	PR D11 987	G.R. Kalbfleisch, R.C. Strand, J.W. Chapman	(BNL+)	960 ± 10		28	BUGG	94	RVUE	$\bar{p}p \rightarrow \eta 2\pi^0$
DUANE	74	PRL 32 425	A. Duane <i>et al.</i>	(LOIC, SHMP)	994 ± 5		29	KAMINSKI	94	RVUE	$\pi\pi \rightarrow \pi\pi, K\bar{K}$
KALBFLEISCH	74	PR D10 916	G.R. Kalbfleisch	(BNL)	~ 996		30	ZOU	94B	RVUE	
DANBURG	73	PR D8 3744	J.S. Danburg <i>et al.</i>	(BRAN, UMD, SYRA+)	987 ± 6		31	MORGAN	93	RVUE	$\pi\pi(K\bar{K}) \rightarrow \pi\pi(K\bar{K}), J/\psi \rightarrow \phi\pi\pi(K\bar{K}), D_s \rightarrow \pi(K\pi)$
JACOBS	73	PR D8 18	S.M. Jacobs <i>et al.</i>	(KARLK, KARL, PISA)	1015 ± 15		20	AGUILAR...	91	EHS	$400 \rho\rho$
APEL	72	PL 40B 680	W.D. Apel <i>et al.</i>	(CERN)	979 ± 4		32	ARMSTRONG	91	OMEG	$300 \rho\rho \rightarrow \rho\rho\pi\pi, \rho\rho K\bar{K}$
DALPIAZ	72	PL 42B 377	P.F. Dalpiaz <i>et al.</i>	(CERN)	956 ± 12		BREAKSTONE	90	SFM	$\rho\rho \rightarrow \rho\rho\pi^+\pi^-$	
BASILE	71	NC 3A 371	M. Basile <i>et al.</i>	(CERN, BGNA, STRB)	959.4 ± 6.5		20	AUGUSTIN	89	DM2	$J/\psi \rightarrow \omega\pi^+\pi^-$
HARVEY	71	PRL 27 885	E.H. Harvey <i>et al.</i>	(MINN, MICH)	978 ± 9		20	ABACHI	86B	HRS	$e^+e^- \rightarrow \pi^+\pi^-\pi^0 X$
BENSINGER	70	PL 33B 505	J.R. Bensingier <i>et al.</i>	(WISC)	985.0 ± 9.0		ETKIN	82B	MPS	$23 \pi^-p \rightarrow n 2K_S^0$	
RITTENBERG	69	Thesis UCRL 18863	A. Rittenberg	(LRL) I	974 ± 4		32	GIDAL	81	MRK2	$J/\psi \rightarrow \pi^+\pi^- X$
DAVIS	68	PL 27B 532	R. Davis <i>et al.</i>	(NWES, ANL)	975		33	ACHASOV	80	RVUE	
LONDON	66	PR 143 1034	G.W. London <i>et al.</i>	(BNL, SYRA)	986 ± 10		32	AGUILAR...	78	HBC	$0.7 \bar{p}p \rightarrow K_S^0 K_S^0$
BADIER	65B	PL 17 337	J. Badier <i>et al.</i>	(EPOL, SACL, AMST)	969 ± 5		32	LEEPER	77	ASPK	$2-2.4 \pi^-p \rightarrow \pi^+\pi^-\pi^0 n, K^+K^-\pi^- n$
RITTENBERG	65	PRL 15 556	A. Rittenberg, G.R. Kalbfleisch	(LRL, BNL)	987 ± 7		32	BINNIE	73	CNTR	$\pi^-p \rightarrow nMM$
DAUBER	64	PRL 13 449	P.M. Dauber <i>et al.</i>	(UCLA) JP	1012 ± 6		34	GRAYER	73	ASPK	$17 \pi^-p \rightarrow \pi^+\pi^-\pi^- n$
					1007 ± 20		34	HYAMS	73	ASPK	$17 \pi^-p \rightarrow \pi^+\pi^-\pi^- n$
					997 ± 6		34	PROTOPOP...	73	HBC	$7 \pi^+p \rightarrow \pi^+\pi^+\pi^-\pi^-$

OTHER RELATED PAPERS

AMBROSINO	07A	PL B648 267	F. Ambrosino <i>et al.</i>	(KLOE Collab.)	971.1 ± 4.0
ESCRIBANO	07	JHEP 0705 006	E. Escribano, J. Nadal		979 ± 4
HUANG	07A	EPJ C50 771	T. Huang, X. Wu		956 ± 12
AUBERT	06M	PR D74 012002	B. Aubert <i>et al.</i>	(BABAR Collab.)	959.4 ± 6.5
BORASOY	06	PL B643 41	B. Borasoy, U.-G. Meissner, R. Nisler		978 ± 9
BENAYOUN	05B	EPJ C31 525	M. Benayoun <i>et al.</i>		985.0 ± 9.0
BENAYOUN	99B	PR D59 114027	M. Benayoun <i>et al.</i>		-39.0
PROKOSHKIN	99	PAN 62 356	Yu.D. Prokoshkin		974 ± 4
Translated from YAF 62	336				975
GRONBERG	98	PR D57 33	J. Gronberg <i>et al.</i>	(CLEO Collab.)	986 ± 10
ABELE	97B	PL B402 195	A. Abele <i>et al.</i>	(Crystal Barrel Collab.)	969 ± 5
GENOVESE	94	ZPHY C61 425	M. Genovese, D.B. Lichtenberg, E. Predazzi	(TORI+)	987 ± 7
BENAYOUN	93	ZPHY C58 31	M. Benayoun <i>et al.</i>	(CDEF, CERN, BARI)	1012 ± 6
KAMAL	92	PL B284 421	A.N. Kamal, Q.P. Xu	(ALBE)	1007 ± 20
BICKERSTAFF	82	ZPHY C16 171	R.P. Bickerstaff, B.H.J. McKellar	(MELB)	997 ± 6
KIENZLE	65	PL 19 438	H. Kienzle <i>et al.</i>	(CERN)	
TRILLING	65	PL 19 427	G.H. Trilling <i>et al.</i>	(LRL)	
GOLDBERG	64	PRL 12 546	M. Goldberg <i>et al.</i>	(SYRA, BNL)	
GOLDBERG	64B	PRL 13 249	M. Goldberg <i>et al.</i>	(SYRA, BNL)	
KALBFLEISCH	64	PRL 12 527	G.R. Kalbfleisch <i>et al.</i>	(LRL) JP	
KALBFLEISCH	64B	PRL 13 349	G.R. Kalbfleisch, O.J. Dahl, A. Rittenberg	(LRL) JP	

 $f_0(980)$

$$I^G(J^{PC}) = 0^+(0^{++})$$

See also the minireview on scalar mesons under $f_0(600)$. (See the index for the page number.) $f_0(980)$ MASS

VALUE (MeV)	EVTS	DOCUMENT ID	TECN	COMMENT
980 ± 10	OUR ESTIMATE			
• • •	We do not use the following data for averages, fits, limits, etc. • • •			
976.8 ± 0.3 ^{+10.1} _{-0.6}	64k	1	AMBROSINO 07 KLOE	1.02 $e^+e^- \rightarrow \pi^0\pi^0\gamma$
984.7 ± 0.4 ^{+2.4} _{-3.7}	64k	2	AMBROSINO 07 KLOE	1.02 $e^+e^- \rightarrow \pi^0\pi^0\gamma$
973 ± 3	262 ± 30	3	AUBERT 07AKBABR	10.6 $e^+e^- \rightarrow \phi\pi^+\pi^-\gamma$
970 ± 7	54 ± 9	3	AUBERT 07AKBABR	10.6 $e^+e^- \rightarrow \phi\pi^0\pi^0\gamma$
953 ± 20	2.6k	4	BONVICINI 07 CLEO	$D^+ \rightarrow \pi^-\pi^+\pi^+$
985.6 ^{+1.2} _{-1.5} ^{+1.1} _{-1.6}		5	MORI 07 BELL	10.6 $e^+e^- \rightarrow e^+e^-\pi^+\pi^-$
983.0 ± 0.6 ^{+4.0} _{-3.0}		6	AMBROSINO 06B KLOE	1.02 $e^+e^- \rightarrow \pi^+\pi^-\gamma$
977.3 ± 0.9 ^{+3.7} _{-4.3}		7	AMBROSINO 06B KLOE	1.02 $e^+e^- \rightarrow \pi^+\pi^-\gamma$
950 ± 9	4286	8	GARMASH 06 BELL	$B^+ \rightarrow K^+\pi^+\pi^-$
965 ± 10			ABLKIM 05 BES2	$J/\psi \rightarrow \phi\pi^+\pi^-, \phi K^+K^-$
1031 ± 8		9	ANISOVICH 03 RVUE	
1037 ± 31			TIKHOMIROV 03 SPEC	$40.0 \pi^-C \rightarrow K_S^0 K_S^0 K_S^0 X$
973 ± 1	2438	10	ALOISIO 02D KLOE	$e^+e^- \rightarrow \pi^0\pi^0\gamma$
977 ± 3 ± 2	848	11	AITALA 01A E791	$D_S^+ \rightarrow \pi^-\pi^+\pi^+$
969.8 ± 4.5	419	12	ACHASOV 00H SND	$e^+e^- \rightarrow \pi^0\pi^0\gamma$
985 ⁺¹⁶ ₋₁₂	419	13,14	ACHASOV 00H SND	$e^+e^- \rightarrow \pi^0\pi^0\gamma$
976 ± 5 ± 6		15	AKHMETSHIN 99B CMD2	$e^+e^- \rightarrow \pi^+\pi^-\gamma$
977 ± 3 ± 6	268	15	AKHMETSHIN 99C CMD2	$e^+e^- \rightarrow \pi^0\pi^0\gamma$
975 ± 4 ± 6		16	AKHMETSHIN 99C CMD2	$e^+e^- \rightarrow \pi^0\pi^0\gamma$

- In the kaon-loop fit.
- In the no-structure fit.
- Systematic errors not estimated.
- FLATTE 76 parameterization. $g_{f_0\pi\pi} = 329 \pm 96$ MeV/c² assuming $g_{f_0 K\bar{K}}/g_{f_0\pi\pi} = 2$.
- Breit-Wigner mass. Using finite width corrections according to FLATTE 76 and ACHASOV 05, and the ratio $g_{f_0 K\bar{K}}^2/g_{f_0\pi\pi}^2$ from ABLKIM 05.
- In the kaon-loop fit following formalism of ACHASOV 89.
- In the no-structure fit assuming a direct coupling of ϕ to $f_0\gamma$.
- FLATTE 76 parameterization. Supersedes GARMASH 05.
- K-matrix pole from combined analysis of $\pi^-p \rightarrow \pi^0\pi^0 n$, $\pi^-p \rightarrow K\bar{K}n$, $\pi^+\pi^- \rightarrow \pi^+\pi^-, \bar{p}p \rightarrow \pi^0\pi^0\pi^0, \pi^0\eta\eta, \pi^0\pi^0\eta, \pi^+\pi^-\pi^0, K^+K^-\pi^0, K_S^0 K_S^0\pi^0, K^+K_S^0\pi^-$ at rest, $\bar{p}n \rightarrow \pi^-\pi^+\pi^+, K_S^0 K^-\pi^0, K_S^0 K_S^0\pi^-$ at rest.
- From the negative interference with the $f_0(600)$ meson of AITALA 01B using the ACHASOV 89 parameterization for the $f_0(980)$, a Breit-Wigner for the $f_0(600)$, and ACHASOV 01F for the $\rho\pi$ contribution.
- Coupled-channel Breit-Wigner, couplings $g_\pi = 0.09 \pm 0.01 \pm 0.01$, $g_K = 0.02 \pm 0.04 \pm 0.03$.
- Supersedes ACHASOV 98I. Using the model of ACHASOV 89.
- Supersedes ACHASOV 98I.
- In the "narrow resonance" approximation.
- Assuming $\Gamma(f_0) = 40$ MeV.
- From a narrow pole fit taking into account $f_0(980)$ and $f_0(1200)$ intermediate mechanisms.
- From the combined fit of the photon spectra in the reactions $e^+e^- \rightarrow \pi^+\pi^-\gamma$, $\pi^0\pi^0\gamma$.
- Supersedes BARBERIS 99 and BARBERIS 99B
- T-matrix pole.
- From invariant mass fit.
- On sheet II in a 2 pole solution. The other pole is found on sheet III at (1039–93i) MeV.
- On sheet II in a 2 pole solution. The other pole is found on sheet III at (963–29i) MeV.
- Reanalysis of data from HYAMS 73, GRAYER 74, SRINIVASAN 75, and ROSSELET 77 using the interfering amplitude method.
- At high $|t|$.
- At low $|t|$.
- On sheet II in a 4-pole solution, the other poles are found on sheet III at (953–55i) MeV and on sheet IV at (938–35i) MeV.

Meson Particle Listings

$f_0(980)$

- 27 Combined fit of ALDE 95B, ANISOVICH 94, AMSLER 94D.
- 28 On sheet II in a 2 pole solution. The other pole is found on sheet III at (996–103i) MeV.
- 29 From sheet II pole position.
- 30 On sheet II in a 2 pole solution. The other pole is found on sheet III at (797–185i) MeV and can be interpreted as a shadow pole.
- 31 On sheet II in a 2 pole solution. The other pole is found on sheet III at (978–28i) MeV.
- 32 From coupled channel analysis.
- 33 Coupled channel analysis with finite width corrections.
- 34 Included in AGUILAR-BENITEZ 78 fit.

$f_0(980)$ WIDTH

Width determination very model dependent. Peak width in $\pi\pi$ is about 50 MeV, but decay width can be much larger.

VALUE (MeV)	EVTs	DOCUMENT ID	TECN	COMMENT
40 to 100 OUR ESTIMATE				
• • • We do not use the following data for averages, fits, limits, etc. • • •				
65 ± 13	262 ± 30	35 AUBERT	07AK BABR	10.6 $e^+e^- \rightarrow \phi\pi^+\pi^-\gamma$
81 ± 21	54 ± 9	35 AUBERT	07AK BABR	10.6 $e^+e^- \rightarrow \phi\pi^0\pi^0\gamma$
51.3 ^{+20.8+13.2} _{-17.7-3.8}		36 MORI	07 BELL	10.6 $e^+e^- \rightarrow e^+e^-\pi^+\pi^-$
61 ± 9 ⁺¹⁴ ₋₈	2584	37 GARMASH	05 BELL	$B^+ \rightarrow K^+\pi^+\pi^-$
64 ± 16		38 ANISOVICH	03 RVUE	
121 ± 23		TIKHOMIROV	03 SPEC	40.0 $\pi^-C \rightarrow K_S^0 K_S^0 K_L^0 X$
~ 70		39 BRAMON	02 RVUE	1.02 $e^+e^- \rightarrow \pi^0\pi^0\gamma$
44 ± 2 ± 2	848	40 AITALA	01A E791	$D^+ \rightarrow \pi^-\pi^+\pi^+$
201 ± 28	419	41 ACHASOV	00H SND	$e^+e^- \rightarrow \pi^0\pi^0\gamma$
122 ± 13	419, 42, 43	ACHASOV	00H SND	$e^+e^- \rightarrow \pi^0\pi^0\gamma$
56 ± 20		44 AKHMETSHIN	99C CMD2	$e^+e^- \rightarrow \pi^0\pi^0\gamma$
65 ± 20		BARBERIS	99 OMEG	450 $pp \rightarrow p_S p_f K^+ K^-$
80 ± 10		BARBERIS	99B OMEG	450 $pp \rightarrow p_S p_f \pi^+ \pi^-$
80 ± 10		BARBERIS	99C OMEG	450 $pp \rightarrow p_S p_f \pi^0 \pi^0$
48 ± 12 ± 8		45 BARBERIS	99D OMEG	450 $pp \rightarrow K^+ K^-, \pi^+ \pi^-$
65 ± 25		BELLAZZINI	99 GAM4	450 $pp \rightarrow pp\pi^0\pi^0$
71 ± 14		46 KAMINSKI	99 RVUE	$\pi\pi \rightarrow \pi\pi, K\bar{K}, \sigma\sigma$
~ 28		46 OLLER	99 RVUE	$\pi\pi \rightarrow \pi\pi, K\bar{K}$
~ 25		OLLER	99B RVUE	$\pi\pi \rightarrow \pi\pi, K\bar{K}$
~ 14		46 OLLER	99C RVUE	$\pi\pi \rightarrow \pi\pi, K\bar{K}, \eta\eta$
70 ± 20		ALDE	98 GAM4	
86 ± 16		46 ANISOVICH	98B RVUE	Compilation
54		47 LOCHER	98 RVUE	$\pi\pi \rightarrow \pi\pi, K\bar{K}$
69 ± 15		48 ALDE	97 GAM2	450 $pp \rightarrow pp\pi^0\pi^0$
38 ± 20		49 BERTIN	97C OBLX	0.0 $\bar{p}p \rightarrow \pi^+\pi^-\pi^0$
~ 100		50 SHIDA	96 RVUE	$\pi\pi \rightarrow \pi\pi, K\bar{K}$
34		TORNQVIST	96 RVUE	$\pi\pi \rightarrow \pi\pi, K\bar{K}, K\pi,$ $\eta\pi$
48 ± 10	3k	51 ALDE	95B GAM2	38 $\pi^-p \rightarrow \pi^0\pi^0n$
95 ± 20	10k	52 ALDE	95B GAM2	38 $\pi^-p \rightarrow \pi^0\pi^0n$
26 ± 10		AMSLER	95B CBAR	0.0 $\bar{p}p \rightarrow 3\pi^0$
~ 112		53 AMSLER	95D CBAR	0.0 $\bar{p}p \rightarrow \pi^0\pi^0\pi^0,$ $\pi^0\eta\eta, \pi^0\pi^0\eta$
80 ± 12		54 ANISOVICH	95 RVUE	
30		JANSSEN	95 RVUE	$\pi\pi \rightarrow \pi\pi, K\bar{K}$
74		55 BUGG	94 RVUE	$\bar{p}p \rightarrow \eta 2\pi^0$
29 ± 2		56 KAMINSKI	94 RVUE	$\pi\pi \rightarrow \pi\pi, K\bar{K}$
46		57 ZOU	94B RVUE	
48 ± 12		58 MORGAN	93 RVUE	$\pi\pi(K\bar{K}) \rightarrow \pi\pi(K\bar{K}), J/\psi \rightarrow \phi\pi\pi(K\bar{K}), D_S \rightarrow \pi(\pi\pi)$
37.4 ± 10.6		48 AGUILAR-...	91 EHS	400 pp
72 ± 8		59 ARMSTRONG	91 OMEG	300 $pp \rightarrow pp\pi\pi,$ $ppK\bar{K}$
110 ± 30		BREAKSTONE	90 SFM	$pp \rightarrow pp\pi^+\pi^-$
29 ± 13		48 ABACHI	86B HRS	$e^+e^- \rightarrow \pi^+\pi^-X$
120 ± 281 ± 20		ETKIN	82B MPS	23 $\pi^-p \rightarrow n 2K_S^0$
28 ± 10		59 GIDAL	81 MRK2	$J/\psi \rightarrow \pi^+\pi^-X$
70 to 300		60 ACHASOV	80 RVUE	
100 ± 80		61 AGUILAR-...	78 HBC	0.7 $\bar{p}p \rightarrow K_S^0 K_S^0$
30 ± 8		59 LEEPER	77 ASPK	2–2.4 $\pi^-p \rightarrow \pi^+\pi^-n, K^+K^-n$
48 ± 14		59 BINNIE	73 CNTR	$\pi^-p \rightarrow nMM$
32 ± 10		62 GRAYER	73 ASPK	17 $\pi^-p \rightarrow \pi^+\pi^-n$
30 ± 10		62 HYAMS	73 ASPK	17 $\pi^-p \rightarrow \pi^+\pi^-n$
54 ± 16		62 PROTOPOP...	73 HBC	7 $\pi^+p \rightarrow \pi^+p\pi^+\pi^-$

- 35 Systematic errors not estimated.
- 36 Breit-Wigner $\pi\pi$ width. Using finite width corrections according to FLATTE 76 and ACHASOV 05, and the ratio $g_{f_0}^2 K K / g_{f_0}^2 \pi\pi$ from ABLIKIM 05.
- 37 Breit-Wigner, solution 1, PWA ambiguous.
- 38 K-matrix pole from combined analysis of $\pi^-p \rightarrow \pi^0\pi^0n, \pi^-p \rightarrow K\bar{K}n, \pi^+\pi^- \rightarrow \pi^+\pi^-, \bar{p}p \rightarrow \pi^0\pi^0\pi^0, \pi^0\eta\eta, \pi^0\pi^0\eta, \pi^+\pi^-\pi^0, K^+K^-\pi^0, K_S^0 K_S^0\pi^0, K^+K_S^0\pi^-$ at rest, $\bar{p}n \rightarrow \pi^-\pi^-\pi^+, K_S^0 K^-\pi^0, K_S^0 K_S^0\pi^-$ at rest.
- 39 Using the data of AKHMETSHIN 99c, ACHASOV 00H, and ALOISIO 02D.
- 40 Breit-Wigner width.
- 41 Supersedes ACHASOV 98i. Using the model of ACHASOV 89.
- 42 Supersedes ACHASOV 98i.
- 43 In the “narrow resonance” approximation.
- 44 From the combined fit of the photon spectra in the reactions $e^+e^- \rightarrow \pi^+\pi^-\gamma, \pi^0\pi^0\gamma$.
- 45 Supersedes BARBERIS 99 and BARBERIS 99B
- 46 T-matrix pole.
- 47 On sheet II in a 2 pole solution. The other pole is found on sheet III at (1039–93i) MeV.
- 48 From invariant mass fit.
- 49 On sheet II in a 2 pole solution. The other pole is found on sheet III at (963–29i) MeV.
- 50 Reanalysis of data from HYAMS 73, GRAYER 74, SRINIVASAN 75, and ROSSELET 77 using the interfering amplitude method.
- 51 At high $|t|$.
- 52 At low $|t|$.
- 53 On sheet II in a 4-pole solution, the other poles are found on sheet III at (953–55i) MeV and on sheet IV at (938–35i) MeV.
- 54 Combined fit of ALDE 95B, ANISOVICH 94,
- 55 On sheet II in a 2 pole solution. The other pole is found on sheet III at (996–103i) MeV.
- 56 From sheet II pole position.
- 57 On sheet II in a 2 pole solution. The other pole is found on sheet III at (797–185i) MeV and can be interpreted as a shadow pole.
- 58 On sheet II in a 2 pole solution. The other pole is found on sheet III at (978–28i) MeV.
- 59 From coupled channel analysis.
- 60 Coupled channel analysis with finite width corrections.
- 61 From coupled channel fit to the HYAMS 73 and PROTOPODESCU 73 data. With a simultaneous fit to the $\pi\pi$ phase-shifts, inelasticity and to the $K_S^0 K_S^0$ invariant mass.
- 62 Included in AGUILAR-BENITEZ 78 fit.

$f_0(980)$ DECAY MODES

Mode	Fraction (Γ_i/Γ)
$\Gamma_1 \pi\pi$	dominant
$\Gamma_2 K\bar{K}$	seen
$\Gamma_3 \gamma\gamma$	seen
$\Gamma_4 e^+e^-$	

$f_0(980)$ PARTIAL WIDTHS

$\Gamma(\gamma\gamma)$	VALUE (keV)	DOCUMENT ID	TECN	COMMENT	Γ_3
0.29 ± 0.07 ± 0.09 OUR AVERAGE					
	0.205 ^{+0.095+0.147} _{-0.083-0.117}	63 MORI	07 BELL	10.6 $e^+e^- \rightarrow e^+e^-\pi^+\pi^-$	
	0.28 ^{+0.09} _{-0.13}	64 BOGLIONE	99 RVUE	$\gamma\gamma \rightarrow \pi^+\pi^-, \pi^0\pi^0$	
	0.42 ± 0.06 ± 0.18	65 OEST	90 JADE	$e^+e^- \rightarrow e^+e^-\pi^0\pi^0$	
• • • We do not use the following data for averages, fits, limits, etc. • • •					
	0.29 ± 0.07 ± 0.12	66, 67 BOYER	90 MRK2	$e^+e^- \rightarrow e^+e^-\pi^+\pi^-$	
	0.31 ± 0.14 ± 0.09	66, 67 MARSISKE	90 CBAL	$e^+e^- \rightarrow e^+e^-\pi^0\pi^0$	
	0.63 ± 0.14	68 MORGAN	90 RVUE	$\gamma\gamma \rightarrow \pi^+\pi^-, \pi^0\pi^0$	
63 Using finite width corrections according to FLATTE 76 and ACHASOV 05, and the ratio $g_{f_0}^2 K K / g_{f_0}^2 \pi\pi$ from ABLIKIM 05.					
64 Supersedes MORGAN 90.					
65 OEST 90 quote systematic errors ^{+0.08} _{-0.18} . We use ±0.18. Observed 60 events.					
66 From analysis allowing arbitrary background unconstrained by unitarity.					
67 Data included in MORGAN 90, BOGLIONE 99 analyses.					
68 From amplitude analysis of BOYER 90 and MARSISKE 90, data corresponds to resonance parameters $m = 989$ MeV, $\Gamma = 61$ MeV.					

$\Gamma(e^+e^-)$

VALUE (eV)	CL%	DOCUMENT ID	TECN	COMMENT	Γ_4
< 8.4	90	VOROBYEV	88 ND	$e^+e^- \rightarrow \pi^0\pi^0$	

See key on page 373

Meson Particle Listings
 $f_0(980)$, $a_0(980)$ $f_0(980)$ BRANCHING RATIOS

$\Gamma(\pi\pi)/[\Gamma(\pi\pi) + \Gamma(K\bar{K})]$	VALUE	EVTS	DOCUMENT ID	TECN	COMMENT	$\Gamma_1/(\Gamma_1 + \Gamma_2)$
0.52 ± 0.12	9.9k	69	AUBERT	06o	BABR	$B^\pm \rightarrow K^\pm \pi^\pm \pi^\mp$
$0.75^{+0.11}_{-0.13}$		70	ABLIKIM	05q	BES2	$\chi_{c0} \rightarrow 2\pi^+ 2\pi^-$
0.84 ± 0.02		71	ANISOVICH	02d	SPEC	Combined fit
~ 0.68			OLLER	99b	RVUE	$\pi\pi \rightarrow \pi\pi, K\bar{K}$
0.67 ± 0.09		72	LOVERRE	80	HBC	$4\pi^- p \rightarrow n2K_0^0$
$0.81^{+0.09}_{-0.04}$		72	CASON	78	STRC	$7\pi^- p \rightarrow n2K_0^0$
0.78 ± 0.03		72	WETZEL	76	OSPK	$8.9\pi^- p \rightarrow n2K_0^0$

⁶⁹ Recalculated by us using $\Gamma(K^+ K^-) / \Gamma(\pi^+ \pi^-) = 0.69 \pm 0.32$ from AUBERT 06o and isospin relations.

⁷⁰ Using data from ABLIKIM 04g.

⁷¹ From a combined K-matrix analysis of Crystal Barrel ($0. p\bar{p} \rightarrow \pi^0 \pi^0 \pi^0, \pi^0 \eta, \pi^0 \eta \eta$), GAMS ($\pi p \rightarrow \pi^0 \pi^0 n, \eta \eta n, \eta \eta' n$), and BNL ($\pi p \rightarrow K\bar{K} n$) data.

⁷² Measure $\pi\pi$ elasticity assuming two resonances coupled to the $\pi\pi$ and $K\bar{K}$ channels only.

 $f_0(980)$ REFERENCES

AMBROSINO	07	EPJ C49 473	F. Ambrosino et al.	(KLOE Collab.)
AUBERT	07AK	PR D76 012008	B. Aubert et al.	(BABAR Collab.)
BOVICINI	07	PR D76 012001	G. Bonvicini et al.	(CLEO Collab.)
MORI	07	PR D75 051101R	T. Mori et al.	(BELLE Collab.)
AMBROSINO	06B	PL B634 148	F. Ambrosino et al.	(KLOE Collab.)
AUBERT	06O	PR D74 032003	B. Aubert et al.	(BABAR Collab.)
GARMASH	06	PRL 96 251803	A. Garmash et al.	(BELLE Collab.)
ABLIKIM	05	PL B607 243	M. Ablikim et al.	(BES Collab.)
ABLIKIM	05Q	PR D72 092002	M. Ablikim et al.	(BES Collab.)
ACHASOV	05	PR D72 013006	N.N. Achasov, G.N. Shestakov	(BELLE Collab.)
GARMASH	05	PR D71 092003	A. Garmash et al.	(BES Collab.)
ABLIKIM	04G	PR D70 092002	M. Ablikim et al.	(BES Collab.)
ANISOVICH	03	EPJ A16 229	V.V. Anisovich et al.	
TIKHOMIROV	03	PAN 66 828	G.D. Tikhomirov et al.	
		Translated from YAF 66 860.		
ALOISIO	02D	PL B537 21	A. Aloisio et al.	(KLOE Collab.)
ANISOVICH	02D	PAN 65 1545	V.V. Anisovich et al.	
		Translated from YAF 65 1583.		
BRAMON	02	EPJ C26 253	A. Bramon et al.	
ACHASOV	01F	PR D63 094007	N.N. Achasov, V.V. Gubin (Novosibirsk SND Collab.)	
AITALA	01A	PRL 86 765	E.M. Aitala et al. (FNAL E791 Collab.)	
AITALA	01B	PRL 86 770	E.M. Aitala et al. (FNAL E791 Collab.)	
ACHASOV	00H	PL B485 349	N.N. Achasov et al. (Novosibirsk SND Collab.)	
AKHMETSHIN	99B	PL B462 371	R.R. Akhmetshin et al. (Novosibirsk CMD-2 Collab.)	
AKHMETSHIN	99C	PL B462 380	R.R. Akhmetshin et al. (Novosibirsk CMD-2 Collab.)	
BARBERIS	99	PL B453 305	D. Barberis et al. (Omega Expt.)	
BARBERIS	99B	PL B453 316	D. Barberis et al. (Omega Expt.)	
BARBERIS	99C	PL B453 325	D. Barberis et al. (Omega Expt.)	
BARBERIS	99D	PL B462 462	D. Barberis et al. (Omega Expt.)	
BELLAZZINI	99	PL B467 296	R. Bellazzini et al.	
BOGLIONE	99	EPJ C9 11	M. Boglione, M.R. Pennington	
KAMINSKI	99	EPJ C9 141	R. Kaminski, L. Lesniak, B. Loiseau (CRAC, PARIN)	
OLLER	99	PR D60 099906 (erratum)	J.A. Oller et al.	
OLLER	99B	NP A652 407 (erratum)	J.A. Oller, E. Oset	
OLLER	99C	PR D60 074023	J.A. Oller, E. Oset	
ACHASOV	98I	PL B440 442	N.N. Achasov et al.	
ACKERSTAFF	98Q	EPJ C4 19	K. Ackerstaff et al.	(OPAL Collab.)
ALDE	98	EPJ A3 361	D. Alde et al.	(GAMMA Collab.)
		PAN 62 405	D. Alde et al.	(GAMS Collab.)
		Translated from YAF 62 446.		
ANISOVICH	98B	SPU 41 419	V.V. Anisovich et al.	
		Translated from UFN 168 481.		
LOCHER	98	EPJ C4 317	M.P. Locher et al.	(PSI)
ALDE	97	PL B397 350	D.M. Alde et al.	(GAMS Collab.)
BERTIN	97C	PL B408 476	A. Bertin et al.	(OBELIX Collab.)
ISHIDA	96	PTP 95 745	S. Ishida et al.	(TOKY, MINA, KEK)
TORNVIST	96	PRL 76 1575	N.A. Tornqvist, M. Roos	(HEL5)
ALDE	95B	ZPHY C66 375	D.M. Alde et al.	(GAMS Collab.)
AMSLER	95B	PL B342 433	C. Amisler et al.	(Crystal Barrel Collab.)
AMSLER	95D	PL B355 425	C. Amisler et al.	(Crystal Barrel Collab.)
ANISOVICH	95	PL B355 363	V.V. Anisovich et al.	(PNPI, SERP)
JANSSEN	95	PR D52 2690	G. Janssen et al.	(STON, ADD, JULI)
AMSLER	94D	PL B333 277	C. Amisler et al.	(Crystal Barrel Collab.)
ANISOVICH	94	PL B323 233	V.V. Anisovich et al.	(Crystal Barrel Collab.)
BUGG	94	PR D50 4412	D.V. Bugg et al.	(LOQM)
KAMINSKI	94	PR D50 3145	R. Kaminski, L. Lesniak, J.P. Maillet (CRAC+)	
ZOU	94B	PR D50 591	B.S. Zou, D.V. Bugg (LOQM)	
MORGAN	93	PR D48 1185	D. Morgan, M.R. Pennington (RAL, DURH)	
AGUILAR...	91	ZPHY C60 405	M. Aguilar-Benitez et al. (LEBC-CHS Collab.)	
ARMSTRONG	91	ZPHY C51 351	T.A. Armstrong et al. (ATHU, BARI, BIRH+)	
BOYER	90	PR D42 1350	J. Boyer et al. (Mark II Collab.)	
BREAKSTONE	90	ZPHY C48 569	A.M. Breakstone et al. (ISU, BGNA, CERN+)	
MARISKE	90	PR D41 3324	H. Mariske et al. (Crystal Ball Collab.)	
MORGAN	90	ZPHY C48 623	D. Morgan, M.R. Pennington (RAL, DURH)	
OEST	90	ZPHY C47 343	T. Oest et al. (JADE, Collab.)	
ACHASOV	89	NP B315 465	N.N. Achasov, V.N. Ivanchenko	
AUGUSTIN	89	NP B320 1	J.E. Augustin, G. Cosme (DM2 Collab.)	
VOROBIEV	88	SJNP 48 273	P.V. Vorobiev et al. (NOVO)	
		Translated from YAF 48 436.		
ABACHI	86B	PRL 57 1990	S. Abachi et al. (PURD, ANL, IND, MICH+)	
ETKIN	82B	PR D25 1786	A. Etkin et al. (BNL, CUNY, TUFTS, VAND)	
GIDAL	81	PL 107B 153	G. Gidal et al. (SLAC, LBL)	
ACHASOV	80	SJNP 32 566	N.N. Achasov, S.A. Devyanin, G.N. Shestakov (NOVM)	
		Translated from YAF 32 1098.		
LOVERRE	80	ZPHY C6 187	P.F. Loverre et al. (CERN, CDEF, MADR+)	
AGUILAR...	78	NP B140 73	M. Aguilar-Benitez et al. (MADR, BOMB+)	
CASON	78	PRL 41 271	N.M. Cason et al. (NDAM, ANL)	
LEEPER	77	PR D16 2054	R.J. Leeper et al. (ISU)	
ROSSELET	77	PR D15 574	L. Rosselet et al. (GEVA, SAFL)	
FLATTE	76	PL 63B 224	S.M. Flatte (CERN)	
WETZEL	76	NP B115 208	W. Wetzel et al. (ETH, CERN, LOIC)	
SRINIVASAN	75	PR D12 681	V. Srinivasan et al. (NDAM, ANL)	
GRAY	74	NP B75 189	G. Gray et al. (CERN, MPIM)	
BINNIE	73	PRL 31 1534	D.M. Binnie et al. (LOIC, SHMP)	
GRAY	73	Tallahassee	G. Gray et al. (CERN, MPIM)	
HYAMS	73	NP B64 134	B.D. Hyams et al. (CERN, MPIM)	
PROTOPOP...	73	PR D7 1279	S.D. Protopopescu et al. (LBL)	

OTHER RELATED PAPERS

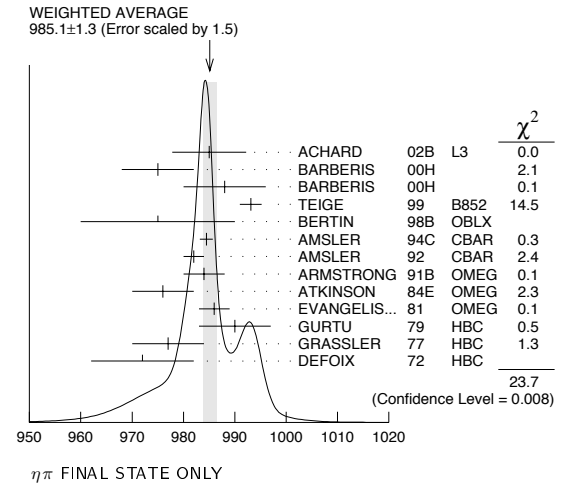
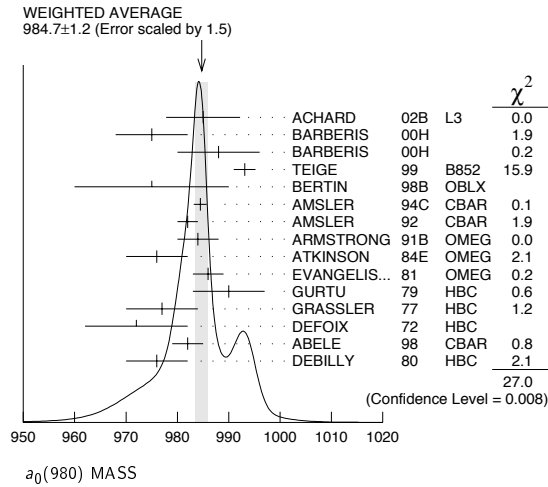
ACHASOV	07C	PR D76 077501	N.N. Achasov, A.V. Kiselev	
CHEN	07E	PR D76 094025	H.-X. Chen, A. Hosaka, S.L. Zhu	
GARMASH	07F	PR D75 012006	A. Garmash et al.	(BELLE Collab.)
GIACOSA	07	PR D75 054007	F. Giacosa	
GUO	07B	PR D76 056004	X.-H. Guo, X.-H. Wu	
HANHART	07	PR D75 074015	C. Hanhart et al.	
HANHART	07B	PR D76 074028	C. Hanhart, B. Kubis, J.R. Pelaez	
LEMMER	07	PL B650 152	R.H. Lemmer	
SANTOPINTO	07	PR C75 045206	E. Santopinto, G. Galata	
TESHIMA	07	PR D76 054002	T. Teshima, I. Kitamura, N. Morisita	
ACHASOV	06A	PR D73 054029	N.N. Achasov, A.V. Kiselev	
BUGG	06A	EPJ C47 45	D.V. Bugg	
		Translated from YAF 69 542.		
CHENG	06	PR D73 014017	H.-Y. Cheng, C.-K. Chua, K.-C. Yang	
FARIBORZ	06	PR D74 054030	A.H. Fariborz	
KALASHNIK...	06	PR C73 045203	Yu. Kalashnikova et al.	
ROSNER	06C	PR D74 076006	J.L. Rosner	
WANG	06B	PR D74 114010	W. Wang et al.	
ANISOVICH	05B	PAN 68 1594	V.V. Anisovich, V.V. Anisovich, V.N. Markov	
		Translated from YAF 68 1614.		
AUBERT.B	05G	PR D72 052002	B. Aubert et al.	(BABAR Collab.)
BARU	05	EPJ A23 523	V.V. Baru, J. Haidenbauer, C. Hanhart	
BRITO	05	PL B608 69	T.V. Brito et al.	
KALASHNIK...	05	EPJ A24 437	Yu.S. Kalashnikova, A.E. Kudryatsev, A.V. Nefediev	
LI	05B	EPJ A25 263	D.-M. Li, K.-W. Wei, H. Yu	
RODRIGUEZ	05	PR D71 074008	S. Rodriguez, M. Napsuciale	
TESHIMA	05	NP A759 151	T. Teshima, I. Kitamura, N. Morisita	
VIJANDE	05	PR D72 034025	J. Vijande, A. Valcaro, F. Fernandez	
WANG	05C	EPJ C42 89	Z.-G. Wang, W.-M. Yang	
ABLIKIM	04A	PL B598 149	M. Ablikim et al.	(BES Collab.)
AUBERT.B	04P	PR D70 092001	B. Aubert et al.	(BABAR Collab.)
BARU	04	PL B586 53	V. Baru et al.	
BEDIAGA	04	PL B579 59	I. Bediaga et al.	
BUGG	04B	PL B598 8	D.V. Bugg	
KREWALD	04	PR D69 016003	S. Krewald, R.H. Lemmer, F.P. Sassen	
LINK	04	PL B585 200	J.M. Link et al.	(FNAL FOCUS Collab.)
PELAEZ	04	PRL 92 102001	J.R. Pelaez	
PELAEZ	04A	MPL A19 2879	J.R. Pelaez et al.	
WANG	04B	EPJ C37 223	Z.-G. Wang et al.	
ANISOVICH	03B	PAN 66 741	V.V. Anisovich, V.A. Nikonov, A.V. Sarantsev	
		Translated from YAF 66 772.		
ANISOVICH	03D	PAN 66 928	V.V. Anisovich, A.V. Sarantsev	
		Translated from YAF 66 960.		
BEDAIGA	03	PR D68 036001	I. Bedaiga, M. Nielsen	
BOGLIONE	03	EPJ C30 503	M. Boglione, M.R. Pennington	
CHEN	03	PR D67 094011	C.-H. Chen	
COLANGELO	03	PL B559 19	P. Colangelo, F. De Fazio	
PALOMAR	03	NP A729 743	J.E. Palomar et al.	
ACHASOV	02C	PL B534 83	N.N. Achasov, A.V. Kiselev	
ANISOVICH	02G	PAN 65 497	A.V. Anisovich et al.	
		Translated from YAF 65 523.		
BLACK	02	PRL 88 181603	D. Black, M. Harada, J. Schechter	
CLOSE	02B	EPJ Direct C4 1	F.E. Close, N. Tornqvist	
KAMINSKI	02	PR D66 034007	R. Kaminski, L. Lesniak, K. Rybicki	
KLEEFELD	02	PR D66 034007	F. Kleefeld et al.	
RUPP	02	PR D65 078501	G. Rupp, E. van Beveren, M.D. Scadron	
SHAKIN	02	PR D65 078502	C.M. Shakin, H. Wang	
TESHIMA	02	JPG 28 1391	T. Teshima, I. Kitamura, N. Morisita	
VOLKOV	02	PAN 65 1657	M.K. Volkov, V.L. Yudinchev	
		Translated from YAF 65 1701.		
ACHASOV	01F	PR D63 094007	N.N. Achasov, V.V. Gubin (Novosibirsk SND Collab.)	
CLOSE	01	PL B515 13	F.E. Close, A. Kirk	
GOKALP	01	PR D64 053017	A. Gokalp, O. Yilmaz	
SUROVITSEV	01	PR D63 054024	Y.S. Surovitshev, D. Krupa, M. Nagy	
MARKUSHIN	00	EPJ B8 389	V.E. Markushin	
WANG	00A	PR D62 017503	Z. Wang	
ABREU	99J	PL B449 364	P. Abreu et al.	(DELPHI Collab.)
ANISOVICH	99D	PL B452 180	A.V. Anisovich et al.	
		NP A651 253	A.V. Anisovich et al.	
ANISOVICH	99H	PL B467 289	A.V. Anisovich, V.V. Anisovich	
BLACK	99	PR D59 074026	D. Black et al.	
DELBORGO	99	PL B446 332	R. Delbourgo, D. Liu, M. Scadron	
MARCO	99	PL B470 20	E. Marco et al.	
MINKOWSKI	99	EPJ C9 283	P. Minkowski, W. Ochs	
ACHASOV	98G	JETPL 67 464	N.N. Achasov et al.	
ACHASOV	98G	SPU 41 1149	N.N. Achasov	
CHLIAPNIK...	98	PL B423 401	P.V. Chliapnikov, V.A. Uvarov	
PROKOSHKIN	97	SPD 42 117	Y.D. Prokoshkin et al.	(SERP)
		Translated from DANS 353 323.		
AU	87	PR D35 1633	K.L. Au, D. Morgan, M.R. Pennington (DURH, RAL)	
AKESSON	86	NP B264 154	T. Akesson et al. (Axial Field Spec. Collab.)	
VANBEVEREN	86	ZPHY C30 615	E. van Beveren et al. (NIJM, BIEL)	
MENNESSIER	83	ZPHY C16 241	G. Mennessier (MOBP)	
BARBER	82	ZPHY C12 1	D.P. Barber et al. (DARE, LANC, SHEP)	
ETKIN	82C	PR D25 2446	A. Etkin et al. (BNL, CUNY, TUFTS, VAND)	
SRINIVASAN	75	PR D12 681	V. Srinivasan et al. (NDAM, ANL)	
BIGI	62	CERN Conf. 247	A. Bigi et al. (CERN)	
BINGHAM	62	CERN Conf. 240	H.H. Bingham et al. (EPOL, CERN)	
ERWIN	62	PRL 9 34	A.R. Erwin et al. (WISC, BNL)	
WANG	61	JETP 13 323	K.-C. Wang et al. (JINR)	
		Translated from ZETF 40 464.		

 $a_0(980)$

$$I^G(J^{PC}) = 1^$$

Meson Particle Listings

$a_0(980)$



$\eta\pi$ FINAL STATE ONLY

VALUE (MeV) EVTS DOCUMENT ID TECN CHG COMMENT
The data in this block is included in the average printed for a previous datablock.

VALUE (MeV)	EVTS	DOCUMENT ID	TECN	CHG	COMMENT
985.1 ± 1.3 OUR AVERAGE					Error includes scale factor of 1.5. See the ideogram below.
985 ± 4 ± 6	318	ACHARD	02B L3		183-209 $e^+e^- \rightarrow e^+e^-\eta\pi^+\pi^-$
975 ± 7		BARBERIS	00H		450 $pp \rightarrow \rho_f\eta\pi^0\rho_s$
988 ± 8		BARBERIS	00H		450 $pp \rightarrow \Delta_f^+\eta\pi^-\rho_s$
993.1 ± 2.1		¹ TEIGE	99 B852		18.3 $\pi^-p \rightarrow \eta\pi^+\pi^-n$
975 ± 15		BERTIN	98B OBLX		0.0 $\bar{p}p \rightarrow K^\pm K_S^0\pi^\mp$
984.45 ± 1.23 ± 0.34		AMSLER	94C CBAR		0.0 $\bar{p}p \rightarrow \omega\eta\pi^0$
982 ± 2		² AMSLER	92 CBAR		0.0 $\bar{p}p \rightarrow \eta\eta\pi^0$
984 ± 4	1040	² ARMSTRONG	91B OMEG ±		300 $pp \rightarrow \rho\rho\eta\pi^+\pi^-$
976 ± 6		ATKINSON	84E OMEG ±		25-55 $\gamma p \rightarrow \eta\pi n$
986 ± 3	500	³ EVANGELIS...	81 OMEG ±		12 $\pi^-p \rightarrow \eta\pi^+\pi^-\pi^0 p$
990 ± 7	145	³ GURTU	79 HBC ±		4.2 $K^-p \rightarrow \Lambda\eta 2\pi$
977 ± 7		GRASSLER	77 HBC		16 $\pi^+p \rightarrow \rho\eta 3\pi$
972 ± 10	150	DEFOIX	72 HBC ±		0.7 $\bar{p}p \rightarrow 7\pi$
••• We do not use the following data for averages, fits, limits, etc. •••					
995 $\begin{smallmatrix} +52 \\ -10 \end{smallmatrix}$	36	⁴ ACHASOV	00F SND		$e^+e^- \rightarrow \eta\pi^0\gamma$
994 $\begin{smallmatrix} +33 \\ -8 \end{smallmatrix}$	36	⁵ ACHASOV	00F SND		$e^+e^- \rightarrow \eta\pi^0\gamma$
~ 1053		⁶ OLLER	99 RVUE		$\eta\pi, K\bar{K}$
~ 1009.2		⁶ OLLER	99B RVUE		$\pi\pi \rightarrow \pi\pi, K\bar{K}$
988 ± 6		⁶ ANISOVICH	98B RVUE		Compilation
987		TORNQVIST	96 RVUE		$\pi\pi \rightarrow \pi\pi, K\bar{K}, K\pi, \eta\pi$
991		JANSSEN	95 RVUE		$\eta\pi \rightarrow \eta\pi, K\bar{K}, K\pi, \eta\pi$
980 ± 11	47	CONFORTO	78 OSPK		4.5 $\pi^-p \rightarrow \rho X^-$
978 ± 16	50	CORDEN	78 OMEG ±		12-15 $\pi^-p \rightarrow n\eta 2\pi$
989 ± 4	70	WELLS	75 HBC		3.1-6 $K^-p \rightarrow \Lambda\eta 2\pi$
970 ± 15	20	BARNES	69c HBC		4-5 $K^-p \rightarrow \Lambda\eta 2\pi$
980 ± 10		CAMPBELL	69 DBC ±		2.7 π^+d
980 ± 10	15	MILLER	69B HBC		4.5 $K^-N \rightarrow \eta\pi\Lambda$
980 ± 10	30	AMMAR	68 HBC ±		5.5 $K^-p \rightarrow \Lambda\eta 2\pi$

¹ Breit-Wigner fit, average between a_0^+ and a_0^0 . The fit favors a slightly heavier a_0^+ .
² From a single Breit-Wigner fit.
³ From $f_1(1285)$ decay.
⁴ Supersedes ACHASOV 98B. Using the model of ACHASOV 89.
⁵ Supersedes ACHASOV 98B. Using the model of JAFFE 77.
⁶ T-matrix pole.

$K\bar{K}$ ONLY

VALUE (MeV) EVTS DOCUMENT ID TECN CHG COMMENT
The data in this block is included in the average printed for a previous datablock.

VALUE (MeV)	EVTS	DOCUMENT ID	TECN	CHG	COMMENT
980.8 ± 2.7 OUR AVERAGE					
982 ± 3		⁷ ABELE	98 CBAR		0.0 $\bar{p}p \rightarrow K_L^0 K^\pm \pi^\mp$
976 ± 6	316	DEBILLY	80 HBC ±		1.2-2 $\bar{p}p \rightarrow f_1(1285)\omega$
••• We do not use the following data for averages, fits, limits, etc. •••					
~ 1053		⁸ OLLER	99c RVUE		$\pi\pi \rightarrow \pi\pi, K\bar{K}$
1016 ± 10	100	⁹ ASTIER	67 HBC ±		0.0 $\bar{p}p$
1003.3 ± 7.0	143	¹⁰ ROSENFELD	65 RVUE ±		
⁷ T-matrix pole on sheet II, the pole on sheet III is at 1006-i49 MeV. ⁸ T-matrix pole. ⁹ ASTIER 67 includes data of BARLOW 67, CONFORTO 67, ARMENTEROS 65. ¹⁰ Plus systematic errors.					

$a_0(980)$ WIDTH

VALUE (MeV)	EVTS	DOCUMENT ID	TECN	CHG	COMMENT
50 to 100 OUR ESTIMATE					Width determination very model dependent. Peak width in $\eta\pi$ is about 60 MeV, but decay width can be much larger.
50 ± 13 ± 4	318	ACHARD	02B L3		183-209 $e^+e^- \rightarrow e^+e^-\eta\pi^+\pi^-$
72 ± 16		BARBERIS	00H		450 $pp \rightarrow \rho_f\eta\pi^0\rho_s$
61 ± 19		BARBERIS	00H		450 $pp \rightarrow \Delta_f^+\eta\pi^-\rho_s$
~ 42		¹¹ OLLER	99 RVUE		$\eta\pi, K\bar{K}$
~ 112		¹¹ OLLER	99B RVUE		$\pi\pi \rightarrow \eta\pi, K\bar{K}$
71 ± 7		TEIGE	99 B852		18.3 $\pi^-p \rightarrow \eta\pi^+\pi^-n$
92 ± 20		¹¹ ANISOVICH	98B RVUE		Compilation
65 ± 10		BERTIN	98B OBLX		0.0 $\bar{p}p \rightarrow K^\pm K_S^0\pi^\mp$
~ 100		TORNQVIST	96 RVUE		$\pi\pi \rightarrow \pi\pi, K\bar{K}, K\pi, \eta\pi$
202		JANSSEN	95 RVUE		$\eta\pi \rightarrow \eta\pi, K\bar{K}, K\pi, \eta\pi$
54.12 ± 0.34 ± 0.12		AMSLER	94C CBAR		0.0 $\bar{p}p \rightarrow \omega\eta\pi^0$
54 ± 10		¹² AMSLER	92 CBAR		0.0 $\bar{p}p \rightarrow \eta\eta\pi^0$
95 ± 14	1040	¹² ARMSTRONG	91B OMEG ±		300 $pp \rightarrow \rho\rho\eta\pi^+\pi^-$
62 ± 15	500	¹³ EVANGELIS...	81 OMEG ±		12 $\pi^-p \rightarrow \eta\pi^+\pi^-\pi^0 p$
60 ± 20	145	¹³ GURTU	79 HBC ±		4.2 $K^-p \rightarrow \Lambda\eta 2\pi$
60 $\begin{smallmatrix} +50 \\ -30 \end{smallmatrix}$	47	CONFORTO	78 OSPK		4.5 $\pi^-p \rightarrow \rho X^-$
86.0 $\begin{smallmatrix} +60.0 \\ -50.0 \end{smallmatrix}$	50	CORDEN	78 OMEG ±		12-15 $\pi^-p \rightarrow n\eta 2\pi$
44 ± 22		GRASSLER	77 HBC		16 $\pi^+p \rightarrow \rho\eta 3\pi$
80 to 300		¹⁴ FLATTE	76 RVUE		4.2 $K^-p \rightarrow \Lambda\eta 2\pi$
16.0 $\begin{smallmatrix} +25.0 \\ -16.0 \end{smallmatrix}$	70	WELLS	75 HBC		3.1-6 $K^-p \rightarrow \Lambda\eta 2\pi$
30 ± 5	150	DEFOIX	72 HBC ±		0.7 $\bar{p}p \rightarrow 7\pi$
40 ± 15		CAMPBELL	69 DBC ±		2.7 π^+d
60 ± 30	15	MILLER	69B HBC		4.5 $K^-N \rightarrow \eta\pi\Lambda$
80 ± 30	30	AMMAR	68 HBC ±		5.5 $K^-p \rightarrow \Lambda\eta 2\pi$

See key on page 373

Meson Particle Listings

 $a_0(980)$ ¹¹T-matrix pole.¹²From a single Breit-Wigner fit.¹³From $f_1(1285)$ decay.¹⁴Using a two-channel resonance parametrization of GAY 76b data. $K\bar{K}$ ONLY

VALUE (MeV)	EVTS	DOCUMENT ID	TECN	CHG	COMMENT
92 ± 8		¹⁵ ABELE	98	CBAR	$0.0 \bar{p}p \rightarrow K_S^0 K^\pm \pi^\mp$
~ 24		¹⁶ OLLER	99c	RVUE	$\pi\pi \rightarrow \pi\pi, K\bar{K}$
~ 25	100	¹⁷ ASTIER	67	HBC \pm	
57 ± 13	143	¹⁸ ROSENFELD	65	RVUE \pm	

• • • We do not use the following data for averages, fits, limits, etc. • • •

¹⁶ OLLER 99c RVUE $\pi\pi \rightarrow \pi\pi, K\bar{K}$ ¹⁷ ASTIER 67 includes data of BARLOW 67, CONFORTO 67, ARMENTEROS 65.¹⁸ Plus systematic errors.¹⁵T-matrix pole on sheet II, the pole on sheet III is at 1006-i49 MeV.¹⁶T-matrix pole.¹⁷ ASTIER 67 includes data of BARLOW 67, CONFORTO 67, ARMENTEROS 65.¹⁸ Plus systematic errors. $a_0(980)$ DECAY MODES

Mode	Fraction (Γ_i/Γ)
Γ_1 $\eta\pi$	dominant
Γ_2 $K\bar{K}$	seen
Γ_3 $\rho\pi$	
Γ_4 $\gamma\gamma$	seen
Γ_5 e^+e^-	

 $a_0(980)$ PARTIAL WIDTHS

$\Gamma(\gamma)$	VALUE (keV)	DOCUMENT ID	TECN	CHG	COMMENT
Γ_4					
• • • We do not use the following data for averages, fits, limits, etc. • • •					
0.30 ± 0.10		¹⁹ AMSLER	98	RVUE	
$0.19 \pm 0.07^{+0.10}_{-0.07}$					

¹⁹Using $\Gamma_{\gamma\gamma}B(a_0(980) \rightarrow \eta\pi) = 0.24 \pm 0.08$ keV. $a_0(980)$ $\Gamma(i)\Gamma(\gamma\gamma)/\Gamma(\text{total})$

$\Gamma(\eta\pi) \times \Gamma(\gamma\gamma)/\Gamma_{\text{total}}$	VALUE (keV)	EVTS	DOCUMENT ID	TECN	COMMENT	$\Gamma_1\Gamma_4/\Gamma$
OUR AVERAGE	0.24 ± 0.09	0.07				
$0.28 \pm 0.04 \pm 0.10$		44	OEST	90	JADE $e^+e^- \rightarrow e^+e^-\pi^0\eta$	
$0.19 \pm 0.07^{+0.10}_{-0.07}$			ANTREASYAN	86	CBAL $e^+e^- \rightarrow e^+e^-\pi^0\eta$	

$\Gamma(\eta\pi) \times \Gamma(e^+e^-)/\Gamma_{\text{total}}$	VALUE (eV)	CL%	DOCUMENT ID	TECN	COMMENT	$\Gamma_1\Gamma_5/\Gamma$
<1.5		90	VOROBYEV	88	ND $e^+e^- \rightarrow \pi^0\eta$	

 $a_0(980)$ BRANCHING RATIOS

$\Gamma(K\bar{K})/\Gamma(\eta\pi)$	VALUE	DOCUMENT ID	TECN	CHG	COMMENT	Γ_2/Γ_1
OUR AVERAGE	0.183 ± 0.024				Error includes scale factor of 1.2.	
0.57 ± 0.16		²⁰ BARGIOTTI	03	OBLX	$\bar{p}p$	
0.23 ± 0.05		²¹ ABELE	98	CBAR	$0.0 \bar{p}p \rightarrow K_S^0 K^\pm \pi^\mp$	
$0.166 \pm 0.01 \pm 0.02$		²² BARBERIS	98c	OMEG	$450 \rho\rho \rightarrow \rho_f f_1(1285) \rho_S$	

• • • We do not use the following data for averages, fits, limits, etc. • • •

 ~ 0.60 OLLER 99b RVUE $\pi\pi \rightarrow \eta\pi, K\bar{K}$ 1.16 ± 0.18 BUGG 94 RVUE $\bar{p}p \rightarrow \eta\eta\pi^0$ 0.7 ± 0.3 ²² CORDEN 78 OMEG $12-15 \pi^-p \rightarrow n\eta 2\pi$ 0.25 ± 0.08 ²² DEFOIX 72 HBC \pm $0.7 \bar{p} \rightarrow 7\pi$

$\Gamma(\rho\pi)/\Gamma(\eta\pi)$	VALUE	CL%	DOCUMENT ID	TECN	CHG	COMMENT	Γ_3/Γ_1
$\rho\pi$ forbidden.							
<0.25		70	AMMAR	70	HBC \pm	$4.1, 5.5 K^-p \rightarrow \Lambda\eta 2\pi$	

• • • We do not use the following data for averages, fits, limits, etc. • • •

 <0.25 70 AMMAR 70 HBC \pm $4.1, 5.5 K^-p \rightarrow \Lambda\eta 2\pi$ ²⁰ Coupled channel analysis of $\pi^+\pi^-\pi^0, K^+K^-\pi^0$, and $K^\pm K_S^0 \pi^\mp$.²¹ Using $\pi^0\pi^0\eta$ from AMSLER 94d.²² From the decay of $f_1(1285)$.²³ BUGG 94 uses AMSLER 94c data. This is a ratio of couplings. $a_0(980)$ REFERENCES

BARGIOTTI	03	EPJ C26 371	M. Bargiotti et al.	(OBELIX Collab.)
ACHARD	02B	PL B526 269	P. Achard et al.	(L3 Collab.)
ACHASOV	00F	PL B479 53	M.N. Achasov et al.	(Novosibirsk SND Collab.)
BARBERIS	00H	PL B488 225	D. Barberis et al.	(WA 102 Collab.)
OLLER	99	PR D60 099906 (erratum)	J.A. Oller et al.	
OLLER	99B	NP A652 407 (erratum)	J.A. Oller, E. Oset	
OLLER	99C	PR D60 074023	J.A. Oller, E. Oset	
TEIGE	99	PR D59 012001	S. Teige et al.	(BNL E852 Collab.)
ABELE	98	PR D57 3860	A. Abele et al.	(Crystal Barrel Collab.)
ACHASOV	98B	PL B438 441	M.N. Achasov et al.	(Novosibirsk SND Collab.)
AMSLER	98	RMP 70 1293	C. Amisler	
ANISOVICH	98B	SPU 41 419	V.V. Anisovich et al.	
BARBERIS	98C	PL B440 225	D. Barberis et al.	(WA 102 Collab.)
BERTIN	98B	PL B434 180	A. Bertin et al.	(OBELIX Collab.)
TORNQVIST	96	PRL 76 1575	N.A. Tornqvist, M. Roos	(HELS)
JANSSEN	95	PR D52 2690	G. Janssen et al.	(STON, ADDL, JULI)
AMSLER	94C	PL B327 425	C. Amisler et al.	(Crystal Barrel Collab.)
AMSLER	94D	PL B333 277	C. Amisler et al.	(Crystal Barrel Collab.)
BUGG	94	PR D50 4412	D.V. Bugg et al.	(LOQM)
AMSLER	92	PL B291 347	C. Amisler et al.	(Crystal Barrel Collab.)
ARMSTRONG	91B	ZPHY C52 389	T.A. Armstrong et al.	(ATHU, BARI, BIRH+)
OEST	90	ZPHY C47 343	T. Oest et al.	(JADE Collab.)
ACHASOV	89	NP B315 465	M.N. Achasov, V.N. Ivanchenko	
VOROBYEV	88	SJNP 48 273	P.V. Vorobyev et al.	(NOVO)
ANTREASYAN	86	PR D33 1847	D. Antreasyan et al.	(Crystal Ball Collab.)
ATKINSON	84E	PL 138B 459	M. Atkinson et al.	(BONN, CERN, GLAS+)
EVANGELIS...	81	NP B178 197	C. Evangelista et al.	(BARI, BONN, CERN+)
DEBILLY	80	NP B176 1	L. de Billy et al.	(CURIN, LAUS, NEUC+)
GURTU	79	NP B151 181	A. Gurtu et al.	(CERN, ZEEM, NIJM, OXF)
CONFORTO	78	LNC 23 419	B. Conforto et al.	(RHEL, TNTO, CHIC+)
CORDEN	78	NP B144 253	M.J. Corden et al.	(BIRM, RHEL, TELA+)
GRASSLER	77	NP B121 189	H. Grassler et al.	(AACH3, BERL, BONN+)
JAFFE	77	PR D15 267,281	R. Jaffe	(MIT)
FLATTE	76	PL 63B 224	S.M. Flatte	(CERN)
GAY	76B	PL 63B 220	J.B. Gay et al.	(CERN, AMST, NIJM, JP)
WELLS	75	NP B101 333	J. Wells et al.	(OXF)
DEFOIX	72	NP B44 125	C. Defoix et al.	(CDEF, CERN)
AMMAR	70	PR D2 430	R. Ammar et al.	(KANS, NWES, ANL, WIS C)
BARNES	69C	PRL 23 610	V.E. Barnes et al.	(BNL, SYRA)
CAMPBELL	69	PRL 22 1204	J.H. Campbell et al.	(PURD)
MILLER	69B	PL 29B 255	D.H. Miller et al.	(PURD)
Alto		PR 188 2011	W.L. Yen et al.	(PURD)
AMMAR	68	PRL 21 1832	R. Ammar et al.	(NWES, ANL)
ASTIER	67	PL 25B 294	A. Astier et al.	(CDEF, CERN, IRAD)
BARLOW	67	NC 50A 701	J. Barlow et al.	(CERN, CDEF, IRAD, LVP)
CONFORTO	67	NP B3 469	G. Conforto et al.	(CERN, CDEF, IPNP+)
ARMENTEROS	65	PL 17 344	R. Armenteros et al.	(CERN, CDEF)
ROSENFELD	65	Oxford Conf. 58	A.H. Rosenfeld	(LRL)

OTHER RELATED PAPERS

ACHASOV	07C	PR D76 077501	N.N. Achasov, A.V. Kiselev	
CHEN	07E	PR D76 094025	H.-X. Chen, A. Hosaka, S.L. Zhu	
GIACOSA	07	PR D75 054007	F. Giacosa	
GUO	07B	PR D76 056004	X.-H. Guo, X.-H. Wu	
HANHART	07B	PR D76 074028	C. Hanhart, B. Kubis, J.R. Pelaez	
SANTOPINTO	07	PR D75 045206	E. Santopinto, G. Galata	
TESHIMA	07	PR D76 054002	T. Teshima, I. Kitamura, N. Morisita	
BUGG	06A	EPJ C47 45	D.V. Bugg	
CHENG	06	PR D73 014017	H.-Y. Cheng, C.-K. Chua, K.-C. Yang	
FEDORETS	06	PAN 69 306	P. Fedorets et al.	
KALASHNIK...	06	PR C73 045203	Yu. Kalashnikova et al.	
MCNEILE	06	PR D74 014508	C. McNeile, C. Michael	
AUBERT,B	05J	PR D72 052008	B. Aubert et al.	(BABAR Collab.)
BARU	05	EPJ A23 523	V.V. Baru, J. Haidenbauer, C. Hanhart	
BRITO	05	PL B608 69	T.V. Brito et al.	
KALASHNIK...	05	EPJ A24 437	Yu.S. Kalashnikova, A.E. Kudryavtsev, A.V. Nefediev	
LI	05B	EPJ A25 263	D.-M. Li, K.-W. Wei, H. Yu	
RODRIGUEZ	05	PR D71 074008	S. Rodriguez, M. Napsuciale	
TESHIMA	05	NP A759 131	T. Teshima, I. Kitamura, N. Morisita	
WANG	05C	EPJ C42 89	Z.-G. Wang, V.-M. Yang	
BARU	04	PL B586 53	V. Baru et al.	
PELAEZ	04	PRL 92 102001	J.R. Pelaez	
PELAEZ	04A	MPL A19 2879	J.R. Pelaez	
WANG	04B	EPJ C37 223	Z.-G. Wang et al.	
ACHASOV	03B	PR D68 014006	N.N. Achasov, A.V. Kiselev	
PALOMAR	03	NP A729 743	J.E. Palomar et al.	
ACHASOV	02G	PL B534 83	N.N. Achasov, A.V. Kiselev	
BLACK	02	PRL 88 181603	D. Black, M. Harada, J. Schechter	
BOGLIONE	02	PR D65 114010	M. Boglione, M.R. Pennington	
CLOSE	02B	JPG 28 R249	F.E. Close, N. Tornqvist	
FURMAN	02	PL B538 266	A. Furman, L. Lesniak	
ACHASOV	01F	PR D63 094007	M.N. Achasov, V.V. Gubin	(Novosibirsk SND Collab.)
CLOSE	01	PL B515 13	F.E. Close, A. Kirk	
ANISOVICH	99D	PL B452 180	A.V. Anisovich et al.	
Alto		NP A651 253	A.V. Anisovich et al.	
MARCO	99	PL B470 20	E. Marco et al.	
ACHASOV	98J	SPU 41 1149	N.N. Achasov	
TORNQVIST	90	NPBPS 21 196	N.A. Tornqvist	(HELS)
WEINSTEIN	90	PR D41 2236	J. Weinstein, N. Isgur	(TNTO)
ACHASOV	88B	ZPHY C41 309	N.N. Achasov, G.N. Shestakov	(NOVM)
VANBEVEREN	86	ZPHY C30 615	E. van Beveren et al.	(NIJM, BIEL)
TORNQVIST	82	PRL 49 624	N.A. Tornqvist	(HELS)
BRAMON	80	PL 93B 65	A. Bramon, E. Masso	(BARC)
TURKOT	63	Siena Conf. 1 661	F. Turkot et al.	(BNL, PITT)

Meson Particle Listings

$\phi(1020)$

$\phi(1020)$

$$J^{PC} = 0^{-}(1^{- -})$$

$\phi(1020)$ MASS

VALUE (MeV)	EVTS	DOCUMENT ID	TECN	COMMENT
1019.455 ± 0.020 OUR AVERAGE		Error includes scale factor of 1.1.		
1019.30 ± 0.02 ± 0.10	105k	AKHMETSHIN 06	CMD2	0.98-1.06 $e^+e^- \rightarrow \pi^+\pi^-\pi^0$
1019.52 ± 0.05 ± 0.05	17.4k	AKHMETSHIN 05	CMD2	0.60-1.38 $e^+e^- \rightarrow \eta\gamma$
1019.483 ± 0.011 ± 0.025	272k	1 AKHMETSHIN 04	CMD2	$e^+e^- \rightarrow K_L^0 K_S^0$
1019.42 ± 0.05	1900k	2 ACHASOV 01E	SND	$e^+e^- \rightarrow K^+K^-$, $K_S K_L, \pi^+\pi^-\pi^0$
1019.40 ± 0.04 ± 0.05	23k	AKHMETSHIN 01B	CMD2	$e^+e^- \rightarrow \eta\gamma$
1019.36 ± 0.12		3 ACHASOV 00B	SND	$e^+e^- \rightarrow \eta\gamma$
1019.38 ± 0.07 ± 0.08	2200	4 AKHMETSHIN 99F	CMD2	$e^+e^- \rightarrow \pi^+\pi^- \geq 2\gamma$
1019.51 ± 0.07 ± 0.10	11169	AKHMETSHIN 98	CMD2	$e^+e^- \rightarrow \pi^+\pi^-\pi^0$
1019.5 ± 0.4		BARBERIS 98	OMEG	450 $pp \rightarrow pp2K^+2K^-$
1019.42 ± 0.06	55600	AKHMETSHIN 95	CMD2	$e^+e^- \rightarrow$ hadrons
1019.7 ± 0.3	2012	DAVENPORT 86	MPSF	400 $pA \rightarrow 4KX$
1019.7 ± 0.1 ± 0.1	5079	ALBRECHT 85D	ARG	10 $e^+e^- \rightarrow K^+K^-X$
1019.3 ± 0.1	1500	ARENTON 82	AEMS	11.8 polar. $pp \rightarrow KK$
1019.67 ± 0.17	25080	5 PELLINEN 82	RVUE	
1019.52 ± 0.13	3681	BUKIN 78c	OLYA	$e^+e^- \rightarrow$ hadrons
••• We do not use the following data for averages, fits, limits, etc. •••				
1019.63 ± 0.07	12540	6 AUBERT,B	05J	BABR $D^0 \rightarrow \bar{K}^0 K^+ K^-$
1019.8 ± 0.7		ARMSTRONG 86	OMEG	85 $\pi^+ / p p \rightarrow \pi^+ / p 4K p$
1020.1 ± 0.11	5526	6 ATKINSON 86	OMEG	20-70 γp
1019.7 ± 1.0		BEBEK 86	CLEO	$e^+e^- \rightarrow \Upsilon(4S)$
1019.411 ± 0.008	642k	7 DIJKSTRA 86	SPEC	100-200 $\pi^\pm, \bar{p}, p, K^\pm$, on Be
1020.9 ± 0.2		6 FRAME 86	OMEG	13 $K^+ p \rightarrow \phi K^+ p$
1021.0 ± 0.2		6 ARMSTRONG 83B	OMEG	18.5 $K^- p \rightarrow K^- K^+ \Lambda$
1020.0 ± 0.5		6 ARMSTRONG 83B	OMEG	18.5 $K^- p \rightarrow K^- K^+ \Lambda$
1019.7 ± 0.3		6 BARATE 83	GOLI	190 $\pi^- Be \rightarrow 2\mu X$
1019.8 ± 0.2 ± 0.5	766	IVANOV 81	OLYA	1-1.4 $e^+e^- \rightarrow K^+K^-$
1019.4 ± 0.5	337	COOPER 78B	HBC	0.7-0.8 $\bar{p} p \rightarrow K_S^0 K_L^0 \pi^+ \pi^-$
1020 ± 1	383	6 BALDI 77	CNTR	10 $\pi^- p \rightarrow \pi^- \phi p$
1018.9 ± 0.6	800	COHEN 77	ASPK	6 $\pi^\pm N \rightarrow K^+ K^- N$
1019.7 ± 0.5	454	KALBFLEISCH 76	HBC	2.18 $K^- p \rightarrow \Lambda K \bar{K}$
1019.4 ± 0.8	984	BESCH 74	CNTR	2 $\gamma p \rightarrow p K^+ K^-$
1020.3 ± 0.4	100	BALLAM 73	HBC	2.8-9.3 γp
1019.4 ± 0.7		BINNIE 73B	CNTR	$\pi^- p \rightarrow \phi n$
1019.6 ± 0.5	120	8 AGUILAR-...	72B	HBC 3.9,4.6 $K^- p \rightarrow K^- p K^+ K^-$
1019.9 ± 0.5	100	8 AGUILAR-...	72B	HBC 3.9,4.6 $K^- p \rightarrow K^- p K^+ K^-$
1020.4 ± 0.5	131	COLLEY 72	HBC	10 $K^+ p \rightarrow K^+ p \phi$
1019.9 ± 0.3	410	STOTTLE...	71	HBC 2.9 $K^- p \rightarrow \Sigma / \Lambda K \bar{K}$

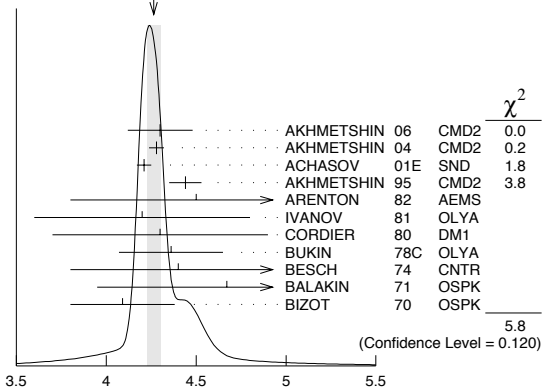
1 Update of AKHMETSHIN 99d
 2 From the combined fit assuming that the total $\phi(1020)$ production cross section is saturated by those of K^+K^- , $K_S K_L$, $\pi^+\pi^-\pi^0$, and $\eta\gamma$ decays modes and using ACHASOV 00B for the $\eta\gamma$ decay mode.
 3 Using a total width of 4.43 ± 0.05 MeV. Systematic uncertainty included.
 4 Using a total width of 4.43 ± 0.05 MeV.
 5 PELLINEN 82 review includes AKERLOF 77, DAUM 81, BALDI 77, AYRES 74, DE-GROOT 74.
 6 Systematic errors not evaluated.
 7 Weighted and scaled average of 12 measurements of DIJKSTRA 86.
 8 Mass errors enlarged by us to Γ/\sqrt{N} ; see the note with the $K^*(892)$ mass.

$\phi(1020)$ WIDTH

VALUE (MeV)	EVTS	DOCUMENT ID	TECN	COMMENT
4.26 ± 0.04 OUR AVERAGE		Error includes scale factor of 1.4. See the ideogram below.		
4.30 ± 0.06 ± 0.17	105k	AKHMETSHIN 06	CMD2	0.98-1.06 $e^+e^- \rightarrow \pi^+\pi^-\pi^0$
4.280 ± 0.033 ± 0.025	272k	9 AKHMETSHIN 04	CMD2	$e^+e^- \rightarrow K_L^0 K_S^0$
4.21 ± 0.04	1900k	10 ACHASOV 01E	SND	$e^+e^- \rightarrow K^+K^-$, $K_S K_L, \pi^+\pi^-\pi^0$
4.44 ± 0.09	55600	AKHMETSHIN 95	CMD2	$e^+e^- \rightarrow$ hadrons
4.5 ± 0.7	1500	ARENTON 82	AEMS	11.8 polar. $pp \rightarrow KK$
4.2 ± 0.6	766	11 IVANOV 81	OLYA	1-1.4 $e^+e^- \rightarrow K^+K^-$

4.3 ± 0.6		11 CORDIER 80	DM1	$e^+e^- \rightarrow \pi^+\pi^-\pi^0$
4.36 ± 0.29	3681	11 BUKIN 78c	OLYA	$e^+e^- \rightarrow$ hadrons
4.4 ± 0.6	984	11 BESCH 74	CNTR	2 $\gamma p \rightarrow p K^+ K^-$
4.67 ± 0.72	681	11 BALAKIN 71	OSPK	$e^+e^- \rightarrow$ hadrons
4.09 ± 0.29		BIZOT 70	OSPK	$e^+e^- \rightarrow$ hadrons
••• We do not use the following data for averages, fits, limits, etc. •••				
4.28 ± 0.13	12540	12 AUBERT,B	05J	BABR $D^0 \rightarrow \bar{K}^0 K^+ K^-$
4.45 ± 0.06	271k	DIJKSTRA 86	SPEC	100 $\pi^- Be$
3.6 ± 0.8	337	11 COOPER 78B	HBC	0.7-0.8 $\bar{p} p \rightarrow K_S^0 K_L^0 \pi^+ \pi^-$
4.5 ± 0.50	1300	11,12 AKERLOF 77	SPEC	400 $pA \rightarrow K^+ K^- X$
4.5 ± 0.8	500	11,12 AYRES 74	ASPK	3-6 $\pi^- p \rightarrow K^+ K^- n, K^- p \rightarrow K^+ K^- \Lambda / \Sigma^0$
3.81 ± 0.37		COSME 74B	OSPK	$e^+e^- \rightarrow K_L^0 K_S^0$
3.8 ± 0.7	454	11 BORENSTEIN 72	HBC	2.18 $K^- p \rightarrow K \bar{K} n$

WEIGHTED AVERAGE
 4.26±0.04 (Error scaled by 1.4)



9 Update of AKHMETSHIN 99d
 10 From the combined fit assuming that the total $\phi(1020)$ production cross section is saturated by those of K^+K^- , $K_S K_L$, $\pi^+\pi^-\pi^0$, and $\eta\gamma$ decays modes and using ACHASOV 00B for the $\eta\gamma$ decay mode.
 11 Width errors enlarged by us to $4\Gamma/\sqrt{N}$; see the note with the $K^*(892)$ mass.
 12 Systematic errors not evaluated.

$\phi(1020)$ DECAY MODES

Mode	Fraction (Γ_i/Γ)	Scale factor/ Confidence level
$K^+ K^-$	(49.2 ± 0.6) %	S=1.2
$K_L^0 K_S^0$	(34.0 ± 0.5) %	S=1.1
$\rho\pi^+ + \pi^+\pi^-\pi^0$	(15.25 ± 0.35) %	S=1.1
$\rho\pi^-$		
$\pi^+\pi^-\pi^0$		
$\eta\gamma$	(1.304 ± 0.025) %	S=1.1
$\pi^0\gamma$	(1.26 ± 0.06) × 10 ⁻³	
$\ell^+\ell^-$		
e^+e^-	(2.97 ± 0.04) × 10 ⁻⁴	S=1.1
$\mu^+\mu^-$	(2.86 ± 0.19) × 10 ⁻⁴	
ηe^+e^-	(1.15 ± 0.10) × 10 ⁻⁴	
$\pi^+\pi^-$	(7.3 ± 1.3) × 10 ⁻⁵	
$\omega\pi^0$	(5.2 ± 1.3) × 10 ⁻⁵	
$\omega\gamma$	< 5 %	CL=84%
$\rho\gamma$	< 1.2 × 10 ⁻⁵	CL=90%
$\pi^+\pi^-\gamma$	(4.1 ± 1.3) × 10 ⁻⁵	
$f_0(980)\gamma$	(3.22 ± 0.19) × 10 ⁻⁴	S=1.1
$\pi^0\pi^0\gamma$	(1.07 ± 0.06) × 10 ⁻⁴	
$\pi^+\pi^-\pi^+\pi^-$	(3.9 ± 2.8) × 10 ⁻⁶	
$\pi^+\pi^+\pi^-\pi^-\pi^0$	< 4.6 × 10 ⁻⁶	CL=90%
$\pi^0 e^+ e^-$	(1.12 ± 0.28) × 10 ⁻⁵	
$\pi^0 \eta\gamma$	(8.3 ± 0.5) × 10 ⁻⁵	
$a_0(980)\gamma$	(7.6 ± 0.6) × 10 ⁻⁵	
$\eta'(958)\gamma$	(6.23 ± 0.21) × 10 ⁻⁵	
$\eta\pi^0\pi^0\gamma$	< 2 × 10 ⁻⁵	CL=90%
$\mu^+\mu^-\gamma$	(1.4 ± 0.5) × 10 ⁻⁵	

Meson Particle Listings

 $\phi(1020)$

$\Gamma(\pi^+\pi^-) \times \Gamma(e^+e^-)/\Gamma_{\text{total}}^2$		$\Gamma_{12}\Gamma_9/\Gamma^2$	
VALUE (units 10^{-8})	DOCUMENT ID	TECN	COMMENT
2.2 ± 0.4 OUR FIT			
2.2 ± 0.4 OUR AVERAGE			
2.1 ± 0.3 ± 0.3	24 ACHASOV	00c	SND $e^+e^- \rightarrow \pi^+\pi^-$
1.95 ^{+1.15} _{-0.87}	18 GOLUBEV	86	ND $e^+e^- \rightarrow \pi^+\pi^-$
6.01 ^{+3.19} _{-2.51}	18 VASSERMAN	81	OLYA $e^+e^- \rightarrow \pi^+\pi^-$

$\Gamma(\pi^0\pi^0\gamma) \times \Gamma(e^+e^-)/\Gamma_{\text{total}}^2$		$\Gamma_{18}\Gamma_9/\Gamma^2$	
VALUE (units 10^{-8})	DOCUMENT ID	TECN	COMMENT
3.33 ± 0.04 ± 0.19	27 AMBROSINO	07	KLOE $e^+e^- \rightarrow \pi^0\pi^0\gamma$
3.33 ± 0.04 ± 0.20			

$\Gamma(\pi^+\pi^-\pi^+\pi^-) \times \Gamma(e^+e^-)/\Gamma_{\text{total}}^2$		$\Gamma_{19}\Gamma_9/\Gamma^2$	
VALUE (units 10^{-9})	EVTS	DOCUMENT ID	TECN
1.2 ± 0.8 OUR FIT			
1.17 ± 0.52 ± 0.64	3285	24 AKHMETSHIN	00e CMD2 $e^+e^- \rightarrow \pi^+\pi^-\pi^+\pi^-$

- ¹⁶From the combined fit assuming that the total $\phi(1020)$ production cross section is saturated by those of K^+K^- , $K_S K_L$, $\pi^+\pi^-\pi^0$, and $\eta\gamma$ decays modes and using ACHASOV 00b for the $\eta\gamma$ decay mode.
- ¹⁷Update of AKHMETSHIN 99d
- ¹⁸Recalculated by us from the cross section in the peak.
- ¹⁹From a combined fit of $\sigma(e^+e^- \rightarrow \eta\gamma)$ with $\eta \rightarrow 3\pi^0$ and $\eta \rightarrow \pi^+\pi^-\pi^0$, and fixing $B(\eta \rightarrow 3\pi^0) / B(\eta \rightarrow \pi^+\pi^-\pi^0) = 1.44 \pm 0.04$. Recalculated by us from the cross section at the peak. Supersedes ACHASOV 00d and ACHASOV 06a.
- ²⁰From the $\eta \rightarrow 2\gamma$ decay and using $B(\eta \rightarrow \gamma\gamma) = 39.43 \pm 0.26\%$.
- ²¹From the $\eta \rightarrow 3\pi^0$ decay and using $B(\eta \rightarrow 3\pi^0) = (32.24 \pm 0.29) \times 10^{-2}$.
- ²²The combined fit from 600 to 1380 MeV taking into account $\rho(770)$, $\omega(782)$, $\phi(1020)$, and $\rho(1450)$ (mass and width fixed at 1450 MeV and 310 MeV respectively).
- ²³From the $\eta \rightarrow 2\gamma$ decay and using $B(\eta \rightarrow 2\gamma) = (39.21 \pm 0.34) \times 10^{-2}$.
- ²⁴Recalculated by the authors from the cross section in the peak.
- ²⁵From the $\eta \rightarrow \pi^+\pi^-\pi^0$ decay and using $B(\eta \rightarrow \pi^+\pi^-\pi^0) = (23.1 \pm 0.5) \times 10^{-2}$.
- ²⁶From the $\pi^0 \rightarrow 2\gamma$ decay and using $B(\pi^0 \rightarrow 2\gamma) = (98.798 \pm 0.032) \times 10^{-2}$.
- ²⁷Calculated by the authors from the cross section at the peak.

 $\phi(1020)$ BRANCHING RATIOS

$\Gamma(K^+K^-)/\Gamma_{\text{total}}$		Γ_1/Γ	
VALUE	EVTS	DOCUMENT ID	TECN
0.492 ± 0.006 OUR FIT			Error includes scale factor of 1.2.
0.493 ± 0.010 OUR AVERAGE			
0.492 ± 0.012	2913	AKHMETSHIN	95 CMD2 $e^+e^- \rightarrow K^+K^-$
0.44 ± 0.05	321	KALBFLEISCH	76 HBC $2.18 K^-p \rightarrow \Lambda K^+K^-$
0.49 ± 0.06	270	DEGROOT	74 HBC $4.2 K^-p \rightarrow \Lambda\phi$
0.540 ± 0.034	565	BALAKIN	71 OSPK $e^+e^- \rightarrow K^+K^-$
0.48 ± 0.04	252	LINDSEY	66 HBC $2.1-2.7 K^-p \rightarrow \Lambda K^+K^-$
• • • We do not use the following data for averages, fits, limits, etc. • • •			
0.476 ± 0.017	1000k	28 ACHASOV	01e SND $e^+e^- \rightarrow K^+K^-, K_S K_L, \pi^+\pi^-\pi^0$

$\Gamma(K_L^0 K_S^0)/\Gamma_{\text{total}}$		Γ_2/Γ	
VALUE	EVTS	DOCUMENT ID	TECN
0.340 ± 0.005 OUR FIT			Error includes scale factor of 1.1.
0.331 ± 0.009 OUR AVERAGE			
0.335 ± 0.010	40644	AKHMETSHIN	95 CMD2 $e^+e^- \rightarrow K_L^0 K_S^0$
0.326 ± 0.035		DOLINSKY	91 ND $e^+e^- \rightarrow K_L^0 K_S^0$
0.310 ± 0.024		DRUZHININ	84 ND $e^+e^- \rightarrow K_L^0 K_S^0$
• • • We do not use the following data for averages, fits, limits, etc. • • •			
0.351 ± 0.013	500k	28 ACHASOV	01e SND $e^+e^- \rightarrow K^+K^-, K_S K_L, \pi^+\pi^-\pi^0$
0.27 ± 0.03	133	KALBFLEISCH	76 HBC $2.18 K^-p \rightarrow \Lambda K_L^0 K_S^0$
0.257 ± 0.030	95	BALAKIN	71 OSPK $e^+e^- \rightarrow K_L^0 K_S^0$
0.40 ± 0.04	167	LINDSEY	66 HBC $2.1-2.7 K^-p \rightarrow \Lambda K_L^0 K_S^0$

$\Gamma(K_L^0 K_S^0)/\Gamma(K^+K^-)$		Γ_2/Γ_1	
VALUE	EVTS	DOCUMENT ID	TECN
0.692 ± 0.017 OUR FIT			Error includes scale factor of 1.1.
0.740 ± 0.031 OUR AVERAGE			
0.70 ± 0.06	2732	BUKIN	78c OLYA $e^+e^- \rightarrow K_L^0 K_S^0$
0.82 ± 0.08		LOSTY	78 HBC $4.2 K^-p \rightarrow \phi$ hyperon
0.71 ± 0.05		LAVEN	77 HBC $10 K^-p \rightarrow K^+K^- \Lambda$
0.71 ± 0.08		LYONS	77 HBC $3-4 K^-p \rightarrow \Lambda\phi$
0.89 ± 0.10	144	AGUILAR...	72b HBC $3.9, 4.6 K^-p$
• • • We do not use the following data for averages, fits, limits, etc. • • •			
0.68 ± 0.03		29 AKHMETSHIN	95 CMD2 $e^+e^- \rightarrow K_L^0 K_S^0, K^+K^-$

$\Gamma(K_L^0 K_S^0)/\Gamma(K^+K^-)$		$\Gamma_2/(\Gamma_1+\Gamma_2)$	
VALUE	EVTS	DOCUMENT ID	TECN
0.409 ± 0.006 OUR FIT			Error includes scale factor of 1.1.
0.45 ± 0.04 OUR AVERAGE			
0.44 ± 0.07		LONDON	66 HBC $2.24 K^-p \rightarrow \Lambda K^+K^-$
0.48 ± 0.07	52	BADIER	65b HBC $3 K^-p$
0.40 ± 0.10	34	SCHLEIN	63 HBC $1.95 K^-p \rightarrow \Lambda K^+K^-$

$[\Gamma(\rho\pi) + \Gamma(\pi^+\pi^-\pi^0)]/\Gamma_{\text{total}}$		Γ_3/Γ	
VALUE	EVTS	DOCUMENT ID	TECN
0.1525 ± 0.0035 OUR FIT			Error includes scale factor of 1.1.
0.151 ± 0.009 OUR AVERAGE			Error includes scale factor of 1.7.
0.161 ± 0.008	11761	AKHMETSHIN	95 CMD2 $e^+e^- \rightarrow \pi^+\pi^-\pi^0$
0.143 ± 0.007		DOLINSKY	91 ND $e^+e^- \rightarrow \pi^+\pi^-\pi^0$
• • • We do not use the following data for averages, fits, limits, etc. • • •			
0.159 ± 0.008	400k	28 ACHASOV	01e SND $e^+e^- \rightarrow K^+K^-, K_S K_L, \pi^+\pi^-\pi^0$
0.145 ± 0.009 ± 0.003	11169	30 AKHMETSHIN	98 CMD2 $e^+e^- \rightarrow \pi^+\pi^-\pi^0$
0.139 ± 0.007		31 PARROUR	76b OSPK e^+e^-

$[\Gamma(\rho\pi) + \Gamma(\pi^+\pi^-\pi^0)]/\Gamma(K^+K^-)$		Γ_3/Γ_1	
VALUE	EVTS	DOCUMENT ID	TECN
0.310 ± 0.010 OUR FIT			Error includes scale factor of 1.2.
0.28 ± 0.09	34	AGUILAR...	72b HBC $3.9, 4.6 K^-p$

$[\Gamma(\rho\pi) + \Gamma(\pi^+\pi^-\pi^0)]/\Gamma(K^+K^-)$		$\Gamma_3/(\Gamma_1+\Gamma_2)$	
VALUE	EVTS	DOCUMENT ID	TECN
0.183 ± 0.005 OUR FIT			Error includes scale factor of 1.1.
0.24 ± 0.04 OUR AVERAGE			
0.237 ± 0.039		CERRADA	77b HBC $4.2 K^-p \rightarrow \Lambda 3\pi$
0.30 ± 0.15		LONDON	66 HBC $2.24 K^-p \rightarrow \Lambda \pi^+\pi^-\pi^0$

$[\Gamma(\rho\pi) + \Gamma(\pi^+\pi^-\pi^0)]/\Gamma(K_L^0 K_S^0)$		Γ_3/Γ_2	
VALUE	EVTS	DOCUMENT ID	TECN
0.448 ± 0.012 OUR FIT			Error includes scale factor of 1.1.
0.51 ± 0.05 OUR AVERAGE			
0.56 ± 0.07	3681	BUKIN	78c OLYA $e^+e^- \rightarrow K_L^0 K_S^0, \pi^+\pi^-\pi^0$
0.47 ± 0.06	516	COSME	74 OSPK $e^+e^- \rightarrow \pi^+\pi^-\pi^0$

$\Gamma(\pi^+\pi^-\pi^0)/\Gamma_{\text{total}}$		Γ_5/Γ	
VALUE	CL% EVTS	DOCUMENT ID	TECN
• • • We do not use the following data for averages, fits, limits, etc. • • •			
≈ 0.0087	1.98M ^{32,33}	ALOISIO	03 KLOE $1.02 e^+e^- \rightarrow \pi^+\pi^-\pi^0$
< 0.0006	90	34 ACHASOV	02 SND $1.02 e^+e^- \rightarrow \pi^+\pi^-\pi^0$
< 0.23	90	34 CORDIER	80 DMI $e^+e^- \rightarrow \pi^+\pi^-\pi^0$
< 0.20	90	34 PARROUR	76b OSPK $e^+e^- \rightarrow \pi^+\pi^-\pi^0$

$\Gamma(\eta\gamma)/\Gamma_{\text{total}}$		Γ_6/Γ	
VALUE (units 10^{-2})	EVTS	DOCUMENT ID	TECN
1.304 ± 0.025 OUR FIT			Error includes scale factor of 1.1.
1.26 ± 0.04 OUR AVERAGE			
1.246 ± 0.025 ± 0.057	10k	35 ACHASOV	98f SND $e^+e^- \rightarrow \eta\gamma$
1.18 ± 0.11	279	36 AKHMETSHIN	95 CMD2 $e^+e^- \rightarrow \pi^+\pi^-\pi^0$
1.30 ± 0.06		37 DRUZHININ	84 ND $e^+e^- \rightarrow 3\gamma$
1.4 ± 0.2		38 DRUZHININ	84 ND $e^+e^- \rightarrow 6\gamma$
0.88 ± 0.20	290	KURDADZE	83c OLYA $e^+e^- \rightarrow 3\gamma$
1.35 ± 0.29		ANDREWS	77 CNTR $6.7-10 \gamma\text{Cu}$
1.5 ± 0.4	54	37 COSME	76 OSPK e^+e^-
• • • We do not use the following data for averages, fits, limits, etc. • • •			
1.36 ± 0.05 ± 0.02	33k	39 ACHASOV	07b SND $0.6-1.38 e^+e^- \rightarrow \eta\gamma$
1.373 ± 0.014 ± 0.085	17.4k	40,41 AKHMETSHIN	05 CMD2 $0.60-1.38 e^+e^- \rightarrow \eta\gamma$
1.287 ± 0.013 ± 0.063	42,43	AKHMETSHIN	01b CMD2 $e^+e^- \rightarrow \eta\gamma$
1.338 ± 0.012 ± 0.052	44	ACHASOV	00 SND $e^+e^- \rightarrow \eta\gamma$
1.18 ± 0.03 ± 0.06	2200	45 AKHMETSHIN	99f CMD2 $e^+e^- \rightarrow \eta\gamma$
1.21 ± 0.07	46	BENAYOUN	96 RVUE $0.54-1.04 e^+e^- \rightarrow \eta\gamma$

$\Gamma(\pi^0\gamma)/\Gamma_{\text{total}}$		Γ_7/Γ	
VALUE (units 10^{-3})	EVTS	DOCUMENT ID	TECN
1.26 ± 0.06 OUR FIT			
1.31 ± 0.13 OUR AVERAGE			
1.30 ± 0.13		DRUZHININ	84 ND $e^+e^- \rightarrow 3\gamma$
1.4 ± 0.5	32	COSME	76 OSPK e^+e^-
• • • We do not use the following data for averages, fits, limits, etc. • • •			
1.258 ± 0.037 ± 0.077	18680	47,48 AKHMETSHIN	05 CMD2 $0.60-1.38 e^+e^- \rightarrow \pi^0\gamma$
1.226 ± 0.036 ± 0.096 ± 0.089	49	ACHASOV	00 SND $e^+e^- \rightarrow \pi^0\gamma$
1.26 ± 0.17	46	BENAYOUN	96 RVUE $0.54-1.04 e^+e^- \rightarrow \pi^0\gamma$

$\Gamma(\eta\gamma)/\Gamma(\pi^0\gamma)$		Γ_6/Γ_7	
VALUE	DOCUMENT ID	TECN	COMMENT
• • • We do not use the following data for averages, fits, limits, etc. • • •			
10.9 ± 0.3 ± 0.7 ± 0.8	ACHASOV	00	SND $e^+e^- \rightarrow \eta\gamma, \pi^0\gamma$

$\Gamma(e^+e^-)/\Gamma_{total}$		Γ_9/Γ			
VALUE (units 10^{-4})	EVTS	DOCUMENT ID	TECN	COMMENT	
2.97±0.04 OUR FIT	Error includes scale factor of 1.1.				
2.98±0.07 OUR AVERAGE	Error includes scale factor of 1.1.				
2.93±0.14	1900k	⁵⁰ ACHASOV	01E	SND	$e^+e^- \rightarrow K^+K^-, K_S^0K_L^0, \pi^+\pi^-\pi^0$
2.88±0.09	55600	AKHMETSHIN 95	CMD2		$e^+e^- \rightarrow$ hadrons
3.00±0.21	3681	BUKIN	78c	OLYA	$e^+e^- \rightarrow$ hadrons
3.10±0.14		⁵¹ PARROUR	76	OSPK	$e^+e^- \rightarrow$ hadrons
3.3 ±0.3		COSME	74	OSPK	$e^+e^- \rightarrow$ hadrons
2.81±0.25	681	BALAKIN	71	OSPK	$e^+e^- \rightarrow$ hadrons
3.50±0.27		CHATELUS	71	OSPK	$e^+e^- \rightarrow$ hadrons

$\Gamma(\mu^+\mu^-)/\Gamma_{total}$		Γ_{10}/Γ			
VALUE (units 10^{-4})	EVTS	DOCUMENT ID	TECN	COMMENT	
2.86±0.19 OUR FIT	Error includes scale factor of 1.1.				
2.5 ±0.4 OUR AVERAGE					
2.69±0.46		⁵² HAYES	71	CNTR	$8.3, 9.8 \gamma C \rightarrow \mu^+\mu^- X$
2.17±0.60		⁵² EARLES	70	CNTR	$6.0 \gamma C \rightarrow \mu^+\mu^- X$
••• We do not use the following data for averages, fits, limits, etc. •••					
2.87±0.20±0.14		⁵³ ACHASOV	01G	SND	$e^+e^- \rightarrow \mu^+\mu^-$
3.30±0.45±0.32		³⁰ ACHASOV	99c	SND	$e^+e^- \rightarrow \mu^+\mu^-$
4.83±1.02		⁵⁴ VASSERMAN	81	OLYA	$e^+e^- \rightarrow \mu^+\mu^-$
2.87±1.98		⁵⁴ AUGUSTIN	73	OSPK	$e^+e^- \rightarrow \mu^+\mu^-$

$\Gamma(\eta e^+e^-)/\Gamma_{total}$		Γ_{11}/Γ			
VALUE (units 10^{-4})	EVTS	DOCUMENT ID	TECN	COMMENT	
1.15±0.10 OUR AVERAGE					
1.19±0.19±0.12	213	⁵⁵ ACHASOV	01B	SND	$e^+e^- \rightarrow \gamma\eta e^+e^-$
1.14±0.10±0.06	355	⁵⁶ AKHMETSHIN 01	CMD2		$e^+e^- \rightarrow \eta e^+e^-$
1.3 $\begin{smallmatrix} +0.8 \\ -0.6 \end{smallmatrix}$	7	GOLUBEV	85	ND	$e^+e^- \rightarrow \gamma\eta e^+e^-$
••• We do not use the following data for averages, fits, limits, etc. •••					
1.13±0.14±0.07	183	⁵⁷ AKHMETSHIN 01	CMD2		$e^+e^- \rightarrow \eta e^+e^-$
1.21±0.14±0.09	130	⁵⁸ AKHMETSHIN 01	CMD2		$e^+e^- \rightarrow \eta e^+e^-$
1.04±0.20±0.08	42	⁵⁹ AKHMETSHIN 01	CMD2		$e^+e^- \rightarrow \eta e^+e^-$

$\Gamma(\pi^+\pi^-)/\Gamma_{total}$		Γ_{12}/Γ			
VALUE (units 10^{-4})	CL%	DOCUMENT ID	TECN	COMMENT	
••• We do not use the following data for averages, fits, limits, etc. •••					
0.71±0.11±0.09		³⁰ ACHASOV	00c	SND	$e^+e^- \rightarrow \pi^+\pi^-$
0.65 $\begin{smallmatrix} +0.38 \\ -0.29 \end{smallmatrix}$		³⁰ GOLUBEV	86	ND	$e^+e^- \rightarrow \pi^+\pi^-$
2.01 $\begin{smallmatrix} +1.07 \\ -0.84 \end{smallmatrix}$		³⁰ VASSERMAN	81	OLYA	$e^+e^- \rightarrow \pi^+\pi^-$
<6.6	95	BUKIN	78b	OLYA	$e^+e^- \rightarrow \pi^+\pi^-$
<2.7	95	ALVENSLEB...	72	CNTR	$6.7 \gamma C \rightarrow C\pi^+\pi^-$

$\Gamma(\omega\pi^0)/\Gamma_{total}$		Γ_{13}/Γ			
VALUE (units 10^{-5})	CL%	DOCUMENT ID	TECN	COMMENT	
5.2±1.1		^{60,61} AULCHENKO	00A	SND	$e^+e^- \rightarrow \pi^+\pi^-\pi^0\pi^0$
••• We do not use the following data for averages, fits, limits, etc. •••					
~5.4		⁶² ACHASOV	00E	SND	$e^+e^- \rightarrow \pi^0\pi^0\gamma$
5.5 $\begin{smallmatrix} +1.6 \\ -1.4 \end{smallmatrix}$ ±0.3		^{61,63} AULCHENKO	00A	SND	$e^+e^- \rightarrow \pi^+\pi^-\pi^0\pi^0$
4.8 $\begin{smallmatrix} +1.9 \\ -1.7 \end{smallmatrix}$ ±0.8		⁶² ACHASOV	99	SND	$e^+e^- \rightarrow \pi^+\pi^-\pi^0\pi^0$

$\Gamma(\omega\gamma)/\Gamma_{total}$		Γ_{14}/Γ			
VALUE	CL%	DOCUMENT ID	TECN	COMMENT	
<0.05	84	LINDSEY	66	HBC	$2.1-2.7 K^-p \rightarrow \Lambda\pi^+\pi^-$ neutrals

$\Gamma(\rho\gamma)/\Gamma_{total}$		Γ_{15}/Γ			
VALUE (units 10^{-4})	CL%	DOCUMENT ID	TECN	COMMENT	
< 0.12	90	⁶⁴ AKHMETSHIN 99B	CMD2		$e^+e^- \rightarrow \pi^+\pi^-\gamma$
••• We do not use the following data for averages, fits, limits, etc. •••					
< 7	90	AKHMETSHIN 97c	CMD2		$e^+e^- \rightarrow \pi^+\pi^-\gamma$
<200	84	LINDSEY	66	HBC	$2.1-2.7 K^-p \rightarrow \Lambda\pi^+\pi^-$ neutrals

$\Gamma(\pi^+\pi^-\gamma)/\Gamma_{total}$		Γ_{16}/Γ				
VALUE (units 10^{-4})	CL%	EVTS	DOCUMENT ID	TECN	COMMENT	
0.41±0.12±0.04		30175	⁶⁵ AKHMETSHIN 99B	CMD2	$e^+e^- \rightarrow \pi^+\pi^-\gamma$	
••• We do not use the following data for averages, fits, limits, etc. •••						
< 0.3	90		⁶⁶ AKHMETSHIN 97c	CMD2	$e^+e^- \rightarrow \pi^+\pi^-\gamma$	
<600	90		KALBFLEISCH 75	HBC	$2.18 K^-p \rightarrow \Lambda\pi^+\pi^-$ neutrals	
< 70	90		COSME	74	OSPK	$e^+e^- \rightarrow \pi^+\pi^-\gamma$
<400	90		LINDSEY	65	HBC	$2.1-2.7 K^-p \rightarrow \Lambda\pi^+\pi^-$ neutrals

$\Gamma(f_0(980)\gamma)/\Gamma_{total}$		Γ_{17}/Γ			
VALUE (units 10^{-4})	CL%	EVTS	DOCUMENT ID	TECN	COMMENT
3.22±0.19 OUR FIT	Error includes scale factor of 1.1.				
3.21±0.19 OUR AVERAGE					
3.21 $\begin{smallmatrix} +0.03 \\ -0.09 \end{smallmatrix}$ ±0.18			⁶⁷ AMBROSINO 07	KLOE	$e^+e^- \rightarrow \pi^0\pi^0\gamma$
2.90±0.21±1.54			⁶⁸ AKHMETSHIN 99c	CMD2	$e^+e^- \rightarrow \pi^+\pi^-\gamma, \pi^0\pi^0\gamma$
••• We do not use the following data for averages, fits, limits, etc. •••					
4.47±0.21	2438	⁶⁹ ALOISIO 02D	KLOE		$e^+e^- \rightarrow \pi^0\pi^0\gamma$
3.5 ±0.3 $\begin{smallmatrix} +1.3 \\ -0.5 \end{smallmatrix}$	419	^{70,71} ACHASOV	00H	SND	$e^+e^- \rightarrow \pi^0\pi^0\gamma$
1.93±0.46±0.50	27188	⁷² AKHMETSHIN 99B	CMD2		$e^+e^- \rightarrow \pi^+\pi^-\gamma$
3.05±0.25±0.72	268	⁷³ AKHMETSHIN 99c	CMD2		$e^+e^- \rightarrow \pi^0\pi^0\gamma$
1.5 ±0.5	268	⁷⁴ AKHMETSHIN 99c	CMD2		$e^+e^- \rightarrow \pi^0\pi^0\gamma$
3.42±0.30±0.36	164	⁷⁰ ACHASOV	98I	SND	$e^+e^- \rightarrow 5\gamma$
< 1	90	⁷⁵ AKHMETSHIN 97c	CMD2		$e^+e^- \rightarrow \pi^+\pi^-\gamma$
< 7	90	⁷⁶ AKHMETSHIN 97c	CMD2		$e^+e^- \rightarrow \pi^+\pi^-\gamma$
< 20	90	DRUZHININ 87	ND		$e^+e^- \rightarrow \pi^0\pi^0\gamma$

$\Gamma(f_0(980)\gamma)/\Gamma(\eta\gamma)$		Γ_{17}/Γ_6			
VALUE (units 10^{-2})	EVTS	DOCUMENT ID	TECN	COMMENT	
2.47±0.16 OUR FIT	Error includes scale factor of 1.1.				
2.6 ±0.2 $\begin{smallmatrix} +0.8 \\ -0.3 \end{smallmatrix}$	419	⁷⁰ ACHASOV	00H	SND	$e^+e^- \rightarrow \pi^0\pi^0\gamma$

$\Gamma(\pi^0\pi^0\gamma)/\Gamma_{total}$		Γ_{18}/Γ			
VALUE (units 10^{-4})	CL%	EVTS	DOCUMENT ID	TECN	COMMENT
1.07 ±0.06 OUR AVERAGE					
1.07 $\begin{smallmatrix} +0.01 \\ -0.03 \end{smallmatrix}$ $\begin{smallmatrix} +0.06 \\ -0.06 \end{smallmatrix}$			⁷⁷ AMBROSINO 07	KLOE	$e^+e^- \rightarrow \pi^0\pi^0\gamma$
1.08 ±0.17 ±0.09	268		AKHMETSHIN 99c	CMD2	$e^+e^- \rightarrow \pi^0\pi^0\gamma$
••• We do not use the following data for averages, fits, limits, etc. •••					
1.09 ±0.03 ±0.05	2438		ALOISIO 02D	KLOE	$e^+e^- \rightarrow \pi^0\pi^0\gamma$
1.158±0.093±0.052	419	^{71,78} ACHASOV	00H	SND	$e^+e^- \rightarrow \pi^0\pi^0\gamma$
<10	90		DRUZHININ 87	ND	$e^+e^- \rightarrow 5\gamma$

$\Gamma(\pi^0\pi^0\gamma)/\Gamma(\eta\gamma)$		Γ_{18}/Γ_6			
VALUE (units 10^{-2})	EVTS	DOCUMENT ID	TECN	COMMENT	
0.865 ±0.070 ±0.017	419	⁷⁸ ACHASOV	00H	SND	$e^+e^- \rightarrow \pi^0\pi^0\gamma$
••• We do not use the following data for averages, fits, limits, etc. •••					
0.90 ±0.08 ±0.07	164		ACHASOV 98I	SND	$e^+e^- \rightarrow 5\gamma$

$\Gamma(\pi^+\pi^-\pi^+\pi^-)/\Gamma_{total}$		Γ_{19}/Γ			
VALUE (units 10^{-6})	CL%	EVTS	DOCUMENT ID	TECN	COMMENT
••• We do not use the following data for averages, fits, limits, etc. •••					
3.93±1.74±2.14	3285		AKHMETSHIN 00E	CMD2	$e^+e^- \rightarrow \pi^+\pi^-\pi^+\pi^-$
< 870	90		CORDIER 79	WIRE	$e^+e^- \rightarrow \pi^+\pi^-\pi^+\pi^-$

$\Gamma(\pi^+\pi^-\pi^-\pi^0)/\Gamma_{total}$		Γ_{20}/Γ			
VALUE (units 10^{-6})	CL%	EVTS	DOCUMENT ID	TECN	COMMENT
< 4.6	90		AKHMETSHIN 00E	CMD2	$e^+e^- \rightarrow \pi^+\pi^-\pi^-\pi^0$
••• We do not use the following data for averages, fits, limits, etc. •••					
<150	95		BARKOV 88	CMD	$e^+e^- \rightarrow \pi^+\pi^-\pi^-\pi^0$

$\Gamma(\pi^0 e^+ e^-)/\Gamma_{total}$		Γ_{21}/Γ				
VALUE (units 10^{-5})	CL%	EVTS	DOCUMENT ID	TECN	COMMENT	
1.12±0.28 OUR AVERAGE						
1.01±0.28±0.29	52		⁷⁹ ACHASOV	02D	SND	$e^+e^- \rightarrow \pi^0 e^+ e^-$
1.22±0.34±0.21	46		⁸⁰ AKHMETSHIN 01c	CMD2	$e^+e^- \rightarrow \pi^0 e^+ e^-$	
••• We do not use the following data for averages, fits, limits, etc. •••						
<12	90		DOLINSKY 88	ND	$e^+e^- \rightarrow \pi^0 e^+ e^-$	

$\Gamma(\pi^0\eta\gamma)/\Gamma_{total}$		Γ_{22}/Γ			
VALUE (units 10^{-5})	CL%	EVTS	DOCUMENT ID	TECN	COMMENT
8.3 ±0.5 OUR AVERAGE					
8.51±0.51±0.57	607		⁸¹ ALOISIO 02c	KLOE	$e^+e^- \rightarrow \eta\pi^0\gamma$
7.96±0.60±0.40	197		⁸² ALOISIO 02c	KLOE	$e^+e^- \rightarrow \eta\pi^0\gamma$
8.8 ±1.4 ±0.9	36		⁸³ ACHASOV 00f	SND	$e^+e^- \rightarrow \eta\pi^0\gamma$
9.0 ±2.4 ±1.0	80		AKHMETSHIN 99c	CMD2	$e^+e^- \rightarrow \eta\pi^0\gamma$
••• We do not use the following data for averages, fits, limits, etc. •••					
8.3 ±2.3 ±1.2	20		ACHASOV 98B	SND	$e^+e^- \rightarrow 5\gamma$
<250	90		DOLINSKY 91	ND	$e^+e^- \rightarrow \pi^0\eta\gamma$

$\Gamma(a_0(980)\gamma)/\Gamma_{total}$		Γ_{23}/Γ			
VALUE (units 10^{-5})	CL%	EVTS	DOCUMENT ID	TECN	COMMENT
7.6±0.6 OUR FIT					
7.6±0.6 OUR AVERAGE					
7.4±0.7			⁸⁴ ALOISIO 02c	KLOE	$e^+e^- \rightarrow \eta\pi^0\gamma$
8.8±1.7	36		⁸⁵ ACHASOV 00f	SND	$e^+e^- \rightarrow \eta\pi^0\gamma$
••• We do not use the following data for averages, fits, limits, etc. •••					
11 ±2			⁸⁶ GOKALP 02	RVUE	$e^+e^- \rightarrow \eta\pi^0\gamma$
<500	90		DOLINSKY 91	ND	$e^+e^- \rightarrow \pi^0\eta\gamma$

Meson Particle Listings

 $\phi(1020)$ $\Gamma(f_0(980)\gamma)/\Gamma(a_0(980)\gamma)$

VALUE	DOCUMENT ID	TECN	COMMENT	Γ_{17}/Γ_{23}
6.1 ± 0.6	87 ALOISIO	02C	KLOE $e^+e^- \rightarrow \eta\pi^0\gamma$	

 $\Gamma(\eta'(958)\gamma)/\Gamma_{\text{total}}$

VALUE (units 10^{-5})	CL%	EVTs	DOCUMENT ID	TECN	COMMENT	Γ_{24}/Γ
6.23 ± 0.21					OUR FIT	
6.23 ± 0.30					OUR AVERAGE	
$6.22 \pm 0.27 \pm 0.12$		3407	88 AMBROSINO	07A	KLOE $1.02 e^+e^- \rightarrow \pi^+\pi^-7\gamma$	
$6.7^{+2.8}_{-2.4} \pm 0.8$		12	89 AULCHENKO	03B	SND $e^+e^- \rightarrow \eta'\gamma$	
$6.7^{+5.0}_{-4.2} \pm 1.5$		7	AULCHENKO	03B	SND $e^+e^- \rightarrow 7\gamma$	
$6.10 \pm 0.61 \pm 0.43$		120	90 ALOISIO	02E	KLOE $1.02 e^+e^- \rightarrow \pi^+\pi^-3\gamma$	
$8.2^{+2.1}_{-1.9} \pm 1.1$		21	91 AKHMETSHIN	00B	CMD2 $e^+e^- \rightarrow \pi^+\pi^-3\gamma$	
$4.9^{+2.2}_{-1.8} \pm 0.6$		9	92 AKHMETSHIN	00F	CMD2 $e^+e^- \rightarrow \pi^+\pi^-\pi^+\pi^- \geq 2\gamma$	
6.4 ± 1.6		30	93 AKHMETSHIN	00F	CMD2 $e^+e^- \rightarrow \eta'(958)\gamma$	
$6.7^{+3.4}_{-2.9} \pm 1.0$		5	94 AULCHENKO	99	SND $e^+e^- \rightarrow \pi^+\pi^-3\gamma$	
<11		90	AULCHENKO	98	SND $e^+e^- \rightarrow 7\gamma$	
$12^{+7}_{-5} \pm 2$		6	91 AKHMETSHIN	97B	CMD2 $e^+e^- \rightarrow \pi^+\pi^-3\gamma$	
<41		90	DRUZHININ	87	ND $e^+e^- \rightarrow \gamma\eta\pi^+\pi^-$	

 $\Gamma(\eta'(958)\gamma)/\Gamma(K_S^0 K_S^0)$

VALUE (units 10^{-4})	EVTs	DOCUMENT ID	TECN	COMMENT	Γ_{24}/Γ_2
1.83 ± 0.06				OUR FIT	
$1.46^{+0.64}_{-0.54} \pm 0.18$		9	95 AKHMETSHIN	00F	CMD2 $e^+e^- \rightarrow \pi^+\pi^-\pi^+\pi^- \geq 2\gamma$

 $\Gamma(\eta'(958)\gamma)/\Gamma(\eta\gamma)$

VALUE (units 10^{-3})	EVTs	DOCUMENT ID	TECN	COMMENT	Γ_{24}/Γ_6
4.77 ± 0.15				OUR FIT	
4.78 ± 0.20				OUR AVERAGE	
$4.77 \pm 0.09 \pm 0.19$		3407	AMBROSINO	07A	KLOE $1.02 e^+e^- \rightarrow \pi^+\pi^-7\gamma$
$4.70 \pm 0.47 \pm 0.31$		120	96 ALOISIO	02E	KLOE $1.02 e^+e^- \rightarrow \pi^+\pi^-3\gamma$
$6.5^{+1.7}_{-1.5} \pm 0.8$		21	AKHMETSHIN	00B	CMD2 $e^+e^- \rightarrow \pi^+\pi^-3\gamma$
$9.5^{+5.2}_{-4.0} \pm 1.4$		6	97 AKHMETSHIN	97B	CMD2 $e^+e^- \rightarrow \pi^+\pi^-3\gamma$

 $\Gamma(\eta\pi^0\pi^0\gamma)/\Gamma_{\text{total}}$

VALUE (units 10^{-5})	CL%	DOCUMENT ID	TECN	COMMENT	Γ_{25}/Γ
<2		90	AULCHENKO	98	SND $e^+e^- \rightarrow 7\gamma$

 $\Gamma(\mu^+\mu^-\gamma)/\Gamma_{\text{total}}$

VALUE (units 10^{-5})	EVTs	DOCUMENT ID	TECN	COMMENT	Γ_{26}/Γ
$1.43 \pm 0.45 \pm 0.14$		27188	72 AKHMETSHIN	99B	CMD2 $e^+e^- \rightarrow \mu^+\mu^-\gamma$
2.3 ± 1.0		824 ± 33	98 AKHMETSHIN	97C	CMD2 $e^+e^- \rightarrow \mu^+\mu^-\gamma$

 $\Gamma(\rho\gamma\gamma)/\Gamma_{\text{total}}$

VALUE (units 10^{-4})	CL%	DOCUMENT ID	TECN	COMMENT	Γ_{27}/Γ
<5		90	AKHMETSHIN	98	CMD2 $e^+e^- \rightarrow \pi^+\pi^-\gamma\gamma$

 $\Gamma(\eta\pi^+\pi^-)/\Gamma_{\text{total}}$

VALUE (units 10^{-5})	CL%	DOCUMENT ID	TECN	COMMENT	Γ_{28}/Γ
< 1.8		90	AKHMETSHIN	00E	CMD2 $e^+e^- \rightarrow \pi^+\pi^-\pi^+\pi^-0$
<30		90	AKHMETSHIN	98	CMD2 $e^+e^- \rightarrow \pi^+\pi^-\gamma\gamma$

 $\Gamma(\eta\mu^+\mu^-)/\Gamma_{\text{total}}$

VALUE (units 10^{-6})	CL%	DOCUMENT ID	TECN	COMMENT	Γ_{29}/Γ
<9.4		90	AKHMETSHIN	01	CMD2 $e^+e^- \rightarrow \eta e^+e^-$

- 28 Using $B(\phi \rightarrow e^+e^-) = (2.93 \pm 0.14) \times 10^{-4}$.
- 29 Theoretical analysis of BRAMON 00 taking into account phase-space difference, electromagnetic radiative corrections, as well as isospin breaking, predicts 0.62. FISCHBACH 02 calculates additional corrections caused by the close threshold and predicts 0.68.
- 30 Using $B(\phi \rightarrow e^+e^-) = (2.99 \pm 0.08) \times 10^{-4}$.
- 31 Using $\Gamma(\phi) = 4.1$ MeV. If interference between the $\rho\pi$ and 3π modes is neglected, the fraction of the $\rho\pi$ is more than 80% at the 90% confidence level.
- 32 From a fit without limitations on charged and neutral ρ masses and widths.
- 33 Adding the direct and $\omega\pi$ contributions and considering the interference between the $\rho\pi$ and $\pi^+\pi^-\pi^0$.
- 34 Neglecting the interference between the $\rho\pi$ and $\pi^+\pi^-\pi^0$.
- 35 Using $B(\phi \rightarrow e^+e^-) = (2.99 \pm 0.08) \times 10^{-4}$ and $B(\eta \rightarrow 3\pi^0) = (32.2 \pm 0.4) \times 10^{-2}$.
- 36 From $\pi^+\pi^-\pi^0$ decay mode of η .
- 37 From 2γ decay mode of η .
- 38 From $3\pi^0$ decay mode of η .

- 39 ACHASOV 07b reports $[B(\phi(1020) \rightarrow \eta\gamma)] \times [B(\phi(1020) \rightarrow e^+e^-)] = (4.05 \pm 0.067 \pm 0.118) \times 10^{-6}$. We divide by our best value $B(\phi(1020) \rightarrow e^+e^-) = (2.97 \pm 0.04) \times 10^{-4}$. Our first error is their experiment's error and our second error is the systematic error from using our best value. Supersedes ACHASOV 00b and ACHASOV 06a.
- 40 Using $B(\phi \rightarrow e^+e^-) = (2.98 \pm 0.04) \times 10^{-4}$ and $B(\eta \rightarrow \gamma\gamma) = 39.43 \pm 0.26\%$.
- 41 Not independent of the corresponding $\Gamma(e^+e^-) \times \Gamma(\eta\gamma)/\Gamma_{\text{total}}^2$.
- 42 Using $B(\phi \rightarrow e^+e^-) = (2.99 \pm 0.08) \times 10^{-4}$ and $B(\eta \rightarrow 3\pi^0) = (32.24 \pm 0.29) \times 10^{-2}$.
- 43 The combined fit from 600 to 1380 MeV taking into account $\rho(770)$, $\omega(782)$, $\phi(1020)$, and $\rho(1450)$ (mass and width fixed at 1450 MeV and 310 MeV respectively).
- 44 From the $\eta \rightarrow 2\gamma$ decay and using $B(\phi \rightarrow e^+e^-) = (2.99 \pm 0.08) \times 10^{-4}$.
- 45 From $\pi^+\pi^-\pi^0$ decay mode of η and using $B(\phi \rightarrow e^+e^-) = (2.99 \pm 0.08) \times 10^{-4}$.
- 46 Reanalysis of DRUZHININ 84, DOLINSKY 89, and DOLINSKY 91 taking into account a triangle anomaly contribution.
- 47 Using $B(\phi \rightarrow e^+e^-) = (2.98 \pm 0.04) \times 10^{-4}$.
- 48 Not independent of the corresponding $\Gamma(e^+e^-) \times \Gamma(\pi^0\gamma)/\Gamma_{\text{total}}^2$.
- 49 From the $\pi^0 \rightarrow 2\gamma$ decay and using $B(\phi \rightarrow e^+e^-) = (2.99 \pm 0.08) \times 10^{-4}$.
- 50 From the combined fit assuming that the total $\phi(1020)$ production cross section is saturated by those of K^+K^- , $K_S^0 K_L^0$, $\pi^+\pi^-\pi^0$, and $\eta\gamma$ decays modes and using ACHASOV 00b for the $\eta\gamma$ decay mode.
- 51 Using total width 4.2 MeV. They detect 3π mode and observe significant interference with ω tail. This is accounted for in the result quoted above.
- 52 Neglecting interference between resonance and continuum.
- 53 Using $B(\phi \rightarrow e^+e^-) = (2.91 \pm 0.07) \times 10^{-4}$.
- 54 Recalculated by us using $B(\phi \rightarrow e^+e^-) = (2.99 \pm 0.08) \times 10^{-4}$.
- 55 Using $B(\eta \rightarrow \gamma\gamma) = (39.25 \pm 0.32)\%$, $B(\phi \rightarrow \eta\gamma) = (1.26 \pm 0.06)\%$, and $B(\phi \rightarrow e^+e^-) = (3.00 \pm 0.06) \times 10^{-4}$.
- 56 The average of the branching ratios separately obtained from the $\eta \rightarrow \gamma\gamma$, $3\pi^0$, $\pi^+\pi^-\pi^0$ decays.
- 57 From $\eta \rightarrow \gamma\gamma$ decays and using $B(\eta \rightarrow \gamma\gamma) = (39.33 \pm 0.25) \times 10^{-2}$, $B(\eta \rightarrow \pi^+\pi^-\gamma) = (4.75 \pm 11) \times 10^{-2}$, and $B(\phi \rightarrow \eta\gamma) = (1.297 \pm 0.033) \times 10^{-2}$.
- 58 From $\eta \rightarrow 3\pi^0$ decays and using $B(\pi^0 \rightarrow \gamma\gamma) = (98.798 \pm 0.033) \times 10^{-2}$, $B(\eta \rightarrow 3\pi^0) = (32.24 \pm 0.29) \times 10^{-2}$, $B(\eta \rightarrow \pi^+\pi^-\gamma) = (4.75 \pm 0.11) \times 10^{-2}$, and $B(\phi \rightarrow \eta\gamma) = (1.297 \pm 0.033) \times 10^{-2}$.
- 59 From $\eta \rightarrow \pi^+\pi^-\pi^0$ decays and using $B(\pi^0 \rightarrow \gamma\gamma) = (98.798 \pm 0.033) \times 10^{-2}$, $B(\pi^0 \rightarrow e^+e^-\gamma) = (1.198 \pm 0.032) \times 10^{-2}$, $B(\eta \rightarrow \pi^+\pi^-\pi^0) = (23.0 \pm 0.4) \times 10^{-2}$, $B(\phi \rightarrow \pi^+\pi^-\pi^0) = (15.5 \pm 0.6) \times 10^{-2}$, and $B(\phi \rightarrow \eta\gamma) = (1.297 \pm 0.033) \times 10^{-2}$.
- 60 Using the 1996 and 1998 data.
- 61 $(2.3 \pm 0.3)\%$ correction for other decay modes of the $\omega(782)$ applied.
- 62 Using the 1996 data.
- 63 Using the 1998 data.
- 64 Supersedes AKHMETSHIN 97c.
- 65 For $E_\gamma > 20$ MeV and assuming that $B(\phi(1020) \rightarrow f_0(980)\gamma)$ is negligible. Supersedes AKHMETSHIN 97c.
- 66 For $E_\gamma > 20$ MeV and assuming that $B(\phi(1020) \rightarrow f_0(980)\gamma)$ is negligible.
- 67 Obtained by the authors taking into account the $\pi^+\pi^-$ decay mode. Includes a component due to $\pi\pi$ production via the $f_0(600)$ meson. Supersedes ALOISIO 02d.
- 68 From the combined fit of the photon spectra in the reactions $e^+e^- \rightarrow \pi^+\pi^-\gamma$, $\pi^0\pi^0\gamma$.
- 69 From the negative interference with the $f_0(600)$ meson of AITALA 01b using the ACHASOV 89 parameterization for the $f_0(980)$, a Breit-Wigner for the $f_0(600)$, and ACHASOV 01f for the $\rho\pi$ contribution. Superseded by AMBROSINO 07.
- 70 Assuming that the $\pi^0\pi^0\gamma$ final state is completely determined by the $f_0\gamma$ mechanism, neglecting the decay $B(\phi \rightarrow K\bar{K}\gamma)$ and using $B(f_0 \rightarrow \pi^+\pi^-) = 2B(f_0 \rightarrow \pi^0\pi^0)$.
- 71 Using the value $B(\phi \rightarrow \eta\gamma) = (1.338 \pm 0.053) \times 10^{-2}$.
- 72 For $E_\gamma > 20$ MeV. Supersedes AKHMETSHIN 97c.
- 73 Neglecting other intermediate mechanisms ($\rho\pi$, $\sigma\gamma$).
- 74 A narrow pole fit taking into account $f_0(980)$ and $f_0(1200)$ intermediate mechanisms.
- 75 For destructive interference with the Bremsstrahlung process
- 76 For constructive interference with the Bremsstrahlung process
- 77 Supersedes ALOISIO 02d.
- 78 Supersedes ACHASOV 98i. Excluding $\omega\pi^0$.
- 79 Using various branching ratios from the 2000 Edition of this Review (PDG 00).
- 80 Using $B(\pi^0 \rightarrow \gamma\gamma) = 0.98798 \pm 0.00032$, $B(\phi \rightarrow \eta\gamma) = (1.297 \pm 0.033) \times 10^{-2}$, and $B(\eta \rightarrow \pi^+\pi^-\gamma) = (4.75 \pm 0.11) \times 10^{-2}$.
- 81 From the decay mode $\eta \rightarrow \gamma\gamma$.
- 82 From the decay mode $\eta \rightarrow \pi^+\pi^-\pi^0$.
- 83 Supersedes ACHASOV 98b.
- 84 Using $M_{a_0(980)} = 984.8$ MeV and assuming $a_0(980)\gamma$ dominance.
- 85 Assuming $a_0(980)\gamma$ dominance in the $\eta\pi^0\gamma$ final state.
- 86 Using data of ACHASOV 00f.
- 87 Using results of ALOISIO 02b and assuming that $f_0(980)$ decays into $\pi\pi$ only and $a_0(980)$ into $\eta\pi$ only.
- 88 AMBROSINO 07a reports $[B(\phi(1020) \rightarrow \eta'(958)\gamma)] / [B(\phi(1020) \rightarrow \eta\gamma)] = (4.77 \pm 0.09 \pm 0.19) \times 10^{-3}$. We multiply by our best value $B(\phi(1020) \rightarrow \eta\gamma) = (1.304 \pm 0.025) \times 10^{-2}$. Our first error is their experiment's error and our second error is the systematic error from using our best value.
- 89 Averaging AULCHENKO 03b with AULCHENKO 99.
- 90 Using $B(\phi \rightarrow \eta\gamma) = (1.297 \pm 0.033)\%$.
- 91 Using the value $B(\phi \rightarrow \eta\gamma) = (1.26 \pm 0.06) \times 10^{-2}$.
- 92 Using $B(\phi \rightarrow K_S^0 K_L^0) = (33.8 \pm 0.6)\%$.
- 93 Averaging AKHMETSHIN 00b with AKHMETSHIN 00f.
- 94 Using the value $B(\eta' \rightarrow \eta\pi^+\pi^-) = (43.7 \pm 1.5) \times 10^{-2}$ and $B(\eta \rightarrow \gamma\gamma) = (39.25 \pm 0.31) \times 10^{-2}$.
- 95 Using various branching ratios of K_S^0 , K_L^0 , η , η' from the 2000 edition (The European Physical Journal **C15** 1 (2000)) of this Review.
- 96 From the decay mode $\eta' \rightarrow \eta\pi^+\pi^-$, $\eta \rightarrow \gamma\gamma$.
- 97 Superseded by AKHMETSHIN 00b.
- 98 For $E_\gamma > 20$ MeV.

See key on page 373

Meson Particle Listings

 $\phi(1020)$, $h_1(1170)$ $\pi^+ \pi^- \pi^0 / \rho \pi$ AMPLITUDE RATIO a_1 IN DECAY OF $\phi \rightarrow \pi^+ \pi^- \pi^0$

VALUE (units 10^{-2})	CL% EVTS	DOCUMENT ID	TECN	COMMENT
9.1 ± 1.2 OUR AVERAGE				
10.1 ± 4.4 ± 1.7	80k	⁹⁹ AKHMETSHIN 06	CMD2	1.017-1.021 $e^+ e^- \rightarrow \pi^+ \pi^- \pi^0$
9.0 ± 1.1 ± 0.6	1.98M ^{100,101}	ALOISIO 03	KLOE	1.02 $e^+ e^- \rightarrow \pi^+ \pi^- \pi^0$
• • • We do not use the following data for averages, fits, limits, etc. • • •				
-6 < a_1 < 6	500k	¹⁰¹ ACHASOV 02	SND	$e^+ e^- \rightarrow \pi^+ \pi^- \pi^0$
-16 < a_1 < 11	90	9.8k ^{99,102} AKHMETSHIN 98	CMD2	$e^+ e^- \rightarrow \pi^+ \pi^- \gamma \gamma$
⁹⁹ Dalitz plot analysis taking into account interference between the contact and $\rho \pi$ amplitudes.				
¹⁰⁰ From a fit without limitations on charged and neutral ρ masses and widths.				
¹⁰¹ Recalculated by us to match the notations of AKHMETSHIN 98.				
¹⁰² Assuming zero phase for the contact term.				

 $\phi(1020)$ REFERENCES

ACHASOV 07B	PR D76 077101	M.N. Achasov et al.	(SND Collab.)
AMBROSINO 07	EPJ C49 473	F. Ambrosino et al.	(KLOE Collab.)
AMBROSINO 07A	PL B648 267	F. Ambrosino et al.	(KLOE Collab.)
ACHASOV 06A	PR D74 014016	M.N. Achasov et al.	(SND Collab.)
AKHMETSHIN 06	PL B642 203	R.R. Akhmetshin et al.	(CMD-2 Collab.)
AKHMETSHIN 05	PL B605 26	R.R. Akhmetshin et al.	(Novosibirsk CMD-2 Collab.)
AMBROSINO 05	PL B608 199	F. Ambrosino et al.	(KLOE Collab.)
AUBERT_B 05J	PR D72 052008	B. Aubert et al.	(BABAR Collab.)
AKHMETSHIN 04	PL B578 285	R.R. Akhmetshin et al.	(Novosibirsk CMD-2 Collab.)
AUBERT_B 04N	PR D70 072004	B. Aubert et al.	(BABAR Collab.)
ALOISIO 02E	PL B561 35	A. Aloisio et al.	(KLOE Collab.)
AULCHENKO 03B	JETP 97 24	V.M. Aulchenko et al.	(Novosibirsk SND Collab.)
ACHASOV 02	PR D65 032002	M.N. Achasov et al.	(Novosibirsk SND Collab.)
ACHASOV 02D	JETPL 75 449	M.N. Achasov et al.	(Novosibirsk SND Collab.)
ACHASOV 02C	PL B536 209	A. Aloisio et al.	(KLOE Collab.)
ALOISIO 02D	PL B537 21	A. Aloisio et al.	(KLOE Collab.)
ALOISIO 02E	PL B541 45	A. Aloisio et al.	(KLOE Collab.)
FISCHBAACH 02	PL B526 355	E. Fischbach, A.W. Overhauser, B. Woodshi	(KLOE Collab.)
GOKALP 02	JPG 28 2783	A. Gokalp et al.	
ACHASOV 01B	PL B504 275	M.N. Achasov et al.	(Novosibirsk SND Collab.)
ACHASOV 01E	PR D63 072002	M.N. Achasov et al.	(Novosibirsk SND Collab.)
ACHASOV 01F	PR D63 094007	M.N. Achasov, V.V. Gubin	(Novosibirsk SND Collab.)
ACHASOV 01G	PRL 86 1698	M.N. Achasov et al.	(Novosibirsk SND Collab.)
AITALA 01B	PRL 86 770	E.M. Aitala et al.	(FNAL E791 Collab.)
AKHMETSHIN 01	PL B501 191	R.R. Akhmetshin et al.	(Novosibirsk CMD-2 Collab.)
AKHMETSHIN 01B	PL B509 217	R.R. Akhmetshin et al.	(Novosibirsk CMD-2 Collab.)
AKHMETSHIN 01C	PL B503 237	R.R. Akhmetshin et al.	(Novosibirsk CMD-2 Collab.)
ACHASOV 00	EPJ C12 25	M.N. Achasov et al.	(Novosibirsk SND Collab.)
ACHASOV 00B	JETP 90 17	M.N. Achasov et al.	(Novosibirsk SND Collab.)
ACHASOV 00C	Translated from ZETF 117 22	M.N. Achasov et al.	(Novosibirsk SND Collab.)
ACHASOV 00D	JETPL 72 282	M.N. Achasov et al.	(Novosibirsk SND Collab.)
ACHASOV 00E	Translated from ZETFP 72 411	M.N. Achasov et al.	(Novosibirsk SND Collab.)
ACHASOV 00F	NP B569 158	M.N. Achasov et al.	(Novosibirsk SND Collab.)
ACHASOV 00G	PL B479 53	M.N. Achasov et al.	(Novosibirsk SND Collab.)
ACHASOV 00H	PL B405 349	M.N. Achasov et al.	(Novosibirsk SND Collab.)
AKHMETSHIN 00B	PL B473 337	R.R. Akhmetshin et al.	(Novosibirsk CMD-2 Collab.)
AKHMETSHIN 00E	PL B491 81	R.R. Akhmetshin et al.	(Novosibirsk CMD-2 Collab.)
AKHMETSHIN 00F	PL B494 26	R.R. Akhmetshin et al.	(Novosibirsk CMD-2 Collab.)
AULCHENKO 00A	JETP 90 927	V.M. Aulchenko et al.	(Novosibirsk SND Collab.)
BRAMON 00	PL B486 406	A. Bramon et al.	
PDG 00	EPJ C15 1	D.E. Groom et al.	
ACHASOV 99	PL B449 122	M.N. Achasov et al.	(Novosibirsk SND Collab.)
ACHASOV 99C	PL B456 304	M.N. Achasov et al.	(Novosibirsk SND Collab.)
AKHMETSHIN 99B	PL B462 371	R.R. Akhmetshin et al.	(Novosibirsk CMD-2 Collab.)
AKHMETSHIN 99C	PL B462 380	R.R. Akhmetshin et al.	(Novosibirsk CMD-2 Collab.)
AKHMETSHIN 99D	PL B466 385	R.R. Akhmetshin et al.	(Novosibirsk CMD-2 Collab.)
Also	PL B508 217 (erratum)	R.R. Akhmetshin et al.	(Novosibirsk CMD-2 Collab.)
AKHMETSHIN 99F	PL B460 242	R.R. Akhmetshin et al.	(Novosibirsk CMD-2 Collab.)
AULCHENKO 99	JETPL 69 97	V.M. Aulchenko et al.	(Novosibirsk SND Collab.)
ACHASOV 98B	PL B438 441	M.N. Achasov et al.	(Novosibirsk SND Collab.)
ACHASOV 98F	JETPL 68 573	M.N. Achasov et al.	(Novosibirsk SND Collab.)
ACHASOV 98I	PL B440 442	M.N. Achasov et al.	(Novosibirsk SND Collab.)
AKHMETSHIN 98	PL B434 426	R.R. Akhmetshin et al.	(Novosibirsk CMD-2 Collab.)
AULCHENKO 98	PL B436 199	V.M. Aulchenko et al.	(Novosibirsk SND Collab.)
BARBERIS 98	PL B432 436	D. Barberis et al.	(Omega Expt.)
AKHMETSHIN 97B	PL B415 445	R.R. Akhmetshin et al.	(NOVO, BOST, PITT+)
AKHMETSHIN 97C	PL B415 452	R.R. Akhmetshin et al.	(Novosibirsk CMD-2 Collab.)
BENAYOUN 96	ZPHY C72 221	M. Benayoun et al.	(IPNP, NOVO)
AKHMETSHIN 95	PL B364 199	R.R. Akhmetshin et al.	(Novosibirsk CMD-2 Collab.)
DOLINSKY 91	PRPL 202 99	S.I. Dolinsky et al.	(NOVO)
ACHASOV 89	NP B315 465	M.N. Achasov, V.N. Ivanchenko	(NOVO)
DOLINSKY 89	ZPHY C42 511	S.I. Dolinsky et al.	(NOVO)
BARKOV 88	SJNP 47 248	L.M. Barkov et al.	(NOVO)
DOLINSKY 88	Translated from YAF 47 393	S.I. Dolinsky et al.	(NOVO)
DRUZHININ 87	ZPHY C37 1	V.P. Druzhinin et al.	(NOVO)
ARMSTRONG 86	PL 166B 245	T.A. Armstrong et al.	(ATHU, BARI, BIRM+)
ATKINSON 86	ZPHY C30 521	M. Atkinson et al.	(BONN, CERN, GLAS+)
BEBEK 86	PRL 56 1893	C. Bebek et al.	(CLEO Collab.)
DAVENPORT 86	PR D33 2519	T.F. Davenport et al.	(TUFTS, ARIZ, FNAL, FSU, NDAM+)
DIJKSTRA 86	ZPHY C31 375	H. Dijkstra et al.	(ANIK, BRIS, CERN+)
FRAME 86	NP B276 667	D. Frame et al.	(GLAS)
GOLUBEV 86	SJNP 44 409	V.B. Golubev et al.	(NOVO)
ALBRECHT 85D	Translated from YAF 44 633	H. Albrecht et al.	(ARGUS Collab.)
GOLUBEV 85	PL 153B 343	V.B. Golubev et al.	(NOVO)
DRUZHININ 84	PL 144B 136	V.P. Druzhinin et al.	(NOVO)
ARMSTRONG 83B	NP B224 193	T.A. Armstrong et al.	(BARI, BIRM, CERN+)
BARATE 83	PL 121B 449	R. Barate et al.	(SACL, LOIC, SHMP, IND)
KURDADZE 83C	JETPL 38 366	L.M. Kurdadze et al.	(NOVO)
ARENTON 82	PR D25 2241	M.W. Arenton et al.	(ANL, ILL)
PELLINEN 82	PS 25 599	A. Pellinen, M. Roos	(HEL5)
DAUM 81	PL 100B 439	C. Daum et al.	(AMST, BRIS, CERN, CRAC+)
IVANOV 81	PL 107B 297	P.M. Ivanov et al.	(NOVO)
Also	Private Comm.	S.I. Edelman	(NOVO)
VASSERMAN 81	PL 99B 62	I.B. Vasserman et al.	(NOVO)
Also	SJNP 35 240	L.M. Kurdadze et al.	(NOVO)
Also	Translated from YAF 35 352		

CORDIER 80	NP B172 13	A. Cordier et al.	(LALO)
CORDIER 79	PL 81B 389	A. Cordier et al.	(LALO)
BUKIN 78B	SJNP 27 521	A.D. Bukin et al.	(NOVO)
BUKIN 78C	Translated from YAF 27 985	A.D. Bukin et al.	(NOVO)
BUKIN 78C	SJNP 27 516	A.D. Bukin et al.	(NOVO)
COOPER 78B	Translated from YAF 27 976	A.M. Cooper et al.	(TATA, CERN, CDEF+)
LOSTY 78	NP B133 38	M.J. Losty et al.	(CERN, AMST, NIJM+)
AKERLOF 77	PRL 39 861	C.W. Akerlof et al.	(FNAL, MICH, PURD)
ANDREWS 77	PRL 38 198	D.E. Andrews et al.	(ROCH)
BALDI 77	PL 68B 381	R. Baldi et al.	(GEVA)
CERRADA 77B	NP B126 241	M. Cerrada et al.	(AMST, CERN, NIJM+)
COHEN 77	PRL 38 269	D. Cohen et al.	(ANL)
LAVEN 77	NP B127 43	H. Laven et al.	(AACH3, BERL, CERN, LOIC+)
LYONS 77	NP B125 207	L. Lyons, A.M. Cooper, A.G. Clark	(OXF)
COSME 76	PL 63B 352	G. Cosme et al.	(ORSAY)
KALBFLEISCH 76	PR D13 22	G.R. Kalbfleisch, R.C. Strand, J.W. Chapman	(BNL+)
PAROUR 76	PL 63B 357	G. Parour et al.	(ORSAY)
PAROUR 76B	PL 63B 362	G. Parour et al.	(ORSAY)
KALBFLEISCH 75	PR D11 987	G.R. Kalbfleisch, R.C. Strand, J.W. Chapman	(BNL+)
AYRES 75	PRL 32 1463	D.S. Ayres et al.	(ANL)
BESCH 74	NP B70 257	H.J. Besch et al.	(BOBN)
COSME 74	PL 48B 155	G. Cosme et al.	(ORSAY)
COSME 74B	PL 48B 159	G. Cosme et al.	(ORSAY)
DEGROOT 74	NP B74 77	A.J. de Groot et al.	(AMST, NIJM)
AUGUSTIN 73	PRL 30 462	J.E. Augustin et al.	(ORSAY)
BALLAM 73	PR D7 3150	J. Ballam et al.	(SLAC, LBL)
BINNIE 73B	PR D8 2789	D.M. Binnie et al.	(LOIC, SHMP)
AGUILAR... 72B	PR D6 29	M. Aguilar-Benitez et al.	(ORSAY)
ALVENSLEB... 72	PRL 28 66	H. Alvensleben et al.	(MIT, DESY)
BORENSTEIN 72	PR D5 1559	S.R. Borenstein et al.	(BNL, MICH)
COLLEY 72	NP B50 1	D.C. Colley et al.	(BIRM, GLAS)
BALAKIN 71	PL 34B 328	V.E. Balakin et al.	(NOVO)
CHATELUS 71	Thesis LAL 1247	Y. Chateaus	(STRB)
Also	PL 32B 416	J.C. Bizot et al.	(ORSAY)
HAYES 71	PR D4 899	S. Hayes et al.	(CORN)
STOTTLE... 71	Thesis ORO 2504 170	A.R. Stottlemeyer	(UMD)
BIZOT 70	PL 32B 416	J.C. Bizot et al.	(ORSAY)
Also	Liverpool Sym. 69	J.P. Perez-y-Jorba	
EARLES 70	PRL 25 1312	D.R. Earles et al.	(NEAS)
LINDSEY 66	PR 147 913	J.S. Lindsey, G. Smith	(LRL)
LONDON 66	PR 143 1034	G.W. London et al.	(BNL, SYRA) IGJPC
BADIER 65B	PL 17 337	J. Badier et al.	(EPOL, SACL, AMST)
LINDSEY 65	PRL 15 221	J.S. Lindsey, G.A. Smith	(LRL)
LINDSEY 65	data included in LINDSEY 66		
SCHLEIN 63	PRL 10 368	P.E. Schlein et al.	(UCLA) IGJP

OTHER RELATED PAPERS

AMBROSINO 06G	PL B634 148	F. Ambrosino et al.	(KLOE Collab.)
AMBROSINO 06B	PL B642 315	F. Ambrosino et al.	(KLOE Collab.)
ANISOVICH 05B	PAN 68 1554	A.V. Anisovich, V.V. Anisovich, V.N. Markov	
AMBROSINO 05A	EPJ A24 437	Yu.S. Kalashnikova, A.E. Kudryatsev, A.V. Nefediev	
VALOSHIN 05A	PAN 68 771	M.B. Voloshin	
ACHASOV 03B	PR D68 014006	M.N. Achasov, A.V. Kiselev	
BOGLIONE 03	EPJ C30 503	M. Boglione, M.R. Pennington	
ACHASOV 02L	PAN 65 1887	M.N. Achasov et al.	
ANISOVICH 02C	PAN 65 497	A.V. Anisovich et al.	
BRAMON 02E	EPJ C26 253	A. Bramon et al.	
ACHASOV 01F	PR D63 094007	M.N. Achasov, V.V. Gubin	(Novosibirsk SND Collab.)
BENAYOUN 01	EPJ C22 503	M. Benayoun, H.B. O'Connell	
CLOSE 01	PL B515 13	F.E. Close, A. Kirk	
GOKALP 01	PR D64 053017	A. Gokalp, O. Yilmaz	
MARKUSHIN 00	EPJ A8 389	V.E. Markushin	
ACHASOV 99B	PAN 62 442	M.N. Achasov et al.	
MARCO 99	PL B470 20	E. Marco et al.	
OLLER 98B	PL B426 7	J.A. Oller	
ACHASOV 95	PL B363 106	M.N. Achasov, V.V. Gubin	(NOVM)
KAMAL 92	PL B284 421	A.N. Kamal, Q.P. Xu	(ALBE)
GEORGIO... 85B	PL 152B 428	C. Georgiopoulos et al.	(TUFTS, ARIZ, FNAL+)
GELFAND 83B	PRL 11 438	N. Gelfand et al.	(COLU, RUTG)
BERTANZA 62	PRL 9 180	L. Bertanza et al.	(BNL, SYRA)

 $h_1(1170)$

$$J^{PC} = 0^-(1^+ -)$$

 $h_1(1170)$ MASS

VALUE (MeV)	DOCUMENT ID	TECN	CHG	COMMENT
1170 ± 20 OUR ESTIMATE				
• • • We do not use the following data for averages, fits, limits, etc. • • •				
1168 ± 4	ANDO	92	SPEC	$8 \pi^- p \rightarrow \pi^+ \pi^- \pi^0 n$
1166 ± 5 ± 3	1 ANDO	92	SPEC	$8 \pi^- p \rightarrow \pi^+ \pi^- \pi^0 n$
1190 ± 60	2 DANKOWY...	81	SPEC	$8 \pi^- p \rightarrow 3 \pi n$
¹ Average and spread of values using 2 variants of the model of BOWLER 75.				
² Uses the model of BOWLER 75.				

 $h_1(1170)$ WIDTH

VALUE (MeV)	DOCUMENT ID	TECN	CHG	COMMENT
360 ± 40 OUR ESTIMATE				
• • • We do not use the following data for averages, fits, limits, etc. • • •				
345 ± 6	ANDO	92	SPEC	$8 \pi^- p \rightarrow \pi^+ \pi^- \pi^0 n$
375 ± 6 ± 34	3 ANDO	92	SPEC	$8 \pi^- p \rightarrow \pi^+ \pi^- \pi^0 n$
320 ± 50	4 DANKOWY...	81	SPEC	$8 \pi^- p \rightarrow 3 \pi n$
³ Average and spread of values using 2 variants of the model of BOWLER 75.				
⁴ Uses the model of BOWLER 75.				

Meson Particle Listings

$h_1(1170)$, $b_1(1235)$

$h_1(1170)$ DECAY MODES

Mode	Fraction (Γ_i/Γ)
Γ_1 $\rho\pi$	seen

$h_1(1170)$ BRANCHING RATIOS

$\Gamma(\rho\pi)/\Gamma_{\text{total}}$	DOCUMENT ID	TECN	COMMENT	Γ_1/Γ
VALUE				
••• We do not use the following data for averages, fits, limits, etc. •••				
seen	ANDO 92	SPEC	$8\pi^-p \rightarrow \pi^+\pi^-\pi^0 n$	
seen	ATKINSON 84	OMEG	$20-70\gamma p \rightarrow \pi^+\pi^-\pi^0 p$	
seen	DANKOWY... 81	SPEC	$8\pi p \rightarrow 3\pi n$	

$h_1(1170)$ REFERENCES

ANDO 92	PL B291 496	A. Ando et al.	(KEK, KYOT, NIRS, SAGA+)
ATKINSON 84	NP B231 15	M. Atkinson et al.	(BONN, CERN, GLAS+)
DANKOWY... 81	PRL 46 580	J.A. Dankowycz et al.	(TNTO, BNL, CARL+)
BOWLER 75	NP B97 227	M.G. Bowler et al.	(OXFTP, DARE)

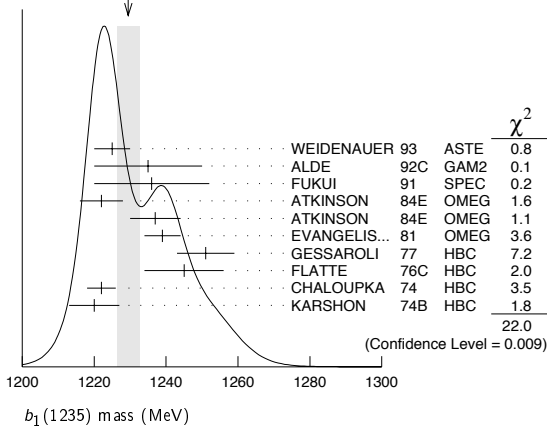
$b_1(1235)$

$I^G(J^{PC}) = 1^+(1^{+-})$

$b_1(1235)$ MASS

VALUE (MeV)	EVTS	DOCUMENT ID	TECN	CHG	COMMENT
1229.5 ± 3.2 OUR AVERAGE		Error includes scale factor of 1.6. See the ideogram below.			
1225 ± 5		WEIDENAUER 93	ASTE		$\bar{p}p \rightarrow 2\pi^+2\pi^-\pi^0$
1235 ± 15		ALDE 92C	GAM2		$38,100\pi^-p \rightarrow \omega\pi^0 n$
1236 ± 16		FUKUI 91	SPEC		$8.95\pi^-p \rightarrow \omega\pi^0 n$
1222 ± 6		ATKINSON 84E	OMEG ±		$25-55\gamma p \rightarrow \omega\pi X$
1237 ± 7		ATKINSON 84E	OMEG 0		$25-55\gamma p \rightarrow \omega\pi X$
1239 ± 5		EVANGELIS... 81	OMEG -		$12\pi^-p \rightarrow \omega\pi p$
1251 ± 8	450	GESSAROLI 77	HBC -		$11\pi^-p \rightarrow \pi^-\omega p$
1245 ± 11	890	FLATTE 76C	HBC -		$4.2K^-p \rightarrow \pi^-\omega\Sigma^+$
1222 ± 4	1400	CHALOUPKA 74	HBC -		$3.9\pi^-p$
1220 ± 7	600	KARSHON 74B	HBC +		$4.9\pi^+p$
••• We do not use the following data for averages, fits, limits, etc. •••					
1190 ± 10		AUGUSTIN 89	DM2 ±		$e^+e^- \rightarrow 5\pi$
1213 ± 5		ATKINSON 84c	OMEG 0		$20-70\gamma p$
1271 ± 11		COLLICK 84	SPEC +		$200\pi^+Z \rightarrow Z\pi\omega$

WEIGHTED AVERAGE
1229.5±3.2 (Error scaled by 1.6)



$b_1(1235)$ WIDTH

VALUE (MeV)	EVTS	DOCUMENT ID	TECN	CHG	COMMENT
142 ± 9 OUR AVERAGE		Error includes scale factor of 1.2.			
113 ± 12		WEIDENAUER 93	ASTE		$\bar{p}p \rightarrow 2\pi^+2\pi^-\pi^0$
160 ± 30		ALDE 92C	GAM2		$38,100\pi^-p \rightarrow \omega\pi^0 n$
151 ± 31		FUKUI 91	SPEC		$8.95\pi^-p \rightarrow \omega\pi^0 n$
170 ± 15		EVANGELIS... 81	OMEG -		$12\pi^-p \rightarrow \omega\pi p$
170 ± 50	225	BALTAY 78B	HBC +		$15\pi^+p \rightarrow p4\pi$
155 ± 32	450	GESSAROLI 77	HBC -		$11\pi^-p \rightarrow \pi^-\omega p$
182 ± 45	890	FLATTE 76C	HBC -		$4.2K^-p \rightarrow \pi^-\omega\Sigma^+$
135 ± 20	1400	CHALOUPKA 74	HBC -		$3.9\pi^-p$
156 ± 22	600	KARSHON 74B	HBC +		$4.9\pi^+p$

••• We do not use the following data for averages, fits, limits, etc. •••

210 ± 19	AUGUSTIN 89	DM2 ±	$e^+e^- \rightarrow 5\pi$
231 ± 14	ATKINSON 84c	OMEG 0	$20-70\gamma p$
232 ± 29	COLLICK 84	SPEC +	$200\pi^+Z \rightarrow Z\pi\omega$

$b_1(1235)$ DECAY MODES

Mode	Fraction (Γ_i/Γ)	Confidence level
Γ_1 $\omega\pi$	dominant	
Γ_2 $\pi^\pm\gamma$	$[D/S \text{ amplitude ratio} = 0.277 \pm 0.027]$	
Γ_3 $\eta\rho$	$(1.6 \pm 0.4) \times 10^{-3}$	
Γ_4 $\pi^\pm\pi^+\pi^-\pi^0$	seen	
Γ_4 $\pi^\pm\pi^+\pi^-\pi^0$	< 50	% 84%
Γ_5 $(KK)^\pm\pi^0$	< 8	% 90%
Γ_6 $K_S^0 K_S^0\pi^\pm$	< 6	% 90%
Γ_7 $K_S^0 K_S^0\pi^\pm$	< 2	% 90%
Γ_8 $\phi\pi$	< 1.5	% 84%

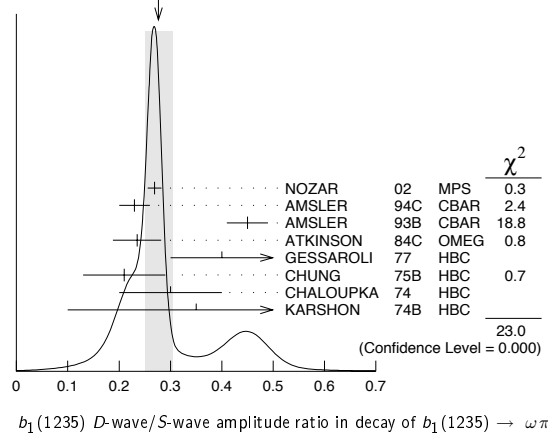
$b_1(1235)$ PARTIAL WIDTHS

$\Gamma(\pi^\pm\gamma)$	DOCUMENT ID	TECN	CHG	COMMENT	Γ_2
VALUE (keV)					
230 ± 60	COLLICK 84	SPEC +		$200\pi^+Z \rightarrow Z\pi\omega$	

$b_1(1235)$ D-wave/S-wave AMPLITUDE RATIO IN DECAY OF $b_1(1235) \rightarrow \omega\pi$

VALUE	EVTS	DOCUMENT ID	TECN	CHG	COMMENT
0.277 ± 0.027 OUR AVERAGE		Error includes scale factor of 2.4. See the ideogram below.			
0.269 ± 0.009 ± 0.010		NOZAR 02	MPS -		$18\pi^-p \rightarrow \omega\pi^-p$
0.23 ± 0.03		AMSLER 94C	CBAR		$0.0\bar{p}p \rightarrow \omega\eta\pi^0$
0.45 ± 0.04		AMSLER 93B	CBAR		$0.0\bar{p}p \rightarrow \omega\eta\pi^0$
0.235 ± 0.047		ATKINSON 84c	OMEG		$20-70\gamma p$
0.4 ± 0.1		GESSAROLI 77	HBC -		$11\pi^-p \rightarrow \pi^-\omega p$
0.21 ± 0.08		CHUNG 75B	HBC +		$7.1\pi^+p$
0.3 ± 0.1		CHALOUPKA 74	HBC -		$3.9-7.5\pi^-p$
0.35 ± 0.25	600	KARSHON 74B	HBC +		$4.9\pi^+p$

WEIGHTED AVERAGE
0.277±0.027 (Error scaled by 2.4)



$b_1(1235)$ D-wave/S-wave AMPLITUDE PHASE DIFFERENCE IN DECAY OF $b_1(1235) \rightarrow \omega\pi$

VALUE (°)	DOCUMENT ID	TECN	CHG	COMMENT
10.5 ± 2.4 ± 3.9				
	NOZAR 02	MPS -		$18\pi^-p \rightarrow \omega\pi^-p$

$b_1(1235)$ BRANCHING RATIOS

$\Gamma(\eta\rho)/\Gamma(\omega\pi)$	DOCUMENT ID	TECN	COMMENT	Γ_3/Γ_1
VALUE				
< 0.10	ATKINSON 84D	OMEG	$20-70\gamma p$	

$\Gamma(\pi^+\pi^+\pi^-\pi^0)/\Gamma(\omega\pi)$	DOCUMENT ID	TECN	CHG	COMMENT	Γ_4/Γ_1
VALUE					
< 0.5	ABOLINS 63	HBC +		$3.5\pi^+p$	

See key on page 373

Meson Particle Listings

$b_1(1235)$, $a_1(1260)$

$\Gamma((K\bar{K})^\pm \pi^0)/\Gamma(\omega\pi)$					Γ_5/Γ_1
VALUE	CL%	DOCUMENT ID	TECN	CHG	COMMENT
<0.08	90	BALTAY	67	HBC	\pm 0.0 $\bar{p}p$

$\Gamma(K_S^0 K_L^0 \pi^\pm)/\Gamma(\omega\pi)$					Γ_6/Γ_1
VALUE	CL%	DOCUMENT ID	TECN	CHG	COMMENT
<0.06	90	BALTAY	67	HBC	\pm 0.0 $\bar{p}p$

$\Gamma(K_S^0 K_S^0 \pi^\pm)/\Gamma(\omega\pi)$					Γ_7/Γ_1
VALUE	CL%	DOCUMENT ID	TECN	CHG	COMMENT
<0.02	90	BALTAY	67	HBC	\pm 0.0 $\bar{p}p$

$\Gamma(\phi\pi)/\Gamma(\omega\pi)$					Γ_8/Γ_1
VALUE	CL%	DOCUMENT ID	TECN	CHG	COMMENT
<0.004	95	VIKTOROV	96	SPEC	0 32.5 $\pi^- p \rightarrow K^+ K^- \pi^0 n$

• • • We do not use the following data for averages, fits, limits, etc. • • •

<0.04	95	BIZZARRI	69	HBC	\pm 0.0 $\bar{p}p$
<0.015		DAHL	67	HBC	1.6-4.2 $\pi^- p$

$b_1(1235)$ REFERENCES

NOZAR	02	PL B541 35	M. Nozar et al.		
VIKTOROV	96	PAN 59 1184 Translated from YAF 59 1239	V.A. Viktorov et al.	(SERP)	
AMSLER	94C	PL B327 425	C. Amisler et al.	(Crystal Barrel Collab.)	
AMSLER	93B	PL B311 362	C. Amisler et al.	(Crystal Barrel Collab.)	
WEIDENAUER	93	ZPHY C59 387	P. Weidenauer et al.	(ASTERIX Collab.)	
ALDE	92C	ZPHY C54 553	D.M. Alde et al.	(BELG, SERP, KEK, LANL+)	
FUKUI	91	PL B257 241	S. Fukui et al.	(SUGI, NAGO, KEK, KYOT+)	
AUGUSTIN	89	NP B320 1	J.E. Augustin, G. Cosme	(DM2 Collab.)	
ATKINSON	84C	NP B243 1	M. Atkinson et al.	(BONN, CERN, GLAS+)	JP
ATKINSON	84D	NP B242 269	M. Atkinson et al.	(BONN, CERN, GLAS+)	
ATKINSON	84E	PL 130B 459	M. Atkinson et al.	(BONN, CERN, GLAS+)	
COLLICK	84	PRL 53 2374	B. Collick et al.	(MINN, ROCH, FNAL)	
EVANGELISTA...	81	NP B178 197	C. Evangelista et al.	(BARI, BONN, CERN+)	
BALTAY	75B	PR D17 62	C. Baltay et al.	(COLU, BING)	
GESSAROLI	77	NP B126 382	R. Gessaroli et al.	(BGNA, FIRZ, GENO+)	JP
FLATTE	76C	PL 64B 225	S.M. Flatte et al.	(CERN, AMST, NIJM+)	JP
CHUNG	75B	PR D11 2426	S.U. Chung et al.	(BNL, LBL, UCSC)	JP
CHALOUPKA	74	PL 51B 407	V. Chaloupka et al.	(CERN)	JP
KARSHON	74B	PR D10 3608	U. Karshon et al.	(REHO)	JP
BIZZARRI	69	NP B14 169	R. Bizzarri et al.	(CERN, CDEF)	
BALTAY	67	PRL 18 93	C. Baltay et al.	(COLU)	
DAHL	67	PR 163 1377	O.I. Dahl et al.	(LRL)	
ABOLINS	63	PRL 11 381	M.A. Abolins et al.	(UCSD)	

OTHER RELATED PAPERS

ABLIKIM	04A	PL B598 149	M. Ablikim et al.	(BES Collab.)	
GOLOVKIN	97	ZPHY A359 435	S.V. Golovkin et al.	(SERP, ITEP)	
BRAU	88	PR D37 2379	J.E. Brau et al.		JP
ATKINSON	84C	NP B243 1	M. Atkinson et al.	(BONN, CERN, GLAS+)	JP
GOLDBABER	65	PRL 15 118	G. Goldhaber et al.	(LRL)	
CARMONY	64	PRL 12 254	D.D. Carmony et al.	(UCB)	JP
BONDAR	63B	PL 5 209	L. Bondar et al.	(AACH, BIRM, HAMB, LOIC+)	

$a_1(1260)$

$$J^{PC} = 1^-(1^{++})$$

$a_1(1260)$ MASS

VALUE (MeV)	EVTS	DOCUMENT ID	TECN	CHG	COMMENT
1230±40 OUR ESTIMATE					
• • • We do not use the following data for averages, fits, limits, etc. • • •					
1243±12±20		1 AUBERT	07AU	BABR	10.6 $e^+e^- \rightarrow \rho^0 \rho^\pm \pi^\mp \gamma$
1230-1270	6360	2 LINK	07A	FOCS	$D^0 \rightarrow \pi^- \pi^+ \pi^- \pi^+$
1203±3		3 GOMEZ-DUMM04		RVUE	$\tau^+ \rightarrow \pi^+ \pi^+ \pi^- \nu_\tau$
1331±10±3	37k	4 ASNER	00	CLE2	10.6 $e^+e^- \rightarrow \tau^+ \tau^-$, $\tau^- \rightarrow \pi^- \pi^0 \pi^0 \nu_\tau$
1255±7±6	5904	5 ABREU	98G	DLPH	e^+e^-
1207±5±8	5904	6 ABREU	98G	DLPH	e^+e^-
1196±4±5	5904	7,8 ABREU	98G	DLPH	e^+e^-
1240±10		BARBERIS	98B		450 $pp \rightarrow p_f \pi^+ \pi^- \pi^0 p_S$
1262±9±7		5,9 ACKERSTAFF	97R	OPAL	$E_{cm}^{ee} = 88-94, \tau \rightarrow 3\pi\nu$
1210±7±2		6,9 ACKERSTAFF	97R	OPAL	$E_{cm}^{ee} = 88-94, \tau \rightarrow 3\pi\nu$
1211±7±50	-0	6 ALBRECHT	93C	ARG	$\tau^+ \rightarrow \pi^+ \pi^+ \pi^- \nu$
1121±8		10 ANDO	92	SPEC	8 $\pi^- p \rightarrow \pi^+ \pi^- \pi^0 n$
1242±37		11 IVANOV	91	RVUE	$\tau \rightarrow \pi^+ \pi^+ \pi^- \nu$
1260±14		12 IVANOV	91	RVUE	$\tau \rightarrow \pi^+ \pi^+ \pi^- \nu$
1250±9		13 IVANOV	91	RVUE	$\tau \rightarrow \pi^+ \pi^+ \pi^- \nu$
1208±15		ARMSTRONG	90	OMEG 0	300.0 $pp \rightarrow p \rho \pi^+ \pi^- \pi^0$
1220±15		14 ISGUR	89	RVUE	$\tau^+ \rightarrow \pi^+ \pi^+ \pi^- \nu$
1260±25		15 BOWLER	88	RVUE	
1166±18±11		BAND	87	MAC	$\tau^+ \rightarrow \pi^+ \pi^+ \pi^- \nu$
1164±41±23		BAND	87	MAC	$\tau^+ \rightarrow \pi^+ \pi^0 \pi^0 \nu$

1250±40	14 TORNQVIST	87	RVUE		
1046±11	ALBRECHT	86B	ARG		$\tau^+ \rightarrow \pi^+ \pi^+ \pi^- \nu$
1056±20±15	RUCKSTUHL	86	DLCO		$\tau^+ \rightarrow \pi^+ \pi^+ \pi^- \nu$
1194±14±10	SCHMIDKE	86	MRK2		$\tau^+ \rightarrow \pi^+ \pi^+ \pi^- \nu$
1255±23	BELLINI	85	SPEC		40 $\pi^- A \rightarrow \pi^- \pi^+ \pi^- A$
1240±80	16 DANKOWY...	81	SPEC	0	8.45 $\pi^- p \rightarrow n3\pi$
1280±30	16 DAUM	81B	CNTR		63.94 $\pi^- p \rightarrow p3\pi$
1041±13	17 GAVILLET	77	HBC	+	4.2 $K^- p \rightarrow \Sigma 3\pi$

- The $\rho^\pm \pi^\mp$ state can be also due to the $\pi(1300)$.
- Using the Breit-Wigner parameterization; strong correlation between mass and width.
- Using the data of BARATE 98R.
- From a fit to the 3π mass spectrum including the $K\bar{K}^*(892)$ threshold.
- Uses the model of KUHN 90.
- Uses the model of ISGUR 89.
- Includes the effect of a possible a_1' state.
- Uses the model of FEINDT 90.
- Supersedes AKERS 95P.
- Average and spread of values using 2 variants of the model of BOWLER 75.
- Reanalysis of RUCKSTUHL 86.
- Reanalysis of SCHMIDKE 86.
- Reanalysis of ALBRECHT 86B.
- From a combined reanalysis of ALBRECHT 86B, SCHMIDKE 86, and RUCKSTUHL 86.
- From a combined reanalysis of ALBRECHT 86B and DAUM 81B.
- Uses the model of BOWLER 75.
- Produced in K^- backward scattering.

$a_1(1260)$ WIDTH

VALUE (MeV)	EVTS	DOCUMENT ID	TECN	CHG	COMMENT	
250 to 600 OUR ESTIMATE						
• • • We do not use the following data for averages, fits, limits, etc. • • •						
410±31±30		18 AUBERT	07AU	BABR	10.6 $e^+e^- \rightarrow \rho^0 \rho^\pm \pi^\mp \gamma$	
520-680	6360	19 LINK	07A	FOCS	$D^0 \rightarrow \pi^- \pi^+ \pi^- \pi^+$	
480±20		20 GOMEZ-DUMM04		RVUE	$\tau^+ \rightarrow \pi^+ \pi^+ \pi^- \nu_\tau$	
460±85	205	21 DRUTSKOY	02	BELL	$B \rightarrow D(*) K^- K^*0$	
814±36±13	37k	22 ASNER	00	CLE2	10.6 $e^+e^- \rightarrow \tau^+ \tau^-$, $\tau^- \rightarrow \pi^- \pi^0 \pi^0 \nu_\tau$	
450±50	22k	23 AKHMETSHIN	99E	CMD2	1.05-1.38 $e^+e^- \rightarrow \pi^+ \pi^- \pi^0 \pi^0$	
570±10		24 BONDAR	99	RVUE	$e^+e^- \rightarrow 4\pi, \tau \rightarrow 3\pi\nu_\tau$	
587±27±21	5904	25 ABREU	98G	DLPH	e^+e^-	
478±3±15	5904	26 ABREU	98G	DLPH	e^+e^-	
425±14±8	5904	27,28 ABREU	98G	DLPH	e^+e^-	
400±35		BARBERIS	98B		450 $pp \rightarrow p_f \pi^+ \pi^- \pi^0 p_S$	
621±32±58		25,29 ACKERSTAFF	97R	OPAL	$E_{cm}^{ee} = 88-94, \tau \rightarrow 3\pi\nu$	
457±15±17		26,29 ACKERSTAFF	97R	OPAL	$E_{cm}^{ee} = 88-94, \tau \rightarrow 3\pi\nu$	
446±21±140	-0	26 ALBRECHT	93C	ARG	$\tau^+ \rightarrow \pi^+ \pi^+ \pi^- \nu$	
239±11		ANDO	92	SPEC	8 $\pi^- p \rightarrow \pi^+ \pi^- \pi^0 n$	
266±13±4		30 ANDO	92	SPEC	8 $\pi^- p \rightarrow \pi^+ \pi^- \pi^0 n$	
465±228	-143	31 IVANOV	91	RVUE	$\tau \rightarrow \pi^+ \pi^+ \pi^- \nu$	
298±40	-34	32 IVANOV	91	RVUE	$\tau \rightarrow \pi^+ \pi^+ \pi^- \nu$	
488±32		33 IVANOV	91	RVUE	$\tau \rightarrow \pi^+ \pi^+ \pi^- \nu$	
430±50		ARMSTRONG	90	OMEG 0	300.0 $pp \rightarrow p \rho \pi^+ \pi^- \pi^0$	
420±40		34 ISGUR	89	RVUE	$\tau^+ \rightarrow \pi^+ \pi^+ \pi^- \nu$	
396±43		35 BOWLER	88	RVUE		
405±75±25		BAND	87	MAC	$\tau^+ \rightarrow \pi^+ \pi^+ \pi^- \nu$	
419±108±57		BAND	87	MAC	$\tau^+ \rightarrow \pi^+ \pi^0 \pi^0 \nu$	
521±27		ALBRECHT	86B	ARG	$\tau^+ \rightarrow \pi^+ \pi^+ \pi^- \nu$	
476±132	-120	RUCKSTUHL	86	DLCO	$\tau^+ \rightarrow \pi^+ \pi^+ \pi^- \nu$	
462±56±30		SCHMIDKE	86	MRK2	$\tau^+ \rightarrow \pi^+ \pi^+ \pi^- \nu$	
292±40		BELLINI	85	SPEC	40 $\pi^- A \rightarrow \pi^- \pi^+ \pi^- A$	
380±100		36 DANKOWY...	81	SPEC	0 8.45 $\pi^- p \rightarrow n3\pi$	
300±50		36 DAUM	81B	CNTR	63.94 $\pi^- p \rightarrow p3\pi$	
230±50		37 GAVILLET	77	HBC	+	4.2 $K^- p \rightarrow \Sigma 3\pi$

- The $\rho^\pm \pi^\mp$ state can be also due to the $\pi(1300)$.
- Using the Breit-Wigner parameterization; strong correlation between mass and width.
- Using the data of BARATE 98R.
- From a fit of the $K^- K^*0$ distribution assuming $m_{a_1} = 1230$ MeV and purely resonant production of the $K^- K^*0$ system.
- From a fit to the 3π mass spectrum including the $K\bar{K}^*(892)$ threshold.
- Using the $a_1(1260)$ mass of 1230 MeV.
- From AKHMETSHIN 99E and ASNER 00 data using the $a_1(1260)$ mass of 1230 MeV.
- Uses the model of KUHN 90.
- Uses the model of ISGUR 89.
- Includes the effect of a possible a_1' state.
- Uses the model of FEINDT 90.
- Supersedes AKERS 95P.
- Average and spread of values using 2 variants of the model of BOWLER 75.
- Reanalysis of RUCKSTUHL 86.

Meson Particle Listings

 $a_1(1260)$

- ³² Reanalysis of SCHMIDKE 86.
³³ Reanalysis of ALBRECHT 86b.
³⁴ From a combined reanalysis of ALBRECHT 86b, SCHMIDKE 86, and RUCKSTUHL 86.
³⁵ From a combined reanalysis of ALBRECHT 86b and DAUM 81b.
³⁶ Uses the model of BOWLER 75.
³⁷ Produced in K^- backward scattering.

 $a_1(1260)$ DECAY MODES

Mode	Fraction (Γ_i/Γ)
Γ_1 $\pi^+\pi^-\pi^0$	
Γ_2 $\pi^0\pi^0\pi^0$	
Γ_3 $(\rho\pi)S$ -wave	seen
Γ_4 $(\rho\pi)D$ -wave	seen
Γ_5 $(\rho(1450)\pi)S$ -wave	seen
Γ_6 $(\rho(1450)\pi)D$ -wave	seen
Γ_7 $\sigma\pi$	seen
Γ_8 $f_0(980)\pi$	not seen
Γ_9 $f_0(1370)\pi$	seen
Γ_{10} $f_2(1270)\pi$	seen
Γ_{11} $K\bar{K}^*(892) + c.c.$	seen
Γ_{12} $\pi\gamma$	seen

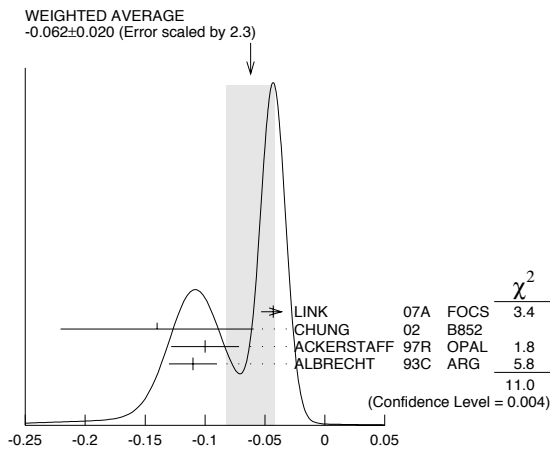
 $a_1(1260)$ PARTIAL WIDTHS

$\Gamma(\pi\gamma)$	VALUE (keV)	DOCUMENT ID	TECN	COMMENT	Γ_{12}
	640 ± 246	ZIELINSKI	84c	SPEC	200 $\pi^+\pi^-Z \rightarrow Z3\pi$

 D -wave/ S -wave AMPLITUDE RATIO IN DECAY OF $a_1(1260) \rightarrow \rho\pi$

VALUE	DOCUMENT ID	TECN	COMMENT
-0.062 ± 0.020 OUR AVERAGE			Error includes scale factor of 2.3. See the ideogram below.
$-0.043 \pm 0.009 \pm 0.005$	LINK	07A	FOCS $D^0 \rightarrow \pi^-\pi^+\pi^-\pi^+$
$-0.14 \pm 0.04 \pm 0.07$	³⁸ CHUNG	02	B852 $18.3 \pi^-\rho \rightarrow \pi^+\pi^-\pi^-\rho$
$-0.10 \pm 0.02 \pm 0.02$	^{39,40} ACKERSTAFF	97R	OPAL $E_{cm}^{ee} = 88-94, \tau \rightarrow 3\pi\nu$
-0.11 ± 0.02	³⁹ ALBRECHT	93C	ARG $\tau^+ \rightarrow \pi^+\pi^+\pi^-\nu$

³⁸ Deck-type background not subtracted.
³⁹ Uses the model of ISGUR 89.
⁴⁰ Supersedes AKERS 95p.

 D -wave/ S -wave AMPLITUDE RATIO IN DECAY OF $a_1(1260) \rightarrow \rho\pi$ $a_1(1260)$ BRANCHING RATIOS

$\Gamma((\rho\pi)S\text{-wave})/\Gamma_{\text{total}}$	VALUE (units 10^{-2})	EVTS	DOCUMENT ID	TECN	COMMENT	Γ_3/Γ
	60.19	37k	⁴¹ ASNER	00	CLE2 $10.6 e^+e^- \rightarrow \tau^+\tau^-, \tau^- \rightarrow \pi^-\pi^0\pi^0\nu_\tau$	

• • • We do not use the following data for averages, fits, limits, etc. • • •

$\Gamma((\rho\pi)D\text{-wave})/\Gamma_{\text{total}}$	VALUE (units 10^{-2})	EVTS	DOCUMENT ID	TECN	COMMENT	Γ_4/Γ
	$1.30 \pm 0.60 \pm 0.22$	37k	⁴¹ ASNER	00	CLE2 $10.6 e^+e^- \rightarrow \tau^+\tau^-, \tau^- \rightarrow \pi^-\pi^0\pi^0\nu_\tau$	

• • • We do not use the following data for averages, fits, limits, etc. • • •

$\Gamma((\rho(1450)\pi)S\text{-wave})/\Gamma_{\text{total}}$	VALUE (units 10^{-2})	EVTS	DOCUMENT ID	TECN	COMMENT	Γ_5/Γ
	$0.56 \pm 0.84 \pm 0.32$	37k	^{41,42} ASNER	00	CLE2 $10.6 e^+e^- \rightarrow \tau^+\tau^-, \tau^- \rightarrow \pi^-\pi^0\pi^0\nu_\tau$	

• • • We do not use the following data for averages, fits, limits, etc. • • •

$\Gamma((\rho(1450)\pi)D\text{-wave})/\Gamma_{\text{total}}$	VALUE (units 10^{-2})	EVTS	DOCUMENT ID	TECN	COMMENT	Γ_6/Γ
	$2.04 \pm 1.20 \pm 0.28$	37k	^{41,42} ASNER	00	CLE2 $10.6 e^+e^- \rightarrow \tau^+\tau^-, \tau^- \rightarrow \pi^-\pi^0\pi^0\nu_\tau$	

• • • We do not use the following data for averages, fits, limits, etc. • • •

$\Gamma(\sigma\pi)/\Gamma_{\text{total}}$	VALUE (units 10^{-2})	EVTS	DOCUMENT ID	TECN	COMMENT	Γ_7/Γ
	seen		CHUNG	02	B852 $18.3 \pi^-\rho \rightarrow \pi^+\pi^-\pi^-\rho$	
	$18.76 \pm 4.29 \pm 1.48$	37k	^{41,43} ASNER	00	CLE2 $10.6 e^+e^- \rightarrow \tau^+\tau^-, \tau^- \rightarrow \pi^-\pi^0\pi^0\nu_\tau$	

• • • We do not use the following data for averages, fits, limits, etc. • • •

$\Gamma(f_0(980)\pi)/\Gamma_{\text{total}}$	VALUE (units 10^{-2})	EVTS	DOCUMENT ID	TECN	COMMENT	Γ_8/Γ
	not seen	37k	ASNER	00	CLE2 $10.6 e^+e^- \rightarrow \tau^+\tau^-, \tau^- \rightarrow \pi^-\pi^0\pi^0\nu_\tau$	

• • • We do not use the following data for averages, fits, limits, etc. • • •

$\Gamma(f_0(1370)\pi)/\Gamma_{\text{total}}$	VALUE (units 10^{-2})	EVTS	DOCUMENT ID	TECN	COMMENT	Γ_9/Γ
	$7.40 \pm 2.71 \pm 1.26$	37k	^{41,44} ASNER	00	CLE2 $10.6 e^+e^- \rightarrow \tau^+\tau^-, \tau^- \rightarrow \pi^-\pi^0\pi^0\nu_\tau$	

• • • We do not use the following data for averages, fits, limits, etc. • • •

$\Gamma(f_2(1270)\pi)/\Gamma_{\text{total}}$	VALUE (units 10^{-2})	EVTS	DOCUMENT ID	TECN	COMMENT	Γ_{10}/Γ
	$1.19 \pm 0.49 \pm 0.17$	37k	^{41,45} ASNER	00	CLE2 $10.6 e^+e^- \rightarrow \tau^+\tau^-, \tau^- \rightarrow \pi^-\pi^0\pi^0\nu_\tau$	

• • • We do not use the following data for averages, fits, limits, etc. • • •

$\Gamma(K\bar{K}^*(892) + c.c.)/\Gamma_{\text{total}}$	VALUE (units 10^{-2})	EVTS	DOCUMENT ID	TECN	COMMENT	Γ_{11}/Γ
	2.2 ± 0.5	2255	⁴⁶ COAN	04	CLEO $\tau^- \rightarrow K^-\pi^-K^+\nu_\tau$	
	8 to 15	205	⁴⁷ DRUTSKOY	02	BELL $B \rightarrow D^{(*)}K^-K^{*0}$	
	$3.3 \pm 0.5 \pm 0.1$	37k	⁴⁸ ASNER	00	CLE2 $10.6 e^+e^- \rightarrow \tau^+\tau^-, \tau^- \rightarrow \pi^-\pi^0\pi^0\nu_\tau$	
	2.6 ± 0.3	49	BARATE	99R	ALEP $\tau \rightarrow K\bar{K}\pi\nu_\tau$	

• • • We do not use the following data for averages, fits, limits, etc. • • •

$\Gamma(\sigma\pi)/\Gamma((\rho\pi)S\text{-wave})$	VALUE	EVTS	DOCUMENT ID	TECN	COMMENT	Γ_7/Γ_3
	~ 0.3	28k	AKHMETSHIN 99E	CMD2	$1.05-1.38 e^+e^- \rightarrow \pi^+\pi^-\pi^+\pi^-$	
	0.003 ± 0.003	50	LONGACRE	82	RVUE	

• • • We do not use the following data for averages, fits, limits, etc. • • •

$\Gamma(\pi^0\pi^0\pi^0)/\Gamma(\pi^+\pi^-\pi^0)$	VALUE	CL%	DOCUMENT ID	COMMENT	Γ_2/Γ_1
	< 0.008	90	⁵¹ BARBERIS	01 450 $p\rho \rightarrow \rho_f 3\pi^0 p_S$	

• • • We do not use the following data for averages, fits, limits, etc. • • •

- ⁴¹ From a fit to the Dalitz plot.
⁴² Assuming for $\rho(1450)$ mass and width of 1370 and 386 MeV respectively.
⁴³ Assuming for σ mass and width of 860 and 880 MeV respectively.
⁴⁴ Assuming for $f_0(1370)$ mass and width of 1186 and 350 MeV respectively.
⁴⁵ Assuming for $f_2(1270)$ mass and width of 1275 and 185 MeV respectively.
⁴⁶ Using structure functions from KUHN 92 and DECKER 93a and $B(\tau^- \rightarrow K^-\pi^-K^+\nu_\tau) = (0.155 \pm 0.006 \pm 0.009)\%$ from BRIERE 03.
⁴⁷ From a comparison to ALAM 94 assuming purely resonant production of the K^-K^{*0} system.
⁴⁸ From a fit to the 3π mass spectrum including the $K\bar{K}^*(892)$ threshold.
⁴⁹ Assuming $a_1(1260)$ dominance and taking $B(\tau \rightarrow a_1(1260)\nu_\tau)$ from BUSKULIC 96.
⁵⁰ Uses multichannel Aitchison-Bowler model (BOWLER 75). Uses data from GAVILLET 77, DAUM 80, and DANKOWYCH 81.
⁵¹ Inconsistent with observations of $\sigma\pi$, $f_0(1370)\pi$, and $f_2(1270)\pi$ decay modes.

See key on page 373

Meson Particle Listings

 $a_1(1260)$, $f_2(1270)$ $a_1(1260)$ REFERENCES

AUBERT	07AU	PR D76 092005	B. Aubert et al.	(BABAR Collab.)
LINK	07A	PR D75 052003	J.M. Link et al.	(FNAL FOCUS Collab.)
COAN	04	PRL 92 232001	T.E. Coan et al.	(CLEO Collab.)
GOMEZ-DUMM	04	PR D69 073002	D. Gomez Dumm, A. Pich, J. Portoles	(CLEO Collab.)
BRIERE	03	PRL 90 181802	R. A. Briere et al.	(CLEO Collab.)
CHUNG	02	PR D65 072001	S.U. Chung et al.	(BNL E852 Collab.)
DRUTSKOY	02	PL B542 171	A. Drutskoy et al.	(BELLE Collab.)
BARBERIS	01	PL B507 14	D. Barberis et al.	(CLEO Collab.)
ASNER	00	PR D61 012002	D.M. Asner et al.	(CLEO Collab.)
AKHMETSHIN	99E	PL B466 392	R.R. Akhmetshin et al.	(Novosibirsk CMD-2 Collab.)
BARATE	99R	EPJ C11 599	R. Barate et al.	(ALEPH Collab.)
BONDAR	99	PL B466 403	A.E. Bondar et al.	(Novosibirsk CMD-2 Collab.)
ABREU	98G	PL B426 411	P. Abreu et al.	(DELPHI Collab.)
BARATE	98R	EPJ C4 409	R. Barate et al.	(ALEPH Collab.)
BARBERIS	98B	PL B422 399	D. Barberis et al.	(WA 102 Collab.)
ACKERSTAFF	97R	ZPHY C75 593	K. Ackerstaff et al.	(OPAL Collab.)
BUSKULIC	96	ZPHY C70 579	D. Buskalic et al.	(ALEPH Collab.)
AKERS	95P	ZPHY C67 45	R. Akers et al.	(OPAL Collab.)
ALAM	94	PR D50 43	M.S. Alam et al.	(CLEO Collab.)
ALBRECHT	93C	ZPHY C58 61	H. Albrecht et al.	(ARGUS Collab.)
DECKER	93A	ZPHY C58 445	R. Decker et al.	(KEK, KYOT, NIRS, SAGA+)
ANDO	92	PL B291 496	A. Ando et al.	(KEK, KYOT, NIRS, SAGA+)
KUHN	92	ZPHY C56 661	J.H. Kuhn, E. Mirkes	(JINR)
IVANOV	91	ZPHY C49 563	Y.P. Ivanov, A.A. Osipov, M.K. Volkov	(JINR)
ARMSTRONG	90	ZPHY C48 213	T.A. Armstrong, M. Benayoun, W. Beusch	(HAMB)
FEINDT	90	ZPHY C48 681	M. Feindt	(MPIM)
KUHN	90	ZPHY C48 445	J.H. Kuhn et al.	(TNT0)
ISGUR	89	PR D39 1357	N. Isgur, C. Morningstar, C. Reader	(OXF)
BOWLER	88	PL B209 99	M.G. Bowler	(MAC Collab.)
BAND	87	PL B198 297	H.R. Band et al.	(HELS)
TORNQVIST	87	ZPHY C36 695	N.A. Tornqvist	(ARGUS Collab.)
ALBRECHT	86B	ZPHY C33 7	H. Albrecht et al.	(DELCO Collab.)
RUCKSTUHL	86	PRL 56 2132	W. Ruckstuhl et al.	(Mark II Collab.)
SCHMIDKE	86	PRL 57 527	W.B. Schmidke et al.	(Mark II Collab.)
BELLINI	85	SJNP 41 781	D. Bellini et al.	(ROCH, MINN, FNAL)
ZIELINSKI	84C	PRL 52 1195	M. Zielinski et al.	(BNL)
LONGACRE	82	PR D26 82	R.S. Longacre	(TNT0, BNL, CARL+)
DANKOWYCH	81	PRL 46 580	J.A. Dankowycz et al.	(AMST, CERN, CRAC, MPIM+)
DAUM	81B	NP B182 269	C. Daum et al.	(AMST, CERN, CRAC, MPIM+)
DAUM	80	PL B9B 281	C. Daum et al.	(AMST, CERN, NIJM+)
GAVILLET	77	PL B9B 119	P. Gavillet et al.	(OXFPT, DARE)
BOWLER	75	NP B97 227	M.G. Bowler et al.	(OXFPT, DARE)

OTHER RELATED PAPERS

DZIERBA	06	PR D73 072001	A.R. Dzierba et al.	(BNL E852 Collab.)
BAKER	03	PL B563 140	C.A. Baker et al.	(BNL E852 Collab.)
CHUNG	02	PR D65 072001	S.U. Chung et al.	(BNL E852 Collab.)
FEUILLAT	01	PL B501 37	M. Feuillat, J.L. Lucio, M.J. Pestieau	(FNAL SELEX Collab.)
MOLCHANOV	01	PL B521 171	V.V. Molchanov et al.	(FNAL SELEX Collab.)
BAKER	99	PL B449 114	C.A. Baker et al.	(FNAL SELEX Collab.)
ZAIMIDOROGA	99	PAN 30 1	O.A. Zaimidoriga	(ORNL, RAL, MCHS)
BARNES	97	PR D55 4157	T. Barnes et al.	(SERP, TBIL)
AMELIN	95B	PL B356 595	D.V. Amelin et al.	(ITEP)
BOLONKIN	95	PAN 58 1535	B.V. Bolonkin et al.	(COLO, FSU)
WINGATE	95	PRL 74 4596	M. Wingate, T. de Grand	(SLAC Hybrid Collab.)
CONDO	93	PR D48 3045	G.T. Condo et al.	(VES Collab.)
GOUZ	92	Dallas HEP 92, p. 672	Yu.P. Gouz et al.	(NAGO, IBAR+)
Proceedings XXVI Int. Conf. on High Energy Physics				(OXF)
IIZUKA	89	PR D39 3357	J. Iizuka, H. Koibuchi, F. Masuda	(FNAL, ANL) JP
BOWLER	86	PL B182 400	M.G. Bowler	(FNAL, ANL) JP
BASDEVANT	78	PRL 40 994	J.L. Basdevant, E.L. Berger	(AAACH3, BERL, BIRM+)
BASDEVANT	77	PR D16 657	J.L. Basdevant, E.L. Berger	(LRL, UCB)
ADERHOLZ	64	PL 10 226	G. Aderholz et al.	(UCSD) JP
GOLDBABER	64	PRL 12 336	G. Goldhaber et al.	(MILA)
LANDER	64	PRL 13 346A	R.L. Lander et al.	(MILA)
BELLINI	63	NC 29 896	G. Bellini et al.	(MILA)

 $f_2(1270)$

$$J^G(J^{PC}) = 0^+(2^{++})$$

 $f_2(1270)$ MASS

VALUE (MeV)	EVTs	DOCUMENT ID	TECN	COMMENT
1275.1 ± 1.2 OUR AVERAGE		Error includes scale factor of 1.1.		
1262 ± 1/2 ± 8		ABLIKIM 06v	BES2	$e^+e^- \rightarrow J/\psi \rightarrow \gamma\pi^+\pi^-$
1275 ± 15		ABLIKIM 05	BES2	$J/\psi \rightarrow \phi\pi^+\pi^-$
1283 ± 5		ALDE 98	GAM4	$100\pi^-p \rightarrow \pi^0\pi^0n$
1278 ± 5		1 BERTIN 97C	OBLX	$0.0\bar{p}p \rightarrow \pi^+\pi^-\pi^0$
1272 ± 8		200k	PROKOSHKIN 94	$38\pi^-p \rightarrow \pi^0\pi^0n$
1269.7 ± 5.2		5730	AUGUSTIN 89	$e^+e^- \rightarrow 5\pi$
1283 ± 8		400	2 ALDE 87	$GAM4 100\pi^-p \rightarrow 4\pi^0n$
1274 ± 5			2 AUGUSTIN 87	$DM2 J/\psi \rightarrow \gamma\pi^+\pi^-$
1283 ± 6			3 LONGACRE 86	$MPS 22\pi^-p \rightarrow n2K_S^0$
1276 ± 7			84 COURAU	$DLCO e^+e^- \rightarrow e^+e^-\pi^+\pi^-$
1273.3 ± 2.3			4 CHABAUD 83	$ASPK 17\pi^-p$ polarized
1280 ± 4			5 CASON 82	$STRC 8\pi^+p \rightarrow \Delta^{++}\pi^0\pi^0$
1281 ± 7		11600	GIDAL 81	MRK2 J/ψ decay
1282 ± 5			6 CORDEN 79	OMEG 12-15 $\pi^-p \rightarrow n2\pi$
1269 ± 4		10k	APEL 75	NICE $40\pi^-p \rightarrow n2\pi^0$
1272 ± 4		4600	ENGLER 74	DBC $6\pi^+n \rightarrow \pi^+\pi^-p$
1277 ± 4		5300	FLATTE 71	HBC $7\pi^+p \rightarrow \Delta^{++}f_2$
1273 ± 8			2 STUNTEBECK 70	HBC $8\pi^-p, 5.4\pi^+d$
1265 ± 8			BOESEBECK 68	HBC $8\pi^+p$

••• We do not use the following data for averages, fits, limits, etc. •••

1277 ± 6	870	7 SCHEGELSKY 06A	RVUE	$\gamma\gamma \rightarrow K_S^0 K_S^0$
1251 ± 10		TIKHOMIROV 03	SPEC	$40.0\pi^-C \rightarrow K_S^0 K_S^0 K_L^0 X$
1260 ± 10		8 ALDE 97	GAM2	$450pp \rightarrow pp\pi^0\pi^0$
1278 ± 6		8 GRYGOREV 96	SPEC	$40\pi^-N \rightarrow K_S^0 K_S^0 X$
1262 ± 11		AGUILAR....	91	EHS $400pp$
1275 ± 10		AKER	91	CBAR $0.0\bar{p}p \rightarrow 3\pi^0$
1220 ± 10		BREAKSTONE 90	SFM	$pp \rightarrow pp\pi^+\pi^-$
1288 ± 12		ABACHI 86B	HRS	$e^+e^- \rightarrow \pi^+\pi^-X$
1284 ± 30	3k	BINON 83	GAM2	$38\pi^-p \rightarrow n2\eta$
1280 ± 20		APEL 82	CNTR	$25\pi^-p \rightarrow n2\pi^0$
1284 ± 10	16000	DEUTSCH...	76	HBC $16\pi^+p$
1258 ± 10	600	TAKAHASHI 72	HBC	$8\pi^-p \rightarrow n2\pi$
1275 ± 13		ARMENISE 70	HBC	$9\pi^+n \rightarrow p\pi^+\pi^-$
1261 ± 5	1960	2 ARMENISE 68	DBC	$5.1\pi^+n \rightarrow p\pi^+MM^-$
1270 ± 10	360	2 ARMENISE 68	DBC	$5.1\pi^+n \rightarrow p\pi^0MM$
1268 ± 6		9 JOHNSON 68	HBC	$3.7-4.2\pi^-p$

1 T-matrix pole.

2 Mass errors enlarged by us to Γ/\sqrt{N} ; see the note with the $K^*(892)$ mass.

3 From a partial-wave analysis of data using a K-matrix formalism with 5 poles.

4 From an energy-independent partial-wave analysis.

5 From an amplitude analysis of the reaction $\pi^+\pi^- \rightarrow 2\pi^0$.6 From an amplitude analysis of $\pi^+\pi^- \rightarrow \pi^+\pi^-$ scattering data.

7 From analysis of L3 data at 91 and 183-209 GeV.

8 Systematic uncertainties not estimated.

9 JOHNSON 68 includes BONDAR 63, LEE 64, DERADO 65, EISNER 67.

 $f_2(1270)$ WIDTH

VALUE (MeV)	EVTs	DOCUMENT ID	TECN	COMMENT
185.0 ± 2.9 OUR FIT		Error includes scale factor of 1.5.		
184.2 ± 3.7 OUR AVERAGE		Error includes scale factor of 1.5. See the ideogram below.		
175 ± 4 ± 10		ABLIKIM 06v	BES2	$e^+e^- \rightarrow J/\psi \rightarrow \gamma\pi^+\pi^-$
190 ± 20		ABLIKIM 05	BES2	$J/\psi \rightarrow \phi\pi^+\pi^-$
171 ± 10		ALDE 98	GAM4	$100\pi^-p \rightarrow \pi^0\pi^0n$
204 ± 20		10 BERTIN 97C	OBLX	$0.0\bar{p}p \rightarrow \pi^+\pi^-\pi^0$
192 ± 5	200k	PROKOSHKIN 94	GAM2	$38\pi^-p \rightarrow \pi^0\pi^0n$
180 ± 24		AGUILAR....	91	EHS $400pp$
169 ± 9	5730	11 AUGUSTIN 89	DM2	$e^+e^- \rightarrow 5\pi$
150 ± 30	400	11 ALDE 87	GAM4	$100\pi^-p \rightarrow 4\pi^0n$
186 ± 9		12 LONGACRE 86	MPS	$22\pi^-p \rightarrow n2K_S^0$
179.2 ± 6.9 ± 6.6		13 CHABAUD 83	ASPK	$17\pi^-p$ polarized
160 ± 11		DENNEY 83	LASS	$10\pi^+N$
196 ± 10	3k	APEL 82	CNTR	$25\pi^-p \rightarrow n2\pi^0$
152 ± 9		14 CASON 82	STRC	$8\pi^+p \rightarrow \Delta^{++}\pi^0\pi^0$
186 ± 27	11600	GIDAL 81	MRK2	J/ψ decay
216 ± 13		15 CORDEN 79	OMEG	12-15 $\pi^-p \rightarrow n2\pi$
190 ± 10	10k	APEL 75	NICE	$40\pi^-p \rightarrow n2\pi^0$
192 ± 16	4600	ENGLER 74	DBC	$6\pi^+n \rightarrow \pi^+\pi^-p$
183 ± 15	5300	FLATTE 71	HBC	$7\pi^+p \rightarrow \Delta^{++}f_2$
196 ± 30		11 STUNTEBECK 70	HBC	$8\pi^-p, 5.4\pi^+d$
216 ± 20	1960	11 ARMENISE 68	DBC	$5.1\pi^+n \rightarrow p\pi^+MM^-$
128 ± 27		11 BOESEBECK 68	HBC	$8\pi^+p$
176 ± 21		11,16 JOHNSON 68	HBC	$3.7-4.2\pi^-p$

••• We do not use the following data for averages, fits, limits, etc. •••

195 ± 15	870	17 SCHEGELSKY 06A	RVUE	$\gamma\gamma \rightarrow K_S^0 K_S^0$
121 ± 26		TIKHOMIROV 03	SPEC	$40.0\pi^-C \rightarrow K_S^0 K_S^0 K_L^0 X$
187 ± 20		18 ALDE 97	GAM2	$450pp \rightarrow pp\pi^0\pi^0$
184 ± 10		18 GRYGOREV 96	SPEC	$40\pi^-N \rightarrow K_S^0 K_S^0 X$
200 ± 10		AKER	91	CBAR $0.0\bar{p}p \rightarrow 3\pi^0$
240 ± 40	3k	BINON 83	GAM2	$38\pi^-p \rightarrow n2\eta$
187 ± 30	650	11 ANTIPOV 77	CIBS	$25\pi^-p \rightarrow p3\pi$
225 ± 38	16000	DEUTSCH...	76	HBC $16\pi^+p$
166 ± 28	600	11 TAKAHASHI 72	HBC	$8\pi^-p \rightarrow n2\pi$
173 ± 53		11 ARMENISE 70	HBC	$9\pi^+n \rightarrow p\pi^+\pi^-$

10 T-matrix pole.

11 Width errors enlarged by us to $4\Gamma/\sqrt{N}$; see the note with the $K^*(892)$ mass.

12 From a partial-wave analysis of data using a K-matrix formalism with 5 poles.

13 From an energy-independent partial-wave analysis.

14 From an amplitude analysis of the reaction $\pi^+\pi^- \rightarrow 2\pi^0$.15 From an amplitude analysis of $\pi^+\pi^- \rightarrow \pi^+\pi^-$ scattering data.

16 JOHNSON 68 includes BONDAR 63, LEE 64, DERADO 65, EISNER 67.

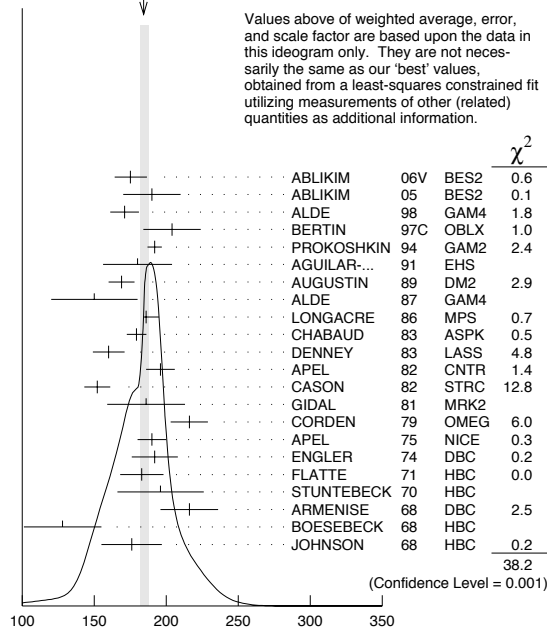
17 From analysis of L3 data at 91 and 183-209 GeV.

18 Systematic uncertainties not estimated.

Meson Particle Listings

 $f_2(1270)$

WEIGHTED AVERAGE
184.2±3.7-2.4
(Error scaled by 1.5)

 $f_2(1270)$ width (MeV) $f_2(1270)$ DECAY MODES

Mode	Fraction (Γ_i/Γ)	Scale factor/ Confidence level
Γ_1 $\pi\pi$	(84.8 \pm 2.4 $-$ 1.2) %	S=1.2
Γ_2 $\pi^+\pi^-2\pi^0$	(7.1 \pm 1.4 $-$ 2.7) %	S=1.3
Γ_3 $K\bar{K}$	(4.6 \pm 0.4) %	S=2.7
Γ_4 $2\pi^+2\pi^-$	(2.8 \pm 0.4) %	S=1.2
Γ_5 $\eta\eta$	(4.0 \pm 0.8) $\times 10^{-3}$	S=2.1
Γ_6 $4\pi^0$	(3.0 \pm 1.0) $\times 10^{-3}$	
Γ_7 $\gamma\gamma$	(1.41 \pm 0.13) $\times 10^{-5}$	
Γ_8 $\eta\pi\pi$	< 8 $\times 10^{-3}$	CL=95%
Γ_9 $K^0 K^- \pi^+ + c.c.$	< 3.4 $\times 10^{-3}$	CL=95%
Γ_{10} e^+e^-	< 6 $\times 10^{-10}$	CL=90%

CONSTRAINED FIT INFORMATION

An overall fit to the total width, 4 partial widths, a combination of partial widths obtained from integrated cross sections, and 6 branching ratios uses 45 measurements and one constraint to determine 8 parameters. The overall fit has a $\chi^2 = 80.0$ for 38 degrees of freedom.

The following *off-diagonal* array elements are the correlation coefficients $\langle \delta p_i \delta p_j \rangle / (\delta p_i \delta p_j)$, in percent, from the fit to parameters p_i , including the branching fractions, $x_i \equiv \Gamma_i/\Gamma_{\text{total}}$. The fit constrains the x_i whose labels appear in this array to sum to one.

x_2	-91						
x_3	11	-38					
x_4	10	-37	1				
x_5	1	-6	0	0			
x_6	0	-7	0	0	0		
x_7	10	-7	-9	1	0	0	
Γ	-78	72	-11	-8	-1	0	-14
	x_1	x_2	x_3	x_4	x_5	x_6	x_7

Mode	Rate (MeV)	Scale factor
Γ_1 $\pi\pi$	156.9 \pm 3.8 $-$ 1.2	
Γ_2 $\pi^+\pi^-2\pi^0$	13.1 \pm 2.7 $-$ 5.0	1.3
Γ_3 $K\bar{K}$	8.5 \pm 0.8	2.7
Γ_4 $2\pi^+2\pi^-$	5.2 \pm 0.7	1.2

Γ_5 $\eta\eta$	0.74 \pm 0.14	2.1
Γ_6 $4\pi^0$	0.55 \pm 0.18	
Γ_7 $\gamma\gamma$	0.00260 \pm 0.00024	

 $f_2(1270)$ PARTIAL WIDTHS

VALUE (MeV)	EVTS	DOCUMENT ID	TECN	COMMENT	Γ_1
156.9 \pm 3.8 $-$ 1.2				OUR FIT	

157.0 \pm 6.0 $-$ 1.0 $\times 10^2$ 19 LONGACRE 86 MPS $22\pi^-p \rightarrow n2K_S^0$

••• We do not use the following data for averages, fits, limits, etc. •••

152 \pm 8 870 20 SCHEGELSKY 06A RVUE $\gamma\gamma \rightarrow K_S^0 K_S^0$

VALUE (MeV)	EVTS	DOCUMENT ID	TECN	COMMENT	Γ_3
8.5 \pm 0.8				OUR FIT Error includes scale factor of 2.7.	

9.0 \pm 0.7 $-$ 0.3 $\times 10^2$ 19 LONGACRE 86 MPS $22\pi^-p \rightarrow n2K_S^0$

••• We do not use the following data for averages, fits, limits, etc. •••

7.5 \pm 2.0 870 20 SCHEGELSKY 06A RVUE $\gamma\gamma \rightarrow K_S^0 K_S^0$

VALUE (MeV)	EVTS	DOCUMENT ID	TECN	COMMENT	Γ_5
0.74 \pm 0.14				OUR FIT Error includes scale factor of 2.1.	

1.0 \pm 0.1 $\times 10^2$ 19 LONGACRE 86 MPS $22\pi^-p \rightarrow n2K_S^0$

••• We do not use the following data for averages, fits, limits, etc. •••

1.8 \pm 0.4 870 20 SCHEGELSKY 06A RVUE $\gamma\gamma \rightarrow K_S^0 K_S^0$

VALUE (keV)	EVTS	DOCUMENT ID	TECN	COMMENT	Γ_7
2.60 \pm 0.24				OUR FIT	

2.71 \pm 0.26 $-$ 0.23 $\times 10^2$ **OUR AVERAGE**

2.84 \pm 0.35 BOGLIONE 99 RVUE $\gamma\gamma \rightarrow \pi^+\pi^-, \pi^0\pi^0$

2.58 \pm 0.13 \pm 0.36 $-$ 0.27 21 BEHREND 92 CELL $e^+e^- \rightarrow e^+e^-\pi^+\pi^-$

••• We do not use the following data for averages, fits, limits, etc. •••

2.55 \pm 0.15 870 20 SCHEGELSKY 06A RVUE $\gamma\gamma \rightarrow K_S^0 K_S^0$

2.93 \pm 0.23 \pm 0.32 22 YABUKI 95 VNS

3.10 \pm 0.35 \pm 0.35 23 BLINOV 92 MD1 $e^+e^- \rightarrow e^+e^-\pi^+\pi^-$

2.27 \pm 0.47 \pm 0.11 ADACHI 90D TOPZ $e^+e^- \rightarrow e^+e^-\pi^+\pi^-$

3.15 \pm 0.04 \pm 0.39 BOYER 90 MRK2 $e^+e^- \rightarrow e^+e^-\pi^+\pi^-$

3.19 \pm 0.16 \pm 0.29 $-$ 0.28 MARSISKE 90 CBAL $e^+e^- \rightarrow e^+e^-\pi^0\pi^0$

2.35 \pm 0.65 24 MORGAN 90 RVUE $\gamma\gamma \rightarrow \pi^+\pi^-, \pi^0\pi^0$

3.19 \pm 0.09 \pm 0.22 $-$ 0.38 2177 OEST 90 JADE $e^+e^- \rightarrow e^+e^-\pi^0\pi^0$

3.2 \pm 0.1 \pm 0.4 25 AIHARA 86B TPC $e^+e^- \rightarrow e^+e^-\pi^+\pi^-$

2.5 \pm 0.1 \pm 0.5 BEHREND 84B CELL $e^+e^- \rightarrow e^+e^-\pi^+\pi^-$

2.85 \pm 0.25 \pm 0.5 26 BERGER 84 PLUT $e^+e^- \rightarrow e^+e^-\pi^+\pi^-$

2.70 \pm 0.05 \pm 0.20 COURAU 84 DLCO $e^+e^- \rightarrow e^+e^-\pi^+\pi^-$

2.52 \pm 0.13 \pm 0.38 27 SMITH 84c MRK2 $e^+e^- \rightarrow e^+e^-\pi^+\pi^-$

2.7 \pm 0.2 \pm 0.6 EDWARDS 82F CBAL $e^+e^- \rightarrow e^+e^-\pi^0\pi^0$

2.9 \pm 0.6 $-$ 0.4 \pm 0.6 28 EDWARDS 82F CBAL $e^+e^- \rightarrow e^+e^-\pi^0\pi^0$

3.2 \pm 0.2 \pm 0.6 BRANDELIK 81B TASS $e^+e^- \rightarrow e^+e^-\pi^+\pi^-$

3.6 \pm 0.3 \pm 0.5 ROUSSARIE 81 MRK2 $e^+e^- \rightarrow e^+e^-\pi^+\pi^-$

2.3 \pm 0.8 29 BERGER 80B PLUT $e^+e^- \rightarrow e^+e^-\pi^+\pi^-$

2.5 \pm 0.1 \pm 0.5 BEHREND 84B CELL $e^+e^- \rightarrow e^+e^-\pi^+\pi^-$

2.85 \pm 0.25 \pm 0.5 26 BERGER 84 PLUT $e^+e^- \rightarrow e^+e^-\pi^+\pi^-$

2.70 \pm 0.05 \pm 0.20 COURAU 84 DLCO $e^+e^- \rightarrow e^+e^-\pi^+\pi^-$

2.52 \pm 0.13 \pm 0.38 27 SMITH 84c MRK2 $e^+e^- \rightarrow e^+e^-\pi^+\pi^-$

2.7 \pm 0.2 \pm 0.6 EDWARDS 82F CBAL $e^+e^- \rightarrow e^+e^-\pi^0\pi^0$

2.9 \pm 0.6 $-$ 0.4 \pm 0.6 28 EDWARDS 82F CBAL $e^+e^- \rightarrow e^+e^-\pi^0\pi^0$

3.2 \pm 0.2 \pm 0.6 BRANDELIK 81B TASS $e^+e^- \rightarrow e^+e^-\pi^+\pi^-$

3.6 \pm 0.3 \pm 0.5 ROUSSARIE 81 MRK2 $e^+e^- \rightarrow e^+e^-\pi^+\pi^-$

2.3 \pm 0.8 29 BERGER 80B PLUT $e^+e^- \rightarrow e^+e^-\pi^+\pi^-$

VALUE (eV)	CL%	DOCUMENT ID	TECN	COMMENT	Γ_{10}
<0.11		90 ACHASOV 00k SND $e^+e^- \rightarrow \pi^0\pi^0$			

••• We do not use the following data for averages, fits, limits, etc. •••

<1.7 90 VOROBYEV 88 ND $e^+e^- \rightarrow \pi^0\pi^0$

19 From a partial-wave analysis of data using a K-matrix formalism with 5 poles.

20 From analysis of L3 data at 91 and 183-209 GeV and using SU(3) relations.

21 Using a unitarized model with a 300 - 500 keV wide scalar at 1100 MeV.

22 With a narrow scalar state around 1220 MeV.

23 Using the unitarized model of LYTH 85.

24 Error includes spread of different solutions. Data of MARK2 and CRYSTAL BALL used in the analysis. Authors report strong correlations with $\gamma\gamma$ width of $f_0(1370)$: $\Gamma(f_2) +$

$1/4 \Gamma(f^0) = 3.6 \pm 0.3$ KeV.

25 Radiative corrections modify the partial widths; for instance the COURAU 84 value becomes 2.66 ± 0.21 in the calculation of LANDRO 86.

26 Using the MENNESSIER 83 model.

27 Superseded by BOYER 90.

28 If helicity = 2 assumption is not made.

29 Using mass, width and $B(f_2(1270) \rightarrow 2\pi)$ from PDG 78.

See key on page 373

Meson Particle Listings

 $f_2(1270)$

$f_2(1270) \Gamma(i)\Gamma(\gamma\gamma)/\Gamma(\text{total})$				$\Gamma_3\Gamma_7/\Gamma$
VALUE (keV)	DOCUMENT ID	TECN	COMMENT	
0.120 ± 0.014 OUR FIT			Error includes scale factor of 1.3.	
$0.091 \pm 0.007 \pm 0.027$	³⁰ ALBRECHT	90G	ARG	$e^+e^- \rightarrow e^+e^-K^+K^-$
• • • We do not use the following data for averages, fits, limits, etc. • • •				
$0.104 \pm 0.007 \pm 0.072$	³¹ ALBRECHT	90G	ARG	$e^+e^- \rightarrow e^+e^-K^+K^-$
³⁰ Using an incoherent background.				
³¹ Using a coherent background.				

$f_2(1270)$ BRANCHING RATIOS					Γ_1/Γ
VALUE	EVTS	DOCUMENT ID	TECN	COMMENT	
0.848 ± 0.024 OUR FIT				Error includes scale factor of 1.2.	
0.837 ± 0.020 OUR AVERAGE					
0.849 ± 0.025		CHABAUD	83	ASPK	$17 \pi^- p$ polarized
0.85 ± 0.05	250	BEAUPRE	71	HBC	$8 \pi^+ p \rightarrow \Delta^{++} f_2$
0.8 ± 0.04	600	OH	70	HBC	$1.26 \pi^- p \rightarrow \pi^+ \pi^- n$

$\Gamma(\pi^+ \pi^- 2\pi^0)/\Gamma(\pi\pi)$					Γ_2/Γ_1
VALUE	EVTS	DOCUMENT ID	TECN	COMMENT	
0.083 ± 0.018 OUR FIT				Error includes scale factor of 1.3.	
0.15 ± 0.06	600	EISENBERG	74	HBC	$4.9 \pi^+ p \rightarrow \Delta^{++} f_2$
• • • We do not use the following data for averages, fits, limits, etc. • • •					
0.07		EMMS	75D	DBC	$4 \pi^+ n \rightarrow p f_2$

$\Gamma(K^+K^-)/\Gamma(\pi\pi)$					Γ_3/Γ_1
VALUE	EVTS	DOCUMENT ID	TECN	COMMENT	
0.054 ± 0.005 OUR FIT				Error includes scale factor of 2.7.	
0.041 ± 0.004 OUR AVERAGE					
0.045 ± 0.01		³² BARGIOTTI	03	OBLX	$\bar{p} p$
0.037 ± 0.008		ETKIN	82B	MPS	$23 \pi^- p \rightarrow n 2K_S^0$
0.045 ± 0.009		CHABAUD	81	ASPK	$17 \pi^- p$ polarized
0.039 ± 0.008		LOVERRE	80	HBC	$4 \pi^- p \rightarrow K^+K^- n$
• • • We do not use the following data for averages, fits, limits, etc. • • •					
0.052 ± 0.025		ABLIKIM	04E	BES2	$J/\psi \rightarrow \omega K^+K^-$
0.036 ± 0.005		³³ COSTA...	80	OMEG	$1-2.2 \pi^- p \rightarrow K^+K^- n$
0.030 ± 0.005		³⁴ MARTIN	79	RVUE	
0.027 ± 0.009		³⁵ POLYCHRO...	79	STRC	$7 \pi^- p \rightarrow n 2K_S^0$
0.025 ± 0.015		EMMS	75D	DBC	$4 \pi^+ n \rightarrow p f_2$
0.031 ± 0.012	20	ADERHOLZ	69	HBC	$8 \pi^+ p \rightarrow K^+K^- \pi^+ p$

$\Gamma(2\pi^+ 2\pi^-)/\Gamma(\pi\pi)$					Γ_4/Γ_1
VALUE	EVTS	DOCUMENT ID	TECN	COMMENT	
0.033 ± 0.005 OUR FIT				Error includes scale factor of 1.2.	
0.033 ± 0.004 OUR AVERAGE				Error includes scale factor of 1.1.	
0.024 ± 0.006	160	EMMS	75D	DBC	$4 \pi^+ n \rightarrow p f_2$
0.051 ± 0.025	70	EISENBERG	74	HBC	$4.9 \pi^+ p \rightarrow \Delta^{++} f_2$
0.043 ± 0.007	285	LOUIE	74	HBC	$3.9 \pi^- p \rightarrow n f_2$
0.037 ± 0.007	154	ANDERSON	73	DBC	$6 \pi^+ n \rightarrow p f_2$
0.047 ± 0.013		OH	70	HBC	$1.26 \pi^- p \rightarrow \pi^+ \pi^- n$

$\Gamma(\eta\eta)/\Gamma(\text{total})$					Γ_5/Γ
VALUE (units 10^{-3})	DOCUMENT ID	TECN	COMMENT		
4.0 ± 0.8 OUR FIT				Error includes scale factor of 2.1.	
2.9 ± 0.5 OUR AVERAGE					
2.7 ± 0.7		BINON	05	GAMS	$33 \pi^- p \rightarrow \eta\eta n$
2.8 ± 0.7		ALDE	86D	GAM4	$100 \pi^- p \rightarrow 2\eta n$
5.2 ± 1.7		BINON	83	GAM2	$38 \pi^- p \rightarrow 2\eta n$

$\Gamma(\eta\eta)/\Gamma(\pi\pi)$					Γ_5/Γ_1
VALUE	CL%	DOCUMENT ID	TECN	COMMENT	
0.003 ± 0.001		BARBERIS	00E		$450 p p \rightarrow p f_1 \eta p_S$
• • • We do not use the following data for averages, fits, limits, etc. • • •					
<0.05	95	EDWARDS	82F	CBAL	$e^+e^- \rightarrow e^+e^- 2\eta$
<0.016	95	EMMS	75D	DBC	$4 \pi^+ n \rightarrow p f_2$
<0.09	95	EISENBERG	74	HBC	$4.9 \pi^+ p \rightarrow \Delta^{++} f_2$

$\Gamma(4\pi^0)/\Gamma_{\text{total}}$			Γ_6/Γ		
VALUE	EVTS	DOCUMENT ID	TECN	COMMENT	
0.0030 ± 0.0010 OUR FIT					
0.003 ± 0.001		ALDE	87	GAM4	$100 \pi^- p \rightarrow 4\pi^0 n$
					400 \pm 50

$\Gamma(\eta\pi\pi)/\Gamma(\pi\pi)$			Γ_8/Γ_1		
VALUE	CL%	DOCUMENT ID	TECN	COMMENT	
<0.010	95	EMMS	75D	DBC	$4 \pi^+ n \rightarrow p f_2$

$\Gamma(K^0 K^- \pi^+ + \text{c.c.})/\Gamma(\pi\pi)$			Γ_9/Γ_1		
VALUE	CL%	DOCUMENT ID	TECN	COMMENT	
<0.004	95	EMMS	75D	DBC	$4 \pi^+ n \rightarrow p f_2$

$\Gamma(e^+e^-)/\Gamma_{\text{total}}$			Γ_{10}/Γ		
VALUE (units 10^{-10})	CL%	DOCUMENT ID	TECN	COMMENT	
<6	90	ACHASOV	00K	SND	$e^+e^- \rightarrow \pi^0 \pi^0$

³² Coupled channel analysis of $\pi^+ \pi^- \pi^0$, $K^+ K^- \pi^0$, and $K^+ K_S^0 \pi^+$.

³³ Re-evaluated by CHABAUD 83.

³⁴ Includes PAWLICKI 77 data.

³⁵ Takes into account the $f_2(1270)$ - $f_2'(1525)$ interference.

 $f_2(1270)$ REFERENCES

ABLIKIM	06V	PL B642 441	M. Ablikim et al.	(BES Collab.)
SCHEGELSKY	06A	EPJ A27 207	V.A. Schegelsky et al.	
ABLIKIM	05	PL B607 243	M. Ablikim et al.	(BES Collab.)
BINON	05	PAN 68 960	F. Binon et al.	
		Translated from YAF 68 998.		
ABLIKIM	04E	PL B603 138	M. Ablikim et al.	(BES Collab.)
BARGIOTTI	03	EPJ C26 371	M. Bargiotti et al.	(OBELIX Collab.)
TIKHOMIROV	03	PAN 66 828	G.D. Tikhomirov et al.	
		Translated from YAF 66 860.		
ACHASOV	00K	PL B492 8	M.N. Achasov et al.	(Novosibirsk SND Collab.)
BARBERIS	00E	PL B479 59	D. Barberis et al.	(WA 102 Collab.)
BOGLIONE	99	EPJ C9 11	M. Boglione, M.R. Pennington	
ALDE	98	EPJ A3 361	D. Alde et al.	(GAM4 Collab.)
		Also PAN 62 405	D. Alde et al.	(GAMS Collab.)
		Translated from YAF 62 446.		
ALDE	97	PL B397 350	D.M. Alde et al.	(GAMS Collab.)
BERTIN	97C	PL B408 476	A. Bertin et al.	(OBELIX Collab.)
GRYGOREV	96	PAN 59 2105	V.K. Grigoriev, O.N. Baloshin, B.P. Barkov	(ITEP)
		Translated from YAF 59 2187.		
YABUKI	95	JPJ 64 435	F. Yabuki et al.	(VENUS Collab.)
PROKOSHNIK	94	SPD 39 420	Y.D. Prokoshkin, A.A. Kondashov	(SERP)
		Translated from DANS 336 613.		
BEHREND	92	ZPHY C56 381	H.J. Behrend	(CELLO Collab.)
BLINOV	92	ZPHY C53 33	A.E. Blinov et al.	(NOVO)
AGUILAR...	91	ZPHY C50 405	M. Aguilar-Benitez et al.	(LEBC-EHS Collab.)
AKER	91	PL B260 249	E. Aker et al.	(Crystal Barrel Collab.)
ADACHI	90D	PL B234 185	I. Adachi et al.	(TOPAZ Collab.)
ALBRECHT	90G	ZPHY C48 183	H. Albrecht et al.	(ARGUS Collab.)
BOYER	90	PR D42 1350	J. Boyer et al.	(Mark II Collab.)
BREAKSTONE	90	ZPHY C48 569	A.M. Breakstone et al.	(ISU, BGNA, CERN+)
MARISISKE	90	PR D41 3324	H. Marisiske et al.	(Crystal Ball Collab.)
MORGAN	90	ZPHY C48 623	D. Morgan, M.R. Pennington	(RAL, DURH)
OEST	90	ZPHY C47 343	T. Oest et al.	(JADE Collab.)
AUGUSTIN	89	NP B320 1	J.E. Augustin, G. Cosme	(DM2 Collab.)
VOROBYEV	88	SJNP 48 273	P.V. Vorobyev et al.	(NOVO)
		Translated from YAF 48 436.		
ALDE	87	PL B198 286	D.M. Alde et al.	(LANL, BRUX, SERP, LAPP)
AUGUSTIN	87	ZPHY C36 369	J.E. Augustin et al.	(LALO, CLER, FRAS+)
ABACHI	86B	PRL 57 1990	S. Abachi et al.	(PURD, ANL, IND, MICH+)
AIHARA	86D	PRL 57 404	H. Aihara et al.	(TPC-2 γ Collab.)
ALDE	86D	NP B269 485	D.M. Alde et al.	(BELG, LAPP, SERP, CERN+)
LANDRO	86	PL B172 445	M. Landro, K.J. Mork, H.A. Olsen	(UTRO)
LONGACRE	86	PL B177 223	R.S. Longacre et al.	(BNL, BRAN, CUNY+)
LYTH	85	JPG 11 459	D.H. Lyth	
BEHREND	84B	ZPHY C23 223	H.J. Behrend et al.	(CELLO Collab.)
BERGER	84	ZPHY C26 199	C. Berger et al.	(PLUTO Collab.)
GOURAU	84	PL 1479 227	A. Gourau et al.	(CIT, SLAC)
SMITH	84C	PR D30 851	J.R. Smith et al.	(SLAC, LBL, HARV)
BINON	83	NC 78A 313	F.G. Binon et al.	(BELG, LAPP, SERP+)
		Also SJNP 38 561	F.G. Binon et al.	(BELG, LAPP, SERP+)
		Translated from YAF 38 934.		
CHABAUD	83	NP B223 1	V. Chabaud et al.	(CERN, CRAC, MPIM)
DENNEY	83	PR D28 2726	D.L. Denney et al.	(IOWA, MICH)
MENNESSIER	83	ZPHY C16 241	G. Mennessier	(MONP)
APEL	82F	NP B201 197	W.D. Apel et al.	(KARLK, KARLE, PISA, SERP+)
CASON	82	PRL 48 1316	N.M. Cason et al.	(NDAM, ANL)
EDWARDS	82F	PL 110B 82	C. Edwards et al.	(CIT, HARV, PRIN+)
ETKIN	82B	PR D25 1786	A. Etkin et al.	(BNL, CUNY, TUFTS, VAND)
BRANDELK	81B	ZPHY C10 117	R. Brandelik et al.	(TASSO Collab.)
CHABAUD	81	APP B12 575	V. Chabaud et al.	(CERN, CRAC, MPIM)
GIDAL	81	PL 107B 153	G. Gidal et al.	(SLAC, LBL)
ROUSSARIE	81	PL 105B 304	A. Roussarie et al.	(SLAC, LBL)
BERGER	80B	PL 94B 254	C. Berger et al.	(PLUTO Collab.)
COSTA...	80	NP B175 402	G. Costa de Beauregard et al.	(BARI, BONN+)
LOVERRE	80	ZPHY C6 187	P.F. Loverre et al.	(CERN, COFE, MADR+)
CORDEN	79	NP B157 250	M.J. Corden et al.	(BIRM, RHEL, TELA+)
MARTIN	79	NP B158 520	A.D. Martin, E.N. Ozmutlu	(DURH)
POLYCHRO...	79	PR D19 1317	V.A. Polychronakos et al.	(NDAM, ANL)
PDG	78	PL 75B 1	C. Bricman et al.	
ANTIPOV	77	NP B119 45	Y.M. Antipov et al.	(SERP, GEVA)
PAWLICKI	77	PR D15 3196	A.J. Pawlicki et al.	(ANL)
DEUTSCH...	76	NP B103 426	M. Deuschmann et al.	(AACH3, BERL, BONN+)
APEL	75	PL 57B 398	W.D. Apel et al.	(KARLK, KARLE, PISA, SERP+)
EMMS	75D	NP B96 155	M.J. Emms et al.	(BIRM, DURH, RHEL)
EISENBERG	74	PL 52B 239	Y. Eisenberg et al.	(REHO)
ENGLER	74	PR D10 2070	A. Engler et al.	(CMU, CASE)
LOUIE	74	PL 48B 385	J. Louie et al.	(SACL, CERN)
ANDERSON	73	PRL 31 562	J.C. Anderson et al.	(CMU, CASE)
TAKAHASHI	72	PR D6 1266	K. Takahashi et al.	(TOHOK, PENN, NDAM+)
BEAUPRE	71	NP B28 77	J.V. Beaupre et al.	(AACH, BERL, CERN)
FLATTE	71	PL 34B 551	S.M. Flatte et al.	(LBL)
ARMENISE	70	LNC 4 199	N. Armenise et al.	(BARI, BGNA, FIRZ)
OH	70	PR D1 2494	B.Y. Oh et al.	(WISC, TUNTO) JP
STUNTEBECK	70	PL 32B 311	P.H. Stuntebeck et al.	(NDAM)
ADERHOLZ	69	NP B11 259	M. Aderholz et al.	(AACH3, BERL, CERN+)
ARMENISE	68	NC 54A 999	N. Armenise et al.	(BARI, BGNA, FIRZ+)

Meson Particle Listings

$f_2(1270)$, $f_1(1285)$

ASCOLI	68D	PRL 21 1712	G. Ascoli <i>et al.</i>	(ILL)
BOESEBECK	68	NP B4 501	K. Boesebeck <i>et al.</i>	(AACH, BERL, CERN)
JOHNSON	68	PR 176 1651	P.B. Johnson <i>et al.</i>	(NDAM, PURD, SLAC)
EISNER	67	PR 164 1699	R.L. Eisner <i>et al.</i>	(PURD)
DERADO	65	PRL 14 872	I. Derado <i>et al.</i>	(NDAM)
LEE	64	PRL 12 342	Y.Y. Lee <i>et al.</i>	(MICH)
BONDAR	63	PL 5 153	L. Bondar <i>et al.</i>	(AACH, BIRM, BONN, DESY+)

OTHER RELATED PAPERS

ANISOVICH	05	JETPL 80 715	V.V. Anisovich	
ABLIKIM	04A	Translated from ZETFP 80 845	M. Ablikim <i>et al.</i>	(BES Collab.)
GARMASH	02	PL B598 149	A. Garmash <i>et al.</i>	(BELLE Collab.)
LI	01	PR D65 092005	D.-M. Li, H. Yu, Q.-X. Shen	
		JPG 27 807		

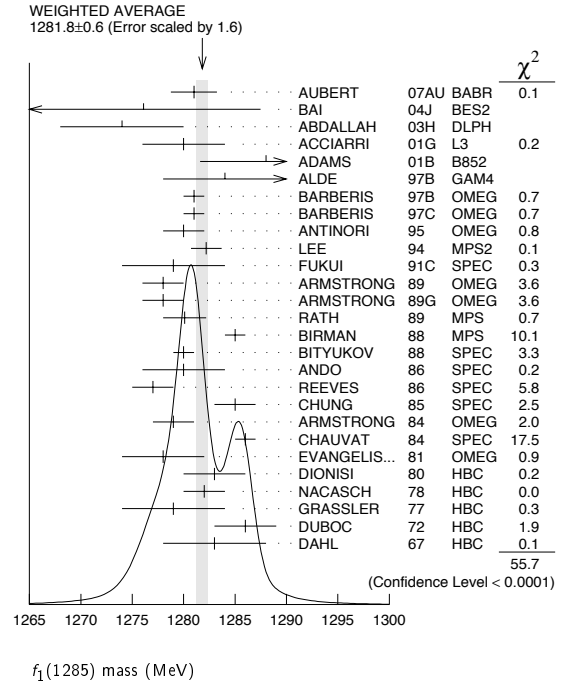
$f_1(1285)$

$$J^G(J^{PC}) = 0^+(1^{++})$$

$f_1(1285)$ MASS

VALUE (MeV)	EVTS	DOCUMENT ID	TECN	COMMENT
1281.8 ± 0.6 OUR AVERAGE				Error includes scale factor of 1.6. See the ideogram below.
1281 ± 2 ± 1		AUBERT	07AU BABR	10.6 $e^+e^- \rightarrow f_1(1285)\pi^+\pi^-\gamma$
1276.1 ± 8.1 ± 8.0	203	BAI	04J BES2	$J/\psi \rightarrow \gamma\gamma\pi^+\pi^-$
1274 ± 6	237	ABDALLAH	03H DLPH	91.2 $e^+e^- \rightarrow K_S^0 K^\pm\pi^\mp + X$
1280 ± 4		ACCIARRI	01G L3	
1288 ± 4 ± 5	20k	ADAMS	01B B852	18 GeV $\pi^-p \rightarrow K^+K^-\pi^0n$
1284 ± 6	1400	ALDE	97B GAM4	100 $\pi^-p \rightarrow \eta\pi^0\pi^0n$
1281 ± 1		BARBERIS	97B OMEG	450 $pp \rightarrow pp2(\pi^+\pi^-)$
1281 ± 1		BARBERIS	97C OMEG	450 $pp \rightarrow ppK_S^0K^\pm\pi^\mp$
1280 ± 2		¹ ANTINORI	95 OMEG	300,450 $pp \rightarrow pp2(\pi^+\pi^-)$
1282.2 ± 1.5		LEE	94 MPS2	18 $\pi^-p \rightarrow K^+\bar{K}^02\pi^-p$
1279 ± 5		FUKUI	91C SPEC	8.95 $\pi^-p \rightarrow \eta\pi^+\pi^-n$
1278 ± 2	140	ARMSTRONG	89 OMEG	300 $pp \rightarrow K\bar{K}\pi pp$
1278 ± 2		ARMSTRONG	89G OMEG	85 $\pi^+p \rightarrow 4\pi\pi p, pp \rightarrow 4\pi pp$
1280.1 ± 2.1	60	RATH	89 MPS	21.4 $\pi^-p \rightarrow K_S^0K_S^0\pi^0n$
1285 ± 1	4750	² BIRMAN	88 MPS	8 $\pi^-p \rightarrow K^+\bar{K}^0\pi^-n$
1280 ± 1	504	BITYUKOV	88 SPEC	32.5 $\pi^-p \rightarrow K^+K^-\pi^0n$
1280 ± 4		ANDO	86 SPEC	8 $\pi^-p \rightarrow \eta\pi^+\pi^-n$
1277 ± 2	420	REEVES	86 SPEC	6.6 $p\bar{p} \rightarrow K\bar{K}\pi X$
1285 ± 2		CHUNG	85 SPEC	8 $\pi^-p \rightarrow N\bar{K}\bar{K}\pi$
1279 ± 2	604	ARMSTRONG	84 OMEG	85 $\pi^+p \rightarrow K\bar{K}\pi\pi p, pp \rightarrow K\bar{K}\pi pp$
1286 ± 1		CHAUVAT	84 SPEC	ISR 31.5 pp
1278 ± 4		EVANGELIS...	81 OMEG	12 $\pi^-p \rightarrow \eta\pi^+\pi^-\pi^-p$
1283 ± 3	103	DIONISI	80 HBC	4 $\pi^-p \rightarrow K\bar{K}\pi n$
1282 ± 2	320	NACASCH	78 HBC	0.7,0.76 $p\bar{p} \rightarrow K\bar{K}3\pi$
1279 ± 5	210	GRASSLER	77 HBC	16 $\pi^+\pi^-p$
1286 ± 3	180	DUBOC	72 HBC	1.2 $p\bar{p} \rightarrow 2K4\pi$
1283 ± 5		DAHL	67 HBC	1.6-4.2 π^-p
• • • We do not use the following data for averages, fits, limits, etc. • • •				
1281.9 ± 0.5		³ SOSA	99 SPEC	$pp \rightarrow p_{\text{slow}}(K_S^0K^+\pi^-)p_{\text{fast}}$
1282.8 ± 0.6		³ SOSA	99 SPEC	$pp \rightarrow p_{\text{slow}}(K_S^0K^-\pi^+)p_{\text{fast}}$
1270 ± 10		AMELIN	95 VES	37 $\pi^-N \rightarrow \pi^-\pi^+\pi^-\gamma N$
1280 ± 2		ABATZIS	94 OMEG	450 $pp \rightarrow pp2(\pi^+\pi^-)$
1282 ± 4		ARMSTRONG	93C E760	$p\bar{p} \rightarrow \pi^0\eta\eta \rightarrow 6\gamma$
1270 ± 6 ± 10		ARMSTRONG	92C OMEG	300 $pp \rightarrow pp\pi^+\pi^-\gamma$
1281 ± 1		ARMSTRONG	89E OMEG	300 $pp \rightarrow pp2(\pi^+\pi^-)$
1279 ± 6 ± 10	16	BECKER	87 MRK3	$e^+e^- \rightarrow \phi K\bar{K}\pi$
1286 ± 9		GIDAL	87 MRK2	$e^+e^- \rightarrow \phi K\bar{K}\pi$
1287 ± 5	353	BITYUKOV	84B SPEC	32 $\pi^-p \rightarrow K^+K^-\pi^0n$
~ 1279		⁴ TORNQVIST	82B RVUE	
1275 ± 6	31	BROMBERG	80 SPEC	100 $\pi^-p \rightarrow K\bar{K}\pi X$
1288 ± 9	200	GURTU	79 HBC	4.2 $K^-p \rightarrow n\eta2\pi$
~ 1275.0	46	⁵ STANTON	79 CNTR	8.5 $\pi^-p \rightarrow n2\gamma2\pi$
1271 ± 10	34	CORDEN	78 OMEG	12-15 $\pi^-p \rightarrow K^+K^-\pi n$
1295 ± 12	85	CORDEN	78 OMEG	12-15 $\pi^-p \rightarrow n5\pi$
1292 ± 10	150	DOFOX	72 HBC	0.7 $p\bar{p} \rightarrow 7\pi$
1280 ± 3	500	⁶ THUN	72 MMS	13.4 π^-p
1303 ± 8		BARDADIN...	71 HBC	8 $\pi^+p \rightarrow p6\pi$
1283 ± 6		BOESEBECK	71 HBC	16.0 $\pi^-p \rightarrow p5\pi$
1270 ± 10		CAMPBELL	69 DBC	2.7 π^+d
1285 ± 7		LORSTAD	69 HBC	0.7 $p\bar{p}, 4,5$ -body
1290 ± 7		D'ANDLAU	68 HBC	1.2 $p\bar{p}, 5-6$ body

- Supersedes ABATZIS 94, ARMSTRONG 89E.
- From partial wave analysis of $K^+\bar{K}^0\pi^-$ system.
- No systematic error given.
- From a unitarized quark-model calculation.
- From phase shift analysis of $\eta\pi^+\pi^-$ system.
- Seen in the missing mass spectrum.



$f_1(1285)$ WIDTH

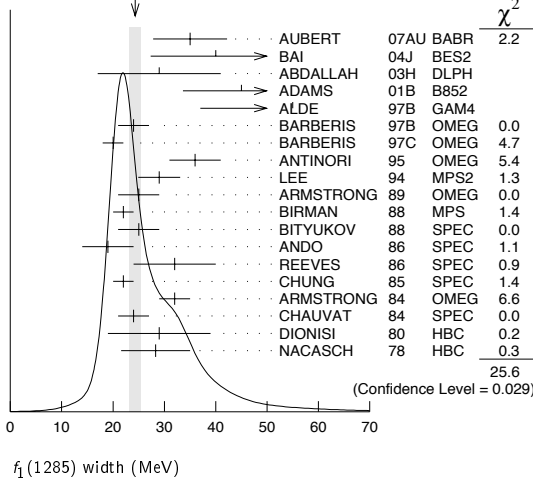
Only experiments giving width error less than 20 MeV are kept for averaging.

VALUE (MeV)	EVTS	DOCUMENT ID	TECN	COMMENT
24.3 ± 1.1 OUR AVERAGE				Error includes scale factor of 1.4. See the ideogram below.
35 ± 6 ± 4		AUBERT	07AU BABR	10.6 $e^+e^- \rightarrow f_1(1285)\pi^+\pi^-\gamma$
40.0 ± 8.6 ± 9.3	203	BAI	04J BES2	$J/\psi \rightarrow \gamma\gamma\pi^+\pi^-$
29 ± 12	237	ABDALLAH	03H DLPH	91.2 $e^+e^- \rightarrow K_S^0 K^\pm\pi^\mp + X$
45 ± 9 ± 7	20k	ADAMS	01B B852	18 GeV $\pi^-p \rightarrow K^+K^-\pi^0n$
55 ± 18	1400	ALDE	97B GAM4	100 $\pi^-p \rightarrow \eta\pi^0\pi^0n$
24 ± 3		BARBERIS	97B OMEG	450 $pp \rightarrow pp2(\pi^+\pi^-)$
20 ± 2		BARBERIS	97C OMEG	450 $pp \rightarrow ppK_S^0K^\pm\pi^\mp$
36 ± 5		⁷ ANTINORI	95 OMEG	300,450 $pp \rightarrow pp2(\pi^+\pi^-)$
29.0 ± 4.1		LEE	94 MPS2	18 $\pi^-p \rightarrow K^+\bar{K}^02\pi^-p$
25 ± 4	140	ARMSTRONG	89 OMEG	300 $pp \rightarrow K\bar{K}\pi pp$
22 ± 2	4750	⁸ BIRMAN	88 MPS	8 $\pi^-p \rightarrow K^+\bar{K}^0\pi^-n$
25 ± 4	504	BITYUKOV	88 SPEC	32.5 $\pi^-p \rightarrow K^+K^-\pi^0n$
19 ± 5		ANDO	86 SPEC	8 $\pi^-p \rightarrow \eta\pi^+\pi^-n$
32 ± 8	420	REEVES	86 SPEC	6.6 $p\bar{p} \rightarrow K\bar{K}\pi X$
22 ± 2		CHUNG	85 SPEC	8 $\pi^-p \rightarrow N\bar{K}\bar{K}\pi$
32 ± 3	604	ARMSTRONG	84 OMEG	85 $\pi^+p \rightarrow K\bar{K}\pi\pi p, pp \rightarrow K\bar{K}\pi pp$
24 ± 3		CHAUVAT	84 SPEC	ISR 31.5 pp
29 ± 10	103	DIONISI	80 HBC	4 $\pi^-p \rightarrow K\bar{K}\pi n$
28.3 ± 6.7	320	NACASCH	78 HBC	0.7,0.76 $p\bar{p} \rightarrow K\bar{K}3\pi$
• • • We do not use the following data for averages, fits, limits, etc. • • •				
18.2 ± 1.2		⁹ SOSA	99 SPEC	$pp \rightarrow p_{\text{slow}}(K_S^0K^+\pi^-)p_{\text{fast}}$
19.4 ± 1.5		⁹ SOSA	99 SPEC	$pp \rightarrow p_{\text{slow}}(K_S^0K^-\pi^+)p_{\text{fast}}$
40 ± 5		ABATZIS	94 OMEG	450 $pp \rightarrow pp2(\pi^+\pi^-)$
31 ± 5		ARMSTRONG	89E OMEG	300 $pp \rightarrow pp2(\pi^+\pi^-)$
41 ± 12		ARMSTRONG	89G OMEG	85 $\pi^+p \rightarrow 4\pi\pi p, pp \rightarrow 4\pi pp$
17.9 ± 10.9	60	RATH	89G MPS	21.4 $\pi^-p \rightarrow K_S^0K_S^0\pi^0n$
14 + ²⁰ / ₋₁₄ ± 10	16	BECKER	87 MRK3	$e^+e^- \rightarrow \phi K\bar{K}\pi$
26 ± 12		EVANGELIS...	81 OMEG	12 $\pi^-p \rightarrow \eta\pi^+\pi^-\pi^-p$
25 ± 15	200	GURTU	79 HBC	4.2 $K^-p \rightarrow n\eta2\pi$

~10		10 STANTON	79 CNTR	8.5 $\pi^- p \rightarrow n 2\gamma 2\pi$
24 ± 18	210	GRASSLER	77 HBC	16 $\pi^\mp p$
28 ± 5	150	11 DEFOIX	72 HBC	0.7 $\bar{p} p \rightarrow 7\pi$
46 ± 9	180	11 DUBOC	72 HBC	1.2 $\bar{p} p \rightarrow 2K 4\pi$
37 ± 5	500	12 THUN	72 MMS	13.4 $\pi^- p$
10 ± 10		BOESEBECK	71 HBC	16.0 $\pi p \rightarrow p 5\pi$
30 ± 15		CAMPBELL	69 DBC	2.7 $\pi^+ d$
60 ± 15		11 LORSTAD	69 HBC	0.7 $\bar{p} p, 4,5$ -body
35 ± 10		11 DAHL	67 HBC	1.6-4.2 $\pi^- p$

- 7 Supersedes ABATZIS 94, ARMSTRONG 89E.
- 8 From partial wave analysis of $K^+ \bar{K}^0 \pi^-$ system.
- 9 No systematic error given.
- 10 From phase shift analysis of $\eta \pi^+ \pi^-$ system.
- 11 Resolution is not unfolded.
- 12 Seen in the missing mass spectrum.

WEIGHTED AVERAGE
24.3±1.1 (Error scaled by 1.4)



$f_1(1285)$ DECAY MODES

Mode	Fraction (Γ_i/Γ)	Scale factor/ Confidence level
Γ_1 4π	$(33.1 \pm 2.1) \%$	S=1.3
Γ_2 $\pi^0 \pi^0 \pi^+ \pi^-$	$(22.0 \pm 1.4) \%$	S=1.3
Γ_3 $2\pi^+ 2\pi^-$	$(11.0 \pm 0.7) \%$	S=1.3
Γ_4 $\rho^0 \pi^+ \pi^-$	$(11.0 \pm 0.7) \%$	S=1.3
Γ_5 $\rho^0 \rho^0$	seen	
Γ_6 $4\pi^0$	$< 7 \times 10^{-4}$	CL=90%
Γ_7 $\eta \pi \pi$	$(52 \pm 16) \%$	
Γ_8 $a_0(980) \pi$ [ignoring $a_0(980) \rightarrow K \bar{K}$]	$(36 \pm 7) \%$	
Γ_9 $\eta \pi \pi$ [excluding $a_0(980) \pi$]	$(16 \pm 7) \%$	
Γ_{10} $K \bar{K} \pi$	$(9.0 \pm 0.4) \%$	S=1.1
Γ_{11} $K \bar{K}^*(892)$	not seen	
Γ_{12} $\gamma \rho^0$	$(5.5 \pm 1.3) \%$	S=2.8
Γ_{13} $\phi \gamma$	$(7.4 \pm 2.6) \times 10^{-4}$	
Γ_{14} $\gamma \gamma^*$		
Γ_{15} $\gamma \gamma$		

CONSTRAINED FIT INFORMATION

An overall fit to 7 branching ratios uses 16 measurements and one constraint to determine 5 parameters. The overall fit has a $\chi^2 = 24.7$ for 12 degrees of freedom.

The following *off-diagonal* array elements are the correlation coefficients $\langle \delta x_i \delta x_j \rangle / (\delta x_i \delta x_j)$, in percent, from the fit to the branching fractions, $x_i \equiv \Gamma_i/\Gamma_{total}$. The fit constrains the x_i whose labels appear in this array to sum to one.

x_8	-17			
x_9	-8	-95		
x_{10}	46	-9	-4	
x_{12}	-36	-4	-2	-34
	x_1	x_8	x_9	x_{10}

$f_1(1285) \Gamma(i)\Gamma(\gamma\gamma)/\Gamma_{total}$

VALUE (keV)	CL%	DOCUMENT ID	TECN	COMMENT
<0.62	95	GIDAL	87	MRK2 $e^+ e^- \rightarrow e^+ e^- \eta \pi^+ \pi^-$

$\Gamma(\eta\pi\pi) \times \Gamma(\gamma\gamma^*)/\Gamma_{total}$

VALUE (keV)	EVTS	DOCUMENT ID	TECN	COMMENT
1.4 ± 0.4 OUR AVERAGE				Error includes scale factor of 1.4.
1.18 ± 0.25 ± 0.20	26	13,14 AIHARA	88B	TPC $e^+ e^- \rightarrow e^+ e^- \eta \pi^+ \pi^-$
2.30 ± 0.61 ± 0.42	13,15	GIDAL	87	MRK2 $e^+ e^- \rightarrow e^+ e^- \eta \pi^+ \pi^-$
• • • We do not use the following data for averages, fits, limits, etc. • • •				
1.8 ± 0.3 ± 0.3	420	16 ACHARD	02B L3	183-209 $e^+ e^- \rightarrow e^+ e^- \eta \pi^+ \pi^-$

- 13 Assuming a ρ -pole form factor.
- 14 Published value multiplied by $\eta \pi \pi$ branching ratio 0.49.
- 15 Published value divided by 2 and multiplied by the $\eta \pi \pi$ branching ratio 0.49.
- 16 Published value multiplied by the $\eta \pi \pi$ branching ratio 0.52.

$f_1(1285)$ BRANCHING RATIOS

$\Gamma(K \bar{K} \pi)/\Gamma(4\pi)$

VALUE	DOCUMENT ID	TECN	COMMENT
0.271 ± 0.016 OUR FIT			Error includes scale factor of 1.3.
0.271 ± 0.016 OUR AVERAGE			Error includes scale factor of 1.2.
0.265 ± 0.014	17	BARBERIS 97C	OMEG 450 $p p \rightarrow p p K_S^0 K^\pm \pi^\mp$
0.28 ± 0.05	18	ARMSTRONG 89E	OMEG 300 $p p \rightarrow p p f_1(1285)$
0.37 ± 0.03 ± 0.05	19	ARMSTRONG 89G	OMEG 85 $p p \rightarrow 4\pi X$
17 Using $2(\pi^+ \pi^-)$ data from BARBERIS 97B.			
18 Assuming $\rho \pi \pi$ and $a_0(980) \pi$ intermediate states.			
19 4π consistent with being entirely $\rho \pi \pi$.			

$\Gamma(\rho^0 \pi^0 \pi^+ \pi^-)/\Gamma_{total}$

VALUE	DOCUMENT ID
0.220 ± 0.014 OUR FIT	
	Error includes scale factor of 1.3.

$\Gamma(2\pi^+ 2\pi^-)/\Gamma_{total}$

VALUE	DOCUMENT ID
0.110 ± 0.007 OUR FIT	
	Error includes scale factor of 1.3.

$\Gamma(\rho^0 \pi^+ \pi^-)/\Gamma_{total}$

VALUE	DOCUMENT ID
0.110 ± 0.007 OUR FIT	
	Error includes scale factor of 1.3.

$\Gamma(\rho^0 \rho^0)/\Gamma_{total}$

VALUE	DOCUMENT ID	COMMENT
seen	BARBERIS 00c	450 $p p \rightarrow p_f 4\pi p_s$

$\Gamma(4\pi^0)/\Gamma_{total}$

VALUE (units 10^{-4})	CL%	DOCUMENT ID	TECN	COMMENT
<7	90	ALDE	87	GAM4 100 $\pi^- p \rightarrow 4\pi^0 n$

$\Gamma(K \bar{K} \pi)/\Gamma(\eta \pi \pi)$

VALUE	DOCUMENT ID	TECN	COMMENT
0.171 ± 0.013 OUR FIT			Error includes scale factor of 1.1.
0.170 ± 0.012 OUR AVERAGE			
0.166 ± 0.01 ± 0.008	BARBERIS 98c	OMEG 450	$p p \rightarrow p_f f_1(1285) p_s$
0.42 ± 0.15	GURTU 79	HBC	4.2 $K^- p$
0.5 ± 0.2	20 CORDEN 78	OMEG	12-15 $\pi^- p$
0.20 ± 0.08	21 DEFOIX 72	HBC	0.7 $\bar{p} p \rightarrow 7\pi$
0.16 ± 0.08	CAMPBELL 69	DBC	2.7 $\pi^+ d$

- 20 CORDEN 78 assumes low-mass $\eta \pi \pi$ region is dominantly 1^{++} . See BARBERIS 98c and MANAK 00a for discussion.
- 21 $K \bar{K}$ system characterized by the $I = 1$ threshold enhancement. (See under $a_0(980)$).

$\Gamma(a_0(980) \pi$ [ignoring $a_0(980) \rightarrow K \bar{K}$])/ $\Gamma(\eta \pi \pi)$

VALUE	CL%	EVTS	DOCUMENT ID	TECN	COMMENT
0.69 ± 0.13 OUR FIT					
0.69 ± 0.13 OUR AVERAGE					
0.72 ± 0.15			GURTU 79	HBC	4.2 $K^- p$
0.6 + 0.3 - 0.2			CORDEN 78	OMEG	12-15 $\pi^- p$
• • • We do not use the following data for averages, fits, limits, etc. • • •					
>0.69	95	318	ACHARD 02B	L3	183-209 $e^+ e^- \rightarrow e^+ e^- \eta \pi^+ \pi^-$
0.28 ± 0.07		1400	ALDE 97B	GAM4	100 $\pi^- p \rightarrow \eta \pi^0 \pi^0 n$
1.0 ± 0.3			GRASSLER 77	HBC	16 $\pi^\mp p$

Meson Particle Listings

 $f_1(1285), \eta(1295)$ $\Gamma(4\pi)/\Gamma(\eta\pi\pi)$

VALUE	DOCUMENT ID	TECN	COMMENT
0.63 ± 0.06 OUR FIT	Error includes scale factor of 1.2.		
0.41 ± 0.14 OUR AVERAGE			
$0.37 \pm 0.11 \pm 0.11$	BOLTON 92	MRK3	$J/\psi \rightarrow \gamma f_1(1285)$
0.64 ± 0.40	GURTU 79	HBC	$4.2 K^- p$
• • • We do not use the following data for averages, fits, limits, etc. • • •			
0.93 ± 0.30	22 GRASSLER 77	HBC	$16 \pi^+ \pi^- p$
22 Assuming $\rho\pi\pi$ and $a_0(980)\pi$ intermediate states.			

 $\Gamma(K\bar{K}^*(892))/\Gamma_{\text{total}}$

VALUE	DOCUMENT ID	TECN	COMMENT
not seen	NACASCH 78	HBC	$0.7, 0.76 \bar{p} p \rightarrow K\bar{K}^* 3\pi$
• • • We do not use the following data for averages, fits, limits, etc. • • •			
seen	23 ACHARD 07	L3	$183-209 e^+ e^- \rightarrow e^+ e^- K_S^0 K^\pm \pi^\mp$
23 A clear signal of 19.8 ± 4.4 events observed at high Q^2 .			

 $\Gamma(\rho^0 \pi^+ \pi^-)/\Gamma(2\pi^+ 2\pi^-)$

VALUE	DOCUMENT ID	TECN	COMMENT
1.0 ± 0.4	GRASSLER 77	HBC	$16 \text{ GeV } \pi^\pm p$
• • • We do not use the following data for averages, fits, limits, etc. • • •			

 $\Gamma(\phi\gamma)/\Gamma(K\bar{K}\pi)$

VALUE (units 10^{-2})	CL%	EVTS	DOCUMENT ID	TECN	COMMENT
$0.82 \pm 0.21 \pm 0.20$	19		BITYUKOV 88	SPEC	$32.5 \pi^- p \rightarrow K^+ K^- \pi^0 n$
• • • We do not use the following data for averages, fits, limits, etc. • • •					
<0.50	95		BARBERIS 98c	OMEG	$450 pp \rightarrow p_f f_1(1285) p_S$
<0.93	95		AMELIN 95	VES	$37 \pi^- N \rightarrow \pi^- \pi^+ \pi^- \gamma N$

 $\Gamma(\gamma\rho^0)/\Gamma(K\bar{K}\pi)$

VALUE	CL%	DOCUMENT ID	TECN	COMMENT
>0.035	90	24 COFFMAN 90	MRK3	$J/\psi \rightarrow \gamma\gamma\pi^+\pi^-$
24 Using $B(J/\psi \rightarrow \gamma f_1(1285)) \rightarrow \gamma\gamma\rho^0 = 0.25 \times 10^{-4}$ and $B(J/\psi \rightarrow \gamma f_1(1285)) \rightarrow \gamma K\bar{K}\pi = < 0.72 \times 10^{-3}$.				

 $\Gamma(\gamma\rho^0)/\Gamma(2\pi^+ 2\pi^-)$

VALUE	DOCUMENT ID	TECN	COMMENT
0.50 ± 0.13 OUR FIT	Error includes scale factor of 2.5.		
0.45 ± 0.18	25 COFFMAN 90	MRK3	$J/\psi \rightarrow \gamma\gamma\pi^+\pi^-$
25 Using $B(J/\psi \rightarrow \gamma f_1(1285)) \rightarrow \gamma\gamma\rho^0 = 0.25 \times 10^{-4}$ and $B(J/\psi \rightarrow \gamma f_1(1285)) \rightarrow \gamma 2\pi^+ 2\pi^- = 0.55 \times 10^{-4}$ given by MIR 88.			

 $\Gamma(\gamma\rho^0)/\Gamma_{\text{total}}$

VALUE (units 10^{-2})	CL%	DOCUMENT ID	TECN	COMMENT
5.5 ± 1.3 OUR FIT	Error includes scale factor of 2.8.			
$2.8 \pm 0.7 \pm 0.6$		AMELIN 95	VES	$37 \pi^- N \rightarrow \pi^- \pi^+ \pi^- \gamma N$
• • • We do not use the following data for averages, fits, limits, etc. • • •				
<5	95	BITYUKOV 91b	SPEC	$32 \pi^- p \rightarrow \pi^+ \pi^- \gamma n$

 $\Gamma(\eta\pi\pi)/\Gamma(\gamma\rho^0)$

VALUE	DOCUMENT ID	TECN	COMMENT
9.5 ± 2.0 OUR FIT	Error includes scale factor of 2.5.		
7.9 ± 0.9 OUR AVERAGE			
$10.0 \pm 1.0 \pm 2.0$	BARBERIS 98c	OMEG	$450 pp \rightarrow p_f f_1(1285) p_S$
7.5 ± 1.0	26 ARMSTRONG 92c	OMEG	$300 pp \rightarrow pp\pi^+\pi^-\gamma, pp\eta\pi^+\pi^-$
26 Published value multiplied by 1.5.			

 $f_1(1285)$ REFERENCES

ACHARD 07	JHEP 0703 018	P. Achard et al.	(L3 Collab.)
AUBERT 07AU	PR D76 092005	B. Aubert et al.	(BABAR Collab.)
BAI 04J	PL B594 47	J.Z. Bai et al.	(BES Collab.)
ABDALLAH 03H	PL B569 129	J. Abdallah et al.	(DELPHI Collab.)
ACHARD 02B	PL B526 269	P. Achard et al.	(L3 Collab.)
ACCIARRI 01G	PL B501 1	M. Acciarri et al.	(L3 Collab.)
ADAMS 01B	PL B516 264	G.S. Adams et al.	(BNL E852 Collab.)
BARBERIS 00C	PL B471 440	D. Barberis et al.	(WA 102 Collab.)
MANAK 00A	PR D62 012003	J.J. Manak et al.	(BNL E852 Collab.)
SOSA 99	PRL 83 913	M. Sosa et al.	
BARBERIS 98C	PL B440 225	D. Barberis et al.	(WA 102 Collab.)
ALDE 97B	PAN 60 386	D. Alde et al.	(GAMS Collab.)
Translated from YAF 60 458.			
BARBERIS 97B	PL B413 217	D. Barberis et al.	(WA 102 Collab.)
BARBERIS 97C	PL B413 225	D. Barberis et al.	(WA 102 Collab.)
AMELIN 95	ZPHY C66 71	D.V. Amelin et al.	(VES Collab.)
ANTINORI 95	PL B353 589	F. Antinori et al.	(ATHU, BARI, BIRM+)
ABATZIS 94	PL B324 509	S. Abatzis et al.	(ATHU, BARI, BIRM+)
LEE 94	PL B323 227	J.H. Lee et al.	(BNL, IND, KYUN, MASN+)
ARMSTRONG 93C	PL B307 394	T.A. Armstrong et al.	(FNAL, FERR, MASN+)
ARMSTRONG 92C	ZPHY C54 371	T.A. Armstrong et al.	(ATHU, BARI, BIRM+)
BOLTON 92	PL B278 495	T. Bolton et al.	(Mark III Collab.)
BITYUKOV 91B	SJNP 54 318	S.I. Bityukov et al.	(SERP)
Translated from YAF 54 529.			

FUKUI 91C	PL B267 293	S. Fukui et al.	(SUGI, NAGO, KEK, KYOT+)
COFFMAN 90	PR D41 1410	D.M. Coffman et al.	(Mark III Collab.)
ARMSTRONG 89	PL B221 216	T.A. Armstrong et al.	(CERN, CDEF, BIRM+) JPC
ARMSTRONG 89E	PL B228 536	T.A. Armstrong, M. Benayoun	(ATHU, BARI, BIRM+)
ARMSTRONG 89G	ZPHY C43 55	T.A. Armstrong et al.	(CERN, BIRM, BARI+)
RATH 89	PR D40 693	M.G. Rath et al.	(NDAM, BRAN, BNL, CUNY+)
AIHARA 88B	PL B209 107	H. Aihara et al.	(TPC-2\gamma Collab.)
BIRMAN 88	PRL 61 1557	A. Birman et al.	(BNL, FSU, IND, MASN) JP
BITYUKOV 88	PL B203 327	S.I. Bityukov et al.	(SERP)
MIR 88	Photon-Photon 88, 126	R. Mir	(Mark III Collab.)
Conference			
ALDE 87	PL B198 286	D.M. Alde et al.	(LANL, BRUX, SERP, LAPP)
BECKER 87	PRL 59 186	J.J. Becker et al.	(Mark III Collab.)
GIDAL 87	PRL 59 2012	G. Gidal et al.	(LBL, SLAC, HARV)
ANDO 86	PRL 57 1296	A. Ando et al.	(KEK, KYOT, NIRS, SAGA+) IJP
REEVES 86	PR D34 1960	D.F. Reeves et al.	(FLOR, BNL, IND+) JP
CHUNG 85	PRL 55 779	S.U. Chung et al.	(BNL, FLOR, IND+) JP
ARMSTRONG 84	PL 146B 273	T.A. Armstrong et al.	(ATHU, BARI, BIRM+) JP
BITYUKOV 84B	PL 144B 133	S.I. Bityukov et al.	(SERP)
CHAUVAT 84	PL 145B 382	P. Chauvat et al.	(CERN, CLER, UCLA+)
TORNQVIST 82B	NP B203 268	N.A. Tornqvist	(HELS)
EVANGELISTA 81	NP B178 197	C. Evangelista et al.	(BARI, BONN, CERN+)
BROMBERG 80	PR D22 1513	C.M. Bromberg et al.	(CIT, FNAL, ILL+)
DIONISI 80	NP B169 1	C. Dionisi et al.	(CERN, MADR, CDEF+)
GURTU 79	NP B151 181	A. Gurtu et al.	(CERN, ZEEM, NIJM, OXF)
STANTON 79	PRL 42 346	N.R. Stanton et al.	(OSU, CARL, MCGI+) JP
CORDEN 78	NP B144 253	M.J. Corden et al.	(BIRM, RHEL, TELA+) JP
NACASCH 78	NP B135 203	R. Nacasch et al.	(PARIS, MADR, CERN)
GRASSLER 77	NP B121 189	H. Grassler et al.	(AACH3, BERL, BONN+)
DEFOIX 72	NP B44 125	C. Defoix et al.	(CDEF, CERN)
DUBOC 72	NP B46 429	J. Duboc et al.	(PARIS, LIVP)
THUN 72	PRL 28 1733	R. Thun et al.	(STON, NEAS)
BARDADIN... 71	PR D4 2711	M. Bardadin-Otwinowska et al.	(WARS)
BOESEBECK 71	PL 34B 659	K. Boesebeck	(AACH, BERL, BONN, CERN, CERN+)
CAMPBELL 69	PRL 22 1204	J.H. Campbell et al.	(PURD)
LORSTAD 69	NP B14 63	B. Lorstad et al.	(CDEF, CERN) JP
D'ANDLAU 68	NP B5 693	C. d'Andlau et al.	(CDEF, CERN, IRAD+) IJP
DAHL 67	PR 163 1377	O.I. Dahl et al.	(LRL) IJP

OTHER RELATED PAPERS

AHOHE 05	PR D71 072001	R. Ahohe et al.	(CLEO Collab.)
AIHARA 88C	PR D38 1	H. Aihara et al.	(TPC-2\gamma Collab.) JPC
ASTON 85	PR D32 2255	D. Aston et al.	(SLAC, CARL, CNR)
ATKINSON 84E	PL 138B 459	M. Atkinson et al.	(BONN, CERN, GLAS+)
GAVILLET 82	ZPHY C16 119	P. Gavillet et al.	(CERN, CDEF, PADO+)
D'ANDLAU 65	PL 17 347	C. d'Andlau et al.	(CDEF, CERN, IRAD+)
MILLER 65	PRL 14 1074	D.H. Miller et al.	(LRL, UCB)

 $\eta(1295)$

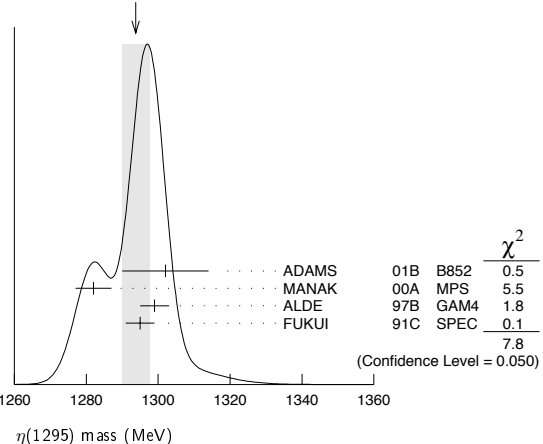
$$I^G(J^{PC}) = 0^+(0^-+)$$

See also the mini-review under non- $q\bar{q}$ candidates in PDG 06, Journal of Physics, G 33 1 (2006).

 $\eta(1295)$ MASS

VALUE (MeV)	EVTS	DOCUMENT ID	TECN	COMMENT
1294 ± 4 OUR AVERAGE	Error includes scale factor of 1.6. See the ideogram below.			
$1302 \pm 9 \pm 8$	20k	ADAMS	01B B852	$18 \text{ GeV } \pi^- p \rightarrow K^+ K^- \pi^0 n$
1282 ± 5	9082	MANAK	00A MPS	$18 \pi^- p \rightarrow \eta\pi^+\pi^- n$
1299 ± 4	2100	ALDE	97B GAM4	$100 \pi^- p \rightarrow \eta\pi^0\pi^0 n$
1295 ± 4		FUKUI	91C SPEC	$8.95 \pi^- p \rightarrow \eta\pi^+\pi^- n$
• • • We do not use the following data for averages, fits, limits, etc. • • •				
1264 ± 8		1 AUGUSTIN 90	DM2	$J/\psi \rightarrow \gamma\eta\pi^+\pi^-$
~ 1275		STANTON 79	CNTR	$8.4 \pi^- p \rightarrow n\eta 2\pi$

WEIGHTED AVERAGE
1294±4 (Error scaled by 1.6)



1 PWA analysis of AUGUSTIN 92 assigns 0^{++} quantum numbers to this state rather than 1^{++} as before.

$\eta(1295)$ WIDTH

VALUE (MeV)	EVTS	DOCUMENT ID	TECN	COMMENT
55 ± 5 OUR AVERAGE				
57 ± 23 ± 21	20k	ADAMS	01B B852	18 GeV $\pi^- p \rightarrow K^+ K^- \pi^0 n$
66 ± 13	9082	MANAK	00A MPS	18 $\pi^- p \rightarrow \eta \pi^+ \pi^- n$
53 ± 6		FUKUI	91c SPEC	8.95 $\pi^- p \rightarrow \eta \pi^+ \pi^- n$
• • • We do not use the following data for averages, fits, limits, etc. • • •				
<40	2100	ALDE	97B GAM4	100 $\pi^- p \rightarrow \eta \pi^0 \pi^0 n$
44 ± 20		AUGUSTIN	90 DM2	$J/\psi \rightarrow \gamma \eta \pi^+ \pi^-$
~ 70		STANTON	79 CNTR	8.4 $\pi^- p \rightarrow n \eta 2\pi$
² PWA analysis of AUGUSTIN 92 assigns 0^{-+} quantum numbers to this state rather than 1^{++} as before.				

 $\eta(1295)$ DECAY MODES

Mode	Fraction (Γ_i/Γ)
Γ_1 $\eta \pi^+ \pi^-$	seen
Γ_2 $a_0(980) \pi$	seen
Γ_3 $\gamma \gamma$	
Γ_4 $\eta \pi^0 \pi^0$	seen
Γ_5 $\eta(\pi\pi)S$ -wave	seen
Γ_6 $\sigma \eta$	
Γ_7 $K \bar{K} \pi$	

 $\eta(1295)$ $\Gamma(i)\Gamma(\gamma\gamma)/\Gamma(\text{total})$

VALUE (keV)	CL%	DOCUMENT ID	TECN	COMMENT	$\Gamma_1 \Gamma_3/\Gamma$
<0.066	95	ACCIARRI	01G L3	183-202 $e^+ e^- \rightarrow e^+ e^- \eta \pi^+ \pi^-$	
• • • We do not use the following data for averages, fits, limits, etc. • • •					
<0.6	90	AIHARA	88c TPC	$e^+ e^- \rightarrow e^+ e^- \eta \pi^+ \pi^-$	
<0.3		ANTREASYAN	87 CBAL	$e^+ e^- \rightarrow e^+ e^- \eta \pi \pi$	
$\Gamma(K \bar{K} \pi) \times \Gamma(\gamma\gamma)/\Gamma(\text{total})$ $\Gamma_7 \Gamma_3/\Gamma$					
VALUE (keV)	CL%	DOCUMENT ID	TECN	COMMENT	
<0.014	90	^{3,4} AHOHE	05 CLE2	10.6 $e^+ e^- \rightarrow e^+ e^- K_S^0 K^\pm \pi^\mp$	

³ Using $\eta(1295)$ mass and width 1294 MeV and 55 MeV, respectively.⁴ Assuming three-body phase-space decay to $K_S^0 K^\pm \pi^\mp$. $\eta(1295)$ BRANCHING RATIOS

$\Gamma(a_0(980)\pi)/\Gamma(\text{total})$	Γ_2/Γ			
not seen				
seen				
large				
large				
$\Gamma(a_0(980)\pi)/\Gamma(\eta\pi^0\pi^0)$ Γ_2/Γ_4				
VALUE	DOCUMENT ID	TECN	COMMENT	
0.65 ± 0.10	⁵ ALDE	97B GAM4	100 $\pi^- p \rightarrow \eta \pi^0 \pi^0 n$	
⁵ Assuming that $a_0(980)$ decays only to $\eta \pi$.				
$\Gamma(\eta(\pi\pi)S\text{-wave})/\Gamma(\eta\pi^0\pi^0)$ Γ_5/Γ_4				
VALUE	DOCUMENT ID	TECN	COMMENT	
0.35 ± 0.10	ALDE	97B GAM4	100 $\pi^- p \rightarrow \eta \pi^0 \pi^0 n$	
$\Gamma(a_0(980)\pi)/\Gamma(\sigma\eta)$ Γ_2/Γ_6				
VALUE	EVTS	DOCUMENT ID	TECN	COMMENT
0.48 ± 0.22	9082	MANAK	00A MPS	18 $\pi^- p \rightarrow \eta \pi^+ \pi^- n$

 $\eta(1295)$ REFERENCES

PDG	06	JPG 33 1	W.-M. Yao et al.	(PDG Collab.)
AHOHE	05	PR D71 072001	R. Ahohe et al.	(CLEO Collab.)
ACCIARRI	01G	PL B501 1	M. Acciari et al.	(L3 Collab.)
ADAMS	01B	PL B516 264	G.S. Adams et al.	(BNL E852 Collab.)
MANAK	00A	PR D62 012003	J.J. Manak et al.	(BNL E852 Collab.)
ALDE	97B	PAN 60 386	D. Alde et al.	(GAMS Collab.)
Translated from YAF 60 458.				
BERTIN	97	PL B400 226	A. Bertin et al.	(OBELIX Collab.)
AUGUSTIN	92	PR D46 1951	J.E. Augustin, G. Cosme	(DM2 Collab.)
FUKUI	91C	PL B267 293	S. Fukui et al.	(SUGI, NAGO, KEK, KYOT+)
AUGUSTIN	90	PR D42 10	J.E. Augustin et al.	(DM2 Collab.)
AIHARA	88C	PR D38 1	H. Aihara et al.	(TPC-2 γ Collab.)
BIRMAN	88	PRL 61 1557	A. Birman et al.	(BNL, FSU, IND, MASH)JP
ANTREASYAN	87	PR D36 2633	D. Antreasyan et al.	(Crystal Ball Collab.)
ANDO	86	PRL 57 1296	A. Ando et al.	(KEK, KYOT, NIRS, SAGA+)IJP
STANTON	79	PRL 42 346	N.R. Stanton et al.	(OSU, CARL, MCGI+)JP

OTHER RELATED PAPERS

KLEMP	07	PRPL 454 1	E. Klempt, A. Zaitsev	
MASONI	06	JPG 32 R293	A. Masoni, C. Cicalo, G.L. Usai	(INFN, CAGL)
AMSLER	04B	EPJ C33 23	C. Amisler et al.	(Crystal Barrel Collab.)
ANISOVICH	00F	EPJ A6 247	A.V. Anisovich et al.	

 $\pi(1300)$

$$J^G(J^{PC}) = 1^-(0^{-+})$$

 $\pi(1300)$ MASS

VALUE (MeV)	EVTS	DOCUMENT ID	TECN	COMMENT
1300 ± 100 OUR ESTIMATE				
• • • We do not use the following data for averages, fits, limits, etc. • • •				
1345 ± 8 ± 10	18k	¹ SCHEGELSKY	06 RVUE	$\gamma \gamma \rightarrow \pi^+ \pi^- \pi^0$
1343 ± 15 ± 24		CHUNG	02 B852	18.3 $\pi^- p \rightarrow \pi^+ \pi^- \pi^- p$
1375 ± 40		ABELE	01 CBAR	0.0 $\bar{p} d \rightarrow \pi^- 4\pi^0 p$
1275 ± 15		BERTIN	97D OBLX	0.05 $\bar{p} p \rightarrow 2\pi^+ 2\pi^-$
~ 1114		ABELE	96 CBAR	0.0 $\bar{p} p \rightarrow 5\pi^0$
1190 ± 30		ZIELINSKI	84 SPEC	200 $\pi^+ Z \rightarrow Z 3\pi$
1240 ± 30		BELLINI	82 SPEC	40 $\pi^- A \rightarrow A 3\pi$
1273 ± 50		² AARON	81 RVUE	
1342 ± 20		BONESINI	81 OMEG	12 $\pi^- p \rightarrow p 3\pi$
~ 1400		DAUM	81B SPEC	63.94 $\pi^- p$
¹ From analysis of L3 data at 183-209 GeV.				
² Uses multichannel Aitchison-Bowler model (BOWLER 75). Uses data from DAUM 80 and DANKOWYCH 81.				

 $\pi(1300)$ WIDTH

VALUE (MeV)	EVTS	DOCUMENT ID	TECN	COMMENT
200 to 600 OUR ESTIMATE				
• • • We do not use the following data for averages, fits, limits, etc. • • •				
260 ± 20 ± 30	18k	³ SCHEGELSKY	06 RVUE	$\gamma \gamma \rightarrow \pi^+ \pi^- \pi^0$
449 ± 39 ± 47		CHUNG	02 B852	18.3 $\pi^- p \rightarrow \pi^+ \pi^- \pi^- p$
268 ± 50		ABELE	01 CBAR	0.0 $\bar{p} d \rightarrow \pi^- 4\pi^0 p$
218 ± 100		BERTIN	97D OBLX	0.05 $\bar{p} p \rightarrow 2\pi^+ 2\pi^-$
~ 340		ABELE	96 CBAR	0.0 $\bar{p} p \rightarrow 5\pi^0$
440 ± 80		ZIELINSKI	84 SPEC	200 $\pi^+ Z \rightarrow Z 3\pi$
360 ± 120		BELLINI	82 SPEC	40 $\pi^- A \rightarrow A 3\pi$
580 ± 100		⁴ AARON	81 RVUE	
220 ± 70		BONESINI	81 OMEG	12 $\pi^- p \rightarrow p 3\pi$
~ 600		DAUM	81B SPEC	63.94 $\pi^- p$
³ From analysis of L3 data at 183-209 GeV.				
⁴ Uses multichannel Aitchison-Bowler model (BOWLER 75). Uses data from DAUM 80 and DANKOWYCH 81.				

 $\pi(1300)$ DECAY MODES

Mode	Fraction (Γ_i/Γ)
Γ_1 $\rho \pi$	seen
Γ_2 $\pi(\pi\pi)S$ -wave	seen
Γ_3 $\gamma \gamma$	

 $\pi(1300)$ $\Gamma(i)\Gamma(\gamma\gamma)/\Gamma(\text{total})$

VALUE (keV)	CL%	DOCUMENT ID	TECN	COMMENT	$\Gamma_1 \Gamma_3/\Gamma$
<0.085	90	ACCIARRI	97T L3	$e^+ e^- \rightarrow e^+ e^- \pi^+ \pi^- \pi^0$	
• • • We do not use the following data for averages, fits, limits, etc. • • •					
<0.8	95	⁵ SCHEGELSKY	06 RVUE	$\gamma \gamma \rightarrow \pi^+ \pi^- \pi^0$	
<0.54	90	ALBRECHT	97b ARG	$e^+ e^- \rightarrow e^+ e^- \pi^+ \pi^- \pi^0$	
⁵ From analysis of L3 data at 183-209 GeV.					

 $\pi(1300)$ BRANCHING RATIOS

$\Gamma(\pi(\pi\pi)S\text{-wave})/\Gamma(\rho\pi)$	Γ_2/Γ_1			
not seen				
0.15				
2.12				
$\Gamma(\pi(\pi\pi)S\text{-wave})/\Gamma(\rho\pi)$ Γ_2/Γ_1				
VALUE	CL%	DOCUMENT ID	TECN	COMMENT
<0.15	90	CHUNG	02 B852	18.3 $\pi^- p \rightarrow \pi^+ \pi^- \pi^- p$
		ABELE	01 CBAR	0.0 $\bar{p} d \rightarrow \pi^- 4\pi^0 p$
		⁶ AARON	81 RVUE	
⁶ Uses multichannel Aitchison-Bowler model (BOWLER 75). Uses data from DAUM 80 and DANKOWYCH 81.				

Meson Particle Listings

 $\pi(1300)$, $a_2(1320)$ $\pi(1300)$ REFERENCES

SCHEGELSKY 06	EPJ A27 199	V.A. Schegelsky et al.	(BNL E852 Collab.)
CHUNG 02	PR D65 072001	S.U. Chung et al.	(Crystal Barrel Collab.)
ABELE 01	EPJ C19 667	A. Abele et al.	(L3 Collab.)
ACCIARRI 97T	PL B413 147	M. Acciari et al.	(ARGUS Collab.)
ALBRECHT 97B	ZPHY C74 469	H. Albrecht et al.	(OBELIX Collab.)
BERTIN 97D	PL B414 220	A. Bertin et al.	(Crystal Barrel Collab.)
ABELE 96	PL B380 453	A. Abele et al.	(ROCH, MINN, FNAL)
ZIELINSKI 84	PR D30 1855	M. Zielinski et al.	(MILA, BGNA, JINR)
BELLINI 82	PRL 48 1697	G. Bellini et al.	(NEAS, BNL)
AARON 81	PR D24 1207	R.A. Aaron, R.S. Longacre	(MILA, LIVP, DARE+)
BONESINI 81	PL 103B 75	M. Bonesini et al.	(TNT0, BNL, CARL+)
DANKOWY... 81	PRL 46 500	J.A. Dankowycz et al.	(AMST, CERN, CRAC, MPIM+)
DAUM 81B	NP B182 269	C. Daum et al.	(AMST, CERN, CRAC, MPIM+)
DAUM 80	PL 89B 281	C. Daum et al.	(OXFDP, DARE)
BOWLER 75	NP B97 227	M.G. Bowler et al.	

OTHER RELATED PAPERS

EBERT 05	MPL A20 1887	D. Ebert, R.N. Faustov, V.O. Galkin	
KATAEV 05	PAN 68 567	A.L. Kataev	
ASNER 00	PR D61 012002	D.M. Asner et al.	(CLEO Collab.)
ZAIMIDOROGA 99	PAN 30 1	O.A. Zaimidoriga	
ACKERSTAFF 97R	ZPHY C75 593	K. Ackerstaff et al.	(OPAL Collab.)
ALBRECHT 95C	PL B349 576	H. Albrecht et al.	(ARGUS Collab.)

 $a_2(1320)$

$$I^G(J^{PC}) = 1^-(2^{++})$$

 $a_2(1320)$ MASS

1318.3 ± 0.6 OUR AVERAGE Includes data from the 4 datablocks that follow this one. Error includes scale factor of 1.2.

3 π MODE

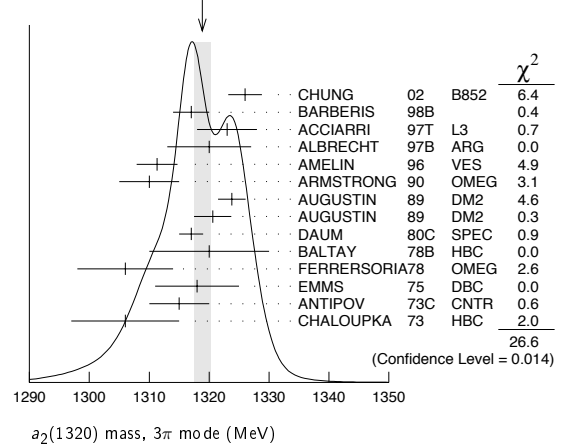
VALUE (MeV)	EVTS	DOCUMENT ID	TECN	CHG	COMMENT
-------------	------	-------------	------	-----	---------

The data in this block is included in the average printed for a previous datablock.

1318.9 ± 1.4 OUR AVERAGE Error includes scale factor of 1.4. See the ideogram below.

1326 ± 2 ± 2		CHUNG 02 B852			18.3 $\pi^- p \rightarrow \pi^+ \pi^- \pi^- p$
1317 ± 3		BARBERIS 98B			45.0 $pp \rightarrow p_f \pi^+ \pi^- \pi^0 p_s$
1323 ± 4 ± 3		ACCIARRI 97T L3			$e^+ e^- \rightarrow e^+ \pi^+ \pi^- \pi^- \pi^0$
1320 ± 7		ALBRECHT 97B ARG			$e^+ e^- \rightarrow e^+ \pi^+ \pi^- \pi^- \pi^0$
1311.3 ± 1.6 ± 3.0	72.4k	AMELIN 96 VES			36 $\pi^- p \rightarrow \pi^+ \pi^- \pi^0 n$
1310 ± 5		ARMSTRONG 90 OMEG 0			300.0 $pp \rightarrow p p \pi^+ \pi^- \pi^0$
1323.8 ± 2.3	4022	AUGUSTIN 89 DM2 ±			$J/\psi \rightarrow \rho^\pm a_2^\mp$
1320.6 ± 3.1	3562	AUGUSTIN 89 DM2 0			$J/\psi \rightarrow \rho^0 a_2^0$
1317 ± 2	25k	¹ DAUM 80C SPEC -			63,94 $\pi^- p \rightarrow 3\pi p$
1320 ± 10	1097	¹ BALTAY 78B HBC +0			15 $\pi^+ p \rightarrow p 4\pi$
1306 ± 8		FERRERSORIA 78 OMEG -			9 $\pi^- p \rightarrow p 3\pi$
1318 ± 7	1.6k	¹ EMMS 75 DBC 0			4 $\pi^+ n \rightarrow p(3\pi)^0$
1315 ± 5		¹ ANTIPOV 73C CNTR -			25,40 $\pi^- p \rightarrow p \eta \pi^-$
1306 ± 9	1580	CHALOUPKA 73 HBC -			3.9 $\pi^- p \rightarrow \Delta^+ \eta \pi^- p_s$
••• We do not use the following data for averages, fits, limits, etc. •••					
1300 ± 2 ± 4	18k	² SCHEGELSKY 06 RVUE 0			$\gamma\gamma \rightarrow \pi^+ \pi^- \pi^0$
1305 ± 14		CONDO 93 SHF			$\gamma p \rightarrow \eta \pi^+ \pi^+ \pi^-$
1310 ± 2		¹ EVANGELIS... 81 OMEG -			12 $\pi^- p \rightarrow 3\pi p$
1343 ± 11	490	BALTAY 78B HBC 0			15 $\pi^+ p \rightarrow \Delta 3\pi$
1309 ± 5	5k	BINNIE 71 MMS -			$\pi^- p$ near a_2 threshold
1299 ± 6	28k	BOWEN 71 MMS -			5 $\pi^- p$
1300 ± 6	24k	BOWEN 71 MMS +			5 $\pi^+ p$
1309 ± 4	17k	BOWEN 71 MMS -			7 $\pi^- p$
1306 ± 4	941	ALSTON... 70 HBC +			7.0 $\pi^+ p \rightarrow 3\pi p$

¹ From a fit to $J^P = 2^+ \pi\pi$ partial wave.
² From analysis of L3 data at 183–209 GeV.

WEIGHTED AVERAGE
1318.9 ± 1.4 (Error scaled by 1.4) $K\bar{K}$ MODE

VALUE (MeV)	EVTS	DOCUMENT ID	TECN	CHG	COMMENT
-------------	------	-------------	------	-----	---------

The data in this block is included in the average printed for a previous datablock.

1318.1 ± 0.7 OUR AVERAGE

1319 ± 5	4700	^{3,4} CLELAND 82B SPEC +			50 $\pi^+ p \rightarrow K_S^0 K^+ p$
1324 ± 6	5200	^{3,4} CLELAND 82B SPEC -			50 $\pi^- p \rightarrow K_S^0 K^- p$
1320 ± 2	4000	CHABAUD 80C SPEC -			17 $\pi^- A \rightarrow K_S^0 K^- A$
1312 ± 4	11000	CHABAUD 78 SPEC -			9.8 $\pi^- p \rightarrow K^- K_S^0 p$
1316 ± 2	4730	CHABAUD 78 SPEC -			18.8 $\pi^- p \rightarrow K^- K_S^0 p$
1318 ± 1		^{3,5} MARTIN 78D SPEC -			10 $\pi^- p \rightarrow K_S^0 K^- p$
1320 ± 2	2724	MARGULIE 76 SPEC -			23 $\pi^- p \rightarrow K^- K_S^0 p$
1313 ± 4	730	FOLEY 72 CNTR -			20.3 $\pi^- p \rightarrow K^- K_S^0 p$
1319 ± 3	1500	⁵ GRAYER 71 ASPK -			17.2 $\pi^- p \rightarrow K^- K_S^0 p$
••• We do not use the following data for averages, fits, limits, etc. •••					
1304 ± 10	870	⁶ SCHEGELSKY 06A RVUE 0			$\gamma\gamma \rightarrow K_S^0 K_S^0$
1330 ± 11	1000	^{3,4} CLELAND 82B SPEC +			30 $\pi^+ p \rightarrow K_S^0 K^+ p$
1324 ± 5	350	HYAMS 78 ASPK +			12.7 $\pi^+ p \rightarrow K^+ K_S^0 p$

³ From a fit to $J^P = 2^+$ partial wave.
⁴ Number of events evaluated by us.
⁵ Systematic error in mass scale subtracted.
⁶ From analysis of L3 data at 91 and 183–209 GeV.

 $\eta\pi$ MODE

VALUE (MeV)	EVTS	DOCUMENT ID	TECN	CHG	COMMENT
-------------	------	-------------	------	-----	---------

The data in this block is included in the average printed for a previous datablock.

1317.7 ± 1.4 OUR AVERAGE

1308 ± 9		BARBERIS 00H			450 $pp \rightarrow p_f \eta \pi^0 p_s$
1316 ± 9		BARBERIS 00H			450 $pp \rightarrow \Delta^+ \eta \pi^- p_s$
1317 ± 1 ± 2		THOMPSON 97 MPS			18 $\pi^- p \rightarrow \eta \pi^- p$
1315 ± 5 ± 2		⁷ AMSLER 94D CBAR			0.0 $\bar{p} p \rightarrow \pi^0 \pi^0 \eta$
1325.1 ± 5.1		AOYAGI 93 BKEI			$\pi^- p \rightarrow \eta \pi^- p$
1317.7 ± 1.4 ± 2.0		BELADIDZE 93 VES			37 $\pi^- N \rightarrow \eta \pi^- N$
1323 ± 8	1000	⁸ KEY 73 OSPK -			6 $\pi^- p \rightarrow p \pi^- \eta$
••• We do not use the following data for averages, fits, limits, etc. •••					
1324 ± 5		ARMSTRONG 93C E760 0			$\bar{p} p \rightarrow \pi^0 \eta \eta \rightarrow 6\gamma$
1336.2 ± 1.7	2561	DELFOSSSE 81 SPEC +			$\pi^\pm p \rightarrow p \pi^\pm \eta$
1330.7 ± 2.4	1653	DELFOSSSE 81 SPEC -			$\pi^\pm p \rightarrow p \pi^\pm \eta$
1324 ± 8	6200	^{8,9} CONFORTO 73 OSPK -			6 $\pi^- p \rightarrow p \pi^- \eta$

⁷ The systematic error of 2 MeV corresponds to the spread of solutions.
⁸ Error includes 5 MeV systematic mass-scale error.
⁹ Missing mass with enriched MMS = $\eta\pi^-$, $\eta = 2\gamma$.

 η'/π MODE

VALUE (MeV)	DOCUMENT ID	TECN	COMMENT
-------------	-------------	------	---------

The data in this block is included in the average printed for a previous datablock.

1322 ± 7 OUR AVERAGE

1318 ± 8	$^{+3}_{-5}$	IVANOV 01 B852	18 $\pi^- p \rightarrow \eta' \pi^- p$
1327.0 ± 10.7		BELADIDZE 93 VES	37 $\pi^- N \rightarrow \eta' \pi^- N$

$a_2(1320)$ WIDTH 3π MODE

VALUE (MeV)	EVTS	DOCUMENT ID	TECN	CHG	COMMENT
104.7 ± 1.9 OUR AVERAGE					
108 ± 3 ± 15		CHUNG	02	B852	18.3 $\pi^- p \rightarrow \pi^+ \pi^- \pi^- p$
120 ± 10		BARBERIS	98B		450 $\rho p \rightarrow \rho_f \pi^+ \pi^- \pi^0 p_S$
105 ± 10 ± 11		ACCIARRI	97T	L3	$e^+ e^- \rightarrow \pi^+ \pi^- \pi^+ \pi^- \pi^0$
120 ± 10		ALBRECHT	97B	ARG	$e^+ e^- \rightarrow \pi^+ \pi^- \pi^+ \pi^- \pi^0$
103.0 ± 6.0 ± 3.3 72.4k		AMELIN	96	VES	36 $\pi^- p \rightarrow \pi^+ \pi^- \pi^0 n$
120 ± 10		ARMSTRONG	90	OMEG 0	300.0 $\rho p \rightarrow \rho p \pi^+ \pi^- \pi^0$
107.0 ± 9.7	4022	AUGUSTIN	89	DM2 ±	$J/\psi \rightarrow \rho^\pm a_2^\mp$
118.5 ± 12.5	3562	AUGUSTIN	89	DM2 0	$J/\psi \rightarrow \rho^0 a_2^0$
97 ± 5		¹⁰ EVANGELIS...	81	OMEG -	12 $\pi^- p \rightarrow 3\pi p$
96 ± 9	25k	¹⁰ DAUM	80c	SPEC -	63,94 $\pi^- p \rightarrow 3\pi p$
110 ± 15	1097	¹⁰ BALTAY	78B	HBC +0	15 $\pi^+ p \rightarrow p 4\pi$
112 ± 18	1.6k	¹⁰ EMMS	75	DBC 0	4 $\pi^+ n \rightarrow \rho(3\pi)^0$
122 ± 14	1.2k	^{10,11} WAGNER	75	HBC 0	7 $\pi^+ p \rightarrow \Delta^{++}(3\pi)^0$
115 ± 15		¹⁰ ANTIPOV	73c	CNTR -	25,40 $\pi^- p \rightarrow \rho \eta \pi^-$
99 ± 15	1580	CHALOUPKA	73	HBC -	3.9 $\pi^- p$
105 ± 5	28k	BOWEN	71	MMS -	5 $\pi^- p$
99 ± 5	24k	BOWEN	71	MMS +	5 $\pi^+ p$
103 ± 5	17k	BOWEN	71	MMS -	7 $\pi^- p$

• • • We do not use the following data for averages, fits, limits, etc. • • •

117 ± 6 ± 20	18k	¹² SCHEGELSKY	06	RVUE 0	$\gamma\gamma \rightarrow \pi^+ \pi^- \pi^0$
120 ± 40		CONDO	93	SHF	$\gamma p \rightarrow \eta \pi^+ \pi^+ \pi^-$
115 ± 14	490	BALTAY	78B	HBC 0	15 $\pi^+ p \rightarrow \Delta 3\pi$
72 ± 16	5k	BINNIE	71	MMS -	$\pi^- p$ near a_2 thresh-old
79 ± 12	941	ALSTON...	70	HBC +	7.0 $\pi^+ p \rightarrow 3\pi p$

¹⁰From a fit to $J^P = 2^+ \rho\pi$ partial wave.

¹¹Width errors enlarged by us to $4\Gamma/\sqrt{N}$; see the note with the $K^*(892)$ mass.

¹²From analysis of L3 data at 183–209 GeV.

 $K\bar{K}$ AND $\eta\pi$ MODES

VALUE (MeV)	DOCUMENT ID
107 ± 5 OUR ESTIMATE	
110.4 ± 1.7 OUR AVERAGE	Includes data from the 2 datablocks that follow this one.

 $K\bar{K}$ MODE

VALUE (MeV)	EVTS	DOCUMENT ID	TECN	CHG	COMMENT
The data in this block is included in the average printed for a previous datablock.					

 109.8 ± 2.4 OUR AVERAGE

112 ± 20	4700	^{13,14} CLELAND	82B	SPEC +	50 $\pi^+ p \rightarrow K_S^0 K^+ p$
120 ± 25	5200	^{13,14} CLELAND	82B	SPEC -	50 $\pi^- p \rightarrow K_S^0 K^- p$
106 ± 4	4000	CHABAUD	80	SPEC -	17 $\pi^- A \rightarrow K_S^0 K^- A$
126 ± 11	11000	CHABAUD	78	SPEC -	9.8 $\pi^- p \rightarrow K^- K_S^0 p$
101 ± 8	4730	CHABAUD	78	SPEC -	18.8 $\pi^- p \rightarrow K^- K_S^0 p$
113 ± 4		^{13,15} MARTIN	78D	SPEC -	10 $\pi^- p \rightarrow K_S^0 K^- p$
105 ± 8	2724	¹⁵ MARGULIE	76	SPEC -	23 $\pi^- p \rightarrow K^- K_S^0 p$
113 ± 19	730	FOLEY	72	CNTR -	20.3 $\pi^- p \rightarrow K^- K_S^0 p$
123 ± 13	1500	¹⁵ GRAYR	71	ASPK -	17.2 $\pi^- p \rightarrow K^- K_S^0 p$

• • • We do not use the following data for averages, fits, limits, etc. • • •

120 ± 15	870	¹⁶ SCHEGELSKY	06A	RVUE 0	$\gamma\gamma \rightarrow K_S^0 K_S^0$
121 ± 51	1000	^{13,14} CLELAND	82B	SPEC +	30 $\pi^+ p \rightarrow K_S^0 K^+ p$
110 ± 18	350	HYAMS	78	ASPK +	12.7 $\pi^+ p \rightarrow K^+ K_S^0 p$

¹³From a fit to $J^P = 2^+$ partial wave.

¹⁴Number of events evaluated by us.

¹⁵Width errors enlarged by us to $4\Gamma/\sqrt{N}$; see the note with the $K^*(892)$ mass.

¹⁶From analysis of L3 data at 91 and 183–209 GeV.

 $\eta\pi$ MODE

VALUE (MeV)	EVTS	DOCUMENT ID	TECN	CHG	COMMENT
The data in this block is included in the average printed for a previous datablock.					

 111.1 ± 2.4 OUR AVERAGE

115 ± 20		BARBERIS	00H		450 $\rho p \rightarrow \rho_f \eta \pi^0 p_S$
112 ± 14		BARBERIS	00H		450 $\rho p \rightarrow \Delta_f^{++} \eta \pi^- p_S$
112 ± 3 ± 2		¹⁷ AMSLER	94D	CBAR	0.0 $\bar{p} p \rightarrow \pi^0 \pi^0 \eta$
103 ± 6 ± 3		BELADIDZE	93	VES	37 $\pi^- N \rightarrow \eta \pi^- N$
112.2 ± 5.7	2561	DELFOSSSE	81	SPEC +	$\pi^\pm p \rightarrow \rho \pi^\pm \eta$
116.6 ± 7.7	1653	DELFOSSSE	81	SPEC -	$\pi^\pm p \rightarrow \rho \pi^\pm \eta$
108 ± 9	1000	KEY	73	OSPK -	6 $\pi^- p \rightarrow \rho \pi^- \eta$

• • • We do not use the following data for averages, fits, limits, etc. • • •

127 ± 2 ± 2		¹⁸ THOMPSON	97	MPS	18 $\pi^- p \rightarrow \eta \pi^- p$
118 ± 10		ARMSTRONG	93c	E760 0	$\bar{p} p \rightarrow \pi^0 \eta \pi^- \rightarrow 6\gamma$
104 ± 9	6200	¹⁹ CONFORTO	73	OSPK -	6 $\pi^- p \rightarrow \rho \text{MM}^-$

¹⁷The systematic error of 2 MeV corresponds to the spread of solutions.

¹⁸Resolution is not unfolded.

¹⁹Missing mass with enriched MMS = $\eta \pi^-$, $\eta = 2\gamma$.

 η/π MODE

VALUE (MeV)	DOCUMENT ID	TECN	COMMENT
119 ± 25 OUR AVERAGE			
140 ± 35 ± 20	IVANOV	01	B852 18 $\pi^- p \rightarrow \eta/\pi^- p$
106 ± 32	BELADIDZE	93	VES 37 $\pi^- N \rightarrow \eta/\pi^- N$

 $a_2(1320)$ DECAY MODES

Mode	Fraction (Γ_i/Γ)	Scale factor/ Confidence level
Γ_1 3 π	(70.1 ± 2.7) %	S=1.2
Γ_2 $\rho(770)\pi$		
Γ_3 $f_2(1270)\pi$		
Γ_4 $\rho(1450)\pi$		
Γ_5 $\eta\pi$	(14.5 ± 1.2) %	
Γ_6 $\omega\pi\pi$	(10.6 ± 3.2) %	S=1.3
Γ_7 $K\bar{K}$	(4.9 ± 0.8) %	
Γ_8 $\eta'(958)\pi$	(5.3 ± 0.9) × 10 ⁻³	
Γ_9 $\pi^\pm\gamma$	(2.68 ± 0.31) × 10 ⁻³	
Γ_{10} $\gamma\gamma$	(9.4 ± 0.7) × 10 ⁻⁶	
Γ_{11} e^+e^-	< 6 × 10 ⁻⁹	CL=90%

CONSTRAINED FIT INFORMATION

An overall fit to 5 branching ratios uses 18 measurements and one constraint to determine 4 parameters. The overall fit has a $\chi^2 = 9.3$ for 15 degrees of freedom.

The following *off-diagonal* array elements are the correlation coefficients $\langle \delta x_i \delta x_j \rangle / (\delta x_i \delta x_j)$, in percent, from the fit to the branching fractions, $x_i \equiv \Gamma_i/\Gamma_{\text{total}}$. The fit constrains the x_i whose labels appear in this array to sum to one.

x_5	10		
x_6	-89	-46	
x_7	-1	-2	-24
	x_1	x_5	x_6

 $a_2(1320)$ PARTIAL WIDTHS

VALUE (MeV)	EVTS	DOCUMENT ID	TECN	CHG	COMMENT
$\Gamma(\eta\pi)$					Γ_5
18.5 ± 3.0	870	²⁰ SCHEGELSKY	06A	RVUE 0	$\gamma\gamma \rightarrow K_S^0 K_S^0$

• • • We do not use the following data for averages, fits, limits, etc. • • •

18.5 ± 3.0	870	²⁰ SCHEGELSKY	06A	RVUE 0	$\gamma\gamma \rightarrow K_S^0 K_S^0$
------------	-----	--------------------------	-----	--------	--

²⁰From analysis of L3 data at 91 and 183–209 GeV, using $\Gamma(a_2(1320) \rightarrow \gamma\gamma) = 0.91$ keV and SU(3) relations.

 $\Gamma(K\bar{K})$

VALUE (MeV)	EVTS	DOCUMENT ID	TECN	CHG	COMMENT
$\Gamma(K\bar{K})$					Γ_7
7.0 ± 2.0	870	²¹ SCHEGELSKY	06A	RVUE 0	$\gamma\gamma \rightarrow K_S^0 K_S^0$

• • • We do not use the following data for averages, fits, limits, etc. • • •

7.0 ± 2.0	870	²¹ SCHEGELSKY	06A	RVUE 0	$\gamma\gamma \rightarrow K_S^0 K_S^0$
-----------	-----	--------------------------	-----	--------	--

²¹From analysis of L3 data at 91 and 183–209 GeV, using $\Gamma(a_2(1320) \rightarrow \gamma\gamma) = 0.91$ keV and SU(3) relations.

 $\Gamma(\pi^\pm\gamma)$

VALUE (keV)	EVTS	DOCUMENT ID	TECN	CHG	COMMENT
287 ± 30 OUR AVERAGE					Γ_9
284 ± 25 ± 25	7100	MOLCHANOV	01	SELX	600 $\pi^- A \rightarrow \pi^+ \pi^- \pi^- A$
295 ± 60		CIHANGIR	82	SPEC +	200 $\pi^+ A$

• • • We do not use the following data for averages, fits, limits, etc. • • •

461 ± 110		²² MAY	77	SPEC ±	9.7 γA
-----------	--	-------------------	----	--------	----------------

²²Assuming one-pion exchange.

Meson Particle Listings

 $a_2(1320)$ $\Gamma(\gamma\gamma)$

VALUE (keV)	EVTS	DOCUMENT ID	TECN	CHG	COMMENT	Γ_{10}
1.00±0.06 OUR AVERAGE						
0.98±0.05±0.09		ACCIARRI 97T	L3		$e^+e^- \rightarrow e^+e^-\pi^+\pi^-\pi^0$	
0.96±0.03±0.13		ALBRECHT 97B	ARG		$e^+e^- \rightarrow e^+e^-\pi^+\pi^-\pi^0$	
1.26±0.26±0.18	36	BARU 90	MD1		$e^+e^- \rightarrow e^+e^-\pi^+\pi^-\pi^0$	
1.00±0.07±0.15	415	BEHREND 90C	CELL	0	$e^+e^- \rightarrow e^+e^-\pi^+\pi^-\pi^0$	
1.03±0.13±0.21		BUTLER 90	MRK2		$e^+e^- \rightarrow e^+e^-\pi^+\pi^-\pi^0$	
1.01±0.14±0.22	85	OEST 90	JADE		$e^+e^- \rightarrow e^+e^-\pi^+\pi^-\pi^0\eta$	
0.90±0.27±0.15	56	²³ ALTHOFF 86	TASS	0	$e^+e^- \rightarrow e^+e^-\pi^+\pi^-\pi^0$	
1.14±0.20±0.26		²⁴ ANTREASIAN 86	CBAL	0	$e^+e^- \rightarrow e^+e^-\pi^+\pi^-\pi^0\eta$	
1.06±0.18±0.19		BERGER 84C	PLUT	0	$e^+e^- \rightarrow e^+e^-\pi^+\pi^-\pi^0$	
••• We do not use the following data for averages, fits, limits, etc. •••						
0.81±0.19 ^{+0.42} _{-0.11}	35	²³ BEHREND 83B	CELL	0	$e^+e^- \rightarrow e^+e^-\pi^+\pi^-\pi^0$	
0.77±0.18±0.27	22	²⁴ EDWARDS 82F	CBAL	0	$e^+e^- \rightarrow e^+e^-\pi^+\pi^-\pi^0\eta$	
²³ From $\rho\pi$ decay mode.						
²⁴ From $\eta\pi^0$ decay mode.						

 $\Gamma(e^+e^-)$

VALUE (eV)	CL%	DOCUMENT ID	TECN	COMMENT	Γ_{11}
< 0.56					
	90	ACHASOV 00K	SND	$e^+e^- \rightarrow \pi^0\pi^0$	
••• We do not use the following data for averages, fits, limits, etc. •••					
<25	90	VOROBYEV 88	ND	$e^+e^- \rightarrow \pi^0\eta$	

 $a_2(1320) \Gamma(i)\Gamma(\gamma\gamma)/\Gamma(\text{total})$

VALUE (keV)	EVTS	DOCUMENT ID	TECN	COMMENT	Γ_{10}/Γ
••• We do not use the following data for averages, fits, limits, etc. •••					
0.65±0.02±0.02	18k	²⁵ SCHEGELSKY 06	RVUE	$\gamma\gamma \rightarrow \pi^+\pi^-\pi^0$	
²⁵ From analysis of L3 data at 183–209 GeV.					

 $\Gamma(K\bar{K}) \times \Gamma(\gamma\gamma)/\Gamma_{\text{total}}$

VALUE (keV)	DOCUMENT ID	TECN	COMMENT	$\Gamma_{7}/\Gamma_{10}/\Gamma$
0.126±0.007±0.028				
	²⁶ ALBRECHT 90G	ARG	$e^+e^- \rightarrow e^+e^-K^+K^-$	
••• We do not use the following data for averages, fits, limits, etc. •••				
0.081±0.006±0.027	²⁷ ALBRECHT 90G	ARG	$e^+e^- \rightarrow e^+e^-K^+K^-$	
²⁶ Using an incoherent background.				
²⁷ Using a coherent background.				

 $a_2(1320) \text{ BRANCHING RATIOS}$

VALUE	CL%	DOCUMENT ID	TECN	CHG	COMMENT	$(\Gamma_3+\Gamma_4)/\Gamma_2$
$[\Gamma(f_2(1270)\pi) + \Gamma(\rho(1450)\pi)]/\Gamma(\rho(770)\pi)$						
<0.12	90	ABRAMOVI... 70B	HBC	-	$3.93\pi^-\rho$	

 $\Gamma(\eta\pi)/\Gamma(3\pi)$

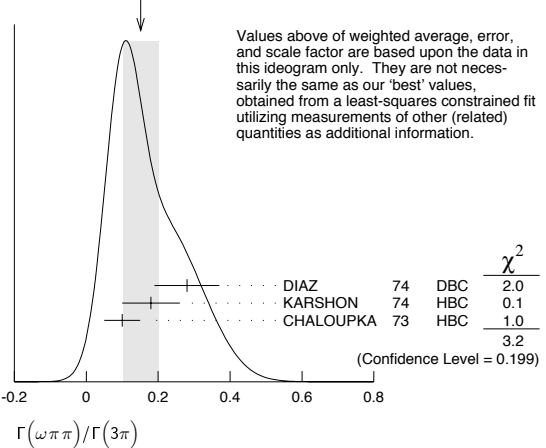
VALUE	EVTS	DOCUMENT ID	TECN	CHG	COMMENT	Γ_5/Γ_1
0.207±0.018 OUR FIT						
0.213±0.020 OUR AVERAGE						
0.18±0.05		FORINO 76	HBC		$11\pi^-\rho$	
0.22±0.05	52	ANTIP OV 73	CNTR	-	$40\pi^-\rho$	
0.211±0.044	149	CHALOUPKA 73	HBC	-	$3.9\pi^-\rho$	
0.246±0.042	167	ALSTON... 71	HBC	+	$7.0\pi^+\rho$	
0.25±0.09	15	BOECKMANN 70	HBC	+	$5.0\pi^+\rho$	
0.23±0.08	22	ASCOLI 68	HBC	-	$5\pi^-\rho$	
0.12±0.08		CHUNG 68	HBC	-	$3.2\pi^-\rho$	
0.22±0.09		CONTE 67	HBC	-	$11.0\pi^-\rho$	

 $\Gamma(\omega\pi\pi)/\Gamma(3\pi)$

VALUE	EVTS	DOCUMENT ID	TECN	CHG	COMMENT	Γ_6/Γ_1
0.15±0.05 OUR FIT						
Error includes scale factor of 1.3.						
0.15±0.05 OUR AVERAGE						
Error includes scale factor of 1.3. See the ideogram below.						
0.28±0.09	60	DIAZ 74	DBC	0	$6\pi^+\eta$	
0.18±0.08		²⁸ KARSHON 74	HBC		Avg. of above two	
0.10±0.05	279	CHALOUPKA 73	HBC	-	$3.9\pi^-\rho$	
••• We do not use the following data for averages, fits, limits, etc. •••						
0.29±0.08	140	²⁸ KARSHON 74	HBC	0	$4.9\pi^+\rho$	
0.10±0.04	60	²⁸ KARSHON 74	HBC	+	$4.9\pi^+\rho$	
0.19±0.08		DEFOIX 73	HBC	0	$0.7\bar{p}\rho$	

²⁸ KARSHON 74 suggest an additional $l=0$ state strongly coupled to $\omega\pi\pi$ which could explain discrepancies in branching ratios and masses. We use a central value and a systematic spread.

WEIGHTED AVERAGE
0.15±0.05 (Error scaled by 1.3)

 $\Gamma(K\bar{K})/\Gamma(3\pi)$

VALUE	EVTS	DOCUMENT ID	TECN	CHG	COMMENT	Γ_7/Γ_1
0.070±0.012 OUR FIT						
0.078±0.017						
••• We do not use the following data for averages, fits, limits, etc. •••						
0.011±0.003		²⁹ BERTIN 98B	OBLX	-	$0.0\bar{p}\rho \rightarrow K^\pm K_S \pi^\mp$	
0.056±0.014	50	³⁰ CHALOUPKA 73	HBC	-	$3.9\pi^-\rho$	
0.097±0.018	113	³⁰ ALSTON... 71	HBC	+	$7.0\pi^+\rho$	
0.06±0.03		³⁰ ABRAMOVI... 70B	HBC	-	$3.93\pi^-\rho$	
0.054±0.022		³⁰ CHUNG 68	HBC	-	$3.2\pi^-\rho$	
²⁹ Using 4π data from BERTIN 97D.						
³⁰ Included in CHABAUD 78 review.						

 $\Gamma(K\bar{K})/\Gamma(\eta\pi)$

VALUE	DOCUMENT ID	TECN	COMMENT	Γ_7/Γ_5
••• We do not use the following data for averages, fits, limits, etc. •••				
0.08±0.02	³¹ BERTIN 98B	OBLX	$0.0\bar{p}\rho \rightarrow K^\pm K_S \pi^\mp$	
³¹ Using $\eta\pi\pi$ data from AMSLER 94D.				

 $\Gamma(\eta\pi)/[\Gamma(3\pi) + \Gamma(\eta\pi) + \Gamma(K\bar{K})]$

VALUE	EVTS	DOCUMENT ID	TECN	CHG	COMMENT	$\Gamma_5/(\Gamma_1+\Gamma_5+\Gamma_7)$
0.162±0.012 OUR FIT						
0.140±0.028 OUR AVERAGE						
0.13±0.04		ESPIGAT 72	HBC	±	$0.0\bar{p}\rho$	
0.15±0.04	34	BARNHAM 71	HBC	+	$3.7\pi^+\rho$	

 $\Gamma(K\bar{K})/[\Gamma(3\pi) + \Gamma(\eta\pi) + \Gamma(K\bar{K})]$

VALUE	EVTS	DOCUMENT ID	TECN	CHG	COMMENT	$\Gamma_7/(\Gamma_1+\Gamma_5+\Gamma_7)$
0.054±0.009 OUR FIT						
0.048±0.012 OUR AVERAGE						
0.05±0.02		TOET 73	HBC	+	$5\pi^+\rho$	
0.09±0.04		TOET 73	HBC	0	$5\pi^+\rho$	
0.03±0.02	8	DAMERI 72	HBC	-	$11\pi^-\rho$	
0.06±0.03	17	BARNHAM 71	HBC	+	$3.7\pi^+\rho$	
••• We do not use the following data for averages, fits, limits, etc. •••						
0.020±0.004		³² ESPIGAT 72	HBC	±	$0.0\bar{p}\rho$	
³² Not averaged because of discrepancy between masses from $K\bar{K}$ and $\rho\pi$ modes.						

 $\Gamma(\eta'(958)\pi)/\Gamma_{\text{total}}$

VALUE	CL%	DOCUMENT ID	TECN	CHG	COMMENT	Γ_8/Γ
••• We do not use the following data for averages, fits, limits, etc. •••						
<0.006	95	ALDE 92B	GAM2		$38,100\pi^-\rho \rightarrow \eta'\pi^0 n$	
<0.02	97	BARNHAM 71	HBC	+	$3.7\pi^+\rho$	
0.004±0.004		BOESEBECK 68	HBC	+	$8\pi^+\rho$	

 $\Gamma(\eta'(958)\pi)/\Gamma(3\pi)$

VALUE	CL%	DOCUMENT ID	TECN	CHG	COMMENT	Γ_8/Γ_1
••• We do not use the following data for averages, fits, limits, etc. •••						
<0.011	90	EISENSTEIN 73	HBC	-	$5\pi^-\rho$	
<0.04		ALSTON... 71	HBC	+	$7.0\pi^+\rho$	
0.04 ^{+0.03} _{-0.04}		BOECKMANN 70	HBC	0	$5.0\pi^+\rho$	

See key on page 373

Meson Particle Listings

 $a_2(1320)$, $f_0(1370)$ $\Gamma(\eta'(958)\pi)/\Gamma(\eta\pi)$

VALUE	DOCUMENT ID	TECN	COMMENT	Γ_8/Γ_5
0.037±0.006 OUR AVERAGE				
0.032±0.009	ABELE	97C	CBAR	0.0 $\bar{p}p \rightarrow \pi^+ \pi^0 \eta'$
0.047±0.010±0.004	³³ BELADIDZE	93	VES	37 $\pi^- N \rightarrow a_2^- N$
0.034±0.008±0.005	BELADIDZE	92	VES	36 $\pi^- C \rightarrow a_2^- C$

³³ Using $B(\eta' \rightarrow \pi^+ \pi^- \eta) = 0.441$, $B(\eta \rightarrow \gamma\gamma) = 0.389$ and $B(\eta \rightarrow \pi^+ \pi^- \pi^0) = 0.236$.

 $\Gamma(\pi^\pm\gamma)/\Gamma_{\text{total}}$

VALUE	DOCUMENT ID	TECN	COMMENT	Γ_9/Γ
••• We do not use the following data for averages, fits, limits, etc. •••				
0.005 ^{+0.005} _{-0.003}	³⁴ EISENBERG	72	HBC	4,3,5,25,7,5 γp

³⁴ Pion-exchange model used in this estimation.

 $\Gamma(e^+e^-)/\Gamma_{\text{total}}$

VALUE (units 10 ⁻⁹)	CL%	DOCUMENT ID	TECN	COMMENT	Γ_{11}/Γ
<6	90	ACHASOV	00K	SND	$e^+e^- \rightarrow \pi^0 \pi^0$

 $a_2(1320)$ REFERENCES

SCHEGELSKY	06	EPL A27 199	V.A. Schegelsky et al.	
SCHEGELSKY	06A	EPL A27 207	V.A. Schegelsky et al.	
CHUNG	02	PR D65 072001	S.U. Chung et al.	(BNL E852 Collab.)
IVANOV	01	PRL 86 3977	E.I. Ivanov et al.	(BNL E852 Collab.)
MOLCHANOV	01	PL B521 171	V.V. Molchanov et al.	(FNAL SELEX Collab.)
ACHASOV	00K	PL B492 8	M.N. Achasov et al.	(Novosibirsk SND Collab.)
BARBERIS	00H	PL B488 225	D. Barberis et al.	(WA 102 Collab.)
BARBERIS	98B	PL B422 399	D. Barberis et al.	(WA 102 Collab.)
BERTIN	98B	PL B434 180	A. Bertin et al.	(OBELIX Collab.)
ABELE	97C	PL B404 179	A. Abele et al.	(Crystal Barrel Collab.)
ACCIARRI	97T	PL B413 147	M. Acciari et al.	(L3 Collab.)
ALBRECHT	97B	ZPHY C74 469	H. Albrecht et al.	(ARGUS Collab.)
THOMPSON	97	PRL 79 1630	D.R. Thompson et al.	(BNL E852 Collab.)
AMELIN	96	ZPHY C70 71	D.V. Amelin et al.	(SERP, TIBL)
AMSLER	94D	PL B333 277	C. Amstler et al.	(Crystal Barrel Collab.)
AOYAGI	93	PL B314 246	H. Aoyagi et al.	(BKEI Collab.)
ARMSTRONG	93C	PL B307 394	T.A. Armstrong et al.	(FNAL, FERR, GENO+)
BELADIDZE	93	PL B313 276	G.M. Beladidze et al.	(VES Collab.)
CONDO	93	PR D48 3045	G.T. Condo et al.	(SLAC Hybrid Collab.)
ALDE	92B	ZPHY C54 549	D.M. Alde et al.	(SERP, BELG, LANL, LAPP+)
BELADIDZE	92	ZPHY C54 235	G.M. Beladidze et al.	(VES Collab.)
ALBRECHT	90G	ZPHY C48 183	H. Albrecht et al.	(ARGUS Collab.)
ARMSTRONG	90	ZPHY C48 213	T.A. Armstrong, M. Benayoun, W. Busch	(ARGUS Collab.)
BARU	90	ZPHY C48 581	S.E. Baru et al.	(MD-1 Collab.)
BEHREND	90C	ZPHY C46 583	H.J. Behrend et al.	(CELLO Collab.)
BUTLER	90	PR D42 1368	F. Butler et al.	(Mark II Collab.)
OEST	90	ZPHY C47 343	T. Oest et al.	(JADE Collab.)
AUGUSTIN	89	NP B320 1	J.E. Augustin, G. Cosme	(DM2 Collab.)
VOROBYEV	88	SJNP 48 273	P.V. Vorobyev et al.	(NOVO)
ALTHOFF	86	ZPHY C31 537	M. Althoff et al.	(TASSO Collab.)
ANTREASIAN	86	PR D33 1847	D. Antreasian et al.	(Crystal Ball Collab.)
BERGER	84C	PL 149B 427	C. Berger et al.	(PLUTO Collab.)
BEHREND	83B	PL 125B 518 (erratum)	H.J. Behrend et al.	(CELLO Collab.)
CHANGIR	82	PL 117B 123	S. Changir et al.	(FNAL, MINN, ROCH)
CLELAND	82B	NP B208 228	W.E. Cleland, GEA, LAUS+	(DURH, NEVA, LAUS+)
EDWARDS	82F	PL 110B 82	C. Edwards et al.	(CIT, HARV, PRIN+)
DELFOSE	81	NP B183 349	A. Delfosse et al.	(GEVA, LAUS)
EVANGELIS...	81	NP B178 197	C. Evangelista et al.	(BARI, BONN, CERN+)
CHABAUD	80	NP B175 189	V. Chabaud et al.	(CERN, MPIM, AMST)
DAUM	80C	PL 89B 276	C. Daum et al.	(AMST, CERN, CRAC, MPIM+)
BALTAY	78B	PR D17 62	C. Baltay et al.	(COLU, BING)
CHABAUD	78	NP B145 349	V. Chabaud et al.	(CERN, MPIM)
FERRESDORIA	78	PL 74B 287	A. Ferrer-Soria et al.	(ORSAY, CERN, CDF+)
HYAMS	78	NP B146 303	B.D. Hyams et al.	(CERN, MPIM, ATEN)
MARTIN	76D	PL 74B 417	A.D. Martin et al.	(DURH, GEVA, JP)
MAY	77	PR D16 1983	E.N. May et al.	(ROCH, CORN)
FORINO	76	NC 35A 465	A. Forino et al.	(BGNA, FIRZ, GENO, MILA+)
MARGULIE	76	PR D14 667	M. Margulies et al.	(BNL, CUNY)
EMMS	75	PL 58B 117	M.J. Emms et al.	(BIRM, DURH, RHEL) JP
WAGNER	75	PL 58B 201	F. Wagner, M. Tabak, D.M. Chew	(LBL) JP
DIAZ	74	PRL 32 260	J. Diaz et al.	(CASE, CHU)
KARSHON	74	PRL 32 852	U. Karshon et al.	(REHO)
ANTIPOV	73	NP B63 175	Y.M. Antipov et al.	(CERN, SERP) JP
ANTIPOV	73C	NP B63 153	Y.M. Antipov et al.	(CERN, SERP) JP
CHALOUKPA	73	PL 44B 211	V. Chaloukpa et al.	(CERN)
CONFORTO	73	PL 45B 154	G. Conforto et al.	(EFI, FNAL, TINTO+)
DEFOIX	73	PL 43B 141	C. Defoix et al.	(CDEF)
EISENSTEIN	73	PR D7 278	L. Eisenstein et al.	(ILL)
KEY	73	PRL 30 503	A.W. Key et al.	(TINTO, EFI, FNAL, WIS C)
TOET	73	NP B63 248	D.Z. Toet et al.	(NIJ, BONN, DURH, TORI)
DAMERI	72	NC 9A 1	M. Dameri et al.	(GENO, MILA, SAEL)
EISENBERG	72	PR D5 15	Y. Eisenberg et al.	(REHO, SLAC, TELA)
ESPIGAT	72	NP B36 93	P. Espigat et al.	(CERN, CDEF)
FOLEY	72	PR D6 747	K.J. Foley et al.	(BNL, CUNY)
ALSTON...	71	PL 34B 156	M. Alston-Garnjost et al.	(LRL)
BARNHAM	71	PRL 26 1494	K.W.J. Barnham et al.	(LRL)
BINNIE	71	PL 36B 257	D.M. Binnie et al.	(LOIC, SHMP)
BOWEN	71	PRL 26 1663	D.R. Bowen et al.	(NEAS, STON)
GRAYER	71	PL 34B 333	G. Graye et al.	(CERN, MPIM)
ABRAMOV...	70B	NP B23 466	M. Abramovich et al.	(CERN) JP
ALSTON...	70	PL 33B 607	M. Alston-Garnjost et al.	(LRL)
BOECKMANN	70	NP B16 221	K. Boeckmann et al.	(BONN, DURH, NIJ+)
ASCOLI	68	PRL 20 1321	G. Ascoli et al.	(ILL) JP
BOESEBECK	68	NP B4 501	K. Boesebeck et al.	(AACH, BERL, CERN)
CHUNG	68	PR 165 1491	S.U. Chung et al.	(LRL)
CONTE	67	NC 51A 175	F. Conte et al.	(GENO, HAMB, MILA, SAEL)

OTHER RELATED PAPERS

DZIERBA	06	PR D73 072001	A.R. Dzierba et al.	(BNL E852 Collab.)
ALDE	99B	PAN 62 421	D. Alde et al.	(GAMS Collab.)
JENNI	83	PR D27 1031	P. Jenni et al.	(SLAC, LBL)
BEHREND	82C	PL 114B 378	H.J. Behrend et al.	(CELLO Collab.)
ADERHOLZ	65	PR 138 B897	M. Aderholz (AACH3, BERL, BIRM, BONN, HAMB+)	
ALITTI	65	PL 15 69	J. Alitti et al.	(SAEL, BGNA) JP
CHUNG	65	PRL 15 325	S.U. Chung et al.	(LRL)

FORINO	65B	PL 19 68	A. Forino et al.	(BGNA, BARI, FIRZ, ORSAY+)
LEFEBVRES	65	PL 19 434	F. Lefebvres et al.	
SEIDLITZ	65	PRL 15 217	L. Seidlitz, O.I. Dahl, D.H. Miller	(LRL)
ADERHOLZ	64	PL 10 226	M. Aderholz et al.	(AACH3, BERL, BIRM+)
CHUNG	64	PRL 12 621	S.U. Chung et al.	(LRL)
GOLDBABER	64	PRL 12 336	G. Goldhaber et al.	(LRL, UCB)
LANDER	64	PRL 13 346A	R.L. Lander et al.	(UCSD)

 $f_0(1370)$

$$I_G(J^{PC}) = 0^+(0^+ +)$$

See also the mini-reviews on scalar mesons under $f_0(600)$ (see the index for the page number) and on non- $q\bar{q}$ candidates in PDG 06, Journal of Physics, G **33** 1 (2006).

 $f_0(1370)$ T-MATRIX POLE POSITION

Note that $\Gamma \approx 2 \text{Im}(\sqrt{s_{\text{pole}}})$.

VALUE (MeV)	DOCUMENT ID	TECN	COMMENT
(1200-1500)-i(150-250) OUR ESTIMATE			

••• We do not use the following data for averages, fits, limits, etc. •••

(1373 ± 15) - i(137 ± 10)	¹ BARGIOTTI	03	OBLX	$\bar{p}p$
(1302 ± 17) - i(166 ± 18)	² BARBERIS	00C		450 $pp \rightarrow p_f 4\pi p_s$
(1312 ± 25 ± 10) - i(109 ± 22 ± 15)	BARBERIS	99D	OMEG	450 $pp \rightarrow K^+ K^-$, $\pi^+ \pi^-$
(1406 ± 19) - i(80 ± 6)	³ KAMINSKI	99	RVUE	$\pi\pi \rightarrow \pi\pi, K\bar{K}, \sigma\sigma$
(1300 ± 20) - i(120 ± 20)	ANISOVICH	98B	RVUE	Compilation
(1290 ± 15) - i(145 ± 15)	BARBERIS	97B	OMEG	450 $pp \rightarrow p\bar{p} 2(\pi^+ \pi^-)$
(1548 ± 40) - i(560 ± 40)	BERTIN	97C	OBLX	0.0 $\bar{p}p \rightarrow \pi^+ \pi^- \pi^0$
(1380 ± 40) - i(180 ± 25)	ABELE	96B	CBAR	0.0 $\bar{p}p \rightarrow \pi^0 K_S^0 K_S^0$
(1300 ± 15) - i(115 ± 8)	BUGG	96	RVUE	
(1330 ± 50) - i(150 ± 40)	⁴ AMSLER	95B	CBAR	$\bar{p}p \rightarrow 3\pi^0$
(1360 ± 35) - i(150-300)	⁴ AMSLER	95C	CBAR	$\bar{p}p \rightarrow \pi^0 \eta\eta$
(1390 ± 30) - i(190 ± 40)	⁵ AMSLER	95D	CBAR	$\bar{p}p \rightarrow 3\pi^0, \pi^0 \eta\eta$, $\pi^0 \pi^0 \eta$
1346 - i249	^{6,7} JANSSEN	95	RVUE	$\pi\pi \rightarrow \pi\pi, K\bar{K}$
1214 - i168	^{7,8} TORNQVIST	95	RVUE	$\pi\pi \rightarrow \pi\pi, K\bar{K}, K\pi$, $\eta\pi$
1364 - i139	AMSLER	94D	CBAR	$\bar{p}p \rightarrow \pi^0 \pi^0 \eta$
(1365 ± 20) - i(134 ± 35)	ANISOVICH	94	CBAR	$\bar{p}p \rightarrow 3\pi^0, \pi^0 \eta\eta$
(1340 ± 40) - i(127 ± 30)	⁹ BUGG	94	RVUE	$\bar{p}p \rightarrow 3\pi^0, \eta\eta\pi^0$, $\eta\pi^0 \pi^0$
(1430 ± 5) - i(73 ± 13)	¹⁰ KAMINSKI	94	RVUE	$\pi\pi \rightarrow \pi\pi, K\bar{K}$
1515 - i214	^{7,11} ZOU	93	RVUE	$\pi\pi \rightarrow \pi\pi, K\bar{K}$
1420 - i220	¹² AU	87	RVUE	$\pi\pi \rightarrow \pi\pi, K\bar{K}$

¹ Coupled channel analysis of $\pi^+ \pi^- \pi^0, K^+ K^- \pi^0$, and $K^\pm K_S^0 \pi^\mp$.

² Average between $\pi^+ \pi^- 2\pi^0$ and $2(\pi^+ \pi^-)$.

³ T-matrix pole on sheet -- --.

⁴ Supersedes ANISOVICH 94.

⁵ Coupled-channel analysis of $\bar{p}p \rightarrow 3\pi^0, \pi^0 \eta\eta$, and $\pi^0 \pi^0 \eta$ on sheet IV. Demonstrates explicitly that $f_0(600)$ and $f_0(1370)$ are two different poles.

⁶ Analysis of data from FALVARD 88.

⁷ The pole is on Sheet III. Demonstrates explicitly that $f_0(600)$ and $f_0(1370)$ are two different poles.

⁸ Uses data from BEIER 72b, OCHS 73, HYAMS 73, GRAYER 74, ROSSELET 77, CASON 83, ASTON 88, and ARMSTRONG 91b. Coupled channel analysis with flavor symmetry and all light two-pseudoscalars systems.

⁹ Reanalysis of ANISOVICH 94 data.

¹⁰ T-matrix pole on sheet III.

¹¹ Analysis of data from OCHS 73, GRAYER 74, and ROSSELET 77.

¹² Analysis of data from OCHS 73, GRAYER 74, BECKER 79, and CASON 83.

 $f_0(1370)$ BREIT-WIGNER MASS OR K-MATRIX POLE PARAMETER

VALUE (MeV)	DOCUMENT ID
1200 to 1500 OUR ESTIMATE	

 $\pi\pi$ MODE

VALUE (MeV)	EVTS	DOCUMENT ID	TECN	COMMENT
••• We do not use the following data for averages, fits, limits, etc. •••				
1259 ± 55	2.6k	BONVICINI	07	CLEO $D^+ \rightarrow \pi^- \pi^+ \pi^+$
1449 ± 13	4286	¹³ GARMASH	06	BELL $B^+ \rightarrow K^+ \pi^+ \pi^-$
1350 ± 50		ABLKIM	05	BES2 $J/\psi \rightarrow \phi \pi^+ \pi^-$
1265 ± 30 ⁺²⁰ ₋₃₅		ABLKIM	05q	BES2 $\psi(2S) \rightarrow \gamma \pi^+ \pi^- K^+ K^-$
1434 ± 18 ± 9	848	AITALA	01A	E791 $D_s^+ \rightarrow \pi^- \pi^+ \pi^+$
1308 ± 10		BARBERIS	99B	OMEG 450 $pp \rightarrow p_s p_f \pi^+ \pi^-$
1315 ± 50		BELLAZZINI	99	GAM4 450 $pp \rightarrow p\bar{p} \pi^0 \pi^0$
1315 ± 30		ALDE	98	GAM4 100 $\pi^- p \rightarrow \pi^0 \pi^0 n$
1280 ± 55		BERTIN	98	OBLX 0.05-0.405 $\bar{p}p \rightarrow \pi^+ \pi^+ \pi^-$
1186		^{14,15} TORNQVIST	95	RVUE $\pi\pi \rightarrow \pi\pi, K\bar{K}, K\pi, \eta\pi$
1472 ± 12		ARMSTRONG	91	OMEG 300 $pp \rightarrow p\bar{p} \pi\pi, p\bar{p} K\bar{K}$
1275 ± 20		BREAKSTONE	90	SFM 62 $pp \rightarrow p\bar{p} \pi^+ \pi^-$
1420 ± 20		AKESSON	86	SPEC 63 $pp \rightarrow p\bar{p} \pi^+ \pi^-$
1256		FROGGATT	77	RVUE $\pi^+ \pi^-$ channel

Meson Particle Listings

 $f_0(1370)$

¹³ Also observed by GARMASH 07 in $B^0 \rightarrow K_S^0 \pi^+ \pi^-$ decays. Supersedes GARMASH 05.

¹⁴ Uses data from BEIER 72b, OCHS 73, HYAMS 73, GRAYER 74, ROSSELET 77, CA-SON 83, ASTON 88, and ARMSTRONG 91b. Coupled channel analysis with flavor symmetry and all light two-pseudoscalars systems.

¹⁵ Also observed by ASNER 00 in $\tau^- \rightarrow \pi^- \pi^0 \pi^0 \nu_\tau$ decays

 $K\bar{K}$ MODE

VALUE (MeV)	DOCUMENT ID	TECN	COMMENT
• • • We do not use the following data for averages, fits, limits, etc. • • •			
1440 ± 6	VLADIMIRSK...06	SPEC	40 $\pi^- p \rightarrow K_S^0 K_S^0 n$
1391 ± 10	TIKHOMIROV 03	SPEC	40.0 $\pi^- C \rightarrow K_S^0 K_S^0 K_L^0 X$
1440 ± 50	BOLONKIN 88	SPEC	40 $\pi^- p \rightarrow K_S^0 K_S^0 n$
1463 ± 9	ETKIN 82b	MPS	23 $\pi^- p \rightarrow n 2K_S^0$
1425 ± 15	WICKLUND 80	SPEC	6 $\pi N \rightarrow K^+ K^- N$
~ 1300	POLYCHRO... 79	STRC	7 $\pi^- p \rightarrow n 2K_S^0$

 4π MODE $2(\pi\pi)_S + \rho\rho$

VALUE (MeV)	EVTS	DOCUMENT ID	TECN	COMMENT
• • • We do not use the following data for averages, fits, limits, etc. • • •				
1395 ± 40		ABELE 01	CBAR	0.0 $\bar{p} d \rightarrow \pi^- 4\pi^0 p$
1374 ± 38		AMSLER 94	CBAR	0.0 $\bar{p} p \rightarrow \pi^+ \pi^- 3\pi^0$
1345 ± 12		ADAMO 93	OBLX	$\bar{p} p \rightarrow 3\pi^+ 2\pi^-$
1386 ± 30		GASPERO 93	DBC	0.0 $\bar{p} n \rightarrow 2\pi^+ 3\pi^-$
~ 1410	5751	¹⁶ BETTINI 66	DBC	0.0 $\bar{p} n \rightarrow 2\pi^+ 3\pi^-$
¹⁶ $\rho\rho$ dominant.				

 $\eta\eta$ MODE

VALUE (MeV)	DOCUMENT ID	TECN	COMMENT
• • • We do not use the following data for averages, fits, limits, etc. • • •			
1430	AMSLER 92	CBAR	0.0 $\bar{p} p \rightarrow \pi^0 \eta\eta$
1220 ± 40	ALDE 86D	GAM4	100 $\pi^- p \rightarrow n 2\eta$

COUPLED CHANNEL MODE

VALUE (MeV)	DOCUMENT ID	TECN
• • • We do not use the following data for averages, fits, limits, etc. • • •		
1306 ± 20	¹⁷ ANISOVICH 03	RVUE
¹⁷ K-matrix pole from combined analysis of $\pi^- p \rightarrow \pi^0 \pi^0 n$, $\pi^- p \rightarrow K\bar{K}n$, $\pi^+ \pi^- \rightarrow \pi^+ \pi^-$, $\bar{p} p \rightarrow \pi^0 \pi^0 \pi^0$, $\pi^0 \eta\eta$, $\pi^0 \pi^0 \eta$, $\pi^+ \pi^- \pi^0$, $K^+ K^- \pi^0$, $K_S^0 K_S^0 \pi^0$, $K^+ K_S^0 \pi^-$ at rest, $\bar{p} n \rightarrow \pi^- \pi^- \pi^+$, $K_S^0 K^- \pi^0$, $K_S^0 K_S^0 \pi^-$ at rest.		

 $f_0(1370)$ BREIT-WIGNER WIDTH

VALUE (MeV)	DOCUMENT ID
200 to 500 OUR ESTIMATE	

 $\pi\pi$ MODE

VALUE (MeV)	EVTS	DOCUMENT ID	TECN	COMMENT
• • • We do not use the following data for averages, fits, limits, etc. • • •				
298 ± 21	2.6k	BONVICINI 07	CLEO	$D^+ \rightarrow \pi^- \pi^+ \pi^+$
126 ± 25	4286	¹⁸ GARMASH 06	BELL	$B^+ \rightarrow K^+ \pi^+ \pi^-$
265 ± 40		ABLIKIM 05	BES2	$J/\psi \rightarrow \phi \pi^+ \pi^-$
350 ± 100 ± 105 / 60		ABLIKIM 05Q	BES2	$\psi(2S) \rightarrow \gamma \pi^+ \pi^- K^+ K^-$
173 ± 32 ± 6	848	AITALA 01A	E791	$D_S^+ \rightarrow \pi^- \pi^+ \pi^+$
222 ± 20		BARBERIS 99B	OMEG	450 $pp \rightarrow p_S p_f \pi^+ \pi^-$
255 ± 60		BELLAZZINI 99	GAM4	450 $pp \rightarrow p p \pi^0 \pi^0$
190 ± 50		ALDE 98	GAM4	100 $\pi^- p \rightarrow \pi^0 \pi^0 n$
323 ± 13		BERTIN 98	OBLX	0.05-0.405 $\bar{p} p \rightarrow \pi^+ \pi^+ \pi^-$
350		^{19,20} TORNVIST 95	RVUE	$\pi\pi \rightarrow \pi\pi, K\bar{K}, K\pi, \eta\pi$
195 ± 33		ARMSTRONG 91	OMEG	300 $pp \rightarrow p p \pi\pi, p p K\bar{K}$
285 ± 60		BREAKSTONE 90	SFM	62 $pp \rightarrow p p \pi^+ \pi^-$
460 ± 50		AKESSON 86	SPEC	63 $pp \rightarrow p p \pi^+ \pi^-$
~ 400		²¹ FROGGATT 77	RVUE	$\pi^+ \pi^-$ channel

¹⁸ Also observed by GARMASH 07 in $B^0 \rightarrow K_S^0 \pi^+ \pi^-$ decays. Supersedes GARMASH 05.

¹⁹ Uses data from BEIER 72b, OCHS 73, HYAMS 73, GRAYER 74, ROSSELET 77, CA-SON 83, ASTON 88, and ARMSTRONG 91b. Coupled channel analysis with flavor symmetry and all light two-pseudoscalars systems.

²⁰ Also observed by ASNER 00 in $\tau^- \rightarrow \pi^- \pi^0 \pi^0 \nu_\tau$ decays

²¹ Width defined as distance between 45 and 135° phase shift.

 $K\bar{K}$ MODE

VALUE (MeV)	DOCUMENT ID	TECN	COMMENT
• • • We do not use the following data for averages, fits, limits, etc. • • •			
121 ± 15	VLADIMIRSK...06	SPEC	40 $\pi^- p \rightarrow K_S^0 K_S^0 n$
55 ± 26	TIKHOMIROV 03	SPEC	40.0 $\pi^- C \rightarrow K_S^0 K_S^0 K_L^0 X$
250 ± 80	BOLONKIN 88	SPEC	40 $\pi^- p \rightarrow K_S^0 K_S^0 n$
118 ± 138 / 16	ETKIN 82b	MPS	23 $\pi^- p \rightarrow n 2K_S^0$
160 ± 30	WICKLUND 80	SPEC	6 $\pi N \rightarrow K^+ K^- N$
~ 150	POLYCHRO... 79	STRC	7 $\pi^- p \rightarrow n 2K_S^0$

 4π MODE $2(\pi\pi)_S + \rho\rho$

VALUE (MeV)	EVTS	DOCUMENT ID	TECN	COMMENT
• • • We do not use the following data for averages, fits, limits, etc. • • •				
275 ± 55		ABELE 01	CBAR	0.0 $\bar{p} d \rightarrow \pi^- 4\pi^0 p$
375 ± 61		AMSLER 94	CBAR	0.0 $\bar{p} p \rightarrow \pi^+ \pi^- 3\pi^0$
398 ± 26		ADAMO 93	OBLX	$\bar{p} p \rightarrow 3\pi^+ 2\pi^-$
310 ± 50		GASPERO 93	DBC	0.0 $\bar{p} n \rightarrow 2\pi^+ 3\pi^-$
~ 90	5751	²² BETTINI 66	DBC	0.0 $\bar{p} n \rightarrow 2\pi^+ 3\pi^-$
²² $\rho\rho$ dominant.				

 $\eta\eta$ MODE

VALUE (MeV)	DOCUMENT ID	TECN	COMMENT
• • • We do not use the following data for averages, fits, limits, etc. • • •			
250	AMSLER 92	CBAR	0.0 $\bar{p} p \rightarrow \pi^0 \eta\eta$
320 ± 40	ALDE 86D	GAM4	100 $\pi^- p \rightarrow n 2\eta$

COUPLED CHANNEL MODE

VALUE (MeV)	DOCUMENT ID	TECN
• • • We do not use the following data for averages, fits, limits, etc. • • •		
147 ± 30 / -50	²³ ANISOVICH 03	RVUE
²³ K-matrix pole from combined analysis of $\pi^- p \rightarrow \pi^0 \pi^0 n$, $\pi^- p \rightarrow K\bar{K}n$, $\pi^+ \pi^- \rightarrow \pi^+ \pi^-$, $\bar{p} p \rightarrow \pi^0 \pi^0 \pi^0$, $\pi^0 \eta\eta$, $\pi^0 \pi^0 \eta$, $\pi^+ \pi^- \pi^0$, $K^+ K^- \pi^0$, $K_S^0 K_S^0 \pi^0$, $K^+ K_S^0 \pi^-$ at rest, $\bar{p} n \rightarrow \pi^- \pi^- \pi^+$, $K_S^0 K^- \pi^0$, $K_S^0 K_S^0 \pi^-$ at rest.		

 $f_0(1370)$ DECAY MODES

Mode	Fraction (Γ_i/Γ)
Γ_1 $\pi\pi$	seen
Γ_2 4π	seen
Γ_3 $4\pi^0$	seen
Γ_4 $2\pi^+ 2\pi^-$	seen
Γ_5 $\pi^+ \pi^- 2\pi^0$	seen
Γ_6 $\rho\rho$	dominant
Γ_7 $2(\pi\pi)_S$ -wave	seen
Γ_8 $\pi(1300)\pi$	seen
Γ_9 $a_1(1260)\pi$	seen
Γ_{10} $\eta\eta$	seen
Γ_{11} $K\bar{K}$	seen
Γ_{12} $K\bar{K}n\pi$	not seen
Γ_{13} 6π	not seen
Γ_{14} $\omega\omega$	not seen
Γ_{15} $\gamma\gamma$	seen
Γ_{16} $e^+ e^-$	not seen

 $f_0(1370)$ PARTIAL WIDTHS

$\Gamma(\gamma\gamma)$	Γ_{15}
See $\gamma\gamma$ widths under $f_0(600)$ and MORGAN 90.	

$\Gamma(e^+ e^-)$	Γ_{16}
VALUE (eV) CL% DOCUMENT ID TECN COMMENT	
<20 90 VOROBYEV 88 ND	$e^+ e^- \rightarrow \pi^0 \pi^0$

 $f_0(1370)$ BRANCHING RATIOS

$\Gamma(\pi\pi)/\Gamma_{\text{total}}$	Γ_1/Γ
VALUE DOCUMENT ID TECN COMMENT	
• • • We do not use the following data for averages, fits, limits, etc. • • •	
0.26 ± 0.09	BUGG 96 RVUE
<0.15	²⁴ AMSLER 94 CBAR $\bar{p} p \rightarrow \pi^+ \pi^- 3\pi^0$
<0.06	GASPERO 93 DBC 0.0 $\bar{p} n \rightarrow$ hadrons
²⁴ Using AMSLER 95B (3 π^0).	

$\Gamma(4\pi)/\Gamma_{\text{total}}$	$\Gamma_2/\Gamma = (\Gamma_3 + \Gamma_4 + \Gamma_5)/\Gamma$
VALUE DOCUMENT ID TECN COMMENT	
• • • We do not use the following data for averages, fits, limits, etc. • • •	
>0.72	GASPERO 93 DBC 0.0 $\bar{p} n \rightarrow$ hadrons

$\Gamma(4\pi^0)/\Gamma(4\pi)$	Γ_3/Γ_2
VALUE DOCUMENT ID TECN COMMENT	
• • • We do not use the following data for averages, fits, limits, etc. • • •	
seen	ABELE 96 CBAR 0.0 $\bar{p} p \rightarrow 5\pi^0$
0.068 ± 0.005	²⁵ GASPERO 93 DBC 0.0 $\bar{p} n \rightarrow$ hadrons
²⁵ Model-dependent evaluation.	

$\Gamma(2\pi^+2\pi^-)/\Gamma(4\pi)$

VALUE	DOCUMENT ID	TECN	COMMENT
0.420±0.014	²⁶ GASPERO	93	DBC 0.0 $p\bar{n} \rightarrow 2\pi^+3\pi^-$

²⁶ Model-dependent evaluation.

 $\Gamma(\pi^+\pi^-2\pi^0)/\Gamma(4\pi)$

VALUE	DOCUMENT ID	TECN	COMMENT
0.512±0.019	²⁷ GASPERO	93	DBC 0.0 $p\bar{n} \rightarrow$ hadrons

²⁷ Model-dependent evaluation.

 $\Gamma(\rho\rho)/\Gamma(4\pi)$

VALUE	DOCUMENT ID	TECN	COMMENT
0.26±0.07	ABELE	01B	CBAR 0.0 $p\bar{d} \rightarrow 5\pi p$

 $\Gamma(2(\pi\pi)s\text{-wave})/\Gamma(\pi\pi)$

VALUE	DOCUMENT ID	TECN	COMMENT
5.6±2.6	²⁸ ABELE	01	CBAR 0.0 $p\bar{d} \rightarrow \pi^-4\pi^0 p$

²⁸ From the combined data of ABELE 96 and ABELE 96c.

 $\Gamma(2(\pi\pi)s\text{-wave})/\Gamma(4\pi)$

VALUE	DOCUMENT ID	TECN	COMMENT
0.51±0.09	ABELE	01B	CBAR 0.0 $p\bar{d} \rightarrow 5\pi p$

 $\Gamma(\rho\rho)/\Gamma(2(\pi\pi)s\text{-wave})$

VALUE	DOCUMENT ID	TECN	COMMENT
large 1.6 ± 0.2 ~ 0.65	BARBERIS AMSLER GASPERO	00c 94 93	DBC CBAR DBC

 $\Gamma(\pi(1300)\pi)/\Gamma(4\pi)$

VALUE	DOCUMENT ID	TECN	COMMENT
0.17±0.06	ABELE	01B	CBAR 0.0 $p\bar{d} \rightarrow 5\pi p$

 $\Gamma(a_1(1260)\pi)/\Gamma(4\pi)$

VALUE	DOCUMENT ID	TECN	COMMENT
0.06±0.02	ABELE	01B	CBAR 0.0 $p\bar{d} \rightarrow 5\pi p$

 $\Gamma(\eta\eta)/\Gamma(4\pi)$

VALUE	DOCUMENT ID	TECN	COMMENT
(28 ± 11) × 10 ⁻³ (4.7 ± 2.0) × 10 ⁻³	²⁹ ANISOVICH BARBERIS	02D 00E	SPEC CBAR

²⁹ From a combined K-matrix analysis of Crystal Barrel (0. $p\bar{p} \rightarrow \pi^0\pi^0\pi^0, \pi^0\eta\eta, \pi^0\pi^0\eta$), GAMS ($\pi\rho \rightarrow \pi^0\pi^0 n, \eta\eta n, \eta\eta' n$), and BNL ($\pi\rho \rightarrow K\bar{K}n$) data.

 $\Gamma(K\bar{K})/\Gamma_{\text{total}}$

VALUE	DOCUMENT ID	TECN	COMMENT
0.35±0.13	BUGG	96	RVUE

 $\Gamma(K\bar{K})/\Gamma(\pi\pi)$

VALUE	DOCUMENT ID	TECN	COMMENT
0.08±0.08	ABLIKIM	05	BES2 $J/\psi \rightarrow \phi\pi^+\pi^-, \phi K^+K^-$
0.91±0.20	³⁰ BARGIOTTI	03	OBLX $p\bar{p}$
0.12±0.06	³¹ ANISOVICH	02D	SPEC Combined fit
0.46±0.15±0.11	BARBERIS	99D	OMEG 450 $p\rho \rightarrow K^+K^-, \pi^+\pi^-$

³⁰ Coupled channel analysis of $\pi^+\pi^-\pi^0, K^+K^-\pi^0$, and $K^\pm K_S^0 \pi^\mp$.

³¹ From a combined K-matrix analysis of Crystal Barrel (0. $p\bar{p} \rightarrow \pi^0\pi^0\pi^0, \pi^0\eta\eta, \pi^0\pi^0\eta$), GAMS ($\pi\rho \rightarrow \pi^0\pi^0 n, \eta\eta n, \eta\eta' n$), and BNL ($\pi\rho \rightarrow K\bar{K}n$) data.

 $\Gamma(K\bar{K}n\pi)/\Gamma_{\text{total}}$

VALUE	DOCUMENT ID	TECN	COMMENT
<0.03	GASPERO	93	DBC 0.0 $p\bar{n} \rightarrow$ hadrons

 $\Gamma(6\pi)/\Gamma_{\text{total}}$

VALUE	DOCUMENT ID	TECN	COMMENT
<0.22	GASPERO	93	DBC 0.0 $p\bar{n} \rightarrow$ hadrons

 $\Gamma(\omega\omega)/\Gamma_{\text{total}}$

VALUE	DOCUMENT ID	TECN	COMMENT
<0.13	GASPERO	93	DBC 0.0 $p\bar{n} \rightarrow$ hadrons

 $f_0(1370)$ REFERENCES

BONVICINI	07	PR D76 012001	G. Bonvicini <i>et al.</i>	(CLEO Collab.)
GARMASH	07	PR D75 012006	A. Garmash <i>et al.</i>	(BELLE Collab.)
GARMASH	06	PRL 96 251803	A. Garmash <i>et al.</i>	(BELLE Collab.)
PDG	06	JPG 33 1	W.-M. Yao <i>et al.</i>	(PDG Collab.)
VLADIMIRSK...	06	PAN 69 493	V.V. Vladimirov <i>et al.</i>	(ITEP, Moscow)
ABLIKIM	05	PL B607 243	M. Ablikim <i>et al.</i>	(BES Collab.)
ABLIKIM	05Q	PR D72 092002	M. Ablikim <i>et al.</i>	(BES Collab.)
GARMASH	05	PR D71 092003	A. Garmash <i>et al.</i>	(BELLE Collab.)
ANISOVICH	03	EPJ A16 229	V.V. Anisovich <i>et al.</i>	(BES Collab.)
BARGIOTTI	03	EPJ C26 371	M. Bargiotti <i>et al.</i>	(OBELIX Collab.)
TIKHOMIROV	03	PAN 66 828	G.D. Tikhomirov <i>et al.</i>	
ANISOVICH	02D	Translated from YAF 66 860.	V.V. Anisovich <i>et al.</i>	
ABELE	01	EPJ C19 667	A. Abele <i>et al.</i>	(Crystal Barrel Collab.)
ABELE	01B	EPJ C21 261	A. Abele <i>et al.</i>	(Crystal Barrel Collab.)
AITALA	01A	PRL 86 765	E.M. Aitala <i>et al.</i>	(FNAL E791 Collab.)
ASNER	00	PR D61 012002	D.M. Asner <i>et al.</i>	(CLEO Collab.)
BARBERIS	00C	PL B471 440	D. Barberis <i>et al.</i>	(WA 102 Collab.)
BARBERIS	00E	PL B479 59	D. Barberis <i>et al.</i>	(WA 102 Collab.)
BARBERIS	99B	PL B453 316	D. Barberis <i>et al.</i>	(Omega Expt.)
BARBERIS	99D	PL B462 462	D. Barberis <i>et al.</i>	(Omega Expt.)
BELLAZZINI	99	PL B467 296	R. Bellazzini <i>et al.</i>	
KAMINSKI	99	EPJ C9 141	R. Kaminski, L. Lesniak, B. Loiseau	(CRAC, PARIN)
ALDE	98	EPJ A3 361	D. Alde <i>et al.</i>	(GAM4 Collab.)
ANISOVICH	98B	SPU 41 419	V.V. Anisovich <i>et al.</i>	
BERTIN	98	PR D57 55	A. Bertin <i>et al.</i>	(OBELIX Collab.)
BARBERIS	97B	PL B413 217	D. Barberis <i>et al.</i>	(WA 102 Collab.)
BERTIN	97C	PL B408 476	A. Bertin <i>et al.</i>	(OBELIX Collab.)
ABELE	96	PL B380 453	A. Abele <i>et al.</i>	(Crystal Barrel Collab.)
ABELE	96B	PL B385 425	A. Abele <i>et al.</i>	(Crystal Barrel Collab.)
ABELE	96C	NP A609 562	A. Abele <i>et al.</i>	(Crystal Barrel Collab.)
BUGG	96	NP B471 59	D.V. Bugg, A.V. Sarantsev, B.S. Zou	(LOQM, PNPI)
AMSLER	95B	PL B342 433	C. Amstler <i>et al.</i>	(Crystal Barrel Collab.)
AMSLER	95C	PL B353 571	C. Amstler <i>et al.</i>	(Crystal Barrel Collab.)
AMSLER	95D	PL B355 425	C. Amstler <i>et al.</i>	(Crystal Barrel Collab.)
JANSEN	95	PR D52 2690	G. Janssen <i>et al.</i>	(STON, ADL, JULI)
TORNOVIST	95	ZPHY C68 647	N.A. Tornqvist	(HELS)
AMSLER	94	PL B322 421	C. Amstler <i>et al.</i>	(Crystal Barrel Collab.)
AMSLER	94D	PL B333 277	C. Amstler <i>et al.</i>	(Crystal Barrel Collab.)
ANISOVICH	94	PL B323 233	V.V. Anisovich <i>et al.</i>	(Crystal Barrel Collab.)
BUGG	94	PR D50 4412	D.V. Bugg <i>et al.</i>	(LOQM)
KAMINSKI	94	PR D50 3145	R. Kaminski, L. Lesniak, J.P. Maillat	(CRA C+)
ADAMO	93	NP A558 13C	A. Adamo <i>et al.</i>	(OBELIX Collab.)
GASPERO	93	NP A562 407	M. Gaspero	(ROMA1) JPC
ZOU	93	PR D48 R3948	B.S. Zou, D.V. Bugg	(LOQM)
AMSLER	92	PL B291 347	C. Amstler <i>et al.</i>	(Crystal Barrel Collab.)
ARMSTRONG	91B	ZPHY C51 351	T.A. Armstrong <i>et al.</i>	(ATHU, BARI, BIRM+)
ARMSTRONG	91B	ZPHY C52 389	T.A. Armstrong <i>et al.</i>	(ATHU, BARI, BIRM+)
BREKSTONE	90	ZPHY C48 569	A.M. Brekstone <i>et al.</i>	(ISU, BGM, CERN+)
MORGAN	90	ZPHY C48 623	D. Morgan, M.R. Pennington	(RAL, DURH)
ASTON	88	NP B296 493	D. Aston <i>et al.</i>	(SLAC, NAGO, CIN, INUS)
BOLONKIN	88	NP B309 426	B.V. Bolonkin <i>et al.</i>	(ITEP, SERP)
FALWARD	88	PR D38 2706	A. Falward <i>et al.</i>	(CLER, FRAS, LALO+)
VOROBYEV	88	SJNP 48 273	P.V. Vorobyev <i>et al.</i>	(NOVO)
AU	87	PR D35 1633	K.L. Au, D. Morgan, M.R. Pennington	(DURH, RAL)
AKESSON	86	NP B264 154	T. Akesson <i>et al.</i>	(Axial Field Spec. Collab.)
ALDE	86D	NP B269 485	D.M. Alde <i>et al.</i>	(BELG, LAPP, SERP, CERN+)
CASON	83	PR D28 1584	N.M. Cason <i>et al.</i>	(NDAM, ANL)
ETKIN	82B	PR D25 1786	A. Etkin <i>et al.</i>	(BNL, CUNY, TUFTS, VAND)
WICKLUND	80	PRL 45 1469	A.B. Wicklund <i>et al.</i>	(ANL)
BECKER	79	NP B151 46	H. Becker <i>et al.</i>	(MPIM, CERN, ZEEM, CRAC)
POLYCHRO...	79	PR D19 1317	V.A. Polychronakos <i>et al.</i>	(NDAM, ANL)
FROGGATT	77	NP B129 89	C.D. Froggatt, J.L. Petersen	(GLAS, NORD)
ROSSELET	77	PR D15 574	L. Rosselet <i>et al.</i>	(GEVA, SAEL)
GRAYER	74	NP B75 189	G. Grayer <i>et al.</i>	(CERN, MPIM)
HYAMS	73	NP B64 134	B.D. Hyams <i>et al.</i>	(CERN, MPIM)
OCHS	73	Thisis	W. Ochs	(MPIM, MUNI)
BEIER	72B	PRL 29 511	E.W. Beier <i>et al.</i>	(PENN)
BETTINI	66	NC 42A 695	A. Bettini <i>et al.</i>	(PADO, PISA)
AUBERT	07AX	PRL 99 161802	B. Aubert <i>et al.</i>	(BABAR Collab.)
AUBERT	07BB	PRL 99 221801	B. Aubert <i>et al.</i>	(BABAR Collab.)
BUGG	07	EPJ C52 35	D. Bugg	
KLEMP	07	PR D75 012005	E. Klemp, A. Zaitsev	
FARIBORZ	06	PR D74 054030	A.H. Fariborz	
AUBERT.B	05G	PR D72 052002	B. Aubert <i>et al.</i>	(BABAR Collab.)
AUBERT.B	05J	PR D72 052008	B. Aubert <i>et al.</i>	(BABAR Collab.)
BINON	05	PAN 68 960	F. Binon <i>et al.</i>	
CLOSE	05	PR D71 094022	F.E. Close, Q. Zhao	
GIACOSA	05	PR C71 025202	F. Giacosa <i>et al.</i>	
GIACOSA	05A	PL B622 277	F. Giacosa <i>et al.</i>	
RODRIGUEZ	05	PR D71 074008	S. Rodriguez, M. Napsuciale	
VIJANDE	05	PR D72 034025	J. Vijande, A. Valarce, F. Fernandez	
ZHAO	05	PR D72 074001	Q. Zhao	
ZHAO	05A	PL B631 22	Q. Zhao, B.-S. Zou, Z.-B. Ma	
LINK	04	PL B585 200	J.M. Link <i>et al.</i>	(FNAL FOCUS Collab.)
ANISOVICH	03B	PAN 66 741	V.V. Anisovich, V.A. Nikonov, A.V. Sarantsev	
ANISOVICH	03D	PAN 66 928	V.V. Anisovich, A.V. Sarantsev	
GARMASH	02	PR D65 092005	A. Garmash <i>et al.</i>	(BELLE Collab.)
JIN	02	PR D66 057505	H. Jin, X. Zhang	
KLEEFELD	02	PR D66 034007	F. Kleefeld <i>et al.</i>	
RUPP	02	PR D65 078501	G. Rupp, E. van Beveren, M.D. Scadron	
SHAKIN	02	PR D65 078502	C.M. Shakin, H. Wang	
TESHIMA	02	JPG 28 1391	T. Teshima, I. Kiamura, N. Morisita	
VOLKOV	02	PAN 65 1657	M.K. Volkov, V.L. Yudichev	
OTHER RELATED PAPERS				

OTHER RELATED PAPERS

Meson Particle Listings

$f_0(1370)$, $h_1(1380)$, $\pi_1(1400)$

KOPP	01	PR D63 092001	S. Kopp <i>et al.</i>	(CLEO Collab.)
LI	01B	EPJ C19 529	D.-M. Li, H. Yu, Q.-X. Shen	
SUROVTSV	01	PR D63 054024	Y.S. Surovtsev, D. Krupa, M. Nagy	
AKHMETSHIN	00C	PL B476 33	R.R. Akhmetshin <i>et al.</i>	(Novosibirsk CMD-2 Collab.)
KAMINSKI	00	APP B31 895	R. Kaminski, L. Lesniak, K. Rybicki	
SADOVSKY	00	NP A665 131c	S.A. Sadovsky	
ISHIDA	99	PTP 101 661	M. Ishida	
MINKOWSKI	99	EPJ C9 283	P. Minkowski, W. Ochs	
VANBEVEREN	99	EPJ C10 469	E. van Beveren, G. Rupp	
ACHASOV	98D	PAN 61 224	N.N. Achasov, V.V. Gubin	
ACHASOV	98E	PR D58 054011	N.N. Achasov, G.N. Shestakov	
AMSLER	98	RMP 70 1293	C. Amster	
ANISOVICH	98	PL B437 209	V.V. Anisovich <i>et al.</i>	
BLACK	98	PR D58 054012	D. Black <i>et al.</i>	
LOCHER	98	EPJ C4 317	M.P. Locher <i>et al.</i>	(PSI)
NARISON	98	NP B509 312	S. Narison	
ANISOVICH	97	PL B395 123	A.V. Anisovich, A.V. Sarantsev	(PNPI)
KAMINSKI	97	ZPHY C74 79	R. Kaminski, L. Lesniak, K. Rybicki	(CRAC)
PROKOSHKIN	97	SPD 42 117	Y.D. Prokoshkin <i>et al.</i>	(SERP)
TORNQVIST	96	PRL 76 1575	V.A. Tornqvist, M. Roos	(HELS)
GASPERO	95	NP A588 861	M. Gaspero	(ROMA)
KLEMPET	95	PL B361 160	E. Klempet <i>et al.</i>	
ZOU	94B	PR D50 591	B.S. Zou, D.V. Bugg	(LOQM)
CLOSE	93A	PL B319 291	F.E. Close <i>et al.</i>	
CLOSE	93B	NP B389 513	F.E. Close, N. Isgur, S. Kumano	
MORGAN	93	PR D48 1185	D. Morgan, M.R. Pennington	(RAL, DURH)
LI	91	PR D43 2161	Z.P. Li <i>et al.</i>	(TENN)
BARNES	85	PL B165 434	T. Barnes	
BIZZARRI	69	NP B14 169	R. Bizzarri <i>et al.</i>	(CERN, CDEF)

$\pi_1(1400)$

$$I^G(J^{PC}) = 1^-(1^+)$$

See also the mini-review under non- $q\bar{q}$ candidates in PDG 06, Journal of Physics, G **33** 1 (2006).

$\pi_1(1400)$ MASS

VALUE (MeV)	EVTS	DOCUMENT ID	TECN	CHG	COMMENT
1351 ± 30	OUR AVERAGE	Error includes scale factor of 2.0. See the ideogram below.			
1257 ± 20	± 25	23.5k	ADAMS	07B B852	18 $\pi^- p \rightarrow \eta\pi^0 n$
1360 ± 25			ABELE	99 CBAR	0.0 $\bar{p} p \rightarrow \pi^0 \pi^0 \eta$
1400 ± 20	± 20		ABELE	98B CBAR	0.0 $\bar{p} n \rightarrow \pi^- \pi^0 \eta$
1370 ± 16	+50 -30		1 THOMPSON	97 MPS	18 $\pi^- p \rightarrow \eta\pi^- p$
1323.1 ± 4.6			2 AOYAGI	93 BKEI	$\pi^- p \rightarrow \eta\pi^- p$
1406 ± 20			3 ALDE	88B GAM4 0	100 $\pi^- p \rightarrow \eta\pi^0 n$

••• We do not use the following data for averages, fits, limits, etc. •••

1 Natural parity exchange, questioned by DZIERBA 03.

2 Unnatural parity exchange.

3 Seen in the P_0 -wave intensity of the $\eta\pi^0$ system, unnatural parity exchange.

$h_1(1380)$

$$I^G(J^{PC}) = ?^-(1^+)$$

OMITTED FROM SUMMARY TABLE

Seen in partial-wave analysis of the $K\bar{K}\pi$ system. Needs confirmation.

$h_1(1380)$ MASS

VALUE (MeV)	DOCUMENT ID	TECN	COMMENT
1386 ± 19	OUR AVERAGE	Error includes scale factor of 1.1.	
1440 ± 60	ABELE	97H CBAR	$\bar{p} p \rightarrow K_L^0 K_S^0 \pi^0 \pi^0$
1380 ± 20	ASTON	88c LASS	11 $K^- p \rightarrow K_S^0 K^\pm \pi^\mp \Lambda$

$h_1(1380)$ WIDTH

VALUE (MeV)	DOCUMENT ID	TECN	COMMENT
91 ± 30	OUR AVERAGE	Error includes scale factor of 1.1.	
170 ± 80	ABELE	97H CBAR	$\bar{p} p \rightarrow K_L^0 K_S^0 \pi^0 \pi^0$
80 ± 30	ASTON	88c LASS	11 $K^- p \rightarrow K_S^0 K^\pm \pi^\mp \Lambda$

$h_1(1380)$ DECAY MODES

Mode	Fraction (Γ_i/Γ)
Γ_1 $K\bar{K}^*(892) + c.c.$	seen

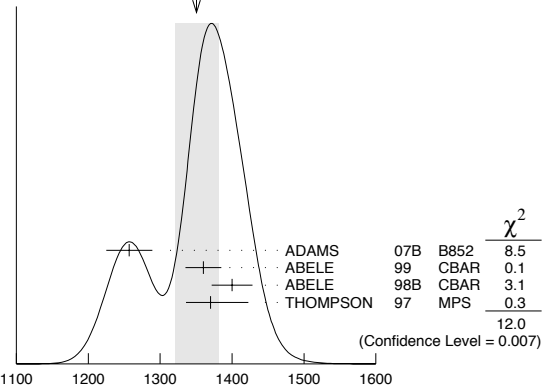
$h_1(1380)$ REFERENCES

ABELE	97H	PL B415 280	A. Abele <i>et al.</i>	(Crystal Barrel Collab.)
ASTON	88c	PL B201 573	D. Aston <i>et al.</i>	(SLAC, NAGO, CINC, INUS)

OTHER RELATED PAPERS

LI	05D	EPJ A26 141	D.-M. Li, B. Ma, H. Yu	
----	-----	-------------	------------------------	--

WEIGHTED AVERAGE
1351±30 (Error scaled by 2.0)



THE IDEOGRAM SUBTITLE IS MISSING.

$\pi_1(1400)$ WIDTH

VALUE (MeV)	EVTS	DOCUMENT ID	TECN	CHG	COMMENT
313 ± 40	OUR AVERAGE	Error includes scale factor of 1.1.			
354 ± 64	± 58	23.5k	ADAMS	07B B852	18 $\pi^- p \rightarrow \eta\pi^0 n$
220 ± 90			ABELE	99 CBAR	0.0 $\bar{p} p \rightarrow \pi^0 \pi^0 \eta$
310 ± 50	+50 -30		ABELE	98B CBAR	0.0 $\bar{p} n \rightarrow \pi^- \pi^0 \eta$
385 ± 40	+65 -105		4 THOMPSON	97 MPS	18 $\pi^- p \rightarrow \eta\pi^- p$
143.2 ± 12.5			5 AOYAGI	93 BKEI	$\pi^- p \rightarrow \eta\pi^- p$
180 ± 20			6 ALDE	88B GAM4 0	100 $\pi^- p \rightarrow \eta\pi^0 n$

••• We do not use the following data for averages, fits, limits, etc. •••

4 Resolution is not unfolded, natural parity exchange, questioned by DZIERBA 03.

5 Unnatural parity exchange.

6 Seen in the P_0 -wave intensity of the $\eta\pi^0$ system, unnatural parity exchange.

$\pi_1(1400)$ DECAY MODES

Mode	Fraction (Γ_i/Γ)
Γ_1 $\eta\pi^0$	seen
Γ_2 $\eta\pi^-$	seen
Γ_3 $\eta'\pi$	

$\pi_1(1400)$ BRANCHING RATIOS

$\Gamma(\eta\pi^0)/\Gamma_{total}$	VALUE	DOCUMENT ID	TECN	CHG	COMMENT	Γ_1/Γ
not seen		PROKOSHKIN 95B	GAM4		100 $\pi^- p \rightarrow \eta\pi^0 n$	
not seen		7 BUGG	94	RVUE	$\bar{p} p \rightarrow \eta 2\pi^0$	
not seen		8 APEL	81	NICE 0	40 $\pi^- p \rightarrow \eta\pi^0 n$	

7 Using Crystal Barrel data.

8 A general fit allowing S, D, and P waves (including $m=0$) is not done because of limited statistics.

$\Gamma(\eta\pi^-)/\Gamma_{\text{total}}$				Γ_2/Γ
VALUE	DOCUMENT ID	TECN	COMMENT	
• • • We do not use the following data for averages, fits, limits, etc. • • •				
possibly seen	BELADIDZE	93	VES	$37\pi^- N \rightarrow \eta\pi^- N$

$\Gamma(\eta'\pi)/\Gamma(\eta\pi^0)$				Γ_3/Γ_1
VALUE	CL%	DOCUMENT ID	TECN	COMMENT
• • • We do not use the following data for averages, fits, limits, etc. • • •				
<0.80	95	BOUTEMEUR	90	GAM4 100 $\pi^- p \rightarrow 4\gamma n$

 $\pi_1(1400)$ REFERENCES

ADAMS	07B	PL B657 27	G.S. Adams <i>et al.</i>	(BNL E852 Collab.)
PDG	06	JPG 33 1	W.-M. Yao <i>et al.</i>	(PDG Collab.)
DZIERBA	03	PR D67 094015	A.R. Dzierba <i>et al.</i>	
ABELE	99	PL B446 349	A. Abele <i>et al.</i>	(Crystal Barrel Collab.)
ABELE	98B	PL B423 175	A. Abele <i>et al.</i>	(Crystal Barrel Collab.)
THOMPSON	97	PRL 79 1630	D.R. Thompson <i>et al.</i>	(BNL E852 Collab.)
PROKOSHKIN	95B	PAN 58 606	Y.D. Prokoshkin, S.A. Sadovsky	(SERP)
		Translated from YAF 58 662		
BUGG	94	PR D50 4412	D.V. Bugg <i>et al.</i>	(LOQM)
AOYAGI	93	PL B314 246	H. Aoyagi <i>et al.</i>	(BKEI Collab.)
BELADIDZE	93	PL B313 276	G.M. Beladidze <i>et al.</i>	(VES Collab.)
BOUTEMEUR	90	Hadron 89 Conf. p 119	M. Boutemeur, M. Poulet	(SERP, BELG, LANL+)
ALDE	88B	PL B205 397	D.M. Alde <i>et al.</i>	(SERP, BELG, LANL, LAPP)
APEL	81	NP B193 269	W.D. Apel <i>et al.</i>	(SERP, CERN)

OTHER RELATED PAPERS

GENERAL	07	EPJ C51 347	L.J. General, S.R. Contanch, F.J. Llanes-Estrada	
GENERAL	07A	PL B653 216	L.J. General <i>et al.</i>	
YANG	07	PR D76 094001	K.-C. Yang	
COOK	06	PR D74 094501	M.S. Cook, H.R. Fiebig	
CUI	06	PR D73 014018	Y. Cui <i>et al.</i>	
HEDDITCH	05	PR D72 114507	J.N. Hedditch <i>et al.</i>	
ZHANG	05	PR D71 011502R	Z.F. Zhang, H.Y. Jin	
BERNARD	03	PR D68 074505	C. Bernard <i>et al.</i>	
JIN	03	PR D67 014025	H.Y. Jin, J.G. Körner, T.G. Steele	
SZCZEPANIAK	03B	PRL 91 092002	A.P. Szczepaniak <i>et al.</i>	
ZHANG	03	PR D67 074020	A. Zhang, T.G. Steele	
ACHASOV	02J	PAN 65 852	N.N. Achasov, G.N. Shestakov	
		Translated from YAF 65 579		
CHUNG	02C	EPJ A15 539	S.U. Chung, E. Klempt, J.G. Körner	
ZHANG	02	PR D65 096005	R. Zhang <i>et al.</i>	
IDDIR	01	PL B507 183	F. Iddir, A.S. Safir	
SADOVSKY	00	NP A655 131c	S.A. Sadovsky	(GAMS Collab.)
ALDE	99B	PAN 62 421	D. Alde <i>et al.</i>	
		Translated from YAF 62 462		
CHUNG	99	PR D60 092001	S.U. Chung <i>et al.</i>	(BNL E852 Collab.)
DONNACHIE	98	PR D58 114012	A. Donnachie <i>et al.</i>	
LACOCK	97	PL B401 308	P. Lacock <i>et al.</i>	(EDIN, LIVP)
SVEC	97C	PR D56 4355	M. Svec	(MCGI)
PROKOSHKIN	95C	PAN 58 853	Y.D. Prokoshkin, S.A. Sadovsky	(SERP)
		Translated from YAF 58 921		
KALASHNIK...	94	ZPHY C62 323	V.S. Kalashnikova	(ITEP)
TUAN	88	PL B213 537	S.F. Tuan, T. Ferbel, R.H. Dalitz	(HAWA, ROCH+)
ZIELINSKI	87	ZPHY C34 255	M. Zielinski	(ROCH)

 $\eta(1405)$

$$I^G(J^{PC}) = 0^+(0^{-+})$$

THE $\eta(1405)$, $\eta(1475)$, $f_1(1420)$, AND $f_1(1510)$

Revised January 2008 by C. Amsler (Zürich) and A. Masoni (INFN Cagliari).

The first observation of the $\eta(1440)$ was made in $p\bar{p}$ annihilation at rest into $\eta(1440)\pi^+\pi^-$, $\eta(1440) \rightarrow K\bar{K}\pi$ (BAILLON 67). This state was reported to decay through $a_0(980)\pi$ and $K^*(892)\bar{K}$ with roughly equal contributions. The $\eta(1440)$ was also observed in radiative $J/\psi(1S)$ decay to $K\bar{K}\pi$ (SCHARRE 80, EDWARDS 82E, AUGUSTIN 90) and $\gamma\rho$ (BAI 04J). There is now evidence for the existence of two pseudoscalars in this mass region, the $\eta(1405)$ and $\eta(1475)$. The former decays mainly through $a_0(980)\pi$ (or direct $K\bar{K}\pi$) and the latter mainly to $K^*(892)\bar{K}$.

The simultaneous observation of two pseudoscalars is reported in three production mechanisms: π^-p (RATH 89, ADAMS 01); radiative $J/\psi(1S)$ decay (BAI 90C, AUGUSTIN 92); and $p\bar{p}$ annihilation at rest (BERTIN 95, BERTIN 97, CICALO 99, NICHITIU 02). All of them give values for the masses, widths, and decay modes in reasonable agreement. However, AUGUSTIN 92 favors a state decaying into $K^*(892)\bar{K}$ at a lower mass than the state decaying into $a_0(980)\pi$, although agreement with MARK-III is not excluded.

In $J/\psi(1S)$ radiative decay, the $\eta(1405)$ decays into $K\bar{K}\pi$ through $a_0(980)\pi$, and hence a signal is also expected in the $\eta\pi\pi$ mass spectrum. This was indeed observed by MARK III in $\eta\pi^+\pi^-$ (BOLTON 92B), which reports a mass of 1400 MeV, in line with the existence of the $\eta(1405)$ decaying to $a_0(980)\pi$. This state is also observed in $p\bar{p}$ annihilation at rest into $\eta\pi^+\pi^-\pi^0\pi^0$, where it decays into $\eta\pi\pi$ (AMSLER 95F). The intermediate $a_0(980)\pi$ accounts for roughly half of the $\eta\pi\pi$ signal, in agreement with MARK III (BOLTON 92B) and DM2 (AUGUSTIN 90).

The existence of the $\eta(1295)$ is questioned by KLEMPPT 05. In KLEMPPT 07, the authors also question the existence of the $\eta(1295)$, and claim a single pseudoscalar meson in the 1400 MeV region. This conclusion is based on properties of the wave functions in the 3P_0 model, and on an unpublished analysis of the annihilation $p\bar{p} \rightarrow 4\pi\eta$. The pseudoscalar signal around 1400 MeV is then attributed to the first radial excitation of the η . However, the $\eta(1295)$ has been observed by four π^-p experiments (ADAMS 01, FUKUI 91C, ALDE 97B, MANAK 00A), and evidence is reported in $p\bar{p}$ annihilation (ANISOVICH 01, ABELE 98, AMSLER 04B). In J/ψ radiative decay, an $\eta(1295)$ signal is evident in the 0^{-+} $\eta\pi\pi$ wave of DM2 data (AUGUSTIN 92).

Assuming establishment of the $\eta(1295)$, the $\eta(1475)$ could be the first radial excitation of the η' , with the $\eta(1295)$ being the first radial excitation of the η . Ideal mixing, suggested by the $\eta(1295)$ and $\pi(1300)$ mass degeneracy, would then imply that the second isoscalar in the nonet is mainly $s\bar{s}$, and hence couples to $K^*\bar{K}$, in agreement with the $\eta(1475)$. Also its width matches the expected width for the radially excited $s\bar{s}$ state (CLOSE 97, BARNES 97).

The $K\bar{K}\pi$ and $\eta\pi\pi$ channels were studied in $\gamma\gamma$ collisions by L3 (ACCIARRI 01G). The analysis leads to a clear $\eta(1475)$ signal in $K\bar{K}\pi$, decaying to $K^*\bar{K}$, very well identified in the untagged data sample, where contamination from spin 1 resonances is not allowed. At the same time, ACCIARRI 01G did not observe $\eta(1405)$, either in $K\bar{K}\pi$ or $\eta\pi\pi$. The observation of the $\eta(1475)$, combined with the absence of an $\eta(1405)$ signal, strengthens the two-resonances hypothesis. Since gluonium production is presumably suppressed in $\gamma\gamma$ collisions, the ACCIARRI 01G results suggest that $\eta(1405)$ has a large gluonic content (see also CLOSE 97B, LI 03C).

The ACCIARRI 01G result is somewhat in disagreement with that of CLEO-II, which did not observe any pseudoscalar signal in $\gamma\gamma \rightarrow \eta(1475) \rightarrow K_S^0 K^\pm \pi^\mp$ (AHOHE 05). However, more data are required. Moreover, after the CLEO-II result, L3 performed a further analysis with full statistics (ACHARD 07), confirming the evidence of the $\eta(1475)$ observed by ACCIARRI 01G. The CLEO upper limit (AHOHE 05) for $\Gamma_{\gamma\gamma}(\eta(1475))$, and the L3 results (ACHARD 07), are consistent with the world average for the $\eta(1475)$ width.

The gluonium interpretation is not favored by lattice gauge theories which predict the 0^{-+} state above 2 GeV (BALI 93). However, the $\eta(1405)$ is an excellent candidate for the 0^{-+}

Meson Particle Listings

$\eta(1405)$

glueball in the fluxtube model (FADDEEV 04). In this model, the 0^{++} $f_0(1500)$ glueball is also naturally related to a 0^{-++} glueball with mass degeneracy broken in QCD.

A detailed review of the experimental situation is available in MASONI 06.

Let us now deal with 1^{++} isoscalars. The $f_1(1420)$, decaying to $K^*\bar{K}$, was first reported in π^-p reactions at 4 GeV/c (DIONISI 80). However, later analyses found that the 1400–1500 MeV region was far more complex (CHUNG 85, REEVES 86, BIRMAN 88). A reanalysis of the MARK III data in radiative $J/\psi(1S)$ decay to $K\bar{K}\pi$ (BAI 90C) shows the $f_1(1420)$, decaying into $K^*\bar{K}$. Also, a $C=+1$ state is observed in tagged $\gamma\gamma$ collisions (*e.g.*, BEHREND 89).

In $\pi^-p \rightarrow \eta\pi\pi n$ charge-exchange reactions at 8–9 GeV/c, the $\eta\pi\pi$ mass spectrum is dominated by the $\eta(1440)$ and $\eta(1295)$ (ANDO 86, FUKUI 91C), and at 100 GeV/c, ALDE 97B reports the $\eta(1295)$ and $\eta(1440)$ decaying to $\eta\pi^0\pi^0$ with a weak $f_1(1285)$ signal, and no evidence for the $f_1(1420)$.

Axial (1^{++}) mesons are not observed in $\bar{p}p$ annihilation at rest in liquid hydrogen, which proceeds dominantly through S -wave annihilation. However, in gaseous hydrogen, P -wave annihilation is enhanced and, indeed, BERTIN 97 reports $f_1(1420)$ decaying to $K^*\bar{K}$.

The $f_1(1420)$, decaying into $K\bar{K}\pi$, is also seen in pp central production, together with the $f_1(1285)$. The latter decays via $a_0(980)\pi$, and the former only via $K^*\bar{K}$, while the $\eta(1440)$ is absent (ARMSTRONG 89, BARBERIS 97C). The $K_S K_S \pi^0$ decay mode of $f_1(1420)$ establishes unambiguously $C=+1$. On the other hand, there is no evidence for any state decaying to $\eta\pi\pi$ around 1400 MeV, and hence the $\eta\pi\pi$ mode of the $f_1(1420)$ must be suppressed (ARMSTRONG 91B).

We now turn to the experimental evidence for the $f_1(1510)$. Two states, the $f_1(1420)$ and $f_1(1510)$, decaying to $K^*\bar{K}$, compete for the $s\bar{s}$ assignment in the 1^{++} nonet. The $f_1(1510)$ was seen in $K^-p \rightarrow \Lambda K\bar{K}\pi$ at 4 GeV/c (GAVILLET 82), and at 11 GeV/c (ASTON 88C). Evidence is also reported in π^-p at 8 GeV/c, based on the phase motion of the 1^{++} $K^*\bar{K}$ wave (BIRMAN 88). A somewhat broader 1^{++} signal is also observed in J/ψ radiative decay to $\eta\pi^+\pi^-$ (BAI 99).

The absence of the $f_1(1420)$ in K^-p (ASTON 88C) argues against the $f_1(1420)$ being the $s\bar{s}$ member of the 1^{++} nonet. However, the $f_1(1420)$ was reported in K^-p but not in π^-p (BITYUKOV 84), while two experiments do not observe the $f_1(1510)$ in K^-p (BITYUKOV 84, KING 91). It is also not seen in radiative $J/\psi(1S)$ decay (BAI 90C, AUGUSTIN 92), central collisions (BARBERIS 97C), or $\gamma\gamma$ collisions (AIHARA 88C), although, surprisingly for an $s\bar{s}$ state, a signal is reported in 4π decays (BAUER 93B). These facts lead to the conclusion that $f_1(1510)$ is not well established (CLOSE 97D).

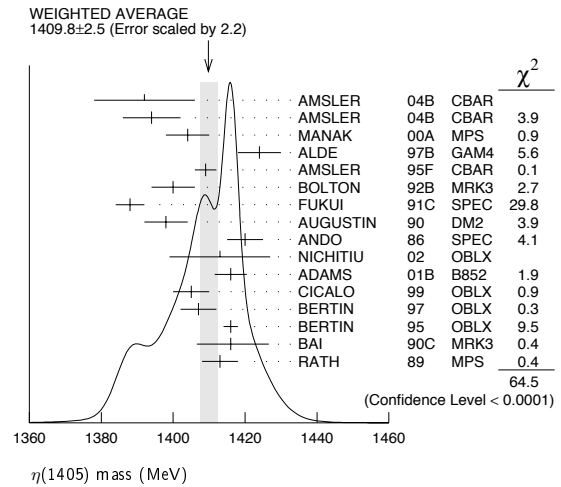
Assigning the $f_1(1420)$ to the 1^{++} nonet, one finds a nonet mixing angle of $\sim 50^\circ$ (CLOSE 97D). However, arguments favoring the $f_1(1420)$ being a hybrid $q\bar{q}g$ meson, or a four-quark state, were put forward by ISHIDA 89 and CALDWELL 90, respectively, while LONGACRE 90 argued for a molecular state

formed by the π orbiting in a P -wave around an S -wave $K\bar{K}$ state.

Summarizing, there is convincing evidence for the $f_1(1420)$ decaying to $K^*\bar{K}$, and for two pseudoscalars in the $\eta(1440)$ region, the $\eta(1405)$ and $\eta(1475)$, decaying to $a_0(980)\pi$ and $K^*\bar{K}$, respectively. The $f_1(1510)$ is not well established.

$\eta(1405)$ MASS

VALUE (MeV) DOCUMENT ID
1409.8 ± 2.5 OUR AVERAGE Includes data from the 2 datablocks that follow this one. Error includes scale factor of 2.2. See the ideogram below.



$\eta\pi\pi$ MODE

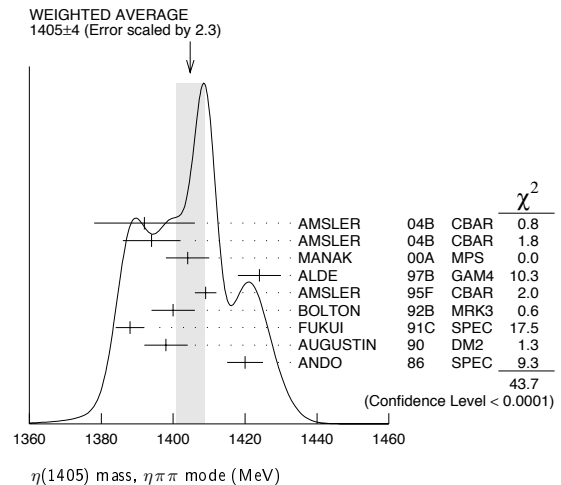
VALUE (MeV) EVTS DOCUMENT ID TECN COMMENT
 The data in this block is included in the average printed for a previous datablock.

1405 ± 4 OUR AVERAGE Error includes scale factor of 2.3. See the ideogram below.

1392 ± 14	900 ± 375	AMSLER	04B	CBAR	$0 \bar{p}p \rightarrow \pi^+\pi^-\pi^+\pi^-\eta$
1394 ± 8	6.6 ± 2.0k	AMSLER	04B	CBAR	$0 \bar{p}p \rightarrow \pi^+\pi^-\pi^0\pi^0\eta$
1404 ± 6	9082	MANAK	00A	MPS	$18 \pi^-p \rightarrow \eta\pi^+\pi^-n$
1424 ± 6	2200	ALDE	97B	GAM4	$100 \pi^-p \rightarrow \eta\pi^0\pi^0n$
1409 ± 3		AMSLER	95F	CBAR	$0 \bar{p}p \rightarrow \pi^+\pi^-\pi^0\pi^0\eta$
1400 ± 6		1 BOLTON	92B	MRK3	$J/\psi \rightarrow \gamma\eta\pi^+\pi^-$
1388 ± 4		FUKUI	91C	SPEC	$8.95 \pi^-p \rightarrow \eta\pi^+\pi^-n$
1398 ± 6	261	2 AUGUSTIN	90	DM2	$J/\psi \rightarrow \gamma\eta\pi^+\pi^-$
1420 ± 5		ANDO	86	SPEC	$8 \pi^-p \rightarrow \eta\pi^+\pi^-n$

••• We do not use the following data for averages, fits, limits, etc. •••

1385 ± 7		BAI	99	BES	$J/\psi \rightarrow \gamma\eta\pi^+\pi^-$
----------	--	-----	----	-----	---



$K\bar{K}\pi$ MODE ($a_0(980)\pi$ or direct $K\bar{K}\pi$)

VALUE (MeV) EVTS DOCUMENT ID TECN COMMENT
The data in this block is included in the average printed for a previous datablock.

VALUE (MeV)	EVTS	DOCUMENT ID	TECN	COMMENT
1413.9 ± 1.7 OUR AVERAGE				Error includes scale factor of 1.1.
1413 ± 14	3651	³ NICHITIU 02	OBLX	
1416 ± 4 ± 2	20k	ADAMS 01B	B852	18 GeV $\pi^- p \rightarrow K^+ K^- \pi^0 n$
1405 ± 5		⁴ CICALO 99	OBLX	$0 \bar{p} p \rightarrow K^\pm K_S^0 \pi^\mp \pi^+ \pi^-$
1407 ± 5		⁴ BERTIN 97	OBLX	$0 \bar{p} p \rightarrow K^\pm (K^0) \pi^\mp \pi^+ \pi^-$
1416 ± 2		⁴ BERTIN 95	OBLX	$0 \bar{p} p \rightarrow K \bar{K} \pi \pi \pi$
1416 ± 8 $\pm \frac{7}{-5}$	700	⁵ BAI 90c	MRK3	$J/\psi \rightarrow \gamma K_S^0 K^\pm \pi^\mp$
1413 ± 5		⁵ RATH 89	MPS	21.4 $\pi^- p \rightarrow n K_S^0 K_S^0 \pi^0$
1459 ± 5		⁶ AUGUSTIN 92	DM2	$J/\psi \rightarrow \gamma K \bar{K} \pi$

 $\pi\pi\gamma$ MODE

VALUE (MeV)	EVTS	DOCUMENT ID	TECN	COMMENT
1390 ± 12	235 ± 91	AMSLER 04B	CBAR	$0 \bar{p} p \rightarrow \pi^+ \pi^- \pi^+ \pi^- \gamma$
••• We do not use the following data for averages, fits, limits, etc. •••				
1424 ± 10 ± 11	547	BAI 04J	BES2	$J/\psi \rightarrow \gamma \gamma \pi^+ \pi^-$
1401 ± 18		^{7,8} AUGUSTIN 90	DM2	$J/\psi \rightarrow \pi^+ \pi^- \gamma \gamma$
1432 ± 8		⁸ COFFMAN 90	MRK3	$J/\psi \rightarrow \pi^+ \pi^- 2\gamma$

4 π MODE

VALUE (MeV)	EVTS	DOCUMENT ID	TECN	COMMENT
••• We do not use the following data for averages, fits, limits, etc. •••				
1420 ± 20		BUGG 95	MRK3	$J/\psi \rightarrow \gamma \pi^+ \pi^- \pi^+ \pi^-$
1489 ± 12	3270	⁹ BISELLO 89B	DM2	$J/\psi \rightarrow 4\pi\gamma$

 $K\bar{K}\pi$ MODE (unresolved)

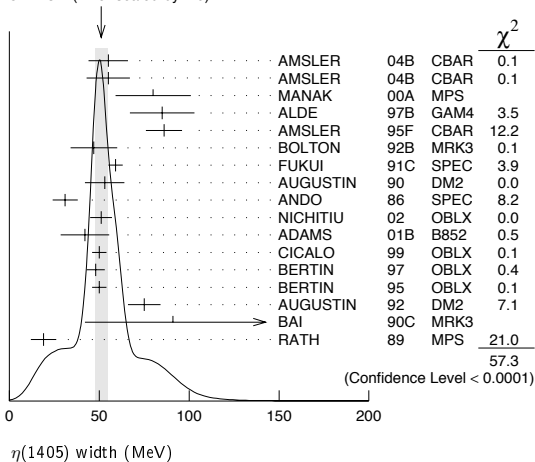
VALUE (MeV)	EVTS	DOCUMENT ID	TECN	COMMENT
••• We do not use the following data for averages, fits, limits, etc. •••				
1437.6 ± 3.2	249 ± 35	^{10,11} ABLIKIM 08E	BES2	$J/\psi \rightarrow \omega K_S^0 K^+ \pi^- + c.c.$
1445.9 ± 5.7	62 ± 18	^{10,11} ABLIKIM 08E	BES2	$J/\psi \rightarrow \omega K^+ K^- \pi^0$
1442 ± 10	410	¹⁰ BAI 98c	BES	$J/\psi \rightarrow \gamma K^+ K^- \pi^0$
1445 ± 8	693	¹⁰ AUGUSTIN 90	DM2	$J/\psi \rightarrow \gamma K_S^0 K^\pm \pi^\mp$
1433 ± 8	296	¹⁰ AUGUSTIN 90	DM2	$J/\psi \rightarrow \gamma K^+ K^- \pi^0$
1413 ± 8	500	¹⁰ DUCH 89	ASTE	$\bar{p} p \rightarrow \pi^+ \pi^- K^\pm \pi^\mp K^0$
1453 ± 7	170	¹⁰ RATH 89	MPS	21.4 $\pi^- p \rightarrow K_S^0 K_S^0 \pi^0 n$
1419 ± 1	8800	¹⁰ BIRMAN 88	MPS	8 $\pi^- p \rightarrow K^+ \bar{K}^0 \pi^- n$
1424 ± 3	620	¹⁰ REEVES 86	SPEC	6.6 $p\bar{p} \rightarrow K \bar{K} \pi \pi$
1421 ± 2		¹⁰ CHUNG 85	SPEC	8 $\pi^- p \rightarrow K \bar{K} \pi n$
1440 $\pm \frac{20}{-15}$	174	¹⁰ EDWARDS 82E	CBAL	$J/\psi \rightarrow \gamma K^+ K^- \pi^0$
1440 $\pm \frac{10}{-15}$		¹⁰ SCHARRE 80	MRK2	$J/\psi \rightarrow \gamma K_S^0 K^\pm \pi^\mp$
1425 ± 7	800	^{10,12} BAILLON 67	HBC	$0 \bar{p} p \rightarrow K \bar{K} \pi \pi \pi$

- From fit to the $a_0(980)\pi 0^-+$ partial wave.
- Best fit with a single Breit Wigner.
- Decaying dominantly directly to $K^+ K^- \pi^0$.
- Decaying into $(K\bar{K})_S \pi$, $(K\pi)_S \bar{K}$, and $a_0(980)\pi$.
- From fit to the $a_0(980)\pi 0^-+$ partial wave. Cannot rule out a $a_0(980)\pi 1^++$ partial wave.
- Excluded from averaging because averaging would be meaningless.
- Best fit with a single Breit Wigner.
- This peak in the $\gamma\pi$ channel may not be related to the $\eta(1405)$.
- Estimated by us from various fits.
- These experiments identify only one pseudoscalar in the 1400–1500 range. Data could also refer to $\eta(1475)$.
- Systematic uncertainty not evaluated.
- From best fit of 0^-+ partial wave, 50% $K^*(892)K$, 50% $a_0(980)\pi$.

 $\eta(1405)$ WIDTH

VALUE (MeV)	DOCUMENT ID
51.1 ± 3.4 OUR AVERAGE	Includes data from the 2 datablocks that follow this one. Error includes scale factor of 2.0. See the ideogram below.

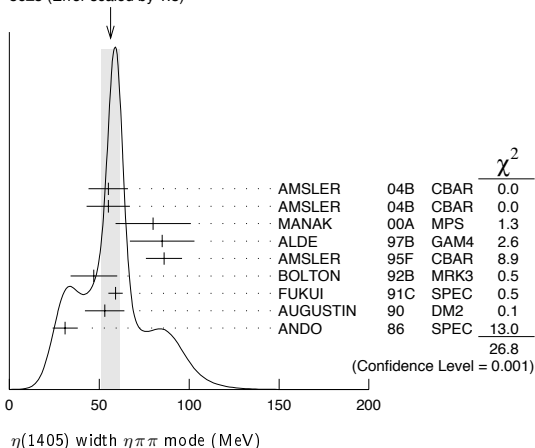
WEIGHTED AVERAGE
51.1 ± 3.4 (Error scaled by 2.0)

 **$\eta\pi\pi$ MODE**

VALUE (MeV) EVTS DOCUMENT ID TECN COMMENT
The data in this block is included in the average printed for a previous datablock.

VALUE (MeV)	EVTS	DOCUMENT ID	TECN	COMMENT
56 ± 5 OUR AVERAGE				Error includes scale factor of 1.8. See the ideogram below.
55 ± 11	900 ± 375	AMSLER 04B	CBAR	$0 \bar{p} p \rightarrow \pi^+ \pi^- \pi^+ \pi^- \eta$
55 ± 12	6.6 ± 2.0k	AMSLER 04B	CBAR	$0 \bar{p} p \rightarrow \pi^+ \pi^- \pi^0 \pi^0 \gamma$
80 ± 21	9082	MANAK 00A	MPS	18 $\pi^- p \rightarrow \eta \pi^+ \pi^- n$
85 ± 18	2200	ALDE 97B	GAM4	100 $\pi^- p \rightarrow \eta \pi^0 \pi^0 n$
86 ± 10		AMSLER 95F	CBAR	$0 \bar{p} p \rightarrow \pi^+ \pi^- \pi^0 \pi^0 \eta$
47 ± 13		¹³ BOLTON 92B	MRK3	$J/\psi \rightarrow \gamma \eta \pi^+ \pi^-$
59 ± 4		FUKUI 91C	SPEC	8.95 $\pi^- p \rightarrow \eta \pi^+ \pi^- n$
53 ± 11		¹⁴ AUGUSTIN 90	DM2	$J/\psi \rightarrow \gamma \eta \pi^+ \pi^-$
31 ± 7		ANDO 86	SPEC	8 $\pi^- p \rightarrow \eta \pi^+ \pi^- n$

WEIGHTED AVERAGE
56 ± 5 (Error scaled by 1.8)

 **$K\bar{K}\pi$ MODE ($a_0(980)\pi$ or direct $K\bar{K}\pi$)**

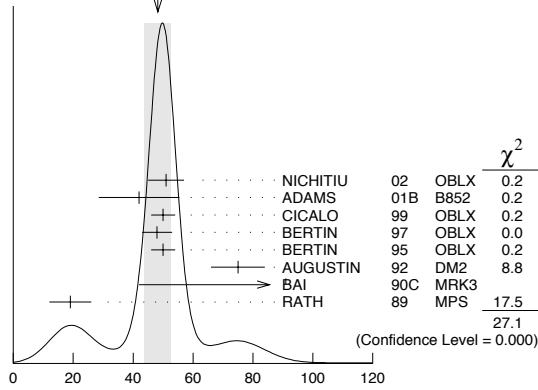
VALUE (MeV) EVTS DOCUMENT ID TECN COMMENT
The data in this block is included in the average printed for a previous datablock.

VALUE (MeV)	EVTS	DOCUMENT ID	TECN	COMMENT
48 ± 4 OUR AVERAGE				Error includes scale factor of 2.1. See the ideogram below.
51 ± 6	3651	¹⁵ NICHITIU 02	OBLX	
42 ± 10 ± 9	20k	ADAMS 01B	B852	18 GeV $\pi^- p \rightarrow K^+ K^- \pi^0 n$
50 ± 4		CICALO 99	OBLX	$0 \bar{p} p \rightarrow K^\pm K_S^0 \pi^\mp \pi^+ \pi^-$
48 ± 5		¹⁶ BERTIN 97	OBLX	$0 \bar{p} p \rightarrow K^\pm (K^0) \pi^\mp \pi^+ \pi^-$
50 ± 4		¹⁶ BERTIN 95	OBLX	$0 \bar{p} p \rightarrow K \bar{K} \pi \pi \pi$
75 ± 9		AUGUSTIN 92	DM2	$J/\psi \rightarrow \gamma K \bar{K} \pi$
91 $\pm \frac{67}{-31} \pm \frac{15}{-38}$		¹⁷ BAI 90c	MRK3	$J/\psi \rightarrow \gamma K_S^0 K^\pm \pi^\mp$
19 ± 7		¹⁷ RATH 89	MPS	21.4 $\pi^- p \rightarrow n K_S^0 K_S^0 \pi^0$

Meson Particle Listings

$\eta(1405)$

WEIGHTED AVERAGE
48±4 (Error scaled by 2.1)



$\eta(1405)$ width $K\bar{K}\pi$ mode ($a_0(980)\pi$ dominant)

$\pi\pi\gamma$ MODE

VALUE (MeV)	EVTS	DOCUMENT ID	TECN	COMMENT
64 ± 18	235 ± 91	AMSLER	04B CBAR	$0\bar{p}p \rightarrow \pi^+\pi^-\pi^+\pi^-\gamma$
••• We do not use the following data for averages, fits, limits, etc. •••				
101.0 ± 8.8 ± 8.8	547	BAI	04J BES2	$J/\psi \rightarrow \gamma\gamma\pi^+\pi^-$
174 ± 44		AUGUSTIN	90 DM2	$J/\psi \rightarrow \pi^+\pi^-\gamma\gamma$
90 ± 26		18 COFFMAN	90 MRK3	$J/\psi \rightarrow \pi^+\pi^-2\gamma$

4π MODE

VALUE (MeV)	EVTS	DOCUMENT ID	TECN	COMMENT
••• We do not use the following data for averages, fits, limits, etc. •••				
160 ± 30		BUGG	95 MRK3	$J/\psi \rightarrow \gamma\pi^+\pi^-\pi^+\pi^-$
144 ± 13	3270	19 BISELLO	89B DM2	$J/\psi \rightarrow 4\pi\gamma$

$K\bar{K}\pi$ MODE (unresolved)

VALUE (MeV)	EVTS	DOCUMENT ID	TECN	COMMENT
••• We do not use the following data for averages, fits, limits, etc. •••				
48.9 ± 9.0	249 ± 35	20,21 ABLIKIM	08E BES2	$J/\psi \rightarrow \omega K_S^0 K^+\pi^- + c.c.$
34.2 ± 18.5	62 ± 18	20,21 ABLIKIM	08E BES2	$J/\psi \rightarrow \omega K_S^0 K^-\pi^0$
93 ± 14	296	20 AUGUSTIN	90 DM2	$J/\psi \rightarrow \gamma K^+ K^-\pi^0$
105 ± 10	693	20 AUGUSTIN	90 DM2	$J/\psi \rightarrow \gamma K_S^0 K^\pm\pi^\mp$
62 ± 16	500	20 DUCH	89 ASTE	$\bar{p}p \rightarrow K\bar{K}\pi\pi\pi$
100 ± 11	170	20 RATH	89 MPS	$21.4\pi^-p \rightarrow K_S^0 K_S^0 \pi^0 n$
66 ± 2	8800	20 BIRMAN	88 MPS	$8\pi^-p \rightarrow K^+ \bar{K}^0 \pi^- n$
60 ± 10	620	20 REEVES	86 SPEC	$6.6\bar{p}p \rightarrow K K\pi X$
60 ± 10		20 CHUNG	85 SPEC	$8\pi^-p \rightarrow K\bar{K}\pi n$
55 +20 -30	174	20 EDWARDS	82E CBAL	$J/\psi \rightarrow \gamma K^+ K^-\pi^0$
50 +30 -20		20 SCHARRE	80 MRK2	$J/\psi \rightarrow \gamma K_S^0 K^\pm\pi^\mp$
80 ± 10	800	20,22 BAILLON	67 HBC	$0.0\bar{p}p \rightarrow K\bar{K}\pi\pi\pi$

13 From fit to the $a_0(980)\pi 0^-+$ partial wave.
 14 From $\eta\pi^+\pi^-$ mass distribution - mainly $a_0(980)\pi$ - no spin-parity determination available.
 15 Decaying dominantly directly to $K^+K^-\pi^0$.
 16 Decaying into $(K\bar{K})_S\pi, (K\pi)_S\bar{K}$, and $a_0(980)\pi$.
 17 From fit to the $a_0(980)\pi 0^-+$ partial wave, but $a_0(980)\pi 1^++$ cannot be excluded.
 18 This peak in the $\gamma\rho$ channel may not be related to the $\eta(1405)$.
 19 Estimated by us from various fits.
 20 These experiments identify only one pseudoscalar in the 1400–1500 range. Data could also refer to $\eta(1475)$.
 21 Systematic uncertainty not evaluated.
 22 From best fit to 0^-+ partial wave, 50% $K^*(892)K$, 50% $a_0(980)\pi$.

$\eta(1405)$ DECAY MODES

Mode	Fraction (Γ_i/Γ)	Confidence level
Γ_1	$K\bar{K}\pi$	seen
Γ_2	$\eta\pi\pi$	seen
Γ_3	$a_0(980)\pi$	seen
Γ_4	$\eta(\pi\pi)S$ -wave	seen
Γ_5	$f_0(980)\eta$	seen
Γ_6	4π	seen
Γ_7	$\rho\rho$	<58% 99.85%
Γ_8	$\gamma\gamma$	
Γ_9	$\rho^0\gamma$	
Γ_{10}	$\phi\gamma$	
Γ_{11}	$K^*(892)K$	seen

$\eta(1405) \Gamma(i)\Gamma(\gamma\gamma)/\Gamma(\text{total})$

VALUE (keV)	CL%	DOCUMENT ID	TECN	COMMENT	$\Gamma_1\Gamma_8/\Gamma$
••• We do not use the following data for averages, fits, limits, etc. •••					
<0.035		90 23,24 AHOHE	05 CLE2	$10.6 e^+e^- \rightarrow e^+e^-K_S^0 K^\pm\pi^\mp$	

VALUE (keV)	CL%	DOCUMENT ID	TECN	COMMENT	$\Gamma_2\Gamma_8/\Gamma$
••• We do not use the following data for averages, fits, limits, etc. •••					
<0.095		95 ACCIARRI	01G L3	$183-202 e^+e^- \rightarrow e^+e^-\eta\pi^+\pi^-$	

VALUE (keV)	CL%	DOCUMENT ID	TECN	COMMENT	$\Gamma_9\Gamma_8/\Gamma$
••• We do not use the following data for averages, fits, limits, etc. •••					
<1.5		95 ALTHOFF	84E TASS	$e^+e^- \rightarrow e^+e^-\pi^+\pi^-\gamma$	

23 Using $\eta(1405)$ mass and width 1410 MeV and 51 MeV, respectively.

24 Assuming three-body phase-space decay to $K_S^0 K^\pm\pi^\mp$.

$\eta(1405)$ BRANCHING RATIOS

$\Gamma(\eta\pi\pi)/\Gamma(K\bar{K}\pi)$	VALUE	CL%	DOCUMENT ID	TECN	COMMENT	Γ_2/Γ_1
••• We do not use the following data for averages, fits, limits, etc. •••						
	1.09 ± 0.48		25 AMSLER	04B CBAR	$0\bar{p}p \rightarrow \pi^+\pi^-\pi^+\pi^-\eta$	
	<0.5		90 EDWARDS	83B CBAL	$J/\psi \rightarrow \eta\pi\pi\gamma$	
	<1.1		90 SCHARRE	80 MRK2	$J/\psi \rightarrow \eta\pi\pi\gamma$	
	<1.5		95 FOSTER	68B HBC	$0.0\bar{p}p$	

$\Gamma(\rho^0\gamma)/\Gamma(\eta\pi\pi)$	VALUE	CL%	DOCUMENT ID	TECN	COMMENT	Γ_9/Γ_2
••• We do not use the following data for averages, fits, limits, etc. •••						
	0.111 ± 0.064		AMSLER	04B CBAR	$0\bar{p}p$	

$\Gamma(a_0(980)\pi)/\Gamma(K\bar{K}\pi)$	VALUE	EVTS	DOCUMENT ID	TECN	COMMENT	Γ_3/Γ_1
••• We do not use the following data for averages, fits, limits, etc. •••						
	~0.15		26 BERTIN	95 OBLX	$0\bar{p}p \rightarrow K\bar{K}\pi\pi\pi$	
	~0.8	500	26 DUCH	89 ASTE	$\bar{p}p \rightarrow \pi^+\pi^-\pi^+\pi^-\pi^0$	
	~0.75		26 REEVES	86 SPEC	$6.6\bar{p}p \rightarrow K K\pi X$	

$\Gamma(a_0(980)\pi)/\Gamma(\eta\pi\pi)$	VALUE	EVTS	DOCUMENT ID	TECN	COMMENT	Γ_3/Γ_2
••• We do not use the following data for averages, fits, limits, etc. •••						
	0.29 ± 0.10		ABELE	98E CBAR	$0\bar{p}p \rightarrow \eta\pi^0\pi^0\pi^0$	
	0.19 ± 0.04	2200	27 ALDE	97B GAM4	$100\pi^-p \rightarrow \eta\pi^0\pi^0 n$	
	0.56 ± 0.04 ± 0.03		27 AMSLER	95F CBAR	$0\bar{p}p \rightarrow \pi^+\pi^-\pi^0\pi^0\eta$	

$\Gamma(a_0(980)\pi)/\Gamma(\eta(\pi\pi)S\text{-wave})$	VALUE	EVTS	DOCUMENT ID	TECN	COMMENT	Γ_3/Γ_4
••• We do not use the following data for averages, fits, limits, etc. •••						
	0.91 ± 0.12		ANISOVICH	01 SPEC	$0.0\bar{p}p \rightarrow \eta\pi^+\pi^-\pi^+\pi^-$	
	0.15 ± 0.04	9082	MANAK	00A MPS	$18\pi^-p \rightarrow \eta\pi^+\pi^-\pi^- n$	
	0.70 ± 0.12 ± 0.20		28 BAI	99 BES	$J/\psi \rightarrow \gamma\eta\pi^+\pi^-$	

$\Gamma(\rho^0\gamma)/\Gamma(K\bar{K}\pi)$	VALUE	CL%	DOCUMENT ID	TECN	COMMENT	Γ_9/Γ_1
••• We do not use the following data for averages, fits, limits, etc. •••						
	0.0152 ± 0.0038		29 COFFMAN	90 MRK3	$J/\psi \rightarrow \gamma\gamma\pi^+\pi^-$	

$\Gamma(\eta(\pi\pi)S\text{-wave})/\Gamma(\eta\pi\pi)$	VALUE	EVTS	DOCUMENT ID	TECN	COMMENT	Γ_4/Γ_2
••• We do not use the following data for averages, fits, limits, etc. •••						
	0.81 ± 0.04	2200	ALDE	97B GAM4	$100\pi^-p \rightarrow \eta\pi^0\pi^0 n$	

$\Gamma(a_0(980)\pi)/\Gamma(\eta(\pi\pi)S\text{-wave})$	VALUE	EVTS	DOCUMENT ID	TECN	COMMENT	Γ_3/Γ_4
••• We do not use the following data for averages, fits, limits, etc. •••						
	0.32 ± 0.07		30 ANISOVICH	99I SPEC	$0.9-1.2\bar{p}p \rightarrow \eta 3\pi^0$	

$\Gamma(\rho\rho)/\Gamma(\text{total})$	VALUE	CL%	DOCUMENT ID	TECN	COMMENT	Γ_7/Γ
••• We do not use the following data for averages, fits, limits, etc. •••						
	<0.58	99.85 ± 0.31	AMSLER	04B CBAR	$0\bar{p}p$	

$\Gamma(K^*(892)K)/\Gamma(a_0(980)\pi)$	VALUE	CL%	DOCUMENT ID	TECN	COMMENT	Γ_{11}/Γ_3
••• We do not use the following data for averages, fits, limits, etc. •••						
	0.084 ± 0.024		32 ADAMS	01B B852	$18\text{ GeV } \pi^-p \rightarrow K^+K^-\pi^0 n$	

See key on page 373

Meson Particle Listings
 $\eta(1405)$, $f_1(1420)$ $\Gamma(\phi\gamma)/\Gamma(\rho^0\gamma)$ Γ_{10}/Γ_9

VALUE CL% DOCUMENT ID TECN COMMENT

• • • We do not use the following data for averages, fits, limits, etc. • • •
 <0.77 95 ³³BAI 04J BES2 $J/\psi \rightarrow \gamma\gamma K^+ K^-$

²⁵ Using the data of BAILLON 67 on $\bar{p}p \rightarrow K\bar{K}\pi$.
²⁶ Assuming that the $a_0(980)$ decays only into $K\bar{K}$.
²⁷ Assuming that the $a_0(980)$ decays only into $\eta\pi$.
²⁸ Assuming that the $a_0(980)$ decays only into $\eta\pi$.
²⁹ Using $B(J/\psi \rightarrow \gamma\eta(1405) \rightarrow \gamma K\bar{K})=4.2 \times 10^{-3}$ and $B(J/\psi \rightarrow \gamma\eta(1405) \rightarrow \gamma\rho^0)=6.4 \times 10^{-5}$ and assuming that the $\gamma\rho^0$ signal does not come from the $f_1(1420)$.
³⁰ Using preliminary Crystal Barrel data.
³¹ Assuming that the $\eta(1405)$ decays are saturated by the $\pi\pi\eta$, $K\bar{K}\pi$ and $\rho\rho$ modes.
³² Statistical error only.
³³ Calculated by us from $B(J/\psi \rightarrow \eta(1405)\gamma \rightarrow \phi\gamma\gamma) < 0.82 \times 10^{-4}$ and $B(J/\psi \rightarrow \eta(1405)\gamma \rightarrow \rho^0\gamma\gamma) = (1.07 \pm 0.11) \times 10^{-4}$.

 $\eta(1405)$ REFERENCES

ABLIKIM	08E	PR D77 032005	M. Ablikim et al.	(BES Collab.)
AHOHE	05	PR D71 072001	R. Ahohe et al.	(CLEO Collab.)
AMSLER	04B	EPJ C33 23	C. Amisler et al.	(Crystal Barrel Collab.)
BAI	04J	PL B594 47	J.Z. Bai et al.	(BES Collab.)
NICHITIU	02	PL B545 261	F. Nitchiu et al.	(OBELIX Collab.)
ACCIARRI	01G	PL B501 1	M. Acciari et al.	(L3 Collab.)
ADAMS	01B	PL B516 264	G.S. Adams et al.	(BNL E852 Collab.)
ANISOVICH	01	NP A690 567	A.V. Anisovich et al.	(BES Collab.)
MANAK	00A	PR D62 012003	J.J. Manak et al.	(BNL E852 Collab.)
ANISOVICH	99I	PL B468 304	A.V. Anisovich et al.	(BES Collab.)
BAI	99	PL B446 356	J.Z. Bai et al.	(BES Collab.)
CICALO	99	PL B462 453	C. Cicalo et al.	(OBELIX Collab.)
ABELE	98E	NP B514 45	A. Abele et al.	(Crystal Barrel Collab.)
BAI	98C	PL B440 217	J.Z. Bai et al.	(BES Collab.)
ALDE	97B	PAN 60 386	D. Alde et al.	(GAMS Collab.)
		Translated from YAF 60 458.		
BERTIN	97	PL B400 226	A. Bertin et al.	(OBELIX Collab.)
AMSLER	95F	PL B358 389	C. Amisler et al.	(Crystal Barrel Collab.)
BERTIN	95	PL B361 187	A. Bertin et al.	(OBELIX Collab.)
BUGG	95	PL B353 378	D.V. Bugg et al.	(LOQM, PNP1, WASH)
AUGUSTIN	92	PR D46 1951	J.E. Augustin, G. Cosme	(DM2 Collab.)
BOLTON	92B	PRL 69 1328	T. Bolton et al.	(Mark III Collab.)
FUKUI	91C	PL B267 293	S. Fukui et al.	(SUGI, NAGO, KEK, KYOT)
AUGUSTIN	90	PR D42 10	J.E. Augustin et al.	(DM2 Collab.)
BAI	90C	PRL 65 2507	Z. Bai et al.	(Mark III Collab.)
COFFMAN	90	PR D41 1410	D.M. Coffman et al.	(Mark III Collab.)
BISELLO	89B	PR D39 701	G. Busetto et al.	(DM2 Collab.)
DUCH	89	ZPHY C45 223	K.D. Duch et al.	(ASTERIX Collab.) JP
RATH	89	PR D40 693	M.G. Rath et al.	(NDAM, BRAN, BNL, CUNY)
BIRMAN	88	PRL 61 1557	A. Birman et al.	(BNL, FSU, IND, MASH) JP
ANDO	86	PRL 57 1236	A. Ando et al.	(KEK, KYOT, NIRS, SAGA) JIP
REEVES	86	PR D34 1960	D.F. Reeves et al.	(FLOR, BNL, IND) JP
CHUNG	85	PRL 55 779	S.U. Chung et al.	(BNL, FLOR, IND) JP
ALTHOFF	84E	PL 147B 487	M. Althoff et al.	(TASSO Collab.)
EDWARDS	83B	PRL 51 859	C. Edwards et al.	(CIT, HARV, PRIN)
EDWARDS	82E	PRL 49 259	C. Edwards et al.	(CIT, HARV, PRIN)
		Also		
SCHARRE	80	PL 97B 329	D.L. Scharre et al.	(SLAC, LBL)
FOSTER	68B	NP B8 174	M. Foster et al.	(CERN, CDEF)
BAILLON	67	NC 50A 393	P.H. Baillon et al.	(CERN, CDEF, IRAD)

OTHER RELATED PAPERS

ACHARD	07	JHEP 0703 018	P. Achard et al.	(L3 Collab.)
KLEMP	07	PRPL 454 1	E. Klemp, A. Zaitsev	
MASONI	06	JPG 32 R293	A. Masoni, C. Cicalo, G.L. Usai	(INFN, CAGL)
FADDEEV	04	PR D70 114033	L. Faddeev et al.	
LI	03C	EPJ C28 335	D.M. Li et al.	
LI	03D	IMP A18 3335	D.M. Li et al.	
ADAMS	01	PRL 87 041001	T. Adams et al.	(NuTeV Collab.)
ANISOVICH	00F	EPJ A6 247	A.V. Anisovich et al.	
CARVALHO	99	EPJ C7 95	W.S. Carvalho et al.	
ABELE	98	PR D57 3860	A. Abele et al.	(Crystal Barrel Collab.)
NEKRASOV	98	EPJ C5 507	M.L. Nekrasov	
BARBERIS	97C	PL B413 225	D. Barberis et al.	(WA 102 Collab.)
BARNES	97	PR D55 4157	T. Barnes et al.	(ORNL, RAL, MCHS)
CLOSE	97	PL B397 333	F. Close et al.	(RAL, BIRM)
CLOSE	97B	PR D55 5749	F. Close et al.	(RAL, RUTG, BEIJ)
CLOSE	97D	ZPHY C76 469	F.E. Close et al.	
BERTIN	96	PL B385 493	A. Bertin et al.	(Obelix Collab.)
FARRAR	96	PRL 76 4111	G.R. Farrar	(RUTG)
AMELIN	95	ZPHY C66 71	D.V. Amelin et al.	(VES Collab.)
GENOVESE	94	ZPHY C61 425	M. Genovese, D.B. Lichtenberg, E. Predazzi	(TORI)
BALI	93	PL B309 378	G.S. Bali et al.	(LIVP)
BAUER	93B	PR D48 3976	D.A. Bauer et al.	(SLAC)
ARMSTRONG	91B	ZPHY C52 389	T.A. Armstrong et al.	(ATHU, BARI, BIRM)
KING	91	NPBPS B21 11	E. King et al.	(FSU, BNL)
CALDWELL	90	Hadron 89 Conf. p 127	D.O. Caldwell	(UCSB)
LONGACRE	90	PR D42 874	R.S. Longacre	(BNL)
AHMAD	89	NP B (PROC.) 8 50	S. Ahmad et al.	(ASTERIX Collab.)
ARMSTRONG	89	PL B221 216	T.A. Armstrong et al.	(CERN, CDEF, BIRM)
BEHREND	89	ZPHY C42 367	H.J. Behrend et al.	(CELLO Collab.)
ISHIDA	89	PTP 82 119	S. Ishida et al.	(NIHO)
ASTON	88C	PL B201 573	D. Aston et al.	(SLAC, NAGO, CIN, INUS)
ARMSTRONG	87	ZPHY C34 23	T.A. Armstrong et al.	(CERN, BIRM, BARI)
ARMSTRONG	84	PL 146B 273	T.A. Armstrong et al.	(ATHU, BARI, BIRM)
BITYUKOV	84	SJNP 39 735	S. Bityukov et al.	(SERP)
		Translated from YAF 39 1165.		
GAVILLET	82	ZPHY C16 119	P. Gavillet et al.	(CERN, CDEF, PADO)
DIONISI	80	NP B169 1	C. Dionisi et al.	(CERN, MADR, CDEF)
DEFOIX	72	NP B44 125	C. Defoix et al.	(CDEF, CERN)
DUBOC	72	NP B46 429	J. Duboc et al.	(PARIS, LIVP)
LORSTAD	69	NP B14 63	B. Lorstad et al.	(CDEF, CERN)

 $f_1(1420)$ $J^{PC} = 0^+(1^{++})$ See the minireview under $\eta(1405)$. $f_1(1420)$ MASS

VALUE (MeV)	EVTS	DOCUMENT ID	TECN	COMMENT
1426.4 ± 0.9 OUR AVERAGE				Error includes scale factor of 1.1.
1434 ± 5 ± 5	133	¹ ACHARD	07 L3	183-209 $e^+e^- \rightarrow e^+e^-K_S^0 K^\pm\pi^\mp$
1426 ± 6	711	ABDALLAH	03H DLPH	91.2 $e^+e^- \rightarrow K_S^0 K^\pm\pi^\mp + X$
1420 ± 14	3651	NICHITIU	02 OBLX	
1428 ± 4 ± 2	20k	ADAMS	01B B852	18 GeV $\pi^-p \rightarrow K^+K^- \pi^0 n$
1426 ± 1		BARBERIS	97C OMEG	450 $pp \rightarrow pp K_S^0 K^\pm\pi^\mp$
1425 ± 8		BERTIN	97 OBLX	0.0 $\bar{p}p \rightarrow K^\pm(K^0)\pi^\mp\pi^+\pi^-$
1435 ± 9		PROKOSHKIN	97B GAM4	100 $\pi^-p \rightarrow \eta\pi^0\pi^0 n$
1430 ± 4		² ARMSTRONG	92E OMEG	85,300 $\pi^+p, pp \rightarrow \pi^+p, pp(K\bar{K}\pi)$
1462 ± 20		³ AUGUSTIN	92 DM2	$J/\psi \rightarrow \gamma K\bar{K}\pi$
1443 $^{+7}_{-6} \pm 3_{-2}$	1100	BAI	90C MRK3	$J/\psi \rightarrow \gamma K_S^0 K^\pm\pi^\mp$
1425 ± 10	17	BEHREND	89 CELL	$\gamma\gamma \rightarrow K_S^0 K^\pm\pi^\mp$
1442 ± 5 $^{+10}_{-17}$	111	BECKER	87 MRK3	$e^+e^- \rightarrow \omega K\bar{K}\pi$
1423 ± 4		GIDAL	87B MRK2	$e^+e^- \rightarrow e^+e^-K\bar{K}\pi$
1417 ± 13	13	AIHARA	86C TPC	$e^+e^- \rightarrow e^+e^-K\bar{K}\pi$
1422 ± 3		CHAUVAT	84 SPEC	ISR 31.5 pp
1440 ± 10		⁴ BROMBERG	80 SPEC	100 $\pi^-p \rightarrow K\bar{K}\pi X$
1426 ± 6	221	DIONISI	80 HBC	4 $\pi^-p \rightarrow K\bar{K}\pi n$
1420 ± 20		DAHL	67 HBC	1.6-4.2 π^-p
1430.8 ± 0.9		⁵ SOSA	99 SPEC	$pp \rightarrow p_{\text{slow}}(K_S^0 K^\pm\pi^\mp) p_{\text{fast}}$
1433.4 ± 0.8		⁵ SOSA	99 SPEC	$pp \rightarrow p_{\text{slow}}(K_S^0 K^\pm\pi^\mp) p_{\text{fast}}$
1429 ± 3	389	ARMSTRONG	89 OMEG	300 $pp \rightarrow K\bar{K}\pi pp$
1425 ± 2	1520	ARMSTRONG	84 OMEG	85 $\pi^+p, pp \rightarrow (\pi^+, p)(K\bar{K}\pi)p$
~ 1420		BITYUKOV	84 SPEC	32 $K^-p \rightarrow K^+K^- \pi^0 \gamma$

¹ From a fit with a width fixed at 55 MeV.
² This result supersedes ARMSTRONG 84, ARMSTRONG 89.
³ From fit to the $K^*(892) K 1^{++}$ partial wave.
⁴ Mass error increased to account for $a_0(980)$ mass cut uncertainties.
⁵ No systematic error given.

 $f_1(1420)$ WIDTH

VALUE (MeV)	EVTS	DOCUMENT ID	TECN	COMMENT
54.9 ± 2.6 OUR AVERAGE				
51 ± 14	711	ABDALLAH	03H DLPH	91.2 $e^+e^- \rightarrow K_S^0 K^\pm\pi^\mp + X$
61 ± 8	3651	NICHITIU	02 OBLX	
38 ± 9 ± 6	20k	ADAMS	01B B852	18 GeV $\pi^-p \rightarrow K^+K^- \pi^0 n$
58 ± 4		BARBERIS	97C OMEG	450 $pp \rightarrow pp K_S^0 K^\pm\pi^\mp$
45 ± 10		BERTIN	97 OBLX	0.0 $\bar{p}p \rightarrow K^\pm(K^0)\pi^\mp\pi^+\pi^-$
90 ± 25		PROKOSHKIN	97B GAM4	100 $\pi^-p \rightarrow \eta\pi^0\pi^0 n$
58 ± 10		⁶ ARMSTRONG	92E OMEG	85,300 $\pi^+p, pp \rightarrow \pi^+p, pp(K\bar{K}\pi)$
129 ± 41		⁷ AUGUSTIN	92 DM2	$J/\psi \rightarrow \gamma K\bar{K}\pi$
68 $^{+29}_{-18} \pm 8_{-9}$	1100	BAI	90C MRK3	$J/\psi \rightarrow \gamma K_S^0 K^\pm\pi^\mp$
42 ± 22	17	BEHREND	89 CELL	$\gamma\gamma \rightarrow K_S^0 K^\pm\pi^\mp$
40 $^{+17}_{-13} \pm 5$	111	BECKER	87 MRK3	$e^+e^- \rightarrow \omega K\bar{K}\pi$
35 $^{+47}_{-20}$	13	AIHARA	86C TPC	$e^+e^- \rightarrow e^+e^-K\bar{K}\pi$
47 ± 10		CHAUVAT	84 SPEC	ISR 31.5 pp
62 ± 14		BROMBERG	80 SPEC	100 $\pi^-p \rightarrow K\bar{K}\pi X$
40 ± 15	221	DIONISI	80 HBC	4 $\pi^-p \rightarrow K\bar{K}\pi n$
60 ± 20		DAHL	67 HBC	1.6-4.2 π^-p

Meson Particle Listings

 $f_1(1420)$

• • • We do not use the following data for averages, fits, limits, etc. • • •

68.7 ± 2.9	⁸ SOSA	99	SPEC	$pp \rightarrow p_{\text{slow}} (K_S^0 K^+ \pi^-) p_{\text{fast}}$
58.8 ± 3.3	⁸ SOSA	99	SPEC	$pp \rightarrow p_{\text{slow}} (K_S^0 K^- \pi^+) p_{\text{fast}}$
58 ± 8	389	ARMSTRONG	89	OMEG $300 pp \rightarrow K \bar{K} \pi pp$
62 ± 5	1520	ARMSTRONG	84	OMEG $85 \pi^+ p, pp \rightarrow (\pi^+, \rho) (K \bar{K} \pi) p$
~ 50		BITYUKOV	84	SPEC $32 K^- p \rightarrow K^+ K^- \pi^0 \gamma$

⁶This result supersedes ARMSTRONG 84, ARMSTRONG 89.

⁷From fit to the $K^*(892) K 1^+ +$ partial wave.

⁸No systematic error given.

 $f_1(1420)$ DECAY MODES

Mode	Fraction (Γ_i/Γ)
Γ_1 $K \bar{K} \pi$	dominant
Γ_2 $K \bar{K}^*(892) + \text{c.c.}$	dominant
Γ_3 $\eta \pi \pi$	possibly seen
Γ_4 $a_0(980) \pi$	
Γ_5 $\pi \pi \rho$	
Γ_6 4π	
Γ_7 $\rho^0 \gamma$	
Γ_8 $\phi \gamma$	seen

 $f_1(1420) \Gamma(i)\Gamma(\gamma\gamma)/\Gamma(\text{total})$

VALUE (keV)	CL%	EVTS	DOCUMENT ID	TECN	COMMENT
1.9 ± 0.4					OUR AVERAGE
$3.2 \pm 0.6 \pm 0.7$		133	9,10	ACHARD	07 L3 $183-209 e^+ e^- \rightarrow e^+ e^- K_S^0 K^\pm \pi^\mp$
$3.0 \pm 0.9 \pm 0.7$			11,12	BEHREND	89 CELL $e^+ e^- \rightarrow e^+ e^- K_S^0 K \pi$
$2.3^{+1.0}_{-0.9} \pm 0.8$				HILL	89 JADE $e^+ e^- \rightarrow e^+ e^- K^\pm K_S^0 \pi^\mp$
$1.3 \pm 0.5 \pm 0.3$				AIHARA	88B TPC $e^+ e^- \rightarrow e^+ e^- K^\pm K_S^0 \pi^\mp$
$1.6 \pm 0.7 \pm 0.3$			11,13	GIDAL	87B MRK2 $e^+ e^- \rightarrow e^+ e^- K \bar{K} \pi$

• • • We do not use the following data for averages, fits, limits, etc. • • •

< 8.0	95	JENNI	83	MRK2	$e^+ e^- \rightarrow e^+ e^- K \bar{K} \pi$
---------	----	-------	----	------	---

⁹From a fit with a width fixed at 55 MeV.

¹⁰The form factor parameter from the fit is 926 ± 78 MeV.

¹¹Assume a ρ -pole form factor.

¹²A ϕ -pole form factor gives considerably smaller widths.

¹³Published value divided by 2.

 $f_1(1420)$ BRANCHING RATIOS

VALUE	DOCUMENT ID	TECN	COMMENT	Γ_2/Γ_1	
0.76 ± 0.06	BROMBERG	80	SPEC	$100 \pi^- p \rightarrow K \bar{K} \pi X$	
0.86 ± 0.12	DIONISI	80	HBC	$4 \pi^- p \rightarrow K \bar{K} \pi n$	

VALUE	CL%	DOCUMENT ID	TECN	COMMENT	Γ_5/Γ_1
< 0.3	95	CORDEN	78	OMEG $12-15 \pi^- p$	
< 2.0		DAHL	67	HBC $1.6-4.2 \pi^- p$	

VALUE	CL%	DOCUMENT ID	TECN	COMMENT	Γ_3/Γ_1
< 0.1	95	ARMSTRONG	91B	OMEG $300 pp \rightarrow pp \eta \pi^+ \pi^-$	

• • • We do not use the following data for averages, fits, limits, etc. • • •

1.35 ± 0.75		KOPKE	89	MRK3 $J/\psi \rightarrow \omega \eta \pi \pi (K \bar{K} \pi)$	
< 0.6	90	GIDAL	87	MRK2 $e^+ e^- \rightarrow e^+ e^- \eta \pi^+ \pi^-$	

VALUE	CL%	DOCUMENT ID	TECN	COMMENT	Γ_4/Γ_3
< 0.5	95	CORDEN	78	OMEG $12-15 \pi^- p$	
1.5 ± 0.8		DEFOIX	72	HBC $0.7 \bar{p} p$	

VALUE	CL%	DOCUMENT ID	TECN	COMMENT	Γ_4/Γ_3
> 0.1	90	PROKOSHKIN	97B	GAM4 $100 \pi^- p \rightarrow \eta \pi^0 \pi^0 n$	

• • • We do not use the following data for averages, fits, limits, etc. • • •

not seen in either mode		ANDO	86	SPEC $8 \pi^- p$	
not seen in either mode		CORDEN	78	OMEG $12-15 \pi^- p$	
0.4 ± 0.2		DEFOIX	72	HBC $0.7 \bar{p} p \rightarrow 7\pi$	

 $\Gamma(4\pi)/\Gamma(K \bar{K}^*(892) + \text{c.c.})$ Γ_6/Γ_2

VALUE	CL%	DOCUMENT ID	TECN	COMMENT
< 0.90	95	DIONISI	80	HBC $4 \pi^- p$

• • • We do not use the following data for averages, fits, limits, etc. • • •

 $\Gamma(K \bar{K} \pi) / [\Gamma(K \bar{K}^*(892) + \text{c.c.}) + \Gamma(a_0(980) \pi)]$ $\Gamma_1/(\Gamma_2 + \Gamma_4)$

VALUE	CL%	DOCUMENT ID	TECN	COMMENT
0.65 ± 0.27		14	DIONISI	80 HBC $4 \pi^- p$

• • • We do not use the following data for averages, fits, limits, etc. • • •

¹⁴Calculated using $\Gamma(K \bar{K})/\Gamma(\eta \pi) = 0.24 \pm 0.07$ for $a_0(980)$ fractions.

 $\Gamma(a_0(980) \pi) / \Gamma(K \bar{K}^*(892) + \text{c.c.})$ Γ_4/Γ_2

VALUE	CL%	DOCUMENT ID	TECN	COMMENT
$0.04 \pm 0.01 \pm 0.01$		BARBERIS	98C	OMEG $450 pp \rightarrow p_f f_1(1420) p_s$

• • • We do not use the following data for averages, fits, limits, etc. • • •

< 0.04	68	ARMSTRONG	84	OMEG $85 \pi^+ p$
----------	----	-----------	----	-------------------

 $\Gamma(4\pi)/\Gamma(K \bar{K} \pi)$ Γ_6/Γ_1

VALUE	CL%	DOCUMENT ID	TECN	COMMENT
< 0.62	95	ARMSTRONG	89G	OMEG $85 \pi p \rightarrow 4\pi X$

 $\Gamma(\rho^0 \gamma) / \Gamma_{\text{total}}$ Γ_7/Γ

VALUE	CL%	DOCUMENT ID	TECN	COMMENT
< 0.08	95	15	ARMSTRONG	92C SPEC $300 pp \rightarrow pp \pi^+ \pi^- \gamma$

¹⁵Using the data on the $\bar{K} K \pi$ mode from ARMSTRONG 89.

 $\Gamma(\rho^0 \gamma) / \Gamma(K \bar{K} \pi)$ Γ_7/Γ_1

VALUE	CL%	DOCUMENT ID	TECN	COMMENT
< 0.02	95	BARBERIS	98C	OMEG $450 pp \rightarrow p_f f_1(1420) p_s$

 $\Gamma(\phi \gamma) / \Gamma(K \bar{K} \pi)$ Γ_8/Γ_1

VALUE	DOCUMENT ID	TECN	COMMENT
$0.003 \pm 0.001 \pm 0.001$	BARBERIS	98C	OMEG $450 pp \rightarrow p_f f_1(1420) p_s$

 $f_1(1420)$ REFERENCES

ACHARD	07	JHEP 0703 018	P. Achard <i>et al.</i>	(L3 Collab.)
ABDALLAH	03H	PL B569 129	J. Abdallah <i>et al.</i>	(DELPHI Collab.)
NICHITIU	02	PL B545 261	F. Nichitiu <i>et al.</i>	(OBELIX Collab.)
ADAMS	01B	PL B516 264	G.S. Adams <i>et al.</i>	(BNL E852 Collab.)
SOSA	99	PRL 83 913	M. Sosa <i>et al.</i>	
BARBERIS	98C	PL B440 225	D. Barberis <i>et al.</i>	(WA 102 Collab.)
BARBERIS	97C	PL B413 225	D. Barberis <i>et al.</i>	(WA 102 Collab.)
BERTIN	97	PL B400 226	A. Bertin <i>et al.</i>	(OBELIX Collab.)
PROKOSHKIN	97B	SPD 42 298	Yu.D. Prokoshkin, S.A. Sadovsky	
ARMSTRONG	92C	ZPHY C54 371	T.A. Armstrong <i>et al.</i>	(ATHU, BARI, BIRM+)
ARMSTRONG	92E	ZPHY C56 29	T.A. Armstrong <i>et al.</i>	(ATHU, BARI, BIRM+)
AUGUSTIN	92	PR D46 1951	J.E. Augustin, G. Cosme	(DM2 Collab.)
ARMSTRONG	91B	ZPHY C52 389	T.A. Armstrong <i>et al.</i>	(ATHU, BARI, BIRM+)
BAI	90C	PRL 65 2507	Z. Bai <i>et al.</i>	(Mark III Collab.)
ARMSTRONG	89	PL B221 216	T.A. Armstrong <i>et al.</i>	(CERN, CDF, BIRM+)
ARMSTRONG	89G	ZPHY C43 55	T.A. Armstrong <i>et al.</i>	(CERN, BIRM, BARI+)
BEHREND	89	ZPHY C42 367	H.J. Behrend <i>et al.</i>	(CELLO Collab.)
HILL	89	ZPHY C42 355	P. Hill <i>et al.</i>	(JADE Collab.)
KOPKE	89	PRPL 174 67	L. Kopke <i>et al.</i>	(CERN)
AIHARA	88B	PL B209 107	H. Aihara <i>et al.</i>	(TPC-2 γ Collab.)
BECKER	87	PRL 59 186	J.J. Becker <i>et al.</i>	(Mark III Collab.)
GIDAL	87	PRL 59 2012	G. Gidal <i>et al.</i>	(LBL, SLAC, HARV)
GIDAL	87B	PRL 59 2016	G. Gidal <i>et al.</i>	(LBL, SLAC, HARV)
AIHARA	86C	PRL 57 2500	H. Aihara <i>et al.</i>	(TPC-2 γ Collab.)
ANDO	86	PRL 57 1296	A. Ando <i>et al.</i>	(KEK, KYOT, NIRS, SAGA+)
ARMSTRONG	84	PL 146B 273	T.A. Armstrong <i>et al.</i>	(ATHU, BARI, BIRM+)
BITYUKOV	84	SJNP 39 735	S. Bitukov <i>et al.</i>	(SERP)
CHAUVAT	84	PL 146B 302	YAF 39 1165	Translated from
JENNI	83	PR D27 1031	P. Jenni <i>et al.</i>	(CERN, CLER, UCLA+)
BROMBERG	80	PR D22 1513	C.M. Bromberg <i>et al.</i>	(SLAC, LBL)
DIONISI	80	NP B169 1	C. Dionisi <i>et al.</i>	(CIT, FNAL, ILLC+)
CORDEN	78	NP B144 253	C. Corden <i>et al.</i>	(CERN, MADR, CDF+)
DEFOIX	72	NP B44 125	C. Defoix <i>et al.</i>	(BIRM, RHEL, TEA+)
DAHL	67	PR 163 1377	O.I. Dahl <i>et al.</i>	(CDFE, CERN)
Also		PRL 14 1074	D.H. Miller <i>et al.</i>	(LRL) IUP

OTHER RELATED PAPERS

AHOHE	05	PR D71 072001	R. Ahohe <i>et al.</i>	(CLEO Collab.)
KANADA-EN...	05	PR D71 094005	Y. Kanada-Enyo, O. Morimatsu, T. Nishikawa	
ACCIARRI	01G	PL B501 1	M. Acciari <i>et al.</i>	(L3 Collab.)
PROKOSHKIN	99	PAN 62 356	Yu.D. Prokoshkin	
IIZUKA	91	PTP 86 885	J. Iizuka, H. Koibuchi	(NAGO)
ISHIDA	89	PTP 82 119	S. Ishida <i>et al.</i>	(NIHO)
AIHARA	88C	PL D38 1	H. Aihara <i>et al.</i>	(TPC-2 γ Collab.)
BITYUKOV	88	PL B203 327	S.I. Bitukov <i>et al.</i>	(SERP)
PROTOPOP...	87B	Hadron 87 Conf.	S.D. Protopopescu, S.U. Chung	(BNL)

$\omega(1420)$

$$J^{PC} = 0^-(1^--)$$

 $\omega(1420)$ MASS

VALUE (MeV)	EVTS	DOCUMENT ID	TECN	COMMENT
-------------	------	-------------	------	---------

(1400-1450) OUR ESTIMATE

1382 ± 23 ± 70		AUBERT	07AU BABR	10.6 e ⁺ e ⁻ → ωπ ⁺ π ⁻ γ
1350 ± 20 ± 20		AUBERT,B	04N BABR	10.6 e ⁺ e ⁻ → π ⁺ π ⁻ π ⁰ γ
1400 ± 50 ± 130	1.2M	¹ ACHASOV	03D RVUE	0.44-2.00 e ⁺ e ⁻ → π ⁺ π ⁻ π ⁰
1450 ± 10		² HENNER	02 RVUE	1.2-2.0 e ⁺ e ⁻ → ρπ, ωππ
1373 ± 70	177	³ AKHMETSHIN	00D CMD2	1.2-1.38 e ⁺ e ⁻ → ωπ ⁺ π ⁻
1370 ± 25	5095	ANISOVICH	00H SPEC	0.0 pπ̄ → ωπ ⁰ π ⁰ π ⁰
1400 ⁺¹⁰⁰ ₋₂₀₀		⁴ ACHASOV	98H RVUE	e ⁺ e ⁻ → π ⁺ π ⁻ π ⁰
~1400		⁵ ACHASOV	98H RVUE	e ⁺ e ⁻ → ωπ ⁺ π ⁻
~1460		⁶ ACHASOV	98H RVUE	e ⁺ e ⁻ → K ⁺ K ⁻
1440 ± 70		⁷ CLEGG	94 RVUE	
1419 ± 31	315	⁸ ANTONELLI	92 DM2	1.34-2.4 e ⁺ e ⁻ → ρπ

¹ From the combined fit of ANTONELLI 92, ACHASOV 01E, ACHASOV 02E, and ACHASOV 03D data on the π⁺π⁻π⁰ and ANTONELLI 92 on the ωπ⁺π⁻ final states. Supersedes ACHASOV 99E and ACHASOV 02E.

² Using results of CORDIER 81 and preliminary data of DOLINSKY 91 and ANTONELLI 92.

³ Using the data of AKHMETSHIN 00D and ANTONELLI 92. The ρπ dominance for the energy dependence of the ω(1420) and ω(1650) width assumed.

⁴ Using data from BARKOV 87, DOLINSKY 91, and ANTONELLI 92.

⁵ Using the data from ANTONELLI 92.

⁶ Using the data from IVANOV 81 and BISELLO 88b.

⁷ From a fit to two Breit-Wigner functions and using the data of DOLINSKY 91 and ANTONELLI 92.

⁸ From a fit to two Breit-Wigner functions interfering between them and with the ω,φ tails with fixed (+,-,+) phases.

 $\omega(1420)$ WIDTH

VALUE (MeV)	EVTS	DOCUMENT ID	TECN	COMMENT
-------------	------	-------------	------	---------

(180-250) OUR ESTIMATE

130 ± 50 ± 100		AUBERT	07AU BABR	10.6 e ⁺ e ⁻ → ωπ ⁺ π ⁻ γ
450 ± 70 ± 70		AUBERT,B	04N BABR	10.6 e ⁺ e ⁻ → π ⁺ π ⁻ π ⁰ γ
870 ⁺⁵⁰⁰ ₋₃₀₀ ± 450	1.2M	⁹ ACHASOV	03D RVUE	0.44-2.00 e ⁺ e ⁻ → π ⁺ π ⁻ π ⁰
199 ± 15		¹⁰ HENNER	02 RVUE	1.2-2.0 e ⁺ e ⁻ → ρπ, ωππ
188 ± 45	177	¹¹ AKHMETSHIN	00D CMD2	1.2-1.38 e ⁺ e ⁻ → ωπ ⁺ π ⁻
360 ⁺¹⁰⁰ ₋₆₀	5095	ANISOVICH	00H SPEC	0.0 pπ̄ → ωπ ⁰ π ⁰ π ⁰
240 ± 70		¹² CLEGG	94 RVUE	
174 ± 59	315	¹³ ANTONELLI	92 DM2	1.34-2.4 e ⁺ e ⁻ → ρπ

⁹ From the combined fit of ANTONELLI 92, ACHASOV 01E, ACHASOV 02E, and ACHASOV 03D data on the π⁺π⁻π⁰ and ANTONELLI 92 on the ωπ⁺π⁻ final states. Supersedes ACHASOV 99E and ACHASOV 02E.

¹⁰ Using results of CORDIER 81 and preliminary data of DOLINSKY 91 and ANTONELLI 92.

¹¹ Using the data of AKHMETSHIN 00D and ANTONELLI 92. The ρπ dominance for the energy dependence of the ω(1420) and ω(1650) width assumed.

¹² From a fit to two Breit-Wigner functions and using the data of DOLINSKY 91 and ANTONELLI 92.

¹³ From a fit to two Breit-Wigner functions interfering between them and with the ω,φ tails with fixed (+,-,+) phases.

 $\omega(1420)$ DECAY MODES

Mode	Fraction (Γ _i /Γ)
Γ ₁ ρπ	dominant
Γ ₂ ωππ	seen
Γ ₃ b ₁ (1235)π	seen
Γ ₄ e ⁺ e ⁻	seen
Γ ₅ π ⁰ γ	

 $\omega(1420)$ Γ(Γ_iΓ_j)/Γ²(total)

VALUE (units 10 ⁻⁶)	EVTS	DOCUMENT ID	TECN	COMMENT
---------------------------------	------	-------------	------	---------

0.82 ± 0.05 ± 0.06		AUBERT,B	04N BABR	10.6 e ⁺ e ⁻ → π ⁺ π ⁻ π ⁰ γ
0.65 ± 0.13 ± 0.21	1.2M	^{14,15} ACHASOV	03D RVUE	0.44-2.00 e ⁺ e ⁻ → π ⁺ π ⁻ π ⁰
0.625 ± 0.160		^{16,17} CLEGG	94 RVUE	
0.466 ± 0.178		^{18,19} ANTONELLI	92 DM2	1.34-2.4 e ⁺ e ⁻ → ρπ

¹⁴ Calculated by us from the cross section at the peak.

¹⁵ From the combined fit of ANTONELLI 92, ACHASOV 01E, ACHASOV 02E, and ACHASOV 03D data on the π⁺π⁻π⁰ and ANTONELLI 92 on the ωπ⁺π⁻ final states. Supersedes ACHASOV 99E and ACHASOV 02E.

¹⁶ From a fit to two Breit-Wigner functions and using the data of DOLINSKY 91 and ANTONELLI 92.

¹⁷ From the partial and leptonic width given by the authors.

¹⁸ From a fit to two Breit-Wigner functions interfering between them and with the ω,φ tails with fixed (+,-,+) phases.

¹⁹ From the product of the leptonic width and partial branching ratio given by the authors.

$$\Gamma(\omega\pi\pi) \times \Gamma(e^+e^-)/\Gamma_{\text{total}}^2 \quad \Gamma_2\Gamma_4/\Gamma^2$$

VALUE (units 10 ⁻⁸)	DOCUMENT ID	TECN	COMMENT
---------------------------------	-------------	------	---------

19.7 ± 5.7	AUBERT	07AU BABR	10.6 e ⁺ e ⁻ → ωπ ⁺ π ⁻ γ
1.9 ± 1.9	²⁰ AKHMETSHIN	00D CMD2	1.2-2.4 e ⁺ e ⁻ → ωπ ⁺ π ⁻

²⁰ Using the data of AKHMETSHIN 00D and ANTONELLI 92. The ρπ dominance for the energy dependence of the ω(1420) and ω(1650) width assumed.

$$\Gamma(\pi^0\gamma) \times \Gamma(e^+e^-)/\Gamma_{\text{total}}^2 \quad \Gamma_5\Gamma_4/\Gamma^2$$

VALUE (units 10 ⁻⁸)	DOCUMENT ID	TECN	COMMENT
---------------------------------	-------------	------	---------

2.03 ^{+0.70} _{-0.75}	²¹ AKHMETSHIN	05 CMD2	0.60-1.38 e ⁺ e ⁻ → π ⁰ γ
--	--------------------------	---------	--

²¹ Using 1420 MeV and 220 MeV for the ω(1420) mass and width.

 $\omega(1420)$ BRANCHING RATIOS

$$\Gamma(\omega\pi\pi)/\Gamma_{\text{total}} \quad \Gamma_2/\Gamma$$

VALUE	DOCUMENT ID	TECN	COMMENT
-------	-------------	------	---------

0.301 ± 0.029	²² HENNER	02 RVUE	1.2-2.0 e ⁺ e ⁻ → ρπ, ωππ possibly seen
	AKHMETSHIN	00D CMD2	e ⁺ e ⁻ → ωπ ⁺ π ⁻

$$\Gamma(\omega\pi\pi)/\Gamma(b_1(1235)\pi) \quad \Gamma_2/\Gamma_3$$

VALUE	EVTS	DOCUMENT ID	TECN	COMMENT
-------	------	-------------	------	---------

0.60 ± 0.16	5095	ANISOVICH	00H SPEC	0.0 pπ̄ → ωπ ⁰ π ⁰ π ⁰
-------------	------	-----------	----------	---

$$\Gamma(\rho\pi)/\Gamma_{\text{total}} \quad \Gamma_1/\Gamma$$

VALUE	DOCUMENT ID	TECN	COMMENT
-------	-------------	------	---------

0.699 ± 0.029	²² HENNER	02 RVUE	1.2-2.0 e ⁺ e ⁻ → ρπ, ωππ
---------------	----------------------	---------	---

$$\Gamma(e^+e^-)/\Gamma_{\text{total}} \quad \Gamma_4/\Gamma$$

VALUE (units 10 ⁻⁷)	EVTS	DOCUMENT ID	TECN	COMMENT
---------------------------------	------	-------------	------	---------

~ 6.6	1.2M	^{23,24} ACHASOV	03D RVUE	0.44-2.00 e ⁺ e ⁻ → π ⁺ π ⁻ π ⁰
23 ± 1		²² HENNER	02 RVUE	1.2-2.0 e ⁺ e ⁻ → ρπ, ωππ

²² Assuming that the ω(1420) decays into ρπ and ωππ only.

²³ Calculated by us from the cross section at the peak.

²⁴ Assuming that the ω(1420) decays into ρπ only.

 $\omega(1420)$ REFERENCES

AUBERT	07AU	PR D76 092005	B. Aubert <i>et al.</i>	(BABAR Collab.)
AKHMETSHIN	05	PL B605 26	R.R. Akhmetshin <i>et al.</i>	(Novosibirsk CMD-2 Collab.)
AUBERT,B	04N	PR D70 072004	B. Aubert <i>et al.</i>	(BABAR Collab.)
ACHASOV	03D	PR D68 052006	M.N. Achasov <i>et al.</i>	(Novosibirsk SND Collab.)
ACHASOV	02E	PR D66 032001	M.N. Achasov <i>et al.</i>	(Novosibirsk SND Collab.)
HENNER	02	EPJ C26 3	V.K. Henner <i>et al.</i>	
ACHASOV	01E	PR D63 072002	M.N. Achasov <i>et al.</i>	(Novosibirsk SND Collab.)
AKHMETSHIN	00D	PL B489 125	R.R. Akhmetshin <i>et al.</i>	(Novosibirsk CMD-2 Collab.)
ANISOVICH	00H	PL B485 341	A.V. Anisovich <i>et al.</i>	
ACHASOV	99E	PL B462 365	M.N. Achasov <i>et al.</i>	(Novosibirsk SND Collab.)
ACHASOV	98H	PR D57 1334	M.N. Achasov, A.A. Kozhevnikov	
CLEGG	94	ZPHY C62 455	A.B. Clegg, A. Donnachie	(LANC, MCHS)
ANTONELLI	92	ZPHY C56 15	A. Antonelli <i>et al.</i>	(DM2 Collab.)
DOLINSKY	91	PR D202 99	S.I. Dolinsky <i>et al.</i>	(NOVO)
BISELLO	88B	ZPHY C39 13	D. Bisello <i>et al.</i>	(PADO, CLER, FRAS+)
BARKOV	87	JETPL 46 164	L.M. Barkov <i>et al.</i>	(NOVO)
		Translated from ZETFP 46 132.		
CORDIER	81	PL 106B 155	A. Cordier <i>et al.</i>	(ORSAY)
IVANOV	81	PL 107B 297	P.M. Ivanov <i>et al.</i>	(NOVO)

OTHER RELATED PAPERS

ACHASOV	07A	PR D76 072012	M.N. Achasov <i>et al.</i>	(SND Collab.)
ACHASOV	02B	PAN 65 153	M.N. Achasov, A.A. Kozhevnikov	
		Translated from YAF 65 150.		
CLOSE	02	PR D65 092003	F.E. Close, A. Donnachie, Yu.S. Kalashnikova	
ACHASOV	00J	PR D62 117503	M.N. Achasov, A.A. Kozhevnikov	
ABELE	98D	PL B468 178	A. Abele <i>et al.</i>	(Crystal Barrel Collab.)
BELOZEROVA	99	PPN 29 63	T.S. Belozerovala, V.K. Henner	
		Translated from FEACV 29 148.		
ACHASOV	97F	PAN 60 2029	M.N. Achasov, A.A. Kozhevnikov	(NOVM)
		Translated from YAF 60 2212.		
ATKINSON	87	ZPHY C34 157	M. Atkinson <i>et al.</i>	(BONN, CERN, GLAS+)
ATKINSON	84	NP B231 15	M. Atkinson <i>et al.</i>	(BONN, CERN, GLAS+)
ATKINSON	83B	PL 127B 132	M. Atkinson <i>et al.</i>	(BONN, CERN, GLAS+)

Meson Particle Listings

 $f_2(1430)$, $a_0(1450)$ $f_2(1430)$

$$J^{PC} = 0^+(2^{++})$$

OMITTED FROM SUMMARY TABLE

This entry lists nearby peaks observed in the D wave of the $K\bar{K}$ and $\pi^+\pi^-$ systems. Needs confirmation. $f_2(1430)$ MASS

VALUE (MeV)	DOCUMENT ID	TECN	COMMENT
≈ 1430 OUR ESTIMATE			
• • • We do not use the following data for averages, fits, limits, etc. • • •			
1453 ± 4	2 VLADIMIRSK...01	SPEC	40 $\pi^- p \rightarrow K_S^0 K_S^0 n$
1421 ± 5	AUGUSTIN 87	DM2	$J/\psi \rightarrow \gamma \pi^+ \pi^-$
1480 ± 5.0	AKESSON 86	SPEC	$pp \rightarrow pp \pi^+ \pi^-$
1436 $^{+26}_{-16}$	DAUM 84	CNTR	17-18 $\pi^- p \rightarrow$ $K^+ K^- n$
1412 ± 3	DAUM 84	CNTR	63 $\pi^- p \rightarrow K_S^0 K_S^0 n$, $K^+ K^- n$
1439 $^{+5}_{-6}$	1 BEUSCH 67	OSPK	5,7,12 $\pi^- p \rightarrow$ $K_S^0 K_S^0 n$
1 Not seen by WETZEL 76. 2 $J^{PC} = 0^{++}$ or 2^{++} .			

 $f_2(1430)$ WIDTH

VALUE (MeV)	DOCUMENT ID	TECN	COMMENT
• • • We do not use the following data for averages, fits, limits, etc. • • •			
13 ± 5	4 VLADIMIRSK...01	SPEC	40 $\pi^- p \rightarrow K_S^0 K_S^0 n$
30 ± 9	AUGUSTIN 87	DM2	$J/\psi \rightarrow \gamma \pi^+ \pi^-$
150 ± 5.0	AKESSON 86	SPEC	$pp \rightarrow pp \pi^+ \pi^-$
81 $^{+5.6}_{-2.9}$	DAUM 84	CNTR	17-18 $\pi^- p \rightarrow$ $K^+ K^- n$
14 ± 6	DAUM 84	CNTR	63 $\pi^- p \rightarrow K_S^0 K_S^0 n$, $K^+ K^- n$
43 $^{+17}_{-18}$	3 BEUSCH 67	OSPK	5,7,12 $\pi^- p \rightarrow$ $K_S^0 K_S^0 n$
3 Not seen by WETZEL 76. 4 $J^{PC} = 0^{++}$ or 2^{++} .			

 $f_2(1430)$ DECAY MODES

Mode	Fraction (Γ_i/Γ)
Γ_1 $K\bar{K}$	seen
Γ_2 $\pi\pi$	seen

 $f_2(1430)$ REFERENCES

VLADIMIRSK...01	PAN 64 1895	V.V. Vladimirov <i>et al.</i>
AUGUSTIN 87	ZPHY C36 369	J.E. Augustin <i>et al.</i>
AKESSON 86	NP B264 154	T. Akesson <i>et al.</i>
DAUM 84	ZPHY C23 339	C. Daum <i>et al.</i>
WETZEL 76	NP B115 208	W. Wetzel <i>et al.</i>
BEUSCH 67	PL 25B 357	W. Beusch <i>et al.</i>

 $a_0(1450)$

$$J^{PC} = 1^-(0^{++})$$

See minireview on scalar mesons under $f_0(600)$. $a_0(1450)$ MASS

VALUE (MeV)	EVTS	DOCUMENT ID	TECN	COMMENT
1474 ± 19 OUR AVERAGE				
1480 ± 30		ABELE 98	CBAR	0.0 $\bar{p}p \rightarrow K_L^0 K^{\pm} \pi^{\mp}$
1470 ± 25		1 AMSLER 95D	CBAR	0.0 $\bar{p}p \rightarrow \pi^0 \pi^0 \pi^0$, $\pi^0 \eta \eta$, $\pi^0 \pi^0 \eta$
• • • We do not use the following data for averages, fits, limits, etc. • • •				
1477 ± 10	80k	2 UMAN 06	E835	5.2 $\bar{p}p \rightarrow \eta \eta \pi^0$
1441 $^{+40}_{-15}$	35280	5 BAKER 03	SPEC	$\bar{p}p \rightarrow \omega \pi^+ \pi^- \pi^0$
1303 ± 16		6 BARGIOTTI 03	OBLX	$\bar{p}p$
1296 ± 10		3 AMSLER 02	CBAR	0.9 $\bar{p}p \rightarrow \pi^0 \pi^0 \eta$
1565 ± 30		3 ANISOVICH 98B	RVUE	Compilation
1290 ± 10		BERTIN 98B	OBLX	0.0 $\bar{p}p \rightarrow K^{\pm} K_S^0 \pi^{\mp}$
1450 ± 40		AMSLER 94D	CBAR	0.0 $\bar{p}p \rightarrow \pi^0 \pi^0 \eta$
1435 ± 40		BUGG 94	RVUE	$\bar{p}p \rightarrow \eta 2\pi^0$
1410 ± 25		ETKIN 82C	MPS	23 $\pi^- p \rightarrow n 2K_S^0$
~1300		MARTIN 78	SPEC	10 $K^{\pm} p \rightarrow K_S^0 \pi^{\mp}$
1255 ± 5		4 CASON 76		

- 1 Coupled-channel analysis of AMSLER 95B, AMSLER 95C, and AMSLER 94D.
- 2 Statistical error only.
- 3 T-matrix pole.
- 4 Isospin 0 not excluded.
- 5 From the pole position.
- 6 Coupled channel analysis of $\pi^+ \pi^- \pi^0$, $K^+ K^- \pi^0$, and $K^{\pm} K_S^0 \pi^{\mp}$.

 $a_0(1450)$ WIDTH

VALUE (MeV)	EVTS	DOCUMENT ID	TECN	COMMENT
265 ± 13 OUR AVERAGE				
265 ± 15		ABELE 98	CBAR	0.0 $\bar{p}p \rightarrow K_L^0 K^{\pm} \pi^{\mp}$
265 ± 30		7 AMSLER 95D	CBAR	0.0 $\bar{p}p \rightarrow \pi^0 \pi^0 \pi^0$, $\pi^0 \eta \eta$, $\pi^0 \pi^0 \eta$
• • • We do not use the following data for averages, fits, limits, etc. • • •				
267 ± 11	80k	8 UMAN 06	E835	5.2 $\bar{p}p \rightarrow \eta \eta \pi^0$
110 ± 14	35280	11 BAKER 03	SPEC	$\bar{p}p \rightarrow \omega \pi^+ \pi^- \pi^0$
92 ± 16		12 BARGIOTTI 03	OBLX	$\bar{p}p$
81 ± 21		9 AMSLER 02	CBAR	0.9 $\bar{p}p \rightarrow \pi^0 \pi^0 \eta$
292 ± 40		9 ANISOVICH 98B	RVUE	Compilation
80 ± 5		BERTIN 98B	OBLX	0.0 $\bar{p}p \rightarrow K^{\pm} K_S^0 \pi^{\mp}$
270 ± 40		AMSLER 94D	CBAR	0.0 $\bar{p}p \rightarrow \pi^0 \pi^0 \eta$
270 ± 40		BUGG 94	RVUE	$\bar{p}p \rightarrow \eta 2\pi^0$
230 ± 30		ETKIN 82C	MPS	23 $\pi^- p \rightarrow n 2K_S^0$
~250		MARTIN 78	SPEC	10 $K^{\pm} p \rightarrow K_S^0 \pi^{\mp}$
79 ± 10		10 CASON 76		

- 7 Coupled-channel analysis of AMSLER 95B, AMSLER 95C, and AMSLER 94D.
- 8 Statistical error only.
- 9 T-matrix pole.
- 10 Isospin 0 not excluded.
- 11 From the pole position.
- 12 Coupled channel analysis of $\pi^+ \pi^- \pi^0$, $K^+ K^- \pi^0$, and $K^{\pm} K_S^0 \pi^{\mp}$.

 $a_0(1450)$ DECAY MODES

Mode	Fraction (Γ_i/Γ)
Γ_1 $\pi\eta$	seen
Γ_2 $\pi\eta'(958)$	seen
Γ_3 $K\bar{K}$	seen
Γ_4 $\omega\pi\pi$	seen

 $\Gamma(\pi\eta'(958))/\Gamma(\pi\eta)$

VALUE	DOCUMENT ID	TECN	COMMENT	Γ_2/Γ_1
0.35 ± 0.16	13 ABELE 98	CBAR	0.0 $\bar{p}p \rightarrow K_L^0 K^{\pm} \pi^{\mp}$	
• • • We do not use the following data for averages, fits, limits, etc. • • •				
0.43 ± 0.19	ABELE 97c	CBAR	0.0 $\bar{p}p \rightarrow \pi^0 \pi^0 \eta'$	
13 Using $\pi^0 \eta$ from AMSLER 94D.				

 $\Gamma(K\bar{K})/\Gamma(\pi\eta)$

VALUE	DOCUMENT ID	TECN	COMMENT	Γ_3/Γ_1
0.88 ± 0.23	13 ABELE 98	CBAR	0.0 $\bar{p}p \rightarrow K_L^0 K^{\pm} \pi^{\mp}$	

 $\Gamma(\omega\pi\pi)/\Gamma(\pi\eta)$

VALUE	EVTS	DOCUMENT ID	TECN	COMMENT	Γ_4/Γ_1
• • • We do not use the following data for averages, fits, limits, etc. • • •					
10.7 ± 2.3	35280	14 BAKER 03	SPEC	$\bar{p}p \rightarrow \omega \pi^+ \pi^- \pi^0$	
14 Using results on $\bar{p}p \rightarrow a_0(1450)^0 \pi^0$, $a_0(1450) \rightarrow \eta \pi^0$ from ABELE 96c and assuming the $\omega\pi\pi$ mechanism for the $\omega\pi\pi$ state.					

 $a_0(1450)$ REFERENCES

UMAN 06	PR D73 052009	I. Uman <i>et al.</i>	(FNAL E835)
BAKER 03	PL B563 140	C.A. Baker <i>et al.</i>	(OBELIX Collab.)
BARGIOTTI 03	EPJ C26 371	M. Bargiotti <i>et al.</i>	(Crystal Barrel Collab.)
AMSLER 02	EPJ C23 29	C. Amisler <i>et al.</i>	(Crystal Barrel Collab.)
ABELE 98	PR D57 2860	A. Abele <i>et al.</i>	(Crystal Barrel Collab.)
ANISOVICH 98B	SPU 41 419	V.V. Anisovich <i>et al.</i>	(Crystal Barrel Collab.)
BERTIN 98B	PL B434 180	A. Bertin <i>et al.</i>	(OBLX Collab.)
ABELE 97C	PL B404 179	A. Abele <i>et al.</i>	(Crystal Barrel Collab.)
ABELE 96C	NP A609 562	A. Abele <i>et al.</i>	(Crystal Barrel Collab.)
AMSLER 95B	PL B342 433	C. Amisler <i>et al.</i>	(Crystal Barrel Collab.)
AMSLER 95C	PL B353 571	C. Amisler <i>et al.</i>	(Crystal Barrel Collab.)
AMSLER 95D	PL B355 425	C. Amisler <i>et al.</i>	(Crystal Barrel Collab.)
AMSLER 94D	PL B333 277	C. Amisler <i>et al.</i>	(Crystal Barrel Collab.)
BUGG 94	PR D50 4412	D.V. Bugg <i>et al.</i>	(LOQM)
ETKIN 82C	PR D25 2446	A. Etkin <i>et al.</i>	(BNL, CUNY, TUFTS, VAND)
MARTIN 78	NP B134 392	A.D. Martin <i>et al.</i>	(DURH, GEVA)
CASON 76	PRL 36 1485	N.M. Cason <i>et al.</i>	(NDAM, ANL)

OTHER RELATED PAPERS

CHENG 06	PR D73 014017	H.-Y. Cheng, C.-K. Chua, K.-C. Yang
KATAEV 05	PAN 68 567	A.L. Kataev
RODRIGUEZ 05	PR D71 074008	S. Rodriguez, M. Napsuciale
FURMAN 02	PL B538 266	A. Furman, L. Lesniak
BARBERIS 00H	PL B498 225	D. Barberis <i>et al.</i>
MASONI 99	EPJ C8 385	A. Masoni
AMSLER 98	RMP 70 1293	C. Amisler

$\rho(1450)$

$$I^G(J^{PC}) = 1^+(1^{--})$$

See our mini-review under the $\rho(1700)$. **$\rho(1450)$ MASS**

VALUE (MeV)	DOCUMENT ID
1465 ± 25 OUR ESTIMATE	This is only an educated guess; the error given is larger than the error on the average of the published values.

 $\eta\rho^0$ MODE

VALUE (MeV)	DOCUMENT ID	TECN	COMMENT
••• We do not use the following data for averages, fits, limits, etc. •••			
1497 ± 14	1 AKHMETSHIN 01B	CMD2	$e^+e^- \rightarrow \eta\gamma$
1421 ± 15	2 AKHMETSHIN 00D	CMD2	$e^+e^- \rightarrow \eta\pi^+\pi^-$
1470 ± 20	ANTONELLI 88	DM2	$e^+e^- \rightarrow \eta\pi^+\pi^-$
1446 ± 10	FUKUI 88	SPEC	$8.95 \pi^-p \rightarrow \eta\pi^+\pi^-n$

¹ Using the data of AKHMETSHIN 01B on $e^+e^- \rightarrow \eta\gamma$, AKHMETSHIN 00D and ANTONELLI 88 on $e^+e^- \rightarrow \eta\pi^+\pi^-$.

² Using the data of ANTONELLI 88, DOLINSKY 91, and AKHMETSHIN 00D. The energy-independent width of the $\rho(1450)$ and $\rho(1700)$ mesons assumed.

 $\omega\pi$ MODE

VALUE (MeV)	EVTS	DOCUMENT ID	TECN	COMMENT
••• We do not use the following data for averages, fits, limits, etc. •••				
1582 ± 17 ± 25	2382	3 AKHMETSHIN 03B	CMD2	$e^+e^- \rightarrow \pi^0\pi^0\gamma$
1349 ± 25 ± 10	341	4 ALEXANDER 01B	CLE2	$B \rightarrow D^{(*)}\omega\pi^-$
1523 ± 10		5 EDWARDS 00A	CLE2	$\tau^- \rightarrow \omega\pi^- \nu_\tau$
1463 ± 25		6 CLEGG 94	RVUE	
1250		7 ASTON 80C	OMEG	20-70 $\gamma p \rightarrow \omega\pi^0 p$
1290 ± 40		7 BARBER 80C	SPEC	3-5 $\gamma p \rightarrow \omega\pi^0 p$

³ Using the data of AKHMETSHIN 03B and BISELLO 91B assuming the $\omega\pi^0$ and $\pi^+\pi^-$ mass dependence of the total width. $\rho(1700)$ mass and width fixed at 1700 MeV and 240 MeV, respectively.

⁴ Using Breit-Wigner parameterization of the $\rho(1450)$ and assuming the $\omega\pi^-$ mass dependence for the total width.

⁵ Mass-independent width parameterization. $\rho(1700)$ mass and width fixed at 1700 MeV and 235 MeV respectively.

⁶ Using data from BISELLO 91B, DOLINSKY 86 and ALBRECHT 87L.

⁷ Not separated from $b_1(1235)$, not pure $J^P = 1^-$ effect.

 4π MODE

VALUE (MeV)	DOCUMENT ID	TECN	COMMENT
••• We do not use the following data for averages, fits, limits, etc. •••			
1435 ± 40	ABELE 01B	CBAR	$0.0 \bar{p}n \rightarrow 2\pi^- 2\pi^0 \pi^+$
1350 ± 50	ACHASOV 97	RVUE	$e^+e^- \rightarrow 2(\pi^+\pi^-)$
1449 ± 4	8 ARMSTRONG 89E	OMEG	300 $pp \rightarrow p\rho 2(\pi^+\pi^-)$

⁸ Not clear whether this observation has $l=1$ or 0.

 $\pi\pi$ MODE

VALUE (MeV)	EVTS	DOCUMENT ID	TECN	COMMENT
••• We do not use the following data for averages, fits, limits, etc. •••				
1328 ± 15		9 SCHAEEL 05C	ALEP	$\tau^- \rightarrow \pi^-\pi^0\nu_\tau$
1406 ± 15	87k 10,11	ANDERSON 00A	CLE2	$\tau^- \rightarrow \pi^-\pi^0\nu_\tau$
~ 1368		12 ABELE 99C	CBAR	$0.0 \bar{p}d \rightarrow \pi^+\pi^-\pi^-p$
1348 ± 33		BERTIN 98	OBLX	$0.05-0.405 \bar{p}p \rightarrow \pi^+\pi^+\pi^-$
1411 ± 14		13 ABELE 97	CBAR	$\bar{p}n \rightarrow \pi^-\pi^0\pi^0$
1370 ± 90		ACHASOV 97	RVUE	$e^+e^- \rightarrow \pi^+\pi^-$
1359 ± 40		11 BERTIN 97C	OBLX	$0.0 \bar{p}p \rightarrow \pi^+\pi^-\pi^0$
1282 ± 37		BERTIN 97D	OBLX	$0.05 \bar{p}p \rightarrow 2\pi^+ 2\pi^-$
1424 ± 25		BISELLO 89	DM2	$e^+e^- \rightarrow \pi^+\pi^-$
1265.5 ± 75.3		DUBNICKA 89	RVUE	$e^+e^- \rightarrow \pi^+\pi^-$
1292 ± 17		14 KURDADZE 83	OLYA	$0.64-1.4 e^+e^- \rightarrow \pi^+\pi^-$

⁹ From the combined fit of the τ^- data from ANDERSON 00A and SCHAEEL 05C and e^+e^- data from the compilation of BARKOV 85, AKHMETSHIN 04, and ALOISIO 05. $\rho(1700)$ mass and width fixed at 1713 MeV and 235 MeV, respectively. Supersedes BARATE 97M.

¹⁰ From the GOUNARIS 68 parametrization of the pion form factor.

¹¹ $\rho(1700)$ mass and width fixed at 1700 MeV and 235 MeV, respectively.

¹² $\rho(1700)$ mass and width fixed at 1780 MeV and 275 MeV respectively.

¹³ T-matrix pole.

¹⁴ Using for $\rho(1700)$ mass and width 1600 ± 20 and 300 ± 10 MeV respectively.

 $K\bar{K}$ MODE

VALUE (MeV)	EVTS	DOCUMENT ID	TECN	CHG	COMMENT
••• We do not use the following data for averages, fits, limits, etc. •••					
1422.8 ± 6.5	27k	15 ABELE 99D	CBAR ±	0.0	$\bar{p}p \rightarrow K^+ K^- \pi^0$

¹⁵ K-matrix pole. Isospin not determined, could be $\omega(1420)$.

 $K\bar{K}^*(892) + c.c.$ MODE

VALUE (MeV)	DOCUMENT ID	TECN	COMMENT
••• We do not use the following data for averages, fits, limits, etc. •••			
1505 ± 19 ± 7	AUBERT 08s	BABR	10.6 $e^+e^- \rightarrow K\bar{K}^*(892)\gamma$

 $\rho(1450)$ WIDTH

VALUE (MeV)	DOCUMENT ID
400 ± 60 OUR ESTIMATE	This is only an educated guess; the error given is larger than the error on the average of the published values.

 $\eta\rho^0$ MODE

VALUE (MeV)	DOCUMENT ID	TECN	COMMENT
••• We do not use the following data for averages, fits, limits, etc. •••			
226 ± 44	16 AKHMETSHIN 01B	CMD2	$e^+e^- \rightarrow \eta\gamma$
211 ± 31	17 AKHMETSHIN 00D	CMD2	$e^+e^- \rightarrow \eta\pi^+\pi^-$
230 ± 30	ANTONELLI 88	DM2	$e^+e^- \rightarrow \eta\pi^+\pi^-$
60 ± 15	FUKUI 88	SPEC	$8.95 \pi^-p \rightarrow \eta\pi^+\pi^-n$

¹⁶ Using the data of AKHMETSHIN 01B on $e^+e^- \rightarrow \eta\gamma$, AKHMETSHIN 00D and ANTONELLI 88 on $e^+e^- \rightarrow \eta\pi^+\pi^-$.

¹⁷ Using the data of ANTONELLI 88, DOLINSKY 91, and AKHMETSHIN 00D. The energy-independent width of the $\rho(1450)$ and $\rho(1700)$ mesons assumed.

 $\omega\pi$ MODE

VALUE (MeV)	EVTS	DOCUMENT ID	TECN	COMMENT
••• We do not use the following data for averages, fits, limits, etc. •••				
429 ± 42 ± 10	2382	18 AKHMETSHIN 03B	CMD2	$e^+e^- \rightarrow \pi^0\pi^0\gamma$
547 ± 86 ± 46	341	19 ALEXANDER 01B	CLE2	$B \rightarrow D^{(*)}\omega\pi^-$
400 ± 35		20 EDWARDS 00A	CLE2	$\tau^- \rightarrow \omega\pi^- \nu_\tau$
311 ± 62		21 CLEGG 94	RVUE	
300		22 ASTON 80C	OMEG	20-70 $\gamma p \rightarrow \omega\pi^0 p$
320 ± 100		22 BARBER 80C	SPEC	3-5 $\gamma p \rightarrow \omega\pi^0 p$

¹⁸ Using the data of AKHMETSHIN 03B and BISELLO 91B assuming the $\omega\pi^0$ and $\pi^+\pi^-$ mass dependence of the total width. $\rho(1700)$ mass and width fixed at 1700 MeV and 240 MeV, respectively.

¹⁹ Using Breit-Wigner parameterization of the $\rho(1450)$ and assuming the $\omega\pi^-$ mass dependence for the total width.

²⁰ Mass-independent width parameterization. $\rho(1700)$ mass and width fixed at 1700 MeV and 235 MeV respectively.

²¹ Using data from BISELLO 91B, DOLINSKY 86 and ALBRECHT 87L.

²² Not separated from $b_1(1235)$, not pure $J^P = 1^-$ effect.

 4π MODE

VALUE (MeV)	DOCUMENT ID	TECN	COMMENT
••• We do not use the following data for averages, fits, limits, etc. •••			
325 ± 100	ABELE 01B	CBAR	$0.0 \bar{p}n \rightarrow 2\pi^- 2\pi^0 \pi^+$

 $\pi\pi$ MODE

VALUE (MeV)	EVTS	DOCUMENT ID	TECN	COMMENT
••• We do not use the following data for averages, fits, limits, etc. •••				
468 ± 41		23 SCHAEEL 05C	ALEP	$\tau^- \rightarrow \pi^-\pi^0\nu_\tau$
455 ± 41	87k 24,25	ANDERSON 00A	CLE2	$\tau^- \rightarrow \pi^-\pi^0\nu_\tau$
~ 374		26 ABELE 99C	CBAR	$0.0 \bar{p}d \rightarrow \pi^+\pi^-\pi^-p$
275 ± 10		BERTIN 98	OBLX	$0.05-0.405 \bar{p}p \rightarrow \pi^+\pi^+\pi^-$
343 ± 20		27 ABELE 97	CBAR	$\bar{p}n \rightarrow \pi^-\pi^0\pi^0$
310 ± 40		25 BERTIN 97C	OBLX	$0.0 \bar{p}p \rightarrow \pi^+\pi^-\pi^0$
236 ± 36		BERTIN 97D	OBLX	$0.05 \bar{p}p \rightarrow 2\pi^+ 2\pi^-$
269 ± 31		BISELLO 89	DM2	$e^+e^- \rightarrow \pi^+\pi^-$
391 ± 70		DUBNICKA 89	RVUE	$e^+e^- \rightarrow \pi^+\pi^-$
218 ± 46		28 KURDADZE 83	OLYA	$0.64-1.4 e^+e^- \rightarrow \pi^+\pi^-$

²³ From the combined fit of the τ^- data from ANDERSON 00A and SCHAEEL 05C and e^+e^- data from the compilation of BARKOV 85, AKHMETSHIN 04, and ALOISIO 05. $\rho(1700)$ mass and width fixed at 1713 MeV and 235 MeV, respectively. Supersedes BARATE 97M.

²⁴ From the GOUNARIS 68 parametrization of the pion form factor.

²⁵ $\rho(1700)$ mass and width fixed at 1700 MeV and 235 MeV, respectively.

²⁶ $\rho(1700)$ mass and width fixed at 1780 MeV and 275 MeV respectively.

²⁷ T-matrix pole.

²⁸ Using for $\rho(1700)$ mass and width 1600 ± 20 and 300 ± 10 MeV respectively.

 $K\bar{K}$ MODE

VALUE (MeV)	EVTS	DOCUMENT ID	TECN	CHG	COMMENT
••• We do not use the following data for averages, fits, limits, etc. •••					
146.5 ± 10.5	27k	29 ABELE 99D	CBAR ±	0.0	$\bar{p}p \rightarrow K^+ K^- \pi^0$

²⁹ K-matrix pole. Isospin not determined, could be $\omega(1420)$.

 $K\bar{K}^*(892) + c.c.$ MODE

VALUE (MeV)	DOCUMENT ID	TECN	COMMENT
••• We do not use the following data for averages, fits, limits, etc. •••			
418 ± 25 ± 4	AUBERT 08s	BABR	10.6 $e^+e^- \rightarrow K\bar{K}^*(892)\gamma$

Meson Particle Listings

 $\rho(1450)$ $\rho(1450)$ DECAY MODES

Mode	Fraction (Γ_i/Γ)
Γ_1 $\pi\pi$	seen
Γ_2 4π	seen
Γ_3 $\omega\pi$	
Γ_4 $a_1(1260)\pi$	
Γ_5 $h_1(1170)\pi$	
Γ_6 $\pi(1300)\pi$	
Γ_7 $\rho\rho$	
Γ_8 $\rho(\pi\pi)$ s-wave	
Γ_9 e^+e^-	seen
Γ_{10} $\eta\rho$	possibly seen
Γ_{11} $a_2(1320)\pi$	not seen
Γ_{12} $K\bar{K}$	not seen
Γ_{13} $K\bar{K}^*(892) + c.c.$	possibly seen
Γ_{14} $\eta\gamma$	possibly seen

 $\rho(1450)$ $\Gamma(i)\Gamma(e^+e^-)/\Gamma(\text{total})$

$\Gamma(\pi\pi) \times \Gamma(e^+e^-)/\Gamma_{\text{total}}$	$\Gamma_1\Gamma_9/\Gamma$
VALUE (keV)	DOCUMENT ID TECN COMMENT
••• We do not use the following data for averages, fits, limits, etc. •••	
0.12	³⁰ DIEKMANN 88 RVUE $e^+e^- \rightarrow \pi^+\pi^-$
$0.027^{+0.015}_{-0.010}$	³¹ KURDADZE 83 OLYA $0.64-1.4 e^+e^- \rightarrow \pi^+\pi^-$

$\Gamma(\eta\rho) \times \Gamma(e^+e^-)/\Gamma_{\text{total}}$	$\Gamma_{10}\Gamma_9/\Gamma$
VALUE (eV)	DOCUMENT ID TECN COMMENT
••• We do not use the following data for averages, fits, limits, etc. •••	
74 ± 20	³² AKHMETSHIN 00D CMD2 $e^+e^- \rightarrow \eta\pi^+\pi^-$
91 ± 19	ANTONELLI 88 DM2 $e^+e^- \rightarrow \eta\pi^+\pi^-$

$\Gamma(\eta\gamma) \times \Gamma(e^+e^-)/\Gamma_{\text{total}}$	$\Gamma_{14}\Gamma_9/\Gamma$
VALUE (eV)	DOCUMENT ID TECN COMMENT
••• We do not use the following data for averages, fits, limits, etc. •••	
<16.4	³³ AKHMETSHIN 05 CMD2 $0.60-1.38 e^+e^- \rightarrow \eta\gamma$
$2.2 \pm 0.5 \pm 0.3$	³⁴ AKHMETSHIN 01B CMD2 $e^+e^- \rightarrow \eta\gamma$

$\Gamma(K\bar{K}^*(892) + c.c.) \times \Gamma(e^+e^-)/\Gamma_{\text{total}}$	$\Gamma_{13}\Gamma_9/\Gamma$
VALUE (eV)	DOCUMENT ID TECN COMMENT
••• We do not use the following data for averages, fits, limits, etc. •••	
$127 \pm 15 \pm 6$	AUBERT 08s BABR $10.6 e^+e^- \rightarrow K\bar{K}^*(892)\gamma$
³⁰ Using total width = 235 MeV.	
³¹ Using for $\rho(1700)$ mass and width 1600 ± 20 and 300 ± 10 MeV respectively.	
³² Using the data of ANTONELLI 88, DOLINSKY 91, and AKHMETSHIN 00D. The energy-independent width of the $\rho(1450)$ and $\rho(1700)$ mesons assumed.	
³³ From 2γ decay mode of η using 1465 MeV and 310 MeV for the $\rho(1450)$ mass and width. Recalculated by us.	
³⁴ Using the data of AKHMETSHIN 01B on $e^+e^- \rightarrow \eta\gamma$, AKHMETSHIN 00D and ANTONELLI 88 on $e^+e^- \rightarrow \eta\pi^+\pi^-$. Recalculated by us using width of 226 MeV.	

 $\rho(1450)$ BRANCHING RATIOS

$\Gamma(\pi\pi)/\Gamma(4\pi)$	Γ_1/Γ_2
VALUE	DOCUMENT ID TECN COMMENT
••• We do not use the following data for averages, fits, limits, etc. •••	
0.37 ± 0.10	^{35,36} ABELE 01B CBAR $0.0 \bar{p}n \rightarrow 5\pi$

$\Gamma(\omega\pi)/\Gamma_{\text{total}}$	Γ_3/Γ
VALUE	DOCUMENT ID TECN COMMENT
••• We do not use the following data for averages, fits, limits, etc. •••	
~ 0.21	CLEGG 94 RVUE

$\Gamma(\pi\pi)/\Gamma(\omega\pi)$	Γ_1/Γ_3
VALUE	DOCUMENT ID TECN COMMENT
••• We do not use the following data for averages, fits, limits, etc. •••	
~ 0.32	CLEGG 94 RVUE

$\Gamma(\omega\rho)/\Gamma(4\pi)$	Γ_3/Γ_2
VALUE	DOCUMENT ID TECN COMMENT
••• We do not use the following data for averages, fits, limits, etc. •••	
<0.14	CLEGG 88 RVUE

$\Gamma(a_1(1260)\pi)/\Gamma(4\pi)$	Γ_4/Γ_2
VALUE	DOCUMENT ID TECN COMMENT
••• We do not use the following data for averages, fits, limits, etc. •••	
0.27 ± 0.08	³⁵ ABELE 01B CBAR $0.0 \bar{p}n \rightarrow 5\pi$

 $\Gamma(h_1(1170)\pi)/\Gamma(4\pi)$

VALUE	DOCUMENT ID	TECN	COMMENT	Γ_5/Γ_2
••• We do not use the following data for averages, fits, limits, etc. •••				
0.08 ± 0.04	³⁵ ABELE	01B	CBAR $0.0 \bar{p}n \rightarrow 5\pi$	

 $\Gamma(\pi(1300)\pi)/\Gamma(4\pi)$

VALUE	DOCUMENT ID	TECN	COMMENT	Γ_6/Γ_2
••• We do not use the following data for averages, fits, limits, etc. •••				
0.37 ± 0.13	³⁵ ABELE	01B	CBAR $0.0 \bar{p}n \rightarrow 5\pi$	

 $\Gamma(\rho\rho)/\Gamma(4\pi)$

VALUE	DOCUMENT ID	TECN	COMMENT	Γ_7/Γ_2
••• We do not use the following data for averages, fits, limits, etc. •••				
0.11 ± 0.05	³⁵ ABELE	01B	CBAR $0.0 \bar{p}n \rightarrow 5\pi$	

 $\Gamma(\rho(\pi\pi)\text{s-wave})/\Gamma(4\pi)$

VALUE	DOCUMENT ID	TECN	COMMENT	Γ_8/Γ_2
••• We do not use the following data for averages, fits, limits, etc. •••				
0.17 ± 0.09	³⁵ ABELE	01B	CBAR $0.0 \bar{p}n \rightarrow 5\pi$	

 $\Gamma(\eta\rho)/\Gamma_{\text{total}}$

VALUE	DOCUMENT ID	TECN	COMMENT	Γ_{10}/Γ
••• We do not use the following data for averages, fits, limits, etc. •••				
<0.04	DONNACHIE 87B	RVUE		

 $\Gamma(\eta\rho)/\Gamma(\omega\pi)$

VALUE	DOCUMENT ID	TECN	COMMENT	Γ_{10}/Γ_3
••• We do not use the following data for averages, fits, limits, etc. •••				
~ 0.24	³⁷ DONNACHIE 91	RVUE		
>2	FUKUI 91	SPEC	$8.95 \pi^- \rho \rightarrow \omega\pi^0 n$	

 $\Gamma(a_2(1320)\pi)/\Gamma_{\text{total}}$

VALUE	DOCUMENT ID	TECN	COMMENT	Γ_{11}/Γ
••• We do not use the following data for averages, fits, limits, etc. •••				
not seen	AMELIN 00	VES	$37 \pi^- \rho \rightarrow \eta\pi^+\pi^- n$	

 $\Gamma(K\bar{K})/\Gamma(\omega\pi)$

VALUE	DOCUMENT ID	TECN	COMMENT	Γ_{12}/Γ_3
••• We do not use the following data for averages, fits, limits, etc. •••				
<0.08	³⁷ DONNACHIE 91	RVUE		

 $\Gamma(K\bar{K}^*(892) + c.c.)/\Gamma_{\text{total}}$

VALUE	DOCUMENT ID	TECN	COMMENT	Γ_{13}/Γ
••• We do not use the following data for averages, fits, limits, etc. •••				
possibly seen	COAN 04	CLEO	$\tau^- \rightarrow K^- \pi^- K^+ \nu_\tau$	
³⁵ $\omega\pi$ not included.				
³⁶ Using ABELE 97.				
³⁷ Using data from BISELLO 91B, DOLINSKY 86 and ALBRECHT 87L.				

 $\rho(1450)$ REFERENCES

AUBERT 08s	PR D77 092002	B. Aubert <i>et al.</i>	(BABAR Collab.)
AKHMETSHIN 05	PL B605 26	R.R. Akhmetshin <i>et al.</i>	(Novosibirsk CMD-2 Collab.)
ALOISIO 05	PL B606 12	A. Aloisio <i>et al.</i>	(KLOE Collab.)
SCHAEEL 05C	PRPL 421 191	S. Schaeel <i>et al.</i>	(ALEPH Collab.)
AKHMETSHIN 04	PL B578 285	R.R. Akhmetshin <i>et al.</i>	(Novosibirsk CMD-2 Collab.)
COAN 04	PRL 92 232001	T.E. Coan <i>et al.</i>	(CLEO Collab.)
AKHMETSHIN 03B	PL B562 173	R.R. Akhmetshin <i>et al.</i>	(Novosibirsk CMD-2 Collab.)
ABELE 01B	EPJ C21 261	A. Abele <i>et al.</i>	(Crystal Barrel Collab.)
AKHMETSHIN 01B	PL B509 217	R.R. Akhmetshin <i>et al.</i>	(Novosibirsk CMD-2 Collab.)
ALEXANDER 01B	PR D64 092001	J.P. Alexander <i>et al.</i>	(CLEO Collab.)
AKHMETSHIN 00D	PL B489 125	R.R. Akhmetshin <i>et al.</i>	(Novosibirsk CMD-2 Collab.)
AMELIN 00	NP A668 83	D. Amelin <i>et al.</i>	(VES Collab.)
ANDERSON 00A	PR D61 112002	S. Anderson <i>et al.</i>	(CLEO Collab.)
EDWARDS 00A	PR D61 072003	K.W. Edwards <i>et al.</i>	(CLEO Collab.)
ABELE 99C	PL B450 275	A. Abele <i>et al.</i>	(Crystal Barrel Collab.)
ABELE 99D	PL B468 178	A. Abele <i>et al.</i>	(Crystal Barrel Collab.)
BERTIN 98	PR D57 55	A. Bertin <i>et al.</i>	(OBELIX Collab.)
ABELE 97	PL B391 191	A. Abele <i>et al.</i>	(Crystal Barrel Collab.)
ACHASOV 97	PR D55 2663	N.M. Achasov <i>et al.</i>	(NOVO Collab.)
BARATE 97M	ZPHY C76 15	R. Barate <i>et al.</i>	(ALEPH Collab.)
BERTIN 97C	PL B408 476	A. Bertin <i>et al.</i>	(OBELIX Collab.)
BERTIN 97D	PL B414 220	A. Bertin <i>et al.</i>	(OBELIX Collab.)
CLEGG 94	ZPHY C62 455	A.B. Clegg, A. Donnachie	(LANC, MCHS)
BISELLO 91B	NPBPS B21 111	D. Biseillo	(DM2 Collab.)
DOLINSKY 91	PRPL 202 99	S.I. Dolinsky <i>et al.</i>	(NOVO Collab.)
DONNACHIE 91	ZPHY C51 689	A. Donnachie, A.B. Clegg	(MCHS, LANC)
FUKUI 91	PL B257 241	S. Fukui <i>et al.</i>	(SUGI, NAGO, KEK, KYOT+)
ARMSTRONG 89E	PL B228 536	T.A. Armstrong, M. Benayoun	(ATHU, BARI, BIRM+)
BISELLO 89	PL B220 321	D. Biseillo <i>et al.</i>	(DM2 Collab.)
DUBNICKA 89	JPG 15 1349	S. Dubnicka <i>et al.</i>	(JINR, SLOV)
ANTONELLI 88	PL B212 133	A. Antonelli <i>et al.</i>	(DM2 Collab.)
CLEGG 88	ZPHY C40 313	A.B. Clegg, A. Donnachie	(MCHS, LANC)
DIEKMANN 88	PRPL 159 99	B. Diekmann	(BONN)
FUKUI 88	PL B202 441	S. Fukui <i>et al.</i>	(SUGI, NAGO, KEK, KYOT+)
ALBRECHT 87L	PL B185 223	H. Albrecht <i>et al.</i>	(ARGUS Collab.)
DONNACHIE 87B	ZPHY C34 257	A. Donnachie, A.B. Clegg	(MCHS, LANC)
DOLINSKY 86	PL B174 453	S.I. Dolinsky <i>et al.</i>	(NOVO Collab.)
BARKOV 85	NP B256 365	L.M. Barkov <i>et al.</i>	(NOVO Collab.)
KURDADZE 83	JETPL 37 733	L.M. Kurdadze <i>et al.</i>	(NOVO Collab.)
ASTON 80C	PL 928 211	D. Aston	(BONN, CERN, EPOL, GLAS, LANC+)
BARBER 80C	ZPHY C4 169	D.P. Barber <i>et al.</i>	(DARE, LANC, SHEF)
GOUNARIS 68	PRL 21 244	G.J. Gounaris, J.J. Sakurai	

See key on page 373

Meson Particle Listings

 $\rho(1450)$, $\eta(1475)$

OTHER RELATED PAPERS

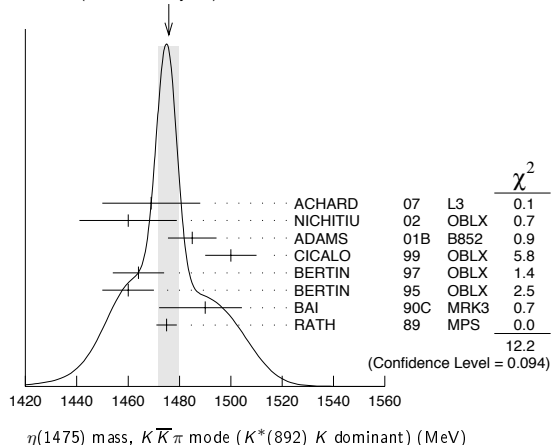
ACHASOV	07A	PR D76 072012	M.N. Achasov et al.	(SND Collab.)
AKHMETSHPIN	07	PL B648 28	R. Akhmetshin et al.	(Novosibirsk CMD-2 Collab.)
FUJIKAWA	07	NPBPS 169 36	M. Fujikawa et al.	(BELLE Collab.)
LI	07A	PR D76 094016	B.A. Li	
LIU	07B	PR D75 074017	X. Liu et al.	
ZHANG	07C	PR D76 036004	A. Zhang et al.	
ABLIKIM	06S	PRL 97 142002	M. Ablikim et al.	(BES Collab.)
ACHASOV	06D	JETP 103 720	N.N. Achasov et al.	(SND Collab.)
		Translated from ZETF 130 831.		
AUBERT	06L	PR D74 012001	B. Aubert et al.	(BABAR Collab.)
DAVIER	06	RMP 78 1043	M. Davier, A. Hocker, Z. Zhang	(LALO, PARIN+)
DING	06	PL B643 33	G.-J. Ding, M.-L. Yan	(CST)
GUO	06	NP A773 78	F.K. Guo et al.	
ACHASOV	05A	JETP 101 1053	M.N. Achasov et al.	(Novosibirsk SND Collab.)
		Translated from ZETF 128 1201.		
AUBERT	05D	PR D71 052001	B. Aubert et al.	(BABAR Collab.)
AULCHENKO	05	JETPL 82 743	V.M. Aulchenko et al.	(Novosibirsk CMD-2 Collab.)
		Translated from ZETFP 82 841.		
EBERT	05	MPL A20 1887	D. Ebert, R.N. Faustov, V.O. Galkin	
AKHMETSHPIN	04C	PL B595 101	R.R. Akhmetshin et al.	(Novosibirsk CMD-2 Collab.)
AMSLER	04A	NP A740 130	C. Amstler et al.	
ACHASOV	03C	JETP 96 789	M.N. Achasov et al.	(Novosibirsk SND Collab.)
		Translated from ZETF 123 899.		
ACHASOV	02B	PAN 65 153	M.M. Achasov, A.A. Kozhevnikov	
		Translated from YAF 65 158.		
CLOSE	02	PR D65 092003	F.E. Close, A. Donnachie, Yu.S. Kalashnikova	
ADAMS	01B	PL B516 264	G.S. Adams et al.	(BNL E852 Collab.)
ACHASOV	00I	PL B486 29	M.N. Achasov et al.	(Novosibirsk SND Collab.)
ACHASOV	00J	PR D62 117503	N.N. Achasov, A.A. Kozhevnikov	
AULCHENKO	00A	JETP 90 927	V.M. Aulchenko et al.	(Novosibirsk SND Collab.)
		Translated from ZETF 117 1067.		
BELOZEROVA	98	PPN 29 63	T.S. Belozeroval, V.K. Henner	
		Translated from FECAV 29 148.		
ABELE	97H	PL B415 280	A. Abele et al.	(Crystal Barrel Collab.)
BARNES	97	PR D55 4157	T. Barnes et al.	(ORNL, RAL, MCHS)
CLOSE	97C	PR D56 1584	F.E. Close et al.	(RAL, MCHS)
URHEIM	97	NPBPS 55C 359	J. Urheim	(CLEO Collab.)
ACHASOV	96B	PAN 59 1262	N.N. Achasov, G.N. Shestakov	(NOVM)
		Translated from YAF 59 1319.		
MURADOV	94	PAN 57 064	R.K. Muradov	(BAKU)
LANDSBERG	92	SJNP 55 1051	L.G. Landsberg	(SERP)
		Translated from YAF 55 1836.		
BRAU	88	PR D37 2379	J.E. Brau et al.	
AULCHENKO	87B	JETPL 45 145	V.M. Aulchenko et al.	(NOVO)
		Translated from ZETFP 45 118.		
KURDADZE	86	JETPL 43 943	L.M. Kurdadze et al.	(NOVO)
		Translated from ZETFP 43 497.		
BARKOV	85	NP B256 365	L.M. Barkov et al.	(NOVO)
BISELLO	85	LAL 85-15	D. Bisello et al.	(PADO, LALO, CLER+)
ABE	84B	PRL 53 751	K. Abe et al.	
ATKINSON	84C	NP B243 1	M. Atkinson et al.	(BONN, CERN, GLAS+)
CORDIER	82	PL 109B 129	A. Cordier et al.	(LALO)
BISELLO	81	PL 107B 145	D. Bisello et al.	(DM1 Collab.)
KILLIAN	80	PR D21 3005	T.J. Killian et al.	(CORN)
COSME	76	PL 63B 352	G. Cosme et al.	(ORSAY)
BINGHAM	72B	PL 41B 635	H.H. Bingham et al.	(LBL, UCBL, SLAC)
FRENKIEL	72	NP B47 61	P. Frankiel et al.	(CDEF, CERN)
LAYSSAC	71	NC 6A 134	J. Layssac, F.M. Renard	(MONP)

 $\eta(1475)$

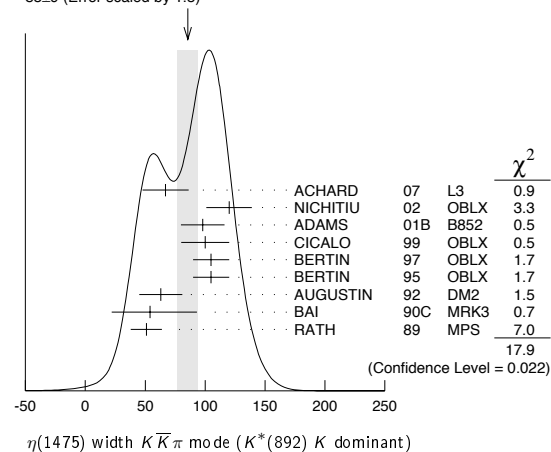
$$J^{PC} = 0^+(0^-+)$$

See also the $\eta(1405)$. $\eta(1475)$ MASS $K\bar{K}\pi$ MODE ($K^*(892)$ K dominant)

VALUE (MeV)	EVTS	DOCUMENT ID	TECN	COMMENT
1476 ± 4 OUR AVERAGE				Error includes scale factor of 1.3. See the ideogram below.
1469 ± 14 ± 13	74	ACHARD	07 L3	183-209 $e^+e^- \rightarrow e^+e^- K_S^0 K^\pm \pi^\mp$
1460 ± 19	3651	NICHITIU	02 OBLX	
1485 ± 8 ± 5	20k	ADAMS	01B B852	18 GeV $\pi^- p \rightarrow K^+ K^- \pi^0 n$
1500 ± 10		CICALO	99 OBLX	0 $\bar{p}p \rightarrow K^\pm K_S^0 \pi^\mp \pi^+ \pi^-$
1464 ± 10		BERTIN	97 OBLX	0 $\bar{p}p \rightarrow K^\pm (K^0) \pi^\mp \pi^+ \pi^-$
1460 ± 10		BERTIN	95 OBLX	0 $\bar{p}p \rightarrow K\bar{K}\pi\pi\pi$
1490 ± 14 + 3 - 8 - 16	1100	BAI	90C MRK3	$J/\psi \rightarrow \gamma K_S^0 K^\pm \pi^\mp$
1475 ± 4		RATH	89 MPS	21.4 $\pi^- p \rightarrow n K_S^0 K_S^0 \pi^0$
• • • We do not use the following data for averages, fits, limits, etc. • • •				
1421 ± 14		AUGUSTIN	92 DM2	$J/\psi \rightarrow \gamma K\bar{K}\pi$

WEIGHTED AVERAGE
1476 ± 4 (Error scaled by 1.3) $\eta(1475)$ WIDTH $K\bar{K}\pi$ MODE ($K^*(892)$ K dominant)

VALUE (MeV)	EVTS	DOCUMENT ID	TECN	COMMENT
85 ± 9 OUR AVERAGE				Error includes scale factor of 1.5. See the ideogram below.
67 ± 18 ± 7	74	ACHARD	07 L3	183-209 $e^+e^- \rightarrow e^+e^- K_S^0 K^\pm \pi^\mp$
120 ± 19	3651	NICHITIU	02 OBLX	
98 ± 18 ± 3	20k	ADAMS	01B B852	18 GeV $\pi^- p \rightarrow K^+ K^- \pi^0 n$
100 ± 20		CICALO	99 OBLX	0 $\bar{p}p \rightarrow K^\pm K_S^0 \pi^\mp \pi^+ \pi^-$
105 ± 15		BERTIN	97 OBLX	0.0 $\bar{p}p \rightarrow K^\pm (K^0) \pi^\mp \pi^+ \pi^-$
105 ± 15		BERTIN	95 OBLX	0 $\bar{p}p \rightarrow K\bar{K}\pi\pi\pi$
63 ± 18		AUGUSTIN	92 DM2	$J/\psi \rightarrow \gamma K\bar{K}\pi$
54 + 37 + 13 - 21 - 24		BAI	90C MRK3	$J/\psi \rightarrow \gamma K_S^0 K^\pm \pi^\mp$
51 ± 13		RATH	89 MPS	21.4 $\pi^- p \rightarrow n K_S^0 K_S^0 \pi^0$

WEIGHTED AVERAGE
85 ± 9 (Error scaled by 1.5) $\eta(1475)$ DECAY MODES

Mode	Fraction (Γ_i/Γ)
Γ_1 $K\bar{K}\pi$	dominant
Γ_2 $K\bar{K}^*(892) + c.c.$	seen
Γ_3 $a_0(980)\pi$	seen
Γ_4 $\gamma\gamma$	seen

 $\eta(1475)$ $\Gamma(i)\Gamma(\gamma\gamma)/\Gamma(\text{total})$

VALUE (keV)	CL%	EVTS	DOCUMENT ID	TECN	COMMENT	$\Gamma_1\Gamma_4/\Gamma$
0.23 ± 0.05 ± 0.05		74	1 ACHARD	07 L3	183-209 $e^+e^- \rightarrow e^+e^- K_S^0 K^\pm \pi^\mp$	
• • • We do not use the following data for averages, fits, limits, etc. • • •						
< 0.089	90	2,3	AHOHE	05 CLE2	10.6 $e^+e^- \rightarrow e^+e^- K_S^0 K^\pm \pi^\mp$	

Meson Particle Listings

$\eta(1475)$, $f_0(1500)$

- ¹ Supersedes ACCIARRI 01G. Compatible with K^*K decay. Using $B(K_S^0 \rightarrow \pi^+\pi^-) = 0.6895$.
- ² Using $\eta(1475)$ mass of 1481 MeV and width of 48 MeV. The upper limit increases to 0.140 keV if the world average value, 87 MeV, of the width is used.
- ³ Assuming three-body phase-space decay to $K_S^0 K^\pm \pi^\mp$.

$\eta(1475)$ BRANCHING RATIOS

$\Gamma(K\bar{K}^*(892) + c.c.)/\Gamma(K\bar{K}\pi)$				Γ_2/Γ_1
VALUE	DOCUMENT ID	TECN	COMMENT	
•••	We do not use the following data for averages, fits, limits, etc. •••			
0.50±0.10	⁴ BAILLON	67	HBC	0.0 $\bar{p}p \rightarrow K\bar{K}\pi\pi$

$\Gamma(K\bar{K}^*(892) + c.c.)/[\Gamma(K\bar{K}^*(892) + c.c.) + \Gamma(a_0(980)\pi)]$				$\Gamma_2/(\Gamma_2+\Gamma_3)$
VALUE	CL%	DOCUMENT ID	TECN	COMMENT
•••	We do not use the following data for averages, fits, limits, etc. •••			
<0.25	90	EDWARDS	82E	CBAL $J/\psi \rightarrow K^+K^-\pi^0\gamma$
⁴ Data could also refer to $\eta(1405)$.				

$\eta(1475)$ REFERENCES

ACHARD 07 JHEP 0703 018	P. Achard et al.	(L3 Collab.)
AHOHE 05 PR D71 072001	R. Ahohe et al.	(CLEO Collab.)
NICHTIU 02 PL B545 261	F. Nichtiu et al.	(OBELIX Collab.)
ACCIARRI 01G PL B501 1	M. Acciari et al.	(L3 Collab.)
ADAMS 01B PL B516 264	G.S. Adams et al.	(BNL E852 Collab.)
CICALO 99 PL B462 453	C. Cicalo et al.	(OBELIX Collab.)
BERTIN 97 PL B400 226	A. Bertin et al.	(OBELIX Collab.)
BERTIN 95 PL B361 187	A. Bertin et al.	(OBELIX Collab.)
AUGUSTIN 92 PR D46 1951	J.E. Augustin, G. Cosme	(DM2 Collab.)
BAI 90C PRL 65 2507	Z. Bai et al.	(Mark III Collab.)
RATH 89 PR D40 693	M.G. Rath et al.	(NDAM, BRAN, BNL, CUNY+)
EDWARDS 82E PRL 49 259	C. Edwards et al.	(CIT, HARV, PRIN+)
BAILLON 67 NC 50A 393	P.H. Baillon et al.	(CERN, CDEF, IRAD)

OTHER RELATED PAPERS

ABLIKIM 08E PR D77 032005	M. Ablikim et al.	(BES Collab.)
MASONI 06 JPG 32 R293	A. Masoni, C. Cicato, G.L. Usai	(INFN, CAGL)

$f_0(1500)$

$$I^G(J^{PC}) = 0^+(0^{++})$$

See also the mini-reviews on scalar mesons under $f_0(600)$ (see the index for the page number) and on non- $q\bar{q}$ candidates in PDG 06, Journal of Physics, G **33** 1 (2006).

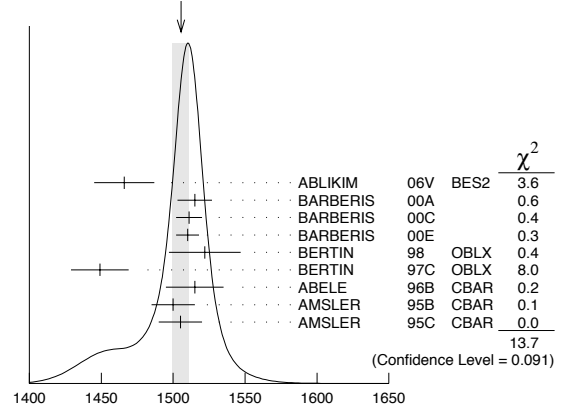
$f_0(1500)$ MASS

VALUE (MeV)	EVTS	DOCUMENT ID	TECN	COMMENT
1505 ± 6 OUR AVERAGE		Error includes scale factor of 1.3. See the ideogram below.		
1466 ± 6 ± 20		ABLIKIM 06V BES2		$e^+e^- \rightarrow J/\psi \rightarrow \gamma\pi^+\pi^-$
1515 ± 12		¹ BARBERIS 00A		$450 pp \rightarrow p_f\eta\eta p_S$
1511 ± 9		^{1,2} BARBERIS 00C		$450 pp \rightarrow p_f 4\pi p_S$
1510 ± 8		¹ BARBERIS 00E		$450 pp \rightarrow p_f\eta\eta p_S$
1522 ± 25		BERTIN 98	OBLX	$0.05-0.405 \bar{p}p \rightarrow \pi^+\pi^+\pi^-$
1449 ± 20		¹ BERTIN 97C	OBLX	$0.0 \bar{p}p \rightarrow \pi^+\pi^-\pi^0$
1515 ± 20		ABELE 96B	CBAR	$0.0 \bar{p}p \rightarrow \pi^0 K_L^0 K_L^0$
1500 ± 15		³ AMSLER 95B	CBAR	$0.0 \bar{p}p \rightarrow 3\pi^0$
1505 ± 15		⁴ AMSLER 95C	CBAR	$0.0 \bar{p}p \rightarrow \eta\eta\pi^0$
•••	We do not use the following data for averages, fits, limits, etc. •••			
1495 ± 4		AMSLER 06	CBAR	$0.9 \bar{p}p \rightarrow K^+K^-\pi^0$
1539 ± 20	9.9k	AUBERT 06O	BABR	$B^\pm \rightarrow K^\pm\pi^\pm\pi^\mp$
1473 ± 5	80k	^{5,6} UMAN 06	E835	$5.2 \bar{p}p \rightarrow \eta\eta\pi^0$
1478 ± 6		VLADIMIRSK...06	SPEC	$40 \pi^-p \rightarrow K_S^0 K_S^0 n$
1493 ± 7		⁵ BINON 05	GAMS	$33 \pi^-p \rightarrow \eta\eta n$
1524 ± 14	1400	⁷ GARMASH 05	BELL	$B^+ \rightarrow K^+K^+K^-$
1489 ± 8		¹⁵ ANISOVICH 03	RVUE	
1490 ± 30		⁵ ABELE 01	CBAR	$0.0 \bar{p}d \rightarrow \pi^- 4\pi^0 p$
1497 ± 10		⁵ BARBERIS 99	OMEG	$450 pp \rightarrow p_S p_f K^+ K^-$
1502 ± 10		⁵ BARBERIS 99B	OMEG	$450 pp \rightarrow p_S p_f \pi^+ \pi^-$
1502 ± 12 ± 10		⁸ BARBERIS 99D	OMEG	$450 pp \rightarrow K^+ K^-, \pi^+ \pi^-$
1530 ± 45		⁵ BELLAZZINI 99	GAM4	$450 pp \rightarrow p p \pi^0 \pi^0$
1505 ± 18		⁵ FRENCH 99		$300 pp \rightarrow p_f(K^+K^-)p_S$
1447 ± 27		⁹ KAMINSKI 99	RVUE	$\pi\pi \rightarrow \pi\pi, K\bar{K}, \sigma\sigma$
1580 ± 80		⁵ ALDE 98	GAM4	$100 \pi^-p \rightarrow \pi^0 \pi^0 n$
1499 ± 8		¹ ANISOVICH 98B	RVUE	Compilation
~ 1520		REYES 98	SPEC	$800 pp \rightarrow p_S p_f K_S^0 K_S^0$
1510 ± 20		¹ BARBERIS 97B	OMEG	$450 pp \rightarrow p p 2(\pi^+\pi^-)$
~ 1475		FRABETTI 97D	E687	$D_S^\pm \rightarrow \pi^\mp \pi^\pm \pi^\pm$
~ 1505		ABELE 96	CBAR	$0.0 \bar{p}p \rightarrow 5\pi^0$
1500 ± 8		¹ ABELE 96C	RVUE	Compilation
1460 ± 20	120	⁵ AMELIN 96B	VES	$37 \pi^-A \rightarrow \eta\eta\pi^-A$
1500 ± 8		BUGG 96	RVUE	

1500 ± 10	¹⁰ AMSLER 95D	CBAR	$0.0 \bar{p}p \rightarrow \pi^0 \pi^0 \pi^0, \pi^0 \eta\eta, \pi^0 \pi^0 \eta$	
1445 ± 5	¹¹ ANTINORI 95	OMEG	$300,450 pp \rightarrow p p 2(\pi^+\pi^-)$	
1497 ± 30	⁵ ANTINORI 95	OMEG	$300,450 pp \rightarrow p p \pi^+\pi^-$	
~ 1505	BUGG 95	MRK3	$J/\psi \rightarrow \gamma\pi^+\pi^-\pi^+\pi^-$	
1446 ± 5	⁵ ABATZIS 94	OMEG	$450 pp \rightarrow p p 2(\pi^+\pi^-)$	
1545 ± 25	⁵ AMSLER 94E	CBAR	$0.0 \bar{p}p \rightarrow \pi^0 \eta\eta'$	
1520 ± 25	^{1,12} ANISOVICH 94	CBAR	$0.0 \bar{p}p \rightarrow 3\pi^0, \pi^0 \eta\eta$	
1505 ± 20	^{1,13} BUGG 94	RVUE	$\bar{p}p \rightarrow 3\pi^0, \eta\eta\pi^0, \eta\pi^0 \pi^0$	
1560 ± 25	⁵ AMSLER 92	CBAR	$0.0 \bar{p}p \rightarrow \pi^0 \eta\eta$	
1550 ± 45 ± 30	⁵ BELADIDZE 92C	VES	$36 \pi^-Be \rightarrow \pi^- \eta' \eta Be$	
1449 ± 4	⁵ ARMSTRONG 89E	OMEG	$300 pp \rightarrow p p 2(\pi^+\pi^-)$	
1610 ± 20	⁵ ALDE 88	GAM4	$300 \pi^-N \rightarrow \pi^- N 2\eta$	
~ 1525	ASTON 88D	LASS	$11 K^-p \rightarrow K_S^0 K_S^0 \Lambda$	
1570 ± 20	600	⁵ ALDE 87	GAM4	$100 \pi^-p \rightarrow 4\pi^0 n$
1575 ± 45	¹⁴ ALDE 86D	GAM4	$100 \pi^-p \rightarrow 2\eta n$	
1568 ± 33	⁵ BINON 84C	GAM2	$38 \pi^-p \rightarrow \eta\eta' n$	
1592 ± 25	⁵ BINON 83	GAM2	$38 \pi^-p \rightarrow 2\eta n$	
1525 ± 5	⁵ GRAY 83	DBC	$0.0 \bar{p}N \rightarrow 3\pi$	

- ¹ T-matrix pole.
- ² Average between $\pi^+\pi^-2\pi^0$ and $2(\pi^+\pi^-)$.
- ³ T-matrix pole, supersedes ANISOVICH 94.
- ⁴ T-matrix pole, supersedes ANISOVICH 94 and AMSLER 92.
- ⁵ Breit-Wigner mass.
- ⁶ Statistical error only.
- ⁷ Breit-Wigner, solution 1, PWA ambiguous.
- ⁸ Supersedes BARBERIS 99 and BARBERIS 99B.
- ⁹ T-matrix pole on sheet $--+$.
- ¹⁰ T-matrix pole. Coupled-channel analysis of AMSLER 95B, AMSLER 95C, and AMSLER 94D.
- ¹¹ Supersedes ABATZIS 94, ARMSTRONG 89E. Breit-Wigner mass.
- ¹² From a simultaneous analysis of the annihilations $\bar{p}p \rightarrow 3\pi^0, \pi^0 \eta\eta$.
- ¹³ Reanalysis of ANISOVICH 94 data.
- ¹⁴ From central value and spread of two solutions. Breit-Wigner mass.

WEIGHTED AVERAGE
1505±6 (Error scaled by 1.3)



- ¹⁵ K-matrix pole from combined analysis of $\pi^-p \rightarrow \pi^0 \pi^0 n$, $\pi^-p \rightarrow K\bar{K}n$, $\pi^+\pi^- \rightarrow \pi^+\pi^-$, $\bar{p}p \rightarrow \pi^0 \pi^0 \pi^0, \pi^0 \eta\eta, \pi^0 \pi^0 \eta, \pi^+\pi^-\pi^0, K^+K^-\pi^0, K_S^0 K_S^0 \pi^0, K^+K_S^0 \pi^-$ at rest, $\bar{p}n \rightarrow \pi^-\pi^-\pi^+$, $K_S^0 K^-\pi^0, K_S^0 K_S^0 \pi^-$ at rest.

$f_0(1500)$ WIDTH

VALUE (MeV)	EVTS	DOCUMENT ID	TECN	COMMENT
109 ± 7 OUR AVERAGE				
108 ± ¹⁴ / ₁₁ ± 25		ABLIKIM 06V	BES2	$e^+e^- \rightarrow J/\psi \rightarrow \gamma\pi^+\pi^-$
110 ± 24		¹⁶ BARBERIS 00A		$450 pp \rightarrow p_f\eta\eta p_S$
102 ± 18		^{16,17} BARBERIS 00C		$450 pp \rightarrow p_f 4\pi p_S$
110 ± 16		¹⁶ BARBERIS 00E		$450 pp \rightarrow p_f\eta\eta p_S$
108 ± 33		BERTIN 98	OBLX	$0.05-0.405 \bar{p}p \rightarrow \pi^+\pi^+\pi^-$
114 ± 30		¹⁶ BERTIN 97C	OBLX	$0.0 \bar{p}p \rightarrow \pi^+\pi^-\pi^0$
105 ± 15		ABELE 96B	CBAR	$0.0 \bar{p}p \rightarrow \pi^0 K_L^0 K_L^0$
120 ± 25		¹⁸ AMSLER 95B	CBAR	$0.0 \bar{p}p \rightarrow 3\pi^0$
120 ± 30		¹⁹ AMSLER 95C	CBAR	$0.0 \bar{p}p \rightarrow \eta\eta\pi^0$
•••	We do not use the following data for averages, fits, limits, etc. •••			
121 ± 8		AMSLER 06	CBAR	$0.9 \bar{p}p \rightarrow K^+K^-\pi^0$
257 ± 33	9.9k	AUBERT 06O	BABR	$B^\pm \rightarrow K^\pm\pi^\pm\pi^\mp$
108 ± 9	80k, 20,21	UMAN 06	E835	$5.2 \bar{p}p \rightarrow \eta\eta\pi^0$

119± 10		VLADIMIRSK...06	SPEC	40	$\pi^- p \rightarrow K_S^0 K_S^0 n$
90± 15		20 BINON	05	GAMS	33 $\pi^- p \rightarrow \eta \eta n$
136± 23	1400	22 GARMASH	05	BELL	$B^+ \rightarrow K^+ K^+ K^-$
102± 10		30 ANISOVICH	03	RVUE	
140± 40		20 ABELE	01	CBAR	$0.0 \bar{p} d \rightarrow \pi^- 4\pi^0 p$
104± 25		20 BARBERIS	99	OMEG	$450 pp \rightarrow p_S p_f K^+ K^-$
131± 15		20 BARBERIS	99B	OMEG	$450 pp \rightarrow p_S p_f \pi^+ \pi^-$
98± 18± 16		23 BARBERIS	99D	OMEG	$450 pp \rightarrow K^+ K^-, \pi^+ \pi^-$
160± 50		20 BELLAZZINI	99	GAM4	$450 pp \rightarrow p p \pi^0 \pi^0$
100± 33		20 FRENCH	99		$300 pp \rightarrow p_f (K^+ K^-) p_S$
108± 46		24 KAMINSKI	99	RVUE	$\pi \pi \rightarrow \pi \pi, K\bar{K}, \sigma \sigma$
280± 100		20 ALDE	98	GAM4	$100 \pi^- p \rightarrow \pi^0 \pi^0 n$
130± 20		16 ANISOVICH	98B	RVUE	Compilation
120± 35		16 BARBERIS	97B	OMEG	$450 pp \rightarrow p p 2(\pi^+ \pi^-)$
~ 100		FRABETTI	97D	E687	$D_S^\pm \rightarrow \pi^\mp \pi^\pm \pi^\pm$
~ 169		ABELE	96	CBAR	$0.0 \bar{p} p \rightarrow 5\pi^0$
100± 30	120	20 AMELIN	96B	VES	$37 \pi^- A \rightarrow \eta \eta \pi^- A$
132± 15		BUGG	96	RVUE	
154± 30		25 AMSLER	95D	CBAR	$0.0 \bar{p} p \rightarrow \pi^0 \pi^0 \pi^0, \pi^0 \eta \eta,$ $\pi^0 \pi^0 \eta$
65± 10		26 ANTINORI	95	OMEG	$300,450 pp \rightarrow p p 2(\pi^+ \pi^-)$
199± 30		20 ANTINORI	95	OMEG	$300,450 pp \rightarrow p p \pi^+ \pi^-$
56± 12		20 ABATZIS	94	OMEG	$450 pp \rightarrow p p 2(\pi^+ \pi^-)$
100± 40		20 AMSLER	94E	CBAR	$0.0 \bar{p} p \rightarrow \pi^0 \eta \eta'$
148± 20	16,27	ANISOVICH	94	CBAR	$0.0 \bar{p} p \rightarrow 3\pi^0, \pi^0 \eta \eta$
25					
150± 20	16,28	BUGG	94	RVUE	$\bar{p} p \rightarrow 3\pi^0, \eta \eta \pi^0, \eta \pi^0 \pi^0$
245± 50		20 AMSLER	92	CBAR	$0.0 \bar{p} p \rightarrow \pi^0 \eta \eta$
153± 67± 50		20 BELADIDZE	92C	VES	$36 \pi^- \text{Be} \rightarrow \pi^- \eta' \eta \text{Be}$
78± 18		20 ARMSTRONG	89E	OMEG	$300 pp \rightarrow p p 2(\pi^+ \pi^-)$
170± 40		20 ALDE	88	GAM4	$300 \pi^- N \rightarrow \pi^- N 2\eta$
150± 20	600	20 ALDE	87	GAM4	$100 \pi^- p \rightarrow 4\pi^0 n$
265± 65		29 ALDE	86D	GAM4	$100 \pi^- p \rightarrow 2\eta n$
260± 60		20 BINON	84C	GAM2	$38 \pi^- p \rightarrow \eta \eta' n$
210± 40		20 BINON	83	GAM2	$38 \pi^- p \rightarrow 2\eta n$
101± 13		20 GRAY	83	DBC	$0.0 \bar{p} N \rightarrow 3\pi$
16					T-matrix pole.
17					Average between $\pi^+ \pi^- 2\pi^0$ and $2(\pi^+ \pi^-)$.
18					T-matrix pole, supersedes ANISOVICH 94.
19					T-matrix pole, supersedes ANISOVICH 94 and AMSLER 92.
20					Breit-Wigner width.
21					Statistical error only.
22					Breit-Wigner, solution 1, PWA ambiguous.
23					Supersedes BARBERIS 99 and BARBERIS 99B.
24					T-matrix pole on sheet -- +.
25					T-matrix pole. Coupled-channel analysis of AMSLER 95B, AMSLER 95C, and AMSLER 94b.
26					Supersedes ABATZIS 94, ARMSTRONG 89E. Breit-Wigner mass.
27					From a simultaneous analysis of the annihilations $\bar{p} p \rightarrow 3\pi^0, \pi^0 \eta \eta$.
28					Reanalysis of ANISOVICH 94 data.
29					From central value and spread of two solutions. Breit-Wigner mass.
30					K-matrix pole from combined analysis of $\pi^- p \rightarrow \pi^0 \pi^0 n, \pi^- p \rightarrow K\bar{K} n, \pi^+ \pi^- \rightarrow \pi^+ \pi^-, \bar{p} p \rightarrow \pi^0 \pi^0 \pi^0, \pi^0 \eta \eta, \pi^0 \pi^0 \eta, \pi^+ \pi^- \pi^0, K^+ K^- \pi^0, K_S^0 K_S^0 \pi^0, K^+ K_S^0 \pi^-$ at rest, $\bar{p} n \rightarrow \pi^- \pi^- \pi^+, K_S^0 K^- \pi^0, K_S^0 K_S^0 \pi^-$ at rest.

 $f_0(1500)$ DECAY MODES

Mode	Fraction (Γ_i/Γ)	Scale factor
Γ_1 $\pi \pi$	(34.9±2.3) %	1.2
Γ_2 $\pi^+ \pi^-$	seen	
Γ_3 $2\pi^0$	seen	
Γ_4 4π	(49.5±3.3) %	1.2
Γ_5 $4\pi^0$	seen	
Γ_6 $2\pi^+ 2\pi^-$	seen	
Γ_7 $2(\pi\pi)S\text{-wave}$		
Γ_8 $\rho\rho$		
Γ_9 $\pi(1300)\pi$		
Γ_{10} $a_1(1260)\pi$		
Γ_{11} $\eta\eta$	(5.1±0.9) %	1.4
Γ_{12} $\eta\eta'(958)$	(1.9±0.8) %	1.7
Γ_{13} $K\bar{K}$	(8.6±1.0) %	1.1
Γ_{14} $\gamma\gamma$	not seen	

CONSTRAINED FIT INFORMATION

An overall fit to 6 branching ratios uses 10 measurements and one constraint to determine 5 parameters. The overall fit has a $\chi^2 = 11.4$ for 6 degrees of freedom.

The following *off-diagonal* array elements are the correlation coefficients $\langle \delta x_i \delta x_j \rangle / (\delta x_i \delta x_j)$, in percent, from the fit to the branching fractions, $x_i \equiv \Gamma_i / \Gamma_{\text{total}}$. The fit constrains the x_i whose labels appear in this array to sum to one.

x_4	-83			
x_{11}	11	-52		
x_{12}	-5	-31	29	
x_{13}	39	-67	33	6
	x_1	x_4	x_{11}	x_{12}

 $f_0(1500)$ $\Gamma(i)\Gamma(\gamma\gamma)/\Gamma(\text{total})$

$\Gamma(\pi\pi) \times \Gamma(\gamma\gamma)/\Gamma_{\text{total}}$	CL%	DOCUMENT ID	TECN	COMMENT	Γ_{14}/Γ
VALUE (keV)					
• • • We do not use the following data for averages, fits, limits, etc. • • •					
not seen		ACCIARRI	01H L3	$\gamma\gamma \rightarrow K_S^0 K_S^0, E_{\text{cm}}^{\text{ex}} = 91, 183-209 \text{ GeV}$	
<0.46	95	BARATE	00E ALEP	$\gamma\gamma \rightarrow \pi^+ \pi^-$	

 $f_0(1500)$ BRANCHING RATIOS

$\Gamma(\pi\pi)/\Gamma_{\text{total}}$	DOCUMENT ID	TECN	Γ_1/Γ	
VALUE				
• • • We do not use the following data for averages, fits, limits, etc. • • •				
0.454±0.104	BUGG	96 RVUE		
$\Gamma(\pi^+ \pi^-)/\Gamma_{\text{total}}$	DOCUMENT ID	TECN	COMMENT	Γ_2/Γ
VALUE				
seen	BERTIN	98 OBLX	0.05-0.405 $\bar{p} p \rightarrow \pi^+ \pi^+ \pi^-$	
• • • We do not use the following data for averages, fits, limits, etc. • • •				
possibly seen	FRABETTI	97D E687	$D_S^\pm \rightarrow \pi^\mp \pi^\pm \pi^\pm$	

$\Gamma(4\pi)/\Gamma(\pi\pi)$	DOCUMENT ID	TECN	COMMENT	Γ_4/Γ_1
VALUE				
1.42±0.18 OUR FIT			Error includes scale factor of 1.2.	
1.42±0.18 OUR AVERAGE			Error includes scale factor of 1.2.	
1.37±0.16	BARBERIS	00D	450 $pp \rightarrow p_f 4\pi p_S$	
2.1 ± 0.6	31 AMSLER	98 RVUE		
• • • We do not use the following data for averages, fits, limits, etc. • • •				
2.1 ± 0.2	32 ANISOVICH	02D SPEC	Combined fit	
3.4 ± 0.8	31 ABELE	96 CBAR	$0.0 \bar{p} p \rightarrow 5\pi^0$	

$\Gamma(2(\pi\pi)S\text{-wave})/\Gamma(\pi\pi)$	DOCUMENT ID	TECN	COMMENT	Γ_7/Γ_1
VALUE				
• • • We do not use the following data for averages, fits, limits, etc. • • •				
0.42±0.26	33 ABELE	01 CBAR	$0.0 \bar{p} d \rightarrow \pi^- 4\pi^0 p$	

$\Gamma(2(\pi\pi)S\text{-wave})/\Gamma(4\pi)$	DOCUMENT ID	TECN	COMMENT	Γ_7/Γ_4
VALUE				
• • • We do not use the following data for averages, fits, limits, etc. • • •				
0.26±0.07	ABELE	01B CBAR	$0.0 \bar{p} d \rightarrow 5\pi p$	

$\Gamma(\rho\rho)/\Gamma(4\pi)$	DOCUMENT ID	TECN	COMMENT	Γ_8/Γ_4
VALUE				
• • • We do not use the following data for averages, fits, limits, etc. • • •				
0.13±0.08	ABELE	01B CBAR	$0.0 \bar{p} d \rightarrow 5\pi p$	

$\Gamma(\rho\rho)/\Gamma(2(\pi\pi)S\text{-wave})$	DOCUMENT ID	COMMENT	Γ_8/Γ_7
VALUE			
• • • We do not use the following data for averages, fits, limits, etc. • • •			
3.3±0.5	BARBERIS	00C 450 $pp \rightarrow p_f \pi^+ \pi^- 2\pi^0 p_S$	
2.6±0.4	BARBERIS	00C 450 $pp \rightarrow p_f 2(\pi^+ \pi^-) p_S$	

$\Gamma(\pi(1300)\pi)/\Gamma(4\pi)$	DOCUMENT ID	TECN	COMMENT	Γ_9/Γ_4
VALUE				
• • • We do not use the following data for averages, fits, limits, etc. • • •				
0.50±0.25	ABELE	01B CBAR	$0.0 \bar{p} d \rightarrow 5\pi p$	

$\Gamma(a_1(1260)\pi)/\Gamma(4\pi)$	DOCUMENT ID	TECN	COMMENT	Γ_{10}/Γ_4
VALUE				
• • • We do not use the following data for averages, fits, limits, etc. • • •				
0.12±0.05	ABELE	01B CBAR	$0.0 \bar{p} d \rightarrow 5\pi p$	

Meson Particle Listings

 $f_0(1500)$

$\Gamma(\eta\eta)/\Gamma_{\text{total}}$	DOCUMENT ID	TECN	COMMENT	Γ_{11}/Γ
--	-------------	------	---------	----------------------

• • • We do not use the following data for averages, fits, limits, etc. • • •

large	ALDE	88	GAM4	300 $\pi^- N \rightarrow \eta\eta\pi^- N$
large	BINON	83	GAM2	38 $\pi^- p \rightarrow 2\eta n$

$\Gamma(\eta\eta)/\Gamma(\pi\pi)$	DOCUMENT ID	TECN	COMMENT	Γ_{11}/Γ_1
-----------------------------------	-------------	------	---------	------------------------

0.145 ± 0.027 OUR FIT Error includes scale factor of 1.5.

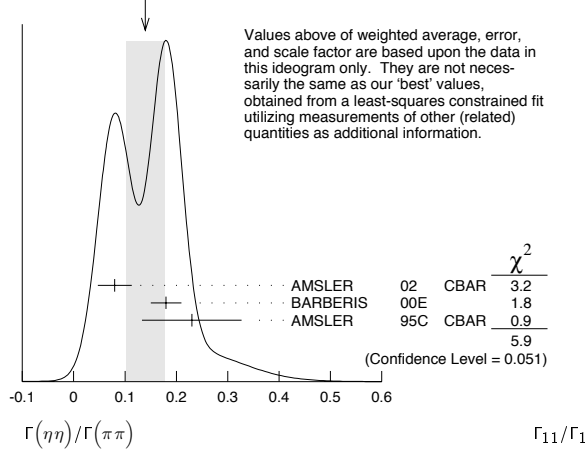
0.14 ± 0.04 OUR AVERAGE Error includes scale factor of 1.7. See the ideogram below.

0.080 ± 0.033	A MSLE	02	CBAR	0.9 $\bar{p}p \rightarrow \pi^0 \eta\eta, \pi^0 \pi^0 \pi^0$
0.18 ± 0.03	BARBERIS	00E		450 $pp \rightarrow \rho_f \eta\eta \rho_s$
0.230 ± 0.097	34 A MSLE	95C	CBAR	0.0 $\bar{p}p \rightarrow \eta\eta\pi^0$

• • • We do not use the following data for averages, fits, limits, etc. • • •

0.11 ± 0.03	32 A NISOVICH	02D	SPEC	Combined fit
0.078 ± 0.013	35 ABELE	96C	RVUE	Compilation
0.157 ± 0.060	36 A MSLE	95D	CBAR	0.0 $\bar{p}p \rightarrow \pi^0 \pi^0 \pi^0, \pi^0 \eta\eta, \pi^0 \pi^0 \eta$

WEIGHTED AVERAGE
0.14 ± 0.04 (Error scaled by 1.7)



$\Gamma(4\pi^0)/\Gamma(\eta\eta)$	DOCUMENT ID	TECN	COMMENT	Γ_5/Γ_{11}
-----------------------------------	-------------	------	---------	------------------------

• • • We do not use the following data for averages, fits, limits, etc. • • •

0.8 ± 0.3	ALDE	87	GAM4	100 $\pi^- p \rightarrow 4\pi^0 n$
-----------	------	----	------	------------------------------------

$\Gamma(\eta\eta'(958))/\Gamma(\pi\pi)$	DOCUMENT ID	TECN	COMMENT	Γ_{12}/Γ_1
---	-------------	------	---------	------------------------

0.055 ± 0.024 OUR FIT Error includes scale factor of 1.8.

0.095 ± 0.026

0.05 ± 0.003	32 ANISOVICH	02D	SPEC	Combined fit
--------------	--------------	-----	------	--------------

• • • We do not use the following data for averages, fits, limits, etc. • • •

$\Gamma(\eta\eta'(958))/\Gamma(\eta\eta)$	DOCUMENT ID	TECN	COMMENT	Γ_{12}/Γ_{11}
---	-------------	------	---------	---------------------------

0.38 ± 0.16 OUR FIT Error includes scale factor of 1.9.

0.29 ± 0.10

0.05 ± 0.03	37 A MSLE	95C	CBAR	0.0 $\bar{p}p \rightarrow \eta\eta\pi^0$
-------------	-----------	-----	------	--

• • • We do not use the following data for averages, fits, limits, etc. • • •

0.84 ± 0.23	32 ANISOVICH	02D	SPEC	Combined fit
2.7 ± 0.8	ABELE	96C	RVUE	Compilation
	BINON	84C	GAM2	38 $\pi^- p \rightarrow \eta\eta' n$

$\Gamma(K\bar{K})/\Gamma_{\text{total}}$	DOCUMENT ID	TECN	COMMENT	Γ_{13}/Γ
--	-------------	------	---------	----------------------

• • • We do not use the following data for averages, fits, limits, etc. • • •

0.044 ± 0.021	BUGG	96	RVUE	
---------------	------	----	------	--

$\Gamma(K\bar{K})/\Gamma(\pi\pi)$	DOCUMENT ID	TECN	COMMENT	Γ_{13}/Γ_1
-----------------------------------	-------------	------	---------	------------------------

0.246 ± 0.026 OUR FIT

0.241 ± 0.028 OUR AVERAGE

0.25 ± 0.03	38 BARGIOTTI	03	OBLX	$\bar{p}p$
0.19 ± 0.07	39 ABELE	98	CBAR	0.0 $\bar{p}p \rightarrow K_L^0 K_{\pm}^{\pm} \pi^{\mp}$

• • • We do not use the following data for averages, fits, limits, etc. • • •

0.16 ± 0.05	32 ANISOVICH	02D	SPEC	Combined fit
0.33 ± 0.03 ± 0.07	BARBERIS	99D	OMEG	450 $pp \rightarrow K^+ K^-, \pi^+ \pi^-$
0.20 ± 0.08	40 ABELE	96B	CBAR	0.0 $\bar{p}p \rightarrow \pi^0 K_L^0 K_L^0$

$\Gamma(K\bar{K})/\Gamma(\eta\eta)$	CL%	DOCUMENT ID	TECN	COMMENT	Γ_{13}/Γ_{11}
-------------------------------------	-----	-------------	------	---------	---------------------------

1.69 ± 0.33 OUR FIT Error includes scale factor of 1.4.

1.85 ± 0.41

1.5 ± 0.6	32 ANISOVICH	02D	SPEC	Combined fit
<0.4	41 PROKOSHKIN	91	GAM4	300 $\pi^- p \rightarrow \pi^- \rho\eta\eta$
<0.6	42 BINON	83	GAM2	38 $\pi^- p \rightarrow 2\eta n$

• • • We do not use the following data for averages, fits, limits, etc. • • •

31 Excluding $\rho\rho$ contribution to 4π .

32 From a combined K-matrix analysis of Crystal Barrel (0. $\rho\bar{p} \rightarrow \pi^0 \pi^0 \pi^0, \pi^0 \eta\eta, \pi^0 \pi^0 \eta$), GAMS ($\pi p \rightarrow \pi^0 \pi^0 n, \eta\eta n, \eta\eta' n$), and BNL ($\pi p \rightarrow K\bar{K} n$) data.

33 From the combined data of ABELE 96 and ABELE 96c.

34 Using A MSLE 95B ($3\pi^0$).

35 2 π width determined to be 60 ± 12 MeV.

36 Coupled-channel analysis of AMSLER 95B, AMSLER 95C, and AMSLER 94D.

37 Using A MSLE 94E ($\eta\eta' \pi^0$).

38 Coupled channel analysis of $\pi^+ \pi^- \pi^0, K^+ K^- \pi^0$, and $K_S^{\pm} K_S^{\mp} \pi^{\mp}$.

39 Using $\pi^0 \pi^0$ from AMSLER 95B.

40 Using A MSLE 95B ($3\pi^0$), AMSLER 94C ($2\pi^0 \eta$) and SU(3).

41 Combining results of GAM4 with those of WA76 on $K\bar{K}$ central production.

42 Using ETKIN 82B and COHEN 80.

 $f_0(1500)$ REFERENCES

ABLIKIM	06V	PL B642 441	M. Ablikim <i>et al.</i>	(BES Collab.)
AMSLER	06	PL B639 165	C. Amshler <i>et al.</i>	(CBAR Collab.)
AUBERT	06O	PR D74 032003	B. Aubert <i>et al.</i>	(BABAR Collab.)
PDG	06	JPG 33 1	W.-M. Yao <i>et al.</i>	(PDG Collab.)
UMAN	06	PR D73 052009	I. Uman <i>et al.</i>	(FNAL E835)
VLADIMIRSK...	06	PAN 69 493	V.V. Vladimirov <i>et al.</i>	(ITEP, Moscow)
BINON	05	PAN 68 960	F. Binon <i>et al.</i>	
GARMASH	05	PR D71 092003	A. Garmash <i>et al.</i>	(BELLE Collab.)
ANISOVICH	03	EPJ A16 229	V.V. Anisovich <i>et al.</i>	
BARGIOTTI	03	EPJ C26 371	M. Bargiotti <i>et al.</i>	(OBELIX Collab.)
AMSLER	02	EPJ C23 29	C. Amshler <i>et al.</i>	
ANISOVICH	02D	PAN 65 1545	V.V. Anisovich <i>et al.</i>	
ABELE	01	EPJ C19 667	A. Abele <i>et al.</i>	(Crystal Barrel Collab.)
ABELE	01B	EPJ C21 261	A. Abele <i>et al.</i>	(Crystal Barrel Collab.)
ACCIARRI	01H	PL B501 173	M. Acciari <i>et al.</i>	(L3 Collab.)
BARATE	00E	PL B472 189	R. Barate <i>et al.</i>	(ALEPH Collab.)
BARBERIS	00A	PL B471 429	D. Barberis <i>et al.</i>	(WA 102 Collab.)
BARBERIS	00C	PL B471 440	D. Barberis <i>et al.</i>	(WA 102 Collab.)
BARBERIS	00D	PL B474 423	D. Barberis <i>et al.</i>	(WA 102 Collab.)
BARBERIS	00E	PL B479 59	D. Barberis <i>et al.</i>	(WA 102 Collab.)
BARBERIS	99	PL B453 305	D. Barberis <i>et al.</i>	(Omega Expt.)
BARBERIS	99B	PL B453 316	D. Barberis <i>et al.</i>	(Omega Expt.)
BARBERIS	99D	PL B462 462	D. Barberis <i>et al.</i>	(Omega Expt.)
BELLAZZINI	99	PL B467 296	R. Bellazzini <i>et al.</i>	
FRENCH	99	PL B460 213	B. French <i>et al.</i>	(WA76 Collab.)
KAMINSKI	99	EPJ C9 141	R. Kaminski, L. Lesniak, B. Loiseau	(CRAC, PARIN)
ABELE	98	PR D57 3860	A. Abele <i>et al.</i>	(Crystal Barrel Collab.)
ALDE	98	EPJ A3 361	D. Alde <i>et al.</i>	(GAM4 Collab.)
Also		PAN 62 405	D. Alde <i>et al.</i>	(GAMS Collab.)
AMSLER	98	RMP 70 1293	C. Amshler	
ANISOVICH	98B	SPU 41 419	V.V. Anisovich <i>et al.</i>	
BERTIN	98	PR D57 55	A. Bertin <i>et al.</i>	(OBELIX Collab.)
REYES	98	PRL 81 4079	M.A. Reyes <i>et al.</i>	
BARBERIS	97B	PL B413 217	D. Barberis <i>et al.</i>	(WA 102 Collab.)
BERTIN	97C	PL B408 476	A. Bertin <i>et al.</i>	(OBELIX Collab.)
FRABETTI	97D	PL B407 79	P.L. Frabetti <i>et al.</i>	(FNAL E687 Collab.)
ABELE	96	PL B380 453	A. Abele <i>et al.</i>	(Crystal Barrel Collab.)
ABELE	96B	PL B385 425	A. Abele <i>et al.</i>	(Crystal Barrel Collab.)
ABELE	96C	NP A609 562	A. Abele <i>et al.</i>	(Crystal Barrel Collab.)
AMELIN	96B	PAN 59 976	D.V. Amelin <i>et al.</i>	(SERP, TBL)
BUGG	96	NP B471 59	D.V. Bugg, A.V. Sarantsev, B.S. Zou	(LOQM, PNPI)
AMSLER	95B	PL B342 433	C. Amshler <i>et al.</i>	(Crystal Barrel Collab.)
AMSLER	95C	PL B353 571	C. Amshler <i>et al.</i>	(Crystal Barrel Collab.)
AMSLER	95D	PL B355 425	C. Amshler <i>et al.</i>	(Crystal Barrel Collab.)
ANTINORI	95	PL B353 589	F. Antinori <i>et al.</i>	(ATHU, BARI, BIRM+)
BUGG	95	PL B353 378	D.V. Bugg <i>et al.</i>	(LOQM, PNPI, WASH)
ABATZIS	94	PL B324 509	S. Abatzis <i>et al.</i>	(ATHU, BARI, BIRM+)
AMSLER	94C	PL B327 425	C. Amshler <i>et al.</i>	(Crystal Barrel Collab.)
AMSLER	94D	PL B333 277	C. Amshler <i>et al.</i>	(Crystal Barrel Collab.)
AMSLER	94E	PL B340 259	C. Amshler <i>et al.</i>	(Crystal Barrel Collab.)
ANISOVICH	94	PL B323 233	V.V. Anisovich <i>et al.</i>	(Crystal Barrel Collab.)
BUGG	94	PR D50 4412	D.V. Bugg <i>et al.</i>	(LOQM)
AMSLER	92	PL B291 347	C. Amshler <i>et al.</i>	(Crystal Barrel Collab.)
BELADIDZE	92C	SJNP 55 1535	G.M. Beladidze, S.I. Bityukov, G.V. Borisov	(SERP+)
PROKOSHKIN	91	SPD 36 155	Y.D. Prokoshkin	(GAM2, GAM4 Collab.)
ARMSTRONG	89E	PL B228 536	T.A. Armstrong, M. Benayoun	(ATHU, BARI, BIRM+)
ALDE	88	PL B201 160	D.M. Alde <i>et al.</i>	(SERP, BELG, LANL, LAPP+)
ASTON	88D	NP B301 525	D. Aston <i>et al.</i>	(SLAC, NAGO, CINC, INUS)
ALDE	87	PL B198 286	D.M. Alde <i>et al.</i>	(LANL, BRUX, SERP, LAPP)
ALDE	86D	NP B269 485	D.M. Alde <i>et al.</i>	(BELG, LAPP, SERP, CERN+)
BINON	84C	NC 80A 363	F.G. Binon <i>et al.</i>	(BELG, LAPP, SERP+)
BINON	83C	NC 78A 313	F.G. Binon <i>et al.</i>	(BELG, LAPP, SERP+)
Also		SJNP 38 561	F.G. Binon <i>et al.</i>	(BELG, LAPP, SERP+)
GRAY	83	PR D27 307	L. Gray <i>et al.</i>	(SYR)
ETKIN	82B	PR D25 1786	A. Etkin <i>et al.</i>	(BNL, CUNY, TUFTS, YAND)
COHEN	80	PR D22 2595	D. Cohen <i>et al.</i>	(ANL)

See key on page 373

Meson Particle Listings
 $f_0(1500)$, $f_1(1510)$, $f_2'(1525)$

OTHER RELATED PAPERS

NAME	EVTS	DOCUMENT ID	TECN	COMMENT
AUBERT	07AX	PRL 99 161802		B. Aubert <i>et al.</i> (BABAR Collab.)
AUBERT	07BB	PRL 99 221801		B. Aubert <i>et al.</i> (BABAR Collab.)
BUGG	07	EPJ C52 55		D. Bugg
FARIBORZ	06	PR D74 054030		A.H. Fariborz
WANG	06B	PR D74 114010		W. Wang <i>et al.</i>
ABLIKIM	05	PL B607 243		M. Ablikim <i>et al.</i> (BES Collab.)
ABLIKIM	05Q	PR D72 092002		M. Ablikim <i>et al.</i> (BES Collab.)
CLOSE	05	PR D71 094022		F.E. Close, Q. Zhao
GIACOSA	05	PR C71 025202		F. Giacosa <i>et al.</i>
GIACOSA	05A	PL B622 277		F. Giacosa <i>et al.</i>
GIACOSA	05B	PR D72 094006		F. Giacosa <i>et al.</i>
IWASAKI	05A	PR D72 094016		M. Iwasaki, T. Fukutome
RODRIGUEZ	05	PR D71 074008		S. Rodríguez, M. Napsuciale
VJANDE	05	PR D72 034025		J. Vijande, A. Valarce, F. Fernandez
ZHAO	05	PR D72 074001		Q. Zhao
ZHAO	05A	PL B631 22		Q. Zhao, B.-S. Zou, Z.-B. Ma
LINK	04	PL B585 200		J.M. Link <i>et al.</i> (FNAL FOCUS Collab.)
ANSOVICH	03B	PAN 66 741		V.V. Anisovich, V.A. Nikonov, A.V. Sarantsev
DEWITT	03	Translated from YAF 66 772		M.A. DeWitt, H.M. Choi, C.R. Ji
AMSLER	02B	PR D68 054026		C. Amstler
GARMASH	02	PR D65 092005		A. Garmash <i>et al.</i> (BELLE Collab.)
JIN	02	PR D66 057505		H. Jin, X. Zhang
KLEEFELD	02	PR D66 034007		F. Kleefeld <i>et al.</i>
RUPP	02	PR D65 078501		G. Rupp, E. vanBeveren, M.D. Scadron
SHAKIN	02	PR D65 078502		C.M. Shakin, H. Wang
TESHIMA	02	JPG 28 1391		T. Teshima, I. Kitamura, N. Morisita
VOLKOV	02	PAN 65 1657		M.K. Volkov, V.L. Yudichev
LI	01B	Translated from YAF 65 1701		D.-M. Li, H. Yu, Q.-X. Shen
SUROVITSEV	01	PR D63 054024		Y.S. Surovtsev, D. Krupa, M. Nagy
BAI	00A	PL B472 207		J.Z. Bai <i>et al.</i> (BES Collab.)
ANSOVICH	99H	PL B467 289		A.V. Anisovich, V.V. Anisovich
AMSLER	98	RMP 70 1293		C. Amstler
STROHMEIER	98	PL B438 21		M. Strohmeier <i>et al.</i>
ANSOVICH	97	PL B395 123		A.V. Anisovich, A.V. Sarantsev (PNPI)
KAMINSKI	97B	PL B413 130		R. Kaminski, L. Lesniak, B. Loiseau (CRAC, IPN)
PROKOSHKIN	97	SPD 42 117		Y.D. Prokoshkin <i>et al.</i> (SERP)
AMSLER	96	PR D53 295		C. Amstler, F.E. Close (ZURI, RAL)
GASPERO	95	NP A588 861		M. Gaspero (ROMA)
SLAUGHTER	88	MPL A3 1361		M.D. Slaughter (LANL)
BRIDGES	86B	PRL 56 215		D.L. Bridges <i>et al.</i> (SYRA, CASE)

 $f_1(1510)$

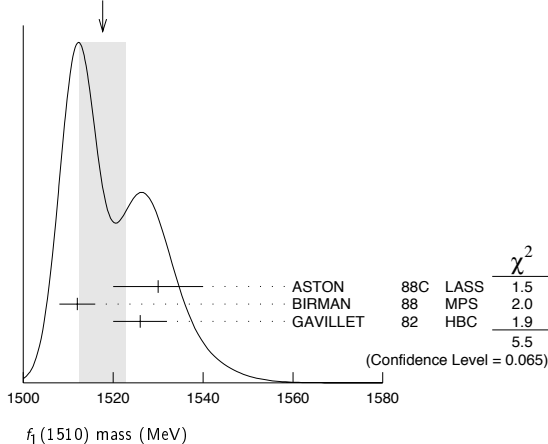
$$J^{PC} = 0^{++}$$

OMITTED FROM SUMMARY TABLE

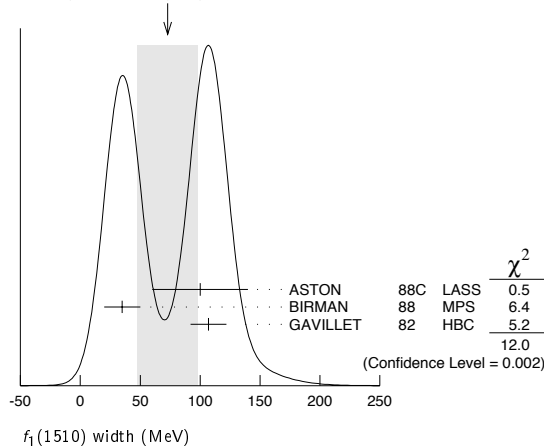
See the minireview under $\eta(1405)$. $f_1(1510)$ MASS

VALUE (MeV)	EVTS	DOCUMENT ID	TECN	COMMENT
1518 ± 5 OUR AVERAGE		Error includes scale factor of 1.7. See the ideogram below.		
1530 ± 10		ASTON	88c LASS	11 $K^- p \rightarrow K_S^0 K^\pm \pi^\mp \Lambda$
1512 ± 4	600	¹ BIRMAN	88 MPS	8 $\pi^- p \rightarrow K^+ \bar{K}^0 \pi^- n$
1526 ± 6	271	GAVILLET	82 HBC	4.2 $K^- p \rightarrow \Lambda K K \pi$
~ 1525		² BAUER	93B	$\gamma \gamma^* \rightarrow \pi^+ \pi^- \pi^0 \pi^0$

• • • We do not use the following data for averages, fits, limits, etc. • • •

¹ From partial wave analysis of $K^+ \bar{K}^0 \pi^-$ state.² Not seen by AIHARA 88c in the $K_S^0 K^\pm \pi^\mp$ final state.WEIGHTED AVERAGE
1518 ± 5 (Error scaled by 1.7) $f_1(1510)$ WIDTH

VALUE (MeV)	EVTS	DOCUMENT ID	TECN	COMMENT
73 ± 25 OUR AVERAGE		Error includes scale factor of 2.5. See the ideogram below.		
100 ± 40		ASTON	88c LASS	11 $K^- p \rightarrow K_S^0 K^\pm \pi^\mp \Lambda$
35 ± 15	600	³ BIRMAN	88 MPS	8 $\pi^- p \rightarrow K^+ \bar{K}^0 \pi^- n$
107 ± 15	271	GAVILLET	82 HBC	4.2 $K^- p \rightarrow \Lambda K K \pi$

³ From partial wave analysis of $K^+ \bar{K}^0 \pi^-$ state.WEIGHTED AVERAGE
73 ± 25 (Error scaled by 2.5) $f_1(1510)$ DECAY MODES

Mode	Fraction (Γ_i/Γ)
Γ_1 $K \bar{K}^*(892) + c.c.$	seen

 $f_1(1510)$ REFERENCES

BAUER	93B	PR D48 3976	D.A. Bauer <i>et al.</i> (SLAC)
AIHARA	88C	PR D38 1	H. Aihara <i>et al.</i> (TPC-2 γ Collab.)
ASTON	88C	PL B201 573	D. Aston <i>et al.</i> (SLAC, NAG, CINC, INUS) JP
BIRMAN	88	PRL 61 1557	A. Birman <i>et al.</i> (BNL, FSU, IND, MASD) JP
GAVILLET	82	ZPHY C16 119	P. Gavillet <i>et al.</i> (CERN, CDEF, PADO+)

OTHER RELATED PAPERS

ACHARD	07	JHEP 0703 018	P. Achard <i>et al.</i> (L3 Collab.)
KANADA-EN...	05	PR D71 094005	Y. Kanada-En'yo, O. Morimatsu, T. Nishikawa
ABELE	97G	PL B415 289	A. Abele <i>et al.</i>
CLOSE	97D	ZPHY C76 469	F.E. Close <i>et al.</i>
KING	91	NPBPS B21 11	E. King <i>et al.</i> (FSU, BNL+)
AIHARA	88C	PR D38 1	H. Aihara <i>et al.</i> (TPC-2 γ Collab.)
BITYUKOV	84	SJNP 39 735	S. Bityukov <i>et al.</i> (SERP)
		Translated from YAF 39 1165.	

 $f_2'(1525)$

$$J^{PC} = 0^{++}$$

 $f_2'(1525)$ MASS

VALUE (MeV)	DOCUMENT ID
1525 ± 5 OUR ESTIMATE	This is only an educated guess; the error given is larger than the error on the average of the published values.

PRODUCED BY PION BEAM

VALUE (MeV)	EVTS	DOCUMENT ID	TECN	COMMENT
• • • We do not use the following data for averages, fits, limits, etc. • • •				
1521 ± 13		TIKHOMIROV	03 SPEC	40.0 $\pi^- C \rightarrow K_S^0 K_S^0 K_S^0 X$
1547 \pm $\frac{10}{2}$		¹ LONGACRE	86 MPS	22 $\pi^- p \rightarrow K_S^0 K_S^0 n$
1496 \pm $\frac{9}{8}$		² CHABAUD	81 ASP K	6 $\pi^- p \rightarrow K^+ K^- n$
1497 \pm $\frac{8}{9}$		CHABAUD	81 ASP K	18.4 $\pi^- p \rightarrow K^+ K^- n$
1492 ± 29		GORLICH	80 ASP K	17 $\pi^- p$ polarized $\rightarrow K^+ K^- n$
1502 ± 25		³ CORDEN	79 OMEG	12-15 $\pi^- p \rightarrow \pi^+ \pi^- n$
1480	14	CRENNELL	66 HBC	6.0 $\pi^- p \rightarrow K_S^0 K_S^0 n$

Meson Particle Listings

 $f_2'(1525)$ PRODUCED BY K^\pm BEAM

VALUE (MeV)	EVTS	DOCUMENT ID	TECN	COMMENT
1523.4 ± 1.3 OUR AVERAGE Includes data from the datablock that follows this one.				
Error includes scale factor of 1.1.				
1526.8 ± 4.3		ASTON	88D LASS	11 $K^- p \rightarrow K_S^0 K_S^0 \Lambda$
1504 ± 12		BOLONKIN	86 SPEC	40 $K^- p \rightarrow K_S^0 K_S^0 Y$
1529 ± 3		ARMSTRONG	83B OMEG	18.5 $K^- p \rightarrow K^- K^+ \Lambda$
1521 ± 6	650	AGUILAR...	81B HBC	4.2 $K^- p \rightarrow \Lambda K^+ K^-$
1521 ± 3	572	ALHARRAN	81 HBC	8.25 $K^- p \rightarrow \Lambda K \bar{K}$
1522 ± 6	123	BARREIRO	77 HBC	4.15 $K^- p \rightarrow \Lambda K_S^0 K_S^0$
1528 ± 7	166	EVANGELIS...	77 OMEG	10 $K^- p \rightarrow K^+ K^- (\Lambda, \Sigma)$
1527 ± 3	120	BRANDENB...	76C ASPK	13 $K^- p \rightarrow K^+ K^- (\Lambda, \Sigma)$
1519 ± 7	100	AGUILAR...	72B HBC	3.9, 4.6 $K^- p \rightarrow K \bar{K} (\Lambda, \Sigma)$
••• We do not use the following data for averages, fits, limits, etc. •••				
1514 ± 8	61	BINON	07 GAMS	32.5 $K^- p \rightarrow \eta \eta (\Lambda / \Sigma^0)$
1513 ± 10	4	BARKOV	99 SPEC	40 $K^- p \rightarrow K_S^0 K_S^0 Y$

PRODUCED IN $e^+ e^-$ ANNIHILATION

VALUE (MeV)	EVTS	DOCUMENT ID	TECN	COMMENT
The data in this block is included in the average printed for a previous datablock.				

1520.7 ± 2.0 OUR AVERAGE

1521 ± 5		ABLIKIM	05 BES2	$J/\psi \rightarrow \phi K^+ K^-$
1518 ± 1 ± 3		ABE	04 BELL	10.6 $e^+ e^- \rightarrow e^+ e^- K^+ K^-$
1519 ± 2 ± $\frac{+15}{-5}$		BAI	03G BES	$J/\psi \rightarrow \gamma K \bar{K}$
1523 ± 6	331	5 ACCIARRI	01H L3	91, 183-209 $e^+ e^- \rightarrow e^+ e^- K_S^0 K_S^0$
1535 ± 5 ± 4		ABREU	96c DLPH	$Z^0 \rightarrow K^+ K^- + X$
1516 ± 5 ± $\frac{+9}{-15}$		BAI	96c BES	$J/\psi \rightarrow \gamma K^+ K^-$
1531.6 ± 10.0		AUGUSTIN	88 DM2	$J/\psi \rightarrow \gamma K^+ K^-$
1515 ± 5	6	FALVARD	88 DM2	$J/\psi \rightarrow \phi K^+ K^-$
1525 ± 10 ± 10		BALTRUSAIT...	87 MRK3	$J/\psi \rightarrow \gamma K^+ K^-$
••• We do not use the following data for averages, fits, limits, etc. •••				
1523 ± 5	870	7 SCHEGELSKY	06A RVUE	$\gamma \gamma \rightarrow K_S^0 K_S^0$
1496 ± 2	8	FALVARD	88 DM2	$J/\psi \rightarrow \phi K^+ K^-$

PRODUCED IN $\bar{p} p$ ANNIHILATION

VALUE (MeV)	DOCUMENT ID	TECN	COMMENT
••• We do not use the following data for averages, fits, limits, etc. •••			
1513 ± 4	AMSLER	06 CBAR	0.9 $\bar{p} p \rightarrow K^+ K^- \pi^0$
1508 ± 9	9 AMSLER	02 CBAR	0.9 $\bar{p} p \rightarrow \pi^0 \eta \eta, \pi^0 \pi^0 \pi^0$

CENTRAL PRODUCTION

VALUE (MeV)	DOCUMENT ID	TECN	COMMENT
1515 ± 15	BARBERIS	99 OMEG	450 $p p \rightarrow p_S p_f K^+ K^-$

PRODUCED IN $e p$ COLLISIONS

VALUE (MeV)	EVTS	DOCUMENT ID	TECN	COMMENT
••• We do not use the following data for averages, fits, limits, etc. •••				
1537 ± $\frac{+9}{-8}$	84	10 CHEKANOV	04 ZEUS	$e p \rightarrow K_S^0 K_S^0 X$

- From a partial-wave analysis of data using a K-matrix formalism with 5 poles.
- CHABAUD 81 is a reanalysis of PAWLICKI 77 data.
- From an amplitude analysis where the $f_2'(1525)$ width and elasticity are in complete disagreement with the values obtained from $K \bar{K}$ channel, making the solution dubious.
- Systematic errors not estimated.
- Supersedes ACCIARRI 95j.
- From an analysis ignoring interference with $f_0(1710)$.
- From analysis of L3 data at 91 and 183-209 GeV.
- From an analysis including interference with $f_0(1710)$.
- T-matrix pole.
- Systematic errors not estimated.

 $f_2'(1525)$ WIDTH

VALUE (MeV)	DOCUMENT ID	COMMENT
73 ± $\frac{6}{5}$ OUR FIT		
76 ± 10	PDG	90 For fitting

PRODUCED BY PION BEAM

VALUE (MeV)	DOCUMENT ID	TECN	COMMENT
••• We do not use the following data for averages, fits, limits, etc. •••			
102 ± 4.2	TIKHOMIROV	03 SPEC	40.0 $\pi^- C \rightarrow K_S^0 K_S^0 K_S^0 X$
108 ± $\frac{+5}{-2}$	11 LONGACRE	86 MPS	22 $\pi^- p \rightarrow K_S^0 K_S^0 n$
69 ± $\frac{+22}{-16}$	12 CHABAUD	81 ASPK	6 $\pi^- p \rightarrow K^+ K^- n$
137 ± $\frac{+23}{-21}$	CHABAUD	81 ASPK	18.4 $\pi^- p \rightarrow K^+ K^- n$
150 ± $\frac{+83}{-50}$	GORLICH	80 ASPK	17 $\pi^- p$ polarized $\rightarrow K^+ K^- n$
165 ± 4.2	13 CORDEN	79 OMEG	12-15 $\pi^- p \rightarrow \pi^+ \pi^- n$
92 ± $\frac{+39}{-22}$	14 POLYCHRO...	79 STRC	7 $\pi^- p \rightarrow n K_S^0 K_S^0$

PRODUCED BY K^\pm BEAM

VALUE (MeV)	EVTS	DOCUMENT ID	TECN	COMMENT
80.2 ± 2.6 OUR AVERAGE Includes data from the datablock that follows this one.				
90 ± 12		ASTON	88D LASS	11 $K^- p \rightarrow K_S^0 K_S^0 \Lambda$
73 ± 18		BOLONKIN	86 SPEC	40 $K^- p \rightarrow K_S^0 K_S^0 Y$
83 ± 15		ARMSTRONG	83B OMEG	18.5 $K^- p \rightarrow K^- K^+ \Lambda$
85 ± 16	650	AGUILAR...	81B HBC	4.2 $K^- p \rightarrow \Lambda K^+ K^-$
80 ± $\frac{+14}{-11}$	572	ALHARRAN	81 HBC	8.25 $K^- p \rightarrow \Lambda K \bar{K}$
72 ± 25	166	EVANGELIS...	77 OMEG	10 $K^- p \rightarrow K^+ K^- (\Lambda, \Sigma)$
69 ± 22	100	AGUILAR...	72B HBC	3.9, 4.6 $K^- p \rightarrow K \bar{K} (\Lambda, \Sigma)$
••• We do not use the following data for averages, fits, limits, etc. •••				
92 ± $\frac{+25}{-16}$	61	BINON	07 GAMS	32.5 $K^- p \rightarrow \eta \eta (\Lambda / \Sigma^0)$
75 ± 20	15	BARKOV	99 SPEC	40 $K^- p \rightarrow K_S^0 K_S^0 Y$
62 ± $\frac{+19}{-14}$	123	BARREIRO	77 HBC	4.15 $K^- p \rightarrow \Lambda K_S^0 K_S^0$
61 ± 8	120	BRANDENB...	76C ASPK	13 $K^- p \rightarrow K^+ K^- (\Lambda, \Sigma)$

PRODUCED IN $e^+ e^-$ ANNIHILATION

VALUE (MeV)	EVTS	DOCUMENT ID	TECN	COMMENT
The data in this block is included in the average printed for a previous datablock.				

77.9 ± 3.3 OUR AVERAGE

Error includes scale factor of 1.1.				
79 ± 15		ABLIKIM	05 BES2	$J/\psi \rightarrow \phi K^+ K^-$
82 ± 2 ± 3		ABE	04 BELL	10.6 $e^+ e^- \rightarrow e^+ e^- K^+ K^-$
75 ± 4 ± $\frac{+15}{-5}$		BAI	03G BES	$J/\psi \rightarrow \gamma K \bar{K}$
100 ± 15	331	16 ACCIARRI	01H L3	91, 183-209 $e^+ e^- \rightarrow e^+ e^- K_S^0 K_S^0$
60 ± 20 ± 19		ABREU	96c DLPH	$Z^0 \rightarrow K^+ K^- + X$
60 ± 23 ± $\frac{+13}{-20}$		BAI	96c BES	$J/\psi \rightarrow \gamma K^+ K^-$
103 ± 30		AUGUSTIN	88 DM2	$J/\psi \rightarrow \gamma K^+ K^-$
62 ± 10	17	FALVARD	88 DM2	$J/\psi \rightarrow \phi K^+ K^-$
85 ± 35		BALTRUSAIT...	87 MRK3	$J/\psi \rightarrow \gamma K^+ K^-$
••• We do not use the following data for averages, fits, limits, etc. •••				
104 ± 10	870	18 SCHEGELSKY	06A RVUE	$\gamma \gamma \rightarrow K_S^0 K_S^0$
100 ± 3	19	FALVARD	88 DM2	$J/\psi \rightarrow \phi K^+ K^-$

PRODUCED IN $\bar{p} p$ ANNIHILATION

VALUE (MeV)	DOCUMENT ID	TECN	COMMENT
••• We do not use the following data for averages, fits, limits, etc. •••			
79 ± 8	20 AMSLER	02 CBAR	0.9 $\bar{p} p \rightarrow \pi^0 \eta \eta, \pi^0 \pi^0 \pi^0$
76 ± 6	AMSLER	06 CBAR	0.9 $\bar{p} p \rightarrow K^+ K^- \pi^0$

CENTRAL PRODUCTION

VALUE (MeV)	DOCUMENT ID	TECN	COMMENT
70 ± 25	BARBERIS	99 OMEG	450 $p p \rightarrow p_S p_f K^+ K^-$

PRODUCED IN $e p$ COLLISIONS

VALUE (MeV)	EVTS	DOCUMENT ID	TECN	COMMENT
••• We do not use the following data for averages, fits, limits, etc. •••				
50 ± $\frac{+34}{-22}$	84	21 CHEKANOV	04 ZEUS	$e p \rightarrow K_S^0 K_S^0 X$

- From a partial-wave analysis of data using a K-matrix formalism with 5 poles.
- CHABAUD 81 is a reanalysis of PAWLICKI 77 data.
- From an amplitude analysis where the $f_2'(1525)$ width and elasticity are in complete disagreement with the values obtained from $K \bar{K}$ channel, making the solution dubious.
- From a fit to the D with $f_2(1270)$ - $f_2'(1525)$ interference. Mass fixed at 1516 MeV.
- Systematic errors not estimated.
- Supersedes ACCIARRI 95j.
- From an analysis ignoring interference with $f_0(1710)$.
- From analysis of L3 data at 91 and 183-209 GeV.
- From an analysis including interference with $f_0(1710)$.
- T-matrix pole.
- Systematic errors not estimated.

 $f_2'(1525)$ DECAY MODES

Mode	Fraction (Γ_i/Γ)
Γ_1 $K \bar{K}$	(88.7 ± 2.2) %
Γ_2 $\eta \eta$	(10.4 ± 2.2) %
Γ_3 $\pi \pi$	(8.2 ± 1.5) × 10 ⁻³
Γ_4 $K \bar{K}^*(892) + \text{c.c.}$	
Γ_5 $\pi K \bar{K}$	
Γ_6 $\pi \pi \eta$	
Γ_7 $\pi^+ \pi^+ \pi^- \pi^-$	
Γ_8 $\gamma \gamma$	(1.11 ± 0.14) × 10 ⁻⁶

CONSTRAINED FIT INFORMATION

An overall fit to the total width, 2 partial widths, a combination of partial widths obtained from integrated cross sections, and 3 branching ratios uses 16 measurements and one constraint to determine 5 parameters. The overall fit has a $\chi^2 = 14.0$ for 12 degrees of freedom.

The following *off-diagonal* array elements are the correlation coefficients $\langle \delta p_i \delta p_j \rangle / (\delta p_i \delta p_j)$, in percent, from the fit to parameters p_i , including the branching fractions, $x_i \equiv \Gamma_i / \Gamma_{\text{total}}$. The fit constrains the x_i whose labels appear in this array to sum to one.

x_2	-100			
x_3	-6	-1		
x_8	-6	6	1	
Γ	-23	23	-1	-55
	x_1	x_2	x_3	x_8

Mode	Rate (MeV)
Γ_1 $K\bar{K}$	65 $^{+5}_{-4}$
Γ_2 $\eta\eta$	7.6 ± 1.8
Γ_3 $\pi\pi$	0.60 ± 0.12
Γ_8 $\gamma\gamma$	(8.1 ± 0.9) $\times 10^{-5}$

 $f_2'(1525)$ PARTIAL WIDTHS

$\Gamma(K\bar{K})$	Γ_1		
VALUE (MeV)	DOCUMENT ID	TECN	COMMENT

65 $^{+5}_{-4}$ OUR FIT63 $^{+6}_{-5}$ 22 LONGACRE 86 MPS 22 $\pi^- p \rightarrow K_S^0 K_S^0 n$

$\Gamma(\eta\eta)$	Γ_2			
VALUE (MeV)	EVTS	DOCUMENT ID	TECN	COMMENT

7.6 ± 1.8 OUR FIT5.0 ± 0.8 870 23 SCHEGELSKY 06A RVUE $\gamma\gamma \rightarrow K_S^0 K_S^0$ 24 $^{+3}_{-1}$ 22 LONGACRE 86 MPS 22 $\pi^- p \rightarrow K_S^0 K_S^0 n$

$\Gamma(\pi\pi)$	Γ_3			
VALUE (MeV)	EVTS	DOCUMENT ID	TECN	COMMENT

0.60 ± 0.12 OUR FIT1.4 $^{+1.0}_{-0.5}$ 22 LONGACRE 86 MPS 22 $\pi^- p \rightarrow K_S^0 K_S^0 n$ 0.2 $^{+1.0}_{-0.2}$ 870 23 SCHEGELSKY 06A RVUE $\gamma\gamma \rightarrow K_S^0 K_S^0$

$\Gamma(\gamma\gamma)$	Γ_8			
VALUE (keV)	EVTS	DOCUMENT ID	TECN	COMMENT

0.081 ± 0.009 OUR FIT0.13 ± 0.03 870 23 SCHEGELSKY 06A RVUE $\gamma\gamma \rightarrow K_S^0 K_S^0$

22 From a partial-wave analysis of data using a K-matrix formalism with 5 poles.

23 From analysis of L3 data at 91 and 183–209 GeV, using $\Gamma(f_2'(1525) \rightarrow K\bar{K}) = 68$ MeV and SU(3) relations. $f_2'(1525)$ $\Gamma(i)\Gamma(\gamma\gamma)/\Gamma(\text{total})$

$\Gamma(K\bar{K}) \times \Gamma(\gamma\gamma)/\Gamma_{\text{total}}$	$\Gamma_1\Gamma_8/\Gamma$			
VALUE (keV)	EVTS	DOCUMENT ID	TECN	COMMENT

0.072 ± 0.007 OUR FIT0.072 ± 0.007 OUR AVERAGE0.0564 $\pm 0.0048 \pm 0.0116$ ABE 04 BELL 10.6 $e^+e^- \rightarrow e^+e^- K^+K^-$ 0.076 $\pm 0.006 \pm 0.011$ 331 24 ACCIARRI 01H L3 $e^+e^- \rightarrow e^+e^- K_S^0 K_S^0$ 0.067 $\pm 0.008 \pm 0.015$ 25 ALBRECHT 90G ARG $e^+e^- \rightarrow e^+e^- K^+K^-$ 0.11 $^{+0.03}_{-0.02} \pm 0.02$ BEHREND 89C CELL $e^+e^- \rightarrow e^+e^- K_S^0 K_S^0$ 0.10 $^{+0.04}_{-0.03} \pm 0.03$ BERGER 88 PLUT $e^+e^- \rightarrow e^+e^- K_S^0 K_S^0$ 0.12 $\pm 0.07 \pm 0.04$ 25 AIHARA 86B TPC $e^+e^- \rightarrow e^+e^- K^+K^-$ 0.11 $\pm 0.02 \pm 0.04$ 25 ALTHOFF 83 TASS $e^+e^- \rightarrow e^+e^- K\bar{K}$ 0.0314 $\pm 0.0050 \pm 0.0077$ 26 ALBRECHT 90G ARG $e^+e^- \rightarrow e^+e^- K^+K^-$

24 Supersedes ACCIARRI 95J. From analysis of L3 data at 91 and 183–209 GeV,

25 Using an incoherent background.

26 Using a coherent background.

 $f_2'(1525)$ BRANCHING RATIOS

$\Gamma(\eta\eta)/\Gamma_{\text{total}}$	Γ_2/Γ		
VALUE	DOCUMENT ID	TECN	COMMENT

0.10 ± 0.03 27 PROKOSHKIN 91 GAM4 300 $\pi^- p \rightarrow \pi^- \rho \eta \eta$ 27 Combining results of GAM4 with those of WA76 on $K\bar{K}$ central production and results of CBAL, MRK3 and DM2 on $J/\psi \rightarrow \gamma \eta \eta$.

$\Gamma(\eta\eta)/\Gamma(K\bar{K})$	Γ_2/Γ_1				
VALUE	CL%	EVTS	DOCUMENT ID	TECN	COMMENT

0.115 ± 0.028 OUR FIT0.115 ± 0.028 OUR AVERAGE0.119 $\pm 0.015 \pm 0.036$ 61 28 BINON 07 GAMS 32.5 $K^- p \rightarrow \eta \eta (\Lambda/\Sigma^0)$ 0.11 ± 0.04 29 PROKOSHKIN 91 GAM4 300 $\pi^- p \rightarrow \pi^- \rho \eta \eta$ < 0.14 90 BARBERIS 00E 450 $p p \rightarrow p_f \eta \eta p_s$ < 0.50 67 BARNES HBC 4.6,5.0 $K^- p$ 28 Using the compilation of the cross sections for $f_2'(1525)$ production in $K^- p$ collisions from ASTON 88D.29 Combining results of GAM4 with those of WA76 on $K\bar{K}$ central production and results of CBAL, MRK3 and DM2 on $J/\psi \rightarrow \gamma \eta \eta$.

$\Gamma(\pi\pi)/\Gamma_{\text{total}}$	Γ_3/Γ			
VALUE	CL%	DOCUMENT ID	TECN	COMMENT

0.0082 ± 0.0016 OUR FIT0.0075 ± 0.0016 OUR AVERAGE0.007 ± 0.002 COSTA... 80 OMEG 10 $\pi^- p \rightarrow K^+ K^- n$ 0.027 $^{+0.071}_{-0.013}$ 30 GORLICH 80 ASPK 17,18 $\pi^- p$ 0.0075 ± 0.0025 30,31 MARTIN 79 RVUE< 0.06 95 AGUILAR... 81B HBC 4.2 $K^- p \rightarrow \Lambda K^+ K^-$ 0.19 ± 0.03 CORDEEN 79 OMEG 12–15 $\pi^- p \rightarrow \pi^+ \pi^- n$ < 0.045 95 BARREIRO 77 HBC 4.15 $K^- p \rightarrow \Lambda K_S^0 K_S^0$ 0.012 ± 0.004 30 PAWLICKI 77 SPEC 6 $\pi N \rightarrow K^+ K^- N$ < 0.063 90 BRANDENB... 76C ASPK 13 $K^- p \rightarrow K^+ K^- (\Lambda, \Sigma)$ < 0.0086 30 BEUSCH 75B OSPK 8.9 $\pi^- p \rightarrow K^0 \bar{K}^0 n$ 30 Assuming that the $f_2'(1525)$ is produced by a one-pion exchange production mechanism.31 MARTIN 79 uses the PAWLICKI 77 data with different input value of the $f_2'(1525) \rightarrow K\bar{K}$ branching ratio.

$\Gamma(\pi\pi)/\Gamma(K\bar{K})$	Γ_3/Γ_1		
VALUE	DOCUMENT ID	TECN	COMMENT

0.0092 ± 0.0018 OUR FIT0.075 ± 0.035 AUGUSTIN 87 DM2 $J/\psi \rightarrow \gamma \pi^+ \pi^-$

$[\Gamma(K\bar{K}^*(892) + \text{c.c.}) + \Gamma(\pi K\bar{K})]/\Gamma(K\bar{K})$	$(\Gamma_4 + \Gamma_5)/\Gamma_1$			
VALUE	CL%	DOCUMENT ID	TECN	COMMENT

< 0.35 95 AGUILAR... 72B HBC 3.9,4.6 $K^- p$

< 0.4 67 AMMAR 67 HBC

$\Gamma(\pi\pi\eta)/\Gamma(K\bar{K})$	Γ_6/Γ_1			
VALUE	CL%	DOCUMENT ID	TECN	COMMENT

< 0.41 95 AGUILAR... 72B HBC 3.9,4.6 $K^- p$

< 0.3 67 AMMAR 67 HBC

$\Gamma(\pi^+ \pi^+ \pi^- \pi^-)/\Gamma(K\bar{K})$	Γ_7/Γ_1			
VALUE	CL%	DOCUMENT ID	TECN	COMMENT

< 0.32 95 AGUILAR... 72B HBC 3.9,4.6 $K^- p$ $f_2'(1525)$ REFERENCES

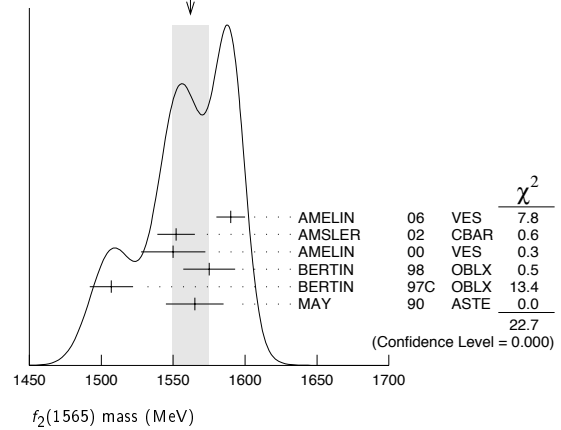
BINON	07	PAN 70 1713	F. Binon et al.	(GAMS Collab.)
		Translated from YAF 70 1758.		
AMSLER	06	PL B639 165	C. Amstler et al.	(CBAR Collab.)
SCHEGELSKY	06A	EPJ A27 207	V.A. Schegelsky et al.	
ABLIKIM	05	PL B607 243	M. Ablikim et al.	(BES Collab.)
ABE	04	EPJ C32 323	K. Abe et al.	(BELLE Collab.)
CHEKANOV	04	PL B578 33	S. Chekanov et al.	(ZEUS Collab.)
BAI	03G	PR D68 052003	J.Z. Bai et al.	(BES Collab.)
TIKHOMIROV	03	PAN 66 828	G.D. Tikhomirov et al.	
		Translated from YAF 66 860.		
AMSLER	02	EPJ C23 29	C. Amstler et al.	
ACCIARRI	01H	PL B501 173	M. Acciari et al.	(L3 Collab.)
BARBERIS	00E	PL B479 59	D. Barberis et al.	(WA 102 Collab.)
BARBERIS	99	PL B453 305	D. Barberis et al.	(Omega Expt.)
BARKOV	99	JETPL 70 248	B.P. Barkov et al.	
		Translated from ZETFF 70 242.		
ABREU	96C	PL B379 309	P. Abreu et al.	(DELPHI Collab.)
BAI	96C	PRL 77 3959	J.Z. Bai et al.	(BES Collab.)
ACCIARRI	95J	PL B363 118	M. Acciari et al.	(L3 Collab.)
PROKOSHKIN	91	SPD 36 155	Y.D. Prokoshkin	(GAM2, GAM4 Collab.)
		Translated from DANS 316 900.		

Meson Particle Listings

$f_2'(1525), f_2(1565)$

ALBRECHT 90G ZPHY C48 183 H. Albrecht et al. (ARGUS Collab.)	PDG 90 PL B239 1 J.J. Hernandez et al. (IFIC, BOST, CIT+)	
BEHREND 89C ZPHY C43 91 H.J. Behrend et al. (CELLO Collab.)	ASTON 88D NP B301 525 D. Aston et al. (SLAC, NAGO, CINC, INUS)	
AUGUSTIN 88 PRL 60 2238 J.E. Augustin et al. (DM2 Collab.)	BERGER 88 ZPHY C37 329 C. Berger et al. (PLUTO Collab.)	
FALVARD 88 PR D38 2706 A. Falvard et al. (CLER, FRAS, LALO+)	AUGUSTIN 87 ZPHY C36 369 J.E. Augustin et al. (LALO, CLER, FRAS+)	
BALTUSAITIS... 87 PR D35 2077 R.M. Baltusaitis et al. (Mark III Collab.)	AIHARA 86B PRL 57 404 H. Aihara et al. (TPC-2 γ Collab.)	
BOLONKIN 86 SJNP 43 776 B.V. Bolonkin et al. (ITEP) JP	Translated from YAF 43 1211.	
LONGACRE 86 PL B177 223 R.S. Longacre et al. (BNL, BRAN, CUNY+)	ALTHOFF 83 PL 121B 216 M. Althoff et al. (TASSO Collab.)	
ARMSTRONG 83B NP B224 193 T.A. Armstrong et al. (BARI, BIRM, CERN+)	AGUILAR... 81B ZPHY C8 313 M. Aguilar-Benitez et al. (CERN, CDEF+)	
ALHARRAN 81 NP B191 26 S. Al-Harran et al. (BIRM, CERN, GLAS+)	CHABAUD 81 APP B12 575 V. Chabaud et al. (CERN, CRAC, MPIM)	
COSTA... 80 NP B175 402 G. Costa de Beauregard et al. (BARI, BONN+)	GORLICH 80 NP B174 16 L. Gorlich et al. (CRAC, MPIM, CERN+)	
CORDEN 79 NP B157 250 M.J. Corden et al. (BIRM, RHEL, TELA+ JP)	MARTIN 79 NP B158 520 A.D. Martin, E.N. Ozmutlu (DURH)	
POLYCHRO... 79 PR D19 1317 V.A. Polychronakos et al. (NDAM, ANL)	BARREIRO 77 NP B121 237 F. Barreiro et al. (CERN, AMST, NIJN+)	
EVANGELIS... 77 NP B127 384 C. Evangelista et al. (BARI, BONN, CERN+)	PAWLICKI 77 PR D15 3196 A.J. Pawlicki et al. (ANL) IJP	
BRANDENB... 76C NP B104 413 G.W. Brandenburg et al. (SLAC)	BEUSCH 75B PL 60B 101 W. Beusch et al. (CERN, ETH)	
AGUILAR... 72B PR D6 29 M. Aguilar-Benitez et al. (BNL)	AMMAR 67 PRL 19 1071 R. Ammar et al. (NWES, ANL) JP	
BARNES 67 PRL 19 964 V.E. Barnes et al. (BNL, SYRA) IJP	CRENNELL 66 PRL 16 1025 D.J. Crennell et al. (BNL) I	

WEIGHTED AVERAGE
1562±13 (Error scaled by 2.1)



OTHER RELATED PAPERS

ANISOVICH 05 JETPL 80 715 V.V. Anisovich	LI 01 JPG 27 807 Translated from ZETFP 80 845	D.-M. Li, H. Yu, Q.-X. Shen (Obelix Collab.)
ALBERICO 98 PL B438 430 A. Alberico et al. (SLAC, LBL)	JENNI 83 PR D27 1031 P. Jenni et al. (SLAC, LBL)	ARMSTRONG 82 PL 110B 77 T.A. Armstrong et al. (BARI, BIRM, CERN+)
ETKIN 82B PR D25 1786 A. Etkin et al. (BNL, CUNY, TUFTS, VAND)	ABRAMS 67B PRL 18 620 G.S. Abrams et al. (UMD)	BARNES 65 PRL 15 322 V.E. Barnes et al. (BNL, SYRA)

$f_2(1565)$

$$J^{PC} = 0^+(2^{++})$$

OMITTED FROM SUMMARY TABLE

Seen in antinucleon-nucleon annihilation at rest. Needs confirmation.

$f_2(1565)$ MASS

VALUE (MeV)	DOCUMENT ID	TECN	COMMENT
1562±13 OUR AVERAGE	Error includes scale factor of 2.1. See the ideogram below.		
1590±10	1 AMELIN 06 VES	36 $\pi^- p \rightarrow \omega \eta n$	
1552±13	2 AMSLER 02 CBAR	0.9 $\bar{p} p \rightarrow \pi^0 \eta \eta, \pi^0 \pi^0 \pi^0$	
1550±10±20	AMELIN 00 VES	37 $\pi^- p \rightarrow \eta \pi^+ \pi^- n$	
1575±18	BERTIN 98 OBLX	0.05-0.405 $\bar{p} p \rightarrow \pi^+ \pi^+ \pi^-$	
1507±15	2 BERTIN 97C OBLX	0.0 $\bar{p} p \rightarrow \pi^+ \pi^- \pi^0$	
1565±20	MAY 90 ASTE	0.0 $\bar{p} p \rightarrow \pi^+ \pi^- \pi^0$	
1598±11±9	BAKER 99B SPEC	0 $\bar{p} p \rightarrow \omega \omega \pi^0$	
1534±20	3 ABELE 96C RVUE	Compilation	
~1552	4 AMSLER 95D CBAR	0.0 $\bar{p} p \rightarrow \pi^0 \pi^0 \pi^0, \pi^0 \eta \eta, \pi^0 \pi^0 \eta$	
1598±72	BALOSHIN 95 SPEC	40 $\pi^- C \rightarrow K_S^0 K_S^0 X$	
1566 ⁺⁸⁰ ₋₅₀	5 ANISOVICH 94 CBAR	0.0 $\bar{p} p \rightarrow 3\pi^0, \eta \eta \pi^0$	
1502±9	ADAMO 93 OBLX	$\bar{p} p \rightarrow \pi^+ \pi^+ \pi^-$	
1488±10	6 ARMSTRONG 93C E760	$\bar{p} p \rightarrow \pi^0 \eta \eta \rightarrow 6\gamma$	
1508±10	6 ARMSTRONG 93D E760	$\bar{p} p \rightarrow 3\pi^0 \rightarrow 6\gamma$	
1525±10	6 ARMSTRONG 93D E760	$\bar{p} p \rightarrow \eta \pi^0 \pi^0 \rightarrow 6\gamma$	
~1504	7 WEIDENAUER 93 ASTE	0.0 $\bar{p} N \rightarrow 3\pi^- 2\pi^+$	
1540±15	6 ADAMO 92 OBLX	$\bar{p} p \rightarrow \pi^+ \pi^+ \pi^-$	
1515±10	8 AKER 91 CBAR	0.0 $\bar{p} p \rightarrow 3\pi^0$	
1477±5	BRIDGES 86C DBC	0.0 $\bar{p} N \rightarrow 3\pi^- 2\pi^+$	

- 1 Supersedes the $\omega \omega$ state of BELADIDZE 92b earlier assigned to the $f_2(1640)$.
- 2 T-matrix pole.
- 3 T-matrix pole, large coupling to $\rho \rho$ and $\omega \omega$, could be $f_2(1640)$.
- 4 Coupled-channel analysis of AMSLER 95b, AMSLER 95c, and AMSLER 94d.
- 5 From a simultaneous analysis of the annihilations $\bar{p} p \rightarrow 3\pi^0, \pi^0 \eta \eta$ including AKER 91 data.
- 6 J^P not determined, could be partly $f_0(1500)$.
- 7 J^P not determined.
- 8 Superseded by AMSLER 95b.

$f_2(1565)$ WIDTH

VALUE (MeV)	DOCUMENT ID	TECN	COMMENT
134±8 OUR AVERAGE			
140±11	9 AMELIN 06 VES	36 $\pi^- p \rightarrow \omega \eta n$	
113±23	10 AMSLER 02 CBAR	0.9 $\bar{p} p \rightarrow \pi^0 \eta \eta, \pi^0 \pi^0 \pi^0$	
130±20±40	AMELIN 00 VES	37 $\pi^- p \rightarrow \eta \pi^+ \pi^- n$	
119±24	BERTIN 98 OBLX	0.05-0.405 $\bar{p} p \rightarrow \pi^+ \pi^+ \pi^-$	
130±20	10 BERTIN 97C OBLX	0.0 $\bar{p} p \rightarrow \pi^+ \pi^- \pi^0$	
170±40	MAY 90 ASTE	0.0 $\bar{p} p \rightarrow \pi^+ \pi^- \pi^0$	
180±60	11 ABELE 96C RVUE	Compilation	
~142	12 AMSLER 95D CBAR	0.0 $\bar{p} p \rightarrow \pi^0 \pi^0 \pi^0, \pi^0 \eta \eta, \pi^0 \pi^0 \eta$	
263±101	BALOSHIN 95 SPEC	40 $\pi^- C \rightarrow K_S^0 K_S^0 X$	
166 ⁺⁸⁰ ₋₂₀	13 ANISOVICH 94 CBAR	0.0 $\bar{p} p \rightarrow 3\pi^0, \eta \eta \pi^0$	
130±10	14 ADAMO 93 OBLX	$\bar{p} p \rightarrow \pi^+ \pi^+ \pi^-$	
148±27	15 ARMSTRONG 93C E760	$\bar{p} p \rightarrow \pi^0 \eta \eta \rightarrow 6\gamma$	
103±15	15 ARMSTRONG 93D E760	$\bar{p} p \rightarrow 3\pi^0 \rightarrow 6\gamma$	
111±10	15 ARMSTRONG 93D E760	$\bar{p} p \rightarrow \eta \pi^0 \pi^0 \rightarrow 6\gamma$	
~206	16 WEIDENAUER 93 ASTE	0.0 $\bar{p} N \rightarrow 3\pi^- 2\pi^+$	
132±37	15 ADAMO 92 OBLX	$\bar{p} p \rightarrow \pi^+ \pi^+ \pi^-$	
120±10	17 AKER 91 CBAR	0.0 $\bar{p} p \rightarrow 3\pi^0$	
116±9	BRIDGES 86C DBC	0.0 $\bar{p} N \rightarrow 3\pi^- 2\pi^+$	

- 9 Supersedes the $\omega \omega$ state of BELADIDZE 92b earlier assigned to the $f_2(1640)$.
- 10 T-matrix pole.
- 11 T-matrix pole, large coupling to $\rho \rho$ and $\omega \omega$, could be $f_2(1640)$.
- 12 Coupled-channel analysis of AMSLER 95b, AMSLER 95c, and AMSLER 94d.
- 13 From a simultaneous analysis of the annihilations $\bar{p} p \rightarrow 3\pi^0, \pi^0 \eta \eta$ including AKER 91 data.
- 14 Supersedes ADAMO 92.
- 15 J^P not determined, could be partly $f_0(1500)$.
- 16 J^P not determined.
- 17 Superseded by AMSLER 95b.

$f_2(1565)$ DECAY MODES

Mode	Fraction (Γ_i/Γ)
Γ_1 $\pi \pi$	seen
Γ_2 $\pi^+ \pi^-$	seen
Γ_3 $\pi^0 \pi^0$	seen
Γ_4 $\rho^0 \rho^0$	seen
Γ_5 $2\pi^+ 2\pi^-$	seen
Γ_6 $\eta \eta$	seen
Γ_7 $a_2(1320) \pi$	
Γ_8 $\omega \omega$	seen
Γ_9 $K \bar{K}$	
Γ_{10} $\gamma \gamma$	

$f_2(1565)$ PARTIAL WIDTHS

$\Gamma(\eta \eta)$	VALUE (MeV)	EVTS	DOCUMENT ID	TECN	COMMENT
	1.2±0.3	870	18 SCHEGELSKY 06A	RVUE	$\gamma \gamma \rightarrow K_S^0 K_S^0$

- • • We do not use the following data for averages, fits, limits, etc. • • •

See key on page 373

Meson Particle Listings

 $f_2(1565)$, $\rho(1570)$ $\Gamma(K\bar{K})$ Γ_9

VALUE (MeV)	EVTS	DOCUMENT ID	TECN	COMMENT
••• We do not use the following data for averages, fits, limits, etc. •••				
2.0±1.0	870	¹⁸ SCHEGELSKY 06A	RVUE	$\gamma\gamma \rightarrow K_S^0 K_S^0$

 $\Gamma(\gamma\gamma)$ Γ_{10}

VALUE (keV)	EVTS	DOCUMENT ID	TECN	COMMENT
••• We do not use the following data for averages, fits, limits, etc. •••				
0.70±0.14	870	¹⁸ SCHEGELSKY 06A	RVUE	$\gamma\gamma \rightarrow K_S^0 K_S^0$
¹⁸ From analysis of L3 data at 91 and 183–209 GeV, using $f_2(1565)$ mass of 1570 MeV, width of 160 MeV, $\Gamma(\pi\pi) = 25$ MeV, and SU(3) relations.				

 $f_2(1565)$ BRANCHING RATIOS $\Gamma(\pi\pi)/\Gamma_{\text{total}}$ Γ_1/Γ

VALUE	DOCUMENT ID	TECN	COMMENT
••• We do not use the following data for averages, fits, limits, etc. •••			
seen	BAKER 99B	SPEC	$0 \bar{p}p \rightarrow \omega\omega\pi^0$

 $\Gamma(\pi^+\pi^-)/\Gamma_{\text{total}}$ Γ_2/Γ

VALUE	DOCUMENT ID	TECN	COMMENT
••• We do not use the following data for averages, fits, limits, etc. •••			
seen	BERTIN 98	OBLX	$0.05-0.405 \bar{p}p \rightarrow \pi^+\pi^+\pi^-$
not seen	¹⁹ ANISOVICH 94B	RVUE	$\bar{p}p \rightarrow \pi^+\pi^-\pi^0$
seen	MAY 89	ASTE	$\bar{p}p \rightarrow \pi^+\pi^-\pi^0$
¹⁹ ANISOVICH 94B is from a reanalysis of MAY 90.			

 $\Gamma(\pi^0\pi^0)/\Gamma_{\text{total}}$ Γ_3/Γ

VALUE	DOCUMENT ID	TECN	COMMENT
seen	AMSLER 95B	CBAR	$0.0 \bar{p}p \rightarrow 3\pi^0$

 $\Gamma(\pi^+\pi^-)/\Gamma(\rho^0\rho^0)$ Γ_2/Γ_4

VALUE	DOCUMENT ID	TECN	COMMENT
••• We do not use the following data for averages, fits, limits, etc. •••			
0.042±0.013	BRIDGES 86B	DBC	$\bar{p}N \rightarrow 3\pi^- 2\pi^+$

 $\Gamma(\eta\eta)/\Gamma(\pi^0\pi^0)$ Γ_6/Γ_3

VALUE	DOCUMENT ID	TECN	COMMENT
••• We do not use the following data for averages, fits, limits, etc. •••			
0.024±0.005±0.012	²⁰ ARMSTRONG 93C	E760	$\bar{p}p \rightarrow \pi^0\eta\eta \rightarrow 6\gamma$
²⁰ J ^P not determined, could be partly $f_0(1500)$.			

 $\Gamma(\omega\omega)/\Gamma_{\text{total}}$ Γ_8/Γ

VALUE	DOCUMENT ID	TECN	COMMENT
••• We do not use the following data for averages, fits, limits, etc. •••			
seen	BAKER 99B	SPEC	$0 \bar{p}p \rightarrow \omega\omega\pi^0$

 $f_2(1565)$ REFERENCES

AMELIN 06	PAN 69 690	D.V. Amelin et al.	(VES Collab.)
SCHEGELSKY 06A	EPJ A27 207	V.A. Schegelsky et al.	(VES Collab.)
AMSLER 02	EPJ C23 29	C. Amstler et al.	
AMELIN 00	NP A668 83	D. Amelin et al.	(VES Collab.)
BAKER 99B	PL B467 147	C.A. Baker et al.	
BERTIN 98	PR D57 55	A. Bertin et al.	(OBELIX Collab.)
BERTIN 97C	PL B408 476	A. Bertin et al.	(OBELIX Collab.)
ABELE 96C	NP A609 562	A. Abele et al.	(Crystal Barrel Collab.)
AMSLER 95B	PL B342 433	C. Amstler et al.	(Crystal Barrel Collab.)
AMSLER 95C	PL B353 571	C. Amstler et al.	(Crystal Barrel Collab.)
AMSLER 95D	PL B355 425	C. Amstler et al.	(Crystal Barrel Collab.)
BALOSHIN 95	PAN 58 46	O.N. Baloshin et al.	(ITEP)
Translated from YAF 58 50.			
AMSLER 94D	PL B333 277	C. Amstler et al.	(Crystal Barrel Collab.)
ANISOVICH 94	PL B323 233	V.V. Anisovich et al.	(Crystal Barrel Collab.)
ANISOVICH 94B	PR D50 1972	V.V. Anisovich et al.	(LOQM)
ADAMO 93	NP A558 13C	A. Adamo et al.	(OBELIX Collab.)
ARMSTRONG 93C	PL B307 394	T.A. Armstrong et al.	(FNAL, FERR, GENO+)
ARMSTRONG 93D	PL B307 399	T.A. Armstrong et al.	(FNAL, FERR, GENO+)
WEIDENAUER 93	ZPHY C59 387	P. Weidenauer et al.	(ASTERIX Collab.)
ADAMO 92	PL B287 368	A. Adamo et al.	(OBELIX Collab.)
BELADIDZE 92B	ZPHY C54 367	G.M. Beladidze et al.	(VES Collab.)
AKER 91	PL B260 249	E. Aker et al.	(Crystal Barrel Collab.)
MAY 90	ZPHY C46 203	B. May et al.	(ASTERIX Collab.)
MAY 89	PL B225 450	B. May et al.	(ASTERIX Collab.)
BRIDGES 86B	PRL 56 215	D.L. Bridges et al.	(SYRA, CASE)
BRIDGES 86C	PRL 57 1534	D.L. Bridges et al.	(SYRA)

OTHER RELATED PAPERS

BUGG 07	EPJ C52 55	D. Bugg	
ANISOVICH 05	JETPL 80 715	V.V. Anisovich	
Translated from ZETFP 80 845.			

 $\rho(1570)$

$$I^G(J^{PC}) = 1^+(1^-)$$

OMITTED FROM SUMMARY TABLE

May be an OZI-violating decay mode of $\rho(1700)$. See our review in $\rho(1700)$ section. $\rho(1570)$ MASS

VALUE (MeV)	EVTS	DOCUMENT ID	TECN	COMMENT
1570±36±62	54	¹ AUBERT 08S	BABR	$10.6 e^+e^- \rightarrow \phi\pi^0\gamma$
••• We do not use the following data for averages, fits, limits, etc. •••				
1480±40		² BITYUKOV 87	SPEC	$32.5 \pi^-p \rightarrow \phi\pi^0n$
¹ From the fit with two resonances.				
² Systematic errors not estimated.				

 $\rho(1570)$ WIDTH

VALUE (MeV)	EVTS	DOCUMENT ID	TECN	COMMENT
144±75±43	54	³ AUBERT 08S	BABR	$10.6 e^+e^- \rightarrow \phi\pi^0\gamma$
••• We do not use the following data for averages, fits, limits, etc. •••				
130±60		⁴ BITYUKOV 87	SPEC	$32.5 \pi^-p \rightarrow \phi\pi^0n$
³ From the fit with two resonances.				
⁴ Systematic errors not estimated.				

 $\rho(1570)$ DECAY MODES

Mode	Fraction (Γ_i/Γ)
Γ_1 e^+e^-	
Γ_2 $\phi\pi$	not seen
Γ_3 $\omega\pi$	

 $\rho(1570)$ $\Gamma(i)\Gamma(e^+e^-)/\Gamma(\text{total})$

VALUE (eV)	CL%	EVTS	DOCUMENT ID	TECN	COMMENT
3.5±0.9±0.3		54	⁵ AUBERT 08S	BABR	$10.6 e^+e^- \rightarrow \phi\pi^0\gamma$
••• We do not use the following data for averages, fits, limits, etc. •••					
<70		90	⁶ AULCHENKO 87B	ND	$e^+e^- \rightarrow K_S^0 K_L^0 \pi^0$
⁵ From the fit with two resonances.					
⁶ Using mass and width of BITYUKOV 87.					

 $\rho(1570)$ BRANCHING RATIOS

$\Gamma(\phi\pi)/\Gamma_{\text{total}}$	DOCUMENT ID	TECN	COMMENT
not seen	ABELE 97H	CBAR	$\bar{p}p \rightarrow K_L^0 K_S^0 \pi^0 \pi^0$
••• We do not use the following data for averages, fits, limits, etc. •••			
<0.01	⁷ DONNACHIE 91	RVUE	
⁷ Using data from BISELLO 91B, DOLINSKY 86, and ALBRECHT 87L.			

 $\Gamma(\phi\pi)/\Gamma(\omega\pi)$ Γ_2/Γ_3

VALUE	CL%	DOCUMENT ID	TECN	COMMENT
••• We do not use the following data for averages, fits, limits, etc. •••				
>0.5	95	BITYUKOV 87	SPEC	$32.5 \pi^-p \rightarrow \phi\pi^0n$

 $\rho(1570)$ REFERENCES

AUBERT 08S	PR D77 092002	B. Aubert et al.	(BABAR Collab.)
ABELE 97H	PL B415 280	A. Abele et al.	(Crystal Barrel Collab.)
BISELLO 91B	NPBPS B21 111	D. Bisello	(DM2 Collab.)
DONNACHIE 91	ZPHY C51 689	A. Donnachie, A.B. Clegg	(MCHS, LANC)
ALBRECHT 87L	PL B185 223	H. Albrecht et al.	(ARGUS Collab.)
AULCHENKO 87B	JETPL 45 145	V.M. Aulchenko et al.	(NOVO)
Translated from ZETFP 45 118.			
BITYUKOV 87	PL B188 383	S.I. Bityukov et al.	(SERP)
DOLINSKY 86	PL B174 453	S.I. Dolinsky et al.	(NOVO)

Meson Particle Listings

 $h_1(1595)$, $\pi_1(1600)$ $h_1(1595)$

$$J^{PC} = 0^-(1^{+-})$$

OMITTED FROM SUMMARY TABLE

Seen in a partial-wave analysis of the $\omega\eta$ system produced in the reaction $\pi^-p \rightarrow \omega\eta n$ at 18 GeV/c. $h_1(1595)$ MASS

VALUE (MeV)	DOCUMENT ID	TECN	COMMENT
$1594 \pm 15^{+10}_{-60}$	EUGENIO	01	SPEC 18 $\pi^-p \rightarrow \omega\eta n$

 $h_1(1595)$ WIDTH

VALUE (MeV)	DOCUMENT ID	TECN	COMMENT
$384 \pm 60^{+70}_{-100}$	EUGENIO	01	SPEC 18 $\pi^-p \rightarrow \omega\eta n$

 $h_1(1595)$ DECAY MODES

Mode	Fraction (Γ_i/Γ)
Γ_1 $\omega\eta$	seen

 $h_1(1595)$ REFERENCES

EUGENIO 01 PL B497 190 P. Eugenio et al.

 $\pi_1(1600)$

$$J^{PC} = 1^-(1^{-+})$$

 $\pi_1(1600)$ MASS

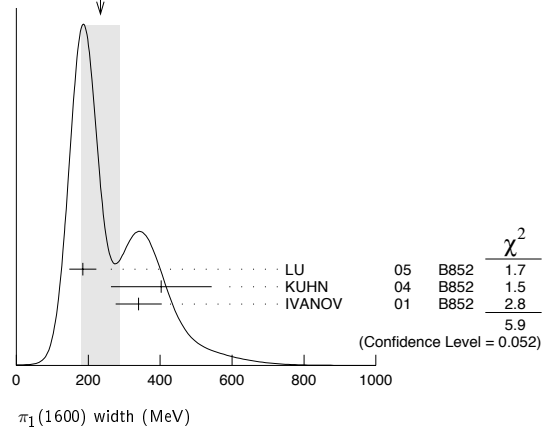
VALUE (MeV)	EVTS	DOCUMENT ID	TECN	COMMENT
$1662 \pm 15^{+11}$ OUR AVERAGE				Error includes scale factor of 1.2.
$1664 \pm 8 \pm 10$	145k	1 LU	05	B852 18 $\pi^-p \rightarrow \omega\pi^-\pi^0p$
$1709 \pm 24 \pm 41$	69k	2 KUHN	04	B852 18 $\pi^-p \rightarrow \eta\pi^+\pi^-\pi^-p$
$1597 \pm 10^{+45}_{-10}$		2 IVANOV	01	B852 18 $\pi^-p \rightarrow \eta'\pi^-p$

••• We do not use the following data for averages, fits, limits, etc. •••

 $1593 \pm 8^{+29}_{-47}$ 2,3 ADAMS 98B B852 18.3 $\pi^-p \rightarrow \pi^+\pi^-\pi^-p$ ¹ May be a different state: natural and unnatural parity exchanges.² Natural parity exchange.³ Superseded by DZIERBA 06 excluding this state in a more refined PWA analysis, with 2.6 M events of $\pi^-p \rightarrow \pi^-\pi^-\pi^+p$ and 3 M events of $\pi^-p \rightarrow \pi^-\pi^0\pi^0p$ of E852 data. $\pi_1(1600)$ WIDTH

VALUE (MeV)	EVTS	DOCUMENT ID	TECN	COMMENT
234 ± 50 OUR AVERAGE				Error includes scale factor of 1.7. See the ideogram below.
$185 \pm 25 \pm 28$	145k	4 LU	05	B852 18 $\pi^-p \rightarrow \omega\pi^-\pi^0p$
$403 \pm 80 \pm 115$	69k	5 KUHN	04	B852 18 $\pi^-p \rightarrow \eta\pi^+\pi^-\pi^-p$
$340 \pm 40 \pm 50$		5 IVANOV	01	B852 18 $\pi^-p \rightarrow \eta'\pi^-p$
$168 \pm 20^{+150}_{-12}$		5,6 ADAMS	98B	B852 18.3 $\pi^-p \rightarrow \pi^+\pi^-\pi^-p$

••• We do not use the following data for averages, fits, limits, etc. •••

⁴ May be a different state: natural and unnatural parity exchanges.⁵ Natural parity exchange.⁶ Superseded by DZIERBA 06 excluding this state in a more refined PWA analysis, with 2.6 M events of $\pi^-p \rightarrow \pi^-\pi^-\pi^+p$ and 3 M events of $\pi^-p \rightarrow \pi^-\pi^0\pi^0p$ of E852 data.WEIGHTED AVERAGE
234±50 (Error scaled by 1.7) $\pi_1(1600)$ DECAY MODES

Mode	Fraction (Γ_i/Γ)
Γ_1 $\pi\pi\pi$	not seen
Γ_2 $\rho^0\pi^-$	not seen
Γ_3 $f_2(1270)\pi^-$	not seen
Γ_4 $b_1(1235)\pi$	seen
Γ_5 $\eta'(958)\pi^-$	seen
Γ_6 $f_1(1285)\pi$	seen

 $\pi_1(1600)$ BRANCHING RATIOS

$\Gamma(\rho^0\pi^-)/\Gamma_{total}$	DOCUMENT ID	TECN	COMMENT	Γ_2/Γ
not seen	7 DZIERBA	06	B852 18 π^-p	

⁷ From the PWA analysis of 2.6 M $\pi^-p \rightarrow \pi^-\pi^-\pi^+p$ and 3 M events of $\pi^-p \rightarrow \pi^-\pi^0\pi^0p$ of E852 data. Supersedes ADAMS 98B.

$\Gamma(f_2(1270)\pi^-)/\Gamma_{total}$	DOCUMENT ID	TECN	COMMENT	Γ_3/Γ
not seen	8 DZIERBA	06	B852 18 π^-p	

⁸ From the PWA analysis of 2.6 M $\pi^-p \rightarrow \pi^-\pi^-\pi^+p$ and 3 M events of $\pi^-p \rightarrow \pi^-\pi^0\pi^0p$ of E852 data. Supersedes CHUNG 02.

$\Gamma(b_1(1235)\pi)/\Gamma_{total}$	EVTS	DOCUMENT ID	TECN	COMMENT	Γ_4/Γ
seen	35280	9 BAKER	03	SPEC $\bar{p}p \rightarrow \omega\pi^+\pi^-\pi^0$	

••• We do not use the following data for averages, fits, limits, etc. •••

$\Gamma(\eta'(958)\pi^-)/\Gamma_{total}$	DOCUMENT ID	TECN	COMMENT	Γ_5/Γ	
seen	145k	LU	05	B852 18 $\pi^-p \rightarrow \omega\pi^-\pi^0p$	
seen		IVANOV	01	B852 18 $\pi^-p \rightarrow \eta'\pi^-p$	

$\Gamma(f_1(1285)\pi)/\Gamma(\eta'(958)\pi^-)$	EVTS	DOCUMENT ID	TECN	COMMENT	Γ_6/Γ_5
3.80 ± 0.78	69k	10 KUHN	04	B852 18 $\pi^-p \rightarrow \eta\pi^+\pi^-\pi^-p$	

⁹ $B((b_1\pi)_{D-wave})/B((b_1\pi)_{S-wave}) = 0.3 \pm 0.1$.¹⁰ Using $\eta'(958)\pi$ data from IVA NOV 01. $\pi_1(1600)$ REFERENCES

DZIERBA	06	PR D73 072001	A.R. Dzierba et al.	(BNL E852 Collab.)
LU	05	PRL 94 032002	M. Lu et al.	(BNL E852 Collab.)
KUHN	04	PL B595 109	J. Kuhn et al.	(BNL E852 Collab.)
BAKER	03	PL B563 140	C.A. Baker et al.	
CHUNG	02	PR D65 072001	S.U. Chung et al.	(BNL E852 Collab.)
IVANOV	01	PRL 86 3977	E.I. Ivanov et al.	(BNL E852 Collab.)
ADAMS	98B	PRL 81 5760	G.S. Adams et al.	(BNL E852 Collab.)

OTHER RELATED PAPERS

GENERAL	07	EPJ C51 347	L.J. General, S.R. Contanch, F.J. Llanes-Estrada	
GENERAL	07A	PL B653 216	L.J. General et al.	
BUISSERET	06	EPJ A29 343	F. Buisseret, V. Mathieu	(UMH)
BURNS	06	PR D74 034003	T.J. Burns, F.E. Close	
COOK	06	PR D74 034001	M.S. Cook, H.R. Fiebig	
CUI	06	PR D73 014018	Y. Cui et al.	
HEDDITCH	05	PR D72 114507	J.N. Hedditch et al.	
POPLAWSKI	05	PR D71 056003	N.J. Poplawski, A.P. Szczepaniak, J.T. Londergan	
CLOSE	04A	PR D70 094015	F.E. Close, J.J. Dudek	

See key on page 373

Meson Particle Listings
 $\pi_1(1600)$, $a_1(1640)$, $f_2(1640)$

BERNARD	03	PR D68 074505	C. Bernard et al.
JIN	03	PR D67 014025	H.Y. Jin, J.G. Korener, T.G. Steele
SZCZEPANIAK	03B	PRL 91 092002	A.P. Szczepaniak et al.
ZHANG	03	PR D67 074020	A. Zhang, T.G. Steele
ACHASOV	02J	PAN 65 552	N.N. Achasov, G.N. Shestakov
Translated from YAF 65 579.			
CHUNG	02C	EPJ A15 539	S.U. Chung, E. Klempf, J.G. Korener
ZHANG	02	PR D65 096005	R. Zhang et al.
IDDIR	01	PL B507 183	F. Idir, A.S. Safir

 $a_1(1640)$

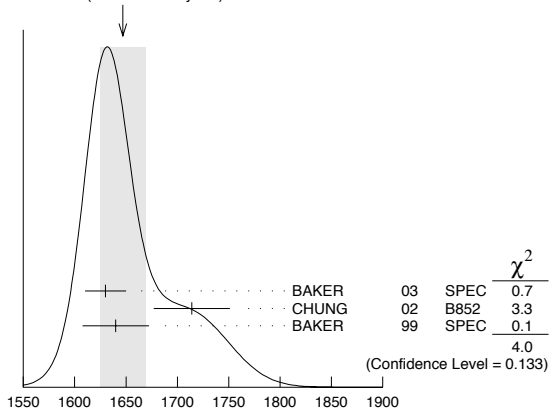
$$I^G(J^{PC}) = 1^-(1^{++})$$

OMITTED FROM SUMMARY TABLE

Seen in the amplitude analysis of the $3\pi^0$ system produced in $\bar{p}p \rightarrow 4\pi^0$. Possibly seen in the study of the hadronic structure in decay $\tau \rightarrow 3\pi\nu_\tau$ (ABREU 98G and ASNER 00). Needs confirmation.

 $a_1(1640)$ MASS

VALUE (MeV)	EVTs	DOCUMENT ID	TECN	COMMENT
1647 ± 22 OUR AVERAGE		Error includes scale factor of 1.4. See the ideogram below.		
1630 ± 20	35280	¹ BAKER	03	SPEC $\bar{p}p \rightarrow \omega\pi^+\pi^-\pi^0$
1714 ± 9 ± 36		CHUNG	02	B852 $18.3\pi^-p \rightarrow \pi^+\pi^-\pi^-p$
1640 ± 12 ± 30		BAKER	99	SPEC $1.94\bar{p}p \rightarrow 4\pi^0$
• • • We do not use the following data for averages, fits, limits, etc. • • •				
1670 ± 90		BELLINI	85	SPEC $40\pi^-A \rightarrow \pi^-\pi^+\pi^-A$

WEIGHTED AVERAGE
1647 ± 22 (Error scaled by 1.4)¹ Using the $a_1(1260)$ mass and width results of BOWLER 88. $a_1(1640)$ WIDTH

VALUE (MeV)	EVTs	DOCUMENT ID	TECN	COMMENT
254 ± 30 OUR AVERAGE		Error includes scale factor of 1.1.		
225 ± 30	35280	² BAKER	03	SPEC $\bar{p}p \rightarrow \omega\pi^+\pi^-\pi^0$
308 ± 37 ± 62		CHUNG	02	B852 $18.3\pi^-p \rightarrow \pi^+\pi^-\pi^-p$
300 ± 22 ± 40		BAKER	99	SPEC $1.94\bar{p}p \rightarrow 4\pi^0$
• • • We do not use the following data for averages, fits, limits, etc. • • •				
300 ± 100		BELLINI	85	SPEC $40\pi^-A \rightarrow \pi^-\pi^+\pi^-A$

² Using the $a_1(1260)$ mass and width results of BOWLER 88. $a_1(1640)$ DECAY MODES

Mode	Fraction (Γ_i/Γ)
Γ_1 $\pi\pi\pi$	seen
Γ_2 $f_2(1270)\pi$	seen
Γ_3 $\sigma\pi$	seen
Γ_4 $\rho\pi S$ -wave	seen
Γ_5 $\rho\pi D$ -wave	seen
Γ_6 $\omega\pi\pi$	seen
Γ_7 $f_1(1285)\pi$	seen
Γ_8 $a_1(1260)\eta$	not seen

 $a_1(1640)$ BRANCHING RATIOS

$\Gamma(f_2(1270)\pi)/\Gamma(\sigma\pi)$	DOCUMENT ID	TECN	COMMENT	Γ_2/Γ_3
0.24 ± 0.07	BAKER	99	SPEC $1.94\bar{p}p \rightarrow 4\pi^0$	

 $\Gamma(\rho\pi D\text{-wave})/\Gamma_{\text{total}}$ Γ_5/Γ

VALUE	DOCUMENT ID	TECN	COMMENT
• • • We do not use the following data for averages, fits, limits, etc. • • •			
seen	CHUNG	02	B852 $18.3\pi^-p \rightarrow \pi^+\pi^-\pi^-p$
seen	AMELIN	95B	VES $36\pi^-A \rightarrow \pi^+\pi^-\pi^-A$

 $\Gamma(\omega\pi\pi)/\Gamma_{\text{total}}$ Γ_6/Γ

VALUE	EVTs	DOCUMENT ID	TECN	COMMENT
• • • We do not use the following data for averages, fits, limits, etc. • • •				
seen	35280	³ BAKER	03	SPEC $\bar{p}p \rightarrow \omega\pi^+\pi^-\pi^0$

 $\Gamma(f_1(1285)\pi)/\Gamma_{\text{total}}$ Γ_7/Γ

VALUE	DOCUMENT ID	TECN	COMMENT
• • • We do not use the following data for averages, fits, limits, etc. • • •			
not seen	KUHN	04	B852 $18\pi^-p \rightarrow \eta\pi^+\pi^-\pi^-p$
seen	LEE	94	MPS2 $18\pi^-p \rightarrow K^+\bar{K}^0\pi^-\pi^-p$

 $\Gamma(a_1(1260)\eta)/\Gamma_{\text{total}}$ Γ_8/Γ

VALUE	DOCUMENT ID	TECN	COMMENT
not seen	KUHN	04	B852 $18\pi^-p \rightarrow \eta\pi^+\pi^-\pi^-p$
³ Assuming the $\omega\rho$ mechanism for the $\omega\pi\pi$ state.			

 $a_1(1640)$ REFERENCES

KUHN	04	PL B595 109	J. Kuhn et al.	(BNL E852 Collab.)
BAKER	03	PL B563 140	C.A. Baker et al.	
CHUNG	02	PR D65 072001	S.U. Chung et al.	(BNL E852 Collab.)
ASNER	00	PR D61 012002	D.M. Asner et al.	(CLEO Collab.)
BAKER	99	PL B449 114	C.A. Baker et al.	
ABREU	98G	PL B426 411	P. Abreu et al.	(DELPHI Collab.)
AMELIN	95B	PL B356 595	D.V. Amelin et al.	(SERP, TBL)
LEE	94	PL B323 227	J.H. Lee et al.	(BNL, IND, KYUN, MASD+)
BOWLER	88	PL B209 99	M.G. Bowler	(OXF)
BELLINI	85	SJNP 41 781	D. Bellini et al.	
Translated from YAF 41 1223.				

OTHER RELATED PAPERS

BARNES	97	PR D55 4157	T. Barnes et al.	(ORNL, RAL, MCHS)
GOUZ	92	Dallas HEP 92, p. 572	Yu.P. Gouz et al.	(VES Collab.)
Proceedings XXVI Int. Conf. on High Energy Physics				

 $f_2(1640)$

$$I^G(J^{PC}) = 0^+(2^{++})$$

OMITTED FROM SUMMARY TABLE

 $f_2(1640)$ MASS

VALUE (MeV)	DOCUMENT ID	TECN	COMMENT
1639 ± 6 OUR AVERAGE	Error includes scale factor of 1.2.		
1620 ± 16	BUGG	95	MRK3 $J/\psi \rightarrow \gamma\pi^+\pi^-\pi^+\pi^-$
1647 ± 7	ADAMO	92	OBLX $\bar{p}p \rightarrow 3\pi^+2\pi^-$
1635 ± 7	ALDE	90	GAM2 $38\pi^-p \rightarrow \omega\omega n$
• • • We do not use the following data for averages, fits, limits, etc. • • •			
1640 ± 5	AMSLER	06	CBAR $0.9\bar{p}p \rightarrow K^+K^-\pi^0$
1659 ± 6	VLADIMIRSK...06	SPEC	$40\pi^-p \rightarrow K_S^0 K_S^0 n$
1643 ± 7	¹ ALDE	89B	GAM2 $38\pi^-p \rightarrow \omega\omega n$

¹ Superseded by ALDE 90. $f_2(1640)$ WIDTH

VALUE (MeV)	CL%	DOCUMENT ID	TECN	COMMENT
99 ⁺⁶⁰ -40 OUR AVERAGE		Error includes scale factor of 2.9.		
140 ⁺⁶⁰ -20		BUGG	95	MRK3 $J/\psi \rightarrow \gamma\pi^+\pi^-\pi^+\pi^-$
58 ± 20		ADAMO	92	OBLX $\bar{p}p \rightarrow 3\pi^+2\pi^-$
• • • We do not use the following data for averages, fits, limits, etc. • • •				
44 ± 9		AMSLER	06	CBAR $0.9\bar{p}p \rightarrow K^+K^-\pi^0$
152 ± 18		VLADIMIRSK...06	SPEC	$40\pi^-p \rightarrow K_S^0 K_S^0 n$
< 70	90	ALDE	90	GAM2 $38\pi^-p \rightarrow \omega\omega n$

 $f_2(1640)$ DECAY MODES

Mode	Fraction (Γ_i/Γ)
Γ_1 $\omega\omega$	seen
Γ_2 4π	seen
Γ_3 $K\bar{K}$	seen

 $f_2(1640)$ BRANCHING RATIOS

$\Gamma(K\bar{K})/\Gamma_{\text{total}}$	DOCUMENT ID	TECN	COMMENT	Γ_3/Γ
seen	AMSLER	06	CBAR $0.9\bar{p}p \rightarrow K^+K^-\pi^0$	

Meson Particle Listings

$f_2(1640), \eta_2(1645), \omega(1650)$

$\eta_2(1640)$ REFERENCES

AMSLER	06	PL B639 165	C. Anisler et al.	(CBAR Collab.)
VLADIMIRSK...	06	PAN 69 493	V.V. Vladimirov et al.	(ITEP, Moscow)
		Translated from YAF 69 515		
BUGG	95	PL B353 378	D.V. Bugg et al.	(LOQM, PNPI, WASH) JP
ADAMO	92	PL B287 368	A. Adamo et al.	(OBELIX Collab.)
ALDE	90	PL B241 600	D.M. Alde et al.	(SERP, BELG, LANL, LAPP+)
ALDE	89B	PL B216 451	D.M. Alde et al.	(SERP, BELG, LANL, LAPP+) IJGPC

OTHER RELATED PAPERS

ABLIKIM	06H	PR D73 112007	M. Ablikim et al.	(BES Collab.)
ANISOVICH	05	JETPL 80 715	V.V. Anisovich	
		Translated from ZETFP 80 845		
PROKOSHKIN	99	PAN 62 356	Yu.D. Prokoshkin	
		Translated from YAF 62 336		

$\eta_2(1645)$

$$J^{PC} = 0^+(2^-+)$$

$\eta_2(1645)$ MASS

VALUE (MeV)	DOCUMENT ID	TECN	CHG	COMMENT
1617 ± 5 OUR AVERAGE				
1613 ± 8	BARBERIS	00B		450 $pp \rightarrow \rho_f \eta \pi^+ \pi^- p_S$
1617 ± 8	BARBERIS	00c		450 $pp \rightarrow \rho_f 4\pi p_S$
1620 ± 20	BARBERIS	97B	OMEG	450 $pp \rightarrow \rho p 2(\pi^+ \pi^-)$
1645 ± 14 ± 15	ADOMEIT	96	CBAR 0	1.94 $\bar{p}p \rightarrow \eta 3\pi^0$
• • • We do not use the following data for averages, fits, limits, etc. • • •				
1645 ± 6 ± 20	ANISOVICH	00E	SPEC	1.94 $\bar{p}p \rightarrow \eta 3\pi^0$

$\eta_2(1645)$ WIDTH

VALUE (MeV)	DOCUMENT ID	TECN	CHG	COMMENT
181 ± 11 OUR AVERAGE				
185 ± 17	BARBERIS	00B		450 $pp \rightarrow \rho_f \eta \pi^+ \pi^- p_S$
177 ± 18	BARBERIS	00c		450 $pp \rightarrow \rho_f 4\pi p_S$
180 ± 25	BARBERIS	97B	OMEG	450 $pp \rightarrow \rho p 2(\pi^+ \pi^-)$
180 ⁺⁴⁰ ₋₂₁ ± 25	ADOMEIT	96	CBAR 0	1.94 $\bar{p}p \rightarrow \eta 3\pi^0$
• • • We do not use the following data for averages, fits, limits, etc. • • •				
200 ± 25	ANISOVICH	00E	SPEC	1.94 $\bar{p}p \rightarrow \eta 3\pi^0$

$\eta_2(1645)$ DECAY MODES

Mode	Fraction (Γ_i/Γ)
Γ_1 $a_2(1320)\pi$	seen
Γ_2 $K\bar{K}\pi$	seen
Γ_3 $K^*\bar{K}$	seen
Γ_4 $\eta\pi^+\pi^-$	seen
Γ_5 $a_0(980)\pi$	seen
Γ_6 $f_2(1270)\eta$	not seen

$\eta_2(1645)$ BRANCHING RATIOS

$\Gamma(K\bar{K}\pi)/\Gamma(a_2(1320)\pi)$	Γ_2/Γ_1
0.07 ± 0.03	
1 BARBERIS	97c
450 $pp \rightarrow \rho p K\bar{K}\pi$	
1 Using $2(\pi^+\pi^-)$ data from BARBERIS 97b.	
$\Gamma(a_2(1320)\pi)/\Gamma(a_0(980)\pi)$	Γ_1/Γ_5
13.0 ± 2.7	
BARBERIS	00B
450 $pp \rightarrow \rho_f \eta \pi^+ \pi^- p_S$	
$\Gamma(f_2(1270)\eta)/\Gamma_{total}$	Γ_6/Γ
not seen	
BARBERIS	00B
450 $pp \rightarrow \rho_f \eta \pi^+ \pi^- p_S$	
• • • We do not use the following data for averages, fits, limits, etc. • • •	

$\eta_2(1645)$ REFERENCES

ANISOVICH	00E	PL B477 19	A.V. Anisovich et al.	
BARBERIS	00B	PL B471 435	D. Barberis et al.	(WA 102 Collab.)
BARBERIS	00C	PL B471 440	D. Barberis et al.	(WA 102 Collab.)
BARBERIS	97B	PL B413 217	D. Barberis et al.	(WA 102 Collab.)
BARBERIS	97C	PL B413 225	D. Barberis et al.	(WA 102 Collab.)
ADOMEIT	96	ZPHY C71 227	J. Adomeit et al.	(Crystal Barrel Collab.)

$\omega(1650)$

$$J^{PC} = 0^-(1^-)$$

$\omega(1650)$ MASS

VALUE (MeV)	EVTS	DOCUMENT ID	TECN	COMMENT
1670 ± 30 OUR ESTIMATE				
• • • We do not use the following data for averages, fits, limits, etc. • • •				
1667 ± 13 ± 6		AUBERT	07AU BABR	10.6 $e^+e^- \rightarrow \omega\pi^+\pi^-\gamma$
1645 ± 8	13	AUBERT	06D BABR	10.6 $e^+e^- \rightarrow \omega\eta\gamma$
1660 ± 10 ± 2		AUBERT,B	04N BABR	10.6 $e^+e^- \rightarrow \pi^+\pi^-\pi^0\gamma$
1770 ± 50 ± 60	1.2M	1 ACHASOV	03D RVUE	0.44-2.00 $e^+e^- \rightarrow \pi^+\pi^-\pi^0$
1619 ± 5		2 HENNER	02 RVUE	1.2-2.0 $e^+e^- \rightarrow \rho\pi, \omega\pi\pi$
1700 ± 20		EUGENIO	01 SPEC	18 $\pi^-\rho \rightarrow \omega\eta\eta$
1705 ± 26	612	3 AKHMETSHIN	00D CMD2	$e^+e^- \rightarrow \omega\pi^+\pi^-$
1820 ⁺¹⁹⁰ ₋₁₅₀		4 ACHASOV	98H RVUE	$e^+e^- \rightarrow \pi^+\pi^-\pi^0$
1840 ⁺¹⁰⁰ ₋₇₀		5 ACHASOV	98H RVUE	$e^+e^- \rightarrow \omega\pi^+\pi^-$
1780 ⁺¹⁷⁰ ₋₃₀₀		6 ACHASOV	98H RVUE	$e^+e^- \rightarrow K^+K^-$
~ 2100		7 ACHASOV	98H RVUE	$e^+e^- \rightarrow K_S^0 K^\pm \pi^\mp$
1606 ± 9		8 CLEGG	94 RVUE	
1662 ± 13	750	9 ANTONELLI	92 DM2	1.34-2.4 $e^+e^- \rightarrow \rho\pi, \omega\pi\pi$
1670 ± 20		ATKINSON	83B OMEG	20-70 $\gamma\rho \rightarrow 3\pi X$
1657 ± 13		CORDIER	81 DM1	$e^+e^- \rightarrow \omega 2\pi$
1679 ± 34	21	ESPOSITO	80 FRAM	$e^+e^- \rightarrow 3\pi$
1652 ± 17		COSME	79 OSPK	$e^+e^- \rightarrow 3\pi$

- From the combined fit of ANTONELLI 92, ACHASOV 01E, ACHASOV 02E, and ACHASOV 03D data on the $\pi^+\pi^-\pi^0$ and ANTONELLI 92 on the $\omega\pi^+\pi^-$ final states. Supersedes ACHASOV 99E and ACHASOV 02E.
- Using results of CORDIER 81 and preliminary data of DOLINSKY 91 and ANTONELLI 92.
- Using the data of AKHMETSHIN 00D and ANTONELLI 92. The $\rho\pi$ dominance for the energy dependence of the $\omega(1420)$ and $\omega(1650)$ width assumed.
- Using data from BARKOV 87, DOLINSKY 91, and ANTONELLI 92.
- Using the data from ANTONELLI 92.
- Using the data from IVANOV 81 and BISELLO 88b.
- Using the data from BISELLO 91c.
- From a fit to two Breit-Wigner functions and using the data of DOLINSKY 91 and ANTONELLI 92.
- From the combined fit of the $\rho\pi$ and $\omega\pi\pi$ final states.

$\omega(1650)$ WIDTH

VALUE (MeV)	EVTS	DOCUMENT ID	TECN	COMMENT
315 ± 35 OUR ESTIMATE				
• • • We do not use the following data for averages, fits, limits, etc. • • •				
222 ± 25 ± 20		AUBERT	07AU BABR	10.6 $e^+e^- \rightarrow \omega\pi^+\pi^-\gamma$
114 ± 14	13	AUBERT	06D BABR	10.6 $e^+e^- \rightarrow \omega\eta\gamma$
230 ± 30 ± 20		AUBERT,B	04N BABR	10.6 $e^+e^- \rightarrow \pi^+\pi^-\pi^0\gamma$
490 ⁺²⁰⁰ ₋₁₅₀ ± 130	1.2M	10 ACHASOV	03D RVUE	0.44-2.00 $e^+e^- \rightarrow \pi^+\pi^-\pi^0$
250 ± 14		11 HENNER	02 RVUE	1.2-2.0 $e^+e^- \rightarrow \rho\pi, \omega\pi\pi$
250 ± 50		EUGENIO	01 SPEC	18 $\pi^-\rho \rightarrow \omega\eta\eta$
370 ± 25	612	12 AKHMETSHIN	00D CMD2	$e^+e^- \rightarrow \omega\pi^+\pi^-$
113 ± 20		13 CLEGG	94 RVUE	
280 ± 24	750	14 ANTONELLI	92 DM2	1.34-2.4 $e^+e^- \rightarrow \rho\pi, \omega\pi\pi$
160 ± 20		ATKINSON	83B OMEG	20-70 $\gamma\rho \rightarrow 3\pi X$
136 ± 46		CORDIER	81 DM1	$e^+e^- \rightarrow \omega 2\pi$
99 ± 49	21	ESPOSITO	80 FRAM	$e^+e^- \rightarrow 3\pi$
42 ± 17		COSME	79 OSPK	$e^+e^- \rightarrow 3\pi$
10 From the combined fit of ANTONELLI 92, ACHASOV 01E, ACHASOV 02E, and ACHASOV 03D data on the $\pi^+\pi^-\pi^0$ and ANTONELLI 92 on the $\omega\pi^+\pi^-$ final states. Supersedes ACHASOV 99E and ACHASOV 02E.				
11 Using results of CORDIER 81 and preliminary data of DOLINSKY 91 and ANTONELLI 92.				
12 Using the data of AKHMETSHIN 00D and ANTONELLI 92. The $\rho\pi$ dominance for the energy dependence of the $\omega(1420)$ and $\omega(1650)$ width assumed.				
13 From a fit to two Breit-Wigner functions and using the data of DOLINSKY 91 and ANTONELLI 92.				
14 From the combined fit of the $\rho\pi$ and $\omega\pi\pi$ final states.				

$\omega(1650)$ DECAY MODES

Mode	Fraction (Γ_i/Γ)
Γ_1 $\rho\pi$	seen
Γ_2 $\omega\pi\pi$	seen
Γ_3 $\omega\eta$	seen
Γ_4 e^+e^-	seen

See key on page 373

Meson Particle Listings

$\omega(1650), \omega_3(1670)$

$\omega(1650) \Gamma(i)\Gamma(e^+e^-)/\Gamma^2(\text{total})$

$\Gamma(\rho\pi) \times \Gamma(e^+e^-)/\Gamma_{\text{total}}^2$	VALUE (units 10^{-6})	EVTS	DOCUMENT ID	TECN	COMMENT	$\Gamma_1\Gamma_4/\Gamma^2$	
••• We do not use the following data for averages, fits, limits, etc. •••							
1.3 ± 0.1	± 0.1		AUBERT,B	04N	BABR	$10.6 e^+e^- \rightarrow \pi^+\pi^-\pi^0\gamma$	
1.2 $\begin{smallmatrix} +0.4 \\ -0.1 \end{smallmatrix}$	± 0.8	1.2M	15,16	ACHASOV	03D	RVUE	$0.44-2.00 e^+e^- \rightarrow \pi^+\pi^-\pi^0$
0.921 ± 0.230			17,18	CLEGG	94	RVUE	
0.479 ± 0.050		750	19,20	ANTONELLI	92	DM2	$1.34-2.4e^+e^- \rightarrow \rho\pi, \omega\pi\pi$

$\Gamma(\omega\pi\pi) \times \Gamma(e^+e^-)/\Gamma_{\text{total}}^2$	VALUE (units 10^{-7})	EVTS	DOCUMENT ID	TECN	COMMENT	$\Gamma_2\Gamma_4/\Gamma^2$	
••• We do not use the following data for averages, fits, limits, etc. •••							
7.0 ± 0.5			AUBERT	07AU	BABR	$10.6 e^+e^- \rightarrow \omega\pi^+\pi^-\gamma$	
4.1 $\pm 0.9 \pm 1.3$		1.2M	15,16	ACHASOV	03D	RVUE	$0.44-2.00 e^+e^- \rightarrow \pi^+\pi^-\pi^0$
5.40 ± 0.95			21	AKHMETSHIN	00D	CMD2	$1.2-1.38 e^+e^- \rightarrow \omega\pi^+\pi^-$
3.18 ± 0.80			17,18	CLEGG	94	RVUE	
6.07 ± 0.61		750	19,20	ANTONELLI	92	DM2	$1.34-2.4 e^+e^- \rightarrow \rho\pi, \omega\pi\pi$

$\Gamma(\omega\eta) \times \Gamma(e^+e^-)/\Gamma_{\text{total}}^2$	VALUE (units 10^{-6})	CL%	EVTS	DOCUMENT ID	TECN	COMMENT	$\Gamma_3\Gamma_4/\Gamma^2$	
••• We do not use the following data for averages, fits, limits, etc. •••								
0.57 ± 0.06			13	AUBERT	06D	BABR	$10.6 e^+e^- \rightarrow \omega\eta\gamma$	
<6			90	22	AKHMETSHIN	03B	CMD2	$e^+e^- \rightarrow \eta\pi^0\gamma$

- 15 Calculated by us from the cross section at the peak.
- 16 From the combined fit of ANTONELLI 92, ACHASOV 01E, ACHASOV 02E, and ACHASOV 03D data on the $\pi^+\pi^-\pi^0$ and ANTONELLI 92 on the $\omega\pi^+\pi^-$ final states. Supersedes ACHASOV 99E and ACHASOV 02E.
- 17 From a fit to two Breit-Wigner functions and using the data of DOLINSKY 91 and ANTONELLI 92.
- 18 From the partial and leptonic width given by the authors.
- 19 From the combined fit of the $\rho\pi$ and $\omega\pi\pi$ final states.
- 20 From the product of the leptonic width and partial branching ratio given by the authors.
- 21 Using the data of AKHMETSHIN 00D and ANTONELLI 92. The $\rho\pi$ dominance for the energy dependence of the $\omega(1420)$ and $\omega(1650)$ width assumed.
- 22 $\omega(1650)$ mass and width fixed at 1700 MeV and 250 MeV, respectively.

$\omega(1650)$ BRANCHING RATIOS

$\Gamma(\omega\pi\pi)/\Gamma_{\text{total}}$	VALUE	EVTS	DOCUMENT ID	TECN	COMMENT	Γ_2/Γ	
••• We do not use the following data for averages, fits, limits, etc. •••							
~ 0.35		1.2M	23	ACHASOV	03D	RVUE	$0.44-2.00 e^+e^- \rightarrow \pi^+\pi^-\pi^0$
0.620 ± 0.014			24	HENNER	02	RVUE	$1.2-2.0 e^+e^- \rightarrow \rho\pi, \omega\pi\pi$

$\Gamma(\rho\pi)/\Gamma_{\text{total}}$	VALUE	EVTS	DOCUMENT ID	TECN	COMMENT	Γ_1/Γ	
••• We do not use the following data for averages, fits, limits, etc. •••							
~ 0.65		1.2M	23	ACHASOV	03D	RVUE	$0.44-2.00 e^+e^- \rightarrow \pi^+\pi^-\pi^0$
0.380 ± 0.014			24	HENNER	02	RVUE	$1.2-2.0 e^+e^- \rightarrow \rho\pi, \omega\pi\pi$

$\Gamma(e^+e^-)/\Gamma_{\text{total}}$	VALUE (units 10^{-7})	EVTS	DOCUMENT ID	TECN	COMMENT	Γ_4/Γ	
••• We do not use the following data for averages, fits, limits, etc. •••							
~ 18		1.2M	24,25	ACHASOV	03D	RVUE	$0.44-2.00 e^+e^- \rightarrow \pi^+\pi^-\pi^0$
32 ± 1			24	HENNER	02	RVUE	$1.2-2.0 e^+e^- \rightarrow \rho\pi, \omega\pi\pi$

- 23 From the combined fit of ANTONELLI 92, ACHASOV 01E, ACHASOV 02E, and ACHASOV 03D data on the $\pi^+\pi^-\pi^0$ and ANTONELLI 92 on the $\omega\pi^+\pi^-$ final states. Supersedes ACHASOV 99E and ACHASOV 02E.
- 24 Assuming that the $\omega(1650)$ decays into $\rho\pi$ and $\omega\pi\pi$ only.
- 25 Calculated by us from the cross section at the peak.

$\omega(1650)$ REFERENCES

AUBERT 07AU PR D76 092005	B. Aubert et al.	(BABAR Collab.)
AUBERT 06D PR D73 052003	B. Aubert et al.	(BABAR Collab.)
AUBERT,B 04N PR D70 072004	B. Aubert et al.	(BABAR Collab.)
ACHASOV 03D PR D68 052006	M.N. Achasov et al.	(Novosibirsk SND Collab.)
AKHMETSHIN 03B PL B562 173	R.R. Akhmetshin et al.	(Novosibirsk CMD-2 Collab.)
ACHASOV 02E PR D66 032001	M.N. Achasov et al.	(Novosibirsk SND Collab.)
HENNER 02 EPJ C26 3	V.K. Henner et al.	
ACHASOV 01E PR D63 072002	M.N. Achasov et al.	(Novosibirsk SND Collab.)
EUGENIO 01 PL B497 190	P. Eugenio et al.	
AKHMETSHIN 00D PL B489 125	R.R. Akhmetshin et al.	(Novosibirsk CMD-2 Collab.)
ACHASOV 99E PL B462 365	M.N. Achasov et al.	(Novosibirsk SND Collab.)
ACHASOV 98H PR D57 4334	M.N. Achasov, A.A. Kozhevnikov	
CLEGG 94 ZPHY C62 455	A.B. Clegg, A. Donnachie	(LANC, MCHS)
ANTONELLI 92 ZPHY C56 15	A. Antonelli et al.	(DM2 Collab.)
BISELLO 91C ZPHY C52 227	D. Bisello et al.	(DM2 Collab.)
DOLINSKY 91 PRPL 202 99	S.I. Dolinsky et al.	(NOVO)
BISELLO 86B ZPHY C39 13	D. Bisello et al.	(NOVO)
BARKOV 87 JETPL 46 164	L.M. Barkov et al.	(PADO, CLER, FRAS+)
	Translated from ZETFP 46 132.	(NOVO)
ATKINSON 83B PL 127B 132	M. Atkinson et al.	(BONN, CERN, GLAS+)
CORDIER 81 PL 106B 155	A. Cordier et al.	(ORSAY)
IVANOV 81 PL 107B 297	P.M. Ivanov et al.	(NOVO)
ESPOSITO 80 LNC 28 195	B. Esposito et al.	(FRAS, NAPL, PADO+)
COSME 79 NP B152 215	G. Cosme et al.	(IPN)

OTHER RELATED PAPERS

ACHASOV 07A PR D76 072012	M.N. Achasov et al.	(SND Collab.)
AKHMETSHIN 03 PL B551 27	R.R. Akhmetshin et al.	(Novosibirsk CMD-2 Collab.)
Also PAN 65 1222	E.V. Anashkin, V.M. Aulchenko, R.R. Akhmetshin	
	Translated from YAF 65 1255.	
ACHASOV 02B PAN 65 153	M.N. Achasov, A.A. Kozhevnikov	
	Translated from YAF 65 158.	
CLOSE 02 PR D65 092003	F.E. Close, A. Donnachie, Yu.S. Kalashnikova	
ACHASOV 00J PR D62 117503	N.N. Achasov, A.A. Kozhevnikov	
ANISOVICH 00H PL B485 341	A.V. Anisovich et al.	
ABELE 99D PL B468 178	A. Abele et al.	(Crystal Barrel Collab.)
BELOZEROVA 98 PPN 29 63	T.S. Belozerovala, V.K. Henner	
	Translated from FECAF 29 148.	
ACHASOV 97F PAN 60 2029	M.N. Achasov, A.A. Kozhevnikov	(NOVM)
	Translated from YAF 60 2212.	
DOLINSKY 91 PRPL 202 99	S.I. Dolinsky et al.	(NOVO)
ATKINSON 87 ZPHY C34 157	M. Atkinson et al.	(BONN, CERN, GLAS+)
ATKINSON 84 NP B231 15	M. Atkinson et al.	(BONN, CERN, GLAS+)

$\omega_3(1670)$

$$I^G(J^{PC}) = 0^-(3^--)$$

$\omega_3(1670)$ MASS

VALUE (MeV)	EVTS	DOCUMENT ID	TECN	COMMENT
1667 ± 4 OUR AVERAGE				
1665.3 $\pm 5.2 \pm 4.5$	23400	AMELIN	96	VES
1685 ± 20	60	BAUBILLIER	79	HBC
1673 ± 12	430	1,2 BALTAY	78E	HBC
1650 ± 12		CORDEEN	78B	OMEG
1669 ± 11	600	2 WAGNER	75	HBC
1678 ± 14	500	DIAZ	74	DBC
1660 ± 13	200	DIAZ	74	DBC
1679 ± 17	200	MATTHEWS	71D	DBC
1670 ± 20		KENYON	69	DBC
~ 1700	110	1 CERRADA	77B	HBC
1695 ± 20		BARNES	69B	HBC
1636 ± 20		ARMENISE	68B	DBC

- We do not use the following data for averages, fits, limits, etc. •••
- 1 Phase rotation seen for $J^P = 3^- \rho\pi$ wave.
- 2 From a fit to $I(J^P) = 0(3^-) \rho\pi$ partial wave.

$\omega_3(1670)$ WIDTH

VALUE (MeV)	EVTS	DOCUMENT ID	TECN	COMMENT
168 ± 10 OUR AVERAGE				
149 $\pm 19 \pm 7$	23400	AMELIN	96	VES
160 ± 80	60	3 BAUBILLIER	79	HBC
173 ± 16	430	4,5 BALTAY	78E	HBC
253 ± 39		CORDEEN	78B	OMEG
173 ± 28	600	3,5 WAGNER	75	HBC
167 ± 40	500	DIAZ	74	DBC
122 ± 39	200	DIAZ	74	DBC
155 ± 40	200	3 MATTHEWS	71D	DBC
90 ± 20		BARNES	69B	HBC
100 ± 40		KENYON	69	DBC
112 ± 60		ARMENISE	68B	DBC

- We do not use the following data for averages, fits, limits, etc. •••
- 3 Width errors enlarged by us to $4\Gamma/\sqrt{N}$; see the note with the $K^*(892)$ mass.
- 4 Phase rotation seen for $J^P = 3^- \rho\pi$ wave.
- 5 From a fit to $I(J^P) = 0(3^-) \rho\pi$ partial wave.

$\omega_3(1670)$ DECAY MODES

Mode	Fraction (Γ_i/Γ)
$\Gamma_1 \rho\pi$	seen
$\Gamma_2 \omega\pi\pi$	seen
$\Gamma_3 b_1(1235)\pi$	possibly seen

$\omega_3(1670)$ BRANCHING RATIOS

$\Gamma(\omega\pi\pi)/\Gamma(\rho\pi)$	VALUE	EVTS	DOCUMENT ID	TECN	COMMENT	Γ_2/Γ_1
••• We do not use the following data for averages, fits, limits, etc. •••						
0.71 ± 0.27		100	DIAZ	74	DBC	$6\pi^+\pi^- \rightarrow p_5\pi^0$

$\Gamma(b_1(1235)\pi)/\Gamma(\rho\pi)$	VALUE	DOCUMENT ID	TECN	COMMENT	Γ_3/Γ_1
possibly seen		DIAZ	74	DBC	$6\pi^+\pi^- \rightarrow p_5\pi^0$

$\Gamma(b_1(1235)\pi)/\Gamma(\omega\pi\pi)$	VALUE	CL%	DOCUMENT ID	TECN	COMMENT	Γ_3/Γ_2
••• We do not use the following data for averages, fits, limits, etc. •••						
>0.75		68	BAUBILLIER	79	HBC	$8.2 K^-\rho$ backward

Meson Particle Listings

$\omega_3(1670), \pi_2(1670)$

$\omega_3(1670)$ REFERENCES

AMELIN	96	ZPHY C70 71	D.V. Amelin et al.	(SERP, TBIL)
BAUBILLIER	79	PL 09B 131	M. Baubillier et al.	(BIRM, CERN, GLAS+)
BALTAY	78E	PRL 40 87	C. Baltay, C.V. Cautis, M. Kalelkar	(COLU) JP
CORDEN	78B	NP B138 235	M.J. Corden et al.	(BIRM, RHEL, TELA+)
CERRADA	77B	NP B126 241	M. Cerrada et al.	(AMST, CERN, NIJM+) JP
WAGNER	75	PL 58B 201	F. Wagner, M. Tabak, D.M. Chew	(LBL) JP
DIAZ	74	PRL 32 260	J. Diaz et al.	(CASE, CMU)
MATTHEWS	71D	PR D3 2561	J.A.J. Matthews et al.	(TNT0, WIS C)
BARNES	69B	PRL 23 142	V.E. Barnes et al.	(BNL)
KENYON	69	PRL 23 146	I.R. Kenyon et al.	(BNL, UCND, ORNL)
ARMENISE	68B	PL 26B 336	N. Armenise et al.	(BARI, BGNA, FIRZ+)

OTHER RELATED PAPERS

MATTHEWS	71	LNC 1 361	J.A.J. Matthews et al.	(TNT0, WIS C)
ARMENISE	70	LNC 4 199	N. Armenise et al.	(BARI, BGNA, FIRZ)

$\pi_2(1670)$

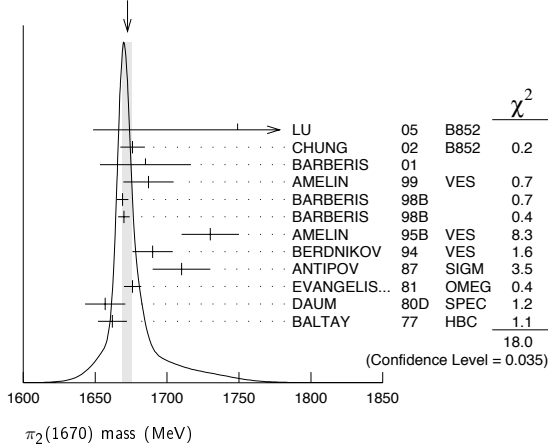
$$I^G(J^{PC}) = 1^-(2^{-+})$$

$\pi_2(1670)$ MASS

VALUE (MeV)	EVTS	DOCUMENT ID	TECN	CHG	COMMENT
1672.4 ± 3.2 OUR AVERAGE		Error includes scale factor of 1.4. See the ideogram below.			
1749 ± 10 ± 100	145k	LU	05	B852	18 $\pi^- \rho \rightarrow \omega \pi^- \pi^0 \rho$
1676 ± 3 ± 8		1 CHUNG	02	B852	18.3 $\pi^- \rho \rightarrow \pi^+ \pi^- \pi^- \rho$
1685 ± 10 ± 30		2 BARBERIS	01		450 $\rho \rho \rightarrow \rho_f 3\pi^0 \rho_S$
1687 ± 9 ± 15		AMELIN	99	VES	37 $\pi^- A \rightarrow \omega \pi^- \pi^0 A^*$
1669 ± 4		BARBERIS	98B		450 $\rho \rho \rightarrow \rho_f \rho \pi \rho_S$
1670 ± 4		BARBERIS	98B		450 $\rho \rho \rightarrow \rho_f f_2(1270) \pi \rho_S$
1730 ± 20		3 AMELIN	95B	VES	36 $\pi^- A \rightarrow \pi^+ \pi^- \pi^- A$
1690 ± 14		4 BERDNIKOV	94	VES	37 $\pi^- A \rightarrow K^+ K^- \pi^- A$
1710 ± 20	700	ANTIPOV	87	SIGM	50 $\pi^- \text{Cu} \rightarrow \mu^+ \mu^- \pi^- \text{Cu}$
1676 ± 6		4 EVANGELIS...	81	OMEG	12 $\pi^- \rho \rightarrow 3\pi \rho$
1657 ± 14		4,5 DAUM	80D	SPEC	63-94 $\pi \rho \rightarrow 3\pi X$
1662 ± 10	2000	4 BALTAY	77	HBC	15 $\pi^+ \rho \rightarrow \rho 3\pi$
• • • We do not use the following data for averages, fits, limits, etc. • • •					
1742 ± 31 ± 49		ANTREASYAN	90	CBAL	$e^+ e^- \rightarrow e^+ e^- \pi^0 \pi^0 \pi^0$
1624 ± 21		1 BELLINI	85	SPEC	40 $\pi^- A \rightarrow \pi^- \pi^+ \pi^- A$
1622 ± 35		6 BELLINI	85	SPEC	40 $\pi^- A \rightarrow \pi^- \pi^+ \pi^- A$
1693 ± 28		7 BELLINI	85	SPEC	40 $\pi^- A \rightarrow \pi^- \pi^+ \pi^- A$
1710 ± 20		8 DAUM	81B	SPEC	63,94 $\pi^- \rho$
1660 ± 10		4 ASCOLI	73	HBC	5-25 $\pi^- \rho \rightarrow \rho \pi_2$

- From $f_2(1270) \pi$ decay.
- From a fit to the invariant mass distribution.
- From a fit to $J^{PC} = 2^{-+} f_2(1270) \pi, f_0(1370) \pi$ waves.
- From a fit to $J^P = 2^- S$ -wave $f_2(1270) \pi$ partial wave.
- Clear phase rotation seen in $2^- S, 2^- P, 2^- D$ waves. We quote central value and spread of single-resonance fits to three channels.
- From $\rho \pi$ decay.
- From $\sigma \pi$ decay.
- From a two-resonance fit to four $2^- 0^+$ waves. This should not be averaged with all the single resonance fits.

WEIGHTED AVERAGE
1672.4 ± 3.2 (Error scaled by 1.4)

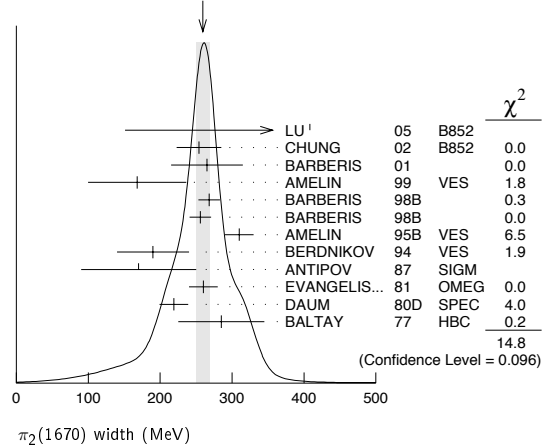


$\pi_2(1670)$ WIDTH

VALUE (MeV)	EVTS	DOCUMENT ID	TECN	CHG	COMMENT
259 ± 9 OUR AVERAGE		Error includes scale factor of 1.3. See the ideogram below.			
408 ± 60 ± 250	145k	LU	05	B852	18 $\pi^- \rho \rightarrow \omega \pi^- \pi^0 \rho$
254 ± 3 ± 31		9 CHUNG	02	B852	18.3 $\pi^- \rho \rightarrow \pi^+ \pi^- \pi^- \rho$
265 ± 30 ± 40		10 BARBERIS	01		450 $\rho \rho \rightarrow \rho_f 3\pi^0 \rho_S$
168 ± 43 ± 53		AMELIN	99	VES	37 $\pi^- A \rightarrow \omega \pi^- \pi^0 A^*$
268 ± 15		BARBERIS	98B		450 $\rho \rho \rightarrow \rho_f \rho \pi \rho_S$
256 ± 15		BARBERIS	98B		450 $\rho \rho \rightarrow \rho_f f_2(1270) \pi \rho_S$
310 ± 20		11 AMELIN	95B	VES	36 $\pi^- A \rightarrow \pi^+ \pi^- \pi^- A$
190 ± 50		12 BERDNIKOV	94	VES	37 $\pi^- A \rightarrow K^+ K^- \pi^- A$
170 ± 80	700	ANTIPOV	87	SIGM	50 $\pi^- \text{Cu} \rightarrow \mu^+ \mu^- \pi^- \text{Cu}$
260 ± 20		12 EVANGELIS...	81	OMEG	12 $\pi^- \rho \rightarrow 3\pi \rho$
219 ± 20		12,13 DAUM	80D	SPEC	63-94 $\pi \rho \rightarrow 3\pi X$
285 ± 60	2000	12 BALTAY	77	HBC	15 $\pi^+ \rho \rightarrow \rho 3\pi$
• • • We do not use the following data for averages, fits, limits, etc. • • •					
236 ± 49 ± 36		ANTREASYAN	90	CBAL	$e^+ e^- \rightarrow e^+ e^- \pi^0 \pi^0 \pi^0$
304 ± 22		9 BELLINI	85	SPEC	40 $\pi^- A \rightarrow \pi^- \pi^+ \pi^- A$
404 ± 108		14 BELLINI	85	SPEC	40 $\pi^- A \rightarrow \pi^- \pi^+ \pi^- A$
330 ± 90		15 BELLINI	85	SPEC	40 $\pi^- A \rightarrow \pi^- \pi^+ \pi^- A$
312 ± 50		16 DAUM	81B	SPEC	63,94 $\pi^- \rho$
270 ± 60		12 ASCOLI	73	HBC	5-25 $\pi^- \rho \rightarrow \rho \pi_2$

- From $f_2(1270) \pi$ decay.
- From a fit to the invariant mass distribution.
- From a fit to $J^{PC} = 2^{-+} f_2(1270) \pi, f_0(1370) \pi$ waves.
- From a fit to $J^P = 2^- f_2(1270) \pi$ partial wave.
- Clear phase rotation seen in $2^- S, 2^- P, 2^- D$ waves. We quote central value and spread of single-resonance fits to three channels.
- From $\rho \pi$ decay.
- From $\sigma \pi$ decay.
- From a two-resonance fit to four $2^- 0^+$ waves. This should not be averaged with all the single resonance fits.

WEIGHTED AVERAGE
259 ± 9 (Error scaled by 1.3)



$\pi_2(1670)$ DECAY MODES

Mode	Fraction (Γ_i/Γ)	Confidence level
Γ_1 3π	(95.8 ± 1.4) %	
Γ_2 $\pi^+ \pi^- \pi^0$		
Γ_3 $\pi^0 \pi^0 \pi^0$		
Γ_4 $f_2(1270) \pi$	(56.3 ± 3.2) %	
Γ_5 $\rho \pi$	(31 ± 4) %	
Γ_6 $\sigma \pi$	(10.9 ± 3.4) %	
Γ_7 $(\pi \pi)_S$ -wave	(8.7 ± 3.4) %	
Γ_8 $K \bar{K}^*(892) + \text{c.c.}$	(4.2 ± 1.4) %	
Γ_9 $\omega \rho$	(2.7 ± 1.1) %	
Γ_{10} $\gamma \gamma$	< 2.8	$\times 10^{-7}$
Γ_{11} $\eta \pi$		90%
Γ_{12} $\pi^\pm 2\pi^+ 2\pi^-$		

Γ_{13}	$\rho(1450)\pi$	< 3.6	$\times 10^{-3}$	97.7%
Γ_{14}	$b_1(1235)\pi$	< 1.9	$\times 10^{-3}$	97.7%
Γ_{15}	$\eta 3\pi$			
Γ_{16}	$f_1(1285)\pi$	possibly seen		
Γ_{17}	$a_2(1320)\pi$	not seen		

CONSTRAINED FIT INFORMATION

An overall fit to 4 branching ratios uses 6 measurements and one constraint to determine 4 parameters. The overall fit has a $\chi^2 = 1.9$ for 3 degrees of freedom.

The following *off-diagonal* array elements are the correlation coefficients $\langle \delta x_i \delta x_j \rangle / (\delta x_i \delta x_j)$, in percent, from the fit to the branching fractions, $x_i \equiv \Gamma_i / \Gamma_{\text{total}}$. The fit constrains the x_i whose labels appear in this array to sum to one.

x_5	-53		
x_7	-29	-59	
x_8	-8	-21	-9
	x_4	x_5	x_7

 $\pi_2(1670)$ PARTIAL WIDTHS

$\Gamma(\gamma\gamma)$	CL%	DOCUMENT ID	TECN	CHG	COMMENT	Γ_{10}
<0.072	90	17 ACCIARRI	97T	L3	$e^+e^- \rightarrow \pi^+\pi^-\pi^0$	
••• We do not use the following data for averages, fits, limits, etc. •••						
<0.19	90	17 ALBRECHT	97B	ARG	$e^+e^- \rightarrow \pi^+\pi^-\pi^0$	
1.41 \pm 0.23 \pm 0.28		ANTREASYAN	90	CBAL	0	
0.8 \pm 0.3 \pm 0.12		18 BEHREND	90c	CELL	0	
1.3 \pm 0.3 \pm 0.2		19 BEHREND	90c	CELL	0	

¹⁷Decaying into $f_2(1270)\pi$ and $\rho\pi$.

¹⁸Constructive interference between $f_2(1270)\pi, \rho\pi$ and background.

¹⁹Incoherent Ansatz.

 $\pi_2(1670)$ $\Gamma(i)\Gamma(\gamma\gamma)/\Gamma(\text{total})$

$\Gamma(\pi^+\pi^-\pi^0) \times \Gamma(\gamma\gamma)/\Gamma_{\text{total}}$	CL%	DOCUMENT ID	TECN	COMMENT	$\Gamma_{2}\Gamma_{10}/\Gamma$
<0.1	95	20 SCHEGELSKY	06	RVUE	$\gamma\gamma \rightarrow \pi^+\pi^-\pi^0$

²⁰From analysis of L3 data at 183–209 GeV.

 $\pi_2(1670)$ BRANCHING RATIOS

$\Gamma(3\pi)/\Gamma_{\text{total}}$	DOCUMENT ID	$\Gamma_1/\Gamma = (\Gamma_4 + \Gamma_5 + \Gamma_7)/\Gamma$
0.958 \pm 0.014 OUR FIT		
$\Gamma(\pi^0\pi^0\pi^0)/\Gamma(\pi^+\pi^-\pi^0)$	DOCUMENT ID	COMMENT
0.29 \pm 0.03 \pm 0.05	21 BARBERIS	01 450 $p\rho \rightarrow \rho_f 3\pi^0 \rho_s$

$\Gamma(\rho\pi)/0.565\Gamma(f_2(1270)\pi)$	DOCUMENT ID	TECN	COMMENT	$\Gamma_5/0.565\Gamma_4$
(With $f_2(1270) \rightarrow \pi^+\pi^-$.)				
0.97 \pm 0.09 OUR AVERAGE	Error includes scale factor of 1.9.			
0.76 \pm 0.07 \pm 0.10	CHUNG	02	B852	18.3 $\pi^-p \rightarrow \pi^+\pi^-\pi^-p$
1.01 \pm 0.05	BARBERIS	98b		45.0 $p\rho \rightarrow \rho_f \pi^+\pi^-\pi^0 \rho_s$

$\Gamma(\sigma\pi)/\Gamma(f_2(1270)\pi)$	DOCUMENT ID	TECN	COMMENT	Γ_6/Γ_4
0.19 \pm 0.06 OUR AVERAGE				
0.17 \pm 0.02 \pm 0.07	CHUNG	02	B852	18.3 $\pi^-p \rightarrow \pi^+\pi^-\pi^-p$
0.24 \pm 0.10	22,23 BAKER	99	SPEC	1.94 $\bar{p}p \rightarrow 4\pi^0$

$\frac{1}{2}\Gamma(\rho\pi)/\Gamma(\pi^+\pi^-\pi^-)$	DOCUMENT ID	TECN	CHG	COMMENT	$\frac{1}{2}\Gamma_5/(0.565\Gamma_4 + \frac{1}{2}\Gamma_5 + 0.624\Gamma_7)$
0.29 \pm 0.04 OUR FIT					
0.29 \pm 0.05	24 DAUM	81b	SPEC	63,94 π^-p	
••• We do not use the following data for averages, fits, limits, etc. •••					
<0.3	BARTSCH	68	HBC	+	8 $\pi^+p \rightarrow 3\pi p$

$$0.565\Gamma(f_2(1270)\pi)/\Gamma(\pi^+\pi^-\pi^-) \quad 0.565\Gamma_4/(0.565\Gamma_4 + \frac{1}{2}\Gamma_5 + 0.624\Gamma_7)$$

(With $f_2(1270) \rightarrow \pi^+\pi^-$.)

VALUE	DOCUMENT ID	TECN	CHG	COMMENT	
0.604 \pm 0.035 OUR FIT					
0.60 \pm 0.05 OUR AVERAGE	Error includes scale factor of 1.3.				
0.61 \pm 0.04	24 DAUM	81b	SPEC	63,94 π^-p	
0.76 $\begin{smallmatrix} +0.24 \\ -0.34 \end{smallmatrix}$	ARMENISE	69	DBC	+	5.1 $\pi^+d \rightarrow d 3\pi$
0.35 \pm 0.20	BALTAY	68	HBC	+	7–8.5 π^+p
••• We do not use the following data for averages, fits, limits, etc. •••					
0.59	BARTSCH	68	HBC	+	8 $\pi^+p \rightarrow 3\pi p$

$$0.624\Gamma((\pi\pi)_{S\text{-wave}})/\Gamma(\pi^+\pi^-\pi^-) \quad 0.624\Gamma_7/(0.565\Gamma_4 + \frac{1}{2}\Gamma_5 + 0.624\Gamma_7)$$

(With $(\pi\pi)_{S\text{-wave}} \rightarrow \pi^+\pi^-$.)

VALUE	DOCUMENT ID	TECN	COMMENT	
0.10 \pm 0.04 OUR FIT				
0.10 \pm 0.05	24 DAUM	81b	SPEC	63,94 π^-p

$$\Gamma(K\bar{K}^*(892) + \text{c.c.})/\Gamma(f_2(1270)\pi) \quad \Gamma_8/\Gamma_4$$

VALUE	DOCUMENT ID	TECN	CHG	COMMENT	
0.075 \pm 0.025 OUR FIT					
0.075 \pm 0.025	25 ARMSTRONG	82b	OMEG	-	16 $\pi^-p \rightarrow K^+K^-\pi^-p$

$$\Gamma(\omega\rho)/\Gamma_{\text{total}} \quad \Gamma_9/\Gamma$$

VALUE	DOCUMENT ID	TECN	COMMENT	
0.027 \pm 0.004 \pm 0.010	26 AMELIN	99	VES	37 $\pi^-A \rightarrow \omega\pi^-\pi^0 A^*$

$$\Gamma(\eta\pi)/\Gamma(\pi^+\pi^-\pi^-) \quad \Gamma_{11}/(0.565\Gamma_4 + \frac{1}{2}\Gamma_5 + 0.624\Gamma_7)$$

(All η decays.)

VALUE	DOCUMENT ID	TECN	CHG	COMMENT	
<0.09	BALTAY	68	HBC	+	7–8.5 π^+p
••• We do not use the following data for averages, fits, limits, etc. •••					
<0.10	CRENNELL	70	HBC	-	6 $\pi^-p \rightarrow f_2\pi^-N$

$$\Gamma(\pi^+2\pi^+2\pi^-)/\Gamma(\pi^+\pi^-\pi^-) \quad \Gamma_{12}/(0.565\Gamma_4 + \frac{1}{2}\Gamma_5 + 0.624\Gamma_7)$$

VALUE	DOCUMENT ID	TECN	CHG	COMMENT	
<0.10	CRENNELL	70	HBC	-	6 $\pi^-p \rightarrow f_2\pi^-N$
<0.1	BALTAY	68	HBC	+	7.8.5 π^+p

$$\Gamma(\rho(1450)\pi)/\Gamma_{\text{total}} \quad \Gamma_{13}/\Gamma$$

VALUE	CL%	DOCUMENT ID	TECN	COMMENT	
<0.0036	97.7	AMELIN	99	VES	37 $\pi^-A \rightarrow \omega\pi^-\pi^0 A^*$

$$\Gamma(b_1(1235)\pi)/\Gamma_{\text{total}} \quad \Gamma_{14}/\Gamma$$

VALUE	CL%	DOCUMENT ID	TECN	COMMENT	
<0.0019	97.7	AMELIN	99	VES	37 $\pi^-A \rightarrow \omega\pi^-\pi^0 A^*$

$$\Gamma(f_1(1285)\pi)/\Gamma_{\text{total}} \quad \Gamma_{16}/\Gamma$$

VALUE	EVTS	DOCUMENT ID	TECN	COMMENT	
possibly seen	69k	KUHN	04	B852	18 $\pi^-p \rightarrow \eta\pi^+\pi^-\pi^-p$

$$\Gamma(a_2(1320)\pi)/\Gamma_{\text{total}} \quad \Gamma_{17}/\Gamma$$

VALUE	EVTS	DOCUMENT ID	TECN	COMMENT	
not seen	69k	KUHN	04	B852	18 $\pi^-p \rightarrow \eta\pi^+\pi^-\pi^-p$

D-wave/S-wave RATIO FOR $\pi_2(1670) \rightarrow f_2(1270)\pi$

VALUE	DOCUMENT ID	TECN	COMMENT	
-0.18 \pm 0.06	22 BAKER	99	SPEC	1.94 $\bar{p}p \rightarrow 4\pi^0$
••• We do not use the following data for averages, fits, limits, etc. •••				
0.22 \pm 0.10	24 DAUM	81b	SPEC	63,94 π^-p

F-wave/P-wave RATIO FOR $\pi_2(1670) \rightarrow \rho\pi$

VALUE	DOCUMENT ID	TECN	COMMENT	
-0.72 \pm 0.07 \pm 0.14	CHUNG	02	B852	18.3 $\pi^-p \rightarrow \pi^+\pi^-\pi^-p$

²¹Using BARBERIS 98b.

²²Using preliminary CBAR data.

²³With the $\sigma\pi$ in $L=2$ and the $f_2(1270)\pi$ in $L=0$.

²⁴From a two-resonance fit to four 2^-0^+ waves.

²⁵From a partial-wave analysis of $K^+K^-\pi^-$ system.

²⁶Normalized to the $B(\pi_2(1670) \rightarrow f_2\pi)$.

Meson Particle Listings

 $\pi_2(1670)$, $\phi(1680)$ $\pi_2(1670)$ REFERENCES

SCHEGELSKY	06	EPL A27 199	V.A. Schegelsky et al.		
LU	05	PRL 94 032002	M. Lu et al.	(BNL E852 Collab.)	
KUHN	04	PL B595 109	J. Kuhn et al.	(BNL E852 Collab.)	
CHUNG	02	PR D65 072001	S.U. Chung et al.	(BNL E852 Collab.)	
BARBERIS	01	PL B507 14	D. Barberis et al.		
AMELIN	99	PAN 62 445	D.V. Amelin et al.	(VES Collab.)	
BAKER	99	PL B449 114	C.A. Baker et al.		
BARBERIS	98B	PL B422 399	D. Barberis et al.	(WA 102 Collab.)	
ACCIARI	97T	PL B413 147	M. Acciari et al.	(L3 Collab.)	
ALBRECHT	97B	ZPHY C74 469	H. Albrecht et al.	(ARGUS Collab.)	
AMELIN	95B	PL B356 595	D.V. Amelin et al.	(SERP, TBIL)	
BERDNIKOV	94	PL B337 219	E.B. Berdnikov et al.	(SERP, TBIL)	
ANTREASYAN	90	ZPHY C48 561	D. Antreasyan et al.	(Crystal Ball Collab.)	
BEHREND	90C	ZPHY C46 583	H.J. Behrend et al.	(CELLO Collab.)	
ANTIPOV	87	EPL 4 403	Y.M. Antipov et al.	(SERP, JINR, INRM+)	
BELLINI	85	SJNP 41 781	D. Bellini et al.		
ARMSTRONG	82B	NP B202 1	T.A. Armstrong, B. Baccafi	(AACH3, BARI, BONN+)	
DAUM	81B	NP B182 269	C. Daum et al.	(AMST, CERN, CRAC, MPIM+)	
EVANGELIS...	81	NP B178 197	C. Evangelista et al.	(BARI, BONN, CERN+)	
Also		NP B186 594	C. Evangelista		
DAUM	80D	PL 89B 285	C. Daum et al.	(AMST, CERN, CRAC, MPIM+)	JP
BALTAY	77	PRL 39 591	C. Baltay, C.V. Cautis, M. Kalelkar	(COLU)JP	
ASCOLI	73	PR D7 669	G. Ascoli	(ILL, TATO, GENO, HAMB, MILA+)	JP
CRENNELL	70	PRL 24 781	D.J. Crennell et al.	(BNL)	
ARMENISE	69	LCN 2 501	N. Armenise et al.	(BARI, BGNA, FIRZ)	
BALTAY	68	PRL 20 887	C. Baltay et al.	(COLU, ROCH, RUTG, YALE)I	
BARTSCH	68	NP B7 345	J. Bartsch et al.	(AACH, BERL, CERN)JP	

OTHER RELATED PAPERS

DZIERBA	06	PR D73 072001	A.R. Dzierba et al.	(BNL E852 Collab.)	
PAGE	03	PL B566 108	P. Page, S. Capstick		
ZAIMIDOROGA	99	PAN 30 1	O.A. Zaimidoriga		
CHEN	83B	PR D38 2304	T.Y. Chen et al.	(ARIZ, FNAL, FLOR, NDAM+)	
LEEDOM	83	PR D27 1426	I.D. Leedom et al.	(PURD, TATO)	
BELLINI	82B	NP B199 1	G. Bellini et al.	(CERN, MILA, JINR+)	
DAUM	81B	NP B182 269	C. Daum et al.	(AMST, CERN, CRAC, MPIM+)	
PERNEGR	78	NP B134 436	J. Pernegr et al.	(ETH, CERN, LOIC+)	
FOCACCI	66	PRL 17 890	M.N. Focacci et al.	(CERN)	
LEVRAT	66	PL 22 714	B. Levrat et al.		
VETLITSKY	66	PL 21 579	I.A. Vetlitsky et al.	(ITEP)	
FORINO	65B	PL 19 68	A. Forino et al.	(BGNA, BARI, FIRZ, ORSAY+)	

 $\phi(1680)$

$$J^G(J^{PC}) = 0^-(1^{--})$$

 $\phi(1680)$ MASS e^+e^- PRODUCTION

VALUE (MeV)	EVTS	DOCUMENT ID	TECN	COMMENT
1680 ± 20 OUR ESTIMATE				
• • • We do not use the following data for averages, fits, limits, etc. • • •				
1709 ± 20 ± 43		¹ AUBERT 08s BABR	10.6 $e^+e^- \rightarrow$ hadrons	
1623 ± 20	948	² AKHMETSHIN 03 CMD2	1.05–1.38 $e^+e^- \rightarrow K_L^0 K_S^0$	
~ 1500		³ ACHASOV 98H RVUE	$e^+e^- \rightarrow \pi^+\pi^-\pi^0$, $\omega\pi^+\pi^-$, K^+K^-	
~ 1900		⁴ ACHASOV 98H RVUE	$e^+e^- \rightarrow K_S^0 K^\pm\pi^\mp$	
1700 ± 20		⁵ CLEGG 94 RVUE	$e^+e^- \rightarrow K^+K^-, K_S^0 K\pi$	
1657 ± 27	367	⁶ BISELLO 91c DM2	$e^+e^- \rightarrow K_S^0 K^\pm\pi^\mp$	
1655 ± 17		⁶ BISELLO 88B DM2	$e^+e^- \rightarrow K^+K^-$	
1680 ± 10		⁷ BUON 82 DM1	$e^+e^- \rightarrow$ hadrons	
1677 ± 12		⁸ MANE 82 DM1	$e^+e^- \rightarrow K_S^0 K\pi$	

PHOTOPRODUCTION

VALUE (MeV)	DOCUMENT ID	TECN	COMMENT
• • • We do not use the following data for averages, fits, limits, etc. • • •			
1753 ± 3	⁹ LINK 02k FOCS	20–160 $\gamma p \rightarrow K^+K^-p$	
1726 ± 22	⁹ BUSENITZ 89 TPS	$\gamma p \rightarrow K^+K^-X$	
1760 ± 20	⁹ ATKINSON 85c OMEG	20–70 $\gamma p \rightarrow K\bar{K}X$	
1690 ± 10	⁹ ASTON 81F OMEG	25–70 $\gamma p \rightarrow K^+K^-X$	

 $p\bar{p}$ ANNIHILATION

VALUE (MeV)	DOCUMENT ID	TECN	COMMENT
• • • We do not use the following data for averages, fits, limits, etc. • • •			
1700 ± 8	¹⁰ AMSLER 06 CBAR	0.9 $\bar{p}p \rightarrow K^+K^-\pi^0$	
¹ From the simultaneous fit to the $K\bar{K}^*(892) +$ c.c. and $\phi\eta$ data from AUBERT 08s using the results of AUBERT 07AK.			
² From the combined fit of AKHMETSHIN 03 and MANE 81 also including ρ, ω , and ϕ . Neither isospin nor flavor structure known.			
³ Using data from IVANOV 81, BARKOV 87, BISELLO 88B, DOLINSKY 91, and ANTONELLI 92.			
⁴ Using the data from BISELLO 91c.			
⁵ Using BISELLO 88B and MANE 82 data.			
⁶ From global fit including ρ, ω, ϕ and $\rho(1700)$ assume mass 1570 MeV and width 510 MeV for ρ radial excitation.			
⁷ From global fit of ρ, ω, ϕ and their radial excitations to channels $\omega\pi^+\pi^-, K^+K^-, K_S^0 K_L^0, K_S^0 K^\pm\pi^\mp$. Assume mass 1570 MeV and width 510 MeV for ρ radial excitations, mass 1570 and width 500 MeV for ω radial excitation.			
⁸ Fit to one channel only, neglecting interference with $\omega, \rho(1700)$.			
⁹ We list here a state decaying into K^+K^- possibly different from $\phi(1680)$.			
¹⁰ Could also be $\rho(1700)$.			

 $\phi(1680)$ WIDTH e^+e^- PRODUCTION

VALUE (MeV)	EVTS	DOCUMENT ID	TECN	COMMENT
150 ± 50 OUR ESTIMATE This is only an educated guess; the error given is larger than the error on the average of the published values.				
• • • We do not use the following data for averages, fits, limits, etc. • • •				
322 ± 77 ± 160		¹¹ AUBERT 08s BABR	10.6 $e^+e^- \rightarrow$ hadrons	
139 ± 60	948	¹² AKHMETSHIN 03 CMD2	1.05–1.38 $e^+e^- \rightarrow K_L^0 K_S^0$	
300 ± 60		¹³ CLEGG 94 RVUE	$e^+e^- \rightarrow K^+K^-, K_S^0 K\pi$	
146 ± 55	367	¹³ BISELLO 91c DM2	$e^+e^- \rightarrow K_S^0 K^\pm\pi^\mp$	
207 ± 45		¹⁴ BISELLO 88B DM2	$e^+e^- \rightarrow K^+K^-$	
185 ± 22		¹⁵ BUON 82 DM1	$e^+e^- \rightarrow$ hadrons	
102 ± 36		¹⁶ MANE 82 DM1	$e^+e^- \rightarrow K_S^0 K\pi$	

PHOTOPRODUCTION

VALUE (MeV)	DOCUMENT ID	TECN	COMMENT
• • • We do not use the following data for averages, fits, limits, etc. • • •			
122 ± 63	¹⁷ LINK 02k FOCS	20–160 $\gamma p \rightarrow K^+K^-p$	
121 ± 47	¹⁷ BUSENITZ 89 TPS	$\gamma p \rightarrow K^+K^-X$	
80 ± 40	¹⁷ ATKINSON 85c OMEG	20–70 $\gamma p \rightarrow K\bar{K}X$	
100 ± 40	¹⁷ ASTON 81F OMEG	25–70 $\gamma p \rightarrow K^+K^-X$	

 $p\bar{p}$ ANNIHILATION

VALUE (MeV)	DOCUMENT ID	TECN	COMMENT
• • • We do not use the following data for averages, fits, limits, etc. • • •			
143 ± 24	¹⁸ AMSLER 06 CBAR	0.9 $\bar{p}p \rightarrow K^+K^-\pi^0$	
¹¹ From the simultaneous fit to the $K\bar{K}^*(892) +$ c.c. and $\phi\eta$ data from AUBERT 08s using the results of AUBERT 07AK.			
¹² From the combined fit of AKHMETSHIN 03 and MANE 81 also including ρ, ω , and ϕ . Neither isospin nor flavor structure known.			
¹³ Using BISELLO 88B and MANE 82 data.			
¹⁴ From global fit including ρ, ω, ϕ and $\rho(1700)$.			
¹⁵ From global fit of ρ, ω, ϕ and their radial excitations to channels $\omega\pi^+\pi^-, K^+K^-, K_S^0 K_L^0, K_S^0 K^\pm\pi^\mp$. Assume mass 1570 MeV and width 510 MeV for ρ radial excitations, mass 1570 and width 500 MeV for ω radial excitation.			
¹⁶ Fit to one channel only, neglecting interference with $\omega, \rho(1700)$.			
¹⁷ We list here a state decaying into K^+K^- possibly different from $\phi(1680)$.			
¹⁸ Could also be $\rho(1700)$.			

 $\phi(1680)$ DECAY MODES

Mode	Fraction (Γ_i/Γ)
Γ_1 $K\bar{K}^*(892) +$ c.c.	dominant
Γ_2 $K_S^0 K\pi$	seen
Γ_3 $K\bar{K}$	seen
Γ_4 $K_L^0 K_S^0$	
Γ_5 e^+e^-	seen
Γ_6 $\omega\pi\pi$	not seen
Γ_7 $\phi\eta$	
Γ_8 $K^+K^-\pi^0$	

 $\phi(1680)$ $\Gamma(i)\Gamma(e^+e^-)/\Gamma^2(\text{total})$

This combination of a branching ratio into channel (i) and branching ratio into e^+e^- is directly measured and obtained from the cross section at the peak. We list only data that have not been used to determine the branching ratio into (i) or e^+e^- .

$$\Gamma(K_L^0 K_S^0) \times \Gamma(e^+e^-)/\Gamma_{\text{total}}^2 \quad \Gamma_4\Gamma_5/\Gamma^2$$

VALUE (units 10^{-6})	EVTS	DOCUMENT ID	TECN	COMMENT
• • • We do not use the following data for averages, fits, limits, etc. • • •				
0.131 ± 0.059	948	¹⁹ AKHMETSHIN 03 CMD2	1.05–1.38 $e^+e^- \rightarrow K_L^0 K_S^0$	
¹⁹ From the combined fit of AKHMETSHIN 03 and MANE 81 also including ρ, ω , and ϕ . Neither isospin nor flavor structure known. Recalculated by us.				

$$\Gamma(K\bar{K}^*(892) + \text{c.c.}) \times \Gamma(e^+e^-)/\Gamma_{\text{total}}^2 \quad \Gamma_1\Gamma_5/\Gamma^2$$

VALUE (units 10^{-6})	EVTS	DOCUMENT ID	TECN	COMMENT
• • • We do not use the following data for averages, fits, limits, etc. • • •				
1.15 ± 0.16 ± 0.01		²⁰ AUBERT 08s BABR	10.6 $e^+e^- \rightarrow K\bar{K}^*(892)\gamma +$ c.c.	
3.29 ± 1.57	367	²¹ BISELLO 91c DM2	1.35–2.40 $e^+e^- \rightarrow K_S^0 K^\pm\pi^\mp$	
²⁰ From the simultaneous fit to the $K\bar{K}^*(892) +$ c.c. and $\phi\eta$ data from AUBERT 08s using the results of AUBERT 07AK.				
²¹ Recalculated by us with the published value of $B(K\bar{K}^*(892) + \text{c.c.}) \times \Gamma(e^+e^-)$.				

$$\Gamma(\phi\eta) \times \Gamma(e^+e^-)/\Gamma_{\text{total}}^2 \quad \Gamma_7\Gamma_5/\Gamma^2$$

VALUE (units 10^{-6})	DOCUMENT ID	TECN	COMMENT
• • • We do not use the following data for averages, fits, limits, etc. • • •			
0.43 ± 0.10 ± 0.09	²² AUBERT 08s BABR	10.6 $e^+e^- \rightarrow \phi\eta\gamma$	
²² From the simultaneous fit to the $K\bar{K}^*(892) +$ c.c. and $\phi\eta$ data from AUBERT 08s using the results of AUBERT 07AK.			

See key on page 373

Meson Particle Listings

 $\phi(1680), \rho_3(1690)$ $\phi(1680)$ BRANCHING RATIOS

$\Gamma(K\bar{K}^*(892) + c.c.) / \Gamma(K_S^0 K \pi)$				Γ_1 / Γ_2
VALUE	DOCUMENT ID	TECN	COMMENT	
dominant	MANE	82	DM1	$e^+ e^- \rightarrow K_S^0 K^\pm \pi^\mp$

$\Gamma(K\bar{K}) / \Gamma(K\bar{K}^*(892) + c.c.)$				Γ_3 / Γ_1
VALUE	DOCUMENT ID	TECN	COMMENT	
• • • We do not use the following data for averages, fits, limits, etc. • • •				
0.07 ± 0.01	BUON	82	DM1	$e^+ e^-$

$\Gamma(\omega \pi \pi) / \Gamma(K\bar{K}^*(892) + c.c.)$				Γ_6 / Γ_1
VALUE	DOCUMENT ID	TECN	COMMENT	
<0.10	BUON	82	DM1	$e^+ e^-$

$\Gamma(\phi \eta) / \Gamma(K\bar{K}^*(892) + c.c.)$				Γ_7 / Γ_1
VALUE	DOCUMENT ID	TECN	COMMENT	
• • • We do not use the following data for averages, fits, limits, etc. • • •				
≈ 0.37	²³ AUBERT	08s	BABR	10.6 $e^+ e^- \rightarrow$ hadrons
²³ From the fit including data from AUBERT 07AK.				

 $\phi(1680)$ REFERENCES

AUBERT	08S	PR D77 092002	B. Aubert et al.	(BABAR Collab.)
AUBERT	07AK	PR D76 012008	B. Aubert et al.	(BABAR Collab.)
AMSLER	06	PL B639 165	C. Amstutz et al.	(CBAR Collab.)
AKHMETSHIN	03	PL B551 27	R.R. Akhmetshin et al.	(Novosibirsk CMD-2 Collab.)
Also		PAN 65 1222	E.Y. Anashkin, V.M. Aulchenko, R.R. Akhmetshin	
		Translated from YAF 65 1258.		
LINK	02K	PL B545 50	J.M. Link et al.	(FNAL FOCUS Collab.)
ACHASOV	98H	PR D57 4334	N.N. Achasov, A.A. Kozhevnikov	
CLEGG	94	ZPHY C62 455	A.B. Clegg, A. Donnachie	(LANC, MCHS)
ANTONELLI	92	ZPHY C56 15	A. Antonelli et al.	(DM2 Collab.)
BISELLO	91C	ZPHY C52 227	D. Bisello et al.	(DM2 Collab.)
DOLINSKY	91	PRPL 202 99	S.I. Dolinsky et al.	(NOVO)
BUSENITZ	89	PR D40 1	J.K. Busenitz et al.	(ILL, FNAL)
BISELLO	88B	ZPHY C39 13	D. Bisello et al.	(PADO, CLER, FRAS+)
BARKOV	87	JETPL 46 164	L.M. Barkov et al.	(NOVO)
		Translated from ZETFP 46 132.		
ATKINSON	85C	ZPHY C27 233	M. Atkinson et al.	(BONN, CERN, GLAS+)
BUON	82	PL 118B 221	J. Buon et al.	(LALO, MONP)
MANE	82	PL 112B 178	F. Mane et al.	(LALO)
ASTON	81F	PL 104B 231	D. Aston	(BONN, CERN, EPOL, GLAS, LANC+)
IVANOV	81	PL 107B 297	P.M. Ivanov et al.	(NOVO)
MANE	81	PL 99B 261	F. Mane et al.	(ORSAY)

OTHER RELATED PAPERS

ACHASOV	07A	PR D76 072012	N.N. Achasov et al.	(SND Collab.)
ACHASOV	06D	JETP 103 720	N.N. Achasov et al.	(SND Collab.)
		Translated from ZETF 130 831.		
AUBERT	06D	PR D73 052003	B. Aubert et al.	(BABAR Collab.)
CLOSE	02	PR D65 092003	F.E. Close, A. Donnachie, Yu.S. Kalashnikova	
LINK	02K	PL B545 50	J.M. Link et al.	(FNAL FOCUS Collab.)
ABELE	99D	PL B468 178	A. Abele et al.	(Crystal Barrel Collab.)
ACHASOV	97F	PAN 60 2029	N.N. Achasov, A.A. Kozhevnikov	(NOVM)
		Translated from YAF 60 2212.		
ATKINSON	86C	ZPHY C30 541	M. Atkinson et al.	(BONN, CERN, GLAS+)
ATKINSON	84	NP B231 15	M. Atkinson et al.	(BONN, CERN, GLAS+)
ATKINSON	84B	NP B231 1	M. Atkinson et al.	(BONN, CERN, GLAS+)
ATKINSON	83C	NP B229 269	M. Atkinson et al.	(BONN, CERN, GLAS+)
CORDIER	81	PL 106B 155	A. Cordier et al.	(ORSAY)
MANE	81	PL 99B 261	F. Mane et al.	(ORSAY)
ASTON	80F	NP B174 269	D. Aston	(BONN, CERN, EPOL, GLAS, LANC+)

 $\rho_3(1690)$

$$J^G(J^{PC}) = 1^+(3^{--})$$

 $\rho_3(1690)$ MASS

VALUE (MeV)	DOCUMENT ID	TECN	CHG	COMMENT
1688.8 ± 2.1 OUR AVERAGE	Includes data from the 5 datablocks that follow this one.			

2 π MODE

VALUE (MeV)	EVTS	DOCUMENT ID	TECN	CHG	COMMENT
-------------	------	-------------	------	-----	---------

The data in this block is included in the average printed for a previous datablock.

1686 ± 4 OUR AVERAGE

1677 ± 14		EVANGELIS...	81	OMEG -	12 $\pi^- p \rightarrow 2\pi p$
1679 ± 11	476	BALTAY	78B	HBC 0	15 $\pi^+ p \rightarrow$ $\pi^+ \pi^- n$
1678 ± 12	175	¹ ANTIPOV	77	CIBS 0	25 $\pi^- p \rightarrow p 3\pi$
1690 ± 7	600	¹ ENGLER	74	DBC 0	6 $\pi^+ n \rightarrow$ $\pi^+ \pi^- p$
1693 ± 8		² GRAYER	74	ASPK 0	17 $\pi^- p \rightarrow$ $\pi^+ \pi^- n$
1678 ± 12		MATTHEWS	71c	DBC 0	7 $\pi^+ N$
• • • We do not use the following data for averages, fits, limits, etc. • • •					
1734 ± 10		³ CORDEN	79	OMEG	12-15 $\pi^- p \rightarrow$ $n 2\pi$
1692 ± 12		^{2,4} ESTABROOKS	75	RVUE	17 $\pi^- p \rightarrow$ $\pi^+ \pi^- n$
1737 ± 23		ARMENISE	70	DBC 0	9 $\pi^+ N$
1650 ± 35	122	BARTSCH	70B	HBC +	8 $\pi^+ p \rightarrow N 2\pi$
1687 ± 21		STUNTEBECK	70	HDBC 0	8 $\pi^- p, 5.4 \pi^+ d$
1683 ± 13		ARMENISE	68	DBC 0	5.1 $\pi^+ d$
1670 ± 30		GOLDBERG	65	HBC 0	6 $\pi^+ d, 8 \pi^- p$

¹ Mass errors enlarged by us to Γ/\sqrt{N} ; see the note with the $K^*(892)$ mass.² Uses same data as HYAMS 75.³ From a phase shift solution containing a $f_2'(1525)$ width two times larger than the $K\bar{K}$ result.⁴ From phase-shift analysis. Error takes account of spread of different phase-shift solutions. $K\bar{K}$ AND $K\bar{K}\pi$ MODES

VALUE (MeV)	EVTS	DOCUMENT ID	TECN	CHG	COMMENT
-------------	------	-------------	------	-----	---------

The data in this block is included in the average printed for a previous datablock.

1696 ± 4 OUR AVERAGE

1699 ± 5		ALPER	80	CNTR 0	62 $\pi^- p \rightarrow$ $K^+ K^- n$
1698 ± 12	6k	^{5,6} MARTIN	78D	SPEC	10 $\pi p \rightarrow$ $K_S^0 K^- p$
1692 ± 6		BLUM	75	ASPK 0	18.4 $\pi^- p \rightarrow$ $n K^+ K^-$
1690 ± 16		ADERHOLZ	69	HBC +	8 $\pi^+ p \rightarrow K\bar{K}\pi$
• • • We do not use the following data for averages, fits, limits, etc. • • •					
1694 ± 8		⁷ COSTA...	80	OMEG	10 $\pi^- p \rightarrow$ $K^+ K^- n$

⁵ From a fit to $J^P = 3^-$ partial wave.⁶ Systematic error on mass scale subtracted.⁷ They cannot distinguish between $\rho_3(1690)$ and $\omega_3(1670)$.(4 π) $^\pm$ MODE

VALUE (MeV)	EVTS	DOCUMENT ID	TECN	CHG	COMMENT
-------------	------	-------------	------	-----	---------

The data in this block is included in the average printed for a previous datablock.

1686 ± 5 OUR AVERAGE Error includes scale factor of 1.1.

1694 ± 6		⁸ EVANGELIS...	81	OMEG -	12 $\pi^- p \rightarrow p 4\pi$
1665 ± 15	177	BALTAY	78B	HBC +	15 $\pi^+ p \rightarrow p 4\pi$
1670 ± 10		THOMPSON	74	HBC +	13 $\pi^+ p$
1687 ± 20		CASON	73	HBC -	8,18.5 $\pi^- p$
1685 ± 14		⁹ CASON	73	HBC -	8,18.5 $\pi^- p$
1680 ± 40	144	BARTSCH	70B	HBC +	8 $\pi^+ p \rightarrow N 4\pi$
1689 ± 20	102	⁹ BARTSCH	70B	HBC +	8 $\pi^+ p \rightarrow N 2p$
1705 ± 21		CASO	70	HBC -	11.2 $\pi^- p \rightarrow$ $n p 2\pi$
• • • We do not use the following data for averages, fits, limits, etc. • • •					
1718 ± 10		¹⁰ EVANGELIS...	81	OMEG -	12 $\pi^- p \rightarrow p 4\pi$
1673 ± 9		¹¹ EVANGELIS...	81	OMEG -	12 $\pi^- p \rightarrow p 4\pi$
1733 ± 9	66	⁹ KLIGER	74	HBC -	4.5 $\pi^- p \rightarrow$ $p 4\pi$

⁸ From $\rho^- \rho^0$ mode, not independent of the other two EVANGELISTA 81 entries.⁹ From $\rho^\pm \rho^0$ mode.¹⁰ From $a_2(1320) \pi^0$ mode, not independent of the other two EVANGELISTA 81 entries.¹¹ From $a_2(1320) \pi^-$ mode, not independent of the other two EVANGELISTA 81 entries. $\omega \pi$ MODE

VALUE (MeV)	DOCUMENT ID	TECN	CHG	COMMENT
-------------	-------------	------	-----	---------

The data in this block is included in the average printed for a previous datablock.

1681 ± 7 OUR AVERAGE

1670 ± 25		¹² ALDE	95	GAM2	38 $\pi^- p \rightarrow$ $\omega \pi^0 n$
1690 ± 15		EVANGELIS...	81	OMEG -	12 $\pi^- p \rightarrow \omega \pi p$
1666 ± 14		GESSAROLI	77	HBC	11 $\pi^- p \rightarrow \omega \pi p$
1686 ± 9		THOMPSON	74	HBC +	13 $\pi^+ p$
• • • We do not use the following data for averages, fits, limits, etc. • • •					
1654 ± 24		BARNHAM	70	HBC +	10 $K^+ p \rightarrow$ $\omega \pi X$

¹² Supersedes ALDE 92c. $\eta \pi^+ \pi^-$ MODE(For difficulties with MMS experiments, see the $a_2(1320)$ mini-review in the 1973 edition.)

VALUE (MeV)	DOCUMENT ID	TECN	CHG	COMMENT
-------------	-------------	------	-----	---------

The data in this block is included in the average printed for a previous datablock.

1682 ± 12 OUR AVERAGE

1685 ± 10 ± 20		AMELIN	00	VES	37 $\pi^- p \rightarrow$ $\eta \pi^+ \pi^- n$
1680 ± 15		FUKUI	88	SPEC 0	8.95 $\pi^- p \rightarrow$ $\eta \pi^+ \pi^- n$
• • • We do not use the following data for averages, fits, limits, etc. • • •					
1700 ± 47		¹³ ANDERSON	69	MMS -	16 $\pi^- p$ back- ward
1632 ± 15		^{13,14} FOCACCI	66	MMS -	7-12 $\pi^- p \rightarrow$ ρMM
1700 ± 15		^{13,14} FOCACCI	66	MMS -	7-12 $\pi^- p \rightarrow$ ρMM
1748 ± 15		^{13,14} FOCACCI	66	MMS -	7-12 $\pi^- p \rightarrow$ ρMM

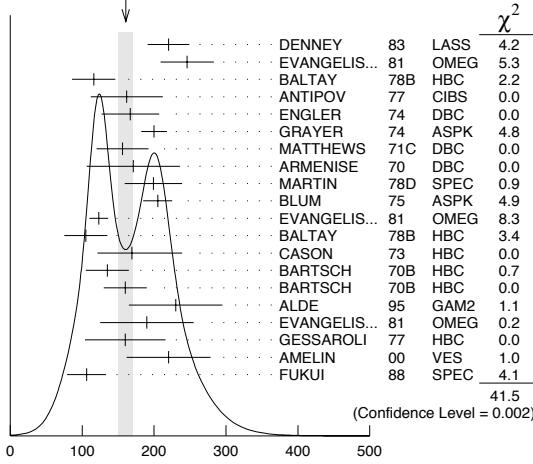
¹³ Seen in 2.5-3 GeV/c $\bar{p}p$. $2\pi^+ 2\pi^-$, with 0, 1, 2 $\pi^+ \pi^-$ pairs in ρ band not seen by OREN 74 (2.3 GeV/c $\bar{p}p$) with more statistics. (Jan. 1976)¹⁴ Not seen by BOWEN 72.

Meson Particle Listings

 $\rho_3(1690)$ $\rho_3(1690)$ WIDTH $2\pi, K\bar{K},$ AND $K\bar{K}\pi$ MODES

161±10 OUR AVERAGE Includes data from the 5 datablocks that follow this one. Error includes scale factor of 1.5. See the ideogram below.

WEIGHTED AVERAGE
161±10 (Error scaled by 1.5)



$\rho_3(1690)$ width, $2\pi, K\bar{K},$ and $K\bar{K}\pi$ modes (MeV)

 2π MODE

186±14 OUR AVERAGE Error includes scale factor of 1.3. See the ideogram below.

VALUE (MeV)	EVTS	DOCUMENT ID	TECN	CHG	COMMENT
220±29		DENNEY 83 LASS			$10 \pi^+ N$
246±37		EVANGELIS... 81 OMEG	-		$12 \pi^- p \rightarrow 2\pi p$
116±30	476	BALTAY 78B HBC	0		$15 \pi^+ p \rightarrow \pi^+ \pi^- n$
162±50	175	15 ANTIPOV 77 CIBS	0		$25 \pi^- p \rightarrow p 3\pi$
167±40	600	ENGLER 74 DBC	0		$6 \pi^+ n \rightarrow \pi^+ \pi^- p$
200±18		16 GRAYER 74 ASPK	0		$17 \pi^- p \rightarrow \pi^+ \pi^- n$
156±36		MATTHEWS 71C DBC	0		$7 \pi^+ N$
171±65		ARMENISE 70 DBC	0		$9 \pi^+ d$
322±35		17 CORDEN 79 OMEG			$12-15 \pi^- p \rightarrow n 2\pi$
240±30		16,18 ESTABROOKS 75 RVUE			$17 \pi^- p \rightarrow \pi^+ \pi^- n$
180±30	122	BARTSCH 70B HBC	+		$8 \pi^+ p \rightarrow N 2\pi$
267 ⁺⁷² ₋₄₆		STUNTEBECK 70 HDHC	0		$8 \pi^- p, 5.4 \pi^+ d$
188±49		ARMENISE 68 DBC	0		$5.1 \pi^+ d$
180±40		GOLDBERG 65 HBC	0		$6 \pi^+ d, 8 \pi^- p$

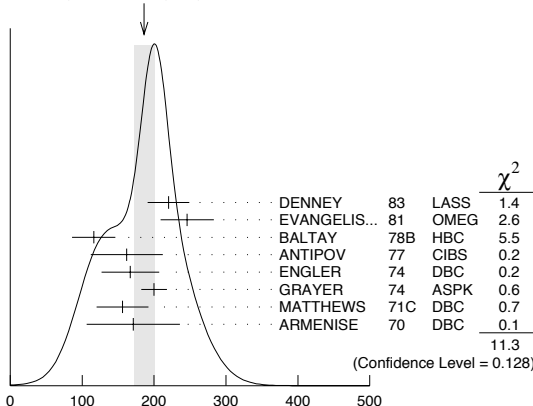
¹⁵ Width errors enlarged by us to $4\Gamma/\sqrt{N}$; see the note with the $K^*(892)$ mass.

¹⁶ Uses same data as HYAMS 75 and BECKER 79.

¹⁷ From a phase shift solution containing a $f_2'(1525)$ width two times larger than the $K\bar{K}$ result.

¹⁸ From phase-shift analysis. Error takes account of spread of different phase-shift solutions.

WEIGHTED AVERAGE
186±14 (Error scaled by 1.3)



$\rho_3(1690)$ width, 2π mode (MeV)

 $K\bar{K}$ AND $K\bar{K}\pi$ MODES

VALUE (MeV) EVTS DOCUMENT ID TECN CHG COMMENT
The data in this block is included in the average printed for a previous datablock.

 204 ± 18 OUR AVERAGE

VALUE (MeV)	EVTS	DOCUMENT ID	TECN	CHG	COMMENT
199±40	6000	19 MARTIN 78D	SPEC		$10 \pi p \rightarrow K_S^0 K^- p$
205±20		BLUM 75	ASPK	0	$18.4 \pi^- p \rightarrow n K^+ K^-$
219±4		ALPER 80	CNTR	0	$62 \pi^- p \rightarrow K^+ K^- n$
186±11		20 COSTA... 80	OMEG		$10 \pi^- p \rightarrow K^+ K^- n$
112±60		ADERHOLZ 69	HBC	+	$8 \pi^+ p \rightarrow K\bar{K}\pi$

• • • We do not use the following data for averages, fits, limits, etc. • • •
¹⁹ From a fit to $J^P = 3^-$ partial wave.
²⁰ They cannot distinguish between $\rho_3(1690)$ and $\omega_3(1670)$.

 $(4\pi)^\pm$ MODE

VALUE (MeV) EVTS DOCUMENT ID TECN CHG COMMENT
The data in this block is included in the average printed for a previous datablock.

 129 ± 10 OUR AVERAGE

VALUE (MeV)	EVTS	DOCUMENT ID	TECN	CHG	COMMENT
123±13		21 EVANGELIS... 81	OMEG	-	$12 \pi^- p \rightarrow p 4\pi$
105±30	177	BALTAY 78B	HBC	+	$15 \pi^+ p \rightarrow p 4\pi$
169 ⁺⁷⁰ ₋₄₈		CASON 73	HBC	-	$8, 18.5 \pi^- p$
135±30	144	BARTSCH 70B	HBC	+	$8 \pi^+ p \rightarrow N 4\pi$
160±30	102	BARTSCH 70B	HBC	+	$8 \pi^+ p \rightarrow N 2\rho$
230±28		22 EVANGELIS... 81	OMEG	-	$12 \pi^- p \rightarrow p 4\pi$
184±33		23 EVANGELIS... 81	OMEG	-	$12 \pi^- p \rightarrow p 4\pi$
150	66	24 KLIGER 74	HBC	-	$4.5 \pi^- p \rightarrow p 4\pi$
106±25		THOMPSON 74	HBC	+	$13 \pi^+ p$
125 ⁺⁸³ ₋₃₅		24 CASON 73	HBC	-	$8, 18.5 \pi^- p$
130±30		HOLMES 72	HBC	+	$10-12 K^+ p$
180±30	90	24 BARTSCH 70B	HBC	+	$8 \pi^+ p \rightarrow N 2\pi$
100±35		BALTAY 68	HBC	+	$7, 8.5 \pi^+ p$

• • • We do not use the following data for averages, fits, limits, etc. • • •
²¹ From $\rho^- \rho^0$ mode, not independent of the other two EVANGELISTA 81 entries.
²² From $a_2(1320) \pi^0$ mode, not independent of the other two EVANGELISTA 81 entries.
²³ From $a_2(1320) \pi^0$ mode, not independent of the other two EVANGELISTA 81 entries.
²⁴ From $\rho^\pm \rho^0$ mode.

 $\omega\pi$ MODE

VALUE (MeV) DOCUMENT ID TECN CHG COMMENT
The data in this block is included in the average printed for a previous datablock.

 190 ± 40 OUR AVERAGE

VALUE (MeV)	EVTS	DOCUMENT ID	TECN	CHG	COMMENT
230±65		25 ALDE 95	GAM2		$38 \pi^- p \rightarrow \omega \pi^0 n$
190±65		EVANGELIS... 81	OMEG	-	$12 \pi^- p \rightarrow \omega \pi p$
160±56		GESSAROLI 77	HBC		$11 \pi^- p \rightarrow \omega \pi p$
89±25		THOMPSON 74	HBC	+	$13 \pi^+ p$
130 ⁺⁷³ ₋₄₃		BARNHAM 70	HBC	+	$10 K^+ p \rightarrow \omega \pi X$

²⁵ Supersedes ALDE 92c.

 $\eta\pi^+\pi^-$ MODE

(For difficulties with MMS experiments, see the $a_2(1320)$ mini-review in the 1973 edition.)

VALUE (MeV) DOCUMENT ID TECN CHG COMMENT
The data in this block is included in the average printed for a previous datablock.

 126 ± 40 OUR AVERAGE Error includes scale factor of 1.8.

VALUE (MeV)	EVTS	DOCUMENT ID	TECN	CHG	COMMENT
220±30±50		AMELIN 00	VES		$37 \pi^- p \rightarrow \eta \pi^+ \pi^- n$
106±27		FUKUI 88	SPEC	0	$8.95 \pi^- p \rightarrow \eta \pi^+ \pi^- n$
195		26 ANDERSON 69	MMS	-	$16 \pi^- p$ backward
< 21		26,27 FOCACCI 66	MMS	-	$7-12 \pi^- p \rightarrow pMM$
< 30		26,27 FOCACCI 66	MMS	-	$7-12 \pi^- p \rightarrow pMM$
< 38		26,27 FOCACCI 66	MMS	-	$7-12 \pi^- p \rightarrow pMM$

• • • We do not use the following data for averages, fits, limits, etc. • • •
²⁶ Seen in 2.5-3 GeV/c $\bar{p}p$. $2\pi^+ 2\pi^-$, with 0, 1, $2 \pi^+ \pi^-$ pairs in ρ^0 band not seen by OREN 74 (2.3 GeV/c $\bar{p}p$) with more statistics. (Jan. 1979)

²⁷ Not seen by BOWEN 72.

$\rho_3(1690)$ DECAY MODES

Mode	Fraction (Γ_i/Γ)	Scale factor
Γ_1 4π	(71.1 ± 1.9) %	
Γ_2 $\pi^\pm \pi^+ \pi^- \pi^0$	(67 ± 22) %	
Γ_3 $\omega \pi$	(16 ± 6) %	
Γ_4 $\pi \pi$	(23.6 ± 1.3) %	
Γ_5 $K \bar{K} \pi$	(3.8 ± 1.2) %	
Γ_6 $K \bar{K}$	(1.58 ± 0.26) %	1.2
Γ_7 $\eta \pi^+ \pi^-$	seen	
Γ_8 $\rho(770) \eta$	seen	
Γ_9 $\pi \pi \rho$	seen	
Γ_{10} $a_2(1320) \pi$	seen	
Γ_{11} $\rho \rho$	seen	
Γ_{12} $\phi \pi$		
Γ_{13} $\eta \pi$		
Γ_{14} $\pi^\pm 2\pi^+ 2\pi^- \pi^0$		

CONSTRAINED FIT INFORMATION

An overall fit to 5 branching ratios uses 10 measurements and one constraint to determine 4 parameters. The overall fit has a $\chi^2 = 14.7$ for 7 degrees of freedom.

The following *off-diagonal* array elements are the correlation coefficients $\langle \delta x_i \delta x_j \rangle / (\delta x_i \delta x_j)$, in percent, from the fit to the branching fractions, $x_i \equiv \Gamma_i / \Gamma_{\text{total}}$. The fit constrains the x_i whose labels appear in this array to sum to one.

x_4	-77		
x_5	-74	17	
x_6	-15	2	0
	x_1	x_4	x_5

 $\rho_3(1690)$ BRANCHING RATIOS

$\Gamma(\pi\pi)/\Gamma_{\text{total}}$	Γ_4/Γ			
VALUE	DOCUMENT ID	TECN	CHG	COMMENT
0.236 ± 0.013 OUR FIT				
0.243 ± 0.013 OUR AVERAGE				

0.259 ^{+0.018} _{-0.019}	BECKER	79	ASPK	0	17 $\pi^- \rho$ polarized
0.23 ± 0.02	CORDEN	79	OMEG		12-15 $\pi^- \rho \rightarrow n 2\pi$
0.22 ± 0.04	²⁸ MATTHEWS	71C	HDBC	0	7 $\pi^+ n \rightarrow \pi^- p$
••• We do not use the following data for averages, fits, limits, etc. •••					
0.245 ± 0.006	²⁹ ESTABROOKS	75	RVUE		17 $\pi^- \rho \rightarrow \pi^+ \pi^- n$

²⁸ One-pion-exchange model used in this estimation.

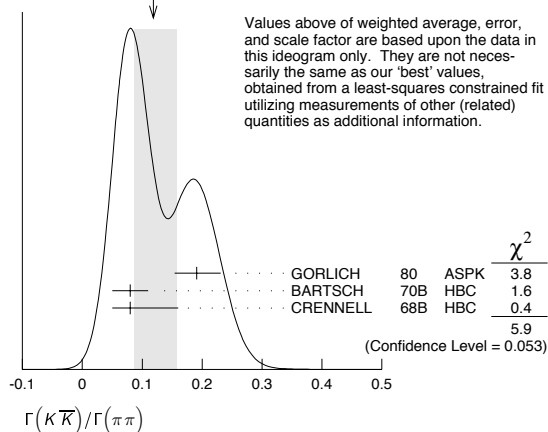
²⁹ From phase-shift analysis of HYAMS 75 data.

$\Gamma(\pi\pi)/\Gamma(\pi^\pm \pi^+ \pi^- \pi^0)$	Γ_4/Γ_2				
VALUE	DOCUMENT ID	TECN	CHG	COMMENT	
0.35 ± 0.11	CASON	73	HBC	-	8,18.5 $\pi^- \rho$
••• We do not use the following data for averages, fits, limits, etc. •••					
<0.2	HOLMES	72	HBC	+	10-12 $K^+ p$
<0.12	BALLAM	71B	HBC	-	16 $\pi^- \rho$

$\Gamma(\pi\pi)/\Gamma(4\pi)$	Γ_4/Γ_1				
VALUE	DOCUMENT ID	TECN	CHG	COMMENT	
0.332 ± 0.026 OUR FIT				Error includes scale factor of 1.1.	
0.30 ± 0.10	BALTAY	78B	HBC	0	15 $\pi^+ \rho \rightarrow p 4\pi$

$\Gamma(K\bar{K})/\Gamma(\pi\pi)$	Γ_6/Γ_4				
VALUE	DOCUMENT ID	TECN	CHG	COMMENT	
0.067 ± 0.011 OUR FIT				Error includes scale factor of 1.2.	
0.118 ± 0.039 -0.032 OUR AVERAGE				Error includes scale factor of 1.7. See the ideogram below.	
0.191 ^{+0.040} _{-0.037}	GORLICH	80	ASPK	0	17,18 $\pi^- \rho$ polarized
0.08 ± 0.03	BARTSCH	70B	HBC	+	8 $\pi^+ p$
0.08 ± 0.08 -0.03	CRENNELL	68B	HBC		6.0 $\pi^- p$

WEIGHTED AVERAGE
0.118±0.039-0.032 (Error scaled by 1.7)



Values above of weighted average, error, and scale factor are based upon the data in this ideogram only. They are not necessarily the same as our 'best' values, obtained from a least-squares constrained fit utilizing measurements of other (related) quantities as additional information.

 $\Gamma(K\bar{K}\pi)/\Gamma(\pi\pi)$ Γ_5/Γ_4

VALUE	DOCUMENT ID	TECN	CHG	COMMENT	
0.16 ± 0.05 OUR FIT					
0.16 ± 0.05	³⁰ BARTSCH	70B	HBC	+	8 $\pi^+ p$
³⁰ Increased by us to correspond to $B(\rho_3(1690) \rightarrow \pi\pi) = 0.24$.					

 $[\Gamma(\pi\pi\rho) + \Gamma(a_2(1320)\pi) + \Gamma(\rho\rho)]/\Gamma(\pi^\pm \pi^+ \pi^- \pi^0)$ $(\Gamma_9 + \Gamma_{10} + \Gamma_{11})/\Gamma_2$

VALUE	DOCUMENT ID	TECN	CHG	COMMENT	
0.94 ± 0.09 OUR AVERAGE					
0.96 ± 0.21	BALTAY	78B	HBC	+	15 $\pi^+ \rho \rightarrow p 4\pi$
0.88 ± 0.15	BALLAM	71B	HBC	-	16 $\pi^- \rho$
1 ± 0.15	BARTSCH	70B	HBC	+	8 $\pi^+ p$
consistent with 1	CASO	68	HBC	-	11 $\pi^- p$

 $\Gamma(\rho\rho)/\Gamma(\pi^\pm \pi^+ \pi^- \pi^0)$ Γ_{11}/Γ_2

VALUE	EVTS	DOCUMENT ID	TECN	CHG	COMMENT	
••• We do not use the following data for averages, fits, limits, etc. •••						
0.12 ± 0.11		BALTAY	78B	HBC	+	15 $\pi^+ \rho \rightarrow p 4\pi$
0.56	66	KLIGER	74	HBC	-	4.5 $\pi^- \rho \rightarrow p 4\pi$
0.13 ± 0.09	³¹	THOMPSON	74	HBC	+	13 $\pi^+ p$
0.7 ± 0.15		BARTSCH	70B	HBC	+	8 $\pi^+ p$
³¹ $\rho\rho$ and $a_2(1320)\pi$ modes are indistinguishable.						

 $\Gamma(\rho\rho)/[\Gamma(\pi\pi\rho) + \Gamma(a_2(1320)\pi) + \Gamma(\rho\rho)]$ $\Gamma_{11}/(\Gamma_9 + \Gamma_{10} + \Gamma_{11})$

VALUE	DOCUMENT ID	TECN	CHG	COMMENT	
••• We do not use the following data for averages, fits, limits, etc. •••					
0.48 ± 0.16	CASO	68	HBC	-	11 $\pi^- p$

 $\Gamma(a_2(1320)\pi)/\Gamma(\pi^\pm \pi^+ \pi^- \pi^0)$ Γ_{10}/Γ_2

VALUE	DOCUMENT ID	TECN	CHG	COMMENT	
••• We do not use the following data for averages, fits, limits, etc. •••					
0.66 ± 0.08	BALTAY	78B	HBC	+	15 $\pi^+ \rho \rightarrow p 4\pi$
0.36 ± 0.14	³² THOMPSON	74	HBC	+	13 $\pi^+ p$
not seen	CASON	73	HBC	-	8,18.5 $\pi^- \rho$
0.6 ± 0.15	BARTSCH	70B	HBC	+	8 $\pi^+ p$
0.6	BALTAY	68	HBC	+	7,8.5 $\pi^+ p$
³² $\rho\rho$ and $a_2(1320)\pi$ modes are indistinguishable.					

 $\Gamma(\omega\pi)/\Gamma(\pi^\pm \pi^+ \pi^- \pi^0)$ Γ_3/Γ_2

VALUE	CL%	DOCUMENT ID	TECN	CHG	COMMENT	
0.23 ± 0.05 OUR AVERAGE					Error includes scale factor of 1.2.	
0.33 ± 0.07		THOMPSON	74	HBC	+	13 $\pi^+ p$
0.12 ± 0.07		BALLAM	71B	HBC	-	16 $\pi^- \rho$
0.25 ± 0.10		BALTAY	68	HBC	+	7,8.5 $\pi^+ p$
0.25 ± 0.10		JOHNSTON	68	HBC	-	7.0 $\pi^- p$
••• We do not use the following data for averages, fits, limits, etc. •••						
<0.11	95	BALTAY	78B	HBC	+	15 $\pi^+ \rho \rightarrow p 4\pi$
<0.09		KLIGER	74	HBC	-	4.5 $\pi^- \rho \rightarrow p 4\pi$

 $\Gamma(\phi\pi)/\Gamma(\pi^\pm \pi^+ \pi^- \pi^0)$ Γ_{12}/Γ_2

VALUE	DOCUMENT ID	TECN	CHG	COMMENT	
••• We do not use the following data for averages, fits, limits, etc. •••					
<0.11	BALTAY	68	HBC	+	7,8.5 $\pi^+ p$

 $\Gamma(\pi^\pm 2\pi^+ 2\pi^- \pi^0)/\Gamma(\pi^\pm \pi^+ \pi^- \pi^0)$ Γ_{14}/Γ_2

VALUE	DOCUMENT ID	TECN	CHG	COMMENT	
••• We do not use the following data for averages, fits, limits, etc. •••					
<0.15	BALTAY	68	HBC	+	7,8.5 $\pi^+ p$

Meson Particle Listings

 $\rho_3(1690), \rho(1700)$

$\Gamma(\eta\pi)/\Gamma(\pi^+\pi^-\pi^0)$					Γ_{13}/Γ_2
VALUE	DOCUMENT ID	TECN	CHG	COMMENT	
••• We do not use the following data for averages, fits, limits, etc. •••					
<0.02	THOMPSON	74	HBC	+	13 $\pi^+\pi^-$
$\Gamma(K\bar{K})/\Gamma_{\text{total}}$					Γ_6/Γ
VALUE	DOCUMENT ID	TECN	CHG	COMMENT	
0.0158 ± 0.0026 OUR FIT Error includes scale factor of 1.2.					
0.0130 ± 0.0024 OUR AVERAGE					
0.013 ± 0.003	COSTA...	80	OMEG	0	10 $\pi^-\rho \rightarrow K^+K^-n$
0.013 ± 0.004	³³ MARTIN	78B	SPEC	-	10 $\pi\rho \rightarrow K_S^0 K^-\rho$
³³ From $(\Gamma_4\Gamma_6)^{1/2} = 0.056 \pm 0.034$ assuming $B(\rho_3(1690) \rightarrow \pi\pi) = 0.24$.					
$\Gamma(\omega\pi)/[\Gamma(\omega\pi) + \Gamma(\rho\rho)]$					$\Gamma_3/(\Gamma_3 + \Gamma_{11})$
VALUE	DOCUMENT ID	TECN	CHG	COMMENT	
••• We do not use the following data for averages, fits, limits, etc. •••					
0.22 ± 0.08	CASON	73	HBC	-	8.185 $\pi^-\rho$
$\Gamma(\eta\pi^+\pi^-)/\Gamma_{\text{total}}$					Γ_7/Γ
VALUE	DOCUMENT ID	TECN	COMMENT		
seen	FUKUI	88	SPEC	8.95 $\pi^-\rho \rightarrow \eta\pi^+\pi^-n$	
$\Gamma(\rho_2(1320)\pi)/\Gamma(\rho(770)\eta)$					Γ_{10}/Γ_8
VALUE	DOCUMENT ID	TECN	COMMENT		
5.5 ± 2.0	AMELIN	00	VES	37 $\pi^-\rho \rightarrow \eta\pi^+\pi^-n$	

 $\rho_3(1690)$ REFERENCES

AMELIN	00	NP A668 83	D. Amelin et al.	(VES Collab.)
ALDE	95	ZPHY C66 379	D.M. Alde et al.	(GAMS Collab.) JP
ALDE	92C	ZPHY C54 553	D.M. Alde et al.	(BELG, SERP, KEK, LANL+)
FUKUI	88	PL B202 441	S. Fukui et al.	(SUGI, NAGO, KEK, KYOT+)
DENNEY	83	PR D28 2726	D.L. Denney et al.	(IOWA, MICH)
EVANGELIS...	81	NP B178 197	C. Evangelista et al.	(BARI, BONN, CERN+)
ALPER	80	PL 94B 422	B. Alper et al.	(AMST, CERN, CRAC, MPIM+)
COSTA...	80	NP B175 402	G. Costa de Beauregard et al.	(BARI, BONN+)
GORLICH	80	NP B174 16	L. Gorlich et al.	(CRAC, MPIM, CERN+)
BECKER	79	NP B151 46	H. Becker et al.	(MPIM, CERN, ZEEM, CRAC)
CORDEN	79	NP B157 250	M.J. Corden et al.	(BIRM, RHEL, TEL+)
BALTAY	78B	PR D17 62	C. Baltay et al.	(COLU, BING)
MARTIN	78B	NP B140 158	A.D. Martin et al.	(DURH, GEVA)
MARTIN	78D	PL 74B 417	A.D. Martin et al.	(DURH, GEVA)
ANTIPOV	77	NP B119 45	Y.M. Antipov et al.	(SERP, GEVA)
GESSAROLI	77	NP B126 382	R. Gessaroli et al.	(BGNA, FIRZ, GENO+)
BLUM	75	PL 57B 403	W. Blum et al.	(CERN, MPIM) JP
ESTABROOKS	75	NP B95 322	P.G. Estabrooks, A.D. Martin	(DURH)
HYAMS	75	NP B100 205	B.D. Hyams et al.	(CERN, MPIM)
ENGLER	74	PR D10 2070	A. Engler et al.	(CMU, CASE)
GRAYER	74	NP B75 189	G. Grayer et al.	(CERN, MPIM)
KLIGER	74	SJNP 19 428	G.K. Kliger et al.	(ITEP)
		Translated from YAF 19 839		
OREN	74	NP B71 189	Y. Oren et al.	(ANL, OXF)
THOMPSON	74	NP B69 220	G. Thompson et al.	(PURD)
CASON	73	PR D7 1971	N.M. Cason et al.	(NDAM)
BOWEN	72	PRL 29 890	D.R. Bowen et al.	(NEAS, STON)
HOLMES	72	PR D6 3336	R. Holmes et al.	(ROCH)
BALLAM	71B	PR D3 2606	J. Ballam et al.	(SLAC)
MATTHEWS	71C	NP B33 1	J.A.J. Matthews et al.	(TNTO, WISC) JP
ARMENISE	70	LNC 4 199	N. Armenise et al.	(BARI, BGNA, FIRZ)
BARNHAM	70	PRL 24 1083	K.W.J. Barnham et al.	(BIRM)
BARTSCH	70B	NP B22 109	J. Bartsch et al.	(AACH, BERL, CERN)
CASO	70	LNC 3 707	C. Caso et al.	(GENO, HAMB, MILA, SACL)
STUNTEBECK	70	PL 32B 391	P.H. Stuntebeck et al.	(NDAM)
ADERHOLZ	69	NP B11 259	M. Aderholz et al.	(AACH3, BERL, CERN+)
ANDERSON	69	PRL 22 1390	E.W. Anderson et al.	(BNL, CMU)
ARMENISE	68	NC 54A 999	N. Armenise et al.	(BARI, BGNA, FIRZ+)
BALTAY	68	PRL 20 887	C. Baltay et al.	(COLU, ROCH, RUTG, YALE)
CASO	68	NC 54A 983	C. Caso et al.	(GENO, HAMB, MILA, SACL)
CRENNELL	68B	PL 28B 136	D.J. Crennell et al.	(BNL)
JOHNSTON	68	PRL 20 1414	T.F. Johnston et al.	(TNTO, WISC) JP
FOCACCI	66	PRL 17 990	M.N. Focacci et al.	(CERN)
GOLDBERG	65	PL 17 354	M. Goldberg et al.	(CERN, EPOL, ORSAY+)

OTHER RELATED PAPERS

BUGG	07	EPJ C52 55	D. Bugg	
BARNETT	83B	PL 120B 455	B. Barnett et al.	(JHU)
EHRlich	66	PR 152 1194	R. Ehrlich, W. Selove, H. Yuta	(PERN)
LEVRAI	66	PL 22 714	B. Levrat et al.	
SEGUINOT	66	PL 19 712	J. Seguinot et al.	
BELLINI	65	NC 40A 948	G. Bellini et al.	(MILA)
DEUTSCH...	65	PL 18 351	M. Deuschmann et al.	(AACH3, BERL, CERN)
FORINO	65	PL 19 65	A. Forino et al.	(BGNA, ORSAY, SACL)

 $\rho(1700)$

$$I^G(J^{PC}) = 1^+(1^-)$$

THE $\rho(1450)$ AND THE $\rho(1700)$

Updated April 2008 by S. Eidelman (Novosibirsk).

In our 1988 edition, we replaced the $\rho(1600)$ entry with two new ones, the $\rho(1450)$ and the $\rho(1700)$, because there was emerging evidence that the 1600-MeV region actually contains two ρ -like resonances. ERKAL 86 had pointed out this possibility with a theoretical analysis on the consistency of 2π and 4π electromagnetic form factors and the $\pi\pi$ scattering length. DONNACHIE 87, with a full analysis of data on the 2π and 4π final states in e^+e^- annihilation and photoproduction reactions, had also argued that in order to obtain a consistent picture, two resonances were necessary. The existence of $\rho(1450)$ was supported by the analysis of $\eta\rho^0$ mass spectra obtained in photoproduction and e^+e^- annihilation (DONNACHIE 87B), as well as that of $e^+e^- \rightarrow \omega\pi$ (DONNACHIE 91).

The analysis of DONNACHIE 87 was further extended by CLEGG 88, 94 to include new data on 4π -systems produced in e^+e^- annihilation, and in τ -decays (τ decays to 4π , and e^+e^- annihilation to 4π can be related by the Conserved Vector Current assumption). These systems were successfully analyzed using interfering contributions from two ρ -like states, and from the tail of the $\rho(770)$ decaying into two-body states. While specific conclusions on $\rho(1450) \rightarrow 4\pi$ were obtained, little could be said about the $\rho(1700)$.

Independent evidence for two 1^- states is provided by KILLIAN 80 in 4π electroproduction at $\langle Q^2 \rangle = 1$ (GeV/c)², and by FUKUI 88 in a high-statistics sample of the $\eta\pi\pi$ system in π^-p charge exchange.

This scenario with two overlapping resonances is supported by other data. BISELLO 89 measured the pion form factor in the interval 1.35–2.4 GeV, and observed a deep minimum around 1.6 GeV. The best fit was obtained with the hypothesis of ρ -like resonances at 1420 and 1770 MeV, with widths of about 250 MeV. ANTONELLI 88 found that the $e^+e^- \rightarrow \eta\pi^+\pi^-$ cross section is better fitted with two fully interfering Breit-Wigners, with parameters in fair agreement with those of DONNACHIE 87 and BISELLO 89. These results can be considered as a confirmation of the $\rho(1450)$.

Decisive evidence for the $\pi\pi$ decay mode of both $\rho(1450)$ and $\rho(1700)$ came from recent results in $\bar{p}p$ annihilation at rest (ABELE 97). It was shown that these resonances also possess a $K\bar{K}$ decay mode (ABELE 98, BERTIN 98B, ABELE 99D). High-statistics studies of the decays $\tau \rightarrow \pi\pi\nu_\tau$ (BARATE 97M, URHEIM 97), and $\tau \rightarrow 4\pi\nu_\tau$ (EDWARDS 00A), also require the $\rho(1450)$, but are not sensitive to the $\rho(1700)$, because it is too close to the τ mass. Recently, in a very-high-statistics study of the $\tau \rightarrow \pi\pi\nu_\tau$ decay performed at Belle (FUJIKAWA 07), both $\rho(1450)$ and $\rho(1700)$ were observed for the first time in τ decays.

The structure of these ρ states is not yet completely clear. BARNES 97 and CLOSE 97C claim that $\rho(1450)$ has a mass

consistent with radial $2S$, but its decays show characteristics of hybrids, and suggest that this state may be a $2S$ -hybrid mixture. DONNACHIE 99 argues that hybrid states could have a 4π decay mode dominated by the $a_1\pi$. Such behavior has recently been observed by AKHMETSHIN 99E in $e^+e^- \rightarrow 4\pi$ in the energy range 1.05–1.38 GeV, and by EDWARDS 00 in $\tau \rightarrow 4\pi$ decays. ALEXANDER 01B observed the $\rho(1450) \rightarrow \omega\pi$ decay mode in B -meson decays, however, did not find $\rho(1700) \rightarrow \omega\pi^0$. A similar conclusion is made by AKHMETSHIN 03B, who studied the process $e^+e^- \rightarrow \omega\pi^0$. Various decay modes of the $\rho(1450)$ and $\rho(1700)$ were observed in $\bar{p}n$ and $\bar{p}p$ annihilation (ABELE 01B, BARGIOTTI 03B), but no definite conclusions could be drawn. More data should be collected to clarify the nature of the ρ states, particularly in the energy range above 1.6 GeV.

We now list under a separate entry the $\rho(1570)$, the $\phi\pi$ state with $J^{PC} = 1^{--}$ earlier observed by BITYUKOV 87 (referred to as $C(1480)$) and recently confirmed by AUBERT 08S. While ACHASOV 96B shows that it may be a threshold effect, CLEGG 88 and LANDSBERG 92 suggest two independent vector states with this decay mode. The $C(1480)$ was not seen by $\bar{p}p$ (ABELE 97H) and e^+e^- (AULCHENKO 87B, BISELLO 91C) experiments. However, the sensitivity of the two latter was an order of magnitude lower than that of AUBERT 08S. Note that AUBERT 08S can not exclude that their observation is due to an OZI-suppressed decay mode of the $\rho(1700)$.

Several observations on the $\omega\pi$ system in the 1200-MeV region (FRENKIEL 72, COSME 76, BARBER 80C, ASTON 80C, ATKINSON 84C, BRAU 88, AMSLER 93B) may be interpreted in terms of either $J^P = 1^- \rho(770) \rightarrow \omega\pi$ production (LAYSSAC 71), or $J^P = 1^+ b_1(1235)$ production (BRAU 88, AMSLER 93B). We argue that no special entry for a $\rho(1250)$ is needed. The LASS amplitude analysis (ASTON 91B) showing evidence for $\rho(1270)$ is preliminary and needs confirmation. For completeness, the relevant observations are listed under the $\rho(1450)$.

Recently ABLIKIM 06S reported a very broad 1^{--} resonance-like K^+K^- state in $J/\psi \rightarrow K^+K^-\pi^0$ decays. Its pole position corresponds to mass of 1576 MeV and width of 818 MeV. DING 06, GUO 06, and ZHANG 07C suggest its exotic structure (molecular or multiquark), while LI 07A and LIU 07B explain it by the interference between the $\rho(1450)$ and $\rho(1700)$. We quote ABLIKIM 06S as $X(1575)$ in the section "Further States."

Evidence for ρ -like mesons decaying into 6π states was first noted by CLEGG 90 in the analysis of 6π mass spectra from e^+e^- annihilation (BISELLO 81, CASTRO 88) and diffractive photoproduction (ATKINSON 85). CLEGG 90 argued that two states at about 2.1 and 1.8 GeV exist: while the former is a candidate for a new resonance ($\rho(2150)$), the latter could be a manifestation of the $\rho(1700)$ distorted by threshold effects. Recently, the E687 Collaboration at Fermilab reported an observation of a narrow-dip structure at 1.9 GeV in the $3\pi^+3\pi^-$ diffractive photoproduction (FRABETTI 01). A similar effect

of the dip in the cross section of $e^+e^- \rightarrow 6\pi$ around 1.9 GeV has been earlier reported by DM2 (CASTRO 88), where 6π included both $3\pi^+3\pi^-$ and $2\pi^+2\pi^-2\pi^0$. Later the dip in the R value (the total cross section of $e^+e^- \rightarrow$ hadrons divided by the cross section of $e^+e^- \rightarrow \mu^+\mu^-$) was observed by ANTONELLI 96, again around 1.9 GeV. This energy is close to the $N\bar{N}$ threshold, which hints at the possible relation between the dip and $N\bar{N}$, *e.g.*, the frequently discussed narrow $N\bar{N}$ resonance or just a threshold effect. Such behaviour is also characteristic of exotic objects like vector $q\bar{q}$ hybrids. Note that AGNELLO 02 failed to find this state in the reaction $\bar{n}p \rightarrow 3\pi^+2\pi^-\pi^0$. A reanalysis of the E687 data by FRABETTI 04 shows that a dip may arise due to interference of a narrow object with a broad $\rho(1700)$ independently of the nature of the former. Recently, BaBar studied the processes $e^+e^- \rightarrow 3\pi^+3\pi^-$ and $e^+e^- \rightarrow 2\pi^+2\pi^-2\pi^0$ using the radiative return, and observed a structure around 1.9 GeV in both final states (AUBERT 06D). The data are not well described by a single Breit-Wigner state, and a good fit is achieved while taking into account the interference of such a structure with a Jacob-Slansky amplitude for continuum. The mass of this state obtained by BaBar is consistent with ANTONELLI 96 and FRABETTI 01, but the width is substantially larger. Recently AUBERT 08S observed a structure at 1.9 GeV in the radiative return to the $\phi\pi$ final state, with a much smaller width of 48 ± 17 MeV consistent with that of ANTONELLI 96 and FRABETTI 04. We list these observations under a separate particle $\rho(1900)$, which needs confirmation.

 $\rho(1700)$ MASS **$\eta\rho^0$ AND $\pi^+\pi^-\pi^0$ MODES**

VALUE (MeV)

DOCUMENT ID

1720 ± 20 OUR ESTIMATE **$\eta\rho^0$ MODE**

VALUE (MeV)

DOCUMENT ID

TECN COMMENT

The data in this block is included in the average printed for a previous datablock.

• • • We do not use the following data for averages, fits, limits, etc. • • •

1740 ± 20	ANTONELLI	88	DM2	$e^+e^- \rightarrow \eta\pi^+\pi^-$
1701 ± 15	1 FUKUI	88	SPEC	$8.95 \pi^-\rho \rightarrow \eta\pi^+\pi^-n$

 $\pi\pi$ MODE

VALUE (MeV)

DOCUMENT ID

TECN COMMENT

The data in this block is included in the average printed for a previous datablock.

• • • We do not use the following data for averages, fits, limits, etc. • • •

1780 $\begin{smallmatrix} +37 \\ -29 \end{smallmatrix}$	2 ABELE	97	CBAR	$\bar{p}n \rightarrow \pi^-\pi^0\pi^0$
1719 ± 15	2 BERTIN	97c	OBLX	$0.0 \bar{p}p \rightarrow \pi^+\pi^-\pi^0$
1730 ± 30	CLEGG	94	RVUE	$e^+e^- \rightarrow \pi^+\pi^-$
1768 ± 21	BISELLO	89	DM2	$e^+e^- \rightarrow \pi^+\pi^-$
1745.7 ± 91.9	DUBNICKA	89	RVUE	$e^+e^- \rightarrow \pi^+\pi^-$
1546 ± 26	GESHKEN...	89	RVUE	
1650	3 ERKAL	85	RVUE	$20-70 \gamma p \rightarrow \gamma\pi$
1550 ± 70	ABE	84B	HYBR	$20 \gamma p \rightarrow \pi^+\pi^-p$
1590 ± 20	4 ASTON	80	OMEG	$20-70 \gamma p \rightarrow p2\pi$
1600 ± 10	5 ATIYA	79B	SPEC	$50 \gamma C \rightarrow C2\pi$
1598 $\begin{smallmatrix} +24 \\ -22 \end{smallmatrix}$	BECKER	79	ASPK	$17 \pi^- p$ polarized
1659 ± 25	3 LANG	79	RVUE	
1575	3 MARTIN	78c	RVUE	$17 \pi^- p \rightarrow \pi^+\pi^-n$
1610 ± 30	3 FROGGATT	77	RVUE	$17 \pi^- p \rightarrow \pi^+\pi^-n$
1590 ± 20	6 HYAMS	73	ASPK	$17 \pi^- p \rightarrow \pi^+\pi^-n$

Meson Particle Listings

 $\rho(1700)$ $\pi\omega$ MODE

VALUE (MeV)	DOCUMENT ID	TECN	COMMENT
1550 to 1620	7 ACHASOV	00i	SND $e^+e^- \rightarrow \pi^0\pi^0\gamma$
1580 to 1710	8 ACHASOV	00i	SND $e^+e^- \rightarrow \pi^0\pi^0\gamma$
1710±90	ACHASOV	97	RVUE $e^+e^- \rightarrow \omega\pi^0$

 $K\bar{K}$ MODE

VALUE (MeV)	EVTS	DOCUMENT ID	TECN	CHG	COMMENT
1740.8±22.2	27k	9 ABELE	99D	CBAR ±	0.0 $\bar{p}p \rightarrow K^+K^-\pi^0$
1582 ±36	1600	CLELAND	82B	SPEC ±	50 $\pi p \rightarrow K_S^0 K^\pm p$

 $2(\pi^+\pi^-)$ MODE

VALUE (MeV)	EVTS	DOCUMENT ID	TECN	COMMENT
1851 ± 27 24		ACHASOV	97	RVUE $e^+e^- \rightarrow 2(\pi^+\pi^-)$
1570 ± 20		10 CORDIER	82	DM1 $e^+e^- \rightarrow 2(\pi^+\pi^-)$
1520 ± 30		4 ASTON	81E	OMEG 20-70 $\gamma p \rightarrow p4\pi$
1654 ± 25		11 DIBIANCA	81	DBC $\pi^+d \rightarrow pp2(\pi^+\pi^-)$
1666 ± 39		10 BACCI	80	FRAG $e^+e^- \rightarrow 2(\pi^+\pi^-)$
1780	34	KILLIAN	80	SPEC 11 $e^-p \rightarrow 2(\pi^+\pi^-)$
1500		12 ATIYA	79B	SPEC 50 $\gamma C \rightarrow C4\pi^\pm$
1570 ± 60	65	13 ALEXANDER	75	HBC 7.5 $\gamma p \rightarrow p4\pi$
1550 ± 60		4 CONVERSI	74	OSPK $e^+e^- \rightarrow 2(\pi^+\pi^-)$
1550 ± 50	160	SCHACHT	74	STRC 5.5-9 $\gamma p \rightarrow p4\pi$
1450±100	340	SCHACHT	74	STRC 9-18 $\gamma p \rightarrow p4\pi$
1430 ± 50	400	BINGHAM	72B	HBC 9.3 $\gamma p \rightarrow p4\pi$

 $\pi^+\pi^-\pi^0$ MODE

VALUE (MeV)	DOCUMENT ID	TECN	COMMENT
1660±30	ATKINSON	85B	OMEG 20-70 γp

 $3(\pi^+\pi^-)$ AND $2(\pi^+\pi^-\pi^0)$ MODES

VALUE (MeV)	DOCUMENT ID	TECN	COMMENT
1730±34	14 FRABETTI	04	E687 $\gamma p \rightarrow 3\pi^+3\pi^-p$
1783±15	CLEGG	90	RVUE $e^+e^- \rightarrow 3(\pi^+\pi^-)2(\pi^+\pi^-\pi^0)$

- Assuming $\rho^+ f_0(1370)$ decay mode interferes with $a_1(1260)^+\pi$ background. From a two Breit-Wigner fit.
- T-matrix pole.
- From phase shift analysis of HYAMS 73 data.
- Simple relativistic Breit-Wigner fit with constant width.
- An additional 40 MeV uncertainty in both the mass and width is present due to the choice of the background shape.
- Included in BECKER 79 analysis.
- Taking into account both $\rho(1450)$ and $\rho(1700)$ contributions. Using the data of ACHASOV 00i on $e^+e^- \rightarrow \omega\pi^0$ and of EDWARDS 00A on $\tau^- \rightarrow \omega\pi^-\nu_\tau$. $\rho(1450)$ mass and width fixed at 1400 MeV and 500 MeV respectively.
- Taking into account the $\rho(1700)$ contribution only. Using the data of ACHASOV 00i on $e^+e^- \rightarrow \omega\pi^0$ and of EDWARDS 00A on $\tau^- \rightarrow \omega\pi^-\nu_\tau$.
- K-matrix pole. Isospin not determined, could be $\omega(1650)$ or $\phi(1680)$.
- Simple relativistic Breit-Wigner fit with model dependent width.
- One peak fit result.
- Parameters roughly estimated, not from a fit.
- Skew mass distribution compensated by Ross-Stodolsky factor.
- From a fit with two resonances with the JACOB 72 continuum.

 $\rho(1700)$ WIDTH $\eta\rho^0$ AND $\pi^+\pi^-$ MODES

VALUE (MeV)	DOCUMENT ID
250±100 OUR ESTIMATE	

 $\eta\rho^0$ MODE

VALUE (MeV)	DOCUMENT ID	TECN	COMMENT
150±30	ANTONELLI	88	DM2 $e^+e^- \rightarrow \eta\pi^+\pi^-$
282±44	15 FUKUI	88	SPEC 8.95 $\pi^-p \rightarrow \eta\pi^+\pi^-n$

• • • We do not use the following data for averages, fits, limits, etc. • • •

 $\pi\pi$ MODE

VALUE (MeV)	DOCUMENT ID	TECN	COMMENT
The data in this block is included in the average printed for a previous datablock.			

• • • We do not use the following data for averages, fits, limits, etc. • • •

275 ± 45	16 ABELE	97	CBAR $\bar{p}n \rightarrow \pi^-\pi^0\pi^0$
310 ± 40	16 BERTIN	97C	OBLX 0.0 $\bar{p}p \rightarrow \pi^+\pi^-\pi^0$
400 ±100	CLEGG	94	RVUE $e^+e^- \rightarrow \pi^+\pi^-$
224 ± 22	BISELLO	89	DM2 $e^+e^- \rightarrow \pi^+\pi^-$
242.5±163.0	DUBNICKA	89	RVUE $e^+e^- \rightarrow \pi^+\pi^-$
620 ± 60	GESHKEN...	89	RVUE
<315	17 ERKAL	85	RVUE 20-70 $\gamma p \rightarrow \gamma\pi$
280 ± 30 - 80	ABE	84B	HYBR 20 $\gamma p \rightarrow \pi^+\pi^-p$
230 ± 80	18 ASTON	80	OMEG 20-70 $\gamma p \rightarrow p2\pi$
283 ± 14	19 ATIYA	79B	SPEC 50 $\gamma C \rightarrow C2\pi$
175 ± 98 53	BECKER	79	ASPK 17 π^-p polarized
232 ± 34	17 LANG	79	RVUE
340	17 MARTIN	78C	RVUE 17 $\pi^-p \rightarrow \pi^+\pi^-n$
300 ±100	17 FROGGATT	77	RVUE 17 $\pi^-p \rightarrow \pi^+\pi^-n$
180 ± 50	20 HYAMS	73	ASPK 17 $\pi^-p \rightarrow \pi^+\pi^-n$

 $K\bar{K}$ MODE

VALUE (MeV)	EVTS	DOCUMENT ID	TECN	CHG	COMMENT
187.2± 26.7	27k	21 ABELE	99D	CBAR ±	0.0 $\bar{p}p \rightarrow K^+K^-\pi^0$
265 ±120	1600	CLELAND	82B	SPEC ±	50 $\pi p \rightarrow K_S^0 K^\pm p$

 $2(\pi^+\pi^-)$ MODE

VALUE (MeV)	EVTS	DOCUMENT ID	TECN	COMMENT
510 ± 40		22 CORDIER	82	DM1 $e^+e^- \rightarrow 2(\pi^+\pi^-)$
400 ± 50		18 ASTON	81E	OMEG 20-70 $\gamma p \rightarrow p4\pi$
400±146		23 DIBIANCA	81	DBC $\pi^+d \rightarrow pp2(\pi^+\pi^-)$
700±160		22 BACCI	80	FRAG $e^+e^- \rightarrow 2(\pi^+\pi^-)$
100	34	KILLIAN	80	SPEC 11 $e^-p \rightarrow 2(\pi^+\pi^-)$
600		24 ATIYA	79B	SPEC 50 $\gamma C \rightarrow C4\pi^\pm$
340±160	65	25 ALEXANDER	75	HBC 7.5 $\gamma p \rightarrow p4\pi$
360±100		18 CONVERSI	74	OSPK $e^+e^- \rightarrow 2(\pi^+\pi^-)$
400±120	160	26 SCHACHT	74	STRC 5.5-9 $\gamma p \rightarrow p4\pi$
850±200	340	26 SCHACHT	74	STRC 9-18 $\gamma p \rightarrow p4\pi$
650±100	400	BINGHAM	72B	HBC 9.3 $\gamma p \rightarrow p4\pi$

 $\pi^+\pi^-\pi^0$ MODE

VALUE (MeV)	DOCUMENT ID	TECN	COMMENT
300±50	ATKINSON	85B	OMEG 20-70 γp

 $\omega\rho^0$ MODE

VALUE (MeV)	DOCUMENT ID	TECN	COMMENT
350 to 580	27 ACHASOV	00i	SND $e^+e^- \rightarrow \pi^0\pi^0\gamma$
490 to 1040	28 ACHASOV	00i	SND $e^+e^- \rightarrow \pi^0\pi^0\gamma$

 $3(\pi^+\pi^-)$ AND $2(\pi^+\pi^-\pi^0)$ MODES

VALUE (MeV)	DOCUMENT ID	TECN	COMMENT
315±100	29 FRABETTI	04	E687 $\gamma p \rightarrow 3\pi^+3\pi^-p$
285 ± 20	CLEGG	90	RVUE $e^+e^- \rightarrow 3(\pi^+\pi^-)2(\pi^+\pi^-\pi^0)$

- Assuming $\rho^+ f_0(1370)$ decay mode interferes with $a_1(1260)^+\pi$ background. From a two Breit-Wigner fit.
- T-matrix pole.
- From phase shift analysis of HYAMS 73 data.
- Simple relativistic Breit-Wigner fit with constant width.
- An additional 40 MeV uncertainty in both the mass and width is present due to the choice of the background shape.
- Included in BECKER 79 analysis.
- K-matrix pole. Isospin not determined, could be $\omega(1650)$ or $\phi(1680)$.
- Simple relativistic Breit-Wigner fit with model-dependent width.
- One peak fit result.
- Parameters roughly estimated, not from a fit.
- Skew mass distribution compensated by Ross-Stodolsky factor.
- Width errors enlarged by us to $4\Gamma/\sqrt{N}$; see the note with the $K^*(892)$ mass.
- Taking into account both $\rho(1450)$ and $\rho(1700)$ contributions. Using the data of ACHASOV 00i on $e^+e^- \rightarrow \omega\pi^0$ and of EDWARDS 00A on $\tau^- \rightarrow \omega\pi^-\nu_\tau$. $\rho(1450)$ mass and width fixed at 1400 MeV and 500 MeV respectively.
- Taking into account the $\rho(1700)$ contribution only. Using the data of ACHASOV 00i on $e^+e^- \rightarrow \omega\pi^0$ and of EDWARDS 00A on $\tau^- \rightarrow \omega\pi^-\nu_\tau$.
- From a fit with two resonances with the JACOB 72 continuum.

$\rho(1700)$ DECAY MODES

Mode	Fraction (Γ_i/Γ)
Γ_1 4π	
Γ_2 $2(\pi^+\pi^-)$	large
Γ_3 $\rho\pi\pi$	dominant
Γ_4 $\rho^0\pi^+\pi^-$	large
Γ_5 $\rho^0\pi^0\pi^0$	
Γ_6 $\rho^\pm\pi^\mp\pi^0$	large
Γ_7 $a_1(1260)\pi$	seen
Γ_8 $h_1(1170)\pi$	seen
Γ_9 $\pi(1300)\pi$	seen
Γ_{10} $\rho\rho$	seen
Γ_{11} $\pi^+\pi^-$	seen
Γ_{12} $\pi\pi$	seen
Γ_{13} $K\bar{K}^*(892) + c.c.$	seen
Γ_{14} $\eta\rho$	seen
Γ_{15} $a_2(1320)\pi$	not seen
Γ_{16} $K\bar{K}$	seen
Γ_{17} e^+e^-	seen
Γ_{18} $\pi^0\omega$	seen

 $\rho(1700)$ $\Gamma(i)\Gamma(e^+e^-)/\Gamma(\text{total})$

This combination of a partial width with the partial width into e^+e^- and with the total width is obtained from the cross-section into channel i in e^+e^- annihilation.

 $\Gamma(2(\pi^+\pi^-)) \times \Gamma(e^+e^-)/\Gamma_{\text{total}}$ $\Gamma_2\Gamma_{17}/\Gamma$

VALUE (keV)	DOCUMENT ID	TECN	COMMENT
••• We do not use the following data for averages, fits, limits, etc. •••			
2.6 ± 0.2	DEL COURT	81B	DM1 $e^+e^- \rightarrow 2(\pi^+\pi^-)$
2.83 ± 0.42	BACCI	80	FRAG $e^+e^- \rightarrow 2(\pi^+\pi^-)$

 $\Gamma(\pi^+\pi^-) \times \Gamma(e^+e^-)/\Gamma_{\text{total}}$ $\Gamma_{11}\Gamma_{17}/\Gamma$

VALUE (keV)	DOCUMENT ID	TECN	COMMENT
••• We do not use the following data for averages, fits, limits, etc. •••			
0.13	³⁰ DIEKMAN	88	RVUE $e^+e^- \rightarrow \pi^+\pi^-$
$0.029^{+0.016}_{-0.012}$	KURDADZE	83	OLYA $0.64-1.4 e^+e^- \rightarrow \pi^+\pi^-$

 $\Gamma(K\bar{K}^*(892) + c.c.) \times \Gamma(e^+e^-)/\Gamma_{\text{total}}$ $\Gamma_{13}\Gamma_{17}/\Gamma$

VALUE (keV)	DOCUMENT ID	TECN	COMMENT
••• We do not use the following data for averages, fits, limits, etc. •••			
0.305 ± 0.071	³¹ BIZOT	80	DM1 e^+e^-

 $\Gamma(\eta\rho) \times \Gamma(e^+e^-)/\Gamma_{\text{total}}$ $\Gamma_{14}\Gamma_{17}/\Gamma$

VALUE (eV)	DOCUMENT ID	TECN	COMMENT
••• We do not use the following data for averages, fits, limits, etc. •••			
7 ± 3	ANTONELLI	88	DM2 $e^+e^- \rightarrow \eta\pi^+\pi^-$

 $\Gamma(K\bar{K}) \times \Gamma(e^+e^-)/\Gamma_{\text{total}}$ $\Gamma_{16}\Gamma_{17}/\Gamma$

VALUE (keV)	DOCUMENT ID	TECN	COMMENT
••• We do not use the following data for averages, fits, limits, etc. •••			
0.035 ± 0.029	³¹ BIZOT	80	DM1 e^+e^-

 $\Gamma(\rho\pi\pi) \times \Gamma(e^+e^-)/\Gamma_{\text{total}}$ $\Gamma_3\Gamma_{17}/\Gamma$

VALUE (keV)	DOCUMENT ID	TECN	COMMENT
••• We do not use the following data for averages, fits, limits, etc. •••			
3.510 ± 0.090	³¹ BIZOT	80	DM1 e^+e^-

³⁰ Using total width = 220 MeV.

³¹ Model dependent.

 $\rho(1700)$ BRANCHING RATIOS $\Gamma(\rho\pi\pi)/\Gamma(4\pi)$ Γ_3/Γ_1

VALUE	DOCUMENT ID	TECN	COMMENT
••• We do not use the following data for averages, fits, limits, etc. •••			
0.28 ± 0.06	³² ABELE	01B	CBAR $0.0 \bar{p}n \rightarrow 5\pi$

 $\Gamma(\rho^0\pi^+\pi^-)/\Gamma(2(\pi^+\pi^-))$ Γ_4/Γ_2

VALUE	EVTS	DOCUMENT ID	TECN	COMMENT
••• We do not use the following data for averages, fits, limits, etc. •••				
~ 1.0		DEL COURT	81B	DM1 $e^+e^- \rightarrow 2(\pi^+\pi^-)$
0.7 ± 0.1	500	SCHACHT	74	STRC $5.5-18 \gamma p \rightarrow p4\pi$
0.80		³³ BINGHAM	72B	HBC $9.3 \gamma p \rightarrow p4\pi$

 $\Gamma(\rho^0\pi^0\pi^0)/\Gamma(\rho^\pm\pi^\mp\pi^0)$ Γ_5/Γ_6

VALUE	DOCUMENT ID	TECN	CHG	COMMENT
••• We do not use the following data for averages, fits, limits, etc. •••				
<0.10	AT KINSON	85B	OMEG	$20-70 \gamma p$
<0.15	AT KINSON	82	OMEG	$0 \quad 20-70 \gamma p \rightarrow p4\pi$

 $\Gamma(a_1(1260)\pi)/\Gamma(4\pi)$ Γ_7/Γ_1

VALUE	DOCUMENT ID	TECN	COMMENT
••• We do not use the following data for averages, fits, limits, etc. •••			
0.16 ± 0.05	³² ABELE	01B	CBAR $0.0 \bar{p}n \rightarrow 5\pi$

 $\Gamma(h_1(1170)\pi)/\Gamma(4\pi)$ Γ_8/Γ_1

VALUE	DOCUMENT ID	TECN	COMMENT
••• We do not use the following data for averages, fits, limits, etc. •••			
0.17 ± 0.06	³² ABELE	01B	CBAR $0.0 \bar{p}n \rightarrow 5\pi$

 $\Gamma(\pi(1300)\pi)/\Gamma(4\pi)$ Γ_9/Γ_1

VALUE	DOCUMENT ID	TECN	COMMENT
••• We do not use the following data for averages, fits, limits, etc. •••			
0.30 ± 0.10	³² ABELE	01B	CBAR $0.0 \bar{p}n \rightarrow 5\pi$

 $\Gamma(\rho\rho)/\Gamma(4\pi)$ Γ_{10}/Γ_1

VALUE	DOCUMENT ID	TECN	COMMENT
••• We do not use the following data for averages, fits, limits, etc. •••			
0.09 ± 0.03	³² ABELE	01B	CBAR $0.0 \bar{p}n \rightarrow 5\pi$

 $\Gamma(\pi^+\pi^-)/\Gamma_{\text{total}}$ Γ_{11}/Γ

VALUE	DOCUMENT ID	TECN	COMMENT
••• We do not use the following data for averages, fits, limits, etc. •••			
$0.287^{+0.043}_{-0.042}$	BECKER	79	ASPK $17 \pi^- p$ polarized
0.15 to 0.30	³⁴ MARTIN	78C	RVUE $17 \pi^- p \rightarrow \pi^+\pi^- n$
<0.20	³⁵ COSTA...	77B	RVUE $e^+e^- \rightarrow 2\pi, 4\pi$
0.30 ± 0.05	³⁴ FROGGATT	77	RVUE $17 \pi^- p \rightarrow \pi^+\pi^- n$
<0.15	³⁶ EISENBERG	73	HBC $5 \pi^+ p \rightarrow \Delta^+ + 2\pi$
0.25 ± 0.05	³⁷ HYAMS	73	ASPK $17 \pi^- p \rightarrow \pi^+\pi^- n$

 $\Gamma(\pi^+\pi^-)/\Gamma(2(\pi^+\pi^-))$ Γ_{11}/Γ_2

VALUE	DOCUMENT ID	TECN	COMMENT
••• We do not use the following data for averages, fits, limits, etc. •••			
0.13 ± 0.05	ASTON	80	OMEG $20-70 \gamma p \rightarrow p2\pi$
<0.14	³⁸ DAVIER	73	STRC $6-18 \gamma p \rightarrow p4\pi$
<0.2	³⁹ BINGHAM	72B	HBC $9.3 \gamma p \rightarrow p2\pi$

 $\Gamma(\pi\pi)/\Gamma(4\pi)$ Γ_{12}/Γ_1

VALUE	DOCUMENT ID	TECN	COMMENT
••• We do not use the following data for averages, fits, limits, etc. •••			
0.16 ± 0.04	^{32,40} ABELE	01B	CBAR $0.0 \bar{p}n \rightarrow 5\pi$

 $\Gamma(K\bar{K}^*(892) + c.c.)/\Gamma_{\text{total}}$ Γ_{13}/Γ

VALUE	DOCUMENT ID	TECN	COMMENT
••• We do not use the following data for averages, fits, limits, etc. •••			
possibly seen	COAN	04	CLEO $\tau^- \rightarrow K^- \pi^- K^+ \nu_\tau$

 $\Gamma(K\bar{K}^*(892) + c.c.)/\Gamma(2(\pi^+\pi^-))$ Γ_{13}/Γ_2

VALUE	DOCUMENT ID	TECN	COMMENT
••• We do not use the following data for averages, fits, limits, etc. •••			
0.15 ± 0.03	⁴¹ DEL COURT	81B	DM1 $e^+e^- \rightarrow \bar{K} K \pi$

 $\Gamma(\eta\rho)/\Gamma_{\text{total}}$ Γ_{14}/Γ

VALUE	CL%	DOCUMENT ID	TECN	COMMENT
••• We do not use the following data for averages, fits, limits, etc. •••				
possibly seen		AKHMETSHIN	00D	CMD2 $e^+e^- \rightarrow \eta\pi^+\pi^-$
<0.04		DONNACHIE	87B	RVUE
<0.02	58	AT KINSON	86B	OMEG $20-70 \gamma p$

 $\Gamma(\eta\rho)/\Gamma(2(\pi^+\pi^-))$ Γ_{14}/Γ_2

VALUE	DOCUMENT ID	TECN	COMMENT
••• We do not use the following data for averages, fits, limits, etc. •••			
0.123 ± 0.027	DEL COURT	82	DM1 $e^+e^- \rightarrow \pi^+\pi^- MM$
~ 0.1	ASTON	80	OMEG $20-70 \gamma p$

 $\Gamma(\pi^+\pi^- \text{ neutrals})/\Gamma(2(\pi^+\pi^-))$ $(\Gamma_5 + \Gamma_6 + 0.714\Gamma_{14})/\Gamma_2$

VALUE	DOCUMENT ID	TECN	COMMENT
••• We do not use the following data for averages, fits, limits, etc. •••			
2.6 ± 0.4	⁴² BALLAM	74	HBC $9.3 \gamma p$

 $\Gamma(a_2(1320)\pi)/\Gamma_{\text{total}}$ Γ_{15}/Γ

VALUE	DOCUMENT ID	TECN	COMMENT
••• We do not use the following data for averages, fits, limits, etc. •••			
not seen	AMELIN	00	VES $37 \pi^- p \rightarrow \eta\pi^+\pi^- n$

Meson Particle Listings

$\rho(1700)$, $a_2(1700)$

$\Gamma(K\bar{K})/\Gamma(2\pi^+\pi^-)$		Γ_{16}/Γ_2			
VALUE	CL%	DOCUMENT ID	TECN	CHG	COMMENT

••• We do not use the following data for averages, fits, limits, etc. •••

0.015±0.010		⁴³ DELCOURT	81B	DM1	$e^+e^- \rightarrow \bar{K}K$
<0.04	95	BINGHAM	72B	HBC	0 9.3 $\gamma\rho$

$\Gamma(K\bar{K})/\Gamma(K\bar{K}^*(892)+c.c.)$		Γ_{16}/Γ_{13}			
VALUE	CL%	DOCUMENT ID	TECN	CHG	COMMENT

••• We do not use the following data for averages, fits, limits, etc. •••

0.052±0.026		BUON	82	DM1	$e^+e^- \rightarrow \text{hadrons}$
-------------	--	------	----	-----	-------------------------------------

$\Gamma(\pi^0\omega)/\Gamma_{\text{total}}$		Γ_{18}/Γ			
VALUE	EVTS	DOCUMENT ID	TECN	CHG	COMMENT

••• We do not use the following data for averages, fits, limits, etc. •••

not seen	2382	AKHMETSHIN	03B	CMD2	$e^+e^- \rightarrow \pi^0\pi^0\gamma$
seen		ACHASOV	97	RVUE	$e^+e^- \rightarrow \omega\pi^0$

- ³² $\omega\pi$ not included.
- ³³ The $\pi\pi$ system is in S-wave.
- ³⁴ From phase shift analysis of HYAMS 73 data.
- ³⁵ Estimate using unitarity, time reversal invariance, Breit-Wigner.
- ³⁶ Estimated using one-pion-exchange model.
- ³⁷ Included in BECKER 79 analysis.
- ³⁸ Upper limit is estimate.
- ³⁹ 2σ upper limit.
- ⁴⁰ Using ABELE 97.
- ⁴¹ Assuming $\rho(1700)$ and ω radial excitations to be degenerate in mass.
- ⁴² Upper limit. Background not subtracted.
- ⁴³ Assuming $\rho(1700)$ and ω radial excitations to be degenerate in mass.

$\rho(1700)$ REFERENCES

COAN	04	PRL 92 232001	T.E. Coan et al.	(CLEO Collab.)
FRABETTI	04	PL B578 290	P.L. Frabetti et al.	(FNAL E687 Collab.)
AKHMETSHIN	03B	PL B562 173	R.R. Akhmetshin et al.	(Novosibirsk CMD-2 Collab.)
ABELE	01B	EPJ C21 261	A. Abele et al.	(Crystal Barrel Collab.)
ACHASOV	001	PL B486 29	M.N. Achasov et al.	(Novosibirsk SND Collab.)
AKHMETSHIN	00D	PL B489 125	R.R. Akhmetshin et al.	(Novosibirsk CMD-2 Collab.)
AMELIN	00	NP A668 83	D. Amelin et al.	(VES Collab.)
EDWARDS	00A	PR D61 072003	K.W. Edwards et al.	(CLEO Collab.)
ABELE	99D	PL B468 178	A. Abele et al.	(Crystal Barrel Collab.)
ABELE	97	PL B391 181	A. Abele et al.	(Crystal Barrel Collab.)
ACHASOV	97	PR D55 2663	N.N. Achasov et al.	(NOVM)
BERTIN	97C	PL B408 474	A. Bertin et al.	(OBELIX Collab.)
CLEGG	94	ZPHY C62 455	A.B. Clegg, A. Donnachie	(LANC, MCHS)
CLEGG	90	ZPHY C45 677	A.B. Clegg, A. Donnachie	(LANC, MCHS)
BISELLO	89	PL B220 321	D. Bisello et al.	(DM2 Collab.)
DUBNICKA	89	JPG 15 1349	S. Dubnicka et al.	(JINR, SLOV)
GESHKEN...	89	ZPHY C45 351	B.V. Geshkenbein	(ITEP)
ANTONELLI	88	PL B212 133	A. Antonelli et al.	(DM2 Collab.)
DIEKMANN	88	PRPL 159 99	B. Diekmann	(BONN)
FUKUI	88	PL B202 441	S. Fukui et al.	(SUGI, NAGO, KEK, KYOT+)
DONNACHIE	87B	ZPHY C34 257	A. Donnachie, A.B. Clegg	(MCHS, LANC)
ATKINSON	86B	ZPHY C30 511	A. Atkinson et al.	(BONN, CERN, GLAS+)
ATKINSON	85B	ZPHY C26 499	M. Atkinson et al.	(BONN, CERN, GLAS+)
ERKAL	85	ZPHY C29 485	C. Erkal, M.G. Olsson	(WIS C)
ABE	84B	PRL 53 751	K. Abe et al.	
KURDADZE	83	JETPL 37 733	L.M. Kurdadze et al.	(NOVO)

Translated from ZETFP 37 613.

ATKINSON	82	PL 108B 55	M. Atkinson et al.	(BONN, CERN, GLAS+)
BUON	82	PL 118B 221	J. Buon et al.	(LALO, MONP)
CLELAND	82B	NP B308 228	W.E. Cleland et al.	(DURH, GEVA, LAUS+)
CORDIER	82	PL 109B 129	A. Cordier et al.	(LALO)
DELCOURT	82	PL 113B 93	B. Delcourt et al.	(LALO)
ASTON	81E	NP B189 15	D. Aston	(BONN, CERN, EPOL, GLAS, LAN C+)
DELCOURT	81B	Bonn Conf. 205	B. Delcourt	(ORSAY)

Also

DIBIANCA	81	PL 109B 129	A. Cordier et al.	(LALO)
ASTON	80	PL 92B 215	F.A. di Bianca et al.	(CASE, CMU)
BACCI	80	PL 95B 139	D. Aston	(BONN, CERN, EPOL, GLAS, LAN C+)
BIZOT	80	Madison Conf. 546	C. Bacci et al.	(ROMA, FRAS)
KILLIAN	80	PR D21 3005	J.C. Bizot et al.	(LALO, MONP)
ATIYA	79B	PRL 43 1691	T.J. Killian et al.	(CORN)
BECKER	79	NP B151 46	M.S. Atiya et al.	(COLU, ILL, FNAL)
LANG	79	PR D19 956	H. Becker et al.	(MPIP, CERN, ZEEM, CRAC)
MARTIN	76C	ANP 114 1	C.B. Lang, A. Mas-Parada	(MCHS, LAN C)
COSTA...	77B	PL 71B 345	A.D. Martin, M.R. Pennington	(CERN)
FROGGATT	77	NP B129 89	B. Costa de Beauregard, B. Pire, T.N. Truong	(EPOL)
ALEXANDER	75	PL 57B 487	C.D. Froggatt, J.L. Petersen	(GLAS, NORD)
BALLAM	74	NP B76 375	G. Alexander et al.	(TELA)
CONVERSI	74	PL 52B 493	J. Ballam et al.	(SLAC, LBL, MPIM)
SCHACHT	74	NP B81 205	M. Conversi et al.	(ROMA, FRAS)
DAVIER	73	NP B58 31	P. Schacht et al.	(MPIM)
EISENBERG	73	PL 43B 149	M. Davier et al.	(SLAC)
HYAMS	73	NP B64 134	Y. Eisenberg et al.	(REHO)
BINGHAM	72B	PL 41B 635	B.D. Hyams et al.	(CERN, MPIM)
JACOB	72	PR D5 1847	H.H. Bingham et al.	(LBL, UCB, SLAC) IGP
			M. Jacob, R. Slansky	

OTHER RELATED PAPERS

AUBERT	08S	PR D77 092002	B. Aubert et al.	(BABAR Collab.)
ACHASOV	07A	PR D76 072012	M.N. Achasov et al.	(SND Collab.)
LIU	07A	PR D76 094016	B. Li et al.	
LIU	07B	PR D75 074017	X. Liu et al.	
ABLIKIM	06S	PRL 97 142002	M. Ablikim et al.	(BES Collab.)
ACHASOV	06D	JETP 103 720	N.N. Achasov et al.	(SND Collab.)

Translated from ZETFP 130 831.

AUBERT	06D	PR D73 052003	B. Aubert et al.	(BABAR Collab.)
DAVIER	06	RMP 78 1043	M. Davier, A. Hocker, Z. Zhang	(LALO, PARIN+)
ABE	05H	hep-ex/0512071	K. Abe et al.	(BELLE Collab.)
ACHASOV	05A	JETP 101 1053	M.N. Achasov et al.	(Novosibirsk SND Collab.)

Translated from ZETFP 128 1201.

AUBERT	05D	PR D71 052001	B. Aubert et al.	(BABAR Collab.)
AULCHENKO	05	JETPL 82 743	V.M. Aulchenko et al.	(Novosibirsk CMD-2 Collab.)

Translated from ZETFP 82 841.

SCHAEEL	05C	PRPL 421 191	S. Schaeel et al.	(ALEPH Collab.)
AKHMETSHIN	04C	PL B595 101	R.R. Akhmetshin et al.	(Novosibirsk CMD-2 Collab.)
AMSLER	04A	NP A740 130	C. Amshler et al.	
ACHASOV	03C	JETP 96 789	M.N. Achasov et al.	(Novosibirsk SND Collab.)

Translated from ZETFP 123 899.

AKHMETSHIN	03	PL B551 27	R.R. Akhmetshin et al.	(Novosibirsk CMD-2 Collab.)
Also		PAN 65 1222	E.V. Anashkin, V.M. Aulchenko, R.R. Akhmetshin	

Translated from YAF 65 1255.

BARGIOTTI	03B	PL B561 233	M. Bargiotti et al.	
ACHASOV	02B	PAN 65 153	N.N. Achasov, A.A. Kozhevnikov	

Translated from YAF 65 158.

AGNELLO	02	PL B527 39	M. Agnello et al.	(OBELIX Collab.)
CLOSE	02	PR D65 092003	F.E. Close, A. Donnachie, Yu.S. Kalashnikova	
ALEXANDER	01B	PR D64 092001	J.P. Alexander et al.	(CLEO Collab.)
FRABETTI	01	PL B514 240	P.L. Frabetti et al.	(FNAL E687 Collab.)
ACHASOV	00J	PR D62 117503	M.N. Achasov, A.A. Kozhevnikov	
ANDERSON	00A	PR D61 112002	S. Anderson et al.	(CLEO Collab.)
ABELE	99C	PL B450 275	A. Abele et al.	(Crystal Barrel Collab.)
AKHMETSHIN	99E	PL B466 392	R.R. Akhmetshin et al.	(Novosibirsk CMD-2 Collab.)
DONNACHIE	99	PR D60 114011	A. Donnachie, Yu.S. Kalashnikova	
KULZINGER	99	EPJ C7 73	G. Kulzinger et al.	
ABELE	98	PR D57 3860	A. Abele et al.	(Crystal Barrel Collab.)
ANTONELLI	98	NP B517 3	A. Antonelli et al.	(FENICE Collab.)
BELOZEROVA	98	PPN 29 63	T.S. Belozerova, V.K. Henner	

Translated from FECAF 29 148.

BERTIN	98B	PL B434 180	A. Bertin et al.	(OBELIX Collab.)
BARATE	97M	ZPHY C76 15	R. Barate et al.	(ALEPH Collab.)
BARNES	97	PR D55 4157	T. Barnes et al.	(ORNL, RAL, MCHS)
CLOSE	97C	PR D56 1584	F.E. Close et al.	(RAL, MCHS)
URHEIM	97	NPBPS 55C 359	J. Urheim	(CLEO Collab.)
ACHASOV	96B	PAN 59 1262	N.N. Achasov, G.N. Shestakov	(NOVM)

Translated from YAF 59 1319.

ANTONELLI	96	PL B365 427	A. Antonelli et al.	(FENICE Collab.)
AMSLER	93B	PL B311 362	C. Amshler et al.	(Crystal Barrel Collab.)
LANDSBERG	92	SJNP 55 1051	L.G. Landsberg	(SERP)

Translated from YAF 55 1896.

ASTON	91B	NPBPS 21 105	D. Aston et al.	(LASS Collab.)
BISELLO	91C	ZPHY C52 227	D. Bisello et al.	(DM2 Collab.)
DOLINSKY	91	PRPL 202 99	S.I. Dolinsky et al.	(NOVO)
DONNACHIE	91	ZPHY C51 689	A. Donnachie, A.B. Clegg	(MCHS, LAN C)
ACHASOV	88C	PL B209 373	N.N. Achasov, A.A. Kozhevnikov	(NOVM)
BRAU	88	PR D37 2379	J.E. Brau et al.	
CASTRO	88	Preprint LAL-88-58	A. Castro et al.	(DM2 Collab.)
AMSLER	88	ZPHY C40 313	A.B. Clegg, A. Donnachie	(MCHS, LAN C)
BITYUKOV	87	PL B188 383	S.I. Bityukov et al.	(SERP)
DONNACHIE	87	ZPHY C33 407	A. Donnachie, H. Mirzaie	(MCHS)
ERKAL	86	ZPHY C31 615	C. Erkal, M.G. Olsson	(WIS C)
ATKINSON	85	ZPHY C29 333	M. Atkinson et al.	(BONN, CERN, GLAS+)
BARKOV	85	NP B256 365	L.M. Barkov et al.	(NOVO)
ATKINSON	84C	NP B243 1	M. Atkinson et al.	(BONN, CERN, GLAS+)
ATKINSON	83B	PL 127B 132	M. Atkinson et al.	(BONN, CERN, GLAS+)
ATKINSON	83C	NP B229 269	M. Atkinson et al.	(BONN, CERN, GLAS+)
AUGUSTIN	83	LAL 83-21	J.E. Augustin et al.	(LALO, PADO, FRAS)
SHAMBROOM	82	PR D26 1	W.D. Shambroom et al.	(HARV, EFI, ILL+)
BISELLO	81	PL 107B 145	D. Bisello et al.	(DM2 Collab.)
ASTON	80C	PL 92B 211	D. Aston	(BONN, CERN, EPOL, GLAS, LAN C+)
BARBER	80C	ZPHY C4 169	D.P. Barber et al.	(DARE, LAN C, SHEF)
KILLIAN	80	PR D21 3005	T.J. Killian et al.	(CORN)
COSME	76	PL 63B 352	G. Cosme et al.	(ORSAY)
FRENKIEL	72	NP B47 61	P. Frenkiel et al.	(CDFE, MIT)
ALVENSLEB...	71	PRL 26 273	H. Alvensleben et al.	(DESY, CERN)
BRAUN	71	NP B30 213	H.M. Braun et al.	(STRB J)
BULOS	71	PRL 26 149	F. Bulos et al.	(SLAC, UMD, IBM, LBL) G
LAYSSAC	71	NC 6A 134	J. Layssac, F.M. Renard	(MONP)

$a_2(1700)$

$$J^{PC} = 1^-(2^{++})$$

OMITTED FROM SUMMARY TABLE

$a_2(1700)$ MASS

VALUE (MeV)	EVTS	DOCUMENT ID	TECN	CHG	COMMENT
1732±16 OUR AVERAGE					
Error includes scale factor of 1.9.					
1737 ± 5 ± 7		ABE	04	BELL	10.6 $e^+e^- \rightarrow K^+K^-$ $e^+e^- \rightarrow K^+K^-$
1698±44		¹ AMSLER	02	CBAR	$0.9 \bar{p}p \rightarrow \pi^0 \eta \eta$
1660±40		ABELE	99B	CBAR	1.94 $\bar{p}p \rightarrow \pi^0 \eta \eta$
••• We do not use the following data for averages, fits, limits, etc. •••					
1722 ± 9 ± 15	18k	² SCHEGELSKY	06	RVUE 0	$\gamma\gamma \rightarrow \pi^+\pi^-\pi^0$
1702 ± 7	80k	³ UMA N	06	E835	$5.2 \bar{p}p \rightarrow \eta \eta \pi^0$
1721 ± 13 ± 44	145k	LU	05	B852	$1.8 \pi^-\pi^+ \rightarrow \omega \pi^-\pi^0 \rho$
1767 ± 14	221	⁴ ACCIARRI	01H	L3	$\gamma\gamma \rightarrow K_S^0 K_S^0, E_{cm} = 91, 183-209 \text{ GeV}$
~ 1775		⁵ GRYGOREV	99	SPEC	$40 \pi^-\pi^+ \rightarrow K_S^0 K_S^0 \eta$
1752±21 ± 4		ACCIARRI	97T	L3	$\gamma\gamma \rightarrow \pi^+\pi^-\pi^0$

- ¹ T-matrix pole.
- ² From analysis of L3 data at 183–209 GeV.
- ³ Statistical error only.
- ⁴ Spin 2 dominant, isospin not determined, could also be I=1.
- ⁵ Possibly two $J^P = 2^+$ resonances with isospins 0 and 1.

$a_2(1700)$ WIDTH

VALUE (MeV)	EVTS	DOCUMENT ID	TECN	CHG	COMMENT
194 ± 40 OUR AVERAGE					
Error includes scale factor of 1.6. See the ideogram below.					
151 ± 22 ± 24		ABE	04	BELL	10.6 $e^+e^- \rightarrow K^+K^-$ $e^+e^- \rightarrow K^+K^-$
265 ± 55		⁶ AMSLER	02	CBAR	$0.9 \bar{p}p \rightarrow \pi^0 \eta \eta$
280 ± 70		ABELE	99B	CBAR	1.94 $\bar{p}p \rightarrow \pi^0 \eta \eta$

See key on page 373

Meson Particle Listings

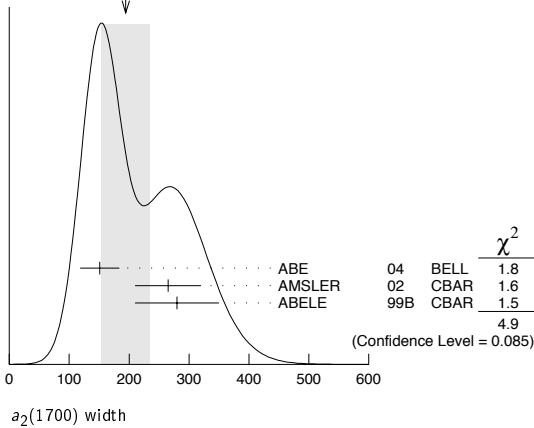
$a_2(1700)$, $f_0(1710)$

• • • We do not use the following data for averages, fits, limits, etc. • • •

336 ± 20 ± 20	18k	7	SCHEGELSKY	06	RVUE	0	$\gamma\gamma \rightarrow \pi^+\pi^-\pi^0$
417 ± 19	80k	8	UMAN	06	E835		$5.2 \bar{p}p \rightarrow \eta\eta\pi^0$
279 ± 49 ± 66	145k		LU	05	B852		$18 \pi^-p \rightarrow \omega\pi^-\pi^0p$
187 ± 60	221	9	ACCIARRI	01H	L3		$\gamma\gamma \rightarrow K_S^0 K_S^0, E_{cm}^{eg} = 91, 183-209 \text{ GeV}$
150 ± 110 ± 34			ACCIARRI	97T	L3		$\gamma\gamma \rightarrow \pi^+\pi^-\pi^0$

⁶T-matrix pole.
⁷From analysis of L3 data at 183–209 GeV.
⁸Statistical error only.
⁹Spin 2 dominant, isospin not determined, could also be $I=1$.

WEIGHTED AVERAGE
194±40 (Error scaled by 1.6)



$a_2(1700)$ DECAY MODES

Mode	Fraction (Γ_i/Γ)
Γ_1 $\eta\pi$	seen
Γ_2 $\gamma\gamma$	
Γ_3 $\rho\pi$	
Γ_4 $f_2(1270)\pi$	
Γ_5 $K\bar{K}$	seen
Γ_6 $\omega\pi^-\pi^0$	seen
Γ_7 $\omega\rho$	seen

$a_2(1700)$ PARTIAL WIDTHS

$\Gamma(\eta\pi)$ Γ_1

VALUE (MeV)	EVTS	DOCUMENT ID	TECN	COMMENT
9.5 ± 2.0	870	¹⁰ SCHEGELSKY 06A	RVUE	$\gamma\gamma \rightarrow K_S^0 K_S^0$

• • • We do not use the following data for averages, fits, limits, etc. • • •

$\Gamma(\gamma\gamma)$ Γ_2

VALUE (keV)	EVTS	DOCUMENT ID	TECN	COMMENT
0.30 ± 0.05	870	¹⁰ SCHEGELSKY 06A	RVUE	$\gamma\gamma \rightarrow K_S^0 K_S^0$

• • • We do not use the following data for averages, fits, limits, etc. • • •

$\Gamma(K\bar{K})$ Γ_5

VALUE (MeV)	EVTS	DOCUMENT ID	TECN	COMMENT
5.0 ± 3.0	870	¹⁰ SCHEGELSKY 06A	RVUE	$\gamma\gamma \rightarrow K_S^0 K_S^0$

¹⁰From analysis of L3 data at 91 and 183–209 GeV, using $a_2(1700)$ mass of 1730 MeV and width of 340 MeV, and SU(3) relations.

$a_2(1700)$ $\Gamma(i)\Gamma(\gamma\gamma)/\Gamma(\text{total})$

$[\Gamma(\rho\pi) + \Gamma(f_2(1270)\pi)] \times \Gamma(\gamma\gamma)/\Gamma(\text{total})$ $(\Gamma_3 + \Gamma_4)\Gamma_2/\Gamma$

VALUE (keV)	EVTS	DOCUMENT ID	TECN	COMMENT
0.29 ± 0.04 ± 0.02		ACCIARRI 97T L3	L3	$\gamma\gamma \rightarrow \pi^+\pi^-\pi^0$
0.37 ^{+0.12} _{-0.08} ± 0.10	18k	¹¹ SCHEGELSKY 06	RVUE	$\gamma\gamma \rightarrow \pi^+\pi^-\pi^0$

• • • We do not use the following data for averages, fits, limits, etc. • • •

¹¹From analysis of L3 data at 183–209 GeV.

$\Gamma(K\bar{K}) \times \Gamma(\gamma\gamma)/\Gamma(\text{total})$ $\Gamma_5\Gamma_2/\Gamma$

VALUE (eV)	DOCUMENT ID	TECN	COMMENT
20.6 ± 4.2 ± 4.6	¹² ABE 04	BELL	$10.6 e^+e^- \rightarrow e^+e^-K^+K^-$
49 ± 11 ± 13	¹³ ACCIARRI 01H L3	L3	$\gamma\gamma \rightarrow K_S^0 K_S^0, E_{cm}^{eg} = 91, 183-209 \text{ GeV}$

¹² Assuming spin 2.
¹³ Spin 2 dominant, isospin not determined, could also be $I=1$.

$a_2(1700)$ BRANCHING RATIOS

$\Gamma(\rho\pi)/\Gamma(f_2(1270)\pi)$ Γ_3/Γ_4

• • • We do not use the following data for averages, fits, limits, etc. • • •

3.4 ± 0.4 ± 0.1	18k	¹⁴ SCHEGELSKY 06	RVUE	$\gamma\gamma \rightarrow \pi^+\pi^-\pi^0$
-----------------	-----	-----------------------------	------	--

¹⁴ From analysis of L3 data at 183–209 GeV.

$a_2(1700)$ REFERENCES

SCHEGELSKY 06	EPJ A27 199	V.A. Schegelsky <i>et al.</i>
SCHEGELSKY 06A	EPJ A27 207	V.A. Schegelsky <i>et al.</i>
UMAN 06	PR D73 052009	I. Uman <i>et al.</i>
LU 05	PRL 94 032002	M. Lu <i>et al.</i>
ABE 04	EPJ C32 323	K. Abe <i>et al.</i>
AMSLER 02	EPJ C23 29	C. Amsler <i>et al.</i>
ACCIARRI 01H	PL B501 173	M. Acciarrì <i>et al.</i>
ABELE 99B	EPJ C8 67	A. Abele <i>et al.</i>
GRYGOREV 99	PAN 62 470	V.K. Grygorev <i>et al.</i>
ACCIARRI 97T	Translated from YAF 62 513.	M. Acciarrì <i>et al.</i>
	PL B413 147	

(FNAL E835)
 (BNL E852 Collab.)
 (BELLE Collab.)
 (L3 Collab.)
 (Crystal Barrel Collab.)
 (L3 Collab.)

OTHER RELATED PAPERS

BAKER 03	PL B563 140	C.A. Baker <i>et al.</i>
BARBERIS 00H	PL B488 225	D. Barberis <i>et al.</i>

(WA 102 Collab.)

$f_0(1710)$

$$J^{PC} = 0^+(0^+)$$

See our mini-review in the 2004 edition of this Review, PDG 04.

$f_0(1710)$ MASS

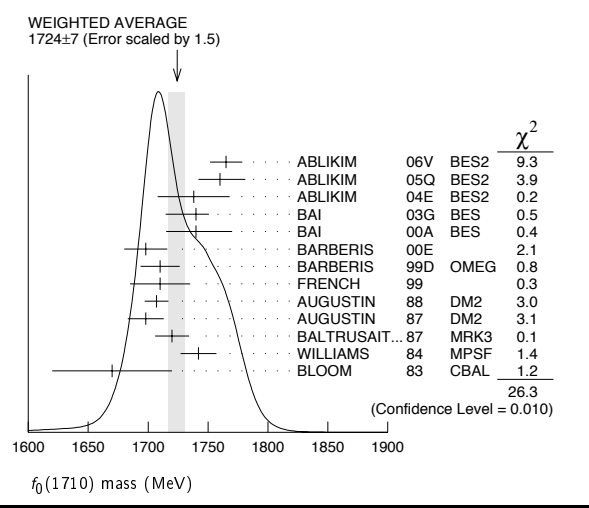
VALUE (MeV)	EVTS	DOCUMENT ID	TECN	COMMENT
1724 ± 7	OUR AVERAGE	Error includes scale factor of 1.5. See the ideogram below.		
1765 ⁺⁴ ₋₃ ± 13		ABLIKIM	06v	BES2 $e^+e^- \rightarrow J/\psi \rightarrow \gamma\pi^+\pi^-$
1760 ± 15	⁺¹⁵ ₋₁₀	¹ ABLIKIM	05Q	BES2 $\psi(2S) \rightarrow \gamma\pi^+\pi^-K^+K^-$
1738 ± 30		ABLIKIM	04E	BES2 $J/\psi \rightarrow \omega K^+K^-$
1740 ± 4	⁺¹⁰ ₋₂₅	² BAI	03G	BES $J/\psi \rightarrow \gamma K\bar{K}$
1740 ⁺³⁰ ₋₂₅		² BAI	00A	BES $J/\psi \rightarrow \gamma(\pi^+\pi^-\pi^+\pi^-)$
1698 ± 18		³ BARBERIS	00E	$450 pp \rightarrow p_f \eta \eta p_s$
1710 ± 12	± 11	⁴ BARBERIS	99D	OMEG $450 pp \rightarrow K^+K^-, \pi^+\pi^-$
1710 ± 25		⁵ FRENCH	99	$300 pp \rightarrow p_f(K^+K^-)p_s$
1707 ± 10		⁶ AUGUSTIN	88	DM2 $J/\psi \rightarrow \gamma K^+K^-, K_S^0 K_S^0$
1698 ± 15		⁶ AUGUSTIN	87	DM2 $J/\psi \rightarrow \gamma\pi^+\pi^-$
1720 ± 10	± 10	⁷ BALTRUSAIT..87	MRK3	$J/\psi \rightarrow \gamma K^+K^-$
1742 ± 15		⁶ WILLIAMS	84	MP SF $200 \pi^- N \rightarrow 2K_S^0 X$
1670 ± 50		BLOOM	83	CBAL $J/\psi \rightarrow \gamma 2\eta$
1750 ± 13		AMSLER	06	CBAR $1.64 \bar{p}p \rightarrow K^+K^-\pi^0$
1747 ± 5	80k	^{8,9} UMAN	06	E835 $5.2 \bar{p}p \rightarrow \eta\eta\pi^0$
1776 ± 15		VLADIMIRSK..06	SPEC	$40 \pi^-p \rightarrow K_S^0 K_S^0 n$
1790 ⁺⁴⁰ ₋₃₀		¹ ABLIKIM	05	BES2 $J/\psi \rightarrow \phi\pi^+\pi^-$
1670 ± 20		⁸ BINON	05	GAMS $33 \pi^-p \rightarrow \eta\eta n$
1726 ± 7	74	⁹ CHEKANOV	04	ZEUS $e p \rightarrow K_S^0 K_S^0 X$
1732 ± 15		¹⁰ ANISOVICH	03	RVEC
1682 ± 16		TIKHOMIROV	03	SPEC $40.0 \pi^- C \rightarrow K_S^0 K_S^0 K_L^0 X$
1670 ± 26	3651	^{2,11} NICHITIU	02	OBLX
1770 ± 12		^{12,13} ANISOVICH	99B	SPEC $0.6-1.2 p\bar{p} \rightarrow \eta\eta\pi^0$
1730 ± 15		² BARBERIS	99	OMEG $450 pp \rightarrow p_s p_f K^+K^-$
1750 ± 20		² BARBERIS	99B	OMEG $450 pp \rightarrow p_s p_f \pi^+\pi^-$
1750 ± 30		¹⁴ ANISOVICH	98B	RVUE Compilation
1720 ± 39		BAI	98H	BES $J/\psi \rightarrow \gamma\pi^0\pi^0$
1775 ± 15	57	¹⁵ BARKOV	98	$\pi^-p \rightarrow K_S^0 K_S^0 n$
1690 ± 11		¹⁶ ABREU	96C	DLPH $Z^0 \rightarrow K^+K^- + X$
1696 ± 5	⁺⁹ ₋₃₄	⁷ BAI	96C	BES $J/\psi \rightarrow \gamma K^+K^-$
1781 ± 8	⁺¹⁰ ₋₃₁	² BAI	96C	BES $J/\psi \rightarrow \gamma K^+K^-$
1768 ± 14		BALOSHIN	95	SPEC $40 \pi^- C \rightarrow K_S^0 K_S^0 X$

Meson Particle Listings

$f_0(1710)$

1750 ± 15	17	BUGG	95	MRK3	$J/\psi \rightarrow \gamma \pi^+ \pi^- \pi^+ \pi^-$
1620 ± 16	7	BUGG	95	MRK3	$J/\psi \rightarrow \gamma \pi^+ \pi^- \pi^+ \pi^-$
1748 ± 10	6	ARMSTRONG	93c	E760	$\bar{p}p \rightarrow \pi^0 \eta \eta \rightarrow 6\gamma$
~ 1750		BREAKSTONE	93	SFM	$pp \rightarrow pp \pi^+ \pi^- \pi^+ \pi^-$
1744 ± 15	18	ALDE	92d	GAM2	$38 \pi^- p \rightarrow \eta \eta n$
1713 ± 10	19	ARMSTRONG	89d	OMEG	$300 pp \rightarrow pp K^+ K^-$
1706 ± 10	19	ARMSTRONG	89d	OMEG	$300 pp \rightarrow pp K_S^0 K_S^0$
1700 ± 15	7	BOLONKIN	88	SPEC	$40 \pi^- p \rightarrow K_S^0 K_S^0 n$
1720 ± 60	2	BOLONKIN	88	SPEC	$40 \pi^- p \rightarrow K_S^0 K_S^0 n$
1638 ± 10	20	FALVARD	88	DM2	$J/\psi \rightarrow \phi K^+ K^-, K_S^0 K_S^0$
1690 ± 4	21	FALVARD	88	DM2	$J/\psi \rightarrow \phi K^+ K^-, K_S^0 K_S^0$
1755 ± 8	22	ALDE	86c	GAM2	$38 \pi^- p \rightarrow n 2\eta$
1730 ⁺ ₋₁₀	23	LONGACRE	86	RVUE	$22 \pi^- p \rightarrow n 2K_S^0$
1650 ± 50		BURKE	82	MRK2	$J/\psi \rightarrow \gamma 2\rho$
1640 ± 50	24,25	EDWARDS	82d	CBAL	$J/\psi \rightarrow \gamma 2\eta$
1730 ± 10 ± 20	26	ETKIN	82c	MPS	$23 \pi^- p \rightarrow n 2K_S^0$

- 1 This state may be different from $f_0(1710)$, see CLOSE 05.
- 2 $J^P = 0^+$.
- 3 T-matrix pole.
- 4 Supersedes BARBERIS 99 and BARBERIS 99b.
- 5 $J^P = 0^+$, supersedes by ARMSTRONG 89d.
- 6 No J^{PC} determination.
- 7 $J^P = 2^+$.
- 8 Breit-Wigner mass.
- 9 Systematic errors not estimated.
- 10 K-matrix pole, assuming $J^P = 0^+$, from combined analysis of $\pi^- p \rightarrow \pi^0 \pi^0 n, \pi^- p \rightarrow K \bar{K} n, \pi^+ \pi^- \rightarrow \pi^+ \pi^-, \bar{p}p \rightarrow \pi^0 \pi^0 \pi^0, \pi^0 \eta \eta, \pi^0 \pi^0 \eta, \pi^+ \pi^- \pi^0, K^+ K^- \pi^0, K_S^0 K_S^0 \pi^0, K^+ K_S^0 \pi^-$ at rest, $\bar{p}n \rightarrow \pi^- \pi^- \pi^+, K_S^0 K^- \pi^0, K_S^0 K_S^0 \pi^-$ at rest.
- 11 Decaying to $f_0(1370) \pi \pi$.
- 12 $J^P = 0^+$.
- 13 Not seen by AMSLER 02.
- 14 T-matrix pole, assuming $J^P = 0^+$.
- 15 No J^{PC} determination.
- 16 No J^{PC} determination, width not determined.
- 17 From a fit to the 0^+ partial wave.
- 18 ALDE 92d combines all the GAMS-2000 data.
- 19 $J^P = 2^+$, superseded by FRENCH 99.
- 20 From an analysis ignoring interference with $f_2'(1525)$.
- 21 From an analysis including interference with $f_2'(1525)$.
- 22 Superseded by ALDE 92d.
- 23 Uses MRK3 data. From a partial-wave analysis of data using a K-matrix formalism with 5 poles, but assuming spin 2. Fit with constrained inelasticity.
- 24 $J^P = 2^+$ preferred.
- 25 From fit neglecting nearby $f_2'(1525)$. Replaced by BLOOM 83.
- 26 Superseded by LONGACRE 86.



$f_0(1710)$ WIDTH

VALUE (MeV)	EVTs	DOCUMENT ID	TECN	COMMENT
137 ± 8	OUR AVERAGE			Error includes scale factor of 1.1.
145 ± 8 ± 69		ABLIKIM 06v	BES2	$e^+ e^- \rightarrow J/\psi \rightarrow \gamma \pi^+ \pi^-$
125 ± 25 ⁺¹⁰ ₋₁₅		27 ABLIKIM 05q	BES2	$\psi(2S) \rightarrow \gamma \pi^+ \pi^- K^+ K^-$
125 ± 20		ABLIKIM 04E	BES2	$J/\psi \rightarrow \omega K^+ K^-$
166 ± 5 ⁺¹⁵ ₋₈		28 BAI 03g	BES	$J/\psi \rightarrow \gamma K \bar{K}$
120 ± 50 ₋₄₀		28 BAI 00A	BES	$J/\psi \rightarrow \gamma(\pi^+ \pi^- \pi^+ \pi^-)$
120 ± 26		29 BARBERIS 00E	450	$pp \rightarrow p f \eta \eta p_S$
126 ± 16 ± 18		30 BARBERIS 99d	OMEG	$450 pp \rightarrow K^+ K^-, \pi^+ \pi^-$

105 ± 34	31	FRENCH	99		$300 pp \rightarrow p f(K^+ K^-) p_S$
166.4 ± 33.2	32	AUGUSTIN	88	DM2	$J/\psi \rightarrow \gamma K^+ K^-, K_S^0 K_S^0$
136 ± 28	32	AUGUSTIN	87	DM2	$J/\psi \rightarrow \gamma \pi^+ \pi^-$
130 ± 20	33	BALTRUSAIT..87	MRK3		$J/\psi \rightarrow \gamma K^+ K^-$
57 ± 38	6	WILLIAMS	84	MP SF	$200 \pi^- N \rightarrow 2K_S^0 X$
160 ± 80		BLOOM	83	CBAL	$J/\psi \rightarrow \gamma 2\eta$
148 ± 40 ₋₃₀		AMSLER	06	CBAR	$1.64 \bar{p}p \rightarrow K^+ K^- \pi^0$
188 ± 13	80k 27,34	UMAN	06	E835	$5.2 \bar{p}p \rightarrow \eta \eta \pi^0$
250 ± 30		VLADIMIRSK..06		SPEC	$40 \pi^- p \rightarrow K_S^0 K_S^0 n$
270 ± 60 ₋₃₀	35	ABLIKIM	05	BES2	$J/\psi \rightarrow \phi \pi^+ \pi^-$
260 ± 50	27	BINON	05	GAMS	$33 \pi^- p \rightarrow \eta \eta n$
38 ± 20	74 34	CHEKANOV	04	ZEUS	$e p \rightarrow K_S^0 K_S^0 X$
144 ± 30	36,37	ANISOVICH	03	RVUE	
320 ± 50 ₋₂₀	37,38	ANISOVICH	03	RVUE	
102 ± 26		TIKHOMIROV	03	SPEC	$40.0 \pi^- C \rightarrow K_S^0 K_S^0 K_S^0 X$
267 ± 44	3651 28,39	NICHITIU	02	OBLX	
220 ± 40	40,41	ANISOVICH	99b	SPEC	$0.6-1.2 p \bar{p} \rightarrow \eta \eta \pi^0$
100 ± 25	28	BARBERIS	99	OMEG	$450 pp \rightarrow p_S p f K^+ K^-$
160 ± 30	28	BARBERIS	99b	OMEG	$450 pp \rightarrow p_S p f \pi^+ \pi^-$
250 ± 140	42	ANISOVICH	98b	RVUE	Compilation
30 ± 7	43	BARKOV	98		$\pi^- p \rightarrow K_S^0 K_S^0 n$
103 ± 18 ⁺³⁰ ₋₁₁	33	BAI	96c	BES	$J/\psi \rightarrow \gamma K^+ K^-$
85 ± 24 ⁺²² ₋₁₉	28	BAI	96c	BES	$J/\psi \rightarrow \gamma K^+ K^-$
56 ± 19		BALOSHIN	95	SPEC	$40 \pi^- C \rightarrow K_S^0 K_S^0 X$
160 ± 40	44	BUGG	95	MRK3	$J/\psi \rightarrow \gamma \pi^+ \pi^- \pi^+ \pi^-$
160 ± 60 ₋₂₀	33	BUGG	95	MRK3	$J/\psi \rightarrow \gamma \pi^+ \pi^- \pi^+ \pi^-$
264 ± 25	32	ARMSTRONG	93c	E760	$\bar{p}p \rightarrow \pi^0 \eta \eta \rightarrow 6\gamma$
200 ± 300		BREAKSTONE	93	SFM	$pp \rightarrow pp \pi^+ \pi^- \pi^+ \pi^-$
< 80 % CL	45	ALDE	92d	GAM2	$38 \pi^- p \rightarrow \eta \eta N^*$
181 ± 30	46	ARMSTRONG	89d	OMEG	$300 pp \rightarrow pp K^+ K^-$
104 ± 30	46	ARMSTRONG	89d	OMEG	$300 pp \rightarrow pp K_S^0 K_S^0$
30 ± 20	33	BOLONKIN	88	SPEC	$40 \pi^- p \rightarrow K_S^0 K_S^0 n$
350 ± 150	28	BOLONKIN	88	SPEC	$40 \pi^- p \rightarrow K_S^0 K_S^0 n$
148 ± 17	47	FALVARD	88	DM2	$J/\psi \rightarrow \phi K^+ K^-, K_S^0 K_S^0$
184 ± 6	48	FALVARD	88	DM2	$J/\psi \rightarrow \phi K^+ K^-, K_S^0 K_S^0$
122 ± 74 ₋₁₅	49	LONGACRE	86	RVUE	$22 \pi^- p \rightarrow n 2K_S^0$
200 ± 100		BURKE	82	MRK2	$J/\psi \rightarrow \gamma 2\rho$
220 ± 100 ₋₇₀	50,51	EDWARDS	82d	CBAL	$J/\psi \rightarrow \gamma 2\eta$
200 ± 156 ₋₉	52	ETKIN	82b	MPS	$23 \pi^- p \rightarrow n 2K_S^0$

- 27 Breit-Wigner width.
- 28 $J^P = 0^+$.
- 29 T-matrix pole.
- 30 Supersedes BARBERIS 99 and BARBERIS 99b.
- 31 $J^P = 0^+$, supersedes by ARMSTRONG 89d.
- 32 No J^{PC} determination.
- 33 $J^P = 2^+$.
- 34 Systematic errors not estimated.
- 35 This state may be different from $f_0(1710)$, see CLOSE 05.
- 36 (Solution I)
- 37 K-matrix pole, assuming $J^P = 0^+$, from combined analysis of $\pi^- p \rightarrow \pi^0 \pi^0 n, \pi^- p \rightarrow K \bar{K} n, \pi^+ \pi^- \rightarrow \pi^+ \pi^-, \bar{p}p \rightarrow \pi^0 \pi^0 \pi^0, \pi^0 \eta \eta, \pi^0 \pi^0 \eta, \pi^+ \pi^- \pi^0, K^+ K^- \pi^0, K_S^0 K_S^0 \pi^0, K^+ K_S^0 \pi^-$ at rest, $\bar{p}n \rightarrow \pi^- \pi^- \pi^+, K_S^0 K^- \pi^0, K_S^0 K_S^0 \pi^-$ at rest.
- 38 (Solution I)
- 39 Decaying to $f_0(1370) \pi \pi$.
- 40 $J^P = 0^+$.
- 41 Not seen by AMSLER 02.
- 42 T-matrix pole, assuming $J^P = 0^+$.
- 43 No J^{PC} determination.
- 44 From a fit to the 0^+ partial wave.
- 45 ALDE 92d combines all the GAMS-2000 data.
- 46 $J^P = 2^+$, (0^+ excluded).
- 47 From an analysis ignoring interference with $f_2'(1525)$.
- 48 From an analysis including interference with $f_2'(1525)$.
- 49 Uses MRK3 data. From a partial-wave analysis of data using a K-matrix formalism with 5 poles, but assuming spin 2. Fit with constrained inelasticity.
- 50 $J^P = 2^+$ preferred.
- 51 From fit neglecting nearby $f_2'(1525)$. Replaced by BLOOM 83.
- 52 From an amplitude analysis of the $K_S^0 K_S^0$ system, superseded by LONGACRE 86.

See key on page 373

Meson Particle Listings

 $f_0(1710)$

$f_0(1710)$ DECAY MODES		
Mode		Fraction (Γ_i/Γ)
Γ_1	$K\bar{K}$	seen
Γ_2	$\eta\eta$	seen
Γ_3	$\pi\pi$	seen
Γ_4	$\gamma\gamma$	
Γ_5	$\omega\omega$	seen

$f_0(1710)$ $\Gamma(i)\Gamma(\gamma\gamma)/\Gamma(\text{total})$		
$\Gamma(K\bar{K}) \times \Gamma(\gamma\gamma)/\Gamma_{\text{total}}$		Γ_1/Γ
VALUE (eV)	CL%	DOCUMENT ID TECN COMMENT
<110	95	54 BEHREND 89C CELL $\gamma\gamma \rightarrow K_S^0 K_S^0$
• • • We do not use the following data for averages, fits, limits, etc. • • •		
<480	95	ALBRECHT 90G ARG $\gamma\gamma \rightarrow K^+ K^-$
<280	95	54 ALTHOFF 85B TASS $\gamma\gamma \rightarrow K\bar{K}\pi$
$\Gamma(\pi\pi) \times \Gamma(\gamma\gamma)/\Gamma_{\text{total}}$		Γ_3/Γ
VALUE (keV)	CL%	DOCUMENT ID TECN COMMENT
<0.82	95	53 BARATE 00E ALEP $\gamma\gamma \rightarrow \pi^+ \pi^-$
53 Assuming spin 0.		
54 Assuming helicity 2.		

$f_0(1710)$ BRANCHING RATIOS		
$\Gamma(K\bar{K})/\Gamma_{\text{total}}$		Γ_1/Γ
VALUE	DOCUMENT ID TECN COMMENT	
• • • We do not use the following data for averages, fits, limits, etc. • • •		
0.36 ± 0.09 0.19	55,56 LONGACRE 86 MPS	$22 \pi^- \rho \rightarrow n 2 K_S^0$
$\Gamma(\eta\eta)/\Gamma_{\text{total}}$		Γ_2/Γ
VALUE	DOCUMENT ID TECN COMMENT	
• • • We do not use the following data for averages, fits, limits, etc. • • •		
0.18 ± 0.03 0.13	55,56 LONGACRE 86 RVUE	
$\Gamma(\pi\pi)/\Gamma_{\text{total}}$		Γ_3/Γ
VALUE	DOCUMENT ID TECN COMMENT	
• • • We do not use the following data for averages, fits, limits, etc. • • •		
not seen	AMSLER 02 CBAR	$0.9 \bar{p} p \rightarrow \pi^0 \eta\eta, \pi^0 \pi^0 \pi^0$
0.039 ± 0.002 0.024	55,56 LONGACRE 86 RVUE	

$\Gamma(\pi\pi)/\Gamma(K\bar{K})$		
VALUE	CL%	DOCUMENT ID TECN COMMENT
0.41 ± 0.11 0.17		ABLIKIM 06v BES2 $e^+ e^- \rightarrow J/\psi \rightarrow \gamma\pi^+ \pi^-$
• • • We do not use the following data for averages, fits, limits, etc. • • •		
< 0.11	95	57 ABLIKIM 04E BES2 $J/\psi \rightarrow \omega K^+ K^-$
5.8 ± 9.1 -5.5		58 ANISOVICH 02D SPEC Combined fit
$0.2 \pm 0.024 \pm 0.036$ 0.39 ± 0.14		BARBERIS 99D OMEG 450 $pp \rightarrow K^+ K^-, \pi^+ \pi^-$ ARMSTRONG 91 OMEG 300 $pp \rightarrow pp\pi\pi, p\rho K\bar{K}$
$\Gamma(\eta\eta)/\Gamma(K\bar{K})$		Γ_2/Γ_1
VALUE	CL%	DOCUMENT ID TECN COMMENT
0.48 ± 0.15		BARBERIS 00E 450 $pp \rightarrow \rho\eta\eta\rho_S$
• • • We do not use the following data for averages, fits, limits, etc. • • •		
0.46 ± 0.70 0.38		58 ANISOVICH 02D SPEC Combined fit
< 0.02	90	59 PROKOSHKIN 91 GA24 $300 \pi^- p \rightarrow \pi^- \rho\eta\eta$
$\Gamma(\omega\omega)/\Gamma_{\text{total}}$		Γ_5/Γ
VALUE	EVTs	DOCUMENT ID TECN COMMENT
seen	180	ABLIKIM 06H BES $J/\psi \rightarrow \gamma\omega\omega$

55 From a partial-wave analysis of data using a K-matrix formalism with 5 poles, but assuming spin 2.

56 Fit with constrained inelasticity.

57 Using data from ABLIKIM 04A.

58 From a combined K-matrix analysis of Crystal Barrel (0. $p\bar{p} \rightarrow \pi^0 \pi^0 \pi^0, \pi^0 \eta\eta, \pi^0 \pi^0 \eta$), GAMS ($\pi p \rightarrow \pi^0 \pi^0 n, \eta\eta n, \eta\eta' n$), and BNL ($\pi p \rightarrow K\bar{K}n$) data.

59 Combining results of GAM4 with those of ARMSTRONG 89D.

 $f_0(1710)$ REFERENCES

ABLIKIM 06H	PR D73 112007	M. ABLIKIM <i>et al.</i>	(BES Collab.)
ABLIKIM 06V	PL B642 441	M. ABLIKIM <i>et al.</i>	(BES Collab.)
AMSLER 06	PL B639 165	C. AMSLER <i>et al.</i>	(CBAR Collab.)
UMAN 06	PR D73 052009	I. UMAN <i>et al.</i>	(FNAL E835)
VLADIMIRSK... 06	PAN 69 493	V.V. Vladimirov <i>et al.</i>	(ITEP, Moscow)
ABLIKIM 05	PL B607 243	M. ABLIKIM <i>et al.</i>	(BES Collab.)
ABLIKIM 05Q	PR D72 092002	M. ABLIKIM <i>et al.</i>	(BES Collab.)
BINON 05	PAN 68 960	F. Binon <i>et al.</i>	
CLOSE 05	PR D71 094022	F.E. Close, Q. Zhao	
ABLIKIM 04A	PL B598 149	M. ABLIKIM <i>et al.</i>	(BES Collab.)
ABLIKIM 04E	PL B603 138	M. ABLIKIM <i>et al.</i>	(BES Collab.)
CHEKANOV 04	PL B578 33	S. Chekanov <i>et al.</i>	(ZEUS Collab.)
PDG 04	PL B592 1	S. Eidelman <i>et al.</i>	
ANISOVICH 03	EPJ A16 229	V.V. Anisovich <i>et al.</i>	
BAI 03G	PR D68 052003	J.Z. Bai <i>et al.</i>	(BES Collab.)
TIKHOMIROV 03	PAN 66 828	G.D. Tikhomirov <i>et al.</i>	
AMSLER 02D	Translated from YAF 66 980.	C. AMSLER <i>et al.</i>	
ANISOVICH 02D	PAN 65 1545	V.V. Anisovich <i>et al.</i>	
NICHTIU 02	PL B545 261	F. Nichtiu <i>et al.</i>	(OBELIX Collab.)
BAI 00A	PL B472 207	J.Z. Bai <i>et al.</i>	(BES Collab.)
BARATE 00E	PL B472 189	R. Barate <i>et al.</i>	(ALEPH Collab.)
BARBERIS 00B	PL B479 159	D. Barberis <i>et al.</i>	(WA 102 Collab.)
ANISOVICH 99B	PL B449 354	A.V. Anisovich <i>et al.</i>	(Omega Expt.)
BARBERIS 99	PL B453 305	D. Barberis <i>et al.</i>	(Omega Expt.)
BARBERIS 99B	PL B453 316	D. Barberis <i>et al.</i>	(Omega Expt.)
BARBERIS 99D	PL B462 462	D. Barberis <i>et al.</i>	(Omega Expt.)
FRENCH 99	PL B460 213	B. French <i>et al.</i>	(WA76 Collab.)
ANISOVICH 98B	SPU 41 419	V.V. Anisovich <i>et al.</i>	
BAI 98H	PRL 81 1179	J.Z. Bai <i>et al.</i>	(BES Collab.)
BARKOV 98	JETPL 68 764	B.P. Barkov <i>et al.</i>	
ABREU 96C	PL B379 309	P. Abreu <i>et al.</i>	(DELPHI Collab.)
BAI 96C	PRL 77 3159	J.Z. Bai <i>et al.</i>	(BES Collab.)
BALOSHIN 95	PAN 58 46	O.N. Baloshin <i>et al.</i>	(ITEP)
BUGG 95	PL B353 378	D.V. Bugg <i>et al.</i>	(LOQM, PNPI, WASH)
ARMSTRONG 93C	PL B307 394	T.A. Armstrong <i>et al.</i>	(FNAL, FERR, GENO+)
BREAKSTONE 93	ZPHY C58 251	A.M. Breakstone <i>et al.</i>	(IOWA, CERN, DORT+)
ALDE 92D	PL B284 457	D.M. Alde <i>et al.</i>	(GAM2 Collab.)
ALDE 92D	SJNP 54 451	D.M. Alde <i>et al.</i>	(GAM2 Collab.)
ARMSTRONG 91	ZPHY C51 351	T.A. Armstrong <i>et al.</i>	(ATHU, BARI, BIRM+)
PROKOSHKIN 91	SPD 36 155	Y.D. Prokoshkin	(GAM2, GAM4 Collab.)
ALBRECHT 90D	ZPHY C48 183	H. Albrecht <i>et al.</i>	(ARGUS Collab.)
ARMSTRONG 89G	PL B227 186	T.A. Armstrong, M. Benayoun	(ATHU, BARI, BIRM+)
BEHREND 89C	ZPHY C43 91	H.J. Behrend <i>et al.</i>	(CELLO Collab.)
AUGUSTIN 88	PRL 60 2238	J.E. Augustin <i>et al.</i>	(DM2 Collab.)
BOLONKIN 88	NP B309 426	B.V. Bolonkin <i>et al.</i>	(ITEP, SERP)
FALVARD 88	PR D38 2706	A. Falvard <i>et al.</i>	(CLER, FRAS, LALO+)
AUGUSTIN 87	ZPHY C36 369	J.E. Augustin <i>et al.</i>	(LALO, CLER, FRAS+)
BALTRUSAIT... 87	PR D35 2077	R.M. Baltrusaitis <i>et al.</i>	(Mark III Collab.)
ALDE 86C	PL B182 105	D.M. Alde <i>et al.</i>	(SERP, BELG, LANL, LAPP)
LONGACRE 86	PL B177 223	R.S. Longacre <i>et al.</i>	(BNL, BRAN, CUNY+)
ALTHOFF 85B	ZPHY C29 189	M. Althoff <i>et al.</i>	(TASSO Collab.)
WILLIAMS 84	PR D30 877	E.G.H. Williams <i>et al.</i>	(VAND, NDAM, TUFTS+)
BLOOM 83	ARNS 33 143	E.D. Bloom, C. Peck	(SLAC, CIT)
BURKE 82D	PRL 49 632	D.L. Burke <i>et al.</i>	(LBL, SLAC)
EDWARDS 82B	PRL 48 458	C. Edwards <i>et al.</i>	(CIT, HARV, PRIN+)
ETKIN 82B	PR D25 1786	A. Etkin <i>et al.</i>	(BNL, CUNY, TUFTS, VAND)
ETKIN 82C	PR D25 2446	A. Etkin <i>et al.</i>	(BNL, CUNY, TUFTS, VAND)

OTHER RELATED PAPERS

POZDNYAKOV 07	PPNL 4 289	V.N. Pozdnyakov	
ABLIKIM 06H	PR D73 112007	M. ABLIKIM <i>et al.</i>	(BES Collab.)
CHEN 06	PR D73 014516	Y. Chen, A. Alexandru, S.J. Dong	
FARBORZ 06	PR D74 054030	A.H. Fariborz	
GLOZMAN 06	PR D73 015003	I.Ya. Glozman	
HE 06	PR D73 051502R	X.-G. He, X.-Q. Li, X.-Q. Zeng	
CHANOWITZ 05	PRL 95 172001	M. Chanowitz	
GIACOSA 05	PR C71 025202	F. Giacosa <i>et al.</i>	
GIACOSA 05A	PL B622 277	F. Giacosa <i>et al.</i>	
GIACOSA 05B	PR D72 094006	F. Giacosa <i>et al.</i>	
VIJANDE 05	PR D72 034025	J. Vijande, A. Valarce, F. Fernandez	
ZHAO 05	PR D72 074001	Q. Zhao	
ZHAO 05A	PL B631 222	Q. Zhao, B.-S. Zou, Z.-B. Ma	
LINK 04	PL B585 200	J.M. Link <i>et al.</i>	(FNAL FOCUS Collab.)
TESHIMA 04	JPG 30 663	T. Teshima <i>et al.</i>	
ANISOVICH 03B	PAN 66 741	V.V. Anisovich, V.A. Nikonov, A.V. Sarantsev	
AMSLER 02B	PL B541 22	C. AMSLER	
JIN 02	PR D66 057505	H. Jin, X. Zhang	
KLEEFELD 02	PR D66 034007	F. Kleefeld <i>et al.</i>	
RUPP 02	PR D65 078501	G. Rupp, E. van Beveren, M.D. Scadron	
SHAKIN 02	PR D65 078502	C.M. Shakin, H. Wang	
TESHIMA 02	JPG 28 1391	T. Teshima, I. Kitamura, N. Morisita	
VOLKOV 02	PAN 65 1657	M.K. Volkov, V.L. Yudichev	
LI 01B	EPJ C19 529	D.-M. Li, H. Yu, Q.-X. Shen	
VOLKOV 01	PAN 64 2006	M.K. Volkov, V.L. Yudichev	
ANISOVICH 99H	PL B467 289	A.V. Anisovich, V.V. Anisovich	
GRYGOREV 99	PAN 62 470	V.K. Grygorev <i>et al.</i>	
PROKOSHKIN 99	PAN 62 356	Y.D. Prokoshkin	
ANISOVICH 97	PL B395 123	A.V. Anisovich, A.V. Sarantsev	(PNPI)
LINDENBAUM 92	PL B274 492	S.J. Lindenbaum, R.S. Longacre	(BNL)
BISELLO 89D	PR D39 701	G. Busetto <i>et al.</i>	(DM2 Collab.)
ASTON 88B	NP B301 525	D. Aston <i>et al.</i>	(SLAC, NAGO, CINC, INUS)
AKESSON 86	NP B264 154	T. Akesson <i>et al.</i>	(Axial Field Spec. Collab.)
ARMSTRONG 86B	PL 167B 133	T.A. Armstrong <i>et al.</i>	(ATHU, BARI, BIRM+)
BALTRUSAIT... 86B	PR D33 1222	R.M. Baltrusaitis <i>et al.</i>	(Mark III Collab.)
ALTHOFF 83B	PL 121B 216	M. Althoff <i>et al.</i>	(TASSO Collab.)
BARNETT 83B	PL 120B 455	B. Barnett <i>et al.</i>	(JHU)
BARNES 82B	NP B198 380	T. Barnes, F.E. Close, S. Monaghan	(RHEL, OXFPT)
TANIMOTO 82	PL 116B 198	M. Tanimoto	(BIEL)

Meson Particle Listings

 $\eta(1760), \pi(1800)$ $\eta(1760)$

$$I^G(J^{PC}) = 0^+(0^{-+})$$

OMITTED FROM SUMMARY TABLE

Seen by DM2 in the $\rho\rho$ system (BISELLO 89B). Structure in this region has been reported before in the same system (BALTRUSAITIS 86B) and in the $\omega\omega$ system (BALTRUSAITIS 85C, BISELLO 87). Needs confirmation.

 $\eta(1760)$ MASS

VALUE (MeV)	EVTs	DOCUMENT ID	TECN	COMMENT
1756 ± 9 OUR AVERAGE				
1744 ± 10 ± 15	1045	¹ ABLIKIM	06H BES	$J/\psi \rightarrow \gamma\omega\omega$
1760 ± 11	320	² BISELLO	89B DM2	$J/\psi \rightarrow 4\pi\gamma$

¹ From a partial wave analysis including $\eta(1760)$, $f_0(1710)$, $f_2(1640)$, and $f_2(1910)$.

² Estimated by us from various fits.

 $\eta(1760)$ WIDTH

VALUE (MeV)	EVTs	DOCUMENT ID	TECN	COMMENT
96 ± 7 OUR AVERAGE	Error includes scale factor of 5.1.			
244 \pm 24 \pm 25	1045	³ ABLIKIM	06H BES	$J/\psi \rightarrow \gamma\omega\omega$
60 ± 16	320	⁴ BISELLO	89B DM2	$J/\psi \rightarrow 4\pi\gamma$

³ From a partial wave analysis including $\eta(1760)$, $f_0(1710)$, $f_2(1640)$, and $f_2(1910)$.

⁴ Estimated by us from various fits.

 $\eta(1760)$ REFERENCES

ABLIKIM	06H	PR D73 112007	M. Ablikim <i>et al.</i>	(BES Collab.)
BISELLO	89B	PR D39 701	G. Busetto <i>et al.</i>	(DM2 Collab.)
BISELLO	87	PL B192 239	D. Bisello <i>et al.</i>	(PADO, CLER, FRAS+)
BALTRUSAITIS...	86B	PR D33 1222	R. M. Baltrusaitis <i>et al.</i>	(Mark III Collab.)
BALTRUSAITIS...	85C	PRL 55 1723	R. M. Baltrusaitis <i>et al.</i>	(CIT, UCSC+)

OTHER RELATED PAPERS

BAI	99	PL B446 356	J.Z. Bai <i>et al.</i>	(BES Collab.)
-----	----	-------------	------------------------	---------------

 $\pi(1800)$

$$I^G(J^{PC}) = 1^-(0^{-+})$$

See also minireview under non- $q\bar{q}$ candidates in PDG 06, Journal of Physics, G **33** 1 (2006).

 $\pi(1800)$ MASS

VALUE (MeV)	EVTs	DOCUMENT ID	TECN	CHG	COMMENT
1816 ± 14 OUR AVERAGE	Error includes scale factor of 2.3. See the ideogram below.				
1876 ± 18 ± 16	4k	¹ EUGENIO	08 B852	-	18 $\pi^- p \rightarrow \eta\eta\pi^- p$
1774 ± 18 ± 20		² CHUNG	02 B852		18.3 $\pi^- p \rightarrow \pi^+ \pi^- \pi^- p$

1863 ± 9 ± 10		³ CHUNG	02 B852		18.3 $\pi^- p \rightarrow \pi^+ \pi^- \pi^- p$
1840 ± 10 ± 10	1200	AMELIN	96B VES	-	37 $\pi^- A \rightarrow \eta\eta\pi^- A$
1775 ± 7 ± 10		⁴ AMELIN	95B VES	-	36 $\pi^- A \rightarrow \pi^+ \pi^- \pi^- A$
1790 ± 14		⁵ BERDNIKOV	94 VES	-	37 $\pi^- A \rightarrow K^+ K^- \pi^- A$

1873 ± 33 ± 20		BELADIDZE	92c VES	-	36 $\pi^- Be \rightarrow \pi^- \eta/\eta Be$
1814 ± 10 ± 23	426 ± 57	BITYUKOV	91 VES	-	36 $\pi^- C \rightarrow \pi^- \eta\eta C$
1770 ± 30	1100	BELLINI	82 SPEC	-	40 $\pi^- A \rightarrow 3\pi A$

••• We do not use the following data for averages, fits, limits, etc. •••

1737 ± 5 ± 15 AMELIN 99 VES 37 $\pi^- A \rightarrow \omega\pi^- \pi^0 A^*$

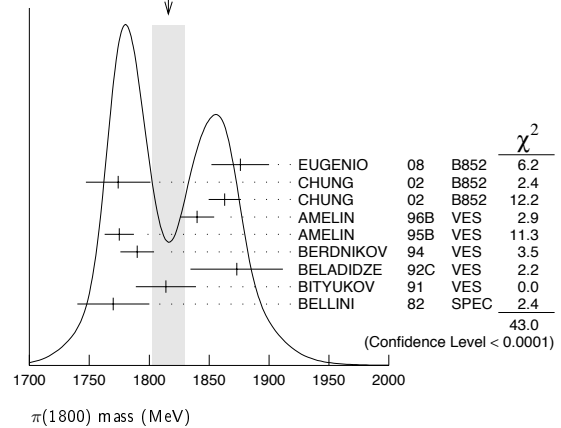
¹ From a single-pole fit.

² In the $f_0(980)$ π wave.

³ In the $f_0(600)$ π wave.

⁴ From a fit to $J^{PC} = 0^{-+} f_0(980)\pi$, $f_0(1370)\pi$ waves.

⁵ From a fit to $J^{PC} = 0^{-+} K_0^*(1430)K^-$ and $f_0(980)\pi^-$ waves.

WEIGHTED AVERAGE
1816 ± 14 (Error scaled by 2.3) $\pi(1800)$ WIDTH

VALUE (MeV)	EVTs	DOCUMENT ID	TECN	CHG	COMMENT
208 ± 12 OUR AVERAGE					
221 ± 26 ± 38	4k	⁶ EUGENIO	08 B852	-	18 $\pi^- p \rightarrow \eta\eta\pi^- p$
223 ± 48 ± 50		⁷ CHUNG	02 B852		18.3 $\pi^- p \rightarrow \pi^+ \pi^- \pi^- p$
191 ± 21 ± 20		⁸ CHUNG	02 B852		18.3 $\pi^- p \rightarrow \pi^+ \pi^- \pi^- p$
210 ± 30 ± 30	1200	AMELIN	96B VES	-	37 $\pi^- A \rightarrow \eta\eta\pi^- A$
190 ± 15 ± 15		⁹ AMELIN	95B VES	-	36 $\pi^- A \rightarrow \pi^+ \pi^- \pi^- A$
210 ± 70		¹⁰ BERDNIKOV	94 VES	-	37 $\pi^- A \rightarrow K^+ K^- \pi^- A$
225 ± 35 ± 20		BELADIDZE	92c VES	-	36 $\pi^- Be \rightarrow \pi^- \eta/\eta Be$
205 ± 18 ± 32	426 ± 57	BITYUKOV	91 VES	-	36 $\pi^- C \rightarrow \pi^- \eta\eta C$
310 ± 50	1100	BELLINI	82 SPEC	-	40 $\pi^- A \rightarrow 3\pi A$
259 ± 19 ± 6		AMELIN	99 VES		37 $\pi^- A \rightarrow \omega\pi^- \pi^0 A^*$

••• We do not use the following data for averages, fits, limits, etc. •••

⁶ From a single-pole fit.

⁷ In the $f_0(980)$ π wave.

⁸ In the $f_0(600)$ π wave.

⁹ From a fit to $J^{PC} = 0^{-+} f_0(980)\pi$, $f_0(1370)\pi$ waves.

¹⁰ From a fit to $J^{PC} = 0^{-+} K_0^*(1430)K^-$ and $f_0(980)\pi^-$ waves.

 $\pi(1800)$ DECAY MODES

Mode	Fraction (Γ_i/Γ)
Γ_1 $\pi^+ \pi^- \pi^-$	seen
Γ_2 $f_0(600)\pi^-$	seen
Γ_3 $f_0(980)\pi^-$	seen
Γ_4 $f_0(1370)\pi^-$	seen
Γ_5 $f_0(1500)\pi^-$	not seen
Γ_6 $\rho\pi^-$	not seen
Γ_7 $\eta\eta\pi^-$	seen
Γ_8 $a_0(980)\eta$	seen
Γ_9 $a_2(1320)\eta$	not seen
Γ_{10} $f_2(1270)\pi$	not seen
Γ_{11} $f_0(1300)\pi$	not seen
Γ_{12} $f_0(1500)\pi^-$	seen
Γ_{13} $\eta\eta'(958)\pi^-$	seen
Γ_{14} $K_0^*(1430)K^-$	seen
Γ_{15} $K^*(892)K^-$	not seen

 $\pi(1800)$ BRANCHING RATIOS

VALUE	DOCUMENT ID	TECN	COMMENT	Γ_3/Γ_2
0.44 ± 0.08 ± 0.38	¹¹ CHUNG	02 B852	18.3 $\pi^- p \rightarrow \pi^+ \pi^- \pi^- p$	

VALUE	DOCUMENT ID	TECN	CHG	COMMENT	Γ_3/Γ_4
1.7 ± 1.3	¹² AMELIN	95B VES	-	36 $\pi^- A \rightarrow \pi^+ \pi^- \pi^- A$	

••• We do not use the following data for averages, fits, limits, etc. •••

VALUE	DOCUMENT ID	TECN	CHG	COMMENT	$\Gamma_4/\Gamma_{\text{total}}$
seen	BELLINI	82 SPEC	-	40 $\pi^- A \rightarrow 3\pi A$	

See key on page 373

Meson Particle Listings

 $\pi(1800)$, $f_2(1810)$

$\Gamma(f_0(1500)\pi^-)/\Gamma_{\text{total}}$		Γ_5/Γ	
VALUE	DOCUMENT ID	TECN	COMMENT
not seen	CHUNG	02	B852 18.3 $\pi^- p \rightarrow \pi^+ \pi^- \pi^- p$

$\Gamma(\rho\pi^-)/\Gamma_{\text{total}}$		Γ_6/Γ	
VALUE	DOCUMENT ID	TECN	CHG COMMENT
not seen	BELLINI	82	SPEC - 40 $\pi^- A \rightarrow 3\pi A$

$\Gamma(\rho\pi^-)/\Gamma(f_0(980)\pi^-)$		Γ_6/Γ_3	
VALUE	CL%	DOCUMENT ID	TECN CHG COMMENT
• • • We do not use the following data for averages, fits, limits, etc. • • •			
<0.25		CHUNG	02 B852 18.3 $\pi^- p \rightarrow \pi^+ \pi^- \pi^- p$
<0.14	90	AMELIN	95B VES - 36 $\pi^- A \rightarrow \pi^+ \pi^- \pi^- A$

$\Gamma(\eta\eta\pi^-)/\Gamma(\pi^+ \pi^- \pi^-)$		Γ_7/Γ_1	
VALUE	EVTS	DOCUMENT ID	TECN CHG COMMENT
• • • We do not use the following data for averages, fits, limits, etc. • • •			
0.5 ± 0.1	1200	12 AMELIN	96B VES - 37 $\pi^- A \rightarrow \eta\eta\pi^- A$

$\Gamma(a_2(1320)\eta)/\Gamma_{\text{total}}$		Γ_9/Γ	
VALUE	DOCUMENT ID	TECN	COMMENT
not seen	EUGENIO	08	B852 18 $\pi^- p \rightarrow \eta\eta\pi^- p$

$\Gamma(f_2(1270)\pi)/\Gamma_{\text{total}}$		Γ_{10}/Γ	
VALUE	DOCUMENT ID	TECN	COMMENT
not seen	EUGENIO	08	B852 18 $\pi^- p \rightarrow \eta\eta\pi^- p$

$\Gamma(f_0(1300)\pi)/\Gamma_{\text{total}}$		Γ_{11}/Γ	
VALUE	DOCUMENT ID	TECN	COMMENT
not seen	EUGENIO	08	B852 18 $\pi^- p \rightarrow \eta\eta\pi^- p$

$\Gamma(f_0(1500)\pi^-)/\Gamma(a_0(980)\eta)$		Γ_{12}/Γ_8	
VALUE	EVTS	DOCUMENT ID	TECN CHG COMMENT
• • • We do not use the following data for averages, fits, limits, etc. • • •			
0.48 ± 0.17	4k	12,13 EUGENIO	08 B852 - 18 $\pi^- p \rightarrow \eta\eta\pi^- p$
0.030 +0.014 -0.011		12 ANISOVICH	01B SPEC 0 0.6-1.94 $\rho\bar{p} \rightarrow \eta\eta\pi^0\pi^0$
0.08 ± 0.03	1200	12,14 AMELIN	96B VES - 37 $\pi^- A \rightarrow \eta\eta\pi^- A$

$\Gamma(\eta\eta'(958)\pi^-)/\Gamma(\eta\eta\pi^-)$		Γ_{13}/Γ_7	
VALUE	EVTS	DOCUMENT ID	TECN CHG COMMENT
• • • We do not use the following data for averages, fits, limits, etc. • • •			
0.29 ± 0.07		12 BELADIDZE	92c VES - 36 $\pi^- \text{Be} \rightarrow \pi^- \eta' \eta \text{Be}$
0.3 ± 0.1	426 ± 57	12 BITYUKOV	91 VES - 36 $\pi^- \text{C} \rightarrow \pi^- \eta\eta \text{C}$

$\Gamma(K_0^*(1430)K^-)/\Gamma_{\text{total}}$		Γ_{14}/Γ	
VALUE	DOCUMENT ID	TECN	CHG COMMENT
seen	BERDNIKOV	94	VES - 37 $\pi^- A \rightarrow K^+ K^- \pi^- A$

$\Gamma(K^*(892)K^-)/\Gamma_{\text{total}}$		Γ_{15}/Γ	
VALUE	DOCUMENT ID	TECN	CHG COMMENT
not seen	BERDNIKOV	94	VES - 37 $\pi^- A \rightarrow K^+ K^- \pi^- A$

¹¹ Assuming that $f_0(980)$ decays only to $\pi\pi$.

¹² Systematic errors not estimated.

¹³ From a single-pole fit.

¹⁴ Assuming that $f_0(1500)$ decays only to $\eta\eta$ and $a_0(980)$ decays only to $\eta\pi$.

 $\pi(1800)$ REFERENCES

EUGENIO	08	PL B660 466	P. Eugenio <i>et al.</i>	(BNL E852 Collab.)
PDG	06	JPG 33 1	W.-M. Yao <i>et al.</i>	(PDG Collab.)
CHUNG	02	PR D65 072001	S.U. Chung <i>et al.</i>	(BNL E852 Collab.)
ANISOVICH	01B	PL B500 222	A.V. Anisovich <i>et al.</i>	
AMELIN	99	PAN 62 445	D.V. Amelin <i>et al.</i>	(VES Collab.)
		Translated from YAF 62 487.		
AMELIN	96B	PAN 59 976	D.V. Amelin <i>et al.</i>	(SERP, TBIL)IGJPC
		Translated from YAF 59 1021.		
AMELIN	95B	PL B356 595	D.V. Amelin <i>et al.</i>	(SERP, TBIL)
BERDNIKOV	94	PL B337 219	E.B. Berdnikov <i>et al.</i>	(SERP, TBIL)
BELADIDZE	92C	SJNP 55 1535	G.M. Beladidze, S.I. Bitjukov, G.V. Borisov	(SERP+)
		Translated from YAF 55 2748.		
BITYUKOV	91	PL B268 137	S.I. Bitjukov <i>et al.</i>	(SERP, TBIL)
BELLINI	82	PRL 48 1697	G. Bellini <i>et al.</i>	(MILA, BGNA, JINR)

OTHER RELATED PAPERS

EBERT	05	MPL A20 1887	D. Ebert, R.N. Faustov, V.O. Galkin	
ZAIMIDOROGA	99	PAN 30 1	O.A. Zaimidorga	
		Translated from SJNP 30 5.		
BORISOV	92	SJNP 55 1441	G.V. Borisov, S.S. Gershtein, A.M. Zaitsev	(SERP)
		Translated from YAF 55 2583.		

 $f_2(1810)$

$$I^G(J^{PC}) = 0^+(2^{++})$$

OMITTED FROM SUMMARY TABLE
Needs confirmation.

 $f_2(1810)$ MASS

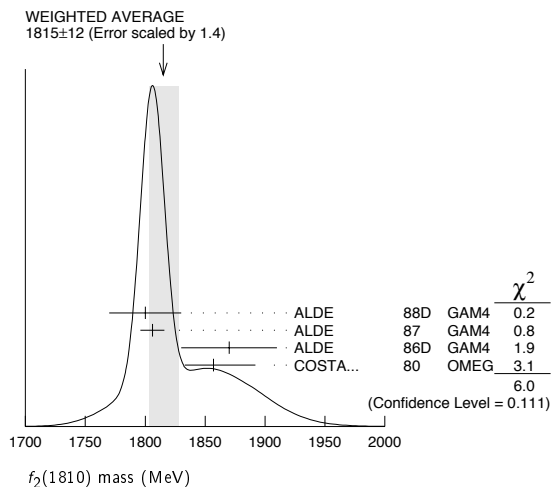
VALUE (MeV)	EVTS	DOCUMENT ID	TECN	COMMENT
1815 ± 12 OUR AVERAGE Error includes scale factor of 1.4. See the ideogram below.				
1800 ± 30	40	ALDE	88D	GAM4 300 $\pi^- p \rightarrow \pi^- p 4\pi^0$
1806 ± 10	1600	ALDE	87	GAM4 100 $\pi^- p \rightarrow 4\pi^0 n$
1870 ± 40		¹ ALDE	86D	GAM4 100 $\pi^- p \rightarrow \eta\eta n$
1857 +35 -24		² COSTA...	80	OMEG 10 $\pi^- p \rightarrow K^+ K^- n$
• • • We do not use the following data for averages, fits, limits, etc. • • •				
1858 +18 -71		³ LONGACRE	86	RVUE Compilation
1799 ± 15		⁴ CASON	82	STRC 8 $\pi^+ p \rightarrow \Delta^{++} \pi^0$

¹ Seen in only one solution.

² Error increased by spread of two solutions. Included in LONGACRE 86 global analysis.

³ From a partial-wave analysis of data using a K-matrix formalism with 5 poles. Includes compilation of several other experiments.

⁴ From an amplitude analysis of the reaction $\pi^+ \pi^- \rightarrow 2\pi^0$. The resonance in the $2\pi^0$ final state is not confirmed by PROKOSHKIN 97.

 $f_2(1810)$ WIDTH

VALUE (MeV)	EVTS	DOCUMENT ID	TECN	COMMENT
197 ± 22 OUR AVERAGE Error includes scale factor of 1.5. See the ideogram below.				
160 ± 30	40	ALDE	88D	GAM4 300 $\pi^- p \rightarrow \pi^- p 4\pi^0$
190 ± 20	1600	ALDE	87	GAM4 100 $\pi^- p \rightarrow 4\pi^0 n$
250 ± 30		⁵ ALDE	86D	GAM4 100 $\pi^- p \rightarrow \eta\eta n$
185 +102 -139		⁶ COSTA...	80	OMEG 10 $\pi^- p \rightarrow K^+ K^- n$
• • • We do not use the following data for averages, fits, limits, etc. • • •				
388 +15 -21		⁷ LONGACRE	86	RVUE Compilation
280 +42 -35		⁸ CASON	82	STRC 8 $\pi^+ p \rightarrow \Delta^{++} \pi^0$

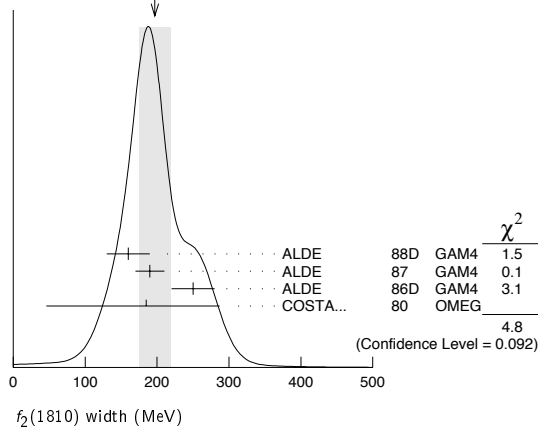
⁵ Seen in only one solution.

⁶ Error increased by spread of two solutions. Included in LONGACRE 86 global analysis.

⁷ From a partial-wave analysis of data using a K-matrix formalism with 5 poles. Includes compilation of several other experiments.

⁸ From an amplitude analysis of the reaction $\pi^+ \pi^- \rightarrow 2\pi^0$. The resonance in the $2\pi^0$ final state is not confirmed by PROKOSHKIN 97.

Meson Particle Listings

 $f_2(1810)$, $X(1835)$ WEIGHTED AVERAGE
197±22 (Error scaled by 1.5) $f_2(1810)$ DECAY MODES

Mode	Fraction (Γ_i/Γ)
Γ_1 $\pi\pi$	
Γ_2 $\eta\eta$	
Γ_3 $4\pi^0$	seen
Γ_4 K^+K^-	

 $f_2(1810)$ BRANCHING RATIOS

$\Gamma(\pi\pi)/\Gamma_{\text{total}}$	DOCUMENT ID	TECN	COMMENT	Γ_1/Γ
••• We do not use the following data for averages, fits, limits, etc. •••				
not seen	AMSLER 02	CBAR	$0.9 \bar{p}p \rightarrow \pi^0 \eta \eta$	
not seen	PROKOSHKIN 97	GAM2	$38 \pi^- p \rightarrow \pi^0 \pi^0 n$	
$0.21^{+0.02}_{-0.03}$	⁹ LONGACRE 86	RVUE	Compilation	
0.44 ± 0.03	¹⁰ CASON 82	STRC	$8 \pi^+ p \rightarrow \Delta^{++} \pi^0 \pi^0$	

⁹From a partial-wave analysis of data using a K-matrix formalism with 5 poles. Includes compilation of several other experiments.
¹⁰Included in LONGACRE 86 global analysis.

$\Gamma(\eta\eta)/\Gamma_{\text{total}}$	DOCUMENT ID	TECN	COMMENT	Γ_2/Γ
••• We do not use the following data for averages, fits, limits, etc. •••				
$0.008^{+0.028}_{-0.003}$	⁹ LONGACRE 86	RVUE	Compilation	

$\Gamma(\pi\pi)/\Gamma(4\pi^0)$	DOCUMENT ID	TECN	COMMENT	Γ_1/Γ_3
••• We do not use the following data for averages, fits, limits, etc. •••				
<0.75	ALDE 87	GAM4	$100 \pi^- p \rightarrow 4\pi^0 n$	

$\Gamma(4\pi^0)/\Gamma(\eta\eta)$	DOCUMENT ID	TECN	COMMENT	Γ_3/Γ_2
••• We do not use the following data for averages, fits, limits, etc. •••				
0.8 ± 0.3	ALDE 87	GAM4	$100 \pi^- p \rightarrow 4\pi^0 n$	

$\Gamma(K^+K^-)/\Gamma_{\text{total}}$	DOCUMENT ID	TECN	COMMENT	Γ_4/Γ
••• We do not use the following data for averages, fits, limits, etc. •••				
$0.003^{+0.019}_{-0.002}$	⁹ LONGACRE 86	RVUE	Compilation	
seen	COSTA... 80	OMEG	$10 \pi^- p \rightarrow K^+K^- n$	

 $f_2(1810)$ REFERENCES

AMSLER 02	EPJ C23 29	C. Amser <i>et al.</i>	
PROKOSHKIN 97	SPD 42 117 Translated from DANS 353 323.	Y.D. Prokoshkin <i>et al.</i>	(SERP)
ALDE 88D	SJNP 47 810 Translated from YAF 47 1275.	D.M. Alde <i>et al.</i>	(SERP, BELG, LANL, LAPP+)
ALDE 87	PL B198 286	D.M. Alde <i>et al.</i>	(LANL, BRUX, SERP, LAPP)
ALDE 86D	NP B269 485	D.M. Alde <i>et al.</i>	(BELG, LAPP, SERP, CERN+)
LONGACRE 86	PL B177 223	R.S. Longacre <i>et al.</i>	(BNL, BRAN, CUNY+)
CASON 82	PRL 48 1316	N.M. Cason <i>et al.</i>	(NDAM, ANL)
COSTA... 80	NP B175 402	G. Costa de Beauregard <i>et al.</i>	(BARI, BONN+)

OTHER RELATED PAPERS

ANISOVICH 05	JETPL 80 715 Translated from ZETFP 80 845.	V.V. Anisovich	
AKER 91	PL B260 249	E. Aker <i>et al.</i>	(Crystal Barrel Collab.)
CASON 83	PR D28 1586	N.M. Cason <i>et al.</i>	(NDAM, ANL)
ETKIN 82B	PR D25 1786	A. Etkin <i>et al.</i>	(BNL, CUNY, TUFTS, VAND)

 $X(1835)$

$$I^G(J^{PC}) = ?^?(?^-+)$$

OMITTED FROM SUMMARY TABLE

Needs confirmation. Seen by BAI 03F and ABLIKIM 05R in radiative decays of the J/ψ . Evidence for a threshold enhancement in the $p\bar{p}$ mass spectrum was also reported by ABE 02K, AUBERT, B 05L, and WANG 05A in $B^+ \rightarrow p\bar{p}K^+$, WANG 05A in $B^0 \rightarrow p\bar{p}K_S^0$, ABE 02W in $\bar{B}^0 \rightarrow p\bar{p}D^0$, and WEI 08 in $B^+ \rightarrow p\bar{p}\pi^+$ decays. Not seen by ATHAR 06 in $\mathcal{T}(1S) \rightarrow p\bar{p}\gamma$.

 $X(1835)$ MASS

VALUE (MeV)	EVTS	DOCUMENT ID	TECN	COMMENT
1833.7 ± 6.1 ± 2.7	264	ABLIKIM	05R BES2	$J/\psi \rightarrow \gamma\pi^+\pi^-\eta'$
••• We do not use the following data for averages, fits, limits, etc. •••				
1812 $^{+19}_{-26}$ ± 18	95	¹ ABLIKIM	06J BES2	$J/\psi \rightarrow \gamma\omega\phi$
1831 ± 7		² ABLIKIM	05R BES2	$J/\psi \rightarrow \gamma\rho\bar{p}$

¹Favors $J^{PC} = 0^{++}$ quantum numbers assignment.
²From the fit including final state interaction effects in isospin 0 S-wave according to SIBIRTSEV 05A. Systematic errors not estimated.

 $X(1835)$ WIDTH

VALUE (MeV)	CL%	EVTS	DOCUMENT ID	TECN	COMMENT
67.7 ± 20.3 ± 7.7		264	ABLIKIM	05R BES2	$J/\psi \rightarrow \gamma\pi^+\pi^-\eta'$
••• We do not use the following data for averages, fits, limits, etc. •••					
105 ± 20 ± 28		95	³ ABLIKIM	06J BES2	$J/\psi \rightarrow \gamma\omega\phi$
< 153		90	⁴ ABLIKIM	05R BES2	$J/\psi \rightarrow \gamma\rho\bar{p}$

³Favors $J^{PC} = 0^{++}$ quantum numbers assignment.
⁴From the fit including final state interaction effects in isospin 0 S-wave according to SIBIRTSEV 05A. Systematic errors not estimated.

 $X(1835)$ DECAY MODES

Mode	Fraction (Γ_i/Γ)
Γ_1 $p\bar{p}$	seen
Γ_2 $\pi^+\pi^-\eta'$	seen
Γ_3 $\omega\phi$	seen

 $X(1835)$ BRANCHING RATIOS

$\Gamma(\rho\bar{p})/\Gamma(\pi^+\pi^-\eta')$	DOCUMENT ID	TECN	COMMENT	Γ_1/Γ_2
••• We do not use the following data for averages, fits, limits, etc. •••				
0.333	ABLIKIM 05R	BES2	$J/\psi \rightarrow \gamma\pi^+\pi^-\eta'$	

$\Gamma(\omega\phi)/\Gamma_{\text{total}}$	DOCUMENT ID	TECN	COMMENT	Γ_3/Γ
seen	ABLIKIM 06J	BES2	$J/\psi \rightarrow \gamma\omega\phi$	

 $X(1835)$ REFERENCES

WEI 08	PL B659 80	J.-T. Wei <i>et al.</i>	(BELLE Collab.)
ABLIKIM 06J	PRL 96 162002	M. Ablikim <i>et al.</i>	(BES Collab.)
ATHAR 06	PR D73 032001	S.B. Athar <i>et al.</i>	(CLEO Collab.)
ABLIKIM 05R	PRL 95 262001	M. Ablikim <i>et al.</i>	(BES Collab.)
AUBERT.B 05L	PR D72 051101R	B. Aubert <i>et al.</i>	(BABAR Collab.)
SIBIRTSEV 05A	PR D71 054010	A. Sibirtsev, J. Haidenbauer	
WANG 05A	PL B617 141	M.-Z. Wang <i>et al.</i>	(BELLE Collab.)
BAI 03F	PRL 91 022001	J.Z. Bai <i>et al.</i>	(BES Collab.)
ABE 02K	PRL 88 181803	K. Abe <i>et al.</i>	(BELLE Collab.)
ABE 02W	PRL 89 151802	K. Abe <i>et al.</i>	(BELLE Collab.)

OTHER RELATED PAPERS

ABLIKIM 08	EPJ C53 15	M. Ablikim <i>et al.</i>	(BES Collab.)
BICUDO 07	EPJ C52 363	P. Bicudo <i>et al.</i>	
CHEN 07F	JPG 34 2679	H. Chen, R.-G. Ping	
ENTEM 07	PR D75 014004	D.R. Entem, F. Fernandez	
HE 07	EPJ C49 731	H.-G. He <i>et al.</i>	
LAPORTA 07	IJMP A22 5401	V. Laporta	
WANG 07A	JPG 34 505	Z.-J. Wang, S.-L. Wan	
HAIDENBAU... 06	PR D74 017501	J. Haidenbauer <i>et al.</i>	
HAIDENBAU... 06A	PL B643 29	J. Haidenbauer <i>et al.</i>	
HUANG 06A	PRL 96 032003	G.S. Huang <i>et al.</i>	(CLEO Collab.)
KOCHELEV 06	PL B633 283	N. Kochelev, D.-P. Min	(SEOUL, JINR)
LI 06	PR D74 034019	B.A. Li	
LI 06A	PR D74 054017	B.A. Li	
ZHAO 06	PR D74 114025	Q. Zhao, B.S. Zhou	
KOCHELEV 05	PR D72 097502	N. Kochelev, D.-P. Min	(SEOUL, JINR)
LOISEAU 05	PR C72 011001	B. Loiseau, S. Wycech	(CURCP, WIRN)
BUGG 04A	EPJ C36 161	D.V. Bugg	
BUGG 04B	PL B598 8	D.V. Bugg	
GAO 04	CTP 42 844	G.-S. Gao, S.-L. Zhu	
KERBIKOV 04	PR C69 055205	B. Kerbikov <i>et al.</i>	
ZOU 04	PR D69 034004	B.S. Zou, H.C. Chiang	
DATTA 03B	PL B567 273	A. Datta, P.J. O'Donnell	

See key on page 373

Meson Particle Listings

 $\phi_3(1850), \eta_2(1870), \pi_2(1880)$

$\phi_3(1850)$		$I^G(J^{PC}) = 0^-(3^{--})$	
$\phi_3(1850)$ MASS			
VALUE (MeV)	EVTS	DOCUMENT ID	TECN COMMENT
1854 ± 7 OUR AVERAGE			
1855 ± 10		ASTON	88E LASS 11 $K^- p \rightarrow K^- K^+ \Lambda, K_S^0 K^\pm \pi^\mp \Lambda$
1870 ⁺³⁰ ₋₂₀	430	ARMSTRONG	82 OMEG 18.5 $K^- p \rightarrow K^- K^+ \Lambda$
1850 ± 10	123	ALHARRAN	81B HBC 8.25 $K^- p \rightarrow K \bar{K} \Lambda$
$\phi_3(1850)$ WIDTH			
VALUE (MeV)	EVTS	DOCUMENT ID	TECN COMMENT
87⁺²⁸₋₂₃ OUR AVERAGE Error includes scale factor of 1.2.			
64 ± 31		ASTON	88E LASS 11 $K^- p \rightarrow K^- K^+ \Lambda, K_S^0 K^\pm \pi^\mp \Lambda$
160 ⁺⁹⁰ ₋₅₀	430	ARMSTRONG	82 OMEG 18.5 $K^- p \rightarrow K^- K^+ \Lambda$
80 ⁺⁴⁰ ₋₃₀	123	ALHARRAN	81B HBC 8.25 $K^- p \rightarrow K \bar{K} \Lambda$
$\phi_3(1850)$ DECAY MODES			
Mode	Fraction (Γ_i/Γ)		
Γ_1 $K \bar{K}$	seen		
Γ_2 $K \bar{K}^*(892) + c.c.$	seen		
$\phi_3(1850)$ BRANCHING RATIOS			
$\Gamma(K \bar{K}^*(892) + c.c.)/\Gamma(K \bar{K})$		Γ_2/Γ_1	
VALUE	DOCUMENT ID	TECN	COMMENT
0.55^{+0.85}_{-0.45}	ASTON	88E LASS	11 $K^- p \rightarrow K^- K^+ \Lambda, K_S^0 K^\pm \pi^\mp \Lambda$
• • • We do not use the following data for averages, fits, limits, etc. • • •			
0.8 ± 0.4	ALHARRAN	81B HBC	8.25 $K^- p \rightarrow K \bar{K} \Lambda$

 $\phi_3(1850)$ REFERENCES

ASTON	88E	PL B208 324	D. Aston <i>et al.</i>	(SLAC, NAGO, CINC, INUS)IGJPC
ARMSTRONG	82	PL 110B 77	T.A. Armstrong <i>et al.</i>	(BARI, BIRM, CERN+)JP
ALHARRAN	81B	PL 101B 357	S. Al-Harran <i>et al.</i>	(BIRM, CERN, GLAS+)

OTHER RELATED PAPERS

CORDIER	82B	PL 110B 335	A. Cordier <i>et al.</i>	(LALO)
ASTON	80B	PL 92B 219	D. Aston	(BONN, CERN, EPOL, GLAS, LANC+)

$\eta_2(1870)$		$I^G(J^{PC}) = 0^+(2^{-+})$	
OMITTED FROM SUMMARY TABLE			
Needs confirmation.			

 $\eta_2(1870)$ MASS

VALUE (MeV)	EVTS	DOCUMENT ID	TECN	CHG	COMMENT
1842 ± 8 OUR AVERAGE					
1835 ± 12		BARBERIS	00B		450 $pp \rightarrow \rho_f \eta \pi^+ \pi^- p_S$
1844 ± 13		BARBERIS	00C		450 $pp \rightarrow \rho_f 4\pi p_S$
1840 ± 25		BARBERIS	97B OMEG		450 $pp \rightarrow pp2(\pi^+ \pi^-)$
1875 ± 20 ± 35		ADOMEIT	96 CBAR 0		1.94 $\bar{p}p \rightarrow \eta 3\pi^0$
1881 ± 32 ± 40	26	KARCH	92 CBAL		$e^+ e^- \rightarrow e^+ e^- \eta \pi^0 \pi^0$
• • • We do not use the following data for averages, fits, limits, etc. • • •					
1860 ± 5 ± 15		ANISOVICH	00E SPEC		1.94 $\bar{p}p \rightarrow \eta 3\pi^0$
1840 ± 15		BAI	99 BES		$J/\psi \rightarrow \gamma \eta \pi^+ \pi^-$

 $\eta_2(1870)$ WIDTH

VALUE (MeV)	EVTS	DOCUMENT ID	TECN	CHG	COMMENT
225 ± 14 OUR AVERAGE					
235 ± 22		BARBERIS	00B		450 $pp \rightarrow \rho_f \eta \pi^+ \pi^- p_S$
228 ± 23		BARBERIS	00C		450 $pp \rightarrow \rho_f 4\pi p_S$
200 ± 40		BARBERIS	97B OMEG		450 $pp \rightarrow pp2(\pi^+ \pi^-)$
200 ± 25 ± 45		ADOMEIT	96 CBAR 0		1.94 $\bar{p}p \rightarrow \eta 3\pi^0$
221 ± 92 ± 44	26	KARCH	92 CBAL		$e^+ e^- \rightarrow e^+ e^- \eta \pi^0 \pi^0$
• • • We do not use the following data for averages, fits, limits, etc. • • •					
250 ± 25 ⁺⁵⁰ ₋₃₅		ANISOVICH	00E SPEC		1.94 $\bar{p}p \rightarrow \eta 3\pi^0$
170 ± 40		BAI	99 BES		$J/\psi \rightarrow \gamma \eta \pi^+ \pi^-$

 $\eta_2(1870)$ DECAY MODES

Mode					
Γ_1 $\eta \pi \pi$					
Γ_2 $a_2(1320) \pi$					
Γ_3 $f_2(1270) \eta$					
Γ_4 $a_0(980) \pi$					

 $\eta_2(1870)$ BRANCHING RATIOS

$\Gamma(a_2(1320)\pi)/\Gamma(f_2(1270)\eta)$		Γ_2/Γ_3			
VALUE	DOCUMENT ID	TECN	CHG COMMENT		
6 ± 5 OUR AVERAGE Error includes scale factor of 2.3.					
20.4 ± 6.6	BARBERIS	00B	450 $pp \rightarrow \rho_f \eta \pi^+ \pi^- p_S$		
4.1 ± 2.3	ADOMEIT	96 CBAR 0	1.94 $\bar{p}p \rightarrow \eta 3\pi^0$		
$\Gamma(a_2(1320)\pi)/\Gamma(a_0(980)\pi)$		Γ_2/Γ_4			
VALUE	DOCUMENT ID	COMMENT			
32.6 ± 12.6	BARBERIS	00B	450 $pp \rightarrow \rho_f \eta \pi^+ \pi^- p_S$		

 $\eta_2(1870)$ REFERENCES

ANISOVICH	00E	PL B477 19	A.V. Anisovich <i>et al.</i>	
BARBERIS	00B	PL B471 435	D. Barberis <i>et al.</i>	(WA 102 Collab.)
BARBERIS	00C	PL B471 440	D. Barberis <i>et al.</i>	(WA 102 Collab.)
BAI	99	PL B446 356	J.Z. Bai <i>et al.</i>	(BES Collab.)
BARBERIS	97B	PL B413 217	D. Barberis <i>et al.</i>	(WA 102 Collab.)
ADOMEIT	96	ZPHY C71 227	J. Adomeit <i>et al.</i>	(Crystal Barrel Collab.)
KARCH	92	ZPHY C54 33	K. Karch <i>et al.</i>	(Crystal Ball Collab.)

OTHER RELATED PAPERS

KARCH	90	PL B249 353	K. Karch <i>et al.</i>	(Crystal Ball Collab.)
-------	----	-------------	------------------------	------------------------

$\pi_2(1880)$		$I^G(J^{PC}) = 1^-(2^{-+})$	
---------------	--	-----------------------------	--

 $\pi(1880)$ MASS

VALUE (MeV)	EVTS	DOCUMENT ID	TECN	CHG	COMMENT
1895 ± 16 OUR AVERAGE					
1929 ± 24 ± 18	4k	EUGENIO	08 B852	-	18 $\pi^- p \rightarrow \eta \eta \pi^- p$
1876 ± 11 ± 67	145k	LU	05 B852	-	18 $\pi^- p \rightarrow \omega \pi^- \pi^0 p$
2003 ± 88 ± 148	69k	KUHN	04 B852	-	18 $\pi^- p \rightarrow \eta \pi^+ \pi^- \pi^- p$
1880 ± 20		ANISOVICH	01B SPEC	0	0.6-1.94 $\bar{p}p \rightarrow \eta \eta \pi^0 \pi^0$

 $\pi(1880)$ WIDTH

VALUE (MeV)	EVTS	DOCUMENT ID	TECN	CHG	COMMENT
235 ± 34 OUR AVERAGE					
323 ± 87 ± 43	4k	EUGENIO	08 B852	-	18 $\pi^- p \rightarrow \eta \eta \pi^- p$
146 ± 17 ± 62	145k	LU	05 B852	-	18 $\pi^- p \rightarrow \omega \pi^- \pi^0 p$
306 ± 132 ± 121	69k	KUHN	04 B852	-	18 $\pi^- p \rightarrow \eta \pi^+ \pi^- \pi^- p$
255 ± 45		ANISOVICH	01B SPEC	0	0.6-1.94 $\bar{p}p \rightarrow \eta \eta \pi^0 \pi^0$

Meson Particle Listings

 $\pi_2(1880)$, $\rho(1900)$, $f_2(1910)$ $\pi_2(1880)$ DECAY MODES

Mode	
Γ_1	$\eta\eta\pi^-$
Γ_2	$a_0(980)\eta$
Γ_3	$a_2(1320)\eta$
Γ_4	$f_0(1500)\pi$
Γ_5	$f_1(1285)\pi$
Γ_6	$\omega\pi^-\pi^0$

 $\Gamma(a_2(1320)\eta)/\Gamma(f_1(1285)\pi)$ Γ_3/Γ_5

VALUE	EVTs	DOCUMENT ID	TECN	CHG	COMMENT
22.7 ± 7.3	69k	KUHN	04	B852	- $18\pi^-\rho \rightarrow \eta\pi^+\pi^-\pi^-\rho$

 $\Gamma(f_0(1500)\pi)/\Gamma(a_0(980)\eta)$ Γ_4/Γ_2

VALUE	DOCUMENT ID	TECN	CHG	COMMENT
$0.28^{+0.20}_{-0.15}$	¹ ANISOVICH 01B	SPEC	0	$0.6-1.94 \bar{p}p \rightarrow \eta\eta\pi^0\pi^0$

¹ Systematic errors not estimated.

 $\pi_2(1880)$ REFERENCES

EUGENIO	08	PL B660 466	P. Eugenio et al.	(BNL E852 Collab.)
LU	05	PRL 94 032002	M. Lu et al.	(BNL E852 Collab.)
KUHN	04	PL B595 109	J. Kuhn et al.	(BNL E852 Collab.)
ANISOVICH	01B	PL B500 222	A.V. Anisovich et al.	

 $\rho(1900)$

$$I^G(J^{PC}) = 1^+(1^{--})$$

OMITTED FROM SUMMARY TABLE

 $\rho(1900)$ MASS

VALUE (MeV)	EVTs	DOCUMENT ID	TECN	COMMENT
$1909 \pm 17 \pm 25$	54	¹ AUBERT 08s	BABR	$10.6 e^+e^- \rightarrow \phi\pi^0\gamma$
1880 ± 30		AUBERT 06d	BABR	$10.6 e^+e^- \rightarrow 3\pi^+3\pi^-\gamma$
1860 ± 20		AUBERT 06d	BABR	$10.6 e^+e^- \rightarrow 2(\pi^+\pi^-\pi^0)\gamma$
1910 ± 10		^{2,3} FRABETTI 04	E687	$\gamma p \rightarrow 3\pi^+3\pi^-\rho$
1870 ± 10		ANTONELLI 96	SPEC	$e^+e^- \rightarrow$ hadrons

- ¹ From the fit with two resonances.
² From a fit with two resonances with the JACOB 72 continuum.
³ Supersedes FRABETTI 01.

 $\rho(1900)$ WIDTH

VALUE (MeV)	EVTs	DOCUMENT ID	TECN	COMMENT
$48 \pm 17 \pm 2$	54	⁴ AUBERT 08s	BABR	$10.6 e^+e^- \rightarrow \phi\pi^0\gamma$
130 ± 30		AUBERT 06d	BABR	$10.6 e^+e^- \rightarrow 3\pi^+3\pi^-\gamma$
160 ± 20		AUBERT 06d	BABR	$10.6 e^+e^- \rightarrow 2(\pi^+\pi^-\pi^0)\gamma$
37 ± 13		^{5,6} FRABETTI 04	E687	$\gamma p \rightarrow 3\pi^+3\pi^-\rho$
10 ± 5		ANTONELLI 96	SPEC	$e^+e^- \rightarrow$ hadrons

- ⁴ From the fit with two resonances.
⁵ From a fit with two resonances with the JACOB 72 continuum.
⁶ Supersedes FRABETTI 01.

 $\rho(1900)$ $\Gamma(i)\Gamma(e^+e^-)/\Gamma^2(\text{total})$

VALUE (units 10^{-8})	EVTs	DOCUMENT ID	TECN	COMMENT
$4.2 \pm 1.2 \pm 0.8$	54	⁷ AUBERT 08s	BABR	$10.6 e^+e^- \rightarrow \phi\pi^0\gamma$

- ⁷ From the fit with two resonances.

 $\rho(1900)$ DECAY MODES

Mode	Fraction (Γ_i/Γ)
Γ_1	6π seen
Γ_2	$3\pi^+3\pi^-$ seen
Γ_3	$2\pi^+2\pi^-2\pi^0$
Γ_4	$\phi\pi$
Γ_5	hadrons seen
Γ_6	e^+e^- seen
Γ_7	$N\bar{N}$ not seen

 $\rho(1900)$ BRANCHING RATIOS

$\Gamma(6\pi)/\Gamma_{\text{total}}$	VALUE	DOCUMENT ID	TECN	COMMENT	Γ_1/Γ
not seen		AGNELLO 02	OBLX	$\bar{p}p \rightarrow 3\pi^+2\pi^-\pi^0$	
seen		FRABETTI 01	E687	$\gamma p \rightarrow 3\pi^+3\pi^-\rho$	
seen		ANTONELLI 96	SPEC	$e^+e^- \rightarrow$ hadrons	

 $\rho(1900)$ REFERENCES

AUBERT	08s	PR D77 092002	B. Aubert et al.	(BABAR Collab.)
AUBERT	06d	PR D73 052003	B. Aubert et al.	(BABAR Collab.)
FRABETTI	04	PL B578 290	PL Frabetti et al.	(FNAL E687 Collab.)
AGNELLO	02	PL B527 39	M. Agnello et al.	(OBELIX Collab.)
FRABETTI	01	PL B514 240	P.L. Frabetti et al.	(FNAL E687 Collab.)
ANTONELLI	96	PL B365 427	A. Antonelli et al.	(FENICE Collab.)
JACOB	72	PR D5 1847	M. Jacob, R. Slansky	

OTHER RELATED PAPERS

DATTA	03B	PL B567 273	A. Datta, P.J. O'Donnell	
PAGE	99	PR D59 034016	P.R. Page, E.S. Swanson, A.P. Szczepaniak	
CLEGG	90	ZPHY C45 677	A.B. Clegg, A. Donnachie	(LANC, MCHS)
CASTRO	88	Preprint LAL-88-58	A. Castro et al.	(DM2 Collab.)

 $f_2(1910)$

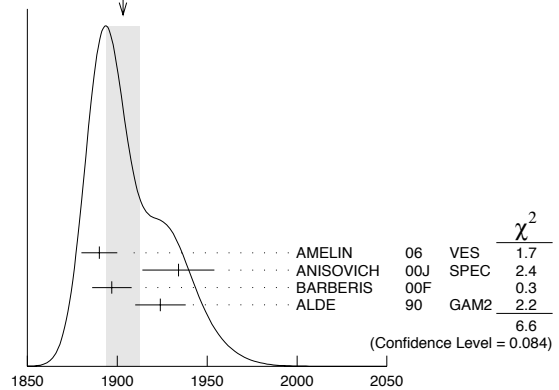
$$I^G(J^{PC}) = 0^+(2^{++})$$

OMITTED FROM SUMMARY TABLE

We list here three different peaks with close masses and widths seen in the mass distributions of $\omega\omega$, $\eta\eta'$, and K^+K^- final states. ALDE 91B argues that they are of different nature.

 $f_2(1910)$ MASS $f_2(1910)$ $\omega\omega$ MODE

VALUE (MeV)	DOCUMENT ID	TECN	COMMENT
1903 ± 9 OUR AVERAGE	Error includes scale factor of 1.5. See the ideogram below.		
1890 ± 10	¹ AMELIN 06	VES	$36\pi^-\rho \rightarrow \omega\omega n$
1934 ± 20	ANISOVICH 00j	SPEC	
1897 ± 11	BARBERIS 00F		$450 p\rho \rightarrow p_f\omega\omega p_s$
1924 ± 14	ALDE 90	GAM2	$38\pi^-\rho \rightarrow \omega\omega n$

¹ Supersedes BELADIDZE 92b.WEIGHTED AVERAGE
1903±9 (Error scaled by 1.5) $f_2(1910)$ $\omega\omega$ MODE MASS (MeV) $f_2(1910)$ $\eta\eta'$ MODE

VALUE (MeV)	DOCUMENT ID	TECN	COMMENT
1934 ± 16	² BARBERIS 00A		$450 p\rho \rightarrow p_f\eta\eta' p_s$

² Also compatible with $J^{PC}=1^-+$.

 $f_2(1910)$ K^+K^- MODE

VALUE (MeV)	DOCUMENT ID	TECN	COMMENT
1941 ± 18	AMSLER 06	CBAR	$1.64 \bar{p}p \rightarrow K^+K^-\pi^0$

See key on page 373

Meson Particle Listings

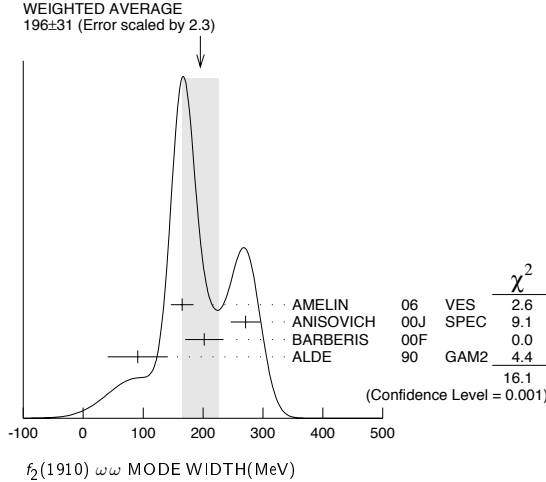
$f_2(1910)$, $f_2(1950)$

$f_2(1910)$ WIDTH

$f_2(1910)$ $\omega\omega$ MODE

VALUE (MeV)	DOCUMENT ID	TECN	COMMENT
196±31 OUR AVERAGE	Error includes scale factor of 2.3. See the ideogram below.		
165±19	³ AMELIN	06 VES	36 $\pi^- p \rightarrow \omega\omega n$
271±25	ANISOVICH	00J SPEC	
202±32	BARBERIS	00F	450 $pp \rightarrow p_f \omega \rho_S$
91±5.0	ALDE	90 GAM2	38 $\pi^- p \rightarrow \omega\omega n$

³ Supersedes BELADIDZE 92b.



$f_2(1910)$ $\eta\eta'$ MODE

VALUE (MeV)	DOCUMENT ID	TECN	COMMENT
141±41	⁴ BARBERIS	00A	450 $pp \rightarrow p_f \eta \eta' \rho_S$
90±35	ALDE	91B GAM2	38 $\pi^- p \rightarrow \eta \eta' n$

⁴ Also compatible with $J^{PC}=1^-+$.

$f_2(1910)$ K^+K^- MODE

VALUE (MeV)	DOCUMENT ID	TECN	COMMENT
120±4.0	AMSLER	06 CBAR	1.64 $\bar{p}p \rightarrow K^+ K^- \pi^0$

$f_2(1910)$ DECAY MODES

Mode	Fraction (Γ_i/Γ)
Γ_1 $\pi^0 \pi^0$	
Γ_2 $K^+ K^-$	seen
Γ_3 $K_S^0 K_S^0$	
Γ_4 $\eta\eta$	seen
Γ_5 $\omega\omega$	seen
Γ_6 $\eta\eta'$	seen
Γ_7 $\eta'\eta'$	
Γ_8 $\rho\rho$	seen

$f_2(1910)$ BRANCHING RATIOS

$\Gamma(K^+K^-)/\Gamma_{total}$	Γ_2/Γ
seen	AMSLER 06 CBAR 1.64 $\bar{p}p \rightarrow K^+ K^- \pi^0$

$\Gamma(\pi^0 \pi^0)/\Gamma(\eta\eta')$	Γ_1/Γ_6
<0.1	ALDE 89 GAM2 38 $\pi^- p \rightarrow \eta \eta' n$

$\Gamma(K_S^0 K_S^0)/\Gamma(\eta\eta')$	Γ_3/Γ_6
<0.066	90 BALOSHIN 86 SPEC 40 $\pi p \rightarrow K_S^0 K_S^0 n$

$\Gamma(\eta)/\Gamma(\eta\eta')$	Γ_4/Γ_6
<0.05	90 ALDE 91B GAM2 38 $\pi^- p \rightarrow \eta \eta' n$

$\Gamma(\omega\omega)/\Gamma(\eta\eta')$

VALUE	DOCUMENT ID	COMMENT	Γ_5/Γ_6
2.6±0.6	BARBERIS 00F	450 $pp \rightarrow p_f \omega \rho_S$	

$\Gamma(\eta'\eta')/\Gamma_{total}$

VALUE	DOCUMENT ID	TECN	COMMENT	Γ_7/Γ
probably not seen	BARBERIS 00A		450 $pp \rightarrow p_f \eta' \eta' \rho_S$	
possibly seen	BELADIDZE 92D	VES	37 $\pi^- p \rightarrow \eta' \eta' n$	

$\Gamma(\rho\rho)/\Gamma(\omega\omega)$

VALUE	DOCUMENT ID	COMMENT	Γ_8/Γ_5
2.6±0.4	BARBERIS 00F	450 $pp \rightarrow p_f \omega \rho_S$	

$f_2(1910)$ REFERENCES

AMELIN 06	PAN 69 690	D.V. Amelin et al.	(VES Collab.)
AMSLER 06	PL B639 165	Translated from YAF 69 715	(CBAR Collab.)
ANISOVICH 00J	PL B491 47	A.V. Anisovich et al.	
BARBERIS 00A	PL B471 429	D. Barberis et al.	(WA 102 Collab.)
BARBERIS 00F	PL B484 198	D. Barberis et al.	(WA 102 Collab.)
BELADIDZE 92B	ZPHY C54 367	G.M. Beladidze et al.	(VES Collab.)
BELADIDZE 92D	ZPHY C57 13	G.M. Beladidze et al.	(VES Collab.)
ALDE 91B	SJNP 54 455	D.M. Alde et al.	(SERP, BELG, LANL, LAPP+)
	Translated from YAF 54 751		
	PL B276 375	D.M. Alde et al.	(BELG, SERP, KEK, LANL+)
ALDE 90	PL B241 600	D.M. Alde et al.	(SERP, BELG, LANL, LAPP+)
ALDE 89	PL B216 447	D.M. Alde et al.	(SERP, BELG, LANL, LAPP)
	Also SJNP 48 1035	D.M. Alde et al.	(BELG, SERP, LANL, LAPP)
BALOSHIN 86	SJNP 43 959	O.N. Baloshin et al.	(ITEP)
	Translated from YAF 43 1487		

OTHER RELATED PAPERS

ABLIKIM 06H	PR D73 112007	M. Ablikim et al.	(BES Collab.)
ANISOVICH 05	JETPL 80 715	V.V. Anisovich	
	Translated from ZETFP 80 845		
ANISOVICH 05A	JETPL 81 417	V.V. Anisovich, A.V. Sarantsev	
	Translated from ZETFP 81 531		
ANISOVICH 05C	IJMP A20 6327	V.V. Anisovich, M.A. Matveev, A.V. Sarantsev	
LEE 94	PL B323 227	J.H. Lee et al.	(BNL, IND, KYUN, MASD+)

$f_2(1950)$

$$J^G(J^{PC}) = 0^+(2^{++})$$

$f_2(1950)$ MASS

VALUE (MeV)	DOCUMENT ID	TECN	CHG	COMMENT
1944±12 OUR AVERAGE	Error includes scale factor of 1.5. See the ideogram below.			
1930±25	¹ BINON	05 GAMS		33 $\pi^- p \rightarrow \eta \eta n$
2010±25	ANISOVICH	00J SPEC		
1940±5.0	BAI	00A BES		$J/\psi \rightarrow \gamma(\pi^+ \pi^- \pi^+ \pi^-)$
1980±22	² BARBERIS	00c		450 $pp \rightarrow pp4\pi$
1940±22	³ BARBERIS	00c		450 $pp \rightarrow pp2\pi 2\pi^0$
1980±5.0	ANISOVICH	99B SPEC		1.35-1.94 $\bar{p}p \rightarrow \eta \eta \pi^0$
1960±30	BARBERIS	97B OMEG		450 $pp \rightarrow pp2(\pi^+ \pi^-)$
1918±12	ANTINORI	95 OMEG		300,450 $pp \rightarrow \rho\rho 2(\pi^+ \pi^-)$

• • • We do not use the following data for averages, fits, limits, etc. • • •

1980± 2±14	ABE	04 BELL		10.6 $e^+ e^- \rightarrow e^+ e^- K^+ K^-$
1867±46	⁴ AMSLER	02 CBAR		0.9 $\bar{p}p \rightarrow \pi^0 \eta \eta, \pi^0 \pi^0 \pi^0$
~ 1996	HASAN	94 RVUE		$\bar{p}p \rightarrow \pi \pi$
~ 1990	⁵ OAKDEN	94 RVUE		0.36-1.55 $\bar{p}p \rightarrow \pi \pi$
1950±15	⁶ ASTON	91 LASS 0		11 $K^- p \rightarrow \Lambda K \bar{K} \pi \pi$

¹ First solution, PWA is ambiguous.

² Decaying into $\pi^+ \pi^- 2\pi^0$.

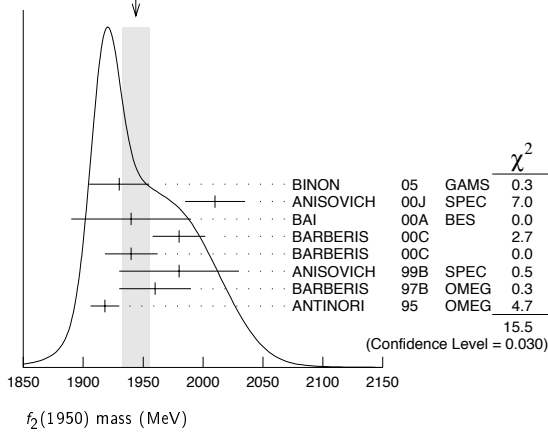
³ Decaying into $2(\pi^+ \pi^-)$.

⁴ T-matrix pole.

⁵ From solution B of amplitude analysis of data on $\bar{p}p \rightarrow \pi \pi$. See however KLOET 96 who fit $\pi^+ \pi^-$ only and find waves only up to $J=3$ to be important but not significantly resonant.

⁶ Cannot determine spin to be 2.

Meson Particle Listings

 $f_2(1950), \rho_3(1990)$ WEIGHTED AVERAGE
1944±12 (Error scaled by 1.5) $f_2(1950)$ WIDTH

VALUE (MeV)	DOCUMENT ID	TECN	CHG	COMMENT
472±18 OUR AVERAGE				
450±50	⁷ BINON 05	GAMS		33 $\pi^- p \rightarrow \eta\eta n$
495±35	ANISOVICH 00J	SPEC		
380 ⁺¹²⁰ ₋₉₀	BAI 00A	BES		$J/\psi \rightarrow \gamma(\pi^+\pi^-\pi^+\pi^-)$
520±50	⁸ BARBERIS 00C			450 $pp \rightarrow pp4\pi$
485±55	⁹ BARBERIS 00C			450 $pp \rightarrow pp4\pi$
500±100	ANISOVICH 99B	SPEC		1.35-1.94 $p\bar{p} \rightarrow \eta\eta\pi^0$
460±40	BARBERIS 97B	OMEG		450 $pp \rightarrow pp2(\pi^+\pi^-)$
390±60	ANTINORI 95	OMEG		300,450 $pp \rightarrow pp2(\pi^+\pi^-)$
••• We do not use the following data for averages, fits, limits, etc. •••				
297±12±6	ABE 04	BELL		10.6 $e^+e^- \rightarrow e^+e^-K^+K^-$
385±58	¹⁰ AMSLER 02	CBAR		0.9 $\bar{p}p \rightarrow \pi^0\eta\eta, \pi^0\pi^0\pi^0$
~134	HASAN 94	RVUE		$\bar{p}p \rightarrow \pi\pi$
~100	¹¹ OAKDEN 94	RVUE		0.36-1.55 $\bar{p}p \rightarrow \pi\pi$
250±50	¹² ASTON 91	LASS	0	11 $K^-p \rightarrow \Lambda K\bar{K}\pi\pi$

⁷ First solution, PWA is ambiguous.
⁸ Decaying into $\pi^+\pi^-\pi^0$.
⁹ Decaying into $2(\pi^+\pi^-)$.
¹⁰ T-matrix pole.
¹¹ From solution B of amplitude analysis of data on $\bar{p}p \rightarrow \pi\pi$. See however KLOET 96 who fit $\pi^+\pi^-$ only and find waves only up to $J=3$ to be important but not significantly resonant.
¹² Cannot determine spin to be 2.

 $f_2(1950)$ DECAY MODES

Mode	Fraction (Γ_i/Γ)
Γ_1 $K^*(892)\bar{K}^*(892)$	seen
Γ_2 $\pi^+\pi^-$	seen
Γ_3 4π	seen
Γ_4 $\pi^+\pi^-\pi^+\pi^-$	
Γ_5 $a_2(1320)\pi$	
Γ_6 $f_2(1270)\pi\pi$	
Γ_7 $\eta\eta$	seen
Γ_8 $K\bar{K}$	seen
Γ_9 $\gamma\gamma$	seen

 $f_2(1950)$ $\Gamma(i)\Gamma(\gamma\gamma)/\Gamma(\text{total})$

VALUE (eV)	DOCUMENT ID	TECN	CHG	COMMENT	$\Gamma_8\Gamma_9/\Gamma$
••• We do not use the following data for averages, fits, limits, etc. •••					
122±4±26	¹³ ABE 04	BELL		10.6 $e^+e^- \rightarrow e^+e^-K^+K^-$	

¹³ Assuming spin 2.

 $f_2(1950)$ BRANCHING RATIOS

VALUE	DOCUMENT ID	TECN	CHG	COMMENT	Γ_1/Γ
seen	ASTON 91	LASS	0	11 $K^-p \rightarrow \Lambda K\bar{K}\pi\pi$	

 $\Gamma(a_2(1320)\pi)/\Gamma_{\text{total}}$

VALUE	DOCUMENT ID	TECN	COMMENT	Γ_5/Γ
••• We do not use the following data for averages, fits, limits, etc. •••				
not seen	BARBERIS 00B		450 $pp \rightarrow p_f\eta\pi^+\pi^-\rho_3$	
not seen	BARBERIS 00C		450 $pp \rightarrow p_f4\pi\rho_3$	
possibly seen	BARBERIS 97B	OMEG	450 $pp \rightarrow p_f2(\pi^+\pi^-)$	

 $\Gamma(\eta\eta)/\Gamma(4\pi)$

VALUE	CL%	DOCUMENT ID	COMMENT	Γ_7/Γ_3
••• We do not use the following data for averages, fits, limits, etc. •••				
<5.0 × 10 ⁻³	90	BARBERIS 00E	450 $pp \rightarrow p_f\eta\eta\rho_3$	

 $\Gamma(\eta\eta)/\Gamma(\pi^+\pi^-)$

VALUE	DOCUMENT ID	TECN	COMMENT	Γ_7/Γ_2
••• We do not use the following data for averages, fits, limits, etc. •••				
0.14±0.05	AMSLER 02	CBAR	0.9 $\bar{p}p \rightarrow \pi^0\eta\eta, \pi^0\pi^0\pi^0$	

 $f_2(1950)$ REFERENCES

BINON 05	PAN 68 960	F. Binon et al.	
ABE 04	EPJ C32 323	K. Abe et al.	(BELLE Collab.)
AMSLER 02	EPJ C23 29	C. Amisler et al.	
ANISOVICH 00J	PL B491 47	A.V. Anisovich et al.	
BAI 00A	PL B472 207	J.Z. Bai et al.	(BES Collab.)
BARBERIS 00B	PL B471 435	D. Barberis et al.	(WA 102 Collab.)
BARBERIS 00C	PL B471 440	D. Barberis et al.	(WA 102 Collab.)
BARBERIS 00E	PL B479 59	D. Barberis et al.	(WA 102 Collab.)
ANISOVICH 99B	PL B449 154	A.V. Anisovich et al.	
BARBERIS 97B	PL B413 217	D. Barberis et al.	(WA 102 Collab.)
KLOET 96	PR D53 6120	W.J.M. Kloet, F. Myhrer	(RUTG. NORD)
ANTINORI 95	PL B353 589	F. Antinori et al.	(ATHU, BARI, BIRM+JP)
HASAN 94	PL B334 215	A. Hasan, D.V. Bugg	(LOQM)
OAKDEN 94	NP A574 731	M.N. Oakden, M.R. Pennington	(DURH)
ASTON 91	NPBPS B21 5	D. Aston et al.	(LASS Collab.)

OTHER RELATED PAPERS

ANISOVICH 05	JETPL 80 715	V.V. Anisovich	
	Translated from ZETFP 80 845		
ANISOVICH 05A	JETPL 81 417	V.V. Anisovich, A.V. Sarantsev	
	Translated from ZETFP 81 531		
ANISOVICH 05C	IJMP A20 6327	V.V. Anisovich, M.A. Matveev, A.V. Sarantsev	
LONGACRE 04	PR D70 094041	R.S. Longacre, S.J. Lindenbaum	
ALBRECHT 88N	PL B212 528	H. Albrecht et al.	(ARGUS Collab.)
ALBRECHT 87Q	PL B198 255	H. Albrecht et al.	(ARGUS Collab.)
ARMSTRONG 87C	ZPHY C34 33	T.A. Armstrong et al.	(CERN, BIRM, BARI+)

 $\rho_3(1990)$

$$I^G(J^{PC}) = 1^+(3^{--})$$

OMITTED FROM SUMMARY TABLE

 $\rho_3(1990)$ MASS

VALUE (MeV)	DOCUMENT ID	TECN	COMMENT
••• We do not use the following data for averages, fits, limits, etc. •••			
1982±14	¹ ANISOVICH 02	SPEC	0.6-1.9 $p\bar{p} \rightarrow \omega\pi^0, \omega\eta\pi^0, \pi^+\pi^-$
~2007	HASAN 94		

¹ From the combined analysis of ANISOVICH 00J, ANISOVICH 01D, ANISOVICH 01E, and ANISOVICH 02.

 $\rho_3(1990)$ WIDTH

VALUE (MeV)	DOCUMENT ID	TECN	COMMENT
••• We do not use the following data for averages, fits, limits, etc. •••			
188±24	² ANISOVICH 02	SPEC	0.6-1.9 $p\bar{p} \rightarrow \omega\pi^0, \omega\eta\pi^0, \pi^+\pi^-$
~267	HASAN 94		

² From the combined analysis of ANISOVICH 00J, ANISOVICH 01D, ANISOVICH 01E, and ANISOVICH 02.

 $\rho_3(1990)$ REFERENCES

ANISOVICH 02	PL B542 8	A.V. Anisovich et al.	
ANISOVICH 01D	PL B508 6	A.V. Anisovich et al.	
ANISOVICH 01E	PL B513 281	A.V. Anisovich et al.	
ANISOVICH 00J	PL B491 47	A.V. Anisovich et al.	
HASAN 94	PL B334 215	A. Hasan, D.V. Bugg	(LOQM)

OTHER RELATED PAPERS

BUGG 07	EPJ C52 55	D. Bugg	
---------	------------	---------	--

See key on page 373

Meson Particle Listings

$f_2(2010)$, $f_0(2020)$, $a_4(2040)$

$f_2(2010)$

$$I^G(J^{PC}) = 0^+(2^{++})$$

$f_2(2010)$ MASS					
VALUE (MeV)	DOCUMENT ID	TECN	COMMENT		
2011 ± 62 76	1	ETKIN	88	MPS	22 $\pi^- p \rightarrow \phi \phi n$
• • • We do not use the following data for averages, fits, limits, etc. • • •					
2005 ± 12		VLADIMIRSK...06		SPEC	40 $\pi^- p \rightarrow K_S^0 K_S^0 n$
1980 ± 20	2	BOLONKIN	88	SPEC	40 $\pi^- p \rightarrow K_S^0 K_S^0 n$
2050 ± 90 50		ETKIN	85	MPS	22 $\pi^- p \rightarrow 2\phi n$
2120 ± 20 120		LINDENBAUM	84	RVUE	
2160 ± 50		ETKIN	82	MPS	22 $\pi^- p \rightarrow 2\phi n$

¹ Includes data of ETKIN 85. The percentage of the resonance going into $\phi\phi$ $2^+ + S_2$, D_2 , and D_0 is 98^{+1}_-3 , 0^{+1}_-0 , and 2^{+2}_-1 , respectively.
² Statistically very weak, only 1.4 s.d.

$f_2(2010)$ WIDTH					
VALUE (MeV)	DOCUMENT ID	TECN	COMMENT		
202 ± 67 62	3	ETKIN	88	MPS	22 $\pi^- p \rightarrow \phi \phi n$
• • • We do not use the following data for averages, fits, limits, etc. • • •					
209 ± 32		VLADIMIRSK...06		SPEC	40 $\pi^- p \rightarrow K_S^0 K_S^0 n$
145 ± 50	4	BOLONKIN	88	SPEC	40 $\pi^- p \rightarrow K_S^0 K_S^0 n$
200 ± 160 50		ETKIN	85	MPS	22 $\pi^- p \rightarrow 2\phi n$
300 ± 150 50		LINDENBAUM	84	RVUE	
310 ± 70		ETKIN	82	MPS	22 $\pi^- p \rightarrow 2\phi n$

³ Includes data of ETKIN 85.
⁴ Statistically very weak, only 1.4 s.d.

$f_2(2010)$ DECAY MODES		
Mode	Fraction (Γ_i/Γ)	
Γ_1 $\phi\phi$	seen	
Γ_2 $K\bar{K}$	seen	

$f_2(2010)$ BRANCHING RATIOS			
$\Gamma(K\bar{K})/\Gamma_{total}$	DOCUMENT ID	TECN	COMMENT
seen	VLADIMIRSK...06	SPEC	40 $\pi^- p \rightarrow K_S^0 K_S^0 n$

$f_2(2010)$ REFERENCES				
VLADIMIRSK... 06	PAN 69 493	V.V. Vladimirov et al.		(ITEP, Moscow)
	Translated from YAF 69 515			
BOLONKIN 88	NP B309 426	B.V. Bolonkin et al.		(ITEP, SERP)
ETKIN 88	PL B201 568	A. Etkin et al.		(BNL, CUNY)
ETKIN 85	PL 165B 217	A. Etkin et al.		(BNL, CUNY)
LINDENBAUM 84	CNPP 13 285	S.J. Lindenbaum		(CUNY)
ETKIN 82	PRL 49 1620	A. Etkin et al.		(BNL, CUNY)
	Also Brighton Conf. 351	S.J. Lindenbaum		(BNL, CUNY)

OTHER RELATED PAPERS				
ANISOVICH 05	JETPL 80 715	V.V. Anisovich		
	Translated from ZETFP 80 845			
ANISOVICH 05A	JETPL 81 417	V.V. Anisovich, A.V. Sarantsev		
	Translated from ZETFP 81 531			
ANISOVICH 05C	IMP A20 6327	V.V. Anisovich, M.A. Matveev, A.V. Sarantsev		
LONGACRE 04	PR D70 094041	R.S. Longacre, S.J. Lindenbaum		
ANISOVICH 99D	PL B452 180	A.V. Anisovich et al.		
	Also NP A651 253	A.V. Anisovich et al.		
ANISOVICH 99F	NP A651 253	A.V. Anisovich et al.		
LANDBERG 96	PR D53 2839	C. Landberg et al.		(BNL, CUNY, RPI)
GREEN 86	PRL 56 1639	D.R. Green et al.		(FNAL, ARIZ, FSU+)
BOOTH 84	NP B242 51	P.S.L. Booth et al.		(LIVP, GLAS, CERN)
EISENHAND... 75	NP B96 109	E. Eisenhandler et al.		(LOQM, LIVP, DARE+)

$f_0(2020)$

$$I^G(J^{PC}) = 0^+(0^{++})$$

OMITTED FROM SUMMARY TABLE
Needs confirmation.

$f_0(2020)$ MASS				
VALUE (MeV)	EVTS	DOCUMENT ID	TECN	COMMENT
1992 ± 16		1,2 BARBERIS	00c	450 $pp \rightarrow p_f 4\pi p_s$
• • • We do not use the following data for averages, fits, limits, etc. • • •				
2037 ± 8	80k	3 UMAN	06	E835 5.2 $\bar{p}p \rightarrow \eta\eta\pi^0$
2040 ± 38		ANISOVICH	00J	SPEC
2010 ± 60		ALDE	98	GAM4 100 $\pi^- p \rightarrow \pi^0 \pi^0 n$
2020 ± 35		BARBERIS	97B	OMEG 450 $pp \rightarrow pp 2(\pi^+ \pi^-)$

¹ Average between $\pi^+ \pi^- 2\pi^0$ and $2(\pi^+ \pi^-)$.
² T-matrix pole.
³ Statistical error only.

$f_0(2020)$ WIDTH				
VALUE (MeV)	EVTS	DOCUMENT ID	TECN	COMMENT
442 ± 60		4,5 BARBERIS	00c	450 $pp \rightarrow p_f 4\pi p_s$
• • • We do not use the following data for averages, fits, limits, etc. • • •				
296 ± 17	80k	6 UMAN	06	E835 5.2 $\bar{p}p \rightarrow \eta\eta\pi^0$
405 ± 40		ANISOVICH	00J	SPEC
240 ± 100		ALDE	98	GAM4 100 $\pi^- p \rightarrow \pi^0 \pi^0 n$
410 ± 50		BARBERIS	97B	OMEG 450 $pp \rightarrow pp 2(\pi^+ \pi^-)$

⁴ Average between $\pi^+ \pi^- 2\pi^0$ and $2(\pi^+ \pi^-)$.
⁵ T-matrix pole.
⁶ Statistical error only.

$f_0(2020)$ DECAY MODES		
Mode	Fraction (Γ_i/Γ)	
Γ_1 $\rho\pi\pi$	seen	
Γ_2 $\pi^0\pi^0$	seen	
Γ_3 $\rho\rho$	seen	
Γ_4 $\omega\omega$	seen	
Γ_5 $\eta\eta$	seen	

$f_0(2020)$ BRANCHING RATIOS			
$\Gamma(\rho\rho)/\Gamma(\omega\omega)$	DOCUMENT ID	TECN	COMMENT
seen	BARBERIS	00f	450 $pp \rightarrow p_f \omega\omega p_s$

$f_0(2020)$ BRANCHING RATIOS			
$\Gamma(\eta\eta)/\Gamma_{total}$	DOCUMENT ID	TECN	COMMENT
seen	UMAN	06	E835 5.2 $\bar{p}p \rightarrow \eta\eta\pi^0$

$f_0(2020)$ REFERENCES				
UMAN	06	PR D73 052009	I. Uman et al.	(FNAL E835)
ANISOVICH	00J	PL B491 47	A.V. Anisovich et al.	
BARBERIS	00C	PL B471 440	D. Barberis et al.	(WA 102 Collab.)
BARBERIS	00F	PL B484 198	D. Barberis et al.	(WA 102 Collab.)
ALDE	98	EPJ A3 361	D. Alde et al.	(GAMMA Collab.)
	Also	PAN 62 405	D. Alde et al.	(GAMS Collab.)
		Translated from YAF 62 446		
BARBERIS	97B	PL B413 217	D. Barberis et al.	(WA 102 Collab.)

OTHER RELATED PAPERS				
IWASAKI	05A	PR D72 094016	M. Iwasaki, T. Fukutome	

$a_4(2040)$

$$I^G(J^{PC}) = 1^-(4^{++})$$

$a_4(2040)$ MASS					
VALUE (MeV)	EVTS	DOCUMENT ID	TECN	CHG	COMMENT
2001 ± 10 OUR AVERAGE					
1985 ± 10 ± 13	145k	LU	05	B852	18 $\pi^- p \rightarrow \omega \pi^- \pi^0 p$
1996 ± 25 ± 43		CHUNG	02	B852	18.3 $\pi^- p \rightarrow 3\pi p$
2000 ± 40 ± 60 20		IVANOV	01	B852	18 $\pi^- p \rightarrow \eta' \pi^- p$
1944 ± 8 ± 50		1 AMELIN	99	VES	37 $\pi^- A \rightarrow \omega \pi^- \pi^0 A^*$
2005 ± 25		ANISOVICH	99E	SPEC	
2010 ± 20		2 DONSKOV	96	GAM2 0	38 $\pi^- p \rightarrow \eta\eta\pi^0 n$
2040 ± 30		3 CLELAND	82B	SPEC ±	50 $\pi p \rightarrow K_S^0 K_S^0 p$
2030 ± 50		4 CORDEN	78c	OMEG 0	15 $\pi^- p \rightarrow 3\pi n$
• • • We do not use the following data for averages, fits, limits, etc. • • •					
2004 ± 6	80k	5 UMAN	06	E835	5.2 $\bar{p}p \rightarrow \eta\eta\pi^0$
2005 ± 25 45		ANISOVICH	01F	SPEC	2.0 $\bar{p}p \rightarrow 3\pi^0, \pi^0\eta,$ $\pi^0\eta'$
1903 ± 10		6 BALDI	78	SPEC -	10 $\pi^- p \rightarrow \rho K_S^0 K^-$

Meson Particle Listings

 $a_4(2040)$, $f_4(2050)$

- ¹ May be a different state.
² From a simultaneous fit to the G_{\perp} and G_0 wave intensities.
³ From an amplitude analysis.
⁴ $J^P = 4^+$ is favored, though $J^P = 2^+$ cannot be excluded.
⁵ Statistical error only.
⁶ From a fit to the Y_8^0 moment. Limited by phase space.

 $a_4(2040)$ WIDTH

VALUE (MeV)	EVTS	DOCUMENT ID	TECN	CHG	COMMENT
313 ± 31 OUR AVERAGE					
231 ± 30 ± 46	145k	LU	05	B852	$18 \pi^- \rho \rightarrow \omega \pi^- \pi^0 \rho$
298 ± 81 ± 85		CHUNG	02	B852	$18.3 \pi^- \rho \rightarrow 3 \pi \rho$
350 ± 100 ⁺⁷⁰ ₋₅₀		IVANOV	01	B852	$18 \pi^- \rho \rightarrow \eta' \pi^- \rho$
324 ± 26 ± 75		⁷ AMELIN	99	VES	$37 \pi^- A \rightarrow \omega \pi^- \pi^0 A^*$
360 ± 80		ANISOVICH	99E	SPEC	
370 ± 80		⁸ DONSKOV	96	GAM2 0	$38 \pi^- \rho \rightarrow \eta \pi^0 n$
380 ± 150		⁹ CLELAND	82B	SPEC ±	$50 \pi \rho \rightarrow K_S^0 K^{\pm} \rho$
510 ± 200		¹⁰ CORDEN	78C	OMEG 0	$15 \pi^- \rho \rightarrow 3 \pi n$
• • • We do not use the following data for averages, fits, limits, etc. • • •					
401 ± 16	80k	¹¹ UMAN	06	E835	$5.2 \bar{p} \rho \rightarrow \eta \eta \pi^0$
180 ± 30		ANISOVICH	01F	SPEC	$2.0 \bar{p} \rho \rightarrow 3 \pi^0, \pi^0 \eta, \pi^0 \eta'$
166 ± 43		¹² BALDI	78	SPEC -	$10 \pi^- \rho \rightarrow \rho K_S^0 K^-$

- ⁷ May be a different state.
⁸ From a simultaneous fit to the G_{\perp} and G_0 wave intensities.
⁹ From an amplitude analysis.
¹⁰ $J^P = 4^+$ is favored, though $J^P = 2^+$ cannot be excluded.
¹¹ Statistical error only.
¹² From a fit to the Y_8^0 moment. Limited by phase space.

 $a_4(2040)$ DECAY MODES

Mode	Fraction (Γ_i/Γ)
Γ_1 $K \bar{K}$	seen
Γ_2 $\pi^+ \pi^- \pi^0$	seen
Γ_3 $\rho \pi$	seen
Γ_4 $f_2(1270) \pi$	seen
Γ_5 $\omega \pi^- \pi^0$	seen
Γ_6 $\omega \rho$	seen
Γ_7 $\eta \pi^0$	seen
Γ_8 $\eta'(958) \pi$	seen

 $a_4(2040)$ BRANCHING RATIOS

$\Gamma(K \bar{K})/\Gamma_{\text{total}}$	Γ_1/Γ				
VALUE	DOCUMENT ID	TECN	CHG	COMMENT	
seen	BALDI	78	SPEC ±	$10 \pi^- \rho \rightarrow K_S^0 K^- \rho$	
$\Gamma(\pi^+ \pi^- \pi^0)/\Gamma_{\text{total}}$	Γ_2/Γ				
VALUE	DOCUMENT ID	TECN	CHG	COMMENT	
seen	CORDEN	78C	OMEG 0	$15 \pi^- \rho \rightarrow 3 \pi n$	
$\Gamma(\rho \pi)/\Gamma(f_2(1270) \pi)$	Γ_3/Γ_4				
VALUE	DOCUMENT ID	TECN	COMMENT		
1.1 ± 0.2 ± 0.2	CHUNG	02	B852	$18.3 \pi^- \rho \rightarrow 3 \pi \rho$	
$\Gamma(\eta \pi^0)/\Gamma_{\text{total}}$	Γ_7/Γ				
VALUE	DOCUMENT ID	TECN	CHG	COMMENT	
seen	DONSKOV	96	GAM2 0	$38 \pi^- \rho \rightarrow \eta \pi^0 n$	
$\Gamma(\omega \rho)/\Gamma_{\text{total}}$	Γ_6/Γ				
VALUE	EVTS	DOCUMENT ID	TECN	COMMENT	
seen	145k	LU	05	B852	$18 \pi^- \rho \rightarrow \omega \pi^- \pi^0 \rho$

 $a_4(2040)$ REFERENCES

UMAN	06	PR D73 052009	I. Uman et al.	(FNAL E835)
LU	05	PRL 94 032002	M. Lu et al.	(BNL E852 Collab.)
CHUNG	02	PR D45 072001	S.U. Chung et al.	(BNL E852 Collab.)
ANISOVICH	01F	PL B517 261	A.V. Anisovich et al.	
IVANOV	01	PRL 86 3977	E.I. Ivanov et al.	(BNL E852 Collab.)
AMELIN	99	PAN 62 445	D.V. Amelin et al.	(VES Collab.)
ANISOVICH	99E	PL B452 187	A.V. Anisovich et al.	
DONSKOV	96	PAN 59 982	S.V. Donskov et al.	(GAMS Collab.)
CLELAND	82B	NP B208 228	W.E. Cleland et al.	(DURH, REHL, LAUS+)
BALDI	78	PL 74B 413	R. Baldi et al.	(GEVA)JP
CORDEN	78C	NP B136 77	M.J. Corden et al.	(BIRM, GHEL, TELA+)JP

OTHER RELATED PAPERS

DZIERBA	06	PR D73 072001	A.R. Dzierba et al.	(BNL E852 Collab.)
DELFOSSÉ	81	NP B183 349	A. Delfosse et al.	(GEVA, LAUS)

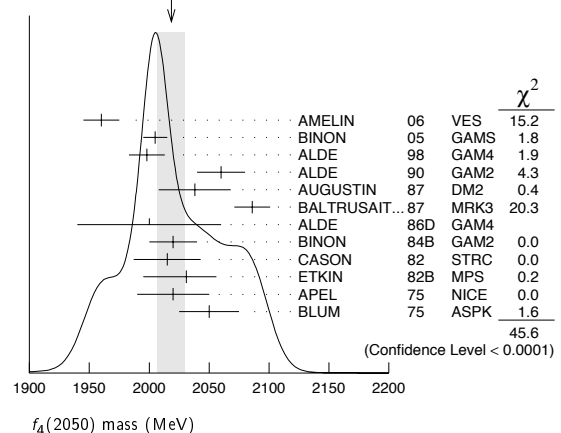
 $f_4(2050)$

$$I^G(J^{PC}) = 0^+(4^{++})$$

 $f_4(2050)$ MASS

VALUE (MeV)	EVTS	DOCUMENT ID	TECN	COMMENT
2018 ± 11 OUR AVERAGE				Error includes scale factor of 2.1. See the ideogram below.
1960 ± 15		AMELIN	06	VES $36 \pi^- \rho \rightarrow \omega \omega n$
2005 ± 10		¹ BINON	05	GAMS $33 \pi^- \rho \rightarrow \eta \eta n$
1998 ± 15		ALDE	98	GAM4 $100 \pi^- \rho \rightarrow \pi^0 \pi^0 n$
2060 ± 20		ALDE	90	GAM2 $38 \pi^- \rho \rightarrow \omega \omega n$
2038 ± 30		AUGUSTIN	87	DM2 $J/\psi \rightarrow \gamma \pi^+ \pi^-$
2086 ± 15		BALTRUSAIT..87	MRK3	$J/\psi \rightarrow \gamma \pi^+ \pi^-$
2000 ± 60		ALDE	86D	GAM4 $100 \pi^- \rho \rightarrow n 2 \eta$
2020 ± 20	40k	² BINON	84B	GAM2 $38 \pi^- \rho \rightarrow n 2 \pi^0$
2015 ± 28		³ CASON	82	STRC $8 \pi^+ \rho \rightarrow \Delta^+ \pi^0 \pi^0$
2031 ⁺²⁵ ₋₃₆		ETKIN	82B	MPS $23 \pi^- \rho \rightarrow n 2 K_S^0$
2020 ± 30	700	APEL	75	NICE $40 \pi^- \rho \rightarrow n 2 \pi^0$
2050 ± 25		BLUM	75	ASPK $18.4 \pi^- \rho \rightarrow n K^+ K^-$
• • • We do not use the following data for averages, fits, limits, etc. • • •				
2018 ± 6		ANISOVICH	00J	SPEC $2.0 \bar{p} \rho \rightarrow \eta \pi^0 \pi^0, \pi^0 \pi^0, \eta \eta, \eta \eta', \pi \pi$
~ 2000		⁴ MARTIN	98	RVUE $N \bar{N} \rightarrow \pi \pi$
~ 2010		⁵ MARTIN	97	RVUE $N \bar{N} \rightarrow \pi \pi$
~ 2040		⁶ OAKDEN	94	RVUE $0.36-1.55 \bar{p} \rho \rightarrow \pi \pi$
~ 1990		⁷ OAKDEN	94	RVUE $0.36-1.55 \bar{p} \rho \rightarrow \pi \pi$
1978 ± 5		⁸ ALPER	80	CNTR $62 \pi^- \rho \rightarrow K^+ K^- n$
2040 ± 10		⁸ ROZANSKA	80	SPRK $18 \pi^- \rho \rightarrow \rho \bar{p} n$
1935 ± 13		⁸ CORDEN	79	OMEG $12-15 \pi^- \rho \rightarrow n 2 \pi$
1988 ± 7		EVANGELIS...	79B	OMEG $10 \pi^- \rho \rightarrow K^+ K^- n$
1922 ± 14		⁹ ANTIPOV	77	CIBS $25 \pi^- \rho \rightarrow \rho 3 \pi$

- ¹ From the first PWA solution.
² From a partial-wave analysis of the data.
³ From an amplitude analysis of the reaction $\pi^+ \pi^- \rightarrow 2 \pi^0$.
⁴ Energy-dependent analysis.
⁵ Single energy analysis.
⁶ From solution A of amplitude analysis of data on $\bar{p} \rho \rightarrow \pi \pi$. See however KLOET 96 who fit $\pi^+ \pi^-$ only and find waves only up to $J = 3$ to be important but not significantly resonant.
⁷ From solution B of amplitude analysis of data on $\bar{p} \rho \rightarrow \pi \pi$. See however KLOET 96 who fit $\pi^+ \pi^-$ only and find waves only up to $J = 3$ to be important but not significantly resonant.
⁸ $I(J^P) = 0(4^+)$ from amplitude analysis assuming one-pion exchange.
⁹ Width errors enlarged by us to $4\Gamma/\sqrt{N}$; see the note with the $K^*(892)$ mass.

WEIGHTED AVERAGE
2018 ± 11 (Error scaled by 2.1) $f_4(2050)$ WIDTH

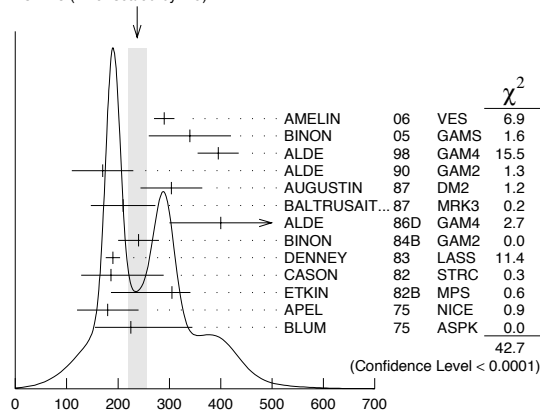
VALUE (MeV)	EVTS	DOCUMENT ID	TECN	COMMENT
237 ± 18 OUR AVERAGE				Error includes scale factor of 1.9. See the ideogram below.
290 ± 20		AMELIN	06	VES $36 \pi^- \rho \rightarrow \omega \omega n$
340 ± 80		¹⁰ BINON	05	GAMS $33 \pi^- \rho \rightarrow \eta \eta n$
395 ± 40		ALDE	98	GAM4 $100 \pi^- \rho \rightarrow \pi^0 \pi^0 n$
170 ± 60		ALDE	90	GAM2 $38 \pi^- \rho \rightarrow \omega \omega n$
304 ± 60		AUGUSTIN	87	DM2 $J/\psi \rightarrow \gamma \pi^+ \pi^-$
210 ± 63		BALTRUSAIT..87	MRK3	$J/\psi \rightarrow \gamma \pi^+ \pi^-$
400 ± 100		ALDE	86D	GAM4 $100 \pi^- \rho \rightarrow n 2 \eta$

See key on page 373

Meson Particle Listings

 $f_4(2050)$

Value	Source	Mode	Value	Source	Mode
240 ± 40	40k	11 BINON	84B	GAM2	$38 \pi^- p \rightarrow n 2\pi^0$
190 ± 14		DENNEY	83	LASS	$10 \pi^+ n/\pi^+ p$
186_{-58}^{+103}		12 CASON	82	STRC	$8 \pi^+ p \rightarrow \Delta^{++} \pi^0 \pi^0$
305_{-119}^{+36}		ETKIN	82B	MPS	$23 \pi^- p \rightarrow n 2K_S^0$
180 ± 60	700	APEL	75	NICE	$40 \pi^- p \rightarrow n 2\pi^0$
225_{-70}^{+120}		BLUM	75	ASPK	$18.4 \pi^- p \rightarrow n K^+ K^-$
182 ± 7		ANISOVICH	00J	SPEC	$2.0 \bar{p} p \rightarrow \eta \pi^0 \pi^0, \pi^0 \pi^0$
~ 170		13 MARTIN	98	RVUE	$N \bar{N} \rightarrow \pi \pi$
~ 200		14 MARTIN	97	RVUE	$\bar{N} N \rightarrow \pi \pi$
~ 60		15 OAKDEN	94	RVUE	$0.36-1.55 \bar{p} p \rightarrow \pi \pi$
~ 80		16 OAKDEN	94	RVUE	$0.36-1.55 \bar{p} p \rightarrow \pi \pi$
243 ± 16		17 ALPER	80	CNTR	$62 \pi^- p \rightarrow K^+ K^- n$
140 ± 15		17 ROZANSKA	80	SPRK	$18 \pi^- p \rightarrow p \bar{p} n$
263 ± 57		17 CORDEN	79	OMEG	$12-15 \pi^- p \rightarrow n 2\pi$
100 ± 28		EVANGELIS...	79B	OMEG	$10 \pi^- p \rightarrow K^+ K^- n$
107 ± 56		18 ANTIPOV	77	CIBS	$25 \pi^- p \rightarrow p 3\pi$

¹⁰From the first PWA solution.¹¹From a partial-wave analysis of the data.¹²From an amplitude analysis of the reaction $\pi^+ \pi^- \rightarrow 2\pi^0$.¹³Energy-dependent analysis.¹⁴Single energy analysis.¹⁵From solution A of amplitude analysis of data on $\bar{p} p \rightarrow \pi \pi$. See however KLOET 96 who fit $\pi^+ \pi^-$ only and find waves only up to $J = 3$ to be important but not significantly resonant.¹⁶From solution B of amplitude analysis of data on $\bar{p} p \rightarrow \pi \pi$. See however KLOET 96 who fit $\pi^+ \pi^-$ only and find waves only up to $J = 3$ to be important but not significantly resonant.¹⁷ $I(J^P) = 0(4^+)$ from amplitude analysis assuming one-pion exchange.¹⁸Width errors enlarged by us to $4\Gamma/\sqrt{N}$; see the note with the $K^*(892)$ mass.WEIGHTED AVERAGE
 237 ± 18 (Error scaled by 1.9) $f_4(2050)$ WIDTH $f_4(2050)$ DECAY MODES

Mode	Fraction (Γ_i/Γ)
Γ_1 $\omega\omega$	seen
Γ_2 $\pi\pi$	$(17.0 \pm 1.5) \%$
Γ_3 $K\bar{K}$	$(6.8_{-1.8}^{+3.4}) \times 10^{-3}$
Γ_4 $\eta\eta$	$(2.1 \pm 0.8) \times 10^{-3}$
Γ_5 $4\pi^0$	$< 1.2 \%$
Γ_6 $\gamma\gamma$	seen
Γ_7 $a_2(1320)\pi$	seen

 $f_4(2050)$ $\Gamma(i)\Gamma(\gamma\gamma)/\Gamma(\text{total})$

Mode	Value (keV)	CL%	Document ID	TECN	Comment
$\Gamma(K\bar{K}) \times \Gamma(\gamma\gamma)/\Gamma_{\text{total}}$					
< 0.29		95	ALTHOFF	85B	TASS $\gamma\gamma \rightarrow K\bar{K}\pi$

• • • We do not use the following data for averages, fits, limits, etc. • • •

Mode	Value (keV)	CL%	EVTS	Document ID	TECN	Comment
$\Gamma(\pi\pi) \times \Gamma(\gamma\gamma)/\Gamma_{\text{total}}$						
< 1.1		95	13 ± 4	OEST	90	JADE $e^+e^- \rightarrow e^+e^-\pi^0\pi^0$

 $f_4(2050)$ BRANCHING RATIOS $\Gamma(\omega\omega)/\Gamma_{\text{total}}$ Γ_1/Γ

Value	Document ID	TECN	Comment
seen	AMELIN	06	VES $36 \pi^- p \rightarrow \omega\omega n$

• • • We do not use the following data for averages, fits, limits, etc. • • •

not seen BARBERIS 00F $450 p p \rightarrow p_f \omega p_s$ $\Gamma(\omega\omega)/\Gamma(\pi\pi)$ Γ_1/Γ_2

Value	Document ID	TECN	Comment
1.5 ± 0.3	ALDE	90	GAM2 $38 \pi^- p \rightarrow \omega\omega n$

 $\Gamma(\pi\pi)/\Gamma_{\text{total}}$ Γ_2/Γ

Value	Document ID	TECN	Comment
0.170 ± 0.015 OUR AVERAGE			

0.18 ± 0.03 ¹⁹BINON 83C GAM2 $38 \pi^- p \rightarrow n 4\gamma$ 0.16 ± 0.03 ¹⁹CASON 82 STRC $8 \pi^+ p \rightarrow \Delta^{++} \pi^0 \pi^0$ 0.17 ± 0.02 ¹⁹CORDEN 79 OMEG $12-15 \pi^- p \rightarrow n 2\pi$ ¹⁹Assuming one pion exchange. $\Gamma(K\bar{K})/\Gamma(\pi\pi)$ Γ_3/Γ_2

Value	Document ID	TECN	Comment
$0.04_{-0.01}^{+0.02}$	ETKIN	82B	MPS $23 \pi^- p \rightarrow n 2K_S^0$

 $\Gamma(\eta\eta)/\Gamma_{\text{total}}$ Γ_4/Γ

Value (units 10^{-3})	Document ID	TECN	Comment
2.1 ± 0.8	ALDE	86D	GAM4 $100 \pi^- p \rightarrow n 4\gamma$

 $\Gamma(4\pi^0)/\Gamma_{\text{total}}$ Γ_5/Γ

Value	Document ID	TECN	Comment
< 0.012	ALDE	87	GAM4 $100 \pi^- p \rightarrow 4\pi^0 n$

 $\Gamma(a_2(1320)\pi)/\Gamma_{\text{total}}$ Γ_7/Γ

Value	Document ID	TECN	Comment
seen	AMELIN	00	VES $37 \pi^- p \rightarrow \eta \pi^+ \pi^- n$

 $f_4(2050)$ REFERENCES

AMELIN	06	PAN 69 690	D.V. Amelin et al.	(VES Collab.)
		Translated from YAF 69 715.		
BINON	05	PAN 68 960	F. Binon et al.	
		Translated from YAF 68 998.		
AMELIN	00	NP A668 83	D. Amelin et al.	(VES Collab.)
ANISOVICH	00J	PL B491 47	A.V. Anisovich et al.	
BARBERIS	00F	PL B484 198	D. Barberis et al.	(WA 102 Collab.)
ALDE	98	EPJ A3 361	D. Alde et al.	(GAM4 Collab.)
		Also PAN 62 405	D. Alde et al.	(GAMS Collab.)
		Translated from YAF 62 446.		
MARTIN	98	PR C57 3492	B.R. Martin et al.	
MARTIN	97	PR C56 1114	B.R. Martin, G.C. Oades	(LOUC, AARH)
KLOET	96	PR D53 6120	W.M. Kloet, F. Myhrer	(RUTG, NORD)
OAKDEN	94	NP A574 731	M.N. Oakden, M.R. Pennington	(DUPH)
ALDE	90	PL B241 600	D.M. Alde et al.	(SERP, BELG, LANL, LAPP+)
OEST	90	ZPHY C47 343	T. Oest et al.	(JADE Collab.)
ALDE	87	PL B198 286	D.M. Alde et al.	(LANL, BRUX, SERP, LAPP)
AUGUSTIN	87	ZPHY C36 369	J.E. Augustin et al.	(LALO, CLER, FRAS+)
BALTRUSAIT...	87	PR D35 2077	R.M. Baltrusaitis et al.	(Mark III Collab.)
ALDE	86D	NP B269 485	D.M. Alde et al.	(BELG, LAPP, SERP, CERN+)
ALTHOFF	85B	ZPHY C29 189	M. Althoff et al.	(TASSO Collab.)
BINON	84B	LNC 39 41	F.G. Binon et al.	(SERP, BELG, LAPP)
BINON	83C	SJNP 38 723	F.G. Binon et al.	(SERP, BRUX+)
		Translated from YAF 38 1199.		
DENNEY	83	PR D28 2726	D.L. Denney et al.	(IOWA, MICH)
CASON	82	PRL 48 1316	N.M. Cason et al.	(NDAM, ANL)
ETKIN	82B	PR D25 1786	A. Etkin et al.	(BNL, CUNY, TUFTS, VAND)
ALPER	80	PL 94B 422	B. Alper et al.	(AMST, CERN, CRAC, MPIM+)
ROZANSKA	80	NP B162 505	M. Rozanska et al.	(MPIM, CERN)
CORDEN	79	NP B157 250	M.J. Corden et al.	(BIRM, RHEL, TELA+JP)
EVANGELIS...	79B	NP B154 381	C. Evangelista et al.	(BARI, BONN, CERN+)
ANTIPOV	77	NP B119 45	Y.M. Antipov et al.	(SERP, GEVA)
APEL	75	PL 57B 398	W.D. Apel et al.	(KARLK, KARLE, PISA, SERP+JP)
BLUM	75	PL 57B 403	W. Blum et al.	(CERN, MPIM)JP

OTHER RELATED PAPERS

BUGG	07	EPJ C52 55	D. Bugg	
ANISOVICH	99D	PL B452 180	A.V. Anisovich et al.	
		Also NP A651 253	A.V. Anisovich et al.	
ANISOVICH	99F	NP A651 253	A.V. Anisovich et al.	
PROKOSHIN	97	SPD 42 117	Y.D. Prokoshin et al.	(SERP)
		Translated from DANS 353 323.		
CASON	83	PR D28 1586	N.M. Cason et al.	(NDAM, ANL)
GOTTESMAN	80	PR D22 1503	S.R. Gottesman et al.	(SYRA, BRAN, BNL+)
EISENHANDL...	75	NP B96 109	E. Eisenhandler et al.	(LOQM, LIPP, DARE+)
WAGNER	74	London Conf. 2 27	F. Wagner	(MPIM)

Meson Particle Listings

 $\pi_2(2100)$, $f_0(2100)$, $f_2(2150)$ $\pi_2(2100)$

$$I^G(J^{PC}) = 1^-(2^{-+})$$

OMITTED FROM SUMMARY TABLE
Needs confirmation.

 $\pi_2(2100)$ MASS

VALUE (MeV)	DOCUMENT ID	TECN	COMMENT
2090 ± 29 OUR AVERAGE			
2090 ± 30	¹ AMELIN	95B VES	36 $\pi^- A \rightarrow \pi^+ \pi^- \pi^- A$
2100 ± 150	² DAUM	81B CNTR	63,94 $\pi^- \rho \rightarrow 3\pi X$

¹ From a fit to $J^{PC} = 2^{-+} f_2(1270)\pi$, $(\pi\pi)_S\pi$ waves.
² From a two-resonance fit to four 2^{-0+} waves.

 $\pi_2(2100)$ WIDTH

VALUE (MeV)	DOCUMENT ID	TECN	COMMENT
625 ± 50 OUR AVERAGE			Error includes scale factor of 1.2.
520 ± 100	³ AMELIN	95B VES	36 $\pi^- A \rightarrow \pi^+ \pi^- \pi^- A$
651 ± 50	⁴ DAUM	81B CNTR	63,94 $\pi^- \rho \rightarrow 3\pi X$

³ From a fit to $J^{PC} = 2^{-+} f_2(1270)\pi$, $(\pi\pi)_S\pi$ waves.
⁴ From a two-resonance fit to four 2^{-0+} waves.

 $\pi_2(2100)$ DECAY MODES

Mode	Fraction (Γ_j/Γ)
Γ_1 3π	seen
Γ_2 $\rho\pi$	seen
Γ_3 $f_2(1270)\pi$	seen
Γ_4 $(\pi\pi)_S\pi$	seen

 $\pi_2(2100)$ BRANCHING RATIOS

$\Gamma(\rho\pi)/\Gamma(3\pi)$	DOCUMENT ID	TECN	COMMENT	Γ_2/Γ_1
0.19 ± 0.05	⁵ DAUM	81B CNTR	63,94 $\pi^- \rho$	

$\Gamma(f_2(1270)\pi)/\Gamma(3\pi)$	DOCUMENT ID	TECN	COMMENT	Γ_3/Γ_1
0.36 ± 0.09	⁵ DAUM	81B CNTR	63,94 $\pi^- \rho$	

$\Gamma((\pi\pi)_S\pi)/\Gamma(3\pi)$	DOCUMENT ID	TECN	COMMENT	Γ_4/Γ_1
0.45 ± 0.07	⁵ DAUM	81B CNTR	63,94 $\pi^- \rho$	

D-wave/S-wave RATIO FOR $\pi_2(2100) \rightarrow f_2(1270)\pi$

VALUE	DOCUMENT ID	TECN	COMMENT
0.39 ± 0.23	⁵ DAUM	81B CNTR	63,94 $\pi^- \rho$

⁵ From a two-resonance fit to four 2^{-0+} waves.

 $\pi_2(2100)$ REFERENCES

AMELIN	95B	PL B356 595	D.V. Amelin et al.	(SERP, TBIL)
DAUM	81B	NP B182 269	C. Daum et al.	(AMST, CERN, CRAC, MPIM+)

 $f_0(2100)$

$$I^G(J^{PC}) = 0^+(0^{++})$$

OMITTED FROM SUMMARY TABLE
Needs confirmation.

 $f_0(2100)$ MASS

VALUE (MeV)	EVTS	DOCUMENT ID	TECN	COMMENT
2103 ± 8 OUR AVERAGE				
2102 ± 13		¹ ANISOVICH	00J SPEC	2.0 $\bar{p}p \rightarrow \eta\pi^0\pi^0, \pi^0\pi^0, \eta\eta, \eta\eta', \pi^+\pi^-$
2090 ± 30		BAI	00A BES	$J/\psi \rightarrow \gamma(\pi^+\pi^-\pi^+\pi^-)$
2105 ± 10		ANISOVICH	99K SPEC	0.6-1.94 $\bar{p}p \rightarrow \eta\eta, \eta\eta'$
••• We do not use the following data for averages, fits, limits, etc. •••				
2105 ± 8	80k	² UMAN	06 E835	5.2 $\bar{p}p \rightarrow \eta\eta\pi^0$
~2104		BUGG	95	$J/\psi \rightarrow \gamma\pi^+\pi^-\pi^+\pi^-$

¹ Includes the data of ANISOVICH 00B.
² Statistical error only.

 $f_0(2100)$ WIDTH

VALUE (MeV)	EVTS	DOCUMENT ID	TECN	COMMENT
209 ± 19 OUR AVERAGE				
211 ± 29		³ ANISOVICH	00J SPEC	2.0 $\bar{p}p \rightarrow \eta\pi^0\pi^0, \pi^0\pi^0, \eta\eta, \eta\eta', \pi^+\pi^-$
330 ± 100		BAI	00A BES	$J/\psi \rightarrow \gamma(\pi^+\pi^-\pi^+\pi^-)$
200 ± 25		ANISOVICH	99K SPEC	0.6-1.94 $\bar{p}p \rightarrow \eta\eta, \eta\eta'$
••• We do not use the following data for averages, fits, limits, etc. •••				
236 ± 14	80k	⁴ UMAN	06 E835	5.2 $\bar{p}p \rightarrow \eta\eta\pi^0$
~203		BUGG	95	$J/\psi \rightarrow \gamma\pi^+\pi^-\pi^+\pi^-$

³ Includes the data of ANISOVICH 00B.
⁴ Statistical error only.

 $f_0(2100)$ REFERENCES

UMAN	06	PR D73 052009	I. Uman et al.	(FNAL E835)
ANISOVICH	00B	NP A662 319	A.V. Anisovich et al.	
ANISOVICH	00J	PL B491 47	A.V. Anisovich et al.	
BAI	00A	PL B472 207	J.Z. Bai et al.	(BES Collab.)
ANISOVICH	99K	PL B468 309	A.V. Anisovich et al.	
BUGG	95	PL B353 378	D.V. Bugg et al.	(LOQM, PNPI, WASH)

OTHER RELATED PAPERS

VIJANDE	05	PR D72 034025	J. Vijande, A. Valarce, F. Fernandez
---------	----	---------------	--------------------------------------

 $f_2(2150)$

$$I^G(J^{PC}) = 0^+(2^{++})$$

OMITTED FROM SUMMARY TABLE
This entry was previously called T_0 .

 $f_2(2150)$ MASS

VALUE (MeV)	EVTS	DOCUMENT ID	TECN	COMMENT
2156 ± 11 OUR AVERAGE				Includes data from the 2 datablocks that follow this one.
••• We do not use the following data for averages, fits, limits, etc. •••				
2170 ± 6	80k	¹ UMAN	06 E835	5.2 $\bar{p}p \rightarrow \eta\eta\pi^0$

¹ Statistical error only.

 $\eta\eta$ MODE

VALUE (MeV)	DOCUMENT ID	TECN	COMMENT
			The data in this block is included in the average printed for a previous datablock.

2157 ± 12 OUR AVERAGE

2151 ± 16	BARBERIS	00E	450 $pp \rightarrow p_f\eta\eta p_S$
2175 ± 20	PROKOSHKIN	95D GAM4	300 $\pi^- N \rightarrow \pi^- N 2\eta$, 450 $pp \rightarrow pp 2\eta$
2130 ± 35	SINGOVSKI	94 GAM4	450 $pp \rightarrow pp 2\eta$
••• We do not use the following data for averages, fits, limits, etc. •••			
2140 ± 30	² ABELE	99B CBAR	
seen	³ ANISOVICH	99B SPEC	1.35-1.94 $\bar{p}p \rightarrow \eta\eta\pi^0$
2105 ± 10	³ ANISOVICH	99K RVUE	0.6-1.94 $\bar{p}p \rightarrow \eta\eta, \eta\eta'$
2104 ± 20	⁴ ARMSTRONG	93C E760	$\bar{p}p \rightarrow \pi^0\eta\eta \rightarrow 6\gamma$

² Spin not determined.
³ $J^{PC} = 0^{++}$.
⁴ No J^{PC} determination.

 $\eta\pi\pi$ MODE

VALUE (MeV)	DOCUMENT ID	TECN	CHG	COMMENT
				The data in this block is included in the average printed for a previous datablock.

2135 ± 20 ± 45	ADOMEIT	96 CBAR	0	1.94 $\bar{p}p \rightarrow \eta 3\pi^0$
-----------------------	---------	---------	---	---

 $\bar{p}p \rightarrow \pi\pi$

VALUE (MeV)	DOCUMENT ID	TECN	COMMENT
••• We do not use the following data for averages, fits, limits, etc. •••			
~2226	HASAN	94 RVUE	$\bar{p}p \rightarrow \pi\pi$
~2090	⁵ OAKDEN	94 RVUE	0.36-1.55 $\bar{p}p \rightarrow \pi\pi$
~2120	⁶ OAKDEN	94 RVUE	0.36-1.55 $\bar{p}p \rightarrow \pi\pi$
~2170	⁷ MARTIN	80B RVUE	
~2150	⁷ MARTIN	80C RVUE	
~2150	⁸ DULUDE	78B OSPK	1-2 $\bar{p}p \rightarrow \pi^0\pi^0$

⁵ OAKDEN 94 makes an amplitude analysis of LEAR data on $\bar{p}p \rightarrow \pi\pi$ using a method based on Barrelet zeros. This is solution A. The amplitude analysis of HASAN 94 includes earlier data as well, and assume that the data can be parametrized in terms of towers of nearly degenerate resonances on the leading Regge trajectory. See also KLOET 96 and MARTIN 97 who make related analyses.
⁶ From solution B of amplitude analysis of data on $\bar{p}p \rightarrow \pi\pi$.
⁷ $I(J^P) = 0(2^+)$ from simultaneous analysis of $p\bar{p} \rightarrow \pi^-\pi^+$ and $\pi^0\pi^0$.
⁸ $I^G(J^P) = 0^+(2^+)$ from partial-wave amplitude analysis.

See key on page 373

Meson Particle Listings

 $f_2(2150)$ **S-CHANNEL $\bar{p}p$, $\bar{N}N$ or $\bar{K}K$**

VALUE (MeV)	DOCUMENT ID	TECN	CHG	COMMENT
-------------	-------------	------	-----	---------

2139^{+8}_{-9}	⁹ EVANGELIS...	97	SPEC	0.6-2.4 $\bar{p}p \rightarrow K_S^0 K_S^0$
~ 2190	⁹ CUTTS	78B	CNTR	0.97-3 $\bar{p}p \rightarrow \bar{N}N$
2155 ± 15	^{9,10} COUPLAND	77	CNTR 0	0.7-2.4 $\bar{p}p \rightarrow \bar{p}p$
2193 ± 2	^{9,11} ALSPECTOR	73	CNTR	$\bar{p}p$ S channel

⁹Isospins 0 and 1 not separated.¹⁰From a fit to the total elastic cross section.¹¹Referred to as T or \bar{T} region by ALSPECTOR 73. **$K\bar{K}$ MODE**

VALUE (MeV)	DOCUMENT ID	TECN	COMMENT
-------------	-------------	------	---------

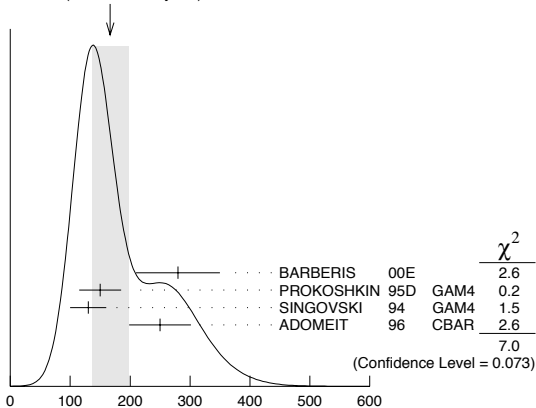
2200 ± 13	VLADIMIRSK...06	SPEC	40 $\pi^- p \rightarrow K_S^0 K_S^0 n$
2150 ± 20	ABLIKIM	04E BES2	$J/\psi \rightarrow \omega K^+ K^-$
2130 ± 35	BARBERIS	99 OMEG	450 $pp \rightarrow p_S p_f K^+ K^-$

 $f_2(2150)$ WIDTH **$f_2(2150)$ WIDTH, COMBINED MODES (MeV)**

VALUE (MeV)	EVTS	DOCUMENT ID	TECN	COMMENT
-------------	------	-------------	------	---------

167±30 OUR AVERAGE Includes data from the 2 datablocks that follow this one. Error includes scale factor of 1.5. See the ideogram below.

182 ± 11	80k	¹² UMAN	06 E835	5.2 $\bar{p}p \rightarrow \eta\eta\pi^0$
--------------	-----	--------------------	---------	--

¹²Statistical error only.WEIGHTED AVERAGE
167±30 (Error scaled by 1.5) $f_2(2150)$ WIDTH, COMBINED MODES (MeV) **$\eta\eta$ MODE**

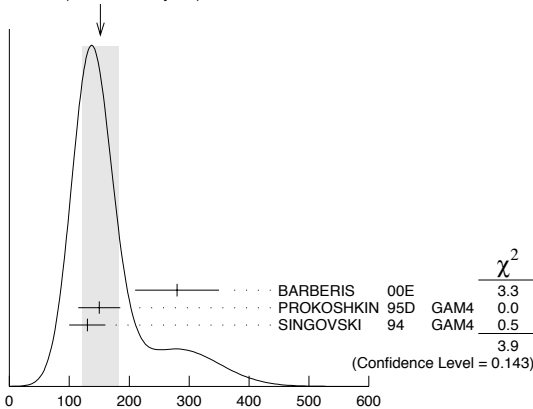
VALUE (MeV)	DOCUMENT ID	TECN	COMMENT
-------------	-------------	------	---------

The data in this block is included in the average printed for a previous datablock.

152±30 OUR AVERAGE Error includes scale factor of 1.4. See the ideogram below.

280 ± 70	BARBERIS	00E	450 $pp \rightarrow p_f \eta \eta p_S$
150 ± 35	PROKOSHKIN	95D GAM4	300 $\pi^- N \rightarrow \pi^- N 2\eta$, 450 $pp \rightarrow pp 2\eta$
130 ± 30	SINGOVSKI	94 GAM4	450 $pp \rightarrow pp 2\eta$

310 ± 50	¹³ ABELE	99B	CBAR
--------------	---------------------	-----	------

¹⁴ANISOVICH 99B SPEC 1.35-1.94 $\bar{p}p \rightarrow \eta\eta\pi^0$ ¹⁵ANISOVICH 99K RVUE 0.6-1.94 $\bar{p}p \rightarrow \eta\eta, \eta\eta'$ ¹⁶ARMSTRONG 93c E760 $\bar{p}p \rightarrow \pi^0 \eta\eta \rightarrow 6\gamma$ ¹³Spin not determined.¹⁴ $J^{PC} = 0^{++}$ ¹⁵PWA gives $J^{PC} = 0^{++}$.¹⁶No J^{PC} determination.WEIGHTED AVERAGE
152±30 (Error scaled by 1.4) $f_2(2150)$ WIDTH, $\eta\eta$ MODE (MeV) **$\eta\pi\pi$ MODE**

VALUE (MeV)	DOCUMENT ID	TECN	CHG	COMMENT
-------------	-------------	------	-----	---------

The data in this block is included in the average printed for a previous datablock.

$250 \pm 25 \pm 45$	ADOMEIT	96	CBAR 0	1.94 $\bar{p}p \rightarrow \eta 3\pi^0$
---------------------	---------	----	--------	---

 $\bar{p}p \rightarrow \pi\pi$

VALUE (MeV)	DOCUMENT ID	TECN	COMMENT
-------------	-------------	------	---------

250 OUR ESTIMATE

~ 226	HASAN	94	RVUE	$\bar{p}p \rightarrow \pi\pi$
------------	-------	----	------	-------------------------------

 ~ 70 ¹⁷OAKDEN 94 RVUE 0.36-1.55 $\bar{p}p \rightarrow \pi\pi$ ~ 250 ¹⁸MARTIN 80B RVUE ~ 250 ¹⁸MARTIN 80C RVUE ~ 250 ¹⁹DULUDE 78B OSPK 1-2 $\bar{p}p \rightarrow \pi^0 \pi^0$ ¹⁷See however KLOET 96 who fit $\pi^+ \pi^-$ only and find waves only up to $J = 3$ to be important but not significantly resonant.¹⁸ $I(J^{PC}) = 0(2^+)$ from simultaneous analysis of $p\bar{p} \rightarrow \pi^- \pi^+$ and $\pi^0 \pi^0$.¹⁹ $I(J^{PC}) = 0^+(2^+)$ from partial-wave amplitude analysis.**S-CHANNEL $\bar{p}p$, $\bar{N}N$ or $\bar{K}K$**

VALUE (MeV)	DOCUMENT ID	TECN	CHG	COMMENT
-------------	-------------	------	-----	---------

56^{+31}_{-16}	²⁰ EVANGELIS...	97	SPEC	0.6-2.4 $\bar{p}p \rightarrow K_S^0 K_S^0$
135 ± 75	^{21,22} COUPLAND	77	CNTR 0	0.7-2.4 $\bar{p}p \rightarrow \bar{p}p$
98 ± 8	²² ALSPECTOR	73	CNTR	$\bar{p}p$ S channel

²⁰Isospin 0 and 2 not separated.²¹From a fit to the total elastic cross section.²²Isospins 0 and 1 not separated. **$K\bar{K}$ MODE**

VALUE (MeV)	DOCUMENT ID	TECN	COMMENT
-------------	-------------	------	---------

91 ± 62	VLADIMIRSK...06	SPEC	40 $\pi^- p \rightarrow K_S^0 K_S^0 n$
150 ± 30	ABLIKIM	04E BES2	$J/\psi \rightarrow \omega K^+ K^-$
270 ± 50	BARBERIS	99 OMEG	450 $pp \rightarrow p_S p_f K^+ K^-$

 $f_2(2150)$ DECAY MODES

Mode	Fraction (Γ_i/Γ)
Γ_1 $\pi\pi$	
Γ_2 $\eta\eta$	seen
Γ_3 $K\bar{K}$	seen
Γ_4 $f_2(1270)\eta$	seen
Γ_5 $a_2(1320)\pi$	seen

 $f_2(2150)$ BRANCHING RATIOS

VALUE	CL%	DOCUMENT ID	TECN	COMMENT	Γ_3/Γ_2
-------	-----	-------------	------	---------	---------------------

1.28±0.23 BARBERIS 00E 450 $pp \rightarrow p_f \eta \eta p_S$

< 0.1	95	²³ PROKOSHKIN	95D GAM4	300 $\pi^- N \rightarrow \pi^- N 2\eta$, 450 $pp \rightarrow pp 2\eta$
---------	----	--------------------------	----------	--

< 0.1	95	²³ PROKOSHKIN	95D GAM4	300 $\pi^- N \rightarrow \pi^- N 2\eta$, 450 $pp \rightarrow pp 2\eta$
---------	----	--------------------------	----------	--

²³Using data from ARMSTRONG 89D.

Meson Particle Listings

 $f_2(2150)$, $\rho(2150)$ $\Gamma(\pi\pi)/\Gamma(\eta\eta)$

VALUE	CL%	DOCUMENT ID	TECN	COMMENT
-------	-----	-------------	------	---------

••• We do not use the following data for averages, fits, limits, etc. •••

<0.33	95	²⁴ PROKOSHKIN 95D	GAM4	300 $\pi^- N \rightarrow \pi^- N 2\eta$, 450 $p p \rightarrow p p 2\eta$
-------	----	------------------------------	------	--

²⁴ Derived from a $\pi^0 \pi^0 / \eta\eta$ limit.

 $\Gamma(f_2(1270)\eta)/\Gamma(a_2(1320)\pi)$

VALUE	DOCUMENT ID	TECN	COMMENT
-------	-------------	------	---------

0.79±0.11 ²⁵ ADOMEIT 96 CBAR 1.94 $\bar{p} p \rightarrow \eta 3\pi^0$

²⁵ Using $B(a_2(1320) \rightarrow \eta\pi) = 0.145$

 $f_2(2150)$ REFERENCES

UMAN	06	PR D73 052009	I. Uman <i>et al.</i>	(FNAL E835)
VLADIMIRSK...	06	PAN 69 492	V.V. Vladimirovsky <i>et al.</i>	(ITEP, Moscow)
ABLIKIM	04E	PL B603 138	M. Ablikim <i>et al.</i>	(BES Collab.)
BARBERIS	00E	PL B479 59	D. Barberis <i>et al.</i>	(WA 102 Collab.)
ABELE	99B	EPJ C8 67	A. Abele <i>et al.</i>	(Crystal Barrel Collab.)
ANISOVICH	99B	PL B449 154	A.V. Anisovich <i>et al.</i>	
ANISOVICH	99K	PL B468 309	A.V. Anisovich <i>et al.</i>	
BARBERIS	99	PL B453 305	D. Barberis <i>et al.</i>	(Omega Expt.)
EVANGELIS...	97	PR D56 3803	C. Evangelista <i>et al.</i>	(LEAR Collab.)
MARTIN	97	PR C56 1114	B.R. Martin, G.C. Oades	(LOUC, AARH)
ADOMEIT	96	ZPHY C71 227	J. Adomeit <i>et al.</i>	(Crystal Barrel Collab.)
KLOET	96	PR D53 6120	W.M. Kloet, F. Myhrer	(RUTG, WORD)
PROKOSHKIN	95D	SPD 40 495	Y.D. Prokoshkin	(SERP) IJGPC
		Translated from DANS 344 469.		
HASAN	94	PL B334 215	A. Hasan, D.V. Bugg	(LOQM)
OAKDEN	94	NP A574 731	M.N. Oakden, M.R. Pennington	(DURH)
SINGOVSKI	94	NC 107A 1911	A.V. Singovsky	(SERP)
ARMSTRONG	93C	PL B307 394	T.A. Armstrong <i>et al.</i>	(FNAL, FERR, GENO+)
ARMSTRONG	89D	PL B227 186	T.A. Armstrong, M. Benayoun	(ATHU, BARI, BIRM+)
MARTIN	80B	NP B176 355	B.R. Martin, D. Morgan	(LOUC, RHEL) JP
MARTIN	80C	NP B169 216	A.D. Martin, M.R. Pennington	(DURH) JP
CUTTS	78B	PR D17 16	D. Cutts <i>et al.</i>	(STON, WISC)
DULUDE	78B	PL 79B 335	R.S. Dulude <i>et al.</i>	(BROW, MIT, BARI) JP
COUPLAND	77	PL 71B 460	M. Coupland <i>et al.</i>	(LOQM, RHEL)
ALSPECTOR	73	PRL 30 511	J. Alspector <i>et al.</i>	(RUTG, UPNJ)

OTHER RELATED PAPERS

ANISOVICH	05	JETPL 80 715	V.V. Anisovich	
		Translated from ZETFP 80 845		
ANISOVICH	05A	JETPL 81 417	V.V. Anisovich, A.V. Sarantsev	
		Translated from ZETFP 81 531		
ANISOVICH	05C	JMP A20 6327	V.V. Anisovich, M.A. Matveev, A.V. Sarantsev	
EISENHAND...	75	NP B96 109	E. Eisenhandler <i>et al.</i>	(LOQM, LIPV, DARE+)
FIELDS	71	PRL 27 1749	T. Fields <i>et al.</i>	(ANL, OXF)
YOH	71	PRL 26 922	J.K. Yoh <i>et al.</i>	(CIT, BNL, ROCH)

 $\rho(2150)$

$$J^{G(J^{PC})} = 1^+(1^{--})$$

OMITTED FROM SUMMARY TABLE

This entry was previously called $T_1(2190)$.

 $\rho(2150)$ MASS e^+e^- PRODUCED

VALUE (MeV)	DOCUMENT ID	TECN	COMMENT
-------------	-------------	------	---------

2149±17 OUR AVERAGE Includes data from the datablock that follows this one.

2150±40±50	AUBERT	07AU BABR	10.6 $e^+e^- \rightarrow f_1(1285)\pi^+\pi^-\gamma$
2153±37	BIAGINI	91 RVUE	$e^+e^- \rightarrow \pi^+\pi^-, K^+K^-$
2110±50	¹ CLEGG	90 RVUE	$e^+e^- \rightarrow 3(\pi^+\pi^-), 2(\pi^+\pi^-\pi^0)$

••• We do not use the following data for averages, fits, limits, etc. •••

1990±80	AUBERT	07AU BABR	10.6 $e^+e^- \rightarrow \eta'\pi^+\pi^-\gamma$
---------	--------	-----------	---

 $\bar{p}p \rightarrow \pi\pi$

VALUE (MeV)	DOCUMENT ID	TECN	COMMENT
-------------	-------------	------	---------

••• We do not use the following data for averages, fits, limits, etc. •••

~2191	HASAN	94 RVUE	$\bar{p}p \rightarrow \pi\pi$
~1988	HASAN	94 RVUE	$\bar{p}p \rightarrow \pi\pi$
~2070	² OAKDEN	94 RVUE	0.36–1.55 $\bar{p}p \rightarrow \pi\pi$
~2170	³ MARTIN	80B RVUE	
~2100	³ MARTIN	80C RVUE	

S-CHANNEL $\bar{N}N$

VALUE (MeV)	DOCUMENT ID	TECN	COMMENT
-------------	-------------	------	---------

••• We do not use the following data for averages, fits, limits, etc. •••

2110±35	⁴ ANISOVICH	02 SPEC	0.6–1.9 $p\bar{p} \rightarrow \omega\pi^0, \omega\eta\pi^0, \pi^+\pi^-$
~2190	⁵ CUTTS	78B CNTR	0.97–3 $\bar{p}p \rightarrow \bar{N}N$
2155±15	^{5,6} COUPLAND	77 CNTR	0.7–2.4 $\bar{p}p \rightarrow \bar{p}p$
2193±2	^{5,7} ALSPECTOR	73 CNTR	$\bar{p}p$ S channel
2190±10	⁸ ABRAMS	70 CNTR	S channel $\bar{p}N$

 $\pi^-p \rightarrow \omega\pi^0 n$

VALUE (MeV)	DOCUMENT ID	TECN	COMMENT
-------------	-------------	------	---------

The data in this block is included in the average printed for a previous datablock.

2155±21 OUR AVERAGE

2140±30	ALDE	95 GAM2	38 $\pi^-p \rightarrow \omega\pi^0 n$
2170±30	ALDE	92C GAM4	100 $\pi^-p \rightarrow \omega\pi^0 n$

¹ Includes ATKINSON 85.

² See however KLOET 96 who fit $\pi^+\pi^-$ only and find waves only up to $J = 3$ to be important but not significantly resonant.

³ $I(J^{PC}) = 1(1^-)$ from simultaneous analysis of $p\bar{p} \rightarrow \pi^-\pi^+$ and $\pi^0\pi^0$.

⁴ From the combined analysis of ANISOVICH 00I, ANISOVICH 01D, ANISOVICH 01E, and ANISOVICH 02.

⁵ Isospins 0 and 1 not separated.

⁶ From a fit to the total elastic cross section.

⁷ Referred to as T or T region by ALSPECTOR 73.

⁸ Seen as bump in $l = 1$ state. See also COOPER 68. PEASLEE 75 confirm $\bar{p}p$ results of ABRAMS 70, no narrow structure.

 $\rho(2150)$ WIDTH e^+e^- PRODUCED

VALUE (MeV)	DOCUMENT ID	TECN	COMMENT
-------------	-------------	------	---------

359±40 OUR AVERAGE Includes data from the datablock that follows this one.

350±40±50	AUBERT	07AU BABR	10.6 $e^+e^- \rightarrow f_1(1285)\pi^+\pi^-\gamma$
389±79	BIAGINI	91 RVUE	$e^+e^- \rightarrow \pi^+\pi^-, K^+K^-$
410±100	⁹ CLEGG	90 RVUE	$e^+e^- \rightarrow 3(\pi^+\pi^-), 2(\pi^+\pi^-\pi^0)$

••• We do not use the following data for averages, fits, limits, etc. •••

310±140	AUBERT	07AU BABR	10.6 $e^+e^- \rightarrow \eta'\pi^+\pi^-\gamma$
---------	--------	-----------	---

 $\bar{p}p \rightarrow \pi\pi$

VALUE (MeV)	DOCUMENT ID	TECN	COMMENT
-------------	-------------	------	---------

••• We do not use the following data for averages, fits, limits, etc. •••

~296	HASAN	94 RVUE	$\bar{p}p \rightarrow \pi\pi$
~244	HASAN	94 RVUE	$\bar{p}p \rightarrow \pi\pi$
~40	¹⁰ OAKDEN	94 RVUE	0.36–1.55 $\bar{p}p \rightarrow \pi\pi$
~250	¹¹ MARTIN	80B RVUE	
~200	¹¹ MARTIN	80C RVUE	

S-CHANNEL $\bar{N}N$

VALUE (MeV)	DOCUMENT ID	TECN	COMMENT
-------------	-------------	------	---------

••• We do not use the following data for averages, fits, limits, etc. •••

230±50	¹² ANISOVICH	02 SPEC	0.6–1.9 $p\bar{p} \rightarrow \omega\pi^0, \omega\eta\pi^0, \pi^+\pi^-$
135±75	^{13,14} COUPLAND	77 CNTR	0.7–2.4 $\bar{p}p \rightarrow \bar{p}p$
98±8	¹⁴ ALSPECTOR	73 CNTR	$\bar{p}p$ S channel
~85	¹⁵ ABRAMS	70 CNTR	S channel $\bar{p}N$

 $\pi^-p \rightarrow \omega\pi^0 n$

VALUE (MeV)	DOCUMENT ID	TECN	COMMENT
-------------	-------------	------	---------

The data in this block is included in the average printed for a previous datablock.

320±70 ALDE 95 GAM2 38 $\pi^-p \rightarrow \omega\pi^0 n$

••• We do not use the following data for averages, fits, limits, etc. •••

~300 ALDE 92C GAM4 100 $\pi^-p \rightarrow \omega\pi^0 n$

⁹ Includes ATKINSON 85.

¹⁰ See however KLOET 96 who fit $\pi^+\pi^-$ only and find waves only up to $J = 3$ to be important but not significantly resonant.

¹¹ $I(J^{PC}) = 1(1^-)$ from simultaneous analysis of $p\bar{p} \rightarrow \pi^-\pi^+$ and $\pi^0\pi^0$.

¹² From the combined analysis of ANISOVICH 00I, ANISOVICH 01D, ANISOVICH 01E, and ANISOVICH 02.

¹³ From a fit to the total elastic cross section.

¹⁴ Isospins 0 and 1 not separated.

¹⁵ Seen as bump in $l = 1$ state. See also COOPER 68. PEASLEE 75 confirm $\bar{p}p$ results of ABRAMS 70, no narrow structure.

 $\rho(2150)$ DECAY MODES

Mode	Fraction (Γ_i/Γ)
Γ_1 e^+e^-	
Γ_2 $\pi^+\pi^-$	seen
Γ_3 K^+K^-	seen
Γ_4 $3(\pi^+\pi^-)$	seen
Γ_5 $2(\pi^+\pi^-\pi^0)$	seen
Γ_6 $\eta'\pi^+\pi^-$	seen
Γ_7 $f_1(1285)\pi^+\pi^-$	seen
Γ_8 $\omega\pi^0$	seen
Γ_9 $\omega\pi^0\eta$	seen
Γ_{10} $\rho\bar{p}$	

 $\rho(2150)$ $\Gamma(i)\Gamma(e^+e^-)/\Gamma^2(\text{total})$

$\Gamma(f_1(1285)\pi^+\pi^-) \times \Gamma(e^+e^-)/\Gamma_{\text{total}}^2$ $\Gamma_7\Gamma_1/\Gamma^2$

VALUE (units 10^{-7})	DOCUMENT ID	TECN	COMMENT
--------------------------	-------------	------	---------

3.1±0.6±0.5 ¹⁶ AUBERT 07AU BABR 10.6 $e^+e^- \rightarrow f_1(1285)\pi^+\pi^-\gamma$

¹⁶ Calculated by us from the reported value of cross section at the peak.

$\Gamma(\eta'\pi^+\pi^-) \times \Gamma(e^+e^-)/\Gamma_{\text{total}}^2$ $\Gamma_6\Gamma_1/\Gamma^2$

VALUE (units 10^{-8})	DOCUMENT ID	TECN	COMMENT
--------------------------	-------------	------	---------

••• We do not use the following data for averages, fits, limits, etc. •••

4.9±1.9 ¹⁷ AUBERT 07AU BABR 10.6 $e^+e^- \rightarrow \eta'\pi^+\pi^-\gamma$

¹⁷ Calculated by us from the reported value of cross section at the peak.

See key on page 373

Meson Particle Listings

$\rho(2150)$, $\phi(2170)$, $f_0(2200)$

 $\rho(2150)$ REFERENCES

AUBERT	07AU	PR D76 092005	B. Aubert et al.	(BABAR Collab.)
ANISOVICH	02	PL B542 9	A.V. Anisovich et al.	
ANISOVICH	01D	PL B508 6	A.V. Anisovich et al.	
ANISOVICH	01E	PL B513 281	A.V. Anisovich et al.	
ANISOVICH	00J	PL B491 47	A.V. Anisovich et al.	
KLOET	96	PR D53 6120	W.M. Kloet, F. Myhrer	(RUTG, NORD)
ALDE	95	ZPHY C66 379	D.M. Alde et al.	(GAMS Collab.) JP
HASAN	94	PL B334 215	A. Hasan, D.V. Bugg	(LOQM)
OAKDEN	94	NP A574 731	M.N. Oakden, M.R. Pennington	(DURH)
ALDE	92C	ZPHY C54 553	D.M. Alde et al.	(BELG, SERP, KEK, LANL+)
BIAGINI	91	NC 104A 363	M.E. Biagini et al.	(FRAS, PRAG)
CLEGG	90	ZPHY C45 677	A.B. Clegg, A. Donnachie	(LANC, MCHS)
ATKINSON	85	ZPHY C29 333	M. Atkinson et al.	(BONN, CERN, GLAS+)
MARTIN	80B	NP B176 355	B.R. Martin, D. Morgan	(LOUC, RHEL) JP
MARTIN	80C	NP B169 216	A.D. Martin, M.R. Pennington	(DURH) JP
CUTTS	78B	PR D17 16	D. Cutts et al.	(STON, WISC)
COUPLAND	77	PL 71B 460	M. Coupland et al.	(LOQM, RHEL)
PEASLEE	75	PL 57B 189	D.C. Peaslee et al.	(CANB, BARI, BROW+)
ALSPECTOR	73	PRL 30 511	J. Alspector et al.	(RUTG, UPNJ)
ABRAMS	70	PR D1 1917	R.J. Abrams et al.	(BNL)
COOPER	68	PRL 20 1059	W.A. Cooper et al.	(ANL)

OTHER RELATED PAPERS

AMELIN	00	NP A668 83	D. Amelin et al.	(VES Collab.)
EISENHAND...	75	NP B96 109	E. Eisenhandler et al.	(LOQM, LVP, DARE+)
BRICMAN	69	PL 29B 451	C. Bricman et al.	(CERN, CAEN, SACL)
ABRAMS	67C	PRL 18 1209	R.J. Abrams et al.	(BNL)

 $\phi(2170)$

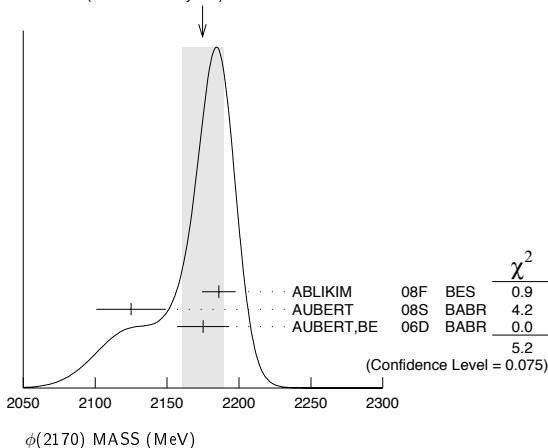
$$I^G(J^{PC}) = 0^-(1^{--})$$

OMITTED FROM SUMMARY TABLE

Observed by AUBERT, BE 06D in the initial-state radiation process
 $e^+e^- \rightarrow \phi f_0(980)\gamma$.

 $\phi(2170)$ MASS

VALUE (MeV)	EVTS	DOCUMENT ID	TECN	COMMENT
2175 ± 15 OUR AVERAGE		Error includes scale factor of 1.6. See the ideogram below.		
2186 ± 10 ± 6	52	ABLIKIM 08F	BES	$J/\psi \rightarrow \eta \phi f_0(980)$
2125 ± 22 ± 10	483	AUBERT 08s	BABR	10.6 $e^+e^- \rightarrow \phi \eta \gamma$
2175 ± 10 ± 15	201	¹ AUBERT, BE 06D	BABR	10.6 $e^+e^- \rightarrow K^+ K^- \pi \pi \gamma$
••• We do not use the following data for averages, fits, limits, etc. •••				
2192 ± 14	116 ± 95	² AUBERT 07AK	BABR	10.6 $e^+e^- \rightarrow K^+ K^- \pi^+ \pi^- \gamma$
2169 ± 20	149 ± 36	² AUBERT 07AK	BABR	10.6 $e^+e^- \rightarrow K^+ K^- \pi^0 \pi^0 \gamma$

¹ From the $\phi f_0(980)$ component.² From the $K^+ K^- f_0(980)$ component.WEIGHTED AVERAGE
2175±15 (Error scaled by 1.6) **$\phi(2170)$ WIDTH**

VALUE (MeV)	EVTS	DOCUMENT ID	TECN	COMMENT
61 ± 18 OUR AVERAGE				
65 ± 23 ± 17	52	ABLIKIM 08F	BES	$J/\psi \rightarrow \eta \phi f_0(980)$
61 ± 50 ± 13	483	AUBERT 08s	BABR	10.6 $e^+e^- \rightarrow \phi \eta \gamma$
58 ± 16 ± 20	201	³ AUBERT, BE 06D	BABR	10.6 $e^+e^- \rightarrow K^+ K^- \pi \pi \gamma$
••• We do not use the following data for averages, fits, limits, etc. •••				
71 ± 21	116 ± 95	⁴ AUBERT 07AK	BABR	10.6 $e^+e^- \rightarrow K^+ K^- \pi^+ \pi^- \gamma$
102 ± 27	149 ± 36	⁴ AUBERT 07AK	BABR	10.6 $e^+e^- \rightarrow K^+ K^- \pi^0 \pi^0 \gamma$

³ From the $\phi f_0(980)$ component.⁴ From the $K^+ K^- f_0(980)$ component. **$\phi(2170)$ DECAY MODES**

Mode	Fraction (Γ_i/Γ)
Γ_1 e^+e^-	seen
Γ_2 $\phi \eta$	
Γ_3 $\phi f_0(980)$	seen
Γ_4 $K^+ K^- \pi^+ \pi^-$	
Γ_5 $K^+ K^- f_0(980) \rightarrow K^+ K^- \pi^+ \pi^-$	seen
Γ_6 $K^+ K^- \pi^0 \pi^0$	
Γ_7 $K^+ K^- f_0(980) \rightarrow K^+ K^- \pi^0 \pi^0$	seen
Γ_8 $K^*0 K^\pm \pi^\mp$	not seen

 $\phi(2170)$ $\Gamma(i)\Gamma(e^+e^-)/\Gamma(\text{total})$

$\Gamma(\phi \eta) \times \Gamma(e^+e^-)/\Gamma_{\text{total}}$	VALUE (eV)	EVTS	DOCUMENT ID	TECN	COMMENT	$\Gamma_2 \Gamma_1/\Gamma$
---	------------	------	-------------	------	---------	----------------------------

••• We do not use the following data for averages, fits, limits, etc. •••

1.7 ± 0.7 ± 1.3 483 AUBERT 08s BABR 10.6 $e^+e^- \rightarrow \phi \eta \gamma$

$\Gamma(\phi f_0(980)) \times \Gamma(e^+e^-)/\Gamma_{\text{total}}$	VALUE (eV)	EVTS	DOCUMENT ID	TECN	COMMENT	$\Gamma_3 \Gamma_1/\Gamma$
---	------------	------	-------------	------	---------	----------------------------

2.5 ± 0.8 ± 0.4 201 ⁵AUBERT, BE 06D BABR 10.6 $e^+e^- \rightarrow K^+ K^- \pi \pi \gamma$ ⁵ From the $\phi f_0(980)$ component. **$\phi(2170)$ BRANCHING RATIOS**

$\Gamma(K^+ K^- f_0(980) \rightarrow K^+ K^- \pi^+ \pi^-)/\Gamma_{\text{total}}$	VALUE	DOCUMENT ID	TECN	COMMENT	Γ_5/Γ
--	-------	-------------	------	---------	-------------------

seen AUBERT 07AK BABR 10.6 $e^+e^- \rightarrow K^+ K^- \pi^+ \pi^- \gamma$

$\Gamma(K^+ K^- f_0(980) \rightarrow K^+ K^- \pi^0 \pi^0)/\Gamma_{\text{total}}$	VALUE	DOCUMENT ID	TECN	COMMENT	Γ_7/Γ
--	-------	-------------	------	---------	-------------------

seen AUBERT 07AK BABR 10.6 $e^+e^- \rightarrow K^+ K^- \pi^0 \pi^0 \gamma$

$\Gamma(K^*0 K^\pm \pi^\mp)/\Gamma_{\text{total}}$	VALUE	DOCUMENT ID	TECN	COMMENT	Γ_8/Γ
--	-------	-------------	------	---------	-------------------

not seen AUBERT 07AK BABR 10.6 GeV e^+e^- **$\phi(2170)$ REFERENCES**

ABLIKIM 08F	PRL 100 102003	M. Ablikim et al.	(BES Collab.)
AUBERT 08S	PR D77 092002	B. Aubert et al.	(BABAR Collab.)
AUBERT 07AK	PR D76 012008	B. Aubert et al.	(BABAR Collab.)
AUBERT, BE 06D	PR D74 091103R	B. Aubert et al.	(BABAR Collab.)

OTHER RELATED PAPERS

DING 07	PL B650 390	G.-J. Ding, M.-L. Yan
DING 07A	PL B657 49	G.-J. Ding, M.-L. Yan

 $f_0(2200)$

$$I^G(J^{PC}) = 0^+(0^{++})$$

OMITTED FROM SUMMARY TABLE

Seen in $K_S^0 K_S^0$ (AUGUSTIN 88), $K^+ K^-$ (ABLIKIM 05Q) and $\eta \eta$ (BINON 05) system. Not seen in $\Upsilon(1S)$ radiative decays (BARU 89).

 $f_0(2200)$ MASS

VALUE (MeV)	DOCUMENT ID	TECN	COMMENT
2189 ± 13 OUR AVERAGE			
2170 ± 20 ± $^{+10}_{-15}$	ABLIKIM 05Q	BES2	$\psi(2S) \rightarrow \gamma \pi^+ \pi^- K^+ K^-$
2210 ± 50	¹ BINON 05	GAMS	$33 \pi^- p \rightarrow \eta \eta n$
2197 ± 17	² AUGUSTIN 88	DM2	$J/\psi \rightarrow \gamma K_S^0 K_S^0$

••• We do not use the following data for averages, fits, limits, etc. •••

~ 2122 HASAN 94 RVUE $\bar{p}p \rightarrow \pi \pi$
 ~ 2321 HASAN 94 RVUE $\bar{p}p \rightarrow \pi \pi$

¹ First solution, PWA is ambiguous.² Cannot determine spin to be 0. **$f_0(2200)$ WIDTH**

VALUE (MeV)	DOCUMENT ID	TECN	COMMENT
238 ± 50 OUR AVERAGE	Error includes scale factor of 1.2.		
220 ± 60 ± $^{+40}_{-45}$	ABLIKIM 05Q	BES2	$\psi(2S) \rightarrow \gamma \pi^+ \pi^- K^+ K^-$
380 ± 90	³ BINON 05	GAMS	$33 \pi^- p \rightarrow \eta \eta n$
201 ± 51	⁴ AUGUSTIN 88	DM2	$J/\psi \rightarrow \gamma K_S^0 K_S^0$

••• We do not use the following data for averages, fits, limits, etc. •••

~ 273 HASAN 94 RVUE $\bar{p}p \rightarrow \pi \pi$
 ~ 223 HASAN 94 RVUE $\bar{p}p \rightarrow \pi \pi$

Meson Particle Listings

$f_0(2200)$, $f_J(2220)$

³ First solution, PWA is ambiguous.

⁴ Cannot determine spin to be 0.

$f_0(2200)$ REFERENCES

ABLIKIM	05Q	PR D72 092002	M. Ablikim <i>et al.</i>	(BES Collab.)
BINON	05	PAN 68 960	F. Binon <i>et al.</i>	
Translated from YAF 68 938.				
HASAN	94	PL B334 215	A. Hasan, D.V. Bugg	(LOQM)
BARU	89	ZPHY C42 505	S.E. Baru <i>et al.</i>	(NOVO)
AUGUSTIN	88	PRL 60 2238	J.E. Augustin <i>et al.</i>	(DM2 Collab.)

OTHER RELATED PAPERS

WASAKI	05A	PR D72 094016	M. Iwasaki, T. Fukutome	
VIJANDE	05	PR D72 034025	J. Vijande, A. Valcaro, F. Fernandez	
EISENHAND...	75	NP B96 109	E. Eisenhandler <i>et al.</i>	(LOQM, LIVP, DARE+)

$f_J(2220)$

$$I^G(J^{PC}) = 0^+(2^{++} \text{ or } 4^{++})$$

OMITTED FROM SUMMARY TABLE

Needs confirmation. See our mini-review in the 2004 edition of this Review, PDG 04.

$f_J(2220)$ MASS

VALUE (MeV)	EVTS	DOCUMENT ID	TECN	COMMENT
2231.1 ± 3.5 OUR AVERAGE				
2235 ± 4 ± 6	74	BAI	96B BES	$e^+e^- \rightarrow J/\psi \rightarrow \gamma\pi^+\pi^-$
2230 ± $\frac{6}{7}$ ± 16	46	BAI	96B BES	$e^+e^- \rightarrow J/\psi \rightarrow \gamma K^+K^-$
2232 ± $\frac{8}{7}$ ± 15	23	BAI	96B BES	$e^+e^- \rightarrow J/\psi \rightarrow \gamma K_S^0 K_S^0$
2235 ± 4 ± 5	32	BAI	96B BES	$e^+e^- \rightarrow J/\psi \rightarrow \gamma\rho\bar{\rho}$
2209 ± $\frac{17}{15}$ ± 10		ASTON	88F LASS	11 $K^-p \rightarrow K^+K^-A$
2230 ± 20		BOLONKIN	88 SPEC	40 $\pi^-p \rightarrow K_S^0 K_S^0 n$
2220 ± 10	41	¹ ALDE	86B GA24	38-100 $\pi p \rightarrow n\eta\eta'$
2230 ± 6 ± 14	93	BALTRUSAIT...86D	MRK3	$e^+e^- \rightarrow \gamma K^+K^-$
2232 ± 7 ± 7	23	BALTRUSAIT...86D	MRK3	$e^+e^- \rightarrow \gamma K_S^0 K_S^0$
••• We do not use the following data for averages, fits, limits, etc. •••				
2246 ± 36		BAI	98H BES	$J/\psi \rightarrow \gamma\pi^0\pi^0$
¹ ALDE 86B uses data from both the GAMS-2000 and GAMS-4000 detectors.				

$f_J(2220)$ WIDTH

VALUE (MeV)	CL%	EVTS	DOCUMENT ID	TECN	COMMENT
23 ± $\frac{8}{9}$ OUR AVERAGE					
19 ± $\frac{13}{11}$ ± 12		74	BAI	96B BES	$e^+e^- \rightarrow J/\psi \rightarrow \gamma\pi^+\pi^-$
20 ± $\frac{20}{15}$ ± 17		46	BAI	96B BES	$e^+e^- \rightarrow J/\psi \rightarrow \gamma K^+K^-$
20 ± $\frac{25}{16}$ ± 14		23	BAI	96B BES	$e^+e^- \rightarrow J/\psi \rightarrow \gamma K_S^0 K_S^0$
15 ± $\frac{12}{9}$ ± 9		32	BAI	96B BES	$e^+e^- \rightarrow J/\psi \rightarrow \gamma\rho\bar{\rho}$
60 ± $\frac{107}{57}$			ASTON	88F LASS	11 $K^-p \rightarrow K^+K^-A$
80 ± 30			BOLONKIN	88 SPEC	40 $\pi^-p \rightarrow K_S^0 K_S^0 n$
26 ± $\frac{20}{16}$ ± 17		93	BALTRUSAIT...86D	MRK3	$e^+e^- \rightarrow \gamma K^+K^-$
18 ± $\frac{23}{15}$ ± 10		23	BALTRUSAIT...86D	MRK3	$e^+e^- \rightarrow \gamma K_S^0 K_S^0$
••• We do not use the following data for averages, fits, limits, etc. •••					
<80	90		ALDE	87C GAM2	38 $\pi^-p \rightarrow \eta'\eta n$

$f_J(2220)$ DECAY MODES

Mode	Fraction (Γ_i/Γ)
Γ_1 $\pi\pi$	seen
Γ_2 $\pi^+\pi^-$	seen
Γ_3 $K\bar{K}$	seen
Γ_4 $\rho\bar{\rho}$	
Γ_5 $\gamma\gamma$	not seen
Γ_6 $\eta\eta'(958)$	seen
Γ_7 $\phi\phi$	not seen
Γ_8 $\eta\eta$	not seen

$f_J(2220)$ $\Gamma(i)\Gamma(\gamma\gamma)/\Gamma(\text{total})$

VALUE (eV)	CL%	DOCUMENT ID	TECN	COMMENT	$\Gamma_3/\Gamma_5/\Gamma$
< 1.4	95	² ACCIARRI	01H L3	$\gamma\gamma \rightarrow K_S^0 K_S^0, E_{cm}^{ee} = 91, 183-209$ GeV	
••• We do not use the following data for averages, fits, limits, etc. •••					
< 5.6	95	² GODANG	97 CLE2	$\gamma\gamma \rightarrow K_S^0 K_S^0$	
< 86	95	² ALBRECHT	90G ARG	$\gamma\gamma \rightarrow K^+K^-$	
<1000	95	³ ALTHOFF	85B TASS	$\gamma\gamma, K\bar{K}\pi$	

$\Gamma(\pi\pi) \times \Gamma(\gamma\gamma)/\Gamma(\text{total})$

VALUE (eV)	CL%	DOCUMENT ID	TECN	COMMENT	$\Gamma_1/\Gamma_5/\Gamma$
<2.5	95	ALAM	98C CLE2	$\gamma\gamma \rightarrow \pi^+\pi^-$	
² Assuming $J^P = 2^+$.					
³ True for $J^P = 0^+$ and $J^P = 2^+$.					

$f_J(2220)$ $\Gamma(i)\Gamma(\rho\bar{\rho})/\Gamma^2(\text{total})$

VALUE (units 10^{-5})	CL%	DOCUMENT ID	TECN	COMMENT	$\Gamma_4/\Gamma_1/\Gamma^2$
<18	95	⁴ AMSLER	01 CBAR	1.4-1.5 $\rho\bar{\rho} \rightarrow \pi^0\pi^0$	
••• We do not use the following data for averages, fits, limits, etc. •••					
<(11-42)	99	⁵ HASAN	96 SPEC	1.35-1.55 $\rho\bar{\rho} \rightarrow \pi^+\pi^-$	

$\Gamma(\rho\bar{\rho}) \times \Gamma(\phi\phi)/\Gamma^2(\text{total})$

VALUE (units 10^{-5})	CL%	DOCUMENT ID	TECN	COMMENT	$\Gamma_4/\Gamma_7/\Gamma^2$
<6	95	⁶ EVANGELIS...	98 SPEC	1.1-2.0 $\rho\bar{\rho} \rightarrow \phi\phi$	

$\Gamma(\rho\bar{\rho}) \times \Gamma(\eta\eta)/\Gamma^2(\text{total})$

VALUE (units 10^{-5})	CL%	DOCUMENT ID	TECN	COMMENT	$\Gamma_4/\Gamma_8/\Gamma^2$
<4	95	⁴ AMSLER	01 CBAR	1.4-1.5 $\rho\bar{\rho} \rightarrow \eta\eta$	
⁴ For $J^P = 2^+$ in the mass range 2222-2240 MeV and the total width between 10 and 20 MeV.					
⁵ For $J^P = 2^+$ and $J^P = 4^+$ in the mass range 2220-2245 MeV and the total width of 15 MeV.					
⁶ For $J^P = 2^+$, the mass of 2235 MeV and the total width of 15 MeV.					

$f_J(2220)$ BRANCHING RATIOS

VALUE (units 10^{-4})	CL%	DOCUMENT ID	TECN	COMMENT	Γ_4/Γ
••• We do not use the following data for averages, fits, limits, etc. •••					
not seen		⁷ AUBERT	07AV BABR	$B \rightarrow \rho\bar{\rho}K^{(*)}$	
not seen		WANG	05A BELL	$B^+ \rightarrow \bar{\rho}\rho K^+$	
<3.0	95	⁸ EVANGELIS...	97 SPEC	1.96-2.40 $\bar{\rho}\rho \rightarrow K_S^0 K_S^0$	
<1.1	99.7	⁹ BARNES	93 SPEC	1.3-1.57 $\bar{\rho}\rho \rightarrow K_S^0 K_S^0$	
<2.6	99.7	⁹ BARDIN	87 CNTR	1.3-1.5 $\bar{\rho}\rho \rightarrow K^+K^-$	
<3.6	99.7	⁹ SCULLI	87 CNTR	1.29-1.55 $\bar{\rho}\rho \rightarrow K^+K^-$	
⁷ Assuming $\Gamma < 30$ MeV.					
⁸ Assuming $\Gamma \sim 20$ MeV, $J^P = 2^+$ and $B(f_J(2220) \rightarrow K\bar{K}) = 100\%$.					
⁹ Assuming $\Gamma = 30-35$ MeV, $J^P = 2^+$ and $B(f_J(2220) \rightarrow K\bar{K}) = 100\%$.					

$\Gamma(\pi\pi)/\Gamma(K\bar{K})$

VALUE	DOCUMENT ID	TECN	COMMENT	Γ_1/Γ_3
1.0 ± 0.5	BAI	96B BES	$e^+e^- \rightarrow J/\psi \rightarrow \gamma 2\pi, K\bar{K}$	

$\Gamma(\rho\bar{\rho})/\Gamma(K\bar{K})$

VALUE	DOCUMENT ID	TECN	COMMENT	Γ_4/Γ_3
0.17 ± 0.09	BAI	96B BES	$e^+e^- \rightarrow J/\psi \rightarrow \gamma\rho\bar{\rho}, K\bar{K}$	

$f_J(2220)$ REFERENCES

AUBERT	07AV	PR D76 092004	B. Aubert <i>et al.</i>	(BABAR Collab.)
WANG	05A	PL B617 141	M.-Z. Wang <i>et al.</i>	(BELLE Collab.)
PDG	04	PL B592 1	S. Eidelman <i>et al.</i>	
ACCIARRI	01H	PL B501 173	M. Acciarri <i>et al.</i>	(L3 Collab.)
AMSLER	01	PL B520 175	C. Amisler <i>et al.</i>	(Crystal Barrel Collab.)
ALAM	98C	PRL 81 3328	M.S. Alam <i>et al.</i>	(CLEO Collab.)
BAI	98H	PRL 81 1179	J.Z. Bai <i>et al.</i>	(BES Collab.)
EVANGELIS...	98	PR D57 5370	C. Evangelista <i>et al.</i>	(JETSSET Collab.)
GODANG	97	PRL 79 3829	R. Godang <i>et al.</i>	(LEAR Collab.)
BAI	96B	PRL 76 3502	J.Z. Bai <i>et al.</i>	(CLEO Collab.)
HASAN	96	PL B388 376	A. Hasan, D.V. Bugg	(BRUN, LOQM)
BARNES	93	PL B309 469	P.D. Barnes, P. Binin, W.H. Breunlich	
ALBRECHT	90G	ZPHY C48 183	H. Albrecht <i>et al.</i>	(ARGUS Collab.)
ASTON	88F	PL B215 199	D. Aston <i>et al.</i>	(SLAC, NAGO, CIN, INUS JP)
BOLONKIN	88	NP B309 426	B.V. Bolonkin <i>et al.</i>	(ITEP, SERP)
ALDE	87C	SJNP 45 255	D. Alde <i>et al.</i>	
Translated from YAF 45 405.				
BARDIN	87	PL B195 292	G. Bardin <i>et al.</i>	(SACL, FERR, CERN, PADO+)
SCULLI	87	PRL 58 1715	J. Sculli <i>et al.</i>	(NYU, BNL)
ALDE	86B	PL B177 120	D.M. Alde <i>et al.</i>	(SERP, BELG, LANL, LAPP)
BALTRUSAIT...	86D	PRL 56 107	R.M. Baltrusaitis	(CIT, UCSC, ILL, SLAC+)
ALTHOFF	85B	ZPHY C29 189	M. Althoff <i>et al.</i>	(TASSO Collab.)

See key on page 373

Meson Particle Listings
 $f_J(2220)$, $\eta(2225)$, $\rho_3(2250)$

OTHER RELATED PAPERS

CHUA	02	PL B544 139	C.-K. Chua, W.-S. Hou, S.U. Tsai	
MASEK	02	PR D65 072002	G. Masek et al.	(CLEO Collab.)
LIU	00A	JPG 26 L59	L.C. Liu, W.H. Ma	
WANG	00A	PR D62 017503	Z. Wang	
ANISOVICH	99D	PL B452 180	A.V. Anisovich et al.	
Also		NP A651 253	A.V. Anisovich et al.	
ANISOVICH	99F	NP A651 253	A.V. Anisovich et al.	
PROKOSHKIN	99	PAN 62 356	Yu. D. Prokoshkin	
		Translated from YAF 62 336		
HUANG	96	PL B380 189	T. Huang et al.	(BHEP, BEIJ)
BARDIN	87	PL B195 292	G. Bardin et al.	(SACL, FERR, CERN, PADO+)
LEYAOUANC	85	ZPHY C28 309	A. Le Yaouanc et al.	(ORSAY, TOKY)
GODFREY	84	PL 141B 439	S. Godfrey, R. Kokoski, N. Isgur	(TNTO)
SHATZ	84	PL 138B 209	M.P. Shatz	(CIT)
WILLEY	84	PRL 52 585	R.S. Willey	(PITT)
EISENHAND...	75	NP B96 109	E. Eisenhandler et al.	(LOQM, LIVP, DARE+)

 $\eta(2225)$

$$I^G(J^{PC}) = 0^+(0^-)$$

OMITTED FROM SUMMARY TABLE

Seen in $J/\psi \rightarrow \gamma\phi\phi$. Needs confirmation. $\eta(2225)$ MASS

VALUE (MeV)	DOCUMENT ID	TECN	CHG	COMMENT
2220 ± 18 OUR AVERAGE				
2230 ± 25 ± 15	BAI	90B	MRK3	$J/\psi \rightarrow \gamma K^+ K^- K^+ K^-$
2214 ± 20 ± 13	BAI	90B	MRK3	$J/\psi \rightarrow \gamma K^+ K^- K_S^0 K_L^0$
••• We do not use the following data for averages, fits, limits, etc. •••				
~ 2220	BISELLO	86B	DM2	$J/\psi \rightarrow \gamma K^+ K^- K^+ K^-$

 $\eta(2225)$ WIDTH

VALUE (MeV)	DOCUMENT ID	TECN	CHG	COMMENT
150 ± 300 ± 60 ± 60	BAI	90B	MRK3	$J/\psi \rightarrow \gamma K^+ K^- K^+ K^-$
••• We do not use the following data for averages, fits, limits, etc. •••				
~ 80	BISELLO	86B	DM2	$J/\psi \rightarrow \gamma K^+ K^- K^+ K^-$

 $\eta(2225)$ REFERENCES

BAI	90B	PRL 65 1309	Z. Bai et al.	(Mark III Collab.)
BISELLO	86B	PL B179 294	D. Bisello et al.	(DM2 Collab.)

 $\rho_3(2250)$

$$I^G(J^{PC}) = 1^+(3^-)$$

OMITTED FROM SUMMARY TABLE

Contains results mostly from formation experiments. For further production experiments see the Further States entry. See also $\rho(2150)$, $f_2(2150)$, $f_4(2300)$, $\rho_5(2350)$. $\rho_3(2250)$ MASS

VALUE (MeV)	DOCUMENT ID	TECN	CHG	COMMENT
••• We do not use the following data for averages, fits, limits, etc. •••				
~ 2232	HASAN	94	RVUE	$\bar{p}p \rightarrow \pi\pi$
~ 2090	1 OAKDEN	94	RVUE	0.36-1.55 $\bar{p}p \rightarrow \pi\pi$
~ 2250	2 MARTIN	80B	RVUE	
~ 2300	2 MARTIN	80C	RVUE	
~ 2140	3 CARTER	78B	CNTR 0	0.7-2.4 $\bar{p}p \rightarrow K^- K^+$
~ 2150	4 CARTER	77	CNTR 0	0.7-2.4 $\bar{p}p \rightarrow \pi\pi$

- 1 See however KLOET 96 who fit $\pi^+\pi^-$ only and find waves only up to $J = 3$ to be important but not significantly resonant.
 2 $I(J^P) = 1(3^-)$ from simultaneous analysis of $p\bar{p} \rightarrow \pi^-\pi^+$ and $\pi^0\pi^0$.
 3 $I = 0, 1, J^P = 3^-$ from Barrelet-zero analysis.
 4 $I(J^P) = 1(3^-)$ from amplitude analysis.

S-CHANNEL $\bar{N}N$

VALUE (MeV)	DOCUMENT ID	TECN	CHG	COMMENT
••• We do not use the following data for averages, fits, limits, etc. •••				
2260 ± 20	5 ANISOVICH	02	SPEC	0.6-1.9 $p\bar{p} \rightarrow \omega\pi^0, \omega\eta\pi^0, \pi^+\pi^-$
~ 2190	6 CUTTS	78B	CNTR	0.97-3 $\bar{p}p \rightarrow \bar{N}N$
2155 ± 15	6,7 COUPLAND	77	CNTR 0	0.7-2.4 $\bar{p}p \rightarrow \bar{p}p$
2193 ± 2	6,8 ALSPECTOR	73	CNTR	$\bar{p}p$ S channel
2190 ± 10	9 ABRAMS	70	CNTR	S channel $\bar{p}N$

- 5 From the combined analysis of ANISOVICH 00J, ANISOVICH 01D, ANISOVICH 01E, and ANISOVICH 02.
 6 Isospins 0 and 1 not separated.
 7 From a fit to the total elastic cross section.
 8 Referred to as T or T region by ALSPECTOR 73.
 9 Seen as bump in $l = 1$ state. See also COOPER 68. PEASLEE 75 confirm $\bar{p}p$ results of ABRAMS 70, no narrow structure.

 $\pi^-p \rightarrow \eta\pi\pi$

VALUE (MeV)	DOCUMENT ID	TECN	CHG	COMMENT
••• We do not use the following data for averages, fits, limits, etc. •••				
2290 ± 20 ± 30	AMELIN	00	VES	37 $\pi^-p \rightarrow \eta\pi^+\pi^-n$

 $\rho_3(2250)$ WIDTH $\bar{p}p \rightarrow \pi\pi$ or $K\bar{K}$

VALUE (MeV)	DOCUMENT ID	TECN	CHG	COMMENT
••• We do not use the following data for averages, fits, limits, etc. •••				
~ 220	HASAN	94	RVUE	$\bar{p}p \rightarrow \pi\pi$
~ 60	10 OAKDEN	94	RVUE	0.36-1.55 $\bar{p}p \rightarrow \pi\pi$
~ 250	11 MARTIN	80B	RVUE	
~ 200	11 MARTIN	80C	RVUE	
~ 150	12 CARTER	78B	CNTR 0	0.7-2.4 $\bar{p}p \rightarrow K^- K^+$
~ 200	13 CARTER	77	CNTR 0	0.7-2.4 $\bar{p}p \rightarrow \pi\pi$
10 See however KLOET 96 who fit $\pi^+\pi^-$ only and find waves only up to $J = 3$ to be important but not significantly resonant. 11 $I(J^P) = 1(3^-)$ from simultaneous analysis of $p\bar{p} \rightarrow \pi^-\pi^+$ and $\pi^0\pi^0$. 12 $I = 0, 1, J^P = 3^-$ from Barrelet-zero analysis. 13 $I(J^P) = 1(3^-)$ from amplitude analysis.				

S-CHANNEL $\bar{N}N$

VALUE (MeV)	DOCUMENT ID	TECN	CHG	COMMENT
••• We do not use the following data for averages, fits, limits, etc. •••				
160 ± 25	14 ANISOVICH	02	SPEC	0.6-1.9 $p\bar{p} \rightarrow \omega\pi^0, \omega\eta\pi^0, \pi^+\pi^-$
135 ± 75	15,16 COUPLAND	77	CNTR 0	0.7-2.4 $\bar{p}p \rightarrow \bar{p}p$
98 ± 8	16 ALSPECTOR	73	CNTR	$\bar{p}p$ S channel
~ 85	17 ABRAMS	70	CNTR	S channel $\bar{p}N$

- 14 From the combined analysis of ANISOVICH 00J, ANISOVICH 01D, ANISOVICH 01E, and ANISOVICH 02.
 15 From a fit to the total elastic cross section.
 16 Isospins 0 and 1 not separated.
 17 Seen as bump in $l = 1$ state. See also COOPER 68. PEASLEE 75 confirm $\bar{p}p$ results of ABRAMS 70, no narrow structure.

 $\pi^-p \rightarrow \eta\pi\pi$

VALUE (MeV)	DOCUMENT ID	TECN	CHG	COMMENT
••• We do not use the following data for averages, fits, limits, etc. •••				
230 ± 50 ± 80	AMELIN	00	VES	37 $\pi^-p \rightarrow \eta\pi^+\pi^-n$

 $\rho_3(2250)$ REFERENCES

ANISOVICH	02	PL B542 8	A.V. Anisovich et al.	
ANISOVICH	01D	PL B508 6	A.V. Anisovich et al.	
ANISOVICH	01E	PL B513 281	A.V. Anisovich et al.	
AMELIN	00	NP A668 83	D. Amelin et al.	(VES Collab.)
ANISOVICH	00J	PL B491 47	A.V. Anisovich et al.	
KLOET	96	PR D53 6120	W.M. Kloet, F. Myhrer	(RUTG, NORD)
HASAN	94	PL B334 215	A. Hasan, D.V. Bugg	(LOQM)
OAKDEN	94	NP A574 731	M.N. Oakden, M.R. Pennington	(DURH)
MARTIN	80B	NP B176 355	B.R. Martin, D. Morgan	(LOUC, RHEL) JP
MARTIN	80C	NP B169 216	A.D. Martin, M.R. Pennington	(DURH) JP
CARTER	78B	NP B141 467	A.A. Carter	(LOQM)
CUTTS	78B	PR D17 16	D. Cutts et al.	(STON, WISC)
CARTER	77	PL 67B 117	A.A. Carter et al.	(LOQM, RHEL) JP
COUPLAND	77	PL 71B 460	M. Coupland et al.	(LOQM, RHEL)
PEASLEE	75	PL 57B 189	D.C. Peaslee et al.	(CANB, BARI, BROW+)
ALSPECTOR	73	PRL 30 511	J. Alspector et al.	(RUTG, UPNJ)
ABRAMS	70	PR D1 1917	R.J. Abrams et al.	(BNL)
COOPER	68	PRL 20 1059	W.A. Cooper et al.	(ANL)

OTHER RELATED PAPERS

MARTIN	79B	PL 86B 93	A.D. Martin, M.R. Pennington	(DURH) JP
CARTER	78	NP B132 176	A.A. Carter	(LOQM) JP
CARTER	77B	PL 67B 122	A.A. Carter	(LOQM) JP
CARTER	77C	NP B127 202	A.A. Carter et al.	(LOQM, DARE, RHEL)
ZEMANY	76	NP B103 537	P.D. Zemany et al.	(MSU)
EISENHAND...	75	NP B96 109	E. Eisenhandler et al.	(LOQM, LIVP, DARE+)
BERTANZA	74	NC 23A 209	L. Bertanza et al.	(PISA, PADO, TORI)
BETTINI	73	NC 15A 563	A. Bettini et al.	(PADO, LBL, PISA+)
DONNACHE	73	LNC 7 285	A. Donnachie, P.R. Thomas	(MCHS)
NICHOLSON	73	PR D7 2572	H. Nicholson et al.	(CIT, ROCH, BNL)
FIELDS	71	PRL 27 1749	T. Fields et al.	(ANL, OXF)
YOH	71	PRL 26 922	J.K. Yoh et al.	(CIT, BNL, ROCH)
ABRAMS	67C	PRL 18 1209	R.J. Abrams et al.	(BNL)

Meson Particle Listings

 $f_2(2300)$, $f_4(2300)$ $f_2(2300)$

$$I^G(J^{PC}) = 0^+(2^{++})$$

 $f_2(2300)$ MASS

VALUE (MeV)	DOCUMENT ID	TECN	COMMENT
2297 ± 28	¹ ETKIN 88	MPS	$22 \pi^- p \rightarrow \phi \phi n$
• • • We do not use the following data for averages, fits, limits, etc. • • •			
2270 ± 12	VLADIMIRSK...06	SPEC	$40 \pi^- p \rightarrow K_S^0 K_S^0 n$
2327 ± 9 ± 6	ABE 04	BELL	$10.6 e^+ e^- \rightarrow e^+ e^- K^+ K^-$
2240 ± 15	ANISOVICH 00j	SPEC	$p \bar{p} \rightarrow \pi^0 \pi^0 \eta$
2231 ± 10	BOOTH 86	OMEG	$85 \pi^- \text{Be} \rightarrow 2\phi \text{Be}$
2220 ⁺⁹⁰ ₋₂₀	LINDENBAUM 84	RVUE	
2320 ± 40	ETKIN 82	MPS	$22 \pi^- p \rightarrow 2\phi n$

¹Includes data of ETKIN 85. The percentage of the resonance going into $\phi \phi 2^{++} S_2$, D_2 , and D_0 is 6^{+15}_{-5} , 25^{+18}_{-14} , and 69^{+16}_{-27} , respectively.

 $f_2(2300)$ WIDTH

VALUE (MeV)	DOCUMENT ID	TECN	COMMENT
149 ± 41	² ETKIN 88	MPS	$22 \pi^- p \rightarrow \phi \phi n$
• • • We do not use the following data for averages, fits, limits, etc. • • •			
90 ± 29	VLADIMIRSK...06	SPEC	$40 \pi^- p \rightarrow K_S^0 K_S^0 n$
275 ± 36 ± 20	ABE 04	BELL	$10.6 e^+ e^- \rightarrow e^+ e^- K^+ K^-$
241 ± 30	ANISOVICH 00j	SPEC	$p \bar{p} \rightarrow \pi^0 \pi^0 \eta$
133 ± 5.0	BOOTH 86	OMEG	$85 \pi^- \text{Be} \rightarrow 2\phi \text{Be}$
200 ± 5.0	LINDENBAUM 84	RVUE	
220 ± 7.0	ETKIN 82	MPS	$22 \pi^- p \rightarrow 2\phi n$

²Includes data of ETKIN 85.

 $f_2(2300)$ DECAY MODES

Mode	Fraction (Γ_i/Γ)
Γ_1 $\phi \phi$	seen
Γ_2 $K \bar{K}$	seen
Γ_3 $\gamma \gamma$	seen

 $f_2(2300)$ $\Gamma(i)\Gamma(\gamma\gamma)/\Gamma(\text{total})$

$\Gamma(K\bar{K}) \times \Gamma(\gamma\gamma)/\Gamma_{\text{total}}$	DOCUMENT ID	TECN	COMMENT	$\Gamma_2/\Gamma_3/\Gamma$
44 ± 6 ± 12	³ ABE 04	BELL	$10.6 e^+ e^- \rightarrow e^+ e^- K^+ K^-$	

³Assuming spin 2.

 $f_2(2300)$ REFERENCES

VLADIMIRSK... 06	PAN 69 493	V.V. Vladimirov et al.	(ITEP, Moscow)
ABE 04	EPJ C32 323	K. Abe et al.	(BELLE Collab.)
ANISOVICH 00j	PL B491 47	A.V. Anisovich et al.	
ETKIN 88	PL B201 568	A. Etkin et al.	(BNL, CUNY)
BOOTH 86	NP B273 677	P.S.L. Booth et al.	(LIVP, GLAS, CERN)
ETKIN 85	PL 165B 217	A. Etkin et al.	(BNL, CUNY)
LINDENBAUM 84	CNPP 13 285	S.J. Lindenbaum	(CUNY)
ETKIN 82	PRL 49 1620	A. Etkin et al.	(BNL, CUNY)

OTHER RELATED PAPERS

ANISOVICH 05	JETPL 80 715	V.V. Anisovich	
	Translated from ZETFP 80 845.		
ANISOVICH 05A	JETPL 81 417	V.V. Anisovich, A.V. Sarantsev	
	Translated from ZETFP 81 531.		
ANISOVICH 05C	JIMP A20 6327	V.V. Anisovich, M.A. Matveev, A.V. Sarantsev	
LONGACRE 04	PR D70 094041	R.S. Longacre, S.J. Lindenbaum	
AMELIN 00	NP A668 83	D. Amelin et al.	(VES Collab.)
BOLONKIN 00	JETPL 72 166	B.V. Bolonkin et al.	
	Translated from ZETFP 72 240.		
BARBERIS 98	PL B432 436	D. Barberis et al.	(Omega Expt.)
LANDBERG 96	PR D53 2839	C. Landberg et al.	(BNL, CUNY, RPI)
GREEN 86	PRL 56 1639	D.R. Green et al.	(FNAL, ARIZ, FSU+)
BOOTH 84	NP B242 51	P.S.L. Booth et al.	(LIVP, GLAS, CERN)
EISENHAND... 75	NP B96 109	E. Eisenhandler et al.	(LOQM, LIVP, DARE+)

 $f_4(2300)$

$$I^G(J^{PC}) = 0^+(4^{++})$$

OMITTED FROM SUMMARY TABLE

This entry was previously called $U_0(2350)$. Contains results mostly from formation experiments. For further production experiments see the Further States entry. See also $\rho(2150)$, $f_2(2150)$, $\rho_3(2250)$, $\rho_5(2350)$.

 $f_4(2300)$ MASS $\bar{p}p \rightarrow \pi\pi$ or $\bar{K}K$

VALUE (MeV)	DOCUMENT ID	TECN	COMMENT
• • • We do not use the following data for averages, fits, limits, etc. • • •			
~ 2314	HASAN 94	RVUE	$\bar{p}p \rightarrow \pi\pi$
~ 2300	¹ MARTIN 80B	RVUE	
~ 2300	¹ MARTIN 80C	RVUE	
~ 2340	² CARTER 78B	CNTR	$0.7\text{--}2.4 \bar{p}p \rightarrow K^- K^+$
~ 2330	DULUDE 78B	OSP K	$1\text{--}2 \bar{p}p \rightarrow \pi^0 \pi^0$
~ 2310	³ CARTER 77	CNTR	$0.7\text{--}2.4 \bar{p}p \rightarrow \pi\pi$
¹ $I(J^P) = 0(4^+)$ from simultaneous analysis of $p\bar{p} \rightarrow \pi^- \pi^+$ and $\pi^0 \pi^0$.			
² $I(J^P) = 0(4^+)$ from Barrelet-zero analysis.			
³ $I(J^P) = 0(4^+)$ from amplitude analysis.			

S-CHANNEL $\bar{p}p$ or $\bar{N}N$

VALUE (MeV)	DOCUMENT ID	TECN	COMMENT
• • • We do not use the following data for averages, fits, limits, etc. • • •			
2283 ± 17	⁴ ANISOVICH 00j	SPEC	
~ 2380	⁵ CUTTS 78B	CNTR	$0.97\text{--}3 \bar{p}p \rightarrow \bar{N}N$
2345 ± 15	^{5,6} COUPLAND 77	CNTR	$0.7\text{--}2.4 \bar{p}p \rightarrow \bar{p}p$
2359 ± 2	^{5,7} ALSPECTOR 73	CNTR	$\bar{p}p$ S channel
2375 ± 10	ABRAMS 70	CNTR	S channel $\bar{N}N$
⁴ From the combined analysis of ANISOVICH 99c and ANISOVICH 99f on $\bar{p}p \rightarrow \eta \pi^0 \pi^0$, $\pi^0 \pi^0$, $\eta \eta$, $\eta \eta'$, $\pi^+ \pi^-$.			
⁵ Isospins 0 and 1 not separated.			
⁶ From a fit to the total elastic cross section.			
⁷ Referred to as U or U region by ALSPECTOR 73.			

 $\pi^- p \rightarrow \eta \pi \pi n$

VALUE (MeV)	DOCUMENT ID	TECN	COMMENT
• • • We do not use the following data for averages, fits, limits, etc. • • •			
2330 ± 20 ± 40	AMELIN 00	VES	$37 \pi^- p \rightarrow \eta \pi^+ \pi^- n$

 $p\bar{p}$ CENTRAL PRODUCTION

VALUE (MeV)	DOCUMENT ID	COMMENT
2320 ± 60 OUR ESTIMATE		
• • • We do not use the following data for averages, fits, limits, etc. • • •		
2332 ± 15	BARBERIS 00f	450 $p\bar{p} \rightarrow p_f \omega \omega p_S$

 $f_4(2300)$ WIDTH $\bar{p}p \rightarrow \pi\pi$ or $\bar{K}K$

VALUE (MeV)	DOCUMENT ID	TECN	COMMENT
• • • We do not use the following data for averages, fits, limits, etc. • • •			
~ 278	HASAN 94	RVUE	$\bar{p}p \rightarrow \pi\pi$
~ 200	⁸ MARTIN 80C	RVUE	
~ 150	⁹ CARTER 78B	CNTR	$0.7\text{--}2.4 \bar{p}p \rightarrow K^- K^+$
~ 210	¹⁰ CARTER 77	CNTR	$0.7\text{--}2.4 \bar{p}p \rightarrow \pi\pi$
⁸ $I(J^P) = 0(4^+)$ from simultaneous analysis of $p\bar{p} \rightarrow \pi^- \pi^+$ and $\pi^0 \pi^0$.			
⁹ $I(J^P) = 0(4^+)$ from Barrelet-zero analysis.			
¹⁰ $I(J^P) = 0(4^+)$ from amplitude analysis.			

S-CHANNEL $\bar{p}p$ or $\bar{N}N$

VALUE (MeV)	DOCUMENT ID	TECN	COMMENT
• • • We do not use the following data for averages, fits, limits, etc. • • •			
310 ± 25	¹¹ ANISOVICH 00j	SPEC	
135^{+150}_{-65}	^{12,13} COUPLAND 77	CNTR	$0.7\text{--}2.4 \bar{p}p \rightarrow \bar{p}p$
165^{+18}_{-8}	¹³ ALSPECTOR 73	CNTR	$\bar{p}p$ S channel
~ 190	ABRAMS 70	CNTR	S channel $\bar{N}N$
¹¹ From the combined analysis of ANISOVICH 99c and ANISOVICH 99f on $\bar{p}p \rightarrow \eta \pi^0 \pi^0$, $\pi^0 \pi^0$, $\eta \eta$, $\eta \eta'$, $\pi^+ \pi^-$.			
¹² From a fit to the total elastic cross section.			
¹³ Isospins 0 and 1 not separated.			

 $\pi^- p \rightarrow \eta \pi \pi n$

VALUE (MeV)	DOCUMENT ID	TECN	COMMENT
• • • We do not use the following data for averages, fits, limits, etc. • • •			
235 ± 5.0 ± 4.0	AMELIN 00	VES	$37 \pi^- p \rightarrow \eta \pi^+ \pi^- n$

See key on page 373

Meson Particle Listings
 $f_4(2300)$, $f_0(2330)$, $f_2(2340)$ **$p\bar{p}$ CENTRAL PRODUCTION**

VALUE (MeV) DOCUMENT ID COMMENT

250±80 OUR ESTIMATE

• • • We do not use the following data for averages, fits, limits, etc. • • •

260±57 BARBERIS 00F 450 $p\bar{p} \rightarrow p_f \omega \omega p_S$ **$f_4(2300)$ DECAY MODES**

Mode	Fraction (Γ_i/Γ)
Γ_1 $\rho\rho$	seen
Γ_2 $\omega\omega$	seen
Γ_3 $\eta\pi\pi$	seen
Γ_4 $\pi\pi\pi$	seen
Γ_5 $K\bar{K}$	seen
Γ_6 $N\bar{N}$	seen

 $f_4(2300)$ BRANCHING RATIOS $\Gamma(\rho\rho)/\Gamma(\omega\omega)$ Γ_1/Γ_2

VALUE DOCUMENT ID COMMENT

• • • We do not use the following data for averages, fits, limits, etc. • • •

2.8±0.5 BARBERIS 00F 450 $p\bar{p} \rightarrow p_f \omega \omega p_S$ **$f_4(2300)$ REFERENCES**

AMELIN 00 NP A668 83	D. Amelin et al.	(VES Collab.)
ANISOVICH 00J PL B491 47	A.V. Anisovich et al.	
BARBERIS 00F PL B484 198	D. Barberis et al.	(WA 102 Collab.)
ANISOVICH 99C PL B452 173	A.V. Anisovich et al.	
ANISOVICH 99F NP A651 253	A.V. Anisovich et al.	
HASAN 94 PL B334 215	A. Hasan, D.V. Bugg	(LOQM)
MARTIN 80B NP B176 355	B.R. Martin, D. Morgan	(LOUC, RHEL) JP
MARTIN 80C NP B169 216	A.D. Martin, M.R. Pennington	(DURH) JP
CARTER 78B NP B141 467	A.A. Carter	(LOQM)
CUTTS 78B PR D17 16	D. Cutts et al.	(STON, WISC)
DULUDE 78B PL 79B 335	R.S. Dulude et al.	(BROW, MIT, BARI) JP
CARTER 77 PL 67B 117	A.A. Carter et al.	(LOQM, RHEL) JP
COUPLAND 77 PL 71B 460	M. Coupland et al.	(LOQM, RHEL)
ALSPECTOR 73 PRL 30 511	J. Alspector et al.	(RUTG, UPNJ)
ABRAMS 70 PR D1 1917	R.J. Abrams et al.	(BNL)

OTHER RELATED PAPERS

ANISOVICH 99D PL B452 180	A.V. Anisovich et al.	
Also NP A651 253	A.V. Anisovich et al.	
ANISOVICH 99F NP A651 253	A.V. Anisovich et al.	
EISENHAND... 75 NP B96 109	E. Eisenhandler et al.	(LOQM, LIVP, DARE+)
FIELDS 71 PRL 27 1749	T. Fields et al.	(ANL, OXF)
YOH 71 PRL 26 922	J.K. Yoh et al.	(CIT, BNL, ROCH)
BRICMAN 69 PL 29B 451	C. Bricman et al.	(CERN, CAEN, SACL)

 $f_0(2330)$

$$I^G(J^{PC}) = 0^+(0^{++})$$

OMITTED FROM SUMMARY TABLE

 $f_0(2330)$ MASS

VALUE (MeV) DOCUMENT ID TECN COMMENT

• • • We do not use the following data for averages, fits, limits, etc. • • •

2314±25	¹ BUGG 04A RVUE
2337±14	ANISOVICH 00J SPEC 2.0 $\bar{p}p \rightarrow \pi\pi, \eta\eta$
~ 2321	HASAN 94 RVUE $\bar{p}p \rightarrow \pi\pi$

¹ Partial wave analysis of the data on $p\bar{p} \rightarrow \bar{\Lambda}\Lambda$ from BARNES 00. **$f_0(2330)$ WIDTH**

VALUE (MeV) DOCUMENT ID TECN COMMENT

• • • We do not use the following data for averages, fits, limits, etc. • • •

144±20	² BUGG 04A RVUE
217±33	ANISOVICH 00J SPEC 2.0 $\bar{p}p \rightarrow \pi\pi, \eta\eta$
~ 223	HASAN 94 RVUE $\bar{p}p \rightarrow \pi\pi$

² Partial wave analysis of the data on $p\bar{p} \rightarrow \bar{\Lambda}\Lambda$ from BARNES 00. **$f_0(2330)$ REFERENCES**

BUGG 04A EPJ C36 161	D.V. Bugg	
ANISOVICH 00J PL B491 47	A.V. Anisovich et al.	
BARNES 00 PR C62 055203	P.D. Barnes et al.	
HASAN 94 PL B334 215	A. Hasan, D.V. Bugg	(LOQM)

 $f_2(2340)$

$$I^G(J^{PC}) = 0^+(2^{++})$$

 $f_2(2340)$ MASS

VALUE (MeV) EVTS DOCUMENT ID TECN COMMENT

2339±55	¹ ETKIN 88 MPS 22 $\pi^- p \rightarrow \phi\phi n$
----------------	---

• • • We do not use the following data for averages, fits, limits, etc. • • •

2350±7	80k	² UMAN 06 E835 5.2 $\bar{p}p \rightarrow \eta\eta\pi^0$
2392±10		BOOTH 86 OMEG 85 $\pi^- Be \rightarrow 2\phi Be$
2360±20		LINDENBAUM 84 RVUE

¹ Includes data of ETKIN 85. The percentage of the resonance going into $\phi\phi 2^{++} S_2$, D_2 , and D_0 is 37 ± 19 , 4 ± 12 , and 59 ± 21 , respectively.² Statistical error only. **$f_2(2340)$ WIDTH**

VALUE (MeV) EVTS DOCUMENT ID TECN COMMENT

319+⁻81/69	³ ETKIN 88 MPS 22 $\pi^- p \rightarrow \phi\phi n$
------------------------------	---

• • • We do not use the following data for averages, fits, limits, etc. • • •

218±16	80k	⁴ UMAN 06 E835 5.2 $\bar{p}p \rightarrow \eta\eta\pi^0$
198±50		BOOTH 86 OMEG 85 $\pi^- Be \rightarrow 2\phi Be$
150+ ⁻ 150/50		LINDENBAUM 84 RVUE

³ Includes data of ETKIN 85.⁴ Statistical error only. **$f_2(2340)$ DECAY MODES**

Mode	Fraction (Γ_i/Γ)
Γ_1 $\phi\phi$	seen
Γ_2 $\eta\eta$	seen

 $f_2(2340)$ BRANCHING RATIOS $\Gamma(\eta\eta)/\Gamma_{total}$ Γ_2/Γ

VALUE DOCUMENT ID TECN COMMENT

seen	UMAN 06 E835 5.2 $\bar{p}p \rightarrow \eta\eta\pi^0$
------	---

 $f_2(2340)$ REFERENCES

UMAN 06 PR D73 052009	I. Uman et al.	(FNAL E835)
ETKIN 88 PL B201 568	A. Etkin et al.	(BNL, CUNY)
BOOTH 86 NP B273 677	P.S.L. Booth et al.	(LIVP, GLAS, CERN)
ETKIN 85 PL 165B 217	A. Etkin et al.	(BNL, CUNY)
LINDENBAUM 84 CNPP 13 285	S.J. Lindenbaum	(CUNY)

OTHER RELATED PAPERS

ANISOVICH 05 JETPL 80 715	V.V. Anisovich	
Translated from ZETFP 80 845.		
ANISOVICH 05A JETPL 81 417	V.V. Anisovich, A.V. Sarantsev	
Translated from ZETFP 81 531.		
ANISOVICH 05C IJMP A20 6327	V.V. Anisovich, M.A. Matveev, A.V. Sarantsev	
BUGG 04A EPJ C36 161	D.V. Bugg	
LONGACRE 04 PR D70 094041	R.S. Longacre, S.J. Lindenbaum	
BOLONKIN 00 JETPL 72 166	B.V. Bolonkin et al.	
Translated from ZETFP 72 240.		
ANISOVICH 99D PL B452 180	A.V. Anisovich et al.	
Also NP A651 253	A.V. Anisovich et al.	
ANISOVICH 99F NP A651 253	A.V. Anisovich et al.	
LANDBERG 96 PR D53 2839	C. Landberg et al.	(BNL, CUNY, RPI)
GREEN 86 PRL 56 1639	D.R. Green et al.	(FNAL, ARIZ, FSU+)
BOOTH 84 NP B242 51	P.S.L. Booth et al.	(LIVP, GLAS, CERN)
EISENHAND... 75 NP B96 109	E. Eisenhandler et al.	(LOQM, LIVP, DARE+)

Meson Particle Listings

 $\rho_5(2350)$, $a_6(2450)$ $\rho_5(2350)$

$$I^G(J^{PC}) = 1^+(5^{- -})$$

OMITTED FROM SUMMARY TABLE

This entry was previously called $U_1(2400)$. See also $\rho(2150)$, $f_2(2150)$, $\rho_3(2250)$, $f_4(2300)$. $\rho_5(2350)$ MASS $\pi^- p \rightarrow \omega \pi^0 n$

VALUE (MeV)	DOCUMENT ID	TECN	CHG	COMMENT
2330 ± 35	ALDE	95	GAM2	$38 \pi^- p \rightarrow \omega \pi^0 n$

VALUE (MeV)	DOCUMENT ID	TECN	CHG	COMMENT
-------------	-------------	------	-----	---------

• • • We do not use the following data for averages, fits, limits, etc. • • •

~ 2303	HASAN	94	RVUE	$\bar{p} p \rightarrow \pi \pi$
~ 2300	1 MARTIN	80B	RVUE	
~ 2250	1 MARTIN	80C	RVUE	
~ 2500	2 CARTER	78B	CNTR	0
~ 2480	3 CARTER	77	CNTR	0

S-CHANNEL $\bar{N} N$

VALUE (MeV)	DOCUMENT ID	TECN	CHG	COMMENT
-------------	-------------	------	-----	---------

• • • We do not use the following data for averages, fits, limits, etc. • • •

2300 ± 45	4 ANISOVICH	02	SPEC	0.6–1.9 $\rho \bar{p} \rightarrow \omega \pi^0, \omega \eta \pi^0, \pi^+ \pi^-$
2295 ± 30	ANISOVICH	00J	SPEC	
~ 2380	5 CUTTS	78B	CNTR	0.97–3 $\bar{p} p \rightarrow \bar{N} N$
2345 ± 15	5,6 COUPLAND	77	CNTR	0
2359 ± 2	5,7 ALSPECTOR	73	CNTR	$\bar{p} p$ S channel
2350 ± 10	8 ABRAMS	70	CNTR	S channel $\bar{N} N$
2360 ± 25	9 OH	70B	HDBC	–0 $\bar{p}(\rho n), K^* K 2\pi$

 $\pi^- p \rightarrow K^+ K^- n$

VALUE (MeV)	DOCUMENT ID	TECN	CHG	COMMENT
-------------	-------------	------	-----	---------

• • • We do not use the following data for averages, fits, limits, etc. • • •

2307 ± 6	ALPER	80	CNTR	0
----------	-------	----	------	---

1 $I(J^P) = 1(5^-)$ from simultaneous analysis of $\rho \bar{p} \rightarrow \pi^- \pi^+$ and $\pi^0 \pi^0$.2 $I = 0(1); J^P = 5^-$ from Barrelet-zero analysis.3 $I(J^P) = 1(5^-)$ from amplitude analysis.

4 From the combined analysis of ANISOVICH 00J, ANISOVICH 01D, ANISOVICH 01E, and ANISOVICH 02.

5 Isospins 0 and 1 not separated.

6 From a fit to the total elastic cross section.

7 Referred to as U or U region by ALSPECTOR 73.8 For $I = 1 \bar{N} N$.9 No evidence for this bump seen in the $\bar{p} p$ data of CHAPMAN 71B. Narrow state not confirmed by OH 73 with more data. $\rho_5(2350)$ WIDTH $\pi^- p \rightarrow \omega \pi^0 n$

VALUE (MeV)	DOCUMENT ID	TECN	CHG	COMMENT
400 ± 100	ALDE	95	GAM2	$38 \pi^- p \rightarrow \omega \pi^0 n$

 $\bar{p} p \rightarrow \pi \pi$ or $\bar{K} K$

VALUE (MeV)	DOCUMENT ID	TECN	CHG	COMMENT
-------------	-------------	------	-----	---------

• • • We do not use the following data for averages, fits, limits, etc. • • •

~ 169	HASAN	94	RVUE	$\bar{p} p \rightarrow \pi \pi$
~ 250	10 MARTIN	80B	RVUE	
~ 300	10 MARTIN	80C	RVUE	
~ 150	11 CARTER	78B	CNTR	0
~ 210	12 CARTER	77	CNTR	0

S-CHANNEL $\bar{N} N$

VALUE (MeV)	DOCUMENT ID	TECN	CHG	COMMENT
-------------	-------------	------	-----	---------

• • • We do not use the following data for averages, fits, limits, etc. • • •

260 ± 75	13 ANISOVICH	02	SPEC	0.6–1.9 $\rho \bar{p} \rightarrow \omega \pi^0, \omega \eta \pi^0, \pi^+ \pi^-$
235 ⁺ _{–40}	ANISOVICH	00J	SPEC	
135 ⁺ _{–65}	14,15 COUPLAND	77	CNTR	0
165 ⁺ _{–18}	15 ALSPECTOR	73	CNTR	$\bar{p} p$ S channel
< 60	16 OH	70B	HDBC	–0 $\bar{p}(\rho n), K^* K 2\pi$
~ 140	ABRAMS	67C	CNTR	S channel $\bar{N} N$

 $\pi^- p \rightarrow K^+ K^- n$

VALUE (MeV)	DOCUMENT ID	TECN	CHG	COMMENT
-------------	-------------	------	-----	---------

• • • We do not use the following data for averages, fits, limits, etc. • • •

245 ± 20	ALPER	80	CNTR	0
----------	-------	----	------	---

10 $I(J^P) = 1(5^-)$ from simultaneous analysis of $\rho \bar{p} \rightarrow \pi^- \pi^+$ and $\pi^0 \pi^0$.11 $I = 0(1); J^P = 5^-$ from Barrelet-zero analysis.12 $I(J^P) = 1(5^-)$ from amplitude analysis.

13 From the combined analysis of ANISOVICH 00J, ANISOVICH 01D, ANISOVICH 01E, and ANISOVICH 02.

14 From a fit to the total elastic cross section.

15 Isospins 0 and 1 not separated.

16 No evidence for this bump seen in the $\bar{p} p$ data of CHAPMAN 71B. Narrow state not confirmed by OH 73 with more data. $\rho_5(2350)$ REFERENCES

ANISOVICH 02	PL B542 8	A.V. Anisovich et al.	
ANISOVICH 01D	PL B508 6	A.V. Anisovich et al.	
ANISOVICH 01E	PL B513 281	A.V. Anisovich et al.	
ANISOVICH 00J	PL B491 47	A.V. Anisovich et al.	
ALDE 95	ZPHY C66 379	D.M. Alde et al.	(GAMS Collab.) JP
HASAN 94	PL B334 215	A. Hasan, D.V. Bugg	(LOQM)
ALPER 80	PL 94B 422	B. Alper et al.	(AMST, CERN, CRAC, MPIM+)
MARTIN 80B	NP B176 355	B.R. Martin, D. Morgan	(LOUC, RHEL) JP
MARTIN 80C	NP B169 216	A.D. Martin, M.R. Pennington	(DURH) JP
CARTER 78B	NP B141 467	A.A. Carter	(LOQM)
CUTTS 78B	PR D17 16	D. Cutts et al.	(STON, WIS C)
CARTER 77	PL 67B 117	A.A. Carter et al.	(LOQM, RHEL) JP
COUPLAND 77	PL 71B 460	M. Coupland et al.	(LOQM, RHEL)
ALSPECTOR 73	PRL 30 511	J. Alspector et al.	(RUTG, UPNJ)
OH 73	NP B51 57	B.Y. Oh et al.	(MSU)
CHAPMAN 71B	PR D4 1275	J.W. Chapman et al.	(MICH)
ABRAMS 70	PR D1 1917	R.J. Abrams et al.	(BNL)
OH 70B	PRL 24 1257	B.Y. Oh et al.	(MSU)
ABRAMS 67C	PRL 18 1209	R.J. Abrams et al.	(BNL)

OTHER RELATED PAPERS

EISENHAND... 75	NP B96 109	E. Eisenhandler et al.	(LOQM, LIVP, DARE+)
CASO 70	LCN 3 707	C. Caso et al.	(GENO, HAMB, MILA, SAEL)
BRICMAN 69	PL 29B 451	C. Bricman et al.	(CERN, CAEN, SAEL)

 $a_6(2450)$

$$I^G(J^{PC}) = 1^-(6^{+ +})$$

OMITTED FROM SUMMARY TABLE

Needs confirmation.

 $a_6(2450)$ MASS

VALUE (MeV)	DOCUMENT ID	TECN	CHG	COMMENT
2450 ± 130	1 CLELAND	82B	SPEC	±

1 From an amplitude analysis.

 $a_6(2450)$ WIDTH

VALUE (MeV)	DOCUMENT ID	TECN	CHG	COMMENT
400 ± 250	2 CLELAND	82B	SPEC	±

2 From an amplitude analysis.

 $a_6(2450)$ DECAY MODES

Mode	Γ_1
$K \bar{K}$	

 $a_6(2450)$ REFERENCES

CLELAND 82B	NP B208 228	W.E. Cleland et al.	(DURH, GEVA, LAUS+)
-------------	-------------	---------------------	---------------------

See key on page 373

 $f_6(2510)$

$$J^G(J^{PC}) = 0^+(6^{++})$$

OMITTED FROM SUMMARY TABLE
Needs confirmation. $f_6(2510)$ MASS

VALUE (MeV)	DOCUMENT ID	TECN	COMMENT
2465 ± 50 OUR AVERAGE	Error includes scale factor of 2.1.		
2420 ± 30	ALDE 98	GAM4	100 $\pi^- p \rightarrow \pi^0 \pi^0 n$
2510 ± 30	BINON 84B	GAM2	38 $\pi^- p \rightarrow n 2\pi^0$

 $f_6(2510)$ WIDTH

VALUE (MeV)	DOCUMENT ID	TECN	COMMENT
255 ± 40 OUR AVERAGE			
270 ± 60	ALDE 98	GAM4	100 $\pi^- p \rightarrow \pi^0 \pi^0 n$
240 ± 60	BINON 84B	GAM2	38 $\pi^- p \rightarrow n 2\pi^0$

 $f_6(2510)$ DECAY MODES

Mode	Fraction (Γ_i/Γ)
$\Gamma_1 \pi\pi$	(6.0 ± 1.0) %

 $f_6(2510)$ BRANCHING RATIOS

$\Gamma(\pi\pi)/\Gamma_{total}$	DOCUMENT ID	TECN	COMMENT	Γ_1/Γ
0.06 ± 0.01	¹ BINON 83c	GAM2	38 $\pi^- p \rightarrow n 4\gamma$	

¹ Assuming one pion exchange and using data of BOLOTOV 74. $f_6(2510)$ REFERENCES

ALDE 98	EPJ A3 361	D. Alde <i>et al.</i>	(GAM4 Collab.)
Also	PAN 62 405	D. Alde <i>et al.</i>	(GAMS Collab.)
	Translated from YAF 62 446.		
BINON 84B	LNC 39 41	F.G. Binon <i>et al.</i>	(SERP, BELG, LAPP) JP
BINON 83C	SJNP 38 723	F.G. Binon <i>et al.</i>	(SERP, BRUX+)
	Translated from YAF 38 1199.		
BOLOTOV 74	PL 52B 489	V.N. Bolotov <i>et al.</i>	(SERP)

OTHER RELATED PAPERS

BOLONKIN 00	JETPL 72 166	B.V. Bolonkin <i>et al.</i>	
	Translated from ZETFP 72 240.		
PROKOSHKIN 99	PAN 62 356	Yu.D. Prokoshkin	
	Translated from YAF 62 396.		
EISENHAND... 75	NP B96 109	E. Eisenhandler <i>et al.</i>	(LOQM, LIVP, DARE+)

Meson Particle Listings

Further States

OTHER LIGHT MESONS

Further States

OMITTED FROM SUMMARY TABLE

This section contains states observed by a single group or states poorly established that thus need confirmation. Publications that exclude earlier claims in this section are listed under 'Other Related Papers.'

QUANTUM NUMBERS, MASSES, WIDTHS, AND BRANCHING RATIOS

X(1070) $I^G(J^{PC}) = ?^?(0^{++})$					
MASS (MeV)	WIDTH (MeV)	DOCUMENT ID	TECN	COMMENT	
1072.4 ± 0.8	3.5 ^{+1.5} _{-1.0}	GRIGOR'EV 05		40 $\pi^- p \rightarrow K_S^0 K_S^0 n$	

X(1110) $I^G(J^{PC}) = 0^+(\text{even}^{++})$					
MASS (MeV)	WIDTH (MeV)	DOCUMENT ID	TECN	COMMENT	
1107 ± 4	111 ± 8 ± 15	DAFTARI 87	DBC	0. $\bar{p} n \rightarrow \rho^- \pi^+ \pi^-$	

$\eta_0(1200-1600)$ $I^G(J^{PC}) = 0^+(0^{++})$					
MASS (MeV)	WIDTH (MeV)	DOCUMENT ID	TECN	COMMENT	
1323 ± 8	237 ± 20	VLADIMIRSK...06	SPEC	40 $\pi^- p \rightarrow K_S^0 K_S^0 n$	
1480 ⁺¹⁰⁰ ₋₁₅₀	1030 ⁺⁸⁰ ₋₁₇₀	1 ANISOVICH 03	SPEC		
1530 ⁺⁹⁰ ₋₂₅₀	560 ± 40	2 ANISOVICH 03	SPEC		

¹ K-matrix pole from combined analysis of $\pi^- p \rightarrow \pi^0 \pi^0 n$, $\pi^- p \rightarrow K \bar{K} n$, $\pi^+ \pi^- \rightarrow \pi^+ \pi^-$, $\bar{p} p \rightarrow \pi^0 \pi^0 \pi^0$, $\pi^0 \eta \eta$, $\pi^0 \pi^0 \eta$, $\pi^+ \pi^- \pi^0$, $K^+ K^- \pi^0$, $K_S^0 K_S^0 \pi^0$, $K^+ K_S^0 \pi^-$ at rest, $\bar{p} n \rightarrow \pi^- \pi^- \pi^+$, $K_S^0 K^- \pi^0$, $K_S^0 K_S^0 \pi^-$ at rest.

² K-matrix pole from combined analysis of $\pi^- p \rightarrow \pi^0 \pi^0 n$, $\pi^- p \rightarrow K \bar{K} n$, $\bar{p} p \rightarrow \pi^0 \pi^0 \pi^0$, $\pi^0 \eta \eta$, $\pi^0 \pi^0 \eta$ at rest.

X(1420) $I^G(J^{PC}) = 2^+(0^{++})$					
MASS (MeV)	WIDTH (MeV)	DOCUMENT ID	TECN	COMMENT	
1420 ± 20	160 ± 10	FILIPPI 00	OBLX	0 $\bar{p} p \rightarrow \pi^+ \pi^+ \pi^-$	

X(1545) $I^G(J^{PC}) = ?^?(?^{+-})$					
MASS (MeV)	WIDTH (MeV)	DOCUMENT ID	TECN	COMMENT	
1544.7 ± 3.0	10.3 ± 3.0	VLADIMIRSKII 00	SPEC	40 $\pi^- p \rightarrow K_S^0 K_S^0 X$	

X(1575) $I^G(J^{PC}) = ?^?(1^{--})$					
MASS (MeV)	WIDTH (MeV)	DOCUMENT ID	TECN	COMMENT	
1576 ⁺⁴⁹⁺⁹⁸ ₋₅₅₋₉₁	818 ⁺²²⁺⁶⁴ ₋₂₃₋₁₃₃	3 ABLIKIM 06s	BES	$J/\psi \rightarrow K^+ K^- \pi^0$	

³ A broad peak observed at $K^+ K^-$ invariant mass. Mass and width above are its pole position. The observed branching ratio is $B(J/\psi \rightarrow X \pi^0) B(X \rightarrow K^+ K^-) = (8.5 \pm 0.6^{+2.7}_{-3.6}) \times 10^{-4}$.

X(1600) $I^G(J^{PC}) = 2^+(2^{++})$					
MASS (MeV)	WIDTH (MeV)	DOCUMENT ID	TECN	COMMENT	
1600 ± 100	400 ± 200	4 ALBRECHT 91F	ARG	10.2 $e^+ e^- \rightarrow e^+ e^- 2(\pi^+ \pi^-)$	

⁴ Our estimate.

X(1650) $I^G(J^{PC}) = 0^-(?^{--})$					
MASS (MeV)	WIDTH (MeV)	EVTS	DOCUMENT ID	TECN	COMMENT
1652 ± 7	<50	100	PROKOSHKIN 96	GAM2	32,38 $\pi p \rightarrow \omega \eta n$

X(1730) $I^G(J^{PC}) = ?^?(?^{+-})$					
MASS (MeV)	WIDTH (MeV)	EVTS	DOCUMENT ID	TECN	COMMENT
1731.0 ± 1.2 ± 2.0	3.2 ± 0.8 ± 1.3	58	VLADIMIRSK...07	SPEC	40 $\pi^- p \rightarrow K_S^0 K_S^0 X$

X(1750) $I^G(J^{PC}) = ?^?(1^{--})$					
MASS (MeV)	WIDTH (MeV)	DOCUMENT ID	TECN	COMMENT	
1753.5 ± 1.5 ± 2.3	122.2 ± 6.2 ± 8.0	LINK 02k	FOCS	20-160 $\gamma p \rightarrow K^+ K^- p$	

$B(X(1750) \rightarrow \bar{K}^*(892)^0 K^0 \rightarrow K^\pm \pi^\mp K_S^0) / B(X(1750) \rightarrow K^+ K^-)$

VALUE	CL%	DOCUMENT ID	TECN
<0.065	90	LINK	02k FOCS

$B(X(1750) \rightarrow \bar{K}^*(892)^\pm K^\mp \rightarrow K^\pm \pi^\mp K_S^0) / B(X(1750) \rightarrow K^+ K^-)$

VALUE	CL%	DOCUMENT ID	TECN
<0.183	90	LINK	02k FOCS

$\eta_2(1750)$ $I^G(J^{PC}) = 0^+(2^{++})$					
MASS (MeV)	WIDTH (MeV)	EVTS	DOCUMENT ID	TECN	COMMENT
1755 ± 10	67 ± 12	870	5 SCHEGELSKY 06A	RVUE	$\gamma \gamma \rightarrow K_S^0 K_S^0$

$\Gamma(K \bar{K})$					
VALUE (MeV)	EVTS	DOCUMENT ID	TECN	COMMENT	
17 ± 5	870	6 SCHEGELSKY 06A	RVUE	$\gamma \gamma \rightarrow K_S^0 K_S^0$	

$\Gamma(\gamma \gamma)$					
VALUE (keV)	EVTS	DOCUMENT ID	TECN	COMMENT	
0.13 ± 0.04	870	6 SCHEGELSKY 06A	RVUE	$\gamma \gamma \rightarrow K_S^0 K_S^0$	

$\Gamma(\pi \pi)$					
VALUE (MeV)	EVTS	DOCUMENT ID	TECN	COMMENT	
1.3 ± 1.0	870	6 SCHEGELSKY 06A	RVUE	$\gamma \gamma \rightarrow K_S^0 K_S^0$	

$\Gamma(\eta \eta)$					
VALUE (MeV)	EVTS	DOCUMENT ID	TECN	COMMENT	
2.0 ± 0.5	870	6 SCHEGELSKY 06A	RVUE	$\gamma \gamma \rightarrow K_S^0 K_S^0$	

⁵ From analysis of L3 data at 91 and 183-209 GeV.

⁶ From analysis of L3 data at 91 and 183-209 GeV and using SU(3) relations.

X(1775) $I^G(J^{PC}) = 1^-(?^{+-})$					
MASS (MeV)	WIDTH (MeV)	DOCUMENT ID	TECN	COMMENT	
1763 ± 20	192 ± 60	CONDO 91	SHF	$\gamma p \rightarrow (p \pi^+) (\pi^+ \pi^- \pi^-)$	
1787 ± 18	118 ± 60	CONDO 91	SHF	$\gamma p \rightarrow n \pi^+ \pi^+ \pi^-$	

X(1855) $I^G(J^{PC}) = ?^?(?^{??})$					
MASS (MeV)	WIDTH (MeV)	DOCUMENT ID	TECN	COMMENT	
1856.6 ± 5	20 ± 5	BRIDGES 86D	SPEC	0. $\bar{p} d \rightarrow \pi \pi N$	

X(1870) $I^G(J^{PC}) = ?^?(2^{??})$					
MASS (MeV)	WIDTH (MeV)	DOCUMENT ID	TECN	COMMENT	
1870 ± 40	250 ± 30	ALDE 86D	GAM4	100 $\pi^- p \rightarrow 2\eta X$	

$a_3(1875)$ $I^G(J^{PC}) = 1^-(3^{+-})$					
MASS (MeV)	WIDTH (MeV)	DOCUMENT ID	TECN	COMMENT	
1874 ± 43 ± 96	385 ± 121 ± 114	CHUNG 02	B852	18.3 $\pi^- p \rightarrow \pi^+ \pi^- \pi^- p$	

$B(a_3(1875) \rightarrow f_2(1270) \pi) / B(a_3(1875) \rightarrow \rho \pi)$

VALUE	DOCUMENT ID	TECN	COMMENT
0.8 ± 0.2	7 CHUNG 02	B852	18.3 $\pi^- p \rightarrow \pi^+ \pi^- \pi^- p$

⁷ Using the observable fractions of 50.0% $\rho \pi$, 56.5% $f_2 \pi$, and 11.8% $\rho_3 \pi$.

$B(a_3(1875) \rightarrow \rho_3(1690) \pi) / B(a_3(1875) \rightarrow \rho \pi)$

VALUE	DOCUMENT ID	TECN	COMMENT
0.9 ± 0.3	8 CHUNG 02	B852	18.3 $\pi^- p \rightarrow \pi^+ \pi^- \pi^- p$

⁸ Using the observable fractions of 50.0% $\rho \pi$, 56.5% $f_2 \pi$, and 11.8% $\rho_3 \pi$.

$a_1(1930)$ $I^G(J^{PC}) = 1^-(1^{+-})$					
MASS (MeV)	WIDTH (MeV)	DOCUMENT ID	TECN	COMMENT	
1930 ⁺³⁰ ₋₇₀	155 ± 45	ANISOVICH 01F	SPEC	2.0 $\bar{p} p \rightarrow 3\pi^0, \pi^0 \eta, \pi^0 \eta'$	

X(1935) $I^G(J^{PC}) = 1^+(1^{--})$					
MASS (MeV)	WIDTH (MeV)	DOCUMENT ID	TECN	COMMENT	
1935 ± 20	215 ± 30	EVANGELIS... 79	OMEG	10,16 $\pi^- p \rightarrow \bar{p} p n$	

$\rho_2(1940)$ $I^G(J^{PC}) = 1^+(2^{--})$					
MASS (MeV)	WIDTH (MeV)	DOCUMENT ID	TECN	COMMENT	
1940 ± 40	155 ± 40	9 ANISOVICH 02	SPEC	0.6-1.9 $p \bar{p} \rightarrow \omega \pi^0, \omega \eta \pi^0, \pi^+ \pi^-$	

⁹ From the combined analysis of ANISOVICH 00J, ANISOVICH 01D, ANISOVICH 01E, and ANISOVICH 02.

$\omega_3(1945)$ $I^G(J^{PC}) = 0^-(3^{--})$					
MASS (MeV)	WIDTH (MeV)	DOCUMENT ID	TECN	COMMENT	
1945 ± 20	115 ± 22	10 ANISOVICH 02B	SPEC	0.6-1.9 $p \bar{p} \rightarrow \omega \eta, \omega \pi^0 \pi^0$	

¹⁰ From the combined analysis of ANISOVICH 00b, ANISOVICH 01c, and ANISOVICH 02b.

$\omega(1960)$ $I^G(J^{PC}) = 0^-(1^{--})$					
MASS (MeV)	WIDTH (MeV)	DOCUMENT ID	TECN	COMMENT	
1960 ± 25	195 ± 60	¹¹ ANISOVICH	02B	SPEC	0.6–1.9 $p\bar{p} \rightarrow \omega\eta, \omega\pi^0\pi^0$

¹¹ From the combined analysis of ANISOVICH 00b, ANISOVICH 01c, and ANISOVICH 02b.

$b_1(1960)$ $I^G(J^{PC}) = 1^+(1^{+-})$					
MASS (MeV)	WIDTH (MeV)	DOCUMENT ID	TECN	COMMENT	
1960 ± 35	230 ± 50	¹² ANISOVICH	02	SPEC	0.6–1.9 $p\bar{p} \rightarrow \omega\pi^0, \omega\eta\pi^0, \pi^+\pi^-$

¹² From the combined analysis of ANISOVICH 00j, ANISOVICH 01d, ANISOVICH 01e, and ANISOVICH 02.

$h_1(1965)$ $I^G(J^{PC}) = 0^-(1^{+-})$					
MASS (MeV)	WIDTH (MeV)	DOCUMENT ID	TECN	COMMENT	
1965 ± 45	345 ± 75	¹³ ANISOVICH	02B	SPEC	0.6–1.9 $p\bar{p} \rightarrow \omega\eta, \omega\pi^0\pi^0$

¹³ From the combined analysis of ANISOVICH 00b, ANISOVICH 01c, and ANISOVICH 02b.

$f_1(1970)$ $I^G(J^{PC}) = 0^+(1^{++})$					
MASS (MeV)	WIDTH (MeV)	DOCUMENT ID	TECN	COMMENT	
1971 ± 15	240 ± 45	ANISOVICH	00J	SPEC	

$X(1970)$ $I^G(J^{PC}) = ?^?(?^{??})$					
MASS (MeV)	WIDTH (MeV)	DOCUMENT ID	TECN	COMMENT	
1970 ± 10	40 ± 20	CHLIAPNIK...	80	HBC	32 $K^+p \rightarrow 2K_S^0 2\pi X$

$X(1975)$ $I^G(J^{PC}) = ?^?(?^{??})$					
MASS (MeV)	WIDTH (MeV)	EVTs	DOCUMENT ID	TECN	COMMENT
1973 ± 15	80	30	CASO	70	HBC 11.2 $\pi^-\pi^0 \rightarrow \rho 2\pi$

$\omega_2(1975)$ $I^G(J^{PC}) = 0^-(2^{--})$					
MASS (MeV)	WIDTH (MeV)	DOCUMENT ID	TECN	COMMENT	
1975 ± 20	175 ± 25	¹⁴ ANISOVICH	02B	SPEC	0.6–1.9 $p\bar{p} \rightarrow \omega\eta, \omega\pi^0\pi^0$

¹⁴ From the combined analysis of ANISOVICH 00b, ANISOVICH 01c, and ANISOVICH 02b.

$a_2(1990)$ $I^G(J^{PC}) = 1^-(2^{+-})$					
MASS (MeV)	WIDTH (MeV)	EVTs	DOCUMENT ID	TECN	COMMENT
2050 ± 10 ± 40	190 ± 22 ± 100	18k	¹⁵ SCHEGELSKY	06	RVUE $\gamma\gamma \rightarrow \pi^+\pi^-\pi^0$
2003 ± 10 ± 19	249 ± 23 ± 32		LU	05	B852 $18 \pi^-\pi^0 p \rightarrow \omega\pi^-\pi^0 p$
1990 ± ¹⁵ ₃₀	190 ± 50		ANISOVICH	99c	SPEC

¹⁵ From analysis of L3 data at 183–209 GeV.

$\Gamma(\gamma\gamma) \Gamma(\pi^+\pi^-\pi^0) / \Gamma(\text{total})$					
VALUE (keV)	EVTs	DOCUMENT ID	TECN	COMMENT	
0.11 ± 0.04 ± 0.05	18k	¹⁶ SCHEGELSKY	06	RVUE	$\gamma\gamma \rightarrow \pi^+\pi^-\pi^0$

¹⁶ From analysis of L3 data at 183–209 GeV.

$\rho(2000)$ $I^G(J^{PC}) = 1^+(1^{--})$					
MASS (MeV)	WIDTH (MeV)	DOCUMENT ID	TECN	COMMENT	
2000 ± 30	260 ± 45	¹⁷ BUGG	04c	RVUE	

¹⁷ From the combined analysis of ANISOVICH 00j, ANISOVICH 01d, ANISOVICH 01e, and ANISOVICH 02.

$f_2(2000)$ $I^G(J^{PC}) = 0^+(2^{++})$					
MASS (MeV)	WIDTH (MeV)	DOCUMENT ID	TECN	COMMENT	
2001 ± 10	312 ± 32	ANISOVICH	00J	SPEC	

$X(2000)$ $I^G(J^{PC}) = 1^-(2^{+-})$					
MASS (MeV)	WIDTH (MeV)	DOCUMENT ID	TECN	CHG	COMMENT
1964 ± 35	225 ± 50	¹⁸ ARMSTRONG	93D	E760	$\bar{p}p \rightarrow 3\pi^0 \rightarrow 6\gamma$
~ 2100	~ 500	¹⁸ ANTIPOV	77	CIBS	– 25 $\pi^-\pi^0 \rightarrow \rho\pi^-\rho_3$
2214 ± 15	355 ± 21	¹⁹ BALTAY	77	HBC	0 15 $\pi^-\pi^0 \rightarrow \Delta^{++} 3\pi$
2080 ± 40	340 ± 80	KALELKAR	75	HBC	+ 15 $\pi^+\pi^0 \rightarrow \rho\pi^+\rho_3$

¹⁸ Cannot determine spin to be 3.
¹⁹ BALTAY 77 favors $J^P = ,3^+$.

$X(2000)$ $I^G(J^{PC}) = ?^?(4^{++})$					
MASS (MeV)	WIDTH (MeV)	DOCUMENT ID	TECN	COMMENT	
1998 ± 3 ± 5	<15	VLADIMIRSK...03	SPEC		$\pi^-\pi^0 \rightarrow K_S^0 K_S^0 MM$

$\pi_2(2005)$ $I^G(J^{PC}) = 1^-(2^{+-})$					
MASS (MeV)	WIDTH (MeV)	EVTs	DOCUMENT ID	TECN	COMMENT
1974 ± 14 ± 83	341 ± 61 ± 139	145k	LU	05	B852 $18 \pi^-\pi^0 \rightarrow \omega\pi^-\pi^0 p$
2005 ± 15	200 ± 40		ANISOVICH	01F	SPEC $2.0 \bar{p}p \rightarrow 3\pi^0, \pi^0\eta, \pi^0\eta'$

$\eta(2010)$ $I^G(J^{PC}) = 0^+(0^{--})$					
MASS (MeV)	WIDTH (MeV)	DOCUMENT ID	TECN	COMMENT	
2010 ± ³⁵ ₆₀	270 ± 60	ANISOVICH	00J	SPEC	

$\pi_1(2015)$ $I^G(J^{PC}) = 1^-(1^{+-})$					
MASS (MeV)	WIDTH (MeV)	EVTs	DOCUMENT ID	TECN	COMMENT
2014 ± 20 ± 16	230 ± 32 ± 73	145k	LU	05	B852 $18 \pi^-\pi^0 \rightarrow \omega\pi^-\pi^0 p$
2001 ± 30 ± 92	333 ± 52 ± 49	69k	KUHN	04	B852 $18 \pi^-\pi^0 \rightarrow \eta\pi^+\pi^-\pi^0 p$

$a_0(2020)$ $I^G(J^{PC}) = 1^-(0^{++})$					
MASS (MeV)	WIDTH (MeV)	DOCUMENT ID	TECN	COMMENT	
2025 ± 30	330 ± 75	ANISOVICH	99c	SPEC	

$X(2020)$ $I^G(J^{PC}) = ?^?(?^{??})$					
MASS (MeV)	WIDTH (MeV)	DOCUMENT ID	TECN	COMMENT	
2015 ± 3	10 ± 4	FERRER	99	RVUE	$\pi p \rightarrow p\rho\bar{p}\pi(\pi)$

$h_3(2025)$ $I^G(J^{PC}) = 0^-(3^{+-})$					
MASS (MeV)	WIDTH (MeV)	DOCUMENT ID	TECN	COMMENT	
2025 ± 20	145 ± 30	²⁰ ANISOVICH	02B	SPEC	0.6–1.9 $p\bar{p} \rightarrow \omega\eta, \omega\pi^0\pi^0$

²⁰ From the combined analysis of ANISOVICH 00b, ANISOVICH 01c, and ANISOVICH 02b.

$b_3(2025)$ $I^G(J^{PC}) = 1^+(3^{+-})$					
MASS (MeV)	WIDTH (MeV)	DOCUMENT ID	TECN	COMMENT	
2032 ± 12	117 ± 11	²¹ ANISOVICH	02	SPEC	0.6–1.9 $p\bar{p} \rightarrow \omega\pi^0, \omega\eta\pi^0, \pi^+\pi^-$

²¹ From the combined analysis of ANISOVICH 00j, ANISOVICH 01d, ANISOVICH 01e, and ANISOVICH 02.

$\eta_2(2030)$ $I^G(J^{PC}) = 0^+(2^{+-})$					
MASS (MeV)	WIDTH (MeV)	DOCUMENT ID	TECN	COMMENT	
2030 ± 5 ± 15	205 ± 10 ± 15	ANISOVICH	00E	SPEC	

$B(a_2\pi)_L=0/B(a_2\pi)_L=2$					
VALUE	DOCUMENT ID	TECN	COMMENT		
0.74 ± 0.17	²² ANISOVICH	00E	SPEC		

$B(a_0\pi)/B(a_2\pi)_L=2$					
VALUE	DOCUMENT ID	TECN	COMMENT		
0.072 ± 0.016	²² ANISOVICH	00E	SPEC		

$B(f_2\eta)/B(a_2\pi)_L=2$					
VALUE	DOCUMENT ID	TECN	COMMENT		
0.074 ± 0.026	²² ANISOVICH	00E	SPEC		

²² Corrected for all decay modes.

$f_3(2050)$ $I^G(J^{PC}) = 0^+(3^{+-})$					
MASS (MeV)	WIDTH (MeV)	DOCUMENT ID	TECN	COMMENT	
2048 ± 8	213 ± 34	ANISOVICH	00J	SPEC	2.0 $p\bar{p} \rightarrow \eta\pi^0\pi^0$

$f_0(2060)$ $I^G(J^{PC}) = 0^+(0^{++})$					
MASS (MeV)	WIDTH (MeV)	DOCUMENT ID	TECN	COMMENT	
~ 2050	~ 120	²³ OAKDEN	94	RVUE	0.36–1.55 $\bar{p}p \rightarrow \pi\pi$
~ 2060	~ 50	²³ OAKDEN	94	RVUE	0.36–1.55 $\bar{p}p \rightarrow \pi\pi$

Meson Particle Listings

Further States

²³ See SEMENOV 99 and KLOET 96.

$\pi(2070)$		$I^G(J^{PC}) = 1^-(0^-+)$			
MASS (MeV)	WIDTH (MeV)	DOCUMENT ID	TECN	COMMENT	
2070 ± 35	310 ⁺¹⁰⁰ ₋₅₀	ANISOVICH	01F	SPEC	2.0 $\bar{p}p \rightarrow 3\pi^0, \pi^0\eta, \pi^0\eta'$

$a_3(2070)$		$I^G(J^{PC}) = 1^-(3^+)$			
MASS (MeV)	WIDTH (MeV)	DOCUMENT ID	TECN	COMMENT	
2070 ± 20	170 ± 40	ANISOVICH	99C	SPEC	

$X(2075)$		$I^G(J^{PC}) = ?^?(?^{??})$			
MASS (MeV)	WIDTH (MeV)	DOCUMENT ID	TECN	COMMENT	
2075 ± 12 ± 5	90 ± 35 ± 9	24 ABLIKIM	04J	BES2	$J/\psi \rightarrow K^- \rho \bar{\Lambda}$
²⁴ From a fit in the region $M_{\rho\bar{\Lambda}} - M_p - M_\Lambda < 150$ MeV. S-wave in the $\rho\bar{\Lambda}$ system preferred.					

$a_2(2080)$		$I^G(J^{PC}) = 1^-(2^+)$			
MASS (MeV)	WIDTH (MeV)	DOCUMENT ID	TECN	COMMENT	
2060 ± 20	195 ± 30	ANISOVICH	99C	SPEC	
2100 ⁺¹⁰ ₋₃₀	360 ⁺⁴⁰ ₋₁₀₀	ANISOVICH	99E	SPEC	

$X(2080)$		$I^G(J^{PC}) = ?^?(?^{??})$			
MASS (MeV)	WIDTH (MeV)	DOCUMENT ID	TECN	COMMENT	
2080 ± 10	110 ± 20	KREYMER	80	STRC	13 $\pi^- d \rightarrow p \bar{p} n(n_S)$

$X(2080)$		$I^G(J^{PC}) = ?^?(3^-)$			
MASS (MeV)	WIDTH (MeV)	DOCUMENT ID	TECN	COMMENT	
2080 ± 10	190 ± 15	ROZANSKA	80	SPRK	18 $\pi^- p \rightarrow p \bar{p} n$

$a_1(2095)$		$I^G(J^{PC}) = 1^-(1^+)$			
MASS (MeV)	WIDTH (MeV)	EVT S	DOCUMENT ID	TECN	COMMENT
2096 ± 17 ± 121	451 ± 41 ± 81	69k	KUHN	04	B852 18 $\pi^- p \rightarrow \eta \pi^+ \pi^- \pi^- p$

$B(a_1(2095) \rightarrow f_1(1285)\pi) / B(a_1(2095) \rightarrow a_1(1260))$					
VALUE	EVT S	DOCUMENT ID	TECN	COMMENT	
3.18 ± 0.64	69k	KUHN	04	B852	18 $\pi^- p \rightarrow \eta \pi^+ \pi^- \pi^- p$

$\eta(2100)$		$I^G(J^{PC}) = 0^+(0^-)$			
MASS (MeV)	WIDTH (MeV)	EVT S	DOCUMENT ID	TECN	COMMENT
2103 ± 50	187 ± 75	586	25 BISELLO	89B	DM2 $J/\psi \rightarrow 4\pi\gamma$
²⁵ ASTON 81B sees no peak, has 850 events in Ajinenko+Barth bins. ARESTOV 80 sees no peak.					

$X(2100)$		$I^G(J^{PC}) = ?^?(0^{??})$			
MASS (MeV)	WIDTH (MeV)	DOCUMENT ID	TECN	COMMENT	
2100 ± 40	250 ± 40	ALDE	86D	GAM4	100 $\pi^- p \rightarrow 2\eta X$

$X(2110)$		$I^G(J^{PC}) = 1^+(3^-)$			
MASS (MeV)	WIDTH (MeV)	DOCUMENT ID	TECN	COMMENT	
2110 ± 10	330 ± 20	EVANGELIS...	79	OMEG	10,16 $\pi^- p \rightarrow \bar{p} p n$

$f_2(2140)$		$I^G(J^{PC}) = 0^+(2^+)$			
MASS (MeV)	WIDTH (MeV)	EVT S	DOCUMENT ID	TECN	COMMENT
2141 ± 12	49 ± 28	389	GREEN	86	MPSF 400 $pA \rightarrow 4KX$

$X(2150)$		$I^G(J^{PC}) = ?^?(2^+)$			
MASS (MeV)	WIDTH (MeV)	DOCUMENT ID	TECN	COMMENT	
2150 ± 10	260 ± 10	ROZANSKA	80	SPRK	18 $\pi^- p \rightarrow p \bar{p} n$

$a_2(2175)$		$I^G(J^{PC}) = 1^-(2^+)$			
MASS (MeV)	WIDTH (MeV)	DOCUMENT ID	TECN	COMMENT	
2175 ± 40	310 ⁺⁹⁰ ₋₄₅	ANISOVICH	01F	SPEC	2.0 $\bar{p}p \rightarrow 3\pi^0, \pi^0\eta, \pi^0\eta'$

$\eta(2190)$		$I^G(J^{PC}) = 0^+(0^-)$			
MASS (MeV)	WIDTH (MeV)	DOCUMENT ID	TECN	COMMENT	
2190 ± 50	850 ± 100	BUGG	99	BES	

$\omega_2(2195)$		$I^G(J^{PC}) = 0^-(2^-)$			
MASS (MeV)	WIDTH (MeV)	DOCUMENT ID	TECN	COMMENT	
2195 ± 30	225 ± 40	26 ANISOVICH	02B	SPEC	0.6-1.9 $p\bar{p} \rightarrow \omega\eta, \omega\pi^0\pi^0$

²⁶ From the combined analysis of ANISOVICH 00b, ANISOVICH 01c, and ANISOVICH 02b.

$\omega(2205)$		$I^G(J^{PC}) = 0^-(1^-)$			
MASS (MeV)	WIDTH (MeV)	DOCUMENT ID	TECN	COMMENT	
2205 ± 30	350 ± 90	27 ANISOVICH	02B	SPEC	0.6-1.9 $p\bar{p} \rightarrow \omega\eta, \omega\pi^0\pi^0$
²⁷ From the combined analysis of ANISOVICH 00b, ANISOVICH 01c, and ANISOVICH 02b.					

$X(2210)$		$I^G(J^{PC}) = ?^?(?^{??})$			
MASS (MeV)	WIDTH (MeV)	DOCUMENT ID	TECN	COMMENT	
2210 ⁺⁷⁹ ₋₂₁	203 ⁺⁴³⁷ ₋₈₇	EVANGELIS...	79B	OMEG	10 $\pi^- p \rightarrow K^+ K^- n$

$X(2210)$		$I^G(J^{PC}) = ?^?(?^{??})$			
MASS (MeV)	WIDTH (MeV)	DOCUMENT ID	TECN	COMMENT	
2207 ± 22	130	CASO	70	HBC	11.2 $\pi^- p$

$h_1(2215)$		$I^G(J^{PC}) = 0^-(1^+)$			
MASS (MeV)	WIDTH (MeV)	DOCUMENT ID	TECN	COMMENT	
2215 ± 40	325 ± 55	28 ANISOVICH	02B	SPEC	0.6-1.9 $p\bar{p} \rightarrow \omega\eta, \omega\pi^0\pi^0$
²⁸ From the combined analysis of ANISOVICH 00b, ANISOVICH 01c, and ANISOVICH 02b.					

$b_1(2240)$		$I^G(J^{PC}) = 1^+(1^+)$			
MASS (MeV)	WIDTH (MeV)	DOCUMENT ID	TECN	COMMENT	
2240 ± 35	320 ± 85	29 ANISOVICH	02	SPEC	0.6-1.9 $p\bar{p} \rightarrow \omega\pi^0, \omega\eta\pi^0, \pi^+\pi^-$

²⁹ From the combined analysis of ANISOVICH 00j, ANISOVICH 01d, ANISOVICH 01e, and ANISOVICH 02.

$\rho_2(2240)$		$I^G(J^{PC}) = 1^+(2^-)$			
MASS (MeV)	WIDTH (MeV)	DOCUMENT ID	TECN	COMMENT	
2225 ± 35	335 ⁺¹⁰⁰ ₋₅₀	30 ANISOVICH	02	SPEC	0.6-1.9 $p\bar{p} \rightarrow \omega\pi^0, \omega\eta\pi^0, \pi^+\pi^-$

³⁰ From the combined analysis of ANISOVICH 00j, ANISOVICH 01d, ANISOVICH 01e, and ANISOVICH 02.

$\rho_4(2240)$		$I^G(J^{PC}) = 1^+(4^-)$			
MASS (MeV)	WIDTH (MeV)	DOCUMENT ID	TECN	COMMENT	
2230 ± 25	210 ± 30	31 ANISOVICH	02	SPEC	0.6-1.9 $p\bar{p} \rightarrow \omega\pi^0, \omega\eta\pi^0, \pi^+\pi^-$

³¹ From the combined analysis of ANISOVICH 00j, ANISOVICH 01d, ANISOVICH 01e, and ANISOVICH 02.

$\pi_2(2245)$		$I^G(J^{PC}) = 1^-(2^-)$			
MASS (MeV)	WIDTH (MeV)	DOCUMENT ID	TECN	COMMENT	
2245 ± 60	320 ⁺¹⁰⁰ ₋₄₀	ANISOVICH	01F	SPEC	2.0 $\bar{p}p \rightarrow 3\pi^0, \pi^0\eta, \pi^0\eta'$

$b_3(2245)$		$I^G(J^{PC}) = 1^+(3^-)$			
MASS (MeV)	WIDTH (MeV)	DOCUMENT ID	TECN	COMMENT	
2245 ± 50	320 ± 70	32 BUGG	04c	RVUE	

³² From the combined analysis of ANISOVICH 00j, ANISOVICH 01d, ANISOVICH 01e, and ANISOVICH 02.

$\eta_2(2250)$		$I^G(J^{PC}) = 0^+(2^-)$			
MASS (MeV)	WIDTH (MeV)	DOCUMENT ID	TECN	COMMENT	
2248 ± 20	280 ± 20	A NISOVICH	00i	SPEC	
2267 ± 14	290 ± 50	A NISOVICH	00j	SPEC	

$\pi_4(2250)$		$I^G(J^{PC}) = 1^-(4^-)$			
MASS (MeV)	WIDTH (MeV)	DOCUMENT ID	TECN	COMMENT	
2250 ± 15	215 ± 25	ANISOVICH	01F	SPEC	2.0 $\bar{p}p \rightarrow 3\pi^0, \pi^0\eta, \pi^0\eta'$

$\omega_4(2250)$		$I^G(J^{PC}) = 0^-(4^-)$			
MASS (MeV)	WIDTH (MeV)	DOCUMENT ID	TECN	COMMENT	
2250 ± 30	150 ± 50	33 ANISOVICH	02B	SPEC	0.6-1.9 $p\bar{p} \rightarrow \omega\eta, \omega\pi^0\pi^0$

³³ From the combined analysis of ANISOVICH 00b, ANISOVICH 01c, and ANISOVICH 02b.

$\omega_5(2250)$		$I^G(J^{PC}) = 0^-(5^-)$			
MASS (MeV)	WIDTH (MeV)	DOCUMENT ID	TECN	COMMENT	
2250 ± 70	320 ± 95	34 BUGG	04	RVUE	

See key on page 373

Meson Particle Listings
Further States³⁴ From the combined analysis of ANISOVICH 00b, ANISOVICH 01c, and ANISOVICH 02b.

$\omega_3(2255) \quad I^G(J^{PC}) = 0^-(3^{--})$					
MASS (MeV)	WIDTH (MeV)	DOCUMENT ID	TECN	COMMENT	
2255 ± 15	175 ± 30	³⁵ ANISOVICH 02B	SPEC	0.6-1.9 $p\bar{p} \rightarrow \omega\eta, \omega\pi^0\pi^0$	

³⁵ From the combined analysis of ANISOVICH 00b, ANISOVICH 01c, and ANISOVICH 02b.

$X(2260) \quad I^G(J^{PC}) = 0^+(4^{+?})$					
MASS (MeV)	WIDTH (MeV)	DOCUMENT ID	TECN	COMMENT	
2260 ± 20	400 ± 100	EVANGELIS... 79	OMEG	10,16 $\pi^-p \rightarrow \bar{p}\rho n$	

$\rho(2270) \quad I^G(J^{PC}) = 1^+(1^{--})$					
MASS (MeV)	WIDTH (MeV)	DOCUMENT ID	TECN	COMMENT	
2265 ± 40	325 ± 80	³⁶ ANISOVICH 02	SPEC	0.6-1.9 $p\bar{p} \rightarrow \omega\pi^0, \omega\eta\pi^0, \pi^+\pi^-$	
2280 ± 50	440 ± 110	ATKINSON 85	OMEG	20-70 $\gamma p \rightarrow \rho\omega\pi^+\pi^-\pi^0$	

³⁶ From the combined analysis of ANISOVICH 00j, ANISOVICH 01d, ANISOVICH 01e, and ANISOVICH 02.

$a_1(2270) \quad I^G(J^{PC}) = 1^-(1^{++})$					
MASS (MeV)	WIDTH (MeV)	DOCUMENT ID	TECN	COMMENT	
2270 $^{+55}_{-40}$	305 $^{+70}_{-40}$	ANISOVICH 01F	SPEC	2.0 $\bar{p}p \rightarrow 3\pi^0, \pi^0\eta, \pi^0\eta'$	

$a_2(2270) \quad I^G(J^{PC}) = 1^-(2^{++})$					
MASS (MeV)	WIDTH (MeV)	DOCUMENT ID	TECN	COMMENT	
2265 ± 20	235 $^{+60}_{-35}$	ANISOVICH 99c	SPEC		
2280 ± 30	280 ± 50	ANISOVICH 99e	SPEC		

$h_3(2275) \quad I^G(J^{PC}) = 0^-(3^{+-})$					
MASS (MeV)	WIDTH (MeV)	DOCUMENT ID	TECN	COMMENT	
2275 ± 25	190 ± 45	³⁷ ANISOVICH 02B	SPEC	0.6-1.9 $p\bar{p} \rightarrow \omega\eta, \omega\pi^0\pi^0$	

³⁷ From the combined analysis of ANISOVICH 00b, ANISOVICH 01c, and ANISOVICH 02b.

$a_4(2280) \quad I^G(J^{PC}) = 1^-(4^{++})$					
MASS (MeV)	WIDTH (MeV)	DOCUMENT ID	TECN	COMMENT	
2300 ± 20	230 ± 40	ANISOVICH 99c	SPEC		
2260 ± 15	180 ± 20	ANISOVICH 99e	SPEC		
• • • We do not use the following data for averages, fits, limits, etc. • • •					
2237 ± 5	291 ± 12	³⁸ UMAN	06 E835	5.2 $\bar{p}p \rightarrow \eta\eta\pi^0$	

³⁸ Statistical error only.

$\eta(2280) \quad I^G(J^{PC}) = 0^+(0^{-+})$					
MASS (MeV)	WIDTH (MeV)	DOCUMENT ID	TECN	COMMENT	
2320 ± 15	230 ± 35	³⁹ ANISOVICH 00m	SPEC		

³⁹ From the combined analysis of $\bar{p}p \rightarrow \eta\eta\eta$ from ANISOVICH 00m and $\bar{p}p \rightarrow \eta\pi^0\pi^0$ from ANISOVICH 00j.

$\omega_3(2285) \quad I^G(J^{PC}) = 0^-(3^{--})$					
MASS (MeV)	WIDTH (MeV)	DOCUMENT ID	TECN	COMMENT	
2278 ± 28	224 ± 50	⁴⁰ BUGG 04A	RVUE		
2285 ± 60	230 ± 40	⁴¹ ANISOVICH 02B	SPEC	0.6-1.9 $p\bar{p} \rightarrow \omega\eta, \omega\pi^0\pi^0$	

⁴⁰ Partial wave analysis of the data on $p\bar{p} \rightarrow \bar{\Lambda}\Lambda$ from BARNES 00.⁴¹ From the combined analysis of ANISOVICH 00b, ANISOVICH 01c, and ANISOVICH 02b.

$\omega(2290) \quad I^G(J^{PC}) = 0^-(1^{--})$					
MASS (MeV)	WIDTH (MeV)	DOCUMENT ID	TECN	COMMENT	
2290 ± 20	275 ± 35	⁴² BUGG 04A	RVUE		

⁴² Partial wave analysis of the data on $p\bar{p} \rightarrow \bar{\Lambda}\Lambda$ from BARNES 00.

$f_3(2300) \quad I^G(J^{PC}) = 0^+(3^{++})$					
MASS (MeV)	WIDTH (MeV)	DOCUMENT ID	TECN	COMMENT	
2334 ± 25	200 ± 20	⁴³ BUGG 04A	RVUE		
2303 ± 15	214 ± 29	ANISOVICH 00j	SPEC	2.0 $p\bar{p} \rightarrow \eta\pi^0\pi^0$	

⁴³ Partial wave analysis of the data on $p\bar{p} \rightarrow \bar{\Lambda}\Lambda$ from BARNES 00.

$\rho_3(2300) \quad I^G(J^{PC}) = 1^+(3^{--})$					
MASS (MeV)	WIDTH (MeV)	DOCUMENT ID	TECN	COMMENT	
2300 $^{+50}_{-80}$	340 ± 50	ANISOVICH 00j	SPEC		

$a_3(2310) \quad I^G(J^{PC}) = 1^-(3^{++})$					
MASS (MeV)	WIDTH (MeV)	DOCUMENT ID	TECN	COMMENT	
2310 ± 40	180 $^{+120}_{-60}$	ANISOVICH 99c	SPEC		

$f_1(2310) \quad I^G(J^{PC}) = 0^+(1^{++})$					
MASS (MeV)	WIDTH (MeV)	DOCUMENT ID	TECN	COMMENT	
2310 ± 60	255 ± 70	ANISOVICH 00j	SPEC		

$\eta_4(2330) \quad I^G(J^{PC}) = 0^+(4^{-+})$					
MASS (MeV)	WIDTH (MeV)	DOCUMENT ID	TECN	COMMENT	
2328 ± 38	240 ± 90	ANISOVICH 00j	SPEC	2.0 $p\bar{p} \rightarrow \eta\pi^0\pi^0$	

$\omega(2330) \quad I^G(J^{PC}) = 0^-(1^{--})$					
MASS (MeV)	WIDTH (MeV)	DOCUMENT ID	TECN	COMMENT	
2330 ± 30	435 ± 75	ATKINSON 88	OMEG	25-50 $\gamma p \rightarrow \rho^\pm\rho^0\pi^\mp$	

$a_1(2340) \quad I^G(J^{PC}) = 1^-(1^{++})$					
MASS (MeV)	WIDTH (MeV)	DOCUMENT ID	TECN	COMMENT	
2340 ± 40	230 ± 70	ANISOVICH 99e	SPEC		

$X(2340) \quad I^G(J^{PC}) = ?^?(?^{??})$					
MASS (MeV)	WIDTH (MeV)	EVS	DOCUMENT ID	TECN	COMMENT
2340 ± 20	180 ± 60	126	⁴⁴ BALTAY 75	HBC	15 $\pi^+p \rightarrow \rho^0\pi^+$

⁴⁴ Dominant decay into $\rho^0\rho^0\pi^+$. BALTAY 78 finds confirmation in $2\pi^+\pi^-2\pi^0$ events which contain $\rho^+\rho^0\pi^0$ and $2\rho^+\pi^-$.

$\pi(2360) \quad I^G(J^{PC}) = 1^-(0^{-+})$					
MASS (MeV)	WIDTH (MeV)	DOCUMENT ID	TECN	COMMENT	
2360 ± 25	300 $^{+100}_{-50}$	ANISOVICH 01F	SPEC	2.0 $\bar{p}p \rightarrow 3\pi^0, \pi^0\eta, \pi^0\eta'$	

$X(2360) \quad I^G(J^{PC}) = ?^?(4^{+?})$					
MASS (MeV)	WIDTH (MeV)	DOCUMENT ID	TECN	COMMENT	
2360 ± 10	430 ± 30	ROZANSKA 80	SPRK	18 $\pi^-p \rightarrow \rho\bar{p}n$	

$X(2440) \quad I^G(J^{PC}) = ?^?(5^{-?})$					
MASS (MeV)	WIDTH (MeV)	DOCUMENT ID	TECN	COMMENT	
2440 ± 10	310 ± 20	ROZANSKA 80	SPRK	18 $\pi^-p \rightarrow \rho\bar{p}n$	

$X(2632) \quad I^G(J^{PC}) = ?^?(?^{??})$					
MASS (MeV)	WIDTH (MeV)	DOCUMENT ID	TECN	COMMENT	
2635.2 ± 3.3		⁴⁵ EVDOKIMOV 04	SELX	$X(2632) \rightarrow D_s^+\eta$	
2631.6 ± 2.1	< 17	⁴⁶ EVDOKIMOV 04	SELX	$X(2632) \rightarrow D_s^0K^+$	

⁴⁵ From a mass difference to D_s^+ of 666.9 ± 3.3 MeV.⁴⁶ From a mass difference to D_s^0 of 767.0 ± 2.0 MeV.

$B(X(2632) \rightarrow D_s^0K^+)/B(X(2632) \rightarrow D_s^+\eta)$					
VALUE	DOCUMENT ID	TECN	COMMENT		
0.14 ± 0.06	⁴⁷ EVDOKIMOV 04	SELX			

⁴⁷ Possible interpretation of this decay pattern is discussed by YASUI 07.

$X(2680) \quad I^G(J^{PC}) = ?^?(?^{??})$					
MASS (MeV)	WIDTH (MeV)	DOCUMENT ID	TECN	COMMENT	
2676 ± 27	150	CASO 70	HBC	11.2 $\pi^-p \rightarrow \rho^-\pi^+\pi^-p$	

$X(2710) \quad I^G(J^{PC}) = ?^?(6^{+?})$					
MASS (MeV)	WIDTH (MeV)	DOCUMENT ID	TECN	COMMENT	
2710 ± 20	170 ± 40	ROZANSKA 80	SPRK	18 $\pi^-p \rightarrow \rho\bar{p}n$	

$X(2750) \quad I^G(J^{PC}) = ?^?(7^{-?})$					
MASS (MeV)	WIDTH (MeV)	DOCUMENT ID	TECN	COMMENT	
2747 ± 32	195 ± 75	DENNEY 83	LASS	10 $\pi^+p \rightarrow K^+K^-\pi^+p$	

Meson Particle Listings

Further States

Table for X(2860) with columns: MASS (MeV), WIDTH (MeV), DOCUMENT ID, TECN, COMMENT. Row 1: 2856.6 ± 1.5 ± 5.0, 47 ± 7 ± 10, 48,49 AUBERT,BE 06E BABR e+ e- -> D K X

48 Conventional cS nature suggested by LI 07 and ZHANG 07. 49 Observed in the D0 K+ and D+ K0 final states. JP is natural.

Table for f0(3100) with columns: MASS (MeV), WIDTH (MeV), DOCUMENT ID, TECN, COMMENT. Row 1: 3100 ± 100, 700 ± 130, BINON 05 GAMS 33 pi- p -> eta eta n

Table for X(3250) with columns: MASS (MeV), WIDTH (MeV), DOCUMENT ID, TECN, COMMENT. Rows: 3250 ± 8 ± 20, 45 ± 18, ALEEVE 93 BIS2 X(3250) -> Lambda pbar K+; 3265 ± 7 ± 20, 40 ± 18, ALEEVE 93 BIS2 X(3250) -> Lambda bar p K-

Table for X(3250) with columns: MASS (MeV), WIDTH (MeV), DOCUMENT ID, TECN, COMMENT. Rows: 3245 ± 8 ± 20, 25 ± 11, ALEEVE 93 BIS2 X(3250) -> Lambda pbar K+ pi±; 3250 ± 9 ± 20, 50 ± 20, ALEEVE 93 BIS2 X(3250) -> Lambda bar p K- pi±; 3270 ± 8 ± 20, 25 ± 11, ALEEVE 93 BIS2 X(3250) -> KS0 Lambda pbar K±

Table for X(3350) with columns: MASS (MeV), WIDTH (MeV), EVTS, DOCUMENT ID, TECN, COMMENT. Row 1: 3350 +10 -20 ± 20, 70 +40 -20 ± 40, 50 ± 10, GABYSHEV 06A BELL B- -> Lambda c+ pbar pi-

REFERENCES for Further States

LI 07 EPJ C51 359, VLADMIRSK... 07 PAN 70 1706, YASUJ 07 PR D76 034009, ZHANG 07 EPJ C50 617, ABLIKIM 06S PRL 97 142002, AUBERT,BE 06E PRL 97 222001, GABYSHEV 06A PRL 97 242001, SCHEGELSKY 06 EPJ A27 199, SCHEGELSKY 06A EPJ A27 200, UMAN 06 PR D73 052009, VLADMIRSK... 06 PAN 69 493, BINON 05 PAN 68 960, GRIGOR'EV 05 PAN 68 1271, LU 05 PRL 94 032002, ABLIKIM 04J PRL 93 112002, BUGG 04 PL B595 556, BUGG 04A EPJ C36 161, EVDOKIMOV 04 PRL 93 242001, KUHN 04 PL B595 109, ANISOVICH 03 EPJ A16 229, VLADMIRSK... 03 PAN 66 700, ANISOVICH 02 PL B542 8, ANISOVICH 02B PL B542 19, CHUNG 02 PR D65 072001, LIRK 02K PL B545 50, ANISOVICH 01C PL B507 23, ANISOVICH 01D PL B508 6, ANISOVICH 01E PL B513 281, ANISOVICH 01F PL B517 261, ANISOVICH 00D PL B476 15, ANISOVICH 00E PL B477 19, ANISOVICH 00I PL B491 40, ANISOVICH 00J PL B491 47, ANISOVICH 00M PL B496 145, BARNES 00 PR C62 055203, FILIPPI 00 PL B495 284, VLADMIRSKII 00 JETPL 72 486, ANISOVICH 99C PL B452 173, ANISOVICH 99E PL B452 187, BUGG 99 PL B458 511, FERRER 99 EPJ C10 249, SEMENOV 99 SPU 42 847, KLOET 96 Translated from UFN 42 937, PROKOSHNIK 96 SPD 41 247, OAKDEN 94 NP A574 731, ALEEVE 93 PAN 56 1358, ARMSTRONG 93D PL B307 399, ALBRECHT 91F PR D53 0911, CONDO 91 PR D43 2787, BISELLO 89B PR D39 701, ATKINSON 88 ZPHY C38 535, DAFTARI 87 PRL 58 859, ALDE 86D NP B269 485, BRIDGES 86D PL B180 313, GREEN 86 PRL 56 1639, ATKINSON 85 ZPHY C29 333, DENNEY 83 PR D28 2726, ASTON 81B NP B189 205, ARESTOV 80 IHEP 90-165, CHLAPNIK... 80 ZPHY C3 285, KREYMER 80 PR D22 36, ROZANSKA 80 NP B162 505, EVANGELISTA... 79 NP B153 253, EVANGELIS... 79B NP B154 381, BALTAY 78 PR D17 52, ANTIPOV 77 NP B119 45, BALTAY 77 PRL 39 591, D.M. Li et al., V. Vladimirov et al., S. Yasu, M. Oka, B. Zhang et al., M. Ablikim et al., M. Aubert et al., N. Gabyshev et al., V.A. Schegelsky et al., U. Aman et al., V.V. Vladimirov et al., Binon et al., V.K. Grigor'ev et al., M. Lu et al., M. Ablikim et al., D.V. Bugg, D.V. Bugg, D.V. Bugg, V.V. Evdokimov et al., J. Kuhn et al., V.V. Anisovich et al., V.V. Vladimirov et al., A.V. Anisovich et al., A.V. Anisovich et al., S.U. Chung et al., J.M. Link et al., A.V. Anisovich et al., P.D. Barnes et al., A. Filippi et al., V.V. Vladimirov et al., A.V. Anisovich et al., A.V. Anisovich et al., A.V. Anisovich et al., A.V. Anisovich et al., W.M. Kloe, F. Myhrer, D. Prokoshnik, V.D. Samoilenko, M.N. Oaiden, M.R. Pennington, A.N. Aleev et al., T.A. Armstrong et al., H. Albrecht et al., G.T. Condo et al., G. Busetto et al., M. Atkinson et al., I.K. Daftari et al., M. Alde et al., D.L. Bridges et al., D.R. Green et al., M. Atkinson et al., D.L. Denney et al., D. Aston et al., Y.I. Arestov et al., P.V. Chlapnikov et al., A.E. Kreymmer et al., M. Rozanska et al., C. Evangelista et al., C. Evangelista et al., C. Baltay et al., Y.M. Antipov et al., C. Baltay, C.V. Cautis, M. Kalelkar, (BES Collab.), (BABAR Collab.), (BELLE Collab.), (FNAL E835), (ITEP, Moscow), (BNL E852 Collab.), (BES Collab.), (BNL E852 Collab.), (FNAL FOCUS Collab.), (OBELIX Experiment), (RUTG, NORD), (SERP), (DURH), (BIS-2 Collab.), (FNAL, FERR, GEWO+), (ARGUS Collab.), (SLAC Hybrid Collab.), (DM2 Collab.), (BONN, CERN, GLAS+), (SYRA), (BELG, LAPP, SERP, CERN+), (SYRA, BNL, CASE+), (FNAL, ARIZ, FSU+), (BONN, CERN, GLAS+), (IOWA, MICH), (BONN, CERN, EPOL, GLAS+), (SERP), (SERP, BRUX, MONS), (IND, PURD, SLAC+), (MPIM, CERN), (BARI, BONN, CERN+), (BARI, BONN, CERN+), (COLU, BING), (SERP, GEVA), (COLU)

BALTAY 75 PRL 35 891, KALELKAR 75 Thesis Nevis 207, CASO 70 LNC 3 707, C. Baltay et al., M.S. Kalelkar, C. Caso et al., (COLU, BING), (COLU), (GENO, HAMB, MILA, SAEL)

OTHER RELATED PAPERS

AFONIN 07 MPL A22 1359, AFONIN 07A PR C76 015202, CLOSE 07 PL B647 159, GLOZMAN 07 PRPL 444 1, LI 07A PR D76 094016, LIU 07B PR D75 074017, ZHANG 07C PR D76 036004, AFONIN 06 EPJ A29 327, COLANGELO 06 PL B642 48, DINI 06 PL B645 33, GUO 06A PR D74 097503, VANBEVEREN 06B PRL 97 202001, WEI 06A JUMP A21 4617, CHANG 05B PL B623 218, DIMITRASINO... 05 PRL 94 162002, GUPTA 05 JUMP A20 5891, HUANG 05A PR D71 114015, MAIANI 05 PR D71 014028, YAN 05 PR C71 025204, ZHANG 05C PRL D72 017902, ANISOVICH 04 SPU 47 45, Translated from UFN 174 49, BARNES 04 PL B600 223, BUGG 04B PL B598 8, BUGG 04C PRPL 397 257, CHAO 04A PL B599 43, CHEN 04C PRL 93 232001, DAI 04 JHEP 0411 043, GAO 04 CTP 42 844, KERBIKOV 04 PR C69 055205, LIU 04 PR D70 094009, MAIANI 04 PR D70 054009, SIMONOV 04 PR D70 114013, SWANSON 04 PL B582 167, VANBEVEREN 04A PRL 93 202001, ZOU 04 PR D69 034004, DATTA 03B PL B567 273, ROSNER 03B PR D68 014004, WANG 03 PRL 90 201802, ABE 02K PRL 88 181803, ABE 02W PRL 89 151802, ANISOVICH 01E PL B513 281, ABELE 00B EPJ C17 583, BARNES 00 PR C62 055203, BOLONKIN 00 JETPL 72 166, Translated from ZETFP 72 240, ANISOVICH 99F NP A651 253, CHIBA 99 PR C60 035204, BUZZO 97 ZPHY C76 475, CHIBA 97 NP D55 410, BARNES 94 PL B331 203, CARBONELL 93 PL B306 407, FERRER 93 NP A558 191c, CHIBA 91 PR D44 1933, GRAF 91 PR D44 1945, TANIMORI 90 PR D41 744, ALBRECHT 89D PL B217 205, BEHREND 89M PL B218 493, BUSENITZ 89 PR D40 1, CHIBA 88 PR B202 447, CHIBA 87 PR D36 3321, FRANKLIN 87 PR B184 111, LIU 87 PRL 58 2288, ADIELS 86 PL B182 405, ANGELOPOULOS... 86 PL B178 441, ARMSTRONG 86C PL B175 383, BRIDGES 86 PRL 56 211, BRIDGES 86B PRL 56 215, BRIDGES 86C PRL 57 1534, BRIDGES 86D PL B180 313, DOVER 86 PRL 57 1207, ANGELOPOULOS... 85 PL 159B 210, BODENKAMP 85 NP B255 717, ADIELS 84 PL 138B 235, ATKINSON 84F NP B239 1, AZOOZ 84 NP B244 277, CLOUGH 84 PL 146B 299, AZOOZ 83 PL 122B 471, BARNETT 83 PR D27 493, BODENKAMP 83 PL 133B 275, RICHTER 83 PL 126B 284, AJALTOUNI 82 NP B209 301, ASTON 81B NP B189 205, BARNES 81 NP B189 191, CHUNG 81 PRL 46 395, HARRIS 81 ZPHY C9 275, ARESTOV 80 IHEP 80-165, ASTON 80D PL 93B 517, BIONTA 80 PRL 44 909, CARROLL 80 PRL 44 1572, DALLM 80E PL 90B 475, DEFOIX 80 NP B162 12, HAMILTON 80 PRL 44 1179, HAMILTON 80B PRL 44 1182, KREYMER 80 PR D22 36, ALBERI 79 PR 83B 247, ARMSTRONG 79 PL B85 304, BARTALUCCI 79 NC 49A 207, DELCOURT 79 PL 86B 395, GIBBARD 79 PRL 42 1593, SAKAMOTO 79 NP B158 410, CARTER 78B NP B141 467, ESPOSITO 78 LNC 22 305, PAVLOPOULOS... 78 PL 72B 415, PETERSON 78 PR D18 395, BENKHEIRI 77 PL 83B 393, BRUCKNER 77 PL 67B 222, ABASHIAN 76 PR D13 5, BRAUN 76 PL 60B 481, CHALOUKPA 76 PL 61B 487, ALSTON... 75 PRL 35 1685, D'ANDLAW 75 PR 58B 223, KALOGEROPOULOS... 75 PRL 34 1047, CARROLL 74 PRL 32 247, THOMPSON 74 NP B69 220, S.S. Afonin, S.S. Afonin, F.E. Close et al., L.Ya. Glzman, B.A. Li, X. Liu et al., A. Zhang et al., S.S. Afonin, P. Colangelo et al., G.-J. Ding, M.-L. Yan, F.-K. Guo, P.-N. Shen, E. van Beveren, G. Rupp, W. Wei, L. Zhang, S.L. Zhu, C.-H. Chang, C.S. Kim, G. Wang, V. Dmitrasinovic, V. Gupta, M.Q. Huang, D.W. Wang, L. Maiani et al., Y. Yan et al., A. Zhang, V.V. Anisovich, T. Barnes et al., D.V. Bugg, D.V. Bugg, K.-T. Chao, Y.-Q. Chen, X.-Q. Li, Y.-B. Dai et al., G.-S. Gao, S.-L. Zhu, B. Kerbikov et al., Y.-R. Liu, L. Maiani et al., Yu.A. Simonov, J.A. Tjon, E. Swanson, E. van Beveren, G. Rupp, B.S. Zou, H.C. Chiang, A. Datta, P.J. O'Donnell, J.L. Rosner, M.-Z. Wang et al., K. Abe et al., A.V. Anisovich et al., A. Abele et al., P.D. Barnes et al., B.V. Bolonkin et al., A.V. Anisovich et al., M. Chiba et al., M. Chiba et al., (JETSET Collab.), M. Chiba et al., (FUKI, INUS, KEK, SANG+), P.D. Barnes et al., (PS18s Collab.), J. Carbonell, K.V. Protasov, O.D. Dalkarov, (ISN+), A. Ferrer, A.A. Grigorian, (WA56 Collab.), M. Chiba et al., (FUKI, KEK, SANG, OSAK+), N.A. Graf et al., (UCI, PENN, NMSU, KARLK+), T. Tanimori et al., (KEK, INUS, KYOT+), H. Albrecht et al., (ARGUS Collab.), H.J. Behrend et al., (CELLO Collab.), J.K. Busenitz et al., (ILL, FNAL), M. Chiba, K. Doi, (FUKI, INUS, KEK, SANG, OSAK+), M. Chiba et al., (FUKI, INUS, KEK, SANG+), J. Franklin, (K.F. Liu, B.A. Li, (STON), L. Adiels et al., (STOH, BASL, LASL, THES+), A. Angelopoulos et al., (ATHU, UCI, KARLK+), T.A. Armstrong et al., (BNL, HOUS, PENN+), D.L. Bridges et al., (BLSU, BNL, CASE+), D.L. Bridges et al., (SYRA, CASE), D.L. Bridges et al., (SYRA), D.L. Bridges et al., (SYRA, BNL, CASE+), C.B. Dover et al., (BNL), A. Angelopoulos et al., (ATHU, UCI, UNM+), J. Bodenkamp et al., (KARLK, KARLE, DESY), L. Adiels et al., (BASL, KARLK, KARLE, STO+), M. Atkinson et al., (BONN, CERN, GLAS+), F. Azooz, I. Butterworth, (LOIC, RHEL, SACL+), A.S. Clough et al., (SURRE, LOQM, ANIK+), F. Azooz, I. Butterworth, (LOIC, RHEL, SACL+), B. Barnett et al., (JHY), J. Bodenkamp et al., (KARLK, KARLE, DESY), B. Richter, L. Adiels, (BASL, KARLK, KARLE, STO+), Z. Ajaltouni et al., (CERN, NEUC+), D. Aston et al., (BONN, CERN, EPOL, GLAS+), A.D. Banks et al., (LIVP, CERN), S.U. Chung et al., (BNL, BRAN, CINC+), R.M. Harris et al., (SEAT, UCB), Y.I. Arestov et al., (SERP), D. Aston, (BONN, CERN, EPOL, GLAS, LAN+C), R.M. Bionta et al., (BNL, CMU, FNAL+), A.S. Carroll et al., (BNL, PRIN), C. Daum et al., (AMST, CERN, CRAC, MPIM+), C. Defoix et al., (CDEF, PISA), R.P. Hamilton et al., (LBL, BNL, MTHO), R.P. Hamilton et al., (LBL, BNL, MTHO), A.E. Kreymmer et al., (IND, PURD, SLAC+), G. Alberi et al., (TRST, CERN, IFRJ), T.A. Armstrong et al., (DESY, GLAS), S. Bartalucci et al., (DESY, FRAS), B. Delcourt et al., (LALO), B.G. Gibbard et al., (CORN), S. Sakamoto et al., (INUS), A.A. Carter, (LOQM), B. Esposito, F. Felicetti, (FRAS, NAPL, PADO+), P. Pavlooulos et al., (KARLK, KARLE, BASL+), D. Peterson et al., (CORN, HARV), P. Benkheiri et al., (CERN, CDEF, EPOL+), W. Bruckner et al., (MPH, HEIDP, CERN), A. Abashian et al., (ILL, ANL, CHIC+), H.M. Braun et al., (STRB), V. Chaloukpa et al., (CERN, LIVP, MONS+), M. Alston-Garnjost et al., (LBL, MTHO), C. d'Andlaw et al., (CDEF, PISA), T. Kalogeropoulos, G.S. Tzanakos, (BNL), A.S. Carroll et al., (PURD), G. Thompson et al.

Meson Particle Listings

Further States

See key on page 373

DONALD	73	NP B61 333	R.A. Donald <i>et al.</i>	(LIVP, PARIS)	BOESEBECK	68	NP B4 501	K. Boesebeck <i>et al.</i>	(AACH, BERL, CERN)
ALEXANDER	72	NP B45 29	G. Alexander <i>et al.</i>	(TELA)	HUSON	68	PL 28B 208	R. Huson <i>et al.</i>	(ORSAY, MILA, UCLA)
ANTIPOV	72	PL 40B 147	Y.M. Antipov <i>et al.</i>	(SERP)	ALLES-...	67B	NC 50A 776	V. Alles-Borelli <i>et al.</i>	(CERN, BONN)
TAKAHASHI	72	PR D6 1266	K. Takahashi <i>et al.</i>	(TOHOK, PENN, NDAM+)	DANYSZ	67B	NC 51A 801	J.A. Danysz, B.R. French, V. Simak	(CERN)
BENVENUTI	71	PRL 27 283	A.C. Benvenuti <i>et al.</i>	(WISC)	CHIKOVANI	66	PL 22 233	G.E. Chikovani <i>et al.</i>	(SERP)
SABAU	71	LNC 1 514	M. Sabau, J.L. Uretsky	(BUCH, ANL)	FOCACCI	66	PRL 17 890	M.N. Focacci <i>et al.</i>	(CERN)
BAUD	70	PL 31B 549	R. Baud <i>et al.</i>	(CERN Boson Spectrometer Collab.)					
ANDERSON	69	PRL 22 1390	E.W. Anderson <i>et al.</i>	(BNL, CMU)					

Meson Particle Listings

 K^\pm

STRANGE MESONS
($S = \pm 1, C = B = 0$)

$K^+ = u\bar{s}, K^0 = d\bar{s}, \bar{K}^0 = \bar{d}s, K^- = \bar{u}s,$ similarly for K^{*} 's

 K^\pm $I(J^P) = \frac{1}{2}(0^-)$ **THE CHARGED KAON MASS**

Revised 1994 by T.G. Trippe (LBNL).

The average of the six charged kaon mass measurements which we use in the Particle Listings is

$$m_{K^\pm} = 493.677 \pm 0.013 \text{ MeV } (S = 2.4), \quad (1)$$

where the error has been increased by the scale factor S . The large scale factor indicates a serious disagreement between different input data. The average before scaling the error is

$$m_{K^\pm} = 493.677 \pm 0.005 \text{ MeV}, \quad (2)$$

$$\chi^2 = 22.9 \text{ for } 5 \text{ D.F.}, \text{ Prob.} = 0.04\%,$$

where the high χ^2 and correspondingly low χ^2 probability further quantify the disagreement.

The main disagreement is between the two most recent and precise results,

$$m_{K^\pm} = 493.696 \pm 0.007 \text{ MeV} \quad \text{DENISOV 91}$$

$$m_{K^\pm} = 493.636 \pm 0.011 \text{ MeV } (S = 1.5) \quad \text{GALL 88}$$

$$\text{Average} = 493.679 \pm 0.006 \text{ MeV}$$

$$\chi^2 = 21.2 \text{ for } 1 \text{ D.F.}, \text{ Prob.} = 0.0004\%, \quad (3)$$

both of which are measurements of x-ray energies from kaonic atoms. Comparing the average in Eq. (3) with the overall average in Eq. (2), it is clear that DENISOV 91 and GALL 88 dominate the overall average, and that their disagreement is responsible for most of the high χ^2 .

The GALL 88 measurement was made using four different kaonic atom transitions, $K^- \text{Pb } (9 \rightarrow 8)$, $K^- \text{Pb } (11 \rightarrow 10)$, $K^- \text{W } (9 \rightarrow 8)$, and $K^- \text{W } (11 \rightarrow 10)$. The m_{K^\pm} values they obtain from each of these transitions is shown in the Particle Listings and in Fig. 1. Their $K^- \text{Pb } (9 \rightarrow 8)$ m_{K^\pm} is below and somewhat inconsistent with their other three transitions. The average of their four measurements is

$$m_{K^\pm} = 493.636 \pm 0.007,$$

$$\chi^2 = 7.0 \text{ for } 3 \text{ D.F.}, \text{ Prob.} = 7.2\%. \quad (4)$$

This is a low but acceptable χ^2 probability so, to be conservative, GALL 88 scaled up the error on their average by $S=1.5$ to obtain their published error ± 0.011 shown in Eq. (3) above and used in the Particle Listings average.

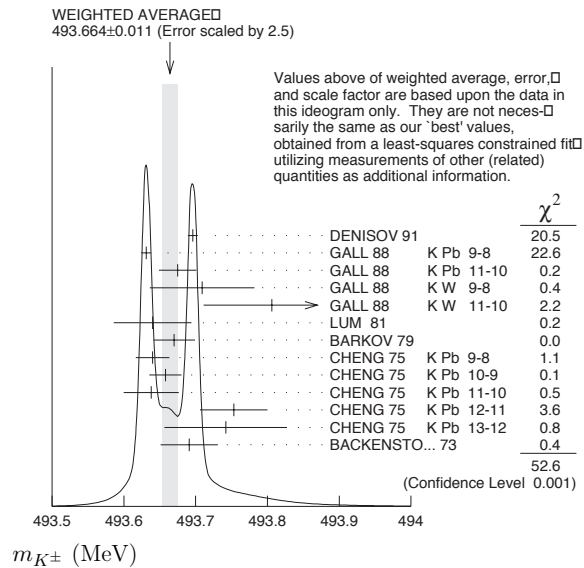


Figure 1: Ideogram of m_{K^\pm} mass measurements. GALL 88 and CHENG 75 measurements are shown separately for each transition they measured.

The ideogram in Fig. 1 shows that the DENISOV 91 measurement and the GALL 88 $K^- \text{Pb } (9 \rightarrow 8)$ measurement yield two well-separated peaks. One might suspect the GALL 88 $K^- \text{Pb } (9 \rightarrow 8)$ measurement since it is responsible both for the internal inconsistency in the GALL 88 measurements and the disagreement with DENISOV 91.

To see if the disagreement could result from a systematic problem with the $K^- \text{Pb } (9 \rightarrow 8)$ transition, we have separated the CHENG 75 data, which also used $K^- \text{Pb}$, into its separate transitions. Figure 1 shows that the CHENG 75 and GALL 88 $K^- \text{Pb } (9 \rightarrow 8)$ values are consistent, suggesting the possibility of a common effect such as contaminant nuclear γ rays near the $K^- \text{Pb } (9 \rightarrow 8)$ transition energy, although the CHENG 75 errors are too large to make a strong conclusion. The average of all 13 measurements has a χ^2 of 52.6 as shown in Fig. 1 and the first line of Table 1, yielding an unacceptable χ^2 probability of 0.00005%. The second line of Table 1 excludes both the GALL 88 and CHENG 75 measurements of the $K^- \text{Pb } (9 \rightarrow 8)$ transition and yields a χ^2 probability of 43%. The third [fourth] line of Table 1 excludes only the GALL 88 $K^- \text{Pb } (9 \rightarrow 8)$ [DENISOV 91] measurement and yields a χ^2 probability of 20% [8.6%]. Table 1 shows that removing both measurements of the $K^- \text{Pb } (9 \rightarrow 8)$ transition produces the most consistent set of data, but that excluding only the GALL 88 $K^- \text{Pb } (9 \rightarrow 8)$ transition or DENISOV 91 also produces acceptable probabilities.

Table 1: m_{K^\pm} averages for some combinations of Fig. 1 data.

m_{K^\pm} (MeV)	χ^2	D.F.	Prob. (%)	Measurements used
493.664 ± 0.004	52.6	12	0.00005	all 13 measurements
493.690 ± 0.006	10.1	10	43	no K^- Pb(9→8)
493.687 ± 0.006	14.6	11	20	no GALL 88 K^- Pb(9→8)
493.642 ± 0.006	17.8	11	8.6	no DENISOV 91

Yu.M. Ivanov, representing DENISOV 91, has estimated corrections needed for the older experiments because of improved ^{192}Ir and ^{198}Au calibration γ -ray energies. He estimates that CHENG 75 and BACKENSTOSS 73 m_{K^\pm} values could be raised by about 15 keV and 22 keV, respectively. With these estimated corrections, Table 1 becomes Table 2. The last line of Table 2 shows that if such corrections are assumed, then GALL 88 K^- Pb (9 → 8) is inconsistent with the rest of the data even when DENISOV 91 is excluded. Yu.M. Ivanov warns that these are rough estimates. Accordingly, we do not use Table 2 to reject the GALL 88 K^- Pb (9 → 8) transition, but we note that a future reanalysis of the CHENG 75 data could be useful because it might provide supporting evidence for such a rejection.

Table 2: m_{K^\pm} averages for some combinations of Fig. 1 data after raising CHENG 75 and BACKENSTOSS 73 values by 0.015 and 0.022 MeV respectively.

m_{K^\pm} (MeV)	χ^2	D.F.	Prob. (%)	Measurements used
493.666 ± 0.004	53.9	12	0.00003	all 13 measurements
493.693 ± 0.006	9.0	10	53	no K^- Pb(9→8)
493.690 ± 0.006	11.5	11	40	no GALL 88 K^- Pb(9→8)
493.645 ± 0.006	23.0	11	1.8	no DENISOV 91

The GALL 88 measurement uses a Ge semiconductor spectrometer which has a resolution of about 1 keV, so they run the risk of some contaminant nuclear γ rays. Studies of γ rays following stopped π^- and Σ^- absorption in nuclei (unpublished) do not show any evidence for contaminants according to GALL 88 spokesperson, B.L. Roberts. The DENISOV 91 measurement uses a crystal diffraction spectrometer with a resolution of 6.3 eV for radiation at 22.1 keV to measure the 4f-3d transition in K^- ^{12}C . The high resolution and the light nucleus reduce the probability for overlap by contaminant γ rays, compared with the measurement of GALL 88. The DENISOV 91 measurement is supported by their high-precision measurement of the 4d-2p transition energy in π^- ^{12}C , which is good agreement with the calculated energy.

While we suspect that the GALL 88 K^- Pb (9 → 8) measurements could be the problem, we are unable to find clear grounds for rejecting it. Therefore, we retain their measurement in the average and accept the large scale factor until further information can be obtained from new measurements and/or from reanalysis of GALL 88 and CHENG 75 data.

We thank B.L. Roberts (Boston Univ.) and Yu.M. Ivanov (Petersburg Nuclear Physics Inst.) for their extensive help in understanding this problem.

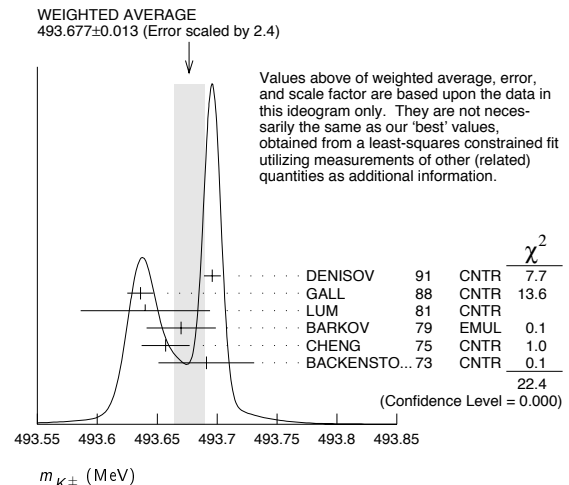
 K^\pm MASS

VALUE (MeV)	DOCUMENT ID	TECN	CHG	COMMENT
493.677 ± 0.016 OUR FIT	Error includes scale factor of 2.8.			
493.677 ± 0.013 OUR AVERAGE	Error includes scale factor of 2.4. See the ideogram below.			
493.696 ± 0.007	1 DENISOV	91	CNTR	— Kaonic atoms
493.636 ± 0.011	2 GALL	88	CNTR	— Kaonic atoms
493.640 ± 0.054	LUM	81	CNTR	— Kaonic atoms
493.670 ± 0.029	BARKOV	79	EMUL	± $e^+ e^- \rightarrow K^+ K^-$
493.657 ± 0.020	2 CHENG	75	CNTR	— Kaonic atoms
493.691 ± 0.040	BACKENSTOSS 73	CNTR	—	Kaonic atoms
• • • We do not use the following data for averages, fits, limits, etc. • • •				
493.631 ± 0.007	GALL	88	CNTR	— K^- Pb (9 → 8)
493.675 ± 0.026	GALL	88	CNTR	— K^- Pb (11 → 10)
493.709 ± 0.073	GALL	88	CNTR	— K^- W (9 → 8)
493.806 ± 0.095	GALL	88	CNTR	— K^- W (11 → 10)
$493.640 \pm 0.022 \pm 0.008$	3 CHENG	75	CNTR	— K^- Pb (9 → 8)
$493.658 \pm 0.019 \pm 0.012$	3 CHENG	75	CNTR	— K^- Pb (10 → 9)
$493.638 \pm 0.035 \pm 0.016$	3 CHENG	75	CNTR	— K^- Pb (11 → 10)
$493.753 \pm 0.042 \pm 0.021$	3 CHENG	75	CNTR	— K^- Pb (12 → 11)
$493.742 \pm 0.081 \pm 0.027$	3 CHENG	75	CNTR	— K^- Pb (13 → 12)

¹ Error increased from 0.0059 based on the error analysis in IVANOV 92.

² This value is the authors' combination of all of the separate transitions listed for this paper.

³ The CHENG 75 values for separate transitions were calculated from their Table 7 transition energies. The first error includes a 20% systematic error in the nonrelativistic contaminant shift. The second error is due to a ± 5 eV uncertainty in the theoretical transition energies.

 **$m_{K^+} - m_{K^-}$**

Test of CPT.

VALUE (MeV)	EVTS	DOCUMENT ID	TECN	CHG
-0.032 ± 0.090	1.5M	4 FORD	72	ASPK ±

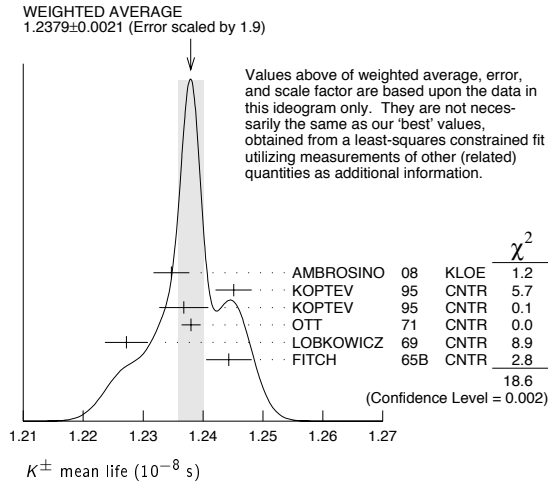
⁴ FORD 72 uses $m_{\pi^+} - m_{\pi^-} = +28 \pm 70$ keV.

 K^\pm MEAN LIFE

VALUE (10^{-8} s)	EVTS	DOCUMENT ID	TECN	CHG	COMMENT
1.2380 ± 0.0021 OUR FIT	Error includes scale factor of 1.9.				
1.2379 ± 0.0021 OUR AVERAGE	Error includes scale factor of 1.9. See the ideogram below.				
1.2347 ± 0.0030	15M	5 AMBROSINO	08	KLOE ±	$\phi \rightarrow K^+ K^-$
1.2451 ± 0.0030	250k	KOPTEV	95	CNTR	K at rest, U target
1.2368 ± 0.0041	150k	KOPTEV	95	CNTR	K at rest, Cu target
1.2380 ± 0.0016	3M	OTT	71	CNTR	+ K at rest
1.2272 ± 0.0036		LOBKOWICZ	69	CNTR	+ K in flight
1.2443 ± 0.0038		FITCH	65B	CNTR	+ K at rest
• • • We do not use the following data for averages, fits, limits, etc. • • •					
1.2415 ± 0.0024	400k	6 KOPTEV	95	CNTR	K at rest
1.221 ± 0.011		FORD	67	CNTR	±
1.231 ± 0.011		BOYARSKI	62	CNTR	+

⁵ Result obtained by averaging the decay length and decay time analyses taking correlations into account.

⁶ KOPTEV 95 report this weighted average of their U-target and Cu-target results, where they have weighted by $1/\sigma$ rather than $1/\sigma^2$.



$$\frac{(\tau_{K^+} - \tau_{K^-})}{\tau_{\text{average}}}$$

This quantity is a measure of CPT invariance in weak interactions.

VALUE (%)	DOCUMENT ID	TECN
0.11 ± 0.09 OUR AVERAGE	Error includes scale factor of 1.2.	
0.090 ± 0.078	LOBKOWICZ 69	CNTR
0.47 ± 0.30	FORD 67	CNTR

RARE KAON DECAYS

Revised November 2007 by L. Littenberg (BNL) and G. Valencia (Iowa State University).

A. Introduction: There are several useful reviews on rare kaon decays and related topics [1–15]. Activity in rare kaon decays can be divided roughly into four categories:

1. Searches for explicit violations of the Standard Model
2. Measurements of Standard Model parameters
3. Searches for CP violation
4. Studies of strong interactions at low energy.

The paradigm of Category 1 is the lepton flavor violating decay $K_L \rightarrow \mu e$. Category 2 includes processes such as $K^+ \rightarrow \pi^+ \nu \bar{\nu}$, which is sensitive to $|V_{td}|$. Much of the interest in Category 3 is focused on the decays $K_L \rightarrow \pi^0 \ell \bar{\ell}$, where $\ell \equiv e, \mu, \nu$. Category 4 includes reactions like $K^+ \rightarrow \pi^+ \ell^+ \ell^-$ which constitute a testing ground for the ideas of chiral perturbation theory. Category 4 also includes $K_L \rightarrow \pi^0 \gamma \gamma$ and $K_L \rightarrow \ell^+ \ell^- \gamma$. The former is important in understanding a CP -conserving contribution to $K_L \rightarrow \pi^0 \ell^+ \ell^-$, whereas the latter could shed light on long distance contributions to $K_L \rightarrow \mu^+ \mu^-$.

The interplay between Categories 2-4 can be illustrated in Fig. 1. The modes $K \rightarrow \pi \nu \bar{\nu}$ are the cleanest ones theoretically. They can provide accurate determinations of certain CKM parameters (shown in the figure). In combination with alternate determinations of these parameters, they also constrain new interactions. The modes $K_L \rightarrow \pi^0 e^+ e^-$ and $K_L \rightarrow \mu^+ \mu^-$ are also sensitive to CKM parameters. However, they suffer from a series of hadronic uncertainties that can be addressed, at least in part, through a systematic study of the additional modes indicated in the figure.

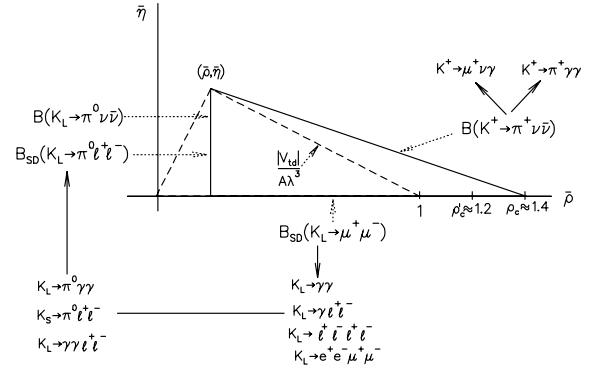


Figure 1: Role of rare kaon decays in determining the unitarity triangle. The solid arrows point to auxiliary modes needed to interpret the main results, or potential backgrounds to them.

B. Explicit violations of the Standard Model: Much activity has focussed on searches for lepton flavor violation (LFV). This is motivated by the fact that many extensions of the minimal Standard Model violate lepton flavor and by the potential to access very high energy scales. For example, the tree-level exchange of a LFV vector boson of mass M_X that couples to left-handed fermions with electroweak strength and without mixing angles yields $B(K_L \rightarrow \mu e) = 4.7 \times 10^{-12} (148 \text{ TeV}/M_X)^4$ [6]. This simple dimensional analysis may be read from Table 1 that the reaction $K_L \rightarrow \mu e$ is already probing scales of over 100 TeV. Table 1 summarizes the present experimental situation vis a vis LFV. The decays $K_L \rightarrow \mu^\pm e^\mp$ and $K^+ \rightarrow \pi^+ e^\mp \mu^\pm$ (or $K_L \rightarrow \pi^0 e^\mp \mu^\pm$) provide complementary information on potential family number violating interactions, since the former is sensitive to parity-odd couplings and the latter is sensitive to parity-even couplings. Limits on certain lepton-number violating kaon decays [16,17] also exist. Related searches in μ and τ processes are discussed in our section “Tests of Conservation Laws.”

Table 1: Searches for lepton flavor violation in K decay

Mode	90% CL upper limit	Exp't	Yr./Ref.
$K^+ \rightarrow \pi^+ e^- \mu^+$	1.2×10^{-11}	BNL-865	2003/Ref. 18
$K^+ \rightarrow \pi^+ e^+ \mu^-$	5.2×10^{-10}	BNL-865	2001/Ref. 16
$K_L \rightarrow \mu e$	4.7×10^{-12}	BNL-871	1998/Ref. 19
$K_L \rightarrow \pi^0 e \mu$	7.6×10^{-11}	KTeV (prelim.)	2007/Ref. 20
$K_L \rightarrow \pi^0 \pi^0 e \mu$	1.6×10^{-10}	KTeV (prelim.)	2007/Ref. 20

Physics beyond the SM is also pursued through the search for $K^+ \rightarrow \pi^+ X^0$, where X^0 is a very light, long-lived particle (e.g., hyperphoton, axion, familon, etc.). The 90% CL upper limit on this process is 5.9×10^{-11} [21].

C. Measurements of Standard Model parameters:

In the SM, the decay $K^+ \rightarrow \pi^+ \nu \bar{\nu}$ is dominated by one-loop diagrams with top-quark intermediate states and long-distance contributions are known to be quite small [2,22,23]. This permits a precise calculation [24] of this rate in terms of SM parameters. Studies of this process are thus motivated by the possibility of detecting non-SM physics when comparing with the results of global fits [25,26].

BNL-787 has observed two candidate events [21,27], and BNL-949 has observed one more, yielding a branching ratio of $(1.47^{+1.30}_{-0.89}) \times 10^{-10}$ [28]. A new experiment with a sensitivity goal of $\sim 10^{-12}$ /event was proposed [29] at CERN in 2005. In the future, this mode may provide grounds for precision tests of the flavor structure of the Standard Model [30]. The branching ratio can be written in terms of the very well-measured K_{e3} rate as [2]:

$$B(K^+ \rightarrow \pi^+ \nu \bar{\nu}) = \frac{\alpha^2 B(K^+ \rightarrow \pi^0 e^+ \nu)}{V_{us}^2 2\pi^2 \sin^4 \theta_W} \times \sum_{l=e,\mu,\tau} |V_{cs}^* V_{cd} X_{NL}^\ell + V_{ts}^* V_{td} X(m_t)|^2 \quad (1)$$

to eliminate the *a priori* unknown hadronic matrix element. Isospin breaking corrections to the ratio of matrix elements reduce this rate by 10% [31]. In Eq. (1), the Inami-Lim function $X(m_t)$ is of order 1 [32], and X_{NL}^ℓ is several hundred times smaller. This form exhibits the strong dependence of this branching ratio on $|V_{td}|$. QCD corrections, which mainly affect X_{NL}^ℓ , lead to a residual error of $< 5\%$ for the decay amplitude [13,23,33,34]. Evaluating the constants in Eq. (1), one can cast this result in terms of the CKM parameters λ , V_{cb} , $\bar{\rho}$ and $\bar{\eta}$ (see our Section on “The Cabibbo-Kobayashi-Maskawa mixing matrix”) [13]:

$$B(K^+ \rightarrow \pi^+ \nu \bar{\nu}) \approx 1.6 \times 10^{-5} |V_{cb}|^4 [\sigma \bar{\eta}^2 + (\rho_c - \bar{\rho})^2], \quad (2)$$

where $\rho_c \equiv 1 + (\frac{2}{3} X_{NL}^e + \frac{1}{3} X_{NL}^\tau) / (|V_{cb}|^2 X(m_t)) \approx 1.4$ and $\sigma \equiv 1 / (1 - \frac{1}{2} \lambda^2)^2$. Thus, $B(K^+ \rightarrow \pi^+ \nu \bar{\nu})$ determines an ellipse in the $\bar{\rho}$, $\bar{\eta}$ plane with center $(\rho_c, 0)$ and semi-axes $\approx \frac{1}{|V_{cb}|^2} \sqrt{\frac{B(K^+ \rightarrow \pi^+ \nu \bar{\nu})}{1.6 \times 10^{-5}}}$ and $\frac{1}{\sigma |V_{cb}|^2} \sqrt{\frac{B(K^+ \rightarrow \pi^+ \nu \bar{\nu})}{1.6 \times 10^{-5}}}$. Current constraints on the CKM parameters lead to a predicted branching ratio $(8.0 \pm 1.1) \times 10^{-11}$ [34], near the lower end of the BNL-787 measurement.

The decay $K_L \rightarrow \mu^+ \mu^-$ also has a short distance contribution sensitive to the CKM parameter $\bar{\rho}$, given by [13]:

$$B_{SD}(K_L \rightarrow \mu^+ \mu^-) \approx 2.7 \times 10^{-4} |V_{cb}|^4 (\rho'_c - \bar{\rho})^2 \quad (3)$$

where ρ'_c depends on the charm quark mass and is approximately 1.2. This decay, however, is dominated by a long-distance contribution from a two-photon intermediate state. The absorptive (imaginary) part of the long-distance component is determined by the measured rate for $K_L \rightarrow \gamma \gamma$ to be $B_{\text{abs}}(K_L \rightarrow \mu^+ \mu^-) = (6.64 \pm 0.07) \times 10^{-9}$; and it almost completely saturates the observed rate $B(K_L \rightarrow \mu^+ \mu^-) = (6.87 \pm 0.11) \times 10^{-9}$ [35].

The difference between the observed rate and the absorptive component can be attributed to the (coherent) sum of the short-distance amplitude and the real part of the long-distance amplitude. The latter cannot be derived directly from experiment [36], but can be estimated with certain assumptions [37,38]. The decay $K_L \rightarrow e^+ e^-$ is completely dominated by long distance physics and is easier to estimate. The result, $B(K_L \rightarrow e^+ e^-) \sim 9 \times 10^{-12}$ [36,39], is in good agreement with the BNL-871 measurement, $(8.7^{+5.7}_{-4.1}) \times 10^{-12}$ [40].

D. Searches for direct CP violation: The mode $K_L \rightarrow \pi^0 \nu \bar{\nu}$ is dominantly *CP*-violating and free of hadronic uncertainties [2,41,42]. In the Standard Model, this mode is dominated by an intermediate top-quark state and does not suffer from the small uncertainty associated with the charm-quark intermediate state that affects the mode $K^+ \rightarrow \pi^+ \nu \bar{\nu}$. The branching ratio is given approximately by Ref. 13:

$$B(K_L \rightarrow \pi^0 \nu \bar{\nu}) \approx 7.6 \times 10^{-5} |V_{cb}|^4 \bar{\eta}^2. \quad (4)$$

With current constraints on the CKM parameters this leads to a predicted branching ratio $(3.0 \pm 0.6) \times 10^{-11}$ [43]. The 90% CL bound on $K^+ \rightarrow \pi^+ \nu \bar{\nu}$ provides a nearly model-independent bound $B(K_L \rightarrow \pi^0 \nu \bar{\nu}) < 1.4 \times 10^{-9}$ [44]. KEK-391a, which began data-taking in early 2004, aims to reach this level, and has published a result of $B(K_L \rightarrow \pi^0 \nu \bar{\nu}) \leq 2.1 \times 10^{-7}$ [45] based on a fraction of their data. A proposal for an experiment to reach the 10^{-11} /event level has been submitted to the J-PARC PAC [46].

There has been much theoretical work on possible contributions to rare *K* decays beyond the SM. While in the simplest case of the MSSM with no new sources of flavor or *CP* violation, the main effect is a suppression of the rare *K* decays [2,3,47], substantial enhancements are possible in more general SUSY models [48]. A comprehensive discussion of these and several other models can be found in Refs. [43] and [49].

The decay $K_L \rightarrow \pi^0 e^+ e^-$ also has sensitivity to the CKM parameter η through its *CP*-violating component. There are both direct and indirect *CP*-violating amplitudes which can interfere. The direct *CP*-violating amplitude is short distance dominated and has been calculated in detail within the SM [10]. The indirect *CP*-violating amplitude can be inferred from a measurement of $K_S \rightarrow \pi^0 e^+ e^-$. The complete *CP*-violating contribution to the rate can be written as [50]:

$$B_{CPV} \approx 10^{-12} \left[15.7 |a_S|^2 \pm 1.45 \left(\frac{|V_{cb}|^2 \bar{\eta}}{10^{-4}} \right) |a_S| + 0.129 \left(\frac{|V_{cb}|^2 \bar{\eta}}{10^{-4}} \right)^2 \right] \quad (5)$$

where the three terms correspond to the indirect CP violation, the interference, and the direct CP violation respectively. The parameter a_S has been extracted by NA48 from a measurement of the decay $K_S \rightarrow \pi^0 e^+ e^-$ with the result $|a_S| = 1.06^{+0.26}_{-0.21} \pm$

Meson Particle Listings

K^\pm

0.07 [51]. With current constraints on the CKM parameters this implies that

$$B_{\text{CPV}} \approx (17.2 \pm 9.4 + 4.7) \times 10^{-12}. \quad (6)$$

The indirect CP violation is larger than the direct CP violation. While the sign of the interference is *a priori* unknown, arguments in favor of a positive sign have been put forward in Ref. 52 and Ref. 53. NA48 has also obtained the value $a_s = 1.54^{+0.40}_{-0.32} \pm 0.06$ [54] from a measurement of the $K_S \rightarrow \pi^0 \mu^+ \mu^-$ rate, in agreement with the value extracted from $K_S \rightarrow \pi^0 e^+ e^-$.

$K_L \rightarrow \pi^0 \gamma \gamma$ also has a CP -conserving component dominated by a two-photon intermediate state. This component can be decomposed into an absorptive and a dispersive part. The absorptive part can be extracted from the measurement of the low $m_{\gamma\gamma}$ region of the $K_L \rightarrow \pi^0 \gamma \gamma$ spectrum. The rate and the shape of the distribution $d\Gamma/dm_{\gamma\gamma}$ in $K_L \rightarrow \pi^0 \gamma \gamma$ are well described in chiral perturbation theory in terms of three (*a priori*) unknown parameters [55,56].

Both KTeV and NA48 have studied the mode $K_L \rightarrow \pi^0 \gamma \gamma$, reporting similar results. KTeV finds $B(K_L \rightarrow \pi^0 \gamma \gamma) = (1.30 \pm 0.03_{\text{stat}} \pm 0.04_{\text{sys}}) \times 10^{-6}$ [57], while NA48 finds $B(K_L \rightarrow \pi^0 \gamma \gamma) = (1.36 \pm 0.03_{\text{stat}} \pm 0.03_{\text{sys}} \pm 0.03_{\text{norm}}) \times 10^{-6}$ [58]. Both experiments are consistent with a negligible rate in the low $m_{\gamma\gamma}$ region, suggesting a very small CP -conserving component $B_{\text{CP}}(K_L \rightarrow \pi^0 e^+ e^-) \sim \mathcal{O}(10^{-13})$ [52,56,58]. There remains some model dependence in the estimate of the dispersive part of the CP -conserving $K_L \rightarrow \pi^0 e^+ e^-$ [52].

The related process, $K_L \rightarrow \pi^0 \gamma e^+ e^-$, is potentially an additional background in some region of phase space [59]. This process has been observed with a branching ratio of $(1.62 \pm 0.14_{\text{stat}} \pm 0.09_{\text{sys}}) \times 10^{-8}$ [60].

The decay $K_L \rightarrow \gamma e^+ e^-$ constitutes the dominant background to $K_L \rightarrow \pi^0 e^+ e^-$. It was first observed by BNL-845 [61], and subsequently confirmed with a much larger sample by FNAL-799 [62]. It has been estimated that this background will enter at about the 10^{-10} level [63,64], comparable to or larger than the signal level. Because of this, the observation of $K_L \rightarrow \pi^0 e^+ e^-$ at the SM level will depend on background subtraction with good statistics. Possible alternative strategies are discussed in Ref. 52 and references cited therein.

The 90% CL upper bound for the process $K_L \rightarrow \pi^0 e^+ e^-$ is 2.8×10^{-10} [64]. For the closely related muonic process, the published upper bound is $B(K_L \rightarrow \pi^0 \mu^+ \mu^-) \leq 3.8 \times 10^{-10}$ [65], compared with the SM prediction of $(1.5 \pm 0.3) \times 10^{-11}$ [66] (assuming positive interference between the direct and indirect- CP violating components). KTeV has additional data corresponding to about a factor 1.3 in sensitivity for the latter reaction that is under analysis.

A study of $K_L \rightarrow \pi^0 \mu^+ \mu^-$ has indicated that it might be possible to extract the direct CP -violating contribution by a joint study of the Dalitz plot variables and the components of the μ^+ polarization [67]. The latter tends to be quite substantial so that large statistics may not be necessary.

Combined information from the two $K_L \rightarrow \pi^0 \ell^+ \ell^-$ modes complements the $K \rightarrow \pi \nu \bar{\nu}$ measurements in constraining physics beyond the SM [68].

E. Other long distance dominated modes:

The decays $K^+ \rightarrow \pi^+ \ell^+ \ell^-$ ($\ell = e$ or μ) have received considerable attention. The rate and spectrum have been measured for both the electron and muon modes [69,70]. Ref. 50 has proposed a parametrization inspired by chiral perturbation theory, which provides a successful description of data but indicates the presence of large corrections beyond leading order. More work is needed to fully understand the origin of these large corrections.

Much information has been recorded by KTeV and NA48 on the rates and spectrum for the Dalitz pair conversion modes $K_L \rightarrow \ell^+ \ell^- \gamma$ [71,72], and $K_L \rightarrow \ell^+ \ell^- \ell'^+ \ell'^-$ for $\ell, \ell' = e$ or μ [17,73–75]. All these results are used to test hadronic models and could further our understanding of the long distance component in $K_L \rightarrow \mu^+ \mu^-$.

References

1. D. Bryman, Int. J. Mod. Phys. **A4**, 79 (1989).
2. J. Hagelin and L. Littenberg, Prog. in Part. Nucl. Phys. **23**, 1 (1989).
3. I. Bigi and F. Gabbiani, Nucl. Phys. **B367**, 3 (1991).
4. R. Battiston *et al.*, Phys. Reports **214**, 293 (1992).
5. L. Littenberg and G. Valencia, Ann. Rev. Nucl. and Part. Sci. **43**, 729 (1993).
6. J. Ritchie and S. Wojcicki, Rev. Mod. Phys. **65**, 1149 (1993).
7. B. Winstein and L. Wolfenstein, Rev. Mod. Phys. **65**, 1113 (1993).
8. G. D'Ambrosio, G. Ecker, G. Isidori and H. Neufeld, *Radiative Non-Leptonic Kaon Decays*, in The DAΦNE Physics Handbook (second edition), eds. L. Maiani, G. Pancheri, and N. Paver (Frascati), Vol. I, 265 (1995).
9. A. Pich, Rept. on Prog. in Phys. **58**, 563 (1995).
10. G. Buchalla, A.J. Buras, and M.E. Lautenbacher, Rev. Mod. Phys. **68**, 1125 (1996).
11. G. D'Ambrosio and G. Isidori, Int. J. Mod. Phys. **A13**, 1 (1996).
12. P. Buchholz and B. Renk Prog. in Part. Nucl. Phys. **39**, 253 (1997).
13. A.J. Buras and R. Fleischer, TUM-HEP-275-97, hep-ph/9704376, *Heavy Flavours II*, World Scientific, eds. A.J. Buras and M. Lindner (1997), 65–238.
14. A.J. Buras, TUM-HEP-349-99, Lectures given at Lake Louise Winter Institute: Electroweak Physics, Lake Louise, Alberta, Canada, 14–20 Feb. 1999.
15. A.R. Barker and S.H. Kettell, Ann. Rev. Nucl. and Part. Sci. **50**, 249 (2000).
16. R. Appel *et al.*, Phys. Rev. Lett. **85**, 2877 (2000).
17. A. Alavi-Harati *et al.*, Phys. Rev. Lett. **90**, 141801 (2003).
18. A. Sher *et al.*, Phys. Rev. **D72**, 012005 (2005).
19. D. Ambrose *et al.*, Phys. Rev. Lett. **81**, 5734 (1998).
20. R. Tschirhart “Search for Lepton Flavor Violating Kaon Decays from the KTeV Experiment at Fermilab,” KAON 07, 21–25 May 07, INFN, Frascati, Italy.
21. S. Adler *et al.*, Phys. Rev. Lett. **88**, 041803 (2002).

See key on page 373

22. M. Lu and M.B. Wise, Phys. Lett. **B324**, 461 (1994); A.F. Falk, A. Lewandowski, and A.A. Petrov, Phys. Lett. **B505**, 107 (2001).
23. G. Isidori, F. Mescia, and C. Smith, Nucl. Phys. **B718**, 319 (2005).
24. F. Mescia and C. Smith, "Improved estimates of rare K decay matrix-elements from $K(13)$ decays," arXiv:0705.2025 [hep-ph].
25. CKMfitter Group (J. Charles *et al.*), Eur. Phys. J. **C41**, 1 (2005), [hep-ph/0406184], updated results and plots available at: <http://ckmfitter.in2p3.fr>.
26. M. Bona *et al.*, [UTfit Collaboration] "Model-independent constraints on Delta F=2 operators and the scale of New Physics," arXiv:0707.0636 [hep-ph].
27. S. Adler *et al.*, Phys. Rev. Lett. **84**, 3768 (2000).
28. V.V. Anisimovsky *et al.*, Phys. Rev. Lett. **93**, 031801 (2004).
29. G. Anelli *et al.*, CERN-SPSC-2005-013, 11 June 2005.
30. G. D'Ambrosio and G. Isidori, Phys. Lett. **B530**, 108 (2002).
31. W. Marciano and Z. Parsa, Phys. Rev. **D53**, 1 (1996).
32. T. Inami and C.S. Lim, Prog. Theor. Phys. **65**, 297 (1981); Erratum Prog. Theor. Phys. **65**, 172 (1981).
33. G. Buchalla and A.J. Buras, Nucl. Phys. **B548**, 309 (1999); M. Misiak and J. Urban, Phys. Lett. **B451**, 161 (1999).
34. A.J. Buras *et al.*, Phys. Rev. Lett. **95**, 261805 (2005).
35. D. Ambrose *et al.*, Phys. Rev. Lett. **84**, 1389 (2000).
36. G. Valencia, Nucl. Phys. **B517**, 339 (1998).
37. G. D'Ambrosio, G. Isidori, and J. Portoles, Phys. Lett. **B423**, 385 (1998).
38. G. Isidori and R. Unterdorfer, JHEP **0401**, 009 (2004).
39. D. Gomez-Dumm and A. Pich, Phys. Rev. Lett. **80**, 4633 (1998).
40. D. Ambrose *et al.*, Phys. Rev. Lett. **81**, 4309 (1998).
41. L. Littenberg, Phys. Rev. **D39**, 3322 (1989).
42. G. Buchalla and G. Isidori, Phys. Lett. **B440**, 170 (1998).
43. A.J. Buras, F. Schwab, and S. Uhlig, hep-ph/0405132.
44. Y. Grossman and Y. Nir, Phys. Lett. **B398**, 163 (1997).
45. J. K. Ahn *et al.*, Phys. Rev. **D74**, 051105 (2006), Erratum *ibid.*, 079901 (2006).
46. J. Comfort *et al.*, "Proposal for $K_L^0 \rightarrow \pi^0 \nu \bar{\nu}$ Experiment at J-Parc," J-PARC Proposal 14 (2006).
47. A.J. Buras *et al.*, Nucl. Phys. **B592**, 55 (2001).
48. A.J. Buras *et al.*, Nucl. Phys. **B566**, 3 (2000).
49. D. Bryman *et al.*, Int. J. Mod. Phys. **A21**, 487 (2006).
50. G. D'Ambrosio *et al.*, JHEP **9808**, 004 (1998); C.O. Dib, I. Duniety, and F.J. Gilman, Phys. Rev. **D39**, 2639 (1989).
51. J.R. Batley *et al.*, Phys. Lett. **B576**, 43 (2003).
52. G. Buchalla, G. D'Ambrosio, and G. Isidori, Nucl. Phys. **B672**, 387 (2003).
53. S. Friot, D. Greynat, and E. de Rafael, Phys. Lett. **B595**, 301 (2004).
54. J.R. Batley *et al.*, Phys. Lett. **B599**, 197 (2004).
55. G. Ecker, A. Pich, and E. de Rafael, Phys. Lett. **237B**, 481 (1990); L. Cappiello, G. D'Ambrosio, and M. Miragliuolo, Phys. Lett. **B298**, 423 (1993); A. Cohen, G. Ecker, and A. Pich, Phys. Lett. **B304**, 347 (1993).
56. F. Gabbiani and G. Valencia, Phys. Rev. **D64**, 094008 (2001); F. Gabbiani and G. Valencia, Phys. Rev. **D66**, 074006 (2002).
57. E. Cheu, "KTeV results on chiral perturbation theory," In the *Proceedings of International Conference on Heavy Quarks and Leptons* (HQL 06), Munich, Germany, 16-20 Oct 2006, pp 010 [hep-ex/0610078].
58. A. Lai *et al.*, Phys. Lett. **B536**, 229 (2002).
59. J. Donoghue and F. Gabbiani, Phys. Rev. **D56**, 1605 (1997).
60. E. Abouzaid *et al.*, Phys. Rev. **D76**, 052001 (2007).
61. W.M. Morse *et al.*, Phys. Rev. **D45**, 36 (1992).
62. A. Alavi-Harati *et al.*, Phys. Rev. **D64**, 012003 (2001).
63. H.B. Greenlee, Phys. Rev. **D42**, 3724 (1990).
64. A. Alavi-Harati *et al.*, Phys. Rev. Lett. **93**, 021805 (2004).
65. A. Alavi-Harati *et al.*, Phys. Rev. Lett. **84**, 5279 (2000).
66. G. Isidori, C. Smith, and R. Unterdorfer, Eur. Phys. J. **C36**, 57 (2004).
67. M.V. Diwan, H. Ma, and T.L. Trueman, Phys. Rev. **D65**, 054020 (2002).
68. F. Mescia, C. Smith, and S. Trine, JHEP **0608**, 088 (2006).
69. R. Appel *et al.*, Phys. Rev. Lett. **83**, 4482 (1999).
70. S.C. Adler *et al.*, Phys. Rev. Lett. **79**, 4756 (1997); R. Appel *et al.*, Phys. Rev. Lett. **84**, 2580 (2000); H.K. Park *et al.*, Phys. Rev. Lett. **88**, 111801 (2002).
71. A. Alavi-Harati *et al.*, Phys. Rev. Lett. **87**, 071801 (2001).
72. A. Abouzaid *et al.*, Phys. Rev. Lett. **99**, 051804 (2007).
73. J.R. LaDue "Understanding Dalitz Decays of the K_L in particular the decays of $K_L \rightarrow e^+ e^- \gamma$ and $K_L \rightarrow e^+ e^- e^+ e^-$ " University of Colorado Thesis, May 2003. The preliminary result for $K_L \rightarrow e^+ e^- \gamma$ in this thesis has been superseded by the final result in [72].
74. A. Alavi-Harati *et al.*, Phys. Rev. Lett. **86**, 5425 (2001).
75. V. Fanti *et al.*, Phys. Lett. **B458**, 458 (1999).

 K^+ DECAY MODES K^- modes are charge conjugates of the modes below.

Mode	Fraction (Γ_i/Γ)	Scale factor/ Confidence level
Leptonic and semileptonic modes		
Γ_1 $K^+ \rightarrow e^+ \nu_e$	$(1.55 \pm 0.07) \times 10^{-5}$	
Γ_2 $K^+ \rightarrow \mu^+ \nu_\mu$	$(63.54 \pm 0.14) \%$	S=1.3
Γ_3 $K^+ \rightarrow \pi^0 e^+ \nu_e$	$(5.08 \pm 0.05) \%$	S=2.1
Called K_{e3}^+ .		
Γ_4 $K^+ \rightarrow \pi^0 \mu^+ \nu_\mu$	$(3.35 \pm 0.04) \%$	S=1.9
Called $K_{\mu 3}^+$.		
Γ_5 $K^+ \rightarrow \pi^0 \pi^0 e^+ \nu_e$	$(2.2 \pm 0.4) \times 10^{-5}$	
Γ_6 $K^+ \rightarrow \pi^+ \pi^- e^+ \nu_e$	$(4.09 \pm 0.10) \times 10^{-5}$	
Γ_7 $K^+ \rightarrow \pi^+ \pi^- \mu^+ \nu_\mu$	$(1.4 \pm 0.9) \times 10^{-5}$	
Γ_8 $K^+ \rightarrow \pi^0 \pi^0 \pi^0 e^+ \nu_e$	$< 3.5 \times 10^{-6}$	CL=90%
Hadronic modes		
Γ_9 $K^+ \rightarrow \pi^+ \pi^0$	$(20.68 \pm 0.13) \%$	S=1.6
Γ_{10} $K^+ \rightarrow \pi^+ \pi^0 \pi^0$	$(1.761 \pm 0.022) \%$	S=1.1
Γ_{11} $K^+ \rightarrow \pi^+ \pi^+ \pi^-$	$(5.59 \pm 0.04) \%$	S=1.5

Meson Particle Listings

 K^\pm

Leptonic and semileptonic modes with photons

Γ_{12}	$K^+ \rightarrow \mu^+ \nu_\mu \gamma$	[a,b]	$(6.2 \pm 0.8) \times 10^{-3}$	
Γ_{13}	$K^+ \rightarrow \mu^+ \nu_\mu \gamma (SD^+)$	[c,d]	< 3.0	CL=90%
Γ_{14}	$K^+ \rightarrow \mu^+ \nu_\mu \gamma (SD^+ INT)$	[c,d]	< 2.7	CL=90%
Γ_{15}	$K^+ \rightarrow \mu^+ \nu_\mu \gamma (SD^- + SD^- INT)$	[c,d]	< 2.6	CL=90%
Γ_{16}	$K^+ \rightarrow e^+ \nu_e \gamma (SD^+)$	[c,d]	$(1.52 \pm 0.23) \times 10^{-5}$	
Γ_{17}	$K^+ \rightarrow e^+ \nu_e \gamma (SD^-)$	[c,d]	< 1.6	CL=90%
Γ_{18}	$K^+ \rightarrow \pi^0 e^+ \nu_e \gamma$	[a,b]	$(2.56 \pm 0.16) \times 10^{-4}$	
Γ_{19}	$K^+ \rightarrow \pi^0 e^+ \nu_e \gamma (SD)$	[c,d]	< 5.3	CL=90%
Γ_{20}	$K^+ \rightarrow \pi^0 \mu^+ \nu_\mu \gamma$	[a,b]	$(1.5 \pm 0.4) \times 10^{-5}$	
Γ_{21}	$K^+ \rightarrow \pi^0 \pi^0 e^+ \nu_e \gamma$		< 5	CL=90%

Hadronic modes with photons or $\ell\bar{\ell}$ pairs

Γ_{22}	$K^+ \rightarrow \pi^+ \pi^0 \gamma$	[a,b]	$(2.75 \pm 0.15) \times 10^{-4}$	
Γ_{23}	$K^+ \rightarrow \pi^+ \pi^0 \gamma (DE)$	[b,e]	$(4.3 \pm 0.7) \times 10^{-6}$	
Γ_{24}	$K^+ \rightarrow \pi^+ \pi^0 \pi^0 \gamma$	[a,b]	$(7.6 \pm 5.6 \pm 3.0) \times 10^{-6}$	
Γ_{25}	$K^+ \rightarrow \pi^+ \pi^+ \pi^- \gamma$	[a,b]	$(1.04 \pm 0.31) \times 10^{-4}$	
Γ_{26}	$K^+ \rightarrow \pi^+ \gamma \gamma$	[b]	$(1.10 \pm 0.32) \times 10^{-6}$	
Γ_{27}	$K^+ \rightarrow \pi^+ 3\gamma$	[b]	< 1.0	CL=90%
Γ_{28}	$K^\pm \rightarrow \pi^+ e^\pm e^- \gamma$		$(1.19 \pm 0.13) \times 10^{-8}$	

Leptonic modes with $\ell\bar{\ell}$ pairs

Γ_{29}	$K^+ \rightarrow e^+ \nu_e \nu \bar{\nu}$		< 6	$\times 10^{-5}$	CL=90%
Γ_{30}	$K^+ \rightarrow \mu^+ \nu_\mu \nu \bar{\nu}$		< 6.0	$\times 10^{-6}$	CL=90%
Γ_{31}	$K^+ \rightarrow e^+ \nu_e e^+ e^-$		$(2.48 \pm 0.20) \times 10^{-8}$		
Γ_{32}	$K^+ \rightarrow \mu^+ \nu_\mu e^+ e^-$		$(7.06 \pm 0.31) \times 10^{-8}$		
Γ_{33}	$K^+ \rightarrow e^+ \nu_e \mu^+ \mu^-$		$(1.7 \pm 0.5) \times 10^{-8}$		
Γ_{34}	$K^+ \rightarrow \mu^+ \nu_\mu \mu^+ \mu^-$		< 4.1	$\times 10^{-7}$	CL=90%

Lepton Family number (LF), Lepton number (L), $\Delta S = \Delta Q$ (SQ) violating modes, or $\Delta S = 1$ weak neutral current (S1) modes

Γ_{35}	$K^+ \rightarrow \pi^+ \pi^+ e^- \bar{\nu}_e$	SQ	< 1.2	$\times 10^{-8}$	CL=90%
Γ_{36}	$K^+ \rightarrow \pi^+ \pi^+ \mu^- \bar{\nu}_\mu$	SQ	< 3.0	$\times 10^{-6}$	CL=95%
Γ_{37}	$K^+ \rightarrow \pi^+ e^+ e^-$	S1	$(2.88 \pm 0.13) \times 10^{-7}$		
Γ_{38}	$K^+ \rightarrow \pi^+ \mu^+ \mu^-$	S1	$(8.1 \pm 1.4) \times 10^{-8}$		S=2.7
Γ_{39}	$K^+ \rightarrow \pi^+ \nu \bar{\nu}$	S1	$(1.5 \pm 1.3 \pm 0.9) \times 10^{-10}$		
Γ_{40}	$K^+ \rightarrow \pi^+ \pi^0 \nu \bar{\nu}$	S1	< 4.3	$\times 10^{-5}$	CL=90%
Γ_{41}	$K^+ \rightarrow \mu^- \nu e^+ e^+$	LF	< 2.0	$\times 10^{-8}$	CL=90%
Γ_{42}	$K^+ \rightarrow \mu^+ \nu e^-$	LF	[f] < 4	$\times 10^{-3}$	CL=90%
Γ_{43}	$K^+ \rightarrow \pi^+ \mu^+ e^-$	LF	< 1.3	$\times 10^{-11}$	CL=90%
Γ_{44}	$K^+ \rightarrow \pi^+ \mu^- e^+$	LF	< 5.2	$\times 10^{-10}$	CL=90%
Γ_{45}	$K^+ \rightarrow \pi^- \mu^+ e^+$	L	< 5.0	$\times 10^{-10}$	CL=90%
Γ_{46}	$K^+ \rightarrow \pi^- e^+ e^+$	L	< 6.4	$\times 10^{-10}$	CL=90%
Γ_{47}	$K^+ \rightarrow \pi^- \mu^+ \mu^+$	L	[f] < 3.0	$\times 10^{-9}$	CL=90%
Γ_{48}	$K^+ \rightarrow \mu^+ \bar{\nu}_e$	L	[f] < 3.3	$\times 10^{-3}$	CL=90%
Γ_{49}	$K^+ \rightarrow \pi^0 e^+ \bar{\nu}_e$	L	< 3	$\times 10^{-3}$	CL=90%
Γ_{50}	$K^+ \rightarrow \pi^+ \gamma$	[g]	< 2.3	$\times 10^{-9}$	CL=90%

[a] Most of this radiative mode, the low-momentum γ part, is also included in the parent mode listed without γ 's.

[b] See the Particle Listings below for the energy limits used in this measurement.

[c] See the "Note on $\pi^\pm \rightarrow \ell^\pm \nu \gamma$ and $K^\pm \rightarrow \ell^\pm \nu \gamma$ Form Factors" in the π^\pm Particle Listings for definitions and details.

[d] Structure-dependent part.

[e] Direct-emission branching fraction.

[f] Derived from an analysis of neutrino-oscillation experiments.

[g] Violates angular-momentum conservation.

CONSTRAINED FIT INFORMATION

An overall fit to the mean life, a decay rate, and 13 branching ratios uses 31 measurements and one constraint to determine 8 parameters. The overall fit has a $\chi^2 = 51.7$ for 24 degrees of freedom.

The following *off-diagonal* array elements are the correlation coefficients $\langle \delta p_i \delta p_j \rangle / (\delta p_i \delta p_j)$, in percent, from the fit to parameters p_i , including the branching fractions, $x_i \equiv \Gamma_i / \Gamma_{\text{total}}$. The fit constrains the x_i whose labels appear in this array to sum to one.

x_3	-42							
x_4	-40	91						
x_5	-2	4	4					
x_9	-77	-13	-15	-1				
x_{10}	-4	-5	-5	0	-11			
x_{11}	-8	-10	-10	0	-21	5		
Γ	2	2	2	0	4	-1	-20	
		x_2	x_3	x_4	x_5	x_9	x_{10}	x_{11}

Mode	Rate (10^8 s^{-1})	Scale factor
Γ_2 $K^+ \rightarrow \mu^+ \nu_\mu$	0.5132 ± 0.0014	1.4
Γ_3 $K^+ \rightarrow \pi^0 e^+ \nu_e$	0.0410 ± 0.0004	2.1
Called K_{e3}^+ .		
Γ_4 $K^+ \rightarrow \pi^0 \mu^+ \nu_\mu$	0.02709 ± 0.00030	1.9
Called $K_{\mu 3}^+$.		
Γ_5 $K^+ \rightarrow \pi^0 \pi^0 e^+ \nu_e$	$(1.77 \pm 0.35 \pm 0.30) \times 10^{-5}$	
Γ_9 $K^+ \rightarrow \pi^+ \pi^0$	0.1670 ± 0.0011	1.6
Γ_{10} $K^+ \rightarrow \pi^+ \pi^0 \pi^0$	0.01423 ± 0.00018	1.1
Γ_{11} $K^+ \rightarrow \pi^+ \pi^+ \pi^-$	0.04518 ± 0.00035	1.5

 K^\pm DECAY RATES $\Gamma(\mu^+ \nu_\mu)$

VALUE (10^6 s^{-1}) DOCUMENT ID TECN CHG
51.32 ± 0.14 OUR FIT Error includes scale factor of 1.4.

• • • We do not use the following data for averages, fits, limits, etc. • • •

51.2 ± 0.8 FORD 67 CNTR ±

 $\Gamma(\pi^+ \pi^+ \pi^-)$

VALUE (10^6 s^{-1}) EVTS DOCUMENT ID TECN CHG
4.518 ± 0.035 OUR FIT Error includes scale factor of 1.5.

4.511 ± 0.024 ⁷FORD 70 ASPK

• • • We do not use the following data for averages, fits, limits, etc. • • •

4.529 ± 0.032 3.2M ⁷FORD 70 ASPK

4.496 ± 0.030 ⁷FORD 67 CNTR ±

⁷First FORD 70 value is second FORD 70 combined with FORD 67.

 $(\Gamma(K^+) - \Gamma(K^-)) / \Gamma(K)$ $K^\pm \rightarrow \mu^\pm \nu_\mu$ RATE DIFFERENCE/AVERAGE

Test of *CPT* conservation.

VALUE (%) DOCUMENT ID TECN
-0.54 ± 0.41 FORD 67 CNTR

 $K^\pm \rightarrow \pi^\pm \pi^+ \pi^-$ RATE DIFFERENCE/AVERAGE

Test of *CP* conservation.

VALUE (%) EVTS DOCUMENT ID TECN CHG
0.08 ± 0.12 ⁸FORD 70 ASPK

• • • We do not use the following data for averages, fits, limits, etc. • • •

-0.02 ± 0.16 ⁹SMITH 73 ASPK ±

0.10 ± 0.14 3.2M ⁸FORD 70 ASPK

-0.50 ± 0.90 FLETCHER 67 OSPK

-0.04 ± 0.21 ⁸FORD 67 CNTR

⁸First FORD 70 value is second FORD 70 combined with FORD 67.

⁹SMITH 73 value of $K^\pm \rightarrow \pi^\pm \pi^+ \pi^-$ rate difference is derived from SMITH 73 value of $K^\pm \rightarrow \pi^\pm 2\pi^0$ rate difference.

 $K^\pm \rightarrow \pi^\pm \pi^0 \pi^0$ RATE DIFFERENCE/AVERAGE

Test of *CP* conservation.

VALUE (%) EVTS DOCUMENT ID TECN CHG
0.0 ± 0.6 OUR AVERAGE

0.08 ± 0.58 SMITH 73 ASPK ±

-1.1 ± 1.8 1802 HERZO 69 OSPK

 $K^\pm \rightarrow \pi^\pm \pi^0$ RATE DIFFERENCE/AVERAGE

Test of *CPT* conservation.

VALUE (%) DOCUMENT ID TECN
0.8 ± 1.2 HERZO 69 OSPK

$K^\pm \rightarrow \pi^\pm \pi^0 \gamma$ RATE DIFFERENCE/AVERAGE

Test of CP conservation.					
VALUE (%)	EVTS	DOCUMENT ID	TECN	CHG	COMMENT
0.9 ± 3.3 OUR AVERAGE					
0.8 ± 5.8	2461	SMITH	76	WIRE	$\pm E_\pi$ 55–90 MeV
1.0 ± 4.0	4000	ABRAMS	73B	ASPK	$\pm E_\pi$ 51–100 MeV

K⁺ BRANCHING RATIOS

Leptonic and semileptonic modes

 $\Gamma(e^+ \nu_e)/\Gamma(\mu^+ \nu_\mu)$ Γ_1/Γ_2 See the note on “Decay Constants of Charged Pseudoscalar Mesons” in the D_S^\pm Listings.

VALUE (units 10^{-5})	EVTS	DOCUMENT ID	TECN	CHG	COMMENT
2.45 ± 0.11 OUR AVERAGE					
2.51 ± 0.15	404	HEINTZE	76	SPEC	+
2.37 ± 0.17	534	HEARD	75B	SPEC	+
2.42 ± 0.42	112	CLARK	72	OSPK	+

 $\Gamma(\mu^+ \nu_\mu)/\Gamma_{\text{total}}$ Γ_2/Γ See the note on “Decay Constants of Charged Pseudoscalar Mesons” in the D_S^\pm Listings.

VALUE (units 10^{-2})	EVTS	DOCUMENT ID	TECN	CHG	COMMENT
63.54 ± 0.14 OUR FIT					Error includes scale factor of 1.3.
63.60 ± 0.16 OUR AVERAGE					
63.66 ± 0.09 ± 0.15	865k	¹⁰ AMBROSINO	06A	KLOE	+
63.24 ± 0.44	62k	CHIANG	72	OSPK	+ 1.84 GeV/c K^+

¹⁰ Fully inclusive. Used tagged kaons from ϕ decays. $\Gamma(\pi^0 e^+ \nu_e)/\Gamma_{\text{total}}$ Γ_3/Γ

VALUE (units 10^{-2})	EVTS	DOCUMENT ID	TECN	CHG	COMMENT
5.08 ± 0.05 OUR FIT					Error includes scale factor of 2.1.
4.94 ± 0.05 OUR AVERAGE					
4.965 ± 0.037 ± 0.037		¹¹ AMBROSINO	08A	KLOE	\pm
4.86 ± 0.10	3516	CHIANG	72	OSPK	+ 1.84 GeV/c K^+

• • • We do not use the following data for averages, fits, limits, etc. • • •

4.7 ± 0.3	429	SHAKLEE	64	HLBC	+
5.0 ± 0.5		ROE	61	HLBC	+

¹¹ Depends on K^+ lifetime τ . AMBROSINO 08A uses PDG 06 value of $\tau = (1.2385 \pm 0.0024) \times 10^{-8}$ sec. The correlation between K_{e3}^+ and $K_{\mu 3}^+$ branching fraction measurements is 62.7%. $\Gamma(\pi^0 e^+ \nu_e)/\Gamma(\mu^+ \nu_\mu)$ Γ_3/Γ_2

VALUE	EVTS	DOCUMENT ID	TECN	CHG	COMMENT
0.0799 ± 0.0008 OUR FIT					Error includes scale factor of 1.8.
0.069 ± 0.006	350	ZELLER	69	ASPK	+
0.0775 ± 0.0033	960	BOTTERILL	68c	ASPK	+
0.069 ± 0.006	561	GARLAND	68	OSPK	+
0.0791 ± 0.0054	295	¹² AUERBACH	67	OSPK	+

¹² AUERBACH 67 changed from 0.0797 ± 0.0054. See comment with ratio $\Gamma(\pi^0 \mu^+ \nu_\mu)/\Gamma(\mu^+ \nu_\mu)$. The value 0.0785 ± 0.0025 given in AUERBACH 67 is an average of AUERBACH 67 $\Gamma(\pi^0 e^+ \nu_e)/\Gamma(\mu^+ \nu_\mu)$ and CESTER 66 $\Gamma(\pi^0 e^+ \nu_e)/[\Gamma(\mu^+ \nu_\mu) + \Gamma(\pi^+ \pi^0)]$. $\Gamma(\pi^0 e^+ \nu_e)/[\Gamma(\mu^+ \nu_\mu) + \Gamma(\pi^+ \pi^0)]$ $\Gamma_3/(\Gamma_2 + \Gamma_9)$

VALUE (units 10^{-2})	EVTS	DOCUMENT ID	TECN	CHG	COMMENT
6.03 ± 0.06 OUR FIT					Error includes scale factor of 2.1.
6.02 ± 0.15 OUR AVERAGE					
6.16 ± 0.22	5110	ESCHSTRUTH	68	OSPK	+
5.89 ± 0.21	1679	CESTER	66	OSPK	+

• • • We do not use the following data for averages, fits, limits, etc. • • •

¹³ Value calculated from WEISSENBERG 76 ($\pi^0 e \nu$), ($\mu \nu$), and ($\pi \pi^0$) values to eliminate dependence on our 1974 ($\pi 2\pi^0$) and ($\pi \pi^+ \pi^-$) fractions. $\Gamma(\pi^0 e^+ \nu_e)/[\Gamma(\pi^0 \mu^+ \nu_\mu) + \Gamma(\pi^+ \pi^0) + \Gamma(\pi^+ \pi^0 \pi^0)]$ $\Gamma_3/(\Gamma_4 + \Gamma_9 + \Gamma_{10})$

VALUE	EVTS	DOCUMENT ID	TECN	CHG	COMMENT
0.1968 ± 0.0020 OUR FIT					Error includes scale factor of 3.0.
0.1962 ± 0.0008 ± 0.0035					
	71k	SHER	03	B865	+

 $\Gamma(\pi^0 e^+ \nu_e)/\Gamma(\pi^+ \pi^0)$ Γ_3/Γ_9

VALUE	EVTS	DOCUMENT ID	TECN	CHG	COMMENT
0.2455 ± 0.0029 OUR FIT					Error includes scale factor of 3.2.
0.2470 ± 0.0009 ± 0.0004					
	87k	BATLEY	07A	NA48	\pm

• • • We do not use the following data for averages, fits, limits, etc. • • •

¹⁴ LUCAS 73B gives $N(K_{e3}) = 786 \pm 3.1\%$, $N(2\pi) = 3564 \pm 3.1\%$. We use these values to obtain quoted result. $\Gamma(\pi^0 e^+ \nu_e)/\Gamma(\pi^+ \pi^+ \pi^-)$ Γ_3/Γ_{11}

VALUE	EVTS	DOCUMENT ID	TECN	CHG	COMMENT
0.907 ± 0.012 OUR FIT					Error includes scale factor of 1.8.
0.867 ± 0.027	2768	BARMIN	87	XEBC	+
0.856 ± 0.040	2827	BRAUN	75	HLBC	+
0.850 ± 0.019	4385	¹⁵ HAIDT	71	HLBC	+
0.846 ± 0.021	4385	¹⁵ EICHTEN	68	HLBC	+
0.94 ± 0.09	854	BELLOTTI	67B	HLBC	+
0.90 ± 0.06	230	BORREANI	64	HBC	+

¹⁵ HAIDT 71 is a reanalysis of EICHTEN 68. Not included in average because of large discrepancy in $\Gamma(\pi^0 \mu^+ \nu)/\Gamma(\pi^0 e^+ \nu)$ with more precise results. $\Gamma(\pi^0 \mu^+ \nu_\mu)/\Gamma_{\text{total}}$ Γ_4/Γ

VALUE (units 10^{-2})	EVTS	DOCUMENT ID	TECN	CHG	COMMENT
3.35 ± 0.04 OUR FIT					Error includes scale factor of 1.9.
3.24 ± 0.04 OUR AVERAGE					
3.233 ± 0.029 ± 0.026		¹⁶ AMBROSINO	08A	KLOE	\pm
3.33 ± 0.16	2345	CHIANG	72	OSPK	+ 1.84 GeV/c K^+

• • • We do not use the following data for averages, fits, limits, etc. • • •

¹⁶ Depends on K^+ lifetime τ . AMBROSINO 08A uses PDG 06 value of $\tau = (1.2385 \pm 0.0024) \times 10^{-8}$ sec. The correlation between K_{e3}^+ and $K_{\mu 3}^+$ branching fraction measurements is 62.7%.¹⁷ Earlier experiments not averaged. $\Gamma(\pi^0 \mu^+ \nu_\mu)/\Gamma(\mu^+ \nu_\mu)$ Γ_4/Γ_2

VALUE	EVTS	DOCUMENT ID	TECN	CHG	COMMENT
0.0528 ± 0.0006 OUR FIT					Error includes scale factor of 1.7.
0.054 ± 0.009	240	ZELLER	69	ASPK	+
0.0480 ± 0.0037	424	¹⁸ GARLAND	68	OSPK	+
0.0486 ± 0.0040	307	¹⁹ AUERBACH	67	OSPK	+

• • • We do not use the following data for averages, fits, limits, etc. • • •

¹⁸ GARLAND 68 changed from 0.055 ± 0.004 in agreement with μ -spectrum calculation of GAILLARD 70 appendix B. L.G.Pondrom, (private communication 73).¹⁹ AUERBACH 67 changed from 0.0602 ± 0.0046 by erratum which brings the μ -spectrum calculation into agreement with GAILLARD 70 appendix B. $\Gamma(\pi^0 \mu^+ \nu_\mu)/\Gamma(\pi^0 e^+ \nu_e)$ Γ_4/Γ_3

VALUE	EVTS	DOCUMENT ID	TECN	CHG	COMMENT
0.6608 ± 0.0030 OUR FIT					Error includes scale factor of 1.1.
0.6618 ± 0.0027 OUR AVERAGE					
0.6511 ± 0.0064		²⁰ AMBROSINO	08A	KLOE	\pm
0.663 ± 0.003 ± 0.001	77k	BATLEY	07A	NA48	\pm
0.671 ± 0.007 ± 0.008	24k	HORIE	01	SPEC	
0.670 ± 0.014		²¹ HEINTZE	77	SPEC	+
0.667 ± 0.017	5601	BOTTERILL	68B	ASPK	+

• • • We do not use the following data for averages, fits, limits, etc. • • •

0.608 ± 0.014	1585	²² BRAUN	75	HLBC	+
0.705 ± 0.063	554	²³ LUCAS	73B	HBC	– Dalitz pairs only
0.698 ± 0.025	3480	²⁴ CHIANG	72	OSPK	+ 1.84 GeV/c K^+
0.596 ± 0.025		²⁵ HAIDT	71	HLBC	+
0.604 ± 0.022	1398	²⁵ EICHTEN	68	HLBC	+
0.703 ± 0.056	1509	CALLAHAN	66B	HLBC	

²⁰ Not used in the fit. This result enters the fit via correlation of K_{e3}^+ and $K_{\mu 3}^+$ branching fraction measurements of AMBROSINO 08A.²¹ HEINTZE 77 value from fit to λ_0 . Assumes μ -e universality.²² BRAUN 75 value is from form factor fit. Assumes μ -e universality.²³ LUCAS 73B gives $N(K_{\mu 3}) = 554 \pm 7.6\%$, $N(K_{e3}) = 786 \pm 3.1\%$. We divide.²⁴ CHIANG 72 $\Gamma(\pi^0 \mu^+ \nu_\mu)/\Gamma(\pi^0 e^+ \nu_e)$ is statistically independent of CHIANG 72 $\Gamma(\pi^0 \mu^+ \nu_\mu)/\Gamma_{\text{total}}$ and $\Gamma(\pi^0 e^+ \nu_e)/\Gamma_{\text{total}}$.²⁵ HAIDT 71 is a reanalysis of EICHTEN 68. Not included in average because of large discrepancy with more precise results. $[\Gamma(\pi^0 \mu^+ \nu_\mu) + \Gamma(\pi^+ \pi^0 \pi^0)]/\Gamma_{\text{total}}$ $(\Gamma_4 + \Gamma_9)/\Gamma$

We combine these two modes for experiments measuring them in xenon bubble chamber because of difficulties of separating them there.

VALUE (units 10^{-2})	EVTS	DOCUMENT ID	TECN	CHG	COMMENT
24.03 ± 0.13 OUR FIT					Error includes scale factor of 1.4.
25.4 ± 0.9	886	SHAKLEE	64	HLBC	+
23.4 ± 1.1		ROE	61	HLBC	+

 $\Gamma(\pi^0 \mu^+ \nu_\mu)/\Gamma(\pi^+ \pi^0)$ Γ_4/Γ_9

VALUE	EVTS	DOCUMENT ID	TECN	CHG	COMMENT
0.1637 ± 0.0006 ± 0.0003					
	77k	BATLEY	07A	NA48	\pm

 $\Gamma(\pi^0 \mu^+ \nu_\mu)/\Gamma(\pi^+ \pi^+ \pi^-)$ Γ_4/Γ_{11}

VALUE	EVTS	DOCUMENT ID	TECN	CHG	COMMENT
0.600 ± 0.008 OUR FIT					Error includes scale factor of 1.7.
0.503 ± 0.019	1505	²⁶ HAIDT	71	HLBC	+
0.510 ± 0.017	1505	²⁶ EICHTEN	68	HLBC	+
0.63 ± 0.07	2845	²⁷ BISI	65B	BC	+ HBC+HLBC

• • • We do not use the following data for averages, fits, limits, etc. • • •

²⁶ HAIDT 71 is a reanalysis of EICHTEN 68. Not included in average because of large discrepancy in $\Gamma(\pi^0 \mu^+ \nu)/\Gamma(\pi^0 e^+ \nu)$ with more precise results.²⁷ Error enlarged for background problems. See GAILLARD 70.

Meson Particle Listings

 K^\pm

$\Gamma(\pi^0 \pi^0 e^+ \nu_e)/\Gamma_{\text{total}}$		Γ_5/Γ		
VALUE (units 10^{-5})	EVTS	DOCUMENT ID	TECN	CHG
2.2 ± 0.4 OUR FIT				
2.54 ± 0.89	10	BARMIN	88B	HLBC +

$\Gamma(\pi^0 \pi^0 e^+ \nu_e)/\Gamma(\pi^0 e^+ \nu_e)$		Γ_5/Γ_3		
VALUE (units 10^{-4})	EVTS	DOCUMENT ID	TECN	CHG
4.3 ± 0.9 OUR FIT				
4.1 ± 1.0 OUR AVERAGE				
4.2 ± 1.0	25	BOLOTOV	86B	CALO -
3.8 ± 1.2	2	LJUNG	73	HLBC +

$\Gamma(\pi^+ \pi^- e^+ \nu_e)/\Gamma(\pi^+ \pi^+ \pi^-)$		Γ_6/Γ_{11}		
VALUE (units 10^{-4})	EVTS	DOCUMENT ID	TECN	CHG
7.31 ± 0.16 OUR AVERAGE				
7.35 ± 0.01 ± 0.19	388k	²⁸ PISLAK	01	B865
7.21 ± 0.32	30k	ROSSELET	77	SPEC +
7.36 ± 0.68	500	BOURQUIN	71	ASPK
7.0 ± 0.9	106	SCHWEINB...	71	HLBC +
5.83 ± 0.63	269	ELY	69	HLBC +

²⁸PISLAK 01 reports $\Gamma(\pi^+ \pi^- e^+ \nu_e)/\Gamma_{\text{total}} = (4.109 \pm 0.008 \pm 0.110) \times 10^{-5}$ using the PDG 00 value $\Gamma(\pi^+ \pi^+ \pi^-)/\Gamma_{\text{total}} = (5.59 \pm 0.05) \times 10^{-2}$. We divide by the PDG value and unfold its error from the systematic error. PISLAK 03 gives additional details on the branching ratio measurement and gives improved errors on the S-wave $\pi\pi$ scattering length: $a_0^0 = 0.216 \pm 0.013(\text{stat.}) \pm 0.002(\text{syst.}) \pm 0.002(\text{theor.})$.

$\Gamma(\pi^+ \pi^- \mu^+ \nu_\mu)/\Gamma_{\text{total}}$		Γ_7/Γ		
VALUE (units 10^{-5})	EVTS	DOCUMENT ID	TECN	CHG
0.77 ± 0.54 OUR FIT				
0.77 ± 0.54	1	CLINE	65	FBC +

$\Gamma(\pi^+ \pi^- \mu^+ \nu_\mu)/\Gamma(\pi^+ \pi^+ \pi^-)$		Γ_7/Γ_{11}		
VALUE (units 10^{-4})	EVTS	DOCUMENT ID	TECN	CHG
2.57 ± 1.55	7	BISI	67	DBC +
~ 2.5	1	GREINER	64	EMUL +

$\Gamma(\pi^0 \pi^0 e^+ \nu_e)/\Gamma_{\text{total}}$		Γ_8/Γ			
VALUE (units 10^{-6})	CL%	EVTS	DOCUMENT ID	TECN	CHG
< 3.5	90	0	BOLOTOV	88	SPEC -
< 9	90	0	BARMIN	92	XEBC +

Hadronic modes

$\Gamma(\pi^+ \pi^0)/\Gamma_{\text{total}}$		Γ_9/Γ			
VALUE (units 10^{-2})	EVTS	DOCUMENT ID	TECN	CHG	COMMENT
20.68 ± 0.13 OUR FIT					Error includes scale factor of 1.6.
21.18 ± 0.28	16k	CHIANG	72	OSPK +	1.84 GeV/c K^+
21.0 ± 0.6		CALLAHAN	65	HLBC	See $\Gamma(\pi^+ \pi^0)/\Gamma(\pi^+ \pi^+ \pi^-)$

$\Gamma(\pi^+ \pi^0)/\Gamma(\pi^+ \pi^+ \pi^-)$		Γ_9/Γ_{11}		
VALUE	EVTS	DOCUMENT ID	TECN	CHG
3.70 ± 0.04 OUR FIT				
3.96 ± 0.15	1045	CALLAHAN	66	FBC +

$\Gamma(\pi^+ \pi^0)/\Gamma(\mu^+ \nu_\mu)$		Γ_9/Γ_2			
VALUE	EVTS	DOCUMENT ID	TECN	CHG	COMMENT
0.3254 ± 0.0026 OUR FIT					Error includes scale factor of 1.4.
0.3325 ± 0.0032 OUR AVERAGE					
0.3329 ± 0.0047 ± 0.0010	45k	USHER	92	SPEC +	$p\bar{p}$ at rest
0.3355 ± 0.0057		²⁹ WEISSENBERG...	76	SPEC +	
0.3277 ± 0.0065	4517	³⁰ AUERBACH	67	OSPK +	
0.328 ± 0.005	25k	²⁹ WEISSENBERG...	74	STRC +	
0.305 ± 0.018	1600	ZELLER	69	ASPK +	

²⁹WEISSENBERG 76 revises WEISSENBERG 74.
³⁰AUERBACH 67 changed from 0.3253 ± 0.0065. See comment with ratio $\Gamma(\pi^0 \mu^+ \nu_\mu)/\Gamma(\mu^+ \nu_\mu)$.

$\Gamma(\pi^+ \pi^0 \pi^0)/\Gamma_{\text{total}}$		Γ_{10}/Γ			
VALUE (units 10^{-2})	EVTS	DOCUMENT ID	TECN	CHG	COMMENT
1.761 ± 0.022 OUR FIT					Error includes scale factor of 1.1.
1.775 ± 0.028 OUR AVERAGE					Error includes scale factor of 1.2.
1.763 ± 0.013 ± 0.022		ALOISIO	04A	KLOE ±	
1.84 ± 0.06	1307	CHIANG	72	OSPK +	1.84 GeV/c K^+
1.53 ± 0.11	198	³¹ PANDOULAS	70	EMUL +	
1.8 ± 0.2	108	SHAKLEE	64	HLBC +	
1.7 ± 0.2		ROE	61	HLBC +	
1.5 ± 0.2		³² TAYLOR	59	EMUL +	

$\Gamma(\pi^+ \pi^0 \pi^0)/\Gamma(\pi^+ \pi^0)$		Γ_{10}/Γ_9			
VALUE	EVTS	DOCUMENT ID	TECN	CHG	COMMENT
0.0852 ± 0.0013 OUR FIT					Error includes scale factor of 1.1.
0.081 ± 0.005	574	³³ LUCAS	73B	HBC -	Dalitz pairs only
0.393 ± 0.099	17	YOUNG	65	EMUL +	

$\Gamma(\pi^+ \pi^0 \pi^0)/\Gamma(\pi^+ \pi^+ \pi^-)$		Γ_{10}/Γ_{11}			
VALUE	EVTS	DOCUMENT ID	TECN	CHG	COMMENT
0.315 ± 0.005 OUR FIT					Error includes scale factor of 1.1.
0.303 ± 0.009	2027	BISI	65	BC +	HBC+HLBC
0.393 ± 0.099	17	YOUNG	65	EMUL +	

$\Gamma(\pi^+ \pi^+ \pi^-)/\Gamma_{\text{total}}$		Γ_{11}/Γ			
VALUE (units 10^{-2})	EVTS	DOCUMENT ID	TECN	CHG	COMMENT
5.59 ± 0.04 OUR FIT					Error includes scale factor of 1.5.
5.56 ± 0.20	2330	³⁴ CHIANG	72	OSPK +	1.84 GeV/c K^+
5.34 ± 0.21	693	³⁵ PANDOULAS	70	EMUL +	
5.71 ± 0.15		DEMARCO	65	HBC	
6.0 ± 0.4	44	YOUNG	65	EMUL +	
5.54 ± 0.12	2332	CALLAHAN	64	HLBC +	
5.1 ± 0.2	540	SHAKLEE	64	HLBC +	
5.7 ± 0.3		ROE	61	HLBC +	

³⁴Value is not independent of CHIANG 72 $\Gamma(\mu^+ \nu_\mu)/\Gamma_{\text{total}}$, $\Gamma(\pi^+ \pi^0)/\Gamma_{\text{total}}$, $\Gamma(\pi^+ \pi^0 \pi^0)/\Gamma_{\text{total}}$, $\Gamma(\pi^0 \mu^+ \nu_\mu)/\Gamma_{\text{total}}$, and $\Gamma(\pi^0 e^+ \nu_e)/\Gamma_{\text{total}}$.
³⁵Includes events of TAYLOR 59.

Leptonic and semileptonic modes with photons

$\Gamma(\mu^+ \nu_\mu \gamma)/\Gamma_{\text{total}}$		Γ_{12}/Γ			
VALUE (units 10^{-3})	EVTS	DOCUMENT ID	TECN	CHG	COMMENT
6.2 ± 0.8 OUR AVERAGE					
6.6 ± 1.5	36,37	DEMIDOV	90	XEBC	$P(\mu) < 231.5$ MeV/c
6.0 ± 0.9		BARMIN	88	HLBC +	$P(\mu) < 231.5$ MeV/c
3.5 ± 0.8	37,38	DEMIDOV	90	XEBC	$E(\gamma) > 20$ MeV
3.2 ± 0.5	57	³⁹ BARMIN	88	HLBC +	$E(\gamma) > 20$ MeV
5.4 ± 0.3	40	AKIBA	85	SPEC	$P(\mu) < 231.5$ MeV/c

³⁶ $P(\mu)$ cut given in DEMIDOV 90 paper, 235.1 MeV/c, is a misprint according to authors (private communication).
³⁷DEMIDOV 90 quotes only inner bremsstrahlung (IB) part.
³⁸Not independent of above DEMIDOV 90 value. Cuts differ.
³⁹Not independent of above BARMIN 88 value. Cuts differ.
⁴⁰Assumes μ -e universality and uses constraints from $K \rightarrow e\nu\gamma$.

$\Gamma(\mu^+ \nu_\mu \gamma(\text{SD}^+))/\Gamma_{\text{total}}$		Γ_{13}/Γ		
VALUE (units 10^{-5})	CL%	DOCUMENT ID	TECN	CHG
< 3.0	90	AKIBA	85	SPEC

$\Gamma(\mu^+ \nu_\mu \gamma(\text{SD}^+ \text{INT}))/\Gamma_{\text{total}}$		Γ_{14}/Γ		
VALUE (units 10^{-5})	CL%	DOCUMENT ID	TECN	CHG
< 2.7	90	AKIBA	85	SPEC

$\Gamma(\mu^+ \nu_\mu \gamma(\text{SD}^- + \text{SD}^- \text{INT}))/\Gamma_{\text{total}}$		Γ_{15}/Γ		
VALUE (units 10^{-4})	CL%	DOCUMENT ID	TECN	CHG
< 2.6	90	⁴¹ AKIBA	85	SPEC

⁴¹Assumes μ -e universality and uses constraints from $K \rightarrow e\nu\gamma$.

$\Gamma(e^+ \nu_e \gamma(SD^+))/\Gamma_{total}$ Γ_{16}/Γ

Structure-dependent part with $+\gamma$ helicity (SD^+ term). See the "Note on $\pi^\pm \rightarrow \ell^\pm \nu_\ell \gamma$ and $K^\pm \rightarrow \ell^\pm \nu_\ell \gamma$ Form Factors" in the π^\pm section of the Particle Data Listings above.

VALUE (units 10^{-5})	CL%	DOCUMENT ID	TECN	CHG	COMMENT
--------------------------	-----	-------------	------	-----	---------

• • • We do not use the following data for averages, fits, limits, etc. • • •

<7.1 90 MACEK 70 OSPK + P(e) 234-247

 $\Gamma(e^+ \nu_e \gamma(SD^+))/\Gamma(e^+ \nu_e)$ Γ_{16}/Γ_1

Structure-dependent part with $+\gamma$ helicity (SD^+ term). See the "Note on $\pi^\pm \rightarrow \ell^\pm \nu_\ell \gamma$ and $K^\pm \rightarrow \ell^\pm \nu_\ell \gamma$ Form Factors" in the π^\pm section of the Particle Data Listings above.

VALUE	EVTS	DOCUMENT ID	TECN	CHG	COMMENT
-------	------	-------------	------	-----	---------

• • • We do not use the following data for averages, fits, limits, etc. • • •

$1.05^{+0.25}_{-0.30}$ 56 42 HEARD 75 SPEC + P(e) 236-247

⁴² This value is included in the first HEINTZE 79 value in the section on $\Gamma(e^+ \nu_e \gamma(SD^+))/\Gamma(\mu^+ \nu_\mu)$ above.

 $\Gamma(e^+ \nu_e \gamma(SD^+))/\Gamma(\mu^+ \nu_\mu)$ Γ_{16}/Γ_2

Structure-dependent part with $+\gamma$ helicity (SD^+ term). See the "Note on $\pi^\pm \rightarrow \ell^\pm \nu_\ell \gamma$ and $K^\pm \rightarrow \ell^\pm \nu_\ell \gamma$ Form Factors" in the π^\pm section of the Particle Data Listings above.

VALUE (units 10^{-5})	EVTS	DOCUMENT ID	TECN	CHG	COMMENT
--------------------------	------	-------------	------	-----	---------

• • • We do not use the following data for averages, fits, limits, etc. • • •

2.40 ± 0.36 107 43 HEINTZE 79 SPEC +

2.33 ± 0.42 51 43 HEINTZE 79 SPEC +

⁴³ First HEINTZE 79 result is second combined with HEARD 75 result from section $\Gamma(e^+ \nu_e \gamma(SD^+))/\Gamma(e^+ \nu_e)$ below.

 $\Gamma(e^+ \nu_e \gamma(SD^-))/\Gamma_{total}$ Γ_{17}/Γ

Structure-dependent part with $-\gamma$ helicity (SD^- term). See the "Note on $\pi^\pm \rightarrow \ell^\pm \nu_\ell \gamma$ and $K^\pm \rightarrow \ell^\pm \nu_\ell \gamma$ Form Factors" in the π^\pm section of the Particle Data Listings above.

VALUE (units 10^{-4})	CL%	DOCUMENT ID	TECN	CHG	COMMENT
--------------------------	-----	-------------	------	-----	---------

<1.6 90 44 HEINTZE 79 SPEC +

⁴⁴ Implies (axial vector/vector) amplitude ratio outside range from -1.8 to -0.54 .

 $\Gamma(\pi^0 e^+ \nu_e \gamma)/\Gamma(\pi^0 e^+ \nu_e)$ Γ_{18}/Γ_3

VALUE (units 10^{-2})	EVTS	DOCUMENT ID	TECN	CHG	COMMENT
--------------------------	------	-------------	------	-----	---------

0.505 ± 0.032 OUR AVERAGE Error includes scale factor of 1.3. See the ideogram below.

$0.47 \pm 0.02 \pm 0.03$ 4476 45 AKIMENKO 07 ISTR - $E_\gamma > 10$ MeV, $0.6 < \cos(\theta_{e\gamma}) < 0.9$

0.46 ± 0.08 82 46 BARMIN 91 XEBC $E_\gamma > 10$ MeV, $0.6 < \cos(\theta_{e\gamma}) < 0.9$

0.56 ± 0.04 192 47 BOLOTOV 86B CALO - $E_\gamma > 10$ MeV

• • • We do not use the following data for averages, fits, limits, etc. • • •

$1.81 \pm 0.03 \pm 0.07$ 4476 45 AKIMENKO 07 ISTR - $E_\gamma > 10$ MeV, $\theta_{e\gamma} > 10^\circ$

$0.63 \pm 0.02 \pm 0.03$ 4476 45 AKIMENKO 07 ISTR - $E_\gamma > 30$ MeV, $\theta_{e\gamma} > 20^\circ$

1.51 ± 0.25 82 46 BARMIN 91 XEBC $E_\gamma > 10$ MeV, $\cos(\theta_{e\gamma}) < 0.98$

0.48 ± 0.20 16 48 LJUNG 73 HLBC + $E_\gamma > 30$ MeV

$0.22^{+0.15}_{-0.10}$ 48 LJUNG 73 HLBC + $E_\gamma > 30$ MeV

0.76 ± 0.28 13 49 ROMANO 71 HLBC $E_\gamma > 10$ MeV

0.53 ± 0.22 49 ROMANO 71 HLBC + $E_\gamma > 30$ MeV

1.2 ± 0.8 BELLOTTI 67 HLBC $E_\gamma > 30$ MeV

⁴⁵ AKIMENKO 07 provides values for three kinematic regions. For averaging, we use value with $E_\gamma > 10$ MeV and $0.6 < \cos(\theta_{e\gamma}) < 0.9$.

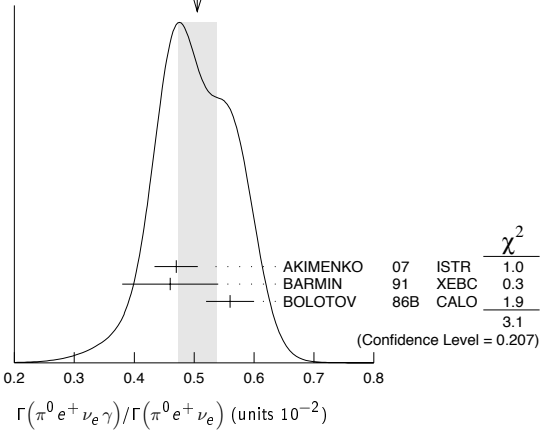
⁴⁶ BARMIN 91 quotes branching ratio $\Gamma(K \rightarrow e\pi^0 \nu_e \gamma)/\Gamma_{all}$. The measured normalization is $[\Gamma(K \rightarrow e\pi^0 \nu_e) + \Gamma(K \rightarrow \pi^+ \pi^+ \pi^-)]$. For comparison with other experiments we used $\Gamma(K \rightarrow e\pi^0 \nu_e)/\Gamma_{all} = 0.0482$ to calculate the values quoted here.

⁴⁷ $\cos(\theta_{e\gamma})$ between 0.6 and 0.9.

⁴⁸ First LJUNG 73 value is for $\cos(\theta_{e\gamma}) < 0.9$, second value is for $\cos(\theta_{e\gamma})$ between 0.6 and 0.9 for comparison with ROMANO 71.

⁴⁹ Both ROMANO 71 values are for $\cos(\theta_{e\gamma})$ between 0.6 and 0.9. Second value is for comparison with second LJUNG 73 value. We use lowest E_γ cut for Summary Table value. See ROMANO 71 for E_γ dependence.

WEIGHTED AVERAGE
 0.505 ± 0.032 (Error scaled by 1.3)

 $\Gamma(\pi^0 e^+ \nu_e \gamma(SD))/\Gamma_{total}$ Γ_{19}/Γ

Structure-dependent part.

VALUE (units 10^{-5})	CL%	DOCUMENT ID	TECN	CHG	COMMENT
--------------------------	-----	-------------	------	-----	---------

<5.3 90 BOLOTOV 86B CALO -

 $\Gamma(\pi^0 \mu^+ \nu_\mu \gamma)/\Gamma_{total}$ Γ_{20}/Γ

VALUE (units 10^{-5})	CL%	EVTS	DOCUMENT ID	TECN	CHG	COMMENT
--------------------------	-----	------	-------------	------	-----	---------

$1.46 \pm 0.22 \pm 0.32$ 153 ⁵⁰ TCHIKILEV 07 ISTR - $30 < E_\gamma < 60$ MeV

• • • We do not use the following data for averages, fits, limits, etc. • • •

$2.4 \pm 0.5 \pm 0.6$ 125 SHIMIZU 06 K470 + $E_\gamma > 30$ MeV;

< 6.1 90 0 LJUNG 73 HLBC + $E(\gamma) > 30$ MeV

⁵⁰ Obtained from measuring $B(K_{\mu 3\gamma})/B(K_{\mu 3})$ and using PDG 02 value $B(K_{\mu 3}) = 3.27\%$.

$B(K_{\mu 3\gamma}) = (8.82 \pm 0.94 \pm 0.86) \times 10^{-5}$ is obtained for $5 \text{ MeV} < E_\gamma < 30 \text{ MeV}$.

$B(K_{\mu 3\gamma}) = (8.82 \pm 0.94 \pm 0.86) \times 10^{-5}$ is obtained for $5 \text{ MeV} < E_\gamma < 30 \text{ MeV}$.

 $\Gamma(\pi^0 \pi^0 e^+ \nu_e \gamma)/\Gamma_{total}$ Γ_{21}/Γ

VALUE (units 10^{-6})	CL%	EVTS	DOCUMENT ID	TECN	CHG	COMMENT
--------------------------	-----	------	-------------	------	-----	---------

<5 90 0 BARMIN 92 XEBC + $E_\gamma > 10$ MeV

Hadronic modes with photons

 $\Gamma(\pi^+ \pi^0 \gamma)/\Gamma_{total}$ Γ_{22}/Γ

VALUE (units 10^{-4})	CL%	EVTS	DOCUMENT ID	TECN	CHG	COMMENT
--------------------------	-----	------	-------------	------	-----	---------

2.75 ± 0.15 OUR AVERAGE

2.71 ± 0.45 140 BOLOTOV 87 WIRE - $T_{\pi^+} 55-90$ MeV

2.87 ± 0.32 2461 SMITH 76 WIRE \pm $T_{\pi^\pm} 55-90$ MeV

2.71 ± 0.19 2100 ABRAMS 72 ASPK \pm $T_{\pi^+} 55-90$ MeV

• • • We do not use the following data for averages, fits, limits, etc. • • •

$1.5^{+1.1}_{-0.6}$ 51 LJUNG 73 HLBC + $T_{\pi^+} 55-80$ MeV

$2.6^{+1.5}_{-1.1}$ 51 LJUNG 73 HLBC + $T_{\pi^+} 55-90$ MeV

$6.8^{+3.7}_{-2.1}$ 17 51 LJUNG 73 HLBC + $T_{\pi^+} 55-102$ MeV

2.4 ± 0.8 24 EDWARDS 72 OSPK $T_{\pi^+} 58-90$ MeV

<1.0 0 52 MALTSEV 70 HLBC + $T_{\pi^+} < 55$ MeV

<1.9 90 0 EMMERSON 69 OSPK $T_{\pi^+} 55-80$ MeV

2.2 ± 0.7 18 CLINE 64 FBC + $T_{\pi^+} 55-80$ MeV

⁵¹ The LJUNG 73 values are not independent.

⁵² MALTSEV 70 selects low π^+ energy to enhance direct emission contribution.

 $\Gamma(\pi^+ \pi^0 \gamma(DE))/\Gamma_{total}$ Γ_{23}/Γ

Direct emission (DE) part of $\Gamma(\pi^+ \pi^0 \gamma)/\Gamma_{total}$, assuming that interference (INT) component is zero.

VALUE (units 10^{-6})	EVTS	DOCUMENT ID	TECN	CHG	COMMENT
--------------------------	------	-------------	------	-----	---------

4.3 ± 0.7 OUR AVERAGE

$3.8 \pm 0.8 \pm 0.7$ 10k ALIEV 06 K470 + $T_{\pi^+} 55-90$ MeV

$3.7 \pm 3.9 \pm 1.0$ 930 UVAROV 06 ISTR - $T_{\pi^+} 55-90$ MeV

$4.7 \pm 0.8 \pm 0.3$ 20k 53 ADLER 00C B787 + $T_{\pi^+} 55-90$ MeV

• • • We do not use the following data for averages, fits, limits, etc. • • •

$3.2 \pm 1.3 \pm 1.0$ 4k ALIEV 03 K470 + $T_{\pi^+} 55-90$ MeV

$6.1 \pm 2.5 \pm 1.9$ 4k ALIEV 03 K470 + T_{π^+} full range

$20.5 \pm 4.6^{+3.9}_{-2.3}$ BOLOTOV 87 WIRE - $T_{\pi^+} 55-90$ MeV

$15.6 \pm 3.5 \pm 5.0$ ABRAMS 72 ASPK \pm $T_{\pi^\pm} 55-90$ MeV

⁵³ ADLER 00C measures the INT component to be $(-0.4 \pm 1.6)\%$ of the inner bremsstrahlung (IB) component.

Meson Particle Listings

K^\pm

$\Gamma(\pi^+\pi^0\pi^0\gamma)/\Gamma(\pi^+\pi^0\pi^0)$ Γ_{24}/Γ_{10}

VALUE (units 10^{-4})	DOCUMENT ID	TECN	CHG	COMMENT
$4.3^{+3.2}_{-1.7}$	BOLOTOV	85	SPEC	$E(\gamma) > 10$ MeV

$\Gamma(\pi^+\pi^+\pi^-\gamma)/\Gamma_{total}$ Γ_{25}/Γ

VALUE (units 10^{-4})	EVTS	DOCUMENT ID	TECN	CHG	COMMENT
1.04 ± 0.31 OUR AVERAGE					
1.10 ± 0.48	7	BARMIN	89	XEBC	$E(\gamma) > 5$ MeV
1.0 ± 0.4		STAMER	65	EMUL	$E(\gamma) > 11$ MeV

$\Gamma(\pi^+\pi^+\pi^-\gamma)/\Gamma_{total}$ Γ_{26}/Γ

VALUE (units 10^{-7})	CL%	EVTS	DOCUMENT ID	TECN	CHG	COMMENT
$11 \pm 3 \pm 1$		31	54 KITCHING	97	B787	
••• We do not use the following data for averages, fits, limits, etc. •••						
< 0.083	90	55	ARTAMONOV	05	B949	$P_\pi > 213$ MeV/c
< 10	90	0	ATIYA	90b	B787	T_π 117–127 MeV
< 84	90	0	ASANO	82	CNTR	T_π 117–127 MeV
-420 ± 520	0	0	ABRAMS	77	SPEC	$T_\pi < 92$ MeV
< 350	90	0	LJUNG	73	HLBC	6–102, 114–127 MeV
< 500	90	0	KLEMS	71	OSPK	$T_\pi < 117$ MeV
-100 ± 600			CHEN	68	OSPK	T_π 60–90 MeV

⁵⁴ KITCHING 97 is extrapolated from their model-independent branching fraction $(6.0 \pm 1.5 \pm 0.7) \times 10^{-7}$ for 100 MeV/c $P_{\pi^+} < 180$ MeV/c using Chiral Perturbation Theory.

⁵⁵ ARTAMONOV 05 limit assumes ChPT with $\tilde{c} = 1.8$ with unitarity corrections. With $\tilde{c} = 1.6$ and no unitarity corrections they obtain $< 2.3 \times 10^{-8}$ at 90% CL. This partial branching ratio is predicted to be 6.10×10^{-9} and 0.49×10^{-9} for the cases with and without unitarity correction.

$\Gamma(\pi^+\pi^+\pi^-\gamma)/\Gamma_{total}$ Γ_{27}/Γ

Values given here assume a phase space pion energy spectrum.

VALUE (units 10^{-4})	CL%	DOCUMENT ID	TECN	CHG	COMMENT
< 1.0	90	ASANO	82	CNTR	$T(\pi)$ 117–127 MeV
••• We do not use the following data for averages, fits, limits, etc. •••					
< 3.0	90	KLEMS	71	OSPK	$T(\pi) > 117$ MeV

$\Gamma(\pi^+e^+e^-\gamma)/\Gamma_{total}$ Γ_{28}/Γ

VALUE (units 10^{-8})	EVTS	DOCUMENT ID	TECN	COMMENT
$1.19 \pm 0.12 \pm 0.04$	113	⁵⁶ BATLEY	08	NA48 $m_{e^+e^-} > 260$ MeV

⁵⁶ BATLEY 08 also reports the Chiral Perturbation Theory parameter $\tilde{c} = 0.9 \pm 0.45$ obtained using the shape of the $e^+e^-\gamma$ invariant mass spectrum. By extrapolating the theoretical amplitude to $m_{e^+e^-} < 260$ MeV, it obtains the inclusive $B(K^+ \rightarrow \pi^+e^+e^-\gamma) = (1.29 \pm 0.13 \pm 0.03) \times 10^{-8}$, where the first error is the combined statistical and systematic errors and the second error is from the uncertainty in \tilde{c} .

Leptonic modes with $\ell\bar{\ell}$ pairs

$\Gamma(e^+\nu_e\nu\bar{\nu})/\Gamma(e^+\nu_e)$ Γ_{29}/Γ_1

VALUE	CL%	EVTS	DOCUMENT ID	TECN	CHG
< 3.8	90	0	HEINTZE	79	SPEC

$\Gamma(\mu^+\nu_\mu\nu\bar{\nu})/\Gamma_{total}$ Γ_{30}/Γ

VALUE (units 10^{-6})	CL%	EVTS	DOCUMENT ID	TECN	CHG
< 6.0	90	0	⁵⁷ PANG	73	CNTR

⁵⁷ PANG 73 assumes μ spectrum from ν - ν interaction of BARDIN 70.

$\Gamma(e^+\nu_e e^+e^-)/\Gamma_{total}$ Γ_{31}/Γ

VALUE (units 10^{-8})	EVTS	DOCUMENT ID	TECN	CHG	COMMENT
$2.48 \pm 0.14 \pm 0.14$	410	POBLAGUEV	02	B865	$m_{e^+e^-} > 150$ MeV
••• We do not use the following data for averages, fits, limits, etc. •••					
20 ± 20	4	DIAMANT...	76	SPEC	$m_{e^+e^-} > 140$ MeV

$\Gamma(\mu^+\nu_\mu e^+e^-)/\Gamma_{total}$ Γ_{32}/Γ

VALUE (units 10^{-8})	EVTS	DOCUMENT ID	TECN	CHG	COMMENT
$7.06 \pm 0.16 \pm 0.26$	2.7k	POBLAGUEV	02	B865	$m_{e^+e^-} > 145$ MeV
••• We do not use the following data for averages, fits, limits, etc. •••					
100 ± 30	14	DIAMANT....	76	SPEC	$m_{e^+e^-} > 140$ MeV

$\Gamma(e^+\nu_e\mu^+\mu^-)/\Gamma_{total}$ Γ_{33}/Γ

VALUE (units 10^{-8})	CL%	DOCUMENT ID	TECN	COMMENT
1.72 ± 0.45		MA	06	B865
••• We do not use the following data for averages, fits, limits, etc. •••				
< 50	90	ADLER	98	B787

$\Gamma(\mu^+\nu_\mu\mu^+\mu^-)/\Gamma_{total}$ Γ_{34}/Γ

VALUE (units 10^{-7})	CL%	DOCUMENT ID	TECN	CHG
< 4.1	90	ATIYA	89	B787

Lepton Family number (LF), Lepton number (L), $\Delta S = \Delta Q$ (SQ) violating modes, or $\Delta S = 1$ weak neutral current (S1) modes

$\Gamma(\pi^+\pi^+e^-\nu_e)/\Gamma_{total}$ Γ_{35}/Γ

Test of $\Delta S = \Delta Q$ rule.

VALUE (units 10^{-7})	CL%	EVTS	DOCUMENT ID	TECN	CHG
••• We do not use the following data for averages, fits, limits, etc. •••					
< 9.0	95	0	SCHWEINB...	71	HLBC
< 6.9	95	0	ELY	69	HLBC
< 20	95		BIRGE	65	FBC

$\Gamma(\pi^+\pi^+e^-\nu_e)/\Gamma(\pi^+\pi^-e^+\nu_e)$ Γ_{35}/Γ_6

Test of $\Delta S = \Delta Q$ rule.

VALUE (units 10^{-4})	CL%	EVTS	DOCUMENT ID	TECN
< 3	90	3	⁵⁸ BLOCH	76
••• We do not use the following data for averages, fits, limits, etc. •••				
< 130	95	0	BOURQUIN	71

⁵⁸ BLOCH 76 quotes 3.6×10^{-4} at CL = 95%, we convert.

$\Gamma(\pi^+\pi^+\mu^-\nu_\mu)/\Gamma_{total}$ Γ_{36}/Γ

Test of $\Delta S = \Delta Q$ rule.

VALUE (units 10^{-6})	CL%	EVTS	DOCUMENT ID	TECN	CHG
< 3.0	95	0	BIRGE	65	FBC

$\Gamma(\pi^+e^+e^-)/\Gamma_{total}$ Γ_{37}/Γ

Test for $\Delta S = 1$ weak neutral current. Allowed by combined first-order weak and electromagnetic interactions.

VALUE (units 10^{-7})	EVTS	DOCUMENT ID	TECN	CHG
2.88 ± 0.13 OUR AVERAGE				
$2.94 \pm 0.05 \pm 0.14$	10300	⁵⁹ APPEL	99	SPEC
$2.75 \pm 0.23 \pm 0.13$	500	⁶⁰ ALLIEGRO	92	SPEC
2.7 ± 0.5	41	⁶¹ BLOCH	75	SPEC

⁵⁹ APPEL 99 establishes vector nature of this decay and determines form factor $f(Z) = f_0(1+\delta Z)$, $Z = M_{e^+e^-}^2/m_K^2$, $\delta = 2.14 \pm 0.13 \pm 0.15$.

⁶⁰ ALLIEGRO 92 assumes a vector interaction with a form factor given by $\lambda = 0.105 \pm 0.035 \pm 0.015$ and a correlation coefficient of -0.82 .

⁶¹ BLOCH 75 assumes a vector interaction.

$\Gamma(\pi^+\mu^+\mu^-)/\Gamma_{total}$ Γ_{38}/Γ

Test for $\Delta S = 1$ weak neutral current. Allowed by higher-order electroweak interactions.

VALUE (units 10^{-8})	CL%	EVTS	DOCUMENT ID	TECN	CHG
8.1 ± 1.4 OUR AVERAGE					
Error includes scale factor of 2.7. See the ideogram below.					
$9.8 \pm 1.0 \pm 0.5$		110	⁶² PARK	02	HYCP
$9.22 \pm 0.60 \pm 0.49$		402	⁶³ MA	00	B865
$5.0 \pm 0.4 \pm 0.9$		207	⁶⁴ ADLER	97c	B787

••• We do not use the following data for averages, fits, limits, etc. •••

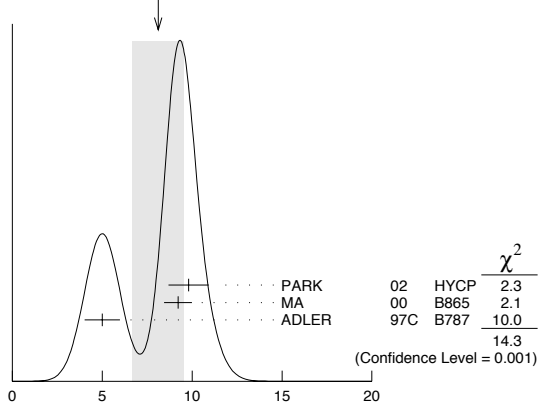
$9.7 \pm 1.2 \pm 0.4$		65	PARK	02	HYCP
$10.0 \pm 1.9 \pm 0.7$		35	PARK	02	HYCP
< 23		90	ATIYA	89	B787

⁶² PARK 02 "±" result comes from combining $K^+ \rightarrow \pi^+\mu^+\mu^-$ and $K^- \rightarrow \pi^-\mu^+\mu^-$, assuming CP is conserved.

⁶³ MA 00 establishes vector nature of this decay and determines form factor $f(Z) = f_0(1+\delta Z)$, $Z = M_{\mu\mu}^2/m_K^2$, $\delta = 2.45^{+1.30}_{-0.95}$.

⁶⁴ ADLER 97c gives systematic error 0.7×10^{-8} and theoretical uncertainty 0.6×10^{-8} , which we combine in quadrature to obtain our second error.

WEIGHTED AVERAGE
8.1±1.4 (Error scaled by 2.7)



$\Gamma(\pi^+\mu^+\mu^-)/\Gamma_{total}$ Γ_{38}/Γ

$\Gamma(\pi^+ \nu \bar{\nu})/\Gamma_{\text{total}}$ Γ_{39}/Γ

Test for $\Delta S = 1$ weak neutral current. Allowed by higher-order electroweak interactions. Branching ratio values are extrapolated from the momentum or energy regions shown in the comments assuming Standard Model phase space except for those labeled "Scalar" or "Tensor" to indicate the assumed non-Standard-Model interaction.

VALUE (units 10^{-9})	CL%	EVTS	DOCUMENT ID	TECN	CHG	COMMENT
0.147 ± 0.130 -0.089		3	65 ANISOVSK...04	B949	+	$211 < P_\pi < 229$ MeV
< 2.2	90		66 ADLER	04	B787	+ $140 < P_\pi < 195$ MeV
0.157 ± 0.175 -0.082		2	ADLER	02	B787	$P_\pi > 211$ MeV/c
< 4.2	90	1	ADLER	02c	B787	$140 < P_\pi < 195$ MeV
< 4.7	90		ADLER	02c	B787	Scalar
< 2.5	90		ADLER	02c	B787	Tensor
0.15 ± 0.34 -0.12		1	ADLER	00	B787	In ADLER 02
0.42 ± 0.97 -0.35		1	ADLER	97	B787	
< 2.4	90		ADLER	96	B787	
< 7.5	90		ATIYA	93	B787	+ $\mathcal{T}(\pi)$ 115–127 MeV
< 5.2	90		67 ATIYA	93	B787	+
< 17	90	0	ATIYA	93B	B787	+ $\mathcal{T}(\pi)$ 60–100 MeV
< 34	90		ATIYA	90	B787	+
< 140	90		ASANO	81B	CNTR	+ $\mathcal{T}(\pi)$ 116–127 MeV

⁶⁵ Value obtained combining the previous E787 result ADLER 02 with 2 evts and the present E949 with 1 evt. The additional event has a signal-to-background ratio 0.9.

⁶⁶ Value obtained combining the previous result ADLER 02c with 1 event and the present result with 0 events to obtain an expected background 1.22 ± 0.24 evts and 1 evt observed.

⁶⁷ Combining ATIYA 93 and ATIYA 93B results. Superseded by ADLER 96.

 $\Gamma(\pi^+ \pi^0 \nu \bar{\nu})/\Gamma_{\text{total}}$ Γ_{40}/Γ

Test for $\Delta S = 1$ weak neutral current. Allowed by higher-order electroweak interactions.

VALUE (units 10^{-5})	CL%	DOCUMENT ID	TECN
< 4.3	90	68 ADLER 01	SPEC

⁶⁸ Search region defined by $90 \text{ MeV}/c < P_{\pi^+} < 188 \text{ MeV}/c$ and $135 \text{ MeV} < E_{\pi^0} < 180 \text{ MeV}$.

 $\Gamma(\mu^- \nu e^+ e^+)/\Gamma(\pi^+ \pi^- e^+ \nu_e)$ Γ_{41}/Γ_6

Test of lepton family number conservation.

VALUE (units 10^{-3})	CL%	EVTS	DOCUMENT ID	TECN	CHG
< 0.5	90	0	69 DIAMANT-... 76	SPEC	+

⁶⁹ DIAMANT-BERGER 76 quotes this result times our 1975 $\pi^+ \pi^- e \nu$ BR ratio.

 $\Gamma(\mu^+ \nu_e)/\Gamma_{\text{total}}$ Γ_{42}/Γ

Forbidden by lepton family number conservation.

VALUE	CL%	EVTS	DOCUMENT ID	TECN	COMMENT
< 0.004	90	0	70 LYONS	81	HLBC 200 GeV K^+ narrow band ν beam

• • • We do not use the following data for averages, fits, limits, etc. • • •

< 0.012 90 70 COOPER 82 HLBC Wideband ν beam

⁷⁰ COOPER 82 and LYONS 81 limits on ν_e observation are here interpreted as limits on lepton family number violation in the absence of mixing.

 $\Gamma(\pi^+ \mu^+ e^-)/\Gamma_{\text{total}}$ Γ_{43}/Γ

Test of lepton family number conservation.

VALUE (units 10^{-10})	CL%	EVTS	DOCUMENT ID	TECN	CHG
< 0.13	90	0	71 SHER	05	RVUE +

• • • We do not use the following data for averages, fits, limits, etc. • • •

< 0.21 90 SHER 05 B865 +

< 0.39 90 APPEL 00 B865 +

< 2.1 90 LEE 90 SPEC +

⁷¹ This result combines SHER 05 1998 data, APPEL 00 1996 data, and data from BERGMAN 97 and PISLAK 97 theses, all from BNL-E865, with LEE 90 BNL-E777 data.

 $\Gamma(\pi^+ \mu^- e^+)/\Gamma_{\text{total}}$ Γ_{44}/Γ

Test of lepton family number conservation.

VALUE (units 10^{-10})	CL%	EVTS	DOCUMENT ID	TECN	CHG
< 5.2	90	0	APPEL	00B	B865 +

• • • We do not use the following data for averages, fits, limits, etc. • • •

< 70 90 0 ⁷² DIAMANT-... 76 SPEC +

⁷² Measurement actually applies to the sum of the $\pi^+ \mu^- e^+$ and $\pi^- \mu^+ e^+$ modes.

 $\Gamma(\pi^- \mu^+ e^+)/\Gamma_{\text{total}}$ Γ_{45}/Γ

Test of total lepton number conservation.

VALUE (units 10^{-10})	CL%	EVTS	DOCUMENT ID	TECN	CHG
< 5.0	90	0	APPEL	00B	B865 +

• • • We do not use the following data for averages, fits, limits, etc. • • •

< 70 90 0 ⁷³ DIAMANT-... 76 SPEC +

⁷³ Measurement actually applies to the sum of the $\pi^+ \mu^- e^+$ and $\pi^- \mu^+ e^+$ modes.

 $\Gamma(\pi^- e^+ e^+)/\Gamma_{\text{total}}$ Γ_{46}/Γ

Test of total lepton number conservation.

VALUE	CL%	EVTS	DOCUMENT ID	TECN	CHG
< 6.4×10^{-10}	90	0	APPEL	00B	B865 +

• • • We do not use the following data for averages, fits, limits, etc. • • •

< 9.2×10^{-9} 90 0 DIAMANT-... 76 SPEC +

< 1.5×10^{-5} CHANG 68 HBC -

 $\Gamma(\pi^- \mu^+ \mu^+)/\Gamma_{\text{total}}$ Γ_{47}/Γ

Forbidden by total lepton number conservation.

VALUE	CL%	EVTS	DOCUMENT ID	TECN	CHG
< 3.0×10^{-9}	90	0	APPEL	00B	B865 +

• • • We do not use the following data for averages, fits, limits, etc. • • •

< 1.5×10^{-4} 90 ⁷⁴ LITTEBERG 92 HBC

⁷⁴ LITTEBERG 92 is from retroactive data analysis of CHANG 68 bubble chamber data.

 $\Gamma(\mu^+ \bar{\nu}_e)/\Gamma_{\text{total}}$ Γ_{48}/Γ

Forbidden by total lepton number conservation.

VALUE (units 10^{-3})	CL%	DOCUMENT ID	TECN	COMMENT
< 3.3	90	⁷⁵ COOPER 82	HLBC	Wideband ν beam

⁷⁵ COOPER 82 limit on $\bar{\nu}_e$ observation is here interpreted as a limit on lepton number violation in the absence of mixing.

 $\Gamma(\pi^0 e^+ \bar{\nu}_e)/\Gamma_{\text{total}}$ Γ_{49}/Γ

Forbidden by total lepton number conservation.

VALUE	CL%	DOCUMENT ID	TECN	COMMENT
< 0.003	90	⁷⁶ COOPER 82	HLBC	Wideband ν beam

⁷⁶ COOPER 82 limit on $\bar{\nu}_e$ observation is here interpreted as a limit on lepton number violation in the absence of mixing.

 $\Gamma(\pi^+ \gamma)/\Gamma_{\text{total}}$ Γ_{50}/Γ

Violates angular momentum conservation and gauge invariance. Current interest in this decay is as a search for non-commutative space-time effects as discussed in ARTAMONOV 05 and for exotic physics such as a vacuum expectation value of a new vector field, non-local Superstring effects, or departures from Lorentz invariance, as discussed in ADLER 02b.

VALUE (units 10^{-3})	CL%	DOCUMENT ID	TECN	CHG
< 2.3	90	ARTAMONOV 05	B949	+

• • • We do not use the following data for averages, fits, limits, etc. • • •

< 360 90 ADLER 02B B787 +

< 1400 90 ASANO 82 CNTR +

< 4000 90 ⁷⁷ KLEMS 71 OSPK +

⁷⁷ Test of model of Selleri, Nuovo Cimento **60A** 291 (1969).

 K^+ LONGITUDINAL POLARIZATION OF EMITTED μ^+

VALUE	CL%	DOCUMENT ID	TECN	CHG	COMMENT
< -0.990	90	⁷⁸ AOKI 94	SPEC	+	

• • • We do not use the following data for averages, fits, limits, etc. • • •

< -0.990 90 IMAZATO 92 SPEC + Repl. by AOKI 94

-0.970 \pm 0.047 ⁷⁹ YAMANAKA 86 SPEC +

-1.0 \pm 0.1 ⁷⁹ CUTTS 69 SPRK +

-0.96 \pm 0.12 ⁷⁹ COOMBES 57 CNTR +

⁷⁸ AOKI 94 measures $\xi P_\mu = -0.9996 \pm 0.0030 \pm 0.0048$. The above limit is obtained by summing the statistical and systematic errors in quadrature, normalizing to the physically significant region ($|\xi P_\mu| < 1$) and assuming that $\xi=1$, its maximum value.

⁷⁹ Assumes $\xi=1$.

DALITZ PLOT PARAMETERS FOR

 $K \rightarrow 3\pi$ DECAYS

Revised 1999 by T.G. Trippe (LBNL).

The Dalitz plot distribution for $K^\pm \rightarrow \pi^\pm \pi^\pm \pi^\mp$, $K^\pm \rightarrow \pi^0 \pi^0 \pi^\pm$, and $K_L^0 \rightarrow \pi^+ \pi^- \pi^0$ can be parameterized by a series expansion such as that introduced by Weinberg [1]. We use the form

$$\begin{aligned}
 |M|^2 \propto & 1 + g \frac{(s_3 - s_0)}{m_{\pi^+}^2} + h \left[\frac{s_3 - s_0}{m_{\pi^+}^2} \right]^2 \\
 & + j \frac{(s_2 - s_1)}{m_{\pi^+}^2} + k \left[\frac{s_2 - s_1}{m_{\pi^+}^2} \right]^2 \\
 & + f \frac{(s_2 - s_1)(s_3 - s_0)}{m_{\pi^+}^2 m_{\pi^+}^2} + \dots, \quad (1)
 \end{aligned}$$

Meson Particle Listings

 K^\pm

where $m_{\pi^+}^2$ has been introduced to make the coefficients g , h , j , and k dimensionless, and

$$s_i = (P_K - P_i)^2 = (m_K - m_i)^2 - 2m_K T_i, \quad i = 1, 2, 3,$$

$$s_0 = \frac{1}{3} \sum_i s_i = \frac{1}{3} (m_K^2 + m_1^2 + m_2^2 + m_3^2).$$

Here the P_i are four-vectors, m_i and T_i are the mass and kinetic energy of the i^{th} pion, and the index 3 is used for the odd pion.

The coefficient g is a measure of the slope in the variable s_3 (or T_3) of the Dalitz plot, while h and k measure the quadratic dependence on s_3 and $(s_2 - s_1)$, respectively. The coefficient j is related to the asymmetry of the plot and must be zero if CP invariance holds. Note also that if CP is good, g , h , and k must be the same for $K^+ \rightarrow \pi^+\pi^+\pi^-$ as for $K^- \rightarrow \pi^-\pi^-\pi^+$.

Since different experiments use different forms for $|M|^2$, in order to compare the experiments we have converted to g , h , j , and k whatever coefficients have been measured. Where such conversions have been done, the measured coefficient a_y , a_t , a_u , or a_v is given in the comment at the right. For definitions of these coefficients, details of this conversion, and discussion of the data, see the April 1982 version of this note [2].

References

1. S. Weinberg, Phys. Rev. Lett. **4**, 87 (1960).
2. Particle Data Group, Phys. Lett. **111B**, 69 (1982).

ENERGY DEPENDENCE OF K^\pm DALITZ PLOT

$$|\text{matrix element}|^2 = 1 + gu + hu^2 + kv^2$$

where $u = (s_3 - s_0) / m_{\pi^+}^2$ and $v = (s_2 - s_1) / m_{\pi^+}^2$

LINEAR COEFFICIENT g FOR $K^\pm \rightarrow \pi^\pm\pi^+\pi^-$

Some experiments use Dalitz variables x and y . In the comments we give $a_y =$ coefficient of y term. See note above on "Dalitz Plot Parameters for $K \rightarrow 3\pi$ Decays." For discussion of the conversion of a_y to g , see the earlier version of the same note in the Review published in Physics Letters **111B** 70 (1982).

VALUE	EVTS	DOCUMENT ID	TECN	CHG	COMMENT
-0.21134 ± 0.00017	471M	⁸⁰ BATLEY	07B	NA48	\pm
••• We do not use the following data for averages, fits, limits, etc. •••					
-0.2221 ± 0.0065	225k	DEVAUX	77	SPEC	$+$ $a_y = -0.2814 \pm 0.0082$
-0.199 ± 0.008	81k	⁸¹ LUCAS	73	HBC	$-$ $a_y = 0.252 \pm 0.011$
-0.2157 ± 0.0028	750k	FORD	72	ASPK	$+$ $a_y = -0.2734 \pm 0.0035$
-0.2186 ± 0.0028	750k	FORD	72	ASPK	$-$ $a_y = -0.2770 \pm 0.0035$
-0.200 ± 0.009	39819	⁸² HOFFMASTER	72	HLBC	$+$
-0.196 ± 0.012	17898	⁸³ GRAUMAN	70	HLBC	$+$ $a_y = -0.228 \pm 0.030$
-0.193 ± 0.010	50919	MAST	69	HBC	$-$ $a_y = 0.244 \pm 0.013$
-0.218 ± 0.016	9994	⁸⁴ BUTLER	68	HBC	$+$ $a_y = -0.277 \pm 0.020$
-0.190 ± 0.023	5778	^{84,85} MOSCOSO	68	HBC	$-$ $a_y = -0.242 \pm 0.029$
-0.22 ± 0.024	5428	^{84,85} ZINCHENKO	67	HBC	$+$ $a_y = -0.28 \pm 0.03$
-0.220 ± 0.035	1347	⁸⁶ FERRO-LUZZI	61	HBC	$-$ $a_y = 0.28 \pm 0.045$

⁸⁰ Final state strong interaction and radiative corrections not included in the fit.

⁸¹ Quadratic dependence is required by K_L^0 experiments.

⁸² HOFFMASTER 72 includes GRAUMAN 70 data.

⁸³ Emulsion data added — all events included by HOFFMASTER 72.

⁸⁴ Experiments with large errors not included in average.

⁸⁵ Also includes DBC events.

⁸⁶ No radiative corrections included.

QUADRATIC COEFFICIENT h FOR $K^\pm \rightarrow \pi^\pm\pi^+\pi^-$

VALUE (units 10^{-2})	EVTS	DOCUMENT ID	TECN	CHG
1.848 ± 0.040	471M	⁸⁷ BATLEY	07B	NA48
••• We do not use the following data for averages, fits, limits, etc. •••				
-0.06 ± 1.43	225k	DEVAUX	77	SPEC
1.87 ± 0.62	750k	FORD	72	ASPK
1.25 ± 0.62	750k	FORD	72	ASPK
-0.9 ± 1.4	39819	HOFFMASTER	72	HLBC
-0.1 ± 1.2	50919	MAST	69	HBC

⁸⁷ Final state strong interaction and radiative corrections not included in the fit.

QUADRATIC COEFFICIENT k FOR $K^\pm \rightarrow \pi^\pm\pi^+\pi^-$

VALUE (units 10^{-3})	EVTS	DOCUMENT ID	TECN	CHG
-4.63 ± 0.14	471M	⁸⁸ BATLEY	07B	NA48
••• We do not use the following data for averages, fits, limits, etc. •••				
-20.5 ± 3.9	225k	DEVAUX	77	SPEC
-7.5 ± 1.9	750k	FORD	72	ASPK
-8.3 ± 1.9	750k	FORD	72	ASPK
-10.5 ± 4.5	39819	HOFFMASTER	72	HLBC
-14 ± 12	50919	MAST	69	HBC

⁸⁸ Final state strong interaction and radiative corrections not included in the fit.

 $(g_+ - g_-) / (g_+ + g_-)$ FOR $K^\pm \rightarrow \pi^\pm\pi^+\pi^-$

This is a CP violating asymmetry between linear coefficients g_+ for $K^+ \rightarrow \pi^+\pi^+\pi^-$ decay and g_- for $K^- \rightarrow \pi^-\pi^-\pi^+$ decay.

VALUE (units 10^{-4})	EVTS	DOCUMENT ID	TECN
$-1.5 \pm 1.5 \pm 1.6$	3.1G	⁸⁹ BATLEY	07E NA48
••• We do not use the following data for averages, fits, limits, etc. •••			
$1.7 \pm 2.1 \pm 2.0$	1.7G	⁹⁰ BATLEY	06 NA48
-70.0 ± 53	3.2M	FORD	70 ASPK

⁸⁹ BATLEY 07E includes data from BATLEY 06. Uses quadratic parametrization and value $g_+ + g_- = 2g$ from BATLEY 07B. This measurement neglects any possible charge asymmetries in higher order slope parameters h or k .

⁹⁰ This measurement neglects any possible charge asymmetries in higher order slope parameters h or k .

LINEAR COEFFICIENT g FOR $K^\pm \rightarrow \pi^\pm\pi^0\pi^0$

Unless otherwise stated, all experiments include terms quadratic in $(s_3 - s_0) / m_{\pi^+}^2$. See note above on "Dalitz Plot Parameters for $K \rightarrow 3\pi$ Decays."

See BATUSOV 98 for a discussion of the discrepancy between their result and others, especially BOLOTOV 86. At this time we have no way to resolve the discrepancy so we depend on the large scale factor as a warning.

VALUE	EVTS	DOCUMENT ID	TECN	CHG	COMMENT
0.626 ± 0.007	OUR AVERAGE				
$0.6259 \pm 0.0043 \pm 0.0093$	493k	AKOPDZHAN.	05B	TNF	\pm
$0.627 \pm 0.004 \pm 0.010$	252k	^{91,92} AJINENKO	03B	ISTR	$-$
••• We do not use the following data for averages, fits, limits, etc. •••					
$0.736 \pm 0.014 \pm 0.012$	33k	BATUSOV	98	SPEC	$+$
0.582 ± 0.021	43k	BOLOTOV	86	CALO	$-$
0.670 ± 0.054	3263	BRAUN	76B	HLBC	$+$
0.630 ± 0.038	5635	SHEAFF	75	HLBC	$+$
0.510 ± 0.060	27k	SMITH	75	WIRE	$+$
0.67 ± 0.06	1365	AUBERT	72	HLBC	$+$
0.544 ± 0.048	4048	DAVISON	69	HLBC	$+$ Also emulsion

⁹¹ Measured using in-flight decays of the 25 GeV negative secondary beam.

⁹² They form new world averages $g_- = (0.617 \pm 0.018)$ and $g_+ = (0.684 \pm 0.033)$ which give $\Delta g_{\pi^0} = 0.051 \pm 0.028$.

QUADRATIC COEFFICIENT h FOR $K^\pm \rightarrow \pi^\pm\pi^0\pi^0$

VALUE	EVTS	DOCUMENT ID	TECN	CHG	COMMENT
0.052 ± 0.008	OUR AVERAGE				
$0.0551 \pm 0.0044 \pm 0.0086$	493k	AKOPDZHAN.	05B	TNF	\pm
$0.046 \pm 0.004 \pm 0.012$	252k	⁹³ AJINENKO	03B	ISTR	$-$
••• We do not use the following data for averages, fits, limits, etc. •••					
$0.128 \pm 0.015 \pm 0.024$	33k	BATUSOV	98	SPEC	$+$
0.037 ± 0.024	43k	BOLOTOV	86	CALO	$-$
0.152 ± 0.082	3263	BRAUN	76B	HLBC	$+$
0.041 ± 0.030	5635	SHEAFF	75	HLBC	$+$
0.009 ± 0.040	27k	SMITH	75	WIRE	$+$
-0.01 ± 0.08	1365	AUBERT	72	HLBC	$+$
0.026 ± 0.050	4048	DAVISON	69	HLBC	$+$ Also emulsion

⁹³ Measured using in-flight decays of the 25 GeV negative secondary beam.

QUADRATIC COEFFICIENT k FOR $K^\pm \rightarrow \pi^\pm\pi^0\pi^0$

VALUE	EVTS	DOCUMENT ID	TECN	CHG
0.0054 ± 0.0035	OUR AVERAGE			
$0.0082 \pm 0.0011 \pm 0.0014$	493k	AKOPDZHAN.	05B	TNF
$0.001 \pm 0.001 \pm 0.002$	252k	⁹⁴ AJINENKO	03B	ISTR
••• We do not use the following data for averages, fits, limits, etc. •••				
$0.0197 \pm 0.0045 \pm 0.0029$	33k	BATUSOV	98	SPEC

⁹⁴ Measured using in-flight decays of the 25 GeV negative secondary beam.

 $(g_+ - g_-) / (g_+ + g_-)$ FOR $K^\pm \rightarrow \pi^\pm\pi^0\pi^0$

A nonzero value for this quantity indicates CP violation.

VALUE (units 10^{-4})	EVTS	DOCUMENT ID	TECN
1.8 ± 1.8	OUR AVERAGE		
$1.8 \pm 1.7 \pm 0.6$	91.3M	⁹⁵ BATLEY	07E NA48
$2 \pm 18 \pm 5$	619k	⁹⁶ AKOPDZHAN.	05B TNF
••• We do not use the following data for averages, fits, limits, etc. •••			
$1.8 \pm 2.2 \pm 1.3$	47M	⁹⁷ BATLEY	06A NA48

⁹⁵ BATLEY 07E includes data from BATLEY 06A. Uses quadratic parametrization and PDG 06 value $g = 0.626 \pm 0.007$ to obtain $g_+ - g_- = (2.2 \pm 2.1 \pm 0.7) \times 10^{-4}$. Neglects any possible charge asymmetries in higher order slope parameters h or k .

⁹⁶ Asymmetry obtained assuming that $g_+ + g_- = 2 \times 0.652$ (PDG 02) and that asymmetries in h and k are zero.

⁹⁷ Linear and quadratic slopes from PDG 04 are used. Any possible charge asymmetries in higher order slope parameters h or k are neglected.

ALTERNATIVE PARAMETERIZATION OF $K^\pm \rightarrow \pi^\pm \pi^0 \pi^0$ DALITZ PLOT

The following functional form for the matrix element suggested by $\pi\pi$ rescattering in $K^+ \rightarrow \pi^+ \pi^+ \pi^- \nu \rightarrow \pi^+ \pi^0 \pi^0$ is used for this fit (CABIBBO 04A, CABIBBO 05): Matrix element = $M_0 + M_1$ where $M_0 = 1 + (1/2)g_0 u + (1/2)h' u^2$ with $u = (s_3 - s_0)/(m_{\pi^+})^2$ and where M_1 takes into account the non-analytic piece due to $\pi^0 \pi^0$ rescattering amplitudes a_0 and a_2 ; The parameters g_0 and h' are related to the parameters g and h of the matrix element squared given in the previous section by the approximations $g_0 \sim g^{PDG}$ and $h' \sim h^{PDG} - (g/2)^2$.

LINEAR COEFFICIENT g_0 FOR $K^\pm \rightarrow \pi^\pm \pi^0 \pi^0$

VALUE	EVT5	DOCUMENT ID	TECN	CHG
$0.645 \pm 0.004 \pm 0.009$	23M	⁹⁸ BATLEY	06b	NA48 ±

⁹⁸This fit is obtained with the CABIBBO 05 matrix element in the $2\pi^0$ invariant mass squared range $0.074 \text{ GeV}^2 < m_{2\pi^0}^2 < 0.097 \text{ GeV}^2$, assuming $k = 0$ (no term proportional to $(s_2 - s_1)^2$) and excluding the kinematic region around the cusp ($m_{2\pi^0}^2 = (2m_{\pi^+})^2 \pm 0.000525 \text{ GeV}^2$). Also $\pi\pi$ phase shifts a_0 and a_2 are measured: $(a_0 - a_2)m_{\pi^+} = 0.268 \pm 0.010 \pm 0.004 \pm 0.013(\text{external})$ and $a_2 m_{\pi^+} = -0.041 \pm 0.022 \pm 0.014$.

QUADRATIC COEFFICIENT h' FOR $K^\pm \rightarrow \pi^\pm \pi^0 \pi^0$

VALUE	EVT5	DOCUMENT ID	TECN	CHG
$-0.047 \pm 0.012 \pm 0.011$	23M	⁹⁹ BATLEY	06b	NA48 ±

⁹⁹This fit is obtained with the CABIBBO 05 matrix element in the $2\pi^0$ invariant mass squared range $0.074 \text{ GeV}^2 < m_{2\pi^0}^2 < 0.097 \text{ GeV}^2$, assuming $k = 0$ (no term proportional to $(s_2 - s_1)^2$) and excluding the kinematic region around the cusp ($m_{2\pi^0}^2 = (2m_{\pi^+})^2 \pm 0.000525 \text{ GeV}^2$). Also $\pi\pi$ phase shifts a_0 and a_2 are measured: $(a_0 - a_2)m_{\pi^+} = 0.268 \pm 0.010 \pm 0.004 \pm 0.013(\text{external})$ and $a_2 m_{\pi^+} = -0.041 \pm 0.022 \pm 0.014$.

 $K_{\ell 3}^\pm$ AND $K_{\ell 3}^0$ FORM FACTORS

Revised May 2008 by T.G. Trippe (LBNL) and C.-J. Lin (LBNL).

Assuming that only the vector current contributes to $K \rightarrow \pi \ell \nu$ decays, we write the matrix element as

$$M \propto f_+(t) [(P_K + P_\pi)_\mu \bar{\ell} \gamma_\mu (1 + \gamma_5) \nu] + f_-(t) [m_\ell \bar{\ell} (1 + \gamma_5) \nu], \quad (1)$$

where P_K and P_π are the four-momenta of the K and π mesons, m_ℓ is the lepton mass, and f_+ and f_- are dimensionless form factors which can depend only on $t = (P_K - P_\pi)^2$, the square of the four-momentum transfer to the leptons. If time-reversal invariance holds, f_+ and f_- are relatively real. $K_{\mu 3}$ experiments, discussed immediately below, measure f_+ and f_- , while $K_{e 3}$ experiments, discussed further below, are sensitive only to f_+ because the small electron mass makes the f_- term negligible.

$K_{\mu 3}$ Experiments. Analyses of $K_{\mu 3}$ data frequently assume a linear dependence of f_+ and f_- on t , i.e.,

$$f_\pm(t) = f_\pm(0) [1 + \lambda_\pm(t/m_{\pi^+}^2)]. \quad (2)$$

Most $K_{\mu 3}$ data are adequately described by Eq. (2) for f_+ and a constant f_- (i.e., $\lambda_- = 0$).

There are two equivalent parametrizations commonly used in these analyses:

(1) λ_+ , $\xi(0)$ parametrization. Older analyses of $K_{\mu 3}$ data often introduce the ratio of the two form factors

$$\xi(t) = f_-(t)/f_+(t). \quad (3)$$

The $K_{\mu 3}$ decay distribution is then described by the two parameters λ_+ and $\xi(0)$ (assuming time reversal invariance and $\lambda_- = 0$).

(2) λ_+ , λ_0 parametrization. More recent $K_{\mu 3}$ analyses have parametrized in terms of the form factors f_+ and f_0 , which are associated with vector and scalar exchange, respectively, to the lepton pair. f_0 is related to f_+ and f_- by

$$f_0(t) = f_+(t) + [t/(m_K^2 - m_\pi^2)] f_-(t). \quad (4)$$

Here $f_0(0)$ must equal $f_+(0)$ unless $f_-(t)$ diverges at $t = 0$. The earlier assumption that f_+ is linear in t and f_- is constant leads to f_0 linear in t :

$$f_0(t) = f_0(0) [1 + \lambda_0(t/m_{\pi^+}^2)]. \quad (5)$$

With the assumption that $f_0(0) = f_+(0)$, the two parametrizations, $(\lambda_+, \xi(0))$ and (λ_+, λ_0) are equivalent as long as correlation information is retained. (λ_+, λ_0) correlations tend to be less strong than $(\lambda_+, \xi(0))$ correlations.

Since the 2006 edition of the *Review* [4], we no longer quote results in the $(\lambda_+, \xi(0))$ parametrization. We have removed many older low statistics results from the Listings. See the 2004 version of this note [5] for these older results, and the 1982 version [6] for additional discussion of the $K_{\mu 3}^0$ parameters, correlations, and conversion between parametrizations.

Quadratic Parametrization. More recent high-statistics experiments have included a quadratic term in the expansion of $f_+(t)$,

$$f_+(t) = f_+(0) \left[1 + \lambda'_+(t/m_{\pi^+}^2) + \frac{\lambda''_+}{2}(t/m_{\pi^+}^2)^2 \right]. \quad (6)$$

If there is a non-vanishing quadratic term, then λ_+ of Eq. (2) represents the average slope, which is then different from λ'_+ . Our convention is to include the factor $\frac{1}{2}$ in the quadratic term, and to use m_{π^+} even for $K_{e 3}^+$ and $K_{\mu 3}^+$ decays. We have converted other's parametrizations to match our conventions, as noted in the beginning of the " $K_{\ell 3}^\pm$ and $K_{\ell 3}^0$ Form Factors" sections of the Listings.

Pole Parametrization. The pole model describes the t -dependence of $f_+(t)$ and $f_0(t)$ in terms of the exchange of the lightest vector and scalar K^* mesons with masses M_v and M_s , respectively:

$$f_+(t) = f_+(0) \left[\frac{M_v^2}{M_v^2 - t} \right], \quad f_0(t) = f_0(0) \left[\frac{M_s^2}{M_s^2 - t} \right]. \quad (7)$$

Dispersive Parametrization [7,8]. This approach uses dispersive techniques and the known low-energy $K\pi$ phases to parametrize the vector and scalar form factors:

$$f_+(t) = f_+(0) \exp \left[\frac{t}{m_\pi^2} (\Lambda_+ + H(t)) \right]; \quad (8)$$

$$f_0(t) = f_+(0) \exp \left[\frac{t}{(m_K^2 - m_\pi^2)} (\ln[C] - G(t)) \right], \quad (9)$$

where Λ_+ is the slope of the vector form factor, and $\ln[C] = \ln[f_0(m_K^2 - m_\pi^2)]$ is the logarithm of the scalar form factor at the Callan-Treiman point. The functions $H(t)$ and $G(t)$ are dispersive integrals.

Meson Particle Listings

K^\pm

K_{e3} Experiments: Analysis of K_{e3} data is simpler than that of $K_{\mu 3}$ because the second term of the matrix element assuming a pure vector current [Eq. (1) above] can be neglected. Here f_+ can be assumed to be linear in t , in which case the linear coefficient λ_+ of Eq. (2) is determined, or quadratic, in which case the linear coefficient λ'_+ and quadratic coefficient λ''_+ of Eq. (6) are determined.

If we remove the assumption of a pure vector current, then the matrix element for the decay, in addition to the terms in Eq. (1), would contain

$$+2m_K f_S \bar{\ell}(1 + \gamma_5)\nu + (2f_T/m_K)(P_K)_\lambda(P_\pi)_\mu \bar{\ell}\sigma_{\lambda\mu}(1 + \gamma_5)\nu, \quad (10)$$

where f_S is the scalar form factor, and f_T is the tensor form factor. In the case of the K_{e3} decays where the f_- term can be neglected, experiments have yielded limits on $|f_S/f_+|$ and $|f_T/f_+|$.

Fits for K_{e3} Form Factors. For K_{e3} data, we determine best values for the three parametrizations: linear (λ_+), quadratic (λ'_+ , λ''_+) and pole (M_v). For $K_{\mu 3}$ data, we determine best values for the three parametrizations: linear (λ_+ , λ_0), quadratic (λ'_+ , λ''_+ , λ_0) and pole (M_v , M_s). We then assume $\mu - e$ universality so that we can combine K_{e3} and $K_{\mu 3}$ data, and again determine best values for the three parametrizations: linear (λ_+ , λ_0), quadratic (λ'_+ , λ''_+ , λ_0), and pole (M_v , M_s). When there is more than one parameter, fits are done including input correlations. Simple averages suffice in the two K_{e3} cases where there is only one parameter: linear (λ_+) and pole (M_v).

Both KTeV and KLOE see an improvement in the quality of their fits relative to linear fits when a quadratic term is introduced, as well as when the pole parametrization is used. The quadratic parametrization has the disadvantage that the quadratic parameter λ''_+ is highly correlated with the linear parameter λ'_+ , in the neighborhood of 95%, and that neither parameter is very well determined. The pole fit has the same number of parameters as the linear fit, but yields slightly better fit probabilities, so that it would be advisable for all experiments to include the pole parametrization as one of their choices [9].

The ‘‘Kaon Particle Listings’’ show the results with and without assuming $\mu - e$ universality. The ‘‘Meson Summary Tables’’ show all of the results assuming $\mu - e$ universality, but most results not assuming $\mu - e$ universality are given only in the Listings.

References

1. L.M. Chounet, J.M. Gaillard, and M.K. Gaillard, Phys. Reports **4C**, 199 (1972).
2. H.W. Fearing, E. Fischbach, and J. Smith, Phys. Rev. **D2**, 542 (1970).
3. N. Cabibbo and A. Maksymowicz, Phys. Lett. **9**, 352 (1964).
4. W.-M. Yao *et al.*, Particle Data Group, J. Phys. **G33**, 1 (2006).
5. S. Eidelman *et al.*, Particle Data Group, Phys. Lett. **B592**, 1 (2004).

6. M. Roos *et al.*, Particle Data Group, Phys. Lett. **111B**, 73 (1982).
7. V. Bernard *et al.*, Phys. Lett. **B638**, 48 (2006).
8. A. Lai *et al.*, Phys. Lett. **B647**, 341 (2007), and references therein.
9. We thank P. Franzini (Rome U. and Frascati) for useful discussions on this point.

K_{e3}^\pm FORM FACTORS

In the form factor comments, the following symbols are used.

f_+ and f_- are form factors for the vector matrix element.

f_S and f_T refer to the scalar and tensor term.

$f_0 = f_+ + f_- t/(m_{K^\pm}^2 - m_{\pi^0}^2)$.

t = momentum transfer to the π .

λ_+ and λ_0 are the linear expansion coefficients of f_+ and f_0 :

$f_+(t) = f_+(0) (1 + \lambda_+ t/m_{\pi^\pm}^2)$

For quadratic expansion

$f_+(t) = f_+(0) (1 + \lambda'_+ t/m_{\pi^\pm}^2 + \frac{\lambda''_+}{2} t^2/m_{\pi^\pm}^4)$

as used by KTeV. If there is a non-vanishing quadratic term, then λ_+ represents an average slope, which is then different from λ'_+ .

NA48 and ISTRA quadratic expansion coefficients are converted with $\lambda'_+{}^{PDG} = \lambda_+{}^{NA48}$ and $\lambda''_+{}^{PDG} = 2\lambda'_+{}^{NA48}$

$\lambda'_+{}^{PDG} = (\frac{m_{\pi^\pm}}{m_{\pi^0}})^2 \lambda_+{}^{ISTRA}$ and

$\lambda''_+{}^{PDG} = 2(\frac{m_{\pi^\pm}}{m_{\pi^0}})^4 \lambda'_+{}^{ISTRA}$

ISTRA linear expansion coefficients are converted with $\lambda_+{}^{PDG} = (\frac{m_{\pi^\pm}}{m_{\pi^0}})^2 \lambda_+{}^{ISTRA}$ and $\lambda_0{}^{PDG} = (\frac{m_{\pi^\pm}}{m_{\pi^0}})^2 \lambda_0{}^{ISTRA}$

The pole parametrization is

$f_+(t) = f_+(0) (\frac{M_V^2}{M_V^2 - t})$

$f_0(t) = f_0(0) (\frac{M_S^2}{M_S^2 - t})$

where M_V and M_S are the vector and scalar pole masses.

The following abbreviations are used:

DP = Dalitz plot analysis.

PI = π spectrum analysis.

MU = μ spectrum analysis.

POL = μ polarization analysis.

BR = $K_{\mu 3}^\pm/K_{e3}^\pm$ branching ratio analysis.

E = positron or electron spectrum analysis.

RC = radiative corrections.

λ_+ (LINEAR ENERGY DEPENDENCE OF f_+ IN K_{e3}^\pm DECAY)

These results are for a linear expansion only. See the next section for fits including a quadratic term. For radiative correction of the K_{e3}^\pm Dalitz plot, see GINSBERG 67, BECHERRAWY 70, CIRIGLIANO 02, CIRIGLIANO 04, and ANDRE 04. Results labeled OUR FIT are discussed in the review ‘‘ K_{e3}^\pm and $K_{\mu 3}^0$ Form Factors’’ above. For earlier, lower statistics results, see the 2004 edition of this review, Physics Letters **B592** 1 (2004).

VALUE (units 10^{-2})	EVTS	DOCUMENT ID	TECN	CHG	COMMENT
2.96 ± 0.06 OUR FIT	Assuming $\mu - e$ universality				
2.96 ± 0.06 OUR AVERAGE					
2.96 ± 0.050 ± 0.034	919k	100 YUSHCHENKO04B	ISTR	—	DP
2.78 ± 0.26 ± 0.30	41k	SHIMIZU 00	SPEC	+	DP
2.84 ± 0.27 ± 0.20	32k	101 AKIMENKO 91	SPEC	PI, no RC	
2.9 ± 0.4	62k	102 BOLOTOV 88	SPEC	PI, no RC	
• • •	We do not use the following data for averages, fits, limits, etc. • • •				
3.06 ± 0.09 ± 0.06	550k	100,103 AJINENKO 03c	ISTR	—	DP
2.93 ± 0.15 ± 0.2	130k	103 AJINENKO 02	SPEC		DP
100	Rescaled to agree with our conventions as noted above.				
101	AKIMENKO 91 state that radiative corrections would raise λ_+ by 0.0013.				
102	BOLOTOV 88 state radiative corrections of GINSBERG 67 would raise λ_+ by 0.002.				
103	Superseded by YUSHCHENKO 04B.				

λ_+ (LINEAR ENERGY DEPENDENCE OF f_+ IN $K_{\mu 3}^\pm$ DECAY)

Results labeled OUR FIT are discussed in the review ‘‘ K_{e3}^\pm and $K_{\mu 3}^0$ Form Factors’’ above. For earlier, lower statistics results, see the 2004 edition of this review, Physics Letters **B592** 1 (2004).

VALUE (units 10^{-2})	EVTS	DOCUMENT ID	TECN	CHG	COMMENT
2.96 ± 0.06 OUR FIT	Assuming $\mu - e$ universality				
2.96 ± 0.17 OUR FIT	Not assuming $\mu - e$ universality				
2.96 ± 0.14 ± 0.10	540k	104 YUSHCHENKO04	ISTR	—	DP
• • •	We do not use the following data for averages, fits, limits, etc. • • •				
3.21 ± 0.45	112k	105 AJINENKO 03	ISTR	—	DP

¹⁰⁴ Rescaled to agree with our conventions as noted above.

¹⁰⁵ Superseded by YUSHCHENKO 04.

λ_0 (LINEAR ENERGY DEPENDENCE OF f_0 IN $K_{\mu 3}^\pm$ DECAY)

Results labeled OUR FIT are discussed in the review " $K_{\mu 3}^\pm$ and $K_{\mu 3}^0$ Form Factors" above. For earlier, lower statistics results, see the 2004 edition of this review, Physics Letters **B592** 1 (2004).

VALUE (units 10^{-2})	$d\lambda_0/d\lambda_+$	EVTS	DOCUMENT ID	TECN	CHG	COMMENT
1.96 ± 0.12 OUR FIT	Assuming μ -e universality					
1.96 ± 0.13 OUR FIT	Not assuming μ -e universality					
+1.96 ± 0.12 ± 0.06	-0.348	540k	¹⁰⁶ YUSHCHENKO04	ISTR	-	DP
••• We do not use the following data for averages, fits, limits, etc. •••						
+2.09 ± 0.45	-0.46	112k	¹⁰⁷ AJINENKO	03	ISTR	- DP
+1.9 ± 0.64		24k	¹⁰⁸ HORIE	01	SPEC	+ BR
+1.9 ± 1.0	+0.03	55k	¹⁰⁹ HEINTZE	77	SPEC	+ BR

¹⁰⁶ Rescaled to agree with our conventions as noted above.
¹⁰⁷ Superseded by YUSHCHENKO 04.
¹⁰⁸ HORIE 01 assumes μ -e universality in $K_{\mu 3}^\pm$ decay and uses SHIMIZU 00 value $\lambda = 0.0278 \pm 0.0040$ from $K_{e 3}^\pm$ decay.
¹⁰⁹ HEINTZE 77 uses $\lambda_+ = 0.029 \pm 0.003$. $d\lambda_0/d\lambda_+$ estimated by us.

λ_+^+ (LINEAR $K_{e 3}^\pm$ FORM FACTOR FROM QUADRATIC FIT)

VALUE (units 10^{-2})	EVTS	DOCUMENT ID	TECN	CHG	COMMENT
2.485 ± 0.163 ± 0.034	919k	110,111 YUSHCHENKO04B	ISTR	-	DP
••• We do not use the following data for averages, fits, limits, etc. •••					
3.07 ± 0.21	550k	110,112 AJINENKO	03c	ISTR	- DP

¹¹⁰ Rescaled to agree with our conventions as noted above.
¹¹¹ YUSHCHENKO 04B λ_+^+ and λ_+'' are strongly correlated with coefficient $\rho(\lambda_+^+, \lambda_+''+) = -0.95$.
¹¹² Superseded by YUSHCHENKO 04B.

λ_+'' (QUADRATIC $K_{e 3}^\pm$ FORM FACTOR)

VALUE (units 10^{-2})	EVTS	DOCUMENT ID	TECN	CHG	COMMENT
0.192 ± 0.062 ± 0.071	919k	113,114 YUSHCHENKO04B	ISTR	-	DP
••• We do not use the following data for averages, fits, limits, etc. •••					
-0.5 ± 0.7 ± 1.5	550k	113,115 AJINENKO	03c	ISTR	- DP

¹¹³ Rescaled to agree with our conventions as noted above.
¹¹⁴ YUSHCHENKO 04B λ_+^+ and λ_+'' are strongly correlated with coefficient $\rho(\lambda_+^+, \lambda_+''+) = -0.95$.
¹¹⁵ Superseded by YUSHCHENKO 04B.

$|f_S/f_+|$ FOR $K_{e 3}^\pm$ DECAY

Ratio of scalar to f_+ couplings.

VALUE (units 10^{-2})	CL%	EVTS	DOCUMENT ID	TECN	CHG	COMMENT
-0.3 ± 0.8 OUR AVERAGE						
-0.37 ± 0.66 ± 0.41		919k	YUSHCHENKO04B	ISTR	-	λ_+^+ , λ_+'' , f_S fit
0.2 ± 2.6 ± 1.4		41k	SHIMIZU	00	SPEC	+ λ_+ , f_S , f_T fit
••• We do not use the following data for averages, fits, limits, etc. •••						
0.2 ± 2.0 ± 2.2 ± 0.3		550k	¹¹⁶ AJINENKO	03c	ISTR	- λ_+ , f_S , f_T fit
-1.9 ± 2.5 ± 1.6		130k	¹¹⁶ AJINENKO	02	SPEC	λ_+ , f_S fit
7.0 ± 1.6 ± 1.6		32k	AKIMENKO	91	SPEC	λ_+ , f_S , f_T , ϕ fit
0 ± 10		2827	¹¹⁷ BRAUN	75	HLBC	+
< 13		90	4017 CHIANG	72	OSPK	+
14 ± 3 ± 4		2707	¹¹⁷ STEINER	71	HLBC	+ λ_+ , f_S , f_T , ϕ fit
< 23		90	BOTTERILL	68c	ASPK	
< 18		90	BELLOTTI	67b	HLBC	
< 30		95	KALMUS	67	HLBC	+

¹¹⁶ Superseded by YUSHCHENKO 04B.
¹¹⁷ Statistical errors only.

$|f_T/f_+|$ FOR $K_{e 3}^\pm$ DECAY

Ratio of tensor to f_+ couplings.

VALUE (units 10^{-2})	CL%	EVTS	DOCUMENT ID	TECN	CHG	COMMENT
-1.2 ± 2.3 OUR AVERAGE						
-1.2 ± 2.1 ± 1.1		919k	YUSHCHENKO04B	ISTR	-	λ_+^+ , λ_+'' , f_T fit
1 ± 14 ± 9		41k	SHIMIZU	00	SPEC	+ λ_+ , f_S , f_T fit
••• We do not use the following data for averages, fits, limits, etc. •••						
2.1 ± 6.4 ± 7.5 ± 2.6		550k	¹¹⁸ AJINENKO	03c	ISTR	- λ_+ , f_S , f_T fit
-4.5 ± 6.0 ± 5.7		130k	¹¹⁸ AJINENKO	02	SPEC	λ_+ , f_T fit
53 ± 9 ± 10		32k	AKIMENKO	91	SPEC	λ_+ , f_S , f_T , ϕ fit
7 ± 37		2827	¹¹⁹ BRAUN	75	HLBC	+
< 75		90	4017 CHIANG	72	OSPK	+
24 ± 16 ± 14		2707	¹¹⁹ STEINER	71	HLBC	+ λ_+ , f_S , f_T , ϕ fit
< 58		90	BOTTERILL	68c	ASPK	
< 58		90	BELLOTTI	67b	HLBC	
< 110		95	KALMUS	67	HLBC	+

¹¹⁸ Superseded by YUSHCHENKO 04B.
¹¹⁹ Statistical errors only.

f_S/f_+ FOR $K_{\mu 3}^\pm$ DECAY

Ratio of scalar to f_+ couplings.

VALUE (units 10^{-2})	EVTS	DOCUMENT ID	TECN	CHG	COMMENT
0.17 ± 0.14 ± 0.54	540k	¹²⁰ YUSHCHENKO04	ISTR	-	DP
••• We do not use the following data for averages, fits, limits, etc. •••					
0.4 ± 0.5 ± 0.5	112k	¹²¹ AJINENKO	03	ISTR	- DP

¹²⁰ The second error is the theoretical error from the uncertainty in the chiral perturbation theory prediction for λ_0 , ± 0.0053 , combined in quadrature with the systematic error ± 0.0009 .

¹²¹ The second error is the theoretical error from the uncertainty in the chiral perturbation theory prediction for λ_0 . Superseded by YUSHCHENKO 04.

f_T/f_+ FOR $K_{\mu 3}^\pm$ DECAY

Ratio of tensor to f_+ couplings.

VALUE (units 10^{-2})	EVTS	DOCUMENT ID	TECN	CHG	COMMENT
-0.07 ± 0.71 ± 0.20	540k	YUSHCHENKO04	ISTR	-	DP
••• We do not use the following data for averages, fits, limits, etc. •••					
-2.1 ± 2.8 ± 1.4	112k	¹²² AJINENKO	03	ISTR	- DP
2 ± 12	1585	BRAUN	75	HLBC	

¹²² The second error is the theoretical error from the uncertainty in the chiral perturbation theory prediction for λ_0 . Superseded by YUSHCHENKO 04.

DECAY FORM FACTORS FOR $K^\pm \rightarrow \pi^+ \pi^- e^\pm \nu_e$

Given in PISLAK 01, ROSSELET 77, BEIER 73, and BASILE 71c.

DECAY FORM FACTOR FOR $K^\pm \rightarrow \pi^0 \pi^0 e^\pm \nu_e$

Given in BOLOTOV 86B, BARMIN 88B, and SHIMIZU 04.

$K^\pm \rightarrow \ell^\pm \nu \gamma$ FORM FACTORS

For definitions of the axial-vector F_A and vector F_V form factor, see the "Note on $\pi^\pm \rightarrow \ell^\pm \nu \gamma$ and $K^\pm \rightarrow \ell^\pm \nu \gamma$ Form Factors" in the π^\pm section. In the kaon literature, often different definitions $a_K = F_A/m_K$ and $v_K = F_V/m_K$ are used.

$F_A + F_V$, SUM OF AXIAL-VECTOR AND VECTOR FORM FACTOR FOR $K \rightarrow e \nu_e \gamma$

VALUE	EVTS	DOCUMENT ID	TECN
0.148 ± 0.010 OUR AVERAGE			
0.147 ± 0.011	51	¹²³ HEINTZE	79 SPEC
0.150 ± 0.018 ± 0.023	56	¹²⁴ HEARD	75 SPEC

¹²³ HEINTZE 79 quotes absolute value of $|F_A + F_V| \sin \theta_c$. We use $\sin \theta_c = V_{US} = 0.2205$.

¹²⁴ HEARD 75 quotes absolute value of $|F_A + F_V| \sin \theta_c$. We use $\sin \theta_c = V_{US} = 0.2205$.

$F_A + F_V$, SUM OF AXIAL-VECTOR AND VECTOR FORM FACTOR FOR $K \rightarrow \mu \nu \mu \gamma$

VALUE	CL%	EVTS	DOCUMENT ID	TECN	CHG
0.165 ± 0.007 ± 0.011		2588	¹²⁵ ADLER	00b	B787 +
••• We do not use the following data for averages, fits, limits, etc. •••					
-1.2 to 1.1		90	DEMIDOV	90	XEBC
< 0.23		90	¹²⁵ AKIBA	85	SPEC

¹²⁵ Quotes absolute value. Sign not determined.

$F_A - F_V$, DIFFERENCE OF AXIAL-VECTOR AND VECTOR FORM FACTOR FOR $K \rightarrow e \nu_e \gamma$

VALUE	EVTS	DOCUMENT ID	TECN
< 0.49	90	¹²⁶ HEINTZE	79 SPEC

¹²⁶ HEINTZE 79 quotes $|F_A - F_V| < \sqrt{11} |F_A + F_V|$.

$F_A - F_V$, DIFFERENCE OF AXIAL-VECTOR AND VECTOR FORM FACTOR FOR $K \rightarrow \mu \nu \mu \gamma$

VALUE	CL%	EVTS	DOCUMENT ID	TECN	CHG
-0.24 to 0.04		90	2588 ADLER	00b	B787 +
••• We do not use the following data for averages, fits, limits, etc. •••					
-2.2 to 0.6		90	DEMIDOV	90	XEBC
-2.5 to 0.3		90	AKIBA	85	SPEC

K^\pm CHARGE RADIUS

VALUE (fm)	DOCUMENT ID	COMMENT
0.560 ± 0.031 OUR AVERAGE		
0.580 ± 0.040	AMENDOLIA	86B $Ke \rightarrow Ke$
0.530 ± 0.050	DALLY	80 $Ke \rightarrow Ke$
••• We do not use the following data for averages, fits, limits, etc. •••		
0.620 ± 0.037	BLATNIK	79 VMD + dispersion relations

CP VIOLATION TESTS IN K^+ AND K^- DECAYS

$$\Delta(K_{\pi\mu\mu}^\pm) = \frac{\Gamma(K_{\pi\mu\mu}^+) - \Gamma(K_{\pi\mu\mu}^-)}{\Gamma(K_{\pi\mu\mu}^+) + \Gamma(K_{\pi\mu\mu}^-)}$$

VALUE	DOCUMENT ID	TECN
-0.02 ± 0.11 ± 0.04	PARK	02 HYCP

Meson Particle Listings

 K^\pm T VIOLATION TESTS IN K^+ AND K^- DECAYS P_T in $K^+ \rightarrow \pi^0 \mu^+ \nu_\mu$

T-violating muon polarization. Sensitive to new sources of CP violation beyond the Standard Model.

VALUE (units 10^{-3})	EVTS	DOCUMENT ID	TECN	CHG
$-1.7 \pm 2.3 \pm 1.1$	127	ABE	04F	K246 +
••• We do not use the following data for averages, fits, limits, etc. •••				
$-4.2 \pm 4.9 \pm 0.9$	3.9M	ABE	99s	K246 +

127 Includes three sets of data: 96-97 (ABE 99s), 98, and 99-00 totaling about three times the ABE 99s data sample. Corresponds to $P_T < 5.0 \times 10^{-3}$ at 90% CL.

 P_T in $K^+ \rightarrow \mu^+ \nu_\mu \gamma$

T-violating muon polarization. Sensitive to new sources of CP violation beyond the Standard Model.

VALUE (units 10^{-2})	EVTS	DOCUMENT ID	TECN	CHG
$-0.64 \pm 1.85 \pm 0.10$	114k	128 ANISIMOVSK...03	K246	+

128 Muons stopped and polarization measured from decay to positrons.

 $\text{Im}(\xi)$ in $K^+ \rightarrow \pi^0 \mu^+ \nu_\mu$ DECAY (from transverse μ pol.)

Test of T reversal invariance.

VALUE	EVTS	DOCUMENT ID	TECN	CHG	COMMENT
-0.006 ± 0.008	OUR AVERAGE				
$-0.0053 \pm 0.0071 \pm 0.0036$	129	ABE	04F	K246	+
-0.016 ± 0.025	20M	CAMPBELL	81	CNTR	+ Pol.
••• We do not use the following data for averages, fits, limits, etc. •••					
$-0.013 \pm 0.016 \pm 0.003$	3.9M	ABE	99s	CNTR	+ $P_T K^+$ at rest

129 Includes three sets of data: 96-97 (ABE 99s), 98, and 99-00 totaling about three times the ABE 99s data sample. Corresponds to $\text{Im}(\xi) < 0.016$ at 90% CL.

 K^\pm REFERENCES

AMBROSINO 08	JHEP 0801 073	F. Ambrosino et al.	(KLOE Collab.)
AMBROSINO 08A	JHEP 0802 098	F. Ambrosino et al.	(KLOE Collab.)
BATLEY 08	PL B659 493	J.R. Batley et al.	(CERN NA48/2 Collab.)
AKIMENKO 07	PAN 70 702	S.A. Akimenko et al.	(ISTRA+ Collab.)
BATLEY 07A	Translated from YAF 70 734.	J.R. Batley et al.	(CERN NA48/2 Collab.)
Also	EPJ C50 329	J.R. Batley et al.	(CERN NA48/2 Collab.)
BATLEY 07B	PL B649 349	J.R. Batley et al.	(CERN NA48/2 Collab.)
BATLEY 07E	EPJ C52 875	J.R. Batley et al.	(CERN NA48/2 Collab.)
TCHIKILEV 07	PAN 70 29	O.G. Tchikilev et al.	(ISTRA+ Collab.)
ALIEV 06	EPJ C46 61	M.A. Aliev et al.	(KEK E470 Collab.)
AMBROSINO 06A	PL B632 76	F. Ambrosino et al.	(KLOE Collab.)
BATLEY 06	PL B634 474	J.R. Batley et al.	(CERN NA48/2 Collab.)
BATLEY 06A	PL B638 22	J.R. Batley et al.	(CERN NA48/2 Collab.)
Also	PL B640 297 (erratum)	J.R. Batley et al.	(CERN NA48/2 Collab.)
BATLEY 06B	PL B633 173	J.R. Batley et al.	(CERN NA48/2 Collab.)
MA 06	PR D73 037101	H. Ma et al.	(BNL E246 Collab.)
PDG 06	JPG 33 1	W.-M. Yao et al.	(PDG Collab.)
SHIMIZU 06	PL B633 190	S. Shimizu et al.	(KEK E470 Collab.)
UVAROV 06	PAN 69 26	V.A. Uvarov et al.	(ISTRA+ Collab.)
AKOPDZHAN...05	EPJ C40 343	G.A. Akopdzhyanov et al.	(IHEP Collab.)
Also	PAN 68 948	G.A. Akopdzhyanov et al.	(IHEP Collab.)
AKOPDZHAN...05B	JETPL 82 875	G.A. Akopdzhyanov et al.	(IHEP Collab.)
Also	Translated from ZETFP 82 771.		
ARTAMONOV 05	PL B623 192	V.Y. Artamonov et al.	(BNL E949 Collab.)
CABIBBO 05	JHEP 0503 021	N. Cabibbo, G. Isidori	(CERN, ROMAI, FRAS)
SHER 05	PR D72 012005	A. Sher et al.	(BNL E865 Collab.)
ABE 04F	PL R3 131601	M. Abe et al.	(KEK E246 Collab.)
Also	PR D73 072005	M. Abe et al.	(KEK E246 Collab.)
ADLER 04	PR D70 037102	S. Adler et al.	(BNL E787 Collab.)
ALOISIO 04A	PL B597 139	A. Aloisio et al.	(KLOE Collab.)
ANDRE 04	hep-ph/0406006	T. Andre	(EFI Collab.)
ANISIMOVSK...04	PRL 93 031801	V.V. Anisimovskiy et al.	(BNL E949 Collab.)
CABIBBO 04A	PRL 93 121801	N. Cabibbo	(CERN, ROMAI)
CIRIGLIANO 04	EPJ C35 53	S. Cirigliano, H. Neufeld, H. Pichl	(CIT, VALE+)
PDG 04	PL B592 1	V. Eidelman et al.	(PDG Collab.)
SHIMIZU 04	PR D70 037101	S. Shimizu et al.	(KEK E470 Collab.)
YUSHCHEENKO 04	PL B581 31	O.P. Yushchenko et al.	(INRM, INRM)
YUSHCHEENKO 04B	PL B589 111	O.P. Yushchenko et al.	(INRM)
AJINENKO 03	PAN 66 105	I.V. Ajinenko et al.	(IHEP, INRM)
Also	Translated from YAF 66 107.		
AJINENKO 03B	PL B567 159	I.V. Ajinenko et al.	(IHEP, INRM)
AJINENKO 03C	PL B574 14	I.V. Ajinenko et al.	(IHEP, INRM)
ALIEV 03	PL B554 7	M.A. Aliev et al.	(KEK E470 Collab.)
ANISIMOVSK...03	PL B562 166	V.V. Anisimovskiy et al.	(BNL E865 Collab.)
PISLAK 03	PR D67 072004	S. Pislak et al.	(BNL E865 Collab.)
SHER 03	PRL 91 261802	A. Sher et al.	(BNL E865 Collab.)
ADLER 02	PRL 88 041803	S. Adler et al.	(BNL E787 Collab.)
ADLER 02B	PR D65 052009	S. Adler et al.	(BNL E787 Collab.)
ADLER 02C	PL B537 211	S. Adler et al.	(BNL E787 Collab.)
AJINENKO 02	PAN 65 2064	I.V. Ajinenko et al.	(IHEP, INRM)
Also	Translated from YAF 65 2125.		
CIRIGLIANO 02	EPJ C23 121	V. Cirigliano et al.	(VIEN, VALE, MARS)
PARK 02	PRL 88 111801	H.K. Park et al.	(FNAL HyperCP Collab.)
PDG 02	PR D66 010001	K. Hagiwara et al.	(PDG Collab.)
POBLAGUEV 02	PRL 89 061803	A.A. Poblaguev et al.	(BNL E865 Collab.)
ADLER 01	PR D63 032004	S. Adler et al.	(BNL E787 Collab.)
HORIE 01	PL B513 311	K. Horie et al.	(KEK E426 Collab.)
PISLAK 01	PRL 87 221801	S. Pislak et al.	(BNL E865 Collab.)
Also	PR D67 072004	S. Pislak et al.	(BNL E865 Collab.)
ADLER 00	PRL 84 3768	S. Adler et al.	(BNL E787 Collab.)
ADLER 00B	PRL 85 2256	S. Adler et al.	(BNL E787 Collab.)
ADLER 00C	PRL 85 4856	S. Adler et al.	(BNL E787 Collab.)
APPEL 00	PRL 85 2450	R. Appel et al.	(BNL E865 Collab.)
Also	Thesis, Yale Univ.	D.R. Bergman	
Also	Thesis, Univ. Zurich	S. Pislak	
APPEL 00B	PRL 85 2877	R. Appel et al.	(BNL E865 Collab.)
MA 00	PRL 84 2580	H. Ma et al.	(BNL E865 Collab.)
PDG 00	EPJ C15 1	D.E. Groom et al.	(PDG Collab.)
SHIMIZU 00	PL B495 33	S. Shimizu et al.	(KEK E246 Collab.)
ABE 99S	PRL 83 4253	M. Abe et al.	(KEK E246 Collab.)
APPEL 99	PRL 83 4482	R. Appel et al.	(BNL E865 Collab.)
ADLER 98	PR D58 012003	S. Adler et al.	(BNL E787 Collab.)
BATUSOV 98	NP B516 3	V.Y. Batusov et al.	(BNL E787 Collab.)
ADLER 97	PRL 79 2204	S. Adler et al.	(BNL E787 Collab.)
ADLER 97C	PRL 79 4756	S. Adler et al.	(BNL E787 Collab.)

BERGMAN 97	Thesis, Yale Univ.	D.R. Bergman	
KITCHING 97	PRL 79 4079	P. Kitching et al.	(BNL E787 Collab.)
PISLAK 97	Thesis, Univ. Zurich	S. Pislak	
ADLER 96	PRL 76 1421	S. Adler et al.	(BNL E787 Collab.)
KOPTEV 95	JETPL 61 877	V.P. Kopiev et al.	(PNPI)
Also	Translated from ZETFP 61 865.		
AOKI 94	PR D50 69	M. Aoki et al.	(INUS, KEK, TOKMS)
ATIYA 93	PRL 70 2521	M.S. Atiya et al.	(BNL E787 Collab.)
Also	PRL 71 305 (erratum)	M.S. Atiya et al.	(BNL E787 Collab.)
ATIYA 93B	PR D48 R1	M.S. Atiya et al.	(BNL E787 Collab.)
ALLIEGRO 92	PRL 68 278	C. Alliegro et al.	(BNL, FNAL, PSI+)
BARMIN 92	SJNP 55 547	V.V. Barmin et al.	(ITEP)
Also	Translated from YAF 55 976.		
IMAZATO 92	PRL 69 877	J. Imazato et al.	(KEK, INUS, TOKY+)
IVANOV 92	THEISIS	Yu.M. Ivanov	(PNPI)
LITTENBERG 92	PR 68 443	L.S. Littenberg, R.E. Shrock	(BNL, ST-ON)
USHER 92	PR D45 3961	T. Usher et al.	(UCI)
AKIMENKO 91	PL B259 225	S.A. Akimenko et al.	(SERP, JINR, TBI+)
BARMIN 91	SJNP 53 606	V.V. Barmin et al.	(ITEP)
Also	Translated from YAF 53 981.		
DENISOV 91	JETPL 54 558	A.S. Denisov et al.	(PNPI)
Also	THEISIS	Yu.M. Ivanov	(PNPI)
ATIYA 90	PRL 64 21	M.S. Atiya et al.	(BNL E787 Collab.)
ATIYA 90B	PRL 65 1188	M.S. Atiya et al.	(BNL E787 Collab.)
DEMIDOV 90	SJNP 52 1006	V.S. Demidov et al.	(ITEP)
Also	Translated from YAF 52 1595.		
LEE 90	PRL 64 165	A.M. Lee et al.	(BNL, FNAL, VILL, WAS H+)
ATIYA 89	PRL 63 2177	M.S. Atiya et al.	(BNL E787 Collab.)
BARMIN 89	SJNP 50 421	V.V. Barmin et al.	(ITEP)
Also	Translated from YAF 50 678.		
BARMIN 88	SJNP 47 643	V.V. Barmin et al.	(ITEP)
BARMIN 88B	SJNP 48 1032	V.V. Barmin et al.	(ITEP)
Also	Translated from YAF 48 1719.		
BOLOTOV 88	JETPL 47 7	V.N. Bolotov et al.	(ASCI)
Also	Translated from ZETFP 47 8		
GALL 88	PRL 60 186	K.P. Gall et al.	(BOST, MIT, WILL, CIT+)
BARMIN 87	SJNP 45 62	V.V. Barmin et al.	(ITEP)
Also	Translated from YAF 45 97.		
BOLOTOV 87	SJNP 45 1023	V.N. Bolotov et al.	(INRM)
Also	Translated from YAF 45 1652.		
AMENDOLIA 86B	PL B178 435	S.R. Amendolia et al.	(CERN NA7 Collab.)
BOLOTOV 86	SJNP 43 73	V.N. Bolotov et al.	(INRM)
Also	Translated from YAF 44 117.		
BOLOTOV 86B	SJNP 44 68	V.N. Bolotov et al.	(INRM)
Also	Translated from YAF 44 108.		
YAMANAKA 86	PR D34 85	T. Yamanaka et al.	(KEK, TOKY)
Also	PRL 52 329	R.S. Hayano et al.	(TOKY, KEK)
AKIBA 85	PR D32 2911	Y. Akiba et al.	(TOKY, TINT, TSUK, KEK)
BOLOTOV 85	JETPL 42 481	V.N. Bolotov et al.	(INRM)
Also	Translated from ZETFP 42 390.		
ASANO 82	PL 113B 195	Y. Asano et al.	(KEK, TOKY, INUS, OSAK)
COOPER 82	PL 112B 97	A.M. Cooper et al.	(RL)
PDG 82B	PL 111B 70	M. Roos et al.	(HEL5, CIT, CERN)
ASANO 81B	PL 107B 159	Y. Asano et al.	(KEK, TOKY, INUS, OSAK)
CAMPBELL 81	PRL 47 1032	M.K. Campbell et al.	(VALE, BNL)
Also	PR D27 1056	S.R. Blatt et al.	(YALE, BNL)
LUM 81	PR D23 2522	G.K. Lum et al.	(LBL, NBS+)
LYONS 81	ZPHY C10 215	L. Lyons, C. Albajar, G. Myatt	(CERN, UA1)
DALLY 80	DALY 45 232	D. Dally et al.	(CERN, UA1)
BARKOV 79	NP B148 53	S.L. Barkov et al.	(NOVO, KIAE)
BLATNIK 79	LNC 24 39	B. Blatnik, J. Stahov, C.B. Lang	(TUZL, GRAZ)
HEINTZE 79	NP B149 365	J. Heintze et al.	(HEIDP, CERN)
ABRAMS 77	PR D15 22	R.J. Abrams et al.	(BNL)
DEVAUX 77	NP B126 11	B. Devaux et al.	(SACL, GEVA)
HEINTZE 77	PL 70B 482	J. Heintze et al.	(HEIDP, CERN)
ROSSELET 77	PR D15 574	L. Rosselet et al.	(GEVA, SACL)
BLOCH 76	PL 60B 393	P. Bloch et al.	(GEVA, SACL)
BRAUN 76B	LNC 17 521	H.M. Braun et al.	(AACH3, BARI, BELG+)
DIAMANT... 76	PL 62B 485	A.M. Diamant-Berger et al.	(SACL, GEVA)
HEINTZE 76	PL 60B 302	J. Heintze et al.	(HEIDP)
SMITH 76	NP B109 173	K.M. Smith et al.	(GLAS, LIVP, OXF+)
WEISSENBERG... 76	NP B115 55	A.O. Weissenberg et al.	(ITEP, LEDB)
BLOCH 75	PL 56B 201	P. Bloch et al.	(SACL, GEVA)
BRAUN 75	NP B89 210	H.M. Braun et al.	(AACH3, BARI, BRUX+)
CHENG 75	NP A254 381	S.C. Cheng et al.	(COLU, YALE)
HEARD 75	PL 55B 324	K.S. Heard et al.	(CERN, HEID)
HEARD 75B	PL 55B 327	K.S. Heard et al.	(CERN, HEID)
SHEAFF 75	PR D12 2570	M. Sheaff et al.	(WIS C)
SMITH 75	NP B91 45	K.M. Smith et al.	(GLAS, LIVP, OXF+)
WEISSENBERG... 74	PL 48B 474	A.O. Weissenberg et al.	(ITEP, LEDB)
ABRAMS 73B	PL 30 600	R.J. Abrams et al.	(BNL)
BACKENSTOSS... 73	PL 43B 431	G. Backenstoss et al.	(CERN, KARLK, KARLE+)
BEIER 73	PR 30 399	E.W. Beier et al.	(PENN)
LUJUNG 73	PR D8 1307	D. Ljung, D. Cline	(WIS C)
Also	PRL 28 523	D. Ljung	(WIS C)
Also	PRL 28 1287	D. Cline, D. Ljung	(WIS C)
Also	PRL 23 326	U. Camerini et al.	(WIS C)
LUCAS 73	PR D8 719	P.W. Lucas, H.D. Taft, W.J. Willis	(YALE)
LUCAS 73B	PR D8 727	P.W. Lucas, H.D. Taft, W.J. Willis	(YALE)
PANG 73	PR D8 1989	C.Y. Pang et al.	(EFI, LBL, LBL)
Also	PL 40B 699	G.D. Cable et al.	(EFI, LBL)
SMITH 73	NP B60 411	K.M. Smith et al.	(GLAS, LIVP, OXF+)
ABRAMS 72	PRL 29 1118	R.J. Abrams et al.	(GLAS, LIVP, OXF+)
ALBERT 72	NC 12A 509	B. Aubert et al.	(ORSAY, BRUX, EPOL)
CHIANG 72	PR D6 1254	I.H. Chiang et al.	(ROCH, WIS C)
CLARK 72	PRL 29 1274	A.R. Clark et al.	(LBL)
EDWARDS 72	PR D5 2720	R.T. Edwards et al.	(ILL)
FORD 72	PL 38B 335	W.T. Ford et al.	(PRIN)
HOFFMASTER 72	NP B36 1	S. Hoffmaster et al.	(STEV, SETO, LEHI)
BASEL 71C	PL 36B 619	P. Basile et al.	(SACL, GEVA)
BOURQUIN 71	PL 36B 615	M.H. Bourquin et al.	(GEVA, SACL)
HAIDI 71	PR D3 10	D. Haidt et al.	(AACH, BARI, CERN, EPOL+)
Also	PR D3 10	(AACH, BARI, CERN, EPOL+)	
KLEMS 71	PR D4 66	J.H. Klems, R.H. Hildebrand, R. Stiening	(CHIC+)
Also	PRL 24 1086	J.H. Klems, R.H. Hildebrand, R. Stiening	(CHIC+)
Also	PRL 25 473	J.H. Klems, R.H. Hildebrand, R. Stiening	(LRL+)
OTT 71	PR D3 52	R.J. Ott, T.W. Pritchard	(LOQM)
ROMANO 71	PL 36B 525	F. Romano et al.	(BARI, CERN, ORSAY)
SCHWEINBERG... 71	PL 36B 246	W. Schweinberger	(AACH, BELG, CERN, NIJM+)
STEINER 71	PL 36B 521	H.J. Steiner	(AACH, BARI, CERN, EPOL, ORSAY+)
BARDIN 70	PL 32B 121	D.Y. Bardin, S.N. Bilenky, B.M. Pontecorno	(JINR)
BECHERRAWY 70	PR D1 1452	T. Becherrawy	(ROCH)
FORD 70	PR D1 137		

PANDOLAS 70 PR D2 1205	D. Pandoulas et al.	(STEV, SETO)
CUTTS 69 PR 184 1380	D. Cutts et al.	(LRL, MIT)
Also PRL 20 955	D. Cutts et al.	(LRL, MIT)
DAVISON 69 PR 180 1333	D.C. Davison et al.	(UCR)
ELY 69 PR 180 1319	R.P.J. Ely et al.	(LOUC, WISC, LRL)
EMMERSON 69 PRL 23 393	J.M.L. Emmerson, T.W. Quirk	(OXF)
HERZO 69 PR 186 1403	D. Herzo et al.	(ILL)
LOBKOWICZ 69 PR 185 1576	F. Lobkowicz et al.	(ROCH, BNL)
Also PRL 17 548	F. Lobkowicz et al.	(ROCH, BNL)
MAST 69 PR 183 1200	T.S. Mast et al.	(LRL)
SELLERI 69 NC 60A 291	F. Selleri	
ZELLER 69 PR 182 1420	M.E. Zeller et al.	(UCLA, LRL)
BOTTERILL 68B PRL 21 766	D.R. Botterill et al.	(OXF)
BOTTERILL 68C PR 174 1661	D.R. Botterill et al.	(OXF)
BUTLER 68 UCRL 18420	W.D. Butler et al.	(LRL)
CHANG 68 PRL 20 510	C.Y. Chang et al.	(UMD, RUTG)
CHEN 68 PRL 20 73	M. Chen et al.	(LRL, MIT)
EICHTEN 68 PL 27B 586	T. Eichten (AACH, BARI, CERN, EPOL, ORSAY+)	
ESCHSTRUTH 68 PR 165 1487	T.T. Eschstruth et al.	(PRIN, PENN)
GARLAND 68 PR 167 1225	R.T. Garland et al.	(COLU, RUTG, WISC)
MOSCOSO 68 Thesis	L. Moscoso	(ORSAY)
AUERBACH 67 PR 155 1505	L.B. Auerbach et al.	(PENN, PRIN)
Also PR D9 3216	L.B. Auerbach	
Erratum.		
BELLOTTI 67 Heidelberg Conf.	E. Bellotti, A. Pullia	(MILA)
BELLOTTI 67B NC 52A 1287	E. Bellotti, E. Fiorini, A. Pullia	(MILA)
Also PL 20 690	E. Bellotti et al.	(MILA)
BISI 67 PL 25B 572	V. Bisi et al.	(TORI)
FLETCHER 67 PRL 19 98	C.R. Fletcher et al.	(ILL)
FORD 67 PRL 18 1214	W.T. Ford et al.	(PRIN)
GINSBERG 67 PR 162 1570	E.S. Ginsberg	(MASB)
KALMUS 67 PR 159 1187	G.E. Kalmus, A. Kernan	(LRL)
ZINCHENKO 67 Thesis Rutgers	A.I. Zinchenko	(RUTG)
CALLAHAN 66 NC 44A 90	A.C. Callahan	(WISC)
CALLAHAN 66B PR 150 1153	A.C. Callahan et al.	(WISC, LRL, UCR+)
CESTER 66 PL 21 343	R. Cester et al.	(PPA)
See footnote 1 in AUERBACH 67.		
Also PR 155 1505	L.B. Auerbach et al.	(PENN, PRIN)
BIRGE 65 PR 139 B1600	R.W. Birge et al.	(LRL, WISC)
BISI 65 NC 35 768	V. Bisi et al.	(TORI)
BISI 65B PR 139 B1068	V. Bisi et al.	(TORI)
CALLAHAN 65 PRL 15 129	A. Callahan, D. Cline	(WISC)
CLINE 65 PL 15 293	D. Cline, W.F. Fry	(WISC)
DEMARCO 65 PR 140B 1430	A. de Marco, C. Grosso, G. Rinaudo	(TORI, CERN)
FITCH 65B PR 140B 1088	V.L. Fitch, C.A. Quarles, H.C. Wilkins	(PRIN+)
STAMER 65 PR 138 B440	P. Stamer et al.	(STEV)
YOUNG 65 Thesis UCRL 16362	P.S. Young	(LRL)
Also PR 156 1464	P.S. Young, W.Z. Osborne, W.H. Barkas	(LRL)
BORREANI 64 PL 12 123	G. Borreani, G. Rinaudo, A.E. Werbrouck	(TORI)
CALLAHAN 64 PR 136 B1463	A. Callahan, R. March, R. Stark	(WISC)
CLINE 64 PRL 13 101	D. Cline, W.F. Fry	(WISC)
GREINER 64 PRL 13 284	D.E. Greiner, W.Z. Osborne, W.H. Barkas	(LRL)
SHAKLEE 64 PR 136 B1423	F.S. Shaklee et al.	(MICH)
BOYARSKI 62 PR 128 2398	A.M. Boyarski et al.	(MIT)
FERRI-LUZZI 61 NC 22 1087	M. Ferro-Luzzi et al.	(LRL)
ROE 61 PRL 7 346	B.P. Roe et al.	(MICH, LRL)
TAYLOR 59 PR 114 359	S. Taylor et al.	(COLU)
COOMBES 57 PR 108 1348	C.A. Coombes et al.	(LBL)

OTHER RELATED PAPERS

LITTENBERG 93 ARNPS 43 729	L.S. Littenberg, G. Valencia	(BNL, FNAL)
Rare and Radiative Kaon Decays		
RITCHIE 93 RMP 65 1149	J.L. Ritchie, S.G. Wojcicki	
"Rare K Decays"		
BATTISTON 92 PRPL 214 293	R. Battiston et al.	(PGIA, CERN, TRSTT)
Status and Perspectives of K Decay Physics		
BRYMAN 89 JIMP A4 79	D.A. Bryman	(TRIU)
"Rare Kaon Decays"		
CHOUNET 72 PRPL 4C 199	L.M. Chounet, J.M. Gaillard, M.K. Gaillard	(ORSAY+)
FEARING 70 PR D2 542	H.W. Fearing, E. Fischbach, J. Smith	(STON, BOHR)
HAIDT 69B PL 29B 696	D. Haidt et al.	(AACH, BARI, CERN, EPOL+)
CRONIN 68B Vienna Conf. 241	J.W. Cronin	(PRIN)
Rapporteur talk.		
WILLIS 67 Heidelberg Conf. 273	W.J. Willis	(YALE)
Rapporteur talk.		
CABIBBO 66 Berkeley Conf. 33	N. Cabibbo	(CERN)
ADAIR 64 PL 12 67	R.K. Adair, L.B. Leipuner	(YALE, BNL)
CABIBBO 64 PL 9 352	N. Cabibbo, A. Maksymowicz	(CERN)
Also PL 11 360	N. Cabibbo, A. Maksymowicz	(CERN)
Also PL 14 72	N. Cabibbo, A. Maksymowicz	(CERN)
BIRGE 63 PRL 11 35	R.W. Birge et al.	(LRL, WISC, BARI)
BLOCK 62B CERN Conf. 371	M.M. Block, L. Lendinara, L. Monari	(NWES, BGNA)
BRENE 61 NP 22 553	N. Brene, L. Egardt, B. Qvist	(NORD)

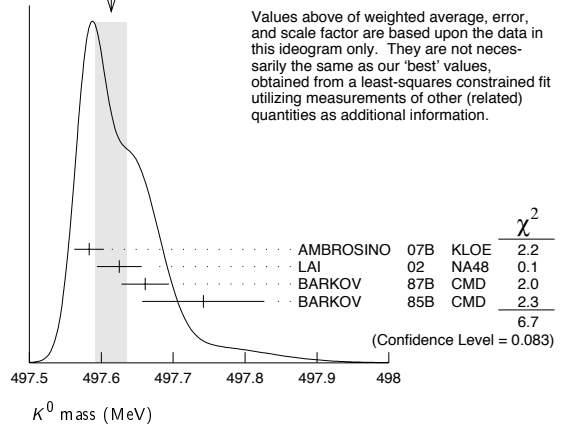


$$I(J^P) = \frac{1}{2}(0^-)$$

K^0 MASS

VALUE (MeV)	EVTS	DOCUMENT ID	TECN	COMMENT
497.614 ± 0.024 OUR FIT		Error includes scale factor of 1.6.		
497.614 ± 0.022 OUR AVERAGE		Error includes scale factor of 1.5. See the ideogram below.		
497.583 ± 0.005 ± 0.020	35k	AMBROSINO 07B	KLOE	$e^+e^- \rightarrow K_L^0 K_S^0$
497.625 ± 0.001 ± 0.031	655k	LAI 02	NA48	K_L^0 beam
497.661 ± 0.033	3713	BARKOV 87B	CMD	$e^+e^- \rightarrow K_L^0 K_S^0$
497.742 ± 0.085	780	BARKOV 85B	CMD	$e^+e^- \rightarrow K_L^0 K_S^0$
• • • We do not use the following data for averages, fits, limits, etc. • • •				
497.44 ± 0.50		FITCH 67	OSPK	
498.9 ± 0.5	4500	BALTAY 66	HBC	K^0 from $\bar{p}p$
497.44 ± 0.33	2223	KIM 65B	HBC	K^0 from $\bar{p}p$
498.1 ± 0.4		CHRISTENS... 64	OSPK	

WEIGHTED AVERAGE
497.614 ± 0.022 (Error scaled by 1.5)



Values above of weighted average, error, and scale factor are based upon the data in this ideogram only. They are not necessarily the same as our 'best' values, obtained from a least-squares constrained fit utilizing measurements of other (related) quantities as additional information.

		χ^2
AMBROSINO 07B	KLOE	2.2
LAI 02	NA48	0.1
BARKOV 87B	CMD	2.0
BARKOV 85B	CMD	2.3
		6.7
		(Confidence Level = 0.083)

$m_{K^0} - m_{K^\pm}$

VALUE (MeV)	EVTS	DOCUMENT ID	TECN	CHG	COMMENT
3.937 ± 0.028 OUR FIT		Error includes scale factor of 1.8.			
• • • We do not use the following data for averages, fits, limits, etc. • • •					
3.95 ± 0.21	417	HILL 68B	DBC	+	$K^+d \rightarrow K^0 p p$
3.90 ± 0.25	9	BURNSTEIN 65	HBC	-	
3.71 ± 0.35	7	KIM 65B	HBC	-	$K^-p \rightarrow n \bar{K}^0$
5.4 ± 1.1		CRAWFORD 59	HBC	+	
3.9 ± 0.6		ROSENFELD 59	HBC	-	

K^0 MEAN SQUARE CHARGE RADIUS

VALUE (fm ²)	EVTS	DOCUMENT ID	TECN	COMMENT
-0.077 ± 0.010 OUR AVERAGE				
-0.077 ± 0.007 ± 0.011	5037	ABOUZAID 06	KTEV	$K^0 \rightarrow \pi^+ \pi^- e^+ e^-$
-0.090 ± 0.021		LAI 03C	NA48	$K_L^0 \rightarrow \pi^+ \pi^- e^+ e^-$
-0.054 ± 0.026		MOLZON 78		K_S^0 regen. by electrons
• • • We do not use the following data for averages, fits, limits, etc. • • •				
-0.087 ± 0.046		BLATNIK 79		VMD + dispersion relations
-0.050 ± 0.130		FOETH 69B		K_S^0 regen. by electrons

T-VIOLATION PARAMETER IN K^0 - \bar{K}^0 MIXING

The asymmetry $A_T = \frac{\Gamma(\bar{K}^0 \rightarrow K^0) - \Gamma(K^0 \rightarrow \bar{K}^0)}{\Gamma(\bar{K}^0 \rightarrow K^0) + \Gamma(K^0 \rightarrow \bar{K}^0)}$ must vanish if T invariance holds.

ASYMMETRY A_T IN K^0 - \bar{K}^0 MIXING

VALUE (units 10 ⁻³)	EVTS	DOCUMENT ID	TECN
6.6 ± 1.3 ± 1.0	640k	1 ANGELOPO... 98E	CPLR

¹ ANGELOPOULOS 98E measures the asymmetry $A_T = [\Gamma(\bar{K}^0_{t=0} \rightarrow e^+ \pi^- \nu_{t=\tau}) - \Gamma(K^0_{t=0} \rightarrow e^- \pi^+ \bar{\nu}_{t=\tau})] / [\Gamma(\bar{K}^0_{t=0} \rightarrow e^+ \pi^- \nu_{t=\tau}) + \Gamma(K^0_{t=0} \rightarrow e^- \pi^+ \bar{\nu}_{t=\tau})]$ as a function of the neutral-kaon eigentime τ . The initial strangeness of the neutral kaon is tagged by the charge of the accompanying charged kaon in the reactions $p\bar{p} \rightarrow K^- \pi^+ K^0$ and $p\bar{p} \rightarrow K^+ \pi^- \bar{K}^0$. The strangeness at the time of the decay is tagged by the lepton charge. The reported result is the average value of A_T over the interval $1\tau_S < \tau < 20\tau_S$. From this value of A_T ANGELOPOULOS 01b, assuming CPT invariance in the $e\nu$ decay amplitude, determine the T-violating as $\Delta S = \Delta S$ conserving parameter (for its definition, see Review below) $4\text{Re}(\epsilon) = (6.2 \pm 1.4 \pm 1.0) \times 10^{-3}$.

CPT INVARIANCE TESTS IN NEUTRAL KAON DECAY

Written November 2007 by M. Antonelli (LNF-INFN, Frascati) and G. D'Ambrosio (INFN Sezione di Napoli).

CPT theorem is based on three assumptions: quantum field theory, locality, and Lorentz invariance, and thus it is a fundamental probe of our basic understanding of particle physics. Strangeness oscillation in $K^0 - \bar{K}^0$ system, described by the equation

$$i \frac{d}{dt} \begin{bmatrix} K^0 \\ \bar{K}^0 \end{bmatrix} = [M - i\Gamma/2] \begin{bmatrix} K^0 \\ \bar{K}^0 \end{bmatrix},$$

Meson Particle Listings

K^0

where M and Γ are hermitian matrices (see PDG review [1], references [2,3], and KLOE paper [4] for notations and previous literature), allows a very accurate test of CPT symmetry; indeed since CPT requires $M_{11} = M_{22}$ and $\Gamma_{11} = \Gamma_{22}$, the mass and width eigenstates, $K_{S,L}$, have a CPT -violating piece, δ , in addition to the usual CPT -conserving parameter ϵ :

$$K_{S,L} = \frac{1}{\sqrt{2(1+|\epsilon_{S,L}|^2)}} \left[(1+\epsilon_{S,L}) K^0 + (1-\epsilon_{S,L}) \bar{K}^0 \right]$$

$$\epsilon_{S,L} = \frac{-i\Im(M_{12}) - \frac{1}{2}\Im(\Gamma_{12}) \mp \frac{1}{2} \left[M_{11} - M_{22} - \frac{i}{2}(\Gamma_{11} - \Gamma_{22}) \right]}{m_L - m_S + i(\Gamma_S - \Gamma_L)/2}$$

$$\equiv \epsilon \pm \delta. \quad (1)$$

Using the phase convention $\Im(\Gamma_{12}) = 0$, we determine the phase of ϵ to be $\varphi_{SW} \equiv \arctan \frac{2(m_L - m_S)}{\Gamma_S - \Gamma_L}$. Imposing unitarity to an arbitrary combination of K^0 and \bar{K}^0 wave functions, we obtain the Bell-Steinberger relation [5] connecting CP and CPT violation in the mass matrix to CP and CPT violation in the decay; in fact, neglecting $\mathcal{O}(\epsilon)$ corrections to the coefficient of the CPT -violating parameter, δ , we can write [4]

$$\left[\frac{\Gamma_S + \Gamma_L}{\Gamma_S - \Gamma_L} + i \tan \phi_{SW} \right] \left[\frac{\Re(\epsilon)}{1+|\epsilon|^2} - i\Im(\delta) \right] =$$

$$\frac{1}{\Gamma_S - \Gamma_L} \sum_f A_L(f) A_S^*(f), \quad (2)$$

where $A_{L,S}(f) \equiv A(K_{L,S} \rightarrow f)$. We stress that this relation is phase-convention-independent. The advantage of the neutral kaon system is that only a few decay modes give significant contributions to the r.h.s. in Eq. (2); in fact, defining for the hadronic modes

$$\alpha_i \equiv \frac{1}{\Gamma_S} \langle \mathcal{A}_L(i) \mathcal{A}_S^*(i) \rangle = \eta_i \mathcal{B}(K_S \rightarrow i),$$

$$i = \pi^0 \pi^0, \pi^+ \pi^-(\gamma), 3\pi^0, \pi^0 \pi^+ \pi^-(\gamma), \quad (3)$$

the recent data from CPLEAR, KLOE, KTeV, and NA48 have led to the following determinations (the analysis described in Ref. 4 has been updated by using the recent measurements of K_L branching ratios from KTeV [6] and NA48 [7,8])

$$\alpha_{\pi^+ \pi^-} = \left((1.112 \pm 0.013) + i(1.061 \pm 0.014) \right) \times 10^{-3},$$

$$\alpha_{\pi^0 \pi^0} = \left((0.493 \pm 0.007) + i(0.471 \pm 0.007) \right) \times 10^{-3},$$

$$\alpha_{\pi^+ \pi^- \pi^0} = \left((0 \pm 2) + i(0 \pm 2) \right) \times 10^{-6},$$

$$|\alpha_{\pi^0 \pi^0 \pi^0}| < 7 \times 10^{-6} \quad \text{at 95\% CL.} \quad (4)$$

The semileptonic contribution to the right-handed side of Eq. (2) requires the determination of several observables: we define [2,3]

$$\mathcal{A}(K^0 \rightarrow \pi^- l^+ \nu) = \mathcal{A}_0(1 - y),$$

$$\mathcal{A}(K^0 \rightarrow \pi^+ l^- \nu) = \mathcal{A}_0^*(1 + y^*)(x_+ - x_-)^*,$$

$$\mathcal{A}(\bar{K}^0 \rightarrow \pi^+ l^- \nu) = \mathcal{A}_0^*(1 + y^*),$$

$$\mathcal{A}(\bar{K}^0 \rightarrow \pi^- l^+ \nu) = \mathcal{A}_0(1 - y)(x_+ + x_-), \quad (5)$$

where x_+ (x_-) describes the violation of the $\Delta S = \Delta Q$ rule in CPT -conserving (violating) decay amplitudes, and y parametrizes CPT violation for $\Delta S = \Delta Q$ transitions. Taking advantage of their tagged $K^0(\bar{K}^0)$ beams, CPLEAR has measured $\Im(x_+)$, $\Re(x_-)$, $\Im(\delta)$, and $\Re(\delta)$ [10]. These determinations have been improved in Ref. 4 by including the information $A_S - A_L = 4[\Re(\delta) + \Re(x_-)]$, where $A_{L,S}$ are the K_L and K_S semileptonic charge asymmetries, respectively, from the PDG [11] and KLOE [12]. Here we are also including the T -violating asymmetry measurement from CPLEAR [13].

Table 1: Values, errors, and correlation coefficients for $\Re(\delta)$, $\Im(\delta)$, $\Re(x_-)$, $\Im(x_+)$, and $A_S + A_L$ obtained from a combined fit, including KLOE [4] and CPLEAR [13].

	value	Correlations coefficients			
$\Re(\delta)$	$(3.0 \pm 2.3) \times 10^{-4}$	1			
$\Im(\delta)$	$(-0.66 \pm 0.65) \times 10^{-2}$	-0.21	1		
$\Re(x_-)$	$(-0.30 \pm 0.21) \times 10^{-2}$	-0.21	-0.60	1	
$\Im(x_+)$	$(0.02 \pm 0.22) \times 10^{-2}$	-0.38	-0.14	0.47	1
$A_S + A_L$	$(-0.40 \pm 0.83) \times 10^{-2}$	-0.10	-0.63	0.99	0.43 1

The value $A_S + A_L$ in Table 1 can be directly included in the semileptonic contributions to the Bell Steinberger relations in Eq. (2)

$$\sum_{\pi l \nu} \langle \mathcal{A}_L(\pi l \nu) \mathcal{A}_S^*(\pi l \nu) \rangle$$

$$= 2\Gamma(K_L \rightarrow \pi l \nu) \left((\Re(\epsilon) - \Re(y) - i(\Im(x_+) + \Im(\delta))) \right)$$

$$= 2\Gamma(K_L \rightarrow \pi l \nu) \left((A_S + A_L)/4 - i(\Im(x_+) + \Im(\delta)) \right). \quad (6)$$

Defining

$$\alpha_{\pi l \nu} \equiv \frac{1}{\Gamma_S} \sum_{\pi l \nu} \langle \mathcal{A}_L(\pi l \nu) \mathcal{A}_S^*(\pi l \nu) \rangle + 2i \frac{\tau_{K_S}}{\tau_{K_L}} \mathcal{B}(K_L \rightarrow \pi l \nu) \Im(\delta), \quad (7)$$

we find:

$$\alpha_{\pi l \nu} = \left((-0.2 \pm 0.5) + i(0.1 \pm 0.5) \right) \times 10^{-5}.$$

Inserting the values of the α parameters into Eq. (2), we find

$$\Re(\epsilon) = (161.2 \pm 0.6) \times 10^{-5},$$

$$\Im(\delta) = (-0.6 \pm 1.9) \times 10^{-5}. \quad (8)$$

The complete information on Eq. (8) is given in Table 2.

Table 2: Summary of results: values, errors, and correlation coefficients for $\Re(\epsilon)$, $\Im(\delta)$, $\Re(\delta)$, and $\Re(x_-)$.

	value	Correlations coefficients			
$\Re(\epsilon)$	$(161.2 \pm 0.6) \times 10^{-5}$	+1			
$\Im(\delta)$	$(-0.6 \pm 1.9) \times 10^{-5}$	+0.26	1		
$\Re(\delta)$	$(2.5 \pm 2.3) \times 10^{-4}$	+0.08	-0.09	1	
$\Re(x_-)$	$(-4.2 \pm 1.7) \times 10^{-3}$	+0.13	0.17	-0.43	1

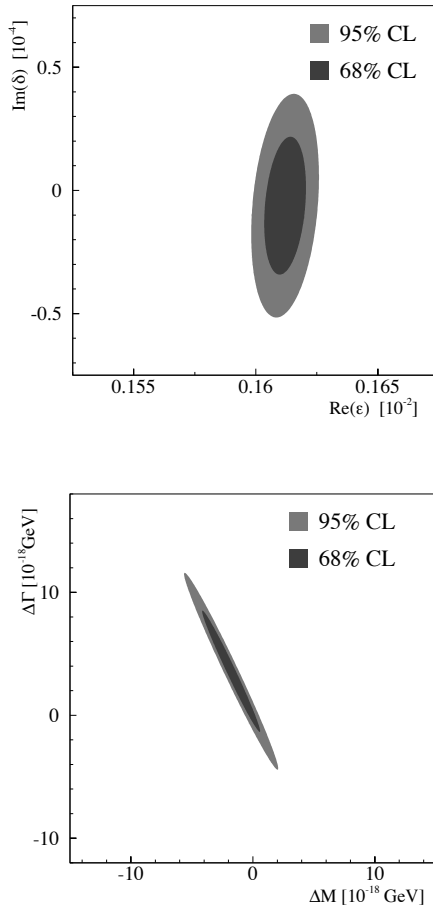


Figure 1: Top: allowed region at 68% and 95% C.L. in the $\Re(\epsilon)$, $\Im(\delta)$ plane. Bottom: allowed region at 68% and 95% C.L. in the ΔM , $\Delta\Gamma$ plane.

Now the agreement with CPT conservation, $\Im(\delta) = \Re(\delta) = \Re(x_-) = 0$, is at 30% C.L.

The allowed region in the $\Re(\epsilon) - \Im(\delta)$ plane at 68% CL and 95% C.L. is shown in the top panel of Fig. 1.

The process giving the largest contribution to the size of the allowed region is $K_L \rightarrow \pi^+\pi^-$, through the uncertainty on ϕ_{+-} .

The limits on $\Im(\delta)$ and $\Re(\delta)$ can be used to constrain the $K^0 - \bar{K}^0$ mass and width difference

$$\delta = \frac{i(m_{K^0} - m_{\bar{K}^0}) + \frac{1}{2}(\Gamma_{K^0} - \Gamma_{\bar{K}^0})}{\Gamma_S - \Gamma_L} \cos \phi_{SW} e^{i\phi_{SW}} [1 + \mathcal{O}(\epsilon)].$$

The allowed region in the $\Delta M = (m_{K^0} - m_{\bar{K}^0})$, $\Delta\Gamma = (\Gamma_{K^0} - \Gamma_{\bar{K}^0})$ plane is shown in the bottom panel of Fig. 1. As a result, we improve on the previous limits (see for instance, P. Bloch in Ref. 11) and in the limit $\Gamma_{K^0} - \Gamma_{\bar{K}^0} = 0$ we obtain

$$-5.1 \times 10^{-19} \text{ GeV} < m_{K^0} - m_{\bar{K}^0} < 5.1 \times 10^{-19} \text{ GeV} \text{ at } 95 \% \text{ C.L.}$$

References

1. See the “ CP Violation in Meson Decays,” in this *Review*.
2. L. Maiani, “ CP And CPT Violation In Neutral Kaon Decays,” L. Maiani, G. Pancheri, and N. Paver, *The Second Daphne Physics Handbook*, Vol. 1, 2.
3. G. D’Ambrosio, G. Isidori, and A. Pugliese, “ CP and CPT measurements at DAΦNE,” L. Maiani, G. Pancheri, and N. Paver, *The Second Daphne Physics Handbook*, Vol. 1, 2.
4. F. Ambrosino *et al.*, [KLOE Collaboration], JHEP **0612**, 011 (2006) [arXiv:hep-ex/0610034].
5. J. S. Bell and J. Steinberger, In Wolfenstein, L. (ed.): *CP violation*, 42-57. (In *Oxford International Symposium Conference on Elementary Particles*, September 1965, 195-208, 221-222). (See Book Index).
6. T. Alexopoulos *et al.*, [KTeV Collaboration], Phys. Rev. **D70**, 092006 (1998).
7. A. Lai *et al.*, [NA48 Collaboration], Phys. Lett. **B645**, 26 (2007); A. Lai *et al.*, [NA48 Collaboration], Phys. Lett. **B602**, 41 (2004).
8. We thank G. Isidori and M. Palutan for their contribution to the original analysis [4] performed with KLOE data.
9. A. Angelopoulos *et al.*, [CLEAR Collaboration], Phys. Reports **374**, 165 (2003).
10. A. Angelopoulos *et al.*, [CLEAR Collaboration], Phys. Lett. **B444**, 52 (1998).
11. W. M. Yao *et al.*, [Particle Data Group], J. Phys. **G33**, 1 (2006).
12. F. Ambrosino *et al.*, [KLOE Collaboration], Phys. Lett. **B636**, 173 (2006) [arXiv:hep-ex/0601026].
13. P. Bloch, M. Fidencaro, private communication of the data in a finer binning format; A. Angelopoulos *et al.*, [CLEAR Collaboration], Phys. Lett. **B444**, 43 (1998).

CP-VIOLATION PARAMETERS

Re(ϵ)

VALUE (units 10^{-3})	DOCUMENT ID	TECN
1.596 ± 0.013	² AMBROSINO 06H	KLOE
••• We do not use the following data for averages, fits, limits, etc. •••		
1.664 ± 0.010	³ LAI	05A NA48

² AMBROSINO 06H uses Bell-Steinberger relations with the following measurements: $B(K_L^0 \rightarrow \pi^+\pi^-)$ in AMBROSINO 06F, $B(K_S^0 \rightarrow \pi^0\pi^0\pi^0)$ in AMBROSINO 05B, the K_S^0 -semileptonic charge asymmetry in AMBROSINO 06E, and K^0 -semileptonic results in ANGELOPOULOS 98F.

³ LAI 05A values are obtained through unitarity (Bell-Steinberger relations), improving determination of η_{000} and combining other data from PDG 04 and APOSTOLAKIS 99B.

Meson Particle Listings

K^0

CPT-VIOLATION PARAMETERS

In K^0 - \bar{K}^0 mixing, if CP -violating interactions include a T conserving part then

$$|K_S\rangle = [|K_1\rangle + (\epsilon + \delta)|K_2\rangle] / \sqrt{1 + |\epsilon + \delta|^2}$$

$$|K_L\rangle = [|K_2\rangle + (\epsilon - \delta)|K_1\rangle] / \sqrt{1 + |\epsilon - \delta|^2}$$

where

$$|K_1\rangle = [(|K^0\rangle + |\bar{K}^0\rangle) / \sqrt{2}]$$

$$|K_2\rangle = [(|K^0\rangle - |\bar{K}^0\rangle) / \sqrt{2}]$$

and

$$|\bar{K}^0\rangle = CP|K^0\rangle.$$

The parameter δ specifies the CPT -violating part.

Estimates of δ are given below assuming the validity of the $\Delta S = \Delta Q$ rule. See also THOMSON 95 for a test of CPT -symmetry conservation in K^0 decays using the Bell-Steinberger relation.

REAL PART OF δ

A nonzero value violates CPT invariance.

VALUE (units 10^{-4})	EVTS	DOCUMENT ID	TECN	COMMENT
2.3 ± 2.7		⁴ AMBROSINO 06H	KLOE	
••• We do not use the following data for averages, fits, limits, etc. •••				
2.4 ± 2.8		⁵ APOSTOLA... 99B	RVUE	
2.9 ± 2.6 ± 0.6	1.3M	⁶ ANGELOPO... 98F	CPLR	
180 ± 200	6481	⁷ DEMIDOV 95		$K_{\ell 3}$ reanalysis

- ⁴ AMBROSINO 06H uses Bell-Steinberger relations with the following measurements: $B(K_L^0 \rightarrow \pi^+ \pi^-)$ in AMBROSINO 06F, $B(K_S^0 \rightarrow \pi^0 \pi^0 \pi^0)$ in AMBROSINO 05B, the K_S^0 -semileptonic charge asymmetry in AMBROSINO 06E, and K^0 -semileptonic results in ANGELOPOULOS 98F.
- ⁵ APOSTOLAKIS 99B assumes only unitarity and combines CPLEAR and other results.
- ⁶ ANGELOPOULOS 98F use $\Delta S = \Delta Q$. If $\Delta S = \Delta Q$ is not assumed, they find $\text{Re}\delta = (3.0 \pm 3.3 \pm 0.6) \times 10^{-4}$.
- ⁷ DEMIDOV 95 reanalyzes data from HART 73 and NIEBERGALL 74.

IMAGINARY PART OF δ

A nonzero value violates CPT invariance.

VALUE (units 10^{-5})	EVTS	DOCUMENT ID	TECN	COMMENT
0.4 ± 2.1		⁸ AMBROSINO 06H	KLOE	
••• We do not use the following data for averages, fits, limits, etc. •••				
- 0.2 ± 2.0		⁹ LAI 05A	NA48	
2.4 ± 5.0		¹⁰ APOSTOLA... 99B	RVUE	
- 90 ± 290 ± 100	1.3M	¹¹ ANGELOPO... 98F	CPLR	
2100 ± 3700	6481	¹² DEMIDOV 95		$K_{\ell 3}$ reanalysis

- ⁸ AMBROSINO 06H uses Bell-Steinberger relations with the following measurements: $B(K_L^0 \rightarrow \pi^+ \pi^-)$ in AMBROSINO 06F, $B(K_S^0 \rightarrow \pi^0 \pi^0 \pi^0)$ in AMBROSINO 05B, the K_S^0 -semileptonic charge asymmetry in AMBROSINO 06E, and K^0 -semileptonic results in ANGELOPOULOS 98F.
- ⁹ LAI 05A values are obtained through unitarity (Bell-Steinberger relations), improving determination of η_{000} and combining other data from PDG 04 and APOSTOLAKIS 99B.
- ¹⁰ APOSTOLAKIS 99B assumes only unitarity and combines CPLEAR and other results.
- ¹¹ If $\Delta S = \Delta Q$ is not assumed, ANGELOPOULOS 98F finds $\text{Im}\delta = (-15 \pm 23 \pm 3) \times 10^{-3}$.
- ¹² DEMIDOV 95 reanalyzes data from HART 73 and NIEBERGALL 74.

Re(η)

A non-zero value would violate CPT invariance in $\Delta S = \Delta Q$ amplitude. Re(η) is the following combination of K_{e3} decay amplitudes:

$$\text{Re}(\eta) = \text{Re} \left(\frac{A(K^0 \rightarrow e^- \pi^+ \bar{\nu}_e)^* - A(K^0 \rightarrow e^+ \pi^- \nu_e)}{A(K^0 \rightarrow e^- \pi^+ \bar{\nu}_e)^* + A(K^0 \rightarrow e^+ \pi^- \nu_e)} \right)$$

VALUE (units 10^{-3})	EVTS	DOCUMENT ID	TECN	COMMENT
0.4 ± 2.5	13k	¹³ AMBROSINO 06E	KLOE	
••• We do not use the following data for averages, fits, limits, etc. •••				
0.3 ± 3.1		¹⁴ APOSTOLA... 99B	CPLR	

- ¹³ They use the PDG 04 for the K_L^0 semileptonic charge asymmetry and PDG 04 (CPL review, CPT NOT ASSUMED) for Re(ϵ).
- ¹⁴ Constrained by Bell-Steinberger (or unitarity) relation.

Re(x_{-})

A non-zero value would violate CPT invariance in decay amplitudes with $\Delta S \neq \Delta Q$. x_{-} , used here to define Re(x_{-}), and x_{+} , used below in the $\Delta S = \Delta Q$ section are the following combinations of K_{e3} decay amplitudes:

$$x_{\pm} = \frac{1}{2} \left(\frac{A(K^0 \rightarrow \pi^- e^+ \nu_e)}{A(K^0 \rightarrow \pi^- e^+ \nu_e)} \pm \frac{A(K^0 \rightarrow \pi^+ e^- \bar{\nu}_e)^*}{A(K^0 \rightarrow \pi^+ e^- \bar{\nu}_e)^*} \right).$$

VALUE (units 10^{-3})	EVTS	DOCUMENT ID	TECN	COMMENT
-2.9 ± 2.0		¹⁵ AMBROSINO 06H	KLOE	
••• We do not use the following data for averages, fits, limits, etc. •••				
-0.8 ± 2.5	13k	¹⁶ AMBROSINO 06E	KLOE	
-0.5 ± 3.0		¹⁷ APOSTOLA... 99B	CPLR	Strangeness tagged
2 ± 13 ± 3	650k	ANGELOPO... 98F	CPLR	Strangeness tagged

- ¹⁵ AMBROSINO 06H uses Bell-Steinberger relations with the following measurements: $B(K_L^0 \rightarrow \pi^+ \pi^-)$ in AMBROSINO 06F, $B(K_S^0 \rightarrow \pi^0 \pi^0 \pi^0)$ in AMBROSINO 05B, the K_S^0 -semileptonic charge asymmetry in AMBROSINO 06E, and K^0 -semileptonic results in ANGELOPOULOS 98F.
- ¹⁶ Uses PDG 04 for the K_L^0 semileptonic charge asymmetry and Re(δ) from CPLEAR, ANGELOPOULOS 98F.
- ¹⁷ Constrained by Bell-Steinberger (or unitarity) relation.

$$|m_{K^0} - m_{\bar{K}^0}| / m_{\text{average}}$$

A test of CPT invariance. "Our Evaluation" is described in the "Tests of Conservation Laws" section. It assumes CPT invariance in the decay and neglects some contributions from decay channels other than $\pi\pi$.

VALUE	CL%	DOCUMENT ID	TECN
$< 8 \times 10^{-19}$	90	PDG	08
••• We do not use the following data for averages, fits, limits, etc. •••			
$(-3 \pm 4) \times 10^{-18}$		¹⁸ ANGELOPO... 99B	RVUE

- ¹⁸ ANGELOPOULOS 99B assumes only unitarity and combines CPLEAR and other results.

$$(\Gamma_{K^0} - \Gamma_{\bar{K}^0}) / m_{\text{average}}$$

A test of CPT invariance.

VALUE	DOCUMENT ID	TECN
$(7.8 \pm 8.4) \times 10^{-18}$	¹⁹ ANGELOPO... 99B	RVUE

- ¹⁹ ANGELOPOULOS 99B assumes only unitarity and combines CPLEAR with other results. Correlated with $(m_{K^0} - m_{\bar{K}^0}) / m_{\text{average}}$ with a correlation coefficient of -0.95 .

TESTS OF $\Delta S = \Delta Q$ RULE

Re(x_{+})

A non-zero value would violate the $\Delta S = \Delta Q$ rule in CPT conserving transitions. x_{+} is defined above in the Re(x_{-}) section.

VALUE (units 10^{-3})	EVTS	DOCUMENT ID	TECN
-0.9 ± 3.0 OUR AVERAGE			
-2 ± 10		²⁰ BATLEY 07D	NA48
-0.5 ± 3.6	13k	²¹ AMBROSINO 06E	KLOE
-1.8 ± 6.1		²² ANGELOPO... 98D	CPLR

- ²⁰ Result obtained from the measurement $\Gamma(K_S^0 \rightarrow \pi e \nu) / \Gamma(K_L^0 \rightarrow \pi e \nu) = 0.993 \pm 0.34$, neglecting possible CPT non-invariance and using PDG 06 values of $B(K_L^0 \rightarrow \pi e \nu) = 0.4053 \pm 0.0015$, $\tau_L = (5.114 \pm 0.021) \times 10^{-8}$ s and $\tau_S = (0.8958 \pm 0.0005) \times 10^{-10}$ s.
- ²¹ Re(x_{+}) can be shown to be equal to the following combination of rates:

$$\text{Re}(x_{+}) = \frac{1}{2} \frac{\Gamma(K_S^0 \rightarrow \pi e \nu) - \Gamma(K_L^0 \rightarrow \pi e \nu)}{\Gamma(K_S^0 \rightarrow \pi e \nu) + \Gamma(K_L^0 \rightarrow \pi e \nu)}$$

which is valid up to first order in terms violating CPT and/or the $\Delta S = \Delta Q$ rule.

- ²² Obtained neglecting CPT violating amplitudes.

K^0 REFERENCES

PDG 08	PL B667 1	C. Amstutz et al.	(PDG Collab.)
AMBROSINO 07B	JHEP 0712 073	F. Ambrosino et al.	(KLOE Collab.)
BATLEY 07D	PL B653 145	J.R. Batley et al.	(CERN NA48 Collab.)
ABOUZAIID 06	PRL 96 101801	E. Abouzaid et al.	(KTeV Collab.)
AMBROSINO 06E	PL B636 173	F. Ambrosino et al.	(KLOE Collab.)
AMBROSINO 06F	PL B638 140	F. Ambrosino et al.	(KLOE Collab.)
AMBROSINO 06H	JHEP 0612 011	F. Ambrosino et al.	(KLOE Collab.)
PDG 06	JPG 33 1	W.-M. Yao et al.	(PDG Collab.)
AMBROSINO 05B	PL B619 61	F. Ambrosino et al.	(KLOE Collab.)
LAI 05A	PL B610 165	A. Lai et al.	(CERN NA48 Collab.)
PDG 04	PL B592 1	S. Eidelman et al.	(CERN NA48 Collab.)
LAI 03C	EPJ C30 33	A. Lai et al.	(CERN NA48 Collab.)
LAI 02	PL B533 196	A. Lai et al.	(CERN NA48 Collab.)
ANGELOPO... 01B	EPJ C22 55	A. Angelopoulos et al.	(CPLEAR Collab.)
ANGELOPO... 99B	PL B471 332	A. Angelopoulos et al.	(CPLEAR Collab.)
APOSTOLA... 99B	PL B456 297	A. Apostolakis et al.	(CPLEAR Collab.)
ANGELOPO... 98D	PL B444 38	A. Angelopoulos et al.	(CPLEAR Collab.)
Also	EPJ C22 55	A. Angelopoulos et al.	(CPLEAR Collab.)
ANGELOPO... 98F	PL B444 43	A. Angelopoulos et al.	(CPLEAR Collab.)
ANGELOPO... 98F	PL B444 52	A. Angelopoulos et al.	(CPLEAR Collab.)
Also	EPJ C22 55	A. Angelopoulos et al.	(CPLEAR Collab.)
DEMIDOV 95	PAN 58 968	V. Demidov, K. Gusev, E. Shabalina	(ITEP)
From YAF 58	1041		
THOMSON 95	PR D51 1412	G.B. Thomson, Y. Zou	(RUTG)
BARKOV 87B	SJNP 46 630	L.M. Barkov et al.	(NOVO)
BARKOV 85B	JETPL 42 138	L.M. Barkov et al.	(NOVO)
Translated from	YAF 46 1088		
Translated from	ZETFP 42 113		
BLATNIK 79	LNC 24 39	S. Blatnik, J. Stahov, C.B. Lang	(TUZL, GRAZ)
MOLZON 78	PRL 41 1213	W.R. Molzon et al.	(EFI-I)
NIEBERGALL 74	PL 49B 103	F. Niebergall et al.	(CERN, ORSAY, VIEN)
HART 73	NP B66 317	J.C. Hart et al.	(CAVE, RHEL)
FOETH 69B	PL 30B 276	H. Foeth et al.	(AACH, CERN, TORI)
HILL 68B	PR 168 1534	D.G. Hill et al.	(BNL, CMU)
FITCH 67	PR 164 1711	V.L. Fitch et al.	(BNL)
BALTAY 66	PR 142 932	C. Baltay et al.	(YALE, PRIN)
BURNSTEIN 65	PR 138 B895	R.A. Burnstein, H.A. Rubin	(UMD)
KIM 65B	PR 140B 1334	J.K. Kim, L. Kirsch, D. Miller	(COLU)
CHRISTENS... 64	PRL 13 138	J.H. Christenson et al.	(PRIN)
CRAWFORD 59	PRL 2 112	F.S. Crawford et al.	(LRL)
ROSENFELD 59	PRL 2 110	A.H. Rosenfeld, F.T. Solmitz, R.D. Tripp	(LRL)



$$I(J^P) = \frac{1}{2}(0^-)$$

K_S^0 MEAN LIFE

For earlier measurements, beginning with BOLDT 58B, see our 1986 edition, Physics Letters **170B** 130 (1986).

OUR FIT is described in the note on "CP violation in K_L decays" in the K^0 Particle Listings. The result labeled "OUR FIT Assuming CPT" ["OUR FIT Not assuming CPT"] includes all measurements except those with the comment "Not assuming CPT" ["Assuming CPT"]. Measurements with neither comment do not assume CPT and enter both fits.

VALUE (10^{-10} s)	EVTS	DOCUMENT ID	TECN	COMMENT
0.8953 ± 0.0005	OUR FIT	Error includes scale factor of 1.1. Assuming CPT		
0.8958 ± 0.0005	OUR FIT	Not assuming CPT		
0.8965 ± 0.0007		1,2 ALAVI-HARATI03	KTEV	Assuming CPT
0.8958 ± 0.0013		2,3 ALAVI-HARATI03	KTEV	Not assuming CPT
0.89598 ± 0.00048 ± 0.00051	16M	LAI	02c	NA48
0.8971 ± 0.0021		BERTANZA	97	NA31
0.8941 ± 0.0014 ± 0.0009		SCHWINGEN..95	E773	Assuming CPT
0.8929 ± 0.0016		GIBBONS	93	E731 Assuming CPT
• • • We do not use the following data for averages, fits, limits, etc. • • •				
0.8920 ± 0.0044	214k	GROSSMAN	87	SPEC
0.905 ± 0.007		4 ARONSON	82B	SPEC
0.881 ± 0.009	26k	ARONSON	76	SPEC
0.8926 ± 0.0032 ± 0.0002		5 CARITHERS	75	SPEC
0.8937 ± 0.0048	6M	GEWENIGER	74B	ASP K
0.8958 ± 0.0045	50k	6 SKJEGGEST..	72	HBC
0.856 ± 0.008	19994	7 DONALD	68B	HBC
0.872 ± 0.009	20000	7,8 HILL	68	DBC

¹ This ALAVI-HARATI 03 fit has Δm and τ_S free but constrains ϕ_{+-} to the Superweak value, i.e. assumes CPT. This τ_S value is correlated with their $\Delta m = m_{K_L^0} - m_{K_S^0}$ measurement in the K_L^0 listings. The correlation coefficient $\rho(\tau_S, \Delta m) = -0.396$.

² The two ALAVI-HARATI 03 values use the same data. The first enters the "assuming CPT" fit and the second enters the "not assuming CPT" fit.

³ This ALAVI-HARATI 03 fit has Δm , ϕ_{+-} , and τ_{K_S} free. See ϕ_{+-} in the " K_L CP violation" section for correlation information.

⁴ ARONSON 82 find that K_S^0 mean life may depend on the kaon energy.

⁵ CARITHERS 75 measures the Δm dependence of the total decay rate (inverse mean life) to be $\Gamma(K_S^0) = [(1.122 \pm 0.004) + 0.16(\Delta m - 0.5348)/\Delta m]10^{10}/s$, or, in terms of mean life, CARITHERS 75 measures $\tau_S = (0.8913 \pm 0.0032) - 0.238[\Delta m - 0.5348](10^{-10} s)$. We have adjusted the measurement to use our best values of ($\Delta m = 0.5292 \pm 0.0009$) ($10^{10} \hbar s^{-1}$). Our first error is their experiment's error and our second error is the systematic error from using our best values.

⁶ HILL 68 has been changed by the authors from the published value (0.865 ± 0.009) because of a correction in the shift due to η_{+-} . SKJEGGESTAD 72 and HILL 68 give detailed discussions of systematics encountered in this type of experiment.

⁷ Pre-1971 experiments are excluded from the average because of disagreement with later more precise experiments.

⁸ HILL 68 has been changed by the authors from the published value (0.865 ± 0.009) because of a correction in the shift due to η_{+-} . SKJEGGESTAD 72 and HILL 68 give detailed discussions of systematics encountered in this type of experiment.

K_S^0 DECAY MODES

Mode	Fraction (Γ_i/Γ)	Confidence level
------	--------------------------------	------------------

Hadronic modes

Γ_1	$\pi^0 \pi^0$	(30.69 ± 0.05) %
Γ_2	$\pi^+ \pi^-$	(69.20 ± 0.05) %
Γ_3	$\pi^+ \pi^- \pi^0$	(3.5 $\frac{+1.1}{-0.9}$) × 10 ⁻⁷

Modes with photons or $\ell\bar{\ell}$ pairs

Γ_4	$\pi^+ \pi^- \gamma$	[a,b] (1.79 ± 0.05) × 10 ⁻³
Γ_5	$\pi^+ \pi^- e^+ e^-$	(4.69 ± 0.30) × 10 ⁻⁵
Γ_6	$\pi^0 \gamma \gamma$	[b] (4.9 ± 1.8) × 10 ⁻⁸
Γ_7	$\gamma \gamma$	(2.71 ± 0.06) × 10 ⁻⁶

Semileptonic modes

Γ_8	$\pi^\pm e^\mp \nu_e$	[c] (7.04 ± 0.08) × 10 ⁻⁴
Γ_9	$\pi^\pm \mu^\mp \nu_\mu$	[c,d] (4.69 ± 0.05) × 10 ⁻⁴

CP violating (CP) and $\Delta S = 1$ weak neutral current (S1) modes

Γ_{10}	$3\pi^0$	CP	< 1.2	× 10 ⁻⁷	90%
Γ_{11}	$\mu^+ \mu^-$	S1	< 3.2	× 10 ⁻⁷	90%
Γ_{12}	$e^+ e^-$	S1	< 1.4	× 10 ⁻⁷	90%
Γ_{13}	$\pi^0 e^+ e^-$	S1	[b] (3.0 $\frac{+1.5}{-1.2}$)	× 10 ⁻⁹	
Γ_{14}	$\pi^0 \mu^+ \mu^-$	S1	(2.9 $\frac{+1.5}{-1.2}$)	× 10 ⁻⁹	

[a] Most of this radiative mode, the low-momentum γ part, is also included in the parent mode listed without γ 's.

[b] See the Particle Listings below for the energy limits used in this measurement.

[c] The value is for the sum of the charge states or particle/antiparticle states indicated.

[d] Not a measurement. Calculated as 0.666·B($\pi^\pm e^\mp \nu_e$).

CONSTRAINED FIT INFORMATION

An overall fit to 4 branching ratios uses 5 measurements and one constraint to determine 4 parameters. The overall fit has a $\chi^2 = 0.1$ for 2 degrees of freedom.

The following *off-diagonal* array elements are the correlation coefficients $\langle \delta x_i \delta x_j \rangle / (\delta x_i \delta x_j)$, in percent, from the fit to the branching fractions, $x_i \equiv \Gamma_i / \Gamma_{\text{total}}$. The fit constrains the x_i whose labels appear in this array to sum to one.

x_2	-100		
x_8	-6	3	
x_9	-6	3	100
	x_1	x_2	x_8

K_S^0 DECAY RATES

$\Gamma(\pi^\pm e^\mp \nu_e)$

 Γ_8

VALUE ($10^6 s^{-1}$)	EVTS	DOCUMENT ID	TECN	COMMENT
• • • We do not use the following data for averages, fits, limits, etc. • • •				
8.1 ± 1.6	75	9 AKHMETSHIN 99	CMD2	Tagged K_S^0 using $\phi \rightarrow K_L^0 K_S^0$
7.50 ± 0.08		10 PDG	98	
seen		BURGUN	72	HBC $K^+ p \rightarrow K^0 p \pi^+$
9.3 ± 2.5		AUBERT	65	HLBC $\Delta S = \Delta Q$, CP cons. not assumed

⁹ AKHMETSHIN 99 is from a measured branching ratio $B(K_S^0 \rightarrow \pi e \nu_e) = (7.2 \pm 1.4) \times 10^{-4}$ and $\tau_{K_S^0} = (0.8934 \pm 0.0008) \times 10^{-10}$ s. Not independent of measured branching ratio.

¹⁰ PDG 98 from K_L^0 measurements, assuming that $\Delta S = \Delta Q$ in K^0 decay so that $\Gamma(K_S^0 \rightarrow \pi^\pm e^\mp \nu_e) = \Gamma(K_L^0 \rightarrow \pi^\pm e^\mp \nu_e)$.

$\Gamma(\pi^\pm \mu^\mp \nu_\mu)$

 Γ_9

VALUE ($10^6 s^{-1}$)	EVTS	DOCUMENT ID	TECN	COMMENT
• • • We do not use the following data for averages, fits, limits, etc. • • •				
5.25 ± 0.07		11 PDG	98	
¹¹ PDG 98 from K_L^0 measurements, assuming that $\Delta S = \Delta Q$ in K^0 decay so that $\Gamma(K_S^0 \rightarrow \pi^\pm \mu^\mp \nu_\mu) = \Gamma(K_L^0 \rightarrow \pi^\pm \mu^\mp \nu_\mu)$.				

K_S^0 BRANCHING RATIOS

Hadronic modes

$\Gamma(\pi^0 \pi^0) / \Gamma_{\text{total}}$

 Γ_1 / Γ

VALUE	EVTS	DOCUMENT ID	TECN	COMMENT
0.3069 ± 0.0005	OUR FIT	• • • We do not use the following data for averages, fits, limits, etc. • • •		
0.335 ± 0.014	1066	BROWN	63	HLBC
0.288 ± 0.021	198	CHRETIEN	63	HLBC
0.30 ± 0.035		BROWN	61	HLBC

$\Gamma(\pi^+ \pi^-) / \Gamma_{\text{total}}$

 Γ_2 / Γ

VALUE	EVTS	DOCUMENT ID	TECN	COMMENT
0.6920 ± 0.0005	OUR FIT	• • • We do not use the following data for averages, fits, limits, etc. • • •		
0.670 ± 0.010	3447	DOYLE	69	HBC $\pi^- p \rightarrow \Lambda K^0$

$\Gamma(\pi^+ \pi^-) / \Gamma(\pi^0 \pi^0)$

 Γ_2 / Γ_1

VALUE	EVTS	DOCUMENT ID	TECN	COMMENT
2.255 ± 0.005	OUR FIT	• • • We do not use the following data for averages, fits, limits, etc. • • •		
2.2549 ± 0.0054		12 AMBROSINO	06c	KLOE
2.2555 ± 0.0012 ± 0.0054		13 AMBROSINO	06c	KLOE
2.236 ± 0.003 ± 0.015	766k	13 ALOISIO	02B	KLOE
2.11 ± 0.09	1315	EVERHART	76	WIRE $\pi^- p \rightarrow \Lambda K^0$
2.169 ± 0.094	16k	COWELL	74	OSPK $\pi^- p \rightarrow \Lambda K^0$
2.16 ± 0.08	4799	HILL	73	DBC $K^+ d \rightarrow K^0 p p$
2.22 ± 0.10	3068	ALITTI	72	HBC $K^+ p \rightarrow \pi^+ p K^0$
2.22 ± 0.08	6380	MORSE	72B	DBC $K^+ n \rightarrow K^0 p$

Meson Particle Listings

 K_S^0

2.10 ± 0.11	701	15	NAGY	72	HLBC	$K^+ n \rightarrow K^0 p$
2.22 ± 0.095	6150	16	BALTAY	71	HBC	$K p \rightarrow K^0 \text{ neutrals}$
2.282 ± 0.043	7944	17	MOFFETT	70	OSPK	$K^+ n \rightarrow K^0 p$
2.12 ± 0.17	267	15	BOZOKI	69	HLBC	
2.285 ± 0.055	3016	17	GOBBI	69	OSPK	$K^+ n \rightarrow K^0 p$
2.10 ± 0.06	3700		MORFIN	69	HLBC	$K^+ n \rightarrow K^0 p$

¹²This result combines AMBROSINO 06c KLOE 2001-02 data with ALOISIO 02b KLOE 2000 data. $K_S^0 \rightarrow \pi^+ \pi^-$ fully inclusive.

¹³Includes radiative decays $\pi^+ \pi^- \gamma$.

¹⁴The directly measured quantity is $K_S^0 \rightarrow \pi^+ \pi^- / \text{all } K^0 = 0.345 \pm 0.005$.

¹⁵NAGY 72 is a final result which includes BOZOKI 69.

¹⁶The directly measured quantity is $K_S^0 \rightarrow \pi^+ \pi^- / \text{all } \bar{K}^0 = 0.345 \pm 0.005$.

¹⁷MOFFETT 70 is a final result which includes GOBBI 69.

 $\Gamma(\pi^+ \pi^- \pi^0) / \Gamma_{\text{total}}$ Γ_3 / Γ

VALUE (units 10^{-7})	EVTS	DOCUMENT ID	TECN	COMMENT
3.5 ± 1.1				OUR AVERAGE
4.7 ± 2.2 + 1.7 - 1.7 - 1.5		18	BATLEY	05 NA48
2.5 ± 1.3 + 0.5 - 1.0 - 0.6	500k	19	ADLER	97B CPLR
4.8 ± 2.2 - 1.6 ± 1.1		20	ZOU	96 E621

• • • We do not use the following data for averages, fits, limits, etc. • • •

4.1 ± 2.5 + 0.5 - 1.9 - 0.6		21	ADLER	96E CPLR Sup. by ADLER 97B
3.9 ± 5.4 + 0.9 - 1.8 - 0.7		22	THOMSON	94 E621 Sup. by ZOU 96

¹⁸BATLEY 05 is obtained by measuring the interference parameters in $K_S, K_L \rightarrow \pi^+ \pi^- \pi^0$; $\text{Re}(\lambda) = 0.038 \pm 0.008 \pm 0.006$ and $\text{Im}(\lambda) = -0.013 \pm 0.005 \pm 0.004$; the correlation coeff. between $\text{Re}(\lambda)$ and $\text{Im}(\lambda)$ is 0.66 (statistical only).

¹⁹ADLER 97B find the CP -conserving parameters $\text{Re}(\lambda) = (28 \pm 7 \pm 3) \times 10^{-3}$, $\text{Im}(\lambda) = (-10 \pm 8 \pm 2) \times 10^{-3}$. They estimate $B(K_S^0 \rightarrow \pi^+ \pi^- \pi^0)$ from $\text{Re}(\lambda)$ and the K_L^0 decay parameters. See also ANGELOPOULOS 98c.

²⁰ZOU 96 is from the the measured quantities $|\rho_{+-0}| = 0.039^{+0.009}_{-0.006} \pm 0.005$ and $\phi_\rho = (-9 \pm 18)^\circ$.

²¹ADLER 96E is from the measured quantities $\text{Re}(\lambda) = 0.036 \pm 0.010^{+0.002}_{-0.003}$ and $\text{Im}(\lambda)$ consistent with zero. Note that the quantity λ is the same as ρ_{+-0} used in other footnotes.

²²THOMSON 94 calculates this branching ratio from their measurements $|\rho_{+-0}| = 0.035^{+0.019}_{-0.011} \pm 0.004$ and $\phi_\rho = (-59 \pm 48)^\circ$ where $|\rho_{+-0}| e^{i\phi_\rho} = A(K_S^0 \rightarrow \pi^+ \pi^- \pi^0, I = 2) / A(K_L^0 \rightarrow \pi^+ \pi^- \pi^0)$.

Modes with photons or $\ell\bar{\ell}$ pairs $\Gamma(\pi^+ \pi^- \gamma) / \Gamma(\pi^+ \pi^-)$ Γ_4 / Γ_2

VALUE (units 10^{-3})	EVTS	DOCUMENT ID	TECN	COMMENT
2.59 ± 0.08				OUR AVERAGE
2.56 ± 0.09	1286		RAMBERG	93 E731 $p_\gamma > 50 \text{ MeV}/c$
2.68 ± 0.15		23	TAUREG	76 SPEC $p_\gamma > 50 \text{ MeV}/c$

• • • We do not use the following data for averages, fits, limits, etc. • • •

7.10 ± 0.22	3723		RAMBERG	93 E731 $p_\gamma > 20 \text{ MeV}/c$
3.0 ± 0.6	29	24	BOBISUT	74 HLBC $p_\gamma > 40 \text{ MeV}/c$
2.8 ± 0.6		25	BURGUN	73 HBC $p_\gamma > 50 \text{ MeV}/c$

²³TAUREG 76 find direct emission contribution < 0.06 , $CL = 90\%$.

²⁴BOBISUT 74 not included in average because p_γ cut differs. Estimates direct emission contribution to be 0.5 or less, $CL = 95\%$.

²⁵BURGUN 73 estimates that direct emission contribution is 0.3 ± 0.6 .

 $\Gamma(\pi^+ \pi^- e^+ e^-) / \Gamma_{\text{total}}$ Γ_5 / Γ

VALUE (units 10^{-5})	EVTS	DOCUMENT ID	TECN	COMMENT
4.69 ± 0.30	676	26	LAI	03c NA48 1998+1999 data

• • • We do not use the following data for averages, fits, limits, etc. • • •

4.71 ± 0.23 ± 0.22	620	26,27	LAI	03c NA48 1999 data
4.5 ± 0.7 ± 0.4	56		LAI	00b NA48 1998 data

²⁶Uses normalization $\text{BR}(K_L \rightarrow \pi^+ \pi^- \pi^0) * \text{BR}(\pi^0 \rightarrow e^+ e^-) = (1.505 \pm 0.047) \times 10^{-3}$ from our 2000 Edition.

²⁷Second error is $0.16(\text{syst}) \pm 0.15(\text{norm})$ combined in quadrature.

 $\Gamma(\pi^0 \gamma \gamma) / \Gamma_{\text{total}}$ Γ_6 / Γ

VALUE (units 10^{-8})	CL%	EVTS	DOCUMENT ID	TECN	COMMENT
4.9 ± 1.6 ± 0.9		17	28	LAI	04 NA48 $m_\gamma^2 / m_K^2 > 0.2$

• • • We do not use the following data for averages, fits, limits, etc. • • •

< 33	90		LAI	03b NA48 $m_\gamma^2 / m_K^2 > 0.2$
--------	----	--	-----	-------------------------------------

²⁸Spectrum also measured and found consistent with the one generated by a constant matrix element.

 $\Gamma(\gamma \gamma) / \Gamma_{\text{total}}$ Γ_7 / Γ

VALUE (units 10^{-6})	CL%	EVTS	DOCUMENT ID	TECN
2.713 ± 0.063 ± 0.005	7.5k	29	LAI	03 NA48

• • • We do not use the following data for averages, fits, limits, etc. • • •

2.58 ± 0.36 ± 0.22	149		LAI	00 NA48
2.2 ± 1.1	16	30	BARR	95B NA31
2.4 ± 0.9	35	31	BARR	95B NA31
< 13	90		BALATS	89 SPEC
2.4 ± 1.2	19		BURKHARDT	87 NA31
< 133	90		BARMIN	86B XEBC

²⁹LAI 03 reports $[B(K_S^0 \rightarrow \gamma \gamma)] / [B(K_S^0 \rightarrow \pi^0 \pi^0)] = (8.84 \pm 0.18 \pm 0.10) \times 10^{-6}$.

We multiply by our best value $B(K_S^0 \rightarrow \pi^0 \pi^0) = (30.69 \pm 0.05) \times 10^{-2}$. Our first error is their experiment's error and our second error is the systematic error from using our best value.

³⁰BARR 95B result is calculated using $B(K_L \rightarrow \gamma \gamma) = (5.86 \pm 0.17) \times 10^{-4}$.

³¹BARR 95B quotes this as the combined BARR 95B + BURKHARDT 87 result after rescaling BURKHARDT 87 to use same branching ratios and lifetimes as BARR 95B.

Semileptonic modes

 $\Gamma(\pi^\pm e^\mp \nu_e) / \Gamma_{\text{total}}$ Γ_8 / Γ

VALUE (units 10^{-4})	EVTS	DOCUMENT ID	TECN	COMMENT
7.04 ± 0.08				OUR FIT
7.04 ± 0.08				OUR AVERAGE

7.046 ± 0.18 ± 0.16	32	BATLEY	07D NA48	$K^0(\bar{K}^0)(t) \rightarrow \pi e \nu$
7.05 ± 0.09	13k	33	AMBROSINO	06E KLOE Not fitted
6.91 ± 0.34 ± 0.15	624	34	ALOISIO	02 KLOE Tagged K_S^0 using $\phi \rightarrow K_L^0 K_S^0$

• • • We do not use the following data for averages, fits, limits, etc. • • •

7.2 ± 1.4	75		AKHMETSHIN	99 CMD2 Tagged K_S^0 using $\phi \rightarrow K_L^0 K_S^0$
-----------	----	--	------------	---

³²Reconstructed from $K^0(\bar{K}^0)(t) \rightarrow \pi e \nu$ distributions using PDG values of $B(K_L^0 \rightarrow \pi e \nu) = 0.4053 \pm 0.0015$, $\tau_L = (5.114 \pm 0.021) \times 10^{-8}$ s and $\tau_S = (0.8958 \pm 0.0005) \times 10^{-10}$ s.

³³Obtained by imposing $\sum_i B(K_S^0 \rightarrow i) = 1$, where i runs over all the four branching ratios $\pi^+ \pi^-$, $\pi^0 \pi^0$, $\pi e \nu$, and $\pi \mu \nu$. Input value of $B(K_S^0 \rightarrow \pi^+ \pi^-) / B(K_S^0 \rightarrow \pi^0 \pi^0)$ from AMBROSINO 06c is used. To derive $\Gamma(K_S^0 \rightarrow \pi^+ \mu \nu) / \Gamma(K_S^0 \rightarrow \pi^+ e \nu)$, lepton universality is assumed, radiative corrections from ANDRE 04 are used, and phase space integrals are taken from KTeV, ALEXOPOULOS 04A. This branching fraction enters our fit via their $\Gamma(\pi^\pm e^\mp \nu_e) / \Gamma(\pi^+ \pi^-)$ branching ratio measurement.

³⁴Uses the PDG 00 value for $B(K_S^0 \rightarrow \pi^+ \pi^-)$.

 $\Gamma(\pi^\pm \mu^\mp \nu_\mu) / \Gamma_{\text{total}}$ Γ_9 / Γ

The PDG 06 value below has not been measured but is computed to be 0.666 times the $K_S \rightarrow \pi^\pm e^\mp \nu_e$ branching fraction. It is included in the fit that constrains the four branching ratios $\pi^+ \pi^-$, $\pi^0 \pi^0$, $\pi e \nu$, and $\pi \mu \nu$ to sum to 1. This treatment, used by AMBROSINO 06E, is preferable to our previous practice of constraining the $\pi^+ \pi^-$ and $\pi^0 \pi^0$ modes to sum to 1. The 0.666 factor is obtained from AMBROSINO 06E and assumes lepton universality, radiative corrections from ANDRE 04, and phase space integrals from KTeV, ALEXOPOULOS 04A.

VALUE (units 10^{-4})	DOCUMENT ID	COMMENT
4.69 ± 0.06		OUR FIT
4.691 ± 0.001 ± 0.056	35	PDG 06 calculated from $\pi^\pm e^\mp \nu_e$

³⁵The PDG 06 value is computed to be $B_{\text{PDG06}}(\pi \mu \nu) = 0.666 B_{\text{FIT}}(\pi e \nu)$. The first error specifies the arbitrarily small error, 0.001×10^{-4} , on $B_{\text{PDG06}}(\pi \mu \nu)$ for fixed $B_{\text{FIT}}(\pi e \nu)$. The second error is that due to the uncertainty in $B_{\text{FIT}}(\pi e \nu)$.

 $\Gamma(\pi^\pm e^\mp \nu_e) / \Gamma(\pi^+ \pi^-)$ Γ_8 / Γ_2

VALUE (units 10^{-4})	EVTS	DOCUMENT ID	TECN
10.18 ± 0.12			OUR FIT
10.19 ± 0.11 ± 0.07	13k	AMBROSINO	06E KLOE

CP violating (CP) and $\Delta S = 1$ weak neutral current (S1) modes $\Gamma(3\pi^0) / \Gamma_{\text{total}}$ Γ_{10} / Γ

VALUE (units 10^{-7})	CL%	EVTS	DOCUMENT ID	TECN
< 1.2	90	37.8M	AMBROSINO	05B KLOE

• • • We do not use the following data for averages, fits, limits, etc. • • •

< 7.4	90	4.9M	36	LAI	05A NA48
< 140	90	7M		ACHASOV	99D SND
< 190	90	17300	37	ANGELOPO...	98B CPLR
< 370	90			BARMIN	83 HLBC

³⁶LAI 05A value is obtained from their bound on $|\eta_{000}|$ (not assuming $CP T$) and $B(K_L^0 \rightarrow 3\pi^0) = 0.211 \pm 0.003$, and PDG 04 values for K_L^0 and K_S^0 lifetimes. If $CP T$ is assumed then $B(K_S^0 \rightarrow 3\pi^0)_{CP T} < 2.3 \times 10^{-7}$ at 90% CL

³⁷ANGELOPOULOS 98B is from $\text{Im}(\eta_{000}) = -0.05 \pm 0.12 \pm 0.05$, assuming $\text{Re}(\eta_{000}) = \text{Re}(e) = 1.635 \times 10^{-3}$ and using the value $B(K_L^0 \rightarrow \pi^0 \pi^0) = 0.2112 \pm 0.0027$.

 $\Gamma(\mu^+ \mu^-) / \Gamma_{\text{total}}$ Γ_{11} / Γ

Test for $\Delta S = 1$ weak neutral current. Allowed by first-order weak interaction combined with electromagnetic interaction.

VALUE (units 10^{-5})	CL%	DOCUMENT ID	TECN
< 0.032	90	GJESDAL	73 ASPK

• • • We do not use the following data for averages, fits, limits, etc. • • •

< 0.7	90		HYAMS	69B OSPK
---------	----	--	-------	----------

$\Gamma(e^+e^-)/\Gamma_{\text{total}}$ Γ_{12}/Γ
 Test for $\Delta S = 1$ weak neutral current. Allowed by first-order weak interaction combined with electromagnetic interaction.

VALUE (units 10^{-7})	CL%	EVTS	DOCUMENT ID	TECN	COMMENT
< 1.4	90		ANGELOPO... 97	CPLR	
••• We do not use the following data for averages, fits, limits, etc. •••					
< 28	90	0	BLICK 94	CNTR	Hyperon facility
< 100	90		BARMIN 86	XEBC	

$\Gamma(\pi^0 e^+ e^-)/\Gamma_{\text{total}}$ Γ_{13}/Γ
 Test for $\Delta S = 1$ weak neutral current. Allowed by first-order weak interaction combined with electromagnetic interaction.

VALUE (units 10^{-9})	CL%	EVTS	DOCUMENT ID	TECN	COMMENT
$3.0 \pm 1.5 \pm 0.2$		7	³⁸ BATLEY 03	NA48	$m_{ee} > 0.165 \text{ GeV}$
••• We do not use the following data for averages, fits, limits, etc. •••					
< 140	90		LAI 01	NA48	
< 1100	90	0	BARR 93B	NA31	
< 45 000	90		GIBBONS 88	E731	
³⁸ BATLEY 03 extrapolate also to the full kinematical region using a constant form factor and a vector matrix element. The resulting branching ratio is $(5.8 \pm 2.9) \times 10^{-9}$.					

$\Gamma(\pi^0 \mu^+ \mu^-)/\Gamma_{\text{total}}$ Γ_{14}/Γ
 Test for $\Delta S = 1$ weak neutral current. Allowed by first-order weak interaction combined with electromagnetic interaction.

VALUE (units 10^{-9})	EVTS	DOCUMENT ID	TECN	COMMENT
$2.9 \pm 1.5 \pm 0.2$	6	³⁹ BATLEY 04A	NA48	NA48/1 K_S^0 beam
³⁹ Background estimate is 0.22 ± 0.18 events. Branching ratio assumes a vector matrix element and unit form factor.				

K_S^0 FORM FACTORS

For discussion, see note on K_{e3} form factors in the K^\pm section of the Particle Listings above. Because the semileptonic branching fraction is smaller in K_S^0 than K_L^0 by the ratio of the mean lives, the K_S^0 semileptonic form factor has so far been measured only in the K_{e3} mode using the linear expansion $f_+(t) = f_+(0) (1 + \lambda_+ t/m_\pi^2)$, which gives the vector form factor $f_+(t)$ relative to its value at $t = 0$.

λ_+ (LINEAR ENERGY DEPENDENCE OF f_+ IN K_{e3}^0 DECAY)

VALUE (units 10^{-2})	EVTS	DOCUMENT ID	TECN
3.39 ± 0.41	15k	AMBROSINO 06E	KLOE

CP VIOLATION IN $K_S \rightarrow 3\pi$

Written 1996 by T. Nakada (Paul Scherrer Institute) and L. Wolfenstein (Carnegie-Mellon University).

The possible final states for the decay $K^0 \rightarrow \pi^+ \pi^- \pi^0$ have isospin $I = 0, 1, 2$, and 3 . The $I = 0$ and $I = 2$ states have $CP = +1$ and K_S can decay into them without violating CP symmetry, but they are expected to be strongly suppressed by centrifugal barrier effects. The $I = 1$ and $I = 3$ states, which have no centrifugal barrier, have $CP = -1$ so that the K_S decay to these requires CP violation.

In order to see CP violation in $K_S \rightarrow \pi^+ \pi^- \pi^0$, it is necessary to observe the interference between K_S and K_L decay, which determines the amplitude ratio

$$\eta_{+-0} = \frac{A(K_S \rightarrow \pi^+ \pi^- \pi^0)}{A(K_L \rightarrow \pi^+ \pi^- \pi^0)}. \quad (1)$$

If η_{+-0} is obtained from an integration over the whole Dalitz plot, there is no contribution from the $I = 0$ and $I = 2$ final states and a nonzero value of η_{+-0} is entirely due to CP violation.

Only $I = 1$ and $I = 3$ states, which are $CP = -1$, are allowed for $K^0 \rightarrow \pi^0 \pi^0 \pi^0$ decays and the decay of K_S into $3\pi^0$ is an unambiguous sign of CP violation. Similarly to η_{+-0} , η_{000} is defined as

$$\eta_{000} = \frac{A(K_S \rightarrow \pi^0 \pi^0 \pi^0)}{A(K_L \rightarrow \pi^0 \pi^0 \pi^0)}. \quad (2)$$

If one assumes that CPT invariance holds and that there are no transitions to $I = 3$ (or to nonsymmetric $I = 1$ states), it can be shown that

$$\begin{aligned} \eta_{+-0} &= \eta_{000} \\ &= \epsilon + i \frac{\text{Im } a_1}{\text{Re } a_1}. \end{aligned} \quad (3)$$

With the Wu-Yang phase convention, a_1 is the weak decay amplitude for K^0 into $I = 1$ final states; ϵ is determined from CP violation in $K_L \rightarrow 2\pi$ decays. The real parts of η_{+-0} and η_{000} are equal to $\text{Re}(\epsilon)$. Since currently-known upper limits on $|\eta_{+-0}|$ and $|\eta_{000}|$ are much larger than $|\epsilon|$, they can be interpreted as upper limits on $\text{Im}(\eta_{+-0})$ and $\text{Im}(\eta_{000})$ and so as limits on the CP -violating phase of the decay amplitude a_1 .

CP-VIOLATION PARAMETERS IN K_S^0 DECAY

$A_S = [\Gamma(K_S^0 \rightarrow \pi^- e^+ \nu_e) - \Gamma(K_S^0 \rightarrow \pi^+ e^- \bar{\nu}_e)] / \text{SUM}$
 Such asymmetry violates CP . If CPT is assumed then $A_S = 2 \text{Re}(\epsilon)$.

VALUE (units 10^{-3})	EVTS	DOCUMENT ID	TECN
$1.5 \pm 9.6 \pm 2.9$	13k	AMBROSINO 06E	KLOE

PARAMETERS FOR $K_S^0 \rightarrow 3\pi$ DECAY

$\text{Im}(\eta_{+-0})^2 = \Gamma(K_S^0 \rightarrow \pi^+ \pi^- \pi^0, CP\text{-violating}) / \Gamma(K_L^0 \rightarrow \pi^+ \pi^- \pi^0)$
 $CP T$ assumed valid (i.e. $\text{Re}(\eta_{+-0}) \simeq 0$).

VALUE	CL%	EVTS	DOCUMENT ID	TECN
< 0.23	90	601	⁴⁰ BARMIN 85	HLBC
< 0.12	90	384	METCALF 72	ASPK

⁴⁰BARMIN 85 find $\text{Re}(\eta_{+-0}) = (0.05 \pm 0.17)$ and $\text{Im}(\eta_{+-0}) = (0.15 \pm 0.33)$. Includes events of BALDO-CEOLIN 75.

$\text{Im}(\eta_{+-0}) = \text{Im}(A(K_S^0 \rightarrow \pi^+ \pi^- \pi^0, CP\text{-violating}) / A(K_L^0 \rightarrow \pi^+ \pi^- \pi^0))$

VALUE	EVTS	DOCUMENT ID	TECN	COMMENT
$-0.002 \pm 0.009 \pm 0.002$	500k	⁴¹ ADLER 97B	97B	CPLR

••• We do not use the following data for averages, fits, limits, etc. •••

$-0.002 \pm 0.018 \pm 0.003$	137k	⁴² ADLER 96D	96D	CPLR Sup. by ADLER 97B
$-0.015 \pm 0.017 \pm 0.025$	272k	⁴³ ZOU 94	94	SPEC

⁴¹ADLER 97B also find $\text{Re}(\eta_{+-0}) = -0.002 \pm 0.007 \pm 0.004$. See also ANGELOPOULOS 98C.

⁴²The ADLER 96D fit also yields $\text{Re}(\eta_{+-0}) = 0.006 \pm 0.013 \pm 0.001$ with a correlation +0.66 between real and imaginary parts. Their results correspond to $|\eta_{+-0}| < 0.037$ with 90% CL.

⁴³ZOU 94 use theoretical constraint $\text{Re}(\eta_{+-0}) = \text{Re}(\epsilon) = 0.0016$. Without this constraint they find $\text{Im}(\eta_{+-0}) = 0.019 \pm 0.061$ and $\text{Re}(\eta_{+-0}) = 0.019 \pm 0.027$.

$\text{Im}(\eta_{000})^2 = \Gamma(K_S^0 \rightarrow 3\pi^0) / \Gamma(K_L^0 \rightarrow 3\pi^0)$

$CP T$ assumed valid (i.e. $\text{Re}(\eta_{000}) \simeq 0$). This limit determines branching ratio $\Gamma(3\pi^0)/\Gamma_{\text{total}}$ above.

VALUE	CL%	EVTS	DOCUMENT ID	TECN	COMMENT
< 0.1	90	632	⁴⁴ BARMIN 83	HLBC	
< 0.28	90		⁴⁵ GJESDAL 74B	SPEC	Indirect meas.

••• We do not use the following data for averages, fits, limits, etc. •••

⁴⁴BARMIN 83 find $\text{Re}(\eta_{000}) = (-0.08 \pm 0.18)$ and $\text{Im}(\eta_{000}) = (-0.05 \pm 0.27)$. Assuming $CP T$ invariance they obtain the limit quoted above.

⁴⁵GJESDAL 74B uses $K_{2\pi}$, $K_{\mu 3}$, and K_{e3} decay results, unitarity, and $CP T$. Calculates $|\langle \eta_{000} \rangle| = 0.26 \pm 0.20$. We convert to upper limit.

$\text{Im}(\eta_{000}) = \text{Im}(A(K_S^0 \rightarrow \pi^0 \pi^0 \pi^0) / A(K_L^0 \rightarrow \pi^0 \pi^0 \pi^0))$

$K_S^0 \rightarrow \pi^0 \pi^0 \pi^0$ violates CP conservation, in contrast to $K_S^0 \rightarrow \pi^+ \pi^- \pi^0$ which has a CP -conserving part.

VALUE	EVTS	DOCUMENT ID	TECN	COMMENT
$(-0.1 \pm 1.6) \times 10^{-2}$		OUR AVERAGE		

$0.000 \pm 0.009 \pm 0.013$	4.9M	⁴⁶ LAI 05A	05A	NA48 Assumes $CP T$
$-0.05 \pm 0.12 \pm 0.05$	17300	⁴⁷ ANGELOPO... 98B	98B	CPLR Assumes $CP T$

⁴⁶LAI 05A assumes $\text{Re}(\eta_{000}) = \text{Re}(\epsilon) = 1.66 \times 10^{-3}$. The equivalent limit is $|\eta_{000}|_{CPT} < 0.025$ at 90% CL. Without assuming $CP T$ invariance, they obtain $\text{Re}(\eta_{000}) = -0.002 \pm 0.011 \pm 0.015$ and $\text{Im}(\eta_{000}) = -0.003 \pm 0.013 \pm 0.017$ with a statistical correlation coefficient of 0.77 and an overall correlation coefficient of 0.57 between imaginary and real part. The equivalent limit is $|\eta_{000}| < 0.045$ at 90% CL.

⁴⁷ANGELOPOULOS 98B assumes $\text{Re}(\eta_{000}) = \text{Re}(\epsilon) = 1.635 \times 10^{-3}$. Without assuming $CP T$ invariance, they obtain $\text{Re}(\eta_{000}) = 0.18 \pm 0.14 \pm 0.06$ and $\text{Im}(\eta_{000}) = 0.15 \pm 0.20 \pm 0.03$.

Meson Particle Listings

K_S^0, K_L^0

$$|\eta_{000}| = |A(K_S^0 \rightarrow 3\pi^0)/A(K_L^0 \rightarrow 3\pi^0)|$$

A non-zero value violates CP invariance.

VALUE	CL%	EVTs	DOCUMENT ID	TECN
<0.018	90	37.8M	AMBROSINO 05B	KLOE

••• We do not use the following data for averages, fits, limits, etc. •••

<0.045	90	4.9M	LAI	05A NA48
--------	----	------	-----	----------

DECAY-PLANE ASYMMETRY IN $\pi^+\pi^-e^+e^-$ DECAYS

This is the CP-violating asymmetry

$$A = \frac{N_{\sin\phi\cos\phi>0.0} - N_{\sin\phi\cos\phi<0.0}}{N_{\sin\phi\cos\phi>0.0} + N_{\sin\phi\cos\phi<0.0}}$$

where ϕ is the angle between the e^+e^- and $\pi^+\pi^-$ planes in the K_S^0 rest frame.

CP asymmetry A in $K_S^0 \rightarrow \pi^+\pi^-e^+e^-$

VALUE (%)	DOCUMENT ID	TECN	COMMENT
-1.1 ± 4.1	LAI	03C NA48	1998+1999 data

••• We do not use the following data for averages, fits, limits, etc. •••

0.5 ± 4.0 ± 1.6	LAI	03C NA48	1999 data
-----------------	-----	----------	-----------

K_S^0 REFERENCES

BATLEY	07D	PL B653 145	J.R. Batley et al.	(CERN NA48 Collab.)
AMBROSINO	06C	EPJ C48 767	F. Ambrosino et al.	(KLOE Collab.)
AMBROSINO	06E	PL B636 173	F. Ambrosino et al.	(KLOE Collab.)
PDG	06	JPG 33 1	W.-M. Yao et al.	(PDG Collab.)
AMBROSINO	05B	PL B619 61	F. Ambrosino et al.	(KLOE Collab.)
BATLEY	05	PL B630 31	J.R. Batley et al.	(NA48 Collab.)
LAI	05A	PL B610 165	A. Lai et al.	(CERN NA48 Collab.)
ALEXOPOU...	04A	PR D70 092007	T. Alexopoulos et al.	(FNAL KTeV Collab.)
ANDRE	04	hep-ph/0406006	T. Andre	(EFI)
BATLEY	04A	PL B599 197	J.R. Batley et al.	(NA48 Collab.)
LAI	04	PL B578 276	A. Lai et al.	(CERN NA48 Collab.)
PDG	04	PL B592 1	S. Edelman et al.	(NA48 Collab.)
ALAVI-HARATI	03	PR D67 012005	A. Alavi-Harati et al.	(FNAL KTeV Collab.)
Also		PR D70 079904 (errata)	A. Alavi-Harati et al.	(FNAL KTeV Collab.)
BATLEY	03	PL B576 43	J.R. Batley et al.	(CERN NA48 Collab.)
LAI	03	PL B561 7	A. Lai et al.	(CERN NA48 Collab.)
LAI	03B	PL B556 105	A. Lai et al.	(CERN NA48 Collab.)
LAI	03A	EPJ C30 33	A. Lai et al.	(CERN NA48 Collab.)
ALOISIO	02	PL B535 37	A. Aloisio et al.	(KLOE Collab.)
ALOISIO	02B	PL B538 21	A. Aloisio et al.	(KLOE Collab.)
LAI	02C	PL B537 28	A. Lai et al.	(CERN NA48 Collab.)
LAI	01	PL B514 253	A. Lai et al.	(CERN NA48 Collab.)
LAI	00	PL B493 29	A. Lai et al.	(CERN NA48 Collab.)
LAI	00B	PL B496 137	A. Lai et al.	(CERN NA48 Collab.)
PDG	00	EPJ C15 1	D.E. Groom et al.	
ACHASOV	99D	PL B459 674	M.N. Achasov et al.	
AKHMETSHIN	99	PL B456 90	R.R. Akhmetshin et al.	(Novosibirsk CMD-2 Collab.)
ANGELOPO...	98B	PL B425 391	A. Angelopoulos et al.	(CLEAR Collab.)
ANGELOPO...	98C	EPJ C5 389	A. Angelopoulos et al.	(CLEAR Collab.)
PDG	98	EPJ C3 1	C. Caso et al.	
ADLER	97B	PL B407 193	R. Adler et al.	(CLEAR Collab.)
ANGELOPO...	97	PL B413 232	A. Angelopoulos et al.	(CLEAR Collab.)
BERTANZA	97	ZPHY C73 629	L. Bertanza (PISA, CERN, EDIN, MANZ, ORSAY+)	
ADLER	96D	PL B370 167	R. Adler et al.	(CLEAR Collab.)
ADLER	96E	PL B374 313	R. Adler et al.	(CLEAR Collab.)
ZOU	96	PL B369 362	Y. Zou et al.	(RUTG, MINN, MICH)
BARR	95B	PL B351 579	G.D. Barr et al.	(CERN, EDIN, MANZ, LALO+)
SCHWINGEN...	95	PRL 74 4376	B. Schwingerheuer et al.	(EFI, CHIC+)
BLICK	94	PL B334 234	A.M. Blick et al.	(SERP, JINR)
THOMSON	94	PL B337 411	G.B. Thomson et al.	(RUTG, MINN, MICH)
ZOU	94	PL B329 519	Y. Zou et al.	(RUTG, MINN, MICH)
BARR	93B	PL B304 381	G.D. Barr et al.	(CERN, EDIN, MANZ, LALO+)
GIBBONS	93	PRL 70 1199	L.K. Gibbons et al.	(FNAL E731 Collab.)
Also		PR D55 6625	L.K. Gibbons et al.	(FNAL E731 Collab.)
RAMBERG	93	PRL 70 2525	E. Ramberg et al.	(FNAL E731 Collab.)
BALATS	89	SJNP 49 828	M.Y. Balats et al.	(ITEP)
Translated from YAF		49 1332		
GIBBONS	88	PRL 61 2661	L.K. Gibbons et al.	(FNAL E731 Collab.)
BURKHARDT	87	PL B199 139	H. Burkhardt et al.	(CERN, EDIN, MANZ+)
GROSSMAN	87	PRL 59 389	N. Grossman et al.	(MINN, MICH, RUTG)
BARMAN	86	SJNP 44 622	V.V. Barmin et al.	(ITEP)
Translated from YAF		44 965		
BARMAN	86B	NC 96A 159	V.V. Barmin et al.	(ITEP, PADO)
PDG	86B	PL 170B 130	M. Aguilar-Benitez et al.	(CERN, CIT+)
BARMAN	85	NC 85A 67	V.V. Barmin et al.	(ITEP, PADO)
Also		SJNP 41 759	V.V. Barmin et al.	(ITEP)
BARMAN	83	Translated from YAF	V.V. Barmin et al.	(ITEP, PADO)
Also		PL 129B 129	V.V. Barmin et al.	(ITEP, PADO)
Translated from YAF		39 428		
ARONSON	82	PRL 48 1078	S.H. Aronson et al.	(BNL, CHIC, STAN+)
ARONSON	82B	PRL 48 1306	S.H. Aronson et al.	(BNL, CHIC, PURD)
Also		PL 116B 73	E. Fischbach et al.	(PURD, BNL, CHIC)
Also		PR D28 476	S.H. Aronson et al.	(BNL, CHIC, PURD)
Also		PR D28 495	S.H. Aronson et al.	(BNL, CHIC, PURD)
ARONSON	76	NC 32A 236	S.H. Aronson et al.	(WISC, EFI, UCSD+)
EVERHART	76	PR D14 661	G.C. Everhart et al.	(PERN)
TAUREG	76	PL 65B 92	H. Taureg et al.	(HEIDH, CERN, DORT)
BALDO...	75	NC 25A 688	M. Baldo-Ceolin et al.	(PADO, WISC)
CARITHERS	75	PRL 34 1244	W.C.J. Carithers et al.	(COLU, NYU)
BOBISUT	74	LNC 11 646	F. Bobisut et al.	(PADO)
COWELL	74	PR D10 2083	P.L. Cowell et al.	(STON, COLU)
GEWENIGER	74B	PL 48B 487	C. Geweniger et al.	(CERN, HEIDH)
GJESDAL	74B	PL 52B 119	S. Gjesdal et al.	(CERN, HEIDH)
BURGUN	73	PL 46B 481	G. Burgun et al.	(SACL, CERN)
GJESDAL	73	PL 44B 217	S. Gjesdal et al.	(CERN, HEIDH)
HILL	73	PR D9 1290	D.G. Hill et al.	(BNL, CHU)
ALITTI	72	PL 39B 568	J. Alitti, E. Lesquoy, A. Muller	(SACL)
BURGUN	72	NP B50 194	G. Burgun et al.	(SACL, CERN, OSLO)
METCALF	72	PL 40B 703	M. Metcalf et al.	(CERN, IPN, WIEN)
MORSE	72B	PRL 28 388	R. Morse et al.	(COLO, PRIN, UMD)
NAGY	72	NP B47 94	E. Nagy, F. Telbisz, G. Vesztegombi	(BUDA)
Also		PL 30B 498	G. Bozoki et al.	(BUDA)
SKJEGGEST...	72	NP B48 343	O. Skjeggestad et al.	(OSLO, CERN, SACL)
BALTAY	71	PRL 27 1678	C. Baltay et al.	(COLU)
Also		Thesis Nevis 187	W.A. Cooper	(COLU)

MOFFETT	70	BAPS 15 512	R. Moffett et al.	(ROCH)
BOZOKI	69	PL 30B 498	G. Bozoki et al.	(BUDA)
DOYLE	69	Thesis UCLR 18139	J.C. Doyle	(LRL)
GOBBI	69	PRL 22 682	B. Gobbi et al.	(ROCH)
HYAMS	69B	PL 29B 521	B.D. Hyams et al.	(CERN, MPIM)
MORFIN	69	PRL 23 660	J.G. Morfin, D. Sinclair	(MICH)
DONALD	68B	PL 27B 58	R.A. Donald et al.	(LIVP, CERN, IPNP+)
HILL	68	PR 171 1418	D.G. Hill et al.	(BNL, CMU)
AUBERT	65	PL 17 59	B. Aubert et al.	(EPOL, ORSAY)
BROWN	63	PR 130 769	J.L. Brown et al.	(LRL, MICH)
CHRETIEN	63	PR 131 2208	M. Chretien et al.	(BRAN, BROW, HARY+)
BROWN	61	NC 19 1155	J.L. Brown et al.	(MICH)
BOLDT	58B	PRL 1 150	E. Boldt, D.O. Caldwell, Y. Pal	(MIT)

OTHER RELATED PAPERS

LITTENBERG	93	ARNPS 43 729	L.S. Littenberg, G. Valencia	(BNL, FNAL)
BATTISTON	92	PRPL 214 293	R. Battiston et al.	(PGIA, CERN, TRSTT)
TRILLING	65B	UCRL 16473	G.N. Trilling	(LRL)
Updated from 1965 Argonne Conference,		page 115.		
CRAWFORD	62	CERN Conf. 827	F.S. Crawford	(LRL)
FITCH	61	NC 22 1160	V.L. Fitch, P.A. Piroue, R.B. Perkins	(PRIN+)
GOOD	61	PR 124 1223	R.H. Good et al.	(LRL)
BIRGE	60	Rochester Conf. 601	R.W. Birge et al.	(LRL, WISC)
MULLER	60	PRL 4 438	F. Muller et al.	(LRL, BNL)



$$J(J^P) = \frac{1}{2}(0^-)$$

$$m_{K_L^0} - m_{K_S^0}$$

For earlier measurements, beginning with GOOD 61 and FITCH 61, see our 1986 edition, Physics Letters **170B** 132 (1986).

OUR FIT is described in the note on "CP violation in K_L decays" in the K_L^0 Particle Listings. The result labeled "OUR FIT Assuming CPT " ["OUR FIT Not assuming CPT "] includes all measurements except those with the comment "Not assuming CPT " ["Assuming CPT "]. Measurements with neither comment do not assume CPT and enter both fits.

VALUE (10^{10} s^{-1})	DOCUMENT ID	TECN	COMMENT
0.5292 ± 0.0009 OUR FIT			Error includes scale factor of 1.2. Assuming CPT
0.5290 ± 0.0015 OUR FIT			Error includes scale factor of 1.1. Not assuming CPT
0.5261 ± 0.0015	^{1,2} ALAVI-HARATI03	KTEV	Assuming CPT
0.5288 ± 0.0043	^{2,3} ALAVI-HARATI03	KTEV	Not assuming CPT
0.5240 ± 0.0044 ± 0.0033	APOSTOLA...	99c CPLR	$K^0 \bar{K}^0$ to $\pi^+\pi^-$
0.5297 ± 0.0030 ± 0.0022	⁴ SCHWINGEN...95	E773	20-160 GeV K beams
0.5286 ± 0.0028	⁵ GIBBONS 93	E731	Assuming CPT
0.5257 ± 0.0049 ± 0.0021	⁴ GIBBONS 93c	E731	Not assuming CPT
0.5340 ± 0.00255 ± 0.0015	⁶ GEWENIGER 74c	SPEC	Gap method
0.5334 ± 0.0040 ± 0.0015	^{6,7} GJESDAL 74	SPEC	Assuming CPT
••• We do not use the following data for averages, fits, limits, etc. •••			
0.5343 ± 0.0063 ± 0.0025	⁸ ANGELOPO... 01	CPLR	
0.5295 ± 0.0020 ± 0.0003	⁹ ANGELOPO... 98D	CPLR	Assuming CPT
0.5307 ± 0.0013	¹⁰ ADLER 96c	RVUE	
0.5274 ± 0.0029 ± 0.0005	⁹ ADLER 95c	CPLR	Sup. by ANGELOPOULOS 98D
0.482 ± 0.014	¹¹ ARONSON 82b	SPEC	$E=30-110$ GeV
0.534 ± 0.007	¹² CARNEGIE 71	ASPK	Gap method
0.542 ± 0.006	¹² ARONSON 70	ASPK	Gap method
0.542 ± 0.006	CULLEN 70	CNTR	

- ALAVI-HARATI 03 fit Δm and $\tau_{K_S^0}$ simultaneously. ϕ_{+-} is constrained to the Superweak value, i.e. CPT is assumed. See " K_S^0 Mean Life" section for correlation information.
- The two ALAVI-HARATI 03 values use the same data. The first enters the "Assuming CPT " fit and the second enters the "Not assuming CPT " fit. They use 40-160 GeV K beams.
- ALAVI-HARATI 03 fit Δm , ϕ_{+-} , and $\tau_{K_S^0}$ simultaneously. See ϕ_{+-} in the " K_L CP violation" section for correlation information.
- Fits Δm and ϕ_{+-} simultaneously. GIBBONS 93c systematic error is from B. Winstein via private communication. 20-160 GeV K beams.
- GIBBONS 93 value assume $\phi_{+-} = \phi_{00} = \phi_{SW} = (43.7 \pm 0.2)^\circ$, i.e. assumes CPT . 20-160 GeV K beams.
- These two experiments have a common systematic error due to the uncertainty in the momentum scale, as pointed out in WAHL 89.
- GJESDAL 74 uses charge asymmetry in K_{e3}^0 decays.
- ANGELOPOULOS 01 uses strong interactions strangeness tagging at two different times.
- Uses \bar{K}^0 and K_{e3}^0 strangeness tagging at production and decay. Assumes CPT conservation on $\Delta S = -\Delta Q$ transitions.
- ADLER 96c is the result of a fit which includes nearly the same data as entered into the "OUR FIT" value above.
- ARONSON 82 find that Δm may depend on the kaon energy.
- ARONSON 70 and CARNEGIE 71 use K_S^0 mean life = $(0.862 \pm 0.006) \times 10^{-10}$ s. We have not attempted to adjust these values for the subsequent change in the K_S^0 mean life or in η_{+-} .

K_L^0 MEAN LIFE

VALUE (10^{-8} s)	EVTS	DOCUMENT ID	TECN	COMMENT
5.116 ± 0.020 OUR FIT				
5.099 ± 0.021 OUR AVERAGE				
5.072 ± 0.011 ± 0.035	13M	13 AMBROSINO	06 KLOE	$\sum_i B_i = 1$
5.092 ± 0.017 ± 0.025	15M	AMBROSINO	05c KLOE	
5.154 ± 0.044	0.4M	VOSBURGH	72 CNTR	

• • • We do not use the following data for averages, fits, limits, etc. • • •

5.15 ± 0.14
 13 AMBROSINO 06 uses $\phi \rightarrow K_L K_S$ with K_L tagged by $K_S \rightarrow \pi^+ \pi^-$. The four major K_L BR's are measured, the small remainder ($\pi^+ \pi^-, \pi^0 \pi^0, \gamma \gamma$) is taken from PDG 04. This KLOE K_L lifetime is obtained by imposing $\sum_i B_i = 1$. The correlation matrix among the four measured K_L BR's and this K_L lifetime is

	K_{e3}	$K_{\mu 3}$	$3\pi^0$	$\pi^+ \pi^- \pi^0$	τ_{K_L}
K_{e3}	1	-0.25	-0.56	-0.07	0.25
$K_{\mu 3}$		1	-0.43	-0.20	0.33
$3\pi^0$			1	-0.39	-0.21
$\pi^+ \pi^- \pi^0$				1	-0.39
τ_{K_L}					1

These correlations are taken into account in our fit. The average of this KLOE mean life measurement and the independent KLOE measurement in AMBROSINO 05c is $(5.084 \pm 0.023) \times 10^{-8}$ s.

 K_L^0 DECAY MODES

Mode	Fraction (Γ_i/Γ)	Scale factor/ Confidence level
Semileptonic modes		
Γ_1 $\pi^\pm e^\mp \nu_e$ Called K_{e3}^0 .	[a] (40.55 ± 0.12) %	S=1.8
Γ_2 $\pi^\pm \mu^\mp \nu_\mu$ Called $K_{\mu 3}^0$.	[a] (27.04 ± 0.07) %	S=1.1
Γ_3 ($\pi \mu$ atom) ν	(1.05 ± 0.11) × 10 ⁻⁷	
Γ_4 $\pi^0 \pi^\pm e^\mp \nu$	[a] (5.20 ± 0.11) × 10 ⁻⁵	
Γ_5 $\pi^\pm e^\mp \nu e^+ e^-$	[a] (1.28 ± 0.04) × 10 ⁻⁵	

Hadronic modes, including Charge conjugation × Parity Violating (CPV) modes

Γ_6 $3\pi^0$	(19.52 ± 0.12) %	S=1.7
Γ_7 $\pi^+ \pi^- \pi^0$	(12.54 ± 0.05) %	
Γ_8 $\pi^+ \pi^-$	CPV [b] (1.966 ± 0.010) × 10 ⁻³	S=1.6
Γ_9 $\pi^0 \pi^0$	CPV (8.65 ± 0.06) × 10 ⁻⁴	S=1.8

Semileptonic modes with photons

Γ_{10} $\pi^\pm e^\mp \nu_e \gamma$	[a,c,d] (3.80 ± 0.08) × 10 ⁻³	
Γ_{11} $\pi^\pm \mu^\mp \nu_\mu \gamma$	(5.65 ± 0.23) × 10 ⁻⁴	

Hadronic modes with photons or $\ell\bar{\ell}$ pairs

Γ_{12} $\pi^0 \pi^0 \gamma$	< 5.6	× 10 ⁻⁶	CL=90%
Γ_{13} $\pi^+ \pi^- \gamma$	[c,d] (4.15 ± 0.15) × 10 ⁻⁵		S=2.8
Γ_{14} $\pi^+ \pi^- \gamma$ (DE)	(2.84 ± 0.11) × 10 ⁻⁵		S=2.0
Γ_{15} $\pi^0 2\gamma$	[d] (1.32 ± 0.14) × 10 ⁻⁶		S=3.6
Γ_{16} $\pi^0 \gamma e^+ e^-$	(1.62 ± 0.17) × 10 ⁻⁸		

Other modes with photons or $\ell\bar{\ell}$ pairs

Γ_{17} 2γ	(5.47 ± 0.04) × 10 ⁻⁴	S=1.2	
Γ_{18} 3γ	< 2.4	× 10 ⁻⁷	CL=90%
Γ_{19} $e^+ e^- \gamma$	(9.50 ± 0.35) × 10 ⁻⁶	S=1.7	
Γ_{20} $\mu^+ \mu^- \gamma$	(3.59 ± 0.11) × 10 ⁻⁷	S=1.3	
Γ_{21} $e^+ e^- \gamma \gamma$	[d] (5.95 ± 0.33) × 10 ⁻⁷		
Γ_{22} $\mu^+ \mu^- \gamma \gamma$	[d] (1.0 ± 0.8/-0.6) × 10 ⁻⁸		

Charge conjugation × Parity (CP) or Lepton Family number (LF) violating modes, or $\Delta S = 1$ weak neutral current (SI) modes

Γ_{23} $\mu^+ \mu^-$	SI (6.84 ± 0.11) × 10 ⁻⁹		
Γ_{24} $e^+ e^-$	SI (9 ± 4) × 10 ⁻¹²		
Γ_{25} $\pi^+ \pi^- e^+ e^-$	SI [d] (3.11 ± 0.19) × 10 ⁻⁷		
Γ_{26} $\pi^0 \pi^0 e^+ e^-$	SI < 6.6	× 10 ⁻⁹	CL=90%
Γ_{27} $\mu^+ \mu^- e^+ e^-$	SI (2.69 ± 0.27) × 10 ⁻⁹		
Γ_{28} $e^+ e^- e^+ e^-$	SI (3.56 ± 0.21) × 10 ⁻⁸		
Γ_{29} $\pi^0 \mu^+ \mu^-$	CP,SI [e] < 3.8	× 10 ⁻¹⁰	CL=90%
Γ_{30} $\pi^0 e^+ e^-$	CP,SI [e] < 2.8	× 10 ⁻¹⁰	CL=90%
Γ_{31} $\pi^0 \nu \bar{\nu}$	CP,SI [f] < 2.1	× 10 ⁻⁷	CL=90%
Γ_{32} $\pi^0 \pi^0 \nu \bar{\nu}$	SI < 4.7	× 10 ⁻⁵	CL=90%
Γ_{33} $e^\pm \mu^\mp$	LF [a] < 4.7	× 10 ⁻¹²	CL=90%
Γ_{34} $e^\pm e^\pm \mu^\mp \mu^\mp$	LF [a] < 4.12	× 10 ⁻¹¹	CL=90%
Γ_{35} $\pi^0 \mu^\pm e^\mp$	LF [a] < 6.2	× 10 ⁻⁹	CL=90%

[a] The value is for the sum of the charge states or particle/antiparticle states indicated.

[b] This mode includes gammas from inner bremsstrahlung but not the direct emission mode $K_L^0 \rightarrow \pi^+ \pi^- \gamma$ (DE).

[c] Most of this radiative mode, the low-momentum γ part, is also included in the parent mode listed without γ 's.

[d] See the Particle Listings below for the energy limits used in this measurement.

[e] Allowed by higher-order electroweak interactions.

[f] Violates CP in leading order. Test of direct CP violation since the indirect CP-violating and CP-conserving contributions are expected to be suppressed.

CONSTRAINED FIT INFORMATION

An overall fit to the mean life and 15 branching ratios uses 27 measurements and one constraint to determine 11 parameters. The overall fit has a $\chi^2 = 35.7$ for 17 degrees of freedom.

The following *off-diagonal* array elements are the correlation coefficients $\langle \delta p_i \delta p_j \rangle / (\delta p_i \delta p_j)$, in percent, from the fit to parameters p_i , including the branching fractions, $x_i \equiv \Gamma_i / \Gamma_{\text{total}}$. The fit constrains the x_i whose labels appear in this array to sum to one.

x_2	-17									
x_6	-80	-31								
x_7	-21	-20	-10							
x_8	56	-9	-51	-1						
x_9	30	-23	-11	-15	62					
x_{13}	7	-1	-7	0	13	8				
x_{14}	6	-1	-6	0	12	7	93			
x_{17}	-50	-24	66	-9	-25	7	-3	-3		
x_{19}	-8	-3	10	-1	-5	-1	-1	-1	7	
Γ	-9	-10	9	13	-4	-2	-1	-1	6	1
	x_1	x_2	x_6	x_7	x_8	x_9	x_{13}	x_{14}	x_{17}	x_{19}

Mode	Rate (10^8 s^{-1})	Scale factor
Γ_1 $\pi^\pm e^\mp \nu_e$ Called K_{e3}^0 .	[a] 0.0793 ± 0.0004	1.2
Γ_2 $\pi^\pm \mu^\mp \nu_\mu$ Called $K_{\mu 3}^0$.	[a] 0.05286 ± 0.00024	
Γ_6 $3\pi^0$	0.03816 ± 0.00029	1.4
Γ_7 $\pi^+ \pi^- \pi^0$	0.02451 ± 0.00015	
Γ_8 $\pi^+ \pi^-$	[b] (3.844 ± 0.024) × 10 ⁻⁴	1.2
Γ_9 $\pi^0 \pi^0$	(1.690 ± 0.013) × 10 ⁻⁴	1.4
Γ_{13} $\pi^+ \pi^- \gamma$	[c,d] (8.11 ± 0.29) × 10 ⁻⁶	2.7
Γ_{14} $\pi^+ \pi^- \gamma$ (DE)	(5.55 ± 0.22) × 10 ⁻⁶	2.0
Γ_{17} 2γ	(1.069 ± 0.009) × 10 ⁻⁴	1.1
Γ_{19} $e^+ e^- \gamma$	(1.86 ± 0.07) × 10 ⁻⁶	1.7

 K_L^0 DECAY RATES

VALUE (10^6 s^{-1})	EVTS	DOCUMENT ID	TECN	COMMENT	Γ_7
2.451 ± 0.015 OUR FIT					

• • • We do not use the following data for averages, fits, limits, etc. • • •

2.32 +0.13/-0.15	192	BALDO-...	75	HLBC	Assumes CP
2.35 ± 0.20	180	14 JAMES	72	HBC	Assumes CP
2.71 ± 0.28	99	CHO	71	DBC	Assumes CP
2.5 ± 0.3	98	14 JAMES	71	HBC	Assumes CP
2.12 ± 0.33	50	MEISNER	71	HBC	Assumes CP
2.20 ± 0.35	53	WEBBER	70	HBC	Assumes CP
2.62 +0.28/-0.27	136	BEHR	66	HLBC	Assumes CP
3.26 ± 0.77	18	ANDERSON	65	HBC	
1.4 ± 0.4	14	FRANZINI	65	HBC	

14 JAMES 72 is a final measurement and includes JAMES 71.

VALUE (10^6 s^{-1})	EVTS	DOCUMENT ID	TECN	COMMENT	Γ_1
7.93 ± 0.04 OUR FIT				Error includes scale factor of 1.2.	

• • • We do not use the following data for averages, fits, limits, etc. • • •

7.81 ± 0.56	620	CHAN	71	HBC	
7.52 +0.85/-0.72		AUBERT	65	HLBC	$\Delta S = \Delta Q, CP$ assumed

Meson Particle Listings

 K_L^0 $\Gamma(\pi^\pm e^\mp \nu_e) + \Gamma(\pi^\pm \mu^\mp \nu_\mu)$ $(\Gamma_1 + \Gamma_2)$

VALUE (10^6 s^{-1})	EVTS	DOCUMENT ID	TECN	COMMENT
13.21 ± 0.05 OUR FIT	Error includes scale factor of 1.1.			
••• We do not use the following data for averages, fits, limits, etc. •••				
12.4 ± 0.7	410	15 BURGUN	72 HBC	$K^+ p \rightarrow K^0 p \pi^+$
8.47 ± 1.69	126	15 MANN	72 HBC	$K^- p \rightarrow n \bar{K}^0$
13.1 ± 1.3	252	15 WEBBER	71 HBC	$K^- p \rightarrow n \bar{K}^0$
11.6 ± 0.9	393	15,16 CHO	70 DBC	$K^+ n \rightarrow K^0 p$
10.3 ± 0.8	335	16 HILL	67 DBC	$K^+ n \rightarrow K^0 p$
9.85 ± 1.15 -1.05	109	15 FRANZINI	65 HBC	

¹⁵ Assumes $\Delta S = \Delta Q$ rule.

¹⁶ CHO 70 includes events of HILL 67.

 K_L^0 BRANCHING RATIOS

Semileptonic modes

 $\Gamma(\pi^\pm e^\mp \nu_e)/\Gamma_{\text{total}}$ Γ_1/Γ

VALUE	EVTS	DOCUMENT ID	TECN	COMMENT
0.4055 ± 0.0012 OUR FIT	Error includes scale factor of 1.8.			
0.4047 ± 0.0028 OUR AVERAGE	Error includes scale factor of 3.1.			
0.4007 ± 0.0005 ± 0.0015	13M	17 AMBROSINO 06	KLOE	Not fitted
0.4067 ± 0.0011		18 ALEXOPOU... 04	KTEV	Not fitted

¹⁷ There are correlations between these five KLOE measurements: $B(K_L \rightarrow \pi e \nu)$, $B(K_L \rightarrow \pi \mu \nu)$, $B(K_L \rightarrow 3\pi^0)$, $B(K_L \rightarrow \pi^+ \pi^- \pi^0)$, and τ_{K_L} measured in AMBROSINO 06. See the footnote for the τ_{K_L} measurement for the correlation matrix.

¹⁸ ALEXOPOULOS 04 constrains $\sum_j B_j = 0.9993$ for the six major K_L branching fractions. The correlations among these branching fractions are taken into account in our fit. The correlation matrix is

	K_{e3}	$K_{\mu 3}$	$3\pi^0$	$\pi^+ \pi^- \pi^0$	$\pi^+ \pi^-$	$\pi^0 \pi^0$
K_{e3}	1					
$K_{\mu 3}$	0.15	1				
$3\pi^0$	-0.77	-0.62	1			
$\pi^+ \pi^- \pi^0$	0.18	0.08	-0.54	1		
$\pi^+ \pi^-$	0.28	0.22	-0.48	0.49	1	
$\pi^0 \pi^0$	-0.72	-0.54	0.89	-0.46	-0.39	1

 $\Gamma(\pi^\pm \mu^\mp \nu_\mu)/\Gamma_{\text{total}}$ Γ_2/Γ

VALUE	EVTS	DOCUMENT ID	TECN	COMMENT
0.2704 ± 0.0007 OUR FIT	Error includes scale factor of 1.1.			
0.2700 ± 0.0008 OUR AVERAGE				
0.2698 ± 0.0005 ± 0.0015	13M	19 AMBROSINO 06	KLOE	
0.2701 ± 0.0009		20 ALEXOPOU... 04	KTEV	

¹⁹ There are correlations between these five KLOE measurements: $B(K_L \rightarrow \pi e \nu)$, $B(K_L \rightarrow \pi \mu \nu)$, $B(K_L \rightarrow 3\pi^0)$, $B(K_L \rightarrow \pi^+ \pi^- \pi^0)$, and τ_{K_L} measured in AMBROSINO 06. See the footnote for the τ_{K_L} measurement for the correlation matrix.

²⁰ For correlations with other ALEXOPOULOS 04 measurements, see the footnote with their $B(K_L \rightarrow \pi e \nu)$ measurement.

 $[\Gamma(\pi^\pm e^\mp \nu_e) + \Gamma(\pi^\pm \mu^\mp \nu_\mu)]/\Gamma_{\text{total}}$ $(\Gamma_1 + \Gamma_2)/\Gamma$

VALUE	DOCUMENT ID	TECN	COMMENT
0.6760 ± 0.0013 OUR FIT	Error includes scale factor of 1.7.		

 $\Gamma(\pi^\pm \mu^\mp \nu_\mu)/\Gamma(\pi^\pm e^\mp \nu_e)$ Γ_2/Γ_1

VALUE	EVTS	DOCUMENT ID	TECN	COMMENT
0.6669 ± 0.0028 OUR FIT	Error includes scale factor of 1.3.			
0.666 ± 0.004 OUR AVERAGE	Error includes scale factor of 1.6.			
0.6740 ± 0.0059	13M	21 AMBROSINO 06	KLOE	Not in fit
0.6640 ± 0.0014 ± 0.0022	394K	22 ALEXOPOU... 04	KTEV	Not in fit
••• We do not use the following data for averages, fits, limits, etc. •••				
0.702 ± 0.011	33k	CHO	80 HBC	
0.662 ± 0.037	10k	WILLIAMS	74 ASPK	
0.741 ± 0.044	6700	BRANDENB...	73 HBC	
0.662 ± 0.030	1309	EVANS	73 HLBC	
0.68 ± 0.08	3548	BASILE	70 OSPK	
0.71 ± 0.05	770	BUDAGOV	68 HLBC	

²¹ AMBROSINO 06 enters the fit via their separate measurements of these two modes.

²² ALEXOPOULOS 04 enters the fit via their separate measurements of these two modes.

 $\Gamma((\pi \mu \text{atom})\nu)/\Gamma(\pi^\pm \mu^\mp \nu_\mu)$ Γ_3/Γ_2

VALUE (units 10^{-7})	EVTS	DOCUMENT ID	TECN	COMMENT
3.90 ± 0.39	155	23 ARONSON 86	SPEC	
••• We do not use the following data for averages, fits, limits, etc. •••				
seen	18	COOMBES 76	WIRE	
²³ ARONSON 86 quote theoretical value of $(4.31 \pm 0.08) \times 10^{-7}$.				

 $\Gamma(\pi^0 \pi^\pm e^\mp \nu)/\Gamma_{\text{total}}$ Γ_4/Γ

VALUE (units 10^{-5})	CL%	EVTS	DOCUMENT ID	TECN	COMMENT
5.20 ± 0.11 OUR AVERAGE					
5.21 ± 0.07 ± 0.09		5402	BATLEY 04	NA48	
5.16 ± 0.20 ± 0.22		729	MAKOFF 93	E731	
••• We do not use the following data for averages, fits, limits, etc. •••					
6.2 ± 2.0		16	CARROLL 80c	SPEC	
< 220		90	24 DONALDSON 74	SPEC	
²⁴ DONALDSON 74 uses $K_L^0 \rightarrow \pi^+ \pi^- \pi^0$ / (all K_L^0 decays) = 0.126.					

 $\Gamma(\pi^\pm e^\mp \nu e^+ e^-)/\Gamma(\pi^+ \pi^- \pi^0)$ Γ_5/Γ_7

VALUE (units 10^{-5})	EVTS	DOCUMENT ID	TECN	COMMENT
10.23 ± 0.18 ± 0.28	19k	25 ABOUZAID 07c	KTEV	$M_{ee} > 5 \text{ MeV}$, $E_{ee}^* > 30 \text{ MeV}$
²⁵ E_{ee}^* is the energy of the $e^+ e^-$ pair in the kaon rest frame. ABOUZAID 07c reports $[\Gamma(K_L^0 \rightarrow \pi^\pm e^\mp \nu e^+ e^-)/\Gamma(K_L^0 \rightarrow \pi^+ \pi^- \pi^0)] / [B(\pi^0 \rightarrow e^+ e^- \gamma)] = (8.54 \pm 0.07 \pm 0.13) \times 10^{-3}$. We multiply by our best value $B(\pi^0 \rightarrow e^+ e^- \gamma) = (1.198 \pm 0.032) \times 10^{-2}$. Our first error is their experiment's error and our second error is the systematic error from using our best value.				

Hadronic modes,

including Charge conjugation × Parity Violating (CPV) modes

 $\Gamma(3\pi^0)/\Gamma_{\text{total}}$ Γ_6/Γ

VALUE	EVTS	DOCUMENT ID	TECN	COMMENT
0.1952 ± 0.0012 OUR FIT	Error includes scale factor of 1.7.			
0.1969 ± 0.0026 OUR AVERAGE	Error includes scale factor of 2.0.			
0.1997 ± 0.0003 ± 0.0019	13M	26 AMBROSINO 06	KLOE	Not fitted
0.1945 ± 0.0018		26 ALEXOPOU... 04	KTEV	Not fitted

²⁶ We exclude these $B(K_L \rightarrow 3\pi^0)$ measurements from our fit because the authors have constrained K_L branching fractions to sum to one. It enters our fit via the other measurements from the experiment and their correlations, along with our constraint that the fitted branching fractions sum to one.

 $\Gamma(3\pi^0)/\Gamma(\pi^\pm e^\mp \nu_e)$ Γ_6/Γ_1

VALUE	EVTS	DOCUMENT ID	TECN	COMMENT
0.481 ± 0.004 OUR FIT	Error includes scale factor of 1.9.			
0.4782 ± 0.0014 ± 0.0053	209K	27 ALEXOPOU... 04	KTEV	Not in fit
••• We do not use the following data for averages, fits, limits, etc. •••				
0.545 ± 0.004 ± 0.009	38k	KREUTZ 95	NA31	

²⁷ This measurement enters the fit via their separate measurements of these two modes.

 $\Gamma(3\pi^0)/[\Gamma(\pi^\pm e^\mp \nu_e) + \Gamma(\pi^\pm \mu^\mp \nu_\mu) + \Gamma(\pi^+ \pi^- \pi^0)]$ $\Gamma_6/(\Gamma_1 + \Gamma_2 + \Gamma_7)$

VALUE	EVTS	DOCUMENT ID	TECN	COMMENT
0.2436 ± 0.0019 OUR FIT	Error includes scale factor of 1.7.			
••• We do not use the following data for averages, fits, limits, etc. •••				
0.251 ± 0.014	549	BUDAGOV 68	HLBC	ORSAY measur.
0.277 ± 0.021	444	BUDAGOV 68	HLBC	Ecole polytec.meas
0.31 ± 0.07 -0.06	29	KULYUKINA 68	CC	
0.24 ± 0.08	24	ANIKINA 64	CC	

 $\Gamma(3\pi^0)/\Gamma(\pi^+ \pi^- \pi^0)$ Γ_6/Γ_7

VALUE	EVTS	DOCUMENT ID	TECN	COMMENT
1.557 ± 0.012 OUR FIT	Error includes scale factor of 1.3.			
1.582 ± 0.027	13M	28 AMBROSINO 06	KLOE	Not in fit
••• We do not use the following data for averages, fits, limits, etc. •••				
1.611 ± 0.014 ± 0.034	28k	KREUTZ 95	NA31	
1.65 ± 0.07	883	BARMIN 72b	HLBC	Error statistical only
1.80 ± 0.13	1010	BUDAGOV 68	HLBC	
2.0 ± 0.6	188	ALEKSANYAN 64b	FBC	

²⁸ AMBROSINO 06 enters the fit via their separate measurements of these two modes.

 $\Gamma(\pi^+ \pi^- \pi^0)/\Gamma_{\text{total}}$ Γ_7/Γ

VALUE	EVTS	DOCUMENT ID	TECN	COMMENT
0.1254 ± 0.0005 OUR FIT	Error includes scale factor of 1.7.			
0.1255 ± 0.0006 OUR AVERAGE				
0.1263 ± 0.0004 ± 0.0011	13M	29 AMBROSINO 06	KLOE	
0.1252 ± 0.0007		30 ALEXOPOU... 04	KTEV	

²⁹ There are correlations between these five KLOE measurements: $B(K_L \rightarrow \pi e \nu)$, $B(K_L \rightarrow \pi \mu \nu)$, $B(K_L \rightarrow 3\pi^0)$, $B(K_L \rightarrow \pi^+ \pi^- \pi^0)$, and τ_{K_L} measured in AMBROSINO 06. See the footnote for the τ_{K_L} measurement for the correlation matrix.

³⁰ For correlations with other ALEXOPOULOS 04 measurements, see the footnote with their $B(K_L \rightarrow \pi e \nu)$ measurement.

 $\Gamma(\pi^+ \pi^- \pi^0)/\Gamma(\pi^\pm e^\mp \nu_e)$ Γ_7/Γ_1

VALUE	EVTS	DOCUMENT ID	TECN	COMMENT
0.3092 ± 0.0017 OUR FIT	Error includes scale factor of 1.2.			
0.3078 ± 0.0005 ± 0.0017	799K	31 ALEXOPOU... 04	KTEV	Not in fit
••• We do not use the following data for averages, fits, limits, etc. •••				
0.336 ± 0.003 ± 0.007	28k	KREUTZ 95	NA31	

³¹ This measurement enters the fit via their separate measurements for the two modes.

 $\Gamma(\pi^+ \pi^- \pi^0)/[\Gamma(\pi^\pm e^\mp \nu_e) + \Gamma(\pi^\pm \mu^\mp \nu_\mu) + \Gamma(\pi^+ \pi^- \pi^0)]$ $\Gamma_7/(\Gamma_1 + \Gamma_2 + \Gamma_7)$

VALUE	EVTS	DOCUMENT ID	TECN	COMMENT
0.1565 ± 0.0007 OUR FIT	Error includes scale factor of 1.1.			
••• We do not use the following data for averages, fits, limits, etc. •••				
0.163 ± 0.003	6499	CHO 77	HBC	
0.1605 ± 0.0038	1590	ALEXANDER 73b	HBC	
0.146 ± 0.004	3200	BRANDENB... 73	HBC	
0.159 ± 0.010	558	EVANS 73	HLBC	
0.167 ± 0.016	1402	KULYUKINA 68	CC	
0.161 ± 0.005		HOPKINS 67	HBC	
0.162 ± 0.015	126	HAWKINS 66	HBC	
0.159 ± 0.015	326	ASTBURY 65b	CC	
0.178 ± 0.017	566	GUIDONI 65	HBC	
0.144 ± 0.004	1729	HOPKINS 65	HBC	See HOPKINS 67

$\Gamma(\pi^+\pi^-)/\Gamma_{total}$ Γ_8/Γ

Violates CP conservation.
 VALUE (units 10^{-3}) DOCUMENT ID TECN COMMENT
1.966 ± 0.010 OUR FIT Error includes scale factor of 1.6.
1.975 ± 0.012 ³² ALEXOPOU... 04 KTEV
³² For correlations with other ALEXOPOULOS 04 measurements, see the footnote with their $B(K_L \rightarrow \pi e \nu)$ measurement.

$\Gamma(\pi^+\pi^-)/\Gamma(\pi^\pm e^\mp \nu_e)$ Γ_8/Γ_1

VALUE (units 10^{-3}) EVTS DOCUMENT ID TECN COMMENT
4.849 ± 0.020 OUR FIT Error includes scale factor of 1.1.
4.840 ± 0.020 OUR AVERAGE
 4.826 ± 0.022 ± 0.016 47k ³³ LAI 07 NA48
 4.856 ± 0.017 ± 0.023 84k ³⁴ ALEXOPOU... 04 KTEV Not in fit

³³ The LAI 07 central value of 4.835×10^{-3} has been reduced by 0.19% to 4.826×10^{-3} to subtract the contribution from the direct emission mode $K_L^0 \rightarrow \pi^+\pi^-\gamma(DE)$.

³⁴ This measurement enters the fit via their separate measurements for the two modes.

$[\Gamma(\pi^+\pi^-) + \Gamma(\pi^+\pi^-\gamma(DE))]/\Gamma(\pi^\pm \mu^\mp \nu_\mu)$ $(\Gamma_8 + \Gamma_{14})/\Gamma_2$

VALUE (units 10^{-3}) EVTS DOCUMENT ID TECN COMMENT
7.38 ± 0.04 OUR FIT Error includes scale factor of 1.4.
7.275 ± 0.042 ± 0.054 45k ³⁵ AMBROSINO 06F KLOE

³⁵ Fully inclusive. Taking $B(K_L^0 \rightarrow \pi \mu \nu)$ from KLOE, AMBROSINO 06, $B(K_L^0 \rightarrow \pi^+\pi^- + \pi^+\pi^-\gamma(DE)) = (1.963 \pm 0.012 \pm 0.017) \times 10^{-3}$ is obtained.

$\Gamma(\pi^+\pi^-)/[\Gamma(\pi^\pm e^\mp \nu_e) + \Gamma(\pi^\pm \mu^\mp \nu_\mu)]$ $\Gamma_8/(\Gamma_1 + \Gamma_2)$

Violates CP conservation.
 VALUE (units 10^{-3}) EVTS DOCUMENT ID TECN COMMENT
2.909 ± 0.013 OUR FIT Error includes scale factor of 1.3.

• • • We do not use the following data for averages, fits, limits, etc. • • •
 3.13 ± 0.14 1687 COUPAL 85 SPEC $\eta_{+-} = 2.28 \pm 0.06$
 3.04 ± 0.14 2703 DEVOE 77 SPEC $\eta_{+-} = 2.25 \pm 0.05$
 2.51 ± 0.23 309 ³⁶ DEBOUARD 67 OSPK $\eta_{+-} = 2.00 \pm 0.09$
 2.35 ± 0.19 525 ³⁶ FITCH 67 OSPK $\eta_{+-} = 1.94 \pm 0.08$

³⁶ Old experiments excluded from fit. See subsection on η_{+-} in section on "PARAMETERS FOR $K_L^0 \rightarrow 2\pi$ DECAY" below for average η_{+-} of these experiments and for note on discrepancy.

$\Gamma(\pi^\pm e^\mp \nu_e)/\Gamma(2 \text{ tracks})$ $\Gamma_1/(\Gamma_1 + \Gamma_2 + 0.03508\Gamma_6 + \Gamma_7 + \Gamma_8)$

$\Gamma(2 \text{ tracks}) = \Gamma(\pi^\pm e^\mp \nu_e) + \Gamma(\pi^\pm \mu^\mp \nu_\mu) + 0.03508 \Gamma(3\pi^0) + \Gamma(\pi^+\pi^-\pi^0) + \Gamma(\pi^+\pi^-)$ where 0.03508 is the fraction of $3\pi^0$ events with one Dalitz decay ($\pi^0 \rightarrow \gamma e^+ e^-$).

VALUE EVTS DOCUMENT ID TECN COMMENT
0.5006 ± 0.0010 OUR FIT Error includes scale factor of 1.4.
0.4978 ± 0.0035 6.8M LAI 04B NA48

$\Gamma(\pi^+\pi^-)/[\Gamma(\pi^\pm e^\mp \nu_e) + \Gamma(\pi^\pm \mu^\mp \nu_\mu) + \Gamma(\pi^+\pi^-\pi^0)]$ $\Gamma_8/(\Gamma_1 + \Gamma_2 + \Gamma_7)$

Violates CP conservation.
 VALUE (units 10^{-3}) EVTS DOCUMENT ID TECN COMMENT
2.454 ± 0.011 OUR FIT Error includes scale factor of 1.3.

• • • We do not use the following data for averages, fits, limits, etc. • • •
 2.60 ± 0.07 4200 ³⁷ MESSNER 73 ASPK $\eta_{+-} = 2.23 \pm 0.05$

³⁷ From same data as $\Gamma(\pi^+\pi^-)/\Gamma(\pi^+\pi^-\pi^0)$ MESSNER 73, but with different normalization.

$\Gamma(\pi^+\pi^-)/\Gamma(\pi^+\pi^-\pi^0)$ Γ_8/Γ_7

Violates CP conservation.
 VALUE (units 10^{-2}) EVTS DOCUMENT ID TECN COMMENT
1.568 ± 0.010 OUR FIT Error includes scale factor of 1.3.

• • • We do not use the following data for averages, fits, limits, etc. • • •
 1.64 ± 0.04 4200 MESSNER 73 ASPK $\eta_{+-} = 2.23$

$\Gamma(\pi^0\pi^0)/\Gamma_{total}$ Γ_9/Γ

Violates CP conservation.
 VALUE (units 10^{-3}) DOCUMENT ID TECN COMMENT
0.865 ± 0.006 OUR FIT Error includes scale factor of 1.8.
0.865 ± 0.012 ³⁸ ALEXOPOU... 04 KTEV

³⁸ For correlations with other ALEXOPOULOS 04 measurements, see the footnote with their $B(K_L \rightarrow \pi e \nu)$ measurement.

$\Gamma(\pi^0\pi^0)/\Gamma(\pi^+\pi^-)$ Γ_9/Γ_8

Violates CP conservation.
 VALUE DOCUMENT ID TECN COMMENT
0.4397 ± 0.0024 OUR FIT Error includes scale factor of 1.9.
0.4391 ± 0.0013 ETAFIT 08

$\Gamma(\pi^0\pi^0)/\Gamma(3\pi^0)$ Γ_9/Γ_6

Violates CP conservation.
 VALUE (units 10^{-2}) EVTS DOCUMENT ID TECN COMMENT
0.443 ± 0.004 OUR FIT Error includes scale factor of 2.2.
0.4446 ± 0.0016 ± 0.0019 100K ³⁹ ALEXOPOU... 04 KTEV Not in fit

• • • We do not use the following data for averages, fits, limits, etc. • • •
 0.37 ± 0.08 29 BARMIN 70 HLBC $\eta_{00} = 2.02 \pm 0.23$
 0.32 ± 0.15 30 BUDAGOV 70 HLBC $\eta_{00} = 1.9 \pm 0.5$
 0.46 ± 0.11 57 BANNER 69 OSPK $\eta_{00} = 2.2 \pm 0.3$

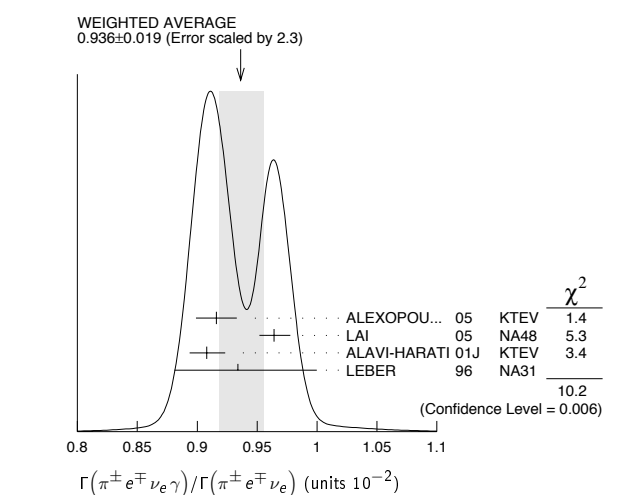
³⁹ This measurement enters the fit via their separate measurements for the two modes.

Semileptonic modes with photons $\Gamma(\pi^\pm e^\mp \nu_e \gamma)/\Gamma(\pi^\pm e^\mp \nu_e)$ Γ_{10}/Γ_1

VALUE (units 10^{-2}) EVTS DOCUMENT ID TECN COMMENT
0.936 ± 0.019 OUR AVERAGE Error includes scale factor of 2.3. See the ideogram below.
 0.916 ± 0.017 4309 ⁴⁰ ALEXOPOU... 05 KTEV $E_\gamma^* > 30 \text{ MeV}, \theta_{e\gamma}^* > 20^\circ$

0.964 ± 0.008 $^{+0.011}_{-0.009}$ 19K LAI 05 NA48 $E_\gamma^* > 30 \text{ MeV}, \theta_{e\gamma}^* > 20^\circ$
 0.908 ± 0.008 $^{+0.013}_{-0.012}$ 15k ALAVI-HARATI01J KTEV $E_\gamma^* \geq 30 \text{ MeV}, \theta_{e\gamma}^* \geq 20^\circ$
 0.934 ± 0.036 $^{+0.055}_{-0.039}$ 1384 LEBER 96 NA31 $E_\gamma^* \geq 30 \text{ MeV}, \theta_{e\gamma}^* \geq 20^\circ$

⁴⁰ Also measured cut $E_\gamma^* > 10 \text{ MeV}, \theta_{e\gamma}^* > 0^\circ$ 14221 evts: $\Gamma(\pi^\pm e^\mp \nu_e \gamma) / \Gamma(\pi^\pm e^\mp \nu_e) = (4.942 \pm 0.062)\%$.



$\Gamma(\pi^\pm \mu^\mp \nu_\mu \gamma)/\Gamma(\pi^\pm \mu^\mp \nu_\mu)$ Γ_{11}/Γ_2

VALUE (units 10^{-3}) EVTS DOCUMENT ID TECN COMMENT
2.09 ± 0.08 OUR AVERAGE
 2.09 ± 0.09 ⁴¹ ALEXOPOU... 05 KTEV $E_\gamma^* > 30 \text{ MeV}$

2.08 ± 0.17 $^{+0.16}_{-0.21}$ 252 BENDER 98 NA48 $E_\gamma^* \geq 30 \text{ MeV}$

⁴¹ Also measured cut $E_\gamma^* > 10 \text{ MeV}$, 1385 evts: $\Gamma(\pi^\pm \mu^\mp \nu_\mu \gamma) / \Gamma(\pi^\pm \mu^\mp \nu_\mu) = (0.530 \pm 0.014 \pm 0.012)\%$.

Hadronic modes with photons or $e\bar{e}$ pairs $\Gamma(\pi^0\pi^0\gamma)/\Gamma_{total}$ Γ_{12}/Γ

VALUE (units 10^{-6}) CL% DOCUMENT ID TECN COMMENT
< 5.6 90 BARR 94 NA31

• • • We do not use the following data for averages, fits, limits, etc. • • •
 <230 90 ROBERTS 94 E799

$\Gamma(\pi^+\pi^-\gamma)/\Gamma(\pi^+\pi^-\pi^0)$ Γ_{13}/Γ_7

For earlier limits see our 1992 edition Physical Review **D45** S1 (1992).
 VALUE (units 10^{-4}) EVTS DOCUMENT ID TECN COMMENT

• • • We do not use the following data for averages, fits, limits, etc. • • •
 1.23 ± 0.13 516 ^{42,43} CARROLL 80B SPEC $E_\gamma^* > 20 \text{ MeV}$

2.33 ± 0.23 546 ^{42,44} CARROLL 80B SPEC
 3.56 ± 0.26 1062 ^{42,45} CARROLL 80B SPEC $E_\gamma^* > 20 \text{ MeV}$

⁴² CARROLL 80B quotes $B(\pi^+\pi^-\gamma)$ using normalization $B(\pi^+\pi^-\pi^0) = 0.1239$. We divide by this value to obtain their measured $\Gamma(\pi^+\pi^-\gamma) / \Gamma(\pi^+\pi^-\pi^0)$.

⁴³ Internal Bremsstrahlung component only.

⁴⁴ Direct γ emission component only.

⁴⁵ Both IB and DE components.

$\Gamma(\pi^+\pi^-\gamma)/\Gamma(\pi^+\pi^-)$ Γ_{13}/Γ_8

VALUE (units 10^{-2}) EVTS DOCUMENT ID TECN COMMENT
2.11 ± 0.08 OUR FIT Error includes scale factor of 2.9.
2.11 ± 0.08 OUR AVERAGE Error includes scale factor of 2.9.

2.08 ± 0.02 ± 0.02 8669 ⁴⁶ ALAVI-HARATI01B KTEV $E_\gamma^* > 20 \text{ MeV}$
 2.30 ± 0.07 3136 RAMBERG 93 E731 $E_\gamma^* > 20 \text{ MeV}$

⁴⁶ ALAVI-HARATI 01B includes both Direct Emission (DE) and Inner Bremsstrahlung (IB) processes.

Meson Particle Listings

 K_L^0 $\Gamma(\pi^+\pi^-\gamma(\text{DE}))/\Gamma(\pi^+\pi^-)$ Γ_{14}/Γ_{13}

These values assume that $\Gamma(K_L^0 \rightarrow \pi^+\pi^-\gamma) = \Gamma(K_L^0 \rightarrow \pi^+\pi^-\gamma(\text{DE})) + \Gamma(K_L^0 \rightarrow \pi^+\pi^-\gamma(\text{IB}))$, the sum of widths for the direct emission (DE) and inner bremsstrahlung (IB) processes, with no IB-DE interference. DE assumes a form factor as described in RAMBERG 93.

VALUE	EVTS	DOCUMENT ID	TECN	COMMENT
0.684±0.009 OUR FIT				
0.684±0.009 OUR AVERAGE				
0.689±0.021	111k	ABOUZAID	06A	KTEV $E_\gamma^* > 20$ MeV
0.683±0.011	8669	ALAVI-HARATI01B	KTEV	$E_\gamma^* > 20$ MeV
0.685±0.041	3136	RAMBERG	93	E731 $E_\gamma^* > 20$ MeV

 $\Gamma(\pi^0 2\gamma)/\Gamma_{\text{total}}$ Γ_{15}/Γ

VALUE (units 10^{-6})	CL%	EVTS	DOCUMENT ID	TECN	COMMENT
1.32±0.14 OUR AVERAGE					Error includes scale factor of 3.6.
1.27±0.04±0.01		2.5k	47 LAI	02B	NA48
1.68±0.07±0.08		884	48 ALAVI-HARATI99B	KTEV	
• • • We do not use the following data for averages, fits, limits, etc. • • •					
1.7 ± 0.2 ± 0.2		63	49 BARR	92	NA31
1.86±0.60±0.60		60	PAPADIMITR...91	E731	$m_{\gamma\gamma} > 280$ MeV
<5.1		90	PAPADIMITR...91	E731	$m_{\gamma\gamma} < 264$ MeV
2.1 ± 0.6		14	50 BARR	90c	NA31 $m_{\gamma\gamma} > 280$ MeV
47 LAI 02B reports $[B(K_L^0 \rightarrow \pi^0 2\gamma)] / [B(K_L^0 \rightarrow \pi^0 \pi^0)] = (1.467 \pm 0.032 \pm 0.032) \times 10^{-3}$. We multiply by our best value $B(K_L^0 \rightarrow \pi^0 \pi^0) = (8.65 \pm 0.06) \times 10^{-4}$. Our first error is their experiment's error and our second error is the systematic error from using our best value. They also find that $B(\pi^0 2\gamma, m_{\gamma\gamma} < 110 \text{ MeV}) < 0.6 \times 10^{-8}$ (90% CL).					
48 ALAVI-HARATI 99B finds that $\Gamma(\pi^0 2\gamma, m_{\gamma\gamma} < 240 \text{ MeV}) / \Gamma(\pi^0 2\gamma) = (17.3 \pm 1.3 \pm 1.5)\%$.					
49 BARR 92 find that $\Gamma(\pi^0 2\gamma, m_{\gamma\gamma} < 240 \text{ MeV}) / \Gamma(\pi^0 2\gamma) < 0.09$ (90% CL).					
50 BARR 90c superseded by BARR 92.					

 $\Gamma(\pi^0 \gamma e^+ e^-)/\Gamma_{\text{total}}$ Γ_{16}/Γ

VALUE (units 10^{-8})	CL%	EVTS	DOCUMENT ID	TECN	COMMENT
1.62±0.14±0.09		125	51 ABOUZAID	07D	KTEV
• • • We do not use the following data for averages, fits, limits, etc. • • •					
2.34±0.35±0.13		44	ALAVI-HARATI01E	KTEV	
<71		90	MURAKAMI	99	SPEC
51 ABOUZAID 07D includes 1997 (ALAVI-HARATI 01E) and 1999 data. It measures the ratio of $B(K_L^0 \rightarrow \pi^0 \gamma e^+ e^-) / B(K_L^0 \rightarrow \pi^0 \pi^0)$, where π_D^0 is the Dalitz decaying π^0 , and uses PDG 06 values $B(K_L^0 \rightarrow \pi^0 \pi^0) = (8.69 \pm 0.04) \times 10^{-4}$, and $B(\pi_D^0 \rightarrow e^+ e^- \gamma) = (1.198 \pm 0.032) \times 10^{-2}$. Supersedes ALAVI-HARATI 01E result.					

Other modes with photons or $\ell\bar{\ell}$ pairs $\Gamma(2\gamma)/\Gamma_{\text{total}}$ Γ_{17}/Γ

VALUE (units 10^{-4})	EVTS	DOCUMENT ID	TECN	COMMENT
5.47±0.04 OUR FIT				Error includes scale factor of 1.2.
• • • We do not use the following data for averages, fits, limits, etc. • • •				
4.54±0.84		52 BANNER	72B	OSPK
4.5 ± 1.0	23	ENSTROM	71	OSPK K_L^0 1.5–9 GeV/c
5.0 ± 1.0		53 REPELLIN	71	OSPK
5.5 ± 1.1	90	KUNZ	68	OSPK Norm.to $3\pi(C+N)$
52 This value uses $(\eta_{00}/\eta_{+-})^2 = 1.05 \pm 0.14$. In general, $\Gamma(2\gamma)/\Gamma_{\text{total}} = [(4.32 \pm 0.55) \times 10^{-4}] / [(\eta_{00}/\eta_{+-})^2]$.				
53 Assumes regeneration amplitude in copper at 2 GeV is 22 mb. To evaluate for a given regeneration amplitude and error, multiply by (regeneration amplitude/22mb) ² .				

 $\Gamma(2\gamma)/\Gamma(3\pi^0)$ Γ_{17}/Γ_6

VALUE (units 10^{-3})	EVTS	DOCUMENT ID	TECN	COMMENT
2.802±0.017 OUR FIT				
2.802±0.018 OUR AVERAGE				
2.79 ± 0.02 ± 0.02	27k	ADINOLFI	03	KLOE
2.81 ± 0.01 ± 0.02		LAI	03	NA48
• • • We do not use the following data for averages, fits, limits, etc. • • •				
2.13 ± 0.43	28	BARMIN	71	HLBC
2.24 ± 0.28	115	BANNER	69	OSPK
2.5 ± 0.7	16	ARNOLD	68B	HLBC Vacuum decay

 $\Gamma(2\gamma)/\Gamma(\pi^0 \pi^0)$ Γ_{17}/Γ_9

VALUE	EVTS	DOCUMENT ID	TECN	COMMENT
0.633±0.006 OUR FIT				Error includes scale factor of 1.5.
0.632±0.004±0.008	110k	BURKHARDT	87	NA31

 $\Gamma(3\gamma)/\Gamma_{\text{total}}$ Γ_{18}/Γ

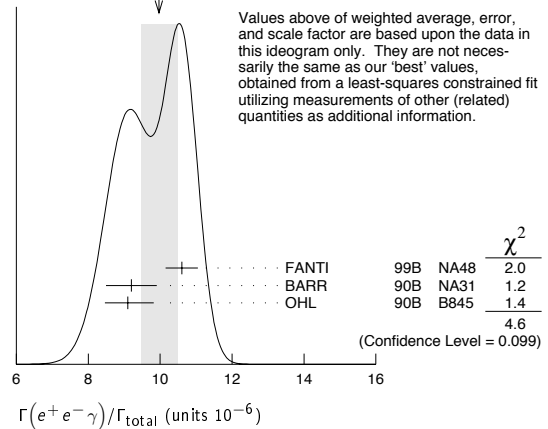
VALUE	CL%	EVTS	DOCUMENT ID	TECN	COMMENT
<2.4 × 10⁻⁷		90	54 BARR	95c	NA31
54 Assumes a phase-space decay distribution.					

 $\Gamma(e^+ e^- \gamma)/\Gamma_{\text{total}}$ Γ_{19}/Γ

VALUE (units 10^{-6})	EVTS	DOCUMENT ID	TECN	COMMENT
9.50±0.35 OUR FIT				Error includes scale factor of 1.7.
10.0 ± 0.5 OUR AVERAGE				Error includes scale factor of 1.5. See the ideogram below.
10.6 ± 0.2 ± 0.4	6864	55 FANTI	99B	NA48
9.2 ± 0.5 ± 0.5	1053	BARR	90B	NA31
9.1 ± 0.4 ± 0.6	919	OHL	90B	B845

55 For FANTI 99B, the ± 0.4 systematic error includes for uncertainties in the calculation, primarily uncertainties in the $\pi^0 \rightarrow e^+ e^- \gamma$ and $K_L^0 \rightarrow \pi^0 \pi^0$ branching ratios, evaluated using our 1999 Web edition values.

WEIGHTED AVERAGE
10.0±0.5 (Error scaled by 1.5)

 $\Gamma(e^+ e^- \gamma)/\Gamma(3\pi^0)$ Γ_{19}/Γ_6

VALUE (units 10^{-3})	EVTS	DOCUMENT ID	TECN	COMMENT
4.87±0.18 OUR FIT				Error includes scale factor of 1.7.
4.72±0.04±0.13	83k	56 ABOUZAID	07B	KTEV
56 ABOUZAID 07B reports $[\Gamma(K_L^0 \rightarrow e^+ e^- \gamma)/\Gamma(K_L^0 \rightarrow 3\pi^0)] / [3\Gamma(\pi^0 \rightarrow 2\gamma) \times \Gamma(\pi^0 \rightarrow e^+ e^- \gamma)/\Gamma_{\text{total}}^2] = (1.3302 \pm 0.0046 \pm 0.0103) \times 10^{-3}$. We multiply by our best value $3\Gamma(\pi^0 \rightarrow 2\gamma) \times \Gamma(\pi^0 \rightarrow e^+ e^- \gamma)/\Gamma_{\text{total}}^2 = (3.55 \pm 0.09) \times 10^{-2}$. Our first error is their experiment's error and our second error is the systematic error from using our best value.				

 $\Gamma(\mu^+ \mu^- \gamma)/\Gamma_{\text{total}}$ Γ_{20}/Γ

VALUE (units 10^{-7})	EVTS	DOCUMENT ID	TECN	COMMENT
3.59±0.11 OUR AVERAGE				Error includes scale factor of 1.3.
3.62±0.04±0.08	9100	ALAVI-HARATI01G	KTEV	
3.4 ± 0.6 ± 0.4	45	FANTI	97	NA48
3.23±0.23±0.19	197	SPENCER	95	E799

 $\Gamma(e^+ e^- \gamma \gamma)/\Gamma_{\text{total}}$ Γ_{21}/Γ

VALUE (units 10^{-7})	EVTS	DOCUMENT ID	TECN	COMMENT
5.95±0.33 OUR AVERAGE				
5.84±0.15±0.32	1543	ALAVI-HARATI01F	KTEV	$E_\gamma^* > 5$ MeV
8.0 ± 1.5 ± 1.4	40	SETZU	98	NA31 $E_\gamma^* > 5$ MeV
6.5 ± 1.2 ± 0.6	58	NAKAYA	94	E799 $E_\gamma^* > 5$ MeV
6.6 ± 3.2		MORSE	92	B845 $E_\gamma^* > 5$ MeV

 $\Gamma(\mu^+ \mu^- \gamma \gamma)/\Gamma_{\text{total}}$ Γ_{22}/Γ

VALUE (units 10^{-3})	EVTS	DOCUMENT ID	TECN	COMMENT
10.4^{+7.5}_{-5.9} ± 0.7	4	ALAVI-HARATI00E	KTEV	$m_{\gamma\gamma} \geq 1$ MeV/c ²

Charge conjugation × Parity (CP) or Lepton Family number (LF) violating modes, or $\Delta S = 1$ weak neutral current (S1) modes $\Gamma(\mu^+ \mu^-)/\Gamma(\pi^+ \pi^-)$ Γ_{23}/Γ_8

VALUE (units 10^{-6})	EVTS	DOCUMENT ID	TECN	COMMENT
3.48 ± 0.05 OUR AVERAGE				
3.474 ± 0.057	6210	AMBROSE	00	B871
3.87 ± 0.30	179	57 AKAGI	95	SPEC
3.38 ± 0.17	707	HEINSON	95	B791
• • • We do not use the following data for averages, fits, limits, etc. • • •				
3.9 ± 0.3 ± 0.1	178	58 AKAGI	91B	SPEC In AKAGI 95
3.45 ± 0.18 ± 0.13	368	59 HEINSON	91B	SPEC In HEINSON 95
4.1 ± 0.5	54	INAGAKI	89	SPEC In AKAGI 91B
2.8 ± 0.3 ± 0.2	87	MATHIAZHA...89B	SPEC	In HEINSON 91

⁵⁷AKAGI 95 gives this number multiplied by the PDG 1992 average for $\Gamma(K_L^0 \rightarrow \pi^+\pi^-)/\Gamma(\text{total})$.

⁵⁸AKAGI 91B give this number multiplied by the 1990 PDG average for $\Gamma(K_L^0 \rightarrow \pi^+\pi^-)/\Gamma(\text{total})$.

⁵⁹HEINSON 91 give $\Gamma(K_L^0 \rightarrow \mu\mu)/\Gamma_{\text{total}}$. We divide out the $\Gamma(K_L^0 \rightarrow \pi^+\pi^-)/\Gamma_{\text{total}}$ PDG average which they used.

$\Gamma(e^+e^-)/\Gamma_{\text{total}}$ Γ_{24}/Γ
 Test for $\Delta S = 1$ weak neutral current. Allowed by higher-order electroweak interaction.

VALUE (units 10^{-10})	CL%	EVTS	DOCUMENT ID	TECN
0.087 ± 0.057 -0.041		4	AMBROSE 98 B871	

• • • We do not use the following data for averages, fits, limits, etc. • • •

<1.6	90	1	AKAGI 95 SPEC
<0.41	90	0	⁶⁰ ARISAKA 93B B791

⁶⁰ARISAKA 93B includes all events with <6 MeV radiated energy.

$\Gamma(\pi^+\pi^-e^+e^-)/\Gamma_{\text{total}}$ Γ_{25}/Γ
 Test for $\Delta S = 1$ weak neutral current. Allowed by higher-order electroweak interaction.

VALUE (units 10^{-7})	CL%	EVTS	DOCUMENT ID	TECN	COMMENT
3.11 ± 0.19 OUR AVERAGE					
3.08 ± 0.09 ± 0.18		1125	⁶¹ LAI 03c NA48		
3.2 ± 0.6 ± 0.4		37	ADAMS 98 KTEV		
4.4 ± 1.3 ± 0.5		13	TAKEUCHI 98 SPEC		

• • • We do not use the following data for averages, fits, limits, etc. • • •

<4.6	90		NOMURA 97 SPEC $m_{e^+e^-} > 4$ MeV
------	----	--	-------------------------------------

⁶¹LAI 03c second error is $0.15(\text{syst}) \pm 0.10(\text{norm})$ combined in quadrature. The normalization uses $\text{BR}(K_L^0 \rightarrow \pi^+\pi^-\pi^0) * \text{BR}(\pi^0 \rightarrow e^+e^-) = (1.505 \pm 0.047) \times 10^{-3}$ from our 2000 Edition.

$\Gamma(\pi^0\pi^0e^+e^-)/\Gamma_{\text{total}}$ Γ_{26}/Γ
 Test for $\Delta S = 1$ weak neutral current. Allowed by higher-order electroweak interaction.

VALUE (units 10^{-9})	CL%	EVTS	DOCUMENT ID	TECN
<6.6	90	1	ALAVI-HARATI02c E799	

$\Gamma(\mu^+\mu^-e^+e^-)/\Gamma_{\text{total}}$ Γ_{27}/Γ
 Test for $\Delta S = 1$ weak neutral current. Allowed by higher-order electroweak interaction.

VALUE (units 10^{-9})	CL%	EVTS	DOCUMENT ID	TECN	COMMENT
2.69 ± 0.27 OUR AVERAGE					
2.69 ± 0.24 ± 0.12		131	⁶² ALAVI-HARATI03B KTEV		
2.9 + 6.7 - 2.4		1	GU 96 E799		

• • • We do not use the following data for averages, fits, limits, etc. • • •

2.62 ± 0.40 ± 0.17		43	ALAVI-HARATI01H KTEV Sup. by ALAVI-HARATI 03B
<4900	90		BALATS 83 SPEC

⁶²ALAVI-HARATI 03B also measures the linear slope $\alpha = -1.59 \pm 0.37$.

$\Gamma(e^+e^-e^+e^-)/\Gamma_{\text{total}}$ Γ_{28}/Γ
 Test for $\Delta S = 1$ weak neutral current. Allowed by higher-order electroweak interaction.

VALUE (units 10^{-8})	EVTS	DOCUMENT ID	TECN	COMMENT
3.56 ± 0.21 OUR AVERAGE				
3.30 ± 0.24 ± 0.25	200	⁶³ LAI 05B NA48		
3.72 ± 0.18 ± 0.23	441	ALAVI-HARATI01D KTEV		
3.96 ± 0.78 ± 0.32	27	GU 94 E799		
3.07 ± 1.25 ± 0.26	6	VAGINS 93 B845		

• • • We do not use the following data for averages, fits, limits, etc. • • •

6 ± 2 ± 1	18	⁶⁴ AKAGI 95 SPEC $m_{e^+e^-} > 470$ MeV
7 ± 3 ± 2	6	⁶⁴ AKAGI 95 SPEC $m_{e^+e^-} > 470$ MeV
10.4 ± 3.7 ± 1.1	8	⁶⁵ BARR 95 NA31
6 ± 2 ± 1	18	AKAGI 93 CNTR Sup. by AKAGI 95
4 ± 3	2	BARR 91 NA31 Sup. by BARR 95

⁶³LAI 05B uses 1998 and 1999 data. Data are normalized to the observed events of $K_L^0 \rightarrow \pi^+\pi^-\pi^0$ (π^0 into Dalitz pair) and PDG 04 values are used for $\text{B}(K_L^0 \rightarrow \pi^+\pi^-\pi^0)$ and $\text{B}(\pi^0 \rightarrow e^+e^-\gamma)$. The systematic error includes a normalization error of ± 0.10 .

⁶⁴Values are for the total branching fraction, acceptance-corrected for the m_{ee} cuts shown.

⁶⁵Distribution of angles between two e^+e^- pair planes favors $CP = -1$ for K_L^0 .

$\Gamma(\pi^0\mu^+\mu^-)/\Gamma_{\text{total}}$ Γ_{29}/Γ
 Violates CP in leading order. Test for $\Delta S = 1$ weak neutral current. Allowed by higher-order electroweak interaction.

VALUE (units 10^{-9})	CL%	EVTS	DOCUMENT ID	TECN
<0.38	90		ALAVI-HARATI00D KTEV	

• • • We do not use the following data for averages, fits, limits, etc. • • •

<5.1	90	0	HARRIS 93 E799
------	----	---	----------------

$\Gamma(\pi^0e^+e^-)/\Gamma_{\text{total}}$ Γ_{30}/Γ
 Violates CP in leading order. Direct and indirect CP -violating contributions are expected to be comparable and to dominate the CP -conserving part. LAI 02B result suggests that CP -violation effects dominate. Test for $\Delta S = 1$ weak neutral current. Allowed by higher-order electroweak interaction.

VALUE (units 10^{-10})	CL%	EVTS	DOCUMENT ID	TECN	COMMENT
< 2.8	90		⁶⁶ ALAVI-HARATI04A KTEV		combined result

• • • We do not use the following data for averages, fits, limits, etc. • • •

< 3.5	90		ALAVI-HARATI04A KTEV
0.0047 + 0.0022 - 0.0018			⁶⁷ LAI 02B NA48 CP -conserving part
< 5.1	90	2	ALAVI-HARATI01 KTEV
< 0.01 to 0.02			ALAVI-HARATI 99B KTEV CP -conserving part
< 43	90	0	HARRIS 93B E799
< 75	90	0	BARKER 90 E731
< 55	90	0	OHL 90 B845
< 400	90		BARR 88 NA31
< 3200	90		JASTRZEM... 88 SPEC

⁶⁶Combined result of ALAVI-HARATI 04A 1999-2000 data set and ALAVI-HARATI 01 1997 data set.

⁶⁷LAI 02B uses the absence of a signal in $K_L^0 \rightarrow \pi^0\gamma\gamma$ with $m(\gamma\gamma) < m(\pi^0)$ and their a_V value to predict this value.

$\Gamma(\pi^0\nu\bar{\nu})/\Gamma_{\text{total}}$ Γ_{31}/Γ
 Violates CP in leading order. Test of direct CP violation since the indirect CP -violating and CP -conserving contributions are expected to be suppressed. Test of $\Delta S = 1$ weak neutral current.

VALUE (units 10^{-7})	CL%	EVTS	DOCUMENT ID	TECN
< 2.1	90	0	⁶⁸ AHN 06 K391	

• • • We do not use the following data for averages, fits, limits, etc. • • •

< 5.9	90	0	ALAVI-HARATI00 KTEV
< 16	90	0	ADAMS 99 KTEV
< 580	90	0	WEAVER 94 E799
< 2200	90	0	GRAHAM 92 CNTR

⁶⁸Value obtained analyzing 10% of data of RUN 1 (performed in 2004).

$\Gamma(\pi^0\pi^0\nu\bar{\nu})/\Gamma_{\text{total}}$ Γ_{32}/Γ

VALUE	CL%	DOCUMENT ID	TECN
< 4.7 × 10⁻⁵	90	⁶⁹ NIX 07 K391	

⁶⁹Observed 1 event with expected background of 0.43 ± 0.35 events.

$\Gamma(e^\pm\mu^\mp)/\Gamma_{\text{total}}$ Γ_{33}/Γ
 Test of lepton family number conservation.

VALUE (units 10^{-11})	CL%	EVTS	DOCUMENT ID	TECN
< 0.47	90		AMBROSE 98B B871	

• • • We do not use the following data for averages, fits, limits, etc. • • •

< 9.4	90	0	AKAGI 95 SPEC
< 3.9	90	0	ARISAKA 93 B791
< 3.3	90	0	⁷⁰ ARISAKA 93 B791

⁷⁰This is the combined result of ARISAKA 93 and MATHIAZHAGAN 89.

$\Gamma(e^\pm e^\pm\mu^\mp\mu^\mp)/\Gamma_{\text{total}}$ Γ_{34}/Γ
 Test of lepton family number conservation.

VALUE (units 10^{-11})	CL%	EVTS	DOCUMENT ID	TECN	COMMENT
< 4.12	90	0	ALAVI-HARATI03B KTEV		

• • • We do not use the following data for averages, fits, limits, etc. • • •

< 12.3	90	0	⁷¹ ALAVI-HARATI01H KTEV Sup. by ALAVI-HARATI 03B
< 610	90	0	⁷¹ GU 96 E799

⁷¹Assuming uniform phase space distribution.

$\Gamma(\pi^0\mu^\pm e^\mp)/\Gamma_{\text{total}}$ Γ_{35}/Γ
 Test of lepton family number conservation.

VALUE	CL%	DOCUMENT ID	TECN
< 6.2 × 10⁻⁹	90	ARISAKA 98 E799	

V_{ud} , V_{us} , THE CABIBBO ANGLE, AND CKM UNITARITY

Updated November 2007 by E. Blucher (Univ. of Chicago) and W.J. Marciano (BNL)

The Cabibbo-Kobayashi-Maskawa (CKM) [1,2] three-generation quark mixing matrix written in terms of the Wolfenstein parameters (λ, A, ρ, η) [3] nicely illustrates the orthonormality constraint of unitarity and central role played by λ .

$$V_{\text{CKM}} = \begin{pmatrix} V_{ud} & V_{us} & V_{ub} \\ V_{cd} & V_{cs} & V_{cb} \\ V_{td} & V_{ts} & V_{tb} \end{pmatrix}$$

$$= \begin{pmatrix} 1 - \lambda^2/2 & \lambda & A\lambda^3(\rho - i\eta) \\ -\lambda & 1 - \lambda^2/2 & A\lambda^2 \\ A\lambda^3(1 - \rho - i\eta) & -A\lambda^2 & 1 \end{pmatrix} + \mathcal{O}(\lambda^4). \quad (1)$$

Meson Particle Listings

K_L^0

That cornerstone is a carryover from the two-generation Cabibbo angle, $\lambda = \sin(\theta_{\text{Cabibbo}}) = V_{us}$. Its value is a critical ingredient in determinations of the other parameters and in tests of CKM unitarity.

Unfortunately, the precise value of λ has been somewhat controversial in the past, with kaon decays suggesting [4] $\lambda \simeq 0.220$, while hyperon decays [5] and indirect determinations via nuclear β -decays imply a somewhat larger $\lambda \simeq 0.225 - 0.230$. That discrepancy is often discussed in terms of a deviation from the unitarity requirement

$$|V_{ud}|^2 + |V_{us}|^2 + |V_{ub}|^2 = 1. \quad (2)$$

For many years, using a value of V_{us} derived from $K \rightarrow \pi e \nu$ (K_{e3}) decays, that sum was consistently 2–2.5 sigma below unity, a potential signal [6] for new physics effects. Below, we discuss the current status of V_{ud} , V_{us} , and their associated unitarity test in Eq. (2). (Since $|V_{ub}|^2 \simeq 1 \times 10^{-5}$ is negligibly small, it is ignored in this discussion.)

V_{ud}

The value of V_{ud} has been obtained from superallowed nuclear, neutron, and pion decays. Currently, the most precise determination of V_{ud} comes from superallowed nuclear beta-decays [6] ($0^+ \rightarrow 0^+$ transitions). Measuring their half-lives, t , and Q values which give the decay rate factor, f , leads to a precise determination of V_{ud} via the master formula [7–9]

$$|V_{ud}|^2 = \frac{2984.48(5) \text{ sec}}{ft(1 + \text{RC})} \quad (3)$$

where RC denotes the entire effect of electroweak radiative corrections, nuclear structure, and isospin violating nuclear effects. RC is nucleus-dependent, ranging from about +3.0% to +3.6% for the nine best measured superallowed decays. In Table 1, we give updated [10] ft values along with their implied V_{ud} for the nine best measured superallowed decays [6, 10]. They collectively give a weighted average (with errors combined in quadrature) of

$$V_{ud} = 0.97418(27) \text{ (superallowed)}, \quad (4)$$

which, assuming unitarity, corresponds to $\lambda = 0.226(1)$. We note that the new average value of V_{ud} is shifted upward compared to our 2005 value of 0.97377(27) primarily because of a recent reevaluation of the isospin breaking Coulomb corrections by Towner and Hardy [10].

Combined measurements of the neutron lifetime, τ_n , and the ratio of axial-vector/vector couplings, $g_A \equiv G_A/G_V$, via neutron decay asymmetries can also be used to determine V_{ud} :

$$|V_{ud}|^2 = \frac{4908.7(1.9) \text{ sec}}{\tau_n(1 + 3g_A^2)}, \quad (5)$$

where the error stems from uncertainties in the electroweak radiative corrections [8] due to hadronic loop effects. Those effects have been recently updated and their error was reduced by about a factor of 2 [9], leading to a ± 0.0002 theoretical

Table 1: Values of V_{ud} implied by various precisely measured superallowed nuclear beta decays. The ft values and Coulomb isospin breaking corrections are taken from Towner and Hardy [10]. Uncertainties in V_{ud} correspond to 1) nuclear structure and $Z^2\alpha^3$ uncertainties [6, 11] added in quadrature with the ft error; 2) a common error assigned to nuclear Coulomb distortion effects [11]; and 3) a common uncertainty in the radiative corrections from quantum loop effects [9]. Only the first error is used to obtain the weighted average.

Nucleus	ft (sec)	V_{ud}
^{10}C	3039.5(47)	0.97370(80)(14)(19)
^{14}O	3042.5(27)	0.97411(51)(14)(19)
^{26}Al	3037.0(11)	0.97400(24)(14)(19)
^{34}Cl	3050.0(11)	0.97417(34)(14)(19)
^{38}K	3051.1(10)	0.97413(39)(14)(19)
^{42}Sc	3046.4(14)	0.97423(44)(14)(19)
^{46}V	3049.6(16)	0.97386(49)(14)(19)
^{50}Mn	3044.4(12)	0.97487(45)(14)(19)
^{54}Co	3047.6(15)	0.97490(54)(14)(19)
Weighted Ave.		0.97418(13)(14)(19)

uncertainty in V_{ud} (common to all V_{ud} extractions). Using the world averages from this *Review*

$$\begin{aligned} \tau_n^{\text{ave}} &= 885.7(8) \text{ sec} \\ g_A^{\text{ave}} &= 1.2695(29) \end{aligned} \quad (6)$$

leads to

$$V_{ud} = 0.9746(4)\tau_n(18)g_A(2)\text{RC} \quad (7)$$

with the error dominated by g_A uncertainties (which have been expanded due to experimental inconsistencies). We note that a recent precise measurement [12] of $\tau_n = 878.5(7)(3)$ sec is also inconsistent with the world average from this *Review* and would lead to a considerably larger $V_{ud} = 0.9786(4)(18)(2)$. Future neutron studies are expected to resolve these inconsistencies and significantly reduce the uncertainties in g_A and τ_n , potentially making them the best way to determine V_{ud} .

The recently completed PIBETA experiment at PSI measured the very small ($\mathcal{O}(10^{-8})$) branching ratio for $\pi^+ \rightarrow \pi^0 e^+ \nu_e$ with about $\pm 1/2\%$ precision. Their result gives [13]

$$V_{ud} = 0.9749(26) \left[\frac{BR(\pi^+ \rightarrow e^+ \nu_e(\gamma))}{1.2352 \times 10^{-4}} \right]^{\frac{1}{2}} \quad (8)$$

which is normalized using the very precisely determined theoretical prediction for $BR(\pi^+ \rightarrow e^+ \nu_e(\gamma)) = 1.2352(5) \times 10^{-4}$ [7], rather than the experimental branching ratio from this *Review* of $1.230(4) \times 10^{-4}$ which would lower the value to $V_{ud} = 0.9728(30)$. Theoretical uncertainties in that determination are very small; however, much higher statistics would be required to make this approach competitive with others.

V_{us}

$|V_{us}|$ may be determined from kaon decays, hyperon decays, and tau decays. Previous determinations have most often used $K\ell 3$ decays:

$$\Gamma_{K\ell 3} = \frac{G_F^2 M_K^5}{192\pi^3} S_{EW} (1 + \delta_K^\ell + \delta_{SU2}) C^2 |V_{us}|^2 f_+^2(0) I_K^\ell. \quad (9)$$

Here, ℓ refers to either e or μ , G_F is the Fermi constant, M_K is the kaon mass, S_{EW} is the short-distance radiative correction, δ_K^ℓ is the mode-dependent long-distance radiative correction, $f_+(0)$ is the calculated form factor at zero momentum transfer for the $\ell\nu$ system, and I_K^ℓ is the phase-space integral, which depends on measured semileptonic form factors. For charged kaon decays, δ_{SU2} is the deviation from one of the ratio of $f_+(0)$ for the charged to neutral kaon decay; it is zero for the neutral kaon. C^2 is 1 (1/2) for neutral (charged) kaon decays. Most determinations of $|V_{us}|$ have been based only on $K \rightarrow \pi e \nu$ decays; $K \rightarrow \pi \mu \nu$ decays have not been used because of large uncertainties in I_K^μ . The experimental measurements are the semileptonic decay widths (based on the semileptonic branching fractions and lifetime) and form factors (allowing calculation of the phase space integrals). Theory is needed for S_{EW} , δ_K^ℓ , δ_{SU2} , and $f_+(0)$.

Many new measurements during the last few years have resulted in a significant shift in V_{us} . Most importantly, recent measurements of the $K \rightarrow \pi e \nu$ branching fractions are significantly different than earlier PDG averages, probably as a result of inadequate treatment of radiation in older experiments. This effect was first observed by BNL E865 [14] in the charged kaon system and then by KTeV [15,16] in the neutral kaon system; subsequent measurements were made by KLOE [17–20], NA48 [21–23], and ISTRA+ [24]. Current averages (*e.g.*, by the PDG [25] or Flavianet [26]) of the semileptonic branching fractions are based only on recent, high-statistics experiments where the treatment of radiation is clear. In addition to measurements of branching fractions, new measurements of lifetimes [27] and form factors [28–32], have resulted in improved precision for all of the experimental inputs to V_{us} . Precise measurements of form factors for $K_{\mu 3}$ decay now make it possible to use both semileptonic decay modes to extract V_{us} .

Following the analysis of the Flavianet group [26], one finds the values of $|V_{us}|f_+(0)$ in Table 2. The average of these measurements gives

$$f_+(0)|V_{us}| = 0.21668(45). \quad (10)$$

Figure 1 shows a comparison of these results with the PDG evaluation from 2002 [33], as well as $f_+(0)(1 - |V_{ud}|^2 - |V_{ub}|^2)^{1/2}$, the expectation for $f_+(0)|V_{us}|$ assuming unitarity, based on $|V_{ud}| = 0.9742 \pm 0.0003$, $|V_{ub}| = (3.6 \pm 0.7) \times 10^{-3}$, and the widely used Leutwyler-Roos calculation of $f_+(0) = 0.961 \pm 0.008$ [34]. Using the result in Eq. (10) with the Leutwyler-Roos calculation of $f_+(0)$ gives

$$|V_{us}| = \lambda = 0.2255 \pm 0.0019. \quad (11)$$

Similar results for $f_+(0)$ were recently obtained from lattice gauge theory calculations [35,36]. For example, and recent 2+1 fermion dynamical wall calculation [36] gave $f_+(0) = 0.9609(51)$. Other calculations of $f_+(0)$ result in $|V_{us}|$ values that differ by as much as 2% from the result in Eq. (11). For example, a recent chiral perturbation theory calculation [37, 38] gives $f_+(0) = 0.974 \pm 0.012$, which implies a lower value of $|V_{us}| = 0.2225 \pm 0.0028$ [39].

Table 2: $|V_{us}|f_+(0)$ from $K\ell 3$.

Decay Mode	$ V_{us} f_+(0)$
$K^\pm e 3$	0.21746 ± 0.00085
$K^\pm \mu 3$	0.21810 ± 0.00114
$K_L e 3$	0.21638 ± 0.00055
$K_L \mu 3$	0.21678 ± 0.00067
$K_S e 3$	0.21554 ± 0.00142
Average	0.21668 ± 0.00045

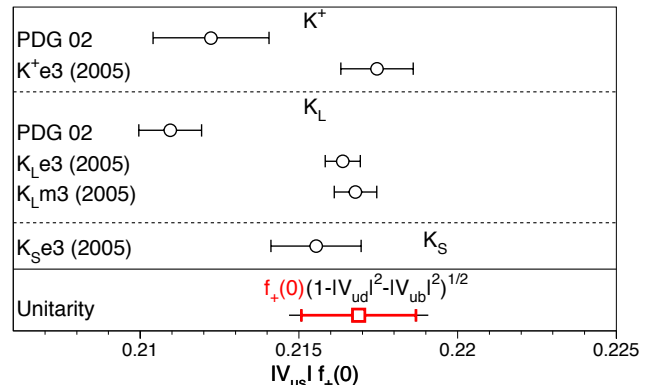


Figure 1: Comparison of determinations of $|V_{us}|f_+(0)$ from this review (labeled 2005), from the PDG 2002, and with the prediction from unitarity using $|V_{ud}|$ and the Leutwyler-Roos calculation of $f_+(0)$ [34]. For $f_+(0)(1 - |V_{ud}|^2 - |V_{ub}|^2)^{1/2}$, the inner error bars are from the quoted uncertainty in $f_+(0)$; the total uncertainties include the $|V_{ud}|$ and $|V_{ub}|$ errors.

A value of V_{us} can also be obtained from a comparison of the radiative inclusive decay rates for $K \rightarrow \mu\nu(\gamma)$ and $\pi \rightarrow \mu\nu(\gamma)$ combined with a lattice gauge theory calculation of f_K/f_π via [40]

$$\frac{|V_{us}|f_K}{|V_{ud}|f_\pi} = 0.2387(4) \left[\frac{\Gamma(K \rightarrow \mu\nu(\gamma))}{\Gamma(\pi \rightarrow \mu\nu(\gamma))} \right]^{\frac{1}{2}} \quad (12)$$

with the small error coming from electroweak radiative corrections. Employing

$$\frac{\Gamma(K \rightarrow \mu\nu(\gamma))}{\Gamma(\pi \rightarrow \mu\nu(\gamma))} = 1.3337(46), \quad (13)$$

Meson Particle Listings

K_L^0

which averages in the KLOE result [41], $B(K \rightarrow \mu\nu(\gamma)) = 63.66(9)(15)\%$ and [42, 43]

$$f_K/f_\pi = 1.208(2)(+7/-14) \quad (14)$$

along with the value of V_{ud} in Eq. (4) leads to

$$|V_{us}| = 0.2223(5)(1.208f_\pi/f_K). \quad (15)$$

It should be mentioned that hyperon decay fits suggest [5]

$$|V_{us}| = 0.2250(27) \text{ Hyperon Decays} \quad (16)$$

modulo SU(3) breaking effects that could shift that value up or down. We note that a recent representative effort [44] that incorporates SU(3) breaking found $V_{us} = 0.226(5)$. Similarly, strangeness changing tau decays give [45]

$$|V_{us}| = 0.2208(34) \text{ Tau Decays} \quad (17)$$

where the central value depends on the strange quark mass.

Employing the value of V_{ud} in Eq. (4) and V_{us} in Eq. (11) leads to the unitarity consistency check

$$|V_{ud}|^2 + |V_{us}|^2 + |V_{ub}|^2 = 0.9999(5)(9), \quad (18)$$

where the first error is the uncertainty from $|V_{ud}|^2$ and the second error is the uncertainty from $|V_{us}|^2$. The result is in good agreement with unitarity. Averaging the direct determination of λ (V_{us}) with the determination derived from unitarity and V_{ud} gives $\lambda = 0.226(1)$. Although unitarity now seems well established, issues regarding the Q values in superallowed nuclear β -decays, $\tau_n, g_A, f_+(0)$ and f_K/f_π must still be resolved before a definitive confirmation is possible.

CKM Unitarity Constraints

The current good experimental agreement with unitarity, $|V_{ud}|^2 + |V_{us}|^2 + |V_{ub}|^2 = 0.9999(10)$ provides strong confirmation of Standard Model radiative corrections (which range between 3-4% depending on the nucleus used) at better than the 30 sigma level [46]. In addition, it implies constraints on “New Physics” effects at both the tree and quantum loop levels. Those effects could be in the form of contributions to nuclear beta decays, $K_{\ell 3}$ decays and/or muon decays, with the last of these providing normalization via the muon lifetime [47], which is used to obtain the Fermi constant, $G_\mu = 1.166371(6) \times 10^{-5} \text{GeV}^{-2}$.

We illustrate the implications of CKM unitarity for: 1) exotic muon decays [48] (beyond ordinary muon decay $\mu^+ \rightarrow e^+ \nu_e \bar{\nu}_\mu$); and 2) new heavy quark mixing V_{uD} [49]. Other examples in the literature [50,51] include Z_χ boson quantum loop effects, supersymmetry, leptoquarks, compositeness etc.

Exotic Muon Decays

If additional lepton flavor violating decays such as $\mu^+ \rightarrow e^+ \bar{\nu}_e \nu_\mu$ (wrong neutrinos) occur, they would cause confusion in searches for neutrino oscillations at, for example, muon storage rings/neutrino factories or other neutrino sources from muon

decays. Calling the rate for all such decays $\Gamma(\text{exotic } \mu \text{ decays})$, they should be subtracted before the extraction of G_μ and normalization of the CKM matrix. Since that is not done and unitarity works, one has (at one-sided 95% CL)

$$|V_{ud}|^2 + |V_{us}|^2 + |V_{ub}|^2 = 1 - BR(\text{exotic } \mu \text{ decays}) \geq 0.9982 \quad (19)$$

or

$$BR(\text{exotic } \mu \text{ decays}) < 0.0018. \quad (20)$$

That bound is a factor of 6-7 better than the direct experimental bound on $\mu^+ \rightarrow e^+ \bar{\nu}_e \nu_\mu$.

New Heavy Quark Mixing

Heavy D quarks naturally occur in fourth quark generation models and some heavy quark “new physics” scenarios such as E_6 grand unification. Their mixing with ordinary quarks gives rise to V_{uD} which is constrained by unitarity (one sided 95% CL)

$$|V_{ud}|^2 + |V_{us}|^2 + |V_{ub}|^2 = 1 - |V_{uD}|^2 > 0.9982 \\ |V_{uD}| < 0.04. \quad (21)$$

A similar constraint applies to heavy neutrino mixing and the couplings $V_{\mu N}$ and V_{eN} .

References

1. N. Cabibbo, Phys. Rev. Lett. **10**, 531 (1963).
2. M. Kobayashi and T. Maskawa, Prog. Theor. Phys. **49**, 652 (1973).
3. L. Wolfenstein, Phys. Rev. Lett. **51**, 1945 (1983).
4. S. Eidelman *et al.*, [Particle Data Group], Phys. Lett. **B592**, 1 (2004).
5. N. Cabibbo, E.C. Swallow, and R. Winston, Phys. Rev. Lett. **92**, 251803 (2004) [[hep-ph/0307214](#)].
6. J.C. Hardy and I.S. Towner, Phys. Rev. Lett. **94**, 092502 (2005) [[nucl-th/0412050](#)].
7. W.J. Marciano and A. Sirlin, Phys. Rev. Lett. **71**, 3629 (1993).
8. A. Czarnecki, W.J. Marciano, and A. Sirlin, Phys. Rev. **D70**, 093006 (2004) [[hep-ph/0406324](#)].
9. W.J. Marciano and A. Sirlin, Phys. Rev. Lett. **96**, 032002 (2006) [[hep-ph/0510099](#)].
10. I.S. Towner and J.C. Hardy, [arXiv:0710.3181](#) [[nucl-th](#)].
11. I.S. Towner and J.C. Hardy, [[nucl-th/0209014](#)].
12. A. Serebrov *et al.*, Phys. Lett. **B605**, 72 (2005) [[nucl-ex/0408009](#)].
13. D. Poganic *et al.*, Phys. Rev. Lett. **93**, 181803 (2004) [[hep-ex/0312030](#)].
14. A. Sher *et al.*, Phys. Rev. Lett. **91**, 261802 (2003).
15. T. Alexopoulos *et al.*, [KTeV Collab.], Phys. Rev. Lett. **93**, 181802 (2004) [[hep-ex/0406001](#)].
16. T. Alexopoulos *et al.*, [KTeV Collab.], Phys. Rev. **D70**, 092006 (2004) [[hep-ex/0406002](#)].

17. F. Ambrosino *et al.*, [KLOE Collab.], Phys. Lett. **B632**, 43 (2006) [hep-ex/0508027].
18. F. Ambrosino *et al.*, [KLOE Collab.], Phys. Lett. **B638**, 140 (2006) [hep-ex/0603041].
19. F. Ambrosino *et al.*, [KLOE Collab.], Phys. Lett. **B636**, 173 (2006) [hep-ex/0601026].
20. F. Ambrosino *et al.*, [KLOE Collab.], PoS **HEP2005**, 287 (2006) [Frascati Phys. Ser. **41**, 69 (2006)] [hep-ex/0510028].
21. A. Lai *et al.*, [NA48 Collab.], Phys. Lett. **B602**, 41 (2004) [hep-ex/0410059].
22. A. Lai *et al.*, [NA48 Collab.], Phys. Lett. **B645**, 26 (2007) [hep-ex/0611052].
23. J.R. Batley *et al.*, [NA48/2 Collab.], Eur. Phys. J. C **50**, 329 (2007) [hep-ex/0702015].
24. V.I. Romanovsky *et al.*, [hep-ex/0704.2052].
25. W.M. Yao *et al.*, [Particle Data Group], J. Phys. G **33**, 1 (2006).
26. Flavianet Working Group on Precise SM Tests in K Decays, <http://www.lnf.infn.it/wg/vus>.
27. F. Ambrosino *et al.*, [KLOE Collab.], Phys. Lett. **B626**, 15 (2005) [hep-ex/0507088].
28. T. Alexopoulos *et al.*, [KTeV Collab.], Phys. Rev. **D70**, 092007 (2004) [hep-ex/0406003].
29. E. Abouzaid *et al.*, [KTeV Collab.], Phys. Rev. **D74**, 097101 (2006) [hep-ex/0608058].
30. F. Ambrosino *et al.*, [KLOE Collab.], Phys. Lett. **B636**, 166 (2006) [hep-ex/0601038].
31. A. Lai *et al.*, [NA48 Collab.], Phys. Lett. **B604**, 1 (2004) [hep-ex/0410065].
32. O.P. Yushchenko *et al.*, Phys. Lett. **B589**, 111 (2004) [hep-ex/0404030].
33. K. Hagiwara *et al.*, [Particle Data Group], Phys. Rev. **D66**, 1 (2002).
34. H. Leutwyler and M. Roos, Z. Phys. **C25**, 91 (1984).
35. D. Becirevic *et al.*, Nucl. Phys. **B705**, 339 (2005) [hep-ph/0403217].
36. D.J. Antonio *et al.*, [hep-lat/0702026].
37. J. Bijnens and P. Talavera, Nucl. Phys. **B669**, 341 (2003).
38. V. Cirigliano *et al.*, JHEP **0504**, 006 (2005) [hep-ph/0503108].
39. M. Jamin, J.A. Oller, and A. Pich, JHEP **02**, 047 (2004).
40. W.J. Marciano, Phys. Rev. Lett. **93**, 231803 (2004) [hep-ph/0402299].
41. F. Ambrosino *et al.*, [KLOE Collab.], Phys. Lett. **B632**, 76 (2006) [hep-ex/0509045].
42. C. Aubin *et al.*, [MILC Collab.], Phys. Rev. **D70**, 114501 (2004) [hep-lat/0407028].
43. C. Bernard *et al.*, [MILC Collab.], PoS **LAT 2005**, 025 (2005) [hep-lat/0509137]; C. Bernard *et al.*, hep-lat/0611024.
44. V. Mateu and A. Pich, JHEP **0510**, 041 (2005) [hep-ph/0509045].
45. E. Gamiz *et al.*, Phys. Rev. Lett. **94**, 011803 (2005) [hep-ph/0408044]; E. Gamiz *et al.*, arXiv:0709.0282 [hep-ph].
46. A. Sirlin, Rev. Mod. Phys. **50**, 573 (1978).
47. D.B. Chitwood *et al.*, Phys. Rev. Lett. **99**, 032001 (2007).
48. K.S. Babu and S. Pakvasa, hep-ph/0204236.

49. W. Marciano and A. Sirlin, Phys. Rev. Lett. **56**, 22 (1986); P. Langacker and D. London, Phys. Rev. **D38**, 886 (1988).
50. W. Marciano and A. Sirlin, Phys. Rev. **D35**, 1672 (1987).
51. R. Barbieri *et al.*, Phys. Lett. **156B**, 348 (1985); K. Hagiwara *et al.*, Phys. Rev. Lett. **75**, 3605 (1995); A. Kurylov and M. Ramsey-Musolf, Phys. Rev. Lett. **88**, 071804 (2000).

ENERGY DEPENDENCE OF K_L^0 DALITZ PLOT

For discussion, see note on Dalitz plot parameters in the K^\pm section of the Particle Listings above. For definitions of a_V , a_T , a_U , and a_Y , see the earlier version of the same note in the 1982 edition of this Review published in Physics Letters **111B** 70 (1982).

$$|\text{matrix element}|^2 = 1 + gu + hu^2 + jv + kv^2 + fuv$$

where $u = (s_3 - s_0) / m_\pi^2$ and $v = (s_2 - s_1) / m_\pi^2$

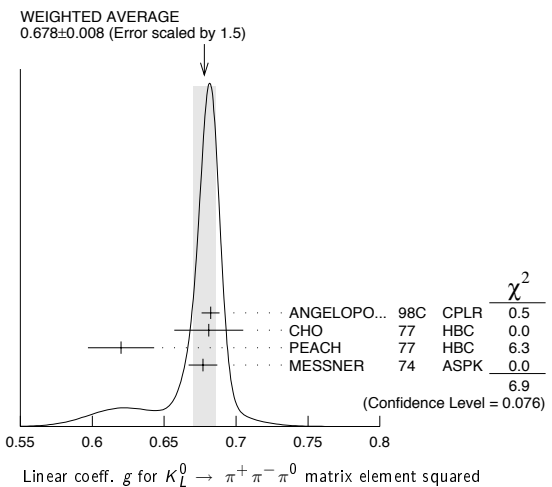
LINEAR COEFFICIENT g FOR $K_L^0 \rightarrow \pi^+ \pi^- \pi^0$

VALUE	EVTS	DOCUMENT ID	TECN	COMMENT
0.678 ± 0.008 OUR AVERAGE				Error includes scale factor of 1.5. See the ideogram below.
0.6823 ± 0.0044 ± 0.0044	500k	ANGELOPO...	98c CPLR	
0.681 ± 0.024	6499	CHO	77 HBC	
0.620 ± 0.023	4709	PEACH	77 HBC	
0.677 ± 0.010	509k	MESSNER	74 ASPK	$a_Y = -0.917 \pm 0.013$
• • • We do not use the following data for averages, fits, limits, etc. • • •				
0.69 ± 0.07	192	⁷² BALDO...	75 HLBC	
0.590 ± 0.022	56k	⁷² BUCHANAN	75 SPEC	$a_U = -0.277 \pm 0.010$
0.619 ± 0.027	20k	^{72,73} BISI	74 ASPK	$a_T = -0.282 \pm 0.011$
0.612 ± 0.032		⁷² ALEXANDER	73B HBC	
0.73 ± 0.04	3200	⁷² BRANDEN...	73 HBC	
0.608 ± 0.043	1486	⁷² KRENZ	72 HLBC	$a_T = -0.277 \pm 0.018$
0.650 ± 0.012	29k	⁷² ALBROW	70 ASPK	$a_Y = -0.858 \pm 0.015$
0.593 ± 0.022	36k	^{72,74} BUCHANAN	70 SPEC	$a_U = -0.278 \pm 0.010$
0.664 ± 0.056	4400	⁷² SMITH	70 OSPK	$a_T = -0.306 \pm 0.024$
0.400 ± 0.045	2446	⁷² BASILE	68B OSPK	$a_T = -0.188 \pm 0.020$
0.649 ± 0.044	1350	⁷² HOPKINS	67 HBC	$a_T = -0.294 \pm 0.018$
0.428 ± 0.055	1198	⁷² NEFKENS	67 OSPK	$a_U = -0.204 \pm 0.025$

⁷²Quadratic dependence required by some experiments. (See sections on "QUADRATIC COEFFICIENT h " and "QUADRATIC COEFFICIENT k " below.) Correlations prevent us from averaging results of fits not including g , h , and k terms.

⁷³BISI 74 value comes from quadratic fit with quad. term consistent with zero. g error is thus larger than if linear fit were used.

⁷⁴BUCHANAN 70 result revised by BUCHANAN 75 to include radiative correlations and to use more reliable K_L^0 momentum spectrum of second experiment (had same beam).

QUADRATIC COEFFICIENT h FOR $K_L^0 \rightarrow \pi^+ \pi^- \pi^0$

VALUE	EVTS	DOCUMENT ID	TECN
0.076 ± 0.006 OUR AVERAGE			
0.061 ± 0.004 ± 0.015	500k	ANGELOPO...	98c CPLR
0.095 ± 0.032	6499	CHO	77 HBC
0.048 ± 0.036	4709	PEACH	77 HBC
0.079 ± 0.007	509k	MESSNER	74 ASPK
• • • We do not use the following data for averages, fits, limits, etc. • • •			
-0.011 ± 0.018	29k	⁷⁵ ALBROW	70 ASPK
0.043 ± 0.052	4400	⁷⁵ SMITH	70 OSPK

See notes in section "LINEAR COEFFICIENT g FOR $K_L^0 \rightarrow \pi^+ \pi^- \pi^0$ | MATRIX ELEMENT²" above.

Meson Particle Listings

 K_L^0

⁷⁵ Quadratic coefficients h and k required by some experiments. (See section on "QUADRATIC COEFFICIENT k " below.) Correlations prevent us from averaging results of fits not including g , h , and k terms.

QUADRATIC COEFFICIENT k FOR $K_L^0 \rightarrow \pi^+ \pi^- \pi^0$

VALUE	EVTS	DOCUMENT ID	TECN
0.0099 ± 0.0015 OUR AVERAGE			
0.0104 ± 0.0017 ± 0.0024	500k	ANGELOPO...	98c CPLR
0.024 ± 0.010	6499	CHO	77 HBC
-0.008 ± 0.012	4709	PEACH	77 HBC
0.0097 ± 0.0018	509k	MESSNER	74 ASPK

LINEAR COEFFICIENT j FOR $K_L^0 \rightarrow \pi^+ \pi^- \pi^0$ (CP-VIOLATING TERM)

Listed in CP-violation section below.

QUADRATIC COEFFICIENT f FOR $K_L^0 \rightarrow \pi^+ \pi^- \pi^0$ (CP-VIOLATING TERM)

Listed in CP-violation section below.

QUADRATIC COEFFICIENT h FOR $K_L^0 \rightarrow \pi^0 \pi^0 \pi^0$

VALUE (units 10^{-3})	EVTS	DOCUMENT ID	TECN
-5.0 ± 1.4 OUR AVERAGE			
-6.1 ± 0.9 ± 0.5	14.7M	LAI	01B NA48
-3.3 ± 1.1 ± 0.7	5M	⁷⁶ SOMALWAR	92 E731

⁷⁶ SOMALWAR 92 chose m_{π^+} as normalization to make it compatible with the Particle Data Group $K_L^0 \rightarrow \pi^+ \pi^- \pi^0$ definitions.

 K_L^0 FORM FACTORS

For discussion, see note on form factors in the K^\pm section of the Particle Listings above.

In the form factor comments, the following symbols are used.

f_+ and f_- are form factors for the vector matrix element.

f_S and f_T refer to the scalar and tensor term.

$f_0(t) = f_+(t) + f_-(t) t / (m_{K^0}^2 - m_{\pi^+}^2)$.

$t =$ momentum transfer to the π .

λ_+ and λ_0 are the linear expansion coefficients of f_+ and f_0 :

$f_+(t) = f_+(0) (1 + \lambda_+ t / m_{\pi^+}^2)$

For quadratic expansion

$f_+(t) = f_+(0) (1 + \lambda'_+ t / m_{\pi^+}^2 + \frac{\lambda''_+}{2} t^2 / m_{\pi^+}^4)$

as used by KTeV. If there is a non-vanishing quadratic term, then λ_+

represents an average slope, which is then different from λ'_+ .

NA48 (K_{e3}) and ISTRA quadratic expansion coefficients are converted with

$\lambda'_+{}^{PDG} = \lambda_+{}^{NA48}$ and $\lambda''_+{}^{PDG} = 2 \lambda'_+{}^{NA48}$

$\lambda'_+{}^{PDG} = (\frac{m_{\pi^+}}{m_{\pi^0}})^2 \lambda_+{}^{ISTRA}$ and

$\lambda''_+{}^{PDG} = 2 (\frac{m_{\pi^+}}{m_{\pi^0}})^4 \lambda'_+{}^{ISTRA}$

ISTRA linear expansion coefficients are converted with

$\lambda_+{}^{PDG} = (\frac{m_{\pi^+}}{m_{\pi^0}})^2 \lambda_+{}^{ISTRA}$ and $\lambda_0{}^{PDG} = (\frac{m_{\pi^+}}{m_{\pi^0}})^2 \lambda_0{}^{ISTRA}$

The pole parametrization is

$f_+(t) = f_+(0) (\frac{M_V^2}{M_V^2 - t})$

$f_0(t) = f_0(0) (\frac{M_S^2}{M_S^2 - t})$

where M_V and M_S are the vector and scalar pole masses.

The dispersive parametrization is

$f_+(t) = f_+(0) \exp[\frac{t}{m_\pi^2} (A_+ + H(t))];$

$f_0(t) = f_+(0) \exp[\frac{t}{m_K^2 - m_\pi^2} (\ln[C] - G(t))],$

where A_+ is the slope parameter and $\ln[C] = \ln[f_0(m_K^2 - m_\pi^2)]$

is the logarithm of the scalar form factor at the Callan-Treiman point.

$H(t)$ and $G(t)$ are dispersive integrals.

The following abbreviations are used:

DP = Dalitz plot analysis.

PI = π spectrum analysis.

MU = μ spectrum analysis.

POL = μ polarization analysis.

BR = $K_{\mu 3}^0 / K_{e 3}^0$ branching ratio analysis.

E = positron or electron spectrum analysis.

RC = radiative corrections.

 λ_+ (LINEAR ENERGY DEPENDENCE OF f_+ IN $K_{e 3}^0$ DECAY)

For radiative correction of $K_{e 3}^0$ DP, see GINSBERG 67, BECHERRAWY 70, CIRIGLIANO 02, CIRIGLIANO 04, and ANDRE 04. Results labeled OUR FIT are discussed in the review " $K_{e 3}^\pm$ and $K_{\mu 3}^0$ Form Factors" in the K^\pm Listings. For earlier, lower statistics results, see the 2004 edition of this review, Physics Letters **B592 1** (2004).

VALUE (units 10^{-2})	EVTS	DOCUMENT ID	TECN	COMMENT
2.82 ± 0.04 OUR FIT				Error includes scale factor of 1.1. Assuming μ -e universality
2.85 ± 0.04 OUR AVERAGE				
2.86 ± 0.05 ± 0.04	2M	AMBROSINO	06D KLOE	
2.832 ± 0.037 ± 0.043	1.9M	ALEXOPOU...	04A KTEV	PI, no $\mu = e$
2.88 ± 0.04 ± 0.11	5.6M	⁷⁷ LAI	04c NA48	DP
• • • We do not use the following data for averages, fits, limits, etc. • • •				
2.84 ± 0.07 ± 0.13	5.6M	⁷⁸ LAI	04c NA48	DP
2.45 ± 0.12 ± 0.22	366k	APOSTOLA...	00 CPLR	DP
3.06 ± 0.34	74k	BIRULEV	81 SPEC	DP
3.12 ± 0.25	500k	GJESDAL	76 SPEC	DP
2.70 ± 0.28	25k	BLUMENTHAL	75 SPEC	DP

⁷⁷ Results from linear fit and assuming only vector and axial couplings.

⁷⁸ Results from linear fit with $|f_S/f_+|$ and $|f_T/f_+|$ free.

 λ_+ (LINEAR ENERGY DEPENDENCE OF f_+ IN $K_{\mu 3}^0$ DECAY)

Results labeled OUR FIT are discussed in the review " $K_{e 3}^\pm$ and $K_{\mu 3}^0$ Form Factors" in the K^\pm Listings. For earlier, lower statistics results, see the 2004 edition of this review, Physics Letters **B592 1** (2004).

VALUE (units 10^{-2})	EVTS	DOCUMENT ID	TECN	COMMENT
2.82 ± 0.04 OUR FIT				Error includes scale factor of 1.1. Assuming μ -e universality
2.71 ± 0.10 OUR FIT				Error includes scale factor of 1.4. Not assuming μ -e universality
2.67 ± 0.06 ± 0.08	2.3M	⁷⁹ LAI	07A NA48	DP
2.745 ± 0.088 ± 0.063	1.5M	ALEXOPOU...	04A KTEV	DP, no $\mu = e$
2.813 ± 0.051	3.4M	ALEXOPOU...	04A KTEV	PI, DP, $\mu = e$
3.0 ± 0.3	1.6M	DONALDSON	74B SPEC	DP
• • • We do not use the following data for averages, fits, limits, etc. • • •				
4.27 ± 0.44	150k	BIRULEV	81 SPEC	DP
⁷⁹ LAI 07A gives a correlation -0.40 between their λ_0 and λ_+ measurements.				

 λ_0 (LINEAR ENERGY DEPENDENCE OF f_0 IN $K_{\mu 3}^0$ DECAY)

Wherever possible, we have converted the above values of $\xi(0)$ into values of λ_0 using the associated λ_+^μ and $d\xi(0)/d\lambda_+$. Results labeled OUR FIT are discussed in the review " $K_{e 3}^\pm$ and $K_{\mu 3}^0$ Form Factors" in the K^\pm Listings. For earlier, lower statistics results, see the 2004 edition of this review, Physics Letters **B592 1** (2004).

VALUE (units 10^{-2})	$d\lambda_0/d\lambda_+$	EVTS	DOCUMENT ID	TECN	COMMENT
1.38 ± 0.18 OUR FIT					Error includes scale factor of 2.2. Assuming μ -e universality
1.42 ± 0.23 OUR FIT					Error includes scale factor of 2.8. Not assuming μ -e universality
1.17 ± 0.07 ± 0.10		2.3M	⁸⁰ LAI	07A NA48	DP
1.657 ± 0.125	-0.44	1.5M	⁸¹ ALEXOPOU...	04A KTEV	DP, no $\mu = e$
1.635 ± 0.121	-0.85	3.4M	⁸² ALEXOPOU...	04A KTEV	PI, DP, $\mu = e$
+1.9 ± 0.4	-0.47	1.6M	⁸³ DONALDSON	74B SPEC	DP
• • • We do not use the following data for averages, fits, limits, etc. • • •					
3.41 ± 0.67	unknown	150k	⁸⁴ BIRULEV	81 SPEC	DP
⁸⁰ LAI 07A gives a correlation -0.40 between their λ_0 and λ_+ measurements.					
⁸¹ ALEXOPOULOS 04A gives a correlation -0.38 between their λ_0 and λ_+ measurements.					
⁸² ALEXOPOULOS 04A gives a correlation -0.36 between their λ_0 and λ_+ measurements.					
⁸³ DONALDSON 74B $d\lambda_0/d\lambda_+$ obtained from figure 18.					
⁸⁴ BIRULEV 81 gives $d\lambda_0/d\lambda_+ = -1.5$, giving an unreasonably narrow error ellipse which dominates all other results. We use $d\lambda_0/d\lambda_+ = 0$.					

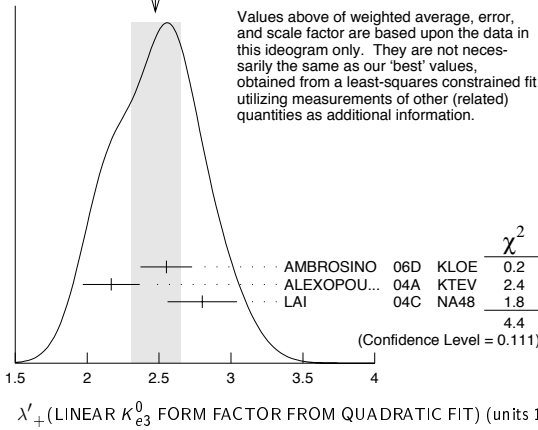
 λ'_+ (LINEAR $K_{e 3}^0$ FORM FACTOR FROM QUADRATIC FIT)

VALUE (units 10^{-2})	EVTS	DOCUMENT ID	TECN	COMMENT
2.40 ± 0.12 OUR FIT				Error includes scale factor of 1.2. Assuming μ -e universality
2.49 ± 0.13 OUR FIT				Error includes scale factor of 1.1. Not assuming μ -e universality
2.48 ± 0.17 OUR AVERAGE				Error includes scale factor of 1.5. See the ideogram below.
2.55 ± 0.15 ± 0.10	2M	⁸⁵ AMBROSINO	06D KLOE	
2.167 ± 0.137 ± 0.143	1.9M	⁸⁶ ALEXOPOU...	04A KTEV	PI, no $\mu = e$
2.80 ± 0.19 ± 0.15	5.6M	⁸⁷ LAI	04c NA48	DP

⁸⁵ We use AMBROSINO 06D result in the fit not assuming μ -e universality. This result enters the fit assuming μ -e universality via AMBROSINO 07C measurement of λ'_+ in $K_{\mu 3}$ decays. AMBROSINO 06D gives a correlation -0.95 between their λ'_+ and λ''_+ .

⁸⁶ ALEXOPOULOS 04A gives a correlation -0.97 between their λ'_+ and λ''_+ .

⁸⁷ For LAI 04c we calculate a correlation -0.88 between their λ'_+ and λ''_+ .

WEIGHTED AVERAGE
2.48±0.17 (Error scaled by 1.5)

Values above of weighted average, error, and scale factor are based upon the data in this ideogram only. They are not necessarily the same as our 'best' values, obtained from a least-squares constrained fit utilizing measurements of other (related) quantities as additional information.

 λ_+^0 (QUADRATIC K_{e3}^0 FORM FACTOR)

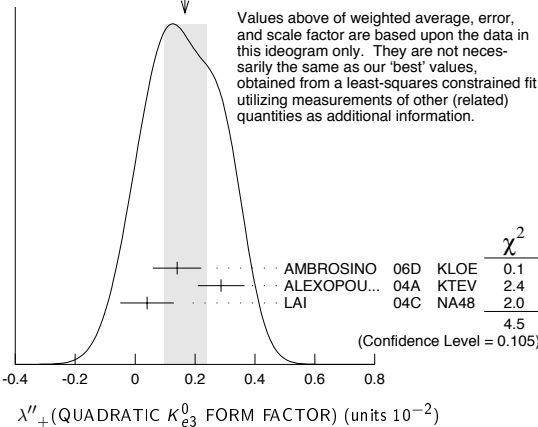
VALUE (units 10^{-2})	EVTS	DOCUMENT ID	TECN	COMMENT
0.20 ± 0.05 OUR FIT				Error includes scale factor of 1.2. Assuming μ -e universality
0.16 ± 0.05 OUR FIT				Error includes scale factor of 1.1. Not assuming μ -e universality
0.17 ± 0.07 OUR AVERAGE				Error includes scale factor of 1.5. See the ideogram below.
0.14 ± 0.07 ± 0.04	2M	⁸⁸ AMBROSINO 06D	KLOE	
0.287 ± 0.057 ± 0.053	1.9M	⁸⁹ ALEXOPOU... 04A	KTEV	PI, no $\mu = e$
0.04 ± 0.08 ± 0.04	5.6M	^{90,91} LAI 04C	NA48	DP

⁸⁸We use AMBROSINO 06D result in the fit not assuming μ -e universality. This result enters the fit assuming μ -e universality via AMBROSINO 07C measurement of λ_+^0 in $K_{\mu 3}$ decays. AMBROSINO 06D gives a correlation -0.95 between their λ_+^0 and $\lambda_+^{\prime\prime}$.

⁸⁹ALEXOPOULOS 04A gives a correlation -0.97 between their λ_+^0 and $\lambda_+^{\prime\prime}$.

⁹⁰Values doubled to agree with PDG conventions described above.

⁹¹LAI 04C gives a correlation -0.88 between their λ_+^0 and $\lambda_+^{\prime\prime}$.

WEIGHTED AVERAGE
0.17±0.07 (Error scaled by 1.5)

Values above of weighted average, error, and scale factor are based upon the data in this ideogram only. They are not necessarily the same as our 'best' values, obtained from a least-squares constrained fit utilizing measurements of other (related) quantities as additional information.

 λ_+^0 (LINEAR $K_{\mu 3}^0$ FORM FACTOR FROM QUADRATIC FIT)

VALUE (units 10^{-2})	EVTS	DOCUMENT ID	TECN	COMMENT
2.40 ± 0.12 OUR FIT				Error includes scale factor of 1.2. Assuming μ -e universality
1.89 ± 0.24 OUR FIT				Not assuming μ -e universality
2.23 ± 0.98 ± 0.37	1.8M	⁹² AMBROSINO 07C	KLOE	no $\mu = e$
2.56 ± 0.15 ± 0.09	3.8M	⁹² AMBROSINO 07C	KLOE	$\mu = e$
2.05 ± 0.22 ± 0.24	2.3M	⁹² LAI 07A	NA48	DP
1.703 ± 0.319 ± 0.177	1.5M	⁹² ALEXOPOU... 04A	KTEV	DP, no $\mu = e$
2.064 ± 0.175	3.4M	⁹² ALEXOPOU... 04A	KTEV	PI, DP, $\mu = e$

⁹²See section λ_0 below for correlations.

 $\lambda_+^{\prime\prime}$ (QUADRATIC $K_{\mu 3}^0$ FORM FACTOR)

VALUE (units 10^{-2})	EVTS	DOCUMENT ID	TECN	COMMENT
0.20 ± 0.05 OUR FIT				Error includes scale factor of 1.2. Assuming μ -e universality
0.37 ± 0.12 OUR FIT				Error includes scale factor of 1.3. Not assuming μ -e universality
0.48 ± 0.49 ± 0.16	1.8M	⁹³ AMBROSINO 07C	KLOE	no $\mu = e$
0.15 ± 0.07 ± 0.04	3.8M	⁹³ AMBROSINO 07C	KLOE	$\mu = e$
0.26 ± 0.09 ± 0.10	2.3M	⁹³ LAI 07A	NA48	DP
0.443 ± 0.131 ± 0.072	1.5M	⁹³ ALEXOPOU... 04A	KTEV	DP, no $\mu = e$
0.320 ± 0.069	3.4M	⁹³ ALEXOPOU... 04A	KTEV	PI, DP, $\mu = e$

⁹³See section λ_0 below for correlations.

 λ_0 (LINEAR $f_0 K_{\mu 3}^0$ FORM FACTOR FROM QUADRATIC FIT)

VALUE (units 10^{-2})	EVTS	DOCUMENT ID	TECN	COMMENT
1.16 ± 0.09 OUR FIT				Error includes scale factor of 1.2. Assuming μ -e universality
1.07 ± 0.14 OUR FIT				Error includes scale factor of 1.3. Not assuming μ -e universality
0.91 ± 0.59 ± 0.26	1.8M	⁹⁴ AMBROSINO 07C	KLOE	no $\mu = e$
1.54 ± 0.18 ± 0.13	3.8M	⁹⁵ AMBROSINO 07C	KLOE	$\mu = e$
0.95 ± 0.11 ± 0.08	2.3M	⁹⁶ LAI 07A	NA48	DP
1.281 ± 0.136 ± 0.122	1.5M	⁹⁷ ALEXOPOU... 04A	KTEV	DP, no $\mu = e$
1.372 ± 0.131	3.4M	⁹⁸ ALEXOPOU... 04A	KTEV	PI, DP, $\mu = e$

⁹⁴AMBROSINO 07C, not assuming μ -e universality, gives a correlation matrix

$$\begin{matrix} \lambda_+^{\prime\prime} & \lambda_+^{\prime\prime} & \\ \lambda_+^{\prime\prime} & -0.97 & 1 \\ \lambda_0 & 0.81 & -0.91 \end{matrix}$$

⁹⁵AMBROSINO 07C, assuming μ -e universality, gives a correlation matrix

$$\begin{matrix} \lambda_+^{\prime\prime} & \lambda_+^{\prime\prime} & \\ \lambda_+^{\prime\prime} & -0.95 & 1 \\ \lambda_0 & 0.29 & -0.38 \end{matrix}$$

⁹⁶LAI 07A gives a correlation matrix

$$\begin{matrix} \lambda_+^{\prime\prime} & \lambda_+^{\prime\prime} & \\ \lambda_+^{\prime\prime} & -0.96 & 1 \\ \lambda_0 & 0.63 & -0.73 \end{matrix}$$

⁹⁷ALEXOPOULOS 04A, not assuming μ -e universality, gives a correlation matrix

$$\begin{matrix} \lambda_+^{\prime\prime} & \lambda_+^{\prime\prime} & \lambda_0 \\ \lambda_+^{\prime\prime} & 1 & \\ \lambda_+^{\prime\prime} & -0.96 & 1 \\ \lambda_0 & 0.65 & -0.75 & 1 \end{matrix}$$

⁹⁸ALEXOPOULOS 04A, assuming μ -e universality, gives a correlation matrix

$$\begin{matrix} \lambda_+^{\prime\prime} & \lambda_+^{\prime\prime} & \lambda_0 \\ \lambda_+^{\prime\prime} & 1 & \\ \lambda_+^{\prime\prime} & -0.97 & 1 \\ \lambda_0 & 0.34 & -0.44 & 1 \end{matrix}$$

 M_V^e (POLE MASS FOR K_{e3}^0 DECAY)

VALUE (MeV)	EVTS	DOCUMENT ID	TECN	COMMENT
878 ± 6 OUR FIT				Error includes scale factor of 1.1. Assuming μ -e universality
875 ± 5 OUR AVERAGE				
870 ± 6 ± 7	2M	AMBROSINO 06D	KLOE	
881.03 ± 5.12 ± 4.94	1.9M	ALEXOPOU... 04A	KTEV	PI, no $\mu = e$
859 ± 18	5.6M	LAI 04C	NA48	

 M_V^{μ} (POLE MASS FOR $K_{\mu 3}^0$ DECAY)

VALUE (MeV)	EVTS	DOCUMENT ID	TECN	COMMENT
878 ± 6 OUR FIT				Error includes scale factor of 1.1. Assuming μ -e universality
900 ± 21 OUR FIT				Error includes scale factor of 1.7. Not assuming μ -e universality
905 ± 9 ± 17	2.3M	⁹⁹ LAI 07A	NA48	DP
889.19 ± 12.81 ± 9.92	1.5M	⁹⁹ ALEXOPOU... 04A	KTEV	DP, no $\mu = e$
882.32 ± 6.54	3.4M	⁹⁹ ALEXOPOU... 04A	KTEV	PI, DP, $\mu = e$

⁹⁹See section M_S^{μ} below for correlations.

 M_S^{μ} (POLE MASS FOR $K_{\mu 3}^0$ DECAY)

VALUE (MeV)	EVTS	DOCUMENT ID	TECN	COMMENT
1222 ± 80 OUR FIT				Error includes scale factor of 2.3. Not assuming μ -e universality
1252 ± 90 OUR FIT				Error includes scale factor of 2.6. Assuming μ -e universality
1400 ± 46 ± 53	2.3M	¹⁰⁰ LAI 07A	NA48	DP
1167.14 ± 28.30 ± 31.04	1.5M	¹⁰¹ ALEXOPOU... 04A	KTEV	PI, no $\mu = e$
1173.80 ± 39.47	3.4M	¹⁰² ALEXOPOU... 04A	KTEV	PI, DP, $\mu = e$

¹⁰⁰LAI 07A gives a correlation -0.47 between their M_S^{μ} and M_V^{μ} measurements, not assuming μ -e universality.

¹⁰¹ALEXOPOULOS 04A gives a correlation -0.46 between their M_S^{μ} and M_V^{μ} measurements, not assuming μ -e universality.

¹⁰²ALEXOPOULOS 04A gives a correlation -0.40 between their M_S^{μ} and M_V^{μ} measurements, assuming μ -e universality.

 Λ_+ (DISPERSIVE VECTOR FORM FACTOR FOR $K_{\mu 3}^0$ DECAY)

See the review on " $K_{\ell 3}^{\pm}$ and $K_{\ell 3}^0$ Form Factors" for details of the dispersive parametrization.

VALUE (units 10^{-1})	EVTS	DOCUMENT ID	TECN	COMMENT
0.251 ± 0.011 OUR AVERAGE				Error includes scale factor of 2.2.
0.257 ± 0.004 ± 0.004	3.8M	¹⁰³ AMBROSINO 07C	KLOE	$\mu = e$
0.233 ± 0.005 ± 0.008	2.3M	¹⁰⁴ LAI 07A	NA48	DP

¹⁰³AMBROSINO 07C results include 2M K_{e3} events from AMBROSINO 06D. The correlation between Λ_+ and $\ln(C)$ is -0.26 .

¹⁰⁴LAI 07A gives a correlation -0.44 between their Λ_+ and $\ln(C)$ measurements.

Meson Particle Listings

 K_L^0 $\ln(C)$ (DISPERSIVE SCALAR FORM FACTOR FOR $K_{\mu 3}^0$ DECAY)

See the review on " $K_{\mu 3}^0$ and $K_{e 3}^0$ Form Factors" for details of the dispersive parametrization.

VALUE (units 10^{-1})	EVTS	DOCUMENT ID	TECN	COMMENT
1.59 ± 0.26 OUR AVERAGE				Error includes scale factor of 2.2.
$2.04 \pm 0.19 \pm 0.15$	3.8M	105 AMBROSINO 07C	KLOE	$\mu = e$
$1.438 \pm 0.080 \pm 0.112$	2.3M	106 LAI	07A NA48 DP	

105 AMBROSINO 07C results include 2M $K_{\mu 3}$ events from AMBROSINO 06D. We convert (A_+, A_0) to $(A_+, \ln(C))$ parametrization using $\ln(C) = (A_0 \cdot 11.713 + 0.0398) \pm 0.0041$, where the error is due to theory parametrization of the form factor. The correlation between A_+ and $\ln(C)$ is -0.26 .

106 LAI 07A gives a correlation -0.44 between their A_+ and $\ln(C)$ measurements.

 $a_1(t_0, Q^2)$ FORM FACTOR PARAMETER

See HILL 06 for a definition of this parameter.

VALUE	EVTS	DOCUMENT ID	TECN
$1.023 \pm 0.028 \pm 0.029$	2M	107 ABOUZAID 06C	KTEV

107 $Q^2 = 2 \text{ GeV}^2$, $t_0 = 0.49 (m_K - m_\pi)^2$. Correlation between a_1 and a_2 : $\rho_{12} = -0.064$.

 $a_2(t_0, Q^2)$ FORM FACTOR PARAMETER

See HILL 06 for a definition of this parameter.

VALUE	EVTS	DOCUMENT ID	TECN
$0.75 \pm 1.58 \pm 1.47$	2M	108 ABOUZAID 06C	KTEV

108 $Q^2 = 2 \text{ GeV}^2$, $t_0 = 0.49 (m_K - m_\pi)^2$. Correlation between a_1 and a_2 : $\rho_{12} = -0.064$.

 $|f_S/f_+|$ FOR $K_{e 3}^0$ DECAY

Ratio of scalar to f_+ couplings.

VALUE (units 10^{-2})	CL%	EVTS	DOCUMENT ID	TECN	COMMENT
1.5 ± 0.7 -1.0 ± 1.2		5.6M	109 LAI	04C NA48	
•••					We do not use the following data for averages, fits, limits, etc. •••
<9.5	95	18k	HILL	78	STRC
<7.	68	48k	BIRULEV	76	SPEC See also BIRULEV 81
<4.	68	25k	BLUMENTHAL75		SPEC

109 Results from linear fit with $|f_S/f_+|$ and $|f_T/f_+|$ free.

 $|f_T/f_+|$ FOR $K_{e 3}^0$ DECAY

Ratio of tensor to f_+ couplings.

VALUE (units 10^{-2})	CL%	EVTS	DOCUMENT ID	TECN	COMMENT
5 ± 3 -4 ± 3		5.6M	110 LAI	04C NA48	
•••					We do not use the following data for averages, fits, limits, etc. •••
<40.	95	18k	HILL	78	STRC
<34.	68	48k	BIRULEV	76	SPEC See also BIRULEV 81
<23.	68	25k	BLUMENTHAL75		SPEC

110 Results from linear fit with $|f_S/f_+|$ and $|f_T/f_+|$ free.

 $|f_T/f_+|$ FOR $K_{\mu 3}^0$ DECAY

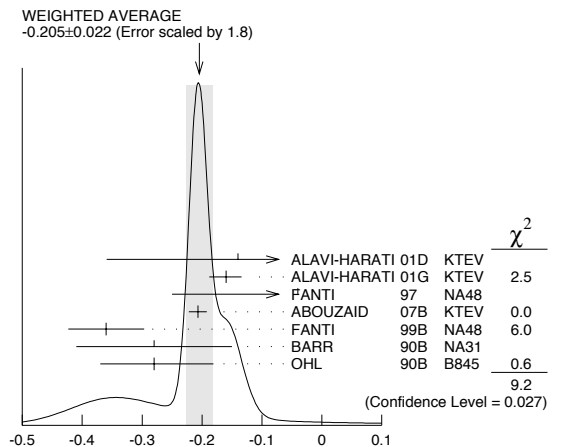
Ratio of tensor to f_+ couplings.

VALUE (units 10^{-2})	DOCUMENT ID	TECN
12 ± 12	BIRULEV 81	SPEC

 α_{K^*} DECAY FORM FACTOR FOR $K_L \rightarrow \ell^+ \ell^- \gamma$, $K_L^0 \rightarrow \ell^+ \ell^- \ell'^+ \ell'^-$

Average of all α_{K^*} measurements (from each of three datablocks following this one) assuming lepton universality.

VALUE	DOCUMENT ID
-0.205 ± 0.022 OUR AVERAGE	Includes data from the 3 datablocks that follow this one. Error includes scale factor of 1.8. See the ideogram below.

 α_{K^*} DECAY FORM FACTOR FOR $K_L \rightarrow e^+ e^- \gamma$

α_{K^*} is the constant in the model of BERGSTROM 83 which measures the relative strength of the vector-vector transition $K_L \rightarrow K^* \gamma$ with $K^* \rightarrow \rho, \omega, \phi \rightarrow \gamma^*$ and the pseudoscalar-pseudoscalar transition $K_L \rightarrow \pi, \eta, \eta' \rightarrow \gamma \gamma^*$.

VALUE	EVTS	DOCUMENT ID	TECN
The data in this block is included in the average printed for a previous datablock.			

-0.217 ± 0.034 OUR AVERAGE Error includes scale factor of 2.4.

$-0.207 \pm 0.012 \pm 0.009$	83k	111 ABOUZAID 07B	KTEV
$-0.36 \pm 0.06 \pm 0.02$	6864	FANTI	99B NA48
-0.28 ± 0.13		BARR	90B NA31
-0.280 ± 0.099 -0.090		OHL	90B B845

111 ABOUZAID 07B measures $C \cdot \alpha_{K^*} = -0.517 \pm 0.030 \pm 0.022$. We assume $C = 2.5$, as in all other measurements.

 α_{K^*} DECAY FORM FACTOR FOR $K_L \rightarrow \mu^+ \mu^- \gamma$

α_{K^*} is the constant in the model of BERGSTROM 83 described in the previous section.

VALUE	EVTS	DOCUMENT ID	TECN
The data in this block is included in the average printed for a previous datablock.			

-0.158 ± 0.027 OUR AVERAGE

-0.160 ± 0.026 -0.028	9100	ALAVI-HARATI 01G	KTEV
-0.04 ± 0.24 -0.21		FANTI	97 NA48

 $\alpha_{K^*}^{\text{eff}}$ DECAY FORM FACTOR FOR $K_L \rightarrow e^+ e^- e^+ e^-$

$\alpha_{K^*}^{\text{eff}}$ is the parameter describing the relative strength of an intermediate pseudoscalar decay amplitude and a vector meson decay amplitude in the model of BERGSTROM 83. It takes into account both the radiative effects and the form factor. Since there are two $e^+ e^-$ pairs here compared with one in $e^+ e^- \gamma$ decays, a factorized expression is used for the $e^+ e^- e^+ e^-$ decay form factor.

VALUE	EVTS	DOCUMENT ID	TECN
The data in this block is included in the average printed for a previous datablock.			

$-0.14 \pm 0.16 \pm 0.15$ 441 ALAVI-HARATI 01D KTEV

 α_{DIP} DECAY FORM FACTOR FOR $K_L^0 \rightarrow \ell^+ \ell^- \gamma$, $K_L^0 \rightarrow \ell^+ \ell^- \ell'^+ \ell'^-$

Average of all α_{DIP} measurements (from each of three datablocks following this one) assuming lepton universality.

VALUE	DOCUMENT ID
-1.69 ± 0.08 OUR AVERAGE	Includes data from the 3 datablocks that follow this one. Error includes scale factor of 1.7.

 α_{DIP} DECAY FORM FACTOR FOR $K_L^0 \rightarrow e^+ e^- \gamma$

α_{DIP} parameter in $K_L^0 \rightarrow \gamma^* \gamma^*$ form factor by DAMBROSIO 98, motivated by vector meson dominance and a proper short distance behavior.

VALUE	EVTS	DOCUMENT ID	TECN
The data in this block is included in the average printed for a previous datablock.			

$-1.729 \pm 0.043 \pm 0.028$ 83k ABOUZAID 07B KTEV

 α_{DIP} DECAY FORM FACTOR FOR $K_L^0 \rightarrow \mu^+ \mu^- \gamma$

α_{DIP} is a constant in the model of DAMBROSIO 98 described in the previous section.

VALUE	EVTS	DOCUMENT ID	TECN
The data in this block is included in the average printed for a previous datablock.			

-1.54 ± 0.10 9100 ALAVI-HARATI 01G KTEV

 α_{DIP} DECAY FORM FACTOR FOR $K_L^0 \rightarrow e^+ e^- \mu^+ \mu^-$

α_{DIP} is a constant in the model of DAMBROSIO 98 described in the previous section.

VALUE	EVTS	DOCUMENT ID	TECN
The data in this block is included in the average printed for a previous datablock.			

-1.59 ± 0.37 131 ALAVI-HARATI 03B KTEV

 a_1/a_2 FORM FACTOR FOR M1 DIRECT EMISSION AMPLITUDE

Form factor = $\bar{g}_{M1} \left[1 + \frac{a_1/a_2}{(M_\rho^2 - M_K^2) + 2M_K E_\gamma^*} \right]$ as described in ALAVI-HARATI 00B.

VALUE (GeV 2)	EVTS	DOCUMENT ID	TECN	COMMENT
-0.737 ± 0.014 OUR AVERAGE				

$-0.744 \pm 0.027 \pm 0.032$	5241	112 ABOUZAID 06	KTEV	$\pi^+ \pi^- e^+ e^-$
$-0.738 \pm 0.007 \pm 0.018$	111k	113 ABOUZAID 06A	KTEV	$\pi^+ \pi^+ \gamma$
$-0.81 \pm 0.07 \pm 0.02$ -0.13		114 LAI	03C NA48	$\pi^+ \pi^- e^+ e^-$
$-0.737 \pm 0.026 \pm 0.022$		115 ALAVI-HARATI 01B		$\pi^+ \pi^- \gamma$
$-0.720 \pm 0.028 \pm 0.009$	1766	116 ALAVI-HARATI 00B	KTEV	$\pi^+ \pi^- e^+ e^-$

112 ABOUZAID 06 also measured $|\bar{g}_{M1}| = 1.11 \pm 0.14$.

113 ABOUZAID 06A also measured $|\bar{g}_{M1}| = 1.198 \pm 0.035 \pm 0.086$.

114 LAI 03c also measured $\bar{g}_{M1} = 0.99 \pm 0.28 \pm 0.07$.

115 ALAVI-HARATI 01B fit gives $\chi^2/\text{DOF} = 38.8/27$. Linear and quadratic fits give $\chi^2/\text{DOF} = 43.2/27$ and $37.6/26$ respectively.

116 ALAVI-HARATI 00B also measured $|\bar{g}_{M1}| = 1.35 \pm 0.20 \pm 0.17$.

 \bar{f}_S DECAY FORM FACTOR FOR $K_L^0 \rightarrow \pi^\pm \pi^0 e^\mp \nu_e$

VALUE	DOCUMENT ID	TECN
0.049 ± 0.011 OUR AVERAGE	Error includes scale factor of 1.7.	
$0.052 \pm 0.006 \pm 0.002$	BATLEY 04	NA48
$0.010 \pm 0.016 \pm 0.017$	MAKOFF 93	E731

\bar{F}_P DECAY FORM FACTOR FOR $K_L^0 \rightarrow \pi^\pm \pi^0 e^\mp \nu_e$

VALUE	DOCUMENT ID	TECN
-0.052 ± 0.012 OUR AVERAGE		
$-0.051 \pm 0.011 \pm 0.005$	BATLEY 04	NA48
$-0.079 \pm 0.049 \pm 0.022$	MAKOFF 93	E731

 λ_g DECAY FORM FACTOR FOR $K_L^0 \rightarrow \pi^\pm \pi^0 e^\mp \nu_e$

VALUE	DOCUMENT ID	TECN
0.085 ± 0.020 OUR AVERAGE		
$0.087 \pm 0.019 \pm 0.006$	BATLEY 04	NA48
$0.014 \pm 0.087 \pm 0.070$	MAKOFF 93	E731

 \bar{h} DECAY FORM FACTOR FOR $K_L^0 \rightarrow \pi^\pm \pi^0 e^\mp \nu_e$

VALUE	DOCUMENT ID	TECN
-0.30 ± 0.13 OUR AVERAGE		
$-0.32 \pm 0.12 \pm 0.07$	BATLEY 04	NA48
$-0.07 \pm 0.31 \pm 0.31$	MAKOFF 93	E731

 L_3 CHIRAL PERT. THEO. PARAM. FOR $K_L^0 \rightarrow \pi^\pm \pi^0 e^\mp \nu_e$

VALUE (units 10^{-3})	DOCUMENT ID	TECN
-3.96 ± 0.28 OUR AVERAGE		
-4.1 ± 0.2	BATLEY 04	NA48
-3.4 ± 0.4	117 MAKOFF 93	E731

117 MAKOFF 93 sign has been changed to negative to agree with the sign convention used in BATLEY 04.

 a_V , VECTOR MESON EXCHANGE CONTRIBUTION

VALUE	DOCUMENT ID	TECN	COMMENT
-0.54 ± 0.12 OUR AVERAGE			Error includes scale factor of 2.8.
$-0.46 \pm 0.03 \pm 0.04$	LAI 02B	NA48	$K_L^0 \rightarrow \pi^0 2\gamma$
$-0.67 \pm 0.21 \pm 0.12$	ALAVI-HARATI 01E	KTEV	$K_L^0 \rightarrow \pi^0 e^+ e^- \gamma$
$-0.72 \pm 0.05 \pm 0.06$	ALAVI-HARATI 99B	KTEV	$K_L^0 \rightarrow \pi^0 2\gamma$

CP VIOLATION IN K_L DECAYS

Revised May 2008 by L. Wolfenstein (Carnegie-Mellon University), T.G. Trippe (LBNL), and C.-J. Lin (LBNL).

The symmetries C (particle-antiparticle interchange) and P (space inversion) hold for strong and electromagnetic interactions. After the discovery of large C and P violation in the weak interactions, it appeared that the product CP was a good symmetry. In 1964 CP violation was observed in K^0 decays at a level given by the parameter $\epsilon \approx 2.3 \times 10^{-3}$.

A unified treatment of CP violation in K , D , B , and B_s mesons is given in “ CP Violation in Meson Decays” by D. Kirkby and Y. Nir in this *Review*. A more detailed review including a thorough discussion of the experimental techniques used to determine CP violation parameters is given in a book by K. Kleinknecht [1]. Here we give a concise summary of the formalism needed to define the parameters of CP violation in K_L decays, and a description of our fits for the best values of these parameters.

1. Formalism for CP violation in Kaon decay:

CP violation has been observed in the semi-leptonic decays $K_L^0 \rightarrow \pi^\mp \ell^\pm \nu$, and in the nonleptonic decay $K_L^0 \rightarrow 2\pi$. The experimental numbers that have been measured are

$$A_L = \frac{\Gamma(K_L^0 \rightarrow \pi^- \ell^+ \nu) - \Gamma(K_L^0 \rightarrow \pi^+ \ell^- \nu)}{\Gamma(K_L^0 \rightarrow \pi^- \ell^+ \nu) + \Gamma(K_L^0 \rightarrow \pi^+ \ell^- \nu)} \quad (1a)$$

$$\eta_{+-} = A(K_L^0 \rightarrow \pi^+ \pi^-) / A(K_S^0 \rightarrow \pi^+ \pi^-) = |\eta_{+-}| e^{i\phi_{+-}} \quad (1b)$$

$$\eta_{00} = A(K_L^0 \rightarrow \pi^0 \pi^0) / A(K_S^0 \rightarrow \pi^0 \pi^0) = |\eta_{00}| e^{i\phi_{00}} \quad (1c)$$

CP violation can occur either in the $K^0 - \bar{K}^0$ mixing or in the decay amplitudes. Assuming CPT invariance, the mass eigenstates of the $K^0 - \bar{K}^0$ system can be written

$$|K_S\rangle = p|K^0\rangle + q|\bar{K}^0\rangle, \quad |K_L\rangle = p|K^0\rangle - q|\bar{K}^0\rangle. \quad (2)$$

If CP invariance held, we would have $q = p$ so that K_S would be CP -even and K_L CP -odd. (We define $|\bar{K}^0\rangle$ as $CP |K^0\rangle$.) CP violation in $K^0 - \bar{K}^0$ mixing is then given by the parameter $\tilde{\epsilon}$ where

$$\frac{p}{q} = \frac{(1 + \tilde{\epsilon})}{(1 - \tilde{\epsilon})}. \quad (3)$$

CP violation can also occur in the decay amplitudes

$$A(K^0 \rightarrow \pi\pi(I)) = A_I e^{i\delta_I}, \quad A(\bar{K}^0 \rightarrow \pi\pi(I)) = A_I^* e^{i\delta_I}, \quad (4)$$

where I is the isospin of $\pi\pi$, δ_I is the final-state phase shift, and A_I would be real if CP invariance held. The CP -violating observables are usually expressed in terms of ϵ and ϵ' defined by

$$\eta_{+-} = \epsilon + \epsilon', \quad \eta_{00} = \epsilon - 2\epsilon'. \quad (5a)$$

One can then show [2]

$$\epsilon = \tilde{\epsilon} + i (\text{Im } A_0 / \text{Re } A_0), \quad (5b)$$

$$\sqrt{2}\epsilon' = ie^{i(\delta_2 - \delta_0)} (\text{Re } A_2 / \text{Re } A_0) (\text{Im } A_2 / \text{Re } A_2 - \text{Im } A_0 / \text{Re } A_0), \quad (5c)$$

$$A_L = 2\text{Re } \epsilon / (1 + |\epsilon|^2) \approx 2\text{Re } \epsilon. \quad (5d)$$

In Eqs. (5a), small corrections [3] of order $\epsilon' \times \text{Re}(A_2/A_0)$ are neglected, and Eq. (5d) assumes the $\Delta S = \Delta Q$ rule.

The quantities $\text{Im } A_0$, $\text{Im } A_2$, and $\text{Im } \tilde{\epsilon}$ depend on the choice of phase convention, since one can change the phases of K^0 and \bar{K}^0 by a transformation of the strange quark state $|s\rangle \rightarrow |s\rangle e^{i\alpha}$; of course, observables are unchanged. It is possible by a choice of phase convention to set $\text{Im } A_0$ or $\text{Im } A_2$ or $\text{Im } \tilde{\epsilon}$ to zero, but none of these is zero with the usual phase conventions in the Standard Model. The choice $\text{Im } A_0 = 0$ is called the Wu-Yang phase convention [4], in which case $\epsilon = \tilde{\epsilon}$. The value of ϵ' is independent of phase convention, and a nonzero value demonstrates CP violation in the decay amplitudes, referred to as direct CP violation. The possibility that direct CP violation is essentially zero, and that CP violation occurs only in the mixing matrix, was referred to as the superweak theory [5].

By applying CPT invariance and unitarity the phase of ϵ is given approximately by

$$\phi_\epsilon \approx \tan^{-1} \frac{2(m_{K_L} - m_{K_S})}{\Gamma_{K_S} - \Gamma_{K_L}} \approx 43.51 \pm 0.05^\circ, \quad (6a)$$

while Eq. (5c) gives the phase of ϵ' to be

$$\phi_{\epsilon'} = \delta_2 - \delta_0 + \frac{\pi}{2} \approx 42.3 \pm 1.5^\circ, \quad (6b)$$

where the numerical value is based on an analysis of $\pi - \pi$ scattering using chiral perturbation theory [6]. The approximation in Eq. (6a) depends on the assumption that direct CP violation is very small in all K^0 decays. This is expected to be good to a few tenths of a degree, as indicated by the small value of ϵ' and

Meson Particle Listings

K_L^0

of η_{+-0} and η_{000} , the CP -violation parameters in the decays $K_S \rightarrow \pi^+\pi^-\pi^0$ [7], and $K_S \rightarrow \pi^0\pi^0\pi^0$ [8]. The relation in Eq. (6a) is exact in the superweak theory, so this is sometimes called the superweak-phase ϕ_{SW} . An important point for the analysis is that $\cos(\phi_{e'}-\phi_e) \simeq 1$. The consequence is that only two real quantities need be measured, the magnitude of ϵ and the value of (ϵ'/ϵ) , including its sign. The measured quantity $|\eta_{00}/\eta_{+-}|^2$ is very close to unity so that we can write

$$|\eta_{00}/\eta_{+-}|^2 \approx 1 - 6\text{Re}(\epsilon'/\epsilon) \approx 1 - 6\epsilon'/\epsilon, \quad (7a)$$

$$\text{Re}(\epsilon'/\epsilon) \approx \frac{1}{3}(1 - |\eta_{00}/\eta_{+-}|). \quad (7b)$$

From the experimental measurements in this edition of the *Review*, and the fits discussed in the next section, one finds

$$|\epsilon| = (2.229 \pm 0.012) \times 10^{-3}, \quad (8a)$$

$$\phi_\epsilon = (43.5 \pm 0.7)^\circ, \quad (8b)$$

$$\text{Re}(\epsilon'/\epsilon) \approx \epsilon'/\epsilon = (1.65 \pm 0.26) \times 10^{-3}, \quad (8c)$$

$$\phi_{+-} = (43.4 \pm 0.7)^\circ, \quad (8d)$$

$$\phi_{00} - \phi_{+-} = (0.2 \pm 0.4)^\circ, \quad (8e)$$

$$A_L = (3.32 \pm 0.06) \times 10^{-3}. \quad (8f)$$

Direct CP violation, as indicated by ϵ'/ϵ , is expected in the Standard Model. However, the numerical value cannot be reliably predicted because of theoretical uncertainties [9]. The value of A_L agrees with Eq. (5d). The values of ϕ_{+-} and $\phi_{00} - \phi_{+-}$ are used to set limits on CPT violation [see “Tests of Conservation Laws”].

2. Fits for K_L^0 CP -violation parameters:

In recent years, K_L^0 CP -violation experiments have improved our knowledge of CP -violation parameters, and their consistency with the expectations of CPT invariance and unitarity. To determine the best values of the CP -violation parameters in $K_L^0 \rightarrow \pi^+\pi^-$ and $\pi^0\pi^0$ decay, we make two types of fits, one for the phases ϕ_{+-} and ϕ_{00} jointly with Δm and τ_S , and the other for the amplitudes $|\eta_{+-}|$ and $|\eta_{00}|$ jointly with the $K_L^0 \rightarrow \pi\pi$ branching fractions.

Fits to ϕ_{+-} , ϕ_{00} , $\Delta\phi$, Δm , and τ_S data: These are joint fits to the data on ϕ_{+-} , ϕ_{00} , the phase difference $\Delta\phi = \phi_{00} - \phi_{+-}$, the $K_L^0 - K_S^0$ mass difference Δm , and the K_S^0 mean life τ_S , including the effects of correlations.

Measurements of ϕ_{+-} and ϕ_{00} are highly correlated with Δm and τ_S . Some measurements of τ_S are correlated with Δm . The correlations are given in the footnotes of the ϕ_{+-} and ϕ_{00} sections of the K_L^0 Listings, and the τ_S section of the K_S^0 Listings.

In most cases, the correlations are quoted as 100%, *i.e.*, with the value and error of ϕ_{+-} or ϕ_{00} given at a fixed value of Δm and τ_S , with additional terms specifying the dependence of the value on Δm and τ_S . These cases lead to diagonal bands in Figs. [1] and [2]. The KTeV experiment [10] quotes its results as values of ϕ_{+-} , Δm , and τ_S with correlations, leading to the ellipses labeled “b.”

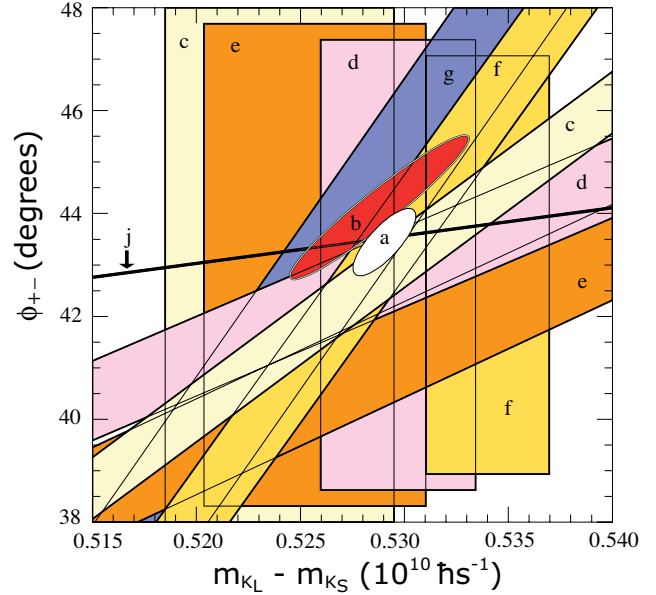


Figure 1: ϕ_{+-} vs Δm for experiments which do not assume CPT invariance. Δm measurements appear as vertical bands spanning $\Delta m \pm 1\sigma$, cut near the top and bottom to aid the eye. Most ϕ_{+-} measurements appear as diagonal bands spanning $\phi_{+-} \pm \sigma_\phi$. Data are labeled by letters: “b”–FNAL KTeV, “c”–CERN CPLEAR, “d”–FNAL E773, “e”–FNAL E731, “f”–CERN, “g”–CERN NA31, and are cited in Table 1. The narrow band “j” shows ϕ_{SW} . The ellipse “a” shows the $\chi^2 = 1$ contour of the fit result. Color version at end of book.

Table 1: References, Document ID’s, and sources corresponding to the letter labels in the figures. The data are given in the ϕ_{+-} and Δm sections of the K_L Listings, and the τ_S section of the K_S Listings.

Label	Source	PDG Document ID	Ref.
a	this <i>Review</i>	OUR FIT	
b	FNAL KTeV	ALAVI-HARATI 03	[10]
c	CERN CPLEAR	APOSTOLAKIS 99C	[11]
d	FNAL E773	SCHWINGENHEUER 95	[12]
e	FNAL E731	GIBBONS 93,93C	[13,14]
f	CERN	GEWENIGER 74B,74C	[15,16]
g	CERN NA31	CAROSI 90	[17]
h	CERN NA48	LAI 02C	[18]
i	CERN NA31	BERTANZA 97	[19]
j	this <i>Review</i>	SUPERWEAK 08	

The data on τ_S , Δm , and ϕ_{+-} shown in Figs. [1] and [2] are combined with data on ϕ_{00} and $\phi_{00} - \phi_{+-}$ in two fits, one without assuming CPT , and the other with this assumption. The results without assuming CPT are shown as ellipses labeled

“a.” These ellipses are seen to be in good agreement with the superweak phase

$$\phi_{\text{SW}} = \tan^{-1} \left(\frac{2\Delta m}{\Delta\Gamma} \right) = \tan^{-1} \left(\frac{2\Delta m \tau_S \tau_L}{\hbar(\tau_L - \tau_S)} \right). \quad (9)$$

In Figs. [1] and [2], ϕ_{SW} is shown as narrow bands labeled “j.”

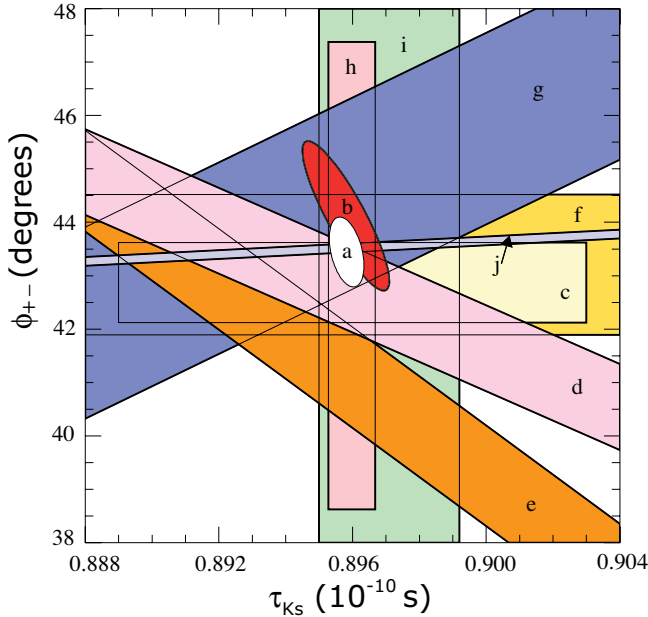


Figure 2: ϕ_{+-} vs τ_S . τ_S measurements appear as vertical bands spanning $\tau_S \pm 1\sigma$, some of which are cut near the top and bottom to aid the eye. Most ϕ_{+-} measurements appear as diagonal or horizontal bands spanning $\phi_{+-} \pm \sigma_\phi$. Data are labeled by letters: “b”–FNAL KTeV, “c”–CERN CPLEAR, “d”–FNAL E773, “e”–FNAL E731, “f”–CERN, “g”–CERN NA31, “h”–CERN NA48, “i”–CERN NA31, and are cited in Table 1. The narrow band “j” shows ϕ_{SW} . The ellipse “a” shows the fit result’s $\chi^2 = 1$ contour. Color version at end of book.

Table 2 column 2, “Fit w/o *CPT*,” gives the resulting fitted parameters, while Table 3 gives the correlation matrix for this fit. The white ellipses labeled “a” in Fig. 1 and Fig. 2 are the $\chi^2 = 1$ contours for this fit.

For experiments which have dependencies on unseen fit parameters, that is, parameters other than those shown on the x or y axis of the figure, their band positions are evaluated using the fit results and their band widths include the fitted uncertainty in the unseen parameters. This is also true for the ϕ_{SW} bands.

If *CPT* invariance and unitarity are assumed, then by Eq. (6a), the phase of ϵ is constrained to be approximately equal to

$$\phi_{\text{SW}} = (43.5165 \pm 0.0002)^\circ + 54.1(\Delta m - 0.5290)^\circ + 32.0(\tau_S - 0.8958) \quad (10)$$

where we have linearized the Δm and τ_S dependence of Eq. (9). The error ± 0.0002 is due to the uncertainty in τ_L . Here Δm has units $10^{10} \hbar \text{ s}^{-1}$ and τ_S has units 10^{-10} s .

If in addition we use the observation that $\text{Re}(\epsilon'/\epsilon) \ll 1$ and $\cos(\phi_{\epsilon'} - \phi_\epsilon) \simeq 1$, as well as the numerical value of $\phi_{\epsilon'}$ given in Eq. (6b), then Eqs. (5a), which are sketched in Fig. 3, lead to the constraint

$$\begin{aligned} \phi_{00} - \phi_{+-} &\approx -3 \text{Im} \left(\frac{\epsilon'}{\epsilon} \right) \\ &\approx -3 \text{Re} \left(\frac{\epsilon'}{\epsilon} \right) \tan(\phi_{\epsilon'} - \phi_\epsilon) \\ &\approx 0.006^\circ \pm 0.008^\circ, \end{aligned} \quad (11)$$

so that $\phi_{+-} \approx \phi_{00} \approx \phi_\epsilon \approx \phi_{\text{SW}}$.

Table 2: Fit results for ϕ_{+-} , Δm , τ_S , ϕ_{00} , $\Delta\phi = \phi_{00} - \phi_{+-}$, and ϕ_ϵ without and with the *CPT* assumption.

Quantity(units)	Fit w/o <i>CPT</i>	Fit w/ <i>CPT</i>
$\phi_{+-}(\text{°})$	43.4 ± 0.7 (S=1.3)	43.51 ± 0.05 (S=1.1)
$\Delta m(10^{10} \hbar \text{ s}^{-1})$	0.5290 ± 0.0015 (S=1.1)	0.5292 ± 0.0009 (S=1.2)
$\tau_S(10^{-10} \text{ s})$	0.8958 ± 0.0005	0.8953 ± 0.0005 (S=1.1)
$\phi_{00}(\text{°})$	43.7 ± 0.8 (S=1.2)	43.52 ± 0.05 (S=1.1)
$\Delta\phi(\text{°})$	0.2 ± 0.4	0.006 ± 0.014 (S=1.8)
$\phi_\epsilon(\text{°})$	43.5 ± 0.7 (S=1.3)	43.51 ± 0.05 (S=1.1)
χ^2	17.4	21.9
# Deg. Free.	13	17

In the fit assuming *CPT*, we constrain $\phi_\epsilon = \phi_{\text{SW}}$ using the linear expression in Eq. (10), and constrain $\phi_{00} - \phi_{+-}$ using Eq. (11). These constraints are inserted into the Listings with the Document ID of SUPERWEAK 08. Some additional data for which the authors assumed *CPT* are added to this fit or substitute for other less precise data for which the authors did not make this assumption. See the Listings for details.

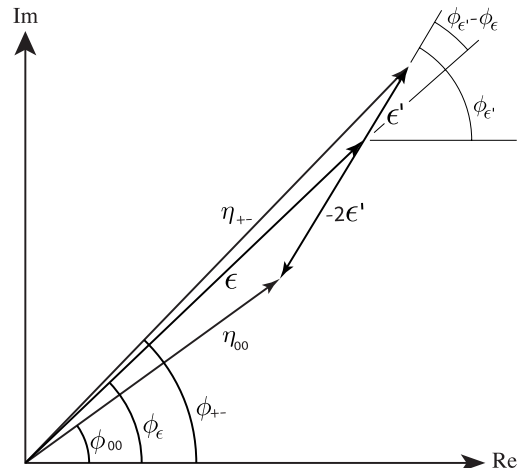


Figure 3: Sketch of Eqs. (5a). Not to scale.

Meson Particle Listings

 K_L^0

The results of this fit are shown in Table 2, column 3, “Fit w/*CPT*,” and the correlation matrix is shown in Table 4. The Δm precision is improved by the *CPT* assumption.

Table 3: Correlation matrix for the results of the fit without the *CPT* assumption

	ϕ_{+-}	Δm	τ_S	ϕ_{00}	$\Delta\phi$	ϕ_ϵ
ϕ_{+-}	1.000	0.778	-0.391	0.837	-0.002	0.977
Δm	0.778	1.000	-0.424	0.665	0.024	0.766
τ_S	-0.391	-0.424	1.000	-0.327	0.001	-0.382
ϕ_{00}	0.837	0.665	-0.327	1.000	0.546	0.934
$\Delta\phi$	-0.002	0.024	0.001	0.546	1.000	0.211
ϕ_ϵ	0.977	0.766	-0.382	0.934	0.211	1.000

Table 4: Correlation matrix for the results of the fit with the *CPT* assumption

	ϕ_{+-}	Δm	τ_S	ϕ_{00}	$\Delta\phi$	ϕ_ϵ
ϕ_{+-}	1.000	0.924	0.054	0.711	-0.283	0.964
Δm	0.924	1.000	-0.231	0.834	-0.020	0.958
τ_S	0.054	-0.231	1.000	0.056	0.009	0.059
ϕ_{00}	0.711	0.834	0.056	1.000	0.473	0.873
$\Delta\phi$	-0.283	-0.020	0.009	0.473	1.000	-0.018
ϕ_ϵ	0.964	0.958	0.059	0.873	-0.018	1.000

Fits for ϵ'/ϵ , $|\eta_{+-}|$, $|\eta_{00}|$, and $B(K_L \rightarrow \pi\pi)$

We list measurements of $|\eta_{+-}|$, $|\eta_{00}|$, $|\eta_{00}/\eta_{+-}|$, and ϵ'/ϵ . Independent information on $|\eta_{+-}|$ and $|\eta_{00}|$ can be obtained from measurements of the K_L^0 and K_S^0 lifetimes (τ_L , τ_S), and branching ratios (B) to $\pi\pi$, using the relations

$$|\eta_{+-}| = \left[\frac{B(K_L^0 \rightarrow \pi^+\pi^-)}{\tau_L} \frac{\tau_S}{B(K_S^0 \rightarrow \pi^+\pi^-)} \right]^{1/2}, \quad (12a)$$

$$|\eta_{00}| = \left[\frac{B(K_L^0 \rightarrow \pi^0\pi^0)}{\tau_L} \frac{\tau_S}{B(K_S^0 \rightarrow \pi^0\pi^0)} \right]^{1/2}. \quad (12b)$$

For historical reasons, the branching ratio fits and the *CP*-violation fits are done separately, but we want to include the influence of $|\eta_{+-}|$, $|\eta_{00}|$, $|\eta_{00}/\eta_{+-}|$, and ϵ'/ϵ measurements on $B(K_L^0 \rightarrow \pi^+\pi^-)$ and $B(K_L^0 \rightarrow \pi^0\pi^0)$ and vice versa. We approximate a global fit to all of these measurements by first performing two independent fits: 1) BRFIT, a fit to the K_L^0 branching ratios, rates, and mean life, and 2) ETAFIT, a fit to the $|\eta_{+-}|$, $|\eta_{00}|$, $|\eta_{+-}/\eta_{00}|$, and ϵ'/ϵ measurements. The results from fit 1, along with the K_S^0 values from this edition, are used to compute values of $|\eta_{+-}|$ and $|\eta_{00}|$, which are included as measurements in the $|\eta_{00}|$ and $|\eta_{+-}|$ sections with a document ID of BRFIT 08. Thus, the fit values of $|\eta_{+-}|$ and $|\eta_{00}|$ given in this edition include both the direct measurements and the results from the branching ratio fit.

The process is reversed in order to include the direct $|\eta|$ measurements in the branching ratio fit. The results from fit 2 above (before including BRFIT 08 values) are used along with the K_L^0 and K_S^0 mean lives and the $K_S^0 \rightarrow \pi\pi$ branching fractions to compute the K_L^0 branching ratio $\Gamma(K_L^0 \rightarrow \pi^0\pi^0)/\Gamma(K_L^0 \rightarrow \pi^+\pi^-)$. This branching ratio value is included as a measurement in the branching ratio section with a document ID of ETAFIT 08. Thus, the K_L^0 branching ratio fit values in this edition include the results of the direct measurement of $|\eta_{00}/\eta_{+-}|$ and ϵ'/ϵ . Most individual measurements of $|\eta_{+-}|$ and $|\eta_{00}|$ enter our fits directly via the corresponding measurements of $\Gamma(K_L^0 \rightarrow \pi^+\pi^-)/\Gamma(\text{total})$ and $\Gamma(K_L^0 \rightarrow \pi^0\pi^0)/\Gamma(\text{total})$, and those that do not have too large errors to have any influence on the fitted values of these branching ratios. A more detailed discussion of these fits is given in the 1990 edition of this *Review* [20].

References

1. K. Kleinknecht, “Uncovering *CP* violation: experimental clarification in the neutral *K* meson and *B* meson systems,” *Springer Tracts in Modern Physics*, vol. 195 (Springer Verlag 2003).
2. B. Winstein and L. Wolfenstein, *Rev. Mod. Phys.* **65**, 1113 (1993).
3. M.S. Sozzi, *Eur. Phys. J.* **C36**, 37 (2004).
4. T.T. Wu and C.N. Yang, *Phys. Rev. Lett.* **13**, 380 (1964).
5. L. Wolfenstein, *Phys. Rev. Lett.* **13**, 562 (1964); L. Wolfenstein, *Comm. Nucl. Part. Phys.* **21**, 275 (1994).
6. G. Colangelo, J. Gasser, and H. Leutwyler, *Nucl. Phys.* **B603**, 125 (2001).
7. R. Adler *et al.*, (CLEAR Collaboration), *Phys. Lett.* **B407**, 193 (1997); P. Bloch, *Proceedings of Workshop on K Physics* (Orsay 1996), ed. L. Iconomidou-Fayard, Edition Frontieres, Gif-sur-Yvette, France (1997) p. 307.
8. A. Lai *et al.*, *Phys. Lett.* **B610**, 165 (2005).
9. G. Buchalla, A.J. Buras, and M.E. Lautenbacher, *Rev. Mod. Phys.* **68**, 1125 (1996); S. Bosch *et al.*, *Nucl. Phys.* **B565**, 3 (2000); S. Bertolini, M. Fabrichesi, and J.O. Egg, *Rev. Mod. Phys.* **72**, 65 (2000).
10. A. Alavi-Harati *et al.*, *Phys. Rev.* **D67**, 012005 (2003); See also *erratum*, Alavi-Harati *et al.*, *Phys. Rev.* **D**, to be published, for corrections to correlation coefficients.
11. A. Apostolakis *et al.*, *Phys. Lett.* **B458**, 545 (1999).
12. B. Schwingerheuer *et al.*, *Phys. Rev. Lett.* **74**, 4376 (1995).
13. L.K. Gibbons *et al.*, *Phys. Rev. Lett.* **70**, 1199 (1993) and footnote in Ref. 12.
14. L.K. Gibbons, Thesis, RX-1487, Univ. of Chicago, 1993.
15. C. Geweniger *et al.*, *Phys. Lett.* **48B**, 487 (1974).
16. C. Geweniger *et al.*, *Phys. Lett.* **52B**, 108 (1974).
17. R. Carosi *et al.*, *Phys. Lett.* **B237**, 303 (1990).
18. A. Lai *et al.*, *Phys. Lett.* **B537**, 28 (2002).
19. L. Bertanza *et al.*, *Z. Phys.* **C73**, 629 (1997).
20. J.J. Hernandez *et al.*, Particle Data Group, *Phys. Lett.* **B239**, 1 (1990).

CP-VIOLATION PARAMETERS IN K_L^0 DECAYSCHARGE ASYMMETRY IN K_{L3}^0 DECAYS

Such asymmetry violates CP. It is related to $\text{Re}(\epsilon)$.

 $A_L =$ weighted average of $A_L(\mu)$ and $A_L(e)$

In previous editions and in the literature the symbol used for this asymmetry was δ_L or δ . We use A_L for consistency with B^0 asymmetry notation and with recent K_S^0 notation.

VALUE (%)	EVTS	DOCUMENT ID	TECN	COMMENT
0.332±0.006 OUR AVERAGE		Includes data from the 2 datablocks that follow this one.		
0.333±0.050	33M	WILLIAMS	73	ASPK $K_{\mu 3} + K_{e 3}$

 $A_L(\mu) = [\Gamma(\pi^- \mu^+ \nu_\mu) - \Gamma(\pi^+ \mu^- \bar{\nu}_\mu)]/\text{SUM}$

Only the combined value below is put into the Meson Summary Table.

VALUE (%)	EVTS	DOCUMENT ID	TECN	COMMENT
The data in this block is included in the average printed for a previous datablock.				

0.304±0.025 OUR AVERAGE

0.313±0.029	15M	GEWENIGER	74	ASPK
0.278±0.051	7.7M	PICCIONI	72	ASPK

• • • We do not use the following data for averages, fits, limits, etc. • • •

0.60 ± 0.14	4.1M	MCCARTHY	73	CNTR
0.57 ± 0.17	1M	118 PACIOTTI	69	OSPK
0.403±0.134	1M	118 DORFAN	67	OSPK

118 PACIOTTI 69 is a reanalysis of DORFAN 67 and is corrected for $\mu^+ \mu^-$ range difference in MCCARTHY 72.

 $A_L(e) = [\Gamma(\pi^- e^+ \nu_e) - \Gamma(\pi^+ e^- \bar{\nu}_e)]/\text{SUM}$

Only the combined value below is put into the Meson Summary Table.

VALUE (%)	EVTS	DOCUMENT ID	TECN	COMMENT
The data in this block is included in the average printed for a previous datablock.				

0.334 ± 0.007 OUR AVERAGE

0.3322±0.0058±0.0047	298M	ALAVI-HARATI02		
0.341 ± 0.018	34M	GEWENIGER	74	ASPK
0.318 ± 0.038	40M	FITCH	73	ASPK
0.346 ± 0.033	10M	MARX	70	CNTR

• • • We do not use the following data for averages, fits, limits, etc. • • •

0.36 ± 0.18	600k	ASHFORD	72	ASPK
0.246 ± 0.059	10M	119 SAAL	69	CNTR
0.224 ± 0.036	10M	119 BENNETT	67	CNTR

119 SAAL 69 is a reanalysis of BENNETT 67.

PARAMETERS FOR $K_L^0 \rightarrow 2\pi$ DECAY

$$\eta_{+-} = A(K_L^0 \rightarrow \pi^+ \pi^-) / A(K_S^0 \rightarrow \pi^+ \pi^-)$$

$$\eta_{00} = A(K_L^0 \rightarrow \pi^0 \pi^0) / A(K_S^0 \rightarrow \pi^0 \pi^0)$$

The fitted values of $|\eta_{+-}|$ and $|\eta_{00}|$ given below are the results of a fit to $|\eta_{+-}|$, $|\eta_{00}|$, $|\eta_{00}/\eta_{+-}|$, and $\text{Re}(\epsilon'/\epsilon)$. Independent information on $|\eta_{+-}|$ and $|\eta_{00}|$ can be obtained from the fitted values of the $K_L^0 \rightarrow \pi\pi$ and $K_S^0 \rightarrow \pi\pi$ branching ratios and the K_L^0 and K_S^0 lifetimes. This information is included as data in the $|\eta_{+-}|$ and $|\eta_{00}|$ sections with a Document ID "BRFIT." See the note "CP violation in K_L^0 decays" above for details.

 $|\eta_{00}| = |A(K_L^0 \rightarrow 2\pi^0) / A(K_S^0 \rightarrow 2\pi^0)|$

VALUE (units 10^{-3})	DOCUMENT ID	TECN	COMMENT
2.222±0.012 OUR FIT	Error includes scale factor of 1.7.		
2.243±0.014	BRFIT	08	

• • • We do not use the following data for averages, fits, limits, etc. • • •

2.47 ± 0.31 ± 0.24	ANGELOPO...	98	CPLR
2.49 ± 0.40	120 ADLER	96B	CPLR Sup. by ANGELOPOULOS 98
2.33 ± 0.18	CHRISTENS...	79	ASPK
2.71 ± 0.37	121 WOLFF	71	OSPK Cu reg., 4γ 's
2.95 ± 0.63	121 CHOLLET	70	OSPK Cu reg., 4γ 's

120 Error is statistical only.

121 CHOLLET 70 gives $|\eta_{00}| = (1.23 \pm 0.24) \times (\text{regeneration amplitude, } 2 \text{ GeV}/c \text{ Cu})/10000\text{mb}$. WOLFF 71 gives $|\eta_{00}| = (1.13 \pm 0.12) \times (\text{regeneration amplitude, } 2 \text{ GeV}/c \text{ Cu})/10000\text{mb}$. We compute both $|\eta_{00}|$ values for (regeneration amplitude, 2 GeV/c Cu) = 24 ± 2mb. This regeneration amplitude results from averaging over FAISSNER 69, extrapolated using optical-model calculations of Bohm et al., Physics Letters **27B** 594 (1968) and the data of BALATS 71. (From H. Faissner, private communication).

 $|\eta_{+-}| = |A(K_L^0 \rightarrow \pi^+ \pi^-) / A(K_S^0 \rightarrow \pi^+ \pi^-)|$

VALUE (units 10^{-3})	EVTS	DOCUMENT ID	TECN	COMMENT
2.233±0.012 OUR FIT	Error includes scale factor of 1.7.			
2.226±0.008		BRFIT	08	

• • • We do not use the following data for averages, fits, limits, etc. • • •

2.223±0.012	122 LAI	07	NA48
2.219±0.013	123 AMBROSINO	06F	KLOE
2.228±0.010	124 ALEXOPOU...	04	KTEV
2.286±0.023±0.026	70M	125 APOSTOLA...	99c CPLR $K^0\text{-}\bar{K}^0$ asymmetry
2.310±0.043±0.031		126 ADLER	95B CPLR $K^0\text{-}\bar{K}^0$ asymmetry
2.32 ± 0.14 ± 0.03	10 ⁵	ADLER	92B CPLR $K^0\text{-}\bar{K}^0$ asymmetry
2.30 ± 0.035		GEWENIGER	74B ASPK

122 Value obtained from the NA48 measurements of $\Gamma(K_L^0 \rightarrow \pi^+ \pi^-)/\Gamma(K_L^0 \rightarrow \pi^+ \nu_e)$ and $\tau_{K_S^0}$ and KLOE measurements of $B(K_S^0 \rightarrow \pi^+ \pi^-)$ and $\tau_{K_L^0}$. $\Gamma(K_L^0 \rightarrow \pi^+ \pi^-)$

is defined to include the inner bremsstrahlung component $\Gamma(K_L^0 \rightarrow \pi^+ \pi^- \gamma(\text{IB}))$ but exclude the direct emission component $B(K_S^0 \rightarrow \pi^+ \pi^- (\text{DE}))$. Their $|\eta_{+-}|$ value is not directly used in our fit, but enters the fit via their branching ratio and lifetime measurements.

123 AMBROSINO 06F uses KLOE branching ratios and τ_L together with τ_S from PDG 04. Their $|\eta_{+-}|$ value is not directly used in our fit, but enters the fit via their branching ratio and lifetime measurements.

124 ALEXOPOULOS 04 $|\eta_{+-}|$ uses their $K_L^0 \rightarrow \pi\pi$ branching fractions, $\tau_S = (0.8963 \pm 0.0005) \times 10^{-10}$ s from the average of KTeV and NA48 τ_S measurements, and assumes that $\Gamma(K_S^0 \rightarrow \pi\ell\nu_\ell) = \Gamma(K_L^0 \rightarrow \pi\ell\nu_\ell)$ giving $B(K_S^0 \rightarrow \pi\ell\nu_\ell) = 0.118\%$. Their η_{+-} is not directly used in our fit, but enters our fit via their branching ratio measurements.

125 APOSTOLAKIS 99c report $(2.264 \pm 0.023 \pm 0.026 + 9.1[\tau_S - 0.8934]) \times 10^{-3}$. We evaluate for our 2006 best value $\tau_S = (0.8958 \pm 0.0005) \times 10^{-10}$ s.

126 ADLER 95B report $(2.312 \pm 0.043 \pm 0.030 - 1[\Delta m - 0.5274] + 9.1[\tau_S - 0.8926]) \times 10^{-3}$. We evaluate for our 1996 best values $\Delta m = (0.5304 \pm 0.0014) \times 10^{-10} \text{hs}^{-1}$ and $\tau_S = (0.8927 \pm 0.0009) \times 10^{-10}$ s. Superseded by APOSTOLAKIS 99c.

 $|\epsilon| = (2|\eta_{+-}| + |\eta_{00}|)/3$

This expression is a very good approximation, good to about one part in 10^{-4} because of the small measured value of $\phi_{00} - \phi_{+-}$ and small theoretical ambiguities.

VALUE (units 10^{-3})	DOCUMENT ID	COMMENT
2.229±0.012 OUR FIT	Error includes scale factor of 1.7.	

 $|\eta_{00}/\eta_{+-}|$

VALUE	EVTS	DOCUMENT ID	TECN	COMMENT
0.9951±0.0008 OUR FIT	Error includes scale factor of 1.6.			
0.9930±0.0020 OUR AVERAGE				

0.9931 ± 0.0020	127,128 BARR	93D	NA31
0.9904 ± 0.0084 ± 0.0036	129 WOODS	88	E731

• • • We do not use the following data for averages, fits, limits, etc. • • •

0.9939 ± 0.0013 ± 0.0015	1M	127 BARR	93D	NA31
0.9899 ± 0.0020 ± 0.0025		127 BURKHARDT	88	NA31

127 This is the square root of the ratio R given by BURKHARDT 88 and BARR 93D.

128 This is the combined results from BARR 93D and BURKHARDT 88, taking into account a common systematic uncertainty of 0.0014.

129 We calculate $|\eta_{00}/\eta_{+-}| = 1 - 3(\epsilon'/\epsilon)$ from WOODS 88 (ϵ'/ϵ) value.

 $\text{Re}(\epsilon'/\epsilon) = (1 - |\eta_{00}/\eta_{+-}|)/3$

We have neglected terms of order $\omega \cdot \text{Re}(\epsilon'/\epsilon)$, where $\omega = \text{Re}(A_2)/\text{Re}(A_0) \approx 1/22$. If included, this correction would lower $\text{Re}(\epsilon'/\epsilon)$ by about 0.04×10^{-3} . See SOZZI 04.

VALUE (units 10^{-3})	DOCUMENT ID	TECN	COMMENT
1.65 ± 0.26 OUR FIT	Error includes scale factor of 1.6.		
1.67 ± 0.23 OUR AVERAGE	Error includes scale factor of 1.4. See the ideogram below.		

2.07 ± 0.28	ALAVI-HARATI03	KTEV
1.47 ± 0.22	BATLEY	02 NA48
2.3 ± 0.65	130,131 BARR	93D NA31
0.74 ± 0.52 ± 0.29	GIBBONS	93B E731

• • • We do not use the following data for averages, fits, limits, etc. • • •

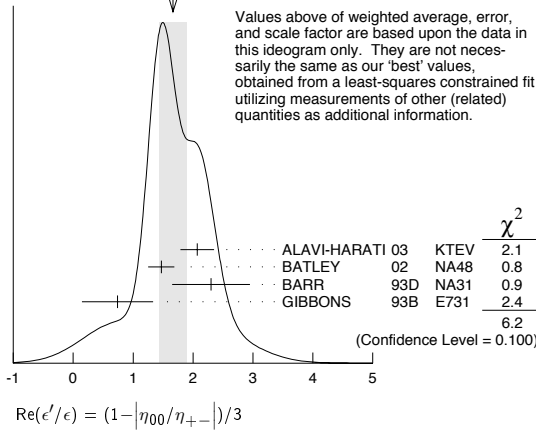
1.53 ± 0.26	LAI	01c	NA48 Incl. in BATLEY 02
2.80 ± 0.30 ± 0.28	ALAVI-HARATI99D	KTEV	In ALAVI-HARATI 03
1.85 ± 0.45 ± 0.58	FANTI	99c	NA48 In LAI 01c
2.0 ± 0.7	132 BARR	93D	NA31
-0.4 ± 1.4 ± 0.6	PATTERSON	90	E731 in GIBBONS 93B
3.3 ± 1.1	132 BURKHARDT	88	NA31
3.2 ± 2.8 ± 1.2	130 WOODS	88	E731

130 These values are derived from $|\eta_{00}/\eta_{+-}|$ measurements. They enter the average in this section but enter the fit via the $|\eta_{00}/\eta_{+-}|$ only.

131 This is the combined results from BARR 93D and BURKHARDT 88, taking into account their common systematic uncertainty.

132 These values are derived from $|\eta_{00}/\eta_{+-}|$ measurements.

Meson Particle Listings

 K_L^0 WEIGHTED AVERAGE
1.67±0.23 (Error scaled by 1.4) ϕ_{+-} , PHASE OF η_{+-}

The dependence of the phase on Δm and τ_S is given for each experiment in the comments below, where Δm is the $K_L^0 - K_S^0$ mass difference in units $10^{10} \hbar s^{-1}$ and τ_S is the K_S mean life in units 10^{-10} s. We also give the regeneration phase ϕ_f in the comments below.

OUR FIT is described in the note on "CP violation in K_L decays" in the K_L^0 Particle Listings. Most experiments in this section are included in both the "Not Assuming CPT" and "Assuming CPT" fits. In the latter fit, they have little direct influence on ϕ_{+-} because their errors are large compared to that assuming CPT, but they influence Δm and τ_S through their dependencies on these parameters, which are given in the footnotes. Only ALAVI-HARATI 03 is excluded from the "Assuming CPT" fit because we explicitly include their Δm and τ_S measurements which assume CPT.

VALUE (°)	EVTS	DOCUMENT ID	TECN	COMMENT
43.51 ± 0.05 OUR FIT	Error includes scale factor of 1.1. Assuming CPT			
43.4 ± 0.7 OUR FIT	Error includes scale factor of 1.3. Not assuming CPT			
44.12 ± 0.72 ± 1.20	133	ALAVI-HARATI 03	KTEV	Not assuming CPT
42.9 ± 0.6 ± 0.3	70M 134	APOSTOLA...	CPLR	$K^0 - \bar{K}^0$ asymmetry
43.0 ± 0.8 ± 0.2	135,136	SCHWINGENHEUER 95	E773	CH _{1,1} regenerator
41.4 ± 0.9 ± 0.3	136,137	GIBBONS 93	E731	B ₄ C regenerator
44.4 ± 1.6 ± 0.6	138	CAROSI 90	NA31	Vacuum regen.
43.3 ± 1.0 ± 0.5	139	GEWENIGER 74B	ASP K	Vacuum regen.
• • • We do not use the following data for averages, fits, limits, etc. • • •				
42.5 ± 0.4 ± 0.3	140,141	ADLER 96C	RVUE	
43.4 ± 1.1 ± 0.3	142	ADLER 95B	CPLR	$K^0 - \bar{K}^0$ asymmetry
42.3 ± 4.4 ± 1.4	10 ⁵ 143	ADLER 92B	CPLR	$K^0 - \bar{K}^0$ asymmetry
47.7 ± 2.0 ± 0.9	136,144	KARLSSON 90	E731	
44.3 ± 2.8 ± 0.2	145	CARITHERS 75	SPEC	C regenerator

133 ALAVI-HARATI 03 ϕ_{+-} is correlated with their $\Delta m = m_{K_L^0} - m_{K_S^0}$ and τ_{K_S} measurements in the K_L^0 and K_S^0 sections respectively. The correlation coefficients are $\rho(\phi_{+-}, \Delta m) = +0.955$, $\rho(\phi_{+-}, \tau_S) = -0.871$, and $\rho(\tau_S, \Delta m) = -0.840$. CPT is not assumed. Uses scintillator Pb regenerator.

134 APOSTOLAKIS 99C measures $\phi_{+-} = (43.19 \pm 0.53 \pm 0.28) + 300 [\Delta m - 0.5301] (^\circ)$. We have adjusted the measurement to use our best values of ($\Delta m = 0.5292 \pm 0.0009$) ($10^{10} \hbar s^{-1}$). Our first error is their experiment's error and our second error is the systematic error from using our best values.

135 SCHWINGENHEUER 95 measures $\phi_{+-} = (43.53 \pm 0.76) + 173 [\Delta m - 0.5282] - 275 [\tau_S - 0.8922] (^\circ)$. We have adjusted the measurement to use our best values of ($\Delta m = 0.5292 \pm 0.0009$) ($10^{10} \hbar s^{-1}$), ($\tau_S = 0.8953 \pm 0.0005$) (10^{-10} s). Our first error is their experiment's error and our second error is the systematic error from using our best values.

136 These experiments measure $\phi_{+-} - \phi_f$ and calculate the regeneration phase from the power law momentum dependence of the regeneration amplitude using analyticity and dispersion relations. SCHWINGENHEUER 95 [GIBBONS 93] includes a systematic error of 0.35° [0.5°] for uncertainties in their modeling of the regeneration amplitude.

137 GIBBONS 93 measures $\phi_{+-} = (42.21 \pm 0.9) + 189 [\Delta m - 0.5257] - 460 [\tau_S - 0.8922] (^\circ)$. We have adjusted the measurement to use our best values of ($\Delta m = 0.5292 \pm 0.0009$) ($10^{10} \hbar s^{-1}$), ($\tau_S = 0.8953 \pm 0.0005$) (10^{-10} s). Our first error is their experiment's error and our second error is the systematic error from using our best values. This is actually reported in SCHWINGENHEUER 95, footnote 8. GIBBONS 93 reports $\phi_{+-} (42.2 \pm 1.4)^\circ$. They measure $\phi_{+-} - \phi_f$ and calculate the regeneration phase ϕ_f from the power law momentum dependence of the regeneration amplitude using analyticity. An error of 0.6° is included for possible uncertainties in the regeneration phase.

138 CAROSI 90 measures $\phi_{+-} = (46.9 \pm 1.4 \pm 0.7) + 579 [\Delta m - 0.5351] + 303 [\tau_S - 0.8922] (^\circ)$. We have adjusted the measurement to use our best values of ($\Delta m = 0.5292 \pm 0.0009$) ($10^{10} \hbar s^{-1}$), ($\tau_S = 0.8953 \pm 0.0005$) (10^{-10} s). Our first error is their experiment's error and our second error is the systematic error from using our best values.

139 GEWENIGER 74B measures $\phi_{+-} = (49.4 \pm 1.0) + 565 [\Delta m - 0.540] (^\circ)$. We have adjusted the measurement to use our best values of ($\Delta m = 0.5292 \pm 0.0009$) ($10^{10} \hbar s^{-1}$). Our first error is their experiment's error and our second error is the systematic error from using our best values.

140 ADLER 96C measures $\phi_{+-} = (43.82 \pm 0.41) + 339 [\Delta m - 0.5307] - 252 [\tau_S - 0.8922] (^\circ)$. We have adjusted the measurement to use our best values of ($\Delta m = 0.5292 \pm 0.0009$) ($10^{10} \hbar s^{-1}$), ($\tau_S = 0.8953 \pm 0.0005$) (10^{-10} s). Our first error is their experiment's error and our second error is the systematic error from using our best values.

141 ADLER 96C is the result of a fit which includes nearly the same data as entered into the "OUR FIT" value in the 1996 edition of this Review (Physical Review D54 1 (1996)).

142 ADLER 95B measures $\phi_{+-} = (42.7 \pm 0.9 \pm 0.6) + 316 [\Delta m - 0.5274] + 30 [\tau_S - 0.8926] (^\circ)$. We have adjusted the measurement to use our best values of ($\Delta m = 0.5292 \pm 0.0009$) ($10^{10} \hbar s^{-1}$), ($\tau_S = 0.8953 \pm 0.0005$) (10^{-10} s). Our first error is their experiment's error and our second error is the systematic error from using our best values.

143 ADLER 92B quote separately two systematic errors: ± 0.4 from their experiment and ± 1.0 degrees due to the uncertainty in the value of Δm .

144 KARLSSON 90 systematic error does not include regeneration phase uncertainty.

145 CARITHERS 75 measures $\phi_{+-} = (45.5 \pm 2.8) + 224 [\Delta m - 0.5348] (^\circ)$. We have adjusted the measurement to use our best values of ($\Delta m = 0.5292 \pm 0.0009$) ($10^{10} \hbar s^{-1}$). Our first error is their experiment's error and our second error is the systematic error from using our best values. $\phi_f = -40.9 \pm 2.6^\circ$.

 ϕ_{00} , PHASE OF η_{00}

See comment in ϕ_{+-} header above for treatment of Δm and τ_S dependence, as well as for the inclusion of data in both the "Assuming CPT" and "Not Assuming CPT" fits.

OUR FIT is described in the note on "CP violation in K_L decays" in the K_L^0 Particle Listings.

VALUE (°)	DOCUMENT ID	TECN	COMMENT
43.52 ± 0.05 OUR FIT	Error includes scale factor of 1.1. Assuming CPT		
43.7 ± 0.8 OUR FIT	Error includes scale factor of 1.2. Not assuming CPT		
44.5 ± 2.3 ± 0.6	146	CAROSI 90	NA31
• • • We do not use the following data for averages, fits, limits, etc. • • •			
41.6 ± 5.9 ± 0.2	147	ANGELOPOULOS 98	CPLR
50.8 ± 7.1 ± 1.7	148	ADLER 96B	CPLR
47.4 ± 1.4 ± 0.9	149	KARLSSON 90	E731

146 CAROSI 90 measures $\phi_{00} = (47.1 \pm 2.1 \pm 1.0) + 579 [\Delta m - 0.5351] + 252 [\tau_S - 0.8922] (^\circ)$. We have adjusted the measurement to use our best values of ($\Delta m = 0.5292 \pm 0.0009$) ($10^{10} \hbar s^{-1}$), ($\tau_S = 0.8953 \pm 0.0005$) (10^{-10} s). Our first error is their experiment's error and our second error is the systematic error from using our best values.

147 ANGELOPOULOS 98 measures $\phi_{00} = (42.0 \pm 5.6 \pm 1.9) + 240 [\Delta m - 0.5307] (^\circ)$. We have adjusted the measurement to use our best values of ($\Delta m = 0.5292 \pm 0.0009$) ($10^{10} \hbar s^{-1}$). Our first error is their experiment's error and our second error is the systematic error from using our best values. The τ_S dependence is negligible.

148 ADLER 96B identified initial neutral kaon individually as being a K^0 or a \bar{K}^0 . The systematic uncertainty is $\pm 1.5^\circ$ combined in quadrature with $\pm 0.8^\circ$ due to Δm .

149 KARLSSON 90 systematic error does not include regeneration phase uncertainty.

 $\phi_\epsilon = (2\phi_{+-} + \phi_{00})/3$

This expression is a very good approximation, good to about 10^{-3} degrees because of the small measured values of $\phi_{00} - \phi_{+-}$ and $\text{Re } \epsilon'/\epsilon$, and small theoretical ambiguities.

VALUE (°)	DOCUMENT ID	COMMENT
43.51 ± 0.05 OUR FIT	Error includes scale factor of 1.1. Assuming CPT	
43.5 ± 0.7 OUR FIT	Error includes scale factor of 1.3. Not assuming CPT	
43.5136 ± 0.0002 ± 0.0533	150	SUPERWEAK 08 Assuming CPT

150 SUPERWEAK 08 is a fake measurement used to impose the CPT or Superweak constraint $\phi_{+-} = \phi_{SW} = \tan^{-1} [2 \frac{\Delta m}{\hbar} (\frac{\tau_S \tau_L}{\tau_L - \tau_S})]$. This "measurement" is linearized using values near the RPP 2004 edition values of Δm , τ_S and τ_L , and then adjusted to our current values as described in the following "measurement". SUPERWEAK 08 measures $\phi_\epsilon = (43.51647 \pm 0.00020) + 54.1 [\Delta m - 0.5290] + 32.0 [\tau_S - 0.8958] (^\circ)$. We have adjusted the measurement to use our best values of ($\Delta m = 0.5292 \pm 0.0009$) ($10^{10} \hbar s^{-1}$), ($\tau_S = 0.8953 \pm 0.0005$) (10^{-10} s). Our first error is their experiment's error and our second error is the systematic error from using our best values.

DECAY-PLANE ASYMMETRY IN $\pi^+ \pi^- e^+ e^-$ DECAYS

This is the CP-violating asymmetry

$$A = \frac{N_{\sin\phi\cos\phi>0.0} - N_{\sin\phi\cos\phi<0.0}}{N_{\sin\phi\cos\phi>0.0} + N_{\sin\phi\cos\phi<0.0}}$$

where ϕ is the angle between the $e^+ e^-$ and $\pi^+ \pi^-$ planes in the K_L^0 rest frame.

CP ASYMMETRY A IN $K_L^0 \rightarrow \pi^+ \pi^- e^+ e^-$

VALUE (%)	DOCUMENT ID	TECN
13.7 ± 1.5 OUR AVERAGE		
13.6 ± 1.4 ± 1.5	ABOUZAID 06	KTEV
14.2 ± 3.0 ± 1.9	LAI 03C	NA48
13.6 ± 2.5 ± 1.2	ALAVI-HARATI 00B	KTEV

PARAMETERS FOR $e^+ e^- e^+ e^-$ DECAYS

These are the CP-violating parameters in the ϕ distribution, where ϕ is the angle between the planes of the two $e^+ e^-$ pairs in the kaon rest frame:

$$d\Gamma/d\phi \propto 1 + \beta_{CP} \cos(2\phi) + \gamma_{CP} \sin(2\phi)$$

 β_{CP} from $K_L^0 \rightarrow e^+ e^- e^+ e^-$

VALUE (%)	EVTS	DOCUMENT ID	TECN	COMMENT
-0.19 ± 0.07 OUR AVERAGE				
-0.13 ± 0.10 ± 0.03	200	151 LAI 05B	NA48	
-0.23 ± 0.09 ± 0.02	441	ALAVI-HARATI 01D	KTEV	$M_{e^+ e^-} > 8 \text{ MeV}/c^2$
151 LAI 05B obtains $\beta_{CP} = -0.13 \pm 0.10$ (stat) if $\gamma_{CP} = 0$ is assumed.				

γ_{CP} from $K_L^0 \rightarrow e^+ e^- e^+ e^-$

VALUE	EVTS	DOCUMENT ID	TECN	COMMENT
0.01 ± 0.11 OUR AVERAGE	Error	includes scale factor of 1.6.		
+0.13 ± 0.10 ± 0.03	200	LAI 05B	NA48	
-0.09 ± 0.09 ± 0.02	441	ALAVI-HARATI01D	KTEV	$M_{e e} > 8 \text{ MeV}/c^2$

CHARGE ASYMMETRY IN $\pi^+ \pi^- \pi^0$ DECAYS

These are CP -violating charge-asymmetry parameters, defined at beginning of section "LINEAR COEFFICIENT g FOR $K_L^0 \rightarrow \pi^+ \pi^- \pi^0$ " above.

See also note on Dalitz plot parameters in K^\pm section and note on " CP violation in K_L decays" above.

LINEAR COEFFICIENT j FOR $K_L^0 \rightarrow \pi^+ \pi^- \pi^0$

VALUE	EVTS	DOCUMENT ID	TECN
0.0012 ± 0.0008 OUR AVERAGE			
0.0010 ± 0.0024 ± 0.0030	500k	ANGELOPO...	98c CPLR
-0.001 ± 0.011	6499	CHO	77
0.001 ± 0.003	4709	PEACH	77
0.0013 ± 0.0009	3M	SCRIBANO	70
0.0 ± 0.017	4400	SMITH	70 OSPK
0.001 ± 0.004	238k	BLANPIED	68

QUADRATIC COEFFICIENT f FOR $K_L^0 \rightarrow \pi^+ \pi^- \pi^0$

VALUE	EVTS	DOCUMENT ID	TECN
0.0045 ± 0.0024 ± 0.0059	500k	ANGELOPO...	98c CPLR

PARAMETERS for $K_L^0 \rightarrow \pi^+ \pi^- \gamma$ DECAY

$$|\eta_{+-\gamma}| = |A(K_L^0 \rightarrow \pi^+ \pi^- \gamma, CP \text{ violating})/A(K_S^0 \rightarrow \pi^+ \pi^- \gamma)|$$

VALUE (units 10^{-3})	EVTS	DOCUMENT ID	TECN
2.35 ± 0.07 OUR AVERAGE			
2.359 ± 0.062 ± 0.040	9045	MATTHEWS 95	E773
2.15 ± 0.26 ± 0.20	3671	RAMBERG 93B	E731

 $\phi_{+-\gamma} = \text{phase of } \eta_{+-\gamma}$

VALUE (°)	EVTS	DOCUMENT ID	TECN
44 ± 4 OUR AVERAGE			
43.8 ± 3.5 ± 1.9	9045	MATTHEWS 95	E773
72 ± 23 ± 17	3671	RAMBERG 93B	E731

 $|\epsilon'_{+-\gamma}|/\epsilon$ for $K_L^0 \rightarrow \pi^+ \pi^- \gamma$

VALUE	CL%	EVTS	DOCUMENT ID	TECN
<0.3	90	3671	152 RAMBERG 93B	E731

152 RAMBERG 93B limit on $|\epsilon'_{+-\gamma}|/\epsilon$ assumes that any difference between η_{+-} and $\eta_{+-\gamma}$ is due to direct CP violation.

 $|\xi_{E1}|$ for $K_L^0 \rightarrow \pi^+ \pi^- \gamma$

This parameter is the amplitude of the direct emission of a CP violating E1 electric dipole photon.

VALUE	CL%	EVTS	DOCUMENT ID	TECN	COMMENT
<0.21	90	111k	ABOUZAID 06A	KTEV	$E_\gamma > 20 \text{ MeV}$

T VIOLATION TESTS IN K_L^0 DECAYS **$\text{Im}(\xi)$ in $K_{\mu 3}^0$ DECAY (from transverse μ pol.)**

VALUE	EVTS	DOCUMENT ID	TECN	COMMENT
-0.007 ± 0.026 OUR AVERAGE				
0.009 ± 0.030	12M	MORSE 80	CNTR	Polarization
0.35 ± 0.30	207k	153 CLARK 77	SPEC	POL, $t=0$
-0.085 ± 0.064	2.2M	154 SANDWEISS 73	CNTR	POL, $t=0$
-0.02 ± 0.08		LONGO 69	CNTR	POL, $t=3.3$
-0.2 ± 0.6		ABRAMS 68B	OSPK	Polarization
••• We do not use the following data for averages, fits, limits, etc. •••				
0.012 ± 0.026		SCHMIDT 79	CNTR	Repl. by MORSE 80
153 CLARK 77 value has additional $\xi(0)$ dependence $+0.21\text{Re}\{\xi(0)\}$.				
154 SANDWEISS 73 value corrected from value quoted in their paper due to new value of $\text{Re}(\xi)$. See footnote 4 of SCHMIDT 79.				

 CP -INVARIANCE TESTS IN K_L^0 DECAYS**PHASE DIFFERENCE $\phi_{00} - \phi_{+-}$**

Test of CPT .

OUR FIT is described in the note on " CP violation in K_L decays" in the K_L^0 Particle Listings.

VALUE (°)	DOCUMENT ID	TECN	COMMENT
0.006 ± 0.014 OUR FIT	Error	includes scale factor of 1.8. Assuming CPT	
0.2 ± 0.4 OUR FIT	Not assuming CPT		
0.006 ± 0.008	155 SUPERWEAK 08		Assuming CPT
0.39 ± 0.22 ± 0.45	156 ALAVI-HARATI03	KTEV	
-0.30 ± 0.88	157 SCHWINGEN...95		Combined E731, E773

••• We do not use the following data for averages, fits, limits, etc. •••

0.62 ± 0.71 ± 0.75	SCHWINGEN...95	E773
-1.6 ± 1.2	158 GIBBONS 93	E731
0.2 ± 2.6 ± 1.2	159 CAROSI 90	NA31
-0.3 ± 2.4 ± 1.2	KARLSSON 90	E731
155 SUPERWEAK 08 is a fake experiment to constrain $\phi_{00}-\phi_{+-}$ to a small value as described in the note " CP violation in K_L decays."		
156 ALAVI-HARATI 03 fit $\text{Re}(\epsilon'/\epsilon)$, $\text{Im}(\epsilon'/\epsilon)$, Δm , τ_S , and ϕ_{+-} simultaneously, not assuming CPT . Phase difference is obtained from $\phi_{00} - \phi_{+-} \approx -3\text{Im}(\epsilon'/\epsilon)$ for small $ \epsilon'/\epsilon $.		
157 This SCHWINGENHEUER 95 values is the combined result of SCHWINGENHEUER 95 and GIBBONS 93, accounting for correlated systematic errors.		
158 GIBBONS 93 give detailed dependence of systematic error on lifetime (see the section on the K_S^0 mean life) and mass difference (see the section on $m_{K_L^0} - m_{K_S^0}$).		
159 CAROSI 90 is excluded from the fit because it is not independent of ϕ_{+-} and ϕ_{00} values.		

PHASE DIFFERENCE $\phi_{+-} - \phi_{SW}$

Test of CPT . The Superweak phase $\phi_{SW} \equiv \tan^{-1}(2\Delta m/\Delta\Gamma)$ where $\Delta m = m_{K_L^0} - m_{K_S^0}$ and $\Delta\Gamma = \hbar(\tau_L - \tau_S)/(\tau_L\tau_S)$.

VALUE (°)	DOCUMENT ID	TECN
0.61 ± 0.62 ± 1.01	160 ALAVI-HARATI03	KTEV

160 ALAVI-HARATI 03 fit is the same as their ϕ_{+-} , τ_{K_S} , Δm fit, except that the parameter $\phi_{+-} - \phi_{SW}$ is used in place of ϕ .

 $\text{Re}(\frac{2}{3}\eta_{+-} + \frac{1}{3}\eta_{00}) - \frac{A_f}{A_i}$

VALUE (units 10^{-6})	DOCUMENT ID	TECN	COMMENT
-3 ± 35	161 ALAVI-HARATI02	E799	Uses A_L from K_{e3} decays
161 ALAVI-HARATI 02 uses PDG 00 values of η_{+-} and η_{00} .			

 $\Delta S = \Delta Q$ IN K^0 DECAYS

The relative amount of $\Delta S \neq \Delta Q$ component present is measured by the parameter x , defined as

$$x = A(\bar{K}^0 \rightarrow \pi^- \ell^+ \nu)/A(K^0 \rightarrow \pi^- \ell^+ \nu)$$

We list $\text{Re}\{x\}$ and $\text{Im}\{x\}$ for K_{e3} and $K_{\mu 3}$ combined.

$$x = A(\bar{K}^0 \rightarrow \pi^- \ell^+ \nu)/A(K^0 \rightarrow \pi^- \ell^+ \nu) = A(\Delta S = -\Delta Q)/A(\Delta S = \Delta Q)$$

REAL PART OF x

VALUE	EVTS	DOCUMENT ID	TECN	COMMENT
-0.0018 ± 0.0041 ± 0.0045		ANGELOPO... 98D	CPLR	K_{e3} from K^0
••• We do not use the following data for averages, fits, limits, etc. •••				
0.10 ± 0.18	79	SMITH 75B	WIRE	$\pi^- p \rightarrow K^0 \Lambda$
-0.19				
0.04 ± 0.03	4724	NIEBERGALL 74	ASPK	$K^+ p \rightarrow K^0 p \pi^+$
-0.008 ± 0.044	1757	FACKLER 73	OSPK	K_{e3} from K^0
-0.03 ± 0.07	1367	HART 73	OSPK	K_{e3} from $K^0 \Lambda$
-0.070 ± 0.036	1079	MALLARY 73	OSPK	K_{e3} from $K^0 \Lambda X$
0.03 ± 0.06	410	162 BURGUN 72	HBC	$K^+ p \rightarrow K^0 p \pi^+$
0.04 ± 0.10	100	163 GRAHAM 72	OSPK	$K_{\mu 3}$ from $K^0 \Lambda$
-0.13				
-0.05 ± 0.09	442	163 GRAHAM 72	OSPK	$\pi^- p \rightarrow K^0 \Lambda$
0.26 ± 0.10	126	MANN 72	HBC	$K^- p \rightarrow n \bar{K}^0$
-0.14				
-0.13 ± 0.11	342	163 MANTSCH 72	OSPK	K_{e3} from $K^0 \Lambda$
0.04 ± 0.07	222	162 BURGUN 71	HBC	$K^+ p \rightarrow K^0 p \pi^+$
-0.08				
0.25 ± 0.07	252	WEBBER 71	HBC	$K^- p \rightarrow n \bar{K}^0$
-0.09				
0.12 ± 0.09	215	164 CHO 70	DBC	$K^+ d \rightarrow K^0 p p$
-0.020 ± 0.025	165 BENNETT 69	CNTR		Charge asym + Cu regen.
0.09 ± 0.14	686	LITTENBERG 69	OSPK	$K^+ n \rightarrow K^0 p$
-0.16				
0.03 ± 0.03	165 BENNETT 68	CNTR		
0.09 ± 0.07	121	JAMES 68	HBC	$\bar{p} p$
-0.09				
0.17 ± 0.16	116	FELDMAN 67B	OSPK	$\pi^- p \rightarrow K^0 \Lambda$
-0.35				
0.17 ± 0.10	335	164 HILL 67	DBC	$K^+ d \rightarrow K^0 p p$
0.035 ± 0.11	196	AUBERT 65	HLBC	K^+ charge exch.
-0.13				
0.06 ± 0.18	152	166 BALDO... 65	HLBC	K^+ charge exch.
-0.44				
-0.08 ± 0.16	109	167 FRANZINI 65	HBC	$\bar{p} p$
-0.28				
162 BURGUN 72 is a final result which includes BURGUN 71.				
163 First GRAHAM 72 value is second GRAHAM 72 value combined with MANTSCH 72.				
164 CHO 70 is analysis of unambiguous events in new data and HILL 67.				
165 BENNETT 69 is a reanalysis of BENNETT 68.				
166 BALDO-CEOLIN 65 gives x and θ converted by us to $\text{Re}(x)$ and $\text{Im}(x)$.				
167 FRANZINI 65 gives x and θ for $\text{Re}(x)$ and $\text{Im}(x)$. See SCHMIDT 67.				

Meson Particle Listings

K^0_L

IMAGINARY PART OF χ

Assumes $m_{K^0_L} - m_{K^0_S}$ positive. See Listings above.

VALUE	EVTs	DOCUMENT ID	TECN	COMMENT
$0.0012 \pm 0.0019 \pm 0.0009$	640k	ANGELOPO... 01B	CPLR	K_{e3} from K^0
••• We do not use the following data for averages, fits, limits, etc. •••				
0.0012 ± 0.0019	640k	168 ANGELOPO...	98E	CPLR K_{e3} from K^0
-0.10 ± 0.16 -0.19	79	SMITH	75B	WIRE $\pi^- p \rightarrow K^0 \Lambda$
-0.06 ± 0.05	4724	NIEBERGALL	74	ASPK $K^+ p \rightarrow K^0 p \pi^+$
-0.017 ± 0.060	1757	FACKLER	73	OSPK K_{e3} from K^0
0.09 ± 0.07	1367	HART	73	OSPK K_{e3} from $K^0 \Lambda$
0.107 ± 0.092 -0.074	1079	MALLARY	73	OSPK K_{e3} from $K^0 \Lambda X$
0.07 ± 0.06 -0.07	410	169 BURGUN	72	HBC $K^+ p \rightarrow K^0 p \pi^+$
0.12 ± 0.17 -0.16	100	170 GRAHAM	72	OSPK $K_{\mu 3}$ from $K^0 \Lambda$
0.05 ± 0.13	442	170 GRAHAM	72	OSPK $\pi^- p \rightarrow K^0 \Lambda$
0.21 ± 0.15 -0.12	126	MANN	72	HBC $K^- p \rightarrow n \bar{K}^0$
-0.04 ± 0.16	342	170 MANTSCH	72	OSPK K_{e3} from $K^0 \Lambda$
0.12 ± 0.08 -0.09	222	169 BURGUN	71	HBC $K^+ p \rightarrow K^0 p \pi^+$
0.0 ± 0.08	252	WEBBER	71	HBC $K^- p \rightarrow n \bar{K}^0$
-0.08 ± 0.07	215	171 CHO	70	DBC $K^+ d \rightarrow K^0 p p$
-0.11 ± 0.10 -0.11	686	LITTENBERG	69	OSPK $K^+ n \rightarrow K^0 p$
+0.22 ± 0.37 -0.29	121	JAMES	68	HBC $\bar{p} p$
0.0 ± 0.25	116	FELDMAN	67B	OSPK $\pi^- p \rightarrow K^0 \Lambda$
-0.20 ± 0.10	335	171 HILL	67	DBC $K^+ d \rightarrow K^0 p p$
-0.21 ± 0.11 -0.15	196	AUBERT	65	HLBC K^+ charge exch.
-0.44 ± 0.32 -0.19	152	172 BALDO...	65	HLBC K^+ charge exch.
+0.24 ± 0.40 -0.30	109	173 FRANZINI	65	HBC $\bar{p} p$

168 Superseded by ANGELOPOULOS 01B.
 169 BURGUN 72 is a final result which includes BURGUN 71.
 170 First GRAHAM 72 value is second GRAHAM 72 value combined with MANTSCH 72.
 171 Footnote 10 of HILL 67 should read +0.58, not -0.58 (private communication) CHO 70 is analysis of unambiguous events in new data and HILL 67.
 172 BALDO-CEOLIN 65 gives x and θ converted by us to $\text{Re}(x)$ and $\text{Im}(x)$.
 173 FRANZINI 65 gives x and θ for $\text{Re}(x)$ and $\text{Im}(x)$. See SCHMIDT 67.

K^0_L REFERENCES

BRFIT 08	RPP 2008 edition	T.G. Trippe	(PDG Collab.)
ETAFIT 08	RPP 2008 edition	T.G. Trippe	(PDG Collab.)
SUPERWEAK 08	RPP 2008 edition	T.G. Trippe	(PDG Collab.)
CP violation in K_L decays			
ABOUZAIID 07B	PRL 99 051804	E. Abouzaid et al.	(FNAL KTeV Collab.)
ABOUZAIID 07C	PRL 99 081803	E. Abouzaid et al.	(FNAL KTeV Collab.)
ABOUZAIID 07D	PR D76 052001	E. Abouzaid et al.	(FNAL KTeV Collab.)
AMBROSINO 07C	JHEP 0712 105	F. Ambrosino et al.	(KLOE Collab.)
LAI 07	PL B645 26	A. Lai et al.	(CERN NA48 Collab.)
LAI 07A	PL B647 341	A. Lai et al.	(CERN NA48 Collab.)
NIX 07	PR D76 011101R	J. Nix et al.	(KEK E91a Collab.)
ABOUZAIID 06	PRL 96 101801	E. Abouzaid et al.	(KTeV Collab.)
ABOUZAIID 06A	PR D74 032004	E. Abouzaid et al.	(KTeV Collab.)
Also	PR D74 039905 (err.)	E. Abouzaid et al.	(KTeV Collab.)
ABOUZAIID 06C	PR D74 097101	E. Abouzaid et al.	(KTeV Collab.)
AHN 06	PR D74 051105R	J.K. Ahn et al.	(KEK E91a Collab.)
Also	PR D74 079901 (err.)	J.K. Ahn et al.	(KEK E91a Collab.)
AMBROSINO 06	PL B632 43	F. Ambrosino et al.	(KLOE Collab.)
AMBROSINO 06D	PL B636 166	F. Ambrosino et al.	(KLOE Collab.)
AMBROSINO 06F	PL B638 140	F. Ambrosino et al.	(KLOE Collab.)
HILL 06	PR D74 096006	R.J. Hill	(FNAL (PDG Collab.)
PDG 06	JPG 33 1	W.-M. Yao et al.	(PDG Collab.)
ALEXOPOU... 05	PR D71 012001	T. Alexopoulos et al.	(FNAL KTeV Collab.)
AMBROSINO 05C	PL B626 15	F. Ambrosino et al.	(KLOE Collab.)
LAI 05	PL B605 247	A. Lai et al.	(CERN NA48 Collab.)
LAI 05B	PL B615 31	A. Lai et al.	(CERN NA48 Collab.)
ALAVI-HARATI 04A	PRL 93 021805	A. Alavi-Harati et al.	(FNAL KTeV/E799 Collab.)
ALEXOPOU... 04	PR D70 092006	T. Alexopoulos et al.	(FNAL KTeV Collab.)
ALEXOPOU... 04A	PR D70 092007	T. Alexopoulos et al.	(FNAL KTeV Collab.)
ANDRE 04	hep-ph/0406006	T. Andre	(EFT)
BATLEY 04	PL B595 75	J.R. Batley et al.	(CERN NA48 Collab.)
CIRIGLIANO 04	EPJ C35 53	V. Cirigliano, H. Neufeld, H. Pichl	(CIT, VALE+)
LAI 04B	PL B602 41	A. Lai et al.	(CERN NA48 Collab.)
LAI 04C	PL B604 1	A. Lai et al.	(CERN NA48 Collab.)
PDG 04	PL B592 1	S. Eidelman et al.	(PDG Collab.)
SOZZI 04	EPJ C36 37	M. Sozzi	(PISA)
ADINOLFI 03	PL B566 61	M. Adinolfi et al.	(KLOE Collab.)
ALAVI-HARATI 03	PR D67 012005	A. Alavi-Harati et al.	(FNAL KTeV Collab.)
Also	PR D70 079904 (err.)	A. Alavi-Harati et al.	(FNAL KTeV Collab.)
ALAVI-HARATI 03B	PRL 90 141801	A. Alavi-Harati et al.	(FNAL KTeV Collab.)
LAI 03	PL B551 7	A. Lai et al.	(CERN NA48 Collab.)
LAI 03C	EPJ C30 33	A. Lai et al.	(CERN NA48 Collab.)
ALAVI-HARATI 02G	PRL 88 181601	A. Alavi-Harati et al.	(FNAL KTeV Collab.)
ALAVI-HARATI 02C	PRL 89 211801	A. Alavi-Harati et al.	(FNAL KTeV Collab.)
BATLEY 02	PL B544 97	J.R. Batley et al.	(CERN NA48 Collab.)
CIRIGLIANO 02	EPJ C23 121	V. Cirigliano et al.	(VIEN, VALE, MARS)
LAI 02B	PL B536 229	A. Lai et al.	(CERN NA48 Collab.)
ALAVI-HARATI 01	PRL 86 397	A. Alavi-Harati et al.	(FNAL KTeV Collab.)
ALAVI-HARATI 01B	PRL 86 761	A. Alavi-Harati et al.	(FNAL KTeV Collab.)
ALAVI-HARATI 01D	PRL 86 5425	A. Alavi-Harati et al.	(FNAL KTeV Collab.)
ALAVI-HARATI 01E	PRL 87 021801	A. Alavi-Harati et al.	(FNAL KTeV Collab.)
ALAVI-HARATI 01F	PR D64 012003	A. Alavi-Harati et al.	(FNAL KTeV Collab.)
ALAVI-HARATI 01G	PRL 87 071801	A. Alavi-Harati et al.	(FNAL KTeV Collab.)
ALAVI-HARATI 01H	PRL 87 111802	A. Alavi-Harati et al.	(FNAL KTeV Collab.)
ALAVI-HARATI 01J	PR D64 112004	A. Alavi-Harati et al.	(FNAL KTeV Collab.)
ANGELOPO... 01	PL B503 49	A. Angelopoulos et al.	(CLEEAR Collab.)
ANGELOPO... 01B	EPJ C22 55	A. Angelopoulos et al.	(CLEEAR Collab.)
LAI 01B	PL B515 261	A. Lai et al.	(CERN NA48 Collab.)

LAI 01C	EPJ C22 231	A. Lai et al.	(CERN NA48 Collab.)
ALAVI-HARATI 00B	PR D61 072006	A. Alavi-Harati et al.	(FNAL KTeV Collab.)
ALAVI-HARATI 00B	PRL 84 408	A. Alavi-Harati et al.	(FNAL KTeV Collab.)
ALAVI-HARATI 00E	PRL 84 5279	A. Alavi-Harati et al.	(FNAL KTeV Collab.)
ALAVI-HARATI 00E	PR D62 112001	A. Alavi-Harati et al.	(FNAL KTeV Collab.)
AMBROSE 00	PRL 84 1389	D. Ambrose et al.	(BNL E871 Collab.)
APOSTOLA... 00	PL B473 186	A. Apostolakis et al.	(CLEEAR Collab.)
PDG 00	EPJ C15 1	D.E. Groom et al.	(CLEEAR Collab.)
ADAMS 99	PL B447 240	J. Adams et al.	(FNAL KTeV Collab.)
ALAVI-HARATI 99B	PRL 83 917	A. Alavi-Harati et al.	(FNAL KTeV Collab.)
ALAVI-HARATI 99D	PRL 83 22	A. Alavi-Harati et al.	(FNAL KTeV Collab.)
APOSTOLA... 99C	PL B458 545	A. Apostolakis et al.	(CLEEAR Collab.)
Also	EPJ C18 41	A. Apostolakis et al.	(CLEEAR Collab.)
FANTI 99B	PL B458 553	V. Fanti et al.	(CERN NA48 Collab.)
FANTI 99C	PL B465 335	V. Fanti et al.	(CERN NA48 Collab.)
MURAKAMI 99	PL B463 333	K. Murakami et al.	(KEK E162 Collab.)
ADAMS 98	PRL 80 4123	J. Adams et al.	(FNAL KTeV Collab.)
AMBROSE 98	PRL 81 4309	D. Ambrose et al.	(BNL E871 Collab.)
AMBROSE 98B	PRL 81 5734	D. Ambrose et al.	(BNL E871 Collab.)
ANGELOPO... 98	PL B420 191	A. Angelopoulos et al.	(CLEEAR Collab.)
ANGELOPO... 98D	EPJ C5 339	A. Angelopoulos et al.	(CLEEAR Collab.)
ANGELOPO... 98D	PL B444 38	A. Angelopoulos et al.	(CLEEAR Collab.)
Also	EPJ C22 55	A. Angelopoulos et al.	(CLEEAR Collab.)
ANGELOPO... 98E	PL B444 43	A. Angelopoulos et al.	(CLEEAR Collab.)
ARISAKA 98	PL B432 230	K. Arisaka et al.	(FNAL E799 Collab.)
BENDER 98	PL B418 411	M. Bender et al.	(CERN NA48 Collab.)
DAMBROSIO 98	PL B423 385	G. D'Ambrosio, G. Isidori, J. Portoles	(CERN NA48 Collab.)
SETZU 98	PL B420 205	M.G. Setzu et al.	(CLEEAR Collab.)
TAKEUCHI 98	PL B443 409	Y. Takeuchi et al.	(KYOT, KEK, HIRO)
FANTI 97	ZPHY C76 653	V. Fanti et al.	(CERN NA48 Collab.)
NOMURA 97	PL B408 445	T. Nomura et al.	(KYOT, KEK, HIRO)
ADLER 96B	ZPHY C70 211	R. Adler et al.	(CLEEAR Collab.)
ADLER 96C	PL B369 367	R. Adler et al.	(CLEEAR Collab.)
GU 96	PRL 76 4312	P. Gu et al.	(RUTG, UCLA, EFI, COLO+)
LEBER 96	PL B369 69	F. Leber et al.	(MANZ, CERN, EDIN, ORSAY+)
PDG 96	PR D54 1	R. M. Barnett et al.	(CLEEAR Collab.)
ADLER 95B	PL B363 237	R. Adler et al.	(CLEEAR Collab.)
ADLER 95B	PL B363 243	R. Adler et al.	(CLEEAR Collab.)
AKAGI 95	PR D51 2061	T. Akagi et al.	(TOHOK, TOKY, KYOT, KEK)
BARR 95	ZPHY C65 361	G.D. Barr et al.	(CERN, EDIN, MANZ, LALO+)
BARR 95C	PL B358 399	G.D. Barr et al.	(CERN, EDIN, MANZ, LALO+)
HEINSON 95	PR D51 985	A.P. Heinson et al.	(BNL E791 Collab.)
KREUTZ 95	ZPHY C65 67	A. Kreuz et al.	(SIEG, EDIN, MANZ, ORSAY+)
MATTHEWS 95	PRL 75 2803	J.N. Matthews et al.	(RUTG, EFI, ELMT+)
SCHWINGEN... 95	PRL 74 4376	B. Schwingenheuer et al.	(EFI, CHIC+)
SPENCER 95	PRL 74 3323	M.B. Spencer et al.	(UCLA, EFI, COLO+)
BARR 94	PL B328 528	G.D. Barr et al.	(CERN, EDIN, MANZ, LALO+)
GU 94	PRL 72 3000	P. Gu et al.	(RUTG, UCLA, EFI, COLO+)
NAKAYA 94	PRL 73 2169	T. Nakaya et al.	(OSAK, UCLA, EFI, COLO+)
ROBERTS 94	PR D50 1874	D. Roberts et al.	(UCLA, EFI, COLO+)
WEAVER 94	PRL 72 3758	M. Weaver et al.	(UCLA, EFI, COLU, ELMT+)
AKAGI 93	PR D47 2644	T. Akagi et al.	(TOHOK, TOKY, KYOT, KEK)
ARISAKA 93B	PRL 70 1049	K. Arisaka et al.	(BNL E791 Collab.)
ARISAKA 93B	PRL 70 3910	K. Arisaka et al.	(BNL E791 Collab.)
BARR 93D	PL B317 233	G.D. Barr et al.	(CERN, EDIN, MANZ, LALO+)
GIBBONS 93	PRL 70 1199	L.K. Gibbons et al.	(FNAL E731 Collab.)
Also	PR D55 6625	L.K. Gibbons et al.	(FNAL E731 Collab.)
GIBBONS 93B	PRL 70 1203	L.K. Gibbons et al.	(FNAL E731 Collab.)
GIBBONS 93C	Thesis RX-1487	L.K. Gibbons et al.	(CHIC)
Also	PR D55 6625	L.K. Gibbons et al.	(FNAL E731 Collab.)
HARRIS 93B	PRL 71 3914	D.A. Harris et al.	(EFI, UCLA, COLO+)
HARRIS 93B	PRL 71 3918	D.A. Harris et al.	(EFI, UCLA, COLO+)
MAKOFF 93	PRL 70 1591	G. Makoff et al.	(FNAL E731 Collab.)
Also	PRL 75 2059 (erratum)	G. Makoff et al.	(FNAL E731 Collab.)
RAMBERG 93	PRL 70 2525	E. Ramberg et al.	(FNAL E731 Collab.)
RAMBERG 93B	PRL 70 2529	E.J. Ramberg et al.	(FNAL E731 Collab.)
VAGINS 93	PRL 71 35	M.R. Vagins et al.	(BNL E845 Collab.)
ADLER 92B	PL B286 180	R. Adler et al.	(CLEEAR Collab.)
Also	SJNP 55 840	R. Adler et al.	(CLEEAR Collab.)
BARR 92	PL B284 440	G.D. Barr et al.	(CERN, EDIN, MANZ, LALO+)
GRAHAM 92	PL B295 169	G.E. Graham et al.	(FNAL E731 Collab.)
MORSE 92	PR D45 36	W.M. Morse et al.	(BNL, YALE, VASS+)
PDG 92	PR D45 51	K. Hikasa et al.	(KEK, LBL, BOST)
SOMALWAR 92	PRL 68 2580	S.V. Somalwar et al.	(FNAL E731 Collab.)
AKAGI 91B	PRL 67 2618	T. Akagi et al.	(TOHOK, TOKY, KYOT, KEK)
BARR 91	PR D259 389	G.D. Barr et al.	(CERN, EDIN, MANZ, LALO+)
HEINSON 91	PR D41 81	A.P. Heinson et al.	(UCL, UCLA, LANL+)
PAPADIMITRI... 91	PR D44 8573	V. Papadimitriou et al.	(UCL, UCLA, LANL+)
BARKER 90	PR D41 3546	A.R. Barker et al.	(FNAL E731 Collab.)
Also	PRL 61 2661	L.K. Gibbons et al.	(FNAL E731 Collab.)
BARR 90C	PL B240 283	G.D. Barr et al.	(CERN, EDIN, MANZ, LALO+)
BARR 90B	PL B242 523	G.D. Barr et al.	(CERN, EDIN, MANZ, LALO+)
CAROSI 90	PL B237 303	R. Carosi et al.	(CERN, EDIN, MANZ, LALO+)
KARLSSON 90	PRL 64 2976	M. Karlsson et al.	(FNAL E731 Collab.)
OHL 90	PRL 64 2755	K.E. Ohl et al.	(BNL E845 Collab.)
OHL 90B	PRL 65 1407	K.E. Ohl et al.	(BNL E845 Collab.)
PATTERSON 90	PRL 64 1491	J.R. Patterson et al.	(FNAL E731 Collab.)
INAGAKI 89	PR D40 1712	T. Inagaki et al.	(KEK, TOKY, KYOT)
MATHIAZHAGAN 89	PR 63 2181	C. Mathiazhagan et al.	(UCL, UCLA, LANL+)
MATHIAZHAGAN 89B	PR 63 2185	C. Mathiazhagan et al.	(UCL, UCLA, LANL+)
WAHL 89	CERN-EP/89-86	H. Wahl	(CERN)
BARR 88	PL B214 303	G.D. Barr et al.	(CERN, EDIN, MANZ, LALO+)
BURKHARDT 88	PL B206 169	H. Burkhardt et al.	(CERN, EDIN, MANZ+)
JASTRZEM... 88	PRL 61 2390	E. Jastrzembski et al.	(BNL, YALE)
WOODS 88	PRL 60 1695	M. Woods et al.	(FNAL E731 Collab.)
BURKHARDT 87	PL B199 139	H. Burkhardt et al.	(CERN, EDIN, MANZ+)
ARONSON 86	PR D33 3180	S.H. Aronson et al.	(BNL, CHIC, STAN+)
Also	PRL 49 1078	S.H. Aronson et al.	(BNL, CHIC, STAN+)
PDG 86C	PL 170B 132	H.M. Aguilar-Benitez et al.	(CERN, CIT+)
COUPLAL 85	PRL 55 566	D.P. Couplal et al.	(CHIC, SACL)
BALATS 83	SJNP 38 556	M.Y. Balats et al.	(ITEP)
BERGSTROM 83	PL 131B 229	L. Bergstrom, E. Masso, P. Singer	(CERN)
ARONSON 82	PRL 48 1078	S.H. Aronson et al.	(BNL, CHIC, STAN+)
ARONSON 82B	PRL 48 1306	S.H. Aronson et al.	(BNL, CHIC, PURD)
Also	PL 116B 73	E. Fischbach et al.	(PURD, BNL, CHIC)
Also	PR D28 476	S.H. Aronson et al.	(BNL, CHIC, PURD)
Also	PR D28 495	S.H. Aronson et al.	(

See key on page 373

Meson Particle Listings

$K_L^0, K_S^0(800)$

Table listing meson particles with columns for name, reference number, author(s), and experimental details. Includes sections for 'OTHER RELATED PAPERS' and 'K0*(800) MASS'.

$K_0^*(800)$
or κ

$I(J^P) = \frac{1}{2}(0^+)$

OMITTED FROM SUMMARY TABLE
Needs confirmation.

$K_0^*(800)$ MASS

Table with columns: VALUE (MeV), EVTS, DOCUMENT ID, TECN, COMMENT. Lists experimental results for K0*(800) mass.

- 1 S-matrix pole. GUO 06 in a chiral unitary approach report a mass of 757 ± 33 MeV and a width of 558 ± 82 MeV.
2 A fit in the K0*(800) + K*(892) + K*(1410) model with mass and width of the K0*(800) from ABLIKIM 06c well describes the left slope of the K0S pi- invariant mass spectrum in tau- -> K0S pi- nu- decay studied by EPIFANOV 07.
3 S-matrix pole. Using Roy-Steiner equations (ROY 71) as well as unitarity, analyticity and crossing symmetry constraints.
4 Not seen by KOPP 01 using 7070 events of D0 -> K- pi+ pi0. LINK 02e and LINK 05i show clear evidence for a constant non-resonant scalar amplitude rather than K0*(800) in their high statistics analysis of D+ -> K- pi+ nu+ nu-.
5 AUBERT 07r does not find evidence for the charged K0*(800) using 11k events of D0 -> K- K+ pi0.
6 A Breit-Wigner mass and width.
7 S-matrix pole. Reanalysis of ASTON 88, AITALA 02, and ABLIKIM 06c using for the kappa an s-dependent width with an Adler zero near threshold.

Meson Particle Listings

$K_0^*(800)$, $K^*(892)$

- ⁸Breit-Wigner parameters. A significant S-wave can be also modeled as a non-resonant contribution.
- ⁹S-matrix pole.
- ¹⁰Using ASTON 88.
- ¹¹T-matrix pole. Reanalysis of data from LINGLIN 73, ESTABROOKS 78, and ASTON 88 in the unitarized ChPT model.
- ¹²T-matrix pole. Reanalysis of ASTON 88 data.
- ¹³Reanalysis of ASTON 88 using interfering Breit-Wigner amplitudes.

LINK	02L	PL B544 89	J.M. Link et al.	(FNAL FOCUS Collab.)
VANBEVEREN	01B	EPJ C22 493	E. van Beveren	
JAMIN	00	NP B587 331	M. Jamin et al.	

$K^*(892)$

$$I(J^P) = \frac{1}{2}(1^-)$$

$K_0^*(800)$ WIDTH

VALUE (MeV)	EVTS	DOCUMENT ID	TECN	COMMENT
550 ± 34 OUR AVERAGE		Error includes scale factor of 1.5.		
618 ± 20 ⁺⁹⁶ ₋₁₄₄	25k	14.15 ABLIKIM	06c BES2	$J/\psi \rightarrow \bar{K}^*(892)^0 K^+ \pi^-$
557 ± 24		16 DESCOTES-G.	06 RVUE	$\pi K \rightarrow \pi K$
410 ± 43 ± 87	15090	17.18 AITALA	02 E791	$D^+ \rightarrow K^- \pi^+ \pi^+$
• • • We do not use the following data for averages, fits, limits, etc. • • •				
464 ± 28 ± 22	54k	19 LINK	07b FOCUS	$D^+ \rightarrow K^- \pi^+ \pi^+$
684 ± 120		20 BUGG	06 RVUE	
251 ± 48	627 ± 30	21 CAWFIELD	06a CLEO	$D^0 \rightarrow K^+ K^- \pi^0$
606 ± 59		14.22 ZHOU	06 RVUE	$K\rho \rightarrow K^- \pi^+ n$
470 ± 66		23 PELAEZ	04a RVUE	$K\pi \rightarrow K\pi$
724 ± 332		22 ZHENG	04 RVUE	$K^- \rho \rightarrow K^- \pi^+ n$
772 ± 100		24 BUGG	03 RVUE	$11 K^- \rho \rightarrow K^- \pi^+ n$
545 ⁺²³⁵ ₋₁₁₀		25 ISHIDA	97b RVUE	$11 K^- \rho \rightarrow K^- \pi^+ n$

- ¹⁴S-matrix pole.
- ¹⁵A fit in the $K_0^*(800) + K^*(892) + K^*(1410)$ model with mass and width of the $K_0^*(800)$ from ABLIKIM 06c well describes the left slope of the $K_S^0 \pi^-$ invariant mass spectrum in $\tau^- \rightarrow K_S^0 \pi^- \nu_\tau$ decay studied by EPIFANOV 07.
- ¹⁶S-matrix pole. Using Roy-Steiner equations (ROY 71) as well as unitarity, analyticity and crossing symmetry constraints.
- ¹⁷Not seen by KOPP 01 using 7070 events of $D^0 \rightarrow K^- \pi^+ \pi^0$. LINK 02e and LINK 05i show clear evidence for a constant non-resonant scalar amplitude rather than $K_0^*(800)$ in their high statistics analysis of $D^+ \rightarrow K^- \pi^+ \mu^+ \nu_\mu$.
- ¹⁸AUBERT 07T does not find evidence for the charged $K_0^*(800)$ using 11k events of $D^0 \rightarrow K^- K^+ \pi^0$.
- ¹⁹A Breit-Wigner mass and width.
- ²⁰S-matrix pole. Reanalysis of ASTON 88, AITALA 02, and ABLIKIM 06c using for the κ an s-dependent width with an Adler zero near threshold.
- ²¹Statistical error only. A fit to the Dalitz plot including the $K_0^*(800)^\pm$, $K^*(892)^\pm$, and ϕ resonances modeled as Breit-Wigners. A significant S-wave can be also modeled as a non-resonant contribution.
- ²²Using ASTON 88.
- ²³T-matrix pole. Reanalysis of data from LINGLIN 73, ESTABROOKS 78, and ASTON 88 in the unitarized ChPT model.
- ²⁴T-matrix pole. Reanalysis of ASTON 88 data.
- ²⁵Reanalysis of ASTON 88 using interfering Breit-Wigner amplitudes.

$K_0^*(800)$ REFERENCES

AUBERT	07T	PR D76 011102R	B. Aubert et al.	(BABAR Collab.)
EPIFANOV	07	PL B654 65	D. Epifanov et al.	(BELLE Collab.)
LINK	07B	PL B653 1	J.M. Link et al.	(FNAL FOCUS Collab.)
ABLIKIM	06C	PL B633 681	M. Ablikim et al.	(BES Collab.)
BUGG	06	PL B632 471	D.V. Bugg	(LOQM)
CAWFIELD	06A	PR D74 031108R	C. Kawfield et al.	(CLEO Collab.)
DESCOTES-G.	06	EPJ C48 553	S. Descotes-Genon, B. Moussallam	
GUO	06	NP A773 78	F.K. Guo et al.	
ZHOU	06	NP A775 212	Z.Y. Zhou, H.Q. Zheng	
LINK	05A	PL B621 72	J.M. Link et al.	(FNAL FOCUS Collab.)
PELAEZ	04A	MPL A19 2879	J.R. Pelaez	
ZHENG	04	NP A733 235	H.Q. Zheng et al.	
BUGG	03	PL B572 1	D.V. Bugg	
AITALA	02	PRL 89 121801	E.M. Aitala et al.	(FNAL E791 Collab.)
LINK	02E	PL B535 43	J.M. Link et al.	(FNAL FOCUS Collab.)
KOPP	01	PR D63 092001	S. Kopp et al.	(CLEO Collab.)
ISHIDA	97B	PTP 98 621	S. Ishida et al.	
ASTON	88	NP B296 493	D. Aston et al.	(SLAC, NAGO, CINC, INUS)
ESTABROOKS	78	NP B133 490	P.G. Estabrooks et al.	(MCGI, CARL, DURH+)
LINGLIN	73	NP B95 408	D. Linglin	(CERN)
ROY	71	PL 36B 353	S.M. Roy	

OTHER RELATED PAPERS

CHEN	07E	PR D76 094025	H.-X. Chen, A. Hosaka, S.L. Zhu	
GIACOSA	07	PR D75 054007	F. Giacosa	
MAJANI	07	EPJ C50 609	L. Majani et al.	
WADA	07	PL B652 250	H. Wada et al.	
AITALA	06	PR D73 032004	E.M. Aitala et al.	(FNAL E791 Collab.)
Also		PR D74 059901 (erratum)	E.M. Aitala et al.	(FNAL E791 Collab.)
CHENG	06	PR D73 014017	H.-Y. Cheng, C.-K. Chua, K.-C. Yang	
JAMIN	06	PR D74 074009	M. Jamin, J.A. Oller, A. Pich	
LINK	06	PL B633 183	J.M. Link et al.	(FNAL FOCUS Collab.)
MCNEILE	06	PR D74 014508	C. McNeile, C. Michael	
VANBEVEREN	06A	PR D74 037501	E. van Beveren et al.	
VANBEVEREN	06B	PRL 97 202001	E. van Beveren, G. Rupp	
ABLIKIM	05Q	PR D72 092002	M. Ablikim et al.	(BES Collab.)
BRITO	05	PL B608 69	T.V. Brito et al.	
BUGG	05A	EPJ A25 107	D.V. Bugg	(LOQM)
Also		EPJ A26 151 (erratum)	D.V. Bugg	(LOQM)
BUGG	05B	EPJ A26 151 (erratum)	D.V. Bugg	(LOQM)
GARMASH	05	PR D71 092003	A. Garmash et al.	(BELLE Collab.)
LI	05B	EPJ A25 263	D.-M. Li, K.-W. Wei, H. Yu	
ABLIKIM	04E	PL B603 138	M. Ablikim et al.	(BES Collab.)
PELAEZ	04	PRL 92 102001	J.R. Pelaez	
YNDURAIN	04	PL B578 99	F.J. Yndurain	
Also		PL B586 439 (erratum)	F.J. Yndurain	
SEMENOV	03	PAN 66 526	S.V. Semenov	

Translated from YAF 66 553.

$K^*(892)$ MASS

CHARGED ONLY, HADROPRODUCED

VALUE (MeV)	EVTS	DOCUMENT ID	TECN	CHG	COMMENT
891.66 ± 0.26 OUR AVERAGE		Error includes scale factor of 1.5.			
892.6 ± 0.5	5840	BAUBILLIER	84B HBC	-	8.25 $K^- \rho \rightarrow \bar{K}^0 \pi^- \rho$
888 ± 3		NAPIER	84 SPEC	+	200 $\pi^- \rho \rightarrow 2K_S^0 X$
891 ± 1		NAPIER	84 SPEC	-	200 $\pi^- \rho \rightarrow 2K_S^0 X$
891.7 ± 2.1	3700	BARTH	83 HBC	+	70 $K^+ \rho \rightarrow K^0 \pi^+ X$
891 ± 1	4100	TOAFF	81 HBC	-	6.5 $K^- \rho \rightarrow \bar{K}^0 \pi^- X$
892.8 ± 1.6		AJINENKO	80 HBC	+	32 $K^+ \rho \rightarrow K^0 \pi^+ X$
890.7 ± 0.9	1800	AGUILAR...	78B HBC	±	0.76 $\bar{p} \rho \rightarrow K^\mp K_S^0 \pi^\pm$
886.6 ± 2.4	1225	BALAND	78 HBC	±	12 $\bar{p} \rho \rightarrow (K\pi)^\pm X$
891.7 ± 0.6	6706	COOPER	78 HBC	±	0.76 $\bar{p} \rho \rightarrow (K\pi)^\pm X$
891.9 ± 0.7	9000	1 PALER	75 HBC	-	14.3 $K^- \rho \rightarrow (K\pi)^\mp X$
892.2 ± 1.5	4404	AGUILAR...	71B HBC	-	3.9,4.6 $K^- \rho \rightarrow (K\pi)^\mp$
891 ± 2	1000	CRENNELL	69D DBC	-	3.9 $K^- N \rightarrow K^0 \pi^- X$
890 ± 3.0	720	BARLOW	67 HBC	±	1.2 $\bar{p} \rho \rightarrow (K^0 \pi)^\pm K^\mp$
889 ± 3.0	600	BARLOW	67 HBC	±	1.2 $\bar{p} \rho \rightarrow (K^0 \pi)^\pm K\pi$
891 ± 2.3	620	2 DEBAERE	67B HBC	+	3.5 $K^+ \rho \rightarrow K^0 \pi^+ \rho$
891.0 ± 1.2	1700	3 WOJCICKI	64 HBC	-	1.7 $K^- \rho \rightarrow \bar{K}^0 \pi^- \rho$
• • • We do not use the following data for averages, fits, limits, etc. • • •					
893.5 ± 1.1	27k	4 ABELE	99D CBAR	±	0.0 $\bar{p} \rho \rightarrow K^+ K^- \pi^0$
890.4 ± 0.2 ± 0.5	80 ± 0.8k	5 BIRD	89 LASS	-	11 $K^- \rho \rightarrow \bar{K}^0 \pi^- \rho$
890.0 ± 2.3	800	2,3 CLELAND	82 SPEC	+	30 $K^+ \rho \rightarrow K_S^0 \pi^+ \rho$
896.0 ± 1.1	3200	2,3 CLELAND	82 SPEC	+	50 $K^+ \rho \rightarrow K_S^0 \pi^+ \rho$
893 ± 1	3600	2,3 CLELAND	82 SPEC	-	50 $K^+ \rho \rightarrow K_S^0 \pi^- \rho$
896.0 ± 1.9	380	DELFOSSÉ	81 SPEC	+	50 $K^\pm \rho \rightarrow K^\pm \pi^0 \rho$
886.0 ± 2.3	187	DELFOSSÉ	81 SPEC	-	50 $K^\pm \rho \rightarrow K^\pm \pi^0 \rho$
894.2 ± 2.0	765	2 CLARK	73 HBC	-	3.13 $K^- \rho \rightarrow \bar{K}^0 \pi^- \rho$
894.3 ± 1.5	1150	2,3 CLARK	73 HBC	-	3.3 $K^- \rho \rightarrow \bar{K}^0 \pi^- \rho$
892.0 ± 2.6	341	2 SCHWEING...	68 HBC	-	5.5 $K^- \rho \rightarrow \bar{K}^0 \pi^- \rho$

CHARGED ONLY, PRODUCED IN τ LEPTON DECAYS

VALUE (MeV)	EVTS	DOCUMENT ID	TECN	COMMENT
895.47 ± 0.20 ± 0.74	53k	6 EPIFANOV	07 BELL	$\tau^- \rightarrow K_S^0 \pi^- \nu_\tau$
• • • We do not use the following data for averages, fits, limits, etc. • • •				
896.4 ± 0.9	11970	7 BONVICINI	02 CLEO	$\tau^- \rightarrow K^- \pi^0 \nu_\tau$
895 ± 2		8 BARATE	99R ALEP	$\tau^- \rightarrow K^- \pi^0 \nu_\tau$

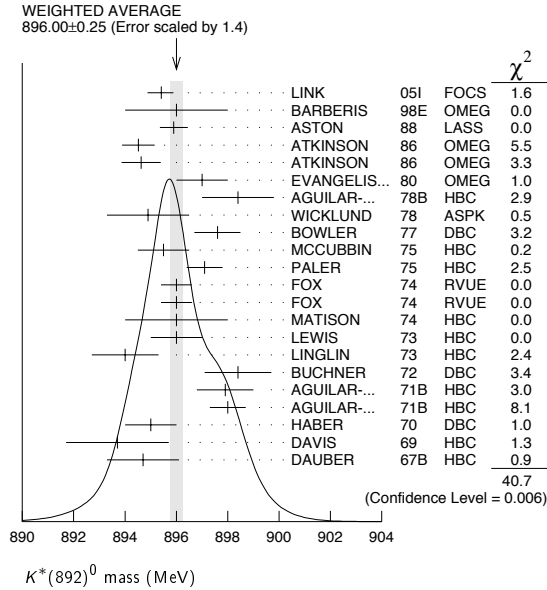
NEUTRAL ONLY

VALUE (MeV)	EVTS	DOCUMENT ID	TECN	COMMENT
896.00 ± 0.25 OUR AVERAGE		Error includes scale factor of 1.4. See the ideogram below.		
895.41 ± 0.32 ^{+0.35} _{-0.43}	18k	9 LINK	05I FOCUS	$D^+ \rightarrow K^- \pi^+ \mu^+ \nu_\mu$
896 ± 2		BARBERIS	98E OMEG	450 $pp \rightarrow p_f p_s K^* \bar{K}^*$
895.9 ± 0.5 ± 0.2		ASTON	88 LASS	11 $K^- \rho \rightarrow K^- \pi^+ n$
894.52 ± 0.63	25k	1 ATKINSON	86 OMEG	20-70 $\gamma\rho$
894.63 ± 0.76	20k	1 ATKINSON	86 OMEG	20-70 $\gamma\rho$
897 ± 1	28k	EVANGELIS...	80 OMEG	10 $\pi^- \rho \rightarrow K^+ \pi^- (\Lambda, \Sigma)$
898.4 ± 1.4	1180	AGUILAR...	78B HBC	0.76 $\bar{p} \rho \rightarrow K^\mp K_S^0 \pi^\pm$
894.9 ± 1.6		WICKLUND	78 ASPK	3,4,6 $K^\pm N \rightarrow (K\pi)^0 N$
897.6 ± 0.9		BOWLER	77 DBC	5.4 $K^+ d \rightarrow K^+ \pi^- p\rho$
895.5 ± 1.0	3600	MCCUBBIN	75 HBC	3.6 $K^- \rho \rightarrow K^- \pi^+ n$
897.1 ± 0.7	22k	1 PALER	75 HBC	14.3 $K^- \rho \rightarrow (K\pi)^0 X$
896.0 ± 0.6	10k	FOX	74 RVUE	2 $K^- \rho \rightarrow K^- \pi^+ n$
896.0 ± 0.6		FOX	74 RVUE	2 $K^+ n \rightarrow K^+ \pi^- p$
896 ± 2		10 MATISON	74 HBC	12 $K^+ \rho \rightarrow K^+ \pi^- \Delta$
896 ± 1	3186	LEWIS	73 HBC	2.1-2.7 $K^+ \rho \rightarrow K\pi p\rho$
894.0 ± 1.3		10 LINGLIN	73 HBC	2-13 $K^+ \rho \rightarrow K^+ \pi^- \pi^+ \rho$
898.4 ± 1.3	1700	2 BUCHNER	72 DBC	4.6 $K^+ n \rightarrow K^+ \pi^- p$
897.9 ± 1.1	2934	2 AGUILAR...	71B HBC	3.9,4.6 $K^- \rho \rightarrow K^- \pi^+ n$
898.0 ± 0.7	5362	2 AGUILAR...	71B HBC	3.9,4.6 $K^- \rho \rightarrow K^- \pi^+ \pi^- \rho$
895 ± 1	4300	3 HABER	70 DBC	3 $K^- N \rightarrow K^- \pi^+ X$
893.7 ± 2.0	10k	DAVIS	69 HBC	12 $K^+ \rho \rightarrow K^+ \pi^- \pi^+ \rho$
894.7 ± 1.4	1040	2 DAUBER	67B HBC	2.0 $K^- \rho \rightarrow K^- \pi^+ \pi^- \rho$
• • • We do not use the following data for averages, fits, limits, etc. • • •				
896.2 ± 0.3	20k	11 AUBERT	07AK BABR	10.6 $e^+ e^- \rightarrow K^* K^\pm \pi^\mp \gamma$
900.7 ± 1.1	5900	BARTH	83 HBC	70 $K^+ \rho \rightarrow K^+ \pi^- X$

See key on page 373

Meson Particle Listings

$K^*(892)$



- 1 Inclusive reaction. Complicated background and phase-space effects.
- 2 Mass errors enlarged by us to Γ/\sqrt{N} . See note.
- 3 Number of events in peak reevaluated by us.
- 4 K-matrix pole.
- 5 From a partial wave amplitude analysis.
- 6 From a fit in the $K_S^0(800) + K^*(892) + K^*(1410)$ model.
- 7 Calculated by us from the shift by 4.7 ± 0.9 MeV (statistical uncertainty only) reported in BONVICINI 02 with respect to the world average value from PDG 00.
- 8 With mass and width of the $K^*(1410)$ fixed at 1412 MeV and 227 MeV, respectively.
- 9 Fit to $K\pi$ mass spectrum includes a non-resonant scalar component.
- 10 From pole extrapolation.
- 11 Systematic errors not estimated.

$K^*(892)$ MASSES AND MASS DIFFERENCES

Unrealistically small errors have been reported by some experiments. We use simple “realistic” tests for the minimum errors on the determination of a mass and width from a sample of N events:

$$\delta_{\min}(m) = \frac{\Gamma}{\sqrt{N}}, \quad \delta_{\min}(\Gamma) = 4 \frac{\Gamma}{\sqrt{N}}. \quad (1)$$

We consistently increase unrealistic errors before averaging. For a detailed discussion, see the 1971 edition of this Note.

VALUE (MeV)	EVTS	DOCUMENT ID	TECN	CHG	COMMENT
6.7 ± 1.2 OUR AVERAGE					
7.7 ± 1.7	2980	AGUILAR-...	78B	HBC	±0 0.76 $\bar{p}p \rightarrow K^\mp K_S^0 \pi^\pm$
5.7 ± 1.7	7338	AGUILAR-...	71B	HBC	-0 3.9,4.6 K^-p
6.3 ± 4.1	283	12 BARASH	67B	HBC	0.0 $\bar{p}p$

12 Number of events in peak reevaluated by us.

$K^*(892)$ RANGE PARAMETER

All from partial wave amplitude analyses.

VALUE (GeV^{-1})	EVTS	DOCUMENT ID	TECN	CHG	COMMENT
3.96 ± 0.54 +1.31 -0.90	18k	13 LINK	051	FOCS	0 $D^+ \rightarrow K^- \pi^+ \mu^+ \nu_\mu$
3.4 ± 0.7		ASTON	88	LASS	0 11 $K^-p \rightarrow K^- \pi^+ n$
12.1 ± 3.2 ± 3.0		BIRD	89	LASS	- 11 $K^-p \rightarrow \bar{K}^0 \pi^- p$

13 Fit to $K\pi$ mass spectrum includes a non-resonant scalar component.

$K^*(892)$ WIDTH

CHARGED ONLY, HADROPRODUCED

VALUE (MeV)	EVTS	DOCUMENT ID	TECN	CHG	COMMENT
50.8 ± 0.9 OUR FIT					
50.8 ± 0.9 OUR AVERAGE					
49 ± 2	5840	BAUBILLIER	84B	HBC	- 8.25 $K^-p \rightarrow \bar{K}^0 \pi^- p$
56 ± 4		NAPIER	84	SPEC	- 200 $\pi^- p \rightarrow 2K_S^0 X$
51 ± 2	4100	TOAFF	81	HBC	- 6.5 $K^-p \rightarrow \bar{K}^0 \pi^- p$
50.5 ± 5.6		AJINENKO	80	HBC	+ 32 $K^+p \rightarrow K^0 \pi^+ X$
45.8 ± 3.6	1800	AGUILAR-...	78B	HBC	± 0.76 $\bar{p}p \rightarrow K^\mp K_S^0 \pi^\pm$
52.0 ± 2.5	6706	14 COOPER	78	HBC	± 0.76 $\bar{p}p \rightarrow (K\pi)^\pm X$
52.1 ± 2.2	9000	15 PALER	75	HBC	- 14.3 $K^-p \rightarrow (K\pi)^- X$
46.3 ± 6.7	765	14 CLARK	73	HBC	- 3.13 $K^-p \rightarrow \bar{K}^0 \pi^- p$
48.2 ± 5.7	1150	14,16 CLARK	73	HBC	- 3.3 $K^-p \rightarrow \bar{K}^0 \pi^- p$
54.3 ± 3.3	4404	14 AGUILAR-...	71B	HBC	- 3.9,4.6 $K^-p \rightarrow (K\pi)^- p$
46 ± 5	1700	14,16 WOJICKI	64	HBC	- 1.7 $K^-p \rightarrow \bar{K}^0 \pi^- p$
• • • We do not use the following data for averages, fits, limits, etc. • • •					
54.8 ± 1.7	27k	17 ABELE	99D	CBAR	± 0.0 $\bar{p}p \rightarrow K^+ K^- \pi^0$
45.2 ± 1 ± 2	79.7 ± 0.8k	18 BIRD	89	LASS	- 11 $K^-p \rightarrow \bar{K}^0 \pi^- p$
42.8 ± 7.1	3700	BARTH	83	HBC	+ 70 $K^+p \rightarrow K^0 \pi^+ X$
64.0 ± 9.2	800	14,16 CLELAND	82	SPEC	+ 30 $K^+p \rightarrow K_S^0 \pi^+ p$
62.0 ± 4.4	3200	14,16 CLELAND	82	SPEC	+ 50 $K^+p \rightarrow K_S^0 \pi^+ p$
55 ± 4	3600	14,16 CLELAND	82	SPEC	- 50 $K^+p \rightarrow K_S^0 \pi^+ p$
62.6 ± 3.8	380	DELFOSE	81	SPEC	+ 50 $K^\pm p \rightarrow K^\pm \pi^0 p$
50.5 ± 3.9	187	DELFOSE	81	SPEC	+ 50 $K^\pm p \rightarrow K^\pm \pi^0 p$

CHARGED ONLY, PRODUCED IN τ LEPTON DECAYS

VALUE	EVTS	DOCUMENT ID	TECN	CHG	COMMENT
46.2 ± 0.6 ± 1.2	53k	19 EPIFANOV	07	BELL	$\tau^- \rightarrow K_S^0 \pi^- \nu_\tau$
• • • We do not use the following data for averages, fits, limits, etc. • • •					
55 ± 8		20 BARATE	99R	ALEP	$\tau^- \rightarrow K^- \pi^0 \nu_\tau$

NEUTRAL ONLY

VALUE (MeV)	EVTS	DOCUMENT ID	TECN	CHG	COMMENT
50.3 ± 0.6 OUR FIT					Error includes scale factor of 1.1.
50.3 ± 0.6 OUR AVERAGE					Error includes scale factor of 1.1.
47.79 ± 0.86 +1.32 -1.06	18k	21 LINK	051	FOCS	0 $D^+ \rightarrow K^- \pi^+ \mu^+ \nu_\mu$
54 ± 3		BARBERIS	98E	OMEG	450 $pp \rightarrow p_f p_S K^* \bar{K}^*$
50.8 ± 0.8 ± 0.9		ASTON	88	LASS	0 11 $K^-p \rightarrow K^- \pi^+ n$
46.5 ± 4.3	5900	BARTH	83	HBC	0 70 $K^+p \rightarrow K^+ \pi^- X$
54 ± 2	28k	EVANGELIS...	80	OMEG	0 10 $\pi^- p \rightarrow K^+ \pi^- (\Lambda, \Sigma)$
45.9 ± 4.8	1180	AGUILAR-...	78B	HBC	0 0.76 $\bar{p}p \rightarrow K^\mp K_S^0 \pi^\pm$
51.2 ± 1.7		WICKLUND	78	ASPK	0 3,4,6 $K^\pm N \rightarrow (K\pi)^0 N$
48.9 ± 2.5		BOWLER	77	DBC	0 5.4 $K^+ d \rightarrow K^+ \pi^- pp$
48 +3 -2	3600	MCCUBBIN	75	HBC	0 3.6 $K^-p \rightarrow K^- \pi^+ n$
50.6 ± 2.5	22k	15 PALER	75	HBC	0 14.3 $K^-p \rightarrow (K\pi)^0 X$
47 ± 2	10k	FOX	74	RVUE	0 2 $K^-p \rightarrow K^- \pi^+ n$
51 ± 2		FOX	74	RVUE	0 2 $K^+n \rightarrow K^+ \pi^- p$
46.0 ± 3.3	3186	14 LEWIS	73	HBC	0 2.1-2.7 $K^+p \rightarrow K\pi\pi p$
51.4 ± 5.0	1700	14 BUCHNER	72	DBC	0 4.6 $K^+n \rightarrow K^+ \pi^- p$
55.8 +4.2 -3.4	2934	14 AGUILAR-...	71B	HBC	0 3.9,4.6 $K^-p \rightarrow K^- \pi^+ n$
48.5 ± 2.7	5362	AGUILAR-...	71B	HBC	0 3.9,4.6 $K^-p \rightarrow K^- \pi^+ \pi^- p$
54.0 ± 3.3	4300	14,16 HABER	70	DBC	0 3 $K^-N \rightarrow K^- \pi^+ X$
53.2 ± 2.1	10k	14 DAVIS	69	HBC	0 12 $K^+p \rightarrow K^+ \pi^- \pi^+ p$
44 ± 5.5	1040	14 DAUBER	67B	HBC	0 2.0 $K^-p \rightarrow K^- \pi^+ \pi^- p$
• • • We do not use the following data for averages, fits, limits, etc. • • •					
50.6 ± 0.9	20k	22 AUBERT	07AK	BABR	10.6 $e^+ e^- \rightarrow K^* \pi^0 K^\pm \pi^\mp \gamma$

- 14 Width errors enlarged by us to $4 \times \Gamma/\sqrt{N}$; see note.
- 15 Inclusive reaction. Complicated background and phase-space effects.
- 16 Number of events in peak reevaluated by us.
- 17 K-matrix pole.
- 18 From a partial wave amplitude analysis.
- 19 From a fit in the $K_S^0(800) + K^*(892) + K^*(1410)$ model.
- 20 With mass and width of the $K^*(1410)$ fixed at 1412 MeV and 227 MeV, respectively.
- 21 Fit to $K\pi$ mass spectrum includes a non-resonant scalar component.
- 22 Systematic errors not estimated.

$K^*(892)$ DECAY MODES

Mode	Fraction (Γ_i/Γ)	Confidence level
Γ_1 $K\pi$	~ 100	%
Γ_2 $(K\pi)^\pm$	(99.901 ± 0.009)	%
Γ_3 $(K\pi)^0$	(99.769 ± 0.020)	%
Γ_4 $K_S^0 \gamma$	(2.31 ± 0.20)	$\times 10^{-3}$
Γ_5 $K^\pm \gamma$	(9.9 ± 0.9)	$\times 10^{-4}$
Γ_6 $K\pi\pi$	< 7	$\times 10^{-4}$ 95%

Meson Particle Listings

 $K^*(892)$, $K_1(1270)$

CONSTRAINED FIT INFORMATION

An overall fit to the total width and a partial width uses 13 measurements and one constraint to determine 3 parameters. The overall fit has a $\chi^2 = 7.8$ for 11 degrees of freedom.

The following *off-diagonal* array elements are the correlation coefficients $\langle \delta p_i \delta p_j \rangle / (\delta p_i \delta p_j)$, in percent, from the fit to parameters p_i , including the branching fractions, $x_i \equiv \Gamma_i / \Gamma_{\text{total}}$. The fit constrains the x_i whose labels appear in this array to sum to one.

$$\Gamma \begin{array}{|c|} \hline -100 \\ \hline 19 \quad -19 \\ \hline x_2 \quad x_5 \\ \hline \end{array}$$

Mode	Rate (MeV)
Γ_2 ($K\pi$) $^\pm$	50.7 \pm 0.9
Γ_5 $K^\pm \gamma$	0.050 \pm 0.005

CONSTRAINED FIT INFORMATION

An overall fit to the total width and a partial width uses 20 measurements and one constraint to determine 3 parameters. The overall fit has a $\chi^2 = 22.6$ for 18 degrees of freedom.

The following *off-diagonal* array elements are the correlation coefficients $\langle \delta p_i \delta p_j \rangle / (\delta p_i \delta p_j)$, in percent, from the fit to parameters p_i , including the branching fractions, $x_i \equiv \Gamma_i / \Gamma_{\text{total}}$. The fit constrains the x_i whose labels appear in this array to sum to one.

$$\Gamma \begin{array}{|c|} \hline -100 \\ \hline 14 \quad -14 \\ \hline x_3 \quad x_4 \\ \hline \end{array}$$

Mode	Rate (MeV)	Scale factor
Γ_3 ($K\pi$) 0	50.2 \pm 0.6	1.1
Γ_4 $K^0 \gamma$	0.117 \pm 0.010	

 $K^*(892)$ PARTIAL WIDTHS

$\Gamma(K^0 \gamma)$	Γ_4			
VALUE (keV)	DOCUMENT ID	TECN	CHG	COMMENT
116 \pm 10 OUR FIT				
116.5 \pm 9.9	584	CARLSMITH	86	SPEC 0 $K_L^0 A \rightarrow K_S^0 \pi^0 A$

$\Gamma(K^\pm \gamma)$	Γ_5			
VALUE (keV)	DOCUMENT ID	TECN	CHG	COMMENT
50 \pm 5 OUR FIT				
50 \pm 5 OUR AVERAGE				
48 \pm 11	BERG	83	SPEC -	156 $K^- A \rightarrow \bar{K} \pi A$
51 \pm 5	CHANDLEE	83	SPEC +	200 $K^+ A \rightarrow K \pi A$

 $K^*(892)$ BRANCHING RATIOS

$\Gamma(K^0 \gamma) / \Gamma_{\text{total}}$	Γ_4 / Γ			
VALUE (units 10^{-3})	DOCUMENT ID	TECN	CHG	COMMENT
2.31 \pm 0.20 OUR FIT				
••• We do not use the following data for averages, fits, limits, etc. •••				
1.5 \pm 0.7	CARITHERS	75B	CNTR 0	8-16 $\bar{K}^0 A$

$\Gamma(K^\pm \gamma) / \Gamma_{\text{total}}$	Γ_5 / Γ			
VALUE (units 10^{-3})	DOCUMENT ID	TECN	CHG	COMMENT
0.99 \pm 0.09 OUR FIT				
••• We do not use the following data for averages, fits, limits, etc. •••				
<1.6	95	BEMPORAD	73	CNTR + 10-16 $K^+ A$

$\Gamma(K\pi\pi) / \Gamma((K\pi)^\pm)$	Γ_6 / Γ_2			
VALUE	DOCUMENT ID	TECN	CHG	COMMENT
< 7 $\times 10^{-4}$	95	JONGEJANS	78	HBC 4 $K^- p \rightarrow p \bar{K}^0 \pi$
••• We do not use the following data for averages, fits, limits, etc. •••				
<20 $\times 10^{-4}$		WOJCICKI	64	HBC - 1.7 $K^- p \rightarrow \bar{K}^0 \pi^- p$

 $K^*(892)$ REFERENCES

AUBERT	07AK	PR D76 012008	B. Aubert et al.	(BABAR Collab.)
EPIFANOV	07	PL B654 65	D. Epifanov et al.	(BELLE Collab.)
LINK	05I	PL B621 72	J.M. Link et al.	(FNAL FOCUS Collab.)
BONVICINI	02	PRL 88 111803	G. Bonvicini et al.	(CLEO Collab.)
PDG	00	EPJ C15 1	D.E. Groom et al.	
ABELE	99D	PL B468 178	A. Abele et al.	(Crystal Barrel Collab.)
BARATE	99R	EPJ C11 599	R. Barate et al.	(ALEPH Collab.)
BARBERIS	98E	PL B436 204	D. Barberis et al.	(Omega Expt.)
BIRD	89	SLAC-332	P.F. Bird	(SLAC)
ASTON	88	NP B296 493	D. Aston et al.	(SLAC, NAGO, CINC, INUS)
ATKINSON	86	ZPHY C30 521	M. Atkinson et al.	(BONN, CERN, GLAS+)
CARLSMITH	86	PRL 56 38	D. Carlsmith et al.	(EFI, SACL)
BAUBILLIER	84B	ZPHY C26 37	M. Baubillier et al.	(BIRM, CERN, GLAS+)
NAPIER	84	PL 149B 514	A. Napier et al.	(TUFTS, ARIZ, FNAL, FLOR+)
BARTH	83	NP B223 296	M. Barth et al.	(BRUX, CERN, GENO, MONS+)
BERG	83	Thesis UMI 83-21652	D.M. Berg	(ROCH)
CHANDLEE	83	PRL 51 168	C. Chandlee et al.	(ROCH, FNAL, MINN)
CLELAND	82	NP B208 189	W.E. Cleland et al.	(DURH, GEVA, LAUS+)
DELFOSE	81	NP B183 349	A. Delfosse et al.	(GEVA, LAUS)
TOAFF	81	PR D23 1500	S. Toaff et al.	(ANL, KANS)
AJINENKO	80	ZPHY C5 177	I.V. Ajinenko et al.	(SERP, BRUX, MONS+)
EVANGELIS...	80	NP B165 383	C. Evangelista et al.	(BARI, BONN, CERN+)
AGUILAR...	78B	NP B341 101	M. Aguilar-Benitez et al.	(MADR, TATA+)
BALAND	78	NP B340 220	J.F. Baland et al.	(MONS, BELG, CERN+)
COOPER	78	NP B136 365	A.M. Cooper et al.	(TATA, CERN, CDEF+)
JONGEJANS	78	NP B139 383	B. Jongejans et al.	(ZEEM, CERN, NIUM+)
WICKLUND	78	PR D17 1197	A.B. Wicklund et al.	(ANL)
BOWLER	77	NP B126 31	M.G. Bowler et al.	(OXF)
CARITHERS	75B	PRL 35 349	W.C.J. Carithers et al.	(ROCH, MCGI)
MCCUBBIN	75	NP B86 13	N.A. McCubbin, L. Lyons	(OXF)
PALER	75	NP B96 1	K. Paler et al.	(RHEL, SACL, EPOL)
FOX	74	NP B80 403	G.C. Fox, M.L. Griss	(CIT)
MATISON	74	PR D9 1872	M.J. Matison et al.	(LBL)
BEMPORAD	73	NP B51 1	C. Bemporad et al.	(CERN, ETH, LOIC)
CLARK	73	NP B54 432	A.C. Clark, L. Lyons, D. Radojicic	(OXF)
LEWIS	73	NP B60 283	P.H. Lewis et al.	(LOWC, LOIC, CDEF)
LINGLIN	73	NP B55 408	D. Linglin et al.	(CERN)
BUCHNER	72	NP B45 333	K. Buchner et al.	(MPIM, CERN, BRUX)
AGUILAR...	71B	PR D4 2583	M. Aguilar-Benitez, R.L. Eisner, J.B. Kinson	(BNL)
HABER	70	NP B17 289	B. Haber et al.	(REHO, SACL, BGNA, EPOL)
CRENNELL	69D	PRL 22 487	D.J. Crennell et al.	(BNL)
DAVIS	69	PRL 23 1071	P.J. Davis et al.	(LRL)
SCHWEING...	68	PR 166 1317	F. Schweingruber et al.	(ANL, NWES)
BARASH	67B	PR 156 1399	N. Barash et al.	(COLU)
BARLOW	67	NC 50A 701	J. Barlow et al.	(CERN, CDEF, IRAD, LIPP)
DAUBER	67B	PR 153 1403	P.M. Dauber et al.	(UCLA)
DEBAERE	67B	NC 51A 401	W. de Baere et al.	(BRUX, CERN)
WOJCICKI	64	PR 135 B484	S.G. Wojcicki	(LRL)

OTHER RELATED PAPERS

ABLIKIM	05Q	PR D72 092002	M. Ablikim et al.	(BES Collab.)
BENAYOUN	99B	PR D59 114027	M. Benayoun et al.	
KAMAL	92	PL B284 421	A.N. Kamal, Q.P. Xu	(ALBE)
NAPIER	84	PL 149B 514	A. Napier et al.	(TUFTS, ARIZ, FNAL, FLOR+)
CLELAND	82	NP B208 189	W.E. Cleland et al.	(DURH, GEVA, LAUS+)
ALEXANDER	82	PRL 8 447	G. Alexander et al.	(LRL)
ALSTON	61	PRL 6 300	M.H. Alston et al.	(LRL)

 $K_1(1270)$

$$J(P) = \frac{1}{2}(1^+)$$

 $K_1(1270)$ MASS

VALUE (MeV)	DOCUMENT ID
1272 \pm 7 OUR AVERAGE	Includes data from the 2 datablocks that follow this one.

PRODUCED BY K^- , BACKWARD SCATTERING, HYPERON EXCHANGE

VALUE (MeV)	EVTS	DOCUMENT ID	TECN	CHG	COMMENT
1275 \pm 10	700	GAVILLET	78	HBC +	4.2 $K^- p \rightarrow \Xi^- (K\pi\pi)^+$

1275 \pm 10	700	GAVILLET	78	HBC +	4.2 $K^- p \rightarrow \Xi^- (K\pi\pi)^+$
---------------------------------	-----	----------	----	-------	---

PRODUCED BY K BEAMS

VALUE (MeV)	DOCUMENT ID	TECN	CHG	COMMENT
1270 \pm 10	¹ DAUM	81C	CNTR -	63 $K^- p \rightarrow K^- 2\pi p$
••• We do not use the following data for averages, fits, limits, etc. •••				
~1276	² TORNQVIST	82B	RVUE	
~1300	VERGEEST	79	HBC -	4.2 $K^- p \rightarrow (\bar{K}\pi\pi)^- p$
1289 \pm 25	³ CARNEGIE	77	ASPK \pm	13 $K^\pm p \rightarrow (K\pi\pi)^\pm p$
~1300	BRANDENB...	76	ASPK \pm	13 $K^\pm p \rightarrow (K\pi\pi)^\pm p$
~1270	OTTER	76	HBC -	10,14,16 $K^- p \rightarrow (\bar{K}\pi\pi)^- p$
1260	DAVIS	72	HBC +	12 $K^+ p$
1234 \pm 12	FIRESTONE	72B	DBC +	12 $K^+ d$

¹ Well described in the chiral unitary approach of GENG 07 with two poles at 1195 and 1284 MeV and widths of 246 and 146 MeV, respectively.

² From a unitarized quark-model calculation.

³ From a model-dependent fit with Gaussian background to BRANDENBURG 76 data.

PRODUCED BY BEAMS OTHER THAN K MESONS

VALUE (MeV)	EVTS	DOCUMENT ID	TECN	CHG	COMMENT
1279 \pm 10	25k	⁴ ABLIKIM	06c	BES2	$J/\psi \rightarrow \bar{K}^*(892)^0 K^+ \pi^-$
1294 \pm 10	310	RODEBACK	81	HBC	4 $\pi^- p \rightarrow \Lambda K 2\pi$
1300	40	CRENNELL	72	HBC 0	4.5 $\pi^- p \rightarrow \Lambda K 2\pi$
1242 \pm ⁹ ₁₀		⁵ ASTIER	69	HBC 0	$\bar{p} p$
1300	45	CRENNELL	67	HBC 0	6 $\pi^- p \rightarrow \Lambda K 2\pi$

See key on page 373

Meson Particle Listings

 $K_1(1270)$ ⁴ Systematic errors not estimated.⁵ This was called the C meson.PRODUCED IN τ LEPTON DECAYS

VALUE (MeV)	EVTS	DOCUMENT ID	TECN	CHG	COMMENT
$1254 \pm 33 \pm 34$	7k	ASNER	00B	CLEO	$\tau^- \rightarrow K^- \pi^+ \pi^- \nu_\tau$

 $K_1(1270)$ WIDTH

VALUE (MeV)	DOCUMENT ID
90 ± 20 OUR ESTIMATE	This is only an educated guess; the error given is larger than the error on the average of the published values.
87 ± 7 OUR AVERAGE	Includes data from the 2 datablocks that follow this one.

PRODUCED BY K^- , BACKWARD SCATTERING, HYPERON EXCHANGE

VALUE (MeV)	EVTS	DOCUMENT ID	TECN	CHG	COMMENT
75 ± 15	700	GAVILLET	78	HBC	$4.2 K^- p \rightarrow \Xi^- K \pi \pi$

PRODUCED BY K BEAMS

VALUE (MeV)	DOCUMENT ID	TECN	CHG	COMMENT
90 ± 8	⁶ DAUM 81c CNTR	-		$63 K^- p \rightarrow K^- 2\pi p$
~ 150	VERGEEST 79 HBC	-		$4.2 K^- p \rightarrow (\bar{K} \pi \pi)^- p$
150 ± 71	⁷ CARNEGIE 77 ASPK	\pm		$13 K^\pm p \rightarrow (K \pi \pi)^\pm p$
~ 200	BRANDENB... 76 ASPK	\pm		$13 K^\pm p \rightarrow (K \pi \pi)^\pm p$
120	DAVIS 72 HBC	+		$12 K^+ p$
188 ± 21	FIRESTONE 72B DBC	+		$12 K^+ d$

⁶ Well described in the chiral unitary approach of GENG 07 with two poles at 1195 and 1284 MeV and widths of 246 and 146 MeV, respectively.⁷ From a model-dependent fit with Gaussian background to BRANDENBURG 76 data.

PRODUCED BY BEAMS OTHER THAN K MESONS

VALUE (MeV)	EVTS	DOCUMENT ID	TECN	CHG	COMMENT
131 ± 21	25k	⁸ ABLIKIM 06c BES2			$J/\psi \rightarrow \bar{K}^*(892)^0 K^+ \pi^-$
66 ± 15	310	RODEBACK 81 HBC			$4 \pi^- p \rightarrow \Lambda K 2\pi$
60	40	CRENNELL 72 HBC	0		$4.5 \pi^- p \rightarrow \Lambda K 2\pi$
127^{+7}_{-25}		ASTIER 69 HBC	0		$\bar{p} p$
60	45	CRENNELL 67 HBC	0		$6 \pi^- p \rightarrow \Lambda K 2\pi$

⁸ Systematic errors not estimated.PRODUCED IN τ LEPTON DECAYS

VALUE (MeV)	EVTS	DOCUMENT ID	TECN	CHG	COMMENT
$260^{+90}_{-70} \pm 80$	7k	ASNER	00B	CLEO	$\tau^- \rightarrow K^- \pi^+ \pi^- \nu_\tau$

 $K_1(1270)$ DECAY MODES

Mode	Fraction (Γ_i/Γ)
$\Gamma_1 K \rho$	(42 \pm 6) %
$\Gamma_2 K_0^*(1430) \pi$	(28 \pm 4) %
$\Gamma_3 K^*(892) \pi$	(16 \pm 5) %
$\Gamma_4 K \omega$	(11.0 \pm 2.0) %
$\Gamma_5 K f_0(1370)$	(3.0 \pm 2.0) %
$\Gamma_6 \gamma K^0$	seen

 $K_1(1270)$ PARTIAL WIDTHS

$\Gamma(K \rho)$	Γ_1
VALUE (MeV)	DOCUMENT ID TECN CHG COMMENT
57 ± 5	MAZZUCATO 79 HBC + $4.2 K^- p \rightarrow \Xi^- (K \pi \pi)^+$
75 ± 6	CARNEGIE 77B ASPK \pm $13 K^\pm p \rightarrow (K \pi \pi)^\pm p$
$\Gamma(K_0^*(1430) \pi)$	Γ_2
VALUE (MeV)	DOCUMENT ID TECN CHG COMMENT
26 ± 6	CARNEGIE 77B ASPK \pm $13 K^\pm p \rightarrow (K \pi \pi)^\pm p$
$\Gamma(K^*(892) \pi)$	Γ_3
VALUE (MeV)	DOCUMENT ID TECN CHG COMMENT
14 ± 11	MAZZUCATO 79 HBC + $4.2 K^- p \rightarrow \Xi^- (K \pi \pi)^+$
2 ± 2	CARNEGIE 77B ASPK \pm $13 K^\pm p \rightarrow (K \pi \pi)^\pm p$

 $\Gamma(K \omega)$

VALUE (MeV)	DOCUMENT ID	TECN	CHG	COMMENT
4 ± 4	MAZZUCATO 79 HBC	+		$4.2 K^- p \rightarrow \Xi^- (K \pi \pi)^+$
24 ± 3	CARNEGIE 77B ASPK	\pm		$13 K^\pm p \rightarrow (K \pi \pi)^\pm p$

 $\Gamma(K f_0(1370))$

VALUE (MeV)	DOCUMENT ID	TECN	CHG	COMMENT
22 ± 5	CARNEGIE 77B ASPK	\pm		$13 K^\pm p \rightarrow (K \pi \pi)^\pm p$

 $\Gamma(\gamma K^0)$

VALUE (keV)	DOCUMENT ID	TECN	COMMENT
$73.2 \pm 6.1 \pm 28.3$	ALAVI-HARATI 02B KTEV		$K^+ A \rightarrow K^* + A$

 $K_1(1270)$ BRANCHING RATIOS

$\Gamma(K \rho)/\Gamma_{\text{total}}$	Γ_1/Γ
VALUE	DOCUMENT ID TECN COMMENT
0.42 ± 0.06	⁹ DAUM 81c CNTR $63 K^- p \rightarrow K^- 2\pi p$
< 0.30	RODEBACK 81 HBC $4 \pi^- p \rightarrow \Lambda K 2\pi$

$\Gamma(K_0^*(1430) \pi)/\Gamma_{\text{total}}$	Γ_2/Γ
VALUE	DOCUMENT ID TECN COMMENT
0.28 ± 0.04	⁹ DAUM 81c CNTR $63 K^- p \rightarrow K^- 2\pi p$

$\Gamma(K^*(892) \pi)/\Gamma_{\text{total}}$	Γ_3/Γ
VALUE	DOCUMENT ID TECN COMMENT
0.16 ± 0.05	⁹ DAUM 81c CNTR $63 K^- p \rightarrow K^- 2\pi p$

$\Gamma(K \omega)/\Gamma_{\text{total}}$	Γ_4/Γ
VALUE	DOCUMENT ID TECN COMMENT
0.11 ± 0.02	⁹ DAUM 81c CNTR $63 K^- p \rightarrow K^- 2\pi p$

$\Gamma(K \omega)/\Gamma(K \rho)$	Γ_4/Γ_1
VALUE	CL% DOCUMENT ID TECN COMMENT
< 0.30	95 RODEBACK 81 HBC $4 \pi^- p \rightarrow \Lambda K 2\pi$

$\Gamma(K f_0(1370))/\Gamma_{\text{total}}$	Γ_5/Γ
VALUE	DOCUMENT ID TECN COMMENT
0.03 ± 0.02	⁹ DAUM 81c CNTR $63 K^- p \rightarrow K^- 2\pi p$

D-wave/S-wave RATIO FOR $K_1(1270) \rightarrow K^*(892) \pi$

VALUE	DOCUMENT ID	TECN	COMMENT
1.0 ± 0.7	⁹ DAUM 81c CNTR		$63 K^- p \rightarrow K^- 2\pi p$

⁹ Average from low and high t data. $K_1(1270)$ REFERENCES

GENG 07	PR D75 014017	L.S. Geng <i>et al.</i>	
ABLIKIM 06C	PL B633 681	M. Ablikim <i>et al.</i>	(BES Collab.)
ALAVI-HARATI 02B	PRL 89 072001	A. Alavi-Harati <i>et al.</i>	(FNAL KTeV Collab.)
ASNER 00B	PR D62 072006	D.M. Asner <i>et al.</i>	(CLEO Collab.)
TORNQVIST 82B	NP B203 268	N.A. Tornqvist	(HELS)
DAUM 81C	NP B187 1	C. Daum <i>et al.</i>	(AMST, CERN, CRAC, MPIM+)
RODEBACK 81	ZPHY C9 9	S. Rodeback <i>et al.</i>	(CERN, CDEF, MADR+)
MAZZUCATO 79	NP B156 532	M. Mazzucato <i>et al.</i>	(CERN, ZEEM, NIJM+)
VERGEEST 79	NP B158 265	J.S.M. Vergeest <i>et al.</i>	(NIJM, AMST, CERN+)
GAVILLET 78	PL 76B 517	P. Gavillet <i>et al.</i>	(AMST, CERN, NIJM+)
CARNEGIE 77	NP B127 509	R.K. Carnegie <i>et al.</i>	(SLAC)
CARNEGIE 77B	PL 68B 287	R.K. Carnegie <i>et al.</i>	(SLAC)
BRANDENB... 76	PRL 36 703	G.W. Brandenburg <i>et al.</i>	(SLAC) JP
OTTER 76	NP B106 77	G. Otter <i>et al.</i>	(AACH3, BERL, CERN, LOIC+)
CRENNELL 72	PR D6 1220	D.J. Crennell <i>et al.</i>	(BNL)
DAVIS 72	PR D5 2688	P.J. Davis <i>et al.</i>	(LBL)
FIRESTONE 72B	PR D5 505	A. Firestone <i>et al.</i>	(LBL)
ASTIER 69	NP B10 65	A. Astier <i>et al.</i>	(CDEF, CERN, IPNP, LIVP) IJP
CRENNELL 67	PRL 19 44	D.J. Crennell <i>et al.</i>	(BNL) I

OTHER RELATED PAPERS

AUBERT 07R	PRL 98 211804	B. Aubert <i>et al.</i>	(BABAR Collab.)
ABLIKIM 05Q	PR D72 092002	M. Ablikim <i>et al.</i>	(BES Collab.)
ROCA 05	PR D72 014002	L. Roca <i>et al.</i>	
SUZUKI 93	PR D47 1252	M. Suzuki	(LBL)
BAUBILLIER 82B	NP B202 21	M. Baubillier <i>et al.</i>	(BIRM, CERN, GLAS+)
FERNANDEZ 82	ZPHY C16 95	C. Fernandez <i>et al.</i>	(MADR, CERN, CDEF+)
GAVILLET 82	ZPHY C16 119	P. Gavillet <i>et al.</i>	(CERN, CDEF, PADO+)
SHEN 66	PRL 17 726	B.C. Shen <i>et al.</i>	(LBL)
Albo	Private Comm.	G. Goldhaber	(LRL)
ALMEIDA 65	PL 16 184	S.F. Almeida <i>et al.</i>	(CAVE)
ARMENTEROS 64	PL 9 207	R. Armenteros <i>et al.</i>	(CERN, CDEF)
Albo	PR 145 1095	N. Barash <i>et al.</i>	(COLU)

Meson Particle Listings

 $K_1(1400)$ $K_1(1400)$

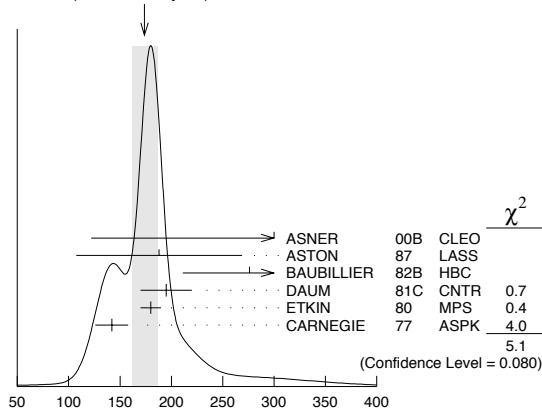
$$I(J^P) = \frac{1}{2}(1^+)$$

 $K_1(1400)$ MASS

VALUE (MeV)	EVTs	DOCUMENT ID	TECN	CHG	COMMENT
1403 ± 7 OUR AVERAGE					
1463 ± 64 ± 68	7k	ASNER	00B	CLEO ±	$\tau^- \rightarrow K^- \pi^+ \pi^- \nu_\tau$
1373 ± 14 ± 18		¹ ASTON	87	LASS 0	$11 K^- p \rightarrow \bar{K}^0 \pi^+ \pi^- n$
1392 ± 18		BAUBILLIER	82B	HBC 0	$8.25 K^- p \rightarrow K_S^0 \pi^+ \pi^- n$
1410 ± 25		DAUM	81C	CNTR -	$63 K^- p \rightarrow K^- 2\pi p$
1415 ± 15		ETKIN	80	MPS 0	$6 K^- p \rightarrow \bar{K}^0 \pi^+ \pi^- n$
1404 ± 10		² CARNEGIE	77	ASPK ±	$13 K^\pm p \rightarrow (K\pi\pi)^\pm p$
• • • We do not use the following data for averages, fits, limits, etc. • • •					
1418 ± 8	25k	³ ABLIKIM	06c	BES2	$J/\psi \rightarrow \bar{K}^*(892)^0 K^+ \pi^-$
~ 1350		⁴ TORNQVIST	82B	RVUE	
~ 1400		VERGEEST	79	HBC -	$4.2 K^- p \rightarrow (\bar{K}\pi\pi)^- p$
~ 1400		BRANDENB...	76	ASPK ±	$13 K^\pm p \rightarrow (K\pi\pi)^\pm p$
1420		DAVIS	72	HBC +	$12 K^+ p$
1368 ± 18		FIRESTONE	72B	DBC +	$12 K^+ d$

¹ From partial-wave analysis of $K^0 \pi^+ \pi^-$ system.² From a model-dependent fit with Gaussian background to BRANDENBURG 76 data.³ Systematic errors not estimated.⁴ From a unitarized quark-model calculation. $K_1(1400)$ WIDTH

VALUE (MeV)	EVTs	DOCUMENT ID	TECN	CHG	COMMENT
174 ± 13 OUR AVERAGE					Error includes scale factor of 1.6. See the ideogram below.
300 ± 370 -110	7k	ASNER	00B	CLEO ±	$\tau^- \rightarrow K^- \pi^+ \pi^- \nu_\tau$
188 ± 54 ± 60		⁵ ASTON	87	LASS 0	$11 K^- p \rightarrow \bar{K}^0 \pi^+ \pi^- n$
276 ± 65		BAUBILLIER	82B	HBC 0	$8.25 K^- p \rightarrow K_S^0 \pi^+ \pi^- n$
195 ± 25		DAUM	81C	CNTR -	$63 K^- p \rightarrow K^- 2\pi p$
180 ± 10		ETKIN	80	MPS 0	$6 K^- p \rightarrow \bar{K}^0 \pi^+ \pi^- n$
142 ± 16		⁶ CARNEGIE	77	ASPK ±	$13 K^\pm p \rightarrow (K\pi\pi)^\pm p$
• • • We do not use the following data for averages, fits, limits, etc. • • •					
152 ± 16	25k	⁷ ABLIKIM	06c	BES2	$J/\psi \rightarrow \bar{K}^*(892)^0 K^+ \pi^-$
~ 200		VERGEEST	79	HBC -	$4.2 K^- p \rightarrow (\bar{K}\pi\pi)^- p$
~ 160		BRANDENB...	76	ASPK ±	$13 K^\pm p \rightarrow (K\pi\pi)^\pm p$
80		DAVIS	72	HBC +	$12 K^+ p$
241 ± 30		FIRESTONE	72B	DBC +	$12 K^+ d$

⁵ From partial-wave analysis of $K^0 \pi^+ \pi^-$ system.⁶ From a model-dependent fit with Gaussian background to BRANDENBURG 76 data.⁷ Systematic errors not estimated.WEIGHTED AVERAGE
174±13 (Error scaled by 1.6) $K_1(1400)$ width (MeV) $K_1(1400)$ DECAY MODES

Mode	Fraction (Γ_i/Γ)
Γ_1 $K^*(892)\pi$	(94 ± 6) %
Γ_2 $K\rho$	(3.0 ± 3.0) %
Γ_3 $K f_0(1370)$	(2.0 ± 2.0) %
Γ_4 $K\omega$	(1.0 ± 1.0) %
Γ_5 $K_0^*(1430)\pi$	not seen
Γ_6 γK^0	seen

 $K_1(1400)$ PARTIAL WIDTHS

$\Gamma(K^*(892)\pi)$	DOCUMENT ID	TECN	CHG	COMMENT	Γ_1
VALUE (MeV)					
117 ± 10	CARNEGIE	77	ASPK ±	$13 K^\pm p \rightarrow (K\pi\pi)^\pm p$	
$\Gamma(K\rho)$	DOCUMENT ID	TECN	CHG	COMMENT	Γ_2
VALUE (MeV)					
2 ± 1	CARNEGIE	77	ASPK ±	$13 K^\pm p \rightarrow (K\pi\pi)^\pm p$	
$\Gamma(K\omega)$	DOCUMENT ID	TECN	CHG	COMMENT	Γ_4
VALUE (MeV)					
23 ± 12	CARNEGIE	77	ASPK ±	$13 K^\pm p \rightarrow (K\pi\pi)^\pm p$	
$\Gamma(\gamma K^0)$	DOCUMENT ID	TECN	COMMENT	Γ_6	
VALUE (MeV)					
280.8 ± 23.2 ± 40.4	ALAVI-HARATI02B	KTEV	$K^+ A \rightarrow K^* + A$		

 $K_1(1400)$ BRANCHING RATIOS

$\Gamma(K^*(892)\pi)/\Gamma_{\text{total}}$	DOCUMENT ID	TECN	COMMENT	Γ_1/Γ
VALUE				
0.94 ± 0.06	⁸ DAUM	81c	CNTR $63 K^- p \rightarrow K^- 2\pi p$	
$\Gamma(K\rho)/\Gamma_{\text{total}}$	DOCUMENT ID	TECN	COMMENT	Γ_2/Γ
VALUE				
0.03 ± 0.03	⁸ DAUM	81c	CNTR $63 K^- p \rightarrow K^- 2\pi p$	
$\Gamma(K f_0(1370))/\Gamma_{\text{total}}$	DOCUMENT ID	TECN	COMMENT	Γ_3/Γ
VALUE				
0.02 ± 0.02	⁸ DAUM	81c	CNTR $63 K^- p \rightarrow K^- 2\pi p$	
$\Gamma(K\omega)/\Gamma_{\text{total}}$	DOCUMENT ID	TECN	COMMENT	Γ_4/Γ
VALUE				
0.01 ± 0.01	⁸ DAUM	81c	CNTR $63 K^- p \rightarrow K^- 2\pi p$	
$\Gamma(K_0^*(1430)\pi)/\Gamma_{\text{total}}$	DOCUMENT ID	TECN	COMMENT	Γ_5/Γ
VALUE				
not seen	⁸ DAUM	81c	CNTR $63 K^- p \rightarrow K^- 2\pi p$	

D-wave/S-wave RATIO FOR $K_1(1400) \rightarrow K^*(892)\pi$

VALUE	DOCUMENT ID	TECN	COMMENT
0.04 ± 0.01	⁸ DAUM	81c	CNTR $63 K^- p \rightarrow K^- 2\pi p$

⁸ Average from low and high t data. $K_1(1400)$ REFERENCES

ABLIKIM	06c	PL B633 681	M. Ablikim <i>et al.</i>	(BES Collab.)
ALAVI-HARATI	02B	PRL 89 072001	A. Alavi-Harati <i>et al.</i>	(FNAL KTeV Collab.)
ASNER	00B	PR D62 072006	D.M. Asner <i>et al.</i>	(CLEO Collab.)
ASTON	87	NP B292 693	D. Aston <i>et al.</i>	(SLAC, NAGO, CINC, INUS)
BAUBILLIER	82B	NP B202 21	M. Baubillier <i>et al.</i>	(BIRM, CERN, GLAS+)
TORNQVIST	82B	NP B203 268	M.A. Torngvist	(HELS)
DAUM	81C	NP B187 1	C. Daum <i>et al.</i>	(AMST, CERN, CRA, MPIM+)
ETKIN	80	PR D22 42	A. Etkin <i>et al.</i>	(BNL, CUNY) JP
VERGEEST	79	NP B158 265	J.S.M. Vergeest <i>et al.</i>	(NIJ, AMST, CERN+)
CARNEGIE	77	NP B127 509	R.K. Carnegie <i>et al.</i>	(SLAC)
BRANDENB...	76	PRL 36 703	G.W. Brandenburg <i>et al.</i>	(SLAC) JP
DAVIS	72	PR D5 2688	P.J. Davis <i>et al.</i>	(LBL)
FIRESTONE	72B	PR D5 505	A. Firestone <i>et al.</i>	(LBL)

OTHER RELATED PAPERS

ABLIKIM	05Q	PR D72 092002	M. Ablikim <i>et al.</i>	(BES Collab.)
SUZUKI	93	PR D47 1252	M. Suzuki	(LBL)
FERNANDEZ	82	ZPHY C16 95	C. Fernandez <i>et al.</i>	(MADR, CERN, CDEF+)
SHEN	66	PRL 17 726	B.C. Shen <i>et al.</i>	(LRL)
Also		Private Comm.	G. Goldhaber	(LRL)
ALMEIDA	65	PL 16 184	S.P. Almeida <i>et al.</i>	(CAVE)
ARMENTEROS	64	PL 9 207	R. Armenteros <i>et al.</i>	(CERN, CDEF)
Also		PR 145 1095	N. Barash <i>et al.</i>	(COLU)

$K^*(1410)$, $K_0^*(1430)$ $K^*(1410)$

$$I(J^P) = \frac{1}{2}(1^-)$$

 $K^*(1410)$ MASS

VALUE (MeV)	DOCUMENT ID	TECN	CHG	COMMENT
1414 ± 15 OUR AVERAGE	Error includes scale factor of 1.3.			
1380 ± 21 ± 19	ASTON	88	LASS	0 11 $K^- p \rightarrow K^- \pi^+ n$
1420 ± 7 ± 10	ASTON	87	LASS	0 11 $K^- p \rightarrow \bar{K}^0 \pi^+ \pi^- n$
• • • We do not use the following data for averages, fits, limits, etc. • • •				
1367 ± 54	BIRD	89	LASS	- 11 $K^- p \rightarrow \bar{K}^0 \pi^- p$
1474 ± 25	BAUBILLIER	82B	HBC	0 8.25 $K^- p \rightarrow \bar{K}^0 2\pi n$
1500 ± 30	ETKIN	80	MPS	0 6 $K^- p \rightarrow \bar{K}^0 \pi^+ \pi^- n$

 $K^*(1410)$ WIDTH

VALUE (MeV)	DOCUMENT ID	TECN	CHG	COMMENT
232 ± 21 OUR AVERAGE	Error includes scale factor of 1.1.			
176 ± 52 ± 22	ASTON	88	LASS	0 11 $K^- p \rightarrow K^- \pi^+ n$
240 ± 18 ± 12	ASTON	87	LASS	0 11 $K^- p \rightarrow \bar{K}^0 \pi^+ \pi^- n$
• • • We do not use the following data for averages, fits, limits, etc. • • •				
114 ± 101	BIRD	89	LASS	- 11 $K^- p \rightarrow \bar{K}^0 \pi^- p$
275 ± 65	BAUBILLIER	82B	HBC	0 8.25 $K^- p \rightarrow \bar{K}^0 2\pi n$
500 ± 100	ETKIN	80	MPS	0 6 $K^- p \rightarrow \bar{K}^0 \pi^+ \pi^- n$

 $K^*(1410)$ DECAY MODES

Mode	Fraction (Γ_j/Γ)	Confidence level
Γ_1 $K^*(892)\pi$	> 40 %	95%
Γ_2 $K\pi$	(6.6 ± 1.3) %	
Γ_3 $K\rho$	< 7 %	95%
Γ_4 γK^0	seen	

 $K^*(1410)$ PARTIAL WIDTHS

VALUE (keV)	CL%	DOCUMENT ID	TECN	COMMENT
<52.9	90	ALAVI-HARATI02B	KTEV	$K + A \rightarrow K^* + A$

 $K^*(1410)$ BRANCHING RATIOS

VALUE	CL%	DOCUMENT ID	TECN	CHG	COMMENT
$\Gamma(K\rho)/\Gamma(K^*(892)\pi)$					Γ_3/Γ_1
<0.17	95	ASTON	84	LASS	0 11 $K^- p \rightarrow \bar{K}^0 2\pi n$

VALUE	CL%	DOCUMENT ID	TECN	CHG	COMMENT
$\Gamma(K\pi)/\Gamma(K^*(892)\pi)$					Γ_2/Γ_1
<0.16	95	ASTON	84	LASS	0 11 $K^- p \rightarrow \bar{K}^0 2\pi n$

VALUE	DOCUMENT ID	TECN	CHG	COMMENT
$\Gamma(K\pi)/\Gamma_{\text{total}}$				Γ_2/Γ
0.066 ± 0.010 ± 0.008	ASTON	88	LASS	0 11 $K^- p \rightarrow K^- \pi^+ n$

 $K^*(1410)$ REFERENCES

ALAVI-HARATI 02B	PRL 89 072001	A. Alavi-Harati et al.	(FNAL KTeV Collab.)
BIRD	89 SLAC-332	P.F. Bird	(SLAC)
ASTON	88 NP B296 493	D. Aston et al.	(SLAC, NAGO, CINC, INUS)
ASTON	87 NP B292 693	D. Aston et al.	(SLAC, NAGO, CINC, INUS)
ASTON	84 PL 149B 258	D. Aston et al.	(SLAC, CARL, OTTA) JP
BAUBILLIER	82B NP B202 21	M. Baubillier et al.	(BIRM, CERN, GLAS+)
ETKIN	80 PR D22 42	A. Etkin et al.	(BNL, CUNY) JP

OTHER RELATED PAPERS

YANG	07 PR D76 094001	K.-C. Yang
LI	05E MPL A20 2497	D.-M. Li et al.

 $K_0^*(1430)$

$$I(J^P) = \frac{1}{2}(0^+)$$

See our minireview in the 1994 edition and in this edition under the $f_0(600)$.

 $K_0^*(1430)$ MASS

VALUE (MeV)	EVTS	DOCUMENT ID	TECN	CHG	COMMENT
1425 ± 50 OUR ESTIMATE	• • • We do not use the following data for averages, fits, limits, etc. • • •				
~ 1412	1	LINK	07	FOCS	0 $D^+ \rightarrow K^- K^+ \pi^+$
1461.0 ± 4.0 ± 2.1	54k	2	LINK	07B	FOCS $D^+ \rightarrow K^- \pi^+ \pi^+$
1406 ± 29	3	BUGG	06	RVUE	
1435 ± 6	4	ZHOU	06	RVUE	$K\rho \rightarrow K^- \pi^+ n$
1455 ± 20 ± 15		ABLIKIM	05Q	BES2	$\psi(2S) \rightarrow \gamma \pi^+ \pi^- K^+ K^-$
1456 ± 8	5	ZHENG	04	RVUE	$K^- p \rightarrow K^- \pi^+ n$
~ 1419	6	BUGG	03	RVUE	11 $K^- p \rightarrow K^- \pi^+ n$
~ 1440	7	LI	03	RVUE	11 $K^- p \rightarrow K^- \pi^+ n$
1459 ± 9	15k	8	AITALA	02	E791 $D^+ \rightarrow K^- \pi^+ \pi^+$
~ 1440	9	JAMIN	00	RVUE	$K\rho \rightarrow K\rho$
1436 ± 8	10	BARBERIS	98E	OMEG	450 $pp \rightarrow p_f p_s K^+ K^- \pi^+ \pi^-$
1415 ± 25	6	ANISOVICH	97C	RVUE	11 $K^- p \rightarrow K^- \pi^+ n$
~ 1450	11	TORNQVIST	96	RVUE	$\pi\pi \rightarrow \pi\pi, K\bar{K}, K\pi$
1412 ± 6	12	ASTON	88	LASS	0 11 $K^- p \rightarrow K^- \pi^+ n$
~ 1430		BAUBILLIER	84B	HBC	- 8.25 $K^- p \rightarrow \bar{K}^0 \pi^- p$
~ 1425	13,14	ESTABROOKS	78	ASPK	13 $K^\pm p \rightarrow K^\pm \pi^\pm(n, \Delta)$
~ 1450.0		MARTIN	78	SPEC	10 $K^\pm p \rightarrow K_S^0 \pi p$

- From a non-parametric analysis.
- A Breit-Wigner mass and width.
- S-matrix pole. Reanalysis of ASTON 88, AITALA 02, and ABLIKIM 06c including the κ with an s -dependent width and an Adler zero near threshold.
- S-matrix pole. Using ASTON 88 and assuming $K_0^*(800)$, $K_0^*(1950)$.
- Using ASTON 88 and assuming $K_0^*(800)$.
- T-matrix pole. Reanalysis of ASTON 88 data.
- Breit-Wigner fit. Using ASTON 88.
- Assuming a low-mass scalar $K\pi$ resonance, $\kappa(800)$.
- T-matrix pole. Using data from ESTABROOKS 78 and ASTON 88.
- J^P not determined, could be $K_2^*(1430)$.
- T-matrix pole.
- Uses a model for the background, without this background they get a mass 1340 MeV, where the phase shift passes 90°.
- Mass defined by pole position.
- From elastic $K\pi$ partial-wave analysis.

 $K_0^*(1430)$ WIDTH

VALUE (MeV)	EVTS	DOCUMENT ID	TECN	CHG	COMMENT
270 ± 80 OUR ESTIMATE	• • • We do not use the following data for averages, fits, limits, etc. • • •				
~ 500	15	LINK	07	FOCS	0 $D^+ \rightarrow K^- K^+ \pi^+$
177.0 ± 8.0 ± 3.4	54k	16	LINK	07B	FOCS $D^+ \rightarrow K^- \pi^+ \pi^+$
350 ± 40	17	BUGG	06	RVUE	
288 ± 22	18	ZHOU	06	RVUE	$K\rho \rightarrow K^- \pi^+ n$
270 ± 45 ± 30		ABLIKIM	05Q	BES2	$\psi(2S) \rightarrow \gamma \pi^+ \pi^- K^+ K^-$
217 ± 31	19	ZHENG	04	RVUE	$K^- p \rightarrow K^- \pi^+ n$
~ 316	20	BUGG	03	RVUE	11 $K^- p \rightarrow K^- \pi^+ n$
~ 350	21	LI	03	RVUE	11 $K^- p \rightarrow K^- \pi^+ n$
175 ± 17	15k	22	AITALA	02	E791 $D^+ \rightarrow K^- \pi^+ \pi^+$
~ 300	23	JAMIN	00	RVUE	$K\rho \rightarrow K\rho$
196 ± 45	24	BARBERIS	98E	OMEG	450 $pp \rightarrow p_f p_s K^+ K^- \pi^+ \pi^-$
330 ± 50	20	ANISOVICH	97C	RVUE	11 $K^- p \rightarrow K^- \pi^+ n$
~ 320	25	TORNQVIST	96	RVUE	$\pi\pi \rightarrow \pi\pi, K\bar{K}, K\pi$
294 ± 23		ASTON	88	LASS	0 11 $K^- p \rightarrow K^- \pi^+ n$
~ 200		BAUBILLIER	84B	HBC	- 8.25 $K^- p \rightarrow \bar{K}^0 \pi^- p$
200 to 300	26	ESTABROOKS	78	ASPK	13 $K^\pm p \rightarrow K^\pm \pi^\pm(n, \Delta)$

- From a non-parametric analysis.
- A Breit-Wigner mass and width.
- S-matrix pole. Reanalysis of ASTON 88, AITALA 02, and ABLIKIM 06c including the κ with an s -dependent width and an Adler zero near threshold.
- S-matrix pole. Using ASTON 88 and assuming $K_0^*(800)$, $K_0^*(1950)$.
- Using ASTON 88 and assuming $K_0^*(800)$.
- T-matrix pole. Reanalysis of ASTON 88 data.
- Breit-Wigner fit. Using ASTON 88.
- Assuming a low-mass scalar $K\pi$ resonance, $\kappa(800)$.
- T-matrix pole. Using data from ESTABROOKS 78 and ASTON 88.
- J^P not determined, could be $K_2^*(1430)$.
- T-matrix pole.
- From elastic $K\pi$ partial-wave analysis.

Meson Particle Listings

 $K_0^*(1430)$, $K_2^*(1430)$ $K_0^*(1430)$ DECAY MODES

Mode	Fraction (Γ_i/Γ)
Γ_1 $K\pi$	(93±10) %

 $K_0^*(1430)$ BRANCHING RATIOS

$\Gamma(K\pi)/\Gamma_{\text{total}}$	DOCUMENT ID	TECN	CHG	COMMENT	Γ_1/Γ
0.93±0.04±0.09	ASTON	88	LASS	0	11 $K^-p \rightarrow K^-\pi^+n$

 $K_0^*(1430)$ REFERENCES

LINK	07	PL B648 156	J.M. Link et al.	(FNAL FOCUS Collab.)
LINK	07B	PL B653 1	J.M. Link et al.	(FNAL FOCUS Collab.)
ABLIKIM	06C	PL B633 681	M. Ablikim et al.	(BES Collab.)
BUGG	06	PL B632 471	D.V. Bugg	(LOQM)
ZHOU	06	NP A775 212	Z.Y. Zhou, H.Q. Zheng	
ABLIKIM	05Q	PR D72 092002	M. Ablikim et al.	(BES Collab.)
ZHENG	04	NP A733 235	H.Q. Zheng et al.	
BUGG	03	PL B572 1	D.V. Bugg	
LI	03	PR D67 034025	L. Li, B. Zou, G. Li	
AITALA	02	PRL 89 121801	E.M. Aitala et al.	(FNAL E791 Collab.)
JAMIN	00	NP B587 331	M. Jamin et al.	
BARBERIS	96E	PL B436 204	D. Barberis et al.	(Omega Expt.)
ANISOVICH	97C	PL B413 137	A.V. Anisovich, A.V. Sarantsev	
TORNQVIST	96	PRL 76 1575	N.A. Tornqvist, M. Roos	(HELS)
ASTON	88	NP B296 493	D. Aston et al.	(SLAC, NAGO, CINC, INUS)
BAUBILLIER	84B	ZPHY C26 37	M. Baubillier et al.	(BIRM, CERN, GLAS+)
ESTABROOKS	78	NP B133 490	P.G. Estabrooks et al.	(MCGI, CARL, DURH+)
MARTIN	78	NP B134 392	A.D. Martin et al.	(DURH, GEVA)

OTHER RELATED PAPERS

MCNEILE	06	PR D74 014508	C. McNeile, C. Michael	
YANG	06	MPL A21 1625	M.Z. Yang	
AUBERT,B	05N	PR D72 072003	B. Aubert et al.	(BABAR Collab.)
BUGG	05A	EPJ A25 107	D.V. Bugg	(LOQM)
Also		EPJ A26 151 (erratum)	D.V. Bugg	(LOQM)
BUGG	05B	EPJ A26 151 (erratum)	D.V. Bugg	(LOQM)
AUBERT,B	04O	PR D70 091103R	B. Aubert et al.	(BABAR Collab.)
AUBERT,B	04P	PR D70 092001	B. Aubert et al.	(BABAR Collab.)
SHAKIN	00	PR D62 114014	C.M. Shakin, H. Wang	
OLLER	99	PR D60 099906 (erratum)	J.A. Oller et al.	
OLLER	99C	PR D60 074023	J.A. Oller, E. Oset	
VANBEVEREN	99	EPJ C10 469	E. van Beveren, G. Rupp	
TORNQVIST	82	PRL 49 624	N.A. Tornqvist	(HELS)
GOLDBERG	69	PL 30B 434	J. Goldberg et al.	(SABRE Collab.)
TRIPPE	68	PL 28B 203	T.G. Trippie et al.	(UCLA)

 $K_2^*(1430)$

$$J(P) = \frac{1}{2}(2^+)$$

We consider that phase-shift analyses provide more reliable determinations of the mass and width.

 $K_2^*(1430)$ MASSCHARGED ONLY, WITH FINAL STATE $K\pi$

VALUE (MeV)	EVTS	DOCUMENT ID	TECN	CHG	COMMENT
1425.6±1.5 OUR AVERAGE					Error includes scale factor of 1.1.
1420 ± 4	1587	BAUBILLIER	84B	HBC	- 8.25 $K^-p \rightarrow \bar{K}^0\pi^-p$
1436 ± 5.5	400	^{1,2} CLELAND	82	SPEC	+ 30 $K^+p \rightarrow K_S^0\pi^+p$
1430 ± 3.2	1500	^{1,2} CLELAND	82	SPEC	+ 50 $K^+p \rightarrow K_S^0\pi^+p$
1430 ± 3.2	1200	^{1,2} CLELAND	82	SPEC	- 50 $K^+p \rightarrow K_S^0\pi^-p$
1423 ± 5	935	TOAFF	81	HBC	- 6.5 $K^-p \rightarrow \bar{K}^0\pi^-p$
1428.0±4.6		³ MARTIN	78	SPEC	+ 10 $K^\pm p \rightarrow K_S^0\pi p$
1423.8±4.6		³ MARTIN	78	SPEC	- 10 $K^\pm p \rightarrow K_S^0\pi p$
1420.0±3.1	1400	AGUILAR-...	71B	HBC	- 3.9,4.6 K^-p
1425 ± 8.0	225	^{1,2} BARNHAM	71C	HBC	+ $K^+p \rightarrow K^0\pi^+p$
1416 ± 10	220	CRENNELL	69D	DBC	- 3.9 $K^-N \rightarrow \bar{K}^0\pi^-N$
1414 ± 13.0	60	¹ LIND	69	HBC	+ 9 $K^+p \rightarrow K^0\pi^+p$
1427 ± 12	63	¹ SCHWEING...	68	HBC	- 4.5 $K^-p \rightarrow \bar{K}\pi N$
1423 ± 11.0	39	¹ BASSANO	67	HBC	- 5.6-5.0 $K^-p \rightarrow \bar{K}^0\pi^-p$

••• We do not use the following data for averages, fits, limits, etc. •••

1423.4±2±3	24809±820	⁴ BIRD	89	LASS	- 11 $K^-p \rightarrow \bar{K}^0\pi^-p$
------------	-----------	-------------------	----	------	---

NEUTRAL ONLY

VALUE (MeV)	EVTS	DOCUMENT ID	TECN	COMMENT
1432.4±1.3 OUR AVERAGE				
1431.2±1.8±0.7		⁵ ASTON	88	LASS 11 $K^-p \rightarrow K^-\pi^+n$
1434 ± 4 ± 6		⁵ ASTON	87	LASS 11 $K^-p \rightarrow \bar{K}^0\pi^+\pi^-n$
1433 ± 6 ± 10		⁵ ASTON	84B	LASS 11 $K^-p \rightarrow \bar{K}^02\pi n$
1471 ± 12		⁵ BAUBILLIER	82B	HBC 8.25 $K^-p \rightarrow NK_S^0\pi\pi$
1428 ± 3		⁵ ASTON	81C	LASS 11 $K^-p \rightarrow K^-\pi^+n$
1434 ± 2		⁵ ESTABROOKS	78	ASPK 13 $K^\pm p \rightarrow pK\pi$
1440 ± 10		⁵ BOWLER	77	DBC 5.5 $K^+d \rightarrow K\pi pp$

••• We do not use the following data for averages, fits, limits, etc. •••

1428.5±3.9	1786±127	⁶ AUBERT	07AK	BABR	10.6 $e^+e^- \rightarrow K^{*0}K^\pm\pi^\mp\gamma$
1420 ± 7	300	HENDRICK	76	DBC	8.25 $K^+N \rightarrow K^+\pi N$
1421.6±4.2	800	MCCUBBIN	75	HBC	3.6 $K^-p \rightarrow K^-\pi^+n$
1420.1±4.3		⁷ LINGLIN	73	HBC	2-13 $K^+p \rightarrow K^+\pi^-X$
1419.1±3.7	1800	AGUILAR-...	71B	HBC	3.9,4.6 K^-p
1416 ± 6	600	CORDS	71	DBC	9 $K^+n \rightarrow K^+\pi^-p$
1421.1±2.6	2200	DAVIS	69	HBC	12 $K^+p \rightarrow K^+\pi^-X$

¹ Errors enlarged by us to Γ/\sqrt{N} ; see the note with the $K^*(892)$ mass.

² Number of events in peak re-evaluated by us.

³ Systematic error added by us.

⁴ From a partial wave amplitude analysis.

⁵ From phase shift or partial-wave analysis.

⁶ Systematic errors not estimated.

⁷ From pole extrapolation, using world K^+p data summary tape.

 $K_2^*(1430)$ WIDTHCHARGED ONLY, WITH FINAL STATE $K\pi$

VALUE (MeV)	EVTS	DOCUMENT ID	TECN	CHG	COMMENT
98.5±2.7 OUR FIT					Error includes scale factor of 1.1.
98.5±2.9 OUR AVERAGE					Error includes scale factor of 1.1.
109 ± 22	400	^{8,9} CLELAND	82	SPEC	+ 30 $K^+p \rightarrow K_S^0\pi^+p$
124 ± 12.8	1500	^{8,9} CLELAND	82	SPEC	+ 50 $K^+p \rightarrow K_S^0\pi^+p$
113 ± 12.8	1200	^{8,9} CLELAND	82	SPEC	- 50 $K^+p \rightarrow K_S^0\pi^-p$
85 ± 16	935	TOAFF	81	HBC	- 6.5 $K^-p \rightarrow \bar{K}^0\pi^-p$
96.5±3.8		MARTIN	78	SPEC	+ 10 $K^\pm p \rightarrow K_S^0\pi p$
97.7±4.0		MARTIN	78	SPEC	- 10 $K^\pm p \rightarrow K_S^0\pi p$
94.7±15.1-12.5	1400	AGUILAR-...	71B	HBC	- 3.9,4.6 K^-p

••• We do not use the following data for averages, fits, limits, etc. •••

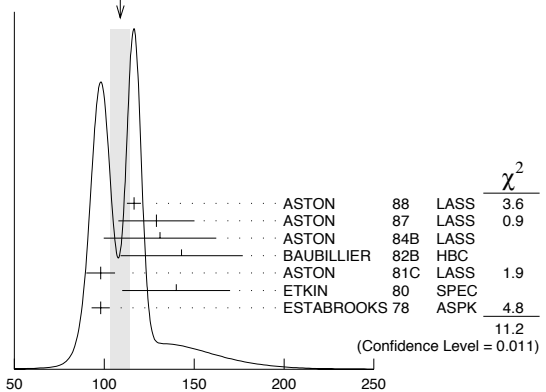
98 ± 4 ± 4	24809±820	¹⁰ BIRD	89	LASS	- 11 $K^-p \rightarrow \bar{K}^0\pi^-p$
------------	-----------	--------------------	----	------	---

NEUTRAL ONLY

VALUE (MeV)	EVTS	DOCUMENT ID	TECN	COMMENT
109 ± 5 OUR AVERAGE				Error includes scale factor of 1.9. See the ideogram below.
116.5±3.6±1.7		¹¹ ASTON	88	LASS 11 $K^-p \rightarrow K^-\pi^+n$
129 ± 15 ± 15		¹¹ ASTON	87	LASS 11 $K^-p \rightarrow \bar{K}^0\pi^+\pi^-n$
131 ± 24 ± 20		¹¹ ASTON	84B	LASS 11 $K^-p \rightarrow \bar{K}^02\pi n$
143 ± 34		¹¹ BAUBILLIER	82B	HBC 8.25 $K^-p \rightarrow NK_S^0\pi\pi$
98 ± 8		¹¹ ASTON	81C	LASS 11 $K^-p \rightarrow K^-\pi^+n$
140 ± 30		¹¹ ETKIN	80	SPEC 6 $K^-p \rightarrow \bar{K}^0\pi^+\pi^-n$
98 ± 5		¹¹ ESTABROOKS	78	ASPK 13 $K^\pm p \rightarrow pK\pi$

••• We do not use the following data for averages, fits, limits, etc. •••

113.7±9.2	1786±127	¹² AUBERT	07AK	BABR	10.6 $e^+e^- \rightarrow K^{*0}K^\pm\pi^\mp\gamma$
125 ± 29	300	⁸ HENDRICK	76	DBC	8.25 $K^+N \rightarrow K^+\pi N$
116 ± 18	800	MCCUBBIN	75	HBC	3.6 $K^-p \rightarrow K^-\pi^+n$
61 ± 14		¹³ LINGLIN	73	HBC	2-13 $K^+p \rightarrow K^+\pi^-X$
116.6±10.3-15.5	1800	AGUILAR-...	71B	HBC	3.9,4.6 K^-p
144 ± 24.0	600	⁸ CORDS	71	DBC	9 $K^+n \rightarrow K^+\pi^-p$
101 ± 10	2200	DAVIS	69	HBC	12 $K^+p \rightarrow K^+\pi^-X$

WEIGHTED AVERAGE
109±5 (Error scaled by 1.9)

⁸ Errors enlarged by us to $4\Gamma/\sqrt{N}$; see the note with the $K^*(892)$ mass.

⁹ Number of events in peak re-evaluated by us.

¹⁰ From a partial wave amplitude analysis.

¹¹ From phase shift or partial-wave analysis.

¹² Systematic errors not estimated.

¹³ From pole extrapolation, using world K^+p data summary tape.

See key on page 373

Meson Particle Listings

$K_2^*(1430)$

$K_2^*(1430)$ DECAY MODES

Mode	Fraction (Γ_i/Γ)	Scale factor/ Confidence level
Γ_1 $K\pi$	$(49.9 \pm 1.2) \%$	
Γ_2 $K^*(892)\pi$	$(24.7 \pm 1.5) \%$	
Γ_3 $K^*(892)\pi\pi$	$(13.4 \pm 2.2) \%$	
Γ_4 $K\rho$	$(8.7 \pm 0.8) \%$	S=1.2
Γ_5 $K\omega$	$(2.9 \pm 0.8) \%$	
Γ_6 $K^+\gamma$	$(2.4 \pm 0.5) \times 10^{-3}$	S=1.1
Γ_7 $K\eta$	$(1.5^{+3.4}_{-1.0}) \times 10^{-3}$	S=1.3
Γ_8 $K\omega\pi$	$< 7.2 \times 10^{-4}$	CL=95%
Γ_9 $K^0\gamma$	$< 9 \times 10^{-4}$	CL=90%

CONSTRAINED FIT INFORMATION

An overall fit to the total width, a partial width, and 10 branching ratios uses 31 measurements and one constraint to determine 8 parameters. The overall fit has a $\chi^2 = 20.2$ for 24 degrees of freedom.

The following off-diagonal array elements are the correlation coefficients $\langle \delta p_i \delta p_j \rangle / (\delta p_i \delta p_j)$, in percent, from the fit to parameters p_i , including the branching fractions, $x_i \equiv \Gamma_i/\Gamma_{\text{total}}$. The fit constrains the x_i whose labels appear in this array to sum to one.

x_2	-9						
x_3	-40	-73					
x_4	-8	36	-52				
x_5	-11	-3	-26	-7			
x_6	-1	-1	-1	-1	0		
x_7	-4	-7	-5	-5	-2	0	
Γ	0	0	0	0	0	-13	0
	x_1	x_2	x_3	x_4	x_5	x_6	x_7

Mode	Rate (MeV)	Scale factor
Γ_1 $K\pi$	49.1 ± 1.8	
Γ_2 $K^*(892)\pi$	24.3 ± 1.6	
Γ_3 $K^*(892)\pi\pi$	13.2 ± 2.2	
Γ_4 $K\rho$	8.5 ± 0.8	1.2
Γ_5 $K\omega$	2.9 ± 0.8	
Γ_6 $K^+\gamma$	0.24 ± 0.05	1.1
Γ_7 $K\eta$	$0.15^{+0.33}_{-0.10}$	1.3

$K_2^*(1430)$ PARTIAL WIDTHS

$\Gamma(K^+\gamma)$		Γ_6			
VALUE (keV)	DOCUMENT ID	TECN	CHG	COMMENT	
241 ± 50 OUR FIT					Error includes scale factor of 1.1.
240 ± 45	CIHANGIR	82	SPEC	+	$200 K^+ Z \rightarrow Z K^+ \pi^0, Z K_S^0 \pi^+$

$\Gamma(K^0\gamma)$		Γ_9			
VALUE (keV)	CL%	DOCUMENT ID	TECN	CHG	COMMENT
< 5.4	90	ALAVI-HARATI02b	KTEV		$K + A \rightarrow K^* + A$
••• We do not use the following data for averages, fits, limits, etc. •••					
< 84	90	CARLSMITH	87	SPEC	0 $60-200 K_L^0 A \rightarrow K_S^0 \pi^0 A$

$K_2^*(1430)$ BRANCHING RATIOS

$\Gamma(K\pi)/\Gamma_{\text{total}}$		Γ_1/Γ			
VALUE	DOCUMENT ID	TECN	CHG	COMMENT	
0.499 ± 0.012 OUR FIT					
0.488 ± 0.014 OUR AVERAGE					
$0.485 \pm 0.006 \pm 0.020$	¹⁴ ASTON	88	LASS	0	$11 K^- p \rightarrow K^- \pi^+ n$
0.49 ± 0.02	¹⁴ ESTABROOKS	78	ASPK	\pm	$13 K^\pm p \rightarrow p K\pi$

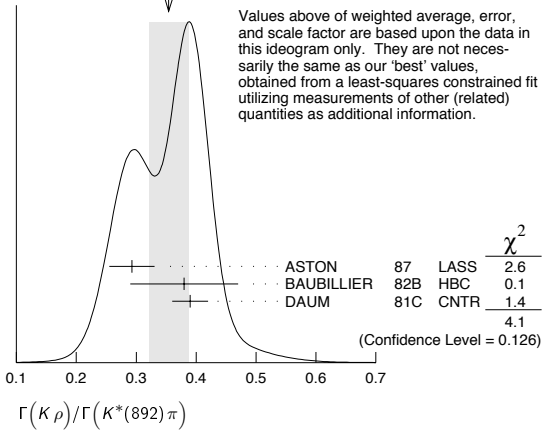
$\Gamma(K^*(892)\pi)/\Gamma(K\pi)$		Γ_2/Γ_1			
VALUE	DOCUMENT ID	TECN	CHG	COMMENT	
0.496 ± 0.034 OUR FIT					
0.47 ± 0.04 OUR AVERAGE					
0.44 ± 0.09	ASTON	84b	LASS	0	$11 K^- p \rightarrow \bar{K}^0 2\pi n$
0.62 ± 0.19	LAUSCHER	75	HBC	0	$10,16 K^- p \rightarrow K^- \pi^+ n$
0.54 ± 0.16	DEHM	74	DBC	0	$4.6 K^+ N$
0.47 ± 0.08	AGUILAR-...	71b	HBC		$3.9, 4.6 K^- p$
0.47 ± 0.10	BASSANO	67	HBC	-0	$4.6, 5.0 K^- p$
0.45 ± 0.13	BADIER	65c	HBC	-	$3 K^- p$

$\Gamma(K\omega)/\Gamma(K\pi)$		Γ_5/Γ_1			
VALUE	DOCUMENT ID	TECN	CHG	COMMENT	
0.059 ± 0.017 OUR FIT					
0.070 ± 0.035 OUR AVERAGE					
0.05 ± 0.04	AGUILAR-...	71b	HBC		$3.9, 4.6 K^- p$
0.13 ± 0.07	BASSOMPIE...	69	HBC	0	$5 K^+ p$

$\Gamma(K\rho)/\Gamma(K\pi)$		Γ_4/Γ_1			
VALUE	DOCUMENT ID	TECN	CHG	COMMENT	
0.174 ± 0.017 OUR FIT					Error includes scale factor of 1.2.
0.150 ± 0.029 OUR AVERAGE					
0.18 ± 0.05	ASTON	84b	LASS	0	$11 K^- p \rightarrow \bar{K}^0 2\pi n$
$0.02^{+0.10}_{-0.02}$	DEHM	74	DBC	0	$4.6 K^+ N$
0.16 ± 0.05	AGUILAR-...	71b	HBC		$3.9, 4.6 K^- p$
0.14 ± 0.10	BASSANO	67	HBC	-0	$4.6, 5.0 K^- p$
0.14 ± 0.07	BADIER	65c	HBC	-	$3 K^- p$

$\Gamma(K\rho)/\Gamma(K^*(892)\pi)$		Γ_4/Γ_2			
VALUE	DOCUMENT ID	TECN	CHG	COMMENT	
0.350 ± 0.031 OUR FIT					Error includes scale factor of 1.4.
0.354 ± 0.033 OUR AVERAGE					Error includes scale factor of 1.4. See the ideogram below.
$0.293 \pm 0.032 \pm 0.020$	ASTON	87	LASS	0	$11 K^- p \rightarrow \bar{K}^0 \pi^+ \pi^- n$
0.38 ± 0.09	BAUBILLIER	82b	HBC	0	$8.25 K^- p \rightarrow N K_S^0 \pi\pi$
0.39 ± 0.03	DAUM	81c	CNTR		$63 K^- p \rightarrow K^- 2\pi p$

WEIGHTED AVERAGE
0.354±0.033 (Error scaled by 1.4)



$\Gamma(K\omega)/\Gamma(K^*(892)\pi)$		Γ_5/Γ_2			
VALUE	DOCUMENT ID	TECN	CHG	COMMENT	
0.118 ± 0.034 OUR FIT					
0.10 ± 0.04	FIELD	67	HBC	-	$3.8 K^- p$

$\Gamma(K\eta)/\Gamma(K^*(892)\pi)$		Γ_7/Γ_2			
VALUE	DOCUMENT ID	TECN	CHG	COMMENT	
0.006 ± 0.014 OUR FIT					Error includes scale factor of 1.2.
0.07 ± 0.04	FIELD	67	HBC	-	$3.8 K^- p$

$\Gamma(K\eta)/\Gamma(K\pi)$		Γ_7/Γ_1			
VALUE	CL%	DOCUMENT ID	TECN	CHG	COMMENT
0.0030 ± 0.0068 OUR FIT					Error includes scale factor of 1.3.
0 ± 0.0056		¹⁵ ASTON	88b	LASS	- $11 K^- p \rightarrow K^- \eta p$
••• We do not use the following data for averages, fits, limits, etc. •••					
< 0.04	95	AGUILAR-...	71b	HBC	$3.9, 4.6 K^- p$
< 0.065		¹⁶ BASSOMPIE...	69	HBC	$5.0 K^+ p$
< 0.02		BISHOP	69	HBC	$3.5 K^+ p$

$\Gamma(K^*(892)\pi\pi)/\Gamma_{\text{total}}$		Γ_3/Γ			
VALUE	DOCUMENT ID	TECN	CHG	COMMENT	
0.134 ± 0.022 OUR FIT					
0.12 ± 0.04	¹⁷ GOLDBERG	76	HBC	-	$3 K^- p \rightarrow p \bar{K}^0 \pi\pi$

$\Gamma(K^*(892)\pi\pi)/\Gamma(K\pi)$		Γ_3/Γ_1			
VALUE	DOCUMENT ID	TECN	CHG	COMMENT	
0.27 ± 0.05 OUR FIT					
0.21 ± 0.08	^{16,17} JONGEJANS	78	HBC	-	$4 K^- p \rightarrow p \bar{K}^0 \pi\pi$

Meson Particle Listings

 $K_2^*(1430)$, $K(1460)$, $K_2(1580)$

$\Gamma(K\omega\pi)/\Gamma_{\text{total}}$ Γ_8/Γ

VALUE (units 10^{-3})	CL%	EVTs	DOCUMENT ID	TECN	COMMENT
<0.72	95	0	JONGEJANS	78	HBC 4 $K^-p \rightarrow p\bar{K}^0 4\pi$

¹⁴ From phase shift analysis.

¹⁵ ASTON 88B quote < 0.0092 at CL=95%. We convert this to a central value and 1 sigma error in order to be able to use it in our constrained fit.

¹⁶ Restated by us.

¹⁷ Assuming $\pi\pi$ system has isospin 1, which is supported by the data.

 $K_2^*(1430)$ REFERENCES

AUBERT	07AK	PR D76 012008	B. Aubert et al.	(BABAR Collab.)
ALAVI-HARATI	02B	PRL 89 072001	A. Alavi-Harati et al.	(FNAL KTeV Collab.)
BIRD	89	SLAC-332	P.F. Bird	(SLAC)
ASTON	88	NP B296 493	D. Aston et al.	(SLAC, NAGO, CINC, INUS)
ASTON	88B	PL B201 169	D. Aston et al.	(SLAC, NAGO, CINC, INUS)
ASTON	87	NP B292 693	D. Aston et al.	(SLAC, NAGO, CINC, INUS)
CARLSMITH	87	PR D36 3502	D. Carlsmith et al.	(EFI, SACL)
ASTON	84B	NP B247 261	D. Aston et al.	(SLAC, CARL, OTTA)
BAUBILLIER	84B	ZPHY C26 37	M. Baubillier et al.	(BIRM, CERN, GLAS+)
BAUBILLIER	82B	NP B202 21	M. Baubillier et al.	(BIRM, CERN, GLAS+)
CHANGIR	82	PL 117B 123	S. Changir et al.	(FNAL, MINN, ROCH)
CLELAND	82	NP B208 189	W.F. Cleland et al.	(DURH, GEVA, LAUS+)
ASTON	81C	PL 106B 235	D. Aston et al.	(SLAC, CARL, OTTA JP)
DAUM	81C	NP B187 1	C. Daum et al.	(AMST, CERN, CRAC, MPIM+)
TOAFF	81	PR D23 1500	S. Toaff et al.	(ANL, KANS)
ETKIN	80	PR D22 42	A. Etkin et al.	(BNL, CUNY) JP
ESTABROOKS	78	NP B133 490	P.G. Estabrooks et al.	(MCGI, CARL, DURH+)
Also		PR D17 658	P.G. Estabrooks et al.	(MCGI, CARL, DURH+)
JONGEJANS	78	NP B139 383	B. Jongejans et al.	(ZEEM, CERN, NIJM+)
MARTIN	78	NP B134 392	A.D. Martin et al.	(DURH, GEVA)
BOWLER	77	NP B126 31	M.G. Bowler et al.	(OXF)
GOLDBERG	76	LNC 17 253	J. Goldberg	(HAIF)
HENDRICK	76	NP B112 189	P. Hendrick et al.	(MONS, SACL, PARIS+)
LAUSCHER	75	NP B86 189	P. Lauscher et al.	(ABCLV Collab.) JP
MCCUBBIN	75	NP B86 13	N.A. McCubbin, L. Lyons	(OXF)
DEHM	74	NP B75 47	G. Dehm et al.	(MPIM, BRUX, MONS, CERN)
LINGLIN	73	NP B55 408	D. Linglin	(CERN)
AGUILAR...	71B	PR D4 2583	M. Aguilar-Benitez, R.L. Eisner, J.B. Kinson	(BNL)
BARNHAM	71C	NP B28 171	K.W.J. Barnham et al.	(BIRM, GLAS)
CORDS	71	PR D4 1974	D. Cords et al.	(PURD, UCD, IUPU)
BASSOMPIE...	69	NP B13 189	G. Bassompierre et al.	(CERN, BRUX) JP
BISHOP	69	NP B9 403	J.M. Bishop et al.	(WISC)
CRENNELL	69D	PRL 22 487	D.L. Crennell et al.	(BNL)
DAVIS	69	PRL 23 1071	P.J. Davis et al.	(LRL)
LIND	69	NP B14 1	V.G. Lind et al.	(LRL) JP
SCHWEING...	68	PR 166 1317	F. Schweingruber et al.	(ANL, NWES)
Also		Thesis	F.L. Schweingruber	(NWES, NWES)
BASSANO	67	PRL 19 968	D. Bassano et al.	(BNL, SYRA)
FIELD	67	PL 24B 638	J.H. Field et al.	(UCSD)
BADIER	65C	PL 19 612	J. Badier et al.	(EPOL, SACL, AMST)

OTHER RELATED PAPERS

ABLIKIM	05Q	PR D72 092002	M. Ablikim et al.	(BES Collab.)
AUBERT.B	04O	PR D70 091103R	B. Aubert et al.	(BABAR Collab.)
AUBERT.B	04P	PR D70 092001	B. Aubert et al.	(BABAR Collab.)
VANBEVEREN	01B	EPJ C22 493	E. van Beveren	
BARBERIS	98E	PL B436 204	D. Barberis et al.	(Omega Expt.)
ATKINSON	86	ZPHY C30 521	M. Atkinson et al.	(BONN, CERN, GLAS+)
BAUBILLIER	82B	NP B202 21	M. Baubillier et al.	(BIRM, CERN, GLAS+)
CHUNG	65	PRL 15 325	S.U. Chung et al.	(LRL)
FOCARDI	65	PL 16 351	S. Focardi et al.	(BGNA, SACL)
HAQUE	65	PL 14 338	N. Haque et al.	
HARDY	65	PRL 14 401	L.M. Hardy et al.	(LRL)

 $K(1460)$

$$I(J^P) = \frac{1}{2}(0^-)$$

OMITTED FROM SUMMARY TABLE

Observed in $K\pi\pi$ partial-wave analysis.

 $K(1460)$ MASS

VALUE (MeV)	DOCUMENT ID	TECN	CHG	COMMENT
-------------	-------------	------	-----	---------

• • • We do not use the following data for averages, fits, limits, etc. • • •

~ 1460	DAUM	81c	CNTR	— 63 $K^-p \rightarrow K^-2\pi p$
~ 1400	¹ BRANDENB...	76B	ASPK ±	13 $K^\pm p \rightarrow K^\pm 2\pi p$

¹ Coupled mainly to $K f_0(1370)$. Decay into $K^*(892)\pi$ seen.

 $K(1460)$ WIDTH

VALUE (MeV)	DOCUMENT ID	TECN	CHG	COMMENT
-------------	-------------	------	-----	---------

• • • We do not use the following data for averages, fits, limits, etc. • • •

~ 260	DAUM	81c	CNTR	— 63 $K^-p \rightarrow K^-2\pi p$
~ 250	² BRANDENB...	76B	ASPK ±	13 $K^\pm p \rightarrow K^\pm 2\pi p$

² Coupled mainly to $K f_0(1370)$. Decay into $K^*(892)\pi$ seen.

 $K(1460)$ DECAY MODES

Mode	Fraction (Γ_i/Γ)
Γ_1 $K^*(892)\pi$	seen
Γ_2 $K\rho$	seen
Γ_3 $K_0^*(1430)\pi$	seen

 $K(1460)$ PARTIAL WIDTHS $\Gamma(K^*(892)\pi)$

VALUE (MeV)	DOCUMENT ID	TECN	COMMENT	Γ_1
• • • We do not use the following data for averages, fits, limits, etc. • • •				
~ 109	DAUM	81c	CNTR 63 $K^-p \rightarrow K^-2\pi p$	

 $\Gamma(K\rho)$

VALUE (MeV)	DOCUMENT ID	TECN	COMMENT	Γ_2
• • • We do not use the following data for averages, fits, limits, etc. • • •				
~ 34	DAUM	81c	CNTR 63 $K^-p \rightarrow K^-2\pi p$	

 $\Gamma(K_0^*(1430)\pi)$

VALUE (MeV)	DOCUMENT ID	TECN	COMMENT	Γ_3
• • • We do not use the following data for averages, fits, limits, etc. • • •				
~ 117	DAUM	81c	CNTR 63 $K^-p \rightarrow K^-2\pi p$	

 $K(1460)$ REFERENCES

DAUM	81C	NP B187 1	C. Daum et al.	(AMST, CERN, CRAC, MPIM+)
BRANDENB...	76B	PRL 36 1239	G.W. Brandenburg et al.	(SLAC) JP

OTHER RELATED PAPERS

ABLIKIM	05Q	PR D72 092002	M. Ablikim et al.	(BES Collab.)
TANIMOTO	82	PL 116B 198	M. Tanimoto	(BIEL)
VERGEEST	79	NP B158 265	J.S.M. Vergeest et al.	(NIJM, AMST, CERN+)

 $K_2(1580)$

$$I(J^P) = \frac{1}{2}(2^-)$$

OMITTED FROM SUMMARY TABLE

Seen in partial-wave analysis of the $K^-\pi^+\pi^-$ system. Needs confirmation.

 $K_2(1580)$ MASS

VALUE (MeV)	DOCUMENT ID	CHG	COMMENT
-------------	-------------	-----	---------

• • • We do not use the following data for averages, fits, limits, etc. • • •

~ 1580	OTTER	79	— 10,14,16 K^-p
--------	-------	----	-------------------

 $K_2(1580)$ WIDTH

VALUE (MeV)	DOCUMENT ID	CHG	COMMENT
-------------	-------------	-----	---------

• • • We do not use the following data for averages, fits, limits, etc. • • •

~ 110	OTTER	79	— 10,14,16 K^-p
-------	-------	----	-------------------

 $K_2(1580)$ DECAY MODES

Mode	Fraction (Γ_i/Γ)
Γ_1 $K^*(892)\pi$	seen
Γ_2 $K_2^*(1430)\pi$	possibly seen

 $K_2(1580)$ BRANCHING RATIOS

$\Gamma(K^*(892)\pi)/\Gamma_{\text{total}}$	Γ_1/Γ			
VALUE	DOCUMENT ID	TECN	CHG	COMMENT
seen	OTTER	79	HBC	— 10,14,16 K^-p

$\Gamma(K_2^*(1430)\pi)/\Gamma_{\text{total}}$	Γ_2/Γ			
VALUE	DOCUMENT ID	TECN	CHG	COMMENT
possibly seen	OTTER	79	HBC	— 10,14,16 K^-p

 $K_2(1580)$ REFERENCES

OTTER	79	NP B147 1	G. Otter et al.	(AACH3, BERL, CERN, LOIC+) JP
-------	----	-----------	-----------------	-------------------------------

See key on page 373

Meson Particle Listings
 $K(1630)$, $K_1(1650)$, $K^*(1680)$ $K(1630)$

$$I(J^P) = \frac{1}{2}(??)$$

OMITTED FROM SUMMARY TABLE

Seen as a narrow peak, compatible with the experimental resolution, in the invariant mass of the $K_S^0 \pi^+ \pi^-$ system produced in $\pi^- p$ interactions at high momentum transfers.

 $K(1630)$ MASS

VALUE (MeV)	EVTS	DOCUMENT ID	TECN	CHG	COMMENT
1629±7	~ 75	KARNAUKHOV98	BC		16.0 $\pi^- p \rightarrow$ ($K_S^0 \pi^+ \pi^-$) $\chi^+ \pi^- \chi^0$

 $K(1630)$ WIDTH

VALUE (MeV)	EVTS	DOCUMENT ID	TECN	CHG	COMMENT
16⁺¹⁹₋₁₆	~ 75	¹ KARNAUKHOV98	BC		16.0 $\pi^- p \rightarrow$ ($K_S^0 \pi^+ \pi^-$) $\chi^+ \pi^- \chi^0$

¹ Compatible with an experimental resolution of 14 ± 1 MeV. $K(1630)$ DECAY MODES

Mode	Fraction (Γ_i/Γ)
Γ_1 $K_S^0 \pi^+ \pi^-$	

 $K(1630)$ REFERENCES

KARNAUKHOV 98 PAN 61 203 V.M. Karnaukhov, C. Coca, V.J. Moroz
Translated from YAF 61 252.

OTHER RELATED PAPERS

KARNAUKHOV 00 PAN 63 588 V.M. Karnaukhov, C. Coca, V.J. Moroz
Translated from YAF 63 652.

 $K_1(1650)$

$$I(J^P) = \frac{1}{2}(1^+)$$

OMITTED FROM SUMMARY TABLE

This entry contains various peaks in strange meson systems ($K^+ \phi$, $K \pi \pi$) reported in partial-wave analysis in the 1600–1900 mass region.

 $K_1(1650)$ MASS

VALUE (MeV)	DOCUMENT ID	TECN	CHG	COMMENT
1650±50	FRAME	86	OMEG +	13 $K^+ p \rightarrow \phi K^+ p$
~ 1840	ARMSTRONG	83	OMEG -	18.5 $K^- p \rightarrow 3 K p$
~ 1800	DAUM	81c	CNTR -	63 $K^- p \rightarrow K^- 2\pi p$

• • • We do not use the following data for averages, fits, limits, etc. • • •

 $K_1(1650)$ WIDTH

VALUE (MeV)	DOCUMENT ID	TECN	CHG	COMMENT
150±50	FRAME	86	OMEG +	13 $K^+ p \rightarrow \phi K^+ p$
~ 250	DAUM	81c	CNTR -	63 $K^- p \rightarrow K^- 2\pi p$

• • • We do not use the following data for averages, fits, limits, etc. • • •

 $K_1(1650)$ DECAY MODES

Mode	Fraction (Γ_i/Γ)
Γ_1 $K \pi \pi$	
Γ_2 $K \phi$	

 $K_1(1650)$ REFERENCES

FRAME 86 NP B276 667 D. Frame et al. (SLAC)
ARMSTRONG 83 NP B221 1 T.A. Armstrong et al. (BARI, BIRM, CERN+)
DAUM 81c NP B187 1 C. Daum et al. (AMST, CERN, CRAC, MPIM+)

 $K^*(1680)$

$$I(J^P) = \frac{1}{2}(1^-)$$

 $K^*(1680)$ MASS

VALUE (MeV)	DOCUMENT ID	TECN	CHG	COMMENT
1717±27 OUR AVERAGE	Error includes scale factor of 1.4.			
1677±10±32	ASTON	88	LASS 0	11 $K^- p \rightarrow K^- \pi^+ n$
1735±10±20	ASTON	87	LASS 0	11 $K^- p \rightarrow \bar{K}^0 \pi^+ \pi^- n$
• • •	We do not use the following data for averages, fits, limits, etc. • • •			
1678±64	BIRD	89	LASS -	11 $K^- p \rightarrow \bar{K}^0 \pi^- p$
1800±70	ETKIN	80	MPS 0	6 $K^- p \rightarrow \bar{K}^0 \pi^+ \pi^- n$
~ 1650	ESTABROOKS 78	ASPK 0		13 $K^\pm p \rightarrow K^\pm \pi^\pm n$

 $K^*(1680)$ WIDTH

VALUE (MeV)	DOCUMENT ID	TECN	CHG	COMMENT
322±110 OUR AVERAGE	Error includes scale factor of 4.2.			
205± 16±34	ASTON	88	LASS 0	11 $K^- p \rightarrow K^- \pi^+ n$
423± 18±30	ASTON	87	LASS 0	11 $K^- p \rightarrow \bar{K}^0 \pi^+ \pi^- n$
• • •	We do not use the following data for averages, fits, limits, etc. • • •			
454±270	BIRD	89	LASS -	11 $K^- p \rightarrow \bar{K}^0 \pi^- p$
170± 30	ETKIN	80	MPS 0	6 $K^- p \rightarrow \bar{K}^0 \pi^+ \pi^- n$
250 to 300	ESTABROOKS 78	ASPK 0		13 $K^\pm p \rightarrow K^\pm \pi^\pm n$

 $K^*(1680)$ DECAY MODES

Mode	Fraction (Γ_i/Γ)
Γ_1 $K \pi$	(38.7±2.5) %
Γ_2 $K \rho$	(31.4 ^{+4.7} _{-2.1}) %
Γ_3 $K^*(892)\pi$	(29.9 ^{+2.2} _{-4.7}) %

CONSTRAINED FIT INFORMATION

An overall fit to 4 branching ratios uses 4 measurements and one constraint to determine 3 parameters. The overall fit has a $\chi^2 = 2.9$ for 2 degrees of freedom.

The following *off-diagonal* array elements are the correlation coefficients $\langle \delta x_i \delta x_j \rangle / (\delta x_i \delta x_j)$, in percent, from the fit to the branching fractions, $x_i \equiv \Gamma_i/\Gamma_{\text{total}}$. The fit constrains the x_i whose labels appear in this array to sum to one.

$$\begin{array}{cc|cc} x_2 & & -36 & \\ x_3 & & -39 & -72 \\ \hline & x_1 & x_2 & \end{array}$$

 $K^*(1680)$ BRANCHING RATIOS

$\Gamma(K\pi)/\Gamma_{\text{total}}$	Γ_1/Γ
0.387±0.026 OUR FIT	
0.388±0.014±0.022	ASTON 88 LASS 0 11 $K^- p \rightarrow K^- \pi^+ n$
$\Gamma(K\pi)/\Gamma(K^*(892)\pi)$	Γ_1/Γ_3
1.30^{+0.23}_{-0.14} OUR FIT	
2.8 ±1.1	ASTON 84 LASS 0 11 $K^- p \rightarrow \bar{K}^0 2\pi n$
$\Gamma(K\rho)/\Gamma(K\pi)$	Γ_2/Γ_1
0.81^{+0.14}_{-0.09} OUR FIT	
1.2 ±0.4	ASTON 84 LASS 0 11 $K^- p \rightarrow \bar{K}^0 2\pi n$
$\Gamma(K\rho)/\Gamma(K^*(892)\pi)$	Γ_2/Γ_3
1.05^{+0.27}_{-0.11} OUR FIT	
0.97±0.09^{+0.30}_{-0.10}	ASTON 87 LASS 0 11 $K^- p \rightarrow \bar{K}^0 \pi^+ \pi^- n$

 $K^*(1680)$ REFERENCES

BIRD 89 SLAC-332 P.F. Bird (SLAC)
ASTON 88 NP B296 493 D. Aston et al. (SLAC, NAGO, CINC, INUS)
ASTON 87 NP B292 693 D. Aston et al. (SLAC, NAGO, CINC, INUS)
ASTON 84 PL 149B 258 D. Aston et al. (SLAC, CARL, OTTA) JP
ETKIN 80 PR D22 42 A. Etkin et al. (BNL, CUNY) JP
ESTABROOKS 78 NP B133 490 P.G. Estabrooks et al. (MCGI, CARL, DURH+) JP

Meson Particle Listings

 $K^*(1680)$, $K_2(1770)$, $K_3^*(1780)$

OTHER RELATED PAPERS

ABLUKIM	05Q	PR D72 092002	M. Ablukim et al.	(BES Collab.)
EBERT	05	MPL A20 1887	D. Ebert, R.N. Fauslov, V.O. Galkin	
LI	05E	MPL A20 2497	D.-M. Li et al.	

 $K_2(1770)$

$$I(J^P) = \frac{1}{2}(2^-)$$

See our mini-review in the 2004 edition of this Review, PDG 04.

 $K_2(1770)$ MASS

VALUE (MeV)	EVTS	DOCUMENT ID	TECN	CHG	COMMENT
1773 ± 8		¹ ASTON 93	LASS		$11K^-p \rightarrow K^- \omega p$
••• We do not use the following data for averages, fits, limits, etc. •••					
1743 ± 15		TIKHOMIROV 03	SPEC		$40.0 \frac{\pi^- C}{K_S^0 K_S^0 K_L^0 X}$
1810 ± 20		FRAME 86	OMEG +		$13 K^+ p \rightarrow \phi K^+ p$
~ 1730		ARMSTRONG 83	OMEG -		$18.5 K^- p \rightarrow 3Kp$
~ 1780		² DAUM 81c	CNTR -		$63 K^- p \rightarrow K^- 2\pi p$
1710 ± 15	60	CHUNG 74	HBC -		$7.3 K^- p \rightarrow K^- \omega p$
1767 ± 6		BLIEDEN 72	MMS -		$11-16 K^- p$
1730 ± 20	306	³ FIRESTONE 72b	DBC +		$12 K^+ d$
1765 ± 40		⁴ COLLEY 71	HBC +		$10 K^+ p \rightarrow K 2\pi N$
1740		DENEGRI 71	DBC -		$12.6 K^- d \rightarrow \bar{K} 2\pi d$
1745 ± 20		AGUILAR-... 70c	HBC -		$4.6 K^- p$
1780 ± 15		BARTSCH 70c	HBC -		$10.1 K^- p$
1760 ± 15		LUDLAM 70	HBC -		$12.6 K^- p$

¹ From a partial wave analysis of the $K^- \omega$ system.

² From a partial wave analysis of the $K^- 2\pi$ system.

³ Produced in conjunction with excited deuteron.

⁴ Systematic errors added correspond to spread of different fits.

 $K_2(1770)$ WIDTH

VALUE (MeV)	EVTS	DOCUMENT ID	TECN	CHG	COMMENT
186 ± 14		⁵ ASTON 93	LASS		$11K^-p \rightarrow K^- \omega p$
••• We do not use the following data for averages, fits, limits, etc. •••					
147 ± 70		TIKHOMIROV 03	SPEC		$40.0 \frac{\pi^- C}{K_S^0 K_S^0 K_L^0 X}$
140 ± 40		FRAME 86	OMEG +		$13 K^+ p \rightarrow \phi K^+ p$
~ 220		ARMSTRONG 83	OMEG -		$18.5 K^- p \rightarrow 3Kp$
~ 210		⁶ DAUM 81c	CNTR -		$63 K^- p \rightarrow K^- 2\pi p$
110 ± 50	60	CHUNG 74	HBC -		$7.3 K^- p \rightarrow K^- \omega p$
100 ± 26		BLIEDEN 72	MMS -		$11-16 K^- p$
210 ± 30	306	⁷ FIRESTONE 72b	DBC +		$12 K^+ d$
90 ± 70		⁸ COLLEY 71	HBC +		$10 K^+ p \rightarrow K 2\pi N$
130		DENEGRI 71	DBC -		$12.6 K^- d \rightarrow \bar{K} 2\pi d$
100 ± 50		AGUILAR-... 70c	HBC -		$4.6 K^- p$
138 ± 40		BARTSCH 70c	HBC -		$10.1 K^- p$
50 ± 40		LUDLAM 70	HBC -		$12.6 K^- p$

⁵ From a partial wave analysis of the $K^- \omega$ system.

⁶ From a partial wave analysis of the $K^- 2\pi$ system.

⁷ Produced in conjunction with excited deuteron.

⁸ Systematic errors added correspond to spread of different fits.

 $K_2(1770)$ DECAY MODES

Mode	Fraction (Γ_i/Γ)
Γ_1 $K \pi \pi$	
Γ_2 $K_2^*(1430) \pi$	dominant
Γ_3 $K^*(892) \pi$	seen
Γ_4 $K f_2(1270)$	seen
Γ_5 $K f_0(980)$	
Γ_6 $K \phi$	seen
Γ_7 $K \omega$	seen

 $K_2(1770)$ BRANCHING RATIOS

$$\Gamma(K_2^*(1430)\pi)/\Gamma(K\pi\pi) \quad \Gamma_2/\Gamma_1$$

$$(K_2^*(1430) \rightarrow K\pi)$$

VALUE	DOCUMENT ID	TECN	CHG	COMMENT
••• We do not use the following data for averages, fits, limits, etc. •••				
~ 0.03	DAUM 81c	CNTR		$63 K^- p \rightarrow K^- 2\pi p$
~ 1.0	⁹ FIRESTONE 72b	DBC +		$12 K^+ d$
< 1.0	COLLEY 71	HBC		$10 K^+ p$
0.2 ± 0.2	AGUILAR-... 70c	HBC -		$4.6 K^- p$
< 1.0	BARTSCH 70c	HBC -		$10.1 K^- p$
1.0	BARBARO-... 69	HBC +		$12.0 K^+ p$

⁹ Produced in conjunction with excited deuteron.

 $\Gamma(K^*(892)\pi)/\Gamma(K\pi\pi)$

VALUE	DOCUMENT ID	TECN	CHG	COMMENT
••• We do not use the following data for averages, fits, limits, etc. •••				
~ 0.23	DAUM 81c	CNTR		$63 K^- p \rightarrow K^- 2\pi p$

 $\Gamma(K f_2(1270))/\Gamma(K\pi\pi)$

VALUE	DOCUMENT ID	TECN	CHG	COMMENT
••• We do not use the following data for averages, fits, limits, etc. •••				
~ 0.74	DAUM 81c	CNTR		$63 K^- p \rightarrow K^- 2\pi p$

 $\Gamma(K f_0(980))/\Gamma_{total}$

VALUE	DOCUMENT ID	TECN	CHG	COMMENT
••• We do not use the following data for averages, fits, limits, etc. •••				
possibly seen	TIKHOMIROV 03	SPEC		$40.0 \frac{\pi^- C}{K_S^0 K_S^0 K_L^0 X}$

 $\Gamma(K\phi)/\Gamma_{total}$

VALUE	DOCUMENT ID	TECN	CHG	COMMENT
seen	ARMSTRONG 83	OMEG -		$18.5 K^- p \rightarrow K^- \phi N$

 $\Gamma(K\omega)/\Gamma_{total}$

VALUE	DOCUMENT ID	TECN	CHG	COMMENT
seen	OTTER 81	HBC	±	$8.25, 10, 16 K^\pm p$
seen	CHUNG 74	HBC -		$7.3 K^- p \rightarrow K^- \omega p$

 $K_2(1770)$ REFERENCES

PDG 04	PL B592 1	S. Eidelman et al.
TIKHOMIROV 03	PAN 66 828	G.D. Tikhomirov et al.
ASTON 93	PL B308 186	D. Aston et al.
FRAME 86	NP B276 667	D. Frame et al.
ARMSTRONG 83	NP B221 1	T.A. Armstrong et al.
DAUM 81c	NP B187 1	C. Daum et al.
OTTER 81	NP B181 1	G. Otter
CHUNG 74	PL 51B 413	S.U. Chung et al.
BLIEDEN 72	PL 39B 668	H.R. Blieden et al.
FIRESTONE 72b	PR D5 505	A. Firestone et al.
COLLEY 71	NP B26 71	D.C. Colley et al.
DENEGRI 71	NP B28 13	D. Denegri et al.
AGUILAR-... 70c	PL 25 54	M. Aguilar-Benitez et al.
BARTSCH 70c	PL 33B 186	J. Bartsch et al.
LUDLAM 70	PR D2 1234	T. Ludlam, J. Sandweiss, A.J. Slaughter
BARBARO-... 69	PL 22 1207	A. Barbaro-Galieri et al.

OTHER RELATED PAPERS

BERLINGHIERI 67	PRL 18 1087	J.C. Berlinghieri et al.
CARMONY 67	PRL 18 615	D.D. Carmony, T. Hendricks, R.L. Lander
JOBS 67	PL 26B 49	M. Jobs et al.
BARTSCH 66	PL 22 357	J. Bartsch et al.

 $K_3^*(1780)$

$$I(J^P) = \frac{1}{2}(3^-)$$

 $K_3^*(1780)$ MASS

VALUE (MeV)	EVTS	DOCUMENT ID	TECN	CHG	COMMENT
1776 ± 7 OUR AVERAGE		Error includes scale factor of 1.1.			
1781 ± 8 ± 4		¹ ASTON 88	LASS	0	$11 K^- p \rightarrow K^- \pi^+ n$
1740 ± 14 ± 15		¹ ASTON 87	LASS	0	$11 K^- p \rightarrow \bar{K}^0 \pi^+ \pi^- n$
1779 ± 11		² BALDI 76	SPEC +		$10 K^+ p \rightarrow K^0 \pi^+ p$
1776 ± 26		³ BRANDENB... 76d	ASPK	0	$13 K^\pm p \rightarrow K^\pm \pi^\mp N$
••• We do not use the following data for averages, fits, limits, etc. •••					
1720 ± 10 ± 15	6111	⁴ BIRD 89	LASS -		$11 K^- p \rightarrow \bar{K}^0 \pi^- p$
1749 ± 10		ASTON 88b	LASS -		$11 K^- p \rightarrow K^- \eta p$
1780 ± 9	300	BAUBILLIER 84b	HBC -		$8.25 K^- p \rightarrow \bar{K}^0 \pi^- p$
1790 ± 15		BAUBILLIER 82b	HBC	0	$8.25 K^- p \rightarrow K_S^0 2\pi N$
1784 ± 9	2060	CLELAND 82	SPEC ±		$50 K^+ p \rightarrow K_S^0 \pi^\pm p$
1786 ± 15		⁵ ASTON 81d	LASS	0	$11 K^- p \rightarrow K^- \pi^+ n$
1762 ± 9	190	TOAFF 81	HBC -		$6.5 K^- p \rightarrow \bar{K}^0 \pi^- p$
1850 ± 50		ETKIN 80	MPS	0	$6 K^- p \rightarrow \bar{K}^0 \pi^+ \pi^-$
1812 ± 28		BEUSCH 78	OMEG		$10 K^- p \rightarrow \bar{K}^0 \pi^+ \pi^-$
1786 ± 8		CHUNG 78	MPS	0	$6 K^- p \rightarrow K^- \pi^+ n$

¹ From energy-independent partial-wave analysis.

² From a fit to Y_2^2 moment. $J^P = 3^-$ found.

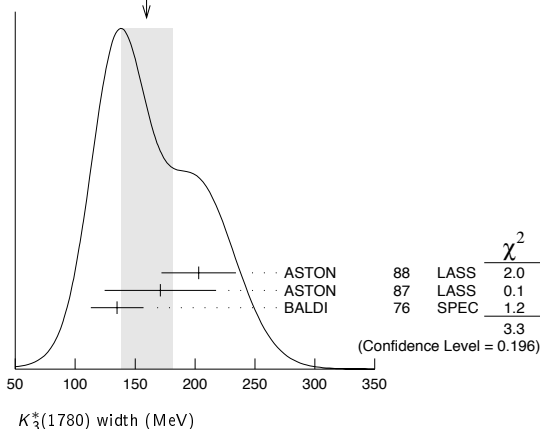
³ Confirmed by phase shift analysis of ESTABROOKS 78, yields $J^P = 3^-$.

⁴ From a partial wave amplitude analysis.

⁵ From a fit to the Y_0^0 moment.

$K_3^*(1780)$ WIDTH

VALUE (MeV)	EVTS	DOCUMENT ID	TECN	CHG	COMMENT	
159±21 OUR AVERAGE		Error includes scale factor of 1.3. See the ideogram below.				
203±30±8		⁶ ASTON	88	LASS	0	11 $K^- p \rightarrow K^- \pi^+ n$
171±42±20		⁶ ASTON	87	LASS	0	11 $K^- p \rightarrow \bar{K}^0 \pi^+ \pi^- n$
135±22		⁷ BALDI	76	SPEC	+	10 $K^+ p \rightarrow K^0 \pi^+ \pi^- n$
••• We do not use the following data for averages, fits, limits, etc. •••						
187±31±20	6111	⁸ BIRD	89	LASS	-	11 $K^- p \rightarrow \bar{K}^0 \pi^- p$
193 ⁺⁵¹ / ₋₃₇		ASTON	88B	LASS	-	11 $K^- p \rightarrow K^- \eta p$
99±30	300	BAUBILLIER	84B	HBC	-	8.25 $K^- p \rightarrow \bar{K}^0 \pi^- p$
~ 130		BAUBILLIER	82B	HBC	0	8.25 $K^- p \rightarrow K_S^0 2\pi N$
191±24	2060	CLELAND	82	SPEC	±	50 $K^+ p \rightarrow K_S^0 \pi^\pm p$
225±60		⁹ ASTON	81D	LASS	0	11 $K^- p \rightarrow K^- \pi^+ n$
~ 80	190	TOAFF	81	HBC	-	6.5 $K^- p \rightarrow \bar{K}^0 \pi^- p$
240±50		ETKIN	80	MPS	0	6 $K^- p \rightarrow \bar{K}^0 \pi^+ \pi^- n$
181±44		¹⁰ BEUSCH	78	OMEG		10 $K^- p \rightarrow \bar{K}^0 \pi^+ \pi^- n$
96±31		CHUNG	78	MPS	0	6 $K^- p \rightarrow K^- \pi^+ n$
270±70		¹¹ BRANDENB...	76D	ASPK	0	13 $K^\pm p \rightarrow K^\pm \pi^\mp N$

⁶ From energy-independent partial-wave analysis.⁷ From a fit to Y_6^2 moment. $J^P = 3^-$ found.⁸ From a partial wave amplitude analysis.⁹ From a fit to Y_6^0 moment.¹⁰ Errors enlarged by us to $4\Gamma/\sqrt{N}$; see the note with the $K^*(892)$ mass.¹¹ ESTABROOKS 78 find that BRANDENBURG 76d data are consistent with 175 MeV width. Not averaged.WEIGHTED AVERAGE
159±21 (Error scaled by 1.3) $K_3^*(1780)$ DECAY MODES

Mode	Fraction (Γ_i/Γ)	Confidence level
Γ_1 $K\rho$	(31 ± 9) %	
Γ_2 $K^*(892)\pi$	(20 ± 5) %	
Γ_3 $K\pi$	(18.8 ± 1.0) %	
Γ_4 $K\eta$	(30 ± 13) %	
Γ_5 $K_2^*(1430)\pi$	< 16 %	95%

CONSTRAINED FIT INFORMATION

An overall fit to 3 branching ratios uses 4 measurements and one constraint to determine 4 parameters. The overall fit has a $\chi^2 = 0.0$ for 1 degrees of freedom.

The following *off-diagonal* array elements are the correlation coefficients $\langle \delta x_i \delta x_j \rangle / (\delta x_i \delta x_j)$, in percent, from the fit to the branching fractions, $x_i \equiv \Gamma_i/\Gamma_{\text{total}}$. The fit constrains the x_i whose labels appear in this array to sum to one.

x_2	85		
x_3	18	21	
x_4	-98	-94	-27
	x_1	x_2	x_3

 $K_3^*(1780)$ BRANCHING RATIOS

$\Gamma(K\rho)/\Gamma(K^*(892)\pi)$	VALUE	DOCUMENT ID	TECN	CHG	COMMENT	Γ_1/Γ_2
1.52±0.23 OUR FIT						
1.52±0.21±0.10		ASTON	87	LASS	0	11 $K^- p \rightarrow \bar{K}^0 \pi^+ \pi^- n$

$\Gamma(K^*(892)\pi)/\Gamma(K\pi)$	VALUE	DOCUMENT ID	TECN	CHG	COMMENT	Γ_2/Γ_3
1.09±0.26 OUR FIT						
1.09±0.26		ASTON	84B	LASS	0	11 $K^- p \rightarrow \bar{K}^0 2\pi n$

$\Gamma(K\pi)/\Gamma_{\text{total}}$	VALUE	DOCUMENT ID	TECN	CHG	COMMENT	Γ_3/Γ
0.188±0.010 OUR FIT						
0.188±0.010 OUR AVERAGE						
0.187±0.008±0.008		ASTON	88	LASS	0	11 $K^- p \rightarrow K^- \pi^+ n$
0.19 ± 0.02		ESTABROOKS 78	ASPK	0		13 $K^\pm p \rightarrow K\pi N$

$\Gamma(K\eta)/\Gamma(K\pi)$	VALUE	DOCUMENT ID	TECN	CHG	COMMENT	Γ_4/Γ_3
1.6 ± 0.7 OUR FIT						

••• We do not use the following data for averages, fits, limits, etc. •••

0.41±0.050		¹² BIRD	89	LASS	-	11 $K^- p \rightarrow \bar{K}^0 \pi^- p$
0.50±0.18		ASTON	88B	LASS	-	11 $K^- p \rightarrow K^- \eta p$

¹² This result supersedes ASTON 88B.

$\Gamma(K_2^*(1430)\pi)/\Gamma(K^*(892)\pi)$	VALUE	CL%	DOCUMENT ID	TECN	CHG	COMMENT	Γ_5/Γ_2
<0.78		95	ASTON	87	LASS	0	11 $K^- p \rightarrow \bar{K}^0 \pi^+ \pi^- n$

 $K_3^*(1780)$ REFERENCES

BIRD	89	SLAC-332	P.F. Bird		(SLAC)
ASTON	88	NP B296 493	D. Aston et al.		(SLAC, NAGO, CINC, INUS)
ASTON	88B	PL B201 169	D. Aston et al.		(SLAC, NAGO, CINC, INUS) JP
ASTON	87	NP B292 693	D. Aston et al.		(SLAC, NAGO, CINC, INUS)
ASTON	84B	NP B247 261	D. Aston et al.		(SLAC, CARL, OTTA)
BAUBILLIER	84B	ZPHY C26 37	M. Baubillier et al.		(BIRM, CERN, GLAS+)
BAUBILLIER	82B	NP B202 21	M. Baubillier et al.		(BIRM, CERN, GLAS+)
CLELAND	82	NP B208 189	W.E. Cleland et al.		(DURH, GEVA, LAUS+)
ASTON	81D	PL 99B 502	D. Aston et al.		(SLAC, CARL, OTTA) JP
TOAFF	81	PR D23 1500	S. Toaff et al.		(ANL, KANS)
ETKIN	80	PR D22 42	A. Etkin et al.		(BNL, CUNY) JP
BEUSCH	78	PL 74B 282	W. Beusch et al.		(CERN, AACH3, ETH) JP
CHUNG	78	PRL 40 355	S.U. Chung et al.		(BNL, BRAN, CUNY+) JP
ESTABROOKS	78	NP B133 490	P.G. Estabrooks et al.		(MCGI, CARL, DURH+) JP
Also		PR D17 658	P.G. Estabrooks et al.		(MCGI, CARL, DURH+)
BALDI	76	PL 63B 344	R. Baldi et al.		(GEVA) JP
BRANDENB...	76D	PL 60B 478	G.W. Brandenburg et al.		(SLAC) JP

OTHER RELATED PAPERS

AGUILAR...	73	PRL 30 672	M. Aguilar-Benitez et al.		(BNL)
WALUCH	73	PR D8 2837	V. Waluch, S.M. Flatte, J.H. Friedman		(LBL)
CARMONY	71	PRL 27 1160	D.D. Carmony et al.		(PURD, UCD, IUPU)
FIRESTONE	71	PL 36B 513	A. Firestone et al.		(LBL)

Meson Particle Listings

 $K_2(1820)$, $K(1830)$, $K_0^*(1950)$ $K_2(1820)$

$$I(J^P) = \frac{1}{2}(2^-)$$

See our mini-review in the 2004 edition of this *Review* (PDG 04) under $K_2(1770)$.

 $K_2(1820)$ MASS

VALUE (MeV)	DOCUMENT ID	TECN	CHG	COMMENT
1816 ± 13	¹ ASTON 93	LASS		$11K^-p \rightarrow K^- \omega p$
••• We do not use the following data for averages, fits, limits, etc. •••				
~ 1840	² DAUM 81c	CNTR	63	$K^-p \rightarrow K^- 2\pi p$
¹ From a partial wave analysis of the $K^- \omega$ system.				
² From a partial wave analysis of the $K^- 2\pi$ system.				

 $K_2(1820)$ WIDTH

VALUE (MeV)	DOCUMENT ID	TECN	CHG	COMMENT
276 ± 35	³ ASTON 93	LASS		$11K^-p \rightarrow K^- \omega p$
••• We do not use the following data for averages, fits, limits, etc. •••				
~ 230	⁴ DAUM 81c	CNTR	63	$K^-p \rightarrow K^- 2\pi p$
³ From a partial wave analysis of the $K^- \omega$ system.				
⁴ From a partial wave analysis of the $K^- 2\pi$ system.				

 $K_2(1820)$ DECAY MODES

Mode	Fraction (Γ_i/Γ)
Γ_1 $K \pi \pi$	
Γ_2 $K_2^*(1430) \pi$	seen
Γ_3 $K^*(892) \pi$	seen
Γ_4 $K f_2(1270)$	seen
Γ_5 $K \omega$	seen

 $K_2(1820)$ BRANCHING RATIOS

$\Gamma(K_2^*(1430)\pi)/\Gamma(K\pi\pi)$	Γ_2/Γ_1			
VALUE	DOCUMENT ID	TECN	CHG	COMMENT
••• We do not use the following data for averages, fits, limits, etc. •••				
~ 0.77	DAUM 81c	CNTR	63	$K^-p \rightarrow \bar{K}2\pi p$
$\Gamma(K^*(892)\pi)/\Gamma(K\pi\pi)$	Γ_3/Γ_1			
VALUE	DOCUMENT ID	TECN	CHG	COMMENT
••• We do not use the following data for averages, fits, limits, etc. •••				
~ 0.05	DAUM 81c	CNTR	63	$K^-p \rightarrow \bar{K}2\pi p$
$\Gamma(K f_2(1270))/\Gamma(K\pi\pi)$	Γ_4/Γ_1			
VALUE	DOCUMENT ID	TECN	CHG	COMMENT
••• We do not use the following data for averages, fits, limits, etc. •••				
~ 0.18	DAUM 81c	CNTR	63	$K^-p \rightarrow \bar{K}2\pi p$

 $K_2(1820)$ REFERENCES

PDG 04	PL B592 1	S. Eidelman <i>et al.</i>	
ASTON 93	PL B308 186	D. Aston <i>et al.</i>	(SLAC, NAGO, CINC, INUS)
DAUM 81c	NP B187 1	C. Daum <i>et al.</i>	(AMST, CERN, CRAC, MPIM+)

 $K(1830)$

$$I(J^P) = \frac{1}{2}(0^-)$$

OMITTED FROM SUMMARY TABLE

Seen in partial-wave analysis of $K^- \phi$ system. Needs confirmation.

 $K(1830)$ MASS

VALUE (MeV)	DOCUMENT ID	TECN	CHG	COMMENT
••• We do not use the following data for averages, fits, limits, etc. •••				
~ 1830	ARMSTRONG 83	OMEG	-	$18.5 K^-p \rightarrow 3Kp$

 $K(1830)$ WIDTH

VALUE (MeV)	DOCUMENT ID	TECN	CHG	COMMENT
••• We do not use the following data for averages, fits, limits, etc. •••				
~ 250	ARMSTRONG 83	OMEG	-	$18.5 K^-p \rightarrow 3Kp$

 $K(1830)$ DECAY MODES

Mode	Fraction (Γ_i/Γ)
Γ_1 $K \phi$	

 $K(1830)$ REFERENCES

ARMSTRONG 83	NP B221 1	T.A. Armstrong <i>et al.</i>	(BARI, BIRM, CERN+)JP
--------------	-----------	------------------------------	-----------------------

OTHER RELATED PAPERS

KATAEV 05	PAN 68 567	A.L. Kataev	
Translated from YAF 68 597.			

 $K_0^*(1950)$

$$I(J^P) = \frac{1}{2}(0^+)$$

OMITTED FROM SUMMARY TABLE

Seen in partial-wave analysis of the $K^- \pi^+$ system. Needs confirmation.

 $K_0^*(1950)$ MASS

VALUE (MeV)	DOCUMENT ID	TECN	CHG	COMMENT
1945 ± 10 ± 20	¹ ASTON 88	LASS	0	$11 K^-p \rightarrow K^- \pi^+ n$
••• We do not use the following data for averages, fits, limits, etc. •••				
1917 ± 12	² ZHOU 06	RVUE		$Kp \rightarrow K^- \pi^+ n$
1820 ± 40	³ ANISOVICH 97c	RVUE		$11 K^-p \rightarrow K^- \pi^+ n$
¹ We take the central value of the two solutions and the larger error given.				
² S-matrix pole. Using ASTON 88 and assuming $K_0^*(800)$, $K_0^*(1430)$.				
³ T-matrix pole. Reanalysis of ASTON 88 data.				

 $K_0^*(1950)$ WIDTH

VALUE (MeV)	DOCUMENT ID	TECN	CHG	COMMENT
201 ± 34 ± 79	⁴ ASTON 88	LASS	0	$11 K^-p \rightarrow K^- \pi^+ n$
••• We do not use the following data for averages, fits, limits, etc. •••				
145 ± 38	⁵ ZHOU 06	RVUE		$Kp \rightarrow K^- \pi^+ n$
250 ± 100	⁶ ANISOVICH 97c	RVUE		$11 K^-p \rightarrow K^- \pi^+ n$
⁴ We take the central value of the two solutions and the larger error given.				
⁵ S-matrix pole. Using ASTON 88 and assuming $K_0^*(800)$, $K_0^*(1430)$.				
⁶ T-matrix pole. Reanalysis of ASTON 88 data.				

 $K_0^*(1950)$ DECAY MODES

Mode	Fraction (Γ_i/Γ)
Γ_1 $K \pi$	(52 ± 14) %

 $K_0^*(1950)$ BRANCHING RATIOS

$\Gamma(K\pi)/\Gamma_{\text{total}}$	Γ_1/Γ			
VALUE	DOCUMENT ID	TECN	CHG	COMMENT
0.52 ± 0.08 ± 0.12	⁷ ASTON 88	LASS	0	$11 K^-p \rightarrow K^- \pi^+ n$
••• We do not use the following data for averages, fits, limits, etc. •••				
~ 0.60	⁸ ZHOU 06	RVUE		$Kp \rightarrow K^- \pi^+ n$
⁷ We take the central value of the two solutions and the larger error given.				
⁸ S-matrix pole. Using ASTON 88 and assuming $K_0^*(800)$, $K_0^*(1430)$.				

 $K_0^*(1950)$ REFERENCES

ZHOU 06	NP A775 212	Z.Y. Zhou, H.Q. Zheng	
ANISOVICH 97c	PL B413 137	A.V. Anisovich, A.V. Sarantsev	
ASTON 88	NP B296 493	D. Aston <i>et al.</i>	(SLAC, NAGO, CINC, INUS)

OTHER RELATED PAPERS

ABLIKIM 05q	PR D72 092002	M. Ablikim <i>et al.</i>	(BES Collab.)
KATAEV 05	PAN 68 567	A.L. Kataev	
Translated from YAF 68 597.			
JAMIN 00	NP B587 331	M. Jamin <i>et al.</i>	
SHAKIN 00	PR D62 114014	C.M. Shakin, H. Wang	

See key on page 373

Meson Particle Listings

 $K_2^*(1980)$, $K_4^*(2045)$ $K_2^*(1980)$

$$I(J^P) = \frac{1}{2}(2^+)$$

OMITTED FROM SUMMARY TABLE
Needs confirmation. $K_2^*(1980)$ MASS

VALUE (MeV)	EVTS	DOCUMENT ID	TECN	CHG	COMMENT	
1973 ± 8 ± 25		ASTON	87	LASS	0	11 $K^- p \rightarrow \bar{K}^0 \pi^+ \pi^- n$
• • • We do not use the following data for averages, fits, limits, etc. • • •						
2020 ± 20		TIKHOMIROV	03	SPEC		40.0 $\pi^- C \rightarrow K_S^0 K_S^0 K_L^0 X$
1978 ± 40	241 ± 47	BIRD	89	LASS	-	11 $K^- p \rightarrow \bar{K}^0 \pi^- p$

 $K_2^*(1980)$ WIDTH

VALUE (MeV)	EVTS	DOCUMENT ID	TECN	CHG	COMMENT	
373 ± 33 ± 60		ASTON	87	LASS	0	11 $K^- p \rightarrow \bar{K}^0 \pi^+ \pi^- n$
• • • We do not use the following data for averages, fits, limits, etc. • • •						
180 ± 70		TIKHOMIROV	03	SPEC		40.0 $\pi^- C \rightarrow K_S^0 K_S^0 K_L^0 X$
398 ± 47	241 ± 47	BIRD	89	LASS	-	11 $K^- p \rightarrow \bar{K}^0 \pi^- p$

 $K_2^*(1980)$ DECAY MODES

Mode	Fraction (Γ_i/Γ)
Γ_1 $K^*(892)\pi$	(9.9 ± 1.2) %
Γ_2 $K\rho$	(9 ± 5) %
Γ_3 $K f_2(1270)$	(7 ± 5) %

 $K_2^*(1980)$ BRANCHING RATIOS

$\Gamma(K\rho)/\Gamma(K^*(892)\pi)$	Γ_2/Γ_1
1.49 ± 0.24 ± 0.09	
ASTON	87
LASS	0
11 $K^- p \rightarrow \bar{K}^0 \pi^+ \pi^- n$	

$\Gamma(K f_2(1270))/\Gamma_{\text{total}}$	Γ_3/Γ
• • • We do not use the following data for averages, fits, limits, etc. • • •	
possibly seen	
TIKHOMIROV	03
SPEC	
40.0 $\pi^- C \rightarrow K_S^0 K_S^0 K_L^0 X$	

 $K_2^*(1980)$ REFERENCES

TIKHOMIROV	03	PAN 66 828	G.D. Tikhomirov et al.	
		Translated from YAF 66 860.		
BIRD	89	SLAC-332	P.F. Bird	(SLAC)
ASTON	87	NP B292 693	D. Aston et al.	(SLAC, NAGO, CINC, INUS)

 $K_4^*(2045)$

$$I(J^P) = \frac{1}{2}(4^+)$$

 $K_4^*(2045)$ MASS

VALUE (MeV)	EVTS	DOCUMENT ID	TECN	CHG	COMMENT	
2045 ± 9 OUR AVERAGE		Error includes scale factor of 1.1.				
2062 ± 14 ± 13		1 ASTON	86	LASS	0	11 $K^- p \rightarrow K^- \pi^+ n$
2039 ± 10	400	2,3 CLELAND	82	SPEC	±	50 $K^+ p \rightarrow K_S^0 \pi^\pm p$
2070 +100 -40		4 ASTON	81c	LASS	0	11 $K^- p \rightarrow K^- \pi^+ n$
• • • We do not use the following data for averages, fits, limits, etc. • • •						
2079 ± 7	431	TORRES	86	MPSF		400 $pA \rightarrow 4KX$
2088 ± 20	650	BAUBILLIER	82	HBC	-	8.25 $K^- p \rightarrow K_S^0 \pi^- p$
2115 ± 46	488	CARMONY	77	HBC	0	9 $K^+ d \rightarrow K^+ \pi^+ X$

¹ From a fit to all moments.² From a fit to 8 moments.³ Number of events evaluated by us.⁴ From energy-independent partial-wave analysis. $K_4^*(2045)$ WIDTH

VALUE (MeV)	EVTS	DOCUMENT ID	TECN	CHG	COMMENT	
198 ± 30 OUR AVERAGE						
221 ± 48 ± 27		5 ASTON	86	LASS	0	11 $K^- p \rightarrow K^- \pi^+ n$
189 ± 35	400	6,7 CLELAND	82	SPEC	±	50 $K^+ p \rightarrow K_S^0 \pi^\pm p$
• • • We do not use the following data for averages, fits, limits, etc. • • •						
61 ± 58	431	TORRES	86	MPSF		400 $pA \rightarrow 4KX$
170 +100 -50	650	BAUBILLIER	82	HBC	-	8.25 $K^- p \rightarrow K_S^0 \pi^- p$
240 +500 -100		8 ASTON	81c	LASS	0	11 $K^- p \rightarrow K^- \pi^+ n$
300 ± 200		CARMONY	77	HBC	0	9 $K^+ d \rightarrow K^+ \pi^+ X$

⁵ From a fit to all moments.
⁶ From a fit to 8 moments.
⁷ Number of events evaluated by us.
⁸ From energy-independent partial-wave analysis.

 $K_4^*(2045)$ DECAY MODES

Mode	Fraction (Γ_i/Γ)
Γ_1 $K\pi$	(9.9 ± 1.2) %
Γ_2 $K^*(892)\pi\pi$	(9 ± 5) %
Γ_3 $K^*(892)\pi\pi\pi$	(7 ± 5) %
Γ_4 $\rho K\pi$	(5.7 ± 3.2) %
Γ_5 $\omega K\pi$	(5.0 ± 3.0) %
Γ_6 $\phi K\pi$	(2.8 ± 1.4) %
Γ_7 $\phi K^*(892)$	(1.4 ± 0.7) %

 $K_4^*(2045)$ BRANCHING RATIOS

$\Gamma(K\pi)/\Gamma_{\text{total}}$	Γ_1/Γ
0.099 ± 0.012	
ASTON	88
LASS	0
11 $K^- p \rightarrow K^- \pi^+ n$	

$\Gamma(K^*(892)\pi\pi)/\Gamma(K\pi)$	Γ_2/Γ_1
0.89 ± 0.53	
BAUBILLIER	82
HBC	-
8.25 $K^- p \rightarrow \rho K_S^0 3\pi$	

$\Gamma(K^*(892)\pi\pi\pi)/\Gamma(K\pi)$	Γ_3/Γ_1
0.75 ± 0.49	
BAUBILLIER	82
HBC	-
8.25 $K^- p \rightarrow \rho K_S^0 3\pi$	

$\Gamma(\rho K\pi)/\Gamma(K\pi)$	Γ_4/Γ_1
0.58 ± 0.32	
BAUBILLIER	82
HBC	-
8.25 $K^- p \rightarrow \rho K_S^0 3\pi$	

$\Gamma(\omega K\pi)/\Gamma(K\pi)$	Γ_5/Γ_1
0.50 ± 0.30	
BAUBILLIER	82
HBC	-
8.25 $K^- p \rightarrow \rho K_S^0 3\pi$	

$\Gamma(\phi K\pi)/\Gamma_{\text{total}}$	Γ_6/Γ
0.028 ± 0.014	
9 TORRES	86
MPSF	400
$pA \rightarrow 4KX$	

$\Gamma(\phi K^*(892))/\Gamma_{\text{total}}$	Γ_7/Γ
0.014 ± 0.007	
9 TORRES	86
MPSF	400
$pA \rightarrow 4KX$	
⁹ Error determination is model dependent.	

 $K_4^*(2045)$ REFERENCES

ASTON	88	NP B296 493	D. Aston et al.	(SLAC, NAGO, CINC, INUS)
ASTON	86	PL B180 308	D. Aston et al.	(SLAC, NAGO, CINC, INUS)
TORRES	86	PR D34 707	S. Torres et al.	(VPI, ARIZ, FNAL, FSU+)
BAUBILLIER	82	PL 118B 447	M. Baubillier et al.	(BIRM, CERN, GLAS+)
CLELAND	82	NP B208 189	W.E. Cleland et al.	(DURH, GEVA, LAUS+)
ASTON	81c	PL 106B 235	D. Aston et al.	(SLAC, CARL, OTTA)JP
CARMONY	77	PR D16 1251	D.D. Carmony et al.	(PURD, UCD, IUUP)

OTHER RELATED PAPERS

BROMBERG	80	PR D22 1513	C.M. Bromberg et al.	(CIT, FNAL, ILLC+)
CARMONY	71	PRL 27 1160	D.D. Carmony et al.	(PURD, UCD, IUUP)

Meson Particle Listings

 $K_2(2250)$, $K_3(2320)$, $K_5^*(2380)$, $K_4(2500)$ **$K_2(2250)$**

$$I(J^P) = \frac{1}{2}(2^-)$$

OMITTED FROM SUMMARY TABLE

This entry contains various peaks in strange meson systems reported in the 2150–2260 MeV region, as well as enhancements seen in the antihyperon-nucleon system, either in the mass spectra or in the $J^P = 2^-$ wave.

 $K_2(2250)$ MASS

VALUE (MeV)	EVTS	DOCUMENT ID	TECN	CHG	COMMENT
2247 ± 17 OUR AVERAGE					
2200 ± 40		¹ ARMSTRONG 83c	OMEG	–	18 $K^- p \rightarrow \Lambda \bar{p} X$
2235 ± 50		¹ BAUBILLIER 81	HBC	–	8 $K^- p \rightarrow \Lambda \bar{p} X$
2260 ± 20		¹ CLELAND 81	SPEC	±	50 $K^+ p \rightarrow \Lambda \bar{p} X$
• • •		We do not use the following data for averages, fits, limits, etc. • • •			
2280 ± 20		TIKHOMIROV 03	SPEC		$40.0 \frac{\pi^- C}{K_S^0 K_S^0 K_L^0 X}$
2147 ± 4	37	CHLIAPNIK... 79	HBC	+	32 $K^+ p \rightarrow \Lambda \bar{p} X$
2240 ± 20	20	LISSAUER 70	HBC		9 $K^+ p$
¹ $J^P = 2^-$ from moments analysis.					

 $K_2(2250)$ WIDTH

VALUE (MeV)	EVTS	DOCUMENT ID	TECN	CHG	COMMENT
180 ± 30 OUR AVERAGE					Error includes scale factor of 1.4.
150 ± 30		² ARMSTRONG 83c	OMEG	–	18 $K^- p \rightarrow \Lambda \bar{p} X$
210 ± 30		² CLELAND 81	SPEC	±	50 $K^+ p \rightarrow \Lambda \bar{p} X$
• • •		We do not use the following data for averages, fits, limits, etc. • • •			
180 ± 60		TIKHOMIROV 03	SPEC		$40.0 \frac{\pi^- C}{K_S^0 K_S^0 K_L^0 X}$
~ 200		² BAUBILLIER 81	HBC	–	8 $K^- p \rightarrow \Lambda \bar{p} X$
~ 40	37	CHLIAPNIK... 79	HBC	+	32 $K^+ p \rightarrow \Lambda \bar{p} X$
80 ± 20	20	LISSAUER 70	HBC		9 $K^+ p$
² $J^P = 2^-$ from moments analysis.					

 $K_2(2250)$ DECAY MODES

Mode	Γ_1
$K \pi \pi$	
$K f_2(1270)$	
$K^*(892) f_0(980)$	
$\rho \bar{\Lambda}$	

 $K_2(2250)$ REFERENCES

TIKHOMIROV 03	PAN 66 828	G.D. Tikhomirov et al.	
ARMSTRONG 83c	NP B227 365	T.A. Armstrong et al.	(BARI, BIRM, CERN+)
BAUBILLIER 81	NP B183 1	M. Baubillier et al.	(BIRM, CERN, GLAS+)
CLELAND 81	NP B184 1	W.E. Cleland et al.	(PITT, GEVA, LAUS+)
CHLIAPNIK... 79	NP B158 253	P.V. Chliapnikov et al.	(CERN, BELG, MONS)
LISSAUER 70	NP B18 491	D. Lissauer et al.	(LBL)

OTHER RELATED PAPERS

ALEXANDER 68B	PRL 20 755	G. Alexander et al.	(LRL)
---------------	------------	---------------------	-------

 $K_3(2320)$

$$I(J^P) = \frac{1}{2}(3^+)$$

OMITTED FROM SUMMARY TABLE

Seen in the $J^P = 3^+$ wave of the antihyperon-nucleon system. Needs confirmation.

 $K_3(2320)$ MASS

VALUE (MeV)	DOCUMENT ID	TECN	CHG	COMMENT
2324 ± 24 OUR AVERAGE				
2330 ± 40	¹ ARMSTRONG 83c	OMEG	–	18 $K^- p \rightarrow \Lambda \bar{p} X$
2320 ± 30	¹ CLELAND 81	SPEC	±	50 $K^+ p \rightarrow \Lambda \bar{p} X$
¹ $J^P = 3^+$ from moments analysis.				

 $K_3(2320)$ WIDTH

VALUE (MeV)	DOCUMENT ID	TECN	CHG	COMMENT
150 ± 30	² ARMSTRONG 83c	OMEG	–	18 $K^- p \rightarrow \Lambda \bar{p} X$
• • •	We do not use the following data for averages, fits, limits, etc. • • •			
~ 250	² CLELAND 81	SPEC	±	50 $K^+ p \rightarrow \Lambda \bar{p} X$
² $J^P = 3^+$ from moments analysis.				

 $K_3(2320)$ DECAY MODES

Mode	Γ_1
$\rho \bar{\Lambda}$	

 $K_3(2320)$ REFERENCES

ARMSTRONG 83c	NP B227 365	T.A. Armstrong et al.	(BARI, BIRM, CERN+)
CLELAND 81	NP B184 1	W.E. Cleland et al.	(PITT, GEVA, LAUS+)

OTHER RELATED PAPERS

ABLIKIM 05Q	PR D72 092002	M. Ablikim et al.	(BES Collab.)
-------------	---------------	-------------------	---------------

 $K_5^*(2380)$

$$I(J^P) = \frac{1}{2}(5^-)$$

OMITTED FROM SUMMARY TABLE

Needs confirmation.

 $K_5^*(2380)$ MASS

VALUE (MeV)	DOCUMENT ID	TECN	CHG	COMMENT
2382 ± 14 ± 19	¹ ASTON 86	LASS	0	11 $K^- p \rightarrow K^- \pi^+ n$
¹ From a fit to all the moments.				

 $K_5^*(2380)$ WIDTH

VALUE (MeV)	DOCUMENT ID	TECN	CHG	COMMENT
178 ± 37 ± 32	² ASTON 86	LASS	0	11 $K^- p \rightarrow K^- \pi^+ n$
² From a fit to all the moments.				

 $K_5^*(2380)$ DECAY MODES

Mode	Fraction (Γ_i/Γ)
$K \pi$	(6.1 ± 1.2) %

 $K_5^*(2380)$ BRANCHING RATIOS

$\Gamma(K\pi)/\Gamma_{\text{total}}$	DOCUMENT ID	TECN	CHG	COMMENT	Γ_1/Γ
0.061 ± 0.012	ASTON 88	LASS	0	11 $K^- p \rightarrow K^- \pi^+ n$	

 $K_5^*(2380)$ REFERENCES

ASTON 88	NP B296 493	D. Aston et al.	(SLAC, NAGO, CINC, INUS)
ASTON 86	PL B180 308	D. Aston et al.	(SLAC, NAGO, CINC, INUS)

OTHER RELATED PAPERS

ABLIKIM 05Q	PR D72 092002	M. Ablikim et al.	(BES Collab.)
-------------	---------------	-------------------	---------------

 $K_4(2500)$

$$I(J^P) = \frac{1}{2}(4^-)$$

OMITTED FROM SUMMARY TABLE

Needs confirmation.

 $K_4(2500)$ MASS

VALUE (MeV)	DOCUMENT ID	TECN	CHG	COMMENT
2490 ± 20	¹ CLELAND 81	SPEC	±	50 $K^+ p \rightarrow \Lambda \bar{p}$
¹ $J^P = 4^-$ from moments analysis.				

 $K_4(2500)$ WIDTH

VALUE (MeV)	DOCUMENT ID	TECN	CHG	COMMENT
• • •	We do not use the following data for averages, fits, limits, etc. • • •			
~ 250	² CLELAND 81	SPEC	±	50 $K^+ p \rightarrow \Lambda \bar{p}$
² $J^P = 4^-$ from moments analysis.				

 $K_4(2500)$ DECAY MODES

Mode	Γ_1
$\rho \bar{\Lambda}$	

 $K_4(2500)$ REFERENCES

CLELAND 81	NP B184 1	W.E. Cleland et al.	(PITT, GEVA, LAUS+)
------------	-----------	---------------------	---------------------

K(3100)

$$I^G(J^{PC}) = ?^?(?^{??})$$

K(3100) WIDTH

OMITTED FROM SUMMARY TABLE

Narrow peak observed in several ($\Lambda\bar{p}$ + pions) and ($\bar{\Lambda}p$ + pions) states in Σ^- Be reactions by BOURQUIN 86 and in np and nA reactions by ALEEV 93. Not seen by BOEHNLEIN 91. If due to strong decays, this state has exotic quantum numbers ($B=0, Q=+1, S=-1$ for $\Lambda\bar{p}\pi^+\pi^+$ and $I \geq 3/2$ for $\Lambda\bar{p}\pi^-$). Needs confirmation.

K(3100) MASS

VALUE (MeV)	DOCUMENT ID	TECN	COMMENT
≈ 3100 OUR ESTIMATE			
3-BODY DECAYS			
3054 \pm 11 OUR AVERAGE			
3060 \pm 7 \pm 20	¹ ALEEV 93	BIS2	$K(3100) \rightarrow \Lambda\bar{p}\pi^+$
3056 \pm 7 \pm 20	¹ ALEEV 93	BIS2	$K(3100) \rightarrow \bar{\Lambda}p\pi^-$
3055 \pm 8 \pm 20	¹ ALEEV 93	BIS2	$K(3100) \rightarrow \Lambda\bar{p}\pi^-$
3045 \pm 8 \pm 20	¹ ALEEV 93	BIS2	$K(3100) \rightarrow \bar{\Lambda}p\pi^+$
4-BODY DECAYS			
3059 \pm 11 OUR AVERAGE			
3067 \pm 6 \pm 20	¹ ALEEV 93	BIS2	$K(3100) \rightarrow \Lambda\bar{p}\pi^+\pi^+$
3060 \pm 8 \pm 20	¹ ALEEV 93	BIS2	$K(3100) \rightarrow \Lambda\bar{p}\pi^+\pi^-$
3055 \pm 7 \pm 20	¹ ALEEV 93	BIS2	$K(3100) \rightarrow \bar{\Lambda}p\pi^-\pi^-$
3052 \pm 8 \pm 20	¹ ALEEV 93	BIS2	$K(3100) \rightarrow \bar{\Lambda}p\pi^-\pi^+$
• • • We do not use the following data for averages, fits, limits, etc. • • •			
3105 \pm 30	BOURQUIN 86	SPEC	$K(3100) \rightarrow \Lambda\bar{p}\pi^+\pi^+$
3115 \pm 30	BOURQUIN 86	SPEC	$K(3100) \rightarrow \Lambda\bar{p}\pi^+\pi^-$
5-BODY DECAYS			
3095 \pm 30	BOURQUIN 86	SPEC	$K(3100) \rightarrow \Lambda\bar{p}\pi^+\pi^+\pi^-$
¹ Supersedes ALEEV 90.			

3-BODY DECAYS

VALUE (MeV)	DOCUMENT ID	TECN	COMMENT
• • • We do not use the following data for averages, fits, limits, etc. • • •			
42 \pm 16	² ALEEV 93	BIS2	$K(3100) \rightarrow \Lambda\bar{p}\pi^+$
36 \pm 15	² ALEEV 93	BIS2	$K(3100) \rightarrow \bar{\Lambda}p\pi^-$
50 \pm 18	² ALEEV 93	BIS2	$K(3100) \rightarrow \Lambda\bar{p}\pi^-$
30 \pm 15	² ALEEV 93	BIS2	$K(3100) \rightarrow \bar{\Lambda}p\pi^+$

4-BODY DECAYS

VALUE (MeV)	CL%	DOCUMENT ID	TECN	COMMENT
• • • We do not use the following data for averages, fits, limits, etc. • • •				
22 \pm 8		² ALEEV 93	BIS2	$K(3100) \rightarrow \Lambda\bar{p}\pi^+\pi^+$
28 \pm 12		² ALEEV 93	BIS2	$K(3100) \rightarrow \Lambda\bar{p}\pi^+\pi^-$
32 \pm 15		² ALEEV 93	BIS2	$K(3100) \rightarrow \bar{\Lambda}p\pi^-\pi^-$
30 \pm 15		² ALEEV 93	BIS2	$K(3100) \rightarrow \bar{\Lambda}p\pi^-\pi^+$
<30	90	BOURQUIN 86	SPEC	$K(3100) \rightarrow \Lambda\bar{p}\pi^+\pi^+$
<80	90	BOURQUIN 86	SPEC	$K(3100) \rightarrow \Lambda\bar{p}\pi^+\pi^-$

5-BODY DECAYS

VALUE (MeV)	CL%	DOCUMENT ID	TECN	COMMENT
• • • We do not use the following data for averages, fits, limits, etc. • • •				
<30	90	BOURQUIN 86	SPEC	$K(3100) \rightarrow \Lambda\bar{p}\pi^+\pi^+\pi^-$

² Supersedes ALEEV 90.**K(3100) DECAY MODES**

Mode
Γ_1 $K(3100)^0 \rightarrow \Lambda\bar{p}\pi^+$
Γ_2 $K(3100)^{--} \rightarrow \Lambda\bar{p}\pi^-$
Γ_3 $K(3100)^- \rightarrow \Lambda\bar{p}\pi^+\pi^-$
Γ_4 $K(3100)^+ \rightarrow \Lambda\bar{p}\pi^+\pi^+$
Γ_5 $K(3100)^0 \rightarrow \Lambda\bar{p}\pi^+\pi^+\pi^-$
Γ_6 $K(3100)^0 \rightarrow \Sigma(1385)^+\bar{p}$

 $\Gamma(\Sigma(1385)^+\bar{p})/\Gamma(\Lambda\bar{p}\pi^+)$

VALUE	CL%	DOCUMENT ID	TECN	COMMENT	Γ_6/Γ_1
<0.04	90	ALEEV 93	BIS2	$K(3100)^0 \rightarrow \Sigma(1385)^+\bar{p}$	

K(3100) REFERENCES

ALEEV 93	PAN 56 1358 Translated from YAF 56 100.	A.N. Aleev <i>et al.</i>	(BIS-2 Collab.)
BOEHNLEIN 91	NPBPS B21 174	A. Boehnlein <i>et al.</i>	(FLOR, BNL, IND+)
ALEEV 90	ZPHY C47 533	A.N. Aleev <i>et al.</i>	(BIS-2 Collab.)
BOURQUIN 86	PL B172 113	M.H. Bourquin <i>et al.</i>	(GEVA, RAL, HEIDP+)

Meson Particle Listings

D MESONS, D^\pm

CHARMED MESONS

($C = \pm 1$)

$D^+ = c\bar{d}$, $D^0 = c\bar{u}$, $\bar{D}^0 = \bar{c}u$, $D^- = \bar{c}d$, similarly for D^{*s}

D^\pm

$$I(J^P) = \frac{1}{2}(0^-)$$

D^\pm MASS

The fit includes D^\pm , D^0 , D_S^\pm , D^{*s} , D^{*0} , and D_S^{*s} mass and mass difference measurements.

VALUE (MeV)	EVTS	DOCUMENT ID	TECN	COMMENT
1869.62 ± 0.20 OUR FIT	Error includes scale factor of 1.1.			
1869.5 ± 0.5 OUR AVERAGE				
1870.0 ± 0.5 ± 1.0	317	BARLAG	90c ACCM	π^- Cu 230 GeV
1869.4 ± 0.6	1	TRILLING	81 RVUE	e^+e^- 3.77 GeV
• • • We do not use the following data for averages, fits, limits, etc. • • •				
1875 ± 10	9	ADAMOVICH	87 EMUL	Photoproduction
1860 ± 16	6	ADAMOVICH	84 EMUL	Photoproduction
1863 ± 4		DERRICK	84 HRS	e^+e^- 29 GeV
1868.4 ± 0.5	1	SCHINDLER	81 MRK2	e^+e^- 3.77 GeV
1874 ± 5		GOLDBABER	77 MRK1	D^0 , D^+ recoil spectra
1868.3 ± 0.9	1	PERUZZI	77 LGW	e^+e^- 3.77 GeV
1874 ± 11		PICCOLO	77 MRK1	e^+e^- 4.03, 4.41 GeV
1876 ± 15	50	PERUZZI	76 MRK1	$K^\mp\pi^\pm\pi^\pm$

¹PERUZZI 77 and SCHINDLER 81 errors do not include the 0.13% uncertainty in the absolute SPEAR energy calibration. TRILLING 81 uses the high precision $J/\psi(1S)$ and $\psi(2S)$ measurements of ZHOLENTZ 80 to determine this uncertainty and combines the PERUZZI 77 and SCHINDLER 81 results to obtain the value quoted.

D^\pm MEAN LIFE

Measurements with an error $> 100 \times 10^{-15}$ s have been omitted from the Listings.

VALUE (10^{-15} s)	EVTS	DOCUMENT ID	TECN	COMMENT
1040 ± 7 OUR AVERAGE				
1039.4 ± 4.3 ± 7.0	110k	LINK	02F FOCS	γ nucleus, ≈ 180 GeV
1033.6 ± 22.1 ^{+9.9} _{-12.7}	3777	BONVICINI	99 CLEO	$e^+e^- \approx \Upsilon(4S)$
1048 ± 15 ± 11	9k	FRABETTI	94d E687	$D^+ \rightarrow K^-\pi^+\pi^+$
• • • We do not use the following data for averages, fits, limits, etc. • • •				
1075 ± 40 ± 18	2455	FRABETTI	91 E687	γ Be, $D^+ \rightarrow K^-\pi^+\pi^+$
1030 ± 80 ± 60	200	ALVAREZ	90 NA14	γ , $D^+ \rightarrow K^-\pi^+\pi^+$
1050 ⁺⁷⁷ ₋₇₂	317	² BARLAG	90c ACCM	π^- Cu 230 GeV
1050 ± 80 ± 70	363	ALBRECHT	88i ARG	e^+e^- 10 GeV
1090 ± 30 ± 25	2992	RAAB	88 E691	Photoproduction

²BARLAG 90c estimates the systematic error to be negligible.

D^+ DECAY MODES

Most decay modes (other than the semileptonic modes) that involve a neutral K meson are now given as K_S^0 modes, not as \bar{K}^0 modes. Nearly always it is a K_S^0 that is measured, and interference between Cabibbo-allowed and doubly Cabibbo-suppressed modes can invalidate the assumption that $2\Gamma(K_S^0) = \Gamma(\bar{K}^0)$.

Mode	Fraction (Γ_i/Γ)	Scale factor/ Confidence level
Inclusive modes		
Γ_1 e^+ anything	(16.0 ± 0.4) %	
Γ_2 μ^+ anything		
Γ_3 K^- anything	(25.7 ± 1.4) %	
Γ_4 \bar{K}^0 anything + K^0 anything	(61 ± 5) %	
Γ_5 K^+ anything	(5.9 ± 0.8) %	
Γ_6 $K^*(892)^-$ anything	(6 ± 5) %	
Γ_7 $\bar{K}^*(892)^0$ anything	(23 ± 5) %	
Γ_8 $K^*(892)^+$ anything		
Γ_9 $K^*(892)^0$ anything	< 6.6 %	CL=90%
Γ_{10} η anything	(6.3 ± 0.7) %	
Γ_{11} η' anything	(1.04 ± 0.18) %	
Γ_{12} ϕ anything	(1.03 ± 0.12) %	

Leptonic and semileptonic modes

Γ_{13} $e^+\nu_e$	< 2.4	$\times 10^{-5}$	CL=90%
Γ_{14} $\mu^+\nu_\mu$	(4.4 ± 0.7)	$\times 10^{-4}$	
Γ_{15} $\tau^+\nu_\tau$	< 2.1	$\times 10^{-3}$	
Γ_{16} $\bar{K}^0\ell^+\nu_\ell$	[a]		
Γ_{17} $\bar{K}^0e^+\nu_e$	(8.6 ± 0.5) %		
Γ_{18} $\bar{K}^0\mu^+\nu_\mu$	(9.3 ± 0.8) %		S=1.1
Γ_{19} $K^-\pi^+e^+\nu_e$	(4.1 ± 0.6) %		S=1.1
Γ_{20} $\bar{K}^*(892)^0e^+\nu_e$ $\bar{K}^*(892)^0 \rightarrow K^-\pi^+$	(3.66 ± 0.21) %		
Γ_{21} $K^-\pi^+e^+\nu_e$ nonresonant	< 7	$\times 10^{-3}$	CL=90%
Γ_{22} $K^-\pi^+\mu^+\nu_\mu$	(3.9 ± 0.5) %		
Γ_{23} $\bar{K}^*(892)^0\mu^+\nu_\mu$ $\bar{K}^*(892)^0 \rightarrow K^-\pi^+$	(3.6 ± 0.3) %		
Γ_{24} $K^-\pi^+\mu^+\nu_\mu$ nonresonant	(2.1 ± 0.5) $\times 10^{-3}$		
Γ_{25} $(\bar{K}^*(892)\pi)^0e^+\nu_e$			
Γ_{26} $(\bar{K}\pi\pi)^0e^+\nu_e$ non- $\bar{K}^*(892)$			
Γ_{27} $K^-\pi^+\pi^0\mu^+\nu_\mu$	< 1.6	$\times 10^{-3}$	CL=90%
Γ_{28} $\pi^0e^+\nu_e$	(4.4 ± 0.7) $\times 10^{-3}$		
Γ_{29} $\pi^0\ell^+\nu_\ell$	[a]		
Γ_{30} $\rho^0e^+\nu_e$	(2.2 ± 0.4) $\times 10^{-3}$		
Γ_{31} $\rho^0\mu^+\nu_\mu$	(2.4 ± 0.4) $\times 10^{-3}$		
Γ_{32} $\omega e^+\nu_e$	(1.6 ^{+0.7} _{-0.6}) $\times 10^{-3}$		
Γ_{33} $\phi e^+\nu_e$	< 2.01 %		CL=90%
Γ_{34} $\phi\mu^+\nu_\mu$	< 2.04 %		CL=90%
Γ_{35} $\eta\ell^+\nu_\ell$	< 7	$\times 10^{-3}$	CL=90%
Γ_{36} $\eta'(958)\mu^+\nu_\mu$	< 1.1 %		CL=90%

Fractions of some of the following modes with resonances have already appeared above as submodes of particular charged-particle modes.

Γ_{37} $\bar{K}^*(892)^0e^+\nu_e$	(5.49 ± 0.31) %	S=1.2
Γ_{38} $\bar{K}^*(892)^0\mu^+\nu_\mu$	(5.4 ± 0.4) %	S=1.1
Γ_{39} $\bar{K}_1(1270)^0\mu^+\nu_\mu$		
Γ_{40} $\bar{K}^*(1410)^0\mu^+\nu_\mu$		
Γ_{41} $\bar{K}_0^*(1430)^0\mu^+\nu_\mu$	< 2.5	$\times 10^{-4}$
Γ_{42} $\bar{K}_2^*(1430)^0\mu^+\nu_\mu$		
Γ_{43} $\bar{K}^*(1680)^0\mu^+\nu_\mu$	< 1.5	$\times 10^{-3}$

Hadronic modes with a \bar{K} or $\bar{K}K\bar{K}$

Γ_{44} $K^0\pi^+$	(1.45 ± 0.04) %	S=1.3
Γ_{45} $K_L^0\pi^+$	(1.46 ± 0.05) %	
Γ_{46} $K^-\pi^+\pi^+$	[b] (9.22 ± 0.21) %	S=1.1
Γ_{47} $(K^-\pi^+)_{S\text{-wave}}\pi^+$	(7.54 ± 0.26) %	
Γ_{48} $\bar{K}_0^*(800)^0\pi^+$, $\bar{K}_0^*(800) \rightarrow K^-\pi^+$	[c]	
Γ_{49} $\bar{K}_0^*(1430)^0\pi^+$, $\bar{K}_0^*(1430)^0 \rightarrow K^-\pi^+$	[c]	
Γ_{50} $\bar{K}^*(892)^0\pi^+$, $\bar{K}^*(892)^0 \rightarrow K^-\pi^+$	(1.22 ± 0.09) %	
Γ_{51} $\bar{K}_2^*(1430)^0\pi^+$, $\bar{K}_2^*(1430)^0 \rightarrow K^-\pi^+$	[c] (3.0 ± 0.8) $\times 10^{-4}$	
Γ_{52} $\bar{K}^*(1680)^0\pi^+$, $\bar{K}^*(1680)^0 \rightarrow K^-\pi^+$	[c] (1.6 ± 0.6) $\times 10^{-3}$	
Γ_{53} $K^-\pi^+\pi^+$ nonresonant	[c]	
Γ_{54} $K_S^0\pi^+\pi^0$	[b] (6.8 ± 0.5) %	S=1.9
Γ_{55} $K_S^0\rho^+$	(4.6 ± 1.0) %	
Γ_{56} $\bar{K}^*(892)^0\pi^+$, $\bar{K}^*(892)^0 \rightarrow K_S^0\pi^0$	(1.3 ± 0.6) %	
Γ_{57} $K_S^0\pi^+\pi^0$ nonresonant	(9 ± 7) $\times 10^{-3}$	
Γ_{58} $K^-\pi^+\pi^+\pi^0$	[b] (6.00 ± 0.20) %	S=1.2
Γ_{59} $\bar{K}^*(892)^0\rho^+$ total, $\bar{K}^*(892)^0 \rightarrow K^-\pi^+$	(1.3 ± 0.8) %	
Γ_{60} $\bar{K}_1(1400)^0\pi^+$, $\bar{K}_1(1400)^0 \rightarrow K^-\pi^+\pi^0$	(1.8 ± 0.7) %	
Γ_{61} $K^-\rho^+\pi^+$ total	(2.9 ^{+1.0} _{-0.9}) %	
Γ_{62} $K^-\rho^+\pi^+$ 3-body	(1.0 ± 0.4) %	
Γ_{63} $\bar{K}^*(892)^0\pi^+\pi^0$ total, $\bar{K}^*(892)^0 \rightarrow K^-\pi^+$	(4.2 ± 0.6) %	
Γ_{64} $\bar{K}^*(892)^0\pi^+\pi^0$ 3-body, $\bar{K}^*(892)^0 \rightarrow K^-\pi^+$	(2.7 ± 0.8) %	
Γ_{65} $K^*(892)^-\pi^+\pi^+$ 3-body, $K^*(892)^- \rightarrow K^-\pi^0$	(6 ± 3) $\times 10^{-3}$	

See key on page 373

Meson Particle Listings

 D^\pm

Γ_{66}	$K^- \pi^+ \pi^+ \pi^0$ nonresonant	[d]	(1.1 \pm 0.5) %		Γ_{119}	$\eta \rho^+$	< 7	$\times 10^{-3}$	CL=90%
Γ_{67}	$K_S^0 \pi^+ \pi^+ \pi^-$	[b]	(3.02 \pm 0.12) %	S=1.3	Γ_{120}	$\eta'(958) \pi^+$	(5.1 \pm 1.0)	$\times 10^{-3}$	
Γ_{68}	$K_S^0 a_1(1260)^+$,		(1.8 \pm 0.3) %		Γ_{121}	$\eta'(958) \rho^+$	< 5	$\times 10^{-3}$	CL=90%
Γ_{69}	$a_1(1260)^+ \rightarrow \pi^+ \pi^+ \pi^-$		(1.8 \pm 0.7) %		Hadronic modes with a $K\bar{K}$ pair				
Γ_{70}	$\bar{K}_1(1400)^0 \pi^+$,		(1.3 \pm 0.6) %		Γ_{122}	$K^+ K_S^0$	(2.89 \pm 0.17)	$\times 10^{-3}$	
Γ_{71}	$\bar{K}_1(1400)^0 \rightarrow K_S^0 \pi^+ \pi^-$		(1.8 \pm 0.6) %		Γ_{123}	$K^+ K^- \pi^+$	[b] (9.63 \pm 0.31)	$\times 10^{-3}$	S=1.3
Γ_{72}	$K^*(892)^- \pi^+ \pi^+ 3\text{-body}$,		(2.1 \pm 2.2) $\times 10^{-3}$		Γ_{124}	$\phi \pi^+, \phi \rightarrow K^+ K^-$	(3.06 \pm 0.34)	$\times 10^{-3}$	
Γ_{73}	$K^*(892)^- \rightarrow K_S^0 \pi^-$		(3.6 \pm 1.8) $\times 10^{-3}$		Γ_{125}	$K^+ \bar{K}^*(892)^0$,	(2.90 \pm 0.32)	$\times 10^{-3}$	
Γ_{74}	$K_S^0 \rho^+ \pi^+$ total		(1.2 \pm 0.4) $\times 10^{-3}$		Γ_{126}	$\bar{K}^*(892)^0 \rightarrow K^- \pi^+$	(3.6 \pm 0.4)	$\times 10^{-3}$	
Γ_{75}	$K_S^0 \rho^+ \pi^+ 3\text{-body}$		(5.6 \pm 0.5) $\times 10^{-3}$	S=1.1	Γ_{127}	$K^+ K^- \pi^+$ nonresonant	—		
Γ_{76}	$K^- 3\pi^+ \pi^-$	[b]	(1.2 \pm 0.4) $\times 10^{-3}$		Γ_{128}	$K_S^0 K_S^0 \pi^+$	(5.3 \pm 2.3)	$\times 10^{-3}$	
Γ_{77}	$\bar{K}^*(892)^0 \pi^+ \pi^+ \pi^-$,		(2.3 \pm 0.4) $\times 10^{-3}$		Γ_{129}	$K^*(892)^+ K_S^0$,	(2.32 \pm 0.18)	$\times 10^{-3}$	
Γ_{78}	$\bar{K}^*(892)^0 \rightarrow K^- \pi^+$		(1.69 \pm 0.28) $\times 10^{-3}$		Γ_{130}	$K^*(892)^+ \rightarrow K_S^0 \pi^+$	—		
Γ_{79}	$\bar{K}^*(892)^0 \rho^0 \pi^+$,		(3.9 \pm 2.9) $\times 10^{-4}$		Γ_{131}	$K^+ K^- \pi^+ \pi^0$	(1.1 \pm 0.5) %		
Γ_{80}	$\bar{K}^*(892)^0 \rightarrow K^- \pi^+$		(4.5 \pm 2.1) $\times 10^{-3}$		Γ_{132}	$\phi \pi^+ \pi^0, \phi \rightarrow K^+ K^-$	< 7	$\times 10^{-3}$	CL=90%
Γ_{81}	$\bar{K}^*(892)^0 \pi^+ \pi^+ \pi^- \text{ no-}\rho$,		(2.3 \pm 0.5) $\times 10^{-4}$		Γ_{133}	$\phi \rho^+, \phi \rightarrow K^+ K^-$	(1.5 \pm 0.7)	$\times 10^{-3}$	
	$K^- \rho^0 \pi^+ \pi^+$		(1.69 \pm 0.28) $\times 10^{-3}$		Γ_{134}	$K^+ K^- \pi^+ \pi^0 \text{ non-}\phi$	(1.5 \pm 0.6) %		
	$K^- 3\pi^+ \pi^-$ nonresonant		(3.9 \pm 2.9) $\times 10^{-4}$		Γ_{135}	$K^+ K_S^0 \pi^+ \pi^-$	(1.69 \pm 0.18)	$\times 10^{-3}$	
	$K^+ 2K_S^0$		(4.5 \pm 2.1) $\times 10^{-3}$		Γ_{136}	$K_S^0 K^- \pi^+ \pi^+$	(2.32 \pm 0.18)	$\times 10^{-3}$	
	$K^+ K^- K_S^0 \pi^+$		(2.3 \pm 0.5) $\times 10^{-4}$		Γ_{137}	$K_S^0 K^- \pi^+ \pi^+ (\text{non-}K^* \bar{K}^*)$	(2.3 \pm 1.2)	$\times 10^{-4}$	

Fractions of some of the following modes with resonances have already appeared above as submodes of particular charged-particle modes.

Γ_{82}	$K_S^0 a_1(1260)^+$		(3.5 \pm 0.6) %	
Γ_{83}	$K_S^0 a_2(1320)^+$		< 1.5	$\times 10^{-3}$ CL=90%
Γ_{84}	$\bar{K}^*(892)^0 \rho^+$ total	[d]	(2.0 \pm 1.2) %	
Γ_{85}	$\bar{K}^*(892)^0 \rho^+$ S-wave	[d]	(1.5 \pm 1.5) %	
Γ_{86}	$\bar{K}^*(892)^0 \rho^+$ P-wave		< 1	$\times 10^{-3}$ CL=90%
Γ_{87}	$\bar{K}^*(892)^0 \rho^+$ D-wave		(9 \pm 6)	$\times 10^{-3}$ CL=90%
Γ_{88}	$\bar{K}^*(892)^0 \rho^+$ D-wave longitudinal		< 7	$\times 10^{-3}$ CL=90%
Γ_{89}	$\bar{K}_1(1270)^0 \pi^+$		< 7	$\times 10^{-3}$ CL=90%
Γ_{90}	$\bar{K}_1(1400)^0 \pi^+$		(3.8 \pm 1.3) %	
Γ_{91}	$\bar{K}^*(1410)^0 \pi^+$		(6.3 \pm 0.8) %	
Γ_{92}	$\bar{K}^*(892)^0 \pi^+ \pi^0$ total		(4.0 \pm 1.2) %	
Γ_{93}	$\bar{K}^*(892)^0 \pi^+ \pi^0 3\text{-body}$	[d]	(1.4 \pm 0.9) %	
Γ_{94}	$K^*(892)^- \pi^+ \pi^+$ total		(9.1 \pm 1.8)	$\times 10^{-3}$
Γ_{95}	$K^*(892)^- \pi^+ \pi^+ 3\text{-body}$		(9.1 \pm 1.8)	$\times 10^{-3}$
Γ_{96}	$K_S^0 f_0(980) \pi^+$		(9.1 \pm 1.8)	$\times 10^{-3}$
Γ_{97}	$\bar{K}^*(892)^0 a_1(1260)^+$		(9.1 \pm 1.8)	$\times 10^{-3}$

Pionic modes

Γ_{98}	$\pi^+ \pi^0$		(1.24 \pm 0.07)	$\times 10^{-3}$
Γ_{99}	$\pi^+ \pi^+ \pi^-$		(3.21 \pm 0.19)	$\times 10^{-3}$
Γ_{100}	$\rho^0 \pi^+$		(8.2 \pm 1.5)	$\times 10^{-4}$
Γ_{101}	$\pi^+ (\pi^+ \pi^-)_{S\text{-wave}}$		(1.80 \pm 0.16)	$\times 10^{-3}$
Γ_{102}	$\sigma \pi^+, \sigma \rightarrow \pi^+ \pi^-$		(1.35 \pm 0.12)	$\times 10^{-3}$
Γ_{103}	$f_0(980) \pi^+$,		(1.54 \pm 0.33)	$\times 10^{-4}$
Γ_{104}	$f_0(980) \rightarrow \pi^+ \pi^-$		(8 \pm 4)	$\times 10^{-5}$
Γ_{105}	$f_0(1370) \pi^+$,		(5.0 \pm 0.9)	$\times 10^{-4}$
Γ_{106}	$f_0(1370) \rightarrow \pi^+ \pi^-$		< 8	$\times 10^{-5}$ CL=95%
Γ_{107}	$f_2(1270) \pi^+$,		(1.1 \pm 0.4)	$\times 10^{-4}$
Γ_{108}	$f_2(1270) \rightarrow \pi^+ \pi^-$		< 5	$\times 10^{-5}$ CL=95%
Γ_{109}	$\rho(1450)^0 \pi^+$,		< 6	$\times 10^{-5}$ CL=95%
Γ_{110}	$\rho(1450)^0 \rightarrow \pi^+ \pi^-$		< 1.2	$\times 10^{-4}$ CL=95%
Γ_{111}	$\rho(1500) \pi^+$,		< 1.1	$\times 10^{-4}$ CL=95%
Γ_{112}	$\rho(1500) \rightarrow \pi^+ \pi^-$		(4.6 \pm 0.4)	$\times 10^{-3}$
Γ_{113}	$f_0(1710) \pi^+$,		(1.14 \pm 0.08) %	
Γ_{114}	$f_0(1710) \rightarrow \pi^+ \pi^-$		(7.7 \pm 0.7)	$\times 10^{-4}$
Γ_{115}	$f_0(1790) \pi^+$,		< 3	$\times 10^{-4}$ CL=90%
Γ_{116}	$f_0(1790) \rightarrow \pi^+ \pi^-$		(1.63 \pm 0.16)	$\times 10^{-3}$ S=1.1
Γ_{117}	$(\pi^+ \pi^+)_{S\text{-wave}} \pi^-$		< 1.2	$\times 10^{-4}$ CL=95%
Γ_{118}	$\pi^+ \pi^+ \pi^-$ nonresonant		< 1.1	$\times 10^{-4}$ CL=95%
	$\pi^+ 2\pi^0$		(4.6 \pm 0.4)	$\times 10^{-3}$
	$\pi^+ \pi^+ \pi^- \pi^0$		(1.14 \pm 0.08) %	
	$\eta \pi^+, \eta \rightarrow \pi^+ \pi^- \pi^0$		(7.7 \pm 0.7)	$\times 10^{-4}$
	$\omega \pi^+, \omega \rightarrow \pi^+ \pi^- \pi^0$		< 3	$\times 10^{-4}$ CL=90%
	$3\pi^+ 2\pi^-$		(1.63 \pm 0.16)	$\times 10^{-3}$ S=1.1

Fractions of some of the following modes with resonances have already appeared above as submodes of particular charged-particle modes.

Γ_{117}	$\eta \pi^+$		(3.39 \pm 0.29)	$\times 10^{-3}$
Γ_{118}	$\omega \pi^+$		< 3.4	$\times 10^{-4}$ CL=90%

Γ_{119}	$\eta \rho^+$	< 7	$\times 10^{-3}$	CL=90%
Γ_{120}	$\eta'(958) \pi^+$	(5.1 \pm 1.0)	$\times 10^{-3}$	
Γ_{121}	$\eta'(958) \rho^+$	< 5	$\times 10^{-3}$	CL=90%

Hadronic modes with a $K\bar{K}$ pair

Γ_{122}	$K^+ K_S^0$	(2.89 \pm 0.17)	$\times 10^{-3}$	
Γ_{123}	$K^+ K^- \pi^+$	[b] (9.63 \pm 0.31)	$\times 10^{-3}$	S=1.3
Γ_{124}	$\phi \pi^+, \phi \rightarrow K^+ K^-$	(3.06 \pm 0.34)	$\times 10^{-3}$	
Γ_{125}	$K^+ \bar{K}^*(892)^0$,	(2.90 \pm 0.32)	$\times 10^{-3}$	
Γ_{126}	$\bar{K}^*(892)^0 \rightarrow K^- \pi^+$	(3.6 \pm 0.4)	$\times 10^{-3}$	
Γ_{127}	$K^+ K^- \pi^+$ nonresonant	—		
Γ_{128}	$K_S^0 K_S^0 \pi^+$	(5.3 \pm 2.3)	$\times 10^{-3}$	
Γ_{129}	$K^*(892)^+ K_S^0$,	(2.32 \pm 0.18)	$\times 10^{-3}$	
Γ_{130}	$K^*(892)^+ \rightarrow K_S^0 \pi^+$	—		
Γ_{131}	$K^+ K^- \pi^+ \pi^0$	(1.1 \pm 0.5) %		
Γ_{132}	$\phi \pi^+ \pi^0, \phi \rightarrow K^+ K^-$	< 7	$\times 10^{-3}$	CL=90%
Γ_{133}	$\phi \rho^+, \phi \rightarrow K^+ K^-$	(1.5 \pm 0.7)	$\times 10^{-3}$	
Γ_{134}	$K^+ K^- \pi^+ \pi^0 \text{ non-}\phi$	(1.5 \pm 0.6) %		
Γ_{135}	$K^+ K_S^0 \pi^+ \pi^-$	(1.69 \pm 0.18)	$\times 10^{-3}$	
Γ_{136}	$K_S^0 K^- \pi^+ \pi^+$	(2.32 \pm 0.18)	$\times 10^{-3}$	
Γ_{137}	$K_S^0 K^- \pi^+ \pi^+ (\text{non-}K^* \bar{K}^*)$	(2.3 \pm 1.2)	$\times 10^{-4}$	

Fractions of the following modes with resonances have already appeared above as submodes of particular charged-particle modes.

Γ_{138}	$\phi \pi^+$	(6.2 \pm 0.7)	$\times 10^{-3}$	
Γ_{139}	$\phi \pi^+ \pi^0$	(2.3 \pm 1.0) %		
Γ_{140}	$\phi \rho^+$	< 1.5	%	CL=90%
Γ_{141}	$K^+ \bar{K}^*(892)^0$	(4.4 \pm 0.5)	$\times 10^{-3}$	
Γ_{142}	$K^*(892)^+ K_S^0$	(1.6 \pm 0.7) %		
Γ_{143}	$K^*(892)^+ \bar{K}^*(892)^0$			

Doubly Cabibbo-suppressed modes

Γ_{144}	$K^+ \pi^0$	(2.37 \pm 0.32)	$\times 10^{-4}$	
Γ_{145}	$K^+ \pi^+ \pi^-$	(6.2 \pm 0.7)	$\times 10^{-4}$	
Γ_{146}	$K^+ \rho^0$	(2.4 \pm 0.6)	$\times 10^{-4}$	
Γ_{147}	$K^*(892)^0 \pi^+, K^*(892)^0 \rightarrow$	(2.9 \pm 0.6)	$\times 10^{-4}$	
Γ_{148}	$K^+ f_0(980), f_0(980) \rightarrow$	(5.6 \pm 3.4)	$\times 10^{-5}$	
Γ_{149}	$K_S^+ \pi^+ \pi^- \pi^0, K_S^+(1430)^0 \rightarrow$	(5.0 \pm 3.4)	$\times 10^{-5}$	
Γ_{150}	$K^+ \pi^+ \pi^-$ nonresonant	(8.7 \pm 2.0)	$\times 10^{-5}$	
Γ_{151}	$K^+ K^+ K^-$	(8.7 \pm 2.0)	$\times 10^{-5}$	

 $\Delta C = 1$ weak neutral current (CI) modes, or Lepton Family number (LF) or Lepton number (L) violating modes

Γ_{152}	$\pi^+ e^+ e^-$	CI	< 7.4	$\times 10^{-6}$	CL=90%
Γ_{153}	$\pi^+ \phi, \phi \rightarrow e^+ e^-$	[e]	(2.7 \pm 3.6)	$\times 10^{-6}$	
Γ_{154}	$\pi^+ \mu^+ \mu^-$	CI	< 3.9	$\times 10^{-6}$	CL=90%
Γ_{155}	$\rho^+ \mu^+ \mu^-$	CI	< 5.6	$\times 10^{-4}$	CL=90%
Γ_{156}	$K^+ e^+ e^-$	[f]	< 6.2	$\times 10^{-6}$	CL=90%
Γ_{157}	$K^+ \mu^+ \mu^-$	[f]	< 9.2	$\times 10^{-6}$	CL=90%
Γ_{158}	$\pi^+ e^\pm \mu^\mp$	LF	[g] < 3.4	$\times 10^{-5}$	CL=90%
Γ_{159}	$\pi^+ e^+ \mu^-$				
Γ_{160}	$\pi^+ e^- \mu^+$				
Γ_{161}	$K^+ e^\pm \mu^\mp$	LF	[g] < 6.8	$\times 10^{-5}$	CL=90%
Γ_{162}	$K^+ e^+ \mu^-$				
Γ_{163}	$K^+ e^- \mu^+$				
Γ_{164}	$\pi^- e^+ e^+$	L	< 3.6	$\times 10^{-6}$	CL=90%
Γ_{165}	$\pi^- \mu^+ \mu^+$	L	< 4.8	$\times 10^{-6}$	CL=90%
Γ_{166}	$\pi^- e^+ \mu^+$	L	< 5.0	$\times 10^{-5}$	CL=90%
Γ_{167}	$\rho^- \mu^+ \mu^+$	L	< 5.6	$\times 10^{-4}$	CL=90%
Γ_{168}	$K^- e^+ e^+$	L	< 4.5	$\times 10^{-6}$	CL=90%
Γ_{169}	$K^- \mu^+ \mu^+$	L	< 1.3	$\times 10^{-5}$	CL=90%
Γ_{170}	$K^- e^+ \mu^+$	L	< 1.3	$\times 10^{-4}$	CL=90%
Γ_{171}	$K^*(892)^- \mu^+ \mu^+$	L	< 8.5	$\times 10^{-4}$	CL=90%

Γ_{172} A dummy mode used by the fit. (37.3 \pm 1.6) %

See key on page 373

Meson Particle Listings

 D^{\pm} $\Gamma(K^*(892)^+ \text{ anything})/\Gamma_{\text{total}}$ Γ_8/Γ

VALUE	CL%	DOCUMENT ID	TECN	COMMENT
• • • We do not use the following data for averages, fits, limits, etc. • • •				
<0.203	90	¹⁰ ABLIKIM	06U BES2	e^+e^- at 3773 MeV
¹⁰ One-third of the $K^*(892)^+$ would decay to $K^+\pi^0$, and one-third of this ABLIKIM 06U limit is < 0.068, which is larger than the measured K^+X branching fraction.				

 $\Gamma(K^*(892)^0 \text{ anything})/\Gamma_{\text{total}}$ Γ_9/Γ

VALUE	CL%	DOCUMENT ID	TECN	COMMENT
<0.066	90	ABLIKIM	05P BES	$e^+e^- \approx 3773$ MeV

 $\Gamma(\eta \text{ anything})/\Gamma_{\text{total}}$ Γ_{10}/Γ

This ratio includes η particles from η' decays.

VALUE (units 10^{-2})	EVTS	DOCUMENT ID	TECN	COMMENT
6.3 ± 0.5 ± 0.5	1972 ± 142	HUANG	06B CLEO	e^+e^- at $\psi(3770)$

 $\Gamma(\eta' \text{ anything})/\Gamma_{\text{total}}$ Γ_{11}/Γ

VALUE (units 10^{-2})	EVTS	DOCUMENT ID	TECN	COMMENT
1.04 ± 0.16 ± 0.09	82 ± 13	HUANG	06B CLEO	e^+e^- at $\psi(3770)$

 $\Gamma(\phi \text{ anything})/\Gamma_{\text{total}}$ Γ_{12}/Γ

VALUE (units 10^{-2})	EVTS	DOCUMENT ID	TECN	COMMENT
1.03 ± 0.10 ± 0.07	248 ± 21	HUANG	06B CLEO	e^+e^- at $\psi(3770)$

Leptonic and semileptonic modes

 $\Gamma(e^+ \nu_e)/\Gamma_{\text{total}}$ Γ_{13}/Γ

VALUE	CL%	DOCUMENT ID	TECN	COMMENT
<2.4 × 10 ⁻⁵	90	ARTUSO	05A CLEO	e^+e^- at $\psi(3770)$

 $\Gamma(\mu^+ \nu_\mu)/\Gamma_{\text{total}}$ Γ_{14}/Γ

See the note on "Decay Constants of Charged Pseudoscalar Mesons" in the D_S^+ Listings.

VALUE (units 10^{-4})	EVTS	DOCUMENT ID	TECN	COMMENT
4.40 ± 0.66 ± 0.09 ± 0.12	47 ± 7	¹¹ ARTUSO	05A CLEO	e^+e^- at $\psi(3770)$

• • • We do not use the following data for averages, fits, limits, etc. • • •

12.2 $\frac{+11.1}{-5.3}$ ± 1.0	3	¹² ABLIKIM	05D BES	$e^+e^- \approx 3.773$ GeV
3.5 ± 1.4 ± 0.6	7	¹³ BONVICINI	04A CLEO	Incl. in ARTUSO 05A
8 $\frac{+16}{-5}$ $\frac{+5}{-2}$	1	¹⁴ BAI	98B BES	$e^+e^- \rightarrow D^{*+} D^-$

- ¹¹ ARTUSO 05A obtains $f_{D^+} = 222.6 \pm 16.7 \pm 2.8 \pm 3.4$ MeV from this measurement.
- ¹² ABLIKIM 05D finds a background-subtracted 2.67 ± 1.74 $D^+ \rightarrow \mu^+ \nu_\mu$ events, and from this obtains $f_{D^+} = 371 \pm 129 \pm 25$ MeV.
- ¹³ BONVICINI 04A finds eight events with an estimated background of one, and from the branching fraction obtains $f_{D^+} = 202 \pm 41 \pm 17$ MeV.
- ¹⁴ BAI 98B obtains $f_{D^+} = (300 \pm 180 \pm 80 \pm 150 \pm 40)$ MeV from this measurement.

 $\Gamma(\tau^+ \nu_\tau)/\Gamma_{\text{total}}$ Γ_{15}/Γ

VALUE	EVTS	DOCUMENT ID	TECN	COMMENT
<2.1 × 10 ⁻³	90	RUBIN	06A CLEO	e^+e^- at $\psi(3770)$

 $\Gamma(\bar{K}^0 e^+ \nu_e)/\Gamma_{\text{total}}$ Γ_{17}/Γ

VALUE	EVTS	DOCUMENT ID	TECN	COMMENT
0.086 ± 0.005 OUR FIT				
0.087 ± 0.005 OUR AVERAGE				
0.0895 ± 0.0159 ± 0.0067	34 ± 6	¹⁵ ABLIKIM	05A BES	e^+e^- at $\psi(3770)$
0.0871 ± 0.0038 ± 0.0037	545 ± 24	¹⁶ HUANG	05B CLEO	e^+e^- at $\psi(3770)$

- ¹⁵ The ABLIKIM 05A result together with the $D^0 \rightarrow K^- e^+ \nu_e$ branching fraction of ABLIKIM 04C and Particle Data Group lifetimes gives $\Gamma(D^0 \rightarrow K^- e^+ \nu_e) / \Gamma(D^+ \rightarrow \bar{K}^0 e^+ \nu_e) = 1.08 \pm 0.22 \pm 0.07$; isospin invariance predicts the ratio is 1.0.
- ¹⁶ HUANG 05B finds $\Gamma(D^0 \rightarrow K^- e^+ \nu_e) / \Gamma(D^+ \rightarrow \bar{K}^0 e^+ \nu_e) = 1.00 \pm 0.05 \pm 0.04$; isospin invariance predicts the ratio is 1.0.

 $\Gamma(\bar{K}^0 e^+ \nu_e)/\Gamma(K_S^0 \pi^+)$ Γ_{17}/Γ_{44}

VALUE	EVTS	DOCUMENT ID	TECN	COMMENT
5.91 ± 0.35 OUR FIT				
5.20 ± 0.70 ± 0.52	186	¹⁷ BEAN	93C CLEO	$e^+e^- \approx \mathcal{T}(4S)$

- ¹⁷ BEAN 93C uses $\bar{K}^0 \mu^+ \nu_\mu$ as well as $\bar{K}^0 e^+ \nu_e$ events and makes a small phase-space adjustment to the number of the μ^+ events to use them as e^+ events. The value given is twice that in BEAN 93C because we are using $K_S^0 \pi^+$ and not $\bar{K}^0 \pi^+$, in the denominator.

 $\Gamma(\bar{K}^0 \mu^+ \nu_\mu)/\Gamma_{\text{total}}$ Γ_{18}/Γ

VALUE	EVTS	DOCUMENT ID	TECN	COMMENT
0.093 ± 0.008 OUR FIT				Error includes scale factor of 1.1.
0.103 ± 0.023 ± 0.008	29 ± 6	ABLIKIM	07 BES2	e^+e^- at 3773 MeV

 $\Gamma(\bar{K}^0 \mu^+ \nu_\mu)/\Gamma(K^- \pi^+ \pi^+)$ Γ_{18}/Γ_{46}

VALUE	EVTS	DOCUMENT ID	TECN	COMMENT
1.01 ± 0.08 OUR FIT				Error includes scale factor of 1.1.
1.019 ± 0.076 ± 0.065	555 ± 39	LINK	04E FOCUS	γ nucleus, $\bar{E}_{\gamma} \approx 180$ GeV

 $\Gamma(\bar{K}^0 \mu^+ \nu_\mu)/\Gamma(\mu^+ \text{ anything})$ Γ_{18}/Γ_2

VALUE	EVTS	DOCUMENT ID	COMMENT
• • • We do not use the following data for averages, fits, limits, etc. • • •			
0.76 ± 0.06	84	¹⁸ AOKI	88 π^- emulsion
¹⁸ From topological branching ratios in emulsion with an identified muon.			

 $\Gamma(K^- \pi^+ e^+ \nu_e)/\Gamma_{\text{total}}$ Γ_{19}/Γ

VALUE (units 10^{-2})	EVTS	DOCUMENT ID	TECN	COMMENT
4.1 ± 0.6 OUR FIT				Error includes scale factor of 1.1.
3.5 $\frac{+0.7}{-0.6}$ OUR AVERAGE				
3.50 ± 0.75 ± 0.27	29 ± 6	ABLIKIM	06o BES2	e^+e^- at 3773 MeV
3.5 $\frac{+1.2}{-0.7}$ ± 0.4	14	BAI	91 MRK3	$e^+e^- \approx 3.77$ GeV

 $\Gamma(\bar{K}^*(892)^0 e^+ \nu_e)/\Gamma_{\text{total}}$ Γ_{37}/Γ

Unseen decay modes of $\bar{K}^*(892)^0$ are included. See the end of the D^+ Listings for measurements of $D^+ \rightarrow \bar{K}^*(892)^0 e^+ \nu_e$ form-factor ratios.

VALUE (units 10^{-2})	EVTS	DOCUMENT ID	TECN	COMMENT
5.49 ± 0.31 OUR FIT				Error includes scale factor of 1.2.
5.52 ± 0.34 OUR AVERAGE				

5.06 ± 1.21 ± 0.40	28 ± 7	ABLIKIM	06o BES2	e^+e^- at 3773 MeV
5.56 ± 0.27 ± 0.23	422 ± 21	¹⁹ HUANG	05B CLEO	e^+e^- at $\psi(3770)$

- ¹⁹ HUANG 05B finds $\Gamma(D^0 \rightarrow K^{*-} e^+ \nu_e) / \Gamma(D^+ \rightarrow \bar{K}^{*0} e^+ \nu_e) = 0.98 \pm 0.08 \pm 0.04$; isospin invariance predicts the ratio is 1.0.

 $\Gamma(\bar{K}^*(892)^0 e^+ \nu_e)/\Gamma(K^- \pi^+ e^+ \nu_e)$ Γ_{37}/Γ_{19}

Unseen decay modes of the $\bar{K}^*(892)^0$ are included. See the end of the D^+ Listings for measurements of $D^+ \rightarrow \bar{K}^*(892)^0 e^+ \nu_e$ form-factor ratios.

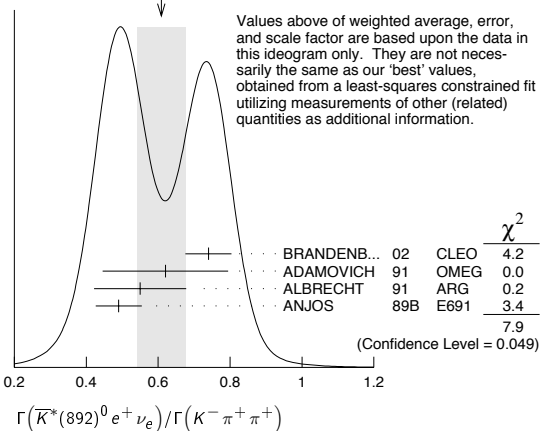
VALUE	EVTS	DOCUMENT ID	TECN	COMMENT
1.35 ± 0.22 OUR FIT				Error includes scale factor of 1.2.
1.0 ± 0.3	35	ADAMOVIICH	91 OMEG	π^- 340 GeV

 $\Gamma(\bar{K}^*(892)^0 e^+ \nu_e)/\Gamma(K^- \pi^+ \pi^+)$ Γ_{37}/Γ_{46}

Unseen decay modes of the $\bar{K}^*(892)^0$ are included. See the end of the D^+ Listings for measurements of $D^+ \rightarrow \bar{K}^*(892)^0 e^+ \nu_e$ form-factor ratios.

VALUE	EVTS	DOCUMENT ID	TECN	COMMENT
0.596 ± 0.035 OUR FIT				Error includes scale factor of 1.3.
0.61 ± 0.07 OUR AVERAGE				Error includes scale factor of 1.6. See the ideogram below.
0.74 ± 0.04 ± 0.05		BRANDENB...	02 CLEO	$e^+e^- \approx \mathcal{T}(4S)$
0.62 ± 0.15 ± 0.09	35	ADAMOVIICH	91 OMEG	π^- 340 GeV
0.55 ± 0.08 ± 0.10	880	ALBRECHT	91 ARG	$e^+e^- \approx 10.4$ GeV
0.49 ± 0.04 ± 0.05		ANJOS	89B E691	Photoproduction

WEIGHTED AVERAGE
0.61 ± 0.07 (Error scaled by 1.6)

 $\Gamma(K^- \pi^+ e^+ \nu_e \text{ nonresonant})/\Gamma_{\text{total}}$ Γ_{21}/Γ

VALUE	CL%	DOCUMENT ID	TECN	COMMENT
<0.007	90	ANJOS	89B E691	Photoproduction

 $\Gamma(K^- \pi^+ \mu^+ \nu_\mu)/\Gamma(\bar{K}^0 \mu^+ \nu_\mu)$ Γ_{22}/Γ_{18}

VALUE	EVTS	DOCUMENT ID	TECN	COMMENT
0.417 ± 0.030 ± 0.023	555 ± 39	LINK	04E FOCUS	γ nucleus, $\bar{E}_{\gamma} \approx 180$ GeV

 $\Gamma(\bar{K}^*(892)^0 \mu^+ \nu_\mu)/\Gamma(\bar{K}^0 \mu^+ \nu_\mu)$ Γ_{38}/Γ_{18}

Unseen decay modes of the $\bar{K}^*(892)^0$ are included. See the end of the D^+ Listings for measurements of $D^+ \rightarrow \bar{K}^*(892)^0 e^+ \nu_e$ form-factor ratios.

VALUE	EVTS	DOCUMENT ID	TECN	COMMENT
0.58 ± 0.05 OUR FIT				
0.594 ± 0.043 ± 0.033	555 ± 39	LINK	04E FOCUS	γ nucleus, $\bar{E}_{\gamma} \approx 180$ GeV

Meson Particle Listings

 D^\pm $\Gamma(\bar{K}^*(892)^0 \mu^+ \nu_\mu) / \Gamma(K^- \pi^+ \pi^+)$ $\Gamma_{38} / \Gamma_{46}$

Unseen decay modes of the $\bar{K}^*(892)^0$ are included. See the end of the D^+ Listings for measurements of $D^+ \rightarrow \bar{K}^*(892)^0 \ell^+ \nu_\ell$ form-factor ratios.

VALUE	EVTs	DOCUMENT ID	TECN	COMMENT
0.58 ± 0.05 OUR FIT				Error includes scale factor of 1.1.
0.57 ± 0.06 OUR AVERAGE				Error includes scale factor of 1.2.
0.72 ± 0.10 ± 0.05		BRANDENB... 02	CLEO	$e^+ e^- \approx \gamma(4S)$
0.56 ± 0.04 ± 0.06	875	FRABETTI 93E	E687	γ Be $\bar{E}_\gamma \approx 200$ GeV
0.46 ± 0.07 ± 0.08	224	KODAMA 92C	E653	π^- emulsion 600 GeV
• • •				We do not use the following data for averages, fits, limits, etc. • • •
0.602 ± 0.010 ± 0.021	12k	20 LINK 02J	FOCS	γ nucleus, ≈ 180 GeV

²⁰This LINK 02J result includes the effects of an interference of a small S -wave $K^- \pi^+$ amplitude with the dominant \bar{K}^{*0} amplitude. (The interference effect is reported in LINK 02E.) This result is redundant with results of LINK 04E elsewhere in these Listings.

 $\Gamma(K^- \pi^+ \mu^+ \nu_\mu \text{ nonresonant}) / \Gamma(K^- \pi^+ \mu^+ \nu_\mu)$ $\Gamma_{24} / \Gamma_{22}$

VALUE	EVTs	DOCUMENT ID	TECN	COMMENT
0.0530 ± 0.0074 ± 0.0099	14k	LINK 05I	FOCS	γ nucleus, $\bar{E}_\gamma \approx 180$ GeV

 $\Gamma(\pi^0 e^+ \nu_e) / \Gamma_{\text{total}}$ Γ_{28} / Γ

VALUE	EVTs	DOCUMENT ID	TECN	COMMENT
0.0044 ± 0.0006 ± 0.0003	63 ± 9	21 HUANG 05B	CLEO	$e^+ e^-$ at $\psi(3770)$

²¹HUANG 05B finds $\Gamma(D^0 \rightarrow \pi^- e^+ \nu_e) / 2 \Gamma(D^+ \rightarrow \pi^0 e^+ \nu_e) = 0.75 \pm 0.14$ ± 0.04; isospin invariance predicts the ratio is 1.0.

 $\Gamma(\pi^0 \ell^+ \nu_\ell) / \Gamma(\bar{K}^{*0} \ell^+ \nu_\ell)$ $\Gamma_{29} / \Gamma_{16}$

VALUE	EVTs	DOCUMENT ID	TECN	COMMENT
0.046 ± 0.014 ± 0.017	100	22 BARTELT 97	CLEO	$e^+ e^- \approx \gamma(4S)$
• • •				We do not use the following data for averages, fits, limits, etc. • • •

0.085 ± 0.027 ± 0.014 53 ²³ALAM 93 CLEO See BARTELT 97

²²BARTELT 97 thus directly measures the product of ratios squared of CKM matrix elements and form factors at $q^2=0$: $|V_{cd}/V_{cs}|^2 \cdot |f_+^\pi(0)/f_+^K(0)|^2 = 0.046 \pm 0.014 \pm 0.017$.

²³ALAM 93 thus directly measures the product of ratios squared of CKM matrix elements and form factors at $q^2=0$: $|V_{cd}/V_{cs}|^2 \cdot |f_+^\pi(0)/f_+^K(0)|^2 = 0.085 \pm 0.027 \pm 0.014$.

 $\Gamma(\rho^0 e^+ \nu_e) / \Gamma_{\text{total}}$ Γ_{30} / Γ

VALUE	EVTs	DOCUMENT ID	TECN	COMMENT
0.0022 ± 0.0004 OUR FIT				
0.0021 ± 0.0004 ± 0.0001	27 ± 6	24 HUANG 05B	CLEO	$e^+ e^-$ at $\psi(3770)$

²⁴HUANG 05B finds $\Gamma(D^0 \rightarrow \rho^- e^+ \nu_e) / 2 \Gamma(D^+ \rightarrow \rho^0 e^+ \nu_e) = 1.2 \pm 0.4$ ± 0.1; isospin invariance predicts the ratio is 1.0.

 $\Gamma(\rho^0 e^+ \nu_e) / \Gamma(\bar{K}^*(892)^0 e^+ \nu_e)$ $\Gamma_{30} / \Gamma_{37}$

VALUE	EVTs	DOCUMENT ID	TECN	COMMENT
0.039 ± 0.007 OUR FIT				
0.045 ± 0.014 ± 0.009	49	25 AITALA 97	E791	π^- nucleus, 500 GeV

²⁵AITALA 97 explicitly subtracts $D^+ \rightarrow \eta' e^+ \nu_e$ and other backgrounds to get this result.

 $\Gamma(\rho^0 \mu^+ \nu_\mu) / \Gamma(\bar{K}^*(892)^0 \mu^+ \nu_\mu)$ $\Gamma_{31} / \Gamma_{38}$

VALUE	EVTs	DOCUMENT ID	TECN	COMMENT
0.045 ± 0.007 OUR AVERAGE				Error includes scale factor of 1.1.
0.041 ± 0.006 ± 0.004	320 ± 44	LINK 06B	FOCS	γ A, $\bar{E}_\gamma \approx 180$ GeV

0.051 ± 0.015 ± 0.009 54 ²⁶AITALA 97 E791 π^- nucleus, 500 GeV

0.079 ± 0.019 ± 0.013 39 ²⁷FRABETTI 97 E687 γ Be, $\bar{E}_\gamma \approx 220$ GeV

²⁶AITALA 97 explicitly subtracts $D^+ \rightarrow \eta' \mu^+ \nu_\mu$ and other backgrounds to get this result.

²⁷Because the reconstruction efficiency for photons is low, this FRABETTI 97 result also includes any $D^+ \rightarrow \eta' \mu^+ \nu_\mu \rightarrow \gamma \rho^0 \mu^+ \nu_\mu$ events in the numerator.

 $\Gamma(\omega e^+ \nu_e) / \Gamma_{\text{total}}$ Γ_{32} / Γ

VALUE	EVTs	DOCUMENT ID	TECN	COMMENT
0.0016 ± 0.0007 ± 0.0006	7.6 ± 3.3	2,7 HUANG 05B	CLEO	$e^+ e^-$ at $\psi(3770)$

 $\Gamma(\phi e^+ \nu_e) / \Gamma_{\text{total}}$ Γ_{33} / Γ

Unseen decay modes of the ϕ are included.

VALUE	CL%	DOCUMENT ID	TECN	COMMENT
< 0.0201	90	ABLIKIM 06P	BES2	$e^+ e^-$ at 3773 MeV
• • •				We do not use the following data for averages, fits, limits, etc. • • •

< 0.0209 90 BAI 91 MRK3 $e^+ e^- \approx 3.77$ GeV

 $\Gamma(\phi \mu^+ \nu_\mu) / \Gamma_{\text{total}}$ Γ_{34} / Γ

Unseen decay modes of the ϕ are included.

VALUE	CL%	DOCUMENT ID	TECN	COMMENT
< 0.0204	90	ABLIKIM 06P	BES2	$e^+ e^-$ at 3773 MeV
• • •				We do not use the following data for averages, fits, limits, etc. • • •

< 0.0372 90 BAI 91 MRK3 $e^+ e^- \approx 3.77$ GeV

 $\Gamma(\eta \ell^+ \nu_\ell) / \Gamma(\pi^0 \ell^+ \nu_\ell)$ $\Gamma_{35} / \Gamma_{29}$

VALUE	CL%	DOCUMENT ID	TECN	COMMENT
< 1.5	90	BARTELT 97	CLEO	$e^+ e^- \approx \gamma(4S)$

 $\Gamma(\eta'(958) \mu^+ \nu_\mu) / \Gamma(\bar{K}^*(892)^0 \mu^+ \nu_\mu)$ $\Gamma_{36} / \Gamma_{38}$

Decay modes of the $\eta'(958)$ not included in the search are corrected for.

VALUE	CL%	DOCUMENT ID	TECN	COMMENT
< 0.20	90	KODAMA 93B	E653	π^- emulsion 600 GeV

 $\Gamma((\bar{K}^*(892) \pi)^0 e^+ \nu_e) / \Gamma_{\text{total}}$ Γ_{25} / Γ

Unseen decay modes of the $\bar{K}^*(892)$ are included.

VALUE	CL%	DOCUMENT ID	TECN	COMMENT
• • •				We do not use the following data for averages, fits, limits, etc. • • •

< 0.012 90 ANJOS 92 E691 Photoproduction

 $\Gamma((\bar{K} \pi \pi)^0 e^+ \nu_e \text{ non-}\bar{K}^*(892)) / \Gamma_{\text{total}}$ Γ_{26} / Γ

VALUE	CL%	DOCUMENT ID	TECN	COMMENT
• • •				We do not use the following data for averages, fits, limits, etc. • • •

< 0.009 90 ANJOS 92 E691 Photoproduction

 $\Gamma(K^- \pi^+ \pi^0 \mu^+ \nu_\mu) / \Gamma(K^- \pi^+ \mu^+ \nu_\mu)$ $\Gamma_{27} / \Gamma_{22}$

VALUE	CL%	DOCUMENT ID	TECN	COMMENT
< 0.042	90	FRABETTI 93E	E687	γ Be $\bar{E}_\gamma \approx 200$ GeV

 $\Gamma(\bar{K}_1^*(1270)^0 \mu^+ \nu_\mu) / \Gamma(\bar{K}^*(892)^0 \mu^+ \nu_\mu)$ $\Gamma_{39} / \Gamma_{38}$

VALUE	CL%	DOCUMENT ID	TECN	COMMENT
• • •				We do not use the following data for averages, fits, limits, etc. • • •

< 0.78 95 ABE 99P CDF $\bar{p}p$ 1.8 TeV

 $\Gamma(\bar{K}^*(1410)^0 \mu^+ \nu_\mu) / \Gamma(\bar{K}^*(892)^0 \mu^+ \nu_\mu)$ $\Gamma_{40} / \Gamma_{38}$

VALUE	CL%	DOCUMENT ID	TECN	COMMENT
• • •				We do not use the following data for averages, fits, limits, etc. • • •

< 0.60 95 ABE 99P CDF $\bar{p}p$ 1.8 TeV

 $\Gamma(\bar{K}_0^*(1430)^0 \mu^+ \nu_\mu) / \Gamma(K^- \pi^+ \mu^+ \nu_\mu)$ $\Gamma_{41} / \Gamma_{22}$

Unseen decay modes of the $\bar{K}_0^*(1430)^0$ are included.

VALUE	EVTs	DOCUMENT ID	TECN	COMMENT
< 0.0064	90	LINK 05I	FOCS	γ nucleus, $\bar{E}_\gamma \approx 180$ GeV

 $\Gamma(\bar{K}_2^*(1430)^0 \mu^+ \nu_\mu) / \Gamma(\bar{K}^*(892)^0 \mu^+ \nu_\mu)$ $\Gamma_{42} / \Gamma_{38}$

VALUE	CL%	DOCUMENT ID	TECN	COMMENT
• • •				We do not use the following data for averages, fits, limits, etc. • • •

< 0.19 95 ABE 99P CDF $\bar{p}p$ 1.8 TeV

 $\Gamma(\bar{K}^*(1680)^0 \mu^+ \nu_\mu) / \Gamma(K^- \pi^+ \mu^+ \nu_\mu)$ $\Gamma_{43} / \Gamma_{22}$

Unseen decay modes of the $\bar{K}^*(1680)^0$ are included.

VALUE	EVTs	DOCUMENT ID	TECN	COMMENT
< 0.04	90	LINK 05I	FOCS	γ nucleus, $\bar{E}_\gamma \approx 180$ GeV

Hadronic modes with a \bar{K} or $\bar{K} \bar{K}$ $\Gamma(K_S^0 \pi^+) / \Gamma_{\text{total}}$ Γ_{44} / Γ

VALUE (units 10^{-2})	EVTs	DOCUMENT ID	TECN	COMMENT
1.45 ± 0.04 OUR FIT				Error includes scale factor of 1.3.
1.526 ± 0.022 ± 0.038	28	DOBBS 07	CLEO	$e^+ e^-$ at $\psi(3770)$

• • • We do not use the following data for averages, fits, limits, etc. • • •

1.55 ± 0.05 ± 0.06 2230 ± 60 ²⁸HE 05 CLEO See DOBBS 07

1.6 ± 0.3 ± 0.1 161 ADLER 88C MRK3 $e^+ e^-$ 3.77 GeV

²⁸DOBBS 07 and HE 05 use single- and double-tagged events in an overall fit. DOBBS 07 supersedes HE 05.

 $\Gamma(K_S^0 \pi^+) / \Gamma(K^- \pi^+ \pi^+)$ $\Gamma_{44} / \Gamma_{46}$

VALUE	EVTs	DOCUMENT ID	TECN	COMMENT
0.157 ± 0.005 OUR FIT				Error includes scale factor of 2.1.
0.1530 ± 0.0023 ± 0.0016	10.6k	LINK 02B	FOCS	γ nucleus, $\bar{E}_\gamma \approx 180$ GeV

• • • We do not use the following data for averages, fits, limits, etc. • • •

0.174 ± 0.012 ± 0.011 473 ²⁹BISHAI 97 CLEO $e^+ e^- \approx \gamma(4S)$

0.137 ± 0.015 ± 0.016 264 ANJOS 90C E691 Photoproduction

²⁹See BISHAI 97 for an isospin analysis of $D^+ \rightarrow \bar{K} \pi$ amplitudes.

 $\Gamma(K_L^0 \pi^+) / \Gamma_{\text{total}}$ Γ_{45} / Γ

VALUE (units 10^{-2})	EVTs	DOCUMENT ID	TECN	COMMENT
1.460 ± 0.040 ± 0.035	2023 ± 54	30 HE 08	CLEO	$e^+ e^-$ at $\psi(3770)$

³⁰The difference of CLEO $D^+ \rightarrow K_S^0 \pi^+$ and $K_L^0 \pi^+$ branching fractions over the sum (DOBBS 07 and HE 08) is $+0.022 \pm 0.016 \pm 0.018$.

$\Gamma(K^- \pi^+ \pi^+)/\Gamma_{\text{total}}$					Γ_{46}/Γ
VALUE (units 10^{-2})	EVTS	DOCUMENT ID	TECN	COMMENT	
9.22 ± 0.21 OUR FIT	Error includes scale factor of 1.1.				
9.14 ± 0.10 ± 0.17		³¹ DOBBS	07 CLEO	$e^+ e^-$ at $\psi(3770)$	
• • • We do not use the following data for averages, fits, limits, etc. • • •					
9.5 ± 0.2 ± 0.3	15.1k ± 130	³¹ HE	05 CLEO	See DOBBS 07	
9.3 ± 0.6 ± 0.8	1502	³² BALEST	94 CLEO	$e^+ e^- \approx \Upsilon(4S)$	
6.4 +1.5 -1.4		³³ BARLAG	92c ACCM	π^- Cu 230 GeV	
9.1 ± 1.3 ± 0.4	1164	ADLER	88c MRK3	$e^+ e^-$ 3.77 GeV	
9.1 ± 1.9	239	³⁴ SCHINDLER	81 MRK2	$e^+ e^-$ 3.771 GeV	
³¹ DOBBS 07 and HE 05 use single- and double-tagged events in an overall fit. DOBBS 07 supersedes HE 05.					
³² BALEST 94 measures the ratio of $D^+ \rightarrow K^- \pi^+ \pi^+$ and $D^0 \rightarrow K^- \pi^+$ branching fractions to be $2.35 \pm 0.16 \pm 0.16$ and uses their absolute measurement of the $D^0 \rightarrow K^- \pi^+$ fraction (AKERIB 93).					
³³ BARLAG 92c computes the branching fraction by topological normalization.					
³⁴ SCHINDLER 81 (MARK-2) measures $\sigma(e^+ e^- \rightarrow \psi(3770)) \times$ branching fraction to be 0.38 ± 0.05 nb. We use the MARK-3 (ADLER 88c) value of $\sigma = 4.2 \pm 0.6 \pm 0.3$ nb.					

DALITZ PLOT ANALYSIS FORMALISM

Written January 2006 by D. Asner (Carleton University)

Introduction: Weak nonleptonic decays of D and B mesons are expected to proceed dominantly through resonant two-body decays [1]; see Ref. [2] for a review of resonance phenomenology. The amplitudes are typically calculated with the Dalitz-plot analysis technique [3], which uses the minimum number of independent observable quantities. For three-body decays of a spin-0 particle to all pseudo-scalar final states, D or $B \rightarrow abc$, the decay rate [4] is

$$\Gamma = \frac{1}{(2\pi)^3 32\sqrt{s^3}} |\mathcal{M}|^2 dm_{ab}^2 dm_{bc}^2, \quad (1)$$

where m_{ij} is the invariant mass of particles i and j . The coefficient of the amplitude includes all kinematic factors, and $|\mathcal{M}|^2$ contains the dynamics. The scatter plot in m_{ab}^2 versus m_{bc}^2 is the Dalitz plot. If $|\mathcal{M}|^2$ is constant, the kinematically allowed region of the plot will be populated uniformly with events. Any variation in the population over the Dalitz plot is due to dynamical rather than kinematical effects. It is straightforward to extend the formalism beyond three-body final states. For N -body final states with only spin-0 particles, phase space has dimension $3N - 7$. Other decays of interest include one vector particle or a fermion/anti-fermion pair (*e.g.*, $B \rightarrow D^* \pi \pi$, $B \rightarrow \bar{A}_c p \pi$, $B \rightarrow K \ell \ell$) in the final state. For the first case, phase space has dimension $3N - 5$, and for the latter two the dimension is $3N - 4$.

Formalism: The amplitude for the process, $R \rightarrow rc, r \rightarrow ab$ where R is a D or B , r is an intermediate resonance, and a, b, c are pseudo-scalars, is given by

$$\begin{aligned} \mathcal{M}_r(J, L, l, m_{ab}, m_{bc}) &= \sum_{\lambda} \langle ab|r_{\lambda} \rangle T_r(m_{ab}) \langle cr_{\lambda}|R_J \rangle \quad (2) \\ &= Z(J, L, l, \vec{p}, \vec{q}) B_L^R(|\vec{p}|) B_L^r(|\vec{q}|) T_r(m_{ab}). \end{aligned}$$

The sum is over the helicity states λ of r , J is the total angular momentum of R (for D and B decays, $J=0$), L is the orbital angular momentum between r and c , l is the orbital angular momentum between a and b (the spin of r), \vec{p} and \vec{q} are the momenta of c and of a in the r rest frame, Z describes the

angular distribution of the final-state particles, B_L^R and B_L^r are the barrier factors for the production of rc and of ab , and T_r is the dynamical function describing the resonance r . The amplitude for modeling the Dalitz plot is a phenomenological object. Differences in the parametrizations of Z , B_L , and T_r , as well as in the set of resonances r , complicate the comparison of results from different experiments.

Usually the resonances are modeled with a Breit-Wigner form, although some more recent analyses use a K -matrix formalism [5,6,7] with the P -vector approximation [8] to describe the $\pi\pi$ S-wave.

The nonresonant (NR) contribution to $D \rightarrow abc$ is parametrized as constant (S-wave) with no variation in magnitude or phase across the Dalitz plot. The available phase space is much greater for B decays, and the nonresonant contribution to $B \rightarrow abc$ requires a more sophisticated parametrization. Theoretical models of the NR amplitude [9-12] do not reproduce the distributions observed in the data. Experimentally, several parametrizations have been used [13,14].

Barrier Factor B_L : The maximum angular momentum L in a strong decay is limited by the linear momentum q . Decay particles moving slowly with an impact parameter (meson radius) d of order 1 fm have difficulty generating sufficient angular momentum to conserve the spin of the resonance. The Blatt-Weisskopf [15,16] functions B_L , given in Table 1, weight the reaction amplitudes to account for this spin-dependent effect. These functions are normalized to give $B_L = 1$ for $z = (|q|d)^2 = 1$. Another common formulation, B_L' , also in Table 1, is normalized to give $B_L' = 1$ for $z = z_0 = (|q_0|d)^2$ where q_0 is the value of q when $m_{ab} = m_r$.

Table 1: Blatt-Weisskopf barrier factors.

L	$B_L(q)$	$B_L'(q, q_0)$
0	1	1
1	$\sqrt{\frac{2z}{1+z}}$	$\sqrt{\frac{1+z_0}{1+z}}$
2	$\sqrt{\frac{13z^2}{(z-3)^2+9z}}$	$\sqrt{\frac{(z_0-3)^2+9z_0}{(z-3)^2+9z}}$
where $z = (q d)^2$ and $z_0 = (q_0 d)^2$		

Angular distribution: The tensor or Zemach formalism [17,18] and the helicity formalism [19,18] yield identical descriptions of the angular distributions for the decay process $R \rightarrow rc, r \rightarrow ab$ when a, b and c all have spin-0. The angular distributions for $L = 0, 1$, and 2 are given in Table 2. For final-state particles with non-zero spin (*e.g.*, radiative decays), the helicity formalism is required.

Meson Particle Listings

D^\pm

Table 2: Angular distributions for $L = 0, 1, 2$ where θ is the angle between particles a and c in the rest frame of resonance r , $\sqrt{1+\zeta^2} = E_r/m_{ab}$ is a relativistic correction, and $E_r = (m_R^2 + m_{ab}^2 - m_c^2)/2m_R$.

$J \rightarrow L+l$	Angular distribution
$0 \rightarrow 0+0$	uniform
$0 \rightarrow 1+1$	$(1+\zeta^2) \cos^2 \theta$
$0 \rightarrow 2+2$	$\left(\zeta^2 + \frac{3}{2}\right)^2 (\cos^2 \theta - 1/3)^2$

Dynamical Function T_r : The dynamical function T_r is derived from the S -matrix formalism. In general, the amplitude that a final state f couples to an initial state i is $S_{fi} = \langle f|S|i\rangle$, where the scattering operator S is unitary and satisfies $SS^\dagger = S^\dagger S = I$. The Lorentz-invariant transition operator \hat{T} is defined by separating the probability that $f = i$, yielding

$$S = I + 2iT = I + 2i\{\rho\}^{1/2} \hat{T} \{\rho\}^{1/2}, \quad (3)$$

where I is the identity operator, ρ is the diagonal phase-space matrix, with $\rho_{ii} = 2q_i/m$, and q_i is the momentum of a in the r rest frame for decay channel i . In the single-channel S-wave case, $S = e^{2i\delta}$ satisfies unitarity and

$$\hat{T} = \frac{1}{\rho} e^{i\delta} \sin \delta. \quad (4)$$

There are three common formulations of the dynamical function. The Breit-Wigner formalism—the first term in a Taylor expansion about a T -matrix pole—is the simplest formulation. The K -matrix formalism [5] is more general (allowing more than one T -matrix pole and coupled channels while preserving unitarity). The Flatté distribution [20] is used to parametrize resonances near threshold and is equivalent to a one-pole, two-channel K -matrix.

Breit-Wigner Formulation: The common formulation of a Breit-Wigner resonance decaying to spin-0 particles a and b is

$$T_r(m_{ab}) = \frac{1}{m_r^2 - m_{ab}^2 - im_r \Gamma_{ab}(q)}. \quad (5)$$

The “mass-dependent” width Γ is

$$\Gamma = \Gamma_r \left(\frac{q}{q_r}\right)^{2L+1} \left(\frac{m_r}{m_{ab}}\right) B'_L(q, q_0)^2, \quad (6)$$

and $B'_L(q, q_0)$ is the Blatt-Weisskopf barrier factor from Table 1. A Breit-Wigner parametrization best describes isolated, non-overlapping resonances far from the threshold of additional decay channels. For the ρ and $\rho(1450)$ a more complex parametrization suggested by Gounaris-Sakurai [21] is often used [22–26]. Unitarity can be violated when the dynamical function is parametrized as the sum of two or more overlapping Breit-Wigners. The proximity of a threshold to a resonance distorts the line shape from a simple Breit-Wigner. Here the Flatté formula provides a better description and is discussed below.

K -matrix Formalism: The T matrix can be written as

$$\hat{T} = (I - i\hat{K}\rho)^{-1} \hat{K}, \quad (7)$$

where \hat{K} is the Lorentz-invariant K -matrix describing the scattering process and ρ is the phase-space factor. Resonances appear as poles in the K -matrix:

$$\hat{K}_{ij} = \sum_\alpha \frac{\sqrt{m_\alpha \Gamma_{\alpha i}(m) m_\alpha \Gamma_{\alpha j}(m)}}{(m_\alpha^2 - m^2) \sqrt{\rho_i \rho_j}}. \quad (8)$$

The K -matrix is real by construction, and so the associated T -matrix respects unitarity.

For a single pole in a single channel, K is

$$K = \frac{m_0 \Gamma(m)}{m_0^2 - m^2} \quad (9)$$

and

$$T = K(1 - iK)^{-1} = \frac{m_0 \Gamma(m)}{m_0^2 - m^2 - im_0 \Gamma(m)}, \quad (10)$$

which is the relativistic Breit-Wigner formula. For two poles in a single channel, K is

$$K = \frac{m_\alpha \Gamma_\alpha(m)}{m_\alpha^2 - m^2} + \frac{m_\beta \Gamma_\beta(m)}{m_\beta^2 - m^2}. \quad (11)$$

If m_α and m_β are far apart relative to the widths, the T matrix is approximately the sum of two Breit-Wigners, $T(K_\alpha + K_\beta) \approx T(K_\alpha) + T(K_\beta)$, each of the form of Eq. (10). This approximation is not valid for two nearby resonances, in which case T can violate unitarity.

This formulation, which applies to S -channel production in two-body scattering, $ab \rightarrow cd$, can be generalized to describe the production of resonances in processes such as the decay of charm mesons. The key assumption here is that the two-body system described by the K -matrix does *not* interact with the rest of the final state [8]. The validity of this assumption varies with the production process and is appropriate for reactions such as $\pi^- p \rightarrow \pi^0 \pi^0 n$ and semileptonic decays such as $D \rightarrow K \pi \ell \nu$. The assumption may be of limited validity for production processes such as $p\bar{p} \rightarrow \pi\pi\pi$ or $D \rightarrow \pi\pi\pi$. In these cases, the two-body Lorentz-invariant amplitude, \hat{F} , is given by

$$\hat{F}_i = (I - i\hat{K}\rho)^{-1} \hat{P}_j = (\hat{T}\hat{K}^{-1})_{ij} \hat{P}_j, \quad (12)$$

where P is the production vector that parametrizes the resonance production in the open channels.

For the $\pi\pi$ S-wave, a common formulation of the K -matrix [7,24,25] is

$$K_{ij}(s) = \left[\sum_\alpha \left(\frac{g_i^{(\alpha)} g_j^{(\alpha)}}{m_\alpha^2 - s} \right) + f_{ij}^{sc} \frac{1 - s_0^{sc}}{s - s_0^{sc}} \right] \left[\frac{(s - s_A m_\pi^2 / 2)(1 - s_{A0})}{(s - s_{A0})} \right]. \quad (13)$$

The factor $g_i^{(\alpha)}$ is the real coupling constant of the K -matrix pole m_α to meson channel i ; the parameters f_{ij}^{sc} and s_0^{sc} describe a smooth part of the K -matrix elements; the second factor in square brackets suppresses a false kinematical singularity near

the $\pi\pi$ threshold (the Adler zero); and the number 1 has units GeV^2 .

The production vector, with $i = 1$ denoting $\pi\pi$, is

$$P_j(s) = \left[\sum_{\alpha} \left(\frac{\beta_{\alpha} g_j^{(\alpha)}}{m_{\alpha}^2 - s} \right) + f_{1j}^{pr} \frac{1 - s_0^{pr}}{s - s_0^{pr}} \right] \left[\frac{(s - s_A m_{\pi}^2 / 2)(1 - s_{A0})}{(s - s_{A0})} \right]. \quad (14)$$

where the free parameters of the Dalitz plot fit are the complex production couplings β_{α} and the production-vector background parameters f_{1j}^{pr} and s_0^{pr} . All other parameters are fixed by scattering experiments. Ref. [6] describes the $\pi\pi$ scattering data with a 4-pole, 2-channel ($\pi\pi$, $K\bar{K}$) model, while Ref. [7] describes the scattering data with 5-pole, 5-channel ($\pi\pi$, $K\bar{K}$, $\eta\eta$, $\eta'\eta'$ and 4π) model. The former has been implemented by CLEO [27] and the latter by FOCUS [25] and BABAR [24]. In both cases, only the $\pi\pi$ channel was analyzed. A more complete coupled-channel analysis would simultaneously fit all final states accessible by rescattering.

Flatté Formalism: The Flatté formulation is used when a second channel opens close to a resonance:

$$\hat{T}(m_{ab}) = \frac{1}{m_r^2 - m_{ab}^2 - i(\rho_1 g_1^2 + \rho_2 g_2^2)}, \quad (15)$$

where $g_1^2 + g_2^2 = m_0 \Gamma_r$. This situation occurs in the $\pi\pi$ S-wave where the $f_0(980)$ is near the $K\bar{K}$ threshold, and in the $\pi\eta$ channel where the $a_0(980)$ also lies near the $K\bar{K}$ threshold. For the $a_0(980)$ resonance, the relevant coupling constants are $g_1 = g_{\pi\eta}$ and $g_2 = g_{KK}$, and the phase space terms are $\rho_1 = \rho_{\pi\eta}$ and $\rho_2 = \rho_{KK}$, where

$$\rho_{ab} = \sqrt{\left(1 - \left(\frac{m_a - m_b}{m_{ab}}\right)^2\right) \left(1 + \left(\frac{m_a - m_b}{m_{ab}}\right)^2\right)}. \quad (16)$$

For the $f_0(980)$ the relevant coupling constants are $g_1 = g_{\pi\pi}$ and $g_2 = g_{KK}$, and the phase space terms are $\rho_1 = \rho_{\pi\pi}$ and $\rho_2 = \rho_{KK}$. The charged and neutral K channels are usually assumed to have the same coupling constant but different phase space factors, due to $m_{K^+} \neq m_{K^0}$; the result is

$$\rho_{KK} = \frac{1}{2} \left(\sqrt{1 - \left(\frac{2m_{K^\pm}}{m_{KK}}\right)^2} + \sqrt{1 - \left(\frac{2m_{K^0}}{m_{KK}}\right)^2} \right). \quad (17)$$

Branching Ratios from Dalitz Plot Fits: A fit to the Dalitz plot distribution using either a Breit-Wigner or a K -matrix formalism factorizes into a resonant contribution to the amplitude \mathcal{M}_j and a complex coefficient, $a_j e^{i\delta_j}$, where a_j and δ_j are real. The definition of a rate of a single process, given a set of amplitudes a_j and phases δ_j , is the square of the relevant matrix element (see Eq. (1)). The “fit fraction” is usually defined as the integral over the Dalitz plot (m_{ab} vs. m_{bc}) of a single amplitude squared divided by the integral over the Dalitz plot of the square of the coherent sum of all amplitudes, or

$$\text{fit fraction}_j = \frac{\int |a_j e^{i\delta_j} \mathcal{M}_j|^2 dm_{ab}^2 dm_{bc}^2}{\int \left| \sum_k a_k e^{i\delta_k} \mathcal{M}_k \right|^2 dm_{ab}^2 dm_{bc}^2}, \quad (18)$$

where \mathcal{M}_j is defined in Eq. (2) and described in Ref. [28]. In general, the sum of the fit fractions for all components will not be unity due to interference.

When the K -matrix of Eq. (12) is used to describe a wave (e.g., the $\pi\pi$ S-wave), then \mathcal{M}_j refers to the entire wave. In this case, it may not be straightforward to separate \mathcal{M}_j into a sum of individual resonances unless these are narrow and well separated.

Reconstruction Efficiency and Resolution: The efficiency for reconstructing an event as a function of position on the Dalitz plot is in general non-uniform. Typically, a Monte Carlo sample generated with a uniform distribution in phase space is used to determine the efficiency. The variation in efficiency across the Dalitz plot varies with experiment and decay mode. Most recent analyses utilize a full GEANT [29] detector simulation.

Finite detector resolution can usually be safely neglected as most resonances are comparatively broad. Notable exceptions where detector resolution effects must be modeled are $\phi \rightarrow K^+ K^-$, $\omega \rightarrow \pi^+ \pi^-$, and $a_0 \rightarrow \eta \pi^0$. One approach is to convolve the resolution function in the Dalitz-plot variables m_{ab}^2 and m_{bc}^2 with the function that parametrizes the resonant amplitudes. In high-statistics data samples, resolution effects near the phase-space boundary typically contribute to a poor goodness of fit. The momenta of the final-state particles can be recalculated with a D or B mass constraint, which forces the kinematic boundaries of the Dalitz plot to be strictly respected. If the three-body mass is not constrained, then the efficiency (and the parametrization of background) may also depend on the reconstructed mass.

Backgrounds: The contribution of background to the D and B samples varies by experiment and final state. The background naturally falls into five categories: (i) purely combinatoric background containing no resonances; (ii) combinatoric background containing intermediate resonances, such as a real K^{*-} or ρ , plus additional random particles; (iii) final states containing identical particles as in $D^0 \rightarrow K_S^0 \pi^0$ background to $D^0 \rightarrow \pi^+ \pi^- \pi^0$ and $B \rightarrow D\pi$ background to $B \rightarrow K\pi\pi$; (iv) mistagged decays such as a real \bar{D}^0 or \bar{B}^0 incorrectly identified as a D^0 or B^0 ; and (v) particle misidentification of the decay products such as $D^+ \rightarrow \pi^- \pi^+ \pi^+$ or $D_s^+ \rightarrow K^- K^+ \pi^+$ reconstructed as $D^+ \rightarrow K^- \pi^+ \pi^+$.

The contribution from combinatoric background with intermediate resonances is distinct from the resonances in the signal because the former do *not* interfere with the latter since they are not from true resonances. Similarly, $D^0 \rightarrow \rho\pi$ and $D^0 \rightarrow K_S^0 \pi^0$ do not interfere since strong and weak transitions proceed on different time scales. The usual identification tag of the initial particle as a D^0 or a \bar{D}^0 is the charge of the distinctive slow pion in the decay sequence $D^{*+} \rightarrow D^0 \pi_s^+$ or $D^{*-} \rightarrow \bar{D}^0 \pi_s^-$. Another possibility is the identification or “tagging” of one of the D mesons from $\psi(3770) \rightarrow D^0 \bar{D}^0$, as is done for B mesons from $\Upsilon(4S)$. The mistagged background is subtle and may be

Meson Particle Listings

 D^\pm

mistakenly enumerated in the *signal* fraction determined by a D^0 mass fit. Mistagged decays contain true \overline{D}^0 's or B^0 's and so the resonances in the mistagged sample exhibit interference on the Dalitz plot.

References

1. M Bauer, B. Stech and M. Wirbel, Z. Phys. C **34**, 103 (1987); P. Bedaque, A. Das and V.S. Mathur, Phys. Rev. D **49**, 269 (1994); L.-L. Chau and H.-Y. Cheng, Phys. Rev. D **36**, 137 (1987); K. Terasaki, Int. J. Mod. Phys. A **10**, 3207 (1995); F. Buccella, M. Lusignoli and A. Pugliese, Phys. Lett. B **379**, 249 (1996).
2. J. D. Jackson, Nuovo Cim. **34**, 1644 (1964).
3. R. H. Dalitz, *Phil. Mag.* **44**, 1068 (1953).
4. See the note on Kinematics in this *Review*.
5. S.U. Chung *et al.*, Ann. Physik. **4**, 404 (1995).
6. K. L. Au, D. Morgan and M. R. Pennington, Phys. Rev. D **35**, 1633 (1987).
7. V. V. Anisovich and A. V. Sarantsev, Eur. Phys. J. A **16**, 229 (2003).
8. I. J. R. Aitchison, Nucl. Phys. A **189**, 417 (1972).
9. S. Fajfer, R. J. Oakes and T. N. Pham, Phys. Rev. D **60**, 054029 (1999).
10. H. Y. Cheng and K. C. Yang, Phys. Rev. D **66**, 054015 (2002).
11. S. Fajfer, T. N. Pham and A. Prapotnik, Phys. Rev. D **70**, 034033 (2004).
12. H. Y. Cheng, C. K. Chua and A. Soni, arXiv:hep-ph/0506268.
13. A. Garmash *et al.* (Belle Collab.), Phys. Rev. D **71**, 092003 (2005).
14. B. Aubert *et al.* (BABAR Collab.), arXiv:hep-ex/0507094.
15. J. Blatt and V. Weisskopf, *Theoretical Nuclear Physics*, New York: John Wiley & Sons (1952).
16. F. von Hippel and C. Quigg, Phys. Rev. D **5**, 624, (1972).
17. C. Zemach, Phys. Rev. B **133**, 1201 (1964); C. Zemach, Phys. Rev. B **140**, 97 (1965).
18. V. Filippini, A. Fontana and A. Rotondi, Phys. Rev. D **51**, 2247 (1995).
19. M. Jacob and G. C. Wick, Annals Phys. **7**, 404 (1959) [Annals Phys. **281**, 774 (2000)]; S. U. Chung, Phys. Rev. D **48**, 1225, (1993); J. D. Richman, CALT-68-1148.
20. S. M. Flatté, Phys. Lett. B **63**, 224 (1976).
21. G. J. Gounaris and J. J. Sakarai, Phys. Rev. Lett. **21** 244, (1968).
22. B. Aubert *et al.* (BABAR Collab.), arXiv:hep-ex/0408073.
23. K. Abe *et al.* (Belle Collab.), arXiv:hep-ex/0504013.
24. B. Aubert *et al.* (BABAR Collab.), arXiv:hep-ex/0507101.
25. J. M. Link *et al.* (FOCUS Collab.), Phys. Lett. B **585**, 200 (2004).
26. B. Aubert *et al.* (BABAR Collab.), arXiv:hep-ex/0408099.
27. D. Cronin-Hennessy *et al.* (CLEO Collab.), Phys. Rev. D **72**, 031102 (2005).
28. S. Kopp *et al.* (CLEO Collab.), Phys. Rev. D **63**, 092001 (2001).
29. R. Brun *et al.*, GEANT 3.15, CERN Report No. DD/EE/84-1 (1987); R. Brun *et al.*, GEANT 3.21, CERN Program Library Long Writeup W5013 (1993), unpublished; S. Agostinelli *et al.* (GEANT4 Collab.), Nucl. Instrum. Meth. A **506**, 250 (2003).

REVIEW OF D-MESON DALITZ PLOT ANALYSES

Revised April 2008 by D. Asner (Carleton University)

The formalism of Dalitz-Plot analysis is reviewed in the preceding note. Recent studies of multi-body decays of charm mesons probe a variety of physics including γ/ϕ_3 , D^0 - \overline{D}^0 mixing, searches for CP violation, doubly Cabibbo-suppressed decays, and properties of S-wave $\pi\pi$, $K\pi$, and KK resonances. In the following, we discuss: (1) $D^0 \rightarrow K_S^0\pi^+\pi^-$; (2) doubly Cabibbo-suppressed decays; and (3) CP violation.

$D^0 \rightarrow K_S^0\pi^+\pi^-$: Several experiments have analyzed $D^0 \rightarrow K_S^0\pi^+\pi^-$ decay. A CLEO analysis [1] of this process included ten resonances: $K_S^0\rho^0$, $K_S^0\omega$, $K_S^0f_0(980)$, $K_S^0f_2(1270)$, $K_S^0f_0(1370)$, $K^*(892)^-\pi^+$, $K_0^*(1430)^-\pi^+$, $K_2^*(1430)^-\pi^+$, $K^*(1680)^-\pi^+$, and the doubly Cabibbo-suppressed (DCS) mode $K^*(892)^+\pi^-$. A BABAR analysis [2-4] added to these ten the $K^*(1410)^-\pi^+$, $K_S^0\rho(1450)$, the DCS resonances $K_0^*(1430)^+\pi^-$ and $K_2^*(1430)^+\pi^-$, and two Breit-Wigner $\pi\pi$ S-wave contributions. A Belle analysis [5-7] included all the components of BABAR and added two more DCS contributions, $K^*(1410)^+\pi^-$ and $K^*(1680)^+\pi^-$.

The primary motivation for the analysis of the decay $D^0 \rightarrow K_S^0\pi^+\pi^-$ is to study $D^0 - \overline{D}^0$ oscillations and the CKM angles. The quasi-two-body intermediate states include both CP -even and CP -odd eigenstates as well as doubly Cabibbo-suppressed channels. A time-dependent analysis of the Dalitz plot from CLEO [8] and Belle [9] allows simultaneous determination of the strong transition amplitudes and phases, the mixing parameters x and y without phase or sign ambiguity, and the CP -violating parameter $|q/p|$ and $\text{Arg}(q/p)$. See the note on “ $D^0 - \overline{D}^0$ Mixing” for a discussion.

The CKM angle γ/ϕ_3 [10] and the quark-mixing parameter $\cos 2\beta/\phi_1$ [11] can be determined with the process $B^- \rightarrow D^{(*)}K^{(*)-}$ and $\overline{B}^0 \rightarrow Dh^0$, respectively, followed by the decay $D \rightarrow K_S^0\pi^+\pi^-$. The Belle and BABAR experiments measured γ/ϕ_3 (Belle [5-7] and BABAR [2-4]) and $\cos 2\beta/\phi_1$ (Belle [12], BABAR [13]). In these analyses, a large systematic uncertainty in the relative phase between the D^0 and \overline{D}^0 amplitudes point by point across the Dalitz plot remains to be fully understood.

The CLEO model with only ten submodes does not provide a good description of the higher-statistics BABAR and Belle data samples. An improved description is obtained in two ways: First, by adding more Breit-Wigner resonances, including two $\pi\pi$ resonances with arbitrary mass and width. Second, following the methodology of FOCUS [14], by applying a K -matrix model to the $\pi\pi$ S-wave [9,2].

The quantum entangled production of D 's from $\psi(3770)$ enables a model-independent determination of the $D^0 - \overline{D}^0$ relative phase. Studying CP -tagged Dalitz plots [15,16] provides sensitivity to the cosine of the relative phase, while studying double-tagged Dalitz plots [16] probes both the cosine and sine of the $D^0 - \overline{D}^0$ phase difference. CLEO analyzed [17] the

$D^0 \rightarrow K_S^0 \pi^+ \pi^-$ and $D^0 \rightarrow K_L^0 \pi^+ \pi^-$ samples using the CP -even tag modes $K^+ K^-$, $\pi^+ \pi^-$, $K_L^0 \pi^0$ (vs. $K_S^0 \pi^+ \pi^-$ only), the CP -odd tag modes $K_S^0 \pi^0$, $K_S^0 \eta$, and the double-tag modes $(K_S^0 \pi^+ \pi^-)^2$ and $(K_S^0 \pi^+ \pi^-)(K_L^0 \pi^+ \pi^-)$. These measurements can reduce the model uncertainty on γ/ϕ_3 to about 3° .

Doubly Cabibbo-Suppressed Decays: There are two classes of multibody doubly Cabibbo-suppressed (DCS) decays of D mesons. The first consists of those in which the DCS and corresponding Cabibbo-favored (CF) decays populate distinct Dalitz plots; the pairs $D^0 \rightarrow K^+ \pi^- \pi^0$ and $D^0 \rightarrow K^- \pi^+ \pi^0$, or $D^+ \rightarrow K^+ \pi^+ \pi^-$ and $D^+ \rightarrow K^- \pi^+ \pi^+$, are examples. Our average of three measurements of $\Gamma(D^0 \rightarrow K^+ \pi^- \pi^0)/\Gamma(D^0 \rightarrow K^- \pi^+ \pi^0)$ is $(2.20 \pm 0.10) \times 10^{-3}$. Our average of three measurements of $\Gamma(D^+ \rightarrow K^+ \pi^- \pi^+)/\Gamma(D^+ \rightarrow K^- \pi^+ \pi^+)$ is $(6.8 \pm 0.8) \times 10^{-3}$; see the Particle Listings.

The second class consists of decays in which the DCS and CF modes populate the same Dalitz plot; for example, $D^0 \rightarrow K^{*-} \pi^+$ and $D^0 \rightarrow K^{*+} \pi^-$ both contribute to $D^0 \rightarrow K_S^0 \pi^+ \pi^-$. In this class, the potential for interference of DCS and CF amplitudes increases the sensitivity to the DCS amplitude and allows direct measurement of the relative strong phases between amplitudes. CLEO [1] and Belle [9] have measured the relative phase between $D^0 \rightarrow K^*(892)^+ \pi^-$ and $D^0 \rightarrow K^*(892)^- \pi^+$ to be $(189 \pm 10 \pm 3_{-5}^{+15})^\circ$ and $(171.9 \pm 1.3)^\circ$ (statistical error only). These results are close to the 180° expected from Cabibbo factors and a small strong phase.

Additionally, Belle [9] has reported results for both the relative phase (statistical errors only) and ratio R (central values only) of the DCS fit fraction relative to the CF fit fractions for $K^*(892)^+ \pi^-$, $K_0^*(1430)^+ \pi^-$, $K_2^*(1430)^+ \pi^-$, $K^*(1410)^+ \pi^-$, and $K^*(1680)^+ \pi^-$. The reported values for R , in units of $\tan^4 \theta_c$, are 2.94 ± 0.12 , 22.0 ± 1.6 , 34 ± 4 , 87 ± 13 , and $(5 \pm 5) \times 10^2$. For $K^+ \pi^-$, the corresponding value for R is $(1.28 \pm 0.02) \times \tan^4 \theta_c$. Similarly, BABAR [2] has reported central values for R for $K^*(892)^+ \pi^-$, $K_0^*(1430)^+ \pi^-$, and $K_2^*(1430)^+ \pi^-$. In units of $\tan^4 \theta_c$, R is 3.45 ± 0.31 , 7.7 ± 3.0 , and 1.7 ± 1.7 . The systematic uncertainties on these values remain to be evaluated. The large differences in R among these final states, if significant, could point to an interesting role for hadronic effects that deserves theoretical attention.

(There are other ways, not involving DCS decays, in which D^0 and \bar{D}^0 decays can populate the same Dalitz plot. Examples are D^0 and \bar{D}^0 decays to $K_S^0 K^+ \pi^-$, or to $K_S^0 K^- \pi^+$. These final states can be used to study D^0 - \bar{D}^0 mixing and the CKM angle γ/ϕ_3 .)

CP Violation: In the limit of CP conservation, charge conjugate decays will have the same Dalitz-plot distribution. The D^\pm tag enables the discrimination between D^0 and \bar{D}^0 . The integrated CP violation across the Dalitz plot is determined in two ways. The first uses

$$\mathcal{A}_{CP} = \int \left(\frac{|\mathcal{M}|^2 - |\overline{\mathcal{M}}|^2}{|\mathcal{M}|^2 + |\overline{\mathcal{M}}|^2} \right) dm_{ab}^2 dm_{bc}^2 / \int dm_{ab}^2 dm_{bc}^2, \quad (1)$$

where \mathcal{M} and $\overline{\mathcal{M}}$ are the D^0 and \bar{D}^0 Dalitz-plot amplitudes for the three-body decay $D \rightarrow abc$, and m_{ab} (m_{bc}) is the invariant mass of ab (bc). The second uses the asymmetry in the efficiency-corrected D^0 and \bar{D}^0 yields,

$$\mathcal{A}_{CP} = \frac{N_{D^0} - N_{\bar{D}^0}}{N_{D^0} + N_{\bar{D}^0}}. \quad (2)$$

These expressions are less sensitive to CP violation than are the individual resonant submodes [18]. Our Particle Listings give limits on CP violation for 11 D^+ , 25 D^0 , and 12 D_S^+ decay modes.

The possibility of interference between CP -conserving and CP -violating amplitudes provides a more sensitive probe of CP violation. The constraints on the square of the CP -violating amplitude obtained in the resonant submodes of $D^0 \rightarrow K_S^0 \pi^+ \pi^-$ range from 3.5×10^{-4} to 28.4×10^{-4} at 95% confidence level [18].

References

1. H. Muramatsu *et al.* (CLEO Collab.), Phys. Rev. Lett. **89**, 251802 (2002).
2. B. Aubert *et al.* (BABAR Collab.), Phys. Rev. Lett. **95**, 121802 (2005).
3. B. Aubert *et al.* (BABAR Collab.), hep-ex/0507101.
4. B. Aubert *et al.* (BABAR Collab.), arXiv:hep-ex/0607104.
5. A. Poluektov *et al.* (Belle Collab.), Phys. Rev. D **70**, 072003 (2004).
6. K. Abe *et al.* (Belle Collab.), hep-ex/0411049.
7. A. Poluektov *et al.* (Belle Collab.), Phys. Rev. **D73**, 112009 (2006).
8. D.M. Asner *et al.* (CLEO Collab.), Phys. Rev. **D72**, 012001 (2005).
9. L.M. Zhang *et al.* (Belle Collab.), Phys. Rev. Lett. **99**, 131803 (2007).
10. A. Giri *et al.*, Phys. Rev. **D68**, 054018 (2003).
11. A. Bondar, T. Gershon, and P. Krokovny, Phys. Lett. **B624**, 1 (2005).
12. P. Krokovny *et al.* (Belle Collab.), Phys. Rev. Lett. **97**, 081801 (2006).
13. B. Aubert *et al.* (BABAR Collab.), arXiv:hep-ex/0607105.
14. J.M. Link *et al.* (FOCUS Collab.), Phys. Lett. **B585**, 200 (2004).
15. A. Bondar and A. Poluektov, Eur. Phys. J. **C47**, 347 (2006).
16. A. Bondar and A. Poluektov, arXiv:hep-ph/0703267.
17. E. White and Q. He (CLEO Collab.), arXiv:0711.2285 [hep-ex].
18. D.M. Asner *et al.* (CLEO Collab.), Phys. Rev. **D70**, 091101R (2004).

$\Gamma((K^- \pi^+)_{S\text{-wave}} \pi^+)/\Gamma(K^- \pi^+ \pi^+)$

Γ_{47}/Γ_{46}

This is the "fit fraction" from the Dalitz-plot analysis. The $K^- \pi^+$ S-wave includes a broad scalar κ ($\overline{K}_0^*(800)$), the $\overline{K}_0^*(1430)^0$, and non-resonant background.

VALUE	DOCUMENT ID	TECN	COMMENT
0.818 ± 0.021 OUR AVERAGE	Error includes scale factor of 1.7.		
0.8323 ± 0.0150 ± 0.0008	35 LINK	07B FOCUS	K-matrix fit, 50.5k ± 248 evts
0.786 ± 0.014 ± 0.018	AITALA	06 E791	Dalitz fit, 15.1k events

³⁵ This LINK 07B fit uses a K matrix. The $K^- \pi^+$ S-wave fit fraction given above breaks down into (207.3 ± 25.5 ± 12.4)% isospin-1/2 and (40.5 ± 9.6 ± 3.2)% isospin-3/2 — with large interference between the two. The isospin-1/2 component includes the κ (or $\overline{K}_0^*(800)^0$) and $\overline{K}_0^*(1430)^0$.

Meson Particle Listings

 D^\pm

$\Gamma(\bar{K}_S^0(800)^0 \pi^+, \bar{K}_S^0(800)^0 \rightarrow K^- \pi^+)/\Gamma(K^- \pi^+ \pi^+)$ Γ_{48}/Γ_{46}
This is the "fit fraction" from the Dalitz-plot analysis.

VALUE	DOCUMENT ID	TECN	COMMENT
$0.478 \pm 0.121 \pm 0.053$	AITALA	02	E791 See AITALA 06

$\Gamma(\bar{K}_S^0(1430)^0 \pi^+, \bar{K}_S^0(1430)^0 \rightarrow K^- \pi^+)/\Gamma(K^- \pi^+ \pi^+)$ Γ_{49}/Γ_{46}
This is the "fit fraction" from the Dalitz-plot analysis.

VALUE	DOCUMENT ID	TECN	COMMENT
$0.125 \pm 0.014 \pm 0.005$	AITALA	02	E791 See AITALA 06
$0.284 \pm 0.022 \pm 0.059$	FRABETTI	94G	E687 γ Be, $\bar{E}_\gamma \approx 220$ GeV
$0.248 \pm 0.019 \pm 0.017$	ANJOS	93	E691 γ Be 90–260 GeV

$\Gamma(\bar{K}^*(892)^0 \pi^+, \bar{K}^*(892)^0 \rightarrow K^- \pi^+)/\Gamma(K^- \pi^+ \pi^+)$ Γ_{50}/Γ_{46}
This is the "fit fraction" from the Dalitz-plot analysis.

VALUE	DOCUMENT ID	TECN	COMMENT
0.133 ± 0.009 OUR AVERAGE			
$0.1361 \pm 0.0098 \pm 0.0030$	LINK	07B	FOCS K-matrix fit, 50.5k \pm 248 evts
$0.119 \pm 0.002 \pm 0.020$	AITALA	06	E791 Dalitz fit, 15.1k events
$0.123 \pm 0.010 \pm 0.009$	AITALA	02	E791 See AITALA 06
$0.137 \pm 0.006 \pm 0.009$	FRABETTI	94G	E687 γ Be, $\bar{E}_\gamma \approx 220$ GeV
$0.170 \pm 0.009 \pm 0.034$	ANJOS	93	E691 γ Be 90–260 GeV
$0.14 \pm 0.04 \pm 0.04$	ALVAREZ	91B	NA14 Photoproduction
$0.13 \pm 0.01 \pm 0.07$	ADLER	87	MRK3 $e^+ e^-$ 3.77 GeV

$\Gamma(\bar{K}^*(1410)^0 \pi^+)/\Gamma(K^- \pi^+ \pi^+)$ Γ_{91}/Γ_{46}

VALUE (units 10^{-3})	DOCUMENT ID	TECN	COMMENT
$4.8 \pm 2.1 \pm 1.7$	LINK	07B	FOCS K-matrix fit, 50.5k \pm 248 evts

$\Gamma(\bar{K}_2^*(1430)^0 \pi^+, \bar{K}_2^*(1430)^0 \rightarrow K^- \pi^+)/\Gamma(K^- \pi^+ \pi^+)$ Γ_{51}/Γ_{46}
This is the "fit fraction" from the Dalitz-plot analysis.

VALUE	DOCUMENT ID	TECN	COMMENT
0.0032 ± 0.0009 OUR AVERAGE			
$0.0039 \pm 0.0009 \pm 0.0005$	LINK	07B	FOCS K-matrix fit, 50.5k \pm 248 evts
$0.002 \pm 0.001 \pm 0.001$	AITALA	06	E791 Dalitz fit, 15.1k events
$0.005 \pm 0.001 \pm 0.002$	AITALA	02	E791 See AITALA 06

$\Gamma(\bar{K}^*(1680)^0 \pi^+, \bar{K}^*(1680)^0 \rightarrow K^- \pi^+)/\Gamma(K^- \pi^+ \pi^+)$ Γ_{52}/Γ_{46}
This is the "fit fraction" from the Dalitz-plot analysis.

VALUE	DOCUMENT ID	TECN	COMMENT
0.017 ± 0.007 OUR AVERAGE			
$0.0190 \pm 0.0063 \pm 0.0043$	LINK	07B	FOCS K-matrix fit, 50.5k \pm 248 evts
$0.012 \pm 0.006 \pm 0.012$	AITALA	06	E791 Dalitz fit, 15.1k events
$0.025 \pm 0.007 \pm 0.003$	AITALA	02	E791 See AITALA 06
$0.047 \pm 0.006 \pm 0.007$	FRABETTI	94G	E687 γ Be, $\bar{E}_\gamma \approx 220$ GeV
$0.030 \pm 0.004 \pm 0.013$	ANJOS	93	E691 γ Be 90–260 GeV

$\Gamma(K^- \pi^+ \pi^+ \text{ nonresonant})/\Gamma(K^- \pi^+ \pi^+)$ Γ_{53}/Γ_{46}
This is the "fit fraction" from the Dalitz-plot analysis.

VALUE	DOCUMENT ID	TECN	COMMENT
$0.130 \pm 0.058 \pm 0.044$	AITALA	02	E791 See AITALA 06
$0.998 \pm 0.037 \pm 0.072$	FRABETTI	94G	E687 γ Be, $\bar{E}_\gamma \approx 220$ GeV
$0.838 \pm 0.088 \pm 0.275$	ANJOS	93	E691 γ Be 90–260 GeV
$0.79 \pm 0.07 \pm 0.15$	ADLER	87	MRK3 $e^+ e^-$ 3.77 GeV

$\Gamma(K_S^0 \pi^+ \pi^0)/\Gamma_{\text{total}}$ Γ_{54}/Γ

VALUE (units 10^{-2})	EVTS	DOCUMENT ID	TECN	COMMENT
6.8 ± 0.5 OUR FIT				Error includes scale factor of 1.9.
$6.99 \pm 0.09 \pm 0.25$	36	DOBBS	07	CLEO $e^+ e^-$ at $\psi(3770)$
$7.2 \pm 0.2 \pm 0.4$	5090 \pm 100	36	HE	05 CLEO See DOBBS 07
$5.1 \pm 1.3 \pm 0.8$	159	ADLER	88c	MRK3 $e^+ e^-$ 3.77 GeV

³⁶DOBBS 07 and HE 05 use single- and double-tagged events in an overall fit. DOBBS 07 supersedes HE 05.

$\Gamma(K_S^0 \rho^+)/\Gamma(K_S^0 \pi^+ \pi^0)$ Γ_{55}/Γ_{54}

VALUE	DOCUMENT ID	TECN	COMMENT
$0.68 \pm 0.08 \pm 0.12$	ADLER	87	MRK3 $e^+ e^-$ 3.77 GeV

$\Gamma(\bar{K}^*(892)^0 \pi^+, \bar{K}^*(892)^0 \rightarrow K_S^0 \pi^0)/\Gamma(K_S^0 \pi^+ \pi^0)$ Γ_{56}/Γ_{54}
This is the "fit fraction" from the Dalitz-plot analysis.

VALUE	DOCUMENT ID	TECN	COMMENT
$0.19 \pm 0.06 \pm 0.06$	ADLER	87	MRK3 $e^+ e^-$ 3.77 GeV

$\Gamma(K_S^0 \pi^+ \pi^0 \text{ nonresonant})/\Gamma(K_S^0 \pi^+ \pi^0)$ Γ_{57}/Γ_{54}
This is the "fit fraction" from the Dalitz-plot analysis.

VALUE	DOCUMENT ID	TECN	COMMENT
$0.13 \pm 0.07 \pm 0.08$	ADLER	87	MRK3 $e^+ e^-$ 3.77 GeV

$\Gamma(K^- \pi^+ \pi^+ \pi^0)/\Gamma_{\text{total}}$ Γ_{58}/Γ

VALUE (units 10^{-2})	EVTS	DOCUMENT ID	TECN	COMMENT
6.00 ± 0.20 OUR FIT				Error includes scale factor of 1.2.
$5.98 \pm 0.08 \pm 0.16$	37	DOBBS	07	CLEO $e^+ e^-$ at $\psi(3770)$
$6.0 \pm 0.2 \pm 0.2$	4840 \pm 100	37	HE	05 CLEO See DOBBS 07
$5.8 \pm 1.2 \pm 1.2$	142	COFFMAN	92B	MRK3 $e^+ e^-$ 3.77 GeV
$6.3 \pm 1.4 \pm 1.3$	175	BALTRUSAIT.	86E	MRK3 See COFFMAN 92B

³⁷DOBBS 07 and HE 05 use single- and double-tagged events in an overall fit. DOBBS 07 supersedes HE 05.

$\Gamma(K^- \pi^+ \pi^+ \pi^0)/\Gamma(K^- \pi^+ \pi^+)$ Γ_{58}/Γ_{46}

VALUE	EVTS	DOCUMENT ID	TECN	COMMENT
$0.76 \pm 0.11 \pm 0.12$	91	ANJOS	92C	E691 γ Be 90–260 GeV
$0.69 \pm 0.10 \pm 0.16$		ANJOS	89E	E691 See ANJOS 92C

$\Gamma(\bar{K}^*(892)^0 \rho^+ \text{ total})/\Gamma(K^- \pi^+ \pi^+ \pi^0)$ Γ_{84}/Γ_{58}

Unseen decay modes of the $\bar{K}^*(892)^0$ are included.

VALUE	DOCUMENT ID	TECN	COMMENT	
$0.33 \pm 0.165 \pm 0.12$	38	ANJOS	92C	E691 γ Be 90–260 GeV

³⁸See, however, the next entry, where the two experiments disagree completely.

$\Gamma(\bar{K}^*(892)^0 \rho^+ S\text{-wave})/\Gamma(K^- \pi^+ \pi^+ \pi^0)$ Γ_{85}/Γ_{58}

Unseen decay modes of the $\bar{K}^*(892)^0$ are included. The two experiments here disagree completely.

VALUE	DOCUMENT ID	TECN	COMMENT	
0.26 ± 0.25 OUR AVERAGE			Error includes scale factor of 3.1.	
$0.15 \pm 0.075 \pm 0.045$		ANJOS	92C	E691 γ Be 90–260 GeV
$0.833 \pm 0.116 \pm 0.165$		COFFMAN	92B	MRK3 $e^+ e^-$ 3.77 GeV

$\Gamma(\bar{K}^*(892)^0 \rho^+ P\text{-wave})/\Gamma_{\text{total}}$ Γ_{86}/Γ

Unseen decay modes of the $\bar{K}^*(892)^0$ are included.

VALUE	CL%	DOCUMENT ID	TECN	COMMENT
<0.001	90	ANJOS	92C	E691 γ Be 90–260 GeV
<0.005	90	COFFMAN	92B	MRK3 $e^+ e^-$ 3.77 GeV

$\Gamma(\bar{K}^*(892)^0 \rho^+ D\text{-wave})/\Gamma(K^- \pi^+ \pi^+ \pi^0)$ Γ_{87}/Γ_{58}

Unseen decay modes of the $\bar{K}^*(892)^0$ are included.

VALUE	DOCUMENT ID	TECN	COMMENT	
$0.15 \pm 0.09 \pm 0.045$		ANJOS	92C	E691 γ Be 90–260 GeV

$\Gamma(\bar{K}^*(892)^0 \rho^+ D\text{-wave longitudinal})/\Gamma_{\text{total}}$ Γ_{88}/Γ

Unseen decay modes of the $\bar{K}^*(892)^0$ are included.

VALUE	CL%	DOCUMENT ID	TECN	COMMENT
<0.007	90	COFFMAN	92B	MRK3 $e^+ e^-$ 3.77 GeV

$\Gamma(\bar{K}_1^*(1400)^0 \pi^+)/\Gamma(K^- \pi^+ \pi^+ \pi^0)$ Γ_{90}/Γ_{58}

Unseen decay modes of the $\bar{K}_1^*(1400)^0$ are included.

VALUE	DOCUMENT ID	TECN	COMMENT	
$0.907 \pm 0.218 \pm 0.180$		COFFMAN	92B	MRK3 $e^+ e^-$ 3.77 GeV

$\Gamma(K^- \rho^+ \pi^+ \text{ total})/\Gamma(K^- \pi^+ \pi^+ \pi^0)$ Γ_{61}/Γ_{58}

This includes $\bar{K}^*(892)^0 \rho^+$, etc. The next entry gives the specifically 3-body fraction.

VALUE	DOCUMENT ID	TECN	COMMENT	
$0.48 \pm 0.13 \pm 0.09$		ANJOS	92C	E691 γ Be 90–260 GeV

$\Gamma(K^- \rho^+ \pi^+ \text{ 3-body})/\Gamma(K^- \pi^+ \pi^+ \pi^0)$ Γ_{62}/Γ_{58}

VALUE	DOCUMENT ID	TECN	COMMENT	
0.17 ± 0.06 OUR AVERAGE				
$0.18 \pm 0.08 \pm 0.04$		ANJOS	92C	E691 γ Be 90–260 GeV
$0.159 \pm 0.065 \pm 0.060$		COFFMAN	92B	MRK3 $e^+ e^-$ 3.77 GeV

$\Gamma(\bar{K}^*(892)^0 \pi^+ \pi^0 \text{ total})/\Gamma(K^- \pi^+ \pi^+ \pi^0)$ Γ_{92}/Γ_{58}

This includes $\bar{K}^*(892)^0 \rho^+$, etc. The next two entries give the specifically 3-body fraction. Unseen decay modes of the $\bar{K}^*(892)^0$ are included.

VALUE	DOCUMENT ID	TECN	COMMENT	
$1.05 \pm 0.11 \pm 0.08$		ANJOS	92C	E691 γ Be 90–260 GeV

$\Gamma(\bar{K}^*(892)^0 \pi^+ \pi^0 \text{ 3-body})/\Gamma_{\text{total}}$ Γ_{93}/Γ

Unseen decay modes of the $\bar{K}^*(892)^0$ are included.

VALUE	CL%	DOCUMENT ID	TECN	COMMENT	
<0.008	90	39	COFFMAN	92B	MRK3 $e^+ e^-$ 3.77 GeV

³⁹See, however, the next entry: ANJOS 92C sees a large signal in this channel.

$\Gamma(\bar{K}^*(892)^0 \pi^+ \pi^0 \text{ 3-body})/\Gamma(K^- \pi^+ \pi^+ \pi^0)$ Γ_{93}/Γ_{58}

Unseen decay modes of the $\bar{K}^*(892)^0$ are included.

VALUE	DOCUMENT ID	TECN	COMMENT	
$0.66 \pm 0.09 \pm 0.17$		ANJOS	92C	E691 γ Be 90–260 GeV

$\Gamma(K^*(892)^-\pi^+\pi^+3\text{-body})/\Gamma(K^-\pi^+\pi^+\pi^0)$ Γ_{95}/Γ_{58}
Unseen decay modes of the $K^*(892)^-$ are included.

VALUE	DOCUMENT ID	TECN	COMMENT
$0.24 \pm 0.12 \pm 0.09$	ANJOS	92c	E691 γ Be 90–260 GeV

$\Gamma(K^-\pi^+\pi^+\pi^0 \text{ nonresonant})/\Gamma_{\text{total}}$ Γ_{66}/Γ

VALUE	CL%	DOCUMENT ID	TECN	COMMENT
<0.002	90	⁴⁰ ANJOS	92c	E691 γ Be 90–260 GeV

⁴⁰Whereas ANJOS 92c finds no signal here, COFFMAN 92B finds a fairly large one; see the next entry.

$\Gamma(K^-\pi^+\pi^+\pi^0 \text{ nonresonant})/\Gamma(K^-\pi^+\pi^+\pi^0)$ Γ_{66}/Γ_{58}

VALUE	DOCUMENT ID	TECN	COMMENT
$0.184 \pm 0.070 \pm 0.050$	COFFMAN	92B	MRK3 e^+e^- 3.77 GeV

$\Gamma(K_S^0\pi^+\pi^-\pi^0)/\Gamma_{\text{total}}$ Γ_{67}/Γ

VALUE (units 10^{-2})	EVTS	DOCUMENT ID	TECN	COMMENT
3.02 ± 0.12	OUR FIT			Error includes scale factor of 1.3.
$3.122 \pm 0.046 \pm 0.096$		⁴¹ DOBBS	07	CLEO e^+e^- at $\psi(3770)$

••• We do not use the following data for averages, fits, limits, etc. **••••**

3.2	± 0.1	± 0.2	3210 \pm 85	⁴¹ HE	05	CLEO	See DOBBS 07
2.1	$+1.0$	-0.9		⁴² BARLAG	92c	ACCM	π^- Cu 230 GeV

3.3 ± 0.8 ± 0.2 168 ADLER 88c MRK3 e^+e^- 3.77 GeV

⁴¹DOBBS 07 and HE 05 use single- and double-tagged events in an overall fit. DOBBS 07 supersedes HE 05.

⁴²BARLAG 92c computes the branching fraction by topological normalization.

$\Gamma(K_S^0\pi^+\pi^+\pi^-)/\Gamma(K^-\pi^+\pi^+\pi^-)$ Γ_{67}/Γ_{46}

VALUE	EVTS	DOCUMENT ID	TECN	COMMENT
$0.39 \pm 0.04 \pm 0.06$	229 \pm 17	ANJOS	92c	E691 γ Be 90–260 GeV

••• We do not use the following data for averages, fits, limits, etc. **••••**

$\Gamma(K_S^0\pi^+\pi^+\pi^- \text{ nonresonant})/\Gamma(K^-\pi^+\pi^+\pi^-)$ Γ_{67}/Γ_{46}

Unseen decay modes of the $a_1(1260)^+$ are included, assuming that the $a_1(1260)^+$ decays entirely to $\rho\pi$ [or at least to $(\pi\pi)_{I=1}\pi$].

VALUE	DOCUMENT ID	TECN	COMMENT
1.15 ± 0.19	OUR AVERAGE		Error includes scale factor of 1.1.
1.66 ± 0.28 ± 0.40	ANJOS	92c	E691 γ Be 90–260 GeV
1.078 ± 0.114 ± 0.140	COFFMAN	92B	MRK3 e^+e^- 3.77 GeV

••• We do not use the following data for averages, fits, limits, etc. **••••**

$\Gamma(K_S^0\pi^+\pi^+\pi^- \text{ nonresonant})/\Gamma(K^-\pi^+\pi^+\pi^-)$ Γ_{67}/Γ_{46}

Unseen decay modes of the $a_2(1320)^+$ are included.

VALUE	CL%	DOCUMENT ID	TECN	COMMENT
<0.0015	90	ANJOS	92c	E691 γ Be 90–260 GeV

••• We do not use the following data for averages, fits, limits, etc. **••••**

$\Gamma(K_S^0\pi^+\pi^+\pi^- \text{ nonresonant})/\Gamma(K^-\pi^+\pi^+\pi^-)$ Γ_{67}/Γ_{46}

Unseen decay modes of the $\bar{K}_1(1270)^0$ are included.

VALUE	CL%	DOCUMENT ID	TECN	COMMENT
<0.007	90	ANJOS	92c	E691 γ Be 90–260 GeV

••• We do not use the following data for averages, fits, limits, etc. **••••**

$\Gamma(\bar{K}_1(1400)^0\pi^+)/\Gamma_{\text{total}}$ Γ_{90}/Γ

Unseen decay modes of the $\bar{K}_1(1400)^0$ are included.

VALUE	CL%	DOCUMENT ID	TECN	COMMENT
<0.009	90	⁴³ ANJOS	92c	E691 γ Be 90–260 GeV

⁴³ANJOS 92c sees no evidence for $\bar{K}_1(1400)^0\pi^+$ in either the $\bar{K}^0\pi^+\pi^+\pi^-$ or $K^-\pi^+\pi^+\pi^0$ channels, whereas COFFMAN 92B finds the $\bar{K}_1(1400)^0\pi^+$ branching fraction to be large; see the next entry.

$\Gamma(\bar{K}_1(1400)^0\pi^+)/\Gamma(K_S^0\pi^+\pi^+\pi^-)$ Γ_{90}/Γ_{67}

Unseen decay modes of the $\bar{K}_1(1400)^0$ are included.

VALUE	DOCUMENT ID	TECN	COMMENT
$1.246 \pm 0.212 \pm 0.360$	COFFMAN	92B	MRK3 e^+e^- 3.77 GeV

$\Gamma(\bar{K}^*(1410)^0\pi^+)/\Gamma_{\text{total}}$ Γ_{91}/Γ

VALUE	CL%	DOCUMENT ID	TECN	COMMENT
<0.007	90	COFFMAN	92B	MRK3 e^+e^- 3.77 GeV

••• We do not use the following data for averages, fits, limits, etc. **••••**

$\Gamma(K^*(892)^-\pi^+\pi^+\pi^0 \text{ total})/\Gamma(K_S^0\pi^+\pi^+\pi^-)$ Γ_{94}/Γ_{67}

Unseen decay modes of the $K^*(892)^-$ are included.

VALUE	EVTS	DOCUMENT ID	TECN	COMMENT
0.82 ± 0.28	14	ALEEV	94	BIS2 nN 20–70 GeV

••• We do not use the following data for averages, fits, limits, etc. **••••**

$\Gamma(K^*(892)^-\pi^+\pi^+3\text{-body})/\Gamma_{\text{total}}$ Γ_{95}/Γ
Unseen decay modes of the $\bar{K}^*(892)^0$ are included.

VALUE	CL%	DOCUMENT ID	TECN	COMMENT
<0.013	90	COFFMAN	92B	MRK3 e^+e^- 3.77 GeV

••• We do not use the following data for averages, fits, limits, etc. **••••**

$\Gamma(K^*(892)^-\pi^+\pi^+3\text{-body})/\Gamma(K_S^0\pi^+\pi^+\pi^-)$ Γ_{95}/Γ_{67}

Unseen decay modes of the $K^*(892)^-$ are included.

VALUE	DOCUMENT ID	TECN	COMMENT
$1.00 \pm 0.18 \pm 0.42$	ANJOS	92c	E691 γ Be 90–260 GeV

$\Gamma(K_S^0\rho^0\pi^+\pi^0 \text{ total})/\Gamma(K_S^0\pi^+\pi^+\pi^-)$ Γ_{71}/Γ_{67}

This includes $\bar{K}^0 a_1(1260)^+$. The next two entries give the specifically 3-body reaction.

VALUE	DOCUMENT ID	TECN	COMMENT
$0.60 \pm 0.10 \pm 0.17$	ANJOS	92c	E691 γ Be 90–260 GeV

$\Gamma(K_S^0\rho^0\pi^+3\text{-body})/\Gamma_{\text{total}}$ Γ_{72}/Γ

VALUE	CL%	DOCUMENT ID	TECN	COMMENT
<0.002	90	COFFMAN	92B	MRK3 e^+e^- 3.77 GeV

••• We do not use the following data for averages, fits, limits, etc. **••••**

$\Gamma(K_S^0\rho^0\pi^+3\text{-body})/\Gamma(K_S^0\pi^+\pi^+\pi^-)$ Γ_{72}/Γ_{67}

VALUE	DOCUMENT ID	TECN	COMMENT
$0.07 \pm 0.04 \pm 0.06$	ANJOS	92c	E691 γ Be 90–260 GeV

••• We do not use the following data for averages, fits, limits, etc. **••••**

$\Gamma(K_S^0 f_0(980)\pi^+)/\Gamma_{\text{total}}$ Γ_{96}/Γ

VALUE	CL%	DOCUMENT ID	TECN	COMMENT
<0.0025	90	ANJOS	92c	E691 γ Be 90–260 GeV

••• We do not use the following data for averages, fits, limits, etc. **••••**

$\Gamma(K_S^0\pi^+\pi^+\pi^- \text{ nonresonant})/\Gamma(K_S^0\pi^+\pi^+\pi^-)$ Γ_{73}/Γ_{67}

VALUE	DOCUMENT ID	TECN	COMMENT
0.12 ± 0.06	OUR AVERAGE		
0.10 ± 0.04 ± 0.06	ANJOS	92c	E691 γ Be 90–260 GeV
0.17 ± 0.056 ± 0.100	COFFMAN	92B	MRK3 e^+e^- 3.77 GeV

••• We do not use the following data for averages, fits, limits, etc. **••••**

$\Gamma(K^-3\pi^+\pi^-)/\Gamma(K^-\pi^+\pi^+)$ Γ_{74}/Γ_{46}

VALUE	EVTS	DOCUMENT ID	TECN	COMMENT
0.061 ± 0.005	OUR FIT			Error includes scale factor of 1.1.
0.062 ± 0.008	OUR AVERAGE			Error includes scale factor of 1.3.
0.058 ± 0.002 ± 0.006	2923	LINK	03D	FOCS γ A, $\bar{E}_\gamma \approx 180$ GeV
0.077 ± 0.008 ± 0.010	239	FRABETTI	97c	E687 γ Be, $\bar{E}_\gamma \approx 200$ GeV

••• We do not use the following data for averages, fits, limits, etc. **••••**

$\Gamma(\bar{K}^*(892)^0\pi^+\pi^+\pi^-, \bar{K}^*(892)^0 \rightarrow K^-\pi^+)/\Gamma(K^-3\pi^+\pi^-)$ Γ_{75}/Γ_{74}

VALUE	DOCUMENT ID	TECN	COMMENT
$0.21 \pm 0.04 \pm 0.06$	LINK	03D	FOCS γ A, $\bar{E}_\gamma \approx 180$ GeV

••• We do not use the following data for averages, fits, limits, etc. **••••**

$\Gamma(\bar{K}^*(892)^0\rho^0\pi^+, \bar{K}^*(892)^0 \rightarrow K^-\pi^+)/\Gamma(K^-\pi^+\pi^+)$ Γ_{76}/Γ_{46}

VALUE	DOCUMENT ID	TECN	COMMENT
$0.40 \pm 0.03 \pm 0.06$	LINK	03D	FOCS γ A, $\bar{E}_\gamma \approx 180$ GeV

••• We do not use the following data for averages, fits, limits, etc. **••••**

$\Gamma(\bar{K}^*(892)^0\rho^0\pi^+, \bar{K}^*(892)^0 \rightarrow K^-\pi^+)/\Gamma(K^-\pi^+\pi^+)$ Γ_{76}/Γ_{46}

VALUE	DOCUMENT ID	TECN	COMMENT
$0.016 \pm 0.007 \pm 0.004$	FRABETTI	97c	E687 γ Be, $\bar{E}_\gamma \approx 200$ GeV

••• We do not use the following data for averages, fits, limits, etc. **••••**

$\Gamma(\bar{K}^*(892)^0\pi^+\pi^+\pi^0 \text{ non-}\rho, \bar{K}^*(892)^0 \rightarrow K^-\pi^+)/\Gamma(K^-\pi^+\pi^+)$ Γ_{77}/Γ_{46}

VALUE	DOCUMENT ID	TECN	COMMENT
$0.032 \pm 0.010 \pm 0.008$	FRABETTI	97c	E687 γ Be, $\bar{E}_\gamma \approx 200$ GeV

••• We do not use the following data for averages, fits, limits, etc. **••~**

$\Gamma(K^-\rho^0\pi^+\pi^+)/\Gamma(K^-\pi^+\pi^+)$ Γ_{78}/Γ_{46}

VALUE	DOCUMENT ID	TECN	COMMENT
$0.034 \pm 0.009 \pm 0.005$	FRABETTI	97c	E687 γ Be, $\bar{E}_\gamma \approx 200$ GeV

••• We do not use the following data for averages, fits, limits, etc. **••~**

$\Gamma(K^-\rho^0\pi^+\pi^+)/\Gamma(K^-3\pi^+\pi^-)$ Γ_{78}/Γ_{74}

VALUE	DOCUMENT ID	TECN	COMMENT
$0.30 \pm 0.04 \pm 0.01$	LINK	03D	FOCS γ A, $\bar{E}_\gamma \approx 180$ GeV

••~ We do not use the following data for averages, fits, limits, etc. **••~**

$\Gamma(\bar{K}^*(892)^0 a_1(1260)^+)/\Gamma(K^-\pi^+\pi^+)$ Γ_{97}/Γ_{46}

Unseen decay modes of the $\bar{K}^*(892)^0$ and $a_1(1260)^+$ are included.

VALUE	DOCUMENT ID	TECN	COMMENT
$0.099 \pm 0.008 \pm 0.018$	LINK	03D	FOCS γ A, $\bar{E}_\gamma \approx 180$ GeV

••~ We do not use the following data for averages, fits, limits, etc. **••~**

$\Gamma(K^-3\pi^+\pi^- \text{ nonresonant})/\Gamma(K^-3\pi^+\pi^-)$ Γ_{79}/Γ_{74}

VALUE	CL%	DOCUMENT ID	TECN	COMMENT
$0.07 \pm 0.05 \pm 0.01$		LINK	03D	FOCS γ A, $\bar{E}_\gamma \approx 180$ GeV

••~ We do not use the following data for averages, fits, limits, etc. **••~**

<0.026 90 FRABETTI 97c E687 γ Be, $\bar{E}_\gamma \approx 200$ GeV

Meson Particle Listings

 D^\pm $\Gamma(K^+ 2K_S^0)/\Gamma(K^- \pi^+ \pi^+)$ Γ_{80}/Γ_{46}

VALUE	EVTS	DOCUMENT ID	TECN	COMMENT
0.049 ± 0.022 OUR AVERAGE				Error includes scale factor of 2.4.
0.035 ± 0.010 ± 0.005	39 ± 9	ALBRECHT 94i	ARG	$e^+ e^- \approx 10$ GeV
0.085 ± 0.018	70 ± 12	AMMAR 91	CLEO	$e^+ e^- \approx 10.5$ GeV

 $\Gamma(K^+ K^- K_S^0 \pi^+)/\Gamma(K_S^0 \pi^+ \pi^+ \pi^-)$ Γ_{81}/Γ_{67}

VALUE (units 10^{-3})	EVTS	DOCUMENT ID	TECN	COMMENT
7.7 ± 1.5 ± 0.9	35 ± 7	LINK	01c	FOCS γ nucleus, $\bar{E}_\gamma \approx 180$ GeV

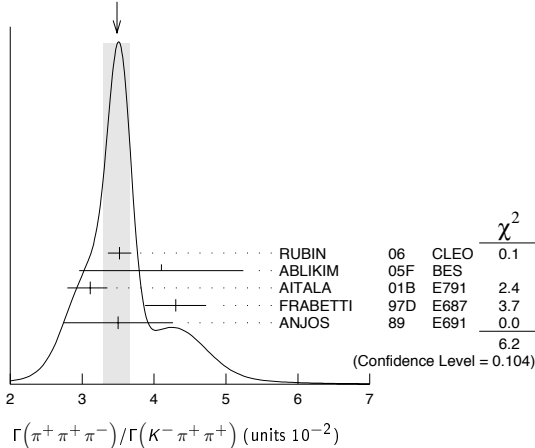
Pionic modes

 $\Gamma(\pi^+ \pi^0)/\Gamma(K^- \pi^+ \pi^+)$ Γ_{98}/Γ_{46}

VALUE (units 10^{-2})	EVTS	DOCUMENT ID	TECN	COMMENT
1.34 ± 0.07 OUR AVERAGE				
1.33 ± 0.11 ± 0.09	1229 ± 99	AUBERT,B	06F	BABR $e^+ e^- \approx \Upsilon(4S)$
1.33 ± 0.07 ± 0.06	914 ± 46	RUBIN	06	CLEO $e^+ e^-$ at $\psi(3770)$
1.44 ± 0.19 ± 0.10	171 ± 22	ARMS	04	CLEO $e^+ e^- \approx 10$ GeV

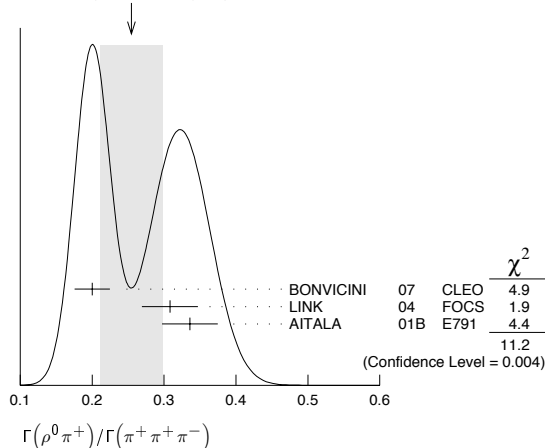
 $\Gamma(\pi^+ \pi^+ \pi^-)/\Gamma(K^- \pi^+ \pi^+)$ Γ_{99}/Γ_{46}

VALUE (units 10^{-2})	EVTS	DOCUMENT ID	TECN	COMMENT
3.48 ± 0.19 OUR AVERAGE				Error includes scale factor of 1.4. See the ideogram below.
3.52 ± 0.11 ± 0.12	3303 ± 95	RUBIN	06	CLEO $e^+ e^-$ at $\psi(3770)$
4.1 ± 1.1 ± 0.3	85 ± 22	ABLIKIM	05F	BES $e^+ e^- \approx \psi(3770)$
3.11 ± 0.18 ± 0.16	1172	AITALA	01B	E791 π^- nucleus, 500 GeV
4.3 ± 0.3 ± 0.3	236	FRABETTI	97D	E687 γ Be ≈ 200 GeV
3.5 ± 0.7 ± 0.3	83	ANJOS	89	E691 Photoproduction

WEIGHTED AVERAGE
3.48 ± 0.19 (Error scaled by 1.4) $\Gamma(\rho^0 \pi^+)/\Gamma(\pi^+ \pi^+ \pi^-)$ Γ_{100}/Γ_{99}

This is the "fit fraction" from the Dalitz-plot analysis.

VALUE	DOCUMENT ID	TECN	COMMENT
0.25 ± 0.04 OUR AVERAGE			Error includes scale factor of 2.4. See the ideogram below.
0.200 ± 0.023 ± 0.009	BONVICINI 07	CLEO	Dalitz fit, ≈ 2240 evts
0.3082 ± 0.0314 ± 0.0230	LINK 04	FOCS	Dalitz fit, 1527 ± 51 evts
0.336 ± 0.032 ± 0.022	AITALA 01B	E791	Dalitz fit, 1172 evts

WEIGHTED AVERAGE
0.25 ± 0.04 (Error scaled by 2.4) $\Gamma(\pi^+ (\pi^+ \pi^-)_{S\text{-wave}})/\Gamma(\pi^+ \pi^+ \pi^-)$ Γ_{101}/Γ_{99}

This is the "fit fraction" from the Dalitz-plot analysis. See also the next three data blocks.

VALUE	DOCUMENT ID	TECN	COMMENT	
0.5600 ± 0.0324 ± 0.0214	44	LINK	04	FOCS Dalitz fit, 1527 ± 51 evts

44 LINK 04 borrows a K-matrix parametrization from ANISOVICH 03 of the full $\pi-\pi$ S-wave isoscalar scattering amplitude to describe the $\pi^+ \pi^-$ S-wave component of the $\pi^+ \pi^+ \pi^-$ state. The fit fraction given above is a sum over five f_0 mesons, the $f_0(980)$, $f_0(1300)$, $f_0(1200-1600)$, $f_0(1500)$, and $f_0(1750)$. See LINK 04 for details and discussion.

 $\Gamma(\sigma \pi^+, \sigma \rightarrow \pi^+ \pi^-)/\Gamma(\pi^+ \pi^+ \pi^-)$ Γ_{102}/Γ_{99}

This is the "fit fraction" from the Dalitz-plot analysis.

VALUE	DOCUMENT ID	TECN	COMMENT
0.422 ± 0.027 OUR AVERAGE			
0.418 ± 0.014 ± 0.025	BONVICINI 07	CLEO	Dalitz fit, ≈ 2240 evts
0.463 ± 0.090 ± 0.021	AITALA 01B	E791	Dalitz fit, 1172 evts

 $\Gamma(f_0(980) \pi^+, f_0(980) \rightarrow \pi^+ \pi^-)/\Gamma(\pi^+ \pi^+ \pi^-)$ Γ_{103}/Γ_{99}

This is the "fit fraction" from the Dalitz-plot analysis.

VALUE	DOCUMENT ID	TECN	COMMENT
0.048 ± 0.010 OUR AVERAGE			Error includes scale factor of 1.3.
0.041 ± 0.009 ± 0.003	BONVICINI 07	CLEO	Dalitz fit, ≈ 2240 evts
0.062 ± 0.013 ± 0.004	AITALA 01B	E791	Dalitz fit, 1172 evts

 $\Gamma(f_0(1370) \pi^+, f_0(1370) \rightarrow \pi^+ \pi^-)/\Gamma(\pi^+ \pi^+ \pi^-)$ Γ_{104}/Γ_{99}

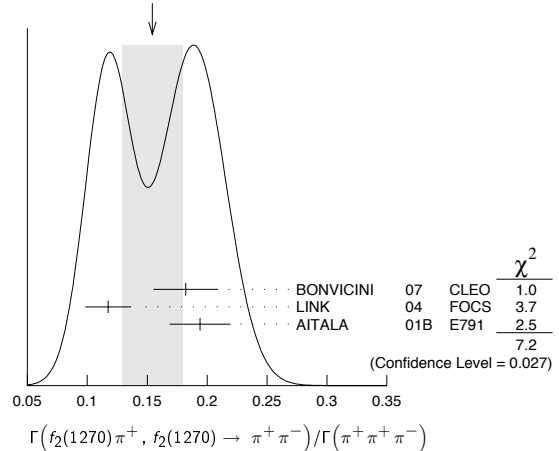
This is the "fit fraction" from the Dalitz-plot analysis.

VALUE	DOCUMENT ID	TECN	COMMENT
0.024 ± 0.013 OUR AVERAGE			
0.026 ± 0.018 ± 0.006	BONVICINI 07	CLEO	Dalitz fit, ≈ 2240 evts
0.023 ± 0.015 ± 0.008	AITALA 01B	E791	Dalitz fit, 1172 evts

 $\Gamma(f_2(1270) \pi^+, f_2(1270) \rightarrow \pi^+ \pi^-)/\Gamma(\pi^+ \pi^+ \pi^-)$ Γ_{105}/Γ_{99}

This is the "fit fraction" from the Dalitz-plot analysis.

VALUE	DOCUMENT ID	TECN	COMMENT
0.154 ± 0.025 OUR AVERAGE			Error includes scale factor of 1.9. See the ideogram below.
0.182 ± 0.026 ± 0.007	BONVICINI 07	CLEO	Dalitz fit, ≈ 2240 evts
0.1174 ± 0.0190 ± 0.0029	LINK 04	FOCS	Dalitz fit, 1527 ± 51 evts
0.194 ± 0.025 ± 0.004	AITALA 01B	E791	Dalitz fit, 1172 evts

WEIGHTED AVERAGE
0.154 ± 0.025 (Error scaled by 1.9) $\Gamma(\rho(1450)^0 \pi^+, \rho(1450)^0 \rightarrow \pi^+ \pi^-)/\Gamma(\pi^+ \pi^+ \pi^-)$ Γ_{106}/Γ_{99}

This is the "fit fraction" from the Dalitz-plot analysis.

VALUE	CL%	DOCUMENT ID	TECN	COMMENT
<0.024	95	BONVICINI 07	CLEO	Dalitz fit, ≈ 2240 evts
0.007 ± 0.007 ± 0.003		AITALA 01B	E791	Dalitz fit, 1172 evts

••• We do not use the following data for averages, fits, limits, etc. •••

 $\Gamma(f_0(1500) \pi^+, f_0(1500) \rightarrow \pi^+ \pi^-)/\Gamma(\pi^+ \pi^+ \pi^-)$ Γ_{107}/Γ_{99}

This is the "fit fraction" from the Dalitz-plot analysis.

VALUE	DOCUMENT ID	TECN	COMMENT
0.034 ± 0.010 ± 0.008	BONVICINI 07	CLEO	Dalitz fit, ≈ 2240 evts

 $\Gamma(f_0(1710) \pi^+, f_0(1710) \rightarrow \pi^+ \pi^-)/\Gamma(\pi^+ \pi^+ \pi^-)$ Γ_{108}/Γ_{99}

This is the "fit fraction" from the Dalitz-plot analysis.

VALUE	CL%	DOCUMENT ID	TECN	COMMENT
<0.016	95	BONVICINI 07	CLEO	Dalitz fit, ≈ 2240 evts

 $\Gamma(f_0(1790) \pi^+, f_0(1790) \rightarrow \pi^+ \pi^-)/\Gamma(\pi^+ \pi^+ \pi^-)$ Γ_{109}/Γ_{99}

This is the "fit fraction" from the Dalitz-plot analysis.

VALUE	CL%	DOCUMENT ID	TECN	COMMENT
<0.02	95	BONVICINI 07	CLEO	Dalitz fit, ≈ 2240 evts

$\Gamma((\pi^+\pi^-)_{S\text{-wave}}\pi^-)/\Gamma(\pi^+\pi^-\pi^-)$ Γ_{110}/Γ_{99}

This is the "fit fraction" from the Dalitz-plot analysis.

VALUE	CL%	DOCUMENT ID	TECN	COMMENT
<0.037	95	BONVICINI 07	CLEO	Dalitz fit, ≈ 2240 evts

 $\Gamma(\pi^+\pi^-\pi^- \text{ nonresonant})/\Gamma(\pi^+\pi^-\pi^-)$ Γ_{111}/Γ_{99}

This is the "fit fraction" from the Dalitz-plot analysis.

VALUE	CL%	DOCUMENT ID	TECN	COMMENT
<0.035	95	BONVICINI 07	CLEO	Dalitz fit, ≈ 2240 evts

• • • We do not use the following data for averages, fits, limits, etc. • • •

0.078 ± 0.060 ± 0.027 AITALA 01B E791 Dalitz fit, 1172 evts

 $\Gamma(\pi^+2\pi^0)/\Gamma(K^-\pi^+\pi^+)$ Γ_{112}/Γ_{46}

VALUE (units 10^{-2})	EVTS	DOCUMENT ID	TECN	COMMENT
5.0 ± 0.3 ± 0.3	1535 ± 89	RUBIN 06	CLEO	e^+e^- at $\psi(3770)$

 $\Gamma(\pi^+\pi^-\pi^0)/\Gamma(K^-\pi^+\pi^+)$ Γ_{113}/Γ_{46}

VALUE (units 10^{-2})	EVTS	DOCUMENT ID	TECN	COMMENT
12.4 ± 0.5 ± 0.6	5701 ± 205	RUBIN 06	CLEO	e^+e^- at $\psi(3770)$

 $\Gamma(\eta\pi^+)/\Gamma(\phi\pi^+)$ $\Gamma_{117}/\Gamma_{138}$ Unseen decay modes of the η are included.

VALUE	CL%	DOCUMENT ID	TECN	COMMENT
0.54 ± 0.06 OUR FIT				
0.49 ± 0.08	275	JESSOP 98	CLEO	$e^+e^- \approx \Upsilon(4S)$

 $\Gamma(\eta\pi^+)/\Gamma(K^-\pi^+\pi^+)$ Γ_{117}/Γ_{46} Unseen decay modes of the η are included.

VALUE (units 10^{-2})	EVTS	DOCUMENT ID	TECN	COMMENT
3.67 ± 0.30 OUR FIT				
3.81 ± 0.26 ± 0.21	377 ± 26	RUBIN 06	CLEO	e^+e^- at $\psi(3770)$

• • • We do not use the following data for averages, fits, limits, etc. • • •

8.3 ± 2.3 ± 1.4 99 DAOUDI 92 CLEO See JESSOP 98

 $\Gamma(\omega\pi^+)/\Gamma_{\text{total}}$ Γ_{118}/Γ Unseen decay modes of the ω are included.

VALUE	CL%	DOCUMENT ID	TECN	COMMENT
<3.4 × 10⁻⁴	90	RUBIN 06	CLEO	e^+e^- at $\psi(3770)$

 $\Gamma(3\pi^+2\pi^-)/\Gamma(K^-\pi^+\pi^+)$ Γ_{116}/Γ_{46}

VALUE (units 10^{-2})	EVTS	DOCUMENT ID	TECN	COMMENT
1.77 ± 0.17 OUR FIT				
1.73 ± 0.20 ± 0.17	732 ± 77	RUBIN 06	CLEO	e^+e^- at $\psi(3770)$

• • • We do not use the following data for averages, fits, limits, etc. • • •

2.3 ± 0.4 ± 0.2 58 FRABETTI 97c E687 $\gamma\text{Be}, \bar{E}_\gamma \approx 200$ GeV $\Gamma(3\pi^+2\pi^-)/\Gamma(K^-\pi^+\pi^-)$ Γ_{116}/Γ_{74}

VALUE	CL%	DOCUMENT ID	TECN	COMMENT
0.289 ± 0.019 OUR FIT				
0.290 ± 0.017 ± 0.011	835	LINK 03D	FOCS	$\gamma A, \bar{E}_\gamma \approx 180$ GeV

 $\Gamma(\eta\rho^+)/\Gamma(\phi\pi^+)$ $\Gamma_{119}/\Gamma_{138}$ Unseen decay modes of the η are included.

VALUE	CL%	DOCUMENT ID	TECN	COMMENT
<1.11	90	JESSOP 98	CLEO	$e^+e^- \approx \Upsilon(4S)$

 $\Gamma(\eta'(958)\pi^+)/\Gamma(\phi\pi^+)$ $\Gamma_{120}/\Gamma_{138}$ Unseen decay modes of the $\eta'(958)$ are included.

VALUE	CL%	DOCUMENT ID	TECN	COMMENT
0.82 ± 0.14	126	JESSOP 98	CLEO	$e^+e^- \approx \Upsilon(4S)$

 $\Gamma(\eta'(958)\rho^+)/\Gamma(\phi\pi^+)$ $\Gamma_{121}/\Gamma_{138}$ Unseen decay modes of the $\eta'(958)$ are included.

VALUE	CL%	DOCUMENT ID	TECN	COMMENT
<0.86	90	JESSOP 98	CLEO	$e^+e^- \approx \Upsilon(4S)$

Hadronic modes with a $K\bar{K}$ pair $\Gamma(K^+K_S^0)/\Gamma(K_S^0\pi^+)$ Γ_{122}/Γ_{44}

VALUE	CL%	DOCUMENT ID	TECN	COMMENT
0.199 ± 0.011 OUR FIT				
0.206 ± 0.014 OUR AVERAGE				

0.222 ± 0.037 ± 0.013 63 ± 10 ABLIKIM 05F BES $e^+e^- \approx \psi(3770)$ 0.1892 ± 0.0155 ± 0.0073 278 ± 21 ARMS 04 CLEO $e^+e^- \approx 10$ GeV0.25 ± 0.04 ± 0.02 129 FRABETTI 95 E687 $\gamma\text{Be}, \bar{E}_\gamma \approx 200$ GeV0.271 ± 0.065 ± 0.039 69 ANJOS 90c E691 γBe 0.317 ± 0.086 ± 0.048 31 BALTRUSAIT...85E MRK3 e^+e^- 3.77 GeV0.25 ± 0.15 6 SCHINDLER 81 MRK2 e^+e^- 3.771 GeV

• • • We do not use the following data for averages, fits, limits, etc. • • •

0.1996 ± 0.0119 ± 0.0096 949 45 LINK 02B FOCS $\gamma A, \bar{E}_\gamma \approx 180$ GeV

0.222 ± 0.041 ± 0.019 70 46 BISHAI 97 CLEO See ARMS 04

45 This LINK 02B result is redundant with a result in the next datablock.

46 This BISHAI 97 result is redundant with results elsewhere in the Listings.

 $\Gamma(K^+K_S^0)/\Gamma(K^-\pi^+\pi^+)$ Γ_{122}/Γ_{46}

VALUE (units 10^{-2})	EVTS	DOCUMENT ID	TECN	COMMENT
3.13 ± 0.17 OUR FIT				Error includes scale factor of 1.1.
3.02 ± 0.18 ± 0.15	949	LINK 02B	FOCS	γ nucleus, $\bar{E}_\gamma \approx 180$ GeV

• • • We do not use the following data for averages, fits, limits, etc. • • •

3.86 ± 0.69 ± 0.37 70 47 BISHAI 97 CLEO See ARMS 04

47 See BISHAI 97 for an isospin analysis of $D^+ \rightarrow K\bar{K}$ amplitudes. $\Gamma(K^+K^-\pi^+)/\Gamma_{\text{total}}$ Γ_{123}/Γ

VALUE (units 10^{-2})	EVTS	DOCUMENT ID	TECN	COMMENT
0.963 ± 0.031 OUR FIT				Error includes scale factor of 1.3.
0.935 ± 0.017 ± 0.024	48	DOBBS 07	CLEO	e^+e^- at $\psi(3770)$

• • • We do not use the following data for averages, fits, limits, etc. • • •

0.97 ± 0.04 ± 0.04 1250 ± 40 48 HE 05 CLEO See DOBBS 07

48 DOBBS 07 and HE 05 use single- and double-tagged events in an overall fit. DOBBS 07 supersedes HE 05.

 $\Gamma(K^+K^-\pi^+)/\Gamma(K^-\pi^+\pi^+)$ Γ_{123}/Γ_{46}

VALUE	CL%	DOCUMENT ID	TECN	COMMENT
0.1045 ± 0.0022 OUR FIT				Error includes scale factor of 1.3.
0.1058 ± 0.0029 OUR AVERAGE				Error includes scale factor of 1.4.

0.117 ± 0.013 ± 0.007 181 ± 20 ABLIKIM 05F BES $e^+e^- \approx \psi(3770)$ 0.107 ± 0.001 ± 0.002 43k AUBERT 05s BABR $e^+e^- \approx \Upsilon(4S)$ 0.093 ± 0.010 ± 0.008 006 JUN 00 SELX Σ^- nucleus, 600 GeV0.0976 ± 0.0042 ± 0.0046 FRABETTI 95B E687 $\gamma\text{Be}, \bar{E}_\gamma \approx 200$ GeV $\Gamma(\phi\pi^+, \phi \rightarrow K^+K^-)/\Gamma(K^+K^-\pi^+)$ $\Gamma_{124}/\Gamma_{123}$

This is the "fit fraction" from the Dalitz-plot analysis.

VALUE	CL%	DOCUMENT ID	TECN	COMMENT
0.318 ± 0.034 OUR FIT				
0.292 ± 0.031 ± 0.030		FRABETTI 95B	E687	Dalitz fit, 915 evts

 $\Gamma(\phi\pi^+, \phi \rightarrow K^+K^-)/\Gamma(\phi\pi^+)$ $\Gamma_{124}/\Gamma_{138}$

VALUE	CL%	DOCUMENT ID	TECN	COMMENT
0.491 ± 0.006 OUR FIT				
0.491 ± 0.006		49 PDG	06	

49 This is, of course, just the $\phi \rightarrow K^+K^-$ branching fraction, but we need it to connect other modes in the fit. $\Gamma(\phi\pi^+)/\Gamma(K^-\pi^+\pi^+)$ Γ_{138}/Γ_{46} Unseen decay modes of the ϕ are included. However, we now get branching fractions for resonant submodes of $K^+K^-\pi^+$ decays from Dalitz-plot analyses.

VALUE	CL%	DOCUMENT ID	TECN	COMMENT
0.057 ± 0.011 ± 0.003	46 ± 9	ABLIKIM 06P	BES2	e^+e^- at 3773 MeV

0.062 ± 0.017 ± 0.006 19 ADAMOVIICH 93 WA82 π^- 340 GeV0.077 ± 0.011 ± 0.005 128 DAOUDI 92 CLEO $e^+e^- \approx 10.5$ GeV

0.098 ± 0.032 ± 0.014 12 ALVAREZ 90c NA14 Photoproduction

0.071 ± 0.008 ± 0.007 84 ANJOS 88 E691 Photoproduction

0.084 ± 0.021 ± 0.011 21 BALTRUSAIT...85E MRK3 e^+e^- 3.77 GeV $\Gamma(K^+\bar{K}^*(892)^0, \bar{K}^*(892)^0 \rightarrow K^-\pi^+)/\Gamma(K^+K^-\pi^+)$ $\Gamma_{125}/\Gamma_{123}$

This is the "fit fraction" from the Dalitz-plot analysis.

VALUE	CL%	DOCUMENT ID	TECN	COMMENT
0.301 ± 0.020 ± 0.025		FRABETTI 95B	E687	Dalitz fit, 915 evts

 $\Gamma(K^+\bar{K}^*(892)^0)/\Gamma(K^-\pi^+\pi^+)$ Γ_{141}/Γ_{46} Unseen decay modes of the $\bar{K}^*(892)^0$ are included. However, we now get branching fractions for resonant submodes of $K^+K^-\pi^+$ decays from Dalitz-plot analyses.

VALUE	CL%	DOCUMENT ID	TECN	COMMENT
0.058 ± 0.009 ± 0.006	73	ANJOS 88	E691	Photoproduction

0.048 ± 0.021 ± 0.011 14 BALTRUSAIT...85E MRK3 e^+e^- 3.77 GeV $\Gamma(K^+\bar{K}_S^0(1430)^0, \bar{K}_S^0(1430)^0 \rightarrow K^-\pi^+)/\Gamma(K^+K^-\pi^+)$ $\Gamma_{126}/\Gamma_{123}$

This is the "fit fraction" from the Dalitz-plot analysis.

VALUE	CL%	DOCUMENT ID	TECN	COMMENT
0.370 ± 0.035 ± 0.018		FRABETTI 95B	E687	Dalitz fit, 915 evts

 $\Gamma(K^+K^-\pi^+ \text{ nonresonant})/\Gamma(K^-\pi^+\pi^+)$ Γ_{127}/Γ_{46}

VALUE	CL%	DOCUMENT ID	TECN	COMMENT
0.049 ± 0.008 ± 0.006	95	ANJOS 88	E691	Photoproduction

0.059 ± 0.026 ± 0.009 37 BALTRUSAIT...85E MRK3 e^+e^- 3.77 GeV $\Gamma(K^*(892)^+K_S^0)/\Gamma(K_S^0\pi^+)$ Γ_{142}/Γ_{44} Unseen decay modes of the $K^*(892)^+$ are included.

VALUE	CL%	DOCUMENT ID	TECN	COMMENT
1.1 ± 0.3 ± 0.4		FRABETTI 95	E687	$\gamma\text{Be}, \bar{E}_\gamma \approx 200$ GeV

Meson Particle Listings

 D^\pm $\Gamma(\phi\pi^+\pi^0)/\Gamma_{\text{total}}$ Γ_{139}/Γ

Unseen decay modes of the ϕ are included.

VALUE	DOCUMENT ID	TECN	COMMENT
0.023 ± 0.010	50 BARLAG	92c ACCM	π^- Cu 230 GeV

⁵⁰BARLAG 92c computes the branching fraction using topological normalization.

 $\Gamma(\phi\rho^+)/\Gamma(K^-\pi^+\pi^+)$ Γ_{140}/Γ_{46}

Unseen decay modes of the ϕ are included.

VALUE	CL%	DOCUMENT ID	TECN	COMMENT
<0.16	90	DAOUDI	92 CLEO	$e^+e^- \approx 10.5$ GeV

 $\Gamma(K^+K^-\pi^+\pi^0 \text{ non-}\phi)/\Gamma_{\text{total}}$ Γ_{133}/Γ

VALUE	DOCUMENT ID	TECN	COMMENT
0.015 ± 0.007 -0.006	51 BARLAG	92c ACCM	π^- Cu 230 GeV

⁵¹BARLAG 92c computes the branching fraction using topological normalization.

 $\Gamma(K^+K^-\pi^+\pi^0 \text{ non-}\phi)/\Gamma(K^-\pi^+\pi^+)$ Γ_{133}/Γ_{46}

VALUE	CL%	DOCUMENT ID	TECN	COMMENT
<0.25	90	ANJOS	89E E691	Photoproduction

• • • We do not use the following data for averages, fits, limits, etc. • • •

 $\Gamma(K^+K_S^0\pi^+\pi^-)/\Gamma(K_S^0\pi^+\pi^+\pi^-)$ Γ_{134}/Γ_{67}

VALUE (units 10^{-2})	EVTS	DOCUMENT ID	TECN	COMMENT
5.62 ± 0.39 ± 0.40	469 ± 32	LINK	01c FOCS	γ nucleus, $\bar{E}_\gamma \approx 180$ GeV

 $\Gamma(K_S^0K^-\pi^+\pi^+)/\Gamma(K_S^0\pi^+\pi^+\pi^-)$ Γ_{135}/Γ_{67}

VALUE (units 10^{-2})	EVTS	DOCUMENT ID	TECN	COMMENT
7.68 ± 0.41 ± 0.32	670 ± 35	LINK	01c FOCS	γ nucleus, $\bar{E}_\gamma \approx 180$ GeV

 $\Gamma(K^+K^-\pi^+\pi^+\pi^-)/\Gamma(K^-\pi^+\pi^+)$ Γ_{137}/Γ_{74}

VALUE	EVTS	DOCUMENT ID	TECN	COMMENT
0.040 ± 0.009 ± 0.019	38	LINK	03d FOCS	γ A, $\bar{E}_\gamma \approx 180$ GeV

Doubly Cabibbo-suppressed modes

 $\Gamma(K^+\pi^0)/\Gamma_{\text{total}}$ Γ_{144}/Γ

VALUE (units 10^{-4})	EVTS	DOCUMENT ID	TECN	COMMENT
2.37 ± 0.32 OUR AVERAGE				
2.52 ± 0.47 ± 0.26	189 ± 37	AUBERT,B	06F BABR	$e^+e^- \approx \Upsilon(4S)$
2.28 ± 0.36 ± 0.17	148 ± 23	DYTMAN	06 CLEO	e^+e^- at $\psi(3770)$

 $\Gamma(K^+\pi^+\pi^-)/\Gamma(K^-\pi^+\pi^+)$ Γ_{145}/Γ_{46}

VALUE	EVTS	DOCUMENT ID	TECN	COMMENT
0.0068 ± 0.0008 OUR AVERAGE				
0.0065 ± 0.0008 ± 0.0004	189 ± 24	LINK	04F FOCS	γ A, $\bar{E}_\gamma \approx 180$ GeV
0.0077 ± 0.0017 ± 0.0008	59 ± 13	AITALA	97c E791	π^- A, 500 GeV
0.0072 ± 0.0023 ± 0.0017	21	FRABETTI	95E E687	γ Be, $\bar{E}_\gamma \approx 220$ GeV

 $\Gamma(K^+\rho^0)/\Gamma(K^+\pi^+\pi^-)$ $\Gamma_{146}/\Gamma_{145}$

This is the "fit fraction" from the Dalitz-plot analysis.

VALUE	DOCUMENT ID	TECN	COMMENT
0.39 ± 0.09 OUR AVERAGE			
0.3943 ± 0.0787 ± 0.0815	LINK	04F FOCS	Dalitz fit, 189 evts
0.37 ± 0.14 ± 0.07	AITALA	97c E791	Dalitz fit, 59 evts

 $\Gamma(K^+\rho_0(980), \rho_0(980) \rightarrow \pi^+\pi^-)/\Gamma(K^+\pi^+\pi^-)$ $\Gamma_{148}/\Gamma_{145}$

This is the "fit fraction" from the Dalitz-plot analysis.

VALUE	DOCUMENT ID	TECN	COMMENT
0.0892 ± 0.0333 ± 0.0412	LINK	04F FOCS	Dalitz fit, 189 evts

 $\Gamma(K^*(892)^0\pi^+, K^*(892)^0 \rightarrow K^+\pi^-)/\Gamma(K^+\pi^+\pi^-)$ $\Gamma_{147}/\Gamma_{145}$

This is the "fit fraction" from the Dalitz-plot analysis.

VALUE	DOCUMENT ID	TECN	COMMENT
0.47 ± 0.08 OUR AVERAGE			
0.5220 ± 0.0684 ± 0.0638	LINK	04F FOCS	Dalitz fit, 189 evts
0.35 ± 0.14 ± 0.01	AITALA	97c E791	Dalitz fit, 59 evts

 $\Gamma(K_S^2(1430)^0\pi^+, K_S^2(1430)^0 \rightarrow K^+\pi^-)/\Gamma(K^+\pi^+\pi^-)$ $\Gamma_{149}/\Gamma_{145}$

This is the "fit fraction" from the Dalitz-plot analysis.

VALUE	DOCUMENT ID	TECN	COMMENT
0.0803 ± 0.0372 ± 0.0391	LINK	04F FOCS	Dalitz fit, 189 evts

 $\Gamma(K^+\pi^+\pi^- \text{ nonresonant})/\Gamma(K^+\pi^+\pi^-)$ $\Gamma_{150}/\Gamma_{145}$

This is the "fit fraction" from the Dalitz-plot analysis.

VALUE	DOCUMENT ID	TECN	COMMENT
<0.36 ± 0.14 ± 0.07	52 AITALA	97c E791	Dalitz fit, 59 evts

⁵²LINK 04F, with three times as many events, finds no need for a nonresonant amplitude.

 $\Gamma(K^+K^+K^-)/\Gamma(K^-\pi^+\pi^+)$ Γ_{151}/Γ_{46}

VALUE (units 10^{-4})	EVTS	DOCUMENT ID	TECN	COMMENT
9.49 ± 2.17 ± 0.22	65	53 LINK	02i FOCS	γ nucleus, ≈ 180 GeV

⁵³LINK 02i finds little evidence for ϕK^+ or $f_0(980) K^+$ submodes.

Rare or forbidden modes

 $\Gamma(\pi^+e^+e^-)/\Gamma_{\text{total}}$ Γ_{152}/Γ

A test for the $\Delta C = 1$ weak neutral current. Allowed by higher-order electroweak interactions.

VALUE	CL%	EVTS	DOCUMENT ID	TECN	COMMENT
<7.4 × 10⁻⁶	90		HE	05A CLEO	e^+e^- at $\psi(3770)$
• • • We do not use the following data for averages, fits, limits, etc. • • •					
<5.2 × 10 ⁻⁵	90		AITALA	99G E791	π^- N 500 GeV
<1.1 × 10 ⁻⁴	90		FRABETTI	97B E687	γ Be, $\bar{E}_\gamma \approx 220$ GeV
<6.6 × 10 ⁻⁵	90		AITALA	96 E791	π^- N 500 GeV
<2.5 × 10 ⁻³	90		WEIR	90B MRK2	e^+e^- 29 GeV
<2.6 × 10 ⁻³	90	39	HAAS	88 CLEO	e^+e^- 10 GeV

 $\Gamma(\pi^+\phi, \phi \rightarrow e^+e^-)/\Gamma_{\text{total}}$ Γ_{153}/Γ

This is *not* a test for the $\Delta C = 1$ weak neutral current, but leads to the $\pi^+e^+e^-$ final state.

VALUE	EVTS	DOCUMENT ID	TECN	COMMENT
(2.7 ± 3.6 ± 0.2) × 10⁻⁶	2	54 HE	05A CLEO	e^+e^- at $\psi(3770)$

⁵⁴This HE 05A result is consistent with the branching fraction for $D^+ \rightarrow \phi\pi^+, \phi \rightarrow K^+K^-$.

 $\Gamma(\pi^+\mu^+\mu^-)/\Gamma_{\text{total}}$ Γ_{154}/Γ

A test for the $\Delta C = 1$ weak neutral current. Allowed by higher-order electroweak interactions.

VALUE	CL%	EVTS	DOCUMENT ID	TECN	COMMENT
<3.9 × 10⁻⁶	90	55	ABAZOV	08D D0	$p\bar{p}$, $E_{\text{cm}} = 1.96$ TeV
• • • We do not use the following data for averages, fits, limits, etc. • • •					
<8.8 × 10 ⁻⁶	90		LINK	03F FOCS	γ nucleus, $\bar{E}_\gamma \approx 180$ GeV
<1.5 × 10 ⁻⁵	90		AITALA	99G E791	π^- N 500 GeV
<8.9 × 10 ⁻⁵	90		FRABETTI	97B E687	γ Be, $\bar{E}_\gamma \approx 220$ GeV
<1.8 × 10 ⁻⁵	90		AITALA	96 E791	π^- N 500 GeV
<2.2 × 10 ⁻⁴	90	0	KODAMA	95 E653	π^- emulsion 600 GeV
<5.9 × 10 ⁻³	90		WEIR	90B MRK2	e^+e^- 29 GeV
<2.9 × 10 ⁻³	90	36	HAAS	88 CLEO	e^+e^- 10 GeV

⁵⁵This ABAZOV 08D limit is for the $\mu^+\mu^-$ mass in the continuum away from the $\phi(1020)$. The branching fraction for $D^+ \rightarrow \phi\pi^+, \phi \rightarrow \mu^+\mu^-$ is $(1.8 \pm 0.5 \pm 0.6) \times 10^{-6}$, consistent with known $D^+ \rightarrow \phi\pi^+$ and $\phi \rightarrow \mu^+\mu^-$ fractions.

 $\Gamma(\rho^+\mu^+\mu^-)/\Gamma_{\text{total}}$ Γ_{155}/Γ

A test for the $\Delta C = 1$ weak neutral current. Allowed by higher-order electroweak interactions.

VALUE	CL%	EVTS	DOCUMENT ID	TECN	COMMENT
<5.6 × 10⁻⁴	90	0	KODA MA	95 E653	π^- emulsion 600 GeV

 $\Gamma(K^+e^+e^-)/\Gamma_{\text{total}}$ Γ_{156}/Γ

Both quarks would have to change flavor for this decay to occur.

VALUE	CL%	DOCUMENT ID	TECN	COMMENT
<6.2 × 10⁻⁶	90	HE	05A CLEO	e^+e^- at $\psi(3770)$
• • • We do not use the following data for averages, fits, limits, etc. • • •				
<2.0 × 10 ⁻⁴	90	AITALA	99G E791	π^- N 500 GeV
<2.0 × 10 ⁻⁴	90	FRABETTI	97B E687	γ Be, $\bar{E}_\gamma \approx 220$ GeV
<4.8 × 10 ⁻³	90	WEIR	90B MRK2	e^+e^- 29 GeV

 $\Gamma(K^+\mu^+\mu^-)/\Gamma_{\text{total}}$ Γ_{157}/Γ

Both quarks would have to change flavor for this decay to occur.

VALUE	CL%	DOCUMENT ID	TECN	COMMENT
<9.2 × 10⁻⁶	90	LINK	03F FOCS	γ nucleus, $\bar{E}_\gamma \approx 180$ GeV
• • • We do not use the following data for averages, fits, limits, etc. • • •				
<4.4 × 10 ⁻⁵	90	AITALA	99G E791	π^- N 500 GeV
<9.7 × 10 ⁻⁵	90	FRABETTI	97B E687	γ Be, $\bar{E}_\gamma \approx 220$ GeV
<3.2 × 10 ⁻⁴	90	KODA MA	95 E653	π^- emulsion 600 GeV
<9.2 × 10 ⁻³	90	WEIR	90B MRK2	e^+e^- 29 GeV

 $\Gamma(\pi^+e^\pm\mu^\mp)/\Gamma_{\text{total}}$ Γ_{158}/Γ

A test of lepton-family-number conservation.

VALUE	CL%	DOCUMENT ID	TECN	COMMENT
<3.4 × 10⁻⁵	90	AITALA	99G E791	π^- N 500 GeV

 $\Gamma(\pi^+e^+\mu^-)/\Gamma_{\text{total}}$ Γ_{159}/Γ

A test of lepton-family-number conservation.

VALUE	CL%	DOCUMENT ID	TECN	COMMENT
• • • We do not use the following data for averages, fits, limits, etc. • • •				
<1.1 × 10 ⁻⁴	90	FRABETTI	97B E687	γ Be, $\bar{E}_\gamma \approx 220$ GeV
<3.3 × 10 ⁻³	90	WEIR	90B MRK2	e^+e^- 29 GeV

 $\Gamma(\pi^+e^-\mu^+)/\Gamma_{\text{total}}$ Γ_{160}/Γ

A test of lepton-family-number conservation.

VALUE	CL%	DOCUMENT ID	TECN	COMMENT
• • • We do not use the following data for averages, fits, limits, etc. • • •				
<1.3 × 10 ⁻⁴	90	FRABETTI	97B E687	γ Be, $\bar{E}_\gamma \approx 220$ GeV
<3.3 × 10 ⁻³	90	WEIR	90B MRK2	e^+e^- 29 GeV

See key on page 373

Meson Particle Listings

 D^\pm $\Gamma(K^+ e^\pm \mu^\mp)/\Gamma_{\text{total}}$ Γ_{161}/Γ

A test of lepton-family-number conservation.

VALUE	CL%	DOCUMENT ID	TECN	COMMENT
$<6.8 \times 10^{-5}$	90	AITALA	99G E791	$\pi^- N$ 500 GeV

 $\Gamma(K^+ e^+ \mu^-)/\Gamma_{\text{total}}$ Γ_{162}/Γ

A test of lepton-family-number conservation.

VALUE	CL%	DOCUMENT ID	TECN	COMMENT
••• We do not use the following data for averages, fits, limits, etc. •••				
$<1.3 \times 10^{-4}$	90	FRABETTI	97B E687	γ Be, $\bar{E}_\gamma \approx 220$ GeV
$<3.4 \times 10^{-3}$	90	WEIR	90B MRK2	$e^+ e^-$ 29 GeV

 $\Gamma(K^+ e^- \mu^+)/\Gamma_{\text{total}}$ Γ_{163}/Γ

A test of lepton-family-number conservation.

VALUE	CL%	DOCUMENT ID	TECN	COMMENT
••• We do not use the following data for averages, fits, limits, etc. •••				
$<1.2 \times 10^{-4}$	90	FRABETTI	97B E687	γ Be, $\bar{E}_\gamma \approx 220$ GeV
$<3.4 \times 10^{-3}$	90	WEIR	90B MRK2	$e^+ e^-$ 29 GeV

 $\Gamma(\pi^- e^+ e^+)/\Gamma_{\text{total}}$ Γ_{164}/Γ

A test of lepton-number conservation.

VALUE	CL%	DOCUMENT ID	TECN	COMMENT
$<3.6 \times 10^{-6}$	90	HE	05A CLEO	$e^+ e^-$ at $\psi(3770)$
••• We do not use the following data for averages, fits, limits, etc. •••				
$<9.6 \times 10^{-5}$	90	AITALA	99G E791	$\pi^- N$ 500 GeV
$<1.1 \times 10^{-4}$	90	FRABETTI	97B E687	γ Be, $\bar{E}_\gamma \approx 220$ GeV
$<4.8 \times 10^{-3}$	90	WEIR	90B MRK2	$e^+ e^-$ 29 GeV

 $\Gamma(\pi^- \mu^+ \mu^+)/\Gamma_{\text{total}}$ Γ_{165}/Γ

A test of lepton-number conservation.

VALUE	CL%	EVTS	DOCUMENT ID	TECN	COMMENT
$<4.8 \times 10^{-6}$	90		LINK	03F FOCUS	γ nucleus, $\bar{E}_\gamma \approx 180$ GeV
••• We do not use the following data for averages, fits, limits, etc. •••					
$<1.7 \times 10^{-5}$	90		AITALA	99G E791	$\pi^- N$ 500 GeV
$<8.7 \times 10^{-5}$	90		FRABETTI	97B E687	γ Be, $\bar{E}_\gamma \approx 220$ GeV
$<2.2 \times 10^{-4}$	90	0	KODAMA	95 E653	π^- emulsion 600 GeV
$<6.8 \times 10^{-3}$	90		WEIR	90B MRK2	$e^+ e^-$ 29 GeV

 $\Gamma(\pi^- e^+ \mu^+)/\Gamma_{\text{total}}$ Γ_{166}/Γ

A test of lepton-number conservation.

VALUE	CL%	DOCUMENT ID	TECN	COMMENT
$<5.0 \times 10^{-5}$	90	AITALA	99G E791	$\pi^- N$ 500 GeV
••• We do not use the following data for averages, fits, limits, etc. •••				
$<1.1 \times 10^{-4}$	90	FRABETTI	97B E687	γ Be, $\bar{E}_\gamma \approx 220$ GeV
$<3.7 \times 10^{-3}$	90	WEIR	90B MRK2	$e^+ e^-$ 29 GeV

 $\Gamma(\rho^- \mu^+ \mu^+)/\Gamma_{\text{total}}$ Γ_{167}/Γ

A test of lepton-number conservation.

VALUE	CL%	EVTS	DOCUMENT ID	TECN	COMMENT
$<5.6 \times 10^{-4}$	90	0	KODAMA	95 E653	π^- emulsion 600 GeV

 $\Gamma(K^- e^+ e^+)/\Gamma_{\text{total}}$ Γ_{168}/Γ

A test of lepton-number conservation.

VALUE	CL%	DOCUMENT ID	TECN	COMMENT
$<4.5 \times 10^{-6}$	90	HE	05A CLEO	$e^+ e^-$ at $\psi(3770)$
••• We do not use the following data for averages, fits, limits, etc. •••				
$<1.2 \times 10^{-4}$	90	FRABETTI	97B E687	γ Be, $\bar{E}_\gamma \approx 220$ GeV
$<9.1 \times 10^{-3}$	90	WEIR	90B MRK2	$e^+ e^-$ 29 GeV

 $\Gamma(K^- \mu^+ \mu^+)/\Gamma_{\text{total}}$ Γ_{169}/Γ

A test of lepton-number conservation.

VALUE	CL%	EVTS	DOCUMENT ID	TECN	COMMENT
$<1.3 \times 10^{-5}$	90		LINK	03F FOCUS	γ nucleus, $\bar{E}_\gamma \approx 180$ GeV
••• We do not use the following data for averages, fits, limits, etc. •••					
$<1.2 \times 10^{-4}$	90		FRABETTI	97B E687	γ Be, $\bar{E}_\gamma \approx 220$ GeV
$<3.2 \times 10^{-4}$	90	0	KODAMA	95 E653	π^- emulsion 600 GeV
$<4.3 \times 10^{-3}$	90		WEIR	90B MRK2	$e^+ e^-$ 29 GeV

 $\Gamma(K^- e^+ \mu^+)/\Gamma_{\text{total}}$ Γ_{170}/Γ

A test of lepton-number conservation.

VALUE	CL%	DOCUMENT ID	TECN	COMMENT
$<1.3 \times 10^{-4}$	90	FRABETTI	97B E687	γ Be, $\bar{E}_\gamma \approx 220$ GeV
••• We do not use the following data for averages, fits, limits, etc. •••				
$<4.0 \times 10^{-3}$	90	WEIR	90B MRK2	$e^+ e^-$ 29 GeV

 $\Gamma(K^*(892)^- \mu^+ \mu^+)/\Gamma_{\text{total}}$ Γ_{171}/Γ

A test of lepton-number conservation.

VALUE	CL%	EVTS	DOCUMENT ID	TECN	COMMENT
$<8.5 \times 10^{-4}$	90	0	KODAMA	95 E653	π^- emulsion 600 GeV

 D^\pm CP-VIOLATING DECAY-RATE ASYMMETRIESThis is the difference between D^+ and D^- partial widths for these modes divided by the sum of the widths. $A_{CP}(K_S^0 \pi^\pm)$ in $D^\pm \rightarrow K_S^0 \pi^\pm$

VALUE	EVTS	DOCUMENT ID	TECN	COMMENT
-0.009 ± 0.009				OUR AVERAGE
$-0.006 \pm 0.010 \pm 0.003$		DOBBS	07 CLEO	$e^+ e^-$ at $\psi(3770)$
$-0.016 \pm 0.015 \pm 0.009$	10.6k	⁵⁶ LINK	02B FOCUS	γ nucleus, $\bar{E}_\gamma \approx 180$ GeV

⁵⁶ LINK 02B measures $N(D^+ \rightarrow K_S^0 \pi^+)/N(D^+ \rightarrow K^- \pi^+ \pi^+)$, the ratio of numbers of events observed, and similarly for the D^- .

 $A_{CP}(K^\mp 2\pi^\pm)$ in $D^+ \rightarrow K^- 2\pi^+$, $D^- \rightarrow K^+ 2\pi^-$

VALUE	DOCUMENT ID	TECN	COMMENT
$-0.005 \pm 0.004 \pm 0.009$	DOBBS	07 CLEO	$e^+ e^-$ at $\psi(3770)$

 $A_{CP}(K^\mp \pi^\pm \pi^\pm \pi^0)$ in $D^+ \rightarrow K^- \pi^+ \pi^+ \pi^0$, $D^- \rightarrow K^+ \pi^- \pi^- \pi^0$

VALUE	DOCUMENT ID	TECN	COMMENT
$+0.010 \pm 0.009 \pm 0.009$	DOBBS	07 CLEO	$e^+ e^-$ at $\psi(3770)$

 $A_{CP}(K_S^0 \pi^\pm \pi^0)$ in $D^+ \rightarrow K_S^0 \pi^+ \pi^0$, $D^- \rightarrow K_S^0 \pi^- \pi^0$

VALUE	DOCUMENT ID	TECN	COMMENT
$+0.003 \pm 0.009 \pm 0.003$	DOBBS	07 CLEO	$e^+ e^-$ at $\psi(3770)$

 $A_{CP}(K_S^0 \pi^\pm \pi^+ \pi^-)$ in $D^+ \rightarrow K_S^0 \pi^+ \pi^+ \pi^-$, $D^- \rightarrow K_S^0 \pi^- \pi^- \pi^+$

VALUE	DOCUMENT ID	TECN	COMMENT
$+0.001 \pm 0.011 \pm 0.006$	DOBBS	07 CLEO	$e^+ e^-$ at $\psi(3770)$

 $A_{CP}(K_S^0 K^\pm)$ in $D^\pm \rightarrow K_S^0 K^\pm$

VALUE	EVTS	DOCUMENT ID	TECN	COMMENT
$+0.071 \pm 0.061 \pm 0.012$	949	⁵⁷ LINK	02B FOCUS	γ nucleus, $\bar{E}_\gamma \approx 180$ GeV
$+0.069 \pm 0.060 \pm 0.015$	949	⁵⁸ LINK	02B FOCUS	γ nucleus, $\bar{E}_\gamma \approx 180$ GeV

⁵⁷ LINK 02B measures $N(D^+ \rightarrow K_S^0 K^+)/N(D^+ \rightarrow K_S^0 \pi^+)$, the ratio of numbers of events observed, and similarly for the D^- .

⁵⁸ LINK 02B measures $N(D^+ \rightarrow K_S^0 K^+)/N(D^+ \rightarrow K^- \pi^+ \pi^+)$, the ratio of numbers of events observed, and similarly for the D^- .

 $A_{CP}(K^+ K^- \pi^\pm)$ in $D^\pm \rightarrow K^+ K^- \pi^\pm$

VALUE	EVTS	DOCUMENT ID	TECN	COMMENT
0.006 ± 0.007				OUR AVERAGE
$-0.001 \pm 0.015 \pm 0.008$		DOBBS	07 CLEO	$e^+ e^-$ at $\psi(3770)$
$+0.014 \pm 0.010 \pm 0.008$	43k±321	⁵⁹ AUBERT	05s BABR	$e^+ e^- \approx \gamma(4S)$
$+0.006 \pm 0.011 \pm 0.005$	14k	⁶⁰ LINK	00B FOCUS	
-0.014 ± 0.029		⁶⁰ AITALA	97B E791	$-0.062 < A_{CP} < +0.034$ (90% CL)
-0.031 ± 0.068		⁶⁰ FRABETTI	94i E687	$-0.14 < A_{CP} < +0.081$ (90% CL)

⁵⁹ AUBERT 05s measures $N(D^+ \rightarrow K^+ K^- \pi^+)/N(D^+ \rightarrow K^+ K^- \pi^+)$, the ratio of the numbers of events observed, and similarly for the D^- .

⁶⁰ FRABETTI 94i, AITALA 98c, and LINK 00b measure $N(D^+ \rightarrow K^- K^+ \pi^+)/N(D^+ \rightarrow K^- \pi^+ \pi^+)$, the ratio of numbers of events observed, and similarly for the D^- .

 $A_{CP}(K^\pm K^* 0)$ in $D^+ \rightarrow K^+ \bar{K}^{*0}$, $D^- \rightarrow K^- K^{*0}$

VALUE	EVTS	DOCUMENT ID	TECN	COMMENT
0.005 ± 0.017				OUR AVERAGE
$+0.009 \pm 0.017 \pm 0.007$	11k±122	⁶¹ AUBERT	05s BABR	$e^+ e^- \approx \gamma(4S)$
-0.010 ± 0.050		⁶² AITALA	97B E791	$-0.092 < A_{CP} < +0.072$ (90% CL)
-0.12 ± 0.13		⁶² FRABETTI	94i E687	$-0.33 < A_{CP} < +0.094$ (90% CL)

⁶¹ AUBERT 05s measures $N(D^+ \rightarrow K^+ \bar{K}^{*0})/N(D^+ \rightarrow K^+ K^- \pi^+)$, the ratio of the numbers of events observed, and similarly for the D^- .

⁶² FRABETTI 94i and AITALA 97b measure $N(D^+ \rightarrow K^+ \bar{K}^{*0}(892)^0)/N(D^+ \rightarrow K^- \pi^+ \pi^+)$, the ratio of numbers of events observed, and similarly for the D^- .

 $A_{CP}(\phi \pi^\pm)$ in $D^\pm \rightarrow \phi \pi^\pm$

VALUE	EVTS	DOCUMENT ID	TECN	COMMENT
-0.001 ± 0.015				OUR AVERAGE
$+0.002 \pm 0.015 \pm 0.006$	10k±136	⁶³ AUBERT	05s BABR	$e^+ e^- \approx \gamma(4S)$
-0.028 ± 0.036		⁶⁴ AITALA	97B E791	$-0.087 < A_{CP} < +0.031$ (90% CL)
$+0.066 \pm 0.086$		⁶⁴ FRABETTI	94i E687	$-0.075 < A_{CP} < +0.21$ (90% CL)

⁶³ AUBERT 05s measures $N(D^+ \rightarrow \phi \pi^+)/N(D^+ \rightarrow K^+ K^- \pi^+)$, the ratio of the numbers of events observed, and similarly for the D^- .

⁶⁴ FRABETTI 94i and AITALA 97b measure $N(D^+ \rightarrow \phi \pi^+)/N(D^+ \rightarrow K^- \pi^+ \pi^+)$, the ratio of numbers of events observed, and similarly for the D^- .

Meson Particle Listings

D^\pm

$A_{CP}(\pi^+\pi^-\pi^\pm)$ in $D^\pm \rightarrow \pi^+\pi^-\pi^\pm$

VALUE	DOCUMENT ID	TECN	COMMENT
-0.017 ± 0.042	65 AITALA	97B E791	$-0.086 < A_{CP} < +0.052$ (90% CL)

65 AITALA 97B measure $N(D^+ \rightarrow \pi^+\pi^-\pi^+)/N(D^+ \rightarrow K^-\pi^+\pi^+)$, the ratio of numbers of events observed, and similarly for the D^- .

$A_{CP}(K_S^0 K^\pm \pi^\mp)$ in $D^\pm \rightarrow K_S^0 K^\pm \pi^\mp$

This is the difference between D^+ and D^- partial widths for these modes divided by the sum of the widths.

VALUE	EVTS	DOCUMENT ID	TECN	COMMENT
$-0.042 \pm 0.064 \pm 0.022$	523 ± 32	LINK	05E FOCS	$\gamma_A, \bar{E}_\gamma \approx 180$ GeV

D^+-D^- T-VIOLATING DECAY-RATE ASYMMETRIES

$A_{Tviol}(K_S^0 K^\pm \pi^\mp)$ in $D^\pm \rightarrow K_S^0 K^\pm \pi^\mp$

$C_T \equiv \bar{p}_{K^+} \cdot (\bar{p}_{\pi^+} \times \bar{p}_{\pi^-})$ is a T -odd correlation of the K^+ , π^+ , and π^- momenta for the D^+ . $\bar{C}_T \equiv \bar{p}_{K^-} \cdot (\bar{p}_{\pi^-} \times \bar{p}_{\pi^+})$ is the corresponding quantity for the D^- . $A_T \equiv [\Gamma(C_T > 0) - \Gamma(C_T < 0)] / [\Gamma(C_T > 0) + \Gamma(C_T < 0)]$ would, in the absence of strong phases, test for T violation in D^+ decays (the Γ 's are partial widths). With $\bar{A}_T \equiv [\Gamma(-\bar{C}_T > 0) - \Gamma(-\bar{C}_T < 0)] / [\Gamma(-\bar{C}_T > 0) + \Gamma(-\bar{C}_T < 0)]$, the asymmetry $A_{Tviol} \equiv \frac{1}{2}(A_T - \bar{A}_T)$ tests for T violation even with nonzero strong phases.

VALUE	EVTS	DOCUMENT ID	TECN	COMMENT
$+0.023 \pm 0.062 \pm 0.022$	523 ± 32	LINK	05E FOCS	$\gamma_A, \bar{E}_\gamma \approx 180$ GeV

$D^+ \rightarrow \bar{K}^*(892)^0 \ell^+ \nu_\ell$ FORM FACTORS

$r_V \equiv V(0)/A_1(0)$ in $D^+ \rightarrow \bar{K}^*(892)^0 \ell^+ \nu_\ell$

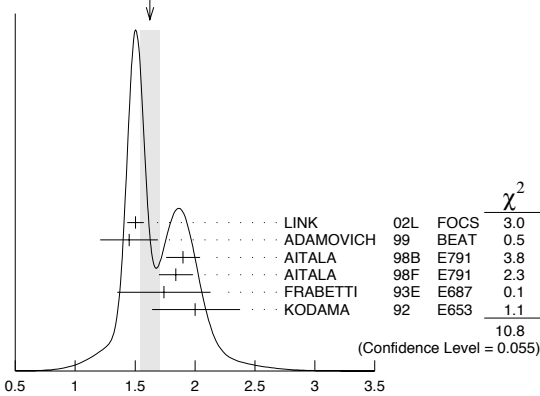
VALUE	EVTS	DOCUMENT ID	TECN	COMMENT
1.62 ± 0.08 OUR AVERAGE				Error includes scale factor of 1.5. See the ideogram below.
$1.504 \pm 0.057 \pm 0.039$	15k	66 LINK	02L FOCS	$\bar{K}^*(892)^0 \mu^+ \nu_\mu$
$1.45 \pm 0.23 \pm 0.07$	763	ADAMOVICH	99 BEAT	$\bar{K}^*(892)^0 \mu^+ \nu_\mu$
$1.90 \pm 0.11 \pm 0.09$	3000	67 AITALA	98B E791	$\bar{K}^*(892)^0 e^+ \nu_e$
$1.84 \pm 0.11 \pm 0.09$	3034	AITALA	98F E791	$\bar{K}^*(892)^0 \mu^+ \nu_\mu$
$1.74 \pm 0.27 \pm 0.28$	874	FRABETTI	93E E687	$\bar{K}^*(892)^0 \mu^+ \nu_\mu$
$2.00 \pm 0.34 \pm 0.32$	305	KODAMA	92 E653	$\bar{K}^*(892)^0 \mu^+ \nu_\mu$
$2.0 \pm 0.6 \pm 0.3$	183	ANJOS	90E E691	$\bar{K}^*(892)^0 e^+ \nu_e$

••• We do not use the following data for averages, fits, limits, etc. •••

66 LINK 02L includes the effects of interference with an S-wave background. This much improves the goodness of fit, but does not much shift the values of the form factors.

67 This is slightly different from the AITALA 98B value: see ref. [5] in AITALA 98F.

WEIGHTED AVERAGE
 1.62 ± 0.08 (Error scaled by 1.5)



$r_V \equiv A_2(0)/A_1(0)$ in $D^+ \rightarrow \bar{K}^*(892)^0 \ell^+ \nu_\ell$

VALUE	EVTS	DOCUMENT ID	TECN	COMMENT
0.83 ± 0.05 OUR AVERAGE				
$0.875 \pm 0.049 \pm 0.064$	15k	68 LINK	02L FOCS	$\bar{K}^*(892)^0 \mu^+ \nu_\mu$
$1.00 \pm 0.15 \pm 0.03$	763	ADAMOVICH	99 BEAT	$\bar{K}^*(892)^0 \mu^+ \nu_\mu$
$0.71 \pm 0.08 \pm 0.09$	3000	AITALA	98B E791	$\bar{K}^*(892)^0 e^+ \nu_e$
$0.75 \pm 0.08 \pm 0.09$	3034	AITALA	98F E791	$\bar{K}^*(892)^0 \mu^+ \nu_\mu$
$0.78 \pm 0.18 \pm 0.10$	874	FRABETTI	93E E687	$\bar{K}^*(892)^0 \mu^+ \nu_\mu$
$0.82 \pm 0.22 \pm 0.11$	305	KODAMA	92 E653	$\bar{K}^*(892)^0 \mu^+ \nu_\mu$
$0.0 \pm 0.5 \pm 0.2$	183	ANJOS	90E E691	$\bar{K}^*(892)^0 e^+ \nu_e$

••• We do not use the following data for averages, fits, limits, etc. •••

68 LINK 02L includes the effects of interference with an S-wave background. This much improves the goodness of fit, but does not much shift the values of the form factors.

$r_3 \equiv A_3(0)/A_1(0)$ in $D^+ \rightarrow \bar{K}^*(892)^0 \ell^+ \nu_\ell$

VALUE	EVTS	DOCUMENT ID	TECN	COMMENT
$0.04 \pm 0.33 \pm 0.29$	3034	AITALA	98F E791	$\bar{K}^*(892)^0 \mu^+ \nu_\mu$

Γ_L/Γ_T in $D^+ \rightarrow \bar{K}^*(892)^0 \ell^+ \nu_\ell$

VALUE	EVTS	DOCUMENT ID	TECN	COMMENT
1.13 ± 0.08 OUR AVERAGE				
$1.09 \pm 0.10 \pm 0.02$	763	ADAMOVICH	99 BEAT	$\bar{K}^*(892)^0 \mu^+ \nu_\mu$
$1.20 \pm 0.13 \pm 0.13$	874	FRABETTI	93E E687	$\bar{K}^*(892)^0 \mu^+ \nu_\mu$
$1.18 \pm 0.18 \pm 0.08$	305	KODA MA	92 E653	$\bar{K}^*(892)^0 \mu^+ \nu_\mu$
$1.8 \pm 0.6 \pm 0.3$	183	ANJOS	90E E691	$\bar{K}^*(892)^0 e^+ \nu_e$

••• We do not use the following data for averages, fits, limits, etc. •••

Γ_+/ Γ_- in $D^+ \rightarrow \bar{K}^*(892)^0 \ell^+ \nu_\ell$

VALUE	EVTS	DOCUMENT ID	TECN	COMMENT
0.22 ± 0.06 OUR AVERAGE				Error includes scale factor of 1.6.
$0.28 \pm 0.05 \pm 0.02$	763	ADAMOVICH	99 BEAT	$\bar{K}^*(892)^0 \mu^+ \nu_\mu$
$0.16 \pm 0.05 \pm 0.02$	305	KODA MA	92 E653	$\bar{K}^*(892)^0 \mu^+ \nu_\mu$
$0.15 \pm 0.07 \pm 0.03$	183	ANJOS	90E E691	$\bar{K}^*(892)^0 e^+ \nu_e$

••• We do not use the following data for averages, fits, limits, etc. •••

D^\pm REFERENCES

ABAZOV	08D	PRL 100 101801	V.M. Abazov et al.	(D0 Collab.)
HE	08	PRL 100 091801	Q. He et al.	(CLEO Collab.)
ABLIKIM	07	PL B644 20	M. Ablikim et al.	(BES Collab.)
ABLIKIM	07G	PL B658 1	M. Ablikim et al.	(BES Collab.)
BONVICINI	07	PR D76 012001	G. Bonvicini et al.	(CLEO Collab.)
DOBBS	07	PR D76 112001	S. Dobbs et al.	(CLEO Collab.)
LINK	07B	PL B653 1	J.M. Link et al.	(FNAL FOCUS Collab.)
ABLIKIM	06O	EPJ C47 31	M. Ablikim et al.	(BES Collab.)
ABLIKIM	06P	EPJ C47 39	M. Ablikim et al.	(BES Collab.)
ABLIKIM	06U	PL B643 246	M. Ablikim et al.	(BES Collab.)
ADAM	06A	PRL 97 251801	N.E. Adam et al.	(CLEO Collab.)
AITALA	06	PR D73 032004	E.M. Aitala et al.	(FNAL E791 Collab.)
		PR D74 059901 (err.)	E.M. Aitala et al.	(FNAL E791 Collab.)
AUBERT,B	06F	PR D74 011107R	B. Aubert et al.	(BABAR Collab.)
DYTMAN	06P	PR D74 071102R	S.A. Dytman et al.	(CLEO Collab.)
HUANG	06B	PR D74 112005	G.S. Huang et al.	(CLEO Collab.)
LINK	06B	PL B637 32	J.M. Link et al.	(FNAL FOCUS Collab.)
PDG	06	JPG 33 1	W.-M. Yao et al.	(PDG Collab.)
RUBIN	06	PRL 96 081802	P. Rubin et al.	(CLEO Collab.)
RUBIN	06A	PR D73 112005	P. Rubin et al.	(CLEO Collab.)
ABLIKIM	05A	PL B608 24	M. Ablikim et al.	(BES Collab.)
ABLIKIM	05D	PL B610 183	M. Ablikim et al.	(BES Collab.)
ABLIKIM	05F	PL B622 6	M. Ablikim et al.	(BES Collab.)
ABLIKIM	05P	PL B625 196	M. Ablikim et al.	(BES Collab.)
ARTUSO	05A	PRL 95 251801	M. Artuso et al.	(CLEO Collab.)
AUBERT	05S	PR D71 091101R	B. Aubert et al.	(BABAR Collab.)
HE	05	PRL 95 121801	Q. He et al.	(CLEO Collab.)
		PRL 96 199903 (err.)	Q. He et al.	(CLEO Collab.)
HE	05B	PRL 95 221802	Q. He et al.	(CLEO Collab.)
HUANG	05A	PRL 95 181801	G.S. Huang et al.	(CLEO Collab.)
KAYIS-TOPAK	05	PL B626 24	A. Kayis-Topaksu et al.	(CERN CHORUS Collab.)
LINK	05E	PL B622 239	J.M. Link et al.	(FNAL FOCUS Collab.)
LINK	05I	PL B621 72	J.M. Link et al.	(FNAL FOCUS Collab.)
ABLIKIM	04C	PL B597 39	M. Ablikim et al.	(BEP/ BES Collab.)
ARMS	04	PR D69 071102R	K. Arms et al.	(CLEO Collab.)
BONVICINI	04A	PR D70 112004	G. Bonvicini et al.	(CLEO Collab.)
LINK	04	PL B585 200	J.M. Link et al.	(FNAL FOCUS Collab.)
LINK	04E	PL B598 33	J.M. Link et al.	(FNAL FOCUS Collab.)
LINK	04F	PL B601 10	J.M. Link et al.	(FNAL FOCUS Collab.)
ANISOVICH	03D	EPJ A16 229	V.V. Anisovich et al.	(FNAL FOCUS Collab.)
LINK	03D	PL B561 225	J.M. Link et al.	(FNAL FOCUS Collab.)
LINK	03F	PL B572 21	J.M. Link et al.	(FNAL FOCUS Collab.)
AITALA	02	PRL 89 121801	E.M. Aitala et al.	(FNAL E791 Collab.)
BRANDENB...	02	PRL 89 222001	G. Brandenburg et al.	(CLEO Collab.)
KAYIS-TOPAK	02	PL B549 48	A. Kayis-Topaksu et al.	(CERN CHORUS Collab.)
LINK	02B	PRL 88 041602	J.M. Link et al.	(FNAL FOCUS Collab.)
		PRL 88 159903 (erratum)	J.M. Link et al.	(FNAL FOCUS Collab.)
LINK	02E	PL B535 43	J.M. Link et al.	(FNAL FOCUS Collab.)
LINK	02F	PL B537 192	J.M. Link et al.	(FNAL FOCUS Collab.)
LINK	02I	PL B541 227	J.M. Link et al.	(FNAL FOCUS Collab.)
LINK	02J	PL B541 243	J.M. Link et al.	(FNAL FOCUS Collab.)
LINK	02L	PL B544 89	J.M. Link et al.	(FNAL FOCUS Collab.)
AITALA	01B	PRL 86 770	E.M. Aitala et al.	(FNAL E791 Collab.)
LINK	01C	PRL 87 162001	J.M. Link et al.	(FNAL FOCUS Collab.)
ABREU	00O	EPJ C12 209	P. Abreu et al.	(DELPHI Collab.)
ASTIER	00D	PL B486 35	P. Astier et al.	(CERN NOMAD Collab.)
JUN	00	PRL 84 1857	S.Y. Jun et al.	(FNAL SELEX Collab.)
LINK	00B	PL B491 232	J.M. Link et al.	(FNAL FOCUS Collab.)
		PL B495 443 (erratum)	J.M. Link et al.	(FNAL FOCUS Collab.)
ABBIENDI	99K	EPJ C8 573	G. Abbiendi et al.	(OPAL Collab.)
ABREU	99P	PR D60 092005	F. Abe et al.	(CDF Collab.)
ADAMOVICH	99	EPJ C6 35	M. Adamovich et al.	(CERN BEATRICE Collab.)
AITALA	99G	PL B462 401	E.M. Aitala et al.	(FNAL E791 Collab.)
BONVICINI	99	PRL 82 4586	G. Bonvicini et al.	(CLEO Collab.)
AITALA	98C	PRL 80 1393	E.M. Aitala et al.	(FNAL E791 Collab.)
AITALA	98B	PL B421 405	E.M. Aitala et al.	(FNAL E791 Collab.)
AITALA	98F	PL B440 435	E.M. Aitala et al.	(FNAL E791 Collab.)
BAI	98B	PL B429 188	J.Z. Bai et al.	(BEP/ BES Collab.)
JESSOP	98	PR D58 052002	C.P. Jessop et al.	(CLEO Collab.)
AITALA	97	PL B397 325	E.M. Aitala et al.	(FNAL E791 Collab.)
AITALA	97C	PL B403 377	E.M. Aitala et al.	(FNAL E791 Collab.)
AITALA	97B	PL B404 187	E.M. Aitala et al.	(FNAL E791 Collab.)
BARTELT	97	PL B405 373	J. Bartelt et al.	(CLEO Collab.)
BISHAI	97	PRL 78 3261	M. Bishai et al.	(CLEO Collab.)
FRABETTI	97	PL B391 235	P.L. Frabetti et al.	(FNAL E687 Collab.)
FRABETTI	97B	PL B398 239	P.L. Frabetti et al.	(FNAL E687 Collab.)
FRABETTI	97C	PL B401 131	P.L. Frabetti et al.	(FNAL E687 Collab.)
FRABETTI	97D	PL B407 79	P.L. Frabetti et al.	(FNAL E687 Collab.)
AITALA	96	PRL 76 364	E.M. Aitala et al.	(FNAL E791 Collab.)
FRABETTI	95	PL B346 199	P.L. Frabetti et al.	(FNAL E687 Collab.)
FRABETTI	95B	PL B351 591	P.L. Frabetti et al.	(FNAL E687 Collab.)
FRABETTI	95	PL B359 403	P.L. Frabetti et al.	(FNAL E687 Collab.)
KODAMA	95	PL B345 85	K. Kodama et al.	(FNAL E653 Collab.)
ALBRECHT	94I	ZPHY C64 375	H. Albrecht et al.	(ARGUS Collab.)
ALEEV	94I	PAN 57 1370	A.N. Aleev et al.	(Serpukhov BIS-2 Collab.)

Translated from YF 57 1443.

BALEST	94	PRL 72 2328	R. Balest <i>et al.</i>	(CLEO Collab.)
FRABETTI	94D	PL B323 459	P.L. Frabetti <i>et al.</i>	(FNAL E687 Collab.)
FRABETTI	94G	PL B331 217	P.L. Frabetti <i>et al.</i>	(FNAL E687 Collab.)
FRABETTI	94I	PR D50 R2953	P.L. Frabetti <i>et al.</i>	(FNAL E687 Collab.)
ADAMOVIICH	93	PL B305 177	M.I. Adamovich <i>et al.</i>	(CERN WA82 Collab.)
AKERIB	93	PRL 71 3070	D.S. Akerib <i>et al.</i>	(CLEO Collab.)
ALAM	93	PRL 71 1311	M.S. Alam <i>et al.</i>	(CLEO Collab.)
ANJOS	93	PR D48 56	J.C. Anjos <i>et al.</i>	(FNAL E691 Collab.)
BEAN	93C	PL B317 647	A. Bean <i>et al.</i>	(FNAL E687 Collab.)
FRABETTI	93E	PL B307 262	P.L. Frabetti <i>et al.</i>	(FNAL E687 Collab.)
KODAMA	93B	PL B313 260	K. Kodama <i>et al.</i>	(FNAL E653 Collab.)
ALBRECHT	92F	PL B278 202	H. Albrecht <i>et al.</i>	(ARGUS Collab.)
ANJOS	92	PR D45 R2177	J.C. Anjos <i>et al.</i>	(FNAL E691 Collab.)
ANJOS	92C	PR D46 1941	J.C. Anjos <i>et al.</i>	(FNAL E691 Collab.)
BARLAG	92C	ZPHY C55 383	S. Barlag <i>et al.</i>	(ACCMOR Collab.)
Also		ZPHY C48 29	S. Barlag <i>et al.</i>	(ACCMOR Collab.)
COFFMAN	92B	PR D45 2196	D.M. Coffman <i>et al.</i>	(Mark III Collab.)
DAOUDI	92	PR D45 3965	M. Daoudi <i>et al.</i>	(CLEO Collab.)
KODAMA	92	PL B274 246	K. Kodama <i>et al.</i>	(FNAL E653 Collab.)
KODAMA	92C	PL B204 187	K. Kodama <i>et al.</i>	(FNAL E653 Collab.)
ADAMOVIICH	91	PL B268 142	M.I. Adamovich <i>et al.</i>	(WA82 Collab.)
ALBRECHT	91	PL B255 634	H. Albrecht <i>et al.</i>	(ARGUS Collab.)
ALVAREZ	91B	ZPHY C50 11	M.P. Alvarez <i>et al.</i>	(CERN NA14/2 Collab.)
AMMAR	91	PR D44 3383	R. Ammar <i>et al.</i>	(CLEO Collab.)
BAI	91	PRL 66 1011	Z. Bai <i>et al.</i>	(Mark III Collab.)
COFFMAN	91	PL B263 135	D.M. Coffman <i>et al.</i>	(Mark III Collab.)
FRABETTI	91	PL B263 584	P.L. Frabetti <i>et al.</i>	(FNAL E687 Collab.)
ALVAREZ	90	ZPHY C47 539	M.P. Alvarez <i>et al.</i>	(CERN NA14/2 Collab.)
ALVAREZ	90C	PL B246 261	M.P. Alvarez <i>et al.</i>	(CERN NA14/2 Collab.)
ANJOS	90C	PR D41 2705	J.C. Anjos <i>et al.</i>	(FNAL E691 Collab.)
ANJOS	90D	PR D42 2414	J.C. Anjos <i>et al.</i>	(FNAL E691 Collab.)
ANJOS	90E	PRL 65 2630	J.C. Anjos <i>et al.</i>	(FNAL E691 Collab.)
BARLAG	90C	ZPHY C46 563	S. Barlag <i>et al.</i>	(ACCMOR Collab.)
WEIR	90B	PR D41 1384	A.J. Weir <i>et al.</i>	(Mark II Collab.)
ANJOS	89	PRL 62 125	J.C. Anjos <i>et al.</i>	(FNAL E691 Collab.)
ANJOS	89B	PRL 62 722	J.C. Anjos <i>et al.</i>	(FNAL E691 Collab.)
ANJOS	89E	PL B223 267	J.C. Anjos <i>et al.</i>	(FNAL E691 Collab.)
ADLER	88C	PRL 60 89	J. Adler <i>et al.</i>	(Mark III Collab.)
ALBRECHT	88I	PL B210 267	H. Albrecht <i>et al.</i>	(ARGUS Collab.)
ANJOS	88	PRL 60 897	J.C. Anjos <i>et al.</i>	(FNAL E691 Collab.)
AOKI	88	PL B209 113	S. Aoki <i>et al.</i>	(WA75 Collab.)
HAAS	88	PRL 60 1614	P. Haas <i>et al.</i>	(CLEO Collab.)
ONG	88	PRL 60 2587	R.A. Ong <i>et al.</i>	(Mark II Collab.)
RAAB	88	PR D37 2391	J.R. Raab <i>et al.</i>	(FNAL E691 Collab.)
ADAMOVIICH	87	EPL 4 887	M.I. Adamovich <i>et al.</i>	(Photon Emission Collab.)
ADLER	87	PL B196 107	J. Adler <i>et al.</i>	(Mark III Collab.)
BARTEL	87	ZPHY C33 339	W. Bartel <i>et al.</i>	(JADE Collab.)
BALTRUSAITIS...	86E	PRL 56 2140	R.M. Baltrusaitis <i>et al.</i>	(Mark III Collab.)
BALTRUSAITIS...	85B	PRL 54 1976	R.M. Baltrusaitis <i>et al.</i>	(Mark III Collab.)
BALTRUSAITIS...	85E	PRL 55 150	R.M. Baltrusaitis <i>et al.</i>	(Mark III Collab.)
BARTEL	85J	PL 163B 277	W. Bartel <i>et al.</i>	(JADE Collab.)
ADAMOVIICH	84	PL 140B 119	M.I. Adamovich <i>et al.</i>	(CERN WA5B Collab.)
ALTHOFF	84G	ZPHY C22 219	M. Althoff <i>et al.</i>	(TASSO Collab.)
DERRICK	84	PRL 53 1971	M. Derrick <i>et al.</i>	(HRS Collab.)
SCHINDLER	81	PR D24 78	R.H. Schindler <i>et al.</i>	(Mark II Collab.)
TRILLING	81	PRPL 75 57	G.H. Trilling	(LBL, UCB/J
ZHOLENTZ	80	PL 96B 214	A.A. Zholents <i>et al.</i>	(NOVO)
Also		SJNP 34 814	A.A. Zholents <i>et al.</i>	(NOVO)
Translated from		YAF 34 1471		
GOLDHABER	77	PL 69B 503	G. Goldhaber <i>et al.</i>	(Mark I Collab.)
PERUZZI	77	PRL 39 1301	I. Peruzzi <i>et al.</i>	(LGV Collab.)
PICCOLO	77	PL 70B 260	M. Piccolo <i>et al.</i>	(Mark I Collab.)
PERUZZI	76	PRL 37 569	I. Peruzzi <i>et al.</i>	(Mark I Collab.)

OTHER RELATED PAPERS

RICHMAN	95	RMP 67 893	J.D. Richman, P.R. Burchat	(UCSB; STAN)
ROSNER	95	CNPP 21 369	J. Rosner	(CHIC)

 D^0

$$I(J^P) = \frac{1}{2}(0^-)$$

 D^0 MASS

The fit includes $D^\pm, D^0, D_s^\pm, D^{*\pm}, D^{*0}$, and $D_s^{*\pm}$ mass and difference measurements.

VALUE (MeV)	EVTS	DOCUMENT ID	TECN	COMMENT
1864.84 ± 0.17 OUR FIT	Error includes scale factor of 1.1.			
1864.84 ± 0.18 OUR AVERAGE				
1864.847 ± 0.150 ± 0.095	319 ± 18	CAWFIELD	07 CLEO	$D^0 \rightarrow K_S^0 \phi$
1864.6 ± 0.3 ± 1.0	641	BARLAG	90c ACCM	$\pi^- \text{Cu } 230 \text{ GeV}$
• • • We do not use the following data for averages, fits, limits, etc. • • •				
1852 ± 7	16	ADAMOVIICH	87 EMUL	Photoproduction
1856 ± 36	22	ADAMOVIICH	84B EMUL	Photoproduction
1861 ± 4		DERRICK	84 HRS	$e^+e^- 29 \text{ GeV}$
1847 ± 7	1	FIORINO	81 EMUL	$\gamma N \rightarrow \bar{D}^0 +$
1863.8 ± 0.5		¹ SCHINDLER	81 MRK2	$e^+e^- 3.77 \text{ GeV}$
1864.7 ± 0.6		¹ TRILLING	81 RVUE	$e^+e^- 3.77 \text{ GeV}$
1863.0 ± 2.5	238	ASTON	80E OMEG	$\gamma p \rightarrow \bar{D}^0$
1860 ± 2	143	² AVERY	80 SPEC	$\gamma N \rightarrow D^{*+}$
1869 ± 4	35	² AVERY	80 SPEC	$\gamma N \rightarrow D^{*+}$
1854 ± 6	94	² ATIYA	79 SPEC	$\gamma N \rightarrow D^0 \bar{D}^0$
1850 ± 15	64	BALTAY	78c HBC	$\nu N \rightarrow K^0 \pi \pi$
1863 ± 3		GOLDHABER	77 MRK1	D^0, D^+ recoil spectra
1863.3 ± 0.9		¹ PERUZZI	77 LGW	$e^+e^- 3.77 \text{ GeV}$
1868 ± 11		PICCOLO	77 MRK1	$e^+e^- 4.03, 4.41 \text{ GeV}$
1865 ± 15	234	GOLDHABER	76 MRK1	$K \pi$ and $K \pi$

¹PERUZZI 77 and SCHINDLER 81 errors do not include the 0.13% uncertainty in the absolute SPEAR energy calibration. TRILLING 81 uses the high precision $J/\psi(1S)$ and $\psi(2S)$ measurements of ZHOLENTZ 80 to determine this uncertainty and combines the PERUZZI 77 and SCHINDLER 81 results to obtain the value quoted. TRILLING 81 enters the fit in the D^\pm mass, and PERUZZI 77 and SCHINDLER 81 enter in the $m_{D^\pm} - m_{D^0}$, below.

²Error does not include possible systematic mass scale shift, estimated to be less than 5 MeV.

 $m_{D^\pm} - m_{D^0}$

The fit includes $D^\pm, D^0, D_s^\pm, D^{*\pm}, D^{*0}$, and $D_s^{*\pm}$ mass and mass difference measurements.

VALUE (MeV)	DOCUMENT ID	TECN	COMMENT
4.78 ± 0.10 OUR FIT	Error includes scale factor of 1.1.		
4.74 ± 0.28 OUR AVERAGE			
4.7 ± 0.3	³ SCHINDLER 81	MRK2	$e^+e^- 3.77 \text{ GeV}$
5.0 ± 0.8	³ PERUZZI 77	LGW	$e^+e^- 3.77 \text{ GeV}$
³ See the footnote on TRILLING 81 in the D^0 and D^\pm sections on the mass.			

 D^0 MEAN LIFE

Measurements with an error $> 10 \times 10^{-15}$ s have been omitted from the average.

VALUE (10^{-15} s)	EVTS	DOCUMENT ID	TECN	COMMENT
410.1 ± 1.5 OUR AVERAGE				
409.6 ± 1.1 ± 1.5	210k	LINK	02F FOCUS	γ nucleus, $\approx 180 \text{ GeV}$
407.9 ± 6.0 ± 4.3	10k	KUSHNIR...	01 SELX	$K^- \pi^+, K^- \pi^+ \pi^+ \pi^-$
413 ± 3 ± 4	35k	AITALA	99E E791	$K^- \pi^+$
408.5 ± 4.1 ± 3.5	25k	BONVICINI	99 CLE2	$e^+e^- \approx \mathcal{T}(4S)$
413 ± 4 ± 3	16k	FRABETTI	94D E687	$K^- \pi^+, K^- \pi^+ \pi^+ \pi^-$
• • • We do not use the following data for averages, fits, limits, etc. • • •				
424 ± 11 ± 7	5118	FRABETTI	91 E687	$K^- \pi^+, K^- \pi^+ \pi^+ \pi^-$
417 ± 18 ± 15	890	ALVAREZ	90 NA14	$K^- \pi^+, K^- \pi^+ \pi^+ \pi^-$
388 +23 -21	641	⁴ BARLAG	90c ACCM	$\pi^- \text{Cu } 230 \text{ GeV}$
480 ± 40 ± 30	776	ALBRECHT	88I ARG	$e^+e^- 10 \text{ GeV}$
422 ± 8 ± 10	4212	RAAB	88 E691	Photoproduction
420 ± 50	90	BARLAG	87B ACCM	K^- and $\pi^- 200 \text{ GeV}$
⁴ BARLAG 90c estimate systematic error to be negligible.				

 $D^0 - \bar{D}^0$ MIXING

Revised April 2008 by D. Asner (Carleton University)

The detailed formalism for $D^0 - \bar{D}^0$ mixing is presented in the "Note on CP Violation in Meson Decays" in this *Review*. For completeness, we present an overview here. The time evolution of the $D^0 - \bar{D}^0$ system is described by the Schrödinger equation

$$i \frac{\partial}{\partial t} \begin{pmatrix} D^0(t) \\ \bar{D}^0(t) \end{pmatrix} = \left(M - \frac{i}{2} \Gamma \right) \begin{pmatrix} D^0(t) \\ \bar{D}^0(t) \end{pmatrix}, \quad (1)$$

where the M and Γ matrices are Hermitian, and CPT invariance requires that $M_{11} = M_{22} \equiv M$ and $\Gamma_{11} = \Gamma_{22} \equiv \Gamma$. The off-diagonal elements of these matrices describe the dispersive and absorptive parts of the mixing.

Because CP violation is expected to be quite small here, it is convenient to label the mass eigenstates by the CP quantum number in the limit of CP conservation. Thus, we write

$$|D_{1,2}\rangle = p|D^0\rangle \pm q|\bar{D}^0\rangle, \quad (2)$$

where

$$\left(\frac{q}{p} \right)^2 = \frac{M_{12}^* - \frac{i}{2}\Gamma_{12}^*}{M_{12} - \frac{i}{2}\Gamma_{12}}, \quad (3)$$

with the normalization condition that $|p|^2 + |q|^2 = 1$ and the sign is chosen so that D_1 has CP even, or nearly so. The corresponding eigenvalues are

$$\omega_{1,2} \equiv m_{1,2} - \frac{i}{2}\Gamma_{1,2} = \left(M - \frac{i}{2}\Gamma \right) \pm \frac{q}{p} \left(M_{12} - \frac{i}{2}\Gamma_{12} \right), \quad (4)$$

Meson Particle Listings

D^0

where $m_{1,2}$ and $\Gamma_{1,2}$ are the masses and widths of the $D_{1,2}$.

We define reduced mixing parameters x and y by

$$x \equiv (m_1 - m_2)/\Gamma = \Delta m/\Gamma \quad (5)$$

and

$$y \equiv (\Gamma_1 - \Gamma_2)/2\Gamma = \Delta\Gamma/2\Gamma, \quad (6)$$

where $\Gamma \equiv (\Gamma_1 + \Gamma_2)/2$. We choose the phase convention $CP|D^0\rangle = +|\overline{D}^0\rangle$. If CP is conserved, then M_{12} and Γ_{12} are real and $\Delta m = 2M_{12}$, $\Delta\Gamma = 2\Gamma_{12}$. The signs of Δm and $\Delta\Gamma$ are to be determined experimentally.

The parameters x and y are measured in several ways. The most precise constraints are obtained using the time-dependence of D decays. Since $D^0\text{--}\overline{D}^0$ mixing is a small effect, the identifying tag of the initial particle as a D^0 or a \overline{D}^0 must be extremely accurate. The usual tag is the charge of the distinctive slow pion in the decay sequence $D^{*+} \rightarrow D^0\pi^+$ or $D^{*-} \rightarrow \overline{D}^0\pi^-$. In current experiments, the probability of mistagging is about 0.1%. The large data samples available from the B -factories allow the production flavor to also be determined by fully reconstructing charm on the ‘‘other side’’ of the event—significantly reducing the mistag rate. Another tag of comparable accuracy is identification of one of the D 's produced from $\psi(3770) \rightarrow D^0\overline{D}^0$. Although time-dependent analyses are not possible at symmetric charm-threshold facilities (the D^0 and \overline{D}^0 do not travel far enough), the quantum-coherent $C = -1$ $\psi(3770) \rightarrow D^0\overline{D}^0$ state provides time-integrated sensitivity [1,2].

Time-Dependent Analyses: We extend the formalism of this Review's note on ‘‘ $B^0\text{--}\overline{B}^0$ Mixing’’ [3]. In addition to the ‘‘right-sign’’ instantaneous decay amplitudes $\overline{A}_f \equiv \langle f|H|\overline{D}^0\rangle$ and $A_{\overline{f}} \equiv \langle \overline{f}|H|D^0\rangle$ for CP conjugate final states $f = K^+\pi^-$, ... and $\overline{f} = K^-\pi^+$, ..., we include ‘‘wrong-sign’’ amplitudes $\overline{A}_{\overline{f}} \equiv \langle \overline{f}|H|\overline{D}^0\rangle$ and $A_f \equiv \langle f|H|D^0\rangle$.

It is conventional to normalize the wrong-sign decay distributions to the integrated rate of right-sign decays and to express time in units of the precisely measured neutral D -meson mean lifetime, $\overline{\tau}_{D^0} = 1/\Gamma = 2/(\Gamma_1 + \Gamma_2)$. Starting from a pure $|D^0\rangle$ or $|\overline{D}^0\rangle$ state at $t = 0$, the time-dependent rates of decay to wrong-sign final states relative to the integrated right-sign decay rates are, to leading order:

$$r(t) \equiv \frac{|\langle f|H|D^0(t)\rangle|^2}{|\overline{A}_f|^2} = \left|\frac{q}{p}\right|^2 \left|g_+(t)\lambda_f^{-1} + g_-(t)\right|^2, \quad (7)$$

and

$$\overline{r}(t) \equiv \frac{|\langle \overline{f}|H|\overline{D}^0(t)\rangle|^2}{|A_{\overline{f}}|^2} = \left|\frac{p}{q}\right|^2 \left|g_+(t)\lambda_{\overline{f}} + g_-(t)\right|^2. \quad (8)$$

where

$$\lambda_f \equiv q\overline{A}_f/pA_f, \quad \lambda_{\overline{f}} \equiv q\overline{A}_{\overline{f}}/pA_{\overline{f}}, \quad (9)$$

and

$$g_{\pm}(t) = \frac{1}{2}(e^{-iz_1t} \pm e^{-iz_2t}), \quad z_{1,2} = \frac{\omega_{1,2}}{\Gamma}. \quad (10)$$

Note that a change in the convention for the relative phase of D^0 and \overline{D}^0 would cancel between q/p and \overline{A}_f/A_f and leave

λ_f unchanged. We expand $r(t)$ and $\overline{r}(t)$ to second order in x and y for modes in which the ratio of decay amplitudes, $R_D = |A_f/\overline{A}_f|^2$, is very small.

Semileptonic decays: In semileptonic D decays, $A_f = \overline{A}_{\overline{f}} = 0$ in the Standard Model, and $r(t)$ is

$$r(t) = |g_-(t)|^2 \left|\frac{q}{p}\right|^2 \approx \frac{e^{-t}}{4}(x^2 + y^2)t^2 \left|\frac{q}{p}\right|^2. \quad (11)$$

For $\overline{r}(t)$ one replaces q/p here with p/q . In the Standard Model, CP violation in charm mixing is small and $|q/p| \approx 1$. In the limit of CP conservation, $r(t) = \overline{r}(t)$, and the time-integrated mixing rate relative to the time-integrated right-sign decay rate is

$$R_M = \int_0^\infty r(t)dt = \frac{1}{2}(x^2 + y^2). \quad (12)$$

Table 1 summarizes results for R_M from semileptonic decays; the world average from the Heavy Flavor Averaging Group (HFAG) [10] is $R_M = (1.7 \pm 3.9) \times 10^{-4}$.

Table 1: Results for R_M in D^0 semileptonic decays.

Year	Exper.	Final state(s)	$R_M (\times 10^{-3})$	90% C.L.
2007	BABAR [4]	$K^{(*)+}e^-\overline{\nu}_e$	$0.04^{+0.70}_{-0.60}$	$< 1.2 \times 10^{-3}$
2005	Belle [5]	$K^{(*)+}e^-\overline{\nu}_e$	$0.02 \pm 0.47 \pm 0.14$	$< 1.0 \times 10^{-3}$
2005	CLEO [6]	$K^{(*)+}e^-\overline{\nu}_e$	$1.6 \pm 2.9 \pm 2.9$	$< 7.8 \times 10^{-3}$
2004*	BABAR [7]	$K^{(*)+}e^-\overline{\nu}_e$	$2.3 \pm 1.2 \pm 0.4$	$< 4.2 \times 10^{-3}$
2002*	FOCUS [8]	$K^+\mu^-\overline{\nu}_\mu$	$-0.76^{+0.99}_{-0.93}$	$< 1.01 \times 10^{-3}$
1996	E791 [9]	$K^+\ell^-\overline{\nu}_\ell$	$(1.1^{+3.0}_{-2.7}) \times 10^{-3}$	$< 5.0 \times 10^{-3}$
HFAG [10]			0.17 ± 0.39	

*These measurements are excluded from the HFAG average. The FOCUS result is unpublished, and the BABAR result has been superseded by Ref. 4.

Wrong-sign decays to hadronic non- CP eigenstates:

Consider the final state $f = K^+\pi^-$, where A_f is doubly Cabibbo-suppressed. The ratio of decay amplitudes is

$$\frac{A_f}{\overline{A}_f} = -\sqrt{R_D}e^{-i\delta_f}, \quad \left|\frac{A_f}{\overline{A}_f}\right| \sim O(\tan^2\theta_c), \quad (13)$$

where R_D is the doubly Cabibbo-suppressed (DCS) decay rate relative to the Cabibbo-favored (CF) rate, δ_f is the strong phase difference between DCS and CF processes, and θ_c is the Cabibbo angle. The minus sign originates from the sign of V_{us} relative to V_{cd} .

We characterize the violation of CP in the mixing amplitude, the decay amplitude, and the interference between mixing and decay, by real-valued parameters A_M , A_D , and ϕ . We adopt the parametrization (see Refs. 12 and 13).

$$\left|\frac{q}{p}\right|^2 = \sqrt{\frac{1 + A_M}{1 - A_M}}, \quad (14)$$

$$\lambda_f^{-1} \equiv \frac{pA_f}{q\bar{A}_f} = -\sqrt{R_D} \left(\frac{(1+A_D)(1-A_M)}{(1-A_D)(1+A_M)} \right)^{1/4} e^{-i(\delta_f+\phi)}, \quad (15)$$

$$\lambda_{\bar{f}} \equiv \frac{q\bar{A}_{\bar{f}}}{pA_{\bar{f}}} = -\sqrt{R_D} \left(\frac{(1-A_D)(1+A_M)}{(1+A_D)(1-A_M)} \right)^{1/4} e^{-i(\delta_f-\phi)}. \quad (16)$$

Since

$$\sqrt{\frac{1+A_D}{1-A_D}} = \frac{|A_f/\bar{A}_f|}{|\bar{A}_{\bar{f}}/A_{\bar{f}}|}, \quad (17)$$

A_D is a measure of direct CP violation, while A_M is a measure of CP violation in mixing. The angle ϕ measures CP violation in interference between mixing and decay. While A_M is independent of the decay process, A_D and ϕ may depend on f .

In general, $\lambda_{\bar{f}}$ and λ_f^{-1} are independent complex numbers. More detail on CP violation in meson decays can be found in Ref. 3. To leading order, for A_D and $A_M \ll 1$,

$$r(t) = e^{-t} \left[R_D(1+A_D) + \sqrt{R_D} \sqrt{1+A_M} \sqrt{1+A_D} y' t + \frac{1}{2}(1+A_M)R_M t^2 \right] \quad (18)$$

and

$$\bar{r}(t) = e^{-t} \left[R_D(1-A_D) + \sqrt{R_D} \sqrt{1-A_M} \sqrt{1-A_D} y' t + \frac{1}{2}(1-A_M)R_M t^2 \right] \quad (19)$$

Here

$$y'_{\pm} \equiv y' \cos \phi \pm x' \sin \phi \\ = y \cos(\delta_{K\pi} \mp \phi) - x \sin(\delta_{K\pi} \mp \phi), \quad (20)$$

where

$$y' \equiv y \cos \delta_{K\pi} - x \sin \delta_{K\pi}, \\ x' \equiv x \cos \delta_{K\pi} + y \sin \delta_{K\pi}, \quad (21)$$

and $R_M \approx (x^2 + y^2)/2 = (x'^2 + y'^2)/2$ is the mixing rate relative to the time-integrated right-sign rate.

The ratio R is the most readily accessible experimental quantity. Table 2 gives recent measurements of R in $D^0 \rightarrow K^+\pi^-$ decay. The average R is $(0.380 \pm 0.005)\%$.

*These measurements are included in the HFAG average of R_D but are excluded from the HFAG average A_D .

The three terms in Eq. (18) and Eq. (19) probe the three fundamental types of CP violation. In the limit of CP conservation, A_M , A_D , and ϕ are all zero. Then

$$r(t) = \bar{r}(t) = e^{-t} \left(R_D + \sqrt{R_D} y' t + \frac{1}{2} R_M t^2 \right), \quad (22)$$

and the time-integrated wrong-sign rate relative to the integrated right-sign rate is

$$R = \int_0^{\infty} r(t) dt = R_D + \sqrt{R_D} y' + R_M. \quad (23)$$

Table 2 gives the limits on A_D , and the HFAG average [10] of R_D and A_D from a general fit; all allow for both mixing and CP violation. Typically, the fit parameters are R_D , x'^2 , and y' . Table 3 summarizes the results for y' and x'^2 . Allowing for CP violation, the separate contributions to R can be extracted by fitting the $D^0 \rightarrow K^+\pi^-$ and $\bar{D}^0 \rightarrow K^-\pi^+$ decay rates.

Table 3: Results on the time-dependence of $r(t)$ in $D^0 \rightarrow K^+\pi^-$ and $\bar{D}^0 \rightarrow K^-\pi^+$ decays. The CDF result assumes no CP violation. The FOCUS and CLEO results restrict x'^2 to the physical region. The confidence intervals from FOCUS and CLEO are obtained from the fit, whereas Belle uses a Feldman-Cousins method, and CDF uses a Bayesian method.

Year	Exper.	y' (%)	$x'^2 (\times 10^{-3})$
2007	CDF [14]	0.85 ± 0.76	-0.12 ± 0.35
2007	BABAR [15]	$0.97 \pm 0.44 \pm 0.31$	$-0.22 \pm 0.30 \pm 0.21$
2006	Belle [16]	$-2.8 < y' < 2.1$	< 0.72 (95% C.L.)
2005	FOCUS [17]	$-11.2 < y' < 6.7$	< 8.0 (95% C.L.)
2000	CLEO [11]	$-5.8 < y' < 1.0$	< 0.81 (95% C.L.)

Table 4 summarizes results for R measured in multibody final states with nonzero strangeness. Here R , defined in Eq. (23), becomes an average over the Dalitz plot.

Table 2: Results for R , R_D , and A_D in $D^0 \rightarrow K^+\pi^-$.

Year	Exper.	$R (\times 10^{-3})$	$R_D (\times 10^{-3})$	A_D (%)
2007	CDF [14]	4.15 ± 0.10	3.04 ± 0.55	—
2007	BABAR [15]	$3.53 \pm 0.08 \pm 0.04$	$3.03 \pm 0.16 \pm 0.10$	$-2.1 \pm 5.2 \pm 1.5$
2006	Belle [16]	$3.77 \pm 0.08 \pm 0.05$	3.64 ± 0.17	2.3 ± 4.7
2005*	FOCUS [17]	$4.29_{-0.61}^{+0.63} \pm 0.28$	$5.17_{-1.58}^{+1.47} \pm 0.76$	$13_{-25}^{+33} \pm 10$
2000*	CLEO [11]	$3.32_{-0.65}^{+0.63} \pm 0.40$	$4.8 \pm 1.2 \pm 0.4$	$-1_{-17}^{+16} \pm 1$
1998	E791 [18]	$6.8_{-3.3}^{+3.4} \pm 0.7$	—	—
Average		3.80 ± 0.05	3.35 ± 0.09 [10]	-2.2 ± 2.5 [10]

Meson Particle Listings

 D^0

Table 4: Results for R in $D^0 \rightarrow K^{(*)+}\pi^-(n\pi)$. The values of R need not be the same for different decay channels.

Year	Exper.	D^0 final state	$R(\%)$
2006	BABAR [22]	$K^+\pi^-\pi^0$	$0.214 \pm 0.008 \pm 0.008$
2005	Belle [23]	$K^+\pi^-\pi^+\pi^-$	$0.320 \pm 0.018^{+0.018}_{-0.013}$
2005	Belle [23]	$K^+\pi^-\pi^0$	$0.229 \pm 0.015^{+0.013}_{-0.009}$
2002	CLEO [19]	$K^{*+}\pi^-$	$0.5 \pm 0.2^{+0.6}_{-0.1}$
2001	CLEO [24]	$K^+\pi^-\pi^+\pi^-$	$0.41^{+0.12}_{-0.11} \pm 0.04$
2001	CLEO [25]	$K^+\pi^-\pi^0$	$0.43^{+0.11}_{-0.10} \pm 0.07$
1998	E791 [18]	$K^+\pi^-\pi^+\pi^-$	$0.68^{+0.34}_{-0.33} \pm 0.07$

Extraction of the mixing parameters x and y from the results in Table 3 requires knowledge of the relative strong phase $\delta_{K\pi}$. An interference effect that provides useful sensitivity to $\delta_{K\pi}$ arises in the decay chain $\psi(3770) \rightarrow D^0 \bar{D}^0 \rightarrow (f_{CP})(K^+\pi^-)$, where f_{CP} denotes a CP -even or -odd eigenstate from D^0 decay, such as K^+K^- [26]. Here, the amplitude relation

$$\sqrt{2} A(D_{\pm} \rightarrow K^-\pi^+) = A(D^0 \rightarrow K^-\pi^+) \pm A(\bar{D}^0 \rightarrow K^-\pi^+). \quad (24)$$

where D_{\pm} denotes a CP -even or -odd eigenstate, implies that

$$\cos \delta_{K\pi} = \frac{|A(D_+ \rightarrow K^-\pi^+)|^2 - |A(D_- \rightarrow K^-\pi^+)|^2}{2\sqrt{R_D} |A(D^0 \rightarrow K^-\pi^+)|^2}. \quad (25)$$

This neglects CP violation and uses $\sqrt{R_D} \ll 1$.

For multibody final states, Eqs. (13)–(23) apply separately to each point in phase-space. Although x and y do not vary across the space, knowledge of the resonant substructure is needed to extrapolate the strong phase difference δ from point to point to determine x and y .

A time-dependent Dalitz-plot analysis of $D^0 \rightarrow K^+\pi^-\pi^0$ from BABAR [22,28] reports $R_M = (2.9 \pm 1.6) \times 10^{-4}$, $x'' = (2.39 \pm 0.61 \pm 0.32)\%$, and $y'' = (-0.14 \pm 0.60 \pm 0.40)\%$, where x'' , y'' , and $\delta_{K\pi\pi^0}$ are defined as

$$x'' \equiv x \cos \delta_{K\pi\pi^0} + y \sin \delta_{K\pi\pi^0}, y'' \equiv y \cos \delta_{K\pi\pi^0} - x \sin \delta_{K\pi\pi^0}, \quad (26)$$

in parallel to x' , y' , and $\delta_{K\pi}$ of Eq. (21). Both strong phases, $\delta_{K\pi}$ and $\delta_{K\pi\pi^0}$, can be determined from time-integrated CP asymmetries in correlated $D^0 \bar{D}^0$ produced at the $\psi(3770)$ [26,27].

Both the sign and magnitude of x and y without phase or sign ambiguity may be measured using the time-dependent resonant substructure of multibody D^0 decays—see CLEO [29]. In $D^0 \rightarrow K_S^0 \pi^+ \pi^-$, the DCS and CF decay amplitudes populate the same Dalitz plot, which allows direct measurement of the relative strong phases. CLEO [19] and Belle [20] have measured the relative phase between $D^0 \rightarrow K^*(892)^+ \pi^-$ and $D^0 \rightarrow K^*(892)^- \pi^+$ to be $(189 \pm 10 \pm 3_{-5}^{+15})^\circ$ and $(171.9 \pm 1.3 \text{ (stat. only)})^\circ$, respectively. These results are close to the 180° expected from Cabibbo factors and a small strong phase. Table 5 summarizes the results from Belle [20] of a time-dependent Dalitz-plot analysis of $D^0 \rightarrow K_S^0 \pi^+ \pi^-$.

Table 5: Belle results from a time-dependent Dalitz-plot analysis of $D^0 \rightarrow K_S^0 \pi^+ \pi^-$ [20]. The errors are statistical, experimental systematic, and decay-model systematic, respectively ($CPV = CP$ violation).

Result	95% C.L. interval
No CP Violation	
$x = (0.80 \pm 0.29^{+0.09+0.10}_{-0.07-0.14})\%$	$(0.0, 1.6)\%$
$y = (0.33 \pm 0.24^{+0.08+0.06}_{-0.12-0.08})\%$	$(-0.34, 0.96)\%$
With CP Violation	
$x = (0.81 \pm 0.30^{+0.10+0.09}_{-0.07-0.16})\%$	$ x < 1.6\%$
$y = (0.37 \pm 0.25^{+0.07+0.07}_{-0.13-0.08})\%$	$ y < 1.04\%$
$ q/p = 0.86^{+0.30+0.06}_{-0.29-0.03} \pm 0.08$	
$\phi = (-14_{-18-3-4}^{+16+5+2})^\circ$	

In addition, Belle [20] has reported results for both the relative phase (statistical errors only) and ratio R (central values only) of the DCS fit fraction relative to the CF fit fractions for $K^*(892)^+ \pi^-$, $K_0^*(1430)^+ \pi^-$, $K_2^*(1430)^+ \pi^-$, $K^*(1410)^+ \pi^-$, and $K^*(1680)^+ \pi^-$. The reported values for R in units of $\tan^4 \theta_c$ are 2.94 ± 0.12 , 22.0 ± 1.6 , 34 ± 4 , 87 ± 13 , and $(5 \pm 5) \times 10^2$. For $K^+ \pi^-$, the corresponding value for R_D is $(1.28 \pm 0.02) \times \tan^4 \theta_c$. Similarly, BABAR [21] has reported central values for R for $K^*(892)^+ \pi^-$, $K_0^*(1430)^+ \pi^-$, and $K_2^*(1430)^+ \pi^-$. The reported values for R in units of $\tan^4 \theta_c$ are 3.45 ± 0.31 , 7.7 ± 3.0 , and 1.7 ± 1.7 , respectively. The systematic uncertainties on these value R must be evaluated. The large differences in R among these final states could point to an interesting role for hadronic effects.

Decays to CP Eigenstates: When the final state f is a CP eigenstate, there is no distinction between f and \bar{f} , and $A_f = A_{\bar{f}}$ and $\bar{A}_{\bar{f}} = \bar{A}_f$. We denote final states with CP eigenvalues ± 1 by f_{\pm} and write λ_{\pm} for $\lambda_{f_{\pm}}$.

The quantity y may be measured by comparing the rate for D^0 decays to non- CP eigenstates such as $K^-\pi^+$ with decays to CP eigenstates such as K^+K^- [13]. If decays to K^+K^- have a shorter effective lifetime than those to $K^-\pi^+$, y is positive.

In the limit of slow mixing, $x, y \ll 1$, and the absence of direct CP violation ($A_D = 0$), but allowing for small indirect CP violation ($|A_M|, |\phi| \ll 1$), we can write

$$\lambda_{\pm} = \left| \frac{q}{p} \right| e^{i\phi}. \quad (27)$$

To a good approximation, the decay rates for states that are initially D^0 and \bar{D}^0 to a CP eigenstate have exponential time dependence

$$r_{\pm}(t) \propto \exp(-t/\tau_{\pm}), \quad (28)$$

$$\bar{r}_{\pm}(t) \propto \exp(-t/\bar{\tau}_{\pm}), \quad (29)$$

where τ is measured in units of $1/\Gamma$.

The effective lifetimes are given by

$$1/\tau_{\pm} = 1 \pm \left| \frac{q}{p} \right| (y \cos \phi - x \sin \phi), \quad (30)$$

$$1/\bar{\tau}_{\pm} = 1 \pm \left| \frac{p}{q} \right| (y \cos \phi + x \sin \phi). \quad (31)$$

The effective decay rate to a CP eigenstate combining both D^0 and \bar{D}^0 decays is

$$r_{\pm}(t) + \bar{r}_{\pm}(t) \propto e^{-(1 \pm y_{CP})t}. \quad (32)$$

Here

$$y_{CP} = \frac{1}{2} \left(\left| \frac{q}{p} \right| + \left| \frac{p}{q} \right| \right) y \cos \phi - \frac{1}{2} \left(\left| \frac{q}{p} \right| - \left| \frac{p}{q} \right| \right) x \sin \phi \quad (33)$$

$$\approx y \cos \phi - A_M x \sin \phi. \quad (34)$$

If CP is conserved, $y_{CP} = y$.

Belle [30] and BaBar [31] have recently updated y_{CP} and the decay-rate asymmetry for CP even final states

$$A_{\Gamma} = \frac{\bar{\tau}_{+} - \tau_{+}}{\bar{\tau}_{+} + \tau_{+}} \quad (35)$$

$$= \frac{1}{2} \left(\left| \frac{q}{p} \right| - \left| \frac{p}{q} \right| \right) y \cos \phi - \frac{1}{2} \left(\left| \frac{q}{p} \right| + \left| \frac{p}{q} \right| \right) x \sin \phi \quad (36)$$

$$\approx A_M y \cos \phi - x \sin \phi. \quad (37)$$

If CP is conserved, $A_{\Gamma} = 0$. All measurements of y_{CP} and A_{Γ} are relative to the $D^0 \rightarrow K^- \pi^+$ decay rate. Table 6 summarizes the current status of measurements. The average of the six y_{CP} measurements is $1.13 \pm 0.27\%$.

Substantial work on the integrated CP asymmetries in decays to CP eigenstates indicates that A_{CP} is consistent with zero at the few-percent level [36]. The expression for the integrated CP asymmetry that includes the possibility of CP violation in mixing is

$$A_{CP} = \frac{\Gamma(D^0 \rightarrow f_{\pm}) - \Gamma(\bar{D}^0 \rightarrow f_{\pm})}{\Gamma(D^0 \rightarrow f_{\pm}) + \Gamma(\bar{D}^0 \rightarrow f_{\pm})} \quad (38)$$

$$= |q|^2 - |p|^2 + 2\text{Re} \left(\frac{1 \mp \lambda_{\pm}}{1 \pm \lambda_{\pm}} \right). \quad (39)$$

Coherent $D^0\bar{D}^0$ Analyses: Measurements of R_D , $\cos \delta_{K\pi}$, x , and y can be made simultaneously in a combined fit to the single-tag (ST) and double-tag (DT) yields, or individually by a series of “targeted” analyses [26,27].

The “comprehensive” analysis simultaneously measures mixing and DCS parameters by examining various ST and DT rates. Due to quantum correlations in the $C = -1$ and $C = +1$ $D^0\bar{D}^0$ pairs produced in the reactions $e^+e^- \rightarrow D^0\bar{D}^0(\pi^0)$ and $e^+e^- \rightarrow D^0\bar{D}^0\gamma(\pi^0)$, respectively, the time-integrated $D^0\bar{D}^0$ decay rates are sensitive to interference between amplitudes for indistinguishable final states. The size of this interference is governed by the relevant amplitude ratios and can include contributions from $D^0\text{--}\bar{D}^0$ mixing.

The following categories of final states are considered:

f or \bar{f} : Hadronic states accessed from either D^0 or \bar{D}^0 decay but that are not CP eigenstates. An example is $K^- \pi^+$, which results from Cabibbo-favored D^0 transitions or DCS \bar{D}^0 transitions.

ℓ^+ or ℓ^- : Semileptonic or purely leptonic final states, which, in the absence of mixing, tag unambiguously the flavor of the parent D^0 .

S_+ or S_- : CP -even and CP -odd eigenstates, respectively.

The decay rates for $D^0\bar{D}^0$ pairs to all possible combinations of the above categories of final states are calculated in Ref. 1, for both $C = -1$ and $C = +1$, reproducing the work of Ref. 2. Such $D^0\bar{D}^0$ combinations, where both D final states are specified, are double tags. In addition, the rates for single tags, where either the D^0 or \bar{D}^0 is identified and the other neutral D decays generically are given in Ref. 1.

CLEO-c has reported results using 281 pb $^{-1}$ of $e^+e^- \rightarrow \psi(3770)$ data [37,38], where the quantum coherent $D^0\bar{D}^0$ pairs are in the $C = -1$ state. The values of y , R_M , and $\cos \delta_{K\pi}$ are determined from a combined fit to the ST (hadronic only) and DT yields. The hadronic final states included are $K^- \pi^+$ (f), $K^+ \pi^-$ (\bar{f}), $K^- K^+$ (S_+), $\pi^+ \pi^-$ (S_+), $K_S^0 \pi^0 \pi^0$ (S_+), $K_L^0 \pi^0$ (S_+), $K_S^0 \pi^0$ (S_-), $K_S^0 \eta$ (S_-), and $K_S^0 \omega$ (S_-). The two flavored final states, $K^- \pi^+$ and $K^+ \pi^-$, can be reached via CF or DCS transitions.

Table 6: Results for y from $D^0 \rightarrow K^+ K^-$ and $\pi^+ \pi^-$.

Year	Exper.	D^0 final state(s)	$y(\%)$	$A_{\Gamma}(\times 10^{-3})$
2007	BABAR [31]	$K^+ K^-$, $\pi^+ \pi^-$	$1.03 \pm 0.33 \pm 0.19$	$2.6 \pm 3.6 \pm 0.8$
2007	Belle [30]	$K^+ K^-$, $\pi^+ \pi^-$	$1.31 \pm 0.32 \pm 0.25$	$0.1 \pm 3.0 \pm 1.5$
2001	CLEO [32]	$K^+ K^-$, $\pi^+ \pi^-$	$-1.2 \pm 2.5 \pm 1.4$	—
2001	Belle [33]	$K^+ K^-$	$-0.5 \pm 1.0_{-0.8}^{+0.7}$	—
2000	FOCUS [34]	$K^+ K^-$	$3.42 \pm 1.39 \pm 0.74$	—
1999	E791 [35]	$K^+ K^-$	$0.8 \pm 2.9 \pm 1.0$	—
HFAG Avg. [10]			1.132 ± 0.266	0.123 ± 0.248

Meson Particle Listings

D^0

Semileptonic DT yields are also included, where one D is fully reconstructed in one of the hadronic modes listed above, and the other D is partially reconstructed, requiring that only the electron be found. When the electron is accompanied by a flavor tag ($D \rightarrow K^- \pi^+$ or $K^+ \pi^-$), only the “right-sign” DT sample, where the electron and kaon charges are the same, is used.

The main results of the CLEO-c analysis are the determination of $\cos \delta_{K\pi} = 1.10 \pm 0.35 \pm 0.07$, and World Averages for the mixing parameters from an “extended” fit that combines the CLEO-c data with previous mixing and branching-ratio measurements [37,38]. In these fits, which allow $\cos \delta_{K\pi}$ and x^2 to be unphysical, the no-mixing result ($x = y = 0$) is excluded at 5.0σ . Constraining $\cos \delta_{K\pi}$ and $\sin \delta_{K\pi}$ to $[-1,+1]$ —that is interpreting $\delta_{K\pi}$ as an angle—yields $\delta_{K\pi} = (22_{-12}^{+11+9})^\circ$. Note that measurements of y (Table 6 and Table 3) and y' (Table 5) contribute to the determination of $\delta_{K\pi}$.

Summary of Experimental Results: Several recent results indicate that charm mixing is at the upper end of the range of Standard Model estimates.

BABAR [15] and CDF [14] find evidence for oscillations in $D^0 \rightarrow K^+ \pi^-$ with 3.9σ ($\Delta \text{Log}\mathcal{L}$) and 3.8σ (Bayesian), respectively. The most precise measurement is from Belle [16], which excludes $x^2 = y^2 = 0$ at 2.1σ .

Belle [30] and BABAR [31] find 3.2σ and 3σ effects for y_{CP} in $D^0 \rightarrow K^+ K^-$ and $\pi^+ \pi^-$. The most sensitive measurement of y is in $D^0 \rightarrow K_S^0 \pi^+ \pi^-$ from Belle [20] and is only 1.2σ significant. In the same analysis, Belle also finds a 2.4σ result for x . The current situation would benefit from better knowledge of the strong phase difference $\delta_{K\pi}$ than provided by the current CLEO-c result [37,38]. This would allow one to unfold x and y from the $D^0 \rightarrow K^+ \pi^-$ measurements of x'^2 and y' , and directly compare them to the $D^0 \rightarrow K_S^0 \pi^+ \pi^-$ results.

The experimental data consistently indicate that the D^0 and \bar{D}^0 do mix. The mixing is presumably dominated by long-range processes. A serious limitation to the interpretation of charm oscillations in terms of New Physics is the theoretical uncertainty of the Standard Model prediction. However, recent evidence opens the window to searches for CP violation, which would provide unequivocal evidence of New Physics.

HFAG Averaging of Charm Mixing Results:

All mixing measurements can be combined to obtain world average values for x and y . The HFAG has done this in two ways [39,40,10]: (a) By adding together log-likelihood functions for x , y , and $\delta_{K\pi}$ from measurements of relevant observables; (b) by making a global fit to the measured observables x , y , $\delta_{K\pi}$, $\delta_{K\pi\pi^0}$, and R_D , being careful to account for the correlations among observables by using the error matrices from the experiments. Both methods use measurements of $D^0 \rightarrow K^+ \ell^- \bar{\nu}$, $K^+ K^-$, $\pi^+ \pi^-$, $K^+ \pi^-$, $K^+ \pi^- \pi^0$, $K^+ \pi^- \pi^+ \pi^-$, and $K_S^0 \pi^+ \pi^-$ decays, as well as CLEO-c results for double-tagged branching fractions measured at the $\psi(3770)$ resonance (see previous sections of this note). Method (a) has the advantage that non-Gaussian errors are accounted for; method (b) has

the advantage that it is readily expanded to allow for CP violation. For that, three additional parameters are included in the fit: $A_D \equiv (R_D^+ - R_D^-)/(R_D^+ + R_D^-)$, $|q/p|$, and $\text{Arg}(q/p) \equiv \phi$. The two methods obtain almost identical results when they are applied to the same set of observables.

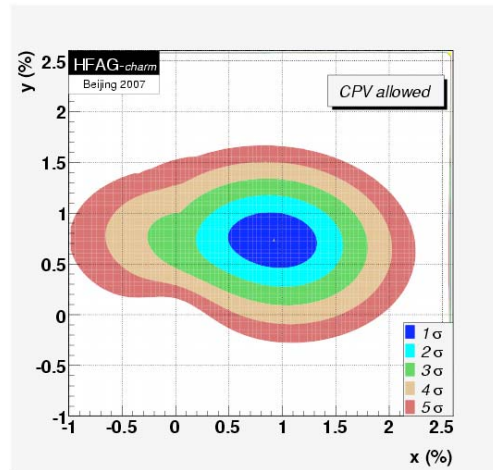


Figure 1: Two-dimensional 1σ - 5σ contours for (x, y) from measurements of $D^0 \rightarrow K^+ \ell \nu$, $h^+ h^-$, $K^+ \pi^-$, $K^+ \pi^- \pi^0$, $K^+ \pi^- \pi^+ \pi^-$, and $K_S^0 \pi^+ \pi^-$ decays, and double-tagged branching fractions measured at the $\psi(3770)$ resonance (from HFAG [10]). Color version at end of book.

Table 7: HFAG Charm Mixing Average allowing for CP violation [10,39,40].

Parameter	HFAG average	95% C.L. interval
$x(\%)$	$0.97_{-0.29}^{+0.27}$	(0.39 – 1.48)
$y(\%)$	$0.78_{-0.19}^{+0.18}$	(0.41 – 1.13)
$R_D(\%)$	0.335 ± 0.009	(0.316 – 0.353)
$\delta_{K\pi}(\circ)$	$21.9_{-12.5}^{+11.5}$	(–6.3 – 44.6)
$\delta_{K\pi\pi^0}(\circ)$	$32.4_{-25.8}^{+25.1}$	(–20.3 – 82.7)
$A_D(\%)$	-2.2 ± 2.5	(–7.10 – 2.67)
$ q/p $	$0.86_{-0.15}^{+0.18}$	(0.59 – 1.23)
$\phi(\circ)$	$-9.6_{-9.5}^{+8.3}$	(–30.3 – 6.5)

For the global fit, confidence contours in the two dimensions (x, y) and $(|q/p|, \phi)$ are obtained by letting, for any point in the two-dimensional plane, all other fit parameters take their preferred values. Figures 1 and 2 show the resulting 1-to-5 σ contours. The fits exclude the no-mixing point ($x = y = 0$) at 6.7σ , whether or not CP violation is allowed. The parameters x and y differ from zero by 3.0σ and 4.1σ , respectively. One-dimensional likelihood functions for parameters are obtained by allowing, for any value of the parameter, all other fit parameters to take their preferred values. The resulting likelihood functions give central values, 68.3% C.L. intervals, and 95% C.L. intervals as listed in Table 7.

See key on page 373

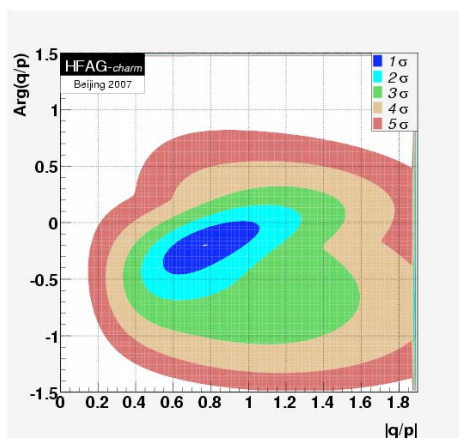


Figure 2: Two-dimensional 1σ - 5σ contours for $(|q/p|, \text{Arg}(q/p))$ from measurements of $D^0 \rightarrow K^+\ell\nu, h^+h^-, K^+\pi^-, K^+\pi^-\pi^0, K^+\pi^-\pi^+\pi^-$, and $K_S^0\pi^+\pi^-$ decays, and double-tagged branching fractions measured at the $\psi(3770)$ resonance (from HFAG [10]). Color version at end of book.

From the results of the HFAG averaging, the following can be concluded: (1) Since CP violation is small and y_{CP} is positive, the CP -even state is shorter-lived, as in the $K^0\bar{K}^0$ system. However, since x appears to be positive, the CP -even state is heavier, unlike in the $K^0\bar{K}^0$ system. (2) There is no evidence yet for CP -violation in the $D^0\bar{D}^0$ system.

References

- D.M. Asner and W.M. Sun, Phys. Rev. **D73**, 034024 (2006); Erratum-*ibid.*, **77**, 019901 (2008).
- D. Atwood and A.A. Petrov, Phys. Rev. **D71**, 054032 (2005) Z.Z. Xing, Phys. Rev. **D55**, 196 (1997) M. Goldhaber and J.L. Rosner, Phys. Rev. **D15**, 1254 (1977).
- See the Note on $B^0\text{-}\bar{B}^0$ mixing in this *Review*.
- B. Aubert *et al.*, Phys. Rev. **D76**, 014018 (2007).
- U. Bitenc *et al.*, Phys. Rev. **D72**, 071101R (2005).
- C. Cawlfeld *et al.*, Phys. Rev. **D71**, 077101 (2005).
- B. Aubert *et al.*, Phys. Rev. **D70**, 091102R (2004).
- K. Stenson, presented at the April Meeting of the American Physical Society (APS 03), Philadelphia, Pennsylvania, April 5-8, 2003; M. Hosack, (FOCUS Collab.), Fermilab-Thesis-2002-25.
- E.M. Aitala *et al.*, Phys. Rev. Lett. **77**, 2384 (1996).
- A.J. Schwartz, for the Heavy Flavor Averaging Group, arXiv:0803.0082 [hep-ex].
- R. Godang *et al.*, Phys. Rev. Lett. **84**, 5038 (2000).
- Y. Nir, Lectures given at 27th SLAC Summer Institute on Particle Physics: CP Violation in and Beyond the Standard Model (SSI 99), Stanford, California, 7-16 Jul 1999. Published in Trieste 1999, *Particle Physics*, pp. 165-243.
- S. Bergmann *et al.*, Phys. Lett. **B486**, 418 (2000).
- T. Aaltonen, Phys. Rev. Lett. **100**, 121802 (2008).
- B. Aubert *et al.*, Phys. Rev. Lett. **98**, 211802 (2007).
- L.M. Zhang *et al.*, Phys. Rev. Lett. **96**, 151801 (2006).
- J.M. Link *et al.*, Phys. Lett. **B607**, 51 (2005).
- E.M. Aitala *et al.*, Phys. Rev. **D57**, 13 (1998).
- H. Muramatsu *et al.*, Phys. Rev. Lett. **89**, 251802 (2002).
- L.M. Zhang *et al.*, Phys. Rev. Lett. **99**, 131803 (2007).
- B. Aubert *et al.*, Phys. Rev. Lett. **95**, 121802 (2005).
- B. Aubert *et al.*, Phys. Rev. Lett. **97**, 221803 (2006).
- X.C. Tian *et al.*, Phys. Rev. Lett. **95**, 231801 (2005).
- S.A. Dytman *et al.*, Phys. Rev. **D64**, 111101R (2001).
- G. Brandenburg *et al.*, Phys. Rev. Lett. **87**, 071802 (2001).
- R.A. Briere *et al.*, (CLEO Collab.), CLNS 01-1742, (2001).
- G. Cavoto *et al.*, Prepared for 3rd Workshop on the Unitarity Triangle: CKM 2005, San Diego, California, 15-18 Mar 2005, hep-ph/0603019.
- BABAR has updated AUBERT 06N (230.4 fb⁻¹) at Lepton-Photon 2007 using 384 fb⁻¹.
http://chep.knu.ac.kr/lp07/htm/S4/S04_13a.pdf.
- D.M. Asner *et al.*, Phys. Rev. **D72**, 012001 (2005).
- M. Staric, Phys. Rev. Lett. **98**, 211803 (2007).
- B. Aubert *et al.*, (BABAR Collab.), arXiv:0712.2249 [hep-ex], Phys. Rev. D (accepted).
- S.E. Csorna *et al.*, Phys. Rev. **D65**, 092001 (2002).
- K. Abe *et al.*, Phys. Rev. Lett. **88**, 162001 (2002).
- J.M. Link *et al.*, Phys. Lett. **B485**, 62 (2000).
- E.M. Aitala *et al.*, Phys. Rev. Lett. **83**, 32 (1999).
- See the tabulation of A_{CP} results in the D^0 and D^+ Listings in this *Review*.
- J.L. Rosner *et al.*, (CLEO Collab.), Phys. Rev. Lett. **100**, 221801 (2008).
- D.M. Asner *et al.*, (CLEO Collab.), arXiv:0802.2264 [hep-ex], accepted by Phys. Rev. D.
- A.J. Schwartz, for the Heavy Flavor Averaging Group, arXiv:0708.4225 [hep-ex], arXiv:0712.1589 [hep-ex].
- B.A. Petersen, in *Proceedings of International Workshop on Charm Physics (Charm 2007)*, Ithaca, New York, 5-8 Aug. 2007, p. 9.

$$|m_{D_1^0} - m_{D_2^0}| = x \Gamma$$

The D_1^0 and D_2^0 are the mass eigenstates of the D^0 meson, as described in the note on " $D^0\text{-}\bar{D}^0$ Mixing," above. The experiments usually present $x \equiv \Delta m/\Gamma$. Then $\Delta m = x \Gamma = x \hbar/\tau$.

VALUE (10^{10} h s^{-1})	CL%	DOCUMENT ID	TECN	COMMENT
$2.37^{+0.66}_{-0.71}$	OUR EVALUATION	HFAG fit; see the note on " $D^0\text{-}\bar{D}^0$ Mixing."		
$1.98 \pm 0.73^{+0.32}_{-0.41}$		⁵ ZHANG	07B BELL	$\Delta m < 3.9, 95\%$ CL
●●● We do not use the following data for averages, fits, limits, etc. ●●●				
< 7	95	⁶ ZHANG	06 BELL	e^+e^-
-11 to +22		⁵ ASNER	05 CLEO	$e^+e^- \approx 10 \text{ GeV}$
< 11	90	BITENC	05 BELL	
< 30	90	CRAWFIELD	05 CLEO	
< 7	95	⁶ LI	05A BELL	See ZHANG 06
< 22	95	⁷ LINK	05H FOCS	γ nucleus
< 23	95	AUBERT	04Q BABR	
< 11	95	⁶ AUBERT	03Z BABR	e^+e^- , 10.6 GeV
< 7	95	⁸ GODANG	00 CLE2	e^+e^-
< 32	90	^{9,10} AITALA	98 E791	π^- nucleus, 500 GeV
< 24	90	¹¹ AITALA	96C E791	π^- nucleus, 500 GeV
< 21	90	^{10,12} ANJOS	88C E691	Photoproduction

Meson Particle Listings

 D^0

- ⁵ The ASNER 05 and ZHANG 07b values are from the time-dependent Dalitz-plot analysis of $D^0 \rightarrow K_S^0 \pi^+ \pi^-$. Decay-time information and interference on the Dalitz plot are used to distinguish doubly Cabibbo-suppressed decays from mixing and to measure the relative phase between $D^0 \rightarrow K^{*+} \pi^-$ and $\bar{D}^0 \rightarrow K^{*+} \pi^-$. This value allows CP violation and is sensitive to the sign of Δm .
- ⁶ The AUBERT 03z, LI 05A, and ZHANG 06 limits are inferred from the D^0 - \bar{D}^0 mixing ratio $\Gamma(K^+ \pi^- \text{ (via } \bar{D}^0)) / \Gamma(K^- \pi^+)$ given near the end of this D^0 Listings. Decay-time information is used to distinguish DCS decays from D^0 - \bar{D}^0 mixing. The limit allows interference between the DCS and mixing ratios, and also allows CP violation. AUBERT 03z assumes the strong phase between $D^0 \rightarrow K^+ \pi^-$ and $\bar{D}^0 \rightarrow K^+ \pi^-$ amplitudes is small; if an arbitrary phase is allowed, the limit degrades by 20%. The LI 05A and ZHANG 06 limits are valid for an arbitrary strong phase.
- ⁷ This LINK 05H limit is inferred from the D^0 - \bar{D}^0 mixing ratio $\Gamma(K^+ \pi^- \text{ (via } \bar{D}^0)) / \Gamma(K^- \pi^+)$ given near the end of this D^0 Listings. Decay-time information is used to distinguish DCS decays from D^0 - \bar{D}^0 mixing. The limit allows interference between the DCS and mixing ratios, and also allows CP violation. The strong phase between $D^0 \rightarrow K^+ \pi^-$ and $\bar{D}^0 \rightarrow K^+ \pi^-$ is assumed to be small. If an arbitrary relative strong phase is allowed, the limit degrades by 25%.
- ⁸ This GODANG 00 limit is inferred from the D^0 - \bar{D}^0 mixing ratio $\Gamma(K^+ \pi^- \text{ (via } \bar{D}^0)) / \Gamma(K^- \pi^+)$ given near the end of this D^0 Listings. Decay-time information is used to distinguish DCS decays from D^0 - \bar{D}^0 mixing. The limit allows interference between the DCS and mixing ratios, and also allows CP violation. The strong phase between $D^0 \rightarrow K^+ \pi^-$ and $\bar{D}^0 \rightarrow K^+ \pi^-$ is assumed to be small. If an arbitrary relative strong phase is allowed, the limit degrades by a factor of two.
- ⁹ AITALA 98 allows interference between the doubly Cabibbo-suppressed and mixing amplitudes, and also allows CP violation in this term, but assumes that $A_D = A_R = 0$. See the note on " D^0 - \bar{D}^0 Mixing," above.
- ¹⁰ This limit is inferred from R_M for $f = K^+ \pi^-$ and $f = K^+ \pi^- \pi^+ \pi^-$. See the note on " D^0 - \bar{D}^0 Mixing," above. Decay-time information is used to distinguish doubly Cabibbo-suppressed decays from D^0 - \bar{D}^0 mixing.
- ¹¹ This limit is inferred from R_M for $f = K^+ \ell^- \bar{\nu}_\ell$. See the note on " D^0 - \bar{D}^0 Mixing," above.
- ¹² ANJOS 88c assumes that $y = 0$. See the note on " D^0 - \bar{D}^0 Mixing," above. Without this assumption, the limit degrades by about a factor of two.

$$(\Gamma_{D_1^0} - \Gamma_{D_2^0}) / \Gamma = 2y$$

The D_1^0 and D_2^0 are the mass eigenstates of the D^0 meson, as described in the note on " D^0 - \bar{D}^0 Mixing," above.

Due to the strong phase difference between $D^0 \rightarrow K^+ \pi^-$ and $\bar{D}^0 \rightarrow K^+ \pi^-$, we exclude from the average those measurements of y' that are inferred from the D^0 - \bar{D}^0 mixing ratio $\Gamma(K^+ \pi^- \text{ via } \bar{D}^0) / \Gamma(K^+ \pi^-)$ given near the end of this D^0 Listings.

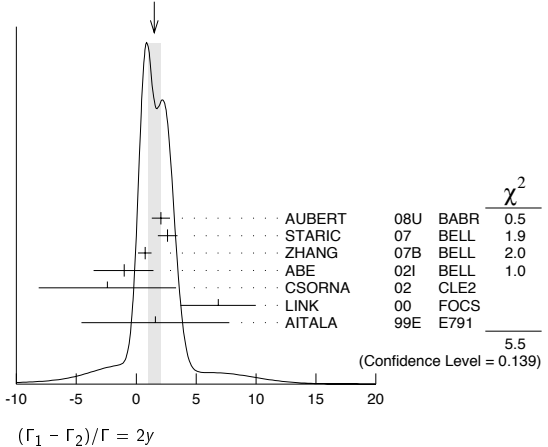
Some early results have been omitted. See our 2006 Review (Journal of Physics, G **33** 1 (2006)).

VALUE (units 10^{-2})	EVTS	DOCUMENT ID	TECN	COMMENT
1.56^{+0.36}_{-0.38}	OUR EVALUATION	HFAG fit; see the note on " D^0 - \bar{D}^0 Mixing."		
1.5 ± 0.5	OUR AVERAGE	Error includes scale factor of 1.4. See the ideogram below.		
2.06 ± 0.66 ± 0.38	13	AUBERT	08u	BABR $e^+ e^- \approx \Upsilon(4S)$
2.62 ± 0.64 ± 0.50	160k	14	STARIC	07 BELL $e^+ e^- \approx \Upsilon(4S)$
0.74 ± 0.50 ^{+0.20} _{-0.31}	534k	15	ZHANG	07b BELL $e^+ e^- \approx \Upsilon(4S)$
-1.0 ± 2.0 ^{+1.4} _{-1.6}	18k	16	ABE	02i BELL $e^+ e^- \approx \Upsilon(4S)$
-2.4 ± 5.0 ± 2.8	3393	17	CSORNA	02 CLE2 $e^+ e^- \approx \Upsilon(4S)$
6.84 ± 2.78 ± 1.48	10k	16	LINK	00 FOCS γ nucleus
+1.6 ± 5.8 ± 2.1		16	AITALA	99e E791 $K^- \pi^+, K^+ K^-$
••• We do not use the following data for averages, fits, limits, etc. •••				
1.70 ± 1.52	12.7 ± 0.3k	18	AALTONEN	08E CDF $p\bar{p}, \sqrt{s} = 1.96$ TeV
1.94 ± 0.88 ± 0.62	4030 ± 90	18	AUBERT	07w BABR $e^+ e^- \approx 10.6$ GeV
-0.7 ± 4.9	4k ± 88	18,19	ZHANG	06 BELL $e^+ e^-$
-3.0 ± 5.0 ± 1.6		15	ASNER	05 CLEO $e^+ e^- \approx 10$ GeV
-0.3 ± 4.7		18,19	LI	05A BELL See ZHANG 06
-5.2 ± 18.4		18,19	LINK	05H FOCS γ nucleus
1.6 ± 0.8 ^{+1.0} _{-0.8}	450k	20	AUBERT	03P BABR See AUBERT 08u
1.6 ± 6.2		18,19	AUBERT	03z BABR $e^+ e^-$, 10.6 GeV
-5.0 ± 2.8 ± 0.6		18	GODANG	00 CLE2 $e^+ e^-$

- ¹³ This value combines the results of AUBERT 08u and AUBERT 03P.
- ¹⁴ STARIC 07 compares the lifetimes of D^0 decay to the CP eigenstates $K^+ K^-$ and $\pi^+ \pi^-$ with D^0 decay to $K^- \pi^+$.
- ¹⁵ The ASNER 05 and ZHANG 07b values are from the time-dependent Dalitz-plot analysis of $D^0 \rightarrow K_S^0 \pi^+ \pi^-$. Decay-time information and interference on the Dalitz plot are used to distinguish doubly Cabibbo-suppressed decays from mixing and to measure the relative phase between $D^0 \rightarrow K^{*+} \pi^-$ and $\bar{D}^0 \rightarrow K^{*+} \pi^-$. This limit allows CP violation.
- ¹⁶ LINK 00, AITALA 99e, and ABE 02i measure the lifetime difference between $D^0 \rightarrow K^- K^+$ (CP even) decays and $D^0 \rightarrow K^- \pi^+$ (CP mixed) decays, or $y_{CP} = [\Gamma(CP+) - \Gamma(CP-)] / [\Gamma(CP+) + \Gamma(CP-)]$. We list $2y_{CP} = \Delta\Gamma/\Gamma$.
- ¹⁷ CSORNA 02 measures the lifetime difference between $D^0 \rightarrow K^- K^+$ and $\pi^- \pi^+$ (CP even) decays and $D^0 \rightarrow K^- \pi^+$ (CP mixed) decays, or $y_{CP} = [\Gamma(CP+) - \Gamma(CP-)] / [\Gamma(CP+) + \Gamma(CP-)]$. We list $2y_{CP} = \Delta\Gamma/\Gamma$.

- ¹⁸ The GODANG 00, AUBERT 03z, LINK 05H, LI 05A, ZHANG 06, AUBERT 07w, and AALTONEN 08E limits are inferred from the D^0 - \bar{D}^0 mixing ratio $\Gamma(K^+ \pi^- \text{ (via } \bar{D}^0)) / \Gamma(K^- \pi^+)$ given near the end of this D^0 Listings. Decay-time information is used to distinguish DCS decays from D^0 - \bar{D}^0 mixing. The limits allow interference between the DCS and mixing ratios, and all except AUBERT 07w and AALTONEN 08E also allow CP violation. The phase between $D^0 \rightarrow K^+ \pi^-$ and $\bar{D}^0 \rightarrow K^+ \pi^-$ is assumed to be small. This is a measurement of y' and is not the same as the y_{CP} of our note above on " D^0 - \bar{D}^0 Mixing."
- ¹⁹ The ranges of AUBERT 03z, LINK 05H, LI 05A, and ZHANG 06 measurements are for 95% confidence level.
- ²⁰ AUBERT 03P measures $Y \equiv 2\tau^0 / (\tau^+ + \tau^-) - 1$, where τ^0 is the $D^0 \rightarrow K^- \pi^+$ (and $\bar{D}^0 \rightarrow K^+ \pi^-$) lifetime, and τ^+ and τ^- are the D^0 and \bar{D}^0 lifetimes to CP -even states (here $K^- K^+$ and $\pi^- \pi^+$). In the limit of CP conservation, $Y = y \equiv \Delta\Gamma / 2\Gamma$ (we list $2y = \Delta\Gamma/\Gamma$). AUBERT 03P also uses $\tau^+ - \tau^-$ to get $\Delta Y = -0.008 \pm 0.006 \pm 0.002$.

WEIGHTED AVERAGE
1.5 ± 0.5 (Error scaled by 1.4)

 $|q/p|$

The mass eigenstates D_1^0 and D_2^0 are related to the $C = \pm 1$ states by $|D_{1,2}^0\rangle = p|D^0\rangle + q|\bar{D}^0\rangle$. See the note on " D^0 - \bar{D}^0 Mixing" above.

VALUE	DOCUMENT ID	TECN	COMMENT
0.86^{+0.30}_{-0.29} ± 0.08	21	ZHANG	07B BELL $e^+ e^- \approx \Upsilon(4S)$

- ²¹ The phase of p/q is $(-14^{+16}_{-18} \pm 5)^\circ$. The ZHANG 07B value is from the time-dependent Dalitz-plot analysis of $D^0 \rightarrow K_S^0 \pi^+ \pi^-$. Decay-time information and interference on the Dalitz plot are used to distinguish doubly Cabibbo-suppressed decays from mixing and to measure the relative phase between $D^0 \rightarrow K^{*+} \pi^-$ and $\bar{D}^0 \rightarrow K^{*+} \pi^-$. This value allows CP violation.

 A_Γ

A_Γ is the decay-rate asymmetry for CP -even final states $A_\Gamma = (\bar{\tau}_+ - \tau_+) / (\bar{\tau}_+ + \tau_+)$. See the note on " D^0 - \bar{D}^0 Mixing" above.

VALUE (units 10^{-3})	DOCUMENT ID	TECN	COMMENT
1.4 ± 2.7	OUR AVERAGE		
+2.6 ± 3.6 ± 0.8	AUBERT 08U	BABR	$e^+ e^- \approx \Upsilon(4S)$
+0.1 ± 3.0 ± 2.5	STARIC 07	BELL	$e^+ e^- \approx \Upsilon(4S)$
••• We do not use the following data for averages, fits, limits, etc. •••			
+8 ± 6 ± 2	AUBERT 03P	BABR	$e^+ e^- \approx \Upsilon(4S)$

 D^0 DECAY MODES

Most decay modes (other than the semileptonic modes) that involve a neutral K meson are now given as K_S^0 modes, not as \bar{K}^0 modes. Nearly always it is a K_S^0 that is measured, and interference between Cabibbo-allowed and doubly Cabibbo-suppressed modes can invalidate the assumption that $2\Gamma(K_S^0) = \Gamma(\bar{K}^0)$.

Mode	Fraction (Γ_i/Γ)	Scale factor / Confidence level
------	--------------------------------	---------------------------------

Topological modes

Γ_1	0-prongs	[a] (15 ± 6) %
Γ_2	2-prongs	(71 ± 6) %
Γ_3	4-prongs	[b] (14.6 ± 0.5) %
Γ_4	6-prongs	(1.2 ^{+1.3} _{-0.7}) × 10 ⁻³

		Inclusive modes				
Γ_5	e^+ anything	[c] (6.53 \pm 0.17) %		Γ_{54}	$K^*(1680)^- \pi^+$, $K^*(1680)^- \rightarrow K^- \pi^0$	(1.8 \pm 0.7) $\times 10^{-3}$
Γ_6	μ^+ anything	(6.7 \pm 0.6) %		Γ_{55}	$K^- \pi^+ \pi^0$ nonresonant	(1.11 \pm 0.53) %
Γ_7	K^- anything	(54.7 \pm 2.8) %	S=1.3	Γ_{56}	$K_S^0 \pi^0 \pi^0$	—
Γ_8	\bar{K}^0 anything + K^0 anything	(47 \pm 4) %		Γ_{57}	$\bar{K}^*(892)^0 \pi^0$, $\bar{K}^*(892)^0 \rightarrow K_S^0 \pi^0$	(6.7 \pm 1.8) $\times 10^{-3}$
Γ_9	K^+ anything	(3.4 \pm 0.4) %		Γ_{58}	$K_S^0 \pi^0 \pi^0$ nonresonant	(4.5 \pm 1.1) $\times 10^{-3}$
Γ_{10}	$K^*(892)^-$ anything	(15 \pm 9) %		Γ_{59}	$K^- \pi^+ \pi^+$	[d] (8.10 \pm 0.20) %
Γ_{11}	$\bar{K}^*(892)^0$ anything	(9 \pm 4) %		Γ_{60}	$K^- \pi^+ \rho^0$ total	(6.76 \pm 0.33) %
Γ_{12}	$K^*(892)^+$ anything	< 3.6 %	CL=90%	Γ_{61}	$K^- \pi^+ \rho^0$ 3-body	(5.1 \pm 2.3) $\times 10^{-3}$
Γ_{13}	$K^*(892)^0$ anything	(2.8 \pm 1.3) %		Γ_{62}	$\bar{K}^*(892)^0 \rho^0$, $\bar{K}^*(892)^0 \rightarrow K^- \pi^+$	(1.00 \pm 0.22) %
Γ_{14}	η anything	(9.5 \pm 0.9) %		Γ_{63}	$K^- a_1(1260)^+$, $a_1(1260)^+ \rightarrow \pi^+ \pi^+ \pi^-$	(3.6 \pm 0.6) %
Γ_{15}	η' anything	(2.48 \pm 0.27) %		Γ_{64}	$\bar{K}^*(892)^0 \pi^+ \pi^-$ total, $\bar{K}^*(892)^0 \rightarrow K^- \pi^+$	(1.5 \pm 0.4) %
Γ_{16}	ϕ anything	(1.05 \pm 0.11) %		Γ_{65}	$\bar{K}^*(892)^0 \pi^+ \pi^-$ 3-body, $\bar{K}^*(892)^0 \rightarrow K^- \pi^+$	(9.7 \pm 2.1) $\times 10^{-3}$
		Semileptonic modes		Γ_{66}	$K_1(1270)^- \pi^+$, $K_1(1270)^- \rightarrow K^- \pi^+ \pi^-$	[f] (2.9 \pm 0.3) $\times 10^{-3}$
Γ_{17}	$K^- \ell^+ \nu_\ell$			Γ_{67}	$K^- \pi^+ \pi^+ \pi^-$ nonresonant	(1.88 \pm 0.26) %
Γ_{18}	$K^- e^+ \nu_e$	(3.58 \pm 0.06) %	S=1.1	Γ_{68}	$K_S^0 \pi^+ \pi^- \pi^0$	[d] (5.4 \pm 0.6) %
Γ_{19}	$K^- \mu^+ \nu_\mu$	(3.31 \pm 0.13) %		Γ_{69}	$K_S^0 \eta, \eta \rightarrow \pi^+ \pi^- \pi^0$	(8.6 \pm 1.4) $\times 10^{-4}$
Γ_{20}	$K^*(892)^- e^+ \nu_e$	(2.18 \pm 0.16) %		Γ_{70}	$K_S^0 \omega, \omega \rightarrow \pi^+ \pi^- \pi^0$	(9.8 \pm 1.8) $\times 10^{-3}$
Γ_{21}	$K^*(892)^- \mu^+ \nu_\mu$	(2.01 \pm 0.25) %		Γ_{71}	$K^*(892)^- \rho^+$, $K^*(892)^- \rightarrow K_S^0 \pi^-$	(2.1 \pm 0.8) %
Γ_{22}	$K^- \pi^0 e^+ \nu_e$	(1.6 \pm 1.3) %		Γ_{72}	$K_1(1270)^- \pi^+$, $K_1(1270)^- \rightarrow K_S^0 \pi^- \pi^0$	[f] (2.2 \pm 0.6) $\times 10^{-3}$
Γ_{23}	$\bar{K}^0 \pi^- e^+ \nu_e$	(2.7 \pm 0.9) %		Γ_{73}	$\bar{K}^*(892)^0 \pi^+ \pi^-$ 3-body, $\bar{K}^*(892)^0 \rightarrow K_S^0 \pi^0$	(2.4 \pm 0.5) $\times 10^{-3}$
Γ_{24}	$K^*(892)^- \ell^+ \nu_\ell$			Γ_{74}	$K_S^0 \pi^+ \pi^- \pi^0$ nonresonant	(1.1 \pm 1.2) %
Γ_{25}	$K^- \pi^+ \pi^- e^+ \nu_e$	(2.8 \pm 1.4) $\times 10^{-4}$		Γ_{75}	$K^- \pi^+ \pi^0 \pi^0$	
Γ_{26}	$K_1(1270)^- e^+ \nu_e$	(7.6 \pm 4.2) $\times 10^{-4}$		Γ_{76}	$K^- \pi^+ \pi^+ \pi^- \pi^0$	(4.2 \pm 0.4) %
Γ_{27}	$K^- \pi^+ \pi^- \mu^+ \nu_\mu$	< 1.2 $\times 10^{-3}$	CL=90%	Γ_{77}	$\bar{K}^*(892)^0 \pi^+ \pi^- \pi^0$, $\bar{K}^*(892)^0 \rightarrow K^- \pi^+$	(1.2 \pm 0.6) %
Γ_{28}	$(\bar{K}^*(892) \pi)^- \mu^+ \nu_\mu$	< 1.4 $\times 10^{-3}$	CL=90%	Γ_{78}	$K^- \pi^+ \omega, \omega \rightarrow \pi^+ \pi^- \pi^0$	(2.7 \pm 0.5) %
Γ_{29}	$\pi^- e^+ \nu_e$	(2.83 \pm 0.17) $\times 10^{-3}$		Γ_{79}	$\bar{K}^*(892)^0 \omega$, $\bar{K}^*(892)^0 \rightarrow K^- \pi^+$, $\omega \rightarrow \pi^+ \pi^- \pi^0$	(6.5 \pm 2.4) $\times 10^{-3}$
Γ_{30}	$\pi^- \mu^+ \nu_\mu$	(2.37 \pm 0.24) $\times 10^{-3}$		Γ_{80}	$K_S^0 \eta \pi^0$	(5.6 \pm 1.2) $\times 10^{-3}$
Γ_{31}	$\rho^- e^+ \nu_e$	(1.9 \pm 0.4) $\times 10^{-3}$		Γ_{81}	$K_S^0 a_0(980), a_0(980) \rightarrow \eta \pi^0$	(6.7 \pm 2.1) $\times 10^{-3}$
		Hadronic modes with one \bar{K}		Γ_{82}	$\bar{K}^*(892)^0 \eta, \bar{K}^*(892)^0 \rightarrow K_S^0 \pi^0$	(1.6 \pm 0.5) $\times 10^{-3}$
Γ_{32}	$K^- \pi^+$	(3.89 \pm 0.05) %	S=1.1	Γ_{83}	$K_S^0 2\pi^+ 2\pi^-$	(2.84 \pm 0.31) $\times 10^{-3}$
Γ_{33}	$K_S^0 \pi^0$	(1.22 \pm 0.06) %	S=1.2	Γ_{84}	$K_S^0 \rho^0 \pi^+ \pi^-$, no $K^*(892)^-$	(1.1 \pm 0.7) $\times 10^{-3}$
Γ_{34}	$K_S^0 \pi^0$	(10.0 \pm 0.7) $\times 10^{-3}$		Γ_{85}	$K^*(892)^- \pi^+ \pi^+ \pi^-$, $K^*(892)^- \rightarrow K_S^0 \pi^-$, no ρ^0	(5 \pm 8) $\times 10^{-4}$
Γ_{35}	$K_S^0 \pi^+ \pi^-$	[d] (2.99 \pm 0.17) %	S=1.1	Γ_{86}	$K^*(892)^- \rho^0 \pi^+$, $K^*(892)^- \rightarrow K_S^0 \pi^-$	(1.7 \pm 0.7) $\times 10^{-3}$
Γ_{36}	$K_S^0 \rho^0$	(7.7 \pm 0.6) $\times 10^{-3}$		Γ_{87}	$K_S^0 2\pi^+ 2\pi^-$ nonresonant	< 1.3 $\times 10^{-3}$
Γ_{37}	$K_S^0 \omega, \omega \rightarrow \pi^+ \pi^-$	(2.2 \pm 0.6) $\times 10^{-4}$		Γ_{88}	$\bar{K}^0 \pi^+ \pi^- \pi^0 \pi^0 (\pi^0)$	
Γ_{38}	$K_S^0 f_0(980), f_0(980) \rightarrow \pi^+ \pi^-$	(1.40 \pm 0.30) $\times 10^{-3}$		Γ_{89}	$K^- 3\pi^+ 2\pi^-$	(2.2 \pm 0.6) $\times 10^{-4}$
Γ_{39}	$K_S^0 f_2(1270), f_2(1270) \rightarrow \pi^+ \pi^-$	(1.3 \pm 1.2) $\times 10^{-4}$		Fractions of many of the following modes with resonances have already appeared above as submodes of particular charged-particle modes. (Modes for which there are only upper limits and $\bar{K}^*(892) \rho$ submodes only appear below.)		
Γ_{40}	$K_S^0 f_0(1370), f_0(1370) \rightarrow \pi^+ \pi^-$	(2.5 \pm 0.6) $\times 10^{-3}$		Γ_{90}	$K_S^0 \eta$	(4.0 \pm 0.5) $\times 10^{-3}$
Γ_{41}	$K^*(892)^- \pi^+$, $K^*(892)^- \rightarrow K_S^0 \pi^-$	(1.97 \pm 0.13) %		Γ_{91}	$K_S^0 \omega$	(1.13 \pm 0.20) %
Γ_{42}	$K^*(892)^+ \pi^-, K^*(892)^+ \rightarrow K_S^0 \pi^+$	[e] (1.0 \pm 1.3) $\times 10^{-4}$		Γ_{92}	$K_S^0 \eta'(958)$	(9.4 \pm 1.4) $\times 10^{-3}$
Γ_{43}	$K_0^*(1430)^- \pi^+$, $K_0^*(1430)^- \rightarrow K_S^0 \pi^-$	(2.9 \pm 0.7) $\times 10^{-3}$		Γ_{93}	$K^- a_1(1260)^+$	(7.8 \pm 1.1) %
Γ_{44}	$K_2^*(1430)^- \pi^+$, $K_2^*(1430)^- \rightarrow K_S^0 \pi^-$	(3.3 \pm 2.2) $\times 10^{-4}$		Γ_{94}	$\bar{K}^0 a_1(1260)^0$	< 1.9 %
Γ_{45}	$K^*(1680)^- \pi^+$, $K^*(1680)^- \rightarrow K_S^0 \pi^-$	(7 \pm 6) $\times 10^{-4}$		Γ_{95}	$K^- a_2(1320)^+$	< 2 $\times 10^{-3}$
Γ_{46}	$K_S^0 \pi^+ \pi^-$ nonresonant	(2.7 \pm 6.1) $\times 10^{-4}$		Γ_{96}	$\bar{K}^*(892)^0 \pi^+ \pi^-$ total	(2.4 \pm 0.5) %
Γ_{47}	$K^- \pi^+ \pi^0$	[d] (13.9 \pm 0.5) %	S=1.6	Γ_{97}	$\bar{K}^*(892)^0 \pi^+ \pi^-$ 3-body	(1.53 \pm 0.34) %
Γ_{48}	$K^- \rho^+$	(10.8 \pm 0.7) %		Γ_{98}	$\bar{K}^*(892)^0 \rho^0$	(1.58 \pm 0.35) %
Γ_{49}	$K^- \rho(1700)^+$, $\rho(1700)^+ \rightarrow \pi^+ \pi^0$	(7.9 \pm 1.7) $\times 10^{-3}$		Γ_{99}	$\bar{K}^*(892)^0 \rho^0$ transverse	(1.6 \pm 0.6) %
Γ_{50}	$K^*(892)^- \pi^+$, $K^*(892)^- \rightarrow K^- \pi^0$	(2.22 \pm 0.36) %		Γ_{100}	$\bar{K}^*(892)^0 \rho^0$ S-wave	(3.0 \pm 0.6) %
Γ_{51}	$\bar{K}^*(892)^0 \pi^0$, $\bar{K}^*(892)^0 \rightarrow K^- \pi^+$	(1.88 \pm 0.23) %		Γ_{101}	$\bar{K}^*(892)^0 \rho^0$ S-wave long.	< 3 $\times 10^{-3}$
Γ_{52}	$K_0^*(1430)^- \pi^+$, $K_0^*(1430)^- \rightarrow K^- \pi^0$	(4.6 \pm 2.1) $\times 10^{-3}$		Γ_{102}	$\bar{K}^*(892)^0 \rho^0$ P-wave	< 3 $\times 10^{-3}$
Γ_{53}	$\bar{K}_0^*(1430)^0 \pi^0$, $\bar{K}_0^*(1430)^0 \rightarrow K^- \pi^+$	(5.7 \pm 4.5) $\times 10^{-3}$		Γ_{103}	$\bar{K}^*(892)^0 \rho^0$ D-wave	(2.1 \pm 0.6) %
				Γ_{104}	$K^*(892)^- \rho^+$	(6.6 \pm 2.6) %

Meson Particle Listings

 D^0

Γ_{105}	$K^*(892)^-\rho^+$ longitudinal	(3.2 \pm 1.3) %	
Γ_{106}	$K^*(892)^-\rho^+$ transverse	(3.5 \pm 2.0) %	
Γ_{107}	$K^*(892)^-\rho^+$ P-wave	< 1.5 %	CL=90%
Γ_{108}	$K^-\pi^+ f_0(980)$		
Γ_{109}	$\bar{K}^*(892)^0 f_0(980)$		
Γ_{110}	$K_1(1270)^-\pi^+$	[f] (1.15 \pm 0.32) %	
Γ_{111}	$K_1(1400)^-\pi^+$	< 1.2 %	CL=90%
Γ_{112}	$\bar{K}_1(1400)^0\pi^0$	< 3.7 %	CL=90%
Γ_{113}	$K^*(1410)^-\pi^+$		
Γ_{114}	$\bar{K}^*(892)^0\pi^+\pi^-\pi^0$	(1.9 \pm 0.9) %	
Γ_{115}	$\bar{K}^*(892)^0\eta$		
Γ_{116}	$K^-\pi^+\omega$	(3.0 \pm 0.6) %	
Γ_{117}	$\bar{K}^*(892)^0\omega$	(1.1 \pm 0.5) %	
Γ_{118}	$K^-\pi^+\eta'(958)$	(7.5 \pm 1.9) $\times 10^{-3}$	
Γ_{119}	$\bar{K}^*(892)^0\eta'(958)$	< 1.1 $\times 10^{-3}$	CL=90%

Hadronic modes with three K's

Γ_{120}	$K_S^0 K^+ K^-$	(4.72 \pm 0.32) $\times 10^{-3}$	
Γ_{121}	$K_S^0 a_0(980)^0, a_0^0 \rightarrow K^+ K^-$	(3.1 \pm 0.4) $\times 10^{-3}$	
Γ_{122}	$K^-\pi^0(980)^+, a_0^+ \rightarrow K^+ K_S^0$	(6.3 \pm 1.9) $\times 10^{-4}$	
Γ_{123}	$K^+\pi^0(980)^-, a_0^- \rightarrow K^- K_S^0$	< 1.2 $\times 10^{-4}$	CL=95%
Γ_{124}	$K_S^0 f_0(980), f_0 \rightarrow K^+ K^-$	< 1.0 $\times 10^{-4}$	CL=95%
Γ_{125}	$K_S^0 \phi, \phi \rightarrow K^+ K^-$	(2.17 \pm 0.15) $\times 10^{-3}$	
Γ_{126}	$K_S^0 f_0(1400), f_0 \rightarrow K^+ K^-$	(1.8 \pm 1.1) $\times 10^{-4}$	
Γ_{127}	$3K_S^0$	(9.6 \pm 1.4) $\times 10^{-4}$	
Γ_{128}	$K^+ K^- K^-\pi^+$	(2.22 \pm 0.32) $\times 10^{-4}$	
Γ_{129}	$K^+ K^- \bar{K}^*(892)^0,$ $\bar{K}^*(892)^0 \rightarrow K^-\pi^+$	(4.4 \pm 1.7) $\times 10^{-5}$	
Γ_{130}	$K^-\pi^+\phi, \phi \rightarrow K^+ K^-$	(4.0 \pm 1.7) $\times 10^{-5}$	
Γ_{131}	$\phi \bar{K}^*(892)^0,$ $\phi \rightarrow K^+ K^-,$ $\bar{K}^*(892)^0 \rightarrow K^-\pi^+$	(1.06 \pm 0.20) $\times 10^{-4}$	
Γ_{132}	$K^+ K^- K^-\pi^+$ nonresonant	(3.3 \pm 1.5) $\times 10^{-5}$	
Γ_{133}	$K_S^0 K_S^0 K^\pm \pi^\mp$	(6.3 \pm 1.3) $\times 10^{-4}$	

Pionic modes

Γ_{134}	$\pi^+\pi^-$	(1.397 \pm 0.027) $\times 10^{-3}$	
Γ_{135}	$\pi^0\pi^0$	(8.0 \pm 0.8) $\times 10^{-4}$	
Γ_{136}	$\pi^+\pi^-\pi^0$	(1.44 \pm 0.06) %	S=1.8
Γ_{137}	$\rho^+\pi^-$	(9.8 \pm 0.4) $\times 10^{-3}$	
Γ_{138}	$\rho^0\pi^0$	(3.73 \pm 0.22) $\times 10^{-3}$	
Γ_{139}	$\rho^-\pi^+$	(4.97 \pm 0.23) $\times 10^{-3}$	
Γ_{140}	$\rho(1450)^+\pi^-, \rho(1450)^+ \rightarrow$ $\rho(1450)^0\pi^0, \rho(1450)^0 \rightarrow$	(1.6 \pm 2.0) $\times 10^{-5}$	
Γ_{141}	$\rho(1450)^0\pi^0, \rho(1450)^0 \rightarrow$ $\rho(1450)^+\pi^-, \rho(1450)^- \rightarrow$	(4.3 \pm 1.9) $\times 10^{-5}$	
Γ_{142}	$\rho(1700)^+\pi^-, \rho(1700)^+ \rightarrow$ $\rho(1700)^0\pi^0, \rho(1700)^0 \rightarrow$	(2.6 \pm 0.4) $\times 10^{-4}$	
Γ_{143}	$\rho(1700)^+\pi^-, \rho(1700)^+ \rightarrow$ $\rho(1700)^0\pi^0, \rho(1700)^0 \rightarrow$	(5.9 \pm 1.4) $\times 10^{-4}$	
Γ_{144}	$\rho(1700)^0\pi^0, \rho(1700)^0 \rightarrow$ $\rho(1700)^-\pi^+, \rho(1700)^- \rightarrow$	(7.2 \pm 1.7) $\times 10^{-4}$	
Γ_{145}	$\rho(1700)^-\pi^+, \rho(1700)^- \rightarrow$ $f_0(980)\pi^0, f_0(980) \rightarrow \pi^+\pi^-$	(4.6 \pm 1.1) $\times 10^{-4}$	
Γ_{146}	$f_0(980)\pi^0, f_0(980) \rightarrow \pi^+\pi^-$	(3.6 \pm 0.8) $\times 10^{-5}$	
Γ_{147}	$f_0(600)\pi^0, f_0(600) \rightarrow \pi^+\pi^-$	(1.18 \pm 0.21) $\times 10^{-4}$	
Γ_{148}	$(\pi^+\pi^-)_{S\text{-wave}}\pi^0$		
Γ_{149}	$f_0(1370)\pi^0, f_0(1370) \rightarrow$	(5.3 \pm 2.1) $\times 10^{-5}$	
Γ_{150}	$f_0(1500)\pi^0, f_0(1500) \rightarrow$	(5.6 \pm 1.5) $\times 10^{-5}$	
Γ_{151}	$f_0(1710)\pi^0, f_0(1710) \rightarrow$	(4.5 \pm 1.5) $\times 10^{-5}$	
Γ_{152}	$f_2(1270)\pi^0, f_2(1270) \rightarrow$	(1.90 \pm 0.20) $\times 10^{-4}$	
Γ_{153}	$\pi^+\pi^-\pi^0$ nonresonant	(1.21 \pm 0.35) $\times 10^{-4}$	
Γ_{154}	$3\pi^0$	< 3.5 $\times 10^{-4}$	CL=90%
Γ_{155}	$2\pi^+2\pi^-$	(7.44 \pm 0.21) $\times 10^{-3}$	S=1.1
Γ_{156}	$a_1(1260)^+\pi^-, a_1^+ \rightarrow$ $\pi^+\pi^-\pi^+$ total	(4.47 \pm 0.31) $\times 10^{-3}$	
Γ_{157}	$a_1(1260)^+\pi^-, a_1^+ \rightarrow$ $\rho^0\pi^+$ S-wave	(3.22 \pm 0.25) $\times 10^{-3}$	
Γ_{158}	$a_1(1260)^+\pi^-, a_1^+ \rightarrow$ $\rho^0\pi^+$ D-wave	(1.9 \pm 0.5) $\times 10^{-4}$	
Γ_{159}	$a_1(1260)^+\pi^-, a_1^+ \rightarrow \sigma\pi^+$	(6.2 \pm 0.7) $\times 10^{-4}$	
Γ_{160}	$2\rho^0$ total	(1.82 \pm 0.13) $\times 10^{-3}$	
Γ_{161}	$2\rho^0$, parallel helicities	(8.2 \pm 3.2) $\times 10^{-5}$	

Γ_{162}	$2\rho^0$, perpendicular helicities	(4.8 \pm 0.6) $\times 10^{-4}$	
Γ_{163}	$2\rho^0$, longitudinal helicities	(1.25 \pm 0.10) $\times 10^{-3}$	
Γ_{164}	Resonant $(\pi^+\pi^-)\pi^+\pi^-$ 3-body total	(1.49 \pm 0.12) $\times 10^{-3}$	
Γ_{165}	$\sigma\pi^+\pi^-$	(6.1 \pm 0.9) $\times 10^{-4}$	
Γ_{166}	$f_0(980)\pi^+\pi^-, f_0 \rightarrow$ $\pi^+\pi^-$	(1.8 \pm 0.5) $\times 10^{-4}$	
Γ_{167}	$f_2(1270)\pi^+\pi^-, f_2 \rightarrow$ $\pi^+\pi^-$	(3.6 \pm 0.6) $\times 10^{-4}$	
Γ_{168}	$\pi^+\pi^-2\pi^0$	(1.00 \pm 0.09) %	
Γ_{169}	$\eta\pi^0$	[g] (5.7 \pm 1.4) $\times 10^{-4}$	
Γ_{170}	$\omega\pi^0$	[g] < 2.6 $\times 10^{-4}$	CL=90%
Γ_{171}	$2\pi^+2\pi^-\pi^0$	(4.2 \pm 0.5) $\times 10^{-3}$	
Γ_{172}	$\eta\pi^+\pi^-$	[g] < 1.9 $\times 10^{-3}$	CL=90%
Γ_{173}	$\omega\pi^+\pi^-$	[g] (1.6 \pm 0.5) $\times 10^{-3}$	
Γ_{174}	$3\pi^+3\pi^-$	(4.2 \pm 1.2) $\times 10^{-4}$	

Hadronic modes with a $K\bar{K}$ pair

Γ_{175}	K^+K^-	(3.93 \pm 0.08) $\times 10^{-3}$	
Γ_{176}	$2K_S^0$	(3.8 \pm 0.7) $\times 10^{-4}$	
Γ_{177}	$K_S^0 K^-\pi^+$	(3.5 \pm 0.5) $\times 10^{-3}$	S=1.1
Γ_{178}	$\bar{K}^*(892)^0 K_S^0, \bar{K}^*(892)^0 \rightarrow$ $K^-\pi^+$	< 6 $\times 10^{-4}$	CL=90%
Γ_{179}	$K_S^0 K^+\pi^-$	(2.7 \pm 0.5) $\times 10^{-3}$	
Γ_{180}	$K^*(892)^0 K_S^0, K^*(892)^0 \rightarrow$ $K^+\pi^-$	< 3.0 $\times 10^{-4}$	CL=90%
Γ_{181}	$K^+K^-\pi^0$	(3.29 \pm 0.14) $\times 10^{-3}$	
Γ_{182}	$K^*(892)^+K^-, K^*(892)^+ \rightarrow$ $K^+\pi^0$	(1.47 \pm 0.07) $\times 10^{-3}$	
Γ_{183}	$K^*(892)^-K^+, K^*(892)^- \rightarrow$ $K^-\pi^0$	(5.1 \pm 0.5) $\times 10^{-4}$	
Γ_{184}	$(K^+\pi^0)_{S\text{-wave}}K^-$	(2.34 \pm 0.17) $\times 10^{-3}$	
Γ_{185}	$(K^-\pi^0)_{S\text{-wave}}K^+$	(1.3 \pm 0.4) $\times 10^{-4}$	
Γ_{186}	$f_0(980)\pi^0, f_0 \rightarrow K^+K^-$	(3.5 \pm 0.6) $\times 10^{-4}$	
Γ_{187}	$\phi\pi^0, \phi \rightarrow K^+K^-$	(6.1 \pm 0.6) $\times 10^{-4}$	
Γ_{188}	$K^+K^-\pi^0$ nonresonant		
Γ_{189}	$K_S^0 K_S^0 \pi^0$	< 5.9 $\times 10^{-4}$	
Γ_{190}	$K^+K^-\pi^+\pi^-$	[h] (2.43 \pm 0.12) $\times 10^{-3}$	
Γ_{191}	$\phi\pi^+\pi^-$ 3-body, $\phi \rightarrow K^+K^-$	(2.4 \pm 2.4) $\times 10^{-5}$	
Γ_{192}	$\phi\rho^0, \phi \rightarrow K^+K^-$	(7.1 \pm 0.6) $\times 10^{-4}$	
Γ_{193}	$K^+K^-\rho^0$ 3-body	(5 \pm 7) $\times 10^{-5}$	
Γ_{194}	$f_0(980)\pi^+\pi^-, f_0 \rightarrow K^+K^-$	(3.6 \pm 0.9) $\times 10^{-4}$	
Γ_{195}	$K^*(892)^0 K^\mp\pi^\pm$ 3-body, [j] $K^{*0} \rightarrow K^\pm\pi^\mp$	(2.7 \pm 0.6) $\times 10^{-4}$	
Γ_{196}	$K^*(892)^0 \bar{K}^*(892)^0, K^{*0} \rightarrow$ $K^\pm\pi^\mp$	(7 \pm 5) $\times 10^{-5}$	
Γ_{197}	$K_1(1270)^\pm K^\mp,$ $K_1(1270)^\pm \rightarrow K^\pm\pi^+\pi^-$	(8.0 \pm 1.8) $\times 10^{-4}$	
Γ_{198}	$K_1(1400)^\pm K^\mp,$ $K_1(1400)^\pm \rightarrow K^\pm\pi^+\pi^-$	(5.4 \pm 1.2) $\times 10^{-4}$	
Γ_{199}	$K^+K^-\pi^+\pi^-$ non- ϕ		
Γ_{200}	$K^+K^-\pi^+\pi^-$ nonresonant		
Γ_{201}	$K_S^0 K_S^0 \pi^+\pi^-$	(1.30 \pm 0.24) $\times 10^{-3}$	
Γ_{202}	$K_S^0 K^-\pi^+\pi^-$	< 1.5 $\times 10^{-4}$	CL=90%
Γ_{203}	$K^+K^-\pi^+\pi^-\pi^0$	(3.1 \pm 2.0) $\times 10^{-3}$	

Fractions of most of the following modes with resonances have already appeared above as submodes of particular charged-particle modes.

Γ_{204}	$\phi\pi^0$	(7.6 \pm 0.5) $\times 10^{-4}$	
Γ_{205}	$\phi\eta$	(1.4 \pm 0.5) $\times 10^{-4}$	
Γ_{206}	$\phi\omega$	< 2.1 $\times 10^{-3}$	CL=90%
Radiative modes			
Γ_{207}	$\rho^0\gamma$	< 2.4 $\times 10^{-4}$	CL=90%
Γ_{208}	$\omega\gamma$	< 2.4 $\times 10^{-4}$	CL=90%
Γ_{209}	$\phi\gamma$	(2.5 \pm 0.7) $\times 10^{-5}$	
Γ_{210}	$\bar{K}^*(892)^0\gamma$	< 7.6 $\times 10^{-4}$	CL=90%

Doubly Cabibbo suppressed (DC) modes or $\Delta C = 2$ forbidden via mixing (CM) modes

Γ_{211}	$K^+\ell^-\bar{\nu}_\ell$ via \bar{D}^0	< 1.8 $\times 10^{-4}$	CL=90%
Γ_{212}	K^+ or $K^*(892)^+ e^-\bar{\nu}_e$ via \bar{D}^0	< 6 $\times 10^{-5}$	CL=90%
Γ_{213}	$K^+\pi^-$	DC (1.48 \pm 0.07) $\times 10^{-4}$	
Γ_{214}	$K^+\pi^-$ via DCS	(1.31 \pm 0.08) $\times 10^{-4}$	
Γ_{215}	$K^+\pi^-$ via \bar{D}^0	< 1.6 $\times 10^{-5}$	CL=95%
Γ_{216}	$K_S^0\pi^+\pi^-$ in $D^0 \rightarrow \bar{D}^0$	< 1.9 $\times 10^{-4}$	CL=95%

Meson Particle Listings

D^0

CONSTRAINED FIT INFORMATION

An overall fit to 3 branching ratios uses 3 measurements and one constraint to determine 4 parameters. The overall fit has a $\chi^2 = 0.0$ for 0 degrees of freedom.

The following *off-diagonal* array elements are the correlation coefficients $\langle \delta x_i \delta x_j \rangle / (\delta x_i \delta x_j)$, in percent, from the fit to the branching fractions, $x_i \equiv \Gamma_i / \Gamma_{\text{total}}$. The fit constrains the x_i whose labels appear in this array to sum to one.

x_2	-100		
x_3	-46	39	
x_4	-2	0	0
	x_1	x_2	x_3

D^0 BRANCHING RATIOS

Some older now obsolete results have been omitted from these Listings.

Topological modes

$\Gamma(0\text{-prongs})/\Gamma_{\text{total}}$ Γ_1/Γ

This value is obtained by subtracting the branching fractions for 2-, 4-, and 6-prongs from unity.

VALUE	DOCUMENT ID
0.15 ± 0.06 OUR FIT	

$\Gamma(4\text{-prongs})/\Gamma_{\text{total}}$ Γ_3/Γ

This is the sum of our $K^- \pi^+ \pi^+ \pi^-$, $K^- \pi^+ \pi^+ \pi^- \pi^0$, $\bar{K}^0 2\pi^+ 2\pi^-$, $2\pi^+ 2\pi^-$, $2\pi^+ 2\pi^- \pi^0$, $K^+ K^- \pi^+ \pi^-$, and $K^+ K^- \pi^+ \pi^- \pi^0$ branching fractions.

VALUE	DOCUMENT ID
0.146 ± 0.005 OUR FIT	
0.146 ± 0.005	PDG 08

$\Gamma(4\text{-prongs})/\Gamma(2\text{-prongs})$ Γ_3/Γ_2

VALUE	EVTs	DOCUMENT ID	TECN	COMMENT
0.207 ± 0.016 OUR FIT				
0.207 ± 0.016 ± 0.004	226	ONENGUT 05	CHRS	ν_μ emulsion, $\bar{E}_\nu \approx 27$ GeV

$\Gamma(6\text{-prongs})/\Gamma_{\text{total}}$ Γ_4/Γ

VALUE (units 10^{-3})	EVTs	DOCUMENT ID	TECN	COMMENT
1.2 ± 1.3 OUR FIT				
1.2 ± 1.3 ± 0.2	3	ONENGUT 05	CHRS	ν_μ emulsion, $\bar{E}_\nu \approx 27$ GeV

Inclusive modes

$\Gamma(e^+ \text{ anything})/\Gamma_{\text{total}}$ Γ_5/Γ

The branching fractions for the $K^- e^+ \nu_e$, $K^*(892)^- e^+ \nu_e$, $\pi^- e^+ \nu_e$, and $\rho^- e^+ \nu_e$ modes add up to 6.24 ± 0.18 %.

VALUE	EVTs	DOCUMENT ID	TECN	COMMENT
0.0653 ± 0.0017 OUR AVERAGE				
0.063 ± 0.007 ± 0.004	290 ± 32	ABLIKIM 07G	BES2	$e^+ e^- \approx \psi(3770)$
0.0646 ± 0.0017 ± 0.0013	2246 ± 57	ADAM 06A	CLEO	$e^+ e^-$ at $\psi(3770)$
0.069 ± 0.003 ± 0.005	1670	ALBRECHT 96C	ARG	$e^+ e^- \approx 10$ GeV
0.0664 ± 0.0018 ± 0.0029	4609	KUBOTA 96B	CLE2	$e^+ e^- \approx \Upsilon(4S)$

²² Using the D^+ and D^0 lifetimes, ADAM 06A finds that the ratio of the D^+ and D^0 inclusive e^+ widths is $0.985 \pm 0.028 \pm 0.015$, consistent with the isospin-invariance prediction of 1.

$\Gamma(\mu^+ \text{ anything})/\Gamma_{\text{total}}$ Γ_6/Γ

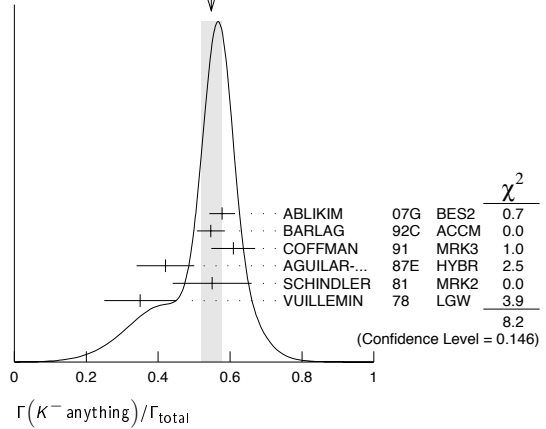
VALUE	EVTs	DOCUMENT ID	TECN	COMMENT
0.067 ± 0.006 OUR FIT				
0.063 ± 0.009 OUR AVERAGE				
0.065 ± 0.012 ± 0.003	36	KAYIS-TOPAK.05	CHRS	ν_μ emulsion
0.060 ± 0.007 ± 0.012	310	ALBRECHT 96C	ARG	$e^+ e^- \approx 10$ GeV

$\Gamma(K^- \text{ anything})/\Gamma_{\text{total}}$ Γ_7/Γ

VALUE	EVTs	DOCUMENT ID	TECN	COMMENT
0.547 ± 0.028 OUR AVERAGE	Error	includes scale factor of 1.3. See the ideogram below.		
0.578 ± 0.016 ± 0.032	2098 ± 59	ABLIKIM 07G	BES2	$e^+ e^- \approx \psi(3770)$
0.546 ± 0.039 - 0.038		²³ BARLAG 92c	ACCM	π^- Cu 230 GeV
0.609 ± 0.032 ± 0.052		COFFMAN 91	MRK3	$e^+ e^-$ 3.77 GeV
0.42 ± 0.08		AGUILAR-... 87E	HYBR	$\pi p, p p$ 360, 400 GeV
0.55 ± 0.11	121	SCHINDLER 81	MRK2	$e^+ e^-$ 3.771 GeV
0.35 ± 0.10	19	VUILLEMIN 78	LGW	$e^+ e^-$ 3.772 GeV

²³ BARLAG 92c computes the branching fraction using topological normalization.

WEIGHTED AVERAGE
0.547 ± 0.028 (Error scaled by 1.3)



$[\Gamma(\bar{K}^0 \text{ anything}) + \Gamma(K^0 \text{ anything})]/\Gamma_{\text{total}}$ Γ_8/Γ

VALUE	EVTs	DOCUMENT ID	TECN	COMMENT
0.47 ± 0.04 OUR AVERAGE	250 ± 25			
0.476 ± 0.048 ± 0.030		ABLIKIM 06u	BES2	$e^+ e^-$ at 3773 MeV
0.455 ± 0.050 ± 0.032		COFFMAN 91	MRK3	$e^+ e^-$ 3.77 GeV

$\Gamma(K^+ \text{ anything})/\Gamma_{\text{total}}$ Γ_9/Γ

VALUE	EVTs	DOCUMENT ID	TECN	COMMENT
0.034 ± 0.004 OUR AVERAGE	119 ± 23			
0.035 ± 0.007 ± 0.003		ABLIKIM 07G	BES2	$e^+ e^- \approx \psi(3770)$
0.034 ± 0.007 - 0.005		²⁴ BARLAG 92c	ACCM	π^- Cu 230 GeV
0.028 ± 0.009 ± 0.004		COFFMAN 91	MRK3	$e^+ e^-$ 3.77 GeV
0.03 ± 0.05 - 0.02		AGUILAR-... 87E	HYBR	$\pi p, p p$ 360, 400 GeV
0.08 ± 0.03	25	SCHINDLER 81	MRK2	$e^+ e^-$ 3.771 GeV

²⁴ BARLAG 92c computes the branching fraction using topological normalization.

$\Gamma(K^*(892)^- \text{ anything})/\Gamma_{\text{total}}$ Γ_{10}/Γ

VALUE	EVTs	DOCUMENT ID	TECN	COMMENT
0.153 ± 0.083 ± 0.019	28 ± 15	ABLIKIM 06u	BES2	$e^+ e^-$ at 3773 MeV

$\Gamma(\bar{K}^*(892)^0 \text{ anything})/\Gamma_{\text{total}}$ Γ_{11}/Γ

VALUE	EVTs	DOCUMENT ID	TECN	COMMENT
0.087 ± 0.040 ± 0.012	96 ± 44	ABLIKIM 05P	BES	$e^+ e^- \approx 3773$ MeV

$\Gamma(K^*(892)^+ \text{ anything})/\Gamma_{\text{total}}$ Γ_{12}/Γ

VALUE	CL%	DOCUMENT ID	TECN	COMMENT
< 0.036	90	ABLIKIM 06u	BES2	$e^+ e^-$ at 3773 MeV

$\Gamma(K^*(892)^0 \text{ anything})/\Gamma_{\text{total}}$ Γ_{13}/Γ

VALUE	EVTs	DOCUMENT ID	TECN	COMMENT
0.028 ± 0.012 ± 0.004	31 ± 12	ABLIKIM 05P	BES	$e^+ e^- \approx 3773$ MeV

$\Gamma(\eta \text{ anything})/\Gamma_{\text{total}}$ Γ_{14}/Γ

VALUE (units 10^{-2})	EVTs	DOCUMENT ID	TECN	COMMENT
9.5 ± 0.4 ± 0.8	4463 ± 197	HUANG 06B	CLEO	$e^+ e^-$ at $\psi(3770)$

$\Gamma(\eta' \text{ anything})/\Gamma_{\text{total}}$ Γ_{15}/Γ

VALUE (units 10^{-2})	EVTs	DOCUMENT ID	TECN	COMMENT
2.48 ± 0.17 ± 0.21	299 ± 21	HUANG 06B	CLEO	$e^+ e^-$ at $\psi(3770)$

$\Gamma(\phi \text{ anything})/\Gamma_{\text{total}}$ Γ_{16}/Γ

VALUE (units 10^{-2})	EVTs	DOCUMENT ID	TECN	COMMENT
1.05 ± 0.08 ± 0.07	368 ± 24	HUANG 06B	CLEO	$e^+ e^-$ at $\psi(3770)$
1.71 ± 0.76 - 0.71	9	BAI 00c	BES	$e^+ e^- \rightarrow D \bar{D}^*, D^* \bar{D}^*$

Semileptonic modes

$\Gamma(K^- e^+ \nu_e)/\Gamma_{\text{total}}$ Γ_{18}/Γ

VALUE (units 10^{-2})	EVTs	DOCUMENT ID	TECN	COMMENT
3.58 ± 0.06 OUR FIT	Error	includes scale factor of 1.1.		
3.46 ± 0.11 OUR AVERAGE				
3.45 ± 0.10 ± 0.19	1318 ± 38	WIDHALM 06	BELL	$e^+ e^- \approx \Upsilon(4S)$
3.44 ± 0.10 ± 0.10	1311 ± 37	COAN 05	CLEO	$e^+ e^-$ at $\psi(3770)$
3.82 ± 0.40 ± 0.27	104 ± 11	ABLIKIM 04c	BES	$e^+ e^-$, 3.773 GeV
3.4 ± 0.5 ± 0.4	55	ADLER 89	MRK3	$e^+ e^-$ 3.77 GeV

$\Gamma(K^- e^+ \nu_e)/\Gamma(K^- \pi^+)$ Γ_{18}/Γ_{32}

VALUE	EVTS	DOCUMENT ID	TECN	COMMENT
0.921 ± 0.012 OUR FIT				
0.930 ± 0.013 OUR AVERAGE				
0.927 ± 0.007 ± 0.012	76k ± 323	25 AUBERT	07B6 BABR	$e^+ e^- \approx \gamma(4S)$
0.978 ± 0.027 ± 0.044	2510	26 BEAN	93C CLE2	$e^+ e^- \approx \gamma(4S)$
0.90 ± 0.06 ± 0.06	584	27 CRAWFORD	91B CLEO	$e^+ e^- \approx 10.5$ GeV
0.91 ± 0.07 ± 0.11	250	28 ANJOS	89F E691	Photoproduction

²⁵ The event samples in this AUBERT 07B6 result include radiative photons. The $D^0 \rightarrow K^- e^+ \nu_e$ form factor at $q^2 = 0$ is $f_+(0) = 0.727 \pm 0.007 \pm 0.005 \pm 0.007$.

²⁶ BEAN 93c uses $K^- \mu^+ \nu_\mu$ as well as $K^- e^+ \nu_e$ events and makes a small phase-space adjustment to the number of the μ^+ events to use them as e^+ events. A pole mass of $2.00 \pm 0.12 \pm 0.18$ GeV/ c^2 is obtained from the q^2 dependence of the decay rate.

²⁷ CRAWFORD 91B uses $K^- e^+ \nu_e$ and $K^- \mu^+ \nu_\mu$ candidates to measure a pole mass of $2.1_{-0.2}^{+0.4+0.3}$ GeV/ c^2 from the q^2 dependence of the decay rate.

²⁸ ANJOS 89F measures a pole mass of $2.1_{-0.2}^{+0.4} \pm 0.2$ GeV/ c^2 from the q^2 dependence of the decay rate.

 $\Gamma(K^- \mu^+ \nu_\mu)/\Gamma_{total}$ Γ_{19}/Γ

VALUE (units 10^{-2})	EVTS	DOCUMENT ID	TECN	COMMENT
3.31 ± 0.13 OUR FIT				
3.45 ± 0.10 ± 0.21	1249 ± 43	WIDHALM	06 BELL	$e^+ e^- \approx \gamma(4S)$

 $\Gamma(K^- \mu^+ \nu_\mu)/\Gamma(K^- \pi^+)$ Γ_{19}/Γ_{32}

VALUE	EVTS	DOCUMENT ID	TECN	COMMENT
0.851 ± 0.033 OUR FIT				
0.84 ± 0.04 OUR AVERAGE				
0.852 ± 0.034 ± 0.028	1897	²⁹ FRABETTI	95G E687	γ Be $\bar{E}_\gamma = 220$ GeV
0.82 ± 0.13 ± 0.13	338	³⁰ FRABETTI	93I E687	γ Be $\bar{E}_\gamma = 221$ GeV
0.79 ± 0.08 ± 0.09	231	³¹ CRAWFORD	91B CLEO	$e^+ e^- \approx 10.5$ GeV

²⁹ FRABETTI 95G extracts the ratio of form factors $f_-(0)/f_+(0) = -1.3_{-3.4}^{+3.6} \pm 0.6$, and measures a pole mass of $1.87_{-0.08}^{+0.11+0.07}$ GeV/ c^2 from the q^2 dependence of the decay rate.

³⁰ FRABETTI 93I measures a pole mass of $2.1_{-0.3}^{+0.7+0.7}$ GeV/ c^2 from the q^2 dependence of the decay rate.

³¹ CRAWFORD 91B measures a pole mass of $2.00 \pm 0.12 \pm 0.18$ GeV/ c^2 from the q^2 dependence of the decay rate.

 $\Gamma(K^- \mu^+ \nu_\mu)/\Gamma(\mu^+ \text{anything})$ Γ_{19}/Γ_6

VALUE	EVTS	DOCUMENT ID	TECN	COMMENT
0.50 ± 0.05 OUR FIT				
0.472 ± 0.051 ± 0.040	232	KODAMA	94 E653	π^- emulsion 600 GeV
• • • We do not use the following data for averages, fits, limits, etc. • • •				
0.32 ± 0.05 ± 0.05	124	KODAMA	91 EMUL	pA 800 GeV

 $\Gamma(K^- \pi^0 e^+ \nu_e)/\Gamma_{total}$ Γ_{22}/Γ

VALUE	EVTS	DOCUMENT ID	TECN	COMMENT
0.016 ± 0.013 ± 0.002	4	³² BAI	91 MRK3	$e^+ e^- \approx 3.77$ GeV

³² BAI 91 finds that a fraction $0.79_{-0.03}^{+0.15+0.09}$ of combined D^+ and D^0 decays to $\bar{K} \pi e^+ \nu_e$ (24 events) are $\bar{K}^*(892) e^+ \nu_e$. BAI 91 uses 56 $K^- e^+ \nu_e$ events to measure a pole mass of $1.8 \pm 0.3 \pm 0.2$ GeV/ c^2 from the q^2 dependence of the decay rate.

 $\Gamma(\bar{K}^0 \pi^- e^+ \nu_e)/\Gamma_{total}$ Γ_{23}/Γ

VALUE (units 10^{-2})	EVTS	DOCUMENT ID	TECN	COMMENT
2.7_{-0.7}^{+0.9} OUR AVERAGE				
2.61 ± 1.04 ± 0.28	9 ± 3	ABLIKIM	06o BES2	$e^+ e^-$ at 3773 MeV
2.8_{-0.8}^{+1.7} ± 0.3	6	³³ BAI	91 MRK3	$e^+ e^- \approx 3.77$ GeV

³³ BAI 91 finds that a fraction $0.79_{-0.03}^{+0.15+0.09}$ of combined D^+ and D^0 decays to $\bar{K} \pi e^+ \nu_e$ (24 events) are $\bar{K}^*(892) e^+ \nu_e$.

 $\Gamma(K^*(892)^- e^+ \nu_e)/\Gamma_{total}$ Γ_{20}/Γ

Both decay modes of the $K^*(892)^-$ are included.

VALUE (units 10^{-2})	EVTS	DOCUMENT ID	TECN	COMMENT
2.18 ± 0.16 OUR FIT				
2.16 ± 0.15 ± 0.08	219 ± 16	³⁴ COAN	05 CLEO	$e^+ e^-$ at $\psi(3770)$

³⁴ COAN 05 uses both $K^- \pi^0$ and $K_S^0 \pi^-$ events.

 $\Gamma(K^*(892)^- e^+ \nu_e)/\Gamma(K_S^0 \pi^+ \pi^-)$ Γ_{20}/Γ_{35}

Unseen decay modes of the $K^*(892)^-$ are included.

VALUE	EVTS	DOCUMENT ID	TECN	COMMENT
0.73 ± 0.06 OUR FIT				
0.76 ± 0.12 ± 0.06	152	³⁵ BEAN	93C CLE2	$e^+ e^- \approx \gamma(4S)$

³⁵ BEAN 93c uses $K^{*-} \mu^+ \nu_\mu$ as well as $K^{*-} e^+ \nu_e$ events and makes a small phase-space adjustment to the number of the μ^+ events to use them as e^+ events.

 $\Gamma(K^*(892)^- e^+ \nu_e)/\Gamma(K^- e^+ \nu_e)$ Γ_{20}/Γ_{18}

Unseen decay modes of the $K^*(892)^-$ are included.

VALUE	EVTS	DOCUMENT ID	TECN	COMMENT
• • • We do not use the following data for averages, fits, limits, etc. • • •				
0.51 ± 0.18 ± 0.06		CRAWFORD	91B CLEO	$e^+ e^- \approx 10.5$ GeV

 $\Gamma(K^*(892)^- \mu^+ \nu_\mu)/\Gamma(K_S^0 \pi^+ \pi^-)$ Γ_{21}/Γ_{35}

Unseen decay modes of the $K^*(892)^-$ are included.

VALUE	EVTS	DOCUMENT ID	TECN	COMMENT
0.674 ± 0.068 ± 0.026	175 ± 17	³⁶ LINK	05B FOCS	$\gamma A, \bar{E}_\gamma \approx 180$ GeV
³⁶ LINK 05B finds that in $D^0 \rightarrow \bar{K}^0 \pi^- \mu^+ \nu_\mu$ the $\bar{K}^0 \pi^-$ system is 6% in S-wave.				

 $\Gamma(K^*(892)^- e^+ \nu_e)/\Gamma(K_S^0 \pi^+ \pi^-)$ Γ_{24}/Γ_{35}

This is an average of the $K^*(892)^- e^+ \nu_e$ and $K^*(892)^- \mu^+ \nu_\mu$ ratios. Unseen decay modes of the $K^*(892)^-$ are included.

VALUE	EVTS	DOCUMENT ID	TECN	COMMENT
• • • We do not use the following data for averages, fits, limits, etc. • • •				
0.48 ± 0.14 ± 0.12	137	³⁷ ALEXANDER	90B CLEO	$e^+ e^-$ 10.5–11 GeV
³⁷ ALEXANDER 90B cannot exclude extra π^0 's in the final state.				

 $\Gamma(K^- \pi^+ \pi^- e^+ \nu_e)/\Gamma_{total}$ Γ_{25}/Γ

VALUE (units 10^{-4})	EVTS	DOCUMENT ID	TECN	COMMENT
2.8 ± 1.4 ± 0.3	8	ARTUSO	07A CLEO	$e^+ e^-$ at $\gamma(3770)$

 $\Gamma(K_1(1270)^- e^+ \nu_e)/\Gamma_{total}$ Γ_{26}/Γ

VALUE (units 10^{-4})	EVTS	DOCUMENT ID	TECN	COMMENT
7.6 ± 4.1 ± 0.9	8	³⁸ ARTUSO	07A CLEO	$e^+ e^-$ at $\gamma(3770)$

³⁸ This ARTUSO 07A result is corrected for all decay modes of the $K_1(1270)^-$.

 $\Gamma(K^- \pi^+ \pi^- \mu^+ \nu_\mu)/\Gamma(K^- \mu^+ \nu_\mu)$ Γ_{27}/Γ_{19}

VALUE	CL%	DOCUMENT ID	TECN	COMMENT
< 0.037	90	KODAMA	93B E653	π^- emulsion 600 GeV

 $\Gamma((\bar{K}^*(892) \pi^-) \mu^+ \nu_\mu)/\Gamma(K^- \mu^+ \nu_\mu)$ Γ_{28}/Γ_{19}

VALUE	CL%	DOCUMENT ID	TECN	COMMENT
< 0.043	90	³⁹ KODAMA	93B E653	π^- emulsion 600 GeV

³⁹ KODAMA 93B searched in $K^- \pi^+ \pi^- \mu^+ \nu_\mu$, but the limit includes other $(\bar{K}^*(892) \pi^-)$ charge states.

 $\Gamma(\pi^- e^+ \nu_e)/\Gamma_{total}$ Γ_{29}/Γ

VALUE (units 10^{-2})	EVTS	DOCUMENT ID	TECN	COMMENT
0.283 ± 0.017 OUR FIT				
0.269 ± 0.020 OUR AVERAGE				
0.279 ± 0.027 ± 0.016	126 ± 12	⁴⁰ WIDHALM	06 BELL	$e^+ e^- \approx \gamma(4S)$
0.262 ± 0.025 ± 0.008	117 ± 11	COAN	05 CLEO	$e^+ e^-$ at $\psi(3770)$

⁴⁰ This result of WIDHALM 06 gives $|\frac{V_{cd}}{V_{cs}} \cdot \frac{f_+^\pi(0)}{f_+^{K^*}(0)}|^2 = 0.042 \pm 0.003 \pm 0.003$.

 $\Gamma(\pi^- e^+ \nu_e)/\Gamma(K^- e^+ \nu_e)$ Γ_{29}/Γ_{18}

VALUE	EVTS	DOCUMENT ID	TECN	COMMENT
0.079 ± 0.005 OUR FIT				
0.085 ± 0.007 OUR AVERAGE				
0.082 ± 0.006 ± 0.005		⁴¹ HUANG	05 CLEO	$e^+ e^- \approx \gamma(4S)$
0.101 ± 0.020 ± 0.003	91	⁴² FRABETTI	96B E687	γ Be, $\bar{E}_\gamma \approx 200$ GeV
0.103 ± 0.039 ± 0.013	87	⁴³ BUTLER	95 CLE2	< 0.156 (90% CL)

⁴¹ HUANG 05 uses both e and μ events, and makes a small correction to the μ events to make them effectively e events. This result gives $|\frac{V_{cd}}{V_{cs}} \cdot \frac{f_+^\pi(0)}{f_+^{K^*}(0)}|^2 = 0.038_{-0.007}^{+0.006+0.005}$.

⁴² FRABETTI 96B uses both e and μ events, and makes a small correction to the μ events to make them effectively e events. This result gives $|\frac{V_{cd}}{V_{cs}} \cdot \frac{f_+^\pi(0)}{f_+^{K^*}(0)}|^2 = 0.050 \pm 0.011 \pm 0.002$.

⁴³ BUTLER 95 has 87 ± 33 $\pi^- e^+ \nu_e$ events. The result gives $|\frac{V_{cd}}{V_{cs}} \cdot \frac{f_+^\pi(0)}{f_+^{K^*}(0)}|^2 = 0.052 \pm 0.020 \pm 0.007$.

 $\Gamma(\pi^- \mu^+ \nu_\mu)/\Gamma_{total}$ Γ_{30}/Γ

VALUE (units 10^{-2})	EVTS	DOCUMENT ID	TECN	COMMENT
0.237 ± 0.024 OUR FIT				
0.231 ± 0.026 ± 0.019	106 ± 13	WIDHALM	06 BELL	$e^+ e^- \approx \gamma(4S)$

 $\Gamma(\pi^- \mu^+ \nu_\mu)/\Gamma(K^- \mu^+ \nu_\mu)$ Γ_{30}/Γ_{19}

VALUE	EVTS	DOCUMENT ID	TECN	COMMENT
0.072 ± 0.007 OUR FIT				
0.074 ± 0.008 ± 0.007	288 ± 29	⁴⁴ LINK	05 FOCS	$\gamma A, \bar{E}_\gamma \approx 180$ GeV

⁴⁴ LINK 05 finds the form-factor ratio $|f_0^\pi(0)/f_0^{K^*}(0)|$ to be $0.85 \pm 0.04 \pm 0.04 \pm 0.01$.

Meson Particle Listings

 D^0

$\Gamma(\rho^- e^+ \nu_e)/\Gamma_{\text{total}}$		Γ_{31}/Γ		
VALUE (units 10^{-2})	EVTS	DOCUMENT ID	TECN	COMMENT
0.194 ± 0.039 ± 0.013	31 ± 6	COAN	05	CLEO $e^+ e^-$ at $\psi(3770)$

Hadronic modes with a single \bar{K}

$\Gamma(K^- \pi^+)/\Gamma_{\text{total}}$		Γ_{32}/Γ		
VALUE (units 10^{-2})	EVTS	DOCUMENT ID	TECN	COMMENT
3.89 ± 0.05 OUR FIT				Error includes scale factor of 1.1.
3.91 ± 0.05 OUR AVERAGE				Error includes scale factor of 1.1.
4.007 ± 0.037 ± 0.072	33.8 ± 0.3k	AUBERT	08L	BABR $e^+ e^-$ at $\Upsilon(4S)$
3.891 ± 0.035 ± 0.069		49 DOBBS	07	CLEO $e^+ e^-$ at $\psi(3770)$
3.82 ± 0.07 ± 0.12		46 ARTUSO	98	CLE2 CLEO average
3.90 ± 0.09 ± 0.12	5392	47 BARATE	97c	ALEP From Z decays
3.41 ± 0.12 ± 0.28	1173 ± 37	47 ALBRECHT	94F	ARG $e^+ e^- \approx \Upsilon(4S)$
3.62 ± 0.34 ± 0.44		47 DECAMP	91J	ALEP From Z decays
• • • We do not use the following data for averages, fits, limits, etc. • • •				
3.91 ± 0.08 ± 0.09	10.3k ± 100	45 HE	05	CLEO See DOBBS 07
3.81 ± 0.15 ± 0.16	1165	48 ARTUSO	98	CLE2 $e^+ e^-$ at $\Upsilon(4S)$
3.69 ± 0.11 ± 0.16		49 COAN	98	CLE2 See ARTUSO 98
4.5 ± 0.6 ± 0.4		50 ALBRECHT	94	ARG $e^+ e^- \approx \Upsilon(4S)$
3.95 ± 0.08 ± 0.17	4208	47.51 AKERIB	93	CLE2 See ARTUSO 98
4.5 ± 0.8 ± 0.5	56	47 ABACHI	88	HRS $e^+ e^-$ 29 GeV
4.2 ± 0.4 ± 0.4	930		88c	MRK3 $e^+ e^-$ 3.77 GeV
4.1 ± 0.6	263 ± 17	52 SCHINDLER	81	MRK2 $e^+ e^-$ 3.771 GeV
4.3 ± 1.0	130	53 PERUZZI	77	LGW $e^+ e^-$ 3.77 GeV

45 DOBBS 07 and HE 05 use single- and double-tagged events in an overall fit. DOBBS 07 supersedes HE 05.

46 This combines the CLEO results of ARTUSO 98, COAN 98, and AKERIB 93.

47 ABACHI 88, DECAMP 91J, AKERIB 93, ALBRECHT 94F, and BARATE 97c use $D^*(2010)^+ \rightarrow D^0 \pi^+$ decays. The π^+ is both slow and of low p_T with respect to the event thrust axis or nearest jet ($\approx D^{*+}$ direction). The excess number of such π^+ 's over background gives the number of $D^*(2010)^+ \rightarrow D^0 \pi^+$ events, and the branching with $D^0 \rightarrow K^- \pi^+$ gives the $D^0 \rightarrow K^- \pi^+$ branching fraction.

48 ARTUSO 98, following ALBRECHT 94, uses D^0 mesons from $\bar{B}^0 \rightarrow D^*(2010)^+ X \ell^- \bar{\nu}_\ell$ decays. Our average uses the CLEO average of this value with the values of COAN 98 and AKERIB 93.

49 COAN 98 assumes that $\Gamma(B \rightarrow \bar{D} X \ell^+ \nu)/\Gamma(B \rightarrow X \ell^+ \nu) = 1.0 - 3|V_{ub}/V_{cb}|^2 - 0.010 \pm 0.005$, the last term accounting for $\bar{B} \rightarrow D_s^+ K X \ell^- \bar{\nu}$. COAN 98 is included in the CLEO average in ARTUSO 98.

50 ALBRECHT 94 uses D^0 mesons from $\bar{B}^0 \rightarrow D^{*+} \ell^- \bar{\nu}_\ell$ decays. This is a different set of events than used by ALBRECHT 94F.

51 This AKERIB 93 value includes radiative corrections; without them, the value is $0.0391 \pm 0.0008 \pm 0.0017$. AKERIB 93 is included in the CLEO average in ARTUSO 98.

52 SCHINDLER 81 (MARK-2) measures $\sigma(e^+ e^- \rightarrow \psi(3770)) \times$ branching fraction to be 0.24 ± 0.02 nb. We use the MARK-3 (ADLER 88c) value of $\sigma = 5.8 \pm 0.5 \pm 0.6$ nb.

53 PERUZZI 77 (MARK-1) measures $\sigma(e^+ e^- \rightarrow \psi(3770)) \times$ branching fraction to be 0.25 ± 0.05 nb. We use the MARK-3 (ADLER 88c) value of $\sigma = 5.8 \pm 0.5 \pm 0.6$ nb.

$\Gamma(K_S^0 \pi^0)/\Gamma_{\text{total}}$		Γ_{33}/Γ		
VALUE (units 10^{-2})	EVTS	DOCUMENT ID	TECN	COMMENT
1.22 ± 0.06 OUR FIT				Error includes scale factor of 1.2.
1.240 ± 0.017 ± 0.056	614	HE	08	CLEO $e^+ e^-$ at $\psi(3770)$

$\Gamma(K_S^0 \pi^0)/\Gamma(K^- \pi^+)$		Γ_{33}/Γ_{32}		
VALUE	EVTS	DOCUMENT ID	TECN	COMMENT
0.314 ± 0.016 OUR FIT				Error includes scale factor of 1.1.
0.68 ± 0.12 ± 0.11	119	ANJOS	92B	E691 γ Be 80–240 GeV

$\Gamma(K_S^0 \pi^0)/\Gamma(K_S^0 \pi^+ \pi^-)$		Γ_{33}/Γ_{35}		
VALUE	EVTS	DOCUMENT ID	TECN	COMMENT
0.409 ± 0.025 OUR FIT				Error includes scale factor of 1.1.
0.378 ± 0.033 OUR AVERAGE				
0.44 ± 0.02 ± 0.05	1942 ± 64	PROCARIO	93B	CLE2 $e^+ e^-$ 10.36–10.7 GeV
0.34 ± 0.04 ± 0.02	92	54 ALBRECHT	92P	ARG $e^+ e^- \approx 10$ GeV
0.36 ± 0.04 ± 0.08	104	KINOSHITA	91	CLEO $e^+ e^- \sim 10.7$ GeV

54 This value is calculated from numbers in Table 1 of ALBRECHT 92P.

$\Gamma(K_L^0 \pi^0)/\Gamma_{\text{total}}$		Γ_{34}/Γ		
VALUE (units 10^{-2})	EVTS	DOCUMENT ID	TECN	COMMENT
0.998 ± 0.049 ± 0.048	1116	55 HE	08	CLEO $e^+ e^-$ at $\psi(3770)$

55 The difference of HE 08 $D^0 \rightarrow K_S^0 \pi^0$ and $K_L^0 \pi^0$ branching fractions over the sum is $0.108 \pm 0.025 \pm 0.024$. This is consistent with U-spin symmetry and the Cabibbo angle.

$\Gamma(K_S^0 \pi^+ \pi^-)/\Gamma_{\text{total}}$		Γ_{35}/Γ		
VALUE (units 10^{-2})	EVTS	DOCUMENT ID	TECN	COMMENT
2.99 ± 0.17 OUR FIT				Error includes scale factor of 1.1.
2.68 ± 0.29 OUR AVERAGE				
2.52 ± 0.20 ± 0.25	284 ± 22	56 ALBRECHT	94F	ARG $e^+ e^- \approx \Upsilon(4S)$
3.2 ± 0.3 ± 0.5		ADLER	87	MRK3 $e^+ e^-$ 3.77 GeV
• • • We do not use the following data for averages, fits, limits, etc. • • •				
2.6 ± 0.8	32 ± 8	57 SCHINDLER	81	MRK2 $e^+ e^-$ 3.771 GeV
4.0 ± 1.2	28	58 PERUZZI	77	LGW $e^+ e^-$ 3.77 GeV

56 See the footnote on the ALBRECHT 94F measurement of $\Gamma(K^- \pi^+)/\Gamma_{\text{total}}$ for the method used.

57 SCHINDLER 81 (MARK-2) measures $\sigma(e^+ e^- \rightarrow \psi(3770)) \times$ branching fraction to be 0.30 ± 0.08 nb. We use the MARK-3 (ADLER 88c) value of $\sigma = 5.8 \pm 0.5 \pm 0.6$ nb.

58 PERUZZI 77 (MARK-1) measures $\sigma(e^+ e^- \rightarrow \psi(3770)) \times$ branching fraction to be 0.46 ± 0.12 nb. We use the MARK-3 (ADLER 88c) value of $\sigma = 5.8 \pm 0.5 \pm 0.6$ nb.

$\Gamma(K_S^0 \pi^+ \pi^-)/\Gamma(K^- \pi^+)$		Γ_{35}/Γ_{32}		
VALUE	EVTS	DOCUMENT ID	TECN	COMMENT
0.77 ± 0.05 OUR FIT				Error includes scale factor of 1.1.
0.81 ± 0.05 ± 0.08	856 ± 35	FRABETTI	94J	E687 γ Be $\bar{E}_\gamma \approx 220$ GeV
• • • We do not use the following data for averages, fits, limits, etc. • • •				
0.85 ± 0.40	35	AVERY	80	SPEC $\gamma N \rightarrow D^{*+}$
1.4 ± 0.5	116	PICCOLO	77	MRK1 $e^+ e^-$ 4.03, 4.41 GeV

$\Gamma(K_S^0 \rho^0)/\Gamma(K_S^0 \pi^+ \pi^-)$		Γ_{36}/Γ_{35}		
VALUE	EVTS	DOCUMENT ID	TECN	COMMENT
0.259 ± 0.014 OUR AVERAGE				Error includes scale factor of 1.1.
0.264 ± 0.009 ± 0.010		MURAMATSU	02	CLE2 Dalitz fit, 5299 evts
0.350 ± 0.028 ± 0.067		FRABETTI	94G	E687 γ Be, $\bar{E}_\gamma \approx 220$ GeV
0.227 ± 0.032 ± 0.009		ALBRECHT	93D	ARG $e^+ e^- \approx 10$ GeV
• • • We do not use the following data for averages, fits, limits, etc. • • •				
0.267 ± 0.011 ± 0.009		ASNER	04A	CLEO See MURAMATSU 02
0.215 ± 0.051 ± 0.037		ANJOS	93	E691 γ Be 90–260 GeV
0.20 ± 0.06 ± 0.03		FRABETTI	92B	E687 γ Be, $\bar{E}_\gamma \approx 221$ GeV
0.12 ± 0.01 ± 0.07		ADLER	87	MRK3 $e^+ e^-$ 3.77 GeV

$\Gamma(K_S^0 \omega, \omega \rightarrow \pi^+ \pi^-)/\Gamma(K_S^0 \pi^+ \pi^-)$		Γ_{37}/Γ_{35}		
VALUE	EVTS	DOCUMENT ID	TECN	COMMENT
0.0072 ± 0.0018 ± 0.0010		MURAMATSU	02	CLE2 Dalitz fit, 5299 evts
• • • We do not use the following data for averages, fits, limits, etc. • • •				
0.0081 ± 0.0019 ± 0.0018		ASNER	04A	CLEO See MURAMATSU 02

$\Gamma(K_S^0 f_0(980), f_0(980) \rightarrow \pi^+ \pi^-)/\Gamma(K_S^0 \pi^+ \pi^-)$		Γ_{38}/Γ_{35}		
VALUE	EVTS	DOCUMENT ID	TECN	COMMENT
0.047 ± 0.010 OUR AVERAGE				Error includes scale factor of 1.1.
0.043 ± 0.005 ± 0.012		MURAMATSU	02	CLE2 Dalitz fit, 5299 evts
0.068 ± 0.016 ± 0.018		FRABETTI	94G	E687 γ Be, $\bar{E}_\gamma \approx 220$ GeV
0.046 ± 0.018 ± 0.006		ALBRECHT	93D	ARG $e^+ e^- \approx 10$ GeV
• • • We do not use the following data for averages, fits, limits, etc. • • •				
0.042 ± 0.005 ± 0.011		ASNER	04A	CLEO See MURAMATSU 02

$\Gamma(K_S^0 f_2(1270), f_2(1270) \rightarrow \pi^+ \pi^-)/\Gamma(K_S^0 \pi^+ \pi^-)$		Γ_{39}/Γ_{35}		
VALUE	EVTS	DOCUMENT ID	TECN	COMMENT
0.0045 ± 0.0039 OUR AVERAGE				Error includes scale factor of 1.1.
0.0027 ± 0.0015 ± 0.0037		MURAMATSU	02	CLE2 Dalitz fit, 5299 evts
0.037 ± 0.014 ± 0.017		FRABETTI	94G	E687 γ Be, $\bar{E}_\gamma \approx 220$ GeV
0.050 ± 0.021 ± 0.008		ALBRECHT	93D	ARG $e^+ e^- \approx 10$ GeV
• • • We do not use the following data for averages, fits, limits, etc. • • •				
0.0036 ± 0.0022 ± 0.0032		ASNER	04A	CLEO See MURAMATSU 02

$\Gamma(K_S^0 f_0(1370), f_0(1370) \rightarrow \pi^+ \pi^-)/\Gamma(K_S^0 \pi^+ \pi^-)$		Γ_{40}/Γ_{35}		
VALUE	EVTS	DOCUMENT ID	TECN	COMMENT
0.085 ± 0.019 OUR AVERAGE				Error includes scale factor of 1.1.
0.099 ± 0.011 ± 0.028		MURAMATSU	02	CLE2 Dalitz fit, 5299 evts
0.077 ± 0.022 ± 0.031		FRABETTI	94G	E687 γ Be, $\bar{E}_\gamma \approx 220$ GeV
0.082 ± 0.028 ± 0.013		ALBRECHT	93D	ARG $e^+ e^- \approx 10$ GeV
• • • We do not use the following data for averages, fits, limits, etc. • • •				
0.098 ± 0.014 ± 0.026		ASNER	04A	CLEO See MURAMATSU 02

$\Gamma(K^*(892)^- \pi^+, K^*(892)^- \rightarrow K_S^0 \pi^-)/\Gamma(K_S^0 \pi^+ \pi^-)$		Γ_{41}/Γ_{35}		
VALUE	EVTS	DOCUMENT ID	TECN	COMMENT
0.660 ± 0.019 OUR AVERAGE				Error includes scale factor of 1.1.
0.657 ± 0.013 ± 0.018		MURAMATSU	02	CLE2 Dalitz fit, 5299 evts
0.625 ± 0.036 ± 0.026		FRABETTI	94G	E687 γ Be, $\bar{E}_\gamma \approx 220$ GeV
0.718 ± 0.042 ± 0.030		ALBRECHT	93D	ARG $e^+ e^- \approx 10$ GeV

• • • We do not use the following data for averages, fits, limits, etc. • • •

$0.663 \pm 0.013 \pm_{-0.043}^{0.024}$	ASNER	04A	CLEO	See MURAMATSU 02
0.480 ± 0.097	ANJOS	93	E691	γ Be 90–260 GeV
$0.56 \pm 0.04 \pm 0.05$	ADLER	87	MRK3	e^+e^- 3.77 GeV

$\Gamma(K^*(892)^+\pi^-, K^*(892)^+ \rightarrow K_S^0\pi^+)/\Gamma(K_S^0\pi^+\pi^-)$ Γ_{217}/Γ_{35}
This is the “fit fraction” from the Dalitz-plot analysis. This is a doubly Cabibbo-suppressed mode.

VALUE (units 10^{-3})	DOCUMENT ID	TECN	COMMENT
$3.4 \pm 1.3 \pm_{-0.4}^{4.1}$	MURAMATSU 02	CLE2	Dalitz fit, 5299 evts

• • • We do not use the following data for averages, fits, limits, etc. • • •

$3.4 \pm 1.3 \pm_{-0.5}^{3.6}$	ASNER	04A	CLEO	See MURAMATSU 02
--------------------------------	-------	-----	------	------------------

$\Gamma(K_S^0(1430)^-\pi^+, K_S^0(1430)^- \rightarrow K_S^0\pi^-)/\Gamma(K_S^0\pi^+\pi^-)$ Γ_{43}/Γ_{35}
This is the “fit fraction” from the Dalitz-plot analysis.

VALUE	DOCUMENT ID	TECN	COMMENT
$0.096 \pm 0.021 \pm_{-0.012}^{0.031}$ OUR AVERAGE			

$0.073 \pm 0.007 \pm_{-0.011}^{0.031}$	MURAMATSU 02	CLE2	Dalitz fit, 5299 evts
--	--------------	------	-----------------------

$0.109 \pm 0.027 \pm 0.029$	FRABETTI 94G	E687	γ Be, $\bar{E}_\gamma \approx 220$ GeV
-----------------------------	--------------	------	---

$0.129 \pm 0.034 \pm 0.021$	ALBRECHT 93D	ARG	$e^+e^- \approx 10$ GeV
-----------------------------	--------------	-----	-------------------------

• • • We do not use the following data for averages, fits, limits, etc. • • •

$0.072 \pm 0.007 \pm_{-0.013}^{0.014}$	ASNER	04A	CLEO	See MURAMATSU 02
--	-------	-----	------	------------------

$\Gamma(K_S^*(1430)^-\pi^+, K_S^*(1430)^- \rightarrow K_S^0\pi^-)/\Gamma(K_S^0\pi^+\pi^-)$ Γ_{44}/Γ_{35}
This is the “fit fraction” from the Dalitz-plot analysis.

VALUE	DOCUMENT ID	TECN	COMMENT
$0.011 \pm 0.002 \pm_{-0.003}^{0.007}$	MURAMATSU 02	CLE2	Dalitz fit, 5299 evts

• • • We do not use the following data for averages, fits, limits, etc. • • •

$0.011 \pm 0.002 \pm_{-0.003}^{0.005}$	ASNER	04A	CLEO	See MURAMATSU 02
--	-------	-----	------	------------------

$\Gamma(K^*(1680)^-\pi^+, K^*(1680)^- \rightarrow K_S^0\pi^-)/\Gamma(K_S^0\pi^+\pi^-)$ Γ_{45}/Γ_{35}
This is the “fit fraction” from the Dalitz-plot analysis.

VALUE	DOCUMENT ID	TECN	COMMENT
$0.022 \pm 0.004 \pm_{-0.015}^{0.018}$	MURAMATSU 02	CLE2	Dalitz fit, 5299 evts

• • • We do not use the following data for averages, fits, limits, etc. • • •

$0.023 \pm 0.005 \pm_{-0.014}^{0.007}$	ASNER	04A	CLEO	See MURAMATSU 02
--	-------	-----	------	------------------

$\Gamma(K_S^0\pi^+\pi^- \text{ nonresonant})/\Gamma(K_S^0\pi^+\pi^-)$ Γ_{46}/Γ_{35}
This is the “fit fraction” from the Dalitz-plot analysis. Neither FRABETTI 94G nor ALBRECHT 93D (quoted in many of the earlier submodes of $K_S^0\pi^+\pi^-$) sees evidence for a nonresonant component.

VALUE	DOCUMENT ID	TECN	COMMENT
$0.009 \pm 0.004 \pm_{-0.004}^{0.020}$	MURAMATSU 02	CLE2	Dalitz fit, 5299 evts

• • • We do not use the following data for averages, fits, limits, etc. • • •

$0.007 \pm 0.007 \pm_{-0.006}^{0.021}$	ASNER	04A	CLEO	See MURAMATSU 02
--	-------	-----	------	------------------

$0.263 \pm 0.024 \pm 0.041$	ANJOS	93	E691	γ Be 90–260 GeV
-----------------------------	-------	----	------	------------------------

$0.26 \pm 0.08 \pm 0.05$	FRABETTI 92B	E687	γ Be, $\bar{E}_\gamma \approx 221$ GeV
--------------------------	--------------	------	---

$0.33 \pm 0.05 \pm 0.10$	ADLER	87	MRK3	e^+e^- 3.77 GeV
--------------------------	-------	----	------	-------------------

$\Gamma(K^-\pi^+\pi^0)/\Gamma_{\text{total}}$ Γ_{47}/Γ

VALUE (units 10^{-2})	EVTS	DOCUMENT ID	TECN	COMMENT
13.9 ± 0.5 OUR FIT	Error includes scale factor of 1.6.			

$14.57 \pm 0.12 \pm 0.38$	⁵⁹ DOBBS	07	CLEO	e^+e^- at $\psi(3770)$
---------------------------	---------------------	----	------	--------------------------

• • • We do not use the following data for averages, fits, limits, etc. • • •

$14.9 \pm 0.3 \pm 0.5$	$19k \pm 150$	⁵⁹ HE	05	CLEO	See DOBBS 07
------------------------	---------------	------------------	----	------	--------------

$13.3 \pm 1.2 \pm 1.3$	931	ADLER	88c	MRK3	e^+e^- 3.77 GeV
------------------------	-----	-------	-----	------	-------------------

11.7 ± 4.3	37	⁶⁰ SCHINDLER	81	MRK2	$e^+e^- \approx 3.771$ GeV
----------------	----	-------------------------	----	------	----------------------------

⁵⁹ DOBBS 07 and HE 05 use single- and double-tagged events in an overall fit. DOBBS 07 supersedes HE 05.

⁶⁰ SCHINDLER 81 (MARK-2) measures $\sigma(e^+e^- \rightarrow \psi(3770)) \times$ branching fraction to be 0.68 ± 0.23 nb. We use the MARK-3 (ADLER 88c) value of $\sigma = 5.8 \pm 0.5 \pm 0.6$ nb.

$\Gamma(K^-\pi^+\pi^0)/\Gamma(K^-\pi^+)$ Γ_{47}/Γ_{32}

VALUE	EVTS	DOCUMENT ID	TECN	COMMENT
3.57 ± 0.13 OUR FIT	Error includes scale factor of 1.9.			

3.44 ± 0.30 OUR AVERAGE Error includes scale factor of 1.5. See the ideogram below.

$3.81 \pm 0.07 \pm 0.26$	10k	BARISH	96	CLE2	$e^+e^- \approx 7(45)$
--------------------------	-----	--------	----	------	------------------------

$3.04 \pm 0.16 \pm 0.34$	931	⁶¹ ALBRECHT	92P	ARG	$e^+e^- \approx 10$ GeV
--------------------------	-----	------------------------	-----	-----	-------------------------

$2.8 \pm 0.14 \pm 0.52$	1050	KINOSHITA	91	CLEO	$e^+e^- \approx 10.7$ GeV
-------------------------	------	-----------	----	------	---------------------------

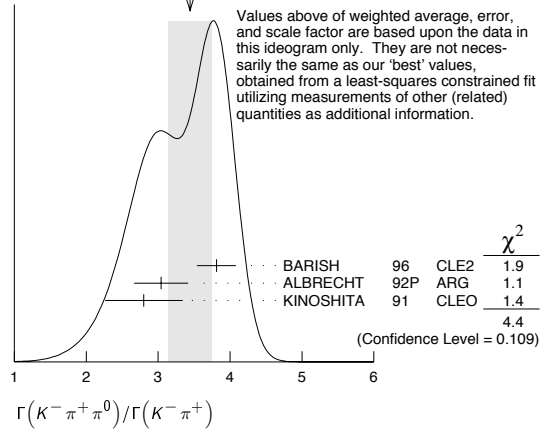
• • • We do not use the following data for averages, fits, limits, etc. • • •

$4.0 \pm 0.9 \pm 1.0$	69	ALVAREZ	91B	NA14	Photoproduction
-----------------------	----	---------	-----	------	-----------------

4.2 ± 1.4	41	SUMMERS	84	E691	Photoproduction
---------------	----	---------	----	------	-----------------

⁶¹ This value is calculated from numbers in Table 1 of ALBRECHT 92P.

WEIGHTED AVERAGE
 3.44 ± 0.30 (Error scaled by 1.5)



$\Gamma(K^-\rho^+)/\Gamma(K^-\pi^+\pi^0)$ Γ_{48}/Γ_{47}
This is the “fit fraction” from the Dalitz-plot analysis.

VALUE	DOCUMENT ID	TECN	COMMENT
0.78 ± 0.04 OUR AVERAGE			

$0.788 \pm 0.019 \pm 0.048$	KOPP	01	CLE2	$e^+e^- \approx 10.6$ GeV
-----------------------------	------	----	------	---------------------------

$0.765 \pm 0.041 \pm 0.054$	FRABETTI 94G	E687	γ Be, $\bar{E}_\gamma \approx 220$ GeV
-----------------------------	--------------	------	---

$0.647 \pm 0.039 \pm 0.150$	ANJOS	93	E691	γ Be 90–260 GeV
-----------------------------	-------	----	------	------------------------

$0.81 \pm 0.03 \pm 0.06$	ADLER	87	MRK3	e^+e^- 3.77 GeV
--------------------------	-------	----	------	-------------------

$\Gamma(K^-\rho(1700)^+, \rho(1700)^+ \rightarrow \pi^+\pi^0)/\Gamma(K^-\pi^+\pi^0)$ Γ_{49}/Γ_{47}
This is the “fit fraction” from the Dalitz-plot analysis.

VALUE	DOCUMENT ID	TECN	COMMENT	
$0.057 \pm 0.008 \pm 0.009$	KOPP	01	CLE2	$e^+e^- \approx 10.6$ GeV

$\Gamma(K^*(892)^-\pi^+, K^*(892)^- \rightarrow K^-\pi^0)/\Gamma(K^-\pi^+\pi^0)$ Γ_{50}/Γ_{47}
This is the “fit fraction” from the Dalitz-plot analysis.

VALUE	DOCUMENT ID	TECN	COMMENT
$0.160 \pm 0.025 \pm_{-0.013}^{0.025}$ OUR AVERAGE			

$0.161 \pm 0.007 \pm_{-0.011}^{0.027}$	KOPP	01	CLE2	$e^+e^- \approx 10.6$ GeV
--	------	----	------	---------------------------

$0.148 \pm 0.028 \pm 0.049$	FRABETTI 94G	E687	γ Be, $\bar{E}_\gamma \approx 220$ GeV
-----------------------------	--------------	------	---

$0.084 \pm 0.011 \pm 0.012$	ANJOS	93	E691	γ Be 90–260 GeV
-----------------------------	-------	----	------	------------------------

$0.12 \pm 0.02 \pm 0.03$	ADLER	87	MRK3	e^+e^- 3.77 GeV
--------------------------	-------	----	------	-------------------

• • • We do not use the following data for averages, fits, limits, etc. • • •

$\Gamma(\bar{K}^*(892)^0\pi^0, \bar{K}^*(892)^0 \rightarrow K^-\pi^+)/\Gamma(K^-\pi^+\pi^0)$ Γ_{51}/Γ_{47}
This is the “fit fraction” from the Dalitz-plot analysis.

VALUE	DOCUMENT ID	TECN	COMMENT
0.135 ± 0.016 OUR AVERAGE			

$0.127 \pm 0.009 \pm 0.016$	KOPP	01	CLE2	$e^+e^- \approx 10.6$ GeV
-----------------------------	------	----	------	---------------------------

$0.165 \pm 0.031 \pm 0.015$	FRABETTI 94G	E687	γ Be, $\bar{E}_\gamma \approx 220$ GeV
-----------------------------	--------------	------	---

$0.142 \pm 0.018 \pm 0.024$	ANJOS	93	E691	γ Be 90–260 GeV
-----------------------------	-------	----	------	------------------------

$0.13 \pm 0.02 \pm 0.03$	ADLER	87	MRK3	e^+e^- 3.77 GeV
--------------------------	-------	----	------	-------------------

• • • We do not use the following data for averages, fits, limits, etc. • • •

$\Gamma(K_S^0(1430)^-\pi^+, K_S^0(1430)^- \rightarrow K^-\pi^0)/\Gamma(K^-\pi^+\pi^0)$ Γ_{52}/Γ_{47}
This is the “fit fraction” from the Dalitz-plot analysis.

VALUE	DOCUMENT ID	TECN	COMMENT	
$0.033 \pm 0.006 \pm 0.014$	KOPP	01	CLE2	$e^+e^- \approx 10.6$ GeV

$0.033 \pm 0.006 \pm 0.014$	KOPP	01	CLE2	$e^+e^- \approx 10.6$ GeV
-----------------------------	------	----	------	---------------------------

$\Gamma(\bar{K}_S^0(1430)^0\pi^0, \bar{K}_S^0(1430)^0 \rightarrow K^-\pi^+)/\Gamma(K^-\pi^+\pi^0)$ Γ_{53}/Γ_{47}
This is the “fit fraction” from the Dalitz-plot analysis.

VALUE	DOCUMENT ID	TECN	COMMENT	
$0.041 \pm 0.006 \pm_{-0.009}^{0.032}$	KOPP	01	CLE2	$e^+e^- \approx 10.6$ GeV

$0.041 \pm 0.006 \pm_{-0.009}^{0.032}$	KOPP	01	CLE2	$e^+e^- \approx 10.6$ GeV
--	------	----	------	---------------------------

$\Gamma(K^*(1680)^-\pi^+, K^*(1680)^- \rightarrow K^-\pi^0)/\Gamma(K^-\pi^+\pi^0)$ Γ_{54}/Γ_{47}
This is the “fit fraction” from the Dalitz-plot analysis.

VALUE	DOCUMENT ID	TECN	COMMENT	
$0.013 \pm 0.003 \pm 0.004$	KOPP	01	CLE2	$e^+e^- \approx 10.6$ GeV

$0.013 \pm 0.003 \pm 0.004$	KOPP	01	CLE2	$e^+e^- \approx 10.6$ GeV
-----------------------------	------	----	------	---------------------------

$\Gamma(K^-\pi^+\pi^0 \text{ nonresonant})/\Gamma(K^-\pi^+\pi^0)$ Γ_{55}/Γ_{47}
This is the “fit fraction” from the Dalitz-plot analysis.

VALUE	EVTS	DOCUMENT ID	TECN	COMMENT
$0.080 \pm 0.038 \pm_{-0.014}^{0.038}$ OUR AVERAGE				

$0.075 \pm 0.009 \pm_{-0.011}^{0.056}$	KOPP	01	CLE2	$e^+e^- \approx 10.6$ GeV
--	------	----	------	---------------------------

$0.101 \pm 0.033 \pm 0.040$	FRABETTI 94G	E687	γ Be, $\bar{E}_\gamma \approx 220$ GeV
-----------------------------	--------------	------	---

Meson Particle Listings

 D^0

• • • We do not use the following data for averages, fits, limits, etc. • • •

$0.036 \pm 0.004 \pm 0.018$	ANJOS	93	E691	γ Be 90–260 GeV
$0.09 \pm 0.02 \pm 0.04$	ADLER	87	MRK3	e^+e^- 3.77 GeV
0.51 ± 0.22	21	SUMMERS	84	E691 Photoproduction

$\Gamma(\bar{K}^*(892)^0 \pi^0, \bar{K}^*(892)^0 \rightarrow K_S^0 \pi^0) / \Gamma(K_S^0 \pi^0)$				$\Gamma_{57} / \Gamma_{33}$
VALUE		DOCUMENT ID	TECN	COMMENT
$0.55^{+0.13}_{-0.10} \pm 0.07$		PROCARIO	93B	CLE2 Dalitz plot fit, 122 evts

$\Gamma(K_S^0 \pi^0 \pi^0 \text{ nonresonant}) / \Gamma(K_S^0 \pi^0)$				$\Gamma_{58} / \Gamma_{33}$
VALUE		DOCUMENT ID	TECN	COMMENT
$0.37 \pm 0.08 \pm 0.04$		PROCARIO	93B	CLE2 Dalitz plot fit, 122 evts

$\Gamma(K^- \pi^+ \pi^+ \pi^-) / \Gamma_{\text{total}}$				Γ_{59} / Γ
VALUE (units 10^{-2})	EVTS	DOCUMENT ID	TECN	COMMENT
8.10 ± 0.20 OUR FIT		Error includes scale factor of 1.3.		
8.17 ± 0.33 OUR AVERAGE		Error includes scale factor of 1.7. See the ideogram below.		
$8.30 \pm 0.07 \pm 0.20$		62 DOBBS	07	CLEO e^+e^- at $\psi(3770)$
$7.9 \pm 1.5 \pm 0.9$		63 ALBRECHT	94	ARG $e^+e^- \approx \Upsilon(4S)$
$6.80 \pm 0.27 \pm 0.57$	1430 \pm 52	64 ALBRECHT	94F	ARG $e^+e^- \approx \Upsilon(4S)$
$9.1 \pm 0.8 \pm 0.8$	992	ADLER	88c	MRK3 e^+e^- 3.77 GeV
• • • We do not use the following data for averages, fits, limits, etc. • • •				
$8.3 \pm 0.2 \pm 0.3$	15k \pm 130	62 HE	05	CLEO See DOBBS 07
11.7 ± 2.5	185	65 SCHINDLER	81	MRK2 e^+e^- 3.771 GeV
6.2 ± 1.9	44	66 PERUZZI	77	LGW e^+e^- 3.77 GeV

62 DOBBS 07 and HE 05 use single- and double-tagged events in an overall fit. DOBBS 07 supersedes HE 05.

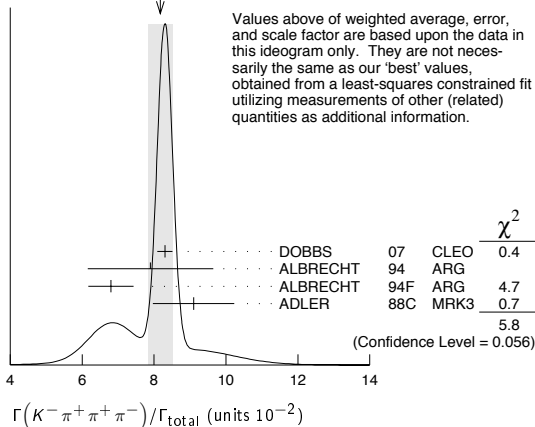
63 ALBRECHT 94 uses D^0 mesons from $\bar{B}^0 \rightarrow D^{*+} \ell^- \bar{\nu}_\ell$ decays. This is a different set of events than used by ALBRECHT 94F.

64 See the footnote on the ALBRECHT 94F measurement of $\Gamma(K^- \pi^+) / \Gamma_{\text{total}}$ for the method used.

65 SCHINDLER 81 (MARK-2) measures $\sigma(e^+e^- \rightarrow \psi(3770)) \times$ branching fraction to be 0.68 ± 0.11 nb. We use the MARK-3 (ADLER 88c) value of $\sigma = 5.8 \pm 0.5 \pm 0.6$ nb.

66 PERUZZI 77 (MARK-1) measures $\sigma(e^+e^- \rightarrow \psi(3770)) \times$ branching fraction to be 0.36 ± 0.10 nb. We use the MARK-3 (ADLER 88c) value of $\sigma = 5.8 \pm 0.5 \pm 0.6$ nb.

WEIGHTED AVERAGE
8.17 \pm 0.33 (Error scaled by 1.7)



$\Gamma(K^- \pi^+ \pi^+ \pi^-) / \Gamma(K^- \pi^+)$				$\Gamma_{59} / \Gamma_{32}$
VALUE	EVTS	DOCUMENT ID	TECN	COMMENT
2.08 ± 0.05 OUR FIT		Error includes scale factor of 1.6.		
1.97 ± 0.09 OUR AVERAGE				

$1.94 \pm 0.07 \pm 0.09$		JUN	00	SELX Σ^- nucleus, 600 GeV
$1.7 \pm 0.2 \pm 0.2$	1745	ANJOS	92c	E691 γ Be 90–260 GeV
$1.90 \pm 0.25 \pm 0.20$	337	ALVAREZ	91B	NA14 Photoproduction
$2.12 \pm 0.16 \pm 0.09$		BORTOLETT	O88	CLEO e^+e^- 10.55 GeV
$2.17 \pm 0.28 \pm 0.23$		ALBRECHT	85F	ARG e^+e^- 10 GeV
• • • We do not use the following data for averages, fits, limits, etc. • • •				
2.0 ± 0.9	48	BAILEY	86	ACCM π^- Be fixed target
2.0 ± 1.0	10	BAILEY	83B	SPEC π^- Be $\rightarrow D^0$
2.2 ± 0.8	214	PICCOLO	77	MRK1 e^+e^- 4.03, 4.41 GeV

$\Gamma(K^- \pi^+ \rho^0 \text{ total}) / \Gamma(K^- \pi^+ \pi^+ \pi^-)$				$\Gamma_{60} / \Gamma_{59}$
VALUE		DOCUMENT ID	TECN	COMMENT
0.835 ± 0.035 OUR AVERAGE				
$0.80 \pm 0.03 \pm 0.05$		ANJOS	92c	E691 γ Be 90–260 GeV
$0.855 \pm 0.032 \pm 0.030$		COFFMAN	92B	MRK3 e^+e^- 3.77 GeV
• • • We do not use the following data for averages, fits, limits, etc. • • •				
$0.98 \pm 0.12 \pm 0.10$		ALVAREZ	91B	NA14 Photoproduction

This includes $K^- a_1(1260)^+$, $\bar{K}^*(892)^0 \rho^0$, etc. The next entry gives the specifically 3-body fraction. We rely on the MARK III and E691 full amplitude analyses of the $K^- \pi^+ \pi^+ \pi^-$ channel for values of the resonant substructure.

$\Gamma(K^- \pi^+ \rho^0 \text{ 3-body}) / \Gamma(K^- \pi^+ \pi^+ \pi^-)$				$\Gamma_{61} / \Gamma_{59}$
VALUE	EVTS	DOCUMENT ID	TECN	COMMENT
0.063 ± 0.028 OUR AVERAGE				
$0.05 \pm 0.03 \pm 0.02$		ANJOS	92c	E691 γ Be 90–260 GeV
$0.084 \pm 0.022 \pm 0.04$		COFFMAN	92B	MRK3 e^+e^- 3.77 GeV

• • • We do not use the following data for averages, fits, limits, etc. • • •				
$0.77 \pm 0.06 \pm 0.06$		67 ALVAREZ	91B	NA14 Photoproduction
$0.85^{+0.11}_{-0.22}$	180	PICCOLO	77	MRK1 e^+e^- 4.03, 4.41 GeV

67 This value is for ρ^0 ($K^- \pi^+$)-nonresonant. ALVAREZ 91B cannot determine what fraction of this is $K^- a_1(1260)^+$.

$\Gamma(\bar{K}^*(892)^0 \rho^0) / \Gamma(K^- \pi^+ \pi^+ \pi^-)$				$\Gamma_{98} / \Gamma_{59}$
VALUE	EVTS	DOCUMENT ID	TECN	COMMENT
$0.195 \pm 0.03 \pm 0.03$		Unseen decay modes of the $\bar{K}^*(892)^0$ are included. We rely on the MARK III and E691 full amplitude analyses of the $K^- \pi^+ \pi^+ \pi^-$ channel for values of the resonant substructure.		

$0.34 \pm 0.09 \pm 0.09$		ALVAREZ	91B	NA14 Photoproduction
0.75 ± 0.3	5	BAILEY	83B	SPEC π Be $\rightarrow D^0$
$0.15^{+0.16}_{-0.15}$	20	PICCOLO	77	MRK1 e^+e^- 4.03, 4.41 GeV

$\Gamma(\bar{K}^*(892)^0 \rho^0 \text{ transverse}) / \Gamma(K^- \pi^+ \pi^+ \pi^-)$				$\Gamma_{99} / \Gamma_{59}$
VALUE	EVTS	DOCUMENT ID	TECN	COMMENT
0.20 ± 0.07 OUR FIT		Unseen decay modes of the $\bar{K}^*(892)^0$ are included.		
$0.213 \pm 0.024 \pm 0.075$		COFFMAN	92B	MRK3 e^+e^- 3.77 GeV

$\Gamma(\bar{K}^*(892)^0 \rho^0 \text{ S-wave}) / \Gamma(K^- \pi^+ \pi^+ \pi^-)$				$\Gamma_{100} / \Gamma_{59}$
VALUE	EVTS	DOCUMENT ID	TECN	COMMENT
$0.375 \pm 0.045 \pm 0.06$		Unseen decay modes of the $\bar{K}^*(892)^0$ are included.		
		ANJOS	92c	E691 γ Be 90–260 GeV

$\Gamma(\bar{K}^*(892)^0 \rho^0 \text{ S-wave long.}) / \Gamma_{\text{total}}$				Γ_{101} / Γ
VALUE	CL%	DOCUMENT ID	TECN	COMMENT
<0.003	90	COFFMAN	92B	MRK3 e^+e^- 3.77 GeV

$\Gamma(\bar{K}^*(892)^0 \rho^0 \text{ P-wave}) / \Gamma_{\text{total}}$				Γ_{102} / Γ
VALUE	CL%	DOCUMENT ID	TECN	COMMENT
<0.003	90	COFFMAN	92B	MRK3 e^+e^- 3.77 GeV
• • • We do not use the following data for averages, fits, limits, etc. • • •				
<0.009	90	ANJOS	92c	E691 γ Be 90–260 GeV

$\Gamma(\bar{K}^*(892)^0 \rho^0 \text{ D-wave}) / \Gamma(K^- \pi^+ \pi^+ \pi^-)$				$\Gamma_{103} / \Gamma_{59}$
VALUE	EVTS	DOCUMENT ID	TECN	COMMENT
$0.255 \pm 0.045 \pm 0.06$		Unseen decay modes of the $\bar{K}^*(892)^0$ are included.		
		ANJOS	92c	E691 γ Be 90–260 GeV

$\Gamma(K^- \pi^+ f_0(980)) / \Gamma_{\text{total}}$				Γ_{108} / Γ
VALUE	CL%	DOCUMENT ID	TECN	COMMENT
<0.011	90	ANJOS	92c	E691 γ Be 90–260 GeV

$\Gamma(\bar{K}^*(892)^0 f_0(980)) / \Gamma_{\text{total}}$				Γ_{109} / Γ
VALUE	CL%	DOCUMENT ID	TECN	COMMENT
<0.007	90	ANJOS	92c	E691 γ Be 90–260 GeV

$\Gamma(K^- a_1(1260)^+) / \Gamma(K^- \pi^+ \pi^+ \pi^-)$				$\Gamma_{93} / \Gamma_{59}$
VALUE	EVTS	DOCUMENT ID	TECN	COMMENT
0.97 ± 0.14 OUR AVERAGE		Unseen decay modes of the $a_1(1260)^+$ are included, assuming that the $a_1(1260)^+$ decays entirely to $\rho\pi$ [or at least to $(\pi\pi)_{J=1} \pi$].		
$0.94 \pm 0.13 \pm 0.20$		ANJOS	92c	E691 γ Be 90–260 GeV
$0.984 \pm 0.048 \pm 0.16$		COFFMAN	92B	MRK3 e^+e^- 3.77 GeV

$\Gamma(K^- a_2(1320)^+) / \Gamma_{\text{total}}$				Γ_{95} / Γ
VALUE	CL%	DOCUMENT ID	TECN	COMMENT
<0.002	90	ANJOS	92c	E691 γ Be 90–260 GeV
• • • We do not use the following data for averages, fits, limits, etc. • • •				
<0.006	90	COFFMAN	92B	MRK3 e^+e^- 3.77 GeV

$\Gamma(K_1(1270)^-\pi^+)/\Gamma(K^-\pi^+\pi^-\pi^-)$ Γ_{110}/Γ_{59}

Unseen decay modes of the $K_1(1270)^-$ are included. The MARK3 and E691 experiments disagree considerably here.

VALUE	CL%	DOCUMENT ID	TECN	COMMENT
0.14 ± 0.04 OUR FIT				
0.194 ± 0.056 ± 0.088		COFFMAN	92B MRK3	e^+e^- 3.77 GeV
••• We do not use the following data for averages, fits, limits, etc. •••				
<0.013	90	ANJOS	92C E691	γ Be 90–260 GeV

 $\Gamma(K_1(1400)^-\pi^+)/\Gamma_{total}$ Γ_{111}/Γ

VALUE	CL%	DOCUMENT ID	TECN	COMMENT
<0.012	90	COFFMAN	92B MRK3	e^+e^- 3.77 GeV

 $\Gamma(K^*(1410)^-\pi^+)/\Gamma_{total}$ Γ_{113}/Γ

VALUE	CL%	DOCUMENT ID	TECN	COMMENT
••• We do not use the following data for averages, fits, limits, etc. •••				
<0.012	90	COFFMAN	92B MRK3	e^+e^- 3.77 GeV

 $\Gamma(\bar{K}^*(892)^0\pi^+\pi^-\pi^-)/\Gamma(K^-\pi^+\pi^-\pi^-)$ Γ_{96}/Γ_{59}

This includes $\bar{K}^*(892)^0\rho^0$, etc. The next entry gives the specifically 3-body fraction. Unseen decay modes of the $\bar{K}^*(892)^0$ are included.

VALUE	DOCUMENT ID	TECN	COMMENT
0.30 ± 0.06 ± 0.03	ANJOS	92C E691	γ Be 90–260 GeV

 $\Gamma(\bar{K}^*(892)^0\pi^+\pi^-\pi^- \text{ 3-body})/\Gamma(K^-\pi^+\pi^-\pi^-)$ Γ_{97}/Γ_{59}

Unseen decay modes of the $\bar{K}^*(892)^0$ are included.

VALUE	DOCUMENT ID	TECN	COMMENT
0.19 ± 0.04 OUR FIT			
0.18 ± 0.04 OUR AVERAGE			
0.165 ± 0.03 ± 0.045	ANJOS	92C E691	γ Be 90–260 GeV
0.210 ± 0.027 ± 0.06	COFFMAN	92B MRK3	e^+e^- 3.77 GeV

 $\Gamma(K^-\pi^+\pi^-\pi^- \text{ nonresonant})/\Gamma(K^-\pi^+\pi^-\pi^-)$ Γ_{67}/Γ_{59}

VALUE	DOCUMENT ID	TECN	COMMENT
0.233 ± 0.032 OUR AVERAGE			
0.23 ± 0.02 ± 0.03	ANJOS	92C E691	γ Be 90–260 GeV
0.242 ± 0.025 ± 0.06	COFFMAN	92B MRK3	e^+e^- 3.77 GeV

 $\Gamma(K_S^0\pi^+\pi^-\pi^0)/\Gamma_{total}$ Γ_{68}/Γ

VALUE (units 10^{-2})	EVTS	DOCUMENT ID	TECN	COMMENT
5.4 ± 0.6 OUR FIT				
5.2 ± 1.1 ± 1.2	140	COFFMAN	92B MRK3	e^+e^- 3.77 GeV
••• We do not use the following data for averages, fits, limits, etc. •••				
6.7 + 1.6 - 1.7	68	BARLAG	92C ACCM	π^- Cu 230 GeV

⁶⁸BARLAG 92c computes the branching fraction using topological normalization.

 $\Gamma(K_S^0\pi^+\pi^-\pi^0)/\Gamma(K_S^0\pi^+\pi^-)$ Γ_{68}/Γ_{35}

VALUE	EVTS	DOCUMENT ID	TECN	COMMENT
1.82 ± 0.20 OUR FIT				
1.86 ± 0.23 OUR AVERAGE				
1.80 ± 0.20 ± 0.21	190	⁶⁹ ALBRECHT	92P ARG	$e^+e^- \approx 10$ GeV
2.8 ± 0.8 ± 0.8	46	ANJOS	92C E691	γ Be 90–260 GeV
1.85 ± 0.26 ± 0.30	158	KINOSHITA	91 CLEO	$e^+e^- \sim 10.7$ GeV

⁶⁹This value is calculated from numbers in Table 1 of ALBRECHT 92P.

 $\Gamma(K_S^0\eta)/\Gamma(K_S^0\pi^0)$ Γ_{90}/Γ_{33}

Unseen decay modes of the η are included.

VALUE	EVTS	DOCUMENT ID	TECN	COMMENT
0.33 ± 0.04 OUR FIT				
0.32 ± 0.04 ± 0.03	225 ± 30	PROCARIO	93B CLE2	$\eta \rightarrow \gamma\gamma$

 $\Gamma(K_S^0\eta)/\Gamma(K_S^0\pi^+\pi^-)$ Γ_{90}/Γ_{35}

Unseen decay modes of the η are included.

VALUE	EVTS	DOCUMENT ID	TECN	COMMENT
0.134 ± 0.017 OUR FIT				
0.14 ± 0.02 ± 0.02	80 ± 12	PROCARIO	93B CLE2	$\eta \rightarrow \pi^+\pi^-\pi^0$

 $\Gamma(K_S^0\omega)/\Gamma(K^-\pi^+)$ Γ_{91}/Γ_{32}

Unseen decay modes of the ω are included.

VALUE	DOCUMENT ID	TECN	COMMENT
0.29 ± 0.05 OUR FIT			
0.50 ± 0.18 ± 0.10	ALBRECHT	89D ARG	e^+e^- 10 GeV

 $\Gamma(K_S^0\omega)/\Gamma(K_S^0\pi^+\pi^-)$ Γ_{91}/Γ_{35}

Unseen decay modes of the ω are included.

VALUE	EVTS	DOCUMENT ID	TECN	COMMENT
0.38 ± 0.06 OUR FIT				
0.33 ± 0.09 OUR AVERAGE				Error includes scale factor of 1.1.
0.29 ± 0.08 ± 0.05	16	⁷⁰ ALBRECHT	92P ARG	$e^+e^- \approx 10$ GeV
0.54 ± 0.14 ± 0.16	40	KINOSHITA	91 CLEO	$e^+e^- \sim 10.7$ GeV

⁷⁰This value is calculated from numbers in Table 1 of ALBRECHT 92P.

 $\Gamma(K_S^0\omega)/\Gamma(K_S^0\pi^+\pi^-\pi^0)$ Γ_{91}/Γ_{68}

Unseen decay modes of the ω are included.

VALUE	DOCUMENT ID	TECN	COMMENT
0.21 ± 0.04 OUR FIT			
0.220 ± 0.048 ± 0.0116	COFFMAN	92B MRK3	e^+e^- 3.77 GeV

 $\Gamma(K_S^0\eta'(958))/\Gamma(K_S^0\pi^+\pi^-)$ Γ_{92}/Γ_{35}

Unseen decay modes of the $\eta'(958)$ are included.

VALUE	EVTS	DOCUMENT ID	TECN	COMMENT
0.32 ± 0.04 OUR AVERAGE				
0.31 ± 0.02 ± 0.04	594	PROCARIO	93B CLE2	$\eta' \rightarrow \eta\pi^+\pi^-, \rho^0\gamma$
0.37 ± 0.13 ± 0.06	18	⁷¹ ALBRECHT	92P ARG	$e^+e^- \approx 10$ GeV

⁷¹This value is calculated from numbers in Table 1 of ALBRECHT 92P.

 $\Gamma(K^*(892)^-\rho^+)/\Gamma(K_S^0\pi^+\pi^-\pi^0)$ Γ_{104}/Γ_{68}

Unseen decay modes of the $K^*(892)^-$ are included.

VALUE	DOCUMENT ID	TECN	COMMENT
1.212 ± 0.376 ± 0.252	COFFMAN	92B MRK3	e^+e^- 3.77 GeV

 $\Gamma(K^*(892)^-\rho^+ \text{ longitudinal})/\Gamma(K_S^0\pi^+\pi^-\pi^0)$ Γ_{105}/Γ_{68}

Unseen decay modes of the $K^*(892)^-$ are included.

VALUE	DOCUMENT ID	TECN	COMMENT
0.580 ± 0.222	COFFMAN	92B MRK3	e^+e^- 3.77 GeV

 $\Gamma(K^*(892)^-\rho^+ \text{ transverse})/\Gamma(K_S^0\pi^+\pi^-\pi^0)$ Γ_{106}/Γ_{68}

Unseen decay modes of the $K^*(892)^-$ are included.

VALUE	DOCUMENT ID	TECN	COMMENT
0.634 ± 0.360	COFFMAN	92B MRK3	e^+e^- 3.77 GeV

 $\Gamma(K^*(892)^-\rho^+ \text{ P-wave})/\Gamma_{total}$ Γ_{107}/Γ

Unseen decay modes of the $K^*(892)^-$ are included.

VALUE	CL%	DOCUMENT ID	TECN	COMMENT
<0.015	90	⁷² COFFMAN	92B MRK3	e^+e^- 3.77 GeV

⁷²Obtained using other $\bar{K}^*(892)\rho$ P-wave limits and isospin relations.

 $\Gamma(\bar{K}^*(892)^0\rho^0 \text{ transverse})/\Gamma(K_S^0\pi^+\pi^-\pi^0)$ Γ_{99}/Γ_{68}

Unseen decay modes of the $\bar{K}^*(892)^0$ are included.

VALUE	DOCUMENT ID	TECN	COMMENT
0.30 ± 0.11 OUR FIT			
0.252 ± 0.222	COFFMAN	92B MRK3	e^+e^- 3.77 GeV

 $\Gamma(\bar{K}^0 a_1(1260)^0)/\Gamma_{total}$ Γ_{94}/Γ

Unseen decay modes of the $a_1(1260)^+$ are included, assuming that the $a_1(1260)^+$ decays entirely to $\rho\pi$ [or at least to $(\pi\pi)_{J=1}$].

VALUE	CL%	DOCUMENT ID	TECN	COMMENT
<0.019	90	COFFMAN	92B MRK3	e^+e^- 3.77 GeV

 $\Gamma(K_1(1270)^-\pi^+)/\Gamma(K_S^0\pi^+\pi^-\pi^0)$ Γ_{110}/Γ_{68}

Unseen decay modes of the $K_1(1270)^-$ are included.

VALUE	DOCUMENT ID	TECN	COMMENT
0.21 ± 0.06 OUR FIT			
0.20 ± 0.06	COFFMAN	92B MRK3	e^+e^- 3.77 GeV

 $\Gamma(\bar{K}_1(1400)^0\pi^0)/\Gamma_{total}$ Γ_{112}/Γ

VALUE	CL%	DOCUMENT ID	TECN	COMMENT
<0.037	90	COFFMAN	92B MRK3	e^+e^- 3.77 GeV

 $\Gamma(\bar{K}^*(892)^0\pi^+\pi^-\pi^0 \text{ 3-body})/\Gamma(K_S^0\pi^+\pi^-\pi^0)$ Γ_{97}/Γ_{68}

Unseen decay modes of the $\bar{K}^*(892)^0$ are included.

VALUE	DOCUMENT ID	TECN	COMMENT
0.28 ± 0.07 OUR FIT			Error includes scale factor of 1.1.
0.382 ± 0.210	COFFMAN	92B MRK3	e^+e^- 3.77 GeV

 $\Gamma(K_S^0\pi^+\pi^-\pi^0 \text{ nonresonant})/\Gamma(K_S^0\pi^+\pi^-)$ Γ_{74}/Γ_{68}

VALUE	DOCUMENT ID	TECN	COMMENT
0.210 ± 0.147 ± 0.150	COFFMAN	92B MRK3	e^+e^- 3.77 GeV

 $\Gamma(K^-\pi^+\pi^0\pi^0)/\Gamma_{total}$ Γ_{75}/Γ

VALUE	EVTS	DOCUMENT ID	TECN	COMMENT
••• We do not use the following data for averages, fits, limits, etc. •••				
0.177 ± 0.029		⁷³ BARLAG	92C ACCM	π^- Cu 230 GeV
0.149 ± 0.037 ± 0.030	24	⁷⁴ ADLER	88C MRK3	e^+e^- 3.77 GeV
0.209 + 0.074 - 0.043 ± 0.012	9	⁷³ AGUILAR-...	87F HYBR	$\pi p, pp$ 360, 400 GeV

⁷³AGUILAR-BENITEZ 87F and BARLAG 92c compute the branching fraction using topological normalization. They do not distinguish the presence of a third π^0 , and thus are not included in the average.

⁷⁴ADLER 88c uses an absolute normalization method finding this decay channel opposite a detected $\bar{D}^0 \rightarrow K^+\pi^-$ in pure $D\bar{D}$ events.

 $\Gamma(K^-\pi^+\pi^+\pi^-\pi^0)/\Gamma(K^-\pi^+)$ Γ_{76}/Γ_{32}

VALUE	EVTS	DOCUMENT ID	TECN	COMMENT
1.09 ± 0.10 OUR FIT				
0.98 ± 0.11 ± 0.11	225	⁷⁵ ALBRECHT	92P ARG	$e^+e^- \approx 10$ GeV

⁷⁵This value is calculated from numbers in Table 1 of ALBRECHT 92P.

Meson Particle Listings

 D^0 $\Gamma(K^- \pi^+ \pi^+ \pi^- \pi^0) / \Gamma(K^- \pi^+ \pi^+ \pi^-)$ $\Gamma_{76} / \Gamma_{59}$

VALUE	EVTs	DOCUMENT ID	TECN	COMMENT
0.52 ± 0.05 OUR FIT				
0.56 ± 0.07 OUR AVERAGE				
0.55 ± 0.07 +0.12 -0.09	167	KINOSHITA	91	CLEO $e^+ e^- \sim 10.7$ GeV
0.57 ± 0.06 ± 0.05	180	ANJOS	90D	E691 Photoproduction

 $\Gamma(\bar{K}^*(892)^0 \pi^+ \pi^- \pi^0) / \Gamma(K^- \pi^+ \pi^+ \pi^- \pi^0)$ $\Gamma_{114} / \Gamma_{76}$ Unseen decay modes of the $\bar{K}^*(892)^0$ are included.

VALUE	EVTs	DOCUMENT ID	TECN	COMMENT
0.45 ± 0.15 ± 0.15				
		ANJOS	90D	E691 Photoproduction

 $\Gamma(\bar{K}^*(892)^0 \eta) / \Gamma(K^- \pi^+ \pi^+)$ $\Gamma_{115} / \Gamma_{32}$ Unseen decay modes of the $\bar{K}^*(892)^0$ and η are included.

VALUE	EVTs	DOCUMENT ID	TECN	COMMENT
0.58 ± 0.19 ± 0.24 -0.28	46	KINOSHITA	91	CLEO $e^+ e^- \sim 10.7$ GeV

 $\Gamma(\bar{K}^*(892)^0 \eta) / \Gamma(K^- \pi^+ \pi^0)$ $\Gamma_{115} / \Gamma_{47}$ Unseen decay modes of the $\bar{K}^*(892)^0$ and η are included.

VALUE	EVTs	DOCUMENT ID	TECN	COMMENT
0.13 ± 0.02 ± 0.03	214	PROCARIO	93B	CLE2 $\bar{K}^{*0} \eta \rightarrow K^- \pi^+ / \gamma \gamma$

 $\Gamma(K_S^0 \eta \pi^0) / \Gamma(K_S^0 \pi^0)$ $\Gamma_{80} / \Gamma_{33}$

VALUE	EVTs	DOCUMENT ID	TECN	COMMENT
0.46 ± 0.07 ± 0.06	155 ± 22	76 RUBIN	04	CLEO $e^+ e^- \approx 10$ GeV

⁷⁶ The η here is detected in its $\gamma \gamma$ mode, but other η modes are included in the value given. $\Gamma(K_S^0 a_0(980), a_0(980) \rightarrow \eta \pi^0) / \Gamma(K_S^0 \eta \pi^0)$ $\Gamma_{81} / \Gamma_{80}$

This is the "fit fraction" from the Dalitz-plot analysis, with interference.

VALUE	EVTs	DOCUMENT ID	TECN	COMMENT
1.19 ± 0.09 ± 0.26	77	RUBIN	04	CLEO Dalitz fit, 155 evts

⁷⁷ In addition to $K_S^0 a_0(980)$ and $\bar{K}^*(892)^0 \eta$ modes, RUBIN 04 finds a fit fraction of $0.246 \pm 0.092 \pm 0.091$ for other, undetermined modes. $\Gamma(\bar{K}^*(892)^0 \eta, \bar{K}^*(892)^0 \rightarrow K_S^0 \pi^0) / \Gamma(K_S^0 \eta \pi^0)$ $\Gamma_{82} / \Gamma_{80}$

This is the "fit fraction" from the Dalitz-plot analysis, with interference.

VALUE	EVTs	DOCUMENT ID	TECN	COMMENT
0.293 ± 0.062 ± 0.035	78	RUBIN	04	CLEO Dalitz fit, 155 evts

⁷⁸ See the note on RUBIN 04 in the preceding data block. $\Gamma(K^- \pi^+ \omega) / \Gamma(K^- \pi^+)$ $\Gamma_{116} / \Gamma_{32}$ Unseen decay modes of the ω are included.

VALUE	EVTs	DOCUMENT ID	TECN	COMMENT
0.78 ± 0.12 ± 0.10	99	79 ALBRECHT	92P	ARG $e^+ e^- \approx 10$ GeV

⁷⁹ This value is calculated from numbers in Table 1 of ALBRECHT 92P. $\Gamma(\bar{K}^*(892)^0 \omega) / \Gamma(K^- \pi^+)$ $\Gamma_{117} / \Gamma_{32}$ Unseen decay modes of the $\bar{K}^*(892)^0$ and ω are included.

VALUE	EVTs	DOCUMENT ID	TECN	COMMENT
0.28 ± 0.11 ± 0.04	17	80 ALBRECHT	92P	ARG $e^+ e^- \approx 10$ GeV

⁸⁰ This value is calculated from numbers in Table 1 of ALBRECHT 92P. $\Gamma(K^- \pi^+ \eta(958)) / \Gamma(K^- \pi^+ \pi^+ \pi^-)$ $\Gamma_{118} / \Gamma_{59}$ Unseen decay modes of the $\eta(958)$ are included.

VALUE	EVTs	DOCUMENT ID	TECN	COMMENT
0.093 ± 0.014 ± 0.019	286	PROCARIO	93B	CLE2 $\eta' \rightarrow \eta \pi^+ \pi^-, \rho^0 \gamma$

 $\Gamma(\bar{K}^*(892)^0 \eta(958)) / \Gamma(K^- \pi^+ \eta(958))$ $\Gamma_{119} / \Gamma_{118}$ Unseen decay modes of the $\bar{K}^*(892)^0$ are included.

VALUE	CL%	DOCUMENT ID	TECN	COMMENT
<0.15	90	PROCARIO	93B	CLE2

 $\Gamma(K_S^0 2\pi^+ 2\pi^-) / \Gamma(K_S^0 \pi^+ \pi^-)$ $\Gamma_{83} / \Gamma_{35}$

VALUE	EVTs	DOCUMENT ID	TECN	COMMENT
0.095 ± 0.005 ± 0.007	1283 ± 57	LINK	04D	FOCS $\gamma A, \bar{E}_\gamma \approx 180$ GeV

• • • We do not use the following data for averages, fits, limits, etc. • • •

0.07 ± 0.02 ± 0.01	11	81 ALBRECHT	92P	ARG $e^+ e^- \approx 10$ GeV
0.149 ± 0.026	56	AMMAR	91	CLEO $e^+ e^- \approx 10.5$ GeV
0.18 ± 0.07 ± 0.04	6	ANJOS	90D	E691 Photoproduction

⁸¹ This value is calculated from numbers in Table 1 of ALBRECHT 92P. $\Gamma(K_S^0 \rho^0 \pi^+ \pi^-, \text{no } K^*(892)^-) / \Gamma(K_S^0 2\pi^+ 2\pi^-)$ $\Gamma_{84} / \Gamma_{83}$

VALUE	DOCUMENT ID	TECN	COMMENT
0.40 ± 0.24 ± 0.07	LINK	04D	FOCS $\gamma A, \bar{E}_\gamma \approx 180$ GeV

 $\Gamma(K^*(892)^- \pi^+ \pi^+ \pi^-, K^*(892)^- \rightarrow K_S^0 \pi^-, \text{no } \rho^0) / \Gamma(K_S^0 2\pi^+ 2\pi^-)$ $\Gamma_{85} / \Gamma_{83}$

VALUE	DOCUMENT ID	TECN	COMMENT
0.17 ± 0.28 ± 0.02	LINK	04D	FOCS $\gamma A, \bar{E}_\gamma \approx 180$ GeV

 $\Gamma(K^*(892)^- \rho^0 \pi^+, K^*(892)^- \rightarrow K_S^0 \pi^-) / \Gamma(K_S^0 2\pi^+ 2\pi^-)$ $\Gamma_{86} / \Gamma_{83}$

VALUE	DOCUMENT ID	TECN	COMMENT
0.60 ± 0.21 ± 0.09	LINK	04D	FOCS $\gamma A, \bar{E}_\gamma \approx 180$ GeV

 $\Gamma(K_S^0 2\pi^+ 2\pi^- \text{ nonresonant}) / \Gamma(K_S^0 2\pi^+ 2\pi^-)$ $\Gamma_{87} / \Gamma_{83}$

VALUE	CL%	DOCUMENT ID	TECN	COMMENT
<0.46	90	LINK	04D	FOCS $\gamma A, \bar{E}_\gamma \approx 180$ GeV

 $\Gamma(K^- 3\pi^+ 2\pi^-) / \Gamma(K^- \pi^+ \pi^+ \pi^-)$ $\Gamma_{89} / \Gamma_{59}$

VALUE (units 10^{-3})	EVTs	DOCUMENT ID	TECN	COMMENT
2.70 ± 0.58 ± 0.38	48 ± 10	LINK	04B	FOCS $\gamma A, \bar{E}_\gamma \approx 180$ GeV

Hadronic modes with three K 's $\Gamma(K_S^0 K^+ K^-) / \Gamma(K_S^0 \pi^+ \pi^-)$ $\Gamma_{120} / \Gamma_{35}$

VALUE	EVTs	DOCUMENT ID	TECN	COMMENT
0.158 ± 0.001 ± 0.005	14k ± 116	AUBERT,B	05J	BABR $e^+ e^- \approx \Upsilon(4S)$

• • • We do not use the following data for averages, fits, limits, etc. • • •

0.20 ± 0.05 ± 0.04	47	FRABETTI	92B	E687 γ Be, $\bar{E}_\gamma = 221$ GeV
0.170 ± 0.022	136	AMMAR	91	CLEO $e^+ e^- \approx 10.5$ GeV
0.24 ± 0.08		BEBEK	86	CLEO $e^+ e^-$ near $\Upsilon(4S)$
0.185 ± 0.055	52	ALBRECHT	85B	ARG $e^+ e^- 10$ GeV

 $\Gamma(K_S^0 a_0(980)^0, a_0^0 \rightarrow K^+ K^-) / \Gamma(K_S^0 K^+ K^-)$ $\Gamma_{121} / \Gamma_{120}$

This is the "fit fraction" from the Dalitz-plot analysis, with interference.

VALUE	DOCUMENT ID	TECN	COMMENT
0.664 ± 0.016 ± 0.070	AUBERT,B	05J	BABR Dalitz fit, 12540 ± 112 evts

 $\Gamma(K^- a_0(980)^+, a_0^+ \rightarrow K^+ K_S^0) / \Gamma(K_S^0 K^+ K^-)$ $\Gamma_{122} / \Gamma_{120}$

This is the "fit fraction" from the Dalitz-plot analysis, with interference.

VALUE	DOCUMENT ID	TECN	COMMENT
0.134 ± 0.011 ± 0.037	AUBERT,B	05J	BABR Dalitz fit, 12540 ± 112 evts

 $\Gamma(K^+ a_0(980)^-, a_0^- \rightarrow K^- K_S^0) / \Gamma(K_S^0 K^+ K^-)$ $\Gamma_{123} / \Gamma_{120}$

This is a doubly Cabibbo-suppressed mode.

VALUE	CL%	DOCUMENT ID	TECN	COMMENT
<0.025	95	AUBERT,B	05J	BABR Dalitz fit, 12540 ± 112 evts

 $\Gamma(K_S^0 f_0(980), f_0 \rightarrow K^+ K^-) / \Gamma(K_S^0 K^+ K^-)$ $\Gamma_{124} / \Gamma_{120}$

VALUE	CL%	DOCUMENT ID	TECN	COMMENT
<0.021	95	AUBERT,B	05J	BABR Dalitz fit, 12540 ± 112 evts

 $\Gamma(K_S^0 \phi, \phi \rightarrow K^+ K^-) / \Gamma(K_S^0 K^+ K^-)$ $\Gamma_{125} / \Gamma_{120}$

This is the "fit fraction" from the Dalitz-plot analysis, with interference.

VALUE	DOCUMENT ID	TECN	COMMENT
0.459 ± 0.007 ± 0.007	AUBERT,B	05J	BABR Dalitz fit, 12540 ± 112 evts

 $\Gamma(K_S^0 f_0(1400), f_0 \rightarrow K^+ K^-) / \Gamma(K_S^0 K^+ K^-)$ $\Gamma_{126} / \Gamma_{120}$

This is the "fit fraction" from the Dalitz-plot analysis, with interference.

VALUE	DOCUMENT ID	TECN	COMMENT
0.038 ± 0.007 ± 0.023	AUBERT,B	05J	BABR Dalitz fit, 12540 ± 112 evts

 $\Gamma(3K_S^0) / \Gamma(K_S^0 \pi^+ \pi^-)$ $\Gamma_{127} / \Gamma_{35}$

VALUE (units 10^{-2})	EVTs	DOCUMENT ID	TECN	COMMENT
3.2 ± 0.4 OUR AVERAGE				

3.58 ± 0.54 ± 0.52	170 ± 26	LINK	05A	FOCS γ Be, $\bar{E}_\gamma \approx 180$ GeV
2.78 ± 0.38 ± 0.48	61	ASNER	96B	CLE2 $e^+ e^- \approx \Upsilon(4S)$
7.0 ± 2.4 ± 1.2	10 ± 3	FRABETTI	94J	E687 γ Be, $\bar{E}_\gamma = 220$ GeV
3.2 ± 1.0	22	AMMAR	91	CLEO $e^+ e^- \approx 10.5$ GeV
3.4 ± 1.4 ± 1.0	5	ALBRECHT	90C	ARG $e^+ e^- \approx 10$ GeV

 $\Gamma(K^+ K^- K^- \pi^+) / \Gamma(K^- \pi^+ \pi^+ \pi^-)$ $\Gamma_{128} / \Gamma_{59}$

VALUE	EVTs	DOCUMENT ID	TECN	COMMENT
0.0027 ± 0.0004 OUR AVERAGE				Error includes scale factor of 1.1.

0.00257 ± 0.00034 ± 0.00024	143	LINK	03G	FOCS $\gamma A, \bar{E}_\gamma \approx 180$ GeV
0.0054 ± 0.0016 ± 0.0008	18	AITALA	01D	E791 $\pi^- A, 500$ GeV
0.0028 ± 0.0007 ± 0.0001	20	FRABETTI	95C	E687 γ Be, $\bar{E}_\gamma \approx 200$ GeV

 $\Gamma(\phi \bar{K}^*(892)^0, \phi \rightarrow K^+ K^-, \bar{K}^*(892)^0 \rightarrow K^- \pi^+) / \Gamma(K^+ K^- K^- \pi^+)$ $\Gamma_{131} / \Gamma_{128}$

VALUE	DOCUMENT ID	TECN	COMMENT
0.48 ± 0.06 ± 0.01	LINK	03G	FOCS $\gamma A, \bar{E}_\gamma \approx 180$ GeV

 $\Gamma(K^- \pi^+ \phi, \phi \rightarrow K^+ K^-) / \Gamma(K^+ K^- K^- \pi^+)$ $\Gamma_{130} / \Gamma_{128}$

VALUE	DOCUMENT ID	TECN	COMMENT
0.18 ± 0.06 ± 0.04	LINK	03G	FOCS $\gamma A, \bar{E}_\gamma \approx 180$ GeV

 $\Gamma(K^+ K^- \bar{K}^*(892)^0, \bar{K}^*(892)^0 \rightarrow K^- \pi^+) / \Gamma(K^+ K^- K^- \pi^+)$ $\Gamma_{129} / \Gamma_{128}$

VALUE	DOCUMENT ID	TECN	COMMENT
0.20 ± 0.07 ± 0.02	LINK	03G	FOCS $\gamma A, \bar{E}_\gamma \approx 180$ GeV

$\Gamma(K^+ K^- K^- \pi^+ \text{ nonresonant})/\Gamma(K^+ K^- K^- \pi^+)$				$\Gamma_{132}/\Gamma_{128}$
VALUE	DOCUMENT ID	TECN	COMMENT	
$0.15 \pm 0.06 \pm 0.02$	LINK	03G	FOCS $\gamma A, \bar{E}_\gamma \approx 180 \text{ GeV}$	

$\Gamma(K_S^0 K_S^0 K^\pm \pi^\mp)/\Gamma(K_S^0 \pi^+ \pi^-)$				Γ_{133}/Γ_{35}
VALUE (units 10^{-2})	EVTS	DOCUMENT ID	TECN	COMMENT
$2.12 \pm 0.38 \pm 0.20$	57 ± 10	LINK	05A	FOCS $\gamma \text{ Be}, \bar{E}_\gamma \approx 180 \text{ GeV}$

Pionic modes

$\Gamma(\pi^+ \pi^-)/\Gamma(K^- \pi^+)$				Γ_{134}/Γ_{32}
VALUE (units 10^{-2})	EVTS	DOCUMENT ID	TECN	COMMENT

3.59 ± 0.05 OUR AVERAGE				
$3.62 \pm 0.10 \pm 0.08$	2085 ± 54	RUBIN	06	CLEO $e^+ e^-$ at $\psi(3770)$
$3.594 \pm 0.054 \pm 0.040$	7334 ± 97	ACOSTA	05c	CDF $p\bar{p}, \sqrt{s} = 1.96 \text{ TeV}$
$3.53 \pm 0.12 \pm 0.06$	3453	LINK	03	FOCS $\gamma A, \bar{E}_\gamma \approx 180 \text{ GeV}$
$3.51 \pm 0.16 \pm 0.17$	710	CSORNA	02	CLE2 $e^+ e^- \approx \Upsilon(4S)$
$4.0 \pm 0.2 \pm 0.3$	2043	AITALA	98c	E791 $\pi^- A, 500 \text{ GeV}$
••• We do not use the following data for averages, fits, limits, etc. •••				
$3.4 \pm 0.7 \pm 0.1$	76 ± 15	ABLIKIM	05F	BES $e^+ e^- \approx \psi(3770)$
$4.3 \pm 0.7 \pm 0.3$	177	FRABETTI	94c	E687 $\gamma \text{ Be } \bar{E}_\gamma = 220 \text{ GeV}$
$3.48 \pm 0.30 \pm 0.23$	227	SELEN	93	CLE2 $e^+ e^- \approx \Upsilon(4S)$
$5.5 \pm 0.8 \pm 0.5$	120	ANJOS	91D	E691 Photoproduction
$5.0 \pm 0.7 \pm 0.5$	110	ALEXANDER	90	CLEO $e^+ e^- 10.5\text{--}11 \text{ GeV}$

$\Gamma(\pi^0 \pi^0)/\Gamma(K^- \pi^+)$				Γ_{135}/Γ_{32}
VALUE (units 10^{-2})	EVTS	DOCUMENT ID	TECN	COMMENT

2.07 ± 0.19 OUR AVERAGE				
$2.05 \pm 0.13 \pm 0.16$	499 ± 32	RUBIN	06	CLEO $e^+ e^-$ at $\psi(3770)$
$2.2 \pm 0.4 \pm 0.4$	40	SELEN	93	CLE2 $e^+ e^- \approx \Upsilon(4S)$

$\Gamma(\pi^+ \pi^- \pi^0)/\Gamma(K^- \pi^+)$				Γ_{136}/Γ_{32}
VALUE (units 10^{-2})	EVTS	DOCUMENT ID	TECN	COMMENT

37.0 ± 1.6 OUR FIT Error includes scale factor of 2.0.				
$34.4 \pm 0.5 \pm 1.2$	$11k \pm 164$	RUBIN	06	CLEO $e^+ e^-$ at $\psi(3770)$

$\Gamma(\pi^+ \pi^- \pi^0)/\Gamma(K^- \pi^+ \pi^0)$				Γ_{136}/Γ_{47}
VALUE (units 10^{-2})	EVTS	DOCUMENT ID	TECN	COMMENT

10.34 ± 0.24 OUR FIT Error includes scale factor of 2.2.				
10.41 ± 0.23 OUR AVERAGE Error includes scale factor of 2.0.				
$10.12 \pm 0.04 \pm 0.18$	$123k \pm 490$	ARINSTEIN	08	BELL $e^+ e^- \approx \Upsilon(4S)$
$10.59 \pm 0.06 \pm 0.13$	$60k \pm 343$	AUBERT,B	06x	BABR $e^+ e^- \approx \Upsilon(4S)$

$\Gamma(\pi^+ \pi^-)/\Gamma(\pi^+ \pi^- \pi^0)$				$\Gamma_{137}/\Gamma_{136}$
VALUE (units 10^{-2})	DOCUMENT ID	TECN	COMMENT	

This is the "fit fraction" from the Dalitz-plot analysis, with interference.				
68.1 ± 0.6 OUR AVERAGE				
$67.8 \pm 0.0 \pm 0.6$	AUBERT	07Bj	BABR	Dalitz fit, 45k events
$76.3 \pm 1.9 \pm 2.5$	CRONIN-HEN..05	CLEO		$e^+ e^- \approx 10 \text{ GeV}$

$\Gamma(\rho^0 \pi^0)/\Gamma(\pi^+ \pi^- \pi^0)$				$\Gamma_{138}/\Gamma_{136}$
VALUE (units 10^{-2})	DOCUMENT ID	TECN	COMMENT	

This is the "fit fraction" from the Dalitz-plot analysis, with interference.				
25.9 ± 1.1 OUR AVERAGE				
$26.2 \pm 0.5 \pm 1.1$	AUBERT	07Bj	BABR	Dalitz fit, 45k events
$24.4 \pm 2.0 \pm 2.1$	CRONIN-HEN..05	CLEO		$e^+ e^- \approx 10 \text{ GeV}$

$\Gamma(\rho^- \pi^+)/\Gamma(\pi^+ \pi^- \pi^0)$				$\Gamma_{139}/\Gamma_{136}$
VALUE (units 10^{-2})	DOCUMENT ID	TECN	COMMENT	

This is the "fit fraction" from the Dalitz-plot analysis, with interference.				
34.6 ± 0.8 OUR AVERAGE				
$34.6 \pm 0.8 \pm 0.3$	AUBERT	07Bj	BABR	Dalitz fit, 45k events
$34.5 \pm 2.4 \pm 1.3$	CRONIN-HEN..05	CLEO		$e^+ e^- \approx 10 \text{ GeV}$

$\Gamma(\rho(1450)^+ \pi^-, \rho(1450)^+ \rightarrow \pi^+ \pi^0)/\Gamma(\pi^+ \pi^- \pi^0)$				$\Gamma_{140}/\Gamma_{136}$
VALUE (units 10^{-2})	DOCUMENT ID	TECN	COMMENT	

$0.11 \pm 0.07 \pm 0.12$	AUBERT	07Bj	BABR	Dalitz fit, 45k events
--------------------------	--------	------	------	------------------------

$\Gamma(\rho(1450)^0 \pi^0, \rho(1450)^0 \rightarrow \pi^+ \pi^-)/\Gamma(\pi^+ \pi^- \pi^0)$				$\Gamma_{141}/\Gamma_{136}$
VALUE (units 10^{-2})	DOCUMENT ID	TECN	COMMENT	

$0.30 \pm 0.11 \pm 0.07$	AUBERT	07Bj	BABR	Dalitz fit, 45k events
--------------------------	--------	------	------	------------------------

$\Gamma(\rho(1450)^- \pi^+, \rho(1450)^- \rightarrow \pi^- \pi^0)/\Gamma(\pi^+ \pi^- \pi^0)$				$\Gamma_{142}/\Gamma_{136}$
VALUE (units 10^{-2})	DOCUMENT ID	TECN	COMMENT	

$1.79 \pm 0.22 \pm 0.12$	AUBERT	07Bj	BABR	Dalitz fit, 45k events
--------------------------	--------	------	------	------------------------

$\Gamma(\rho(1700)^+ \pi^-, \rho(1700)^+ \rightarrow \pi^+ \pi^0)/\Gamma(\pi^+ \pi^- \pi^0)$				$\Gamma_{143}/\Gamma_{136}$
VALUE (units 10^{-2})	DOCUMENT ID	TECN	COMMENT	

$4.1 \pm 0.7 \pm 0.7$	AUBERT	07Bj	BABR	Dalitz fit, 45k events
-----------------------	--------	------	------	------------------------

$\Gamma(\rho(1700)^0 \pi^0, \rho(1700)^0 \rightarrow \pi^+ \pi^-)/\Gamma(\pi^+ \pi^- \pi^0)$				$\Gamma_{144}/\Gamma_{136}$
VALUE (units 10^{-2})	DOCUMENT ID	TECN	COMMENT	

$5.0 \pm 0.6 \pm 1.0$	AUBERT	07Bj	BABR	Dalitz fit, 45k events
-----------------------	--------	------	------	------------------------

$\Gamma(\rho(1700)^- \pi^+, \rho(1700)^- \rightarrow \pi^- \pi^0)/\Gamma(\pi^+ \pi^- \pi^0)$				$\Gamma_{145}/\Gamma_{136}$
VALUE (units 10^{-2})	DOCUMENT ID	TECN	COMMENT	

$3.2 \pm 0.4 \pm 0.6$	AUBERT	07Bj	BABR	Dalitz fit, 45k events
-----------------------	--------	------	------	------------------------

$\Gamma(f_0(980) \pi^0, f_0(980) \rightarrow \pi^+ \pi^-)/\Gamma(\pi^+ \pi^- \pi^0)$				$\Gamma_{146}/\Gamma_{136}$
VALUE (units 10^{-2})	CL%	DOCUMENT ID	TECN	COMMENT

$0.25 \pm 0.04 \pm 0.04$		AUBERT	07Bj	BABR Dalitz fit, 45k events
••• We do not use the following data for averages, fits, limits, etc. •••				
<0.026	95	⁸² CRONIN-HEN..05	CLEO	$e^+ e^- \approx 10 \text{ GeV}$
⁸² The CRONIN-HENNESSY 05 fit here includes, in addition to the three $\rho\pi$ charged states, only the $f_0(980) \pi^0$ mode. See also the next entries for limits obtained in the same way for the $f_0(600) \pi^0$ mode and for an S-wave $\pi^+ \pi^-$ parametrized using a K-matrix. Our $\rho\pi$ branching ratios, given above, use the fit with the K-matrix S wave.				

$\Gamma(f_0(600) \pi^0, f_0(600) \rightarrow \pi^+ \pi^-)/\Gamma(\pi^+ \pi^- \pi^0)$				$\Gamma_{147}/\Gamma_{136}$
VALUE (units 10^{-2})	CL%	DOCUMENT ID	TECN	COMMENT

$0.82 \pm 0.10 \pm 0.10$		AUBERT	07Bj	BABR Dalitz fit, 45k events
••• We do not use the following data for averages, fits, limits, etc. •••				
<0.21	95	⁸³ CRONIN-HEN..05	CLEO	$e^+ e^- \approx 10 \text{ GeV}$
⁸³ See the note on CRONIN-HENNESSY 05 in the preceding data block.				

$\Gamma((\pi^+ \pi^-)_{S\text{-wave}} \pi^0)/\Gamma(\pi^+ \pi^- \pi^0)$				$\Gamma_{148}/\Gamma_{136}$
VALUE	CL%	DOCUMENT ID	TECN	COMMENT

••• We do not use the following data for averages, fits, limits, etc. •••				
<0.019	95	⁸⁴ CRONIN-HEN..05	CLEO	$e^+ e^- \approx 10 \text{ GeV}$
⁸⁴ See the note on CRONIN-HENNESSY 05 two data blocks up.				

$\Gamma(f_0(1370) \pi^0, f_0(1370) \rightarrow \pi^+ \pi^-)/\Gamma(\pi^+ \pi^- \pi^0)$				$\Gamma_{149}/\Gamma_{136}$
VALUE (units 10^{-2})	DOCUMENT ID	TECN	COMMENT	

$0.37 \pm 0.11 \pm 0.09$	AUBERT	07Bj	BABR	Dalitz fit, 45k events
--------------------------	--------	------	------	------------------------

$\Gamma(f_0(1500) \pi^0, f_0(1500) \rightarrow \pi^+ \pi^-)/\Gamma(\pi^+ \pi^- \pi^0)$				$\Gamma_{150}/\Gamma_{136}$
VALUE (units 10^{-2})	DOCUMENT ID	TECN	COMMENT	

$0.39 \pm 0.08 \pm 0.07$	AUBERT	07Bj	BABR	Dalitz fit, 45k events
--------------------------	--------	------	------	------------------------

$\Gamma(f_0(1710) \pi^0, f_0(1710) \rightarrow \pi^+ \pi^-)/\Gamma(\pi^+ \pi^- \pi^0)$				$\Gamma_{151}/\Gamma_{136}$
VALUE (units 10^{-2})	DOCUMENT ID	TECN	COMMENT	

$0.31 \pm 0.07 \pm 0.08$	AUBERT	07Bj	BABR	Dalitz fit, 45k events
--------------------------	--------	------	------	------------------------

$\Gamma(f_2(1270) \pi^0, f_2(1270) \rightarrow \pi^+ \pi^-)/\Gamma(\pi^+ \pi^- \pi^0)$				$\Gamma_{152}/\Gamma_{136}$
VALUE (units 10^{-2})	DOCUMENT ID	TECN	COMMENT	

$1.32 \pm 0.08 \pm 0.10$	AUBERT	07Bj	BABR	Dalitz fit, 45k events
--------------------------	--------	------	------	------------------------

$\Gamma(\pi^+ \pi^- \pi^0 \text{ nonresonant})/\Gamma(\pi^+ \pi^- \pi^0)$				$\Gamma_{153}/\Gamma_{136}$
VALUE (units 10^{-2})	DOCUMENT ID	TECN	COMMENT	

$0.84 \pm 0.21 \pm 0.12$	AUBERT	07Bj	BABR	Dalitz fit, 45k events
--------------------------	--------	------	------	------------------------

$\Gamma(3\pi^0)/\Gamma_{\text{total}}$				Γ_{154}/Γ
VALUE	CL%	DOCUMENT ID	TECN	COMMENT

$<3.5 \times 10^{-4}$	90	RUBIN	06	CLEO $e^+ e^-$ at $\psi(3770)$
-----------------------	----	-------	----	--------------------------------

$\Gamma(2\pi^+ 2\pi^-)/\Gamma(K^- \pi^+)$				Γ_{155}/Γ_{32}
VALUE (units 10^{-2})	EVTS	DOCUMENT ID	TECN	COMMENT

19.1 ± 0.5 OUR FIT Error includes scale factor of 1.1.				
$19.1 \pm 0.4 \pm 0.6$	7331 ± 130	RUBIN	06	CLEO $e^+ e^-$ at $\psi(3770)$

$\Gamma(2\pi^+ 2\pi^-)/\Gamma(K^- \pi^+ \pi^+ \pi^-)$				Γ_{155}/Γ_{59}
VALUE (units 10^{-2})	EVTS	DOCUMENT ID	TECN	COMMENT

9.20 ± 0.23 OUR FIT Error includes scale factor of 1.1.				
9.20 ± 0.26 OUR AVERAGE				
$9.14 \pm 0.18 \pm 0.22$	6360 ± 115	LINK	07A	FOCS $\gamma \text{ Be}, \bar{E}_\gamma \approx 180 \text{ GeV}$
$7.9 \pm 1.8 \pm 0.5$	162	ABLIKIM	05F	BES $e^+ e^- \approx \psi(3770)$
$9.5 \pm 0.7 \pm 0.2$	814	FRABETTI	95c	E687 $\gamma \text{ Be}, \bar{E}_\gamma \approx 200 \text{ GeV}$
10.2 ± 1.3	345	AMMAR	91	CLEO $e^+ e^- \approx 10.5 \text{ GeV}$
••• We do not use the following data for averages, fits, limits, etc. •••				
$11.5 \pm 2.3 \pm 1.6$	64	ADAMOVIICH	92	OMEG $\pi^- 340 \text{ GeV}$
$10.8 \pm 2.4 \pm 0.8$	79	FRABETTI	92	E687 $\gamma \text{ Be}$
$9.6 \pm 1.8 \pm 0.7$	66	ANJOS	91	E691 $\gamma \text{ Be } 80\text{--}240 \text{ GeV}$

$\Gamma(a_1(1260)^+ \pi^-, a_1^+ \rightarrow \pi^+ \pi^- \pi^+ \text{ total})/\Gamma(2\pi^+ 2\pi^-)$				$\Gamma_{156}/\Gamma_{155}$
VALUE (units 10^{-2})	DOCUMENT ID	TECN	COMMENT	

This is the fit fraction from the coherent amplitude analysis.				
$60.0 \pm 3.0 \pm 2.4$	LINK	07A	FOCS	4-body fit, $\approx 5.7k$ evts

$\Gamma(a_1(1260)^+ \pi^-, a_1^+ \rightarrow \rho^0 \pi^+ \text{ S-wave})/\Gamma(2\pi^+ 2\pi^-)$				$\Gamma_{157}/\Gamma_{155}$
VALUE (units 10^{-2})	DOCUMENT ID	TECN	COMMENT	

$43.3 \pm 2.5 \pm 1.9$	LINK	07A	FOCS	4-body fit, $\approx 5.7k$ evts
------------------------	------	-----	------	---------------------------------

Meson Particle Listings

 D^0

$\Gamma(a_1(1260)^+\pi^-, a_1^+ \rightarrow \rho^0\pi^+ D\text{-wave})/\Gamma(2\pi^+2\pi^-)$ $\Gamma_{158}/\Gamma_{155}$

This is the fit fraction from the coherent amplitude analysis.

VALUE (units 10^{-2})	DOCUMENT ID	TECN	COMMENT
$2.5 \pm 0.5 \pm 0.4$	LINK	07A	FOCS 4-body fit, $\approx 5.7k$ evts

$\Gamma(a_1(1260)^+\pi^-, a_1^+ \rightarrow \sigma\pi^+)/\Gamma(2\pi^+2\pi^-)$ $\Gamma_{159}/\Gamma_{155}$

This is the fit fraction from the coherent amplitude analysis.

VALUE (units 10^{-2})	DOCUMENT ID	TECN	COMMENT
$8.3 \pm 0.7 \pm 0.6$	LINK	07A	FOCS 4-body fit, $\approx 5.7k$ evts

$\Gamma(2\rho^0\text{total})/\Gamma(2\pi^+2\pi^-)$ $\Gamma_{160}/\Gamma_{155}$

This is the fit fraction from the coherent amplitude analysis.

VALUE (units 10^{-2})	DOCUMENT ID	TECN	COMMENT
$24.5 \pm 1.3 \pm 1.0$	LINK	07A	FOCS 4-body fit, $\approx 5.7k$ evts

$\Gamma(2\rho^0, \text{parallel helicities})/\Gamma(2\pi^+2\pi^-)$ $\Gamma_{161}/\Gamma_{155}$

This is the fit fraction from the coherent amplitude analysis.

VALUE (units 10^{-2})	DOCUMENT ID	TECN	COMMENT
$1.1 \pm 0.3 \pm 0.3$	LINK	07A	FOCS 4-body fit, $\approx 5.7k$ evts

$\Gamma(2\rho^0, \text{perpendicular helicities})/\Gamma(2\pi^+2\pi^-)$ $\Gamma_{162}/\Gamma_{155}$

This is the fit fraction from the coherent amplitude analysis.

VALUE (units 10^{-2})	DOCUMENT ID	TECN	COMMENT
$6.4 \pm 0.6 \pm 0.5$	LINK	07A	FOCS 4-body fit, $\approx 5.7k$ evts

$\Gamma(2\rho^0, \text{longitudinal helicities})/\Gamma(2\pi^+2\pi^-)$ $\Gamma_{163}/\Gamma_{155}$

This is the fit fraction from the coherent amplitude analysis.

VALUE (units 10^{-2})	DOCUMENT ID	TECN	COMMENT
$16.8 \pm 1.0 \pm 0.8$	LINK	07A	FOCS 4-body fit, $\approx 5.7k$ evts

$\Gamma(\text{Resonant } (\pi^+\pi^-)\pi^+\pi^- \text{ 3-body total})/\Gamma(2\pi^+2\pi^-)$ $\Gamma_{164}/\Gamma_{155}$

This is the fit fraction from the coherent amplitude analysis.

VALUE (units 10^{-2})	DOCUMENT ID	TECN	COMMENT
$20.0 \pm 1.2 \pm 1.0$	LINK	07A	FOCS 4-body fit, $\approx 5.7k$ evts

$\Gamma(\sigma\pi^+\pi^-)/\Gamma(2\pi^+2\pi^-)$ $\Gamma_{165}/\Gamma_{155}$

This is the fit fraction from the coherent amplitude analysis.

VALUE (units 10^{-2})	DOCUMENT ID	TECN	COMMENT
$8.2 \pm 0.9 \pm 0.7$	LINK	07A	FOCS 4-body fit, $\approx 5.7k$ evts

$\Gamma(f_0(980)\pi^+\pi^-, f_0 \rightarrow \pi^+\pi^-)/\Gamma(2\pi^+2\pi^-)$ $\Gamma_{166}/\Gamma_{155}$

This is the fit fraction from the coherent amplitude analysis.

VALUE (units 10^{-2})	DOCUMENT ID	TECN	COMMENT
$2.4 \pm 0.5 \pm 0.4$	LINK	07A	FOCS 4-body fit, $\approx 5.7k$ evts

$\Gamma(f_2(1270)\pi^+\pi^-, f_2 \rightarrow \pi^+\pi^-)/\Gamma(2\pi^+2\pi^-)$ $\Gamma_{167}/\Gamma_{155}$

This is the fit fraction from the coherent amplitude analysis.

VALUE (units 10^{-2})	DOCUMENT ID	TECN	COMMENT
$4.9 \pm 0.6 \pm 0.5$	LINK	07A	FOCS 4-body fit, $\approx 5.7k$ evts

$\Gamma(\pi^+\pi^-2\pi^0)/\Gamma(K^-\pi^+)$ Γ_{168}/Γ_{32}

VALUE (units 10^{-2})	EVTS	DOCUMENT ID	TECN	COMMENT
$25.8 \pm 1.5 \pm 1.8$	2724 ± 166	RUBIN	06	CLEO e^+e^- at $\psi(3770)$

$\Gamma(\eta\pi^0)/\Gamma(K^-\pi^+)$ Γ_{169}/Γ_{32}

Unseen decay modes of the η are included.

VALUE (units 10^{-2})	EVTS	DOCUMENT ID	TECN	COMMENT
$1.47 \pm 0.34 \pm 0.11$	62 ± 14	RUBIN	06	CLEO e^+e^- at $\psi(3770)$

$\Gamma(\omega\pi^0)/\Gamma_{\text{total}}$ Γ_{170}/Γ

Unseen decay modes of the ω are included.

VALUE	CL%	DOCUMENT ID	TECN	COMMENT
$<2.6 \times 10^{-4}$	90	RUBIN	06	CLEO e^+e^- at $\psi(3770)$

$\Gamma(2\pi^+2\pi^-\pi^0)/\Gamma(K^-\pi^+)$ Γ_{171}/Γ_{32}

VALUE (units 10^{-2})	EVTS	DOCUMENT ID	TECN	COMMENT
$10.7 \pm 1.2 \pm 0.5$	1614 ± 171	RUBIN	06	CLEO e^+e^- at $\psi(3770)$

$\Gamma(\eta\pi^+\pi^-)/\Gamma_{\text{total}}$ Γ_{172}/Γ

Unseen decay modes of the η are included.

VALUE	CL%	DOCUMENT ID	TECN	COMMENT
$<1.9 \times 10^{-3}$	90	RUBIN	06	CLEO e^+e^- at $\psi(3770)$

$\Gamma(\omega\pi^+\pi^-)/\Gamma(K^-\pi^+)$ Γ_{173}/Γ_{32}

Unseen decay modes of the ω are included.

VALUE (units 10^{-2})	EVTS	DOCUMENT ID	TECN	COMMENT
$4.1 \pm 1.2 \pm 0.4$	472 ± 132	RUBIN	06	CLEO e^+e^- at $\psi(3770)$

$\Gamma(3\pi^+3\pi^-)/\Gamma(K^-\pi^+\pi^-\pi^-)$ Γ_{174}/Γ_{59}

VALUE (units 10^{-3})	EVTS	DOCUMENT ID	TECN	COMMENT
$5.23 \pm 0.59 \pm 1.35$	149 ± 17	LINK	04B	FOCS $\gamma A, \bar{E}_\gamma \approx 180$ GeV

$\Gamma(3\pi^+3\pi^-)/\Gamma(K^-\pi^+2\pi^-)$ Γ_{174}/Γ_{89}

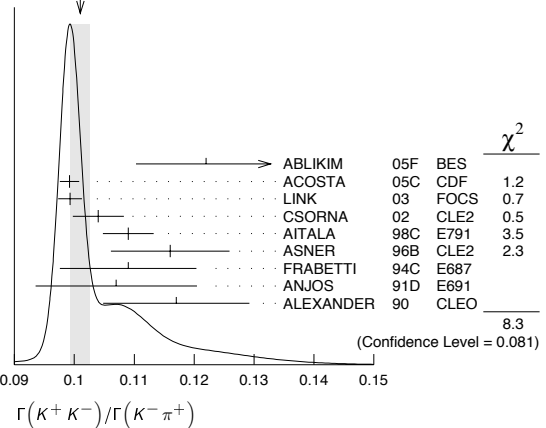
VALUE	DOCUMENT ID	TECN	COMMENT
$1.93 \pm 0.47 \pm 0.48$	⁸⁵ LINK	04B	FOCS $\gamma A, \bar{E}_\gamma \approx 180$ GeV

⁸⁵ This LINK 04B result is not independent of other results in these Listings.Hadronic modes with a $K\bar{K}$ pair

$\Gamma(K^+K^-)/\Gamma(K^-\pi^+)$ Γ_{175}/Γ_{32}

VALUE	EVTS	DOCUMENT ID	TECN	COMMENT
0.1010 ± 0.0016 OUR AVERAGE	Error includes scale factor of 1.4.			See the ideogram below.
$0.122 \pm 0.011 \pm 0.004$	242 ± 20	ABLIKIM	05F	BES $e^+e^- \approx \psi(3770)$
$0.0992 \pm 0.0011 \pm 0.0012$	$16k \pm 200$	ACOSTA	05c	CDF $p\bar{p}, \sqrt{s}=1.96$ TeV
$0.0993 \pm 0.0014 \pm 0.0014$	11k	LINK	03	FOCS γ nucleus, $\bar{E}_\gamma \approx 180$ GeV
$0.1040 \pm 0.0033 \pm 0.0027$	1900	CSORNA	02	CLE2 $e^+e^- \approx \Upsilon(4S)$
$0.109 \pm 0.003 \pm 0.003$	3317	AITALA	98c	E791 π^- nucleus, 500 GeV
$0.116 \pm 0.007 \pm 0.007$	1102	ASNER	96B	CLE2 $e^+e^- \approx \Upsilon(4S)$
$0.109 \pm 0.007 \pm 0.009$	581	FRABETTI	94c	E687 γ Be $\bar{E}_\gamma = 220$ GeV
$0.107 \pm 0.010 \pm 0.009$	193	ANJOS	91D	E691 Photoproduction
$0.117 \pm 0.010 \pm 0.007$	249	ALEXANDER	90	CLEO $e^+e^- 10.5-11$ GeV
$0.107 \pm 0.029 \pm 0.015$	103	ADAMOVICH	92	OMEG $\pi^- 340$ GeV
$0.138 \pm 0.027 \pm 0.010$	155	FRABETTI	92	E687 γ Be
0.16 ± 0.05	34	ALVAREZ	91B	NA14 Photoproduction
$0.10 \pm 0.02 \pm 0.01$	131	ALBRECHT	90c	ARG $e^+e^- \approx 10$ GeV
$0.122 \pm 0.018 \pm 0.012$	118	BALTRUSAITIS	85E	MRK3 $e^+e^- 3.77$ GeV
0.113 ± 0.030		ABRAMS	79D	MRK2 $e^+e^- 3.77$ GeV

WEIGHTED AVERAGE
 0.1010 ± 0.0016 (Error scaled by 1.4)



$\Gamma(K^+K^-)/\Gamma(\pi^+\pi^-)$ $\Gamma_{175}/\Gamma_{134}$

The unused results here are redundant with $\Gamma(K^+K^-)/\Gamma(K^-\pi^+)$ and $\Gamma(\pi^+\pi^-)/\Gamma(K^-\pi^+)$ measurements by the same experiments.

VALUE	EVTS	DOCUMENT ID	TECN	COMMENT
$2.760 \pm 0.040 \pm 0.034$	7334	ACOSTA	05c	CDF $p\bar{p}, \sqrt{s}=1.96$ TeV
$2.81 \pm 0.10 \pm 0.06$		LINK	03	FOCS γ nucleus, $\bar{E}_\gamma \approx 180$ GeV
$2.96 \pm 0.16 \pm 0.15$	710	CSORNA	02	CLE2 $e^+e^- \approx \Upsilon(4S)$
$2.75 \pm 0.15 \pm 0.16$		AITALA	98c	E791 π^- nucleus, 500 GeV
$2.53 \pm 0.46 \pm 0.19$		FRABETTI	94c	E687 γ Be $\bar{E}_\gamma = 220$ GeV
$2.23 \pm 0.81 \pm 0.46$		ADAMOVICH	92	OMEG $\pi^- 340$ GeV
$1.95 \pm 0.34 \pm 0.22$		ANJOS	91D	E691 Photoproduction
2.5 ± 0.7		ALBRECHT	90c	ARG $e^+e^- \approx 10$ GeV
$2.35 \pm 0.37 \pm 0.28$		ALEXANDER	90	CLEO $e^+e^- 10.5-11$ GeV

$\Gamma(K_S^0)/\Gamma(K_L^0\pi^+\pi^-)$ Γ_{176}/Γ_{35}

This is the same as $\Gamma(K^0\bar{K}^0)/\Gamma(\bar{K}^0\pi^+\pi^-)$ because $D^0 \rightarrow K_S^0 K_L^0$ is forbidden by CP conservation.

VALUE	EVTS	DOCUMENT ID	TECN	COMMENT
0.0126 ± 0.0022 OUR AVERAGE				
$0.0144 \pm 0.0032 \pm 0.0016$	79 ± 17	LINK	05A	FOCS γ Be, $\bar{E}_\gamma \approx 180$ GeV
$0.0101 \pm 0.0022 \pm 0.0016$	26	ASNER	96B	CLE2 $e^+e^- \approx \Upsilon(4S)$
$0.039 \pm 0.013 \pm 0.013$	20 ± 7	FRABETTI	94J	E687 γ Be $\bar{E}_\gamma = 220$ GeV
$0.021 \pm 0.011 \pm 0.008$	5	ALEXANDER	90	CLEO $e^+e^- 10.5-11$ GeV

$\Gamma(K_S^0 K^-\pi^+)/\Gamma(K^-\pi^+)$ Γ_{177}/Γ_{32}

VALUE	DOCUMENT ID	TECN	COMMENT
0.090 ± 0.013 OUR FIT			Error includes scale factor of 1.1.
0.08 ± 0.03	⁸⁶ ANJOS	91	E691 γ Be 80-240 GeV

⁸⁶ The factor 100 at the top of column 2 of Table I of ANJOS 91 should be omitted.

$\Gamma(K_S^0 K^- \pi^+)/\Gamma(K_S^0 \pi^+ \pi^-)$ Γ_{177}/Γ_{35}

VALUE	EVTS	DOCUMENT ID	TECN	COMMENT
0.117±0.017 OUR FIT				Error includes scale factor of 1.1.
0.119±0.021 OUR AVERAGE				Error includes scale factor of 1.3.
0.108±0.019	61	AMMAR	91 CLEO	$e^+e^- \approx 10.5$ GeV
0.16 ± 0.03 ± 0.02	39	ALBRECHT	90c ARG	$e^+e^- \approx 10$ GeV

 $\Gamma(\bar{K}^*(892)^0 K_S^0, \bar{K}^*(892)^0 \rightarrow K^- \pi^+)/\Gamma(K_S^0 \pi^+ \pi^-)$ Γ_{178}/Γ_{35}

VALUE	CL%	DOCUMENT ID	TECN	COMMENT
<0.019	90	AMMAR	91 CLEO	$e^+e^- \approx 10.5$ GeV
••• We do not use the following data for averages, fits, limits, etc. ••••				
<0.02	90	ALBRECHT	90c ARG	$e^+e^- \approx 10$ GeV

 $\Gamma(K_S^0 K^+ \pi^-)/\Gamma(K^- \pi^+)$ Γ_{179}/Γ_{32}

VALUE	DOCUMENT ID	TECN	COMMENT
0.068±0.013 OUR FIT			
0.05 ± 0.025	87 ANJOS	91 E691	γ Be 80–240 GeV
87 The factor 100 at the top of column 2 of Table I of ANJOS 91 should be omitted.			

 $\Gamma(K_S^0 K^+ \pi^-)/\Gamma(K_S^0 \pi^+ \pi^-)$ Γ_{179}/Γ_{35}

VALUE	EVTS	DOCUMENT ID	TECN	COMMENT
0.089±0.017 OUR FIT				
0.098±0.020	55	AMMAR	91 CLEO	$e^+e^- \approx 10.5$ GeV

 $\Gamma(K^*(892)^0 K_S^0, K^*(892)^0 \rightarrow K^+ \pi^-)/\Gamma(K_S^0 \pi^+ \pi^-)$ Γ_{180}/Γ_{35}

VALUE	CL%	DOCUMENT ID	TECN	COMMENT
<0.010	90	AMMAR	91 CLEO	$e^+e^- \approx 10.5$ GeV

 $\Gamma(K^+ K^- \pi^0)/\Gamma(K^- \pi^+ \pi^0)$ Γ_{181}/Γ_{47}

VALUE (units 10^{-2})	EVTS	DOCUMENT ID	TECN	COMMENT
2.37±0.03±0.04	11k±122	AUBERT,B	06x BABR	$e^+e^- \approx \Upsilon(4S)$
••• We do not use the following data for averages, fits, limits, etc. ••••				
0.95±0.26	151	ASNER	96b CLE2	$e^+e^- \approx \Upsilon(4S)$

 $\Gamma(K^*(892)^+ K^-, K^*(892)^+ \rightarrow K^+ \pi^0)/\Gamma(K^+ K^- \pi^0)$ $\Gamma_{182}/\Gamma_{181}$

This is the "fit fraction" from the Dalitz-plot analysis with interference.

VALUE (units 10^{-2})	DOCUMENT ID	TECN	COMMENT
44.6^{+1.0}_{-0.9} OUR AVERAGE			
44.4±0.8±0.6	AUBERT	07T BABR	Dalitz fit II, 11k evts
46.1±3.1	88 CAWLFIELD	06A CLEO	Dalitz fit, 627 ± 30 evts
88 The error on this CAWLFIELD 06A result is statistical only.			

 $\Gamma(K^*(892)^- K^+, K^*(892)^- \rightarrow K^- \pi^0)/\Gamma(K^+ K^- \pi^0)$ $\Gamma_{183}/\Gamma_{181}$

This is the "fit fraction" from the Dalitz-plot analysis with interference.

VALUE (units 10^{-2})	DOCUMENT ID	TECN	COMMENT
15.4±1.3 OUR AVERAGE			Error includes scale factor of 1.5.
15.9±0.7±0.6	AUBERT	07T BABR	Dalitz fit II, 11k evts
12.3±2.2	89 CAWLFIELD	06A CLEO	Dalitz fit, 627 ± 30 evts
89 The error on this CAWLFIELD 06A result is statistical only.			

 $\Gamma((K^+ \pi^0)_{S\text{-wave}} K^-)/\Gamma(K^+ K^- \pi^0)$ $\Gamma_{184}/\Gamma_{181}$

This is the "fit fraction" from the Dalitz-plot analysis with interference.

VALUE (units 10^{-2})	DOCUMENT ID	TECN	COMMENT
71.1±3.7±1.9	90 AUBERT	07T BABR	Dalitz fit II, 11k evts
90 The only major difference between fits I and II in the AUBERT 07T analysis is in this mode, where fit-I fraction is (16.3 ± 3.4 ± 2.1)%.			

 $\Gamma((K^- \pi^0)_{S\text{-wave}} K^+)/\Gamma(K^+ K^- \pi^0)$ $\Gamma_{185}/\Gamma_{181}$

This is the "fit fraction" from the Dalitz-plot analysis with interference.

VALUE (units 10^{-2})	DOCUMENT ID	TECN	COMMENT
3.9±0.9±1.0	AUBERT	07T BABR	Dalitz fit II, 11k evts

 $\Gamma(f_0(980) \pi^0, f_0 \rightarrow K^+ K^-)/\Gamma(K^+ K^- \pi^0)$ $\Gamma_{186}/\Gamma_{181}$

This is the "fit fraction" from the Dalitz-plot analysis with interference.

VALUE (units 10^{-2})	DOCUMENT ID	TECN	COMMENT
10.5±1.1±1.2	91 AUBERT	07T BABR	Dalitz fit II, 11k evts
91 When AUBERT 07T replace the $f_0(980) \pi^0$ mode with $a_0(980) \pi^0$, the fit fraction is a negligibly different (11.0 ± 1.5 ± 1.2)%.			

 $\Gamma(\phi \pi^0, \phi \rightarrow K^+ K^-)/\Gamma(K^+ K^- \pi^0)$ $\Gamma_{187}/\Gamma_{181}$

This is the "fit fraction" from the Dalitz-plot analysis with interference.

VALUE (units 10^{-2})	DOCUMENT ID	TECN	COMMENT
18.5±1.8 OUR AVERAGE			Error includes scale factor of 2.5.
19.4±0.6±0.5	AUBERT	07T BABR	Dalitz fit II, 11k evts
14.9±1.6	92 CAWLFIELD	06A CLEO	Dalitz fit, 627 ± 30 evts
92 The error on this CAWLFIELD 06A result is statistical only.			

 $\Gamma(K^+ K^- \pi^0 \text{ nonresonant})/\Gamma(K^+ K^- \pi^0)$ $\Gamma_{188}/\Gamma_{181}$

This is the "fit fraction" from the Dalitz-plot analysis with interference.

VALUE	DOCUMENT ID	TECN	COMMENT
0.360±0.037	93 CAWLFIELD	06A CLEO	Dalitz fit, 627 ± 30 evts
93 The error is statistical only. CAWLFIELD 06A also fits the Dalitz plot replacing this flat nonresonant background with broad S-wave $\kappa^\pm \rightarrow K^\pm \pi^0$ resonances. There is no significant improvement in the fit, and $K^* \pm K^\mp$ and $\phi \pi^0$ results are not much changed.			

 $\Gamma(K_S^0 K_S^0 \pi^0)/\Gamma_{\text{total}}$ Γ_{189}/Γ

VALUE	DOCUMENT ID	TECN	COMMENT
<0.00059	ASNER	96b CLE2	$e^+e^- \approx \Upsilon(4S)$

 $\Gamma(\phi \pi^0)/\Gamma(K^+ K^-)$ $\Gamma_{204}/\Gamma_{175}$

VALUE	EVTS	DOCUMENT ID	TECN	COMMENT
0.194±0.006±0.009	1254	TAJIMA	04 BELL	e^+e^- at $\Upsilon(4S)$

 $\Gamma(\phi \eta)/\Gamma(K^+ K^-)$ $\Gamma_{205}/\Gamma_{175}$

VALUE (units 10^{-2})	EVTS	DOCUMENT ID	TECN	COMMENT
3.59±1.14±0.18	31	TAJIMA	04 BELL	e^+e^- at $\Upsilon(4S)$

 $\Gamma(\phi \omega)/\Gamma_{\text{total}}$ Γ_{206}/Γ

VALUE	CL%	DOCUMENT ID	TECN	COMMENT
<0.0021	90	ALBRECHT	94i ARG	$e^+e^- \approx 10$ GeV

 $\Gamma(K^+ K^- \pi^+ \pi^-)/\Gamma(K^- \pi^+ \pi^+ \pi^-)$ Γ_{190}/Γ_{59}

VALUE (units 10^{-2})	EVTS	DOCUMENT ID	TECN	COMMENT
3.00±0.13 OUR AVERAGE				
2.95±0.11±0.08	2669 ± 101	94 LINK	05G FOCUS	γ Be, $\bar{E}_\gamma \approx 180$ GeV
3.13±0.37±0.36	136 ± 15	AITALA	98D E791	π^- nucleus, 500 GeV
3.5 ± 0.4 ± 0.2	244 ± 26	FRABETTI	95C E687	γ Be, $\bar{E}_\gamma \approx 200$ GeV
••• We do not use the following data for averages, fits, limits, etc. ••••				
4.4 ± 1.8 ± 0.5	19 ± 8	ABLIKIM	05F BES	$e^+e^- \approx \psi(3770)$
4.1 ± 0.7 ± 0.5	114 ± 20	ALBRECHT	94i ARG	$e^+e^- \approx 10$ GeV
3.14±1.0	89 ± 29	AMMAR	91 CLEO	$e^+e^- \approx 10.5$ GeV
2.8 ^{+0.8} _{-0.7}		ANJOS	91 E691	γ Be 80–240 GeV
94 LINK 05G uses a smaller, cleaner subset of 1279 ± 48 events for the amplitude analysis that gives the results in the next data blocks.				

 $\Gamma(\phi \pi^+ \pi^- \text{ 3-body}, \phi \rightarrow K^+ K^-)/\Gamma(K^+ K^- \pi^+ \pi^-)$ $\Gamma_{191}/\Gamma_{190}$

This is the fraction from a coherent amplitude analysis.

VALUE	DOCUMENT ID	TECN	COMMENT
0.01±0.01	LINK	05G FOCUS	1279 ± 48 $K^+ K^- \pi^+ \pi^-$ evts.

 $\Gamma(\phi \rho^0, \phi \rightarrow K^+ K^-)/\Gamma(K^+ K^- \pi^+ \pi^-)$ $\Gamma_{192}/\Gamma_{190}$

This is the fraction from a coherent amplitude analysis.

VALUE	DOCUMENT ID	TECN	COMMENT
0.29±0.02 ± 0.01	LINK	05G FOCUS	1279 ± 48 $K^+ K^- \pi^+ \pi^-$ evts.

 $\Gamma(K^+ K^- \rho^0 \text{ 3-body})/\Gamma(K^+ K^- \pi^+ \pi^-)$ $\Gamma_{193}/\Gamma_{190}$

This is the fraction from a coherent amplitude analysis.

VALUE	DOCUMENT ID	TECN	COMMENT
0.02±0.02 ± 0.02	LINK	05G FOCUS	1279 ± 48 $K^+ K^- \pi^+ \pi^-$ evts.

 $\Gamma(f_0(980) \pi^+ \pi^-, f_0 \rightarrow K^+ K^-)/\Gamma(K^+ K^- \pi^+ \pi^-)$ $\Gamma_{194}/\Gamma_{190}$

This is the fraction from a coherent amplitude analysis.

VALUE	DOCUMENT ID	TECN	COMMENT
0.15±0.03±0.02	LINK	05G FOCUS	1279 ± 48 $K^+ K^- \pi^+ \pi^-$ evts.

 $\Gamma(K^*(892)^0 K^\mp \pi^\pm \text{ 3-body}, K^{*0} \rightarrow K^\pm \pi^\mp)/\Gamma(K^+ K^- \pi^+ \pi^-)$ $\Gamma_{195}/\Gamma_{190}$

This is the fraction from a coherent amplitude analysis.

VALUE	DOCUMENT ID	TECN	COMMENT
0.11±0.02 ± 0.01	LINK	05G FOCUS	1279 ± 48 $K^+ K^- \pi^+ \pi^-$ evts.

 $\Gamma(K^*(892)^0 \bar{K}^*(892)^0, K^{*0} \rightarrow K^\pm \pi^\mp)/\Gamma(K^+ K^- \pi^+ \pi^-)$ $\Gamma_{196}/\Gamma_{190}$

This is the fraction from a coherent amplitude analysis.

VALUE	DOCUMENT ID	TECN	COMMENT
0.03±0.02 ± 0.01	LINK	05G FOCUS	1279 ± 48 $K^+ K^- \pi^+ \pi^-$ evts.

 $\Gamma(K_1(1270)^\pm K^\mp, K_1(1270)^\pm \rightarrow K^\pm \pi^\mp)/\Gamma(K^+ K^- \pi^+ \pi^-)$ $\Gamma_{197}/\Gamma_{190}$

This is the fraction from a coherent amplitude analysis.

VALUE	DOCUMENT ID	TECN	COMMENT
0.33±0.06±0.04	95 LINK	05G FOCUS	1279 ± 48 $K^+ K^- \pi^+ \pi^-$ evts.
95 This LINK 05G value includes $K_1(1270)^\pm \rightarrow \rho^0 K^\pm \rightarrow K_0^0(1430) \pi^\pm$, and $K^*(892) \pi^\pm$.			

 $\Gamma(K_1(1400)^\pm K^\mp, K_1(1400)^\pm \rightarrow K^\pm \pi^\mp)/\Gamma(K^+ K^- \pi^+ \pi^-)$ $\Gamma_{198}/\Gamma_{190}$

This is the fraction from a coherent amplitude analysis.

VALUE	DOCUMENT ID	TECN	COMMENT
0.22±0.03±0.04	LINK	05G FOCUS	1279 ± 48 $K^+ K^- \pi^+ \pi^-$ evts.

Meson Particle Listings

 D^0 $\Gamma(K_S^0 K_S^0 \pi^+ \pi^-) / \Gamma(K_S^0 \pi^+ \pi^-)$ $\Gamma_{201} / \Gamma_{35}$

VALUE (units 10^{-2})	EVTS	DOCUMENT ID	TECN	COMMENT
4.3 ± 0.8 OUR AVERAGE				
4.16 ± 0.70 ± 0.42	113 ± 21	LINK	05A	FOCS γ Be, $\bar{E}_\gamma \approx 180$ GeV
6.2 ± 2.0 ± 1.6	25	ALBRECHT	94i	ARG $e^+ e^- \approx 10$ GeV

 $\Gamma(K_S^0 K^- \pi^+ \pi^+ \pi^-) / \Gamma(K_S^0 2\pi^+ 2\pi^-)$ $\Gamma_{202} / \Gamma_{83}$

VALUE	CL%	DOCUMENT ID	TECN	COMMENT
<0.054	90	LINK	04D	FOCS γ A, $\bar{E}_\gamma \approx 180$ GeV

 $\Gamma(K^+ K^- \pi^+ \pi^- \pi^0) / \Gamma_{total}$ Γ_{203} / Γ

VALUE	DOCUMENT ID	TECN	COMMENT
0.0031 ± 0.0020	96 BARLAG	92c	ACCM π^- Cu 230 GeV

⁹⁶ BARLAG 92c computes the branching fraction using topological normalization.

Radiative modes

 $\Gamma(\rho^0 \gamma) / \Gamma_{total}$ Γ_{207} / Γ

VALUE	CL%	DOCUMENT ID	TECN
<2.4 × 10⁻⁴	90	ASNER	98 CLE2

 $\Gamma(\omega \gamma) / \Gamma_{total}$ Γ_{208} / Γ

VALUE	CL%	DOCUMENT ID	TECN
<2.4 × 10⁻⁴	90	ASNER	98 CLE2

 $\Gamma(\phi \gamma) / \Gamma_{total}$ Γ_{209} / Γ

VALUE	CL%	DOCUMENT ID	TECN
<1.9 × 10⁻⁴	90	ASNER	98 CLE2

• • • We do not use the following data for averages, fits, limits, etc. • • •

 $\Gamma(\phi \gamma) / \Gamma(K^+ K^-)$ $\Gamma_{209} / \Gamma_{175}$

VALUE (units 10^{-3})	EVTS	DOCUMENT ID	TECN	COMMENT
6.31 ± 1.70 + 0.30 -1.48 - 0.36	28	TAJIMA	04	BELL $e^+ e^-$ at $\Upsilon(4S)$

 $\Gamma(K^*(892)^0 \gamma) / \Gamma_{total}$ Γ_{210} / Γ

VALUE	CL%	DOCUMENT ID	TECN
<7.6 × 10⁻⁴	90	ASNER	98 CLE2

Doubly Cabibbo-suppressed / Mixing modes

 $\Gamma(K^+ \ell^- \bar{\nu}_\ell \text{ via } \bar{D}^0) / \Gamma(K^- \ell^+ \nu_\ell)$ $\Gamma_{211} / \Gamma_{17}$

This is a limit on R_M without the complications of possible doubly Cabibbo-suppressed decays that occur when using hadronic modes. For the limits on $|m_1 - m_2|$ and $(\Gamma_1 - \Gamma_2) / \Gamma$ that come from the best mixing limit, see near the beginning of these D^0 Listings.

VALUE	CL%	DOCUMENT ID	TECN	COMMENT
<0.005	90	97 AITALA	96c	E791 π^- nucleus, 500 GeV

⁹⁷ AITALA 96c uses $D^{*+} \rightarrow D^0 \pi^+$ (and charge conjugate) decays to identify the charm at production and $D^0 \rightarrow K^- \ell^+ \nu_\ell$ (and charge conjugate) decays to identify the charm at decay.

 $\Gamma(K^+ \text{ or } K^*(892)^+ e^- \bar{\nu}_e \text{ via } \bar{D}^0) / [\Gamma(K^- e^+ \nu_e) + \Gamma(K^*(892)^- e^+ \nu_e)]$ $\Gamma_{212} / (\Gamma_{18} + \Gamma_{20})$

This is a limit on R_M without the complications of possible doubly Cabibbo-suppressed decays that occur when using hadronic modes. The experiments use $D^{*+} \rightarrow D^0 \pi^+$ (and charge conjugate) decays to identify the charm at production and the charge of the e to identify the charm at decay. These limits do not allow CP violation. For the limits on $|m_1 - m_2|$ and $(\Gamma_1 - \Gamma_2) / \Gamma$ that come from the best mixing limit, see near the beginning of these D^0 Listings.

VALUE	CL%	DOCUMENT ID	TECN	COMMENT
<0.001	90	BITENC	05	BELL $e^+ e^- \approx 10.6$ GeV

• • • We do not use the following data for averages, fits, limits, etc. • • •

-0.0013 < R < +0.0012	90	AUBERT	07AB	BABR $e^+ e^- \approx 10.58$ GeV
<0.0078	90	CAWLFIELD	05	CLEO $e^+ e^- \approx 10.6$ GeV
<0.0042	90	AUBERT,B	04Q	BABR See AUBERT 07AB

 $\Gamma(K^+ \pi^-) / \Gamma(K^- \pi^+)$ $\Gamma_{213} / \Gamma_{32}$

This is R , the time-integrated wrong-sign rate compared to the right-sign rate. See the note on " D^0 - \bar{D}^0 Mixing," near the start of the D^0 Listings.

The experiments here use the charge of the pion in $D^*(2010)^\pm \rightarrow (D^0 \text{ or } \bar{D}^0) \pi^\pm$ decay to tell whether a D^0 or a \bar{D}^0 was born. The $D^0 \rightarrow K^+ \pi^-$ decay can occur directly by doubly Cabibbo-suppressed (DCS) decay, or indirectly by $D^0 \rightarrow \bar{D}^0$ mixing followed by $\bar{D}^0 \rightarrow K^+ \pi^-$ decay. Some of the experiments can use the decay-time information to disentangle the two mechanisms. Here, we list the experimental branching ratio, which if there is no mixing is the DCS ratio. See the next data block for values of the DCS ratio R_D , and the following data block for limits on the mixing ratio R_M . See the section on CP -violating asymmetries near the end of this D^0 Listing for values of A_D , and the note on " D^0 - \bar{D}^0 Mixing" for limits on x' and y' .

Some early limits have been omitted from this Listing; see our 1998 edition (The European Physical Journal **C3** 1 (1998)) and our 2006 edition (Journal of Physics, **G33** 1 (2006)).

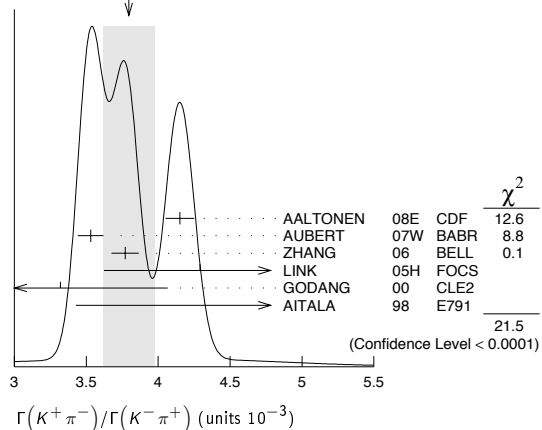
VALUE (units 10^{-3}) EVTS DOCUMENT ID TECN COMMENT

VALUE (units 10^{-3})	EVTS	DOCUMENT ID	TECN	COMMENT
3.80 ± 0.18 OUR AVERAGE	Error	includes scale factor of 3.3. See the ideogram below.		
4.15 ± 0.10	12.7 ± 0.3k	98 AALTONEN	08E	CDF $p\bar{p}$, $\sqrt{s} = 1.96$ TeV
3.53 ± 0.08 ± 0.04	4030 ± 90	99 AUBERT	07W	BABR $e^+ e^- \approx 10.6$ GeV
3.77 ± 0.08 ± 0.05	4024 ± 88	98 ZHANG	06	BELL $e^+ e^-$
4.29 ^{+0.63} _{-0.61} ± 0.27	234	100 LINK	05H	FOCS γ nucleus
3.32 ^{+0.63} _{-0.65} ± 0.40	45	98 GODANG	00	CLE2 $e^+ e^-$
6.8 ^{+3.4} _{-3.3} ± 0.7	34	99 AITALA	98	E791 π^- nucl., 500 GeV

• • • We do not use the following data for averages, fits, limits, etc. • • •

4.05 ± 0.21 ± 0.11	2.0 ± 0.1k	101 ABULENCIA	06x	CDF See AALTONEN 08E
3.81 ± 0.17 ^{+0.08} _{-0.16}	845 ± 40	99 LI	05A	BELL See ZHANG 06
3.57 ± 0.22 ± 0.27		102 AUBERT	03z	BABR See AUBERT 07W
4.04 ± 0.85 ± 0.25	149	103 LINK	01	FOCS γ nucleus

⁹⁸ GODANG 00, ZHANG 06, and AALTONEN 08E allow CP violation.
⁹⁹ AITALA 98, LI 05A, and AUBERT 07W assume no CP violation.
¹⁰⁰ This LINK 05H result assumes no mixing but allows CP violation. If neither mixing nor CP violation is allowed, $R = (4.29 \pm 0.63 \pm 0.28) \times 10^{-3}$.
¹⁰¹ This ABULENCIA 06x result assumes no mixing.
¹⁰² This AUBERT 03z result allows CP violation. If CP violation is not allowed, $R = 0.00359 \pm 0.00020 \pm 0.00027$.
¹⁰³ This LINK 01 result assumes no mixing or CP violation.

WEIGHTED AVERAGE
3.80 ± 0.18 (Error scaled by 3.3) $\Gamma(K^+ \pi^- \text{ via DCS}) / \Gamma(K^- \pi^+)$ $\Gamma_{214} / \Gamma_{32}$

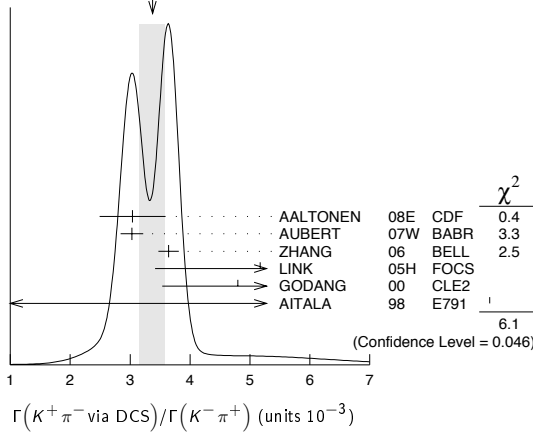
This is R_D , the doubly Cabibbo-suppressed ratio when mixing is allowed.

VALUE (units 10^{-3})	CL%	EVTS	DOCUMENT ID	TECN	COMMENT
3.37 ± 0.21 OUR AVERAGE	Error	includes scale factor of 1.8. See the ideogram below.			
3.04 ± 0.55	12.7 ± 0.3k		AALTONEN	08E	CDF $p\bar{p}$, $\sqrt{s} = 1.96$ TeV
3.03 ± 0.16 ± 0.10	4030 ± 90		104 AUBERT	07W	BABR $e^+ e^- \approx 10.6$ GeV
3.64 ± 0.17	4024 ± 88		105 ZHANG	06	BELL $e^+ e^-$
5.17 ^{+1.47} _{-1.58} ± 0.76	234		106 LINK	05H	FOCS γ nucleus
4.8 ± 1.2 ± 0.4	45		107 GODANG	00	CLE2 $e^+ e^-$
9.0 ^{+12.0} _{-10.9} ± 4.4	34		108 AITALA	98	E791 π^- nucl., 500 GeV

• • • We do not use the following data for averages, fits, limits, etc. • • •

2.87 ± 0.37	845 ± 40		LI	05A	BELL See ZHANG 06
2.3 < R_D < 5.2	95		109 AUBERT	03z	BABR See AUBERT 07W

¹⁰⁴ This AUBERT 07W result is the same whether or not CP violation is allowed.
¹⁰⁵ This ZHANG 06 assumes no CP violation.
¹⁰⁶ This LINK 05H result allows CP violation. Allowing mixing but not CP violation, $R_D = (3.81 \pm 1.67 \pm 0.92) \times 10^{-3}$.
¹⁰⁷ This GODANG 00 result allows CP violation.
¹⁰⁸ This AITALA 98 result assumes no CP violation.
¹⁰⁹ This AUBERT 03z result allows CP violation. If only mixing is allowed, the 95% confidence level interval is $(2.4 < R_D < 4.9) \times 10^{-3}$.

WEIGHTED AVERAGE
3.37±0.21 (Error scaled by 1.8) $\Gamma(K^+\pi^- \text{ via } \bar{D}^0)/\Gamma(K^-\pi^+)$ **Γ215/Γ32**

This is R_M in the note on " D^0 - \bar{D}^0 Mixing" near the start of the D^0 Listings. The experiments here (1) use the charge of the pion in $D^*(2010)^\pm \rightarrow (D^0 \text{ or } \bar{D}^0) \pi^\pm$ decay to tell whether a D^0 or a \bar{D}^0 was born; and (2) use the decay-time distribution to disentangle doubly Cabibbo-suppressed decay and mixing. For the limits on $|m_1 - m_2|$ and $(\Gamma_1 - \Gamma_2)/\Gamma$ that come from the best mixing limit, see near the beginning of these D^0 Listings.

VALUE	CL%	EVTS	DOCUMENT ID	TECN	COMMENT
<0.00040	95	110	ZHANG	06	BELL e^+e^-
•••					We do not use the following data for averages, fits, limits, etc. •••
<0.00046	95	111	LI	05A	BELL See ZHANG 06
<0.0063	95	112	LINK	05H	FOCS γ nucleus
<0.0013	95	113	AUBERT	03Z	BABR e^+e^- , 10.6 GeV
<0.00041	95	114	GODANG	00	CLE2 e^+e^-
<0.0092	95	115	BARATE	98W	ALEP e^+e^- at Z^0
<0.005	90	1 ± 4	ANJOS	88c	E691 Photoproduction

- 110 This ZHANG 06 result allows CP violation, but the result does not change if CP violation is not allowed.
- 111 This LI 05A result allows CP violation. The limit becomes < 0.00042 (95% CL) if CP violation is not allowed.
- 112 LINK 05H obtains the same result whether or not CP violation is allowed.
- 113 This AUBERT 03Z result allows CP violation and assumes that the strong phase between $D^0 \rightarrow K^+\pi^-$ and $\bar{D}^0 \rightarrow K^+\pi^-$ is small, and limits only $D^0 \rightarrow \bar{D}^0$ transitions via off-shell intermediate states. The limit on transitions via on-shell intermediate states is 0.0016.
- 114 This GODANG 00 result allows CP violation and assumes that the strong phase between $D^0 \rightarrow K^+\pi^-$ and $\bar{D}^0 \rightarrow K^+\pi^-$ is small, and limits only $D^0 \rightarrow \bar{D}^0$ transitions via off-shell intermediate states. The limit on transitions via on-shell intermediate states is 0.0017.
- 115 This BARATE 98W result assumes no interference between the DCS and mixing amplitudes ($\gamma' = 0$ in the note on " D^0 - \bar{D}^0 Mixing" near the start of the D^0 Listings). When interference is allowed, the limit degrades to 0.036 (95% CL).
- 116 This ANJOS 88c result assumes no interference between the DCS and mixing amplitudes ($\gamma' = 0$ in the note on " D^0 - \bar{D}^0 Mixing" near the start of the D^0 Listings). When interference is allowed, the limit degrades to 0.019.

 $\Gamma(K_S^0 \pi^+ \pi^- \text{ in } D^0 \rightarrow \bar{D}^0)/\Gamma(K_S^0 \pi^+ \pi^-)$ **Γ216/Γ35**

This is R_M in the note on " D^0 - \bar{D}^0 Mixing" near the start of the D^0 Listings. The experiments here (1) use the charge of the pion in $D^*(2010)^\pm \rightarrow (D^0 \text{ or } \bar{D}^0) \pi^\pm$ decay to tell whether a D^0 or a \bar{D}^0 was born; and (2) use the decay-time distribution to disentangle doubly Cabibbo-suppressed decay and mixing. For the limits on $|m_1 - m_2|$ and $(\Gamma_1 - \Gamma_2)/\Gamma$ that come from the best mixing limit, see near the beginning of these D^0 Listings.

VALUE	CL%	DOCUMENT ID	TECN	COMMENT
<0.0063	95	117	ASNER	05 CLEO $e^+e^- \approx 10$ GeV

- 117 This ASNER 05 limit allows CP violation. If CP violation is not allowed, the limit is 0.0042 at 95% CL.

 $\Gamma(K^+\pi^-\pi^0)/\Gamma(K^-\pi^+\pi^0)$ **Γ218/Γ47**

The experiments here use the charge of the pion in $D^*(2010)^\pm \rightarrow (D^0 \text{ or } \bar{D}^0) \pi^\pm$ decay to tell whether a D^0 or a \bar{D}^0 was born. The $D^0 \rightarrow K^+\pi^-\pi^0$ decay can occur directly by doubly Cabibbo-suppressed (DCS) decay, or indirectly by $D^0 \rightarrow \bar{D}^0$ mixing followed by $\bar{D}^0 \rightarrow K^+\pi^-\pi^0$ decay.

VALUE (units 10^{-3})	CL%	EVTS	DOCUMENT ID	TECN	COMMENT
2.20 ± 0.10 OUR AVERAGE					
2.14 ± 0.08 ± 0.08	763 ± 51	118	AUBERT,B	06N	BABR $e^+e^- \approx \gamma(4S)$
2.29 ± 0.15 ± 0.13 -0.09	1978 ± 104		TIAN	05	BELL $e^+e^- \approx \gamma(4S)$
4.3 ± 1.1 ± 0.7 -1.0	38		BRANDENB...	01	CLE2 $e^+e^- \approx \gamma(4S)$

- 118 This AUBERT,B 06N result assumes no mixing.

 $\Gamma(K^+\pi^-\pi^0 \text{ via } \bar{D}^0)/\Gamma(K^-\pi^+\pi^0)$ **Γ219/Γ47**

This is R_M in the note on " D^0 - \bar{D}^0 Mixing" near the start of the D^0 Listings. The experiments here (1) use the charge of the pion in $D^*(2010)^\pm \rightarrow (D^0 \text{ or } \bar{D}^0) \pi^\pm$ decay to tell whether a D^0 or a \bar{D}^0 was born; and (2) use the decay-time distribution to disentangle doubly Cabibbo-suppressed decay and mixing. For the limits on $|m_1 - m_2|$ and $(\Gamma_1 - \Gamma_2)/\Gamma$ that come from the best mixing limit, see near the beginning of these D^0 Listings.

VALUE	CL%	DOCUMENT ID	TECN	COMMENT	
<5.4 × 10⁻⁴	95	119	AUBERT,B	06N	BABR $e^+e^- \approx \gamma(4S)$

- 119 This AUBERT,B 06N limit assumes no CP violation. The measured value corresponding to the limit is $(2.3^{+1.8}_{-1.4} \pm 0.4) \times 10^{-4}$. If CP violation is allowed, this becomes $(1.0^{+2.2}_{-0.7} \pm 0.3) \times 10^{-4}$.

 $\Gamma(K^+\pi^-\pi^+\pi^-)/\Gamma(K^-\pi^+\pi^+\pi^-)$ **Γ220/Γ59**

The experiments here use the charge of the pion in $D^*(2010)^\pm \rightarrow (D^0 \text{ or } \bar{D}^0) \pi^\pm$ decay to tell whether a D^0 or a \bar{D}^0 was born. The $D^0 \rightarrow K^+\pi^-\pi^+\pi^-$ decay can occur directly by doubly Cabibbo-suppressed (DCS) decay, or indirectly by $D^0 \rightarrow \bar{D}^0$ mixing followed by $\bar{D}^0 \rightarrow K^+\pi^-\pi^+\pi^-$ decay. Some of the experiments can use the decay-time information to disentangle the two mechanisms. Here, we list the experimental branching ratio, which if there is no mixing is the DCS ratio; in the next data block we give the limits on the mixing ratio.

Some early limits have been omitted from this Listing; see our 1998 edition (EPJ C3 1).

VALUE (units 10^{-3})	CL%	EVTS	DOCUMENT ID	TECN	COMMENT
3.23 ± 0.25 OUR AVERAGE -0.22					
3.20 ± 0.18 ± 0.18 -0.13	1721 ± 75	120	TIAN	05	BELL $e^+e^- \approx \gamma(4S)$
4.4 ± 1.3 ± 0.6 -1.2	54	120	DYTMAN	01	CLE2 $e^+e^- \approx \gamma(4S)$
2.5 ± 3.6 ± 0.3 -3.4		121	AITALA	98	E791 π^- nucl., 500 GeV

- We do not use the following data for averages, fits, limits, etc. •••
- <18 90 120 AMMAR 91 CLEO $e^+e^- \approx 10.5$ GeV
- <18 90 5 ± 12 122 ANJOS 88c E691 Photoproduction
- 120 AMMAR 91 cannot and DYTMAN 01 and TIAN 05 do not distinguish between doubly Cabibbo-suppressed decay and D^0 - \bar{D}^0 mixing.
- 121 This AITALA 98 result assumes no D^0 - \bar{D}^0 mixing (R_M in the note on " D^0 - \bar{D}^0 Mixing"). It becomes $-0.0020^{+0.0117}_{-0.0106} \pm 0.0035$ when mixing is allowed and decay-time information is used to distinguish doubly Cabibbo-suppressed decays from mixing.
- 122 ANJOS 88c uses decay-time information to distinguish doubly Cabibbo-suppressed (DCS) decays from D^0 - \bar{D}^0 mixing. However, the result assumes no interference between the DCS and mixing amplitudes ($\gamma' = 0$ in the note on " D^0 - \bar{D}^0 Mixing" near the start of the D^0 Listings). When interference is allowed, the limit degrades to 0.033.

 $\Gamma(K^+\pi^-\pi^+\pi^- \text{ via } \bar{D}^0)/\Gamma(K^-\pi^+\pi^+\pi^-)$ **Γ221/Γ59**

This is a D^0 - \bar{D}^0 mixing limit. The experiments here (1) use the charge of the pion in $D^*(2010)^\pm \rightarrow (D^0 \text{ or } \bar{D}^0) \pi^\pm$ decay to tell whether a D^0 or a \bar{D}^0 was born; and (2) use the decay-time distribution to disentangle doubly Cabibbo-suppressed decay and mixing. For the limits on $|m_{D_1^0} - m_{D_2^0}|$ and $(\Gamma_{D_1^0} - \Gamma_{D_2^0})/\Gamma_{D^0}$ that come from the best mixing limit, see near the beginning of these D^0 Listings.

VALUE	CL%	EVTS	DOCUMENT ID	TECN	COMMENT
<0.005	90	0 ± 4	123	ANJOS	88c E691 Photoproduction

- 123 ANJOS 88c uses decay-time information to distinguish doubly Cabibbo-suppressed (DCS) decays from D^0 - \bar{D}^0 mixing. However, the result assumes no interference between the DCS and mixing amplitudes ($\gamma' = 0$ in the note on " D^0 - \bar{D}^0 Mixing" near the start of the D^0 Listings). When interference is allowed, the limit degrades to 0.007.

 $\Gamma(K^+\pi^- \text{ or } K^+\pi^-\pi^+\pi^- \text{ via } \bar{D}^0)/\Gamma(K^-\pi^+ \text{ or } K^-\pi^+\pi^+\pi^-)$ **Γ222/Γ0**

This is a D^0 - \bar{D}^0 mixing limit. For the limits on $|m_{D_1^0} - m_{D_2^0}|$ and $(\Gamma_{D_1^0} - \Gamma_{D_2^0})/\Gamma_{D^0}$ that come from the best mixing limit, see near the beginning of these D^0 Listings.

VALUE	CL%	DOCUMENT ID	TECN	COMMENT
•••				We do not use the following data for averages, fits, limits, etc. •••
<0.0085	90	124	AITALA	98 E791 π^- nucleus, 500 GeV
<0.0037	90	125	ANJOS	88c E691 Photoproduction

- 124 AITALA 98 uses decay-time information to distinguish doubly Cabibbo-suppressed decays from D^0 - \bar{D}^0 mixing. The fit allows interference between the two amplitudes, and also allows CP violation in this term. The central value obtained is $0.0039^{+0.0036}_{-0.0032} \pm 0.0016$. When interference is disallowed, the result becomes $0.0021 \pm 0.0009 \pm 0.0002$.
- 125 This combines results of ANJOS 88c on $K^+\pi^-$ and $K^+\pi^-\pi^+\pi^-$ (via \bar{D}^0) reported in the data block above (see footnotes there). It assumes no interference.

 $\Gamma(\mu^- \text{ anything via } \bar{D}^0)/\Gamma(\mu^+ \text{ anything})$ **Γ223/Γ6**

This is a D^0 - \bar{D}^0 mixing limit. See the somewhat better limits above.

VALUE	CL%	DOCUMENT ID	TECN	COMMENT
<0.0056	90	LOUIS	86	SPEC π^- W 225 GeV

- We do not use the following data for averages, fits, limits, etc. •••
- <0.012 90 BENVENUTI 85 CNTR μ C, 200 GeV
- <0.044 90 BODEK 82 SPEC π^- , $pFe \rightarrow D^0$

Meson Particle Listings

 D^0

Rare or forbidden modes

$\Gamma(\gamma\gamma)/\Gamma(\pi^0\pi^0)$ $\Gamma_{224}/\Gamma_{135}$
 $D^0 \rightarrow \gamma\gamma$ is a flavor-changing neutral-current decay, forbidden in the Standard Model at the tree level.

VALUE	CL%	EVTS	DOCUMENT ID	TECN	COMMENT
<0.033	90		COAN	03	CLE2 $e^+e^- \approx \gamma(4S)$

$\Gamma(e^+e^-)/\Gamma_{total}$ Γ_{225}/Γ
 A test for the $\Delta C = 1$ weak neutral current. Allowed by first-order weak interaction combined with electromagnetic interaction.

VALUE	CL%	EVTS	DOCUMENT ID	TECN	COMMENT
<1.2 $\times 10^{-6}$	90	3	AUBERT,B	04Y	BABR $e^+e^- \approx \gamma(4S)$
••• We do not use the following data for averages, fits, limits, etc. •••					
<8.19 $\times 10^{-6}$	90		PRIPSTEIN	00	E789 p nucleus, 800 GeV
<6.2 $\times 10^{-6}$	90		AITALA	99G	E791 $\pi^- N$ 500 GeV
<1.3 $\times 10^{-5}$	90	0	FREYBERGER	96	CLE2 $e^+e^- \approx \gamma(4S)$
<1.3 $\times 10^{-4}$	90		ADLER	88	MRK3 e^+e^- 3.77 GeV
<1.7 $\times 10^{-4}$	90	7	ALBRECHT	88G	ARG e^+e^- 10 GeV
<2.2 $\times 10^{-4}$	90	8	HAAS	88	CLEO e^+e^- 10 GeV

$\Gamma(\mu^+\mu^-)/\Gamma_{total}$ Γ_{226}/Γ
 A test for the $\Delta C = 1$ weak neutral current. Allowed by first-order weak interaction combined with electromagnetic interaction.

VALUE	CL%	EVTS	DOCUMENT ID	TECN	COMMENT
<1.3 $\times 10^{-6}$	90	1	AUBERT,B	04Y	BABR $e^+e^- \approx \gamma(4S)$
••• We do not use the following data for averages, fits, limits, etc. •••					
<2.0 $\times 10^{-6}$	90		ABT	04	HERB pA , 920 GeV
<2.5 $\times 10^{-6}$	90		ACOSTA	03F	CDF $p\bar{p}$, $\sqrt{s} = 1.96$ TeV
<1.56 $\times 10^{-5}$	90		PRIPSTEIN	00	E789 p nucleus, 800 GeV
<5.2 $\times 10^{-6}$	90		AITALA	99G	E791 $\pi^- N$ 500 GeV
<4.1 $\times 10^{-6}$	90		ADAMOVICH	97	BEAT π^- Cu, W 350 GeV
<4.2 $\times 10^{-6}$	90		ALEXOPOU...	96	E771 p Si, 800 GeV
<3.4 $\times 10^{-5}$	90	1	FREYBERGER	96	CLE2 $e^+e^- \approx \gamma(4S)$
<7.6 $\times 10^{-6}$	90	0	ADAMOVICH	95	BEAT See ADAMOVICH 97
<4.4 $\times 10^{-5}$	90	0	KODAMA	95	E653 π^- emulsion 600 GeV
<3.1 $\times 10^{-5}$	90	126	MISHRA	94	E789 -4.1 ± 4.8 events
<7.0 $\times 10^{-5}$	90	3	ALBRECHT	88G	ARG e^+e^- 10 GeV
<1.1 $\times 10^{-5}$	90		LOUIS	86	SPEC $\pi^- W$ 225 GeV
<3.4 $\times 10^{-4}$	90		AUBERT	85	EMC Deep inelast. $\mu^- N$

126 Here MISHRA 94 uses "the statistical approach advocated by the PDG." For an alternate approach, giving a limit of 9×10^{-6} at 90% confidence level, see the paper.

$\Gamma(\pi^0 e^+e^-)/\Gamma_{total}$ Γ_{227}/Γ
 A test for the $\Delta C = 1$ weak neutral current. Allowed by higher-order electroweak interactions.

VALUE	CL%	EVTS	DOCUMENT ID	TECN	COMMENT
<4.5 $\times 10^{-5}$	90	0	FREYBERGER	96	CLE2 $e^+e^- \approx \gamma(4S)$

$\Gamma(\pi^0 \mu^+\mu^-)/\Gamma_{total}$ Γ_{228}/Γ
 A test for the $\Delta C=1$ weak neutral current. Allowed by higher-order electroweak interactions.

VALUE	CL%	EVTS	DOCUMENT ID	TECN	COMMENT
<1.8 $\times 10^{-4}$	90	2	KODAMA	95	E653 π^- emulsion 600 GeV
••• We do not use the following data for averages, fits, limits, etc. •••					
<5.4 $\times 10^{-4}$	90	3	FREYBERGER	96	CLE2 $e^+e^- \approx \gamma(4S)$

$\Gamma(\eta e^+e^-)/\Gamma_{total}$ Γ_{229}/Γ
 A test for the $\Delta C = 1$ weak neutral current. Allowed by higher-order electroweak interactions.

VALUE	CL%	EVTS	DOCUMENT ID	TECN	COMMENT
<1.1 $\times 10^{-4}$	90	0	FREYBERGER	96	CLE2 $e^+e^- \approx \gamma(4S)$

$\Gamma(\eta \mu^+\mu^-)/\Gamma_{total}$ Γ_{230}/Γ
 A test for the $\Delta C = 1$ weak neutral current. Allowed by higher-order electroweak interactions.

VALUE	CL%	EVTS	DOCUMENT ID	TECN	COMMENT
<5.3 $\times 10^{-4}$	90	0	FREYBERGER	96	CLE2 $e^+e^- \approx \gamma(4S)$

$\Gamma(\pi^+\pi^-e^+e^-)/\Gamma_{total}$ Γ_{231}/Γ
 A test for the $\Delta C = 1$ weak neutral current. Allowed by higher-order electroweak interactions.

VALUE	CL%	EVTS	DOCUMENT ID	TECN	COMMENT
<3.73 $\times 10^{-4}$	90	9	AITALA	01c	E791 π^- nucleus, 500 GeV

$\Gamma(\rho^0 e^+e^-)/\Gamma_{total}$ Γ_{232}/Γ
 A test for the $\Delta C = 1$ weak neutral current. Allowed by higher-order electroweak interactions.

VALUE	CL%	EVTS	DOCUMENT ID	TECN	COMMENT	
<1.0 $\times 10^{-4}$	90	2	127	FREYBERGER	96	CLE2 $e^+e^- \approx \gamma(4S)$
••• We do not use the following data for averages, fits, limits, etc. •••						
<1.24 $\times 10^{-4}$	90	1	AITALA	01c	E791 π^- nucleus, 500 GeV	
<4.5 $\times 10^{-4}$	90	2	HAAS	88	CLEO e^+e^- 10 GeV	

127 This FREYBERGER 96 limit is obtained using a phase-space model. The limit changes to $<1.8 \times 10^{-4}$ using a photon pole amplitude model.

$\Gamma(\pi^+\pi^-\mu^+\mu^-)/\Gamma_{total}$ Γ_{233}/Γ
 A test for the $\Delta C = 1$ weak neutral current. Allowed by higher-order electroweak interactions.

VALUE	CL%	EVTS	DOCUMENT ID	TECN	COMMENT
<3.0 $\times 10^{-5}$	90	2	AITALA	01c	E791 π^- nucleus, 500 GeV

$\Gamma(\rho^0 \mu^+\mu^-)/\Gamma_{total}$ Γ_{234}/Γ
 A test for the $\Delta C = 1$ weak neutral current. Allowed by higher-order electroweak interactions.

VALUE	CL%	EVTS	DOCUMENT ID	TECN	COMMENT	
<2.2 $\times 10^{-5}$	90	0	AITALA	01c	E791 π^- nucleus, 500 GeV	
••• We do not use the following data for averages, fits, limits, etc. •••						
<4.9 $\times 10^{-4}$	90	1	128	FREYBERGER	96	CLE2 $e^+e^- \approx \gamma(4S)$
<2.3 $\times 10^{-4}$	90	0	KODAMA	95	E653 π^- emulsion 600 GeV	
<8.1 $\times 10^{-4}$	90	5	HAAS	88	CLEO e^+e^- 10 GeV	

128 This FREYBERGER 96 limit is obtained using a phase-space model. The limit changes to $<4.5 \times 10^{-4}$ using a photon pole amplitude model.

$\Gamma(\omega e^+e^-)/\Gamma_{total}$ Γ_{235}/Γ
 A test for the $\Delta C = 1$ weak neutral current. Allowed by higher-order electroweak interactions.

VALUE	CL%	EVTS	DOCUMENT ID	TECN	COMMENT	
<1.8 $\times 10^{-4}$	90	1	129	FREYBERGER	96	CLE2 $e^+e^- \approx \gamma(4S)$

129 This FREYBERGER 96 limit is obtained using a phase-space model. The limit changes to $<2.7 \times 10^{-4}$ using a photon pole amplitude model.

$\Gamma(\omega \mu^+\mu^-)/\Gamma_{total}$ Γ_{236}/Γ
 A test for the $\Delta C = 1$ weak neutral current. Allowed by higher-order electroweak interactions.

VALUE	CL%	EVTS	DOCUMENT ID	TECN	COMMENT	
<8.3 $\times 10^{-4}$	90	0	130	FREYBERGER	96	CLE2 $e^+e^- \approx \gamma(4S)$

130 This FREYBERGER 96 limit is obtained using a phase-space model. The limit changes to $<6.5 \times 10^{-4}$ using a photon pole amplitude model.

$\Gamma(K^- K^+ e^+e^-)/\Gamma_{total}$ Γ_{237}/Γ
 A test for the $\Delta C = 1$ weak neutral current. Allowed by higher-order electroweak interactions.

VALUE	CL%	EVTS	DOCUMENT ID	TECN	COMMENT
<3.15 $\times 10^{-4}$	90	9	AITALA	01c	E791 π^- nucleus, 500 GeV

$\Gamma(\phi e^+e^-)/\Gamma_{total}$ Γ_{238}/Γ
 A test for the $\Delta C = 1$ weak neutral current. Allowed by higher-order electroweak interactions.

VALUE	CL%	EVTS	DOCUMENT ID	TECN	COMMENT	
<5.2 $\times 10^{-5}$	90	2	131	FREYBERGER	96	CLE2 $e^+e^- \approx \gamma(4S)$

••• We do not use the following data for averages, fits, limits, etc. •••

VALUE	CL%	EVTS	DOCUMENT ID	TECN	COMMENT
<5.9 $\times 10^{-5}$	90	0	AITALA	01c	E791 π^- nucleus, 500 GeV

131 This FREYBERGER 96 limit is obtained using a phase-space model. The limit changes to $<7.6 \times 10^{-5}$ using a photon pole amplitude model.

$\Gamma(K^- K^+ \mu^+\mu^-)/\Gamma_{total}$ Γ_{239}/Γ
 A test for the $\Delta C = 1$ weak neutral current. Allowed by higher-order electroweak interactions.

VALUE	CL%	EVTS	DOCUMENT ID	TECN	COMMENT
<3.3 $\times 10^{-5}$	90	0	AITALA	01c	E791 π^- nucleus, 500 GeV

$\Gamma(\phi \mu^+\mu^-)/\Gamma_{total}$ Γ_{240}/Γ
 A test for the $\Delta C = 1$ weak neutral current. Allowed by higher-order electroweak interactions.

VALUE	CL%	EVTS	DOCUMENT ID	TECN	COMMENT
<3.1 $\times 10^{-5}$	90	0	AITALA	01c	E791 π^- nucleus, 500 GeV

••• We do not use the following data for averages, fits, limits, etc. •••

VALUE	CL%	EVTS	DOCUMENT ID	TECN	COMMENT	
<4.1 $\times 10^{-4}$	90	0	132	FREYBERGER	96	CLE2 $e^+e^- \approx \gamma(4S)$

132 This FREYBERGER 96 limit is obtained using a phase-space model. The limit changes to $<2.4 \times 10^{-4}$ using a photon pole amplitude model.

$\Gamma(K^0 e^+e^-)/\Gamma_{total}$ Γ_{241}/Γ
 Not a useful test for $\Delta C=1$ weak neutral current because both quarks must change flavor.

VALUE	CL%	EVTS	DOCUMENT ID	TECN	COMMENT
<1.1 $\times 10^{-4}$	90	0	FREYBERGER	96	CLE2 $e^+e^- \approx \gamma(4S)$

••• We do not use the following data for averages, fits, limits, etc. •••

VALUE	CL%	EVTS	DOCUMENT ID	TECN	COMMENT
<1.7 $\times 10^{-3}$	90		ADLER	89c	MRK3 e^+e^- 3.77 GeV

$\Gamma(K^0 \mu^+\mu^-)/\Gamma_{total}$ Γ_{242}/Γ
 Not a useful test for $\Delta C=1$ weak neutral current because both quarks must change flavor.

VALUE	CL%	EVTS	DOCUMENT ID	TECN	COMMENT
<2.6 $\times 10^{-4}$	90	2	KODAMA	95	E653 π^- emulsion 600 GeV

••• We do not use the following data for averages, fits, limits, etc. •••

VALUE	CL%	EVTS	DOCUMENT ID	TECN	COMMENT
<6.7 $\times 10^{-4}$	90	1	FREYBERGER	96	CLE2 $e^+e^- \approx \gamma(4S)$

$\Gamma(K^- \pi^+ e^+e^-)/\Gamma_{total}$ Γ_{243}/Γ
 A test for the $\Delta C = 1$ weak neutral current. Allowed by higher-order electroweak interactions.

VALUE	CL%	EVTS	DOCUMENT ID	TECN	COMMENT
<3.85 $\times 10^{-4}$	90	6	AITALA	01c	E791 π^- nucleus, 500 GeV

See key on page 373

Meson Particle Listings

 D^0

$\Gamma(K^*(892)^0 e^+ e^-)/\Gamma_{\text{total}}$ Γ_{244}/Γ
Not a useful test for $\Delta C=1$ weak neutral current because both quarks must change flavor.

VALUE	CL%	EVTS	DOCUMENT ID	TECN	COMMENT
$<4.7 \times 10^{-5}$	90	2	AITALA	01c	E791 π^- nucleus, 500 GeV

••• We do not use the following data for averages, fits, limits, etc. •••

$<1.4 \times 10^{-4}$	90	1	133 FREYBERGER 96	CLE2	$e^+ e^- \approx \Upsilon(4S)$
-----------------------	----	---	-------------------	------	--------------------------------

133 This FREYBERGER 96 limit is obtained using a phase-space model. The limit changes to $<2.0 \times 10^{-4}$ using a photon pole amplitude model.

$\Gamma(K^- \pi^+ \mu^+ \mu^-)/\Gamma_{\text{total}}$ Γ_{245}/Γ
A test for the $\Delta C=1$ weak neutral current. Allowed by higher-order electroweak interactions.

VALUE	CL%	EVTS	DOCUMENT ID	TECN	COMMENT
$<3.59 \times 10^{-4}$	90	12	AITALA	01c	E791 π^- nucleus, 500 GeV

$\Gamma(K^*(892)^0 \mu^+ \mu^-)/\Gamma_{\text{total}}$ Γ_{246}/Γ
Not a useful test for $\Delta C=1$ weak neutral current because both quarks must change flavor.

VALUE	CL%	EVTS	DOCUMENT ID	TECN	COMMENT
$<2.4 \times 10^{-5}$	90	3	AITALA	01c	E791 π^- nucleus, 500 GeV

••• We do not use the following data for averages, fits, limits, etc. •••

$<1.18 \times 10^{-3}$	90	1	134 FREYBERGER 96	CLE2	$e^+ e^- \approx \Upsilon(4S)$
------------------------	----	---	-------------------	------	--------------------------------

134 This FREYBERGER 96 limit is obtained using a phase-space model. The limit changes to $<1.0 \times 10^{-3}$ using a photon pole amplitude model.

$\Gamma(\pi^+ \pi^- \pi^0 \mu^+ \mu^-)/\Gamma_{\text{total}}$ Γ_{247}/Γ
A test for the $\Delta C=1$ weak neutral current. Allowed by higher-order electroweak interactions.

VALUE	CL%	EVTS	DOCUMENT ID	TECN	COMMENT
$<8.1 \times 10^{-4}$	90	1	KODAMA	95	E653 π^- emulsion 600 GeV

$\Gamma(\mu^\pm e^\mp)/\Gamma_{\text{total}}$ Γ_{248}/Γ
A test of lepton family number conservation.

VALUE	CL%	EVTS	DOCUMENT ID	TECN	COMMENT
$<8.1 \times 10^{-7}$	90	0	AUBERT,B	04Y	BABR $e^+ e^- \approx \Upsilon(4S)$

••• We do not use the following data for averages, fits, limits, etc. •••

$<1.72 \times 10^{-5}$	90		PRIPSTEIN	00	E789 p nucleus, 800 GeV
$<8.1 \times 10^{-6}$	90		AITALA	99G	E791 $\pi^- N$ 500 GeV
$<1.9 \times 10^{-5}$	90	2	135 FREYBERGER 96	CLE2	$e^+ e^- \approx \Upsilon(4S)$
$<1.0 \times 10^{-4}$	90	4	ALBRECHT	88G	ARG $e^+ e^- 10$ GeV
$<2.7 \times 10^{-4}$	90	9	HAAS	88	CLEO $e^+ e^- 10$ GeV
$<1.2 \times 10^{-4}$	90		BECKER	87c	MRK3 $e^+ e^- 3.77$ GeV
$<9 \times 10^{-4}$	90		PALKA	87	SILI 200 GeV πp
$<21 \times 10^{-4}$	90	0	136 RILES	87	MRK2 $e^+ e^- 29$ GeV

135 This is the corrected result given in the erratum to FREYBERGER 96.

136 RILES 87 assumes $B(D \rightarrow K\pi) = 3.0\%$ and has production model dependency.

$\Gamma(\pi^0 e^\pm \mu^\mp)/\Gamma_{\text{total}}$ Γ_{249}/Γ
A test of lepton family number conservation. The value is for the sum of the two charge states.

VALUE	CL%	EVTS	DOCUMENT ID	TECN	COMMENT
$<8.6 \times 10^{-5}$	90	2	FREYBERGER 96	CLE2	$e^+ e^- \approx \Upsilon(4S)$

$\Gamma(\eta e^\pm \mu^\mp)/\Gamma_{\text{total}}$ Γ_{250}/Γ
A test of lepton family number conservation. The value is for the sum of the two charge states.

VALUE	CL%	EVTS	DOCUMENT ID	TECN	COMMENT
$<1.0 \times 10^{-4}$	90	0	FREYBERGER 96	CLE2	$e^+ e^- \approx \Upsilon(4S)$

$\Gamma(\pi^+ \pi^- e^\pm \mu^\mp)/\Gamma_{\text{total}}$ Γ_{251}/Γ
A test of lepton family-number conservation. The value is for the sum of the two charge states.

VALUE	CL%	EVTS	DOCUMENT ID	TECN	COMMENT
$<1.5 \times 10^{-5}$	90	1	AITALA	01c	E791 π^- nucleus, 500 GeV

$\Gamma(\rho^0 e^\pm \mu^\mp)/\Gamma_{\text{total}}$ Γ_{252}/Γ
A test of lepton family number conservation. The value is for the sum of the two charge states.

VALUE	CL%	EVTS	DOCUMENT ID	TECN	COMMENT
$<4.9 \times 10^{-5}$	90	0	137 FREYBERGER 96	CLE2	$e^+ e^- \approx \Upsilon(4S)$

••• We do not use the following data for averages, fits, limits, etc. •••

$<6.6 \times 10^{-5}$	90	1	AITALA	01c	E791 π^- nucleus, 500 GeV
-----------------------	----	---	--------	-----	-------------------------------

137 This FREYBERGER 96 limit is obtained using a phase-space model. The limit changes to $<5.0 \times 10^{-5}$ using a photon pole amplitude model.

$\Gamma(\omega e^\pm \mu^\mp)/\Gamma_{\text{total}}$ Γ_{253}/Γ
A test of lepton family number conservation. The value is for the sum of the two charge states.

VALUE	CL%	EVTS	DOCUMENT ID	TECN	COMMENT
$<1.2 \times 10^{-4}$	90	0	138 FREYBERGER 96	CLE2	$e^+ e^- \approx \Upsilon(4S)$

138 This FREYBERGER 96 limit is obtained using a phase-space model. The same limit is obtained using a photon pole amplitude model.

$\Gamma(K^- K^+ e^\pm \mu^\mp)/\Gamma_{\text{total}}$ Γ_{254}/Γ
A test of lepton family-number conservation. The value is for the sum of the two charge states.

VALUE	CL%	EVTS	DOCUMENT ID	TECN	COMMENT
$<1.8 \times 10^{-4}$	90	5	AITALA	01c	E791 π^- nucleus, 500 GeV

$\Gamma(\phi e^\pm \mu^\mp)/\Gamma_{\text{total}}$ Γ_{255}/Γ
A test of lepton family number conservation. The value is for the sum of the two charge states.

VALUE	CL%	EVTS	DOCUMENT ID	TECN	COMMENT
$<3.4 \times 10^{-5}$	90	0	139 FREYBERGER 96	CLE2	$e^+ e^- \approx \Upsilon(4S)$

••• We do not use the following data for averages, fits, limits, etc. •••

$<4.7 \times 10^{-5}$	90	0	AITALA	01c	E791 π^- nucleus, 500 GeV
-----------------------	----	---	--------	-----	-------------------------------

139 This FREYBERGER 96 limit is obtained using a phase-space model. The limit changes to $<3.3 \times 10^{-5}$ using a photon pole amplitude model.

$\Gamma(K^0 e^\pm \mu^\mp)/\Gamma_{\text{total}}$ Γ_{256}/Γ
A test of lepton family number conservation. The value is for the sum of the two charge states.

VALUE	CL%	EVTS	DOCUMENT ID	TECN	COMMENT
$<1.0 \times 10^{-4}$	90	0	FREYBERGER 96	CLE2	$e^+ e^- \approx \Upsilon(4S)$

$\Gamma(K^- \pi^+ e^\pm \mu^\mp)/\Gamma_{\text{total}}$ Γ_{257}/Γ
A test of lepton family-number conservation. The value is for the sum of the two charge states.

VALUE	CL%	EVTS	DOCUMENT ID	TECN	COMMENT
$<5.53 \times 10^{-4}$	90	15	AITALA	01c	E791 π^- nucleus, 500 GeV

$\Gamma(K^*(892)^0 e^\pm \mu^\mp)/\Gamma_{\text{total}}$ Γ_{258}/Γ
A test of lepton family number conservation. The value is for the sum of the two charge states.

VALUE	CL%	EVTS	DOCUMENT ID	TECN	COMMENT
$<8.3 \times 10^{-5}$	90	9	AITALA	01c	E791 π^- nucleus, 500 GeV

••• We do not use the following data for averages, fits, limits, etc. •••

$<1.0 \times 10^{-4}$	90	0	140 FREYBERGER 96	CLE2	$e^+ e^- \approx \Upsilon(4S)$
-----------------------	----	---	-------------------	------	--------------------------------

140 This FREYBERGER 96 limit is obtained using a phase-space model. The same limit is obtained using a photon pole amplitude model.

$\Gamma(\pi^- \pi^+ e^+ e^- + \text{c.c.})/\Gamma_{\text{total}}$ Γ_{259}/Γ
A test of lepton-number conservation. The value is for the sum of the two charge states.

VALUE	CL%	EVTS	DOCUMENT ID	TECN	COMMENT
$<1.12 \times 10^{-4}$	90	1	AITALA	01c	E791 π^- nucleus, 500 GeV

$\Gamma(\pi^- \pi^+ \mu^+ \mu^- + \text{c.c.})/\Gamma_{\text{total}}$ Γ_{260}/Γ
A test of lepton-number conservation. The value is for the sum of the two charge states.

VALUE	CL%	EVTS	DOCUMENT ID	TECN	COMMENT
$<2.9 \times 10^{-5}$	90	1	AITALA	01c	E791 π^- nucleus, 500 GeV

$\Gamma(K^- \pi^- e^+ e^- + \text{c.c.})/\Gamma_{\text{total}}$ Γ_{261}/Γ
A test of lepton-number conservation. The value is for the sum of the two charge states.

VALUE	CL%	EVTS	DOCUMENT ID	TECN	COMMENT
$<2.06 \times 10^{-4}$	90	2	AITALA	01c	E791 π^- nucleus, 500 GeV

$\Gamma(K^- \pi^- \mu^+ \mu^- + \text{c.c.})/\Gamma_{\text{total}}$ Γ_{262}/Γ
A test of lepton-number conservation. The value is for the sum of the two charge states.

VALUE	CL%	EVTS	DOCUMENT ID	TECN	COMMENT
$<3.9 \times 10^{-4}$	90	14	AITALA	01c	E791 π^- nucleus, 500 GeV

$\Gamma(K^- K^- e^+ e^- + \text{c.c.})/\Gamma_{\text{total}}$ Γ_{263}/Γ
A test of lepton-number conservation. The value is for the sum of the two charge states.

VALUE	CL%	EVTS	DOCUMENT ID	TECN	COMMENT
$<1.52 \times 10^{-4}$	90	2	AITALA	01c	E791 π^- nucleus, 500 GeV

$\Gamma(K^- K^- \mu^+ \mu^- + \text{c.c.})/\Gamma_{\text{total}}$ Γ_{264}/Γ
A test of lepton-number conservation. The value is for the sum of the two charge states.

VALUE	CL%	EVTS	DOCUMENT ID	TECN	COMMENT
$<9.4 \times 10^{-5}$	90	1	AITALA	01c	E791 π^- nucleus, 500 GeV

$\Gamma(\pi^- \pi^- e^+ \mu^+ + \text{c.c.})/\Gamma_{\text{total}}$ Γ_{265}/Γ
A test of lepton-number conservation. The value is for the sum of the two charge states.

VALUE	CL%	EVTS	DOCUMENT ID	TECN	COMMENT
$<7.9 \times 10^{-5}$	90	4	AITALA	01c	E791 π^- nucleus, 500 GeV

$\Gamma(K^- \pi^- e^+ \mu^+ + \text{c.c.})/\Gamma_{\text{total}}$ Γ_{266}/Γ
A test of lepton-number conservation. The value is for the sum of the two charge states.

VALUE	CL%	EVTS	DOCUMENT ID	TECN	COMMENT
$<2.18 \times 10^{-4}$	90	7	AITALA	01c	E791 π^- nucleus, 500 GeV

Meson Particle Listings

 D^0

$\Gamma(K^- K^+ e^+ \mu^+ + c.c.)/\Gamma_{\text{total}}$ Γ_{267}/Γ
 A test of lepton-number conservation. The value is for the sum of the two charge states.

VALUE	CL%	EVTs	DOCUMENT ID	TECN	COMMENT
$<5.7 \times 10^{-5}$	90	0	AITALA	01c E791	π^- nucleus, 500 GeV

 D^0 CP-VIOLATING DECAY-RATE ASYMMETRIES

This is the difference between D^0 and \bar{D}^0 partial widths for these modes divided by the sum of the widths. The D^0 and \bar{D}^0 are distinguished by the charge of the parent D^* : $D^{*+} \rightarrow D^0 \pi^+$ and $D^{*-} \rightarrow \bar{D}^0 \pi^-$.

 $A_{CP}(K^+ K^-)$ in $D^0, \bar{D}^0 \rightarrow K^+ K^-$

VALUE (units 10^{-2})	EVTs	DOCUMENT ID	TECN	COMMENT
0.1 ± 0.5 OUR AVERAGE				Error includes scale factor of 1.4.
0.00 ± 0.34 ± 0.13	129k	141 AUBERT	08M BABR	$e^+ e^- \approx 10.6$ GeV
+2.0 ± 1.2 ± 0.6		142 ACOSTA	05c CDF	$p\bar{p}, \sqrt{s}=1.96$ TeV
0.0 ± 2.2 ± 0.8	3023	142 CSORNA	02 CLE2	$e^+ e^- \approx \Upsilon(4S)$
-0.1 ± 2.2 ± 1.5	3330	142 LINK	00B FOCS	
-1.0 ± 4.9 ± 1.2	609	142 AITALA	98c E791	$-0.093 < A_{CP} < +0.073$ (90% CL)

141 AUBERT 08M uses corrected numbers of events directly, not ratios with $K^{\mp} \pi^{\pm}$ events.
 142 AITALA 98c, LINK 00b, CSORNA 02, and ACOSTA 05c measure $N(D^0 \rightarrow K^+ K^-)/N(D^0 \rightarrow K^- \pi^+)$, the ratio of numbers of events observed, and similarly for the \bar{D}^0 .

 $A_{CP}(K_S^0 K_S^0)$ in $D^0, \bar{D}^0 \rightarrow K_S^0 K_S^0$

VALUE	EVTs	DOCUMENT ID	TECN	COMMENT
-0.23 ± 0.19	65	BONVICINI	01 CLE2	$e^+ e^- \approx 10.6$ GeV

 $A_{CP}(\pi^+ \pi^-)$ in $D^0, \bar{D}^0 \rightarrow \pi^+ \pi^-$

VALUE (units 10^{-2})	EVTs	DOCUMENT ID	TECN	COMMENT
0.0 ± 0.5 OUR AVERAGE				
-0.24 ± 0.52 ± 0.22	63.7k	143 AUBERT	08M BABR	$e^+ e^- \approx 10.6$ GeV
+1.0 ± 1.3 ± 0.6		144 ACOSTA	05c CDF	$p\bar{p}, \sqrt{s}=1.96$ TeV
+1.9 ± 3.2 ± 0.8	1136	144 CSORNA	02 CLE2	$e^+ e^- \approx \Upsilon(4S)$
+4.8 ± 3.9 ± 2.5	1177	144 LINK	00B FOCS	
-4.9 ± 7.8 ± 3.0	343	144 AITALA	98c E791	$-0.186 < A_{CP} < +0.088$ (90% CL)

143 AUBERT 08M uses corrected numbers of events directly, not ratios with $K^{\mp} \pi^{\pm}$ events.
 144 AITALA 98c, LINK 00b, CSORNA 02, and ACOSTA 05c measure $N(D^0 \rightarrow \pi^+ \pi^-)/N(D^0 \rightarrow K^- \pi^+)$, the ratio of numbers of events observed, and similarly for the \bar{D}^0 .

 $A_{CP}(\pi^0 \pi^0)$ in $D^0, \bar{D}^0 \rightarrow \pi^0 \pi^0$

VALUE	EVTs	DOCUMENT ID	TECN	COMMENT
+0.001 ± 0.048	810	BONVICINI	01 CLE2	$e^+ e^- \approx 10.6$ GeV

 $A_{CP}(\pi^+ \pi^- \pi^0)$ in $D^0, \bar{D}^0 \rightarrow \pi^+ \pi^- \pi^0$

VALUE	EVTs	DOCUMENT ID	TECN	COMMENT
0.004 ± 0.013 OUR AVERAGE				
0.0043 ± 0.0130	123k ± 490	ARINSTEIN	08 BELL	$e^+ e^- \approx \Upsilon(4S)$
0.01 $^{+0.09}_{-0.07}$ ± 0.05		CRONIN-HEN..05	CLEO	$e^+ e^- \approx 10$ GeV

 $A_{CP}(K_S^0 \phi)$ in $D^0, \bar{D}^0 \rightarrow K_S^0 \phi$

VALUE	DOCUMENT ID	TECN	COMMENT
-0.028 ± 0.094	BARTELT 95	CLE2	$-0.182 < A_{CP} < +0.126$ (90% CL)

 $A_{CP}(K_S^0 \pi^0)$ in $D^0, \bar{D}^0 \rightarrow K_S^0 \pi^0$

VALUE	EVTs	DOCUMENT ID	TECN	COMMENT
+0.001 ± 0.013	9099	BONVICINI	01 CLE2	$e^+ e^- \approx 10.6$ GeV
• • • We do not use the following data for averages, fits, limits, etc. • • •				
-0.018 ± 0.030		BARTELT 95	CLE2	See BONVICINI 01

 $A_{CP}(K^{\mp} \pi^{\pm})$ in $D^0 \rightarrow K^- \pi^+, \bar{D}^0 \rightarrow K^+ \pi^-$

VALUE	DOCUMENT ID	TECN	COMMENT
-0.004 ± 0.005 ± 0.009	DOBBS 07	CLEO	$e^+ e^-$ at $\psi(3770)$

 $A_{CP}(K^{\pm} \pi^{\mp})$ in $D^0 \rightarrow K^+ \pi^-, \bar{D}^0 \rightarrow K^- \pi^+$

VALUE	EVTs	DOCUMENT ID	TECN	COMMENT
0.022 ± 0.032 OUR AVERAGE				
-0.021 ± 0.052 ± 0.015	4030 ± 90	AUBERT	07w BABR	$e^+ e^- \approx 10.6$ GeV
+0.023 ± 0.047	4024 ± 88	145 ZHANG	06 BELL	$e^+ e^-$
+0.18 ± 0.14 ± 0.04		146 LINK	05H FOCS	γ nucleus
+0.095 ± 0.061 ± 0.083		147 AUBERT	03z BABR	$e^+ e^-$, 10.6 GeV
+0.02 $^{+0.19}_{-0.20}$ ± 0.01	45	148 GODANG	00 CLE2	$-0.43 < A_{CP} < +0.34$ (95% CL)

• • • We do not use the following data for averages, fits, limits, etc. • • •
 -0.080 ± 0.077 845 ± 40 149 LI 05A BELL See ZHANG 06
 145 This ZHANG 06 result allows mixing.
 146 This LINK 05H result assumes no mixing. If mixing is allowed, it becomes $0.13^{+0.33}_{-0.25} \pm 0.10$.
 147 This AUBERT 03z limit assumes no mixing. If mixing is allowed, the 95% confidence-level interval is $(-2.8 < A_D < 4.9) \times 10^{-3}$.
 148 This GODANG 00 result assumes no D^0 - \bar{D}^0 mixing; it becomes $-0.01^{+0.16}_{-0.17} \pm 0.01$ when mixing is allowed.
 149 This LI 05A result allows mixing.

 $A_{CP}(K^{\mp} \pi^{\pm} \pi^0)$ in $D^0 \rightarrow K^- \pi^+ \pi^0, \bar{D}^0 \rightarrow K^+ \pi^- \pi^0$

VALUE	DOCUMENT ID	TECN	COMMENT
0.002 ± 0.009 OUR AVERAGE			
+0.002 ± 0.004 ± 0.008	DOBBS 07	CLEO	$e^+ e^-$ at $\psi(3770)$
-0.031 ± 0.086	150 KOPP	01 CLE2	$e^+ e^- \approx 10.6$ GeV

150 KOPP 01 fits separately the D^0 and \bar{D}^0 Dalitz plots and then calculates the integrated difference of normalized densities divided by the integrated sum.

 $A_{CP}(K^{\pm} \pi^{\mp} \pi^0)$ in $D^0 \rightarrow K^+ \pi^- \pi^0, \bar{D}^0 \rightarrow K^- \pi^+ \pi^0$

VALUE	EVTs	DOCUMENT ID	TECN	COMMENT
0.00 ± 0.05 OUR AVERAGE				
-0.006 ± 0.053	1978 ± 104	TIAN	05 BELL	$e^+ e^- \approx \Upsilon(4S)$
+0.09 $^{+0.25}_{-0.22}$	38	BRANDENB...	01 CLE2	$e^+ e^- \approx \Upsilon(4S)$

 $A_{CP}(K_S^0 \pi^+ \pi^-)$ in $D^0, \bar{D}^0 \rightarrow K_S^0 \pi^+ \pi^-$

VALUE	EVTs	DOCUMENT ID	TECN	COMMENT
-0.009 ± 0.021 $^{+0.016}_{-0.057}$	4854	151 ASNER	04A CLEO	$e^+ e^- \approx 10$ GeV

151 This is the overall result of ASNER 04A; CP-violating limits are also given below for each of the 10 resonant submodes found in an amplitude analysis of the D^0 and $\bar{D}^0 \rightarrow K_S^0 \pi^+ \pi^-$ Dalitz plots. These limits range from $< 3.5 \times 10^{-4}$ to 28.4×10^{-4} at 95% CL.

 $A_{CP}(K^*(892)^{\mp} \pi^{\pm}) \rightarrow K_S^0 \pi^+ \pi^-$ in $D^0 \rightarrow K^* \pi^+, \bar{D}^0 \rightarrow K^* \pi^-$

VALUE (units 10^{-4})	CL%	DOCUMENT ID	TECN	COMMENT
<3.5	95	152 ASNER	04A CLEO	Dalitz fit, 4854 $D^0 + \bar{D}^0$ evts

152 This ASNER 04A limit comes from an amplitude analysis of the D^0 and $\bar{D}^0 \rightarrow K_S^0 \pi^+ \pi^-$ Dalitz plots.

 $A_{CP}(K^*(892)^{\pm} \pi^{\mp}) \rightarrow K_S^0 \pi^+ \pi^-$ in $D^0 \rightarrow K^+ \pi^-, \bar{D}^0 \rightarrow K^- \pi^+$

VALUE (units 10^{-4})	CL%	DOCUMENT ID	TECN	COMMENT
<7.8	95	153 ASNER	04A CLEO	Dalitz fit, 4854 $D^0 + \bar{D}^0$ evts

153 This ASNER 04A limit comes from an amplitude analysis of the D^0 and $\bar{D}^0 \rightarrow K_S^0 \pi^+ \pi^-$ Dalitz plots.

 $A_{CP}(K_S^0 \rho^0) \rightarrow K_S^0 \pi^+ \pi^-$ in $D^0 \rightarrow \bar{K}^0 \rho^0, \bar{D}^0 \rightarrow K^0 \rho^0$

VALUE (units 10^{-4})	CL%	DOCUMENT ID	TECN	COMMENT
<4.8	95	154 ASNER	04A CLEO	Dalitz fit, 4854 $D^0 + \bar{D}^0$ evts

154 This ASNER 04A limit comes from an amplitude analysis of the D^0 and $\bar{D}^0 \rightarrow K_S^0 \pi^+ \pi^-$ Dalitz plots.

 $A_{CP}(K_S^0 \omega) \rightarrow K_S^0 \pi^+ \pi^-$ in $D^0 \rightarrow \bar{K}^0 \omega, \bar{D}^0 \rightarrow K^0 \omega$

VALUE (units 10^{-4})	CL%	DOCUMENT ID	TECN	COMMENT
<9.2	95	155 ASNER	04A CLEO	Dalitz fit, 4854 $D^0 + \bar{D}^0$ evts

155 This ASNER 04A limit comes from an amplitude analysis of the D^0 and $\bar{D}^0 \rightarrow K_S^0 \pi^+ \pi^-$ Dalitz plots.

 $A_{CP}(K_S^0 f_0(980) \rightarrow K_S^0 \pi^+ \pi^-)$ in $D^0 \rightarrow \bar{K}^0 f_0(980), \bar{D}^0 \rightarrow K^0 f_0(980)$

VALUE (units 10^{-4})	CL%	DOCUMENT ID	TECN	COMMENT
<6.8	95	156 ASNER	04A CLEO	Dalitz fit, 4854 $D^0 + \bar{D}^0$ evts

156 This ASNER 04A limit comes from an amplitude analysis of the D^0 and $\bar{D}^0 \rightarrow K_S^0 \pi^+ \pi^-$ Dalitz plots.

 $A_{CP}(K_S^0 f_2(1270) \rightarrow K_S^0 \pi^+ \pi^-)$ in $D^0 \rightarrow \bar{K}^0 f_2(1270), \bar{D}^0 \rightarrow K^0 f_2(1270)$

VALUE (units 10^{-4})	CL%	DOCUMENT ID	TECN	COMMENT
<13.5	95	157 ASNER	04A CLEO	Dalitz fit, 4854 $D^0 + \bar{D}^0$ evts

157 This ASNER 04A limit comes from an amplitude analysis of the D^0 and $\bar{D}^0 \rightarrow K_S^0 \pi^+ \pi^-$ Dalitz plots.

 $A_{CP}(K_S^0 f_0(1370) \rightarrow K_S^0 \pi^+ \pi^-)$ in $D^0 \rightarrow \bar{K}^0 f_0(1370), \bar{D}^0 \rightarrow K^0 f_0(1370)$

VALUE (units 10^{-4})	CL%	DOCUMENT ID	TECN	COMMENT
<25.5	95	158 ASNER	04A CLEO	Dalitz fit, 4854 $D^0 + \bar{D}^0$ evts

158 This ASNER 04A limit comes from an amplitude analysis of the D^0 and $\bar{D}^0 \rightarrow K_S^0 \pi^+ \pi^-$ Dalitz plots.

 $A_{CP}(K_0^*(1430)^{\mp} \pi^{\pm}) \rightarrow K_S^0 \pi^+ \pi^-$ in $D^0 \rightarrow K_0^*(1430)^- \pi^+, \bar{D}^0 \rightarrow K_0^*(1430)^+ \pi^-$

VALUE (units 10^{-4})	CL%	DOCUMENT ID	TECN	COMMENT
<9.0	95	159 ASNER	04A CLEO	Dalitz fit, 4854 $D^0 + \bar{D}^0$ evts

159 This ASNER 04A limit comes from an amplitude analysis of the D^0 and $\bar{D}^0 \rightarrow K_S^0 \pi^+ \pi^-$ Dalitz plots.

 $A_{CP}(K_2^*(1430)^{\mp} \pi^{\pm}) \rightarrow K_S^0 \pi^+ \pi^-$ in $D^0 \rightarrow K_2^*(1430)^- \pi^+, \bar{D}^0 \rightarrow K_2^*(1430)^+ \pi^-$

VALUE (units 10^{-4})	CL%	DOCUMENT ID	TECN	COMMENT
<6.5	95	160 ASNER	04A CLEO	Dalitz fit, 4854 $D^0 + \bar{D}^0$ evts

160 This ASNER 04A limit comes from an amplitude analysis of the D^0 and $\bar{D}^0 \rightarrow K_S^0 \pi^+ \pi^-$ Dalitz plots.

Meson Particle Listings

 $D^0, D^*(2007)^0$

DECAMP	91J	PL B266 218	D. Decamp <i>et al.</i>	(ALEPH Collab.)
FRABETTI	91	PL B263 584	P.L. Frabetti <i>et al.</i>	(FNAL E687 Collab.)
KINOSHITA	91	PR D43 2836	K. Kinoshita <i>et al.</i>	(CLEO Collab.)
KODAMA	91	PRL 66 1819	K. Kodama <i>et al.</i>	(FNAL E653 Collab.)
ALBRECHT	90C	ZPHY C46 9	H. Albrecht <i>et al.</i>	(ARGUS Collab.)
ALEXANDER	90	PRL 65 1184	J. Alexander <i>et al.</i>	(CLEO Collab.)
ALEXANDER	90B	PRL 65 1531	J. Alexander <i>et al.</i>	(CLEO Collab.)
ALVAREZ	90	ZPHY C47 539	M.P. Alvarez <i>et al.</i>	(CERN NA14/2 Collab.)
ANJOS	90D	PR D42 2414	J.C. Anjos <i>et al.</i>	(FNAL E691 Collab.)
BARLAG	90C	ZPHY C46 563	S. Barlag <i>et al.</i>	(ACCMOR Collab.)
ADLER	89	PRL 62 1821	J. Adler <i>et al.</i>	(Mark III Collab.)
ADLER	89C	PR D40 906	J. Adler <i>et al.</i>	(Mark III Collab.)
ALBRECHT	89D	ZPHY C43 181	H. Albrecht <i>et al.</i>	(ARGUS Collab.)
ANJOS	89F	PRL 62 1587	J.C. Anjos <i>et al.</i>	(FNAL E691 Collab.)
ABACHI	88	PL B205 411	S. Abachi <i>et al.</i>	(HRS Collab.)
ADLER	88	PR D37 2023	J. Adler <i>et al.</i>	(Mark III Collab.)
ADLER	88C	PRL 60 89	J. Adler <i>et al.</i>	(Mark III Collab.)
ALBRECHT	88G	PL B209 380	H. Albrecht <i>et al.</i>	(ARGUS Collab.)
ALBRECHT	88I	PL B210 267	H. Albrecht <i>et al.</i>	(ARGUS Collab.)
ANJOS	88C	PRL 60 1239	J.C. Anjos <i>et al.</i>	(FNAL E691 Collab.)
BORTOLETTO	88	PR D37 1719	D. Bortoletto <i>et al.</i>	(CLEO Collab.)
Also	PR D39 1471 (erratum)	D. Bortoletto <i>et al.</i>	(CLEO Collab.)	
HAAS	88	PRL 60 1614	P. Haas <i>et al.</i>	(CLEO Collab.)
RAAB	88	PR D37 2391	J.R. Raab <i>et al.</i>	(FNAL E691 Collab.)
ADAMOVICH	87	EPL 4 887	M.I. Adamovich <i>et al.</i>	(Photon Emulsion Collab.)
ADLER	87	PL B196 107	J. Adler <i>et al.</i>	(Mark III Collab.)
AGUILAR...	87E	ZPHY C36 551	M. Aguilar-Benitez <i>et al.</i>	(LEBC-EHS Collab.)
Also	ZPHY C40 321	M. Aguilar-Benitez <i>et al.</i>	(LEBC-EHS Collab.)	
AGUILAR...	87F	ZPHY C36 559	M. Aguilar-Benitez <i>et al.</i>	(LEBC-EHS Collab.)
Also	ZPHY C38 520 (erratum)	M. Aguilar-Benitez <i>et al.</i>	(LEBC-EHS Collab.)	
BARLAG	87B	ZPHY C37 17	S. Barlag <i>et al.</i>	(ACCMOR Collab.)
BECKER	87C	PL B193 147	J.J. Becker <i>et al.</i>	(Mark III Collab.)
Also	PL B198 590 (erratum)	J.J. Becker <i>et al.</i>	(Mark III Collab.)	
PALKA	87	PL B189 238	H. Palka <i>et al.</i>	(ACCMOR Collab.)
RILES	87	PR D35 2914	K. Riles <i>et al.</i>	(Mark II Collab.)
BAILEY	86	ZPHY C30 51	R. Bailey <i>et al.</i>	(ACCMOR Collab.)
BEBEK	86	PL 56 1893	C. Bebek <i>et al.</i>	(CLEO Collab.)
LOUIS	86	PRL 56 1027	W.C. Louis <i>et al.</i>	(PRIN, CHIC, ISU)
ALBRECHT	85B	PL 158B 525	H. Albrecht <i>et al.</i>	(ARGUS Collab.)
ALBRECHT	85F	PL 150B 235	H. Albrecht <i>et al.</i>	(ARGUS Collab.)
AUBERT	85	PL 155B 461	J.J. Aubert <i>et al.</i>	(EMC Collab.)
BALTRUSAITIS	85E	PRL 55 150	R.M. Baltrusaitis <i>et al.</i>	(Mark III Collab.)
BENVENUTI	85	PL 150B 531	A.A. Benvenuti <i>et al.</i>	(BCDMS Collab.)
ADAMOVICH	84B	PL 140B 123	M.I. Adamovich <i>et al.</i>	(CERN WA52 Collab.)
DERRICK	84	PRL 53 1971	M. Derrick <i>et al.</i>	(HRS Collab.)
SUMMERS	84	PRL 52 410	D.J. Summers <i>et al.</i>	(UCSB, CARL, COLO+)
BAILEY	83B	PL 132B 237	R. Bailey <i>et al.</i>	(ACCMOR Collab.)
BODEK	82	PL 113B 82	A. Bodek <i>et al.</i>	(ROCH, CIT, CHIC, FNAL+)
FIORINO	81	LNC 30 166	A. Fiorino <i>et al.</i>	
SCHINDLER	81	PR D24 78	R.H. Schindler <i>et al.</i>	(Mark II Collab.)
TRILLING	81	PRPL 75 57	G.H. Trilling	(LBL, UCB) J
ASTON	80E	PL 94B 113	D. Aston <i>et al.</i>	(BONN, CERN, EPOL, GLAS+)
AVERY	80	PRL 44 1309	P. Avery <i>et al.</i>	(ILL, FNAL, COLU)
ZHOLENTZ	80	PL 96B 214	A.A. Zholents <i>et al.</i>	(NOVO)
Also	SJNP 34 814	A.A. Zholents <i>et al.</i>	(NOVO)	
Translated from YAF 34	1471.			
ABRAMS	79D	PRL 43 481	G.S. Abrams <i>et al.</i>	(Mark II Collab.)
ATIYA	79	PRL 43 414	M.S. Atiya <i>et al.</i>	(COLU, ILL, FNAL)
BALTAY	78C	PRL 41 73	C. Baltay <i>et al.</i>	(COLU, BNL)
VUILLEMIN	78	PRL 41 1149	V. Vuillemin <i>et al.</i>	(LGV Collab.)
GOLDHABER	77	PL 69B 503	G. Goldhaber <i>et al.</i>	(Mark I Collab.)
PERUZZI	77	PRL 39 1301	I. Peruzzi <i>et al.</i>	(LGV Collab.)
PICCOLO	77	PL 70B 260	M. Piccolo <i>et al.</i>	(Mark I Collab.)
GOLDHABER	76	PRL 37 255	G. Goldhaber <i>et al.</i>	(Mark I Collab.)

OTHER RELATED PAPERS

RICHMAN	95	RMP 67 893	J.D. Richman, P.R. Burchat	(UCSB, STAN)
ROSNER	95	CNPP 21 369	J. Rosner	(CHIC)

 $D^*(2007)^0$

$$I(J^P) = \frac{1}{2}(1^-)$$

I, J, P need confirmation.

J consistent with 1, value 0 ruled out (NGUYEN 77).

 $D^*(2007)^0$ MASS

The fit includes $D^\pm, D^0, D_S^\pm, D^{*\pm}, D^{*0}$, and $D_S^{*\pm}$ mass and mass difference measurements.

VALUE (MeV)	DOCUMENT ID	TECN	COMMENT
2006.97 ± 0.19 OUR FIT	Error includes scale factor of 1.1.		

• • • We do not use the following data for averages, fits, limits, etc. • • •

2006 ± 1.5	¹ GOLDHABER 77	MRK1	e^+e^-
------------	---------------------------	------	----------

¹ From simultaneous fit to $D^*(2010)^+, D^*(2007)^0, D^+$, and D^0 .

 $m_{D^*(2007)^0} - m_{D^0}$

The fit includes $D^\pm, D^0, D_S^\pm, D^{*\pm}, D^{*0}$, and $D_S^{*\pm}$ mass and mass difference measurements.

VALUE (MeV)	EVTS	DOCUMENT ID	TECN	COMMENT
142.12 ± 0.07 OUR FIT				
142.12 ± 0.07 OUR AVERAGE				

142.2 ± 0.3 ± 0.2	145	ALBRECHT 95F	ARG	$e^+e^- \rightarrow$ hadrons
-------------------	-----	--------------	-----	------------------------------

142.2 ± 0.05 ± 0.05	1176	BORTOLETTO92B	CLE2	$e^+e^- \rightarrow$ hadrons
---------------------	------	---------------	------	------------------------------

• • • We do not use the following data for averages, fits, limits, etc. • • •

142.2 ± 0.2		SADROZINSKI 80	CBAL	$D^{*0} \rightarrow D^0\pi^0$
-------------	--	----------------	------	-------------------------------

142.7 ± 1.7		² GOLDHABER 77	MRK1	e^+e^-
-------------	--	---------------------------	------	----------

² From simultaneous fit to $D^*(2010)^+, D^*(2007)^0, D^+$, and D^0 .

 $D^*(2007)^0$ WIDTH

VALUE (MeV)	CL%	DOCUMENT ID	TECN	COMMENT
<2.1	90	³ ABACHI	88B HRS	$D^{*0} \rightarrow D^+\pi^-$

³ Assuming $m_{D^{*0}} = 2007.2 \pm 2.1$ MeV/ c^2 .

 $D^*(2007)^0$ DECAY MODES

$\bar{D}^*(2007)^0$ modes are charge conjugates of modes below.

Mode	Fraction (Γ_i/Γ)
Γ_1 $D^0\pi^0$	(61.9 ± 2.9) %
Γ_2 $D^0\gamma$	(38.1 ± 2.9) %

CONSTRAINED FIT INFORMATION

An overall fit to a branching ratio uses 3 measurements and one constraint to determine 2 parameters. The overall fit has a $\chi^2 = 0.5$ for 2 degrees of freedom.

The following *off-diagonal* array elements are the correlation coefficients $\langle \delta x_i \delta x_j \rangle / (\delta x_i \delta x_j)$, in percent, from the fit to the branching fractions, $x_i \equiv \Gamma_i/\Gamma_{\text{total}}$. The fit constrains the x_i whose labels appear in this array to sum to one.

$$x_2 \begin{vmatrix} -100 & \\ & x_1 \end{vmatrix}$$

 $D^*(2007)^0$ BRANCHING RATIOS

$\Gamma(D^0\pi^0)/\Gamma(D^0\gamma)$	DOCUMENT ID	TECN	COMMENT	Γ_1/Γ_2
1.74 ± 0.02 ± 0.13	AUBERT, BE	05G BABR	10.6 $e^+e^- \rightarrow$ hadrons	

$\Gamma(D^0\pi^0)/\Gamma_{\text{total}}$	DOCUMENT ID	TECN	COMMENT	Γ_1/Γ
0.619 ± 0.029 OUR FIT				

• • • We do not use the following data for averages, fits, limits, etc. • • •

0.635 ± 0.003 ± 0.017	69k	⁴ AUBERT, BE	05G BABR	10.6 $e^+e^- \rightarrow$ hadrons
0.596 ± 0.035 ± 0.028	858	⁵ ALBRECHT	95F ARG	$e^+e^- \rightarrow$ hadrons
0.636 ± 0.023 ± 0.033	1097	⁵ BUTLER	92 CLE2	$e^+e^- \rightarrow$ hadrons

$\Gamma(D^0\gamma)/\Gamma_{\text{total}}$	DOCUMENT ID	TECN	COMMENT	Γ_2/Γ
0.381 ± 0.029 OUR FIT				
0.381 ± 0.029 OUR AVERAGE				

0.404 ± 0.035 ± 0.028	456	⁵ ALBRECHT	95F ARG	$e^+e^- \rightarrow$ hadrons
-----------------------	-----	-----------------------	---------	------------------------------

0.364 ± 0.023 ± 0.033	621	⁵ BUTLER	92 CLE2	$e^+e^- \rightarrow$ hadrons
-----------------------	-----	---------------------	---------	------------------------------

0.37 ± 0.08 ± 0.08		ADLER	88D MRK3	e^+e^-
--------------------	--	-------	----------	----------

• • • We do not use the following data for averages, fits, limits, etc. • • •

0.365 ± 0.003 ± 0.017	68k	⁴ AUBERT, BE	05G BABR	10.6 $e^+e^- \rightarrow$ hadrons
0.47 ± 0.23		LOW	87 HRS	29 GeV e^+e^-
0.53 ± 0.13		BARTEL	85G JADE	e^+e^- , hadrons
0.47 ± 0.12		COLES	82 MRK2	e^+e^-
0.45 ± 0.15		GOLDHABER	77 MRK1	e^+e^-

⁴ Derived from the ratio $\Gamma(D^0\pi^0)/\Gamma(D^0\gamma)$ assuming that the branching fractions of $D^{*0} \rightarrow D^0\pi^0$ and $D^{*0} \rightarrow D^0\gamma$ decays sum to 100%

⁵ The BUTLER 92 and ALBRECHT 95F branching ratios are not independent, they have been constrained by the authors to sum to 100%.

 $D^*(2007)^0$ REFERENCES

AUBERT, BE	05G	PR D72 091101	B. Aubert <i>et al.</i>	(BABAR Collab.)
ALBRECHT	95F	ZPHY C66 63	H. Albrecht <i>et al.</i>	(ARGUS Collab.)
BORTOLETTO	92B	PRL 69 2046	D. Bortoletto <i>et al.</i>	(CLEO Collab.)
BUTLER	92	PRL 69 2041	F. Butler <i>et al.</i>	(CLEO Collab.)
ABACHI	88B	PL B212 533	S. Abachi <i>et al.</i>	(ANL, IND, MICH, PURD+)
ADLER	88D	PL B208 152	J. Adler <i>et al.</i>	(Mark III Collab.)
LOW	87	PL B193 232	E.H. Low <i>et al.</i>	(HRS Collab.)
BARTEL	85G	PL 161B 197	W. Bartel <i>et al.</i>	(JADE Collab.)
COLES	82	PR D26 2190	M.W. Coles <i>et al.</i>	(LBL, SLAC)
SADROZINSKI	80	Madison Conf. 681	H.F.W. Sadrozinski <i>et al.</i>	(PRIN, CIT+)
GOLDHABER	77	PL 69B 503	G. Goldhaber <i>et al.</i>	(Mark I Collab.)
NGUYEN	77	PRL 39 262	H.K. Nguyen <i>et al.</i>	(LBL, SLAC) J

OTHER RELATED PAPERS

EDWARDS	02	PR D65 012002	K.W. Edwards <i>et al.</i>	(CLEO Collab.)
SEMENOV	99	SPU 42 847	S.V. Semenov	
Translated from UFN 42	937.			
KAMAL	92	PL B284 421	A.N. Kamal, Q.P. Xu	(ALBE)
TRILLING	81	PRPL 75 57	G.H. Trilling	(LBL, UCB)
GOLDHABER	76	PRL 37 255	G. Goldhaber <i>et al.</i>	(Mark I Collab.)

$D^*(2010)^\pm$

$I(J^P) = \frac{1}{2}(1^-)$
 I, J, P need confirmation.

 $D^*(2010)^\pm$ MASS

The fit includes $D^\pm, D^0, D_S^\pm, D^{*\pm}, D^{*0}$, and $D_S^{*\pm}$ mass and mass difference measurements.

VALUE (MeV) DOCUMENT ID TECN CHG COMMENT
2010.27 ± 0.17 OUR FIT Error includes scale factor of 1.1.

• • • We do not use the following data for averages, fits, limits, etc. • • •
 2008 ± 3 ¹ GOLDHABER 77 MRK1 ± e^+e^-
 2008.6 ± 1.0 ² PERUZZI 77 LGW ± e^+e^-
¹ From simultaneous fit to $D^*(2010)^\pm, D^*(2007)^0, D^+,$ and D^0 ; not independent of FELDMAN 77b mass difference below.
² PERUZZI 77 mass not independent of FELDMAN 77b mass difference below and PERUZZI 77 D^0 mass value.

 $m_{D^*(2010)^+} - m_{D^+}$

The fit includes $D^\pm, D^0, D_S^\pm, D^{*\pm}, D^{*0}$, and $D_S^{*\pm}$ mass and mass difference measurements.

VALUE (MeV) EVTS DOCUMENT ID TECN COMMENT
140.64 ± 0.10 OUR FIT Error includes scale factor of 1.1.
140.64 ± 0.08 ± 0.06 620 BORTOLETTO92B CLE2 $e^+e^- \rightarrow$ hadrons

 $m_{D^*(2010)^+} - m_{D^0}$

The fit includes $D^\pm, D^0, D_S^\pm, D^{*\pm}, D^{*0}$, and $D_S^{*\pm}$ mass and mass difference measurements.

VALUE (MeV) EVTS DOCUMENT ID TECN COMMENT
145.421 ± 0.010 OUR FIT Error includes scale factor of 1.1.
145.421 ± 0.010 OUR AVERAGE

VALUE (MeV)	EVTS	DOCUMENT ID	TECN	COMMENT
145.412 ± 0.002 ± 0.012		ANASTASSOV 02	CLE2	$D^{*\pm} \rightarrow D^0 \pi^\pm \rightarrow (K\pi) \pi^\pm$
145.54 ± 0.08	611	³ ADINOLFI 99	BEAT	$D^{*\pm} \rightarrow D^0 \pi^\pm$
145.45 ± 0.02		³ BREITWEG 99	ZEUS	$D^{*\pm} \rightarrow D^0 \pi^\pm \rightarrow (K\pi) \pi^\pm$
145.42 ± 0.05		³ BREITWEG 99	ZEUS	$D^{*\pm} \rightarrow D^0 \pi^\pm \rightarrow (K^- 3\pi^+) \pi^\pm$
145.5 ± 0.15	103	⁴ ADLOFF 97B	H1	$D^{*\pm} \rightarrow D^0 \pi^\pm$
145.44 ± 0.08	152	⁴ BREITWEG 97	ZEUS	$D^{*\pm} \rightarrow D^0 \pi^\pm$
145.42 ± 0.11	199	⁴ BREITWEG 97	ZEUS	$D^{*\pm} \rightarrow D^0 \pi^\pm \rightarrow K^- \pi^+$
145.4 ± 0.2	48	⁴ DERRICK 95	ZEUS	$D^{*\pm} \rightarrow D^0 \pi^\pm$
145.39 ± 0.06 ± 0.03		BARLAG 92B	ACCM	$\pi^- 230$ GeV
145.5 ± 0.2	115	⁴ ALEXANDER 91B	OPAL	$D^{*\pm} \rightarrow D^0 \pi^\pm$
145.30 ± 0.06		⁴ DECAMP 91J	ALEP	$D^{*\pm} \rightarrow D^0 \pi^\pm$
145.40 ± 0.05 ± 0.10		ABACHI 88B	HRS	$D^{*\pm} \rightarrow D^0 \pi^\pm$
145.46 ± 0.07 ± 0.03		ALBRECHT 85F	ARG	$D^{*\pm} \rightarrow D^0 \pi^\pm$
145.5 ± 0.3	28	BAILEY 83	SPEC	$D^{*\pm} \rightarrow D^0 \pi^\pm$
145.5 ± 0.3	60	FITCH 81	SPEC	$\pi^- A$
145.3 ± 0.5	30	FELDMAN 77B	MRK1	$D^{*+} \rightarrow D^0 \pi^+$
• • • We do not use the following data for averages, fits, limits, etc. • • •				
145.44 ± 0.09	122	⁴ BREITWEG 97B	ZEUS	$D^{*+} \rightarrow D^0 \pi^+, D^0 \rightarrow K^- \pi^+$
145.8 ± 1.5	16	AHLEN 83	HRS	$D^{*+} \rightarrow D^0 \pi^+$
145.1 ± 1.8	12	BAILEY 83	SPEC	$D^{*+} \rightarrow D^0 \pi^+$
145.1 ± 0.5	14	BAILEY 83	SPEC	$D^{*+} \rightarrow D^0 \pi^+$
145.5 ± 0.5	14	YELTON 82	MRK2	$29 e^+e^- \rightarrow K^- \pi^+$
~ 145.5		AVERY 80	SPEC	γA
145.2 ± 0.6	2	BLIETSCHAU 79	BEBC	νp
³ Statistical errors only.				
⁴ Systematic error not evaluated.				

 $m_{D^*(2010)^+} - m_{D^*(2007)^0}$

VALUE (MeV) DOCUMENT ID TECN COMMENT
 • • • We do not use the following data for averages, fits, limits, etc. • • •
 2.6 ± 1.8 ⁵ PERUZZI 77 LGW e^+e^-
⁵ Not independent of FELDMAN 77b mass difference above, PERUZZI 77 D^0 mass, and GOLDHABER 77 $D^*(2007)^0$ mass.

 $D^*(2010)^\pm$ WIDTH

VALUE (keV) CL% EVTS DOCUMENT ID TECN COMMENT
96 ± 4 ± 22 ANASTASSOV 02 CLE2 $D^{*\pm} \rightarrow D^0 \pi^\pm \rightarrow (K\pi) \pi^\pm$
 • • • We do not use the following data for averages, fits, limits, etc. • • •
 <131 90 110 BARLAG 92B ACCM $\pi^- 230$ GeV

 $D^*(2010)^\pm$ DECAY MODES

$D^*(2010)^-$ modes are charge conjugates of the modes below.

Mode	Fraction (Γ_i/Γ)
$\Gamma_1 D^0 \pi^+$	(67.7 ± 0.5) %
$\Gamma_2 D^+ \pi^0$	(30.7 ± 0.5) %
$\Gamma_3 D^+ \gamma$	(1.6 ± 0.4) %

CONSTRAINED FIT INFORMATION

An overall fit to 3 branching ratios uses 6 measurements and one constraint to determine 3 parameters. The overall fit has a $\chi^2 = 0.3$ for 4 degrees of freedom.

The following *off-diagonal* array elements are the correlation coefficients $\langle \delta x_i \delta x_j \rangle / (\delta x_i \delta x_j)$, in percent, from the fit to the branching fractions, $x_i \equiv \Gamma_i/\Gamma_{\text{total}}$. The fit constrains the x_i whose labels appear in this array to sum to one.

x_2	-62	
x_3	-43	-44
	x_1	x_2

 $D^*(2010)^+$ BRANCHING RATIOS

$\Gamma(D^0 \pi^+)/\Gamma_{\text{total}}$ Γ_1/Γ

VALUE DOCUMENT ID TECN COMMENT
0.677 ± 0.005 OUR FIT
0.677 ± 0.006 OUR AVERAGE
 0.6759 ± 0.0029 ± 0.0064 ^{6,7,8} BARTELT 98 CLE2 e^+e^-
 0.688 ± 0.024 ± 0.013 ALBRECHT 95F ARG $e^+e^- \rightarrow$ hadrons
 0.681 ± 0.010 ± 0.013 ⁶ BUTLER 92 CLE2 $e^+e^- \rightarrow$ hadrons
 • • • We do not use the following data for averages, fits, limits, etc. • • •

0.57 ± 0.04 ± 0.04	ADLER 88D	MRK3	e^+e^-
0.44 ± 0.10	COLES 82	MRK2	e^+e^-
0.6 ± 0.15	⁸ GOLDHABER 77	MRK1	e^+e^-

$\Gamma(D^+ \pi^0)/\Gamma_{\text{total}}$ Γ_2/Γ

VALUE EVTS DOCUMENT ID TECN COMMENT
0.307 ± 0.005 OUR FIT
0.3073 ± 0.0013 ± 0.0062 ^{6,7,8} BARTELT 98 CLE2 e^+e^-
 • • • We do not use the following data for averages, fits, limits, etc. • • •
 0.312 ± 0.011 ± 0.008 1404 ALBRECHT 95F ARG $e^+e^- \rightarrow$ hadrons
 0.308 ± 0.004 ± 0.008 410 ⁶ BUTLER 92 CLE2 $e^+e^- \rightarrow$ hadrons
 0.26 ± 0.02 ± 0.02 ADLER 88D MRK3 e^+e^-
 0.34 ± 0.07 COLES 82 MRK2 e^+e^-

$\Gamma(D^+ \gamma)/\Gamma_{\text{total}}$ Γ_3/Γ

VALUE CL% EVTS DOCUMENT ID TECN COMMENT
0.016 ± 0.004 OUR FIT
0.016 ± 0.005 OUR AVERAGE
 0.0168 ± 0.0042 ± 0.0029 ^{6,7} BARTELT 98 CLE2 e^+e^-
 0.011 ± 0.014 ± 0.016 12 ⁶ BUTLER 92 CLE2 $e^+e^- \rightarrow$ hadrons
 • • • We do not use the following data for averages, fits, limits, etc. • • •

<0.052	90	ALBRECHT 95F	ARG	$e^+e^- \rightarrow$ hadrons
0.17 ± 0.05 ± 0.05		ADLER 88D	MRK3	$e^+e^- \rightarrow$ hadrons
0.22 ± 0.12		⁹ COLES 82	MRK2	e^+e^-

⁶ The branching ratios are not independent, they have been constrained by the authors to sum to 100%.

⁷ Systematic error includes theoretical error on the prediction of the ratio of hadronic modes.

⁸ Assuming that isospin is conserved in the decay.

⁹ Not independent of $\Gamma(D^0 \pi^+)/\Gamma_{\text{total}}$ and $\Gamma(D^+ \pi^0)/\Gamma_{\text{total}}$ measurement.

 $D^*(2010)^\pm$ REFERENCES

ANASTASSOV 02	PR D65 032003	A. Anastassov et al.	(CLEO Collab.)
ADINOLFI 99	NP B547 3	M. Adinolfi et al.	(Beatrice Collab.)
BREITWEG 99	EPJ C6 67	J. Breitweg et al.	(ZEUS Collab.)
BARTELT 98	PRL 80 3919	J. Bartelt et al.	(CLEO II Collab.)
ADLOFF 97B	ZPHY C72 593	C. Adloff et al.	(HI Collab.)
BREITWEG 97	PL B401 192	J. Breitweg et al.	(ZEUS Collab.)
BREITWEG 97B	PL B407 402	J. Breitweg et al.	(ZEUS Collab.)
ALBRECHT 95F	ZPHY C66 63	H. Albrecht et al.	(ARGUS Collab.)
DERRICK 95	PL B349 225	M. Derrick et al.	(ZEUS Collab.)
BARLAG 92B	PL B278 480	S. Barlag et al.	(ACCMOR Collab.)
BORTOLETTO 92B	PRL 69 2046	D. Bortoletto et al.	(CLEO Collab.)
BUTLER 92	PRL 69 2041	F. Butler et al.	(CLEO Collab.)
ALEXANDER 91B	PL B262 341	G. Alexander et al.	(OPAL Collab.)
DECAMP 91J	PL B266 218	D. Decamp et al.	(ALEPH Collab.)
ABACHI 88B	PL B212 533	S. Abachi et al.	(ANL, IND., MICH., PURD+)
ADLER 88D	PL B208 152	J. Adler et al.	(Mark III Collab.)

Meson Particle Listings

$D^*(2010)^\pm, D_0^*(2400)^0, D_0^*(2400)^\pm, D_1(2420)^0$

ALBRECHT	85F	PL 150B 235	H. Albrecht <i>et al.</i>	(ARGUS Collab.)
AHLEN	83	PRL 51 1147	S.P. Ahlen <i>et al.</i>	(ANL, IND, LBL+)
BAILEY	83	PL 132B 230	R. Bailey <i>et al.</i>	(AMST, BRIS, CERN, CRAC+)
COLES	82	PR D26 2190	M.W. Coles <i>et al.</i>	(LBL, SLAC)
YELTON	82	PRL 49 430	J.M. Yelton <i>et al.</i>	(SLAC, LBL, UCB+)
FITCH	81	PRL 46 761	V.L. Fitch <i>et al.</i>	(PRIN, SACL, TORI+)
AVERY	80	PRL 44 1309	P. Avery <i>et al.</i>	(ILL, FNAL, COLU)
BLIETSCHAU	79	PL 86B 108	J. Blietschau <i>et al.</i>	(AACH3, BONN, CERN+)
FELDMAN	77B	PRL 38 1313	G.J. Feldman <i>et al.</i>	(Mark I Collab.)
GOLDBABER	77	PL 69B 503	G. Goldhaber <i>et al.</i>	(Mark I Collab.)
PERUZZI	77	PRL 39 1301	I. Peruzzi <i>et al.</i>	(LGV Collab.)

OTHER RELATED PAPERS

AHMED	01	PRL 87 251801	S. Ahmed <i>et al.</i>	(CLEO Collab.)
SEMENOV	99	SPU 42 847	S.V. Semenov	
			Translated from UFN 42 937	
NUSSINOV	98	PL B418 383	S. Nussinov	
KAMAL	92	PL B284 421	A.N. Kamal, Q.P. Xu	(ALBE)
ALTHOFF	83C	PL 126B 493	M. Althoff <i>et al.</i>	(TASSO Collab.)
BEBEK	82	PRL 49 610	C. Bebek <i>et al.</i>	(HARV, OSU, ROCH, RUTG+)
TRILLING	81	PRPL 75 57	G.H. Trilling	(LBL, UCB)
PERUZZI	76	PRL 37 569	I. Peruzzi <i>et al.</i>	(Mark I Collab.)

$D_0^*(2400)^0$

$$I(J^P) = \frac{1}{2}(0^+)$$

OMITTED FROM SUMMARY TABLE
 $J = 0^+$ assignment favoured (ABE 04D).

$D_0^*(2400)^0$ MASS

VALUE (MeV)	EVTS	DOCUMENT ID	TECN	COMMENT
2352 ± 50 OUR AVERAGE				Error includes scale factor of 1.8.
2308 ± 17 ± 32		ABE	04D	BELL $B^- \rightarrow D^+ \pi^- \pi^-$
2407 ± 21 ± 35	9.8k	LINK	04A	FOCS γA

$D_0^*(2400)^0$ WIDTH

VALUE (MeV)	EVTS	DOCUMENT ID	TECN	COMMENT
261 ± 50 OUR AVERAGE				
276 ± 21 ± 63		ABE	04D	BELL $B^- \rightarrow D^+ \pi^- \pi^-$
240 ± 55 ± 59	9.8k	LINK	04A	FOCS γA

$D_0^*(2400)^0$ DECAY MODES

Mode	Fraction (Γ_i/Γ)
Γ_1 $D^+ \pi^-$	seen

$D_0^*(2400)^0$ REFERENCES

ABE	04D	PR D69 112002	K. Abe <i>et al.</i>	(BELLE Collab.)
LINK	04A	PL B586 11	J.M. Link <i>et al.</i>	(FOCUS Collab.)

OTHER RELATED PAPERS

ABULENCIA	06A	PR D73 051104	A. Abulencia <i>et al.</i>	(CDF Collab.)
DMITRASINOVIC	06	MPL A21 533	V. Dmitrasinovic	
VIJANDE	06	PR D73 034002	J. Vijande, F. Fernandez, A. Valcarce	
BRACCO	05	PL B624 217	M.E. Bracco, A. Lozea, R.D. Matheus	
DMITRASINOVIC	05	PRL 94 162002	V. Dmitrasinovic	
GODFREY	05	PR D72 054029	S. Godfrey	
ANDERSON	99	CLEO CONF99-6	S. Anderson <i>et al.</i>	(CLEO Collab.)
			Conference Report	
EICHTEN	93	PRL 71 4116	E.J. Eichten, C.T. Hill, C. Quigg	
GODFREY	85	PR D32 189	S. Godfrey, N. Isgur	
SHURYAK	82	NP B198 83	E.V. Shuryak	

$D_0^*(2400)^\pm$

$$I(J^P) = \frac{1}{2}(0^+)$$

OMITTED FROM SUMMARY TABLE
 J, P need confirmation.

$D_0^*(2400)^\pm$ MASS

VALUE (MeV)	EVTS	DOCUMENT ID	TECN	COMMENT
2403 ± 14 ± 35	18.8k	LINK	04A	FOCS γA

$D_0^*(2400)^\pm$ WIDTH

VALUE (MeV)	EVTS	DOCUMENT ID	TECN	COMMENT
283 ± 24 ± 34	18.8k	LINK	04A	FOCS γA

$D_0^*(2400)^\pm$ DECAY MODES

Mode	Fraction (Γ_i/Γ)
Γ_1 $D^0 \pi^+$	seen

$D_0^*(2400)^\pm$ REFERENCES

LINK	04A	PL B586 11	J.M. Link <i>et al.</i>	(FOCUS Collab.)
------	-----	------------	-------------------------	-----------------

OTHER RELATED PAPERS

BRACCO	05	PL B624 217	M.E. Bracco, A. Lozea, R.D. Matheus	
ANDERSON	99	CLEO CONF99-6	S. Anderson <i>et al.</i>	(CLEO Collab.)
			Conference Report	
EICHTEN	93	PRL 71 4116	E.J. Eichten, C.T. Hill, C. Quigg	
GODFREY	85	PR D32 189	S. Godfrey, N. Isgur	
SHURYAK	82	NP B198 83	E.V. Shuryak	

$D_1(2420)^0$

$$I(J^P) = \frac{1}{2}(1^+)$$

I, J, P need confirmation.

Seen in $D^*(2010)^+ \pi^-$. $J^P = 1^+$ according to ALBRECHT 89H.

$D_1(2420)^0$ MASS

VALUE (MeV)	EVTS	DOCUMENT ID	TECN	COMMENT
2422.3 ± 1.3 OUR AVERAGE				Error includes scale factor of 1.2.
2426 ± 3 ± 1	151	ABE	05A	BELL $B^- \rightarrow D^0 \pi^+ \pi^- \pi^-$
2421.4 ± 1.5 ± 0.9		¹ ABE	04D	BELL $B^- \rightarrow D^+ \pi^- \pi^-$
2421 ± $\frac{+1}{-2}$ ± 2	286	AVERY	94C	CLE2 $e^+ e^- \rightarrow D^+ \pi^- X$
2422 ± 2 ± 2	51	FRABETTI	94B	E687 $\gamma Be \rightarrow D^+ \pi^- X$
2428 ± 3 ± 2	279	AVERY	90	CLEO $e^+ e^- \rightarrow D^+ \pi^- X$
2414 ± 2 ± 5	171	ALBRECHT	89H	ARG $e^+ e^- \rightarrow D^+ \pi^- X$
2428 ± 8 ± 5	171	ANJOS	89C	TPS $\gamma N \rightarrow D^+ \pi^- X$
••• We do not use the following data for averages, fits, limits, etc. •••				
2421.7 ± 0.7 ± 0.6	7.5k	ABULENCIA	06A	CDF 1900 $p\bar{p} \rightarrow D^+ \pi^- X$
2425 ± 3	235	² ABREU	98M	DLPH $e^+ e^-$

¹ Fit includes the contribution from $D_1^*(2430)^0$.

² No systematic error given.

$m_{D_1^0} - m_{D^{*+}}$

VALUE	EVTS	DOCUMENT ID	TECN	COMMENT
411.7 ± 0.7 ± 0.4	7.5k	ABULENCIA	06A	CDF 1900 $p\bar{p} \rightarrow D^+ \pi^- X$

$D_1(2420)^0$ WIDTH

VALUE (MeV)	EVTS	DOCUMENT ID	TECN	COMMENT
20.4 ± 1.7 OUR AVERAGE				
20.0 ± 1.7 ± 1.3	7.5k	ABULENCIA	06A	CDF 1900 $p\bar{p} \rightarrow D^+ \pi^- X$
24 ± 7 ± 8	151	ABE	05A	BELL $B^- \rightarrow D^0 \pi^+ \pi^- \pi^-$
23.7 ± 2.7 ± 4.0		³ ABE	04D	BELL $B^- \rightarrow D^+ \pi^- \pi^-$
20 ± $\frac{+6}{-5}$ ± 3	286	AVERY	94C	CLE2 $e^+ e^- \rightarrow D^+ \pi^- X$
15 ± 8 ± 4	51	FRABETTI	94B	E687 $\gamma Be \rightarrow D^+ \pi^- X$
23 ± $\frac{+8}{-6}$ ± 10	279	AVERY	90	CLEO $e^+ e^- \rightarrow D^+ \pi^- X$
13 ± 6 ± $\frac{+10}{-5}$	171	ALBRECHT	89H	ARG $e^+ e^- \rightarrow D^+ \pi^- X$
••• We do not use the following data for averages, fits, limits, etc. •••				
58 ± 14 ± 10	171	ANJOS	89C	TPS $\gamma N \rightarrow D^+ \pi^- X$

³ Fit includes the contribution from $D_1^*(2430)^0$.

$D_1(2420)^0$ DECAY MODES

$\bar{D}_1(2420)^0$ modes are charge conjugates of modes below.

Mode	Fraction (Γ_i/Γ)
Γ_1 $D^*(2010)^+ \pi^-$	seen
Γ_2 $D^0 \pi^+ \pi^-$	seen
Γ_3 $D^0 \rho^0$	
Γ_4 $D^0 f_0(600)$	
Γ_5 $D_0^*(2400)^+ \pi^-$	
Γ_6 $D^+ \pi^-$	not seen
Γ_7 $D^{*0} \pi^+ \pi^-$	not seen

$D_1(2420)^0$ BRANCHING RATIOS

$\Gamma(D^*(2010)^+ \pi^-)/\Gamma_{total}$	DOCUMENT ID	TECN	COMMENT	Γ_i/Γ
seen	ACKERSTAFF	97W	OPAL $e^+ e^- \rightarrow D^+ \pi^- X$	
seen	AVERY	90	CLEO $e^+ e^- \rightarrow D^+ \pi^- X$	
seen	ALBRECHT	89H	ARG $e^+ e^- \rightarrow D^+ \pi^- X$	
seen	ANJOS	89C	TPS $\gamma N \rightarrow D^+ \pi^- X$	

See key on page 373

Meson Particle Listings
 $D_1(2420)^0, D_1(2420)^\pm, D_1(2430)^0$

$\Gamma(D^+\pi^-)/\Gamma(D^*(2010)^+\pi^-)$					Γ_6/Γ_1
VALUE	CL%	DOCUMENT ID	TECN	COMMENT	
<0.24	90	AVERY	90	CLEO $e^+e^- \rightarrow D^+\pi^-\chi$	

 $D_1(2420)^0$ REFERENCES

ABULENCIA	06A	PR D73 051104	A. Abulencia et al.	(CDF Collab.)
ABE	05A	PRL 94 221805	K. Abe et al.	(BELLE Collab.)
ABE	04D	PR D69 112002	K. Abe et al.	(BELLE Collab.)
ABREU	98M	PL B426 231	P. Abreu et al.	(DELPHI Collab.)
ACKERSTAFF	97W	ZPHY C76 425	K. Ackerstaff et al.	(OPAL Collab.)
AVERY	94C	PL B331 236	P. Avery et al.	(CLEO Collab.)
FRABETTI	94B	PRL 72 324	P.L. Frabetti et al.	(FNAL E687 Collab.)
AVERY	90	PR D41 774	P. Avery, D. Besson	(CLEO Collab.)
ALBRECHT	89H	PL B232 398	H. Albrecht et al.	(ARGUS Collab.) JP
ANJOS	89C	PRL 62 1717	J.C. Anjos et al.	(FNAL E691 Collab.)

OTHER RELATED PAPERS

AUBERT	06L	PR D74 012001	B. Aubert et al.	(BABAR Collab.)
ABAZOV	05O	PRL 95 171803	V.M. Abazov et al.	(D0 Collab.)
ACOSTA	05F	PR D71 051103R	D. Acosta et al.	(CDF Collab.)
CLOSE	05C	PR D72 094004	F.E. Close, E.S. Swanson	(OXFTP)
SEME NOV	99	SPU 42 847	S.V. Semenov	

Translated from UFN 42 937.

 $D_1(2420)^\pm$

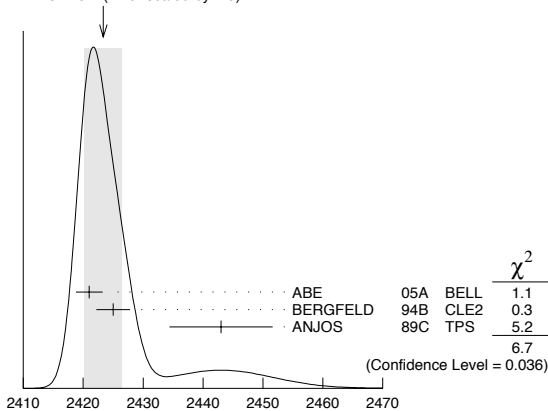
$$I(J^P) = \frac{1}{2}(??)$$

I needs confirmation.

OMITTED FROM SUMMARY TABLE

Seen in $D^*(2007)^0\pi^+$. $J^P = 0^+$ ruled out. $D_1(2420)^\pm$ MASS

VALUE (MeV)	EVTS	DOCUMENT ID	TECN	COMMENT
2423.4 ± 3.1 OUR AVERAGE	Error	includes scale factor of 1.8. See the ideogram below.		
2421 ± 2 ± 1	124	ABE	05A	BELL $\bar{B}^0 \rightarrow D^+\pi^+\pi^-\pi^-$
2425 ± 2 ± 2	146	BERGFELD	94B	CLE2 $e^+e^- \rightarrow D^{*0}\pi^+\chi$
2443 ± 7 ± 5	190	ANJOS	89C	TPS $\gamma N \rightarrow D^0\pi^+\chi^0$

WEIGHTED AVERAGE
2423.4 ± 3.1 (Error scaled by 1.8) $D_1(2420)^\pm$ MASS (MeV) $m_{D_1(2420)^\pm} - m_{D_1^*(2420)^0}$

VALUE (MeV)	DOCUMENT ID	TECN	COMMENT
4 ± 2 ± 3	BERGFELD	94B	CLE2 $e^+e^- \rightarrow$ hadrons

 $D_1(2420)^\pm$ WIDTH

VALUE (MeV)	EVTS	DOCUMENT ID	TECN	COMMENT
25 ± 6 OUR AVERAGE				
21 ± 5 ± 8	124	ABE	05A	BELL $\bar{B}^0 \rightarrow D^+\pi^+\pi^-\pi^-$
26 ± 8 ± 4	146	BERGFELD	94B	CLE2 $e^+e^- \rightarrow D^{*0}\pi^+\chi$
41 ± 19 ± 8	190	ANJOS	89C	TPS $\gamma N \rightarrow D^0\pi^+\chi^0$

 $D_1(2420)^\pm$ DECAY MODES $D_1^*(2420)^-$ modes are charge conjugates of modes below.

Mode	Fraction (Γ_i/Γ)
Γ_1 $D^*(2007)^0\pi^+$	seen
Γ_2 $D^+\pi^+\pi^-$	seen
Γ_3 $D^+\rho^0$	

Γ_4	$D^+f_0(600)$	
Γ_5	$D_0^*(2400)^0\pi^+$	
Γ_6	$D^0\pi^+$	not seen
Γ_7	$D^{*+}\pi^+\pi^-$	not seen

 $D_1(2420)^\pm$ BRANCHING RATIOS

$\Gamma(D^*(2007)^0\pi^+)/\Gamma_{\text{total}}$				Γ_1/Γ
VALUE	DOCUMENT ID	TECN	COMMENT	
seen	ANJOS	89C	TPS	$\gamma N \rightarrow D^0\pi^+\chi^0$

$\Gamma(D^0\pi^+)/\Gamma(D^*(2007)^0\pi^+)$					Γ_6/Γ_1
VALUE	CL%	DOCUMENT ID	TECN	COMMENT	
<0.18	90	BERGFELD	94B	CLE2 $e^+e^- \rightarrow$ hadrons	

• • • We do not use the following data for averages, fits, limits, etc. • • •

 $D_1(2420)^\pm$ REFERENCES

ABE	05A	PRL 94 221805	K. Abe et al.	(BELLE Collab.)
BERGFELD	94B	PL B340 194	T. Bergfeld et al.	(CLEO Collab.)
ANJOS	89C	PRL 62 1717	J.C. Anjos et al.	(FNAL E691 Collab.)

OTHER RELATED PAPERS

CLOSE	05C	PR D72 094004	F.E. Close, E.S. Swanson	(OXFTP)
SEME NOV	99	SPU 42 847	S.V. Semenov	

Translated from UFN 42 937.

 $D_1(2430)^0$

$$I(J^P) = \frac{1}{2}(1^+)$$

OMITTED FROM SUMMARY TABLE

 $J = 1^+$ assignment favored (ABE 04D). $D_1(2430)^0$ MASS

VALUE (MeV)	DOCUMENT ID	TECN	COMMENT
2427 ± 26 ± 25	ABE	04D	BELL $B^- \rightarrow D^{*+}\pi^-\pi^-$
2477 ± 28	¹ AUBERT	06L	BABR $\bar{B}^0 \rightarrow D^{*+}\omega\pi^-$

¹ Systematic errors not estimated. $D_1(2430)^0$ WIDTH

VALUE (MeV)	DOCUMENT ID	TECN	COMMENT
384 ± 107 ± 74	ABE	04D	BELL $B^- \rightarrow D^{*+}\pi^-\pi^-$
266 ± 97	² AUBERT	06L	BABR $\bar{B}^0 \rightarrow D^{*+}\omega\pi^-$

² Systematic errors not estimated. $D_1(2430)^0$ DECAY MODES

Mode	Fraction (Γ_i/Γ)
Γ_1 $D^*(2010)^+\pi^-$	seen

 $D_1(2430)^0$ REFERENCES

AUBERT	06L	PR D74 012001	B. Aubert et al.	(BABAR Collab.)
ABE	04D	PR D69 112002	K. Abe et al.	(BELLE Collab.)

OTHER RELATED PAPERS

ABULENCIA	06A	PR D73 051104	A. Abulencia et al.	(CDF Collab.)
ABAZOV	05O	PRL 95 171803	V.M. Abazov et al.	(D0 Collab.)
CLOSE	05C	PR D72 094004	F.E. Close, E.S. Swanson	(OXFTP)
GODFREY	05	PR D72 054029	S. Godfrey	
ZHANG	05C	PR D72 017902	A. Zhang	
ANDERSON	99	CLEO CONF 99-6	S. Anderson et al.	(CLEO Collab.)
EICHTE N	93	PRL 71 4116	E.J. Eichten, C.T. Hill, C. Quigg	
GODFREY	85	PR D32 189	S. Godfrey, N. Isgur	
SHURYAK	82	NP B198 83	E.V. Shuryak	

Meson Particle Listings

$D_2^*(2460)^0$

$D_2^*(2460)^0$

$$I(J^P) = \frac{1}{2}(2^+)$$

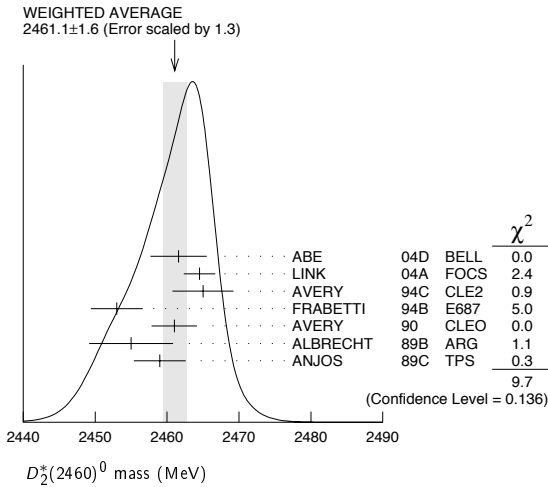
$J^P = 2^+$ assignment strongly favored(ALBRECHT 89B).

$D_2^*(2460)^0$ MASS

VALUE (MeV)	EVTS	DOCUMENT ID	TECN	COMMENT
2461.1 ± 1.6 OUR AVERAGE				Error includes scale factor of 1.3. See the ideogram below.
2461.6 ± 2.1 ± 3.3		¹ ABE 04D BELL		$B^- \rightarrow D^+ \pi^- \pi^-$
2464.5 ± 1.1 ± 1.9	5.8k	¹ LINK 04A FOCS		γA
2465 ± 3 ± 3	486	AVERY 94C CLE2		$e^+ e^- \rightarrow D^+ \pi^- X$
2453 ± 3 ± 2	128	FRABETTI 94B E687		$\gamma Be \rightarrow D^+ \pi^- X$
2461 ± 3 ± 1	440	AVERY 90 CLEO		$e^+ e^- \rightarrow D^{*+} \pi^- X$
2455 ± 3 ± 5	337	ALBRECHT 89B ARG		$e^+ e^- \rightarrow D^+ \pi^- X$
2459 ± 3 ± 2	153	ANJOS 89C TPS		$\gamma N \rightarrow D^+ \pi^- X$
• • • We do not use the following data for averages, fits, limits, etc. • • •				
2463.3 ± 0.6 ± 0.8	20k	ABULENCIA 06A CDF	1900	$p\bar{p} \rightarrow D^+ \pi^- X$
2461 ± 6	126	² ABREU 98M DLPH		$e^+ e^-$
2466 ± 7	1	ASRATYAN 95 BEBC	53,40	$\nu(\bar{\nu}) \rightarrow p + X, d + X$

¹ Fit includes the contribution from $D_0^*(2400)^0$.

² No systematic error given.



$m_{D_2^*} - m_{D^+}$

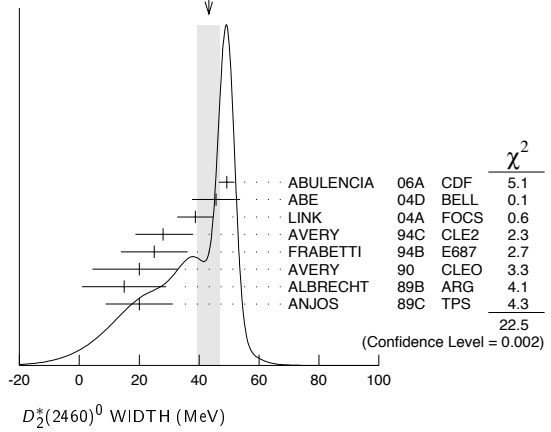
VALUE	EVTS	DOCUMENT ID	TECN	COMMENT
593.9 ± 0.6 ± 0.5	20k	ABULENCIA 06A CDF	1900	$p\bar{p} \rightarrow D^+ \pi^- X$

$D_2^*(2460)^0$ WIDTH

VALUE (MeV)	EVTS	DOCUMENT ID	TECN	COMMENT
43 ± 4 OUR AVERAGE				Error includes scale factor of 1.8. See the ideogram below.
49.2 ± 2.3 ± 1.3	20k	ABULENCIA 06A CDF	1900	$p\bar{p} \rightarrow D^+ \pi^- X$
45.6 ± 4.4 ± 6.7		³ ABE 04D BELL		$B^- \rightarrow D^+ \pi^- \pi^-$
38.7 ± 5.3 ± 2.9	5.8k	³ LINK 04A FOCS		γA
28 ± $\frac{8}{7}$ ± 6	486	AVERY 94C CLE2		$e^+ e^- \rightarrow D^+ \pi^- X$
25 ± 10 ± 5	128	FRABETTI 94B E687		$\gamma Be \rightarrow D^+ \pi^- X$
20 ± $\frac{9}{12}$ ± $\frac{9}{10}$	440	AVERY 90 CLEO		$e^+ e^- \rightarrow D^{*+} \pi^- X$
15 ± $\frac{13}{10}$ ± 5	337	ALBRECHT 89B ARG		$e^+ e^- \rightarrow D^+ \pi^- X$
20 ± 10 ± 5	153	ANJOS 89C TPS		$\gamma N \rightarrow D^+ \pi^- X$

³ Fit includes the contribution from $D_0^*(2400)^0$.

WEIGHTED AVERAGE
43 ± 4 (Error scaled by 1.8)



$D_2^*(2460)^0$ DECAY MODES

$\bar{D}_2^*(2460)^0$ modes are charge conjugates of modes below.

Mode	Fraction (Γ_i/Γ)
Γ_1 $D^+ \pi^-$	seen
Γ_2 $D^*(2010)^+ \pi^-$	seen
Γ_3 $D^0 \pi^+ \pi^-$	not seen
Γ_4 $D^{*0} \pi^+ \pi^-$	not seen

$D_2^*(2460)^0$ BRANCHING RATIOS

$\Gamma(D^+ \pi^-)/\Gamma_{total}$					Γ_1/Γ
VALUE	EVTS	DOCUMENT ID	TECN	COMMENT	
seen	337	ALBRECHT 89B ARG		$e^+ e^- \rightarrow D^+ \pi^- X$	
seen		ANJOS 89C TPS		$\gamma N \rightarrow D^+ \pi^- X$	
$\Gamma(D^*(2010)^+ \pi^-)/\Gamma_{total}$					Γ_2/Γ
VALUE	EVTS	DOCUMENT ID	TECN	COMMENT	
seen		ACKERSTAFF 97W OPAL		$e^+ e^- \rightarrow D^{*+} \pi^- X$	
seen		AVERY 90 CLEO		$e^+ e^- \rightarrow D^{*+} \pi^- X$	
seen		ALBRECHT 89H ARG		$e^+ e^- \rightarrow D^{*+} \pi^- X$	
$\Gamma(D^+ \pi^-)/\Gamma(D^*(2010)^+ \pi^-)$					Γ_1/Γ_2
VALUE	EVTS	DOCUMENT ID	TECN	COMMENT	
2.3 ± 0.6 OUR AVERAGE					
2.2 ± 0.7 ± 0.6		AVERY 94C CLE2		$e^+ e^- \rightarrow D^{*+} \pi^- X$	
2.3 ± 0.8		AVERY 90 CLEO		$e^+ e^-$	
3.0 ± 1.1 ± 1.5		ALBRECHT 89H ARG		$e^+ e^- \rightarrow D^* \pi^- X$	
• • • We do not use the following data for averages, fits, limits, etc. • • •					
1.9 ± 0.5		ABE 04D BELL		$B^- \rightarrow D^{(*)+} \pi^- \pi^-$	

$D_2^*(2460)^0$ REFERENCES

ABULENCIA 06A PR D73 051104	A. Abulencia et al.	(CDF Collab.)
ABE 04D PR D69 112002	K. Abe et al.	(BELLE Collab.)
LINK 04A PL B586 11	J.M. Link et al.	(FOCUS Collab.)
ABREU 90M PL B426 231	P. Abreu et al.	(DELPHI Collab.)
ACKERSTAFF 97W ZPHY C76 425	K. Ackerstaff et al.	(OPAL Collab.)
ASRATYAN 95 ZPHY C68 43	A.E. Asratyan et al.	(BIRM, BELG, CERN+)
AVERY 94C PL B331 236	P. Avery et al.	(CLEO Collab.)
FRABETTI 94B PRL 72 324	P.L. Frabetti et al.	(FNAL E687 Collab.)
AVERY 90 PR D41 774	P. Avery, D. Besson	(CLEO Collab.)
ALBRECHT 89B PL B221 422	H. Albrecht et al.	(ARGUS Collab.) JP
ALBRECHT 89H PL B232 398	H. Albrecht et al.	(ARGUS Collab.) JP
ANJOS 89C PRL 62 1717	J.C. Anjos et al.	(FNAL E691 Collab.)

OTHER RELATED PAPERS

AUBERT 08G PRL 100 171803	B. Aubert et al.	(BABAR Collab.)
ANTIPIN 07 PL B647 164	O. Antipin, G. Valencia	
AUBERT 06L PR D74 012001	B. Aubert et al.	(BABAR Collab.)
ABAZOV 05O PRL 95 171803	V.M. Abazov et al.	(DO Collab.)
ACOSTA 05F PR D71 051103R	D. Acosta et al.	(CDF Collab.)
CLOSE 05C PR D72 094004	F.E. Close, E.S. Swanson	(OXFTP)
SEMENOV 99 SPU 42 947	S.V. Semenov	

Translated from UFN 42 937.

See key on page 373

Meson Particle Listings

$$D_2^*(2460)^\pm, D^*(2640)^\pm$$

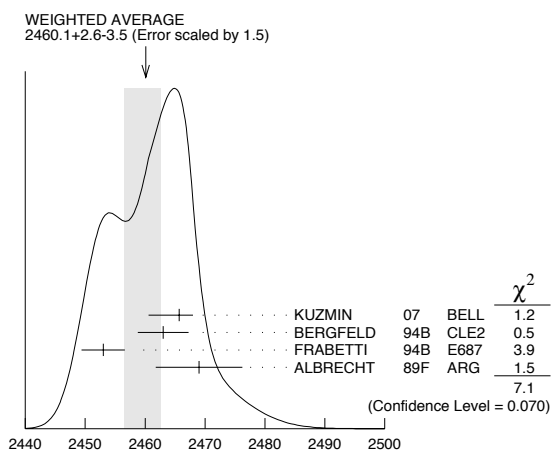
 $D_2^*(2460)^\pm$

$$I(J^P) = \frac{1}{2}(2^+)$$

 $J^P = 2^+$ assignment strongly favored (ALBRECHT 89B). $D_2^*(2460)^\pm$ MASS

VALUE (MeV)	EVTS	DOCUMENT ID	TECN	COMMENT
2460.1 \pm 2.5	OUR AVERAGE	Error includes scale factor of 1.5. See the ideogram below.		
2465.7 \pm 1.8 \pm 1.4	2909	KUZMIN	07 BELL	$e^+e^- \rightarrow$ hadrons
2463 \pm 3 \pm 3	310	BERGFELD	94B CLE2	$e^+e^- \rightarrow D^0\pi^+X$
2453 \pm 3 \pm 2	185	FRABETTI	94B E687	$\gamma\text{Be} \rightarrow D^0\pi^+X$
2469 \pm 4 \pm 6		ALBRECHT	89F ARG	$e^+e^- \rightarrow D^0\pi^+X$
• • • We do not use the following data for averages, fits, limits, etc. • • •				
2467.6 \pm 1.5 \pm 0.8	3.5k	¹ LINK	04A FOCS	γA

¹ Fit includes the contribution from $D_0^*(2400)^\pm$. Not independent of the corresponding mass difference measurement, $(m_{D_2^*(2460)^\pm} - m_{D_2^*(2460)^0})$.

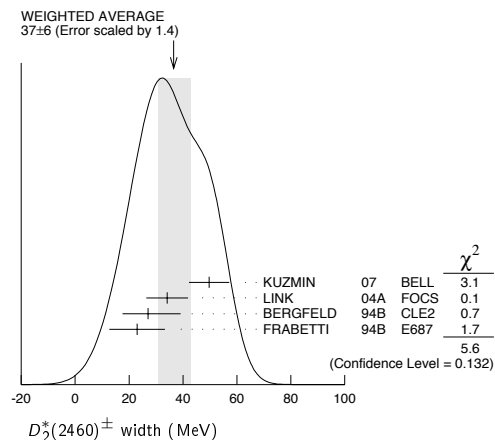
0.9 $D_2^*(2460)^\pm$ mass (MeV) $m_{D_2^*(2460)^\pm} - m_{D_2^*(2460)^0}$

VALUE (MeV)	DOCUMENT ID	TECN	COMMENT
2.4 \pm 1.7	OUR AVERAGE		
3.1 \pm 1.9 \pm 0.9	LINK 04A FOCS	γA	
- 2 \pm 4 \pm 4	BERGFELD 94B CLE2	$e^+e^- \rightarrow$ hadrons	
0 \pm 4	FRABETTI 94B E687	$\gamma\text{Be} \rightarrow D\pi X$	
14 \pm 5 \pm 8	ALBRECHT 89F ARG	$e^+e^- \rightarrow D^0\pi^+X$	

 $D_2^*(2460)^\pm$ WIDTH

VALUE (MeV)	EVTS	DOCUMENT ID	TECN	COMMENT
37 \pm 6	OUR AVERAGE	Error includes scale factor of 1.4. See the ideogram below.		
49.7 \pm 3.8 \pm 6.4	2909	KUZMIN	07 BELL	$e^+e^- \rightarrow$ hadrons
34.1 \pm 6.5 \pm 4.2	3.5k	² LINK	04A FOCS	γA
27 \pm 11 \pm 5	310	BERGFELD	94B CLE2	$e^+e^- \rightarrow D^0\pi^+X$
23 \pm 9 \pm 5	185	FRABETTI	94B E687	$\gamma\text{Be} \rightarrow D^0\pi^+X$

² Fit includes the contribution from $D_0^*(2400)^\pm$.

 $D_2^*(2460)^\pm$ DECAY MODES $D_2^*(2460)^-$ modes are charge conjugates of modes below.

Mode	Fraction (Γ_i/Γ)
$\Gamma_1 D^0\pi^+$	seen
$\Gamma_2 D^{*0}\pi^+$	seen
$\Gamma_3 D^+\pi^+\pi^-$	not seen
$\Gamma_4 D^{*+}\pi^+\pi^-$	not seen

 $D_2^*(2460)^\pm$ BRANCHING RATIOS

$\Gamma(D^0\pi^+)/\Gamma_{\text{total}}$	DOCUMENT ID	TECN	COMMENT	Γ_1/Γ
seen	ALBRECHT 89F ARG		$e^+e^- \rightarrow D^0\pi^+X$	
$\Gamma(D^0\pi^+)/\Gamma(D^{*0}\pi^+)$	DOCUMENT ID	TECN	COMMENT	Γ_1/Γ_2
1.9 \pm 1.1 \pm 0.3	BERGFELD 94B CLE2		$e^+e^- \rightarrow$ hadrons	

 $D_2^*(2460)^\pm$ REFERENCES

KUZMIN 07 PR D76 012006	A. Kuzmin <i>et al.</i>	(BELLE Collab.)
LINK 04A PL B586 11	J.M. Link <i>et al.</i>	(FOCUS Collab.)
BERGFELD 94B PL B340 194	T. Bergfeld <i>et al.</i>	(CLEO Collab.)
FRABETTI 94B PRL 72 324	P.L. Frabetti <i>et al.</i>	(FNAL E687 Collab.)
ALBRECHT 89B PL B221 422	H. Albrecht <i>et al.</i>	(ARGUS Collab.)
ALBRECHT 89F PL B231 208	H. Albrecht <i>et al.</i>	(ARGUS Collab.)

OTHER RELATED PAPERS

CLOSE 05C PR D72 094004	F.E. Close, E.S. Swanson	(OXFPT)
-------------------------	--------------------------	---------

 $D^*(2640)^\pm$

$$I(J^P) = \frac{1}{2}(?^?)$$

OMITTED FROM SUMMARY TABLE

Seen in Z decays by ABREU 98M. Not seen by ABBIENDI 01N.
Needs confirmation.

 $D^*(2640)^\pm$ MASS

VALUE (MeV)	EVTS	DOCUMENT ID	TECN	COMMENT
2637 \pm 2 \pm 6	66 \pm 14	ABREU 98M DLPH		$e^+e^- \rightarrow D^{*+}\pi^+\pi^-X$

 $D^*(2640)^\pm$ WIDTH

VALUE (MeV)	CL%	DOCUMENT ID	TECN	COMMENT
<15	95	ABREU 98M DLPH		$e^+e^- \rightarrow D^{*+}\pi^+\pi^-X$

 $D^*(2640)^+$ DECAY MODES $D^*(2640)^-$ modes are charge conjugates of modes below.

Mode	Fraction (Γ_i/Γ)
$\Gamma_1 D^*(2010)^+\pi^+\pi^-$	seen

 $D^*(2640)^\pm$ REFERENCES

ABBIENDI 01N EPJ C20 445	G. Abbiendi <i>et al.</i>	(OPAL Collab.)
ABREU 98M PL B426 231	P. Abreu <i>et al.</i>	(DELPHI Collab.)

OTHER RELATED PAPERS

CLOSE 05C PR D72 094004	F.E. Close, E.S. Swanson	(OXFPT)
-------------------------	--------------------------	---------

Meson Particle Listings

D_s^\pm

CHARMED, STRANGE MESONS ($C = S = \pm 1$)

$$D_s^+ = c\bar{s}, D_s^- = \bar{c}s, \text{ similarly for } D_s^{*\prime}s$$

D_s^\pm

$$J(P) = 0(0^-)$$

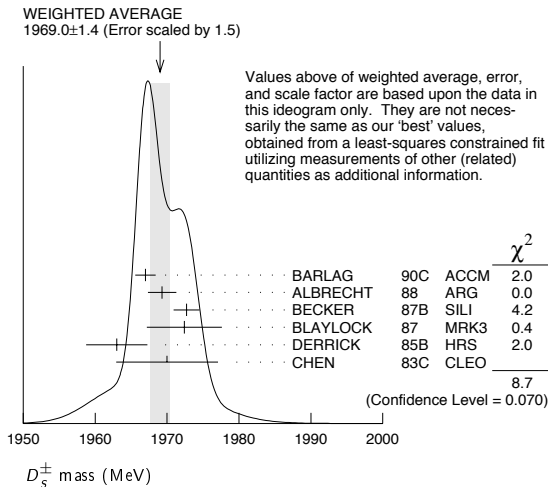
The angular distributions of the decays of the ϕ and $\bar{K}^*(892)^0$ in the $\phi\pi^+$ and $K^+\bar{K}^*(892)^0$ modes strongly indicate that the spin is zero. The parity given is that expected of a $c\bar{s}$ ground state.

D_s^\pm MASS

The fit includes $D_s^\pm, D_s^0, D_s^{*+}, D_s^{*0}$, and $D_s^{*\pm}$ mass and mass difference measurements. Measurements of the D_s^\pm mass with an error greater than 10 MeV are omitted from the fit and average. A number of early measurements have been omitted altogether.

VALUE (MeV)	EVTS	DOCUMENT ID	TECN	COMMENT
1968.49 ± 0.34 OUR FIT				Error includes scale factor of 1.3.
1969.0 ± 1.4 OUR AVERAGE				Error includes scale factor of 1.5. See the ideogram below.
1967.0 ± 1.0 ± 1.0	54	BARLAG	90C ACCM	π^- Cu 230 GeV
1969.3 ± 1.4 ± 1.4		ALBRECHT	88 ARG	e^+e^- 9.4–10.6 GeV
1972.7 ± 1.5 ± 1.0	21	BECKER	87B SILI	200 GeV π, K, p
1972.4 ± 3.7 ± 3.7	27	BLAYLOCK	87 MRK3	e^+e^- 4.14 GeV
1963 ± 3 ± 3	30	DERRICK	85B HRS	e^+e^- 29 GeV
1970 ± 5 ± 5	104	CHEN	83C CLEO	e^+e^- 10.5 GeV
••• We do not use the following data for averages, fits, limits, etc. •••				
1968.3 ± 0.7 ± 0.7	290	¹ ANJOS	88 E691	Photoproduction
1980 ± 15	6	USHIDA	86 EMUL	ν wideband
1973.6 ± 2.6 ± 3.0	163	ALBRECHT	85D ARG	e^+e^- 10 GeV
1948 ± 28 ± 10	65	AIHARA	84D TPC	e^+e^- 29 GeV
1975 ± 9 ± 10	49	ALTHOFF	84 TASS	e^+e^- 14–25 GeV
1975 ± 4	3	BAILEY	84 ACCM	hadron ⁺ Be → $\phi\pi^+X$

¹ ANJOS 88 enters the fit via $m_{D_s^\pm} - m_{D^\pm}$ (see below).



$$m_{D_s^\pm} - m_{D^\pm}$$

The fit includes $D_s^\pm, D_s^0, D_s^{*+}, D_s^{*0}$, and $D_s^{*\pm}$ mass and mass difference measurements.

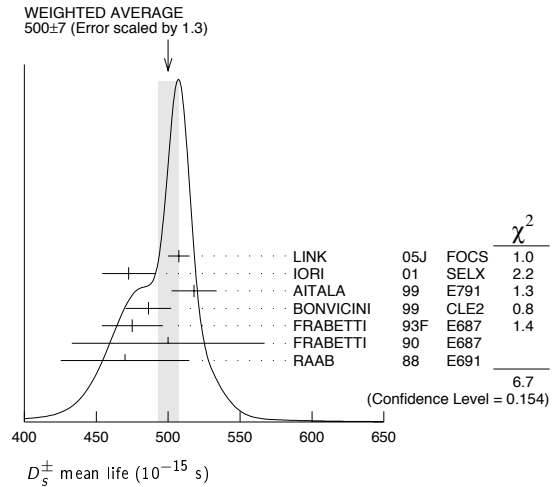
VALUE (MeV)	EVTS	DOCUMENT ID	TECN	COMMENT
98.87 ± 0.30 OUR FIT				Error includes scale factor of 1.4.
98.85 ± 0.25 OUR AVERAGE				Error includes scale factor of 1.1.
99.41 ± 0.38 ± 0.21		ACOSTA	03D CDF2	$\bar{p}p, \sqrt{s} = 1.96$ TeV
98.4 ± 0.1 ± 0.3	48k	AUBERT	02G BABR	$e^+e^- \approx \Upsilon(4S)$
99.5 ± 0.6 ± 0.3		BROWN	94 CLE2	$e^+e^- \approx \Upsilon(4S)$
98.5 ± 1.5	555	CHEN	89 CLEO	e^+e^- 10.5 GeV
99.0 ± 0.8	290	ANJOS	88 E691	Photoproduction

D_s^\pm MEAN LIFE

Measurements with an error greater than 100×10^{-15} s or with fewer than 100 events have been omitted from the Listings.

VALUE (10^{-15} s)	EVTS	DOCUMENT ID	TECN	COMMENT
500 ± 7 OUR AVERAGE				Error includes scale factor of 1.3. See the ideogram below.
507.4 ± 5.5 ± 5.1	13.6k	LINK	05J FOCS	$\phi\pi^+$ and $\bar{K}^{*0}K^+$
472.5 ± 17.2 ± 6.6	760	IORI	01 SELX	600 GeV Σ^-, π^-, p
518 ± 14 ± 7	1662	AITALA	99 E791	π^- nucleus, 500 GeV
486.3 ± 15.0 ⁺ ± 4.9 ⁻	2167	² BONVICINI	99 CLE2	$e^+e^- \approx \Upsilon(4S)$
475 ± 20 ± 7	900	FRABETTI	93F E687	γ Be, $\phi\pi^+$
500 ± 60 ± 30	104	FRABETTI	90 E687	γ Be, $\phi\pi^+$
470 ± 40 ± 20	228	RAAB	88 E691	Photoproduction

² BONVICINI 99 obtains 1.19 ± 0.04 for the ratio of D_s^+ to D^0 lifetimes.



D_s^+ DECAY MODES

Unless otherwise noted, the branching fractions for modes with a resonance in the final state include all the decay modes of the resonance. D_s^- modes are charge conjugates of the modes below.

Mode	Fraction (Γ_i/Γ)	Confidence level
Inclusive modes		
Γ_1 K^- anything	(13 ± 14) ₋₁₂ %	
Γ_2 \bar{K}^0 anything + K^0 anything	(39 ± 28) %	
Γ_3 K^+ anything	(20 ± 18) ₋₁₄ %	
Γ_4 (non- $K\bar{K}$) anything	(64 ± 17) %	
Γ_5 η anything	[a] (24 ± 4) %	
Γ_6 η' anything	(8.7 ± 2.1) %	
Γ_7 ϕ anything	(16.1 ± 1.6) %	
Γ_8 e^+ anything	(8 ± 6) ₋₅ %	
Leptonic and semileptonic modes		
Γ_9 $e^+\nu_e$	< 1.3 × 10 ⁻⁴	90%
Γ_{10} $\mu^+\nu_\mu$	(6.2 ± 0.6) × 10 ⁻³	
Γ_{11} $\tau^+\nu_\tau$	(6.6 ± 0.6) %	
Γ_{12} $\phi\ell^+\nu_\ell$	[b] (2.36 ± 0.26) %	
Γ_{13} $\eta\ell^+\nu_\ell + \eta'(958)\ell^+\nu_\ell$	[b] (3.9 ± 0.7) %	
Γ_{14} $\eta\ell^+\nu_\ell$	[b] (2.9 ± 0.6) %	
Γ_{15} $\eta'(958)\ell^+\nu_\ell$	[b] (1.02 ± 0.33) %	
Hadronic modes with a $K\bar{K}$ pair		
Γ_{16} $K^+K_S^0$	(1.49 ± 0.09) %	
Γ_{17} $K^+K^-\pi^+$	[c] (5.50 ± 0.28) %	
Γ_{18} $\phi\pi^+$	[d,e] (4.38 ± 0.35) %	
Γ_{19} $\phi\pi^+, \phi \rightarrow K^+K^-$	[d] (2.18 ± 0.33) %	
Γ_{20} $K^+\bar{K}^*(892)^0$		
Γ_{21} $K^+\bar{K}^*(892)^0, \bar{K}^{*0} \rightarrow K^-\pi^+$	(2.6 ± 0.4) %	
Γ_{22} $f_0(980)\pi^+, f_0 \rightarrow K^+K^-$	(6.0 ± 2.4) × 10 ⁻³	
Γ_{23} $K^+\bar{K}_0^*(1430)^0, \bar{K}_0^* \rightarrow K^-\pi^+$	(5.1 ± 2.5) × 10 ⁻³	
Γ_{24} $f_0(1710)\pi^+, f_0 \rightarrow K^+K^-$		

Γ ₂₅	$K^+ K^- \pi^+$ nonresonant			
Γ ₂₆	$K^0 \bar{K}^0 \pi^+$	—		
Γ ₂₇	$K^*(892) + \bar{K}^0$	[e] (5.3 ± 1.2) %		
Γ ₂₈	$K^+ K^- \pi^+ \pi^0$	(5.6 ± 0.5) %		
Γ ₂₉	$\phi \pi^+ \pi^0, \phi \rightarrow K^+ K^-$			
Γ ₃₀	$\phi \rho^+, \phi \rightarrow K^+ K^-$	(4.0 ± 1.1) %		
Γ ₃₁	$\phi \pi^+ \pi^0$ 3-body, $\phi \rightarrow K^+ K^-$	< 1.5 %	90%	
Γ ₃₂	$K^+ K^- \pi^+ \pi^0$ non- ϕ	< 11 %	90%	
Γ ₃₃	$K_S^0 K^- \pi^+ \pi^+$	(1.64 ± 0.12) %		
Γ ₃₄	$K^*(892) + \bar{K}^*(892)^0$	[e] (7.0 ± 2.5) %		
Γ ₃₅	$K^0 K^- 2\pi^+$ (non- $K^* + \bar{K}^{*0}$)	< 3.5 %	90%	
Γ ₃₆	$K^+ K_S^0 \pi^+ \pi^-$	(9.6 ± 1.3) × 10 ⁻³		
Γ ₃₇	$K^+ K^- \pi^+ \pi^+ \pi^-$	(8.8 ± 1.6) × 10 ⁻³		
Γ ₃₈	$\phi \pi^+ \pi^+ \pi^-, \phi \rightarrow K^+ K^-$	(5.9 ± 1.1) × 10 ⁻³		
Γ ₃₉	$K^+ K^- \rho^0 \pi^+$ non- ϕ	< 2.6 × 10 ⁻⁴	90%	
Γ ₄₀	$\phi \rho^0 \pi^+, \phi \rightarrow K^+ K^-$	(6.6 ± 1.3) × 10 ⁻³		
Γ ₄₁	$\phi a_1(1260)^+, \phi \rightarrow K^+ K^-, a_1^+ \rightarrow \rho^0 \pi^+$	(7.5 ± 1.3) × 10 ⁻³		
Γ ₄₂	$K^+ K^- \pi^+ \pi^+ \pi^-$ nonresonant	(9 ± 7) × 10 ⁻⁴		
Γ ₄₃	$K_S^0 K_S^0 \pi^+ \pi^+ \pi^-$	(8.4 ± 3.5) × 10 ⁻⁴		

Hadronic modes without K's

Γ ₄₄	$\pi^+ \pi^0$	< 6 × 10 ⁻⁴	90%	
Γ ₄₅	$\pi^+ \pi^+ \pi^-$	(1.11 ± 0.08) %		
Γ ₄₆	$\rho^0 \pi^+$	not seen		
Γ ₄₇	$\pi^+ (\pi^+ \pi^-)_{S\text{-wave}}$	[f] (9.7 ± 1.1) × 10 ⁻³		
Γ ₄₈	$f_0(980) \pi^+, f_0 \rightarrow \pi^+ \pi^-$			
Γ ₄₉	$f_0(1370) \pi^+, f_0 \rightarrow \pi^+ \pi^-$			
Γ ₅₀	$f_0(1500) \pi^+, f_0 \rightarrow \pi^+ \pi^-$			
Γ ₅₁	$f_2(1270) \pi^+, f_2 \rightarrow \pi^+ \pi^-$	(1.1 ± 0.6) × 10 ⁻³		
Γ ₅₂	$\rho(1450)^0 \pi^+, \rho^0 \rightarrow \pi^+ \pi^-$	(7 ± 6) × 10 ⁻⁴		
Γ ₅₃	$\pi^+ \pi^+ \pi^-$ nonresonant			
Γ ₅₄	$\pi^+ \pi^+ \pi^- \pi^0$	< 14 %	90%	
Γ ₅₅	$\eta \pi^+$	[e] (1.58 ± 0.21) %		
Γ ₅₆	$\omega \pi^+$	[e] (2.5 ± 0.9) × 10 ⁻³		
Γ ₅₇	$3\pi^+ 2\pi^-$	(8.0 ± 0.9) × 10 ⁻³		
Γ ₅₈	$\pi^+ \pi^+ \pi^- \pi^0 \pi^0$	—		
Γ ₅₉	$\eta \rho^+$	[e] (13.0 ± 2.2) %		
Γ ₆₀	$\eta \pi^+ \pi^0$ 3-body	[e] < 5 %	90%	
Γ ₆₁	$3\pi^+ 2\pi^- \pi^0$	(4.9 ± 3.2) %		
Γ ₆₂	$\eta'(958) \pi^+$	[e] (3.8 ± 0.4) %		
Γ ₆₃	$3\pi^+ 2\pi^- 2\pi^0$	—		
Γ ₆₄	$\eta'(958) \rho^+$	[e] (12.2 ± 2.0) %		
Γ ₆₅	$\eta'(958) \pi^+ \pi^0$ 3-body	[e] < 1.8 %	90%	

Modes with one or three K's

Γ ₆₆	$K^+ \pi^0$	(8.2 ± 2.2) × 10 ⁻⁴		
Γ ₆₇	$K_S^0 \pi^+$	(1.25 ± 0.15) × 10 ⁻³		
Γ ₆₈	$K^+ \eta$	(1.41 ± 0.31) × 10 ⁻³		
Γ ₆₉	$K^+ \eta'(958)$	(1.6 ± 0.5) × 10 ⁻³		
Γ ₇₀	$K^+ \pi^+ \pi^-$	(6.9 ± 0.5) × 10 ⁻³		
Γ ₇₁	$K^+ \rho^0$	(2.7 ± 0.5) × 10 ⁻³		
Γ ₇₂	$K^+ \rho(1450)^0, \rho^0 \rightarrow \pi^+ \pi^-$	(7.4 ± 2.6) × 10 ⁻⁴		
Γ ₇₃	$K^*(892)^0 \pi^+, K^{*0} \rightarrow K^+ \pi^-$	(1.50 ± 0.26) × 10 ⁻³		
Γ ₇₄	$K^*(1410)^0 \pi^+, K^{*0} \rightarrow K^+ \pi^-$	(1.30 ± 0.31) × 10 ⁻³		
Γ ₇₅	$K^*(1430)^0 \pi^+, K^{*0} \rightarrow K^+ \pi^-$	(5 ± 4) × 10 ⁻⁴		
Γ ₇₆	$K^+ \pi^+ \pi^-$ nonresonant	(1.1 ± 0.4) × 10 ⁻³		
Γ ₇₇	$K_S^0 \pi^+ \pi^+ \pi^-$	(3.0 ± 1.1) × 10 ⁻³		
Γ ₇₈	$K^+ K^+ K^-$	(4.9 ± 1.7) × 10 ⁻⁴		
Γ ₇₉	$\phi K^+, \phi \rightarrow K^+ K^-$	< 2.8 × 10 ⁻⁴	90%	

Doubly Cabibbo-suppressed modes

Γ ₈₀	$K^+ K^+ \pi^-$	(2.9 ± 1.1) × 10 ⁻⁴		
-----------------	-----------------	----------------------------------	--	--

Baryon-antibaryon mode

Γ ₈₁	$p \bar{p}$	(1.3 ± 0.4) × 10 ⁻³		
-----------------	-------------	----------------------------------	--	--

ΔC = 1 weak neutral current (C1) modes, Lepton family number (LF), or Lepton number (L) violating modes

Γ ₈₂	$\pi^+ e^+ e^-$	[g] < 2.7 × 10 ⁻⁴	90%	
Γ ₈₃	$\pi^+ \mu^+ \mu^-$	[g] < 2.6 × 10 ⁻⁵	90%	
Γ ₈₄	$K^+ e^+ e^-$	C1 < 1.6 × 10 ⁻³	90%	
Γ ₈₅	$K^+ \mu^+ \mu^-$	C1 < 3.6 × 10 ⁻⁵	90%	
Γ ₈₆	$K^*(892)^+ \mu^+ \mu^-$	C1 < 1.4 × 10 ⁻³	90%	

Γ ₈₇	$\pi^+ e^\pm \mu^\mp$	LF [h] < 6.1 × 10 ⁻⁴	90%	
Γ ₈₈	$K^+ e^\pm \mu^\mp$	LF [h] < 6.3 × 10 ⁻⁴	90%	
Γ ₈₉	$\pi^- e^+ e^+$	L < 6.9 × 10 ⁻⁴	90%	
Γ ₉₀	$\pi^- \mu^+ \mu^+$	L < 2.9 × 10 ⁻⁵	90%	
Γ ₉₁	$\pi^- e^+ \mu^+$	L < 7.3 × 10 ⁻⁴	90%	
Γ ₉₂	$K^- e^+ e^+$	L < 6.3 × 10 ⁻⁴	90%	
Γ ₉₃	$K^- \mu^+ \mu^+$	L < 1.3 × 10 ⁻⁵	90%	
Γ ₉₄	$K^- e^+ \mu^+$	L < 6.8 × 10 ⁻⁴	90%	
Γ ₉₅	$K^*(892)^- \mu^+ \mu^+$	L < 1.4 × 10 ⁻³	90%	
Γ ₉₆	A dummy mode used by the fit.	(73.6 ± 1.3) %		

[a] This fraction includes η from η' decays.

[b] For now, we average together measurements of the $X e^+ \nu_e$ and $X \mu^+ \nu_\mu$ branching fractions. This is the *average*, not the *sum*.

[c] The branching fraction for this mode may differ from the sum of the submodes that contribute to it, due to interference effects. See the relevant papers.

[d] We decouple the $D_s^+ \rightarrow \phi \pi^+$ branching fraction obtained from mass projections (and used to get some of the other branching fractions) from the $D_s^+ \rightarrow \phi \pi^+, \phi \rightarrow K^+ K^-$ branching fraction obtained from the Dalitz-plot analysis of $D_s^+ \rightarrow K^+ K^- \pi^+$. That is, the ratio of these two branching fractions is not exactly the $\phi \rightarrow K^+ K^-$ branching fraction 0.491.

[e] This branching fraction includes all the decay modes of the final-state resonance.

[f] This comes from a K -matrix parametrization of the $\pi^+ \pi^-$ S -wave and is a sum over the $f_0(980)$, $f_0(1300)$, $f_0(1200-1600)$, $f_0(1500)$, and $f_0(1750)$. Not all of these correspond to particles in our Tables.

[g] This mode is not a useful test for a $\Delta C=1$ weak neutral current because both quarks must change flavor in this decay.

[h] The value is for the sum of the charge states or particle/antiparticle states indicated.

CONSTRAINED FIT INFORMATION

An overall fit to 12 branching ratios uses 15 measurements and one constraint to determine 11 parameters. The overall fit has a $\chi^2 = 2.1$ for 5 degrees of freedom.

The following *off-diagonal* array elements are the correlation coefficients $\langle \delta x_i \delta x_j \rangle / (\delta x_i \delta x_j)$, in percent, from the fit to the branching fractions, $x_i \equiv \Gamma_i / \Gamma_{\text{total}}$. The fit constrains the x_i whose labels appear in this array to sum to one.

x_{16}	0									
x_{17}	0	77								
x_{18}	42	0	0							
x_{28}	0	43	49	0						
x_{33}	0	52	59	0	33					
x_{45}	0	41	46	0	25	31				
x_{55}	0	39	44	0	24	30	23			
x_{62}	0	47	53	0	32	37	28	28		
x_{70}	0	38	45	0	23	29	22	21	26	
x_{96}	-16	-71	-81	-30	-72	-59	-45	-52	-69	-41
	x_{10}	x_{16}	x_{17}	x_{18}	x_{28}	x_{33}	x_{45}	x_{55}	x_{62}	x_{70}

 D_s^+ BRANCHING RATIOS

A number of older, now obsolete results have been omitted. They may be found in earlier editions.

Inclusive modes

$\Gamma(K^- \text{ anything}) / \Gamma_{\text{total}}$				Γ_1 / Γ
VALUE	DOCUMENT ID	TECN	COMMENT	
$0.13^{+0.14}_{-0.12} \pm 0.02$	COFFMAN	91	MRK3	$e^+ e^-$ 4.14 GeV

$[\Gamma(\bar{K}^0 \text{ anything}) + \Gamma(K^0 \text{ anything})] / \Gamma_{\text{total}}$				Γ_2 / Γ
VALUE	DOCUMENT ID	TECN	COMMENT	
$0.39^{+0.29}_{-0.27} \pm 0.04$	COFFMAN	91	MRK3	$e^+ e^-$ 4.14 GeV

$\Gamma(K^+ \text{ anything}) / \Gamma_{\text{total}}$				Γ_3 / Γ
VALUE	DOCUMENT ID	TECN	COMMENT	
$0.20^{+0.18}_{-0.13} \pm 0.04$	COFFMAN	91	MRK3	$e^+ e^-$ 4.14 GeV

Meson Particle Listings

 D_s^\pm

$\Gamma((\text{non-}K\bar{K}) \text{ anything})/\Gamma_{\text{total}}$				Γ_4/Γ
VALUE	DOCUMENT ID	TECN	COMMENT	
$0.64 \pm 0.17 \pm 0.03$	³ COFFMAN	91	MRK3 e^+e^- 4.14 GeV	
³ COFFMAN 91 uses the direct measurements of the kaon content to determine this non- $K\bar{K}$ fraction. This number implies that a large fraction of D_s^\pm decays involve η , η' , and/or non-spectator decays.				
$\Gamma(\eta \text{ anything})/\Gamma_{\text{total}}$				Γ_5/Γ
This ratio includes η particles from η' decays.				
VALUE (units 10^{-2})	EVTS	DOCUMENT ID	TECN	COMMENT
$23.5 \pm 3.1 \pm 2.0$	674 \pm 91	HUANG	06B	CLEO e^+e^- at 4170 MeV
$\Gamma(\eta' \text{ anything})/\Gamma_{\text{total}}$				Γ_6/Γ
VALUE (units 10^{-2})	EVTS	DOCUMENT ID	TECN	COMMENT
$8.7 \pm 1.9 \pm 0.8$	68 \pm 15	HUANG	06B	CLEO e^+e^- at 4170 MeV
$\Gamma(\phi \text{ anything})/\Gamma_{\text{total}}$				Γ_7/Γ
VALUE (units 10^{-2})	EVTS	DOCUMENT ID	TECN	COMMENT
$16.1 \pm 1.2 \pm 1.1$	398 \pm 27	HUANG	06B	CLEO e^+e^- at 4170 MeV
$\Gamma(e^+ \text{ anything})/\Gamma_{\text{total}}$				Γ_8/Γ
VALUE	DOCUMENT ID	TECN	COMMENT	
$0.077 \pm 0.057 \pm 0.024$ $-0.043 - 0.021$	BAI	97	BES $e^+e^- \rightarrow D_s^+ D_s^-$	

Leptonic and semileptonic modes

DECAY CONSTANTS OF CHARGED PSEUDO-SCALAR MESONS

Written May 2008 by J. Rosner (Univ. Chicago) and S. Stone (Syracuse Univ.)

Charged mesons formed from a quark and anti-quark can decay to a charged lepton pair when these objects annihilate via a virtual W^\pm boson. Fig. 1 illustrates this process for the purely leptonic decay of a D^+ meson.

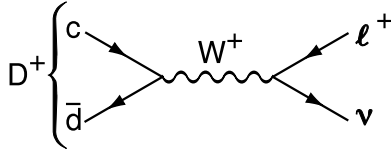


Figure 1: The annihilation process for pure D^+ leptonic decays in the Standard Model.

Similar quark-antiquark annihilations via a virtual W^- to the $\ell^+\nu$ ($\ell^-\bar{\nu}$) final states occur for the π^\pm , K^\pm , D_s^\pm , and B^\pm mesons. Let P be any of these pseudoscalar mesons. To lowest order, the decay width is

$$\Gamma(P \rightarrow \ell\nu) = \frac{G_F^2}{8\pi} f_P^2 m_\ell^2 M_P \left(1 - \frac{m_\ell^2}{M_P^2}\right)^2 |V_{q_1 q_2}|^2. \quad (1)$$

Here M_P is the P mass, m_ℓ is the ℓ mass, $|V_{q_1 q_2}|$ is the Cabibbo-Kobayashi-Maskawa (CKM) matrix element between the constituent quarks $q_1 \bar{q}_2$ in P , and G_F is the Fermi coupling constant. The parameter f_P is the decay constant, and is related to the wave-function overlap of the quark and antiquark.

The decay P^\pm starts with a spin-0 meson, and ends up with a left-handed neutrino or right-handed antineutrino. By angular momentum conservation, the ℓ^\pm must then also be left-handed or right-handed, respectively. In the $m_\ell = 0$ limit, the decay is forbidden, and can only occur as a result of the finite ℓ mass. This helicity suppression is the origin of the m_ℓ^2 dependence of the decay width.

There is a complication in measuring purely leptonic decay rates. The process $P \rightarrow \ell\nu\gamma$ is not simply a radiative correction, although radiative corrections contribute. The P can make a transition to a virtual P^* , emitting a real photon, and the P^* decays into $\ell\nu$, avoiding helicity suppression. The importance of this amplitude depends on the decaying particle and the detection technique. The $\ell\nu\gamma$ rate for a heavy particle such as B decaying into a light particle such as a muon can be larger than the width without photon emission [1]. On the other hand, for decays into a τ^\pm , the helicity suppression is mostly broken and these effects appear to be small.

Measurements of purely leptonic decay branching fractions and lifetimes allow an experimental determination of the product $|V_{q_1 q_2}| f_P$. If the CKM element is well known from other measurements, then f_P can be well measured. If, on the other hand, the CKM element is less well or poorly measured, having theoretical input on f_P can allow a determination of the CKM element. The importance of measuring $\Gamma(P \rightarrow \ell\nu)$ depends on the particle being considered. For the B system, f_B is crucial for using measurements of $B^0\text{-}\bar{B}^0$ mixing to extract information on the fundamental CKM parameters. Knowledge of f_{B_s} is also needed, but this parameter cannot be directly measured as the B_s is neutral, so the violation of the SU(3) relation $f_{B_s} = f_B$ must be estimated theoretically. This difficulty does not occur for D mesons as both the D^+ and D_s^+ are charged, allowing the direct measurement of SU(3) breaking and a direct comparison with theory. (In this note mention of specific particle charge also implies the use of the charge-conjugate partner.)

For B^- and D_s^+ decays, the existence of a charged Higgs boson (or any other charged object beyond the Standard Model) would modify the decay rates; however, this would not necessarily be true for the D^+ [2,3]. More generally, the ratio of $\mu\nu$ to $\tau\nu$ decays can serve as one probe of lepton universality [2,4].

As $|V_{ud}|$ has been quite accurately measured in superallowed β decays [5], with a value of 0.97418(26), measurements of $\Gamma(\pi^+ \rightarrow \mu^+\nu)$ yield a value for f_π . Similarly, $|V_{us}|$ has been well measured in semileptonic kaon decays, so a value for f_K from $\Gamma(K^- \rightarrow \mu^-\bar{\nu})$ can be compared to theoretical calculations. Recently, however, lattice gauge theory calculations have been claimed to be very accurate in determining f_K , and these have been used to predict $|V_{us}|$ [6].

Next we review current measurements, starting with the charm system. The CLEO collaboration has measured the branching fraction for $D^+ \rightarrow \mu^+\nu$ and recently updated their published result [7]. By using the well measured D^+ lifetime of 1.040(7) ps and assuming $|V_{cd}| = |V_{us}| = 0.2255(19)$ [8], they report

$$f_{D^+} = (205.8 \pm 8.5 \pm 2.5) \text{ MeV}. \quad (2)$$

This result includes a 1% correction for the radiative $\mu^+\nu\gamma$ final state based on the estimate by Dobrescu and Kronfeld [9].

Before we compare this result with theoretical predictions, we discuss the D_s^+ . Measurements of f_{D_s} have been made by

Table 1: Experimental results for $\mathcal{B}(D_s^+ \rightarrow \mu^+\nu)$, $\mathcal{B}(D_s^+ \rightarrow \tau^+\nu)$, and $f_{D_s^+}$. Numbers have been updated using the D_s^+ lifetime of 0.50 ps. Results listed below the “Average” line have not been used in our average. The assumed value of $\mathcal{B}_{\phi\pi} \equiv \mathcal{B}(D_s^+ \rightarrow \phi\pi^+)$ is listed if evident. ALEPH averages their two results to obtain a value for $f_{D_s^+}$.

Experiment	Mode	\mathcal{B}	$\mathcal{B}_{\phi\pi}(\%)$	$f_{D_s^+}$ (MeV)
CLEO-c [10]	$\mu^+\nu$	$(5.94 \pm 0.66 \pm 0.31) \times 10^{-3}$		$264 \pm 15 \pm 7$
CLEO-c [10]	$\tau^+\nu$	$(8.0 \pm 1.3 \pm 0.4) \times 10^{-2}$		$310 \pm 25 \pm 8$
CLEO-c [11]	$\tau^+\nu$	$(6.17 \pm 0.71 \pm 0.36) \times 10^{-2}$		$273 \pm 16 \pm 8$
CLEO-c	combined			$274 \pm 10 \pm 5$
Belle [12]	$\mu^+\nu$	$(6.44 \pm 0.76 \pm 0.57) \times 10^{-3}$		$275 \pm 16 \pm 12$
Average		CLEO combined & Belle		275 ± 10
Average		With radiative correction		273 ± 10
CLEO [13]	$\mu^+\nu$	$(6.2 \pm 0.8 \pm 1.3 \pm 1.6) \times 10^{-3}$	3.6 ± 0.9	$273 \pm 19 \pm 27 \pm 33$
BEATRICE [14]	$\mu^+\nu$	$(8.3 \pm 2.3 \pm 0.6 \pm 2.1) \times 10^{-3}$	3.6 ± 0.9	$312 \pm 43 \pm 12 \pm 39$
ALEPH [15]	$\mu^+\nu$	$(6.8 \pm 1.1 \pm 1.8) \times 10^{-3}$	3.6 ± 0.9	$282 \pm 19 \pm 40$
ALEPH [15]	$\tau^+\nu$	$(5.8 \pm 0.8 \pm 1.8) \times 10^{-2}$		
L3 [16]	$\tau^+\nu$	$(7.4 \pm 2.8 \pm 1.6 \pm 1.8) \times 10^{-2}$		$299 \pm 57 \pm 32 \pm 37$
OPAL [17]	$\tau^+\nu$	$(7.0 \pm 2.1 \pm 2.0) \times 10^{-2}$		$283 \pm 44 \pm 41$
BaBar [18]	$\mu^+\nu$	$(6.74 \pm 0.83 \pm 0.26 \pm 0.66) \times 10^{-3}$	4.71 ± 0.46	$283 \pm 17 \pm 7 \pm 14$

Table 2: Theoretical predictions of $f_{D_s^+}$, f_{D^+} , and $f_{D_s^+}/f_{D^+}$. QL indicates a quenched-lattice calculation. (Only selected results having errors are included.)

Model	$f_{D_s^+}$ (MeV)	f_{D^+} (MeV)	$f_{D_s^+}/f_{D^+}$
Experiment (our averages)	273 ± 10	205.8 ± 8.9	1.33 ± 0.07
Lattice (HPQCD+UKQCD) [21]	241 ± 3	208 ± 4	1.162 ± 0.009
Lattice (FNAL+MILC+HPQCD) [22]	$249 \pm 3 \pm 16$	$201 \pm 3 \pm 17$	$1.24 \pm 0.01 \pm 0.07$
QL (QCDSF) [23]	$220 \pm 6 \pm 5 \pm 11$	$206 \pm 6 \pm 3 \pm 22$	$1.07 \pm 0.02 \pm 0.02$
QL (Taiwan) [24]	$266 \pm 10 \pm 18$	$235 \pm 8 \pm 14$	$1.13 \pm 0.03 \pm 0.05$
QL (UKQCD) [25]	$236 \pm 8_{-14}^{+17}$	$210 \pm 10_{-16}^{+17}$	$1.13 \pm 0.02_{-0.02}^{+0.04}$
QL [26]	$231 \pm 12_{-1}^{+6}$	$211 \pm 14_{-12}^{+2}$	1.10 ± 0.02
QCD Sum Rules [27]	205 ± 22	177 ± 21	$1.16 \pm 0.01 \pm 0.03$
QCD Sum Rules [28]	235 ± 24	203 ± 20	1.15 ± 0.04
Field Correlators [29]	210 ± 10	260 ± 10	1.24 ± 0.03
Isospin Splittings [30]		262 ± 29	

Meson Particle Listings

D_s^\pm

several groups and are listed in Table 1 [10–18]. Early measurements actually determined the ratio of the leptonic decay to some hadronic decay, usually $\Gamma(D_s^+ \rightarrow \ell^+\nu)/\Gamma(D_s^+ \rightarrow \phi\pi^+)$. This introduces a large additional source of error since the denominator is not well known. CLEO [10] has published absolute branching fractions for $\mu^+\nu$ and $\tau^+\nu$, $\tau^+ \rightarrow \pi^+\bar{\nu}$, and in a separate paper [11] for $\tau^+\nu$, $\tau^+ \rightarrow e^+\nu\bar{\nu}$; there is also an as-yet-unpublished result from Belle [12] for $\mu^+\nu$.

We extract the decay constant from the measured branching ratios using $|V_{cs}| = 0.9742$, and a D_s lifetime of 0.50 ps. Our experimental average,

$$f_{D_s} = (273 \pm 10) \text{ MeV}, \quad (3)$$

uses only those results that are absolutely normalized [19]. We note that the experiments do not correct explicitly for any $\ell^+\nu\gamma$ that may have been included. We have included the radiative correction of 1% in the $\mu^+\nu$ rates [9] (the $\tau^+\nu$ rates need not be corrected). Other theoretical calculations show that this rate is a factor of 40–100 below the $\mu^+\nu$ rate for charm [20]

Table 2 compares the experimental f_{D_s} with theoretical calculations [21–30]. While most theories give values lower than the f_{D_s} measurement, the errors are sufficiently large, in most cases, to declare success. A recent unquenched lattice calculation [21], however, differs by more than three standard deviations [31]. Remarkably it agrees with f_{D^+} and consequently disagrees in the ratio $f_{D_s^+}/f_{D^+}$.

Akeroyd and Chen [32] first pointed out that leptonic decay widths are modified by new physics. Specifically, for the D^+ and D_s^+ , in the case of the two-Higgs doublet model (2HDM), Eq. (1) is modified by a factor r_q multiplying the right-hand side:

$$r_q = \left[1 + \left(\frac{1}{m_c + m_q} \right) \left(\frac{M_{D_q}}{M_{H^+}} \right)^2 (m_c - m_q \tan^2 \beta) \right]^2, \quad (4)$$

where m_{H^+} is the charged Higgs mass, M_{D_q} is the mass of the D meson (containing the light quark q), m_c is the charm quark mass, m_q is the light-quark mass, and $\tan\beta$ is the ratio of the vacuum expectation values of the two Higgs doublets. (Here we modified the original formula to take into account the charm quark coupling [33].) For the D^+ , $m_d \ll m_c$, and the change due to the H^+ is very small. For the D_s^+ , however, the effect can be substantial. One major concern is that we need to know the value of $f_{D_s^+}$ in the Standard Model (SM). We can take that from a theoretical model. Our most aggressive choice is that of the unquenched lattice calculation [21], because they claim the smallest error. Since the charged Higgs would lower the rate compared to the SM, in principle, experiment gives a lower limit on the charged Higgs mass. However, the value for the predicted decay constant using this model is more than 3 standard deviations *below* the measurement, implying that (a) either the model of Ref. 21 is not representative; or (b) no value of m_{H^+} in the two-Higgs doublet model will satisfy the

constraint at 99.9% confidence level; or (c) there is new physics, different from the 2HDM, that interferes constructively with the SM amplitude [34].

Dobrescu and Kronfeld [9] emphasize that the discrepancy between the theoretical lattice calculation and the CLEO data is substantial and “is worth interpreting in terms of new physics.” They give three possible examples of new physics models that might be responsible. These include a specific two-Higgs doublet model and two leptiquark models.

The Belle [35] and BaBar [36] collaborations have found evidence for $B^- \rightarrow \tau^-\bar{\nu}$ decays. The measurements are

$$\begin{aligned} \mathcal{B}(B^- \rightarrow \tau^-\bar{\nu}) &= (1.79_{-0.49}^{+0.56} \text{ }_{-0.51}^{+0.46}) \times 10^{-4} \text{ (Belle);} \\ &= (1.2 \pm 0.4 \pm 0.3 \pm 0.2) \times 10^{-4} \text{ (BaBar);} \\ &= (1.42 \pm 0.43) \times 10^{-4} \text{ (our average).} \end{aligned} \quad (5)$$

The Belle and BaBar values have 3.5 and 2.6 standard-deviation significances. More data are needed, and the average can only be provisional. Here the effect of a charged Higgs is different as it can either increase or decrease the expected SM branching ratio. The factor r is given in terms of the B meson mass, M_B , by [2]

$$r = \left(1 - \tan^2 \beta \frac{M_B^2}{m_{H^+}^2} \right)^2. \quad (6)$$

In principle, we can get a limit in the $\tan\beta$ - m_{H^+} plane even with this statistically limited set of data. Again, we need to know the SM prediction of this decay rate. We ascertain this value using Eq. (1). Here theory provides a value of $f_B = (216 \pm 22) \text{ MeV}$ [37]. The subject of the value of $|V_{ub}|$ is addressed elsewhere [38]. Taking an average over inclusive and exclusive determinations, and enlarging the error using the PDG prescription because the results differ, we find $|V_{ub}| = (3.9 \pm 0.5) \times 10^{-3}$, where the error is dominantly theoretical. We thus arrive at the SM prediction for the $\tau^-\bar{\nu}$ branching fraction of $(1.25 \pm 0.41) \times 10^{-4}$. Taking the ratio of the experimental value to the predicted branching ratio at its 90% c.l. *upper* limit and using Eq. (6), we find that we can limit $M_{H^+} / \tan\beta > 3.5 \text{ GeV}$. The 90% c.l. *lower* limit also permits us to exclude the region $4.1 \text{ GeV} < M_{H^+} / \tan\beta < 9.6 \text{ GeV}$ [39].

We now discuss the determination of charged pion and kaon decay constants. The sum of branching fractions for $\pi^- \rightarrow \mu^-\bar{\nu}$ and $\pi^- \rightarrow \mu^-\bar{\nu}\gamma$ is 99.98770(4)%. The two modes are difficult to separate experimentally, so we use this sum, with Eq. (1) modified to include photon emission and radiative corrections [40]. The branching fraction together with the lifetime 26.033(5) ns gives

$$f_{\pi^-} = (130.4 \pm 0.04 \pm 0.2) \text{ MeV}. \quad (7)$$

The first error is due to the error on $|V_{ud}|$, 0.97418(26) [5]; the second is due to the higher-order corrections.

Similarly, the sum of branching fractions for $K^- \rightarrow \mu^-\bar{\nu}$ and $K^- \rightarrow \mu^-\bar{\nu}\gamma$ is 63.57(11)%, and the lifetime is 12.3840(193) ns [41]. We use a value for $f_+(0)|V_{us}|$ obtained from the average of semileptonic kaon decays of 0.21661(46). The $f_+(0)$ must be

See key on page 373

determined theoretically. We follow Blucher and Marciano [8] in using the Leutwyler-Roos calculation $f_+(0) = 0.961 \pm 0.008$, that gives $|V_{us}| = 0.2255 \pm 0.0019$, yielding

$$f_{K^-} = (155.5 \pm 0.2 \pm 0.8 \pm 0.2) \text{ MeV} . \quad (8)$$

The first error is due to the error on Γ , the second is due to the CKM factor $|V_{us}|$, and the third is due to the higher-order corrections. The largest source of error in these corrections depends on the QCD part, which is based on one calculation in the large N_c framework. We have doubled the quoted error here; this would probably be unnecessary if other calculations were to come to similar conclusions. A large part of the additional uncertainty vanishes in the ratio of the K^- and π^- decay constants, which is

$$f_{K^-}/f_{\pi^-} = 1.193 \pm 0.002 \pm 0.006 \pm 0.001 . \quad (9)$$

The first error is due to the measured decay rates; the second is due to the uncertainties on the CKM factors; the third is due to the uncertainties in the radiative correction ratio.

These measurements have been used in conjunction with lattice calculations that predict f_K/f_π in order to find a value for $|V_{us}|/|V_{ud}|$. Together with the precisely measured $|V_{ud}|$, this gives an independent measure of $|V_{us}|$ [6,41].

References

- Most predictions for the rate for $B^- \rightarrow \mu^- \bar{\nu} \gamma$ are in the range of 1 to 20 times the rate for $B^- \rightarrow \mu^- \bar{\nu}$. See G. Burdman, T. Goldman, and D. Wyler, Phys. Rev. **D51**, 111 (1995); P. Colangelo, F. De Fazio, and G. Nardulli, Phys. Lett. **B372**, 331 (1996); *ibid.*, **386**, 328 (1996); A. Khodjamirian, G. Stoll, and D. Wyler, Phys. Lett. **B358**, 129 (1995); G. Eilam, I. Halperin, and R. Mendel, Phys. Lett. **B361**, 137 (1995); D. Atwood, G. Eilam, and A. Soni, Mod. Phys. Lett. **A11**, 1061 (1996); C.Q. Geng and C.C. Lih, Phys. Rev. **D57**, 5697 (1998) and Mod. Phys. Lett. **A15**, 2087 (2000); G.P. Korchemsky, D. Pirjol, and T.M. Yang, Phys. Rev. **D61**, 114510 (2000); C.W. Hwang, Eur. Phys. J. **C46**, 379 (2006).
- W.-S. Hou, Phys. Rev. **D48**, 2342 (1993).
- See, for example, A.G. Akeroyd and S. Recksiegel, Phys. Lett. **B554**, 38 (2003); A.G. Akeroyd, Prog. Theor. Phys. **111**, 295 (2004).
- J.L. Hewett, hep-ph/9505246, presented at *Lafex International School on High Energy Physics (LISHEP95)*, Rio de Janeiro, Brazil, Feb. 6-22, 1995.
- I. S. Towner and J. C. Hardy, Phys. Rev. **C77**, 025501 (2008).
- W.J. Marciano, Phys. Rev. Lett. **93**, 231803 (2004); A. Jüttner, [arXiv:0711.1239].
- S. Stone, "Leptonic Decays: Measurements of f_{D^+} and $f_{D_s^+}$," presented at FPCP 2008, Taipei, Taiwan, May, 2008, to appear in the proceedings; we have included the radiative correction here. See also M. Artuso *et al.*, (CLEO Collab.), Phys. Rev. Lett. **95**, 251801 (2005).
- CLEO assumes that $|V_{cd}|$ equals $|V_{us}|$ and take the value from E. Blucher and W. J. Marciano, " V_{ud} , V_{us} , The Cabibbo Angle and CKM Unitarity" in PDG 2008.
- B. A. Dobrescu and A. S. Kronfeld, arXiv:0803.0512 [hep-ph].
- M. Artuso *et al.*, (CLEO Collab.), Phys. Rev. Lett. **99**, 071802 (2007).
- K.M. Ecklund *et al.*, (CLEO Collab.), Phys. Rev. Lett. **100**, 161801 (2008).
- K. Abe *et al.*, (Belle Collab.), [arXiv:0709.1340](2007).
- M. Chadha *et al.*, (CLEO Collab.), Phys. Rev. **D58**, 032002 (1998).
- Y. Alexandrov *et al.*, (BEATRICE Collab.), Phys. Lett. **B478**, 31 (2000).
- A. Heister *et al.*, (ALEPH Collab.), Phys. Lett. **B528**, 1 (2002).
- M. Acciarri *et al.*, (L3 Collab.), Phys. Lett. **B396**, 327 (1997).
- G. Abbiendi *et al.*, (OPAL Collab.), Phys. Lett. **B516**, 236 (2001).
- B. Aubert *et al.*, (BABAR Collab.), Phys. Rev. Lett. **98**, 141801 (2007).
- We exclude measurements with normalizations to other D_s^\pm decay modes, mostly $\phi\pi^+$, because of the large systematic uncertainty that this introduces. Furthermore, due to the complications caused by interferences of resonances in the $K^+K^- \pi^+$ Dalitz plot, the value of $\mathcal{B}(D_s^+ \rightarrow \phi\pi^+)$ depends on the experimental resolution and the width of the K^+K^- mass interval used by each experiment; see J. Alexander *et al.* (CLEO Collaboration), [arXiv:0801.0680](2007).
- See most papers in Ref. 1 and C. D. Lü and G. L. Song, Phys. Lett. **B562**, 75 (2003).
- E. Follana *et al.*, (HPQCD and UKQCD Collabs.), [arXiv:0706.1726](2007). The statistical error is given as 0.6%, with the other systematic errors added in quadrature yielding the 3 MeV total error.
- C. Aubin *et al.*, (MILC Collaboration), Phys. Rev. Lett. **95**, 122002 (2005).
- A. Ali Khan *et al.*, (QCDSF Collaboration), Phys. Lett. **B652**, 150 (2007).
- T.W. Chiu *et al.*, Phys. Lett. **B624**, 31 (2005) [hep-ph/0506266].
- L. Lellouch and C.-J. Lin (UKQCD Collaboration), Phys. Rev. **D64**, 094501 (2001).
- D. Becirevic *et al.*, Phys. Rev. **D60**, 074501 (1999).
- J. Bordes, J. Peñarrocha, and K. Schilcher, JHEP **0511**, 014 (2005).
- S. Narison, [hep-ph/0202200](2002).
- A.M. Badalian *et al.*, Phys. Rev. **D75**, 116001 (2007); see also A.M. Badalian and B.L.G. Bakker, [hep-ph/0702229].
- J. Amundson *et al.*, Phys. Rev. **D47**, 3059 (1993).
- The small errors quoted in Follana *et al.* [21] are being discussed in the lattice community. See, for example, M. Della Morte [arXiv:0711.3160], page 6.
- A.G. Akeroyd and C.H. Chen, Phys. Rev. **D75**, 075004 (2007) [hep-ph/0701078].
- A. Kronfeld, private communication.
- An example of such a model is R-parity violating SUSY; see A. G. Akeroyd and S. Recksiegel, Phys. Lett. **B554**, 38 (2003) [hep-ph/0210376].

Meson Particle Listings

 D_s^\pm

35. K. Ikado *et al.*, (Belle Collaboration), Phys. Rev. Lett. **97**, 251802 (2006).
36. We use the average of the two results from B. Aubert *et al.*, (BaBar Collaboration) [arXiv:0705.1820], and B. Aubert *et al.*, (BaBar Collaboration), Phys. Rev. **D76**, 052002 (2007) [arXiv:0708.2260], presented in the latter reference.
37. A. Gray *et al.*, (HPQCD), Phys. Rev. Lett. **95**, 212001 (2005).
38. Heavy Flavor Averaging Group: see <http://www.slac.stanford.edu/xorg/hfag/>.
39. In supersymmetric models there may be corrections which weaken our bound; a slightly different formula for r is given by Isidori and Paradisi, Phys. Lett. **B639**, 499 (2006) [hep-ph/0605012] that depends on a model dependent value of a parameter ϵ_0 .
40. W.J. Marciano and A. Sirlin, Phys. Rev. Lett. **71**, 3629 (1993); V. Cirigliano and I. Rosell, [arXiv:0707.4464v1].
41. M. Antonelli, "Precision Tests of Standard Model with Leptonic and Semileptonic Kaon Decays," presented at XXIII Int. Symp. on Lepton and Photon Interactions at High Energy, Daegu, Korea (2007) arXiv:0712.0734 [hep-ex].

$\Gamma(e^+ \nu_e)/\Gamma_{\text{total}}$					Γ_9/Γ
VALUE	CL%	DOCUMENT ID	TECN	COMMENT	
$<1.3 \times 10^{-4}$	90	PEDLAR	07A	CLEO $e^+ e^- \rightarrow D_s^+ D_s^{*-}$, 4170 MeV	

$\Gamma(\mu^+ \nu_\mu)/\Gamma_{\text{total}}$					Γ_{10}/Γ
VALUE (units 10^{-3})	EVTS	DOCUMENT ID	TECN	COMMENT	
6.2 ± 0.6 OUR FIT					
5.94 ± 0.66 ± 0.31	88	⁴ PEDLAR	07A	CLEO $e^+ e^- \rightarrow D_s^+ D_s^{*-}$, 4.17 GeV	

- • • We do not use the following data for averages, fits, limits, etc. • • •
- 6.8 ± 1.1 ± 1.8 553 ⁵ HEISTER 02i ALEP Z decays
- ⁴ PEDLAR 07A also fits μ^+ and τ^+ events together and gets an effective $\mu^+ \nu_\mu$ branching fraction of $(6.38 \pm 0.59 \pm 0.33) \times 10^{-3}$
- ⁵ This HEISTER 02i result is not actually an independent measurement of the absolute $\mu^+ \nu_\mu$ branching fraction, but is in fact based on our $\phi \pi^+$ branching fraction of 3.6 ± 0.9%, so it cannot be included in our overall fit. HEISTER 02i combines its $D_s^+ \rightarrow \tau^+ \nu_\tau$ and $\mu^+ \nu_\mu$ branching fractions to get $f_{D_s} = (285 \pm 19 \pm 40)$ MeV.

$\Gamma(\mu^+ \nu_\mu)/\Gamma(\phi \pi^+)$					Γ_{10}/Γ_{18}
VALUE	EVTS	DOCUMENT ID	TECN	COMMENT	
0.142 ± 0.013 OUR FIT					
0.148 ± 0.017 OUR AVERAGE					
0.143 ± 0.018 ± 0.006	489 ± 55	⁶ AUBERT	07v	BABR $e^+ e^- \approx \Upsilon(4S)$	
0.173 ± 0.023 ± 0.035	182	⁷ CHADHA	98	CLE2 $e^+ e^- \approx \Upsilon(4S)$	

- • • We do not use the following data for averages, fits, limits, etc. • • •
- 0.23 ± 0.06 ± 0.04 18 ⁸ ALEXANDROV 00 BEAT π^- nucleus, 350 GeV
- 0.245 ± 0.052 ± 0.074 39 ⁹ ACOSTA 94 CLE2 See CHADHA 98
- ⁶ AUBERT 07v gets $f_{D_s^+} = (283 \pm 17 \pm 16)$ MeV, using $\Gamma(D_s^+ \rightarrow \phi \pi^+)/\Gamma(\text{total}) = (4.71 \pm 0.46)\%$.
- ⁷ CHADHA 98 obtains $f_{D_s} = (280 \pm 19 \pm 28 \pm 34)$ MeV from this measurement, using $\Gamma(D_s^+ \rightarrow \phi \pi^+)/\Gamma(\text{total}) = 0.036 \pm 0.009$.
- ⁸ ALEXANDROV 00 uses $f_D^2/f_{D_s}^2 = 0.82 \pm 0.09$ from a lattice-gauge-theory calculation to get the relative numbers of $D^+ \rightarrow \mu^+ \nu_\mu$ and $D_s^+ \rightarrow \mu^+ \nu_\mu$ events. The present result leads to $f_{D_s} = (323 \pm 44 \pm 36)$ MeV.
- ⁹ ACOSTA 94 obtains $f_{D_s} = (344 \pm 37 \pm 52 \pm 42)$ MeV from this measurement, using $\Gamma(D_s^+ \rightarrow \phi \pi^+)/\Gamma(\text{total}) = 0.037 \pm 0.009$.

$\Gamma(\mu^+ \nu_\mu)/\Gamma(\phi \ell^+ \nu_\ell)$					Γ_{10}/Γ_{12}
VALUE	EVTS	DOCUMENT ID	TECN	COMMENT	
0.16 ± 0.06 ± 0.03	23	¹⁰ KODAMA	96	E653 π^- emulsion, 600 GeV	

- • • We do not use the following data for averages, fits, limits, etc. • • •
- ¹⁰ KODAMA 96 obtains $f_{D_s} = (194 \pm 35 \pm 20 \pm 14)$ MeV from this measurement, using $\Gamma(D_s^+ \rightarrow \phi \ell^+ \nu)/\Gamma_{\text{total}} = 0.0188 \pm 0.0029$. The third error is from the uncertainty on $\phi \ell^+ \nu_\ell$ branching fraction.

$\Gamma(\phi \ell^+ \nu_\ell)/\Gamma(\phi \pi^+)$					Γ_{11}/Γ_{10}
VALUE	EVTS	DOCUMENT ID	TECN	COMMENT	
11.0 ± 1.4 ± 0.6	102	¹⁴ ECKLUND	08	CLEO $e^+ e^- \rightarrow D_s^+ D_s^{*-}$, 4170 MeV	

- • • We do not use the following data for averages, fits, limits, etc. • • •
- ¹¹ HEISTER 02i combines its $D_s^+ \rightarrow \tau^+ \nu_\tau$ and $\mu^+ \nu_\mu$ branching fractions to get $f_{D_s} = (285 \pm 19 \pm 40)$ MeV.
- ¹² This ABBIENDI 01L value gives a decay constant f_{D_s} of $(286 \pm 44 \pm 41)$ MeV.
- ¹³ The second ACCIARRI 97F error here combines in quadrature systematic (0.016) and normalization (0.018) errors. The branching fraction gives $f_{D_s} = (309 \pm 58 \pm 33 \pm 38)$ MeV.

$\Gamma(\tau^+ \nu_\tau)/\Gamma_{\text{total}}$					Γ_{11}/Γ
VALUE (units 10^{-2})	EVTS	DOCUMENT ID	TECN	COMMENT	
6.6 ± 0.6 OUR AVERAGE					
6.17 ± 0.71 ± 0.34	102	ECKLUND	08	CLEO $e^+ e^- \rightarrow D_s^+ D_s^{*-}$, 4170 MeV	
8.0 ± 1.3 ± 0.4	47	PEDLAR	07A	CLEO $e^+ e^- \rightarrow D_s^+ D_s^{*-}$, 4170 MeV	
5.79 ± 0.77 ± 1.84	881	¹¹ HEISTER	02i	ALEP Z decays	
7.0 ± 2.1 ± 2.0	22	¹² ABBIENDI	01L	OPAL $D_s^{*+} \rightarrow \gamma D_s^+$ from Z's	
7.4 ± 2.8 ± 2.4	16	¹³ ACCIARRI	97F	L3 $D_s^{*+} \rightarrow \gamma D_s^+$ from Z's	

- See the note on "Decay Constants of Charged Pseudoscalar Mesons" in the D_s^\pm Listings.
- • • We do not use the following data for averages, fits, limits, etc. • • •
- ¹¹ HEISTER 02i combines its $D_s^+ \rightarrow \tau^+ \nu_\tau$ and $\mu^+ \nu_\mu$ branching fractions to get $f_{D_s} = (285 \pm 19 \pm 40)$ MeV.
- ¹² This ABBIENDI 01L value gives a decay constant f_{D_s} of $(286 \pm 44 \pm 41)$ MeV.
- ¹³ The second ACCIARRI 97F error here combines in quadrature systematic (0.016) and normalization (0.018) errors. The branching fraction gives $f_{D_s} = (309 \pm 58 \pm 33 \pm 38)$ MeV.

$\Gamma(\tau^+ \nu_\tau)/\Gamma(\mu^+ \nu_\mu)$					Γ_{11}/Γ_{10}
VALUE	EVTS	DOCUMENT ID	TECN	COMMENT	
11.0 ± 1.4 ± 0.6	102	¹⁴ ECKLUND	08	CLEO $e^+ e^- \rightarrow D_s^+ D_s^{*-}$, 4170 MeV	

- • • We do not use the following data for averages, fits, limits, etc. • • •
- ¹⁴ This ECKLUND 08 value also uses results from PEDLAR 07A, and it is not independent of other results in these Listings. Combined with earlier CLEO results, the decay constant f_{D_s} is $274 \pm 10 \pm 5$ MeV.

$\Gamma(\phi \ell^+ \nu_\ell)/\Gamma(\phi \pi^+)$					Γ_{12}/Γ_{18}
VALUE	EVTS	DOCUMENT ID	TECN	COMMENT	
0.54 ± 0.04 OUR AVERAGE					
0.540 ± 0.033 ± 0.048	793	LINK	02j	FOCS Uses $\phi \mu^+ \nu_\mu$	
0.54 ± 0.05 ± 0.04	367	BUTLER	94	CLE2 Uses $\phi e^+ \nu_e$ and $\phi \mu^+ \nu_\mu$	
0.58 ± 0.17 ± 0.07	97	FRABETTI	93g	E687 Uses $\phi \mu^+ \nu_\mu$	
0.57 ± 0.15 ± 0.15	104	ALBRECHT	91	ARG Uses $\phi e^+ \nu_e$	
0.49 ± 0.10 ± 0.10	54	ALEXANDER	90b	CLEO Uses $\phi e^+ \nu_e$ and $\phi \mu^+ \nu_\mu$	

- For now, we average together measurements of the $\Gamma(\phi e^+ \nu_e)/\Gamma(\phi \pi^+)$ and $\Gamma(\phi \mu^+ \nu_\mu)/\Gamma(\phi \pi^+)$ ratios. See the end of the D_s^\pm Listings for measurements of $D_s^+ \rightarrow \phi \ell^+ \nu_\ell$ form-factor ratios.
- Unseen decay modes of the η and the ϕ are included.

$\Gamma(\eta \ell^+ \nu_\ell)/\Gamma(\phi \ell^+ \nu_\ell)$					Γ_{14}/Γ_{12}
VALUE	EVTS	DOCUMENT ID	TECN	COMMENT	
1.24 ± 0.12 ± 0.15	440	¹⁵ BRANDENB...	95	CLE2 $e^+ e^- \approx \Upsilon(4S)$	

- ¹⁵ BRANDENBURG 95 uses both e^+ and μ^+ events and makes a phase-space adjustment to use the μ^+ events as e^+ events.

$\Gamma(\eta'(958) \ell^+ \nu_\ell)/\Gamma(\phi \ell^+ \nu_\ell)$					Γ_{15}/Γ_{12}
VALUE	EVTS	DOCUMENT ID	TECN	COMMENT	
0.43 ± 0.11 ± 0.07	29	¹⁶ BRANDENB...	95	CLE2 $e^+ e^- \approx \Upsilon(4S)$	

- Unseen decay modes of the resonances are included.
- ¹⁶ BRANDENBURG 95 uses both e^+ and μ^+ events and makes a phase-space adjustment to use the μ^+ events as e^+ events.

$[\Gamma(\eta \ell^+ \nu_\ell) + \Gamma(\eta'(958) \ell^+ \nu_\ell)]/\Gamma(\phi \ell^+ \nu_\ell)$					$\Gamma_{13}/\Gamma_{12} = (\Gamma_{14} + \Gamma_{15})/\Gamma_{12}$
VALUE	EVTS	DOCUMENT ID	TECN	COMMENT	
1.67 ± 0.17 ± 0.17	17	BRANDENB...	95	CLE2 $e^+ e^- \approx \Upsilon(4S)$	

- ¹⁷ This BRANDENBURG 95 data is redundant with data in previous blocks.

Hadronic modes with a $K\bar{K}$ pair.

$\Gamma(K^+ K_0^0)/\Gamma_{\text{total}}$					Γ_{16}/Γ
VALUE (units 10^{-2})	EVTS	DOCUMENT ID	TECN	COMMENT	
1.49 ± 0.09 OUR FIT					
1.49 ± 0.07 ± 0.05					
0.58 ± 0.16 ± 0.10	68	¹⁸ ALEXANDER	08	CLEO $e^+ e^-$ at 4.17 GeV	

- ¹⁸ ALEXANDER 08 uses single- and double-tagged events in an overall fit. The correlation matrix for the branching fractions is used in the fit.

$\Gamma(K^+ K_0^0)/\Gamma(\phi \pi^+)$					Γ_{16}/Γ_{18}
VALUE	EVTS	DOCUMENT ID	TECN	COMMENT	
0.46 ± 0.16 ± 0.10	68	ANJOS	90c	E691 γ Be	
0.50 ± 0.09 ± 0.05	89	ADLER	89b	MRK3 $e^+ e^-$ 4.14 GeV	
	89	CHEN	89	CLEO $e^+ e^-$ 10 GeV	

- • • We do not use the following data for averages, fits, limits, etc. • • •

$\Gamma(K^+ K^- \pi^+)/\Gamma_{\text{total}}$					Γ_{17}/Γ
VALUE (units 10^{-2})	EVTS	DOCUMENT ID	TECN	COMMENT	
5.50 ± 0.28 OUR FIT					
5.50 ± 0.23 ± 0.16					
5.50 ± 0.23 ± 0.16	19	ALEXANDER	08	CLEO $e^+ e^-$ at 4.17 GeV	

- ¹⁹ ALEXANDER 08 uses single- and double-tagged events in an overall fit. The correlation matrix for the branching fractions is used in the fit.

$\Gamma(\phi\pi^+)/\Gamma_{\text{total}}$ Γ_{18}/Γ

The results here are model-independent. For earlier, model-dependent results, see our PDG 06 edition. See also the header note in the next block of data.

VALUE (units 10^{-2})	EVTS	DOCUMENT ID	TECN	COMMENT
4.38±0.35 OUR FIT				
4.5 ± 0.4 OUR AVERAGE				
4.62±0.36±0.51		20 AUBERT	06N BABR	e^+e^- at $\mathcal{T}(4S)$
4.81±0.52±0.38	212±19	21 AUBERT	05V BABR	$e^+e^- \approx \mathcal{T}(4S)$
3.59±0.77±0.48		22 ARTUSO	96 CLE2	e^+e^- at $\mathcal{T}(4S)$
• • • We do not use the following data for averages, fits, limits, etc. • • •				
3.9 $\begin{smallmatrix} +5.1 & +1.8 \\ -1.9 & -1.1 \end{smallmatrix}$		23 BAI	95c BES	e^+e^- 4.03 GeV

²⁰This AUBERT 06N measurement uses $\bar{B}^0 \rightarrow D_S^{(*)-} D^{(*)+}$ and $B^- \rightarrow D_S^{(*)-} D^{(*)0}$ decays, including some from other papers. However, the result is independent of AUBERT 05V.

²¹AUBERT 05V uses the ratio of $B^0 \rightarrow D^{*-} D_S^{*+}$ events seen in two different ways, in both of which the $D^{*-} \rightarrow \bar{D}^0 \pi^-$ decay is fully reconstructed: (1) The $D_S^{*+} \rightarrow D_S^+ \gamma$, $D_S^+ \rightarrow \phi \pi^+$ decay is fully reconstructed. (2) The number of events in the D_S^+ peak in the missing mass spectrum against the $D^{*-} \gamma$ is measured.

²²ARTUSO 96 uses partially reconstructed $\bar{B}^0 \rightarrow D^{*+} D_S^{*-}$ decays to get a model-independent value for $\Gamma(D_S^- \rightarrow \phi \pi^-)/\Gamma(D^0 \rightarrow K^- \pi^+)$ of $0.92 \pm 0.20 \pm 0.11$.

²³BAI 95c uses $e^+e^- \rightarrow D_S^+ D_S^-$ events in which one or both of the D_S^\pm are observed to obtain the first model-independent measurement of the $D_S^+ \rightarrow \phi \pi^+$ branching fraction, without assumptions about $\sigma(D_S^\pm)$. However, with only two “doubly-tagged” events, the statistical error is very large.

 $\Gamma(\phi\pi^+, \phi \rightarrow K^+ K^-)/\Gamma(K^+ K^- \pi^+)$ Γ_{19}/Γ_{17}

This is the “fit fraction” from the Dalitz-plot analysis. We decouple the $D_S^+ \rightarrow \phi \pi^+$ branching fraction obtained from mass projections (and used to get some of the other branching fractions) from the $D_S^+ \rightarrow \phi \pi^+, \phi \rightarrow K^+ K^-$ branching fraction obtained from the Dalitz-plot analysis of $D_S^+ \rightarrow K^+ K^- \pi^+$. That is, the ratio of these two branching fractions is not exactly the $\phi \rightarrow K^+ K^-$ branching fraction 0.491.

VALUE	DOCUMENT ID	TECN	COMMENT
0.396±0.033±0.047	FRABETTI	95B E687	Dalitz fit, 701 evts

 $\Gamma(K^+ \bar{K}^*(892)^0, \bar{K}^{*0} \rightarrow K^- \pi^+)/\Gamma(K^+ K^- \pi^+)$ Γ_{21}/Γ_{17}

This is the “fit fraction” from the Dalitz-plot analysis.

VALUE	DOCUMENT ID	TECN	COMMENT
0.478±0.046±0.040	FRABETTI	95B E687	Dalitz fit, 701 evts

 $\Gamma(K^+ \bar{K}^*(892)^0)/\Gamma(\phi\pi^+)$ Γ_{20}/Γ_{18}

Unseen decay modes of the resonances are included. However, we now get branching fractions for resonant submodes of 3-body decays from Dalitz-plot analyses.

VALUE	EVTS	DOCUMENT ID	TECN	COMMENT
• • • We do not use the following data for averages, fits, limits, etc. • • •				
0.85±0.34±0.20	9	ALVAREZ	90C NA14	Photoproduction
0.84±0.30±0.22		ADLER	89B MRK3	e^+e^- 4.14 GeV
1.05±0.17±0.12		CHEN	89 CLEO	e^+e^- 10 GeV
0.87±0.13±0.05	117	ANJOS	88 E691	Photoproduction
1.44±0.37	87	ALBRECHT	87F ARG	e^+e^- 10 GeV

 $\Gamma(f_0(980)\pi^+, f_0 \rightarrow K^+ K^-)/\Gamma(K^+ K^- \pi^+)$ Γ_{22}/Γ_{17}

This is the “fit fraction” from the Dalitz-plot analysis.

VALUE	DOCUMENT ID	TECN	COMMENT
0.11±0.035±0.026	FRABETTI	95B E687	Dalitz fit, 701 evts

 $\Gamma(f_0(1710)\pi^+, f_0 \rightarrow K^+ K^-)/\Gamma(K^+ K^- \pi^+)$ Γ_{24}/Γ_{17}

This is the “fit fraction” from the Dalitz-plot analysis.

VALUE	DOCUMENT ID	TECN	COMMENT	
• • • We do not use the following data for averages, fits, limits, etc. • • •				
0.034±0.023±0.035	24	FRABETTI	95B E687	Dalitz fit, 701 evts

²⁴In other words, FRABETTI 95B doesn't see this resonance.

 $\Gamma(K^+ \bar{K}_0^*(1430)^0, \bar{K}_0^{*0} \rightarrow K^- \pi^+)/\Gamma(K^+ K^- \pi^+)$ Γ_{23}/Γ_{17}

This is the “fit fraction” from the Dalitz-plot analysis.

VALUE	DOCUMENT ID	TECN	COMMENT
0.093±0.032±0.032	FRABETTI	95B E687	Dalitz fit, 701 evts

 $\Gamma(K^*(892)+\bar{K}^0)/\Gamma(\phi\pi^+)$ Γ_{27}/Γ_{18}

Unseen decay modes of the resonances are included.

VALUE	DOCUMENT ID	TECN	COMMENT
1.20±0.21±0.13	CHEN	89 CLEO	e^+e^- 10 GeV

 $\Gamma(K^+ K^- \pi^+ \pi^0)/\Gamma_{\text{total}}$ Γ_{28}/Γ

VALUE (units 10^{-2})	DOCUMENT ID	TECN	COMMENT	
5.6 ± 0.5 OUR FIT				
5.65±0.29±0.40	25	ALEXANDER	08 CLEO	e^+e^- at 4.17 GeV

²⁵ALEXANDER 08 uses single- and double-tagged events in an overall fit. The correlation matrix for the branching fractions is used in the fit.

 $\Gamma(\phi\rho^+, \phi \rightarrow K^+ K^-)/\Gamma(\phi\pi^+, \phi \rightarrow K^+ K^-)$ Γ_{30}/Γ_{19}

VALUE	EVTS	DOCUMENT ID	TECN	COMMENT
1.86±0.26±0.29	253	AVERY	92 CLE2	$e^+e^- \approx 10.5$ GeV

 $\Gamma(\phi\pi^+ \pi^0 \text{ 3-body, } \phi \rightarrow K^+ K^-)/\Gamma(\phi\pi^+, \phi \rightarrow K^+ K^-)$ Γ_{31}/Γ_{19}

VALUE	CL%	DOCUMENT ID	TECN	COMMENT
<0.71	90	DAOUDI	92 CLE2	$e^+e^- \approx 10.5$ GeV

 $\Gamma(K^+ K^- \pi^+ \pi^0 \text{ non-}\phi)/\Gamma(\phi\pi^+)$ Γ_{32}/Γ_{18}

VALUE	CL%	DOCUMENT ID	TECN	COMMENT
<2.4	90	ANJOS	89E E691	Photoproduction

 $\Gamma(K_S^0 K^- \pi^+ \pi^+)/\Gamma_{\text{total}}$ Γ_{33}/Γ

VALUE (units 10^{-2})	DOCUMENT ID	TECN	COMMENT	
1.64±0.12 OUR FIT				
1.64±0.10±0.07	26	ALEXANDER	08 CLEO	e^+e^- at 4.17 GeV

²⁶ALEXANDER 08 uses single- and double-tagged events in an overall fit. The correlation matrix for the branching fractions is used in the fit.

 $\Gamma(K^*(892)+\bar{K}^*(892)^0)/\Gamma(\phi\pi^+)$ Γ_{34}/Γ_{18}

Unseen decay modes of the resonances are included.

VALUE	DOCUMENT ID	TECN	COMMENT
1.6±0.4±0.4	ALBRECHT	92B ARG	$e^+e^- \approx 10.4$ GeV

 $\Gamma(K^0 K^- 2\pi^+ \text{ (non-} K^+ \bar{K}^{*0})/)\Gamma(\phi\pi^+)$ Γ_{35}/Γ_{18}

VALUE	CL%	DOCUMENT ID	TECN	COMMENT
<0.80	90	ALBRECHT	92B ARG	$e^+e^- \approx 10.4$ GeV

 $\Gamma(K^+ K_S^0 \pi^+ \pi^-)/\Gamma(K_S^0 K^- \pi^+ \pi^+)$ Γ_{36}/Γ_{33}

VALUE	EVTS	DOCUMENT ID	TECN	COMMENT
0.586±0.052±0.043	476	LINK	01C FOCS	γ nucleus, $\bar{E}_\gamma \approx 180$ GeV

 $\Gamma(K^+ K^- \pi^+ \pi^+ \pi^-)/\Gamma(K^+ K^- \pi^+)$ Γ_{37}/Γ_{17}

VALUE	EVTS	DOCUMENT ID	TECN	COMMENT
0.160±0.027 OUR AVERAGE				
0.150±0.019±0.025	240	LINK	03D FOCS	γ A, $\bar{E}_\gamma \approx 180$ GeV
0.188±0.036±0.040	75	FRABETTI	97C E687	γ Be, $\bar{E}_\gamma \approx 200$ GeV

 $\Gamma(\phi\pi^+ \pi^+ \pi^-, \phi \rightarrow K^+ K^-)/\Gamma(\phi\pi^+, \phi \rightarrow K^+ K^-)$ Γ_{38}/Γ_{19}

VALUE	EVTS	DOCUMENT ID	TECN	COMMENT
0.269±0.027 OUR AVERAGE				
0.249±0.024±0.021	136	LINK	03D FOCS	γ A, $\bar{E}_\gamma \approx 180$ GeV
0.28 ± 0.06 ± 0.01	40	FRABETTI	97C E687	γ Be, $\bar{E}_\gamma \approx 200$ GeV
0.58 ± 0.21 ± 0.10	21	FRABETTI	92 E687	γ Be
0.42 ± 0.13 ± 0.07	19	ANJOS	88 E691	Photoproduction
1.11 ± 0.37 ± 0.28	62	ALBRECHT	85D ARG	e^+e^- 10 GeV

 $\Gamma(\phi\pi^+ \pi^+ \pi^-, \phi \rightarrow K^+ K^-)/\Gamma(K^+ K^- \pi^+ \pi^+ \pi^-)$ Γ_{38}/Γ_{37}

VALUE	EVTS	DOCUMENT ID	TECN	COMMENT
• • • We do not use the following data for averages, fits, limits, etc. • • •				
0.21±0.05±0.06	136	²⁷ LINK	03D FOCS	γ A, $\bar{E}_\gamma \approx 180$ GeV

²⁷This LINK 03D result is redundant with its $\Gamma(\phi\pi^+ \pi^+ \pi^-)/\Gamma(\phi\pi^+)$ result above.

 $\Gamma(K^+ K^- \rho^0 \pi^+ \text{ non-}\phi)/\Gamma(K^+ K^- \pi^+ \pi^+ \pi^-)$ Γ_{39}/Γ_{37}

VALUE	CL%	DOCUMENT ID	TECN	COMMENT
<0.03	90	LINK	03D FOCS	γ A, $\bar{E}_\gamma \approx 180$ GeV

 $\Gamma(\phi\rho^+ \pi^+, \phi \rightarrow K^+ K^-)/\Gamma(K^+ K^- \pi^+ \pi^+ \pi^-)$ Γ_{40}/Γ_{37}

VALUE	DOCUMENT ID	TECN	COMMENT
0.75±0.06±0.04	LINK	03D FOCS	γ A, $\bar{E}_\gamma \approx 180$ GeV

 $\Gamma(\phi a_1(1260)^+, \phi \rightarrow K^+ K^-, a_1^+ \rightarrow \rho^0 \pi^+)/\Gamma(K^+ K^- \pi^+)$ Γ_{41}/Γ_{17}

VALUE	DOCUMENT ID	TECN	COMMENT
0.137±0.019±0.011	LINK	03D FOCS	γ A, $\bar{E}_\gamma \approx 180$ GeV

 $\Gamma(K^+ K^- \pi^+ \pi^+ \pi^- \text{ nonresonant})/\Gamma(K^+ K^- \pi^+ \pi^+ \pi^-)$ Γ_{42}/Γ_{37}

VALUE	DOCUMENT ID	TECN	COMMENT
0.10±0.06±0.05	LINK	03D FOCS	γ A, $\bar{E}_\gamma \approx 180$ GeV

 $\Gamma(K_S^0 K_S^0 \pi^+ \pi^+ \pi^-)/\Gamma(K_S^0 K^- \pi^+ \pi^+)$ Γ_{43}/Γ_{33}

VALUE	EVTS	DOCUMENT ID	TECN	COMMENT
0.051±0.015±0.015	37 ± 10	LINK	04D FOCS	γ A, $\bar{E}_\gamma \approx 180$ GeV

Pionic modes $\Gamma(\pi^+ \pi^0)/\Gamma(K^+ K_S^0)$ Γ_{44}/Γ_{16}

This decay is forbidden by isospin conservation.

VALUE (units 10^{-2})	CL%	DOCUMENT ID	TECN	COMMENT
<4.1	90	ADAMS	07A CLEO	e^+e^- , $E_{\text{cm}}=4.17$ GeV

 $\Gamma(\pi^+ \pi^+ \pi^-)/\Gamma_{\text{total}}$ Γ_{45}/Γ

VALUE (units 10^{-2})	DOCUMENT ID	TECN	COMMENT	
1.11±0.08 OUR FIT				
1.11±0.07±0.04	28	ALEXANDER	08 CLEO	e^+e^- at 4.17 GeV

²⁸ALEXANDER 08 uses single- and double-tagged events in an overall fit. The correlation matrix for the branching fractions is used in the fit.

Meson Particle Listings

 D_s^\pm $\Gamma(\pi^+\pi^+\pi^-)/\Gamma(K^+K^-\pi^+)$ Γ_{45}/Γ_{17}

VALUE	EVTS	DOCUMENT ID	TECN	COMMENT
0.265 ± 0.041 ± 0.031	98	FRABETTI	97D E687	γ Be \approx 200 GeV

 $\Gamma(\pi^+\pi^+\pi^-)/\Gamma(\phi\pi^+)$ Γ_{45}/Γ_{18}

VALUE	EVTS	DOCUMENT ID	TECN	COMMENT
0.245 ± 0.028 ^{+0.019} _{-0.012}	848	AITALA	01A E791	π^- nucleus, 500 GeV
0.33 ± 0.10 ± 0.04	29	ADAMOVICH	93 WA82	π^- 340 GeV
0.44 ± 0.10 ± 0.04	68	ANJOS	89 E691	Photoproduction

 $\Gamma(\rho^0\pi^+)/\Gamma(\pi^+\pi^+\pi^-)$ Γ_{46}/Γ_{45}

VALUE	CL%	DOCUMENT ID	TECN	COMMENT
not seen		LINK	04 FOCS	Dalitz fit, 1475 ± 50 evts
0.058 ± 0.023 ± 0.037		AITALA	01A E791	Dalitz fit, 848 evts
<0.073	90	FRABETTI	97D E687	γ Be \approx 200 GeV

 $\Gamma(\rho^0\pi^+)/\Gamma(\phi\pi^+)$ Γ_{46}/Γ_{18}

VALUE	CL%	DOCUMENT ID	TECN	COMMENT
<0.08	90	ANJOS	89 E691	Photoproduction
<0.22	90	ALBRECHT	87G ARG	e^+e^- 10 GeV

 $\Gamma(\pi^+(\pi^+\pi^-)_{S\text{-wave}})/\Gamma(\pi^+\pi^+\pi^-)$ Γ_{47}/Γ_{45}

This is the "fit fraction" from the Dalitz-plot analysis.

VALUE	DOCUMENT ID	TECN	COMMENT
0.8704 ± 0.0560 ± 0.0438	29 LINK	04 FOCS	Dalitz fit, 1475 ± 50 evts

²⁹LINK 04 borrows a K-matrix parametrization from ANISOVICH 03 of the full $\pi\pi$ -S-wave isoscalar scattering amplitude to describe the $\pi^+\pi^-$ S-wave component of the $\pi^+\pi^+\pi^-$ state. The fit fraction given above is a sum over five f_0 mesons, the $f_0(980)$, $f_0(1300)$, $f_0(1200-1600)$, $f_0(1500)$, and $f_0(1750)$. See LINK 04 for details and discussion.

 $\Gamma(f_0(980)\pi^+, f_0 \rightarrow \pi^+\pi^-)/\Gamma(\pi^+\pi^+\pi^-)$ Γ_{48}/Γ_{45}

This is the "fit fraction" from the Dalitz-plot analysis.

VALUE	DOCUMENT ID	TECN	COMMENT
0.565 ± 0.043 ± 0.047	AITALA	01A E791	Dalitz fit, 848 evts
1.074 ± 0.140 ± 0.043	FRABETTI	97D E687	γ Be \approx 200 GeV

 $\Gamma(f_0(1370)\pi^+, f_0 \rightarrow \pi^+\pi^-)/\Gamma(\pi^+\pi^+\pi^-)$ Γ_{49}/Γ_{45}

This is the "fit fraction" from the Dalitz-plot analysis.

VALUE	DOCUMENT ID	TECN	COMMENT
0.324 ± 0.077 ± 0.017	AITALA	01A E791	Dalitz fit, 848 evts

 $\Gamma(f_0(1500)\pi^+, f_0 \rightarrow \pi^+\pi^-)/\Gamma(\pi^+\pi^+\pi^-)$ Γ_{50}/Γ_{45}

This is the "fit fraction" from the Dalitz-plot analysis.

VALUE	DOCUMENT ID	TECN	COMMENT
0.274 ± 0.114 ± 0.019	³⁰ FRABETTI	97D E687	γ Be \approx 200 GeV

³⁰FRABETTI 97D calls this mode $S(1475)\pi^+$, but finds the mass and width of this $S(1475)$ to be in excellent agreement with those of the $f_0(1500)$.

 $\Gamma(f_2(1270)\pi^+, f_2 \rightarrow \pi^+\pi^-)/\Gamma(\pi^+\pi^+\pi^-)$ Γ_{51}/Γ_{45}

This is the "fit fraction" from the Dalitz-plot analysis.

VALUE	DOCUMENT ID	TECN	COMMENT
0.0974 ± 0.0449 ± 0.0294	LINK	04 FOCS	Dalitz fit, 1475 ± 50 evts
0.197 ± 0.033 ± 0.006	AITALA	01A E791	Dalitz fit, 848 evts
0.123 ± 0.056 ± 0.018	FRABETTI	97D E687	γ Be \approx 200 GeV

 $\Gamma(\rho(1450)^0\pi^+, \rho^0 \rightarrow \pi^+\pi^-)/\Gamma(\pi^+\pi^+\pi^-)$ Γ_{52}/Γ_{45}

This is the "fit fraction" from the Dalitz-plot analysis.

VALUE	DOCUMENT ID	TECN	COMMENT
0.0656 ± 0.0343 ± 0.0440	LINK	04 FOCS	Dalitz fit, 1475 ± 50 evts
0.044 ± 0.021 ± 0.002	AITALA	01A E791	Dalitz fit, 848 evts

 $\Gamma(\pi^+\pi^+\pi^- \text{ nonresonant})/\Gamma(\pi^+\pi^+\pi^-)$ Γ_{53}/Γ_{45}

This is the "fit fraction" from the Dalitz-plot analysis.

VALUE	CL%	DOCUMENT ID	TECN	COMMENT
0.005 ± 0.014 ± 0.017		AITALA	01A E791	π^- nucleus, 500 GeV
<0.269	90	FRABETTI	97D E687	γ Be \approx 200 GeV

 $\Gamma(\pi^+\pi^+\pi^-\pi^0)/\Gamma(\phi\pi^+)$ Γ_{54}/Γ_{18}

VALUE	CL%	DOCUMENT ID	TECN	COMMENT
<3.3	90	ANJOS	89E E691	Photoproduction

 $\Gamma(\eta\pi^+)/\Gamma_{\text{total}}$ Γ_{55}/Γ

Unseen decay modes of the η are included.

VALUE (units 10^{-2})	DOCUMENT ID	TECN	COMMENT
1.58 ± 0.21 OUR FIT			
1.58 ± 0.11 ± 0.18	³¹ ALEXANDER	08 CLEO	e^+e^- at 4.17 GeV

³¹ALEXANDER 08 uses single- and double-tagged events in an overall fit. The correlation matrix for the branching fractions is used in the fit.

 $\Gamma(\eta\pi^+)/\Gamma(\phi\pi^+)$ Γ_{55}/Γ_{18}

Unseen decay modes of the resonances are included.

VALUE	EVTS	DOCUMENT ID	TECN	COMMENT
0.48 ± 0.03 ± 0.04	920	JESSOP	98 CLE2	$e^+e^- \approx \Upsilon(4S)$
0.54 ± 0.09 ± 0.06	165	ALEXANDER	92 CLE2	See JESSOP 98

 $\Gamma(\omega\pi^+)/\Gamma(\eta\pi^+)$ Γ_{56}/Γ_{55}

Unseen decay modes of the resonances are included.

VALUE	DOCUMENT ID	TECN	COMMENT
0.16 ± 0.04 ± 0.03	BALEST	97 CLE2	$e^+e^- \approx \Upsilon(4S)$

 $\Gamma(3\pi^+2\pi^-)/\Gamma(K^+K^-\pi^+)$ Γ_{57}/Γ_{17}

VALUE	EVTS	DOCUMENT ID	TECN	COMMENT
0.146 ± 0.014 OUR AVERAGE				
0.145 ± 0.011 ± 0.010	671	LINK	03D FOCS	γ A, $\bar{E}_\gamma \approx$ 180 GeV
0.158 ± 0.042 ± 0.031	37	FRABETTI	97C E687	γ Be, $\bar{E}_\gamma \approx$ 200 GeV

 $\Gamma(\eta\rho^+)/\Gamma(\phi\pi^+)$ Γ_{59}/Γ_{18}

Unseen decay modes of the resonances are included.

VALUE	EVTS	DOCUMENT ID	TECN	COMMENT
2.98 ± 0.20 ± 0.39	447	JESSOP	98 CLE2	$e^+e^- \approx \Upsilon(4S)$
2.86 ± 0.38 ^{+0.36} _{-0.38}	217	AVERY	92 CLE2	See JESSOP 98

 $\Gamma(\eta\pi^+\pi^0 \text{ 3-body})/\Gamma(\phi\pi^+)$ Γ_{60}/Γ_{18}

Unseen decay modes of the resonances are included.

VALUE	CL%	DOCUMENT ID	TECN	COMMENT
<1.1	90	JESSOP	98 CLE2	$e^+e^- \approx \Upsilon(4S)$
<0.82	90	³² DAOUDI	92 CLE2	See JESSOP 98

³²We use the JESSOP 98 limit, even though the DAOUDI 92 limit, from the same experiment but with a much smaller data sample, is more restrictive.

 $\Gamma(3\pi^+2\pi^-\pi^0)/\Gamma_{\text{total}}$ Γ_{61}/Γ

VALUE	DOCUMENT ID	TECN	COMMENT
0.049 ± 0.033 -0.030	BARLAG	92C ACCM	π^- 230 GeV

 $\Gamma(\eta'(958)\pi^+)/\Gamma_{\text{total}}$ Γ_{62}/Γ

Unseen decay modes of the $\eta'(958)$ are included.

VALUE (units 10^{-2})	DOCUMENT ID	TECN	COMMENT
3.8 ± 0.4 OUR FIT			
3.77 ± 0.25 ± 0.30	³³ ALEXANDER	08 CLEO	e^+e^- at 4.17 GeV

³³ALEXANDER 08 uses single- and double-tagged events in an overall fit. The correlation matrix for the branching fractions is used in the fit.

 $\Gamma(\eta'(958)\pi^+)/\Gamma(\phi\pi^+)$ Γ_{62}/Γ_{18}

Unseen decay modes of the resonances are included.

VALUE	EVTS	DOCUMENT ID	TECN	COMMENT
1.03 ± 0.06 ± 0.07	537	JESSOP	98 CLE2	$e^+e^- \approx \Upsilon(4S)$
1.20 ± 0.15 ± 0.11	281	ALEXANDER	92 CLE2	See JESSOP 98
2.5 ± 1.0 ^{+1.5} _{-0.4}	22	ALVAREZ	91 NA14	Photoproduction
2.5 ± 0.5 ± 0.3	215	ALBRECHT	90D ARG	$e^+e^- \approx$ 10.4 GeV

 $\Gamma(\eta'(958)\rho^+)/\Gamma(\phi\pi^+)$ Γ_{64}/Γ_{18}

Unseen decay modes of the resonances are included.

VALUE	EVTS	DOCUMENT ID	TECN	COMMENT
2.78 ± 0.28 ± 0.30	137	JESSOP	98 CLE2	$e^+e^- \approx \Upsilon(4S)$
3.44 ± 0.62 ^{+0.44} _{-0.46}	68	AVERY	92 CLE2	See JESSOP 98

 $\Gamma(\eta'(958)\pi^+\pi^0 \text{ 3-body})/\Gamma(\phi\pi^+)$ Γ_{65}/Γ_{18}

Unseen decay modes of the resonances are included.

VALUE	CL%	DOCUMENT ID	TECN	COMMENT
<0.4	90	JESSOP	98 CLE2	$e^+e^- \approx \Upsilon(4S)$
<0.85	90	DAOUDI	92 CLE2	See JESSOP 98

Modes with one or three K's

 $\Gamma(K^+\pi^0)/\Gamma(K^+K_s^0)$ Γ_{66}/Γ_{16}

VALUE (units 10^{-2})	EVTS	DOCUMENT ID	TECN	COMMENT
5.5 ± 1.3 ± 0.7	141 ± 34	ADAMS	07A CLEO	e^+e^- , $E_{\text{cm}}=4.17$ GeV

$\Gamma(K_S^0 \pi^+)/\Gamma(K^+ K_S^0)$ Γ_{67}/Γ_{16}

VALUE (units 10^{-2})	EVTS	DOCUMENT ID	TECN	COMMENT
8.4 ± 0.9 OUR AVERAGE				
10.4 ± 2.4 ± 1.4	113 ± 26	LINK	08	FOCS γ A, $\bar{E}_\gamma \approx 180$ GeV
8.2 ± 0.9 ± 0.2	206 ± 22	ADAMS	07A	CLEO $e^+ e^-$, $E_{cm} = 4.17$ GeV

 $\Gamma(K^+ \eta)/\Gamma(\eta \pi^+)$ Γ_{68}/Γ_{55}

VALUE (units 10^{-2})	EVTS	DOCUMENT ID	TECN	COMMENT
8.9 ± 1.5 ± 0.4	113 ± 18	ADAMS	07A	CLEO $e^+ e^-$, $E_{cm} = 4.17$ GeV

 $\Gamma(K^+ \eta'(958))/\Gamma(\eta'(958) \pi^+)$ Γ_{69}/Γ_{62}

VALUE (units 10^{-2})	EVTS	DOCUMENT ID	TECN	COMMENT
4.2 ± 1.3 ± 0.3	28 ± 9	ADAMS	07A	CLEO $e^+ e^-$, $E_{cm} = 4.17$ GeV

 $\Gamma(K^+ \pi^+ \pi^-)/\Gamma_{total}$ Γ_{70}/Γ

VALUE (units 10^{-2})	DOCUMENT ID	TECN	COMMENT
0.69 ± 0.05 OUR FIT			
0.69 ± 0.05 ± 0.03	34 ALEXANDER	08	CLEO $e^+ e^-$ at 4.17 GeV

³⁴ ALEXANDER 08 uses single- and double-tagged events in an overall fit. The correlation matrix for the branching fractions is used in the fit.

 $\Gamma(K^+ \pi^+ \pi^-)/\Gamma(K^+ K^- \pi^+)$ Γ_{70}/Γ_{17}

VALUE	EVTS	DOCUMENT ID	TECN	COMMENT
0.126 ± 0.009 OUR FIT				
0.127 ± 0.007 ± 0.014	567 ± 31	LINK	04F	FOCS γ A, $\bar{E}_\gamma \approx 180$ GeV

 $\Gamma(K^+ \pi^+ \pi^-)/\Gamma(\phi \pi^+)$ Γ_{70}/Γ_{18}

VALUE	EVTS	DOCUMENT ID	TECN	COMMENT
0.28 ± 0.06 ± 0.05	85	FRABETTI	95E	E687 γ Be, $\bar{E}_\gamma = 220$ GeV

 $\Gamma(K^+ \rho^0)/\Gamma(K^+ \pi^+ \pi^-)$ Γ_{71}/Γ_{70}

VALUE	DOCUMENT ID	TECN	COMMENT
0.3883 ± 0.0531 ± 0.0261	LINK	04F	FOCS Dalitz fit, 567 evts

 $\Gamma(K^+ \rho(1450)^0, \rho^0 \rightarrow \pi^+ \pi^-)/\Gamma(K^+ \pi^+ \pi^-)$ Γ_{72}/Γ_{70}

VALUE	DOCUMENT ID	TECN	COMMENT
0.1062 ± 0.0351 ± 0.0104	LINK	04F	FOCS Dalitz fit, 567 evts

 $\Gamma(K^*(892)^0 \pi^+, K^{*0} \rightarrow K^+ \pi^-)/\Gamma(K^+ \pi^+ \pi^-)$ Γ_{73}/Γ_{70}

VALUE	DOCUMENT ID	TECN	COMMENT
0.2164 ± 0.0321 ± 0.0114	LINK	04F	FOCS Dalitz fit, 567 evts

 $\Gamma(K^*(1410)^0 \pi^+, K^{*0} \rightarrow K^+ \pi^-)/\Gamma(K^+ \pi^+ \pi^-)$ Γ_{74}/Γ_{70}

VALUE	DOCUMENT ID	TECN	COMMENT
0.1888 ± 0.0403 ± 0.0122	LINK	04F	FOCS Dalitz fit, 567 evts

 $\Gamma(K^*(1430)^0 \pi^+, K^{*0} \rightarrow K^+ \pi^-)/\Gamma(K^+ \pi^+ \pi^-)$ Γ_{75}/Γ_{70}

VALUE	DOCUMENT ID	TECN	COMMENT
0.0765 ± 0.0500 ± 0.0170	LINK	04F	FOCS Dalitz fit, 567 evts

 $\Gamma(K^+ \pi^+ \pi^- \text{ nonresonant})/\Gamma(K^+ \pi^+ \pi^-)$ Γ_{76}/Γ_{70}

VALUE	DOCUMENT ID	TECN	COMMENT
0.1588 ± 0.0492 ± 0.0153	LINK	04F	FOCS Dalitz fit, 567 evts

 $\Gamma(K_S^0 \pi^+ \pi^-)/\Gamma(K_S^0 K^- \pi^+ \pi^+)$ Γ_{77}/Γ_{33}

VALUE	EVTS	DOCUMENT ID	TECN	COMMENT
0.18 ± 0.04 ± 0.05	179 ± 36	LINK	08	FOCS γ A, $\bar{E}_\gamma \approx 180$ GeV

 $\Gamma(K^+ K^+ K^-)/\Gamma(K^+ K^- \pi^+)$ Γ_{78}/Γ_{17}

VALUE (units 10^{-3})	EVTS	DOCUMENT ID	TECN	COMMENT
8.95 ± 2.12 ± $\frac{2.24}{-2.31}$	31	LINK	02i	FOCS γ nucleus, ≈ 180 GeV

 $\Gamma(\phi K^+, \phi \rightarrow K^+ K^-)/\Gamma(\phi \pi^+, \phi \rightarrow K^+ K^-)$ Γ_{79}/Γ_{19}

VALUE	CL%	DOCUMENT ID	TECN	COMMENT
<0.013	90	FRABETTI	95F	E687 γ Be, $\bar{E}_\gamma \approx 220$ GeV
<0.071	90	ANJOS	92D	E691 γ Be, $\bar{E}_\gamma = 145$ GeV

Doubly Cabibbo-suppressed modes $\Gamma(K^+ K^+ \pi^-)/\Gamma(K^+ K^- \pi^+)$ Γ_{80}/Γ_{17}

VALUE	EVTS	DOCUMENT ID	TECN	COMMENT
0.0052 ± 0.0017 ± 0.0011	27 ± 9	LINK	05k	FOCS $<0.78\%$, CL = 90%

Baryon-antibaryon mode $\Gamma(\rho \bar{n})/\Gamma_{total}$ Γ_{81}/Γ

VALUE (units 10^{-3})	EVTS	DOCUMENT ID	TECN	COMMENT
1.30 ± 0.36 ± $\frac{0.12}{-0.16}$	13.0 ± 3.6	ATHAR	08	CLEO $e^+ e^-$, $E_{cm} \approx 4170$ MeV

Rare or forbidden modes $\Gamma(\pi^+ e^+ e^-)/\Gamma_{total}$ Γ_{82}/Γ

VALUE	CL%	DOCUMENT ID	TECN	COMMENT
<2.7 × 10⁻⁴	90	AITALA	99G	E791 π^- N 500 GeV

 $\Gamma(\pi^+ \mu^+ \mu^-)/\Gamma_{total}$ Γ_{83}/Γ

VALUE	CL%	EVTS	DOCUMENT ID	TECN	COMMENT
<2.6 × 10⁻⁵	90		LINK	03F	FOCS γ nucleus, $\bar{E}_\gamma \approx 180$ GeV

• • • We do not use the following data for averages, fits, limits, etc. • • •

<1.4 × 10 ⁻⁴	90	AITALA	99G	E791	π^- N 500 GeV
<4.3 × 10 ⁻⁴	90	0	KODA MA	95	E653 π^- emulsion 600 GeV

 $\Gamma(K^+ e^+ e^-)/\Gamma_{total}$ Γ_{84}/Γ

VALUE	CL%	DOCUMENT ID	TECN	COMMENT
<1.6 × 10⁻³	90	AITALA	99G	E791 π^- N 500 GeV

 $\Gamma(K^+ \mu^+ \mu^-)/\Gamma_{total}$ Γ_{85}/Γ

VALUE	CL%	EVTS	DOCUMENT ID	TECN	COMMENT
<3.6 × 10⁻⁵	90		LINK	03F	FOCS γ nucleus, $\bar{E}_\gamma \approx 180$ GeV

• • • We do not use the following data for averages, fits, limits, etc. • • •

<1.4 × 10 ⁻⁴	90	AITALA	99G	E791	π^- N 500 GeV
<5.9 × 10 ⁻⁴	90	0	KODA MA	95	E653 π^- emulsion 600 GeV

 $\Gamma(K^*(892)^+ \mu^+ \mu^-)/\Gamma_{total}$ Γ_{86}/Γ

VALUE	CL%	EVTS	DOCUMENT ID	TECN	COMMENT
<1.4 × 10⁻³	90	0	KODA MA	95	E653 π^- emulsion 600 GeV

 $\Gamma(\pi^+ e^\pm \mu^\mp)/\Gamma_{total}$ Γ_{87}/Γ

VALUE	CL%	DOCUMENT ID	TECN	COMMENT
<6.1 × 10⁻⁴	90	AITALA	99G	E791 π^- N 500 GeV

 $\Gamma(K^+ e^\pm \mu^\mp)/\Gamma_{total}$ Γ_{88}/Γ

VALUE	CL%	DOCUMENT ID	TECN	COMMENT
<6.3 × 10⁻⁴	90	AITALA	99G	E791 π^- N 500 GeV

 $\Gamma(\pi^- e^+ e^+)/\Gamma_{total}$ Γ_{89}/Γ

VALUE	CL%	DOCUMENT ID	TECN	COMMENT
<6.9 × 10⁻⁴	90	AITALA	99G	E791 π^- N 500 GeV

 $\Gamma(\pi^- \mu^+ \mu^+)/\Gamma_{total}$ Γ_{90}/Γ

VALUE	CL%	EVTS	DOCUMENT ID	TECN	COMMENT
<2.9 × 10⁻⁵	90		LINK	03F	FOCS γ nucleus, $\bar{E}_\gamma \approx 180$ GeV

• • • We do not use the following data for averages, fits, limits, etc. • • •

<8.2 × 10 ⁻⁵	90	AITALA	99G	E791	π^- N 500 GeV
<4.3 × 10 ⁻⁴	90	0	KODA MA	95	E653 π^- emulsion 600 GeV

 $\Gamma(\pi^- e^+ \mu^+)/\Gamma_{total}$ Γ_{91}/Γ

VALUE	CL%	DOCUMENT ID	TECN	COMMENT
<7.3 × 10⁻⁴	90	AITALA	99G	E791 π^- N 500 GeV

 $\Gamma(K^- e^+ e^+)/\Gamma_{total}$ Γ_{92}/Γ

VALUE	CL%	DOCUMENT ID	TECN	COMMENT
<6.3 × 10⁻⁴	90	AITALA	99G	E791 π^- N 500 GeV

 $\Gamma(K^- \mu^+ \mu^+)/\Gamma_{total}$ Γ_{93}/Γ

VALUE	CL%	EVTS	DOCUMENT ID	TECN	COMMENT
<1.3 × 10⁻⁵	90		LINK	03F	FOCS γ nucleus, $\bar{E}_\gamma \approx 180$ GeV

• • • We do not use the following data for averages, fits, limits, etc. • • •

<1.8 × 10 ⁻⁴	90	AITALA	99G	E791	π^- N 500 GeV
<5.9 × 10 ⁻⁴	90	0	KODA MA	95	E653 π^- emulsion 600 GeV

Meson Particle Listings

 D_s^\pm

$\Gamma(K^- e^+ \mu^+)/\Gamma_{\text{total}}$ Γ_{94}/Γ
A test of lepton-number conservation.

VALUE	CL%	DOCUMENT ID	TECN	COMMENT
$<6.8 \times 10^{-4}$	90	AITALA	99G E791	$\pi^- N$ 500 GeV

$\Gamma(K^*(892)^- \mu^+ \mu^+)/\Gamma_{\text{total}}$ Γ_{95}/Γ
A test of lepton-number conservation.

VALUE	CL%	EVTS	DOCUMENT ID	TECN	COMMENT
$<1.4 \times 10^{-3}$	90	0	KODAMA	95 E653	π^- emulsion 600 GeV

 $D_s^+ - D_s^-$ CP-VIOLATING DECAY-RATE ASYMMETRIES

This is the difference of the D_s^+ and D_s^- partial widths divided by the sum of the widths.

$A_{CP}(K^\pm K_S^0)$ in $D_s^\pm \rightarrow K^\pm K_S^0$

VALUE	DOCUMENT ID	TECN	COMMENT
$+0.049 \pm 0.021 \pm 0.009$	ALEXANDER 08	CLEO	$e^+ e^-$ at 4.17 GeV

$A_{CP}(K^+ K^- \pi^\pm)$ in $D_s^\pm \rightarrow K^+ K^- \pi^\pm$

VALUE	DOCUMENT ID	TECN	COMMENT
$+0.003 \pm 0.011 \pm 0.008$	ALEXANDER 08	CLEO	$e^+ e^-$ at 4.17 GeV

$A_{CP}(K^+ K^- \pi^\pm \pi^0)$ in $D_s^\pm \rightarrow K^+ K^- \pi^\pm \pi^0$

VALUE	DOCUMENT ID	TECN	COMMENT
$-0.059 \pm 0.042 \pm 0.012$	ALEXANDER 08	CLEO	$e^+ e^-$ at 4.17 GeV

$A_{CP}(K_S^0 K^\pm 2\pi^\pm)$ in $D_s^\pm \rightarrow K_S^0 K^\pm 2\pi^\pm$, $D_s^- \rightarrow K_S^0 K^+ 2\pi^-$

VALUE	DOCUMENT ID	TECN	COMMENT
$-0.007 \pm 0.036 \pm 0.011$	ALEXANDER 08	CLEO	$e^+ e^-$ at 4.17 GeV

$A_{CP}(\pi^+ \pi^- \pi^\pm)$ in $D_s^\pm \rightarrow \pi^+ \pi^- \pi^\pm$

VALUE	DOCUMENT ID	TECN	COMMENT
$+0.020 \pm 0.046 \pm 0.007$	ALEXANDER 08	CLEO	$e^+ e^-$ at 4.17 GeV

$A_{CP}(\pi^\pm \eta)$ in $D_s^\pm \rightarrow \pi^\pm \eta$

VALUE	DOCUMENT ID	TECN	COMMENT
$-0.082 \pm 0.052 \pm 0.008$	ALEXANDER 08	CLEO	$e^+ e^-$ at 4.17 GeV

$A_{CP}(\pi^\pm \eta')$ in $D_s^\pm \rightarrow \pi^\pm \eta'$

VALUE	DOCUMENT ID	TECN	COMMENT
$-0.055 \pm 0.037 \pm 0.012$	ALEXANDER 08	CLEO	$e^+ e^-$ at 4.17 GeV

$A_{CP}(K^\pm \pi^0)$ in $D_s^\pm \rightarrow K^\pm \pi^0$

VALUE	DOCUMENT ID	TECN	COMMENT
$+0.02 \pm 0.29$	ADAMS 07A	CLEO	$e^+ e^-$, $E_{\text{cm}}=4.17$ GeV

$A_{CP}(K_S^0 \pi^\pm)$ in $D_s^\pm \rightarrow K_S^0 \pi^\pm$

VALUE	DOCUMENT ID	TECN	COMMENT
$+0.27 \pm 0.11$	ADAMS 07A	CLEO	$e^+ e^-$, $E_{\text{cm}}=4.17$ GeV

$A_{CP}(K^\pm \pi^+ \pi^-)$ in $D_s^\pm \rightarrow K^\pm \pi^+ \pi^-$

VALUE	DOCUMENT ID	TECN	COMMENT
$+0.112 \pm 0.070 \pm 0.009$	ALEXANDER 08	CLEO	$e^+ e^-$ at 4.17 GeV

$A_{CP}(K^\pm \eta)$ in $D_s^\pm \rightarrow K^\pm \eta$

VALUE	DOCUMENT ID	TECN	COMMENT
-0.20 ± 0.18	ADAMS 07A	CLEO	$e^+ e^-$, $E_{\text{cm}}=4.17$ GeV

$A_{CP}(K^\pm \eta'(958))$ in $D_s^\pm \rightarrow K^\pm \eta'(958)$

VALUE	DOCUMENT ID	TECN	COMMENT
-0.17 ± 0.37	ADAMS 07A	CLEO	$e^+ e^-$, $E_{\text{cm}}=4.17$ GeV

 $D_s^+ - D_s^-$ T-VIOLATING DECAY-RATE ASYMMETRIES

$A_{T\text{viol}}(K_S^0 K^\pm \pi^+ \pi^-)$ in $D_s^\pm \rightarrow K_S^0 K^\pm \pi^+ \pi^-$

$C_T \equiv \vec{p}_{K^+} \cdot (\vec{p}_{\pi^+} \times \vec{p}_{\pi^-})$ is a T -odd correlation of the K^+ , π^+ , and π^- momenta for the D_s^+ . $\bar{C}_T \equiv \vec{p}_{K^-} \cdot (\vec{p}_{\pi^-} \times \vec{p}_{\pi^+})$ is the corresponding quantity for the D_s^- . $A_T \equiv [\Gamma(C_T > 0) - \Gamma(C_T < 0)] / [\Gamma(C_T > 0) + \Gamma(C_T < 0)]$ would, in the absence of strong phases, test for T violation in D_s^\pm decays (the Γ 's are partial widths). With $\bar{A}_T \equiv [\Gamma(-\bar{C}_T > 0) - \Gamma(-\bar{C}_T < 0)] / [\Gamma(-\bar{C}_T > 0) + \Gamma(-\bar{C}_T < 0)]$, the asymmetry $A_{T\text{viol}} \equiv \frac{1}{2}(A_T - \bar{A}_T)$ tests for T violation even with nonzero strong phases.

VALUE	EVTS	DOCUMENT ID	TECN	COMMENT
$-0.036 \pm 0.067 \pm 0.023$	508 ± 34	LINK	05E FOCS	γA , $\bar{E}_\gamma \approx 180$ GeV

 $D_s^+ \rightarrow \phi \ell^+ \nu_\ell$ FORM FACTORS

$r_2 \equiv A_2(0)/A_1(0)$ in $D_s^+ \rightarrow \phi \ell^+ \nu_\ell$

VALUE	EVTS	DOCUMENT ID	TECN	COMMENT
1.32 ± 0.24	OUR AVERAGE			Error includes scale factor of 1.2.
$0.713 \pm 0.202 \pm 0.284$	793	LINK	04C FOCS	$\phi \mu^+ \nu_\mu$
$1.57 \pm 0.25 \pm 0.19$	271	AITALA	99D E791	$\phi e^+ \nu_e$, $\phi \mu^+ \nu_\mu$
$1.4 \pm 0.5 \pm 0.3$	308	VERY	94B CLE2	$\phi e^+ \nu_e$
$1.1 \pm 0.8 \pm 0.1$	90	FRABETTI	94F E687	$\phi \mu^+ \nu_\mu$
$2.1^{+0.6}_{-0.5} \pm 0.2$	19	KODAMA	93 E653	$\phi \mu^+ \nu_\mu$

$r_V \equiv V(0)/A_1(0)$ in $D_s^+ \rightarrow \phi \ell^+ \nu_\ell$

VALUE	EVTS	DOCUMENT ID	TECN	COMMENT
1.72 ± 0.21	OUR AVERAGE			
$1.549 \pm 0.250 \pm 0.148$	793	LINK	04C FOCS	$\phi \mu^+ \nu_\mu$
$2.27 \pm 0.35 \pm 0.22$	271	AITALA	99D E791	$\phi e^+ \nu_e$, $\phi \mu^+ \nu_\mu$
$0.9 \pm 0.6 \pm 0.3$	308	VERY	94B CLE2	$\phi e^+ \nu_e$
$1.8 \pm 0.9 \pm 0.2$	90	FRABETTI	94F E687	$\phi \mu^+ \nu_\mu$
$2.3^{+1.1}_{-0.9} \pm 0.4$	19	KODAMA	93 E653	$\phi \mu^+ \nu_\mu$

Γ_L/Γ_T in $D_s^+ \rightarrow \phi \ell^+ \nu_\ell$

VALUE	EVTS	DOCUMENT ID	TECN	COMMENT
0.72 ± 0.18	OUR AVERAGE			
$1.0 \pm 0.3 \pm 0.2$	308	VERY	94B CLE2	$\phi e^+ \nu_e$
$1.0 \pm 0.5 \pm 0.1$	90	FRABETTI	94F E687	$\phi \mu^+ \nu_\mu$
$0.54 \pm 0.21 \pm 0.10$	19	KODAMA	93 E653	$\phi \mu^+ \nu_\mu$

³⁵ FRABETTI 94F and KODAMA 93 evaluate Γ_L/Γ_T for a lepton mass of zero.

 D_s^\pm REFERENCES

ALEXANDER 08	PRL 100 161804	J.P. Alexander et al.	(CLEO Collab.)
ATHAR 08	PRL 100 181802	S.B. Athar et al.	(CLEO Collab.)
ECKLUND 08	PRL 100 161801	K.M. Ecklund et al.	(CLEO Collab.)
LINK 08	PL B660 147	J.M. Link et al.	(FNAL FOCUS Collab.)
ADAMS 07A	PRL 99 191805	G.S. Adams et al.	(CLEO Collab.)
AUBERT 07V	PRL 98 141801	B. Aubert et al.	(BABAR Collab.)
PEDLAR 07A	PR D76 072002	T.K. Pedlar et al.	(CLEO Collab.)
Also	PRL 99 071802	M. Artuso et al.	(CLEO Collab.)
AUBERT 06N	PR D74 031103R	B. Aubert et al.	(BABAR Collab.)
HUANG 06B	PR D74 112005	G.S. Huang et al.	(CLEO Collab.)
PDG 06	JPG 33 3	W.-M. Yao et al.	(PDG Collab.)
AUBERT 05V	PR D71 091104R	B. Aubert et al.	(BABAR Collab.)
LINK 05E	PL B622 239	J.M. Link et al.	(FNAL FOCUS Collab.)
LINK 05J	PRL 95 052003	J.M. Link et al.	(FNAL FOCUS Collab.)
LINK 05K	PL B624 166	J.M. Link et al.	(FNAL FOCUS Collab.)
LINK 04	PL B585 200	J.M. Link et al.	(FNAL FOCUS Collab.)
LINK 04C	PL B586 183	J.M. Link et al.	(FNAL FOCUS Collab.)
LINK 04D	PL B586 191	J.M. Link et al.	(FNAL FOCUS Collab.)
LINK 04F	PL B601 10	J.M. Link et al.	(FNAL FOCUS Collab.)
ACOSTA 03D	PR D68 072004	D. Acosta et al.	(FNAL CDF-II Collab.)
ANISOVICH 03	EPJ A16 229	V.V. Anisovich et al.	(FNAL FOCUS Collab.)
LINK 03D	PL B561 225	J.M. Link et al.	(FNAL FOCUS Collab.)
LINK 03F	PL B572 21	J.M. Link et al.	(FNAL FOCUS Collab.)
AUBERT 02G	PR D65 091104R	B. Aubert et al.	(BABAR Collab.)
HEISTER 02I	PL B528 1	A. Heister et al.	(ALEPH Collab.)
LINK 02I	PL B541 227	J.M. Link et al.	(FNAL FOCUS Collab.)
LINK 02J	PL B541 243	J.M. Link et al.	(FNAL FOCUS Collab.)
ABBIENDI 01L	PL B516 236	G. Abbiendi et al.	(OPAL Collab.)
AITALA 01A	PRL 86 765	E.M. Aitala et al.	(FNAL E791 Collab.)
IORI 01C	PL B523 22	M. Iori et al.	(FNAL SELEX Collab.)
LINK 01C	PRL 87 162001	J.M. Link et al.	(FNAL FOCUS Collab.)
ALEXANDROV 00	PL B478 31	Y. Alexandrov et al.	(CERN BEATRICE Collab.)
AITALA 99	PL B445 449	E.M. Aitala et al.	(FNAL E791 Collab.)
AITALA 99D	PL B450 294	E.M. Aitala et al.	(FNAL E791 Collab.)
AITALA 99G	PL B462 401	E.M. Aitala et al.	(FNAL E791 Collab.)
BONVICINI 99	PRL 82 4586	G. Bonvicini et al.	(CLEO Collab.)
CHADHA 98	PR D58 032002	M. Chada et al.	(CLEO Collab.)
JESSOP 98	PR D58 052002	C.P. Jessop et al.	(CLEO Collab.)
ACCARIARI 97F	PL B396 327	M. Acciarri et al.	(L3 Collab.)
BAI 97	PR D56 3779	J.Z. Bai et al.	(BES Collab.)
BALEST 97	PRL 79 1436	R. Balest et al.	(CLEO Collab.)
FRABETTI 97C	PL B401 131	P.L. Frabetti et al.	(FNAL E687 Collab.)
FRABETTI 97D	PL B407 79	P.L. Frabetti et al.	(FNAL E687 Collab.)
ARTUSO 96	PL B324 255	M. Artuso et al.	(CLEO Collab.)
KODAMA 96	PL B382 299	K. Kodama et al.	(FNAL E653 Collab.)
BAI 95C	PR D52 3781	J.Z. Bai et al.	(BES Collab.)
BRANDENBURG... 95	PRL 75 3804	G.W. Brandenburg et al.	(CLEO Collab.)
FRABETTI 95B	PL B351 591	P.L. Frabetti et al.	(FNAL E687 Collab.)
FRABETTI 95E	PL B359 403	P.L. Frabetti et al.	(FNAL E687 Collab.)
FRABETTI 95F	PL B363 259	P.L. Frabetti et al.	(FNAL E687 Collab.)
KODAMA 95	PL B345 85	K. Kodama et al.	(FNAL E653 Collab.)
ACOSTA 94	PR D49 5690	D. Acosta et al.	(CLEO Collab.)
VERY 94B	PL B337 405	P. Avery et al.	(CLEO Collab.)
BROWN 94	PR D50 1884	D. Brown et al.	(CLEO Collab.)
BUTLER 94	PL B324 255	F. Butler et al.	(CLEO Collab.)
FRABETTI 94F	PL B328 187	P.L. Frabetti et al.	(FNAL E687 Collab.)
ADAMOVIICH 93F	PL B305 177	M.L. Adamovich et al.	(CERN WA82 Collab.)
FRABETTI 93F	PRL 71 827	P.L. Frabetti et al.	(FNAL E687 Collab.)
FRABETTI 93G	PL B313 253	P.L. Frabetti et al.	(FNAL E687 Collab.)
KODAMA 93	PL B309 483	K. Kodama et al.	(FNAL E653 Collab.)
ALBRECHT 92B	ZPHY C53 361	H. Albrecht et al.	(ARGUS Collab.)
ALEXANDER 92B	PRL 68 1275	J. Alexander et al.	(CLEO Collab.)
ANJOS 92D	PRL 69 2892	J.C. Anjos et al.	(FNAL E691 Collab.)
VERY 92D	PRL 68 1279	P. Avery et al.	(CLEO Collab.)
BARLAG 92C	ZPHY C55 383	S. Barlag et al.	(ACCMOR Collab.)
Also	ZPHY C48 29	S. Barlag et al.	(ACCMOR Collab.)
DAOUDI 92	PR D45 3965	M. Daoudi et al.	(CLEO Collab.)
FRABETTI 92	PL B281 167	P.L. Frabetti et al.	(FNAL E687 Collab.)
ALBRECHT 91	PL B255 634	H. Albrecht et al.	(ARGUS Collab.)
ALVAREZ 91	PL B255 639	M.P. Alvarez et al.	(CERN NA14/2 Collab.)
COFFMAN 91	PL B263 135	D.M. Coffman et al.	(Mark III Collab.)
ALBRECHT 90D	PL B245 315	H. Albrecht et al.	(ARGUS Collab.)

ALEXANDER	90B	PRL 65 1531	J. Alexander et al.	(CLEO Collab.)
ALVAREZ	90C	PL B246 261	M.P. Alvarez et al.	(CERN NA14/2 Collab.)
ANJOS	90C	PR D41 2705	J.C. Anjos et al.	(FNAL E691 Collab.)
BARLAG	90C	ZPHY C46 563	S. Barlag et al.	(ACCMOR Collab.)
FRABETTI	90	PL B251 639	P.L. Frabetti et al.	(FNAL E687 Collab.)
ADLER	89B	PRL 63 1211	J. Adler et al.	(Mark III Collab.)
Also		PRL 63 2858 (erratum)	J. Adler et al.	(Mark III Collab.)
ANJOS	89	PRL 62 125	J.C. Anjos et al.	(FNAL E691 Collab.)
ANJOS	89E	PL B223 267	J.C. Anjos et al.	(FNAL E691 Collab.)
CHEN	89	PL B226 192	W.Y. Chen et al.	(CLEO Collab.)
ALBRECHT	88	PL B207 349	H. Albrecht et al.	(ARGUS Collab.)
ANJOS	88	PRL 60 897	J.C. Anjos et al.	(FNAL E691 Collab.)
RAAB	88	PR D37 2391	J.R. Raab et al.	(FNAL E691 Collab.)
ALBRECHT	87F	PL B179 398	H. Albrecht et al.	(ARGUS Collab.)
ALBRECHT	87G	PL B195 102	H. Albrecht et al.	(ARGUS Collab.)
BECKER	87B	PL B184 277	H. Becker et al.	(NA11 and NA32 Collab.)
BLAYLOCK	87	PRL 58 2171	G.T. Blaylock et al.	(Mark III Collab.)
USHIDA	86	PRL 56 1767	N. Ushida et al.	(FNAL E531 Collab.)
ALBRECHT	85D	PL 153B 343	H. Albrecht et al.	(ARGUS Collab.)
DERRICK	85B	PRL 54 2568	M. Derrick et al.	(HRS Collab.)
AIHARA	84D	PRL 53 2465	H. Aihara et al.	(TPC Collab.)
ALTHOFF	84	PL 136B 130	M. Althoff et al.	(TASSO Collab.)
BAILEY	84	PL 139B 320	R. Bailey et al.	(ACCMOR Collab.)
CHEN	83C	PRL 51 634	A. Chen et al.	(CLEO Collab.)

OTHER RELATED PAPERS

RICHMAN	95	RMP 67 893	J.D. Richman, P.R. Burchat	(UCSB, STAN)
---------	----	------------	----------------------------	--------------



$$I(J^P) = 0(?)^?$$

J^P is natural, width and decay modes consistent with 1^- .

 $D_s^{*±}$ MASS

The fit includes $D^\pm, D^0, D_s^{*\pm}, D^{*±}, D^{*0}$, and $D_s^{*\pm}$ mass and mass difference measurements.

VALUE (MeV)	DOCUMENT ID	TECN	COMMENT
2112.3 ± 0.5 OUR FIT	Error includes scale factor of 1.1.		
2106.6 ± 2.1 ± 2.7	¹ BLAYLOCK 87	MRK3	$e^+e^- \rightarrow D_s^{*\pm}\gamma X$

¹ Assuming $D_s^{*\pm}$ mass = 1968.7 ± 0.9 MeV.

 $m_{D_s^{*±}} - m_{D_s^\pm}$

The fit includes $D^\pm, D^0, D_s^{*\pm}, D^{*±}, D^{*0}$, and $D_s^{*\pm}$ mass and mass difference measurements.

VALUE (MeV)	EVTS	DOCUMENT ID	TECN	COMMENT
143.8 ± 0.4 OUR FIT				
143.9 ± 0.4 OUR AVERAGE				
143.76 ± 0.39 ± 0.40		GRONBERG 95	CLE2	e^+e^-
144.22 ± 0.47 ± 0.37		BROWN 94	CLE2	e^+e^-
142.5 ± 0.8 ± 1.5		² ALBRECHT 88	ARG	$e^+e^- \rightarrow D_s^{*\pm}\gamma X$
139.5 ± 8.3 ± 9.7	60	AIHARA 84D	TPC	$e^+e^- \rightarrow$ hadrons
• • • We do not use the following data for averages, fits, limits, etc. • • •				
143.0 ± 18.0	8	ASRATYAN 85	HLBC	FNAL 15-ft, ν^-2H
110 ± 46		BRANDELIK 79	DASP	$e^+e^- \rightarrow D_s^{*\pm}\gamma X$

² Result includes data of ALBRECHT 84B.

 $D_s^{*±}$ WIDTH

VALUE (MeV)	CL %	DOCUMENT ID	TECN	COMMENT
< 1.9	90	GRONBERG 95	CLE2	e^+e^-
< 4.5	90	ALBRECHT 88	ARG	$E_{cm}^{ee} = 10.2$ GeV
• • • We do not use the following data for averages, fits, limits, etc. • • •				
< 4.9	90	BROWN 94	CLE2	e^+e^-
< 22	90	BLAYLOCK 87	MRK3	$e^+e^- \rightarrow D_s^{*\pm}\gamma X$

 $D_s^{*±}$ DECAY MODES

D_s^{*-} modes are charge conjugates of the modes below.

Mode	Fraction (Γ_i/Γ)
Γ_1 $D_s^+\gamma$	(94.2 ± 0.7) %
Γ_2 $D_s^+\pi^0$	(5.8 ± 0.7) %

CONSTRAINED FIT INFORMATION

An overall fit to a branching ratio uses 2 measurements and one constraint to determine 2 parameters. The overall fit has a $\chi^2 = 0.0$ for 1 degrees of freedom.

The following *off-diagonal* array elements are the correlation coefficients $\langle \delta x_i \delta x_j \rangle / (\delta x_i \delta x_j)$, in percent, from the fit to the branching fractions, $X_i \equiv \Gamma_i/\Gamma_{\text{total}}$. The fit constrains the x_i whose labels appear in this array to sum to one.

$$x_2 \begin{vmatrix} & -100 \\ & x_1 \end{vmatrix}$$

 D_s^{*+} BRANCHING RATIOS

$\Gamma(D_s^{*+}\gamma)/\Gamma_{\text{total}}$	VALUE	EVTS	DOCUMENT ID	TECN	COMMENT	Γ_1/Γ
0.942 ± 0.007 OUR FIT						
• • • We do not use the following data for averages, fits, limits, etc. • • •						
0.942 ± 0.004 ± 0.006	16k	³ AUBERT, BE	05G	BABR	10.6 $e^+e^- \rightarrow$ hadrons	
seen		ASRATYAN 91	HLBC	$\bar{\nu}_\mu$ Ne		
seen		ALBRECHT 88	ARG		$e^+e^- \rightarrow D_s^{*+}\gamma X$	
seen		AIHARA 84D				
seen		ALBRECHT 84B				
seen		BRANDELIK 79				

$\Gamma(D_s^{*+}\pi^0)/\Gamma_{\text{total}}$	VALUE	EVTS	DOCUMENT ID	TECN	COMMENT	Γ_2/Γ
• • • We do not use the following data for averages, fits, limits, etc. • • •						
0.059 ± 0.004 ± 0.006	560	³ AUBERT, BE	05G	BABR	10.6 $e^+e^- \rightarrow$ hadrons	
$\Gamma(D_s^{*+}\pi^0)/\Gamma(D_s^{*+}\gamma)$	VALUE	DOCUMENT ID	TECN	COMMENT	Γ_2/Γ_1	
0.062 ± 0.008 OUR FIT						
0.062 ± 0.008 OUR AVERAGE						
0.062 ± 0.005 ± 0.006		AUBERT, BE	05G	BABR	10.6 $e^+e^- \rightarrow$ hadrons	
0.062 ^{+0.020} _{-0.018} ± 0.022		GRONBERG 95	CLE2		e^+e^-	

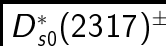
³ Derived from the ratio $\Gamma(D_s^{*+}\pi^0) / \Gamma(D_s^{*+}\gamma)$ assuming that the branching fractions of $D_s^{*+} \rightarrow D_s^+\pi^0$ and $D_s^{*+} \rightarrow D_s^+\gamma$ decays sum to 100%.

 $D_s^{*±}$ REFERENCES

AUBERT, BE	05G	PR D72 091101	B. Aubert et al.	(BABAR Collab.)
GRONBERG	95	PRL 75 3232	J. Gronberg et al.	(CLEO Collab.)
BROWN	94	PR D50 1884	D. Brown et al.	(CLEO Collab.)
ASRATYAN	91	PL B257 525	A.E. Asratyan et al.	(ITEP, BELG, SACL+)
ALBRECHT	88	PL B207 349	H. Albrecht et al.	(ARGUS Collab.)
BLAYLOCK	87	PRL 58 2171	G.T. Blaylock et al.	(Mark III Collab.)
ASRATYAN	85	PL 156B 441	A.E. Asratyan et al.	(ITEP, SERP)
AIHARA	84D	PRL 53 2465	H. Aihara et al.	(TPC Collab.)
ALBRECHT	84B	PL 146B 111	H. Albrecht et al.	(ARGUS Collab.)
BRANDELIK	79	PL 80B 412	R. Brandelik et al.	(DASP Collab.)

OTHER RELATED PAPERS

KAMAL	92	PL B284 421	A.N. Kamal, Q.P. Xu	(ALBE)
BRANDELIK	78C	PL 76B 361	R. Brandelik et al.	(DASP Collab.)
BRANDELIK	77B	PL 70B 132	R. Brandelik et al.	(DASP Collab.)



$$I(J^P) = 0(0^+)$$

J, P need confirmation.

AUBERT 06P does not observe neutral and doubly charged partners of the $D_{s0}^*(2317)^\pm$.

 $D_{s0}^*(2317)^\pm$ MASS

VALUE (MeV)	EVTS	DOCUMENT ID	TECN	COMMENT
2317.8 ± 0.6 OUR FIT				Error includes scale factor of 1.1.
2318.0 ± 1.0 OUR AVERAGE				Error includes scale factor of 1.4.
2319.6 ± 0.2 ± 1.4	3180	AUBERT	06P	BABR 10.6 $e^+e^- \rightarrow D_s^{*+}\pi^0 X$
2317.3 ± 0.4 ± 0.8	1022	¹ AUBERT	04E	BABR 10.6 e^+e^-
• • • We do not use the following data for averages, fits, limits, etc. • • •				
2317.2 ± 1.3	88	² AUBERT, B	04S	BABR $B \rightarrow D_{s0}^{(*)}(2317) + \bar{D}^{(*)}$
2317.2 ± 0.5 ± 0.9	761	³ MIKAMI	04	BELL 10.6 e^+e^-
2316.8 ± 0.4 ± 3.0	1267 ± 53	^{3,4} AUBERT	03G	BABR 10.6 e^+e^-
2317.6 ± 1.3	273 ± 33	^{3,5} AUBERT	03G	BABR 10.6 e^+e^-
2319.8 ± 2.1 ± 2.0	24	³ KROKOVNY	03B	BELL 10.6 e^+e^-

Meson Particle Listings

 $D_{s0}^*(2317)^\pm, D_{s1}(2460)^\pm$

- ¹ Supersedes AUBERT 03G.
² Systematic errors not evaluated.
³ Not independent of the corresponding $m_{D_{s0}^*(2317)} - m_{D_s}$.

- ⁴ From $D_s^+ \rightarrow K^+ K^- \pi^+$ decay.
⁵ From $D_s^+ \rightarrow K^+ K^- \pi^+ \pi^0$ decay.

 $m_{D_{s0}^*(2317)^\pm} - m_{D_s^\pm}$

VALUE (MeV)	EVTS	DOCUMENT ID	TECN	COMMENT
349.3 ± 0.6 OUR FIT	Error includes scale factor of 1.1.			
349.2 ± 0.7 OUR AVERAGE				
348.7 ± 0.5 ± 0.7	761	MIKAMI	04 BELL	10.6 e ⁺ e ⁻
350.0 ± 1.2 ± 1.0	135	BESSION	03 CLE2	10.6 e ⁺ e ⁻
351.3 ± 2.1 ± 1.9	24	⁶ KROKOVNY	03B BELL	10.6 e ⁺ e ⁻
• • • We do not use the following data for averages, fits, limits, etc. • • •				
349.6 ± 0.4 ± 3.0	1267	^{7,8} AUBERT	03G BABR	10.6 e ⁺ e ⁻
350.2 ± 1.3	273	^{9,10} AUBERT	03G BABR	10.6 e ⁺ e ⁻

- ⁶ Recalculated by us using $m_{D_s^+} = 1968.5 \pm 0.6$ MeV.
⁷ From $D_s^+ \rightarrow K^+ K^- \pi^+$ decay.
⁸ Recalculated by us using $m_{D_s^+} = 1967.20 \pm 0.03$ MeV.
⁹ From $D_s^+ \rightarrow K^+ K^- \pi^+ \pi^0$ decay.
¹⁰ Recalculated by us using $m_{D_s^+} = 1967.4 \pm 0.2$ MeV. Systematic errors not estimated.

 $D_{s0}^*(2317)^\pm$ WIDTH

VALUE (MeV)	CL%	EVTS	DOCUMENT ID	TECN	COMMENT
< 3.8	95	3180	AUBERT	06P BABR	10.6 e ⁺ e ⁻ → $D_s^+ \pi^0 X$
• • • We do not use the following data for averages, fits, limits, etc. • • •					
< 4.6	90	761	MIKAMI	04 BELL	10.6 e ⁺ e ⁻
< 10			AUBERT	03G BABR	10.6 e ⁺ e ⁻
< 7	90	135	BESSION	03 CLE2	10.6 e ⁺ e ⁻

 $D_{s0}^*(2317)^\pm$ DECAY MODES

$D_{s0}^*(2317)^-$ modes are charge conjugates of modes below.

Mode	Fraction (Γ_i/Γ)
Γ_1 $D_s^+ \pi^0$	seen
Γ_2 $D_s^+ \gamma$	
Γ_3 $D_s^{*+}(2112)^+ \gamma$	
Γ_4 $D_s^+ \gamma \gamma$	
Γ_5 $D_s^{*+}(2112)^+ \pi^0$	
Γ_6 $D_s^{*+} \pi^+ \pi^-$	
Γ_7 $D_s^+ \pi^0 \pi^0$	not seen

 $D_{s0}^*(2317)^\pm$ BRANCHING RATIOS

$\Gamma(D_s^+ \pi^0)/\Gamma_{\text{total}}$	Γ_1/Γ			
VALUE	EVTS	DOCUMENT ID	TECN	COMMENT
seen	1540 ± 62	AUBERT	03G BABR	10.6 e ⁺ e ⁻

$\Gamma(D_s^+ \gamma)/\Gamma(D_s^+ \pi^0)$	Γ_2/Γ_1			
VALUE	CL%	DOCUMENT ID	TECN	COMMENT
< 0.05	90	MIKAMI	04 BELL	10.6 e ⁺ e ⁻
• • • We do not use the following data for averages, fits, limits, etc. • • •				
< 0.14	95	AUBERT	06P BABR	10.6 e ⁺ e ⁻
< 0.052	90	BESSION	03 CLE2	10.6 e ⁺ e ⁻

$\Gamma(D_s^{*+}(2112)^+ \gamma)/\Gamma(D_s^+ \pi^0)$	Γ_3/Γ_1			
VALUE	CL%	DOCUMENT ID	TECN	COMMENT
< 0.059	90	BESSION	03 CLE2	10.6 e ⁺ e ⁻
• • • We do not use the following data for averages, fits, limits, etc. • • •				
< 0.16	95	AUBERT	06P BABR	10.6 e ⁺ e ⁻
< 0.18	90	MIKAMI	04 BELL	10.6 e ⁺ e ⁻

$\Gamma(D_s^+ \gamma \gamma)/\Gamma(D_s^+ \pi^0)$	Γ_4/Γ_1			
VALUE	CL%	DOCUMENT ID	TECN	COMMENT
< 0.18	95	AUBERT	06P BABR	10.6 e ⁺ e ⁻
• • • We do not use the following data for averages, fits, limits, etc. • • •				
not seen		AUBERT	03G BABR	10.6 e ⁺ e ⁻

$\Gamma(D_s^{*+}(2112)^+ \pi^0)/\Gamma(D_s^+ \pi^0)$	Γ_5/Γ_1			
VALUE	CL%	DOCUMENT ID	TECN	COMMENT
< 0.11	90	BESSION	03 CLE2	10.6 e ⁺ e ⁻

$\Gamma(D_s^{*+} \pi^+ \pi^-)/\Gamma(D_s^+ \pi^0)$	Γ_6/Γ_1			
VALUE	CL%	DOCUMENT ID	TECN	COMMENT
< 0.004	90	MIKAMI	04 BELL	10.6 e ⁺ e ⁻
• • • We do not use the following data for averages, fits, limits, etc. • • •				
< 0.005	95	AUBERT	06P BABR	10.6 e ⁺ e ⁻
< 0.019	90	BESSION	03 CLE2	10.6 e ⁺ e ⁻

$\Gamma(D_s^{*+} \pi^0 \pi^0)/\Gamma(D_s^+ \pi^0)$	Γ_7/Γ_1			
VALUE	CL%	DOCUMENT ID	TECN	COMMENT
< 0.25	95	AUBERT	06P BABR	10.6 e ⁺ e ⁻

 $D_{s0}^*(2317)^\pm$ REFERENCES

AUBERT	06P	PR D74 032007	B. Aubert et al.	(BABAR Collab.)
AUBERT	04E	PR D69 031101R	B. Aubert et al.	(BABAR Collab.)
AUBERT,B	04S	PRL 93 181801	B. Aubert et al.	(BABAR Collab.)
MIKAMI	04	PRL 92 012002	Y. Mikami et al.	(BELLE Collab.)
AUBERT	03G	PRL 90 242001	B. Aubert et al.	(BaBar Collab.)
BESSION	03	PR D68 032002	D. Besson et al.	(CLEO Collab.)
KROKOVNY	03B	PRL 91 262002	P. Krokovny et al.	(BELLE Collab.)

OTHER RELATED PAPERS

FAESSLER	07	PR D76 014003	A. Faessler et al.	
FAESSLER	07A	PR D76 014005	A. Faessler et al.	
FLYNN	07	PR D75 074024	J.M. Flynn, J. Nieves	
LAKHINA	07	PL B650 159	O. Lakhina, E. Swanson	
LI	07	EPJ C51 359	D.M. Li et al.	
WANG	07	PR D75 034013	Z.-G. Wang	
COLANGELO	06	PL B642 48	P. Colangelo et al.	
DMITRASINO...	06	MPL A21 533	V. Dmitrasinovic	
NIELSEN	06	PL B634 35	M. Nielsen	
SWANSON	06	PRPL 429 243	E.S. Swanson	(PITT)
VANBEVEREN	06A	PR D74 037501	E. van Beveren et al.	
VANBEVEREN	06B	PRL 97 202001	E. van Beveren, G. Rupp	
VIJANDJE	06	PR D73 034002	J. Vijandje, F. Fernandez, A. Valcarce	
WANG	06	PR D73 094020	Z.-G. Wang, S.-L. Wan	
WEI	06	PR D73 034004	W. Wei, P.-Z. Huang, S.-L. Zhu	
BICUDO	05	NP A748 537	P. Bicudo	
BRACCO	05	PL B624 217	M.E. Bracco, A. Loza, R.D. Matheus	
CLOSE	05C	PR D72 094004	F.E. Close, E.S. Swanson	(OXFTF)
COLANGELO	05	PR D72 074004	P. Colangelo, F. De Fazio, A. Ozpineci	
DMITRASINO...	05	PRL 94 162002	V. Dmitrasinovic	
GODFREY	05	PR D72 054029	S. Godfrey	
KIM	05A	PR D72 074012	H. Kim, Y. Oh	
MAIANI	05	PR D71 014028	L. Maiani et al.	
ZHANG	05C	PR D72 017902	A. Zhang	
BROWDER	04	PL B578 365	T.E. Browder, S. Pakvasa, A.A. Petrov	
CHEN	04A	PR D69 054002	C.-H. Chen	
CHEN	04C	PRL 93 232001	Y.-Q. Chen, X.-Q. Li	
COHEN	04	PL B578 359	T.D. Cohen et al.	
DMITRASINO...	04	PR D70 096011	V. Dmitrasinovic	
FAYYAZUDDIN	04	PR D69 114008	Fayyazuddin, Riazuddin	
HWANG	04	PL B601 137	D.S. Hwang, D.-W. Kim	
KOLOMEITSEV	04	PL B582 39	E.E. Kolomeitsev, M.F.M. Lutz	
LIPKIN	04	PL B580 50	H.J. Lipkin	
SADZIKOWSKI	04	PL B579 39	M. Satzlikowski	
SIMONOV	04	PR D70 114013	Yu.A. Simonov, J.A. Tjon	
VANBEVEREN	04	MPL A19 1949	E. van Beveren, G. Rupp	
BALI	03	PR D68 071501	G.S. Bali	
BARDEEN	03	PR D68 054024	W.A. Bardeen et al.	
BARNES	03	PR D68 054006	T. Barnes et al.	
CAHN	03	PR D68 037502	R.N. Cahn, J.D. Jackson	
CHENG	03C	PL B566 193	H.-Y. Cheng, W.-S. Hou	
COLANGELO	03B	PL B570 180	P. Colangelo, F. De Fazio	
DATTA	03C	PL B572 164	A. Datta, P.J. O'Donnell	
SZCZEPANIAK	03	PL B567 23	A.P. Szczepaniak	
TERASAKI	03	PR D68 011501	K. Terasaki	
VANBEVEREN	03	PRL 91 012003	E. van Beveren, G. Rupp	

 $D_{s1}(2460)^\pm$

$$I(J^P) = 0(1^+)$$

 $D_{s1}(2460)^\pm$ MASS

VALUE (MeV)	EVTS	DOCUMENT ID	TECN	COMMENT
2459.6 ± 0.6 OUR FIT	Error includes scale factor of 1.1.			
2459.6 ± 0.9 OUR AVERAGE	Error includes scale factor of 1.3.			
2460.1 ± 0.2 ± 0.8		¹ AUBERT	06P BABR	10.6 e ⁺ e ⁻
2458.0 ± 1.0 ± 1.0	195	AUBERT	04E BABR	10.6 e ⁺ e ⁻
• • • We do not use the following data for averages, fits, limits, etc. • • •				
2459.5 ± 1.2 ± 3.7	920	AUBERT	06P BABR	10.6 e ⁺ e ⁻ → $D_s^+ \gamma X$
2458.6 ± 1.0 ± 2.5	560	AUBERT	06P BABR	10.6 e ⁺ e ⁻ → $D_s^+ \pi^0 \gamma X$
2460.2 ± 0.2 ± 0.8	123	AUBERT	06P BABR	10.6 e ⁺ e ⁻ → $D_s^+ \pi^+ \pi^- X$
2458.9 ± 1.5	112	² AUBERT,B	04S BABR	$B \rightarrow D_{s1}(2460) + \overline{D}^{(*)}$
2461.1 ± 1.6	139	³ AUBERT,B	04S BABR	$B \rightarrow D_{s1}(2460) + \overline{D}^{(*)}$
2456.5 ± 1.3 ± 1.3	126	^{4,5} MIKAMI	04 BELL	10.6 e ⁺ e ⁻
2459.5 ± 1.3 ± 2.0	152	^{6,7} MIKAMI	04 BELL	10.6 e ⁺ e ⁻
2459.9 ± 0.9 ± 1.6	60	^{6,7} MIKAMI	04 BELL	10.6 e ⁺ e ⁻
2459.2 ± 1.6 ± 2.0	57	KROKOVNY	03B BELL	10.6 e ⁺ e ⁻

- ¹ The average of the values obtained from the $D_s^+ \pi^0, D_s^+ \pi^0 \gamma, D_s^+ \pi^+ \pi^-$ final state.
² Systematic errors not evaluated. From the decay to $D_s^{*+} \pi^0$.
³ Systematic errors not evaluated. From the decay to $D_s^+ \gamma$.
⁴ Not independent of the corresponding $m_{D_{s1}(2460)^\pm} - m_{D_s^\pm}$.
⁵ Using $m_{D_{s^{++}}} = 2112.4 \pm 0.7$ MeV.

⁶ Not independent of the corresponding $m_{D_{s1}(2460)^{\pm}} - m_{D_s^{\pm}}$.

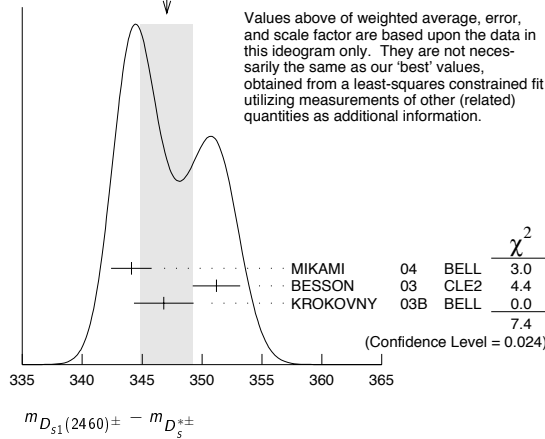
⁷ Using $m_{D_s^+} = 1968.5 \pm 0.6$ MeV.

 $m_{D_{s1}(2460)^{\pm}} - m_{D_s^{\pm}}$

VALUE (MeV)	EVTs	DOCUMENT ID	TECN	COMMENT
347.2 ± 0.8 OUR FIT				Error includes scale factor of 1.2.
347.1 ± 2.2 OUR AVERAGE				Error includes scale factor of 1.9. See the ideogram below.
344.1 ± 1.3 ± 1.1	126	MIKAMI	04 BELL	10.6 e ⁺ e ⁻
351.2 ± 1.7 ± 1.0	41	BESSON	03 CLE2	10.6 e ⁺ e ⁻
346.8 ± 1.6 ± 1.9	57	⁸ KROKOVNY	03B BELL	10.6 e ⁺ e ⁻

⁸ Recalculated by us using $m_{D_s^{*+}} = 2112.4 \pm 0.7$ MeV.

WEIGHTED AVERAGE
347.1 ± 2.2 (Error scaled by 1.9)

 $m_{D_{s1}(2460)^{\pm}} - m_{D_s^{\pm}}$

VALUE (MeV)	EVTs	DOCUMENT ID	TECN	COMMENT
491.1 ± 0.7 OUR FIT				Error includes scale factor of 1.1.
491.3 ± 1.4 OUR AVERAGE				
491.0 ± 1.3 ± 1.9	152	⁹ MIKAMI	04 BELL	10.6 e ⁺ e ⁻
491.4 ± 0.9 ± 1.5	60	¹⁰ MIKAMI	04 BELL	10.6 e ⁺ e ⁻

⁹ From the decay to $D_s^{\pm} \gamma$.

¹⁰ From the decay to $D_s^{\pm} \pi^+ \pi^-$.

 $D_{s1}(2460)^{\pm}$ WIDTH

VALUE (MeV)	CL%	EVTs	DOCUMENT ID	TECN	COMMENT
< 3.5	95	123	AUBERT	06P BABR	10.6 e ⁺ e ⁻ → $D_s^+ \pi^+ \pi^- X$
• • • We do not use the following data for averages, fits, limits, etc. • • •					
< 6.3	95	560	AUBERT	06P BABR	10.6 e ⁺ e ⁻ → $D_s^+ \pi^0 \gamma X$
< 10		195	AUBERT	04E BABR	10.6 e ⁺ e ⁻
< 5.5	90	126	MIKAMI	04 BELL	10.6 e ⁺ e ⁻
< 7	90	41	BESSON	03 CLE2	10.6 e ⁺ e ⁻

 $D_{s1}(2460)^+$ DECAY MODES

$D_{s1}(2460)^-$ modes are charge conjugates of the modes below.

Mode	Fraction (Γ_i/Γ)	Scale factor/ Confidence level
Γ_1 $D_s^{*+} \pi^0$	(48 ± 11) %	
Γ_2 $D_s^+ \gamma$	(18 ± 4) %	
Γ_3 $D_s^+ \pi^+ \pi^-$	(4.3 ± 1.3) %	S=1.1
Γ_4 $D_s^{*+} \gamma$	< 8 %	CL=90%
Γ_5 $D_{s0}^*(2317)^+ \gamma$	(3.7 ^{+5.1} _{-2.4}) %	
Γ_6 $D_s^+ \pi^0$		
Γ_7 $D_s^+ \pi^0 \pi^0$		
Γ_8 $D_s^+ \gamma \gamma$		

CONSTRAINED FIT INFORMATION

An overall fit to 7 branching ratios uses 8 measurements and one constraint to determine 5 parameters. The overall fit has a $\chi^2 = 3.4$ for 4 degrees of freedom.

The following *off-diagonal* array elements are the correlation coefficients $\langle \delta x_i \delta x_j \rangle / (\delta x_i \delta x_j)$, in percent, from the fit to the branching fractions, $x_i \equiv \Gamma_i/\Gamma_{\text{total}}$. The fit constrains the x_i whose labels appear in this array to sum to one.

x_2	80		
x_3	68	62	
x_5	-3	25	26
	x_1	x_2	x_3

 $D_{s1}(2460)^{\pm}$ BRANCHING RATIOS

$\Gamma(D_s^{*+} \pi^0)/\Gamma_{\text{total}}$	EVTs	DOCUMENT ID	TECN	COMMENT	Γ_1/Γ
--	------	-------------	------	---------	-------------------

0.48 ± 0.11 OUR FIT

0.56 ± 0.13 ± 0.09

¹¹ AUBERT 06N BABR $B \rightarrow D_{s1}(2460)^- \bar{D}^{(*)}$

• • • We do not use the following data for averages, fits, limits, etc. • • •

41 BESSON 03 CLE2 10.6 e⁺ e⁻

¹¹ Evaluated in AUBERT 06N including measurements from AUBERT,B 04s.

$\Gamma(D_s^+ \gamma)/\Gamma_{\text{total}}$

VALUE	DOCUMENT ID	TECN	COMMENT	Γ_2/Γ
-------	-------------	------	---------	-------------------

0.18 ± 0.04 OUR FIT

0.16 ± 0.04 ± 0.03

¹² AUBERT 06N BABR $B \rightarrow D_{s1}(2460)^0 \bar{D}^{(*)}$

¹² Evaluated in AUBERT 06N including measurements from AUBERT,B 04s.

$\Gamma(D_s^+ \gamma)/\Gamma(D_s^{*+} \pi^0)$

VALUE	CL%	EVTs	DOCUMENT ID	TECN	COMMENT	Γ_2/Γ_1
-------	-----	------	-------------	------	---------	---------------------

0.38 ± 0.05 OUR FIT

0.44 ± 0.09 OUR AVERAGE

0.55 ± 0.13 ± 0.08 152 MIKAMI 04 BELL 10.6 e⁺ e⁻

0.38 ± 0.11 ± 0.04 38 KROKOVNY 03B BELL 10.6 e⁺ e⁻

• • • We do not use the following data for averages, fits, limits, etc. • • •

0.274 ± 0.045 ± 0.020 251 ¹³ AUBERT,B 04s BABR $B \rightarrow D_{s1}(2460)^+ \bar{D}^{(*)}$

< 0.49 90 BESSON 03 CLE2 10.6 e⁺ e⁻

¹³ Used by AUBERT 06N in their measurement of $B(D_s^{*-} \pi^0)$ and $B(D_s^- \gamma)$.

$\Gamma(D_s^+ \pi^+ \pi^-)/\Gamma(D_s^{*+} \pi^0)$

VALUE	CL%	EVTs	DOCUMENT ID	TECN	COMMENT	Γ_3/Γ_1
-------	-----	------	-------------	------	---------	---------------------

0.090 ± 0.020 OUR FIT Error includes scale factor of 1.2.

0.14 ± 0.04 ± 0.02

60 MIKAMI 04 BELL 10.6 e⁺ e⁻

• • • We do not use the following data for averages, fits, limits, etc. • • •

< 0.08 90 BESSON 03 CLE2 10.6 e⁺ e⁻

$\Gamma(D_s^{*+} \gamma)/\Gamma(D_s^{*+} \pi^0)$

VALUE	CL%	DOCUMENT ID	TECN	COMMENT	Γ_4/Γ_1
-------	-----	-------------	------	---------	---------------------

< 0.16

90 BESSON 03 CLE2 10.6 e⁺ e⁻

• • • We do not use the following data for averages, fits, limits, etc. • • •

< 0.31 90 MIKAMI 04 BELL 10.6 e⁺ e⁻

$\Gamma(D_{s0}^*(2317)^+ \gamma)/\Gamma(D_s^{*+} \pi^0)$

VALUE	CL%	DOCUMENT ID	TECN	COMMENT	Γ_5/Γ_1
-------	-----	-------------	------	---------	---------------------

< 0.22

95 AUBERT 04E BABR 10.6 e⁺ e⁻

• • • We do not use the following data for averages, fits, limits, etc. • • •

< 0.58 90 BESSON 03 CLE2 10.6 e⁺ e⁻

$\Gamma(D_s^{*+} \pi^0)/[\Gamma(D_s^{*+} \pi^0) + \Gamma(D_{s0}^*(2317)^+ \gamma)]$

VALUE	DOCUMENT ID	TECN	COMMENT	$\Gamma_1/(\Gamma_1 + \Gamma_5)$
-------	-------------	------	---------	----------------------------------

0.93 ± 0.09 OUR FIT

0.97 ± 0.09 ± 0.05

AUBERT 06P BABR 10.6 e⁺ e⁻

$\Gamma(D_s^+ \gamma)/[\Gamma(D_s^{*+} \pi^0) + \Gamma(D_{s0}^*(2317)^+ \gamma)]$

VALUE	DOCUMENT ID	TECN	COMMENT	$\Gamma_2/(\Gamma_1 + \Gamma_5)$
-------	-------------	------	---------	----------------------------------

0.35 ± 0.04 OUR FIT

0.337 ± 0.036 ± 0.038

AUBERT 06P BABR 10.6 e⁺ e⁻

$\Gamma(D_s^+ \pi^+ \pi^-)/[\Gamma(D_s^{*+} \pi^0) + \Gamma(D_{s0}^*(2317)^+ \gamma)]$

VALUE	DOCUMENT ID	TECN	COMMENT	$\Gamma_3/(\Gamma_1 + \Gamma_5)$
-------	-------------	------	---------	----------------------------------

0.083 ± 0.017 OUR FIT Error includes scale factor of 1.2.

0.077 ± 0.013 ± 0.008

AUBERT 06P BABR 10.6 e⁺ e⁻

$\Gamma(D_s^{*+} \gamma)/[\Gamma(D_s^{*+} \pi^0) + \Gamma(D_{s0}^*(2317)^+ \gamma)]$

VALUE	CL%	DOCUMENT ID	TECN	COMMENT	$\Gamma_4/(\Gamma_1 + \Gamma_5)$
-------	-----	-------------	------	---------	----------------------------------

< 0.24

95 AUBERT 06P BABR 10.6 e⁺ e⁻

Meson Particle Listings

 $D_{s1}(2460)^\pm, D_{s1}(2536)^\pm$

$\Gamma(D_{s0}^*(2317)^+\gamma)/[\Gamma(D_{s0}^*(2317)^+\gamma) + \Gamma(D_{s0}^*(2317)^+\gamma)]$					$\Gamma_5/(\Gamma_1+\Gamma_5)$
VALUE	CL%	DOCUMENT ID	TECN	COMMENT	
<0.25	95	AUBERT	06P	BABR	$10.6 e^+ e^-$

$\Gamma(D_s^+ \pi^0)/[\Gamma(D_s^+ \pi^0) + \Gamma(D_{s0}^*(2317)^+\gamma)]$					$\Gamma_6/(\Gamma_1+\Gamma_5)$
VALUE	CL%	DOCUMENT ID	TECN	COMMENT	
<0.042	95	AUBERT	06P	BABR	$10.6 e^+ e^-$

$\Gamma(D_s^+ \pi^0 \pi^0)/[\Gamma(D_s^+ \pi^0) + \Gamma(D_{s0}^*(2317)^+\gamma)]$					$\Gamma_7/(\Gamma_1+\Gamma_5)$
VALUE	CL%	DOCUMENT ID	TECN	COMMENT	
<0.68	95	AUBERT	06P	BABR	$10.6 e^+ e^-$

$\Gamma(D_s^+ \gamma\gamma)/[\Gamma(D_s^+ \pi^0) + \Gamma(D_{s0}^*(2317)^+\gamma)]$					$\Gamma_8/(\Gamma_1+\Gamma_5)$
VALUE	CL%	DOCUMENT ID	TECN	COMMENT	
<0.33	95	AUBERT	06P	BABR	$10.6 e^+ e^-$

 $D_{s1}(2460)^\pm$ REFERENCES

AUBERT	06N	PR D74 031103R	B. Aubert et al.	(BABAR Collab.)
AUBERT	06P	PR D74 032007	B. Aubert et al.	(BABAR Collab.)
AUBERT	04E	PR D69 031101R	B. Aubert et al.	(BABAR Collab.)
AUBERT.B	04S	PRL 93 181801	B. Aubert et al.	(BABAR Collab.)
MIKAMI	04	PRL 92 012002	Y. Mikami et al.	(BELLE Collab.)
BESSON	03	PR D68 032002	A. Besson et al.	(CLEO Collab.)
KROKOVNY	03B	PRL 91 262002	P. Krokovny et al.	(BELLE Collab.)

OTHER RELATED PAPERS

FAESSLER	07	PR D76 014003	A. Faessler et al.	
FAESSLER	07B	PR D76 114008	A. Faessler et al.	
GUO	07	PL B647 133	F.-K. Guo et al.	
WANG	07	PR D75 034013	Z.-G. Wang	
COLANGELO	06	PL B642 48	P. Colangelo et al.	
SWANSON	06	PRPL 429 243	E.S. Swanson	(PITT)
VIJANDE	06	PR D73 034002	J. Vijande, F. Fernandez, A. Valcaro	
WEI	06	PR D73 034004	W. Wei, P.-Z. Huang, S.-L. Zhu	
BICUDO	05	NP A748 537	P. Bicudo	
CLOSE	05C	PR D72 094004	F.E. Close, E.S. Swanson	(OXFPT)
COLANGELO	05	PR D72 074004	P. Colangelo, F. De Fazio, A. Ozpineci	
GODFREY	05	PR D72 054029	S. Godfrey	
MAIANI	05	PR D71 014028	L. Maiani et al.	
YAMADA	05	PR C72 065202	Y. Yamada et al.	
ZHANG	05C	PR D72 017902	A. Zhang	
BROWDER	04	PL B578 365	T.E. Browder, S. Pakvasa, A.A. Petrov	
CHEN	04A	PR D69 054002	C.-H. Chen	
CHEN	04C	PRL 93 232001	Y.-Q. Chen, X.-Q. Li	
COHEN	04	PL B576 359	T.D. Cohen et al.	
DMITRASINOV	04	PR D70 096011	V. Dmitrasinovic	
FAYYAZUDDIN	04	PR D69 114008	Fayyazuddin, Riazuddin	
KOLOMEITSEV	04	PL B582 39	E.E. Kolomeitsev, M.F.M. Lutz	
SADZIKOWSKI	04	PL B579 39	M. Sadzikowski	
VANBEVEREN	04B	EPJ C32 493	E. van Beveren, G. Rupp	
AUBERT	03G	PRL 90 242001	B. Aubert et al.	(BaBar Collab.)
BARDEEN	03	PR D68 054024	W.A. Bardeen et al.	
BARNES	03	PR D68 054006	T. Barnes et al.	
CAHN	03	PR D68 037502	R.N. Cahn, J.D. Jackson	
COLANGELO	03B	PL B570 180	P. Colangelo, F. De Fazio	
DATTA	03C	PL B572 164	A. Datta, P.J. O'Donnell	

 $D_{s1}(2536)^\pm$

$$J(J^P) = 0(1^+)$$

 J, P need confirmation.

Seen in $D^*(2010)^+ K^0$, $D^*(2007)^0 K^+$, and $D_s^+ \pi^+ \pi^-$. Not seen in $D^+ K^0$ or $D^0 K^+$. $J^P = 1^+$ assignment strongly favored.

 $D_{s1}(2536)^\pm$ MASS

VALUE (MeV)	EVTS	DOCUMENT ID	TECN	COMMENT
2535.35 ± 0.34 ± 0.5	OUR EVALUATION			
2535.12 ± 0.25	OUR AVERAGE			
2534.78 ± 0.31 ± 0.40	182	AUBERT	08B	BABR $B \rightarrow \bar{D}^{(*)} D^* K$
2534.6 ± 0.3 ± 0.7	193	AUBERT	06P	BABR $10.6 e^+ e^- \rightarrow D_s^+ \pi^+ \pi^- X$
2535.3 ± 0.7	92	¹ HEISTER	02B	ALEP $e^+ e^- \rightarrow D^{*+} K^0 X, D^{*0} K^+ X$
2534.2 ± 1.2	9	ASRATYAN	94	BEBC $\nu N \rightarrow D^* K^0 X, D^{*0} K^\pm X$
2535 ± 0.6 ± 1	75	FRABETTI	94B	E687 $\gamma Be \rightarrow D^{*+} K^0 X, D^{*0} K^+ X$
2535.3 ± 0.2 ± 0.5	134	ALEXANDER	93	CLE2 $e^+ e^- \rightarrow D^{*0} K^+ X$
2534.8 ± 0.6 ± 0.6	44	ALEXANDER	93	CLE2 $e^+ e^- \rightarrow D^{*+} K^0 X$
2535.2 ± 0.5 ± 1.5	28	ALBRECHT	92R	ARG $10.4 e^+ e^- \rightarrow D^{*0} K^+ X$
2536.6 ± 0.7 ± 0.4		AVERY	90	CLEO $e^+ e^- \rightarrow D^{*+} K^0 X$
2535.9 ± 0.6 ± 2.0		ALBRECHT	89E	ARG $D_{s1}^* \rightarrow D^*(2010) K^0$

• • • We do not use the following data for averages, fits, limits, etc. • • •

2535 ± 28 ² ASRATYAN 88 HLBC $\nu N \rightarrow D_s \gamma \gamma X$

¹ Calculated using $m_{D^*(2010)^\pm} = 2010.0 \pm 0.5$ MeV, $m_{D^*(2007)^0} = 2006.7 \pm 0.5$ MeV, and the mass difference below.

² Not seen in $D^* K$.

 $m_{D_{s1}(2536)^\pm} - m_{D_s^*(2111)}$

VALUE (MeV)	DOCUMENT ID	TECN	COMMENT
424 ± 28	ASRATYAN 88	HLBC	$D_s^{*\pm} \gamma$

 $m_{D_{s1}(2536)^\pm} - m_{D^*(2010)^\pm}$

VALUE (MeV)	EVTS	DOCUMENT ID	TECN	COMMENT
525.3 ± 0.6 ± 0.1	41	HEISTER	02B	ALEP $e^+ e^- \rightarrow D^{*+} K^0 X$

 $m_{D_{s1}(2536)^\pm} - m_{D^*(2007)^0}$

VALUE (MeV)	EVTS	DOCUMENT ID	TECN	COMMENT
528.1 ± 1.5	OUR AVERAGE			
528.7 ± 1.9 ± 0.5	51	HEISTER	02B	ALEP $e^+ e^- \rightarrow D^{*0} K^+ X$
527.3 ± 2.2	29	ACKERSTAFF	97W	OPAL $e^+ e^- \rightarrow D^{*0} K^+ X$

 $D_{s1}(2536)^\pm$ WIDTH

VALUE (MeV)	CL%	EVTS	DOCUMENT ID	TECN	COMMENT
<2.3	90		ALEXANDER 93	CLEO	$e^+ e^- \rightarrow D^{*0} K^+ X$
• • • We do not use the following data for averages, fits, limits, etc. • • •					
<2.5	95	193	AUBERT	06P	BABR $10.6 e^+ e^- \rightarrow D_s^+ \pi^+ \pi^- X$
<3.2	90	75	FRABETTI	94B	E687 $\gamma Be \rightarrow D^{*+} K^0 X, D^{*0} K^+ X$
<3.9	90		ALBRECHT 92R	ARG	$10.4 e^+ e^- \rightarrow D^{*0} K^+ X$
<5.44	90		AVERY	90	CLEO $e^+ e^- \rightarrow D^{*+} K^0 X$
<4.6	90		ALBRECHT 89E	ARG	$D_{s1}^* \rightarrow D^*(2010) K^0$

 $D_{s1}(2536)^+$ DECAY MODES

$D_{s1}(2536)^-$ modes are charge conjugates of the modes below.

Mode	Fraction (Γ_i/Γ)
Γ_1 $D^*(2010)^+ K^0$	seen
Γ_2 $(D^*(2010)^+ K^0)_{S\text{-wave}}$	
Γ_3 $(D^*(2010)^+ K^0)_{D\text{-wave}}$	
Γ_4 $D^+ \pi^- K^+$	
Γ_5 $D^*(2007)^0 K^+$	seen
Γ_6 $D^+ K^0$	not seen
Γ_7 $D^0 K^+$	not seen
Γ_8 $D_s^{*+} \gamma$	possibly seen
Γ_9 $D_s^+ \pi^+ \pi^-$	seen

 $D_{s1}(2536)^+$ BRANCHING RATIOS

$\Gamma(D^*(2007)^0 K^+)/\Gamma(D^*(2010)^+ K^0)$					Γ_5/Γ_1
VALUE	EVTS	DOCUMENT ID	TECN	COMMENT	
1.27 ± 0.21	OUR AVERAGE				
1.32 ± 0.47 ± 0.23	92	³ HEISTER	02B	ALEP $e^+ e^- \rightarrow D^{*+} K^0 X, D^{*0} K^+ X$	
1.9 $^{+1.1}_{-0.9}$ ± 0.4	35	³ ACKERSTAFF	97W	OPAL $e^+ e^- \rightarrow D^{*0} K^+ X, D^{*+} K^0 X$	
1.1 ± 0.3		ALEXANDER 93	CLEO	$e^+ e^- \rightarrow D^{*0} K^+ X, D^{*+} K^0 X$	
1.4 ± 0.3 ± 0.2		⁴ ALBRECHT 92R	ARG	$10.4 e^+ e^- \rightarrow D^{*0} K^+ X, D^{*+} K^0 X$	

³ Ratio of the production rates measured in Z^0 decays.

⁴ Evaluated by us from published inclusive cross-sections.

$\Gamma((D^*(2010)^+ K^0)_{S\text{-wave}})/\Gamma(D^*(2010)^+ K^0)$					Γ_2/Γ_1
VALUE	EVTS	DOCUMENT ID	TECN	COMMENT	
0.72 ± 0.05 ± 0.01	5485	BALAGURA 08	BELL	$10.6 e^+ e^- \rightarrow D^{*+} K^0 X$	

$\Gamma(D^+ \pi^- K^+)/\Gamma(D^*(2010)^+ K^0)$					Γ_4/Γ_1
VALUE (units 10^{-2})	EVTS	DOCUMENT ID	TECN	COMMENT	
3.27 ± 0.18 ± 0.37	1264	BALAGURA 08	BELL	$10.6 e^+ e^- \rightarrow D^+ \pi^- K^+ X$	

$\Gamma(D^+ K^0)/\Gamma(D^*(2010)^+ K^0)$					Γ_6/Γ_1
VALUE	CL%	DOCUMENT ID	TECN	COMMENT	
<0.40	90	ALEXANDER 93	CLEO	$e^+ e^- \rightarrow D^{*+} K^0 X$	
<0.43	90	ALBRECHT 89E	ARG	$D_{s1}^* \rightarrow D^*(2010) K^0$	

$\Gamma(D^0 K^+)/\Gamma(D^*(2007)^0 K^+)$					Γ_7/Γ_5
VALUE	CL%	DOCUMENT ID	TECN	COMMENT	
<0.12	90	ALEXANDER 93	CLEO	$e^+ e^- \rightarrow D^{*0} K^+ X$	

$\Gamma(D_s^{*+} \gamma)/\Gamma_{\text{total}}$					Γ_8/Γ
VALUE	DOCUMENT ID	TECN	COMMENT		
possibly seen	ASRATYAN 88	HLBC	$\nu N \rightarrow D_s \gamma \gamma X$		

See key on page 373

Meson Particle Listings

$D_{s1}(2536)^\pm, D_{s2}(2573)^\pm$

$\Gamma(D_s^{*\pm}\gamma)/\Gamma(D^*(2007)^0 K^+)$					Γ_9/Γ_5
VALUE	CL%	DOCUMENT ID	TECN	COMMENT	
<0.42	90	ALEXANDER	93	CLEO	$e^+e^- \rightarrow D^{*0} K^+ X$

$\Gamma(D_s^+ \pi^+ \pi^-)/\Gamma_{total}$					Γ_9/Γ
VALUE	DOCUMENT ID	TECN	COMMENT		
seen	AUBERT	06P	BABR	10.6	$e^+e^- \rightarrow D_s^\pm \pi^+ \pi^- X$

$D_{s1}(2536)^\pm$ REFERENCES

AUBERT	06B	PR D77 011102R	B. Aubert et al.	(BABAR Collab.)
BALAGURA	08	PR D77 032001	V. Balagura et al.	(BELLE Collab.)
AUBERT	06P	PR D74 032007	B. Aubert et al.	(BABAR Collab.)
HEISTER	02B	PL B526 34	A. Heister et al.	(ALEPH Collab.)
ACKERSTAFF	97W	ZPHY C76 425	K. Ackerstaff et al.	(OPAL Collab.)
ASRATYAN	94	ZPHY C61 563	A.E. Asratyan et al.	(BIRM, BELG, CERN+)
FRABETTI	94B	PRL 72 324	P.L. Frabetti et al.	(FNAL E687 Collab.)
ALEXANDER	93	PL B303 377	J. Alexander et al.	(CLEO Collab.)
ALBRECHT	92R	PL B297 425	H. Albrecht et al.	(ARGUS Collab.)
AVERY	90	PR D41 774	P. Avery, D. Besson	(CLEO Collab.)
ALBRECHT	89E	PL B230 162	H. Albrecht et al.	(ARGUS Collab.)
ASRATYAN	88	ZPHY C40 483	A.E. Asratyan et al.	(ITEP, SERP)

OTHER RELATED PAPERS

COLANGELO	06	PL B642 48	P. Colangelo et al.	
VIJANDE	06	PR D73 034002	J. Vijande, F. Fernandez, A. Valcaro	
CLOSE	05C	PR D72 094004	F.E. Close, E.S. Swanson	(OXFTP)
YAMADA	05	PR C72 065202	Y. Yamada et al.	
SEMENOV	99	SPU 42 847	S.V. Semenov	

Translated from UFN 42 937.

$D_{s2}(2573)^\pm$

$I(J^P) = 0(?)^2$

J^P is natural, width and decay modes consistent with 2^+ .

$D_{s2}(2573)^\pm$ MASS

VALUE (MeV)	EVTS	DOCUMENT ID	TECN	CHG	COMMENT
2572.6 ± 0.9 OUR AVERAGE					
2572.2 ± 0.3 ± 1.0		AUBERT,BE	06E	BABR	$e^+e^- \rightarrow D K X$
2574.5 ± 3.3 ± 1.6		ALBRECHT	96	ARG	$e^+e^- \rightarrow D^0 K^+ X$
2573.2 ^{+1.7} _{-1.6} ± 0.9	217	KUBOTA	94	CLE2	+ $e^+e^- \sim 10.5$ GeV

- • • We do not use the following data for averages, fits, limits, etc. • • •
| 2570.0 ± 4.3 | 25 | ¹EVDOKIMOV | 04 | SELX | 600 $\Sigma^- A \rightarrow D^0 K^+ X$ |
| 2568.6 ± 3.2 | 64 | ²HEISTER | 02b | ALEP | $e^+e^- \rightarrow D^0 K^+ X$ |

¹ Not independent of the mass difference below.
² Calculated using $m_{D^0} = 1864.5 \pm 0.5$ MeV and the mass difference below.

$m_{D_{s2}(2573)^\pm} - m_{D^0}$

VALUE (MeV)	EVTS	DOCUMENT ID	TECN	COMMENT
704 ± 3 ± 1	64	HEISTER	02b	ALEP $e^+e^- \rightarrow D^0 K^+ X$
• • • We do not use the following data for averages, fits, limits, etc. • • •				
705.4 ± 4.3	25	³ EVDOKIMOV	04	SELX 600 $\Sigma^- A \rightarrow D^0 K^+ X$

³ Systematic errors not estimated.

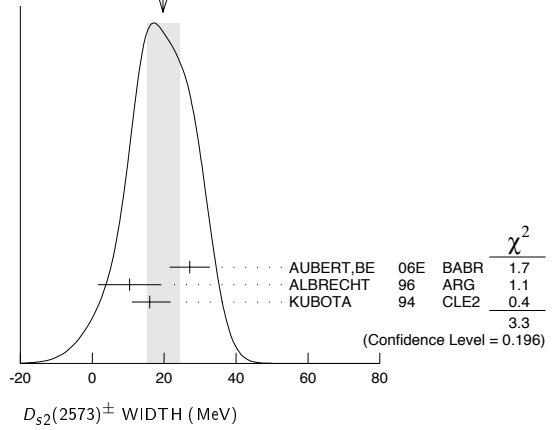
$D_{s2}(2573)^\pm$ WIDTH

VALUE (MeV)	EVTS	DOCUMENT ID	TECN	CHG	COMMENT
20 ± 5 OUR AVERAGE					Error includes scale factor of 1.3. See the ideogram below.
27.1 ± 0.6 ± 5.6		AUBERT,BE	06E	BABR	$e^+e^- \rightarrow D K X$
10.4 ± 8.3 ± 3.0		ALBRECHT	96	ARG	$e^+e^- \rightarrow D^0 K^+ X$
16 ⁺⁵ ₋₄ ± 3	217	KUBOTA	94	CLE2	+ $e^+e^- \sim 10.5$ GeV

- • • We do not use the following data for averages, fits, limits, etc. • • •
| 14⁺⁹₋₆ | 25 | ⁴EVDOKIMOV | 04 | SELX | 600 $\Sigma^- A \rightarrow D^0 K^+ X$ |

⁴ Systematic errors not estimated.

WEIGHTED AVERAGE
20 ± 5 (Error scaled by 1.3)



$D_{s2}(2573)^\pm$ DECAY MODES

$D_{s2}(2573)^-$ modes are charge conjugates of the modes below.

Mode	Fraction (Γ_i/Γ)
Γ_1 $D^0 K^+$	seen
Γ_2 $D^*(2007)^0 K^+$	not seen

$D_{s2}(2573)^\pm$ BRANCHING RATIOS

$\Gamma(D^0 K^+)/\Gamma_{total}$						Γ_1/Γ
VALUE	EVTS	DOCUMENT ID	TECN	CHG	COMMENT	
seen	217	KUBOTA	94	CLE2	\pm $e^+e^- \sim 10.5$ GeV	

$\Gamma(D^*(2007)^0 K^+)/\Gamma(D^0 K^+)$						Γ_2/Γ_1
VALUE	CL%	DOCUMENT ID	TECN	CHG	COMMENT	
<0.33	90	KUBOTA	94	CLE2	+ $e^+e^- \sim 10.5$ GeV	

$D_{s2}(2573)^\pm$ REFERENCES

AUBERT,BE	06E	PRL 97 222001	B. Aubert et al.	(BABAR Collab.)
EVDOKIMOV	04	PRL 93 242001	A.V. Evdokimov et al.	(SLEX Collab.)
HEISTER	02B	PL B526 34	A. Heister et al.	(ALEPH Collab.)
ALBRECHT	96	ZPHY C69 405	H. Albrecht et al.	(ARGUS Collab.)
KUBOTA	94	PRL 72 1972	Y. Kubota et al.	(CLEO Collab.)

OTHER RELATED PAPERS

COLANGELO	06	PL B642 48	P. Colangelo et al.	
CLOSE	05C	PR D72 094004	F.E. Close, E.S. Swanson	(OXFTP)
SEMENOV	99	SPU 42 847	S.V. Semenov	

Translated from UFN 42 937.

Meson Particle Listings

 $D_{s2}(2573)^\pm, D_{s1}(2700)^\pm$ $D_{s1}(2700)^\pm$

$I(J^P) = 0(1^-)$

OMITTED FROM SUMMARY TABLE

 $D_{s1}(2700)^+$ MASS

VALUE (MeV)	EVTS	DOCUMENT ID	TECN	COMMENT
2690 ± 7 OUR AVERAGE		Error includes scale factor of 1.4.		
2708 ± 9 ⁺¹¹ ₋₁₀	182	BRODZICKA	08 BELL	$B^+ \rightarrow D^0 \bar{D}^0 K^+$
2688 ± 4 ± 3		AUBERT,BE	06E BABR	10.6 e ⁺ e ⁻ → DKX

 $D_{s1}(2700)^+$ WIDTH

VALUE (MeV)	EVTS	DOCUMENT ID	TECN	COMMENT
110 ± 27 OUR AVERAGE				
108 ± 23 ⁺³⁶ ₋₃₁	182	BRODZICKA	08 BELL	$B^+ \rightarrow D^0 \bar{D}^0 K^+$
112 ± 7 ± 36		AUBERT,BE	06E BABR	10.6 e ⁺ e ⁻ → DKX

 $D_{s1}(2700)^\pm$ DECAY MODES

Mode
$\Gamma_1 \quad D^0 K^+$

 $D_{s1}(2700)^\pm$ REFERENCES

BRODZICKA	08	PRL 100 092001	J. Brodzicka <i>et al.</i>	(BELLE Collab.)
AUBERT,BE	06E	PRL 97 222001	B. Aubert <i>et al.</i>	(BABAR Collab.)

OTHER RELATED PAPERS

COLANGELO	08	PR D77 014012	P. Colangelo <i>et al.</i>
MATSUKI	07	EPJ A31 701	T. Matsuki, T. Morii, K. Sudo

BOTTOM MESONS

$$(B = \pm 1)$$

$$B^+ = u\bar{d}, B^0 = d\bar{b}, \bar{B}^0 = \bar{d}b, B^- = \bar{u}b, \text{ similarly for } B^{*s}$$

B-particle organization

Many measurements of *B* decays involve admixtures of *B* hadrons. Previously we arbitrarily included such admixtures in the B^\pm section, but because of their importance we have created two new sections: “ B^\pm/B^0 Admixture” for $\Upsilon(4S)$ results and “ $B^\pm/B^0/B_s^0/b$ -baryon Admixture” for results at higher energies. Most inclusive decay branching fractions and χ_b at high energy are found in the Admixture sections. $B^0-\bar{B}^0$ mixing data are found in the B^0 section, while $B_s^0-\bar{B}_s^0$ mixing data and $B-\bar{B}$ mixing data for a B^0/B_s^0 admixture are found in the B_s^0 section. *CP*-violation data are found in the B^\pm , B^0 , and B^\pm/B^0 Admixture sections. *b*-baryons are found near the end of the Baryon section. Recently, we also created a new section: “ V_{cb} and V_{ub} CKM Matrix Elements.”

The organization of the *B* sections is now as follows, where bullets indicate particle sections and brackets indicate reviews.

[Production and Decay of *b*-flavored Hadrons]

[A Short Note on HFAG Activities]

- B^\pm
 - mass, mean life
 - branching fractions
 - polarization in B^\pm decay
 - CP* violation
- B^0
 - mass, mean life
 - branching fractions
 - [Polarization in *B* decay]
 - polarization in B^0 decay
 - [$B-\bar{B}$ Mixing]
 - $B^0-\bar{B}^0$ mixing
 - CP* violation
- B^\pm/B^0 Admixture
 - branching fractions, *CP* violation
 - CP* violation
- $B^\pm/B^0/B_s^0/b$ -baryon Admixture
 - mean life
 - production fractions
 - branching fractions
 - χ_b at high energy
 - production fractions in hadronic *Z* decay
- V_{cb} and V_{ub} CKM Matrix Elements
 - [Determination of V_{cb} and V_{ub}]

- B^*
 - mass
- $B_1(5721)^0$
 - mass
- $B_J^*(5732)$
 - mass, width
- $B_2(5747)^0$
 - mass
- B_s^0
 - mass, mean life
 - branching fractions
 - polarization in B_s^0 decay
 - $B_s^0-\bar{B}_s^0$ mixing
- B_s^*
 - mass
- $B_{s,J}^*(5850)$
 - mass, width
- B_c^\pm
 - mass, mean life
 - branching fractions

At end of Baryon Listings:

- Λ_b
 - mass, mean life
 - branching fractions
- Σ_b, Σ_b^*
 - mass
- Ξ_b^0, Ξ_b^-
 - mean life
- *b*-baryon Admixture
 - mean life
 - branching fractions

PRODUCTION AND DECAY OF *b*-FLAVORED HADRONS

Updated April 2008 by Y. Kwon (Yonsei U., Seoul, Korea), G. Punzi (INFN, Pisa, Italy), and J. G. Smith (U. of Colorado, Boulder, CO, USA).

The *b* quark belongs to the third generation of quarks and is the weak-doublet partner of the *t* quark. The existence of the third-generation quark doublet was proposed in 1973 by Kobayashi and Maskawa [1] in their model of the quark mixing matrix (“CKM” matrix), and confirmed four years later by the first observation of a $b\bar{b}$ meson [2]. In the KM model, *CP* violation is explained within the Standard Model (SM) by an irreducible phase of the 3×3 unitary matrix. The regular pattern of the three lepton and quark families is one of the most intriguing puzzles in particle physics. The existence of families gives rise to many of the free parameters in the SM, including the fermion masses, and the elements of the CKM matrix.

Since the *b* quark is the lighter element of the third-generation quark doublet, the decays of *b*-flavored hadrons occur via generation-changing processes through this matrix. Because of this and the fact that the CKM matrix is close to a 3×3 unit matrix, many interesting features such as loop and box diagrams, $B_{(s)}^0-\bar{B}_{(s)}^0$ mixing, as well as large *CP* asymmetries, can be observed in the weak decays of *b*-flavored hadrons. The CKM matrix is parameterized by three real parameters and one complex phase. This complex phase can become a source of *CP* violation in *B* meson decays. A crucial milestone in 2001 was the first observation of *CP* violation in the *B* meson system by the BaBar [3] and Belle [4] collaborations. They measured a large value for the parameter $\sin 2\beta$ ($= \sin 2\phi_1$) [5], almost four decades after the discovery of a small *CP* asymmetry in neutral kaons. A more detailed discussion of the CKM matrix and *CP* violation can be found elsewhere in this *Review* [6,7].

Recent developments in the physics of *b*-hadrons include the observation of direct *CP* violation, results for rare higher-order-weak decays, investigations of heavier *b*-hadrons (B_s^0 , B_c , baryons, excited states), measurement of the B_s^0 -mixing frequency, increasingly accurate determinations of the CKM matrix elements V_{cb} and V_{ub} , and of the angles α and γ of the unitarity triangle.

The structure of this mini-review is organized as follows. After a brief description of theory and terminology, we discuss *b*-quark production and current results on spectroscopy and lifetimes of *b*-flavored hadrons. We then discuss some basic properties of *B*-meson decays, followed by summaries of

Meson Particle Listings

b-flavored hadrons

hadronic, rare, and electroweak penguin decays of *B*-mesons. There are separate mini-reviews for $B\bar{B}$ mixing [8] and the extraction of the CKM matrix elements V_{cb} and V_{ub} from *B*-meson decays [9] in this *Review*.

Theory and terminology: The ground states of *b*-flavored hadrons decay via weak interactions. In most hadrons, the *b*-quark is accompanied by light-partner quarks (*d*, *u*, or *s*), and the decay modes are well described by the decay of the *b* quark (spectator model) [10]. The dominant decay mode of a *b* quark is $b \rightarrow cW^{*-}$ (referred to as a “tree” or “spectator” decay), where the virtual W^* materializes either into a pair of leptons, $\ell\bar{\nu}$ (“semileptonic decay”), or into a pair of quarks, which then hadronizes. The decays in which the spectator quark combines with one of the quarks from W^* to form one of the final state hadrons are suppressed by a factor $\simeq 1/9$, because the colors of the two quarks from different sources must match (“color-suppression”).

Many aspects of *B* decays can be understood with the use of Heavy Quark Effective Theory (HQET) [11]. This has been particularly successful for semileptonic decays. For further discussion of HQET, see for instance Ref. 9. For hadronic decays, one typically uses effective Hamiltonian calculations that rely on a perturbative expansion with Wilson coefficients. In addition, some form of the factorization hypothesis is commonly used, where, in analogy with semileptonic decays, two-body hadronic decays of *B* mesons are expressed as the product of two independent hadronic currents, one describing the formation of a charm meson (in case of the dominant $b \rightarrow cW^{*-}$ decays), and the other the hadronization of the remaining $\bar{u}d$ (or $\bar{c}s$) system from the virtual W^- . Qualitatively, for a *B* decay with a large energy release, the $\bar{u}d$ pair (produced as a color singlet) travels fast enough to leave the interaction region without influencing the charm meson. This is known to work well for the dominant spectator decays [12]. There are several common implementations of these ideas for hadronic *B* decays, the most common of which are QCD factorization (QCDF) [13], perturbative QCD (pQCD) [14], and soft collinear effective theory (SCET) [15].

The transition $b \rightarrow u$ is suppressed by $|V_{ub}/V_{cb}|^2 \sim (0.1)^2$ relative to $b \rightarrow c$ transitions, and gives way to rarer decay modes, *e.g.*, loop-induced $b \rightarrow s$ decays. The transition $b \rightarrow s$ is a flavor-changing neutral-current (FCNC) process, and although not allowed in the SM as a tree-process, can occur via more complex diagrams (denoted “penguin” decays). The rates for such processes are comparable or larger than CKM-suppressed $b \rightarrow u$ processes. Penguin processes involving $b \rightarrow d$ transitions are also possible, and have recently been observed [16,17]. Other decay processes discussed in this *Review* include *W*-exchange (a *W* is exchanged between initial-state quarks), penguin annihilation (the gluon from a penguin loop attaches to the spectator quark, similar to an exchange diagram), and pure-annihilation (the initial quarks annihilate to a virtual *W*, which then decays).

Production and spectroscopy: The bound states of a \bar{b} antiquark and a *u*, *d*, *s*, or *c* quark are referred to as the B_u (B^+), B_d (B^0), B_s^0 , and B_c^+ mesons, respectively. The B_c^+ is the heaviest of the ground-state *b*-flavored mesons, and the most difficult to produce; it was observed for the first time in the semileptonic mode by CDF in 1998 [18], but its mass was accurately determined only in 2006 from the fully reconstructed mode $B_c^+ \rightarrow J/\psi\pi^+$ [19].

The first excited meson is called the B^* meson. B^{**} is the generic name for the four orbitally excited ($L = 1$) *B*-meson states that correspond to the *P*-wave mesons in the charm system, D^{**} . Of the possible bound $\bar{b}b$ states, the Υ series (*S*-wave) and the χ_b (*P*-wave) are well studied; see Ref. 20 for classification and naming of these and other $\bar{b}b$ states.

Experimental studies of *b* decays have been performed in e^+e^- collisions at the $\Upsilon(4S)$ resonance (ARGUS, CLEO, Belle, and BaBar), as well as at higher energies at the *Z* resonance (SLC and LEP) and in $p\bar{p}$ collisions (Tevatron). The $e^+e^- \rightarrow \bar{b}b$ production cross-section at the *Z* and $\Upsilon(4S)$ resonances are about 6.6 *nb* and 1.1 *nb*, respectively. High-energy $p\bar{p}$ collisions produce *b*-flavored hadrons of all species with a very large cross-section ($\sigma(p\bar{p} \rightarrow bX, |\eta| < 1) \sim 30 \mu\text{b}$ at the Tevatron, which is expected to be ten times larger at the LHC pp collider with $\sqrt{s} = 14$ TeV). The total *b*-production cross section in hadronic collision is an interesting test of our understanding of QCD processes. For many years, experimental measurements have been several times higher than predictions. With improved measurements [21], more accurate input parameters, and more advanced calculations [22], the discrepancy between theory and data is now much reduced, although the presence of inconsistencies among existing measurements makes further data desirable.

As of this writing, BaBar and Belle have accumulated approximately 500 fb^{-1} and 700 fb^{-1} , respectively, and CDF and D0 have each accumulated about 2.5 fb^{-1} . Although these numbers imply that the majority of *b*-quarks are produced in hadron collisions, the large backgrounds cause the hadron collider experiments to have lower efficiency. Only the few decay modes for which triggering and reconstruction are easiest have been studied so far in hadron collisions. These have included final states with leptons, and the exclusive modes into all charged particles. In contrast, detectors operating at the $\Upsilon(4S)$ (“B-Factories”) have a high efficiency for most decays, and have provided large samples of a rich variety of decays of B^0 and B^+ mesons.

In hadron collisions, most production happens as $\bar{b}b$ pairs, either via *s*-channel production or gluon-splitting, with a smaller fraction of single *b*-quarks produced by flavor excitation. After production, each quark of a $\bar{b}b$ pair hadronizes separately and incoherently from the other, but it is still possible, although difficult, to obtain a statistical indication of the charge of a produced b/\bar{b} quark (“flavor tag” or “charge tag”) from the accompanying particles produced in the hadronization process, or from the decay products of the other quark. The momentum

spectrum of produced *b*-quarks typically peaks near the *b*-quark mass, and extends to much higher momenta, dropping by about a decade for every ten GeV. This implies typical decay lengths of a *mm*, that are important to resolve the fast oscillations of B_s^0 mesons.

In e^+e^- colliders, since the *B* mesons are very slow in the $\Upsilon(4S)$ rest frame, asymmetric beam energies are used to boost the decay products to improve the precision of time-dependent measurements that are crucial for the study of *CP* violation. At KEKB, the boost is $\beta\gamma = 0.43$, and the typical *B*-meson decay length is dilated from $\approx 20 \mu\text{m}$ to $\approx 200 \mu\text{m}$. PEP-II uses a slightly larger boost, $\beta\gamma = 0.55$. The two *B* mesons produced in $\Upsilon(4S)$ decay are in a coherent quantum state, which makes it easier than in hadron collision to infer the charge state of one *B* meson from observation of the other; however, the coherence also requires to determine the decay time of both mesons, rather than just one, in order to perform time-dependent *CP*-violation measurements.

For the measurement of branching fractions, the initial composition of the data sample must be known precisely. The $\Upsilon(4S)$ resonance decays predominantly to $B^0\bar{B}^0$ and B^+B^- ; the current experimental upper limit for non- $B\bar{B}$ decays of the $\Upsilon(4S)$ is less than 4% at the 95% confidence level (CL) [23]. The only known modes of this category are decays to lower Υ states and a pion pair, recently observed with branching fractions of order 10^{-4} [24]. The ratio f_+/f_0 of the fractions of charged to neutral *B* productions from $\Upsilon(4S)$ decays has been measured by CLEO, BaBar, and Belle in various ways, typically based on pairs of isospin-related decays of B^+ and B^0 , such that it can be assumed that $\Gamma(B^+ \rightarrow x^+) = \Gamma(B^0 \rightarrow x^0)$. In this way, the ratio of the number of events observed in these modes is proportional to $(f_+\tau_+)/ (f_0\tau_0)$ [25–28]. BaBar has also performed an independent measurement of f_0 with a different method that does not require isospin symmetry or the value of the lifetime ratio, based on the number of events with one or two reconstructed $B^0 \rightarrow D^{*-}\ell^+\nu$ decays [29]. The combined result, from the current average of τ_+/τ_0 , is $f_+/f_0 = 1.065 \pm 0.026$ [30]. This number is currently a bit less consistent with equal production of B^+B^- and $B^0\bar{B}^0$ pairs than it used to be in the past (deviates from unity by 2.5σ), but we still assume $f_+/f_0 = 1$ in this mini-review except where explicitly stated otherwise. This assumption is also supported by the near equality of the B^+ and B^0 masses: our fit of CLEO, ARGUS, and CDF measurements yields $m(B^0) = 5279.50 \pm 0.33 \text{ MeV}/c^2$, $m(B^+) = 5279.13 \pm 0.31 \text{ MeV}/c^2$, and $m(B^0) - m(B^+) = 0.37 \pm 0.24 \text{ MeV}/c^2$.

CLEO and Belle have also collected some data at the $\Upsilon(5S)$ resonance [31,32]. They measured the fraction of events with a pair of B_s^0 mesons over the total number of events with a pair of *b*-flavored hadrons. Their combined result is $f_s[\Upsilon(5S)] = 0.199 \pm 0.029$, thus establishing an alternative way of producing samples of B_s^0 mesons, dominated by production of $B_s^{*0}\bar{B}_s^{*0}$ events. However, the small boost of B_s^0 mesons produced in this way prevents resolution of their fast oscillations

for time-dependent measurements; these are only accessible in hadron collisions or at the *Z* peak.

In high-energy collisions, the produced *b* or \bar{b} quarks can hadronize with different probabilities into the full spectrum of *b*-hadrons, either in their ground or excited states. Table 1 shows the measured fractions f_d , f_u , f_s , and f_{baryon} of B^0 , B^+ , B_s^0 , and *b* baryons, respectively, in an unbiased sample of weakly decaying *b* hadrons produced at the *Z* resonance and in $p\bar{p}$ collisions [30]. The results were obtained from a fit where the sum of the fractions were constrained to equal 1.0, neglecting production of B_c mesons. The observed yields of B_c mesons at the Tevatron [18], provide an estimate $f_c = 0.2\%$, in agreement with expectations [33], which is below the current experimental uncertainties in the other fractions.

The combined values assume identical hadronization in $p\bar{p}$ collisions and in *Z* decay. These could in principle differ, because of the different momentum distributions of the *b*-quark in these processes; the sample used in the $p\bar{p}$ measurements has momenta close to the *b* mass, rather than $m_Z/2$. A test of the agreement between production fractions may be given by comparison of values of the average time-integrated mixing probability parameter $\bar{\chi} = f_d\chi_d + f_s\chi_s$ [8], which is an important input in the determination of the world-averages of production fractions. The current measurements of $\bar{\chi}$ from LEP and Tevatron differ by 1.8σ [30]. This slight discrepancy causes a larger uncertainty in the combined fractions in Table 1. With the availability of increasing large samples of *b*-flavored mesons and baryons at $p\bar{p}$ colliders, the limited knowledge of these fractions has become an important limiting factor in the determination of their branching fractions.

Table 1: Fractions of weakly-decaying *b*-hadron species in $Z \rightarrow b\bar{b}$ decay and in $p\bar{p}$ collisions at $\sqrt{s} = 1.8 \text{ TeV}$.

<i>b</i> hadron	Fraction at <i>Z</i> [%]	Combined with $p\bar{p}$ [%]
B^+, B^0	40.2 ± 0.9	39.9 ± 1.1
B_s^0	10.5 ± 0.9	11.1 ± 1.2
<i>b</i> baryons	9.1 ± 1.5	9.2 ± 1.9

Excited *B*-meson states have been observed by CLEO, LEP, CUSB, D0, and CDF. The current world average of the $B^{*-}B$ mass difference is $45.78 \pm 0.35 \text{ MeV}/c^2$. Evidence for B^{**} (L=1) production has been presented by the LEP and CDF experiments [34], as a broad resonance in the mass of an inclusively reconstructed bottom hadron candidate combined with a charged pion from the primary vertex. Results with exclusive modes have been obtained at the Tevatron, allowing separation of the narrow states, B_1 and B_2^* . The D0 collaboration measures $M(B_1) = 5720.6 \pm 2.4 \pm 1.4 \text{ MeV}/c^2$ and $M(B_2^*) - m(B_1) = 26.2 \pm 3.1 \pm 0.9 \text{ MeV}/c^2$ [35].

The narrow B_s^{**} states, first sighted by OPAL as a single broad enhancement in the B^+K mass spectrum [36], have now been clearly observed and separately measured at the

Meson Particle Listings

b-flavored hadrons

Tevatron [37]: $M(B_{s1}) = 5829.4 \pm 0.7 \text{ MeV}/c^2$ (CDF) and $M(B_{s2}^*) = 5839.7 \pm 0.7 \text{ MeV}/c^2$ (CDF), $M(B_{s2}^*) = 5839.6 \pm 1.1 \pm 0.7 \text{ MeV}/c^2$ (D0).

Baryon states containing a *b* quark are labeled according to the same scheme used for non-*b* baryons, with the addition of a *b* subscript [20]. For many years, the only well-established *b* baryon was the Λ_b^0 (quark composition *udb*); only indirect evidence for Ξ_b (*dsb*) production had been obtained at LEP [38]. This situation is now rapidly changing due to the large samples being accumulated at the Tevatron. Clear signals of four baryon states, Σ_b^+ , Σ_b^{*+} (*ub*), Σ_b^- , Σ_b^{*-} (*ddb*) have been obtained by CDF in $\Lambda_b^0 \pi^\pm$ final state [39]. The strange bottom baryon Ξ_b^\pm has been observed in the exclusive mode $\Xi_b^\pm \rightarrow J/\psi \Xi^\pm$ by D0 [40], and CDF [41]. The masses of all these new baryons have been measured to a precision of a few MeV/c^2 , and found to be in agreement with predictions from HQET. The relative production of Ξ_b and Λ_b baryons has been found to be consistent with the B_s to B_d production ratio [40].

Lifetimes: Precise lifetimes are key in extracting the weak parameters that are important for understanding the role of the CKM matrix in *CP* violation, such as the determination of V_{cb} and $B_s^0 \bar{B}_s^0$ mixing measurements. In the naive spectator model, the heavy quark can decay only via the external spectator mechanism, and thus, the lifetimes of all mesons and baryons containing *b* quarks would be equal. Non-spectator effects, such as the interference between contributing amplitudes, modify this simple picture and give rise to a lifetime hierarchy for *b*-flavored hadrons similar to the one in the charm sector. However, since the lifetime differences are expected to scale as $1/m_Q^2$, where m_Q is the mass of the heavy quark, the variations in the *b* system are expected to be significantly smaller; on the order of 10% or less [42]. We expect:

$$\tau(B^+) \geq \tau(B^0) \approx \tau(B_s^0) > \tau(\Lambda_b^0) \gg \tau(B_c^+) . \quad (1)$$

In the B_c^+ , both quarks can decay weakly, resulting in a much shorter lifetime.

Measurements of lifetimes for the various *b*-flavored hadrons thus provide a means to determine the importance of non-spectator mechanisms in the *b* sector. Over the past years, the precision of silicon vertex detectors, and the increasing availability of fully-reconstructed samples, yielded measurements with much-reduced statistical and systematic uncertainties, at the 1% level. The averaging of precision results from different experiments is a complex task that requires careful treatment of correlated systematic uncertainties; the world averages given in this mini-review (Table 2) have been determined by the Heavy Flavor Averaging Group (HFAG) [30].

Table 2: Summary of inclusive and exclusive world-average *b*-hadron lifetime measurements. For the two B_s^0 averages, see text below.

Particle	Lifetime [ps]
B^+	1.638 ± 0.011
B^0	1.530 ± 0.009
B_s^0	1.417 ± 0.042 (flavor-specific)
B_s^0	$1.437_{-0.030}^{+0.031}$ ($1/\Gamma_s$)
B_c^+	0.463 ± 0.071
Λ_b	$1.383_{-0.048}^{+0.049}$
Ξ_b mixture	$1.42_{-0.24}^{+0.28}$
<i>b</i> -baryon mixture	$1.319_{-0.38}^{+0.39}$
<i>b</i> -hadron mixture	1.568 ± 0.009

The short B_c^+ lifetime is in good agreement with predictions [43]. For precision comparisons with theory, lifetime ratios are more sensitive. Experimentally we find:

$$\frac{\tau_{B^+}}{\tau_{B^0}} = 1.071 \pm 0.009, \quad \frac{\tau_{B_s^0}}{\tau_{B^0}} = 0.939 \pm 0.021,$$

$$\frac{\tau_{\Lambda_b}}{\tau_{B^0}} = 0.904 \pm 0.032,$$

while theory makes the following predictions [42,44]

$$\frac{\tau_{B^+}}{\tau_{B^0}} = 1.06 \pm 0.02, \quad \frac{\tau_{B_s^0}}{\tau_{B^0}} = 1.00 \pm 0.01, \quad \frac{\tau_{\Lambda_b}}{\tau_{B^0}} = 0.88 \pm 0.05.$$

The ratio of B^+ to B^0 is measured to better than 1%, and is significantly different from one, in agreement with predictions [42]. Conversely, the ratio of B_s^0 to B^0 lifetimes is expected to be very close to one, but exhibits a 2.5σ deviation. The Λ_b lifetime has a history of discrepancies. Predictions used to be higher than data, before the introduction of higher-order effects lowered them. The latest measurements, from CDF on the exclusive $J/\psi \Lambda$ mode [45], and from D0 [46] on both semileptonic and $J/\psi \Lambda$ mode, disagree at the 3σ level. Further measurements will help clarify the situation in the future.

Neutral *B* mesons are two-component systems similar to neutral kaons, with a light (L) and a heavy (H) mass eigenstate, and independent decay widths Γ_L and Γ_H . The SM predicts a non-zero width difference $\Delta\Gamma = \Gamma_L - \Gamma_H > 0$ for both B_s and B_d . For B_d , $\Delta\Gamma_d/\Gamma_d$ is expected to be $\sim 0.2\%$. Analysis of BaBar and DELPHI data on *CP*-specific modes of the B^0 yield a combined result: $\Delta\Gamma_d/\Gamma_d = 0.009 \pm 0.037$ [30]. The issue is much more interesting for the B_s , since the SM expectation for $\Delta\Gamma_s/\Gamma_s$ is of order 10%. This potentially non-negligible difference requires care when defining the B_s^0 lifetime.

As indicated in Table 2, two different lifetimes are defined for the B_s^0 meson: one is defined as $1/\Gamma_s$, where Γ_s is the average width of the two mass eigenstates $(\Gamma_L + \Gamma_H)/2$; the other is obtained from “flavor-specific” decays (*e.g.*, semileptonic) and depends both on Γ_s and $\Delta\Gamma_s$. Experimentally, the quantity $\Delta\Gamma_s$ can be accessed by measuring lifetimes in decays into *CP* eigenstates, which are expected to be close approximations to the mass eigenstates. This has been done with the $J/\psi \phi$ mode,

where the two CP eigenstates are distinguished by angular distributions, and in $B_s^0 \rightarrow K^+K^-$ which is dominated by a single CP -state. The current experimental information is dominated by CDF and D0 measurements on the $J/\psi\phi$ mode. By appropriately combining all published measurements of $J/\psi\phi$ lifetimes and flavor-specific lifetimes, the HFAG group obtains a world-average $\Delta\Gamma_s/\Gamma_s = 0.121_{-0.090}^{+0.083}$ [30]; the quoted uncertainties are, however, non-Gaussian, and a better representation of the current uncertainty is given by the 95% CL interval: $-0.06 < \Delta\Gamma_s/\Gamma_s < 0.28$ [30], which is still compatible with zero. The latest predictions yield $\Delta\Gamma_s/\Gamma_s = 0.147 \pm 0.060$ [47], in agreement with the experiment within the large uncertainties on both. The experimental precision can still improve in the near future with the growth of Tevatron samples; a very recent update by CDF, not yet included in the above average yields already a significant improvement: $\Delta\Gamma_s = 0.076_{-0.063}^{+0.059} \pm 0.006 \text{ ps}^{-1}$ [48]. D0 combined the contour in the $(\phi_s, \Delta\Gamma)$ plane (ϕ_s is the B_s^0 mixing phase) with a constraint obtained from the charge asymmetry in B_s^0 oscillations to obtain the result $\Delta\Gamma_s = 0.13 \pm 0.09 \text{ ps}^{-1}$ [49]. Further improvements may come from $B_s^0 \rightarrow K^+K^-$, and alternative (model-dependent) determinations via the $B_s^0 \rightarrow D_s^{(*)+}D_s^{(*)-}$ branching fraction [50].

From the theoretical point of view, the best quantity to use is $\Delta\Gamma_s/\Delta M_s$, which is much less affected by hadronic uncertainties: $\Delta\Gamma_s/\Delta M_s = (49.7 \pm 9.4) \times 10^{-4}$ [47]. Exploiting the very accurate measurement of ΔM_s now available [51], this can be turned into a SM prediction with just 20% uncertainty: $\Delta\Gamma_s/\Gamma_s = 0.127 \pm 0.024$. This is likely to be of importance in future comparisons to improved measurements.

B meson decay properties: Semileptonic B decays $B \rightarrow X_c \ell \nu$ and $B \rightarrow X_u \ell \nu$ provide an excellent way to measure the magnitude of the CKM elements $|V_{cb}|$ and $|V_{ub}|$ respectively, because the strong interaction effects are much simplified due to the two leptons in the final state. Both exclusive and inclusive decays can be used, and the nature of uncertainties are quite complementary. For exclusive decay analysis, knowledge of the form factors for the exclusive hadronic system $X_{c(u)}$ is required. For inclusive analysis, it is usually necessary to restrict the available phase-space of the decay products to suppress backgrounds; subsequently uncertainties are introduced in the extrapolation to the full phase-space. Moreover, restriction to a small corner of the phase-space may result in breakdown of the operator-product expansion scheme, thus making theoretical calculations unreliable. A more detailed discussion of B semileptonic decays and the extraction of $|V_{cb}|$ and $|V_{ub}|$ is given elsewhere in this *Review* [9].

On the other hand, hadronic decays of B are complicated because of strong interaction effects caused by the surrounding cloud of light quarks and gluons. While this complicates the extraction of CKM matrix elements, it also provides a great opportunity to study perturbative and non-perturbative QCD, hadronization, and Final State Interaction (FSI) effects. Pure-penguin decays were first established by the observation of $B \rightarrow$

$K^*\gamma$ [52]. Some observed decay modes such as $B^0 \rightarrow D_s^- K^+$, may be interpreted as evidence of a W -exchange process [53]. The recent evidence for the decay $B^+ \rightarrow \tau^+ \nu$ from Belle [54] and BaBar [55] is the first sign of a pure annihilation decay. There is growing evidence that penguin annihilation processes may be important in decays with two vector mesons in the final state [56].

Hadronic decays:

Most of the hadronic B decays involve $b \rightarrow c$ transition at the quark level, resulting in a charmed hadron or charmonium in the final state. Other types of hadronic decays are very rare and will be discussed separately in the next section. The experimental results on hadronic B decays have steadily improved over the past few years, and the measurements have reached sufficient precision to challenge our understanding of the dynamics of these decays. With the good neutral particle detection and hadron identification capabilities of B -factory detectors, a substantial fraction of hadronic B decay events can be fully reconstructed. Because of the kinematic constraint of $\Upsilon(4S)$, the energy sum of the final-state particles of a B meson decay is always equal to one half of the total energy in the center of mass frame. As a result, the two variables, ΔE (energy difference) and M_B (B candidate mass with a beam-energy constraint) are very effective for suppressing combinatorial background both from $\Upsilon(4S)$ and $e^+e^- \rightarrow q\bar{q}$ continuum events. In particular, the energy-constraint in M_B improves the signal resolution by almost an order of magnitude.

The kinematically clean environment of B meson decays provides an excellent opportunity to search for new states. For instance, quark-level $b \rightarrow c\bar{c}s$ decays have been used to search for new charmonium and charm-strange mesons and study their properties in detail. In 2003, BaBar discovered a new narrow charm-strange state $D_{sJ}^*(2317)$ [57], and CLEO observed a similar state $D_{sJ}(2460)$ [58]. However, the properties of these new states were not well known until Belle observed $B \rightarrow DD_{sJ}^*(2317)$ and $B \rightarrow DD_{sJ}(2460)$, which helped identify some quantum numbers of $D_{sJ}(2460)$ [59]. Further studies of $D_{sJ}^{(*)}$ meson production in B decays have been made by Belle and BaBar. In particular, BaBar has observed $B \rightarrow D_{sJ}^*(2317)^+ \bar{D}^{(*)}$ ($D_{sJ}^*(2317)^+ \rightarrow D_s^+ \pi^0$) and $B \rightarrow D_{sJ}(2460)^+ \bar{D}^{(*)}$ ($D_{sJ}(2460)^+ \rightarrow D_s^{*+} \pi^0$, $D_s^+ \gamma$) decays. The angular analysis of $B \rightarrow D_{sJ}(2460)^+ \bar{D}$ with $D_{sJ}(2460)^+ \rightarrow D_s^+ \gamma$ supports the $J^P = 1^+$ assignment for $D_{sJ}(2460)$. With a sample of 449 million $B\bar{B}$ pairs, Belle has observed a new D_{sJ} meson produced in $B^+ \rightarrow \bar{D}^0 D_{sJ} \rightarrow \bar{D}^0 D^0 K^+$ [60]. The mass and width of this state are measured to be $2708 \pm 9_{-10}^{+11} \text{ MeV}/c^2$ and $108 \pm 23_{-31}^{+36} \text{ MeV}$, respectively. An analysis of the helicity angle distribution determines its spin-parity to be 1^- .

A variety of exotic particles have been discovered in B decays. Belle found the $X(3872)$ state [61], confirmed by CDF [62] and BaBar [64]. Belle has observed a near-threshold enhancement in the $\omega J/\psi$ invariant mass for $B \rightarrow K \omega J/\psi$ decays [65]. BaBar has studied $B \rightarrow J/\psi \pi^+ \pi^- K$, finding an

Meson Particle Listings

b-flavored hadrons

excess of $J/\psi\pi^+\pi^-$ events with a mass just above 4.2 GeV/ c^2 ; this is consistent with the $Y(4260)$ that was observed by BaBar in ISR (Initial State Radiation) events [67]. A Belle study of $B \rightarrow K\pi^\pm\psi'$ [68] finds a state called $Z^\pm(4430)$ that decays to $\pi^\pm\psi'$. Since it is charged, it cannot be a charmonium state. More details about these exotic states are described in a separate mini-review [69] in this *Review*.

There have been hundreds of publications on hadronic B decays to open-charm and charmonium final states mostly from the B -factory experiments. These results are nicely summarized in a recent report by HFAG [30].

Rare B decays: All B -meson decays that do not occur through the $b \rightarrow c$ transition are usually called rare B decays. These include both semileptonic and hadronic $b \rightarrow u$ decays that are suppressed at leading order by the small CKM matrix element V_{ub} , as well as higher-order $b \rightarrow s(d)$ processes such as electroweak and gluonic penguin decays.

Charmless B meson decays into two-body hadronic final states such as $B \rightarrow \pi\pi$ and $K\pi$ are experimentally clean, and provide good opportunities to probe new physics and search for indirect and direct CP violations. Since the final state particles in these decays tend to have larger momenta than average B decay products, the event environment is cleaner than for $b \rightarrow c$ decays. Branching fractions are typically around 10^{-5} . Over the past decade, many such modes have been observed by BaBar, Belle, and CLEO. More recently, comparable samples of the modes with all charged final particles have been reconstructed in $p\bar{p}$ collisions by CDF by triggering on the impact parameter of the charged tracks. This also allowed observation of charmless decays of the B_s for the first time, in the final states $\phi\phi$ [70] and K^+K^- [71].

Because of relatively high-momenta for final state particles, the dominant source of background in e^+e^- collisions is $q\bar{q}$ continuum events; sophisticated background suppression techniques exploiting event shape variables are essential for these analyses. In hadron collisions, the dominant background comes from QCD or partially reconstructed heavy flavors, and is similarly suppressed by a combination of kinematic and isolation requirements. The results are in general consistent among the four experiments.

BaBar [72] and Belle [73] have recently observed the decays $B^+ \rightarrow \bar{K}^0 K^+$ and $B^0 \rightarrow K^0 \bar{K}^0$. The world-average branching fractions are $\mathcal{B}(B^0 \rightarrow K^0 \bar{K}^0) = (0.96_{-0.18}^{+0.20}) \times 10^{-6}$ and $\mathcal{B}(B^+ \rightarrow \bar{K}^0 K^+) = (1.36 \pm 0.27) \times 10^{-6}$. These are the first observations of hadronic $b \rightarrow d$ transitions, with significance $> 5\sigma$ for all four measurements. CP asymmetries have even been measured for these modes, though with large errors.

Most rare decay modes including $B^0 \rightarrow K^+\pi^-$ have contributions from both $b \rightarrow u$ tree and $b \rightarrow sg$ penguin processes. If the size of the two contributions are comparable, the interference between them may result in direct CP violation, seen experimentally as a charge asymmetry in the decay rate measurement. BaBar [74], Belle [75], and CDF [76] have measured

the direct CP violating asymmetry in $B^0 \rightarrow K^+\pi^-$ decays. The BaBar measurement, $A_{CP}(K^+\pi^-) = -0.107 \pm 0.018_{-0.004}^{+0.007}$, constitutes observation of direct CP violation with a significance of 5.5σ . The world average for this quantity is now rather precise, -0.101 ± 0.015 . There are sum rules that relate the decay rates and decay-rate asymmetries between the four $K\pi$ charge states. The experimental measurements of the other three modes are not yet precise enough to test these sum rules.

There is now evidence for direct CP violation in three other decays: $B^+ \rightarrow \rho^0 K^+$ [77], $B^+ \rightarrow \eta K^+$ [78], and $B^0 \rightarrow \eta K^{*0}$ [79]. The significance is typically $3\text{--}4\sigma$. In at least the first two cases, a large direct CP violation might be expected since the penguin amplitude is suppressed so the tree and penguin amplitudes may have comparable magnitudes.

The decay $B^0 \rightarrow \pi^+\pi^-$ can be used to extract the CKM angle α . This is complicated by the presence of significant contributions from penguin diagrams. An isospin analysis [80] can be used to untangle the penguin complications. The decay $B^0 \rightarrow \pi^0\pi^0$, which is now measured by both BaBar and Belle, is crucial in this analysis. Unfortunately the amount of penguin pollution in the $B \rightarrow \pi\pi$ system is rather large. In the past two years, measurements in the $B^0 \rightarrow \rho\rho$ system have produced more precise values of α , since penguin amplitudes are generally smaller for decays with vector mesons. An important ingredient in the analysis is the $B^0 \rightarrow \rho^0\rho^0$ branching fraction. Evidence for this mode has now been found by BaBar [81] with a branching fraction of $(1.07 \pm 0.33 \pm 0.19) \times 10^{-6}$. This is only 4% of the $\rho^+\rho^-$ branching fraction, much smaller than the corresponding ratio in the $\pi\pi$ system.

The decay $B \rightarrow a_1\pi$ has now been seen by BaBar [82]. This decay can be used to constrain the CKM angle α [83] though there are not yet suitable constraints on the penguin pollution in this system.

Since $B \rightarrow \rho\rho$ has two vector mesons in the final state, the CP eigenvalue of the final state depends on the longitudinal polarization fraction f_L for the decay. Therefore, a measurement of f_L is needed to extract the CKM angle α . Both BaBar and Belle have measured the f_L for the decays $\rho^+\rho^-$ and $\rho^+\rho^0$ and in both cases the measurements show $f_L > 0.9$, making a complete angular analysis unnecessary.

By analyzing the angular distributions of the B decays to two vector mesons, we can learn a lot about both weak- and strong-interaction dynamics in B decays. Decays that are penguin-dominated (such as $B \rightarrow \phi K^*$) surprisingly have values of f_L near 0.5. The reasons for this are not understood. A detailed description of the angular analysis of B decays to two vector mesons can be found in a separate mini-review [84] in this *Review*.

There has been substantial progress in measurements of many other rare- B decays. The decay $B \rightarrow \eta'K$ stood out as the largest rare- B decay for many years. The reasons for the large rate are now largely understood [13,85]. However, there are now measurements of several 3-body or quasi-3-body modes with similarly large branching fractions. States seen so

far include $K\pi\pi$ (three charge states) [86], KKK (four charge states) [87], and $K^*\pi\pi$ (two charged states) [88]. Several of these analyses now include quite sophisticated Dalitz plot analyses with many intermediate resonances. There has also been a recent observation of the decay $B^+ \rightarrow K^+K^-\pi^+$ by BaBar [89], noteworthy because an even number of kaons is typically indicative of suppressed $b \rightarrow d$ transitions as discussed above.

Belle [54] and BaBar [55] have found evidence for $B^+ \rightarrow \tau^+\nu$ with a combined branching fraction of $(140 \pm 40) \times 10^{-6}$ in excellent agreement with the value expected in the Standard Model. This is the first evidence for a pure annihilation decay.

The recently observed $B_s \rightarrow K^+K^-$ mode [71] is related to $B^0 \rightarrow \pi^+\pi^-$ by U-spin symmetry, and is similarly determined by a superposition of tree and penguin diagrams. Combining the observables from these two modes is another way of eliminating hadronic uncertainties and extracting relevant CKM information [90].

Electroweak penguin decays:

More than a decade has passed since the CLEO experiment first observed an exclusive radiative $b \rightarrow s\gamma$ transition, $B \rightarrow K^*(892)\gamma$ [52], thus providing the first evidence for the one-loop FCNC electromagnetic penguin decay. Using much larger data samples, both Belle and BaBar have updated this analysis [91], and have added several new decay modes such as $B \rightarrow K_1\gamma$, $K_2^*(1430)\gamma$, *etc.* [92].

Compared to $b \rightarrow s\gamma$, the $b \rightarrow d\gamma$ transitions such as $B \rightarrow \rho\gamma$, are suppressed by the small CKM element V_{td} . Both BaBar and Belle have observed these decays [16,17]. The world average $\mathcal{B}(B \rightarrow (\rho, \omega)\gamma) = (1.28 \pm 0.21) \times 10^{-6}$. This can be used to calculate $|V_{td}/V_{ts}|$ [93]; both BaBar and Belle find a value of 0.20 ± 0.03 .

The observed radiative penguin branching fractions can constrain a large class of SM extensions [94]. However, due to the uncertainties in the hadronization, only the inclusive $b \rightarrow s\gamma$ rate can be reliably compared with theoretical calculations. This rate can be measured from the endpoint of the inclusive photon spectrum in B decay. By combining the measurements of $B \rightarrow X_s\gamma$ from CLEO, Belle, and BaBar experiments [95], HFAG obtains the new average: $\mathcal{B}(B \rightarrow X_s\gamma) = (3.52 \pm 0.23 \pm 0.09) \times 10^{-4}$ [30]. Consistent results have been reported by ALEPH for inclusive b -hadrons produced at the Z . The measured branching fraction can be compared to theoretical calculations [96–98]. They predict $\mathcal{B}(b \rightarrow s\gamma) = (3.29 \pm 0.33) \times 10^{-4}$.

According to the SM, the CP asymmetry in $b \rightarrow s\gamma$ is smaller than 1%, but some non-SM models allow significantly larger CP asymmetry ($\sim 10\%$) without altering the inclusive branching fraction [99–101]. The current world average is $A_{CP} = 0.004 \pm 0.037$, again dominated by BaBar and Belle [102].

In addition, all three experiments have measured the inclusive photon energy spectrum for $b \rightarrow s\gamma$, and by analyzing the shape of the spectrum they obtain the first and second moments for photon energies. These results can be used to extract

non-perturbative HQET parameters that are needed for precise determination of the CKM matrix element V_{ub} .

Additional information on FCNC processes can be obtained from $B \rightarrow X_s\ell^+\ell^-$ decays, which are mediated by electroweak penguin and W -box diagrams. Belle [103] and BaBar [104] have measured the branching fractions for $B \rightarrow K\ell^+\ell^-$ and their average is $(0.39 \pm 0.06) \times 10^{-6}$. Similarly, the branching fraction for $B \rightarrow K^*(892)\ell^+\ell^-$ is also measured by both experiments with an average of $(0.94_{-0.16}^{+0.17}) \times 10^{-6}$, consistent with the SM expectation. Both experiments also measured the branching fractions for inclusive $B \rightarrow X_s\ell^+\ell^-$ decays, with an average of $(4.5 \pm 1.0) \times 10^{-6}$ [105].

Finally the decays $B_{(s)}^0 \rightarrow \mu^+\mu^-$ are interesting since they only proceed at second order in weak interactions in the SM, but may have large contributions from supersymmetric loops, proportional to $(\tan\beta)^6$. CDF and D0 have both obtained results that start to exclude a portion of the region allowed by SUSY models. The most recent limits are: $< 5.8 \times 10^{-8}$ and $< 1.8 \times 10^{-8}$, respectively, for B_s^0 and B^0 [106]. For the B_s^0 mode, the current result is just one order of magnitude above predictions. There are also limits for lepton flavor-violating channels such as $B \rightarrow e\mu$.

Summary and Outlook: The study of B mesons continues to be one of the most productive fields in particle physics. With the two asymmetric B -factory experiments Belle and BaBar, we now have a combined data sample of over $1 ab^{-1}$. CP violation has been observed for the first time outside the kaon system. Evidence for direct CP violations has been observed. Many rare decays such as hadronic $b \rightarrow u$ transitions and $b \rightarrow s(d)$ gluonic penguin decays have been observed, and the emerging pattern is still full of surprises. The coming years look equally promising.

At Fermilab, CDF and D0 have accumulated about $2.5 fb^{-1}$, which is the equivalent of over 10^{11} b -hadrons produced. In spite of the low trigger efficiency of hadronic experiments, a selection of modes have been reconstructed in large quantities, giving a start to a program of studies on B_s^0 and b -flavored baryons, in which a first major step has been the determination of the B_s^0 oscillation frequency.

In addition, the LHC will soon start operating and produce huge samples of b -hadrons. There are also proposals for higher-luminosity B Factories at KEK and Frascati in order to increase the samples to $\sim 50 ab^{-1}$!

These experiments promise a rich spectrum of rare and precise measurements that have the potential to fundamentally affect our understanding of the SM and CP -violating phenomena.

References

1. M. Kobayashi and T. Maskawa, *Prog. Theor. Phys.* **49**, 652 (1973).
2. S. W. Herb *et al.*, *Phys. Rev. Lett.* **39**, 252 (1977).
3. B. Aubert *et al.* (BaBar Collab.), *Phys. Rev. Lett.* **87**, 091801 (2001).

Meson Particle Listings

b-flavored hadrons

4. K. Abe *et al.* (Belle Collab.), Phys. Rev. Lett. **87**, 091802 (2001).
5. Currently two different notations (ϕ_1, ϕ_2, ϕ_3) and (α, β, γ) are used in the literature for CKM unitarity angles. In this mini-review, we use the latter notation following the other mini-reviews in this *Review*. The two notations are related by $\phi_1 = \beta$, $\phi_2 = \alpha$ and $\phi_3 = \gamma$.
6. See the “*CP* Violation in Meson Decays” by D. Kirkby and Y. Nir in this *Review*.
7. See the “CKM Quark Mixing Matrix,” by A. Cecucci, Z. Ligeti, and Y. Sakai, in this *Review*.
8. See the “Review on B - \bar{B} Mixing,” by O. Schneider in this *Review*.
9. See the “Determination of $|V_{cb}|$ and $|V_{ub}|$,” by R. Kowalewski and T. Mannel in this *Review*.
10. The B_c is a special case, where a weak decay of the c quark is also possible, but the spectator model still applies.
11. B. Grinstein, Nucl. Phys. **B339**, 253 (1990); H. Georgi, Phys. Lett. **B240**, 447 (1990); A.F. Falk *et al.*, Nucl. Phys. **B343**, 1 (1990); E. Eichten and B. Hill, Phys. Lett. **B234**, 511 (1990).
12. M. Neubert, “Aspects of QCD Factorization,” hep-ph/0110093, *Proceedings of HF9*, Pasadena (2001) and references therein; Z. Ligeti *et al.*, Phys. Lett. **B507**, 142 (2001).
13. M. Beneke *et al.*, Phys. Rev. Lett. **83**, 1914 (1999); Nucl. Phys. **B591**, 313 (2000); Nucl. Phys. **B606**, 245 (2001); M. Beneke and M. Neubert, Nucl. Phys. **B675**, 333 (2003).
14. Y.Y. Keum, H-n. Li, and A.I. Sanda, Phys. Lett. **B504**, 6 (2001); Phys. Rev. **D63**, 054008 (2001); Y.Y. Keum and H-n. Li, Phys. Rev. **D63**, 074006 (2001); C.D. Lü, K. Ukai, and M.Z. Yang, Phys. Rev. **D63**, 074009 (2001); C.D. Lü and M.Z. Yang, Eur. Phys. J. **C23**, 275 (2002).
15. C.W. Bauer, S. Fleming, and M.E. Luke, Phys. Rev. **D63**, 014006 (2001); C.W. Bauer *et al.*, Phys. Rev. **D63**, 114020 (2001); C.W. Bauer and I.W. Stewart, Phys. Lett. **B516**, 134 (2001).
16. D. Mohapatra *et al.* (Belle Collab.), Phys. Rev. Lett. **96**, 221601 (2006).
17. B. Aubert *et al.* (BaBar Collab.), Phys. Rev. Lett. **98**, 151802 (2007).
18. F. Abe *et al.* (CDF Collab.), Phys. Rev. Lett. **81**, 2432 (1998); F. Abe *et al.* (CDF Collab.), Phys. Rev. **D58**, 112004 (1998).
19. D. Acosta *et al.* (CDF Collab.), Phys. Rev. Lett. **96**, 082002 (2006).
20. See the note on “Naming scheme for hadrons,” by M. Roos and C.G. Wohl in this *Review*.
21. A. Abulencia *et al.* (CDF Collab.), Phys. Rev. **D75**, 012010 (2007), and references therein.
22. M. Cacciari *et al.*, JHEP **9805**, 007 (1998); S. Frixione and B. R. Webber, JHEP **0206**, 029 (2002); M. Cacciari *et al.*, JHEP **0407**, 033 (2004); M. Cacciari *et al.*, JHEP **0604**, 006 (2006), and references therein.
23. B. Barish *et al.* (CLEO Collab.), Phys. Rev. Lett. **76**, 1570 (1996).
24. B. Aubert *et al.* (BaBar Collab.), Phys. Rev. Lett. **96**, 232001 (2006); A. Sokolov *et al.* (Belle Collab.), Phys. Rev. **D75**, 071103 (R) (2007).
25. J.P. Alexander *et al.* (CLEO Collab.), Phys. Rev. Lett. **86**, 2737 (2001).
26. B. Aubert *et al.* (BaBar Collab.), Phys. Rev. **D65**, 032001 (2001); B. Aubert *et al.* (BaBar Collab.), Phys. Rev. **D69**, 071101 (2004).
27. S.B. Athar *et al.* (CLEO Collab.), Phys. Rev. **D66**, 052003 (2002).
28. N.C. Hastings *et al.* (Belle Collab.), Phys. Rev. **D67**, 052004 (2003).
29. B. Aubert *et al.* (BaBar Collab.), Phys. Rev. Lett. **95**, 042001 (2005).
30. E. Barberio *et al.* (Heavy Flavor Averaging Group), “Averages of *b*-hadron properties at the end of 2006,” arXiv:0704.3575 [hep-ex], and 2008 update in <http://www.slac.stanford.edu/xorg/hfag/osc/>.
31. G.S. Huang *et al.* (CLEO Collab.), Phys. Rev. **D75**, 012002 (2007).
32. A. Drutskoy *et al.* (Belle Collab.), Phys. Rev. Lett. **98**, 052001 (2007).
33. M. Lusignoli, M. Masetti, and S. Petrarca, Phys. Lett. **B266**, 142 (1991); K. Cheung, Phys. Lett. **B472**, 408 (2000).
34. P. Abreu *et al.* (DELPHI Collab.), Phys. Lett. **B345**, 598 (1995).
35. V.M. Abazov *et al.* (D0 Collab.), Phys. Rev. Lett. **99**, 172001 (2007).
36. R. Akers *et al.* (OPAL Collab.), Z. Phys. **C66**, 19 (1995).
37. T. Aaltonen *et al.* (CDF Collab.), Phys. Rev. Lett. **100**, 082001 (2008); V.M. Abazov *et al.* (D0 Collab.), Phys. Rev. Lett. **100**, 082002 (2008).
38. D. Buskulic *et al.* (ALEPH Collab.), Phys. Lett. **B384**, 449 (1996); P. Abreu *et al.* (DELPHI Collab.), Z. Phys. **C68**, 541 (1995).
39. T. Aaltonen *et al.* (CDF Collab.), Phys. Rev. Lett. **99**, 202001 (2007).
40. V.M. Abazov *et al.* (Co Collab.), Phys. Rev. Lett. **99**, 052001 (2007).
41. T. Aaltonen *et al.* (CDF Collab.), Phys. Rev. Lett. **99**, 052002 (2007).
42. C. Tarantino, Eur. Phys. J. **C33**, S895 (2004); F. Gabbiani *et al.*, Phys. Rev. **D68**, 114006 (2003); F. Gabbiani *et al.*, Phys. Rev. **D70**, 094031 (2004).
43. C.H. Chang *et al.*, Phys. Rev. **D64**, 014003 (2001); V.V. Kiselev, A.E. Kovalsky, and A.K. Likhoded, Nucl. Phys. **B585**, 353 (2000); V.V. Kiselev, arXiv:hep-ph/0308214, and references therein.
44. I.I. Bigi *et al.*, in *B Decays*, 2nd ed., S. Stone (ed.), World Scientific, Singapore, 1994.
45. A. Abulencia *et al.* (CDF Collab.), Phys. Rev. Lett. **98**, 122001 (2007).
46. V.M. Abazov *et al.* (D0 Collab.), Phys. Rev. Lett. **99**, 182001 (2007); V.M. Abazov *et al.* (D0 Collab.), Phys. Rev. Lett. **99**, 142001 (2007).
47. A. Lenz and U. Nierste, JHEP **0706**, 072 (2007).
48. T. Aaltonen *et al.* (CDF Collab.), Phys. Rev. Lett. **100**, 121803 (2008).

See key on page 373

-
49. V.M. Abazov *et al.* (D0 Collab.), Phys. Rev. **D76**, 057101 (2007).
50. R. Barate *et al.* (ALEPH Collab.), Phys. Lett. **B486**, 286 (2000); V.M. Abazov *et al.* (D0 Collab.), Phys. Rev. Lett. **99**, 241801 (2007).
51. A. Abulencia *et al.* (CDF Collab.), Phys. Rev. Lett. **97**, 242003 (2006).
52. R. Ammar *et al.* (CLEO Collab.), Phys. Rev. Lett. **71**, 674 (1993).
53. P. Krokovny *et al.* (Belle Collab.), Phys. Rev. Lett. **89**, 231804 (2002); B. Aubert *et al.* (BaBar Collab.), Phys. Rev. Lett. **98**, 081801 (2007).
54. K. Ikado *et al.* (Belle Collab.), Phys. Rev. Lett. **97**, 251802 (2006).
55. B. Aubert *et al.* (BaBar Collab.), Phys. Rev. **D77**, 011107 (2008).
56. M. Beneke, J. Rohrer, and D. Yang, Nucl. Phys. **B774**, 64 (2007).
57. B. Aubert *et al.* (BaBar Collab.), Phys. Rev. Lett. **90**, 242001 (2003).
58. D. Besson *et al.* (CLEO Collab.), Phys. Rev. **D68**, 032002 (2003).
59. P. Krokovny *et al.* (Belle Collab.), Phys. Rev. Lett. **91**, 262002 (2003).
60. J. Brodzicka *et al.* (Belle Collab.), Phys. Rev. Lett. **100**, 092001 (2008).
61. S.-K. Choi *et al.* (Belle Collab.), Phys. Rev. Lett. **91**, 262001 (2003).
62. D. Acosta *et al.* (CDF II Collab.), Phys. Rev. Lett. **93**, 072001 (2004); BaBar Collab., B. Aubert *et al.*, Phys. Rev. **D71**, 071103 (2005).
63. G. Gokhroo *et al.* (Belle Collab.), Phys. Rev. Lett. **97**, 162002 (2006).
64. B. Aubert *et al.* (BaBar Collab.), Phys. Rev. **D77**, 011102 (2008); B. Aubert *et al.* (BaBar Collab.), Phys. Rev. **D71**, 031501 (2005).
65. S.-K. Choi *et al.* (Belle Collab.), Phys. Rev. Lett. **94**, 182002 (2005).
66. B. Aubert *et al.* (BaBar Collab.), Phys. Rev. **D73**, 011101 (2006).
67. B. Aubert *et al.* (BaBar Collab.), Phys. Rev. Lett. **95**, 142001 (2005).
68. S.-K. Choi *et al.* (Belle Collab.), Phys. Rev. Lett. **100**, 121803 (2008).
69. See the “Non- $q\bar{q}$ mesons,” by C. Amsler in this *Review*.
70. D. Acosta *et al.* (CDF Collab.), Phys. Rev. Lett. **95**, 031801 (2005).
71. A. Abulencia *et al.* (CDF Collab.), Phys. Rev. Lett. **97**, 211802 (2006).
72. B. Aubert *et al.* (BaBar Collab.), Phys. Rev. Lett. **97**, 171805 (2006).
73. K. Abe *et al.* (Belle Collab.), Phys. Rev. Lett. **95**, 231802 (2005).
74. B. Aubert *et al.* (BaBar Collab.), Phys. Rev. Lett. **99**, 021603 (2007).
75. Y. Chao *et al.* (Belle Collab.), Phys. Rev. Lett. **93**, 191802 (2004).
76. M. Morello (CDF Collab.), Nucl. Phys. **B170**, 39 (2007).
77. B. Aubert *et al.* (BaBar Collab.), Phys. Rev. **D72**, 072003 (2005); A. Garmash *et al.* (Belle Collab.), Phys. Rev. Lett. **96**, 251803 (2006).
78. P. Chang *et al.* (Belle Collab.), Phys. Rev. **D75**, 071104 (2007); B. Aubert *et al.* (BaBar Collab.), Phys. Rev. **D76**, 031103 (2007).
79. B. Aubert *et al.* (BaBar Collab.), Phys. Rev. Lett. **97**, 201802 (2006); C.H. Wang *et al.* (Belle Collab.), Phys. Rev. **D75**, 092005 (2007).
80. M. Gronau and D. London, Phys. Rev. Lett. **65**, 3381 (1990).
81. B. Aubert *et al.* (BaBar Collab.), Phys. Rev. Lett. **98**, 111801 (2007).
82. B. Aubert *et al.* (BaBar Collab.), Phys. Rev. Lett. **98**, 181803 (2007).
83. M. Gronau and J. Zupan, Phys. Rev. **D70**, 074031 (2004).
84. See the “Polarization in *B* Decays,” by A. Gritsan and J. Smith in this *Review*.
85. A. Williamson and J. Zupan, Phys. Rev. **D74**, 014003 (2006).
86. B. Aubert *et al.* (BaBar Collab.), Phys. Rev. **D72**, 072003 (2005); A. Garmash *et al.* (Belle Collab.), Phys. Rev. Lett. **96**, 251803 (2006); P. Chang *et al.* (Belle Collab.), Phys. Lett. **B599**, 148 (2004); B. Aubert *et al.* (BaBar Collab.), Phys. Rev. **D73**, 031101R (2006); A. Garmash *et al.* (Belle Collab.), Phys. Rev. **D75**, 012006 (2007).
87. A. Garmash *et al.* (Belle Collab.), Phys. Rev. **D71**, 092003 (2005); B. Aubert *et al.* (BaBar Collab.), Phys. Rev. **D74**, 032003 (2006); A. Garmash *et al.* (Belle Collab.), Phys. Rev. **D69**, 012001 (2004); B. Aubert *et al.* (BaBar Collab.), Phys. Rev. Lett. **93**, 181805 (2004); B. Aubert *et al.* (BaBar Collab.), Phys. Rev. Lett. **95**, 011801 (2006).
88. B. Aubert *et al.* (BaBar Collab.), Phys. Rev. **D74**, 051104R (2006); B. Aubert *et al.* (BaBar Collab.), Phys. Rev. **D76**, 071104R (2007).
89. B. Aubert *et al.* (BaBar Collab.), Phys. Rev. Lett. **99**, 221801 (2007).
90. R. Fleischer, Phys. Lett. **B459**, 306 (1999); D. London and J. Matias, Phys. Rev. **D70**, 031502 (2004).
91. M. Nakao *et al.* (Belle Collab.), Phys. Rev. **D69**, 112001 (2004); B. Aubert *et al.* (BaBar Collab.), Phys. Rev. **D70**, 112006 (2004).
92. B. Aubert *et al.* (BaBar Collab.), Phys. Rev. **D70**, 091105R (2004); H. Yang *et al.* (Belle Collab.), Phys. Rev. Lett. **94**, 111802 (2005); S. Nishida *et al.* (Belle Collab.), Phys. Lett. **B610**, 23 (2005); B. Aubert *et al.* (Belle Collab.), Phys. Rev. **D74**, 031102R (2004).
93. A. Ali *et al.*, Phys. Lett. **B595**, 323 (2004); P. Ball, G. Jones, and R. Zwicky, Phys. Rev. **D75**, 054004 (2007).
94. J.L. Hewett, Phys. Rev. Lett. **70**, 1045 (1993).
95. S. Chen *et al.* (CLEO Collab.), Phys. Rev. Lett. **87**, 251807 (2001); K. Abe *et al.* (Belle Collab.), Phys. Lett. **B511**, 151 (2001); P. Koppenburg *et al.* (Belle Collab.), Phys. Rev. Lett. **93**, 061803 (2004); B. Aubert *et al.* (BaBar Collab.), Phys. Rev. **D72**, 052004 (2005); B. Aubert *et al.* (BaBar Collab.), Phys. Rev. Lett. **97**, 171803 (2006).
96. K. Chetyrkin *et al.*, Phys. Lett. **B400**, 206 (1997); Erratum-*ibid.*, Phys. Lett. **B425**, 414 (1998).

Meson Particle Listings

b -flavored hadrons, b -flavored hadrons, B^\pm

97. A.J. Buras *et al.*, Phys. Lett. **B414**, 157 (1997); Erratum-*ibid.*, Phys. Lett. **B434**, 459 (1998).
98. A.L. Kagan and Matthias Neubert, Eur. Phys. J. **C7**, 5 (1999).
99. K. Kiers *et al.*, Phys. Rev. **D62**, 116004 (2000).
100. A.L. Kagan and M. Neubert, Phys. Rev. **D58**, 094012 (1998).
101. S. Baek and P. Ko, Phys. Rev. Lett. **83**, 488 (1998).
102. P. Koppenburg *et al.* (Belle Collab.), Phys. Rev. Lett. **93**, 061803 (2004); B. Aubert *et al.* (BaBar Collab.), Phys. Rev. **D72**, 052004 (2005).
103. K. Abe *et al.* (Belle Collab.), Phys. Rev. Lett. **91**, 261601 (2003).
104. B. Aubert *et al.* (BaBar Collab.), Phys. Rev. **D73**, 092001 (2006).
105. M. Iwasaki *et al.* (Belle Collab.), Phys. Rev. **D72**, 092005 (2005); B. Aubert *et al.* (BaBar Collab.), Phys. Rev. Lett. **93**, 081802 (2004).
106. T. Aaltonen *et al.* (CDF Collab.), Phys. Rev. Lett. **100**, 101802 (2008).

A NOTE ON HFAG ACTIVITIES

The Heavy Flavor Averaging Group (HFAG) has been formed, continuing the activities of the LEP Heavy Flavor Steering group, to provide the averages for measurements dedicated to the b -flavor related quantities. The HFAG consists of representatives and contacts from the experimental groups: BaBar, Belle, CDF, CLEO, DØ, LEP, and SLD.

In the averaging the input parameters used in the various analyses are adjusted (rescaled) to common values, and all known correlations are taken into account. The HFAG has five subgroups providing averages for b -hadron lifetimes and B -oscillation parameters, CP -violation measurements, semileptonic parameters, rare branching fractions, and b -hadron decays to charm. The averages provided by the HFAG are listed as “OUR EVALUATION” with a corresponding note.

The most up-to-date and complete listing of averages and more detailed information on the averaging procedures are available at:

<http://www.slac.stanford.edu/xorg/hfag> and also at
<http://belle.kek.jp/mirror/hfag> (KEK mirror site).

B^\pm

$$J(P) = \frac{1}{2}(0^-)$$

Quantum numbers not measured. Values shown are quark-model predictions.

See also the B^\pm/B^0 ADMIXTURE and $B^\pm/B^0/B_s^0/b$ -baryon ADMIXTURE sections.

B^\pm MASS

The fit uses m_{B^\pm} , ($m_{B^0} - m_{B^\pm}$), and m_{B^0} to determine m_{B^\pm} , m_{B^0} , and the mass difference.

VALUE (MeV)	EVTs	DOCUMENT ID	TECN	COMMENT
5279.15 ± 0.31 OUR FIT				
5279.1 ± 0.4 OUR AVERAGE				
5279.10 ± 0.41 ± 0.36		¹ ACOSTA 06	CDF	$p\bar{p}$ at 1.96 TeV
5279.1 ± 0.4 ± 0.4	526	² CSORNA 00	CLE2	$e^+e^- \rightarrow \Upsilon(4S)$
5279.1 ± 1.7 ± 1.4	147	ABE 96B	CDF	$p\bar{p}$ at 1.8 TeV
••• We do not use the following data for averages, fits, limits, etc. •••				
5278.8 ± 0.54 ± 2.0	362	ALAM 94	CLE2	$e^+e^- \rightarrow \Upsilon(4S)$
5278.3 ± 0.4 ± 2.0		BORTOLETTO92	CLEO	$e^+e^- \rightarrow \Upsilon(4S)$
5280.5 ± 1.0 ± 2.0		³ ALBRECHT 90J	ARG	$e^+e^- \rightarrow \Upsilon(4S)$
5275.8 ± 1.3 ± 3.0	32	ALBRECHT 87C	ARG	$e^+e^- \rightarrow \Upsilon(4S)$
5278.2 ± 1.8 ± 3.0	12	⁴ ALBRECHT 87D	ARG	$e^+e^- \rightarrow \Upsilon(4S)$
5278.6 ± 0.8 ± 2.0		BEBEK 87	CLEO	$e^+e^- \rightarrow \Upsilon(4S)$

¹ Uses exclusively reconstructed final states containing a $J/\psi \rightarrow \mu^+\mu^-$ decays.

² CSORNA 00 uses fully reconstructed $526 B^+ \rightarrow J/\psi(\ell^+) K^+$ events and invariant masses without beam constraint.

³ ALBRECHT 90J assumes 10580 for $\Upsilon(4S)$ mass. Supersedes ALBRECHT 87C and ALBRECHT 87D.

⁴ Found using fully reconstructed decays with $J/\psi(1S)$. ALBRECHT 87D assume $m_{\Upsilon(4S)} = 10577$ MeV.

B^\pm MEAN LIFE

See $B^\pm/B^0/B_s^0/b$ -baryon ADMIXTURE section for data on B -hadron mean life averaged over species of bottom particles.

“OUR EVALUATION” is an average using rescaled values of the data listed below. The average and rescaling were performed by the Heavy Flavor Averaging Group (HFAG) and are described at <http://www.slac.stanford.edu/xorg/hfag/>. The averaging/rescaling procedure takes into account correlations between the measurements and asymmetric lifetime errors.

VALUE (10^{-12} s)	EVTs	DOCUMENT ID	TECN	COMMENT
1.638 ± 0.011 OUR EVALUATION				
1.635 ± 0.011 ± 0.011		¹ ABE 05B	BELL	$e^+e^- \rightarrow \Upsilon(4S)$
1.624 ± 0.014 ± 0.018		² ABDALLAH 04E	DLPH	$e^+e^- \rightarrow Z$
1.636 ± 0.058 ± 0.025		³ ACOSTA 02C	CDF	$p\bar{p}$ at 1.8 TeV
1.673 ± 0.032 ± 0.023		⁴ AUBERT 01F	BABR	$e^+e^- \rightarrow \Upsilon(4S)$
1.648 ± 0.049 ± 0.035		⁵ BARATE 00R	ALEP	$e^+e^- \rightarrow Z$
1.643 ± 0.037 ± 0.025		⁶ ABBIENDI 99J	OPAL	$e^+e^- \rightarrow Z$
1.637 ± 0.058 ± 0.045 -0.043		⁵ ABE 98Q	CDF	$p\bar{p}$ at 1.8 TeV
1.66 ± 0.06 ± 0.03		⁶ ACCIARRI 98S	L3	$e^+e^- \rightarrow Z$
1.66 ± 0.06 ± 0.05		⁶ ABE 97J	SLD	$e^+e^- \rightarrow Z$
1.58 ± 0.21 ± 0.04 -0.18 -0.03	94	³ BUSKULIC 96J	ALEP	$e^+e^- \rightarrow Z$
1.61 ± 0.16 ± 0.12		^{5,7} ABREU 95Q	DLPH	$e^+e^- \rightarrow Z$
1.72 ± 0.08 ± 0.06		⁸ ADAM 95	DLPH	$e^+e^- \rightarrow Z$
1.52 ± 0.14 ± 0.09		⁵ AKERS 95T	OPAL	$e^+e^- \rightarrow Z$
••• We do not use the following data for averages, fits, limits, etc. •••				
1.695 ± 0.026 ± 0.015		⁴ ABE 02H	BELL	Repl. by ABE 05B
1.68 ± 0.07 ± 0.02		³ ABE 98B	CDF	Repl. by ACOSTA 02C
1.56 ± 0.13 ± 0.06		⁵ ABE 96C	CDF	Repl. by ABE 98Q
1.58 ± 0.09 ± 0.03		⁹ BUSKULIC 96J	ALEP	$e^+e^- \rightarrow Z$
1.58 ± 0.09 ± 0.04		⁵ BUSKULIC 96J	ALEP	Repl. by BARATE 00R
1.70 ± 0.09		¹⁰ ADAM 95	DLPH	$e^+e^- \rightarrow Z$
1.61 ± 0.16 ± 0.05	148	³ ABE 94D	CDF	Repl. by ABE 98B
1.30 ± 0.33 ± 0.16 -0.29	92	⁵ ABREU 93D	DLPH	Sup. by ABREU 95Q
1.56 ± 0.19 ± 0.13	134	⁸ ABREU 93G	DLPH	Sup. by ADAM 95
1.51 ± 0.30 ± 0.12 -0.28 -0.14	59	⁵ ACTON 93C	OPAL	Sup. by AKERS 95T
1.47 ± 0.22 ± 0.15 -0.19 -0.14	77	⁵ BUSKULIC 93D	ALEP	Sup. by BUSKULIC 96J

¹ Measurement performed using a combined fit of CP -violation, mixing and lifetimes.

² Measurement performed using an inclusive reconstruction and B flavor identification technique.

³ Measured mean life using fully reconstructed decays.

⁴ Events are selected in which one B meson is fully reconstructed while the second B meson is reconstructed inclusively.

⁵ Data analyzed using $D/D^* \ell X$ event vertices.

⁶ Data analyzed using charge of secondary vertex.

⁷ ABREU 95Q assumes $B(B^0 \rightarrow D^{*-} \ell^+ \nu_\ell) = 3.2 \pm 1.7\%$.

⁸ Data analyzed using vertex-charge technique to tag B charge.

⁹ Combined result of $D/D^* \ell X$ analysis and fully reconstructed B analysis.

¹⁰ Combined ABREU 95Q and ADAM 95 result.

B^- DECAY MODES

B^- modes are charge conjugates of the modes below. Modes which do not identify the charge state of the B are listed in the B^\pm/B^0 ADMIXTURE section.

The branching fractions listed below assume 50% $B^0\bar{B}^0$ and 50% B^+B^- production at the $\Upsilon(4S)$. We have attempted to bring older measurements up to date by rescaling their assumed $\Upsilon(4S)$ production ratio to 50:50 and their assumed D, D_s, D^* , and ψ branching ratios to current values whenever this would affect our averages and best limits significantly.

Indentation is used to indicate a subchannel of a previous reaction. All resonant subchannels have been corrected for resonance branching fractions to the final state so the sum of the subchannel branching fractions can exceed that of the final state.

For inclusive branching fractions, e.g., $B \rightarrow D^\pm$ anything, the values usually are multiplicities, not branching fractions. They can be greater than one.

Mode	Fraction (Γ_i/Γ)	Scale factor/ Confidence level
Semileptonic and leptonic modes		
Γ_1 $\ell^+ \nu_\ell$ anything	[a] (10.99 \pm 0.28) %	
Γ_2 $e^+ \nu_e X_c$	(10.8 \pm 0.4) %	
Γ_3 $D \ell^+ \nu_\ell$ anything	(10.4 \pm 0.8) %	
Γ_4 $\bar{D}^0 \ell^+ \nu_\ell$	[a] (2.27 \pm 0.11) %	
Γ_5 $\bar{D}^0 \tau^+ \nu_\tau$	(7 \pm 4) $\times 10^{-3}$	
Γ_6 $\bar{D}^*(2007)^0 \ell^+ \nu_\ell$	[a] (6.07 \pm 0.29) %	
Γ_7 $D^*(2007)^0 \tau^+ \nu_\tau$	(2.2 \pm 0.6) %	
Γ_8 $D^- \pi^+ \ell^+ \nu_\ell$	(4.2 \pm 0.5) $\times 10^{-3}$	
Γ_9 $\bar{D}_0^*(2420)^0 \ell^+ \nu_\ell \times$ $B(\bar{D}_0^{*0} \rightarrow D^+ \pi^-)$	(2.4 \pm 0.7) $\times 10^{-3}$	
Γ_{10} $\bar{D}_2^*(2460)^0 \ell^+ \nu_\ell \times$ $B(\bar{D}_2^{*0} \rightarrow D^+ \pi^-)$	(2.2 \pm 0.5) $\times 10^{-3}$	
Γ_{11} $D^{(*)} n \pi \ell^+ \nu_\ell$ ($n \geq 1$)	(1.99 \pm 0.28) %	
Γ_{12} $D^{*-} \pi^+ \ell^+ \nu_\ell$	(6.1 \pm 0.6) $\times 10^{-3}$	
Γ_{13} $\bar{D}_1(2420)^0 \ell^+ \nu_\ell \times B(\bar{D}_1^0 \rightarrow$ $D^{*+} \pi^-)$	(4.0 \pm 0.7) $\times 10^{-3}$	
Γ_{14} $\bar{D}_1'(2430)^0 \ell^+ \nu_\ell \times B(\bar{D}_1^0 \rightarrow$ $D^{*+} \pi^-)$	< 7 $\times 10^{-4}$	CL=90%
Γ_{15} $\bar{D}_2^*(2460)^0 \ell^+ \nu_\ell \times$ $B(\bar{D}_2^{*0} \rightarrow D^{*+} \pi^-)$	(1.8 \pm 0.7) $\times 10^{-3}$	
Γ_{16} $\pi^0 \ell^+ \nu_\ell$	(7.7 \pm 1.2) $\times 10^{-5}$	
Γ_{17} $\pi^0 e^+ \nu_e$		
Γ_{18} $\eta \ell^+ \nu_\ell$	< 1.01 $\times 10^{-4}$	CL=90%
Γ_{19} $\eta' \ell^+ \nu_\ell$	(2.7 \pm 1.0) $\times 10^{-4}$	
Γ_{20} $\omega \ell^+ \nu_\ell$	[a] (1.3 \pm 0.6) $\times 10^{-4}$	
Γ_{21} $\omega \mu^+ \nu_\mu$		
Γ_{22} $\rho^0 \ell^+ \nu_\ell$	[a] (1.28 \pm 0.18) $\times 10^{-4}$	
Γ_{23} $p \bar{p} e^+ \nu_e$	< 5.2 $\times 10^{-3}$	CL=90%
Γ_{24} $e^+ \nu_e$	< 9.8 $\times 10^{-6}$	CL=90%
Γ_{25} $\mu^+ \nu_\mu$	< 1.7 $\times 10^{-6}$	CL=90%
Γ_{26} $\tau^+ \nu_\tau$	(1.4 \pm 0.4) $\times 10^{-4}$	
Γ_{27} $e^+ \nu_e \gamma$	< 2.0 $\times 10^{-4}$	CL=90%
Γ_{28} $\mu^+ \nu_\mu \gamma$	< 5.2 $\times 10^{-5}$	CL=90%
Inclusive modes		
Γ_{29} $D^0 X$	(8.6 \pm 0.7) %	
Γ_{30} $\bar{D}^0 X$	(79 \pm 4) %	
Γ_{31} $D^+ X$	(2.5 \pm 0.5) %	
Γ_{32} $D^- X$	(9.9 \pm 1.2) %	
Γ_{33} $D_s^+ X$	(7.9 \pm 1.4 -1.3) %	
Γ_{34} $D_s^- X$	(1.10 \pm 0.45 -0.32) %	
Γ_{35} $A_c^+ X$	(2.1 \pm 0.9 -0.6) %	
Γ_{36} $\bar{A}_c^- X$	(2.8 \pm 1.1 -0.9) %	
Γ_{37} $\bar{c} X$	(97 \pm 4) %	
Γ_{38} $c X$	(23.4 \pm 2.2 -1.8) %	
Γ_{39} $\bar{c} c X$	(120 \pm 6) %	

 D, D^* , or D_s modes

Γ_{40} $\bar{D}^0 \pi^+$	(4.84 \pm 0.15) $\times 10^{-3}$	
Γ_{41} $D_{CP(+1)} \pi^+$	[b] (1.96 \pm 0.34) $\times 10^{-3}$	
Γ_{42} $D_{CP(-1)} \pi^+$	[b] (1.8 \pm 0.4) $\times 10^{-3}$	
Γ_{43} $\bar{D}^0 \rho^+$	(1.34 \pm 0.18) %	
Γ_{44} $\bar{D}^0 K^+$	(4.02 \pm 0.21) $\times 10^{-4}$	
Γ_{45} $D_{CP(+1)} K^+$	[b] (1.81 \pm 0.27) $\times 10^{-4}$	
Γ_{46} $D_{CP(-1)} K^+$	[b] (1.73 \pm 0.23) $\times 10^{-4}$	
Γ_{47} $[K^- \pi^+]_D K^+$	[c]	
Γ_{48} $[K^+ \pi^-]_D K^+$	[c]	
Γ_{49} $[K^- \pi^+ \pi^0]_D K^+$		
Γ_{50} $[K^+ \pi^- \pi^0]_D K^+$		
Γ_{51} $[K^- \pi^+]_D K^*(892)^+$	[c]	
Γ_{52} $[K^+ \pi^-]_D K^*(892)^+$	[c]	
Γ_{53} $[K^- \pi^+]_D \pi^+$	[c] (1.7 \pm 0.5) $\times 10^{-5}$	
Γ_{54} $[\pi^+ \pi^- \pi^0]_D K^-$	(4.6 \pm 0.9) $\times 10^{-6}$	
Γ_{55} $\bar{D}^0 K^*(892)^+$	(5.3 \pm 0.4) $\times 10^{-4}$	
Γ_{56} $D_{CP(-1)} K^*(892)^+$	[b] (1.7 \pm 0.7) $\times 10^{-4}$	
Γ_{57} $D_{CP(+1)} K^*(892)^+$	[b] (5.2 \pm 1.2) $\times 10^{-4}$	
Γ_{58} $\bar{D}^0 K^+ \bar{K}^0$	(5.5 \pm 1.6) $\times 10^{-4}$	
Γ_{59} $\bar{D}^0 K^+ \bar{K}^*(892)^0$	(7.5 \pm 1.7) $\times 10^{-4}$	
Γ_{60} $\bar{D}^0 \pi^+ \pi^+ \pi^-$	(1.1 \pm 0.4) %	
Γ_{61} $\bar{D}^0 \pi^+ \pi^+ \pi^-$ nonresonant	(5 \pm 4) $\times 10^{-3}$	
Γ_{62} $\bar{D}^0 \pi^+ \rho^0$	(4.2 \pm 3.0) $\times 10^{-3}$	
Γ_{63} $\bar{D}^0 a_1(1260)^+$	(4 \pm 4) $\times 10^{-3}$	
Γ_{64} $\bar{D}^0 \omega \pi^+$	(4.1 \pm 0.9) $\times 10^{-3}$	
Γ_{65} $D^*(2010)^- \pi^+ \pi^+$	(1.35 \pm 0.22) $\times 10^{-3}$	
Γ_{66} $D^- \pi^+ \pi^+$	(1.02 \pm 0.16) $\times 10^{-3}$	
Γ_{67} $D^+ K^0$	< 5.0 $\times 10^{-6}$	CL=90%
Γ_{68} $\bar{D}^*(2007)^0 \pi^+$	(5.19 \pm 0.26) $\times 10^{-3}$	
Γ_{69} $\bar{D}_{CP(+1)}^0 \pi^+$	[d]	
Γ_{70} $\bar{D}_{CP(-1)}^0 \pi^+$	[d]	
Γ_{71} $\bar{D}^*(2007)^0 \omega \pi^+$	(4.5 \pm 1.2) $\times 10^{-3}$	
Γ_{72} $\bar{D}^*(2007)^0 \rho^+$	(9.8 \pm 1.7) $\times 10^{-3}$	
Γ_{73} $\bar{D}^*(2007)^0 K^+$	(4.16 \pm 0.33) $\times 10^{-4}$	
Γ_{74} $\bar{D}_{CP(+1)}^0 K^+$	[d]	
Γ_{75} $\bar{D}_{CP(-1)}^0 K^+$	[d]	
Γ_{76} $\bar{D}^*(2007)^0 K^*(892)^+$	(8.1 \pm 1.4) $\times 10^{-4}$	
Γ_{77} $\bar{D}^*(2007)^0 K^+ \bar{K}^0$	< 1.06 $\times 10^{-3}$	CL=90%
Γ_{78} $\bar{D}^*(2007)^0 K^+ K^*(892)^0$	(1.5 \pm 0.4) $\times 10^{-3}$	
Γ_{79} $\bar{D}^*(2007)^0 \pi^+ \pi^+ \pi^-$	(1.03 \pm 0.12) %	
Γ_{80} $\bar{D}^*(2007)^0 a_1(1260)^+$	(1.9 \pm 0.5) %	
Γ_{81} $\bar{D}^*(2007)^0 \pi^- \pi^+ \pi^+ \pi^0$	(1.8 \pm 0.4) %	
Γ_{82} $\bar{D}^{*0} 3\pi^+ 2\pi^-$	(5.7 \pm 1.2) $\times 10^{-3}$	
Γ_{83} $D^*(2010)^+ \pi^0$	< 1.7 $\times 10^{-4}$	CL=90%
Γ_{84} $D^*(2010)^+ K^0$	< 9.0 $\times 10^{-6}$	CL=90%
Γ_{85} $D^*(2010)^- \pi^+ \pi^+ \pi^0$	(1.5 \pm 0.7) %	
Γ_{86} $D^*(2010)^- \pi^+ \pi^+ \pi^+ \pi^-$	(2.6 \pm 0.4) $\times 10^{-3}$	
Γ_{87} $\bar{D}^{*0} \pi^+$	[e] (5.9 \pm 1.3) $\times 10^{-3}$	
Γ_{88} $\bar{D}_1^*(2420)^0 \pi^+$	(1.5 \pm 0.6) $\times 10^{-3}$	S=1.3
Γ_{89} $\bar{D}_1(2420)^0 \pi^+ \times B(\bar{D}_1^0 \rightarrow$ $\bar{D}^0 \pi^+ \pi^-)$	(1.9 \pm 0.5 -0.6) $\times 10^{-4}$	
Γ_{90} $\bar{D}_2^*(2462)^0 \pi^+$ $\times B(\bar{D}_2^{*0}(2462)^0 \rightarrow D^- \pi^+)$	(3.4 \pm 0.8) $\times 10^{-4}$	
Γ_{91} $\bar{D}_0^*(2400)^0 \pi^+$ $\times B(\bar{D}_0^{*0}(2400)^0 \rightarrow D^- \pi^+)$	(6.1 \pm 1.9) $\times 10^{-4}$	
Γ_{92} $\bar{D}_1(2421)^0 \pi^+$ $\times B(\bar{D}_1(2421)^0 \rightarrow D^{*-} \pi^+)$	(6.8 \pm 1.5) $\times 10^{-4}$	
Γ_{93} $\bar{D}_2^*(2462)^0 \pi^+$ $\times B(\bar{D}_2^{*0}(2462)^0 \rightarrow D^{*-} \pi^+)$	(1.8 \pm 0.5) $\times 10^{-4}$	
Γ_{94} $\bar{D}_1'(2427)^0 \pi^+$ $\times B(\bar{D}_1'(2427)^0 \rightarrow D^{*-} \pi^+)$	(5.0 \pm 1.2) $\times 10^{-4}$	
Γ_{95} $\bar{D}_1(2420)^0 \pi^+ \times B(\bar{D}_1^0 \rightarrow$ $\bar{D}^{*0} \pi^+ \pi^-)$	< 6 $\times 10^{-6}$	CL=90%
Γ_{96} $\bar{D}_1^*(2420)^0 \rho^+$	< 1.4 $\times 10^{-3}$	CL=90%
Γ_{97} $\bar{D}_2^*(2460)^0 \pi^+$	< 1.3 $\times 10^{-3}$	CL=90%
Γ_{98} $\bar{D}_2^*(2460)^0 \pi^+ \times B(\bar{D}_2^{*0} \rightarrow$ $\bar{D}^{*0} \pi^+ \pi^-)$	< 2.2 $\times 10^{-5}$	CL=90%
Γ_{99} $\bar{D}_2^*(2460)^0 \rho^+$	< 4.7 $\times 10^{-3}$	CL=90%
Γ_{100} $\bar{D}^0 D_s^+$	(1.03 \pm 0.17) %	

Meson Particle Listings

B^\pm

Γ_{101}	$D_{s0}(2317)^+ \bar{D}^0 \times$ $B(D_{s0}(2317)^+ \rightarrow D_s^+ \pi^0)$	$(7.5 \begin{smallmatrix} +2.2 \\ -1.7 \end{smallmatrix}) \times 10^{-4}$	
Γ_{102}	$D_{s0}(2317)^+ \bar{D}^0 \times$ $B(D_{s0}(2317)^+ \rightarrow D_s^{*+} \gamma)$	$< 7.6 \times 10^{-4}$	CL=90%
Γ_{103}	$D_{s0}(2317)^+ \bar{D}^*(2007)^0 \times$ $B(D_{s0}(2317)^+ \rightarrow D_s^+ \pi^0)$	$(9 \pm 7) \times 10^{-4}$	
Γ_{104}	$D_{sJ}(2457)^+ \bar{D}^0$	$(3.1 \begin{smallmatrix} +1.0 \\ -0.9 \end{smallmatrix}) \times 10^{-3}$	
Γ_{105}	$D_{sJ}(2457)^+ \bar{D}^0 \times$ $B(D_{sJ}(2457)^+ \rightarrow D_s^+ \gamma)$	$(4.8 \begin{smallmatrix} +1.3 \\ -1.1 \end{smallmatrix}) \times 10^{-4}$	
Γ_{106}	$D_{sJ}(2457)^+ \bar{D}^0 \times$ $B(D_{sJ}(2457)^+ \rightarrow$ $D_s^+ \pi^+ \pi^-)$	$< 2.2 \times 10^{-4}$	CL=90%
Γ_{107}	$D_{sJ}(2457)^+ \bar{D}^0 \times$ $B(D_{sJ}(2457)^+ \rightarrow D_s^+ \pi^0)$	$< 2.7 \times 10^{-4}$	CL=90%
Γ_{108}	$D_{sJ}(2457)^+ \bar{D}^0 \times$ $B(D_{sJ}(2457)^+ \rightarrow D_s^{*+} \gamma)$	$< 9.8 \times 10^{-4}$	CL=90%
Γ_{109}	$D_{sJ}(2457)^+ \bar{D}^*(2007)^0$	$(1.20 \pm 0.30) \%$	
Γ_{110}	$D_{sJ}(2457)^+ \bar{D}^*(2007)^0 \times$ $B(D_{sJ}(2457)^+ \rightarrow D_s^+ \gamma)$	$(1.4 \begin{smallmatrix} +0.7 \\ -0.6 \end{smallmatrix}) \times 10^{-3}$	
Γ_{111}	$\bar{D}^0 D_{s1}(2536)^+ \times$ $B(D_{s1}(2536)^+ \rightarrow$ $D^*(2007)^0 K^+)$	$(2.2 \pm 0.7) \times 10^{-4}$	
Γ_{112}	$\bar{D}^*(2007)^0 D_{s1}(2536)^+ \times$ $B(D_{s1}(2536)^+ \rightarrow$ $D^*(2007)^0 K^+)$	$(5.5 \pm 1.6) \times 10^{-4}$	
Γ_{113}	$\bar{D}^0 D_{s1}(2536)^+ \times$ $B(D_{s1}(2536)^+ \rightarrow D^{*+} K^0)$	$(2.3 \pm 1.1) \times 10^{-4}$	
Γ_{114}	$\bar{D}^0 D_{sJ}(2700)^+ \times$ $B(D_{sJ}(2700)^+ \rightarrow D^0 K^+)$	$(1.13 \begin{smallmatrix} +0.26 \\ -0.36 \end{smallmatrix}) \times 10^{-3}$	
Γ_{115}	$\bar{D}^{*0} D_{s1}(2536)^+ \times$ $B(D_{s1}(2536)^+ \rightarrow D^{*+} K^0)$	$(3.9 \pm 2.6) \times 10^{-4}$	
Γ_{116}	$\bar{D}^{*0} D_{sJ}(2573)^+ \times$ $B(D_{sJ}(2573)^+ \rightarrow D^0 K^+)$	$< 2 \times 10^{-4}$	CL=90%
Γ_{117}	$\bar{D}^*(2007)^0 D_{sJ}(2573)^+ \times$ $B(D_{sJ}(2573)^+ \rightarrow D^0 K^+)$	$< 5 \times 10^{-4}$	CL=90%
Γ_{118}	$\bar{D}^0 D_s^{*+}$	$(7.8 \pm 1.6) \times 10^{-3}$	
Γ_{119}	$\bar{D}^*(2007)^0 D_s^+$	$(8.4 \pm 1.7) \times 10^{-3}$	
Γ_{120}	$\bar{D}^*(2007)^0 D_s^{*+}$	$(1.75 \pm 0.23) \%$	
Γ_{121}	$D_s^{(*)+} \bar{D}^{*0}$	$(2.7 \pm 1.2) \%$	
Γ_{122}	$\bar{D}^*(2007)^0 D^*(2010)^+$	$(8.1 \pm 1.7) \times 10^{-4}$	
Γ_{123}	$\bar{D}^0 D^*(2010)^+ +$ $\bar{D}^*(2007)^0 D^+$	$< 1.30 \%$	CL=90%
Γ_{124}	$\bar{D}^0 D^*(2010)^+$	$(3.9 \pm 0.5) \times 10^{-4}$	
Γ_{125}	$\bar{D}^0 D^+$	$(4.2 \pm 0.6) \times 10^{-4}$	
Γ_{126}	$\bar{D}^0 D^+ K^0$	$< 2.8 \times 10^{-3}$	CL=90%
Γ_{127}	$D^+ \bar{D}^*(2007)^0$	$(6.3 \pm 1.7) \times 10^{-4}$	
Γ_{128}	$\bar{D}^*(2007)^0 D^+ K^0$	$< 6.1 \times 10^{-3}$	CL=90%
Γ_{129}	$\bar{D}^0 \bar{D}^*(2010)^+ K^0$	$(5.2 \pm 1.2) \times 10^{-3}$	
Γ_{130}	$\bar{D}^*(2007)^0 D^*(2010)^+ K^0$	$(7.8 \pm 2.6) \times 10^{-3}$	
Γ_{131}	$\bar{D}^0 D^0 K^+$	$(2.10 \pm 0.26) \times 10^{-3}$	
Γ_{132}	$\bar{D}^*(2007)^0 D^0 K^+$	$< 3.8 \times 10^{-3}$	CL=90%
Γ_{133}	$\bar{D}^0 D^*(2007)^0 K^+$	$(4.7 \pm 1.0) \times 10^{-3}$	
Γ_{134}	$\bar{D}^*(2007)^0 D^*(2007)^0 K^+$	$(5.3 \pm 1.6) \times 10^{-3}$	
Γ_{135}	$D^- D^+ K^+$	$< 4 \times 10^{-4}$	CL=90%
Γ_{136}	$D^- D^*(2010)^+ K^+$	$< 7 \times 10^{-4}$	CL=90%
Γ_{137}	$D^*(2010)^- D^+ K^+$	$(1.5 \pm 0.4) \times 10^{-3}$	
Γ_{138}	$D^*(2010)^- D^*(2010)^+ K^+$	$< 1.8 \times 10^{-3}$	CL=90%
Γ_{139}	$(\bar{D}^+ \bar{D}^*)(D^+ D^+) K$	$(3.5 \pm 0.6) \%$	
Γ_{140}	$D_s^+ \pi^0$	$(1.6 \pm 0.6) \times 10^{-5}$	
Γ_{141}	$D_s^{*+} \pi^0$	$< 2.7 \times 10^{-4}$	CL=90%
Γ_{142}	$D_s^+ \eta$	$< 4 \times 10^{-4}$	CL=90%
Γ_{143}	$D_s^{*+} \eta$	$< 6 \times 10^{-4}$	CL=90%
Γ_{144}	$D_s^{*+} \rho^0$	$< 3.1 \times 10^{-4}$	CL=90%
Γ_{145}	$D_s^{*+} \rho^0$	$< 4 \times 10^{-4}$	CL=90%
Γ_{146}	$D_s^+ \omega$	$< 4 \times 10^{-4}$	CL=90%
Γ_{147}	$D_s^{*+} \omega$	$< 6 \times 10^{-4}$	CL=90%
Γ_{148}	$D_s^+ a_1(1260)^0$	$< 1.8 \times 10^{-3}$	CL=90%
Γ_{149}	$D_s^{*+} a_1(1260)^0$	$< 1.4 \times 10^{-3}$	CL=90%
Γ_{150}	$D_s^+ \phi$	$< 1.9 \times 10^{-6}$	CL=90%
Γ_{151}	$D_s^{*+} \phi$	$< 1.2 \times 10^{-5}$	CL=90%

Γ_{152}	$D_s^+ \bar{K}^0$	$< 9 \times 10^{-4}$	CL=90%
Γ_{153}	$D_s^{*+} \bar{K}^0$	$< 9 \times 10^{-4}$	CL=90%
Γ_{154}	$D_s^+ \bar{K}^*(892)^0$	$< 4 \times 10^{-4}$	CL=90%
Γ_{155}	$D_s^{*+} \bar{K}^*(892)^0$	$< 4 \times 10^{-4}$	CL=90%
Γ_{156}	$D_s^+ \pi^+ K^+$	$< 7 \times 10^{-4}$	CL=90%
Γ_{157}	$D_s^{*+} \pi^+ K^+$	$< 9.9 \times 10^{-4}$	CL=90%
Γ_{158}	$D_s^+ \pi^+ K^*(892)^+$	$< 5 \times 10^{-3}$	CL=90%
Γ_{159}	$D_s^{*+} \pi^+ K^*(892)^+$	$< 7 \times 10^{-3}$	CL=90%

Charmonium modes

Γ_{160}	$\eta_c K^+$	$(9.1 \pm 1.3) \times 10^{-4}$	
Γ_{161}	$\eta_c K^*(892)^+$	$(1.2 \begin{smallmatrix} +0.7 \\ -0.6 \end{smallmatrix}) \times 10^{-3}$	
Γ_{162}	$\eta_c(2S) K^+$	$(3.4 \pm 1.8) \times 10^{-4}$	
Γ_{163}	$J/\psi(1S) K^+$	$(1.007 \pm 0.035) \times 10^{-3}$	
Γ_{164}	$J/\psi(1S) K^+ \pi^+ \pi^-$	$(1.07 \pm 0.19) \times 10^{-3}$	S=1.9
Γ_{165}	$h_c(1P) K^+ \times B(h_c(1P) \rightarrow$ $J/\psi \pi^+ \pi^-)$	$< 3.4 \times 10^{-6}$	CL=90%
Γ_{166}	$X(3872) K^+$	$< 3.2 \times 10^{-4}$	CL=90%
Γ_{167}	$X(3872) K^+ \times B(X \rightarrow$ $J/\psi \pi^+ \pi^-)$	$(1.14 \pm 0.20) \times 10^{-5}$	
Γ_{168}	$X(3872) K^+ \times B(X \rightarrow J/\psi \gamma)$	$(3.3 \pm 1.0) \times 10^{-6}$	
Γ_{169}	$X(3872) K^+ \times B(X \rightarrow D^0 \bar{D}^0)$	$< 6.0 \times 10^{-5}$	CL=90%
Γ_{170}	$X(3872) K^+ \times B(X \rightarrow D^+ D^-)$	$< 4.0 \times 10^{-5}$	CL=90%
Γ_{171}	$X(3872) K^+ \times B(X \rightarrow$ $D^0 \bar{D}^0 \pi^0)$	$(1.0 \pm 0.4) \times 10^{-4}$	
Γ_{172}	$X(3872) K^+ \times B(X \rightarrow \bar{D}^{*0} D^0)$	$(1.7 \pm 0.6) \times 10^{-4}$	
Γ_{173}	$X(3872) K^+ \times$ $B(X(3872) \rightarrow J/\psi(1S) \eta)$	$< 7.7 \times 10^{-6}$	CL=90%
Γ_{174}	$X(3872)^+ K^0 \times B(X(3872)^+ \rightarrow$ $J/\psi(1S) \pi^+ \pi^0)$	$[r] < 2.2 \times 10^{-5}$	CL=90%
Γ_{175}	$X(4260)^0 K^+ \times B(X^0 \rightarrow$ $J/\psi \pi^+ \pi^-)$	$< 2.9 \times 10^{-5}$	CL=95%
Γ_{176}	$X(3945)^0 K^+ \times B(X^0 \rightarrow$ $J/\psi \gamma)$	$< 1.4 \times 10^{-5}$	CL=90%
Γ_{177}	$Z(3930)^0 K^+ \times B(Z^0 \rightarrow J/\psi \gamma)$	$< 2.5 \times 10^{-6}$	CL=90%
Γ_{178}	$J/\psi(1S) K^*(892)^+$	$(1.43 \pm 0.08) \times 10^{-3}$	
Γ_{179}	$J/\psi(1S) K(1270)^+$	$(1.8 \pm 0.5) \times 10^{-3}$	
Γ_{180}	$J/\psi(1S) K(1400)^+$	$< 5 \times 10^{-4}$	CL=90%
Γ_{181}	$J/\psi(1S) \eta K^+$	$(1.08 \pm 0.33) \times 10^{-4}$	
Γ_{182}	$J/\psi(1S) \eta' K^+$	$< 8.8 \times 10^{-5}$	CL=90%
Γ_{183}	$J/\psi(1S) \phi K^+$	$(5.2 \pm 1.7) \times 10^{-5}$	S=1.2
Γ_{184}	$J/\psi(1S) \pi^+$	$(4.9 \pm 0.6) \times 10^{-5}$	S=1.5
Γ_{185}	$J/\psi(1S) \rho^+$	$(5.0 \pm 0.8) \times 10^{-5}$	
Γ_{186}	$J/\psi(1S) \pi^+ \pi^0$ nonresonant	$< 7.3 \times 10^{-6}$	CL=90%
Γ_{187}	$J/\psi(1S) a_1(1260)^+$	$< 1.2 \times 10^{-3}$	CL=90%
Γ_{188}	$J/\psi(1S) p \bar{\Lambda}$	$(1.18 \pm 0.31) \times 10^{-5}$	
Γ_{189}	$J/\psi(1S) \bar{\Sigma}^0 p$	$< 1.1 \times 10^{-5}$	CL=90%
Γ_{190}	$J/\psi(1S) D^+$	$< 1.2 \times 10^{-4}$	CL=90%
Γ_{191}	$J/\psi(1S) \bar{D}^0 \pi^+$	$< 2.5 \times 10^{-5}$	CL=90%
Γ_{192}	$\psi(2S) K^+$	$(6.48 \pm 0.35) \times 10^{-4}$	
Γ_{193}	$\psi(2S) K^*(892)^+$	$(6.7 \pm 1.4) \times 10^{-4}$	S=1.3
Γ_{194}	$\psi(2S) K^+ \pi^+ \pi^-$	$(1.9 \pm 1.2) \times 10^{-3}$	
Γ_{195}	$\psi(3770) K^+$	$(4.9 \pm 1.3) \times 10^{-4}$	
Γ_{196}	$\psi(3770) K^+ \times B(\psi \rightarrow D^0 \bar{D}^0)$	$(1.6 \pm 0.4) \times 10^{-4}$	S=1.1
Γ_{197}	$\psi(3770) K^+ \times B(\psi \rightarrow D^+ D^-)$	$(9.4 \pm 3.5) \times 10^{-5}$	
Γ_{198}	$\chi_{c0} \pi^+ \times B(\chi_{c0} \rightarrow \pi^+ \pi^-)$	$< 3 \times 10^{-7}$	CL=90%
Γ_{199}	$\chi_{c0}(1P) K^+$	$(1.40 \begin{smallmatrix} +0.23 \\ -0.19 \end{smallmatrix}) \times 10^{-4}$	
Γ_{200}	$\chi_{c0} K^*(892)^+$	$< 2.86 \times 10^{-3}$	CL=90%
Γ_{201}	$\chi_{c2} K^+$	$< 2.9 \times 10^{-5}$	CL=90%
Γ_{202}	$\chi_{c2} K^*(892)^+$	$< 1.2 \times 10^{-5}$	CL=90%
Γ_{203}	$\chi_{c1}(1P) \pi^+$	$(2.2 \pm 0.5) \times 10^{-5}$	
Γ_{204}	$\chi_{c1}(1P) K^+$	$(4.9 \pm 0.5) \times 10^{-4}$	S=1.5
Γ_{205}	$\chi_{c1}(1P) K^*(892)^+$	$(3.6 \pm 0.9) \times 10^{-4}$	
Γ_{206}	$h_c K^+$	$< 3.8 \times 10^{-5}$	

K or K* modes

Γ_{207}	$K^0 \pi^+$	$(2.31 \pm 0.10) \times 10^{-5}$	
Γ_{208}	$K^+ \pi^0$	$(1.29 \pm 0.06) \times 10^{-5}$	
Γ_{209}	$\eta' K^+$	$(7.02 \pm 0.25) \times 10^{-5}$	
Γ_{210}	$\eta' K^*(892)^+$	$(4.9 \pm 2.0) \times 10^{-6}$	
Γ_{211}	ηK^+	$(2.7 \pm 0.9) \times 10^{-6}$	S=3.3
Γ_{212}	$\eta K^*(892)^+$	$(1.93 \pm 0.16) \times 10^{-5}$	
Γ_{213}	$\eta K_0^*(1430)^+$	$(1.8 \pm 0.4) \times 10^{-5}$	
Γ_{214}	$\eta K_2^*(1430)^+$	$(9.1 \pm 3.0) \times 10^{-6}$	

Γ_{215}	ωK^+	(6.7 \pm 0.8) $\times 10^{-6}$	S=1.8	Γ_{274}	$K^+ \phi$	(4.9 $\begin{smallmatrix} +2.4 \\ -2.2 \end{smallmatrix}$) $\times 10^{-6}$	S=2.9
Γ_{216}	$\omega K^*(892)^+$	< 3.4 $\times 10^{-6}$	CL=90%	Γ_{275}	$\eta' \eta' K^+$	< 2.5 $\times 10^{-5}$	CL=90%
Γ_{217}	$a_0(980)^+ K^0 \times B(a_0(980)^+ \rightarrow \eta \pi^+)$	< 3.9 $\times 10^{-6}$	CL=90%	Γ_{276}	$K^*(892)^+ \gamma$	(4.03 \pm 0.26) $\times 10^{-5}$	
Γ_{218}	$a_0(980)^0 K^+ \times B(a_0(980)^0 \rightarrow \eta \pi^0)$	< 2.5 $\times 10^{-6}$	CL=90%	Γ_{277}	$K_1(1270)^+ \gamma$	(4.3 \pm 1.3) $\times 10^{-5}$	
Γ_{219}	$K^*(892)^0 \pi^+$	(1.09 \pm 0.18) $\times 10^{-5}$	S=2.1	Γ_{278}	$\eta K^+ \gamma$	(9.4 \pm 1.1) $\times 10^{-6}$	
Γ_{220}	$K^*(892)^+ \pi^0$	(6.9 \pm 2.4) $\times 10^{-6}$		Γ_{279}	$\eta' K^+ \gamma$	< 4.2 $\times 10^{-6}$	CL=90%
Γ_{221}	$K^+ \pi^- \pi^+$	(5.5 \pm 0.7) $\times 10^{-5}$	S=2.6	Γ_{280}	$\phi K^+ \gamma$	(3.5 \pm 0.6) $\times 10^{-6}$	
Γ_{222}	$K^+ \pi^- \pi^+$ nonresonant	(6 $\begin{smallmatrix} +6 \\ -4 \end{smallmatrix}$) $\times 10^{-6}$	S=6.1	Γ_{281}	$K^+ \pi^- \pi^+ \gamma$	(2.76 \pm 0.22) $\times 10^{-5}$	S=1.2
Γ_{223}	$K^+ f_0(980) \times B(f_0(980) \rightarrow \pi^+ \pi^-)$	(9.2 $\begin{smallmatrix} +0.8 \\ -1.1 \end{smallmatrix}$) $\times 10^{-6}$		Γ_{282}	$K^*(892)^0 \pi^+ \gamma$	(2.0 $\begin{smallmatrix} +0.7 \\ -0.6 \end{smallmatrix}$) $\times 10^{-5}$	
Γ_{224}	$f_2(1270)^0 K^+$	(1.3 $\begin{smallmatrix} +0.4 \\ -0.5 \end{smallmatrix}$) $\times 10^{-6}$		Γ_{283}	$K^+ \rho^0 \gamma$	< 2.0 $\times 10^{-5}$	CL=90%
Γ_{225}	$f_0(1370)^0 K^+ \times B(f_0(1370)^0 \rightarrow \pi^+ \pi^-)$	< 1.07 $\times 10^{-5}$	CL=90%	Γ_{284}	$K^+ \pi^- \pi^+ \gamma$ nonresonant	< 9.2 $\times 10^{-6}$	CL=90%
Γ_{226}	$\rho^0(1450) K^+ \times B(\rho^0(1450) \rightarrow \pi^+ \pi^-)$	< 1.17 $\times 10^{-5}$	CL=90%	Γ_{285}	$K^0 \pi^+ \pi^0 \gamma$	(4.6 \pm 0.5) $\times 10^{-5}$	
Γ_{227}	$f_0(1500) K^+ \times B(f_0(1500) \rightarrow \pi^+ \pi^-)$	< 4.4 $\times 10^{-6}$	CL=90%	Γ_{286}	$K_1(1400)^+ \gamma$	< 1.5 $\times 10^{-5}$	CL=90%
Γ_{228}	$f'_2(1525) K^+ \times B(f'_2(1525) \rightarrow \pi^+ \pi^-)$	< 3.4 $\times 10^{-6}$	CL=90%	Γ_{287}	$K_2^*(1430)^+ \gamma$	(1.4 \pm 0.4) $\times 10^{-5}$	
Γ_{229}	$K^+ \rho^0$	(4.2 \pm 0.5) $\times 10^{-6}$		Γ_{288}	$K^*(1680)^+ \gamma$	< 1.9 $\times 10^{-3}$	CL=90%
Γ_{230}	$K_0^*(1430)^0 \pi^+$	(4.7 \pm 0.5) $\times 10^{-5}$		Γ_{289}	$K_3^*(1780)^+ \gamma$	< 3.9 $\times 10^{-5}$	CL=90%
Γ_{231}	$K_2^*(1430)^0 \pi^+$	< 6.9 $\times 10^{-6}$	CL=90%	Γ_{290}	$K_4^*(2045)^+ \gamma$	< 9.9 $\times 10^{-3}$	CL=90%
Γ_{232}	$K^*(1410)^0 \pi^+$	< 4.5 $\times 10^{-5}$	CL=90%	Light unflavored meson modes			
Γ_{233}	$K^*(1680)^0 \pi^+$	< 1.2 $\times 10^{-5}$	CL=90%	Γ_{291}	$\rho^+ \gamma$	(8.8 $\begin{smallmatrix} +2.9 \\ -2.5 \end{smallmatrix}$) $\times 10^{-7}$	
Γ_{234}	$K^- \pi^+ \pi^+$	< 1.8 $\times 10^{-6}$	CL=90%	Γ_{292}	$\pi^+ \pi^0$	(5.7 \pm 0.5) $\times 10^{-6}$	S=1.4
Γ_{235}	$K^- \pi^+ \pi^+$ nonresonant	< 5.6 $\times 10^{-5}$	CL=90%	Γ_{293}	$\pi^+ \pi^+ \pi^-$	(1.62 \pm 0.15) $\times 10^{-5}$	
Γ_{236}	$K_1(1400)^0 \pi^+$	< 2.6 $\times 10^{-3}$	CL=90%	Γ_{294}	$\rho^0 \pi^+$	(8.7 \pm 1.1) $\times 10^{-6}$	
Γ_{237}	$K^0 \pi^+ \pi^0$	< 6.6 $\times 10^{-5}$	CL=90%	Γ_{295}	$\pi^+ f_0(980) \times B(f_0(980) \rightarrow \pi^+ \pi^-)$	< 3.0 $\times 10^{-6}$	CL=90%
Γ_{238}	$K^0 \rho^+$	(8.0 \pm 1.5) $\times 10^{-6}$		Γ_{296}	$\pi^+ f_2(1270)$	(8.2 \pm 2.5) $\times 10^{-6}$	
Γ_{239}	$K^*(892)^+ \pi^+ \pi^-$	(7.5 \pm 1.0) $\times 10^{-5}$		Γ_{297}	$\rho(1450)^0 \pi^+$	< 2.3 $\times 10^{-6}$	CL=90%
Γ_{240}	$K^*(892)^+ \rho^0$	< 6.1 $\times 10^{-6}$	CL=90%	Γ_{298}	$f_0(1370) \pi^+ \times B(f_0(1370) \rightarrow \pi^+ \pi^-)$	< 3.0 $\times 10^{-6}$	CL=90%
Γ_{241}	$K^*(892)^+ f_0(980)$	(5.2 \pm 1.3) $\times 10^{-6}$		Γ_{299}	$f_0(600) \pi^+ \times B(f_0(600) \rightarrow \pi^+ \pi^-)$	< 4.1 $\times 10^{-6}$	CL=90%
Γ_{242}	$a_1^+ K^0$	(3.5 \pm 0.7) $\times 10^{-5}$		Γ_{300}	$\pi^+ \pi^- \pi^+ \pi^+$ nonresonant	< 4.6 $\times 10^{-6}$	CL=90%
Γ_{243}	$K^*(892)^0 \rho^+$	(9.2 \pm 1.5) $\times 10^{-6}$		Γ_{301}	$\pi^+ \pi^0 \pi^0$	< 8.9 $\times 10^{-4}$	CL=90%
Γ_{244}	$K^*(892)^+ K^*(892)^0$	< 7.1 $\times 10^{-5}$	CL=90%	Γ_{302}	$\rho^+ \pi^0$	(1.09 \pm 0.14) $\times 10^{-5}$	
Γ_{245}	$K_1(1400)^+ \rho^0$	< 7.8 $\times 10^{-4}$	CL=90%	Γ_{303}	$\pi^+ \pi^- \pi^+ \pi^0$	< 4.0 $\times 10^{-3}$	CL=90%
Γ_{246}	$K_2^*(1430)^+ \rho^0$	< 1.5 $\times 10^{-3}$	CL=90%	Γ_{304}	$\rho^+ \rho^0$	(1.8 \pm 0.4) $\times 10^{-5}$	S=1.5
Γ_{247}	$K^+ \bar{K}^0$	(1.36 \pm 0.27) $\times 10^{-6}$		Γ_{305}	$\rho^+ f_0(980) \times B(f_0(980) \rightarrow \pi^+ \pi^-)$	< 1.9 $\times 10^{-6}$	CL=90%
Γ_{248}	$\bar{K}^0 K^+ \pi^0$	< 2.4 $\times 10^{-5}$	CL=90%	Γ_{306}	$a_1(1260)^+ \pi^0$	(2.6 \pm 0.7) $\times 10^{-5}$	
Γ_{249}	$K^+ K_S^0 K_S^0$	(1.15 \pm 0.13) $\times 10^{-5}$		Γ_{307}	$a_1(1260)^0 \pi^+$	(2.0 \pm 0.6) $\times 10^{-5}$	
Γ_{250}	$K_S^0 K_S^0 \pi^+$	< 3.2 $\times 10^{-6}$	CL=90%	Γ_{308}	$b_1^0 \pi^+ \times B(b_1^0 \rightarrow \omega \pi^0)$	(6.7 \pm 2.0) $\times 10^{-6}$	
Γ_{251}	$K^+ K^- \pi^+$	(5.0 \pm 0.7) $\times 10^{-6}$		Γ_{309}	$\omega \pi^+$	(6.9 \pm 0.5) $\times 10^{-6}$	
Γ_{252}	$K^+ K^- \pi^+$ nonresonant	< 7.5 $\times 10^{-5}$	CL=90%	Γ_{310}	$\omega \rho^+$	(1.06 $\begin{smallmatrix} +0.26 \\ -0.23 \end{smallmatrix}$) $\times 10^{-5}$	
Γ_{253}	$K^+ \bar{K}^*(892)^0$	< 1.1 $\times 10^{-6}$	CL=90%	Γ_{311}	$\eta \pi^+$	(4.4 \pm 0.4) $\times 10^{-6}$	S=1.1
Γ_{254}	$K^+ \bar{K}_0^*(1430)^0$	< 2.2 $\times 10^{-6}$	CL=90%	Γ_{312}	$\eta' \pi^+$	(2.7 \pm 1.0) $\times 10^{-6}$	S=2.1
Γ_{255}	$K^+ K^+ \pi^-$	< 1.3 $\times 10^{-6}$	CL=90%	Γ_{313}	$\eta' \rho^+$	(8.7 $\begin{smallmatrix} +3.9 \\ -3.1 \end{smallmatrix}$) $\times 10^{-6}$	
Γ_{256}	$K^+ K^+ \pi^-$ nonresonant	< 8.79 $\times 10^{-5}$	CL=90%	Γ_{314}	$\eta \rho^+$	(5.4 \pm 1.9) $\times 10^{-6}$	S=1.6
Γ_{257}	$b_1^0 K^+ \times B(b_1^0 \rightarrow \omega \pi^0)$	(9.1 \pm 2.0) $\times 10^{-6}$		Γ_{315}	$\phi \pi^+$	< 2.4 $\times 10^{-7}$	CL=90%
Γ_{258}	$K^+ f_J(2220)$			Γ_{316}	$\phi \rho^+$	< 1.6 $\times 10^{-5}$	
Γ_{259}	$K^* \pi^+ K^-$	< 1.18 $\times 10^{-5}$	CL=90%	Γ_{317}	$a_0(980)^0 \pi^+ \times B(a_0(980)^0 \rightarrow \eta \pi^0)$	< 5.8 $\times 10^{-6}$	CL=90%
Γ_{260}	$K^* \pi^+ K^-$	< 6.1 $\times 10^{-6}$	CL=90%	Γ_{318}	$a_0(980)^+ \pi^0 \times B(a_0^+ \rightarrow \eta \pi^+)$	< 1.4 $\times 10^{-6}$	CL=90%
Γ_{261}	$K^+ K^- K^+$	(3.37 \pm 0.22) $\times 10^{-5}$	S=1.4	Γ_{319}	$\pi^+ \pi^+ \pi^+ \pi^- \pi^-$	< 8.6 $\times 10^{-4}$	CL=90%
Γ_{262}	$K^+ \phi$	(8.3 \pm 0.7) $\times 10^{-6}$		Γ_{320}	$\rho^0 a_1(1260)^+$	< 6.2 $\times 10^{-4}$	CL=90%
Γ_{263}	$f_0(980) K^+ \times B(f_0(980) \rightarrow K^+ K^-)$	< 2.9 $\times 10^{-6}$	CL=90%	Γ_{321}	$\rho^0 a_2(1320)^+$	< 7.2 $\times 10^{-4}$	CL=90%
Γ_{264}	$a_2(1320) K^+ \times B(a_2(1320) \rightarrow K^+ K^-)$	< 1.1 $\times 10^{-6}$	CL=90%	Γ_{322}	$\pi^+ \pi^+ \pi^+ \pi^- \pi^- \pi^0$	< 6.3 $\times 10^{-3}$	CL=90%
Γ_{265}	$f'_2(1525) K^+ \times B(f'_2(1525) \rightarrow K^+ K^-)$	< 4.9 $\times 10^{-6}$	CL=90%	Γ_{323}	$a_1(1260)^+ a_1(1260)^0$	< 1.3 %	CL=90%
Γ_{266}	$X_0(1550) K^+ \times B(X_0(1550) \rightarrow K^+ K^-)$	(4.3 \pm 0.7) $\times 10^{-6}$		Charged particle (h^\pm) modes			
Γ_{267}	$\phi(1680) K^+ \times B(\phi(1680) \rightarrow K^+ K^-)$	< 8 $\times 10^{-7}$	CL=90%	$h^\pm = K^\pm \text{ or } \pi^\pm$			
Γ_{268}	$f_0(1710) K^+ \times B(f_0(1710) \rightarrow K^+ K^-)$	(1.7 \pm 1.0) $\times 10^{-6}$		Γ_{324}	$h^+ \pi^0$	(1.6 $\begin{smallmatrix} +0.7 \\ -0.6 \end{smallmatrix}$) $\times 10^{-5}$	
Γ_{269}	$K^+ K^- K^+$ nonresonant	(2.8 $\begin{smallmatrix} +0.9 \\ -1.6 \end{smallmatrix}$) $\times 10^{-5}$	S=3.3	Γ_{325}	ωh^+	(1.38 $\begin{smallmatrix} +0.27 \\ -0.24 \end{smallmatrix}$) $\times 10^{-5}$	
Γ_{270}	$K^*(892)^+ K^+ K^-$	(3.6 \pm 0.5) $\times 10^{-5}$		Γ_{326}	$h^+ X^0$ (Familon)	< 4.9 $\times 10^{-5}$	CL=90%
Γ_{271}	$K^*(892)^+ \phi$	(1.05 \pm 0.15) $\times 10^{-5}$	S=1.4	Baryon modes			
Γ_{272}	$K_1(1400)^+ \phi$	< 1.1 $\times 10^{-3}$	CL=90%	Γ_{327}	$p \bar{p} \pi^+$	(1.62 \pm 0.20) $\times 10^{-6}$	
Γ_{273}	$K_2^*(1430)^+ \phi$	< 3.4 $\times 10^{-3}$	CL=90%	Γ_{328}	$p \bar{p} \pi^+$ nonresonant	< 5.3 $\times 10^{-5}$	CL=90%
				Γ_{329}	$p \bar{p} \pi^+ \pi^+ \pi^-$	< 5.2 $\times 10^{-4}$	CL=90%
				Γ_{330}	$p \bar{p} K^+$	(5.9 \pm 0.5) $\times 10^{-6}$	S=1.5
				Γ_{331}	$\Theta(1710)^{++} \bar{p} \times B(\Theta(1710)^{++} \rightarrow p K^+)$	[g] < 9.1 $\times 10^{-8}$	CL=90%

Meson Particle Listings

 B^\pm

Γ_{332}	$f_J(2220)K^+ \times B(f_J(2220) \rightarrow \rho\bar{\rho})$	$[g] < 4.1$	$\times 10^{-7}$	CL=90%
Γ_{333}	$\rho\bar{\Lambda}(1520)$	< 1.5	$\times 10^{-6}$	CL=90%
Γ_{334}	$\rho\bar{\Lambda}K^+$ nonresonant	< 8.9	$\times 10^{-5}$	CL=90%
Γ_{335}	$\rho\bar{\rho}K^*(892)^+$	(6.6 ± 2.3)	$\times 10^{-6}$	S=1.3
Γ_{336}	$f_J(2220)K^{*+} \times B(f_J(2220) \rightarrow \rho\bar{\rho})$	< 7.7	$\times 10^{-7}$	CL=90%
Γ_{337}	$\rho\bar{\Lambda}$	< 3.2	$\times 10^{-7}$	CL=90%
Γ_{338}	$\rho\bar{\Lambda}\gamma$	(2.5 ± 0.5)	$\times 10^{-6}$	
Γ_{339}	$\rho\bar{\Lambda}\pi^0$	(3.0 ± 0.7)	$\times 10^{-6}$	
Γ_{340}	$\rho\bar{\Sigma}^-(1385)^0$	< 4.7	$\times 10^{-7}$	CL=90%
Γ_{341}	$\Delta^+\bar{\Lambda}$	< 8.2	$\times 10^{-7}$	CL=90%
Γ_{342}	$\rho\bar{\Sigma}^-\gamma$	< 4.6	$\times 10^{-6}$	CL=90%
Γ_{343}	$\rho\bar{\Lambda}\pi^+\pi^-$	< 2.0	$\times 10^{-4}$	CL=90%
Γ_{344}	$\Lambda\bar{\Lambda}\pi^+$	< 2.8	$\times 10^{-6}$	CL=90%
Γ_{345}	$\Lambda\bar{\Lambda}K^+$	(2.9 ± 1.0)	$\times 10^{-6}$	
Γ_{346}	$\bar{\Delta}^0\rho$	< 1.38	$\times 10^{-6}$	CL=90%
Γ_{347}	$\Delta^{++}\bar{\rho}$	< 1.4	$\times 10^{-7}$	CL=90%
Γ_{348}	$D^+\rho\bar{\rho}$	< 1.5	$\times 10^{-5}$	CL=90%
Γ_{349}	$D^*(2010)^+\rho\bar{\rho}$	< 1.5	$\times 10^{-5}$	CL=90%
Γ_{350}	$\bar{\Lambda}_c^-\rho\pi^+$	(2.1 ± 0.6)	$\times 10^{-4}$	
Γ_{351}	$\bar{\Lambda}_c^-\Delta(1232)^{++}$	< 1.9	$\times 10^{-5}$	CL=90%
Γ_{352}	$\bar{\Lambda}_c^-\Delta_X(1600)^{++}$	(5.9 ± 1.9)	$\times 10^{-5}$	
Γ_{353}	$\bar{\Lambda}_c^-\Delta_X(2420)^{++}$	(4.7 ± 1.6)	$\times 10^{-5}$	
Γ_{354}	$(\bar{\Lambda}_c^-\rho)_s\pi^+$	$[h] (3.9 \pm 1.3)$	$\times 10^{-5}$	
Γ_{355}	$\bar{\Lambda}_c^-\rho\pi^+\pi^0$	(1.8 ± 0.6)	$\times 10^{-3}$	
Γ_{356}	$\bar{\Lambda}_c^-\rho\pi^+\pi^+\pi^-$	(2.3 ± 0.7)	$\times 10^{-3}$	
Γ_{357}	$\bar{\Lambda}_c^-\rho\pi^+\pi^+\pi^-\pi^0$	< 1.34	%	CL=90%
Γ_{358}	$\Lambda_c^+\Lambda_c^-K^+$	(7 ± 4)	$\times 10^{-4}$	
Γ_{359}	$\bar{\Sigma}_c^+(2455)^0\rho$	(3.7 ± 1.3)	$\times 10^{-5}$	
Γ_{360}	$\bar{\Sigma}_c^+(2520)^0\rho$	< 2.7	$\times 10^{-5}$	CL=90%
Γ_{361}	$\bar{\Sigma}_c^+(2455)^0\rho\pi^0$	(4.4 ± 1.8)	$\times 10^{-4}$	
Γ_{362}	$\bar{\Sigma}_c^+(2455)^0\rho\pi^-\pi^+$	(4.4 ± 1.7)	$\times 10^{-4}$	
Γ_{363}	$\bar{\Sigma}_c^+(2455)^{-}\rho\pi^+\pi^+$	(2.8 ± 1.2)	$\times 10^{-4}$	
Γ_{364}	$\bar{\Lambda}_c^-(2593)^{-}/\bar{\Lambda}_c^-(2625)^{-}\rho\pi^+$	< 1.9	$\times 10^{-4}$	CL=90%
Γ_{365}	$\bar{\Xi}_c^0\Lambda_c^+ \times B(\bar{\Xi}_c^0 \rightarrow \bar{\Xi}^+\pi^-)$	(5.6 ± 2.7)	$\times 10^{-5}$	
Γ_{366}	$\bar{\Xi}_c^0\Lambda_c^+ \times B(\bar{\Xi}_c^0 \rightarrow \Lambda K^+\pi^-)$	(4.0 ± 1.6)	$\times 10^{-5}$	

Lepton Family number (LF) or Lepton number (L) violating modes, or $\Delta B = 1$ weak neutral current (BI) modes

Γ_{367}	$\pi^+\ell^+\ell^-$	BI	< 1.2	$\times 10^{-7}$	CL=90%
Γ_{368}	$\pi^+e^+e^-$	BI	< 1.8	$\times 10^{-7}$	CL=90%
Γ_{369}	$\pi^+\mu^+\mu^-$	BI	< 2.8	$\times 10^{-7}$	CL=90%
Γ_{370}	$\pi^+\nu\bar{\nu}$	BI	< 1.0	$\times 10^{-4}$	CL=90%
Γ_{371}	$K^+\ell^+\ell^-$	BI	$[a] (4.4 \pm 0.8)$	$\times 10^{-7}$	S=1.1
Γ_{372}	$K^+e^+e^-$	BI	(4.9 ± 1.0)	$\times 10^{-7}$	
Γ_{373}	$K^+\mu^+\mu^-$	BI	(3.9 ± 1.0)	$\times 10^{-7}$	
Γ_{374}	$K^+\bar{\nu}\nu$	BI	< 1.4	$\times 10^{-5}$	CL=90%
Γ_{375}	$\rho^+\nu\bar{\nu}$	BI	< 1.5	$\times 10^{-4}$	CL=90%
Γ_{376}	$K^*(892)^+\ell^+\ell^-$	BI	$[a] (7 \pm 5)$	$\times 10^{-7}$	
Γ_{377}	$K^*(892)^+\nu\bar{\nu}$	BI	< 1.4	$\times 10^{-4}$	CL=90%
Γ_{378}	$K^*(892)^+e^+e^-$	BI	(8 ± 8)	$\times 10^{-7}$	
Γ_{379}	$K^*(892)^+\mu^+\mu^-$	BI	(8 ± 4)	$\times 10^{-7}$	
Γ_{380}	$\pi^+e^+\mu^-$	LF	< 6.4	$\times 10^{-3}$	CL=90%
Γ_{381}	$\pi^+e^-\mu^+$	LF	< 6.4	$\times 10^{-3}$	CL=90%
Γ_{382}	$\pi^+e^\pm\mu^\mp$	LF	< 1.7	$\times 10^{-7}$	CL=90%
Γ_{383}	$K^+e^+\mu^-$	LF	< 9.1	$\times 10^{-8}$	CL=90%
Γ_{384}	$K^+e^-\mu^+$	LF	< 1.3	$\times 10^{-7}$	CL=90%
Γ_{385}	$K^+e^\pm\mu^\mp$	LF	< 9.1	$\times 10^{-8}$	CL=90%
Γ_{386}	$K^+\mu^\pm\tau^\mp$	LF	< 7.7	$\times 10^{-5}$	CL=90%
Γ_{387}	$K^*(892)^+e^+\mu^-$	LF	< 1.3	$\times 10^{-6}$	CL=90%
Γ_{388}	$K^*(892)^+e^-\mu^+$	LF	< 9.9	$\times 10^{-7}$	CL=90%
Γ_{389}	$K^*(892)^+e^\pm\mu^\mp$	LF	< 1.4	$\times 10^{-7}$	CL=90%
Γ_{390}	$\pi^-e^+e^+$	L	< 1.6	$\times 10^{-6}$	CL=90%
Γ_{391}	$\pi^-\mu^+\mu^+$	L	< 1.4	$\times 10^{-6}$	CL=90%
Γ_{392}	$\pi^-e^+\mu^+$	L	< 1.3	$\times 10^{-6}$	CL=90%
Γ_{393}	$\rho^-e^+\mu^+$	L	< 2.6	$\times 10^{-6}$	CL=90%
Γ_{394}	$\rho^-\mu^+\mu^+$	L	< 5.0	$\times 10^{-6}$	CL=90%
Γ_{395}	$\rho^-e^+\mu^+$	L	< 3.3	$\times 10^{-6}$	CL=90%
Γ_{396}	$K^-e^+e^+$	L	< 1.0	$\times 10^{-6}$	CL=90%

Γ_{397}	$K^-\mu^+\mu^+$	L	< 1.8	$\times 10^{-6}$	CL=90%
Γ_{398}	$K^-e^+\mu^+$	L	< 2.0	$\times 10^{-6}$	CL=90%
Γ_{399}	$K^*(892)^-e^+e^+$	L	< 2.8	$\times 10^{-6}$	CL=90%
Γ_{400}	$K^*(892)^-\mu^+\mu^+$	L	< 8.3	$\times 10^{-6}$	CL=90%
Γ_{401}	$K^*(892)^-e^+\mu^+$	L	< 4.4	$\times 10^{-6}$	CL=90%

[a] An ℓ indicates an e or a μ mode, not a sum over these modes.

[b] An $CP(\pm 1)$ indicates the $CP=+1$ and $CP=-1$ eigenstates of the $D^0-\bar{D}^0$ system.

[c] D denotes D^0 or \bar{D}^0 .

[d] $D_{CP^+}^{*0}$ decays into $D^0\pi^0$ with the D^0 reconstructed in CP -even eigenstates K^+K^- and $\pi^+\pi^-$.

[e] \bar{D}^{*+} represents an excited state with $2.2 < M < 2.8$ GeV/ c^2 .

[f] $X(3872)^+$ is a hypothetical charged partner of the $X(3872)$.

[g] $\Theta(1710)^{++}$ is a possible narrow pentaquark state and $G(2220)$ is a possible glueball resonance.

[h] $(\bar{\Lambda}_c^- \rho)_s$ denotes a low-mass enhancement near 3.35 GeV/ c^2 .

CONSTRAINED FIT INFORMATION

An overall fit to 3 branching ratios uses 11 measurements and one constraint to determine 3 parameters. The overall fit has a $\chi^2 = 7.2$ for 9 degrees of freedom.

The following *off-diagonal* array elements are the correlation coefficients $\langle \delta x_i \delta x_j \rangle / (\delta x_i \delta x_j)$, in percent, from the fit to the branching fractions, $x_i \equiv \Gamma_i / \Gamma_{\text{total}}$. The fit constrains the x_i whose labels appear in this array to sum to one.

$$x_{184} \begin{array}{|c} \hline 24 \\ \hline x_{163} \\ \hline \end{array}$$

 B^+ BRANCHING RATIOS

$\Gamma(\ell^+ \nu_\ell \text{ anything}) / \Gamma_{\text{total}}$ Γ_1 / Γ
 "OUR EVALUATION" is an average using rescaled values of the data listed below. The average and rescaling were performed by the Heavy Flavor Averaging Group (HFAG) and are described at <http://www.slac.stanford.edu/xorg/hfag/>. The averaging/rescaling procedure takes into account correlations between the measurements.

VALUE (units 10^{-2})	DOCUMENT ID	TECN	COMMENT
10.99 ± 0.28 OUR EVALUATION			
10.76 ± 0.32 OUR AVERAGE Error includes scale factor of 1.1.			
11.17 ± 0.25 ± 0.28	¹ URQUIJO	07 BELL	$e^+e^- \rightarrow \gamma(4S)$
10.28 ± 0.26 ± 0.39	² AUBERT,B	06Y BABR	$e^+e^- \rightarrow \gamma(4S)$
10.25 ± 0.57 ± 0.65	³ ARTUSO	97 CLE2	$e^+e^- \rightarrow \gamma(4S)$
••• We do not use the following data for averages, fits, limits, etc. •••			
11.15 ± 0.26 ± 0.41	⁴ OKABE	05 BELL	Repl. by URQUIJO 07
10.1 ± 1.8 ± 1.5	ATHANAS	94 CLE2	Sup. by ARTUSO 97

¹ URQUIJO 07 report a measurement of (10.34 ± 0.23 ± 0.25)% for the partial branching fraction of $B^+ \rightarrow e^+\nu_e X_c$ decay with electron energy above 0.6 GeV. We converted the result to $B^+ \rightarrow e^+\nu_e X$ branching fraction.

² The measurements are obtained for charged and neutral B mesons partial rates of semileptonic decay to electrons with momentum above 0.6 GeV/c in the B rest frame. The best precision on the ratio is achieved for a momentum threshold of 1.0 GeV: $B(B^+ \rightarrow e^+\nu_e X) / B(B^0 \rightarrow e^+\nu_e X) = 1.074 \pm 0.041 \pm 0.026$.

³ ARTUSO 97 uses partial reconstruction of $B \rightarrow D^* \ell \nu_\ell$ and inclusive semileptonic branching ratio from BARISH 96B (0.1049 ± 0.0017 ± 0.0043).

⁴ The measurements are obtained for charged and neutral B mesons partial rates of semileptonic decay to electrons with momentum above 0.6 GeV/c in the B rest frame, and their ratio of $B(B^+ \rightarrow e^+\nu_e X)/B(B^0 \rightarrow e^+\nu_e X) = 1.08 \pm 0.05 \pm 0.02$.

VALUE (units 10^{-2})	DOCUMENT ID	TECN	COMMENT
10.79 ± 0.25 ± 0.27			
	¹ URQUIJO	07 BELL	$e^+e^- \rightarrow \gamma(4S)$

¹ Measure the independent B^+ and B^0 partial branching fractions with electron threshold energies of 0.4 GeV.

$\Gamma(\bar{D}^0 \ell^+ \nu_\ell) / \Gamma_{\text{total}}$ Γ_4 / Γ
 "OUR EVALUATION" is an average using rescaled values of the data listed below. The average and rescaling were performed by the Heavy Flavor Averaging Group (HFAG) and are described at <http://www.slac.stanford.edu/xorg/hfag/>. The averaging/rescaling procedure takes into account correlations between the measurements. $\ell = e$ or μ , not sum over e and μ modes.

VALUE	DOCUMENT ID	TECN	COMMENT
0.0227 ± 0.0011 OUR EVALUATION			
0.0228 ± 0.0011 OUR AVERAGE			
0.0233 ± 0.0009 ± 0.0009	¹ AUBERT	08Q BABR	$e^+e^- \rightarrow \gamma(4S)$
0.0221 ± 0.0013 ± 0.0019	² BARTELT	99 CLE2	$e^+e^- \rightarrow \gamma(4S)$
0.016 ± 0.006 ± 0.003	³ FULTON	91 CLEO	$e^+e^- \rightarrow \gamma(4S)$
••• We do not use the following data for averages, fits, limits, etc. •••			
0.0194 ± 0.0015 ± 0.0034	⁴ ATHANAS	97 CLE2	Repl. by BARTELT 99

¹ Uses a fully reconstructed B meson as a tag on the recoil side.

² Assumes equal production of B^+ and B^0 at the $\Upsilon(4S)$.

³ FULTON 91 assumes equal production of $B^0\bar{B}^0$ and B^+B^- at the $\Upsilon(4S)$.

⁴ ATHANAS 97 uses missing energy and missing momentum to reconstruct neutrino.

$\Gamma(\bar{D}^0\pi^+\nu_e)/\Gamma_{\text{total}}$	Γ_5/Γ
VALUE (units 10^{-2})	DOCUMENT ID TECN COMMENT
0.67±0.37±0.13	¹ AUBERT 08N BABR $e^+e^- \rightarrow \Upsilon(4S)$

¹ Uses a fully reconstructed B meson as a tag on the recoil side.

$\Gamma(\bar{D}^0\ell^+\nu_e)/\Gamma(D\ell^+\nu_e\text{anything})$	Γ_4/Γ_3
VALUE	DOCUMENT ID TECN COMMENT
0.227±0.014±0.016	¹ AUBERT 07AN BABR $e^+e^- \rightarrow \Upsilon(4S)$

¹ Uses a fully reconstructed B meson on the recoil side.

$\Gamma(\bar{D}^*(2007)^0\ell^+\nu_e)/\Gamma_{\text{total}}$	Γ_6/Γ
VALUE	EVTs DOCUMENT ID TECN COMMENT
0.0607±0.0029 OUR EVALUATION	
0.0606±0.0031 OUR AVERAGE	Error includes scale factor of 1.2.
0.0583±0.0015±0.0030	¹ AUBERT 08Q BABR $e^+e^- \rightarrow \Upsilon(4S)$
0.0650±0.0020±0.0043	² ADAM 03 CLE2 $e^+e^- \rightarrow \Upsilon(4S)$
0.066±0.016±0.015	³ ALBRECHT 92C ARG $e^+e^- \rightarrow \Upsilon(4S)$
••• We do not use the following data for averages, fits, limits, etc. •••	
0.0650±0.0020±0.0043	⁴ BRIERE 02 CLE2 $e^+e^- \rightarrow \Upsilon(4S)$
0.0513±0.0054±0.0064	302 ⁵ BARISH 95 CLE2 Repl. by ADAM 03
seen	398 ⁶ SANGHERA 93 CLE2 $e^+e^- \rightarrow \Upsilon(4S)$
0.041±0.008+0.008	⁷ FULTON 91 CLEO $e^+e^- \rightarrow \Upsilon(4S)$
-0.009	
0.070±0.018±0.014	⁸ ANTREASIAN 90B CBAL $e^+e^- \rightarrow \Upsilon(4S)$

¹ Uses a fully reconstructed B meson as a tag on the recoil side.

² Simultaneous measurements of both $B^0 \rightarrow D^*(2010)^-\ell\nu$ and $B^+ \rightarrow \bar{D}(2007)^0\ell\nu$.

³ ALBRECHT 92C reports 0.058±0.014±0.013. We rescale using the method described in STONE 94 but with the updated PDG 94 $B(D^0 \rightarrow K^-\pi^+)$. Assumes equal production of $B^0\bar{B}^0$ and B^+B^- at the $\Upsilon(4S)$.

⁴ The results are based on the same analysis and data sample reported in ADAM 03.

⁵ BARISH 95 use $B(D^0 \rightarrow K^-\pi^+) = (3.91 \pm 0.08 \pm 0.17)\%$ and $B(D^{*0} \rightarrow D^0\pi^0) = (63.6 \pm 2.3 \pm 3.3)\%$.

⁶ Combining $\bar{D}^{*0}\ell^+\nu_e$ and $\bar{D}^{*-}\ell^+\nu_e$ SANGHERA 93 test $V-A$ structure and fit the decay angular distributions to obtain $A_{FB} = 3/4*(\Gamma^- - \Gamma^+)/\Gamma = 0.14 \pm 0.06 \pm 0.03$. Assuming a value of V_{cb} , they measure V, A_1 , and A_2 , the three form factors for the $D^*\ell\nu_e$ decay, where results are slightly dependent on model assumptions.

⁷ Assumes equal production of $B^0\bar{B}^0$ and B^+B^- at the $\Upsilon(4S)$. Uncorrected for D and D^* branching ratio assumptions.

⁸ ANTREASIAN 90B is average over B and $\bar{D}^*(2010)$ charge states.

$\Gamma(\bar{D}^*(2007)^0\pi^+\nu_e)/\Gamma_{\text{total}}$	Γ_7/Γ
VALUE (units 10^{-2})	DOCUMENT ID TECN COMMENT
2.25±0.48±0.28	¹ AUBERT 08N BABR $e^+e^- \rightarrow \Upsilon(4S)$

¹ Uses a fully reconstructed B meson as a tag on the recoil side.

$\Gamma(\bar{D}^*(2007)^0\ell^+\nu_e)/\Gamma(D\ell^+\nu_e\text{anything})$	Γ_6/Γ_3
VALUE	DOCUMENT ID TECN COMMENT
0.582±0.018±0.030	¹ AUBERT 07AN BABR $e^+e^- \rightarrow \Upsilon(4S)$

¹ Uses a fully reconstructed B meson on the recoil side.

$\Gamma(D^{(*)}\pi\ell^+\nu_e(n \geq 1))/\Gamma(D\ell^+\nu_e\text{anything})$	Γ_{11}/Γ_3
VALUE	DOCUMENT ID TECN COMMENT
0.191±0.013±0.019	¹ AUBERT 07AN BABR $e^+e^- \rightarrow \Upsilon(4S)$

¹ Uses a fully reconstructed B meson on the recoil side.

$\Gamma(D^-\pi^+\ell^+\nu_e)/\Gamma_{\text{total}}$	Γ_8/Γ
VALUE (units 10^{-3})	DOCUMENT ID TECN COMMENT
4.2±0.5 OUR AVERAGE	
4.2±0.6±0.3	¹ AUBERT 08Q BABR $e^+e^- \rightarrow \Upsilon(4S)$
4.2±0.6±0.2	^{1,2} LIVENTSEV 08 BELL $e^+e^- \rightarrow \Upsilon(4S)$
••• We do not use the following data for averages, fits, limits, etc. •••	
5.4±0.9±0.3	³ LIVENTSEV 05 BELL Repl. by LIVENTSEV 08

¹ Uses a fully reconstructed B meson as a tag on the recoil side.

² LIVENTSEV 08 reports $(4.0 \pm 0.4 \pm 0.6) \times 10^{-3}$ for $B(B^+ \rightarrow \bar{D}^0\ell^+\nu_e) = (2.15 \pm 0.22) \times 10^{-2}$. We rescale to our best value $B(B^+ \rightarrow \bar{D}^0\ell^+\nu_e) = (2.27 \pm 0.11) \times 10^{-2}$. Our first error is their experiment's error and our second error is the systematic error from using our best value.

³ LIVENTSEV 05 reports $[B(B^+ \rightarrow D^-\pi^+\ell^+\nu_e)] / [B(B^0 \rightarrow D^-\ell^+\nu_e)] = 0.25 \pm 0.03 \pm 0.03$. We multiply by our best value $B(B^0 \rightarrow D^-\ell^+\nu_e) = (2.17 \pm 0.12) \times 10^{-2}$. Our first error is their experiment's error and our second error is the systematic error from using our best value.

$\Gamma(\bar{D}_1^0(2420)^0\ell^+\nu_e \times B(\bar{D}_1^0 \rightarrow D^+\pi^-))/\Gamma_{\text{total}}$	Γ_9/Γ
VALUE (units 10^{-3})	DOCUMENT ID TECN COMMENT
2.4±0.4±0.6	¹ LIVENTSEV 08 BELL $e^+e^- \rightarrow \Upsilon(4S)$

¹ Uses a fully reconstructed B meson as a tag on the recoil side.

$\Gamma(\bar{D}_2^0(2460)^0\ell^+\nu_e \times B(\bar{D}_2^0 \rightarrow D^+\pi^-))/\Gamma_{\text{total}}$	Γ_{10}/Γ
VALUE (units 10^{-3})	DOCUMENT ID TECN COMMENT
2.2±0.3±0.4	¹ LIVENTSEV 08 BELL $e^+e^- \rightarrow \Upsilon(4S)$

¹ Uses a fully reconstructed B meson as a tag on the recoil side.

$\Gamma(D^{*+}\pi^+\ell^+\nu_e)/\Gamma_{\text{total}}$	Γ_{12}/Γ
VALUE (units 10^{-3})	DOCUMENT ID TECN COMMENT
6.1±0.6 OUR AVERAGE	
5.9±0.5±0.4	¹ AUBERT 08Q BABR $e^+e^- \rightarrow \Upsilon(4S)$
6.8±1.1±0.3	^{1,2} LIVENTSEV 08 BELL $e^+e^- \rightarrow \Upsilon(4S)$
••• We do not use the following data for averages, fits, limits, etc. •••	
6.2±1.5±0.1	^{3,4} LIVENTSEV 05 BELL Repl. by LIVENTSEV 08

¹ Uses a fully reconstructed B meson as a tag on the recoil side.

² LIVENTSEV 08 reports $(6.4 \pm 0.8 \pm 0.9) \times 10^{-3}$ for $B(B^+ \rightarrow \bar{D}^0\ell^+\nu_e) = (2.15 \pm 0.22) \times 10^{-2}$. We rescale to our best value $B(B^+ \rightarrow \bar{D}^0\ell^+\nu_e) = (2.27 \pm 0.11) \times 10^{-2}$. Our first error is their experiment's error and our second error is the systematic error from using our best value.

³ Excludes D^{*+} contribution to $D\pi$ modes.

⁴ LIVENTSEV 05 reports $[B(B^+ \rightarrow D^{*+}\pi^+\ell^+\nu_e)] / [B(B^0 \rightarrow D^*(2010)^-\ell^+\nu_e)] = 0.12 \pm 0.02 \pm 0.02$. We multiply by our best value $B(B^0 \rightarrow D^*(2010)^-\ell^+\nu_e) = (5.16 \pm 0.11) \times 10^{-2}$. Our first error is their experiment's error and our second error is the systematic error from using our best value.

$\Gamma(\bar{D}_1^-(2420)^0\ell^+\nu_e \times B(\bar{D}_1^- \rightarrow D^{*+}\pi^-))/\Gamma_{\text{total}}$	Γ_{13}/Γ
VALUE (units 10^{-3})	DOCUMENT ID TECN COMMENT
4.0±0.7 OUR AVERAGE	
4.2±0.7±0.7	¹ LIVENTSEV 08 BELL $e^+e^- \rightarrow \Upsilon(4S)$
3.73±0.85±0.57	² ANASTASSOV 98 CLE2 $e^+e^- \rightarrow \Upsilon(4S)$

¹ Uses a fully reconstructed B meson as a tag on the recoil side.

² Assumes equal production of B^+ and B^0 at the $\Upsilon(4S)$.

$\Gamma(\bar{D}_1^-(2430)^0\ell^+\nu_e \times B(\bar{D}_1^- \rightarrow D^{*+}\pi^-))/\Gamma_{\text{total}}$	Γ_{14}/Γ
VALUE (units 10^{-3})	CL% DOCUMENT ID TECN COMMENT
<0.7	90 ¹ LIVENTSEV 08 BELL $e^+e^- \rightarrow \Upsilon(4S)$

¹ Uses a fully reconstructed B meson as a tag on the recoil side.

$\Gamma(\bar{D}_2^-(2460)^0\ell^+\nu_e \times B(\bar{D}_2^- \rightarrow D^{*+}\pi^-))/\Gamma_{\text{total}}$	Γ_{15}/Γ
VALUE (units 10^{-3})	CL% DOCUMENT ID TECN COMMENT
1.8±0.6±0.3	¹ LIVENTSEV 08 BELL $e^+e^- \rightarrow \Upsilon(4S)$
••• We do not use the following data for averages, fits, limits, etc. •••	
<1.6	90 ² ANASTASSOV 98 CLE2 $e^+e^- \rightarrow \Upsilon(4S)$

¹ Uses a fully reconstructed B meson as a tag on the recoil side.

² Assumes equal production of B^+ and B^0 at the $\Upsilon(4S)$.

$\Gamma(\pi^0\ell^+\nu_e)/\Gamma_{\text{total}}$	Γ_{16}/Γ
VALUE (units 10^{-4})	DOCUMENT ID TECN COMMENT
0.77±0.10±0.07 OUR EVALUATION	
0.75±0.09 OUR AVERAGE	
0.77±0.14±0.08	¹ HOKUUE 07 BELL $e^+e^- \rightarrow \Upsilon(4S)$
0.74±0.05±0.10	² AUBERT,B 05o BABR $e^+e^- \rightarrow \Upsilon(4S)$

¹ The signal events are tagged by a second B meson reconstructed in the semileptonic mode $B \rightarrow D^{(*)}\ell\nu_e$.

² B^+ and B^0 decays combined assuming isospin symmetry. Systematic errors include both experimental and form-factor uncertainties.

$\Gamma(\pi^0 e^+ \nu_e)/\Gamma_{\text{total}}$	Γ_{17}/Γ
VALUE (units 10^{-4})	CL% DOCUMENT ID TECN COMMENT
••• We do not use the following data for averages, fits, limits, etc. •••	
0.9±0.2±0.2	¹ ALEXANDER 96T CLE2 $e^+e^- \rightarrow \Upsilon(4S)$
<22	90 ² ANTREASIAN 90B CBAL $e^+e^- \rightarrow \Upsilon(4S)$

¹ Derived based in the reported B^0 result by assuming isospin symmetry: $\Gamma(B^0 \rightarrow \pi^-\ell^+\nu_e) = 2\Gamma(B^+ \rightarrow \pi^0\ell^+\nu_e)$.

$\Gamma(\eta\ell^+\nu_e)/\Gamma_{\text{total}}$	Γ_{18}/Γ
VALUE (units 10^{-4})	CL% DOCUMENT ID TECN COMMENT
<1.01	90 ¹ ADAM 07 CLE2 $e^+e^- \rightarrow \Upsilon(4S)$
••• We do not use the following data for averages, fits, limits, etc. •••	
0.84±0.31±0.18	² ATHAR 03 CLE2 Repl. by ADAM 07

¹ The B^0 and B^+ results are combined assuming the isospin, B lifetimes, and relative charged/neutral B production at the $\Upsilon(4S)$.

² ATHAR 03 reports systematic errors 0.16 ± 0.09 , which are experimental systematic and systematic due to model dependence. We combine these in quadrature.

Meson Particle Listings

 B^\pm $\Gamma(\eta^0 \ell^+ \nu_\ell)/\Gamma_{\text{total}}$ Γ_{19}/Γ

VALUE (units 10^{-4})	CL%	DOCUMENT ID	TECN	COMMENT
$2.66 \pm 0.80 \pm 0.56$	90	1 ADAM 07	CLE2	$e^+ e^- \rightarrow \Upsilon(4S)$

¹The B^0 and B^+ results are combined assuming the isospin, B lifetimes, and relative charged/neutral B production at the $\Upsilon(4S)$. Corresponds to 90% CL interval $(1.20-4.46) \times 10^{-4}$.

 $\Gamma(\omega \ell^+ \nu_\ell)/\Gamma_{\text{total}}$ Γ_{20}/Γ

VALUE (units 10^{-4})	CL%	DOCUMENT ID	TECN	COMMENT
$1.3 \pm 0.4 \pm 0.4$	90	1 SCHVANDA 04	BELL	$e^+ e^- \rightarrow \Upsilon(4S)$

• • • We do not use the following data for averages, fits, limits, etc. • • •
 < 2.1 90 ²BEAN 93B CLE2 $e^+ e^- \rightarrow \Upsilon(4S)$
¹Assumes equal production of B^+ and B^0 at the $\Upsilon(4S)$.
²BEAN 93B limit set using ISGW Model. Using isospin and the quark model to combine $\Gamma(\rho^0 \ell^+ \nu_\ell)$ and $\Gamma(\rho^- \ell^+ \nu_\ell)$ with this result, they obtain a limit $< (1.6-2.7) \times 10^{-4}$ at 90% CL for $B^+ \rightarrow \omega \ell^+ \nu_\ell$. The range corresponds to the ISGW, WSB, and KS models. An upper limit on $|V_{ub}/V_{cb}| < 0.8-0.13$ at 90% CL is derived as well.

 $\Gamma(\omega \mu^+ \nu_\mu)/\Gamma_{\text{total}}$ Γ_{21}/Γ

VALUE	CL%	DOCUMENT ID	TECN	COMMENT
< 2.1	90	1 ALBRECHT 91c	ARG	ARG

• • • We do not use the following data for averages, fits, limits, etc. • • •
 seen ¹In ALBRECHT 91c, one event is fully reconstructed providing evidence for the $b \rightarrow u$ transition.

 $\Gamma(\rho^0 \ell^+ \nu_\ell)/\Gamma_{\text{total}}$ Γ_{22}/Γ

VALUE (units 10^{-4})	CL%	DOCUMENT ID	TECN	COMMENT
1.28 ± 0.18 OUR AVERAGE				

$1.33 \pm 0.23 \pm 0.18$	90	1 HOKUUE 07	BELL	$e^+ e^- \rightarrow \Upsilon(4S)$
$1.16 \pm 0.11 \pm 0.30$	90	2 AUBERT,B 05b	BABR	$e^+ e^- \rightarrow \Upsilon(4S)$
$1.34 \pm 0.15 \pm 0.28$ -0.32	90	3 BEHRENS 00	CLE2	$e^+ e^- \rightarrow \Upsilon(4S)$
$1.40 \pm 0.21 \pm 0.32$ -0.33	90	3 BEHRENS 00	CLE2	$e^+ e^- \rightarrow \Upsilon(4S)$
$1.2 \pm 0.2 \pm 0.3$ -0.4	90	3 ALEXANDER 96T	CLE2	$e^+ e^- \rightarrow \Upsilon(4S)$
< 2.1	90	4 BEAN 93B	CLE2	$e^+ e^- \rightarrow \Upsilon(4S)$

• • • We do not use the following data for averages, fits, limits, etc. • • •
 < 2.1 90 ⁴BEAN 93B limit set using ISGW Model. Using isospin and the quark model to combine $\Gamma(\omega^0 \ell^+ \nu_\ell)$ and $\Gamma(\rho^- \ell^+ \nu_\ell)$ with this result, they obtain a limit $< (1.6-2.7) \times 10^{-4}$ at 90% CL for $B^+ \rightarrow \rho^0 \ell^+ \nu_\ell$. The range corresponds to the ISGW, WSB, and KS models. An upper limit on $|V_{ub}/V_{cb}| < 0.8-0.13$ at 90% CL is derived as well.

 $\Gamma(\rho^0 e^+ \nu_e)/\Gamma_{\text{total}}$ Γ_{23}/Γ

VALUE	CL%	DOCUMENT ID	TECN	COMMENT
$< 5.2 \times 10^{-3}$	90	1 ADAM 03b	CLE2	$e^+ e^- \rightarrow \Upsilon(4S)$

¹Based on phase-space model; if $V-A$ model is used, the 90% CL upper limit becomes $< 1.2 \times 10^{-3}$.

 $\Gamma(e^+ \nu_e)/\Gamma_{\text{total}}$ Γ_{24}/Γ

VALUE (units 10^{-6})	CL%	DOCUMENT ID	TECN	COMMENT
< 9.8	90	1 SATOYAMA 07	BELL	$e^+ e^- \rightarrow \Upsilon(4S)$

• • • We do not use the following data for averages, fits, limits, etc. • • •
 < 15 90 ARTUSO 95 CLE2 $e^+ e^- \rightarrow \Upsilon(4S)$
¹Assumes equal production of B^+ and B^0 at the $\Upsilon(4S)$.

 $\Gamma(\mu^+ \nu_\mu)/\Gamma_{\text{total}}$ Γ_{25}/Γ

VALUE (units 10^{-6})	CL%	DOCUMENT ID	TECN	COMMENT
< 1.7	90	1 SATOYAMA 07	BELL	$e^+ e^- \rightarrow \Upsilon(4S)$

• • • We do not use the following data for averages, fits, limits, etc. • • •
 < 6.6 90 AUBERT 04o BABR $e^+ e^- \rightarrow \Upsilon(4S)$
 < 21 90 ARTUSO 95 CLE2 $e^+ e^- \rightarrow \Upsilon(4S)$

¹Assumes equal production of B^+ and B^0 at the $\Upsilon(4S)$.

 $\Gamma(\tau^+ \nu_\tau)/\Gamma_{\text{total}}$ Γ_{26}/Γ

VALUE (units 10^{-4})	CL%	DOCUMENT ID	TECN	COMMENT
1.4 ± 0.4 OUR AVERAGE				

$1.8 \pm 0.9 \pm 0.45$ -0.8	90	1,2 AUBERT 08D	BABR	$e^+ e^- \rightarrow \Upsilon(4S)$
$0.9 \pm 0.6 \pm 0.1$	90	2,3 AUBERT 07AL	BABR	$e^+ e^- \rightarrow \Upsilon(4S)$
$1.79 \pm 0.56 \pm 0.46$ $-0.49 - 0.51$	90	1,2 IKADO 06	BELL	$e^+ e^- \rightarrow \Upsilon(4S)$

• • • We do not use the following data for averages, fits, limits, etc. • • •

< 2.6	90	2 AUBERT 06K	BABR	$e^+ e^- \rightarrow \Upsilon(4S)$
< 4.2	90	2 AUBERT,B 05b	BABR	Repl. by AUBERT 06K
< 8.3	90	4 BARATE 01E	ALEP	$e^+ e^- \rightarrow Z$
< 8.4	90	2 BROWDER 01	CLE2	$e^+ e^- \rightarrow \Upsilon(4S)$
< 5.7	90	5 ACCIARRI 97F	L3	$e^+ e^- \rightarrow Z$
< 104	90	6 ALBRECHT 95D	ARG	$e^+ e^- \rightarrow \Upsilon(4S)$
< 22	90	ARTUSO 95	CLE2	$e^+ e^- \rightarrow \Upsilon(4S)$
< 18	90	7 BUSKULIC 95	ALEP	$e^+ e^- \rightarrow Z$

¹The analysis is based on a sample of events with one fully reconstructed tag B in a hadronic decay mode $B^- \rightarrow D^{(*)0} X^-$.
²Assumes equal production of B^+ and B^0 at the $\Upsilon(4S)$.
³Requires one reconstructed semileptonic B decay $B^- \rightarrow D^0 \ell^- \bar{\nu}_\ell X$ in the recoil.
⁴The energy-flow and b -tagging algorithms were used.
⁵ACCIARRI 97F uses missing-energy technique and $f(b \rightarrow B^-) = (38.2 \pm 2.5)\%$.
⁶ALBRECHT 95D uses full reconstruction of one B decay as tag.
⁷BUSKULIC 95 uses same missing-energy technique as in $\bar{b} \rightarrow \tau^+ \nu_\tau X$, but analysis is restricted to endpoint region of missing-energy distribution.

 $\Gamma(e^+ \nu_e \gamma)/\Gamma_{\text{total}}$ Γ_{27}/Γ

VALUE	CL%	DOCUMENT ID	TECN	COMMENT
$< 2.0 \times 10^{-4}$	90	1 BROWDER 97	CLE2	$e^+ e^- \rightarrow \Upsilon(4S)$

¹BROWDER 97 uses the hermiticity of the CLEO II detector to reconstruct the neutrino energy and momentum.

 $\Gamma(\mu^+ \nu_\mu \gamma)/\Gamma_{\text{total}}$ Γ_{28}/Γ

VALUE	CL%	DOCUMENT ID	TECN	COMMENT
$< 5.2 \times 10^{-5}$	90	1 BROWDER 97	CLE2	$e^+ e^- \rightarrow \Upsilon(4S)$

¹BROWDER 97 uses the hermiticity of the CLEO II detector to reconstruct the neutrino energy and momentum.

 $\Gamma(D^0 X)/\Gamma_{\text{total}}$ Γ_{29}/Γ

VALUE	CL%	DOCUMENT ID	TECN	COMMENT
$0.086 \pm 0.006 \pm 0.004$	90	1 AUBERT 07N	BABR	$e^+ e^- \rightarrow \Upsilon(4S)$

• • • We do not use the following data for averages, fits, limits, etc. • • •
 $0.098 \pm 0.009 \pm 0.006$ ¹AUBERT, BE 04B BABR Repl. by AUBERT 07N
¹Events are selected by completely reconstructing one B and searching for a reconstructed charmed particle in the rest of the event. The last error includes systematic and charm branching ratio uncertainties.

 $\Gamma(\bar{D}^0 X)/\Gamma_{\text{total}}$ Γ_{30}/Γ

VALUE	CL%	DOCUMENT ID	TECN	COMMENT
$0.786 \pm 0.016 \pm 0.034$ -0.033	90	1 AUBERT 07N	BABR	$e^+ e^- \rightarrow \Upsilon(4S)$

• • • We do not use the following data for averages, fits, limits, etc. • • •
 $0.793 \pm 0.025 \pm 0.045$
 -0.044 ¹AUBERT, BE 04B BABR Repl. by AUBERT 07N
¹Events are selected by completely reconstructing one B and searching for a reconstructed charmed particle in the rest of the event. The last error includes systematic and charm branching ratio uncertainties.

 $\Gamma(D^0 X)/[\Gamma(D^0 X) + \Gamma(\bar{D}^0 X)]$ $\Gamma_{29}/(\Gamma_{29} + \Gamma_{30})$

VALUE	CL%	DOCUMENT ID	TECN	COMMENT
$0.098 \pm 0.007 \pm 0.001$	90	AUBERT 07N	BABR	$e^+ e^- \rightarrow \Upsilon(4S)$

• • • We do not use the following data for averages, fits, limits, etc. • • •
 $0.110 \pm 0.010 \pm 0.003$ AUBERT, BE 04B BABR Repl. by AUBERT 07N

 $\Gamma(D^+ X)/\Gamma_{\text{total}}$ Γ_{31}/Γ

VALUE	CL%	DOCUMENT ID	TECN	COMMENT
$0.025 \pm 0.005 \pm 0.002$	90	1 AUBERT 07N	BABR	$e^+ e^- \rightarrow \Upsilon(4S)$

• • • We do not use the following data for averages, fits, limits, etc. • • •
 $0.038 \pm 0.009 \pm 0.005$ ¹AUBERT, BE 04B BABR Repl. by AUBERT 07N
¹Events are selected by completely reconstructing one B and searching for a reconstructed charmed particle in the rest of the event. The last error includes systematic and charm branching ratio uncertainties.

 $\Gamma(D^- X)/\Gamma_{\text{total}}$ Γ_{32}/Γ

VALUE	CL%	DOCUMENT ID	TECN	COMMENT
$0.099 \pm 0.008 \pm 0.009$	90	1 AUBERT 07N	BABR	$e^+ e^- \rightarrow \Upsilon(4S)$

• • • We do not use the following data for averages, fits, limits, etc. • • •
 $0.098 \pm 0.012 \pm 0.014$ ¹AUBERT, BE 04B BABR Repl. by AUBERT 07N
¹Events are selected by completely reconstructing one B and searching for a reconstructed charmed particle in the rest of the event. The last error includes systematic and charm branching ratio uncertainties.

 $\Gamma(D^+ X)/[\Gamma(D^+ X) + \Gamma(D^- X)]$ $\Gamma_{31}/(\Gamma_{31} + \Gamma_{32})$

VALUE	CL%	DOCUMENT ID	TECN	COMMENT
$0.204 \pm 0.035 \pm 0.001$	90	AUBERT 07N	BABR	$e^+ e^- \rightarrow \Upsilon(4S)$

• • • We do not use the following data for averages, fits, limits, etc. • • •
 $0.278 \pm 0.052 \pm 0.009$ AUBERT, BE 04B BABR Repl. by AUBERT 07N

$\Gamma(D_s^+ X)/\Gamma_{\text{total}}$ Γ_{33}/Γ

VALUE	DOCUMENT ID	TECN	COMMENT
$0.079 \pm 0.006 \pm_{-0.011}^{+0.013}$	¹ AUBERT	07N	BABR $e^+e^- \rightarrow \Upsilon(4S)$
$0.143 \pm 0.016 \pm_{-0.034}^{+0.051}$	¹ AUBERT,BE	04B	BABR Repl. by AUBERT 07N

¹ Events are selected by completely reconstructing one B and searching for a reconstructed charmed particle in the rest of the event. The last error includes systematic and charm branching ratio uncertainties.

$\Gamma(D_s^- X)/\Gamma_{\text{total}}$ Γ_{34}/Γ

VALUE	CL%	DOCUMENT ID	TECN	COMMENT
$0.011 \pm 0.004 \pm_{-0.003}^{+0.002}$		¹ AUBERT	07N	BABR $e^+e^- \rightarrow \Upsilon(4S)$
<0.022	90	¹ AUBERT,BE	04B	BABR Repl. by AUBERT 07N

¹ Events are selected by completely reconstructing one B and searching for a reconstructed charmed particle in the rest of the event. The last error includes systematic and charm branching ratio uncertainties.

$\Gamma(D_s^+ X)/[\Gamma(D_s^+ X) + \Gamma(D_s^- X)]$ $\Gamma_{33}/(\Gamma_{33} + \Gamma_{34})$

VALUE	DOCUMENT ID	TECN	COMMENT
$0.884 \pm 0.038 \pm 0.002$	AUBERT	07N	BABR $e^+e^- \rightarrow \Upsilon(4S)$
$0.966 \pm 0.039 \pm 0.012$	AUBERT,BE	04B	BABR Repl. by AUBERT 07N

• • • We do not use the following data for averages, fits, limits, etc. • • •

$\Gamma(D_s^- X)/[\Gamma(D_s^+ X) + \Gamma(D_s^- X)]$ $\Gamma_{34}/(\Gamma_{33} + \Gamma_{34})$

VALUE	CL%	DOCUMENT ID	TECN	COMMENT
<0.126	90	AUBERT,BE	04B	BABR $e^+e^- \rightarrow \Upsilon(4S)$

$\Gamma(A_c^+ X)/\Gamma_{\text{total}}$ Γ_{35}/Γ

VALUE	DOCUMENT ID	TECN	COMMENT
$0.021 \pm 0.005 \pm_{-0.004}^{+0.008}$	¹ AUBERT	07N	BABR $e^+e^- \rightarrow \Upsilon(4S)$
$0.029 \pm 0.008 \pm_{-0.007}^{+0.011}$	¹ AUBERT,BE	04B	BABR Repl. by AUBERT 07N

¹ Events are selected by completely reconstructing one B and searching for a reconstructed charmed particle in the rest of the event. The last error includes systematic and charm branching ratio uncertainties.

$\Gamma(\bar{A}_c^- X)/\Gamma_{\text{total}}$ Γ_{36}/Γ

VALUE	DOCUMENT ID	TECN	COMMENT
$0.028 \pm 0.005 \pm_{-0.007}^{+0.010}$	¹ AUBERT	07N	BABR $e^+e^- \rightarrow \Upsilon(4S)$
$0.035 \pm 0.008 \pm_{-0.009}^{+0.013}$	¹ AUBERT,BE	04B	BABR Repl. by AUBERT 07N

¹ Events are selected by completely reconstructing one B and searching for a reconstructed charmed particle in the rest of the event. The last error includes systematic and charm branching ratio uncertainties.

$\Gamma(A_c^+ X)/[\Gamma(A_c^+ X) + \Gamma(\bar{A}_c^- X)]$ $\Gamma_{35}/(\Gamma_{35} + \Gamma_{36})$

VALUE	DOCUMENT ID	TECN	COMMENT
$0.427 \pm 0.071 \pm 0.001$	AUBERT	07N	BABR $e^+e^- \rightarrow \Upsilon(4S)$
$0.452 \pm 0.090 \pm 0.003$	AUBERT,BE	04B	BABR Repl. by AUBERT 07N

• • • We do not use the following data for averages, fits, limits, etc. • • •

$\Gamma(\bar{c} X)/\Gamma_{\text{total}}$ Γ_{37}/Γ

VALUE	DOCUMENT ID	TECN	COMMENT
$0.968 \pm 0.019 \pm_{-0.039}^{+0.041}$	¹ AUBERT	07N	BABR $e^+e^- \rightarrow \Upsilon(4S)$
$0.983 \pm 0.030 \pm_{-0.051}^{+0.054}$	¹ AUBERT,BE	04B	BABR Repl. by AUBERT 07N

¹ Events are selected by completely reconstructing one B and searching for a reconstructed charmed particle in the rest of the event. The last error includes systematic and charm branching ratio uncertainties.

$\Gamma(c X)/\Gamma_{\text{total}}$ Γ_{38}/Γ

VALUE	DOCUMENT ID	TECN	COMMENT
$0.234 \pm 0.012 \pm_{-0.014}^{+0.018}$	¹ AUBERT	07N	BABR $e^+e^- \rightarrow \Upsilon(4S)$
$0.330 \pm 0.022 \pm_{-0.037}^{+0.055}$	¹ AUBERT,BE	04B	BABR Repl. by AUBERT 07N

¹ Events are selected by completely reconstructing one B and searching for a reconstructed charmed particle in the rest of the event. The last error includes systematic and charm branching ratio uncertainties.

$\Gamma(\bar{c} c X)/\Gamma_{\text{total}}$ Γ_{39}/Γ

VALUE	DOCUMENT ID	TECN	COMMENT
$1.202 \pm 0.023 \pm_{-0.049}^{+0.053}$	¹ AUBERT	07N	BABR $e^+e^- \rightarrow \Upsilon(4S)$
$1.313 \pm 0.037 \pm_{-0.075}^{+0.088}$	¹ AUBERT,BE	04B	BABR Repl. by AUBERT 07N

¹ Events are selected by completely reconstructing one B and searching for a reconstructed charmed particle in the rest of the event. The last error includes systematic and charm branching ratio uncertainties.

$\Gamma(\bar{D}^0 \pi^+)/\Gamma_{\text{total}}$ Γ_{40}/Γ

VALUE (units 10^{-3})	EVTS	DOCUMENT ID	TECN	COMMENT
4.84 ± 0.15 OUR AVERAGE				
4.90 ± 0.07 ± 0.22		¹ AUBERT	07H	BABR $e^+e^- \rightarrow \Upsilon(4S)$
5.3 ± 0.6 ± 0.3		² ABULENCIA	06J	CDF $p\bar{p}$ at 1.96 TeV
4.49 ± 0.21 ± 0.23		³ AUBERT,BE	06J	BABR $e^+e^- \rightarrow \Upsilon(4S)$
4.97 ± 0.12 ± 0.29		^{1,4} AHMED	02B	CLE2 $e^+e^- \rightarrow \Upsilon(4S)$
5.0 ± 0.7 ± 0.6	54	⁵ BORTOLETTO	92	CLEO $e^+e^- \rightarrow \Upsilon(4S)$
5.4 ± 1.8 ± 1.2	14	⁶ BEBEK	87	CLEO $e^+e^- \rightarrow \Upsilon(4S)$
4.75 ± 0.26 ± 0.06		⁷ AUBERT,B	04P	BABR Repl. by AUBERT 07H
5.5 ± 0.4 ± 0.5	304	⁸ ALAM	94	CLE2 Repl. by AHMED 02B
2.0 ± 0.8 ± 0.6	12	⁵ ALBRECHT	90J	ARG $e^+e^- \rightarrow \Upsilon(4S)$
1.9 ± 1.0 ± 0.6	7	⁹ ALBRECHT	88K	ARG $e^+e^- \rightarrow \Upsilon(4S)$

• • • We do not use the following data for averages, fits, limits, etc. • • •

¹ Assumes equal production of B^+ and B^0 at the $\Upsilon(4S)$.

² ABULENCIA 06J reports $[B(B^+ \rightarrow \bar{D}^0 \pi^+) / [B(B^0 \rightarrow D^- \pi^+)]] = 1.97 \pm 0.10 \pm 0.21$. We multiply by our best value $B(B^0 \rightarrow D^- \pi^+) = (2.68 \pm 0.13) \times 10^{-3}$. Our first error is their experiment's error and our second error is the systematic error from using our best value.

³ Uses a missing-mass method. Does not depend on D branching fractions or B^+/B^0 production rates.

⁴ AHMED 02B reports an additional uncertainty on the branching ratios to account for 4.5% uncertainty on relative production of B^0 and B^+ , which is not included here.

⁵ Assumes equal production of B^+ and B^0 at the $\Upsilon(4S)$ and uses the Mark III branching fractions for the D .

⁶ BEBEK 87 value has been updated in BERKELMAN 91 to use same assumptions as noted for BORTOLETTO 92.

⁷ AUBERT,B 04P reports $[B(B^+ \rightarrow \bar{D}^0 \pi^+) / [B(D^0 \rightarrow K^- \pi^+)]] = (1.846 \pm 0.032 \pm 0.097) \times 10^{-4}$. We divide by our best value $B(D^0 \rightarrow K^- \pi^+) = (3.89 \pm 0.05) \times 10^{-2}$. Our first error is their experiment's error and our second error is the systematic error from using our best value.

⁸ ALAM 94 assume equal production of B^+ and B^0 at the $\Upsilon(4S)$ and use the CLEO II absolute $B(D^0 \rightarrow K^- \pi^+)$ and the PDG 1992 $B(D^0 \rightarrow K^- \pi^+ \pi^0)/B(D^0 \rightarrow K^- \pi^+)$ and $B(D^0 \rightarrow K^- \pi^+ \pi^+ \pi^-)/B(D^0 \rightarrow K^- \pi^+)$.

⁹ ALBRECHT 88K assumes $B^0 \bar{B}^0, B^+ B^-$ ratio is 45:55. Superseded by ALBRECHT 90J.

$\Gamma(\bar{D}^0 \rho^+)/\Gamma_{\text{total}}$ Γ_{43}/Γ

VALUE	EVTS	DOCUMENT ID	TECN	COMMENT
0.0134 ± 0.0018 OUR AVERAGE				
0.0135 ± 0.0012 ± 0.0015	212	¹ ALAM	94	CLE2 $e^+e^- \rightarrow \Upsilon(4S)$
0.013 ± 0.004 ± 0.004	19	² ALBRECHT	90J	ARG $e^+e^- \rightarrow \Upsilon(4S)$
0.021 ± 0.008 ± 0.009	10	³ ALBRECHT	88K	ARG $e^+e^- \rightarrow \Upsilon(4S)$

• • • We do not use the following data for averages, fits, limits, etc. • • •

¹ ALAM 94 assume equal production of B^+ and B^0 at the $\Upsilon(4S)$ and use the CLEO II absolute $B(D^0 \rightarrow K^- \pi^+)$ and the PDG 1992 $B(D^0 \rightarrow K^- \pi^+ \pi^0)/B(D^0 \rightarrow K^- \pi^+)$ and $B(D^0 \rightarrow K^- \pi^+ \pi^+ \pi^-)/B(D^0 \rightarrow K^- \pi^+)$.

² Assumes equal production of B^+ and B^0 at the $\Upsilon(4S)$ and uses the Mark III branching fractions for the D .

³ ALBRECHT 88K assumes $B^0 \bar{B}^0, B^+ B^-$ ratio is 45:55.

$\Gamma(\bar{D}^0 K^+)/\Gamma(\bar{D}^0 \pi^+)$ Γ_{44}/Γ_{40}

VALUE (units 10^{-2})	DOCUMENT ID	TECN	COMMENT
8.30 ± 0.35 OUR AVERAGE			
8.31 ± 0.35 ± 0.20	AUBERT	04N	BABR $e^+e^- \rightarrow \Upsilon(4S)$
9.9 ± 1.4 ± 0.7	BORNHEIM	03	CLE2 $e^+e^- \rightarrow \Upsilon(4S)$
7.7 ± 0.5 ± 0.6	SWAIN	03	BELL $e^+e^- \rightarrow \Upsilon(4S)$
9.4 ± 0.9 ± 0.7	ABE	03D	BELL Repl. by SWAIN 03
7.9 ± 0.9 ± 0.6	ABE	01I	BELL Repl. by ABE 03D
5.5 ± 1.4 ± 0.5	ATHANAS	98	CLE2 Repl. by BORNHEIM 03

$\Gamma(D_{CP(+)} K^+)/\Gamma_{\text{total}}$ Γ_{45}/Γ

VALUE (units 10^{-4})	DOCUMENT ID	TECN	COMMENT
1.81 ± 0.25 ± 0.10	¹ AUBERT	06J	BABR $e^+e^- \rightarrow \Upsilon(4S)$

¹ AUBERT 06J reports $[B(B^+ \rightarrow D_{CP(+)} K^+) / [B(B^+ \rightarrow \bar{D}^0 K^+)]] = 0.45 \pm 0.06 \pm 0.02$. We multiply by our best value $B(B^+ \rightarrow \bar{D}^0 K^+) = (4.02 \pm 0.21) \times 10^{-4}$. Our first error is their experiment's error and our second error is the systematic error from using our best value.

Meson Particle Listings

 B^\pm $\Gamma(D_{CP(-1)} K^+)/\Gamma_{\text{total}}$ Γ_{46}/Γ

VALUE (units 10^{-4})	DOCUMENT ID	TECN	COMMENT
$1.73 \pm 0.22 \pm 0.09$	¹ AUBERT	06j	BABR $e^+e^- \rightarrow \Upsilon(4S)$
¹ AUBERT 06j reports $[B(B^+ \rightarrow D_{CP(-1)} K^+)/B(B^+ \rightarrow \bar{D}^0 K^+)] = 0.43 \pm 0.05 \pm 0.02$. We multiply by our best value $B(B^+ \rightarrow \bar{D}^0 K^+) = (4.02 \pm 0.21) \times 10^{-4}$. Our first error is their experiment's error and our second error is the systematic error from using our best value.			

 $\Gamma(D_{CP(+1)} K^+)/\Gamma(D_{CP(+1)} \pi^+)$ Γ_{45}/Γ_{41}

VALUE	DOCUMENT ID	TECN	COMMENT
0.092 ± 0.008 OUR AVERAGE			
$0.094 \pm 0.008 \pm 0.004$	^{1,2} ABE	06	BELL $e^+e^- \rightarrow \Upsilon(4S)$
$0.088 \pm 0.016 \pm 0.005$	³ AUBERT	04N	BABR $e^+e^- \rightarrow \Upsilon(4S)$
• • • We do not use the following data for averages, fits, limits, etc. • • •			
$0.125 \pm 0.036 \pm 0.010$	³ ABE	03D	BELL Repl. by SWAIN 03
$0.093 \pm 0.018 \pm 0.008$	³ SWAIN	03	BELL Repl. by ABE 06

¹ Reports a double ratio of $B(B^+ \rightarrow D_{CP(+1)} K^+)/B(B^+ \rightarrow D_{CP(+1)} \pi^+)$ and $B(B^+ \rightarrow \bar{D}^0 K^+)/B(B^+ \rightarrow \bar{D}^0 \pi^+)$, $1.13 \pm 0.16 \pm 0.08$. We multiply by our best value of $B(B^+ \rightarrow \bar{D}^0 K^+)/B(B^+ \rightarrow \bar{D}^0 \pi^+) = 0.083 \pm 0.006$. Our first error is their experiment's error and the second error is systematic error from using our best value.

² ABE 06 reports $[\Gamma(B^+ \rightarrow D_{CP(+1)} K^+)/\Gamma(B^+ \rightarrow D_{CP(+1)} \pi^+)] / [\Gamma(B^+ \rightarrow \bar{D}^0 K^+)/\Gamma(B^+ \rightarrow \bar{D}^0 \pi^+)] = 1.13 \pm 0.06 \pm 0.08$. We multiply by our best value $\Gamma(B^+ \rightarrow \bar{D}^0 K^+)/\Gamma(B^+ \rightarrow \bar{D}^0 \pi^+) = (8.30 \pm 0.35) \times 10^{-2}$. Our first error is their experiment's error and our second error is the systematic error from using our best value.

³ $CP=+1$ eigenstate of $D^0 \bar{D}^0$ system is reconstructed via $K^+ K^-$ and $\pi^+ \pi^-$.

 $\Gamma(D_{CP(-1)} K^+)/\Gamma(D_{CP(-1)} \pi^+)$ Γ_{46}/Γ_{42}

VALUE	DOCUMENT ID	TECN	COMMENT
$0.097 \pm 0.016 \pm 0.007$	¹ ABE	06	BELL $e^+e^- \rightarrow \Upsilon(4S)$
• • • We do not use the following data for averages, fits, limits, etc. • • •			
$0.119 \pm 0.028 \pm 0.006$	² ABE	03D	BELL Repl. by SWAIN 03
$0.108 \pm 0.019 \pm 0.007$	² SWAIN	03	BELL Repl. by ABE 06

¹ Reports a double ratio of $B(B^+ \rightarrow D_{CP(-1)} K^+)/B(B^+ \rightarrow D_{CP(-1)} \pi^+)$ and $B(B^+ \rightarrow \bar{D}^0 K^+)/B(B^+ \rightarrow \bar{D}^0 \pi^+)$, $1.17 \pm 0.14 \pm 0.14$. We multiply by our best value of $B(B^+ \rightarrow \bar{D}^0 K^+)/B(B^+ \rightarrow \bar{D}^0 \pi^+) = 0.083 \pm 0.006$. Our first error is their experiment's error and the second error is systematic error from using our best value.

² $CP=-1$ eigenstate of $D^0 \bar{D}^0$ system is reconstructed via $K_S^0 \pi^0$, $K_S^0 \omega$, $K_S^0 \phi$, $K_S^0 \eta$, and $K_S^0 \eta'$.

 $\Gamma([K^- \pi^+]_D K^+)/\Gamma([K^+ \pi^-]_D K^+)$ Γ_{47}/Γ_{48}

VALUE	CL%	DOCUMENT ID	TECN	COMMENT
<0.029	90	¹ AUBERT	05G	BABR $e^+e^- \rightarrow \Upsilon(4S)$
• • • We do not use the following data for averages, fits, limits, etc. • • •				
<0.044	90	² SAIGO	05	BELL $e^+e^- \rightarrow \Upsilon(4S)$
<0.026	90	³ AUBERT,B	04L	BABR Repl. by AUBERT 05G

¹ AUBERT 05G extract a constraint on the magnitude of the ratio of amplitudes $|A(B^+ \rightarrow D^0 K^+)/A(B^+ \rightarrow \bar{D}^0 K^+)| < 0.23$ at 90% CL (Bayesian). Similar measurements from $B^+ \rightarrow D^{*0} K^+$ are also reported.

² SAIGO 05 extract a constraint on the magnitude of the ratio of amplitudes $|A(B^+ \rightarrow D^0 K^+)/A(B^+ \rightarrow \bar{D}^0 K^+)| < 0.27$ at 90% CL.

³ AUBERT,B 04L extract a constraint on the magnitude of the ratio of amplitudes $|A(B^+ \rightarrow D^0 K^+)/A(B^+ \rightarrow \bar{D}^0 K^+)| < 0.22$ at 90% CL.

 $\Gamma([K^- \pi^+ \pi^0]_D K^+)/\Gamma([K^+ \pi^- \pi^0]_D K^+)$ Γ_{49}/Γ_{50}

VALUE	CL%	DOCUMENT ID	TECN	COMMENT
<0.039	95	¹ AUBERT	07BN	BABR $e^+e^- \rightarrow \Upsilon(4S)$

¹ Extracts a constraint on the magnitude of the ratio of amplitudes $|A(B^+ \rightarrow D^0 K^+)/A(B^+ \rightarrow \bar{D}^0 K^+)| < 0.19$ at 95% CL.

 $\Gamma([K^- \pi^+]_D K^*(892)^+)/\Gamma([K^+ \pi^-]_D K^*(892)^+)$ Γ_{51}/Γ_{52}

VALUE	DOCUMENT ID	TECN	COMMENT
$0.046 \pm 0.031 \pm 0.008$	AUBERT,B	05v	BABR $e^+e^- \rightarrow \Upsilon(4S)$

 $\Gamma([K^- \pi^+]_D \pi^+)/\Gamma_{\text{total}}$ Γ_{53}/Γ

VALUE (units 10^{-5})	DOCUMENT ID	TECN	COMMENT
$1.70^{+0.51}_{-0.46} \pm 0.02$	¹ SAIGO	05	BELL $e^+e^- \rightarrow \Upsilon(4S)$

¹ SAIGO 05 reports $[B(B^+ \rightarrow [K^- \pi^+]_D \pi^+)] \times [B(D^0 \rightarrow K^- \pi^+)] = (6.6^{+1.9}_{-1.7} \pm 0.5) \times 10^{-7}$. We divide by our best value $B(D^0 \rightarrow K^- \pi^+) = (3.89 \pm 0.05) \times 10^{-2}$. Our first error is their experiment's error and our second error is the systematic error from using our best value.

 $\Gamma([\pi^+ \pi^- \pi^0]_D K^-)/\Gamma_{\text{total}}$ Γ_{54}/Γ

VALUE (units 10^{-6})	DOCUMENT ID	TECN	COMMENT
$4.6 \pm 0.8 \pm 0.4$	¹ AUBERT	07BJ	BABR $e^+e^- \rightarrow \Upsilon(4S)$

• • • We do not use the following data for averages, fits, limits, etc. • • •

$5.5 \pm 1.0 \pm 0.7$

¹ AUBERT,B 05T BABR Repl. by AUBERT 07BJ

¹ Assumes equal production of B^+ and B^0 at the $\Upsilon(4S)$.

 $\Gamma([K^- \pi^+]_D \pi^+)/\Gamma(\bar{D}^0 \pi^+)$ Γ_{53}/Γ_{40}

VALUE (units 10^{-3})	DOCUMENT ID	TECN	COMMENT
$3.5 \pm 1.0_{-0.3} \pm 0.2$	SAIGO	05	BELL $e^+e^- \rightarrow \Upsilon(4S)$

 $\Gamma(\bar{D}^0 K^*(892)^+)/\Gamma_{\text{total}}$ Γ_{55}/Γ

VALUE (units 10^{-4})	DOCUMENT ID	TECN	COMMENT
5.3 ± 0.4 OUR AVERAGE			
$5.29 \pm 0.30 \pm 0.34$	¹ AUBERT	06z	BABR $e^+e^- \rightarrow \Upsilon(4S)$
$6.1 \pm 1.6 \pm 1.7$	¹ MAHAPATRA	02	CLE2 $e^+e^- \rightarrow \Upsilon(4S)$
• • • We do not use the following data for averages, fits, limits, etc. • • •			
$6.3 \pm 0.7 \pm 0.5$	¹ AUBERT	04Q	BABR Repl. by AUBERT 06z

¹ Assumes equal production of B^+ and B^0 at the $\Upsilon(4S)$.

 $\Gamma(D_{CP(-1)} K^*(892)^+)/\Gamma_{\text{total}}$ Γ_{56}/Γ

VALUE (units 10^{-4})	DOCUMENT ID	TECN	COMMENT
$1.7 \pm 0.7 \pm 0.1$	¹ AUBERT,B	05u	BABR $e^+e^- \rightarrow \Upsilon(4S)$
¹ AUBERT,B 05u reports $[B(B^+ \rightarrow D_{CP(-1)} K^*(892)^+)/B(B^+ \rightarrow \bar{D}^0 K^*(892)^+)] = 0.325 \pm 0.13 \pm 0.04$. We multiply by our best value $B(B^+ \rightarrow \bar{D}^0 K^*(892)^+) = (5.3 \pm 0.4) \times 10^{-4}$. Our first error is their experiment's error and our second error is the systematic error from using our best value.			

 $\Gamma(D_{CP(+1)} K^*(892)^+)/\Gamma_{\text{total}}$ Γ_{57}/Γ

VALUE (units 10^{-4})	DOCUMENT ID	TECN	COMMENT
$5.2 \pm 1.1 \pm 0.4$	¹ AUBERT,B	05u	BABR $e^+e^- \rightarrow \Upsilon(4S)$
¹ AUBERT,B 05u reports $[B(B^+ \rightarrow D_{CP(+1)} K^*(892)^+)/B(B^+ \rightarrow \bar{D}^0 K^*(892)^+)] = 0.98 \pm 0.20 \pm 0.055$. We multiply by our best value $B(B^+ \rightarrow \bar{D}^0 K^*(892)^+) = (5.3 \pm 0.4) \times 10^{-4}$. Our first error is their experiment's error and our second error is the systematic error from using our best value.			

 $\Gamma(\bar{D}^0 K^+ \bar{K}^0)/\Gamma_{\text{total}}$ Γ_{58}/Γ

VALUE (units 10^{-4})	DOCUMENT ID	TECN	COMMENT
$5.5 \pm 1.4 \pm 0.8$	¹ DRUTSKOY	02	BELL $e^+e^- \rightarrow \Upsilon(4S)$
¹ Assumes equal production of B^+ and B^0 at the $\Upsilon(4S)$.			

 $\Gamma(\bar{D}^0 K^+ \bar{K}^*(892)^0)/\Gamma_{\text{total}}$ Γ_{59}/Γ

VALUE (units 10^{-4})	DOCUMENT ID	TECN	COMMENT
$7.5 \pm 1.3 \pm 1.1$	¹ DRUTSKOY	02	BELL $e^+e^- \rightarrow \Upsilon(4S)$
¹ Assumes equal production of B^+ and B^0 at the $\Upsilon(4S)$.			

 $\Gamma(\bar{D}^0 \pi^+ \pi^+ \pi^-)/\Gamma_{\text{total}}$ Γ_{60}/Γ

VALUE	DOCUMENT ID	TECN	COMMENT
$0.0115 \pm 0.0029 \pm 0.0021$	¹ BORTOLETTO	092	CLEO $e^+e^- \rightarrow \Upsilon(4S)$
¹ BORTOLETTO 92 assumes equal production of B^+ and B^0 at the $\Upsilon(4S)$ and uses MarkIII branching fractions for the D .			

 $\Gamma(\bar{D}^0 \pi^+ \pi^+ \pi^- \text{ nonresonant})/\Gamma_{\text{total}}$ Γ_{61}/Γ

VALUE	DOCUMENT ID	TECN	COMMENT
$0.0051 \pm 0.0034 \pm 0.0023$	¹ BORTOLETTO	092	CLEO $e^+e^- \rightarrow \Upsilon(4S)$
¹ BORTOLETTO 92 assumes equal production of B^+ and B^0 at the $\Upsilon(4S)$ and uses MarkIII branching fractions for the D .			

 $\Gamma(\bar{D}^0 \pi^+ \rho^0)/\Gamma_{\text{total}}$ Γ_{62}/Γ

VALUE	DOCUMENT ID	TECN	COMMENT
$0.0042 \pm 0.0023 \pm 0.0020$	¹ BORTOLETTO	092	CLEO $e^+e^- \rightarrow \Upsilon(4S)$
¹ BORTOLETTO 92 assumes equal production of B^+ and B^0 at the $\Upsilon(4S)$ and uses MarkIII branching fractions for the D .			

 $\Gamma(\bar{D}^0 a_1(1260)^+)/\Gamma_{\text{total}}$ Γ_{63}/Γ

VALUE	DOCUMENT ID	TECN	COMMENT
$0.0045 \pm 0.0019 \pm 0.0031$	¹ BORTOLETTO	092	CLEO $e^+e^- \rightarrow \Upsilon(4S)$
¹ BORTOLETTO 92 assumes equal production of B^+ and B^0 at the $\Upsilon(4S)$ and uses MarkIII branching fractions for the D .			

 $\Gamma(\bar{D}^0 \omega \pi^+)/\Gamma_{\text{total}}$ Γ_{64}/Γ

VALUE	DOCUMENT ID	TECN	COMMENT
$0.0041 \pm 0.0007 \pm 0.0006$	¹ ALEXANDER	01B	CLE2 $e^+e^- \rightarrow \Upsilon(4S)$
¹ Assumes equal production of B^+ and B^0 at the $\Upsilon(4S)$. The signal is consistent with all observed $\omega \pi^+$ having proceeded through the ρ^+ resonance at mass $1349 \pm 25^{+10}_{-5}$ MeV and width $547 \pm 86^{+46}_{-45}$ MeV.			

 $\Gamma(D^*(2010)^- \pi^+ \pi^+)/\Gamma_{\text{total}}$ Γ_{65}/Γ

VALUE (units 10^{-3})	CL%	EVTS	DOCUMENT ID	TECN	COMMENT
1.35 ± 0.22 OUR AVERAGE					
$1.25 \pm 0.08 \pm 0.22$			¹ ABE	04D	BELL $e^+e^- \rightarrow \Upsilon(4S)$
$1.9 \pm 0.7 \pm 0.3$	14		² ALAM	94	CLE2 $e^+e^- \rightarrow \Upsilon(4S)$
$2.6 \pm 1.4 \pm 0.7$	11		³ ALBRECHT	90J	ARG $e^+e^- \rightarrow \Upsilon(4S)$
$2.4^{+1.7}_{-1.6} \pm 1.0_{-0.6}$	3		⁴ BEBEK	87	CLEO $e^+e^- \rightarrow \Upsilon(4S)$
• • • We do not use the following data for averages, fits, limits, etc. • • •					
$<4.$	90		⁵ BORTOLETTO	092	CLEO $e^+e^- \rightarrow \Upsilon(4S)$
$5. \pm 2. \pm 3.$	7		⁶ ALBRECHT	87c	ARG $e^+e^- \rightarrow \Upsilon(4S)$

- ¹ Assumes equal production of B^+ and B^0 at the $\Upsilon(4S)$.
² ALAM 94 assume equal production of B^+ and B^0 at the $\Upsilon(4S)$ and use the CLEO II $B(D^*(2010)^+ \rightarrow D^0 \pi^+)$ and absolute $B(D^0 \rightarrow K^- \pi^+)$ and the PDG 1992 $B(D^0 \rightarrow K^- \pi^+ \pi^0)/B(D^0 \rightarrow K^- \pi^+)$ and $B(D^0 \rightarrow K^- \pi^+ \pi^+ \pi^-)/B(D^0 \rightarrow K^- \pi^+)$.
³ Assumes equal production of B^+ and B^0 at the $\Upsilon(4S)$ and uses the MarkIII branching fractions for the D .
⁴ BEBEK 87 value has been updated in BERKELMAN 91 to use same assumptions as noted for BORTOLETTO 92.
⁵ BORTOLETTO 92 assumes equal production of B^+ and B^0 at the $\Upsilon(4S)$ and uses MarkIII branching fractions for the D and $D^*(2010)$. The authors also find the product branching fraction into $D^{**} \pi$ followed by $D^{**} \rightarrow D^*(2010) \pi$ to be $0.0014^{+0.0008}_{-0.0006} \pm 0.0003$ where D^{**} represents all orbitally excited D mesons.
⁶ ALBRECHT 87c use PDG 86 branching ratios for D and $D^*(2010)$ and assume $B(\Upsilon(4S) \rightarrow B^+ B^-) = 55\%$ and $B(\Upsilon(4S) \rightarrow B^0 \bar{B}^0) = 45\%$. Superseded by ALBRECHT 90J.

$\Gamma(D^- \pi^+ \pi^+)/\Gamma_{\text{total}}$		Γ_{66}/Γ	
VALUE (units 10^{-3})	CL%	DOCUMENT ID	TECN COMMENT
1.02 ± 0.04 ± 0.15		¹ ABE 04D BELL	$e^+ e^- \rightarrow \Upsilon(4S)$
• • • We do not use the following data for averages, fits, limits, etc. • • •			
<1.4	90	² ALAM 94	CLE2 $e^+ e^- \rightarrow \Upsilon(4S)$
<7	90	³ BORTOLETTO92	CLEO $e^+ e^- \rightarrow \Upsilon(4S)$
2.5 $\frac{+4.1}{-2.3}$ $\frac{+2.4}{-0.8}$	1	⁴ BEBEK 87	CLEO $e^+ e^- \rightarrow \Upsilon(4S)$

- ¹ Assumes equal production of B^+ and B^0 at the $\Upsilon(4S)$.
² ALAM 94 assume equal production of B^+ and B^0 at the $\Upsilon(4S)$ and use the MarkIII $B(D^+ \rightarrow K^- \pi^+ \pi^+)$.
³ BORTOLETTO 92 assumes equal production of B^+ and B^0 at the $\Upsilon(4S)$ and uses MarkIII branching fractions for the D . The product branching fraction into $D_0^*(2340) \pi$ followed by $D_0^*(2340) \rightarrow D \pi$ is < 0.005 at 90%CL and into $D_2^*(2460) \pi$ followed by $D_2^*(2460) \rightarrow D \pi$ is < 0.004 at 90%CL.
⁴ BEBEK 87 assume the $\Upsilon(4S)$ decays 43% to $B^0 \bar{B}^0$. $B(D^- \rightarrow K^+ \pi^- \pi^-) = (9.1 \pm 1.3 \pm 0.4)\%$ is assumed.

$\Gamma(D^+ K^0)/\Gamma_{\text{total}}$		Γ_{67}/Γ	
VALUE (units 10^{-6})	CL%	DOCUMENT ID	TECN COMMENT
<5.0	90	¹ AUBERT,B	05E BABR $e^+ e^- \rightarrow \Upsilon(4S)$

- ¹ Assumes equal production of B^+ and B^0 at the $\Upsilon(4S)$.

$\Gamma(\bar{D}^*(2007)^0 \pi^+)/\Gamma_{\text{total}}$		Γ_{68}/Γ	
VALUE (units 10^{-3})	EVTS	DOCUMENT ID	TECN COMMENT
5.19 ± 0.26 OUR AVERAGE			
5.52 ± 0.17 ± 0.42		¹ AUBERT 07H BABR	$e^+ e^- \rightarrow \Upsilon(4S)$
5.5 ± 0.4 ± 0.2		^{2,3} AUBERT, BE 06J BABR	$e^+ e^- \rightarrow \Upsilon(4S)$
4.34 ± 0.47 ± 0.18		⁴ BRANDENB... 98	CLE2 $e^+ e^- \rightarrow \Upsilon(4S)$
5.2 ± 0.7 ± 0.7	71	⁵ ALAM 94	CLE2 $e^+ e^- \rightarrow \Upsilon(4S)$
7.2 ± 1.8 ± 1.6		⁶ BORTOLETTO92	CLEO $e^+ e^- \rightarrow \Upsilon(4S)$
4.0 ± 1.4 ± 1.2	9	⁶ ALBRECHT 90J ARG	$e^+ e^- \rightarrow \Upsilon(4S)$
• • • We do not use the following data for averages, fits, limits, etc. • • •			
2.7 ± 4.4		⁷ BEBEK 87	CLEO $e^+ e^- \rightarrow \Upsilon(4S)$

- ¹ Assumes equal production of B^+ and B^0 at the $\Upsilon(4S)$.
² AUBERT, BE 06J reports $[B(B^+ \rightarrow \bar{D}^*(2007)^0 \pi^+)] / [B(B^+ \rightarrow \bar{D}^0 \pi^+)] = 1.14 \pm 0.07 \pm 0.04$. We multiply by our best value $B(B^+ \rightarrow \bar{D}^0 \pi^+) = (4.84 \pm 0.15) \times 10^{-3}$. Our first error is their experiment's error and our second error is the systematic error from using our best value.
³ Uses a missing-mass method. Does not depend on D branching fractions or B^+/B^0 production rates.
⁴ BRANDENBURG 98 assume equal production of B^+ and B^0 at $\Upsilon(4S)$ and use the D^* reconstruction technique. The first error is their experiment's error and the second error is the systematic error from the PDG 96 value of $B(D^* \rightarrow D \pi)$.
⁵ ALAM 94 assume equal production of B^+ and B^0 at the $\Upsilon(4S)$ and use the CLEO II $B(D^*(2007)^0 \rightarrow D^0 \pi^0)$ and absolute $B(D^0 \rightarrow K^- \pi^+)$ and the PDG 1992 $B(D^0 \rightarrow K^- \pi^+ \pi^0)/B(D^0 \rightarrow K^- \pi^+)$ and $B(D^0 \rightarrow K^- \pi^+ \pi^+ \pi^-)/B(D^0 \rightarrow K^- \pi^+)$.
⁶ Assumes equal production of B^+ and B^0 at the $\Upsilon(4S)$ and uses MarkIII branching fractions for the D and $D^*(2010)$.
⁷ This is a derived branching ratio, using the inclusive pion spectrum and other two-body B decays. BEBEK 87 assume the $\Upsilon(4S)$ decays 43% to $B^0 \bar{B}^0$.

$\Gamma(\bar{D}^*(2007)^0 \omega \pi^+)/\Gamma_{\text{total}}$		Γ_{71}/Γ	
VALUE	DOCUMENT ID	TECN	COMMENT
0.0045 ± 0.0010 ± 0.0007	¹ ALEXANDER 01B	CLE2	$e^+ e^- \rightarrow \Upsilon(4S)$

- ¹ Assumes equal production of B^+ and B^0 at the $\Upsilon(4S)$. The signal is consistent with all observed $\omega \pi^+$ having proceeded through the ρ^+ resonance at mass $1349 \pm 25^{+10}_{-5}$ MeV and width $547 \pm 86^{+46}_{-45}$ MeV.

$\Gamma(\bar{D}^*(2007)^0 \rho^+)/\Gamma_{\text{total}}$		Γ_{72}/Γ	
VALUE	EVTS	DOCUMENT ID	TECN COMMENT
0.0098 ± 0.0017 OUR AVERAGE			
0.0098 ± 0.0006 ± 0.0017		¹ CSORNA 03	CLE2 $e^+ e^- \rightarrow \Upsilon(4S)$
0.010 ± 0.006 ± 0.004	7	² ALBRECHT 90J ARG	$e^+ e^- \rightarrow \Upsilon(4S)$
• • • We do not use the following data for averages, fits, limits, etc. • • •			
0.0168 ± 0.0021 ± 0.0028	86	³ ALAM 94	CLE2 $e^+ e^- \rightarrow \Upsilon(4S)$

- ¹ Assumes equal production of B^0 and B^+ at the $\Upsilon(4S)$ resonance. The second error combines the systematic and theoretical uncertainties in quadrature. CSORNA 03 includes data used in ALAM 94. A full angular fit to three complex helicity amplitudes is performed.
² Assumes equal production of B^+ and B^0 at the $\Upsilon(4S)$ and uses MarkIII branching fractions for the D and $D^*(2010)$.
³ ALAM 94 assume equal production of B^+ and B^0 at the $\Upsilon(4S)$ and use the CLEO II $B(D^*(2007)^0 \rightarrow D^0 \pi^0)$ and absolute $B(D^0 \rightarrow K^- \pi^+)$ and the PDG 1992 $B(D^0 \rightarrow K^- \pi^+ \pi^0)/B(D^0 \rightarrow K^- \pi^+)$ and $B(D^0 \rightarrow K^- \pi^+ \pi^+ \pi^-)/B(D^0 \rightarrow K^- \pi^+)$. The nonresonant $\pi^+ \pi^0$ contribution under the ρ^+ is negligible.

$\Gamma(\bar{D}^*(2007)^0 K^+)/\Gamma_{\text{total}}$		Γ_{73}/Γ	
VALUE (units 10^{-4})	DOCUMENT ID	TECN	COMMENT
4.16 ± 0.33 OUR AVERAGE			
4.22 $\frac{+0.30}{-0.26}$ ± 0.21	¹ AUBERT 05N	BABR	$e^+ e^- \rightarrow \Upsilon(4S)$
3.59 ± 0.97 ± 0.31	² ABE 01I	BELL	$e^+ e^- \rightarrow \Upsilon(4S)$

- ¹ AUBERT 05N reports $[B(B^+ \rightarrow \bar{D}^*(2007)^0 K^+)] / [B(B^+ \rightarrow \bar{D}^*(2007)^0 \pi^+)] = 0.0813 \pm 0.0040^{+0.0042}_{-0.0031}$. We multiply by our best value $B(B^+ \rightarrow \bar{D}^*(2007)^0 \pi^+) = (5.19 \pm 0.26) \times 10^{-3}$. Our first error is their experiment's error and our second error is the systematic error from using our best value.
² ABE 01I reports $B(B^+ \rightarrow \bar{D}^*(2007)^0 K^+)/B(B^+ \rightarrow \bar{D}^*(2007)^0 \pi^+) = 0.078 \pm 0.019 \pm 0.009$. We multiply by our best value $B(B^+ \rightarrow \bar{D}^*(2007)^0 \pi^+) = (4.6 \pm 0.4) \times 10^{-3}$. Our first error is their experiment's error and the second error is systematic error from using our best value.

$\Gamma(\bar{D}_{CP(+)}^{*0} K^+)/\Gamma(\bar{D}_{CP(+)}^{*0} \pi^+)$		Γ_{74}/Γ_{69}	
VALUE	DOCUMENT ID	TECN	COMMENT
0.095 ± 0.017 OUR AVERAGE			
0.11 ± 0.02 ± 0.02	¹ ABE 06	BELL	$e^+ e^- \rightarrow \Upsilon(4S)$
0.086 ± 0.021 ± 0.007	² AUBERT 05N	BABR	$e^+ e^- \rightarrow \Upsilon(4S)$

- ¹ Reports a double ratio of $B(B^+ \rightarrow (D_{CP(+)}^{*0})^0 K^+)/B(B^+ \rightarrow (D_{CP(+)}^{*0})^0 \pi^+)$ and $B(B^+ \rightarrow \bar{D}^{*0} K^+)/B(B^+ \rightarrow \bar{D}^{*0} \pi^+)$, $1.41 \pm 0.25 \pm 0.06$. We multiply by our best value of $B(B^+ \rightarrow \bar{D}^{*0} K^+)/B(B^+ \rightarrow \bar{D}^{*0} \pi^+) = 0.080 \pm 0.011$. Our first error is their experiment's error and the second error is systematic error from using our best value.
² Uses $D^{*0} \rightarrow D^0 \pi^0$ with D^0 reconstructed in the CP -even eigenstates $K^+ K^-$ and $\pi^+ \pi^-$.

$\Gamma(\bar{D}_{CP(-)}^{*0} K^+)/\Gamma(\bar{D}_{CP(-)}^{*0} \pi^+)$		Γ_{75}/Γ_{70}	
VALUE	DOCUMENT ID	TECN	COMMENT
0.09 ± 0.03 ± 0.01			
	¹ ABE 06	BELL	$e^+ e^- \rightarrow \Upsilon(4S)$

- ¹ Reports a double ratio of $B(B^+ \rightarrow (D_{CP(-)}^{*0})^0 K^+)/B(B^+ \rightarrow (D_{CP(-)}^{*0})^0 \pi^+)$ and $B(B^+ \rightarrow \bar{D}^{*0} K^+)/B(B^+ \rightarrow \bar{D}^{*0} \pi^+)$, $1.15 \pm 0.31 \pm 0.12$. We multiply by our best value of $B(B^+ \rightarrow \bar{D}^{*0} K^+)/B(B^+ \rightarrow \bar{D}^{*0} \pi^+) = 0.080 \pm 0.011$. Our first error is their experiment's error and the second error is systematic error from using our best value.

$\Gamma(\bar{D}^*(2007)^0 K^*(892)^+)/\Gamma_{\text{total}}$		Γ_{76}/Γ	
VALUE (units 10^{-4})	DOCUMENT ID	TECN	COMMENT
8.1 ± 1.4 OUR AVERAGE			
8.3 ± 1.1 ± 1.0	¹ AUBERT 04K	BABR	$e^+ e^- \rightarrow \Upsilon(4S)$
7.2 ± 2.2 ± 2.6	² MAHAPATRA 02	CLE2	$e^+ e^- \rightarrow \Upsilon(4S)$

- ¹ Assumes equal production of B^+ and B^0 at the $\Upsilon(4S)$.
² Assumes equal production of B^+ and B^0 at the $\Upsilon(4S)$ and an unpolarized final state.

$\Gamma(\bar{D}^*(2007)^0 K^+ \bar{K}^0)/\Gamma_{\text{total}}$		Γ_{77}/Γ	
VALUE (units 10^{-4})	CL%	DOCUMENT ID	TECN COMMENT
<10.6	90	¹ DRUTSKOY 02	BELL $e^+ e^- \rightarrow \Upsilon(4S)$

- ¹ Assumes equal production of B^+ and B^0 at the $\Upsilon(4S)$.

$\Gamma(\bar{D}^*(2007)^0 K^+ K^*(892)^0)/\Gamma_{\text{total}}$		Γ_{78}/Γ	
VALUE (units 10^{-4})	DOCUMENT ID	TECN	COMMENT
15.3 ± 3.1 ± 2.9	¹ DRUTSKOY 02	BELL	$e^+ e^- \rightarrow \Upsilon(4S)$

- ¹ Assumes equal production of B^+ and B^0 at the $\Upsilon(4S)$.

$\Gamma(\bar{D}^*(2007)^0 \pi^+ \pi^+ \pi^-)/\Gamma_{\text{total}}$		Γ_{79}/Γ	
VALUE (units 10^{-2})	EVTS	DOCUMENT ID	TECN COMMENT
1.03 ± 0.12 OUR AVERAGE			
1.055 ± 0.047 ± 0.129		¹ MAJUMDER 04	BELL $e^+ e^- \rightarrow \Upsilon(4S)$
0.94 ± 0.20 ± 0.17	48	^{2,3} ALAM 94	CLE2 $e^+ e^- \rightarrow \Upsilon(4S)$

- ¹ Assumes equal production of B^+ and B^0 at the $\Upsilon(4S)$.
² ALAM 94 assume equal production of B^+ and B^0 at the $\Upsilon(4S)$ and use the CLEO II $B(D^*(2007)^0 \rightarrow D^0 \pi^0)$ and absolute $B(D^0 \rightarrow K^- \pi^+)$ and the PDG 1992 $B(D^0 \rightarrow K^- \pi^+ \pi^0)/B(D^0 \rightarrow K^- \pi^+)$ and $B(D^0 \rightarrow K^- \pi^+ \pi^+ \pi^-)/B(D^0 \rightarrow K^- \pi^+)$.
³ The three pion mass is required to be between 1.0 and 1.6 GeV consistent with an a_1 meson. (If this channel is dominated by a_1^+ , the branching ratio for $\bar{D}^{*0} a_1^+$ is twice that for $\bar{D}^{*0} \pi^+ \pi^+ \pi^-$.)

Meson Particle Listings

 B^\pm

$\Gamma(\overline{D}^*(2007)^0 a_1(1260)^+)/\Gamma_{\text{total}}$ Γ_{80}/Γ

VALUE	DOCUMENT ID	TECN	COMMENT
0.0188 ± 0.0040 ± 0.0034	1,2 ALAM 94	CLE2	$e^+e^- \rightarrow \Upsilon(4S)$

¹ALAM 94 value is twice their $\Gamma(\overline{D}^*(2007)^0 \pi^+ \pi^+ \pi^-)/\Gamma_{\text{total}}$ value based on their observation that the three pions are dominantly in the $a_1(1260)$ mass range 1.0 to 1.6 GeV.

²ALAM 94 assume equal production of B^+ and B^0 at the $\Upsilon(4S)$ and use the CLEO II $B(D^*(2007)^0 \rightarrow D^0 \pi^0)$ and absolute $B(D^0 \rightarrow K^- \pi^+)$ and the PDG 1992 $B(D^0 \rightarrow K^- \pi^+ \pi^0)/B(D^0 \rightarrow K^- \pi^+)$ and $B(D^0 \rightarrow K^- \pi^+ \pi^+ \pi^-)/B(D^0 \rightarrow K^- \pi^+)$.

$\Gamma(\overline{D}^*(2007)^0 \pi^- \pi^+ \pi^+ \pi^0)/\Gamma_{\text{total}}$ Γ_{81}/Γ

VALUE	DOCUMENT ID	TECN	COMMENT
0.0180 ± 0.0024 ± 0.0027	1 ALEXANDER 01B	CLE2	$e^+e^- \rightarrow \Upsilon(4S)$

¹Assumes equal production of B^+ and B^0 at the $\Upsilon(4S)$. The signal is consistent with all observed $\omega \pi^+$ having proceeded through the ρ^+ resonance at mass $1349 \pm 25^{+10}_{-5}$ MeV and width $547 \pm 86^{+46}_{-45}$ MeV.

$\Gamma(\overline{D}^{*0} 3\pi^+ 2\pi^-)/\Gamma_{\text{total}}$ Γ_{82}/Γ

VALUE (units 10^{-3})	DOCUMENT ID	TECN	COMMENT
5.67 ± 0.91 ± 0.85	1 MAJUMDER 04	BELL	$e^+e^- \rightarrow \Upsilon(4S)$

¹Assumes equal production of B^+ and B^0 at the $\Upsilon(4S)$.

$\Gamma(D^*(2010)^+ \pi^0)/\Gamma_{\text{total}}$ Γ_{83}/Γ

VALUE	CL%	DOCUMENT ID	TECN	COMMENT
<0.00017	90	1 BRANDENB... 98	CLE2	$e^+e^- \rightarrow \Upsilon(4S)$

¹BRANDENBURG 98 assume equal production of B^+ and B^0 at $\Upsilon(4S)$ and use the D^* partial reconstruction technique. The first error is their experiment's error and the second error is the systematic error from the PDG 96 value of $B(D^* \rightarrow D \pi)$.

$\Gamma(D^*(2010)^+ K^0)/\Gamma_{\text{total}}$ Γ_{84}/Γ

VALUE	CL%	DOCUMENT ID	TECN	COMMENT
<9.0 × 10⁻⁶	90	1 AUBERT,B 05E	BABR	$e^+e^- \rightarrow \Upsilon(4S)$

• • • We do not use the following data for averages, fits, limits, etc. • • •

VALUE	CL%	DOCUMENT ID	TECN	COMMENT
$<9.5 \times 10^{-5}$	90	1 GRITSAN 01	CLE2	$e^+e^- \rightarrow \Upsilon(4S)$

¹Assumes equal production of B^+ and B^0 at the $\Upsilon(4S)$.

$\Gamma(D^*(2010)^- \pi^+ \pi^+ \pi^0)/\Gamma_{\text{total}}$ Γ_{85}/Γ

VALUE	EVTs	DOCUMENT ID	TECN	COMMENT
0.0152 ± 0.0071 ± 0.0001	26	1 ALBRECHT 90J	ARG	$e^+e^- \rightarrow \Upsilon(4S)$

• • • We do not use the following data for averages, fits, limits, etc. • • •

VALUE	EVTs	DOCUMENT ID	TECN	COMMENT
$0.043 \pm 0.013 \pm 0.026$	24	2 ALBRECHT 87C	ARG	$e^+e^- \rightarrow \Upsilon(4S)$

¹ALBRECHT 90J reports $0.018 \pm 0.007 \pm 0.005$ for $B(D^*(2010)^+ \rightarrow D^0 \pi^+) = 0.57 \pm 0.06$. We rescale to our best value $B(D^*(2010)^+ \rightarrow D^0 \pi^+) = (67.7 \pm 0.5) \times 10^{-2}$. Our first error is their experiment's error and our second error is the systematic error from using our best value. Assumes equal production of B^+ and B^0 at the $\Upsilon(4S)$ and uses MarkIII branching fractions for the D .

²ALBRECHT 87C use PDG 86 branching ratios for D and $D^*(2010)$ and assume $B(\Upsilon(4S) \rightarrow B^+ B^-) = 55\%$ and $B(\Upsilon(4S) \rightarrow B^0 \overline{B}^0) = 45\%$. Superseded by ALBRECHT 90J.

$\Gamma(D^*(2010)^- \pi^+ \pi^+ \pi^+ \pi^-)/\Gamma_{\text{total}}$ Γ_{86}/Γ

VALUE (units 10^{-3})	CL%	DOCUMENT ID	TECN	COMMENT
2.56 ± 0.26 ± 0.33		1 MAJUMDER 04	BELL	$e^+e^- \rightarrow \Upsilon(4S)$

• • • We do not use the following data for averages, fits, limits, etc. • • •

VALUE	CL%	DOCUMENT ID	TECN	COMMENT
<10	90	2 ALBRECHT 90J	ARG	$e^+e^- \rightarrow \Upsilon(4S)$

¹Assumes equal production of B^+ and B^0 at the $\Upsilon(4S)$.

²Assumes equal production of B^+ and B^0 at the $\Upsilon(4S)$ and uses MarkIII branching fractions for the D and $D^*(2010)$.

$\Gamma(\overline{D}^{**0} \pi^+)/\Gamma_{\text{total}}$ Γ_{87}/Γ

D^{**0} represents an excited state with mass $2.2 < M < 2.8$ GeV/ c^2 .

VALUE (units 10^{-3})	DOCUMENT ID	TECN	COMMENT
5.9 ± 1.3 ± 0.2	1,2 AUBERT, BE 06J	BABR	$e^+e^- \rightarrow \Upsilon(4S)$

¹AUBERT, BE 06J reports $[B(B^+ \rightarrow \overline{D}^{**0} \pi^+)] / [B(B^+ \rightarrow \overline{D}^0 \pi^+)] = 1.22 \pm 0.13 \pm 0.23$. We multiply by our best value $B(B^+ \rightarrow \overline{D}^0 \pi^+) = (4.84 \pm 0.15) \times 10^{-3}$. Our first error is their experiment's error and our second error is the systematic error from using our best value.

²Uses a missing-mass method. Does not depend on D branching fractions or B^+/\overline{B}^0 production rates.

$\Gamma(\overline{D}_1^*(2420)^0 \pi^+)/\Gamma_{\text{total}}$ Γ_{88}/Γ

VALUE	EVTs	DOCUMENT ID	TECN	COMMENT
0.0015 ± 0.0006 OUR AVERAGE	Error includes scale factor of 1.3.			

VALUE	EVTs	DOCUMENT ID	TECN	COMMENT
$0.0011 \pm 0.0005 \pm 0.0002$	8	1 ALAM 94	CLE2	$e^+e^- \rightarrow \Upsilon(4S)$
$0.0025 \pm 0.0007 \pm 0.0006$		2 ALBRECHT 94D	ARG	$e^+e^- \rightarrow \Upsilon(4S)$

¹ALAM 94 assume equal production of B^+ and B^0 at the $\Upsilon(4S)$ and use the CLEO II $B(D^*(2010)^+ \rightarrow D^0 \pi^+)$ and absolute $B(D^0 \rightarrow K^- \pi^+)$ and the PDG 1992 $B(D^0 \rightarrow K^- \pi^+ \pi^0)/B(D^0 \rightarrow K^- \pi^+)$ and assuming $B(D_1(2420)^0 \rightarrow D^*(2010)^+ \pi^-) = 67\%$.

²ALBRECHT 94D assume equal production of B^+ and B^0 at the $\Upsilon(4S)$ and use the CLEO II $B(D^*(2010)^+ \rightarrow D^0 \pi^+)$ assuming $B(D_1(2420)^0 \rightarrow D^*(2010)^+ \pi^-) = 67\%$.

$\Gamma(\overline{D}_1(2420)^0 \pi^+ \times B(\overline{D}_1^0 \rightarrow \overline{D}^0 \pi^+ \pi^-))/\Gamma_{\text{total}}$ Γ_{89}/Γ

VALUE (units 10^{-4})	DOCUMENT ID	TECN	COMMENT
1.85 ± 0.29 ± 0.35	1 ABE 05A	BELL	$e^+e^- \rightarrow \Upsilon(4S)$

¹Assumes equal production of B^+ and B^0 at the $\Upsilon(4S)$.

$\Gamma(\overline{D}_2^*(2462)^0 \pi^+ \times B(\overline{D}_2^*(2462)^0 \rightarrow D^- \pi^+))/\Gamma_{\text{total}}$ Γ_{90}/Γ

VALUE (units 10^{-4})	DOCUMENT ID	TECN	COMMENT
3.4 ± 0.3 ± 0.72	1 ABE 04D	BELL	$e^+e^- \rightarrow \Upsilon(4S)$

¹Assumes equal production of B^+ and B^0 at the $\Upsilon(4S)$.

$\Gamma(\overline{D}_0^*(2400)^0 \pi^+ \times B(\overline{D}_0^*(2400)^0 \rightarrow D^- \pi^+))/\Gamma_{\text{total}}$ Γ_{91}/Γ

VALUE (units 10^{-4})	DOCUMENT ID	TECN	COMMENT
6.1 ± 0.6 ± 1.8	1 ABE 04D	BELL	$e^+e^- \rightarrow \Upsilon(4S)$

¹Assumes equal production of B^+ and B^0 at the $\Upsilon(4S)$.

$\Gamma(\overline{D}_1(2421)^0 \pi^+ \times B(\overline{D}_1(2421)^0 \rightarrow D^{*-} \pi^+))/\Gamma_{\text{total}}$ Γ_{92}/Γ

VALUE (units 10^{-4})	DOCUMENT ID	TECN	COMMENT
6.8 ± 0.7 ± 1.3	1 ABE 04D	BELL	$e^+e^- \rightarrow \Upsilon(4S)$

¹Assumes equal production of B^+ and B^0 at the $\Upsilon(4S)$.

$\Gamma(\overline{D}_2^*(2462)^0 \pi^+ \times B(\overline{D}_2^*(2462)^0 \rightarrow D^{*-} \pi^+))/\Gamma_{\text{total}}$ Γ_{93}/Γ

VALUE (units 10^{-4})	DOCUMENT ID	TECN	COMMENT
1.8 ± 0.3 ± 0.4	1 ABE 04D	BELL	$e^+e^- \rightarrow \Upsilon(4S)$

¹Assumes equal production of B^+ and B^0 at the $\Upsilon(4S)$.

$\Gamma(\overline{D}_1^*(2427)^0 \pi^+ \times B(\overline{D}_1^*(2427)^0 \rightarrow D^{*-} \pi^+))/\Gamma_{\text{total}}$ Γ_{94}/Γ

VALUE (units 10^{-4})	DOCUMENT ID	TECN	COMMENT
5.0 ± 0.4 ± 1.1	1 ABE 04D	BELL	$e^+e^- \rightarrow \Upsilon(4S)$

¹Assumes equal production of B^+ and B^0 at the $\Upsilon(4S)$.

$\Gamma(\overline{D}_1(2420)^0 \pi^+ \times B(\overline{D}_1^0 \rightarrow \overline{D}^{*0} \pi^+ \pi^-))/\Gamma_{\text{total}}$ Γ_{95}/Γ

VALUE (units 10^{-4})	CL%	DOCUMENT ID	TECN	COMMENT
<0.06	90	1 ABE 05A	BELL	$e^+e^- \rightarrow \Upsilon(4S)$

¹Assumes equal production of B^+ and B^0 at the $\Upsilon(4S)$.

$\Gamma(\overline{D}_1^*(2420)^0 \rho^+)/\Gamma_{\text{total}}$ Γ_{96}/Γ

VALUE	CL%	DOCUMENT ID	TECN	COMMENT
<0.0014	90	1 ALAM 94	CLE2	$e^+e^- \rightarrow \Upsilon(4S)$

¹ALAM 94 assume equal production of B^+ and B^0 at the $\Upsilon(4S)$ and use the CLEO II $B(D^*(2010)^+ \rightarrow D^0 \pi^+)$ assuming $B(D_1(2420)^0 \rightarrow D^*(2010)^+ \pi^-) = 67\%$.

$\Gamma(\overline{D}_2^*(2460)^0 \pi^+)/\Gamma_{\text{total}}$ Γ_{97}/Γ

VALUE	CL%	DOCUMENT ID	TECN	COMMENT
<0.0013	90	1 ALAM 94	CLE2	$e^+e^- \rightarrow \Upsilon(4S)$

• • • We do not use the following data for averages, fits, limits, etc. • • •

VALUE	CL%	DOCUMENT ID	TECN	COMMENT
<0.0028	90	2 ALAM 94	CLE2	$e^+e^- \rightarrow \Upsilon(4S)$

VALUE	CL%	DOCUMENT ID	TECN	COMMENT
<0.0023	90	3 ALBRECHT 94D	ARG	$e^+e^- \rightarrow \Upsilon(4S)$

¹ALAM 94 assume equal production of B^+ and B^0 at the $\Upsilon(4S)$ and use the MarkIII $B(D^+ \rightarrow K^- \pi^+ \pi^+)$ and $B(D_2^*(2460)^0 \rightarrow D^+ \pi^-) = 30\%$.

²ALAM 94 assume equal production of B^+ and B^0 at the $\Upsilon(4S)$ and use the MarkIII $B(D^+ \rightarrow K^- \pi^+ \pi^+)$, the CLEO II $B(D^*(2010)^+ \rightarrow D^0 \pi^+)$ and $B(D_2^*(2460)^0 \rightarrow D^*(2010)^+ \pi^-) = 20\%$.

³ALBRECHT 94D assume equal production of B^+ and B^0 at the $\Upsilon(4S)$ and use the CLEO II $B(D^*(2010)^+ \rightarrow D^0 \pi^+)$ and $B(D_2^*(2460)^0 \rightarrow D^*(2010)^+ \pi^-) = 30\%$.

$\Gamma(\overline{D}_2^*(2460)^0 \pi^+ \times B(\overline{D}_2^0 \rightarrow \overline{D}^{*0} \pi^+ \pi^-))/\Gamma_{\text{total}}$ Γ_{98}/Γ

VALUE (units 10^{-4})	CL%	DOCUMENT ID	TECN	COMMENT
<0.22	90	1 ABE 05A	BELL	$e^+e^- \rightarrow \Upsilon(4S)$

¹Assumes equal production of B^+ and B^0 at the $\Upsilon(4S)$.

$\Gamma(\overline{D}_2^*(2460)^0 \rho^+)/\Gamma_{\text{total}}$ Γ_{99}/Γ

VALUE	CL%	DOCUMENT ID	TECN	COMMENT
<0.0047	90	1 ALAM 94	CLE2	$e^+e^- \rightarrow \Upsilon(4S)$
<0.005	90	2 ALAM 94	CLE2	$e^+e^- \rightarrow \Upsilon(4S)$

¹ALAM 94 assume equal production of B^+ and B^0 at the $\Upsilon(4S)$ and use the MarkIII $B(D^+ \rightarrow K^- \pi^+ \pi^+)$ and $B(D_2^*(2460)^0 \rightarrow D^+ \pi^-) = 30\%$.

²ALAM 94 assume equal production of B^+ and B^0 at the $\Upsilon(4S)$ and use the MarkIII $B(D^+ \rightarrow K^- \pi^+ \pi^+)$, the CLEO II $B(D^*(2010)^+ \rightarrow D^0 \pi^+)$ and $B(D_2^*(2460)^0 \rightarrow D^*(2010)^+ \pi^-) = 20\%$.

$\Gamma(D^0 D_s^+)/\Gamma_{\text{total}}$		Γ_{100}/Γ		
VALUE	EVTs	DOCUMENT ID	TECN	COMMENT

0.0103 ± 0.0017 OUR AVERAGE

0.0097 ± 0.0020 ± 0.0008	1	AUBERT	06N	BABR $e^+ e^- \rightarrow \Upsilon(4S)$
0.0101 ± 0.0027 ± 0.0008	2	GIBAUT	96	CLE2 $e^+ e^- \rightarrow \Upsilon(4S)$
0.015 ± 0.008 ± 0.001	3	ALBRECHT	92G	ARG $e^+ e^- \rightarrow \Upsilon(4S)$
0.013 ± 0.006 ± 0.001	5	4	BORTOLETTO90	CLEO $e^+ e^- \rightarrow \Upsilon(4S)$

¹ AUBERT 06N reports $(0.92 \pm 0.14 \pm 0.18) \times 10^{-2}$ for $B(D_s^+ \rightarrow \phi\pi^+) = 0.0462 \pm 0.0062$. We rescale to our best value $B(D_s^+ \rightarrow \phi\pi^+) = (4.38 \pm 0.35) \times 10^{-2}$. Our first error is their experiment's error and our second error is the systematic error from using our best value.

² GIBAUT 96 reports 0.0126 ± 0.0022 ± 0.0025 for $B(D_s^+ \rightarrow \phi\pi^+) = 0.035$. We rescale to our best value $B(D_s^+ \rightarrow \phi\pi^+) = (4.38 \pm 0.35) \times 10^{-2}$. Our first error is their experiment's error and our second error is the systematic error from using our best value.

³ ALBRECHT 92G reports 0.024 ± 0.012 ± 0.004 for $B(D_s^+ \rightarrow \phi\pi^+) = 0.027$. We rescale to our best value $B(D_s^+ \rightarrow \phi\pi^+) = (4.38 \pm 0.35) \times 10^{-2}$. Our first error is their experiment's error and our second error is the systematic error from using our best value. Assumes PDG 1990 D^0 branching ratios, e.g., $B(D^0 \rightarrow K^-\pi^+) = 3.71 \pm 0.25\%$.

⁴ BORTOLETTO 90 reports 0.029 ± 0.013 for $B(D_s^+ \rightarrow \phi\pi^+) = 0.02$. We rescale to our best value $B(D_s^+ \rightarrow \phi\pi^+) = (4.38 \pm 0.35) \times 10^{-2}$. Our first error is their experiment's error and our second error is the systematic error from using our best value.

$\Gamma(D_{s0}(2317)^+ \bar{D}^0 \times B(D_{s0}(2317)^+ \rightarrow D_s^+ \pi^0))/\Gamma_{\text{total}}$		Γ_{101}/Γ		
VALUE (units 10^{-3})	CL%	DOCUMENT ID	TECN	COMMENT

0.75 ± 0.22 ± 0.17 OUR AVERAGE

0.82 ± 0.36 ± 0.21 ± 0.07	1,2	AUBERT,B	04s	BABR $e^+ e^- \rightarrow \Upsilon(4S)$
0.67 ± 0.27 ± 0.25 ± 0.05	1,3	KROKOVNY	03B	BELL $e^+ e^- \rightarrow \Upsilon(4S)$

¹ Assumes equal production of B^+ and B^0 at the $\Upsilon(4S)$.

² AUBERT,B 04s reports $(1.0 \pm 0.3 \pm 0.4) \times 10^{-3}$ for $B(D_s^+ \rightarrow \phi\pi^+) = 0.036 \pm 0.009$. We rescale to our best value $B(D_s^+ \rightarrow \phi\pi^+) = (4.38 \pm 0.35) \times 10^{-2}$. Our first error is their experiment's error and our second error is the systematic error from using our best value.

³ KROKOVNY 03B reports $(0.81 \pm 0.30 \pm 0.24) \times 10^{-3}$ for $B(D_s^+ \rightarrow \phi\pi^+) = 0.036 \pm 0.009$. We rescale to our best value $B(D_s^+ \rightarrow \phi\pi^+) = (4.38 \pm 0.35) \times 10^{-2}$. Our first error is their experiment's error and our second error is the systematic error from using our best value.

$\Gamma(D_{s0}(2317)^+ \bar{D}^0 \times B(D_{s0}(2317)^+ \rightarrow D_s^{*+} \gamma))/\Gamma_{\text{total}}$		Γ_{102}/Γ		
VALUE (units 10^{-3})	CL%	DOCUMENT ID	TECN	COMMENT

<0.76

¹ Assumes equal production of B^+ and B^0 at the $\Upsilon(4S)$.

$\Gamma(D_{s0}(2317)^+ \bar{D}^{*0}(2007)^0 \times B(D_{s0}(2317)^+ \rightarrow D_s^+ \pi^0))/\Gamma_{\text{total}}$		Γ_{103}/Γ		
VALUE (units 10^{-3})	CL%	DOCUMENT ID	TECN	COMMENT

0.9 ± 0.6 ± 0.4 ± 0.3

¹ Assumes equal production of B^+ and B^0 at the $\Upsilon(4S)$.

$\Gamma(D_{sJ}(2457)^+ \bar{D}^0)/\Gamma_{\text{total}}$		Γ_{104}/Γ		
VALUE (units 10^{-3})	CL%	DOCUMENT ID	TECN	COMMENT

3.1 ± 1.0 ± 0.9 OUR AVERAGE

4.3 ± 1.6 ± 1.3	1	AUBERT	06N	BABR $e^+ e^- \rightarrow \Upsilon(4S)$
4.6 ± 1.8 ± 1.6 ± 1.0	2,3	AUBERT,B	04s	BABR $e^+ e^- \rightarrow \Upsilon(4S)$
2.1 ± 1.1 ± 0.9 ± 0.5	2,4	KROKOVNY	03B	BELL $e^+ e^- \rightarrow \Upsilon(4S)$

¹ Uses a missing-mass method in the events that one of the B mesons is fully reconstructed.

² Assumes equal production of B^+ and B^0 at the $\Upsilon(4S)$.

³ AUBERT,B 04s reports $[B(B^+ \rightarrow D_{sJ}(2457)^+ \bar{D}^0)] \times [B(D_{s1}(2460)^+ \rightarrow D_s^{*+} \pi^0)] = (2.2 \pm 0.8 \pm 0.3) \times 10^{-3}$. We divide by our best value $B(D_{s1}(2460)^+ \rightarrow D_s^{*+} \pi^0) = (48 \pm 11) \times 10^{-2}$. Our first error is their experiment's error and our second error is the systematic error from using our best value.

⁴ KROKOVNY 03B reports $[B(B^+ \rightarrow D_{sJ}(2457)^+ \bar{D}^0)] \times [B(D_{s1}(2460)^+ \rightarrow D_s^{*+} \pi^0)] = (1.0 \pm 0.5 \pm 0.1) \times 10^{-3}$. We divide by our best value $B(D_{s1}(2460)^+ \rightarrow D_s^{*+} \pi^0) = (48 \pm 11) \times 10^{-2}$. Our first error is their experiment's error and our second error is the systematic error from using our best value.

$\Gamma(D_{sJ}(2457)^+ \bar{D}^0 \times B(D_{sJ}(2457)^+ \rightarrow D_s^+ \gamma))/\Gamma_{\text{total}}$		Γ_{105}/Γ		
VALUE (units 10^{-3})	CL%	DOCUMENT ID	TECN	COMMENT

0.48 ± 0.13 ± 0.11 OUR AVERAGE

0.49 ± 0.20 ± 0.14 ± 0.04	1,2	AUBERT,B	04s	BABR $e^+ e^- \rightarrow \Upsilon(4S)$
0.46 ± 0.15 ± 0.04	1,3	KROKOVNY	03B	BELL $e^+ e^- \rightarrow \Upsilon(4S)$

¹ Assumes equal production of B^+ and B^0 at the $\Upsilon(4S)$.

² AUBERT,B 04s reports $(0.6 \pm 0.2 \pm 0.2) \times 10^{-3}$ for $B(D_s^+ \rightarrow \phi\pi^+) = 0.036 \pm 0.009$.

We rescale to our best value $B(D_s^+ \rightarrow \phi\pi^+) = (4.38 \pm 0.35) \times 10^{-2}$. Our first error is their experiment's error and our second error is the systematic error from using our best value.

³ KROKOVNY 03B reports $(0.56 \pm 0.16 \pm 0.17) \times 10^{-3}$ for $B(D_s^+ \rightarrow \phi\pi^+) = 0.036 \pm 0.009$. We rescale to our best value $B(D_s^+ \rightarrow \phi\pi^+) = (4.38 \pm 0.35) \times 10^{-2}$. Our first error is their experiment's error and our second error is the systematic error from using our best value.

$\Gamma(D_{sJ}(2457)^+ \bar{D}^0 \times B(D_{sJ}(2457)^+ \rightarrow D_s^+ \pi^+ \pi^-))/\Gamma_{\text{total}}$		Γ_{106}/Γ		
VALUE (units 10^{-3})	CL%	DOCUMENT ID	TECN	COMMENT

<0.22

¹ Assumes equal production of B^+ and B^0 at the $\Upsilon(4S)$.

$\Gamma(D_{sJ}(2457)^+ \bar{D}^0 \times B(D_{sJ}(2457)^+ \rightarrow D_s^+ \pi^0))/\Gamma_{\text{total}}$		Γ_{107}/Γ		
VALUE (units 10^{-3})	CL%	DOCUMENT ID	TECN	COMMENT

<0.27

¹ Assumes equal production of B^+ and B^0 at the $\Upsilon(4S)$.

$\Gamma(D_{sJ}(2457)^+ \bar{D}^0 \times B(D_{sJ}(2457)^+ \rightarrow D_s^{*+} \gamma))/\Gamma_{\text{total}}$		Γ_{108}/Γ		
VALUE (units 10^{-3})	CL%	DOCUMENT ID	TECN	COMMENT

<0.98

¹ Assumes equal production of B^+ and B^0 at the $\Upsilon(4S)$.

$\Gamma(D_{sJ}(2457)^+ \bar{D}^{*0}(2007)^0)/\Gamma_{\text{total}}$		Γ_{109}/Γ		
VALUE (units 10^{-3})	CL%	DOCUMENT ID	TECN	COMMENT

12.0 ± 3.0 OUR AVERAGE

11.2 ± 2.6 ± 2.0	1	AUBERT	06N	BABR $e^+ e^- \rightarrow \Upsilon(4S)$
16 ± 8 ± 6 ± 4	2,3	AUBERT,B	04s	BABR $e^+ e^- \rightarrow \Upsilon(4S)$

¹ Uses a missing-mass method in the events that one of the B mesons is fully reconstructed.

² AUBERT,B 04s reports $[B(B^+ \rightarrow D_{sJ}(2457)^+ \bar{D}^{*0}(2007)^0)] \times [B(D_{s1}(2460)^+ \rightarrow D_s^{*+} \pi^0)] = (7.6 \pm 1.7 \pm 3.2 \pm 2.4) \times 10^{-3}$. We divide by our best value $B(D_{s1}(2460)^+ \rightarrow D_s^{*+} \pi^0) = (48 \pm 11) \times 10^{-2}$. Our first error is their experiment's error and our second error is the systematic error from using our best value.

³ Assumes equal production of B^+ and B^0 at the $\Upsilon(4S)$.

$\Gamma(D_{sJ}(2457)^+ \bar{D}^{*0}(2007)^0 \times B(D_{sJ}(2457)^+ \rightarrow D_s^+ \gamma))/\Gamma_{\text{total}}$		Γ_{110}/Γ		
VALUE (units 10^{-3})	CL%	DOCUMENT ID	TECN	COMMENT

1.4 ± 0.4 ± 0.6 ± 0.4

¹ Assumes equal production of B^+ and B^0 at the $\Upsilon(4S)$.

$\Gamma(D^0 D_{s1}(2536)^+ \times B(D_{s1}(2536)^+ \rightarrow D^{*0}(2007)^0 K^+))/\Gamma_{\text{total}}$		Γ_{111}/Γ		
VALUE (units 10^{-4})	CL%	DOCUMENT ID	TECN	COMMENT

2.16 ± 0.52 ± 0.45

¹ AUBERT 08B BABR $e^+ e^- \rightarrow \Upsilon(4S)$

• • • We do not use the following data for averages, fits, limits, etc. • • •

<2 90 AUBERT 03X BABR Repl. by AUBERT 08B

¹ Assumes equal production of B^+ and B^0 at the $\Upsilon(4S)$.

$\Gamma(\bar{D}^{*0}(2007)^0 D_{s1}(2536)^+ \times B(D_{s1}(2536)^+ \rightarrow D^{*0}(2007)^0 K^+))/\Gamma_{\text{total}}$		Γ_{112}/Γ		
VALUE (units 10^{-4})	CL%	DOCUMENT ID	TECN	COMMENT

5.46 ± 1.17 ± 1.04

¹ AUBERT 08B BABR $e^+ e^- \rightarrow \Upsilon(4S)$

• • • We do not use the following data for averages, fits, limits, etc. • • •

<7 90 AUBERT 03X BABR Repl. by AUBERT 08B

¹ Assumes equal production of B^+ and B^0 at the $\Upsilon(4S)$.

$\Gamma(D^0 D_{s1}(2536)^+ \times B(D_{s1}(2536)^+ \rightarrow D^{*+} K^0))/\Gamma_{\text{total}}$		Γ_{113}/Γ		
VALUE (units 10^{-4})	CL%	DOCUMENT ID	TECN	COMMENT

2.30 ± 0.98 ± 0.43

¹ Assumes equal production of B^+ and B^0 at the $\Upsilon(4S)$.

$\Gamma(\bar{D}^0 D_{sJ}(2700)^+ \times B(D_{sJ}(2700)^+ \rightarrow D^0 K^+))/\Gamma_{\text{total}}$		Γ_{114}/Γ		
VALUE (units 10^{-4})	CL%	DOCUMENT ID	TECN	COMMENT

11.3 ± 2.2 ± 1.4 ± 2.8

¹ BRODZICKA 08 BELL $e^+ e^- \rightarrow \Upsilon(4S)$

¹ Assumes equal production of B^+ and B^0 at the $\Upsilon(4S)$.

$\Gamma(\bar{D}^{*0} D_{s1}(2536)^+ \times B(D_{s1}(2536)^+ \rightarrow D^{*+} K^0))/\Gamma_{\text{total}}$		Γ_{115}/Γ		
VALUE (units 10^{-4})	CL%	DOCUMENT ID	TECN	COMMENT

3.92 ± 2.46 ± 0.83

¹ AUBERT 08B BABR $e^+ e^- \rightarrow \Upsilon(4S)$

¹ Assumes equal production of B^+ and B^0 at the $\Upsilon(4S)$.

$\Gamma(\bar{D}^{*0} D_{sJ}(2573)^+ \times B(D_{sJ}(2573)^+ \rightarrow D^0 K^+))/\Gamma_{\text{total}}$		Γ_{116}/Γ		
VALUE (units 10^{-4})	CL%	DOCUMENT ID	TECN	COMMENT

<2

90 AUBERT 03X BABR $e^+ e^- \rightarrow \Upsilon(4S)$

Meson Particle Listings

 B^\pm

$\Gamma(\bar{D}^*(2007)^0 D_{sJ}(2573)^+ \times B(D_{sJ}(2573)^+ \rightarrow D^0 K^+))/\Gamma_{\text{total}}$					Γ_{117}/Γ
VALUE (units 10^{-4})	CL%	DOCUMENT ID	TECN	COMMENT	
<5	90	AUBERT	03x	BABR $e^+ e^- \rightarrow \Upsilon(4S)$	

$\Gamma(\bar{D}^0 D_s^{*+})/\Gamma_{\text{total}}$					Γ_{118}/Γ
VALUE	CL%	DOCUMENT ID	TECN	COMMENT	
0.0078 ± 0.0016 OUR AVERAGE					
0.0081 ± 0.0018 ± 0.0007		¹ AUBERT	06N	BABR $e^+ e^- \rightarrow \Upsilon(4S)$	
0.0070 ± 0.0026 ± 0.0006		² GIBAUT	96	CLE2 $e^+ e^- \rightarrow \Upsilon(4S)$	
0.010 ± 0.008 ± 0.001		³ ALBRECHT	92G	ARG $e^+ e^- \rightarrow \Upsilon(4S)$	

¹ AUBERT 06N reports $(0.77 \pm 0.15 \pm 0.13) \times 10^{-2}$ for $B(D_s^+ \rightarrow \phi\pi^+) = 0.0462 \pm 0.0062$. We rescale to our best value $B(D_s^+ \rightarrow \phi\pi^+) = (4.38 \pm 0.35) \times 10^{-2}$. Our first error is their experiment's error and our second error is the systematic error from using our best value.

² GIBAUT 96 reports $0.0087 \pm 0.0027 \pm 0.0017$ for $B(D_s^+ \rightarrow \phi\pi^+) = 0.035$. We rescale to our best value $B(D_s^+ \rightarrow \phi\pi^+) = (4.38 \pm 0.35) \times 10^{-2}$. Our first error is their experiment's error and our second error is the systematic error from using our best value.

³ ALBRECHT 92G reports $0.016 \pm 0.012 \pm 0.003$ for $B(D_s^+ \rightarrow \phi\pi^+) = 0.027$. We rescale to our best value $B(D_s^+ \rightarrow \phi\pi^+) = (4.38 \pm 0.35) \times 10^{-2}$. Our first error is their experiment's error and our second error is the systematic error from using our best value. Assumes PDG 1990 D^0 branching ratios, e.g., $B(D^0 \rightarrow K^- \pi^+) = 3.71 \pm 0.25\%$.

$\Gamma(\bar{D}^*(2007)^0 D_s^+)/\Gamma_{\text{total}}$					Γ_{119}/Γ
VALUE	CL%	DOCUMENT ID	TECN	COMMENT	
0.0084 ± 0.0017 OUR AVERAGE					
0.0080 ± 0.0018 ± 0.0006		¹ AUBERT	06N	BABR $e^+ e^- \rightarrow \Upsilon(4S)$	
0.011 ± 0.004 ± 0.001		² GIBAUT	96	CLE2 $e^+ e^- \rightarrow \Upsilon(4S)$	
0.008 ± 0.006 ± 0.001		³ ALBRECHT	92G	ARG $e^+ e^- \rightarrow \Upsilon(4S)$	

¹ AUBERT 06N reports $(0.76 \pm 0.15 \pm 0.13) \times 10^{-2}$ for $B(D_s^+ \rightarrow \phi\pi^+) = 0.0462 \pm 0.0062$. We rescale to our best value $B(D_s^+ \rightarrow \phi\pi^+) = (4.38 \pm 0.35) \times 10^{-2}$. Our first error is their experiment's error and our second error is the systematic error from using our best value.

² GIBAUT 96 reports $0.0140 \pm 0.0043 \pm 0.0035$ for $B(D_s^+ \rightarrow \phi\pi^+) = 0.035$. We rescale to our best value $B(D_s^+ \rightarrow \phi\pi^+) = (4.38 \pm 0.35) \times 10^{-2}$. Our first error is their experiment's error and our second error is the systematic error from using our best value.

³ ALBRECHT 92G reports $0.013 \pm 0.009 \pm 0.002$ for $B(D_s^+ \rightarrow \phi\pi^+) = 0.027$. We rescale to our best value $B(D_s^+ \rightarrow \phi\pi^+) = (4.38 \pm 0.35) \times 10^{-2}$. Our first error is their experiment's error and our second error is the systematic error from using our best value. Assumes PDG 1990 D^0 and $D^*(2007)^0$ branching ratios, e.g., $B(D^0 \rightarrow K^- \pi^+) = 3.71 \pm 0.25\%$ and $B(D^*(2007)^0 \rightarrow D^0 \pi^0) = 55 \pm 6\%$.

$\Gamma(\bar{D}^*(2007)^0 D_s^{*+})/\Gamma_{\text{total}}$					Γ_{120}/Γ
VALUE	CL%	DOCUMENT ID	TECN	COMMENT	
0.0175 ± 0.0023 OUR AVERAGE					
0.0171 ± 0.0019 ± 0.0014		¹ AUBERT	06N	BABR $e^+ e^- \rightarrow \Upsilon(4S)$	
0.025 ± 0.009 ± 0.002		² GIBAUT	96	CLE2 $e^+ e^- \rightarrow \Upsilon(4S)$	
0.019 ± 0.010 ± 0.002		³ ALBRECHT	92G	ARG $e^+ e^- \rightarrow \Upsilon(4S)$	

¹ AUBERT 06N reports $(1.62 \pm 0.22 \pm 0.18) \times 10^{-2}$ for $B(D_s^+ \rightarrow \phi\pi^+) = 0.0462 \pm 0.0062$. We rescale to our best value $B(D_s^+ \rightarrow \phi\pi^+) = (4.38 \pm 0.35) \times 10^{-2}$. Our first error is their experiment's error and our second error is the systematic error from using our best value.

² GIBAUT 96 reports $0.0310 \pm 0.0088 \pm 0.0065$ for $B(D_s^+ \rightarrow \phi\pi^+) = 0.035$. We rescale to our best value $B(D_s^+ \rightarrow \phi\pi^+) = (4.38 \pm 0.35) \times 10^{-2}$. Our first error is their experiment's error and our second error is the systematic error from using our best value.

³ ALBRECHT 92G reports $0.031 \pm 0.016 \pm 0.005$ for $B(D_s^+ \rightarrow \phi\pi^+) = 0.027$. We rescale to our best value $B(D_s^+ \rightarrow \phi\pi^+) = (4.38 \pm 0.35) \times 10^{-2}$. Our first error is their experiment's error and our second error is the systematic error from using our best value. Assumes PDG 1990 D^0 and $D^*(2007)^0$ branching ratios, e.g., $B(D^0 \rightarrow K^- \pi^+) = 3.71 \pm 0.25\%$ and $B(D^*(2007)^0 \rightarrow D^0 \pi^0) = 55 \pm 6\%$.

$\Gamma(D_s^{*+} \bar{D}^{*0})/\Gamma_{\text{total}}$					Γ_{121}/Γ
VALUE	CL%	DOCUMENT ID	TECN	COMMENT	
(2.73 ± 0.93 ± 0.68) × 10⁻²					
		¹ AHMED	00B	CLE2 $e^+ e^- \rightarrow \Upsilon(4S)$	

¹ AHMED 00B reports their experiment's uncertainties ($\pm 0.78 \pm 0.48 \pm 0.68\%$), where the first error is statistical, the second is systematic, and the third is the uncertainty in the $D_s \rightarrow \phi\pi$ branching fraction. We combine the first two in quadrature.

$\Gamma(\bar{D}^*(2007)^0 D^*(2010)^+)/\Gamma_{\text{total}}$					Γ_{122}/Γ
VALUE (units 10^{-4})	CL%	DOCUMENT ID	TECN	COMMENT	
8.1 ± 1.2 ± 1.2		¹ AUBERT,B	06A	BABR $e^+ e^- \rightarrow \Upsilon(4S)$	
<110	90	BARATE	98Q	ALEP $e^+ e^- \rightarrow Z$	

¹ Assumes equal production of B^+ and B^0 at the $\Upsilon(4S)$.

$\Gamma(\bar{D}^0 D^*(2010)^+) + \Gamma(\bar{D}^*(2007)^0 D^+)/\Gamma_{\text{total}}$					Γ_{123}/Γ
VALUE (units 10^{-4})	CL%	DOCUMENT ID	TECN	COMMENT	
<130	90	BARATE	98Q	ALEP $e^+ e^- \rightarrow Z$	

$\Gamma(\bar{D}^0 D^*(2010)^+)/\Gamma_{\text{total}}$					Γ_{124}/Γ
VALUE (units 10^{-4})	CL%	DOCUMENT ID	TECN	COMMENT	
3.9 ± 0.5 OUR AVERAGE					
3.6 ± 0.5 ± 0.4		¹ AUBERT,B	06A	BABR $e^+ e^- \rightarrow \Upsilon(4S)$	
4.57 ± 0.71 ± 0.56		¹ MAJUMDER	05	BELL $e^+ e^- \rightarrow \Upsilon(4S)$	

¹ Assumes equal production of B^+ and B^0 at the $\Upsilon(4S)$.

$\Gamma(\bar{D}^0 D^+)/\Gamma_{\text{total}}$					Γ_{125}/Γ
VALUE (units 10^{-4})	CL%	DOCUMENT ID	TECN	COMMENT	
4.2 ± 0.6 OUR AVERAGE					
3.8 ± 0.6 ± 0.5		¹ AUBERT,B	06A	BABR $e^+ e^- \rightarrow \Upsilon(4S)$	
4.83 ± 0.78 ± 0.58		¹ MAJUMDER	05	BELL $e^+ e^- \rightarrow \Upsilon(4S)$	

• • • We do not use the following data for averages, fits, limits, etc. • • •

<67 90 BARATE 98Q ALEP $e^+ e^- \rightarrow Z$

¹ Assumes equal production of B^+ and B^0 at the $\Upsilon(4S)$.

$\Gamma(\bar{D}^0 D^+ K^0)/\Gamma_{\text{total}}$					Γ_{126}/Γ
VALUE (units 10^{-3})	CL%	DOCUMENT ID	TECN	COMMENT	
<2.8	90	¹ AUBERT	03x	BABR $e^+ e^- \rightarrow \Upsilon(4S)$	

¹ Assumes equal production of B^+ and B^0 at the $\Upsilon(4S)$.

$\Gamma(D^+ \bar{D}^*(2007)^0)/\Gamma_{\text{total}}$					Γ_{127}/Γ
VALUE (units 10^{-4})	CL%	DOCUMENT ID	TECN	COMMENT	
6.3 ± 1.4 ± 1.0					
		¹ AUBERT,B	06A	BABR $e^+ e^- \rightarrow \Upsilon(4S)$	

¹ Assumes equal production of B^+ and B^0 at the $\Upsilon(4S)$.

$\Gamma(\bar{D}^*(2007)^0 D^+ K^0)/\Gamma_{\text{total}}$					Γ_{128}/Γ
VALUE (units 10^{-3})	CL%	DOCUMENT ID	TECN	COMMENT	
<6.1	90	¹ AUBERT	03x	BABR $e^+ e^- \rightarrow \Upsilon(4S)$	

¹ Assumes equal production of B^+ and B^0 at the $\Upsilon(4S)$.

$\Gamma(\bar{D}^0 \bar{D}^*(2010)^+ K^0)/\Gamma_{\text{total}}$					Γ_{129}/Γ
VALUE (units 10^{-3})	CL%	DOCUMENT ID	TECN	COMMENT	
5.2 ± 1.0 ± 0.7					
		¹ AUBERT	03x	BABR $e^+ e^- \rightarrow \Upsilon(4S)$	

¹ Assumes equal production of B^+ and B^0 at the $\Upsilon(4S)$.

$\Gamma(\bar{D}^*(2007)^0 D^*(2010)^+ K^0)/\Gamma_{\text{total}}$					Γ_{130}/Γ
VALUE (units 10^{-3})	CL%	DOCUMENT ID	TECN	COMMENT	
7.8 ± 2.3 ± 1.4					
		¹ AUBERT	03x	BABR $e^+ e^- \rightarrow \Upsilon(4S)$	

¹ Assumes equal production of B^+ and B^0 at the $\Upsilon(4S)$.

$\Gamma(\bar{D}^0 D^0 K^+)/\Gamma_{\text{total}}$					Γ_{131}/Γ
VALUE (units 10^{-3})	CL%	DOCUMENT ID	TECN	COMMENT	
2.10 ± 0.26 OUR AVERAGE					
2.22 ± 0.22 ± 0.26 ± 0.24		¹ BRODZICKA	08	BELL $e^+ e^- \rightarrow \Upsilon(4S)$	
1.9 ± 0.3 ± 0.3		¹ AUBERT	03x	BABR $e^+ e^- \rightarrow \Upsilon(4S)$	

• • • We do not use the following data for averages, fits, limits, etc. • • •

1.17 ± 0.21 ± 0.15 ¹ CHISTOV 04 BELL Repl. by BRODZICKA 08

¹ Assumes equal production of B^+ and B^0 at the $\Upsilon(4S)$.

$\Gamma(\bar{D}^*(2007)^0 D^0 K^+)/\Gamma_{\text{total}}$					Γ_{132}/Γ
VALUE (units 10^{-3})	CL%	DOCUMENT ID	TECN	COMMENT	
<3.8	90	¹ AUBERT	03x	BABR $e^+ e^- \rightarrow \Upsilon(4S)$	

¹ Assumes equal production of B^+ and B^0 at the $\Upsilon(4S)$.

$\Gamma(\bar{D}^0 D^*(2007)^0 K^+)/\Gamma_{\text{total}}$					Γ_{133}/Γ
VALUE (units 10^{-3})	CL%	DOCUMENT ID	TECN	COMMENT	
4.7 ± 0.7 ± 0.7					
		¹ AUBERT	03x	BABR $e^+ e^- \rightarrow \Upsilon(4S)$	

¹ Assumes equal production of B^+ and B^0 at the $\Upsilon(4S)$.

$\Gamma(\bar{D}^*(2007)^0 D^*(2007)^0 K^+)/\Gamma_{\text{total}}$					Γ_{134}/Γ
VALUE (units 10^{-3})	CL%	DOCUMENT ID	TECN	COMMENT	
5.3 ± 1.1 ± 1.2					
		¹ AUBERT	03x	BABR $e^+ e^- \rightarrow \Upsilon(4S)$	

¹ Assumes equal production of B^+ and B^0 at the $\Upsilon(4S)$.

$\Gamma(D^- D^+ K^+)/\Gamma_{\text{total}}$					Γ_{135}/Γ
VALUE (units 10^{-3})	CL%	DOCUMENT ID	TECN	COMMENT	
<0.4	90	¹ AUBERT	03x	BABR $e^+ e^- \rightarrow \Upsilon(4S)$	

• • • We do not use the following data for averages, fits, limits, etc. • • •

<0.90 90 ¹ CHISTOV 04 BELL $e^+ e^- \rightarrow \Upsilon(4S)$

¹ Assumes equal production of B^+ and B^0 at the $\Upsilon(4S)$.

$\Gamma(D^- D^*(2010)^+ K^+)/\Gamma_{\text{total}}$					Γ_{136}/Γ
VALUE (units 10^{-3})	CL%	DOCUMENT ID	TECN	COMMENT	
<0.7	90	¹ AUBERT	03x	BABR $e^+ e^- \rightarrow \Upsilon(4S)$	

¹ Assumes equal production of B^+ and B^0 at the $\Upsilon(4S)$.

$\Gamma(D^*(2010)^- D^+ K^+)/\Gamma_{\text{total}}$ Γ_{137}/Γ

VALUE (units 10^{-3})	CL%	DOCUMENT ID	TECN	COMMENT
$1.5 \pm 0.3 \pm 0.2$		¹ AUBERT 03X	BABR	$e^+ e^- \rightarrow \Upsilon(4S)$

¹ Assumes equal production of B^+ and B^0 at the $\Upsilon(4S)$.

 $\Gamma(D^*(2010)^- D^*(2010)^+ K^+)/\Gamma_{\text{total}}$ Γ_{138}/Γ

VALUE (units 10^{-3})	CL%	DOCUMENT ID	TECN	COMMENT
<1.8	90	¹ AUBERT 03X	BABR	$e^+ e^- \rightarrow \Upsilon(4S)$

¹ Assumes equal production of B^+ and B^0 at the $\Upsilon(4S)$.

 $\Gamma((\bar{D} + \bar{D}^*)(D + D^*)K)/\Gamma_{\text{total}}$ Γ_{139}/Γ

VALUE (units 10^{-2})	CL%	DOCUMENT ID	TECN	COMMENT
$3.5 \pm 0.3 \pm 0.5$		¹ AUBERT 03X	BABR	$e^+ e^- \rightarrow \Upsilon(4S)$

¹ Assumes equal production of B^+ and B^0 at the $\Upsilon(4S)$.

 $\Gamma(D_s^+ \pi^0)/\Gamma_{\text{total}}$ Γ_{140}/Γ

VALUE (units 10^{-5})	CL%	DOCUMENT ID	TECN	COMMENT
$1.6 \pm 0.6 \pm 0.1$		¹ AUBERT 07M	BABR	$e^+ e^- \rightarrow \Upsilon(4S)$

- • • We do not use the following data for averages, fits, limits, etc. • • •
- <17 90 ² ALEXANDER 93B CLE2 $e^+ e^- \rightarrow \Upsilon(4S)$
- ¹ AUBERT 07M reports $[B(B^+ \rightarrow D_s^+ \pi^0)] \times [B(D_s^+ \rightarrow \phi \pi^+)] = (7.0^{+2.4+0.6}_{-2.1-0.8}) \times 10^{-7}$. We divide by our best value $B(D_s^+ \rightarrow \phi \pi^+) = (4.38 \pm 0.35) \times 10^{-2}$. Our first error is their experiment's error and our second error is the systematic error from using our best value.
- ² ALEXANDER 93B reports $< 2.0 \times 10^{-4}$ for $B(D_s^+ \rightarrow \phi \pi^+) = 0.037$. We rescale to our best value $B(D_s^+ \rightarrow \phi \pi^+) = 0.0438$.

 $[\Gamma(D_s^+ \pi^0) + \Gamma(D_s^+ \rho^0)]/\Gamma_{\text{total}}$ $(\Gamma_{140} + \Gamma_{141})/\Gamma$

VALUE	CL%	DOCUMENT ID	TECN	COMMENT
<0.0006	90	¹ ALBRECHT 93E	ARG	$e^+ e^- \rightarrow \Upsilon(4S)$

¹ ALBRECHT 93E reports $< 0.9 \times 10^{-3}$ for $B(D_s^+ \rightarrow \phi \pi^+) = 0.027$. We rescale to our best value $B(D_s^+ \rightarrow \phi \pi^+) = 0.0438$.

 $\Gamma(D_s^+ \pi^0)/\Gamma_{\text{total}}$ Γ_{141}/Γ

VALUE	CL%	DOCUMENT ID	TECN	COMMENT
<0.00027	90	¹ ALEXANDER 93B	CLE2	$e^+ e^- \rightarrow \Upsilon(4S)$

¹ ALEXANDER 93B reports $< 3.2 \times 10^{-4}$ for $B(D_s^+ \rightarrow \phi \pi^+) = 0.037$. We rescale to our best value $B(D_s^+ \rightarrow \phi \pi^+) = 0.0438$.

 $\Gamma(D_s^+ \eta)/\Gamma_{\text{total}}$ Γ_{142}/Γ

VALUE	CL%	DOCUMENT ID	TECN	COMMENT
<0.0004	90	¹ ALEXANDER 93B	CLE2	$e^+ e^- \rightarrow \Upsilon(4S)$

¹ ALEXANDER 93B reports $< 4.6 \times 10^{-4}$ for $B(D_s^+ \rightarrow \phi \pi^+) = 0.037$. We rescale to our best value $B(D_s^+ \rightarrow \phi \pi^+) = 0.0438$.

 $\Gamma(D_s^+ \eta)/\Gamma_{\text{total}}$ Γ_{143}/Γ

VALUE	CL%	DOCUMENT ID	TECN	COMMENT
<0.0006	90	¹ ALEXANDER 93B	CLE2	$e^+ e^- \rightarrow \Upsilon(4S)$

¹ ALEXANDER 93B reports $< 7.5 \times 10^{-4}$ for $B(D_s^+ \rightarrow \phi \pi^+) = 0.037$. We rescale to our best value $B(D_s^+ \rightarrow \phi \pi^+) = 0.0438$.

 $\Gamma(D_s^+ \rho^0)/\Gamma_{\text{total}}$ Γ_{144}/Γ

VALUE	CL%	DOCUMENT ID	TECN	COMMENT
<0.00031	90	¹ ALEXANDER 93B	CLE2	$e^+ e^- \rightarrow \Upsilon(4S)$

¹ ALEXANDER 93B reports $< 3.7 \times 10^{-4}$ for $B(D_s^+ \rightarrow \phi \pi^+) = 0.037$. We rescale to our best value $B(D_s^+ \rightarrow \phi \pi^+) = 0.0438$.

 $[\Gamma(D_s^+ \rho^0) + \Gamma(D_s^+ \bar{K}^*(892)^0)]/\Gamma_{\text{total}}$ $(\Gamma_{144} + \Gamma_{154})/\Gamma$

VALUE	CL%	DOCUMENT ID	TECN	COMMENT
<0.0021	90	¹ ALBRECHT 93E	ARG	$e^+ e^- \rightarrow \Upsilon(4S)$

¹ ALBRECHT 93E reports $< 3.4 \times 10^{-3}$ for $B(D_s^+ \rightarrow \phi \pi^+) = 0.027$. We rescale to our best value $B(D_s^+ \rightarrow \phi \pi^+) = 0.0438$.

 $\Gamma(D_s^+ \rho^0)/\Gamma_{\text{total}}$ Γ_{145}/Γ

VALUE	CL%	DOCUMENT ID	TECN	COMMENT
<0.0004	90	¹ ALEXANDER 93B	CLE2	$e^+ e^- \rightarrow \Upsilon(4S)$

¹ ALEXANDER 93B reports $< 4.8 \times 10^{-4}$ for $B(D_s^+ \rightarrow \phi \pi^+) = 0.037$. We rescale to our best value $B(D_s^+ \rightarrow \phi \pi^+) = 0.0438$.

 $[\Gamma(D_s^+ \rho^0) + \Gamma(D_s^+ \bar{K}^*(892)^0)]/\Gamma_{\text{total}}$ $(\Gamma_{145} + \Gamma_{155})/\Gamma$

VALUE	CL%	DOCUMENT ID	TECN	COMMENT
<0.0012	90	¹ ALBRECHT 93E	ARG	$e^+ e^- \rightarrow \Upsilon(4S)$

¹ ALBRECHT 93E reports $< 2.0 \times 10^{-3}$ for $B(D_s^+ \rightarrow \phi \pi^+) = 0.027$. We rescale to our best value $B(D_s^+ \rightarrow \phi \pi^+) = 0.0438$.

 $\Gamma(D_s^+ \omega)/\Gamma_{\text{total}}$ Γ_{146}/Γ

VALUE	CL%	DOCUMENT ID	TECN	COMMENT
<0.0004	90	¹ ALEXANDER 93B	CLE2	$e^+ e^- \rightarrow \Upsilon(4S)$

- • • We do not use the following data for averages, fits, limits, etc. • • •

<0.0021 90 ² ALBRECHT 93E ARG $e^+ e^- \rightarrow \Upsilon(4S)$

¹ ALEXANDER 93B reports $< 4.8 \times 10^{-4}$ for $B(D_s^+ \rightarrow \phi \pi^+) = 0.037$. We rescale to our best value $B(D_s^+ \rightarrow \phi \pi^+) = 0.0438$.

² ALBRECHT 93E reports $< 3.4 \times 10^{-3}$ for $B(D_s^+ \rightarrow \phi \pi^+) = 0.027$. We rescale to our best value $B(D_s^+ \rightarrow \phi \pi^+) = 0.0438$.

 $\Gamma(D_s^+ \omega)/\Gamma_{\text{total}}$ Γ_{147}/Γ

VALUE	CL%	DOCUMENT ID	TECN	COMMENT
<0.0006	90	¹ ALEXANDER 93B	CLE2	$e^+ e^- \rightarrow \Upsilon(4S)$

- • • We do not use the following data for averages, fits, limits, etc. • • •

<0.0012 90 ² ALBRECHT 93E ARG $e^+ e^- \rightarrow \Upsilon(4S)$

¹ ALEXANDER 93B reports $< 6.8 \times 10^{-4}$ for $B(D_s^+ \rightarrow \phi \pi^+) = 0.037$. We rescale to our best value $B(D_s^+ \rightarrow \phi \pi^+) = 0.0438$.

² ALBRECHT 93E reports $< 1.9 \times 10^{-3}$ for $B(D_s^+ \rightarrow \phi \pi^+) = 0.027$. We rescale to our best value $B(D_s^+ \rightarrow \phi \pi^+) = 0.0438$.

 $\Gamma(D_s^+ a_1(1260)^0)/\Gamma_{\text{total}}$ Γ_{148}/Γ

VALUE	CL%	DOCUMENT ID	TECN	COMMENT
<0.0018	90	¹ ALBRECHT 93E	ARG	$e^+ e^- \rightarrow \Upsilon(4S)$

¹ ALBRECHT 93E reports $< 3.0 \times 10^{-3}$ for $B(D_s^+ \rightarrow \phi \pi^+) = 0.027$. We rescale to our best value $B(D_s^+ \rightarrow \phi \pi^+) = 0.0438$.

 $\Gamma(D_s^+ a_1(1260)^0)/\Gamma_{\text{total}}$ Γ_{149}/Γ

VALUE	CL%	DOCUMENT ID	TECN	COMMENT
<0.0014	90	¹ ALBRECHT 93E	ARG	$e^+ e^- \rightarrow \Upsilon(4S)$

¹ ALBRECHT 93E reports $< 2.2 \times 10^{-3}$ for $B(D_s^+ \rightarrow \phi \pi^+) = 0.027$. We rescale to our best value $B(D_s^+ \rightarrow \phi \pi^+) = 0.0438$.

 $\Gamma(D_s^+ \phi)/\Gamma_{\text{total}}$ Γ_{150}/Γ

VALUE	CL%	DOCUMENT ID	TECN	COMMENT
$<1.9 \times 10^{-6}$	90	¹ AUBERT 06F	BABR	$e^+ e^- \rightarrow \Upsilon(4S)$

- • • We do not use the following data for averages, fits, limits, etc. • • •

<0.0010 90 ² ALBRECHT 93E ARG $e^+ e^- \rightarrow \Upsilon(4S)$

<0.00026 90 ³ ALEXANDER 93B CLE2 $e^+ e^- \rightarrow \Upsilon(4S)$

¹ Assumes equal production of B^+ and B^0 at the $\Upsilon(4S)$.

² ALBRECHT 93E reports $< 1.7 \times 10^{-3}$ for $B(D_s^+ \rightarrow \phi \pi^+) = 0.027$. We rescale to our best value $B(D_s^+ \rightarrow \phi \pi^+) = 0.0438$.

³ ALEXANDER 93B reports $< 3.1 \times 10^{-4}$ for $B(D_s^+ \rightarrow \phi \pi^+) = 0.037$. We rescale to our best value $B(D_s^+ \rightarrow \phi \pi^+) = 0.0438$.

 $\Gamma(D_s^+ \phi)/\Gamma_{\text{total}}$ Γ_{151}/Γ

VALUE	CL%	DOCUMENT ID	TECN	COMMENT
$<1.2 \times 10^{-5}$	90	¹ AUBERT 06F	BABR	$e^+ e^- \rightarrow \Upsilon(4S)$

- • • We do not use the following data for averages, fits, limits, etc. • • •

<0.0013 90 ² ALBRECHT 93E ARG $e^+ e^- \rightarrow \Upsilon(4S)$

<0.00035 90 ³ ALEXANDER 93B CLE2 $e^+ e^- \rightarrow \Upsilon(4S)$

¹ Assumes equal production of B^+ and B^0 at the $\Upsilon(4S)$.

² ALBRECHT 93E reports $< 2.1 \times 10^{-3}$ for $B(D_s^+ \rightarrow \phi \pi^+) = 0.027$. We rescale to our best value $B(D_s^+ \rightarrow \phi \pi^+) = 0.0438$.

³ ALEXANDER 93B reports $< 4.2 \times 10^{-4}$ for $B(D_s^+ \rightarrow \phi \pi^+) = 0.037$. We rescale to our best value $B(D_s^+ \rightarrow \phi \pi^+) = 0.0438$.

 $\Gamma(D_s^+ \bar{K}^0)/\Gamma_{\text{total}}$ Γ_{152}/Γ

VALUE	CL%	DOCUMENT ID	TECN	COMMENT
<0.0009	90	¹ ALEXANDER 93B	CLE2	$e^+ e^- \rightarrow \Upsilon(4S)$

- • • We do not use the following data for averages, fits, limits, etc. • • •

<0.0015 90 ² ALBRECHT 93E ARG $e^+ e^- \rightarrow \Upsilon(4S)$

¹ ALEXANDER 93B reports $< 10.3 \times 10^{-4}$ for $B(D_s^+ \rightarrow \phi \pi^+) = 0.037$. We rescale to our best value $B(D_s^+ \rightarrow \phi \pi^+) = 0.0438$.

² ALBRECHT 93E reports $< 2.5 \times 10^{-3}$ for $B(D_s^+ \rightarrow \phi \pi^+) = 0.027$. We rescale to our best value $B(D_s^+ \rightarrow \phi \pi^+) = 0.0438$.

 $\Gamma(D_s^+ \bar{K}^0)/\Gamma_{\text{total}}$ Γ_{153}/Γ

VALUE	CL%	DOCUMENT ID	TECN	COMMENT
<0.0009	90	¹ ALEXANDER 93B	CLE2	$e^+ e^- \rightarrow \Upsilon(4S)$

- • • We do not use the following data for averages, fits, limits, etc. • • •

<0.0019 90 ² ALBRECHT 93E ARG $e^+ e^- \rightarrow \Upsilon(4S)$

¹ ALEXANDER 93B reports $< 10.9 \times 10^{-4}$ for $B(D_s^+ \rightarrow \phi \pi^+) = 0.037$. We rescale to our best value $B(D_s^+ \rightarrow \phi \pi^+) = 0.0438$.

² ALBRECHT 93E reports $< 3.1 \times 10^{-3}$ for $B(D_s^+ \rightarrow \phi \pi^+) = 0.027$. We rescale to our best value $B(D_s^+ \rightarrow \phi \pi^+) = 0.0438$.

Meson Particle Listings

 B^\pm

$\Gamma(D_s^+ \bar{K}^*(892)^0)/\Gamma_{\text{total}}$ Γ_{154}/Γ

VALUE	CL%	DOCUMENT ID	TECN	COMMENT
<0.0004	90	¹ ALEXANDER 93B	CLE2	$e^+e^- \rightarrow \Upsilon(4S)$

¹ ALEXANDER 93B reports $< 4.4 \times 10^{-4}$ for $B(D_s^+ \rightarrow \phi\pi^+) = 0.037$. We rescale to our best value $B(D_s^+ \rightarrow \phi\pi^+) = 0.0438$.

$\Gamma(D_s^+ \bar{K}^*(892)^0)/\Gamma_{\text{total}}$ Γ_{155}/Γ

VALUE	CL%	DOCUMENT ID	TECN	COMMENT
<0.0004	90	¹ ALEXANDER 93B	CLE2	$e^+e^- \rightarrow \Upsilon(4S)$

¹ ALEXANDER 93B reports $< 4.3 \times 10^{-4}$ for $B(D_s^+ \rightarrow \phi\pi^+) = 0.037$. We rescale to our best value $B(D_s^+ \rightarrow \phi\pi^+) = 0.0438$.

$\Gamma(D_s^- \pi^+ K^+)/\Gamma_{\text{total}}$ Γ_{156}/Γ

VALUE	CL%	DOCUMENT ID	TECN	COMMENT
<0.0007	90	¹ ALBRECHT 93E	ARG	$e^+e^- \rightarrow \Upsilon(4S)$

¹ ALBRECHT 93E reports $< 1.1 \times 10^{-3}$ for $B(D_s^- \rightarrow \phi\pi^+) = 0.027$. We rescale to our best value $B(D_s^- \rightarrow \phi\pi^+) = 0.0438$.

$\Gamma(D_s^* \pi^+ K^+)/\Gamma_{\text{total}}$ Γ_{157}/Γ

VALUE	CL%	DOCUMENT ID	TECN	COMMENT
<0.0010	90	¹ ALBRECHT 93E	ARG	$e^+e^- \rightarrow \Upsilon(4S)$

¹ ALBRECHT 93E reports $< 1.6 \times 10^{-3}$ for $B(D_s^+ \rightarrow \phi\pi^+) = 0.027$. We rescale to our best value $B(D_s^+ \rightarrow \phi\pi^+) = 0.0438$.

$\Gamma(D_s^- \pi^+ K^*(892)^+)/\Gamma_{\text{total}}$ Γ_{158}/Γ

VALUE	CL%	DOCUMENT ID	TECN	COMMENT
<0.0005	90	¹ ALBRECHT 93E	ARG	$e^+e^- \rightarrow \Upsilon(4S)$

¹ ALBRECHT 93E reports $< 8.6 \times 10^{-3}$ for $B(D_s^- \rightarrow \phi\pi^+) = 0.027$. We rescale to our best value $B(D_s^- \rightarrow \phi\pi^+) = 0.0438$.

$\Gamma(D_s^* \pi^+ K^*(892)^+)/\Gamma_{\text{total}}$ Γ_{159}/Γ

VALUE	CL%	DOCUMENT ID	TECN	COMMENT
<0.0007	90	¹ ALBRECHT 93E	ARG	$e^+e^- \rightarrow \Upsilon(4S)$

¹ ALBRECHT 93E reports $< 1.1 \times 10^{-2}$ for $B(D_s^+ \rightarrow \phi\pi^+) = 0.027$. We rescale to our best value $B(D_s^+ \rightarrow \phi\pi^+) = 0.0438$.

$\Gamma(\eta_c K^+)/\Gamma_{\text{total}}$ Γ_{160}/Γ

VALUE (units 10^{-3})	DOCUMENT ID	TECN	COMMENT
0.91 ± 0.13 OUR AVERAGE			
0.87 ± 0.15	^{1,2} AUBERT 06E	BABR	$e^+e^- \rightarrow \Upsilon(4S)$
1.4 $^{+0.3}_{-0.2} \pm 0.4$	³ AUBERT,B 05L	BABR	$e^+e^- \rightarrow \Upsilon(4S)$
1.25 ± 0.14 $^{+0.39}_{-0.40}$	⁴ FANG 03	BELL	$e^+e^- \rightarrow \Upsilon(4S)$
0.69 $^{+0.26}_{-0.21} \pm 0.22$	⁵ EDWARDS 01	CLE2	$e^+e^- \rightarrow \Upsilon(4S)$

• • • We do not use the following data for averages, fits, limits, etc. • • •

1.06 ± 0.12 ± 0.18 ^{2,6} AUBERT,B 04B BABR $e^+e^- \rightarrow \Upsilon(4S)$

¹ Perform measurements of absolute branching fractions using a missing mass technique.
² The ratio of $B(B^\pm \rightarrow K^\pm \eta_c) B(\eta_c \rightarrow K \bar{K} \pi) = (7.4 \pm 0.5 \pm 0.7) \times 10^{-5}$ reported in AUBERT,B 04B and $B(B^\pm \rightarrow K^\pm \eta_c) = (8.7 \pm 1.5) \times 10^{-3}$ reported in AUBERT 06E contribute to the determination of $B(\eta_c \rightarrow K \bar{K} \pi)$, which is used by others for normalization.
³ AUBERT,B 05L reports $[B(B^+ \rightarrow \eta_c K^+) \times [B(\eta_c(1S) \rightarrow p\bar{p})] = (1.8^{+0.3}_{-0.2} \pm 0.2) \times 10^{-6}$. We divide by our best value $B(\eta_c(1S) \rightarrow p\bar{p}) = (1.3 \pm 0.4) \times 10^{-3}$. Our first error is their experiment's error and our second error is the systematic error from using our best value.
⁴ Assumes equal production of B^+ and B^0 at the $\Upsilon(4S)$.
⁵ EDWARDS 01 assumes equal production of B^0 and B^+ at the $\Upsilon(4S)$. The correlated uncertainties (28.3)% from $B(J/\psi(1S) \rightarrow \gamma\eta_c)$ in those modes have been accounted for.
⁶ AUBERT,B 04B reports $[B(B^+ \rightarrow \eta_c K^+) \times [B(\eta_c(1S) \rightarrow K \bar{K} \pi)]] = (0.074 \pm 0.005 \pm 0.007) \times 10^{-3}$. We divide by our best value $B(\eta_c(1S) \rightarrow K \bar{K} \pi) = (7.0 \pm 1.2) \times 10^{-2}$. Our first error is their experiment's error and our second error is the systematic error from using our best value.

$\Gamma(\eta_c K^*(892)^+)/\Gamma_{\text{total}}$ Γ_{161}/Γ

VALUE (units 10^{-3})	DOCUMENT ID	TECN	COMMENT
1.2 $^{+0.6}_{-0.4} \pm 0.4$	^{1,2} AUBERT 07AV	BABR	$e^+e^- \rightarrow \Upsilon(4S)$

¹ AUBERT 07AV reports $[B(B^+ \rightarrow \eta_c K^*(892)^+) \times [B(\eta_c(1S) \rightarrow p\bar{p})] = (1.57^{+0.56+0.45}_{-0.46-0.36}) \times 10^{-6}$. We divide by our best value $B(\eta_c(1S) \rightarrow p\bar{p}) = (1.3 \pm 0.4) \times 10^{-3}$. Our first error is their experiment's error and our second error is the systematic error from using our best value.
² Assumes equal production of B^+ and B^0 at the $\Upsilon(4S)$.

$\Gamma(\eta_c(2S) K^+)/\Gamma_{\text{total}}$ Γ_{162}/Γ

VALUE (units 10^{-4})	DOCUMENT ID	TECN	COMMENT
3.4 ± 1.8 ± 0.3	¹ AUBERT 06E	BABR	$e^+e^- \rightarrow \Upsilon(4S)$

¹ Perform measurements of absolute branching fractions using a missing mass technique.

$\Gamma(\eta_c K^+)/\Gamma(J/\psi(1S) K^+)$ $\Gamma_{160}/\Gamma_{163}$

VALUE	DOCUMENT ID	TECN	COMMENT
1.33 ± 0.10 ± 0.43	¹ AUBERT,B 04B	BABR	$e^+e^- \rightarrow \Upsilon(4S)$

¹ Uses BABAR measurement of $B(B^+ \rightarrow J/\psi K^+) = (10.1 \pm 0.3 \pm 0.5) \times 10^{-4}$.

$\Gamma(J/\psi(1S) K^+)/\Gamma_{\text{total}}$ Γ_{163}/Γ

VALUE (units 10^{-4})	EVTS	DOCUMENT ID	TECN	COMMENT
10.07 ± 0.35 OUR FIT				
10.22 ± 0.35 OUR AVERAGE				
8.1 ± 1.3 ± 0.7		¹ AUBERT 06E	BABR	$e^+e^- \rightarrow \Upsilon(4S)$
10.61 ± 0.15 ± 0.48		² AUBERT 05J	BABR	$e^+e^- \rightarrow \Upsilon(4S)$
10.1 ± 1.0 ± 0.3		³ AUBERT,B 05L	BABR	$e^+e^- \rightarrow \Upsilon(4S)$
10.1 ± 0.2 ± 0.7		² ABE 03B	BELL	$e^+e^- \rightarrow \Upsilon(4S)$
10.2 ± 0.8 ± 0.7		² JESSOP 97	CLE2	$e^+e^- \rightarrow \Upsilon(4S)$
9.3 ± 3.1 ± 0.1		⁴ BORTOLETTO92	CLEO	$e^+e^- \rightarrow \Upsilon(4S)$
8.1 ± 3.5 ± 0.1	6	⁵ ALBRECHT 90J	ARG	$e^+e^- \rightarrow \Upsilon(4S)$

• • • We do not use the following data for averages, fits, limits, etc. • • •

10.1 ± 0.3 ± 0.5 ² AUBERT 02 BABR Repl. by AUBERT 05J
 11.0 ± 1.5 ± 0.9 ⁵⁹ ² ALAM 94 CLE2 Repl. by JESSOP 97
 22 ± 10 ± 2 ² BUSKULIC 92G ALEP $e^+e^- \rightarrow Z$
 7 ± 4 ³ ALBRECHT 87D ARG $e^+e^- \rightarrow \Upsilon(4S)$
 10 ± 7 ± 2 ³ BEBEK 87 CLEO $e^+e^- \rightarrow \Upsilon(4S)$
 9 ± 5 ³ ALAM 86 CLEO $e^+e^- \rightarrow \Upsilon(4S)$

¹ Perform measurements of absolute branching fractions using a missing mass technique.
² Assumes equal production of B^+ and B^0 at the $\Upsilon(4S)$.
³ AUBERT,B 05L reports $[B(B^+ \rightarrow J/\psi(1S) K^+) \times [B(J/\psi(1S) \rightarrow p\bar{p})] = (2.2 \pm 0.2 \pm 0.1) \times 10^{-6}$. We divide by our best value $B(J/\psi(1S) \rightarrow p\bar{p}) = (2.17 \pm 0.07) \times 10^{-3}$. Our first error is their experiment's error and our second error is the systematic error from using our best value.
⁴ BORTOLETTO 92 reports $(8 \pm 2 \pm 2) \times 10^{-4}$ for $B(J/\psi(1S) \rightarrow e^+e^-) = 0.069 \pm 0.009$. We rescale to our best value $B(J/\psi(1S) \rightarrow e^+e^-) = (5.94 \pm 0.06) \times 10^{-2}$. Our first error is their experiment's error and our second error is the systematic error from using our best value. Assumes equal production of B^+ and B^0 at the $\Upsilon(4S)$.
⁵ ALBRECHT 90J reports $(7 \pm 3 \pm 1) \times 10^{-4}$ for $B(J/\psi(1S) \rightarrow e^+e^-) = 0.069 \pm 0.009$. We rescale to our best value $B(J/\psi(1S) \rightarrow e^+e^-) = (5.94 \pm 0.06) \times 10^{-2}$. Our first error is their experiment's error and our second error is the systematic error from using our best value. Assumes equal production of B^+ and B^0 at the $\Upsilon(4S)$.
⁶ ALBRECHT 87D assume $B^+B^-/B^0\bar{B}^0$ ratio is 55/45. Superseded by ALBRECHT 90J.
⁷ BEBEK 87 value has been updated in BERKELMAN 91 to use same assumptions as noted for BORTOLETTO 92.
⁸ ALAM 86 assumes B^\pm/B^0 ratio is 60/40.

$\Gamma(J/\psi(1S) K^+ \pi^+ \pi^-)/\Gamma_{\text{total}}$ Γ_{164}/Γ

VALUE (units 10^{-3})	CL%	EVTS	DOCUMENT ID	TECN	COMMENT
1.07 ± 0.19 OUR AVERAGE					Error includes scale factor of 1.9.
1.16 ± 0.07 ± 0.09			¹ AUBERT 05R	BABR	$e^+e^- \rightarrow \Upsilon(4S)$
0.69 ± 0.18 ± 0.12			² ACOSTA 02F	CDF	$p\bar{p}$ 1.8 TeV
1.39 ± 0.82 ± 0.01			³ BORTOLETTO92	CLEO	$e^+e^- \rightarrow \Upsilon(4S)$
1.39 ± 0.91 ± 0.01		6	⁴ ALBRECHT 87D	ARG	$e^+e^- \rightarrow \Upsilon(4S)$

• • • We do not use the following data for averages, fits, limits, etc. • • •

<1.9 ⁹⁰ ⁵ ALBRECHT 90J ARG $e^+e^- \rightarrow \Upsilon(4S)$

¹ Assumes equal production of B^+ and B^0 at the $\Upsilon(4S)$.
² ACOSTA 02F uses as reference of $B(B \rightarrow J/\psi(1S) K^+) = (10.1 \pm 0.6) \times 10^{-4}$. The second error includes the systematic error and the uncertainties of the branching ratio.
³ BORTOLETTO 92 reports $(1.2 \pm 0.6 \pm 0.4) \times 10^{-3}$ for $B(J/\psi(1S) \rightarrow e^+e^-) = 0.069 \pm 0.009$. We rescale to our best value $B(J/\psi(1S) \rightarrow e^+e^-) = (5.94 \pm 0.06) \times 10^{-2}$. Our first error is their experiment's error and our second error is the systematic error from using our best value. Assumes equal production of B^+ and B^0 at the $\Upsilon(4S)$.
⁴ ALBRECHT 87D reports $(1.2 \pm 0.8) \times 10^{-3}$ for $B(J/\psi(1S) \rightarrow e^+e^-) = 0.069 \pm 0.009$. We rescale to our best value $B(J/\psi(1S) \rightarrow e^+e^-) = (5.94 \pm 0.06) \times 10^{-2}$. Our first error is their experiment's error and our second error is the systematic error from using our best value. They actually report 0.0011 ± 0.0007 assuming $B^+B^-/B^0\bar{B}^0$ ratio is 55/45. We rescale to 50/50. Analysis explicitly removes $B^+ \rightarrow \psi(2S) K^+$.
⁵ ALBRECHT 90J reports $< 1.6 \times 10^{-3}$ for $B(J/\psi(1S) \rightarrow e^+e^-) = 0.069$. We rescale to our best value $B(J/\psi(1S) \rightarrow e^+e^-) = 0.0594$. Assumes equal production of B^+ and B^0 at the $\Upsilon(4S)$.

$\Gamma(\eta_c(1P) K^+ \times B(\eta_c(1P) \rightarrow J/\psi \pi^+ \pi^-))/\Gamma_{\text{total}}$ Γ_{165}/Γ

VALUE	CL%	DOCUMENT ID	TECN	COMMENT
<3.4 × 10 ⁻⁶	90	¹ AUBERT 05R	BABR	$e^+e^- \rightarrow \Upsilon(4S)$

¹ Assumes equal production of B^+ and B^0 at the $\Upsilon(4S)$.

$\Gamma(X(3872) K^+)/\Gamma_{\text{total}}$ Γ_{166}/Γ

VALUE	CL%	DOCUMENT ID	TECN	COMMENT
<3.2 × 10 ⁻⁴	90	¹ AUBERT 06E	BABR	$e^+e^- \rightarrow \Upsilon(4S)$

¹ Perform measurements of absolute branching fractions using a missing mass technique.

$\Gamma(X(3872) K^+ \times B(X \rightarrow J/\psi \pi^+ \pi^-))/\Gamma_{\text{total}}$ Γ_{167}/Γ

VALUE (units 10^{-6})	DOCUMENT ID	TECN	COMMENT
11.4 ± 2.0 OUR AVERAGE			
10.1 ± 2.5 ± 1.0	¹ AUBERT 06	BABR	$e^+ e^- \rightarrow \Upsilon(4S)$
13.0 ± 2.9 ± 0.7	² CHOI 03	BELL	$e^+ e^- \rightarrow \Upsilon(4S)$
• • • We do not use the following data for averages, fits, limits, etc. • • •			
12.8 ± 4.1	¹ AUBERT 05R	BABR	Repl. by AUBERT 06

¹ Assumes equal production of B^+ and B^0 at the $\Upsilon(4S)$.
² CHOI 03 reports $[B(B^+ \rightarrow X(3872) K^+ \times B(X \rightarrow J/\psi \pi^+ \pi^-))] / [B(B^+ \rightarrow \psi(2S) K^+)] = 0.0200 \pm 0.0038 \pm 0.0023$. We multiply by our best value $B(B^+ \rightarrow \psi(2S) K^+) = (6.48 \pm 0.35) \times 10^{-4}$. Our first error is their experiment's error and our second error is the systematic error from using our best value.

 $\Gamma(X(3872) K^+ \times B(X \rightarrow J/\psi \gamma))/\Gamma_{\text{total}}$ Γ_{168}/Γ

VALUE (units 10^{-6})	DOCUMENT ID	TECN	COMMENT
3.3 ± 1.0 ± 0.3	¹ AUBERT, BE 06M	BABR	$e^+ e^- \rightarrow \Upsilon(4S)$
¹ Assumes equal production of B^+ and B^0 at the $\Upsilon(4S)$.			

 $\Gamma(X(3872) K^+ \times B(X \rightarrow D^0 \bar{D}^0))/\Gamma_{\text{total}}$ Γ_{169}/Γ

VALUE	CL%	DOCUMENT ID	TECN	COMMENT
< 6.0 × 10⁻⁵	90	¹ CHISTOV 04	BELL	$e^+ e^- \rightarrow \Upsilon(4S)$
¹ Assumes equal production of B^+ and B^0 at the $\Upsilon(4S)$.				

 $\Gamma(X(3872) K^+ \times B(X \rightarrow D^+ D^-))/\Gamma_{\text{total}}$ Γ_{170}/Γ

VALUE	CL%	DOCUMENT ID	TECN	COMMENT
< 4.0 × 10⁻⁵	90	¹ CHISTOV 04	BELL	$e^+ e^- \rightarrow \Upsilon(4S)$
¹ Assumes equal production of B^+ and B^0 at the $\Upsilon(4S)$.				

 $\Gamma(X(3872) K^+ \times B(X \rightarrow D^0 \bar{D}^0 \pi^0))/\Gamma_{\text{total}}$ Γ_{171}/Γ

VALUE (units 10^{-4})	CL%	DOCUMENT ID	TECN	COMMENT
1.02 ± 0.31 ^{+0.21} _{-0.29}		¹ GOKHROO 06	BELL	$e^+ e^- \rightarrow \Upsilon(4S)$
• • • We do not use the following data for averages, fits, limits, etc. • • •				
< 0.6	90	² CHISTOV 04	BELL	Repl. by GOKHROO 06

¹ Measure the near-threshold enhancements in the $(D^0 \bar{D}^0 \pi^0)$ system at a mass $3875.2 \pm 0.7^{+0.3}_{-1.6} \pm 0.8$ MeV/ c^2 .
² Assumes equal production of B^+ and B^0 at the $\Upsilon(4S)$.

 $\Gamma(X(3872) K^+ \times B(X \rightarrow \bar{D}^{*0} D^0))/\Gamma_{\text{total}}$ Γ_{172}/Γ

VALUE (units 10^{-4})	DOCUMENT ID	TECN	COMMENT
1.67 ± 0.36 ± 0.47	¹ AUBERT 08B	BABR	$e^+ e^- \rightarrow \Upsilon(4S)$
¹ Assumes equal production of B^+ and B^0 at the $\Upsilon(4S)$.			

 $\Gamma(X(3872) K^+ \times B(X(3872) \rightarrow J/\psi(1S) \eta))/\Gamma_{\text{total}}$ Γ_{173}/Γ

VALUE	CL%	DOCUMENT ID	TECN	COMMENT
< 7.7 × 10⁻⁶	90	¹ AUBERT 04Y	BABR	$e^+ e^- \rightarrow \Upsilon(4S)$
¹ Assumes equal production of B^+ and B^0 at the $\Upsilon(4S)$.				

 $\Gamma(X(3872)^+ K^0 \times B(X(3872)^+ \rightarrow J/\psi(1S) \pi^+ \pi^0))/\Gamma_{\text{total}}$ Γ_{174}/Γ

VALUE (units 10^{-6})	CL%	DOCUMENT ID	TECN	COMMENT
< 22	90	¹ AUBERT 05B	BABR	$e^+ e^- \rightarrow \Upsilon(4S)$
¹ Assumes equal production of B^+ and B^0 at the $\Upsilon(4S)$. The isovector-X hypothesis is excluded with a likelihood test at 1×10^{-4} level.				

 $\Gamma(X(4260)^0 K^+ \times B(X^0 \rightarrow J/\psi \pi^+ \pi^-))/\Gamma_{\text{total}}$ Γ_{175}/Γ

VALUE (units 10^{-6})	CL%	DOCUMENT ID	TECN	COMMENT
< 29	95	¹ AUBERT 06	BABR	$e^+ e^- \rightarrow \Upsilon(4S)$
¹ Assumes equal production of B^+ and B^0 at the $\Upsilon(4S)$.				

 $\Gamma(X(3945)^0 K^+ \times B(X^0 \rightarrow J/\psi \gamma))/\Gamma_{\text{total}}$ Γ_{176}/Γ

VALUE (units 10^{-6})	CL%	DOCUMENT ID	TECN	COMMENT
< 14	90	¹ AUBERT, BE 06M	BABR	$e^+ e^- \rightarrow \Upsilon(4S)$
¹ Assumes equal production of B^+ and B^0 at the $\Upsilon(4S)$.				

 $\Gamma(Z(3930)^0 K^+ \times B(Z^0 \rightarrow J/\psi \gamma))/\Gamma_{\text{total}}$ Γ_{177}/Γ

VALUE (units 10^{-6})	CL%	DOCUMENT ID	TECN	COMMENT
< 2.5	90	¹ AUBERT, BE 06M	BABR	$e^+ e^- \rightarrow \Upsilon(4S)$
¹ Assumes equal production of B^+ and B^0 at the $\Upsilon(4S)$.				

 $\Gamma(J/\psi(1S) K^*(892)^+)/\Gamma_{\text{total}}$ Γ_{178}/Γ

VALUE (units 10^{-3})	EVTS	DOCUMENT ID	TECN	COMMENT
1.43 ± 0.08 OUR AVERAGE				
1.74 ^{+0.36} _{-0.31} ± 0.06		^{1,2} AUBERT 07AV	BABR	$e^+ e^- \rightarrow \Upsilon(4S)$
1.454 ± 0.047 ± 0.097		² AUBERT 05J	BABR	$e^+ e^- \rightarrow \Upsilon(4S)$
1.28 ± 0.07 ± 0.14		² ABE 02N	BELL	$e^+ e^- \rightarrow \Upsilon(4S)$
1.41 ± 0.23 ± 0.24		² JESSOP 97	CLE2	$e^+ e^- \rightarrow \Upsilon(4S)$
1.58 ± 0.47 ± 0.27		³ ABE 96H	CDF	$p\bar{p}$ at 1.8 TeV
1.51 ± 1.08 ± 0.02		⁴ BORTOLETTO 92	CLEO	$e^+ e^- \rightarrow \Upsilon(4S)$
1.86 ± 1.30 ± 0.02	2	⁵ ALBRECHT 90J	ARG	$e^+ e^- \rightarrow \Upsilon(4S)$
• • • We do not use the following data for averages, fits, limits, etc. • • •				
1.37 ± 0.09 ± 0.11		² AUBERT 02	BABR	Repl. by AUBERT 05J
1.78 ± 0.51 ± 0.23	13	² ALAM 94	CLE2	Sup. by JESSOP 97

¹ AUBERT 07AV reports $[B(B^+ \rightarrow J/\psi(1S) K^*(892)^+)] \times [B(J/\psi(1S) \rightarrow p\bar{p})] = (3.76^{+0.72+0.28}_{-0.64-0.23}) \times 10^{-6}$. We divide by our best value $B(J/\psi(1S) \rightarrow p\bar{p}) = (2.17 \pm 0.07) \times 10^{-3}$. Our first error is their experiment's error and our second error is the systematic error from using our best value.
² Assumes equal production of B^+ and B^0 at the $\Upsilon(4S)$.
³ ABE 96H assumes that $B(B^+ \rightarrow J/\psi K^+) = (1.02 \pm 0.14) \times 10^{-3}$.
⁴ BORTOLETTO 92 reports $(1.3 \pm 0.9 \pm 0.3) \times 10^{-3}$ for $B(J/\psi(1S) \rightarrow e^+ e^-) = 0.069 \pm 0.009$. We rescale to our best value $B(J/\psi(1S) \rightarrow e^+ e^-) = (5.94 \pm 0.06) \times 10^{-2}$. Our first error is their experiment's error and our second error is the systematic error from using our best value. Assumes equal production of B^+ and B^0 at the $\Upsilon(4S)$.
⁵ ALBRECHT 90J reports $(1.6 \pm 1.1 \pm 0.3) \times 10^{-3}$ for $B(J/\psi(1S) \rightarrow e^+ e^-) = 0.069 \pm 0.009$. We rescale to our best value $B(J/\psi(1S) \rightarrow e^+ e^-) = (5.94 \pm 0.06) \times 10^{-2}$. Our first error is their experiment's error and our second error is the systematic error from using our best value. Assumes equal production of B^+ and B^0 at the $\Upsilon(4S)$.

¹ AUBERT 07AV reports $[B(B^+ \rightarrow J/\psi(1S) K^*(892)^+)] \times [B(J/\psi(1S) \rightarrow p\bar{p})] = (3.76^{+0.72+0.28}_{-0.64-0.23}) \times 10^{-6}$. We divide by our best value $B(J/\psi(1S) \rightarrow p\bar{p}) = (2.17 \pm 0.07) \times 10^{-3}$. Our first error is their experiment's error and our second error is the systematic error from using our best value.

² Assumes equal production of B^+ and B^0 at the $\Upsilon(4S)$.
³ ABE 96H assumes that $B(B^+ \rightarrow J/\psi K^+) = (1.02 \pm 0.14) \times 10^{-3}$.
⁴ BORTOLETTO 92 reports $(1.3 \pm 0.9 \pm 0.3) \times 10^{-3}$ for $B(J/\psi(1S) \rightarrow e^+ e^-) = 0.069 \pm 0.009$. We rescale to our best value $B(J/\psi(1S) \rightarrow e^+ e^-) = (5.94 \pm 0.06) \times 10^{-2}$. Our first error is their experiment's error and our second error is the systematic error from using our best value. Assumes equal production of B^+ and B^0 at the $\Upsilon(4S)$.
⁵ ALBRECHT 90J reports $(1.6 \pm 1.1 \pm 0.3) \times 10^{-3}$ for $B(J/\psi(1S) \rightarrow e^+ e^-) = 0.069 \pm 0.009$. We rescale to our best value $B(J/\psi(1S) \rightarrow e^+ e^-) = (5.94 \pm 0.06) \times 10^{-2}$. Our first error is their experiment's error and our second error is the systematic error from using our best value. Assumes equal production of B^+ and B^0 at the $\Upsilon(4S)$.

² Assumes equal production of B^+ and B^0 at the $\Upsilon(4S)$.
³ ABE 96H assumes that $B(B^+ \rightarrow J/\psi K^+) = (1.02 \pm 0.14) \times 10^{-3}$.
⁴ BORTOLETTO 92 reports $(1.3 \pm 0.9 \pm 0.3) \times 10^{-3}$ for $B(J/\psi(1S) \rightarrow e^+ e^-) = 0.069 \pm 0.009$. We rescale to our best value $B(J/\psi(1S) \rightarrow e^+ e^-) = (5.94 \pm 0.06) \times 10^{-2}$. Our first error is their experiment's error and our second error is the systematic error from using our best value. Assumes equal production of B^+ and B^0 at the $\Upsilon(4S)$.
⁵ ALBRECHT 90J reports $(1.6 \pm 1.1 \pm 0.3) \times 10^{-3}$ for $B(J/\psi(1S) \rightarrow e^+ e^-) = 0.069 \pm 0.009$. We rescale to our best value $B(J/\psi(1S) \rightarrow e^+ e^-) = (5.94 \pm 0.06) \times 10^{-2}$. Our first error is their experiment's error and our second error is the systematic error from using our best value. Assumes equal production of B^+ and B^0 at the $\Upsilon(4S)$.

² Assumes equal production of B^+ and B^0 at the $\Upsilon(4S)$.
³ ABE 96H assumes that $B(B^+ \rightarrow J/\psi K^+) = (1.02 \pm 0.14) \times 10^{-3}$.
⁴ BORTOLETTO 92 reports $(1.3 \pm 0.9 \pm 0.3) \times 10^{-3}$ for $B(J/\psi(1S) \rightarrow e^+ e^-) = 0.069 \pm 0.009$. We rescale to our best value $B(J/\psi(1S) \rightarrow e^+ e^-) = (5.94 \pm 0.06) \times 10^{-2}$. Our first error is their experiment's error and our second error is the systematic error from using our best value. Assumes equal production of B^+ and B^0 at the $\Upsilon(4S)$.
⁵ ALBRECHT 90J reports $(1.6 \pm 1.1 \pm 0.3) \times 10^{-3}$ for $B(J/\psi(1S) \rightarrow e^+ e^-) = 0.069 \pm 0.009$. We rescale to our best value $B(J/\psi(1S) \rightarrow e^+ e^-) = (5.94 \pm 0.06) \times 10^{-2}$. Our first error is their experiment's error and our second error is the systematic error from using our best value. Assumes equal production of B^+ and B^0 at the $\Upsilon(4S)$.

² Assumes equal production of B^+ and B^0 at the $\Upsilon(4S)$.
³ ABE 96H assumes that $B(B^+ \rightarrow J/\psi K^+) = (1.02 \pm 0.14) \times 10^{-3}$.
⁴ BORTOLETTO 92 reports $(1.3 \pm 0.9 \pm 0.3) \times 10^{-3}$ for $B(J/\psi(1S) \rightarrow e^+ e^-) = 0.069 \pm 0.009$. We rescale to our best value $B(J/\psi(1S) \rightarrow e^+ e^-) = (5.94 \pm 0.06) \times 10^{-2}$. Our first error is their experiment's error and our second error is the systematic error from using our best value. Assumes equal production of B^+ and B^0 at the $\Upsilon(4S)$.
⁵ ALBRECHT 90J reports $(1.6 \pm 1.1 \pm 0.3) \times 10^{-3}$ for $B(J/\psi(1S) \rightarrow e^+ e^-) = 0.069 \pm 0.009$. We rescale to our best value $B(J/\psi(1S) \rightarrow e^+ e^-) = (5.94 \pm 0.06) \times 10^{-2}$. Our first error is their experiment's error and our second error is the systematic error from using our best value. Assumes equal production of B^+ and B^0 at the $\Upsilon(4S)$.

 $\Gamma(J/\psi(1S) K^*(892)^+)/\Gamma(J/\psi(1S) K^+)$ $\Gamma_{178}/\Gamma_{163}$

VALUE	DOCUMENT ID	TECN	COMMENT
1.39 ± 0.09 OUR AVERAGE			
1.37 ± 0.05 ± 0.08	AUBERT 05J	BABR	$e^+ e^- \rightarrow \Upsilon(4S)$
1.45 ± 0.20 ± 0.17	¹ JESSOP 97	CLE2	$e^+ e^- \rightarrow \Upsilon(4S)$
1.92 ± 0.60 ± 0.17	ABE 96Q	CDF	$p\bar{p}$
• • • We do not use the following data for averages, fits, limits, etc. • • •			
1.37 ± 0.10 ± 0.08	² AUBERT 02	BABR	Repl. by AUBERT 05J

¹ JESSOP 97 assumes equal production of B^+ and B^0 at the $\Upsilon(4S)$. The measurement is actually measured as an average over kaon charged and neutral states.
² Assumes equal production of B^+ and B^0 at the $\Upsilon(4S)$.

 $\Gamma(J/\psi(1S) K(1270)^+)/\Gamma_{\text{total}}$ Γ_{179}/Γ

VALUE (units 10^{-3})	DOCUMENT ID	TECN	COMMENT
1.80 ± 0.34 ± 0.39	¹ ABE 01L	BELL	$e^+ e^- \rightarrow \Upsilon(4S)$
¹ Uses the PDG value of $B(B^+ \rightarrow J/\psi(1S) K^+) = (1.00 \pm 0.10) \times 10^{-3}$.			

 $\Gamma(J/\psi(1S) K(1400)^+)/\Gamma(J/\psi(1S) K(1270)^+)$ $\Gamma_{180}/\Gamma_{179}$

VALUE	CL%	DOCUMENT ID	TECN	COMMENT
< 0.30	90	ABE 01L	BELL	$e^+ e^- \rightarrow \Upsilon(4S)$

 $\Gamma(J/\psi(1S) \eta K^+)/\Gamma_{\text{total}}$ Γ_{181}/Γ

VALUE (units 10^{-5})	DOCUMENT ID	TECN	COMMENT
10.8 ± 2.3 ± 2.4	¹ AUBERT 04Y	BABR	$e^+ e^- \rightarrow \Upsilon(4S)$
¹ Assumes equal production of B^+ and B^0 at the $\Upsilon(4S)$.			

 $\Gamma(J/\psi(1S) \eta' K^+)/\Gamma_{\text{total}}$ Γ_{182}/Γ

VALUE (units 10^{-5})	CL%	DOCUMENT ID	TECN	COMMENT
< 8.8	90	¹ XIE 07	BELL	$e^+ e^- \rightarrow \Upsilon(4S)$
¹ Assumes equal production of B^+ and B^0 at the $\Upsilon(4S)$.				

 $\Gamma(J/\psi(1S) \phi K^+)/\Gamma_{\text{total}}$ Γ_{183}/Γ

VALUE	DOCUMENT ID	TECN	COMMENT
(5.2 ± 1.7) × 10⁻⁵ OUR AVERAGE			Error includes scale factor of 1.2.
(4.4 ± 1.4 ± 0.5) × 10 ⁻⁵	¹ AUBERT 03o	BABR	$e^+ e^- \rightarrow \Upsilon(4S)$
(8.8 ^{+3.5} _{-3.0} ± 1.3) × 10 ⁻⁵	² ANASTASSOV 00	CLE2	$e^+ e^- \rightarrow \Upsilon(4S)$
¹ Assumes equal production of B^+ and B^0 at the $\Upsilon(4S)$.			
² ANASTASSOV 00 finds 10 events on a background of 0.5 ± 0.2 . Assumes equal production of B^0 and B^+ at the $\Upsilon(4S)$, a uniform Dalitz plot distribution, isotropic $J/\psi(1S)$ and ϕ decays, and $B(B^+ \rightarrow J/\psi(1S) \phi K^+) = B(B^0 \rightarrow J/\psi(1S) \phi K^0)$.			

 $\Gamma(J/\psi(1S) \pi^+)/\Gamma_{\text{total}}$ Γ_{184}/Γ

VALUE	DOCUMENT ID	TECN	COMMENT
(4.9 ± 0.6) × 10⁻⁵ OUR FIT			Error includes scale factor of 1.5.
(3.8 ± 0.6 ± 0.3) × 10 ⁻⁵	¹ ABE 03B	BELL	$e^+ e^- \rightarrow \Upsilon(4S)$
¹ Assumes equal production of B^+ and B^0 at the $\Upsilon(4S)$.			

¹ Assumes equal production of B^+ and B^0 at the $\Upsilon(4S)$.

¹ Assumes equal production of B^+ and B^0 at the $\Upsilon(4S)$.
² ANASTASSOV 00 finds 10 events on a background of 0.5 ± 0.2 . Assumes equal production of B^0 and B^+ at the $\Upsilon(4S)$, a uniform Dalitz plot distribution, isotropic $J/\psi(1S)$ and ϕ decays, and $B(B^+ \rightarrow J/\psi(1S) \phi K^+) = B(B^0 \rightarrow J/\psi(1S) \phi K^0)$.

¹ Assumes equal production of B^+ and B^0 at the $\Upsilon(4S)$.
² ANASTASSOV 00 finds 10 events on a background of 0.5 ± 0.2 . Assumes equal production of B^0 and B^+ at the $\Upsilon(4S)$, a uniform Dalitz plot distribution, isotropic $J/\psi(1S)$ and ϕ decays, and $B(B^+ \rightarrow J/\psi(1S) \phi K^+) = B(B^0 \rightarrow J/\psi(1S) \phi K^0)$.

¹ Assumes equal production of B^+ and B^0 at the $\Upsilon(4S)$.
² ANASTASSOV 00 finds 10 events on a background of 0.5 ± 0.2 . Assumes equal production of B^0 and B^+ at the $\Upsilon(4S)$, a uniform Dalitz plot distribution, isotropic $J/\psi(1S)$ and ϕ decays, and $B(B^+ \rightarrow J/\psi(1S) \phi K^+) = B(B^0 \rightarrow J/\psi(1S) \phi K^0)$.

¹ Assumes equal production of B^+ and B^0 at the $\Upsilon(4S)$.
² ANASTASSOV 00 finds 10 events on a background of 0.5 ± 0.2 . Assumes equal production of B^0 and B^+ at the $\Upsilon(4S$

Meson Particle Listings

 B^\pm $\Gamma(J/\psi(1S)\pi^+)/\Gamma(J/\psi(1S)K^+)$ $\Gamma_{184}/\Gamma_{163}$

VALUE	CL%	DOCUMENT ID	TECN	COMMENT
0.049 ± 0.006 OUR FIT				Error includes scale factor of 1.5.
0.053 ± 0.004 OUR AVERAGE				
0.0537 ± 0.0045 ± 0.0011		AUBERT	04P BABR	$e^+e^- \rightarrow \Upsilon(4S)$
0.05 $^{+0.019}_{-0.017}$ ± 0.001		ABE	96R CDF	$p\bar{p}$ 1.8 TeV
0.052 ± 0.024		BISHAI	96 CLE2	$e^+e^- \rightarrow \Upsilon(4S)$
••• We do not use the following data for averages, fits, limits, etc. •••				
0.0391 ± 0.0078 ± 0.0019		AUBERT	02F BABR	Repl. by AUBERT 04P
0.043 ± 0.023		5	1 ALEXANDER 95 CLE2	Sup. by BISHAI 96
1 Assumes equal production of B^+B^- and $B^0\bar{B}^0$ on $\Upsilon(4S)$.				

 $\Gamma(J/\psi(1S)\rho^+)/\Gamma_{total}$ Γ_{185}/Γ

VALUE (units 10^{-5})	CL%	DOCUMENT ID	TECN	COMMENT
5.0 ± 0.7 ± 0.3		1 AUBERT	07AC BABR	$e^+e^- \rightarrow \Upsilon(4S)$
••• We do not use the following data for averages, fits, limits, etc. •••				
<77	90	BISHAI	96 CLE2	$e^+e^- \rightarrow \Upsilon(4S)$
1 Assumes equal production of B^+ and B^0 at the $\Upsilon(4S)$.				

 $\Gamma(J/\psi(1S)\pi^+\pi^0\text{nonresonant})/\Gamma_{total}$ Γ_{186}/Γ

VALUE (units 10^{-5})	CL%	DOCUMENT ID	TECN	COMMENT
<0.73	90	1 AUBERT	07AC BABR	$e^+e^- \rightarrow \Upsilon(4S)$
1 Assumes equal production of B^+ and B^0 at the $\Upsilon(4S)$.				

 $\Gamma(J/\psi(1S)a_1(1260)^+)/\Gamma_{total}$ Γ_{187}/Γ

VALUE	CL%	DOCUMENT ID	TECN	COMMENT
<1.2 × 10⁻³	90	BISHAI	96 CLE2	$e^+e^- \rightarrow \Upsilon(4S)$

 $\Gamma(J/\psi(1S)\rho\bar{\Lambda})/\Gamma_{total}$ Γ_{188}/Γ

VALUE (units 10^{-6})	CL%	DOCUMENT ID	TECN	COMMENT
11.8 ± 3.1 OUR AVERAGE				
11.7 ± 2.8 $^{+1.8}_{-2.3}$		1 XIE	05 BELL	$e^+e^- \rightarrow \Upsilon(4S)$
12 $^{+9}_{-6}$		1 AUBERT	03k BABR	$e^+e^- \rightarrow \Upsilon(4S)$
••• We do not use the following data for averages, fits, limits, etc. •••				
<41	90	ZANG	04 BELL	$e^+e^- \rightarrow \Upsilon(4S)$
1 Assumes equal production of B^+ and B^0 at the $\Upsilon(4S)$.				

 $\Gamma(J/\psi(1S)\Sigma^0\rho)/\Gamma_{total}$ Γ_{189}/Γ

VALUE	CL%	DOCUMENT ID	TECN	COMMENT
<1.1 × 10⁻⁵	90	1 XIE	05 BELL	$e^+e^- \rightarrow \Upsilon(4S)$
1 Assumes equal production of B^+ and B^0 at the $\Upsilon(4S)$.				

 $\Gamma(J/\psi(1S)D^+)/\Gamma_{total}$ Γ_{190}/Γ

VALUE (units 10^{-5})	CL%	DOCUMENT ID	TECN	COMMENT
<12	90	1 AUBERT	05u BABR	$e^+e^- \rightarrow \Upsilon(4S)$
1 Assumes equal production of B^+ and B^0 at the $\Upsilon(4S)$.				

 $\Gamma(J/\psi(1S)\bar{D}^0\pi^+)/\Gamma_{total}$ Γ_{191}/Γ

VALUE (units 10^{-5})	CL%	DOCUMENT ID	TECN	COMMENT
<2.5	90	1 ZHANG	05B BELL	$e^+e^- \rightarrow \Upsilon(4S)$
••• We do not use the following data for averages, fits, limits, etc. •••				
<5.2	90	1 AUBERT	05R BABR	$e^+e^- \rightarrow \Upsilon(4S)$
1 Assumes equal production of B^+ and B^0 at the $\Upsilon(4S)$.				

 $\Gamma(\psi(2S)K^+)/\Gamma_{total}$ Γ_{192}/Γ

VALUE (units 10^{-4})	CL%	EVTS	DOCUMENT ID	TECN	COMMENT
6.48 ± 0.35 OUR AVERAGE					
4.9 ± 1.6 ± 0.4			1 AUBERT	06E BABR	$e^+e^- \rightarrow \Upsilon(4S)$
6.17 ± 0.32 ± 0.44			2 AUBERT	05J BABR	$e^+e^- \rightarrow \Upsilon(4S)$
6.9 ± 0.6			2 ABE	03B BELL	$e^+e^- \rightarrow \Upsilon(4S)$
7.8 ± 0.7 ± 0.9			2 RICHICHI	01 CLE2	$e^+e^- \rightarrow \Upsilon(4S)$
5.5 ± 1.0 ± 0.6			3 ABE	98o CDF	$p\bar{p}$ 1.8 TeV
18 ± 8 ± 4		5	2 ALBRECHT	90J ARG	$e^+e^- \rightarrow \Upsilon(4S)$
••• We do not use the following data for averages, fits, limits, etc. •••					
6.4 ± 0.5 ± 0.8			2 AUBERT	02 BABR	Repl. by AUBERT 05J
6.1 ± 2.3 ± 0.9		7	2 ALAM	94 CLE2	Repl. by RICHICHI 01
<5	90		2 BORTOLETTO	92 CLEO	$e^+e^- \rightarrow \Upsilon(4S)$
22 ± 17		3	4 ALBRECHT	87D ARG	$e^+e^- \rightarrow \Upsilon(4S)$

1 Perform measurements of absolute branching fractions using a missing mass technique.

2 Assumes equal production of B^+ and B^0 at the $\Upsilon(4S)$.

3 ABE 98o reports $[B(B^+ \rightarrow \psi(2S)K^+)]/[B(B^+ \rightarrow J/\psi(1S)K^+)] = 0.558 \pm 0.082 \pm 0.056$. We multiply by our best value $B(B^+ \rightarrow J/\psi(1S)K^+) = (9.9 \pm 1.0) \times 10^{-4}$. Our first error is their experiment's error and our second error is the systematic error from using our best value.

4 ALBRECHT 87D assume $B^+B^-/B^0\bar{B}^0$ ratio is 55/45. Superseded by ALBRECHT 90J.

 $\Gamma(\psi(2S)K^+)/\Gamma(J/\psi(1S)K^+)$ $\Gamma_{192}/\Gamma_{163}$

VALUE	DOCUMENT ID	TECN	COMMENT
0.64 ± 0.06 ± 0.07	1 AUBERT	02 BABR	$e^+e^- \rightarrow \Upsilon(4S)$
1 Assumes equal production of B^+ and B^0 at the $\Upsilon(4S)$.			

 $\Gamma(\psi(2S)K^*(892)^+)/\Gamma_{total}$ Γ_{193}/Γ

VALUE (units 10^{-4})	CL%	DOCUMENT ID	TECN	COMMENT
6.7 ± 1.4 OUR AVERAGE				Error includes scale factor of 1.3.
5.92 ± 0.85 ± 0.89		1 AUBERT	05J BABR	$e^+e^- \rightarrow \Upsilon(4S)$
9.2 ± 1.9 ± 1.2		1 RICHICHI	01 CLE2	$e^+e^- \rightarrow \Upsilon(4S)$
••• We do not use the following data for averages, fits, limits, etc. •••				
<30	90	1 ALAM	94 CLE2	Repl. by RICHICHI 01
<35	90	1 BORTOLETTO	92 CLEO	$e^+e^- \rightarrow \Upsilon(4S)$
<49	90	1 ALBRECHT	90 ARG	$e^+e^- \rightarrow \Upsilon(4S)$
1 Assumes equal production of B^+ and B^0 at the $\Upsilon(4S)$.				

 $\Gamma(\psi(2S)K^*(892)^+)/\Gamma(\psi(2S)K^+)$ $\Gamma_{193}/\Gamma_{192}$

VALUE	DOCUMENT ID	TECN	COMMENT
0.96 ± 0.15 ± 0.09	AUBERT	05J BABR	$e^+e^- \rightarrow \Upsilon(4S)$

 $\Gamma(\psi(2S)K^+\pi^+\pi^-)/\Gamma_{total}$ Γ_{194}/Γ

VALUE	EVTS	DOCUMENT ID	TECN	COMMENT
0.0019 ± 0.0011 ± 0.0004	3	1 ALBRECHT	90J ARG	$e^+e^- \rightarrow \Upsilon(4S)$
1 Assumes equal production of B^+ and B^0 at the $\Upsilon(4S)$.				

 $\Gamma(\psi(3770)K^+)/\Gamma_{total}$ Γ_{195}/Γ

VALUE (units 10^{-3})	DOCUMENT ID	TECN	COMMENT
0.49 ± 0.13 OUR AVERAGE			
3.5 ± 2.5 ± 0.3	1 AUBERT	06E BABR	$e^+e^- \rightarrow \Upsilon(4S)$
0.48 ± 0.11 ± 0.07	2 CHISTOV	04 BELL	$e^+e^- \rightarrow \Upsilon(4S)$
1 Perform measurements of absolute branching fractions using a missing mass technique.			
2 Assumes equal production of B^+ and B^0 at the $\Upsilon(4S)$.			

 $\Gamma(\psi(3770)K^+ \times B(\psi \rightarrow D^0\bar{D}^0))/\Gamma_{total}$ Γ_{196}/Γ

VALUE (units 10^{-4})	DOCUMENT ID	TECN	COMMENT
1.6 ± 0.4 OUR AVERAGE			Error includes scale factor of 1.1.
1.41 ± 0.30 ± 0.22	1 AUBERT	08B BABR	$e^+e^- \rightarrow \Upsilon(4S)$
2.2 ± 0.5 ± 0.3	1 BRODZICKA	08 BELL	$e^+e^- \rightarrow \Upsilon(4S)$
••• We do not use the following data for averages, fits, limits, etc. •••			
3.4 ± 0.8 ± 0.5	1 CHISTOV	04 BELL	Repl. by BRODZICKA 08
1 Assumes equal production of B^+ and B^0 at the $\Upsilon(4S)$.			

 $\Gamma(\psi(3770)K^+ \times B(\psi \rightarrow D^+D^-))/\Gamma_{total}$ Γ_{197}/Γ

VALUE (units 10^{-4})	DOCUMENT ID	TECN	COMMENT
0.94 ± 0.35 OUR AVERAGE			
0.84 ± 0.32 ± 0.21	1 AUBERT	08B BABR	$e^+e^- \rightarrow \Upsilon(4S)$
1.4 ± 0.8 ± 0.2	1 CHISTOV	04 BELL	$e^+e^- \rightarrow \Upsilon(4S)$
1 Assumes equal production of B^+ and B^0 at the $\Upsilon(4S)$.			

 $\Gamma(\chi_{c0}\pi^+ \times B(\chi_{c0} \rightarrow \pi^+\pi^-))/\Gamma_{total}$ Γ_{198}/Γ

VALUE (units 10^{-6})	CL%	DOCUMENT ID	TECN	COMMENT
<0.3	90	1 AUBERT,B	05G BABR	$e^+e^- \rightarrow \Upsilon(4S)$
1 Assumes equal production of B^+ and B^0 at the $\Upsilon(4S)$.				

 $\Gamma(\chi_{c0}(1P)K^+)/\Gamma_{total}$ Γ_{199}/Γ

VALUE (units 10^{-4})	CL%	DOCUMENT ID	TECN	COMMENT
1.40 ± 0.23 ± 0.19 OUR AVERAGE				
1.84 ± 0.32 ± 0.31		1,2 AUBERT	06o BABR	$e^+e^- \rightarrow \Upsilon(4S)$
4.8 ± 2.2 ± 0.4		3 AUBERT,BE	06M BABR	$e^+e^- \rightarrow \Upsilon(4S)$
1.12 ± 0.12 $^{+0.30}_{-0.20}$		2 GARMASH	06 BELL	$e^+e^- \rightarrow \Upsilon(4S)$
1.39 ± 0.49 ± 0.11		4 AUBERT,B	05N BABR	$e^+e^- \rightarrow \Upsilon(4S)$
••• We do not use the following data for averages, fits, limits, etc. •••				
<1.8	90	5 AUBERT	06E BABR	$e^+e^- \rightarrow \Upsilon(4S)$
<8.9	90	2 AUBERT	05K BABR	$e^+e^- \rightarrow \Upsilon(4S)$
1.96 ± 0.35 $^{+2.00}_{-0.42}$		2 GARMASH	05 BELL	Repl. by GARMASH 06
2.7 ± 0.7		6 AUBERT	04T BABR	Repl. by AUBERT,B 04P
3.0 ± 0.8 ± 0.3		7 AUBERT,B	04P BABR	Repl. by AUBERT,B 05N
6.0 $^{+2.1}_{-1.8}$ ± 1.1		8 ABE	02B BELL	Repl. by GARMASH 05
<4.8	90	9 EDWARDS	01 CLE2	$e^+e^- \rightarrow \Upsilon(4S)$

1 Measured in the $B^+ \rightarrow K^+K^-K^+$ decay.

2 Assumes equal production of B^+ and B^0 at the $\Upsilon(4S)$.

3 AUBERT,BE 06M reports $[B(B^+ \rightarrow \chi_{c0}(1P)K^+) \times [B(\chi_{c0}(1P) \rightarrow \gamma J/\psi(1S))] = (6.1 \pm 2.6 \pm 1.1) \times 10^{-6}$. We divide by our best value $B(\chi_{c0}(1P) \rightarrow \gamma J/\psi(1S)) = (1.28 \pm 0.11) \times 10^{-2}$. Our first error is their experiment's error and our second error is the systematic error from using our best value. The significance of the observed signal is 2.4 σ .

4 AUBERT,B 05N reports $(0.66 \pm 0.22 \pm 0.08) \times 10^{-6}$ for $B(B^+ \rightarrow \chi_{c0}^0 K^+) \times B(\chi_{c0}^0 \rightarrow \pi^+\pi^-)$. We compute $B(B^+ \rightarrow \chi_{c0}^0 K^+)$ using the PDG value $B(\chi_{c0}^0 \rightarrow \pi^+\pi^-) = (7.1 \pm 0.6) \times 10^{-3}$ and 2/3 for the $\pi^+\pi^-$ fraction.

⁵ Perform measurements of absolute branching fractions using a missing mass technique.

⁶ The measurement performed using decay channels $\chi_C^0 \rightarrow \pi^+ \pi^-$ and $\chi_C^0 \rightarrow K^+ K^-$. The ratio of the branching ratios for these channels is found to be consistent with world average.

⁷ AUBERT 04P reports $B(B^+ \rightarrow \chi_C^0 K^+) \times B(\chi_C^0 \rightarrow \pi^+ \pi^-) = (1.5 \pm 0.4 \pm 0.1) \times 10^{-6}$ and used PDG value of $B(\chi_C^0 \rightarrow \pi\pi) = (7.4 \pm 0.8) \times 10^{-3}$ and Clebsh-Gordan coefficient to compute $B(B^\pm \rightarrow \chi_C^0 K^\pm)$.

⁸ ABE 02B measures the ratio of $B(B^+ \rightarrow \chi_C^0 K^+)/B(B^+ \rightarrow J/\psi(1S) K^+) = 0.60 \pm 0.21 - 0.18 \pm 0.05 \pm 0.08$, where the third error is due to the uncertainty in the $B(\chi_C^0 \rightarrow \pi^+ \pi^-)$, and uses $B(B^+ \rightarrow J/\psi(1S) K^+) = (10.0 \pm 1.0) \times 10^{-4}$ to obtain the result.

⁹ EDWARDS 01 assumes equal production of B^0 and B^+ at the $\Upsilon(4S)$. The correlated uncertainties (28.3)% from $B(J/\psi(1S) \rightarrow \gamma \eta_C)$ in those modes have been accounted for.

$\Gamma(\chi_{c0} K^*(892)^+)/\Gamma_{\text{total}}$		Γ_{200}/Γ		
VALUE	CL%	DOCUMENT ID	TECN	COMMENT
$<2.86 \times 10^{-3}$	90	¹ AUBERT	05k	BABR $e^+ e^- \rightarrow \Upsilon(4S)$

¹ Assumes equal production of B^+ and B^0 at the $\Upsilon(4S)$.

$\Gamma(\chi_{c2} K^+)/\Gamma_{\text{total}}$		Γ_{201}/Γ		
VALUE	CL%	DOCUMENT ID	TECN	COMMENT
$<2.9 \times 10^{-5}$	90	¹ SONI	06	BELL $e^+ e^- \rightarrow \Upsilon(4S)$

• • • We do not use the following data for averages, fits, limits, etc. • • •

$<2.0 \times 10^{-4}$	90	² AUBERT	06E	BABR $e^+ e^- \rightarrow \Upsilon(4S)$
$<3.0 \times 10^{-5}$	90	¹ AUBERT	05k	BABR Repl. by AUBERT 06E

¹ Assumes equal production of B^+ and B^0 at the $\Upsilon(4S)$.

² Perform measurements of absolute branching fractions using a missing mass technique.

$\Gamma(\chi_{c2} K^*(892)^+)/\Gamma_{\text{total}}$		Γ_{202}/Γ		
VALUE	CL%	DOCUMENT ID	TECN	COMMENT
$<1.2 \times 10^{-5}$	90	¹ AUBERT	05k	BABR $e^+ e^- \rightarrow \Upsilon(4S)$

• • • We do not use the following data for averages, fits, limits, etc. • • •

$<1.27 \times 10^{-4}$	90	¹ SONI	06	BELL $e^+ e^- \rightarrow \Upsilon(4S)$
------------------------	----	-------------------	----	---

¹ Assumes equal production of B^+ and B^0 at the $\Upsilon(4S)$.

$\Gamma(\chi_{c1}(1P) \pi^+)/\Gamma_{\text{total}}$		Γ_{203}/Γ		
VALUE (units 10^{-5})		DOCUMENT ID	TECN	COMMENT
$2.2 \pm 0.4 \pm 0.3$		¹ KUMAR	06	BELL $e^+ e^- \rightarrow \Upsilon(4S)$

¹ Assumes equal production of B^+ and B^0 at the $\Upsilon(4S)$.

$\Gamma(\chi_{c1}(1P) K^+)/\Gamma_{\text{total}}$		Γ_{204}/Γ		
VALUE (units 10^{-4})	EVTS	DOCUMENT ID	TECN	COMMENT
4.9 ± 0.5	OUR AVERAGE	Error includes scale factor of 1.5. See the ideogram below.		

$8.1 \pm 1.4 \pm 0.7$		¹ AUBERT	06E	BABR $e^+ e^- \rightarrow \Upsilon(4S)$
$4.9 \pm 0.4 \pm 0.3$		² AUBERT, BE	06M	BABR $e^+ e^- \rightarrow \Upsilon(4S)$
$4.49 \pm 0.19 \pm 0.53$		³ SONI	06	BELL $e^+ e^- \rightarrow \Upsilon(4S)$
$15.5 \pm 5.4 \pm 2.0$		⁴ ACOSTA	02F	CDF $p\bar{p}$ 1.8 TeV
$5.79 \pm 0.26 \pm 0.65$		³ AUBERT	05J	BABR Repl. by AUBERT, BE 06M
$5.7 \pm 0.9 \pm 0.3$		⁵ AUBERT	02	BABR Repl. by AUBERT 05J
$9.7 \pm 4.0 \pm 0.9$	6	³ ALAM	94	CLE2 $e^+ e^- \rightarrow \Upsilon(4S)$
$19 \pm 13 \pm 6$		⁶ ALBRECHT	92E	ARG $e^+ e^- \rightarrow \Upsilon(4S)$

¹ Perform measurements of absolute branching fractions using a missing mass technique.

² AUBERT, BE 06M reports $[B(B^+ \rightarrow \chi_{c1}(1P) K^+)] \times [B(\chi_{c1}(1P) \rightarrow \gamma J/\psi(1S))] = (1.76 \pm 0.07 \pm 0.12) \times 10^{-4}$. We divide by our best value $B(\chi_{c1}(1P) \rightarrow \gamma J/\psi(1S)) = (36.0 \pm 1.9) \times 10^{-2}$. Our first error is their experiment's error and our second error is the systematic error from using our best value.

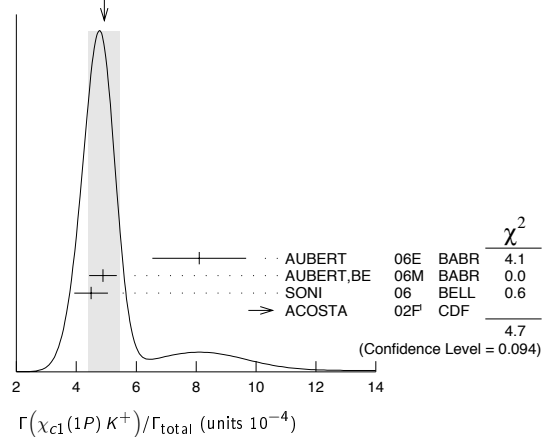
³ Assumes equal production of B^+ and B^0 at the $\Upsilon(4S)$.

⁴ ACOSTA 02F uses as reference of $B(B \rightarrow J/\psi(1S) K^+) = (10.1 \pm 0.6) \times 10^{-4}$. The second error includes the systematic error and the uncertainties of the branching ratio.

⁵ AUBERT 02 reports $(7.5 \pm 0.9 \pm 0.8) \times 10^{-4}$ for $B(\chi_{c1}(1P) \rightarrow \gamma J/\psi(1S)) = 0.273 \pm 0.016$. We rescale to our best value $B(\chi_{c1}(1P) \rightarrow \gamma J/\psi(1S)) = (36.0 \pm 1.9) \times 10^{-2}$. Our first error is their experiment's error and our second error is the systematic error from using our best value. Assumes equal production of B^+ and B^0 at the $\Upsilon(4S)$.

⁶ ALBRECHT 92E assumes no $\chi_{c2}(1P)$ production and $B(\Upsilon(4S) \rightarrow B^+ B^-) = 50\%$.

WEIGHTED AVERAGE
4.9±0.5 (Error scaled by 1.5)



$\Gamma(\chi_{c1}(1P) K^+)/\Gamma(J/\psi(1S) K^+)$		$\Gamma_{204}/\Gamma_{163}$		
VALUE	CL%	DOCUMENT ID	TECN	COMMENT
$0.57 \pm 0.06 \pm 0.03$		¹ AUBERT	02	BABR $e^+ e^- \rightarrow \Upsilon(4S)$

¹ AUBERT 02 reports $0.75 \pm 0.08 \pm 0.05$ for $B(\chi_{c1}(1P) \rightarrow \gamma J/\psi(1S)) = 0.273 \pm 0.016$.

We rescale to our best value $B(\chi_{c1}(1P) \rightarrow \gamma J/\psi(1S)) = (36.0 \pm 1.9) \times 10^{-2}$. Our first error is their experiment's error and our second error is the systematic error from using our best value. Assumes equal production of B^+ and B^0 at the $\Upsilon(4S)$.

$\Gamma(\chi_{c1}(1P) \pi^+)/\Gamma(\chi_{c1}(1P) K^+)$		$\Gamma_{203}/\Gamma_{204}$		
VALUE	CL%	DOCUMENT ID	TECN	COMMENT
$0.043 \pm 0.008 \pm 0.003$		¹ KUMAR	06	BELL $e^+ e^- \rightarrow \Upsilon(4S)$

¹ Assumes equal production of B^+ and B^0 at the $\Upsilon(4S)$.

$\Gamma(\chi_{c1}(1P) K^*(892)^+)/\Gamma_{\text{total}}$		Γ_{205}/Γ		
VALUE (units 10^{-4})	CL%	DOCUMENT ID	TECN	COMMENT
3.6 ± 0.9	OUR AVERAGE			

$4.05 \pm 0.59 \pm 0.95$ ¹ SONI 06 BELL $e^+ e^- \rightarrow \Upsilon(4S)$

$2.94 \pm 0.95 \pm 0.98$ ¹ AUBERT 05J BABR $e^+ e^- \rightarrow \Upsilon(4S)$

• • • We do not use the following data for averages, fits, limits, etc. • • •

<21	90	¹ ALAM	94	CLE2 $e^+ e^- \rightarrow \Upsilon(4S)$
-------	----	-------------------	----	---

¹ Assumes equal production of B^+ and B^0 at the $\Upsilon(4S)$.

$\Gamma(\chi_{c1}(1P) K^*(892)^+)/\Gamma(\chi_{c1}(1P) K^+)$		$\Gamma_{205}/\Gamma_{204}$		
VALUE	CL%	DOCUMENT ID	TECN	COMMENT
$0.51 \pm 0.17 \pm 0.16$		AUBERT	05J	BABR $e^+ e^- \rightarrow \Upsilon(4S)$

$\Gamma(h_c K^+)/\Gamma_{\text{total}}$		Γ_{206}/Γ		
VALUE (units 10^{-5})	EVTS	DOCUMENT ID	TECN	COMMENT
<3.8		¹ FANG	06	BELL $e^+ e^- \rightarrow \Upsilon(4S)$

¹ Assumes equal production of B^+ and B^0 at the $\Upsilon(4S)$ and $B(h_c \rightarrow \eta_c \gamma) = 50\%$.

$\Gamma(K^0 \pi^+)/\Gamma_{\text{total}}$		Γ_{207}/Γ		
VALUE (units 10^{-6})	CL%	DOCUMENT ID	TECN	COMMENT
23.1 ± 1.0	OUR AVERAGE			

$22.8 \pm 0.8 \pm 1.3$ ¹ LIN 07 BELL $e^+ e^- \rightarrow \Upsilon(4S)$

$23.9 \pm 1.1 \pm 1.0$ ¹ AUBERT, BE 06c BABR $e^+ e^- \rightarrow \Upsilon(4S)$

$18.8 \pm 3.7 \pm 2.1$ ¹ BORNHEIM 03 CLE2 $e^+ e^- \rightarrow \Upsilon(4S)$

$18.2 \pm 3.3 \pm 1.8$

• • • We do not use the following data for averages, fits, limits, etc. • • •

$26.0 \pm 1.3 \pm 1.0$ ¹ AUBERT, BE 05E BABR Repl. by AUBERT, BE 06c

$22.3 \pm 1.7 \pm 1.1$ ¹ AUBERT 04M BABR Repl. by AUBERT, BE 05E

$22.0 \pm 1.9 \pm 1.1$ ¹ CHAO 04 BELL Repl. by LIN 07

$19.4 \pm 3.1 \pm 1.6$ ¹ CASEY 02 BELL Repl. by CHAO 04

$13.7 \pm 5.7 \pm 1.9$ ¹ ABE 01H BELL Repl. by CASEY 02

$18.2 \pm 3.3 \pm 2.0$ ¹ AUBERT 01E BABR Repl. by AUBERT 04M

$18.2 \pm 4.6 \pm 1.6$ ¹ CRONIN-HEN.00 CLE2 Repl. by BORNHEIM 03

$23 \pm 11 \pm 3.6$ GODANG 98 CLE2 Repl. by CRONIN-HENNESSY 00

<48 90 ASNER 96 CLE2 Repl. by GODANG 98

<190 90 ALBRECHT 91B ARG $e^+ e^- \rightarrow \Upsilon(4S)$

<100 90 ² AVERY 89B CLEO $e^+ e^- \rightarrow \Upsilon(4S)$

<680 90 AVERY 87 CLEO $e^+ e^- \rightarrow \Upsilon(4S)$

¹ Assumes equal production of B^+ and B^0 at the $\Upsilon(4S)$.

² AVERY 89B reports $<9 \times 10^{-5}$ assuming the $\Upsilon(4S)$ decays 43% to $B^0 \bar{B}^0$. We rescale to 50%.

Meson Particle Listings

 B^\pm $\Gamma(K^+\pi^0)/\Gamma_{\text{total}}$ Γ_{208}/Γ

VALUE (units 10^{-6})	CL%	DOCUMENT ID	TECN	COMMENT
12.9 ± 0.6 OUR AVERAGE				
13.6 ± 0.6 ± 0.7		¹ AUBERT	07BC	BABR $e^+e^- \rightarrow \Upsilon(4S)$
12.4 ± 0.5 ± 0.6		¹ LIN	07A	BELL $e^+e^- \rightarrow \Upsilon(4S)$
12.9 $^{+2.4}_{-2.2} \pm 1.2$		¹ BORNHEIM	03	CLE2 $e^+e^- \rightarrow \Upsilon(4S)$
• • • We do not use the following data for averages, fits, limits, etc. • • •				
12.0 ± 0.7 ± 0.6		¹ AUBERT	05L	BABR Repl. by AUBERT 07bc
12.0 ± 1.3 $^{+1.3}_{-0.9}$		¹ CHAO	04	BELL Repl. by LIN 07A
12.8 $^{+1.2}_{-1.1} \pm 1.0$		¹ AUBERT	03L	BABR Repl. by AUBERT 05L
13.0 $^{+2.5}_{-2.4} \pm 1.3$		¹ CASEY	02	BELL Repl. by CHAO 04
16.3 $^{+3.5}_{-3.3} \pm 1.6$		¹ ABE	01H	BELL Repl. by CASEY 02
10.8 $^{+2.1}_{-1.9} \pm 1.0$		¹ AUBERT	01E	BABR Repl. by AUBERT 03L
11.6 $^{+3.0}_{-2.7} \pm 1.4$		¹ CRONIN-HEN.	00	CLE2 Repl. by BORNHEIM 03
<16	90	GODANG	98	CLE2 Repl. by CRONIN-HENNESSY 00
<14	90	ASNER	96	CLE2 Repl. by GODANG 98
¹ Assumes equal production of B^+ and B^0 at the $\Upsilon(4S)$.				

 $\Gamma(K^+\pi^0)/\Gamma(K^0\pi^+)$ $\Gamma_{208}/\Gamma_{207}$

VALUE	DOCUMENT ID	TECN	COMMENT
0.54 ± 0.03 ± 0.04	LIN	07A	BELL $e^+e^- \rightarrow \Upsilon(4S)$
• • • We do not use the following data for averages, fits, limits, etc. • • •			
2.38 $^{+0.98}_{-1.10} \pm 0.39$	ABE	01H	BELL Repl. by LIN 07A

 $\Gamma(\eta'K^+)/\Gamma_{\text{total}}$ Γ_{209}/Γ

VALUE (units 10^{-6})	DOCUMENT ID	TECN	COMMENT
70.2 ± 2.5 OUR AVERAGE			
70.0 ± 1.5 ± 2.8	¹ AUBERT	07AE	BABR $e^+e^- \rightarrow \Upsilon(4S)$
69.2 ± 2.2 ± 3.7	¹ SCHUEMANN	06	BELL $e^+e^- \rightarrow \Upsilon(4S)$
80 $^{+10}_{-9} \pm 7$	¹ RICHICHI	00	CLE2 $e^+e^- \rightarrow \Upsilon(4S)$
• • • We do not use the following data for averages, fits, limits, etc. • • •			
68.9 ± 2.0 ± 3.2	¹ AUBERT	05m	BABR Repl. by AUBERT 07AE
76.9 ± 3.5 ± 4.4	¹ AUBERT	03w	BABR Repl. by AUBERT 05m
79 $^{+12}_{-11} \pm 9$	¹ ABE	01M	BELL Repl. by SCHUEMANN 06
70 ± 8 ± 5	¹ AUBERT	01G	BABR Repl. by AUBERT 03w
65 $^{+15}_{-14} \pm 9$	BEHRENS	98	CLE2 Repl. by RICHICHI 00
¹ Assumes equal production of B^+ and B^0 at the $\Upsilon(4S)$.			

 $\Gamma(\eta'K^*(892)^+)/\Gamma_{\text{total}}$ Γ_{210}/Γ

VALUE (units 10^{-6})	CL%	DOCUMENT ID	TECN	COMMENT
4.9 $^{+1.9}_{-1.7} \pm 0.8$		¹ AUBERT	07E	BABR $e^+e^- \rightarrow \Upsilon(4S)$
• • • We do not use the following data for averages, fits, limits, etc. • • •				
< 2.9	90	¹ SCHUEMANN	07	BELL $e^+e^- \rightarrow \Upsilon(4S)$
<14	90	¹ AUBERT,B	04D	BABR Repl. by AUBERT 07E
<35	90	¹ RICHICHI	00	CLE2 $e^+e^- \rightarrow \Upsilon(4S)$
<13	90	BEHRENS	98	CLE2 Repl. by RICHICHI 00
¹ Assumes equal production of B^+ and B^0 at the $\Upsilon(4S)$.				

 $\Gamma(\eta K^+)/\Gamma_{\text{total}}$ Γ_{211}/Γ

VALUE (units 10^{-6})	CL%	DOCUMENT ID	TECN	COMMENT
2.7 ± 0.9 OUR AVERAGE				Error includes scale factor of 3.3.
3.7 ± 0.4 ± 0.1		¹ AUBERT	07AE	BABR $e^+e^- \rightarrow \Upsilon(4S)$
1.9 ± 0.3 $^{+0.2}_{-0.1}$		¹ CHANG	07B	BELL $e^+e^- \rightarrow \Upsilon(4S)$
2.2 $^{+2.8}_{-2.2}$		¹ RICHICHI	00	CLE2 $e^+e^- \rightarrow \Upsilon(4S)$
• • • We do not use the following data for averages, fits, limits, etc. • • •				
3.3 ± 0.6 ± 0.3		¹ AUBERT,B	05K	BABR Repl. by AUBERT 07AE
2.1 ± 0.6 ± 0.2		¹ CHANG	05A	BELL Repl. by CHANG 07B
3.4 ± 0.8 ± 0.2		¹ AUBERT	04H	BABR Repl. by AUBERT,B 05K
<14	90	BEHRENS	98	CLE2 Repl. by RICHICHI 00
¹ Assumes equal production of B^+ and B^0 at the $\Upsilon(4S)$.				

 $\Gamma(\eta K^*(892)^+)/\Gamma_{\text{total}}$ Γ_{212}/Γ

VALUE (units 10^{-6})	CL%	DOCUMENT ID	TECN	COMMENT
19.3 ± 1.6 OUR AVERAGE				
19.3 $^{+2.0}_{-1.9} \pm 1.5$		¹ WANG	07B	BELL $e^+e^- \rightarrow \Upsilon(4S)$
18.9 ± 1.8 ± 1.3		¹ AUBERT,B	06H	BABR $e^+e^- \rightarrow \Upsilon(4S)$
26.4 $^{+9.6}_{-8.2} \pm 3.3$		¹ RICHICHI	00	CLE2 $e^+e^- \rightarrow \Upsilon(4S)$
• • • We do not use the following data for averages, fits, limits, etc. • • •				
25.6 ± 4.0 ± 2.4		¹ AUBERT,B	04D	BABR Repl. by AUBERT,B 06H
<30	90	BEHRENS	98	CLE2 Repl. by RICHICHI 00
¹ Assumes equal production of B^+ and B^0 at the $\Upsilon(4S)$.				

 $\Gamma(\eta K_S^0(1430)^+)/\Gamma_{\text{total}}$ Γ_{213}/Γ

VALUE (units 10^{-6})	DOCUMENT ID	TECN	COMMENT
18.2 ± 2.6 ± 2.6	¹ AUBERT,B	06H	BABR $e^+e^- \rightarrow \Upsilon(4S)$
¹ Assumes equal production of B^+ and B^0 at the $\Upsilon(4S)$.			

 $\Gamma(\eta K_S^0(1430)^+)/\Gamma_{\text{total}}$ Γ_{214}/Γ

VALUE (units 10^{-6})	DOCUMENT ID	TECN	COMMENT
9.1 ± 2.7 ± 1.4	¹ AUBERT,B	06H	BABR $e^+e^- \rightarrow \Upsilon(4S)$
¹ Assumes equal production of B^+ and B^0 at the $\Upsilon(4S)$.			

 $\Gamma(\omega K^+)/\Gamma_{\text{total}}$ Γ_{215}/Γ

VALUE (units 10^{-6})	CL%	DOCUMENT ID	TECN	COMMENT
6.7 ± 0.8 OUR AVERAGE				Error includes scale factor of 1.8.
6.3 ± 0.5 ± 0.3		¹ AUBERT	07AE	BABR $e^+e^- \rightarrow \Upsilon(4S)$
8.1 ± 0.6 ± 0.6		¹ JEN	06	BELL $e^+e^- \rightarrow \Upsilon(4S)$
3.2 $^{+2.4}_{-1.9} \pm 0.8$		¹ JESSOP	00	CLE2 $e^+e^- \rightarrow \Upsilon(4S)$
• • • We do not use the following data for averages, fits, limits, etc. • • •				
6.1 ± 0.6 ± 0.4		¹ AUBERT,B	06E	BABR AUBERT 07AE
4.8 ± 0.8 ± 0.4		¹ AUBERT	04H	BABR Repl. by AUBERT,B 06E
6.5 $^{+1.3}_{-1.2} \pm 0.6$		¹ WANG	04A	BELL Repl. by JEN 06
9.2 $^{+2.6}_{-2.3} \pm 1.0$		¹ LU	02	BELL Repl. by WANG 04A
<4	90	¹ AUBERT	01G	BABR $e^+e^- \rightarrow \Upsilon(4S)$
1.5 $^{+7}_{-6} \pm 2$		¹ BERGFELD	98	CLE2 Repl. by JESSOP 00
¹ Assumes equal production of B^+ and B^0 at the $\Upsilon(4S)$.				

 $\Gamma(\omega K^*(892)^+)/\Gamma_{\text{total}}$ Γ_{216}/Γ

VALUE (units 10^{-6})	CL%	DOCUMENT ID	TECN	COMMENT
< 3.4		¹ AUBERT,B	06T	BABR $e^+e^- \rightarrow \Upsilon(4S)$
• • • We do not use the following data for averages, fits, limits, etc. • • •				
< 7.4	90	¹ AUBERT	05o	BABR Repl. by AUBERT,B 06T
<87	90	¹ BERGFELD	98	CLE2
¹ Assumes equal production of B^+ and B^0 at the $\Upsilon(4S)$.				

 $\Gamma(a_0(980)^0 K^+ \times B(a_0(980)^0 \rightarrow \eta\pi^0))/\Gamma_{\text{total}}$ Γ_{218}/Γ

VALUE (units 10^{-6})	CL%	DOCUMENT ID	TECN	COMMENT
<2.5		¹ AUBERT,BE	04	BABR $e^+e^- \rightarrow \Upsilon(4S)$
¹ Assumes equal production of charged and neutral B mesons from $\Upsilon(4S)$ decays.				

 $\Gamma(a_0(980)^+ K^0 \times B(a_0(980)^+ \rightarrow \eta\pi^+))/\Gamma_{\text{total}}$ Γ_{217}/Γ

VALUE (units 10^{-6})	CL%	DOCUMENT ID	TECN	COMMENT
<3.9		¹ AUBERT,BE	04	BABR $e^+e^- \rightarrow \Upsilon(4S)$
¹ Assumes equal production of charged and neutral B mesons from $\Upsilon(4S)$ decays.				

 $\Gamma(K^*(892)^0\pi^+)/\Gamma_{\text{total}}$ Γ_{219}/Γ

VALUE (units 10^{-6})	CL%	DOCUMENT ID	TECN	COMMENT
10.9 ± 1.8 OUR AVERAGE				Error includes scale factor of 2.1.
9.67 ± 0.64 $^{+0.81}_{-0.89}$		¹ GARMASH	06	BELL $e^+e^- \rightarrow \Upsilon(4S)$
13.5 ± 1.2 $^{+0.8}_{-0.9}$		¹ AUBERT,B	05N	BABR $e^+e^- \rightarrow \Upsilon(4S)$
• • • We do not use the following data for averages, fits, limits, etc. • • •				
9.8 ± 0.9 $^{+1.1}_{-1.2}$		¹ GARMASH	05	BELL Repl. by GARMASH 06
15.5 ± 1.8 $^{+1.5}_{-4.0}$		^{1,2} AUBERT,B	04P	BABR Repl. by AUBERT,B 05N
19.4 $^{+4.2}_{-3.9} \pm 4.1$		³ GARMASH	02	BELL Repl. by GARMASH 05
<119	90	⁴ ABE	00c	SLD $e^+e^- \rightarrow Z$
< 16	90	¹ JESSOP	00	CLE2 $e^+e^- \rightarrow \Upsilon(4S)$
<390	90	⁵ ADAM	96D	DLPH $e^+e^- \rightarrow Z$
< 41	90	⁵ ASNER	96	CLE2 Repl. by JESSOP 00
<480	90	⁵ ABREU	95N	DLPH Sup. by ADAM 96D
<170	90	ALBRECHT	91B	ARG $e^+e^- \rightarrow \Upsilon(4S)$
<150	90	⁶ AVERY	89B	CLEO $e^+e^- \rightarrow \Upsilon(4S)$
<260	90	AVERY	87	CLEO $e^+e^- \rightarrow \Upsilon(4S)$

- ¹ Assumes equal production of B^+ and B^0 at the $\Upsilon(4S)$.
- ² AUBERT 04P also report a branching ratio for $B^+ \rightarrow \text{"higher } K^* \text{ resonances"} \pi^+$, $K^* \rightarrow K^+\pi^-$, $(25.1 \pm 2.0^{+11.0}_{-5.7}) \times 10^{-6}$.
- ³ Uses a reference decay mode $B^+ \rightarrow \bar{D}^0\pi^+$ and $\bar{D}^0 \rightarrow K^+\pi^-$ with $B(B^+ \rightarrow \bar{D}^0\pi^+) \cdot B(\bar{D}^0 \rightarrow K^+\pi^-) = (20.3 \pm 2.0) \times 10^{-5}$.
- ⁴ ABE 00c assumes $B(Z \rightarrow b\bar{b}) = (21.7 \pm 0.1)\%$ and the B fractions $f_{B^0} = f_{B^+} = (39.7^{+1.8}_{-2.2})\%$ and $f_{B_S} = (10.5^{+1.8}_{-2.2})\%$.
- ⁵ Assumes a B^0, B^- production fraction of 0.39 and a B_S production fraction of 0.12.
- ⁶ AVERY 89B reports $< 1.3 \times 10^{-4}$ assuming the $\Upsilon(4S)$ decays 43% to $B^0\bar{B}^0$. We rescale to 50%.

$\Gamma(K^*(892)^+\pi^0)/\Gamma_{\text{total}}$ Γ_{220}/Γ

VALUE (units 10^{-6})	CL%	DOCUMENT ID	TECN	COMMENT
$6.9 \pm 2.0 \pm 1.3$		¹ AUBERT	05X BABR	$e^+e^- \rightarrow \Upsilon(4S)$
••• We do not use the following data for averages, fits, limits, etc. •••				
<31	90	¹ JESSOP	00 CLE2	$e^+e^- \rightarrow \Upsilon(4S)$
<99	90	ASNER	96 CLE2	Repl. by JESSOP 00
¹ Assumes equal production of B^+ and B^0 at the $\Upsilon(4S)$.				

 $\Gamma(K^+\pi^-\pi^+)/\Gamma_{\text{total}}$ Γ_{221}/Γ

VALUE (units 10^{-6})	CL%	DOCUMENT ID	TECN	COMMENT
55 ± 7 OUR AVERAGE		Error includes scale factor of 2.6.		
$48.8 \pm 1.1 \pm 3.6$		¹ GARMASH	06 BELL	$e^+e^- \rightarrow \Upsilon(4S)$
$64.1 \pm 2.4 \pm 4.0$		¹ AUBERT,B	05N BABR	$e^+e^- \rightarrow \Upsilon(4S)$
••• We do not use the following data for averages, fits, limits, etc. •••				
$46.6 \pm 2.1 \pm 4.3$		¹ GARMASH	05 BELL	Repl. by GARMASH 06
$53.6 \pm 3.1 \pm 5.1$		² GARMASH	04 BELL	Repl. by GARMASH 05
$59.1 \pm 3.8 \pm 3.2$		² AUBERT	03M BABR	Repl. by AUBERT,B 05N
$55.6 \pm 5.8 \pm 7.7$		³ GARMASH	02 BELL	Repl. by GARMASH 04
¹ Assumes equal production of B^+ and B^0 at the $\Upsilon(4S)$.				
² Assumes equal production of B^0 and B^+ at the $\Upsilon(4S)$; charm and charmonium contributions are subtracted, otherwise no assumptions about intermediate resonances.				
³ Uses a reference decay mode $B^+ \rightarrow \bar{D}^0\pi^+$ and $\bar{D}^0 \rightarrow K^+\pi^-$ with $B(B^+ \rightarrow \bar{D}^0\pi^+) \cdot B(\bar{D}^0 \rightarrow K^+\pi^-) = (20.3 \pm 2.0) \times 10^{-5}$.				

 $\Gamma(K^+\pi^-\pi^+ \text{nonresonant})/\Gamma_{\text{total}}$ Γ_{222}/Γ

VALUE (units 10^{-6})	CL%	DOCUMENT ID	TECN	COMMENT
6 ± 6 OUR AVERAGE		Error includes scale factor of 6.1.		
$16.9 \pm 1.3 \pm 1.7$		¹ GARMASH	06 BELL	$e^+e^- \rightarrow \Upsilon(4S)$
$2.9 \pm 0.6 \pm 0.8$		¹ AUBERT,B	05N BABR	$e^+e^- \rightarrow \Upsilon(4S)$
••• We do not use the following data for averages, fits, limits, etc. •••				
$17.3 \pm 1.7 \pm 17.2$		¹ GARMASH	05 BELL	Repl. by GARMASH 06
< 17	90	¹ AUBERT,B	04P BABR	Repl. by AUBERT,B 05N
<330	90	² ADAM	96D DLPH	$e^+e^- \rightarrow Z$
< 28	90	BERGFELD	96B CLE2	$e^+e^- \rightarrow \Upsilon(4S)$
<400	90	² AUBERT	95N DLPH	Sup. by ADAM 96D
<330	90	ALBRECHT	91E ARG	$e^+e^- \rightarrow \Upsilon(4S)$
<190	90	³ AVERY	89B CLEO	$e^+e^- \rightarrow \Upsilon(4S)$
¹ Assumes equal production of B^+ and B^0 at the $\Upsilon(4S)$.				
² Assumes a B^0, B^- production fraction of 0.39 and a B_S production fraction of 0.12.				
³ AVERY 89B reports $< 1.7 \times 10^{-4}$ assuming the $\Upsilon(4S)$ decays 43% to $B^0\bar{B}^0$. We rescale to 50%.				

 $\Gamma(K^+\rho(980) \times B(\rho(980) \rightarrow \pi^+\pi^-))/\Gamma_{\text{total}}$ Γ_{223}/Γ

VALUE (units 10^{-6})	CL%	DOCUMENT ID	TECN	COMMENT
9.2 ± 0.8 OUR AVERAGE				
$8.78 \pm 0.82 \pm 0.85$		¹ GARMASH	06 BELL	$e^+e^- \rightarrow \Upsilon(4S)$
$9.47 \pm 0.97 \pm 0.62$		¹ AUBERT,B	05N BABR	$e^+e^- \rightarrow \Upsilon(4S)$
••• We do not use the following data for averages, fits, limits, etc. •••				
$7.55 \pm 1.24 \pm 1.63$		¹ GARMASH	05 BELL	Repl. by GARMASH 06
$9.2 \pm 1.2 \pm 2.1$		² AUBERT,B	04P BABR	Repl. by AUBERT,B 05N
$9.6 \pm 2.5 \pm 3.7$		³ GARMASH	02 BELL	Repl. by GARMASH 05
<80	90	⁴ AVERY	89B CLEO	$e^+e^- \rightarrow \Upsilon(4S)$
¹ Assumes equal production of B^+ and B^0 at the $\Upsilon(4S)$.				
² AUBERT,B 04P also reports $B(B^+ \rightarrow \text{"higher } f^0 \text{ resonances"} \pi^+, f(980)^0 \rightarrow \pi^+\pi^-) = (3.2 \pm 1.2 \pm 2.9) \times 10^{-6}$.				
³ Uses a reference decay mode $B^+ \rightarrow \bar{D}^0\pi^+$ and $\bar{D}^0 \rightarrow K^+\pi^-$ with $B(B^+ \rightarrow \bar{D}^0\pi^+) \cdot B(\bar{D}^0 \rightarrow K^+\pi^-) = (20.3 \pm 2.0) \times 10^{-5}$. Only charged pions from the $f_0(980)$ are used.				
⁴ AVERY 89B reports $< 7 \times 10^{-5}$ assuming the $\Upsilon(4S)$ decays 43% to $B^0\bar{B}^0$. We rescale to 50%.				

 $\Gamma(f_2(1270)^0 K^+)/\Gamma_{\text{total}}$ Γ_{224}/Γ

VALUE (units 10^{-6})	CL%	DOCUMENT ID	TECN	COMMENT
$1.33 \pm 0.30 \pm 0.23$ OUR AVERAGE				
$1.33 \pm 0.30 \pm 0.23$		¹ GARMASH	06 BELL	$e^+e^- \rightarrow \Upsilon(4S)$
••• We do not use the following data for averages, fits, limits, etc. •••				
<16	90	² AUBERT,B	05N BABR	$e^+e^- \rightarrow \Upsilon(4S)$
< 2.3	90	³ GARMASH	05 BELL	Repl. by GARMASH 06
¹ Assumes equal production of B^+ and B^0 at the $\Upsilon(4S)$.				
² AUBERT,B 05N reports 8.9×10^{-6} at 90% CL for $B(B^+ \rightarrow f_2(1270)\pi^+) \times B(f_2(1270) \rightarrow \pi^+\pi^-)$. We rescaled it using the PDG value $B(f_2(1270) \rightarrow \pi\pi) = 84.7\%$ and 2/3 for the $K^+\pi^-$ fraction.				
³ GARMASH 05 reports 1.3×10^{-6} at 90% CL for $B(B^+ \rightarrow f_2(1270)\pi^+) \times B(f_2(1270) \rightarrow \pi^+\pi^-)$. We rescaled it using the PDG value $B(f_2(1270) \rightarrow \pi\pi) = 84.7\%$ and 2/3 for the $\pi^+\pi^-$ fraction.				

 $\Gamma(\rho(1370)^0 K^+ \times B(\rho(1370)^0 \rightarrow \pi^+\pi^-))/\Gamma_{\text{total}}$ Γ_{225}/Γ

VALUE	CL%	DOCUMENT ID	TECN	COMMENT
$< 10.7 \times 10^{-6}$	90	¹ AUBERT,B	05N BABR	$e^+e^- \rightarrow \Upsilon(4S)$
¹ Assumes equal production of B^+ and B^0 at the $\Upsilon(4S)$.				

 $\Gamma(\rho^0(1450) K^+ \times B(\rho^0(1450) \rightarrow \pi^+\pi^-))/\Gamma_{\text{total}}$ Γ_{226}/Γ

VALUE	CL%	DOCUMENT ID	TECN	COMMENT
$< 11.7 \times 10^{-6}$	90	¹ AUBERT,B	05N BABR	$e^+e^- \rightarrow \Upsilon(4S)$
¹ Assumes equal production of B^+ and B^0 at the $\Upsilon(4S)$.				

 $\Gamma(f_0(1500) K^+ \times B(f_0(1500) \rightarrow \pi^+\pi^-))/\Gamma_{\text{total}}$ Γ_{227}/Γ

VALUE	CL%	DOCUMENT ID	TECN	COMMENT
$< 4.4 \times 10^{-6}$	90	¹ AUBERT,B	05N BABR	$e^+e^- \rightarrow \Upsilon(4S)$
¹ Assumes equal production of B^+ and B^0 at the $\Upsilon(4S)$.				

 $\Gamma(f_2'(1525) K^+ \times B(f_2'(1525) \rightarrow \pi^+\pi^-))/\Gamma_{\text{total}}$ Γ_{228}/Γ

VALUE	CL%	DOCUMENT ID	TECN	COMMENT
$< 3.4 \times 10^{-6}$	90	¹ AUBERT,B	05N BABR	$e^+e^- \rightarrow \Upsilon(4S)$
¹ Assumes equal production of B^+ and B^0 at the $\Upsilon(4S)$.				

 $\Gamma(K^+\rho^0)/\Gamma_{\text{total}}$ Γ_{229}/Γ

VALUE (units 10^{-6})	CL%	DOCUMENT ID	TECN	COMMENT
4.2 ± 0.5 OUR AVERAGE				
$3.89 \pm 0.47 \pm 0.43$		¹ GARMASH	06 BELL	$e^+e^- \rightarrow \Upsilon(4S)$
$5.07 \pm 0.75 \pm 0.55$		¹ AUBERT,B	05N BABR	$e^+e^- \rightarrow \Upsilon(4S)$
••• We do not use the following data for averages, fits, limits, etc. •••				
$4.78 \pm 0.75 \pm 1.01$		¹ GARMASH	05 BELL	Repl. by GARMASH 06
< 6.2	90	² AUBERT,B	04P BABR	Repl. by AUBERT,B 05N
< 12	90	³ GARMASH	02 BELL	$e^+e^- \rightarrow \Upsilon(4S)$
< 86	90	⁴ ABE	00C SLD	$e^+e^- \rightarrow Z$
< 17	90	¹ JESSOP	00 CLE2	$e^+e^- \rightarrow \Upsilon(4S)$
<120	90	⁵ ADAM	96D DLPH	$e^+e^- \rightarrow Z$
< 19	90	ASNER	96 CLE2	Repl. by JESSOP 00
<190	90	⁵ ABREU	95N DLPH	Sup. by ADAM 96D
<180	90	ALBRECHT	91B ARG	$e^+e^- \rightarrow \Upsilon(4S)$
< 80	90	⁶ AVERY	89B CLEO	$e^+e^- \rightarrow \Upsilon(4S)$
<260	90	AVERY	87 CLEO	$e^+e^- \rightarrow \Upsilon(4S)$

- ¹ Assumes equal production of B^+ and B^0 at the $\Upsilon(4S)$.
- ² AUBERT,B 04P reports a central value of $(3.9 \pm 1.2 \pm 1.3) \times 10^{-6}$ for this branching ratio.
- ³ Uses a reference decay mode $B^+ \rightarrow \bar{D}^0\pi^+$ and $\bar{D}^0 \rightarrow K^+\pi^-$ with $B(B^+ \rightarrow \bar{D}^0\pi^+) \cdot B(\bar{D}^0 \rightarrow K^+\pi^-) = (20.3 \pm 2.0) \times 10^{-5}$.
- ⁴ ABE 00C assumes $B(Z \rightarrow b\bar{b}) = (21.7 \pm 0.1)\%$ and the B fractions $f_{B^0} = f_{B^+} = (39.7 \pm 1.8)\%$ and $f_{B_S} = (10.5 \pm 1.9)\%$.
- ⁵ Assumes production fractions $f_{B^0} = f_{B^-} = 0.39$ and $f_{B_S} = 0.12$.
- ⁶ AVERY 89B reports $< 7 \times 10^{-5}$ assuming the $\Upsilon(4S)$ decays 43% to $B^0\bar{B}^0$. We rescale to 50%.

 $\Gamma(K_2^0(1430)^0 \pi^+)/\Gamma_{\text{total}}$ Γ_{230}/Γ

VALUE (units 10^{-6})	CL%	DOCUMENT ID	TECN	COMMENT
47 ± 5 OUR AVERAGE				
$51.6 \pm 1.7 \pm 7.0$		¹ GARMASH	06 BELL	$e^+e^- \rightarrow \Upsilon(4S)$
$44.4 \pm 2.2 \pm 5.3$		^{1,2} AUBERT,B	05N BABR	$e^+e^- \rightarrow \Upsilon(4S)$
••• We do not use the following data for averages, fits, limits, etc. •••				
$45.0 \pm 2.9 \pm 15.0$		¹ GARMASH	05 BELL	Repl. by GARMASH 06

- ¹ Assumes equal production of B^+ and B^0 at the $\Upsilon(4S)$.
- ² See erratum: AUBERT,BE 06A.

 $\Gamma(K_2^*(1430)^0 \pi^+)/\Gamma_{\text{total}}$ Γ_{231}/Γ

VALUE (units 10^{-6})	CL%	DOCUMENT ID	TECN	COMMENT
< 6.9	90	¹ GARMASH	05 BELL	$e^+e^- \rightarrow \Upsilon(4S)$
••• We do not use the following data for averages, fits, limits, etc. •••				
< 23	90	² AUBERT,B	05N BABR	$e^+e^- \rightarrow \Upsilon(4S)$
<680	90	ALBRECHT	91B ARG	$e^+e^- \rightarrow \Upsilon(4S)$

- ¹ GARMASH 05 reports 2.3×10^{-6} at 90% CL for $B(B^+ \rightarrow K_2^*(1430)^0 \pi^+) \times B(K_2^*(1430)^0 \rightarrow \pi^+\pi^-)$. We rescaled it using the PDG value $B(K_2^*(1430)^0 \rightarrow K\pi) = 49.9\%$ and 2/3 for the $K^+\pi^-$ mode.
- ² AUBERT,B 05N reports 7.7×10^{-6} at 90% CL for $B(B^+ \rightarrow K_2^*(1430)^0 \pi^+) \times B(K_2^*(1430)^0 \rightarrow \pi^+\pi^-)$. We rescaled it using the PDG value $B(K_2^*(1430)^0 \rightarrow K\pi) = 49.9\%$ and 2/3 for the $K^+\pi^-$ fraction.

 $\Gamma(K^*(1410)^0 \pi^+)/\Gamma_{\text{total}}$ Γ_{232}/Γ

VALUE (units 10^{-6})	CL%	DOCUMENT ID	TECN	COMMENT
< 45	90	¹ GARMASH	05 BELL	$e^+e^- \rightarrow \Upsilon(4S)$
¹ GARMASH 05 reports 2.0×10^{-6} at 90% CL for $B(B^+ \rightarrow K^*(1410)^0 \pi^+) \times B(K^*(1410)^0 \rightarrow \pi^+\pi^-)$. We rescaled it using the PDG value $B(K^*(1410)^0 \rightarrow K\pi) = 6.6\%$ and 2/3 for the $K^+\pi^-$ mode.				

Meson Particle Listings

 B^\pm $\Gamma(K^*(1680)^0 \pi^+)/\Gamma_{\text{total}}$ Γ_{233}/Γ

VALUE (units 10^{-6})	CL%	DOCUMENT ID	TECN	COMMENT
<12	90	¹ GARMASH 05	BELL	$e^+e^- \rightarrow \Upsilon(4S)$
••• We do not use the following data for averages, fits, limits, etc. •••				
<15	90	² AUBERT,B 05N	BABR	$e^+e^- \rightarrow \Upsilon(4S)$
¹ GARMASH 05 reports 3.1×10^{-6} at 90% CL for $B(B^+ \rightarrow K^*(1680)^0 \pi^+) \times B(K^*(1680)^0 \rightarrow K^+ \pi^-)$. We rescaled it using the PDG value $B(K^*(1680)^0 \rightarrow K \pi) = 38.7\%$ and 2/3 for the $K^+ \pi^-$ mode.				
² AUBERT,B 05N reports 3.8×10^{-6} at 90% CL for $B(B^+ \rightarrow K^*(1680)^0 \pi^+) \times B(K^*(1680)^0 \rightarrow K^+ \pi^-)$. We rescaled it using the PDG value $B(K^*(1680)^0 \rightarrow K \pi) = 38.7\%$ and 2/3 for the $K^+ \pi^-$ fraction.				

 $\Gamma(K^- \pi^+ \pi^+)/\Gamma_{\text{total}}$ Γ_{234}/Γ

VALUE (units 10^{-6})	CL%	DOCUMENT ID	TECN	COMMENT
<1.8	90	¹ AUBERT 03M	BABR	$e^+e^- \rightarrow \Upsilon(4S)$
••• We do not use the following data for averages, fits, limits, etc. •••				
<4.5	90	² GARMASH 04	BELL	$e^+e^- \rightarrow \Upsilon(4S)$
<7.0	90	³ GARMASH 02	BELL	$e^+e^- \rightarrow \Upsilon(4S)$
¹ Assumes equal production of B^0 and B^+ at the $\Upsilon(4S)$; charm and charmonium contributions are subtracted, otherwise no assumptions about intermediate resonances.				
² Assumes equal production of B^+ and B^0 at the $\Upsilon(4S)$.				
³ Uses a reference decay mode $B^+ \rightarrow \bar{D}^0 \pi^+$ and $\bar{D}^0 \rightarrow K^+ \pi^-$ with $B(B^+ \rightarrow \bar{D}^0 \pi^+) \cdot B(\bar{D}^0 \rightarrow K^+ \pi^-) = (20.3 \pm 2.0) \times 10^{-5}$.				

 $\Gamma(K^- \pi^+ \pi^+ \text{nonresonant})/\Gamma_{\text{total}}$ Γ_{235}/Γ

VALUE (units 10^{-6})	CL%	DOCUMENT ID	TECN	COMMENT
<56	90	BERGFELD 96B	CLE2	$e^+e^- \rightarrow \Upsilon(4S)$

 $\Gamma(K_1^-(1400)^0 \pi^+)/\Gamma_{\text{total}}$ Γ_{236}/Γ

VALUE	CL%	DOCUMENT ID	TECN	COMMENT
<2.6 $\times 10^{-3}$	90	ALBRECHT 91B	ARG	$e^+e^- \rightarrow \Upsilon(4S)$

 $\Gamma(K^0 \pi^+ \pi^0)/\Gamma_{\text{total}}$ Γ_{237}/Γ

VALUE	CL%	DOCUMENT ID	TECN	COMMENT
<66 $\times 10^{-6}$	90	¹ ECKHART 02	CLE2	$e^+e^- \rightarrow \Upsilon(4S)$
¹ Assumes equal production of B^+ and B^0 at the $\Upsilon(4S)$.				

 $\Gamma(K^0 \rho^+)/\Gamma_{\text{total}}$ Γ_{238}/Γ

VALUE (units 10^{-6})	CL%	DOCUMENT ID	TECN	COMMENT
$8.0^{+1.4}_{-1.3} \pm 0.6$		AUBERT 07Z	BABR	$e^+e^- \rightarrow \Upsilon(4S)$
••• We do not use the following data for averages, fits, limits, etc. •••				
<48	90	ASNER 96	CLE2	$e^+e^- \rightarrow \Upsilon(4S)$

 $\Gamma(K^*(892)^+ \pi^+ \pi^-)/\Gamma_{\text{total}}$ Γ_{239}/Γ

VALUE (units 10^{-6})	CL%	DOCUMENT ID	TECN	COMMENT
$75.3 \pm 6.0 \pm 8.1$		¹ AUBERT,B 06U	BABR	$e^+e^- \rightarrow \Upsilon(4S)$
••• We do not use the following data for averages, fits, limits, etc. •••				
<1100	90	ALBRECHT 91E	ARG	$e^+e^- \rightarrow \Upsilon(4S)$
¹ Assumes equal production of B^+ and B^0 at the $\Upsilon(4S)$.				

 $\Gamma(K^*(892)^+ \rho^+)/\Gamma_{\text{total}}$ Γ_{240}/Γ

VALUE (units 10^{-6})	CL%	DOCUMENT ID	TECN	COMMENT
< 6.1	90	¹ AUBERT,B 06G	BABR	$e^+e^- \rightarrow \Upsilon(4S)$
••• We do not use the following data for averages, fits, limits, etc. •••				
$10.6^{+3.0}_{-2.6} \pm 2.4$		¹ AUBERT 03V	BABR	Repl. by AUBERT,B 06G
< 74	90	² GODANG 02	CLE2	$e^+e^- \rightarrow \Upsilon(4S)$
<900	90	ALBRECHT 91B	ARG	$e^+e^- \rightarrow \Upsilon(4S)$
¹ Assumes equal production of B^+ and B^0 at the $\Upsilon(4S)$.				
² Assumes a helicity 00 configuration. For a helicity 11 configuration, the limit decreases to 4.9×10^{-5} .				

 $\Gamma(K^*(892)^+ f_0(980))/\Gamma_{\text{total}}$ Γ_{241}/Γ

VALUE (units 10^{-6})	CL%	DOCUMENT ID	TECN	COMMENT
$5.2 \pm 1.2 \pm 0.5$		¹ AUBERT,B 06G	BABR	$e^+e^- \rightarrow \Upsilon(4S)$
¹ Assumes equal production of B^+ and B^0 at the $\Upsilon(4S)$.				

 $\Gamma(a_1^+ K^0)/\Gamma_{\text{total}}$ Γ_{242}/Γ

VALUE (units 10^{-6})	CL%	DOCUMENT ID	TECN	COMMENT
$34.9 \pm 5.0 \pm 4.4$		^{1,2} AUBERT 08F	BABR	$e^+e^- \rightarrow \Upsilon(4S)$
¹ Assumes equal production of B^+ and B^0 at the $\Upsilon(4S)$.				
² Assumes a_1^\pm decays only to 3π and $B(a_1^\pm \rightarrow \pi^\pm \pi^0 \pi^\pm) = 0.5$.				

 $\Gamma(K^*(892)^0 \rho^+)/\Gamma_{\text{total}}$ Γ_{243}/Γ

VALUE (units 10^{-6})	CL%	DOCUMENT ID	TECN	COMMENT
9.2 ± 1.5 OUR AVERAGE				
$9.6 \pm 1.7 \pm 1.5$		¹ AUBERT,B 06G	BABR	$e^+e^- \rightarrow \Upsilon(4S)$
$8.9 \pm 1.7 \pm 1.2$		¹ ZHANG 05D	BELL	$e^+e^- \rightarrow \Upsilon(4S)$
¹ Assumes equal production of B^+ and B^0 at the $\Upsilon(4S)$.				

 $\Gamma(K^*(892)^+ K^*(892)^0)/\Gamma_{\text{total}}$ Γ_{244}/Γ

VALUE (units 10^{-6})	CL%	DOCUMENT ID	TECN	COMMENT
<71	90	¹ GODANG 02	CLE2	$e^+e^- \rightarrow \Upsilon(4S)$
¹ Assumes a helicity 00 configuration. For a helicity 11 configuration, the limit decreases to 4.8×10^{-5} .				

 $\Gamma(K_1^-(1400)^+ \rho^0)/\Gamma_{\text{total}}$ Γ_{245}/Γ

VALUE	CL%	DOCUMENT ID	TECN	COMMENT
<7.8 $\times 10^{-4}$	90	ALBRECHT 91B	ARG	$e^+e^- \rightarrow \Upsilon(4S)$

 $\Gamma(K_2^-(1430)^+ \rho^0)/\Gamma_{\text{total}}$ Γ_{246}/Γ

VALUE	CL%	DOCUMENT ID	TECN	COMMENT
<1.5 $\times 10^{-3}$	90	ALBRECHT 91B	ARG	$e^+e^- \rightarrow \Upsilon(4S)$

 $\Gamma(K^+ \bar{K}^0)/\Gamma_{\text{total}}$ Γ_{247}/Γ

VALUE (units 10^{-6})	CL%	DOCUMENT ID	TECN	COMMENT
1.36 ± 0.27 OUR AVERAGE				
$1.22^{+0.32+0.13}_{-0.28-0.16}$		¹ LIN 07	BELL	$e^+e^- \rightarrow \Upsilon(4S)$
$1.61 \pm 0.44 \pm 0.09$		¹ AUBERT,BE 06C	BABR	$e^+e^- \rightarrow \Upsilon(4S)$
••• We do not use the following data for averages, fits, limits, etc. •••				
$1.0 \pm 0.4 \pm 0.1$		¹ ABE 05G	BELL	Repl. by LIN 07
$1.5 \pm 0.5 \pm 0.1$		¹ AUBERT,BE 05E	BABR	Repl. by AUBERT,BE 06C
< 2.5	90	¹ AUBERT 04M	BABR	Repl. by AUBERT,BE 05E
< 3.3	90	¹ CHAO 04	BELL	$e^+e^- \rightarrow \Upsilon(4S)$
< 3.3	90	¹ BORNHEIM 03	CLE2	$e^+e^- \rightarrow \Upsilon(4S)$
< 2.0	90	¹ CASEY 02	BELL	Repl. by CHAO 04
< 5.0	90	¹ ABE 01H	BELL	$e^+e^- \rightarrow \Upsilon(4S)$
< 2.4	90	¹ AUBERT 01E	BABR	$e^+e^- \rightarrow \Upsilon(4S)$
< 5.1	90	¹ CRONIN-HEN.00	CLE2	$e^+e^- \rightarrow \Upsilon(4S)$
<21	90	GODANG 98	CLE2	Repl. by CRONIN-HENNESSY 00
¹ Assumes equal production of B^+ and B^0 at the $\Upsilon(4S)$.				

 $\Gamma(\bar{K}^0 K^+ \pi^0)/\Gamma_{\text{total}}$ Γ_{248}/Γ

VALUE	CL%	DOCUMENT ID	TECN	COMMENT
<24 $\times 10^{-6}$	90	¹ ECKHART 02	CLE2	$e^+e^- \rightarrow \Upsilon(4S)$
¹ Assumes equal production of B^+ and B^0 at the $\Upsilon(4S)$.				

 $\Gamma(K^+ K_S^0 K_S^0)/\Gamma_{\text{total}}$ Γ_{249}/Γ

VALUE (units 10^{-6})	CL%	DOCUMENT ID	TECN	COMMENT
11.5 ± 1.3 OUR AVERAGE				
$10.7 \pm 1.2 \pm 1.0$		¹ AUBERT,B 04V	BABR	$e^+e^- \rightarrow \Upsilon(4S)$
$13.4 \pm 1.9 \pm 1.5$		¹ GARMASH 04	BELL	$e^+e^- \rightarrow \Upsilon(4S)$
¹ Assumes equal production of B^+ and B^0 at the $\Upsilon(4S)$.				

 $\Gamma(K_S^0 K_S^0 \pi^+)/\Gamma_{\text{total}}$ Γ_{250}/Γ

VALUE (units 10^{-6})	CL%	DOCUMENT ID	TECN	COMMENT
<3.2	90	¹ GARMASH 04	BELL	$e^+e^- \rightarrow \Upsilon(4S)$
¹ Assumes equal production of B^+ and B^0 at the $\Upsilon(4S)$.				

 $\Gamma(K^+ K^- \pi^+)/\Gamma_{\text{total}}$ Γ_{251}/Γ

VALUE (units 10^{-6})	CL%	DOCUMENT ID	TECN	COMMENT
$5.0 \pm 0.5 \pm 0.5$		¹ AUBERT 07BB	BABR	$e^+e^- \rightarrow \Upsilon(4S)$
••• We do not use the following data for averages, fits, limits, etc. •••				
<13	90	¹ GARMASH 04	BELL	$e^+e^- \rightarrow \Upsilon(4S)$
< 6.3	90	^{1,2} AUBERT 03M	BABR	Repl. by AUBERT 07BB
<12	90	³ GARMASH 02	BELL	$e^+e^- \rightarrow \Upsilon(4S)$
¹ Assumes equal production of B^+ and B^0 at the $\Upsilon(4S)$.				
² Charm and charmonium contributions are subtracted, otherwise no assumptions about intermediate resonances.				
³ Uses a reference decay mode $B^+ \rightarrow \bar{D}^0 \pi^+$ and $\bar{D}^0 \rightarrow K^+ \pi^-$ with $B(B^+ \rightarrow \bar{D}^0 \pi^+) \cdot B(\bar{D}^0 \rightarrow K^+ \pi^-) = (20.3 \pm 2.0) \times 10^{-5}$.				

 $\Gamma(K^+ K^- \pi^+ \text{nonresonant})/\Gamma_{\text{total}}$ Γ_{252}/Γ

VALUE (units 10^{-6})	CL%	DOCUMENT ID	TECN	COMMENT
<75	90	BERGFELD 96B	CLE2	$e^+e^- \rightarrow \Upsilon(4S)$

 $\Gamma(K^+ \bar{K}^*(892)^0)/\Gamma_{\text{total}}$ Γ_{253}/Γ

VALUE (units 10^{-6})	CL%	DOCUMENT ID	TECN	COMMENT
< 1.1	90	¹ AUBERT 07AR	BABR	$e^+e^- \rightarrow \Upsilon(4S)$
••• We do not use the following data for averages, fits, limits, etc. •••				
<129	90	ABBIENDI 00B	OPAL	$e^+e^- \rightarrow Z$
<138	90	² ABE 00C	SLD	$e^+e^- \rightarrow Z$
< 5.3	90	¹ JESSOP 00	CLE2	$e^+e^- \rightarrow \Upsilon(4S)$
¹ Assumes equal production of B^+ and B^0 at the $\Upsilon(4S)$.				
² ABE 00C assumes $B(Z \rightarrow b\bar{b}) = (21.7 \pm 0.1)\%$ and the B fractions $f_{B^0} = f_{B^+} = (39.7^{+1.8}_{-2.2})\%$ and $f_{B_s} = (10.5^{+1.8}_{-2.2})\%$.				

See key on page 373

Meson Particle Listings

 B^{\pm} $\Gamma(K^+ \bar{K}_s^0(1430)^0)/\Gamma_{\text{total}}$ Γ_{254}/Γ

VALUE (units 10^{-6})	CL%	DOCUMENT ID	TECN	COMMENT
<2.2	90	¹ AUBERT	07AR	BABR $e^+e^- \rightarrow \Upsilon(4S)$

¹ Assumes equal production of B^+ and B^0 at the $\Upsilon(4S)$. $\Gamma(K^+ K^+ \pi^-)/\Gamma_{\text{total}}$ Γ_{255}/Γ

VALUE	CL%	DOCUMENT ID	TECN	COMMENT
<1.3 $\times 10^{-6}$	90	¹ AUBERT	03M	BABR $e^+e^- \rightarrow \Upsilon(4S)$
<2.4 $\times 10^{-6}$	90	² GARMASH	04	BELL $e^+e^- \rightarrow \Upsilon(4S)$
<3.2 $\times 10^{-6}$	90	³ GARMASH	02	BELL $e^+e^- \rightarrow \Upsilon(4S)$

¹ Assumes equal production of B^0 and B^+ at the $\Upsilon(4S)$; charm and charmonium contributions are subtracted, otherwise no assumptions about intermediate resonances.² Assumes equal production of B^+ and B^0 at the $\Upsilon(4S)$.³ Uses a reference decay mode $B^+ \rightarrow \bar{D}^0 \pi^+$ and $\bar{D}^0 \rightarrow K^+ \pi^-$ with $B(B^+ \rightarrow \bar{D}^0 \pi^+) \cdot B(\bar{D}^0 \rightarrow K^+ \pi^-) = (20.3 \pm 2.0) \times 10^{-5}$. $\Gamma(K^+ K^+ \pi^- \text{ nonresonant})/\Gamma_{\text{total}}$ Γ_{256}/Γ

VALUE (units 10^{-6})	CL%	DOCUMENT ID	TECN	COMMENT
<87.9	90	ABBIENDI	00B	OPAL $e^+e^- \rightarrow Z$

 $\Gamma(b_1^0 K^+ \times B(b_1^0 \rightarrow \omega \pi^0))/\Gamma_{\text{total}}$ Γ_{257}/Γ

VALUE (units 10^{-6})	DOCUMENT ID	TECN	COMMENT
9.1 $\pm 1.7 \pm 1.0$	¹ AUBERT	07B1	BABR $e^+e^- \rightarrow \Upsilon(4S)$

¹ Assumes equal production of B^+ and B^0 at the $\Upsilon(4S)$. $\Gamma(K^+ f_J(2220))/\Gamma_{\text{total}}$ Γ_{258}/Γ

VALUE (units 10^{-6})	DOCUMENT ID	TECN	COMMENT
not seen	¹ HUANG	03	BELL $e^+e^- \rightarrow \Upsilon(4S)$

¹ No evidence is found for such decay and set a limit on $B(B^+ \rightarrow f_J(2220)) \times B(f_J(2220) \rightarrow \phi\phi) < 1.2 \times 10^{-6}$ at 90%CL where the $f_J(2220)$ is a possible glueball state. $\Gamma(K^{*+} \pi^+ K^-)/\Gamma_{\text{total}}$ Γ_{259}/Γ

VALUE (units 10^{-6})	DOCUMENT ID	TECN	COMMENT
<11.8	¹ AUBERT,B	06U	BABR $e^+e^- \rightarrow \Upsilon(4S)$

¹ Assumes equal production of B^+ and B^0 at the $\Upsilon(4S)$. $\Gamma(K^{*+} K^+ \pi^-)/\Gamma_{\text{total}}$ Γ_{260}/Γ

VALUE (units 10^{-6})	DOCUMENT ID	TECN	COMMENT
<6.1	¹ AUBERT,B	06U	BABR $e^+e^- \rightarrow \Upsilon(4S)$

¹ Assumes equal production of B^+ and B^0 at the $\Upsilon(4S)$. $\Gamma(K^+ K^- K^+)/\Gamma_{\text{total}}$ Γ_{261}/Γ

VALUE (units 10^{-6})	DOCUMENT ID	TECN	COMMENT
33.7 ± 2.2 OUR AVERAGE	Error includes scale factor of 1.4.		
35.2 $\pm 0.9 \pm 1.6$	¹ AUBERT	06O	BABR $e^+e^- \rightarrow \Upsilon(4S)$
30.6 $\pm 1.2 \pm 2.3$	¹ GARMASH	05	BELL $e^+e^- \rightarrow \Upsilon(4S)$
• • • We do not use the following data for averages, fits, limits, etc. • • •			
32.8 $\pm 1.8 \pm 2.8$	¹ GARMASH	04	BELL Repl. by GARMASH 05
29.6 $\pm 2.1 \pm 1.6$	² AUBERT	03M	BABR Repl. by AUBERT 06O
35.3 $\pm 3.7 \pm 4.5$	³ GARMASH	02	BELL Repl. by GARMASH 04
<200	90	ADAM	96D DLPH $e^+e^- \rightarrow Z$
<320	90	ABREU	95N DLPH Sup. by ADAM 96D
<350	90	ALBRECHT	91E ARG $e^+e^- \rightarrow \Upsilon(4S)$

¹ Assumes equal production of B^+ and B^0 at the $\Upsilon(4S)$.² Assumes equal production of B^0 and B^+ at the $\Upsilon(4S)$; charm and charmonium contributions are subtracted, otherwise no assumptions about intermediate resonances.³ Uses a reference decay mode $B^+ \rightarrow \bar{D}^0 \pi^+$ and $\bar{D}^0 \rightarrow K^+ \pi^-$ with $B(B^+ \rightarrow \bar{D}^0 \pi^+) \cdot B(\bar{D}^0 \rightarrow K^+ \pi^-) = (20.3 \pm 2.0) \times 10^{-5}$.⁴ Assumes B^0 and B^- production fractions of 0.39, and B_s production fraction of 0.12. $\Gamma(K^+ \phi)/\Gamma_{\text{total}}$ Γ_{262}/Γ

VALUE (units 10^{-6})	DOCUMENT ID	TECN	COMMENT
8.3 ± 0.7 OUR AVERAGE			
8.4 $\pm 0.7 \pm 0.7$	¹ AUBERT	06O	BABR $e^+e^- \rightarrow \Upsilon(4S)$
7.6 $\pm 1.3 \pm 0.6$	² ACOSTA	05J	CDF $p\bar{p}$ at 1.96 TeV
9.60 $\pm 0.92 \pm 1.05$ -0.85	¹ GARMASH	05	BELL $e^+e^- \rightarrow \Upsilon(4S)$
5.5 ± 2.1 -1.8 ± 0.6	¹ BRIERE	01	CLE2 $e^+e^- \rightarrow \Upsilon(4S)$

¹ We do not use the following data for averages, fits, limits, etc. • • •

10.0 ± 0.9 -0.8 ± 0.5	¹ AUBERT	04A	BABR Repl. by AUBERT 06O
9.4 $\pm 1.1 \pm 0.7$	¹ CHEN	03B	BELL Repl. by GARMASH 05
14.6 ± 3.0 -2.8 ± 2.0	³ GARMASH	02	BELL Repl. by CHEN 03B
7.7 ± 1.6 -1.4 ± 0.8	¹ AUBERT	01D	BABR $e^+e^- \rightarrow \Upsilon(4S)$
<144	90	ABE	00C SLD $e^+e^- \rightarrow Z$
< 5	90	BERGFELD	98 CLE2

<280	90	⁵ ADAM	96D DLPH $e^+e^- \rightarrow Z$
< 12	90	ASNER	96 CLE2 $e^+e^- \rightarrow \Upsilon(4S)$
<440	90	⁶ ABREU	95N DLPH Sup. by ADAM 96D
<180	90	ALBRECHT	91B ARG $e^+e^- \rightarrow \Upsilon(4S)$
< 90	90	⁷ AVERY	89B CLEO $e^+e^- \rightarrow \Upsilon(4S)$
<210	90	AVERY	87 CLEO $e^+e^- \rightarrow \Upsilon(4S)$

¹ Assumes equal production of B^+ and B^0 at the $\Upsilon(4S)$.² Uses $B(B^+ \rightarrow J/\psi K^+) = (1.00 \pm 0.04) \times 10^{-3}$ and $B(J/\psi \rightarrow \mu^+ \mu^-) = 0.0588 \pm 0.0010$.³ Uses a reference decay mode $B^+ \rightarrow \bar{D}^0 \pi^+$ and $\bar{D}^0 \rightarrow K^+ \pi^-$ with $B(B^+ \rightarrow \bar{D}^0 \pi^+) \cdot B(\bar{D}^0 \rightarrow K^+ \pi^-) = (20.3 \pm 2.0) \times 10^{-5}$.⁴ ABE 00c assumes $B(Z \rightarrow b\bar{b}) = (21.7 \pm 0.1)\%$ and the B fractions $f_{B^0} = f_{B^+} = (39.7 \pm 2.2)\%$ and $f_{B_s} = (10.5 \pm 1.8)\%$.⁵ ADAM 96D assumes $f_{B^0} = f_{B^-} = 0.39$ and $f_{B_s} = 0.12$.⁶ Assumes a B^0 , B^- production fraction of 0.39 and a B_s production fraction of 0.12.⁷ AVERY 89B reports $< 8 \times 10^{-5}$ assuming the $\Upsilon(4S)$ decays 43% to $B^0 \bar{B}^0$. We rescale to 50%. $\Gamma(f_0(980) K^+ \times B(f_0(980) \rightarrow K^+ K^-))/\Gamma_{\text{total}}$ Γ_{263}/Γ

VALUE (units 10^{-6})	DOCUMENT ID	TECN	COMMENT
<2.9	90	¹ GARMASH	05 BELL $e^+e^- \rightarrow \Upsilon(4S)$

¹ We do not use the following data for averages, fits, limits, etc. • • •6.5 $\pm 2.5 \pm 1.6$ ¹AUBERT 06O BABR $e^+e^- \rightarrow \Upsilon(4S)$ ¹ Assumes equal production of B^+ and B^0 at the $\Upsilon(4S)$. $\Gamma(a_2(1320) K^+ \times B(a_2(1320) \rightarrow K^+ K^-))/\Gamma_{\text{total}}$ Γ_{264}/Γ

VALUE	DOCUMENT ID	TECN	COMMENT
<1.1 $\times 10^{-6}$	¹ GARMASH	05	BELL $e^+e^- \rightarrow \Upsilon(4S)$

¹ Assumes equal production of B^+ and B^0 at the $\Upsilon(4S)$. $\Gamma(f_2'(1525) K^+ \times B(f_2'(1525) \rightarrow K^+ K^-))/\Gamma_{\text{total}}$ Γ_{265}/Γ

VALUE	DOCUMENT ID	TECN	COMMENT
<4.9 $\times 10^{-6}$	90	¹ GARMASH	05 BELL $e^+e^- \rightarrow \Upsilon(4S)$

¹ Assumes equal production of B^+ and B^0 at the $\Upsilon(4S)$. $\Gamma(X_0(1550) K^+ \times B(X_0(1550) \rightarrow K^+ K^-))/\Gamma_{\text{total}}$ Γ_{266}/Γ $X_0(1550)$ is a possible spin zero state near 1.55 GeV/ c^2 invariant mass of $K^+ K^+ K^-$.

VALUE (units 10^{-6})	DOCUMENT ID	TECN	COMMENT
4.3 $\pm 0.6 \pm 0.3$	¹ AUBERT	06O	BABR $e^+e^- \rightarrow \Upsilon(4S)$

¹ Assumes equal production of B^+ and B^0 at the $\Upsilon(4S)$. $\Gamma(\phi(1680) K^+ \times B(\phi(1680) \rightarrow K^+ K^-))/\Gamma_{\text{total}}$ Γ_{267}/Γ

VALUE	DOCUMENT ID	TECN	COMMENT
<0.8 $\times 10^{-6}$	90	¹ GARMASH	05 BELL $e^+e^- \rightarrow \Upsilon(4S)$

¹ Assumes equal production of B^+ and B^0 at the $\Upsilon(4S)$. $\Gamma(f_0(1710) K^+ \times B(f_0(1710) \rightarrow K^+ K^-))/\Gamma_{\text{total}}$ Γ_{268}/Γ

VALUE (units 10^{-6})	DOCUMENT ID	TECN	COMMENT
1.7 $\pm 1.0 \pm 0.3$	¹ AUBERT	06O	BABR $e^+e^- \rightarrow \Upsilon(4S)$

¹ Assumes equal production of B^+ and B^0 at the $\Upsilon(4S)$. $\Gamma(K^+ K^- K^+ \text{ nonresonant})/\Gamma_{\text{total}}$ Γ_{269}/Γ

VALUE (units 10^{-6})	DOCUMENT ID	TECN	COMMENT
28 ± 9 OUR AVERAGE	Error includes scale factor of 3.3.		
50.0 $\pm 6.0 \pm 4.0$	¹ AUBERT	06O	BABR $e^+e^- \rightarrow \Upsilon(4S)$
24.0 $\pm 1.5 \pm 2.6$ -6.0	¹ GARMASH	05	BELL $e^+e^- \rightarrow \Upsilon(4S)$

¹ We do not use the following data for averages, fits, limits, etc. • • •<38 90 BERGFELD 96B CLE2 $e^+e^- \rightarrow \Upsilon(4S)$ ¹ Assumes equal production of B^+ and B^0 at the $\Upsilon(4S)$. $\Gamma(K^*(892)^+ K^+ K^-)/\Gamma_{\text{total}}$ Γ_{270}/Γ

VALUE (units 10^{-6})	DOCUMENT ID	TECN	COMMENT
36.2 $\pm 3.3 \pm 3.6$	¹ AUBERT,B	06U	BABR $e^+e^- \rightarrow \Upsilon(4S)$

¹ We do not use the following data for averages, fits, limits, etc. • • •<1600 90 ALBRECHT 91E ARG $e^+e^- \rightarrow \Upsilon(4S)$ ¹ Assumes equal production of B^+ and B^0 at the $\Upsilon(4S)$. $\Gamma(K^*(892)^+ \phi)/\Gamma_{\text{total}}$ Γ_{271}/Γ

VALUE (units 10^{-6})	DOCUMENT ID	TECN	COMMENT
10.5 ± 1.5 OUR AVERAGE	Error includes scale factor of 1.4. See the ideogram below.		

11.2 $\pm 1.0 \pm 0.9$ ¹AUBERT 07BA BABR $e^+e^- \rightarrow \Upsilon(4S)$ 12.7 ± 2.2
-2.0 ± 1.1 ¹AUBERT 03V BABR $e^+e^- \rightarrow \Upsilon(4S)$ 6.7 ± 2.1
-1.9 ± 1.0 ¹CHEN 03B BELL $e^+e^- \rightarrow \Upsilon(4S)$

Meson Particle Listings

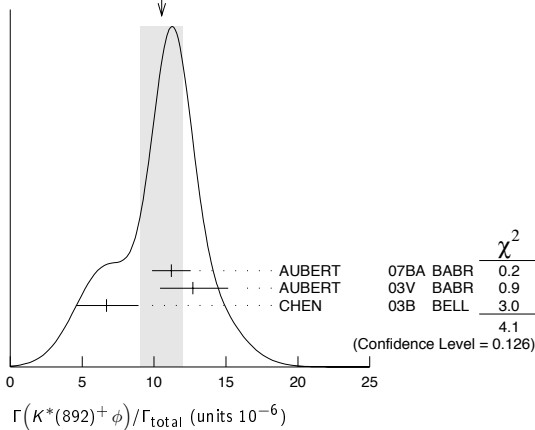
 B^\pm

• • • We do not use the following data for averages, fits, limits, etc. • • •

$9.7^{+4.2}_{-3.4} \pm 1.7$	1	AUBERT	01D	BABR	Repl. by AUBERT 03B
< 22.5	90	1	BRIERE	01	CLE2 $e^+e^- \rightarrow \Upsilon(4S)$
< 41	90	1	BERGFELD	98	CLE2
< 70	90		ASNER	96	CLE2 $e^+e^- \rightarrow \Upsilon(4S)$
< 1300	90		ALBRECHT	91B	ARG $e^+e^- \rightarrow \Upsilon(4S)$

¹ Assumes equal production of B^+ and B^0 at the $\Upsilon(4S)$.

WEIGHTED AVERAGE
10.5±1.5 (Error scaled by 1.4)



$\Gamma(K_1(1400)^+\phi)/\Gamma_{\text{total}}$					χ^2
VALUE (units 10^{-3})	CL%	DOCUMENT ID	TECN	COMMENT	
< 1.1 × 10 ⁻³	90	ALBRECHT	91B	ARG $e^+e^- \rightarrow \Upsilon(4S)$	0.2

Γ_{272}/Γ

$\Gamma(K_2^*(1430)^+\phi)/\Gamma_{\text{total}}$					
VALUE (units 10^{-3})	CL%	DOCUMENT ID	TECN	COMMENT	
< 3.4 × 10 ⁻³	90	ALBRECHT	91B	ARG $e^+e^- \rightarrow \Upsilon(4S)$	0.9

Γ_{273}/Γ

$\Gamma(K^+\phi\phi)/\Gamma_{\text{total}}$					
VALUE (units 10^{-6})	CL%	DOCUMENT ID	TECN	COMMENT	
4.9 ± 2.4	OUR AVERAGE				Error includes scale factor of 2.9.

Γ_{274}/Γ

7.5 ± 1.0 ± 0.7	1	AUBERT, BE	06H	BABR	$e^+e^- \rightarrow \Upsilon(4S)$
2.6 ± 1.1 ± 0.3	1	HUANG	03	BELL	$e^+e^- \rightarrow \Upsilon(4S)$

¹ Assumes equal production of B^0 and B^+ at the $\Upsilon(4S)$ and for a $\phi\phi$ invariant mass below 2.85 GeV/ c^2 .

$\Gamma(\eta'\eta'K^+)/\Gamma_{\text{total}}$					
VALUE (units 10^{-6})	CL%	DOCUMENT ID	TECN	COMMENT	
< 25	90	1	AUBERT, B	06P	BABR $e^+e^- \rightarrow \Upsilon(4S)$

Γ_{275}/Γ

¹ Assumes equal production of B^+ and B^0 at the $\Upsilon(4S)$.

$\Gamma(K^*(892)^+\gamma)/\Gamma_{\text{total}}$					
VALUE (units 10^{-5})	CL%	DOCUMENT ID	TECN	COMMENT	
4.03 ± 0.26	OUR AVERAGE				
3.7 ± 0.28 ± 0.26		1	AUBERT, BE	04A	BABR $e^+e^- \rightarrow \Upsilon(4S)$
4.25 ± 0.31 ± 0.24		2	NAKAO	04	BELL $e^+e^- \rightarrow \Upsilon(4S)$
3.76 ± 0.89 ± 0.28		2	COAN	00	CLE2 $e^+e^- \rightarrow \Upsilon(4S)$

Γ_{276}/Γ

3.83 ± 0.62 ± 0.22	2	AUBERT	02c	BABR	Repl. by AUBERT, BE 04A
5.7 ± 3.1 ± 1.1	3	AMMAR	93	CLE2	Repl. by COAN 00
< 55	90	4	ALBRECHT	89g	ARG $e^+e^- \rightarrow \Upsilon(4S)$
< 55	90	4	AVERY	89B	CLEO $e^+e^- \rightarrow \Upsilon(4S)$
< 180	90		AVERY	87	CLEO $e^+e^- \rightarrow \Upsilon(4S)$

¹ Uses the production ratio of charged and neutral B from $\Upsilon(4S)$ decays $R^{+/-0} = 1.006 \pm 0.048$.

² Assumes equal production of B^+ and B^0 at the $\Upsilon(4S)$.

³ AMMAR 93 observed 4.1 ± 2.3 events above background.

⁴ Assumes the $\Upsilon(4S)$ decays 43% to $B^0\bar{B}^0$.

$\Gamma(K_1(1270)^+\gamma)/\Gamma_{\text{total}}$					
VALUE (units 10^{-5})	CL%	DOCUMENT ID	TECN	COMMENT	
4.3 ± 0.9 ± 0.9		1	YANG	05	BELL $e^+e^- \rightarrow \Upsilon(4S)$

Γ_{277}/Γ

< 9.9	90	1	NISHIDA	02	BELL Repl. by YANG 05
< 730	90	2	ALBRECHT	89g	ARG $e^+e^- \rightarrow \Upsilon(4S)$

¹ Assumes equal production of B^+ and B^0 at the $\Upsilon(4S)$.

² ALBRECHT 89g reports < 0.0066 assuming the $\Upsilon(4S)$ decays 45% to $B^0\bar{B}^0$. We rescale to 50%.

$\Gamma(\eta K^+\gamma)/\Gamma_{\text{total}}$					
VALUE (units 10^{-6})	CL%	DOCUMENT ID	TECN	COMMENT	
9.4 ± 1.1	OUR AVERAGE				
10.0 ± 1.3 ± 0.5		1,2	AUBERT, B	06M	BABR $e^+e^- \rightarrow \Upsilon(4S)$
8.4 ± 1.5 ± 1.2		2,3	NISHIDA	05	BELL $e^+e^- \rightarrow \Upsilon(4S)$

Γ_{278}/Γ

¹ $m_{\eta K} < 3.25$ GeV/ c^2 .

² Assumes equal production of B^+ and B^0 at the $\Upsilon(4S)$.

³ $m_{\eta K} < 2.4$ GeV/ c^2 .

$\Gamma(\eta' K^+\gamma)/\Gamma_{\text{total}}$					
VALUE (units 10^{-6})	CL%	DOCUMENT ID	TECN	COMMENT	
< 4.2	90	1,2	AUBERT, B	06M	BABR $e^+e^- \rightarrow \Upsilon(4S)$

Γ_{279}/Γ

¹ $m_{\eta' K} < 3.25$ GeV/ c^2 .

² Assumes equal production of B^+ and B^0 at the $\Upsilon(4S)$.

$\Gamma(\phi K^+\gamma)/\Gamma_{\text{total}}$					
VALUE (units 10^{-6})	CL%	DOCUMENT ID	TECN	COMMENT	
3.5 ± 0.6	OUR AVERAGE				
3.5 ± 0.6 ± 0.4		1	AUBERT	07Q	BABR $e^+e^- \rightarrow \Upsilon(4S)$
3.4 ± 0.9 ± 0.4		1	DRUTSKOY	04	BELL $e^+e^- \rightarrow \Upsilon(4S)$

Γ_{280}/Γ

¹ Assumes equal production of B^+ and B^0 at $\Upsilon(4S)$.

$\Gamma(K^+\pi^-\pi^+\gamma)/\Gamma_{\text{total}}$					
VALUE (units 10^{-5})	CL%	DOCUMENT ID	TECN	COMMENT	
2.76 ± 0.22	OUR AVERAGE				Error includes scale factor of 1.2.
2.95 ± 0.13 ± 0.20		1,2	AUBERT	07R	BABR $e^+e^- \rightarrow \Upsilon(4S)$
2.50 ± 0.18 ± 0.22		2,3	YANG	05	BELL $e^+e^- \rightarrow \Upsilon(4S)$

Γ_{281}/Γ

• • • We do not use the following data for averages, fits, limits, etc. • • •

2.4 ± 0.5 ± 0.4	2,4	NISHIDA	02	BELL	Repl. by YANG 05
-----------------	-----	---------	----	------	------------------

¹ $M_{K\pi\pi} < 1.8$ GeV/ c^2 .

² Assumes equal production of B^+ and B^0 at the $\Upsilon(4S)$.

³ $M_{K\pi\pi} < 2.0$ GeV/ c^2 .

⁴ $M_{K\pi\pi} < 2.4$ GeV/ c^2 .

$\Gamma(K^*(892)^0\pi^+\gamma)/\Gamma_{\text{total}}$					
VALUE (units 10^{-5})	CL%	DOCUMENT ID	TECN	COMMENT	
(2.0 ± 0.7 ± 0.2) × 10 ⁻⁵		1,2	NISHIDA	02	BELL $e^+e^- \rightarrow \Upsilon(4S)$

Γ_{282}/Γ

¹ Assumes equal production of B^+ and B^0 at the $\Upsilon(4S)$.

² $M_{K\pi\pi} < 2.4$ GeV/ c^2 .

$\Gamma(K^+\rho^0\gamma)/\Gamma_{\text{total}}$					
VALUE (units 10^{-5})	CL%	DOCUMENT ID	TECN	COMMENT	
< 2.0 × 10 ⁻⁵	90	1,2	NISHIDA	02	BELL $e^+e^- \rightarrow \Upsilon(4S)$

Γ_{283}/Γ

¹ Assumes equal production of B^+ and B^0 at the $\Upsilon(4S)$.

² $M_{K\pi\pi} < 2.4$ GeV/ c^2 .

$\Gamma(K^+\pi^-\pi^+\gamma \text{ nonresonant})/\Gamma_{\text{total}}$					
VALUE (units 10^{-6})	CL%	DOCUMENT ID	TECN	COMMENT	
< 9.2 × 10 ⁻⁶	90	1,2	NISHIDA	02	BELL $e^+e^- \rightarrow \Upsilon(4S)$

Γ_{284}/Γ

¹ Assumes equal production of B^+ and B^0 at the $\Upsilon(4S)$.

² $M_{K\pi\pi} < 2.4$ GeV/ c^2 .

$\Gamma(K^0\pi^+\pi^0\gamma)/\Gamma_{\text{total}}$					
VALUE (units 10^{-5})	CL%	DOCUMENT ID	TECN	COMMENT	
4.56 ± 0.42 ± 0.31		1,2	AUBERT	07R	BABR $e^+e^- \rightarrow \Upsilon(4S)$

Γ_{285}/Γ

¹ $M_{K\pi\pi} < 1.8$ GeV/ c^2 .

² Assumes equal production of B^+ and B^0 at the $\Upsilon(4S)$.

$\Gamma(K_1(1400)^+\gamma)/\Gamma_{\text{total}}$					
VALUE (units 10^{-5})	CL%	DOCUMENT ID	TECN	COMMENT	
< 1.5	90	1	YANG	05	BELL $e^+e^- \rightarrow \Upsilon(4S)$

Γ_{286}/Γ

• • • We do not use the following data for averages, fits, limits, etc. • • •

< 5.0	90	1	NISHIDA	02	BELL Repl. by YANG 05
< 220	90	2	ALBRECHT	89g	ARG $e^+e^- \rightarrow \Upsilon(4S)$

¹ Assumes equal production of B^+ and B^0 at the $\Upsilon(4S)$.

² ALBRECHT 89g reports < 0.0020 assuming the $\Upsilon(4S)$ decays 45% to $B^0\bar{B}^0$. We rescale to 50%.

$\Gamma(K_2^*(1430)^+\gamma)/\Gamma_{\text{total}}$					
VALUE (units 10^{-5})	CL%	DOCUMENT ID	TECN	COMMENT	
1.45 ± 0.40 ± 0.15		1	AUBERT, B	04U	BABR $e^+e^- \rightarrow \Upsilon(4S)$

Γ_{287}/Γ

• • • We do not use the following data for averages, fits, limits, etc. • • •

< 140	90	2	ALBRECHT	89g	ARG $e^+e^- \rightarrow \Upsilon(4S)$
-------	----	---	----------	-----	---------------------------------------

¹ Assumes equal production of B^+ and B^0 at the $\Upsilon(4S)$.

² ALBRECHT 89g reports < 0.0013 assuming the $\Upsilon(4S)$ decays 45% to $B^0\bar{B}^0$. We rescale to 50%.

$\Gamma(K^*(1680)^+ \gamma)/\Gamma_{\text{total}}$ Γ_{288}/Γ

VALUE	CL%	DOCUMENT ID	TECN	COMMENT
<0.0019	90	¹ ALBRECHT 89G	ARG	$e^+ e^- \rightarrow \Upsilon(4S)$

¹ ALBRECHT 89G reports < 0.0017 assuming the $\Upsilon(4S)$ decays 45% to $B^0 \bar{B}^0$. We rescale to 50%.

 $\Gamma(K_3^*(1780)^+ \gamma)/\Gamma_{\text{total}}$ Γ_{289}/Γ

VALUE (units 10^{-6})	CL%	DOCUMENT ID	TECN	COMMENT
< 39	90	^{1,2} NISHIDA 05	BELL	$e^+ e^- \rightarrow \Upsilon(4S)$

• • • We do not use the following data for averages, fits, limits, etc. • • •

<5500	90	³ ALBRECHT 89G	ARG	$e^+ e^- \rightarrow \Upsilon(4S)$
-------	----	---------------------------	-----	------------------------------------

¹ Assumes equal production of B^+ and B^0 at the $\Upsilon(4S)$.
² Uses $B(K_3^*(1780) \rightarrow \eta K) = 0.11^{+0.05}_{-0.04}$.
³ ALBRECHT 89G reports < 0.005 assuming the $\Upsilon(4S)$ decays 45% to $B^0 \bar{B}^0$. We rescale to 50%.

 $\Gamma(K_4^*(2045)^+ \gamma)/\Gamma_{\text{total}}$ Γ_{290}/Γ

VALUE	CL%	DOCUMENT ID	TECN	COMMENT
<0.0099	90	¹ ALBRECHT 89G	ARG	$e^+ e^- \rightarrow \Upsilon(4S)$

¹ ALBRECHT 89G reports < 0.0090 assuming the $\Upsilon(4S)$ decays 45% to $B^0 \bar{B}^0$. We rescale to 50%.

 $\Gamma(\rho^+ \gamma)/\Gamma_{\text{total}}$ Γ_{291}/Γ

VALUE (units 10^{-6})	CL%	DOCUMENT ID	TECN	COMMENT
$0.88^{+0.29}_{-0.25}$ OUR AVERAGE				
$1.10^{+0.37}_{-0.33} \pm 0.09$		¹ AUBERT 07L	BABR	$e^+ e^- \rightarrow \Upsilon(4S)$
$0.55^{+0.42+0.09}_{-0.36-0.08}$		¹ MOHAPATRA 06	BELL	$e^+ e^- \rightarrow \Upsilon(4S)$

• • • We do not use the following data for averages, fits, limits, etc. • • •

$0.9^{+0.6}_{-0.5} \pm 0.1$	90	¹ AUBERT 05	BABR	Repl. by AUBERT 07L
< 2.2	90	¹ MOHAPATRA 05	BELL	$e^+ e^- \rightarrow \Upsilon(4S)$
< 2.1	90	¹ AUBERT 90A	BABR	$e^+ e^- \rightarrow \Upsilon(4S)$
<13	90	^{1,2} COAN 00	CLE2	$e^+ e^- \rightarrow \Upsilon(4S)$

¹ Assumes equal production of B^+ and B^0 at $\Upsilon(4S)$.
² No evidence for a nonresonant $K\pi\gamma$ contamination was seen; the central value assumes no contamination.

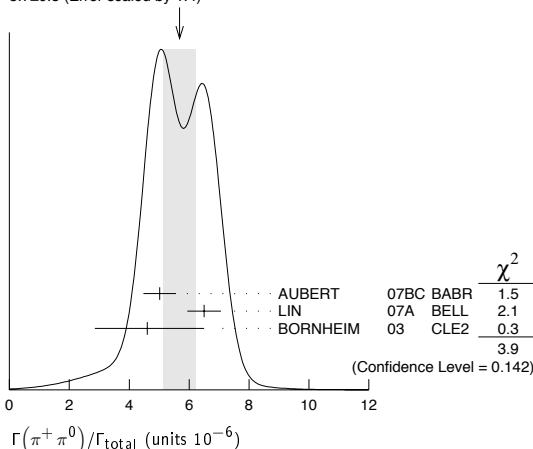
 $\Gamma(\pi^+ \pi^0)/\Gamma_{\text{total}}$ Γ_{292}/Γ

VALUE (units 10^{-6})	CL%	DOCUMENT ID	TECN	COMMENT
5.7 ± 0.5 OUR AVERAGE				Error includes scale factor of 1.4. See the ideogram below.
$5.02 \pm 0.46 \pm 0.29$		¹ AUBERT 07bC	BABR	$e^+ e^- \rightarrow \Upsilon(4S)$
$6.5 \pm 0.4 \pm 0.4$		¹ LIN 07A	BELL	$e^+ e^- \rightarrow \Upsilon(4S)$
$4.6^{+1.8+0.6}_{-1.6-0.7}$		¹ BORNHEIM 03	CLE2	$e^+ e^- \rightarrow \Upsilon(4S)$

• • • We do not use the following data for averages, fits, limits, etc. • • •

$5.8 \pm 0.6 \pm 0.4$		¹ AUBERT 05L	BABR	Repl. by AUBERT 07bC
$5.0 \pm 1.2 \pm 0.5$		¹ CHAO 04	BELL	Repl. by LIN 07A
$5.5^{+1.0}_{-1.9} \pm 0.6$		¹ AUBERT 03L	BABR	Repl. by AUBERT 05L
$7.4^{+2.3}_{-2.2} \pm 0.9$		¹ CASEY 02	BELL	Repl. by CHAO 04
< 13.4	90	¹ ABE 01H	BELL	$e^+ e^- \rightarrow \Upsilon(4S)$
< 9.6	90	¹ AUBERT 01E	BABR	$e^+ e^- \rightarrow \Upsilon(4S)$
< 12.7	90	¹ CRONIN-HEN.00	CLE2	$e^+ e^- \rightarrow \Upsilon(4S)$
< 20	90	GODANG 98	CLE2	Repl. by CRONIN-HENNESSY 00
< 17	90	ASNER 96	CLE2	Repl. by GODANG 98
< 240	90	¹ ALBRECHT 90B	ARG	$e^+ e^- \rightarrow \Upsilon(4S)$
<2300	90	² BEBEK 87	CLEO	$e^+ e^- \rightarrow \Upsilon(4S)$

¹ Assumes equal production of B^+ and B^0 at the $\Upsilon(4S)$.
² BEBEK 87 assume the $\Upsilon(4S)$ decays 43% to $B^0 \bar{B}^0$.

WEIGHTED AVERAGE
5.7±0.5 (Error scaled by 1.4) $\Gamma(\pi^+ \pi^0)/\Gamma(K^0 \pi^+)$ $\Gamma_{292}/\Gamma_{207}$

VALUE	DOCUMENT ID	TECN	COMMENT
$0.285 \pm 0.02 \pm 0.02$	LIN 07A	BELL	$e^+ e^- \rightarrow \Upsilon(4S)$

 $\Gamma(\pi^+ \pi^+ \pi^-)/\Gamma_{\text{total}}$ Γ_{293}/Γ

VALUE (units 10^{-6})	CL%	DOCUMENT ID	TECN	COMMENT
$16.2 \pm 1.2 \pm 0.9$		¹ AUBERT,B 05G	BABR	$e^+ e^- \rightarrow \Upsilon(4S)$

• • • We do not use the following data for averages, fits, limits, etc. • • •

$10.9 \pm 3.3 \pm 1.6$		¹ AUBERT 03M	BABR	Repl. by AUBERT 05G
<130	90	² ADAM 96D	DLPH	$e^+ e^- \rightarrow Z$
<220	90	³ ABREU 95N	DLPH	Sup. by ADAM 96D
<450	90	⁴ ALBRECHT 90B	ARG	$e^+ e^- \rightarrow \Upsilon(4S)$
<190	90	⁵ BORTOLETTO89	CLEO	$e^+ e^- \rightarrow \Upsilon(4S)$

¹ Assumes equal production of B^0 and B^+ at the $\Upsilon(4S)$; charm and charmonium contributions are subtracted, otherwise no assumptions about intermediate resonances.
² ADAM 96D assumes $f_{B^0} = f_{B^-} = 0.39$ and $f_{B_s} = 0.12$.
³ Assumes a B^0, B^- production fraction of 0.39 and a B_s production fraction of 0.12.
⁴ ALBRECHT 90B limit assumes equal production of $B^0 \bar{B}^0$ and $B^+ B^-$ at $\Upsilon(4S)$.
⁵ BORTOLETTO 89 reports < 1.7×10^{-4} assuming the $\Upsilon(4S)$ decays 43% to $B^0 \bar{B}^0$. We rescale to 50%.

 $\Gamma(\rho^0 \pi^+)/\Gamma_{\text{total}}$ Γ_{294}/Γ

VALUE (units 10^{-6})	CL%	DOCUMENT ID	TECN	COMMENT
8.7 ± 1.1 OUR AVERAGE				
$8.8 \pm 1.0^{+0.6}_{-0.9}$		¹ AUBERT,B 05G	BABR	$e^+ e^- \rightarrow \Upsilon(4S)$
$8.0^{+2.3}_{-2.0} \pm 0.7$		¹ GORDON 02	BELL	$e^+ e^- \rightarrow \Upsilon(rs)$
$10.4^{+3.3}_{-3.4} \pm 2.1$		¹ JESSOP 00	CLE2	$e^+ e^- \rightarrow \Upsilon(4S)$

• • • We do not use the following data for averages, fits, limits, etc. • • •

$9.5 \pm 1.1 \pm 0.9$		¹ AUBERT 04Z	BABR	Repl. by AUBERT 05G
< 83	90	² ABE 00C	SLD	$e^+ e^- \rightarrow Z$
<160	90	³ ADAM 96D	DLPH	$e^+ e^- \rightarrow Z$
< 43	90	ASNER 96	CLE2	Repl. by JESSOP 00
<260	90	⁴ ABREU 95N	DLPH	Sup. by ADAM 96D
<150	90	¹ ALBRECHT 90B	ARG	$e^+ e^- \rightarrow \Upsilon(4S)$
<170	90	⁵ BORTOLETTO89	CLEO	$e^+ e^- \rightarrow \Upsilon(4S)$
<230	90	⁵ BEBEK 87	CLEO	$e^+ e^- \rightarrow \Upsilon(4S)$
<600	90	GILES 84	CLEO	Repl. by BEBEK 87

¹ Assumes equal production of B^+ and B^0 at the $\Upsilon(4S)$.
² ABE 00C assumes $B(Z \rightarrow b\bar{b}) = (21.7 \pm 0.1)\%$ and the B fractions $f_{B^0} = f_{B^+} = (39.7^{+1.8}_{-2.2})\%$ and $f_{B_s} = (10.5^{+1.8}_{-2.2})\%$.
³ ADAM 96D assumes $f_{B^0} = f_{B^-} = 0.39$ and $f_{B_s} = 0.12$.
⁴ Assumes a B^0, B^- production fraction of 0.39 and a B_s production fraction of 0.12.
⁵ Papers assume the $\Upsilon(4S)$ decays 43% to $B^0 \bar{B}^0$. We rescale to 50%.

 $[\Gamma(K^*(892)^0 \pi^+) + \Gamma(\rho^0 \pi^+)]/\Gamma_{\text{total}}$ $(\Gamma_{219} + \Gamma_{294})/\Gamma$

VALUE (units 10^{-6})	DOCUMENT ID	TECN	COMMENT
$170^{+120}_{-80} \pm 20$	¹ ADAM 96D	DLPH	$e^+ e^- \rightarrow Z$

¹ ADAM 96D assumes $f_{B^0} = f_{B^-} = 0.39$ and $f_{B_s} = 0.12$.

 $\Gamma(\pi^+ \rho_0(980) \times B(\rho_0(980) \rightarrow \pi^+ \pi^-))/\Gamma_{\text{total}}$ Γ_{295}/Γ

VALUE (units 10^{-6})	CL%	DOCUMENT ID	TECN	COMMENT
< 3.0	90	¹ AUBERT,B 05G	BABR	$e^+ e^- \rightarrow \Upsilon(4S)$

• • • We do not use the following data for averages, fits, limits, etc. • • •

<140	90	² BORTOLETTO89	CLEO	$e^+ e^- \rightarrow \Upsilon(4S)$
------	----	---------------------------	------	------------------------------------

¹ Assumes equal production of B^+ and B^0 at the $\Upsilon(4S)$.
² BORTOLETTO 89 reports < 1.2×10^{-4} assuming the $\Upsilon(4S)$ decays 43% to $B^0 \bar{B}^0$. We rescale to 50%.

Meson Particle Listings

 B^\pm $\Gamma(\pi^+ f_2(1270))/\Gamma_{\text{total}}$ Γ_{296}/Γ

VALUE (units 10^{-6})	CL%	DOCUMENT ID	TECN	COMMENT
$8.2 \pm 2.1 \pm 1.4$		^{1,2} AUBERT,B	05G	BABR $e^+e^- \rightarrow \Upsilon(4S)$

• • • We do not use the following data for averages, fits, limits, etc. • • •

<240	90	³ BORTOLETTO89	CLEO	$e^+e^- \rightarrow \Upsilon(4S)$
------	----	---------------------------	------	-----------------------------------

¹ Reported $B(B^+ \rightarrow f_2(1270)\pi^+) \times B(f_2(1270) \rightarrow \pi^+\pi^-) = (2.3 \pm 0.6 \pm 0.4) \times 10^{-6}$ and rescaled using $B(f_2(1270) \rightarrow \pi^+\pi^-) = 0.28$.

² Assumes equal production of B^+ and B^0 at the $\Upsilon(4S)$.

³ BORTOLETTO 89 reports $< 2.1 \times 10^{-4}$ assuming the $\Upsilon(4S)$ decays 43% to $B^0\bar{B}^0$. We rescale to 50%.

 $\Gamma(\rho(1450)^0\pi^+)/\Gamma_{\text{total}}$ Γ_{297}/Γ

VALUE (units 10^{-6})	CL%	DOCUMENT ID	TECN	COMMENT
<2.3	90	¹ AUBERT,B	05G	BABR $e^+e^- \rightarrow \Upsilon(4S)$

¹ Assumes equal production of B^+ and B^0 at the $\Upsilon(4S)$.

 $\Gamma(f_0(1370)\pi^+ \times B(f_0(1370) \rightarrow \pi^+\pi^-))/\Gamma_{\text{total}}$ Γ_{298}/Γ

VALUE (units 10^{-6})	CL%	DOCUMENT ID	TECN	COMMENT
<3.0	90	¹ AUBERT,B	05G	BABR $e^+e^- \rightarrow \Upsilon(4S)$

¹ Assumes equal production of B^+ and B^0 at the $\Upsilon(4S)$.

 $\Gamma(f_0(600)\pi^+ \times B(f_0(600) \rightarrow \pi^+\pi^-))/\Gamma_{\text{total}}$ Γ_{299}/Γ

VALUE (units 10^{-6})	CL%	DOCUMENT ID	TECN	COMMENT
<4.1	90	¹ AUBERT,B	05G	BABR $e^+e^- \rightarrow \Upsilon(4S)$

¹ Assumes equal production of B^+ and B^0 at the $\Upsilon(4S)$.

 $\Gamma(\pi^+\pi^-\pi^+ \text{ nonresonant})/\Gamma_{\text{total}}$ Γ_{300}/Γ

VALUE (units 10^{-6})	CL%	DOCUMENT ID	TECN	COMMENT
< 4.6	90	¹ AUBERT,B	05G	BABR $e^+e^- \rightarrow \Upsilon(4S)$

• • • We do not use the following data for averages, fits, limits, etc. • • •

<41	90	BERGFELD	96B	CLE2 $e^+e^- \rightarrow \Upsilon(4S)$
-----	----	----------	-----	--

¹ Assumes equal production of B^+ and B^0 at the $\Upsilon(4S)$.

 $\Gamma(\pi^+\pi^0\pi^0)/\Gamma_{\text{total}}$ Γ_{301}/Γ

VALUE	CL%	DOCUMENT ID	TECN	COMMENT
< 8.9×10^{-4}	90	¹ ALBRECHT	90B	ARG $e^+e^- \rightarrow \Upsilon(4S)$

¹ ALBRECHT 90B limit assumes equal production of $B^0\bar{B}^0$ and B^+B^- at $\Upsilon(4S)$.

 $\Gamma(\rho^+\pi^0)/\Gamma_{\text{total}}$ Γ_{302}/Γ

VALUE (units 10^{-6})	CL%	DOCUMENT ID	TECN	COMMENT
10.9 ± 1.4 OUR AVERAGE				

$10.2 \pm 1.4 \pm 0.9$		¹ AUBERT	07X	BABR $e^+e^- \rightarrow \Upsilon(4S)$
------------------------	--	---------------------	-----	--

$13.2 \pm 2.3 \pm 1.4 \pm 1.9$		¹ ZHANG	05A	BELL $e^+e^- \rightarrow \Upsilon(4S)$
--------------------------------	--	--------------------	-----	--

• • • We do not use the following data for averages, fits, limits, etc. • • •

$10.9 \pm 1.9 \pm 1.9$		¹ AUBERT	04Z	BABR Repl. by AUBERT 07X
------------------------	--	---------------------	-----	--------------------------

< 43	90	^{1,2} JESSOP	00	CLE2 $e^+e^- \rightarrow \Upsilon(4S)$
------	----	-----------------------	----	--

< 77	90	ASNER	96	CLE2 Repl. by JESSOP 00
------	----	-------	----	-------------------------

<550	90	¹ ALBRECHT	90B	ARG $e^+e^- \rightarrow \Upsilon(4S)$
------	----	-----------------------	-----	---------------------------------------

¹ Assumes equal production of B^+ and B^0 at the $\Upsilon(4S)$.

² Assumes no nonresonant contributions of $B^+ \rightarrow \pi^+\pi^0\pi^0$.

 $\Gamma(\pi^+\pi^-\pi^+\pi^0)/\Gamma_{\text{total}}$ Γ_{303}/Γ

VALUE	CL%	DOCUMENT ID	TECN	COMMENT
< 4.0×10^{-3}	90	¹ ALBRECHT	90B	ARG $e^+e^- \rightarrow \Upsilon(4S)$

¹ ALBRECHT 90B limit assumes equal production of $B^0\bar{B}^0$ and B^+B^- at $\Upsilon(4S)$.

 $\Gamma(\rho^+\pi^0)/\Gamma_{\text{total}}$ Γ_{304}/Γ

VALUE (units 10^{-6})	CL%	DOCUMENT ID	TECN	COMMENT
18 ± 4 OUR AVERAGE				Error includes scale factor of 1.5.

$16.8 \pm 2.2 \pm 2.3$		¹ AUBERT,BE	06G	BABR $e^+e^- \rightarrow \Upsilon(4S)$
------------------------	--	------------------------	-----	--

$31.7 \pm 7.1 \pm 3.8 \pm 6.7$		^{1,2} ZHANG	03B	BELL $e^+e^- \rightarrow \Upsilon(4S)$
--------------------------------	--	----------------------	-----	--

• • • We do not use the following data for averages, fits, limits, etc. • • •

$22.5 \pm 5.7 \pm 5.8$		¹ AUBERT	03V	BABR Repl. by AUBERT,BE 06G
------------------------	--	---------------------	-----	-----------------------------

<1000	90	¹ ALBRECHT	90B	ARG $e^+e^- \rightarrow \Upsilon(4S)$
-------	----	-----------------------	-----	---------------------------------------

¹ Assumes equal production of B^+ and B^0 at the $\Upsilon(4S)$.

 $\Gamma(\rho^+ f_0(980) \times B(f_0(980) \rightarrow \pi^+\pi^-))/\Gamma_{\text{total}}$ Γ_{305}/Γ

VALUE (units 10^{-6})	CL%	DOCUMENT ID	TECN	COMMENT
<1.9	90	¹ AUBERT,BE	06G	BABR $e^+e^- \rightarrow \Upsilon(4S)$

¹ Assumes equal production of B^+ and B^0 at the $\Upsilon(4S)$.

 $\Gamma(a_1(1260)^+\pi^0)/\Gamma_{\text{total}}$ Γ_{306}/Γ

VALUE (units 10^{-6})	CL%	DOCUMENT ID	TECN	COMMENT
$26.4 \pm 5.4 \pm 4.1$		^{1,2} AUBERT	07BL	BABR $e^+e^- \rightarrow \Upsilon(4S)$

• • • We do not use the following data for averages, fits, limits, etc. • • •

<1700	90	¹ ALBRECHT	90B	ARG $e^+e^- \rightarrow \Upsilon(4S)$
-------	----	-----------------------	-----	---------------------------------------

¹ Assumes equal production of B^+ and B^0 at the $\Upsilon(4S)$.

² Assumes a_1^+ decays only to 3π and $B(a_1^+ \rightarrow \pi^+\pi^-\pi^+) = 0.5$.

 $\Gamma(a_1(1260)^0\pi^+)/\Gamma_{\text{total}}$ Γ_{307}/Γ

VALUE (units 10^{-6})	CL%	DOCUMENT ID	TECN	COMMENT
$20.4 \pm 4.7 \pm 3.4$		^{1,2} AUBERT	07BL	BABR $e^+e^- \rightarrow \Upsilon(4S)$

• • • We do not use the following data for averages, fits, limits, etc. • • •

<900	90	¹ ALBRECHT	90B	ARG $e^+e^- \rightarrow \Upsilon(4S)$
------	----	-----------------------	-----	---------------------------------------

¹ Assumes equal production of B^+ and B^0 at the $\Upsilon(4S)$.

² Assumes a_1^0 decays only to 3π and $B(a_1^0 \rightarrow \pi^+\pi^-\pi^0) = 1.0$.

 $\Gamma(b_1^0\pi^+ \times B(b_1^0 \rightarrow \omega\pi^0))/\Gamma_{\text{total}}$ Γ_{308}/Γ

VALUE (units 10^{-6})	CL%	DOCUMENT ID	TECN	COMMENT
$6.7 \pm 1.7 \pm 1.0$		¹ AUBERT	07BI	BABR $e^+e^- \rightarrow \Upsilon(4S)$

¹ Assumes equal production of B^+ and B^0 at the $\Upsilon(4S)$.

 $\Gamma(\omega\pi^+)/\Gamma_{\text{total}}$ Γ_{309}/Γ

VALUE (units 10^{-6})	CL%	DOCUMENT ID	TECN	COMMENT
6.9 ± 0.5 OUR AVERAGE				

$6.7 \pm 0.5 \pm 0.4$		¹ AUBERT	07AE	BABR $e^+e^- \rightarrow \Upsilon(4S)$
-----------------------	--	---------------------	------	--

$6.9 \pm 0.6 \pm 0.5$		¹ JEN	06	BELL $e^+e^- \rightarrow \Upsilon(4S)$
-----------------------	--	------------------	----	--

$11.3 \pm 3.3 \pm 1.4 \pm 2.9$		¹ JESSOP	00	CLE2 $e^+e^- \rightarrow \Upsilon(4S)$
--------------------------------	--	---------------------	----	--

• • • We do not use the following data for averages, fits, limits, etc. • • •

$6.1 \pm 0.7 \pm 0.4$		¹ AUBERT,B	06E	BABR Repl. by AUBERT 07AE
-----------------------	--	-----------------------	-----	---------------------------

$5.5 \pm 0.9 \pm 0.5$		¹ AUBERT	04H	BABR Repl. by AUBERT,B 06E
-----------------------	--	---------------------	-----	----------------------------

$5.7 \pm 1.4 \pm 1.3 \pm 0.6$		¹ WANG	04A	BELL Repl. by JEN 06
-------------------------------	--	-------------------	-----	----------------------

$4.2 \pm 2.0 \pm 1.8 \pm 0.5$		¹ LU	02	BELL Repl. by WANG 04A
-------------------------------	--	-----------------	----	------------------------

$6.6 \pm 2.1 \pm 1.8 \pm 0.7$		¹ AUBERT	01G	BABR Repl. by AUBERT 04H
-------------------------------	--	---------------------	-----	--------------------------

< 23	90	¹ BERGFELD	98	CLE2 Repl. by JESSOP 00
------	----	-----------------------	----	-------------------------

<400	90	¹ ALBRECHT	90B	ARG $e^+e^- \rightarrow \Upsilon(4S)$
------	----	-----------------------	-----	---------------------------------------

¹ Assumes equal production of B^+ and B^0 at the $\Upsilon(4S)$.

 $\Gamma(\omega\rho^+)/\Gamma_{\text{total}}$ Γ_{310}/Γ

VALUE (units 10^{-6})	CL%	DOCUMENT ID	TECN	COMMENT
$10.6 \pm 2.1 \pm 1.6 \pm 1.0$		¹ AUBERT,B	06T	BABR $e^+e^- \rightarrow \Upsilon(4S)$

• • • We do not use the following data for averages, fits, limits, etc. • • •

$12.6 \pm 3.7 \pm 3.3 \pm 1.6$		¹ AUBERT	05O	BABR Repl. by AUBERT,B 06T
--------------------------------	--	---------------------	-----	----------------------------

<61	90	¹ BERGFELD	98	CLE2
-----	----	-----------------------	----	------

¹ Assumes equal production of B^+ and B^0 at the $\Upsilon(4S)$.

 $\Gamma(\eta\pi^+)/\Gamma_{\text{total}}$ Γ_{311}/Γ

VALUE (units 10^{-6})	CL%	DOCUMENT ID	TECN	COMMENT
4.4 ± 0.4 OUR AVERAGE				Error includes scale factor of 1.1.

$5.0 \pm 0.5 \pm 0.3$		¹ AUBERT	07AE	BABR $e^+e^- \rightarrow \Upsilon(4S)$
-----------------------	--	---------------------	------	--

$4.2 \pm 0.4 \pm 0.2$		¹ CHANG	07B	BELL $e^+e^- \rightarrow \Upsilon(4S)$
-----------------------	--	--------------------	-----	--

$1.2 \pm 2.8 \pm 1.2$		¹ RICHICHI	00	CLE2 $e^+e^- \rightarrow \Upsilon(4S)$
-----------------------	--	-----------------------	----	--

• • • We do not use the following data for averages, fits, limits, etc. • • •

$5.1 \pm 0.6 \pm 0.3$		¹ AUBERT,B	05K	BABR Repl. by AUBERT 07AE
-----------------------	--	-----------------------	-----	---------------------------

$4.8 \pm 0.7 \pm 0.3$		¹ CHANG	05A	BELL Repl. by CHANG 07B
-----------------------	--	--------------------	-----	-------------------------

$5.3 \pm 1.0 \pm 0.3$		¹ AUBERT	04H	BABR Repl. by AUBERT,B 05K
-----------------------	--	---------------------	-----	----------------------------

< 15	90	BEHRENS	98	CLE2 Repl. by RICHICHI 00
------	----	---------	----	---------------------------

<700	90	¹ ALBRECHT	90B	ARG $e^+e^- \rightarrow \Upsilon(4S)$
------	----	-----------------------	-----	---------------------------------------

¹ Assumes equal production of B^+ and B^0 at the $\Upsilon(4S)$.

 $\Gamma(\eta'\pi^+)/\Gamma_{\text{total}}$ Γ_{312}/Γ

VALUE (units 10^{-6})	CL%	DOCUMENT ID	TECN	COMMENT
2.7 ± 1.0 OUR AVERAGE				Error includes scale factor of 2.1.

$3.9 \pm 0.7 \pm 0.3$		¹ AUBERT	07AE	BABR $e^+e^- \rightarrow \Upsilon(4S)$
-----------------------	--	---------------------	------	--

$1.76 \pm 0.67 \pm 0.15 \pm 0.62 \pm 0.14$		¹ SCHUEMANN	06	BELL $e^+e^- \rightarrow \Upsilon(4S)$
--	--	------------------------	----	--

• • • We do not use the following data for averages, fits, limits, etc. • • •

$4.0 \pm 0.8 \pm 0.4$		¹ AUBERT,B	05K	BABR Repl. by AUBERT 07AE
-----------------------	--	-----------------------	-----	---------------------------

< 4.5	90	¹ AUBERT	04H	BABR Repl. by AUBERT,B 05K
-------	----	---------------------	-----	----------------------------

< 7.0	90	¹ ABE	01M	BELL $e^+e^- \rightarrow \Upsilon(4S)$
-------	----	------------------	-----	--

<12	90	¹ AUBERT	01G	BABR $e^+e^- \rightarrow \Upsilon(4S)$
-----	----	---------------------	-----	--

<12	90	¹ RICHICHI	00	CLE2 $e^+e^- \rightarrow \Upsilon(4S)$
-----	----	-----------------------	----	--

<31	90	BEHRENS	98	CLE2 Repl. by RICHICHI 00
-----	----	---------	----	---------------------------

¹ Assumes equal production of B^+ and B^0 at the $\Upsilon(4S)$.

$\Gamma(\eta^{\prime}\rho^+)/\Gamma_{\text{total}}$ Γ_{313}/Γ
 VALUE (units 10^{-6}) CL% DOCUMENT ID TECN COMMENT

$8.7^{+3.1+2.3}_{-2.8-1.3}$ ¹AUBERT 07E BABR $e^+e^- \rightarrow \Upsilon(4S)$

••• We do not use the following data for averages, fits, limits, etc. •••

< 5.8 90 ¹SCHUEMANN 07 BELL $e^+e^- \rightarrow \Upsilon(4S)$
 <22 90 ¹AUBERT,B 04D BABR Repl. by AUBERT 07E
 <33 90 ¹RICHICHI 00 CLE2 $e^+e^- \rightarrow \Upsilon(4S)$
 <47 90 BEHRENS 98 CLE2 Repl. by RICHICHI 00

¹ Assumes equal production of B^+ and B^0 at the $\Upsilon(4S)$.

$\Gamma(\eta\rho^+)/\Gamma_{\text{total}}$ Γ_{314}/Γ
 VALUE (units 10^{-6}) CL% DOCUMENT ID TECN COMMENT

5.4 ± 1.9 OUR AVERAGE Error includes scale factor of 1.6.

$4.1^{+1.4}_{-1.3} \pm 0.4$ ¹WANG 07B BELL $e^+e^- \rightarrow \Upsilon(4S)$

$8.4 \pm 1.9 \pm 1.1$ ¹AUBERT,B 05K BABR $e^+e^- \rightarrow \Upsilon(4S)$

••• We do not use the following data for averages, fits, limits, etc. •••

<14 90 ¹AUBERT,B 04D BABR Repl. by AUBERT,B 05K
 <15 90 ¹RICHICHI 00 CLE2 $e^+e^- \rightarrow \Upsilon(4S)$
 <32 90 BEHRENS 98 CLE2 Repl. by RICHICHI 00

¹ Assumes equal production of B^+ and B^0 at the $\Upsilon(4S)$.

$\Gamma(\phi\pi^+)/\Gamma_{\text{total}}$ Γ_{315}/Γ
 VALUE (units 10^{-6}) CL% DOCUMENT ID TECN COMMENT

< 0.24 90 ¹AUBERT,B 06C BABR $e^+e^- \rightarrow \Upsilon(4S)$

••• We do not use the following data for averages, fits, limits, etc. •••

< 0.41 90 ¹AUBERT 04A BABR Repl. by AUBERT,B 06C
 < 1.4 90 ¹AUBERT 01D BABR $e^+e^- \rightarrow \Upsilon(4S)$
 <15.3 90 ²ABE 00C SLD $e^+e^- \rightarrow Z$
 < 5 90 ¹BERGFELD 98 CLE2

¹ Assumes equal production of B^+ and B^0 at the $\Upsilon(4S)$.

² ABE 00C assumes $B(Z \rightarrow b\bar{b}) = (21.7 \pm 0.1)\%$ and the B fractions $f_{B^0} = f_{B^+} = (39.7^{+1.8}_{-2.2})\%$ and $f_{B_s} = (10.5^{+1.8}_{-2.2})\%$.

$\Gamma(\phi\rho^+)/\Gamma_{\text{total}}$ Γ_{316}/Γ
 VALUE (units 10^{-6}) CL% DOCUMENT ID TECN COMMENT

<16 ¹BERGFELD 98 CLE2

¹ Assumes equal production of B^+ and B^0 at the $\Upsilon(4S)$.

$\Gamma(a_0(980)^0\pi^+ \times B(a_0(980)^0 \rightarrow \eta\pi^0))/\Gamma_{\text{total}}$ Γ_{317}/Γ
 VALUE (units 10^{-6}) CL% DOCUMENT ID TECN COMMENT

<5.8 90 ¹AUBERT,BE 04 BABR $e^+e^- \rightarrow \Upsilon(4S)$

¹ Assumes equal production of charged and neutral B mesons from $\Upsilon(4S)$ decays.

$\Gamma(a_0(980)^+\pi^0 \times B(a_0^+ \rightarrow \eta\pi^+))/\Gamma_{\text{total}}$ Γ_{318}/Γ
 VALUE (units 10^{-6}) CL% DOCUMENT ID TECN COMMENT

<1.4 90 ¹AUBERT 08A BABR $e^+e^- \rightarrow \Upsilon(4S)$

¹ Assumes equal production of B^+ and B^0 at the $\Upsilon(4S)$.

$\Gamma(\pi^+\pi^+\pi^-\pi^-)/\Gamma_{\text{total}}$ Γ_{319}/Γ
 VALUE CL% DOCUMENT ID TECN COMMENT

<8.6 × 10⁻⁴ 90 ¹ALBRECHT 90B ARG $e^+e^- \rightarrow \Upsilon(4S)$

¹ ALBRECHT 90B limit assumes equal production of $B^0\bar{B}^0$ and B^+B^- at $\Upsilon(4S)$.

$\Gamma(\rho^0 a_1(1260)^+)/\Gamma_{\text{total}}$ Γ_{320}/Γ
 VALUE CL% DOCUMENT ID TECN COMMENT

<6.2 × 10⁻⁴ 90 ¹BORTOLETTO89 CLEO $e^+e^- \rightarrow \Upsilon(4S)$

••• We do not use the following data for averages, fits, limits, etc. •••

<6.0 × 10⁻⁴ 90 ²ALBRECHT 90B ARG $e^+e^- \rightarrow \Upsilon(4S)$
 <3.2 × 10⁻³ 90 ¹BEBEK 87 CLEO $e^+e^- \rightarrow \Upsilon(4S)$

¹ BORTOLETTO 89 reports < 5.4 × 10⁻⁴ assuming the $\Upsilon(4S)$ decays 43% to $B^0\bar{B}^0$. We rescale to 50%.

² ALBRECHT 90B limit assumes equal production of $B^0\bar{B}^0$ and B^+B^- at $\Upsilon(4S)$.

$\Gamma(\rho^0 a_2(1320)^+)/\Gamma_{\text{total}}$ Γ_{321}/Γ
 VALUE CL% DOCUMENT ID TECN COMMENT

<7.2 × 10⁻⁴ 90 ¹BORTOLETTO89 CLEO $e^+e^- \rightarrow \Upsilon(4S)$

••• We do not use the following data for averages, fits, limits, etc. •••

<2.6 × 10⁻³ 90 ²BEBEK 87 CLEO $e^+e^- \rightarrow \Upsilon(4S)$

¹ BORTOLETTO 89 reports < 6.3 × 10⁻⁴ assuming the $\Upsilon(4S)$ decays 43% to $B^0\bar{B}^0$. We rescale to 50%.

² BEBEK 87 reports < 2.3 × 10⁻³ assuming the $\Upsilon(4S)$ decays 43% to $B^0\bar{B}^0$. We rescale to 50%.

$\Gamma(\pi^+\pi^+\pi^-\pi^-)/\Gamma_{\text{total}}$ Γ_{322}/Γ
 VALUE CL% DOCUMENT ID TECN COMMENT

<6.3 × 10⁻³ 90 ¹ALBRECHT 90B ARG $e^+e^- \rightarrow \Upsilon(4S)$

¹ ALBRECHT 90B limit assumes equal production of $B^0\bar{B}^0$ and B^+B^- at $\Upsilon(4S)$.

$\Gamma(a_1(1260)^+ a_1(1260)^0)/\Gamma_{\text{total}}$ Γ_{323}/Γ
 VALUE CL% DOCUMENT ID TECN COMMENT

<1.3 × 10⁻² 90 ¹ALBRECHT 90B ARG $e^+e^- \rightarrow \Upsilon(4S)$

¹ ALBRECHT 90B limit assumes equal production of $B^0\bar{B}^0$ and B^+B^- at $\Upsilon(4S)$.

$\Gamma(h^+\pi^0)/\Gamma_{\text{total}}$ Γ_{324}/Γ
 $h^+ = K^+ \text{ or } \pi^+$
 VALUE (units 10^{-6}) CL% DOCUMENT ID TECN COMMENT

$16^{+6}_{-5} \pm 3.6$ GODA NG 98 CLE2 $e^+e^- \rightarrow \Upsilon(4S)$

$\Gamma(\omega h^+)/\Gamma_{\text{total}}$ Γ_{325}/Γ
 $h^+ = K^+ \text{ or } \pi^+$
 VALUE (units 10^{-6}) CL% DOCUMENT ID TECN COMMENT

13.8 ± 2.7 OUR AVERAGE

$13.4^{+3.3}_{-2.9} \pm 1.1$ ¹LU 02 BELL $e^+e^- \rightarrow \Upsilon(4S)$

$14.3^{+3.6}_{-3.2} \pm 2.0$ ¹JESSOP 00 CLE2 $e^+e^- \rightarrow \Upsilon(4S)$

••• We do not use the following data for averages, fits, limits, etc. •••

$25^{+8}_{-7} \pm 3$ ¹BERGFELD 98 CLE2 Repl. by JESSOP 00

¹ Assumes equal production of B^+ and B^0 at the $\Upsilon(4S)$.

$\Gamma(h^+X^0(\text{Familon}))/\Gamma_{\text{total}}$ Γ_{326}/Γ
 VALUE (units 10^{-6}) CL% DOCUMENT ID TECN COMMENT

<49 90 ¹AMMAR 01B CLE2 $e^+e^- \rightarrow \Upsilon(4S)$

¹ AMMAR 01B searched for the two-body decay of the B meson to a massless neutral feebly-interacting particle X^0 such as the familon, the Nambu-Goldstone boson associated with a spontaneously broken global family symmetry.

$\Gamma(\rho\bar{\rho}\pi^+)/\Gamma_{\text{total}}$ Γ_{327}/Γ
 VALUE (units 10^{-6}) CL% DOCUMENT ID TECN COMMENT

1.62 ± 0.20 OUR AVERAGE

$1.60^{+0.22}_{-0.19} \pm 0.12$ ^{1,2,3}WEI 08 BELL $e^+e^- \rightarrow \Upsilon(4S)$

$1.69 \pm 0.29 \pm 0.26$ ¹AUBERT 07Av BABR $e^+e^- \rightarrow \Upsilon(4S)$

••• We do not use the following data for averages, fits, limits, etc. •••

$3.06^{+0.73}_{-0.62} \pm 0.37$ ^{1,3}WANG 04 BELL Repl. by WEI 08

< 3.7 90 ^{1,2}ABE 02K BELL Repl. by WANG 04

<500 90 ⁴ABREU 95N DLPH Repl. by ADAM 96D

<160 90 ⁵BEBEK 89 CLEO $e^+e^- \rightarrow \Upsilon(4S)$

570 ± 150 ± 210 ⁶ALBRECHT 88F ARG $e^+e^- \rightarrow \Upsilon(4S)$

¹ Assumes equal production of B^+ and B^0 at the $\Upsilon(4S)$.

² Explicitly vetoes resonant production of $p\bar{p}$ from Charmonium states.

³ Also provides results with $m_{p\bar{p}} < 2.85 \text{ GeV}/c^2$ and angular asymmetry of $p\bar{p}$ system.

⁴ Assumes a B^0 , B^- production fraction of 0.39 and a B_s production fraction of 0.12.

⁵ BEBEK 89 reports < 1.4 × 10⁻⁴ assuming the $\Upsilon(4S)$ decays 43% to $B^0\bar{B}^0$. We rescale to 50%.

⁶ ALBRECHT 88F reports $(5.2 \pm 1.4 \pm 1.9) \times 10^{-4}$ assuming the $\Upsilon(4S)$ decays 45% to $B^0\bar{B}^0$. We rescale to 50%.

$\Gamma(\rho\bar{\rho}\pi^+\text{nonresonant})/\Gamma_{\text{total}}$ Γ_{328}/Γ
 VALUE (units 10^{-6}) CL% DOCUMENT ID TECN COMMENT

<53 90 BERGFELD 96B CLE2 $e^+e^- \rightarrow \Upsilon(4S)$

$\Gamma(\rho\bar{\rho}\pi^+\pi^-\pi^-)/\Gamma_{\text{total}}$ Γ_{329}/Γ
 VALUE CL% DOCUMENT ID TECN COMMENT

<5.2 × 10⁻⁴ 90 ¹ALBRECHT 88F ARG $e^+e^- \rightarrow \Upsilon(4S)$

¹ ALBRECHT 88F reports < 4.7 × 10⁻⁴ assuming the $\Upsilon(4S)$ decays 45% to $B^0\bar{B}^0$. We rescale to 50%.

$\Gamma(\rho\bar{\rho}K^+)/\Gamma_{\text{total}}$ Γ_{330}/Γ
 VALUE (units 10^{-6}) CL% DOCUMENT ID TECN COMMENT

5.9 ± 0.5 OUR AVERAGE Error includes scale factor of 1.5.

$5.54^{+0.27}_{-0.25} \pm 0.36$ ^{1,2,3}WEI 08 BELL $e^+e^- \rightarrow \Upsilon(4S)$

$6.7 \pm 0.5 \pm 0.4$ ^{1,3}AUBERT,B 05L BABR $e^+e^- \rightarrow \Upsilon(4S)$

••• We do not use the following data for averages, fits, limits, etc. •••

$4.59^{+0.38}_{-0.34} \pm 0.50$ ^{1,2,3}WANG 05A BELL Repl. by WEI 08

$5.66^{+0.67}_{-0.57} \pm 0.62$ ^{1,2,3}WANG 04 BELL Repl. by WANG 05A

$4.3^{+1.1}_{-0.9} \pm 0.5$ ^{1,2}ABE 02K BELL Repl. by WANG 04

¹ Assumes equal production of B^+ and B^0 at the $\Upsilon(4S)$.

² Explicitly vetoes resonant production of $p\bar{p}$ from Charmonium states.

³ Provides also results with $m_{p\bar{p}} < 2.85 \text{ GeV}/c^2$ and angular asymmetry of $p\bar{p}$ system.

Meson Particle Listings

 B^\pm $\Gamma(\Theta(1710)^{++} \bar{p} \times B(\Theta(1710)^{++} \rightarrow \rho K^+))/\Gamma_{\text{total}}$ Γ_{331}/Γ

VALUE (units 10^{-6})	CL%	DOCUMENT ID	TECN	COMMENT
<0.091	90	¹ WANG 05A	BELL	$e^+e^- \rightarrow \Upsilon(4S)$

• • • We do not use the following data for averages, fits, limits, etc. • • •

<0.1	90	^{1,2} AUBERT,B 05L	BABR	$e^+e^- \rightarrow \Upsilon(4S)$
------	----	-----------------------------	------	-----------------------------------

¹ Assumes equal production of B^+ and B^0 at the $\Upsilon(4S)$.

² Provides upper limits depending on the pentaquark masses between 1.43 to 2.0 GeV/ c^2 .

 $\Gamma(f_J(2220) K^+ \times B(f_J(2220) \rightarrow \rho \bar{p}))/\Gamma_{\text{total}}$ Γ_{332}/Γ

VALUE (units 10^{-6})	CL%	DOCUMENT ID	TECN	COMMENT
<0.41	90	¹ WANG 05A	BELL	$e^+e^- \rightarrow \Upsilon(4S)$

¹ Assumes equal production of B^+ and B^0 at the $\Upsilon(4S)$.

 $\Gamma(\rho \bar{\Lambda}(1520))/\Gamma_{\text{total}}$ Γ_{333}/Γ

VALUE (units 10^{-6})	CL%	DOCUMENT ID	TECN	COMMENT
<1.5	90	¹ AUBERT,B 05L	BABR	$e^+e^- \rightarrow \Upsilon(4S)$

¹ Assumes equal production of B^+ and B^0 at the $\Upsilon(4S)$.

 $\Gamma(\rho \bar{p} K^+ \text{ nonresonant})/\Gamma_{\text{total}}$ Γ_{334}/Γ

VALUE (units 10^{-6})	CL%	DOCUMENT ID	TECN	COMMENT
<89	90	BERGFELD 96B	CLE2	$e^+e^- \rightarrow \Upsilon(4S)$

 $\Gamma(\rho \bar{p} K^*(892)^+)/\Gamma_{\text{total}}$ Γ_{335}/Γ

VALUE (units 10^{-6})	CL%	DOCUMENT ID	TECN	COMMENT
6.6 ± 2.3 OUR AVERAGE	Error includes scale factor of 1.3.			
$5.3 \pm 1.5 \pm 1.3$		¹ AUBERT 07AV	BABR	$e^+e^- \rightarrow \Upsilon(4S)$
$10.3^{+3.6}_{-2.8} +1.3_{-1.7}$		^{1,2} WANG 04	BELL	$e^+e^- \rightarrow \Upsilon(4S)$

¹ Assumes equal production of B^+ and B^0 at the $\Upsilon(4S)$.

² Explicitly vetoes resonant production of $\rho \bar{p}$ from charmonium states. The branching fraction for $M_{\rho \bar{p}} < 2.85$ GeV/ c^2 is also reported.

 $\Gamma(f_J(2220) K^{*+} \times B(f_J(2220) \rightarrow \rho \bar{p}))/\Gamma_{\text{total}}$ Γ_{336}/Γ

VALUE (units 10^{-6})	CL%	DOCUMENT ID	TECN	COMMENT
<0.77	90	¹ AUBERT 07AV	BABR	$e^+e^- \rightarrow \Upsilon(4S)$

¹ Assumes equal production of B^+ and B^0 at the $\Upsilon(4S)$.

 $\Gamma(\rho \bar{\Lambda})/\Gamma_{\text{total}}$ Γ_{337}/Γ

VALUE (units 10^{-6})	CL%	DOCUMENT ID	TECN	COMMENT
< 0.32	90	¹ TSAI 07	BELL	$e^+e^- \rightarrow \Upsilon(4S)$
• • • We do not use the following data for averages, fits, limits, etc. • • •				
< 0.49	90	¹ CHANG 05	BELL	Repl. by TSAI 2007
< 1.5	90	¹ BORNHEIM 03	CLE2	$e^+e^- \rightarrow \Upsilon(4S)$
< 2.2	90	¹ ABE 02b	BELL	$e^+e^- \rightarrow \Upsilon(4S)$
< 2.6	90	¹ COAN 99	CLE2	$e^+e^- \rightarrow \Upsilon(4S)$
< 60	90	² AVERY 89B	CLEO	$e^+e^- \rightarrow \Upsilon(4S)$
< 93	90	³ ALBRECHT 88F	ARG	$e^+e^- \rightarrow \Upsilon(4S)$

¹ Assumes equal production of B^+ and B^0 at the $\Upsilon(4S)$.

² AVERY 89B reports $< 5 \times 10^{-5}$ assuming the $\Upsilon(4S)$ decays 43% to $B^0 \bar{B}^0$. We rescale to 50%.

³ ALBRECHT 88F reports $< 8.5 \times 10^{-5}$ assuming the $\Upsilon(4S)$ decays 45% to $B^0 \bar{B}^0$. We rescale to 50%.

 $\Gamma(\rho \bar{\Lambda} \gamma)/\Gamma_{\text{total}}$ Γ_{338}/Γ

VALUE (units 10^{-6})	CL%	DOCUMENT ID	TECN	COMMENT
$2.45^{+0.44}_{-0.38} \pm 0.22$		¹ WANG 07c	BELL	$e^+e^- \rightarrow \Upsilon(4S)$
• • • We do not use the following data for averages, fits, limits, etc. • • •				
$2.16^{+0.58}_{-0.53} \pm 0.20$		¹ LEE 05	BELL	Repl. by WANG 07c
< 3.9	90	² EDWARDS 03	CLE2	$e^+e^- \rightarrow \Upsilon(4S)$

¹ Assumes equal production of B^+ and B^0 at the $\Upsilon(4S)$.

² Corresponds to $E_\gamma > 1.5$ GeV. The limit changes to 3.3×10^{-6} for $E_\gamma > 2.0$ GeV.

 $\Gamma(\rho \bar{\Lambda} \pi^0)/\Gamma_{\text{total}}$ Γ_{339}/Γ

VALUE (units 10^{-6})	CL%	DOCUMENT ID	TECN	COMMENT
$3.00^{+0.61}_{-0.53} \pm 0.33$		¹ WANG 07c	BELL	$e^+e^- \rightarrow \Upsilon(4S)$

¹ Assumes equal production of B^+ and B^0 at the $\Upsilon(4S)$.

 $\Gamma(\rho \Sigma(1385)^0)/\Gamma_{\text{total}}$ Γ_{340}/Γ

VALUE (units 10^{-6})	CL%	DOCUMENT ID	TECN	COMMENT
<0.47	90	¹ WANG 07c	BELL	$e^+e^- \rightarrow \Upsilon(4S)$

¹ Assumes equal production of B^+ and B^0 at the $\Upsilon(4S)$.

 $\Gamma(\Delta^+ \bar{\Lambda})/\Gamma_{\text{total}}$ Γ_{341}/Γ

VALUE (units 10^{-6})	CL%	DOCUMENT ID	TECN	COMMENT
<0.82	90	¹ WANG 07c	BELL	$e^+e^- \rightarrow \Upsilon(4S)$

¹ Assumes equal production of B^+ and B^0 at the $\Upsilon(4S)$.

 $\Gamma(\rho \Sigma^- \gamma)/\Gamma_{\text{total}}$ Γ_{342}/Γ

VALUE (units 10^{-6})	CL%	DOCUMENT ID	TECN	COMMENT
<4.6	90	¹ LEE 05	BELL	$e^+e^- \rightarrow \Upsilon(4S)$

• • • We do not use the following data for averages, fits, limits, etc. • • •

< 7.9	90	² EDWARDS 03	CLE2	$e^+e^- \rightarrow \Upsilon(4S)$
-------	----	-------------------------	------	-----------------------------------

¹ Assumes equal production of B^+ and B^0 at the $\Upsilon(4S)$.

² Corresponds to $E_\gamma > 1.5$ GeV. The limit changes to 6.4×10^{-6} for $E_\gamma > 2.0$ GeV.

 $\Gamma(\rho \bar{\Lambda} \pi^+ \pi^-)/\Gamma_{\text{total}}$ Γ_{343}/Γ

VALUE	CL%	DOCUMENT ID	TECN	COMMENT
< 2.0×10^{-4}	90	¹ ALBRECHT 88F	ARG	$e^+e^- \rightarrow \Upsilon(4S)$

¹ ALBRECHT 88F reports $< 1.8 \times 10^{-4}$ assuming the $\Upsilon(4S)$ decays 45% to $B^0 \bar{B}^0$. We rescale to 50%.

 $\Gamma(\Lambda \bar{\Lambda} \pi^+)/\Gamma_{\text{total}}$ Γ_{344}/Γ

VALUE (units 10^{-6})	CL%	DOCUMENT ID	TECN	COMMENT
< 2.8	90	¹ LEE 04	BELL	$e^+e^- \rightarrow \Upsilon(4S)$

¹ Assumes equal production of B^+ and B^0 at the $\Upsilon(4S)$.

 $\Gamma(\Lambda \bar{\Lambda} K^+)/\Gamma_{\text{total}}$ Γ_{345}/Γ

VALUE (units 10^{-6})	CL%	DOCUMENT ID	TECN	COMMENT
$2.91^{+0.9}_{-0.70} \pm 0.38$		¹ LEE 04	BELL	$e^+e^- \rightarrow \Upsilon(4S)$

¹ Assumes equal production of B^+ and B^0 at the $\Upsilon(4S)$.

 $\Gamma(\bar{\Delta}^0 \rho)/\Gamma_{\text{total}}$ Γ_{346}/Γ

VALUE (units 10^{-6})	CL%	DOCUMENT ID	TECN	COMMENT
< 1.38	90	¹ WEI 08	BELL	$e^+e^- \rightarrow \Upsilon(4S)$
• • • We do not use the following data for averages, fits, limits, etc. • • •				
< 380	90	² BORTOLETTO 89	CLEO	$e^+e^- \rightarrow \Upsilon(4S)$

¹ Assumes equal production of B^+ and B^0 at the $\Upsilon(4S)$.

² BORTOLETTO 89 reports $< 3.3 \times 10^{-4}$ assuming the $\Upsilon(4S)$ decays 43% to $B^0 \bar{B}^0$. We rescale to 50%.

 $\Gamma(\Delta^{++} \bar{p})/\Gamma_{\text{total}}$ Γ_{347}/Γ

VALUE (units 10^{-6})	CL%	DOCUMENT ID	TECN	COMMENT
< 0.14	90	¹ WEI 08	BELL	$e^+e^- \rightarrow \Upsilon(4S)$
• • • We do not use the following data for averages, fits, limits, etc. • • •				
< 150	90	² BORTOLETTO 89	CLEO	$e^+e^- \rightarrow \Upsilon(4S)$

¹ Assumes equal production of B^+ and B^0 at the $\Upsilon(4S)$.

² BORTOLETTO 89 reports $< 1.3 \times 10^{-4}$ assuming the $\Upsilon(4S)$ decays 43% to $B^0 \bar{B}^0$. We rescale to 50%.

 $\Gamma(D^+ \rho \bar{p})/\Gamma_{\text{total}}$ Γ_{348}/Γ

VALUE	CL%	DOCUMENT ID	TECN	COMMENT
< 1.5×10^{-5}	90	¹ ABE 02w	BELL	$e^+e^- \rightarrow \Upsilon(4S)$

¹ Assumes equal production of B^+ and B^0 at the $\Upsilon(4S)$.

 $\Gamma(D^*(2010)^+ \rho \bar{p})/\Gamma_{\text{total}}$ Γ_{349}/Γ

VALUE	CL%	DOCUMENT ID	TECN	COMMENT
< 1.5×10^{-5}	90	¹ ABE 02w	BELL	$e^+e^- \rightarrow \Upsilon(4S)$

¹ Assumes equal production of B^+ and B^0 at the $\Upsilon(4S)$.

 $\Gamma(\bar{\Lambda}_c^- \rho \pi^+)/\Gamma_{\text{total}}$ Γ_{350}/Γ

VALUE (units 10^{-4})	CL%	DOCUMENT ID	TECN	COMMENT
2.1 ± 0.6 OUR AVERAGE				
$2.0 \pm 0.2 \pm 0.5$		¹ GABYSHEV 06A	BELL	$e^+e^- \rightarrow \Upsilon(4S)$
$2.4 \pm 0.6 \pm 0.6$		² DYTMAN 02	CLE2	$e^+e^- \rightarrow \Upsilon(4S)$
• • • We do not use the following data for averages, fits, limits, etc. • • •				
$1.9 \pm 0.5 \pm 0.5$		³ GABYSHEV 02	BELL	Repl. by GABYSHEV 06A
$6.2^{+2.3}_{-2.0} \pm 1.6$		⁴ FU 97	CLE2	Repl. by DYTMAN 02

¹ GABYSHEV 06A reports $(2.01 \pm 0.15 \pm 0.20) \times 10^{-4}$ for $B(\Lambda_c^+ \rightarrow p K^- \pi^+) = 0.05$. We rescale to our best value $B(\Lambda_c^+ \rightarrow p K^- \pi^+) = (5.0 \pm 1.3) \times 10^{-2}$. Our first error is their experiment's error and our second error is the systematic error from using our best value.

² DYTMAN 02 reports $(2.4^{+0.63}_{-0.62}) \times 10^{-4}$ for $B(\Lambda_c^+ \rightarrow p K^- \pi^+) = 0.05$. We rescale to our best value $B(\Lambda_c^+ \rightarrow p K^- \pi^+) = (5.0 \pm 1.3) \times 10^{-2}$. Our first error is their experiment's error and our second error is the systematic error from using our best value.

³ GABYSHEV 02 reports $(1.87^{+0.51}_{-0.49}) \times 10^{-4}$ for $B(\Lambda_c^+ \rightarrow p K^- \pi^+) = 0.05$. We rescale to our best value $B(\Lambda_c^+ \rightarrow p K^- \pi^+) = (5.0 \pm 1.3) \times 10^{-2}$. Our first error is their experiment's error and our second error is the systematic error from using our best value.

⁴ FU 97 uses PDG 96 values of Λ_c branching fraction.

 $\Gamma(\bar{\Lambda}_c^- \Delta(1232)^+)/\Gamma_{\text{total}}$ Γ_{351}/Γ

VALUE (units 10^{-5})	CL%	DOCUMENT ID	TECN	COMMENT
< 1.9	90	GABYSHEV 06A	BELL	$e^+e^- \rightarrow \Upsilon(4S)$

¹ Assumes equal production of B^+ and B^0 at the $\Upsilon(4S)$.

$\Gamma(\bar{A}_c^- \Delta_X(1600)^+)/\Gamma_{\text{total}}$ Γ_{352}/Γ

VALUE (units 10^{-5})	DOCUMENT ID	TECN	COMMENT
$5.9 \pm 1.2 \pm 1.5$	1 GABYSHEV	06A	BELL $e^+e^- \rightarrow \Upsilon(4S)$

¹ GABYSHEV 06A reports $(5.9 \pm 1.0 \pm 0.6) \times 10^{-5}$ for $B(\Lambda_c^+ \rightarrow p K^- \pi^+) = 0.05$. We rescale to our best value $B(\Lambda_c^+ \rightarrow p K^- \pi^+) = (5.0 \pm 1.3) \times 10^{-2}$. Our first error is their experiment's error and our second error is the systematic error from using our best value.

 $\Gamma(\bar{A}_c^- \Delta_X(2420)^+)/\Gamma_{\text{total}}$ Γ_{353}/Γ

VALUE (units 10^{-5})	DOCUMENT ID	TECN	COMMENT
$4.7 \pm 1.1 \pm 1.2$	1 GABYSHEV	06A	BELL $e^+e^- \rightarrow \Upsilon(4S)$

¹ GABYSHEV 06A reports $(4.7 \pm 1.0 \pm 0.4) \times 10^{-5}$ for $B(\Lambda_c^+ \rightarrow p K^- \pi^+) = 0.05$. We rescale to our best value $B(\Lambda_c^+ \rightarrow p K^- \pi^+) = (5.0 \pm 1.3) \times 10^{-2}$. Our first error is their experiment's error and our second error is the systematic error from using our best value.

 $\Gamma(\bar{A}_c^- p_s \pi^+)/\Gamma_{\text{total}}$ Γ_{354}/Γ

$(\bar{A}_c^- p)_s$ denotes a low-mass enhancement near 3.35 GeV/c².

VALUE (units 10^{-5})	DOCUMENT ID	TECN	COMMENT
$3.9 \pm 0.9 \pm 1.0$	1 GABYSHEV	06A	BELL $e^+e^- \rightarrow \Upsilon(4S)$

¹ GABYSHEV 06A reports $(3.9 \pm 0.8 \pm 0.4) \times 10^{-5}$ for $B(\Lambda_c^+ \rightarrow p K^- \pi^+) = 0.05$. We rescale to our best value $B(\Lambda_c^+ \rightarrow p K^- \pi^+) = (5.0 \pm 1.3) \times 10^{-2}$. Our first error is their experiment's error and our second error is the systematic error from using our best value.

 $\Gamma(\bar{A}_c^- p \pi^+ \pi^0)/\Gamma_{\text{total}}$ Γ_{355}/Γ

VALUE (units 10^{-3})	CL%	DOCUMENT ID	TECN	COMMENT
$1.81 \pm 0.29 \pm 0.52$		1,2 DYTMAN	02	CLE2 $e^+e^- \rightarrow \Upsilon(4S)$

• • • We do not use the following data for averages, fits, limits, etc. • • •

<3.12 90 ³FU 97 CLE2 $e^+e^- \rightarrow \Upsilon(4S)$

¹ Assumes equal production of B^+ and B^0 at the $\Upsilon(4S)$.
² DYTMAN 02 measurement uses $B(\Lambda_c^- \rightarrow \bar{p} K^+ \pi^-) = 5.0 \pm 1.3\%$. The second error includes the systematic and the uncertainty of the branching ratio.
³ FU 97 uses PDG 96 values of Λ_c branching ratio.

 $\Gamma(\bar{A}_c^- p \pi^+ \pi^- \pi^0)/\Gamma_{\text{total}}$ Γ_{356}/Γ

VALUE (units 10^{-3})	CL%	DOCUMENT ID	TECN	COMMENT
$2.25 \pm 0.25 \pm 0.63$		1,2 DYTMAN	02	CLE2 $e^+e^- \rightarrow \Upsilon(4S)$

• • • We do not use the following data for averages, fits, limits, etc. • • •

<1.46 90 ³FU 97 CLE2 $e^+e^- \rightarrow \Upsilon(4S)$

¹ Assumes equal production of B^+ and B^0 at the $\Upsilon(4S)$.
² DYTMAN 02 measurement uses $B(\Lambda_c^- \rightarrow \bar{p} K^+ \pi^-) = 5.0 \pm 1.3\%$. The second error includes the systematic and the uncertainty of the branching ratio.
³ FU 97 uses PDG 96 values of Λ_c branching ratio.

 $\Gamma(\bar{A}_c^- p \pi^+ \pi^- \pi^0)/\Gamma_{\text{total}}$ Γ_{357}/Γ

VALUE	CL%	DOCUMENT ID	TECN	COMMENT
$<1.34 \times 10^{-2}$		1 FU	97	CLE2 $e^+e^- \rightarrow \Upsilon(4S)$

¹ FU 97 uses PDG 96 values of Λ_c branching ratio.

 $\Gamma(\Lambda_c^+ \Lambda_c^- K^+)/\Gamma_{\text{total}}$ Γ_{358}/Γ

VALUE (units 10^{-4})	DOCUMENT ID	TECN	COMMENT
$6.5 \pm 1.0 \pm 3.6$	1 GABYSHEV	06	BELL $e^+e^- \rightarrow \Upsilon(4S)$

¹ Assumes equal production of B^+ and B^0 at the $\Upsilon(4S)$ and $B(\Lambda_c^+ \rightarrow p K^- \pi^+) = (5.0 \pm 1.3)\%$.

 $\Gamma(\Sigma_c(2455)^0 p)/\Gamma_{\text{total}}$ Γ_{359}/Γ

VALUE (units 10^{-5})	CL%	DOCUMENT ID	TECN	COMMENT
$3.7 \pm 0.8 \pm 1.0$		1 GABYSHEV	06A	BELL $e^+e^- \rightarrow \Upsilon(4S)$

• • • We do not use the following data for averages, fits, limits, etc. • • •

<8 90 ^{2,3} DYTMAN 02 CLE2 $e^+e^- \rightarrow \Upsilon(4S)$

<9.3 90 ^{2,4} GABYSHEV 02 BELL Repl. by GABYSHEV 06A

¹ GABYSHEV 06A reports $(3.7 \pm 0.7 \pm 0.4) \times 10^{-5}$ for $B(\Lambda_c^+ \rightarrow p K^- \pi^+) = 0.05$. We rescale to our best value $B(\Lambda_c^+ \rightarrow p K^- \pi^+) = (5.0 \pm 1.3) \times 10^{-2}$. Our first error is their experiment's error and our second error is the systematic error from using our best value.

² Assumes equal production of B^+ and B^0 at the $\Upsilon(4S)$.

³ DYTMAN 02 measurement uses $B(\Lambda_c^- \rightarrow \bar{p} K^+ \pi^-) = 5.0 \pm 1.3\%$. The second error includes the systematic and the uncertainty of the branching ratio.

⁴ Uses the value for $\Lambda_c \rightarrow p K^- \pi^+$ branching ratio $(5.0 \pm 1.3)\%$.

 $\Gamma(\Sigma_c(2520)^0 p)/\Gamma_{\text{total}}$ Γ_{360}/Γ

VALUE (units 10^{-5})	CL%	DOCUMENT ID	TECN	COMMENT
<2.7	90	GABYSHEV	06A	BELL $e^+e^- \rightarrow \Upsilon(4S)$

• • • We do not use the following data for averages, fits, limits, etc. • • •

<4.6 90 ^{1,2} GABYSHEV 02 BELL Repl. by GABYSHEV 06A

¹ Assumes equal production of B^+ and B^0 at the $\Upsilon(4S)$.

² Uses the value for $\Lambda_c \rightarrow p K^- \pi^+$ branching ratio $(5.0 \pm 1.3)\%$.

 $\Gamma(\Sigma_c(2455)^0 p \pi^0)/\Gamma_{\text{total}}$ Γ_{361}/Γ

VALUE (units 10^{-4})	DOCUMENT ID	TECN	COMMENT
$4.4 \pm 1.4 \pm 1.1$	1,2 DYTMAN	02	CLE2 $e^+e^- \rightarrow \Upsilon(4S)$

¹ DYTMAN 02 reports $(4.4 \pm 1.4) \times 10^{-4}$ for $B(\Lambda_c^+ \rightarrow p K^- \pi^+) = 0.05$. We rescale to our best value $B(\Lambda_c^+ \rightarrow p K^- \pi^+) = (5.0 \pm 1.3) \times 10^{-2}$. Our first error is their experiment's error and our second error is the systematic error from using our best value.

² Assumes equal production of B^+ and B^0 at the $\Upsilon(4S)$.

 $\Gamma(\Sigma_c(2455)^0 p \pi^- \pi^+)/\Gamma_{\text{total}}$ Γ_{362}/Γ

VALUE (units 10^{-4})	DOCUMENT ID	TECN	COMMENT
$4.4 \pm 1.3 \pm 1.1$	1,2 DYTMAN	02	CLE2 $e^+e^- \rightarrow \Upsilon(4S)$

¹ DYTMAN 02 reports $(4.4 \pm 1.3) \times 10^{-4}$ for $B(\Lambda_c^+ \rightarrow p K^- \pi^+) = 0.05$. We rescale to our best value $B(\Lambda_c^+ \rightarrow p K^- \pi^+) = (5.0 \pm 1.3) \times 10^{-2}$. Our first error is their experiment's error and our second error is the systematic error from using our best value.

² Assumes equal production of B^+ and B^0 at the $\Upsilon(4S)$.

 $\Gamma(\Sigma_c(2455)^{--} p \pi^+ \pi^+)/\Gamma_{\text{total}}$ Γ_{363}/Γ

VALUE (units 10^{-4})	DOCUMENT ID	TECN	COMMENT
$2.8 \pm 1.0 \pm 0.7$	1,2 DYTMAN	02	CLE2 $e^+e^- \rightarrow \Upsilon(4S)$

¹ DYTMAN 02 reports $(2.8 \pm 1.0) \times 10^{-4}$ for $B(\Lambda_c^+ \rightarrow p K^- \pi^+) = 0.05$. We rescale to our best value $B(\Lambda_c^+ \rightarrow p K^- \pi^+) = (5.0 \pm 1.3) \times 10^{-2}$. Our first error is their experiment's error and our second error is the systematic error from using our best value.

² Assumes equal production of B^+ and B^0 at the $\Upsilon(4S)$.

 $\Gamma(\Lambda_c(2593)^- / \Lambda_c(2625)^- p \pi^+)/\Gamma_{\text{total}}$ Γ_{364}/Γ

VALUE	CL%	DOCUMENT ID	TECN	COMMENT
$<1.9 \times 10^{-4}$	90	1,2 DYTMAN	02	CLE2 $e^+e^- \rightarrow \Upsilon(4S)$

¹ Assumes equal production of B^+ and B^0 at the $\Upsilon(4S)$.

² DYTMAN 02 measurement uses $B(\Lambda_c^- \rightarrow \bar{p} K^+ \pi^-) = 5.0 \pm 1.3\%$. The second error includes the systematic and the uncertainty of the branching ratio.

 $\Gamma(\Xi_c^0 \Lambda_c^+ \times B(\Xi_c^0 \rightarrow \Xi^+ \pi^-))/\Gamma_{\text{total}}$ Γ_{365}/Γ

VALUE (units 10^{-5})	DOCUMENT ID	TECN	COMMENT
$5.6 \pm 2.3 \pm 1.5$	1,2 CHISTOV	06A	BELL $e^+e^- \rightarrow \Upsilon(4S)$

¹ CHISTOV 06A reports $(5.6 \pm 1.9 \pm 1.9) \times 10^{-5}$ for $B(\Lambda_c^+ \rightarrow p K^- \pi^+) = (5.0 \pm 1.3) \times 10^{-2}$. We rescale to our best value $B(\Lambda_c^+ \rightarrow p K^- \pi^+) = (5.0 \pm 1.3) \times 10^{-2}$. Our first error is their experiment's error and our second error is the systematic error from using our best value.

² Assumes equal production of B^+ and B^0 at the $\Upsilon(4S)$.

 $\Gamma(\Xi_c^0 \Lambda_c^+ \times B(\Xi_c^0 \rightarrow \Lambda K^+ \pi^-))/\Gamma_{\text{total}}$ Γ_{366}/Γ

VALUE (units 10^{-5})	DOCUMENT ID	TECN	COMMENT
$4.0 \pm 1.2 \pm 1.0$	1,2 CHISTOV	06A	BELL $e^+e^- \rightarrow \Upsilon(4S)$

¹ CHISTOV 06A reports $(4.0 \pm 1.1 \pm 1.3) \times 10^{-5}$ for $B(\Lambda_c^+ \rightarrow p K^- \pi^+) = (5.0 \pm 1.3) \times 10^{-2}$. We rescale to our best value $B(\Lambda_c^+ \rightarrow p K^- \pi^+) = (5.0 \pm 1.3) \times 10^{-2}$. Our first error is their experiment's error and our second error is the systematic error from using our best value.

² Assumes equal production of B^+ and B^0 at the $\Upsilon(4S)$.

 $\Gamma(\pi^+ e^+ e^-)/\Gamma_{\text{total}}$ Γ_{368}/Γ

Test for $\Delta B=1$ weak neutral current. Allowed by higher-order electroweak interactions.

VALUE	CL%	DOCUMENT ID	TECN	COMMENT
$<1.8 \times 10^{-7}$	90	1 AUBERT	07AG	BABR $e^+e^- \rightarrow \Upsilon(4S)$

• • • We do not use the following data for averages, fits, limits, etc. • • •

< 3.9×10^{-3} 90 ² WEIR 90B MRK2 e^+e^- 29 GeV

¹ Assumes equal production of B^+ and B^0 at the $\Upsilon(4S)$.

² WEIR 90B assumes B^+ production cross section from LUND.

 $\Gamma(\pi^+ \mu^+ \mu^-)/\Gamma_{\text{total}}$ Γ_{369}/Γ

Test for $\Delta B=1$ weak neutral current. Allowed by higher-order electroweak interactions.

VALUE	CL%	DOCUMENT ID	TECN	COMMENT
$<2.8 \times 10^{-7}$	90	1 AUBERT	07AG	BABR $e^+e^- \rightarrow \Upsilon(4S)$

• • • We do not use the following data for averages, fits, limits, etc. • • •

< 9.1×10^{-3} 90 ² WEIR 90B MRK2 e^+e^- 29 GeV

¹ Assumes equal production of B^+ and B^0 at the $\Upsilon(4S)$.

² WEIR 90B assumes B^+ production cross section from LUND.

Meson Particle Listings

 B^\pm

$\Gamma(\pi^+ \ell^+ \ell^-)/\Gamma_{\text{total}}$					Γ_{367}/Γ
VALUE	CL%	DOCUMENT ID	TECN	COMMENT	
$<1.2 \times 10^{-7}$	90	1 AUBERT	07AG BABR	$e^+ e^- \rightarrow \Upsilon(4S)$	
1 Assumes equal production of B^+ and B^0 at the $\Upsilon(4S)$.					

$\Gamma(\pi^+ \nu \bar{\nu})/\Gamma_{\text{total}}$					Γ_{370}/Γ
VALUE	CL%	DOCUMENT ID	TECN	COMMENT	
$<1.0 \times 10^{-4}$	90	1 AUBERT	05H BABR	$e^+ e^- \rightarrow \Upsilon(4S)$	
••• We do not use the following data for averages, fits, limits, etc. •••					
$<1.7 \times 10^{-4}$	90	1 CHEN	07D BELL	$e^+ e^- \rightarrow \Upsilon(4S)$	
1 Assumes equal production of B^+ and B^0 at the $\Upsilon(4S)$.					

$\Gamma(K^+ e^+ e^-)/\Gamma_{\text{total}}$					Γ_{372}/Γ
VALUE (units 10^{-7})	CL%	DOCUMENT ID	TECN	COMMENT	
4.9 ± 1.0 OUR AVERAGE					
$4.2^{+1.2}_{-1.1} \pm 0.2$		1 AUBERT,B	06J BABR	$e^+ e^- \rightarrow \Upsilon(4S)$	
$6.3^{+1.9}_{-1.7} \pm 0.3$		2 ISHIKAWA	03 BELL	$e^+ e^- \rightarrow \Upsilon(4S)$	
••• We do not use the following data for averages, fits, limits, etc. •••					
$10.5^{+2.5}_{-2.2} \pm 0.7$		1 AUBERT	03U BABR	Repl. by AUBERT,B 06J	
< 14	90	1 ABE	02 BELL	$e^+ e^- \rightarrow \Upsilon(4S)$	
< 9	90	1 AUBERT	02L BABR	$e^+ e^- \rightarrow \Upsilon(4S)$	
< 24	90	3 ANDERSON	01B CLE2	$e^+ e^- \rightarrow \Upsilon(4S)$	
< 990	90	4 ALBRECHT	91E ARG	$e^+ e^- \rightarrow \Upsilon(4S)$	
< 68000	90	5 WEIR	90B MRK2	$e^+ e^- 29 \text{ GeV}$	
< 600	90	6 AVERY	89B CLEO	$e^+ e^- \rightarrow \Upsilon(4S)$	
< 2500	90	7 AVERY	87 CLEO	$e^+ e^- \rightarrow \Upsilon(4S)$	

- 1 Assumes equal production of B^+ and B^0 at the $\Upsilon(4S)$.
- 2 Assumes equal production of B^0 and B^+ at $\Upsilon(4S)$. The second error is a total of systematic uncertainties including model dependence.
- 3 The result is for di-lepton masses above 0.5 GeV.
- 4 ALBRECHT 91E reports $< 9.0 \times 10^{-5}$ assuming the $\Upsilon(4S)$ decays 45% to $B^0 \bar{B}^0$. We rescale to 50%.
- 5 WEIR 90B assumes B^+ production cross section from LUND.
- 6 AVERY 89B reports $< 5 \times 10^{-5}$ assuming the $\Upsilon(4S)$ decays 43% to $B^0 \bar{B}^0$. We rescale to 50%.
- 7 AVERY 87 reports $< 2.1 \times 10^{-4}$ assuming the $\Upsilon(4S)$ decays 40% to $B^0 \bar{B}^0$. We rescale to 50%.

$\Gamma(K^+ \mu^+ \mu^-)/\Gamma_{\text{total}}$					Γ_{373}/Γ
VALUE (units 10^{-6})	CL%	DOCUMENT ID	TECN	COMMENT	
$0.39^{+0.10}_{-0.09}$ OUR AVERAGE					
$0.31^{+0.15}_{-0.12} \pm 0.03$		1 AUBERT,B	06J BABR	$e^+ e^- \rightarrow \Upsilon(4S)$	
$0.45^{+0.14}_{-0.12} \pm 0.03$		2 ISHIKAWA	03 BELL	$e^+ e^- \rightarrow \Upsilon(4S)$	
••• We do not use the following data for averages, fits, limits, etc. •••					
$0.07^{+0.19}_{-0.11} \pm 0.02$		1 AUBERT	03U BABR	Repl. by AUBERT,B 06J	
$0.98^{+0.46}_{-0.36} \pm 0.16$		1 ABE	02 BELL	Repl. by ISHIKAWA 03	
< 1.2	90	1 AUBERT	02L BABR	$e^+ e^- \rightarrow \Upsilon(4S)$	
< 3.68	90	3 ANDERSON	01B CLE2	$e^+ e^- \rightarrow \Upsilon(4S)$	
< 5.2	90	4 AFFOLDER	99B CDF	$p\bar{p}$ at 1.8 TeV	
< 10	90	5 ABE	96L CDF	Repl. by AFFOLDER 99B	
< 240	90	6 ALBRECHT	91E ARG	$e^+ e^- \rightarrow \Upsilon(4S)$	
< 6400	90	7 WEIR	90B MRK2	$e^+ e^- 29 \text{ GeV}$	
< 170	90	8 AVERY	89B CLEO	$e^+ e^- \rightarrow \Upsilon(4S)$	
< 380	90	9 AVERY	87 CLEO	$e^+ e^- \rightarrow \Upsilon(4S)$	

- 1 Assumes equal production of B^+ and B^0 at the $\Upsilon(4S)$.
- 2 Assumes equal production of B^0 and B^+ at $\Upsilon(4S)$. The second error is a total of systematic uncertainties including model dependence.
- 3 The result is for di-lepton masses above 0.5 GeV.
- 4 AFFOLDER 99B measured relative to $B^+ \rightarrow J/\psi(1S) K^+$.
- 5 ABE 96L measured relative to $B^+ \rightarrow J/\psi(1S) K^+$ using PDG 94 branching ratios.
- 6 ALBRECHT 91E reports $< 2.2 \times 10^{-4}$ assuming the $\Upsilon(4S)$ decays 45% to $B^0 \bar{B}^0$. We rescale to 50%.
- 7 WEIR 90B assumes B^+ production cross section from LUND.
- 8 AVERY 89B reports $< 1.5 \times 10^{-4}$ assuming the $\Upsilon(4S)$ decays 43% to $B^0 \bar{B}^0$. We rescale to 50%.
- 9 AVERY 87 reports $< 3.2 \times 10^{-4}$ assuming the $\Upsilon(4S)$ decays 40% to $B^0 \bar{B}^0$. We rescale to 50%.

$\Gamma(K^+ \ell^+ \ell^-)/\Gamma_{\text{total}}$					Γ_{371}/Γ
VALUE (units 10^{-7})	CL%	DOCUMENT ID	TECN	COMMENT	
$4.4^{+0.8}_{-0.7}$ OUR AVERAGE				Error includes scale factor of 1.1.	
$3.8^{+0.9}_{-0.8} \pm 0.2$		1 AUBERT,B	06J BABR	$e^+ e^- \rightarrow \Upsilon(4S)$	
$5.3^{+1.1}_{-1.0} \pm 0.3$		1 ISHIKAWA	03 BELL	$e^+ e^- \rightarrow \Upsilon(4S)$	

- 1 Assumes equal production of B^+ and B^0 at the $\Upsilon(4S)$.

$\Gamma(K^+ \nu \bar{\nu})/\Gamma_{\text{total}}$					Γ_{374}/Γ
VALUE	CL%	DOCUMENT ID	TECN	COMMENT	
$<1.4 \times 10^{-5}$	90	1 CHEN	07D BELL	$e^+ e^- \rightarrow \Upsilon(4S)$	
••• We do not use the following data for averages, fits, limits, etc. •••					
$<5.2 \times 10^{-5}$	90	1 AUBERT	05H BABR	$e^+ e^- \rightarrow \Upsilon(4S)$	
$<2.4 \times 10^{-4}$	90	1 BROWDER	01 CLE2	$e^+ e^- \rightarrow \Upsilon(4S)$	
1 Assumes equal production of B^+ and B^0 at the $\Upsilon(4S)$.					

$\Gamma(\rho^+ \nu \bar{\nu})/\Gamma_{\text{total}}$					Γ_{375}/Γ
VALUE	CL%	DOCUMENT ID	TECN	COMMENT	
$<1.5 \times 10^{-4}$	90	1 CHEN	07D BELL	$e^+ e^- \rightarrow \Upsilon(4S)$	
1 Assumes equal production of B^+ and B^0 at the $\Upsilon(4S)$.					

$\Gamma(K^*(892)^+ e^+ e^-)/\Gamma_{\text{total}}$					Γ_{378}/Γ
VALUE (units 10^{-6})	CL%	DOCUMENT ID	TECN	COMMENT	
$0.75^{+0.76}_{-0.65} \pm 0.38$		1 AUBERT,B	06J BABR	$e^+ e^- \rightarrow \Upsilon(4S)$	
••• We do not use the following data for averages, fits, limits, etc. •••					
$0.20^{+1.34}_{-0.87} \pm 0.28$		1 AUBERT	03U BABR	$e^+ e^- \rightarrow \Upsilon(4S)$	
< 4.6	90	2 ISHIKAWA	03 BELL	$e^+ e^- \rightarrow \Upsilon(4S)$	
< 8.9	90	1 ABE	02 BELL	Repl. by ISHIKAWA 03	
< 9.5	90	1 AUBERT	02L BABR	$e^+ e^- \rightarrow \Upsilon(4S)$	
< 690	90	3 ALBRECHT	91E ARG	$e^+ e^- \rightarrow \Upsilon(4S)$	

- 1 Assumes equal production of B^+ and B^0 at the $\Upsilon(4S)$.
- 2 Assumes equal production of B^0 and B^+ at $\Upsilon(4S)$. The second error is a total of systematic uncertainties including model dependence.
- 3 ALBRECHT 91E reports $< 6.3 \times 10^{-4}$ assuming the $\Upsilon(4S)$ decays 45% to $B^0 \bar{B}^0$. We rescale to 50%.

$\Gamma(K^*(892)^+ \mu^+ \mu^-)/\Gamma_{\text{total}}$					Γ_{379}/Γ
VALUE (units 10^{-6})	CL%	DOCUMENT ID	TECN	COMMENT	
$0.8^{+0.6}_{-0.4}$ OUR AVERAGE					
$0.97^{+0.94}_{-0.69} \pm 0.14$		1 AUBERT,B	06J BABR	$e^+ e^- \rightarrow \Upsilon(4S)$	
$0.65^{+0.69+0.15}_{-0.53-0.16}$		2 ISHIKAWA	03 BELL	$e^+ e^- \rightarrow \Upsilon(4S)$	
••• We do not use the following data for averages, fits, limits, etc. •••					
$3.07^{+2.58}_{-1.78} \pm 0.42$		1 AUBERT	03U BABR	$e^+ e^- \rightarrow \Upsilon(4S)$	
< 3.9	90	1 ABE	02 BELL	Repl. by ISHIKAWA 03	
< 17.0	90	1 AUBERT	02L BABR	$e^+ e^- \rightarrow \Upsilon(4S)$	
< 1200	90	3 ALBRECHT	91E ARG	$e^+ e^- \rightarrow \Upsilon(4S)$	

- 1 Assumes equal production of B^+ and B^0 at the $\Upsilon(4S)$.
- 2 Assumes equal production of B^0 and B^+ at $\Upsilon(4S)$. The second error is a total of systematic uncertainties including model dependence. The 90% C.L. upper limit is 2.2×10^{-6} .
- 3 ALBRECHT 91E reports $< 1.1 \times 10^{-3}$ assuming the $\Upsilon(4S)$ decays 45% to $B^0 \bar{B}^0$. We rescale to 50%.

$\Gamma(K^*(892)^+ \ell^+ \ell^-)/\Gamma_{\text{total}}$					Γ_{376}/Γ
VALUE (units 10^{-7})	CL%	DOCUMENT ID	TECN	COMMENT	
$7.3^{+5.0}_{-4.2} \pm 2.1$		1 AUBERT,B	06J BABR	$e^+ e^- \rightarrow \Upsilon(4S)$	
••• We do not use the following data for averages, fits, limits, etc. •••					
< 22	90	1 ISHIKAWA	03 BELL	$e^+ e^- \rightarrow \Upsilon(4S)$	
1 Assumes equal production of B^+ and B^0 at the $\Upsilon(4S)$.					

$\Gamma(K^*(892)^+ \nu \bar{\nu})/\Gamma_{\text{total}}$					Γ_{377}/Γ
VALUE	CL%	DOCUMENT ID	TECN	COMMENT	
$<1.4 \times 10^{-4}$	90	1 CHEN	07D BELL	$e^+ e^- \rightarrow \Upsilon(4S)$	
1 Assumes equal production of B^+ and B^0 at the $\Upsilon(4S)$.					

$\Gamma(\pi^+ e^+ \mu^-)/\Gamma_{\text{total}}$					Γ_{380}/Γ
VALUE	CL%	DOCUMENT ID	TECN	COMMENT	
<0.0064		1 WEIR	90B MRK2	$e^+ e^- 29 \text{ GeV}$	
1 WEIR 90B assumes B^+ production cross section from LUND.					

$\Gamma(\pi^+ e^- \mu^+)/\Gamma_{\text{total}}$					Γ_{381}/Γ
VALUE	CL%	DOCUMENT ID	TECN	COMMENT	
<0.0064		1 WEIR	90B MRK2	$e^+ e^- 29 \text{ GeV}$	
1 WEIR 90B assumes B^+ production cross section from LUND.					

$\Gamma(\pi^+ e^\pm \mu^\mp)/\Gamma_{\text{total}}$					Γ_{382}/Γ
VALUE	CL%	DOCUMENT ID	TECN	COMMENT	
$<1.7 \times 10^{-7}$	90	1 AUBERT	07AG BABR	$e^+ e^- \rightarrow \Upsilon(4S)$	
1 Assumes equal production of B^+ and B^0 at the $\Upsilon(4S)$.					

$\Gamma(K^+ e^+ \mu^-)/\Gamma_{\text{total}}$ Γ_{383}/Γ

Test of total lepton family number conservation.

VALUE (units 10^{-7})	CL%	DOCUMENT ID	TECN	COMMENT
<0.91	90	1 AUBERT,B 06j BABR		$e^+ e^- \rightarrow \Upsilon(4S)$
•••				We do not use the following data for averages, fits, limits, etc. •••
<8	90	1 AUBERT 02L BABR		Repl. by AUBERT,B 06j
<6.4 $\times 10^4$	90	2 WEIR 90B MRK2		$e^+ e^- 29 \text{ GeV}$

¹ Assumes equal production of B^+ and B^0 at the $\Upsilon(4S)$.
² WEIR 90B assumes B^+ production cross section from LUND.

 $\Gamma(K^+ e^- \mu^+)/\Gamma_{\text{total}}$ Γ_{384}/Γ

Test of lepton family number conservation.

VALUE (units 10^{-7})	CL%	DOCUMENT ID	TECN	COMMENT
<1.3	90	1 AUBERT,B 06j BABR		$e^+ e^- \rightarrow \Upsilon(4S)$
•••				We do not use the following data for averages, fits, limits, etc. •••
<6.4 $\times 10^4$	90	2 WEIR 90B MRK2		$e^+ e^- 29 \text{ GeV}$

¹ Assumes equal production of B^+ and B^0 at the $\Upsilon(4S)$.
² WEIR 90B assumes B^+ production cross section from LUND.

 $\Gamma(K^+ e^\pm \mu^\mp)/\Gamma_{\text{total}}$ Γ_{385}/Γ

Test of total lepton number conservation.

VALUE (units 10^{-7})	CL%	DOCUMENT ID	TECN	COMMENT
<0.91	90	1 AUBERT,B 06j BABR		$e^+ e^- \rightarrow \Upsilon(4S)$

¹ Assumes equal production of B^+ and B^0 at the $\Upsilon(4S)$.

 $\Gamma(K^+ \mu^\pm \tau^\mp)/\Gamma_{\text{total}}$ Γ_{386}/Γ

Test of lepton family number conservation.

VALUE (units 10^{-6})	CL%	DOCUMENT ID	TECN	COMMENT
<77	90	1 AUBERT 07AZ BABR		$e^+ e^- \rightarrow \Upsilon(4S)$

¹ Uses a fully reconstructed hadronic B decay as a tag on the recoil side.

 $\Gamma(K^*(892)^+ e^+ \mu^-)/\Gamma_{\text{total}}$ Γ_{387}/Γ

Test of total lepton number conservation.

VALUE (units 10^{-7})	CL%	DOCUMENT ID	TECN	COMMENT
<13	90	1 AUBERT,B 06j BABR		$e^+ e^- \rightarrow \Upsilon(4S)$

¹ Assumes equal production of B^+ and B^0 at the $\Upsilon(4S)$.

 $\Gamma(K^*(892)^+ e^- \mu^+)/\Gamma_{\text{total}}$ Γ_{388}/Γ

Test of total lepton number conservation.

VALUE (units 10^{-7})	CL%	DOCUMENT ID	TECN	COMMENT
<9.9	90	1 AUBERT,B 06j BABR		$e^+ e^- \rightarrow \Upsilon(4S)$

¹ Assumes equal production of B^+ and B^0 at the $\Upsilon(4S)$.

 $\Gamma(K^*(892)^+ e^\pm \mu^\mp)/\Gamma_{\text{total}}$ Γ_{389}/Γ

Test of lepton family number conservation.

VALUE (units 10^{-7})	CL%	DOCUMENT ID	TECN	COMMENT
<1.4	90	1 AUBERT,B 06j BABR		$e^+ e^- \rightarrow \Upsilon(4S)$
•••				We do not use the following data for averages, fits, limits, etc. •••
<79	90	1 AUBERT 02L BABR		Repl. by AUBERT,B 06j

¹ Assumes equal production of B^+ and B^0 at the $\Upsilon(4S)$.

 $\Gamma(\pi^- e^+ e^+)/\Gamma_{\text{total}}$ Γ_{390}/Γ

Test of total lepton number conservation.

VALUE	CL%	DOCUMENT ID	TECN	COMMENT
<1.6 $\times 10^{-6}$	90	1 EDWARDS 02B CLE2		$e^+ e^- \rightarrow \Upsilon(4S)$
•••				We do not use the following data for averages, fits, limits, etc. •••
<0.0039	90	2 WEIR 90B MRK2		$e^+ e^- 29 \text{ GeV}$

¹ Assumes equal production of B^+ and B^0 at the $\Upsilon(4S)$.
² WEIR 90B assumes B^+ production cross section from LUND.

 $\Gamma(\pi^- \mu^+ \mu^+)/\Gamma_{\text{total}}$ Γ_{391}/Γ

Test of total lepton number conservation.

VALUE	CL%	DOCUMENT ID	TECN	COMMENT
<1.4 $\times 10^{-6}$	90	1 EDWARDS 02B CLE2		$e^+ e^- \rightarrow \Upsilon(4S)$
•••				We do not use the following data for averages, fits, limits, etc. •••
<0.0091	90	2 WEIR 90B MRK2		$e^+ e^- 29 \text{ GeV}$

¹ Assumes equal production of B^+ and B^0 at the $\Upsilon(4S)$.
² WEIR 90B assumes B^+ production cross section from LUND.

 $\Gamma(\pi^- e^+ \mu^+)/\Gamma_{\text{total}}$ Γ_{392}/Γ

Test of total lepton number conservation.

VALUE	CL%	DOCUMENT ID	TECN	COMMENT
<1.3 $\times 10^{-6}$	90	1 EDWARDS 02B CLE2		$e^+ e^- \rightarrow \Upsilon(4S)$
•••				We do not use the following data for averages, fits, limits, etc. •••
<0.0064	90	2 WEIR 90B MRK2		$e^+ e^- 29 \text{ GeV}$

¹ Assumes equal production of B^+ and B^0 at the $\Upsilon(4S)$.
² WEIR 90B assumes B^+ production cross section from LUND.

 $\Gamma(\rho^- e^+ e^+)/\Gamma_{\text{total}}$ Γ_{393}/Γ

Test of total lepton number conservation.

VALUE (units 10^{-6})	CL%	DOCUMENT ID	TECN	COMMENT
<2.6	90	1 EDWARDS 02B CLE2		$e^+ e^- \rightarrow \Upsilon(4S)$

¹ Assumes equal production of B^+ and B^0 at the $\Upsilon(4S)$.

 $\Gamma(\rho^- \mu^+ \mu^+)/\Gamma_{\text{total}}$ Γ_{394}/Γ

Test of total lepton number conservation.

VALUE (units 10^{-6})	CL%	DOCUMENT ID	TECN	COMMENT
<5.0	90	1 EDWARDS 02B CLE2		$e^+ e^- \rightarrow \Upsilon(4S)$

¹ Assumes equal production of B^+ and B^0 at the $\Upsilon(4S)$.

 $\Gamma(\rho^- e^+ \mu^+)/\Gamma_{\text{total}}$ Γ_{395}/Γ

Test of total lepton number conservation.

VALUE (units 10^{-6})	CL%	DOCUMENT ID	TECN	COMMENT
<3.3	90	1 EDWARDS 02B CLE2		$e^+ e^- \rightarrow \Upsilon(4S)$

¹ Assumes equal production of B^+ and B^0 at the $\Upsilon(4S)$.

 $\Gamma(K^- e^+ e^+)/\Gamma_{\text{total}}$ Γ_{396}/Γ

Test of total lepton number conservation.

VALUE	CL%	DOCUMENT ID	TECN	COMMENT
<1.0 $\times 10^{-6}$	90	1 EDWARDS 02B CLE2		$e^+ e^- \rightarrow \Upsilon(4S)$
•••				We do not use the following data for averages, fits, limits, etc. •••
<0.0039	90	2 WEIR 90B MRK2		$e^+ e^- 29 \text{ GeV}$

¹ Assumes equal production of B^+ and B^0 at the $\Upsilon(4S)$.
² WEIR 90B assumes B^+ production cross section from LUND.

 $\Gamma(K^- \mu^+ \mu^+)/\Gamma_{\text{total}}$ Γ_{397}/Γ

Test of total lepton number conservation.

VALUE	CL%	DOCUMENT ID	TECN	COMMENT
<1.8 $\times 10^{-6}$	90	1 EDWARDS 02B CLE2		$e^+ e^- \rightarrow \Upsilon(4S)$
•••				We do not use the following data for averages, fits, limits, etc. •••
<0.0091	90	2 WEIR 90B MRK2		$e^+ e^- 29 \text{ GeV}$

¹ Assumes equal production of B^+ and B^0 at the $\Upsilon(4S)$.
² WEIR 90B assumes B^+ production cross section from LUND.

 $\Gamma(K^- e^+ \mu^+)/\Gamma_{\text{total}}$ Γ_{398}/Γ

Test of total lepton number conservation.

VALUE	CL%	DOCUMENT ID	TECN	COMMENT
<2.0 $\times 10^{-6}$	90	1 EDWARDS 02B CLE2		$e^+ e^- \rightarrow \Upsilon(4S)$
•••				We do not use the following data for averages, fits, limits, etc. •••
<0.0064	90	2 WEIR 90B MRK2		$e^+ e^- 29 \text{ GeV}$

¹ Assumes equal production of B^+ and B^0 at the $\Upsilon(4S)$.
² WEIR 90B assumes B^+ production cross section from LUND.

 $\Gamma(K^*(892)^- e^+ e^+)/\Gamma_{\text{total}}$ Γ_{399}/Γ

Test of total lepton number conservation.

VALUE (units 10^{-6})	CL%	DOCUMENT ID	TECN	COMMENT
<2.8	90	1 EDWARDS 02B CLE2		$e^+ e^- \rightarrow \Upsilon(4S)$

¹ Assumes equal production of B^+ and B^0 at the $\Upsilon(4S)$.

 $\Gamma(K^*(892)^- \mu^+ \mu^+)/\Gamma_{\text{total}}$ Γ_{400}/Γ

Test of total lepton number conservation.

VALUE (units 10^{-6})	CL%	DOCUMENT ID	TECN	COMMENT
<8.3	90	1 EDWARDS 02B CLE2		$e^+ e^- \rightarrow \Upsilon(4S)$

¹ Assumes equal production of B^+ and B^0 at the $\Upsilon(4S)$.

 $\Gamma(K^*(892)^- e^+ \mu^+)/\Gamma_{\text{total}}$ Γ_{401}/Γ

Test of total lepton number conservation.

VALUE (units 10^{-6})	CL%	DOCUMENT ID	TECN	COMMENT
<4.4	90	1 EDWARDS 02B CLE2		$e^+ e^- \rightarrow \Upsilon(4S)$

¹ Assumes equal production of B^+ and B^0 at the $\Upsilon(4S)$.

POLARIZATION IN B^+ DECAY

In decays involving two vector mesons, one can distinguish among the states in which meson polarizations are both longitudinal (L) or both are transverse and parallel (\parallel) or perpendicular (\perp) to each other with the parameters Γ_L/Γ , Γ_\perp/Γ , and the relative phases ϕ_\parallel and ϕ_\perp . See the definitions in the note on "Polarization in B Decays" review in the B^0 Particle Listings.

 Γ_L/Γ in $B^+ \rightarrow \bar{D}^{*0} \rho^+$

VALUE	DOCUMENT ID	TECN	COMMENT
$0.892 \pm 0.018 \pm 0.016$	CSORNA 03	CLE2	$e^+ e^- \rightarrow \Upsilon(4S)$

 Γ_L/Γ in $B^+ \rightarrow \bar{D}^{*0} K^{*+}$

VALUE	DOCUMENT ID	TECN	COMMENT
$0.86 \pm 0.06 \pm 0.03$	AUBERT 04k	BABR	$e^+ e^- \rightarrow \Upsilon(4S)$

 Γ_L/Γ in $B^+ \rightarrow J/\psi K^{*+}$

VALUE	DOCUMENT ID	TECN	COMMENT
$0.604 \pm 0.015 \pm 0.018$	ITOH 05	BELL	$e^+ e^- \rightarrow \Upsilon(4S)$

 Γ_\perp/Γ in $B^+ \rightarrow J/\psi K^{*+}$

VALUE	DOCUMENT ID	TECN	COMMENT
$0.180 \pm 0.014 \pm 0.010$	ITOH 05	BELL	$e^+ e^- \rightarrow \Upsilon(4S)$

Meson Particle Listings

 B^\pm Γ_L/Γ in $B^+ \rightarrow \phi K^*(892)^+$

VALUE	DOCUMENT ID	TECN	COMMENT
0.50±0.05 OUR AVERAGE			
0.49±0.05±0.03	AUBERT	07BA	BABR $e^+e^- \rightarrow \Upsilon(4S)$
0.52±0.08±0.03	CHEN	05A	BELL $e^+e^- \rightarrow \Upsilon(4S)$
••• We do not use the following data for averages, fits, limits, etc. •••			
0.46±0.12±0.03	AUBERT	03V	BABR Repl. by AUBERT 07BA

 Γ_\perp/Γ in $B^+ \rightarrow \phi K^{*+}$

VALUE	DOCUMENT ID	TECN	COMMENT
0.20±0.05 OUR AVERAGE			
0.21±0.05±0.02	AUBERT	07BA	BABR $e^+e^- \rightarrow \Upsilon(4S)$
0.19±0.08±0.02	CHEN	05A	BELL $e^+e^- \rightarrow \Upsilon(4S)$

 ϕ_\parallel in $B^+ \rightarrow \phi K^{*+}$

VALUE (°)	DOCUMENT ID	TECN	COMMENT
2.34±0.18 OUR AVERAGE			
2.47±0.20±0.07	AUBERT	07BA	BABR $e^+e^- \rightarrow \Upsilon(4S)$
2.10±0.28±0.04	CHEN	05A	BELL $e^+e^- \rightarrow \Upsilon(4S)$

 ϕ_\perp in $B^+ \rightarrow \phi K^{*+}$

VALUE (°)	DOCUMENT ID	TECN	COMMENT
2.58±0.17 OUR AVERAGE			
2.69±0.20±0.03	AUBERT	07BA	BABR $e^+e^- \rightarrow \Upsilon(4S)$
2.31±0.30±0.07	CHEN	05A	BELL $e^+e^- \rightarrow \Upsilon(4S)$

 $\delta_0(B^+ \rightarrow \phi K^{*+})$

VALUE (rad)	DOCUMENT ID	TECN	COMMENT
3.07±0.18±0.06			
	AUBERT	07BA	BABR $e^+e^- \rightarrow \Upsilon(4S)$

 $A_{CP}^0(B^+ \rightarrow \phi K^{*+})$

VALUE	DOCUMENT ID	TECN	COMMENT
0.17±0.11±0.02			
	AUBERT	07BA	BABR $e^+e^- \rightarrow \Upsilon(4S)$

 $A_{CP}^\perp(B^+ \rightarrow \phi K^{*+})$

VALUE	DOCUMENT ID	TECN	COMMENT
0.22±0.24±0.08			
	AUBERT	07BA	BABR $e^+e^- \rightarrow \Upsilon(4S)$

 $\Delta\phi_\parallel(B^+ \rightarrow \phi K^{*+})$

VALUE (rad)	DOCUMENT ID	TECN	COMMENT
0.07±0.20±0.05			
	AUBERT	07BA	BABR $e^+e^- \rightarrow \Upsilon(4S)$

 $\Delta\phi_\perp(B^+ \rightarrow \phi K^{*+})$

VALUE (rad)	DOCUMENT ID	TECN	COMMENT
0.19±0.20±0.07			
	AUBERT	07BA	BABR $e^+e^- \rightarrow \Upsilon(4S)$

 $\Delta\delta_0(B^+ \rightarrow \phi K^{*+})$

VALUE (rad)	DOCUMENT ID	TECN	COMMENT
0.20±0.18±0.03			
	AUBERT	07BA	BABR $e^+e^- \rightarrow \Upsilon(4S)$

 Γ_L/Γ in $B^+ \rightarrow \rho^0 K^*(892)^+$

VALUE	DOCUMENT ID	TECN	COMMENT
••• We do not use the following data for averages, fits, limits, etc. •••			
0.96 $^{+0.04}_{-0.15}$ ±0.04	AUBERT	03V	BABR $e^+e^- \rightarrow \Upsilon(4S)$

 $\Gamma_L/\Gamma(B^+ \rightarrow K^*(892)^0 \rho^+)$

VALUE	DOCUMENT ID	TECN	COMMENT
0.48±0.08 OUR AVERAGE			
0.52±0.10±0.04	AUBERT,B	06G	BABR $e^+e^- \rightarrow \Upsilon(4S)$
0.43±0.11 $^{+0.05}_{-0.02}$	ZHANG	05D	BELL $e^+e^- \rightarrow \Upsilon(4S)$

 Γ_L/Γ in $B^+ \rightarrow \rho^+ \rho^0$

VALUE	DOCUMENT ID	TECN	COMMENT
0.91 ±0.04 OUR AVERAGE			
0.905±0.042 $^{+0.023}_{-0.027}$	AUBERT,BE	06G	BABR $e^+e^- \rightarrow \Upsilon(4S)$
0.948±0.106±0.021	ZHANG	03B	BELL $e^+e^- \rightarrow \Upsilon(4S)$
••• We do not use the following data for averages, fits, limits, etc. •••			
0.97 $^{+0.03}_{-0.07}$ ±0.04	AUBERT	03V	BABR Repl. by AUBERT,BE 06G

 Γ_L/Γ in $B^+ \rightarrow \omega \rho^+$

VALUE	DOCUMENT ID	TECN	COMMENT
0.82±0.11±0.02			
	AUBERT,B	06T	BABR $e^+e^- \rightarrow \Upsilon(4S)$
••• We do not use the following data for averages, fits, limits, etc. •••			
0.88 $^{+0.12}_{-0.15}$ ±0.03	AUBERT	05o	BABR Repl. by AUBERT,B 06T

CP VIOLATION

 A_{CP} is defined as

$$\frac{B(B^- \rightarrow \bar{f}) - B(B^+ \rightarrow f)}{B(B^- \rightarrow \bar{f}) + B(B^+ \rightarrow f)}$$

the CP-violation charge asymmetry of exclusive B^- and B^+ decay. $A_{CP}(B^+ \rightarrow J/\psi(1S) K^+)$

VALUE	DOCUMENT ID	TECN	COMMENT
0.017±0.016 OUR AVERAGE			Error includes scale factor of 1.2.
0.09 ±0.07 ±0.02	¹ WEI	08	BELL $e^+e^- \rightarrow \Upsilon(4S)$
0.030±0.014±0.010	² AUBERT	05J	BABR $e^+e^- \rightarrow \Upsilon(4S)$
-0.026±0.022±0.017	ABE	03B	BELL $e^+e^- \rightarrow \Upsilon(4S)$
0.018±0.043±0.004	³ BONVICINI	00	CLE2 $e^+e^- \rightarrow \Upsilon(4S)$
••• We do not use the following data for averages, fits, limits, etc. •••			
0.03 ±0.015±0.006	AUBERT	04P	BABR Repl. by AUBERT 05J
0.003±0.030±0.004	AUBERT	02F	BABR Repl. by AUBERT 04P
¹ Uses $B^+ \rightarrow J/\psi K^+$, where $J/\psi \rightarrow p\bar{p}$.			
² The result reported corresponds to $-A_{CP}$.			
³ A +0.3% correction is applied due to a slightly higher reconstruction efficiency for the positive kaons.			

 $A_{CP}(B^+ \rightarrow J/\psi(1S) \pi^+)$

VALUE	DOCUMENT ID	TECN	COMMENT
0.09 ±0.08 OUR AVERAGE			
0.123±0.085±0.004	AUBERT	04P	BABR $e^+e^- \rightarrow \Upsilon(4S)$
-0.023±0.164±0.015	ABE	03B	BELL $e^+e^- \rightarrow \Upsilon(4S)$
••• We do not use the following data for averages, fits, limits, etc. •••			
0.01 ±0.22 ±0.01	AUBERT	02F	BABR Repl. by AUBERT 04P

 $A_{CP}(B^+ \rightarrow J/\psi \rho^+)$

VALUE	DOCUMENT ID	TECN	COMMENT
-0.11±0.12±0.08			
	AUBERT	07AC	BABR $e^+e^- \rightarrow \Upsilon(4S)$

 $A_{CP}(B^+ \rightarrow J/\psi K^*(892)^+)$

VALUE	DOCUMENT ID	TECN	COMMENT
-0.048±0.029±0.016			
	¹ AUBERT	05J	BABR $e^+e^- \rightarrow \Upsilon(4S)$
¹ The result reported corresponds to $-A_{CP}$.			

 $A_{CP}(B^+ \rightarrow \eta_c K^+)$

VALUE	DOCUMENT ID	TECN	COMMENT
-0.16±0.08±0.02			
	¹ WEI	08	BELL $e^+e^- \rightarrow \Upsilon(4S)$
¹ Uses $B^+ \rightarrow \eta_c K^+$, where $\eta_c \rightarrow p\bar{p}$.			

 $A_{CP}(B^+ \rightarrow \psi(2S) K^+)$

VALUE	DOCUMENT ID	TECN	COMMENT
-0.025±0.024 OUR AVERAGE			
0.052±0.059±0.020	AUBERT	05J	BABR $e^+e^- \rightarrow \Upsilon(4S)$
-0.042±0.020±0.017	ABE	03B	BELL $e^+e^- \rightarrow \Upsilon(4S)$
0.02 ±0.091±0.01	¹ BONVICINI	00	CLE2 $e^+e^- \rightarrow \Upsilon(4S)$
¹ A +0.3% correction is applied due to a slightly higher reconstruction efficiency for the positive kaons.			

 $A_{CP}(B^+ \rightarrow \psi(2S) K^*(892)^+)$

VALUE	DOCUMENT ID	TECN	COMMENT
0.077±0.207±0.051			
	¹ AUBERT	05J	BABR $e^+e^- \rightarrow \Upsilon(4S)$
¹ The result reported corresponds to $-A_{CP}$.			

 $A_{CP}(B^+ \rightarrow \chi_{c1}(1P) \pi^+)$

VALUE	DOCUMENT ID	TECN	COMMENT
0.07±0.18±0.02			
	KUMAR	06	BELL $e^+e^- \rightarrow \Upsilon(4S)$

 $A_{CP}(B^+ \rightarrow \chi_{c0} K^+)$

VALUE	DOCUMENT ID	TECN	COMMENT
-0.065±0.20$^{+0.035}_{-0.024}$			
	GARMASH	06	BELL $e^+e^- \rightarrow \Upsilon(4S)$

 $A_{CP}(B^+ \rightarrow \chi_{c1} K^+)$

VALUE	DOCUMENT ID	TECN	COMMENT
-0.009±0.033 OUR AVERAGE			
-0.01 ±0.03 ±0.02	KUMAR	06	BELL $e^+e^- \rightarrow \Upsilon(4S)$
-0.003±0.076±0.017	¹ AUBERT	05J	BABR $e^+e^- \rightarrow \Upsilon(4S)$
¹ The result reported corresponds to $-A_{CP}$.			

 $A_{CP}(B^+ \rightarrow \chi_{c1} K^*(892)^+)$

VALUE	DOCUMENT ID	TECN	COMMENT
0.471±0.378±0.268			
	¹ AUBERT	05J	BABR $e^+e^- \rightarrow \Upsilon(4S)$
¹ The result reported corresponds to $-A_{CP}$.			

 $A_{CP}(B^+ \rightarrow \bar{D}^0 \pi^+)$

VALUE	DOCUMENT ID	TECN	COMMENT
-0.008±0.008			
	ABE	06	BELL $e^+e^- \rightarrow \Upsilon(4S)$

$A_{CP}(B^+ \rightarrow D_{CP(+1)}\pi^+)$

VALUE	DOCUMENT ID	TECN	COMMENT
0.035 ± 0.024	ABE	06	BELL $e^+e^- \rightarrow \Upsilon(4S)$

 $A_{CP}(B^+ \rightarrow D_{CP(-1)}\pi^+)$

VALUE	DOCUMENT ID	TECN	COMMENT
0.017 ± 0.026	ABE	06	BELL $e^+e^- \rightarrow \Upsilon(4S)$

 $A_{CP}(B^+ \rightarrow \bar{D}^0 K^+)$

VALUE	DOCUMENT ID	TECN	COMMENT
0.066 ± 0.036	ABE	06	BELL $e^+e^- \rightarrow \Upsilon(4S)$

• • • We do not use the following data for averages, fits, limits, etc. • • •

0.003 ± 0.080 ± 0.037	¹ ABE	03D	BELL Repl. by SWAIN 03
0.04 ± 0.06 ± 0.03	² SWAIN	03	BELL Repl. by ABE 06

¹ Corresponds to 90% confidence range $-0.15 < A_{CP} < 0.16$.

² Corresponds to 90% confidence range $-0.07 < A_{CP} < 0.15$.

 $r_B(B^+ \rightarrow D^0 K^+)$

$r_B^{(*)}$ and $\delta_B^{(*)}$ are the amplitude ratios and relative strong phases between the amplitudes of $A_{CP}(B^+ \rightarrow D^{(*)0} K^+)$ and $A_{CP}(B^+ \rightarrow \bar{D}^{(*)0} K^+)$,

VALUE	DOCUMENT ID	TECN	COMMENT
0.14 ± 0.06 OUR AVERAGE			

0.159 ^{+0.054} _{-0.050} ± 0.050	¹ POLUEKTOV	06	BELL $e^+e^- \rightarrow \Upsilon(4S)$
---	------------------------	----	--

0.12 ± 0.08 ± 0.05	² AUBERT,B	05Y	BABR $e^+e^- \rightarrow \Upsilon(4S)$
--------------------	-----------------------	-----	--

¹ Uses a Dalitz plot analysis of the $\bar{D}^0 \rightarrow K_S^0 \pi^+ \pi^-$ decays; Combines the $D K^+$, $D^* K^+$ and $D K^{*+}$ modes.

² Uses a Dalitz analysis of neutral D decays to $K_S^0 \pi^+ \pi^-$ in the processes $B^{\pm} \rightarrow D^{(*)} K^{\pm}$, $D^* \rightarrow D \pi^0$, $D \gamma$.

 $\delta_B(B^+ \rightarrow D^0 K^+)$

VALUE (degrees)	DOCUMENT ID	TECN	COMMENT
135 ± 26 OUR AVERAGE			

145.7 ^{+19.0} _{-19.7} ± 23.1	¹ POLUEKTOV	06	BELL $e^+e^- \rightarrow \Upsilon(4S)$
--	------------------------	----	--

104 ± 45 ⁺²³ ₋₃₂	² AUBERT,B	05Y	BABR $e^+e^- \rightarrow \Upsilon(4S)$
--	-----------------------	-----	--

¹ Uses a Dalitz plot analysis of the $\bar{D}^0 \rightarrow K_S^0 \pi^+ \pi^-$ decays; Combines the $D K^+$, $D^* K^+$ and $D K^{*+}$ modes.

² Uses a Dalitz analysis of neutral D decays to $K_S^0 \pi^+ \pi^-$ in the processes $B^{\pm} \rightarrow D^{(*)} K^{\pm}$, $D^* \rightarrow D \pi^0$, $D \gamma$.

 $r_B(B^+ \rightarrow D K^{*+})$

r_B and δ_B are the amplitude ratios and relative strong phases between the amplitudes of $A_{CP}(B^+ \rightarrow D K^{*+})$ and $A_{CP}(B^+ \rightarrow \bar{D} K^{*+})$,

VALUE	DOCUMENT ID	TECN	COMMENT
0.564^{+0.216}_{-0.155} ± 0.093	¹ POLUEKTOV	06	BELL $e^+e^- \rightarrow \Upsilon(4S)$

¹ Uses a Dalitz plot analysis of the $\bar{D}^0 \rightarrow K_S^0 \pi^+ \pi^-$ decays; Combines the $D K^+$, $D^* K^+$ and $D K^{*+}$ modes.

 $\delta_B(B^+ \rightarrow D K^{*+})$

VALUE (degrees)	DOCUMENT ID	TECN	COMMENT
242.6^{+20.2}_{-23.2} ± 49.4	¹ POLUEKTOV	06	BELL $e^+e^- \rightarrow \Upsilon(4S)$

¹ Uses a Dalitz plot analysis of the $\bar{D}^0 \rightarrow K_S^0 \pi^+ \pi^-$ decays; Combines the $D K^+$, $D^* K^+$ and $D K^{*+}$ modes.

 $A_{CP}(B^+ \rightarrow [K^-\pi^+]_D K^+)$

VALUE	DOCUMENT ID	TECN	COMMENT
+0.88^{+0.77}_{-0.62} ± 0.06	SAIGO	05	BELL $e^+e^- \rightarrow \Upsilon(4S)$

 $A_{CP}(B^+ \rightarrow [K^-\pi^+]_{\bar{D}} K^{*(892)+})$

VALUE	DOCUMENT ID	TECN	COMMENT
-0.22 ± 0.61 ± 0.17	AUBERT,B	05V	BABR $e^+e^- \rightarrow \Upsilon(4S)$

 $A_{CP}(B^+ \rightarrow [K^-\pi^+]_D \pi^+)$

VALUE	DOCUMENT ID	TECN	COMMENT
+0.30^{+0.29}_{-0.25} ± 0.06	SAIGO	05	BELL $e^+e^- \rightarrow \Upsilon(4S)$

 $A_{CP}(B^+ \rightarrow [\pi^+\pi^-\pi^0]_D K^+)$

VALUE	DOCUMENT ID	TECN	COMMENT
-0.02 ± 0.15 ± 0.03	¹ AUBERT	07Bj	BABR $e^+e^- \rightarrow \Upsilon(4S)$

• • • We do not use the following data for averages, fits, limits, etc. • • •

-0.02 ± 0.16 ± 0.03	AUBERT,B	05T	BABR Repl. by AUBERT 07Bj
---------------------	----------	-----	---------------------------

¹ Uses a Dalitz plot analysis of $D^0 \rightarrow \pi^+ \pi^- \pi^0$. Also reports the one-sigma regions: $0.06 < r_B < 0.78$, $-30^\circ < \gamma < 76^\circ$, and $-27^\circ < \delta < 78^\circ$.

 $A_{CP}(B^+ \rightarrow D_{CP(+1)} K^+)$

VALUE	DOCUMENT ID	TECN	COMMENT
0.22 ± 0.14 OUR AVERAGE	Error		includes scale factor of 1.4.

0.06 ± 0.14 ± 0.05	ABE	06	BELL $e^+e^- \rightarrow \Upsilon(4S)$
0.35 ± 0.13 ± 0.04	AUBERT	06j	BABR $e^+e^- \rightarrow \Upsilon(4S)$

• • • We do not use the following data for averages, fits, limits, etc. • • •

0.07 ± 0.17 ± 0.06	AUBERT	04N	BABR Repl. by AUBERT 06j
0.29 ± 0.26 ± 0.05	¹ ABE	03D	BELL Repl. by SWAIN 03
0.06 ± 0.19 ± 0.04	² SWAIN	03	BELL Repl. by ABE 06

¹ Corresponds to 90% confidence range $-0.14 < A_{CP} < 0.73$.

² Corresponds to 90% confidence range $-0.26 < A_{CP} < 0.38$.

 $A_{CP}(B^+ \rightarrow D_{CP(-1)} K^+)$

VALUE	DOCUMENT ID	TECN	COMMENT
-0.09 ± 0.10 OUR AVERAGE			

-0.12 ± 0.14 ± 0.05	ABE	06	BELL $e^+e^- \rightarrow \Upsilon(4S)$
-0.06 ± 0.13 ± 0.04	AUBERT	06j	BABR $e^+e^- \rightarrow \Upsilon(4S)$

• • • We do not use the following data for averages, fits, limits, etc. • • •

-0.22 ± 0.24 ± 0.04	¹ ABE	03D	BELL Repl. by SWAIN 03
-0.19 ± 0.17 ± 0.05	² SWAIN	03	BELL Repl. by ABE 06

¹ Corresponds to 90% confidence range $-0.62 < A_{CP} < 0.18$.

² Corresponds to 90% confidence range $-0.47 < A_{CP} < 0.11$.

 $A_{CP}(B^+ \rightarrow \bar{D}^{*0} \pi^+)$

VALUE	DOCUMENT ID	TECN	COMMENT
-0.014 ± 0.015	ABE	06	BELL $e^+e^- \rightarrow \Upsilon(4S)$

 $A_{CP}(B^+ \rightarrow (D_{CP(+1)}^*)^0 \pi^+)$

VALUE	DOCUMENT ID	TECN	COMMENT
-0.021 ± 0.045	ABE	06	BELL $e^+e^- \rightarrow \Upsilon(4S)$

 $A_{CP}(B^+ \rightarrow (D_{CP(-1)}^*)^0 \pi^+)$

VALUE	DOCUMENT ID	TECN	COMMENT
-0.090 ± 0.051	ABE	06	BELL $e^+e^- \rightarrow \Upsilon(4S)$

 $A_{CP}(B^+ \rightarrow D^{*0} K^+)$

VALUE	DOCUMENT ID	TECN	COMMENT
-0.089 ± 0.086	ABE	06	BELL $e^+e^- \rightarrow \Upsilon(4S)$

 $r_B^*(B^+ \rightarrow D^{*0} K^+)$

$r_B^{(*)}$ and $\delta_B^{(*)}$ are the amplitude ratios and relative strong phases between the amplitudes of $A_{CP}(B^+ \rightarrow D^{(*)0} K^+)$ and $A_{CP}(B^+ \rightarrow \bar{D}^{(*)0} K^+)$,

VALUE	DOCUMENT ID	TECN	COMMENT
0.17 ± 0.08 OUR AVERAGE			

0.175 ^{+0.108} _{-0.095} ± 0.050	¹ POLUEKTOV	06	BELL $e^+e^- \rightarrow \Upsilon(4S)$
---	------------------------	----	--

0.17 ± 0.10 ± 0.04	² AUBERT,B	05Y	BABR $e^+e^- \rightarrow \Upsilon(4S)$
--------------------	-----------------------	-----	--

¹ Uses a Dalitz plot analysis of the $\bar{D}^0 \rightarrow K_S^0 \pi^+ \pi^-$ decays; Combines the $D K^+$, $D^* K^+$ and $D K^{*+}$ modes.

² Uses a Dalitz analysis of neutral D decays to $K_S^0 \pi^+ \pi^-$ in the processes $B^{\pm} \rightarrow D^{(*)} K^{\pm}$, $D^* \rightarrow D \pi^0$, $D \gamma$.

 $\delta_B^*(B^+ \rightarrow D^{*0} K^+)$

VALUE (degrees)	DOCUMENT ID	TECN	COMMENT
299 ± 31 OUR AVERAGE			

302.0 ^{+33.8} _{-35.1} ± 23.7	¹ POLUEKTOV	06	BELL $e^+e^- \rightarrow \Upsilon(4S)$
--	------------------------	----	--

296 ± 41 ⁺²⁰ ₋₁₉	² AUBERT,B	05Y	BABR $e^+e^- \rightarrow \Upsilon(4S)$
--	-----------------------	-----	--

¹ Uses a Dalitz plot analysis of the $\bar{D}^0 \rightarrow K_S^0 \pi^+ \pi^-$ decays; Combines the $D K^+$, $D^* K^+$ and $D K^{*+}$ modes.

² Uses a Dalitz analysis of neutral D decays to $K_S^0 \pi^+ \pi^-$ in the processes $B^{\pm} \rightarrow D^{(*)} K^{\pm}$, $D^* \rightarrow D \pi^0$, $D \gamma$.

 $A_{CP}(B^+ \rightarrow D_{CP(+1)}^{*0} K^+)$

VALUE	DOCUMENT ID	TECN	COMMENT
-0.15 ± 0.16 OUR AVERAGE			

-0.20 ± 0.22 ± 0.04	ABE	06	BELL $e^+e^- \rightarrow \Upsilon(4S)$
-0.10 ± 0.23 ^{+0.03} _{-0.04}	AUBERT	05N	BABR $e^+e^- \rightarrow \Upsilon(4S)$

 $A_{CP}(B^+ \rightarrow D_{CP(-1)}^{*0} K^+)$

VALUE	DOCUMENT ID	TECN	COMMENT
0.13 ± 0.30 ± 0.08	ABE	06	BELL $e^+e^- \rightarrow \Upsilon(4S)$

 $A_{CP}(B^+ \rightarrow D_{CP(+1)} K^{*(892)+})$

VALUE	DOCUMENT ID	TECN	COMMENT
-0.08 ± 0.19 ± 0.08	AUBERT,B	05U	BABR $e^+e^- \rightarrow \Upsilon(4S)$

 $A_{CP}(B^+ \rightarrow D_{CP(-1)} K^{*(892)+})$

VALUE	DOCUMENT ID	TECN	COMMENT
-0.26 ± 0.40 ± 0.12	AUBERT,B	05U	BABR $e^+e^- \rightarrow \Upsilon(4S)$

Meson Particle Listings

 B^\pm $A_{CP}(B^+ \rightarrow D^{*+} \bar{D}^{*0})$

VALUE	DOCUMENT ID	TECN	COMMENT
$-0.15 \pm 0.11 \pm 0.02$	AUBERT,B	06A	BABR $e^+ e^- \rightarrow \Upsilon(4S)$

 $A_{CP}(B^+ \rightarrow D^{*+} \bar{D}^0)$

VALUE	DOCUMENT ID	TECN	COMMENT
$-0.06 \pm 0.13 \pm 0.02$	AUBERT,B	06A	BABR $e^+ e^- \rightarrow \Upsilon(4S)$

 $A_{CP}(B^+ \rightarrow D^+ \bar{D}^{*0})$

VALUE	DOCUMENT ID	TECN	COMMENT
$0.13 \pm 0.18 \pm 0.04$	AUBERT,B	06A	BABR $e^+ e^- \rightarrow \Upsilon(4S)$

 $A_{CP}(B^+ \rightarrow D^+ \bar{D}^0)$

VALUE	DOCUMENT ID	TECN	COMMENT
$-0.13 \pm 0.14 \pm 0.02$	AUBERT,B	06A	BABR $e^+ e^- \rightarrow \Upsilon(4S)$

 $A_{CP}(B^+ \rightarrow K_S^0 \pi^+)$

VALUE	DOCUMENT ID	TECN	COMMENT
0.009 ± 0.029 OUR AVERAGE	Error includes scale factor of 1.2.		
$0.03 \pm 0.03 \pm 0.01$	LIN	07	BELL $e^+ e^- \rightarrow \Upsilon(4S)$
$-0.029 \pm 0.039 \pm 0.010$	¹ AUBERT,BE	06c	BABR $e^+ e^- \rightarrow \Upsilon(4S)$
0.18 ± 0.24	² CHEN	00	CLE2 $e^+ e^- \rightarrow \Upsilon(4S)$
••• We do not use the following data for averages, fits, limits, etc. •••			
$-0.09 \pm 0.05 \pm 0.01$	³ AUBERT,BE	05E	BABR Repl. by AUBERT,BE 06c
$0.05 \pm 0.05 \pm 0.01$	⁴ CHAO	05A	BELL Repl. by LIN 07
$-0.05 \pm 0.08 \pm 0.01$	⁵ AUBERT	04M	BABR Repl. by AUBERT,BE 05E
$0.07 \pm 0.09 \pm 0.01$	⁶ UNNO	03	BELL Repl. by CHAO 05A
$-0.08 \pm 0.08 \pm 0.03$	⁷ CASEY	02	BELL Repl. by UNNO 03
$0.46 \pm 0.15 \pm 0.02$	⁸ ABE	01k	BELL Repl. by CASEY 02
$0.098 \pm 0.430 \pm 0.020$	⁹ AUBERT	01E	BABR Repl. by AUBERT 04M
$-0.21 \pm 0.18 \pm 0.03$			

¹ Corresponds to 90% confidence range $-0.092 < A_{CP} < 0.036$.² Corresponds to 90% confidence range $-0.22 < A_{CP} < 0.56$.³ Corresponds to 90% confidence range $-0.16 < A_{CP} < -0.02$.⁴ Corresponds to a 90% CL interval of $-0.04 < A_{CP} < 0.13$.⁵ 90% CL interval $-0.18 < A_{CP} < 0.08$.⁶ Corresponds to 90% confidence range $-0.10 < A_{CP} < +0.22$.⁷ Corresponds to 90% confidence range $-0.19 < A_{CP} < +0.72$.⁸ Corresponds to 90% confidence range $-0.53 < A_{CP} < 0.82$.⁹ Corresponds to 90% confidence range $-0.51 < A_{CP} < 0.09$. $A_{CP}(B^+ \rightarrow K^+ \pi^0)$

VALUE	DOCUMENT ID	TECN	COMMENT
0.027 ± 0.032 OUR AVERAGE			
$0.030 \pm 0.039 \pm 0.010$	AUBERT	07Bc	BABR $e^+ e^- \rightarrow \Upsilon(4S)$
$0.04 \pm 0.05 \pm 0.02$	¹ CHAO	04B	BELL $e^+ e^- \rightarrow \Upsilon(4S)$
-0.29 ± 0.23	² CHEN	00	CLE2 $e^+ e^- \rightarrow \Upsilon(4S)$
••• We do not use the following data for averages, fits, limits, etc. •••			
$0.06 \pm 0.06 \pm 0.01$	³ AUBERT	05L	BABR Repl. by AUBERT 07Bc
$0.06 \pm 0.06 \pm 0.02$	³ CHAO	05A	BELL Repl. by CHAO 04B
$-0.09 \pm 0.09 \pm 0.01$	⁴ AUBERT	03L	BABR Repl. by AUBERT 05L
$-0.02 \pm 0.19 \pm 0.02$	⁵ CASEY	02	BELL Repl. by CHAO 04B
$-0.059 \pm 0.222 \pm 0.055$	⁶ ABE	01k	BELL Repl. by CASEY 02
$0.00 \pm 0.18 \pm 0.04$	⁷ AUBERT	01E	BABR Repl. by AUBERT 03L

¹ Corresponds to 90% CL interval of $-0.05 < A_{CP} < 0.13$.² Corresponds to 90% confidence range $-0.67 < A_{CP} < 0.09$.³ Corresponds to a 90% CL interval of $-0.06 < A_{CP} < 0.18$.⁴ Corresponds to 90% confidence range $-0.24 < A_{CP} < 0.06$.⁵ Corresponds to 90% confidence range $-0.35 < A_{CP} < +0.30$.⁶ Corresponds to 90% confidence range $-0.40 < A_{CP} < 0.36$.⁷ Corresponds to 90% confidence range $-0.30 < A_{CP} < +0.30$. $A_{CP}(B^+ \rightarrow \eta' K^+)$

VALUE	DOCUMENT ID	TECN	COMMENT
0.016 ± 0.019 OUR AVERAGE			
$0.010 \pm 0.022 \pm 0.006$	AUBERT	07AE	BABR $e^+ e^- \rightarrow \Upsilon(4S)$
$0.028 \pm 0.028 \pm 0.021$	SCHUEMANN	06	BELL $e^+ e^- \rightarrow \Upsilon(4S)$
0.03 ± 0.12	¹ CHEN	00	CLE2 $e^+ e^- \rightarrow \Upsilon(4S)$
••• We do not use the following data for averages, fits, limits, etc. •••			
$0.033 \pm 0.028 \pm 0.005$	² AUBERT	05M	BABR Repl. by AUBERT 07AE
$0.037 \pm 0.045 \pm 0.011$	³ AUBERT	03W	BABR Repl. by AUBERT 05M
$-0.11 \pm 0.11 \pm 0.02$	⁴ AUBERT	02E	BABR Repl. by AUBERT 05M
$-0.015 \pm 0.070 \pm 0.009$	⁵ CHEN	02B	BELL Repl. by SCHUEMANN 06
$0.06 \pm 0.15 \pm 0.01$	⁶ ABE	01M	BELL Repl. by CHEN 02B

¹ Corresponds to 90% confidence range $-0.17 < A_{CP} < 0.23$.² Corresponds to 90% confidence range $-0.012 < A_{CP} < 0.078$.³ Corresponds to 90% confidence range $-0.04 < A_{CP} < 0.11$.⁴ Corresponds to 90% confidence range $-0.28 < A_{CP} < 0.07$.⁵ Corresponds to 90% confidence range $-0.13 < A_{CP} < 0.10$.⁶ Corresponds to 90% confidence range $-0.20 < A_{CP} < 0.32$. $A_{CP}(B^+ \rightarrow \eta' K^*(892)^+)$

VALUE	DOCUMENT ID	TECN	COMMENT
$0.30 \pm 0.33 \pm 0.02$	AUBERT	07E	BABR $e^+ e^- \rightarrow \Upsilon(4S)$

 $A_{CP}(B^+ \rightarrow \eta K^+)$

VALUE	DOCUMENT ID	TECN	COMMENT
-0.27 ± 0.09 OUR AVERAGE			
$-0.22 \pm 0.11 \pm 0.01$	AUBERT	07AE	BABR $e^+ e^- \rightarrow \Upsilon(4S)$
$-0.39 \pm 0.16 \pm 0.03$	CHANG	07B	BELL $e^+ e^- \rightarrow \Upsilon(4S)$
••• We do not use the following data for averages, fits, limits, etc. •••			
$-0.20 \pm 0.15 \pm 0.01$	AUBERT,B	05k	BABR Repl. by AUBERT 07AE
$-0.49 \pm 0.31 \pm 0.07$	CHANG	05A	BELL Repl. by CHANG 07B
$-0.52 \pm 0.24 \pm 0.01$	AUBERT	04H	BABR Repl. by AUBERT,B 05k

 $A_{CP}(B^+ \rightarrow \eta K^*(892)^+)$

VALUE	DOCUMENT ID	TECN	COMMENT
0.02 ± 0.06 OUR AVERAGE			
$0.03 \pm 0.10 \pm 0.01$	WANG	07B	BELL $e^+ e^- \rightarrow \Upsilon(4S)$
$0.01 \pm 0.08 \pm 0.02$	AUBERT,B	06H	BABR $e^+ e^- \rightarrow \Upsilon(4S)$
••• We do not use the following data for averages, fits, limits, etc. •••			
$0.13 \pm 0.14 \pm 0.02$	AUBERT,B	04D	BABR Repl. by AUBERT,B 06H

 $A_{CP}(B^+ \rightarrow \eta K_0^*(1430)^+)$

VALUE	DOCUMENT ID	TECN	COMMENT
$0.05 \pm 0.13 \pm 0.02$	AUBERT,B	06H	BABR $e^+ e^- \rightarrow \Upsilon(4S)$

 $A_{CP}(B^+ \rightarrow \eta K_2^*(1430)^+)$

VALUE	DOCUMENT ID	TECN	COMMENT
$-0.45 \pm 0.30 \pm 0.02$	AUBERT,B	06H	BABR $e^+ e^- \rightarrow \Upsilon(4S)$

 $A_{CP}(B^+ \rightarrow \omega K^+)$

VALUE	DOCUMENT ID	TECN	COMMENT
0.02 ± 0.05 OUR AVERAGE			
$-0.01 \pm 0.07 \pm 0.01$	AUBERT	07AE	BABR $e^+ e^- \rightarrow \Upsilon(4S)$
$0.05 \pm 0.08 \pm 0.01$	JEN	06	BELL $e^+ e^- \rightarrow \Upsilon(4S)$
••• We do not use the following data for averages, fits, limits, etc. •••			
$0.05 \pm 0.09 \pm 0.01$	AUBERT,B	06E	BABR Repl. by AUBERT 07AE
$-0.09 \pm 0.17 \pm 0.01$	AUBERT	04H	BABR Repl. by AUBERT,B 06E
$0.06 \pm 0.21 \pm 0.01$	¹ WANG	04A	BELL Repl. by JEN 06
$-0.21 \pm 0.28 \pm 0.03$	² LU	02	BELL Repl. by WANG 04A
¹ Corresponds to 90% CL interval $0.15 < A_{CP} < 0.90$			
² Corresponds to 90% confidence range $-0.70 < A_{CP} < +0.38$.			

 $A_{CP}(B^+ \rightarrow K^*(892)^+ \pi^0)$

VALUE	DOCUMENT ID	TECN	COMMENT
$0.04 \pm 0.29 \pm 0.05$	AUBERT	05X	BABR $e^+ e^- \rightarrow \Upsilon(4S)$

 $A_{CP}(B^+ \rightarrow K^{*0} \pi^+)$

VALUE	DOCUMENT ID	TECN	COMMENT
-0.08 ± 0.10 OUR AVERAGE	Error includes scale factor of 1.8.		
$-0.149 \pm 0.064 \pm 0.022$	GARMASH	06	BELL $e^+ e^- \rightarrow \Upsilon(4S)$
$0.068 \pm 0.078 \pm 0.070$	AUBERT,B	05N	BABR $e^+ e^- \rightarrow \Upsilon(4S)$
-0.067			

 $A_{CP}(B^+ \rightarrow K^+ \pi^- \pi^+)$

VALUE	DOCUMENT ID	TECN	COMMENT
0.023 ± 0.031 OUR AVERAGE	Error includes scale factor of 1.2.		
$0.049 \pm 0.026 \pm 0.020$	GARMASH	06	BELL $e^+ e^- \rightarrow \Upsilon(4S)$
$-0.013 \pm 0.037 \pm 0.011$	AUBERT,B	05N	BABR $e^+ e^- \rightarrow \Upsilon(4S)$
••• We do not use the following data for averages, fits, limits, etc. •••			
$0.01 \pm 0.07 \pm 0.03$	AUBERT	03M	BABR Repl. by AUBERT,B 05N

 $A_{CP}(B^+ \rightarrow f_0(980) K^+)$

VALUE	DOCUMENT ID	TECN	COMMENT
$-0.04 \pm 0.08 \pm 0.07$ OUR AVERAGE	Error includes scale factor of 1.1.		
$-0.31 \pm 0.25 \pm 0.08$	¹ AUBERT	06o	BABR $e^+ e^- \rightarrow \Upsilon(4S)$
$-0.077 \pm 0.065 \pm 0.046$	GARMASH	06	BELL $e^+ e^- \rightarrow \Upsilon(4S)$
-0.026			
$0.088 \pm 0.095 \pm 0.097$	AUBERT,B	05N	BABR $e^+ e^- \rightarrow \Upsilon(4S)$
-0.056			
¹ Measured in the $B^+ \rightarrow K^+ K^- K^+$ decay.			

 $A_{CP}(B^+ \rightarrow f_2(1270) K^+)$

VALUE	DOCUMENT ID	TECN	COMMENT
$-0.59 \pm 0.22 \pm 0.036$	GARMASH	06	BELL $e^+ e^- \rightarrow \Upsilon(4S)$

 $A_{CP}(B^+ \rightarrow X_0(1550) K^+)$

VALUE	DOCUMENT ID	TECN	COMMENT
$-0.04 \pm 0.07 \pm 0.02$	¹ AUBERT	06o	BABR $e^+ e^- \rightarrow \Upsilon(4S)$
¹ Measured in the $B^+ \rightarrow K^+ K^- K^+$ decay.			

$A_{CP}(B^+ \rightarrow \rho^0 K^+)$

VALUE	DOCUMENT ID	TECN	COMMENT
$0.31 \pm_{-0.09}^{+0.11}$ OUR AVERAGE			
$0.30 \pm_{-0.04}^{+0.11}$	GARMASH	06	BELL $e^+ e^- \rightarrow \Upsilon(4S)$
$0.32 \pm_{-0.08}^{+0.10}$	AUBERT,B	05N	BABR $e^+ e^- \rightarrow \Upsilon(4S)$

 $A_{CP}(B^+ \rightarrow K_S^0(1430)^0 \pi^+)$

VALUE	DOCUMENT ID	TECN	COMMENT
0.00 ± 0.07 OUR AVERAGE			Error includes scale factor of 2.4.
$0.076 \pm_{-0.022}^{+0.038}$	GARMASH	06	BELL $e^+ e^- \rightarrow \Upsilon(4S)$
$-0.064 \pm_{-0.026}^{+0.032}$	AUBERT,B	05N	BABR $e^+ e^- \rightarrow \Upsilon(4S)$

 $A_{CP}(B^+ \rightarrow K^0 \rho^+)$

VALUE (units 10^{-6})	DOCUMENT ID	TECN	COMMENT
$-0.12 \pm 0.17 \pm 0.02$	AUBERT	07Z	BABR $e^+ e^- \rightarrow \Upsilon(4S)$

 $A_{CP}(B^+ \rightarrow \rho \bar{\Lambda} \pi^0)$

VALUE	DOCUMENT ID	TECN	COMMENT
$+0.01 \pm 0.17 \pm 0.04$	WANG	07C	BELL $e^+ e^- \rightarrow \Upsilon(4S)$

 $A_{CP}(B^+ \rightarrow \rho^0 K^*(892)^+)$

VALUE	DOCUMENT ID	TECN	COMMENT
$0.20 \pm_{-0.29}^{+0.32} \pm 0.04$	AUBERT	03V	BABR $e^+ e^- \rightarrow \Upsilon(4S)$

 $A_{CP}(B^+ \rightarrow K^*(892)^+ \bar{\eta}_0(980))$

VALUE	DOCUMENT ID	TECN	COMMENT
$-0.34 \pm 0.21 \pm 0.03$	AUBERT,B	06G	BABR $e^+ e^- \rightarrow \Upsilon(4S)$

 $A_{CP}(B^+ \rightarrow a_1^+ K^0)$

VALUE	DOCUMENT ID	TECN	COMMENT
$+0.12 \pm 0.11 \pm 0.02$	AUBERT	08F	BABR $e^+ e^- \rightarrow \Upsilon(4S)$

 $A_{CP}(B^+ \rightarrow K^*(892)^0 \rho^+)$

VALUE	DOCUMENT ID	TECN	COMMENT
$-0.01 \pm 0.16 \pm 0.02$	AUBERT,B	06G	BABR $e^+ e^- \rightarrow \Upsilon(4S)$

 $A_{CP}(B^+ \rightarrow K^0 K^+)$

VALUE	DOCUMENT ID	TECN	COMMENT
0.12 ± 0.18 OUR AVERAGE			
$0.13 \pm_{-0.24}^{+0.23} \pm 0.02$	LIN	07	BELL $e^+ e^- \rightarrow \Upsilon(4S)$
$0.10 \pm 0.26 \pm 0.03$	¹ AUBERT,BE	06c	BABR $e^+ e^- \rightarrow \Upsilon(4S)$
$0.15 \pm 0.33 \pm 0.03$	² AUBERT,BE	05E	BABR Repl. by AUBERT,BE 06c
<ul style="list-style-type: none"> ••• We do not use the following data for averages, fits, limits, etc. ••• 			
¹ Corresponds to 90% confidence range $-0.31 < A_{CP} < 0.54$. ² Corresponds to 90% confidence range $-0.43 < A_{CP} < 0.68$.			

 $A_{CP}(B^+ \rightarrow b_1^0 K^+)$

VALUE	DOCUMENT ID	TECN	COMMENT
$-0.46 \pm 0.20 \pm 0.02$	AUBERT	07B1	BABR $e^+ e^- \rightarrow \Upsilon(4S)$

 $A_{CP}(B^+ \rightarrow K^+ K_S^0 K_S^0)$

VALUE	DOCUMENT ID	TECN	COMMENT
$-0.04 \pm 0.11 \pm 0.02$	¹ AUBERT,B	04V	BABR $e^+ e^- \rightarrow \Upsilon(4S)$
¹ Corresponds to 90% confidence range $-0.23 < A_{CP} < 0.15$.			

 $A_{CP}(B^+ \rightarrow K^+ K^- \pi^+)$

VALUE	DOCUMENT ID	TECN	COMMENT
$0.00 \pm 0.10 \pm 0.03$	AUBERT	07Bb	BABR $e^+ e^- \rightarrow \Upsilon(4S)$

 $A_{CP}(B^+ \rightarrow K^+ K^- K^+)$

VALUE	DOCUMENT ID	TECN	COMMENT
$-0.017 \pm 0.026 \pm 0.015$	AUBERT	06o	BABR $e^+ e^- \rightarrow \Upsilon(4S)$
<ul style="list-style-type: none"> ••• We do not use the following data for averages, fits, limits, etc. ••• 			
$0.02 \pm 0.07 \pm 0.03$	AUBERT	03M	BABR Repl. by AUBERT 06o

 $A_{CP}(B^+ \rightarrow K^{*+} K^+ K^-)$

VALUE	DOCUMENT ID	TECN	COMMENT
$0.11 \pm 0.08 \pm 0.03$	AUBERT,B	06u	BABR $e^+ e^- \rightarrow \Upsilon(4S)$

 $A_{CP}(B^+ \rightarrow K^{*+} \pi^+ \pi^-)$

VALUE	DOCUMENT ID	TECN	COMMENT
$0.07 \pm 0.07 \pm 0.04$	AUBERT,B	06u	BABR $e^+ e^- \rightarrow \Upsilon(4S)$

 $A_{CP}(B^+ \rightarrow \phi K^+)$

VALUE	DOCUMENT ID	TECN	COMMENT
-0.01 ± 0.06 OUR AVERAGE			
$0.00 \pm 0.08 \pm 0.02$	AUBERT	06o	BABR $e^+ e^- \rightarrow \Upsilon(4S)$
$-0.07 \pm_{-0.02}^{+0.17}$	ACOSTA	05J	CDF $p\bar{p}$ at 1.96 TeV
$0.01 \pm 0.12 \pm 0.05$	¹ CHEN	03B	BELL $e^+ e^- \rightarrow \Upsilon(4S)$
<ul style="list-style-type: none"> ••• We do not use the following data for averages, fits, limits, etc. ••• 			
$0.04 \pm 0.09 \pm 0.01$	² AUBERT	04A	BABR Repl. by AUBERT 06o
$-0.05 \pm 0.20 \pm 0.03$	³ AUBERT	02E	BABR $e^+ e^- \rightarrow \Upsilon(4S)$
¹ Corresponds to 90% confidence range $-0.20 < A_{CP} < 0.22$. ² Corresponds to 90% confidence range $-0.10 < A_{CP} < 0.18$. ³ Corresponds to 90% confidence range $-0.37 < A_{CP} < 0.28$.			

 $A_{CP}(B^+ \rightarrow \phi K^*(892)^+)$

VALUE	DOCUMENT ID	TECN	COMMENT
-0.01 ± 0.08 OUR AVERAGE			
$0.00 \pm 0.09 \pm 0.04$	AUBERT	07BA	BABR $e^+ e^- \rightarrow \Upsilon(4S)$
$-0.02 \pm 0.14 \pm 0.03$	¹ CHEN	05A	BELL $e^+ e^- \rightarrow \Upsilon(4S)$
<ul style="list-style-type: none"> ••• We do not use the following data for averages, fits, limits, etc. ••• 			
$0.16 \pm 0.17 \pm 0.03$	AUBERT	03V	BABR Repl. by AUBERT 07BA
$-0.13 \pm_{-0.11}^{+0.29}$	² CHEN	03B	BELL Repl. by CHEN 05A
$-0.43 \pm_{-0.30}^{+0.36} \pm 0.06$	³ AUBERT	02E	BABR Repl. by AUBERT 03V
¹ Corresponds to 90% confidence range $-0.25 < A_{CP} < 0.22$. ² Corresponds to 90% confidence range $-0.64 < A_{CP} < 0.36$. ³ Corresponds to 90% confidence range $-0.88 < A_{CP} < 0.18$.			

 $A_{CP}(B^+ \rightarrow \phi K^+ \gamma)$

VALUE	DOCUMENT ID	TECN	COMMENT
$-0.26 \pm 0.14 \pm 0.05$	AUBERT	07Q	BABR $e^+ e^- \rightarrow \Upsilon(4S)$

 $A_{CP}(B^+ \rightarrow \eta K^+ \gamma)$

VALUE	DOCUMENT ID	TECN	COMMENT
-0.13 ± 0.08 OUR AVERAGE			
$-0.09 \pm 0.12 \pm 0.01$	¹ AUBERT,B	06M	BABR $e^+ e^- \rightarrow \Upsilon(4S)$
$-0.16 \pm 0.09 \pm 0.06$	² NISHIDA	05	BELL $e^+ e^- \rightarrow \Upsilon(4S)$
¹ $m_{\eta K} < 3.25 \text{ GeV}/c^2$. ² $m_{\eta K} < 2.4 \text{ GeV}/c^2$			

 $A_{CP}(B^+ \rightarrow \pi^+ \pi^0)$

VALUE	DOCUMENT ID	TECN	COMMENT
0.01 ± 0.06 OUR AVERAGE			
$0.03 \pm 0.08 \pm 0.01$	AUBERT	07Bc	BABR $e^+ e^- \rightarrow \Upsilon(4S)$
$-0.02 \pm 0.10 \pm 0.01$	¹ CHAO	04B	BELL $e^+ e^- \rightarrow \Upsilon(4S)$
<ul style="list-style-type: none"> ••• We do not use the following data for averages, fits, limits, etc. ••• 			
$-0.01 \pm 0.10 \pm 0.02$	² AUBERT	05L	BABR Repl. by AUBERT 07Bc
$0.00 \pm 0.10 \pm 0.02$	³ CHAO	05A	BELL Repl. by CHAO 04B
$-0.03 \pm_{-0.17}^{+0.18} \pm 0.02$	⁴ AUBERT	03L	BABR Repl. by AUBERT 05L
$0.30 \pm_{-0.04}^{+0.30} \pm 0.06$	⁵ CASEY	02	BELL Repl. by CHAO 04B
¹ This corresponds to 90% CL interval of $-0.18 < A_{CP} < 0.14$. ² Corresponds to a 90% CL interval of $-0.19 < A_{CP} < 0.21$. ³ Corresponds to a 90% CL interval of $-0.17 < A_{CP} < 0.16$. ⁴ Corresponds to 90% confidence range $-0.32 < A_{CP} < 0.27$. ⁵ Corresponds to 90% confidence range $-0.23 < A_{CP} < +0.86$.			

 $A_{CP}(B^+ \rightarrow \pi^+ \pi^- \pi^+)$

VALUE	DOCUMENT ID	TECN	COMMENT
$-0.007 \pm 0.077 \pm 0.025$	AUBERT,B	05G	BABR $e^+ e^- \rightarrow \Upsilon(4S)$
<ul style="list-style-type: none"> ••• We do not use the following data for averages, fits, limits, etc. ••• 			
$-0.39 \pm 0.33 \pm 0.12$	AUBERT	03M	BABR Repl. by AUBERT 05G

 $A_{CP}(B^+ \rightarrow \rho^0 \pi^+)$

VALUE	DOCUMENT ID	TECN	COMMENT
$-0.074 \pm 0.120 \pm_{-0.055}^{+0.035}$	AUBERT,B	05G	BABR $e^+ e^- \rightarrow \Upsilon(4S)$
<ul style="list-style-type: none"> ••• We do not use the following data for averages, fits, limits, etc. ••• 			
$-0.19 \pm 0.11 \pm 0.02$	AUBERT	04Z	BABR Repl. by AUBERT,B 05G

 $A_{CP}(B^+ \rightarrow f_2(1270) \pi^+)$

VALUE	DOCUMENT ID	TECN	COMMENT
$-0.004 \pm 0.247 \pm_{-0.032}^{+0.028}$	AUBERT,B	05G	BABR $e^+ e^- \rightarrow \Upsilon(4S)$

 $A_{CP}(B^+ \rightarrow \rho^+ \pi^0)$

VALUE	DOCUMENT ID	TECN	COMMENT
0.02 ± 0.11 OUR AVERAGE			
$-0.01 \pm 0.13 \pm 0.02$	AUBERT	07X	BABR $e^+ e^- \rightarrow \Upsilon(4S)$
$0.06 \pm_{-0.05}^{+0.17}$	ZHANG	05A	BELL $e^+ e^- \rightarrow \Upsilon(4S)$
<ul style="list-style-type: none"> ••• We do not use the following data for averages, fits, limits, etc. ••• 			
$0.24 \pm 0.16 \pm 0.06$	AUBERT	04Z	BABR Repl. by AUBERT 07X

Meson Particle Listings

 B^\pm $A_{CP}(B^+ \rightarrow \rho^+ \rho^0)$

VALUE	DOCUMENT ID	TECN	COMMENT
-0.08 ± 0.13 OUR AVERAGE			
$-0.12 \pm 0.13 \pm 0.10$	AUBERT, BE	06G	BABR $e^+ e^- \rightarrow \Upsilon(4S)$
$0.00 \pm 0.22 \pm 0.03$	ZHANG	03B	BELL $e^+ e^- \rightarrow \Upsilon(4S)$
• • • We do not use the following data for averages, fits, limits, etc. • • •			
$-0.19 \pm 0.23 \pm 0.03$	AUBERT	03V	BABR Repl. by AUBERT, BE 06G

 $A_{CP}(B^+ \rightarrow b_1^0 \pi^+)$

VALUE	DOCUMENT ID	TECN	COMMENT
$+0.05 \pm 0.16 \pm 0.02$	AUBERT	07B1	BABR $e^+ e^- \rightarrow \Upsilon(4S)$

 $A_{CP}(B^+ \rightarrow \omega \pi^+)$

VALUE	DOCUMENT ID	TECN	COMMENT
-0.04 ± 0.06 OUR AVERAGE			
$-0.02 \pm 0.08 \pm 0.01$	AUBERT	07AE	BABR $e^+ e^- \rightarrow \Upsilon(4S)$
$-0.02 \pm 0.09 \pm 0.01$	JEN	06	BELL $e^+ e^- \rightarrow \Upsilon(4S)$
-0.34 ± 0.25	¹ CHEN	00	CLE2 $e^+ e^- \rightarrow \Upsilon(4S)$
• • • We do not use the following data for averages, fits, limits, etc. • • •			
$-0.01 \pm 0.10 \pm 0.01$	AUBERT, B	06E	BABR Repl. by AUBERT 07AE
$0.03 \pm 0.16 \pm 0.01$	AUBERT	04H	BABR Repl. by AUBERT, B 06E
$0.50 \pm 0.23 \pm 0.02$	² WANG	04A	BELL Repl. by JEN 06
$-0.01 \pm 0.29 \pm 0.03$	³ AUBERT	02E	BABR Repl. by AUBERT 04H

¹ Corresponds to 90% confidence range $-0.75 < A_{CP} < 0.07$.

² Corresponds to 90% CL interval $-0.25 < A_{CP} < 0.41$

³ Corresponds to 90% confidence range $-0.50 < A_{CP} < 0.46$.

 $A_{CP}(B^+ \rightarrow \omega \rho^+)$

VALUE	DOCUMENT ID	TECN	COMMENT
$0.04 \pm 0.18 \pm 0.02$	AUBERT, B	06T	BABR $e^+ e^- \rightarrow \Upsilon(4S)$
• • • We do not use the following data for averages, fits, limits, etc. • • •			
$0.05 \pm 0.26 \pm 0.02$	AUBERT	05O	BABR Repl. by AUBERT, B 06T

 $A_{CP}(B^+ \rightarrow \eta \pi^+)$

VALUE	DOCUMENT ID	TECN	COMMENT
-0.16 ± 0.07 OUR AVERAGE	Error includes scale factor of 1.1.		
$-0.08 \pm 0.10 \pm 0.01$	AUBERT	07AE	BABR $e^+ e^- \rightarrow \Upsilon(4S)$
$-0.23 \pm 0.09 \pm 0.02$	CHANG	07B	BELL $e^+ e^- \rightarrow \Upsilon(4S)$
• • • We do not use the following data for averages, fits, limits, etc. • • •			
$-0.13 \pm 0.12 \pm 0.01$	AUBERT, B	05K	BABR Repl. by AUBERT 07AE
$0.07 \pm 0.15 \pm 0.03$	CHANG	05A	BELL Repl. by CHANG 07B
$-0.44 \pm 0.18 \pm 0.01$	AUBERT	04H	BABR Repl. by AUBERT, B 05K

 $A_{CP}(B^+ \rightarrow \eta' \pi^+)$

VALUE	DOCUMENT ID	TECN	COMMENT
0.21 ± 0.15 OUR AVERAGE			
$0.21 \pm 0.17 \pm 0.01$	AUBERT	07AE	BABR $e^+ e^- \rightarrow \Upsilon(4S)$
$0.20 \pm 0.37 \pm 0.04$	SCHUEMANN	06	BELL $e^+ e^- \rightarrow \Upsilon(4S)$
• • • We do not use the following data for averages, fits, limits, etc. • • •			
$0.14 \pm 0.16 \pm 0.01$	AUBERT, B	05K	BABR Repl. by AUBERT 07AE

 $A_{CP}(B^+ \rightarrow \eta \rho^+)$

VALUE	DOCUMENT ID	TECN	COMMENT
0.01 ± 0.16 OUR AVERAGE			
$-0.04 \pm 0.34 \pm 0.01$	WANG	07B	BELL $e^+ e^- \rightarrow \Upsilon(4S)$
$0.02 \pm 0.18 \pm 0.02$	AUBERT, B	05K	BABR $e^+ e^- \rightarrow \Upsilon(4S)$

 $A_{CP}(B^+ \rightarrow \eta' \rho^+)$

VALUE	DOCUMENT ID	TECN	COMMENT
$-0.04 \pm 0.28 \pm 0.02$	AUBERT	07E	BABR $e^+ e^- \rightarrow \Upsilon(4S)$

 $A_{CP}(B^+ \rightarrow \rho \bar{\rho} \pi^+)$

VALUE	DOCUMENT ID	TECN	COMMENT
0.00 ± 0.04 OUR AVERAGE			
$-0.02 \pm 0.05 \pm 0.02$	¹ WEI	08	BELL $e^+ e^- \rightarrow \Upsilon(4S)$
$+0.04 \pm 0.07 \pm 0.04$	AUBERT	07AV	BABR $e^+ e^- \rightarrow \Upsilon(4S)$
• • • We do not use the following data for averages, fits, limits, etc. • • •			
$-0.16 \pm 0.22 \pm 0.01$	WANG	04	BELL Repl. by WEI 08
¹ Requires $m_{\rho \bar{\rho}} < 2.85 \text{ GeV}/c^2$.			

 $A_{CP}(B^+ \rightarrow \rho \bar{\rho} K^+)$

VALUE	DOCUMENT ID	TECN	COMMENT
-0.16 ± 0.07 OUR AVERAGE			
$-0.17 \pm 0.10 \pm 0.02$	¹ WEI	08	BELL $e^+ e^- \rightarrow \Upsilon(4S)$
$-0.16 \pm 0.07 \pm 0.04$	¹ AUBERT, B	05L	BABR $e^+ e^- \rightarrow \Upsilon(4S)$
• • • We do not use the following data for averages, fits, limits, etc. • • •			
$-0.05 \pm 0.11 \pm 0.01$	WANG	04	BELL Repl. by WEI 08
¹ Requires $m_{\rho \bar{\rho}} < 2.85 \text{ GeV}/c^2$.			

 $A_{CP}(B^+ \rightarrow \rho \bar{\rho} K^*(892)^+)$

VALUE	DOCUMENT ID	TECN	COMMENT
$+0.32 \pm 0.13 \pm 0.05$	AUBERT	07AV	BABR $e^+ e^- \rightarrow \Upsilon(4S)$

 $A_{CP}(B^+ \rightarrow \rho \bar{\rho} \gamma)$

VALUE	DOCUMENT ID	TECN	COMMENT
$+0.17 \pm 0.16 \pm 0.05$	WANG	07C	BELL $e^+ e^- \rightarrow \Upsilon(4S)$

 $A_{CP}(B^+ \rightarrow K^+ \ell^+ \ell^-)$

VALUE	DOCUMENT ID	TECN	COMMENT
$-0.07 \pm 0.22 \pm 0.02$	AUBERT, B	06J	BABR $e^+ e^- \rightarrow \Upsilon(4S)$

 $A_{CP}(B^+ \rightarrow K^{*+} \ell^+ \ell^-)$

VALUE	DOCUMENT ID	TECN	COMMENT
$0.03 \pm 0.23 \pm 0.03$	AUBERT, B	06J	BABR $e^+ e^- \rightarrow \Upsilon(4S)$

 $\gamma(B^+ \rightarrow D^{(*)} K(\ell^+)^+)$

For angle $\gamma(\phi_3)$ of the CKM unitarity triangle, see the review on "CP Violation" in the Reviews section.

VALUE (%)	DOCUMENT ID	TECN	COMMENT
57 ± 17 OUR AVERAGE			
$53 \pm 15 \pm 18$	¹ POLUEKTOV	06	BELL $e^+ e^- \rightarrow \Upsilon(4S)$
$70 \pm 31 \pm 15$	² AUBERT, B	05Y	BABR $e^+ e^- \rightarrow \Upsilon(4S)$
• • • We do not use the following data for averages, fits, limits, etc. • • •			
$77 \pm 19 \pm 17$	³ POLUEKTOV	04	BELL Repl. by POLUEKTOV 06

¹ Uses a Dalitz plot analysis of the $\bar{D}^0 \rightarrow K_S^0 \pi^+ \pi^-$ decays; Combines the $D K^+$, $D^* K^+$ and $D K^{*+}$ modes. The corresponding two standard deviations interval for gamma is $8^\circ < \gamma < 111^\circ$.

² Uses a Dalitz plot analysis of neutral $D \rightarrow K_S^0 \pi^+ \pi^-$ decays coming from $B^\pm \rightarrow D K^\pm$ and $B^\pm \rightarrow D^* K^\pm$ followed by $D^{*0} \rightarrow D \pi^0, D \gamma$. The corresponding two standard deviations interval for gamma is $12^\circ < \gamma < 137^\circ$.

³ Uses a Dalitz plot analysis of the 3-body $D \rightarrow K_S^0 \pi^+ \pi^-$ decays coming from $B^\pm \rightarrow D K^\pm$ and $B^\pm \rightarrow D^* K^\pm$ followed by $D^* \rightarrow D \pi^0$; here we use D to denote that the neutral D meson produced in the decay is an admixture of D^0 and \bar{D}^0 . The corresponding two standard deviations interval for γ is $26^\circ < \gamma < 126^\circ$. POLUEKTOV 04 also reports the amplitude ratios and the strong phases.

 B^\pm REFERENCES

AUBERT	08A	PR D77 011101R	B. Aubert et al.	(BABAR Collab.)
AUBERT	08B	PR D77 011102R	B. Aubert et al.	(BABAR Collab.)
AUBERT	08D	PR D77 011107R	B. Aubert et al.	(BABAR Collab.)
AUBERT	08F	PRL 100 051803	B. Aubert et al.	(BABAR Collab.)
AUBERT	08N	PRL 100 021801	B. Aubert et al.	(BABAR Collab.)
AUBERT	08Q	PRL 100 151802	B. Aubert et al.	(BABAR Collab.)
BRODZICKA	08	PRL 100 092001	J. Brodzicka et al.	(BELLE Collab.)
LIVENTSEV	08	PR D77 091503R	D. Liventsev et al.	(BELLE Collab.)
WEI	08	PL B659 80	J.-T. Wei et al.	(BELLE Collab.)
ADAM	07	PRL 99 041802	N.E. Adam et al.	(CLEO Collab.)
	Also	PR D76 012007	D.M. Asner et al.	(CLEO Collab.)
AUBERT	07AC	PR D76 031101R	B. Aubert et al.	(BABAR Collab.)
AUBERT	07AE	PR D76 031103R	B. Aubert et al.	(BABAR Collab.)
AUBERT	07AG	PRL 99 051801	B. Aubert et al.	(BABAR Collab.)
AUBERT	07AL	PR D76 052002	B. Aubert et al.	(BABAR Collab.)
AUBERT	07AN	PR D76 051101R	B. Aubert et al.	(BABAR Collab.)
AUBERT	07AR	PR D76 071103R	B. Aubert et al.	(BABAR Collab.)
AUBERT	07AV	PR D76 092004	B. Aubert et al.	(BABAR Collab.)
AUBERT	07AZ	PRL 99 201801	B. Aubert et al.	(BABAR Collab.)
AUBERT	07BA	PRL 99 201802	B. Aubert et al.	(BABAR Collab.)
AUBERT	07BB	PRL 99 221801	B. Aubert et al.	(BABAR Collab.)
AUBERT	07BC	PR D76 091102R	B. Aubert et al.	(BABAR Collab.)
AUBERT	07B1	PRL 99 241803	B. Aubert et al.	(BABAR Collab.)
AUBERT	07B3	PRL 99 251801	B. Aubert et al.	(BABAR Collab.)
AUBERT	07BL	PRL 99 261801	B. Aubert et al.	(BABAR Collab.)
AUBERT	07BN	PR D76 111101R	B. Aubert et al.	(BABAR Collab.)
AUBERT	07E	PRL 98 051802	B. Aubert et al.	(BABAR Collab.)
AUBERT	07H	PR D75 031101R	B. Aubert et al.	(BABAR Collab.)
AUBERT	07L	PRL 98 181804	B. Aubert et al.	(BABAR Collab.)
AUBERT	07M	PRL 98 171801	B. Aubert et al.	(BABAR Collab.)
AUBERT	07N	PR D75 072002	B. Aubert et al.	(BABAR Collab.)
AUBERT	07Q	PR D75 051102R	B. Aubert et al.	(BABAR Collab.)
AUBERT	07R	PRL 98 211804	B. Aubert et al.	(BABAR Collab.)
AUBERT	07X	PR D75 091103R	B. Aubert et al.	(BABAR Collab.)
AUBERT	07Z	PR D76 011103R	B. Aubert et al.	(BABAR Collab.)
CHANG	07B	PR D75 071104R	P. Chang et al.	(BELLE Collab.)
CHEN	07D	PRL 99 221802	K.-F. Chen et al.	(BELLE Collab.)
HOKUUE	07	PL B648 139	T. Hokuue et al.	(BELLE Collab.)
LIN	07	PRL 98 181804	S.-W. Lin et al.	(BELLE Collab.)
LIN	07A	PRL 99 121601	S.-W. Lin et al.	(BELLE Collab.)
SATOYAMA	07	PL B647 67	N. Satoyama et al.	(BELLE Collab.)
SCHUEMANN	07	PR D75 092002	J. Schuemann et al.	(BELLE Collab.)
TSAI	07	PR D75 111101R	Y.-T. Tsai et al.	(BELLE Collab.)
URQUIJO	07	PR D75 032001	P. Urquijo et al.	(BELLE Collab.)
WANG	07B	PR D75 092005	C.H. Wang et al.	(BELLE Collab.)
WANG	07C	PR D76 052004	M.-Z. Wang et al.	(BELLE Collab.)
XIE	07	PR D75 017101	Q.L. Xie et al.	(BELLE Collab.)
ABE	06	PR D73 051106R	K. Abe et al.	(BELLE Collab.)
ABULENCIA	06J	PRL 96 191801	A. Abulencia et al.	(CDF Collab.)
ACOSTA	06	PRL 96 202001	D. Acosta et al.	(CDF Collab.)
AUBERT	06	PR D73 011101R	B. Aubert et al.	(BABAR Collab.)
AUBERT	06E	PRL 96 052002	B. Aubert et al.	(BABAR Collab.)
AUBERT	06F	PR D73 011103R	B. Aubert et al.	(BABAR Collab.)
AUBERT	06J	PR D73 051105R	B. Aubert et al.	(BABAR Collab.)
AUBERT	06K	PR D73 057101	B. Aubert et al.	(BABAR Collab.)
AUBERT	06N	PR D74 031103R	B. Aubert et al.	(BABAR Collab.)
AUBERT	06O	PR D74 032003	B. Aubert et al.	(BABAR Collab.)
AUBERT	06Z	PR D73 111104R	B. Aubert et al.	(BABAR Collab.)
AUBERT, B	06A	PR D73 112004	B. Aubert et al.	(BABAR Collab.)
AUBERT, B	06C	PR D74 011102R	B. Aubert et al.	(BABAR Collab.)
AUBERT, B	06E	PR D74 011106R	B. Aubert et al.	(BABAR Collab.)
AUBERT, B	06G	PRL 97 201801	B. Aubert et al.	(BABAR Collab.)
AUBERT, B	06H	PRL 97 201802	B. Aubert et al.	(BABAR Collab.)

Meson Particle Listings

 B^\pm, B^0

BARISH	95	PR D51 1014	B.C. Barish et al.	(CLEO Collab.)
BUSKULIC	95	PL B343 444	D. Buskulic et al.	(ALEPH Collab.)
ABE	94D	PRL 72 3456	F. Abe et al.	(CDF Collab.)
ALAM	94	PR D50 43	M.S. Alam et al.	(CLEO Collab.)
ALBRECHT	94D	PL B335 526	H. Albrecht et al.	(ARGUS Collab.)
ATHANAS	94	PRL 73 3503	M. Athanas et al.	(CLEO Collab.)
Also		PRL 74 3090 (erratum)	M. Athanas et al.	(CLEO Collab.)
PDG	94	PR D50 1173	L. Moneta et al.	(CLEO Collab.)
STONE	94	HEPSY 95-11	S. Stone	(CERN, LBL, BOST+)
Published in B Decays, 2nd Edition, World Scientific, Singapore				
ABREU	93D	ZPHY C57 181	P. Abreu et al.	(DELPHI Collab.)
ABREU	93G	PL B312 253	P. Abreu et al.	(DELPHI Collab.)
ACTON	93C	PL B307 247	P.D. Acton et al.	(OPAL Collab.)
ALBRECHT	93E	ZPHY C60 11	H. Albrecht et al.	(ARGUS Collab.)
ALEXANDER	93B	PL B319 365	J. Alexander et al.	(CLEO Collab.)
AMMAR	93	PRL 71 674	R. Ammar et al.	(CLEO Collab.)
BEAN	93B	PRL 70 2681	A. Bean et al.	(CLEO Collab.)
BUSKULIC	93D	PL B307 194	D. Buskulic et al.	(ALEPH Collab.)
Also		PL B325 537 (erratum)	D. Buskulic et al.	(ALEPH Collab.)
SANGHERA	93	PR D47 791	S. Sanghera et al.	(CLEO Collab.)
ALBRECHT	92C	PL B275 195	H. Albrecht et al.	(ARGUS Collab.)
ALBRECHT	92E	PL B277 209	H. Albrecht et al.	(ARGUS Collab.)
ALBRECHT	92G	ZPHY C54 1	H. Albrecht et al.	(ARGUS Collab.)
BORTOLETTO	92	PR D45 21	D. Bortoletto et al.	(CLEO Collab.)
BUSKULIC	92G	PL B295 396	D. Buskulic et al.	(ALEPH Collab.)
ALBRECHT	91B	PL B254 288	H. Albrecht et al.	(ARGUS Collab.)
ALBRECHT	91C	PL B255 297	H. Albrecht et al.	(ARGUS Collab.)
ALBRECHT	91E	PL B262 148	H. Albrecht et al.	(ARGUS Collab.)
BERKELMAN	91	ARNPS 41 1	K. Berkelman, S. Stone	(CORN, SYRA)
"Decays of B Mesons"				
FULTON	91	PR D43 651	R. Fulton et al.	(CLEO Collab.)
ALBRECHT	90B	PL B241 278	H. Albrecht et al.	(ARGUS Collab.)
ALBRECHT	90J	ZPHY C48 543	H. Albrecht et al.	(ARGUS Collab.)
ANTREASAYAN	90B	ZPHY C48 553	D. Antreasayan et al.	(Crystal Ball Collab.)
BORTOLETTO	90	PRL 64 2117	D. Bortoletto et al.	(CLEO Collab.)
Also		PR D45 21	D. Bortoletto et al.	(CLEO Collab.)
WEIR	90B	PR D41 1384	A.J. Weir et al.	(Mark II Collab.)
ALBRECHT	89G	PL B229 304	H. Albrecht et al.	(ARGUS Collab.)
AVERY	89B	PL B223 470	P. Avery et al.	(CLEO Collab.)
BEBEK	89	PRL 62 8	C. Bebek et al.	(CLEO Collab.)
BORTOLETTO	89	PRL 62 2436	D. Bortoletto et al.	(CLEO Collab.)
ALBRECHT	88F	PL B209 119	H. Albrecht et al.	(ARGUS Collab.)
ALBRECHT	88K	PL B215 424	H. Albrecht et al.	(ARGUS Collab.)
ALBRECHT	87C	PL B185 218	H. Albrecht et al.	(ARGUS Collab.)
ALBRECHT	87D	PL B199 451	H. Albrecht et al.	(ARGUS Collab.)
AVERY	87	PL B183 429	P. Avery et al.	(CLEO Collab.)
BEBEK	87	PR D36 1289	C. Bebek et al.	(CLEO Collab.)
ALAM	86	PR D34 3279	M.S. Alam et al.	(CLEO Collab.)
PDG	86	PL 170B 1	M. Aguilar-Benitez et al.	(CERN, CIT+)
GILES	84	PR D30 2279	R. Giles et al.	(CLEO Collab.)

 B^0

$$J(J^P) = \frac{1}{2}(0^-)$$

Quantum numbers not measured. Values shown are quark-model predictions.

See also the B^\pm/B^0 ADMIXTURE and $B^\pm/B^0/B_s^0/b$ -baryon ADMIXTURE sections.

See the Note "Production and Decay of b -flavored Hadrons" at the beginning of the B^\pm Particle Listings and the Note on " B^0 - \bar{B}^0 Mixing" near the end of the B^0 Particle Listings.

 B^0 MASS

The fit uses m_{B^+} , ($m_{B^0} - m_{B^+}$), and m_{B^0} to determine m_{B^+} , m_{B^0} , and the mass difference.

VALUE (MeV)	EVTS	DOCUMENT ID	TECN	COMMENT
5279.53 ± 0.33 OUR FIT				
5279.5 ± 0.5 OUR AVERAGE				
5279.63 ± 0.53 ± 0.33		1 ACOSTA	06 CDF	$p\bar{p}$ at 1.96 TeV
5279.1 ± 0.7 ± 0.3	135	2 CSORNA	00 CLE2	$e^+e^- \rightarrow \Upsilon(4S)$
5281.3 ± 2.2 ± 1.4	51	ABE	96B CDF	$p\bar{p}$ at 1.8 TeV
• • • We do not use the following data for averages, fits, limits, etc. • • •				
5279.2 ± 0.54 ± 2.0	340	ALAM	94 CLE2	$e^+e^- \rightarrow \Upsilon(4S)$
5278.0 ± 0.4 ± 2.0		BORTOLETTO92	CLEO	$e^+e^- \rightarrow \Upsilon(4S)$
5279.6 ± 0.7 ± 2.0	40	3 ALBRECHT	90J ARG	$e^+e^- \rightarrow \Upsilon(4S)$
5278.2 ± 1.0 ± 3.0	40	ALBRECHT	87C ARG	$e^+e^- \rightarrow \Upsilon(4S)$
5279.5 ± 1.6 ± 3.0	7	4 ALBRECHT	87D ARG	$e^+e^- \rightarrow \Upsilon(4S)$
5280.6 ± 0.8 ± 2.0		BEBEK	87 CLEO	$e^+e^- \rightarrow \Upsilon(4S)$

¹ Uses exclusively reconstructed final states containing a $J/\psi \rightarrow \mu^+ \mu^-$ decays.

² CSORNA 00 uses fully reconstructed 135 $B^0 \rightarrow J/\psi(\ell^+) K_S^0$ events and invariant masses without beam constraint.

³ ALBRECHT 90J assumes 10580 for $\Upsilon(4S)$ mass. Supersedes ALBRECHT 87C and ALBRECHT 87D.

⁴ Found using fully reconstructed decays with J/ψ . ALBRECHT 87D assume $m_{\Upsilon(4S)} = 10577$ MeV.

 $m_{B^0} - m_{B^+}$

VALUE (MeV)	DOCUMENT ID	TECN	COMMENT
0.37 ± 0.24 OUR FIT			
0.37 ± 0.26 OUR AVERAGE			
0.53 ± 0.67 ± 0.14	1 ACOSTA	06 CDF	$p\bar{p}$ at 1.96 TeV
0.41 ± 0.25 ± 0.19	ALAM	94 CLE2	$e^+e^- \rightarrow \Upsilon(4S)$
-0.4 ± 0.6 ± 0.5	BORTOLETTO92	CLEO	$e^+e^- \rightarrow \Upsilon(4S)$
-0.9 ± 1.2 ± 0.5	ALBRECHT	90J ARG	$e^+e^- \rightarrow \Upsilon(4S)$
2.0 ± 1.1 ± 0.3	2 BEBEK	87 CLEO	$e^+e^- \rightarrow \Upsilon(4S)$

¹ Uses exclusively reconstructed final states containing a $J/\psi \rightarrow \mu^+ \mu^-$ decays.

² BEBEK 87 actually measure the difference between half of E_{cm} and the B^\pm or B^0 mass, so the $m_{B^0} - m_{B^\pm}$ is more accurate. Assume $m_{\Upsilon(4S)} = 10580$ MeV.

 $m_{B_H^0} - m_{B_L^0}$

See the B^0 - \bar{B}^0 MIXING PARAMETERS section near the end of these B^0 Listings.

 B^0 MEAN LIFE

See $B^\pm/B^0/B_s^0/b$ -baryon ADMIXTURE section for data on B -hadron mean life averaged over species of bottom particles.

"OUR EVALUATION" is an average using rescaled values of the data listed below. The average and rescaling were performed by the Heavy Flavor Averaging Group (HFAG) and are described at <http://www.slac.stanford.edu/xorg/hfag/>. The averaging/rescaling procedure takes into account correlations between the measurements and asymmetric lifetime errors.

VALUE (10^{-12} s)	EVTS	DOCUMENT ID	TECN	COMMENT
1.530 ± 0.009 OUR EVALUATION				
1.501 ± 0.078 ± 0.050		1 ABAZOV	07S D0	$p\bar{p}$ at 1.96 TeV
1.524 ± 0.030 ± 0.016		1 ABULENCIA	07A CDF	$p\bar{p}$ at 1.96 TeV
1.504 ± 0.013 ± 0.018 - 0.013		2 AUBERT	06G BABR	$e^+e^- \rightarrow \Upsilon(4S)$
1.530 ± 0.043 ± 0.023		3 ABAZOV	05W D0	$p\bar{p}$ at 1.96 TeV
1.534 ± 0.008 ± 0.010		4 ABE	05B BELL	$e^+e^- \rightarrow \Upsilon(4S)$
1.54 ± 0.05 ± 0.02		5 ACOSTA	05 CDF	$p\bar{p}$ at 1.96 TeV
1.531 ± 0.021 ± 0.031		6 ABDALLAH	04E DLPH	$e^+e^- \rightarrow Z$
1.533 ± 0.034 ± 0.038		7 AUBERT	03H BABR	$e^+e^- \rightarrow \Upsilon(4S)$
1.497 ± 0.073 ± 0.032		8 ACOSTA	02C CDF	$p\bar{p}$ at 1.8 TeV
1.529 ± 0.012 ± 0.029		9 AUBERT	02H BABR	$e^+e^- \rightarrow \Upsilon(4S)$
1.546 ± 0.032 ± 0.022		10 AUBERT	01F BABR	$e^+e^- \rightarrow \Upsilon(4S)$
1.541 ± 0.028 ± 0.023		9 ABBIENDI,G	00B OPAL	$e^+e^- \rightarrow Z$
1.518 ± 0.053 ± 0.034		11 BARATE	00R ALEP	$e^+e^- \rightarrow Z$
1.523 ± 0.057 ± 0.053		12 ABBIENDI	99J OPAL	$e^+e^- \rightarrow Z$
1.474 ± 0.039 ± 0.052 - 0.051		11 ABE	98Q CDF	$p\bar{p}$ at 1.8 TeV
1.52 ± 0.06 ± 0.04		12 ACCIARRI	98S L3	$e^+e^- \rightarrow Z$
1.64 ± 0.08 ± 0.08		12 ABE	97J SLD	$e^+e^- \rightarrow Z$
1.532 ± 0.041 ± 0.040		13 ABREU	97F DLPH	$e^+e^- \rightarrow Z$
1.25 ± 0.15 - 0.13 ± 0.05	121	8 BUSKULIC	96J ALEP	$e^+e^- \rightarrow Z$
1.49 ± 0.17 + 0.08 - 0.15 - 0.06		14 BUSKULIC	96J ALEP	$e^+e^- \rightarrow Z$
1.61 ± 0.14 - 0.13 ± 0.08	11,15	ABREU	95Q DLPH	$e^+e^- \rightarrow Z$
1.63 ± 0.14 ± 0.13		16 ADAM	95 DLPH	$e^+e^- \rightarrow Z$
1.53 ± 0.12 ± 0.08	11,17	AKERS	95T OPAL	$e^+e^- \rightarrow Z$
• • • We do not use the following data for averages, fits, limits, etc. • • •				
1.473 ± 0.052 - 0.050 ± 0.023		3 ABAZOV	05B D0	Repl. by ABAZOV 05W
1.40 ± 0.11 - 0.10 ± 0.03		1 ABAZOV	05C D0	Repl. by ABAZOV 07S
1.523 ± 0.024 - 0.023 ± 0.022		18 AUBERT	03C BABR	Repl. by AUBERT 06G
1.554 ± 0.030 ± 0.019		10 ABE	02H BELL	Repl. by ABE 05B
1.58 ± 0.09 ± 0.02		8 ABE	98B CDF	Repl. by ACOSTA 02C
1.54 ± 0.08 ± 0.06		11 ABE	96C CDF	Repl. by ABE 98Q
1.55 ± 0.06 ± 0.03		19 BUSKULIC	96J ALEP	$e^+e^- \rightarrow Z$
1.61 ± 0.07 ± 0.04		11 BUSKULIC	96J ALEP	Repl. by BARATE 00R
1.62 ± 0.12		20 ADAM	95 DLPH	$e^+e^- \rightarrow Z$
1.57 ± 0.18 ± 0.08	121	8 ABE	94D CDF	Repl. by ABE 98B
1.17 ± 0.29 - 0.23 ± 0.16	96	11 ABREU	93D DLPH	Sup. by ABREU 95Q
1.55 ± 0.25 ± 0.18	76	16 ABREU	93G DLPH	Sup. by ADAM 95
1.51 ± 0.24 + 0.12 - 0.23 - 0.14	78	11 ACTON	93C OPAL	Sup. by AKERS 95T
1.52 ± 0.20 + 0.07 - 0.18 - 0.13	77	11 BUSKULIC	93D ALEP	Sup. by BUSKULIC 96J
1.20 ± 0.52 + 0.16 - 0.36 - 0.14	15	21 WAGNER	90 MRK2	$E_{cm}^0 = 29$ GeV
0.82 ± 0.57 - 0.37 ± 0.27		22 AVERILL	89 HRS	$E_{cm}^0 = 29$ GeV

¹ Measured mean life using $B^0 \rightarrow J/\psi K_S$ decays.

² Measured using a simultaneous fit of the B^0 lifetime and $\bar{B}^0 B^0$ oscillation frequency Δm_d in the partially reconstructed $B^0 \rightarrow D^{*+} \ell \nu$ decays.

³ Measured mean life using $B^0 \rightarrow J/\psi K^{*0}$ decays.

⁴ Measurement performed using a combined fit of CP -violation, mixing and lifetimes.

⁵ Measured using the time-dependent angular analysis of $B_d^0 \rightarrow J/\psi K^{*0}$ decays.

⁶ Measurement performed using an inclusive reconstruction and B flavor identification technique.

⁷ Measurement performed with decays $B^0 \rightarrow D^{*+} \pi^+$ and $B^0 \rightarrow D^{*+} \rho^+$ using a partial reconstruction technique.

⁸ Measured mean life using fully reconstructed decays.

⁹ Data analyzed using partially reconstructed $\bar{B}^0 \rightarrow D^{*+} \ell^- \bar{\nu}$ decays.

¹⁰ Events are selected in which one B meson is fully reconstructed while the second B meson is reconstructed inclusively.

- 11 Data analyzed using $D/D^* \ell X$ event vertices.
 12 Data analyzed using charge of secondary vertex.
 13 Data analyzed using inclusive $D/D^* \ell X$.
 14 Measured mean life using partially reconstructed $D^{*-} \pi^+ X$ vertices.
 15 ABREU 95Q assumes $B(B^0 \rightarrow D^{*-} \ell^+ \nu_\ell) = 3.2 \pm 1.7\%$.
 16 Data analyzed using vertex-charge technique to tag B charge.
 17 AKERS 95T assumes $B(B^0 \rightarrow D_s^{*} D^0) = 5.0 \pm 0.9\%$ to find B^+/B^0 yield.
 18 AUBERT 03c uses a sample of approximately 14,000 exclusively reconstructed $B^0 \rightarrow D^*(2010)^- \ell \nu$ and simultaneously measures the lifetime and oscillation frequency.
 19 Combined result of $D/D^* \ell X$ analysis, fully reconstructed B analysis, and partially reconstructed $D^{*-} \pi^+ X$ analysis.
 20 Combined ABREU 95Q and ADAM 95 result.
 21 WAGNER 90 tagged B^0 mesons by their decays into $D^{*-} e^+ \nu$ and $D^{*-} \mu^+ \nu$ where the D^{*-} is tagged by its decay into $\pi^- \bar{D}^0$.
 22 AVERILL 89 is an estimate of the B^0 mean lifetime assuming that $B^0 \rightarrow D^{*+} X$ always.

MEAN LIFE RATIO τ_{B^+}/τ_{B^0} τ_{B^+}/τ_{B^0} (direct measurements)

"OUR EVALUATION" is an average using rescaled values of the data listed below. The average and rescaling were performed by the Heavy Flavor Averaging Group (HFAG) and are described at <http://www.slac.stanford.edu/xorg/hfag/>. The averaging/rescaling procedure takes into account correlations between the measurements and asymmetric lifetime errors.

VALUE	EVTS	DOCUMENT ID	TECN	COMMENT
1.071 ± 0.009 OUR EVALUATION				
1.080 ± 0.016 ± 0.014		1 ABAZOV	05D D0	$p\bar{p}$ at 1.96 TeV
1.066 ± 0.008 ± 0.008		2 ABE	05B BELL	$e^+ e^- \rightarrow \Upsilon(4S)$
1.060 ± 0.021 ± 0.024		3 ABDALLAH	04E DLPH	$e^+ e^- \rightarrow Z$
1.093 ± 0.066 ± 0.028		4 ACOSTA	02C CDF	$p\bar{p}$ at 1.8 TeV
1.082 ± 0.026 ± 0.012		5 AUBERT	01F BABR	$e^+ e^- \rightarrow \Upsilon(4S)$
1.085 ± 0.059 ± 0.018		1 BARATE	00R ALEP	$e^+ e^- \rightarrow Z$
1.079 ± 0.064 ± 0.041		6 ABBIENDI	99J OPAL	$e^+ e^- \rightarrow Z$
1.110 ± 0.056 ^{+0.033} _{-0.030}		1 ABE	98Q CDF	$p\bar{p}$ at 1.8 TeV
1.09 ± 0.07 ± 0.03		6 ACCIARRI	98S L3	$e^+ e^- \rightarrow Z$
1.01 ± 0.07 ± 0.06		6 ABE	97J SLD	$e^+ e^- \rightarrow Z$
1.27 ^{+0.23} _{-0.19} ± 0.03 ^{+0.03} _{-0.02}		4 BUSKULIC	96J ALEP	$e^+ e^- \rightarrow Z$
1.00 ^{+0.17} _{-0.15} ± 0.10		1,7 ABREU	95Q DLPH	$e^+ e^- \rightarrow Z$
1.06 ± 0.13 ± 0.10		8 ADAM	95 DLPH	$e^+ e^- \rightarrow Z$
0.99 ± 0.14 ± 0.05 ^{+0.05} _{-0.04}		1,9 AKERS	95T OPAL	$e^+ e^- \rightarrow Z$

- • • We do not use the following data for averages, fits, limits, etc. • • •
- | | | | |
|---|----------------|----------|-------------------------|
| 1.091 ± 0.023 ± 0.014 | 5 ABE | 02H BELL | Repl. by ABE 05B |
| 1.06 ± 0.07 ± 0.02 | 4 ABE | 98B CDF | Repl. by ACOSTA 02C |
| 1.01 ± 0.11 ± 0.02 | 1 ABE | 96C CDF | Repl. by ABE 98Q |
| 1.03 ± 0.08 ± 0.02 | 10 BUSKULIC | 96J ALEP | $e^+ e^- \rightarrow Z$ |
| 0.98 ± 0.08 ± 0.03 | 1 BUSKULIC | 96J ALEP | Repl. by BARATE 00R |
| 1.02 ± 0.16 ± 0.05 | 269 4 ABE | 94D CDF | Repl. by ABE 98B |
| 1.11 ^{+0.51} _{-0.39} ± 0.11 | 188 1 ABREU | 93D DLPH | Sup. by ABREU 95Q |
| 1.01 ± 0.29 ± 0.12 | 253 8 ABREU | 93G DLPH | Sup. by ADAM 95 |
| 1.0 ± 0.33 ± 0.08 | 130 ACTON | 93C OPAL | Sup. by AKERS 95T |
| 0.96 ± 0.19 ± 0.18 ^{+0.18} _{-0.15} ± 0.12 | 154 1 BUSKULIC | 93D ALEP | Sup. by BUSKULIC 96J |
- 1 Data analyzed using $D/D^* \mu X$ vertices.
 2 Measurement performed using a combined fit of CP -violation, mixing and lifetimes.
 3 Measurement performed using an inclusive reconstruction and B flavor identification technique.
 4 Measured using fully reconstructed decays.
 5 Events are selected in which one B meson is fully reconstructed while the second B meson is reconstructed inclusively.
 6 Data analyzed using charge of secondary vertex.
 7 ABREU 95Q assumes $B(B^0 \rightarrow D^{*-} \ell^+ \nu_\ell) = 3.2 \pm 1.7\%$.
 8 Data analyzed using vertex-charge technique to tag B charge.
 9 AKERS 95T assumes $B(B^0 \rightarrow D_s^{*} D^0) = 5.0 \pm 0.9\%$ to find B^+/B^0 yield.
 10 Combined result of $D/D^* \ell X$ analysis and fully reconstructed B analysis.

 τ_{B^+}/τ_{B^0} (inferred from branching fractions)

These measurements are inferred from the branching fractions for semileptonic decay or other spectator-dominated decays by assuming that the rates for such decays are equal for B^0 and B^+ . We do not use measurements which assume equal production of B^0 and B^+ because of the large uncertainty in the production ratio.

VALUE	CL%	EVTS	DOCUMENT ID	TECN	COMMENT
1.076 ± 0.034 OUR EVALUATION					
1.07 ± 0.04 OUR AVERAGE					
1.07 ± 0.04 ± 0.03			URQUIJO	07 BELL	$e^+ e^- \rightarrow \Upsilon(4S)$
1.067 ± 0.041 ± 0.033			AUBERT,B	06Y BABR	$e^+ e^- \rightarrow \Upsilon(4S)$

- • • We do not use the following data for averages, fits, limits, etc. • • •

0.95 ^{+0.117} _{-0.080} ± 0.091	1 ARTUSO	97 CLE2	$e^+ e^- \rightarrow \Upsilon(4S)$
1.15 ± 0.17 ± 0.06	2 JESSOP	97 CLE2	$e^+ e^- \rightarrow \Upsilon(4S)$
0.93 ± 0.18 ± 0.12	3 ATHANAS	94 CLE2	Sup. by ARTUSO 97
0.91 ± 0.27 ± 0.21	4 ALBRECHT	92c ARG	$e^+ e^- \rightarrow \Upsilon(4S)$
1.0 ± 0.4	29 4,5 ALBRECHT	92G ARG	$e^+ e^- \rightarrow \Upsilon(4S)$
0.89 ± 0.19 ± 0.13	4 FULTON	91 CLEO	$e^+ e^- \rightarrow \Upsilon(4S)$
1.00 ± 0.23 ± 0.14	4 ALBRECHT	89L ARG	$e^+ e^- \rightarrow \Upsilon(4S)$
0.49 to 2.3	90 6 BEAN	87B CLEO	$e^+ e^- \rightarrow \Upsilon(4S)$

- 1 ARTUSO 97 uses partial reconstruction of $B \rightarrow D^* \ell \nu_\ell$ and independent of B^0 and B^+ production fraction.
 2 Assumes equal production of B^+ and B^0 at the $\Upsilon(4S)$.
 3 ATHANAS 94 uses events tagged by fully reconstructed B^- decays and partially or fully reconstructed B^0 decays.
 4 Assumes equal production of B^0 and B^+ .
 5 ALBRECHT 92G data analyzed using $B \rightarrow D_s \bar{D}, D_s \bar{D}^*, D_s^* \bar{D}, D_s^* \bar{D}^*$ events.
 6 BEAN 87B assume the fraction of $B^0 \bar{B}^0$ events at the $\Upsilon(4S)$ is 0.41.

 $\text{sgn}(\text{Re}(\lambda_{CP})) \Delta \Gamma_{B_d^0} / \Gamma_{B_d^0}$

$\Gamma_{B_d^0}$ and $\Delta \Gamma_{B_d^0}$ are the decay rate average and difference between two B_d^0 CP eigenstates (light – heavy). The λ_{CP} characterizes B^0 and \bar{B}^0 decays to states of charmonium plus K_L^0 , see the review on "CP Violation" in the reviews section.

"OUR EVALUATION" is an average using rescaled values of the data listed below. The average and rescaling were performed by the Heavy Flavor Averaging Group (HFAG) and are described at <http://www.slac.stanford.edu/xorg/hfag/>. The averaging/rescaling procedure takes into account correlations between the measurements.

VALUE	DOCUMENT ID	TECN	COMMENT
0.009 ± 0.037 OUR EVALUATION			
0.008 ± 0.037 ± 0.018			
	1 AUBERT,B	04c BABR	$e^+ e^- \rightarrow \Upsilon(4S)$

- 1 Corresponds to 90% confidence range $[-0.084, 0.068]$.

 $|\Delta \Gamma_{B_d^0}| / \Gamma_{B_d^0}$

VALUE	CL%	DOCUMENT ID	TECN	COMMENT
The data in this block is included in the average printed for a previous data block.				

< 0.18 95 1 ABDALLAH 03B DLPH $e^+ e^- \rightarrow Z$

- • • We do not use the following data for averages, fits, limits, etc. • • •

< 0.80 95 2,3 BEHRENS 00B CLE2 $e^+ e^- \rightarrow \Upsilon(4S)$

- 1 Using the measured $\tau_{B^0} = 1.55 \pm 0.03$ ps.

- 2 BEHRENS 00B uses high-momentum lepton tags and partially reconstructed $\bar{B}^0 \rightarrow D^{*+} \pi^-, \rho^-$ decays to determine the flavor of the B meson.

- 3 Assumes $\Delta m_d = 0.478 \pm 0.018$ ps⁻¹ and $\tau_{B^0} = 1.548 \pm 0.032$ ps.

 B^0 DECAY MODES

\bar{B}^0 modes are charge conjugates of the modes below. Reactions indicate the weak decay vertex and do not include mixing. Modes which do not identify the charge state of the B are listed in the B^\pm/B^0 ADMIXTURE section.

The branching fractions listed below assume 50% $B^0 \bar{B}^0$ and 50% $B^+ B^-$ production at the $\Upsilon(4S)$. We have attempted to bring older measurements up to date by rescaling their assumed $\Upsilon(4S)$ production ratio to 50:50 and their assumed D, D_s, D^* , and ψ branching ratios to current values whenever this would affect our averages and best limits significantly.

Indentation is used to indicate a subchannel of a previous reaction. All resonant subchannels have been corrected for resonance branching fractions to the final state so the sum of the subchannel branching fractions can exceed that of the final state.

For inclusive branching fractions, e.g., $B \rightarrow D^\pm$ anything, the values usually are multiplicities, not branching fractions. They can be greater than one.

Mode	Fraction (Γ_i/Γ)	Scale factor/ Confidence level
Γ_1 $\ell^+ \nu_\ell$ anything	[a] (10.33 ± 0.28) %	
Γ_2 $e^+ \nu_e X_c$	(10.1 ± 0.4) %	
Γ_3 $D \ell^+ \nu_\ell$ anything	(9.6 ± 0.9) %	
Γ_4 $D^- \ell^+ \nu_\ell$	[a] (2.17 ± 0.12) %	
Γ_5 $D^- \tau^+ \nu_\tau$	(1.0 ± 0.4) %	
Γ_6 $D^*(2010)^- \ell^+ \nu_\ell$	[a] (5.16 ± 0.11) %	
Γ_7 $D^*(2010)^- \tau^+ \nu_\tau$	(1.6 ± 0.5) %	S=1.2
Γ_8 $\bar{D}^0 \pi^- \ell^+ \nu_\ell$	(4.3 ± 0.6) × 10 ⁻³	

Meson Particle Listings

B^0

Γ_9	$D_0^*(2400)^- \ell^+ \nu_\ell \times$ $B(D_0^{*-} \rightarrow \bar{D}^0 \pi^-)$	$(2.0 \pm 0.9) \times 10^{-3}$		Γ_{67}	$D_2^*(2460)^- \pi^+ \times B((D_2^*)^- \rightarrow$ $D^{*-} \pi^+ \pi^-)$	< 2.4	$\times 10^{-5}$	CL=90%	
Γ_{10}	$D_2^*(2460)^- \ell^+ \nu_\ell \times$ $B(D_2^{*-} \rightarrow \bar{D}^0 \pi^-)$	$(2.2 \pm 0.6) \times 10^{-3}$		Γ_{68}	$\bar{D}_2^*(2460)^- \rho^+$	< 4.9	$\times 10^{-3}$	CL=90%	
Γ_{11}	$\bar{D}^{(*)} n \pi \ell^+ \nu_\ell (n \geq 1)$	$(2.4 \pm 0.5) \%$		Γ_{69}	$D_0^+ \bar{D}^0$	< 6	$\times 10^{-5}$	CL=90%	
Γ_{12}	$\bar{D}^{*0} \pi^- \ell^+ \nu_\ell$	$(4.9 \pm 0.8) \times 10^{-3}$		Γ_{70}	$D^{*0} \bar{D}^0$	< 2.9	$\times 10^{-4}$	CL=90%	
Γ_{13}	$D_1(2420)^- \ell^+ \nu_\ell \times$ $B(D_1^- \rightarrow \bar{D}^{*0} \pi^-)$	$(5.4 \pm 2.1) \times 10^{-3}$		Γ_{71}	$D^- D^+$	$(2.11 \pm 0.31) \times 10^{-4}$		S=1.2	
Γ_{14}	$D_1'(2430)^- \ell^+ \nu_\ell \times$ $B(D_1'^- \rightarrow \bar{D}^{*0} \pi^-)$	< 5.0	$\times 10^{-3}$	CL=90%	Γ_{72}	$D^- D_s^+$	$(7.4 \pm 0.7) \times 10^{-3}$		
Γ_{15}	$D_2^*(2460)^- \ell^+ \nu_\ell \times$ $B(D_2^{*-} \rightarrow \bar{D}^{*0} \pi^-)$	< 3.0	$\times 10^{-3}$	CL=90%	Γ_{73}	$D^*(2010)^- D_s^+$	$(8.3 \pm 1.1) \times 10^{-3}$		
Γ_{16}	$\rho^- \ell^+ \nu_\ell$	[a] $(2.47 \pm 0.33) \times 10^{-4}$		Γ_{74}	$D^- D_s^{*+}$	$(7.6 \pm 1.6) \times 10^{-3}$			
Γ_{17}	$\pi^- \ell^+ \nu_\ell$	[a] $(1.36 \pm 0.09) \times 10^{-4}$		Γ_{75}	$D^*(2010)^- D_s^{*+}$	$(1.79 \pm 0.14) \%$			
Γ_{18}	$\pi^- \mu^+ \nu_\mu$			Γ_{76}	$D_{s0}(2317)^- K^+ \times$ $B(D_{s0}(2317)^- \rightarrow D_s^- \pi^0)$	$(4.4 \pm 1.4) \times 10^{-5}$			
Inclusive modes									
Γ_{19}	K^\pm anything	$(78 \pm 8) \%$		Γ_{77}	$D_{s0}(2317)^- \pi^+ \times$ $B(D_{s0}(2317)^- \rightarrow D_s^- \pi^0)$	< 2.5	$\times 10^{-5}$	CL=90%	
Γ_{20}	$D^0 X$	$(8.1 \pm 1.5) \%$		Γ_{78}	$D_{s,J}(2457)^- K^+ \times$ $B(D_{s,J}(2457)^- \rightarrow D_s^- \pi^0)$	< 9.4	$\times 10^{-6}$	CL=90%	
Γ_{21}	$\bar{D}^0 X$	$(47.4 \pm 2.8) \%$		Γ_{79}	$D_{s,J}(2457)^- \pi^+ \times$ $B(D_{s,J}(2457)^- \rightarrow D_s^- \pi^0)$	< 4.0	$\times 10^{-6}$	CL=90%	
Γ_{22}	$D^+ X$	< 3.9	$\%$	CL=90%	Γ_{80}	$D_s^- D_s^+$	< 3.6	$\times 10^{-5}$	CL=90%
Γ_{23}	$D^- X$	$(36.9 \pm 3.3) \%$		Γ_{81}	$D_s^{*-} D_s^+$	< 1.3	$\times 10^{-4}$	CL=90%	
Γ_{24}	$D_s^+ X$	$(10.3 \pm_{-1.8}^{+2.1}) \%$		Γ_{82}	$D_s^- D_s^{*+}$	< 2.4	$\times 10^{-4}$	CL=90%	
Γ_{25}	$D_s^- X$	< 2.6	$\%$	CL=90%	Γ_{83}	$D_{s0}(2317)^+ D^- \times$ $B(D_{s0}(2317)^+ \rightarrow D_s^+ \pi^0)$	$(9.9 \pm_{-3.4}^{+4.2}) \times 10^{-4}$	S=1.5	
Γ_{26}	$\Lambda_c^+ X$	< 3.1	$\%$	CL=90%	Γ_{84}	$D_{s0}(2317)^+ D^- \times$ $B(D_{s0}(2317)^+ \rightarrow D_s^{*+} \gamma)$	< 9.5	$\times 10^{-4}$	CL=90%
Γ_{27}	$\bar{\Lambda}_c^- X$	$(5.0 \pm_{-1.5}^{+2.1}) \%$		Γ_{85}	$D_{s0}(2317)^+ D^*(2010)^- \times$ $B(D_{s0}(2317)^+ \rightarrow D_s^+ \pi^0)$	$(1.5 \pm 0.6) \times 10^{-3}$			
Γ_{28}	$\bar{c} X$	$(95 \pm 5) \%$		Γ_{86}	$D_{s,J}(2457)^+ D^-$	$(3.5 \pm 1.1) \times 10^{-3}$			
Γ_{29}	$c X$	$(24.6 \pm 3.1) \%$		Γ_{87}	$D_{s,J}(2457)^+ D^- \times$ $B(D_{s,J}(2457)^+ \rightarrow D_s^+ \gamma)$	$(6.7 \pm_{-1.4}^{+1.7}) \times 10^{-4}$			
Γ_{30}	$\bar{c} c X$	$(119 \pm 6) \%$		Γ_{88}	$D_{s,J}(2457)^+ D^- \times$ $B(D_{s,J}(2457)^+ \rightarrow D_s^{*+} \gamma)$	< 6.0	$\times 10^{-4}$	CL=90%	
$D, D^*,$ or D_s modes									
Γ_{31}	$D^- \pi^+$	$(2.68 \pm 0.13) \times 10^{-3}$		Γ_{89}	$D_{s,J}(2457)^+ D^- \times$ $B(D_{s,J}(2457)^+ \rightarrow D_s^{*+} \gamma)$	< 2.0	$\times 10^{-4}$	CL=90%	
Γ_{32}	$D^- \rho^+$	$(7.7 \pm 1.3) \times 10^{-3}$		Γ_{90}	$D_{s,J}(2457)^+ D^- \times$ $B(D_{s,J}(2457)^+ \rightarrow D_s^+ \pi^+ \pi^-)$	< 3.6	$\times 10^{-4}$	CL=90%	
Γ_{33}	$D^- K^0 \pi^+$	$(4.9 \pm 0.9) \times 10^{-4}$		Γ_{91}	$D^*(2010)^- D_{s,J}(2457)^+$	$(9.3 \pm 2.2) \times 10^{-3}$			
Γ_{34}	$D^- K^*(892)^+$	$(4.5 \pm 0.7) \times 10^{-4}$		Γ_{92}	$D_{s,J}(2457)^+ D^*(2010) \times$ $B(D_{s,J}(2457)^+ \rightarrow D_s^+ \gamma)$	$(2.3 \pm_{-0.7}^{+0.9}) \times 10^{-3}$			
Γ_{35}	$D^- \omega \pi^+$	$(2.8 \pm 0.6) \times 10^{-3}$		Γ_{93}	$D^- D_{s1}(2536)^+ \times$ $B(D_{s1}(2536)^+ \rightarrow D^{*0} K^+)$	$(1.7 \pm 0.6) \times 10^{-4}$			
Γ_{36}	$D^- K^+$	$(2.0 \pm 0.6) \times 10^{-4}$		Γ_{94}	$D^*(2010)^- D_{s1}(2536)^+ \times$ $B(D_{s1}(2536)^+ \rightarrow D^{*0} K^+)$	$(3.3 \pm 1.1) \times 10^{-4}$			
Γ_{37}	$D^- K^+ \bar{K}^0$	< 3.1	$\times 10^{-4}$	CL=90%	Γ_{95}	$D^- D_{s1}(2536)^+ \times$ $B(D_{s1}(2536)^+ \rightarrow D^{*+} K^0)$	$(2.6 \pm 1.1) \times 10^{-4}$		
Γ_{38}	$D^- K^+ \bar{K}^*(892)^0$	$(8.8 \pm 1.9) \times 10^{-4}$		Γ_{96}	$D^{*-} D_{s1}(2536)^+ \times$ $B(D_{s1}(2536)^+ \rightarrow D^{*+} K^0)$	$(5.0 \pm 1.7) \times 10^{-4}$			
Γ_{39}	$\bar{D}^0 \pi^+ \pi^-$	$(8.4 \pm 0.9) \times 10^{-4}$		Γ_{97}	$D^- D_{s,J}(2573)^+ \times$ $B(D_{s,J}(2573)^+ \rightarrow D^0 K^+)$	< 1	$\times 10^{-4}$	CL=90%	
Γ_{40}	$D^*(2010)^- \pi^+$	$(2.76 \pm 0.13) \times 10^{-3}$		Γ_{98}	$D^*(2010)^- D_{s,J}(2573)^+ \times$ $B(D_{s,J}(2573)^+ \rightarrow D^0 K^+)$	< 2	$\times 10^{-4}$	CL=90%	
Γ_{41}	$D^- \pi^+ \pi^+ \pi^-$	$(8.0 \pm 2.5) \times 10^{-3}$		Γ_{99}	$D_s^+ \pi^-$	$(1.53 \pm 0.35) \times 10^{-5}$			
Γ_{42}	$(D^- \pi^+ \pi^+ \pi^-)$ nonresonant	$(3.9 \pm 1.9) \times 10^{-3}$		Γ_{100}	$D_s^{*+} \pi^-$	$(3.0 \pm 0.7) \times 10^{-5}$			
Γ_{43}	$D^- \pi^+ \rho^0$	$(1.1 \pm 1.0) \times 10^{-3}$		Γ_{101}	$D_s^+ \rho^-$	< 6	$\times 10^{-4}$	CL=90%	
Γ_{44}	$D^- a_1(1260)^+$	$(6.0 \pm 3.3) \times 10^{-3}$		Γ_{102}	$D_s^{*+} \rho^-$	< 6	$\times 10^{-4}$	CL=90%	
Γ_{45}	$D^*(2010)^- \pi^+ \pi^0$	$(1.5 \pm 0.5) \%$		Γ_{103}	$D_s^+ a_0^-$	< 1.9	$\times 10^{-5}$	CL=90%	
Γ_{46}	$D^*(2010)^- \rho^+$	$(6.8 \pm 0.9) \times 10^{-3}$		Γ_{104}	$D_s^{*+} a_0^-$	< 3.6	$\times 10^{-5}$	CL=90%	
Γ_{47}	$D^*(2010)^- K^+$	$(2.14 \pm 0.16) \times 10^{-4}$		Γ_{105}	$D_s^+ a_1(1260)^-$	< 2.2	$\times 10^{-3}$	CL=90%	
Γ_{48}	$D^*(2010)^- K^0 \pi^+$	$(3.0 \pm 0.8) \times 10^{-4}$		Γ_{106}	$D_s^{*+} a_1(1260)^-$	< 1.8	$\times 10^{-3}$	CL=90%	
Γ_{49}	$D^*(2010)^- K^* (892)^+$	$(3.3 \pm 0.6) \times 10^{-4}$		Γ_{107}	$D_s^+ a_2^-$	< 1.9	$\times 10^{-4}$	CL=90%	
Γ_{50}	$D^*(2010)^- K^+ \bar{K}^0$	< 4.7	$\times 10^{-4}$	CL=90%	Γ_{108}	$D_s^{*+} a_2^-$	< 2.0	$\times 10^{-4}$	CL=90%
Γ_{51}	$D^*(2010)^- K^+ \bar{K}^*(892)^0$	$(1.29 \pm 0.33) \times 10^{-3}$		Γ_{109}	$D_s^- K^+$	$(2.9 \pm 0.5) \times 10^{-5}$			
Γ_{52}	$D^*(2010)^- \pi^+ \pi^+ \pi^-$	$(7.0 \pm 0.8) \times 10^{-3}$		Γ_{110}	$D_s^{*-} K^+$	$(2.2 \pm 0.6) \times 10^{-5}$			
Γ_{53}	$(D^*(2010)^- \pi^+ \pi^+ \pi^-)$ non-resonant	$(0.0 \pm 2.5) \times 10^{-3}$		Γ_{111}	$D_s^- K^*(892)^+$	< 8	$\times 10^{-4}$	CL=90%	
Γ_{54}	$D^*(2010)^- \pi^+ \rho^0$	$(5.7 \pm 3.2) \times 10^{-3}$		Γ_{112}	$D_s^{*-} K^*(892)^+$	< 9	$\times 10^{-4}$	CL=90%	
Γ_{55}	$D^*(2010)^- a_1(1260)^+$	$(1.30 \pm 0.27) \%$		Γ_{113}	$D_s^- \pi^+ K^0$	< 5	$\times 10^{-3}$	CL=90%	
Γ_{56}	$D^*(2010)^- \pi^+ \pi^+ \pi^- \pi^0$	$(1.76 \pm 0.27) \%$		Γ_{114}	$D_s^- \pi^+ K^0$	< 2.6	$\times 10^{-3}$	CL=90%	
Γ_{57}	$D^{*-} 3\pi^+ 2\pi^-$	$(4.7 \pm 0.9) \times 10^{-3}$		Γ_{115}	$D_s^- \pi^+ K^*(892)^0$	< 3.1	$\times 10^{-3}$	CL=90%	
Γ_{58}	$D^*(2010)^- \rho \bar{\rho} \pi^+$	$(6.5 \pm 1.6) \times 10^{-4}$							
Γ_{59}	$D^*(2010)^- \rho \bar{\rho}$	$(1.5 \pm 0.4) \times 10^{-3}$							
Γ_{60}	$\bar{D}^*(2010)^- \omega \pi^+$	$(2.89 \pm 0.30) \times 10^{-3}$							
Γ_{61}	$D_1(2430)^0 \omega \times$ $B(D_1(2430)^0 \rightarrow D^{*-} \pi^+)$	$(4.1 \pm 1.6) \times 10^{-4}$							
Γ_{62}	$\bar{D}^{*-} \pi^+$	[b] $(2.1 \pm 1.0) \times 10^{-3}$							
Γ_{63}	$D_1(2420)^- \pi^+ \times B(D_1^- \rightarrow$ $D^- \pi^+ \pi^-)$	$(8.9 \pm_{-3.5}^{+2.3}) \times 10^{-5}$							
Γ_{64}	$D_1(2420)^- \pi^+ \times B(D_1^- \rightarrow$ $D^{*-} \pi^+ \pi^-)$	< 3.3	$\times 10^{-5}$	CL=90%					
Γ_{65}	$\bar{D}_2^*(2460)^- \pi^+ \times$ $B(D_2^*(2460)^- \rightarrow D^0 \pi^-)$	$(2.15 \pm 0.35) \times 10^{-4}$							
Γ_{66}	$\bar{D}_0^*(2400)^- \pi^+ \times$ $B(D_0^*(2400)^- \rightarrow D^0 \pi^-)$	$(6.0 \pm 3.0) \times 10^{-5}$							

Γ_{116}	$D^{*-}\pi^+ K^*(892)^0$	< 1.7	$\times 10^{-3}$	CL=90%	Γ_{182}	$X(3872)K^0 \times B(X \rightarrow D^0 \bar{D}^0 \pi^0)$	(1.7 \pm 0.8)	$\times 10^{-4}$	
Γ_{117}	$\bar{D}^0 K^0$	(5.2 \pm 0.7)	$\times 10^{-5}$		Γ_{183}	$X(3872)K^0 \times B(X \rightarrow \bar{D}^{*0} D^0)$	< 4.37	$\times 10^{-4}$	CL=90%
Γ_{118}	$\bar{D}^0 K^+ \pi^-$	(8.8 \pm 1.7)	$\times 10^{-5}$		Γ_{184}	$J/\psi(1S) p \bar{p}$	< 8.3	$\times 10^{-7}$	CL=90%
Γ_{119}	$\bar{D}^0 K^*(892)^0$	(4.2 \pm 0.6)	$\times 10^{-5}$		Γ_{185}	$J/\psi(1S) \gamma$	< 1.6	$\times 10^{-6}$	CL=90%
Γ_{120}	$D_2^*(2460)^- K^+ \times B(D_2^*(2460)^- \rightarrow \bar{D}^0 \pi^-)$	(1.8 \pm 0.5)	$\times 10^{-5}$		Γ_{186}	$J/\psi(1S) \bar{D}^0$	< 1.3	$\times 10^{-5}$	CL=90%
Γ_{121}	$\bar{D}^0 K^+ \pi^-$ non-resonant	< 3.7	$\times 10^{-5}$	CL=90%	Γ_{187}	$\psi(2S) K^0$	(6.2 \pm 0.6)	$\times 10^{-4}$	
Γ_{122}	$\bar{D}^0 \pi^0$	(2.61 \pm 0.24)	$\times 10^{-4}$		Γ_{188}	$\psi(3770) K^0 \times B(\psi \rightarrow \bar{D}^0 D^0)$	< 1.23	$\times 10^{-4}$	CL=90%
Γ_{123}	$\bar{D}^0 \rho^0$	(3.2 \pm 0.5)	$\times 10^{-4}$		Γ_{189}	$\psi(3770) K^0 \times B(\psi \rightarrow D^- D^+)$	< 1.88	$\times 10^{-4}$	CL=90%
Γ_{124}	$\bar{D}^0 f_2$	(1.2 \pm 0.4)	$\times 10^{-4}$		Γ_{190}	$\psi(2S) K^+ \pi^-$	< 1	$\times 10^{-3}$	CL=90%
Γ_{125}	$\bar{D}^0 \eta$	(2.02 \pm 0.35)	$\times 10^{-4}$	S=1.6	Γ_{191}	$\psi(2S) K^*(892)^0$	(7.2 \pm 0.8)	$\times 10^{-4}$	
Γ_{126}	$\bar{D}^0 \eta'$	(1.25 \pm 0.23)	$\times 10^{-4}$	S=1.1	Γ_{192}	$\chi_{c0}(1P) K^0$	< 1.13	$\times 10^{-4}$	CL=90%
Γ_{127}	$\bar{D}^0 \omega$	(2.59 \pm 0.30)	$\times 10^{-4}$		Γ_{193}	$\chi_{c0} K^*(892)^0$	< 7.7	$\times 10^{-4}$	CL=90%
Γ_{128}	$D^0 \phi$	< 1.16	$\times 10^{-5}$	CL=90%	Γ_{194}	$\chi_{c2} K^0$	< 2.6	$\times 10^{-5}$	CL=90%
Γ_{129}	$D^0 K^+ \pi^-$	< 1.9	$\times 10^{-5}$	CL=90%	Γ_{195}	$\chi_{c2} K^*(892)^0$	< 3.6	$\times 10^{-5}$	CL=90%
Γ_{130}	$D^0 K^*(892)^0$	< 1.1	$\times 10^{-5}$	CL=90%	Γ_{196}	$\chi_{c1}(1P) K^0$	(3.9 \pm 0.4)	$\times 10^{-4}$	
Γ_{131}	$\bar{D}^{*0} \gamma$	< 2.5	$\times 10^{-5}$	CL=90%	Γ_{197}	$\chi_{c1}(1P) K^*(892)^0$	(3.2 \pm 0.6)	$\times 10^{-4}$	
Γ_{132}	$\bar{D}^*(2007)^0 \pi^0$	(1.7 \pm 0.4)	$\times 10^{-4}$	S=1.5	K or K* modes				
Γ_{133}	$\bar{D}^*(2007)^0 \rho^0$	< 5.1	$\times 10^{-4}$	CL=90%	Γ_{198}	$K^+ \pi^-$	(1.94 \pm 0.06)	$\times 10^{-5}$	
Γ_{134}	$\bar{D}^*(2007)^0 \eta$	(1.8 \pm 0.6)	$\times 10^{-4}$	S=1.8	Γ_{199}	$K^0 \pi^0$	(9.8 \pm 0.6)	$\times 10^{-6}$	
Γ_{135}	$\bar{D}^*(2007)^0 \eta'$	(1.23 \pm 0.35)	$\times 10^{-4}$		Γ_{200}	$\eta' K^0$	(6.5 \pm 0.4)	$\times 10^{-5}$	S=1.2
Γ_{136}	$\bar{D}^*(2007)^0 \pi^+ \pi^-$	(6.2 \pm 2.2)	$\times 10^{-4}$		Γ_{201}	$\eta' K^*(892)^0$	(3.8 \pm 1.2)	$\times 10^{-6}$	
Γ_{137}	$\bar{D}^*(2007)^0 K^0$	(3.6 \pm 1.2)	$\times 10^{-5}$		Γ_{202}	ηK^0	< 1.9	$\times 10^{-6}$	CL=90%
Γ_{138}	$\bar{D}^*(2007)^0 K^*(892)^0$	< 6.9	$\times 10^{-5}$	CL=90%	Γ_{203}	$\eta K^*(892)^0$	(1.59 \pm 0.10)	$\times 10^{-5}$	
Γ_{139}	$D^*(2007)^0 K^*(892)^0$	< 4.0	$\times 10^{-5}$	CL=90%	Γ_{204}	$\eta K_0^*(1430)^0$	(1.10 \pm 0.22)	$\times 10^{-5}$	
Γ_{140}	$D^*(2007)^0 \pi^+ \pi^+ \pi^- \pi^-$	(2.7 \pm 0.5)	$\times 10^{-3}$		Γ_{205}	$\eta K_2^*(1430)^0$	(9.6 \pm 2.1)	$\times 10^{-6}$	
Γ_{141}	$D^*(2010)^+ D^*(2010)^-$	(8.2 \pm 0.9)	$\times 10^{-4}$		Γ_{206}	ωK^0	(5.0 \pm 0.6)	$\times 10^{-6}$	
Γ_{142}	$\bar{D}^*(2007)^0 \omega$	(2.7 \pm 0.8)	$\times 10^{-4}$	S=1.5	Γ_{207}	$a_0(980)^0 K^0 \times B(a_0(980)^0 \rightarrow \eta \pi^0)$	< 7.8	$\times 10^{-6}$	CL=90%
Γ_{143}	$D^*(2010)^+ D^-$	(6.1 \pm 1.5)	$\times 10^{-4}$	S=1.6	Γ_{208}	$a_0(980)^\pm K^\mp \times B(a_0(980)^\pm \rightarrow \eta \pi^\pm)$	< 1.9	$\times 10^{-6}$	CL=90%
Γ_{144}	$D^*(2007)^0 \bar{D}^*(2007)^0$	< 9	$\times 10^{-5}$	CL=90%	Γ_{209}	$a_0(1450)^\pm K^\mp \times B(a_0(1450)^\pm \rightarrow \eta \pi^\pm)$	< 3.1	$\times 10^{-6}$	CL=90%
Γ_{145}	$D^- D^0 K^+$	(1.7 \pm 0.4)	$\times 10^{-3}$		Γ_{210}	$K_S^0 \chi^0$ (Familon)	< 5.3	$\times 10^{-5}$	CL=90%
Γ_{146}	$D^- D^*(2007)^0 K^+$	(4.6 \pm 1.0)	$\times 10^{-3}$		Γ_{211}	$\omega K^*(892)^0$	< 4.2	$\times 10^{-6}$	CL=90%
Γ_{147}	$D^*(2010)^- D^0 K^+$	(3.1 \pm 0.6)	$\times 10^{-3}$		Γ_{212}	$K^+ K^-$	< 4.1	$\times 10^{-7}$	CL=90%
Γ_{148}	$D^*(2010)^- D^*(2007)^0 K^+$	(1.18 \pm 0.20)	%		Γ_{213}	$K^0 \bar{K}^0$	(9.6 \pm 2.0)	$\times 10^{-7}$	
Γ_{149}	$D^- D^+ K^0$	< 1.7	$\times 10^{-3}$	CL=90%	Γ_{214}	$K_S^0 K_S^0 K_S^0$	(6.2 \pm 1.2)	$\times 10^{-6}$	S=1.3
Γ_{150}	$D^*(2010)^- D^+ K^0 + D^- D^*(2010)^+ K^0$	(6.5 \pm 1.6)	$\times 10^{-3}$		Γ_{215}	$K_S^0 K_S^0 K_S^0$	< 1.6	$\times 10^{-5}$	CL=90%
Γ_{151}	$D^*(2010)^- D^*(2010)^+ K^0$	(7.8 \pm 1.1)	$\times 10^{-3}$		Γ_{216}	$K^+ \pi^- \pi^0$	(3.7 \pm 0.5)	$\times 10^{-5}$	
Γ_{152}	$D^* D_{s1}(2536)^+ \times B(D_{s1}(2536)^+ \rightarrow D^* K^0)$	(8.0 \pm 2.4)	$\times 10^{-4}$		Γ_{217}	$K^+ \rho^-$	(8.5 \pm 2.8)	$\times 10^{-6}$	S=1.7
Γ_{153}	$\bar{D}^0 D^0 K^0$	< 1.4	$\times 10^{-3}$	CL=90%	Γ_{218}	$(K^+ \pi^- \pi^0)$ non-resonant	< 9.4	$\times 10^{-6}$	CL=90%
Γ_{154}	$\bar{D}^0 D^*(2007)^0 K^0 + \bar{D}^*(2007)^0 D^0 K^0$	< 3.7	$\times 10^{-3}$	CL=90%	Γ_{219}	$K^{*0} \pi^0$	[d] (6.1 \pm 1.6)	$\times 10^{-6}$	
Γ_{155}	$\bar{D}^*(2007)^0 D^*(2007)^0 K^0$	< 6.6	$\times 10^{-3}$	CL=90%	Γ_{220}	$K^0 \pi^+ \pi^-$ charmless	(4.48 \pm 0.26)	$\times 10^{-5}$	
Γ_{156}	$(\bar{D} + \bar{D}^*)(D + D^*) K$	(4.3 \pm 0.7)	%		Γ_{221}	$K^0 \pi^+ \pi^-$ non-resonant	(1.99 \pm 0.31)	$\times 10^{-5}$	
Charmonium modes									
Γ_{157}	$\eta_c K^0$	(8.9 \pm 1.6)	$\times 10^{-4}$		Γ_{222}	$K^0 \rho^0$	(5.4 \pm 0.9)	$\times 10^{-6}$	
Γ_{158}	$\eta_c K^*(892)^0$	(9.6 \pm 3.3)	$\times 10^{-4}$	S=1.1	Γ_{223}	$K^0 f_0(980)$	(5.5 \pm 0.9)	$\times 10^{-6}$	
Γ_{159}	$J/\psi(1S) K^0$	(8.71 \pm 0.32)	$\times 10^{-4}$		Γ_{224}	$K^*(892)^+ \pi^-$	(9.8 \pm 1.3)	$\times 10^{-6}$	S=1.2
Γ_{160}	$J/\psi(1S) K^+ \pi^-$	(1.2 \pm 0.6)	$\times 10^{-3}$		Γ_{225}	$K^*(1430)^+ \pi^-$	(5.0 \pm 0.8)	$\times 10^{-5}$	
Γ_{161}	$J/\psi(1S) K^*(892)^0$	(1.33 \pm 0.06)	$\times 10^{-3}$		Γ_{226}	$K^{*+} \pi^-$	[d] (5.1 \pm 1.6)	$\times 10^{-6}$	
Γ_{162}	$J/\psi(1S) \eta K_S^0$	(8 \pm 4)	$\times 10^{-5}$		Γ_{227}	$K^*(1410)^+ \pi^- \times B(K^*(1410)^+ \rightarrow K^0 \pi^+)$	< 3.8	$\times 10^{-6}$	CL=90%
Γ_{163}	$J/\psi(1S) \eta' K_S^0$	< 2.5	$\times 10^{-5}$	CL=90%	Γ_{228}	$K^*(1680)^+ \pi^- \times B(K^*(1680)^+ \rightarrow K^0 \pi^+)$	< 2.6	$\times 10^{-6}$	CL=90%
Γ_{164}	$J/\psi(1S) \phi K^0$	(9.4 \pm 2.6)	$\times 10^{-5}$		Γ_{229}	$K_2^*(1430)^+ \pi^- \times B(K_2^*(1430)^+ \rightarrow K^0 \pi^+)$	< 2.1	$\times 10^{-6}$	CL=90%
Γ_{165}	$J/\psi(1S) K(1270)^0$	(1.3 \pm 0.5)	$\times 10^{-3}$		Γ_{230}	$f_0(980) K^0 \times B(f_0(980) \rightarrow \pi^+ \pi^-)$	(7.6 \pm 1.9)	$\times 10^{-6}$	
Γ_{166}	$J/\psi(1S) \pi^0$	(2.05 \pm 0.24)	$\times 10^{-5}$		Γ_{231}	$f_2(1270) K^0 \times B(f_2(1270) \rightarrow \pi^+ \pi^-)$	< 1.4	$\times 10^{-6}$	CL=90%
Γ_{167}	$J/\psi(1S) \eta$	(9.5 \pm 1.9)	$\times 10^{-6}$		Γ_{232}	$K^*(892)^0 \pi^0$	< 3.5	$\times 10^{-6}$	CL=90%
Γ_{168}	$J/\psi(1S) \pi^+ \pi^-$	(4.6 \pm 0.9)	$\times 10^{-5}$		Γ_{233}	$K_2^*(1430)^+ \pi^-$	< 1.8	$\times 10^{-5}$	CL=90%
Γ_{169}	$J/\psi(1S) \pi^+ \pi^-$ nonresonant	< 1.2	$\times 10^{-5}$	CL=90%	Γ_{234}	$K^0 K^- \pi^+$	< 1.8	$\times 10^{-5}$	CL=90%
Γ_{170}	$J/\psi(1S) f_2$	< 4.6	$\times 10^{-6}$	CL=90%	Γ_{235}	$\bar{K}^{*0} K^0 + K^{*0} \bar{K}^0$	< 1.9	$\times 10^{-6}$	
Γ_{171}	$J/\psi(1S) \rho^0$	(2.7 \pm 0.4)	$\times 10^{-5}$		Γ_{236}	$K^+ K^- \pi^0$	< 1.9	$\times 10^{-5}$	CL=90%
Γ_{172}	$J/\psi(1S) \omega$	< 2.7	$\times 10^{-4}$	CL=90%	Γ_{237}	$K^0 K^+ K^-$	(2.47 \pm 0.23)	$\times 10^{-5}$	
Γ_{173}	$J/\psi(1S) \phi$	< 9.2	$\times 10^{-6}$	CL=90%	Γ_{238}	$K^0 \phi$	(8.6 \pm 1.3)	$\times 10^{-6}$	
Γ_{174}	$J/\psi(1S) \eta'(958)$	< 6.3	$\times 10^{-5}$	CL=90%	Γ_{239}	$K^+ \pi^- \pi^+ \pi^-$	[e] < 2.3	$\times 10^{-4}$	CL=90%
Γ_{175}	$J/\psi(1S) K^0 \pi^+ \pi^-$	(1.0 \pm 0.4)	$\times 10^{-3}$		Γ_{240}	$K^*(892)^0 \pi^+ \pi^-$	(5.4 \pm 0.5)	$\times 10^{-5}$	
Γ_{176}	$J/\psi(1S) K^0 \rho^0$	(5.4 \pm 3.0)	$\times 10^{-4}$		Γ_{241}	$K^*(892)^0 \rho^0$	(5.6 \pm 1.6)	$\times 10^{-6}$	
Γ_{177}	$J/\psi(1S) K^*(892)^+ \pi^-$	(8 \pm 4)	$\times 10^{-4}$		Γ_{242}	$K^*(892)^0 f_0(980)$	< 4.3	$\times 10^{-6}$	CL=90%
Γ_{178}	$J/\psi(1S) K^*(892)^0 \pi^+ \pi^-$	(6.6 \pm 2.2)	$\times 10^{-4}$						
Γ_{179}	$X(3872)^- K^+$	< 5.6	$\times 10^{-4}$	CL=90%					
Γ_{180}	$X(3872)^- K^+ \times B(X(3872)^- \rightarrow [c] J/\psi(1S) \pi^- \pi^0)$	< 5.4	$\times 10^{-6}$	CL=90%					
Γ_{181}	$X(3872) K^0 \times B(X \rightarrow J/\psi \pi^+ \pi^-)$	< 1.03	$\times 10^{-5}$	CL=90%					

Meson Particle Listings

 B^0

Γ_{243}	$K_1(1400)^+\pi^-$	< 1.1	$\times 10^{-3}$	CL=90%	Γ_{309}	$\rho^0\pi^0$	(1.8 \pm 0.5)	$\times 10^{-6}$	
Γ_{244}	$a_1(1260)^-K^+$	[e] (1.6 \pm 0.4)	$\times 10^{-5}$		Γ_{310}	$\rho^\mp\pi^\pm$	[g] (2.28 \pm 0.25)	$\times 10^{-5}$	
Γ_{245}	$b_1^-K^+ \times B(b_1^- \rightarrow \omega\pi^-)$	(7.4 \pm 1.4)	$\times 10^{-6}$		Γ_{311}	$\pi^+\pi^-\pi^+\pi^-$	< 2.3	$\times 10^{-4}$	CL=90%
Γ_{246}	$K^*(892)^0K^+K^-$	(2.75 \pm 0.26)	$\times 10^{-5}$		Γ_{312}	$\rho^0\rho^0$	(1.1 \pm 0.4)	$\times 10^{-6}$	
Γ_{247}	$K^*(892)^0\phi$	(9.5 \pm 0.8)	$\times 10^{-6}$		Γ_{313}	$\rho^0f_0(980) \times B(f_0(980) \rightarrow \pi^+\pi^-)$	< 5.3	$\times 10^{-7}$	CL=90%
Γ_{248}	$K^*(892)^0K^-\pi^+$	(4.6 \pm 1.4)	$\times 10^{-6}$		Γ_{314}	$f_0(980)f_0(980) \times B(f_0(980) \rightarrow \pi^+\pi^-)^2$	< 1.6	$\times 10^{-7}$	CL=90%
Γ_{249}	$K^*(892)^0\bar{K}^*(892)^0$	(1.28 \pm 0.37)	$\times 10^{-6}$		Γ_{315}	$a_1(1260)^\mp\pi^\pm$	[g] (3.3 \pm 0.5)	$\times 10^{-5}$	
Γ_{250}	$K^*(892)^0K^+\pi^-$	< 2.2	$\times 10^{-6}$	CL=90%	Γ_{316}	$b_1^\mp\pi^\pm \times B(b_1^\mp \rightarrow \omega\pi^\mp)$	(1.09 \pm 0.15)	$\times 10^{-5}$	
Γ_{251}	$K^*(892)^0K^*(892)^0$	< 4.1	$\times 10^{-7}$	CL=90%	Γ_{317}	$a_2(1320)^\mp\pi^\pm$	[g] < 3.0	$\times 10^{-4}$	CL=90%
Γ_{252}	$K^*(892)^+\rho^-$	< 1.20	$\times 10^{-5}$	CL=90%	Γ_{318}	$\pi^+\pi^-\pi^0\pi^0$	< 3.1	$\times 10^{-3}$	CL=90%
Γ_{253}	$K^*(892)^+K^*(892)^-$	< 1.41	$\times 10^{-4}$	CL=90%	Γ_{319}	$\rho^+\rho^-$	(2.42 \pm 0.31)	$\times 10^{-5}$	
Γ_{254}	$K_1(1400)^0\rho^0$	< 3.0	$\times 10^{-3}$	CL=90%	Γ_{320}	$a_1(1260)^0\pi^0$	< 1.1	$\times 10^{-3}$	CL=90%
Γ_{255}	$K_1(1400)^0\phi$	< 5.0	$\times 10^{-3}$	CL=90%	Γ_{321}	$\omega\pi^0$	< 1.2	$\times 10^{-6}$	CL=90%
Γ_{256}	$\phi(K\pi)_0^0$	(5.0 \pm 0.9)	$\times 10^{-6}$		Γ_{322}	$\pi^+\pi^+\pi^-\pi^-\pi^0$	< 9.0	$\times 10^{-3}$	CL=90%
Γ_{257}	$\phi(K\pi)_0^0 (1.60 < m_{K\pi} < 2.15)$	[f] < 1.7	$\times 10^{-6}$	CL=90%	Γ_{323}	$a_1(1260)^+\rho^-$	< 6.1	$\times 10^{-5}$	CL=90%
Γ_{258}	$K_0^*(1430)^0\phi$	(4.6 \pm 0.9)	$\times 10^{-6}$		Γ_{324}	$a_1(1260)^0\rho^0$	< 2.4	$\times 10^{-3}$	CL=90%
Γ_{259}	$K^*(1680)^0\phi$	< 3.5	$\times 10^{-6}$	CL=90%	Γ_{325}	$\pi^+\pi^+\pi^+\pi^-\pi^-\pi^-$	< 3.0	$\times 10^{-3}$	CL=90%
Γ_{260}	$K^*(1780)^0\phi$	< 2.7	$\times 10^{-6}$	CL=90%	Γ_{326}	$a_1(1260)^+a_1(1260)^-$	< 2.8	$\times 10^{-3}$	CL=90%
Γ_{261}	$K^*(2045)^0\phi$	< 1.53	$\times 10^{-5}$	CL=90%	Γ_{327}	$\pi^+\pi^+\pi^+\pi^-\pi^-\pi^-\pi^0$	< 1.1	%	CL=90%
Γ_{262}	$K_2^*(1430)^0\rho^0$	< 1.1	$\times 10^{-3}$	CL=90%	Baryon modes				
Γ_{263}	$K_2^*(1430)^0\phi$	(7.8 \pm 1.3)	$\times 10^{-6}$		Γ_{328}	$\rho\bar{p}$	< 1.1	$\times 10^{-7}$	CL=90%
Γ_{264}	$K^0\phi\phi$	(4.1 \pm 1.7)	$\times 10^{-6}$		Γ_{329}	$\rho\bar{p}\pi^+\pi^-$	< 2.5	$\times 10^{-4}$	CL=90%
Γ_{265}	$\eta'\eta'K^0$	< 3.1	$\times 10^{-5}$	CL=90%	Γ_{330}	$\rho\bar{p}K^0$	(2.7 \pm 0.4)	$\times 10^{-6}$	
Γ_{266}	$K^*(892)^0\gamma$	(4.01 \pm 0.20)	$\times 10^{-5}$		Γ_{331}	$\Theta(1540)^+\bar{p} \times B(\Theta(1540)^+ \rightarrow [h] \rho K_S^0)$	[h] < 5	$\times 10^{-8}$	CL=90%
Γ_{267}	$\eta K^0\gamma$	(1.07 \pm 0.22)	$\times 10^{-5}$		Γ_{332}	$f_J(2220)K^0 \times B(f_J(2220) \rightarrow \rho\bar{p})$	< 4.5	$\times 10^{-7}$	CL=90%
Γ_{268}	$\eta'K^0\gamma$	< 6.6	$\times 10^{-6}$	CL=90%	Γ_{333}	$\rho\bar{p}K^*(892)^0$	(1.5 \pm 0.6)	$\times 10^{-6}$	
Γ_{269}	$K^0\phi\gamma$	< 2.7	$\times 10^{-6}$	CL=90%	Γ_{334}	$f_J(2220)K_0^* \times B(f_J(2220) \rightarrow \rho\bar{p})$	< 1.5	$\times 10^{-7}$	CL=90%
Γ_{270}	$K^+\pi^-\gamma$	(4.6 \pm 1.4)	$\times 10^{-6}$		Γ_{335}	$\rho\bar{\Lambda}\pi^-$	(3.2 \pm 0.4)	$\times 10^{-6}$	
Γ_{271}	$K^*(1410)\gamma$	< 1.3	$\times 10^{-4}$	CL=90%	Γ_{336}	$\rho\bar{\Sigma}^-(1385)^-$	< 2.6	$\times 10^{-7}$	CL=90%
Γ_{272}	$K^+\pi^-\gamma$ nonresonant	< 2.6	$\times 10^{-6}$	CL=90%	Γ_{337}	$\Delta^0\bar{\Lambda}$	< 9.3	$\times 10^{-7}$	CL=90%
Γ_{273}	$K^0\pi^+\pi^-\gamma$	(1.95 \pm 0.22)	$\times 10^{-5}$		Γ_{338}	$\rho\bar{\Lambda}K^-$	< 8.2	$\times 10^{-7}$	CL=90%
Γ_{274}	$K^+\pi^-\pi^0\gamma$	(4.1 \pm 0.4)	$\times 10^{-5}$		Γ_{339}	$\rho\bar{\Sigma}^0\pi^-$	< 3.8	$\times 10^{-6}$	CL=90%
Γ_{275}	$K_1(1270)^0\gamma$	< 5.8	$\times 10^{-5}$	CL=90%	Γ_{340}	$\bar{\Lambda}\bar{\Lambda}$	< 3.2	$\times 10^{-7}$	CL=90%
Γ_{276}	$K_1(1400)^0\gamma$	< 1.5	$\times 10^{-5}$	CL=90%	Γ_{341}	$\Delta^0\bar{\Delta}^0$	< 1.5	$\times 10^{-3}$	CL=90%
Γ_{277}	$K_2^*(1430)^0\gamma$	(1.24 \pm 0.24)	$\times 10^{-5}$		Γ_{342}	$\Delta^{++}\bar{\Delta}^{--}$	< 1.1	$\times 10^{-4}$	CL=90%
Γ_{278}	$K^*(1680)^0\gamma$	< 2.0	$\times 10^{-3}$	CL=90%	Γ_{343}	$\bar{D}^0\rho\bar{p}$	(1.14 \pm 0.09)	$\times 10^{-4}$	
Γ_{279}	$K_3^*(1780)^0\gamma$	< 8.3	$\times 10^{-5}$	CL=90%	Γ_{344}	$D_s^-\bar{\Lambda}\rho$	(2.9 \pm 0.9)	$\times 10^{-5}$	
Γ_{280}	$K_4^*(2045)^0\gamma$	< 4.3	$\times 10^{-3}$	CL=90%	Γ_{345}	$\bar{D}^*(2007)^0\rho\bar{p}$	(1.03 \pm 0.13)	$\times 10^{-4}$	
Light unflavored meson modes					Γ_{346}	$D^-\rho\bar{p}\pi^+$	(3.38 \pm 0.32)	$\times 10^{-4}$	
Γ_{281}	$\rho^0\gamma$	(9.3 \pm 2.1)	$\times 10^{-7}$	S=1.1	Γ_{347}	$D^{*-}\rho\bar{p}\pi^+$	(4.8 \pm 0.5)	$\times 10^{-4}$	
Γ_{282}	$\omega\gamma$	(4.6 \pm 2.0)	$\times 10^{-7}$		Γ_{348}	$\Theta_c\bar{p}\pi^+ \times B(\Theta_c \rightarrow D^-\rho)$	< 9	$\times 10^{-6}$	CL=90%
Γ_{283}	$\phi\gamma$	< 8.5	$\times 10^{-7}$	CL=90%	Γ_{349}	$\Theta_c\bar{p}\pi^+ \times B(\Theta_c \rightarrow D^{*-}\rho)$	< 1.4	$\times 10^{-5}$	CL=90%
Γ_{284}	$\pi^+\pi^-$	(5.13 \pm 0.24)	$\times 10^{-6}$		Γ_{350}	$\bar{\Sigma}_c^{--}\Delta^{++}$	< 1.0	$\times 10^{-3}$	CL=90%
Γ_{285}	$\pi^0\pi^0$	(1.62 \pm 0.31)	$\times 10^{-6}$	S=1.3	Γ_{351}	$\bar{\Lambda}_c^-\rho\pi^+\pi^-$	(1.3 \pm 0.4)	$\times 10^{-3}$	
Γ_{286}	$\eta\pi^0$	< 1.3	$\times 10^{-6}$	CL=90%	Γ_{352}	$\bar{\Lambda}_c^-\rho$	(2.1 \pm 0.7)	$\times 10^{-5}$	
Γ_{287}	$\eta\eta$	< 1.8	$\times 10^{-6}$	CL=90%	Γ_{353}	$\bar{\Lambda}_c^-\rho\pi^0$	< 5.9	$\times 10^{-4}$	CL=90%
Γ_{288}	$\eta'\pi^0$	(1.5 \pm 1.0)	$\times 10^{-6}$	S=1.5	Γ_{354}	$\bar{\Lambda}_c^-\rho\pi^+\pi^-\pi^0$	< 5.07	$\times 10^{-3}$	CL=90%
Γ_{289}	$\eta'\eta'$	< 2.4	$\times 10^{-6}$	CL=90%	Γ_{355}	$\bar{\Lambda}_c^-\rho\pi^+\pi^-\pi^+\pi^-$	< 2.74	$\times 10^{-3}$	CL=90%
Γ_{290}	$\eta'\eta$	< 1.7	$\times 10^{-6}$	CL=90%	Γ_{356}	$\Lambda_c^+\bar{p}\pi^+\pi^-$	(1.12 \pm 0.32)	$\times 10^{-3}$	
Γ_{291}	$\eta'\rho^0$	< 1.3	$\times 10^{-6}$	CL=90%	Γ_{357}	$\Lambda_c^+\bar{p}\pi^+\pi^-$ (nonresonant)	(6.4 \pm 1.9)	$\times 10^{-4}$	
Γ_{292}	$\eta'f_0(980) \times B(f_0(980) \rightarrow \pi^+\pi^-)$	< 1.5	$\times 10^{-6}$	CL=90%	Γ_{358}	$\bar{\Sigma}_c(2520)^{--}\rho\pi^+$	(1.2 \pm 0.4)	$\times 10^{-4}$	
Γ_{293}	$\eta\rho^0$	< 1.5	$\times 10^{-6}$	CL=90%	Γ_{359}	$\bar{\Sigma}_c(2520)^0\rho\pi^-$	< 3.8	$\times 10^{-5}$	CL=90%
Γ_{294}	$\eta f_0(980) \times B(f_0(980) \rightarrow \pi^+\pi^-)$	< 4	$\times 10^{-7}$	CL=90%	Γ_{360}	$\bar{\Sigma}_c(2455)^0\rho\pi^-$	(1.5 \pm 0.5)	$\times 10^{-4}$	
Γ_{295}	$\omega\eta$	< 1.9	$\times 10^{-6}$	CL=90%	Γ_{361}	$\bar{\Sigma}_c(2455)^{--}\rho\pi^+$	(2.2 \pm 0.7)	$\times 10^{-4}$	
Γ_{296}	$\omega\eta'$	< 2.2	$\times 10^{-6}$	CL=90%	Γ_{362}	$\bar{\Lambda}_c^-\Lambda_c^+$	< 6.2	$\times 10^{-5}$	CL=90%
Γ_{297}	$\omega\rho^0$	< 1.5	$\times 10^{-6}$	CL=90%	Γ_{363}	$\bar{\Lambda}_c(2593)^- / \bar{\Lambda}_c(2625)^-\rho$	< 1.1	$\times 10^{-4}$	CL=90%
Γ_{298}	$\omega f_0(980)$	< 1.5	$\times 10^{-6}$	CL=90%	Γ_{364}	$\bar{\Xi}_c^-\Lambda_c^+ \times B(\bar{\Xi}_c^- \rightarrow \bar{\Xi}^+\pi^-\pi^-)$	(9 \pm 5)	$\times 10^{-5}$	
Γ_{299}	$\omega\omega$	< 4.0	$\times 10^{-6}$	CL=90%	Γ_{365}	$\Lambda_c^+\Lambda_c^-K^0$	(8 \pm 5)	$\times 10^{-4}$	
Γ_{300}	$\phi\pi^0$	< 2.8	$\times 10^{-7}$	CL=90%	Lepton Family number (LF) violating modes, or $\Delta B = 1$ weak neutral current (B_1) modes				
Γ_{301}	$\phi\eta$	< 6	$\times 10^{-7}$	CL=90%	Γ_{366}	$\gamma\gamma$	B_1 < 6.2	$\times 10^{-7}$	CL=90%
Γ_{302}	$\phi\eta'$	< 5	$\times 10^{-7}$	CL=90%	Γ_{367}	e^+e^-	B_1 < 1.13	$\times 10^{-7}$	CL=90%
Γ_{303}	$\phi\rho^0$	< 1.3	$\times 10^{-5}$	CL=90%	Γ_{368}	$e^+e^-\gamma$	B_1 < 1.2	$\times 10^{-7}$	CL=90%
Γ_{304}	$\phi\omega$	< 1.2	$\times 10^{-6}$	CL=90%	Γ_{369}	$\mu^+\mu^-$	B_1 < 1.5	$\times 10^{-8}$	CL=90%
Γ_{305}	$\phi\phi$	< 1.5	$\times 10^{-6}$	CL=90%	Γ_{370}	$\mu^+\mu^-\gamma$	B_1 < 1.6	$\times 10^{-7}$	CL=90%
Γ_{306}	$a_0(980)^\pm\pi^\mp \times B(a_0(980)^\pm \rightarrow \eta\pi^\pm)$	< 3.1	$\times 10^{-6}$	CL=90%	Γ_{371}	$\tau^+\tau^-$	B_1 < 4.1	$\times 10^{-3}$	CL=90%
Γ_{307}	$a_0(1450)^\pm\pi^\mp \times B(a_0(1450)^\pm \rightarrow \eta\pi^\pm)$	< 2.3	$\times 10^{-6}$	CL=90%	Γ_{372}	$\pi^0\ell^+\ell^-$	B_1 < 1.2	$\times 10^{-7}$	CL=90%
Γ_{308}	$\pi^+\pi^-\pi^0$	< 7.2	$\times 10^{-4}$	CL=90%					

See key on page 373

Meson Particle Listings

 B^0

Γ_{373}	$\pi^0 \nu \bar{\nu}$	$B1$	< 2.2	$\times 10^{-4}$	CL=90%
Γ_{374}	$\pi^0 e^+ e^-$	$B1$	< 1.4	$\times 10^{-7}$	CL=90%
Γ_{375}	$\pi^0 \mu^+ \mu^-$	$B1$	< 5.1	$\times 10^{-7}$	CL=90%
Γ_{376}	$K^0 \ell^+ \ell^-$	$B1$	[a]	$(2.9^{+1.6}_{-1.3}) \times 10^{-7}$	
Γ_{377}	$K^0 \nu \bar{\nu}$	$B1$	< 1.6	$\times 10^{-4}$	CL=90%
Γ_{378}	$\rho^0 \nu \bar{\nu}$	$B1$	< 4.4	$\times 10^{-4}$	CL=90%
Γ_{379}	$K^0 e^+ e^-$	$B1$	< 1.3	$(1.6^{+1.6}_{-1.1}) \times 10^{-7}$	
Γ_{380}	$K^0 \mu^+ \mu^-$	$B1$	< 5.7	$(2.2^{+2.2}_{-1.8}) \times 10^{-7}$	
Γ_{381}	$K^*(892)^0 \ell^+ \ell^-$	$B1$	[a]	$(9.5 \pm 1.8) \times 10^{-7}$	
Γ_{382}	$K^*(892)^0 e^+ e^-$	$B1$	< 1.04	$(0.35^{+0.35}_{-0.31}) \times 10^{-6}$	
Γ_{383}	$K^*(892)^0 \mu^+ \mu^-$	$B1$	< 1.10	$(0.29^{+0.29}_{-0.26}) \times 10^{-6}$	
Γ_{384}	$K^*(892)^0 \nu \bar{\nu}$	$B1$	< 3.4	$\times 10^{-4}$	CL=90%
Γ_{385}	$\phi \nu \bar{\nu}$	$B1$	< 5.8	$\times 10^{-5}$	CL=90%
Γ_{386}	$e^\pm \mu^\mp$	LF	[g]	< 9.2	$\times 10^{-8}$ CL=90%
Γ_{387}	$\pi^0 e^\pm \mu^\mp$	LF	< 1.4	$\times 10^{-7}$	CL=90%
Γ_{388}	$K^0 e^\pm \mu^\mp$	LF	< 2.7	$\times 10^{-7}$	CL=90%
Γ_{389}	$K^*(892)^0 e^+ \mu^-$	LF	< 5.3	$\times 10^{-7}$	CL=90%
Γ_{390}	$K^*(892)^0 e^- \mu^+$	LF	< 3.4	$\times 10^{-7}$	CL=90%
Γ_{391}	$K^*(892)^0 e^\pm \mu^\mp$	LF	< 5.8	$\times 10^{-7}$	CL=90%
Γ_{392}	$e^\pm \tau^\mp$	LF	[g]	< 1.1	$\times 10^{-4}$ CL=90%
Γ_{393}	$\mu^\pm \tau^\mp$	LF	[g]	< 3.8	$\times 10^{-5}$ CL=90%
Γ_{394}	invisible	$B1$	< 2.2	$\times 10^{-4}$	CL=90%
Γ_{395}	$\nu \bar{\nu} \gamma$	$B1$	< 4.7	$\times 10^{-5}$	CL=90%

- [a] An ℓ indicates an e or a μ mode, not a sum over these modes.
 [b] \bar{D}^{**} represents an excited state with mass $2.2 < M < 2.8$ GeV/c².
 [c] $X(3872)^+$ is a hypothetical charged partner of the $X(3872)$.
 [d] Stands for the possible candidates of $K^*(1410)$, $K_0^*(1430)$ and $K_2^*(1430)$.
 [e] B^0 and B_s^0 contributions not separated. Limit is on weighted average of the two decay rates.
 [f] This decay refers to the coherent sum of resonant and nonresonant $J^P = 0^+ K_\pi$ components with $1.60 < m_{K\pi} < 2.15$ GeV/c².
 [g] The value is for the sum of the charge states or particle/antiparticle states indicated.
 [h] $\Theta(1540)^+$ denotes a possible narrow pentaquark state.

 B^0 BRANCHING RATIOS

For branching ratios in which the charge of the decaying B is not determined, see the B^\pm section.

$\Gamma(\ell^+ \nu_e \text{ anything})/\Gamma_{\text{total}}$ Γ_1/Γ
 "OUR EVALUATION" is an average using rescaled values of the data listed below. The average and rescaling were performed by the Heavy Flavor Averaging Group (HFAG) and are described at <http://www.slac.stanford.edu/xorg/hfag/>. The averaging/rescaling procedure takes into account correlations between the measurements.

VALUE (units 10^{-2})	DOCUMENT ID	TECN	COMMENT
10.33 ± 0.28 OUR EVALUATION			
10.14 ± 0.30 OUR AVERAGE			Error includes scale factor of 1.1.
10.46 ± 0.30 ± 0.23	¹ URQUIJO 07	BELL	$e^+ e^- \rightarrow \Upsilon(4S)$
9.64 ± 0.27 ± 0.33	² AUBERT,B	06Y BABR	$e^+ e^- \rightarrow \Upsilon(4S)$
10.78 ± 0.60 ± 0.69	³ ARTUSO 97	CLE2	$e^+ e^- \rightarrow \Upsilon(4S)$
9.3 ± 1.1 ± 1.5	ALBRECHT 94	ARG	$e^+ e^- \rightarrow \Upsilon(4S)$
9.9 ± 3.0 ± 0.9	HENDERSON 92	CLEO	$e^+ e^- \rightarrow \Upsilon(4S)$
• • • We do not use the following data for averages, fits, limits, etc. • • •			
10.32 ± 0.36 ± 0.35	⁴ OKABE 05	BELL	Repl. by URQUIJO 07
10.9 ± 0.7 ± 1.1	ATHANAS 94	CLE2	Sup. by ARTUSO 97

- ¹ URQUIJO 07 report a measurement of $(9.80 \pm 0.29 \pm 0.21)\%$ for the partial branching fraction of $B \rightarrow e \nu_e X_c$ decay with electron energy above 0.6 GeV. We converted the result to $B \rightarrow e \nu_e X$ branching fraction.
² The measurements are obtained for charged and neutral B mesons partial rates of semileptonic decay to electrons with momentum above 0.6 GeV/c in the B rest frame. The best precision on the ratio is achieved for a momentum threshold of 1.0 GeV: $B(B^+ \rightarrow e^+ \nu_e X)/B(B^0 \rightarrow e^+ \nu_e X) = 1.074 \pm 0.041 \pm 0.026$.
³ ARTUSO 97 uses partial reconstruction of $B \rightarrow D^* \ell \nu_\ell$ and inclusive semileptonic branching ratio from BARISH 96B $(0.1049 \pm 0.0017 \pm 0.0043)$.
⁴ The measurements are obtained for charged and neutral B mesons partial rates of semileptonic decay to electrons with momentum above 0.6 GeV/c in the B rest frame, and their ratio of $B(B^+ \rightarrow e^+ \nu_e X)/B(B^0 \rightarrow e^+ \nu_e X) = 1.08 \pm 0.05 \pm 0.02$.

$\Gamma(e^+ \nu_e X_c)/\Gamma_{\text{total}}$ Γ_2/Γ

VALUE (units 10^{-2})	DOCUMENT ID	TECN	COMMENT
10.08 ± 0.30 ± 0.22	¹ URQUIJO 07	BELL	$e^+ e^- \rightarrow \Upsilon(4S)$

- ¹ Measure the independent B^+ and B^0 partial branching fractions with electron threshold energies of 0.4 GeV.

$\Gamma(D^- \ell^+ \nu_\ell)/\Gamma_{\text{total}}$ Γ_4/Γ
 ℓ denotes e or μ , not the sum.

"OUR EVALUATION" is an average using rescaled values of the data listed below. The average and rescaling were performed by the Heavy Flavor Averaging Group (HFAG) and are described at <http://www.slac.stanford.edu/xorg/hfag/>. The averaging/rescaling procedure takes into account correlations between the measurements.

VALUE	DOCUMENT ID	TECN	COMMENT
0.0217 ± 0.0012 OUR EVALUATION			
0.0218 ± 0.0012 OUR AVERAGE			
0.0221 ± 0.0011 ± 0.0012	¹ AUBERT 08Q	BABR	$e^+ e^- \rightarrow \Upsilon(4S)$
0.0213 ± 0.0012 ± 0.0039	ABE 02E	BELL	$e^+ e^- \rightarrow \Upsilon(4S)$
0.0209 ± 0.0013 ± 0.0018	² BARTELT 99	CLE2	$e^+ e^- \rightarrow \Upsilon(4S)$
0.0235 ± 0.0020 ± 0.0044	³ BUSKULIC 97	ALEP	$e^+ e^- \rightarrow Z$
• • • We do not use the following data for averages, fits, limits, etc. • • •			
0.0187 ± 0.0015 ± 0.0032	⁴ ATHANAS 97	CLE2	Repl. by BARTELT 99
0.018 ± 0.006 ± 0.003	⁵ FULTON 91	CLEO	$e^+ e^- \rightarrow \Upsilon(4S)$
0.020 ± 0.007 ± 0.006	⁶ ALBRECHT 89J	ARG	$e^+ e^- \rightarrow \Upsilon(4S)$

- ¹ Uses a fully reconstructed B meson as a tag on the recoil side.
² Assumes equal production of B^+ and B^0 at the $\Upsilon(4S)$.
³ BUSKULIC 97 assumes fraction (B^+) = fraction (B^0) = $(37.8 \pm 2.2)\%$ and PDG 96 values for B lifetime and branching ratio of D^* and D decays.
⁴ ATHANAS 97 uses missing energy and missing momentum to reconstruct neutrino.
⁵ FULTON 91 assumes assuming equal production of B^0 and B^+ at the $\Upsilon(4S)$ and uses Mark III D and D^* branching ratios.
⁶ ALBRECHT 89J reports $0.018 \pm 0.006 \pm 0.005$. We rescale using the method described in STONE 94 but with the updated PDG 94 $B(D^0 \rightarrow K^- \pi^+)$.

$\Gamma(D^- \tau^+ \nu_\tau)/\Gamma_{\text{total}}$ Γ_5/Γ

VALUE (units 10^{-2})	DOCUMENT ID	TECN	COMMENT
1.04 ± 0.35 ± 0.18	¹ AUBERT 08N	BABR	$e^+ e^- \rightarrow \Upsilon(4S)$

- ¹ Uses a fully reconstructed B meson as a tag on the recoil side.

$\Gamma(D^- \ell^+ \nu_\ell)/\Gamma(D \ell^+ \nu_\ell \text{ anything})$ Γ_4/Γ_3

VALUE	DOCUMENT ID	TECN	COMMENT
0.215 ± 0.016 ± 0.013	¹ AUBERT 07AN	BABR	$e^+ e^- \rightarrow \Upsilon(4S)$

- ¹ Uses a fully reconstructed B meson on the recoil side.

$\Gamma(D^*(2010)^- \ell^+ \nu_\ell)/\Gamma_{\text{total}}$ Γ_6/Γ

"OUR EVALUATION" is an average using rescaled values of the data listed below. The average and rescaling were performed by the Heavy Flavor Averaging Group (HFAG) and are described at <http://www.slac.stanford.edu/xorg/hfag/>. The averaging/rescaling procedure takes into account correlations between the measurements.

VALUE	EVTS	DOCUMENT ID	TECN	COMMENT
0.0516 ± 0.0011 OUR EVALUATION				
0.0523 ± 0.0022 OUR AVERAGE				Error includes scale factor of 1.4. See the ideogram below.
0.0549 ± 0.0016 ± 0.0025	¹ AUBERT 08Q	BABR	$e^+ e^- \rightarrow \Upsilon(4S)$	
0.0469 ± 0.0004 ± 0.0034	² AUBERT 08R	BABR	$e^+ e^- \rightarrow \Upsilon(4S)$	
0.0590 ± 0.0022 ± 0.0050	³ ABDALLAH 04D	DLPH	$e^+ e^- \rightarrow Z^0$	
0.0609 ± 0.0019 ± 0.0040	⁴ ADAM 03	CLE2	$e^+ e^- \rightarrow \Upsilon(4S)$	
0.0459 ± 0.0023 ± 0.0040	⁵ ABE 02F	BELL	$e^+ e^- \rightarrow \Upsilon(4S)$	
0.0470 ± 0.0013 ± 0.0036	⁶ ABREU 01H	DLPH	$e^+ e^- \rightarrow Z$	
0.0526 ± 0.0020 ± 0.0046	⁷ ABBIENDI 00Q	OPAL	$e^+ e^- \rightarrow Z$	
0.0553 ± 0.0026 ± 0.0052	⁸ BUSKULIC 97	ALEP	$e^+ e^- \rightarrow Z$	
• • • We do not use the following data for averages, fits, limits, etc. • • •				
0.0490 ± 0.0007 ± 0.0036	³ AUBERT 05E	BABR	Repl. by AUBERT 08R	
0.0539 ± 0.0011 ± 0.0034	⁹ ABDALLAH 04D	DLPH	$e^+ e^- \rightarrow Z^0$	
0.0609 ± 0.0019 ± 0.0040	¹⁰ BRIERE 02	CLE2	$e^+ e^- \rightarrow \Upsilon(4S)$	
0.0508 ± 0.0021 ± 0.0066	¹¹ ACKERSTAFF 97G	OPAL	Repl. by ABBIENDI 00Q	
0.0552 ± 0.0017 ± 0.0068	¹² ABREU 96P	DLPH	Repl. by ABREU 01H	
0.0449 ± 0.0032 ± 0.0039	³⁷⁶ BARISH 95	CLE2	Repl. by ADAM 03	
0.0518 ± 0.0030 ± 0.0062	⁴¹⁰ BUSKULIC 95N	ALEP	Sup. by BUSKULIC 97	
0.045 ± 0.003 ± 0.004	¹⁵ ALBRECHT 94	ARG	$e^+ e^- \rightarrow \Upsilon(4S)$	
0.047 ± 0.005 ± 0.005	¹⁶ ALBRECHT 93	ARG	$e^+ e^- \rightarrow \Upsilon(4S)$	
seen	¹⁷ SANGHERA 93	CLE2	$e^+ e^- \rightarrow \Upsilon(4S)$	
0.070 ± 0.018 ± 0.014	¹⁸ ANTREASYAN 90B	CBAL	$e^+ e^- \rightarrow \Upsilon(4S)$	
	¹⁹ ALBRECHT 89C	ARG	$e^+ e^- \rightarrow \Upsilon(4S)$	
0.060 ± 0.010 ± 0.014	²⁰ ALBRECHT 89J	ARG	$e^+ e^- \rightarrow \Upsilon(4S)$	
0.040 ± 0.004 ± 0.006	²¹ BORTOLETTO 89B	CLEO	$e^+ e^- \rightarrow \Upsilon(4S)$	
0.070 ± 0.012 ± 0.019	⁴⁷ ALBRECHT 87J	ARG	$e^+ e^- \rightarrow \Upsilon(4S)$	

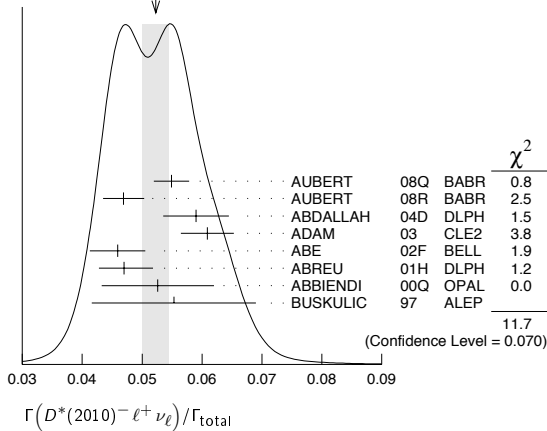
- ¹ Uses a fully reconstructed B meson as a tag on the recoil side.
² Measured using fully reconstructed D^* sample and a simultaneous fit to the Caprini-Lellouch-Neubert form factor parameters: $\rho^2 = 1.191 \pm 0.048 \pm 0.028$, $R_1(1) = 1.429 \pm 0.061 \pm 0.044$, and $R_2(1) = 0.827 \pm 0.038 \pm 0.022$.
³ Measured using fully reconstructed D^* sample.
⁴ Uses the combined fit of both $B^0 \rightarrow D^*(2010)^- \ell \nu$ and $B^+ \rightarrow \bar{D}^*(2007)^0 \ell \nu$ samples.
⁵ Assumes equal production of B^+ and B^0 at the $\Upsilon(4S)$.
⁶ ABREU 01H measured using about 5000 partial reconstructed D^* sample.
⁷ ABBIENDI 00Q assumes the fraction $B(b \rightarrow B^0) = (39.7^{+1.8}_{-2.2})\%$. This result is an average of two methods using exclusive and partial D^* reconstruction.

Meson Particle Listings

B^0

- ⁸ BUSKULIC 97 assumes fraction (B^+) = fraction (B^0) = $(37.8 \pm 2.2)\%$ and PDG 96 values for B lifetime and D^* and D branching fractions.
- ⁹ Combines with previous partial reconstructed D^* measurement.
- ¹⁰ The results are based on the same analysis and data sample reported in ADAM 03.
- ¹¹ ACKERSTAFF 97G assumes fraction (B^+) = fraction (B^0) = $(37.8 \pm 2.2)\%$ and PDG 96 values for B lifetime and branching ratio of D^* and D decays.
- ¹² ABREU 96P result is the average of two methods using exclusive and partial D^* reconstruction.
- ¹³ BARISH 95 use $B(D^0 \rightarrow K^- \pi^+) = (3.91 \pm 0.08 \pm 0.17)\%$ and $B(D^{*+} \rightarrow D^0 \pi^+) = (68.1 \pm 1.0 \pm 1.3)\%$.
- ¹⁴ BUSKULIC 95N assumes fraction (B^+) = fraction (B^0) = $38.2 \pm 1.3 \pm 2.2\%$ and $\tau_{B^0} = 1.58 \pm 0.06$ ps. $\Gamma(D^{*-} \ell^+ \nu_\ell)/\text{total} = [5.18 - 0.13(\text{fraction}(B^0) - 38.2) - 1.5(\tau_{B^0} - 1.58)]\%$.
- ¹⁵ ALBRECHT 94 assumes $B(D^{*+} \rightarrow D^0 \pi^+) = 68.1 \pm 1.0 \pm 1.3\%$. Uses partial reconstruction of D^{*+} and is independent of D^0 branching ratios.
- ¹⁶ ALBRECHT 93 reports $0.052 \pm 0.005 \pm 0.006$. We rescale using the method described in STONE 94 but with the updated PDG 94 $B(D^0 \rightarrow K^- \pi^+)$. We have taken their average e and μ value. They also obtain $\alpha = 2 * \Gamma^0 / (\Gamma^- + \Gamma^+) - 1 = 1.1 \pm 0.4 \pm 0.2$, $A_{AF} = 3/4 * (\Gamma^- - \Gamma^+) / \Gamma = 0.2 \pm 0.08 \pm 0.06$ and a value of $|V_{cb}| = 0.036 - 0.045$ depending on model assumptions.
- ¹⁷ Combining $\bar{D}^{*0} \ell^+ \nu_\ell$ and $\bar{D}^{*-} \ell^+ \nu_\ell$ SANGHERA 93 test $V-A$ structure and fit the decay angular distributions to obtain $A_{FB} = 3/4 * (\Gamma^- - \Gamma^+) / \Gamma = 0.14 \pm 0.06 \pm 0.03$. Assuming a value of V_{cb} , they measure V, A_1 , and A_2 , the three form factors for the $D^* \ell \nu_\ell$ decay, where results are slightly dependent on model assumptions.
- ¹⁸ ANTREASYAN 90B is average over B and \bar{D}^* (2010) charge states.
- ¹⁹ The measurement of ALBRECHT 89C suggests a D^* polarization γ_L/γ_T of 0.85 ± 0.45 or $\alpha = 0.7 \pm 0.9$.
- ²⁰ ALBRECHT 89J is ALBRECHT 87I value rescaled using $B(D^*(2010)^- \rightarrow D^0 \pi^-) = 0.57 \pm 0.04 \pm 0.04$. Superseded by ALBRECHT 93.
- ²¹ We have taken average of the the BORTOLETTO 89B values for electrons and muons, $0.046 \pm 0.005 \pm 0.007$. We rescale using the method described in STONE 94 but with the updated PDG 94 $B(D^0 \rightarrow K^- \pi^+)$. The measurement suggests a D^* polarization parameter value $\alpha = 0.65 \pm 0.66 \pm 0.25$.
- ²² ALBRECHT 87J assume $\mu-e$ universality, the $B(\Upsilon(4S) \rightarrow B^0 \bar{B}^0) = 0.45$, the $B(D^0 \rightarrow K^- \pi^+) = (0.042 \pm 0.004 \pm 0.004)$, and the $B(D^*(2010)^- \rightarrow D^0 \pi^-) = 0.49 \pm 0.08$. Superseded by ALBRECHT 89J.

WEIGHTED AVERAGE
0.0523±0.0022 (Error scaled by 1.4)



$\Gamma(D^*(2010)^- \ell^+ \nu_\ell) / \Gamma(D \ell^+ \nu_\ell \text{ anything})$		Γ_6 / Γ_3	
VALUE	DOCUMENT ID	TECN	COMMENT
0.537 ± 0.031 ± 0.036	¹ AUBERT 07AN BABR		$e^+ e^- \rightarrow \Upsilon(4S)$
¹ Uses a fully reconstructed B meson on the recoil side.			

$\Gamma(D^*(2010)^- \tau^+ \nu_\tau) / \Gamma_{\text{total}}$		Γ_7 / Γ	
VALUE (units 10^{-2})	DOCUMENT ID	TECN	COMMENT
1.6 ± 0.5 OUR AVERAGE	Error includes scale factor of 1.2.		
1.11 ± 0.51 ± 0.06	¹ AUBERT 08N BABR		$e^+ e^- \rightarrow \Upsilon(4S)$
2.02 $^{+0.40}_{-0.37}$	² MATYJA 07 BELL		$e^+ e^- \rightarrow \Upsilon(4S)$

- ¹ Uses a fully reconstructed B meson as a tag on the recoil side.
- ² Observed in the recoil of the accompanying B meson.

$\Gamma(\bar{D}^0 \pi^- \ell^+ \nu_\ell) / \Gamma_{\text{total}}$		Γ_8 / Γ	
VALUE (units 10^{-3})	DOCUMENT ID	TECN	COMMENT
4.3 ± 0.6 OUR AVERAGE			
4.3 ± 0.8 ± 0.3	¹ AUBERT 08Q BABR		$e^+ e^- \rightarrow \Upsilon(4S)$
4.3 ± 0.9 ± 0.2	^{1,2} LIVENTSEV 08 BELL		$e^+ e^- \rightarrow \Upsilon(4S)$
• • • We do not use the following data for averages, fits, limits, etc. • • •			
3.4 ± 1.0 ± 0.2	³ LIVENTSEV 05 BELL		Repl. by LIVENTSEV 08

- ¹ Uses a fully reconstructed B meson as a tag on the recoil side.
- ² LIVENTSEV 08 reports $(4.2 \pm 0.7 \pm 0.6) \times 10^{-3}$ for $B(B^0 \rightarrow D^- \ell^+ \nu_\ell) = (2.12 \pm 0.20) \times 10^{-2}$. We rescale to our best value $B(B^0 \rightarrow D^- \ell^+ \nu_\ell) = (2.17 \pm 0.12) \times 10^{-2}$. Our first error is their experiment's error and our second error is the systematic error from using our best value.
- ³ LIVENTSEV 05 reports $[B(B^0 \rightarrow \bar{D}^0 \pi^- \ell^+ \nu_\ell)] / [B(B^+ \rightarrow \bar{D}^0 \ell^+ \nu_\ell)] = 0.15 \pm 0.03 \pm 0.03$. We multiply by our best value $B(B^+ \rightarrow \bar{D}^0 \ell^+ \nu_\ell) = (2.27 \pm 0.11) \times 10^{-2}$. Our first error is their experiment's error and our second error is the systematic error from using our best value.

$\Gamma(D_s^0(2400)^- \ell^+ \nu_\ell \times B(D_s^{*0} \rightarrow \bar{D}^0 \pi^-)) / \Gamma_{\text{total}}$		Γ_9 / Γ	
VALUE (units 10^{-3})	DOCUMENT ID	TECN	COMMENT
2.0 ± 0.7 ± 0.5	¹ LIVENTSEV 08 BELL		$e^+ e^- \rightarrow \Upsilon(4S)$
¹ Uses a fully reconstructed B meson as a tag on the recoil side.			

$\Gamma(D_s^*(2460)^- \ell^+ \nu_\ell \times B(D_s^{*2-} \rightarrow \bar{D}^0 \pi^-)) / \Gamma_{\text{total}}$		Γ_{10} / Γ	
VALUE (units 10^{-3})	DOCUMENT ID	TECN	COMMENT
2.2 ± 0.4 ± 0.4	¹ LIVENTSEV 08 BELL		$e^+ e^- \rightarrow \Upsilon(4S)$
¹ Uses a fully reconstructed B meson as a tag on the recoil side.			

$\Gamma(\bar{D}^{*0} \pi^- \ell^+ \nu_\ell) / \Gamma_{\text{total}}$		Γ_{12} / Γ	
VALUE (units 10^{-3})	DOCUMENT ID	TECN	COMMENT
4.9 ± 0.8 OUR AVERAGE			
4.8 ± 0.8 ± 0.4	¹ AUBERT 08Q BABR		$e^+ e^- \rightarrow \Upsilon(4S)$
5.7 ± 2.2 ± 0.3	^{1,2} LIVENTSEV 08 BELL		$e^+ e^- \rightarrow \Upsilon(4S)$
• • • We do not use the following data for averages, fits, limits, etc. • • •			
6.1 ± 1.4 ± 0.3	^{3,4} LIVENTSEV 05 BELL		Repl. by LIVENTSEV 08

- ¹ Uses a fully reconstructed B meson as a tag on the recoil side.
- ² LIVENTSEV 08 reports $(5.6 \pm 2.1 \pm 0.8) \times 10^{-3}$ for $B(B^0 \rightarrow D^- \ell^+ \nu_\ell) = (2.12 \pm 0.20) \times 10^{-2}$. We rescale to our best value $B(B^0 \rightarrow D^- \ell^+ \nu_\ell) = (2.17 \pm 0.12) \times 10^{-2}$. Our first error is their experiment's error and our second error is the systematic error from using our best value.
- ³ Excludes D^{*+} contribution to $D \pi$ modes.
- ⁴ LIVENTSEV 05 reports $[B(B^0 \rightarrow \bar{D}^{*0} \pi^- \ell^+ \nu_\ell)] / [B(B^+ \rightarrow \bar{D}^*(2007)^0 \ell^+ \nu_\ell)] = 0.10 \pm 0.02 \pm 0.01$. We multiply by our best value $B(B^+ \rightarrow \bar{D}^*(2007)^0 \ell^+ \nu_\ell) = (6.07 \pm 0.29) \times 10^{-2}$. Our first error is their experiment's error and our second error is the systematic error from using our best value.

$\Gamma(D_1(2420)^- \ell^+ \nu_\ell \times B(D_1^- \rightarrow \bar{D}^{*0} \pi^-)) / \Gamma_{\text{total}}$		Γ_{13} / Γ	
VALUE (units 10^{-3})	DOCUMENT ID	TECN	COMMENT
5.4 ± 1.9 ± 0.9	¹ LIVENTSEV 08 BELL		$e^+ e^- \rightarrow \Upsilon(4S)$
¹ Uses a fully reconstructed B meson as a tag on the recoil side.			

$\Gamma(D_1^*(2430)^- \ell^+ \nu_\ell \times B(D_1^{*2-} \rightarrow \bar{D}^{*0} \pi^-)) / \Gamma_{\text{total}}$		Γ_{14} / Γ	
VALUE (units 10^{-3})	CL%	DOCUMENT ID	TECN
< 5.0	90	¹ LIVENTSEV 08 BELL	$e^+ e^- \rightarrow \Upsilon(4S)$
¹ Uses a fully reconstructed B meson as a tag on the recoil side.			

$\Gamma(D_s^*(2460)^- \ell^+ \nu_\ell \times B(D_s^{*2-} \rightarrow \bar{D}^{*0} \pi^-)) / \Gamma_{\text{total}}$		Γ_{15} / Γ	
VALUE (units 10^{-3})	CL%	DOCUMENT ID	TECN
< 3.0	90	¹ LIVENTSEV 08 BELL	$e^+ e^- \rightarrow \Upsilon(4S)$
¹ Uses a fully reconstructed B meson as a tag on the recoil side.			

$\Gamma(\bar{D}^{*+} n \pi \ell^+ \nu_\ell (n \geq 1)) / \Gamma(D \ell^+ \nu_\ell \text{ anything})$		Γ_{11} / Γ_3	
VALUE	DOCUMENT ID	TECN	COMMENT
0.248 ± 0.032 ± 0.030	¹ AUBERT 07AN BABR		$e^+ e^- \rightarrow \Upsilon(4S)$
¹ Uses a fully reconstructed B meson on the recoil side.			

$\Gamma(\rho^- \ell^+ \nu_\ell) / \Gamma_{\text{total}}$		Γ_{16} / Γ	
VALUE (units 10^{-4})	CL%	DOCUMENT ID	TECN
2.47 ± 0.33 OUR AVERAGE			
2.93 ± 0.37 ± 0.37	¹ ADAM 07 CLE2		$e^+ e^- \rightarrow \Upsilon(4S)$
2.17 ± 0.54 ± 0.32	² HOKUUE 07 BELL		$e^+ e^- \rightarrow \Upsilon(4S)$
2.14 ± 0.21 ± 0.56	³ AUBERT,B 05o BABR		$e^+ e^- \rightarrow \Upsilon(4S)$
• • • We do not use the following data for averages, fits, limits, etc. • • •			
2.17 ± 0.34 $^{+0.62}_{-0.68}$	⁴ ATHAR 03 CLE2		Repl. by ADAM 07
3.29 ± 0.42 ± 0.72	⁵ AUBERT 03E BABR		Repl. by AUBERT,B 05o
2.57 ± 0.29 $^{+0.53}_{-0.62}$	⁶ BEHRENS 00 CLE2		Repl. by ADAM 07
2.69 ± 0.41 $^{+0.61}_{-0.64}$	⁷ BEHRENS 00 CLE2		$e^+ e^- \rightarrow \Upsilon(4S)$
2.5 ± 0.4 $^{+0.7}_{-0.9}$	⁸ ALEXANDER 96T CLE2		Repl. by BEHRENS 00
< 4.1	90	⁹ BEAN 93B CLE2	$e^+ e^- \rightarrow \Upsilon(4S)$

¹ The B^0 and B^+ results are combined assuming the isospin, B lifetimes, and relative charged/neutral B production at the $\Upsilon(4S)$.

² The signal events are tagged by a second B meson reconstructed in the semileptonic mode $B \rightarrow D^{(*)} \ell \nu_\ell$.

³ B^+ and B^0 decays combined assuming isospin symmetry. Systematic errors include both experimental and form-factor uncertainties.

⁴ ATHAR 03 reports systematic errors $^{+0.47}_{-0.50} \pm 0.41 \pm 0.01$, which are experimental systematic, systematic due to residual form-factor uncertainties in the signal, and systematic due to residual form-factor uncertainties in the cross-feed modes, respectively. We combine these in quadrature.

⁵ Uses isospin constraints and extrapolation to all electron energies according to five different form-factor calculations. The second error combines the systematic and theoretical uncertainties in quadrature.

⁶ Averaging with ALEXANDER 96T results including experimental and theoretical correlations considered, BEHRENS 00 reports systematic errors $^{+0.33}_{-0.46} \pm 0.41$, where the second error is theoretical model dependence. We combine these in quadrature.

⁷ BEHRENS 00 reports $^{+0.35}_{-0.40} \pm 0.50$, where the second error is the theoretical model dependence. We combine these in quadrature. B^+ and B^0 decays combined using isospin symmetry: $\Gamma(B^0 \rightarrow \rho^- \ell^+ \nu) = 2\Gamma(B^+ \rightarrow \rho^0 \ell^+ \nu) \approx 2\Gamma(B^+ \rightarrow \omega \ell^+ \nu)$. No evidence for $\omega \ell \nu$ is reported.

⁸ ALEXANDER 96T reports $^{+0.5}_{-0.7} \pm 0.5$ where the second error is the theoretical model dependence. We combine these in quadrature. B^+ and B^0 decays combined using isospin symmetry: $\Gamma(B^0 \rightarrow \rho^- \ell^+ \nu) = 2\Gamma(B^+ \rightarrow \rho^0 \ell^+ \nu) \approx 2\Gamma(B^+ \rightarrow \omega \ell^+ \nu)$. No evidence for $\omega \ell \nu$ is reported.

⁹ BEAN 93B limit set using ISGW Model. Using isospin and the quark model to combine $\Gamma(\rho^0 \ell^+ \nu_\ell)$ and $\Gamma(\omega \ell^+ \nu_\ell)$ with this result, they obtain a limit $<(1.6-2.7) \times 10^{-4}$ at 90% CL for $B^+ \rightarrow (\omega \rho^0) \ell^+ \nu_\ell$. The range corresponds to the ISGW, WSB, and KS models. An upper limit on $|V_{ub}/V_{cb}| < 0.08-0.13$ at 90% CL is derived as well.

$\Gamma(\pi^- \ell^+ \nu_\ell)/\Gamma_{\text{total}}$ Γ_{17}/Γ

"OUR EVALUATION" is an average using rescaled values of the data listed below. The average and rescaling were performed by the Heavy Flavor Averaging Group (HFAG) and are described at <http://www.slac.stanford.edu/xorg/hfag/>. The averaging/rescaling procedure takes into account correlations between the measurements.

VALUE (units 10^{-4})	DOCUMENT ID	TECN	COMMENT
1.36 ± 0.06 ± 0.07 OUR EVALUATION			
1.41 ± 0.08 OUR AVERAGE			
1.37 ± 0.15 ± 0.11	1,2 ADAM 07	CLE2	$e^+ e^- \rightarrow \Upsilon(4S)$
1.46 ± 0.07 ± 0.08	3 AUBERT 07j	BABR	$e^+ e^- \rightarrow \Upsilon(4S)$
1.38 ± 0.19 ± 0.14	4 HOKUUE 07	BELL	$e^+ e^- \rightarrow \Upsilon(4S)$
1.33 ± 0.17 ± 0.11	5 AUBERT,B 06k	BABR	$e^+ e^- \rightarrow \Upsilon(4S)$
• • • We do not use the following data for averages, fits, limits, etc. • • •			
1.38 ± 0.10 ± 0.18	6 AUBERT,B 05o	BABR	Repl. by AUBERT,B 06k
1.33 ± 0.18 ± 0.13	7 ATHAR 03	CLE2	Repl. by ADAM 07
1.8 ± 0.4 ± 0.4	8 ALEXANDER 96T	CLE2	Repl. by ATHAR 03

¹ The B^0 and B^+ results are combined assuming the isospin, B lifetimes, and relative charged/neutral B production at the $\Upsilon(4S)$.

² Also report the rate for $q^2 > 16 \text{ GeV}^2$ of $(0.41 \pm 0.08 \pm 0.04) \times 10^{-4}$ from which they obtain $|V_{ub}| = 3.6 \pm 0.4 \pm 0.2^{+0.6}_{-0.4}$ (last error is from theory).

³ The analysis uses events in which the signal B decays are reconstructed with an innovative loose neutrino reconstruction technique.

⁴ The signal events are tagged by a second B meson reconstructed in the semileptonic mode $B \rightarrow D^{(*)} \ell \nu_\ell$.

⁵ The signals are tagged by a second B meson reconstructed in a semileptonic or hadronic decay. The B^0 and B^+ results are combined assuming the isospin symmetry.

⁶ B^+ and B^0 decays combined assuming isospin symmetry. Systematic errors include both experimental and form-factor uncertainties.

⁷ ATHAR 03 reports systematic errors $0.11 \pm 0.01 \pm 0.07$, which are experimental systematic, systematic due to residual form-factor uncertainties in the signal, and systematic due to residual form-factor uncertainties in the cross-feed modes, respectively. We combine these in quadrature.

⁸ ALEXANDER 96T gives systematic errors $\pm 0.3 \pm 0.2$ where the second error reflects the estimated model dependence. We combine these in quadrature. Assumes isospin symmetry: $\Gamma(B^0 \rightarrow \pi^- \ell^+ \nu) = 2 \times \Gamma(B^+ \rightarrow \pi^0 \ell^+ \nu)$.

$\Gamma(\pi^- \mu^+ \nu_\mu)/\Gamma_{\text{total}}$ Γ_{18}/Γ

VALUE	DOCUMENT ID	TECN	COMMENT
• • • We do not use the following data for averages, fits, limits, etc. • • •			
seen	1 ALBRECHT 91c	ARG	

¹ In ALBRECHT 91c, one event is fully reconstructed providing evidence for the $b \rightarrow u$ transition.

$\Gamma(K^\pm \text{ anything})/\Gamma_{\text{total}}$ Γ_{19}/Γ

VALUE	DOCUMENT ID	TECN	COMMENT
0.78 ± 0.08	1 ALBRECHT 96D	ARG	$e^+ e^- \rightarrow \Upsilon(4S)$

¹ Average multiplicity.

$\Gamma(D^0 X)/\Gamma_{\text{total}}$ Γ_{20}/Γ

VALUE	DOCUMENT ID	TECN	COMMENT
0.081 ± 0.014 ± 0.005	1 AUBERT 07N	BABR	$e^+ e^- \rightarrow \Upsilon(4S)$

• • • We do not use the following data for averages, fits, limits, etc. • • •

0.063 ± 0.019 ± 0.005 ¹ AUBERT, BE 04B BABR Repl. by AUBERT 07N

¹ Events are selected by completely reconstructing one B and searching for a reconstructed charmed particle in the rest of the event. The last error includes systematic and charm branching ratio uncertainties.

$\Gamma(D^0 X)/\Gamma_{\text{total}}$ Γ_{21}/Γ

VALUE	DOCUMENT ID	TECN	COMMENT
0.474 ± 0.020 ± 0.020	1 AUBERT 07N	BABR	$e^+ e^- \rightarrow \Upsilon(4S)$

• • • We do not use the following data for averages, fits, limits, etc. • • •

0.511 ± 0.031 ± 0.028 ¹ AUBERT, BE 04B BABR Repl. by AUBERT 07N

¹ Events are selected by completely reconstructing one B and searching for a reconstructed charmed particle in the rest of the event. The last error includes systematic and charm branching ratio uncertainties.

$\Gamma(D^0 X)/[\Gamma(D^0 X) + \Gamma(D^0 X)]$ $\Gamma_{20}/(\Gamma_{20} + \Gamma_{21})$

VALUE	DOCUMENT ID	TECN	COMMENT
0.146 ± 0.022 ± 0.006	AUBERT 07N	BABR	$e^+ e^- \rightarrow \Upsilon(4S)$

• • • We do not use the following data for averages, fits, limits, etc. • • •

0.110 ± 0.031 ± 0.008 AUBERT, BE 04B BABR Repl. by AUBERT 07N

$\Gamma(D^+ X)/\Gamma_{\text{total}}$ Γ_{22}/Γ

VALUE	CL%	DOCUMENT ID	TECN	COMMENT
<0.039	90	1 AUBERT 07N	BABR	$e^+ e^- \rightarrow \Upsilon(4S)$

• • • We do not use the following data for averages, fits, limits, etc. • • •

<0.051 90 ¹ AUBERT, BE 04B BABR Repl. by AUBERT 07N

¹ Events are selected by completely reconstructing one B and searching for a reconstructed charmed particle in the rest of the event. The last error includes systematic and charm branching ratio uncertainties.

$\Gamma(D^- X)/\Gamma_{\text{total}}$ Γ_{23}/Γ

VALUE	DOCUMENT ID	TECN	COMMENT
0.369 ± 0.016 ± 0.030	1 AUBERT 07N	BABR	$e^+ e^- \rightarrow \Upsilon(4S)$

• • • We do not use the following data for averages, fits, limits, etc. • • •

0.397 ± 0.030 ± 0.040 ¹ AUBERT, BE 04B BABR Repl. by AUBERT 07N

¹ Events are selected by completely reconstructing one B and searching for a reconstructed charmed particle in the rest of the event. The last error includes systematic and charm branching ratio uncertainties.

$\Gamma(D^+ X)/[\Gamma(D^+ X) + \Gamma(D^- X)]$ $\Gamma_{22}/(\Gamma_{22} + \Gamma_{23})$

VALUE	DOCUMENT ID	TECN	COMMENT
0.058 ± 0.028 ± 0.006	AUBERT 07N	BABR	$e^+ e^- \rightarrow \Upsilon(4S)$

• • • We do not use the following data for averages, fits, limits, etc. • • •

0.055 ± 0.040 ± 0.006 AUBERT, BE 04B BABR Repl. by AUBERT 07N

$\Gamma(D_s^+ X)/\Gamma_{\text{total}}$ Γ_{24}/Γ

VALUE	DOCUMENT ID	TECN	COMMENT
0.103 ± 0.012 ± 0.017	1 AUBERT 07N	BABR	$e^+ e^- \rightarrow \Upsilon(4S)$

• • • We do not use the following data for averages, fits, limits, etc. • • •

0.109 ± 0.021 ± 0.039 ¹ AUBERT, BE 04B BABR Repl. by AUBERT 07N

¹ Events are selected by completely reconstructing one B and searching for a reconstructed charmed particle in the rest of the event. The last error includes systematic and charm branching ratio uncertainties.

$\Gamma(D_s^- X)/\Gamma_{\text{total}}$ Γ_{25}/Γ

VALUE	CL%	DOCUMENT ID	TECN	COMMENT
<0.026	90	1 AUBERT 07N	BABR	$e^+ e^- \rightarrow \Upsilon(4S)$

• • • We do not use the following data for averages, fits, limits, etc. • • •

<0.087 90 ¹ AUBERT, BE 04B BABR Repl. by AUBERT 07N

¹ Events are selected by completely reconstructing one B and searching for a reconstructed charmed particle in the rest of the event. The last error includes systematic and charm branching ratio uncertainties.

$\Gamma(D_s^+ X)/[\Gamma(D_s^+ X) + \Gamma(D_s^- X)]$ $\Gamma_{24}/(\Gamma_{24} + \Gamma_{25})$

VALUE	DOCUMENT ID	TECN	COMMENT
0.879 ± 0.066 ± 0.005	AUBERT 07N	BABR	$e^+ e^- \rightarrow \Upsilon(4S)$

• • • We do not use the following data for averages, fits, limits, etc. • • •

0.733 ± 0.092 ± 0.010 AUBERT, BE 04B BABR Repl. by AUBERT 07N

$\Gamma(A_c^+ X)/\Gamma_{\text{total}}$ Γ_{26}/Γ

VALUE	CL%	DOCUMENT ID	TECN	COMMENT
<0.031	90	1 AUBERT 07N	BABR	$e^+ e^- \rightarrow \Upsilon(4S)$

• • • We do not use the following data for averages, fits, limits, etc. • • •

<0.038 90 ¹ AUBERT, BE 04B BABR Repl. by AUBERT 07N

¹ Events are selected by completely reconstructing one B and searching for a reconstructed charmed particle in the rest of the event. The last error includes systematic and charm branching ratio uncertainties.

$\Gamma(\bar{A}_c^- X)/\Gamma_{\text{total}}$ Γ_{27}/Γ

VALUE	DOCUMENT ID	TECN	COMMENT
0.05 ± 0.010 ± 0.019	1 AUBERT 07N	BABR	$e^+ e^- \rightarrow \Upsilon(4S)$

• • • We do not use the following data for averages, fits, limits, etc. • • •

0.049 ± 0.017 ± 0.018 ¹ AUBERT, BE 04B BABR Repl. by AUBERT 07N

¹ Events are selected by completely reconstructing one B and searching for a reconstructed charmed particle in the rest of the event. The last error includes systematic and charm branching ratio uncertainties.

Meson Particle Listings

 B^0

$$\Gamma(\Lambda_c^+ X) / [\Gamma(\Lambda_c^+ X) + \Gamma(\bar{\Lambda}_c^+ X)] \quad \Gamma_{26} / (\Gamma_{26} + \Gamma_{27})$$

VALUE	DOCUMENT ID	TECN	COMMENT
$0.243 \pm 0.119 \pm 0.003$	AUBERT	07N	BABR $e^+ e^- \rightarrow \Upsilon(4S)$
$0.286 \pm 0.142 \pm 0.007$	AUBERT,BE	04B	BABR Repl. by AUBERT 07N

• • • We do not use the following data for averages, fits, limits, etc. • • •

$$\Gamma(\bar{c} X) / \Gamma_{\text{total}} \quad \Gamma_{28} / \Gamma$$

VALUE	DOCUMENT ID	TECN	COMMENT
$0.947 \pm 0.030 \pm 0.045$ -0.040	¹ AUBERT	07N	BABR $e^+ e^- \rightarrow \Upsilon(4S)$

• • • We do not use the following data for averages, fits, limits, etc. • • •

$1.039 \pm 0.051 \pm 0.063$ -0.058	¹ AUBERT,BE	04B	BABR Repl. by AUBERT 07N
---	------------------------	-----	--------------------------

¹ Events are selected by completely reconstructing one B and searching for a reconstructed charmed particle in the rest of the event. The last error includes systematic and charm branching ratio uncertainties.

$$\Gamma(c X) / \Gamma_{\text{total}} \quad \Gamma_{29} / \Gamma$$

VALUE	DOCUMENT ID	TECN	COMMENT
$0.246 \pm 0.024 \pm 0.021$ -0.017	¹ AUBERT	07N	BABR $e^+ e^- \rightarrow \Upsilon(4S)$

• • • We do not use the following data for averages, fits, limits, etc. • • •

$0.237 \pm 0.036 \pm 0.041$ -0.027	¹ AUBERT,BE	04B	BABR Repl. by AUBERT 07N
---	------------------------	-----	--------------------------

¹ Events are selected by completely reconstructing one B and searching for a reconstructed charmed particle in the rest of the event. The last error includes systematic and charm branching ratio uncertainties.

$$\Gamma(\bar{c} c X) / \Gamma_{\text{total}} \quad \Gamma_{30} / \Gamma$$

VALUE	DOCUMENT ID	TECN	COMMENT
$1.193 \pm 0.030 \pm 0.053$ -0.049	¹ AUBERT	07N	BABR $e^+ e^- \rightarrow \Upsilon(4S)$

• • • We do not use the following data for averages, fits, limits, etc. • • •

$1.276 \pm 0.062 \pm 0.088$ -0.074	¹ AUBERT,BE	04B	BABR Repl. by AUBERT 07N
---	------------------------	-----	--------------------------

¹ Events are selected by completely reconstructing one B and searching for a reconstructed charmed particle in the rest of the event. The last error includes systematic and charm branching ratio uncertainties.

$$\Gamma(D^- \pi^+) / \Gamma_{\text{total}} \quad \Gamma_{31} / \Gamma$$

VALUE (units 10^{-3})	EVTS	DOCUMENT ID	TECN	COMMENT
2.68 ± 0.13	OUR AVERAGE			

$2.55 \pm 0.05 \pm 0.16$		¹ AUBERT	07H	BABR $e^+ e^- \rightarrow \Upsilon(4S)$
$3.03 \pm 0.23 \pm 0.23$		² AUBERT,BE	06J	BABR $e^+ e^- \rightarrow \Upsilon(4S)$
$2.68 \pm 0.12 \pm 0.24$		^{1,3} AHMED	02B	CLE2 $e^+ e^- \rightarrow \Upsilon(4S)$
$2.7 \pm 0.6 \pm 0.5$		⁴ BORTOLETTO92	CLEO	$e^+ e^- \rightarrow \Upsilon(4S)$
$4.8 \pm 1.1 \pm 1.1$	22	⁵ ALBRECHT	90J	ARG $e^+ e^- \rightarrow \Upsilon(4S)$
$5.1 \pm 2.8 \pm 1.3$ $-2.5 \quad -1.2$	4	⁶ BEBEK	87	CLEO $e^+ e^- \rightarrow \Upsilon(4S)$

• • • We do not use the following data for averages, fits, limits, etc. • • •

$2.94 \pm 0.21 \pm 0.09$		^{1,7} AUBERT,B	04o	BABR Repl. by AUBERT 07H
$2.9 \pm 0.4 \pm 0.1$	81	⁸ ALAM	94	CLE2 Repl. by AHMED 02B
$3.1 \pm 1.3 \pm 1.0$	7	⁵ ALBRECHT	88k	ARG $e^+ e^- \rightarrow \Upsilon(4S)$

¹ Assumes equal production of B^+ and B^0 at the $\Upsilon(4S)$.

² Uses a missing-mass method. Does not depend on D branching fractions or B^+ / B^0 production rates.

³ AHMED 02B reports an additional uncertainty on the branching ratios to account for 4.5% uncertainty on relative production of B^0 and B^+ , which is not included here.

⁴ BORTOLETTO 92 assumes equal production of B^+ and B^0 at the $\Upsilon(4S)$ and uses Mark III branching fractions for the D .

⁵ ALBRECHT 88k assumes $B^0 \bar{B}^0 : B^+ B^-$ production ratio is 45:55. Superseded by ALBRECHT 90J which assumes 50:50.

⁶ BEBEK 87 value has been updated in BERKELMAN 91 to use same assumptions as noted for BORTOLETTO 92.

⁷ AUBERT,B 04o reports $[B(B^0 \rightarrow D^- \pi^+)] \times [B(D^+ \rightarrow K_S^0 \pi^+)] = (42.7 \pm 2.1 \pm 2.2) \times 10^{-6}$. We divide by our best value $B(D^+ \rightarrow K_S^0 \pi^+) = (1.45 \pm 0.04) \times 10^{-2}$. Our first error is their experiment's error and our second error is the systematic error from using our best value.

⁸ ALAM 94 reports $[B(B^0 \rightarrow D^- \pi^+)] \times [B(D^+ \rightarrow K^- \pi^+ \pi^+)] = (0.265 \pm 0.032 \pm 0.023) \times 10^{-3}$. We divide by our best value $B(D^+ \rightarrow K^- \pi^+ \pi^+) = (9.22 \pm 0.21) \times 10^{-2}$. Our first error is their experiment's error and our second error is the systematic error from using our best value. Assumes equal production of B^+ and B^0 at the $\Upsilon(4S)$.

$$\Gamma(D^- \rho^+) / \Gamma_{\text{total}} \quad \Gamma_{32} / \Gamma$$

VALUE	EVTS	DOCUMENT ID	TECN	COMMENT
0.0077 ± 0.0013	OUR AVERAGE			

$0.0076 \pm 0.0013 \pm 0.0002$	79	¹ ALAM	94	CLE2 $e^+ e^- \rightarrow \Upsilon(4S)$
$0.009 \pm 0.005 \pm 0.003$	9	² ALBRECHT	90J	ARG $e^+ e^- \rightarrow \Upsilon(4S)$

• • • We do not use the following data for averages, fits, limits, etc. • • •

$0.022 \pm 0.012 \pm 0.009$	6	² ALBRECHT	88k	ARG $e^+ e^- \rightarrow \Upsilon(4S)$
-----------------------------	---	-----------------------	-----	--

¹ ALAM 94 reports $[B(B^0 \rightarrow D^- \rho^+)] \times [B(D^+ \rightarrow K^- \pi^+ \pi^+)] = 0.000704 \pm 0.000096 \pm 0.000070$. We divide by our best value $B(D^+ \rightarrow K^- \pi^+ \pi^+) = (9.22 \pm 0.21) \times 10^{-2}$. Our first error is their experiment's error and our second error is the systematic error from using our best value. Assumes equal production of B^+ and B^0 at the $\Upsilon(4S)$.

² ALBRECHT 88k assumes $B^0 \bar{B}^0 : B^+ B^-$ production ratio is 45:55. Superseded by ALBRECHT 90J which assumes 50:50.

$$\Gamma(D^- K^0 \pi^+) / \Gamma_{\text{total}} \quad \Gamma_{33} / \Gamma$$

VALUE (units 10^{-4})	DOCUMENT ID	TECN	COMMENT
$4.9 \pm 0.7 \pm 0.5$	¹ AUBERT,BE	05B	BABR $e^+ e^- \rightarrow \Upsilon(4S)$

¹ Assumes equal production of B^+ and B^0 at the $\Upsilon(4S)$.

$$\Gamma(D^- K^*(892)^+) / \Gamma_{\text{total}} \quad \Gamma_{34} / \Gamma$$

VALUE (units 10^{-4})	DOCUMENT ID	TECN	COMMENT
4.5 ± 0.7	OUR AVERAGE		
$4.6 \pm 0.6 \pm 0.5$	¹ AUBERT,BE	05B	BABR $e^+ e^- \rightarrow \Upsilon(4S)$
$3.7 \pm 1.5 \pm 1.0$	¹ MAHAPATRA	02	CLE2 $e^+ e^- \rightarrow \Upsilon(4S)$

¹ Assumes equal production of B^+ and B^0 at the $\Upsilon(4S)$.

$$\Gamma(D^- \omega \pi^+) / \Gamma_{\text{total}} \quad \Gamma_{35} / \Gamma$$

VALUE	DOCUMENT ID	TECN	COMMENT
$0.0028 \pm 0.0005 \pm 0.0004$	¹ ALEXANDER	01B	CLE2 $e^+ e^- \rightarrow \Upsilon(4S)$

¹ Assumes equal production of B^+ and B^0 at the $\Upsilon(4S)$. The signal is consistent with all observed $\omega \pi^+$ having proceeded through the ρ^+ resonance at mass $1349 \pm 25 \pm 10$ MeV and width $547 \pm 86 \pm 46$ MeV.

$$\Gamma(D^- K^+) / \Gamma_{\text{total}} \quad \Gamma_{36} / \Gamma$$

VALUE	DOCUMENT ID	TECN	COMMENT
$(2.04 \pm 0.50 \pm 0.27) \times 10^{-4}$	¹ ABE	01i	BELL $e^+ e^- \rightarrow \Upsilon(4S)$

¹ ABE 01i reports $B(B^0 \rightarrow D^- K^+) / B(B^0 \rightarrow D^- \pi^+) = 0.068 \pm 0.015 \pm 0.007$. We multiply by our best value $B(B^0 \rightarrow D^- \pi^+) = (3.0 \pm 0.4) \times 10^{-3}$. Our first error is their experiment's error and the second error is systematic error from using our best value.

$$\Gamma(D^- K^+ \bar{K}^0) / \Gamma_{\text{total}} \quad \Gamma_{37} / \Gamma$$

VALUE (units 10^{-4})	CL%	DOCUMENT ID	TECN	COMMENT
< 3.1	90	¹ DRUTSKOY	02	BELL $e^+ e^- \rightarrow \Upsilon(4S)$

¹ Assumes equal production of B^+ and B^0 at the $\Upsilon(4S)$.

$$\Gamma(D^- K^+ \bar{K}^*(892)^0) / \Gamma_{\text{total}} \quad \Gamma_{38} / \Gamma$$

VALUE (units 10^{-4})	DOCUMENT ID	TECN	COMMENT
$8.8 \pm 1.1 \pm 1.5$	¹ DRUTSKOY	02	BELL $e^+ e^- \rightarrow \Upsilon(4S)$

¹ Assumes equal production of B^+ and B^0 at the $\Upsilon(4S)$.

$$\Gamma(D^0 \pi^+ \pi^-) / \Gamma_{\text{total}} \quad \Gamma_{39} / \Gamma$$

VALUE (units 10^{-4})	CL%	EVTS	DOCUMENT ID	TECN	COMMENT
$8.4 \pm 0.4 \pm 0.8$			¹ KUZMIN	07	BELL $e^+ e^- \rightarrow \Upsilon(4S)$

• • • We do not use the following data for averages, fits, limits, etc. • • •

$8.0 \pm 0.6 \pm 1.5$			^{1,2} SATPATHY	03	BELL Repl. by KUZMIN 07
< 16	90		¹ ALAM	94	CLE2 $e^+ e^- \rightarrow \Upsilon(4S)$
< 70	90		³ BORTOLETTO92	CLEO	$e^+ e^- \rightarrow \Upsilon(4S)$
< 340	90		⁴ BEBEK	87	CLEO $e^+ e^- \rightarrow \Upsilon(4S)$
700 ± 500		5	⁵ BEHRENDIS	83	CLEO $e^+ e^- \rightarrow \Upsilon(4S)$

¹ Assumes equal production of B^+ and B^0 at the $\Upsilon(4S)$.

² No assumption about the intermediate mechanism is made in the analysis.

³ BORTOLETTO 92 assumes equal production of B^+ and B^0 at the $\Upsilon(4S)$ and uses Mark III branching fractions for the D . The product branching fraction into $D_S^*(2340) \pi$ followed by $D_S^*(2340) \rightarrow D^0 \pi$ is < 0.0001 at 90% CL and into $D_S^*(2460) \pi$ followed by $D_S^*(2460) \rightarrow D^0 \pi$ is < 0.0004 at 90% CL.

⁴ BEBEK 87 assume the $\Upsilon(4S)$ decays 43% to $B^0 \bar{B}^0$. We rescale to 50%. $B(D^0 \rightarrow K^- \pi^+) = (4.2 \pm 0.4 \pm 0.4)\%$ and $B(D^0 \rightarrow K^- \pi^+ \pi^+ \pi^-) = (9.1 \pm 0.8 \pm 0.8)\%$ were used.

⁵ Corrected by us using assumptions: $B(D^0 \rightarrow K^- \pi^+) = (0.042 \pm 0.006)$ and $B(\Upsilon(4S) \rightarrow B^0 \bar{B}^0) = 50\%$. The product branching ratio is $B(B^0 \rightarrow \bar{D}^0 \pi^+ \pi^-) B(\bar{D}^0 \rightarrow K^+ \pi^-) = (0.39 \pm 0.26) \times 10^{-2}$.

$$\Gamma(D^*(2010)^- \pi^+) / \Gamma_{\text{total}} \quad \Gamma_{40} / \Gamma$$

VALUE (units 10^{-3})	EVTS	DOCUMENT ID	TECN	COMMENT
2.76 ± 0.13	OUR AVERAGE			

$2.79 \pm 0.08 \pm 0.17$		¹ AUBERT	07H	BABR $e^+ e^- \rightarrow \Upsilon(4S)$
$2.7 \pm 0.4 \pm 0.1$		^{2,3} AUBERT,BE	06J	BABR $e^+ e^- \rightarrow \Upsilon(4S)$
$2.81 \pm 0.24 \pm 0.05$		⁴ BRANDENB...	98	CLE2 $e^+ e^- \rightarrow \Upsilon(4S)$
$2.6 \pm 0.3 \pm 0.4$	82	⁵ ALAM	94	CLE2 $e^+ e^- \rightarrow \Upsilon(4S)$
$3.37 \pm 0.96 \pm 0.02$		⁶ BORTOLETTO92	CLEO	$e^+ e^- \rightarrow \Upsilon(4S)$
$2.36 \pm 0.88 \pm 0.02$	12	⁷ ALBRECHT	90J	ARG $e^+ e^- \rightarrow \Upsilon(4S)$
$2.36 \pm 1.5^0 \pm 0.02$ -1.10	5	⁸ BEBEK	87	CLEO $e^+ e^- \rightarrow \Upsilon(4S)$

• • • We do not use the following data for averages, fits, limits, etc. • • •

$10 \pm 4 \pm 1$	8	⁹ AKERS	94J	OPAL $e^+ e^- \rightarrow Z$
$2.7 \pm 1.4 \pm 1.0$	5	¹⁰ ALBRECHT	87c	ARG $e^+ e^- \rightarrow \Upsilon(4S)$
$3.5 \pm 2 \pm 2$		¹¹ ALBRECHT	86F	ARG $e^+ e^- \rightarrow \Upsilon(4S)$
$17 \pm 5 \pm 5$	41	¹² GILES	84	CLEO $e^+ e^- \rightarrow \Upsilon(4S)$

- ¹ Assumes equal production of B^+ and B^0 at the $\Upsilon(4S)$.
- ² AUBERT_BE 06J reports $[B(B^0 \rightarrow D^*(2010)^-\pi^+)]/[B(B^0 \rightarrow D^-\pi^+)] = 0.99 \pm 0.11 \pm 0.08$. We multiply by our best value $B(B^0 \rightarrow D^-\pi^+) = (2.68 \pm 0.13) \times 10^{-3}$. Our first error is their experiment's error and our second error is the systematic error from using our best value.
- ³ Uses a missing-mass method. Does not depend on D branching fractions or B^+ / B^0 production rates.
- ⁴ BRANDENBURG 98 assume equal production of B^+ and B^0 at $\Upsilon(4S)$ and use the D^* reconstruction technique. The first error is their experiment's error and the second error is the systematic error from the PDG 96 value of $B(D^* \rightarrow D\pi)$.
- ⁵ ALAM 94 assume equal production of B^+ and B^0 at the $\Upsilon(4S)$ and use the CLEOII $B(D^*(2010)^+ \rightarrow D^0\pi^+)$ and absolute $B(D^0 \rightarrow K^-\pi^+)$ and the PDG 1992 $B(D^0 \rightarrow K^-\pi^+\pi^0)/B(D^0 \rightarrow K^-\pi^+)$ and $B(D^0 \rightarrow K^-\pi^+\pi^+\pi^-)/B(D^0 \rightarrow K^-\pi^+)$.
- ⁶ BORTOLETTO 92 reports $(4.0 \pm 1.0 \pm 0.7) \times 10^{-3}$ for $B(D^*(2010)^+ \rightarrow D^0\pi^+) = 0.57 \pm 0.06$. We rescale to our best value $B(D^*(2010)^+ \rightarrow D^0\pi^+) = (67.7 \pm 0.5) \times 10^{-2}$. Our first error is their experiment's error and our second error is the systematic error from using our best value. Assumes equal production of B^+ and B^0 at the $\Upsilon(4S)$ and uses Mark III branching fractions for the D .
- ⁷ ALBRECHT 90J reports $(2.8 \pm 0.9 \pm 0.6) \times 10^{-3}$ for $B(D^*(2010)^+ \rightarrow D^0\pi^+) = 0.57 \pm 0.06$. We rescale to our best value $B(D^*(2010)^+ \rightarrow D^0\pi^+) = (67.7 \pm 0.5) \times 10^{-2}$. Our first error is their experiment's error and our second error is the systematic error from using our best value. Assumes equal production of B^+ and B^0 at the $\Upsilon(4S)$ and uses Mark III branching fractions for the D .
- ⁸ BEBEK 87 reports $(2.8^{+1.5+1.0}_{-1.2-0.6}) \times 10^{-3}$ for $B(D^*(2010)^+ \rightarrow D^0\pi^+) = 0.57 \pm 0.06$. We rescale to our best value $B(D^*(2010)^+ \rightarrow D^0\pi^+) = (67.7 \pm 0.5) \times 10^{-2}$. Our first error is their experiment's error and our second error is the systematic error from using our best value. Updated in BERKELMAN 91 to use same assumptions as noted for BORTOLETTO 92 and ALBRECHT 90J.
- ⁹ Assumes $B(Z \rightarrow b\bar{b}) = 0.217$ and 38% B_d production fraction.
- ¹⁰ ALBRECHT 87c use PDG 86 branching ratios for D and $D^*(2010)$ and assume $B(\Upsilon(4S) \rightarrow B^+B^-) = 55\%$ and $B(\Upsilon(4S) \rightarrow B^0\bar{B}^0) = 45\%$. Superseded by ALBRECHT 90J.
- ¹¹ ALBRECHT 86f uses pseudomass that is independent of D^0 and D^+ branching ratios.
- ¹² Assumes $B(D^*(2010)^+ \rightarrow D^0\pi^+) = 0.60^{+0.08}_{-0.15}$. Assumes $B(\Upsilon(4S) \rightarrow B^0\bar{B}^0) = 0.40 \pm 0.02$. Does not depend on D branching ratios.

$$\Gamma(D^-\pi^+\pi^-\pi^-)/\Gamma_{\text{total}} \quad \Gamma_{41}/\Gamma$$

VALUE	DOCUMENT ID	TECN	COMMENT
0.0080 ± 0.0021 ± 0.0014	¹ BORTOLETTO92	CLEO	$e^+e^- \rightarrow \Upsilon(4S)$

- ¹ BORTOLETTO 92 assumes equal production of B^+ and B^0 at the $\Upsilon(4S)$ and uses Mark III branching fractions for the D .

$$\Gamma((D^-\pi^+\pi^+\pi^-) \text{ nonresonant})/\Gamma_{\text{total}} \quad \Gamma_{42}/\Gamma$$

VALUE	DOCUMENT ID	TECN	COMMENT
0.0039 ± 0.0014 ± 0.0013	¹ BORTOLETTO92	CLEO	$e^+e^- \rightarrow \Upsilon(4S)$

- ¹ BORTOLETTO 92 assumes equal production of B^+ and B^0 at the $\Upsilon(4S)$ and uses Mark III branching fractions for the D .

$$\Gamma(D^-\pi^+\rho^0)/\Gamma_{\text{total}} \quad \Gamma_{43}/\Gamma$$

VALUE	DOCUMENT ID	TECN	COMMENT
0.0011 ± 0.0009 ± 0.0004	¹ BORTOLETTO92	CLEO	$e^+e^- \rightarrow \Upsilon(4S)$

- ¹ BORTOLETTO 92 assumes equal production of B^+ and B^0 at the $\Upsilon(4S)$ and uses Mark III branching fractions for the D .

$$\Gamma(D^-\pi^+\pi^+\pi^0)/\Gamma_{\text{total}} \quad \Gamma_{44}/\Gamma$$

VALUE	DOCUMENT ID	TECN	COMMENT
0.0060 ± 0.0022 ± 0.0024	¹ BORTOLETTO92	CLEO	$e^+e^- \rightarrow \Upsilon(4S)$

- ¹ BORTOLETTO 92 assumes equal production of B^+ and B^0 at the $\Upsilon(4S)$ and uses Mark III branching fractions for the D .

$$\Gamma(D^*(2010)^-\pi^+\pi^0)/\Gamma_{\text{total}} \quad \Gamma_{45}/\Gamma$$

VALUE	EVTS	DOCUMENT ID	TECN	COMMENT
0.0152 ± 0.0052 ± 0.0001	51	¹ ALBRECHT 90J	ARG	$e^+e^- \rightarrow \Upsilon(4S)$

- • • We do not use the following data for averages, fits, limits, etc. • • •
- | | | | | |
|-----------------------|---|---------------------------|-----|-----------------------------------|
| 0.015 ± 0.008 ± 0.008 | 8 | ² ALBRECHT 87c | ARG | $e^+e^- \rightarrow \Upsilon(4S)$ |
|-----------------------|---|---------------------------|-----|-----------------------------------|

- ¹ ALBRECHT 90J reports $0.018 \pm 0.004 \pm 0.005$ for $B(D^*(2010)^+ \rightarrow D^0\pi^+) = 0.57 \pm 0.06$. We rescale to our best value $B(D^*(2010)^+ \rightarrow D^0\pi^+) = (67.7 \pm 0.5) \times 10^{-2}$. Our first error is their experiment's error and our second error is the systematic error from using our best value. Assumes equal production of B^+ and B^0 at the $\Upsilon(4S)$ and uses Mark III branching fractions for the D .

- ² ALBRECHT 87c use PDG 86 branching ratios for D and $D^*(2010)$ and assume $B(\Upsilon(4S) \rightarrow B^+B^-) = 55\%$ and $B(\Upsilon(4S) \rightarrow B^0\bar{B}^0) = 45\%$. Superseded by ALBRECHT 90J.

$$\Gamma(D^*(2010)^-\rho^+)/\Gamma_{\text{total}} \quad \Gamma_{46}/\Gamma$$

VALUE	EVTS	DOCUMENT ID	TECN	COMMENT
0.0068 ± 0.0009 OUR AVERAGE				
0.0068 ± 0.0003 ± 0.0009		¹ CSORNA 03	CLE2	$e^+e^- \rightarrow \Upsilon(4S)$
0.0160 ± 0.0113 ± 0.0001		² BORTOLETTO92	CLEO	$e^+e^- \rightarrow \Upsilon(4S)$
0.00589 ± 0.00352 ± 0.00004	19	³ ALBRECHT 90J	ARG	$e^+e^- \rightarrow \Upsilon(4S)$
• • • We do not use the following data for averages, fits, limits, etc. • • •				
0.0074 ± 0.0010 ± 0.0014	76	^{4,5} ALAM 94	CLE2	$e^+e^- \rightarrow \Upsilon(4S)$
0.081 ± 0.029 ± 0.059 ± 0.024	19	⁶ CHEN 85	CLEO	$e^+e^- \rightarrow \Upsilon(4S)$

- ¹ Assumes equal production of B^0 and B^+ at the $\Upsilon(4S)$ resonance. The second error combines the systematic and theoretical uncertainties in quadrature. CSORNA 03 includes data used in ALAM 94. A full angular fit to three complex helicity amplitudes is performed.

- ² BORTOLETTO 92 reports $0.019 \pm 0.008 \pm 0.011$ for $B(D^*(2010)^+ \rightarrow D^0\pi^+) = 0.57 \pm 0.06$. We rescale to our best value $B(D^*(2010)^+ \rightarrow D^0\pi^+) = (67.7 \pm 0.5) \times 10^{-2}$. Our first error is their experiment's error and our second error is the systematic error from using our best value. Assumes equal production of B^+ and B^0 at the $\Upsilon(4S)$ and uses Mark III branching fractions for the D .

- ³ ALBRECHT 90J reports $0.007 \pm 0.003 \pm 0.003$ for $B(D^*(2010)^+ \rightarrow D^0\pi^+) = 0.57 \pm 0.06$. We rescale to our best value $B(D^*(2010)^+ \rightarrow D^0\pi^+) = (67.7 \pm 0.5) \times 10^{-2}$. Our first error is their experiment's error and our second error is the systematic error from using our best value. Assumes equal production of B^+ and B^0 at the $\Upsilon(4S)$ and uses Mark III branching fractions for the D .

- ⁴ ALAM 94 assume equal production of B^+ and B^0 at the $\Upsilon(4S)$ and use the CLEOII $B(D^*(2010)^+ \rightarrow D^0\pi^+)$ and absolute $B(D^0 \rightarrow K^-\pi^+)$ and the PDG 1992 $B(D^0 \rightarrow K^-\pi^+\pi^0)/B(D^0 \rightarrow K^-\pi^+)$ and $B(D^0 \rightarrow K^-\pi^+\pi^+\pi^-)/B(D^0 \rightarrow K^-\pi^+)$.

- ⁵ This decay is nearly completely longitudinally polarized, $\Gamma_L/\Gamma = (93 \pm 5 \pm 5)\%$, as expected from the factorization hypothesis (ROSNER 90). The nonresonant $\pi^+\pi^0$ contribution under the ρ^+ is less than 9% at 90% CL.

- ⁶ Uses $B(D^* \rightarrow D^0\pi^+) = 0.6 \pm 0.15$ and $B(\Upsilon(4S) \rightarrow B^0\bar{B}^0) = 0.4$. Does not depend on D branching ratios.

$$\Gamma(D^*(2010)^-K^+)/\Gamma_{\text{total}} \quad \Gamma_{47}/\Gamma$$

VALUE (units 10^{-4})	DOCUMENT ID	TECN	COMMENT
2.14 ± 0.16 OUR AVERAGE			
2.14 ± 0.12 ± 0.10	¹ AUBERT 06A	BABR	$e^+e^- \rightarrow \Upsilon(4S)$
2.0 ± 0.4 ± 0.1	² ABE 01I	BELL	$e^+e^- \rightarrow \Upsilon(4S)$

- ¹ AUBERT 06A reports $[B(B^0 \rightarrow D^*(2010)^-K^+)]/[B(B^0 \rightarrow D^*(2010)^-\pi^+)] = 0.0776 \pm 0.0034 \pm 0.0029$. We multiply by our best value $B(B^0 \rightarrow D^*(2010)^-\pi^+) = (2.76 \pm 0.13) \times 10^{-3}$. Our first error is their experiment's error and our second error is the systematic error from using our best value.

- ² ABE 01I reports $[B(B^0 \rightarrow D^*(2010)^-K^+)]/[B(B^0 \rightarrow D^*(2010)^-\pi^+)] = 0.074 \pm 0.015 \pm 0.006$. We multiply by our best value $B(B^0 \rightarrow D^*(2010)^-\pi^+) = (2.76 \pm 0.13) \times 10^{-3}$. Our first error is their experiment's error and our second error is the systematic error from using our best value.

$$\Gamma(D^*(2010)^-K^0\pi^+)/\Gamma_{\text{total}} \quad \Gamma_{48}/\Gamma$$

VALUE (units 10^{-4})	DOCUMENT ID	TECN	COMMENT
3.0 ± 0.7 ± 0.3	¹ AUBERT, BE 05B	BABR	$e^+e^- \rightarrow \Upsilon(4S)$

- ¹ Assumes equal production of B^+ and B^0 at the $\Upsilon(4S)$.

$$\Gamma(D^*(2010)^-K^*(892)^+)/\Gamma_{\text{total}} \quad \Gamma_{49}/\Gamma$$

VALUE (units 10^{-4})	DOCUMENT ID	TECN	COMMENT
3.3 ± 0.6 OUR AVERAGE			
3.2 ± 0.6 ± 0.3	¹ AUBERT, BE 05B	BABR	$e^+e^- \rightarrow \Upsilon(4S)$
3.8 ± 1.3 ± 0.8	² MAHAPATRA 02	CLE2	$e^+e^- \rightarrow \Upsilon(4S)$

- ¹ Assumes equal production of B^+ and B^0 at the $\Upsilon(4S)$.
- ² Assumes equal production of B^+ and B^0 at the $\Upsilon(4S)$ and an unpolarized final state.

$$\Gamma(D^*(2010)^-K^+\bar{K}^0)/\Gamma_{\text{total}} \quad \Gamma_{50}/\Gamma$$

VALUE (units 10^{-4})	CL%	DOCUMENT ID	TECN	COMMENT
<4.7	90	¹ DRUTSKOY 02	BELL	$e^+e^- \rightarrow \Upsilon(4S)$

- ¹ Assumes equal production of B^+ and B^0 at the $\Upsilon(4S)$.

$$\Gamma(D^*(2010)^-K^+\bar{K}^*(892)^0)/\Gamma_{\text{total}} \quad \Gamma_{51}/\Gamma$$

VALUE (units 10^{-4})	DOCUMENT ID	TECN	COMMENT
12.9 ± 2.2 ± 2.5	¹ DRUTSKOY 02	BELL	$e^+e^- \rightarrow \Upsilon(4S)$

- ¹ Assumes equal production of B^+ and B^0 at the $\Upsilon(4S)$.

$$\Gamma(D^*(2010)^-\pi^+\pi^+\pi^-)/\Gamma_{\text{total}} \quad \Gamma_{52}/\Gamma$$

VALUE	CL%	DOCUMENT ID	TECN	COMMENT
0.0070 ± 0.0008 OUR AVERAGE				Error includes scale factor of 1.3. See the ideogram below.
0.00681 ± 0.00023 ± 0.00072		¹ MAJUMDER 04	BELL	$e^+e^- \rightarrow \Upsilon(4S)$
0.0063 ± 0.0010 ± 0.0011		^{2,3} ALAM 94	CLE2	$e^+e^- \rightarrow \Upsilon(4S)$
0.0134 ± 0.0036 ± 0.0001		⁴ BORTOLETTO92	CLEO	$e^+e^- \rightarrow \Upsilon(4S)$
0.0101 ± 0.0041 ± 0.0001		⁵ ALBRECHT 90J	ARG	$e^+e^- \rightarrow \Upsilon(4S)$

- • • We do not use the following data for averages, fits, limits, etc. • • •
- | | | | | |
|-----------------------|----|---------------------------|------|-----------------------------------|
| 0.033 ± 0.009 ± 0.016 | | ⁶ ALBRECHT 87c | ARG | $e^+e^- \rightarrow \Upsilon(4S)$ |
| <0.042 | 90 | ⁷ BEBEK 87 | CLEO | $e^+e^- \rightarrow \Upsilon(4S)$ |

- ¹ Assumes equal production of B^+ and B^0 at the $\Upsilon(4S)$.
- ² ALAM 94 assume equal production of B^+ and B^0 at the $\Upsilon(4S)$ and use the CLEOII $B(D^*(2010)^+ \rightarrow D^0\pi^+)$ and absolute $B(D^0 \rightarrow K^-\pi^+)$ and the PDG 1992 $B(D^0 \rightarrow K^-\pi^+\pi^0)/B(D^0 \rightarrow K^-\pi^+)$ and $B(D^0 \rightarrow K^-\pi^+\pi^+\pi^-)/B(D^0 \rightarrow K^-\pi^+)$.

- ³ The three pion mass is required to be between 1.0 and 1.6 GeV consistent with an a_1 meson. (If this channel is dominated by a_1^+ , the branching ratio for $\bar{D}^*-\pi^+\pi^+$ is twice that for $\bar{D}^*-\pi^+\pi^+\pi^-$.)

- ⁴ BORTOLETTO 92 reports $0.0159 \pm 0.0028 \pm 0.0037$ for $B(D^*(2010)^+ \rightarrow D^0\pi^+) = 0.57 \pm 0.06$. We rescale to our best value $B(D^*(2010)^+ \rightarrow D^0\pi^+) = (67.7 \pm 0.5) \times 10^{-2}$. Our first error is their experiment's error and our second error is the systematic error from using our best value. Assumes equal production of B^+ and B^0 at the $\Upsilon(4S)$ and uses Mark III branching fractions for the D .

Meson Particle Listings

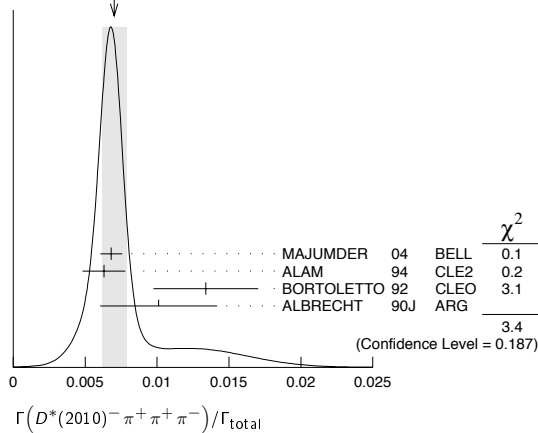
 B^0

⁵ ALBRECHT 90J reports $0.012 \pm 0.003 \pm 0.004$ for $B(D^*(2010)^+ \rightarrow D^0 \pi^+) = 0.57 \pm 0.06$. We rescale to our best value $B(D^*(2010)^+ \rightarrow D^0 \pi^+) = (67.7 \pm 0.5) \times 10^{-2}$. Our first error is their experiment's error and our second error is the systematic error from using our best value. Assumes equal production of B^+ and B^0 at the $\Upsilon(4S)$ and uses Mark III branching fractions for the D .

⁶ ALBRECHT 87C use PDG 86 branching ratios for D and $D^*(2010)$ and assume $B(\Upsilon(4S) \rightarrow B^+ B^-) = 55\%$ and $B(\Upsilon(4S) \rightarrow B^0 \bar{B}^0) = 45\%$. Superseded by ALBRECHT 90J.

⁷ BEBEK 87 value has been updated in BERKELMAN 91 to use same assumptions as noted for BORTOLETTO 92.

WEIGHTED AVERAGE
 0.0070 ± 0.0008 (Error scaled by 1.3)



$\Gamma((D^*(2010)^- \pi^+ \pi^+ \pi^-) \text{ nonresonant})/\Gamma_{\text{total}}$ Γ_{53}/Γ

VALUE	DOCUMENT ID	TECN	COMMENT
$0.0000 \pm 0.0019 \pm 0.0016$	¹ BORTOLETTO92	CLEO	$e^+ e^- \rightarrow \Upsilon(4S)$

¹ BORTOLETTO 92 assumes equal production of B^+ and B^0 at the $\Upsilon(4S)$ and uses Mark III branching fractions for the D and $D^*(2010)$.

$\Gamma(D^*(2010)^- \pi^+ \rho^0)/\Gamma_{\text{total}}$ Γ_{54}/Γ

VALUE	DOCUMENT ID	TECN	COMMENT
$0.00573 \pm 0.00317 \pm 0.00004$	¹ BORTOLETTO92	CLEO	$e^+ e^- \rightarrow \Upsilon(4S)$

¹ BORTOLETTO 92 reports $0.0068 \pm 0.0032 \pm 0.0021$ for $B(D^*(2010)^+ \rightarrow D^0 \pi^+) = 0.57 \pm 0.06$. We rescale to our best value $B(D^*(2010)^+ \rightarrow D^0 \pi^+) = (67.7 \pm 0.5) \times 10^{-2}$. Our first error is their experiment's error and our second error is the systematic error from using our best value. Assumes equal production of B^+ and B^0 at the $\Upsilon(4S)$ and uses Mark III branching fractions for the D .

$\Gamma(D^*(2010)^- a_1(1260)^+)/\Gamma_{\text{total}}$ Γ_{55}/Γ

VALUE	DOCUMENT ID	TECN	COMMENT
0.0130 ± 0.0027 OUR AVERAGE			
$0.0126 \pm 0.0020 \pm 0.0022$	^{1,2} ALAM 94	CLE2	$e^+ e^- \rightarrow \Upsilon(4S)$
$0.0152 \pm 0.0070 \pm 0.0001$	³ BORTOLETTO92	CLEO	$e^+ e^- \rightarrow \Upsilon(4S)$

¹ ALAM 94 value is twice their $\Gamma(D^*(2010)^- \pi^+ \pi^+ \pi^-)/\Gamma_{\text{total}}$ value based on their observation that the three pions are dominantly in the $a_1(1260)$ mass range 1.0 to 1.6 GeV.
² ALAM 94 assume equal production of B^+ and B^0 at the $\Upsilon(4S)$ and use the CLEO II $B(D^*(2010)^+ \rightarrow D^0 \pi^+)$ and absolute $B(D^0 \rightarrow K^- \pi^+)$ and the PDG 1992 $B(D^0 \rightarrow K^- \pi^+ \pi^0)/B(D^0 \rightarrow K^- \pi^+)$ and $B(D^0 \rightarrow K^- \pi^+ \pi^+ \pi^-)/B(D^0 \rightarrow K^- \pi^+)$.
³ BORTOLETTO 92 reports $0.018 \pm 0.006 \pm 0.006$ for $B(D^*(2010)^+ \rightarrow D^0 \pi^+) = 0.57 \pm 0.06$. We rescale to our best value $B(D^*(2010)^+ \rightarrow D^0 \pi^+) = (67.7 \pm 0.5) \times 10^{-2}$. Our first error is their experiment's error and our second error is the systematic error from using our best value. Assumes equal production of B^+ and B^0 at the $\Upsilon(4S)$ and uses Mark III branching fractions for the D .

$\Gamma(D^*(2010)^- \pi^+ \pi^+ \pi^- \pi^0)/\Gamma_{\text{total}}$ Γ_{56}/Γ

VALUE	EVTs	DOCUMENT ID	TECN	COMMENT
0.0176 ± 0.0027 OUR AVERAGE				
$0.0172 \pm 0.0014 \pm 0.0024$	28	¹ ALEXANDER 01B	CLE2	$e^+ e^- \rightarrow \Upsilon(4S)$
$0.0345 \pm 0.0181 \pm 0.0003$		² ALBRECHT 90J	ARG	$e^+ e^- \rightarrow \Upsilon(4S)$

¹ Assumes equal production of B^+ and B^0 at the $\Upsilon(4S)$. The signal is consistent with all observed $\omega \pi^+$ having proceeded through the ρ^{++} resonance at mass $1349 \pm 25^{+10}_{-5}$ MeV and width $547 \pm 86^{+46}_{-45}$ MeV.
² ALBRECHT 90J reports $0.041 \pm 0.015 \pm 0.016$ for $B(D^*(2010)^+ \rightarrow D^0 \pi^+) = 0.57 \pm 0.06$. We rescale to our best value $B(D^*(2010)^+ \rightarrow D^0 \pi^+) = (67.7 \pm 0.5) \times 10^{-2}$. Our first error is their experiment's error and our second error is the systematic error from using our best value. Assumes equal production of B^+ and B^0 at the $\Upsilon(4S)$ and uses Mark III branching fractions for the D .

$\Gamma(D^{*-} 3\pi^+ 2\pi^-)/\Gamma_{\text{total}}$ Γ_{57}/Γ

VALUE (units 10^{-3})	DOCUMENT ID	TECN	COMMENT
$4.72 \pm 0.59 \pm 0.71$	¹ MAJUMDER 04	BELL	$e^+ e^- \rightarrow \Upsilon(4S)$

¹ Assumes equal production of B^+ and B^0 at the $\Upsilon(4S)$.

$\Gamma(D^*(2010)^- \rho \bar{\rho} \pi^+)/\Gamma_{\text{total}}$ Γ_{58}/Γ

VALUE (units 10^{-4})	DOCUMENT ID	TECN	COMMENT
$6.5 \pm 1.3 \pm 1.0$	¹ ANDERSON 01	CLE2	$e^+ e^- \rightarrow \Upsilon(4S)$

¹ Assumes equal production of B^+ and B^0 at the $\Upsilon(4S)$.

$\Gamma(D^*(2010)^- \rho \pi^+)/\Gamma_{\text{total}}$ Γ_{59}/Γ

VALUE (units 10^{-4})	DOCUMENT ID	TECN	COMMENT
$14.5 \pm 3.4 \pm 2.7$	¹ ANDERSON 01	CLE2	$e^+ e^- \rightarrow \Upsilon(4S)$

¹ Assumes equal production of B^+ and B^0 at the $\Upsilon(4S)$.

$\Gamma(\bar{D}^*(2010)^- \omega \pi^+)/\Gamma_{\text{total}}$ Γ_{60}/Γ

VALUE (units 10^{-3})	DOCUMENT ID	TECN	COMMENT
2.89 ± 0.30 OUR AVERAGE			
$2.88 \pm 0.21 \pm 0.31$	¹ AUBERT 06L	BABR	$e^+ e^- \rightarrow \Upsilon(4S)$
$2.9 \pm 0.3 \pm 0.4$	^{1,2} ALEXANDER 01B	CLE2	$e^+ e^- \rightarrow \Upsilon(4S)$

¹ Assumes equal production of B^+ and B^0 at the $\Upsilon(4S)$.
² The signal is consistent with all observed $\omega \pi^+$ having proceeded through the ρ^{++} resonance at mass $1349 \pm 25^{+10}_{-5}$ MeV and width $547 \pm 86^{+46}_{-45}$ MeV.

$\Gamma(D_1(2430)^0 \omega \times B(D_1(2430)^0 \rightarrow D^{*-} \pi^+)/\Gamma_{\text{total}}$ Γ_{61}/Γ

VALUE (units 10^{-4})	DOCUMENT ID	TECN	COMMENT
$4.1 \pm 1.2 \pm 1.1$	¹ AUBERT 06L	BABR	$e^+ e^- \rightarrow \Upsilon(4S)$

¹ Obtained by fitting the events with $\cos \theta_{D^*} < 0.5$ and scaling up the result by a factor of 4/3. No interference effects between $B^0 \rightarrow D_1^+ \omega$ and $D^* \omega \pi$ are assumed.

$\Gamma(\bar{D}^{*-} \pi^+)/\Gamma_{\text{total}}$ Γ_{62}/Γ

\bar{D}^{*-} represents an excited state with mass $2.2 < M < 2.8$ GeV/ c^2 .

VALUE (units 10^{-3})	DOCUMENT ID	TECN	COMMENT
$2.1 \pm 1.0 \pm 0.1$	^{1,2} AUBERT,BE 06J	BABR	$e^+ e^- \rightarrow \Upsilon(4S)$

¹ AUBERT,BE 06J reports $[B(B^0 \rightarrow \bar{D}^{*-} \pi^+)] / [B(B^0 \rightarrow D^- \pi^+)] = 0.77 \pm 0.22 \pm 0.29$. We multiply by our best value $B(B^0 \rightarrow D^- \pi^+) = (2.68 \pm 0.13) \times 10^{-3}$. Our first error is their experiment's error and our second error is the systematic error from using our best value.
² Uses a missing-mass method. Does not depend on D branching fractions or B^+/B^0 production rates.

$\Gamma(D_1(2420)^- \pi^+ \times B(D_1^- \rightarrow D^- \pi^+ \pi^-))/\Gamma_{\text{total}}$ Γ_{63}/Γ

VALUE (units 10^{-4})	DOCUMENT ID	TECN	COMMENT
$0.89 \pm 0.15 \pm 0.17$ -0.32	¹ ABE 05A	BELL	$e^+ e^- \rightarrow \Upsilon(4S)$

¹ Assumes equal production of B^+ and B^0 at the $\Upsilon(4S)$.

$\Gamma(D_1(2420)^- \pi^+ \times B(D_1^- \rightarrow D^{*-} \pi^+ \pi^-))/\Gamma_{\text{total}}$ Γ_{64}/Γ

VALUE (units 10^{-4})	CL%	DOCUMENT ID	TECN	COMMENT
< 0.33	90	¹ ABE 05A	BELL	$e^+ e^- \rightarrow \Upsilon(4S)$

¹ Assumes equal production of B^+ and B^0 at the $\Upsilon(4S)$.

$\Gamma(\bar{D}_2^*(2460)^- \pi^+ \times B(D_2^*(2460)^- \rightarrow D^0 \pi^-))/\Gamma_{\text{total}}$ Γ_{65}/Γ

VALUE (units 10^{-4})	CL%	DOCUMENT ID	TECN	COMMENT
$2.15 \pm 0.17 \pm 0.31$		^{1,2} KUZMIN 07	BELL	$e^+ e^- \rightarrow \Upsilon(4S)$
< 14.7	90	¹ ALAM 94	CLE2	$e^+ e^- \rightarrow \Upsilon(4S)$

••• We do not use the following data for averages, fits, limits, etc. •••
¹ Assumes equal production of B^+ and B^0 at the $\Upsilon(4S)$.
² Our second uncertainty combines systematics and model errors quoted in the paper.

$\Gamma(\bar{D}_2^*(2400)^- \pi^+ \times B(D_2^*(2400)^- \rightarrow D^0 \pi^-))/\Gamma_{\text{total}}$ Γ_{66}/Γ

VALUE (units 10^{-4})	DOCUMENT ID	TECN	COMMENT
$0.60 \pm 0.13 \pm 0.27$	^{1,2} KUZMIN 07	BELL	$e^+ e^- \rightarrow \Upsilon(4S)$

¹ Assumes equal production of B^+ and B^0 at the $\Upsilon(4S)$.
² Our second uncertainty combines systematics and model errors quoted in the paper.

$\Gamma(D_2^*(2460)^- \pi^+ \times B(D_2^*(2460)^- \rightarrow D^{*-} \pi^+ \pi^-))/\Gamma_{\text{total}}$ Γ_{67}/Γ

VALUE (units 10^{-4})	CL%	DOCUMENT ID	TECN	COMMENT
< 0.24	90	¹ ABE 05A	BELL	$e^+ e^- \rightarrow \Upsilon(4S)$

¹ Assumes equal production of B^+ and B^0 at the $\Upsilon(4S)$.

$\Gamma(\bar{D}_2^*(2460)^- \rho^+)/\Gamma_{\text{total}}$ Γ_{68}/Γ

VALUE	CL%	DOCUMENT ID	TECN	COMMENT
< 0.0049	90	¹ ALAM 94	CLE2	$e^+ e^- \rightarrow \Upsilon(4S)$

¹ ALAM 94 assumes equal production of B^+ and B^0 at the $\Upsilon(4S)$ and use the CLEO II absolute $B(D^0 \rightarrow K^- \pi^+)$ and $B(D_2^*(2460)^+ \rightarrow D^0 \pi^+) = 30\%$.

$\Gamma(D^0 \bar{D}^0)/\Gamma_{\text{total}}$ Γ_{69}/Γ

VALUE (units 10^{-4})	CL%	DOCUMENT ID	TECN	COMMENT
< 0.6	90	¹ AUBERT,B 06A	BABR	$e^+ e^- \rightarrow \Upsilon(4S)$

¹ Assumes equal production of B^+ and B^0 at the $\Upsilon(4S)$.

$\Gamma(D^{*0}D^0)/\Gamma_{\text{total}}$		Γ_{70}/Γ	
VALUE (units 10^{-4})	CL%	DOCUMENT ID	TECN COMMENT
<2.9	90	1 AUBERT,B	06A BABR $e^+e^- \rightarrow \Upsilon(4S)$

1 Assumes equal production of B^+ and B^0 at the $\Upsilon(4S)$.

$\Gamma(D^-D^+)/\Gamma_{\text{total}}$		Γ_{71}/Γ	
VALUE (units 10^{-4})	CL%	DOCUMENT ID	TECN COMMENT
2.11 ± 0.31 OUR AVERAGE		Error includes scale factor of 1.2.	
1.97 ± 0.20 ± 0.20		1 FRATINA	07 BELL $e^+e^- \rightarrow \Upsilon(4S)$
2.8 ± 0.4 ± 0.5		1 AUBERT,B	06A BABR $e^+e^- \rightarrow \Upsilon(4S)$

• • • We do not use the following data for averages, fits, limits, etc. • • •

1.91 ± 0.51 ± 0.30		1 MAJUMDER	05 BELL Repl. by FRATINA 07
< 9.4	90	1 LIPELES	00 CLE2 $e^+e^- \rightarrow \Upsilon(4S)$
< 59	90	BARATE	98Q ALEP $e^+e^- \rightarrow Z$
< 12	90	ASNER	97 CLE2 $e^+e^- \rightarrow \Upsilon(4S)$

1 Assumes equal production of B^+ and B^0 at the $\Upsilon(4S)$.

$\Gamma(D^-D_s^+)/\Gamma_{\text{total}}$		Γ_{72}/Γ	
VALUE	EVTS	DOCUMENT ID	TECN COMMENT
0.0074 ± 0.0007 OUR AVERAGE			
0.0075 ± 0.0005 ± 0.0006		1 ZUPANC	07 BELL $e^+e^- \rightarrow \Upsilon(4S)$
0.0068 ± 0.0015 ± 0.0005		2 AUBERT	06N BABR $e^+e^- \rightarrow \Upsilon(4S)$
0.0070 ± 0.0025 ± 0.0006		3 GIBAUT	96 CLE2 $e^+e^- \rightarrow \Upsilon(4S)$
0.010 ± 0.009 ± 0.001		4 ALBRECHT	92G ARG $e^+e^- \rightarrow \Upsilon(4S)$
0.0055 ± 0.0031 ± 0.0004		5 BORTOLETTO92	CLEO $e^+e^- \rightarrow \Upsilon(4S)$

• • • We do not use the following data for averages, fits, limits, etc. • • •

0.012 ± 0.007	3	6 BORTOLETTO90	CLEO $e^+e^- \rightarrow \Upsilon(4S)$
---------------	---	----------------	--

- 1 ZUPANC 07 reports $(7.5 \pm 0.2 \pm 1.1) \times 10^{-3}$ for $B(D_s^+ \rightarrow \phi\pi^+) = (4.4 \pm 0.6) \times 10^{-2}$. We rescale to our best value $B(D_s^+ \rightarrow \phi\pi^+) = (4.38 \pm 0.35) \times 10^{-2}$. Our first error is their experiment's error and our second error is the systematic error from using our best value.
- 2 AUBERT 06N reports $(0.64 \pm 0.13 \pm 0.10) \times 10^{-2}$ for $B(D_s^+ \rightarrow \phi\pi^+) = 0.0462 \pm 0.0062$. We rescale to our best value $B(D_s^+ \rightarrow \phi\pi^+) = (4.38 \pm 0.35) \times 10^{-2}$. Our first error is their experiment's error and our second error is the systematic error from using our best value.
- 3 GIBAUT 96 reports $0.0087 \pm 0.0024 \pm 0.0020$ for $B(D_s^+ \rightarrow \phi\pi^+) = 0.035$. We rescale to our best value $B(D_s^+ \rightarrow \phi\pi^+) = (4.38 \pm 0.35) \times 10^{-2}$. Our first error is their experiment's error and our second error is the systematic error from using our best value.
- 4 ALBRECHT 92G reports $0.017 \pm 0.013 \pm 0.006$ for $B(D_s^+ \rightarrow \phi\pi^+) = 0.027$. We rescale to our best value $B(D_s^+ \rightarrow \phi\pi^+) = (4.38 \pm 0.35) \times 10^{-2}$. Our first error is their experiment's error and our second error is the systematic error from using our best value. Assumes PDG 1990 D^+ branching ratios, e.g., $B(D^+ \rightarrow K^-\pi^+\pi^+) = 7.7 \pm 1.0\%$.
- 5 BORTOLETTO 92 reports $0.0080 \pm 0.0045 \pm 0.0030$ for $B(D_s^+ \rightarrow \phi\pi^+) = 0.030 \pm 0.011$. We rescale to our best value $B(D_s^+ \rightarrow \phi\pi^+) = (4.38 \pm 0.35) \times 10^{-2}$. Our first error is their experiment's error and our second error is the systematic error from using our best value. Assumes equal production of B^+ and B^0 at the $\Upsilon(4S)$ and uses Mark III branching fractions for the D .
- 6 BORTOLETTO 90 assume $B(D_s \rightarrow \phi\pi^+) = 2\%$. Superseded by BORTOLETTO 92.

$\Gamma(D^*(2010)^-D_s^+)/\Gamma_{\text{total}}$		Γ_{73}/Γ	
VALUE	EVTS	DOCUMENT ID	TECN COMMENT
0.0083 ± 0.0011 OUR AVERAGE			
0.0075 ± 0.0013 ± 0.0006		1 AUBERT	06N BABR $e^+e^- \rightarrow \Upsilon(4S)$
0.0085 ± 0.0016 ± 0.0007		2 AUBERT	03i BABR $e^+e^- \rightarrow \Upsilon(4S)$
0.0090 ± 0.0017 ± 0.0007		3 AHMED	00B CLE2 $e^+e^- \rightarrow \Upsilon(4S)$
0.009 ± 0.006 ± 0.001		4 ALBRECHT	92G ARG $e^+e^- \rightarrow \Upsilon(4S)$
0.011 ± 0.006 ± 0.001		5 BORTOLETTO92	CLEO $e^+e^- \rightarrow \Upsilon(4S)$

• • • We do not use the following data for averages, fits, limits, etc. • • •

0.0074 ± 0.0022 ± 0.0006		6 GIBAUT	96 CLE2 Repl. by AHMED 00b
0.024 ± 0.014	3	7 BORTOLETTO90	CLEO $e^+e^- \rightarrow \Upsilon(4S)$

- 1 AUBERT 06N reports $(0.71 \pm 0.13 \pm 0.09) \times 10^{-2}$ for $B(D_s^+ \rightarrow \phi\pi^+) = 0.0462 \pm 0.0062$. We rescale to our best value $B(D_s^+ \rightarrow \phi\pi^+) = (4.38 \pm 0.35) \times 10^{-2}$. Our first error is their experiment's error and our second error is the systematic error from using our best value.
- 2 AUBERT 03i reports $0.0103 \pm 0.0014 \pm 0.0013$ for $B(D_s^+ \rightarrow \phi\pi^+) = 0.036$. We rescale to our best value $B(D_s^+ \rightarrow \phi\pi^+) = (4.38 \pm 0.35) \times 10^{-2}$. Our first error is their experiment's error and our second error is the systematic error from using our best value.
- 3 AHMED 00b reports $0.0110 \pm 0.0018 \pm 0.0011$ for $B(D_s^+ \rightarrow \phi\pi^+) = 0.036$. We rescale to our best value $B(D_s^+ \rightarrow \phi\pi^+) = (4.38 \pm 0.35) \times 10^{-2}$. Our first error is their experiment's error and our second error is the systematic error from using our best value.
- 4 ALBRECHT 92G reports $0.014 \pm 0.010 \pm 0.003$ for $B(D_s^+ \rightarrow \phi\pi^+) = 0.027$. We rescale to our best value $B(D_s^+ \rightarrow \phi\pi^+) = (4.38 \pm 0.35) \times 10^{-2}$. Our first error is their experiment's error and our second error is the systematic error from using our best value. Assumes PDG 1990 D^+ and $D^*(2010)^+$ branching ratios, e.g., $B(D^0 \rightarrow K^-\pi^+) = 3.71 \pm 0.25\%$, $B(D^+ \rightarrow K^-\pi^+\pi^+) = 7.1 \pm 1.0\%$, and $B(D^*(2010)^+ \rightarrow D^0\pi^+) = 55 \pm 4\%$.
- 5 BORTOLETTO 92 reports $0.016 \pm 0.009 \pm 0.006$ for $B(D_s^+ \rightarrow \phi\pi^+) = 0.030 \pm 0.011$. We rescale to our best value $B(D_s^+ \rightarrow \phi\pi^+) = (4.38 \pm 0.35) \times 10^{-2}$. Our first error

is their experiment's error and our second error is the systematic error from using our best value. Assumes equal production of B^+ and B^0 at the $\Upsilon(4S)$ and uses Mark III branching fractions for the D and $D^*(2010)$.

- 6 GIBAUT 96 reports $0.0093 \pm 0.0023 \pm 0.0016$ for $B(D_s^+ \rightarrow \phi\pi^+) = 0.035$. We rescale to our best value $B(D_s^+ \rightarrow \phi\pi^+) = (4.38 \pm 0.35) \times 10^{-2}$. Our first error is their experiment's error and our second error is the systematic error from using our best value.
- 7 BORTOLETTO 90 assume $B(D_s \rightarrow \phi\pi^+) = 2\%$. Superseded by BORTOLETTO 92.

$\Gamma(D^-D_s^+)/\Gamma_{\text{total}}$		Γ_{74}/Γ	
VALUE	DOCUMENT ID	TECN	COMMENT
0.0076 ± 0.0016 OUR AVERAGE			
0.0073 ± 0.0017 ± 0.0006	1 AUBERT	06N BABR	$e^+e^- \rightarrow \Upsilon(4S)$
0.0080 ± 0.0033 ± 0.0006	2 GIBAUT	96 CLE2	$e^+e^- \rightarrow \Upsilon(4S)$
0.017 ± 0.012 ± 0.001	3 ALBRECHT	92G ARG	$e^+e^- \rightarrow \Upsilon(4S)$

- 1 AUBERT 06N reports $(0.69 \pm 0.16 \pm 0.09) \times 10^{-2}$ for $B(D_s^+ \rightarrow \phi\pi^+) = 0.0462 \pm 0.0062$. We rescale to our best value $B(D_s^+ \rightarrow \phi\pi^+) = (4.38 \pm 0.35) \times 10^{-2}$. Our first error is their experiment's error and our second error is the systematic error from using our best value.
- 2 GIBAUT 96 reports $0.0100 \pm 0.0035 \pm 0.0022$ for $B(D_s^+ \rightarrow \phi\pi^+) = 0.035$. We rescale to our best value $B(D_s^+ \rightarrow \phi\pi^+) = (4.38 \pm 0.35) \times 10^{-2}$. Our first error is their experiment's error and our second error is the systematic error from using our best value.
- 3 ALBRECHT 92G reports $0.027 \pm 0.017 \pm 0.009$ for $B(D_s^+ \rightarrow \phi\pi^+) = 0.027$. We rescale to our best value $B(D_s^+ \rightarrow \phi\pi^+) = (4.38 \pm 0.35) \times 10^{-2}$. Our first error is their experiment's error and our second error is the systematic error from using our best value. Assumes PDG 1990 D^+ branching ratios, e.g., $B(D^+ \rightarrow K^-\pi^+\pi^+) = 7.7 \pm 1.0\%$.

$[\Gamma(D^*(2010)^-D_s^+) + \Gamma(D^*(2010)^-D_s^{*+})]/\Gamma_{\text{total}}$		$(\Gamma_{73} + \Gamma_{75})/\Gamma$	
VALUE (units 10^{-2})	EVTS	DOCUMENT ID	TECN COMMENT
2.6 ± 0.4 OUR AVERAGE			
2.5 ± 0.4 ± 0.2		1 AUBERT	03i BABR $e^+e^- \rightarrow \Upsilon(4S)$
3.4 ± 0.9 ± 0.3	22	2 BORTOLETTO90	CLEO $e^+e^- \rightarrow \Upsilon(4S)$

- 1 AUBERT 03i reports $(3.00 \pm 0.19 \pm 0.39) \times 10^{-2}$ for $B(D_s^+ \rightarrow \phi\pi^+) = 0.036$. We rescale to our best value $B(D_s^+ \rightarrow \phi\pi^+) = (4.38 \pm 0.35) \times 10^{-2}$. Our first error is their experiment's error and our second error is the systematic error from using our best value.
- 2 BORTOLETTO 90 reports $(7.5 \pm 2.0) \times 10^{-2}$ for $B(D_s^+ \rightarrow \phi\pi^+) = 0.02$. We rescale to our best value $B(D_s^+ \rightarrow \phi\pi^+) = (4.38 \pm 0.35) \times 10^{-2}$. Our first error is their experiment's error and our second error is the systematic error from using our best value.

$\Gamma(D^*(2010)^-D_s^{*+})/\Gamma_{\text{total}}$		Γ_{75}/Γ	
VALUE	DOCUMENT ID	TECN	COMMENT
0.0179 ± 0.0014 OUR AVERAGE			
0.0177 ± 0.0018 ± 0.0014	1 AUBERT	06N BABR	$e^+e^- \rightarrow \Upsilon(4S)$
0.0188 ± 0.0009 ± 0.0017	2 AUBERT	05v BABR	$e^+e^- \rightarrow \Upsilon(4S)$
0.0162 ± 0.0028 ± 0.0013	3 AUBERT	03i BABR	$e^+e^- \rightarrow \Upsilon(4S)$
0.015 ± 0.004 ± 0.001	4 AHMED	00B CLE2	$e^+e^- \rightarrow \Upsilon(4S)$
0.016 ± 0.009 ± 0.001	5 ALBRECHT	92G ARG	$e^+e^- \rightarrow \Upsilon(4S)$

• • • We do not use the following data for averages, fits, limits, etc. • • •

0.016 ± 0.005 ± 0.001	6 GIBAUT	96 CLE2	Repl. by AHMED 00b
-----------------------	----------	---------	--------------------

- 1 AUBERT 06N reports $(1.68 \pm 0.21 \pm 0.19) \times 10^{-2}$ for $B(D_s^+ \rightarrow \phi\pi^+) = 0.0462 \pm 0.0062$. We rescale to our best value $B(D_s^+ \rightarrow \phi\pi^+) = (4.38 \pm 0.35) \times 10^{-2}$. Our first error is their experiment's error and our second error is the systematic error from using our best value.
- 2 A partial reconstruction technique is used and the result is independent of the particle decay rate of D_s^+ meson. It also provides a model-independent determination of $B(D_s^+ \rightarrow \phi\pi^+) = (4.81 \pm 0.52 \pm 0.38)\%$.
- 3 AUBERT 03i reports $0.0197 \pm 0.0015 \pm 0.0030$ for $B(D_s^+ \rightarrow \phi\pi^+) = 0.036$. We rescale to our best value $B(D_s^+ \rightarrow \phi\pi^+) = (4.38 \pm 0.35) \times 10^{-2}$. Our first error is their experiment's error and our second error is the systematic error from using our best value.
- 4 AHMED 00b reports $0.0182 \pm 0.0037 \pm 0.0025$ for $B(D_s^+ \rightarrow \phi\pi^+) = 0.036$. We rescale to our best value $B(D_s^+ \rightarrow \phi\pi^+) = (4.38 \pm 0.35) \times 10^{-2}$. Our first error is their experiment's error and our second error is the systematic error from using our best value.
- 5 ALBRECHT 92G reports $0.026 \pm 0.014 \pm 0.006$ for $B(D_s^+ \rightarrow \phi\pi^+) = 0.027$. We rescale to our best value $B(D_s^+ \rightarrow \phi\pi^+) = (4.38 \pm 0.35) \times 10^{-2}$. Our first error is their experiment's error and our second error is the systematic error from using our best value. Assumes PDG 1990 D^+ and $D^*(2010)^+$ branching ratios, e.g., $B(D^0 \rightarrow K^-\pi^+) = 3.71 \pm 0.25\%$, $B(D^+ \rightarrow K^-\pi^+\pi^+) = 7.1 \pm 1.0\%$, and $B(D^*(2010)^+ \rightarrow D^0\pi^+) = 55 \pm 4\%$.
- 6 GIBAUT 96 reports $0.0203 \pm 0.0050 \pm 0.0036$ for $B(D_s^+ \rightarrow \phi\pi^+) = 0.035$. We rescale to our best value $B(D_s^+ \rightarrow \phi\pi^+) = (4.38 \pm 0.35) \times 10^{-2}$. Our first error is their experiment's error and our second error is the systematic error from using our best value.

$\Gamma(D_{s0}(2317)^-K^+ \times B(D_{s0}(2317)^- \rightarrow D_s^-\pi^0))/\Gamma_{\text{total}}$		Γ_{76}/Γ	
VALUE (units 10^{-5})	DOCUMENT ID	TECN	COMMENT
4.4 ± 1.3 ± 0.4			
	1 DRUTSKOY	05 BELL	$e^+e^- \rightarrow \Upsilon(4S)$

- 1 DRUTSKOY 05 reports $(5.3^{+1.5}_{-1.3} \pm 1.6) \times 10^{-5}$ for $B(D_s^+ \rightarrow \phi\pi^+) = 0.036 \pm 0.009$. We rescale to our best value $B(D_s^+ \rightarrow \phi\pi^+) = (4.38 \pm 0.35) \times 10^{-2}$. Our first error is their experiment's error and our second error is the systematic error from using our best value.

Meson Particle Listings

 B^0

$\Gamma(D_{S0}(2317)^- \pi^+ \times B(D_{S0}(2317)^- \rightarrow D_s^- \pi^0))/\Gamma_{total}$					Γ_{77}/Γ
VALUE (units 10^{-5})	CL%	DOCUMENT ID	TECN	COMMENT	
<2.5	90	¹ DRUTSKOY 05	BELL	$e^+ e^- \rightarrow \Upsilon(4S)$	

¹ Assumes equal production of B^+ and B^0 at the $\Upsilon(4S)$.

$\Gamma(D_{sJ}(2457)^- K^+ \times B(D_{sJ}(2457)^- \rightarrow D_s^- \pi^0))/\Gamma_{total}$					Γ_{78}/Γ
VALUE (units 10^{-5})	CL%	DOCUMENT ID	TECN	COMMENT	
<0.94	90	¹ DRUTSKOY 05	BELL	$e^+ e^- \rightarrow \Upsilon(4S)$	

¹ Assumes equal production of B^+ and B^0 at the $\Upsilon(4S)$.

$\Gamma(D_{sJ}(2457)^- \pi^+ \times B(D_{sJ}(2457)^- \rightarrow D_s^- \pi^0))/\Gamma_{total}$					Γ_{79}/Γ
VALUE (units 10^{-5})	CL%	DOCUMENT ID	TECN	COMMENT	
<0.40	90	¹ DRUTSKOY 05	BELL	$e^+ e^- \rightarrow \Upsilon(4S)$	

¹ Assumes equal production of B^+ and B^0 at the $\Upsilon(4S)$.

$\Gamma(D_s^- D_s^+)/\Gamma_{total}$					Γ_{80}/Γ
VALUE	CL%	DOCUMENT ID	TECN	COMMENT	
< 3.6×10^{-5}	90	¹ ZUPANC 07	BELL	$e^+ e^- \rightarrow \Upsilon(4S)$	

• • • We do not use the following data for averages, fits, limits, etc. • • •
 < 10×10^{-5} 90 ¹ AUBERT, BE 05F BABR $e^+ e^- \rightarrow \Upsilon(4S)$

¹ Assumes equal production of B^+ and B^0 at the $\Upsilon(4S)$.

$\Gamma(D_s^{*+} D_s^+)/\Gamma_{total}$					Γ_{81}/Γ
VALUE	CL%	DOCUMENT ID	TECN	COMMENT	
< 1.3×10^{-4}	90	¹ AUBERT, BE 05F	BABR	$e^+ e^- \rightarrow \Upsilon(4S)$	

¹ Assumes equal production of B^+ and B^0 at the $\Upsilon(4S)$.

$\Gamma(D_s^{*+} D_s^{*+})/\Gamma_{total}$					Γ_{82}/Γ
VALUE	CL%	DOCUMENT ID	TECN	COMMENT	
< 2.4×10^{-4}	90	¹ AUBERT, BE 05F	BABR	$e^+ e^- \rightarrow \Upsilon(4S)$	

¹ Assumes equal production of B^+ and B^0 at the $\Upsilon(4S)$.

$\Gamma(D_{S0}(2317)^+ D^- \times B(D_{S0}(2317)^+ \rightarrow D_s^+ \pi^0))/\Gamma_{total}$					Γ_{83}/Γ
VALUE (units 10^{-3})	CL%	DOCUMENT ID	TECN	COMMENT	
$0.99 \pm_{-0.34}^{+0.42}$ OUR AVERAGE		Error includes scale factor of 1.5.			

$1.5 \pm_{-0.4}^{+0.5} \pm 0.1$		^{1,2} AUBERT, B 04S	BABR	$e^+ e^- \rightarrow \Upsilon(4S)$	
$0.71 \pm_{-0.25}^{+0.30} \pm 0.06$		^{1,3} KROKOVNY 03B	BELL	$e^+ e^- \rightarrow \Upsilon(4S)$	

¹ Assumes equal production of B^+ and B^0 at the $\Upsilon(4S)$.
² AUBERT, B 04S reports $(1.8 \pm 0.4 \pm_{-0.5}^{+0.7}) \times 10^{-3}$ for $B(D_s^+ \rightarrow \phi \pi^+) = 0.036 \pm 0.009$. We rescale to our best value $B(D_s^+ \rightarrow \phi \pi^+) = (4.38 \pm 0.35) \times 10^{-2}$. Our first error is their experiment's error and our second error is the systematic error from using our best value.
³ KROKOVNY 03B reports $(0.86 \pm_{-0.26}^{+0.33} \pm 0.26) \times 10^{-3}$ for $B(D_s^+ \rightarrow \phi \pi^+) = 0.036 \pm 0.009$. We rescale to our best value $B(D_s^+ \rightarrow \phi \pi^+) = (4.38 \pm 0.35) \times 10^{-2}$. Our first error is their experiment's error and our second error is the systematic error from using our best value.

$\Gamma(D_{S0}(2317)^+ D^- \times B(D_{S0}(2317)^+ \rightarrow D_s^{*+} \gamma))/\Gamma_{total}$					Γ_{84}/Γ
VALUE (units 10^{-3})	CL%	DOCUMENT ID	TECN	COMMENT	
<0.95	90	¹ KROKOVNY 03B	BELL	$e^+ e^- \rightarrow \Upsilon(4S)$	

¹ Assumes equal production of B^+ and B^0 at the $\Upsilon(4S)$.

$\Gamma(D_{S0}(2317)^+ D^*(2010)^- \times B(D_{S0}(2317)^+ \rightarrow D_s^+ \pi^0))/\Gamma_{total}$					Γ_{85}/Γ
VALUE (units 10^{-3})	CL%	DOCUMENT ID	TECN	COMMENT	
$1.5 \pm_{-0.4}^{+0.4} \pm_{-0.4}^{+0.5}$		¹ AUBERT, B 04S	BABR	$e^+ e^- \rightarrow \Upsilon(4S)$	

¹ Assumes equal production of B^+ and B^0 at the $\Upsilon(4S)$.

$\Gamma(D_{sJ}(2457)^+ D^-)/\Gamma_{total}$					Γ_{86}/Γ
VALUE (units 10^{-3})	CL%	DOCUMENT ID	TECN	COMMENT	
3.5 ± 1.1 OUR AVERAGE					

$2.6 \pm 1.5 \pm 0.7$		¹ AUBERT 06N	BABR	$e^+ e^- \rightarrow \Upsilon(4S)$	
$4.8 \pm_{-1.6}^{+2.2} \pm 1.1$		^{2,3} AUBERT, B 04S	BABR	$e^+ e^- \rightarrow \Upsilon(4S)$	
$3.9 \pm_{-1.3}^{+1.5} \pm 0.9$		^{2,4} KROKOVNY 03B	BELL	$e^+ e^- \rightarrow \Upsilon(4S)$	

¹ Uses a missing-mass method in the events that one of the B mesons is fully reconstructed.
² Assumes equal production of B^+ and B^0 at the $\Upsilon(4S)$.
³ AUBERT, B 04S reports $[B(B^0 \rightarrow D_{sJ}(2457)^+ D^-)] \times [B(D_{S1}(2460)^+ \rightarrow D_s^{*+} \pi^0)] = (2.3 \pm_{-0.7}^{+1.0} \pm 0.3) \times 10^{-3}$. We divide by our best value $B(D_{S1}(2460)^+ \rightarrow D_s^{*+} \pi^0) = (48 \pm 11) \times 10^{-2}$. Our first error is their experiment's error and our second error is the systematic error from using our best value.
⁴ KROKOVNY 03B reports $[B(B^0 \rightarrow D_{sJ}(2457)^+ D^-)] \times [B(D_{S1}(2460)^+ \rightarrow D_s^{*+} \pi^0)] = (1.9 \pm_{-0.6}^{+0.7} \pm 0.2) \times 10^{-3}$. We divide by our best value $B(D_{S1}(2460)^+ \rightarrow D_s^{*+} \pi^0) = (48 \pm 11) \times 10^{-2}$. Our first error is their experiment's error and our second error is the systematic error from using our best value.

$\Gamma(D_{sJ}(2457)^+ D^- \times B(D_{sJ}(2457)^+ \rightarrow D_s^+ \gamma))/\Gamma_{total}$					Γ_{87}/Γ
VALUE (units 10^{-3})	CL%	DOCUMENT ID	TECN	COMMENT	
$0.67 \pm_{-0.14}^{+0.17}$ OUR AVERAGE					

$0.66 \pm_{-0.16}^{+0.25} \pm 0.05$		^{1,2} AUBERT, B 04S	BABR	$e^+ e^- \rightarrow \Upsilon(4S)$	
$0.67 \pm_{-0.20}^{+0.22} \pm 0.05$		^{1,3} KROKOVNY 03B	BELL	$e^+ e^- \rightarrow \Upsilon(4S)$	

¹ Assumes equal production of B^+ and B^0 at the $\Upsilon(4S)$.
² AUBERT, B 04S reports $(0.8 \pm 0.2 \pm_{-0.2}^{+0.3}) \times 10^{-3}$ for $B(D_s^+ \rightarrow \phi \pi^+) = 0.036 \pm 0.009$. We rescale to our best value $B(D_s^+ \rightarrow \phi \pi^+) = (4.38 \pm 0.35) \times 10^{-2}$. Our first error is their experiment's error and our second error is the systematic error from using our best value.
³ KROKOVNY 03B reports $(0.82 \pm_{-0.19}^{+0.22} \pm 0.25) \times 10^{-3}$ for $B(D_s^+ \rightarrow \phi \pi^+) = 0.036 \pm 0.009$. We rescale to our best value $B(D_s^+ \rightarrow \phi \pi^+) = (4.38 \pm 0.35) \times 10^{-2}$. Our first error is their experiment's error and our second error is the systematic error from using our best value.

$\Gamma(D_{sJ}(2457)^+ D^- \times B(D_{sJ}(2457)^+ \rightarrow D_s^{*+} \gamma))/\Gamma_{total}$					Γ_{88}/Γ
VALUE (units 10^{-3})	CL%	DOCUMENT ID	TECN	COMMENT	
<0.60	90	¹ KROKOVNY 03B	BELL	$e^+ e^- \rightarrow \Upsilon(4S)$	

¹ Assumes equal production of B^+ and B^0 at the $\Upsilon(4S)$.

$\Gamma(D_{sJ}(2457)^+ D^- \times B(D_{sJ}(2457)^+ \rightarrow D_s^+ \pi^+ \pi^-))/\Gamma_{total}$					Γ_{89}/Γ
VALUE (units 10^{-3})	CL%	DOCUMENT ID	TECN	COMMENT	
<0.20	90	¹ KROKOVNY 03B	BELL	$e^+ e^- \rightarrow \Upsilon(4S)$	

¹ Assumes equal production of B^+ and B^0 at the $\Upsilon(4S)$.

$\Gamma(D_{sJ}(2457)^+ D^- \times B(D_{sJ}(2457)^+ \rightarrow D_s^+ \pi^0))/\Gamma_{total}$					Γ_{90}/Γ
VALUE (units 10^{-3})	CL%	DOCUMENT ID	TECN	COMMENT	
<0.36	90	¹ KROKOVNY 03B	BELL	$e^+ e^- \rightarrow \Upsilon(4S)$	

¹ Assumes equal production of B^+ and B^0 at the $\Upsilon(4S)$.

$\Gamma(D^*(2010)^- D_{sJ}(2457)^+)/\Gamma_{total}$					Γ_{91}/Γ
VALUE (units 10^{-3})	CL%	DOCUMENT ID	TECN	COMMENT	
9.3 ± 2.2 OUR AVERAGE					

$8.8 \pm 2.0 \pm 1.4$		¹ AUBERT 06N	BABR	$e^+ e^- \rightarrow \Upsilon(4S)$	
$11 \pm_{-4}^{+5} \pm 3$		^{2,3} AUBERT, B 04S	BABR	$e^+ e^- \rightarrow \Upsilon(4S)$	

¹ Uses a missing-mass method in the events that one of the B mesons is fully reconstructed.
² AUBERT, B 04S reports $[B(B^0 \rightarrow D^*(2010)^- D_{sJ}(2457)^+)] \times [B(D_{S1}(2460)^+ \rightarrow D_s^{*+} \pi^0)] = (5.5 \pm 1.2 \pm_{-1.6}^{+2.2}) \times 10^{-3}$. We divide by our best value $B(D_{S1}(2460)^+ \rightarrow D_s^{*+} \pi^0) = (48 \pm 11) \times 10^{-2}$. Our first error is their experiment's error and our second error is the systematic error from using our best value.
³ Assumes equal production of B^+ and B^0 at the $\Upsilon(4S)$.

$\Gamma(D_{sJ}(2457)^+ D^*(2010)^- \times B(D_{sJ}(2457)^+ \rightarrow D_s^+ \gamma))/\Gamma_{total}$					Γ_{92}/Γ
VALUE (units 10^{-3})	CL%	DOCUMENT ID	TECN	COMMENT	
$2.3 \pm_{-0.6}^{+0.3} \pm_{-0.6}^{+0.9}$		¹ AUBERT, B 04S	BABR	$e^+ e^- \rightarrow \Upsilon(4S)$	

¹ Assumes equal production of B^+ and B^0 at the $\Upsilon(4S)$.

$\Gamma(D^- D_{S1}(2536)^+ \times B(D_{S1}(2536)^+ \rightarrow D^{*0} K^+))/\Gamma_{total}$					Γ_{93}/Γ
VALUE (units 10^{-4})	CL%	DOCUMENT ID	TECN	COMMENT	
$1.71 \pm_{-0.32}^{+0.48} \pm 0.32$		¹ AUBERT 08B	BABR	$e^+ e^- \rightarrow \Upsilon(4S)$	

• • • We do not use the following data for averages, fits, limits, etc. • • •
 <5 90 AUBERT 03X BABR Repl. by AUBERT 08B

¹ Assumes equal production of B^+ and B^0 at the $\Upsilon(4S)$.

$\Gamma(D^*(2010)^- D_{S1}(2536)^+ \times B(D_{S1}(2536)^+ \rightarrow D^{*0} K^+))/\Gamma_{total}$					Γ_{94}/Γ
VALUE (units 10^{-4})	CL%	DOCUMENT ID	TECN	COMMENT	
$3.32 \pm_{-0.66}^{+0.88} \pm 0.66$		¹ AUBERT 08B	BABR	$e^+ e^- \rightarrow \Upsilon(4S)$	

• • • We do not use the following data for averages, fits, limits, etc. • • •
 <7 90 AUBERT 03X BABR Repl. by AUBERT 08B

¹ Assumes equal production of B^+ and B^0 at the $\Upsilon(4S)$.

$\Gamma(D^- D_{S1}(2536)^+ \times B(D_{S1}(2536)^+ \rightarrow D^{*+} K^0))/\Gamma_{total}$					Γ_{95}/Γ
VALUE (units 10^{-4})	CL%	DOCUMENT ID	TECN	COMMENT	
$2.61 \pm_{-0.31}^{+1.03} \pm 0.31$		¹ AUBERT 08B	BABR	$e^+ e^- \rightarrow \Upsilon(4S)$	

¹ Assumes equal production of B^+ and B^0 at the $\Upsilon(4S)$.

$\Gamma(D^{*-} D_{S1}(2536)^+ \times B(D_{S1}(2536)^+ \rightarrow D^{*+} K^0))/\Gamma_{total}$					Γ_{96}/Γ
VALUE (units 10^{-4})	CL%	DOCUMENT ID	TECN	COMMENT	
$5.00 \pm_{-0.67}^{+1.51} \pm 0.67$		¹ AUBERT 08B	BABR	$e^+ e^- \rightarrow \Upsilon(4S)$	

¹ Assumes equal production of B^+ and B^0 at the $\Upsilon(4S)$.

$\Gamma(D^- D_{sJ}(2573)^+ \times B(D_{sJ}(2573)^+ \rightarrow D^0 K^+))/\Gamma_{total}$					Γ_{97}/Γ
VALUE (units 10^{-4})	CL%	DOCUMENT ID	TECN	COMMENT	
<1	90	AUBERT 03X	BABR	$e^+ e^- \rightarrow \Upsilon(4S)$	

See key on page 373

Meson Particle Listings

 B^0

$\Gamma(D^{*+}(2010)^- D_{sJ}(2573)^+ + B(D_{sJ}(2573)^+ \rightarrow D^0 K^+))/\Gamma_{\text{total}}$					Γ_{98}/Γ
VALUE (units 10^{-4})	CL%	DOCUMENT ID	TECN	COMMENT	
<2	90	AUBERT	03x	BABR $e^+ e^- \rightarrow \Upsilon(4S)$	

$\Gamma(D_s^+ \pi^-)/\Gamma_{\text{total}}$					Γ_{99}/Γ
VALUE (units 10^{-6})	CL%	DOCUMENT ID	TECN	COMMENT	
15.3±3.5 OUR AVERAGE					
14 ± 4 ± 1		1 AUBERT	07k	BABR $e^+ e^- \rightarrow \Upsilon(4S)$	
20 ± $\frac{9}{7}$ ± 2		2 KROKOVNY	02	BELL $e^+ e^- \rightarrow \Upsilon(4S)$	

• • • We do not use the following data for averages, fits, limits, etc. • • •				
VALUE (units 10^{-6})	CL%	DOCUMENT ID	TECN	COMMENT
26 ± 9 ± 2		3 AUBERT	03D	BABR Repl. by AUBERT 07k
< 230	90	4 ALEXANDER	93B	CLE2 $e^+ e^- \rightarrow \Upsilon(4S)$
< 1300	90	5 BORTOLETTO	090	CLEO $e^+ e^- \rightarrow \Upsilon(4S)$

¹ AUBERT 07k reports $[B(B^0 \rightarrow D_s^+ \pi^-)] \times [B(D_s^+ \rightarrow \phi \pi^+)] = (0.63 \pm 0.15 \pm 0.05) \times 10^{-6}$. We divide by our best value $B(D_s^+ \rightarrow \phi \pi^+) = (4.38 \pm 0.35) \times 10^{-2}$. Our first error is their experiment's error and our second error is the systematic error from using our best value.

² KROKOVNY 02 reports $[B(B^0 \rightarrow D_s^+ \pi^-)] \times [B(D_s^+ \rightarrow \phi \pi^+)] = (0.86_{-0.30}^{+0.37} \pm 0.11) \times 10^{-6}$. We divide by our best value $B(D_s^+ \rightarrow \phi \pi^+) = (4.38 \pm 0.35) \times 10^{-2}$. Our first error is their experiment's error and our second error is the systematic error from using our best value.

³ AUBERT 03D reports $[B(B^0 \rightarrow D_s^+ \pi^-)] \times [B(D_s^+ \rightarrow \phi \pi^+)] = (1.13 \pm 0.33 \pm 0.21) \times 10^{-6}$. We divide by our best value $B(D_s^+ \rightarrow \phi \pi^+) = (4.38 \pm 0.35) \times 10^{-2}$. Our first error is their experiment's error and our second error is the systematic error from using our best value.

⁴ ALEXANDER 93B reports < 270×10^{-6} for $B(D_s^+ \rightarrow \phi \pi^+) = 0.037$. We rescale to our best value $B(D_s^+ \rightarrow \phi \pi^+) = 0.0438$.

⁵ BORTOLETTO 90 assume $B(D_s \rightarrow \phi \pi^+) = 2\%$.

$[\Gamma(D_s^+ \pi^-) + \Gamma(D_s^- K^+)]/\Gamma_{\text{total}}$					$(\Gamma_{99} + \Gamma_{109})/\Gamma$
VALUE	CL%	DOCUMENT ID	TECN	COMMENT	
<0.0010	90	1 ALBRECHT	93E	ARG $e^+ e^- \rightarrow \Upsilon(4S)$	

¹ ALBRECHT 93E reports < 1.7×10^{-3} for $B(D_s^+ \rightarrow \phi \pi^+) = 0.027$. We rescale to our best value $B(D_s^+ \rightarrow \phi \pi^+) = 0.0438$.

$\Gamma(D_s^{*+} \pi^-)/\Gamma_{\text{total}}$					Γ_{100}/Γ
VALUE (units 10^{-5})	CL%	DOCUMENT ID	TECN	COMMENT	
3.0±0.7±0.2		1 AUBERT	07k	BABR $e^+ e^- \rightarrow \Upsilon(4S)$	

• • • We do not use the following data for averages, fits, limits, etc. • • •				
VALUE	CL%	DOCUMENT ID	TECN	COMMENT
< 4.1	90	AUBERT	03D	BABR Repl. by AUBERT 07k
< 40	90	2 ALEXANDER	93B	CLE2 $e^+ e^- \rightarrow \Upsilon(4S)$

¹ AUBERT 07k reports $[B(B^0 \rightarrow D_s^{*+} \pi^-)] \times [B(D_s^+ \rightarrow \phi \pi^+)] = (1.32 \pm 0.27 \pm 0.15) \times 10^{-6}$. We divide by our best value $B(D_s^+ \rightarrow \phi \pi^+) = (4.38 \pm 0.35) \times 10^{-2}$. Our first error is their experiment's error and our second error is the systematic error from using our best value.

² ALEXANDER 93B reports < 44×10^{-5} for $B(D_s^+ \rightarrow \phi \pi^+) = 0.037$. We rescale to our best value $B(D_s^+ \rightarrow \phi \pi^+) = 0.0438$.

$[\Gamma(D_s^{*+} \pi^-) + \Gamma(D_s^{*-} K^+)]/\Gamma_{\text{total}}$					$(\Gamma_{100} + \Gamma_{110})/\Gamma$
VALUE	CL%	DOCUMENT ID	TECN	COMMENT	
<0.0007	90	1 ALBRECHT	93E	ARG $e^+ e^- \rightarrow \Upsilon(4S)$	

¹ ALBRECHT 93E reports < 1.2×10^{-3} for $B(D_s^+ \rightarrow \phi \pi^+) = 0.027$. We rescale to our best value $B(D_s^+ \rightarrow \phi \pi^+) = 0.0438$.

$\Gamma(D_s^+ \rho^-)/\Gamma_{\text{total}}$					Γ_{101}/Γ
VALUE	CL%	DOCUMENT ID	TECN	COMMENT	
<0.0006	90	1 ALEXANDER	93B	CLE2 $e^+ e^- \rightarrow \Upsilon(4S)$	

• • • We do not use the following data for averages, fits, limits, etc. • • •				
VALUE	CL%	DOCUMENT ID	TECN	COMMENT
< 0.0014	90	2 ALBRECHT	93E	ARG $e^+ e^- \rightarrow \Upsilon(4S)$

¹ ALEXANDER 93B reports < 6.6×10^{-4} for $B(D_s^+ \rightarrow \phi \pi^+) = 0.037$. We rescale to our best value $B(D_s^+ \rightarrow \phi \pi^+) = 0.0438$.

² ALBRECHT 93E reports < 2.2×10^{-3} for $B(D_s^+ \rightarrow \phi \pi^+) = 0.027$. We rescale to our best value $B(D_s^+ \rightarrow \phi \pi^+) = 0.0438$.

$\Gamma(D_s^{*+} \rho^-)/\Gamma_{\text{total}}$					Γ_{102}/Γ
VALUE	CL%	DOCUMENT ID	TECN	COMMENT	
<0.0006	90	1 ALEXANDER	93B	CLE2 $e^+ e^- \rightarrow \Upsilon(4S)$	

• • • We do not use the following data for averages, fits, limits, etc. • • •				
VALUE	CL%	DOCUMENT ID	TECN	COMMENT
< 0.0015	90	2 ALBRECHT	93E	ARG $e^+ e^- \rightarrow \Upsilon(4S)$

¹ ALEXANDER 93B reports < 7.4×10^{-4} for $B(D_s^+ \rightarrow \phi \pi^+) = 0.037$. We rescale to our best value $B(D_s^+ \rightarrow \phi \pi^+) = 0.0438$.

² ALBRECHT 93E reports < 2.5×10^{-3} for $B(D_s^+ \rightarrow \phi \pi^+) = 0.027$. We rescale to our best value $B(D_s^+ \rightarrow \phi \pi^+) = 0.0438$.

$\Gamma(D_s^+ a_0^-)/\Gamma_{\text{total}}$					Γ_{103}/Γ
VALUE (units 10^{-5})	CL%	DOCUMENT ID	TECN	COMMENT	
<1.9	90	1 AUBERT	06x	BABR $e^+ e^- \rightarrow \Upsilon(4S)$	

¹ Assumes equal production of B^+ and B^0 at the $\Upsilon(4S)$.

$\Gamma(D_s^{*+} a_0^-)/\Gamma_{\text{total}}$					Γ_{104}/Γ
VALUE (units 10^{-5})	CL%	DOCUMENT ID	TECN	COMMENT	
<3.6	90	1 AUBERT	06x	BABR $e^+ e^- \rightarrow \Upsilon(4S)$	

¹ Assumes equal production of B^+ and B^0 at the $\Upsilon(4S)$.

$\Gamma(D_s^+ a_1(1260)^-)/\Gamma_{\text{total}}$					Γ_{105}/Γ
VALUE	CL%	DOCUMENT ID	TECN	COMMENT	
<0.0022	90	1 ALBRECHT	93E	ARG $e^+ e^- \rightarrow \Upsilon(4S)$	

¹ ALBRECHT 93E reports < 3.5×10^{-3} for $B(D_s^+ \rightarrow \phi \pi^+) = 0.027$. We rescale to our best value $B(D_s^+ \rightarrow \phi \pi^+) = 0.0438$.

$\Gamma(D_s^{*+} a_1(1260)^-)/\Gamma_{\text{total}}$					Γ_{106}/Γ
VALUE	CL%	DOCUMENT ID	TECN	COMMENT	
<0.0018	90	1 ALBRECHT	93E	ARG $e^+ e^- \rightarrow \Upsilon(4S)$	

¹ ALBRECHT 93E reports < 2.9×10^{-3} for $B(D_s^+ \rightarrow \phi \pi^+) = 0.027$. We rescale to our best value $B(D_s^+ \rightarrow \phi \pi^+) = 0.0438$.

$\Gamma(D_s^+ a_2^-)/\Gamma_{\text{total}}$					Γ_{107}/Γ
VALUE (units 10^{-5})	CL%	DOCUMENT ID	TECN	COMMENT	
<19	90	1 AUBERT	06x	BABR $e^+ e^- \rightarrow \Upsilon(4S)$	

¹ Assumes equal production of B^+ and B^0 at the $\Upsilon(4S)$.

$\Gamma(D_s^{*+} a_2^-)/\Gamma_{\text{total}}$					Γ_{108}/Γ
VALUE (units 10^{-5})	CL%	DOCUMENT ID	TECN	COMMENT	
<20	90	1 AUBERT	06x	BABR $e^+ e^- \rightarrow \Upsilon(4S)$	

¹ Assumes equal production of B^+ and B^0 at the $\Upsilon(4S)$.

$\Gamma(D_s^- K^+)/\Gamma_{\text{total}}$					Γ_{109}/Γ
VALUE (units 10^{-6})	CL%	DOCUMENT ID	TECN	COMMENT	
29±5 OUR AVERAGE					
28 ± 5 ± 2		1 AUBERT	07k	BABR $e^+ e^- \rightarrow \Upsilon(4S)$	
37 ± $\frac{11}{10}$ ± 3		2 KROKOVNY	02	BELL $e^+ e^- \rightarrow \Upsilon(4S)$	

• • • We do not use the following data for averages, fits, limits, etc. • • •				
VALUE	CL%	DOCUMENT ID	TECN	COMMENT
26 ± 10 ± 2		3 AUBERT	03D	BABR Repl. by AUBERT 07k
< 190	90	4 ALEXANDER	93B	CLE2 $e^+ e^- \rightarrow \Upsilon(4S)$
< 1300	90	5 BORTOLETTO	090	CLEO $e^+ e^- \rightarrow \Upsilon(4S)$

¹ AUBERT 07k reports $[B(B^0 \rightarrow D_s^- K^+)] \times [B(D_s^+ \rightarrow \phi \pi^+)] = (1.21 \pm 0.17 \pm 0.11) \times 10^{-6}$. We divide by our best value $B(D_s^+ \rightarrow \phi \pi^+) = (4.38 \pm 0.35) \times 10^{-2}$. Our first error is their experiment's error and our second error is the systematic error from using our best value.

² KROKOVNY 02 reports $[B(B^0 \rightarrow D_s^- K^+)] \times [B(D_s^+ \rightarrow \phi \pi^+)] = (1.61_{-0.38}^{+0.45} \pm 0.21) \times 10^{-6}$. We divide by our best value $B(D_s^+ \rightarrow \phi \pi^+) = (4.38 \pm 0.35) \times 10^{-2}$. Our first error is their experiment's error and our second error is the systematic error from using our best value.

³ AUBERT 03D reports $[B(B^0 \rightarrow D_s^- K^+)] \times [B(D_s^+ \rightarrow \phi \pi^+)] = (1.16 \pm 0.36 \pm 0.24) \times 10^{-6}$. We divide by our best value $B(D_s^+ \rightarrow \phi \pi^+) = (4.38 \pm 0.35) \times 10^{-2}$. Our first error is their experiment's error and our second error is the systematic error from using our best value.

⁴ ALEXANDER 93B reports < 230×10^{-6} for $B(D_s^+ \rightarrow \phi \pi^+) = 0.037$. We rescale to our best value $B(D_s^+ \rightarrow \phi \pi^+) = 0.0438$.

⁵ BORTOLETTO 90 assume $B(D_s \rightarrow \phi \pi^+) = 2\%$.

$\Gamma(D_s^{*-} K^+)/\Gamma_{\text{total}}$					Γ_{110}/Γ
VALUE (units 10^{-5})	CL%	DOCUMENT ID	TECN	COMMENT	
2.2±0.6±0.2		1 AUBERT	07k	BABR $e^+ e^- \rightarrow \Upsilon(4S)$	

• • • We do not use the following data for averages, fits, limits, etc. • • •				
VALUE	CL%	DOCUMENT ID	TECN	COMMENT
< 2.5	90	AUBERT	03D	BABR Repl. by AUBERT 07k
< 14	90	2 ALEXANDER	93B	CLE2 $e^+ e^- \rightarrow \Upsilon(4S)$

¹ AUBERT 07k reports $[B(B^0 \rightarrow D_s^{*-} K^+)] \times [B(D_s^+ \rightarrow \phi \pi^+)] = (0.97 \pm 0.24 \pm 0.12) \times 10^{-6}$. We divide by our best value $B(D_s^+ \rightarrow \phi \pi^+) = (4.38 \pm 0.35) \times 10^{-2}$. Our first error is their experiment's error and our second error is the systematic error from using our best value.

² ALEXANDER 93B reports < 17×10^{-5} for $B(D_s^+ \rightarrow \phi \pi^+) = 0.037$. We rescale to our best value $B(D_s^+ \rightarrow \phi \pi^+) = 0.0438$.

Meson Particle Listings

 B^0 $\Gamma(D_s^- K^*(892)^+)/\Gamma_{\text{total}}$ Γ_{111}/Γ

VALUE	CL%	DOCUMENT ID	TECN	COMMENT
<0.0008	90	1 ALEXANDER 93B	CLE2	$e^+e^- \rightarrow \Upsilon(4S)$

• • • We do not use the following data for averages, fits, limits, etc. • • •

<0.0028	90	2 ALBRECHT 93E	ARG	$e^+e^- \rightarrow \Upsilon(4S)$
---------	----	----------------	-----	-----------------------------------

¹ ALEXANDER 93B reports $< 9.7 \times 10^{-4}$ for $B(D_s^+ \rightarrow \phi\pi^+) = 0.037$. We rescale to our best value $B(D_s^+ \rightarrow \phi\pi^+) = 0.0438$.

² ALBRECHT 93E reports $< 4.6 \times 10^{-3}$ for $B(D_s^+ \rightarrow \phi\pi^+) = 0.027$. We rescale to our best value $B(D_s^+ \rightarrow \phi\pi^+) = 0.0438$.

 $\Gamma(D_s^{*-} K^*(892)^+)/\Gamma_{\text{total}}$ Γ_{112}/Γ

VALUE	CL%	DOCUMENT ID	TECN	COMMENT
<0.0009	90	1 ALEXANDER 93B	CLE2	$e^+e^- \rightarrow \Upsilon(4S)$

• • • We do not use the following data for averages, fits, limits, etc. • • •

<0.004	90	2 ALBRECHT 93E	ARG	$e^+e^- \rightarrow \Upsilon(4S)$
--------	----	----------------	-----	-----------------------------------

¹ ALEXANDER 93B reports $< 11.0 \times 10^{-4}$ for $B(D_s^+ \rightarrow \phi\pi^+) = 0.037$. We rescale to our best value $B(D_s^+ \rightarrow \phi\pi^+) = 0.0438$.

² ALBRECHT 93E reports $< 5.8 \times 10^{-3}$ for $B(D_s^+ \rightarrow \phi\pi^+) = 0.027$. We rescale to our best value $B(D_s^+ \rightarrow \phi\pi^+) = 0.0438$.

 $\Gamma(D_s^- \pi^+ K^0)/\Gamma_{\text{total}}$ Γ_{113}/Γ

VALUE	CL%	DOCUMENT ID	TECN	COMMENT
<0.0005	90	1 ALBRECHT 93E	ARG	$e^+e^- \rightarrow \Upsilon(4S)$

¹ ALBRECHT 93E reports $< 7.3 \times 10^{-3}$ for $B(D_s^+ \rightarrow \phi\pi^+) = 0.027$. We rescale to our best value $B(D_s^+ \rightarrow \phi\pi^+) = 0.0438$.

 $\Gamma(D_s^- \pi^+ K^0)/\Gamma_{\text{total}}$ Γ_{114}/Γ

VALUE	CL%	DOCUMENT ID	TECN	COMMENT
<0.0026	90	1 ALBRECHT 93E	ARG	$e^+e^- \rightarrow \Upsilon(4S)$

¹ ALBRECHT 93E reports $< 4.2 \times 10^{-3}$ for $B(D_s^+ \rightarrow \phi\pi^+) = 0.027$. We rescale to our best value $B(D_s^+ \rightarrow \phi\pi^+) = 0.0438$.

 $\Gamma(D_s^- \pi^+ K^*(892)^0)/\Gamma_{\text{total}}$ Γ_{115}/Γ

VALUE	CL%	DOCUMENT ID	TECN	COMMENT
<0.0031	90	1 ALBRECHT 93E	ARG	$e^+e^- \rightarrow \Upsilon(4S)$

¹ ALBRECHT 93E reports $< 5.0 \times 10^{-3}$ for $B(D_s^+ \rightarrow \phi\pi^+) = 0.027$. We rescale to our best value $B(D_s^+ \rightarrow \phi\pi^+) = 0.0438$.

 $\Gamma(D_s^{*-} \pi^+ K^*(892)^0)/\Gamma_{\text{total}}$ Γ_{116}/Γ

VALUE	CL%	DOCUMENT ID	TECN	COMMENT
<0.0017	90	1 ALBRECHT 93E	ARG	$e^+e^- \rightarrow \Upsilon(4S)$

¹ ALBRECHT 93E reports $< 2.7 \times 10^{-3}$ for $B(D_s^+ \rightarrow \phi\pi^+) = 0.027$. We rescale to our best value $B(D_s^+ \rightarrow \phi\pi^+) = 0.0438$.

 $\Gamma(D^0 K^0)/\Gamma_{\text{total}}$ Γ_{117}/Γ

VALUE (units 10^{-5})	DOCUMENT ID	TECN	COMMENT
5.2 ± 0.7 OUR AVERAGE			

5.3 ± 0.7 ± 0.3	1 AUBERT,B 06L	BABR	$e^+e^- \rightarrow \Upsilon(4S)$
-----------------	----------------	------	-----------------------------------

5.0 +1.3 -1.2 ± 0.6	1 KROKOVNY 03	BELL	$e^+e^- \rightarrow \Upsilon(4S)$
---------------------	---------------	------	-----------------------------------

¹ Assumes equal production of B^+ and B^0 at the $\Upsilon(4S)$.

 $\Gamma(D^0 K^+ \pi^-)/\Gamma_{\text{total}}$ Γ_{118}/Γ

VALUE (units 10^{-6})	DOCUMENT ID	TECN	COMMENT
88 ± 15 ± 9	1 AUBERT 06A	BABR	$e^+e^- \rightarrow \Upsilon(4S)$

¹ Assumes equal production of B^+ and B^0 at the $\Upsilon(4S)$.

 $\Gamma(D^0 K^*(892)^0)/\Gamma_{\text{total}}$ Γ_{119}/Γ

VALUE (units 10^{-5})	DOCUMENT ID	TECN	COMMENT
4.2 ± 0.6 OUR AVERAGE			

4.0 ± 0.7 ± 0.3	1 AUBERT,B 06L	BABR	$e^+e^- \rightarrow \Upsilon(4S)$
-----------------	----------------	------	-----------------------------------

4.8 +1.1 -1.0 ± 0.5	1 KROKOVNY 03	BELL	$e^+e^- \rightarrow \Upsilon(4S)$
---------------------	---------------	------	-----------------------------------

• • • We do not use the following data for averages, fits, limits, etc. • • •

5.7 ± 0.9 ± 0.6	1 AUBERT 06A	BABR	Repl. by AUBERT,B 06L
-----------------	--------------	------	-----------------------

¹ Assumes equal production of B^+ and B^0 at the $\Upsilon(4S)$.

 $\Gamma(D_2^-(2460) K^- \times B(D_2^+(2460) \bar{D}^0 \pi^-))/\Gamma_{\text{total}}$ Γ_{120}/Γ

VALUE (units 10^{-6})	DOCUMENT ID	TECN	COMMENT
18.3 ± 4.0 ± 3.1	1 AUBERT 06A	BABR	$e^+e^- \rightarrow \Upsilon(4S)$

¹ Assumes equal production of B^+ and B^0 at the $\Upsilon(4S)$.

 $\Gamma(D^0 K^+ \pi^- \text{ non-resonant})/\Gamma_{\text{total}}$ Γ_{121}/Γ

VALUE (units 10^{-6})	CL%	DOCUMENT ID	TECN	COMMENT
<37	90	1 AUBERT 06A	BABR	$e^+e^- \rightarrow \Upsilon(4S)$

¹ Assumes equal production of B^+ and B^0 at the $\Upsilon(4S)$.

 $\Gamma(D^0 \pi^0)/\Gamma_{\text{total}}$ Γ_{122}/Γ

VALUE (units 10^{-4})	CL%	DOCUMENT ID	TECN	COMMENT
2.61 ± 0.24 OUR AVERAGE				

2.25 ± 0.14 ± 0.35	1 BLYTH 06	BELL	$e^+e^- \rightarrow \Upsilon(4S)$
--------------------	------------	------	-----------------------------------

2.9 ± 0.2 ± 0.3	1 AUBERT 04B	BABR	$e^+e^- \rightarrow \Upsilon(4S)$
-----------------	--------------	------	-----------------------------------

2.74 +0.36 -0.32 ± 0.55	1 COAN 02	CLE2	$e^+e^- \rightarrow \Upsilon(4S)$
-------------------------	-----------	------	-----------------------------------

• • • We do not use the following data for averages, fits, limits, etc. • • •

3.1 ± 0.4 ± 0.5	1 ABE 02J	BELL	Repl. by BLYTH 06
-----------------	-----------	------	-------------------

<1.2	90	2 NEMATI 98	CLE2
------	----	-------------	------

<4.8	90	3 ALAM 94	CLE2
------	----	-----------	------

¹ Assumes equal production of B^+ and B^0 at the $\Upsilon(4S)$.

² NEMATI 98 assumes equal production of B^+ and B^0 at the $\Upsilon(4S)$ and use the PDG 96 values for D^0 , D^{*0} , η , η' , and ω branching fractions.

³ ALAM 94 assume equal production of B^+ and B^0 at the $\Upsilon(4S)$ and use the CLEO II absolute $B(D^0 \rightarrow K^- \pi^+)$ and the PDG 1992 $B(D^0 \rightarrow K^- \pi^+ \pi^0)/B(D^0 \rightarrow K^- \pi^+)$ and $B(D^0 \rightarrow K^- \pi^+ \pi^-)/B(D^0 \rightarrow K^- \pi^+)$.

 $\Gamma(D^0 \rho^0)/\Gamma_{\text{total}}$ Γ_{123}/Γ

VALUE (units 10^{-4})	CL%	DOCUMENT ID	TECN	COMMENT
3.19 ± 0.20 ± 0.45		1,2 KUZMIN 07	BELL	$e^+e^- \rightarrow \Upsilon(4S)$

• • • We do not use the following data for averages, fits, limits, etc. • • •

2.9 ± 1.0 ± 0.4	1 SATPATHY 03	BELL	Repl. by KUZMIN 07
-----------------	---------------	------	--------------------

< 3.9	90	3 NEMATI 98	CLE2
-------	----	-------------	------

< 5.5	90	4 ALAM 94	CLE2
-------	----	-----------	------

< 6.0	90	5 BORTOLETTO 92	CLEO
-------	----	-----------------	------

< 27.0	90	6 ALBRECHT 88k	ARG
--------	----	----------------	-----

¹ Assumes equal production of B^+ and B^0 at the $\Upsilon(4S)$.

² Our second uncertainty combines systematics and model errors quoted in the paper.

³ NEMATI 98 assumes equal production of B^+ and B^0 at the $\Upsilon(4S)$ and use the PDG 96 values for D^0 , D^{*0} , η , η' , and ω branching fractions.

⁴ ALAM 94 assume equal production of B^+ and B^0 at the $\Upsilon(4S)$ and use the CLEO II absolute $B(D^0 \rightarrow K^- \pi^+)$ and the PDG 1992 $B(D^0 \rightarrow K^- \pi^+ \pi^0)/B(D^0 \rightarrow K^- \pi^+)$ and $B(D^0 \rightarrow K^- \pi^+ \pi^-)/B(D^0 \rightarrow K^- \pi^+)$.

⁵ BORTOLETTO 92 assumes equal production of B^+ and B^0 at the $\Upsilon(4S)$ and uses Mark III branching fractions for the D .

⁶ ALBRECHT 88k reports < 0.003 assuming $B^0 \bar{B}^0: B^+ B^-$ production ratio is 45:55. We rescale to 50%.

 $\Gamma(D^0 f_2)/\Gamma_{\text{total}}$ Γ_{124}/Γ

VALUE (units 10^{-4})	DOCUMENT ID	TECN	COMMENT
1.20 ± 0.18 ± 0.38	1,2 KUZMIN 07	BELL	$e^+e^- \rightarrow \Upsilon(4S)$

¹ Assumes equal production of B^+ and B^0 at the $\Upsilon(4S)$.

² Our second uncertainty combines systematics and model errors quoted in the paper.

 $\Gamma(D^0 \eta)/\Gamma_{\text{total}}$ Γ_{125}/Γ

VALUE (units 10^{-4})	CL%	DOCUMENT ID	TECN	COMMENT
2.02 ± 0.35 OUR AVERAGE		Error includes scale factor of 1.6.		

1.77 ± 0.16 ± 0.21	1 BLYTH 06	BELL	$e^+e^- \rightarrow \Upsilon(4S)$
--------------------	------------	------	-----------------------------------

2.5 ± 0.2 ± 0.3	1 AUBERT 04B	BABR	$e^+e^- \rightarrow \Upsilon(4S)$
-----------------	--------------	------	-----------------------------------

• • • We do not use the following data for averages, fits, limits, etc. • • •

1.4 +0.5 -0.4 ± 0.3	1 ABE 02J	BELL	Repl. by BLYTH 06
---------------------	-----------	------	-------------------

<1.3	90	2 NEMATI 98	CLE2
------	----	-------------	------

<6.8	90	3 ALAM 94	CLE2
------	----	-----------	------

¹ Assumes equal production of B^+ and B^0 at the $\Upsilon(4S)$.

² NEMATI 98 assumes equal production of B^+ and B^0 at the $\Upsilon(4S)$ and use the PDG 96 values for D^0 , D^{*0} , η , η' , and ω branching fractions.

³ ALAM 94 assume equal production of B^+ and B^0 at the $\Upsilon(4S)$ and use the CLEO II absolute $B(D^0 \rightarrow K^- \pi^+)$ and the PDG 1992 $B(D^0 \rightarrow K^- \pi^+ \pi^0)/B(D^0 \rightarrow K^- \pi^+)$ and $B(D^0 \rightarrow K^- \pi^+ \pi^-)/B(D^0 \rightarrow K^- \pi^+)$.

 $\Gamma(D^0 \eta')/\Gamma_{\text{total}}$ Γ_{126}/Γ

VALUE (units 10^{-4})	CL%	DOCUMENT ID	TECN	COMMENT
1.25 ± 0.23 OUR AVERAGE		Error includes scale factor of 1.1.		

1.14 ± 0.20 +0.10 -0.13	1 SCHUMANN 05	BELL	$e^+e^- \rightarrow \Upsilon(4S)$
-------------------------	---------------	------	-----------------------------------

1.7 ± 0.4 ± 0.2	1 AUBERT 04B	BABR	$e^+e^- \rightarrow \Upsilon(4S)$
-----------------	--------------	------	-----------------------------------

• • • We do not use the following data for averages, fits, limits, etc. • • •

<9.4	90	2 NEMATI 98	CLE2
------	----	-------------	------

<8.6	90	3 ALAM 94	CLE2
------	----	-----------	------

¹ Assumes equal production of B^+ and B^0 at the $\Upsilon(4S)$.

² NEMATI 98 assumes equal production of B^+ and B^0 at the $\Upsilon(4S)$ and use the PDG 96 values for D^0 , D^{*0} , η , η' , and ω branching fractions.

³ ALAM 94 assume equal production of B^+ and B^0 at the $\Upsilon(4S)$ and use the CLEO II absolute $B(D^0 \rightarrow K^- \pi^+)$ and the PDG 1992 $B(D^0 \rightarrow K^- \pi^+ \pi^0)/B(D^0 \rightarrow K^- \pi^+)$ and $B(D^0 \rightarrow K^- \pi^+ \pi^-)/B(D^0 \rightarrow K^- \pi^+)$.

 $\Gamma(D^0 \eta')/\Gamma(D^0 \eta)$ $\Gamma_{126}/\Gamma_{125}$

VALUE	DOCUMENT ID	TECN	COMMENT
0.7 ± 0.2 ± 0.1	AUBERT 04B	BABR	$e^+e^- \rightarrow \Upsilon(4S)$

$\Gamma(D^0\omega)/\Gamma_{\text{total}}$ Γ_{127}/Γ

VALUE (units 10^{-4})	CL%	DOCUMENT ID	TECN	COMMENT
2.59 ± 0.30 OUR AVERAGE				
2.37 ± 0.23 ± 0.28		¹ BLYTH 06	BELL	$e^+e^- \rightarrow \Upsilon(4S)$
3.0 ± 0.3 ± 0.4		¹ AUBERT 04B	BABR	$e^+e^- \rightarrow \Upsilon(4S)$
••• We do not use the following data for averages, fits, limits, etc. •••				
1.8 ± 0.5 $\begin{smallmatrix} +0.4 \\ -0.3 \end{smallmatrix}$		¹ ABE 02J	BELL	Repl. by BLYTH 06
<5.1	90	² NEMAT1 98	CLE2	$e^+e^- \rightarrow \Upsilon(4S)$
<6.3	90	³ ALAM 94	CLE2	Repl. by NEMAT1 98
¹ Assumes equal production of B^+ and B^0 at the $\Upsilon(4S)$.				
² NEMAT1 98 assumes equal production of B^+ and B^0 at the $\Upsilon(4S)$ and use the PDG 96 values for D^0 , D^{*0} , η , η' , and ω branching fractions.				
³ ALAM 94 assume equal production of B^+ and B^0 at the $\Upsilon(4S)$ and use the CLEO II absolute $B(D^0 \rightarrow K^-\pi^+)$ and the PDG 1992 $B(D^0 \rightarrow K^-\pi^+\pi^0)/B(D^0 \rightarrow K^-\pi^+)$ and $B(D^0 \rightarrow K^-\pi^+\pi^-\pi^0)/B(D^0 \rightarrow K^-\pi^+)$.				

 $\Gamma(D^0\phi)/\Gamma_{\text{total}}$ Γ_{128}/Γ

VALUE (units 10^{-6})	CL%	DOCUMENT ID	TECN	COMMENT
<11.6	90	¹ AUBERT 07A0	BABR	$e^+e^- \rightarrow \Upsilon(4S)$
¹ Assumes equal production of B^+ and B^0 at the $\Upsilon(4S)$.				

 $\Gamma(D^0 K^*(892)^0)/\Gamma_{\text{total}}$ Γ_{130}/Γ

VALUE (units 10^{-5})	CL%	DOCUMENT ID	TECN	COMMENT
<1.1	90	¹ AUBERT,B 06L	BABR	$e^+e^- \rightarrow \Upsilon(4S)$
••• We do not use the following data for averages, fits, limits, etc. •••				
<1.8	90	¹ KROKOVNY 03	BELL	$e^+e^- \rightarrow \Upsilon(4S)$
¹ Assumes equal production of B^+ and B^0 at the $\Upsilon(4S)$.				

 $\Gamma(D^0 K^+\pi^-)/\Gamma_{\text{total}}$ Γ_{129}/Γ

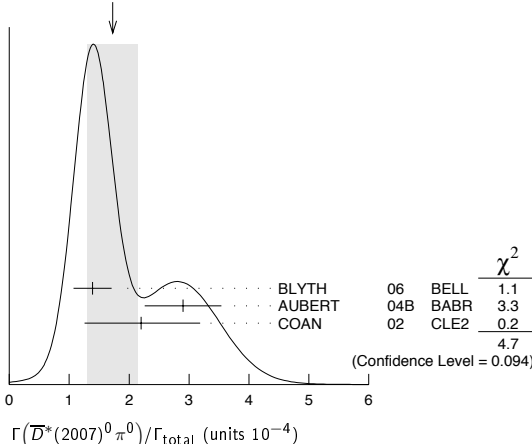
VALUE (units 10^{-6})	CL%	DOCUMENT ID	TECN	COMMENT
<19	90	¹ AUBERT 06A	BABR	$e^+e^- \rightarrow \Upsilon(4S)$
¹ Assumes equal production of B^+ and B^0 at the $\Upsilon(4S)$.				

 $\Gamma(D^{*0}\gamma)/\Gamma_{\text{total}}$ Γ_{131}/Γ

VALUE	CL%	DOCUMENT ID	TECN	COMMENT
<2.5 × 10⁻⁵	90	¹ AUBERT,B 05Q	BABR	$e^+e^- \rightarrow \Upsilon(4S)$
••• We do not use the following data for averages, fits, limits, etc. •••				
<5.0 × 10 ⁻⁵	90	¹ ARTUSO 00	CLE2	$e^+e^- \rightarrow \Upsilon(4S)$
¹ Assumes equal production of B^+ and B^0 at the $\Upsilon(4S)$.				

 $\Gamma(D^*(2007)^0\pi^0)/\Gamma_{\text{total}}$ Γ_{132}/Γ

VALUE (units 10^{-4})	CL%	DOCUMENT ID	TECN	COMMENT
1.7 ± 0.4 OUR AVERAGE				Error includes scale factor of 1.5. See the ideogram below.
1.39 ± 0.18 ± 0.26		¹ BLYTH 06	BELL	$e^+e^- \rightarrow \Upsilon(4S)$
2.9 ± 0.4 ± 0.5		¹ AUBERT 04B	BABR	$e^+e^- \rightarrow \Upsilon(4S)$
2.20 $\begin{smallmatrix} +0.59 \\ -0.52 \end{smallmatrix}$ ± 0.79		¹ COAN 02	CLE2	$e^+e^- \rightarrow \Upsilon(4S)$
••• We do not use the following data for averages, fits, limits, etc. •••				
2.7 $\begin{smallmatrix} +0.8 +0.5 \\ -0.7 -0.6 \end{smallmatrix}$		¹ ABE 02J	BELL	Repl. by BLYTH 06
<4.4	90	² NEMAT1 98	CLE2	Repl. by COAN 02
<9.7	90	³ ALAM 94	CLE2	Repl. by NEMAT1 98
¹ Assumes equal production of B^+ and B^0 at the $\Upsilon(4S)$.				
² NEMAT1 98 assumes equal production of B^+ and B^0 at the $\Upsilon(4S)$ and use the PDG 96 values for D^0 , D^{*0} , η , η' , and ω branching fractions.				
³ ALAM 94 assume equal production of B^+ and B^0 at the $\Upsilon(4S)$ and use the CLEO II $B(D^*(2007)^0 \rightarrow D^0\pi^0)$ and absolute $B(D^0 \rightarrow K^-\pi^+)$ and the PDG 1992 $B(D^0 \rightarrow K^-\pi^+\pi^0)/B(D^0 \rightarrow K^-\pi^+)$ and $B(D^0 \rightarrow K^-\pi^+\pi^-\pi^0)/B(D^0 \rightarrow K^-\pi^+)$.				

WEIGHTED AVERAGE
1.7 ± 0.4 (Error scaled by 1.5) $\Gamma(D^{*0}\pi^0)/\Gamma(D^*(2007)^0\pi^0)$ $\Gamma_{122}/\Gamma_{132}$

VALUE	DOCUMENT ID	TECN	COMMENT
1.14 ± 0.26 OUR AVERAGE			Error includes scale factor of 1.3.
1.62 ± 0.23 ± 0.35	BLYTH 06	BELL	$e^+e^- \rightarrow \Upsilon(4S)$
1.0 ± 0.1 ± 0.2	AUBERT 04B	BABR	$e^+e^- \rightarrow \Upsilon(4S)$

 $\Gamma(D^*(2007)^0\rho^0)/\Gamma_{\text{total}}$ Γ_{133}/Γ

VALUE	CL%	DOCUMENT ID	TECN	COMMENT
<5.1 × 10⁻⁴	90	¹ SATPATHY 03	BELL	$e^+e^- \rightarrow \Upsilon(4S)$
••• We do not use the following data for averages, fits, limits, etc. •••				
<0.00056	90	² NEMAT1 98	CLE2	$e^+e^- \rightarrow \Upsilon(4S)$
<0.00117	90	³ ALAM 94	CLE2	Repl. by NEMAT1 98
¹ Assumes equal production of B^+ and B^0 at the $\Upsilon(4S)$.				
² NEMAT1 98 assumes equal production of B^+ and B^0 at the $\Upsilon(4S)$ and use the PDG 96 values for D^0 , D^{*0} , η , η' , and ω branching fractions.				
³ ALAM 94 assume equal production of B^+ and B^0 at the $\Upsilon(4S)$ and use the CLEO II $B(D^*(2007)^0 \rightarrow D^0\pi^0)$ and absolute $B(D^0 \rightarrow K^-\pi^+)$ and the PDG 1992 $B(D^0 \rightarrow K^-\pi^+\pi^0)/B(D^0 \rightarrow K^-\pi^+)$ and $B(D^0 \rightarrow K^-\pi^+\pi^-\pi^0)/B(D^0 \rightarrow K^-\pi^+)$.				

 $\Gamma(D^*(2007)^0\eta)/\Gamma_{\text{total}}$ Γ_{134}/Γ

VALUE (units 10^{-4})	CL%	DOCUMENT ID	TECN	COMMENT
1.8 ± 0.6 OUR AVERAGE				Error includes scale factor of 1.8.
1.40 ± 0.28 ± 0.26		¹ BLYTH 06	BELL	$e^+e^- \rightarrow \Upsilon(4S)$
2.6 ± 0.4 ± 0.4		¹ AUBERT 04B	BABR	$e^+e^- \rightarrow \Upsilon(4S)$
••• We do not use the following data for averages, fits, limits, etc. •••				
<4.6	90	¹ ABE 02J	BELL	$e^+e^- \rightarrow \Upsilon(4S)$
<2.6	90	² NEMAT1 98	CLE2	$e^+e^- \rightarrow \Upsilon(4S)$
<6.9	90	³ ALAM 94	CLE2	Repl. by NEMAT1 98
¹ Assumes equal production of B^+ and B^0 at the $\Upsilon(4S)$.				
² NEMAT1 98 assumes equal production of B^+ and B^0 at the $\Upsilon(4S)$ and use the PDG 96 values for D^0 , D^{*0} , η , η' , and ω branching fractions.				
³ ALAM 94 assume equal production of B^+ and B^0 at the $\Upsilon(4S)$ and use the CLEO II $B(D^*(2007)^0 \rightarrow D^0\pi^0)$ and absolute $B(D^0 \rightarrow K^-\pi^+)$ and the PDG 1992 $B(D^0 \rightarrow K^-\pi^+\pi^0)/B(D^0 \rightarrow K^-\pi^+)$ and $B(D^0 \rightarrow K^-\pi^+\pi^-\pi^0)/B(D^0 \rightarrow K^-\pi^+)$.				

 $\Gamma(D^0\eta)/\Gamma(D^*(2007)^0\eta)$ $\Gamma_{125}/\Gamma_{134}$

VALUE	DOCUMENT ID	TECN	COMMENT
0.99 ± 0.19 OUR AVERAGE			
1.27 ± 0.29 ± 0.25	BLYTH 06	BELL	$e^+e^- \rightarrow \Upsilon(4S)$
0.9 ± 0.2 ± 0.1	AUBERT 04B	BABR	$e^+e^- \rightarrow \Upsilon(4S)$

 $\Gamma(D^*(2007)^0\eta')/\Gamma(D^*(2007)^0\eta)$ $\Gamma_{135}/\Gamma_{134}$

VALUE	DOCUMENT ID	TECN	COMMENT
0.5 ± 0.3 ± 0.1			
	AUBERT 04B	BABR	$e^+e^- \rightarrow \Upsilon(4S)$

 $\Gamma(D^*(2007)^0\eta'')/\Gamma_{\text{total}}$ Γ_{135}/Γ

VALUE (units 10^{-4})	CL%	DOCUMENT ID	TECN	COMMENT
1.23 ± 0.35 OUR AVERAGE				
1.21 ± 0.34 ± 0.22		¹ SCHUMANN 05	BELL	$e^+e^- \rightarrow \Upsilon(4S)$
1.3 ± 0.7 ± 0.2		^{1,2} AUBERT 04B	BABR	$e^+e^- \rightarrow \Upsilon(4S)$
••• We do not use the following data for averages, fits, limits, etc. •••				
<14	90	BRANDENB...	98	CLE2 $e^+e^- \rightarrow \Upsilon(4S)$
<19	90	³ NEMAT1 98	CLE2	$e^+e^- \rightarrow \Upsilon(4S)$
<27	90	⁴ ALAM 94	CLE2	Repl. by NEMAT1 98
¹ Assumes equal production of B^+ and B^0 at the $\Upsilon(4S)$.				
² Reports an upper limit $< 2.6 \times 10^{-4}$ at 90% CL.				
³ NEMAT1 98 assumes equal production of B^+ and B^0 at the $\Upsilon(4S)$ and use the PDG 96 values for D^0 , D^{*0} , η , η' , and ω branching fractions.				
⁴ ALAM 94 assume equal production of B^+ and B^0 at the $\Upsilon(4S)$ and use the CLEO II $B(D^*(2007)^0 \rightarrow D^0\pi^0)$ and absolute $B(D^0 \rightarrow K^-\pi^+)$ and the PDG 1992 $B(D^0 \rightarrow K^-\pi^+\pi^0)/B(D^0 \rightarrow K^-\pi^+)$ and $B(D^0 \rightarrow K^-\pi^+\pi^-\pi^0)/B(D^0 \rightarrow K^-\pi^+)$.				

 $\Gamma(D^0\eta')/\Gamma(D^*(2007)^0\eta')$ $\Gamma_{126}/\Gamma_{135}$

VALUE	DOCUMENT ID	TECN	COMMENT
1.3 ± 0.8 ± 0.2			
	AUBERT 04B	BABR	$e^+e^- \rightarrow \Upsilon(4S)$

 $\Gamma(D^0\omega)/\Gamma(D^*(2007)^0\omega)$ $\Gamma_{127}/\Gamma_{142}$

VALUE	DOCUMENT ID	TECN	COMMENT
0.78 ± 0.14 OUR AVERAGE			Error includes scale factor of 1.1.
1.04 ± 0.20 ± 0.17	BLYTH 06	BELL	$e^+e^- \rightarrow \Upsilon(4S)$
0.7 ± 0.1 ± 0.1	AUBERT 04B	BABR	$e^+e^- \rightarrow \Upsilon(4S)$

 $\Gamma(D^*(2007)^0\pi^+\pi^-)/\Gamma_{\text{total}}$ Γ_{136}/Γ

VALUE	DOCUMENT ID	TECN	COMMENT
(6.2 ± 1.2 ± 1.8) × 10⁻⁴			
	^{1,2} SATPATHY 03	BELL	$e^+e^- \rightarrow \Upsilon(4S)$
¹ Assumes equal production of B^+ and B^0 at the $\Upsilon(4S)$.			
² No assumption about the intermediate mechanism is made in the analysis.			

 $\Gamma(D^*(2007)^0 K^0)/\Gamma_{\text{total}}$ Γ_{137}/Γ

VALUE (units 10^{-5})	CL%	DOCUMENT ID	TECN	COMMENT
3.6 ± 1.2 ± 0.3		¹ AUBERT,B 06L	BABR	$e^+e^- \rightarrow \Upsilon(4S)$
••• We do not use the following data for averages, fits, limits, etc. •••				
<6.6	90	¹ KROKOVNY 03	BELL	$e^+e^- \rightarrow \Upsilon(4S)$
¹ Assumes equal production of B^+ and B^0 at the $\Upsilon(4S)$.				

Meson Particle Listings

 B^0

$\Gamma(\bar{D}^*(2007)^0 K^*(892)^0)/\Gamma_{\text{total}}$		Γ_{138}/Γ	
VALUE	CL%	DOCUMENT ID	TECN COMMENT
$<6.9 \times 10^{-5}$	90	¹ KROKOVNY 03	BELL $e^+ e^- \rightarrow \Upsilon(4S)$
¹ Assumes equal production of B^+ and B^0 at the $\Upsilon(4S)$.			

$\Gamma(D^*(2007)^0 K^*(892)^0)/\Gamma_{\text{total}}$		Γ_{139}/Γ	
VALUE	CL%	DOCUMENT ID	TECN COMMENT
$<4.0 \times 10^{-5}$	90	¹ KROKOVNY 03	BELL $e^+ e^- \rightarrow \Upsilon(4S)$
¹ Assumes equal production of B^+ and B^0 at the $\Upsilon(4S)$.			

$\Gamma(D^*(2007)^0 \pi^+ \pi^+ \pi^- \pi^-)/\Gamma_{\text{total}}$		Γ_{140}/Γ	
VALUE (units 10^{-3})	CL%	DOCUMENT ID	TECN COMMENT
2.7 ± 0.5		OUR AVERAGE	
$2.60 \pm 0.47 \pm 0.37$		¹ MAJUMDER 04	BELL $e^+ e^- \rightarrow \Upsilon(4S)$
$3.0 \pm 0.7 \pm 0.6$		¹ EDWARDS 02	CLE2 $e^+ e^- \rightarrow \Upsilon(4S)$
¹ Assumes equal production of B^+ and B^0 at the $\Upsilon(4S)$.			

$\Gamma(D^*(2007)^0 \pi^+ \pi^+ \pi^- \pi^-)/\Gamma(D^*(2010)^- \pi^+ \pi^+ \pi^- \pi^0)$		Γ_{140}/Γ_{56}	
VALUE	CL%	DOCUMENT ID	TECN COMMENT
$0.17 \pm 0.04 \pm 0.02$		¹ EDWARDS 02	CLE2 $e^+ e^- \rightarrow \Upsilon(4S)$
¹ Assumes equal production of B^+ and B^0 at the $\Upsilon(4S)$.			

$\Gamma(D^*(2010)^+ D^*(2010)^-)/\Gamma_{\text{total}}$		Γ_{141}/Γ	
VALUE (units 10^{-4})	CL%	DOCUMENT ID	TECN COMMENT
8.2 ± 0.9		OUR AVERAGE	
$8.1 \pm 0.6 \pm 1.0$		¹ AUBERT,B 06A	BABR $e^+ e^- \rightarrow \Upsilon(4S)$
$8.1 \pm 0.8 \pm 1.1$		¹ MIYAKE 05	BELL $e^+ e^- \rightarrow \Upsilon(4S)$
$9.9^{+4.2}_{-3.3} \pm 1.2$		¹ LIPELES 00	CLE2 $e^+ e^- \rightarrow \Upsilon(4S)$
• • • We do not use the following data for averages, fits, limits, etc. • • •			
$8.3 \pm 1.6 \pm 1.2$		^{1,2} AUBERT 02M	BABR Repl. by AUBERT,B 06B
$6.2^{+4.0}_{-2.9} \pm 1.0$		³ ARTUSO 99	CLE2 Repl. by LIPELES 00
<61	90	⁴ BARATE 98Q	ALEP $e^+ e^- \rightarrow Z$
<22	90	⁵ ASNER 97	CLE2 Repl. by ARTUSO 99

- ¹ Assumes equal production of B^+ and B^0 at the $\Upsilon(4S)$.
² AUBERT 02M also assumes the measured CP -odd fraction of the final states is $0.22 \pm 0.18 \pm 0.03$.
³ ARTUSO 99 uses $B(\Upsilon(4S) \rightarrow B^0 \bar{B}^0) = (48 \pm 4)\%$.
⁴ BARATE 98Q (ALEPH) observes 2 events with an expected background of 0.10 ± 0.03 which corresponds to a branching ratio of $(2.3^{+1.9}_{-1.2} \pm 0.4) \times 10^{-3}$.
⁵ ASNER 97 at CLEO observes 1 event with an expected background of 0.022 ± 0.011 . This corresponds to a branching ratio of $(5.3^{+7.1}_{-3.7} \pm 1.0) \times 10^{-4}$.

$\Gamma(\bar{D}^*(2007)^0 \omega)/\Gamma_{\text{total}}$		Γ_{142}/Γ	
VALUE (units 10^{-4})	CL%	DOCUMENT ID	TECN COMMENT
2.7 ± 0.8		OUR AVERAGE	
$2.29 \pm 0.39 \pm 0.40$		¹ BLYTH 06	BELL $e^+ e^- \rightarrow \Upsilon(4S)$
$4.2 \pm 0.7 \pm 0.9$	90	¹ AUBERT 04B	BABR $e^+ e^- \rightarrow \Upsilon(4S)$
• • • We do not use the following data for averages, fits, limits, etc. • • •			
<7.9	90	¹ ABE 02J	BELL $e^+ e^- \rightarrow \Upsilon(4S)$
<7.4	90	² NEMATI 98	CLE2 $e^+ e^- \rightarrow \Upsilon(4S)$
<21	90	³ ALAM 94	CLE2 Repl. by NEMATI 98

- ¹ Assumes equal production of B^+ and B^0 at the $\Upsilon(4S)$.
² NEMATI 98 assumes equal production of B^+ and B^0 at the $\Upsilon(4S)$ and use the PDG 96 values for D^0 , D^{*0} , η , η' , and ω branching fractions.
³ ALAM 94 assume equal production of B^+ and B^0 at the $\Upsilon(4S)$ and use the CLEO II $B(D^*(2007)^0 \rightarrow D^0 \pi^0)$ and absolute $B(D^0 \rightarrow K^- \pi^+)$ and the PDG 1992 $B(D^0 \rightarrow K^- \pi^+ \pi^0)/B(D^0 \rightarrow K^- \pi^+)$ and $B(D^0 \rightarrow K^- \pi^+ \pi^+ \pi^-)/B(D^0 \rightarrow K^- \pi^+)$.

$\Gamma(D^*(2010)^+ D^-)/\Gamma_{\text{total}}$		Γ_{143}/Γ	
VALUE (units 10^{-4})	CL%	DOCUMENT ID	TECN COMMENT
6.1 ± 1.5		OUR AVERAGE	
$5.7 \pm 0.7 \pm 0.7$		¹ AUBERT,B 06A	BABR $e^+ e^- \rightarrow \Upsilon(4S)$
$11.7 \pm 2.6^{+2.2}_{-2.5}$		^{1,2} ABE 02Q	BELL $e^+ e^- \rightarrow \Upsilon(4S)$
• • • We do not use the following data for averages, fits, limits, etc. • • •			
$8.8 \pm 1.0 \pm 1.3$		¹ AUBERT 03J	BABR Repl. by AUBERT,B 06B
$14.8 \pm 3.8^{+2.8}_{-3.1}$		^{1,3} ABE 02Q	BELL $e^+ e^- \rightarrow \Upsilon(4S)$
<6.3	90	¹ LIPELES 00	CLE2 $e^+ e^- \rightarrow \Upsilon(4S)$
<56	90	BARATE 98Q	ALEP $e^+ e^- \rightarrow Z$
<18	90	ASNER 97	CLE2 $e^+ e^- \rightarrow \Upsilon(4S)$

- ¹ Assumes equal production of B^+ and B^0 at the $\Upsilon(4S)$.
² The measurement is performed using fully reconstructed D^* and D^+ decays.
³ The measurement is performed using a partial reconstruction technique for the D^* and fully reconstructed D^+ decays as a cross check.

$\Gamma(D^*(2007)^0 \bar{D}^*(2007)^0)/\Gamma_{\text{total}}$		Γ_{144}/Γ	
VALUE (units 10^{-4})	CL%	DOCUMENT ID	TECN COMMENT
<0.9	90	¹ AUBERT,B 06A	BABR $e^+ e^- \rightarrow \Upsilon(4S)$
• • • We do not use the following data for averages, fits, limits, etc. • • •			
<270	90	BARATE 98Q	ALEP $e^+ e^- \rightarrow Z$
¹ Assumes equal production of B^+ and B^0 at the $\Upsilon(4S)$.			

$\Gamma(D^- D^0 K^+)/\Gamma_{\text{total}}$		Γ_{145}/Γ	
VALUE (units 10^{-3})	CL%	DOCUMENT ID	TECN COMMENT
$1.7 \pm 0.3 \pm 0.3$		¹ AUBERT 03X	BABR $e^+ e^- \rightarrow \Upsilon(4S)$
¹ Assumes equal production of B^+ and B^0 at the $\Upsilon(4S)$.			

$\Gamma(D^- D^*(2007)^0 K^+)/\Gamma_{\text{total}}$		Γ_{146}/Γ	
VALUE (units 10^{-3})	CL%	DOCUMENT ID	TECN COMMENT
$4.6 \pm 0.7 \pm 0.7$		¹ AUBERT 03X	BABR $e^+ e^- \rightarrow \Upsilon(4S)$
¹ Assumes equal production of B^+ and B^0 at the $\Upsilon(4S)$.			

$\Gamma(D^*(2010)^- D^0 K^+)/\Gamma_{\text{total}}$		Γ_{147}/Γ	
VALUE (units 10^{-3})	CL%	DOCUMENT ID	TECN COMMENT
$3.1^{+0.4}_{-0.3} \pm 0.4$		¹ AUBERT 03X	BABR $e^+ e^- \rightarrow \Upsilon(4S)$
¹ Assumes equal production of B^+ and B^0 at the $\Upsilon(4S)$.			

$\Gamma(D^*(2010)^- D^*(2007)^0 K^+)/\Gamma_{\text{total}}$		Γ_{148}/Γ	
VALUE (units 10^{-3})	CL%	DOCUMENT ID	TECN COMMENT
$11.8 \pm 1.0 \pm 1.7$		¹ AUBERT 03X	BABR $e^+ e^- \rightarrow \Upsilon(4S)$
¹ Assumes equal production of B^+ and B^0 at the $\Upsilon(4S)$.			

$\Gamma(D^- D^+ K^0)/\Gamma_{\text{total}}$		Γ_{149}/Γ	
VALUE (units 10^{-3})	CL%	DOCUMENT ID	TECN COMMENT
<1.7	90	¹ AUBERT 03X	BABR $e^+ e^- \rightarrow \Upsilon(4S)$
¹ Assumes equal production of B^+ and B^0 at the $\Upsilon(4S)$.			

$[\Gamma(D^*(2010)^- D^+ K^0) + \Gamma(D^- D^*(2010)^+ K^0)]/\Gamma_{\text{total}}$		Γ_{150}/Γ	
VALUE (units 10^{-3})	CL%	DOCUMENT ID	TECN COMMENT
$6.5 \pm 1.2 \pm 1.0$		¹ AUBERT 03X	BABR $e^+ e^- \rightarrow \Upsilon(4S)$
¹ Assumes equal production of B^+ and B^0 at the $\Upsilon(4S)$.			

$\Gamma(D^*(2010)^- D^*(2010)^+ K^0)/\Gamma_{\text{total}}$		Γ_{151}/Γ	
VALUE (units 10^{-3})	CL%	DOCUMENT ID	TECN COMMENT
7.8 ± 1.1		OUR AVERAGE	
$6.8 \pm 0.8 \pm 1.4$		^{1,2} DALSENO 07	BELL $e^+ e^- \rightarrow \Upsilon(4S)$
$8.8 \pm 0.8 \pm 1.4$		^{1,2} AUBERT,B 06Q	BABR $e^+ e^- \rightarrow \Upsilon(4S)$
• • • We do not use the following data for averages, fits, limits, etc. • • •			
$8.8^{+1.5}_{-1.4} \pm 1.3$		¹ AUBERT 03X	BABR Repl. by AUBERT,B 06Q
¹ Assumes equal production of B^+ and B^0 at the $\Upsilon(4S)$. ² The result is rescaled by a factor of 2 to convert from K_S^0 to K^0 .			

$\Gamma(D^* D_{s1}(2536)^+ \times B(D_{s1}(2536)^+ \rightarrow D^{*+} K^0)/\Gamma_{\text{total}}$		Γ_{152}/Γ	
VALUE (units 10^{-4})	CL%	DOCUMENT ID	TECN COMMENT
8.0 ± 2.4		OUR AVERAGE	
$7.6^{+4.8+1.6}_{-4.2-1.4}$		^{1,2} DALSENO 07	BELL $e^+ e^- \rightarrow \Upsilon(4S)$
$8.2 \pm 2.6 \pm 1.2$		^{1,2} AUBERT,B 06Q	BABR $e^+ e^- \rightarrow \Upsilon(4S)$
¹ Assumes equal production of B^+ and B^0 at the $\Upsilon(4S)$. ² The result is rescaled by a factor of 2 to convert from K_S^0 to K^0 .			

$\Gamma(\bar{D}^0 D^0 K^0)/\Gamma_{\text{total}}$		Γ_{153}/Γ	
VALUE (units 10^{-3})	CL%	DOCUMENT ID	TECN COMMENT
<1.4	90	¹ AUBERT 03X	BABR $e^+ e^- \rightarrow \Upsilon(4S)$
¹ Assumes equal production of B^+ and B^0 at the $\Upsilon(4S)$.			

$[\Gamma(\bar{D}^0 D^*(2007)^0 K^0) + \Gamma(\bar{D}^*(2007)^0 D^0 K^0)]/\Gamma_{\text{total}}$		Γ_{154}/Γ	
VALUE (units 10^{-3})	CL%	DOCUMENT ID	TECN COMMENT
<3.7	90	¹ AUBERT 03X	BABR $e^+ e^- \rightarrow \Upsilon(4S)$
¹ Assumes equal production of B^+ and B^0 at the $\Upsilon(4S)$.			

$\Gamma(\bar{D}^*(2007)^0 D^*(2007)^0 K^0)/\Gamma_{\text{total}}$		Γ_{155}/Γ	
VALUE (units 10^{-3})	CL%	DOCUMENT ID	TECN COMMENT
<6.6	90	¹ AUBERT 03X	BABR $e^+ e^- \rightarrow \Upsilon(4S)$
¹ Assumes equal production of B^+ and B^0 at the $\Upsilon(4S)$.			

$\Gamma((\bar{D} + \bar{D}^*)(D + D^*)K)/\Gamma_{\text{total}}$		Γ_{156}/Γ	
VALUE (units 10^{-2})	CL%	DOCUMENT ID	TECN COMMENT
$4.3 \pm 0.3 \pm 0.6$		¹ AUBERT 03X	BABR $e^+ e^- \rightarrow \Upsilon(4S)$
¹ Assumes equal production of B^+ and B^0 at the $\Upsilon(4S)$.			

See key on page 373

Meson Particle Listings

B^0

$\Gamma(\eta_c K^0)/\Gamma_{total}$		Γ_{157}/Γ	
VALUE (units 10^{-3})	DOCUMENT ID	TECN	COMMENT
0.89 ± 0.16 OUR AVERAGE			
0.64 ^{+0.22} _{-0.20} ± 0.20	1,2 AUBERT	07AV	BABR $e^+ e^- \rightarrow \Upsilon(4S)$
0.93 ± 0.16 ± 0.16	1,3 AUBERT,B	04B	BABR $e^+ e^- \rightarrow \Upsilon(4S)$
1.23 ± 0.23 ^{+0.40} _{-0.41}	1 FANG	03	BELL $e^+ e^- \rightarrow \Upsilon(4S)$
1.09 ^{+0.55} _{-0.42} ± 0.33	4 EDWARDS	01	CLE2 $e^+ e^- \rightarrow \Upsilon(4S)$

- 1 Assumes equal production of B^+ and B^0 at the $\Upsilon(4S)$.
- 2 AUBERT 07AV reports $[B(B^0 \rightarrow \eta_c K^0)] \times [B(\eta_c(1S) \rightarrow p\bar{p})] = (0.83^{+0.28}_{-0.26} \pm 0.05) \times 10^{-6}$. We divide by our best value $B(\eta_c(1S) \rightarrow p\bar{p}) = (1.3 \pm 0.4) \times 10^{-3}$. Our first error is their experiment's error and our second error is the systematic error from using our best value.
- 3 AUBERT,B 04B reports $[B(B^0 \rightarrow \eta_c K^0)] \times [B(\eta_c(1S) \rightarrow K\bar{K}\pi)] = (0.0648 \pm 0.0085 \pm 0.0071) \times 10^{-3}$. We divide by our best value $B(\eta_c(1S) \rightarrow K\bar{K}\pi) = (7.0 \pm 1.2) \times 10^{-2}$. Our first error is their experiment's error and our second error is the systematic error from using our best value.
- 4 EDWARDS 01 assumes equal production of B^0 and B^+ at the $\Upsilon(4S)$. The correlated uncertainties (28.3)% from $B(J/\psi(1S) \rightarrow \gamma\eta_c)$ in those modes have been accounted for.

$\Gamma(\eta_c K^0)/\Gamma(J/\psi(1S) K^0)$		$\Gamma_{157}/\Gamma_{159}$	
VALUE	DOCUMENT ID	TECN	COMMENT
1.39 ± 0.20 ± 0.45			
	1 AUBERT,B	04B	BABR $e^+ e^- \rightarrow \Upsilon(4S)$

- 1 Uses BABAR measurement of $B(B^0 \rightarrow J/\psi K^0) = (8.5 \pm 0.5 \pm 0.6) \times 10^{-4}$.

$\Gamma(\eta_c K^*(892)^0)/\Gamma_{total}$		Γ_{158}/Γ	
VALUE (units 10^{-3})	DOCUMENT ID	TECN	COMMENT
0.96 ± 0.33 OUR AVERAGE			Error includes scale factor of 1.1.
0.79 ^{+0.25} _{-0.23} ± 0.24	1,2 AUBERT	07AV	BABR $e^+ e^- \rightarrow \Upsilon(4S)$
1.62 ± 0.32 ^{+0.55} _{-0.60}	2 FANG	03	BELL $e^+ e^- \rightarrow \Upsilon(4S)$

- 1 AUBERT 07AV reports $[B(B^0 \rightarrow \eta_c K^*(892)^0)] \times [B(\eta_c(1S) \rightarrow p\bar{p})] = (1.03^{+0.27}_{-0.24} \pm 0.17) \times 10^{-6}$. We divide by our best value $B(\eta_c(1S) \rightarrow p\bar{p}) = (1.3 \pm 0.4) \times 10^{-3}$. Our first error is their experiment's error and our second error is the systematic error from using our best value.
- 2 Assumes equal production of B^+ and B^0 at the $\Upsilon(4S)$.

$\Gamma(\eta_c K^*(892)^0)/\Gamma(\eta_c K^0)$		$\Gamma_{158}/\Gamma_{157}$	
VALUE	DOCUMENT ID	TECN	COMMENT
1.33 ± 0.36 ± 0.24			
	FANG	03	BELL $e^+ e^- \rightarrow \Upsilon(4S)$

$\Gamma(J/\psi(1S) K^0)/\Gamma_{total}$		Γ_{159}/Γ	
VALUE (units 10^{-4})	CL% EVTS	DOCUMENT ID	TECN COMMENT
8.71 ± 0.32 OUR AVERAGE			
8.6 ^{+1.3} _{-1.2} ± 0.3		1,2 AUBERT	07AV BABR $e^+ e^- \rightarrow \Upsilon(4S)$
8.69 ± 0.22 ± 0.30		2 AUBERT	05J BABR $e^+ e^- \rightarrow \Upsilon(4S)$
7.9 ± 0.4 ± 0.9		2 ABE	03B BELL $e^+ e^- \rightarrow \Upsilon(4S)$
9.5 ± 0.8 ± 0.6		2 AVERY	00 CLE2 $e^+ e^- \rightarrow \Upsilon(4S)$
11.5 ± 2.3 ± 1.7		3 ABE	96H CDF $p\bar{p}$ at 1.8 TeV
7.0 ± 4.1 ± 0.1		4 BORTOLETTO92	CLEO $e^+ e^- \rightarrow \Upsilon(4S)$
9.3 ± 7.2 ± 0.1		2 5 ALBRECHT	90J ARG $e^+ e^- \rightarrow \Upsilon(4S)$
••• We do not use the following data for averages, fits, limits, etc. •••			
8.3 ± 0.4 ± 0.5		2 AUBERT	02 BABR Repl. by AUBERT 05J
8.5 ^{+1.4} _{-1.2} ± 0.6		2 JESSOP	97 CLE2 Repl. by AVERY 00
7.5 ± 2.4 ± 0.8		4 ALAM	94 CLE2 Sup. by JESSOP 97
<50	90	ALAM	86 CLEO $e^+ e^- \rightarrow \Upsilon(4S)$

- 1 AUBERT 07AV reports $[B(B^0 \rightarrow J/\psi(1S) K^0)] \times [B(J/\psi(1S) \rightarrow p\bar{p})] = (1.87^{+0.28}_{-0.26} \pm 0.07) \times 10^{-6}$. We divide by our best value $B(J/\psi(1S) \rightarrow p\bar{p}) = (2.17 \pm 0.07) \times 10^{-3}$. Our first error is their experiment's error and our second error is the systematic error from using our best value.
- 2 Assumes equal production of B^+ and B^0 at the $\Upsilon(4S)$.
- 3 ABE 96H assumes that $B(B^+ \rightarrow J/\psi K^+) = (1.02 \pm 0.14) \times 10^{-3}$.
- 4 BORTOLETTO 92 reports $(6 \pm 3 \pm 2) \times 10^{-4}$ for $B(J/\psi(1S) \rightarrow e^+ e^-) = 0.069 \pm 0.009$. We rescale to our best value $B(J/\psi(1S) \rightarrow e^+ e^-) = (5.94 \pm 0.06) \times 10^{-2}$. Our first error is their experiment's error and our second error is the systematic error from using our best value. Assumes equal production of B^+ and B^0 at the $\Upsilon(4S)$.
- 5 ALBRECHT 90J reports $(8 \pm 6 \pm 2) \times 10^{-4}$ for $B(J/\psi(1S) \rightarrow e^+ e^-) = 0.069 \pm 0.009$. We rescale to our best value $B(J/\psi(1S) \rightarrow e^+ e^-) = (5.94 \pm 0.06) \times 10^{-2}$. Our first error is their experiment's error and our second error is the systematic error from using our best value. Assumes equal production of B^+ and B^0 at the $\Upsilon(4S)$.

$\Gamma(J/\psi(1S) K^+ \pi^-)/\Gamma_{total}$		Γ_{160}/Γ	
VALUE (units 10^{-3})	CL% EVTS	DOCUMENT ID	TECN COMMENT
1.16 ± 0.56 ± 0.01			
••• We do not use the following data for averages, fits, limits, etc. •••			
<1.3	90	2 ALBRECHT	87D ARG $e^+ e^- \rightarrow \Upsilon(4S)$
<6.3	90	2 GILES	84 CLEO $e^+ e^- \rightarrow \Upsilon(4S)$

- 1 BORTOLETTO 92 reports $(1.0 \pm 0.4 \pm 0.3) \times 10^{-3}$ for $B(J/\psi(1S) \rightarrow e^+ e^-) = 0.069 \pm 0.009$. We rescale to our best value $B(J/\psi(1S) \rightarrow e^+ e^-) = (5.94 \pm 0.06) \times 10^{-2}$. Our first error is their experiment's error and our second error is the systematic error from using our best value. Assumes equal production of B^+ and B^0 at the $\Upsilon(4S)$.
- 2 ALBRECHT 87D assume $B^+ B^- / B^0 \bar{B}^0$ ratio is 55/45. $K\pi$ system is specifically selected as nonresonant.

$\Gamma(J/\psi(1S) K^*(892)^0)/\Gamma_{total}$		Γ_{161}/Γ	
VALUE (units 10^{-3})	EVTS	DOCUMENT ID	TECN COMMENT
1.33 ± 0.06 OUR AVERAGE			
1.30 ^{+0.22} _{-0.21} ± 0.04		1,2 AUBERT	07AV BABR $e^+ e^- \rightarrow \Upsilon(4S)$
1.309 ± 0.026 ± 0.077		2 AUBERT	05J BABR $e^+ e^- \rightarrow \Upsilon(4S)$
1.29 ± 0.05 ± 0.13		2 ABE	02N BELL $e^+ e^- \rightarrow \Upsilon(4S)$
1.74 ± 0.20 ± 0.18		3 ABE	98O CDF $p\bar{p}$ 1.8 TeV
1.32 ± 0.17 ± 0.17		4 JESSOP	97 CLE2 $e^+ e^- \rightarrow \Upsilon(4S)$
1.28 ± 0.66 ± 0.01		5 BORTOLETTO92	CLEO $e^+ e^- \rightarrow \Upsilon(4S)$
1.28 ± 0.60 ± 0.01	6	6 ALBRECHT	90J ARG $e^+ e^- \rightarrow \Upsilon(4S)$
4.07 ± 1.82 ± 0.04	5	7 BEBEK	87 CLEO $e^+ e^- \rightarrow \Upsilon(4S)$
••• We do not use the following data for averages, fits, limits, etc. •••			
1.24 ± 0.05 ± 0.09		2 AUBERT	02 BABR Repl. by AUBERT 05J
1.36 ± 0.27 ± 0.22		8 ABE	96H CDF Sup. by ABE 98O
1.69 ± 0.31 ± 0.18	29	9 ALAM	94 CLE2 Sup. by JESSOP 97
		10 ALBRECHT	94G ARG $e^+ e^- \rightarrow \Upsilon(4S)$
4.0 ± 0.30		11 ALBAJAR	91E UA1 $E_{cm} = 630$ GeV
3.3 ± 0.18	5	12 ALBRECHT	87D ARG $e^+ e^- \rightarrow \Upsilon(4S)$
4.1 ± 0.18	5	13 ALAM	86 CLEO Repl. by BEBEK 87

- 1 AUBERT 07AV reports $[B(B^0 \rightarrow J/\psi(1S) K^*(892)^0)] \times [B(J/\psi(1S) \rightarrow p\bar{p})] = (2.82^{+0.30+0.36}_{-0.28-0.35}) \times 10^{-6}$. We divide by our best value $B(J/\psi(1S) \rightarrow p\bar{p}) = (2.17 \pm 0.07) \times 10^{-3}$. Our first error is their experiment's error and our second error is the systematic error from using our best value.
- 2 Assumes equal production of B^+ and B^0 at the $\Upsilon(4S)$.
- 3 ABE 98O reports $[B(B^0 \rightarrow J/\psi(1S) K^*(892)^0)]/[B(B^+ \rightarrow J/\psi(1S) K^+)] = 1.76 \pm 0.14 \pm 0.15$. We multiply by our best value $B(B^+ \rightarrow J/\psi(1S) K^+) = (9.9 \pm 1.0) \times 10^{-4}$. Our first error is their experiment's error and our second error is the systematic error from using our best value.
- 4 Assumes equal production of B^+ and B^0 at the $\Upsilon(4S)$.
- 5 BORTOLETTO 92 reports $(1.1 \pm 0.5 \pm 0.3) \times 10^{-3}$ for $B(J/\psi(1S) \rightarrow e^+ e^-) = 0.069 \pm 0.009$. We rescale to our best value $B(J/\psi(1S) \rightarrow e^+ e^-) = (5.94 \pm 0.06) \times 10^{-2}$. Our first error is their experiment's error and our second error is the systematic error from using our best value. Assumes equal production of B^+ and B^0 at the $\Upsilon(4S)$.
- 6 ALBRECHT 90J reports $(1.1 \pm 0.5 \pm 0.2) \times 10^{-3}$ for $B(J/\psi(1S) \rightarrow e^+ e^-) = 0.069 \pm 0.009$. We rescale to our best value $B(J/\psi(1S) \rightarrow e^+ e^-) = (5.94 \pm 0.06) \times 10^{-2}$. Our first error is their experiment's error and our second error is the systematic error from using our best value. Assumes equal production of B^+ and B^0 at the $\Upsilon(4S)$.
- 7 BEBEK 87 reports $(3.5 \pm 1.6 \pm 0.3) \times 10^{-3}$ for $B(J/\psi(1S) \rightarrow e^+ e^-) = 0.069 \pm 0.009$. We rescale to our best value $B(J/\psi(1S) \rightarrow e^+ e^-) = (5.94 \pm 0.06) \times 10^{-2}$. Our first error is their experiment's error and our second error is the systematic error from using our best value. Updated in BORTOLETTO 92 to use the same assumptions.
- 8 ABE 96H assumes that $B(B^+ \rightarrow J/\psi K^+) = (1.02 \pm 0.14) \times 10^{-3}$.
- 9 The neutral and charged B events together are predominantly longitudinally polarized, $\Gamma_{\perp}/\Gamma = 0.080 \pm 0.08 \pm 0.05$. This can be compared with a prediction using HJET, 0.73 (KRAMER 92). This polarization indicates that the $B \rightarrow \psi K^*$ decay is dominated by the $CP = -1$ CP eigenstate. Assumes equal production of B^+ and B^0 at the $\Upsilon(4S)$.
- 10 ALBRECHT 94G measures the polarization in the vector-vector decay to be predominantly longitudinal, $\Gamma_{\perp}/\Gamma = 0.03 \pm 0.16 \pm 0.15$ making the neutral decay a CP eigenstate when the K^* decays through $K_S^0 \pi^0$.
- 11 ALBAJAR 91E assumes B_0^0 production fraction of 36%.
- 12 ALBRECHT 87D assume $B^+ B^- / B^0 \bar{B}^0$ ratio is 55/45. Superseded by ALBRECHT 90J.
- 13 ALAM 86 assumes B^{\pm}/B^0 ratio is 60/40. The observation of the decay $B^+ \rightarrow J/\psi K^*(892)^+$ (HAAS 85) has been retracted in this paper.

$\Gamma(J/\psi(1S) K^*(892)^0)/\Gamma(J/\psi(1S) K^0)$		$\Gamma_{161}/\Gamma_{159}$	
VALUE	DOCUMENT ID	TECN	COMMENT
1.50 ± 0.09 OUR AVERAGE			
1.51 ± 0.05 ± 0.08	AUBERT	05J	BABR $e^+ e^- \rightarrow \Upsilon(4S)$
1.39 ± 0.36 ± 0.10	ABE	96Q	CDF $p\bar{p}$
••• We do not use the following data for averages, fits, limits, etc. •••			
1.49 ± 0.10 ± 0.08	1 AUBERT	02	BABR Repl. by AUBERT 05J

- 1 Assumes equal production of B^+ and B^0 at the $\Upsilon(4S)$.

$\Gamma(J/\psi(1S) \eta K_S^0)/\Gamma_{total}$		Γ_{162}/Γ	
VALUE (units 10^{-5})	DOCUMENT ID	TECN	COMMENT
8.4 ± 2.6 ± 2.7			
	1 AUBERT	04Y	BABR $e^+ e^- \rightarrow \Upsilon(4S)$

- 1 Assumes equal production of B^+ and B^0 at the $\Upsilon(4S)$.

$\Gamma(J/\psi(1S) \eta' K_S^0)/\Gamma_{total}$		Γ_{163}/Γ	
VALUE (units 10^{-5})	CL%	DOCUMENT ID	TECN COMMENT
<2.5	90	1 XIE	07 BELL $e^+ e^- \rightarrow \Upsilon(4S)$

- 1 Assumes equal production of B^+ and B^0 at the $\Upsilon(4S)$.

Meson Particle Listings

 B^0 $\Gamma(J/\psi(1S)\phi K^0)/\Gamma_{\text{total}}$ Γ_{164}/Γ

VALUE	DOCUMENT ID	TECN	COMMENT
$(9.4 \pm 2.6) \times 10^{-5}$ OUR AVERAGE			
$(10.2 \pm 3.8 \pm 1.0) \times 10^{-5}$	¹ AUBERT 03o	BABR	$e^+e^- \rightarrow \Upsilon(4S)$
$(8.8^{+3.5}_{-3.0} \pm 1.3) \times 10^{-5}$	² ANASTASSOV 00	CLE2	$e^+e^- \rightarrow \Upsilon(4S)$

- ¹ Assumes equal production of B^+ and B^0 at the $\Upsilon(4S)$.
² ANASTASSOV 00 finds 10 events on a background of 0.5 ± 0.2 . Assumes equal production of B^0 and B^+ at the $\Upsilon(4S)$, a uniform Dalitz plot distribution, isotropic $J/\psi(1S)$ and ϕ decays, and $B(B^+ \rightarrow J/\psi(1S)\phi K^+) = B(B^0 \rightarrow J/\psi(1S)\phi K^0)$.

 $\Gamma(J/\psi(1S)K(1270)^0)/\Gamma_{\text{total}}$ Γ_{165}/Γ

VALUE (units 10^{-3})	DOCUMENT ID	TECN	COMMENT
$1.30 \pm 0.34 \pm 0.32$	¹ ABE 01L	BELL	$e^+e^- \rightarrow \Upsilon(4S)$

- ¹ Assumes equal production of B^+ and B^0 at the $\Upsilon(4S)$ and uses the PDG value of $B(B^+ \rightarrow J/\psi(1S)K^+) = (1.00 \pm 0.10) \times 10^{-3}$.

 $\Gamma(J/\psi(1S)\pi^0)/\Gamma_{\text{total}}$ Γ_{166}/Γ

VALUE (units 10^{-5})	CL%	DOCUMENT ID	TECN	COMMENT
2.05 ± 0.24 OUR AVERAGE				
$1.94 \pm 0.22 \pm 0.17$		¹ AUBERT,B 06B	BABR	$e^+e^- \rightarrow \Upsilon(4S)$
$2.3 \pm 0.5 \pm 0.2$		¹ ABE 03B	BELL	$e^+e^- \rightarrow \Upsilon(4S)$
$2.5^{+1.1}_{-0.9} \pm 0.2$		¹ AVERY 00	CLE2	$e^+e^- \rightarrow \Upsilon(4S)$

- • • We do not use the following data for averages, fits, limits, etc. • • • •
 $2.0 \pm 0.6 \pm 0.2$ ¹ AUBERT 02 BABR Repl. by AUBERT,B 06B
 < 32 90 ² ACCIARRI 97C L3
 < 5.8 90 BISHAI 96 CLE2 Sup. by AVERY 00
 < 690 90 ¹ ALEXANDER 95 CLE2 Sup. by BISHAI 96

- ¹ Assumes equal production of B^+ and B^0 at the $\Upsilon(4S)$.
² ACCIARRI 97C assumes B^0 production fraction ($39.5 \pm 4.0\%$) and B_S ($12.0 \pm 3.0\%$).

 $\Gamma(J/\psi(1S)\eta)/\Gamma_{\text{total}}$ Γ_{167}/Γ

VALUE (units 10^{-6})	CL%	DOCUMENT ID	TECN	COMMENT
$9.5 \pm 1.7 \pm 0.8$		¹ CHANG 07A	BELL	$e^+e^- \rightarrow \Upsilon(4S)$
< 27	90	¹ AUBERT 03o	BABR	$e^+e^- \rightarrow \Upsilon(4S)$
< 1200	90	² ACCIARRI 97C	L3	

- • • We do not use the following data for averages, fits, limits, etc. • • • •
 < 27 90 ¹ AUBERT 03o BABR $e^+e^- \rightarrow \Upsilon(4S)$
 < 1200 90 ² ACCIARRI 97C L3

- ¹ Assumes equal production of B^+ and B^0 at the $\Upsilon(4S)$.
² ACCIARRI 97C assumes B^0 production fraction ($39.5 \pm 4.0\%$) and B_S ($12.0 \pm 3.0\%$).

 $\Gamma(J/\psi(1S)\pi^+\pi^-)/\Gamma_{\text{total}}$ Γ_{168}/Γ

VALUE	DOCUMENT ID	TECN	COMMENT
$(4.6 \pm 0.7 \pm 0.6) \times 10^{-5}$	¹ AUBERT 03B	BABR	$e^+e^- \rightarrow \Upsilon(4S)$

- ¹ Assumes equal production of B^+ and B^0 at the $\Upsilon(4S)$.

 $\Gamma(J/\psi(1S)\pi^+\pi^- \text{ nonresonant})/\Gamma_{\text{total}}$ Γ_{169}/Γ

VALUE (units 10^{-5})	CL%	DOCUMENT ID	TECN	COMMENT
< 1.2	90	¹ AUBERT 07AC	BABR	$e^+e^- \rightarrow \Upsilon(4S)$

- ¹ Assumes equal production of B^+ and B^0 at the $\Upsilon(4S)$.

 $\Gamma(J/\psi(1S)f_2)/\Gamma_{\text{total}}$ Γ_{170}/Γ

VALUE (units 10^{-5})	CL%	DOCUMENT ID	TECN	COMMENT
< 0.46	90	¹ AUBERT 07AC	BABR	$e^+e^- \rightarrow \Upsilon(4S)$

- ¹ Assumes equal production of B^+ and B^0 at the $\Upsilon(4S)$.

 $\Gamma(J/\psi(1S)\rho^0)/\Gamma_{\text{total}}$ Γ_{171}/Γ

VALUE (units 10^{-5})	CL%	DOCUMENT ID	TECN	COMMENT
$2.7 \pm 0.3 \pm 0.2$		¹ AUBERT 07AC	BABR	$e^+e^- \rightarrow \Upsilon(4S)$
$1.6 \pm 0.6 \pm 0.4$		¹ AUBERT 03B	BABR	Repl. by AUBERT 07AC
< 25	90	BISHAI 96	CLE2	$e^+e^- \rightarrow \Upsilon(4S)$

- • • We do not use the following data for averages, fits, limits, etc. • • • •
 < 25 90 BISHAI 96 CLE2 $e^+e^- \rightarrow \Upsilon(4S)$

- ¹ Assumes equal production of B^+ and B^0 at the $\Upsilon(4S)$.

 $\Gamma(J/\psi(1S)\omega)/\Gamma_{\text{total}}$ Γ_{172}/Γ

VALUE	CL%	DOCUMENT ID	TECN	COMMENT
$< 2.7 \times 10^{-4}$	90	BISHAI 96	CLE2	$e^+e^- \rightarrow \Upsilon(4S)$

 $\Gamma(J/\psi(1S)\phi)/\Gamma_{\text{total}}$ Γ_{173}/Γ

VALUE (units 10^{-6})	CL%	DOCUMENT ID	TECN	COMMENT
< 9.2	90	¹ AUBERT 03o	BABR	$e^+e^- \rightarrow \Upsilon(4S)$

- ¹ Assumes equal production of B^+ and B^0 at the $\Upsilon(4S)$.

 $\Gamma(J/\psi(1S)\eta(958))/\Gamma_{\text{total}}$ Γ_{174}/Γ

VALUE (units 10^{-5})	CL%	DOCUMENT ID	TECN	COMMENT
< 6.3	90	¹ AUBERT 03o	BABR	$e^+e^- \rightarrow \Upsilon(4S)$

- ¹ Assumes equal production of B^+ and B^0 at the $\Upsilon(4S)$.

 $\Gamma(J/\psi(1S)K^0\pi^+\pi^-)/\Gamma_{\text{total}}$ Γ_{175}/Γ

VALUE (units 10^{-4})	DOCUMENT ID	TECN	COMMENT
$10.3 \pm 3.3 \pm 1.5$	¹ AFFOLDER 02B	CDF	$p\bar{p}$ 1.8 TeV
			¹ Uses $B^0 \rightarrow J/\psi(1S)K_S^0$ decay as a reference and $B(B^0 \rightarrow J/\psi(1S)K^0) = 8.3 \times 10^{-4}$.

 $\Gamma(J/\psi(1S)K^0\rho^0)/\Gamma_{\text{total}}$ Γ_{176}/Γ

VALUE (units 10^{-4})	DOCUMENT ID	TECN	COMMENT
$5.4 \pm 2.9 \pm 0.9$	¹ AFFOLDER 02B	CDF	$p\bar{p}$ 1.8 TeV
			¹ Uses $B^0 \rightarrow J/\psi(1S)K_S^0$ decay as a reference and $B(B^0 \rightarrow J/\psi(1S)K^0) = 8.3 \times 10^{-4}$.

 $\Gamma(J/\psi(1S)K^*(892)^+\pi^-)/\Gamma_{\text{total}}$ Γ_{177}/Γ

VALUE (units 10^{-4})	DOCUMENT ID	TECN	COMMENT
$7.7 \pm 4.1 \pm 1.3$	¹ AFFOLDER 02B	CDF	$p\bar{p}$ 1.8 TeV
			¹ Uses $B^0 \rightarrow J/\psi(1S)K_S^0$ decay as a reference and $B(B^0 \rightarrow J/\psi(1S)K^0) = 8.3 \times 10^{-4}$.

 $\Gamma(J/\psi(1S)K^*(892)^0\pi^+\pi^-)/\Gamma_{\text{total}}$ Γ_{178}/Γ

VALUE (units 10^{-4})	DOCUMENT ID	TECN	COMMENT
$6.6 \pm 1.9 \pm 1.1$	¹ AFFOLDER 02B	CDF	$p\bar{p}$ 1.8 TeV
			¹ Uses $B^0 \rightarrow J/\psi(1S)K^*(892)^0$ decay as a reference and $B(B^0 \rightarrow J/\psi(1S)K^0) = 12.4 \times 10^{-4}$.

 $\Gamma(X(3872)^-K^+)/\Gamma_{\text{total}}$ Γ_{179}/Γ

VALUE	CL%	DOCUMENT ID	TECN	COMMENT
$< 5 \times 10^{-4}$	90	¹ AUBERT 06E	BABR	$e^+e^- \rightarrow \Upsilon(4S)$
				¹ Perform measurements of absolute branching fractions using a missing mass technique.

 $\Gamma(X(3872)^-K^+ \times B(X(3872)^- \rightarrow J/\psi(1S)\pi^-\pi^0))/\Gamma_{\text{total}}$ Γ_{180}/Γ

VALUE (units 10^{-6})	CL%	DOCUMENT ID	TECN	COMMENT
< 5.4	90	¹ AUBERT 05B	BABR	$e^+e^- \rightarrow \Upsilon(4S)$
				¹ Assumes equal production of B^+ and B^0 at the $\Upsilon(4S)$. The isovector-X hypothesis is excluded with a likelihood test at 1×10^{-4} level.

 $\Gamma(X(3872)K^0 \times B(X \rightarrow J/\psi\pi^+\pi^-))/\Gamma_{\text{total}}$ Γ_{181}/Γ

VALUE (units 10^{-6})	CL%	DOCUMENT ID	TECN	COMMENT
< 10.3	90	^{1,2} AUBERT 06	BABR	$e^+e^- \rightarrow \Upsilon(4S)$
				¹ The lower limit is also given to be 1.34×10^{-6} at 90% CL. ² Assumes equal production of B^+ and B^0 at the $\Upsilon(4S)$.

 $\Gamma(X(3872)K^0 \times B(X \rightarrow D^0\bar{D}^0\pi^0))/\Gamma_{\text{total}}$ Γ_{182}/Γ

VALUE (units 10^{-4})	DOCUMENT ID	TECN	COMMENT
$1.66 \pm 0.70^{+0.32}_{-0.37}$	¹ GOKHROO 06	BELL	$e^+e^- \rightarrow \Upsilon(4S)$
			¹ Measure the near-threshold enhancements in the $(D^0\bar{D}^0\pi^0)$ system at a mass $3875.2 \pm 0.7^{+0.3}_{-1.6} \pm 0.8$ MeV/c ² .

 $\Gamma(X(3872)K^0 \times B(X \rightarrow \bar{D}^{*0}D^0))/\Gamma_{\text{total}}$ Γ_{183}/Γ

VALUE (units 10^{-4})	CL%	DOCUMENT ID	TECN	COMMENT
< 4.37	90	¹ AUBERT 08B	BABR	$e^+e^- \rightarrow \Upsilon(4S)$
				¹ Assumes equal production of B^+ and B^0 at the $\Upsilon(4S)$.

 $\Gamma(J/\psi(1S)\rho\bar{\rho})/\Gamma_{\text{total}}$ Γ_{184}/Γ

VALUE	CL%	DOCUMENT ID	TECN	COMMENT
$< 8.3 \times 10^{-7}$	90	¹ XIE 05	BELL	$e^+e^- \rightarrow \Upsilon(4S)$
$< 1.9 \times 10^{-6}$	90	¹ AUBERT 03K	BABR	$e^+e^- \rightarrow \Upsilon(4S)$
				¹ Assumes equal production of B^+ and B^0 at the $\Upsilon(4S)$.

 $\Gamma(J/\psi(1S)\gamma)/\Gamma_{\text{total}}$ Γ_{185}/Γ

VALUE (units 10^{-6})	CL%	DOCUMENT ID	TECN	COMMENT
< 1.6	90	¹ AUBERT,B 04T	BABR	$e^+e^- \rightarrow \Upsilon(4S)$
				¹ Assumes equal production of B^+ and B^0 at the $\Upsilon(4S)$.

 $\Gamma(J/\psi(1S)\bar{D}^0)/\Gamma_{\text{total}}$ Γ_{186}/Γ

VALUE (units 10^{-5})	CL%	DOCUMENT ID	TECN	COMMENT
< 1.3	90	¹ AUBERT 05U	BABR	$e^+e^- \rightarrow \Upsilon(4S)$
< 2.0	90	¹ ZHANG 05B	BELL	$e^+e^- \rightarrow \Upsilon(4S)$
				¹ Assumes equal production of B^+ and B^0 at the $\Upsilon(4S)$.

 $\Gamma(\psi(2S)K^0)/\Gamma_{\text{total}}$ Γ_{187}/Γ

VALUE (units 10^{-4})	CL%	DOCUMENT ID	TECN	COMMENT
6.2 ± 0.6 OUR AVERAGE				
$6.46 \pm 0.65 \pm 0.51$		¹ AUBERT 05J	BABR	$e^+e^- \rightarrow \Upsilon(4S)$
6.7 ± 1.1		¹ ABE 03B	BELL	$e^+e^- \rightarrow \Upsilon(4S)$
$5.0 \pm 1.1 \pm 0.6$		¹ RICHICHI 01	CLE2	$e^+e^- \rightarrow \Upsilon(4S)$

See key on page 373

Meson Particle Listings
 B^0

• • • We do not use the following data for averages, fits, limits, etc. • • •

VALUE	CL%	DOCUMENT ID	TECN	COMMENT
$6.9 \pm 1.1 \pm 1.1$		¹ AUBERT 02	BABR	Repl. by AUBERT 05J
< 8	90	¹ ALAM	94 CLE2	$e^+e^- \rightarrow \Upsilon(4S)$
< 15	90	¹ BORTOLETTO92	CLEO	$e^+e^- \rightarrow \Upsilon(4S)$
< 28	90	¹ ALBRECHT 90J	ARG	$e^+e^- \rightarrow \Upsilon(4S)$

¹ Assumes equal production of B^+ and B^0 at the $\Upsilon(4S)$.

VALUE (units 10^{-4})	CL%	DOCUMENT ID	TECN	COMMENT
< 1.23	90	¹ AUBERT 08B	BABR	$e^+e^- \rightarrow \Upsilon(4S)$

¹ Assumes equal production of B^+ and B^0 at the $\Upsilon(4S)$.

VALUE (units 10^{-4})	CL%	DOCUMENT ID	TECN	COMMENT
< 1.88	90	¹ AUBERT 08B	BABR	$e^+e^- \rightarrow \Upsilon(4S)$

¹ Assumes equal production of B^+ and B^0 at the $\Upsilon(4S)$.

VALUE	CL%	DOCUMENT ID	TECN	COMMENT
$0.82 \pm 0.13 \pm 0.12$		¹ AUBERT 02	BABR	$e^+e^- \rightarrow \Upsilon(4S)$

¹ Assumes equal production of B^+ and B^0 at the $\Upsilon(4S)$.

VALUE	CL%	DOCUMENT ID	TECN	COMMENT
< 0.001	90	¹ ALBRECHT 90J	ARG	$e^+e^- \rightarrow \Upsilon(4S)$

¹ Assumes equal production of B^+ and B^0 at the $\Upsilon(4S)$.

VALUE	CL%	DOCUMENT ID	TECN	COMMENT
7.2 ± 0.8		OUR AVERAGE		
$6.49 \pm 0.59 \pm 0.97$		¹ AUBERT 05J	BABR	$e^+e^- \rightarrow \Upsilon(4S)$
$7.6 \pm 1.1 \pm 1.0$		¹ RICHICHI 01	CLE2	$e^+e^- \rightarrow \Upsilon(4S)$
$9.0 \pm 2.2 \pm 0.9$		² ABE 980	CDF	$p\bar{p}$ 1.8 TeV

• • • We do not use the following data for averages, fits, limits, etc. • • •

VALUE	CL%	DOCUMENT ID	TECN	COMMENT
< 19	90	¹ ALAM	94 CLE2	Repl. by RICHICHI 01
$14 \pm 8 \pm 4$		¹ BORTOLETTO92	CLEO	$e^+e^- \rightarrow \Upsilon(4S)$
< 23	90	¹ ALBRECHT 90J	ARG	$e^+e^- \rightarrow \Upsilon(4S)$

¹ Assumes equal production of B^+ and B^0 at the $\Upsilon(4S)$.
² ABE 980 reports $[B(B^0 \rightarrow \psi(2S) K^*(892^0))/B(B^+ \rightarrow J/\psi(1S) K^+)] = 0.908 \pm 0.194 \pm 0.10$. We multiply by our best value $B(B^+ \rightarrow J/\psi(1S) K^+) = (9.9 \pm 1.0) \times 10^{-4}$. Our first error is their experiment's error and our second error is the systematic error from using our best value.

VALUE	CL%	DOCUMENT ID	TECN	COMMENT
$1.00 \pm 0.14 \pm 0.09$		AUBERT 05J	BABR	$e^+e^- \rightarrow \Upsilon(4S)$

VALUE (units 10^{-4})	CL%	DOCUMENT ID	TECN	COMMENT
< 1.13	90	¹ GARMASH 07	BELL	$e^+e^- \rightarrow \Upsilon(4S)$

• • • We do not use the following data for averages, fits, limits, etc. • • •

VALUE	CL%	DOCUMENT ID	TECN	COMMENT
< 12.4	90	² AUBERT 05K	BABR	$e^+e^- \rightarrow \Upsilon(4S)$
< 5.0	90	³ EDWARDS 01	CLE2	$e^+e^- \rightarrow \Upsilon(4S)$

¹ Uses Dalitz plot analysis of the $B^0 \rightarrow K^0 \pi^+ \pi^-$ final state decays.

² Assumes equal production of B^+ and B^0 at the $\Upsilon(4S)$.

³ EDWARDS 01 assumes equal production of B^0 and B^+ at the $\Upsilon(4S)$. The correlated uncertainties (28.3%) from $B(J/\psi(1S) \rightarrow \gamma \eta_c)$ in those modes have been accounted for.

VALUE	CL%	DOCUMENT ID	TECN	COMMENT
$< 7.7 \times 10^{-4}$	90	¹ AUBERT 05K	BABR	$e^+e^- \rightarrow \Upsilon(4S)$

¹ Assumes equal production of B^+ and B^0 at the $\Upsilon(4S)$.

VALUE	CL%	DOCUMENT ID	TECN	COMMENT
$< 2.6 \times 10^{-5}$	90	¹ SONI 06	BELL	$e^+e^- \rightarrow \Upsilon(4S)$

• • • We do not use the following data for averages, fits, limits, etc. • • •

VALUE	CL%	DOCUMENT ID	TECN	COMMENT
$< 4.1 \times 10^{-5}$	90	¹ AUBERT 05K	BABR	$e^+e^- \rightarrow \Upsilon(4S)$

¹ Assumes equal production of B^+ and B^0 at the $\Upsilon(4S)$.

VALUE	CL%	DOCUMENT ID	TECN	COMMENT
$< 3.6 \times 10^{-5}$	90	¹ AUBERT 05K	BABR	$e^+e^- \rightarrow \Upsilon(4S)$

• • • We do not use the following data for averages, fits, limits, etc. • • •

VALUE	CL%	DOCUMENT ID	TECN	COMMENT
$< 7.1 \times 10^{-5}$	90	¹ SONI 06	BELL	$e^+e^- \rightarrow \Upsilon(4S)$

¹ Assumes equal production of B^+ and B^0 at the $\Upsilon(4S)$.

VALUE (units 10^{-4})	CL%	DOCUMENT ID	TECN	COMMENT
3.9 ± 0.4		OUR AVERAGE		
$3.51 \pm 0.33 \pm 0.45$		¹ SONI 06	BELL	$e^+e^- \rightarrow \Upsilon(4S)$
$4.53 \pm 0.41 \pm 0.51$		¹ AUBERT 05J	BABR	$e^+e^- \rightarrow \Upsilon(4S)$
$3.0 \pm 1.5 \pm 1.0$		² AVERY 00	CLE2	$e^+e^- \rightarrow \Upsilon(4S)$

• • • We do not use the following data for averages, fits, limits, etc. • • •

VALUE	CL%	DOCUMENT ID	TECN	COMMENT
$4.1 \pm 1.3 \pm 0.2$		³ AUBERT 02	BABR	Repl. by AUBERT 05J
< 27	90	¹ ALAM	94 CLE2	$e^+e^- \rightarrow \Upsilon(4S)$

¹ Assumes equal production of B^+ and B^0 at the $\Upsilon(4S)$.
² AVERY 00 reports $(3.9 \pm 1.9 \pm 0.4) \times 10^{-4}$ for $B(\chi_{c1}(1P) \rightarrow \gamma J/\psi(1S)) = 0.273 \pm 0.016$. We rescale to our best value $B(\chi_{c1}(1P) \rightarrow \gamma J/\psi(1S)) = (36.0 \pm 1.9) \times 10^{-2}$. Our first error is their experiment's error and our second error is the systematic error from using our best value. Assumes equal production of B^+ and B^0 at the $\Upsilon(4S)$.
³ AUBERT 02 reports $(5.4 \pm 1.4 \pm 1.1) \times 10^{-4}$ for $B(\chi_{c1}(1P) \rightarrow \gamma J/\psi(1S)) = 0.273 \pm 0.016$. We rescale to our best value $B(\chi_{c1}(1P) \rightarrow \gamma J/\psi(1S)) = (36.0 \pm 1.9) \times 10^{-2}$. Our first error is their experiment's error and our second error is the systematic error from using our best value. Assumes equal production of B^+ and B^0 at the $\Upsilon(4S)$.

VALUE (units 10^{-4})	CL%	DOCUMENT ID	TECN	COMMENT
3.2 ± 0.6		OUR AVERAGE		
$3.14 \pm 0.34 \pm 0.72$		¹ SONI 06	BELL	$e^+e^- \rightarrow \Upsilon(4S)$
$3.27 \pm 0.42 \pm 0.64$		¹ AUBERT 05J	BABR	$e^+e^- \rightarrow \Upsilon(4S)$

• • • We do not use the following data for averages, fits, limits, etc. • • •

VALUE	CL%	DOCUMENT ID	TECN	COMMENT
$3.6 \pm 1.2 \pm 0.2$		² AUBERT 02	BABR	Repl. by AUBERT 05J
< 21	90	³ ALAM	94 CLE2	$e^+e^- \rightarrow \Upsilon(4S)$

¹ Assumes equal production of B^+ and B^0 at the $\Upsilon(4S)$.
² AUBERT 02 reports $(4.8 \pm 1.4 \pm 0.9) \times 10^{-4}$ for $B(\chi_{c1}(1P) \rightarrow \gamma J/\psi(1S)) = 0.273 \pm 0.016$. We rescale to our best value $B(\chi_{c1}(1P) \rightarrow \gamma J/\psi(1S)) = (36.0 \pm 1.9) \times 10^{-2}$. Our first error is their experiment's error and our second error is the systematic error from using our best value. Assumes equal production of B^+ and B^0 at the $\Upsilon(4S)$.
³ BORTOLETTO 92 assumes equal production of B^+ and B^0 at the $\Upsilon(4S)$.

VALUE	CL%	DOCUMENT ID	TECN	COMMENT
$0.50 \pm 0.15 \pm 0.03$		¹ AUBERT 02	BABR	$e^+e^- \rightarrow \Upsilon(4S)$

¹ AUBERT 02 reports $0.66 \pm 0.11 \pm 0.17$ for $B(\chi_{c1}(1P) \rightarrow \gamma J/\psi(1S)) = 0.273 \pm 0.016$. We rescale to our best value $B(\chi_{c1}(1P) \rightarrow \gamma J/\psi(1S)) = (36.0 \pm 1.9) \times 10^{-2}$. Our first error is their experiment's error and our second error is the systematic error from using our best value. Assumes equal production of B^+ and B^0 at the $\Upsilon(4S)$.

VALUE	CL%	DOCUMENT ID	TECN	COMMENT
$0.72 \pm 0.11 \pm 0.12$		AUBERT 05J	BABR	$e^+e^- \rightarrow \Upsilon(4S)$

• • • We do not use the following data for averages, fits, limits, etc. • • •

VALUE	CL%	DOCUMENT ID	TECN	COMMENT
$0.89 \pm 0.34 \pm 0.17$		¹ AUBERT 02	BABR	Repl. by AUBERT 05J

¹ Assumes equal production of B^+ and B^0 at the $\Upsilon(4S)$.

VALUE (units 10^{-6})	CL%	DOCUMENT ID	TECN	COMMENT
19.4 ± 0.6		OUR AVERAGE		
$19.1 \pm 0.6 \pm 0.6$		¹ AUBERT 07B	BABR	$e^+e^- \rightarrow \Upsilon(4S)$
$19.9 \pm 0.4 \pm 0.8$		¹ LIN 07A	BELL	$e^+e^- \rightarrow \Upsilon(4S)$
$18.0 \pm 2.3 \pm 1.2$		¹ BORNHEIM 03	CLE2	$e^+e^- \rightarrow \Upsilon(4S)$

• • • We do not use the following data for averages, fits, limits, etc. • • •

VALUE	CL%	DOCUMENT ID	TECN	COMMENT
$18.5 \pm 1.0 \pm 0.7$		¹ CHAO 04	BELL	Repl. by LIN 07A
$17.9 \pm 0.9 \pm 0.7$		¹ AUBERT 02Q	BABR	Repl. by AUBERT 07B
$22.5 \pm 1.9 \pm 1.8$		¹ CASEY 02	BELL	Repl. by CHAO 04
$19.3 \pm 3.4 \pm 1.5$		¹ ABE 01H	BELL	Repl. by CASEY 02
$16.7 \pm 1.6 \pm 1.3$		¹ AUBERT 01E	BABR	Repl. by AUBERT 02Q
< 66	90	² ABE 00C	SLD	$e^+e^- \rightarrow Z$
$17.2 \pm 2.5 \pm 1.2$		¹ CRONIN-HEN..00	CLE2	Repl. by BORNHEIM 03

VALUE	CL%	DOCUMENT ID	TECN	COMMENT
$15 \pm 5 \pm 4$		GODANG 98	CLE2	Repl. by CRONIN-HENNESSY 00

• • • We do not use the following data for averages, fits, limits, etc. • • •

VALUE	CL%	DOCUMENT ID	TECN	COMMENT
< 17	90	ASNER 96	CLE2	Sup. by ADAM 96D
< 30	90	⁴ BUSKULIC 96V	ALEP	$e^+e^- \rightarrow Z$
< 90	90	⁵ ABREU 95N	DLPH	Sup. by ADAM 96D
< 81	90	⁶ AKERS 94L	OPAL	$e^+e^- \rightarrow Z$
< 26	90	⁷ BATTLE 93	CLE2	$e^+e^- \rightarrow \Upsilon(4S)$
< 180	90	ALBRECHT 91B	ARG	$e^+e^- \rightarrow \Upsilon(4S)$
< 90	90	⁸ AVERY 89B	CLEO	$e^+e^- \rightarrow \Upsilon(4S)$
< 320	90	AVERY 87	CLEO	$e^+e^- \rightarrow \Upsilon(4S)$

Meson Particle Listings

 B^0

- ¹ Assumes equal production of B^+ and B^0 at the $\Upsilon(4S)$.
² ABE 00C assumes $B(Z \rightarrow b\bar{b}) = (21.7 \pm 0.1)\%$ and the B fractions $f_{B^0} = f_{B^+} = (39.7^{+1.8}_{-2.2})\%$ and $f_{B_s} = (10.5^{+1.3}_{-2.3})\%$.
³ ADAM 96D assumes $f_{B^0} = f_{B^-} = 0.39$ and $f_{B_s} = 0.12$. Contributions from B^0 and B_s decays cannot be separated. Limits are given for the weighted average of the decay rates for the two neutral B mesons.
⁴ BUSKULIC 96V assumes PDG 96 production fractions for B^0, B^+, B_s, b baryons.
⁵ Assumes a B^0, B^- production fraction of 0.39 and a B_s production fraction of 0.12. Contributions from B^0 and B_s^0 decays cannot be separated. Limits are given for the weighted average of the decay rates for the two neutral B mesons.
⁶ Assumes $B(Z \rightarrow b\bar{b}) = 0.217$ and $B_D^0(B_s^0)$ fraction 39.5% (12%).
⁷ BATTLE 93 assumes equal production of $B^0\bar{B}^0$ and B^+B^- at $\Upsilon(4S)$.
⁸ Assumes the $\Upsilon(4S)$ decays 43% to $B^0\bar{B}^0$.

 $\Gamma(K^+\pi^-)/\Gamma(K^0\pi^0)$ $\Gamma_{198}/\Gamma_{199}$

VALUE	DOCUMENT ID	TECN	COMMENT
2.16 ± 0.16 ± 0.16	LIN	07A	BELL $e^+e^- \rightarrow \Upsilon(4S)$
• • • We do not use the following data for averages, fits, limits, etc. • • •			
$1.20^{+0.50+0.22}_{-0.58-0.32}$	¹ ABE	01H	BELL Repl. by LIN 07A

¹ Assumes equal production of B^+ and B^0 at the $\Upsilon(4S)$.

 $[\Gamma(K^+\pi^-) + \Gamma(\pi^+\pi^-)]/\Gamma_{total}$ $(\Gamma_{198} + \Gamma_{284})/\Gamma$

VALUE (units 10^{-6})	EVTS	DOCUMENT ID	TECN	COMMENT
19 ± 6 OUR AVERAGE				
$28^{+15}_{-10} \pm 20$		¹ ADAM	96D	DLPH $e^+e^- \rightarrow Z$
18^{+6+3}_{-5-4}	17.2	ASNER	96	CLE2 $e^+e^- \rightarrow \Upsilon(4S)$
• • • We do not use the following data for averages, fits, limits, etc. • • •				
$24^{+8}_{-7} \pm 2$		² BATTLE	93	CLE2 $e^+e^- \rightarrow \Upsilon(4S)$

- ¹ ADAM 96D assumes $f_{B^0} = f_{B^-} = 0.39$ and $f_{B_s} = 0.12$. Contributions from B^0 and B_s decays cannot be separated. Limits are given for the weighted average of the decay rates for the two neutral B mesons.
² BATTLE 93 assumes equal production of $B^0\bar{B}^0$ and B^+B^- at $\Upsilon(4S)$.

 $\Gamma(K^0\pi^0)/\Gamma_{total}$ Γ_{199}/Γ

VALUE (units 10^{-6})	CL%	DOCUMENT ID	TECN	COMMENT
9.8 ± 0.6 OUR AVERAGE				
$10.3 \pm 0.7 \pm 0.6$		¹ AUBERT	08E	BABR $e^+e^- \rightarrow \Upsilon(4S)$
$9.2 \pm 0.7 \pm 0.6$		¹ LIN	07A	BELL $e^+e^- \rightarrow \Upsilon(4S)$
$12.8^{+4.0+1.7}_{-3.3-1.4}$		¹ BORNHEIM	03	CLE2 $e^+e^- \rightarrow \Upsilon(4S)$
• • • We do not use the following data for averages, fits, limits, etc. • • •				
$11.4 \pm 0.9 \pm 0.6$		¹ AUBERT	05Y	BABR Repl. by AUBERT 08E
$11.4 \pm 1.7 \pm 0.8$		¹ AUBERT	04M	BABR Repl. by AUBERT 05Y
$11.7 \pm 2.3^{+1.2}_{-1.3}$		¹ CHAO	04	BELL Repl. by LIN 07A
$8.0^{+3.3}_{-3.1} \pm 1.6$		¹ CASEY	02	BELL Repl. by CHAO 04
$16.0^{+7.2+2.5}_{-5.9-2.7}$		¹ ABE	01H	BELL Repl. by CASEY 02
$8.2^{+3.1}_{-2.7} \pm 1.2$		¹ AUBERT	01E	BABR Repl. by AUBERT 04M
$14.6^{+5.9+2.4}_{-5.1-3.3}$		¹ CRONIN-HEN.	.00	CLE2 Repl. by BORNHEIM 03
<41	90	GODANG	98	CLE2 Repl. by CRONIN-HENNESSY 00
<40	90	ASNER	96	CLE2 Repl. by GODANG 98

¹ Assumes equal production of B^+ and B^0 at the $\Upsilon(4S)$.

 $\Gamma(\eta'K^0)/\Gamma_{total}$ Γ_{200}/Γ

VALUE (units 10^{-6})	DOCUMENT ID	TECN	COMMENT
65 ± 4 OUR AVERAGE	Error includes scale factor of 1.2.		
$66.6 \pm 2.6 \pm 2.8$	¹ AUBERT	07AE	BABR $e^+e^- \rightarrow \Upsilon(4S)$
$58.9^{+3.6}_{-3.5} \pm 4.3$	¹ SCHUEMANN	06	BELL $e^+e^- \rightarrow \Upsilon(4S)$
$89^{+18}_{-16} \pm 9$	¹ RICHICHI	00	CLE2 $e^+e^- \rightarrow \Upsilon(4S)$
• • • We do not use the following data for averages, fits, limits, etc. • • •			
$67.4 \pm 3.3 \pm 3.2$	¹ AUBERT	05M	BABR AUBERT 07AE
$60.6 \pm 5.6 \pm 4.6$	¹ AUBERT	03W	BABR Repl. by AUBERT 05M
$55^{+19}_{-16} \pm 8$	¹ ABE	01M	BELL Repl. by SCHUEMANN 06
$42^{+13}_{-11} \pm 4$	¹ AUBERT	01G	BABR Repl. by AUBERT 03W
$47^{+27}_{-20} \pm 9$	BEHRENS	98	CLE2 Repl. by RICHICHI 00

¹ Assumes equal production of B^+ and B^0 at the $\Upsilon(4S)$.

 $\Gamma(\eta'K^*(892)^0)/\Gamma_{total}$ Γ_{201}/Γ

VALUE (units 10^{-6})	CL%	DOCUMENT ID	TECN	COMMENT
3.8 ± 1.1 ± 0.5		¹ AUBERT	07E	BABR $e^+e^- \rightarrow \Upsilon(4S)$
• • • We do not use the following data for averages, fits, limits, etc. • • •				
< 2.6	90	¹ SCHUEMANN	07	BELL $e^+e^- \rightarrow \Upsilon(4S)$
< 7.6	90	¹ AUBERT,B	04D	BABR Repl. by AUBERT 07E
< 24	90	¹ RICHICHI	00	CLE2 $e^+e^- \rightarrow \Upsilon(4S)$
< 39	90	BEHRENS	98	CLE2 Repl. by RICHICHI 00

¹ Assumes equal production of B^+ and B^0 at the $\Upsilon(4S)$.

 $\Gamma(\eta K^0)/\Gamma_{total}$ Γ_{202}/Γ

VALUE (units 10^{-6})	CL%	DOCUMENT ID	TECN	COMMENT
< 1.9	90	¹ CHANG	07B	BELL $e^+e^- \rightarrow \Upsilon(4S)$
• • • We do not use the following data for averages, fits, limits, etc. • • •				
< 2.9	90	¹ AUBERT,B	06V	BABR $e^+e^- \rightarrow \Upsilon(4S)$
< 2.5	90	¹ AUBERT,B	05K	BABR $e^+e^- \rightarrow \Upsilon(4S)$
< 2.0	90	¹ CHANG	05A	BELL Repl. by CHANG 07B
< 5.2	90	¹ AUBERT	04H	BABR Repl. by AUBERT,B 05K
< 9.3	90	¹ RICHICHI	00	CLE2 $e^+e^- \rightarrow \Upsilon(4S)$
< 33	90	BEHRENS	98	CLE2 Repl. by RICHICHI 00

¹ Assumes equal production of B^+ and B^0 at the $\Upsilon(4S)$.

 $\Gamma(\eta K^*(892)^0)/\Gamma_{total}$ Γ_{203}/Γ

VALUE (units 10^{-6})	CL%	DOCUMENT ID	TECN	COMMENT
15.9 ± 1.0 OUR AVERAGE				
$15.2 \pm 1.2 \pm 1.0$		¹ WANG	07B	BELL $e^+e^- \rightarrow \Upsilon(4S)$
$16.5 \pm 1.1 \pm 0.8$		¹ AUBERT,B	06H	BABR $e^+e^- \rightarrow \Upsilon(4S)$
$13.8^{+5.5}_{-4.6} \pm 1.6$		¹ RICHICHI	00	CLE2 $e^+e^- \rightarrow \Upsilon(4S)$
• • • We do not use the following data for averages, fits, limits, etc. • • •				
$18.6 \pm 2.3 \pm 1.2$		¹ AUBERT,B	04D	BABR Repl. by AUBERT,B 06H
< 30	90	BEHRENS	98	CLE2 Repl. by RICHICHI 00

¹ Assumes equal production of B^+ and B^0 at the $\Upsilon(4S)$.

 $\Gamma(\eta K_0^*(1430)^0)/\Gamma_{total}$ Γ_{204}/Γ

VALUE (units 10^{-6})	DOCUMENT ID	TECN	COMMENT
11.0 ± 1.6 ± 1.5	¹ AUBERT,B	06H	BABR $e^+e^- \rightarrow \Upsilon(4S)$

¹ Assumes equal production of B^+ and B^0 at the $\Upsilon(4S)$.

 $\Gamma(\eta K_2^*(1430)^0)/\Gamma_{total}$ Γ_{205}/Γ

VALUE (units 10^{-6})	DOCUMENT ID	TECN	COMMENT
9.6 ± 1.8 ± 1.1	¹ AUBERT,B	06H	BABR $e^+e^- \rightarrow \Upsilon(4S)$

¹ Assumes equal production of B^+ and B^0 at the $\Upsilon(4S)$.

 $\Gamma(\omega K^0)/\Gamma_{total}$ Γ_{206}/Γ

VALUE (units 10^{-6})	CL%	DOCUMENT ID	TECN	COMMENT
5.0 ± 0.6 OUR AVERAGE				
$5.4 \pm 0.8 \pm 0.3$		¹ AUBERT	07AE	BABR $e^+e^- \rightarrow \Upsilon(4S)$
$4.4^{+0.8}_{-0.7} \pm 0.4$		¹ JEN	06	BELL $e^+e^- \rightarrow \Upsilon(4S)$
$10.0^{+5.4}_{-4.2} \pm 1.4$		¹ JESSOP	00	CLE2 $e^+e^- \rightarrow \Upsilon(4S)$
• • • We do not use the following data for averages, fits, limits, etc. • • •				
$6.2 \pm 1.0 \pm 0.4$		¹ AUBERT,B	06E	BABR Repl. by AUBERT 07AE
$5.9^{+1.6}_{-1.3} \pm 0.5$		¹ AUBERT	04H	BABR Repl. by AUBERT,B 06E
$4.0^{+1.9}_{-1.6} \pm 0.5$		¹ WANG	04A	BELL Repl. by JEN 06
< 13	90	¹ AUBERT	01G	BABR Repl. by AUBERT 04H
< 57	90	¹ BERGFELD	98	CLE2 Repl. by JESSOP 00

¹ Assumes equal production of B^+ and B^0 at the $\Upsilon(4S)$.

 $\Gamma(a_0(980)^\pm K^\mp \times B(a_0(980)^\pm \rightarrow \eta\pi^\pm))/\Gamma_{total}$ Γ_{208}/Γ

VALUE (units 10^{-6})	CL%	DOCUMENT ID	TECN	COMMENT
< 1.9	90	¹ AUBERT	07Y	BABR $e^+e^- \rightarrow \Upsilon(4S)$
• • • We do not use the following data for averages, fits, limits, etc. • • •				
< 2.1	90	¹ AUBERT,BE	04	BABR Repl. by AUBERT 07Y

¹ Assumes equal production of B^+ and B^0 at the $\Upsilon(4S)$.

 $\Gamma(a_0(1450)^\pm K^\mp \times B(a_0(1450)^\pm \rightarrow \eta\pi^\pm))/\Gamma_{total}$ Γ_{209}/Γ

VALUE (units 10^{-6})	CL%	DOCUMENT ID	TECN	COMMENT
< 3.1	90	¹ AUBERT	07Y	BABR $e^+e^- \rightarrow \Upsilon(4S)$

¹ Assumes equal production of B^+ and B^0 at the $\Upsilon(4S)$.

 $\Gamma(a_0(980)^0 K^0 \times B(a_0(980)^0 \rightarrow \eta\pi^0))/\Gamma_{total}$ Γ_{207}/Γ

VALUE (units 10^{-6})	CL%	DOCUMENT ID	TECN	COMMENT
< 7.8	90	¹ AUBERT,BE	04	BABR $e^+e^- \rightarrow \Upsilon(4S)$

¹ Assumes equal production of charged and neutral B mesons from $\Upsilon(4S)$ decays.

 $\Gamma(K_S^0 X^0 (\text{Familon}))/\Gamma_{total}$ Γ_{210}/Γ

VALUE (units 10^{-6})	CL%	DOCUMENT ID	TECN	COMMENT
< 53	90	¹ AMMAR	01B	CLE2 $e^+e^- \rightarrow \Upsilon(4S)$

¹ AMMAR 01B searched for the two-body decay of the B meson to a massless neutral feebly-interacting particle X^0 such as the familon, the Nambu-Goldstone boson associated with a spontaneously broken global family symmetry.

 $\Gamma(\omega K^*(892)^0)/\Gamma_{total}$ Γ_{211}/Γ

VALUE (units 10^{-6})	CL%	DOCUMENT ID	TECN	COMMENT
< 4.2	90	¹ AUBERT,B	06T	BABR $e^+e^- \rightarrow \Upsilon(4S)$
• • • We do not use the following data for averages, fits, limits, etc. • • •				
< 6.0	90	¹ AUBERT	05O	BABR Repl. by AUBERT,B 06T
< 23	90	¹ BERGFELD	98	CLE2

¹ Assumes equal production of B^+ and B^0 at the $\Upsilon(4S)$.

See key on page 373

Meson Particle Listings

 B^0

$\Gamma(K^+K^-)/\Gamma_{\text{total}}$		Γ_{212}/Γ			
VALUE (units 10^{-6})	CL%	DOCUMENT ID	TECN	COMMENT	
< 0.41	90	¹ LIN	07	BELL	$e^+e^- \rightarrow \Upsilon(4S)$
••• We do not use the following data for averages, fits, limits, etc. •••					
< 0.5	90	¹ AUBERT	07b	BABR	$e^+e^- \rightarrow \Upsilon(4S)$
< 1.8	90	² ABULENCIA,A	06d	CDF	$p\bar{p}$ at 1.96 TeV
< 0.37	90	ABE	05g	BELL	Repl. by LIN 07
< 0.7	90	CHAO	04	BELL	$e^+e^- \rightarrow \Upsilon(4S)$
< 0.8	90	¹ BORNHEIM	03	CLE2	$e^+e^- \rightarrow \Upsilon(4S)$
< 0.6	90	¹ AUBERT	02q	BABR	$e^+e^- \rightarrow \Upsilon(4S)$
< 0.9	90	¹ CASEY	02	BELL	$e^+e^- \rightarrow \Upsilon(4S)$
< 2.7	90	¹ ABE	01h	BELL	$e^+e^- \rightarrow \Upsilon(4S)$
< 2.5	90	¹ AUBERT	01e	BABR	$e^+e^- \rightarrow \Upsilon(4S)$
< 66	90	³ ABE	00c	SLD	$e^+e^- \rightarrow Z$
< 1.9	90	¹ CRONIN-HEN.	00	CLE2	$e^+e^- \rightarrow \Upsilon(4S)$
< 4.3	90	GODANG	98	CLE2	Repl. by CRONIN-HENNESSY 00
< 46		⁴ ADAM	96d	DLPH	$e^+e^- \rightarrow Z$
< 4	90	ASNER	96	CLE2	Repl. by GODANG 98
< 18	90	⁵ BUSKULIC	96v	ALEP	$e^+e^- \rightarrow Z$
< 120	90	⁶ ABREU	95n	DLPH	Sup. by ADAM 96d
< 7	90	¹ BATTLE	93	CLE2	$e^+e^- \rightarrow \Upsilon(4S)$

- ¹ Assumes equal production of B^+ and B^0 at the $\Upsilon(4S)$.
- ² ABULENCIA,A 06d obtains this from $\Gamma(K^+K^-)/\Gamma(K^+\pi^-) < 0.10$ at 90% CL, assuming $B(B^0 \rightarrow K^+\pi^-) = (18.9 \pm 0.7) \times 10^{-6}$.
- ³ ABE 00c assumes $B(Z \rightarrow b\bar{b}) = (21.7 \pm 0.1)\%$ and the B fractions $f_{B^0} = f_{B^+} = (39.7 \pm 1.8)\%$ and $f_{B_s} = (10.5 \pm 1.8)\%$.
- ⁴ ADAM 96d assumes $f_{B^0} = f_{B^-} = 0.39$ and $f_{B_s} = 0.12$. Contributions from B^0 and B_s decays cannot be separated. Limits are given for the weighted average of the decay rates for the two neutral B mesons.
- ⁵ BUSKULIC 96v assumes PDG 96 production fractions for B^0 , B^+ , B_s , b baryons.
- ⁶ Assumes a B^0 , B^- production fraction of 0.39 and a B_s production fraction of 0.12. Contributions from B^0 and B_s decays cannot be separated. Limits are given for the weighted average of the decay rates for the two neutral B mesons.

$\Gamma(K^0\bar{K}^0)/\Gamma_{\text{total}}$		Γ_{213}/Γ			
VALUE (units 10^{-6})	CL%	DOCUMENT ID	TECN	COMMENT	
0.96 ± 0.20		OUR AVERAGE			
$0.87 \pm 0.25 \pm 0.09$		¹ LIN	07	BELL	$e^+e^- \rightarrow \Upsilon(4S)$
$1.08 \pm 0.28 \pm 0.11$		¹ AUBERT,BE	06c	BABR	$e^+e^- \rightarrow \Upsilon(4S)$
••• We do not use the following data for averages, fits, limits, etc. •••					
$0.8 \pm 0.3 \pm 0.9$		¹ ABE	05g	BELL	Repl. by LIN 07
$1.19 \pm 0.40 \pm 0.13$		¹ AUBERT,BE	05e	BABR	Repl. by AUBERT,BE 06c
< 1.8	90	¹ AUBERT	04m	BABR	$e^+e^- \rightarrow \Upsilon(4S)$
< 1.5	90	CHAO	04	BELL	Repl. by ABE 05g
< 3.3	90	¹ BORNHEIM	03	CLE2	$e^+e^- \rightarrow \Upsilon(4S)$
< 4.1	90	¹ CASEY	02	BELL	$e^+e^- \rightarrow \Upsilon(4S)$
< 17	90	GODANG	98	CLE2	$e^+e^- \rightarrow \Upsilon(4S)$

- ¹ Assumes equal production of B^+ and B^0 at the $\Upsilon(4S)$.

$\Gamma(K_S^0 K_S^0)/\Gamma_{\text{total}}$		Γ_{214}/Γ			
VALUE (units 10^{-6})	CL%	DOCUMENT ID	TECN	COMMENT	
6.2 ± 1.2		OUR AVERAGE Error includes scale factor of 1.3.			
$6.9 \pm 0.9 \pm 0.6$		¹ AUBERT,B	05	BABR	$e^+e^- \rightarrow \Upsilon(4S)$
$4.2 \pm 1.6 \pm 0.8$		¹ GARMASH	04	BELL	$e^+e^- \rightarrow \Upsilon(4S)$

- ¹ Assumes equal production of B^+ and B^0 at the $\Upsilon(4S)$.

$\Gamma(K_S^0 K_L^0)/\Gamma_{\text{total}}$		Γ_{215}/Γ			
VALUE (units 10^{-6})	CL%	DOCUMENT ID	TECN	COMMENT	
< 16	90	¹ AUBERT,B	06r	BABR	$e^+e^- \rightarrow \Upsilon(4S)$

- ¹ Assumes equal production of B^+ and B^0 at the $\Upsilon(4S)$.

$\Gamma(K^+\pi^-\pi^0)/\Gamma_{\text{total}}$		Γ_{216}/Γ			
VALUE (units 10^{-6})	CL%	DOCUMENT ID	TECN	COMMENT	
36.6 ± 4.2		¹ CHANG	04	BELL	$e^+e^- \rightarrow \Upsilon(4S)$
4.3 ± 3.0		OUR AVERAGE			

- We do not use the following data for averages, fits, limits, etc. •••
- < 40 90 ¹ECKHART 02 CLE2 $e^+e^- \rightarrow \Upsilon(4S)$

- ¹ Assumes equal production of B^+ and B^0 at the $\Upsilon(4S)$.

$\Gamma(K^+\rho^-)/\Gamma_{\text{total}}$		Γ_{217}/Γ			
VALUE (units 10^{-6})	CL%	DOCUMENT ID	TECN	COMMENT	
8.5 ± 2.8		OUR AVERAGE Error includes scale factor of 1.7.			
$15.1 \pm 3.4 \pm 2.4$		¹ CHANG	04	BELL	$e^+e^- \rightarrow \Upsilon(4S)$
$7.3 \pm 1.3 \pm 1.3$		¹ AUBERT	03t	BABR	$e^+e^- \rightarrow \Upsilon(4S)$

- We do not use the following data for averages, fits, limits, etc. •••
- < 32 90 ¹JESSOP 00 CLE2 $e^+e^- \rightarrow \Upsilon(4S)$
- < 35 90 ASNER 96 CLE2 Repl. by JESSOP 00
- ¹ Assumes equal production of B^+ and B^0 at the $\Upsilon(4S)$.

$\Gamma((K^+\pi^-\pi^0)_{\text{non-resonant}})/\Gamma_{\text{total}}$		Γ_{218}/Γ			
VALUE (units 10^{-6})	CL%	DOCUMENT ID	TECN	COMMENT	
< 9.4	90	¹ CHANG	04	BELL	$e^+e^- \rightarrow \Upsilon(4S)$

- ¹ Assumes equal production of B^+ and B^0 at the $\Upsilon(4S)$.

$\Gamma(K^*_0\pi^0)/\Gamma_{\text{total}}$		Γ_{219}/Γ			
VALUE (units 10^{-6})	CL%	DOCUMENT ID	TECN	COMMENT	
$6.1 \pm 1.6 \pm 0.5$		¹ CHANG	04	BELL	$e^+e^- \rightarrow \Upsilon(4S)$
-1.5 ± 0.6		OUR AVERAGE			

- ¹ Assumes equal production of B^+ and B^0 at the $\Upsilon(4S)$.

$\Gamma(K^0\pi^+\pi^- \text{ charmless})/\Gamma_{\text{total}}$		Γ_{220}/Γ			
VALUE (units 10^{-6})	CL%	DOCUMENT ID	TECN	COMMENT	
44.8 ± 2.6		OUR AVERAGE			
$47.5 \pm 2.4 \pm 3.7$		¹ GARMASH	07	BELL	$e^+e^- \rightarrow \Upsilon(4S)$
$43.0 \pm 2.3 \pm 2.3$		² AUBERT	06i	BABR	$e^+e^- \rightarrow \Upsilon(4S)$
$50 \pm 10 \pm 7$		² ECKHART	02	CLE2	$e^+e^- \rightarrow \Upsilon(4S)$

- We do not use the following data for averages, fits, limits, etc. •••
- $43.7 \pm 3.8 \pm 3.4$ ²AUBERT,B 04o BABR Repl. by AUBERT 06i
- $45.4 \pm 5.2 \pm 5.9$ ²GARMASH 04 BELL Repl. by GARMASH 07
- < 440 90 ALBRECHT 91E ARG $e^+e^- \rightarrow \Upsilon(4S)$
- ¹ Uses Dalitz plot analysis of the $B^0 \rightarrow K^0\pi^+\pi^-$ final state decays.
- ² Assumes equal production of B^+ and B^0 at the $\Upsilon(4S)$.

$\Gamma(K^0\pi^+\pi^- \text{ non-resonant})/\Gamma_{\text{total}}$		Γ_{221}/Γ			
VALUE (units 10^{-6})	CL%	DOCUMENT ID	TECN	COMMENT	
$19.9 \pm 2.5 \pm 2.0$		¹ GARMASH	07	BELL	$e^+e^- \rightarrow \Upsilon(4S)$

- ¹ Uses Dalitz plot analysis of the $B^0 \rightarrow K^0\pi^+\pi^-$ final state decays.

$\Gamma(K^0\rho^0)/\Gamma_{\text{total}}$		Γ_{222}/Γ			
VALUE (units 10^{-6})	CL%	DOCUMENT ID	TECN	COMMENT	
5.4 ± 0.9		OUR AVERAGE			
$4.9 \pm 0.8 \pm 0.9$		¹ AUBERT	07f	BABR	$e^+e^- \rightarrow \Upsilon(4S)$
$6.1 \pm 1.0 \pm 1.1$		² GARMASH	07	BELL	$e^+e^- \rightarrow \Upsilon(4S)$

- We do not use the following data for averages, fits, limits, etc. •••
- < 39 90 ASNER 96 CLEO $e^+e^- \rightarrow \Upsilon(4S)$
- < 320 90 ALBRECHT 91b ARG $e^+e^- \rightarrow \Upsilon(4S)$
- < 500 90 AVERY 89b CLEO $e^+e^- \rightarrow \Upsilon(4S)$
- < 64000 90 AVERY 87 CLEO $e^+e^- \rightarrow \Upsilon(4S)$

- ¹ Assumes equal production of B^+ and B^0 at the $\Upsilon(4S)$.
- ² Uses Dalitz plot analysis of the $B^0 \rightarrow K^0\pi^+\pi^-$ final state decays.
- ³ AVERY 89b reports $< 5.8 \times 10^{-4}$ assuming the $\Upsilon(4S)$ decays 43% to $B^0\bar{B}^0$. We rescale to 50%.
- ⁴ AVERY 87 reports < 0.08 assuming the $\Upsilon(4S)$ decays 40% to $B^0\bar{B}^0$. We rescale to 50%.

$\Gamma(K^0\bar{K}^0(980))/\Gamma_{\text{total}}$		Γ_{223}/Γ			
VALUE (units 10^{-6})	CL%	DOCUMENT ID	TECN	COMMENT	
$5.5 \pm 0.7 \pm 0.6$		¹ AUBERT	06i	BABR	$e^+e^- \rightarrow \Upsilon(4S)$

- We do not use the following data for averages, fits, limits, etc. •••
- < 360 90 ²AVERY 89b CLEO $e^+e^- \rightarrow \Upsilon(4S)$
- ¹ Assumes equal production of B^+ and B^0 at the $\Upsilon(4S)$.
- ² AVERY 89b reports $< 4.2 \times 10^{-4}$ assuming the $\Upsilon(4S)$ decays 43% to $B^0\bar{B}^0$. We rescale to 50%.

$\Gamma(K^*(892)^+\pi^-)/\Gamma_{\text{total}}$		Γ_{224}/Γ			
VALUE (units 10^{-6})	CL%	DOCUMENT ID	TECN	COMMENT	
9.8 ± 1.3		OUR AVERAGE Error includes scale factor of 1.2.			
$8.4 \pm 1.1 \pm 1.0$		¹ GARMASH	07	BELL	$e^+e^- \rightarrow \Upsilon(4S)$
$11.0 \pm 1.5 \pm 0.71$		² AUBERT	06i	BABR	$e^+e^- \rightarrow \Upsilon(4S)$
$16 \pm 6 \pm 2$		² ECKHART	02	CLE2	$e^+e^- \rightarrow \Upsilon(4S)$

Meson Particle Listings

 B^0

• • • We do not use the following data for averages, fits, limits, etc. • • •

$12.9 \pm 2.4 \pm 1.4$	2	AUBERT,B	04a	BABR	Repl. by AUBERT 06i
$14.8 \pm 4.6 \pm 2.8$ $-4.4 - 1.3$	2	CHANG	04	BELL	Repl. by GARMASH 07
< 72	90	ASNER	96	CLE2	$e^+e^- \rightarrow \Upsilon(4S)$
< 620	90	ALBRECHT	91B	ARG	$e^+e^- \rightarrow \Upsilon(4S)$
< 380	90	3 AVERY	89B	CLEO	$e^+e^- \rightarrow \Upsilon(4S)$
< 560	90	4 AVERY	87	CLEO	$e^+e^- \rightarrow \Upsilon(4S)$

- 1 Uses Dalitz plot analysis of the $B^0 \rightarrow K^0 \pi^+ \pi^-$ final state decays.
2 Assumes equal production of B^+ and B^0 at the $\Upsilon(4S)$.
3 AVERY 89B reports $< 4.4 \times 10^{-4}$ assuming the $\Upsilon(4S)$ decays 43% to $B^0 \bar{B}^0$. We rescale to 50%.
4 AVERY 87 reports $< 7 \times 10^{-4}$ assuming the $\Upsilon(4S)$ decays 40% to $B^0 \bar{B}^0$. We rescale to 50%.

$\Gamma(K^*(1430)^+ \pi^-)/\Gamma_{total}$	CL%	DOCUMENT ID	TECN	COMMENT
$49.7 \pm 3.8 \pm 6.8$ -8.2		1 GARMASH 07	BELL	$e^+e^- \rightarrow \Upsilon(4S)$

- 1 Uses Dalitz plot analysis of the $B^0 \rightarrow K^0 \pi^+ \pi^-$ final state decays.

$\Gamma(K_X^{*+} \pi^-)/\Gamma_{total}$	CL%	DOCUMENT ID	TECN	COMMENT
$5.1 \pm 1.5 \pm 0.6$ -0.7		1 CHANG 04	BELL	$e^+e^- \rightarrow \Upsilon(4S)$

- 1 Assumes equal production of B^+ and B^0 at the $\Upsilon(4S)$.

$\Gamma(K^*(1410)^+ \pi^- \times B(K^*(1410)^+ \rightarrow K^0 \pi^+))/\Gamma_{total}$	CL%	DOCUMENT ID	TECN	COMMENT
< 3.8	90	1 GARMASH 07	BELL	$e^+e^- \rightarrow \Upsilon(4S)$

- 1 Uses Dalitz plot analysis of the $B^0 \rightarrow K^0 \pi^+ \pi^-$ final state decays.

$\Gamma(K^*(1680)^+ \pi^- \times B(K^*(1680)^+ \rightarrow K^0 \pi^+))/\Gamma_{total}$	CL%	DOCUMENT ID	TECN	COMMENT
< 2.6	90	1 GARMASH 07	BELL	$e^+e^- \rightarrow \Upsilon(4S)$

- 1 Uses Dalitz plot analysis of the $B^0 \rightarrow K^0 \pi^+ \pi^-$ final state decays.

$\Gamma(K_2^*(1430)^+ \pi^- \times B(K_2^*(1430)^+ \rightarrow K^0 \pi^+))/\Gamma_{total}$	CL%	DOCUMENT ID	TECN	COMMENT
< 2.1	90	1 GARMASH 07	BELL	$e^+e^- \rightarrow \Upsilon(4S)$

- 1 Uses Dalitz plot analysis of the $B^0 \rightarrow K^0 \pi^+ \pi^-$ final state decays.

$\Gamma(f_0(980) K^0 \times B(f_0(980) \rightarrow \pi^+ \pi^-))/\Gamma_{total}$	CL%	DOCUMENT ID	TECN	COMMENT
$7.6 \pm 1.7 \pm 0.9$ -1.3		1 GARMASH 07	BELL	$e^+e^- \rightarrow \Upsilon(4S)$

- 1 Uses Dalitz plot analysis of the $B^0 \rightarrow K^0 \pi^+ \pi^-$ final state decays.

$\Gamma(f_2(1270) K^0 \times B(f_2(1270) \rightarrow \pi^+ \pi^-))/\Gamma_{total}$	CL%	DOCUMENT ID	TECN	COMMENT
< 1.4	90	1 GARMASH 07	BELL	$e^+e^- \rightarrow \Upsilon(4S)$

- 1 Uses Dalitz plot analysis of the $B^0 \rightarrow K^0 \pi^+ \pi^-$ final state decays.

$\Gamma(K^*(892)^0 \pi^0)/\Gamma_{total}$	CL%	DOCUMENT ID	TECN	COMMENT
< 3.5×10^{-6}	90	1 CHANG 04	BELL	$e^+e^- \rightarrow \Upsilon(4S)$

- • • We do not use the following data for averages, fits, limits, etc. • • •
- | | | | | |
|------------------------|----|-----------|------|-----------------------------------|
| < 3.6×10^{-6} | 90 | JESSOP 00 | CLE2 | $e^+e^- \rightarrow \Upsilon(4S)$ |
| < 2.8×10^{-5} | 90 | ASNER 96 | CLE2 | Repl. by JESSOP 00 |
- 1 Assumes equal production of B^+ and B^0 at the $\Upsilon(4S)$.

$\Gamma(K_2^*(1430)^+ \pi^-)/\Gamma_{total}$	CL%	DOCUMENT ID	TECN	COMMENT
< 18	90	1 GARMASH 04	BELL	$e^+e^- \rightarrow \Upsilon(4S)$

- • • We do not use the following data for averages, fits, limits, etc. • • •
- | | | | | |
|--------|----|--------------|-----|-----------------------------------|
| < 2600 | 90 | ALBRECHT 91B | ARG | $e^+e^- \rightarrow \Upsilon(4S)$ |
|--------|----|--------------|-----|-----------------------------------|
- 1 Assumes equal production of B^+ and B^0 at the $\Upsilon(4S)$.

$\Gamma(K^0 K^- \pi^+)/\Gamma_{total}$	CL%	DOCUMENT ID	TECN	COMMENT
< 18×10^{-6}	90	1 GARMASH 04	BELL	$e^+e^- \rightarrow \Upsilon(4S)$

- • • We do not use the following data for averages, fits, limits, etc. • • •
- | | | | | |
|-----------------------|----|--------------|------|-----------------------------------|
| < 21×10^{-6} | 90 | 1 ECKHART 02 | CLE2 | $e^+e^- \rightarrow \Upsilon(4S)$ |
|-----------------------|----|--------------|------|-----------------------------------|
- 1 Assumes equal production of B^+ and B^0 at the $\Upsilon(4S)$.

$[\Gamma(\bar{K}^{*0} K^0) + \Gamma(K^{*0} \bar{K}^0)]/\Gamma_{total}$	CL%	DOCUMENT ID	TECN	COMMENT
< 1.9		1 AUBERT, BE 06N	BABR	$e^+e^- \rightarrow \Upsilon(4S)$

- 1 Assumes equal production of B^+ and B^0 at the $\Upsilon(4S)$.

$\Gamma(K^+ K^- \pi^0)/\Gamma_{total}$	CL%	DOCUMENT ID	TECN	COMMENT
< 19×10^{-6}	90	1 ECKHART 02	CLE2	$e^+e^- \rightarrow \Upsilon(4S)$

- 1 Assumes equal production of B^+ and B^0 at the $\Upsilon(4S)$.

$\Gamma(K^0 K^+ K^-)/\Gamma_{total}$	CL%	DOCUMENT ID	TECN	COMMENT
24.7 ± 2.3 OUR AVERAGE				
23.8 ± 2.0 ± 1.6		1 AUBERT,B 04V	BABR	$e^+e^- \rightarrow \Upsilon(4S)$
28.3 ± 3.3 ± 4.0		1 GARMASH 04	BELL	$e^+e^- \rightarrow \Upsilon(4S)$

- • • We do not use the following data for averages, fits, limits, etc. • • •
- | | | | | |
|--------|----|--------------|-----|-----------------------------------|
| < 1300 | 90 | ALBRECHT 91E | ARG | $e^+e^- \rightarrow \Upsilon(4S)$ |
|--------|----|--------------|-----|-----------------------------------|
- 1 Assumes equal production of B^+ and B^0 at the $\Upsilon(4S)$.

$\Gamma(K^0 \phi)/\Gamma_{total}$	CL%	DOCUMENT ID	TECN	COMMENT
8.6 ± 1.3 OUR AVERAGE				
8.4 ± 1.5 ± 0.5		1 AUBERT 04A	BABR	$e^+e^- \rightarrow \Upsilon(4S)$
9.0 ± 2.2 ± 0.7		1 CHEN 03B	BELL	$e^+e^- \rightarrow \Upsilon(4S)$

- • • We do not use the following data for averages, fits, limits, etc. • • •
- | | | | | |
|-----------------|----|---------------|------|-----------------------------------|
| 8.1 ± 3.1 ± 0.8 | | 1 AUBERT 01D | BABR | $e^+e^- \rightarrow \Upsilon(4S)$ |
| < 12.3 | 90 | 1 BRIERE 01 | CLE2 | $e^+e^- \rightarrow \Upsilon(4S)$ |
| < 31 | 90 | 1 BERGFELD 98 | CLE2 | |
| < 88 | 90 | ASNER 96 | CLE2 | $e^+e^- \rightarrow \Upsilon(4S)$ |
| < 720 | 90 | ALBRECHT 91B | ARG | $e^+e^- \rightarrow \Upsilon(4S)$ |
| < 420 | 90 | 2 AVERY 89B | CLEO | $e^+e^- \rightarrow \Upsilon(4S)$ |
| < 1000 | 90 | 3 AVERY 87 | CLEO | $e^+e^- \rightarrow \Upsilon(4S)$ |

- 1 Assumes equal production of B^+ and B^0 at the $\Upsilon(4S)$.

- 2 AVERY 89B reports $< 4.9 \times 10^{-4}$ assuming the $\Upsilon(4S)$ decays 43% to $B^0 \bar{B}^0$. We rescale to 50%.

- 3 AVERY 87 reports $< 1.3 \times 10^{-3}$ assuming the $\Upsilon(4S)$ decays 40% to $B^0 \bar{B}^0$. We rescale to 50%.

$\Gamma(K^+ \pi^- \pi^+ \pi^-)/\Gamma_{total}$	CL%	DOCUMENT ID	TECN	COMMENT
< 2.3×10^{-4}	90	1 ADAM 96D	DLPH	$e^+e^- \rightarrow Z$
< 2.1×10^{-4}	90	2 ABREU 95N	DLPH	Sup. by ADAM 96D

- • • We do not use the following data for averages, fits, limits, etc. • • •

- 1 ADAM 96D assumes $f_{B^0} = f_{B^-} = 0.39$ and $f_{B_s} = 0.12$. Contributions from B^0 and B_s decays cannot be separated. Limits are given for the weighted average of the decay rates for the two neutral B mesons.

- 2 Assumes a B^0, B^- production fraction of 0.39 and a B_s production fraction of 0.12. Contributions from B^0 and B_s decays cannot be separated. Limits are given for the weighted average of the decay rates for the two neutral B mesons.

$\Gamma(K^*(892)^0 \pi^+ \pi^-)/\Gamma_{total}$	CL%	DOCUMENT ID	TECN	COMMENT
54.5 ± 2.9 ± 4.3		1 AUBERT 07As	BABR	$e^+e^- \rightarrow \Upsilon(4S)$

- • • We do not use the following data for averages, fits, limits, etc. • • •
- | | | | | |
|--------|----|--------------|-----|-----------------------------------|
| < 1400 | 90 | ALBRECHT 91E | ARG | $e^+e^- \rightarrow \Upsilon(4S)$ |
|--------|----|--------------|-----|-----------------------------------|

- 1 Assumes equal production of B^+ and B^0 at the $\Upsilon(4S)$.

$\Gamma(K^*(892)^0 \rho^0)/\Gamma_{total}$	CL%	DOCUMENT ID	TECN	COMMENT
5.6 ± 0.9 ± 1.3		1 AUBERT,B 06G	BABR	$e^+e^- \rightarrow \Upsilon(4S)$

- • • We do not use the following data for averages, fits, limits, etc. • • •
- | | | | | |
|-------|----|--------------|------|-----------------------------------|
| < 34 | 90 | 2 GODANG 02 | CLE2 | $e^+e^- \rightarrow \Upsilon(4S)$ |
| < 286 | 90 | 3 ABE 00C | SLD | $e^+e^- \rightarrow Z$ |
| < 460 | 90 | ALBRECHT 91B | ARG | $e^+e^- \rightarrow \Upsilon(4S)$ |
| < 580 | 90 | 4 AVERY 89B | CLEO | $e^+e^- \rightarrow \Upsilon(4S)$ |
| < 960 | 90 | 5 AVERY 87 | CLEO | $e^+e^- \rightarrow \Upsilon(4S)$ |

- 1 Assumes equal production of B^+ and B^0 at the $\Upsilon(4S)$.

- 2 Assumes a helicity 00 configuration. For a helicity 11 configuration, the limit decreases to 2.4×10^{-5} .

- 3 ABE 00C assumes $B(Z \rightarrow b\bar{b}) = (21.7 \pm 0.1)\%$ and the B fractions $f_{B^0} = f_{B^+} = (39.7 \pm 1.8 \pm 2.2)\%$ and $f_{B_s} = (10.5 \pm 1.8 \pm 2.2)\%$.

- 4 AVERY 89B reports $< 6.7 \times 10^{-4}$ assuming the $\Upsilon(4S)$ decays 43% to $B^0 \bar{B}^0$. We rescale to 50%.

- 5 AVERY 87 reports $< 1.2 \times 10^{-3}$ assuming the $\Upsilon(4S)$ decays 40% to $B^0 \bar{B}^0$. We rescale to 50%.

$\Gamma(K^*(892)^0 f_0(980))/\Gamma_{total}$	CL%	DOCUMENT ID	TECN	COMMENT
< 4.3	90	1 AUBERT,B 06G	BABR	$e^+e^- \rightarrow \Upsilon(4S)$

- • • We do not use the following data for averages, fits, limits, etc. • • •
- | | | | | |
|-------|----|-------------|------|-----------------------------------|
| < 170 | 90 | 2 AVERY 89B | CLEO | $e^+e^- \rightarrow \Upsilon(4S)$ |
|-------|----|-------------|------|-----------------------------------|

- 1 Assumes equal production of B^+ and B^0 at the $\Upsilon(4S)$.

- 2 Assumes a helicity 00 configuration. For a helicity 11 configuration, the limit decreases to 2.4×10^{-5} .

- 3 ABE 00C assumes $B(Z \rightarrow b\bar{b}) = (21.7 \pm 0.1)\%$ and the B fractions $f_{B^0} = f_{B^+} = (39.7 \pm 1.8 \pm 2.2)\%$ and $f_{B_s} = (10.5 \pm 1.8 \pm 2.2)\%$.

- 4 AVERY 89B reports $< 6.7 \times 10^{-4}$ assuming the $\Upsilon(4S)$ decays 43% to $B^0 \bar{B}^0$. We rescale to 50%.

- 5 AVERY 87 reports $< 1.2 \times 10^{-3}$ assuming the $\Upsilon(4S)$ decays 40% to $B^0 \bar{B}^0$. We rescale to 50%.

$\Gamma(K^*(892)^0 \rho^0)/\Gamma_{total}$	CL%	DOCUMENT ID	TECN	COMMENT
< 4.3	90	1 AUBERT,B 06G	BABR	$e^+e^- \rightarrow \Upsilon(4S)$

- • • We do not use the following data for averages, fits, limits, etc. • • •
- | | | | | |
|-------|----|-------------|------|-----------------------------------|
| < 170 | 90 | 2 AVERY 89B | CLEO | $e^+e^- \rightarrow \Upsilon(4S)$ |
|-------|----|-------------|------|-----------------------------------|

- 1 Assumes equal production of B^+ and B^0 at the $\Upsilon(4S)$.

- 2 AVERY 89B reports $< 2.0 \times 10^{-4}$ assuming the $\Upsilon(4S)$ decays 43% to $B^0 \bar{B}^0$. We rescale to 50%.

$\Gamma(K_1(1400)^+\pi^-)/\Gamma_{\text{total}}$				Γ_{243}/Γ
VALUE	CL%	DOCUMENT ID	TECN	COMMENT
$<1.1 \times 10^{-3}$	90	ALBRECHT	91B	ARG $e^+e^- \rightarrow \Upsilon(4S)$

$\Gamma(a_1(1260)^-K^+)/\Gamma_{\text{total}}$				Γ_{244}/Γ
VALUE (units 10^{-6})	CL%	DOCUMENT ID	TECN	COMMENT
$16.3 \pm 2.9 \pm 2.3$		1,2 AUBERT	08F	BABR $e^+e^- \rightarrow \Upsilon(4S)$
$\bullet \bullet \bullet$ We do not use the following data for averages, fits, limits, etc. $\bullet \bullet \bullet$				
<230	90	3 ADAM	96D	DLPH $e^+e^- \rightarrow Z$
<390	90	4 ABREU	95N	DLPH Sup. by ADAM 96D

- 1 Assumes equal production of B^+ and B^0 at the $\Upsilon(4S)$.
 2 Assumes a_1^\pm decays only to 3π and $B(a_1^\pm \rightarrow \pi^\pm \pi^\mp \pi^\pm) = 0.5$.
 3 ADAM 96D assumes $f_{B^0} = f_{B^-} = 0.39$ and $f_{B_s} = 0.12$. Contributions from B^0 and B_s decays cannot be separated. Limits are given for the weighted average of the decay rates for the two neutral B mesons.
 4 Assumes a B^0, B^- production fraction of 0.39 and a B_s production fraction of 0.12. Contributions from B^0 and B_s decays cannot be separated. Limits are given for the weighted average of the decay rates for the two neutral B mesons.

$\Gamma(b_1^-K^+ \times B(b_1^- \rightarrow \omega\pi^-))/\Gamma_{\text{total}}$				Γ_{245}/Γ
VALUE (units 10^{-6})	CL%	DOCUMENT ID	TECN	COMMENT
$7.4 \pm 1.0 \pm 1.0$		1 AUBERT	07B1	BABR $e^+e^- \rightarrow \Upsilon(4S)$
1 Assumes equal production of B^+ and B^0 at the $\Upsilon(4S)$.				

$\Gamma(K^*(892)^0 K^+ K^-)/\Gamma_{\text{total}}$				Γ_{246}/Γ
VALUE (units 10^{-6})	CL%	DOCUMENT ID	TECN	COMMENT
$27.5 \pm 1.3 \pm 2.2$		1 AUBERT	07As	BABR $e^+e^- \rightarrow \Upsilon(4S)$
$\bullet \bullet \bullet$ We do not use the following data for averages, fits, limits, etc. $\bullet \bullet \bullet$				
<610	90	ALBRECHT	91E	ARG $e^+e^- \rightarrow \Upsilon(4S)$
1 Assumes equal production of B^+ and B^0 at the $\Upsilon(4S)$.				

$\Gamma(K^*(892)^0 \phi)/\Gamma_{\text{total}}$				Γ_{247}/Γ
VALUE (units 10^{-6})	CL%	DOCUMENT ID	TECN	COMMENT
9.5 ± 0.8 OUR AVERAGE				
$9.2 \pm 0.7 \pm 0.6$		1 AUBERT	07D	BABR $e^+e^- \rightarrow \Upsilon(4S)$
$10.0^{+1.6+0.7}_{-1.5-0.8}$		1 CHEN	03B	BELL $e^+e^- \rightarrow \Upsilon(4S)$
$11.5^{+4.5+1.8}_{-3.7-1.7}$		1 BRIERE	01	CLE2 $e^+e^- \rightarrow \Upsilon(4S)$
$\bullet \bullet \bullet$ We do not use the following data for averages, fits, limits, etc. $\bullet \bullet \bullet$				
$9.2 \pm 0.9 \pm 0.5$		1 AUBERT,B	04W	BABR Repl. by AUBERT 07D
$11.2 \pm 1.3 \pm 0.8$		1 AUBERT	03V	BABR Repl. by AUBERT,B 04W
$8.7^{+2.5}_{-2.1} \pm 1.1$		1 AUBERT	01D	BABR Repl. by AUBERT 03V
<384	90	2 ABE	00c	SLD $e^+e^- \rightarrow Z$
<21	90	1 BERGFELD	98	CLE2
<43	90	ASNER	96	CLE2 $e^+e^- \rightarrow \Upsilon(4S)$
<320	90	ALBRECHT	91B	ARG $e^+e^- \rightarrow \Upsilon(4S)$
<380	90	3 AVERY	89B	CLEO $e^+e^- \rightarrow \Upsilon(4S)$
<380	90	4 AVERY	87	CLEO $e^+e^- \rightarrow \Upsilon(4S)$

- 1 Assumes equal production of B^+ and B^0 at the $\Upsilon(4S)$.
 2 ABE 00c assumes $B(Z \rightarrow b\bar{b}) = (21.7 \pm 0.1)\%$ and the B fractions $f_{B^0} = f_{B^+} = (39.7^{+1.8}_{-2.2})\%$ and $f_{B_s} = (10.5^{+1.8}_{-2.2})\%$.
 3 AVERY 89B reports $< 4.4 \times 10^{-4}$ assuming the $\Upsilon(4S)$ decays 43% to $B^0\bar{B}^0$. We rescale to 50%.
 4 AVERY 87 reports $< 4.7 \times 10^{-4}$ assuming the $\Upsilon(4S)$ decays 40% to $B^0\bar{B}^0$. We rescale to 50%.

$\Gamma(K^*(892)^0 K^- \pi^+)/\Gamma_{\text{total}}$				Γ_{248}/Γ
VALUE (units 10^{-6})	CL%	DOCUMENT ID	TECN	COMMENT
$4.6 \pm 1.1 \pm 0.8$		1 AUBERT	07As	BABR $e^+e^- \rightarrow \Upsilon(4S)$
1 Assumes equal production of B^+ and B^0 at the $\Upsilon(4S)$.				

$\Gamma(K^*(892)^0 \bar{K}^*(892)^0)/\Gamma_{\text{total}}$				Γ_{249}/Γ
VALUE (units 10^{-6})	CL%	DOCUMENT ID	TECN	COMMENT
$1.28^{+0.35}_{-0.30} \pm 0.11$		1 AUBERT	08i	BABR $e^+e^- \rightarrow \Upsilon(4S)$
$\bullet \bullet \bullet$ We do not use the following data for averages, fits, limits, etc. $\bullet \bullet \bullet$				
<22	90	2 GODANG	02	CLE2 $e^+e^- \rightarrow \Upsilon(4S)$
<469	90	3 ABE	00c	SLD $e^+e^- \rightarrow Z$

- 1 Assumes equal production of B^+ and B^0 at the $\Upsilon(4S)$.
 2 Assumes a helicity 00 configuration. For a helicity 11 configuration, the limit decreases to 1.9×10^{-5} .
 3 ABE 00c assumes $B(Z \rightarrow b\bar{b}) = (21.7 \pm 0.1)\%$ and the B fractions $f_{B^0} = f_{B^+} = (39.7^{+1.8}_{-2.2})\%$ and $f_{B_s} = (10.5^{+1.8}_{-2.2})\%$.

$\Gamma(K^*(892)^0 K^+ \pi^-)/\Gamma_{\text{total}}$				Γ_{250}/Γ
VALUE (units 10^{-6})	CL%	DOCUMENT ID	TECN	COMMENT
<2.2	90	1 AUBERT	07As	BABR $e^+e^- \rightarrow \Upsilon(4S)$
1 Assumes equal production of B^+ and B^0 at the $\Upsilon(4S)$.				

$\Gamma(K^*(892)^0 K^*(892)^0)/\Gamma_{\text{total}}$				Γ_{251}/Γ
VALUE (units 10^{-6})	CL%	DOCUMENT ID	TECN	COMMENT
<0.41	90	1 AUBERT	08i	BABR $e^+e^- \rightarrow \Upsilon(4S)$
$\bullet \bullet \bullet$ We do not use the following data for averages, fits, limits, etc. $\bullet \bullet \bullet$				
<37	90	2 GODANG	02	CLE2 $e^+e^- \rightarrow \Upsilon(4S)$

- 1 Assumes equal production of B^+ and B^0 at the $\Upsilon(4S)$.
 2 Assumes a helicity 00 configuration. For a helicity 11 configuration, the limit decreases to 2.9×10^{-5} .

$\Gamma(K^*(892)^+ \rho^-)/\Gamma_{\text{total}}$				Γ_{252}/Γ
VALUE (units 10^{-6})	CL%	DOCUMENT ID	TECN	COMMENT
<12.0	90	1 AUBERT,B	06G	BABR $e^+e^- \rightarrow \Upsilon(4S)$
1 Assumes equal production of B^+ and B^0 at the $\Upsilon(4S)$.				

$\Gamma(K^*(892)^+ K^*(892)^-)/\Gamma_{\text{total}}$				Γ_{253}/Γ
VALUE (units 10^{-6})	CL%	DOCUMENT ID	TECN	COMMENT
<141	90	1 GODANG	02	CLE2 $e^+e^- \rightarrow \Upsilon(4S)$
1 Assumes a helicity 00 configuration. For a helicity 11 configuration, the limit decreases to 8.9×10^{-5} .				

$\Gamma(K_1(1400)^0 \rho^0)/\Gamma_{\text{total}}$				Γ_{254}/Γ
VALUE	CL%	DOCUMENT ID	TECN	COMMENT
$<3.0 \times 10^{-3}$	90	ALBRECHT	91B	ARG $e^+e^- \rightarrow \Upsilon(4S)$

$\Gamma(\phi(K\pi)_0^0)/\Gamma_{\text{total}}$				Γ_{256}/Γ
VALUE (units 10^{-6})	CL%	DOCUMENT ID	TECN	COMMENT
$5.0 \pm 0.8 \pm 0.3$		1 AUBERT	07D	BABR $e^+e^- \rightarrow \Upsilon(4S)$
This decay refers to the coherent sum of resonant and nonresonant $J^P = 0^+ K\pi$ components with $1.13 < m_{K\pi} < 1.53 \text{ GeV}/c^2$. 1 Assumes equal production of B^+ and B^0 at the $\Upsilon(4S)$.				

$\Gamma(\phi(K\pi)_0^0 (1.60 < m_{K\pi} < 2.15))/\Gamma_{\text{total}}$				Γ_{257}/Γ
VALUE (units 10^{-6})	CL%	DOCUMENT ID	TECN	COMMENT
<1.7	90	1 AUBERT	07A0	BABR $e^+e^- \rightarrow \Upsilon(4S)$
This decay refers to the coherent sum of resonant and nonresonant $J^P = 0^+ K\pi$ components with $1.60 < m_{K\pi} < 2.15 \text{ GeV}/c^2$. 1 Assumes equal production of B^+ and B^0 at the $\Upsilon(4S)$.				

$\Gamma(K_1(1400)^0 \phi)/\Gamma_{\text{total}}$				Γ_{255}/Γ
VALUE	CL%	DOCUMENT ID	TECN	COMMENT
$<5.0 \times 10^{-3}$	90	ALBRECHT	91B	ARG $e^+e^- \rightarrow \Upsilon(4S)$

$\Gamma(K_0^*(1430)^0 \phi)/\Gamma_{\text{total}}$				Γ_{258}/Γ
VALUE (units 10^{-6})	CL%	DOCUMENT ID	TECN	COMMENT
$4.6 \pm 0.7 \pm 0.6$		1 AUBERT	07D	BABR $e^+e^- \rightarrow \Upsilon(4S)$
$\bullet \bullet \bullet$ We do not use the following data for averages, fits, limits, etc. $\bullet \bullet \bullet$				
seen		2 AUBERT,B	04W	BABR Repl. by AUBERT 07D
1 Assumes equal production of B^+ and B^0 at the $\Upsilon(4S)$. 2 Observed 181 ± 17 events with statistical significance greater than 10σ .				

$\Gamma(K^*(1680)^0 \phi)/\Gamma_{\text{total}}$				Γ_{259}/Γ
VALUE (units 10^{-6})	CL%	DOCUMENT ID	TECN	COMMENT
<3.5	90	1 AUBERT	07A0	BABR $e^+e^- \rightarrow \Upsilon(4S)$
1 Assumes equal production of B^+ and B^0 at the $\Upsilon(4S)$.				

$\Gamma(K^*(1780)^0 \phi)/\Gamma_{\text{total}}$				Γ_{260}/Γ
VALUE (units 10^{-6})	CL%	DOCUMENT ID	TECN	COMMENT
<2.7	90	1 AUBERT	07A0	BABR $e^+e^- \rightarrow \Upsilon(4S)$
1 Assumes equal production of B^+ and B^0 at the $\Upsilon(4S)$.				

$\Gamma(K^*(2045)^0 \phi)/\Gamma_{\text{total}}$				Γ_{261}/Γ
VALUE (units 10^{-6})	CL%	DOCUMENT ID	TECN	COMMENT
<15.3	90	1 AUBERT	07A0	BABR $e^+e^- \rightarrow \Upsilon(4S)$
1 Assumes equal production of B^+ and B^0 at the $\Upsilon(4S)$.				

$\Gamma(K_2^*(1430)^0 \rho^0)/\Gamma_{\text{total}}$				Γ_{262}/Γ
VALUE (units 10^{-6})	CL%	DOCUMENT ID	TECN	COMMENT
$<1.1 \times 10^3$	90	ALBRECHT	91B	ARG $e^+e^- \rightarrow \Upsilon(4S)$

$\Gamma(K_2^*(1430)^0 \phi)/\Gamma_{\text{total}}$				Γ_{263}/Γ
VALUE (units 10^{-6})	CL%	DOCUMENT ID	TECN	COMMENT
$7.8 \pm 1.1 \pm 0.6$		1 AUBERT	07D	BABR $e^+e^- \rightarrow \Upsilon(4S)$
$\bullet \bullet \bullet$ We do not use the following data for averages, fits, limits, etc. $\bullet \bullet \bullet$				
seen		2 AUBERT,B	04W	BABR Repl. by AUBERT 07D
<1400	90	ALBRECHT	91B	ARG $e^+e^- \rightarrow \Upsilon(4S)$
1 Assumes equal production of B^+ and B^0 at the $\Upsilon(4S)$. 2 The angular distribution of $B \rightarrow \phi K^*(1430)$ provides evidence with statistical significance of 3.2σ .				

Meson Particle Listings

 B^0

$\Gamma(K^0\phi\phi)/\Gamma_{\text{total}}$ Γ_{264}/Γ
 VALUE (units 10^{-6}) DOCUMENT ID TECN COMMENT

$4.1^{+1.7}_{-1.4} \pm 0.4$ ¹AUBERT,BE 06H BABR $e^+e^- \rightarrow \Upsilon(4S)$
¹ Assumes equal production of B^0 and B^+ at the $\Upsilon(4S)$ and for a $\phi\phi$ invariant mass below 2.85 GeV/c^2 .

$\Gamma(\eta'\eta'K^0)/\Gamma_{\text{total}}$ Γ_{265}/Γ
 VALUE (units 10^{-6}) CL% DOCUMENT ID TECN COMMENT

<31 90 ¹AUBERT,B 06P BABR $e^+e^- \rightarrow \Upsilon(4S)$
¹ Assumes equal production of B^+ and B^0 at the $\Upsilon(4S)$.

$\Gamma(K^*(892)^0\gamma)/\Gamma_{\text{total}}$ Γ_{266}/Γ
 VALUE (units 10^{-6}) CL% DOCUMENT ID TECN COMMENT

40.1 ± 2.0 OUR AVERAGE
 $39.2 \pm 2.0 \pm 2.4$ ¹AUBERT,BE 04A BABR $e^+e^- \rightarrow \Upsilon(4S)$
 $40.1 \pm 2.1 \pm 1.7$ ²NAKAO 04 BELL $e^+e^- \rightarrow \Upsilon(4S)$
 $45.5^{+7.2}_{-6.8} \pm 3.4$ ³COAN 00 CLE2 $e^+e^- \rightarrow \Upsilon(4S)$
 ••• We do not use the following data for averages, fits, limits, etc. •••
 <110 90 ACOSTA 02G CDF $p\bar{p}$ at 1.8 TeV
 $42.3 \pm 4.0 \pm 2.2$ ²AUBERT 02C BABR Repl. by AUBERT,BE 04A
 <210 90 ⁴ADAM 96D DLPH $e^+e^- \rightarrow Z$
 $40 \pm 17 \pm 8$ ⁵AMMAR 93 CLE2 Repl. by COAN 00
 <420 90 ALBRECHT 89G ARG $e^+e^- \rightarrow \Upsilon(4S)$
 <240 90 ⁶AVERY 89B CLEO $e^+e^- \rightarrow \Upsilon(4S)$
 <2100 90 AVERY 87 CLEO $e^+e^- \rightarrow \Upsilon(4S)$

¹ Uses the production ratio of charged and neutral B from $\Upsilon(4S)$ decays $R^{+0} = 1.006 \pm 0.048$.
² Assumes equal production of B^+ and B^0 at the $\Upsilon(4S)$.
³ Assumes equal production of B^+ and B^0 at the $\Upsilon(4S)$. No evidence for a nonresonant $K\pi\gamma$ contamination was seen; the central value assumes no contamination.
⁴ ADAM 96D assumes $f_{B^0} = f_{B^-} = 0.39$ and $f_{B_s} = 0.12$.
⁵ AMMAR 93 observed 6.6 ± 2.8 events above background.
⁶ AVERY 89B reports $< 2.8 \times 10^{-4}$ assuming the $\Upsilon(4S)$ decays 43% to $B^0\bar{B}^0$. We rescale to 50%.

$\Gamma(\eta K^0\gamma)/\Gamma_{\text{total}}$ Γ_{267}/Γ
 VALUE (units 10^{-6}) DOCUMENT ID TECN COMMENT

$10.7^{+2.2}_{-1.5}$ OUR AVERAGE
 $11.3^{+2.8}_{-1.6} \pm 0.6$ ^{1,2}AUBERT,B 06M BABR $e^+e^- \rightarrow \Upsilon(4S)$
 $8.7^{+3.1+1.9}_{-2.7-1.6}$ ^{2,3}NISHIDA 05 BELL $e^+e^- \rightarrow \Upsilon(4S)$
¹ $m_{\eta'K} < 3.25 \text{ GeV}/c^2$.
² Assumes equal production of B^+ and B^0 at the $\Upsilon(4S)$.
³ $m_{\eta K} < 2.4 \text{ GeV}/c^2$

$\Gamma(\eta'K^0\gamma)/\Gamma_{\text{total}}$ Γ_{268}/Γ
 VALUE (units 10^{-6}) CL% DOCUMENT ID TECN COMMENT

<6.6 90 ^{1,2}AUBERT,B 06M BABR $e^+e^- \rightarrow \Upsilon(4S)$
¹ $m_{\eta'K} < 3.25 \text{ GeV}/c^2$.
² Assumes equal production of B^+ and B^0 at the $\Upsilon(4S)$.

$\Gamma(K^0\phi\gamma)/\Gamma_{\text{total}}$ Γ_{269}/Γ
 VALUE (units 10^{-6}) CL% DOCUMENT ID TECN COMMENT

<2.7 90 ¹AUBERT 07Q BABR $e^+e^- \rightarrow \Upsilon(4S)$
 ••• We do not use the following data for averages, fits, limits, etc. •••
 <8.3 90 ¹DRUTSKOY 04 BELL $e^+e^- \rightarrow \Upsilon(4S)$
¹ Assumes equal production of B^+ and B^0 at $\Upsilon(4S)$.

$\Gamma(K^+\pi^-\gamma)/\Gamma_{\text{total}}$ Γ_{270}/Γ
 VALUE DOCUMENT ID TECN COMMENT

$(4.6^{+1.3+0.5}_{-1.2-0.7}) \times 10^{-6}$ ^{1,2}NISHIDA 02 BELL $e^+e^- \rightarrow \Upsilon(4S)$
¹ Assumes equal production of B^+ and B^0 at the $\Upsilon(4S)$.
² $1.25 \text{ GeV}/c^2 < M_{K\pi} < 1.6 \text{ GeV}/c^2$

$\Gamma(K^*(1410)\gamma)/\Gamma_{\text{total}}$ Γ_{271}/Γ
 VALUE CL% DOCUMENT ID TECN COMMENT

$<1.3 \times 10^{-4}$ 90 ¹NISHIDA 02 BELL $e^+e^- \rightarrow \Upsilon(4S)$
¹ Assumes equal production of B^+ and B^0 at the $\Upsilon(4S)$.

$\Gamma(K^+\pi^-\gamma \text{ nonresonant})/\Gamma_{\text{total}}$ Γ_{272}/Γ
 VALUE CL% DOCUMENT ID TECN COMMENT

$<2.6 \times 10^{-6}$ 90 ^{1,2}NISHIDA 02 BELL $e^+e^- \rightarrow \Upsilon(4S)$
¹ Assumes equal production of B^+ and B^0 at the $\Upsilon(4S)$.
² $1.25 \text{ GeV}/c^2 < M_{K\pi} < 1.6 \text{ GeV}/c^2$

$\Gamma(K^0\pi^+\pi^-\gamma)/\Gamma_{\text{total}}$ Γ_{273}/Γ
 VALUE (units 10^{-5}) DOCUMENT ID TECN COMMENT

1.95 ± 0.22 OUR AVERAGE
 $1.85 \pm 0.21 \pm 0.12$ ^{1,2}AUBERT 07R BABR $e^+e^- \rightarrow \Upsilon(4S)$
 $2.40 \pm 0.4 \pm 0.3$ ^{2,3}YANG 05 BELL $e^+e^- \rightarrow \Upsilon(4S)$
¹ $M_{K\pi\pi} < 1.8 \text{ GeV}/c^2$.
² Assumes equal production of B^+ and B^0 at the $\Upsilon(4S)$.
³ $M_{K\pi\pi} < 2.0 \text{ GeV}/c^2$.

$\Gamma(K^+\pi^-\pi^0\gamma)/\Gamma_{\text{total}}$ Γ_{274}/Γ
 VALUE (units 10^{-5}) DOCUMENT ID TECN COMMENT

$4.07 \pm 0.22 \pm 0.31$ ^{1,2}AUBERT 07R BABR $e^+e^- \rightarrow \Upsilon(4S)$
¹ $M_{K\pi\pi} < 1.8 \text{ GeV}/c^2$.
² Assumes equal production of B^+ and B^0 at the $\Upsilon(4S)$.

$\Gamma(K_1(1270)^0\gamma)/\Gamma_{\text{total}}$ Γ_{275}/Γ
 VALUE (units 10^{-5}) CL% DOCUMENT ID TECN COMMENT

< 5.8 90 ¹YANG 05 BELL $e^+e^- \rightarrow \Upsilon(4S)$
 ••• We do not use the following data for averages, fits, limits, etc. •••
 <700 90 ²ALBRECHT 89G ARG $e^+e^- \rightarrow \Upsilon(4S)$
¹ Assumes equal production of B^+ and B^0 at the $\Upsilon(4S)$.
² ALBRECHT 89G reports < 0.0078 assuming the $\Upsilon(4S)$ decays 45% to $B^0\bar{B}^0$. We rescale to 50%.

$\Gamma(K_1(1400)^0\gamma)/\Gamma_{\text{total}}$ Γ_{276}/Γ
 VALUE (units 10^{-5}) CL% DOCUMENT ID TECN COMMENT

< 1.5 90 ¹YANG 05 BELL $e^+e^- \rightarrow \Upsilon(4S)$
 ••• We do not use the following data for averages, fits, limits, etc. •••
 <430 90 ²ALBRECHT 89G ARG $e^+e^- \rightarrow \Upsilon(4S)$
¹ Assumes equal production of B^+ and B^0 at the $\Upsilon(4S)$.
² ALBRECHT 89G reports < 0.0048 assuming the $\Upsilon(4S)$ decays 45% to $B^0\bar{B}^0$. We rescale to 50%.

$\Gamma(K_2^*(1430)^0\gamma)/\Gamma_{\text{total}}$ Γ_{277}/Γ
 VALUE (units 10^{-5}) CL% DOCUMENT ID TECN COMMENT

1.24 ± 0.24 OUR AVERAGE
 $1.22 \pm 0.25 \pm 0.10$ ¹AUBERT,B 04U BABR $e^+e^- \rightarrow \Upsilon(4S)$
 $1.3 \pm 0.5 \pm 0.1$ ¹NISHIDA 02 BELL $e^+e^- \rightarrow \Upsilon(4S)$
 ••• We do not use the following data for averages, fits, limits, etc. •••
 <40 90 ²ALBRECHT 89G ARG $e^+e^- \rightarrow \Upsilon(4S)$
¹ Assumes equal production of B^+ and B^0 at the $\Upsilon(4S)$.
² ALBRECHT 89G reports $< 4.4 \times 10^{-4}$ assuming the $\Upsilon(4S)$ decays 45% to $B^0\bar{B}^0$. We rescale to 50%.

$\Gamma(K^*(1680)^0\gamma)/\Gamma_{\text{total}}$ Γ_{278}/Γ
 VALUE CL% DOCUMENT ID TECN COMMENT

<0.0020 90 ¹ALBRECHT 89G ARG $e^+e^- \rightarrow \Upsilon(4S)$
¹ ALBRECHT 89G reports < 0.0022 assuming the $\Upsilon(4S)$ decays 45% to $B^0\bar{B}^0$. We rescale to 50%.

$\Gamma(K_3^*(1780)^0\gamma)/\Gamma_{\text{total}}$ Γ_{279}/Γ
 VALUE (units 10^{-6}) CL% DOCUMENT ID TECN COMMENT

< 83 90 ^{1,2}NISHIDA 05 BELL $e^+e^- \rightarrow \Upsilon(4S)$
 ••• We do not use the following data for averages, fits, limits, etc. •••
 <10000 90 ³ALBRECHT 89G ARG $e^+e^- \rightarrow \Upsilon(4S)$
¹ Assumes equal production of B^+ and B^0 at the $\Upsilon(4S)$.
² Uses $B(K_3^*(1780) \rightarrow \eta K) = 0.11^{+0.05}_{-0.04}$.
³ ALBRECHT 89G reports < 0.011 assuming the $\Upsilon(4S)$ decays 45% to $B^0\bar{B}^0$. We rescale to 50%.

$\Gamma(K_3^*(2045)^0\gamma)/\Gamma_{\text{total}}$ Γ_{280}/Γ
 VALUE CL% DOCUMENT ID TECN COMMENT

<0.0043 90 ¹ALBRECHT 89G ARG $e^+e^- \rightarrow \Upsilon(4S)$
¹ ALBRECHT 89G reports < 0.0048 assuming the $\Upsilon(4S)$ decays 45% to $B^0\bar{B}^0$. We rescale to 50%.

$\Gamma(\rho^0\gamma)/\Gamma_{\text{total}}$ Γ_{281}/Γ
 VALUE (units 10^{-6}) CL% DOCUMENT ID TECN COMMENT

0.93 ± 0.21 OUR AVERAGE Error includes scale factor of 1.1.
 $0.79^{+0.22}_{-0.20} \pm 0.06$ ¹AUBERT 07L BABR $e^+e^- \rightarrow \Upsilon(4S)$
 $1.25^{+0.37+0.07}_{-0.33-0.06}$ ¹MOHAPATRA 06 BELL $e^+e^- \rightarrow \Upsilon(4S)$
 ••• We do not use the following data for averages, fits, limits, etc. •••
 $0.0 \pm 0.2 \pm 0.1$ 90 ¹AUBERT 05 BABR Repl. by AUBERT 07L
 < 0.8 90 ¹MOHAPATRA 05 BELL $e^+e^- \rightarrow \Upsilon(4S)$
 < 1.2 90 ¹AUBERT 04C BABR $e^+e^- \rightarrow \Upsilon(4S)$
 <17 90 ¹COAN 00 CLE2 $e^+e^- \rightarrow \Upsilon(4S)$
¹ Assumes equal production of B^+ and B^0 at the $\Upsilon(4S)$.

$\Gamma(\omega\gamma)/\Gamma_{total}$				Γ_{282}/Γ
VALUE (units 10^{-6})	CL%	DOCUMENT ID	TECN	COMMENT
0.46 ± 0.20		OUR AVERAGE		
$0.40^{+0.24}_{-0.20} \pm 0.05$		1 AUBERT	07L BABR	$e^+e^- \rightarrow \Upsilon(4S)$
$0.56^{+0.34+0.05}_{-0.27-0.10}$		1 MOHAPATRA	06 BELL	$e^+e^- \rightarrow \Upsilon(4S)$
••• We do not use the following data for averages, fits, limits, etc. •••				
<1.0	90	1 AUBERT	05 BABR	Repl. by AUBERT 07L
<0.8	90	1 MOHAPATRA	05 BELL	Repl. by MOHAPATRA 06
<1.0	90	1 AUBERT	04c BABR	$e^+e^- \rightarrow \Upsilon(4S)$
<9.2	90	1 COAN	00 CLE2	$e^+e^- \rightarrow \Upsilon(4S)$

¹ Assumes equal production of B^+ and B^0 at the $\Upsilon(4S)$.

$\Gamma(\phi\gamma)/\Gamma_{total}$				Γ_{283}/Γ
VALUE	CL%	DOCUMENT ID	TECN	COMMENT
$<8.5 \times 10^{-7}$		OUR AVERAGE		
<0.33 $\times 10^{-5}$	90	1 COAN	00 CLE2	$e^+e^- \rightarrow \Upsilon(4S)$
••• We do not use the following data for averages, fits, limits, etc. •••				
<1.0	90	1 AUBERT, BE	05c BABR	$e^+e^- \rightarrow \Upsilon(4S)$
••• We do not use the following data for averages, fits, limits, etc. •••				
<0.33 $\times 10^{-5}$	90	1 COAN	00 CLE2	$e^+e^- \rightarrow \Upsilon(4S)$
••• We do not use the following data for averages, fits, limits, etc. •••				
<1.0	90	1 AUBERT, BE	05c BABR	$e^+e^- \rightarrow \Upsilon(4S)$
••• We do not use the following data for averages, fits, limits, etc. •••				
<0.33 $\times 10^{-5}$	90	1 COAN	00 CLE2	$e^+e^- \rightarrow \Upsilon(4S)$
••• We do not use the following data for averages, fits, limits, etc. •••				
<1.0	90	1 AUBERT, BE	05c BABR	$e^+e^- \rightarrow \Upsilon(4S)$
••• We do not use the following data for averages, fits, limits, etc. •••				
<0.33 $\times 10^{-5}$	90	1 COAN	00 CLE2	$e^+e^- \rightarrow \Upsilon(4S)$
••• We do not use the following data for averages, fits, limits, etc. •••				
<1.0	90	1 AUBERT, BE	05c BABR	$e^+e^- \rightarrow \Upsilon(4S)$
••• We do not use the following data for averages, fits, limits, etc. •••				
<0.33 $\times 10^{-5}$	90	1 COAN	00 CLE2	$e^+e^- \rightarrow \Upsilon(4S)$

¹ Assumes equal production of B^+ and B^0 at the $\Upsilon(4S)$.

$\Gamma(\pi^+\pi^-)/\Gamma_{total}$				Γ_{284}/Γ
VALUE (units 10^{-6})	CL%	DOCUMENT ID	TECN	COMMENT
5.13 ± 0.24		OUR AVERAGE		
$5.5 \pm 0.4 \pm 0.3$		1 AUBERT	07B BABR	$e^+e^- \rightarrow \Upsilon(4S)$
$5.1 \pm 0.2 \pm 0.2$		1 LIN	07A BELL	$e^+e^- \rightarrow \Upsilon(4S)$
$4.1 \pm 1.1 \pm 0.1$		2 ABULENCIA, A	06d CDF	$p\bar{p}$ at 1.96 TeV
$4.5^{+1.4+0.5}_{-1.2-0.4}$		1 BORNHEIM	03 CLE2	$e^+e^- \rightarrow \Upsilon(4S)$
••• We do not use the following data for averages, fits, limits, etc. •••				
$4.4 \pm 0.6 \pm 0.3$		1 CHAO	04 BELL	Repl. by LIN 07A
$4.7 \pm 0.6 \pm 0.2$		1 AUBERT	02q BABR	Repl. by AUBERT 07b
$5.4 \pm 1.2 \pm 0.5$		1 CASEY	02 BELL	Repl. by CHAO 04
$5.6^{+2.3+0.4}_{-2.0-0.5}$		1 ABE	01H BELL	Repl. by CASEY 02
$4.1 \pm 1.0 \pm 0.7$		1 AUBERT	01e BABR	Repl. by AUBERT 02q
< 67	90	3 ABE	00c SLD	$e^+e^- \rightarrow Z$
$4.3^{+1.6}_{-1.4} \pm 0.5$		1 CRONIN-HEN..	00 CLE2	Repl. by BORNHEIM 03
< 15	90	GODANG	98 CLE2	Repl. by CRONIN-HENNESSY 00
< 45	90	4 ADAM	96d DLPH	$e^+e^- \rightarrow Z$
< 20	90	ASNER	96 CLE2	Repl. by GODANG 98
< 41	90	5 BUSKULIC	96v ALEP	$e^+e^- \rightarrow Z$
< 55	90	6 ABREU	95N DLPH	Sup. by ADAM 96d
< 47	90	7 AKERS	94L OPAL	$e^+e^- \rightarrow Z$
< 29	90	1 BATTLE	93 CLE2	$e^+e^- \rightarrow \Upsilon(4S)$
< 130	90	1 ALBRECHT	90B ARG	$e^+e^- \rightarrow \Upsilon(4S)$
< 77	90	8 BORTOLETTO	89 CLEO	$e^+e^- \rightarrow \Upsilon(4S)$
< 260	90	8 BEBEK	87 CLEO	$e^+e^- \rightarrow \Upsilon(4S)$
< 500	90	GILES	84 CLEO	$e^+e^- \rightarrow \Upsilon(4S)$

¹ Assumes equal production of B^+ and B^0 at the $\Upsilon(4S)$.

² ABULENCIA, A 06d reports $[B(B^0 \rightarrow \pi^+\pi^-)] / [B(B^0 \rightarrow K^+\pi^-)] = 0.21 \pm 0.05 \pm 0.03$. We multiply by our best value $B(B^0 \rightarrow K^+\pi^-) = (1.94 \pm 0.06) \times 10^{-5}$. Our first error is their experiment's error and our second error is the systematic error from using our best value.

³ ABE 00c assumes $B(Z \rightarrow b\bar{b}) = (21.7 \pm 0.1)\%$ and the B fractions $f_{B^0} = f_{B^+} = (39.7^{+1.8}_{-2.2})\%$ and $f_{B_s} = (10.5^{+1.8}_{-2.2})\%$.

⁴ ADAM 96d assumes $f_{B^0} = f_{B^-} = 0.39$ and $f_{B_s} = 0.12$.

⁵ BUSKULIC 96v assumes PDG 96 production fractions for B^0, B^+, B_s, b baryons.

⁶ Assumes a B^0, B^- production fraction of 0.39 and a B_s production fraction of 0.12.

⁷ Assumes $B(Z \rightarrow b\bar{b}) = 0.217$ and $B^0_d (B^0_s)$ fraction 39.5% (12%).

⁸ Paper assumes the $\Upsilon(4S)$ decays 43% to $B^0\bar{B}^0$. We rescale to 50%.

$\Gamma(\pi^+\pi^-)/\Gamma(K^+\pi^-)$				$\Gamma_{284}/\Gamma_{198}$
VALUE	CL%	DOCUMENT ID	TECN	COMMENT
0.257 ± 0.014		OUR AVERAGE		
$0.26 \pm 0.01 \pm 0.01$		LIN	07A BELL	$e^+e^- \rightarrow \Upsilon(4S)$
$0.21 \pm 0.05 \pm 0.03$		ABULENCIA, A	06d CDF	$p\bar{p}$ at 1.96 TeV
••• We do not use the following data for averages, fits, limits, etc. •••				
$0.29^{+0.13+0.01}_{-0.12-0.02}$		ABE	01H BELL	Repl. by LIN 07A

$\Gamma(\pi^0\pi^0)/\Gamma_{total}$				Γ_{285}/Γ
VALUE (units 10^{-6})	CL%	DOCUMENT ID	TECN	COMMENT
1.62 ± 0.31		OUR AVERAGE		
$1.47 \pm 0.25 \pm 0.12$		1 AUBERT	07bc BABR	$e^+e^- \rightarrow \Upsilon(4S)$
$2.3^{+0.4+0.2}_{-0.5-0.3}$		1 CHAO	05 BELL	$e^+e^- \rightarrow \Upsilon(4S)$

Error includes scale factor of 1.3.

$1.17 \pm 0.32 \pm 0.10$		1 AUBERT	05L BABR	Repl. by AUBERT 07bc
< 3.6	90	1 AUBERT	03L BABR	$e^+e^- \rightarrow \Upsilon(4S)$
$2.1 \pm 0.6 \pm 0.3$		1 AUBERT	03s BABR	Repl. by AUBERT 05L
< 4.4	90	1 BORNHEIM	03 CLE2	$e^+e^- \rightarrow \Upsilon(4S)$
$1.7 \pm 0.6 \pm 0.2$		1 LEE	03 BELL	Repl. by CHAO 05
< 5.7	90	1 ASNER	02 CLE2	$e^+e^- \rightarrow \Upsilon(4S)$
< 6.4	90	1 CASEY	02 BELL	$e^+e^- \rightarrow \Upsilon(4S)$
< 9.3	90	GODANG	98 CLE2	Repl. by ASNER 02
< 9.1	90	ASNER	96 CLE2	Repl. by GODANG 98
< 60	90	2 ACCIARRI	95H L3	$e^+e^- \rightarrow Z$

¹ Assumes equal production of B^+ and B^0 at the $\Upsilon(4S)$.

² ACCIARRI 95H assumes $f_{B^0} = 39.5 \pm 4.0$ and $f_{B_s} = 12.0 \pm 3.0\%$.

$\Gamma(\eta\pi^0)/\Gamma_{total}$				Γ_{286}/Γ
VALUE (units 10^{-6})	CL%	DOCUMENT ID	TECN	COMMENT
< 1.3		OUR AVERAGE		
< 2.5	90	1 AUBERT	06w BABR	$e^+e^- \rightarrow \Upsilon(4S)$
••• We do not use the following data for averages, fits, limits, etc. •••				
< 2.5	90	1 CHANG	05A BELL	$e^+e^- \rightarrow \Upsilon(4S)$
< 2.5	90	1 AUBERT, B	04D BABR	Repl. by AUBERT 06w
< 2.9	90	1 RICHICHI	00 CLE2	$e^+e^- \rightarrow \Upsilon(4S)$
< 8	90	BEHRENS	98 CLE2	Repl. by RICHICHI 00
< 250	90	2 ACCIARRI	95H L3	$e^+e^- \rightarrow Z$
< 1800	90	1 ALBRECHT	90B ARG	$e^+e^- \rightarrow \Upsilon(4S)$

¹ Assumes equal production of B^+ and B^0 at the $\Upsilon(4S)$.

² ACCIARRI 95H assumes $f_{B^0} = 39.5 \pm 4.0$ and $f_{B_s} = 12.0 \pm 3.0\%$.

$\Gamma(\eta\eta)/\Gamma_{total}$				Γ_{287}/Γ
VALUE (units 10^{-6})	CL%	DOCUMENT ID	TECN	COMMENT
< 1.8		OUR AVERAGE		
< 2.0	90	1 AUBERT, B	06v BABR	$e^+e^- \rightarrow \Upsilon(4S)$
••• We do not use the following data for averages, fits, limits, etc. •••				
< 2.0	90	1 CHANG	05A BELL	$e^+e^- \rightarrow \Upsilon(4S)$
< 2.8	90	1 AUBERT, B	04X BABR	$e^+e^- \rightarrow \Upsilon(4S)$
< 18	90	BEHRENS	98 CLE2	$e^+e^- \rightarrow \Upsilon(4S)$
< 410	90	2 ACCIARRI	95H L3	$e^+e^- \rightarrow Z$
••• We do not use the following data for averages, fits, limits, etc. •••				
< 5.7	90	1 AUBERT, B	04D BABR	Repl. by AUBERT 06w
< 11	90	1 RICHICHI	00 CLE2	$e^+e^- \rightarrow \Upsilon(4S)$
< 11	90	BEHRENS	98 CLE2	Repl. by RICHICHI 00

¹ Assumes equal production of B^+ and B^0 at the $\Upsilon(4S)$.

² ACCIARRI 95H assumes $f_{B^0} = 39.5 \pm 4.0$ and $f_{B_s} = 12.0 \pm 3.0\%$.

$\Gamma(\eta'\pi^0)/\Gamma_{total}$				Γ_{288}/Γ
VALUE (units 10^{-6})	CL%	DOCUMENT ID	TECN	COMMENT
1.5 ± 1.0		OUR AVERAGE		
$0.8^{+0.8}_{-0.6} \pm 0.1$		1 AUBERT	06w BABR	$e^+e^- \rightarrow \Upsilon(4S)$
$2.8 \pm 1.0 \pm 0.3$		1 SCHUEMANN	06 BELL	$e^+e^- \rightarrow \Upsilon(4S)$
••• We do not use the following data for averages, fits, limits, etc. •••				
$1.0^{+1.4}_{-1.0} \pm 0.8$		1 AUBERT, B	04D BABR	Repl. by AUBERT 06w
< 5.7	90	1 RICHICHI	00 CLE2	$e^+e^- \rightarrow \Upsilon(4S)$
< 11	90	BEHRENS	98 CLE2	Repl. by RICHICHI 00

¹ Assumes equal production of B^+ and B^0 at the $\Upsilon(4S)$.

$\Gamma(\eta'\eta)/\Gamma_{total}$				Γ_{289}/Γ
VALUE (units 10^{-6})	CL%	DOCUMENT ID	TECN	COMMENT
< 2.4		OUR AVERAGE		
< 6.5	90	1 AUBERT, B	06v BABR	$e^+e^- \rightarrow \Upsilon(4S)$
••• We do not use the following data for averages, fits, limits, etc. •••				
< 6.5	90	1 SCHUEMANN	07 BELL	$e^+e^- \rightarrow \Upsilon(4S)$
< 10	90	1 AUBERT, B	04X BABR	Repl. by AUBERT, B 06v
< 47	90	BEHRENS	98 CLE2	$e^+e^- \rightarrow \Upsilon(4S)$

¹ Assumes equal production of B^+ and B^0 at the $\Upsilon(4S)$.

$\Gamma(\eta'\eta)/\Gamma_{total}$				Γ_{290}/Γ
VALUE (units 10^{-6})	CL%	DOCUMENT ID	TECN	COMMENT
< 1.7		OUR AVERAGE		
< 1.7	90	1 AUBERT	06w BABR	$e^+e^- \rightarrow \Upsilon(4S)$
••• We do not use the following data for averages, fits, limits, etc. •••				
< 4.5	90	1 SCHUEMANN	07 BELL	$e^+e^- \rightarrow \Upsilon(4S)$
< 4.6	90	1 AUBERT, B	04X BABR	$e^+e^- \rightarrow \Upsilon(4S)$
< 27	90	BEHRENS	98 CLE2	$e^+e^- \rightarrow \Upsilon(4S)$

¹ Assumes equal production of B^+ and B^0 at the $\Upsilon(4S)$.

$\Gamma(\eta'\rho^0)/\Gamma_{total}$				Γ_{291}/Γ
VALUE (units 10^{-6})	CL%	DOCUMENT ID	TECN	COMMENT
< 1.3		OUR AVERAGE		
< 1.3	90	1 SCHUEMANN	07 BELL	$e^+e^- \rightarrow \Upsilon(4S)$
••• We do not use the following data for averages, fits, limits, etc. •••				
< 3.7	90	AUBERT	07E BABR	$e^+e^- \rightarrow \Upsilon(4S)$
< 4.3	90	1 AUBERT, B	04D BABR	Repl. by AUBERT 07E
< 12	90	1 RICHICHI	00 CLE2	$e^+e^- \rightarrow \Upsilon(4S)$
< 23	90	BEHRENS	98 CLE2	Repl. by RICHICHI 00

¹ Assumes equal production of B^+ and B^0 at the $\Upsilon(4S)$.

Meson Particle Listings

 B^0 $\Gamma(\eta' f_0(980) \times B(f_0(980) \rightarrow \pi^+ \pi^-)) / \Gamma_{\text{total}}$ Γ_{292} / Γ

VALUE (units 10^{-6})	CL%	DOCUMENT ID	TECN	COMMENT
<1.5	90	AUBERT	07E	BABR $e^+ e^- \rightarrow \Upsilon(4S)$

 $\Gamma(\eta \rho^0) / \Gamma_{\text{total}}$ Γ_{293} / Γ

VALUE (units 10^{-6})	CL%	DOCUMENT ID	TECN	COMMENT
< 1.5	90	¹ AUBERT	07Y	BABR $e^+ e^- \rightarrow \Upsilon(4S)$
•••		We do not use the following data for averages, fits, limits, etc. •••		
< 1.9	90	¹ WANG	07B	BELL $e^+ e^- \rightarrow \Upsilon(4S)$
< 1.5	90	¹ AUBERT,B	04D	BABR Repl. by AUBERT 07Y
<10	90	¹ RICHICHI	00	CLE2 $e^+ e^- \rightarrow \Upsilon(4S)$
<13	90	BEHRENS	98	CLE2 Repl. by RICHICHI 00

¹ Assumes equal production of B^+ and B^0 at the $\Upsilon(4S)$.

 $\Gamma(\eta f_0(980) \times B(f_0(980) \rightarrow \pi^+ \pi^-)) / \Gamma_{\text{total}}$ Γ_{294} / Γ

VALUE (units 10^{-6})	CL%	DOCUMENT ID	TECN	COMMENT
<0.4	90	¹ AUBERT	07Y	BABR $e^+ e^- \rightarrow \Upsilon(4S)$

¹ Assumes equal production of B^+ and B^0 at the $\Upsilon(4S)$.

 $\Gamma(\omega \eta) / \Gamma_{\text{total}}$ Γ_{295} / Γ

VALUE (units 10^{-6})	CL%	DOCUMENT ID	TECN	COMMENT
< 1.9	90	¹ AUBERT,B	05K	BABR $e^+ e^- \rightarrow \Upsilon(4S)$
•••		We do not use the following data for averages, fits, limits, etc. •••		
$4.0^{+1.3}_{-1.2} \pm 0.4$		¹ AUBERT,B	04X	BABR Repl. by AUBERT,B 05K
<12	90	¹ BERGFELD	98	CLE2

¹ Assumes equal production of B^+ and B^0 at the $\Upsilon(4S)$.

 $\Gamma(\omega \eta') / \Gamma_{\text{total}}$ Γ_{296} / Γ

VALUE (units 10^{-6})	CL%	DOCUMENT ID	TECN	COMMENT
< 2.2	90	¹ SCHUEMANN	07	BELL $e^+ e^- \rightarrow \Upsilon(4S)$
•••		We do not use the following data for averages, fits, limits, etc. •••		
< 2.8	90	¹ AUBERT,B	04X	BABR $e^+ e^- \rightarrow \Upsilon(4S)$
<60	90	¹ BERGFELD	98	CLE2

¹ Assumes equal production of B^+ and B^0 at the $\Upsilon(4S)$.

 $\Gamma(\omega \rho^0) / \Gamma_{\text{total}}$ Γ_{297} / Γ

VALUE (units 10^{-6})	CL%	DOCUMENT ID	TECN	COMMENT
< 1.5	90	¹ AUBERT,B	06T	BABR $e^+ e^- \rightarrow \Upsilon(4S)$
•••		We do not use the following data for averages, fits, limits, etc. •••		
< 3.3	90	¹ AUBERT	05O	BABR Repl. by AUBERT,B 06T
<11	90	¹ BERGFELD	98	CLE2

¹ Assumes equal production of B^+ and B^0 at the $\Upsilon(4S)$.

 $\Gamma(\omega f_0(980)) / \Gamma_{\text{total}}$ Γ_{298} / Γ

VALUE (units 10^{-6})	CL%	DOCUMENT ID	TECN	COMMENT
<1.5	90	¹ AUBERT,B	06T	BABR $e^+ e^- \rightarrow \Upsilon(4S)$

¹ Assumes equal production of B^+ and B^0 at the $\Upsilon(4S)$.

 $\Gamma(\omega \eta) / \Gamma_{\text{total}}$ Γ_{299} / Γ

VALUE (units 10^{-6})	CL%	DOCUMENT ID	TECN	COMMENT
< 4.0	90	¹ AUBERT,B	06T	BABR $e^+ e^- \rightarrow \Upsilon(4S)$
•••		We do not use the following data for averages, fits, limits, etc. •••		
<19	90	¹ BERGFELD	98	CLE2

¹ Assumes equal production of B^+ and B^0 at the $\Upsilon(4S)$.

 $\Gamma(\phi \pi^0) / \Gamma_{\text{total}}$ Γ_{300} / Γ

VALUE (units 10^{-6})	CL%	DOCUMENT ID	TECN	COMMENT
<0.28	90	¹ AUBERT,B	06C	BABR $e^+ e^- \rightarrow \Upsilon(4S)$
•••		We do not use the following data for averages, fits, limits, etc. •••		
<1.0	90	¹ AUBERT,B	04D	BABR Repl. by AUBERT,B 06C
<5	90	¹ BERGFELD	98	CLE2

¹ Assumes equal production of B^+ and B^0 at the $\Upsilon(4S)$.

 $\Gamma(\phi \eta) / \Gamma_{\text{total}}$ Γ_{301} / Γ

VALUE (units 10^{-6})	CL%	DOCUMENT ID	TECN	COMMENT
<0.6	90	¹ AUBERT,B	06V	BABR $e^+ e^- \rightarrow \Upsilon(4S)$
•••		We do not use the following data for averages, fits, limits, etc. •••		
<1.0	90	¹ AUBERT,B	04X	BABR Repl. by AUBERT,B 06V
<9	90	¹ BERGFELD	98	CLE2

¹ Assumes equal production of B^+ and B^0 at the $\Upsilon(4S)$.

 $\Gamma(\phi \eta') / \Gamma_{\text{total}}$ Γ_{302} / Γ

VALUE (units 10^{-6})	CL%	DOCUMENT ID	TECN	COMMENT
< 0.5	90	¹ SCHUEMANN	07	BELL $e^+ e^- \rightarrow \Upsilon(4S)$
•••		We do not use the following data for averages, fits, limits, etc. •••		
< 1.0	90	¹ AUBERT,B	06V	BABR $e^+ e^- \rightarrow \Upsilon(4S)$
< 4.5	90	¹ AUBERT,B	04X	BABR Repl. by AUBERT,B 06V
<31	90	¹ BERGFELD	98	CLE2

¹ Assumes equal production of B^+ and B^0 at the $\Upsilon(4S)$.

 $\Gamma(\phi \rho^0) / \Gamma_{\text{total}}$ Γ_{303} / Γ

VALUE (units 10^{-6})	CL%	DOCUMENT ID	TECN	COMMENT
< 13	90	¹ BERGFELD	98	CLE2
•••		We do not use the following data for averages, fits, limits, etc. •••		
<156	90	² ABE	00C	SLD $e^+ e^- \rightarrow Z$

¹ Assumes equal production of B^+ and B^0 at the $\Upsilon(4S)$.
² ABE 00C assumes $B(Z \rightarrow b\bar{b}) = (21.7 \pm 0.1)\%$ and the B fractions $f_{B^0} = f_{B^+} = (39.7^{+1.8}_{-2.2})\%$ and $f_{B_s} = (10.5^{+1.8}_{-2.2})\%$.

 $\Gamma(\phi \omega) / \Gamma_{\text{total}}$ Γ_{304} / Γ

VALUE (units 10^{-6})	CL%	DOCUMENT ID	TECN	COMMENT
< 1.2	90	¹ AUBERT,B	06T	BABR $e^+ e^- \rightarrow \Upsilon(4S)$
•••		We do not use the following data for averages, fits, limits, etc. •••		
<21	90	¹ BERGFELD	98	CLE2

¹ Assumes equal production of B^+ and B^0 at the $\Upsilon(4S)$.

 $\Gamma(\phi \phi) / \Gamma_{\text{total}}$ Γ_{305} / Γ

VALUE	CL%	DOCUMENT ID	TECN	COMMENT
<1.5 $\times 10^{-6}$	90	¹ AUBERT,B	04X	BABR $e^+ e^- \rightarrow \Upsilon(4S)$
•••		We do not use the following data for averages, fits, limits, etc. •••		
$< 3.21 \times 10^{-4}$	90	² ABE	00C	SLD $e^+ e^- \rightarrow Z$
$< 1.2 \times 10^{-5}$	90	¹ BERGFELD	98	CLE2
$< 3.9 \times 10^{-5}$	90	ASNER	96	CLE2 $e^+ e^- \rightarrow \Upsilon(4S)$

¹ Assumes equal production of B^+ and B^0 at the $\Upsilon(4S)$.
² ABE 00C assumes $B(Z \rightarrow b\bar{b}) = (21.7 \pm 0.1)\%$ and the B fractions $f_{B^0} = f_{B^+} = (39.7^{+1.8}_{-2.2})\%$ and $f_{B_s} = (10.5^{+1.8}_{-2.2})\%$.

 $\Gamma(a_0(980) \pm \pi^\mp \times B(a_0(980) \pm \rightarrow \eta \pi^\pm)) / \Gamma_{\text{total}}$ Γ_{306} / Γ

VALUE (units 10^{-6})	CL%	DOCUMENT ID	TECN	COMMENT
<3.1	90	¹ AUBERT	07Y	BABR $e^+ e^- \rightarrow \Upsilon(4S)$
•••		We do not use the following data for averages, fits, limits, etc. •••		
<5.1	90	¹ AUBERT,BE	04	BABR Repl. by AUBERT 07Y

¹ Assumes equal production of B^+ and B^0 at the $\Upsilon(4S)$.

 $\Gamma(a_0(1450) \pm \pi^\mp \times B(a_0(1450) \pm \rightarrow \eta \pi^\pm)) / \Gamma_{\text{total}}$ Γ_{307} / Γ

VALUE (units 10^{-6})	CL%	DOCUMENT ID	TECN	COMMENT
<2.3	90	¹ AUBERT	07Y	BABR $e^+ e^- \rightarrow \Upsilon(4S)$

¹ Assumes equal production of B^+ and B^0 at the $\Upsilon(4S)$.

 $\Gamma(\pi^+ \pi^- \pi^0) / \Gamma_{\text{total}}$ Γ_{308} / Γ

VALUE	CL%	DOCUMENT ID	TECN	COMMENT
$< 7.2 \times 10^{-4}$	90	¹ ALBRECHT	90B	ARG $e^+ e^- \rightarrow \Upsilon(4S)$

¹ ALBRECHT 90B limit assumes equal production of $B^0 \bar{B}^0$ and $B^+ B^-$ at $\Upsilon(4S)$.

 $\Gamma(\rho^0 \pi^0) / \Gamma_{\text{total}}$ Γ_{309} / Γ

VALUE (units 10^{-6})	CL%	DOCUMENT ID	TECN	COMMENT
1.8 ± 0.5 OUR AVERAGE				
$3.12^{+0.88+0.60}_{-0.82-0.76}$		¹ DRAGIC	06	BELL $e^+ e^- \rightarrow \Upsilon(4S)$
$1.4 \pm 0.6 \pm 0.3$		¹ AUBERT	04Z	BABR $e^+ e^- \rightarrow \Upsilon(4S)$
$1.6^{+2.0}_{-1.4} \pm 0.8$		¹ JESSOP	00	CLEO $e^+ e^- \rightarrow \Upsilon(4S)$
•••		We do not use the following data for averages, fits, limits, etc. •••		
$5.1 \pm 1.6 \pm 0.9$		DRAGIC	04	BELL Repl. by DRAGIC 06
< 5.3	90	¹ GORDON	02	BELL Repl. by DRAGIC 04
< 24	90	ASNER	96	CLEO Repl. by JESSOP 00
<400	90	¹ ALBRECHT	90B	ARG $e^+ e^- \rightarrow \Upsilon(4S)$

¹ Assumes equal production of B^+ and B^0 at the $\Upsilon(4S)$.

 $\Gamma(\rho^\mp \pi^\pm) / \Gamma_{\text{total}}$ Γ_{310} / Γ

VALUE (units 10^{-6})	CL%	DOCUMENT ID	TECN	COMMENT
22.8 ± 2.5 OUR AVERAGE				
$22.6 \pm 1.8 \pm 2.2$		¹ AUBERT	03T	BABR $e^+ e^- \rightarrow \Upsilon(4S)$
$20.8^{+6.0+2.8}_{-6.3-3.1}$		¹ GORDON	02	BELL $e^+ e^- \rightarrow \Upsilon(4S)$
$27.6^{+8.4}_{-7.4} \pm 4.2$		¹ JESSOP	00	CLE2 $e^+ e^- \rightarrow \Upsilon(4S)$
•••		We do not use the following data for averages, fits, limits, etc. •••		
< 88	90	ASNER	96	CLE2 Repl. by JESSOP 00
< 520	90	¹ ALBRECHT	90B	ARG $e^+ e^- \rightarrow \Upsilon(4S)$
<5200	90	² BEBEK	87	CLEO $e^+ e^- \rightarrow \Upsilon(4S)$

¹ Assumes equal production of B^+ and B^0 at the $\Upsilon(4S)$.
² BEBEK 87 reports $< 6.1 \times 10^{-3}$ assuming the $\Upsilon(4S)$ decays 43% to $B^0 \bar{B}^0$. We rescale to 50%.

See key on page 373

Meson Particle Listings

B^0

$\Gamma(\pi^+\pi^-\pi^+\pi^-)/\Gamma_{\text{total}}$ Γ_{311}/Γ

VALUE	CL%	DOCUMENT ID	TECN	COMMENT
$<2.3 \times 10^{-4}$	90	¹ ADAM 96D	DLPH	$e^+e^- \rightarrow Z$
$<2.8 \times 10^{-4}$	90	² ABREU 95N	DLPH	Sup. by ADAM 96D
$<6.7 \times 10^{-4}$	90	³ ALBRECHT 90B	ARG	$e^+e^- \rightarrow \Upsilon(4S)$

• • • We do not use the following data for averages, fits, limits, etc. • • •
¹ ADAM 96D assumes $f_{B^0} = f_{B^-} = 0.39$ and $f_{B_s} = 0.12$.
² Assumes a B^0, B^- production fraction of 0.39 and a B_s production fraction of 0.12.
³ ALBRECHT 90B limit assumes equal production of $B^0\bar{B}^0$ and B^+B^- at $\Upsilon(4S)$.

$\Gamma(\rho^0\rho^0)/\Gamma_{\text{total}}$ Γ_{312}/Γ

VALUE (units 10^{-6})	CL%	DOCUMENT ID	TECN	COMMENT
$1.07 \pm 0.33 \pm 0.19$		¹ AUBERT 07G	BABR	$e^+e^- \rightarrow \Upsilon(4S)$
< 1.1	90	¹ AUBERT 05i	BABR	Repl. by AUBERT 07G
< 2.1	90	¹ AUBERT 03v	BABR	Repl. by AUBERT 05i
< 18	90	² GODANG 02	CLE2	$e^+e^- \rightarrow \Upsilon(4S)$
<136	90	³ ABE 00c	SLD	$e^+e^- \rightarrow Z$
<280	90	¹ ALBRECHT 90B	ARG	$e^+e^- \rightarrow \Upsilon(4S)$
<290	90	⁴ BORTOLETTO89	CLEO	$e^+e^- \rightarrow \Upsilon(4S)$
<430	90	⁴ BEBEK 87	CLEO	$e^+e^- \rightarrow \Upsilon(4S)$

• • • We do not use the following data for averages, fits, limits, etc. • • •
¹ Assumes equal production of B^+ and B^0 at the $\Upsilon(4S)$.
² Assumes a helicity 00 configuration. For a helicity 11 configuration, the limit decreases to 1.4×10^{-5} .
³ ABE 00c assumes $B(Z \rightarrow b\bar{b}) = (21.7 \pm 0.1)\%$ and the B fractions $f_{B^0} = f_{B^+} = (39.7^{+1.8}_{-2.2}\%)$ and $f_{B_s} = (10.5^{+1.8}_{-2.2}\%)$.
⁴ Paper assumes the $\Upsilon(4S)$ decays 43% to $B^0\bar{B}^0$. We rescale to 50%.

$\Gamma(\rho^0 f_0(980) \times B(f_0(980) \rightarrow \pi^+\pi^-))/\Gamma_{\text{total}}$ Γ_{313}/Γ

VALUE (units 10^{-6})	CL%	DOCUMENT ID	TECN	COMMENT
<0.53	90	¹ AUBERT 07G	BABR	$e^+e^- \rightarrow \Upsilon(4S)$

¹ Assumes equal production of B^+ and B^0 at the $\Upsilon(4S)$.

$\Gamma(f_0(980) f_0(980) \times B(f_0(980) \rightarrow \pi^+\pi^-^2))/\Gamma_{\text{total}}$ Γ_{314}/Γ

VALUE (units 10^{-6})	CL%	DOCUMENT ID	TECN	COMMENT
<0.16	90	¹ AUBERT 07G	BABR	$e^+e^- \rightarrow \Upsilon(4S)$

¹ Assumes equal production of B^+ and B^0 at the $\Upsilon(4S)$.

$\Gamma(a_1(1260)^\mp \pi^\pm)/\Gamma_{\text{total}}$ Γ_{315}/Γ

VALUE (units 10^{-6})	CL%	DOCUMENT ID	TECN	COMMENT
$33.2 \pm 3.8 \pm 3.0$		^{1,2} AUBERT 06v	BABR	$e^+e^- \rightarrow \Upsilon(4S)$
< 630	90	¹ ALBRECHT 90B	ARG	$e^+e^- \rightarrow \Upsilon(4S)$
< 490	90	³ BORTOLETTO89	CLEO	$e^+e^- \rightarrow \Upsilon(4S)$
<1000	90	³ BEBEK 87	CLEO	$e^+e^- \rightarrow \Upsilon(4S)$

• • • We do not use the following data for averages, fits, limits, etc. • • •
¹ Assumes equal production of B^+ and B^0 at the $\Upsilon(4S)$.
² Assumes $a_1(1260)$ decays only to 3π and $B(a_1^\pm \rightarrow \pi^\pm \pi^\mp \pi^\pm) = 0.5$.
³ Paper assumes the $\Upsilon(4S)$ decays 43% to $B^0\bar{B}^0$. We rescale to 50%.

$\Gamma(b_1^\mp \pi^\pm \times B(b_1^\mp \rightarrow \omega \pi^\mp))/\Gamma_{\text{total}}$ Γ_{316}/Γ

VALUE (units 10^{-6})	CL%	DOCUMENT ID	TECN	COMMENT
$10.9 \pm 1.2 \pm 0.9$		¹ AUBERT 07Bi	BABR	$e^+e^- \rightarrow \Upsilon(4S)$

¹ Assumes equal production of B^+ and B^0 at the $\Upsilon(4S)$.

$\Gamma(a_2(1320)^\mp \pi^\pm)/\Gamma_{\text{total}}$ Γ_{317}/Γ

VALUE	CL%	DOCUMENT ID	TECN	COMMENT
$<3.0 \times 10^{-4}$	90	¹ BORTOLETTO89	CLEO	$e^+e^- \rightarrow \Upsilon(4S)$
$<1.4 \times 10^{-3}$	90	¹ BEBEK 87	CLEO	$e^+e^- \rightarrow \Upsilon(4S)$

• • • We do not use the following data for averages, fits, limits, etc. • • •
¹ Paper assumes the $\Upsilon(4S)$ decays 43% to $B^0\bar{B}^0$. We rescale to 50%.

$\Gamma(\pi^+\pi^-\pi^0\pi^0)/\Gamma_{\text{total}}$ Γ_{318}/Γ

VALUE	CL%	DOCUMENT ID	TECN	COMMENT
$<3.1 \times 10^{-3}$	90	¹ ALBRECHT 90B	ARG	$e^+e^- \rightarrow \Upsilon(4S)$

¹ ALBRECHT 90B limit assumes equal production of $B^0\bar{B}^0$ and B^+B^- at $\Upsilon(4S)$.

$\Gamma(\rho^+\rho^-)/\Gamma_{\text{total}}$ Γ_{319}/Γ

VALUE (units 10^{-6})	CL%	DOCUMENT ID	TECN	COMMENT
24.2 ± 3.1 OUR AVERAGE				
$25.5 \pm 2.1^{+3.6}_{-3.9}$		¹ AUBERT 07Bf	BABR	$e^+e^- \rightarrow \Upsilon(4S)$
$22.8 \pm 3.8^{+2.3}_{-2.6}$		¹ SOMOV 06	BELL	$e^+e^- \rightarrow \Upsilon(4S)$
25^{+7}_{-6}		¹ AUBERT 04c	BABR	Repl. by AUBERT, B 04R
$30 \pm 4 \pm 5$		^{1,2} AUBERT, B 04R	BABR	Repl. by AUBERT 07Bf
<2200	90	¹ ALBRECHT 90B	ARG	$e^+e^- \rightarrow \Upsilon(4S)$

• • • We do not use the following data for averages, fits, limits, etc. • • •
¹ Assumes equal production of B^+ and B^0 at the $\Upsilon(4S)$.
² The quoted result is obtained after combining with AUBERT 04c result by AUBERT 04R alone gives $(33 \pm 4 \pm 5) \times 10^{-6}$.

$\Gamma(a_1(1260)^0 \pi^0)/\Gamma_{\text{total}}$ Γ_{320}/Γ

VALUE	CL%	DOCUMENT ID	TECN	COMMENT
$<1.1 \times 10^{-3}$	90	¹ ALBRECHT 90B	ARG	$e^+e^- \rightarrow \Upsilon(4S)$

¹ ALBRECHT 90B limit assumes equal production of $B^0\bar{B}^0$ and B^+B^- at $\Upsilon(4S)$.

$\Gamma(\omega \pi^0)/\Gamma_{\text{total}}$ Γ_{321}/Γ

VALUE (units 10^{-6})	CL%	DOCUMENT ID	TECN	COMMENT
< 1.2	90	¹ AUBERT, B 04D	BABR	$e^+e^- \rightarrow \Upsilon(4S)$
< 2.0	90	¹ JEN 06	BELL	$e^+e^- \rightarrow \Upsilon(4S)$
< 1.9	90	¹ WANG 04A	BELL	$e^+e^- \rightarrow \Upsilon(4S)$
< 3	90	¹ AUBERT 01G	BABR	$e^+e^- \rightarrow \Upsilon(4S)$
< 5.5	90	¹ JESSOP 00	CLE2	$e^+e^- \rightarrow \Upsilon(4S)$
< 14	90	¹ BERGFELD 98	CLE2	Repl. by JESSOP 00
<460	90	² ALBRECHT 90B	ARG	$e^+e^- \rightarrow \Upsilon(4S)$

• • • We do not use the following data for averages, fits, limits, etc. • • •
¹ Assumes equal production of B^+ and B^0 at the $\Upsilon(4S)$.
² ALBRECHT 90B limit assumes equal production of $B^0\bar{B}^0$ and B^+B^- at $\Upsilon(4S)$.

$\Gamma(\pi^+\pi^+\pi^-\pi^0)/\Gamma_{\text{total}}$ Γ_{322}/Γ

VALUE	CL%	DOCUMENT ID	TECN	COMMENT
$<9.0 \times 10^{-3}$	90	¹ ALBRECHT 90B	ARG	$e^+e^- \rightarrow \Upsilon(4S)$

¹ ALBRECHT 90B limit assumes equal production of $B^0\bar{B}^0$ and B^+B^- at $\Upsilon(4S)$.

$\Gamma(a_1(1260)^+ \rho^-)/\Gamma_{\text{total}}$ Γ_{323}/Γ

VALUE (units 10^{-6})	CL%	DOCUMENT ID	TECN	COMMENT
< 61	90	^{1,2} AUBERT, B 06o	BABR	$e^+e^- \rightarrow \Upsilon(4S)$

• • • We do not use the following data for averages, fits, limits, etc. • • •
¹ Assumes equal production of B^+ and B^0 at the $\Upsilon(4S)$.
² Assumes $a_1(1260)$ decays only to 3π and $B(a_1^\pm \rightarrow \pi^\pm \pi^\mp \pi^\pm) = 0.5$.

$\Gamma(a_1(1260)^0 \rho^0)/\Gamma_{\text{total}}$ Γ_{324}/Γ

VALUE	CL%	DOCUMENT ID	TECN	COMMENT
$<2.4 \times 10^{-3}$	90	¹ ALBRECHT 90B	ARG	$e^+e^- \rightarrow \Upsilon(4S)$

¹ ALBRECHT 90B limit assumes equal production of $B^0\bar{B}^0$ and B^+B^- at $\Upsilon(4S)$.

$\Gamma(\pi^+\pi^+\pi^-\pi^-\pi^0)/\Gamma_{\text{total}}$ Γ_{325}/Γ

VALUE	CL%	DOCUMENT ID	TECN	COMMENT
$<3.0 \times 10^{-3}$	90	¹ ALBRECHT 90B	ARG	$e^+e^- \rightarrow \Upsilon(4S)$

¹ ALBRECHT 90B limit assumes equal production of $B^0\bar{B}^0$ and B^+B^- at $\Upsilon(4S)$.

$\Gamma(a_1(1260)^+ a_1(1260)^-)/\Gamma_{\text{total}}$ Γ_{326}/Γ

VALUE	CL%	DOCUMENT ID	TECN	COMMENT
$<2.8 \times 10^{-3}$	90	¹ BORTOLETTO89	CLEO	$e^+e^- \rightarrow \Upsilon(4S)$
$<6.0 \times 10^{-3}$	90	² ALBRECHT 90B	ARG	$e^+e^- \rightarrow \Upsilon(4S)$

• • • We do not use the following data for averages, fits, limits, etc. • • •
¹ BORTOLETTO 89 reports $< 3.2 \times 10^{-3}$ assuming the $\Upsilon(4S)$ decays 43% to $B^0\bar{B}^0$. We rescale to 50%.
² ALBRECHT 90B limit assumes equal production of $B^0\bar{B}^0$ and B^+B^- at $\Upsilon(4S)$.

$\Gamma(\pi^+\pi^+\pi^-\pi^-\pi^-\pi^0)/\Gamma_{\text{total}}$ Γ_{327}/Γ

VALUE	CL%	DOCUMENT ID	TECN	COMMENT
$<1.1 \times 10^{-2}$	90	¹ ALBRECHT 90B	ARG	$e^+e^- \rightarrow \Upsilon(4S)$

¹ ALBRECHT 90B limit assumes equal production of $B^0\bar{B}^0$ and B^+B^- at $\Upsilon(4S)$.

$\Gamma(\rho\bar{\rho})/\Gamma_{\text{total}}$ Γ_{328}/Γ

VALUE (units 10^{-6})	CL%	DOCUMENT ID	TECN	COMMENT
< 0.11	90	¹ TSAI 07	BELL	$e^+e^- \rightarrow \Upsilon(4S)$
< 0.41	90	¹ CHANG 05	BELL	$e^+e^- \rightarrow \Upsilon(4S)$
< 0.27	90	¹ AUBERT 04U	BABR	$e^+e^- \rightarrow \Upsilon(4S)$
< 1.4	90	¹ BORNHEIM 03	CLE2	$e^+e^- \rightarrow \Upsilon(4S)$
< 1.2	90	¹ ABE 02o	BELL	$e^+e^- \rightarrow \Upsilon(4S)$
< 7.0	90	¹ COAN 99	CLE2	$e^+e^- \rightarrow \Upsilon(4S)$
< 18	90	² BUSKULIC 96v	ALEP	$e^+e^- \rightarrow Z$
<350	90	³ ABREU 95N	DLPH	Sup. by ADAM 96D
< 34	90	⁴ BORTOLETTO89	CLEO	$e^+e^- \rightarrow \Upsilon(4S)$
<120	90	⁵ ALBRECHT 88f	ARG	$e^+e^- \rightarrow \Upsilon(4S)$
<170	90	⁴ BEBEK 87	CLEO	$e^+e^- \rightarrow \Upsilon(4S)$

• • • We do not use the following data for averages, fits, limits, etc. • • •
¹ Assumes equal production of B^+ and B^0 at the $\Upsilon(4S)$.
² BUSKULIC 96v assumes PDG 96 production fractions for B^0, B^+, B_s, b baryons.
³ Assumes a B^0, B^- production fraction of 0.39 and a B_s production fraction of 0.12.
⁴ Paper assumes the $\Upsilon(4S)$ decays 43% to $B^0\bar{B}^0$. We rescale to 50%.
⁵ ALBRECHT 88f reports $< 1.3 \times 10^{-4}$ assuming the $\Upsilon(4S)$ decays 45% to $B^0\bar{B}^0$. We rescale to 50%.

Meson Particle Listings

 B^0 $\Gamma(\rho\bar{p}\pi^+\pi^-)/\Gamma_{\text{total}}$ Γ_{329}/Γ

VALUE (units 10^{-4})	CL%	DOCUMENT ID	TECN	COMMENT
<2.5	90	¹ BEBEK 89	CLEO	$e^+e^- \rightarrow \Upsilon(4S)$
<ul style="list-style-type: none"> • • • We do not use the following data for averages, fits, limits, etc. • • • 				
<9.5	90	² ABREU 95N	DLPH	Sup. by ADAM 96D
$5.4 \pm 1.8 \pm 2.0$		³ ALBRECHT 88F	ARG	$e^+e^- \rightarrow \Upsilon(4S)$

- ¹ BEBEK 89 reports $< 2.9 \times 10^{-4}$ assuming the $\Upsilon(4S)$ decays 43% to $B^0\bar{B}^0$. We rescale to 50%.
- ² Assumes a B^0, B^- production fraction of 0.39 and a B_S production fraction of 0.12.
- ³ ALBRECHT 88F reports $6.0 \pm 2.0 \pm 2.2$ assuming the $\Upsilon(4S)$ decays 45% to $B^0\bar{B}^0$. We rescale to 50%.

 $\Gamma(\rho\bar{p}K^0)/\Gamma_{\text{total}}$ Γ_{330}/Γ

VALUE (units 10^{-6})	CL%	DOCUMENT ID	TECN	COMMENT
2.7 ± 0.4 OUR AVERAGE				
$3.0 \pm 0.5 \pm 0.3$		¹ AUBERT 07AV	BABR	$e^+e^- \rightarrow \Upsilon(4S)$
$2.40^{+0.64}_{-0.44} \pm 0.28$		^{1,2,3} WANG 05A	BELL	$e^+e^- \rightarrow \Upsilon(4S)$

- • • We do not use the following data for averages, fits, limits, etc. • • •
- $1.88^{+0.77}_{-0.60} \pm 0.23$ ^{1,2,4} WANG 04 BELL Repl. by WANG 05A
- <7.2 ⁹⁰ ^{1,2} ABE 02K BELL Repl. by WANG 04
- ¹ Assumes equal production of B^+ and B^0 at the $\Upsilon(4S)$.
- ² Explicitly vetoes resonant production of $\rho\bar{p}$ from charmonium states and ρK^0 production from Λ_c .
- ³ Provides also results with $M_{\rho\bar{p}} < 2.85$ GeV/ c^2 and angular asymmetry of $\rho\bar{p}$ system.
- ⁴ The branching fraction for $M_{\rho\bar{p}} < 2.85$ is also reported.

 $\Gamma(\Theta(1540)^+\bar{p} \times B(\Theta(1540)^+ \rightarrow \rho K_S^0))/\Gamma_{\text{total}}$ Γ_{331}/Γ

VALUE (units 10^{-6})	CL%	DOCUMENT ID	TECN	COMMENT
<0.05	90	¹ AUBERT 07AV	BABR	$e^+e^- \rightarrow \Upsilon(4S)$

- • • We do not use the following data for averages, fits, limits, etc. • • •
- <0.23 ⁹⁰ ¹ WANG 05A BELL $e^+e^- \rightarrow \Upsilon(4S)$
- ¹ Assumes equal production of B^+ and B^0 at the $\Upsilon(4S)$.

 $\Gamma(f_J(2220)K^0 \times B(f_J(2220) \rightarrow \rho\bar{p}))/\Gamma_{\text{total}}$ Γ_{332}/Γ

VALUE (units 10^{-6})	CL%	DOCUMENT ID	TECN	COMMENT
<0.45	90	¹ AUBERT 07AV	BABR	$e^+e^- \rightarrow \Upsilon(4S)$

- ¹ Assumes equal production of B^+ and B^0 at the $\Upsilon(4S)$.

 $\Gamma(f_J(2220)K_S^0 \times B(f_J(2220) \rightarrow \rho\bar{p}))/\Gamma_{\text{total}}$ Γ_{333}/Γ

VALUE (units 10^{-6})	CL%	DOCUMENT ID	TECN	COMMENT
$1.47 \pm 0.45 \pm 0.40$		¹ AUBERT 07AV	BABR	$e^+e^- \rightarrow \Upsilon(4S)$

- • • We do not use the following data for averages, fits, limits, etc. • • •
- <7.6 ⁹⁰ ¹ WANG 04 BELL $e^+e^- \rightarrow \Upsilon(4S)$
- ¹ Assumes equal production of B^+ and B^0 at the $\Upsilon(4S)$.

 $\Gamma(f_J(2220)K_S^0 \times B(f_J(2220) \rightarrow \rho\bar{p}))/\Gamma_{\text{total}}$ Γ_{334}/Γ

VALUE (units 10^{-6})	CL%	DOCUMENT ID	TECN	COMMENT
<0.15	90	¹ AUBERT 07AV	BABR	$e^+e^- \rightarrow \Upsilon(4S)$

- ¹ Assumes equal production of B^+ and B^0 at the $\Upsilon(4S)$.

 $\Gamma(\rho\bar{p}\pi^-)/\Gamma_{\text{total}}$ Γ_{335}/Γ

VALUE (units 10^{-6})	CL%	DOCUMENT ID	TECN	COMMENT
$3.23^{+0.33}_{-0.29} \pm 0.29$		¹ WANG 07C	BELL	$e^+e^- \rightarrow \Upsilon(4S)$

- • • We do not use the following data for averages, fits, limits, etc. • • •
- $2.62^{+0.44}_{-0.40} \pm 0.31$ ^{1,2} WANG 05A BELL Repl. by WANG 07C
- $3.97^{+1.00}_{-0.80} \pm 0.56$ ¹ WANG 03 BELL Repl. by WANG 05A
- < 13 ⁹⁰ ¹ COAN 99 CLE2 $e^+e^- \rightarrow \Upsilon(4S)$
- <180 ⁹⁰ ³ ALBRECHT 88F ARG $e^+e^- \rightarrow \Upsilon(4S)$
- ¹ Assumes equal production of B^+ and B^0 at the $\Upsilon(4S)$.
- ² Provides also results with $M_{\rho\bar{p}} < 2.85$ GeV/ c^2 and angular asymmetry of $\rho\bar{p}$ system.
- ³ ALBRECHT 88F reports $< 2.0 \times 10^{-4}$ assuming the $\Upsilon(4S)$ decays 45% to $B^0\bar{B}^0$. We rescale to 50%.

 $\Gamma(\Delta^0\bar{\lambda})/\Gamma_{\text{total}}$ Γ_{337}/Γ

VALUE (units 10^{-6})	CL%	DOCUMENT ID	TECN	COMMENT
<0.93	90	¹ WANG 07C	BELL	$e^+e^- \rightarrow \Upsilon(4S)$

- ¹ Assumes equal production of B^+ and B^0 at the $\Upsilon(4S)$.

 $\Gamma(\rho\bar{\lambda}K^-)/\Gamma_{\text{total}}$ Γ_{338}/Γ

VALUE (units 10^{-6})	CL%	DOCUMENT ID	TECN	COMMENT
<0.82	90	¹ WANG 03	BELL	$e^+e^- \rightarrow \Upsilon(4S)$

- ¹ Assumes equal production of B^+ and B^0 at the $\Upsilon(4S)$.

 $\Gamma(\rho\bar{\Sigma}^0\pi^-)/\Gamma_{\text{total}}$ Γ_{339}/Γ

VALUE	CL%	DOCUMENT ID	TECN	COMMENT
<3.8×10^{-6}	90	¹ WANG 03	BELL	$e^+e^- \rightarrow \Upsilon(4S)$

- ¹ Assumes equal production of B^+ and B^0 at the $\Upsilon(4S)$.

 $\Gamma(\bar{\Lambda})/\Gamma_{\text{total}}$ Γ_{340}/Γ

VALUE (units 10^{-6})	CL%	DOCUMENT ID	TECN	COMMENT
<0.32	90	¹ TSAI 07	BELL	$e^+e^- \rightarrow \Upsilon(4S)$

- • • We do not use the following data for averages, fits, limits, etc. • • •
- <0.69 ⁹⁰ ¹ CHANG 05 BELL Repl. by TSAI 2007
- <1.2 ⁹⁰ ¹ BORNHEIM 03 CLE2 $e^+e^- \rightarrow \Upsilon(4S)$
- <1.0 ⁹⁰ ¹ ABE 020 BELL Repl. by CHANG 05
- <3.9 ⁹⁰ ¹ COAN 99 CLE2 $e^+e^- \rightarrow \Upsilon(4S)$
- ¹ Assumes equal production of B^+ and B^0 at the $\Upsilon(4S)$.

 $\Gamma(\Delta^0\bar{\Delta}^0)/\Gamma_{\text{total}}$ Γ_{341}/Γ

VALUE	CL%	DOCUMENT ID	TECN	COMMENT
<0.0015	90	¹ BORTOLETTO 89	CLEO	$e^+e^- \rightarrow \Upsilon(4S)$

- ¹ BORTOLETTO 89 reports < 0.0018 assuming $\Upsilon(4S)$ decays 43% to $B^0\bar{B}^0$. We rescale to 50%.

 $\Gamma(\Delta^{++}\bar{\Delta}^{--})/\Gamma_{\text{total}}$ Γ_{342}/Γ

VALUE	CL%	DOCUMENT ID	TECN	COMMENT
<1.1×10^{-4}	90	¹ BORTOLETTO 89	CLEO	$e^+e^- \rightarrow \Upsilon(4S)$

- ¹ BORTOLETTO 89 reports $< 1.3 \times 10^{-4}$ assuming $\Upsilon(4S)$ decays 43% to $B^0\bar{B}^0$. We rescale to 50%.

 $\Gamma(\bar{D}^0\rho\bar{p})/\Gamma_{\text{total}}$ Γ_{343}/Γ

VALUE (units 10^{-4})	DOCUMENT ID	TECN	COMMENT
1.14 ± 0.09 OUR AVERAGE			
$1.13 \pm 0.06 \pm 0.08$	¹ AUBERT,B 06s	BABR	$e^+e^- \rightarrow \Upsilon(4S)$
$1.18 \pm 0.15 \pm 0.16$	¹ ABE 02W	BELL	$e^+e^- \rightarrow \Upsilon(4S)$

- ¹ Assumes equal production of B^+ and B^0 at the $\Upsilon(4S)$.

 $\Gamma(D_S^- \bar{\lambda}p)/\Gamma_{\text{total}}$ Γ_{344}/Γ

VALUE (units 10^{-5})	DOCUMENT ID	TECN	COMMENT
$2.9 \pm 0.9 \pm 0.2$	^{1,2} MEDVEDEVA 07	BELL	$e^+e^- \rightarrow \Upsilon(4S)$

- ¹ Assumes equal production of B^+ and B^0 at the $\Upsilon(4S)$.
- ² MEDVEDEVA 07 reports $(2.9 \pm 0.7 \pm 0.5 \pm 0.4) \times 10^{-5}$ for $B(D_S^+ \rightarrow \phi\pi^+) = (4.4 \pm 0.6) \times 10^{-2}$. We rescale to our best value $B(D_S^+ \rightarrow \phi\pi^+) = (4.38 \pm 0.35) \times 10^{-2}$. Our first error is their experiment's error and our second error is the systematic error from using our best value.

 $\Gamma(\bar{D}^*(2007)^0\rho\bar{p})/\Gamma_{\text{total}}$ Γ_{345}/Γ

VALUE (units 10^{-4})	DOCUMENT ID	TECN	COMMENT
1.03 ± 0.13 OUR AVERAGE			
$1.01 \pm 0.10 \pm 0.09$	¹ AUBERT,B 06s	BABR	$e^+e^- \rightarrow \Upsilon(4S)$
$1.20^{+0.33}_{-0.29} \pm 0.21$	¹ ABE 02W	BELL	$e^+e^- \rightarrow \Upsilon(4S)$

- ¹ Assumes equal production of B^+ and B^0 at the $\Upsilon(4S)$.

 $\Gamma(D^- \rho\bar{p}\pi^+)/\Gamma_{\text{total}}$ Γ_{346}/Γ

VALUE (units 10^{-4})	DOCUMENT ID	TECN	COMMENT
$3.38 \pm 0.14 \pm 0.29$	¹ AUBERT,B 06s	BABR	$e^+e^- \rightarrow \Upsilon(4S)$

- ¹ Assumes equal production of B^+ and B^0 at the $\Upsilon(4S)$.

 $\Gamma(D^{*-} \rho\bar{p}\pi^+)/\Gamma_{\text{total}}$ Γ_{347}/Γ

VALUE (units 10^{-4})	DOCUMENT ID	TECN	COMMENT
$4.81 \pm 0.22 \pm 0.44$	¹ AUBERT,B 06s	BABR	$e^+e^- \rightarrow \Upsilon(4S)$

- ¹ Assumes equal production of B^+ and B^0 at the $\Upsilon(4S)$.

 $\Gamma(\Theta_c \bar{p}\pi^+ \times B(\Theta_c \rightarrow D^- \rho))/\Gamma_{\text{total}}$ Γ_{348}/Γ

VALUE (units 10^{-6})	CL%	DOCUMENT ID	TECN	COMMENT
<9	90	¹ AUBERT,B 06s	BABR	$e^+e^- \rightarrow \Upsilon(4S)$

- ¹ Assumes equal production of B^+ and B^0 at the $\Upsilon(4S)$.

 $\Gamma(\Theta_c \bar{p}\pi^+ \times B(\Theta_c \rightarrow D^{*-} \rho))/\Gamma_{\text{total}}$ Γ_{349}/Γ

VALUE (units 10^{-6})	CL%	DOCUMENT ID	TECN	COMMENT
<14	90	¹ AUBERT,B 06s	BABR	$e^+e^- \rightarrow \Upsilon(4S)$

- ¹ Assumes equal production of B^+ and B^0 at the $\Upsilon(4S)$.

See key on page 373

Meson Particle Listings

 B^0

$\Gamma(\Sigma_c^{--} \Delta^{++})/\Gamma_{\text{total}}$		Γ_{350}/Γ	
VALUE	CL%	DOCUMENT ID	TECN COMMENT

<0.0010 90 1 PROCARIO 94 CLE2 $e^+e^- \rightarrow \Upsilon(4S)$
 1 PROCARIO 94 reports < 0.0012 for $B(\Lambda_c^+ \rightarrow pK^-\pi^+) = 0.043$. We rescale to our best value $B(\Lambda_c^+ \rightarrow pK^-\pi^+) = 0.050$.

$\Gamma(\Lambda_c^- \rho\pi^+\pi^-)/\Gamma_{\text{total}}$		Γ_{351}/Γ	
VALUE (units 10^{-3})	CL%	DOCUMENT ID	TECN COMMENT

1.3 ± 0.4 OUR AVERAGE
 1.7 $^{+0.3}_{-0.2} \pm 0.4$ 1 DYTMAN 02 CLE2 $e^+e^- \rightarrow \Upsilon(4S)$
 1.10 $\pm 0.20 \pm 0.29$ 2 GABYSHEV 02 BELL $e^+e^- \rightarrow \Upsilon(4S)$
 • • • We do not use the following data for averages, fits, limits, etc. • • •
 1.33 $^{+0.46}_{-0.42} \pm 0.37$ 3 FU 97 CLE2 Repl. by DYTMAN 02

1 DYTMAN 02 reports $(1.67^{+0.27}_{-0.25}) \times 10^{-3}$ for $B(\Lambda_c^+ \rightarrow pK^-\pi^+) = 0.05$. We rescale to our best value $B(\Lambda_c^+ \rightarrow pK^-\pi^+) = (5.0 \pm 1.3) \times 10^{-2}$. Our first error is their experiment's error and our second error is the systematic error from using our best value.
 2 GABYSHEV 02 reports $(1.1 \pm 0.2) \times 10^{-3}$ for $B(\Lambda_c^+ \rightarrow pK^-\pi^+) = 0.05$. We rescale to our best value $B(\Lambda_c^+ \rightarrow pK^-\pi^+) = (5.0 \pm 1.3) \times 10^{-2}$. Our first error is their experiment's error and our second error is the systematic error from using our best value.
 3 FU 97 uses PDG 96 values of Λ_c branching fraction.

$\Gamma(\Lambda_c^- \rho)/\Gamma_{\text{total}}$		Γ_{352}/Γ	
VALUE (units 10^{-5})	CL%	DOCUMENT ID	TECN COMMENT

2.1 ± 0.7 OUR AVERAGE
 2.10 $^{+0.67+0.77}_{-0.55-0.46}$ 1 AUBERT 07AV BABR $e^+e^- \rightarrow \Upsilon(4S)$
 2.19 $^{+0.56}_{-0.49} \pm 0.65$ 1,2 GABYSHEV 03 BELL $e^+e^- \rightarrow \Upsilon(4S)$
 • • • We do not use the following data for averages, fits, limits, etc. • • •
 < 9 90 1,3 DYTMAN 02 CLE2 $e^+e^- \rightarrow \Upsilon(4S)$
 < 3.1 90 1,4 GABYSHEV 02 BELL $e^+e^- \rightarrow \Upsilon(4S)$
 < 21 90 5 FU 97 CLE2 $e^+e^- \rightarrow \Upsilon(4S)$

1 Assumes equal production of B^+ and B^0 at the $\Upsilon(4S)$.
 2 The second error for GABYSHEV 03 includes the systematic and the error of $\Lambda_c \rightarrow \bar{p}K^+\pi^-$ decay branching fraction.
 3 DYTMAN 02 measurement uses $B(\Lambda_c^- \rightarrow \bar{p}K^+\pi^-) = 5.0 \pm 1.3\%$. The second error includes the systematic and the uncertainty of the branching ratio.
 4 Uses the value for $\Lambda_c \rightarrow pK^-\pi^+$ branching ratio $(5.0 \pm 1.3)\%$.
 5 FU 97 uses PDG 96 values of Λ_c branching ratio.

$\Gamma(\Lambda_c^- \rho\pi^0)/\Gamma_{\text{total}}$		Γ_{353}/Γ	
VALUE	CL%	DOCUMENT ID	TECN COMMENT

$<5.9 \times 10^{-4}$ 90 1 FU 97 CLE2 $e^+e^- \rightarrow \Upsilon(4S)$
 1 FU 97 uses PDG 96 values of Λ_c branching ratio.

$\Gamma(\Lambda_c^- \rho\pi^+\pi^-\pi^0)/\Gamma_{\text{total}}$		Γ_{354}/Γ	
VALUE	CL%	DOCUMENT ID	TECN COMMENT

$<5.07 \times 10^{-3}$ 90 1 FU 97 CLE2 $e^+e^- \rightarrow \Upsilon(4S)$
 1 FU 97 uses PDG 96 values of Λ_c branching ratio.

$\Gamma(\Lambda_c^- \rho\pi^+\pi^-\pi^+)/\Gamma_{\text{total}}$		Γ_{355}/Γ	
VALUE	CL%	DOCUMENT ID	TECN COMMENT

$<2.74 \times 10^{-3}$ 90 1 FU 97 CLE2 $e^+e^- \rightarrow \Upsilon(4S)$
 1 FU 97 uses PDG 96 values of Λ_c branching ratio.

$\Gamma(\Lambda_c^+ \bar{p}\pi^+\pi^-)/\Gamma_{\text{total}}$		Γ_{356}/Γ	
VALUE (units 10^{-4})	CL%	DOCUMENT ID	TECN COMMENT

$11.2 \pm 1.4 \pm 2.9$ 1,2 PARK 07 BELL $e^+e^- \rightarrow \Upsilon(4S)$
 1 Assumes equal production of B^+ and B^0 at the $\Upsilon(4S)$.
 2 PARK 07 reports $(11.2 \pm 0.5 \pm 3.2) \times 10^{-4}$ for $B(\Lambda_c^+ \rightarrow pK^-\pi^+) = (5.0 \pm 1.3) \times 10^{-2}$. We rescale to our best value $B(\Lambda_c^+ \rightarrow pK^-\pi^+) = (5.0 \pm 1.3) \times 10^{-2}$. Our first error is their experiment's error and our second error is the systematic error from using our best value.

$\Gamma(\Lambda_c^+ \bar{p}\pi^+\pi^- (\text{nonresonant}))/\Gamma_{\text{total}}$		Γ_{357}/Γ	
VALUE (units 10^{-4})	CL%	DOCUMENT ID	TECN COMMENT

$6.4 \pm 1.0 \pm 1.7$ 1,2 PARK 07 BELL $e^+e^- \rightarrow \Upsilon(4S)$
 1 Assumes equal production of B^+ and B^0 at the $\Upsilon(4S)$.
 2 PARK 07 reports $(6.4 \pm 0.4 \pm 1.9) \times 10^{-4}$ for $B(\Lambda_c^+ \rightarrow pK^-\pi^+) = (5.0 \pm 1.3) \times 10^{-2}$. We rescale to our best value $B(\Lambda_c^+ \rightarrow pK^-\pi^+) = (5.0 \pm 1.3) \times 10^{-2}$. Our first error is their experiment's error and our second error is the systematic error from using our best value.

$\Gamma(\Sigma_c(2520)^{--} p\pi^+)/\Gamma_{\text{total}}$		Γ_{358}/Γ	
VALUE (units 10^{-4})	CL%	DOCUMENT ID	TECN COMMENT

$1.20 \pm 0.27 \pm 0.31$ 1,2 PARK 07 BELL $e^+e^- \rightarrow \Upsilon(4S)$
 • • • We do not use the following data for averages, fits, limits, etc. • • •
 1.6 $\pm 0.6 \pm 0.4$ 3 GABYSHEV 02 BELL Repl. by PARK 07
 1 Assumes equal production of B^+ and B^0 at the $\Upsilon(4S)$.
 2 PARK 07 reports $(1.2 \pm 0.1 \pm 0.4) \times 10^{-4}$ for $B(\Lambda_c^+ \rightarrow pK^-\pi^+) = (5.0 \pm 1.3) \times 10^{-2}$. We rescale to our best value $B(\Lambda_c^+ \rightarrow pK^-\pi^+) = (5.0 \pm 1.3) \times 10^{-2}$. Our first error is their experiment's error and our second error is the systematic error from using our best value.
 3 GABYSHEV 02 reports $(1.63^{+0.64}_{-0.58}) \times 10^{-4}$ for $B(\Lambda_c^+ \rightarrow pK^-\pi^+) = 0.05$. We rescale to our best value $B(\Lambda_c^+ \rightarrow pK^-\pi^+) = (5.0 \pm 1.3) \times 10^{-2}$. Our first error is their experiment's error and our second error is the systematic error from using our best value.

$\Gamma(\Sigma_c(2520)^0 p\pi^-)/\Gamma_{\text{total}}$		Γ_{359}/Γ	
VALUE	CL%	DOCUMENT ID	TECN COMMENT

$<0.38 \times 10^{-4}$ 90 1 PARK 07 BELL $e^+e^- \rightarrow \Upsilon(4S)$
 • • • We do not use the following data for averages, fits, limits, etc. • • •
 $<1.21 \times 10^{-4}$ 90 1,2 GABYSHEV 02 BELL Repl. by PARK 07
 1 Assumes equal production of B^+ and B^0 at the $\Upsilon(4S)$.
 2 Uses the value for $\Lambda_c \rightarrow pK^-\pi^+$ branching ratio $(5.0 \pm 1.3)\%$.

$\Gamma(\Sigma_c(2455)^0 p\pi^-)/\Gamma_{\text{total}}$		Γ_{360}/Γ	
VALUE (units 10^{-4})	CL%	DOCUMENT ID	TECN COMMENT

1.5 ± 0.5 OUR AVERAGE
 1.4 $\pm 0.3 \pm 0.4$ 1,2 PARK 07 BELL $e^+e^- \rightarrow \Upsilon(4S)$
 2.2 $\pm 0.7 \pm 0.6$ 3 DYTMAN 02 CLE2 $e^+e^- \rightarrow \Upsilon(4S)$
 • • • We do not use the following data for averages, fits, limits, etc. • • •
 0.5 $^{+0.5}_{-0.4} \pm 0.1$ 90 4 GABYSHEV 02 BELL Repl. by PARK 07

1 Assumes equal production of B^+ and B^0 at the $\Upsilon(4S)$.
 2 PARK 07 reports $(1.4 \pm 0.2 \pm 0.4) \times 10^{-4}$ for $B(\Lambda_c^+ \rightarrow pK^-\pi^+) = (5.0 \pm 1.3) \times 10^{-2}$. We rescale to our best value $B(\Lambda_c^+ \rightarrow pK^-\pi^+) = (5.0 \pm 1.3) \times 10^{-2}$. Our first error is their experiment's error and our second error is the systematic error from using our best value.
 3 DYTMAN 02 reports $(2.2 \pm 0.7) \times 10^{-4}$ for $B(\Lambda_c^+ \rightarrow pK^-\pi^+) = 0.05$. We rescale to our best value $B(\Lambda_c^+ \rightarrow pK^-\pi^+) = (5.0 \pm 1.3) \times 10^{-2}$. Our first error is their experiment's error and our second error is the systematic error from using our best value.
 4 GABYSHEV 02 reports $(0.48^{+0.46}_{-0.41}) \times 10^{-4}$ for $B(\Lambda_c^+ \rightarrow pK^-\pi^+) = 0.05$. We rescale to our best value $B(\Lambda_c^+ \rightarrow pK^-\pi^+) = (5.0 \pm 1.3) \times 10^{-2}$. Our first error is their experiment's error and our second error is the systematic error from using our best value.

$\Gamma(\Sigma_c(2455)^{--} p\pi^+)/\Gamma_{\text{total}}$		Γ_{361}/Γ	
VALUE (units 10^{-4})	CL%	DOCUMENT ID	TECN COMMENT

2.2 ± 0.7 OUR AVERAGE
 2.1 $\pm 0.3 \pm 0.5$ 1,2 PARK 07 BELL $e^+e^- \rightarrow \Upsilon(4S)$
 3.7 $\pm 1.1 \pm 1.0$ 3 DYTMAN 02 CLE2 $e^+e^- \rightarrow \Upsilon(4S)$
 • • • We do not use the following data for averages, fits, limits, etc. • • •
 2.4 $\pm 0.7 \pm 0.6$ 4 GABYSHEV 02 BELL Repl. by PARK 07

1 Assumes equal production of B^+ and B^0 at the $\Upsilon(4S)$.
 2 PARK 07 reports $(2.1 \pm 0.2 \pm 0.6) \times 10^{-4}$ for $B(\Lambda_c^+ \rightarrow pK^-\pi^+) = (5.0 \pm 1.3) \times 10^{-2}$. We rescale to our best value $B(\Lambda_c^+ \rightarrow pK^-\pi^+) = (5.0 \pm 1.3) \times 10^{-2}$. Our first error is their experiment's error and our second error is the systematic error from using our best value.
 3 DYTMAN 02 reports $(3.7 \pm 1.1) \times 10^{-4}$ for $B(\Lambda_c^+ \rightarrow pK^-\pi^+) = 0.05$. We rescale to our best value $B(\Lambda_c^+ \rightarrow pK^-\pi^+) = (5.0 \pm 1.3) \times 10^{-2}$. Our first error is their experiment's error and our second error is the systematic error from using our best value.
 4 GABYSHEV 02 reports $(2.38^{+0.75}_{-0.69}) \times 10^{-4}$ for $B(\Lambda_c^+ \rightarrow pK^-\pi^+) = 0.05$. We rescale to our best value $B(\Lambda_c^+ \rightarrow pK^-\pi^+) = (5.0 \pm 1.3) \times 10^{-2}$. Our first error is their experiment's error and our second error is the systematic error from using our best value.

$\Gamma(\Lambda_c^+ \Lambda_c^+)/\Gamma_{\text{total}}$		Γ_{362}/Γ	
VALUE (units 10^{-5})	CL%	DOCUMENT ID	TECN COMMENT

<6.2 90 1 UCHIDA 08 BELL $e^+e^- \rightarrow \Upsilon(4S)$
 1 Assumes equal production of B^+ and B^0 at the $\Upsilon(4S)$.

$\Gamma(\Lambda_c(2593)^- / \Lambda_c(2625)^- \rho)/\Gamma_{\text{total}}$		Γ_{363}/Γ	
VALUE	CL%	DOCUMENT ID	TECN COMMENT

$<1.1 \times 10^{-4}$ 90 1,2 DYTMAN 02 CLE2 $e^+e^- \rightarrow \Upsilon(4S)$
 1 Assumes equal production of B^+ and B^0 at the $\Upsilon(4S)$.
 2 DYTMAN 02 measurement uses $B(\Lambda_c^- \rightarrow \bar{p}K^+\pi^-) = 5.0 \pm 1.3\%$. The second error includes the systematic and the uncertainty of the branching ratio.

Meson Particle Listings

B^0

$\Gamma(\Xi_c^- \Lambda_c^+ \times B(\Xi_c^- \rightarrow \Xi^+ \pi^- \pi^-))/\Gamma_{total}$ Γ 364/Γ

VALUE (units 10^{-5})	DOCUMENT ID	TECN	COMMENT
$9.3^{+4.2}_{-2.6} \pm 2.4$	1,2 CHISTOV	06A BELL	$e^+ e^- \rightarrow \Upsilon(4S)$

- 1 CHISTOV 06A reports $(9.3^{+3.7}_{-2.6} \pm 3.1) \times 10^{-5}$ for $B(\Lambda_c^+ \rightarrow p K^- \pi^+) = (5.0 \pm 1.3) \times 10^{-2}$. We rescale to our best value $B(\Lambda_c^+ \rightarrow p K^- \pi^+) = (5.0 \pm 1.3) \times 10^{-2}$. Our first error is their experiment's error and our second error is the systematic error from using our best value.
 2 Assumes equal production of B^+ and B^0 at the $\Upsilon(4S)$.

$\Gamma(\Lambda_c^+ \Lambda_c^- K^0)/\Gamma_{total}$ Γ 365/Γ

VALUE (units 10^{-4})	DOCUMENT ID	TECN	COMMENT
$7.9^{+2.9}_{-2.3} \pm 4.3$	1 GABYSHEV	06 BELL	$e^+ e^- \rightarrow \Upsilon(4S)$

- 1 Assumes equal production of B^+ and B^0 at the $\Upsilon(4S)$ and $B(\Lambda_c^+ \rightarrow p K^- \pi^+) = (5.0 \pm 1.3)\%$.

$\Gamma(\gamma\gamma)/\Gamma_{total}$ Γ 366/Γ

Test for $\Delta B=1$ weak neutral current. Allowed by higher-order electroweak interactions.

VALUE	CL%	DOCUMENT ID	TECN	COMMENT
$<6.2 \times 10^{-7}$	90	1 VILLA	06 BELL	$e^+ e^- \rightarrow \Upsilon(4S)$

- • • We do not use the following data for averages, fits, limits, etc. • • •
 $<1.7 \times 10^{-6}$ 90 1 AUBERT 01i BABR $e^+ e^- \rightarrow \Upsilon(4S)$
 $<3.9 \times 10^{-5}$ 90 2 ACCIARRI 95i L3 $e^+ e^- \rightarrow Z$

- 1 Assumes equal production of B^+ and B^0 at the $\Upsilon(4S)$.
 2 ACCIARRI 95i assumes $f_{B^0} = 39.5 \pm 4.0$ and $f_{B_s} = 12.0 \pm 3.0\%$.

$\Gamma(e^+ e^-)/\Gamma_{total}$ Γ 367/Γ

Test for $\Delta B=1$ weak neutral current. Allowed by higher-order electroweak interactions.

VALUE	CL%	DOCUMENT ID	TECN	COMMENT
$<11.3 \times 10^{-8}$	90	1 AUBERT 08P	BABR	$e^+ e^- \rightarrow \Upsilon(4S)$
$< 6.1 \times 10^{-8}$	90	1 AUBERT	05W BABR	Repl. by AUBERT 08P
$< 1.9 \times 10^{-7}$	90	1 CHANG	03 BELL	$e^+ e^- \rightarrow \Upsilon(4S)$
$< 8.3 \times 10^{-7}$	90	1 BERGFELD	00B CLE2	$e^+ e^- \rightarrow \Upsilon(4S)$
$< 1.4 \times 10^{-5}$	90	2 ACCIARRI	97B L3	$e^+ e^- \rightarrow Z$
$< 5.9 \times 10^{-6}$	90	AMMAR	94 CLE2	Repl. by BERGFELD 00B
$< 2.6 \times 10^{-5}$	90	3 AVERY	89B CLEO	$e^+ e^- \rightarrow \Upsilon(4S)$
$< 7.6 \times 10^{-5}$	90	4 ALBRECHT	87D ARG	$e^+ e^- \rightarrow \Upsilon(4S)$
$< 6.4 \times 10^{-5}$	90	5 AVERY	87 CLEO	$e^+ e^- \rightarrow \Upsilon(4S)$
$< 3 \times 10^{-4}$	90	GILES	84 CLEO	Repl. by AVERY 87

- 1 Assumes equal production of B^+ and B^0 at the $\Upsilon(4S)$.
 2 ACCIARRI 97B assume PDG 96 production fractions for B^+ , B^0 , B_s , and Λ_b .
 3 AVERY 89B reports $< 3 \times 10^{-5}$ assuming the $\Upsilon(4S)$ decays 43% to $B^0 \bar{B}^0$. We rescale to 50%.
 4 ALBRECHT 87D reports $< 8.5 \times 10^{-5}$ assuming the $\Upsilon(4S)$ decays 45% to $B^0 \bar{B}^0$. We rescale to 50%.
 5 AVERY 87 reports $< 8 \times 10^{-5}$ assuming the $\Upsilon(4S)$ decays 40% to $B^0 \bar{B}^0$. We rescale to 50%.

$\Gamma(e^+ e^- \gamma)/\Gamma_{total}$ Γ 368/Γ

Test for $\Delta B=1$ weak neutral current. Allowed by higher-order electroweak interactions.

VALUE	CL%	DOCUMENT ID	TECN	COMMENT
$<1.2 \times 10^{-7}$	90	AUBERT	08c BABR	$e^+ e^- \rightarrow \Upsilon(4S)$

$\Gamma(\mu^+ \mu^-)/\Gamma_{total}$ Γ 369/Γ

Test for $\Delta B=1$ weak neutral current. Allowed by higher-order electroweak interactions.

VALUE	CL%	DOCUMENT ID	TECN	COMMENT
$<1.5 \times 10^{-8}$	90	1 AALTONEN	08i CDF	$p\bar{p}$ at 1.96 TeV
$<5.2 \times 10^{-8}$	90	2 AUBERT	08P BABR	$e^+ e^- \rightarrow \Upsilon(4S)$
$<3.9 \times 10^{-8}$	90	3 ABULENCIA	05 CDF	Repl. by AALTONEN 08i
$<8.3 \times 10^{-8}$	90	2 AUBERT	05W BABR	$e^+ e^- \rightarrow \Upsilon(4S)$
$<1.5 \times 10^{-7}$	90	4 ACOSTA	04D CDF	$p\bar{p}$ at 1.96 TeV
$<1.6 \times 10^{-7}$	90	2 CHANG	03 BELL	$e^+ e^- \rightarrow \Upsilon(4S)$
$<6.1 \times 10^{-7}$	90	2 BERGFELD	00B CLE2	$e^+ e^- \rightarrow \Upsilon(4S)$
$<4.0 \times 10^{-5}$	90	ABBOTT	98B D0	$p\bar{p}$ 1.8 TeV
$<6.8 \times 10^{-7}$	90	5 ABE	98 CDF	$p\bar{p}$ at 1.8 TeV
$<1.0 \times 10^{-5}$	90	6 ACCIARRI	97B L3	$e^+ e^- \rightarrow Z$
$<1.6 \times 10^{-6}$	90	7 ABE	96L CDF	Repl. by ABE 98
$<5.9 \times 10^{-6}$	90	AMMAR	94 CLE2	$e^+ e^- \rightarrow \Upsilon(4S)$
$<8.3 \times 10^{-6}$	90	8 ALBAJAR	91c UA1	$E_{cm}^{pp} = 630$ GeV
$<1.2 \times 10^{-5}$	90	9 ALBAJAR	91c UA1	$E_{cm}^{pp} = 630$ GeV
$<4.3 \times 10^{-5}$	90	10 AVERY	89B CLEO	$e^+ e^- \rightarrow \Upsilon(4S)$
$<4.5 \times 10^{-5}$	90	11 ALBRECHT	87D ARG	$e^+ e^- \rightarrow \Upsilon(4S)$
$<7.7 \times 10^{-5}$	90	12 AVERY	87 CLEO	$e^+ e^- \rightarrow \Upsilon(4S)$
$<2 \times 10^{-4}$	90	GILES	84 CLEO	Repl. by AVERY 87

- 1 Uses B production ratio $f(\bar{b} \rightarrow B^+)/f(\bar{b} \rightarrow B_s^0) = 3.86 \pm 0.59$, and the number of $B^+ \rightarrow J/\psi K^+$ decays.
 2 Assumes equal production of B^+ and B^0 at the $\Upsilon(4S)$.
 3 Assumes production cross section $\sigma(B^+)/\sigma(B_s) = 3.71 \pm 0.41$ and $B(B^+ \rightarrow J/\psi K^+ \rightarrow \mu^+ \mu^- K^+) = (5.88 \pm 0.26) \times 10^{-5}$.
 4 Assumes production cross-section $\sigma(B_s)/\sigma(B^+) = 0.100/0.391$ and the CDF measured value of $\sigma(B^+) = 3.6 \pm 0.6 \mu b$.
 5 ABE 98 assumes production of $\sigma(B^0) = \sigma(B^+)$ and $\sigma(B_s)/\sigma(B^0) = 1/3$. They normalize to their measured $\sigma(B^0, p_T(B) > 6, |y| < 1.0) = 2.39 \pm 0.32 \pm 0.44 \mu b$.
 6 ACCIARRI 97B assume PDG 96 production fractions for B^+ , B^0 , B_s , and Λ_b .
 7 ABE 96L assumes equal B^0 and B^+ production. They normalize to their measured $\sigma(B^+, p_T(B) > 6 \text{ GeV}/c, |y| < 1) = 2.39 \pm 0.54 \mu b$.
 8 B^0 and B_s^0 are not separated.
 9 Obtained from unseparated B^0 and B_s^0 measurement by assuming a $B^0: B_s^0$ ratio 2:1.
 10 AVERY 89B reports $< 5 \times 10^{-3}$ assuming the $\Upsilon(4S)$ decays 43% to $B^0 \bar{B}^0$. We rescale to 50%.
 11 ALBRECHT 87D reports $< 5 \times 10^{-5}$ assuming the $\Upsilon(4S)$ decays 45% to $B^0 \bar{B}^0$. We rescale to 50%.
 12 AVERY 87 reports $< 9 \times 10^{-5}$ assuming the $\Upsilon(4S)$ decays 40% to $B^0 \bar{B}^0$. We rescale to 50%.

$\Gamma(\mu^+ \mu^- \gamma)/\Gamma_{total}$ Γ 370/Γ

Test for $\Delta B=1$ weak neutral current. Allowed by higher-order electroweak interactions.

VALUE	CL%	DOCUMENT ID	TECN	COMMENT
$<1.6 \times 10^{-7}$	90	AUBERT	08c BABR	$e^+ e^- \rightarrow \Upsilon(4S)$

$\Gamma(\tau^+ \tau^-)/\Gamma_{total}$ Γ 371/Γ

Test for $\Delta B=1$ weak neutral current. Allowed by higher-order electroweak interactions.

VALUE	CL%	DOCUMENT ID	TECN	COMMENT
$<4.1 \times 10^{-3}$	90	1 AUBERT	06s BABR	$e^+ e^- \rightarrow \Upsilon(4S)$

- 1 Assumes equal production of B^+ and B^0 at the $\Upsilon(4S)$.

$\Gamma(\pi^0 e^+ e^-)/\Gamma_{total}$ Γ 374/Γ

VALUE	CL%	DOCUMENT ID	TECN	COMMENT
$<1.4 \times 10^{-7}$	90	1 AUBERT	07AG BABR	$e^+ e^- \rightarrow \Upsilon(4S)$

- 1 Assumes equal production of B^+ and B^0 at the $\Upsilon(4S)$.

$\Gamma(\pi^0 \mu^+ \mu^-)/\Gamma_{total}$ Γ 375/Γ

VALUE	CL%	DOCUMENT ID	TECN	COMMENT
$<5.1 \times 10^{-7}$	90	1 AUBERT	07AG BABR	$e^+ e^- \rightarrow \Upsilon(4S)$

- 1 Assumes equal production of B^+ and B^0 at the $\Upsilon(4S)$.

$\Gamma(\pi^0 \ell^+ \ell^-)/\Gamma_{total}$ Γ 372/Γ

VALUE	CL%	DOCUMENT ID	TECN	COMMENT
$<1.2 \times 10^{-7}$	90	1 AUBERT	07AG BABR	$e^+ e^- \rightarrow \Upsilon(4S)$

- 1 Assumes equal production of B^+ and B^0 at the $\Upsilon(4S)$.

$\Gamma(\pi^0 \nu\bar{\nu})/\Gamma_{total}$ Γ 373/Γ

Test for $\Delta B=1$ weak neutral current. Allowed by higher-order electroweak interaction.

VALUE	CL%	DOCUMENT ID	TECN	COMMENT
$<2.2 \times 10^{-4}$	90	1 CHEN	07D BELL	$e^+ e^- \rightarrow \Upsilon(4S)$

- 1 Assumes equal production of B^+ and B^0 at the $\Upsilon(4S)$.

$\Gamma(K^0 e^+ e^-)/\Gamma_{total}$ Γ 379/Γ

Test for $\Delta B=1$ weak neutral current. Allowed by higher-order electroweak interactions.

VALUE (units 10^{-7})	CL%	DOCUMENT ID	TECN	COMMENT
$1.3^{+1.6}_{-1.1} \pm 0.2$		1 AUBERT,B	06j BABR	$e^+ e^- \rightarrow \Upsilon(4S)$

- • • We do not use the following data for averages, fits, limits, etc. • • •
 $- 2.1^{+2.3}_{-1.6} \pm 0.8$ 1 AUBERT 03U BABR $e^+ e^- \rightarrow \Upsilon(4S)$
 < 5.4 90 2 ISHIKAWA 03 BELL $e^+ e^- \rightarrow \Upsilon(4S)$
 < 27 90 1 ABE 02 BELL Repl. by ISHIKAWA 03
 < 38 90 1 AUBERT 02L BABR $e^+ e^- \rightarrow \Upsilon(4S)$
 < 84.5 90 3 ANDERSON 01B CLE2 $e^+ e^- \rightarrow \Upsilon(4S)$
 < 3000 90 ALBRECHT 91E ARG $e^+ e^- \rightarrow \Upsilon(4S)$
 < 5200 90 4 AVERY 87 CLEO $e^+ e^- \rightarrow \Upsilon(4S)$

- 1 Assumes equal production of B^+ and B^0 at the $\Upsilon(4S)$.
 2 Assumes equal production of B^0 and B^+ at $\Upsilon(4S)$.
 3 The result is for di-lepton masses above 0.5 GeV.
 4 AVERY 87 reports $< 6.5 \times 10^{-4}$ assuming the $\Upsilon(4S)$ decays 40% to $B^0 \bar{B}^0$. We rescale to 50%.

$\Gamma(K^0 \mu^+ \mu^-)/\Gamma_{total}$ Γ 380/Γ

Test for $\Delta B=1$ weak neutral current. Allowed by higher-order electroweak interactions.

VALUE (units 10^{-7})	CL%	DOCUMENT ID	TECN	COMMENT
$5.7^{+2.2}_{-1.8} \pm 0.8$		OUR AVERAGE		

- $5.9^{+3.3}_{-2.6} \pm 0.7$ 1 AUBERT,B 06j BABR $e^+ e^- \rightarrow \Upsilon(4S)$
 $5.6^{+2.9}_{-2.3} \pm 0.5$ 2 ISHIKAWA 03 BELL $e^+ e^- \rightarrow \Upsilon(4S)$

• • • We do not use the following data for averages, fits, limits, etc. • • •

$1.63^{+0.82}_{-0.63} \pm 0.14$	90	1	AUBERT	03u	BABR	Repl. by AUBERT,B 06j
<33	90	1	ABE	02	BELL	Repl. by ISHIKAWA 03
<36	90		AUBERT	02L	BABR	$e^+e^- \rightarrow \Upsilon(4S)$
<66.4	90	3	ANDERSON	01B	CLE2	$e^+e^- \rightarrow \Upsilon(4S)$
<5200	90		ALBRECHT	91E	ARG	$e^+e^- \rightarrow \Upsilon(4S)$
<3600	90	4	AVERY	87	CLEO	$e^+e^- \rightarrow \Upsilon(4S)$

- ¹ Assumes equal production of B⁺ and B⁰ at the $\Upsilon(4S)$.
- ² Assumes equal production of B⁰ and B⁺ at $\Upsilon(4S)$. The second error is a total of systematic uncertainties including model dependence.
- ³ The result is for di-lepton masses above 0.5 GeV.
- ⁴ AVERY 87 reports $< 4.5 \times 10^{-4}$ assuming the $\Upsilon(4S)$ decays 40% to B⁰ \bar{B}^0 . We rescale to 50%.

$\Gamma(K^0 \ell^+ \ell^-) / \Gamma_{total}$ Γ_{376} / Γ

VALUE (units 10 ⁻⁷)	CL%	DOCUMENT ID	TECN	COMMENT
$2.9^{+1.6}_{-1.3} \pm 0.3$		1	AUBERT,B	06j BABR $e^+e^- \rightarrow \Upsilon(4S)$

• • • We do not use the following data for averages, fits, limits, etc. • • •

<6.8	90	1	ISHIKAWA	03	BELL	$e^+e^- \rightarrow \Upsilon(4S)$
------	----	---	----------	----	------	-----------------------------------

- ¹ Assumes equal production of B⁰ and B⁺ at $\Upsilon(4S)$.

$\Gamma(K^0 \nu \bar{\nu}) / \Gamma_{total}$ Γ_{377} / Γ

Test for $\Delta B = 1$ weak neutral current. Allowed by higher-order electroweak interaction.

VALUE	CL%	DOCUMENT ID	TECN	COMMENT
$< 1.6 \times 10^{-4}$	90	1	CHEN	07D BELL $e^+e^- \rightarrow \Upsilon(4S)$

- ¹ Assumes equal production of B⁺ and B⁰ at the $\Upsilon(4S)$.

$\Gamma(\rho^0 \nu \bar{\nu}) / \Gamma_{total}$ Γ_{378} / Γ

Test for $\Delta B = 1$ weak neutral current. Allowed by higher-order electroweak interaction.

VALUE	CL%	DOCUMENT ID	TECN	COMMENT
$< 4.4 \times 10^{-4}$	90	1	CHEN	07D BELL $e^+e^- \rightarrow \Upsilon(4S)$

- ¹ Assumes equal production of B⁺ and B⁰ at the $\Upsilon(4S)$.

$\Gamma(K^*(892)^0 e^+ e^-) / \Gamma_{total}$ Γ_{382} / Γ

Test for $\Delta B = 1$ weak neutral current. Allowed by higher-order electroweak interactions.

VALUE (units 10 ⁻⁶)	CL%	DOCUMENT ID	TECN	COMMENT
$1.04^{+0.33}_{-0.29} \pm 0.11$		1	AUBERT,B	06j BABR $e^+e^- \rightarrow \Upsilon(4S)$

• • • We do not use the following data for averages, fits, limits, etc. • • •

$1.11^{+0.56}_{-0.47} \pm 0.11$		1	AUBERT	03u	BABR	$e^+e^- \rightarrow \Upsilon(4S)$
< 2.4	90	2	ISHIKAWA	03	BELL	$e^+e^- \rightarrow \Upsilon(4S)$
< 6.4	90	1	ABE	02	BELL	Repl. by ISHIKAWA 03
< 6.7	90	1	AUBERT	02L	BABR	$e^+e^- \rightarrow \Upsilon(4S)$
<290	90		ALBRECHT	91E	ARG	$e^+e^- \rightarrow \Upsilon(4S)$

- ¹ Assumes equal production of B⁺ and B⁰ at the $\Upsilon(4S)$.
- ² Assumes equal production of B⁰ and B⁺ at $\Upsilon(4S)$.

$\Gamma(K^*(892)^0 \mu^+ \mu^-) / \Gamma_{total}$ Γ_{383} / Γ

Test for $\Delta B = 1$ weak neutral current. Allowed by higher-order electroweak interactions.

VALUE (units 10 ⁻⁶)	CL%	DOCUMENT ID	TECN	COMMENT
$1.10^{+0.29}_{-0.26} \text{ OUR AVERAGE}$				

$0.87^{+0.38}_{-0.33} \pm 0.12$		1	AUBERT,B	06j	BABR	$e^+e^- \rightarrow \Upsilon(4S)$
$1.33^{+0.42}_{-0.37} \pm 0.11$		2	ISHIKAWA	03	BELL	$e^+e^- \rightarrow \Upsilon(4S)$

• • • We do not use the following data for averages, fits, limits, etc. • • •

$0.86^{+0.79}_{-0.58} \pm 0.11$		1	AUBERT	03u	BABR	Repl. by AUBERT,B 06j
< 4.2	90	1	ABE	02	BELL	$e^+e^- \rightarrow \Upsilon(4S)$
< 3.3	90		AUBERT	02L	BABR	$e^+e^- \rightarrow \Upsilon(4S)$
< 4.0	90	3	AFFOLDER	99B	CDF	$p\bar{p}$ at 1.8 TeV
< 25	90	4	ABE	96L	CDF	Repl. by AFFOLDER 99B
< 23	90	5	ALBAJAR	91c	UA1	$E_{CM}^{pp} = 630$ GeV
<340	90		ALBRECHT	91E	ARG	$e^+e^- \rightarrow \Upsilon(4S)$

- ¹ Assumes equal production of B⁺ and B⁰ at the $\Upsilon(4S)$.
- ² Assumes equal production of B⁰ and B⁺ at $\Upsilon(4S)$. The second error is a total of systematic uncertainties including model dependence.
- ³ AFFOLDER 99B measured relative to B⁰ $\rightarrow J/\psi(1S) K^*(892)^0$.
- ⁴ ABE 96L measured relative to B⁰ $\rightarrow J/\psi(1S) K^*(892)^0$ using PDG 94 branching ratios.
- ⁵ ALBAJAR 91c assumes 36% of \bar{b} quarks give B⁰ mesons.

$\Gamma(K^*(892)^0 \ell^+ \ell^-) / \Gamma_{total}$ Γ_{381} / Γ

Test for $\Delta B = 1$ weak neutral current. Allowed by higher-order electroweak interactions.

VALUE (units 10 ⁻⁷)	CL%	DOCUMENT ID	TECN	COMMENT
$9.5 \pm 1.8 \text{ OUR AVERAGE}$				

$8.1^{+2.1}_{-1.9} \pm 0.9$		1	AUBERT,B	06j	BABR	$e^+e^- \rightarrow \Upsilon(4S)$
$11.7^{+3.0}_{-2.7} \pm 0.9$		1	ISHIKAWA	03	BELL	$e^+e^- \rightarrow \Upsilon(4S)$

- ¹ Assumes equal production of B⁰ and B⁺ at $\Upsilon(4S)$.

$\Gamma(K^*(892)^0 \nu \bar{\nu}) / \Gamma_{total}$ Γ_{384} / Γ

Test for $\Delta B = 1$ weak neutral current. Allowed by higher-order electroweak interactions.

VALUE	CL%	DOCUMENT ID	TECN	COMMENT
$< 3.4 \times 10^{-4}$	90	1	CHEN	07D BELL $e^+e^- \rightarrow \Upsilon(4S)$

• • • We do not use the following data for averages, fits, limits, etc. • • •

$< 1.0 \times 10^{-3}$	90	2	ADAM	96D	DLPH	$e^+e^- \rightarrow Z$
------------------------	----	---	------	-----	------	------------------------

- ¹ Assumes equal production of B⁺ and B⁰ at the $\Upsilon(4S)$.
- ² ADAM 96D assumes $f_{B^0} = f_{B^-} = 0.39$ and $f_{B_s} = 0.12$.

$\Gamma(\phi \nu \bar{\nu}) / \Gamma_{total}$ Γ_{385} / Γ

Test for $\Delta B = 1$ weak neutral current. Allowed by higher-order electroweak interaction.

VALUE	CL%	DOCUMENT ID	TECN	COMMENT
$< 5.8 \times 10^{-5}$	90	1	CHEN	07D BELL $e^+e^- \rightarrow \Upsilon(4S)$

- ¹ Assumes equal production of B⁺ and B⁰ at the $\Upsilon(4S)$.

$\Gamma(e^\pm \mu^\mp) / \Gamma_{total}$ Γ_{386} / Γ

Test of lepton family number conservation. Allowed by higher-order electroweak interactions.

VALUE	CL%	DOCUMENT ID	TECN	COMMENT		
$< 9.2 \times 10^{-8}$	90	1	AUBERT	08P	BABR	$e^+e^- \rightarrow \Upsilon(4S)$

• • • We do not use the following data for averages, fits, limits, etc. • • •

$< 1.8 \times 10^{-7}$	90	1	AUBERT	05W	BABR	$e^+e^- \rightarrow \Upsilon(4S)$
$< 1.7 \times 10^{-7}$	90	1	CHANG	03	BELL	$e^+e^- \rightarrow \Upsilon(4S)$
$< 15 \times 10^{-7}$	90	1	BERGFELD	00B	CLE2	$e^+e^- \rightarrow \Upsilon(4S)$
$< 3.5 \times 10^{-6}$	90		ABE	98V	CDF	$p\bar{p}$ at 1.8 TeV
$< 1.6 \times 10^{-5}$	90	2	ACCIARRI	97B	L3	$e^+e^- \rightarrow Z$
$< 5.9 \times 10^{-6}$	90		AMMAR	94	CLE2	$e^+e^- \rightarrow \Upsilon(4S)$
$< 3.4 \times 10^{-5}$	90	3	AVERY	89B	CLEO	$e^+e^- \rightarrow \Upsilon(4S)$
$< 4.5 \times 10^{-5}$	90	4	ALBRECHT	87D	ARG	$e^+e^- \rightarrow \Upsilon(4S)$
$< 7.7 \times 10^{-5}$	90	5	AVERY	87	CLEO	$e^+e^- \rightarrow \Upsilon(4S)$
$< 3 \times 10^{-4}$	90		GILES	84	CLEO	Repl. by AVERY 87

- ¹ Assumes equal production of B⁺ and B⁰ at the $\Upsilon(4S)$.
- ² ACCIARRI 97B assume PDG 96 production fractions for B⁺, B⁰, B_s, and Λ_b .
- ³ Paper assumes the $\Upsilon(4S)$ decays 43% to B⁰ \bar{B}^0 . We rescale to 50%.
- ⁴ ALBRECHT 87D reports $< 5 \times 10^{-5}$ assuming the $\Upsilon(4S)$ decays 45% to B⁰ \bar{B}^0 . We rescale to 50%.
- ⁵ AVERY 87 reports $< 9 \times 10^{-5}$ assuming the $\Upsilon(4S)$ decays 40% to B⁰ \bar{B}^0 . We rescale to 50%.

$\Gamma(\pi^0 e^\pm \mu^\mp) / \Gamma_{total}$ Γ_{387} / Γ

VALUE	CL%	DOCUMENT ID	TECN	COMMENT		
$< 1.4 \times 10^{-7}$	90	1	AUBERT	07AG	BABR	$e^+e^- \rightarrow \Upsilon(4S)$

- ¹ Assumes equal production of B⁺ and B⁰ at the $\Upsilon(4S)$.

$\Gamma(K^0 e^\pm \mu^\mp) / \Gamma_{total}$ Γ_{388} / Γ

Test of lepton family number conservation.

VALUE (units 10 ⁻⁷)	CL%	DOCUMENT ID	TECN	COMMENT		
< 2.7	90	1	AUBERT,B	06j	BABR	$e^+e^- \rightarrow \Upsilon(4S)$

• • • We do not use the following data for averages, fits, limits, etc. • • •

< 40	90	1	AUBERT	02L	BABR	Repl. by AUBERT,B 06j
--------	----	---	--------	-----	------	-----------------------

- ¹ Assumes equal production of B⁺ and B⁰ at the $\Upsilon(4S)$.

$\Gamma(K^*(892)^0 e^+ \mu^-) / \Gamma_{total}$ Γ_{389} / Γ

VALUE (units 10 ⁻⁷)	CL%	DOCUMENT ID	TECN	COMMENT		
< 5.3	90	1	AUBERT,B	06j	BABR	$e^+e^- \rightarrow \Upsilon(4S)$

- ¹ Assumes equal production of B⁰ and B⁺ at $\Upsilon(4S)$.

$\Gamma(K^*(892)^0 e^- \mu^+) / \Gamma_{total}$ Γ_{390} / Γ

VALUE (units 10 ⁻⁷)	CL%	DOCUMENT ID	TECN	COMMENT		
< 3.4	90	1	AUBERT,B	06j	BABR	$e^+e^- \rightarrow \Upsilon(4S)$

- ¹ Assumes equal production of B⁰ and B⁺ at $\Upsilon(4S)$.

$\Gamma(K^*(892)^0 e^\pm \mu^\mp) / \Gamma_{total}$ Γ_{391} / Γ

Test of lepton family number conservation.

VALUE (units 10 ⁻⁷)	CL%	DOCUMENT ID	TECN	COMMENT		
< 5.8	90	1	AUBERT,B	06j	BABR	$e^+e^- \rightarrow \Upsilon(4S)$

• • • We do not use the following data for averages, fits, limits, etc. • • •

< 34	90	1	AUBERT	02L	BABR	Repl. by AUBERT,B 06j
--------	----	---	--------	-----	------	-----------------------

- ¹ Assumes equal production of B⁺ and B⁰ at the $\Upsilon(4S)$.

$\Gamma(e^\pm \tau^\mp) / \Gamma_{total}$ Γ_{392} / Γ

Test of lepton family number conservation. Allowed by higher-order electroweak interactions.

VALUE	CL%	DOCUMENT ID	TECN	COMMENT		
$< 1.1 \times 10^{-4}$	90		BORNHEIM	04	CLE2	$e^+e^- \rightarrow \Upsilon(4S)$

• • • We do not use the following data for averages, fits, limits, etc. • • •

$< 5.3 \times 10^{-4}$	90		AMMAR	94	CLE2	Repl. by BORNHEIM 04
------------------------	----	--	-------	----	------	----------------------

Meson Particle Listings

 B^0

$\Gamma(\mu^\pm \tau^\mp)/\Gamma_{\text{total}}$		Γ_{393}/Γ		
Test of lepton family number conservation. Allowed by higher-order electroweak interactions.				
VALUE	CL%	DOCUMENT ID	TECN	COMMENT
$<3.8 \times 10^{-5}$	90	BORNHEIM 04	CLE2	$e^+ e^- \rightarrow \Upsilon(4S)$
••• We do not use the following data for averages, fits, limits, etc. •••				
$<8.3 \times 10^{-4}$	90	AMMAR 94	CLE2	Repl. by BORNHEIM 04

$\Gamma(\text{invisible})/\Gamma_{\text{total}}$		Γ_{394}/Γ		
VALUE (units 10^{-5})				
VALUE	CL%	DOCUMENT ID	TECN	COMMENT
<22	90	¹ AUBERT,B	04j	BABR $e^+ e^- \rightarrow \Upsilon(4S)$
¹ Uses the fully reconstructed $B^0 \rightarrow D^{(*)-} \ell^+ \nu_\ell$ events as a tag.				

$\Gamma(\nu \bar{\nu} \gamma)/\Gamma_{\text{total}}$		Γ_{395}/Γ		
VALUE (units 10^{-5})				
VALUE	CL%	DOCUMENT ID	TECN	COMMENT
<4.7	90	¹ AUBERT,B	04j	BABR $e^+ e^- \rightarrow \Upsilon(4S)$
¹ Uses the fully reconstructed $B^0 \rightarrow D^{(*)-} \ell^+ \nu_\ell$ events as a tag.				

POLARIZATION IN B DECAYS

Revised April 2008 by A. V. Gritsan (Johns Hopkins University) and J. G. Smith (University of Colorado at Boulder).

We review the notation used in polarization measurements of B decays and discuss CP -violating observables in polarization measurements. We look at several examples of vector-vector and vector-tensor B meson decays, while more details about the theory and experimental results in B decays can be found in a separate mini-review [1] in this *Review*.

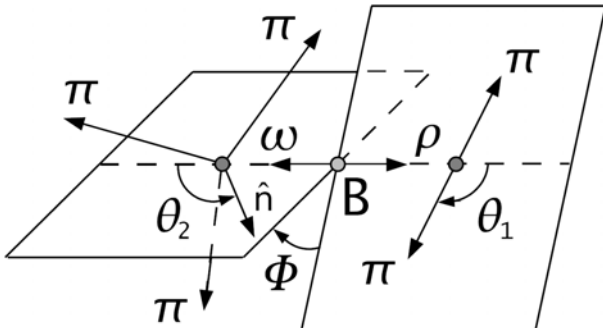


Figure 1: Definition of the helicity angles in the decay $B \rightarrow \rho \omega$ for the two-body (θ_1) and three-body (θ_2) B -daughter decays, where both angles are defined in the rest-frame of the decaying meson. The normal to the three-body decay plane (\hat{n}), and the daughter direction in the two-body decay, serve as analyzers of the polarization.

The angular distribution of the B meson decay to two mesons with non-zero spin is of special interest because it is sensitive to quark-spin alignment in decay transition, and reflects both weak- and strong-interaction dynamics. The angular distribution of decay products can be expressed as a function of three helicity angles which describe the alignment of the particles in the decay chain. The analyzer of the B -daughter polarization is normally chosen for two-body decays, as the direction of the daughters in the center-of-mass of the parent (*e.g.*, $\rho \rightarrow 2\pi$) [2], and for three-body decays as the normal to the decay plane [3] (see Fig. 1). An equivalent set of transversality angles is sometimes used in polarization analyses [4]. The

differential decay width depends on complex amplitudes A_λ , corresponding to the B -daughter helicity states λ .

Most B -decay polarization analyses are limited to the case when the spin of one of the B -meson daughters is 1. In that case, there are only three independent amplitudes corresponding to $\lambda = 0$ or ± 1 [5], where the last two can be expressed in terms of parity-even and parity-odd amplitudes $A_{\parallel,\perp} = (A_{+1} \pm A_{-1})/\sqrt{2}$. The overall decay amplitude would involve three complex terms proportional to the above amplitudes and the d functions of helicity angles. The exact angular dependence would depend on the quantum numbers of the B -meson daughters and of their decay products, and can be found in the literature [5,6]. The differential decay rate would involve six real quantities α_i , including interference terms,

$$\frac{d\Gamma}{\Gamma d \cos \theta_1 d \cos \theta_2 d\Phi} = \sum_i \alpha_i f_i(\cos \theta_1, \cos \theta_2, \Phi), \quad (1)$$

where each $f_i(\cos \theta_1, \cos \theta_2, \Phi)$ has unique angular dependence specific to particle quantum numbers, and the α_i parameters are defined as:

$$\alpha_1 = \frac{|A_0|^2}{\sum |A_\lambda|^2} = f_L, \quad (2)$$

$$\alpha_2 = \frac{|A_{\parallel}|^2 + |A_{\perp}|^2}{\sum |A_\lambda|^2} = (1 - f_L), \quad (3)$$

$$\alpha_3 = \frac{|A_{\parallel}|^2 - |A_{\perp}|^2}{\sum |A_\lambda|^2} = (1 - f_L - 2f_{\perp}), \quad (4)$$

$$\alpha_4 = \frac{\Im m(A_{\perp} A_{\parallel}^*)}{\sum |A_\lambda|^2} = \sqrt{f_{\perp}(1 - f_L - f_{\perp})} \sin(\phi_{\perp} - \phi_{\parallel}), \quad (5)$$

$$\alpha_5 = \frac{\Re e(A_{\parallel} A_0^*)}{\sum |A_\lambda|^2} = \sqrt{f_L(1 - f_L - f_{\perp})} \cos(\phi_{\parallel}), \quad (6)$$

$$\alpha_6 = \frac{\Im m(A_{\perp} A_0^*)}{\sum |A_\lambda|^2} = \sqrt{f_{\perp} f_L} \sin(\phi_{\perp}), \quad (7)$$

where the amplitudes have been expressed with the help of polarization parameters f_L , f_{\perp} , ϕ_{\parallel} , and ϕ_{\perp} defined in Table 1. Note that the terms proportional to $\Re e(A_{\perp} A_{\parallel}^*)$, $\Im m(A_{\parallel} A_0^*)$, and $\Re e(A_{\perp} A_0^*)$ are absent in Eqs. (2-7). However, these terms may appear in some cases of the three-body decay of a B -meson daughter, see Ref. 6.

Overall, six real parameters describe three complex amplitudes A_0 , A_{\parallel} , and A_{\perp} . These could be chosen to be the four polarization parameters f_L , f_{\perp} , ϕ_{\parallel} , and ϕ_{\perp} , one overall size normalization, such as decay rate Γ , or branching fraction \mathcal{B} , and one overall phase δ_0 . The phase convention is arbitrary for an isolated B decay mode. However, for several B decays, the relative phase could produce meaningful and observable effects through interference with other B decays with the same final states, such as for $B \rightarrow VK^*$ with $J = 0, 1, 2, 3, 4, \dots$. The phase could be referenced to the single $B \rightarrow VK_0^*$ amplitude A_{00} in such a case, as shown in Table 1. Here V stands for any spin-one vector meson.

Moreover, CP violation can be tested in the angular distribution of the decay as the difference between the B and \bar{B} . Each of the six real parameters describing the three complex

Table 1: Rate, polarization, and CP -asymmetry parameters defined for the B -meson decays to mesons with non-zero spin. Numerical examples are shown for the $B^0 \rightarrow \varphi K^*(892)^0$ decay. The first six parameters are defined under the assumption of no CP violation in decay, while they are averaged between the \bar{B} and B parameters in general. The last six parameters involve differences between the \bar{B} and B meson decay parameters. The phase convention δ_0 is chosen with respect to a single A_{00} amplitude from a reference B decay mode, which is $B^0 \rightarrow \varphi K_0^*(1430)^0$ for numerical results.

parameter	definition	average
\mathcal{B}	$\Gamma/\Gamma_{\text{total}}$	$(9.5 \pm 0.8) \times 10^{-6}$
f_L	$ A_0 ^2/\Sigma A_\lambda ^2$	0.484 ± 0.033
f_\perp	$ A_\perp ^2/\Sigma A_\lambda ^2$	0.26 ± 0.04
$\phi_\parallel - \pi$	$\arg(A_\parallel/A_0) - \pi$	-0.81 ± 0.14
$\phi_\perp - \pi$	$\arg(A_\perp/A_0) - \pi$	-0.81 ± 0.14
$\delta_0 - \pi$	$\arg(A_{00}/A_0) - \pi$	-0.36 ± 0.19
A_{CP}	$(\bar{\Gamma} - \Gamma)/(\bar{\Gamma} + \Gamma)$	-0.01 ± 0.06
A_{CP}^0	$(\bar{f}_L - f_L)/(f_L + f_L)$	$+0.02 \pm 0.07$
A_{CP}^\perp	$(\bar{f}_\perp - f_\perp)/(f_\perp + f_\perp)$	-0.11 ± 0.12
$\Delta\phi_\parallel$	$(\bar{\phi}_\parallel - \phi_\parallel)/2$	$+0.10 \pm 0.24$
$\Delta\phi_\perp$	$(\bar{\phi}_\perp - \phi_\perp - \pi)/2$	$+0.04 \pm 0.23$
$\Delta\delta_0$	$(\bar{\delta}_0 - \delta_0)/2$	$+0.21 \pm 0.19$

amplitudes would have a counterpart CP -asymmetry term, corresponding to three direct- CP asymmetries in three amplitudes, and three CP -violating phase differences, equivalent to the phase measurements from the mixing-induced CP asymmetries in the time evolution of the B -decays [1]. In Table 1 and Ref. 7, these are chosen to be the direct- CP asymmetries in the overall decay rate \mathcal{A}_{CP} , in the f_L fraction \mathcal{A}_{CP}^0 , and in the f_\perp fraction \mathcal{A}_{CP}^\perp , and three weak phase differences:

$$\Delta\phi_\parallel = \frac{1}{2}\arg(\bar{A}_\parallel A_0/A_\parallel \bar{A}_0), \quad (8)$$

$$\Delta\phi_\perp = \frac{1}{2}\arg(\bar{A}_\perp A_0/A_\perp \bar{A}_0) - \frac{\pi}{2}, \quad (9)$$

$$\Delta\delta_0 = \frac{1}{2}\arg(\bar{A}_{00} A_0/A_{00} \bar{A}_0). \quad (10)$$

The $\frac{\pi}{2}$ term in Eq. (9) reflects the fact that A_\perp and \bar{A}_\perp differ in phase by π if CP is conserved. The two parameters $\Delta\phi_\parallel$ and $\Delta\phi_\perp$ are equivalent to triple-product asymmetries constructed from the vectors describing the decay angular distribution [8]. The CP -violating phase difference in the reference decay mode is, in the Wolfenstein CKM quark-mixing phase convention,

$$\Delta\phi_{00} = \frac{1}{2}\arg(A_{00}/\bar{A}_{00}). \quad (11)$$

This can be measured only together with the mixing-induced phase difference for some of the neutral B -meson decays similar to other mixing-induced CP asymmetry measurements [1].

It may not always be possible to have a phase-reference decay mode which would define δ_0 and $\Delta\delta_0$ parameters. In that

case, it may be possible to define the phase difference directly similarly to Eq. (11):

$$\Delta\phi_0 = \frac{1}{2}\arg(A_0/\bar{A}_0). \quad (12)$$

One can measure the angles of the CKM unitarity triangle, assuming Standard Model contributions to the $\Delta\phi_0$ and B -mixing phases. Examples include measurements of $\beta = \phi_1$ with $B \rightarrow J/\psi K^*$ and $\alpha = \phi_2$ with $B \rightarrow \rho\rho$.

Most of the B decays that arise from tree-level $b \rightarrow c$ transitions have the amplitude hierarchy $|A_0| > |A_+| > |A_-|$ which is expected from analyses based on quark-helicity conservation [9]. The larger the mass of the vector-meson daughters, the weaker the inequality. The B meson decays to heavy vector particles with charm, such as $B \rightarrow J/\psi K^*$, $\psi(2S)K^*$, $\chi_{c1}K^*$, $D^*\rho$, D^*K^* , D^*D^* , and $D^*D_s^*$, show a substantial fraction of the amplitudes corresponding to transverse polarization of the vector mesons ($A_{\pm 1}$), in agreement with the factorization prediction. The detailed amplitude analysis of the $B \rightarrow J/\psi K^*$ decays has been performed by the BABAR [10], Belle [11], CDF [12], and CLEO [13] collaborations. Most analyses are performed under the assumption of the absence of direct CP violation. The parameter values are given in the particle listing of this *Review*. The difference between the strong phases ϕ_\parallel and ϕ_\perp deviates significantly from zero. The recent measurements [10,11] of CP -violating terms similar to those in $B \rightarrow \varphi K^*$ [7] shown in Table 1 are consistent with zero.

In addition, the mixing-induced CP -violating asymmetry is measured in the $B^0 \rightarrow J/\psi K^{*0}$ decay [1,10,11] where angular analysis allows one to separate CP -eigenstate amplitudes. This allows one to resolve the sign ambiguity of the $\cos 2\beta = \cos 2\phi_1$ term that appears in the time-dependent angular distribution due to interference of parity-even and parity-odd terms. This analysis relies on the knowledge of discrete ambiguities in the strong phases ϕ_\parallel and ϕ_\perp , as discussed below. The BABAR experiment used a novel method based on the dependence on the $K\pi$ invariant mass of the interference between the S - and P -waves to resolve the discrete ambiguity in the determination of the strong phases ($\phi_\parallel, \phi_\perp$) in $B \rightarrow J/\psi K^*$ decays [10]. The result is in agreement with the amplitude hierarchy expectation [9]. The CDF [12] and D0 [14] experiments have studied the $B_s^0 \rightarrow J/\psi\varphi$ decay and provided the lifetime, polarization, and phase measurements.

The amplitude hierarchy $|A_0| \gg |A_+| \gg |A_-|$ was expected in the B decays to light vector particles in both the penguin transition [15,16] and the tree-level transition [9]. There is confirmation by BABAR and BELLE experiments of predominantly longitudinal polarization in the tree-level $b \rightarrow u$ transition, such as $B^0 \rightarrow \rho^+\rho^-$ [17], $B^+ \rightarrow \rho^0\rho^+$ [18], and $B^+ \rightarrow \omega\rho^+$ [19], which is consistent with the analysis of the quark helicity conservation [9]. Because the longitudinal amplitude dominates the decay, a detailed amplitude analysis is not possible with current B samples, and limits on the transverse amplitude fraction are obtained. Only limits have been set on

Meson Particle Listings

 B^0

the $B^0 \rightarrow \omega\rho^0, \omega\omega$ [19] and evidence found for $B^0 \rightarrow \rho^0\rho^0$ [20] decays, still indicating that $b \rightarrow d$ penguin pollution is small in the charmless, strangeless vector-vector B decays.

The interest in the polarization and CP -asymmetry measurements in penguin transition, such as $b \rightarrow s$ decays $B \rightarrow \varphi K^*, \rho K^*, \omega K^*$, or $B_s^0 \rightarrow \varphi\varphi$, and $b \rightarrow d$ decay $B \rightarrow K^* \bar{K}^*$, is mainly motivated by their potential sensitivity to physics beyond the Standard Model. The decay amplitudes for $B \rightarrow \varphi K^*$ have been measured by the BABAR and Belle experiments [7,21,22]. The fractions of longitudinal polarization $f_L = 0.50 \pm 0.05$ for the $B^+ \rightarrow \varphi K^{*+}$ decay, and $f_L = 0.484 \pm 0.033$ for the $B^0 \rightarrow \varphi K^{*0}$ decay, indicate significant departure from the naive expectation of predominant longitudinal polarization, and suggest other contributions to the decay amplitude, previously neglected, either within the Standard Model, such as penguin annihilation [24] or QCD rescattering [25], or from physics beyond the Standard Model [26]. The complete set of twelve amplitude parameters measured in the $B^0 \rightarrow \varphi K^{*0}$ decay are given in Table 1. Several other parameters could be constructed from the above twelve parameters, as suggested in Ref. 27.

The discrete ambiguity in the phase ($\phi_{\parallel}, \phi_{\perp}, \Delta\phi_{\parallel}, \Delta\phi_{\perp}$) measurements has been resolved by BABAR in favor of $|A_+| \gg |A_-|$ through interference between the S - and P -waves of $K\pi$. The search for vector-tensor $B \rightarrow \varphi K_J^*$ decays with $J = 2, 3, 4$ revealed a large fraction of longitudinal polarization in the decay $B \rightarrow \varphi K_2^*(1430)$ with $f_L = 0.85 \pm 0.08$ [7,28].

Like $B \rightarrow \varphi K^*$, the decays $B \rightarrow \rho K^*$ and $B \rightarrow \omega K^*$ may be sensitive to New Physics. Measurements of the longitudinal polarization fraction in $B^+ \rightarrow \rho^0 K^{*0}$ and $B^+ \rightarrow \rho^+ K^{*0}$ [29] reveal a polarization anomaly similar to $B \rightarrow \varphi K^*$. At the same time, first measurement of the polarization in the $b \rightarrow d$ penguin decay $B^0 \rightarrow K^{*0} \bar{K}^{*0}$ indicates a large fraction of longitudinal polarization $f_L = 0.81^{+0.12}_{-0.13}$ [30]. There is also evidence for the $B_s^0 \rightarrow \varphi\varphi$ decay [31].

The three-body smileptonic B -meson decays, such as $B \rightarrow V l_1 l_2$, share many features with the two-body $B \rightarrow VV$ decays. Their differential decay width can be parameterized with the two helicity angles defined in the V and $(l_1 l_2)$ frames and with the azimuthal angle, as defined in Fig. 1. However, since the $(l_1 l_2)$ pair does not come from an on-shell particle, the angular distribution is unique to each point in the dilepton mass m_{ll} spectrum. The polarization measurements as a function of m_{ll} provide complementary information on physics beyond the Standard Model, as discussed for $B \rightarrow K^* l^+ l^-$ decay in Ref. 32, though the current data in this mode [33] are not yet sufficient for precise tests.

The examples of the angular distributions and observables in $B \rightarrow K^* l^+ l^-$ are discussed in Ref. 32. With the present statistics only two angular observables have been measured in this decay when integrated over certain ranges of the dilepton mass m_{ll} [33]. One parameter is the fraction of longitudinal polarization F_L , which is determined by the K^* angular distribution and is similar to f_L defined for exclusive two-body

decays. The other parameter is the forward-backward asymmetry of the lepton pair A_{FB} , which is the asymmetry of the decay rate with positive and negative values of $\cos\theta_1$.

In summary, there has been considerable recent interest in the polarization measurements of B -meson decays because they reveal both weak- and strong-interaction dynamics [24–26,34]. New measurements will further elucidate the pattern of spin alignment measurements in rare B decays, and further test the Standard Model and strong interaction dynamics, including the non-factorizable contributions to the B -decay amplitudes.

References

1. Y. Kwon and G. Punzi, “Production and Decay of b -Flavored Hadrons,” mini-review in this *Review*.
2. M. Jacob and G. C. Wick, *Ann. Phys.* **7**, 404 (1959).
3. S. M. Berman and M. Jacob, *Phys. Rev.* **139**, 1023 (1965).
4. I. Dunietz *et al.*, *Phys. Rev.* **D43**, 2193 (1991).
5. G. Kramer and W. F. Palmer, *Phys. Rev.* **D45**, 193 (1992).
6. A. Datta *et al.*, [arXiv:0711.2107](https://arxiv.org/abs/0711.2107) [hep-ph].
7. BABAR Collaboration, B. Aubert *et al.*, *Phys. Rev. Lett.* **93**, 231804 (2004); *Phys. Rev. Lett.* **98**, 051801 (2007).
8. G. Valencia, *Phys. Rev.* **D39**, 3339 (1998); A. Datta and D. London, *Int. J. Mod. Phys.* **A19**, 2505 (2004).
9. A. Ali *et al.*, *Z. Physik* **C1**, 269 (1979); M. Suzuki, *Phys. Rev.* **D64**, 117503 (2001).
10. BABAR Collaboration, B. Aubert *et al.*, *Phys. Rev.* **D71**, 032005 (2005); *Phys. Rev.* **D76**, 031102 (2007).
11. Belle Collaboration, R. Itoh *et al.*, *Phys. Rev. Lett.* **95**, 091601 (2005).
12. CDF Collaboration, T. Affolder *et al.*, *Phys. Rev. Lett.* **85**, 4668 (2000); CDF Collaboration, D. Acosta *et al.*, *Phys. Rev. Lett.* **94**, 101803 (2005).
13. CLEO Collaboration, C. P. Jessop, *Phys. Rev. Lett.* **79**, 4533 (1997).
14. D0 Collaboration, V. M. Abazov *et al.*, *Phys. Rev. Lett.* **98**, 121801 (2007).
15. H. Y. Cheng and K. C. Yang, *Phys. Lett.* **B511**, 40 (2001); C. H. Chen, Y. Y. Keum, and H. n. Li, *Phys. Rev.* **D66**, 054013 (2002).
16. A. L. Kagan, *Phys. Lett.* **B601**, 151 (2004); Y. Grossman, *Int. J. Mod. Phys.* **A19**, 907 (2004).
17. Belle Collaboration, A. Somov *et al.*, *Phys. Rev. Lett.* **96**, 171801 (2006); BABAR Collaboration, B. Aubert *et al.*, *Phys. Rev.* **D76**, 052007 (2007).
18. Belle Collaboration, J. Zhang *et al.*, *Phys. Rev. Lett.* **91**, 221801 (2003); BABAR Collaboration, B. Aubert *et al.*, *Phys. Rev. Lett.* **97**, 261801 (2006).
19. BABAR Collaboration, B. Aubert *et al.*, *Phys. Rev.* **D74**, 051102 (2006).
20. BABAR Collaboration, B. Aubert *et al.*, *Phys. Rev. Lett.* **98**, 111801 (2007).
21. Belle Collaboration, K. F. Chen *et al.*, *Phys. Rev. Lett.* **94**, 221804 (2005).
22. BABAR Collaboration, B. Aubert *et al.*, *Phys. Rev. Lett.* **99**, 201802 (2007).

23. BABAR Collaboration, B. Aubert *et al.*, Phys. Rev. Lett. **91**, 171802 (2003); Belle Collaboration, K. F. Chen *et al.*, Phys. Rev. Lett. **91**, 201801 (2003).
24. A. L. Kagan, Phys. Lett. **B601**, 151 (2004); H. n. Li and S. Mishima, Phys. Rev. **D71**, 054025 (2005); C.-H. Chen *et al.*, Phys. Rev. **D72**, 054011 (2005); M. Beneke *et al.*, Phys. Rev. Lett. **96**, 141801 (2006); C.-H. Chen and C.-Q. Geng, Phys. Rev. **D75**, 054010 (2007); A. Datta *et al.*, Phys. Rev. **D76**, 034015 (2007).
25. C. W. Bauer *et al.*, Phys. Rev. **D70**, 054015 (2004); P. Colangelo *et al.*, Phys. Lett. **B597**, 291 (2004); M. Ladisa *et al.*, Phys. Rev. **D70**, 114025 (2004); H. Y. Cheng *et al.*, Phys. Rev. **D71**, 014030 (2005).
26. Y. Grossman, Int. J. Mod. Phys. A **19**, 907 (2004); E. Alvarez *et al.*, Phys. Rev. **D70**, 115014 (2004); P. K. Das and K. C. Yang, Phys. Rev. **D71**, 094002 (2005); C. H. Chen and C. Q. Geng, Phys. Rev. **D71**, 115004 (2005); Y. D. Yang *et al.*, Phys. Rev. **D72**, 015009 (2005); K. C. Yang, Phys. Rev. **72**, 034009 (2005); S. Baek, Phys. Rev. **D72**, 094008 (2005); C. S. Huang *et al.*, Phys. Rev. **D73**, 034026 (2006); C. H. Chen and H. Hatanaka, Phys. Rev. **D73**, 075003 (2006); A. Faessler *et al.*, Phys. Rev. **D75**, 074029 (2007).
27. D. London, N. Sinha, and R. Sinha, Phys. Rev. **D69**, 114013 (2004).
28. BABAR Collaboration, B. Aubert *et al.*, Phys. Rev. **D76**, 051103 (2007).
29. Belle Collaboration, J. Zhang *et al.*, Phys. Rev. Lett. **95**, 141801 (2005); BABAR Collaboration, B. Aubert *et al.*, Phys. Rev. Lett. **97**, 201801 (2006).
30. BABAR Collaboration, B. Aubert *et al.*, arXiv:0708.2248 [hep-ex].
31. CDF Collaboration, D. Acosta *et al.*, Phys. Rev. Lett. **95**, 031801 (2005).
32. G. Burdman, Phys. Rev. **D52**, 6400 (1995); F. Kruger and J. Matias, Phys. Rev. **D71**, 094009 (2005); E. Lunghi and J. Matias, JHEP **0704**, 058 (2007).
33. Belle Collaboration, A. Ishikawa *et al.*, Phys. Rev. Lett. **96**, 251801 (2006); BABAR Collaboration, B. Aubert *et al.*, Phys. Rev. **D73**, 092001 (2006).
34. C. H. Chen and H. n. Li, Phys. Rev. **D71**, 114008 (2005).

POLARIZATION IN B^0 DECAY

In decays involving two vector mesons, one can distinguish among the states in which meson polarizations are both longitudinal (L) or both are transverse and parallel (\parallel) or perpendicular (\perp) to each other with the parameters Γ_L/Γ , Γ_\perp/Γ , and the relative phases ϕ_\parallel and ϕ_\perp . See the definitions in the note on "Polarization in B Decays" review in the B^0 Particle Listings.

 Γ_L/Γ in $B^0 \rightarrow J/\psi(1S)K^*(892)^0$

VALUE	EVTS	DOCUMENT ID	TECN	COMMENT
0.566±0.010 OUR AVERAGE				
0.556±0.009±0.010		¹ AUBERT	07AD BABR	$e^+e^- \rightarrow \Upsilon(4S)$
0.574±0.012±0.009		ITOH	05 BELL	$e^+e^- \rightarrow \Upsilon(4S)$
0.59 ± 0.06 ± 0.01		² AFFOLDER	00N CDF	$p\bar{p}$ at 1.8 TeV
0.52 ± 0.07 ± 0.04		³ JESSOP	97 CLE2	$e^+e^- \rightarrow \Upsilon(4S)$
0.65 ± 0.10 ± 0.04	65	ABE	95Z CDF	$p\bar{p}$ at 1.8 TeV
0.97 ± 0.16 ± 0.15	13	⁴ ALBRECHT	94G ARG	$e^+e^- \rightarrow \Upsilon(4S)$

••• We do not use the following data for averages, fits, limits, etc. •••

0.566±0.012±0.005		¹ AUBERT	05P BABR	Repl. by AUBERT 07AD
0.62 ± 0.02 ± 0.03		⁵ ABE	02N BELL	Repl. by ITOH 05
0.597±0.028±0.024		⁶ AUBERT	01H BABR	Repl. by AUBERT 07AD
0.80 ± 0.08 ± 0.05	42	⁴ ALAM	94 CLE2	Sup. by JESSOP 97

¹ Obtained by combining the B^0 and B^+ modes.

² AFFOLDER 00N measurements are based on 190 B^0 candidates obtained from a data sample of 89 pb⁻¹. The P -wave fraction is found to be $0.13^{+0.12}_{-0.09} \pm 0.06$.

³ JESSOP 97 is the average over a mixture of B^0 and B^+ decays. The P -wave fraction is found to be $0.16 \pm 0.08 \pm 0.04$.

⁴ Averaged over an admixture of B^0 and B^+ decays.

⁵ Averaged over an admixture of B^0 and B^+ decays and the P wave fraction is $(19 \pm 2 \pm 3)\%$.

⁶ Averaged over an admixture of B^0 and B^- decays and the P wave fraction is $(16.0 \pm 3.2 \pm 1.4) \times 10^{-2}$.

 Γ_\perp/Γ in $B^0 \rightarrow J/\psi K^{*0}$

VALUE	DOCUMENT ID	TECN	COMMENT
0.219±0.018 OUR AVERAGE			Error includes scale factor of 2.1.
0.233±0.010±0.005	¹ AUBERT	07AD BABR	$e^+e^- \rightarrow \Upsilon(4S)$
0.195±0.012±0.008	ITOH	05 BELL	$e^+e^- \rightarrow \Upsilon(4S)$

¹ Obtained by combining the B^0 and B^+ modes.

 ϕ_\parallel in $B^0 \rightarrow J/\psi K^{*0}$

VALUE	DOCUMENT ID	TECN	COMMENT
-2.93±0.08±0.04			
	¹ AUBERT	07AD BABR	$e^+e^- \rightarrow \Upsilon(4S)$

¹ Obtained by combining the B^0 and B^+ modes.

 ϕ_\perp in $B^0 \rightarrow J/\psi K^{*0}$

VALUE	DOCUMENT ID	TECN	COMMENT
2.91±0.05±0.03			
	¹ AUBERT	07AD BABR	$e^+e^- \rightarrow \Upsilon(4S)$

¹ Obtained by combining the B^0 and B^+ modes.

 Γ_L/Γ in $B^0 \rightarrow \psi(2S)K^*(892)^0$

VALUE	DOCUMENT ID	TECN	COMMENT
0.47±0.05 OUR AVERAGE			
0.48±0.05±0.02	¹ AUBERT	07AD BABR	$e^+e^- \rightarrow \Upsilon(4S)$
0.45±0.11±0.04	² RICHICHI	01 CLE2	$e^+e^- \rightarrow \Upsilon(4S)$

¹ Obtained by combining the B^0 and B^+ modes.

² Averages between charged and neutral B mesons.

 Γ_\perp/Γ in $B^0 \rightarrow \psi(2S)K^{*0}$

VALUE	DOCUMENT ID	TECN	COMMENT
0.30±0.06±0.02			
	¹ AUBERT	07AD BABR	$e^+e^- \rightarrow \Upsilon(4S)$

¹ Obtained by combining the B^0 and B^+ modes.

 ϕ_\parallel in $B^0 \rightarrow \psi(2S)K^{*0}$

VALUE	DOCUMENT ID	TECN	COMMENT
-2.8±0.4±0.1			
	¹ AUBERT	07AD BABR	$e^+e^- \rightarrow \Upsilon(4S)$

¹ Obtained by combining the B^0 and B^+ modes.

 ϕ_\perp in $B^0 \rightarrow \psi(2S)K^{*0}$

VALUE	DOCUMENT ID	TECN	COMMENT
2.8±0.3 ± 0.1			
	¹ AUBERT	07AD BABR	$e^+e^- \rightarrow \Upsilon(4S)$

¹ Obtained by combining the B^0 and B^+ modes.

 Γ_L/Γ in $B^0 \rightarrow \chi_{c1} K^*(892)^0$

VALUE	DOCUMENT ID	TECN	COMMENT
0.77±0.07±0.04			
	¹ AUBERT	07AD BABR	$e^+e^- \rightarrow \Upsilon(4S)$

¹ Obtained by combining the B^0 and B^+ modes.

 Γ_\perp/Γ in $B^0 \rightarrow \chi_{c1} K^*(892)^0$

VALUE	DOCUMENT ID	TECN	COMMENT
0.03±0.04±0.02			
	¹ AUBERT	07AD BABR	$e^+e^- \rightarrow \Upsilon(4S)$

¹ Obtained by combining the B^0 and B^+ modes.

 ϕ_\parallel in $B^0 \rightarrow \chi_{c1} K^*(892)^0$

VALUE	DOCUMENT ID	TECN	COMMENT
0.0±0.3 ± 0.1			
	¹ AUBERT	07AD BABR	$e^+e^- \rightarrow \Upsilon(4S)$

¹ Obtained by combining the B^0 and B^+ modes.

 Γ_L/Γ in $B^0 \rightarrow D_s^{*+} D^{*-}$

VALUE	DOCUMENT ID	TECN	COMMENT
0.52 ± 0.05 OUR AVERAGE			
0.519±0.050±0.028	¹ AUBERT	03i BABR	$e^+e^- \rightarrow \Upsilon(4S)$
0.506±0.139±0.036	AHMED	00B CLE2	$e^+e^- \rightarrow \Upsilon(4S)$

¹ Measurement performed using partial reconstruction of D^{*-} decay.

 Γ_\perp/Γ in $B^0 \rightarrow D^{*-} \rho^+$

VALUE	EVTS	DOCUMENT ID	TECN	COMMENT
0.885±0.016±0.012				
		CSORNA	03 CLE2	$e^+e^- \rightarrow \Upsilon(4S)$
0.93 ± 0.05 ± 0.05	76	ALAM	94 CLE2	$e^+e^- \rightarrow \Upsilon(4S)$

••• We do not use the following data for averages, fits, limits, etc. •••

 Γ_L/Γ in $B^0 \rightarrow D^{*+} D^{*-}$

VALUE	DOCUMENT ID	TECN	COMMENT	
0.57±0.08±0.02				
		MIYAKE	05 BELL	$e^+e^- \rightarrow \Upsilon(4S)$

Meson Particle Listings

 B^0 Γ_{\perp}/Γ in $B^0 \rightarrow D^{*+} D^{*-}$

VALUE	DOCUMENT ID	TECN	COMMENT
0.150 ± 0.032 OUR AVERAGE			
0.143 ± 0.034 ± 0.008	AUBERT	07B0	BABR $e^+ e^- \rightarrow \Upsilon(4S)$
0.19 ± 0.08 ± 0.01	MIYAKE	05	BELL $e^+ e^- \rightarrow \Upsilon(4S)$
• • • We do not use the following data for averages, fits, limits, etc. • • •			
0.125 ± 0.044 ± 0.007	AUBERT, BE	05A	BABR Repl. by AUBERT 07B0
0.063 ± 0.055 ± 0.009	AUBERT	03Q	BABR Repl. by AUBERT, BE 05A

 Γ_L/Γ in $B^0 \rightarrow D^{*-} \omega \pi^+$

VALUE	DOCUMENT ID	TECN	COMMENT
0.654 ± 0.042 ± 0.016	¹ AUBERT	06L	BABR $e^+ e^- \rightarrow \Upsilon(4S)$
¹ Invariant mass of the $[\omega \pi]$ system is restricted in the region 1.1 and 1.9 GeV.			

 Γ_L/Γ in $B^0 \rightarrow \phi K^*(892)^0$

VALUE	DOCUMENT ID	TECN	COMMENT
0.484 ± 0.033 OUR AVERAGE			
0.506 ± 0.040 ± 0.015	AUBERT	07D	BABR $e^+ e^- \rightarrow \Upsilon(4S)$
0.45 ± 0.05 ± 0.02	CHEN	05A	BELL $e^+ e^- \rightarrow \Upsilon(4S)$
• • • We do not use the following data for averages, fits, limits, etc. • • •			
0.52 ± 0.05 ± 0.02	¹ AUBERT, B	04W	BABR Repl. by AUBERT 07D
0.65 ± 0.07 ± 0.02	AUBERT	03V	BABR Repl. by AUBERT, B 04W
0.41 ± 0.10 ± 0.04	CHEN	03B	BELL Repl. by CHEN 05A

¹AUBERT, B 04W also measures the fraction of parity-odd transverse contribution $f_{\perp} = 0.22 \pm 0.05 \pm 0.02$ and the phases of the parity-even and parity-odd transverse amplitudes relative to the longitudinal amplitude.

 Γ_L/Γ in $B^0 \rightarrow K^{*0} \bar{K}^{*0}$

VALUE	DOCUMENT ID	TECN	COMMENT
0.80^{+0.10}_{-0.12} ± 0.06	AUBERT	08i	BABR $e^+ e^- \rightarrow \Upsilon(4S)$

 Γ_{\perp}/Γ in $B^0 \rightarrow \phi K^{*0}$

VALUE	DOCUMENT ID	TECN	COMMENT
0.26 ± 0.04 OUR AVERAGE			Error includes scale factor of 1.2.
0.227 ± 0.038 ± 0.013	AUBERT	07D	BABR $e^+ e^- \rightarrow \Upsilon(4S)$
0.31 ^{+0.06} _{-0.05} ± 0.02	¹ CHEN	05A	BELL $e^+ e^- \rightarrow \Upsilon(4S)$
• • • We do not use the following data for averages, fits, limits, etc. • • •			
0.22 ± 0.05 ± 0.02	AUBERT, B	04W	BABR Repl. by AUBERT 07D
¹ This quantity was recalculated by the BELLE authors from numbers in the original paper.			

 ϕ_{\parallel} in $B^0 \rightarrow \phi K^{*0}$

VALUE	DOCUMENT ID	TECN	COMMENT
2.33 ± 0.14 OUR AVERAGE			
2.31 ± 0.14 ± 0.08	AUBERT	07D	BABR $e^+ e^- \rightarrow \Upsilon(4S)$
2.40 ^{+0.28} _{-0.24} ± 0.07	¹ CHEN	05A	BELL $e^+ e^- \rightarrow \Upsilon(4S)$
• • • We do not use the following data for averages, fits, limits, etc. • • •			
2.34 ^{+0.23} _{-0.20} ± 0.05	AUBERT, B	04W	BABR Repl. by AUBERT 07D
¹ This quantity was recalculated by the BELLE authors from numbers in the original paper.			

 ϕ_{\perp} in $B^0 \rightarrow \phi K^{*0}$

VALUE	DOCUMENT ID	TECN	COMMENT
2.33 ± 0.14 OUR AVERAGE			
2.24 ± 0.15 ± 0.09	AUBERT	07D	BABR $e^+ e^- \rightarrow \Upsilon(4S)$
2.51 ± 0.25 ± 0.06	¹ CHEN	05A	BELL $e^+ e^- \rightarrow \Upsilon(4S)$
• • • We do not use the following data for averages, fits, limits, etc. • • •			
2.47 ± 0.25 ± 0.05	AUBERT, B	04W	BABR Repl. by AUBERT 07D
¹ This quantity was recalculated by the BELLE authors from numbers in the original paper.			

 $\delta_0(B^0 \rightarrow \phi K^{*0})$

VALUE	DOCUMENT ID	TECN	COMMENT
2.78 ± 0.17 ± 0.09	AUBERT	07D	BABR $e^+ e^- \rightarrow \Upsilon(4S)$

 A_{CP}^0 in $B^0 \rightarrow \phi K^{*0}$

VALUE	DOCUMENT ID	TECN	COMMENT
0.02 ± 0.07 OUR AVERAGE			Error includes scale factor of 1.1.
-0.03 ± 0.08 ± 0.02	AUBERT	07D	BABR $e^+ e^- \rightarrow \Upsilon(4S)$
0.13 ± 0.12 ± 0.04	¹ CHEN	05A	BELL $e^+ e^- \rightarrow \Upsilon(4S)$
• • • We do not use the following data for averages, fits, limits, etc. • • •			
-0.06 ± 0.10 ± 0.01	AUBERT, B	04W	BABR Repl. by AUBERT 07D
¹ This quantity was recalculated by the BELLE authors from numbers in the original paper.			

 A_{CP}^{\perp} in $B^0 \rightarrow \phi K^{*0}$

VALUE	DOCUMENT ID	TECN	COMMENT
-0.11 ± 0.12 OUR AVERAGE			
-0.03 ± 0.16 ± 0.05	AUBERT	07D	BABR $e^+ e^- \rightarrow \Upsilon(4S)$
-0.20 ± 0.18 ± 0.04	¹ CHEN	05A	BELL $e^+ e^- \rightarrow \Upsilon(4S)$
• • • We do not use the following data for averages, fits, limits, etc. • • •			
-0.10 ± 0.24 ± 0.05	AUBERT, B	04W	BABR Repl. by AUBERT 07D
¹ This quantity was recalculated by the BELLE authors from numbers in the original paper.			

 $\Delta\phi_{\parallel}$ in $B^0 \rightarrow \phi K^{*0}$

VALUE	DOCUMENT ID	TECN	COMMENT
0.10 ± 0.24 OUR AVERAGE			Error includes scale factor of 1.7.
0.24 ± 0.14 ± 0.08	AUBERT	07D	BABR $e^+ e^- \rightarrow \Upsilon(4S)$
-0.32 ± 0.27 ± 0.07	¹ CHEN	05A	BELL $e^+ e^- \rightarrow \Upsilon(4S)$
• • • We do not use the following data for averages, fits, limits, etc. • • •			
0.27 ^{+0.20} _{-0.23} ± 0.05	AUBERT, B	04W	BABR Repl. by AUBERT 07D
¹ This quantity was recalculated by the BELLE authors from numbers in the original paper.			

 $\Delta\phi_{\perp}$ in $B^0 \rightarrow \phi K^{*0}$

VALUE	DOCUMENT ID	TECN	COMMENT
0.04 ± 0.23 OUR AVERAGE			Error includes scale factor of 1.6.
0.19 ± 0.15 ± 0.08	AUBERT	07D	BABR $e^+ e^- \rightarrow \Upsilon(4S)$
-0.30 ± 0.25 ± 0.06	¹ CHEN	05A	BELL $e^+ e^- \rightarrow \Upsilon(4S)$
• • • We do not use the following data for averages, fits, limits, etc. • • •			
0.36 ± 0.25 ± 0.05	AUBERT, B	04W	BABR Repl. by AUBERT 07D
¹ This quantity was recalculated by the BELLE authors from numbers in the original paper.			

 $\Delta\delta_0(B^0 \rightarrow \phi K^{*0})$

VALUE	DOCUMENT ID	TECN	COMMENT
0.21 ± 0.17 ± 0.08	AUBERT	07D	BABR $e^+ e^- \rightarrow \Upsilon(4S)$

 Γ_L/Γ in $B^0 \rightarrow \phi K_2^*(1430)^0$

VALUE	DOCUMENT ID	TECN	COMMENT
0.853^{+0.061}_{-0.069} ± 0.036	AUBERT	07D	BABR $e^+ e^- \rightarrow \Upsilon(4S)$

 Γ_{\perp}/Γ in $B^0 \rightarrow \phi K_2^*(1430)^0$

VALUE	DOCUMENT ID	TECN	COMMENT
0.045^{+0.049}_{-0.040} ± 0.013	AUBERT	07D	BABR $e^+ e^- \rightarrow \Upsilon(4S)$

 ϕ_{\parallel} in $B^0 \rightarrow \phi K_2^*(1430)^0$

VALUE	DOCUMENT ID	TECN	COMMENT
2.90 ± 0.39 ± 0.06	AUBERT	07D	BABR $e^+ e^- \rightarrow \Upsilon(4S)$

 ϕ_{\perp} in $B^0 \rightarrow \phi K_2^*(1430)^0$

VALUE	DOCUMENT ID	TECN	COMMENT
5.72^{+0.55}_{-0.87} ± 0.11	AUBERT	07D	BABR $e^+ e^- \rightarrow \Upsilon(4S)$

 $\delta_0(B^0 \rightarrow \phi K_2^*(1430)^0)$

VALUE	DOCUMENT ID	TECN	COMMENT
3.54^{+0.12}_{-0.14} ± 0.06	AUBERT	07D	BABR $e^+ e^- \rightarrow \Upsilon(4S)$

 Γ_L/Γ in $B^0 \rightarrow K^*(892)^0 \rho^0$

VALUE	DOCUMENT ID	TECN	COMMENT
0.57 ± 0.09 ± 0.08	AUBERT, B	06G	BABR $e^+ e^- \rightarrow \Upsilon(4S)$

 Γ_L/Γ in $B^0 \rightarrow \rho^+ \rho^-$

VALUE	DOCUMENT ID	TECN	COMMENT
0.977^{+0.028}_{-0.024} OUR AVERAGE			
0.992 ± 0.024 ^{+0.026} _{-0.013}	AUBERT	07BF	BABR $e^+ e^- \rightarrow \Upsilon(4S)$
0.941 ^{+0.034} _{-0.040} ± 0.030	SOMOV	06	BELL $e^+ e^- \rightarrow \Upsilon(4S)$
• • • We do not use the following data for averages, fits, limits, etc. • • •			
0.978 ± 0.014 ^{+0.021} _{-0.029}	AUBERT, B	05C	BABR Repl. by AUBERT 07BF
0.98 ^{+0.02} _{-0.08} ± 0.03	AUBERT	04G	BABR Repl. by AUBERT, B 04R
0.99 ± 0.03 ^{+0.04} _{-0.03}	AUBERT, B	04R	BABR Repl. by AUBERT, B 05C

 Γ_L/Γ in $B^0 \rightarrow \rho^0 \rho^0$

VALUE	DOCUMENT ID	TECN	COMMENT
0.87 ± 0.13 ± 0.04	AUBERT	07G	BABR $e^+ e^- \rightarrow \Upsilon(4S)$

 $B^0-\bar{B}^0$ MIXING

Updated April 2008 by O. Schneider (Ecole Polytechnique Fédérale de Lausanne).

There are two neutral $B^0-\bar{B}^0$ meson systems, $B_d^0-\bar{B}_d^0$ and $B_s^0-\bar{B}_s^0$ (generically denoted $B_q^0-\bar{B}_q^0$, $q = s, d$), which exhibit particle-antiparticle mixing [1]. This mixing phenomenon is described in Ref. 2. In the following, we adopt the notation introduced in Ref. 2, and assume CPT conservation throughout. In each system, the light (L) and heavy (H) mass eigenstates,

$$|B_{L,H}\rangle = p|B_q^0\rangle \pm q|\bar{B}_q^0\rangle, \quad (1)$$

have a mass difference $\Delta m_q = m_H - m_L > 0$, and a total decay width difference $\Delta\Gamma_q = \Gamma_L - \Gamma_H$. In the absence of CP violation in the mixing, $|q/p| = 1$, these differences are given by $\Delta m_q = 2|M_{12}|$ and $|\Delta\Gamma_q| = 2|\Gamma_{12}|$, where M_{12} and Γ_{12} are the off-diagonal elements of the mass and decay matrices [2]. The evolution of a pure $|B_q^0\rangle$ or $|\bar{B}_q^0\rangle$ state at $t = 0$ is given by

$$|B_q^0(t)\rangle = g_+(t)|B_q^0\rangle + \frac{q}{p}g_-(t)|\bar{B}_q^0\rangle, \quad (2)$$

$$|\bar{B}_q^0(t)\rangle = g_+(t)|\bar{B}_q^0\rangle + \frac{p}{q}g_-(t)|B_q^0\rangle, \quad (3)$$

which means that the flavor states remain unchanged (+) or oscillate into each other (-) with time-dependent probabilities proportional to

$$|g_{\pm}(t)|^2 = \frac{e^{-\Gamma_q t}}{2} \left[\cosh\left(\frac{\Delta\Gamma_q}{2}t\right) \pm \cos(\Delta m_q t) \right], \quad (4)$$

where $\Gamma_q = (\Gamma_H + \Gamma_L)/2$. In the absence of CP violation, the time-integrated mixing probability $\int |g_-(t)|^2 dt / (\int |g_-(t)|^2 dt + \int |g_+(t)|^2 dt)$ is given by

$$\chi_q = \frac{x_q^2 + y_q^2}{2(x_q^2 + 1)}, \quad \text{where} \quad x_q = \frac{\Delta m_q}{\Gamma_q}, \quad y_q = \frac{\Delta\Gamma_q}{2\Gamma_q}. \quad (5)$$

Standard Model predictions and phenomenology

In the Standard Model, the transitions $B_q^0 \rightarrow \bar{B}_q^0$ and $\bar{B}_q^0 \rightarrow B_q^0$ are due to the weak interaction. They are described, at the lowest order, by box diagrams involving two W bosons and two up-type quarks (see Fig. 1), as is the case for $K^0 - \bar{K}^0$ mixing. However, the long range interactions arising from intermediate virtual states are negligible for the neutral B meson systems, because the large B mass is off the region of hadronic resonances. The calculation of the dispersive and absorptive parts of the box diagrams yields the following predictions for the off-diagonal element of the mass and decay matrices [3],

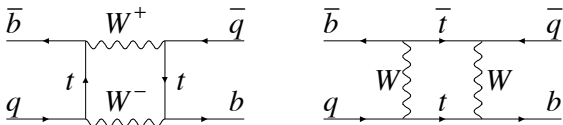


Figure 1: Dominant box diagrams for the $B_q^0 \rightarrow \bar{B}_q^0$ transitions ($q = d$ or s). Similar diagrams exist where one or both t quarks are replaced with c or u quarks.

$$M_{12} = -\frac{G_F^2 m_W^2 \eta_B m_{B_q} B_{B_q} f_{B_q}^2}{12\pi^2} S_0(m_t^2/m_W^2) (V_{tq}^* V_{tb})^2, \quad (6)$$

$$\Gamma_{12} = \frac{G_F^2 m_b^2 \eta'_B m_{B_q} B_{B_q} f_{B_q}^2}{8\pi} \times \left[(V_{tq}^* V_{tb})^2 + V_{tq}^* V_{tb} V_{cq}^* V_{cb} \mathcal{O}\left(\frac{m_c^2}{m_b^2}\right) + (V_{cq}^* V_{cb})^2 \mathcal{O}\left(\frac{m_c^4}{m_b^4}\right) \right], \quad (7)$$

where G_F is the Fermi constant, m_W the W boson mass, and m_i the mass of quark i ; m_{B_q} , f_{B_q} and B_{B_q} are the B_q^0 mass, weak decay constant and bag parameter, respectively. The known function $S_0(x_t)$ can be approximated very well by $0.784 x_t^{0.76}$ [4], and V_{ij} are the elements of the CKM matrix [5]. The QCD corrections η_B and η'_B are of order unity. The only non-negligible contributions to M_{12} are from box diagrams involving two top quarks. The phases of M_{12} and Γ_{12} satisfy

$$\phi_M - \phi_\Gamma = \pi + \mathcal{O}\left(\frac{m_c^2}{m_b^2}\right), \quad (8)$$

implying that the mass eigenstates have mass and width differences of opposite signs. This means that, like in the $K^0 - \bar{K}^0$ system, the heavy state is expected to have a smaller decay width than that of the light state: $\Gamma_H < \Gamma_L$. Hence, $\Delta\Gamma = \Gamma_L - \Gamma_H$ is expected to be positive in the Standard Model.

Furthermore, the quantity

$$\left| \frac{\Gamma_{12}}{M_{12}} \right| \simeq \frac{3\pi}{2} \frac{m_b^2}{m_W^2} \frac{1}{S_0(m_t^2/m_W^2)} \sim \mathcal{O}\left(\frac{m_b^2}{m_t^2}\right) \quad (9)$$

is small, and a power expansion of $|q/p|^2$ yields

$$\left| \frac{q}{p} \right|^2 = 1 + \left| \frac{\Gamma_{12}}{M_{12}} \right| \sin(\phi_M - \phi_\Gamma) + \mathcal{O}\left(\left| \frac{\Gamma_{12}}{M_{12}} \right|^2\right). \quad (10)$$

Therefore, considering both Eqs. (8) and (9), the CP -violating parameter

$$1 - \left| \frac{q}{p} \right|^2 \simeq \text{Im}\left(\frac{\Gamma_{12}}{M_{12}}\right) \quad (11)$$

is expected to be very small: $\sim \mathcal{O}(10^{-3})$ for the $B_d^0 - \bar{B}_d^0$ system and $\lesssim \mathcal{O}(10^{-4})$ for the $B_s^0 - \bar{B}_s^0$ system [6].

In the approximation of negligible CP violation in mixing, the ratio $\Delta\Gamma_q/\Delta m_q$ is equal to the small quantity $|\Gamma_{12}/M_{12}|$ of Eq. (9); it is hence independent of CKM matrix elements, *i.e.*, the same for the $B_d^0 - \bar{B}_d^0$ and $B_s^0 - \bar{B}_s^0$ systems. Recent calculations [7] yield $\sim 5 \times 10^{-3}$ with a $\sim 20\%$ uncertainty. Given the current experimental knowledge on the mixing parameter x_q

$$\begin{cases} x_d = 0.776 \pm 0.008 & (B_d^0 - \bar{B}_d^0 \text{ system}) \\ x_s = 26.1 \pm 0.5 & (B_s^0 - \bar{B}_s^0 \text{ system}) \end{cases}, \quad (12)$$

the Standard Model thus predicts that $\Delta\Gamma_d/\Gamma_d$ is very small (below 1%), but $\Delta\Gamma_s/\Gamma_s$ considerably larger ($\sim 10\%$). These width differences are caused by the existence of final states to which both the B_q^0 and \bar{B}_q^0 mesons can decay. Such decays involve $b \rightarrow c\bar{c}q$ quark-level transitions, which are Cabibbo-suppressed if $q = d$ and Cabibbo-allowed if $q = s$.

A recent and complete set of Standard Model predictions for all mixing parameters in both the $B_d^0 - \bar{B}_d^0$ and $B_s^0 - \bar{B}_s^0$ systems can be found in Ref. 7.

Experimental issues and methods for oscillation analyses

Time-integrated measurements of $B^0 - \bar{B}^0$ mixing were published for the first time in 1987 by UA1 [8] and ARGUS [9], and since then by many other experiments. These measurements are typically based on counting same-sign and opposite-sign lepton

Meson Particle Listings

B^0

pairs from the semileptonic decay of the produced $b\bar{b}$ pairs. Such analyses cannot easily separate the contributions from the different b -hadron species, therefore, the clean environment of $\Upsilon(4S)$ machines (where only B_d^0 and charged B_u mesons are produced) is in principle best suited to measure χ_d .

However, better sensitivity is obtained from time-dependent analyses aiming at the direct measurement of the oscillation frequencies Δm_d and Δm_s , from the proper time distributions of B_d^0 or B_s^0 candidates identified through their decay in (mostly) flavor-specific modes, and suitably tagged as mixed or unmixed. This is particularly true for the B_s^0 - \bar{B}_s^0 system, where the large value of x_s implies maximal mixing, *i.e.*, $\chi_s \simeq 1/2$. In such analyses, the B_d^0 or B_s^0 mesons are either fully reconstructed, partially reconstructed from a charm meson, selected from a lepton with the characteristics of a $b \rightarrow \ell^-$ decay, or selected from a reconstructed displaced vertex. At high-energy colliders (LEP, SLC, Tevatron), the proper time $t = \frac{m_B}{p}L$ is measured from the distance L between the production vertex and the B decay vertex, and from an estimate of the B momentum p . At asymmetric B factories (KEKB, PEP-II), producing $e^+e^- \rightarrow \Upsilon(4S) \rightarrow B_d^0\bar{B}_d^0$ events with a boost $\beta\gamma$ ($= 0.425, 0.55$), the proper time difference between the two B candidates is estimated as $\Delta t \simeq \frac{\Delta z}{\beta\gamma c}$, where Δz is the spatial separation between the two B decay vertices along the boost direction. In all cases, the good resolution needed on the vertex positions is obtained with silicon detectors.

The average statistical significance \mathcal{S} of a B_d^0 or B_s^0 oscillation signal can be approximated as [10]

$$\mathcal{S} \approx \sqrt{N/2} f_{\text{sig}} (1 - 2\eta) e^{-(\Delta m \sigma_t)^2/2}, \quad (13)$$

where N is the number of selected and tagged candidates, f_{sig} is the fraction of signal in that sample, η is the total mistag probability, and σ_t is the resolution on proper time (or proper time difference). The quantity \mathcal{S} decreases very quickly as Δm increases; this dependence is controlled by σ_t , which is therefore a critical parameter for Δm_s analyses. At high-energy colliders, the proper time resolution $\sigma_t \sim \frac{m_B}{\langle p \rangle} \sigma_L \oplus t \frac{\sigma_p}{p}$ includes a constant contribution due to the decay length resolution σ_L (typically 0.05–0.3 ps), and a term due to the relative momentum resolution σ_p/p (typically 10–20% for partially reconstructed decays), which increases with proper time. At B factories, the boost of the B mesons is estimated from the known beam energies, and the term due to the spatial resolution dominates (typically 1–1.5 ps because of the much smaller B boost).

In order to tag a B candidate as mixed or unmixed, it is necessary to determine its flavor both in the initial state and in the final state. The initial and final state mistag probabilities, η_i and η_f , degrade \mathcal{S} by a total factor $(1 - 2\eta) = (1 - 2\eta_i)(1 - 2\eta_f)$. In lepton-based analyses, the final state is tagged by the charge of the lepton from $b \rightarrow \ell^-$ decays; the largest contribution to η_f is then due to $\bar{b} \rightarrow \bar{c} \rightarrow \ell^-$ decays. Alternatively, the charge of a reconstructed charm meson (D^{*-} from B_d^0 or D_s^- from B_s^0), or that of a kaon hypothesized to come from a

$b \rightarrow c \rightarrow s$ decay [11], can be used. For fully-inclusive analyses based on topological vertexing, final-state tagging techniques include jet-charge [12] and charge-dipole [13,14] methods. At high-energy colliders, the methods to tag the initial state (*i.e.*, the state at production), can be divided into two groups: the ones that tag the initial charge of the \bar{b} quark contained in the B candidate itself (same-side tag), and the ones that tag the initial charge of the other b quark produced in the event (opposite-side tag). On the same side, the charge of a track from the primary vertex is correlated with the production state of the B if that track is a decay product of a B^{**} state or the first particle in the fragmentation chain [15,16]. Jet- and vertex-charge techniques work on both sides and on the opposite side, respectively. Finally, the charge of a lepton from $b \rightarrow \ell^-$ or of a kaon from $b \rightarrow c \rightarrow s$ can be used as opposite side tags, keeping in mind that their performance is degraded due to integrated mixing. At SLC, the beam polarization produced a sizeable forward-backward asymmetry in the $Z \rightarrow b\bar{b}$ decays, and provided another very interesting and effective initial state tag based on the polar angle of the B candidate [13]. Initial state tags have also been combined to reach $\eta_i \sim 26\%$ at LEP [16,17], or even 22% at SLD [13] with full efficiency. In the case $\eta_f = 0$, this corresponds to an effective tagging efficiency $Q = \epsilon D^2 = \epsilon(1 - 2\eta)^2$, where ϵ is the tagging efficiency, in the range 23–31%. The equivalent figure achieved by CDF during Tevatron Run I was $\sim 3.5\%$ [18], reflecting the fact that tagging is more difficult at hadron colliders. The current CDF and DØ analyses of Tevatron Run II data reach $\epsilon D^2 = (1.8 \pm 0.1)\%$ [19] and $(2.5 \pm 0.2)\%$ [20] for opposite-side tagging, while same-side kaon tagging (for B_s^0 oscillation analyses) is contributing an additional 3.7–4.8% at CDF [19], and pushes the combined performance to $(4.5 \pm 0.9)\%$ at DØ [21].

At B factories, the flavor of a B_d^0 meson at production cannot be determined, since the two neutral B mesons produced in a $\Upsilon(4S)$ decay evolve in a coherent P -wave state where they keep opposite flavors at any time. However, as soon as one of them decays, the other follows a time-evolution given by Eqs. (2) or (3), where t is replaced with Δt (which will take negative values half of the time). Hence, the “initial state” tag of a B can be taken as the final-state tag of the other B . Effective tagging efficiencies Q of 30% are achieved by BABAR and Belle [22], using different techniques including $b \rightarrow \ell^-$ and $b \rightarrow c \rightarrow s$ tags. It is worth noting that, in this case, mixing of the other B (*i.e.*, the coherent mixing occurring before the first B decay) does not contribute to the mistag probability.

In the absence of experimental observation of a decay-width difference, oscillation analyses typically neglect $\Delta\Gamma$ in Eq. (4), and describe the data with the physics functions $\Gamma e^{-\Gamma t}(1 \pm \cos(\Delta m t))/2$ (high-energy colliders) or $\Gamma e^{-\Gamma|\Delta t|}(1 \pm \cos(\Delta m \Delta t))/4$ (asymmetric $\Upsilon(4S)$ machines). As can be seen from Eq. (4), a non-zero value of $\Delta\Gamma$ would effectively reduce the oscillation amplitude with a small time-dependent factor that would be very difficult to distinguish from time resolution effects. Measurements of Δm_d are usually extracted from the

data using a maximum likelihood fit. To extract information useful for the interpretation of B_s^0 oscillation searches and for the combination of their results, a method [10] is followed in which a B_s^0 oscillation amplitude \mathcal{A} is measured as a function of a fixed test value of Δm_s , using a maximum likelihood fit based on the functions $\Gamma_s e^{-\Gamma_s t} (1 \pm \mathcal{A} \cos(\Delta m_s t))/2$. To a good approximation, the statistical uncertainty on \mathcal{A} is Gaussian and equal to $1/S$ from Eq. (13). If Δm_s is equal to its true value, one expects $\mathcal{A} = 1$ within the total uncertainty $\sigma_{\mathcal{A}}$; in case a signal is seen, its observed (or expected) significance will be defined as $\mathcal{A}/\sigma_{\mathcal{A}}$ (or $1/\sigma_{\mathcal{A}}$). However, if Δm_s is (far) below its true value, a measurement consistent with $\mathcal{A} = 0$ is expected. A value of Δm_s can be excluded at 95% CL if $\mathcal{A} + 1.645 \sigma_{\mathcal{A}} \leq 1$ (since the integral of a normal distribution from $-\infty$ to 1.645 is equal to 0.95). Because of the proper time resolution, the quantity $\sigma_{\mathcal{A}}(\Delta m_s)$ is a steadily increasing function of Δm_s . We define the sensitivity for 95% CL exclusion of Δm_s values (or for a 3σ or 5σ observation of B_s^0 oscillations) as the value of Δm_s for which $1/\sigma_{\mathcal{A}} = 1.645$ (or $1/\sigma_{\mathcal{A}} = 3$ or 5).

B_d^0 mixing studies

Many B_d^0 - \bar{B}_d^0 oscillations analyses have been published [23] by the ALEPH [24], BABAR [25], Belle [26], CDF [15], DØ [20], DELPHI [14,27], L3 [28], and OPAL [29,30] collaborations. Although a variety of different techniques have been used, the individual Δm_d results obtained at high-energy colliders have remarkably similar precision. Their average is compatible with the recent and more precise measurements from asymmetric B factories. The systematic uncertainties are not negligible; they are often dominated by sample composition, mistag probability, or b -hadron lifetime contributions. Before being combined, the measurements are adjusted on the basis of a common set of input values, including the b -hadron lifetimes and fractions published in this *Review*. Some measurements are statistically correlated. Systematic correlations arise both from common physics sources (fragmentation fractions, lifetimes, branching ratios of b hadrons), and from purely experimental or algorithmic effects (efficiency, resolution, tagging, background description). Combining all published measurements [14,15,20,24–30] and accounting for all identified correlations yields $\Delta m_d = 0.507 \pm 0.003(\text{stat}) \pm 0.003(\text{syst}) \text{ ps}^{-1}$ [31], a result dominated by the B factories.

On the other hand, ARGUS and CLEO have published time-integrated measurements [32–34], which average to $\chi_d = 0.182 \pm 0.015$. Following Ref. 34, the width difference $\Delta\Gamma_d$ could in principle be extracted from the measured value of Γ_d and the above averages for Δm_d and χ_d (see Eq. (5)), provided that $\Delta\Gamma_d$ has a negligible impact on the Δm_d measurements. However, direct time-dependent studies published by DELPHI [14] and BABAR [35] provide stronger constraints, which can be combined to yield $\text{sign}(\text{Re}\lambda_{\text{CP}})\Delta\Gamma_d/\Gamma_d = 0.009 \pm 0.037$ [31].

Assuming $\Delta\Gamma_d = 0$ and no CP violation in mixing, and using the measured B_d^0 lifetime of $1.530 \pm 0.009 \text{ ps}$, the Δm_d and χ_d results are combined to yield the world average

$$\Delta m_d = 0.507 \pm 0.005 \text{ ps}^{-1} \quad (14)$$

or, equivalently,

$$\chi_d = 0.1878 \pm 0.0024. \quad (15)$$

Evidence for CP violation in B_d^0 mixing has been searched for, both with flavor-specific and inclusive B_d^0 decays, in samples where the initial flavor state is tagged. In the case of semileptonic (or other flavor-specific) decays, where the final-state tag is also available, the following asymmetry [2]

$$\mathcal{A}_{\text{SL}}^d = \frac{N(\bar{B}_d^0(t) \rightarrow \ell^+ \nu_\ell X) - N(B_d^0(t) \rightarrow \ell^- \bar{\nu}_\ell X)}{N(\bar{B}_d^0(t) \rightarrow \ell^+ \nu_\ell X) + N(B_d^0(t) \rightarrow \ell^- \bar{\nu}_\ell X)} \simeq 1 - |q/p|_d^2 \quad (16)$$

has been measured, either in time-integrated analyses at CLEO [34,36], CDF [37,38] and DØ [39], or in time-dependent analyses at LEP [30,40,41], BABAR [35,42,43] and Belle [44]. In the inclusive case, also investigated at LEP [40,41,45], no final-state tag is used, and the asymmetry [46]

$$\frac{N(B_d^0(t) \rightarrow \text{all}) - N(\bar{B}_d^0(t) \rightarrow \text{all})}{N(B_d^0(t) \rightarrow \text{all}) + N(\bar{B}_d^0(t) \rightarrow \text{all})} \simeq \mathcal{A}_{\text{SL}}^d \left[\frac{x_d}{2} \sin(\Delta m_d t) - \sin^2 \left(\frac{\Delta m_d t}{2} \right) \right] \quad (17)$$

must be measured as a function of the proper time to extract information on CP violation. In all cases, asymmetries compatible with zero have been found, with a precision limited by the available statistics. A simple average of all published results for the B_d^0 meson [30,34–36,39,41,42,44,45] yields $\mathcal{A}_{\text{SL}}^d = -0.0049 \pm 0.0038$, under the assumption of no CP violation in B_s^0 mixing. Published results at B factories only [34–36,42,44], where no B_s^0 is produced, average to

$$\mathcal{A}_{\text{SL}}^d = -0.0005 \pm 0.0056, \text{ or } |q/p|_d = 1.0002 \pm 0.0028, \quad (18)$$

a result which does not yet constrain the Standard Model.

The Δm_d result of Eq. (14) provides an estimate of $2|M_{12}|$, and can be used, together with Eq. (6), to extract the magnitude of the CKM matrix element V_{td} within the Standard Model [47]. The main experimental uncertainties on the resulting estimate of $|V_{td}|$ come from m_t and Δm_d ; however, the extraction is at present completely dominated by the uncertainty on the hadronic matrix element $f_{B_d} \sqrt{B_{B_d}} = 244 \pm 26 \text{ MeV}$ obtained from lattice QCD calculations [48].

B_s^0 mixing studies

In the decade before the Tevatron Run II results became available, B_s^0 - \bar{B}_s^0 oscillations have been the subject of many studies from ALEPH [49], CDF [50], DELPHI [14,17,51], OPAL [52] and SLD [13,53,54]. The most sensitive analyses appeared to be the ones based on inclusive lepton samples. Because of their better proper time resolution, the small data

Meson Particle Listings

 B^0

samples analyzed inclusively at SLD, as well as the fully reconstructed B_s decays at LEP were also very useful to explore the high Δm_s region. However, all results were limited by the available statistics. All published measurements of the B_s^0 oscillation amplitude [13,14,17,49–53] are averaged [31] to yield the combined amplitudes \mathcal{A} shown in Fig. 2 (bottom) as a function of Δm_s . The individual results have been adjusted to common physics inputs, and all known correlations have been accounted for; the sensitivities of the inclusive analyses, which depend directly through Eq. (13) on the assumed fraction f_s of B_s^0 mesons in an unbiased sample of weakly-decaying b hadrons, have also been rescaled to a common average of $f_s = 0.105 \pm 0.009$. The combined sensitivity for 95% CL exclusion of Δm_s values is found to be 18.3 ps^{-1} . All values of Δm_s below 14.6 ps^{-1} are excluded at 95% CL, while the values between 14.6 and 21.7 ps^{-1} cannot be excluded, because the data is compatible with a signal in this region. However, the largest deviation from $\mathcal{A} = 0$ in this range is a 1.9σ effect only, so no signal can be claimed.

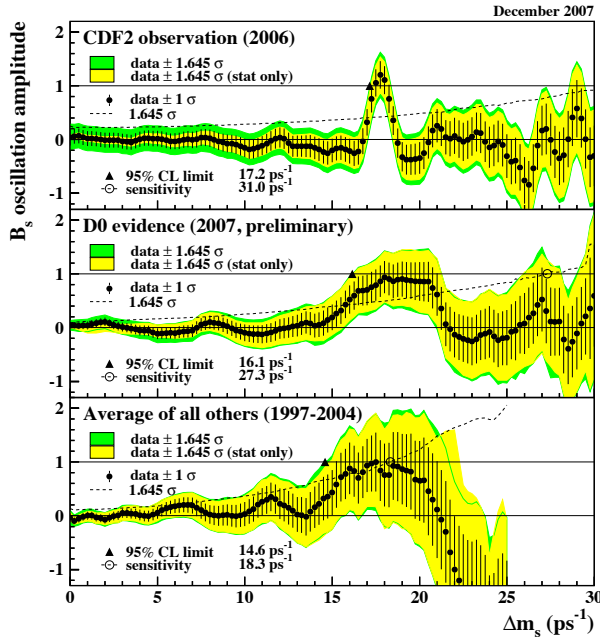


Figure 2: Combined measurements of the B_s^0 oscillation amplitude as a function of Δm_s . Top: CDF result based on Run II data, published in 2006 [19]. Middle: Average of all preliminary D0 results available at the end of 2007 [21]. Bottom: Average of all other results (mainly from LEP and SLD) published between 1997 and 2004. All measurements are dominated by statistical uncertainties. Neighboring points are statistically correlated. Color version at end of book.

Tevatron Run II results based on 1 fb^{-1} of data became available in 2006. After D0 [55] reported $17 < \Delta m_s < 21 \text{ ps}^{-1}$ (90% CL) and a most probable value of 19 ps^{-1} with an observed (expected) significance of 2.5σ (0.9σ), CDF [19] published the first direct evidence of B_s^0 oscillations shortly followed by a

$> 5\sigma$ observation (shown at the top of Fig. 2). The measured value of Δm_s is

$$\Delta m_s = 17.77 \pm 0.10(\text{stat}) \pm 0.07(\text{syst}) \text{ ps}^{-1}, \quad (19)$$

based on samples of flavour-tagged hadronic and semileptonic B_s^0 decays, partially or fully reconstructed in flavour-specific final states. More recently, D0 [21] obtained with 2.4 fb^{-1} an independent 2.9σ preliminary evidence for B_s^0 oscillations (middle of Fig. 2) at $\Delta m_s = 18.53 \pm 0.93(\text{stat}) \pm 0.30(\text{syst}) \text{ ps}^{-1}$ [56], consistent with the CDF measurement.

The information on $|V_{ts}|$ obtained in the framework of the Standard Model is hampered by the hadronic uncertainty, as in the B_d^0 case. However, several uncertainties cancel in the frequency ratio

$$\frac{\Delta m_s}{\Delta m_d} = \frac{m_{B_s}}{m_{B_d}} \xi^2 \left| \frac{V_{ts}}{V_{td}} \right|^2, \quad (20)$$

where $\xi = (f_{B_s} \sqrt{B_{B_s}})/(f_{B_d} \sqrt{B_{B_d}}) = 1.210_{-0.035}^{+0.047}$ is an SU(3) flavor-symmetry breaking factor obtained from lattice QCD calculations [48]. Using the measurements of Eqs. (14) and (19), one can extract

$$\left| \frac{V_{td}}{V_{ts}} \right| = 0.2060 \pm 0.0012(\text{exp})_{-0.0060}^{+0.0080}(\text{lattice}), \quad (21)$$

in good agreement with (but much more precise than) the recent results obtained by the Belle [57] and BABAR [58] collaborations based on the observation of the $b \rightarrow d\gamma$ transition. The CKM matrix can be constrained using experimental results on observables such as Δm_d , Δm_s , $|V_{ub}/V_{cb}|$, ϵ_K , and $\sin(2\beta)$ together with theoretical inputs and unitarity conditions [47,59,60]. The constraint from our knowledge on the ratio $\Delta m_s/\Delta m_d$ is presently more effective in limiting the position of the apex of the CKM unitarity triangle than the one obtained from the Δm_d measurements alone, due to the reduced hadronic uncertainty in Eq. (20). We also note that the measured value of Δm_s is consistent with the Standard Model prediction obtained from CKM fits where no experimental information on Δm_s is used, *e.g.*, $20.6 \pm 2.6 \text{ ps}^{-1}$ [59] or $17.7_{-2.1}^{+6.4} \text{ ps}^{-1}$ [60].

Information on $\Delta\Gamma_s$ can be obtained by studying the proper time distribution of untagged B_s^0 samples [61]. In the case of an inclusive B_s^0 selection [62], or a semileptonic (or flavour-specific) B_s^0 decay selection [17,63,64], both the short- and long-lived components are present, and the proper time distribution is a superposition of two exponentials with decay constants $\Gamma_{L,H} = \Gamma_s \pm \Delta\Gamma_s/2$. In principle, this provides sensitivity to both Γ_s and $(\Delta\Gamma_s/\Gamma_s)^2$. Ignoring $\Delta\Gamma_s$ and fitting for a single exponential leads to an estimate of Γ_s with a relative bias proportional to $(\Delta\Gamma_s/\Gamma_s)^2$. An alternative approach, which is directly sensitive to first order in $\Delta\Gamma_s/\Gamma_s$, is to determine the lifetime of B_s^0 candidates decaying to CP eigenstates; measurements exist for $B_s^0 \rightarrow K^+K^-$ [65], $B_s^0 \rightarrow J/\psi\phi$ [66,67], and $B_s^0 \rightarrow D_s^{(*)+}D_s^{(*)-}$ [68], which are mostly CP -even states [69]. However, in the case of $B_s^0 \rightarrow J/\psi\phi$, this technique has now

been replaced by more sensitive time-dependent angular analyses that allow the simultaneous extraction of $\Delta\Gamma_s/\Gamma_s$ and the CP -even and CP -odd amplitudes [70,71]. Estimates of $\Delta\Gamma_s/\Gamma_s$ have also been obtained directly from measurements of the $B_s^0 \rightarrow D_s^{(*)+} D_s^{(*)-}$ branching ratio [68,72], under the assumption that these decays account for all the CP -even final states (however, no systematic uncertainty due to this assumption is given, so the averages quoted below will not include these estimates).

Applying the combination procedure of Ref. 31 (including the constraint from the flavour-specific lifetime measurements) on the published results [17,63,66,68,70,71] yields

$$\Delta\Gamma_s/\Gamma_s = +0.069_{-0.062}^{+0.058} \quad \text{and} \quad 1/\Gamma_s = 1.470_{-0.027}^{+0.026} \text{ ps}, \quad (22)$$

or equivalently

$$1/\Gamma_L = 1.419_{-0.038}^{+0.039} \text{ ps} \quad \text{and} \quad 1/\Gamma_H = 1.525_{-0.063}^{+0.062} \text{ ps}, \quad (23)$$

under the assumption of no CP violation in B_s^0 mixing.

Recent studies also consider CP violation, either in untagged [70,71] or tagged [73,74] $B_s^0 \rightarrow J/\psi\phi$ decays, and start to constrain the phase difference $-2\beta_s$ between the B_s^0 mixing diagram and the $b \rightarrow c\bar{c}s$ tree decay diagram. In the Standard Model, $\beta_s = \arg(-(V_{ts}V_{tb}^*)/(V_{cs}V_{cb}^*))$ is expected to be about one degree [7]. A proper combination of the current Tevatron constraints on β_s requires extra information not available in the original publications and is being prepared in collaboration between CDF and DØ.

On the other hand CP violation in B_s^0 mixing has been investigated through the asymmetry between positive and negative same-sign muon pairs from semi-leptonic decays of $b\bar{b}$ pairs [37–39], and directly through the charge asymmetry of $B_s^0 \rightarrow D_s\mu\nu X$ decays [75]. Combining all published results [37,39,75] with the knowledge of CP violation in B_d^0 mixing from Eq. (18) leads to

$$\mathcal{A}_{\text{SL}}^s = -0.0030 \pm 0.0101, \quad \text{or} \quad |q/p|_s = 1.0015 \pm 0.0051. \quad (24)$$

A large New Physics phase could possibly contribute to both CP violation in $B_s^0 \rightarrow J/\psi\phi$, and to the mixing phase difference of Eq. (8) on which $\mathcal{A}_{\text{SL}}^s$ depends. Combined fits [76,77] of β_s and $\mathcal{A}_{\text{SL}}^s$ measurements already yield interesting constraints on this New Physics phase. A deviation from the Standard Model, with a significance of more than 3σ , has recently been claimed [77], based on a preliminary analysis including the latest Tevatron B_s^0 mixing results [19,38,39,73–75].

Average b -hadron mixing probability and b -hadron production fractions in Z decays and at high energy

Mixing measurements can significantly improve our knowledge on the fractions f_u , f_d , f_s , and f_{baryon} , defined as the fractions of B_u , B_d^0 , B_s^0 and b -baryon in an unbiased sample of weakly decaying b hadrons produced in high-energy collisions.

Indeed, time-integrated mixing analyses performed with lepton pairs from $b\bar{b}$ events at high energy measure the quantity

$$\bar{\chi} = f'_d \chi_d + f'_s \chi_s, \quad (25)$$

where f'_d and f'_s are the fractions of B_d^0 and B_s^0 hadrons in a sample of semileptonic b -hadron decays. Assuming that all b hadrons have the same semileptonic decay width implies $f'_q = f_q/(\Gamma_q\tau_b)$ ($q = s, d$), where τ_b is the average b -hadron lifetime. Hence $\bar{\chi}$ measurements, together with the χ_d average of Eq. (15) and the very good approximation $\chi_s = 1/2$ (in fact $\chi_s = 0.49927 \pm 0.00003$ from Eqs. (5), (19) and (22)), provide constraints on the fractions f_d and f_s .

The LEP experiments have measured $f_s \times \text{BR}(B_s^0 \rightarrow D_s^- \ell^+ \nu_\ell X)$ [78], $\text{BR}(b \rightarrow A_b^0) \times \text{BR}(A_b^0 \rightarrow A_c^+ \ell^- \bar{\nu}_\ell X)$ [79], and $\text{BR}(b \rightarrow \Xi_b^-) \times \text{BR}(\Xi_b^- \rightarrow \Xi^- \ell^- \bar{\nu}_\ell X)$ [80] from partially reconstructed final states including a lepton, f_{baryon} from protons identified in b events [81], and the production rate of charged b hadrons [82]. The b -hadron fractions measured at CDF using double semileptonic $K^*\mu\mu$ and $\phi\mu\mu$ final states [83] and electron-charm final states [84] are at slight discrepancy with the ones measured at LEP. Furthermore the averages of the $\bar{\chi}$ values measured at LEP, 0.1259 ± 0.0042 [85], and at Tevatron, 0.147 ± 0.011 [39,86], show a 1.8σ deviation with respect to each other. This may be a hint that the fractions at the Tevatron might be different from the ones in Z decays. Combining [31] all the available information under the constraints $f_u = f_d$ and $f_u + f_d + f_s + f_{\text{baryon}} = 1$ yields the two set of averages shown in Table 1. The second set, obtained using both LEP and Tevatron results, has larger errors than the first set, obtained using LEP results only, because we have applied scale factors as advocated by the PDG for the treatment of marginally consistent data.

Table 1: $\bar{\chi}$ and b -hadron fractions (see text).

	in Z decays	at high energy
$\bar{\chi}$	0.1259 ± 0.0042	0.1284 ± 0.0069
$f_u = f_d$	0.402 ± 0.009	0.399 ± 0.011
f_s	0.104 ± 0.009	0.110 ± 0.012
f_{baryon}	0.091 ± 0.015	0.092 ± 0.019

Summary and prospects

B^0 - \bar{B}^0 mixing has been and still is a field of intense study. While fairly little experimental progress was recently achieved in the B_d^0 sector, impressive new B_s^0 results are becoming available from Run II of the Tevatron. B_s^0 oscillations are now established and the mass difference in the B_s^0 - \bar{B}_s^0 system is measured very accurately, with a central value compatible with the Standard Model (SM) expectation and a relative precision (0.7%) matching that in the B_d^0 - \bar{B}_d^0 system (0.9%). However, the extraction of $|V_{td}/V_{ts}|$ from these measurements in the SM framework is limited by the hadronic uncertainty, which will be an important challenge to reduce in the future. New

Meson Particle Listings

 B^0

time-dependent angular analyses of $B_s^0 \rightarrow J/\psi\phi$ decays and measurements of time-integrated B_s^0 asymmetries at CDF and DØ are improving our knowledge of the other B_s^0 mixing parameters: while CP violation in $B_s^0-\bar{B}_s^0$ mixing is consistent with zero, with an uncertainty still large compared to the SM prediction, the relative decay width difference $\Delta\Gamma_s/\Gamma_s$ is now determined to an absolute precision of $\sim 6\%$, smaller than the central value of the SM prediction. The data prefer $\Gamma_L > \Gamma_H$ as predicted in the SM.

Improved B_s^0 results are still to come, with very promising short-term prospects, both for $\Delta\Gamma_s$ and CP -violating phases induced by mixing such as β_s and $\arg(-M_{12}/\Gamma_{12})$. Although first interesting experimental constraints have been published, very little is known yet about these phases, which are predicted to be very small in the SM. A full search for New Physics effects in these observables will require statistics beyond that of the Tevatron. These will eventually become available at CERN's Large Hadron Collider, scheduled to start operation in 2008, where LHCb expects to be able to measure β_s down to the SM value after many years of operations [87].

B mixing may still reveal a surprize, but much effort is needed for this, both on the experimental and theoretical sides, in particular to further reduce the hadronic uncertainties of lattice QCD calculations. In the long term, a stringent check of the consistency of the B_d^0 and B_s^0 mixing amplitudes (magnitudes and phases) with all other measured flavour-physics observables will be possible within the SM, leading to very tight limits (or otherwise new interesting knowledge!) on New Physics.

References

1. T.D. Lee and C.S. Wu, *Ann. Rev. Nucl. Sci.* **16**, 511 (1966); I.I. Bigi and A.I. Sanda, *CP Violation*, Cambridge Univ. Press, 2000; G.C. Branco, L. Lavoura, and J.P. Silva, *CP Violation*, Clarendon Press Oxford, 1999.
2. See the review on “ CP violation in meson decays,” by D. Kirkby and Y. Nir in this publication.
3. A.J. Buras, W. Slominski, and H. Steger, *Nucl. Phys.* **B245**, 369 (1984).
4. T. Inami and C.S. Lim, *Prog. Theor. Phys.* **65**, 297 (1981); for the power-like approximation, see A.J. Buras and R. Fleischer, page 91 in *Heavy Flavours II*, eds., A.J. Buras and M. Lindner, Singapore World Scientific, 1998.
5. M. Kobayashi and K. Maskawa, *Prog. Theor. Phys.* **49**, 652 (1973).
6. I.I. Bigi *et al.*, in *CP violation*, ed. C. Jarlskog, Singapore World Scientific, 1989.
7. A. Lenz and U. Nierste, *JHEP* **0607**, 072 (2007), [arXiv: hep-ph/0612167v3](https://arxiv.org/abs/hep-ph/0612167v3).
8. C. Albajar *et al.* (UA1 Collab.), *Phys. Lett.* **B186**, 247 (1987).
9. H. Albrecht *et al.* (Argus Collab.), *Phys. Lett.* **B192**, 245 (1987).
10. H.-G. Moser and A. Roussarie, *Nucl. Instrum. Methods* **384**, 491 (1997).
11. SLD Collab., SLAC-PUB-7228, SLAC-PUB-7229, and SLAC-PUB-7230, *28th Int. Conf. on High Energy Physics*, Warsaw, 1996; J. Wittlin, PhD thesis, SLAC-R-582, 2001.
12. Aleph Collab., *Int. Europhysics Conf. on High Energy Physics*, Jerusalem, 1997.
13. K. Abe *et al.* (SLD Collab.), *Phys. Rev.* **D67**, 012006 (2003).
14. J. Abdallah *et al.* (DELPHI Collab.), *Eur. Phys. J.* **C28**, 155 (2003).
15. F. Abe *et al.* (CDF Collab.), *Phys. Rev. Lett.* **80**, 2057 (1998) and *Phys. Rev.* **D59**, 032001 (1999); *Phys. Rev.* **D60**, 051101 (1999); *Phys. Rev.* **D60**, 072003 (1999); T. Affolder *et al.* (CDF Collab.), *Phys. Rev.* **D60**, 112004 (1999).
16. R. Barate *et al.* (Aleph Collab.), *Eur. Phys. J.* **C4**, 367 (1998); *Eur. Phys. J.* **C7**, 553 (1999).
17. P. Abreu *et al.* (DELPHI Collab.), *Eur. Phys. J.* **C16**, 555 (2000); *Eur. Phys. J.* **C18**, 229 (2000).
18. See tagging summary on page 160 of K. Anikeev *et al.*, “ B physics at the Tevatron: Run II and beyond,” FERMILAB-PUB-01/97, [hep-ph/0201071](https://arxiv.org/abs/hep-ph/0201071), and references therein.
19. A. Abulencia *et al.* (CDF Collab.), *Phys. Rev. Lett.* **97**, 242003 (2006); this result supersedes A. Abulencia *et al.* (CDF Collab.), *Phys. Rev. Lett.* **97**, 062003 (2006).
20. V.M. Abazov *et al.* (DØ Collab.), *Phys. Rev.* **D74**, 112002 (2006).
21. DØCollab., DØ note 5474-CONF, August 2007, and DØ note 5254-CONF, October 2006.
22. B. Aubert *et al.* (BaBar Collab.), *Phys. Rev. Lett.* **94**, 161803 (2005); K.-F. Chen *et al.* (Belle Collab.), *Phys. Rev.* **D72**, 012004 (2005).
23. Throughout this paper, we omit references of results that have been superseded by new published measurements.
24. D. Buskulic *et al.* (Aleph Collab.), *Z. Phys.* **C75**, 397 (1997).
25. B. Aubert *et al.* (BaBar Collab.), *Phys. Rev. Lett.* **88**, 221802 (2002) and *Phys. Rev.* **D66**, 032003 (2002); *Phys. Rev. Lett.* **88**, 221803 (2002); *Phys. Rev.* **D67**, 072002 (2003); *Phys. Rev.* **D73**, 012004 (2006).
26. N.C. Hastings *et al.* (Belle Collab.), *Phys. Rev.* **D67**, 052004 (2003); Y. Zheng *et al.* (Belle Collab.), *Phys. Rev.* **D67**, 092004 (2003); K. Abe *et al.* (Belle Collab.), *Phys. Rev.* **D71**, 072003 (2005).
27. P. Abreu *et al.* (DELPHI Collab.), *Z. Phys.* **C76**, 579 (1997).
28. M. Acciarri *et al.* (L3 Collab.), *Eur. Phys. J.* **C5**, 195 (1998).
29. G. Alexander *et al.* (OPAL Collab.), *Z. Phys.* **C72**, 377 (1996); K. Ackerstaff *et al.* (OPAL Collab.), *Z. Phys.* **C76**, 417 (1997); G. Abbiendi *et al.* (OPAL Collab.), *Phys. Lett.* **B493**, 266 (2000).
30. K. Ackerstaff *et al.* (OPAL Collab.), *Z. Phys.* **C76**, 401 (1997).
31. E. Barberio *et al.* (HFAG Collab.), “Averages of b -hadron properties at the end of 2006,” [arXiv:0704.3575v1](https://arxiv.org/abs/0704.3575v1) [[hep-ex](https://arxiv.org/abs/hep-ex)], April 2007; the combined results on b -hadron fractions, lifetimes and mixing parameters published in this *Review* have been obtained by the B oscillations working group of the Heavy Flavour Averaging Group (HFAG), using the methods and procedures described in Chapter 3 of the above paper, after updating the list of

See key on page 373

- inputs; for more information, see <http://www.slac.stanford.edu/xorg/hfag/osc/>.
32. H. Albrecht *et al.* (ARGUS Collab.), *Z. Phys.* **C55**, 357 (1992); *Phys. Lett.* **B324**, 249 (1994).
 33. J. Bartelt *et al.* (CLEO Collab.), *Phys. Rev. Lett.* **71**, 1680 (1993).
 34. B.H. Behrens *et al.* (CLEO Collab.), *Phys. Lett.* **B490**, 36 (2000).
 35. B. Aubert *et al.* (BaBar Collab.), *Phys. Rev. Lett.* **92**, 181801 (2004) and *Phys. Rev.* **D70**, 012007 (2004).
 36. D.E. Jaffe *et al.* (CLEO Collab.), *Phys. Rev. Lett.* **86**, 5000 (2001).
 37. F. Abe *et al.* (CDF Collab.), *Phys. Rev.* **D55**, 2546 (1997).
 38. CDF Collab., CDF note 9015, October 2007.
 39. V.M. Abazov *et al.* (D0 Collab.), *Phys. Rev.* **D74**, 092001 (2006).
 40. DELPHI Collab., contrib. 449 to *Int. Europhysics Conf. on High Energy Physics*, Jerusalem, 1997.
 41. R. Barate *et al.* (Aleph Collab.), *Eur. Phys. J.* **C20**, 431 (2001).
 42. B. Aubert *et al.* (BaBar Collab.), *Phys. Rev. Lett.* **96**, 251802 (2006).
 43. BABAR Collab., [arXiv:hep-ex/0607091v1](http://arxiv.org/abs/hep-ex/0607091v1), *33rd Int. Conf. on High Energy Physics*, Moscow, 2006.
 44. E. Nakano *et al.* (Belle Collab.), *Phys. Rev.* **D73**, 112002 (2006).
 45. G. Abbiendi *et al.* (OPAL Collab.), *Eur. Phys. J.* **C12**, 609 (2000).
 46. M. Beneke, G. Buchalla, and I. Dunietz, *Phys. Lett.* **B393**, 132 (1997); I. Dunietz, *Eur. Phys. J.* **C7**, 197 (1999).
 47. See the review on the CKM quark-mixing matrix by A. Ceccucci, Z. Ligeti, and Y. Sakai in this publication.
 48. M. Okamoto, *XXIIIth Int. Symp. on Lattice Field Theory*, Dublin, July 2005, [hep-lat/0510113](http://arxiv.org/abs/hep-lat/0510113); these estimates are obtained by combining the unquenched lattice QCD calculations from A. Gray *et al.* (HPQCD Collab.), *Phys. Rev. Lett.* **95**, 212001 (2005) and S. Aoki *et al.* (JLQCD Collab.), *Phys. Rev. Lett.* **91**, 212001 (2003).
 49. A. Heister *et al.* (Aleph Collab.), *Eur. Phys. J.* **C29**, 143 (2003).
 50. F. Abe *et al.* (CDF Collab.), *Phys. Rev. Lett.* **82**, 3576 (1999).
 51. J. Abdallah *et al.* (DELPHI Collab.), *Eur. Phys. J.* **C35**, 35 (2004).
 52. G. Abbiendi *et al.* (OPAL Collab.), *Eur. Phys. J.* **C11**, 587 (1999); *Eur. Phys. J.* **C19**, 241 (2001).
 53. K. Abe *et al.* (SLD Collab.), *Phys. Rev.* **D66**, 032009 (2002).
 54. SLD Collab., SLAC-PUB-8568, *30th Int. Conf. on High Energy Physics*, Osaka, 2000.
 55. V.M. Abazov *et al.* (D0 Collab.), *Phys. Rev. Lett.* **97**, 021802 (2006).
 56. D0 Collab., D0 note 5618-CONF v1.1, March 2008.
 57. D. Mohapatra *et al.* (Belle Collab.), *Phys. Rev. Lett.* **96**, 221601 (2006), updated in M. Nakao, talk at *23rd Int. Symp. on Lepton and Photon Interactions at High Energy*, Daegu, 2007.
 58. B. Aubert *et al.* (BaBar Collab.), *Phys. Rev. Lett.* **98**, 151802 (2007).
 59. M. Bona *et al.* (UTfit Collab.), [arXiv:hep-ph/0606167v2](http://arxiv.org/abs/hep-ph/0606167v2) and updated results at <http://utfit.roma1.infn.it/>.
 60. J. Charles *et al.* (CKMfitter Collab.), *Eur. Phys. J.* **C41**, 1 (2005) & updated results at <http://ckmfitter.in2p3.fr/>.
 61. K. Hartkorn and H.-G. Moser, *Eur. Phys. J.* **C8**, 381 (1999).
 62. M. Acciarri *et al.* (L3 Collab.), *Phys. Lett.* **B438**, 417 (1998).
 63. D. Buskulic *et al.* (Aleph Collab.), *Phys. Lett.* **B377**, 205 (1996); K. Ackerstaff *et al.* (OPAL Collab.), *Phys. Lett.* **B426**, 161 (1998); F. Abe *et al.* (CDF Collab.), *Phys. Rev.* **D59**, 032004 (1999).
 64. (CDF Collab.), CDF note 7386, March 2005; CDF note 7757, August 2005; V.M. Abazov *et al.* (D0 Collab.), *Phys. Rev. Lett.* **97**, 241801 (2006).
 65. D. Tonelli for the (CDF Collab.), [arXiv:hep-ex/0605038v1](http://arxiv.org/abs/hep-ex/0605038v1), May 2006.
 66. F. Abe *et al.* (CDF Collab.), *Phys. Rev.* **D57**, 5382 (1998).
 67. V.M. Abazov *et al.* (D0 Collab.), *Phys. Rev. Lett.* **94**, 041001 (2005); (CDF Collab.), CDF note 7409, May 2004.
 68. R. Barate *et al.* (Aleph Collab.), *Phys. Lett.* **B486**, 286 (2000).
 69. R. Aleksan *et al.*, *Phys. Lett.* **B316**, 567 (1993).
 70. T. Aaltonen *et al.* (CDF Collab.), *Phys. Rev. Lett.* **100**, 121803 (2008).
 71. V.M. Abazov *et al.* (D0 Collab.), *Phys. Rev. Lett.* **98**, 121801 (2007).
 72. V.M. Abazov *et al.* (D0 Collab.), *Phys. Rev. Lett.* **99**, 241801 (2007); A. Abulencia *et al.* (CDF Collab.), *Phys. Rev. Lett.* **100**, 021803 (2008).
 73. T. Aaltonen *et al.* (CDF Collab.), *Phys. Rev. Lett.* **100**, 161802 (2008).
 74. V.M. Abazov *et al.* (D0 Collab.), [arXiv:0802.2255v1](http://arxiv.org/abs/0802.2255v1) [[hep-ex](http://arxiv.org/abs/hep-ex)], submitted to *Phys. Rev. Lett.*
 75. V.M. Abazov *et al.* (D0 Collab.), *Phys. Rev. Lett.* **98**, 151801 (2007).
 76. V.M. Abazov *et al.* (D0 Collab.), *Phys. Rev.* **D76**, 057101 (2007).
 77. M. Bona *et al.* (UTfit Collab.), [arXiv:0803.0659v1](http://arxiv.org/abs/0803.0659v1) [[hep-ph](http://arxiv.org/abs/hep-ph)], March 2008.
 78. P. Abreu *et al.* (DELPHI Collab.), *Phys. Lett.* **B289**, 199 (1992); P.D. Acton *et al.* (OPAL Collab.), *Phys. Lett.* **B295**, 357 (1992); D. Buskulic *et al.* (Aleph Collab.), *Phys. Lett.* **B361**, 221 (1995).
 79. P. Abreu *et al.* (DELPHI Collab.), *Z. Phys.* **C68**, 375 (1995); R. Barate *et al.* (Aleph Collab.), *Eur. Phys. J.* **C2**, 197 (1998).
 80. D. Buskulic *et al.* (Aleph Collab.), *Phys. Lett.* **B384**, 449 (1996); J. Abdallah *et al.* (DELPHI Collab.), *Eur. Phys. J.* **C44**, 299 (2005).
 81. R. Barate *et al.* (Aleph Collab.), *Eur. Phys. J.* **C5**, 205 (1998).
 82. J. Abdallah *et al.* (DELPHI Collab.), *Phys. Lett.* **B576**, 29 (2003).
 83. F. Abe *et al.* (CDF Collab.), *Phys. Rev.* **D60**, 092005 (1999).
 84. T. Affolder *et al.* (CDF Collab.), *Phys. Rev. Lett.* **84**, 1663 (2000).

Meson Particle Listings

 B^0

85. Aleph, DELPHI, L3, OPAL, and SLD Collabs., "Precision electroweak measurements on the Z resonance," Physics Reports **427**, 257 (2006); we use the $\bar{\chi}$ average given in Eq. (5.39).
86. D. Acosta *et al.* (CDF Collab.), Phys. Rev. **D69**, 012002 (2004).
87. L. Fernández for the LHCb Collab., LHCb note 2006-047, Acta Phys. Pol. **B38**, 931 (2007).

 $B^0\text{-}\bar{B}^0$ MIXING PARAMETERS

For a discussion of $B^0\text{-}\bar{B}^0$ mixing see the note on " $B^0\text{-}\bar{B}^0$ Mixing" in the B^0 Particle Listings above.

χ_d is a measure of the time-integrated $B^0\text{-}\bar{B}^0$ mixing probability that a produced $B^0(\bar{B}^0)$ decays as a $\bar{B}^0(B^0)$. Mixing violates $\Delta B \neq 2$ rule.

$$\chi_d = \frac{x_d^2}{2(1+x_d^2)}$$

$$x_d = \frac{\Delta m_{B^0}}{\Gamma_{B^0}} = (m_{B_H^0} - m_{B_L^0}) \tau_{B^0},$$

where H, L stand for heavy and light states of two B^0 CP eigenstates and

$$\tau_{B^0} = \frac{1}{0.5(\Gamma_{B_H^0} + \Gamma_{B_L^0})}.$$

 χ_d

This $B^0\text{-}\bar{B}^0$ mixing parameter is the probability (integrated over time) that a produced B^0 (or \bar{B}^0) decays as a \bar{B}^0 (or B^0), e.g. for inclusive lepton decays

$$\chi_d = \frac{\Gamma(B^0 \rightarrow \ell^- X \text{ (via } \bar{B}^0)) / \Gamma(B^0 \rightarrow \ell^\pm X)}{\Gamma(\bar{B}^0 \rightarrow \ell^+ X \text{ (via } B^0)) / \Gamma(\bar{B}^0 \rightarrow \ell^\pm X)}$$

Where experiments have measured the parameter $r = \chi/(1-\chi)$, we have converted to χ . Mixing violates the $\Delta B \neq 2$ rule.

Note that the measurement of χ at energies higher than the $\Upsilon(4S)$ have not separated χ_d from χ_s where the subscripts indicate $B^0(\bar{B}^0)$ or $B_s^0(\bar{B}_s^0)$. They are listed in the $B^\pm/B^0/B_s^0/b$ -baryon ADMIXTURE section.

The experiments at $\Upsilon(4S)$ make an assumption about the $B^0\text{-}\bar{B}^0$ fraction and about the ratio of the B^\pm and B^0 semileptonic branching ratios (usually that it equals one).

"OUR EVALUATION" is an average using rescaled values of the data listed below. The average and rescaling were performed by the Heavy Flavor Averaging Group (HFAG) and are described at <http://www.slac.stanford.edu/xorg/hfag/>. The averaging/rescaling procedure takes into account correlations between the measurements, includes χ_d calculated from Δm_{B^0} and τ_{B^0} .

VALUE	CL%	DOCUMENT ID	TECN	COMMENT
0.1878 ± 0.0024				OUR EVALUATION
0.182 ± 0.015				OUR AVERAGE
0.198 ± 0.013 ± 0.014		1 BEHRENS 00b	CLE2	$e^+e^- \rightarrow \Upsilon(4S)$
0.16 ± 0.04 ± 0.04		2 ALBRECHT 94	ARG	$e^+e^- \rightarrow \Upsilon(4S)$
0.149 ± 0.023 ± 0.022		3 BARTELT 93	CLE2	$e^+e^- \rightarrow \Upsilon(4S)$
0.171 ± 0.048		4 ALBRECHT 92L	ARG	$e^+e^- \rightarrow \Upsilon(4S)$
••• We do not use the following data for averages, fits, limits, etc. •••				
0.20 ± 0.13 ± 0.12		5 ALBRECHT 96D	ARG	$e^+e^- \rightarrow \Upsilon(4S)$
0.19 ± 0.07 ± 0.09		6 ALBRECHT 96D	ARG	$e^+e^- \rightarrow \Upsilon(4S)$
0.24 ± 0.12		7 ELSSEN 90	JADE	e^+e^- 35-44 GeV
0.158 $\begin{smallmatrix} +0.052 \\ -0.059 \end{smallmatrix}$		ARTUSO 89	CLEO	$e^+e^- \rightarrow \Upsilon(4S)$
0.17 ± 0.05		8 ALBRECHT 87I	ARG	$e^+e^- \rightarrow \Upsilon(4S)$
<0.19	90	9 BEAN 87B	CLEO	$e^+e^- \rightarrow \Upsilon(4S)$
<0.27	90	10 AVERY 84	CLEO	$e^+e^- \rightarrow \Upsilon(4S)$

1 BEHRENS 00b uses high-momentum lepton tags and partially reconstructed $\bar{B}^0 \rightarrow D^{*+} \pi^-, \rho^-$ decays to determine the flavor of the B meson.

2 ALBRECHT 94 reports $r=0.194 \pm 0.062 \pm 0.054$. We convert to χ for comparison. Uses tagged events (lepton + pion from D^*).

3 BARTELT 93 analysis performed using tagged events (lepton+pion from D^*). Using dilepton events they obtain $0.157 \pm 0.016 \begin{smallmatrix} +0.033 \\ -0.028 \end{smallmatrix}$.

4 ALBRECHT 92L is a combined measurement employing several lepton-based techniques. It uses all previous ARGUS data in addition to new data and therefore supersedes ALBRECHT 87I. A value of $r = 20.6 \pm 7.0\%$ is directly measured. The value can be used to measure $x = \Delta M/\Gamma = 0.72 \pm 0.15$ for the B_d meson. Assumes $f_{+,-}/f_0 = 1.0 \pm 0.05$ and uses $\tau_{B^\pm}/\tau_{B^0} = (0.95 \pm 0.14) (f_{+,-}/f_0)$.

5 Uses $D^{*+} K^\pm$ correlations.

6 Uses $(D^{*+} \ell^-) K^\pm$ correlations.

7 These experiments see a combination of B_s and B_d mesons.

8 ALBRECHT 87I is inclusive measurement with like-sign dileptons, with tagged B decays plus leptons, and one fully reconstructed event. Measures $r=0.21 \pm 0.08$. We convert to χ for comparison. Superseded by ALBRECHT 92L.

9 BEAN 87B measured $r < 0.24$; we converted to χ .

10 Same-sign dilepton events. Limit assumes semileptonic BR for B^+ and B^0 equal. If B^0/B^\pm ratio < 0.58 , no limit exists. The limit was corrected in BEAN 87B from $r < 0.30$ to $r < 0.37$. We converted this limit to χ .

 $\Delta m_{B^0} = m_{B_H^0} - m_{B_L^0}$

Δm_{B^0} is a measure of 2π times the $B^0\text{-}\bar{B}^0$ oscillation frequency in time-dependent mixing experiments.

The second "OUR EVALUATION" is an average using rescaled values of the data listed below. The average and rescaling were performed by the Heavy Flavor Averaging Group (HFAG) and are described at <http://www.slac.stanford.edu/xorg/hfag/>. The averaging/rescaling procedure takes into account correlations between the measurements.

The first "OUR EVALUATION", also provided by the HFAG, includes Δm_d calculated from χ_d measured at $\Upsilon(4S)$.

VALUE (10^{12} h s^{-1})	DOCUMENT ID	TECN	COMMENT
0.507 ± 0.005			OUR EVALUATION First
0.507 ± 0.005			OUR EVALUATION Second
0.506 ± 0.020 ± 0.016	1 ABAZOV 06W	D0	$p\bar{p}$ at 1.96 TeV
0.511 ± 0.007 $\begin{smallmatrix} +0.007 \\ -0.006 \end{smallmatrix}$	2 AUBERT 06G	BABR	$e^+e^- \rightarrow \Upsilon(4S)$
0.511 ± 0.005 ± 0.006	3 ABE 05B	BELL	$e^+e^- \rightarrow \Upsilon(4S)$
0.531 ± 0.025 ± 0.007	4 ABDALLAH 03B	DLPH	$e^+e^- \rightarrow Z$
0.503 ± 0.008 ± 0.010	5 HASTINGS 03	BELL	$e^+e^- \rightarrow \Upsilon(4S)$
0.509 ± 0.017 ± 0.020	6 ZHENG 03	BELL	$e^+e^- \rightarrow \Upsilon(4S)$
0.516 ± 0.016 ± 0.010	7 AUBERT 02I	BABR	$e^+e^- \rightarrow \Upsilon(4S)$
0.493 ± 0.012 ± 0.009	8 AUBERT 02J	BABR	$e^+e^- \rightarrow \Upsilon(4S)$
0.497 ± 0.024 ± 0.025	9 ABBIENDI,G 00B	OPAL	$e^+e^- \rightarrow Z$
0.503 ± 0.064 ± 0.071	10 ABE 99K	CDF	$p\bar{p}$ at 1.8 TeV
0.500 ± 0.052 ± 0.043	11 ABE 99Q	CDF	$p\bar{p}$ at 1.8 TeV
0.516 ± 0.099 $\begin{smallmatrix} +0.029 \\ -0.035 \end{smallmatrix}$	12 AFFOLDER 99C	CDF	$p\bar{p}$ at 1.8 TeV
0.471 $\begin{smallmatrix} +0.078 +0.033 \\ -0.068 -0.034 \end{smallmatrix}$	13 ABE 98C	CDF	$p\bar{p}$ at 1.8 TeV
0.458 ± 0.046 ± 0.032	14 ACCIARRI 98D	L3	$e^+e^- \rightarrow Z$
0.437 ± 0.043 ± 0.044	15 ACCIARRI 98D	L3	$e^+e^- \rightarrow Z$
0.472 ± 0.049 ± 0.053	16 ACCIARRI 98D	L3	$e^+e^- \rightarrow Z$
0.523 ± 0.072 ± 0.043	17 ABREU 97N	DLPH	$e^+e^- \rightarrow Z$
0.493 ± 0.042 ± 0.027	15 ABREU 97N	DLPH	$e^+e^- \rightarrow Z$
0.499 ± 0.053 ± 0.015	18 ABREU 97N	DLPH	$e^+e^- \rightarrow Z$
0.480 ± 0.040 ± 0.051	14 ABREU 97N	DLPH	$e^+e^- \rightarrow Z$
0.444 ± 0.029 $\begin{smallmatrix} +0.020 \\ -0.017 \end{smallmatrix}$	15 ACKERSTAFF 97U	OPAL	$e^+e^- \rightarrow Z$
0.430 ± 0.043 $\begin{smallmatrix} +0.028 \\ -0.030 \end{smallmatrix}$	14 ACKERSTAFF 97V	OPAL	$e^+e^- \rightarrow Z$
0.482 ± 0.044 ± 0.024	19 BUSKULIC 97D	ALEP	$e^+e^- \rightarrow Z$
0.404 ± 0.045 ± 0.027	15 BUSKULIC 97D	ALEP	$e^+e^- \rightarrow Z$
0.452 ± 0.039 ± 0.044	14 BUSKULIC 97D	ALEP	$e^+e^- \rightarrow Z$
0.539 ± 0.060 ± 0.024	20 ALEXANDER 96V	OPAL	$e^+e^- \rightarrow Z$
0.567 ± 0.089 $\begin{smallmatrix} +0.029 \\ -0.023 \end{smallmatrix}$	21 ALEXANDER 96V	OPAL	$e^+e^- \rightarrow Z$
••• We do not use the following data for averages, fits, limits, etc. •••			
0.492 ± 0.018 ± 0.013	22 AUBERT 03C	BABR	Repl. by AUBERT 06G
0.516 ± 0.016 ± 0.010	23 AUBERT 02N	BABR	$e^+e^- \rightarrow \Upsilon(4S)$
0.494 ± 0.012 ± 0.015	24 HARA 02	BELL	Repl. by ABE 05B
0.528 ± 0.017 ± 0.011	25 TOMURA 02	BELL	Repl. by ABE 05B
0.463 ± 0.008 ± 0.016	8 ABE 01D	BELL	Repl. by HASTINGS 03
0.444 ± 0.028 ± 0.028	26 ACCIARRI 98D	L3	$e^+e^- \rightarrow Z$
0.497 ± 0.035	27 ABREU 97N	DLPH	$e^+e^- \rightarrow Z$
0.467 ± 0.022 $\begin{smallmatrix} +0.017 \\ -0.015 \end{smallmatrix}$	28 ACKERSTAFF 97V	OPAL	$e^+e^- \rightarrow Z$
0.446 ± 0.032	29 BUSKULIC 97D	ALEP	$e^+e^- \rightarrow Z$
0.531 $\begin{smallmatrix} +0.050 \\ -0.046 \end{smallmatrix}$ ± 0.078	30 ABREU 96Q	DLPH	Sup. by ABREU 97N
0.496 $\begin{smallmatrix} +0.055 \\ -0.051 \end{smallmatrix}$ ± 0.043	14 ACCIARRI 96E	L3	Repl. by ACCIARRI 98D
0.548 ± 0.050 $\begin{smallmatrix} +0.023 \\ -0.019 \end{smallmatrix}$	31 ALEXANDER 96V	OPAL	$e^+e^- \rightarrow Z$
0.496 ± 0.046	32 AKERS 95J	OPAL	Repl. by ACKERSTAFF 97V
0.462 $\begin{smallmatrix} +0.040 +0.052 \\ -0.053 -0.035 \end{smallmatrix}$	14 AKERS 95J	OPAL	Repl. by ACKERSTAFF 97V
0.50 ± 0.12 ± 0.06	17 ABREU 94M	DLPH	Sup. by ABREU 97N
0.508 ± 0.075 ± 0.025	20 AKERS 94C	OPAL	Repl. by ALEXANDER 96V
0.57 ± 0.11 ± 0.02	21 AKERS 94H	OPAL	Repl. by ALEXANDER 96V
0.50 $\begin{smallmatrix} +0.07 +0.11 \\ -0.06 -0.10 \end{smallmatrix}$	14 BUSKULIC 94B	ALEP	Sup. by BUSKULIC 97D
0.52 $\begin{smallmatrix} +0.10 +0.04 \\ -0.11 -0.03 \end{smallmatrix}$	21 BUSKULIC 93K	ALEP	Sup. by BUSKULIC 97D

1 Uses opposite-side flavor-tagging with $B \rightarrow D^{(*)} \mu \nu_\mu X$ events.

2 Measured using a simultaneous fit of the B^0 lifetime and $\bar{B}^0\text{-}B^0$ oscillation frequency Δm_d in the partially reconstructed $B^0 \rightarrow D^{*-} \ell \nu$ decays.

3 Measurement performed using a combined fit of CP-violation, mixing and lifetimes.

4 Events with a high transverse momentum lepton were removed and an inclusively reconstructed vertex was required.

5 HASTINGS 03 measurement based on the time evolution of dilepton events. It also reports $f_{+}/f_0 = 1.01 \pm 0.03 \pm 0.09$ and CPT violation parameters in $B^0\text{-}\bar{B}^0$ mixing.

6 ZHENG 03 data analyzed using partially reconstructed $\bar{B}^0 \rightarrow D^{*-} \pi^+$ decay and a flavor tag based on the charge of the lepton from the accompanying B decay.

7 Uses a tagged sample of fully-reconstructed neutral B decays at $\Upsilon(4S)$.

8 Measured based on the time evolution of dilepton events in $\Upsilon(4S)$ decays.

9 Data analyzed using partially reconstructed $\bar{B}^0 \rightarrow D^{*+} \ell^- \bar{\nu}$ decay and a combination of flavor tags from the rest of the event.

- 10 Uses di-muon events.
 11 Uses jet-charge and lepton-flavor tagging.
 12 Uses $\ell^- D^{*+} - \ell$ events.
 13 Uses $\pi^- B$ in the same side.
 14 Uses $\ell^- \ell^-$.
 15 Uses $\ell^- Q_{\text{hem}}$.
 16 Uses $\ell^- \ell^-$ with impact parameters.
 17 Uses $D^{*\pm} - Q_{\text{hem}}$.
 18 Uses $\pi_s^\pm \ell^- Q_{\text{hem}}$.
 19 Uses $D^{*\pm} - \ell / Q_{\text{hem}}$.
 20 Uses $D^{*\pm} \ell^- Q_{\text{hem}}$.
 21 Uses $D^{*\pm} - \ell$.
 22 AUBERT 03c uses a sample of approximately 14,000 exclusively reconstructed $B^0 \rightarrow D^*(2010)^- \ell \nu$ and simultaneously measures the lifetime and oscillation frequency.
 23 AUBERT 02N result based on the same analysis and data sample reported in AUBERT 02i.
 24 Uses a tagged sample of B^0 decays reconstructed in the mode $B^0 \rightarrow D^* \ell \nu$.
 25 Uses a tagged sample of fully-reconstructed hadronic B^0 decays at $\mathcal{T}(4S)$.
 26 ACCIARRI 98D combines results from $\ell^- \ell^-$, $\ell^- Q_{\text{hem}}$, and $\ell^- \ell^-$ with impact parameters.
 27 ABREU 97N combines results from $D^{*\pm} - Q_{\text{hem}}$, $\ell^- Q_{\text{hem}}$, $\pi_s^\pm \ell^- Q_{\text{hem}}$, and $\ell^- \ell^-$.
 28 ACKERSTAFF 97v combines results from $\ell^- \ell^-$, $\ell^- Q_{\text{hem}}$, $D^{*\pm} - \ell$, and $D^{*\pm} - Q_{\text{hem}}$.
 29 BUSKULIC 97D combines results from $D^{*\pm} - \ell / Q_{\text{hem}}$, $\ell^- Q_{\text{hem}}$, and $\ell^- \ell^-$.
 30 ABREU 96Q analysis performed using lepton, kaon, and jet-charge tags.
 31 ALEXANDER 96V combines results from $D^{*\pm} - \ell$ and $D^{*\pm} \ell^- Q_{\text{hem}}$.
 32 AKERS 95J combines results from charge measurement, $D^{*\pm} \ell^- Q_{\text{hem}}$ and $\ell^- \ell^-$.

 $\chi_d = \Delta m_{B^0} / \Gamma_{B^0}$

The second "OUR EVALUATION" is an average using rescaled values of the data listed below. The average and rescaling were performed by the Heavy Flavor Averaging Group (HFAG) and are described at <http://www.slac.stanford.edu/xorg/hfag/>. The averaging/rescaling procedure takes into account correlations between the measurements.

The first "OUR EVALUATION", also provided by the HFAG, includes χ_d measured at $\mathcal{T}(4S)$.

VALUE	DOCUMENT ID
0.776 ± 0.008 OUR EVALUATION	First
0.776 ± 0.008 OUR EVALUATION	Second

 $\text{Re}(\lambda_{CP} / |\lambda_{CP}|) \text{Re}(z)$

The λ_{CP} characterizes B^0 and \bar{B}^0 decays to states of charmonium plus K_S^0 . Parameter z is used to describe CPT violation in mixing, see the review on "CP Violation" in the reviews section.

VALUE	DOCUMENT ID	TECN	COMMENT
0.014 ± 0.035 ± 0.034	¹ AUBERT,B	04c	BABR $e^+ e^- \rightarrow \mathcal{T}(4S)$

¹ Corresponds to 90% confidence range $[-0.072, 0.101]$.

 $\Delta\Gamma \text{Re}(z)$

VALUE	DOCUMENT ID	TECN	COMMENT
-0.0071 ± 0.0039 ± 0.0020	AUBERT	06T	BABR $e^+ e^- \rightarrow \mathcal{T}(4S)$

 $\text{Re}(z)$

VALUE	DOCUMENT ID	TECN	COMMENT
0.00 ± 0.12 ± 0.01	¹ HASTINGS	03	BELL $e^+ e^- \rightarrow \mathcal{T}(4S)$

¹ Measured using inclusive dilepton events from B^0 decay.

 $\text{Im}(z)$

VALUE	DOCUMENT ID	TECN	COMMENT
-0.015 ± 0.008 OUR AVERAGE			
-0.0139 ± 0.0073 ± 0.0032	¹ AUBERT	06T	BABR $e^+ e^- \rightarrow \mathcal{T}(4S)$
-0.03 ± 0.01 ± 0.03	² HASTINGS	03	BELL $e^+ e^- \rightarrow \mathcal{T}(4S)$

• • • We do not use the following data for averages, fits, limits, etc. • • •

0.038 ± 0.029 ± 0.025 ³ AUBERT,B 04c BABR Repl. by AUBERT 06T

¹ Assuming $\Delta\Gamma = 0$, the result becomes $\text{Im}(z) = -0.0037 \pm 0.0046$.

² Measured using inclusive dilepton events from B^0 decay.

³ Corresponds to 90% confidence range $[-0.028, 0.104]$.

CP VIOLATION PARAMETERS

 $\text{Re}(\epsilon_{B^0}) / (1 + |\epsilon_{B^0}|^2)$

CP impurity in B_d^0 system. It is obtained from either $a_{\ell\ell}$, the charge asymmetry in like-sign dilepton events or a_{CP} , the time-dependent asymmetry of inclusive B^0 and \bar{B}^0 decays.

The second "OUR EVALUATION" is an average using rescaled values of the data listed below. The average and rescaling were performed by the Heavy Flavor Averaging Group (HFAG) and are described at <http://www.slac.stanford.edu/xorg/hfag/>. The averaging/rescaling procedure takes into account correlations between the measurements. It assumes there is no CP violation in B_s mixing.

The first "OUR EVALUATION", also provided by the HFAG, uses the measurements from B -factories only.

VALUE (units 10^{-3})	DOCUMENT ID	TECN	COMMENT
-0.1 ± 1.4 OUR EVALUATION	First		
-1.2 ± 1.0 OUR EVALUATION	Second		
-0.9 ± 0.9 OUR AVERAGE			
-2.3 ± 1.1 ± 0.8	¹ ABAZOV	06s	D0 $p\bar{p}$ at 1.96 TeV
0.4 ± 1.3 ± 0.9	² AUBERT	06T	BABR $e^+ e^- \rightarrow \mathcal{T}(4S)$
-0.3 ± 2.0 ± 2.1	³ NAKANO	06	BELL $e^+ e^- \rightarrow \mathcal{T}(4S)$
1.2 ± 2.9 ± 3.6	⁴ AUBERT	02k	BABR $e^+ e^- \rightarrow \mathcal{T}(4S)$
-3.2 ± 6.5	⁵ BARATE	01d	ALEP $e^+ e^- \rightarrow Z$
3.5 ± 10.3 ± 1.5	⁶ JAFFE	01	CLE2 $e^+ e^- \rightarrow \mathcal{T}(4S)$
1.2 ± 13.8 ± 3.2	⁷ ABBIENDI	99j	OPAL $e^+ e^- \rightarrow Z$
2 ± 7 ± 3	⁸ ACKERSTAFF	97u	OPAL $e^+ e^- \rightarrow Z$
• • • We do not use the following data for averages, fits, limits, etc. • • •			
-14.7 ± 6.7 ± 5.7	⁹ AUBERT,B	04c	BABR Repl. by AUBERT 06T
4 ± 18 ± 3	¹⁰ BEHRENS	00b	CLE2 Repl. by JAFFE 01
< 45	¹¹ BARTELT	93	CLE2 $e^+ e^- \rightarrow \mathcal{T}(4S)$

¹ Uses the dimuon charge asymmetry.

² AUBERT 06T reports $|q/p| - 1 = (-0.8 \pm 2.7 \pm 1.9) \times 10^{-3}$. We convert to $(1 - |q/p|^2)/4$.

³ Uses the charge asymmetry in like-sign dilepton events and reports $|q/p| = 1.0005 \pm 0.0040 \pm 0.0043$.

⁴ AUBERT 02k uses the charge asymmetry in like-sign dilepton events.

⁵ BARATE 01d measured by investigating time-dependent asymmetries in semileptonic and fully inclusive B_d^0 decays.

⁶ JAFFE 01 finds $a_{\ell\ell} = 0.013 \pm 0.050 \pm 0.005$ and combines with the previous BEHRENS 00b independent measurement.

⁷ Data analyzed using the time-dependent asymmetry of inclusive B^0 decay. The production flavor of B^0 mesons is determined using both the jet charge and the charge of secondary vertex in the opposite hemisphere.

⁸ ACKERSTAFF 97u assumes CPT and is based on measuring the charge asymmetry in a sample of B^0 decays defined by lepton and Q_{hem} tags. If CPT is not invoked, $\text{Re}(\epsilon_B) = -0.006 \pm 0.010 \pm 0.006$ is found. The indirect CPT violation parameter is determined to $\text{Im}(\delta B) = -0.020 \pm 0.016 \pm 0.006$.

⁹ AUBERT 04c reports $|q/p| = 1.029 \pm 0.013 \pm 0.011$ and we converted it to $(1 - |q/p|^2)/4$.

¹⁰ BEHRENS 00b uses high-momentum lepton tags and partially reconstructed $\bar{B}^0 \rightarrow D^{*+} \pi^-$, ρ^- decays to determine the flavor of the B meson.

¹¹ BARTELT 93 finds $a_{\ell\ell} = 0.031 \pm 0.096 \pm 0.032$ which corresponds to $|a_{\ell\ell}| < 0.18$, which yields the above $|\text{Re}(\epsilon_{B^0})| / (1 + |\epsilon_{B^0}|^2)$.

 $A_{T/CP}$

$A_{T/CP}$ is defined as

$$\frac{P(\bar{B}^0 \rightarrow B^0) - P(B^0 \rightarrow \bar{B}^0)}{P(\bar{B}^0 \rightarrow B^0) + P(B^0 \rightarrow \bar{B}^0)}$$

the CPT invariant asymmetry between the oscillation probabilities $P(\bar{B}^0 \rightarrow B^0)$ and $P(B^0 \rightarrow \bar{B}^0)$.

VALUE	DOCUMENT ID	TECN	COMMENT
0.005 ± 0.012 ± 0.014	¹ AUBERT	02k	BABR $e^+ e^- \rightarrow \mathcal{T}(4S)$

¹ AUBERT 02k uses the charge asymmetry in like-sign dilepton events.

 $A_{CP}(B^0 \rightarrow D^{*+}(2010)^+ D^-)$

A_{CP} is defined as

$$\frac{B(\bar{B}^0 \rightarrow \bar{D}^+ B^0 \rightarrow f) - B(B^0 \rightarrow D^+ \bar{B}^0 \rightarrow f)}{B(\bar{B}^0 \rightarrow \bar{D}^+ B^0 \rightarrow f) + B(B^0 \rightarrow D^+ \bar{B}^0 \rightarrow f)}$$

the CP -violation charge asymmetry of exclusive B^0 and \bar{B}^0 decay.

VALUE	DOCUMENT ID	TECN	COMMENT
-0.06 ± 0.09 OUR AVERAGE			Error includes scale factor of 1.7.
-0.12 ± 0.06 ± 0.02	AUBERT	07Ai	BABR $e^+ e^- \rightarrow \mathcal{T}(4S)$
0.07 ± 0.08 ± 0.04	¹ AUSHEV	04	BELL $e^+ e^- \rightarrow \mathcal{T}(4S)$

• • • We do not use the following data for averages, fits, limits, etc. • • •

-0.03 ± 0.10 ± 0.02 AUBERT,B 06A BABR Repl. by AUBERT 07Ai

-0.03 ± 0.11 ± 0.05 AUBERT 03J BABR Repl. by AUBERT,B 06B

¹ Combines results from fully and partially reconstructed $B^0 \rightarrow D^{*\pm} D^\mp$ decays.

 $A_{CP}(B^0 \rightarrow K^+ \pi^-)$

VALUE	DOCUMENT ID	TECN	COMMENT
-0.101 ± 0.015 OUR AVERAGE			
-0.107 ± 0.018 ± 0.007	AUBERT	07Af	BABR $e^+ e^- \rightarrow \mathcal{T}(4S)$
-0.013 ± 0.078 ± 0.012	ABULENCIA,A	06D	CDF $p\bar{p}$ at 1.96 TeV
-0.101 ± 0.025 ± 0.005	¹ CHAO	04B	BELL $e^+ e^- \rightarrow \mathcal{T}(4S)$
-0.04 ± 0.16	² CHEN	00	CLE2 $e^+ e^- \rightarrow \mathcal{T}(4S)$
• • • We do not use the following data for averages, fits, limits, etc. • • •			
-0.088 ± 0.035 ± 0.013	³ CHAO	05A	BELL Repl. by CHAO 04B
-0.133 ± 0.030 ± 0.009	⁴ AUBERT,B	04K	BABR Repl. by AUBERT 07Af
-0.07 ± 0.08 ± 0.02	⁵ AUBERT	02D	BABR Repl. by AUBERT 02Q
-0.102 ± 0.050 ± 0.016	⁶ AUBERT	02Q	BABR Repl. by AUBERT,B 04K
-0.06 ± 0.09 ± 0.01	⁷ CASEY	02	BELL Repl. by CHAO 04B
0.044 ± 0.186 ± 0.018	⁸ ABE	01K	BELL Repl. by CASEY 02
-0.167 ± 0.021	⁹ AUBERT	01E	BABR Repl. by AUBERT 02Q
-0.19 ± 0.10 ± 0.03			

Meson Particle Listings

 B^0

- ¹ CHAO 04b reports significance of 3.9 standard deviation for deviation of A_{CP} from zero.
² Corresponds to 90% confidence range $-0.30 < A_{CP} < 0.22$.
³ Corresponds to a 90% CL interval of $-0.15 < A_{CP} < -0.03$.
⁴ Based on a total signal yield of $N(K^- \pi^+) + N(K^+ \pi^-) = 1606 \pm 51$ events.
⁵ Corresponds to 90% confidence range $-0.21 < A_{CP} < 0.07$.
⁶ Corresponds to 90% confidence range $-0.188 < A_{CP} < -0.016$.
⁷ Corresponds to 90% confidence range $-0.21 < A_{CP} < +0.09$.
⁸ Corresponds to 90% confidence range $-0.25 < A_{CP} < 0.37$.
⁹ Corresponds to 90% confidence range $-0.35 < A_{CP} < -0.03$.

 $A_{CP}(B^0 \rightarrow \eta' K^*(892)^0)$

VALUE	DOCUMENT ID	TECN	COMMENT
$-0.08 \pm 0.25 \pm 0.02$	AUBERT	07E	BABR $e^+ e^- \rightarrow \Upsilon(4S)$

 $A_{CP}(B^0 \rightarrow \eta K^*(892)^0)$

VALUE	DOCUMENT ID	TECN	COMMENT
0.19 ± 0.05 OUR AVERAGE			
$0.17 \pm 0.08 \pm 0.01$	WANG	07B	BELL $e^+ e^- \rightarrow \Upsilon(4S)$
$0.21 \pm 0.06 \pm 0.02$	AUBERT,B	06H	BABR $e^+ e^- \rightarrow \Upsilon(4S)$
••• We do not use the following data for averages, fits, limits, etc. •••			
$0.02 \pm 0.11 \pm 0.02$	AUBERT,B	04D	BABR Repl. by AUBERT,B 06H

 $A_{CP}(B^0 \rightarrow K^0 K^0)$

VALUE (units 10^{-6})	DOCUMENT ID	TECN	COMMENT
$-0.58 \pm 0.73 \pm 0.04$	LIN	07	BELL $e^+ e^- \rightarrow \Upsilon(4S)$

 $A_{CP}(B^0 \rightarrow \eta K_2^*(1430)^0)$

VALUE	DOCUMENT ID	TECN	COMMENT
$0.06 \pm 0.13 \pm 0.02$	AUBERT,B	06H	BABR $e^+ e^- \rightarrow \Upsilon(4S)$

 $A_{CP}(B^0 \rightarrow \eta K_2^*(1430)^0)$

VALUE	DOCUMENT ID	TECN	COMMENT
$-0.07 \pm 0.19 \pm 0.02$	AUBERT,B	06H	BABR $e^+ e^- \rightarrow \Upsilon(4S)$

 $A_{CP}(B^0 \rightarrow \rho^+ K^-)$

VALUE	DOCUMENT ID	TECN	COMMENT
-0.08 ± 0.24 OUR AVERAGE			Error includes scale factor of 1.7.
$0.22 \pm 0.22 \pm 0.06$	¹ CHANG	04	BELL $e^+ e^- \rightarrow \Upsilon(4S)$
$-0.23 \pm 0.23 \pm 0.02$			
$-0.28 \pm 0.17 \pm 0.08$	² AUBERT	03T	BABR $e^+ e^- \rightarrow \Upsilon(4S)$
¹ Corresponds to 90% confidence range $-0.18 < A_{CP} < 0.64$.			
² The result reported corresponds to $-A_{CP}$.			

 $A_{CP}(B^0 \rightarrow K^+ \pi^- \pi^0)$

VALUE	DOCUMENT ID	TECN	COMMENT
$0.07 \pm 0.11 \pm 0.01$	¹ CHANG	04	BELL $e^+ e^- \rightarrow \Upsilon(4S)$
¹ Corresponds to 90% confidence range $-0.12 < A_{CP} < 0.26$.			

 $A_{CP}(B^0 \rightarrow K^*(892)^+ \pi^-)$

VALUE	DOCUMENT ID	TECN	COMMENT
-0.05 ± 0.14 OUR AVERAGE			
$-0.11 \pm 0.14 \pm 0.05$	AUBERT	06i	BABR $e^+ e^- \rightarrow \Upsilon(4S)$
$0.26 \pm 0.33 \pm 0.10$	¹ EISENSTEIN	03	CLE2 $e^+ e^- \rightarrow \Upsilon(4S)$
-0.34 ± 0.08			
••• We do not use the following data for averages, fits, limits, etc. •••			
$0.23 \pm 0.18 \pm 0.09$	AUBERT,B	04o	BABR Repl. by AUBERT 06i
-0.06			
¹ Corresponds to 90% confidence range $-0.31 < A_{CP} < 0.78$.			

 $A_{CP}(B^0 \rightarrow K^*(892)^0 \rho^0)$

VALUE	DOCUMENT ID	TECN	COMMENT
$0.09 \pm 0.19 \pm 0.02$	AUBERT,B	06G	BABR $e^+ e^- \rightarrow \Upsilon(4S)$

 $A_{CP}(B^0 \rightarrow a_1^- K^+)$

VALUE	DOCUMENT ID	TECN	COMMENT
$-0.16 \pm 0.12 \pm 0.01$	AUBERT	08F	BABR $e^+ e^- \rightarrow \Upsilon(4S)$

 $A_{CP}(B^0 \rightarrow K^*(892)^0 \pi^+ \pi^-)$

VALUE	DOCUMENT ID	TECN	COMMENT
$+0.07 \pm 0.04 \pm 0.03$	AUBERT	07As	BABR $e^+ e^- \rightarrow \Upsilon(4S)$

 $A_{CP}(B^0 \rightarrow K^*(892)^0 K^+ K^-)$

VALUE	DOCUMENT ID	TECN	COMMENT
$+0.01 \pm 0.05 \pm 0.02$	AUBERT	07As	BABR $e^+ e^- \rightarrow \Upsilon(4S)$

 $A_{CP}(B^0 \rightarrow K^*(892)^0 \phi)$

VALUE	DOCUMENT ID	TECN	COMMENT
-0.01 ± 0.06 OUR AVERAGE			
$-0.03 \pm 0.07 \pm 0.03$	AUBERT	07D	BABR $e^+ e^- \rightarrow \Upsilon(4S)$
$0.02 \pm 0.09 \pm 0.02$	¹ CHEN	05A	BELL $e^+ e^- \rightarrow \Upsilon(4S)$

- We do not use the following data for averages, fits, limits, etc. •••

$-0.01 \pm 0.09 \pm 0.02$	AUBERT,B	04W	BABR Repl. by AUBERT 07D
$0.04 \pm 0.12 \pm 0.02$	AUBERT	03V	BABR Repl. by AUBERT 04W
$0.07 \pm 0.15 \pm 0.05$	² CHEN	03B	BELL Repl. by CHEN 05A
-0.03			
$0.00 \pm 0.27 \pm 0.03$	³ AUBERT	02E	BABR Repl. by AUBERT 03V
¹ Corresponds to 90% confidence range $-0.14 < A_{CP} < 0.17$.			
² Corresponds to 90% confidence range $-0.18 < A_{CP} < 0.33$.			
³ Corresponds to 90% confidence range $-0.44 < A_{CP} < 0.44$.			

 $A_{CP}(B^0 \rightarrow K^*(892)^0 K^- \pi^+)$

VALUE	DOCUMENT ID	TECN	COMMENT
$+0.22 \pm 0.33 \pm 0.20$	AUBERT	07As	BABR $e^+ e^- \rightarrow \Upsilon(4S)$

 $A_{CP}(B^0 \rightarrow \phi(K\pi)_0^0)$

VALUE	DOCUMENT ID	TECN	COMMENT
$0.17 \pm 0.15 \pm 0.03$	AUBERT	07D	BABR $e^+ e^- \rightarrow \Upsilon(4S)$

 $A_{CP}(B^0 \rightarrow \phi K_2^*(1430)^0)$

VALUE	DOCUMENT ID	TECN	COMMENT
$-0.12 \pm 0.14 \pm 0.04$	AUBERT	07D	BABR $e^+ e^- \rightarrow \Upsilon(4S)$

 $A_{CP}(B^0 \rightarrow \rho^+ \pi^-)$

VALUE	DOCUMENT ID	TECN	COMMENT
0.08 ± 0.12 OUR AVERAGE			Error includes scale factor of 2.0.
$-0.03 \pm 0.07 \pm 0.04$	¹ AUBERT	07AA	BABR $e^+ e^- \rightarrow \Upsilon(4S)$
$0.21 \pm 0.08 \pm 0.04$	KUSAKA	07	BELL $e^+ e^- \rightarrow \Upsilon(4S)$
••• We do not use the following data for averages, fits, limits, etc. •••			
$-0.02 \pm 0.16 \pm 0.05$	WANG	05	BELL Repl. by KUSAKA 07
-0.02			
$0.18 \pm 0.08 \pm 0.03$	¹ AUBERT	03T	BABR Repl. by AUBERT 07AA
¹ The result reported corresponds to $-A_{CP}$.			

 $A_{CP}(B^0 \rightarrow \rho^- \pi^+)$

VALUE	DOCUMENT ID	TECN	COMMENT
-0.16 ± 0.23 OUR AVERAGE			Error includes scale factor of 1.7.
$-0.37 \pm 0.16 \pm 0.09$	AUBERT	07AA	BABR $e^+ e^- \rightarrow \Upsilon(4S)$
-0.10			
$0.08 \pm 0.16 \pm 0.11$	KUSAKA	07	BELL $e^+ e^- \rightarrow \Upsilon(4S)$
••• We do not use the following data for averages, fits, limits, etc. •••			
$-0.53 \pm 0.29 \pm 0.09$	WANG	05	BELL Repl. by KUSAKA 07
-0.04			

 $A_{CP}(B^0 \rightarrow \rho^0 \pi^0)$

VALUE	DOCUMENT ID	TECN	COMMENT
$-0.49 \pm 0.36 \pm 0.28$	KUSAKA	07	BELL $e^+ e^- \rightarrow \Upsilon(4S)$
••• We do not use the following data for averages, fits, limits, etc. •••			
$-0.53 \pm 0.67 \pm 0.10$	DRAGIC	06	BELL Repl. by KUSAKA 07
-0.84 ± 0.15			

 $A_{CP}(B^0 \rightarrow a_1(1260)^\pm \pi^\mp)$

VALUE	DOCUMENT ID	TECN	COMMENT
$-0.07 \pm 0.07 \pm 0.02$	AUBERT	07o	BABR $e^+ e^- \rightarrow \Upsilon(4S)$

 $A_{CP}(B^0 \rightarrow b_1 \pi^+)$

VALUE	DOCUMENT ID	TECN	COMMENT
$-0.05 \pm 0.10 \pm 0.02$	AUBERT	07Bi	BABR $e^+ e^- \rightarrow \Upsilon(4S)$

 $A_{CP}(B^0 \rightarrow K^*(1430) \gamma)$

VALUE	DOCUMENT ID	TECN	COMMENT
$-0.08 \pm 0.15 \pm 0.01$	AUBERT,B	04U	BABR $e^+ e^- \rightarrow \Upsilon(4S)$

 $A_{CP}(B^0 \rightarrow \rho \bar{P} K^*(892)^0)$

VALUE	DOCUMENT ID	TECN	COMMENT
$+0.11 \pm 0.13 \pm 0.06$	AUBERT	07Av	BABR $e^+ e^- \rightarrow \Upsilon(4S)$

 $A_{CP}(B^0 \rightarrow \rho \bar{L} \pi^-)$

VALUE	DOCUMENT ID	TECN	COMMENT
$-0.02 \pm 0.10 \pm 0.03$	WANG	07C	BELL $e^+ e^- \rightarrow \Upsilon(4S)$

 $A_{CP}(B^0 \rightarrow b_1 K^+)$

VALUE	DOCUMENT ID	TECN	COMMENT
$-0.07 \pm 0.12 \pm 0.02$	AUBERT	07Bi	BABR $e^+ e^- \rightarrow \Upsilon(4S)$

 $C_{D^*(2010)^- D^+}(B^0 \rightarrow D^*(2010)^- D^+)$

VALUE	DOCUMENT ID	TECN	COMMENT
0.23 ± 0.13 OUR AVERAGE			
$0.23 \pm 0.15 \pm 0.04$	AUBERT	07Al	BABR $e^+ e^- \rightarrow \Upsilon(4S)$
$0.23 \pm 0.25 \pm 0.06$	¹ AUSHEV	04	BELL $e^+ e^- \rightarrow \Upsilon(4S)$
••• We do not use the following data for averages, fits, limits, etc. •••			
$0.17 \pm 0.24 \pm 0.04$	AUBERT,B	05Z	BABR Repl. by AUBERT 07Al
$-0.22 \pm 0.37 \pm 0.10$	AUBERT	03J	BABR Repl. by AUBERT,B 05Z

- ¹ Combines results from fully and partially reconstructed $B^0 \rightarrow D^{*\pm} D^\mp$ decays.

$S_{D^*(2010)-D^+} (B^0 \rightarrow D^*(2010)^- D^+)$

VALUE	DOCUMENT ID	TECN	COMMENT
-0.55 ± 0.21 OUR AVERAGE			
$-0.44 \pm 0.22 \pm 0.06$	AUBERT	07AI	BABR $e^+ e^- \rightarrow \Upsilon(4S)$
$-0.96 \pm 0.43 \pm 0.12$	¹ AUSHEV	04	BELL $e^+ e^- \rightarrow \Upsilon(4S)$
••• We do not use the following data for averages, fits, limits, etc. •••			
$-0.29 \pm 0.33 \pm 0.07$	AUBERT,B	05Z	BABR Repl. by AUBERT 07AI
$-0.24 \pm 0.69 \pm 0.12$	AUBERT	03J	BABR Repl. by AUBERT,B 05Z
¹ Combines results from fully and partially reconstructed $B^0 \rightarrow D^{*\pm} D^\mp$ decays.			

 $C_{D^*(2010)+D^-} (B^0 \rightarrow D^*(2010)^+ D^-)$

VALUE	DOCUMENT ID	TECN	COMMENT
0.01 ± 0.26 OUR AVERAGE			Error includes scale factor of 2.0.
$0.18 \pm 0.15 \pm 0.04$	AUBERT	07AI	BABR $e^+ e^- \rightarrow \Upsilon(4S)$
$-0.37 \pm 0.22 \pm 0.06$	¹ AUSHEV	04	BELL $e^+ e^- \rightarrow \Upsilon(4S)$
••• We do not use the following data for averages, fits, limits, etc. •••			
$0.09 \pm 0.25 \pm 0.06$	AUBERT,B	05Z	BABR Repl. by AUBERT 07AI
$-0.47 \pm 0.40 \pm 0.12$	AUBERT	03J	BABR Repl. by AUBERT,B 05Z
¹ Combines results from fully and partially reconstructed $B^0 \rightarrow D^{*\pm} D^\mp$ decays.			

 $S_{D^*(2010)+D^-} (B^0 \rightarrow D^*(2010)^+ D^-)$

VALUE	DOCUMENT ID	TECN	COMMENT
-0.74 ± 0.19 OUR AVERAGE			
$-0.79 \pm 0.21 \pm 0.06$	AUBERT	07AI	BABR $e^+ e^- \rightarrow \Upsilon(4S)$
$-0.55 \pm 0.39 \pm 0.12$	¹ AUSHEV	04	BELL $e^+ e^- \rightarrow \Upsilon(4S)$
••• We do not use the following data for averages, fits, limits, etc. •••			
$-0.54 \pm 0.35 \pm 0.07$	AUBERT,B	05Z	BABR Repl. by AUBERT 07AI
$-0.82 \pm 0.75 \pm 0.14$	AUBERT	03J	BABR Repl. by AUBERT,B 05Z
¹ Combines results from fully and partially reconstructed $B^0 \rightarrow D^{*\pm} D^\mp$ decays.			

 $C_{D^{*+}D^{*-}} (B^0 \rightarrow D^{*+} D^{*-})$

VALUE	DOCUMENT ID	TECN	COMMENT
0.02 ± 0.10 OUR AVERAGE			
$-0.02 \pm 0.11 \pm 0.02$	¹ AUBERT	07B0	BABR $e^+ e^- \rightarrow \Upsilon(4S)$
$0.26 \pm 0.26 \pm 0.06$	² MIYAKE	05	BELL $e^+ e^- \rightarrow \Upsilon(4S)$
••• We do not use the following data for averages, fits, limits, etc. •••			
$0.28 \pm 0.23 \pm 0.02$	³ AUBERT	03Q	BABR Repl. by AUBERT 07B0
¹ Assumes both CP -even and CP -odd states having the CP asymmetry.			
² Belle Collab. quotes $A_{D^{*+}D^{*-}}$ which is equal to $-C_{D^{*+}D^{*-}}$.			
³ AUBERT 03Q reports $ \lambda =0.75 \pm 0.19 \pm 0.02$ and $\text{Im}(\lambda)=0.05 \pm 0.29 \pm 0.10$. We convert them to S and C parameters taking into account correlations.			

 $S_{D^{*+}D^{*-}} (B^0 \rightarrow D^{*+} D^{*-})$

VALUE	DOCUMENT ID	TECN	COMMENT
-0.67 ± 0.18 OUR AVERAGE			
$-0.66 \pm 0.19 \pm 0.04$	¹ AUBERT	07B0	BABR $e^+ e^- \rightarrow \Upsilon(4S)$
$-0.75 \pm 0.56 \pm 0.12$	MIYAKE	05	BELL $e^+ e^- \rightarrow \Upsilon(4S)$
••• We do not use the following data for averages, fits, limits, etc. •••			
$0.06 \pm 0.37 \pm 0.13$	² AUBERT	03Q	BABR Repl. by AUBERT 07B0
¹ Assumes both CP -even and CP -odd states having the CP asymmetry.			
² AUBERT 03Q reports $ \lambda =0.75 \pm 0.19 \pm 0.02$ and $\text{Im}(\lambda)=0.05 \pm 0.29 \pm 0.10$. We convert them to S and C parameters taking into account correlations.			

 $C_{\pi^+} (B^0 \rightarrow D^{*+} D^{*-})$ See the note in the $C_{\pi\pi}$ datablock, but for CP even final state.

VALUE	DOCUMENT ID	TECN	COMMENT
$-0.05 \pm 0.14 \pm 0.02$			
$0.06 \pm 0.17 \pm 0.03$	¹ AUBERT,BE	05A	BABR Repl. by AUBERT 07B0
¹ AUBERT,BE 05A reports a CP -odd fraction $R_{\perp} = 0.125 \pm 0.044 \pm 0.007$.			

 $S_{\pi^+} (B^0 \rightarrow D^{*+} D^{*-})$ See the note in the $S_{\pi\pi}$ datablock, but for CP even final state.

VALUE	DOCUMENT ID	TECN	COMMENT
$-0.72 \pm 0.19 \pm 0.05$			
$-0.75 \pm 0.25 \pm 0.03$	¹ AUBERT,BE	05A	BABR Repl. by AUBERT 07B0
¹ AUBERT,BE 05A reports a CP -odd fraction $R_{\perp} = 0.125 \pm 0.044 \pm 0.007$.			

 $C_{\pi^-} (B^0 \rightarrow D^{*+} D^{*-})$ See the note in the $C_{\pi\pi}$ datablock, but for CP odd final state.

VALUE	DOCUMENT ID	TECN	COMMENT
$+0.23 \pm 0.67 \pm 0.10$			
$-0.20 \pm 0.96 \pm 0.11$	¹ AUBERT,BE	05A	BABR Repl. by AUBERT 07B0
¹ AUBERT,BE 05A reports a CP -odd fraction $R_{\perp} = 0.125 \pm 0.044 \pm 0.007$.			

 $S_{\pi^-} (B^0 \rightarrow D^{*+} D^{*-})$ See the note in the $S_{\pi\pi}$ datablock, but for CP odd final state.

VALUE	DOCUMENT ID	TECN	COMMENT
$-1.83 \pm 1.04 \pm 0.23$			
$-1.75 \pm 1.78 \pm 0.22$	¹ AUBERT,BE	05A	BABR Repl. by AUBERT 07B0
¹ AUBERT,BE 05A reports a CP -odd fraction $R_{\perp} = 0.125 \pm 0.044 \pm 0.007$.			

 $C (B^0 \rightarrow D^*(2010)^+ D^*(2010)^- K_S^0)$

VALUE	DOCUMENT ID	TECN	COMMENT
$0.01 \pm 0.28 \pm 0.09$	¹ DALSENO	07	BELL $e^+ e^- \rightarrow \Upsilon(4S)$
¹ Reports value of A which is equal to $-C$.			

 $S (B^0 \rightarrow D^*(2010)^+ D^*(2010)^- K_S^0)$

VALUE	DOCUMENT ID	TECN	COMMENT
$0.06 \pm 0.45 \pm 0.06$	¹ DALSENO	07	BELL $e^+ e^- \rightarrow \Upsilon(4S)$
¹ This value includes an unknown CP dilution factor D due to possible contributions from intermediate resonances and different partial waves.			

 $C_{D^+D^-} (B^0 \rightarrow D^+ D^-)$

VALUE	DOCUMENT ID	TECN	COMMENT
-0.4 ± 0.5 OUR AVERAGE			Error includes scale factor of 3.1.
$0.11 \pm 0.22 \pm 0.07$	AUBERT	07AI	BABR $e^+ e^- \rightarrow \Upsilon(4S)$
$-0.91 \pm 0.23 \pm 0.06$	¹ FRATINA	07	BELL $e^+ e^- \rightarrow \Upsilon(4S)$
••• We do not use the following data for averages, fits, limits, etc. •••			
$0.11 \pm 0.35 \pm 0.06$	AUBERT,B	05Z	BABR Repl. by AUBERT 07AI
¹ The paper reports A , which is equal to $-C$.			

 $S_{D^+D^-} (B^0 \rightarrow D^+ D^-)$

VALUE	DOCUMENT ID	TECN	COMMENT
-0.81 ± 0.29 OUR AVERAGE			Error includes scale factor of 1.1.
$-0.54 \pm 0.34 \pm 0.06$	AUBERT	07AI	BABR $e^+ e^- \rightarrow \Upsilon(4S)$
$-1.13 \pm 0.37 \pm 0.09$	FRATINA	07	BELL $e^+ e^- \rightarrow \Upsilon(4S)$
••• We do not use the following data for averages, fits, limits, etc. •••			
$-0.29 \pm 0.63 \pm 0.06$	AUBERT,B	05Z	BABR Repl. by AUBERT 07AI

 $C_{J/\psi(1S)\pi^0} (B^0 \rightarrow J/\psi(1S)\pi^0)$

VALUE	DOCUMENT ID	TECN	COMMENT
-0.11 ± 0.20 OUR AVERAGE			
$-0.21 \pm 0.26 \pm 0.06$	AUBERT,B	06B	BABR $e^+ e^- \rightarrow \Upsilon(4S)$
$0.01 \pm 0.29 \pm 0.03$	¹ KATAOKA	04	BELL $e^+ e^- \rightarrow \Upsilon(4S)$
••• We do not use the following data for averages, fits, limits, etc. •••			
$0.38 \pm 0.41 \pm 0.09$	AUBERT	03N	BABR Repl. by AUBERT,B 06B
¹ BELLE Collab. quotes $A_{J/\psi\pi^0}$ which is equal to $-C_{J/\psi\pi^0}$.			

 $S_{J/\psi(1S)\pi^0} (B^0 \rightarrow J/\psi(1S)\pi^0)$

VALUE	DOCUMENT ID	TECN	COMMENT
-0.69 ± 0.25 OUR AVERAGE			
$-0.68 \pm 0.30 \pm 0.04$	AUBERT,B	06B	BABR $e^+ e^- \rightarrow \Upsilon(4S)$
$-0.72 \pm 0.42 \pm 0.09$	KATAOKA	04	BELL $e^+ e^- \rightarrow \Upsilon(4S)$
••• We do not use the following data for averages, fits, limits, etc. •••			
$0.05 \pm 0.49 \pm 0.16$	AUBERT	03N	BABR Repl. by AUBERT,B 06B

 $C_{D_{CP}^{(*)}h^0} (B^0 \rightarrow D_{CP}^{(*)}h^0)$

VALUE	DOCUMENT ID	TECN	COMMENT
$-0.23 \pm 0.16 \pm 0.04$			
$0.19 \pm 0.11 \pm 0.05$	AUBERT	07AJ	BABR $e^+ e^- \rightarrow \Upsilon(4S)$

 $S_{D_{CP}^{(*)}h^0} (B^0 \rightarrow D_{CP}^{(*)}h^0)$

VALUE	DOCUMENT ID	TECN	COMMENT
$-0.56 \pm 0.23 \pm 0.05$			
$0.19 \pm 0.11 \pm 0.05$	AUBERT	07AJ	BABR $e^+ e^- \rightarrow \Upsilon(4S)$

 $S_{K_S^0 K_S^0} (B^0 \rightarrow K_S^0 K_S^0)$

VALUE	DOCUMENT ID	TECN	COMMENT
$-1.28 \pm 0.80 \pm 0.11$			
-0.73 ± 0.16	AUBERT,BE	06C	BABR $e^+ e^- \rightarrow \Upsilon(4S)$

 $C_{K_S^0 K_S^0} (B^0 \rightarrow K_S^0 K_S^0)$

VALUE	DOCUMENT ID	TECN	COMMENT
$-0.40 \pm 0.41 \pm 0.06$			
$0.19 \pm 0.11 \pm 0.05$	AUBERT,BE	06C	BABR $e^+ e^- \rightarrow \Upsilon(4S)$

 $C_{\eta(958)\kappa} (B^0 \rightarrow \eta(958) K_S^0)$

VALUE	DOCUMENT ID	TECN	COMMENT
-0.04 ± 0.20 OUR AVERAGE			Error includes scale factor of 2.5.
$-0.21 \pm 0.10 \pm 0.02$	AUBERT	05M	BABR $e^+ e^- \rightarrow \Upsilon(4S)$
$0.19 \pm 0.11 \pm 0.05$	¹ CHEN	05B	BELL $e^+ e^- \rightarrow \Upsilon(4S)$
••• We do not use the following data for averages, fits, limits, etc. •••			
$-0.26 \pm 0.22 \pm 0.03$	¹ ABE	03C	BELL Repl. by ABE 03H
$0.01 \pm 0.16 \pm 0.04$	¹ ABE	03H	BELL Repl. by CHEN 05B
$0.10 \pm 0.22 \pm 0.04$	AUBERT	03W	BABR Repl. by AUBERT 05M
$-0.13 \pm 0.32 \pm 0.06$	¹ CHEN	02B	BELL Repl. by ABE 03C

¹ BELLE Collab. quotes $A_{\eta(958)K_S^0}$ which is equal to $-C_{\eta(958)K_S^0}$.

Meson Particle Listings

 B^0 $S_{\eta(958)K}(B^0 \rightarrow \eta(958)K_S^0)$

VALUE	DOCUMENT ID	TECN	COMMENT
0.43 ± 0.17 OUR AVERAGE	Error includes scale factor of 1.5.		
$0.30 \pm 0.14 \pm 0.02$	AUBERT	05M	BABR $e^+e^- \rightarrow \Upsilon(4S)$
$+0.65 \pm 0.18 \pm 0.04$	CHEN	05B	BELL $e^+e^- \rightarrow \Upsilon(4S)$
• • • We do not use the following data for averages, fits, limits, etc. • • •			
$0.71 \pm 0.37 \pm 0.05$ -0.06	ABE	03C	BELL Repl. by ABE 03H
$0.43 \pm 0.27 \pm 0.05$	ABE	03H	BELL Repl. by CHEN 05B
$0.02 \pm 0.34 \pm 0.03$	AUBERT	03W	BABR Repl. by AUBERT 05M
$0.28 \pm 0.55 \pm 0.07$ -0.08	CHEN	02B	BELL Repl. by ABE 03C

 $C_{\eta K^0}(B^0 \rightarrow \eta K^0)$

VALUE	DOCUMENT ID	TECN	COMMENT
-0.09 ± 0.08 OUR AVERAGE	Error includes scale factor of 1.5.		
$-0.16 \pm 0.07 \pm 0.03$	¹ AUBERT	07A	BABR $e^+e^- \rightarrow \Upsilon(4S)$
$0.01 \pm 0.07 \pm 0.05$	¹ CHEN	07	BELL $e^+e^- \rightarrow \Upsilon(4S)$

¹ The mixing-induced CP violation is reported with a significance of more than 5 standard deviations in this $b \rightarrow s$ penguin dominated mode.

² The paper reports A , which is equal to $-C$.

 $S_{\eta K^0}(B^0 \rightarrow \eta K^0)$

VALUE	DOCUMENT ID	TECN	COMMENT
0.61 ± 0.07 OUR AVERAGE			
$0.58 \pm 0.10 \pm 0.03$	¹ AUBERT	07A	BABR $e^+e^- \rightarrow \Upsilon(4S)$
$0.64 \pm 0.10 \pm 0.04$	¹ CHEN	07	BELL $e^+e^- \rightarrow \Upsilon(4S)$

¹ The mixing-induced CP violation is reported with a significance of more than 5 standard deviations in this $b \rightarrow s$ penguin dominated mode.

 $C_{\omega K_S^0}(B^0 \rightarrow \omega K_S^0)$

VALUE	DOCUMENT ID	TECN	COMMENT
-0.25 ± 0.31 OUR AVERAGE	Error includes scale factor of 1.6.		
$+0.09 \pm 0.29 \pm 0.06$	¹ CHAO	07	BELL $e^+e^- \rightarrow \Upsilon(4S)$
$-0.55 \pm 0.28 \pm 0.03$ -0.26	AUBERT,B	06E	BABR $e^+e^- \rightarrow \Upsilon(4S)$
• • • We do not use the following data for averages, fits, limits, etc. • • •			
$-0.27 \pm 0.48 \pm 0.15$	¹ CHEN	05B	BELL Repl. by CHAO 07

¹ Belle Collab. quotes $A_{\omega K_S^0}$ which is equal to $-C_{\omega K_S^0}$.

 $S_{\omega K_S^0}(B^0 \rightarrow \omega K_S^0)$

VALUE	DOCUMENT ID	TECN	COMMENT
0.35 ± 0.29 OUR AVERAGE			
$+0.11 \pm 0.46 \pm 0.07$	CHAO	07	BELL $e^+e^- \rightarrow \Upsilon(4S)$
$+0.51 \pm 0.35 \pm 0.02$ -0.39	AUBERT,B	06E	BABR $e^+e^- \rightarrow \Upsilon(4S)$
• • • We do not use the following data for averages, fits, limits, etc. • • •			
$+0.76 \pm 0.65 \pm 0.13$ -0.16	CHEN	05B	BELL Repl. by CHAO 07

 $C_{f_0(980)K_S^0}(B^0 \rightarrow f_0(980)K_S^0)$

VALUE	DOCUMENT ID	TECN	COMMENT
-0.03 ± 0.26 OUR AVERAGE	Error includes scale factor of 1.9.		
$-0.41 \pm 0.23 \pm 0.07$	¹ AUBERT	07AX	BABR $e^+e^- \rightarrow \Upsilon(4S)$
$+0.15 \pm 0.15 \pm 0.07$	¹ CHAO	07	BELL $e^+e^- \rightarrow \Upsilon(4S)$
• • • We do not use the following data for averages, fits, limits, etc. • • •			
$+0.39 \pm 0.27 \pm 0.09$	¹ CHEN	05B	BELL Repl. by CHAO 07

¹ Quotes $A_{f_0(980)K_S^0}$ which is equal to $-C_{f_0(980)K_S^0}$.

 $S_{f_0(980)K_S^0}(B^0 \rightarrow f_0(980)K_S^0)$

VALUE	DOCUMENT ID	TECN	COMMENT
-0.02 ± 0.21 OUR AVERAGE	Error includes scale factor of 1.1.		
$-0.25 \pm 0.26 \pm 0.10$	¹ AUBERT	07AX	BABR $e^+e^- \rightarrow \Upsilon(4S)$
$+0.18 \pm 0.23 \pm 0.11$	CHAO	07	BELL $e^+e^- \rightarrow \Upsilon(4S)$
• • • We do not use the following data for averages, fits, limits, etc. • • •			
$+0.47 \pm 0.41 \pm 0.08$	CHEN	05B	BELL Repl. by CHAO 07

¹ Reports β_{eff} . We quote S obtained from epaps: E-PRLTAO-99-076741.

 $C_{K_S K_S K_S}(B^0 \rightarrow K_S K_S K_S)$

VALUE	DOCUMENT ID	TECN	COMMENT
-0.15 ± 0.16 OUR AVERAGE	Error includes scale factor of 1.1.		
$+0.02 \pm 0.21 \pm 0.05$	AUBERT	07AT	BABR $e^+e^- \rightarrow \Upsilon(4S)$
$-0.31 \pm 0.20 \pm 0.07$	¹ CHEN	07	BELL $e^+e^- \rightarrow \Upsilon(4S)$
• • • We do not use the following data for averages, fits, limits, etc. • • •			
$-0.34 \pm 0.28 \pm 0.05$ -0.25	AUBERT,B	05	BABR Repl. by AUBERT 07AT
$-0.54 \pm 0.34 \pm 0.09$	¹ SUMISAWA	05	BELL Repl. by CHEN 07

¹ Belle Collab. quotes $A_{K_S K_S K_S}$ which is equal to $-C_{K_S K_S K_S}$.

 $S_{K_S K_S K_S}(B^0 \rightarrow K_S K_S K_S)$

VALUE	DOCUMENT ID	TECN	COMMENT
-0.4 ± 0.5 OUR AVERAGE	Error includes scale factor of 2.5.		
$-0.71 \pm 0.24 \pm 0.04$	AUBERT	07AT	BABR $e^+e^- \rightarrow \Upsilon(4S)$
$0.30 \pm 0.32 \pm 0.08$	CHEN	07	BELL $e^+e^- \rightarrow \Upsilon(4S)$
• • • We do not use the following data for averages, fits, limits, etc. • • •			
$-0.71 \pm 0.38 \pm 0.04$ -0.32	AUBERT,B	05	BABR Repl. by AUBERT 07AT
$1.26 \pm 0.68 \pm 0.20$	SUMISAWA	05	BELL Repl. by CHEN 07.

 $C_{K^+K^-K_S^0}(B^0 \rightarrow K^+K^-K_S^0)$

VALUE	DOCUMENT ID	TECN	COMMENT
0.07 ± 0.08 OUR AVERAGE			
$0.054 \pm 0.102 \pm 0.060$	^{1,2} AUBERT	07AX	BABR $e^+e^- \rightarrow \Upsilon(4S)$
$0.09 \pm 0.10 \pm 0.05$	^{1,2} CHAO	07	BELL $e^+e^- \rightarrow \Upsilon(4S)$
• • • We do not use the following data for averages, fits, limits, etc. • • •			
$0.10 \pm 0.14 \pm 0.04$	² AUBERT	05T	BABR Repl. by AUBERT 07AX
$0.09 \pm 0.12 \pm 0.07$	¹ CHEN	05B	BELL Repl. by CHAO 07
$-0.10 \pm 0.19 \pm 0.10$	² AUBERT,B	04V	BABR Repl. by AUBERT 05T
$0.40 \pm 0.33 \pm 0.28$ -0.10	¹ ABE	03C	BELL Repl. by ABE 03H
$0.17 \pm 0.16 \pm 0.04$	^{1,2} ABE	03H	BELL Repl. by CHEN 05B

¹ Quotes $A_{K^+K^-K_S^0}$ which is equal to $-C_{K^+K^-K_S^0}$.

² Excludes the events from $B^0 \rightarrow \phi K_S^0$ decay. The results are derived from a combined sample of $K^+K^-K_S^0$ and $K^+K^-K_L^0$ decays.

 $S_{K^+K^-K_S^0}(B^0 \rightarrow K^+K^-K_S^0)$

VALUE	DOCUMENT ID	TECN	COMMENT
-0.74 ± 0.12 OUR AVERAGE -0.10			
$-0.764 \pm 0.111 \pm 0.071$ -0.040	^{1,2} AUBERT	07AX	BABR $e^+e^- \rightarrow \Upsilon(4S)$
$-0.68 \pm 0.15 \pm 0.21$ -0.13	¹ CHAO	07	BELL $e^+e^- \rightarrow \Upsilon(4S)$
• • • We do not use the following data for averages, fits, limits, etc. • • •			
$-0.42 \pm 0.17 \pm 0.03$	^{1,3} AUBERT	05T	BABR Repl. by AUBERT 07AX
$-0.49 \pm 0.18 \pm 0.04$	CHEN	05B	BELL Repl. by CHAO 07
$-0.56 \pm 0.25 \pm 0.04$	^{1,4} AUBERT,B	04V	BABR Repl. by AUBERT 05T
$-0.49 \pm 0.43 \pm 0.11$	ABE	03C	BELL Repl. by ABE 03H
$-0.51 \pm 0.26 \pm 0.05$	^{1,5} ABE	03H	BELL Repl. by CHEN 05B

¹ Excludes events from $B^0 \rightarrow \phi K_S^0$ decay. The results are derived from a combined sample of $K^+K^-K_S^0$ and $K^+K^-K_L^0$ decays.

² Reports β_{eff} . We quote S obtained from epaps: E-PRLTAO-99-076741.

³ The measured CP -even final states fraction is $0.89 \pm 0.08 \pm 0.06$.

⁴ The measured CP -even final states fraction is $0.98 \pm 0.15 \pm 0.04$.

⁵ The measured CP -even final states fraction is $1.03 \pm 0.15 \pm 0.05$.

 $C_{K^+K^-K_S^0}(B^0 \rightarrow K^+K^-K_S^0 \text{ inclusive})$

VALUE	DOCUMENT ID	TECN	COMMENT
$0.015 \pm 0.077 \pm 0.053$	^{1,2} AUBERT	07AX	BABR $e^+e^- \rightarrow \Upsilon(4S)$
• • • We do not use the following data for averages, fits, limits, etc. • • •			
¹ Measured using full Dalitz plot fit including ϕ component.			
² The results are derived from a combined sample of $K^+K^-K_S^0$ and $K^+K^-K_L^0$ decays.			

 $S_{K^+K^-K_S^0}(B^0 \rightarrow K^+K^-K_S^0 \text{ inclusive})$

VALUE	DOCUMENT ID	TECN	COMMENT
$-0.647 \pm 0.116 \pm 0.040$	¹ AUBERT	07AX	BABR $e^+e^- \rightarrow \Upsilon(4S)$
• • • We do not use the following data for averages, fits, limits, etc. • • •			
¹ Measured using full Dalitz plot fit including ϕ component.			

 $C_{\phi K_S^0}(B^0 \rightarrow \phi K_S^0)$

VALUE	DOCUMENT ID	TECN	COMMENT
-0.01 ± 0.12 OUR AVERAGE			
$0.08 \pm 0.18 \pm 0.04$	^{1,2} AUBERT	07AX	BABR $e^+e^- \rightarrow \Upsilon(4S)$
$-0.07 \pm 0.15 \pm 0.05$	^{1,2} CHEN	07	BELL $e^+e^- \rightarrow \Upsilon(4S)$
• • • We do not use the following data for averages, fits, limits, etc. • • •			
$0.00 \pm 0.23 \pm 0.05$	² AUBERT	05T	BABR Repl. by AUBERT 07AX
$-0.08 \pm 0.22 \pm 0.09$	^{1,2} CHEN	05B	BELL Repl. by CHEN 07
$0.01 \pm 0.33 \pm 0.10$	² AUBERT,B	04G	BABR Repl. by AUBERT 05T
$0.56 \pm 0.41 \pm 0.16$	¹ ABE	03C	BELL Repl. by ABE 03H
$0.15 \pm 0.29 \pm 0.07$	¹ ABE	03H	BELL Repl. by CHEN 05B

¹ Quotes $A_{\phi K_S^0}$ which is equal to $-C_{\phi K_S^0}$.

² Result combines B -meson final states ϕK_S^0 and ϕK_L^0 by assuming $S_{\phi K_S^0} = -S_{\phi K_L^0}$.

 $S_{\phi K_S^0}(B^0 \rightarrow \phi K_S^0)$

VALUE	DOCUMENT ID	TECN	COMMENT
0.39 ± 0.17 OUR AVERAGE			
$0.21 \pm 0.26 \pm 0.11$	^{1,2} AUBERT	07AX	BABR $e^+e^- \rightarrow \Upsilon(4S)$
$0.50 \pm 0.21 \pm 0.06$	¹ CHEN	07	BELL $e^+e^- \rightarrow \Upsilon(4S)$

• • • We do not use the following data for averages, fits, limits, etc. • • •

VALUE	DOCUMENT ID	TECN	COMMENT
$0.50 \pm 0.25^{+0.07}_{-0.04}$	¹ AUBERT	05T	BABR Repl. by AUBERT 07AX
$0.08 \pm 0.33 \pm 0.09$	¹ CHEN	05B	BELL Repl. by CHEN 07
$0.47 \pm 0.34^{+0.08}_{-0.06}$	¹ AUBERT,B	04G	BABR Repl. by AUBERT 05T
$-0.73 \pm 0.64 \pm 0.22$	ABE	03C	BELL Repl. by ABE 03H
$-0.96 \pm 0.50^{+0.09}_{-0.11}$	ABE	03H	BELL Repl. by CHEN 05B

¹ Result combines B -meson final states ϕK_S^0 and ϕK_L^0 by assuming $S_{\phi K_S^0} = -S_{\phi K_L^0}$

² Reports β_{eff} . We quote S obtained from epaps: E-PRLTAO-99-076741.

$C_{K_S^0 \pi^0}(B^0 \rightarrow K_S^0 \pi^0)$

VALUE	DOCUMENT ID	TECN	COMMENT
0.14 ± 0.11 OUR AVERAGE			
$+0.24 \pm 0.15 \pm 0.03$	AUBERT	08E	BABR $e^+e^- \rightarrow \Upsilon(4S)$
$+0.05 \pm 0.14 \pm 0.05$	¹ CHAO	07	BELL $e^+e^- \rightarrow \Upsilon(4S)$
• • • We do not use the following data for averages, fits, limits, etc. • • •			
$+0.06 \pm 0.18 \pm 0.03$	AUBERT	05Y	BABR Repl. by AUBERT 08E
$-0.16 \pm 0.29 \pm 0.05$	^{1,2} CHAO	05A	BELL Repl. by CHEN 05B
$+0.11 \pm 0.20 \pm 0.09$	¹ CHEN	05B	BELL Repl. by CHAO 07
$-0.03 \pm 0.36 \pm 0.11$	¹ AUBERT	04M	BABR Repl. by AUBERT,B 04M
$+0.40^{+0.27}_{-0.28} \pm 0.09$	³ AUBERT,B	04M	BABR Repl. by AUBERT 05Y

¹ Reports A which is equal to $-C$.

² Corresponds to a 90% CL interval of $-0.33 < A_{CP} < 0.64$.

³ Based on a total signal yield of 122 ± 16 events.

$S_{K_S^0 \pi^0}(B^0 \rightarrow K_S^0 \pi^0)$

VALUE	DOCUMENT ID	TECN	COMMENT
0.38 ± 0.19 OUR AVERAGE			
$+0.40 \pm 0.23 \pm 0.03$	AUBERT	08E	BABR $e^+e^- \rightarrow \Upsilon(4S)$
$+0.33 \pm 0.35 \pm 0.08$	CHAO	07	BELL $e^+e^- \rightarrow \Upsilon(4S)$
• • • We do not use the following data for averages, fits, limits, etc. • • •			
$+0.35^{+0.30}_{-0.33} \pm 0.04$	AUBERT	05Y	BABR Repl. by AUBERT 08E
$+0.32 \pm 0.61 \pm 0.13$	CHEN	05B	BELL Repl. by CHAO 07
$+0.48^{+0.38}_{-0.47} \pm 0.06$	¹ AUBERT,B	04M	BABR Repl. by AUBERT 05Y

¹ Based on a total signal yield of 122 ± 16 events.

$C(B^0 \rightarrow K_S^0 \pi^0 \pi^0)$

VALUE	DOCUMENT ID	TECN	COMMENT
$0.23 \pm 0.52 \pm 0.13$	AUBERT	07AQ	BABR $e^+e^- \rightarrow \Upsilon(4S)$

$S(B^0 \rightarrow K_S^0 \pi^0 \pi^0)$

VALUE	DOCUMENT ID	TECN	COMMENT
$0.72 \pm 0.71 \pm 0.08$	AUBERT	07AQ	BABR $e^+e^- \rightarrow \Upsilon(4S)$

$C_{K_S^0 \pi^0 \gamma}(B^0 \rightarrow K_S^0 \pi^0 \gamma)$

VALUE	DOCUMENT ID	TECN	COMMENT
0.0 ± 0.4 OUR AVERAGE			Error includes scale factor of 2.1.
$+0.20 \pm 0.20 \pm 0.06$	^{1,2} USHIRODA	06	BELL $e^+e^- \rightarrow \Upsilon(4S)$
$-1.0 \pm 0.5 \pm 0.2$	³ AUBERT,B	05P	BABR $e^+e^- \rightarrow \Upsilon(4S)$
• • • We do not use the following data for averages, fits, limits, etc. • • •			
$-0.03 \pm 0.34 \pm 0.11$	² USHIRODA	05	BELL Repl. by USHIRODA 06
¹ Requires $M_{K_S^0 \pi^0} < 1.8$ GeV/ c^2 .			
² Reports $A_{K_S^0 \pi^0 \gamma}$, which is $-C_{K_S^0 \pi^0 \gamma}$.			
³ Requires $1.1 < M_{K_S^0 \pi^0} < 1.8$ GeV/ c^2 .			

$S_{K_S^0 \pi^0 \gamma}(B^0 \rightarrow K_S^0 \pi^0 \gamma)$

VALUE	DOCUMENT ID	TECN	COMMENT
-0.01 ± 0.30 OUR AVERAGE			
$-0.10 \pm 0.31 \pm 0.07$	¹ USHIRODA	06	BELL $e^+e^- \rightarrow \Upsilon(4S)$
$0.9 \pm 1.0 \pm 0.2$	² AUBERT,B	05P	BABR $e^+e^- \rightarrow \Upsilon(4S)$
• • • We do not use the following data for averages, fits, limits, etc. • • •			
$-0.58^{+0.46}_{-0.38} \pm 0.11$	USHIRODA	05	BELL Repl. by USHIRODA 06

¹ Requires $M_{K_S^0 \pi^0} < 1.8$ GeV/ c^2 .

² Requires $1.1 < M_{K_S^0 \pi^0} < 1.8$ GeV/ c^2 .

$C_{K^*(892)^0 \gamma}(B^0 \rightarrow K^*(892)^0 \gamma)$

VALUE	DOCUMENT ID	TECN	COMMENT
-0.12 ± 0.30 OUR AVERAGE			Error includes scale factor of 1.8.
$+0.20 \pm 0.24 \pm 0.05$	^{1,2} USHIRODA	06	BELL $e^+e^- \rightarrow \Upsilon(4S)$
$-0.40 \pm 0.23 \pm 0.03$	AUBERT,B	05P	BABR $e^+e^- \rightarrow \Upsilon(4S)$
• • • We do not use the following data for averages, fits, limits, etc. • • •			
$-0.57 \pm 0.32 \pm 0.09$	³ AUBERT,B	04Z	BABR Repl. by AUBERT,B 05P

¹ Reports value of A which is equal to $-C$.

² Requires $0.8 < M_{K^*(892)^0} < 1.0$ GeV/ c^2 .

³ Based on a total signal of 105 ± 14 events with $K^*(892)^0 \rightarrow K_S^0 \pi^0$ only.

$S_{K^*(892)^0 \gamma}(B^0 \rightarrow K^*(892)^0 \gamma)$

VALUE	DOCUMENT ID	TECN	COMMENT
-0.27 ± 0.26 OUR AVERAGE			
$-0.32^{+0.36}_{-0.33} \pm 0.05$	¹ USHIRODA	06	BELL $e^+e^- \rightarrow \Upsilon(4S)$
$-0.21 \pm 0.40 \pm 0.05$	AUBERT,B	05P	BABR $e^+e^- \rightarrow \Upsilon(4S)$
• • • We do not use the following data for averages, fits, limits, etc. • • •			
$-0.79^{+0.63}_{-0.50} \pm 0.10$	² USHIRODA	05	BELL Repl. by USHIRODA 06
$0.25 \pm 0.63 \pm 0.14$	³ AUBERT,B	04Z	BABR Repl. by AUBERT,B 05P
¹ Requires $0.8 < M_{K^*(892)^0} < 1.0$ GeV/ c^2 .			
² Assumes $C(B^0 \rightarrow K^*(892)^0 \gamma) = 0$.			
³ Based on a total signal of 105 ± 14 events with $K^*(892)^0 \rightarrow K_S^0 \pi^0$ only.			

$C(B^0 \rightarrow \rho^0 \gamma)$

VALUE	DOCUMENT ID	TECN	COMMENT
$+0.44 \pm 0.49 \pm 0.14$	¹ USHIRODA	08	BELL $e^+e^- \rightarrow \Upsilon(4S)$
¹ Reports value of A which is equal to $-C$.			

$S(B^0 \rightarrow \rho^0 \gamma)$

VALUE	DOCUMENT ID	TECN	COMMENT
$-0.83 \pm 0.65 \pm 0.18$	USHIRODA	08	BELL $e^+e^- \rightarrow \Upsilon(4S)$

$C_{\pi\pi}(B^0 \rightarrow \pi^+ \pi^-)$

$C_{\pi\pi}$ is defined as $(1-|\lambda|^2)/(1+|\lambda|^2)$, where the quantity $\lambda=q/p \bar{A}_f/A_f$ is a phase convention independent observable quantity for the final state f . For details, see the review on "CP Violation" in the Reviews section.

VALUE	DOCUMENT ID	TECN	COMMENT
-0.38 ± 0.17 OUR AVERAGE			Error includes scale factor of 2.6.
$-0.21 \pm 0.09 \pm 0.02$	AUBERT	07AF	BABR $e^+e^- \rightarrow \Upsilon(4S)$
$-0.55 \pm 0.08 \pm 0.05$	¹ ISHINO	07	BELL $e^+e^- \rightarrow \Upsilon(4S)$
• • • We do not use the following data for averages, fits, limits, etc. • • •			
$-0.56 \pm 0.12 \pm 0.06$	¹ ABE	05D	BELL Repl. by ISHINO 07
$-0.09 \pm 0.15 \pm 0.04$	AUBERT,BE	05	BABR Repl. by AUBERT 07AF
$-0.58 \pm 0.15 \pm 0.07$	¹ ABE	04E	BELL Repl. by ABE 05D
$-0.77 \pm 0.27 \pm 0.08$	¹ ABE	03G	BELL Repl. by ABE 04E.
$-0.94^{+0.31}_{-0.25} \pm 0.09$	¹ ABE	02M	BELL Repl. by ABE 03G
$-0.25^{+0.45}_{-0.47} \pm 0.14$	² AUBERT	02D	BABR Repl. by AUBERT 02Q
$-0.30 \pm 0.25 \pm 0.04$	³ AUBERT	02Q	BABR Repl. by AUBERT,BE 05
¹ Paper reports $A_{\pi\pi}$ which equals to $-C_{\pi\pi}$.			
² Corresponds to 90% confidence range $-1.0 < C_{\pi\pi} < 0.47$.			
³ Corresponds to 90% confidence range $-0.72 < C_{\pi\pi} < 0.12$.			

$S_{\pi\pi}(B^0 \rightarrow \pi^+ \pi^-)$

$S_{\pi\pi} = 2\text{Im}\lambda/(1+|\lambda|^2)$, see the note in the $C_{\pi\pi}$ datablock above.

VALUE	DOCUMENT ID	TECN	COMMENT
-0.61 ± 0.08 OUR AVERAGE			
$-0.60 \pm 0.11 \pm 0.03$	AUBERT	07AF	BABR $e^+e^- \rightarrow \Upsilon(4S)$
$-0.61 \pm 0.10 \pm 0.04$	ISHINO	07	BELL $e^+e^- \rightarrow \Upsilon(4S)$
• • • We do not use the following data for averages, fits, limits, etc. • • •			
$-0.67 \pm 0.16 \pm 0.06$	¹ ABE	05D	BELL Repl. by ISHINO 07
$-0.30 \pm 0.17 \pm 0.03$	AUBERT,BE	05	BABR Repl. by AUBERT 07AF
$-1.00 \pm 0.21 \pm 0.07$	² ABE	04E	BELL Repl. by ABE 05D
$-1.23 \pm 0.41^{+0.08}_{-0.07}$	ABE	03G	BELL Repl. by ABE 04E.
$-1.21^{+0.38}_{-0.27} \pm 0.13$	ABE	02M	BELL Repl. by ABE 03G
$0.03^{+0.52}_{-0.56} \pm 0.11$	³ AUBERT	02D	BABR Repl. by AUBERT 02Q
$0.02 \pm 0.34 \pm 0.05$	⁴ AUBERT	02Q	BABR Repl. by AUBERT,BE 05
¹ Rule out the CP -conserving case, $C_{\pi\pi} = S_{\pi\pi} = 0$, at the 5.4 sigma level.			
² Rule out the CP -conserving case, $C_{\pi\pi} = S_{\pi\pi} = 0$, at the 5.2 sigma level.			
³ Corresponds to 90% confidence range $-0.89 < S_{\pi\pi} < 0.85$.			
⁴ Corresponds to 90% confidence range $-0.54 < S_{\pi\pi} < 0.58$.			

$C_{\pi^0 \pi^0}(B^0 \rightarrow \pi^0 \pi^0)$

VALUE	DOCUMENT ID	TECN	COMMENT
-0.48 ± 0.30 OUR AVERAGE			
$-0.49 \pm 0.35 \pm 0.05$	AUBERT	07Bc	BABR $e^+e^- \rightarrow \Upsilon(4S)$
$-0.44^{+0.52}_{-0.53} \pm 0.17$	¹ CHAO	05	BELL $e^+e^- \rightarrow \Upsilon(4S)$
• • • We do not use the following data for averages, fits, limits, etc. • • •			
$-0.12 \pm 0.56 \pm 0.06$	² AUBERT	05L	BABR Repl. by AUBERT 07Bc

¹ BELLE Collab. quotes $A_{\pi^0 \pi^0}$ which is equal to $-C_{\pi^0 \pi^0}$.

² Corresponds to a 90% CL interval of $-0.88 < A_{CP} < 0.64$.

$C_{\rho\pi}(B^0 \rightarrow \rho^+ \pi^-)$

VALUE	DOCUMENT ID	TECN	COMMENT
0.01 ± 0.14 OUR AVERAGE			Error includes scale factor of 1.9.
$0.15 \pm 0.09 \pm 0.05$	AUBERT	07AA	BABR $e^+e^- \rightarrow \Upsilon(4S)$
$-0.13 \pm 0.09 \pm 0.05$	KUSAKA	07	BELL $e^+e^- \rightarrow \Upsilon(4S)$
• • • We do not use the following data for averages, fits, limits, etc. • • •			
$0.25 \pm 0.17^{+0.02}_{-0.06}$	WANG	05	BELL Repl. by KUSAKA 07
$0.36 \pm 0.18 \pm 0.04$	AUBERT	03T	BABR Repl. by AUBERT 07AA

Meson Particle Listings

 B^0 $S_{\rho\pi}(B^0 \rightarrow \rho^+\pi^-)$

VALUE	DOCUMENT ID	TECN	COMMENT
0.01 ± 0.09 OUR AVERAGE			
-0.03 ± 0.11 ± 0.04	AUBERT	07AA	BABR $e^+e^- \rightarrow \Upsilon(4S)$
0.06 ± 0.13 ± 0.05	KUSAKA	07	BELL $e^+e^- \rightarrow \Upsilon(4S)$
••• We do not use the following data for averages, fits, limits, etc. •••			
-0.28 ± 0.23 $^{+0.10}_{-0.08}$	WANG	05	BELL Repl. by KUSAKA 07
0.19 ± 0.24 ± 0.03	AUBERT	03T	BABR Repl. by AUBERT 07AA

 $\Delta C_{\rho\pi}(B^0 \rightarrow \rho^+\pi^-)$

$\Delta C_{\rho\pi}$ describes the asymmetry between the rates $\Gamma(B^0 \rightarrow \rho^+\pi^-) + \Gamma(\bar{B}^0 \rightarrow \rho^-\pi^+)$ and $\Gamma(B^0 \rightarrow \rho^-\pi^+) + \Gamma(\bar{B}^0 \rightarrow \rho^+\pi^-)$.

VALUE	DOCUMENT ID	TECN	COMMENT
0.37 ± 0.08 OUR AVERAGE			
0.39 ± 0.09 ± 0.09	AUBERT	07AA	BABR $e^+e^- \rightarrow \Upsilon(4S)$
0.36 ± 0.10 ± 0.05	KUSAKA	07	BELL $e^+e^- \rightarrow \Upsilon(4S)$
••• We do not use the following data for averages, fits, limits, etc. •••			
0.38 ± 0.18 $^{+0.02}_{-0.04}$	WANG	05	BELL Repl. by KUSAKA 07
0.28 $^{+0.18}_{-0.19}$ ± 0.04	AUBERT	03T	BABR Repl. by AUBERT 07AA

 $\Delta S_{\rho\pi}(B^0 \rightarrow \rho^+\pi^-)$

$\Delta S_{\rho\pi}$ is related to the strong phase difference between the amplitudes contributing to $B^0 \rightarrow \rho^+\pi^-$.

VALUE	DOCUMENT ID	TECN	COMMENT
-0.05 ± 0.10 OUR AVERAGE			
-0.01 ± 0.14 ± 0.06	AUBERT	07AA	BABR $e^+e^- \rightarrow \Upsilon(4S)$
-0.08 ± 0.13 ± 0.05	KUSAKA	07	BELL $e^+e^- \rightarrow \Upsilon(4S)$
••• We do not use the following data for averages, fits, limits, etc. •••			
-0.30 ± 0.24 ± 0.09	WANG	05	BELL Repl. by KUSAKA 07
0.15 ± 0.25 ± 0.03	AUBERT	03T	BABR Repl. by AUBERT 07AA

 $C_{\rho\pi\pi^0}(B^0 \rightarrow \rho^0\pi^0)$

VALUE	DOCUMENT ID	TECN	COMMENT
-0.10 ± 0.40 ± 0.53	AUBERT	07AA	BABR $e^+e^- \rightarrow \Upsilon(4S)$

 $S_{\rho^0\pi^0}(B^0 \rightarrow \rho^0\pi^0)$

VALUE	DOCUMENT ID	TECN	COMMENT
0.1 ± 0.4 OUR AVERAGE			
0.04 ± 0.44 ± 0.18	AUBERT	07AA	BABR $e^+e^- \rightarrow \Upsilon(4S)$
0.17 ± 0.57 ± 0.35	KUSAKA	07	BELL $e^+e^- \rightarrow \Upsilon(4S)$

 $C_{a_1\pi}(B^0 \rightarrow a_1(1260)^+\pi^-)$

VALUE	DOCUMENT ID	TECN	COMMENT
-0.10 ± 0.15 ± 0.09	AUBERT	07o	BABR $e^+e^- \rightarrow \Upsilon(4S)$

 $S_{a_1\pi}(B^0 \rightarrow a_1(1260)^+\pi^-)$

VALUE	DOCUMENT ID	TECN	COMMENT
0.37 ± 0.21 ± 0.07	AUBERT	07o	BABR $e^+e^- \rightarrow \Upsilon(4S)$

 $\Delta C_{a_1\pi}(B^0 \rightarrow a_1(1260)^+\pi^-)$

$\Delta C_{a_1\pi}$ describes the asymmetry between the rates $\Gamma(B^0 \rightarrow a_1^+\pi^-) + \Gamma(\bar{B}^0 \rightarrow a_1^-\pi^+)$ and $\Gamma(B^0 \rightarrow a_1^-\pi^+) + \Gamma(\bar{B}^0 \rightarrow a_1^+\pi^-)$.

VALUE	DOCUMENT ID	TECN	COMMENT
0.26 ± 0.15 ± 0.07	AUBERT	07o	BABR $e^+e^- \rightarrow \Upsilon(4S)$

 $\Delta S_{a_1\pi}(B^0 \rightarrow a_1(1260)^+\pi^-)$

$\Delta S_{a_1\pi}$ is related to the strong phase difference between the amplitudes contributing to $B^0 \rightarrow a_1\pi$ decays.

VALUE	DOCUMENT ID	TECN	COMMENT
-0.14 ± 0.21 ± 0.06	AUBERT	07o	BABR $e^+e^- \rightarrow \Upsilon(4S)$

 $C(B^0 \rightarrow b_1^-K^+)$

VALUE	DOCUMENT ID	TECN	COMMENT
-0.22 ± 0.23 ± 0.05	AUBERT	07Bi	BABR $e^+e^- \rightarrow \Upsilon(4S)$

 $\Delta C(B^0 \rightarrow b_1^-\pi^+)$

VALUE	DOCUMENT ID	TECN	COMMENT
-1.04 ± 0.23 ± 0.08	AUBERT	07Bi	BABR $e^+e^- \rightarrow \Upsilon(4S)$

 $C_{\rho^0 K_S^0}(B^0 \rightarrow \rho^0 K_S^0)$

VALUE	DOCUMENT ID	TECN	COMMENT
0.64 ± 0.41 ± 0.20	AUBERT	07F	BABR $e^+e^- \rightarrow \Upsilon(4S)$

 $S_{\rho^0 K_S^0}(B^0 \rightarrow \rho^0 K_S^0)$

VALUE	DOCUMENT ID	TECN	COMMENT
0.20 ± 0.52 ± 0.24	AUBERT	07F	BABR $e^+e^- \rightarrow \Upsilon(4S)$

 $C_{\rho\rho}(B^0 \rightarrow \rho^+\rho^-)$

VALUE	DOCUMENT ID	TECN	COMMENT
-0.05 ± 0.13 OUR AVERAGE			
0.01 ± 0.15 ± 0.06	AUBERT	07BF	BABR $e^+e^- \rightarrow \Upsilon(4S)$
-0.16 ± 0.21 ± 0.08	¹ SOMOV	07	BELL $e^+e^- \rightarrow \Upsilon(4S)$
••• We do not use the following data for averages, fits, limits, etc. •••			
-0.00 ± 0.30 ± 0.09	¹ SOMOV	06	BELL Repl. by SOMOV 07
-0.03 ± 0.18 ± 0.09	AUBERT,B	05C	BABR Repl. by AUBERT 07BF
-0.17 ± 0.27 ± 0.14	AUBERT,B	04R	BABR Repl. by AUBERT,B 05C
¹ BELLE Collab. quotes A_{CP} which is equal to $-C$.			

 $S_{\rho\rho}(B^0 \rightarrow \rho^+\rho^-)$

VALUE	DOCUMENT ID	TECN	COMMENT
-0.06 ± 0.17 OUR AVERAGE			
-0.17 ± 0.20 $^{+0.05}_{-0.06}$	AUBERT	07BF	BABR $e^+e^- \rightarrow \Upsilon(4S)$
0.19 ± 0.30 ± 0.08	SOMOV	07	BELL $e^+e^- \rightarrow \Upsilon(4S)$
••• We do not use the following data for averages, fits, limits, etc. •••			
0.08 ± 0.41 ± 0.09	SOMOV	06	BELL Repl. by SOMOV 07
-0.33 ± 0.24 $^{+0.08}_{-0.14}$	AUBERT,B	05C	BABR Repl. by AUBERT 07BF
-0.42 ± 0.42 ± 0.14	AUBERT,B	04R	BABR Repl. by AUBERT,B 05C

 $|\lambda|(B^0 \rightarrow c\bar{c}K^0)$

The same λ quantity, defined in the $C_{\pi\pi}$ datablock above.

"OUR EVALUATION" is an average using rescaled values of the data listed below. The average and rescaling were performed by the Heavy Flavor Averaging Group (HFAG) and are described at <http://www.slac.stanford.edu/xorg/hfag/>. The averaging/rescaling procedure takes into account correlations between the measurements.

VALUE	DOCUMENT ID	TECN	COMMENT
0.988 ± 0.020 OUR EVALUATION			
0.964 ± 0.025 OUR AVERAGE			
0.952 ± 0.022 ± 0.017	¹ AUBERT	07AY	BABR $e^+e^- \rightarrow \Upsilon(4S)$
1.007 ± 0.041 ± 0.033	² ABE	05B	BELL $e^+e^- \rightarrow \Upsilon(4S)$
••• We do not use the following data for averages, fits, limits, etc. •••			
0.950 ± 0.031 ± 0.013	³ AUBERT	05F	BABR Repl. by AUBERT 07AY
0.950 ± 0.049 ± 0.025	⁴ ABE	02Z	BELL Repl. by ABE 05B
0.948 ± 0.051 ± 0.030	⁵ AUBERT	02P	BABR Repl. by AUBERT 05F

¹ Measurement based on $B^0 \rightarrow c\bar{c}K^0$ decays.

² Measurement based on $152 \times 10^6 B\bar{B}$ pairs.

³ Measurement based on $227 \times 10^6 B\bar{B}$ pairs.

⁴ Measured with both $\eta_f = \pm 1$ samples.

⁵ Measured with the high purity of $\eta_f = -1$ samples.

 $|\lambda|(B^0 \rightarrow J/\psi K^*(892)^0)$

VALUE	CL%	DOCUMENT ID	TECN	COMMENT
<0.25	95	¹ AUBERT,B	04H	BABR $e^+e^- \rightarrow \Upsilon(4S)$

¹ Uses the measured cosine coefficients C and \bar{C} and assumes $|\eta/p| = 1$.

 $\cos 2\beta(B^0 \rightarrow J/\psi K^*(892)^0)$

$\beta(\phi_1)$ is one of the angles of the CKM unitarity triangle, see the review on "CP" Violation in the Reviews section.

VALUE	DOCUMENT ID	TECN	COMMENT
1.7 $^{+0.7}_{-0.9}$ OUR AVERAGE			Error includes scale factor of 1.6.
2.72 $^{+0.50}_{-0.79}$ ± 0.27	¹ AUBERT	05P	BABR $e^+e^- \rightarrow \Upsilon(4S)$
0.87 ± 0.74 ± 0.12	² ITOH	05	BELL $e^+e^- \rightarrow \Upsilon(4S)$

¹ The measurement is obtained when $\sin 2\beta$ is fixed to 0.726 and the sign of $\cos 2\beta$ is positive with 86% confidence level.

² The measurement is obtained with $\sin 2\beta$ fixed to 0.731.

 $\cos 2\beta(B^0 \rightarrow [K_S^0\pi^+\pi^-]_{D^{(*)}} h^0)$

VALUE	DOCUMENT ID	TECN	COMMENT
1.0 $^{+0.6}_{-0.7}$ OUR AVERAGE			Error includes scale factor of 1.8.
0.42 ± 0.49 ± 0.16	¹ AUBERT	07BH	BABR $e^+e^- \rightarrow \Upsilon(4S)$
1.87 $^{+0.40}_{-0.53}$ ± 0.22	² KROKOVNY	06	BELL $e^+e^- \rightarrow \Upsilon(4S)$

¹ AUBERT 07BH evaluates the likelihoods for the positive and negative solutions assuming $\sin(2\beta_{eff}) = 0.678$. It quotes $L_+/ (L_+ + L_-) = 0.86$ corresponding to a likelihood ratio of $L_+/L_- = 6.14$ in favor of the positive solution.

² KROKOVNY 06 evaluates the likelihoods for the positive and negative solutions assuming $\sin(2\beta_{eff}) = 0.689$. It quotes $L_+/ (L_+ + L_-) = 0.983$ corresponding to a likelihood ratio of $L_+/L_- = 57.8$ in favor of the positive solution.

 $(S_+ + S_-)/2(B^0 \rightarrow D^{*-}\pi^+)$

$S_{\pm} = -\frac{2Im(\lambda_{\pm})}{1+|\lambda_{\pm}|^2}$ where λ_+ and λ_- are defined in the $C_{\pi\pi}$ datablock above for $B^0 \rightarrow D^{*-}\pi^+$ and $\bar{B}^0 \rightarrow D^{*+}\pi^-$.

VALUE	DOCUMENT ID	TECN	COMMENT
-0.037 ± 0.012 OUR AVERAGE			
-0.040 ± 0.023 ± 0.010	¹ AUBERT	06Y	BABR $e^+e^- \rightarrow \Upsilon(4S)$
-0.039 ± 0.020 ± 0.013	² RONGA	06	BELL $e^+e^- \rightarrow \Upsilon(4S)$
-0.034 ± 0.014 ± 0.009	³ AUBERT	05Z	BABR $e^+e^- \rightarrow \Upsilon(4S)$

• • • We do not use the following data for averages, fits, limits, etc. • • •

$-0.030 \pm 0.028 \pm 0.018$	³ GERSHON	05	BELL	Repl. by RONGA 06
$-0.068 \pm 0.038 \pm 0.020$	¹ AUBERT	04V	BABR	Repl. by AUBERT 06Y
$-0.063 \pm 0.024 \pm 0.014$	³ AUBERT	04W	BABR	Repl. by AUBERT 05Z
$0.060 \pm 0.040 \pm 0.019$	¹ SARANGI	04	BELL	Repl. by RONGA 06

¹ Uses fully reconstructed $B^0 \rightarrow D^{*\pm} \pi^\mp$ decays.

² Combines the results from fully reconstructed and partially reconstructed $D^* \pi$ events by taking weighted averages. Assumes that systematic errors from physics parameters and fit biases in the two measurements are 100% correlated.

³ Uses partially reconstructed $B^0 \rightarrow D^{*\pm} \pi^\mp$ decays.

$(S_- - S_+)/2 (B^0 \rightarrow D^{*-} \pi^+)$

VALUE	DOCUMENT ID	TECN	COMMENT
-0.006 ± 0.016 OUR AVERAGE			
$0.049 \pm 0.042 \pm 0.015$	¹ AUBERT	06Y	BABR $e^+ e^- \rightarrow \Upsilon(4S)$
$-0.011 \pm 0.020 \pm 0.013$	² RONGA	06	BELL $e^+ e^- \rightarrow \Upsilon(4S)$
$-0.019 \pm 0.022 \pm 0.013$	³ AUBERT	05Z	BABR $e^+ e^- \rightarrow \Upsilon(4S)$

• • • We do not use the following data for averages, fits, limits, etc. • • •

$-0.005 \pm 0.028 \pm 0.018$	³ GERSHON	05	BELL	Repl. by RONGA 06
$0.031 \pm 0.070 \pm 0.033$	¹ AUBERT	04V	BABR	Repl. by AUBERT 06Y
$-0.004 \pm 0.037 \pm 0.014$	³ AUBERT	04W	BABR	Repl. by AUBERT 05Z
$0.049 \pm 0.040 \pm 0.019$	¹ SARANGI	04	BELL	Repl. by RONGA 06

¹ Uses fully reconstructed $B^0 \rightarrow D^{*\pm} \pi^\mp$ decays.

² Combines the results from fully reconstructed and partially reconstructed $D^* \pi$ events by taking weighted averages. Assumes that systematic errors from physics parameters and fit biases in the two measurements are 100% correlated.

³ Uses partially reconstructed $B^0 \rightarrow D^{*\pm} \pi^\mp$ decays.

$(S_+ + S_-)/2 (B^0 \rightarrow D^- \pi^+)$

VALUE	DOCUMENT ID	TECN	COMMENT
-0.046 ± 0.023 OUR AVERAGE			
$-0.010 \pm 0.023 \pm 0.07$	¹ AUBERT	06Y	BABR $e^+ e^- \rightarrow \Upsilon(4S)$
$-0.050 \pm 0.021 \pm 0.012$	² RONGA	06	BELL $e^+ e^- \rightarrow \Upsilon(4S)$

• • • We do not use the following data for averages, fits, limits, etc. • • •

$-0.022 \pm 0.038 \pm 0.020$	¹ AUBERT	04V	BABR	Repl. by AUBERT 06Y
$-0.062 \pm 0.037 \pm 0.018$	¹ SARANGI	04	BELL	Repl. by RONGA 06

¹ Uses fully reconstructed $B^0 \rightarrow D^\pm \pi^\mp$ decays.

² Combines the results from fully reconstructed and partially reconstructed $D\pi$ events by taking weighted averages. Assumes that systematic errors from physics parameters and fit biases in the two measurements are 100% correlated.

$(S_- - S_+)/2 (B^0 \rightarrow D^- \pi^+)$

VALUE	DOCUMENT ID	TECN	COMMENT
-0.022 ± 0.021 OUR AVERAGE			
$-0.033 \pm 0.042 \pm 0.012$	¹ AUBERT	06Y	BABR $e^+ e^- \rightarrow \Upsilon(4S)$
$-0.019 \pm 0.021 \pm 0.012$	² RONGA	06	BELL $e^+ e^- \rightarrow \Upsilon(4S)$

• • • We do not use the following data for averages, fits, limits, etc. • • •

$0.025 \pm 0.068 \pm 0.033$	¹ AUBERT	04V	BABR	Repl. by AUBERT 06Y
$-0.025 \pm 0.037 \pm 0.018$	¹ SARANGI	04	BELL	Repl. by RONGA 06

¹ Uses fully reconstructed $B^0 \rightarrow D^\pm \pi^\mp$ decays.

² Combines the results from fully reconstructed and partially reconstructed $D\pi$ events by taking weighted averages. Assumes that systematic errors from physics parameters and fit biases in the two measurements are 100% correlated.

$(S_+ + S_-)/2 (B^0 \rightarrow D^- \rho^+)$

VALUE	DOCUMENT ID	TECN	COMMENT
$-0.024 \pm 0.031 \pm 0.009$			
$-0.024 \pm 0.031 \pm 0.009$	¹ AUBERT	06Y	BABR $e^+ e^- \rightarrow \Upsilon(4S)$

¹ Uses fully reconstructed $B^0 \rightarrow D^- \rho^+$ decays.

$(S_- - S_+)/2 (B^0 \rightarrow D^- \rho^+)$

VALUE	DOCUMENT ID	TECN	COMMENT
$-0.098 \pm 0.055 \pm 0.018$			
$-0.098 \pm 0.055 \pm 0.018$	¹ AUBERT	06Y	BABR $e^+ e^- \rightarrow \Upsilon(4S)$

¹ Uses fully reconstructed $B^0 \rightarrow D^- \rho^+$ decays.

$\sin(2\beta)$

For a discussion of CP violation, see the review on “ CP Violation” in the Reviews section. $\sin(2\beta)$ is a measure of the CP -violating amplitude in the $B_d^0 \rightarrow J/\psi(1S) K_S^0$.

“OUR EVALUATION” is an average using rescaled values of the data listed below. The average and rescaling were performed by the Heavy Flavor Averaging Group (HFAG) and are described at <http://www.slac.stanford.edu/xorg/hfag/>. The averaging/rescaling procedure takes into account correlations between the measurements.

VALUE	DOCUMENT ID	TECN	COMMENT
0.678 ± 0.025 OUR EVALUATION			
0.68 ± 0.04 OUR AVERAGE			Error includes scale factor of 1.4.
$0.714 \pm 0.032 \pm 0.018$	¹ AUBERT	07AY	BABR $e^+ e^- \rightarrow \Upsilon(4S)$
$0.642 \pm 0.031 \pm 0.017$	CHEN	07	BELL $e^+ e^- \rightarrow \Upsilon(4S)$
$1.56 \pm 0.42 \pm 0.21$	² AUBERT	04R	BABR $e^+ e^- \rightarrow \Upsilon(4S)$
0.79 ± 0.41 -0.44	³ AFFOLDER	00c	CDF $p\bar{p}$ at 1.8 TeV
0.84 ± 0.82 -1.04	⁴ BARATE	00q	ALEP $e^+ e^- \rightarrow Z$
3.2 ± 1.8 -2.0	⁵ ACKERSTAFF	98z	OPAL $e^+ e^- \rightarrow Z$

• • • We do not use the following data for averages, fits, limits, etc. • • •

$0.728 \pm 0.056 \pm 0.023$	⁶ ABE	05B	BELL	Repl. by CHEN 07
$0.722 \pm 0.040 \pm 0.023$	⁷ AUBERT	05F	BABR	Repl. by AUBERT 07AY
$0.99 \pm 0.14 \pm 0.06$	⁸ ABE	02U	BELL	$e^+ e^- \rightarrow \Upsilon(4S)$
$0.719 \pm 0.074 \pm 0.035$	⁹ ABE	02Z	BELL	Repl. by ABE 05B
$0.59 \pm 0.14 \pm 0.05$	¹⁰ AUBERT	02N	BABR	$e^+ e^- \rightarrow \Upsilon(4S)$
$0.741 \pm 0.067 \pm 0.034$	¹¹ AUBERT	02P	BABR	Repl. by AUBERT 05F
$0.58 \pm 0.32 \pm 0.09$ $-0.34 -0.10$	ABASHIAN	01	BELL	Repl. by ABE 01G
$0.99 \pm 0.14 \pm 0.06$	¹² ABE	01G	BELL	Repl. by ABE 02Z
$0.34 \pm 0.20 \pm 0.05$	AUBERT	01	BABR	Repl. by AUBERT 01B
$0.59 \pm 0.14 \pm 0.05$	¹² AUBERT	01B	BABR	Repl. by AUBERT 02P
$1.8 \pm 1.1 \pm 0.3$	¹³ ABE	98U	CDF	Repl. by AFFOLDER 00c

¹ Measurement based on $B^0 \rightarrow c\bar{c} K^0$ decays.

² Measurement in which the J/ψ decays to hadrons or to muons that do not satisfy the standard identification criteria.

³ AFFOLDER 00c uses about 400 $B^0 \rightarrow J/\psi(1S) K_S^0$ events. The production flavor of B^0 was determined using three tagging algorithms: a same-side tag, a jet-charge tag, and a soft-lepton tag.

⁴ BARATE 00q uses 23 candidates for $B^0 \rightarrow J/\psi(1S) K_S^0$ decays. A combination of jet-charge, vertex-charge, and same-side tagging techniques were used to determine the B^0 production flavor.

⁵ ACKERSTAFF 98z uses 24 candidates for $B_d^0 \rightarrow J/\psi(1S) K_S^0$ decay. A combination of jet-charge and vertex-charge techniques were used to tag the B_d^0 production flavor.

⁶ Measurement based on $152 \times 10^6 B\bar{B}$ pairs.

⁷ Measurement based on $227 \times 10^6 B\bar{B}$ pairs.

⁸ ABE 02U result is based on the same analysis and data sample reported in ABE 01G.

⁹ ABE 02Z result is based on $85 \times 10^6 B\bar{B}$ pairs.

¹⁰ AUBERT 02N result based on the same analysis and data sample reported in AUBERT 01B.

¹¹ AUBERT 02P result is based on $88 \times 10^6 B\bar{B}$ pairs.

¹² First observation of CP violation in B^0 meson system.

¹³ ABE 98U uses $198 \pm 17 B_d^0 \rightarrow J/\psi(1S) K^0$ events. The production flavor of B^0 was determined using the same side tagging technique.

$C_{J/\psi K^0} (B^0 \rightarrow J/\psi K^0)$

VALUE	DOCUMENT ID	TECN	COMMENT
$-0.018 \pm 0.021 \pm 0.014$	¹ CHEN	07	BELL $e^+ e^- \rightarrow \Upsilon(4S)$

¹ The paper reports A , which is equal to $-C$.

$S_{J/\psi K^0} (B^0 \rightarrow J/\psi K^0)$

VALUE	DOCUMENT ID	TECN	COMMENT
$0.642 \pm 0.031 \pm 0.017$	CHEN	07	BELL $e^+ e^- \rightarrow \Upsilon(4S)$

$\sin(2\beta_{\text{eff}}) (B^0 \rightarrow \phi K^0)$

VALUE	DOCUMENT ID	TECN	COMMENT
$0.22 \pm 0.27 \pm 0.12$	AUBERT	07AX	BABR $e^+ e^- \rightarrow \Upsilon(4S)$

• • • We do not use the following data for averages, fits, limits, etc. • • •

$0.50 \pm 0.25 \pm 0.07$ -0.04	¹ AUBERT	05T	BABR	Repl. by AUBERT 07AX
-------------------------------------	---------------------	-----	------	----------------------

¹ Obtained by constraining $C = 0$.

$\sin(2\beta_{\text{eff}}) (B^0 \rightarrow K^+ K^- K_S^0)$

VALUE	DOCUMENT ID	TECN	COMMENT
$0.77 \pm 0.11 \pm 0.07$ -0.04	AUBERT	07AX	BABR $e^+ e^- \rightarrow \Upsilon(4S)$

• • • We do not use the following data for averages, fits, limits, etc. • • •

$0.55 \pm 0.22 \pm 0.12$	¹ AUBERT	05T	BABR	Repl. by AUBERT 07AX
--------------------------	---------------------	-----	------	----------------------

¹ Obtained by constraining $C = 0$.

$\sin(2\beta_{\text{eff}}) (B^0 \rightarrow [K_S^0 \pi^+ \pi^-]_{D^{(*)} h^0})$

VALUE	DOCUMENT ID	TECN	COMMENT
0.45 ± 0.28 OUR AVERAGE			
$0.29 \pm 0.34 \pm 0.06$	AUBERT	07BH	BABR $e^+ e^- \rightarrow \Upsilon(4S)$
$0.78 \pm 0.44 \pm 0.22$	KROKOVNY	06	BELL $e^+ e^- \rightarrow \Upsilon(4S)$

$|\lambda| (B^0 \rightarrow [K_S^0 \pi^+ \pi^-]_{D^{(*)} h^0})$

VALUE	DOCUMENT ID	TECN	COMMENT
$1.01 \pm 0.08 \pm 0.02$	AUBERT	07BH	BABR $e^+ e^- \rightarrow \Upsilon(4S)$

$|\sin(2\beta + \gamma)|$

β (ϕ_1) and γ (ϕ_3) are angles of CKM unitarity triangle, see the review on “ CP Violation” in the Reviews section.

VALUE	CL%	DOCUMENT ID	TECN	COMMENT
>0.40	90	¹ AUBERT	06Y	BABR $e^+ e^- \rightarrow \Upsilon(4S)$

• • • We do not use the following data for averages, fits, limits, etc. • • •

>0.13	95	² RONGA	06	BELL $e^+ e^- \rightarrow \Upsilon(4S)$	
>0.07	95	² RONGA	06	BELL $e^+ e^- \rightarrow \Upsilon(4S)$	
>0.35	90	³ AUBERT	05Z	BABR $e^+ e^- \rightarrow \Upsilon(4S)$	
>0.69	68	⁴ AUBERT	04V	BABR $e^+ e^- \rightarrow \Upsilon(4S)$	
>0.58	95	⁵ AUBERT	04W	BABR	Repl. by AUBERT 05Z

Meson Particle Listings

B^0

- 1 Uses fully reconstructed $B^0 \rightarrow D^{(*)}\pi^{\pm}\pi^{\mp}$ and $D^{\pm}\rho^{\mp}$ decays and some theoretical assumptions.
- 2 Combines the results from fully reconstructed and partially reconstructed $D^{(*)}\pi$ events by taking weighted averages. Assumes that systematic errors from physics parameters and fit biases in the two measurements are 100% correlated.
- 3 Uses partially reconstructed $B^0 \rightarrow D^{*\pm}\pi^{\mp}$ decays and some theoretical assumptions.
- 4 Uses fully reconstructed $B^0 \rightarrow D^{(*)}\pi^{\pm}\pi^{\mp}$ decays and some theoretical assumptions, such as the SU(3) symmetry relation.
- 5 Combining this measurement with the results from AUBERT 04V for fully reconstructed $B^0 \rightarrow D^{(*)}\pi^{\pm}\pi^{\mp}$ and some theoretical assumptions, such as the SU(3) symmetry relation.

α For angle $\alpha(\phi_2)$ of the CKM unitarity triangle, see the review on "CP violation" in the reviews section.

VALUE (%)	DOCUMENT ID	TECN	COMMENT
96 ± 10 OUR AVERAGE			
88 ± 17	¹ SOMOV 06	BELL	$e^+e^- \rightarrow \Upsilon(4S)$
100 ± 13	² AUBERT,B 05c	BABR	$e^+e^- \rightarrow \Upsilon(4S)$
••• We do not use the following data for averages, fits, limits, etc. •••			
78.6 ± 7.3	³ AUBERT 07o	BABR	$e^+e^- \rightarrow \Upsilon(4S)$
102 ⁺¹⁶ ₋₁₂ ± 14	⁴ AUBERT,B 04R	BABR	Repl. by AUBERT,B 05c
<ol style="list-style-type: none"> 1 Obtained using isospin relation and selecting a solution closest to the CKM best fit average; the 90% CL allowed interval is $59^\circ < \phi_2 (\equiv \alpha) < 115^\circ$. 2 Obtained using isospin relation and selecting a solution closest to the CKM best fit average; 90% CL allowed interval is $79^\circ < \alpha < 123^\circ$. 3 The angle α_{eff} is obtained using the measured CP parameters of $B^0 \rightarrow a_1(1260)\pi^{\pm}\pi^{\mp}$ and choosing one of the four solutions that is compatible with the result of SM-based fits. 4 Obtained from the measured CP parameters of the longitudinal polarization by selecting the solution closest to the CKM best fit central value of $\alpha = 95^\circ - 98^\circ$. 			

$B^0 \rightarrow D^{*+} \ell^+ \nu_\ell$ FORM FACTORS

VALUE	DOCUMENT ID	TECN	COMMENT
1.42 ± 0.07 OUR AVERAGE			
1.429 ± 0.061 ± 0.044	AUBERT 08R	BABR	$e^+e^- \rightarrow \Upsilon(4S)$
1.18 ± 0.30 ± 0.12	DUBOSCQ 96	CLE2	$e^+e^- \rightarrow \Upsilon(4S)$
••• We do not use the following data for averages, fits, limits, etc. •••			
1.396 ± 0.060 ± 0.044	AUBERT,B 06Z	BABR	Repl. by AUBERT 08R
R_1 (form factor ratio $\sim V/A_1$)			
VALUE	DOCUMENT ID	TECN	COMMENT
0.82 ± 0.04 OUR AVERAGE			
0.827 ± 0.038 ± 0.022	AUBERT 08R	BABR	$e^+e^- \rightarrow \Upsilon(4S)$
0.71 ± 0.22 ± 0.07	DUBOSCQ 96	CLE2	$e^+e^- \rightarrow \Upsilon(4S)$
••• We do not use the following data for averages, fits, limits, etc. •••			
0.885 ± 0.040 ± 0.026	AUBERT,B 06Z	BABR	Repl. by AUBERT 08R
R_2 (form factor ratio $\sim A_2/A_1$)			
VALUE	DOCUMENT ID	TECN	COMMENT
1.16 ± 0.09 OUR AVERAGE			
1.191 ± 0.048 ± 0.028	AUBERT 08R	BABR	$e^+e^- \rightarrow \Upsilon(4S)$
0.91 ± 0.15 ± 0.06	DUBOSCQ 96	CLE2	$e^+e^- \rightarrow \Upsilon(4S)$
••• We do not use the following data for averages, fits, limits, etc. •••			
1.145 ± 0.059 ± 0.046	AUBERT,B 06Z	BABR	Repl. by AUBERT 08R

B^0 REFERENCES

AALTONEN 08I PRL 100 101802	T. Aaltonen et al.	(CDF Collab.)
AUBERT 08B PR D77 011102R	B. Aubert et al.	(BABAR Collab.)
AUBERT 08C PR D77 011104R	B. Aubert et al.	(BABAR Collab.)
AUBERT 08E PR D77 012003	B. Aubert et al.	(BABAR Collab.)
AUBERT 08F PRL 100 051803	B. Aubert et al.	(BABAR Collab.)
AUBERT 08I PRL 100 081801	B. Aubert et al.	(BABAR Collab.)
AUBERT 08N PRL 100 021801	B. Aubert et al.	(BABAR Collab.)
AUBERT 08P PR D77 032007	B. Aubert et al.	(BABAR Collab.)
AUBERT 08Q PRL 100 151802	B. Aubert et al.	(BABAR Collab.)
AUBERT 08R PR D77 032002	B. Aubert et al.	(BABAR Collab.)
LIVENTSEV 08 PR D77 091503R	D. Liventsev et al.	(BELLE Collab.)
UCHIDA 08 PR D77 051101R	Y. Uchida et al.	(BELLE Collab.)
USHIRODA 08 PRL 100 021602	Y. Ushiroda et al.	(BELLE Collab.)
ABAZOV 07S PRL 99 142001	V.M. Abazov et al.	(DO Collab.)
ABULENCIA 07A PRL 98 122001	A. Abulencia et al.	(FNAL CDF Collab.)
ADAM 07 PRL 99 041802	N.E. Adam et al.	(CLEO Collab.)
Also PR D76 012007	D.M. Asner et al.	(CLEO Collab.)
AUBERT 07A PRL 98 031801	B. Aubert et al.	(BABAR Collab.)
AUBERT 07AA PR D76 012004	B. Aubert et al.	(BABAR Collab.)
AUBERT 07AC PR D76 031101R	B. Aubert et al.	(BABAR Collab.)
AUBERT 07AD PR D76 031102R	B. Aubert et al.	(BABAR Collab.)
AUBERT 07AE PR D76 031103R	B. Aubert et al.	(BABAR Collab.)
AUBERT 07AF PRL 99 021603	B. Aubert et al.	(BABAR Collab.)
AUBERT 07AG PRL 99 051801	B. Aubert et al.	(BABAR Collab.)
AUBERT 07AI PRL 99 071801	B. Aubert et al.	(BABAR Collab.)
AUBERT 07AJ PRL 99 081801	B. Aubert et al.	(BABAR Collab.)
AUBERT 07AN PR D76 051101R	B. Aubert et al.	(BABAR Collab.)
AUBERT 07AO PR D76 051103R	B. Aubert et al.	(BABAR Collab.)
AUBERT 07AQ PR D76 071101R	B. Aubert et al.	(BABAR Collab.)
AUBERT 07AS PR D76 071104R	B. Aubert et al.	(BABAR Collab.)
AUBERT 07AT PR D76 091101R	B. Aubert et al.	(BABAR Collab.)
AUBERT 07AV PR D76 092004	B. Aubert et al.	(BABAR Collab.)
AUBERT 07AX PRL 99 161802	B. Aubert et al.	(BABAR Collab.)
AUBERT 07AY PRL 99 171803	B. Aubert et al.	(BABAR Collab.)
AUBERT 07B PR D75 012008	B. Aubert et al.	(BABAR Collab.)
AUBERT 07BC PR D76 091102R	B. Aubert et al.	(BABAR Collab.)
AUBERT 07BF PR D76 052007	B. Aubert et al.	(BABAR Collab.)

AUBERT 07BH PRL 99 231802	B. Aubert et al.	(BABAR Collab.)
AUBERT 07BI PRL 99 241803	B. Aubert et al.	(BABAR Collab.)
AUBERT 07BO PR D76 111102R	B. Aubert et al.	(BABAR Collab.)
AUBERT 07D PRL 98 051801	B. Aubert et al.	(BABAR Collab.)
AUBERT 07E PRL 98 051802	B. Aubert et al.	(BABAR Collab.)
AUBERT 07F PRL 98 051803	B. Aubert et al.	(BABAR Collab.)
AUBERT 07G PRL 98 111801	B. Aubert et al.	(BABAR Collab.)
AUBERT 07H PR D75 031101R	B. Aubert et al.	(BABAR Collab.)
AUBERT 07I PRL 98 091801	B. Aubert et al.	(BABAR Collab.)
AUBERT 07K PRL 98 081801	B. Aubert et al.	(BABAR Collab.)
AUBERT 07L PRL 98 151802	B. Aubert et al.	(BABAR Collab.)
AUBERT 07N PR D75 072002	B. Aubert et al.	(BABAR Collab.)
AUBERT 07O PRL 98 181803	B. Aubert et al.	(BABAR Collab.)
AUBERT 07Q PR D75 051102R	B. Aubert et al.	(BABAR Collab.)
AUBERT 07R PRL 98 211804	B. Aubert et al.	(BABAR Collab.)
AUBERT 07Y PR D75 111102R	B. Aubert et al.	(BABAR Collab.)
CHANG 07A PRL 98 131803	M.-C. Chang et al.	(BELLE Collab.)
CHANG 07B PR D75 071104R	P. Chang et al.	(BELLE Collab.)
CHEN 07 PR D76 091103R	Y. Chen et al.	(BELLE Collab.)
CHEN 07 PR D75 031802	K.-F. Chen et al.	(BELLE Collab.)
CHEN 07D PRL 99 221802	K.-F. Chen et al.	(BELLE Collab.)
DALSENSO 07 PR D76 072004	J. Dalensio et al.	(BELLE Collab.)
FRATINA 07 PRL 98 221802	S. Fratina et al.	(BELLE Collab.)
GARMASH 07 PR D75 012006	A. Garmash et al.	(BELLE Collab.)
HOKUUE 07 PL B648 139	T. Hokuue et al.	(BELLE Collab.)
ISHINO 07 PRL 98 211801	H. Ishino et al.	(BELLE Collab.)
KUSAKA 07 PRL 98 221602	A. Kusaka et al.	(BELLE Collab.)
KUZMIN 07 PR D76 012006	A. Kuzmin et al.	(BELLE Collab.)
LIN 07 PRL 98 181804	S.-W. Lin et al.	(BELLE Collab.)
LIN 07A PRL 99 121601	S.-W. Lin et al.	(BELLE Collab.)
MATYJA 07 PRL 99 191807	A. Matyja et al.	(BELLE Collab.)
MEDVEDEVA 07 PR D76 051102R	T. Medvedeva et al.	(BELLE Collab.)
PARK 07 PR D75 011101R	K.S. Park et al.	(BELLE Collab.)
SCHUEMANN 07 PR D75 092002	J. Schuemann et al.	(BELLE Collab.)
SOMOV 07 PR D76 011104R	A. Somov et al.	(BELLE Collab.)
TSAI 07 PR D75 111101R	Y.-T. Tsai et al.	(BELLE Collab.)
URQUIJO 07 PR D75 032001	P. Urquijo et al.	(BELLE Collab.)
WANG 07B PR D75 092005	C.H. Wang et al.	(BELLE Collab.)
WANG 07C PR D76 052004	M.-Z. Wang et al.	(BELLE Collab.)
XIE 07 PR D75 017101	Q.L. Xie et al.	(BELLE Collab.)
ZUPANC 07 PR D75 091102R	J. Zupanc et al.	(BELLE Collab.)
ABAZOV 06W PR D74 092001	V.M. Abazov et al.	(DO Collab.)
ABAZOV 06S PR D74 112002	V.M. Abazov et al.	(DO Collab.)
ABULENCIA 06D PRL 97 211802	A. Abulencia et al.	(CDF Collab.)
ACOSTA 06 PR 96 202001	D. Acosta et al.	(CDF Collab.)
AUBERT 06 PR D73 011101R	B. Aubert et al.	(BABAR Collab.)
AUBERT 06A PRL 96 011803	B. Aubert et al.	(BABAR Collab.)
AUBERT 06E PRL 96 052002	B. Aubert et al.	(BABAR Collab.)
AUBERT 06G PR D73 012004	B. Aubert et al.	(BABAR Collab.)
AUBERT 06I PR D73 031101R	B. Aubert et al.	(BABAR Collab.)
AUBERT 06L PR D74 012001	B. Aubert et al.	(BABAR Collab.)
AUBERT 06N PR D74 031103R	B. Aubert et al.	(BABAR Collab.)
AUBERT 06S PRL 96 012002	B. Aubert et al.	(BABAR Collab.)
AUBERT 06T PRL 96 251802	B. Aubert et al.	(BABAR Collab.)
AUBERT 06V PRL 97 051802	B. Aubert et al.	(BABAR Collab.)
AUBERT 06W PR D73 071102R	B. Aubert et al.	(BABAR Collab.)
AUBERT 06X PR D73 071103R	B. Aubert et al.	(BABAR Collab.)
AUBERT 06Y PR D73 111101R	B. Aubert et al.	(BABAR Collab.)
AUBERT,B 06A PR D73 112004	B. Aubert et al.	(BABAR Collab.)
AUBERT,B 06B PR D74 011101R	B. Aubert et al.	(BABAR Collab.)
AUBERT,B 06C PR D74 011102R	B. Aubert et al.	(BABAR Collab.)
AUBERT,B 06E PR D74 011106R	B. Aubert et al.	(BABAR Collab.)
AUBERT,B 06G PRL 97 201801	B. Aubert et al.	(BABAR Collab.)
AUBERT,B 06H PRL 97 011802	B. Aubert et al.	(BABAR Collab.)
AUBERT,B 06J PR D73 092001	B. Aubert et al.	(BABAR Collab.)
AUBERT,B 06K PRL 97 211801	B. Aubert et al.	(BABAR Collab.)
AUBERT,B 06L PR D74 031101R	B. Aubert et al.	(BABAR Collab.)
AUBERT,B 06M PR D74 031102R	B. Aubert et al.	(BABAR Collab.)
AUBERT,B 06O PR D74 031104R	B. Aubert et al.	(BABAR Collab.)
AUBERT,B 06P PR D74 031105R	B. Aubert et al.	(BABAR Collab.)
AUBERT,B 06Q PR D74 091101R	B. Aubert et al.	(BABAR Collab.)
AUBERT,B 06R PR D74 032005	B. Aubert et al.	(BABAR Collab.)
AUBERT,B 06S PR D74 051101R	B. Aubert et al.	(BABAR Collab.)
AUBERT,B 06T PR D74 051102R	B. Aubert et al.	(BABAR Collab.)
AUBERT,B 06U PR D74 031104R	B. Aubert et al.	(BABAR Collab.)
AUBERT,B 06Y PR D74 091105R	B. Aubert et al.	(BABAR Collab.)
AUBERT,B 06Z PR D74 092004	B. Aubert et al.	(BABAR Collab.)
AUBERT,BE 06C PRL 97 171805	B. Aubert et al.	(BABAR Collab.)
AUBERT,BE 06H PRL 97 261803	B. Aubert et al.	(BABAR Collab.)
AUBERT,BE 06J PR D74 111102R	B. Aubert et al.	(BABAR Collab.)
AUBERT,BE 06N PR D74 072008	B. Aubert et al.	(BABAR Collab.)
BLYTH 06 PR D74 092002	S. Blyth et al.	(BELLE Collab.)
CHISTOV 06A PR D74 111105R	R. Chistov et al.	(BELLE Collab.)
DRAGIC 06 PR D73 111105R	J. Dragic et al.	(BELLE Collab.)
GABYSHEV 06 PRL 97 202003	N. Gabyshev et al.	(BELLE Collab.)
GOKHROO 06 PR 97 152002	G. Gokhroo et al.	(BELLE Collab.)
JEN 06 PR D74 111101R	C.-M. Jen et al.	(BELLE Collab.)
KROKOVNY 06 PRL 97 081801	P. Krokovny et al.	(BELLE Collab.)
MOHAPATRA 06 PRL 96 221601	D. Mohapatra et al.	(BELLE Collab.)
NAKANO 06 PR D73 112002	E. Nakano et al.	(BELLE Collab.)
RONGA 06 PR D73 092003	F.J. Ronga et al.	(BELLE Collab.)
SCHUEMANN 06 PRL 97 061802	J. Schuemann et al.	(BELLE Collab.)
SOMOV 06 PR 96 171801	A. Somov et al.	(BELLE Collab.)
SONI 06 PR B634 155	N. Soni et al.	(BELLE Collab.)
USHIRODA 06 PR D74 111104R	Y. Ushiroda et al.	(BELLE Collab.)
VILLA 06 PR D73 051107R	S. Villa et al.	(BELLE Collab.)
ABAZOV 05B PRL 94 042001	V.M. Abazov et al.	(DO Collab.)
ABAZOV 05C PRL 94 102001	V.M. Abazov et al.	(DO Collab.)
ABAZOV 05D PRL 94 182001	V.M. Abazov et al.	(DO Collab.)
ABAZOV 05W PRL 95 171801	V.M. Abazov et al.	(DO Collab.)
ABE 05A PRL 94 221805	K. Abe et al.	(BELLE Collab.)
ABE 05B PR D71 072003	K. Abe et al.	(BELLE Collab.)
Also PR D71 079903 (err.)	K. Abe et al.	(BELLE Collab.)
ABE 05D PRL 95 101801	K. Abe et al.	(BELLE Collab.)
ABE 05G PRL 95 231802	K. Abe et al.	(BELLE Collab.)
ABULENCIA 05 PR 95 221805	A. Abulencia et al.	(CDF Collab.)
Also PRL 95 249305 (erratum)	A. Abulencia et al.	(CDF Collab.)
ACOSTA 05 PR 94 101803	D. Acosta et al.	(CDF Collab.)
AUBERT 05 PR 94 011801	B. Aubert et al.	(BABAR Collab.)
AUBERT 05B PR D71 031501R	B. Aubert et al.	(BABAR Collab.)
AUBERT 05E PR D71 051502R	B. Aubert et al.	(BABAR Collab.)
AUBERT 05F PRL 94 161803	B. Aubert et al.	(BABAR Collab.)
AUBERT 05I PRL 94 131801	B. Aubert et al.	(BABAR Collab.)
AUBERT 05J PRL 94 141801	B. Aubert et al.	(BABAR Collab.)
AUBERT 05K PRL 94 171801	B. Aubert et al.	(BABAR Collab.)
AUBERT 05L PRL 94 181802	B. Aubert et al.	(BABAR Collab.)
AUBERT 05M PRL 94 191802	B. Aubert et al.	(BABAR Collab.)
AUBERT 05O PR D71 031103R	B. Aubert et al.	(BABAR Collab.)
AUBERT 05P PR D71 032005	B. Aubert et al.	(BABAR Collab.)
AUBERT 05T PR D71 091102R	B. Aubert et al.	(BABAR Collab.)
AUBERT 05U PR D71 091103R	B. Aubert et al.	(BABAR Collab.)
AUBERT 05V PR D71 091104R	B. Aubert et al.	(BABAR Collab.)

See key on page 373

Meson Particle Listings

B⁰

AUBERT	05W	PRL 94 221803	B. Aubert et al.	(BABAR Collab.)	HASTINGS	03	PR D67 052004	N.C. Hastings et al.	(BELLE Collab.)
AUBERT	05Y	PR D71 111102	B. Aubert et al.	(BABAR Collab.)	ISHIKAWA	03	PRL 91 261601	A. Ishikawa et al.	(BELLE Collab.)
AUBERT	05Z	PR D71 112003	B. Aubert et al.	(BABAR Collab.)	KROKOVNY	03	PRL 90 141802	P. Krokovny et al.	(BELLE Collab.)
AUBERT,B	05	PRL 95 011801	B. Aubert et al.	(BABAR Collab.)	KROKOVNY	03B	PRL 91 262002	P. Krokovny et al.	(BELLE Collab.)
AUBERT,B	05C	PRL 95 041805	B. Aubert et al.	(BABAR Collab.)	LEE	03	PRL 91 261801	S.H. Lee et al.	(BELLE Collab.)
AUBERT,B	05K	PRL 95 131803	B. Aubert et al.	(BABAR Collab.)	SATPATHY	03	PL B553 159	A. Satpathy et al.	(BELLE Collab.)
AUBERT,B	05O	PR D72 051102R	B. Aubert et al.	(BABAR Collab.)	WAN G	03	PRL 90 201802	M.-Z. Wang et al.	(BELLE Collab.)
AUBERT,B	05P	PR D72 051103R	B. Aubert et al.	(BABAR Collab.)	ZHENG	03	PR D67 092004	Y. Zheng et al.	(BELLE Collab.)
AUBERT,B	05Q	PR D72 051106R	B. Aubert et al.	(BABAR Collab.)	ABE	02	PRL 88 021801	K. Abe et al.	(BELLE Collab.)
AUBERT,B	05Z	PRL 95 131802	B. Aubert et al.	(BABAR Collab.)	ABE	02E	PL B526 258	K. Abe et al.	(BELLE Collab.)
AUBERT,BE	05	PRL 95 151803	B. Aubert et al.	(BABAR Collab.)	ABE	02F	PL B526 247	K. Abe et al.	(BELLE Collab.)
AUBERT,BE	05A	PRL 95 151804	B. Aubert et al.	(BABAR Collab.)	ABE	02H	PRL 88 171801	K. Abe et al.	(BELLE Collab.)
AUBERT,BE	05B	PRL 95 171802	B. Aubert et al.	(BABAR Collab.)	ABE	02J	PRL 88 052002	K. Abe et al.	(BELLE Collab.)
AUBERT,BE	05C	PR D72 091103R	B. Aubert et al.	(BABAR Collab.)	ABE	02K	PRL 88 181803	K. Abe et al.	(BELLE Collab.)
AUBERT,BE	05E	PRL 95 221801	B. Aubert et al.	(BABAR Collab.)	ABE	02M	PRL 89 071801	K. Abe et al.	(BELLE Collab.)
AUBERT,BE	05F	PR D72 111101R	B. Aubert et al.	(BABAR Collab.)	ABE	02N	PL B538 11	K. Abe et al.	(BELLE Collab.)
CHANG	05	PR D71 072007	M.-C. Chang et al.	(BELLE Collab.)	ABE	02Q	PR D65 091103R	K. Abe et al.	(BELLE Collab.)
CHANG	05A	PR D71 091106R	P. Chang et al.	(BELLE Collab.)	ABE	02R	PRL 89 122001	K. Abe et al.	(BELLE Collab.)
CHAO	05	PRL 94 181803	Y. Chao et al.	(BELLE Collab.)	ABE	02U	PR D66 032007	K. Abe et al.	(BELLE Collab.)
CHAO	05A	PR D71 031502R	Y. Chao et al.	(BELLE Collab.)	ABE	02W	PRL 89 151802	K. Abe et al.	(BELLE Collab.)
CHEN	05A	PRL 94 221804	K.-F. Chen et al.	(BELLE Collab.)	ABE	02Z	PR D66 071012R	K. Abe et al.	(BELLE Collab.)
CHEN	05B	PR D72 012004	K.-F. Chen et al.	(BELLE Collab.)	ACOSTA	02C	PR D65 092009	D. Acosta et al.	(CDF Collab.)
DRUTSKOY	05	PRL 94 061802	A. Drutskoy et al.	(BELLE Collab.)	ACOSTA	02G	PR D66 112002	D. Acosta et al.	(CDF Collab.)
GERSHON	05	PL B624 11	T. Gershon et al.	(BELLE Collab.)	AFFOLDER	02B	PRL 88 071801	T. Affolder et al.	(CDF Collab.)
ITOH	05	PRL 95 091601	R. Itoh et al.	(BELLE Collab.)	AHMED	02B	PR D66 031101R	S. Ahmed et al.	(CLEO Collab.)
LIVENTSEV	05	PR D72 051109R	D. Liventsev et al.	(BELLE Collab.)	ASNER	02	PR D65 031103R	D.M. Asner et al.	(CLEO Collab.)
MAJUMDER	05	PRL 95 041803	G. Majumder et al.	(BELLE Collab.)	AUBERT	02	PR D65 032001	B. Aubert et al.	(BaBar Collab.)
MIYAKE	05	PL B618 34	H. Miyake et al.	(BELLE Collab.)	AUBERT	02C	PRL 88 101805	B. Aubert et al.	(BaBar Collab.)
MOHAPATRA	05	PR D72 011101R	D. Mohapatra et al.	(BELLE Collab.)	AUBERT	02D	PR D65 051502R	B. Aubert et al.	(BaBar Collab.)
NISHIDA	05	PL B610 23	S. Nishida et al.	(BELLE Collab.)	AUBERT	02E	PR D65 051101R	B. Aubert et al.	(BaBar Collab.)
OKABE	05	PL B614 27	T. Okabe et al.	(BELLE Collab.)	AUBERT	02H	PRL 89 011802	B. Aubert et al.	(BaBar Collab.)
SCHUMANN	05	PR D72 011103R	J. Schumann et al.	(BELLE Collab.)	Also		PRL 89 169903 (erratum)	B. Aubert et al.	(BaBar Collab.)
SUMISAWA	05	PRL 95 061801	K. Sumisawa et al.	(BELLE Collab.)	AUBERT	02J	PRL 88 221802	B. Aubert et al.	(BaBar Collab.)
USHIRODA	05	PRL 94 231601	Y. Ushiroda et al.	(BELLE Collab.)	AUBERT	02I	PRL 88 221803	B. Aubert et al.	(BaBar Collab.)
WANG	05	PRL 94 121801	C.C. Wang et al.	(BELLE Collab.)	AUBERT	02K	PRL 88 231801	B. Aubert et al.	(BaBar Collab.)
WANG	05A	PL B617 141	M.-Z. Wang et al.	(BELLE Collab.)	AUBERT	02L	PRL 88 241801	B. Aubert et al.	(BaBar Collab.)
XIE	05	PR D72 051105R	Q.L. Xie et al.	(BELLE Collab.)	AUBERT	02M	PRL 89 061801	B. Aubert et al.	(BaBar Collab.)
YANG	05	PRL 94 111802	H. Yang et al.	(BELLE Collab.)	AUBERT	02N	PR D66 032003	B. Aubert et al.	(BaBar Collab.)
ZHANG	05B	PR D71 091107R	L.M. Zhang et al.	(BELLE Collab.)	AUBERT	02P	PRL 89 201802	B. Aubert et al.	(BaBar Collab.)
ABDALLAH	04D	EPJ C33 213	J. Abdallah et al.	(DELPHI Collab.)	AUBERT	02Q	PRL 89 281802	B. Aubert et al.	(BaBar Collab.)
ABDALLAH	04E	EPJ C33 307	J. Abdallah et al.	(DELPHI Collab.)	BRIERE	02	PR D69 081803	R. Briere et al.	(CLEO Collab.)
ABE	04E	PRL 93 021601	K. Abe et al.	(CLEO Collab.)	CHENEY	02	PR D66 092002	R. Cheney et al.	(CLEO Collab.)
ACOSTA	04D	PRL 93 032001	D. Acosta et al.	(CDF Collab.)	CHEN	02B	PL B546 196	K.-F. Chen et al.	(BELLE Collab.)
AUBERT	04A	PR D69 011102	B. Aubert et al.	(BaBar Collab.)	COAN	02	PRL 88 062001	T.E. Coan et al.	(CLEO Collab.)
AUBERT	04B	PR D69 032004	B. Aubert et al.	(BaBar Collab.)	Also		PRL 88 069902 (erratum)	J.T.E. Coan et al.	(CLEO Collab.)
AUBERT	04C	PRL 92 111801	B. Aubert et al.	(BaBar Collab.)	DRUTSKOY	02	PL B542 171	A. Drutskoy et al.	(BELLE Collab.)
AUBERT	04G	PR D69 031102R	B. Aubert et al.	(BaBar Collab.)	DYTMAN	02	PR D66 091101R	S.A. Dytman et al.	(CLEO Collab.)
AUBERT	04H	PRL 92 061801	B. Aubert et al.	(BaBar Collab.)	ECKHART	02	PRL 89 251801	E. Eckhart et al.	(CLEO Collab.)
AUBERT	04M	PRL 92 201802	B. Aubert et al.	(BaBar Collab.)	EDWARDS	02	PR D65 012002	K.W. Edwards et al.	(CLEO Collab.)
AUBERT	04R	PR D69 052001	B. Aubert et al.	(BaBar Collab.)	GABYSHEV	02	PR D66 091102R	N. Gabyshev et al.	(BELLE Collab.)
AUBERT	04U	PR D69 091503R	B. Aubert et al.	(BaBar Collab.)	GODANG	02	PRL 88 021802	R. Godang et al.	(CLEO Collab.)
AUBERT	04V	PRL 92 251801	B. Aubert et al.	(BaBar Collab.)	GORDON	02	PL B542 183	A. Gordon et al.	(BELLE Collab.)
AUBERT	04W	PRL 93 031801	B. Aubert et al.	(BaBar Collab.)	HABA	02	PR D69 251803	K. Hara et al.	(CLEO Collab.)
AUBERT	04Y	PRL 93 041801	B. Aubert et al.	(BaBar Collab.)	KROKOVNY	02	PRL 89 231804	P. Krokovny et al.	(BELLE Collab.)
AUBERT	04Z	PRL 93 051802	B. Aubert et al.	(BaBar Collab.)	MAHAPATRA	02	PRL 88 101803	R. Mahapatra et al.	(CLEO Collab.)
AUBERT,B	04B	PR D70 011101R	B. Aubert et al.	(BABAR Collab.)	NISHIDA	02	PRL 89 231801	S. Nishida et al.	(BELLE Collab.)
AUBERT,B	04C	PR D70 012007	B. Aubert et al.	(BABAR Collab.)	TOMURA	02	PL B542 207	T. Tomura et al.	(BELLE Collab.)
Also		PRL 92 181801	B. Aubert et al.	(BABAR Collab.)	ABASHIAN	01	PRL 86 2509	A. Abashian et al.	(BELLE Collab.)
AUBERT,B	04D	PR D70 032006	B. Aubert et al.	(BABAR Collab.)	ABE	01D	PRL 86 3228	K. Abe et al.	(BELLE Collab.)
AUBERT,B	04G	PRL 93 071801	B. Aubert et al.	(BABAR Collab.)	ABE	01G	PRL 87 091802	K. Abe et al.	(BELLE Collab.)
AUBERT,B	04H	PRL 93 081801	B. Aubert et al.	(BABAR Collab.)	ABE	01H	PRL 87 101801	K. Abe et al.	(BELLE Collab.)
AUBERT,B	04J	PRL 93 091802	B. Aubert et al.	(BABAR Collab.)	ABE	01I	PRL 87 111801	K. Abe et al.	(BELLE Collab.)
AUBERT,B	04K	PRL 93 131801	B. Aubert et al.	(BABAR Collab.)	ABE	01K	PR D64 071101	K. Abe et al.	(BELLE Collab.)
AUBERT,B	04M	PRL 93 131801	B. Aubert et al.	(BABAR Collab.)	ABE	01L	PRL 87 161801	K. Abe et al.	(BELLE Collab.)
AUBERT,B	04O	PR D70 091103R	B. Aubert et al.	(BABAR Collab.)	ABE	01M	PL B517 309	K. Abe et al.	(BELLE Collab.)
AUBERT,B	04R	PRL 93 231801	B. Aubert et al.	(BABAR Collab.)	ABREU	01H	PL B510 55	P. Abreu et al.	(DELPHI Collab.)
AUBERT,B	04S	PRL 93 181801	B. Aubert et al.	(BABAR Collab.)	ALEXANDER	01B	PR D64 092001	J.P. Alexander et al.	(CLEO Collab.)
AUBERT,B	04T	PR D70 091104R	B. Aubert et al.	(BABAR Collab.)	AMMAR	01B	PRL 87 271801	R. Ammar et al.	(CLEO Collab.)
AUBERT,B	04U	PR D70 091105R	B. Aubert et al.	(BABAR Collab.)	ANDERSON	01	PRL 86 2732	S. Anderson et al.	(CLEO Collab.)
AUBERT,B	04V	PRL 93 181805	B. Aubert et al.	(BABAR Collab.)	ANDERSON	01B	PRL 87 181803	S. Anderson et al.	(CLEO Collab.)
AUBERT,B	04W	PRL 93 231804	B. Aubert et al.	(BABAR Collab.)	AUBERT	01	PRL 86 2515	B. Aubert et al.	(BaBar Collab.)
AUBERT,B	04X	PRL 93 181806	B. Aubert et al.	(BABAR Collab.)	AUBERT	01B	PRL 87 091801	B. Aubert et al.	(BaBar Collab.)
AUBERT,B	04Z	PRL 93 201801	B. Aubert et al.	(BABAR Collab.)	AUBERT	01D	PRL 87 151801	B. Aubert et al.	(BaBar Collab.)
AUBERT,BE	04	PR D70 11102R	B. Aubert et al.	(BABAR Collab.)	AUBERT	01E	PRL 87 151802	B. Aubert et al.	(BaBar Collab.)
AUBERT,BE	04A	PR D70 11200R	B. Aubert et al.	(BABAR Collab.)	AUBERT	01F	PRL 87 201802	B. Aubert et al.	(BaBar Collab.)
AUBERT,BE	04B	PR D70 091106	B. Aubert et al.	(BABAR Collab.)	AUBERT	01G	PRL 87 221802	B. Aubert et al.	(BaBar Collab.)
AUSHEV	04	PRL 93 201802	T. Aushev et al.	(BELLE Collab.)	AUBERT	01H	PRL 87 241801	B. Aubert et al.	(BaBar Collab.)
BORNHEIM	04	PRL 93 241802	A. Bornheim et al.	(CLEO Collab.)	AUBERT	01I	PRL 87 241803	B. Aubert et al.	(BaBar Collab.)
CHANG	04	PL B599 148	P. Chang et al.	(BELLE Collab.)	BARATE	01D	EPJ C20 431	R. Barate et al.	(ALEPH Collab.)
CHAO	04	PR D69 111102R	Y. Chao et al.	(BELLE Collab.)	BRIERE	01	PRL 86 3718	R.A. Briere et al.	(CLEO Collab.)
CHAO	04B	PRL 93 191802	Y. Chao et al.	(BELLE Collab.)	EDWARDS	01	PRL 86 30	K.W. Edwards et al.	(CLEO Collab.)
DRAGIC	04	PRL 93 131802	J. Dragic	(BELLE Collab.)	JAFFE	01	PRL 86 5000	D. Jaffe et al.	(CLEO Collab.)
DRUTSKOY	04	PRL 92 051801	A. Drutskoy et al.	(BELLE Collab.)	RICHIHI	01	PR D63 031103R	S.J. Richichi et al.	(CLEO Collab.)
GARMASH	04	PR D69 012001	A. Garmash et al.	(BELLE Collab.)	ABBIENDI	00Q	PL B482 15	G. Abbiendi et al.	(OPAL Collab.)
KATAOKA	04	PRL 93 261801	S.U. Kataoka et al.	(BELLE Collab.)	ABBIENDI,G	00C	PL B493 266	G. Abbiendi et al.	(OPAL Collab.)
MAJUMDER	04	PR D70 11103R	G. Majumder et al.	(BELLE Collab.)	ABE	00C	PR D62 071101R	K. Abe et al.	(CLEO Collab.)
NAKAO	04	PR D69 112001	M. Nakao et al.	(BELLE Collab.)	AFFOLDER	00B	PR D61 072005	T. Affolder et al.	(CDF Collab.)
SARANGI	04	PRL 93 031802	T.R. Sarangi et al.	(BELLE Collab.)	AFFOLDER	00C	PRL 85 4668	T. Affolder et al.	(CDF Collab.)
WANG	04	PRL 92 131801	M.Z. Wang et al.	(BELLE Collab.)	AHMED	00B	PR D62 112003	S. Ahmed et al.	(CLEO Collab.)
WANG	04A	PR D70 012001	C.H. Wang et al.	(BELLE Collab.)	ANASTASSOV	00	PRL 84 1393	A. Anastassov et al.	(CLEO Collab.)
ABDALLAH	03B	EPJ C28 155	J. Abdallah et al.	(DELPHI Collab.)	ARTUSO	00	PRL 84 4292	M. Artuso et al.	(CLEO Collab.)
ABE	03B	PR D67 032003	K. Abe et al.	(BELLE Collab.)	AREY	00	PR D62 051101	P. Arey et al.	(CLEO Collab.)
ABE	03C	PR D67 031102R	K. Abe et al.	(BELLE Collab.)	BARATE	00Q	PL B492 259	R. Barate et al.	(ALEPH Collab.)
ABE	03G	PR D68 012001	K. Abe et al.	(BELLE Collab.)	BARATE	00R	PL B492 275	R. Barate et al.	(ALEPH Collab.)
ABE	03H	PRL 91 261602	K. Abe et al.	(BELLE Collab.)	BEHRENS	00	PR D61 052001	B.H. Behrens et al.	(CLEO Collab.)
ADAM	03	PR D67 032001	N.E. Adam et al.	(CLEO Collab.)	BEHRENS	00B	PL B490 36	B.H. Behrens et al.	(CLEO Collab.)
ATHAR	03	PR D68 072003	S.E. Athar et al.	(CLEO Collab.)	BERGFELD	00B	PR D62 091102R	T. Bergfeld et al.	(CLEO Collab.)
AUBERT	03B	PRL 90 091801	B. Aubert et al.	(BaBar Collab.)	CHEN	00	PRL 85 525	S. Chen et al.	(CLEO Collab.)
AUBERT	03C	PR D67 072002	B. Aubert et al.	(BaBar Collab.)	COAN	00	PRL 84 5283	T.E. Coan et al.	(CLEO Collab.)
AUBERT	03D	PRL 90 181803	B. Aubert et al.	(BaBar Collab.)	CRONIN-HENNESSY	00	PRL 85 515	D. Cronin-Hennessy et al.	(CLEO Collab.)
AUBERT	03E	PRL 90 181801	B. Aubert et al.	(BaBar Collab.)	CSORNA	00	PR D61 111101	S.E. Csorna et al.	(CLEO Collab.)
AUBERT	03H	PR D67 091101R	B. Aubert et al.	(BaBar Collab.)	JESSOP	00	PRL 85 2881	C.P. Jessop et al.	(CLEO Collab.)
AUBERT	03I	PR D67 092003	B. Aubert et al.	(BaBar Collab.)	LIPELES	00	PR D62 032005	E. Lipeles et al.	(CLEO Collab.)
AUBERT	03J	PRL 90 221801	B. Aubert et al.	(BaBar Collab.)	RICHIHI	00	PRL 85 520	S.J. Richichi et al.	(CLEO Collab.)
AUBERT	03K	PRL 90 231801	B. Aubert et al.	(BaBar Collab.)	ABBIENDI	99J	EPJ C12 609	G. Abbiendi et al.	(OPAL Collab.)
AUBERT	03L	PRL 91 021801	B. Aubert et al.	(BaBar Collab.)	ABE	99K	PR D60 051101	F. Abe et al.	(CDF Collab.)
AUBERT	03N	PRL 91 061802	B. Aubert et al.	(BaBar Collab.)	ABE	99Q	PR D60 072003	F. Abe et al.	(CDF Collab.)
AUBERT	03O	PRL 91 071801	B. Aubert et al.	(BaBar Collab.)	AFFOLDER	99B	PRL 83 3378	T. Affolder et al.	(CDF Collab.)
AUBERT	03Q	PRL 91 131801	B. Aubert et al.	(BaBar Collab.)	AFFOLDER	99C	PR D60 112004	T. Affolder et al.	(CDF Collab.)
AUBERT	03S	PRL 91 241801	B. Aubert et al.	(BaBar Collab.)	ARTUSO	99	PRL 82 3020	M. Artuso et al.	(CLEO Collab.)
AUBERT	03T	PRL 91 201802	B. Aubert et al.	(BaBar Collab.)	BARTELT	99	PRL 82 3746	J. Bartelt et al.	(CLEO Collab.)
AUBERT	03U	PRL 91 221802	B. Aubert et al.	(BaBar Collab.)	COAN	99	PR D59 111101	T.E. Coan et al.	(CLEO Collab.)
AUBERT	03V	PRL 91 171802	B. Aubert et al.	(BaBar Collab.)	ABBOTT	98B	PL B423 419	B. Abbott et al.	(DO Collab.)
AUBERT	03W	PRL 91 161801	B. Aubert et al.	(BaBar Collab.)	ABE	98	PR D57 R3811	F. Abe et al.	(CDF Collab.)
AUBERT	03X	PR D68 092001							

Meson Particle Listings

 $B^0, B^\pm/B^0$ ADMIXTURE

Mode	Fraction (Γ_i/Γ)	Scale factor/ Confidence level
B^\pm/B^0 ADMIXTURE		
B DECAY MODES		
The branching fraction measurements are for an admixture of B mesons at the $\Upsilon(4S)$. The values quoted assume that $B(\Upsilon(4S) \rightarrow B\bar{B}) = 100\%$.		
For inclusive branching fractions, e.g., $B \rightarrow D^\pm$ anything, the treatment of multiple D 's in the final state must be defined. One possibility would be to count the number of events with one-or-more D 's and divide by the total number of B 's. Another possibility would be to count the total number of D 's and divide by the total number of B 's, which is the definition of average multiplicity. The two definitions are identical if only one D is allowed in the final state. Even though the "one-or-more" definition seems sensible, for practical reasons inclusive branching fractions are almost always measured using the multiplicity definition. For heavy final state particles, authors call their results inclusive branching fractions while for light particles some authors call their results multiplicities. In the B sections, we list all results as inclusive branching fractions, adopting a multiplicity definition. This means that inclusive branching fractions can exceed 100% and that inclusive partial widths can exceed total widths, just as inclusive cross sections can exceed total cross section.		
\bar{B} modes are charge conjugates of the modes below. Reactions indicate the weak decay vertex and do not include mixing.		
Semileptonic and leptonic modes		
Γ_1	$B \rightarrow e^+ \nu_e$ anything	[a] (10.74 \pm 0.16) %
Γ_2	$B \rightarrow \bar{\nu}_e e^+$ anything	< 5.9 $\times 10^{-4}$ CL=90%
Γ_3	$B \rightarrow \mu^+ \nu_\mu$ anything	[a] (10.74 \pm 0.16) %
Γ_4	$B \rightarrow \ell^+ \nu_\ell$ anything	[a,b] (10.74 \pm 0.16) %
Γ_5	$B \rightarrow D^- \ell^+ \nu_\ell$ anything	[b] (2.8 \pm 0.9) %
Γ_6	$B \rightarrow \bar{D}^0 \ell^+ \nu_\ell$ anything	[b] (7.2 \pm 1.4) %
Γ_7	$B \rightarrow D \tau^+ \nu_\tau$	(8.6 \pm 2.7) $\times 10^{-3}$
Γ_8	$B \rightarrow D^{*-} \ell^+ \nu_\ell$ anything	[c] (6.7 \pm 1.3) $\times 10^{-3}$
Γ_9	$B \rightarrow D^{*0} \ell^+ \nu_\ell$ anything	(1.62 \pm 0.33) %
Γ_{10}	$B \rightarrow D^* \tau^+ \nu_\tau$	(2.7 \pm 0.7) %
Γ_{11}	$B \rightarrow \bar{D}^{*+} \ell^+ \nu_\ell$	[b,d] (3.8 \pm 1.3) $\times 10^{-3}$ S=2.4
Γ_{12}	$B \rightarrow \bar{D}_1(2420) \ell^+ \nu_\ell$ anything	(2.6 \pm 0.5) % S=1.5
Γ_{13}	$B \rightarrow D \pi \ell^+ \nu_\ell$ anything + $D^* \pi \ell^+ \nu_\ell$ anything	(1.5 \pm 0.6) %
Γ_{14}	$B \rightarrow D \pi \ell^+ \nu_\ell$ anything	(1.9 \pm 0.4) %
Γ_{15}	$B \rightarrow D^* \pi \ell^+ \nu_\ell$ anything	(4.4 \pm 1.6) $\times 10^{-3}$
Γ_{16}	$B \rightarrow \bar{D}_2^*(2460) \ell^+ \nu_\ell$ anything	(1.00 \pm 0.34) %
Γ_{17}	$B \rightarrow D^{*-} \pi^+ \ell^+ \nu_\ell$ anything	(1.00 \pm 0.34) %
Γ_{18}	$B \rightarrow D_s^- \ell^+ \nu_\ell$ anything	[b] < 7 $\times 10^{-3}$ CL=90%
Γ_{19}	$B \rightarrow D_s^- \ell^+ \nu_\ell K^+$ anything	[b] < 5 $\times 10^{-3}$ CL=90%
Γ_{20}	$B \rightarrow D_s^- \ell^+ \nu_\ell K^0$ anything	[b] < 7 $\times 10^{-3}$ CL=90%
Γ_{21}	$B \rightarrow \ell^+ \nu_\ell$ charm	(10.57 \pm 0.15) %
Γ_{22}	$B \rightarrow X_u \ell^+ \nu_\ell$	(2.33 \pm 0.22) $\times 10^{-3}$
Γ_{23}	$B \rightarrow \pi \ell \nu_\ell$	(1.35 \pm 0.10) $\times 10^{-4}$
Γ_{24}	$B \rightarrow K^+ \ell^+ \nu_\ell$ anything	[b] (6.2 \pm 0.5) %
Γ_{25}	$B \rightarrow K^- \ell^+ \nu_\ell$ anything	[b] (10 \pm 4) $\times 10^{-3}$
Γ_{26}	$B \rightarrow K^0/\bar{K}^0 \ell^+ \nu_\ell$ anything	[b] (4.5 \pm 0.5) %
D, D*, or D_s modes		
Γ_{27}	$B \rightarrow D^\pm$ anything	(23.5 \pm 1.3) %
Γ_{28}	$B \rightarrow D^0/\bar{D}^0$ anything	(62.5 \pm 2.9) % S=1.3
Γ_{29}	$B \rightarrow D^*(2010)^\pm$ anything	(22.5 \pm 1.5) %
Γ_{30}	$B \rightarrow D^*(2007)^0$ anything	(26.0 \pm 2.7) %
Γ_{31}	$B \rightarrow D_s^\pm$ anything	[e] (8.5 \pm 0.8) %
Γ_{32}	$B \rightarrow D_s^{*\pm}$ anything	(6.5 \pm 1.0) %
Γ_{33}	$B \rightarrow D_s^{*0}$	(3.5 \pm 0.6) %
Γ_{34}	$B \rightarrow \bar{D} D_{s0}(2317)$	

Γ ₃₅	$B \rightarrow \bar{D} D_{sJ}(2457)$		
Γ ₃₆	$B \rightarrow D^{(*)} \bar{D}^{(*)} K^0 + D^{(*)} \bar{D}^{(*)} K^\pm$	[e,f] (7.1 \pm 2.7 \pm 1.7) %	
Γ ₃₇	$b \rightarrow c \bar{c} s$	(22 \pm 4) %	
Γ ₃₈	$B \rightarrow D_s^{(*)} \bar{D}^{(*)}$	[e,f] (4.0 \pm 0.4) %	
Γ ₃₉	$B \rightarrow D^* D^*(2010)^\pm$	[e] < 5.9 $\times 10^{-3}$ CL=90%	
Γ ₄₀	$B \rightarrow D D^*(2010)^\pm + D^* D^\pm$	[e] < 5.5 $\times 10^{-3}$ CL=90%	
Γ ₄₁	$B \rightarrow D D^\pm$	[e] < 3.1 $\times 10^{-3}$ CL=90%	
Γ ₄₂	$B \rightarrow D_s^{(*)} \bar{D}^{(*)} X(n\pi^\pm)$	[e,f] (9 \pm 5 \pm 4) %	
Γ ₄₃	$B \rightarrow D^*(2010)\gamma$	< 1.1 $\times 10^{-3}$ CL=90%	
Γ ₄₄	$B \rightarrow D_s^+ \pi^-, D_s^{*+} \pi^-, D_s^{*+} \rho^-, D_s^{*+} \rho^-, D_s^+ \pi^0, D_s^{*+} \pi^0, D_s^+ \eta, D_s^{*+} \eta, D_s^+ \rho^0, D_s^{*+} \rho^0, D_s^+ \omega, D_s^{*+} \omega$	[e] < 4 $\times 10^{-4}$ CL=90%	
Γ ₄₅	$B \rightarrow D_{s1}(2536)^+ \text{ anything}$	< 9.5 $\times 10^{-3}$ CL=90%	
Charmonium modes			
Γ ₄₆	$B \rightarrow J/\psi(1S) \text{ anything}$	(1.094 \pm 0.032) %	S=1.1
Γ ₄₇	$B \rightarrow J/\psi(1S) \text{ (direct) anything}$	(7.8 \pm 0.4) $\times 10^{-3}$	S=1.1
Γ ₄₈	$B \rightarrow \psi(2S) \text{ anything}$	(3.07 \pm 0.21) $\times 10^{-3}$	
Γ ₄₉	$B \rightarrow \chi_{c1}(1P) \text{ anything}$	(3.86 \pm 0.27) $\times 10^{-3}$	
Γ ₅₀	$B \rightarrow \chi_{c1}(1P) \text{ (direct) anything}$	(3.16 \pm 0.25) $\times 10^{-3}$	
Γ ₅₁	$B \rightarrow \chi_{c2}(1P) \text{ anything}$	(1.3 \pm 0.4) $\times 10^{-3}$	S=1.9
Γ ₅₂	$B \rightarrow \chi_{c2}(1P) \text{ (direct) anything}$	(1.65 \pm 0.31) $\times 10^{-3}$	
Γ ₅₃	$B \rightarrow \eta_c(1S) \text{ anything}$	< 9 $\times 10^{-3}$ CL=90%	
Γ ₅₄	$B^0 \rightarrow X(3872) K \times B(X \rightarrow D^0 \bar{D}^0 \pi^0)$	(1.2 \pm 0.4) $\times 10^{-4}$	
Γ ₅₅	$B \rightarrow KX(3945) \times B(X(3945) \rightarrow \omega J/\psi)$	[g] (7.1 \pm 3.4) $\times 10^{-5}$	
K or K* modes			
Γ ₅₆	$B \rightarrow K^\pm \text{ anything}$	[e] (78.9 \pm 2.5) %	
Γ ₅₇	$B \rightarrow K^+ \text{ anything}$	(78.9 \pm 2.5) %	
Γ ₅₈	$B \rightarrow K^- \text{ anything}$	(13 \pm 4) %	
Γ ₅₉	$B \rightarrow K^0/\bar{K}^0 \text{ anything}$	[e] (64 \pm 4) %	
Γ ₆₀	$B \rightarrow K^*(892)^\pm \text{ anything}$	(18 \pm 6) %	
Γ ₆₁	$B \rightarrow K^*(892)^0/\bar{K}^*(892)^0 \text{ anything}$	[e] (14.6 \pm 2.6) %	
Γ ₆₂	$B \rightarrow K^*(892)\gamma$	(4.2 \pm 0.6) $\times 10^{-5}$	
Γ ₆₃	$B \rightarrow \eta K\gamma$	(8.5 \pm 1.8 \pm 1.6) $\times 10^{-6}$	
Γ ₆₄	$B \rightarrow K_1(1400)\gamma$	< 1.27 $\times 10^{-4}$ CL=90%	
Γ ₆₅	$B \rightarrow K_2^*(1430)\gamma$	(1.7 \pm 0.6 \pm 0.5) $\times 10^{-5}$	
Γ ₆₆	$B \rightarrow K_2(1770)\gamma$	< 1.2 $\times 10^{-3}$ CL=90%	
Γ ₆₇	$B \rightarrow K_3^*(1780)\gamma$	< 3.7 $\times 10^{-5}$ CL=90%	
Γ ₆₈	$B \rightarrow K_4^*(2045)\gamma$	< 1.0 $\times 10^{-3}$ CL=90%	
Γ ₆₉	$B \rightarrow K\eta'(958)$	(8.3 \pm 1.1) $\times 10^{-5}$	
Γ ₇₀	$B \rightarrow K^*(892)\eta'(958)$	(4.1 \pm 1.1) $\times 10^{-6}$	
Γ ₇₁	$B \rightarrow K\eta$	< 5.2 $\times 10^{-6}$ CL=90%	
Γ ₇₂	$B \rightarrow K^*(892)\eta$	(1.8 \pm 0.5) $\times 10^{-5}$	
Γ ₇₃	$B \rightarrow K\phi\phi$	(2.3 \pm 0.9) $\times 10^{-6}$	
Γ ₇₄	$B \rightarrow \bar{b} \rightarrow \bar{s}\gamma$	(3.56 \pm 0.25) $\times 10^{-4}$	
Γ ₇₅	$B \rightarrow \bar{b} \rightarrow \bar{s} \text{ gluon}$	< 6.8 % CL=90%	
Γ ₇₆	$B \rightarrow \eta \text{ anything}$	< 4.4 $\times 10^{-4}$ CL=90%	
Γ ₇₇	$B \rightarrow \eta' \text{ anything}$	(4.2 \pm 0.9) $\times 10^{-4}$	
Light unflavored meson modes			
Γ ₇₈	$B \rightarrow \rho\gamma$	(1.36 \pm 0.30) $\times 10^{-6}$	
Γ ₇₉	$B \rightarrow \rho/\omega\gamma$	(1.28 \pm 0.21) $\times 10^{-6}$	
Γ ₈₀	$B \rightarrow \pi^\pm \text{ anything}$	[e,h] (358 \pm 7) %	
Γ ₈₁	$B \rightarrow \pi^0 \text{ anything}$	(235 \pm 11) %	
Γ ₈₂	$B \rightarrow \eta \text{ anything}$	(17.6 \pm 1.6) %	
Γ ₈₃	$B \rightarrow \rho^0 \text{ anything}$	(21 \pm 5) %	
Γ ₈₄	$B \rightarrow \omega \text{ anything}$	< 81 % CL=90%	
Γ ₈₅	$B \rightarrow \phi \text{ anything}$	(3.43 \pm 0.12) %	
Γ ₈₆	$B \rightarrow \phi K^*(892)$	< 2.2 $\times 10^{-5}$ CL=90%	
Baryon modes			
Γ ₈₇	$B \rightarrow \Lambda_c^+ / \bar{\Lambda}_c^- \text{ anything}$	(4.5 \pm 1.2) %	
Γ ₈₈	$B \rightarrow \Lambda_c^+ \text{ anything}$		
Γ ₈₉	$B \rightarrow \bar{\Lambda}_c^- \text{ anything}$		
Γ ₉₀	$B \rightarrow \bar{\Lambda}_c^- e^+ \text{ anything}$	< 2.3 $\times 10^{-3}$ CL=90%	

Γ ₉₁	$B \rightarrow \bar{\Lambda}_c^- p \text{ anything}$	(2.6 \pm 0.8) %	
Γ ₉₂	$B \rightarrow \bar{\Lambda}_c^- p e^+ \nu_e$	< 1.0 $\times 10^{-3}$ CL=90%	
Γ ₉₃	$B \rightarrow \bar{\Sigma}_c^- \text{ anything}$	(4.2 \pm 2.4) $\times 10^{-3}$	
Γ ₉₄	$B \rightarrow \bar{\Sigma}_c^0 \text{ anything}$	< 9.6 $\times 10^{-3}$ CL=90%	
Γ ₉₅	$B \rightarrow \bar{\Sigma}_c^+ \text{ anything}$	(4.6 \pm 2.4) $\times 10^{-3}$	
Γ ₉₆	$B \rightarrow \bar{\Sigma}_c^0 N(N = p \text{ or } n)$	< 1.5 $\times 10^{-3}$ CL=90%	
Γ ₉₇	$B \rightarrow \Xi_c^- \text{ anything}$ $\times B(\Xi_c^0 \rightarrow \Xi^- \pi^+)$	(1.93 \pm 0.30) $\times 10^{-4}$ S=1.1	
Γ ₉₈	$B \rightarrow \Xi_c^+ \text{ anything}$ $\times B(\Xi_c^+ \rightarrow \Xi^- \pi^+ \pi^+)$	(4.5 \pm 1.3 \pm 1.2) $\times 10^{-4}$	
Γ ₉₉	$B \rightarrow p/\bar{p} \text{ anything}$	[e] (8.0 \pm 0.4) %	
Γ ₁₀₀	$B \rightarrow p/\bar{p} \text{ (direct) anything}$	[e] (5.5 \pm 0.5) %	
Γ ₁₀₁	$B \rightarrow \Lambda/\bar{\Lambda} \text{ anything}$	[e] (4.0 \pm 0.5) %	
Γ ₁₀₂	$B \rightarrow \Lambda \text{ anything}$		
Γ ₁₀₃	$B \rightarrow \bar{\Lambda} \text{ anything}$		
Γ ₁₀₄	$B \rightarrow \Xi^-/\bar{\Xi}^+ \text{ anything}$	[e] (2.7 \pm 0.6) $\times 10^{-3}$	
Γ ₁₀₅	$B \rightarrow \text{baryons anything}$	(6.8 \pm 0.6) %	
Γ ₁₀₆	$B \rightarrow p\bar{p} \text{ anything}$	(2.47 \pm 0.23) %	
Γ ₁₀₇	$B \rightarrow \Lambda\bar{\Lambda} p \text{ anything}$	[e] (2.5 \pm 0.4) %	
Γ ₁₀₈	$B \rightarrow \Lambda\bar{\Lambda} \text{ anything}$	< 5 $\times 10^{-3}$ CL=90%	

Lepton Family number (LF) violating modes or $\Delta B = 1$ weak neutral current (BI) modes

Γ ₁₀₉	$B \rightarrow s e^+ e^-$	BI	(4.7 \pm 1.3) $\times 10^{-6}$
Γ ₁₁₀	$B \rightarrow s \mu^+ \mu^-$	BI	(4.3 \pm 1.2) $\times 10^{-6}$
Γ ₁₁₁	$B \rightarrow s \ell^+ \ell^-$	BI [b]	(4.5 \pm 1.0) $\times 10^{-6}$
Γ ₁₁₂	$B \rightarrow \pi \ell^+ \ell^-$		< 9.1 $\times 10^{-8}$ CL=90%
Γ ₁₁₃	$B \rightarrow K e^+ e^-$	BI	(3.8 \pm 0.8 \pm 0.7) $\times 10^{-7}$
Γ ₁₁₄	$B \rightarrow K^*(892) e^+ e^-$	BI	(1.13 \pm 0.27) $\times 10^{-6}$
Γ ₁₁₅	$B \rightarrow K \mu^+ \mu^-$	BI	(4.2 \pm 0.9 \pm 0.8) $\times 10^{-7}$
Γ ₁₁₆	$B \rightarrow K^*(892) \mu^+ \mu^-$	BI	(1.03 \pm 0.26 \pm 0.23) $\times 10^{-6}$
Γ ₁₁₇	$B \rightarrow K \ell^+ \ell^-$	BI	(3.9 \pm 0.7) $\times 10^{-7}$ S=1.2
Γ ₁₁₈	$B \rightarrow K^*(892) \ell^+ \ell^-$	BI	(9.4 \pm 1.8) $\times 10^{-7}$ S=1.1
Γ ₁₁₉	$B \rightarrow s e^\pm \mu^\mp$	LF [e]	< 2.2 $\times 10^{-5}$ CL=90%
Γ ₁₂₀	$B \rightarrow \pi e^\pm \mu^\mp$	LF	< 9.2 $\times 10^{-8}$ CL=90%
Γ ₁₂₁	$B \rightarrow \rho e^\pm \mu^\mp$	LF	< 3.2 $\times 10^{-6}$ CL=90%
Γ ₁₂₂	$B \rightarrow K e^\pm \mu^\mp$	LF	< 3.8 $\times 10^{-8}$ CL=90%
Γ ₁₂₃	$B \rightarrow K^*(892) e^\pm \mu^\mp$	LF	< 5.1 $\times 10^{-7}$ CL=90%

[a] These values are model dependent.

[b] An ℓ indicates an e or a μ mode, not a sum over these modes.

[c] Here "anything" means at least one particle observed.

[d] D^{**} stands for the sum of the $D(1^1P_1)$, $D(1^3P_0)$, $D(1^3P_1)$, $D(1^3P_2)$, $D(2^1S_0)$, and $D(2^1S_1)$ resonances.

[e] The value is for the sum of the charge states or particle/antiparticle states indicated.

[f] $D^{(*)} \bar{D}^{(*)}$ stands for the sum of $D^* \bar{D}^*$, $D^* \bar{D}$, $D \bar{D}^*$, and $D \bar{D}$.

[g] $X(3945)$ denotes a near-threshold enhancement in the $\omega J/\psi$ mass spectrum.

[h] Inclusive branching fractions have a multiplicity definition and can be greater than 100%.

B^\pm/B^0 ADMIXTURE BRANCHING RATIOS

$\Gamma(e^+ \nu_e \text{ anything})/\Gamma_{\text{total}}$

These branching fraction values are model dependent.

Γ_1/Γ

"OUR EVALUATION" is an average using rescaled values of the data listed below. The average and rescaling were performed by the Heavy Flavor Averaging Group (HFAG) and are described at <http://www.slac.stanford.edu/xorg/hfag/>. The averaging/rescaling procedure takes into account correlations between the measurements.

VALUE DOCUMENT ID TECN COMMENT

The data in this block is included in the average printed for a previous datablock.

0.1074 \pm 0.0016 OUR EVALUATION

0.1044 \pm 0.0025 OUR AVERAGE Error includes scale factor of 1.5. See the ideogram below.

0.1028 \pm 0.0018 \pm 0.0024	¹ URQUIJO	07	BELL	$e^+ e^- \rightarrow \Upsilon(4S)$
0.0996 \pm 0.0019 \pm 0.0032	² AUBERT,B	06Y	BABR	$e^+ e^- \rightarrow \Upsilon(4S)$
0.1091 \pm 0.0009 \pm 0.0024	³ MAHMOOD	04	CLEO	$e^+ e^- \rightarrow \Upsilon(4S)$
0.097 \pm 0.005 \pm 0.004	⁴ ALBRECHT	93H	ARG	$e^+ e^- \rightarrow \Upsilon(4S)$

Meson Particle Listings

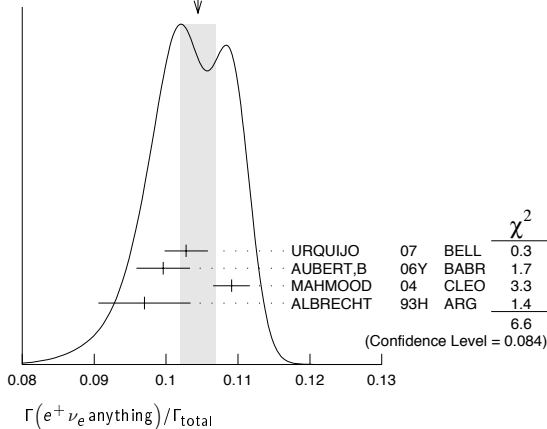
B^\pm/B^0 ADMIXTURE

••• We do not use the following data for averages, fits, limits, etc. •••

0.1085 ± 0.0021 ± 0.0036	5	OKABE	05	BELL	Repl. by URQUIJO 07
0.1083 ± 0.0016 ± 0.0006	6	AUBERT	04X	BABR	Repl. by AUBERT,B 06Y
0.1036 ± 0.0006 ± 0.0023	7	AUBERT,B	04A	BABR	$e^+e^- \rightarrow \Upsilon(4S)$
0.1087 ± 0.0018 ± 0.0030	8	AUBERT	03	BABR	Repl. by AUBERT 04X
0.109 ± 0.0012 ± 0.0049	9	ABE	02Y	BELL	Repl. by OKABE 05
0.1049 ± 0.0017 ± 0.0043	10	BARISH	96B	CLE2	Repl. by MAHMOOD 04
0.100 ± 0.004 ± 0.003	11	YANAGISAWA	91	CSB2	$e^+e^- \rightarrow \Upsilon(4S)$
0.103 ± 0.006 ± 0.002	12	ALBRECHT	90H	ARG	$e^+e^- \rightarrow \Upsilon(4S)$
0.117 ± 0.004 ± 0.010	13	WACHS	89	CBAL	Direct e at $\Upsilon(4S)$
0.120 ± 0.007 ± 0.005		CHEN	84	CLEO	Direct e at $\Upsilon(4S)$
0.132 ± 0.008 ± 0.014	14	KLOPFEN...	83B	CUSB	Direct e at $\Upsilon(4S)$

- URQUIJO 07 report a measurement of $(10.07 \pm 0.18 \pm 0.21)\%$ for the partial branching fraction of $B \rightarrow e\nu_e X_c$ decay with electron energy above 0.6 GeV. We converted the result to $B \rightarrow e\nu_e X$ branching fraction.
- The measurements are obtained for charged and neutral B mesons partial rates of semileptonic decay to electrons with momentum above 0.6 GeV/c in the B rest frame. The best precision on the ratio is achieved for a momentum threshold of 1.0 GeV: $B(B^+ \rightarrow e^+ \nu_e X) / B(B^0 \rightarrow e^+ \nu_e X) = 1.074 \pm 0.041 \pm 0.026$.
- Uses charge and angular correlations in $\Upsilon(4S)$ events with a high-momentum lepton and an additional electron.
- ALBRECHT 93H analysis performed using tagged semileptonic decays of the B . This technique is almost model independent for the lepton branching ratio.
- The measurements are obtained for charged and neutral B mesons partial rates of semileptonic decay to electrons with momentum above 0.6 GeV/c in the B rest frame, and their ratio of $B(B^+ \rightarrow e^+ \nu_e X) / B(B^0 \rightarrow e^+ \nu_e X) = 1.08 \pm 0.05 \pm 0.02$.
- The semileptonic branching ratio, $|V_{cb}|$ and other heavy-quark parameters are determined from a simultaneous fit to moments of the hadronic-mass and lepton-energy distribution.
- Uses the high-momentum lepton tag method and requires the electron energy above 0.6 GeV.
- Uses the high-momentum lepton tag method. They also report $|V_{cb}| = 0.0423 \pm 0.0007(\text{exp}) \pm 0.0020(\text{theo})$.
- Uses the high-momentum lepton tag method. ABE 02Y also reports $|V_{cb}| = 0.0408 \pm 0.0010(\text{exp}) \pm 0.0025(\text{theo})$. The second error is due to uncertainties of theoretical inputs.
- BARISH 96B analysis performed using tagged semileptonic decays of the B . This technique is almost model independent for the lepton branching ratio.
- YANAGISAWA 91 also measures an average semileptonic branching ratio at the $\Upsilon(5S)$ of 9.6–10.5% depending on assumptions about the relative production of different B meson species.
- ALBRECHT 90H uses the model of ALTARELLI 82 to correct over all lepton momenta. 0.099 ± 0.006 is obtained using ISGUR 89b.
- Using data above $p(e) = 2.4$ GeV, WACHS 89 determine $\sigma(B \rightarrow e\nu\mu)/\sigma(B \rightarrow e\nu\text{charm}) < 0.065$ at 90% CL.
- Ratio $\sigma(B \rightarrow e\nu\mu)/\sigma(B \rightarrow e\nu\text{charm}) < 0.055$ at CL = 90%.

WEIGHTED AVERAGE
0.1044±0.0025 (Error scaled by 1.5)



$\Gamma(\bar{p}e^+\nu_e \text{ anything})/\Gamma_{\text{total}}$ Γ_2/Γ

VALUE	CL%	DOCUMENT ID	TECN	COMMENT
$<5.9 \times 10^{-4}$	90	1 ADAM	03B	CLE2 $e^+e^- \rightarrow \Upsilon(4S)$

••• We do not use the following data for averages, fits, limits, etc. •••

<0.0016	90	ALBRECHT	90H	ARG $e^+e^- \rightarrow \Upsilon(4S)$
-----------	----	----------	-----	---------------------------------------

¹Based on V–A model.

$\Gamma(\mu^+\nu_\mu \text{ anything})/\Gamma_{\text{total}}$ Γ_3/Γ

These branching fraction values are model dependent.

“OUR EVALUATION” is an average using rescaled values of the data listed below. The average and rescaling were performed by the Heavy Flavor Averaging Group (HFAG) and are described at <http://www.slac.stanford.edu/xorg/hfag/>. The averaging/rescaling procedure takes into account correlations between the measurements.

VALUE	DOCUMENT ID	TECN	COMMENT
The data in this block is included in the average printed for a previous datablock.			

0.1074 ± 0.0016 OUR EVALUATION

••• We do not use the following data for averages, fits, limits, etc. •••

0.100 ± 0.006 ± 0.002	¹ ALBRECHT	90H	ARG $e^+e^- \rightarrow \Upsilon(4S)$
0.108 ± 0.006 ± 0.01	CHEN	84	CLEO Direct μ at $\Upsilon(4S)$
0.112 ± 0.009 ± 0.01	LEVMAN	84	CUSB Direct μ at $\Upsilon(4S)$

¹ALBRECHT 90H uses the model of ALTARELLI 82 to correct over all lepton momenta. 0.097 ± 0.006 is obtained using ISGUR 89b.

$\Gamma(\ell^+\nu_\ell \text{ anything})/\Gamma_{\text{total}}$ Γ_4/Γ

These branching fraction values are model dependent.

“OUR EVALUATION” is an average using rescaled values of the data listed below. The average and rescaling were performed by the Heavy Flavor Averaging Group (HFAG) and are described at <http://www.slac.stanford.edu/xorg/hfag/>. The averaging/rescaling procedure takes into account correlations between the measurements.

VALUE	DOCUMENT ID	TECN	COMMENT
0.1074 ± 0.0016 OUR EVALUATION			

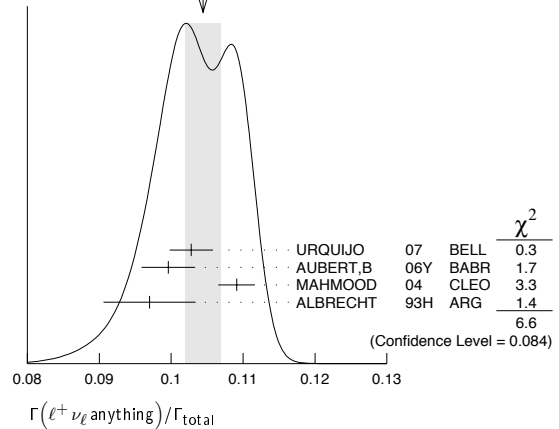
0.1044 ± 0.0025 OUR AVERAGE Includes data from the 2 datablocks that follow this one. Error includes scale factor of 1.5. See the ideogram below.

••• We do not use the following data for averages, fits, limits, etc. •••

0.108 ± 0.002 ± 0.0056	¹ HENDERSON	92	CLEO $e^+e^- \rightarrow \Upsilon(4S)$
------------------------	------------------------	----	--

¹HENDERSON 92 measurement employs e and μ . The systematic error contains 0.004 in quadrature from model dependence. The authors average a variation of the Isgru, Scora, Grinstein, and Wise model with that of the Altarelli-Cabibbo-Corbò-Maiani-Martinelli model for semileptonic decays to correct the acceptance.

WEIGHTED AVERAGE
0.1044±0.0025 (Error scaled by 1.5)



$\Gamma(D^-\ell^+\nu_\ell \text{ anything})/\Gamma(\ell^+\nu_\ell \text{ anything})$ Γ_5/Γ_4

$\ell = e$ or μ .

VALUE	DOCUMENT ID	TECN	COMMENT
0.26 ± 0.07 ± 0.04	¹ FULTON	91	CLEO $e^+e^- \rightarrow \Upsilon(4S)$

¹FULTON 91 uses $B(D^+ \rightarrow K^-\pi^+\pi^+) = (9.1 \pm 1.3 \pm 0.4)\%$ as measured by MARK III.

$\Gamma(D^0\ell^+\nu_\ell \text{ anything})/\Gamma(\ell^+\nu_\ell \text{ anything})$ Γ_6/Γ_4

$\ell = e$ or μ .

VALUE	DOCUMENT ID	TECN	COMMENT
0.67 ± 0.09 ± 0.10	¹ FULTON	91	CLEO $e^+e^- \rightarrow \Upsilon(4S)$

¹FULTON 91 uses $B(D^0 \rightarrow K^-\pi^+) = (4.2 \pm 0.4 \pm 0.4)\%$ as measured by MARK III.

$\Gamma(D^+\tau^+\nu_\tau)/\Gamma_{\text{total}}$ Γ_7/Γ

VALUE (units 10^{-2})	DOCUMENT ID	TECN	COMMENT
0.86 ± 0.24 ± 0.12	¹ AUBERT	08N	BABR $e^+e^- \rightarrow \Upsilon(4S)$

¹Uses a fully reconstructed B meson as a tag on the recoil side.

$\Gamma(D^{*-\ell^+\nu_\ell \text{ anything})/\Gamma_{\text{total}}$ Γ_8/Γ

VALUE (units 10^{-2})	DOCUMENT ID	TECN	COMMENT
0.67 ± 0.08 ± 0.10	ABDALLAH	04D	DLPH $e^+e^- \rightarrow Z^0$

••• We do not use the following data for averages, fits, limits, etc. •••

0.6 ± 0.3 ± 0.1	¹ BARISH	95	CLE2 $e^+e^- \rightarrow \Upsilon(4S)$
-----------------	---------------------	----	--

¹BARISH 95 use $B(D^0 \rightarrow K^-\pi^+) = (3.91 \pm 0.08 \pm 0.17)\%$ and $B(D^{*+} \rightarrow D^0\pi^+) = (68.1 \pm 1.0 \pm 1.3)\%$.

$\Gamma(D^{*0}\ell^+\nu_\ell \text{ anything})/\Gamma_{\text{total}}$ Γ_9/Γ

VALUE (units 10^{-2})	DOCUMENT ID	TECN	COMMENT
0.6 ± 0.6 ± 0.1	¹ BARISH	95	CLE2 $e^+e^- \rightarrow \Upsilon(4S)$

¹BARISH 95 use $B(D^0 \rightarrow K^-\pi^+) = (3.91 \pm 0.08 \pm 0.17)\%$, $B(D^{*+} \rightarrow D^0\pi^+) = (68.1 \pm 1.0 \pm 1.3)\%$, $B(D^{*0} \rightarrow D^0\pi^0) = (63.6 \pm 2.3 \pm 3.3)\%$.

See key on page 373

Meson Particle Listings

B^\pm/B^0 ADMIXTURE

$\Gamma(D^* \tau^+ \nu_\tau)/\Gamma_{\text{total}}$	Γ_{10}/Γ
VALUE (units 10^{-2})	DOCUMENT ID TECN COMMENT
$1.62 \pm 0.31 \pm 0.11$	¹ AUBERT 08N BABR $e^+ e^- \rightarrow \Upsilon(4S)$

¹ Uses a fully reconstructed B meson as a tag on the recoil side. The results are normalized to the B^+ decay rate.

$\Gamma(D^{**} \ell^+ \nu_\ell)/\Gamma_{\text{total}}$	Γ_{11}/Γ
VALUE	DOCUMENT ID TECN COMMENT
$0.027 \pm 0.005 \pm 0.005$	63 ¹ ALBRECHT 93 ARG $e^+ e^- \rightarrow \Upsilon(4S)$

D^{**} stands for the sum of the $D(1^1P_1)$, $D(1^3P_0)$, $D(1^3P_1)$, $D(1^3P_2)$, $D(2^1S_0)$, and $D(2^3S_1)$ resonances. $\ell = e$ or μ , not sum over e and μ modes.

• • • We do not use the following data for averages, fits, limits, etc. • • •

<0.028 95 ² BARISH 95 CLE2 $e^+ e^- \rightarrow \Upsilon(4S)$

¹ ALBRECHT 93 assumes the GISW model to correct for unseen modes. Using the BHKT model, the result becomes $0.023 \pm 0.006 \pm 0.004$. Assumes $B(D^{**} \rightarrow D^0 \pi^+) = 68.1\%$, $B(D^0 \rightarrow K^- \pi^+) = 3.65\%$, $B(D^0 \rightarrow K^- \pi^+ \pi^- \pi^+) = 7.5\%$. We have taken their average e and μ value.

² BARISH 95 use $B(D^0 \rightarrow K^- \pi^+) = (3.91 \pm 0.08 \pm 0.17)\%$, assume all nonresonant channels are zero, and use GISW model for relative abundances of D^{**} states.

$\Gamma(\bar{D}_1(2420) \ell^+ \nu_\ell \text{ anything})/\Gamma_{\text{total}}$	Γ_{12}/Γ
VALUE	DOCUMENT ID TECN COMMENT
0.0038 ± 0.0013 OUR AVERAGE	Error includes scale factor of 2.4.

0.0033 \pm 0.0006 ¹ ABAZOV 05o D0 $p\bar{p}$ at 1.96 TeV

0.0074 \pm 0.0016 ² BUSKULIC 97b ALEP $e^+ e^- \rightarrow Z$

• • • We do not use the following data for averages, fits, limits, etc. • • •

seen ³ BUSKULIC 95b ALEP Repl. by BUSKULIC 97b

¹ Assumes $B(D_1 \rightarrow D^* \pi) = 1$, $B(D_1 \rightarrow D^* \pi^\pm) = 2/3$, and $B(b \rightarrow B) = 0.397$.

² BUSKULIC 97b assumes $B(D_1(2420) \rightarrow D^* \pi) = 1$, $B(D_1(2420) \rightarrow D^* \pi^\pm) = 2/3$, and $B(b \rightarrow B) = 0.378 \pm 0.022$.

³ BUSKULIC 95b reports $f_B \times B(B \rightarrow \bar{D}_1(2420)^0 \ell^+ \nu_\ell \text{ anything}) \times B(\bar{D}_1(2420)^0 \rightarrow \bar{D}^*(2010)^- \pi^+) = (2.04 \pm 0.58 \pm 0.34)10^{-3}$, where f_B is the production fraction for a single B charge state.

$[\Gamma(D \pi \ell^+ \nu_\ell \text{ anything}) + \Gamma(D^* \pi \ell^+ \nu_\ell \text{ anything})]/\Gamma_{\text{total}}$	Γ_{13}/Γ
VALUE	DOCUMENT ID TECN COMMENT
0.026 ± 0.005 OUR AVERAGE	Error includes scale factor of 1.5.

0.0340 \pm 0.0052 \pm 0.0032 ¹ ABREU 00R DLPH $e^+ e^- \rightarrow Z$

0.0226 \pm 0.0029 \pm 0.0033 ² BUSKULIC 97b ALEP $e^+ e^- \rightarrow Z$

¹ Assumes no contribution from B_s and b baryons. Further assumes contributions from single pion ($D \pi$ and $D^* \pi$) states only, allowing isospin conservation to relate the relative π^0 and π^\pm rates.

² BUSKULIC 97b assumes $B(b \rightarrow B) = 0.378 \pm 0.022$ and uses isospin invariance by assuming that all observed $D^0 \pi^+$, $D^{*0} \pi^+$, $D^+ \pi^-$, and $D^{*+} \pi^-$ are from D^{**} states. A correction has been applied to account for the production of B_s^0 and Λ_b^0 .

$\Gamma(D \pi \ell^+ \nu_\ell \text{ anything})/\Gamma_{\text{total}}$	Γ_{14}/Γ
VALUE	DOCUMENT ID TECN COMMENT
0.0154 ± 0.0061	ABREU 00R DLPH $e^+ e^- \rightarrow Z$

$\Gamma(D^* \pi \ell^+ \nu_\ell \text{ anything})/\Gamma_{\text{total}}$	Γ_{15}/Γ
VALUE	DOCUMENT ID TECN COMMENT
0.0186 ± 0.0038	ABREU 00R DLPH $e^+ e^- \rightarrow Z$

$\Gamma(\bar{D}_2^*(2460) \ell^+ \nu_\ell \text{ anything})/\Gamma_{\text{total}}$	Γ_{16}/Γ
VALUE	DOCUMENT ID TECN COMMENT
0.0044 ± 0.0016	¹ ABAZOV 05o D0 $p\bar{p}$ at 1.96 TeV

• • • We do not use the following data for averages, fits, limits, etc. • • •

<0.0065 95 ² BUSKULIC 97b ALEP $e^+ e^- \rightarrow Z$

not seen ³ BUSKULIC 95b ALEP $e^+ e^- \rightarrow Z$

¹ Assumes $B(D_2^* \rightarrow D^* \pi^\pm) = 0.30 \pm 0.06$ and $B(b \rightarrow B) = 0.397$.

² A revised number based on BUSKULIC 97b which assumes $B(D_2^*(2460) \rightarrow D^* \pi^\pm) = 0.20$ and $B(b \rightarrow B) = 0.378 \pm 0.022$.

³ BUSKULIC 95b reports $f_B \times B(B \rightarrow \bar{D}_2^*(2460)^0 \ell^+ \nu_\ell \text{ anything}) \times B(\bar{D}_2^*(2460)^0 \rightarrow \bar{D}^*(2010)^- \pi^+) \leq 0.81 \times 10^{-3}$ at CL=95%, where f_B is the production fraction for a single B charge state.

$\Gamma(B \rightarrow \bar{D}_2^*(2460) \ell^+ \nu_\ell \text{ anything}) \times B(\bar{D}_2^*(2460) \rightarrow D^{*-} \pi^+)$	$\Gamma(B \rightarrow \bar{D}_1(2420) \ell^+ \nu_\ell \text{ anything}) \times B(\bar{D}_1(2420) \rightarrow D^{*-} \pi^+)$
VALUE	DOCUMENT ID TECN COMMENT
$0.39 \pm 0.09 \pm 0.12$	ABAZOV 05o D0 $p\bar{p}$ at 1.96 TeV

$\Gamma(D^{*-} \pi^+ \ell^+ \nu_\ell \text{ anything})/\Gamma_{\text{total}}$	Γ_{17}/Γ
VALUE (units 10^{-3})	DOCUMENT ID TECN COMMENT
$10.0 \pm 2.7 \pm 2.1$	¹ BUSKULIC 95b ALEP $e^+ e^- \rightarrow Z$

Includes resonant and nonresonant contributions.

¹ BUSKULIC 95b reports $f_B \times B(B \rightarrow \bar{D}^*(2010)^- \pi^+ \ell^+ \nu_\ell \text{ anything}) = (3.7 \pm 1.0 \pm 0.7)10^{-3}$. Above value assumes $f_B = 0.37 \pm 0.03$.

$\Gamma(D_s^- \ell^+ \nu_\ell \text{ anything})/\Gamma_{\text{total}}$	Γ_{18}/Γ
VALUE	DOCUMENT ID TECN COMMENT
<0.007	90 ¹ ALBRECHT 93E ARG $e^+ e^- \rightarrow \Upsilon(4S)$

¹ ALBRECHT 93E reports <0.012 for $B(D_s^+ \rightarrow \phi \pi^+) = 0.027$. We rescale to our best value $B(D_s^+ \rightarrow \phi \pi^+) = 0.0438$.

$\Gamma(D_s^- \ell^+ \nu_\ell K^+ \text{ anything})/\Gamma_{\text{total}}$	Γ_{19}/Γ
VALUE	DOCUMENT ID TECN COMMENT
<0.005	90 ¹ ALBRECHT 93E ARG $e^+ e^- \rightarrow \Upsilon(4S)$

¹ ALBRECHT 93E reports <0.008 for $B(D_s^+ \rightarrow \phi \pi^+) = 0.027$. We rescale to our best value $B(D_s^+ \rightarrow \phi \pi^+) = 0.0438$.

$\Gamma(D_s^- \ell^+ \nu_\ell K^0 \text{ anything})/\Gamma_{\text{total}}$	Γ_{20}/Γ
VALUE	DOCUMENT ID TECN COMMENT
<0.007	90 ¹ ALBRECHT 93E ARG $e^+ e^- \rightarrow \Upsilon(4S)$

¹ ALBRECHT 93E reports <0.012 for $B(D_s^+ \rightarrow \phi \pi^+) = 0.027$. We rescale to our best value $B(D_s^+ \rightarrow \phi \pi^+) = 0.0438$.

$\Gamma(\ell^+ \nu_\ell \text{ charm})/\Gamma_{\text{total}}$	Γ_{21}/Γ
VALUE	DOCUMENT ID TECN COMMENT
0.1057 ± 0.0015 OUR AVERAGE	

0.1044 \pm 0.0019 \pm 0.0022 ¹ URQUIJO 07 BELL $e^+ e^- \rightarrow \Upsilon(4S)$

0.1061 \pm 0.0016 \pm 0.0006 ² AUBERT 04x BABR $e^+ e^- \rightarrow \Upsilon(4S)$

¹ Measured the independent B^+ and B^0 partial branching fractions with electron energy above 0.4 GeV.

² The semileptonic branching ratio, $|V_{cb}|$ and other heavy-quark parameters are determined from a simultaneous fit to moments of the hadronic-mass and lepton-energy distribution.

$\Gamma(X_u \ell^+ \nu_\ell)/\Gamma_{\text{total}}$	Γ_{22}/Γ
VALUE (units 10^{-3})	DOCUMENT ID TECN COMMENT
2.33 ± 0.22 OUR AVERAGE	

2.27 \pm 0.26 \pm 0.37 ¹ AUBERT 06H BABR $e^+ e^- \rightarrow \Upsilon(4S)$

2.53 \pm 0.24 \pm 0.24 ² AUBERT,B 05x BABR $e^+ e^- \rightarrow \Upsilon(4S)$

2.80 \pm 0.52 \pm 0.41 ³ LIMOSANI 05 BELL $e^+ e^- \rightarrow \Upsilon(4S)$

1.77 \pm 0.29 \pm 0.38 ⁴ BORNHEIM 02 CLE2 $e^+ e^- \rightarrow \Upsilon(4S)$

• • • We do not use the following data for averages, fits, limits, etc. • • •

2.24 \pm 0.27 \pm 0.47 ^{5,6} AUBERT 04i BABR Repl. by AUBERT,B 05x

¹ Obtained from the partial rate $\Delta B = (0.572 \pm 0.041 \pm 0.065) \times 10^{-3}$ for the electron momentum interval of 2.0–2.6 GeV/c based on BLNP method.

² Determined from the partial rate $\Delta B = (4.41 \pm 0.42 \pm 0.42) \times 10^{-4}$ measured for electron energy > 2 GeV and hadronic mass squared < 3.5 GeV², and calculated acceptance 0.174 in that region. The V_{ub} is measured as $(4.41 \pm 0.30 \pm 0.65 \pm 0.28) \times 10^{-3}$.

³ Uses electrons in the momentum interval 1.9–2.6 GeV/c in the center-of-mass frame. The V_{ub} is found to be $(5.08 \pm 0.47 \pm 0.49) \times 10^{-3}$.

⁴ BORNHEIM 02 uses the observed yield of leptons from semileptonic B decays in the end-point momentum interval 2.2–2.6 GeV/c with recent CLEO-2 data on $B \rightarrow X_s \gamma$. The V_{ub} is found to be $(4.08 \pm 0.34 \pm 0.53) \times 10^{-3}$.

⁵ Used BaBar measurement of Semileptonic branching fraction $B(B \rightarrow X \ell \nu_\ell) = (10.87 \pm 0.18 \pm 0.30)\%$ to convert the ratio of rates to branching fraction.

⁶ The third error includes the systematics and theoretical errors summed in quadrature.

$\Gamma(X_u \ell^+ \nu_\ell)/\Gamma(\ell^+ \nu_\ell \text{ anything})$	Γ_{22}/Γ_4
VALUE (units 10^{-2})	DOCUMENT ID TECN COMMENT
$2.06 \pm 0.25 \pm 0.42$	¹ AUBERT 04i BABR $e^+ e^- \rightarrow \Upsilon(4S)$

• • • We do not use the following data for averages, fits, limits, etc. • • •

<4.0 107 ² ALBRECHT 94c ARG $e^+ e^- \rightarrow \Upsilon(4S)$

<4.0 77 ³ BARTELT 93b CLE2 $e^+ e^- \rightarrow \Upsilon(4S)$

<4.0 41 ⁴ ALBRECHT 91c ARG $e^+ e^- \rightarrow \Upsilon(4S)$

<4.0 76 ⁵ ALBRECHT 90 ARG $e^+ e^- \rightarrow \Upsilon(4S)$

<4.0 90 ⁶ FULTON 90 CLEO $e^+ e^- \rightarrow \Upsilon(4S)$

<4.0 90 ⁷ BEHRENDIS 87 CLEO $e^+ e^- \rightarrow \Upsilon(4S)$

<5.5 90 ⁸ CHEN 84 CLEO Direct e at $\Upsilon(4S)$

<5.5 90 ⁹ KLOPFEN... 83b CUSB Direct e at $\Upsilon(4S)$

¹ The third error includes the systematics and theoretical errors summed in quadrature.

² ALBRECHT 94c find $\Gamma(b \rightarrow c)/\Gamma(b \rightarrow \text{all}) = 0.99 \pm 0.02 \pm 0.04$.

³ BARTELT 93b (CLEO II) measures an excess of $107 \pm 15 \pm 11$ leptons in the lepton momentum interval 2.3–2.6 GeV/c which is attributed to $b \rightarrow u \ell \nu_\ell$. This corresponds to a model-dependent partial branching ratio ΔB_{ub} between $(1.15 \pm 0.16 \pm 0.15) \times 10^{-4}$, as evaluated using the KS model (KOERNER 88), and $(1.54 \pm 0.22 \pm 0.20) \times 10^{-4}$ using the ACCMM model (ARTUSO 93). The corresponding values of $|V_{ub}|/|V_{cb}|$ are 0.056 ± 0.006 and 0.076 ± 0.008 , respectively.

⁴ ALBRECHT 91c result supersedes ALBRECHT 90. Two events are fully reconstructed providing evidence for the $b \rightarrow u$ transition. Using the model of ALTARELLI 82, they obtain $|V_{ub}|/|V_{cb}| = 0.11 \pm 0.012$ from 77 leptons in the 2.3–2.6 GeV momentum range.

⁵ ALBRECHT 90 observes 41 ± 10 excess e and μ (lepton) events in the momentum interval $p = 2.3$ –2.6 GeV signaling the presence of the $b \rightarrow u$ transition. The events correspond to a model-dependent measurement of $|V_{ub}|/|V_{cb}| = 0.10 \pm 0.01$.

⁶ FULTON 90 observe 76 ± 20 excess e and μ (lepton) events in the momentum interval $p = 2.4$ –2.6 GeV signaling the presence of the $b \rightarrow u$ transition. The average branching

Meson Particle Listings

B^\pm/B^0 ADMIXTURE

ratio, $(1.8 \pm 0.4 \pm 0.3) \times 10^{-4}$, corresponds to a model-dependent measurement of approximately $|V_{ub}/V_{cb}| = 0.1$ using $B(b \rightarrow c\ell\nu) = 10.2 \pm 0.2 \pm 0.7\%$.

⁷ The quoted possible limits range from 0.018 to 0.04 for the ratio, depending on which model or momentum range is chosen. We select the most conservative limit they have calculated. This corresponds to a limit on $|V_{ub}|/|V_{cb}| < 0.20$. While the endpoint technique employed is more robust than their previous results in CHEN 84, these results do not provide a numerical improvement in the limit.

$\Gamma(\pi\ell\nu_\ell)/\Gamma_{\text{total}}$ Γ_{23}/Γ

"OUR EVALUATION" is an average using rescaled values of the data listed below. The average and rescaling were performed by the Heavy Flavor Averaging Group (HFAG) and are described at <http://www.slac.stanford.edu/xorg/hfag/>. The averaging/scaling procedure takes into account correlation between the measurements.

VALUE (units 10^{-4})	DOCUMENT ID	TECN	COMMENT
1.35 ± 0.07 ± 0.07 OUR AVERAGE	The result includes measurements of $B^0 \rightarrow \pi^- \ell^+ \nu_\ell$ and $B^+ \rightarrow \pi^0 \ell^+ \nu_\ell$ decay rates.		

$\Gamma(K^+ \ell^+ \nu_\ell \text{ anything})/\Gamma(\ell^+ \nu_\ell \text{ anything})$ Γ_{24}/Γ_4

ℓ denotes e or μ , not the sum.

VALUE	DOCUMENT ID	TECN	COMMENT
0.58 ± 0.05 OUR AVERAGE			
0.594 ± 0.021 ± 0.056	ALBRECHT 94c	ARG	$e^+ e^- \rightarrow \Upsilon(4S)$
0.54 ± 0.07 ± 0.06	1 ALAM 87b	CLEO	$e^+ e^- \rightarrow \Upsilon(4S)$

1 ALAM 87b measurement relies on lepton-kaon correlations.

$\Gamma(K^- \ell^+ \nu_\ell \text{ anything})/\Gamma(\ell^+ \nu_\ell \text{ anything})$ Γ_{25}/Γ_4

ℓ denotes e or μ , not the sum.

VALUE	DOCUMENT ID	TECN	COMMENT
0.092 ± 0.035 OUR AVERAGE			
0.086 ± 0.011 ± 0.044	ALBRECHT 94c	ARG	$e^+ e^- \rightarrow \Upsilon(4S)$
0.10 ± 0.05 ± 0.02	1 ALAM 87b	CLEO	$e^+ e^- \rightarrow \Upsilon(4S)$

1 ALAM 87b measurement relies on lepton-kaon correlations.

$\Gamma(K^0/\bar{K}^0 \ell^+ \nu_\ell \text{ anything})/\Gamma(\ell^+ \nu_\ell \text{ anything})$ Γ_{26}/Γ_4

ℓ denotes e or μ , not the sum. Sum over K^0 and \bar{K}^0 states.

VALUE	DOCUMENT ID	TECN	COMMENT
0.42 ± 0.05 OUR AVERAGE			
0.452 ± 0.038 ± 0.056	1 ALBRECHT 94c	ARG	$e^+ e^- \rightarrow \Upsilon(4S)$
0.39 ± 0.06 ± 0.04	2 ALAM 87b	CLEO	$e^+ e^- \rightarrow \Upsilon(4S)$

1 ALBRECHT 94c assume a K^0/\bar{K}^0 multiplicity twice that of K_S^0 .
2 ALAM 87b measurement relies on lepton-kaon correlations.

$\langle \eta_c \rangle$

VALUE	DOCUMENT ID	TECN	COMMENT
1.10 ± 0.05			
0.98 ± 0.16 ± 0.12	1 GIBBONS 97b	CLE2	$e^+ e^- \rightarrow \Upsilon(4S)$
	2 ALAM 87b	CLEO	$e^+ e^- \rightarrow \Upsilon(4S)$

• • • We do not use the following data for averages, fits, limits, etc. • • •

1 GIBBONS 97b from charm counting using $B(D_S^+ \rightarrow \phi\pi) = 0.036 \pm 0.009$ and $B(\Lambda_c^+ \rightarrow p K^- \pi^+) = 0.044 \pm 0.006$.
2 From the difference between K^- and K^+ widths. ALAM 87b measurement relies on lepton-kaon correlations. It does not consider the possibility of $B\bar{B}$ mixing. We have thus removed it from the average.

$\Gamma(D^\pm \text{ anything})/\Gamma_{\text{total}}$ Γ_{27}/Γ

VALUE	EVTS	DOCUMENT ID	TECN	COMMENT
0.235 ± 0.013 OUR AVERAGE				
0.234 ± 0.012 ± 0.005	1	GIBBONS 97b	CLE2	$e^+ e^- \rightarrow \Upsilon(4S)$
0.25 ± 0.04 ± 0.01	2	BORTOLETTO92	CLEO	$e^+ e^- \rightarrow \Upsilon(4S)$
0.23 ± 0.05 ± 0.01	3	ALBRECHT 91H	ARG	$e^+ e^- \rightarrow \Upsilon(4S)$
• • • We do not use the following data for averages, fits, limits, etc. • • •				
0.206 ± 0.049 ± 0.005	20k	4 BORTOLETTO87	CLEO	Sup. by BORTOLETTO 92

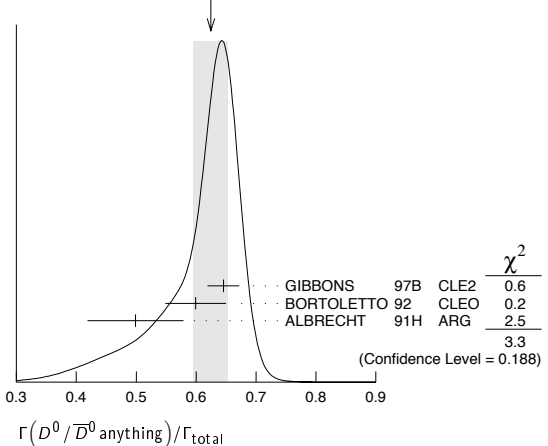
1 GIBBONS 97b reports $[B(B \rightarrow D^\pm \text{ anything})] \times [B(D^+ \rightarrow K^- \pi^+ \pi^+)] = 0.0216 \pm 0.0008 \pm 0.00082$. We divide by our best value $B(D^+ \rightarrow K^- \pi^+ \pi^+) = (9.22 \pm 0.21) \times 10^{-2}$. Our first error is their experiment's error and our second error is the systematic error from using our best value.
2 BORTOLETTO 92 reports $[B(B \rightarrow D^\pm \text{ anything})] \times [B(D^+ \rightarrow K^- \pi^+ \pi^+)] = 0.0226 \pm 0.0030 \pm 0.0018$. We divide by our best value $B(D^+ \rightarrow K^- \pi^+ \pi^+) = (9.22 \pm 0.21) \times 10^{-2}$. Our first error is their experiment's error and our second error is the systematic error from using our best value.
3 ALBRECHT 91H reports $[B(B \rightarrow D^\pm \text{ anything})] \times [B(D^+ \rightarrow K^- \pi^+ \pi^+)] = 0.0209 \pm 0.0027 \pm 0.0040$. We divide by our best value $B(D^+ \rightarrow K^- \pi^+ \pi^+) = (9.22 \pm 0.21) \times 10^{-2}$. Our first error is their experiment's error and our second error is the systematic error from using our best value.
4 BORTOLETTO 87 reports $[B(B \rightarrow D^\pm \text{ anything})] \times [B(D^+ \rightarrow K^- \pi^+ \pi^+)] = 0.019 \pm 0.004 \pm 0.002$. We divide by our best value $B(D^+ \rightarrow K^- \pi^+ \pi^+) = (9.22 \pm 0.21) \times 10^{-2}$. Our first error is their experiment's error and our second error is the systematic error from using our best value.

$\Gamma(D^0/\bar{D}^0 \text{ anything})/\Gamma_{\text{total}}$ Γ_{28}/Γ

VALUE	EVTS	DOCUMENT ID	TECN	COMMENT
0.625 ± 0.029 OUR AVERAGE	Error includes scale factor of 1.3. See the ideogram below.			
0.646 ± 0.025 ± 0.008	1	GIBBONS 97b	CLE2	$e^+ e^- \rightarrow \Upsilon(4S)$
0.60 ± 0.05 ± 0.01	2	BORTOLETTO92	CLEO	$e^+ e^- \rightarrow \Upsilon(4S)$
0.50 ± 0.07 ± 0.01	3	ALBRECHT 91H	ARG	$e^+ e^- \rightarrow \Upsilon(4S)$
• • • We do not use the following data for averages, fits, limits, etc. • • •				
0.54 ± 0.07 ± 0.01	21k	4 BORTOLETTO87	CLEO	$e^+ e^- \rightarrow \Upsilon(4S)$
0.62 ± 0.19 ± 0.01	5	GREEN 83	CLEO	Repl. by BORTOLETTO 87

1 GIBBONS 97b reports $[B(B \rightarrow D^0/\bar{D}^0 \text{ anything})] \times [B(D^0 \rightarrow K^- \pi^+)] = 0.0251 \pm 0.0006 \pm 0.00075$. We divide by our best value $B(D^0 \rightarrow K^- \pi^+) = (3.89 \pm 0.05) \times 10^{-2}$. Our first error is their experiment's error and our second error is the systematic error from using our best value.
2 BORTOLETTO 92 reports $[B(B \rightarrow D^0/\bar{D}^0 \text{ anything})] \times [B(D^0 \rightarrow K^- \pi^+)] = 0.0233 \pm 0.0012 \pm 0.0014$. We divide by our best value $B(D^0 \rightarrow K^- \pi^+) = (3.89 \pm 0.05) \times 10^{-2}$. Our first error is their experiment's error and our second error is the systematic error from using our best value.
3 ALBRECHT 91H reports $[B(B \rightarrow D^0/\bar{D}^0 \text{ anything})] \times [B(D^0 \rightarrow K^- \pi^+)] = 0.0194 \pm 0.0015 \pm 0.0025$. We divide by our best value $B(D^0 \rightarrow K^- \pi^+) = (3.89 \pm 0.05) \times 10^{-2}$. Our first error is their experiment's error and our second error is the systematic error from using our best value.
4 BORTOLETTO 87 reports $[B(B \rightarrow D^0/\bar{D}^0 \text{ anything})] \times [B(D^0 \rightarrow K^- \pi^+)] = 0.0210 \pm 0.0015 \pm 0.0021$. We divide by our best value $B(D^0 \rightarrow K^- \pi^+) = (3.89 \pm 0.05) \times 10^{-2}$. Our first error is their experiment's error and our second error is the systematic error from using our best value.
5 GREEN 83 reports $[B(B \rightarrow D^0/\bar{D}^0 \text{ anything})] \times [B(D^0 \rightarrow K^- \pi^+)] = 0.024 \pm 0.006 \pm 0.004$. We divide by our best value $B(D^0 \rightarrow K^- \pi^+) = (3.89 \pm 0.05) \times 10^{-2}$. Our first error is their experiment's error and our second error is the systematic error from using our best value.

WEIGHTED AVERAGE
0.625 ± 0.029 (Error scaled by 1.3)



$\Gamma(D^*(2010)^\pm \text{ anything})/\Gamma_{\text{total}}$ Γ_{29}/Γ

VALUE	EVTS	DOCUMENT ID	TECN	COMMENT
0.225 ± 0.015 OUR AVERAGE				
0.247 ± 0.019 ± 0.01	1	GIBBONS 97b	CLE2	$e^+ e^- \rightarrow \Upsilon(4S)$
0.205 ± 0.019 ± 0.007	2	ALBRECHT 96d	ARG	$e^+ e^- \rightarrow \Upsilon(4S)$
0.230 ± 0.028 ± 0.009	3	BORTOLETTO92	CLEO	$e^+ e^- \rightarrow \Upsilon(4S)$
• • • We do not use the following data for averages, fits, limits, etc. • • •				
0.283 ± 0.053 ± 0.002	4	ALBRECHT 91H	ARG	Sup. by ALBRECHT 96d
0.22 ± 0.04 $\begin{smallmatrix} +0.07 \\ -0.04 \end{smallmatrix}$	5200	5 BORTOLETTO87	CLEO	$e^+ e^- \rightarrow \Upsilon(4S)$
0.27 ± 0.06 $\begin{smallmatrix} +0.08 \\ -0.06 \end{smallmatrix}$	510	6 CSORNA 85	CLEO	Repl. by BORTOLETTO 87

1 GIBBONS 97b reports $B(B \rightarrow D^*(2010)^\pm \text{ anything}) = 0.239 \pm 0.015 \pm 0.014 \pm 0.009$ using CLEO measured D and D^* branching fractions. We rescale to our PDG 96 values of D and D^* branching ratios. Our first error is their experiment's error and our second error is the systematic error from using our best value.
2 ALBRECHT 96d reports $B(B \rightarrow D^*(2010)^\pm \text{ anything}) = 0.196 \pm 0.019$ using CLEO measured $B(D^*(2010)^\pm \rightarrow D^0 \pi^\pm) = 0.681 \pm 0.01 \pm 0.013$, $B(D^0 \rightarrow K^- \pi^+) = 0.0401 \pm 0.0014$, $B(D^0 \rightarrow K^- \pi^+ \pi^+) = 0.081 \pm 0.005$. We rescale to our PDG 96 values of D and D^* branching ratios. Our first error is their experiment's error and our second error is the systematic error from using our best value.
3 BORTOLETTO 92 reports $B(B \rightarrow D^*(2010)^\pm \text{ anything}) = 0.25 \pm 0.03 \pm 0.04$ using MARK II $B(D^*(2010)^\pm \rightarrow D^0 \pi^\pm) = 0.57 \pm 0.06$ and $B(D^0 \rightarrow K^- \pi^+) = 0.042 \pm 0.008$. We rescale to our PDG 96 values of D and D^* branching ratios. Our first error is their experiment's error and our second error is the systematic error from using our best value.
4 ALBRECHT 91H reports $0.348 \pm 0.060 \pm 0.035$ for $B(D^*(2010)^\pm \rightarrow D^0 \pi^\pm) = 0.55 \pm 0.04$. We rescale to our best value $B(D^*(2010)^\pm \rightarrow D^0 \pi^\pm) = (67.7 \pm 0.5) \times 10^{-2}$. Our first error is their experiment's error and our second error is the systematic error from using our best value. Uses the PDG 90 $B(D^0 \rightarrow K^- \pi^+) = 0.0371 \pm 0.0025$.
5 BORTOLETTO 87 uses old MARK III (BALTRUSAITIS 86e) branching ratios $B(D^0 \rightarrow K^- \pi^+) = 0.056 \pm 0.004 \pm 0.003$ and also assumes $B(D^*(2010)^\pm \rightarrow D^0 \pi^\pm) =$

See key on page 373

Meson Particle Listings

 B^\pm/B^0 ADMIXTURE

$0.60^{+0.08}_{-0.15}$. The product branching ratio for $B(B \rightarrow D^*(2010)^+) B(D^*(2010)^+ \rightarrow D^0 \pi^+)$ is $0.13 \pm 0.02 \pm 0.012$. Superseded by BORTOLETTO 92.

⁶ $V-A$ momentum spectrum used to extrapolate below $p = 1$ GeV. We correct the value assuming $B(D^0 \rightarrow K^- \pi^+) = 0.042 \pm 0.006$ and $B(D^{*+} \rightarrow D^0 \pi^+) = 0.6^{+0.08}_{-0.15}$. The product branching fraction is $B(B \rightarrow D^{*+} X) \cdot B(D^{*+} \rightarrow \pi^+ D^0) \cdot B(D^0 \rightarrow K^- \pi^+) = (68 \pm 15 \pm 9) \times 10^{-4}$.

$\Gamma(D^*(2007)^0 \text{ anything})/\Gamma_{\text{total}}$ Γ_{30}/Γ

VALUE	DOCUMENT ID	TECN	COMMENT
0.260 ± 0.023 ± 0.015	¹ GIBBONS	97B	CLE2 $e^+ e^- \rightarrow \Upsilon(4S)$

¹ GIBBONS 97B reports $B(B \rightarrow D^*(2007)^0 \text{ anything}) = 0.247 \pm 0.012 \pm 0.018 \pm 0.018$ using CLEO measured D and D^* branching fractions. We rescale to our PDG 96 values of D and D^* branching ratios. Our first error is their experiment's error and our second error is the systematic error from using our best value.

$\Gamma(D_s^\pm \text{ anything})/\Gamma_{\text{total}}$ Γ_{31}/Γ

VALUE	EVTS	DOCUMENT ID	TECN	COMMENT
0.085 ± 0.008 OUR AVERAGE				
0.091 ± 0.010 ± 0.007		¹ ARTUSO	05B	CLE2 $e^+ e^- \rightarrow \Upsilon(5S)$
0.090 ± 0.005 ± 0.007		² AUBERT	02G	BABR $e^+ e^- \rightarrow \Upsilon(4S)$
0.067 ± 0.011 ± 0.005		³ ALBRECHT	92G	ARG $e^+ e^- \rightarrow \Upsilon(4S)$
0.070 ± 0.011 ± 0.006	257	⁴ BORTOLETTO	090	CLEO $e^+ e^- \rightarrow \Upsilon(4S)$
0.087 ± 0.023 ± 0.007		⁵ HAAS	86	CLEO $e^+ e^- \rightarrow \Upsilon(4S)$

• • • We do not use the following data for averages, fits, limits, etc. • • •
 0.097 ± 0.008 ± 0.008 ⁶ GIBAUT 96 CLE2 Repl. by ARTUSO 05B
 0.096 ± 0.025 ± 0.008 ⁷ ALBRECHT 87H ARG $e^+ e^- \rightarrow \Upsilon(4S)$

¹ ARTUSO 05B reports $0.0905 \pm 0.0025 \pm 0.0140$ for $B(D_s^+ \rightarrow \phi \pi^+) = (4.4 \pm 0.5) \times 10^{-2}$. We rescale to our best value $B(D_s^+ \rightarrow \phi \pi^+) = (4.38 \pm 0.35) \times 10^{-2}$. Our first error is their experiment's error and our second error is the systematic error from using our best value.

² AUBERT 02G reports $[B(B \rightarrow D_s^\pm \text{ anything})] \times [B(D_s^\pm \rightarrow \phi \pi^+)] = 0.00393 \pm 0.00007 \pm 0.00021$. We divide by our best value $B(D_s^\pm \rightarrow \phi \pi^+) = (4.38 \pm 0.35) \times 10^{-2}$. Our first error is their experiment's error and our second error is the systematic error from using our best value.

³ ALBRECHT 92G reports $[B(B \rightarrow D_s^\pm \text{ anything})] \times [B(D_s^\pm \rightarrow \phi \pi^+)] = 0.00292 \pm 0.00039 \pm 0.00031$. We divide by our best value $B(D_s^\pm \rightarrow \phi \pi^+) = (4.38 \pm 0.35) \times 10^{-2}$. Our first error is their experiment's error and our second error is the systematic error from using our best value.

⁴ BORTOLETTO 90 reports $[B(B \rightarrow D_s^\pm \text{ anything})] \times [B(D_s^\pm \rightarrow \phi \pi^+)] = 0.00306 \pm 0.00047$. We divide by our best value $B(D_s^\pm \rightarrow \phi \pi^+) = (4.38 \pm 0.35) \times 10^{-2}$. Our first error is their experiment's error and our second error is the systematic error from using our best value.

⁵ HAAS 86 reports $[B(B \rightarrow D_s^\pm \text{ anything})] \times [B(D_s^\pm \rightarrow \phi \pi^+)] = 0.0038 \pm 0.0010$. We divide by our best value $B(D_s^\pm \rightarrow \phi \pi^+) = (4.38 \pm 0.35) \times 10^{-2}$. Our first error is their experiment's error and our second error is the systematic error from using our best value. 64 ± 22% decays are 2-body.

⁶ GIBAUT 96 reports $0.1211 \pm 0.0039 \pm 0.0088$ for $B(D_s^+ \rightarrow \phi \pi^+) = 0.035$. We rescale to our best value $B(D_s^+ \rightarrow \phi \pi^+) = (4.38 \pm 0.35) \times 10^{-2}$. Our first error is their experiment's error and our second error is the systematic error from using our best value.

⁷ ALBRECHT 87H reports $[B(B \rightarrow D_s^\pm \text{ anything})] \times [B(D_s^\pm \rightarrow \phi \pi^+)] = 0.0042 \pm 0.0009 \pm 0.0006$. We divide by our best value $B(D_s^\pm \rightarrow \phi \pi^+) = (4.38 \pm 0.35) \times 10^{-2}$. Our first error is their experiment's error and our second error is the systematic error from using our best value. 46 ± 16% of $B \rightarrow D_s X$ decays are 2-body. Superseded by ALBRECHT 92G.

$\Gamma(D_s^\pm \text{ anything})/\Gamma_{\text{total}}$ Γ_{32}/Γ

VALUE	DOCUMENT ID	TECN	COMMENT
0.065 ± 0.009 ± 0.005	¹ AUBERT	02G	BABR $e^+ e^- \rightarrow \Upsilon(4S)$

¹ AUBERT 02G reports $[B(B \rightarrow D_s^\pm \text{ anything})] \times [B(D_s^\pm \rightarrow \phi \pi^+)] = 0.00284 \pm 0.00029 \pm 0.00025$. We divide by our best value $B(D_s^\pm \rightarrow \phi \pi^+) = (4.38 \pm 0.35) \times 10^{-2}$. Our first error is their experiment's error and our second error is the systematic error from using our best value.

$\Gamma(D_s^\pm \bar{D}^{(*)})/\Gamma(D_s^\pm \text{ anything})$ Γ_{33}/Γ_{32}
 Sum over modes

VALUE	DOCUMENT ID	TECN	COMMENT
0.533 ± 0.037 ± 0.037	AUBERT	02G	BABR $e^+ e^- \rightarrow \Upsilon(4S)$

$\Gamma(\bar{D} D_{s0}(2317))/\Gamma_{\text{total}}$ Γ_{34}/Γ

VALUE	DOCUMENT ID	TECN	COMMENT
seen	¹ KROKOVNY	03B	BELL $e^+ e^- \rightarrow \Upsilon(4S)$

¹ The product branching ratio for $B(B \rightarrow \bar{D} D_{s0}(2317)^+) \times B(D_{s0}(2317)^+ \rightarrow D_s \pi^0)$ is measured to be $(8.5^{+2.1}_{-1.9} \pm 2.6) \times 10^{-4}$.

$\Gamma(\bar{D} D_{sJ}(2457))/\Gamma_{\text{total}}$ Γ_{35}/Γ

VALUE	DOCUMENT ID	TECN	COMMENT
seen	¹ KROKOVNY	03B	BELL $e^+ e^- \rightarrow \Upsilon(4S)$

¹ The product branching ratio for $B(B \rightarrow \bar{D} D_{sJ}(2457)^+) \times B(D_{sJ}(2457)^+ \rightarrow D_s^+ \pi^0, D_s^+ \gamma)$ are measured to be $(17.8^{+4.5}_{-3.9} \pm 5.3) \times 10^{-4}$ and $(6.7^{+1.3}_{-1.2} \pm 2.0) \times 10^{-4}$, respectively.

$[\Gamma(D^{(*)} \bar{D}^{(*)} K^0) + \Gamma(D^{(*)} \bar{D}^{(*)} K^\pm)]/\Gamma_{\text{total}}$ Γ_{36}/Γ

VALUE	DOCUMENT ID	TECN	COMMENT
0.071^{+0.025+0.010}_{-0.015-0.009}	¹ BARATE	98Q	ALEP $e^+ e^- \rightarrow Z$

¹ The systematic error includes the uncertainties due to the charm branching ratios.

$\Gamma(c \bar{c} s)/\Gamma_{\text{total}}$ Γ_{37}/Γ

VALUE	DOCUMENT ID	TECN	COMMENT
0.219 ± 0.037	¹ COAN	98	CLE2 $e^+ e^- \rightarrow \Upsilon(4S)$

¹ COAN 98 uses $D-\ell$ correlation.

$\Gamma(D_s^{(*)} \bar{D}^{(*)})/\Gamma(D_s^\pm \text{ anything})$ Γ_{38}/Γ_{31}
 Sum over modes.

VALUE	DOCUMENT ID	TECN	COMMENT
0.469 ± 0.017 OUR AVERAGE			
0.464 ± 0.013 ± 0.015	AUBERT	02G	BABR $e^+ e^- \rightarrow \Upsilon(4S)$
0.56^{+0.21+0.09}_{-0.15-0.08}	¹ BARATE	98Q	ALEP $e^+ e^- \rightarrow Z$
0.457 ± 0.019 ± 0.037	GIBAUT	96	CLE2 $e^+ e^- \rightarrow \Upsilon(4S)$
0.58 ± 0.07 ± 0.09	ALBRECHT	92G	ARG $e^+ e^- \rightarrow \Upsilon(4S)$
0.56 ± 0.10	BORTOLETTO	090	CLEO $e^+ e^- \rightarrow \Upsilon(4S)$

¹ BARATE 98Q measures $B(B \rightarrow D_s^{(*)} \bar{D}^{(*)}) = 0.056^{+0.021+0.009+0.019}_{-0.015-0.008-0.011}$, where the third error results from the uncertainty on the different D branching ratios and is dominated by the uncertainty on $B(D_s^\pm \rightarrow \phi \pi^+)$. We divide $B(B \rightarrow D_s^{(*)} \bar{D}^{(*)})$ by our best value of $B(B \rightarrow D_s \text{ anything}) = 0.1 \pm 0.025$.

$\Gamma(D^* D^*(2010)^\pm)/\Gamma_{\text{total}}$ Γ_{39}/Γ

VALUE	CL%	DOCUMENT ID	TECN	COMMENT
< 5.9 × 10⁻³	90	BARATE	98Q	ALEP $e^+ e^- \rightarrow Z$

$[\Gamma(D D^*(2010)^\pm) + \Gamma(D^* D^\pm)]/\Gamma_{\text{total}}$ Γ_{40}/Γ

VALUE	CL%	DOCUMENT ID	TECN	COMMENT
< 5.5 × 10⁻³	90	BARATE	98Q	ALEP $e^+ e^- \rightarrow Z$

$\Gamma(D D^\pm)/\Gamma_{\text{total}}$ Γ_{41}/Γ

VALUE	CL%	DOCUMENT ID	TECN	COMMENT
< 3.1 × 10⁻³	90	BARATE	98Q	ALEP $e^+ e^- \rightarrow Z$

$\Gamma(D_s^{(*)} \pm \bar{D}^{(*)} X (n\pi^\pm))/\Gamma_{\text{total}}$ Γ_{42}/Γ

VALUE	DOCUMENT ID	TECN	COMMENT
0.094^{+0.040+0.034}_{-0.031-0.024}	¹ BARATE	98Q	ALEP $e^+ e^- \rightarrow Z$

¹ The systematic error includes the uncertainties due to the charm branching ratios.

$\Gamma(D^*(2010)\gamma)/\Gamma_{\text{total}}$ Γ_{43}/Γ

VALUE	CL%	DOCUMENT ID	TECN	COMMENT
< 1.1 × 10⁻³	90	¹ LESIAK	92	CBAL $e^+ e^- \rightarrow \Upsilon(4S)$

¹ LESIAK 92 set a limit on the inclusive process $B(b \rightarrow s \gamma) < 2.8 \times 10^{-3}$ at 90% CL for the range of masses of 892–2045 MeV, independent of assumptions about s-quark hadronization.

$\Gamma(D_s^+ \pi^-, D_s^+ \pi^0, D_s^+ \rho^-, D_s^{*+} \rho^-, D_s^+ \pi^0, D_s^{*+} \pi^0, D_s^+ \eta, D_s^{*+} \eta, D_s^+ \rho^0, D_s^{*+} \rho^0, D_s^+ \omega, D_s^{*+} \omega)/\Gamma_{\text{total}}$ Γ_{44}/Γ
 Sum over modes.

VALUE	CL%	DOCUMENT ID	TECN	COMMENT
< 0.0004	90	¹ ALEXANDER	93B	CLE2 $e^+ e^- \rightarrow \Upsilon(4S)$

¹ ALEXANDER 93B reports $< 4.8 \times 10^{-4}$ for $B(D_s^+ \rightarrow \phi \pi^+) = 0.037$. We rescale to our best value $B(D_s^+ \rightarrow \phi \pi^+) = 0.0438$. This branching ratio limit provides a model-dependent upper limit $|V_{ub}|/|V_{cb}| < 0.16$ at CL=90%.

$\Gamma(D_{s1}(2536)^+ \text{ anything})/\Gamma_{\text{total}}$ Γ_{45}/Γ
 $D_{s1}(2536)^+$ is the narrow P -wave D_s^+ meson with $J^P = 1^+$.

VALUE	CL%	DOCUMENT ID	TECN	COMMENT
< 0.0095	90	¹ BISHAI	98	CLE2 $e^+ e^- \rightarrow \Upsilon(4S)$

¹ Assuming factorization, the decay constant $f_{D_{s1}^+}$ is at least a factor of 2.5 times smaller than $f_{D_s^+}$.

$\Gamma(J/\psi(1S) \text{ anything})/\Gamma_{\text{total}}$ Γ_{46}/Γ

VALUE (units 10 ⁻²)	EVTS	DOCUMENT ID	TECN	COMMENT
1.094 ± 0.032 OUR AVERAGE				Error includes scale factor of 1.1.
1.057 ± 0.012 ± 0.040		¹ AUBERT	03F	BABR $e^+ e^- \rightarrow \Upsilon(4S)$
1.121 ± 0.013 ± 0.042		ANDERSON	02	CLE2 $e^+ e^- \rightarrow \Upsilon(4S)$
1.30 ± 0.45 ± 0.01	27	² MASCHMANN	90	CBAL $e^+ e^- \rightarrow \Upsilon(4S)$
1.24 ± 0.27 ± 0.01	120	³ ALBRECHT	87D	ARG $e^+ e^- \rightarrow \Upsilon(4S)$
1.36 ± 0.24 ± 0.01	52	⁴ ALAM	86	CLEO $e^+ e^- \rightarrow \Upsilon(4S)$

• • • We do not use the following data for averages, fits, limits, etc. • • •

1.13 ± 0.06 ± 0.01 1489 ⁵ BALEST 95B CLE2 $e^+ e^- \rightarrow \Upsilon(4S)$

1.4 ± 0.6 ⁶ ALBRECHT 85H ARG $e^+ e^- \rightarrow \Upsilon(4S)$

1.1 ± 0.21 ± 0.23 46 ⁷ HAAS 85 CLEO Repl. by ALAM 86

Meson Particle Listings

 B^\pm/B^0 ADMIXTURE

- ¹ AUBERT 03F also reports the momentum distribution and helicity of $J/\psi \rightarrow \ell^+ \ell^-$ in the $\Upsilon(4S)$ center-of-mass frame.
- ² MASCHMANN 90 reports $(1.12 \pm 0.33 \pm 0.25) \times 10^{-2}$ for $B(J/\psi(1S) \rightarrow e^+ e^-) = 0.069 \pm 0.009$. We rescale to our best value $B(J/\psi(1S) \rightarrow e^+ e^-) = (5.94 \pm 0.06) \times 10^{-2}$. Our first error is their experiment's error and our second error is the systematic error from using our best value.
- ³ ALBRECHT 87D reports $(1.07 \pm 0.16 \pm 0.22) \times 10^{-2}$ for $B(J/\psi(1S) \rightarrow e^+ e^-) = 0.069 \pm 0.009$. We rescale to our best value $B(J/\psi(1S) \rightarrow e^+ e^-) = (5.94 \pm 0.06) \times 10^{-2}$. Our first error is their experiment's error and our second error is the systematic error from using our best value. ALBRECHT 87D find the branching ratio for J/ψ not from $\psi(2S)$ to be 0.0081 ± 0.0023 .
- ⁴ ALAM 86 reports $(1.09 \pm 0.16 \pm 0.21) \times 10^{-2}$ for $B(J/\psi(1S) \rightarrow \mu^+ \mu^-) = 0.074 \pm 0.012$. We rescale to our best value $B(J/\psi(1S) \rightarrow \mu^+ \mu^-) = (5.93 \pm 0.06) \times 10^{-2}$. Our first error is their experiment's error and our second error is the systematic error from using our best value.
- ⁵ BALEST 95B reports $(1.12 \pm 0.04 \pm 0.06) \times 10^{-2}$ for $B(J/\psi(1S) \rightarrow e^+ e^-) = 0.0599 \pm 0.0025$. We rescale to our best value $B(J/\psi(1S) \rightarrow e^+ e^-) = (5.94 \pm 0.06) \times 10^{-2}$. Our first error is their experiment's error and our second error is the systematic error from using our best value. They measure $J/\psi(1S) \rightarrow e^+ e^-$ and $\mu^+ \mu^-$ and use PDG 1994 values for the branching fractions. The rescaling is the same for either mode so we use $e^+ e^-$.
- ⁶ Statistical and systematic errors were added in quadrature. ALBRECHT 85H also report a CL = 90% limit of 0.007 for $B \rightarrow J/\psi(1S) + X$ where $m_X < 1$ GeV.
- ⁷ Dimuon and dielectron events used.

$\Gamma(J/\psi(1S) \text{ (direct) anything})/\Gamma_{\text{total}}$				Γ_{47}/Γ
VALUE	DOCUMENT ID	TECN	COMMENT	
0.0078 ± 0.0004 OUR AVERAGE	Error includes scale factor of 1.1.			
0.00740 ± 0.00023 ± 0.00043	¹ AUBERT	03F	BABR $e^+ e^- \rightarrow \Upsilon(4S)$	
0.00813 ± 0.00017 ± 0.00037	² ANDERSON	02	CLE2 $e^+ e^- \rightarrow \Upsilon(4S)$	
• • • We do not use the following data for averages, fits, limits, etc. • • •				
0.0080 ± 0.0008	³ BALEST	95B	CLE2 $e^+ e^- \rightarrow \Upsilon(4S)$	

- ¹ AUBERT 03F also reports the helicity of $J/\psi \rightarrow \ell^+ \ell^-$ produced directly in B decay.
- ² Also reports the measurement of $J/\psi \rightarrow \ell^+ \ell^-$ polarization produced directly from B decay.
- ³ BALEST 95B assume PDG 1994 values for sub mode branching ratios. $J/\psi(1S)$ mesons are reconstructed in $J/\psi(1S) \rightarrow e^+ e^-$ and $J/\psi(1S) \rightarrow \mu^+ \mu^-$. The $B \rightarrow J/\psi(1S) X$ branching ratio contains $J/\psi(1S)$ mesons directly from B decays and also from feeddown through $\psi(2S) \rightarrow J/\psi(1S)$, $\chi_{c1}(1P) \rightarrow J/\psi(1S)$, or $\chi_{c2}(1P) \rightarrow J/\psi(1S)$. Using the measured inclusive rates, BALEST 95B corrects for the feeddown and finds the $B \rightarrow J/\psi(1S)$ (direct) X branching ratio.

$\Gamma(\psi(2S) \text{ anything})/\Gamma_{\text{total}}$				Γ_{48}/Γ
VALUE	DOCUMENT ID	TECN	COMMENT	
0.00307 ± 0.00021 OUR AVERAGE				
0.00297 ± 0.00020 ± 0.00020	AUBERT	03F	BABR $e^+ e^- \rightarrow \Upsilon(4S)$	
0.00316 ± 0.00014 ± 0.00028	¹ ANDERSON	02	CLE2 $e^+ e^- \rightarrow \Upsilon(4S)$	
0.0046 ± 0.0017 ± 0.0011	⁸ ALBRECHT	87D	ARG $e^+ e^- \rightarrow \Upsilon(4S)$	
• • • We do not use the following data for averages, fits, limits, etc. • • •				
0.0034 ± 0.0004 ± 0.0003	² BALEST	95B	CLE2 $e^+ e^- \rightarrow \Upsilon(4S)$	
¹ Also reports the measurement of $\psi(2S) \rightarrow \ell^+ \ell^-$ polarization produced directly from B decay.				
² BALEST 95B assume PDG 1994 values for sub mode branching ratios. They find $B(B \rightarrow \psi(2S) X, \psi(2S) \rightarrow \ell^+ \ell^-) = 0.30 \pm 0.05 \pm 0.04$ and $B(B \rightarrow \psi(2S) X, \psi(2S) \rightarrow J/\psi(1S) \pi^+ \pi^-) = 0.37 \pm 0.05 \pm 0.05$. Weighted average is quoted for $B(B \rightarrow \psi(2S) X)$.				

$\Gamma(\chi_{c1}(1P) \text{ anything})/\Gamma_{\text{total}}$				Γ_{49}/Γ
VALUE	DOCUMENT ID	TECN	COMMENT	
0.00386 ± 0.00027 OUR AVERAGE				
0.00367 ± 0.00035 ± 0.00044	AUBERT	03F	BABR $e^+ e^- \rightarrow \Upsilon(4S)$	
0.00363 ± 0.00022 ± 0.00034	¹ ABE	02L	BELL $e^+ e^- \rightarrow \Upsilon(4S)$	
0.00435 ± 0.00029 ± 0.00040	ANDERSON	02	CLE2 $e^+ e^- \rightarrow \Upsilon(4S)$	
• • • We do not use the following data for averages, fits, limits, etc. • • •				
0.00314 ± 0.00034 ± 0.00017	² CHEN	01	CLE2 $e^+ e^- \rightarrow \Upsilon(4S)$	
0.0040 ± 0.0006 ± 0.0004	³ BALEST	95B	CLE2 Repl. by CHEN 01	
0.0105 ± 0.0035 ± 0.0025	⁴ ALBRECHT	92E	ARG $e^+ e^- \rightarrow \Upsilon(4S)$	

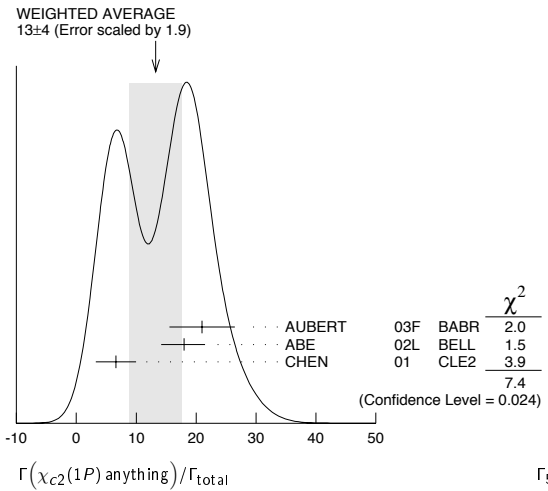
- ¹ ABE 02L uses PDG 01 values for $B(J/\psi(1S) \rightarrow \ell^+ \ell^-)$ and $B(\chi_{c1,c2} \rightarrow J/\psi(1S) \gamma)$.
- ² CHEN 01 reports $0.00414 \pm 0.00031 \pm 0.00040$ for $B(\chi_{c1}(1P) \rightarrow \gamma J/\psi(1S)) = 0.273 \pm 0.016$. We rescale to our best value $B(\chi_{c1}(1P) \rightarrow \gamma J/\psi(1S)) = (36.0 \pm 1.9) \times 10^{-2}$. Our first error is their experiment's error and our second error is the systematic error from using our best value. Assumes equal production of B^+ and B^0 at the $\Upsilon(4S)$.
- ³ BALEST 95B assume $B(\chi_{c1}(1P) \rightarrow J/\psi(1S) \gamma) = (27.3 \pm 1.6) \times 10^{-2}$, the PDG 1994 value. Fit to ψ -photon invariant mass distribution allows for a $\chi_{c1}(1P)$ and a $\chi_{c2}(1P)$ component.
- ⁴ ALBRECHT 92E assumes no $\chi_{c2}(1P)$ production.

$\Gamma(\chi_{c1}(1P) \text{ (direct) anything})/\Gamma_{\text{total}}$				Γ_{50}/Γ
VALUE	DOCUMENT ID	TECN	COMMENT	
0.00316 ± 0.00025 OUR AVERAGE				
0.00341 ± 0.00035 ± 0.00042	AUBERT	03F	BABR $e^+ e^- \rightarrow \Upsilon(4S)$	
0.00332 ± 0.00022 ± 0.00034	¹ ABE	02L	BELL $e^+ e^- \rightarrow \Upsilon(4S)$	
0.00290 ± 0.00034 ± 0.00015	² CHEN	01	CLE2 $e^+ e^- \rightarrow \Upsilon(4S)$	
• • • We do not use the following data for averages, fits, limits, etc. • • •				
0.0037 ± 0.0007	³ BALEST	95B	CLE2 Repl. by CHEN 01	

- ¹ ABE 02L uses PDG 01 values for $B(J/\psi(1S) \rightarrow \ell^+ \ell^-)$ and $B(\chi_{c1,c2} \rightarrow J/\psi(1S) \gamma)$.
- ² CHEN 01 reports $0.00383 \pm 0.00031 \pm 0.00040$ for $B(\chi_{c1}(1P) \rightarrow \gamma J/\psi(1S)) = 0.273 \pm 0.016$. We rescale to our best value $B(\chi_{c1}(1P) \rightarrow \gamma J/\psi(1S)) = (36.0 \pm 1.9) \times 10^{-2}$. Our first error is their experiment's error and our second error is the systematic error from using our best value. Assumes equal production of B^+ and B^0 at the $\Upsilon(4S)$.
- ³ BALEST 95B assume PDG 1994 values. $J/\psi(1S)$ mesons are reconstructed in the $e^+ e^-$ and $\mu^+ \mu^-$ modes. The $B \rightarrow \chi_{c1}(1P) X$ branching ratio contains $\chi_{c1}(1P)$ mesons directly from B decays and also from feeddown through $\psi(2S) \rightarrow \chi_{c1}(1P) \gamma$. Using the measured inclusive rates, BALEST 95B corrects for the feeddown and finds the $B \rightarrow \chi_{c1}(1P)$ (direct) X branching ratio.

$\Gamma(\chi_{c2}(1P) \text{ anything})/\Gamma_{\text{total}}$				Γ_{51}/Γ	
VALUE (units 10^{-4})	CL%	EVTS	DOCUMENT ID	TECN	COMMENT
13 ± 4 OUR AVERAGE			Error includes scale factor of 1.9. See the ideogram below.		
21.0 ± 4.5 ± 3.1			AUBERT	03F	BABR $e^+ e^- \rightarrow \Upsilon(4S)$
18.0 ^{+2.3} _{-2.8} ± 2.6			¹ ABE	02L	BELL $e^+ e^- \rightarrow \Upsilon(4S)$
6.6 ± 3.4 ± 0.3			² CHEN	01	CLE2 $e^+ e^- \rightarrow \Upsilon(4S)$
• • • We do not use the following data for averages, fits, limits, etc. • • •					
<38	90	35	³ BALEST	95B	CLE2 Repl. by CHEN 01

- ¹ ABE 02L uses PDG 01 values for $B(J/\psi(1S) \rightarrow \ell^+ \ell^-)$ and $B(\chi_{c1,c2} \rightarrow J/\psi(1S) \gamma)$.
- ² CHEN 01 reports $(9.8 \pm 4.8 \pm 1.5) \times 10^{-4}$ for $B(\chi_{c2}(1P) \rightarrow \gamma J/\psi(1S)) = 0.135 \pm 0.011$. We rescale to our best value $B(\chi_{c2}(1P) \rightarrow \gamma J/\psi(1S)) = (20.0 \pm 1.0) \times 10^{-2}$. Our first error is their experiment's error and our second error is the systematic error from using our best value. Assumes equal production of B^+ and B^0 at the $\Upsilon(4S)$.
- ³ BALEST 95B assume $B(\chi_{c2}(1P) \rightarrow J/\psi(1S) \gamma) = (13.5 \pm 1.1) \times 10^{-2}$, the PDG 1994 value. $J/\psi(1S)$ mesons are reconstructed in the $e^+ e^-$ and $\mu^+ \mu^-$ modes, and PDG 1994 branching fractions are used. If interpreted as signal, the 35 ± 13 events correspond to $B(B \rightarrow \chi_{c2}(1P) X) = (0.25 \pm 0.10 \pm 0.03) \times 10^{-2}$.



$\Gamma(\chi_{c2}(1P) \text{ (direct) anything})/\Gamma_{\text{total}}$				Γ_{52}/Γ
VALUE	DOCUMENT ID	TECN	COMMENT	
0.00165 ± 0.00031 OUR AVERAGE				
0.00190 ± 0.00045 ± 0.00029	AUBERT	03F	BABR $e^+ e^- \rightarrow \Upsilon(4S)$	
0.00153 ± 0.00023 ± 0.00027	¹ ABE	02L	BELL $e^+ e^- \rightarrow \Upsilon(4S)$	

- ¹ ABE 02L uses PDG 01 values for $B(J/\psi(1S) \rightarrow \ell^+ \ell^-)$ and $B(\chi_{c1,c2} \rightarrow J/\psi(1S) \gamma)$.

$\Gamma(\eta_c(1S) \text{ anything})/\Gamma_{\text{total}}$				Γ_{53}/Γ
VALUE	CL%	DOCUMENT ID	TECN	COMMENT
<0.009	90	¹ BALEST	95B	CLE2 $e^+ e^- \rightarrow \Upsilon(4S)$

- ¹ BALEST 95B assume PDG 1994 values for sub mode branching ratios. $J/\psi(1S)$ mesons are reconstructed in $J/\psi(1S) \rightarrow e^+ e^-$ and $J/\psi(1S) \rightarrow \mu^+ \mu^-$. Search region $2960 < m_{\eta_c(1S)} < 3010$ MeV/ c^2 .

$\Gamma(X(3872) K \times B(X \rightarrow D^0 \bar{D}^0 \pi^0))/\Gamma_{\text{total}}$				Γ_{54}/Γ
VALUE (units 10^{-4})	DOCUMENT ID	TECN	COMMENT	
1.22 ± 0.31 ± 0.23	¹ GOKHROO	06	BELL $e^+ e^- \rightarrow \Upsilon(4S)$	

- ¹ Measure the near-threshold enhancements in the $(D^0 \bar{D}^0 \pi^0)$ system at a mass $3875.2 \pm 0.7^{+0.3}_{-1.6} \pm 0.8$ MeV/ c^2 .

$\Gamma(KX(3945) \times B(X(3945) \rightarrow \omega J/\psi))/\Gamma_{\text{total}}$				Γ_{55}/Γ
VALUE (units 10^{-5})	DOCUMENT ID	TECN	COMMENT	
7.1 ± 1.3 ± 3.1	¹ CHOI	05	BELL $e^+ e^- \rightarrow \Upsilon(4S)$	

- ¹ CHOI 05 reports the observation of a near-threshold enhancement in the $\omega J/\psi$ mass spectrum in exclusive $B \rightarrow K \omega J/\psi$. The new state, denoted as $X(3945)$, has a mass of $3943 \pm 11 \pm 13$ GeV/ c^2 and a width $\Gamma = 87 \pm 22 \pm 26$ MeV.

See key on page 373

Meson Particle Listings

B^\pm/B^0 ADMIXTURE

$\Gamma(K^\pm \text{ anything})/\Gamma_{\text{total}}$				Γ_{56}/Γ
VALUE	DOCUMENT ID	TECN	COMMENT	
0.789 ± 0.025 OUR AVERAGE				
0.82 ± 0.01 ± 0.05	ALBRECHT	94c	ARG $e^+e^- \rightarrow \Upsilon(4S)$	
0.775 ± 0.015 ± 0.025	¹ ALBRECHT	93i	ARG $e^+e^- \rightarrow \Upsilon(4S)$	
0.85 ± 0.07 ± 0.09	ALAM	87B	CLEO $e^+e^- \rightarrow \Upsilon(4S)$	

• • • We do not use the following data for averages, fits, limits, etc. • • •

seen
seen

¹ALBRECHT 93i value is not independent of the sum of $B \rightarrow K^+ \text{ anything}$ and $B \rightarrow K^- \text{ anything}$ ALBRECHT 94c values.
²Assuming $\Upsilon(4S) \rightarrow B\bar{B}$, a total of $3.38 \pm 0.34 \pm 0.68$ kaons per $\Upsilon(4S)$ decay is found (the second error is systematic). In the context of the standard B -decay model, this leads to a value for $(b\text{-quark})/(c\text{-quark})/(b\text{-quark} \rightarrow \text{all})$ of $1.09 \pm 0.33 \pm 0.13$.
³GIANNINI 82 at CESR-CUSB observed $1.58 \pm 0.35 K^0$ per hadronic event much higher than 0.82 ± 0.10 below threshold. Consistent with predominant $b \rightarrow cX$ decay.

$\Gamma(K^+ \text{ anything})/\Gamma_{\text{total}}$				Γ_{57}/Γ
VALUE	DOCUMENT ID	TECN	COMMENT	
0.66 ± 0.05				
• • • We do not use the following data for averages, fits, limits, etc. • • •				
0.620 ± 0.013 ± 0.038	² ALBRECHT	94c	ARG $e^+e^- \rightarrow \Upsilon(4S)$	
0.66 ± 0.05 ± 0.07	² ALAM	87B	CLEO $e^+e^- \rightarrow \Upsilon(4S)$	

¹Measurement relies on lepton-kaon correlations. It is for the weak decay vertex and does not include mixing of the neutral B meson. Mixing effects were corrected for by assuming a mixing parameter r of $(18.1 \pm 4.3)\%$.
²Measurement relies on lepton-kaon correlations. It includes production through mixing of the neutral B meson.

$\Gamma(K^- \text{ anything})/\Gamma_{\text{total}}$				Γ_{58}/Γ
VALUE	DOCUMENT ID	TECN	COMMENT	
0.13 ± 0.04				
• • • We do not use the following data for averages, fits, limits, etc. • • •				
0.165 ± 0.011 ± 0.036	² ALBRECHT	94c	ARG $e^+e^- \rightarrow \Upsilon(4S)$	
0.19 ± 0.05 ± 0.02	² ALAM	87B	CLEO $e^+e^- \rightarrow \Upsilon(4S)$	

¹Measurement relies on lepton-kaon correlations. It is for the weak decay vertex and does not include mixing of the neutral B meson. Mixing effects were corrected for by assuming a mixing parameter r of $(18.1 \pm 4.3)\%$.
²Measurement relies on lepton-kaon correlations. It includes production through mixing of the neutral B meson.

$\Gamma(K^0/\bar{K}^0 \text{ anything})/\Gamma_{\text{total}}$				Γ_{59}/Γ
VALUE	DOCUMENT ID	TECN	COMMENT	
0.64 ± 0.04 OUR AVERAGE				
0.642 ± 0.010 ± 0.042	¹ ALBRECHT	94c	ARG $e^+e^- \rightarrow \Upsilon(4S)$	
0.63 ± 0.06 ± 0.06	ALAM	87B	CLEO $e^+e^- \rightarrow \Upsilon(4S)$	

¹ALBRECHT 94c assume a K^0/\bar{K}^0 multiplicity twice that of K_S^0 .

$\Gamma(K^*(892)^\pm \text{ anything})/\Gamma_{\text{total}}$				Γ_{60}/Γ
VALUE	DOCUMENT ID	TECN	COMMENT	
0.182 ± 0.054 ± 0.024	ALBRECHT	94j	ARG $e^+e^- \rightarrow \Upsilon(4S)$	

$\Gamma(K^*(892)^0/\bar{K}^*(892)^0 \text{ anything})/\Gamma_{\text{total}}$				Γ_{61}/Γ
VALUE	DOCUMENT ID	TECN	COMMENT	
0.146 ± 0.016 ± 0.020	ALBRECHT	94j	ARG $e^+e^- \rightarrow \Upsilon(4S)$	

$\Gamma(K^*(892)\gamma)/\Gamma_{\text{total}}$				Γ_{62}/Γ
VALUE (units 10^{-5})	CL%	DOCUMENT ID	TECN	COMMENT
4.24 ± 0.54 ± 0.32		¹ COAN	00	CLE2 $e^+e^- \rightarrow \Upsilon(4S)$
• • • We do not use the following data for averages, fits, limits, etc. • • •				
<150	90	² LESIAK	92	CBAL $e^+e^- \rightarrow \Upsilon(4S)$
<24	90	ALBRECHT	88H	ARG $e^+e^- \rightarrow \Upsilon(4S)$

¹An average of $B(B^+ \rightarrow K^*(892)^+\gamma)$ and $B(B^0 \rightarrow K^*(892)^0\gamma)$ measurements reported in COAN 00 by assuming full correlated systematic errors.
²LESIAK 92 set a limit on the inclusive process $B(b \rightarrow s\gamma) < 2.8 \times 10^{-3}$ at 90% CL for the range of masses of 892–2045 MeV, independent of assumptions about s-quark hadronization.

$\Gamma(\eta K\gamma)/\Gamma_{\text{total}}$				Γ_{63}/Γ
VALUE (units 10^{-6})	DOCUMENT ID	TECN	COMMENT	
8.5 ± 1.3 ± 1.2 ± 0.9	¹ NISHIDA	05	BELL $e^+e^- \rightarrow \Upsilon(4S)$	

¹ $m_{\eta K} < 2.4 \text{ GeV}/c^2$

$\Delta_{0+}(B \rightarrow K^*(892)\gamma)$
 Δ_{0+} describes the isospin asymmetry between $\Gamma(B^0 \rightarrow K^*(892)^0\gamma)$ and $\Gamma(B^+ \rightarrow K^*(892)^+\gamma)$.

VALUE	DOCUMENT ID	TECN	COMMENT
0.050 ± 0.045 ± 0.037	¹ AUBERT,BE	04A	BABR $e^+e^- \rightarrow \Upsilon(4S)$

¹Uses the production ratio of charged and neutral B from $\Upsilon(4S)$ decays $R^{\pm/0} = 1.006 \pm 0.048$ and the lifetime ratio of $\tau_{B^+} / \tau_{B^0} = 1.083 \pm 0.017$. The 90% CL interval is $-0.046 < \Delta_{0+} < 0.146$.

$\Gamma(K_1(1400)\gamma)/\Gamma_{\text{total}}$				Γ_{64}/Γ
VALUE	CL%	DOCUMENT ID	TECN	COMMENT
<12.7 × 10⁻⁵	90	¹ COAN	00	CLE2 $e^+e^- \rightarrow \Upsilon(4S)$
• • • We do not use the following data for averages, fits, limits, etc. • • •				
< 1.6 × 10 ⁻³	90	² LESIAK	92	CBAL $e^+e^- \rightarrow \Upsilon(4S)$
< 4.1 × 10 ⁻⁴	90	ALBRECHT	88H	ARG $e^+e^- \rightarrow \Upsilon(4S)$

¹Assumes equal production of B^+ and B^0 at the $\Upsilon(4S)$.
²LESIAK 92 set a limit on the inclusive process $B(b \rightarrow s\gamma) < 2.8 \times 10^{-3}$ at 90% CL for the range of masses of 892–2045 MeV, independent of assumptions about s-quark hadronization.

$\Gamma(K_2^*(1430)\gamma)/\Gamma_{\text{total}}$				Γ_{65}/Γ
VALUE (units 10^{-5})	CL%	DOCUMENT ID	TECN	COMMENT
1.66 ± 0.59 ± 0.13		¹ COAN	00	CLE2 $e^+e^- \rightarrow \Upsilon(4S)$
• • • We do not use the following data for averages, fits, limits, etc. • • •				
<83	90	ALBRECHT	88H	ARG $e^+e^- \rightarrow \Upsilon(4S)$
¹ COAN 00 obtains a fitted signal yield of $15.9^{+5.7}_{-5.2}$ events. A search for contamination by $K^*(1410)$ yielded a rate consistent with 0; the central value assumes no contamination.				

$\Gamma(K_2^*(1770)\gamma)/\Gamma_{\text{total}}$				Γ_{66}/Γ
VALUE	CL%	DOCUMENT ID	TECN	COMMENT
<1.2 × 10⁻³	90	¹ LESIAK	92	CBAL $e^+e^- \rightarrow \Upsilon(4S)$
¹ LESIAK 92 set a limit on the inclusive process $B(b \rightarrow s\gamma) < 2.8 \times 10^{-3}$ at 90% CL for the range of masses of 892–2045 MeV, independent of assumptions about s-quark hadronization.				

$\Gamma(K_3^*(1780)\gamma)/\Gamma_{\text{total}}$				Γ_{67}/Γ
VALUE	CL%	DOCUMENT ID	TECN	COMMENT
<3.7 × 10⁻⁵	90	¹ NISHIDA	05	BELL $e^+e^- \rightarrow \Upsilon(4S)$
• • • We do not use the following data for averages, fits, limits, etc. • • •				
<3.0 × 10 ⁻³	90	ALBRECHT	88H	ARG $e^+e^- \rightarrow \Upsilon(4S)$
¹ Uses $B(K_3^*(1780) \rightarrow \eta K) = 0.11^{+0.05}_{-0.04}$.				

$\Gamma(K_3^*(2045)\gamma)/\Gamma_{\text{total}}$				Γ_{68}/Γ
VALUE	CL%	DOCUMENT ID	TECN	COMMENT
<1.0 × 10⁻³	90	¹ LESIAK	92	CBAL $e^+e^- \rightarrow \Upsilon(4S)$
¹ LESIAK 92 set a limit on the inclusive process $B(b \rightarrow s\gamma) < 2.8 \times 10^{-3}$ at 90% CL for the range of masses of 892–2045 MeV, independent of assumptions about s-quark hadronization.				

$\Gamma(K\eta(958))/\Gamma_{\text{total}}$				Γ_{69}/Γ
VALUE	DOCUMENT ID	TECN	COMMENT	
(8.3 ± 0.9 ± 0.7) × 10⁻⁵	¹ RICHICHI	00	CLE2 $e^+e^- \rightarrow \Upsilon(4S)$	

¹Assumes equal production of B^+ and B^0 at the $\Upsilon(4S)$.

$\Gamma(K^*(892)\eta(958))/\Gamma_{\text{total}}$				Γ_{70}/Γ
VALUE (units 10^{-6})	CL%	DOCUMENT ID	TECN	COMMENT
4.1 ± 1.0 ± 0.9 ± 0.5		¹ AUBERT	07E	BABR $e^+e^- \rightarrow \Upsilon(4S)$
• • • We do not use the following data for averages, fits, limits, etc. • • •				
<22	90	¹ RICHICHI	00	CLE2 $e^+e^- \rightarrow \Upsilon(4S)$
¹ Assumes equal production of B^+ and B^0 at the $\Upsilon(4S)$.				

$\Gamma(K\eta)/\Gamma_{\text{total}}$				Γ_{71}/Γ
VALUE	CL%	DOCUMENT ID	TECN	COMMENT
<5.2 × 10⁻⁶	90	¹ RICHICHI	00	CLE2 $e^+e^- \rightarrow \Upsilon(4S)$
¹ Assumes equal production of B^+ and B^0 at the $\Upsilon(4S)$.				

$\Gamma(K^*(892)\eta)/\Gamma_{\text{total}}$				Γ_{72}/Γ
VALUE	DOCUMENT ID	TECN	COMMENT	
(1.80 ± 0.49 ± 0.18) × 10⁻⁵	¹ RICHICHI	00	CLE2 $e^+e^- \rightarrow \Upsilon(4S)$	
¹ Assumes equal production of B^+ and B^0 at the $\Upsilon(4S)$.				

$\Gamma(K\phi\phi)/\Gamma_{\text{total}}$				Γ_{73}/Γ
VALUE (units 10^{-6})	DOCUMENT ID	TECN	COMMENT	
2.3 ± 0.9 ± 0.3	¹ HUANG	03	BELL $e^+e^- \rightarrow \Upsilon(4S)$	
¹ Assumes equal production of charged and neutral B meson pairs and isospin symmetry.				

$\Gamma(\bar{B} \rightarrow \bar{3}\gamma)/\Gamma_{\text{total}}$				Γ_{74}/Γ
VALUE (units 10^{-4})	DOCUMENT ID	TECN	COMMENT	
3.56 ± 0.25 OUR AVERAGE				
3.91 ± 0.91 ± 0.64	^{1,2} AUBERT	08o	BABR $e^+e^- \rightarrow \Upsilon(4S)$	
3.92 ± 0.31 ± 0.47	^{1,3} AUBERT,BE	06b	BABR $e^+e^- \rightarrow \Upsilon(4S)$	
3.49 ± 0.20 ± 0.59 ± 0.46	^{1,4} AUBERT,B	05R	BABR $e^+e^- \rightarrow \Upsilon(4S)$	
3.50 ± 0.32 ± 0.31	^{1,5} KOPPENBURG04	BELL	$e^+e^- \rightarrow \Upsilon(4S)$	
3.29 ± 0.44 ± 0.29	^{1,6} CHEN	01c	CLE2 $e^+e^- \rightarrow \Upsilon(4S)$	
• • • We do not use the following data for averages, fits, limits, etc. • • •				
3.36 ± 0.53 ± 0.65 ± 0.68	⁷ ABE	01f	BELL Repl. by KOPPENBURG 04	
2.32 ± 0.57 ± 0.35	ALAM	95	CLE2 Repl. by CHEN 01c	

Meson Particle Listings

 B^\pm/B^0 ADMIXTURE

¹ We correct it to $E_\gamma > 1.6$ GeV using the method of hep-ph/0507253 (average of three theoretical models).

² Uses a fully reconstructed B meson as a tag on the recoil side. The measurement reported is $(3.66 \pm 0.85 \pm 0.60) \times 10^{-4}$ for $E_\gamma > 1.9$ GeV.

³ The measurement reported is $(3.67 \pm 0.29 \pm 0.45) \times 10^{-4}$ for $E_\gamma > 1.9$ GeV.

⁴ The measurement reported is $(3.27 \pm 0.18^{+0.55}_{-0.42}) \times 10^{-4}$ for $E_\gamma > 1.9$ GeV.

⁵ The measurement reported is $(3.55 \pm 0.32 \pm 0.32) \times 10^{-4}$ for $E_\gamma > 1.8$ GeV.

⁶ The measurement reported is $(3.21 \pm 0.43^{+0.32}_{-0.29}) \times 10^{-4}$ for $E_\gamma > 2.0$ GeV.

⁷ ABE 01F reports their systematic errors $(\pm 0.42^{+0.50}_{-0.54}) \times 10^{-4}$, where the second error is due to the theoretical uncertainty. We combine them in quadrature.

 $\Gamma(B \rightarrow \bar{s}g\text{luon})/\Gamma_{\text{total}}$ Γ_{75}/Γ

VALUE	CL%	EVTS	DOCUMENT ID	TECN	COMMENT
<0.068	90		1 COAN	98 CLE2	$e^+e^- \rightarrow \Upsilon(4S)$

••• We do not use the following data for averages, fits, limits, etc. •••
<0.08 2 2 ALBRECHT 95D ARG $e^+e^- \rightarrow \Upsilon(4S)$

¹ COAN 98 uses D - ℓ correlation.

² ALBRECHT 95D use full reconstruction of one B decay as tag. Two candidate events for charmless B decay can be interpreted as either $b \rightarrow \text{sgluon}$ or $b \rightarrow u$ transition. If interpreted as $b \rightarrow \text{sgluon}$ they find a branching ratio of ~ 0.026 or the upper limit quoted above. Result is highly model dependent.

 $\Gamma(\eta \text{ anything})/\Gamma_{\text{total}}$ Γ_{76}/Γ

VALUE	CL%	DOCUMENT ID	TECN	COMMENT
<4.4 $\times 10^{-4}$	90	1 BROWDER	98 CLE2	$e^+e^- \rightarrow \Upsilon(4S)$

¹ BROWDER 98 search for high momentum $B \rightarrow \eta X_S$ between 2.1 and 2.7 GeV/c.

 $\Gamma(\eta' \text{ anything})/\Gamma_{\text{total}}$ Γ_{77}/Γ

VALUE (units 10^{-4})	DOCUMENT ID	TECN	COMMENT
4.2 \pm 0.9 OUR AVERAGE			

3.9 \pm 0.8 \pm 0.9 1 AUBERT,B 04F BABR $e^+e^- \rightarrow \Upsilon(4S)$

4.6 \pm 1.1 \pm 0.6 2 BONVICINI 03 CLE2 $e^+e^- \rightarrow \Upsilon(4S)$

••• We do not use the following data for averages, fits, limits, etc. •••

6.2 \pm 1.6 $^{+1.3}_{-2.0}$ 3 BROWDER 98 CLE2 $e^+e^- \rightarrow \Upsilon(4S)$

¹ The reported branching ratio is for high momentum η between 2.0 and 2.7 GeV in the $\Upsilon(4S)$ center-of-mass frame. Xs represents a recoil system consisting of a kaon and zero to four pions.

² BONVICINI 03 observed a signal of 61.2 ± 13.9 events in $B \rightarrow \eta' X_{nc}$ production for high momentum η' between 2.0 and 2.7 GeV/c in the $\Upsilon(4S)$ center-of-mass frame. The X_{nc} denotes "charmless" hadronic states recoiling against η' . The second error combines systematic and background subtraction uncertainties in quadrature.

³ BROWDER 98 observed a signal of 39.0 ± 11.6 events in high momentum $B \rightarrow \eta' X_S$ production between 2.0 and 2.7 GeV/c. The branching fraction is based on the interpretation of $b \rightarrow \text{sg}$, where the last error includes additional uncertainties due to the color-suppressed $b \rightarrow \text{backgrounds}$.

 $\Gamma(\rho\gamma)/\Gamma_{\text{total}}$ Γ_{78}/Γ

VALUE (units 10^{-6})	CL%	DOCUMENT ID	TECN	COMMENT
1.36 \pm 0.29 \pm 0.10		AUBERT	07L BABR	$e^+e^- \rightarrow \Upsilon(4S)$

••• We do not use the following data for averages, fits, limits, etc. •••

< 1.9 90 1 AUBERT 04c BABR Repl. by AUBERT 07L

<14 90 2 COAN 00 CLE2 $e^+e^- \rightarrow \Upsilon(4S)$

¹ Assumes $\Gamma(B \rightarrow \rho\gamma) = \Gamma(B^+ \rightarrow \rho^+\gamma) = 2\Gamma(B^0 \rightarrow \rho^0\gamma)$ and uses lifetime ratio of $\tau_{B^+}/\tau_{B^0} = 1.083 \pm 0.017$.

² COAN 00 reports $B(B \rightarrow \rho\gamma)/B(B \rightarrow K^*(892)\gamma) < 0.32$ at 90%CL and scaled by the central value of $B(B \rightarrow K^*(892)\gamma) = (4.24 \pm 0.54 \pm 0.32) \times 10^{-5}$.

 $\Gamma(\rho/\omega\gamma)/\Gamma_{\text{total}}$ Γ_{79}/Γ

VALUE (units 10^{-6})	CL%	DOCUMENT ID	TECN	COMMENT
1.28 \pm 0.21 OUR AVERAGE				

1.25 $^{+0.25}_{-0.24} \pm 0.09$ AUBERT 07L BABR $e^+e^- \rightarrow \Upsilon(4S)$

1.32 $^{+0.34}_{-0.31} \pm 0.10$ MOHAPATRA 06 BELL $e^+e^- \rightarrow \Upsilon(4S)$

••• We do not use the following data for averages, fits, limits, etc. •••

0.6 $\pm 0.3 \pm 0.1$ AUBERT 05 BABR Repl. by AUBERT 07L

<1.4 90 MOHAPATRA 05 BELL $e^+e^- \rightarrow \Upsilon(4S)$

 $\Gamma(\rho/\omega\gamma)/\Gamma(K^*(892)\gamma)$ Γ_{79}/Γ_{62}

VALUE	CL%	DOCUMENT ID	TECN	COMMENT
<0.035	90	1 MOHAPATRA 05	BELL	$e^+e^- \rightarrow \Upsilon(4S)$

¹ A limit of $|V_{td}/V_{ts}| < 0.22$ at 90% CL is also obtained from the measurement.

 $\Gamma(\pi^\pm \text{ anything})/\Gamma_{\text{total}}$ Γ_{80}/Γ

VALUE	DOCUMENT ID	TECN	COMMENT
3.585 \pm 0.025 \pm 0.070	1 ALBRECHT 93i	ARG	$e^+e^- \rightarrow \Upsilon(4S)$

¹ ALBRECHT 93 excludes π^\pm from K_S^0 and Λ decays. If included, they find $4.105 \pm 0.025 \pm 0.080$.

 $\Gamma(\pi^0 \text{ anything})/\Gamma_{\text{total}}$ Γ_{81}/Γ

VALUE	DOCUMENT ID	TECN	COMMENT
2.35 \pm 0.02 \pm 0.11	1 ABE	01j BELL	$e^+e^- \rightarrow \Upsilon(4S)$

¹ From fully inclusive π^0 yield with no corrections from decays of K_S^0 or other particles.

 $\Gamma(\eta \text{ anything})/\Gamma_{\text{total}}$ Γ_{82}/Γ

VALUE	DOCUMENT ID	TECN	COMMENT
0.176 \pm 0.011 \pm 0.012	KUBOTA	96 CLE2	$e^+e^- \rightarrow \Upsilon(4S)$

 $\Gamma(\rho^0 \text{ anything})/\Gamma_{\text{total}}$ Γ_{83}/Γ

VALUE	DOCUMENT ID	TECN	COMMENT
0.208 \pm 0.042 \pm 0.032	ALBRECHT 94j	ARG	$e^+e^- \rightarrow \Upsilon(4S)$

 $\Gamma(\omega \text{ anything})/\Gamma_{\text{total}}$ Γ_{84}/Γ

VALUE	CL%	DOCUMENT ID	TECN	COMMENT
<0.81	90	ALBRECHT 94j	ARG	$e^+e^- \rightarrow \Upsilon(4S)$

 $\Gamma(\phi \text{ anything})/\Gamma_{\text{total}}$ Γ_{85}/Γ

VALUE	DOCUMENT ID	TECN	COMMENT
0.0343 \pm 0.0012 OUR AVERAGE			

0.0353 $\pm 0.0005 \pm 0.0030$ HUANG 07 CLEO $e^+e^- \rightarrow \Upsilon(4S)$

0.0341 $\pm 0.0006 \pm 0.0012$ AUBERT 04s BABR $e^+e^- \rightarrow \Upsilon(4S)$

0.0390 $\pm 0.0030 \pm 0.0035$ ALBRECHT 94j ARG $e^+e^- \rightarrow \Upsilon(4S)$

0.023 $\pm 0.006 \pm 0.005$ BORTOLETTO86 CLEO $e^+e^- \rightarrow \Upsilon(4S)$

 $\Gamma(\phi K^*(892))/\Gamma_{\text{total}}$ Γ_{86}/Γ

VALUE	CL%	DOCUMENT ID	TECN
<2.2 $\times 10^{-5}$	90	1 BERGFELD 98	CLE2

¹ Assumes equal production of B^+ and B^0 at the $\Upsilon(4S)$.

 $\Gamma(\Lambda_c^+ / \bar{\Lambda}_c^- \text{ anything})/\Gamma_{\text{total}}$ Γ_{87}/Γ

VALUE	CL%	DOCUMENT ID	TECN	COMMENT
0.045 \pm 0.004 \pm 0.012		1 AUBERT	07c BABR	$e^+e^- \rightarrow \Upsilon(4S)$

••• We do not use the following data for averages, fits, limits, etc. •••

0.064 $\pm 0.008 \pm 0.008$ 2 CRAWFORD 92 CLEO $e^+e^- \rightarrow \Upsilon(4S)$

0.14 ± 0.09 3 ALBRECHT 88e ARG $e^+e^- \rightarrow \Upsilon(4S)$

<0.112 90 4 ALAM 87 CLEO $e^+e^- \rightarrow \Upsilon(4S)$

¹ AUBERT 07c reports $0.045 \pm 0.003 \pm 0.012$ for $B(\Lambda_c^+ \rightarrow p K^- \pi^+) = (5.0 \pm 1.3) \times 10^{-2}$. We rescale to our best value $B(\Lambda_c^+ \rightarrow p K^- \pi^+) = (5.0 \pm 1.3) \times 10^{-2}$. Our first error is their experiment's error and our second error is the systematic error from using our best value.

² CRAWFORD 92 result derived from lepton baryon correlations. Assumes all charmed baryons in B^0 and B^\pm decay are Λ_c .

³ ALBRECHT 88e measured $B(B \rightarrow \Lambda_c^+ X) \cdot B(\Lambda_c^+ \rightarrow p K^- \pi^+) = (0.30 \pm 0.12 \pm 0.06)\%$ and used $B(\Lambda_c^+ \rightarrow p K^- \pi^+) = (2.2 \pm 1.0)\%$ from ABRAMS 80 to obtain above number.

⁴ Assuming all baryons result from charmed baryons, ALAM 86 conclude the branching fraction is $7.4 \pm 2.9\%$. The limit given above is model independent.

 $\Gamma(\Lambda_c^+ \text{ anything})/\Gamma(\bar{\Lambda}_c^- \text{ anything})$ Γ_{88}/Γ_{89}

VALUE	DOCUMENT ID	TECN	COMMENT
0.19 \pm 0.13 \pm 0.04	1 AMMAR 97	CLE2	$e^+e^- \rightarrow \Upsilon(4S)$

¹ AMMAR 97 uses a high-momentum lepton tag ($P_\ell > 1.4$ GeV/c²).

 $\Gamma(\bar{\Lambda}_c^- e^+ \text{ anything})/\Gamma(\Lambda_c^+ / \bar{\Lambda}_c^- \text{ anything})$ Γ_{90}/Γ_{87}

VALUE	CL%	DOCUMENT ID	TECN	COMMENT
<0.05	90	1 BONVICINI 98	CLE2	$e^+e^- \rightarrow \Upsilon(4S)$

¹ BONVICINI 98 uses the electron with momentum above 0.6 GeV/c.

 $\Gamma(\bar{\Lambda}_c^- p \text{ anything})/\Gamma(\Lambda_c^+ / \bar{\Lambda}_c^- \text{ anything})$ Γ_{91}/Γ_{87}

VALUE	DOCUMENT ID	TECN	COMMENT
0.57 \pm 0.05 \pm 0.05	BONVICINI 98	CLE2	$e^+e^- \rightarrow \Upsilon(4S)$

 $\Gamma(\bar{\Lambda}_c^- p e^+ \nu_e)/\Gamma(\bar{\Lambda}_c^- p \text{ anything})$ Γ_{92}/Γ_{91}

VALUE	CL%	DOCUMENT ID	TECN	COMMENT
<0.04	90	1 BONVICINI 98	CLE2	$e^+e^- \rightarrow \Upsilon(4S)$

¹ BONVICINI 98 uses the electron with momentum above 0.6 GeV/c.

 $\Gamma(\bar{\Sigma}_c^{--} \text{ anything})/\Gamma_{\text{total}}$ Γ_{93}/Γ

VALUE	EVTS	DOCUMENT ID	TECN	COMMENT
0.0042 \pm 0.0021 \pm 0.0011	77	1 PROCARIO 94	CLE2	$e^+e^- \rightarrow \Upsilon(4S)$

¹ PROCARIO 94 reports $[B(B \rightarrow \bar{\Sigma}_c^{--} \text{ anything})] \times [B(\Lambda_c^+ \rightarrow p K^- \pi^+)] = 0.00021 \pm 0.00008 \pm 0.00007$. We divide by our best value $B(\Lambda_c^+ \rightarrow p K^- \pi^+) = (5.0 \pm 1.3) \times 10^{-2}$. Our first error is their experiment's error and our second error is the systematic error from using our best value.

 $\Gamma(\bar{\Sigma}_c^- \text{ anything})/\Gamma_{\text{total}}$ Γ_{94}/Γ

VALUE	CL%	DOCUMENT ID	TECN	COMMENT
<0.010	90	1 PROCARIO 94	CLE2	$e^+e^- \rightarrow \Upsilon(4S)$

¹ PROCARIO 94 reports $[B(B \rightarrow \bar{\Sigma}_c^- \text{ anything})] \times [B(\Lambda_c^+ \rightarrow p K^- \pi^+)] < 0.00048$. We divide by our best value $B(\Lambda_c^+ \rightarrow p K^- \pi^+) = 0.050$.

$\Gamma(\Sigma_c^0 \text{ anything})/\Gamma_{\text{total}}$ Γ_{95}/Γ

VALUE	EVTS	DOCUMENT ID	TECN	COMMENT
0.0046 ± 0.0021 ± 0.0012	76	¹ PROCARIO 94	CLE2	$e^+e^- \rightarrow \Upsilon(4S)$

¹ PROCARIO 94 reports $[B(B \rightarrow \Sigma_c^0 \text{ anything})] \times [B(\Lambda_c^+ \rightarrow pK^-\pi^+)] = 0.00023 \pm 0.00008 \pm 0.00007$. We divide by our best value $B(\Lambda_c^+ \rightarrow pK^-\pi^+) = (5.0 \pm 1.3) \times 10^{-2}$. Our first error is their experiment's error and our second error is the systematic error from using our best value.

$\Gamma(\Sigma_c^0 N(N = p \text{ or } n))/\Gamma_{\text{total}}$ Γ_{96}/Γ

VALUE	CL%	DOCUMENT ID	TECN	COMMENT
<0.0015	90	¹ PROCARIO 94	CLE2	$e^+e^- \rightarrow \Upsilon(4S)$

¹ PROCARIO 94 reports < 0.0017 for $B(\Lambda_c^+ \rightarrow pK^-\pi^+) = 0.043$. We rescale to our best value $B(\Lambda_c^+ \rightarrow pK^-\pi^+) = 0.050$.

$\Gamma(\Xi_c^0 \text{ anything} \times B(\Xi_c^0 \rightarrow \Xi^-\pi^+))/\Gamma_{\text{total}}$ Γ_{97}/Γ

VALUE (units 10^{-3})	DOCUMENT ID	TECN	COMMENT
0.193 ± 0.030 OUR AVERAGE	Error includes scale factor of 1.1.		
0.211 ± 0.019 ± 0.025	¹ AUBERT,B 05M	BABR	$e^+e^- \rightarrow \Upsilon(4S)$
0.144 ± 0.048 ± 0.021	² BARISH 97	CLE2	$e^+e^- \rightarrow \Upsilon(4S)$

¹ The yield is obtained by requiring the momentum $P < 2.15$ GeV/c.

² BARISH 97 find 79 ± 27 Ξ_c^0 events.

$\Gamma(\Xi_c^+ \text{ anything} \times B(\Xi_c^+ \rightarrow \Xi^-\pi^+\pi^+))/\Gamma_{\text{total}}$ Γ_{98}/Γ

VALUE (units 10^{-3})	DOCUMENT ID	TECN	COMMENT
0.453 ± 0.096 ± 0.085 ± 0.065	¹ BARISH 97	CLE2	$e^+e^- \rightarrow \Upsilon(4S)$

¹ BARISH 97 find 125 ± 28 Ξ_c^+ events.

$\Gamma(p/\bar{p} \text{ anything})/\Gamma_{\text{total}}$ Γ_{99}/Γ

VALUE	EVTS	DOCUMENT ID	TECN	COMMENT
0.080 ± 0.004 OUR AVERAGE				
0.080 ± 0.005 ± 0.005		ALBRECHT 93i	ARG	$e^+e^- \rightarrow \Upsilon(4S)$
0.080 ± 0.005 ± 0.003		CRAWFORD 92	CLEO	$e^+e^- \rightarrow \Upsilon(4S)$
0.082 ± 0.005 ± 0.013 ± 0.010	2163	¹ ALBRECHT 89k	ARG	$e^+e^- \rightarrow \Upsilon(4S)$

• • • We do not use the following data for averages, fits, limits, etc. • • •

>0.021 ² ALAM 83b CLEO $e^+e^- \rightarrow \Upsilon(4S)$

¹ ALBRECHT 89k include direct and nondirect protons.

² ALAM 83b reported their result as $> 0.036 \pm 0.006 \pm 0.009$. Data are consistent with equal yields of p and \bar{p} . Using assumed yields below cut, $B(B \rightarrow p + X) = 0.03$ not including protons from Λ decays.

$\Gamma(p/\bar{p}(\text{direct}) \text{ anything})/\Gamma_{\text{total}}$ Γ_{100}/Γ

VALUE	EVTS	DOCUMENT ID	TECN	COMMENT
0.055 ± 0.005 OUR AVERAGE				
0.055 ± 0.005 ± 0.0035		ALBRECHT 93i	ARG	$e^+e^- \rightarrow \Upsilon(4S)$
0.056 ± 0.006 ± 0.005		CRAWFORD 92	CLEO	$e^+e^- \rightarrow \Upsilon(4S)$
0.055 ± 0.016	1220	¹ ALBRECHT 89k	ARG	$e^+e^- \rightarrow \Upsilon(4S)$

¹ ALBRECHT 89k subtract contribution of Λ decay from the inclusive proton yield.

$\Gamma(\Lambda/\bar{\Lambda} \text{ anything})/\Gamma_{\text{total}}$ Γ_{101}/Γ

VALUE	EVTS	DOCUMENT ID	TECN	COMMENT
0.040 ± 0.005 OUR AVERAGE				
0.038 ± 0.004 ± 0.006	2998	CRAWFORD 92	CLEO	$e^+e^- \rightarrow \Upsilon(4S)$
0.042 ± 0.005 ± 0.006	943	ALBRECHT 89k	ARG	$e^+e^- \rightarrow \Upsilon(4S)$

• • • We do not use the following data for averages, fits, limits, etc. • • •

0.022 ± 0.003 ± 0.0022 ¹ ACKERSTAFF 97N OPAL $e^+e^- \rightarrow Z$

>0.011 ² ALAM 83b CLEO $e^+e^- \rightarrow \Upsilon(4S)$

¹ ACKERSTAFF 97N assumes $B(b \rightarrow B) = 0.868 \pm 0.041$, i.e., an admixture of B^0, B^\pm , and B_s .

² ALAM 83b reported their result as $> 0.022 \pm 0.007 \pm 0.004$. Values are for $(B(\Lambda X) + B(\bar{\Lambda} X))/2$. Data are consistent with equal yields of p and \bar{p} . Using assumed yields below cut, $B(B \rightarrow \Lambda X) = 0.03$.

$\Gamma(\Lambda \text{ anything})/\Gamma(\bar{\Lambda} \text{ anything})$ $\Gamma_{102}/\Gamma_{103}$

VALUE	DOCUMENT ID	TECN	COMMENT
0.43 ± 0.09 ± 0.07	¹ AMMAR 97	CLE2	$e^+e^- \rightarrow \Upsilon(4S)$

¹ AMMAR 97 uses a high-momentum lepton tag ($P_\ell > 1.4$ GeV/ c^2).

$\Gamma(\Xi^-/\Xi^+ \text{ anything})/\Gamma_{\text{total}}$ Γ_{104}/Γ

VALUE	EVTS	DOCUMENT ID	TECN	COMMENT
0.0027 ± 0.0006 OUR AVERAGE				
0.0027 ± 0.0005 ± 0.0004	147	CRAWFORD 92	CLEO	$e^+e^- \rightarrow \Upsilon(4S)$
0.0028 ± 0.0014	54	ALBRECHT 89k	ARG	$e^+e^- \rightarrow \Upsilon(4S)$

$\Gamma(\text{baryons anything})/\Gamma_{\text{total}}$ Γ_{105}/Γ

VALUE	DOCUMENT ID	TECN	COMMENT
0.068 ± 0.005 ± 0.003	¹ ALBRECHT 92o	ARG	$e^+e^- \rightarrow \Upsilon(4S)$

• • • We do not use the following data for averages, fits, limits, etc. • • •

0.076 ± 0.014 ² ALBRECHT 89k ARG $e^+e^- \rightarrow \Upsilon(4S)$

¹ ALBRECHT 92o result is from simultaneous analysis of p and Λ yields, $p\bar{p}$ and $\Lambda\bar{\Lambda}$ correlations, and various lepton-baryon and lepton-baryon-antibaryon correlations. Supersedes ALBRECHT 89k.

² ALBRECHT 89k obtain this result by adding their their measurements (5.5 ± 1.6)% for direct protons and (4.2 ± 0.5 ± 0.6)% for inclusive Λ production. They then assume (5.5 ± 1.6)% for neutron production and add it in also. Since each B decay has two baryons, they divide by 2 to obtain (7.6 ± 1.4)%.

$\Gamma(p\bar{p} \text{ anything})/\Gamma_{\text{total}}$ Γ_{106}/Γ

VALUE	EVTS	DOCUMENT ID	TECN	COMMENT
0.0247 ± 0.0023 OUR AVERAGE				
0.024 ± 0.001 ± 0.004		CRAWFORD 92	CLEO	$e^+e^- \rightarrow \Upsilon(4S)$
0.025 ± 0.002 ± 0.002	918	ALBRECHT 89k	ARG	$e^+e^- \rightarrow \Upsilon(4S)$

Includes p and \bar{p} from Λ and $\bar{\Lambda}$ decay.

0.025 ± 0.002 ± 0.002 918 ALBRECHT 89k ARG $e^+e^- \rightarrow \Upsilon(4S)$

0.025 ± 0.002 ± 0.002 918 ALBRECHT 89k ARG $e^+e^- \rightarrow \Upsilon(4S)$

$\Gamma(p\bar{p} \text{ anything})/\Gamma(p/\bar{p} \text{ anything})$ Γ_{106}/Γ_{99}

VALUE	DOCUMENT ID	TECN	COMMENT
0.30 ± 0.02 ± 0.05	¹ CRAWFORD 92	CLEO	$e^+e^- \rightarrow \Upsilon(4S)$

Includes p and \bar{p} from Λ and $\bar{\Lambda}$ decay.

0.30 ± 0.02 ± 0.05 ¹ CRAWFORD 92 CLEO $e^+e^- \rightarrow \Upsilon(4S)$

¹ CRAWFORD 92 value is not independent of their $(p\bar{p} \text{ anything})/\Gamma_{\text{total}}$ value.

$\Gamma(\Lambda\bar{\Lambda} \text{ anything})/\Gamma_{\text{total}}$ Γ_{107}/Γ

VALUE	EVTS	DOCUMENT ID	TECN	COMMENT
0.025 ± 0.004 OUR AVERAGE				
0.029 ± 0.005 ± 0.005		CRAWFORD 92	CLEO	$e^+e^- \rightarrow \Upsilon(4S)$
0.023 ± 0.004 ± 0.003	165	ALBRECHT 89k	ARG	$e^+e^- \rightarrow \Upsilon(4S)$

Includes p and \bar{p} from Λ and $\bar{\Lambda}$ decay.

0.029 ± 0.005 ± 0.005 CRAWFORD 92 CLEO $e^+e^- \rightarrow \Upsilon(4S)$

0.023 ± 0.004 ± 0.003 165 ALBRECHT 89k ARG $e^+e^- \rightarrow \Upsilon(4S)$

$\Gamma(\Lambda\bar{\Lambda} \text{ anything})/\Gamma(\Lambda/\bar{\Lambda} \text{ anything})$ $\Gamma_{107}/\Gamma_{101}$

VALUE	DOCUMENT ID	TECN	COMMENT
0.76 ± 0.11 ± 0.08	¹ CRAWFORD 92	CLEO	$e^+e^- \rightarrow \Upsilon(4S)$

Includes p and \bar{p} from Λ and $\bar{\Lambda}$ decay.

0.76 ± 0.11 ± 0.08 ¹ CRAWFORD 92 CLEO $e^+e^- \rightarrow \Upsilon(4S)$

¹ CRAWFORD 92 value is not independent of their

$[\Gamma(\Lambda\bar{p} \text{ anything}) + \Gamma(\Lambda p \text{ anything})]/\Gamma_{\text{total}}$ value.

$\Gamma(\Lambda\bar{\Lambda} \text{ anything})/\Gamma_{\text{total}}$ Γ_{108}/Γ

VALUE	CL%	EVTS	DOCUMENT ID	TECN	COMMENT
<0.005		90	CRAWFORD 92	CLEO	$e^+e^- \rightarrow \Upsilon(4S)$

• • • We do not use the following data for averages, fits, limits, etc. • • •

<0.0088 90 12 ALBRECHT 89k ARG $e^+e^- \rightarrow \Upsilon(4S)$

$\Gamma(\Lambda\bar{\Lambda} \text{ anything})/\Gamma(\Lambda/\bar{\Lambda} \text{ anything})$ $\Gamma_{108}/\Gamma_{101}$

VALUE	CL%	DOCUMENT ID	TECN	COMMENT
<0.13		90	¹ CRAWFORD 92	CLEO $e^+e^- \rightarrow \Upsilon(4S)$

• • • We do not use the following data for averages, fits, limits, etc. • • •

<0.13 90 ¹ CRAWFORD 92 CLEO $e^+e^- \rightarrow \Upsilon(4S)$

¹ CRAWFORD 92 value is not independent of their $(\Lambda\bar{\Lambda} \text{ anything})/\Gamma_{\text{total}}$ value.

$\Gamma(s e^+ e^-)/\Gamma_{\text{total}}$ Γ_{109}/Γ

VALUE (units 10^{-6})	CL%	DOCUMENT ID	TECN	COMMENT
4.7 ± 1.3 OUR AVERAGE				
4.04 ± 1.30 ± 0.87		¹ IWASAKI 05	BELL	$e^+e^- \rightarrow \Upsilon(4S)$
6.0 ± 1.7 ± 1.3		² AUBERT,B 04i	BABR	$e^+e^- \rightarrow \Upsilon(4S)$

Test for $\Delta B = 1$ weak neutral current. Allowed by higher-order electroweak interactions.

4.7 ± 1.3 OUR AVERAGE

4.04 ± 1.30 ± 0.87 ¹ IWASAKI 05 BELL $e^+e^- \rightarrow \Upsilon(4S)$

6.0 ± 1.7 ± 1.3 ² AUBERT,B 04i BABR $e^+e^- \rightarrow \Upsilon(4S)$

• • • We do not use the following data for averages, fits, limits, etc. • • •

5.0 ± 2.3 ± 1.3 ² KANEKO 03 BELL Repl. by IWASAKI 05

< 57 90 GLENN 98 CLEO $e^+e^- \rightarrow \Upsilon(4S)$

<50000 90 BEBEK 81 CLEO $e^+e^- \rightarrow \Upsilon(4S)$

¹ Requires $M_{\ell^+ \ell^-} > 0.2$ GeV/ c^2 .

² Requires $M_{e^+ e^-} > 0.2$ GeV/ c^2 .

$\Gamma(s \mu^+ \mu^-)/\Gamma_{\text{total}}$ Γ_{110}/Γ

VALUE (units 10^{-6})	CL%	DOCUMENT ID	TECN	COMMENT
4.3 ± 1.2 OUR AVERAGE				
4.13 ± 1.05 ± 0.85		¹ IWASAKI 05	BELL	$e^+e^- \rightarrow \Upsilon(4S)$
5.0 ± 2.8 ± 1.2		AUBERT,B 04i	BABR	$e^+e^- \rightarrow \Upsilon(4S)$

Test for $\Delta B = 1$ weak neutral current. Allowed by higher-order electroweak interactions.

4.3 ± 1.2 OUR AVERAGE

4.13 ± 1.05 ± 0.85 ¹ IWASAKI 05 BELL $e^+e^- \rightarrow \Upsilon(4S)$

5.0 ± 2.8 ± 1.2 AUBERT,B 04i BABR $e^+e^- \rightarrow \Upsilon(4S)$

• • • We do not use the following data for averages, fits, limits, etc. • • •

7.9 ± 2.1 ± 2.1 ² KANEKO 03 BELL Repl. by IWASAKI 05

< 58 90 GLENN 98 CLEO $e^+e^- \rightarrow \Upsilon(4S)$

<17000 90 CHADWICK 81 CLEO $e^+e^- \rightarrow \Upsilon(4S)$

¹ Requires $M_{\ell^+ \ell^-} > 0.2$ GeV/ c^2 .

Meson Particle Listings

 B^\pm/B^0 ADMIXTURE

$[\Gamma(s e^+ e^-) + \Gamma(s \mu^+ \mu^-)]/\Gamma_{\text{total}}$ ($\Gamma_{109} + \Gamma_{110}$)/ Γ
 Test for $\Delta B = 1$ weak neutral current. Allowed by higher-order electroweak interactions.

VALUE	CL%	DOCUMENT ID	TECN	COMMENT
$<4.2 \times 10^{-5}$	90	GLENN 98	CLEO	$e^+ e^- \rightarrow \Upsilon(4S)$
••• We do not use the following data for averages, fits, limits, etc. •••				
<0.0024	90	¹ BEAN 87	CLEO	Repl. by GLENN 98
<0.0062	90	² AVERY 84	CLEO	Repl. by BEAN 87
¹ BEAN 87 reports $[(\mu^+ \mu^-) + (e^+ e^-)]/2$ and we converted it.				
² Determine ratio of B^+ to B^0 semileptonic decays to be in the range 0.25–2.9.				

$\Gamma(s \ell^+ \ell^-)/\Gamma_{\text{total}}$ (Γ_{111})/ Γ
 Test for $\Delta B = 1$ weak neutral current.

VALUE (units 10^{-6})	CL%	DOCUMENT ID	TECN	COMMENT
4.5 ± 1.0		OUR AVERAGE		
$4.11 \pm 0.83^{+0.85}_{-0.81}$		¹ IWASAKI 05	BELL	$e^+ e^- \rightarrow \Upsilon(4S)$
$5.6 \pm 1.5 \pm 1.3$		² AUBERT,B 04i	BABR	$e^+ e^- \rightarrow \Upsilon(4S)$
••• We do not use the following data for averages, fits, limits, etc. •••				
$6.1 \pm 1.4^{+1.4}_{-1.1}$		² KANEKO 03	BELL	Repl. by IWASAKI 05
¹ Requires $M_{\ell^+ \ell^-} > 0.2 \text{ GeV}/c^2$.				
² Requires $M_{e^+ e^-} > 0.2 \text{ GeV}/c^2$.				

$\Gamma(\pi \ell^+ \ell^-)/\Gamma_{\text{total}}$ (Γ_{112})/ Γ

VALUE	CL%	DOCUMENT ID	TECN	COMMENT
$<9.1 \times 10^{-8}$	90	¹ AUBERT 07AG	BABR	$e^+ e^- \rightarrow \Upsilon(4S)$
¹ Assumes equal production of B^+ and B^0 at the $\Upsilon(4S)$.				

$\Gamma(K e^+ e^-)/\Gamma_{\text{total}}$ (Γ_{113})/ Γ
 Test for $\Delta B = 1$ weak neutral current. Allowed by higher-order electroweak interactions.

VALUE (units 10^{-7})	CL%	DOCUMENT ID	TECN	COMMENT
$3.8^{+0.8}_{-0.7}$		OUR AVERAGE		
$3.3^{+0.9}_{-0.8} \pm 0.2$		¹ AUBERT,B 06j	BABR	$e^+ e^- \rightarrow \Upsilon(4S)$
$4.8^{+1.5}_{-1.3} \pm 0.3$		^{1,2} ISHIKAWA 03	BELL	$e^+ e^- \rightarrow \Upsilon(4S)$
••• We do not use the following data for averages, fits, limits, etc. •••				
$7.4^{+1.8}_{-1.6} \pm 0.5$		¹ AUBERT 03u	BABR	Repl. by AUBERT,B 06j
<13	90	ABE 02	BELL	Repl. by ISHIKAWA 03
¹ Assumes equal production of B^+ and B^0 at the $\Upsilon(4S)$.				
² The second error is a total of systematic uncertainties including model dependence.				

$\Gamma(K^*(892) e^+ e^-)/\Gamma_{\text{total}}$ (Γ_{114})/ Γ
 Test for $\Delta B = 1$ weak neutral current. Allowed by higher-order electroweak interactions.

VALUE (units 10^{-7})	CL%	DOCUMENT ID	TECN	COMMENT
11.3 ± 2.7		OUR AVERAGE		
$9.7^{+3.0}_{-2.7} \pm 1.4$		¹ AUBERT,B 06j	BABR	$e^+ e^- \rightarrow \Upsilon(4S)$
$14.9^{+5.2}_{-4.6} \pm 1.2$		² ISHIKAWA 03	BELL	$e^+ e^- \rightarrow \Upsilon(4S)$
••• We do not use the following data for averages, fits, limits, etc. •••				
$9.8^{+5.0}_{-4.2} \pm 1.1$		¹ AUBERT 03u	BABR	Repl. by AUBERT,B 06j
<56	90	ABE 02	BELL	Repl. by ISHIKAWA 03
¹ Assumes equal production of B^+ and B^0 at the $\Upsilon(4S)$.				
² Assumes equal production of B^0 and B^+ at $\Upsilon(4S)$. The second error is a total of systematic uncertainties including model dependence.				

$\Gamma(K \mu^+ \mu^-)/\Gamma_{\text{total}}$ (Γ_{115})/ Γ
 Test for $\Delta B = 1$ weak neutral current. Allowed by higher-order electroweak interactions.

VALUE (units 10^{-7})	CL%	DOCUMENT ID	TECN	COMMENT
$4.2^{+0.9}_{-0.8}$		OUR AVERAGE		
$3.5^{+1.3}_{-1.1} \pm 0.3$		¹ AUBERT,B 06j	BABR	$e^+ e^- \rightarrow \Upsilon(4S)$
$4.8^{+1.2}_{-1.1} \pm 0.4$		^{1,2} ISHIKAWA 03	BELL	$e^+ e^- \rightarrow \Upsilon(4S)$
••• We do not use the following data for averages, fits, limits, etc. •••				
$4.5^{+2.3}_{-1.9} \pm 0.4$		¹ AUBERT 03u	BABR	Repl. by AUBERT,B 06j
$9.9^{+4.0}_{-3.2} \pm 1.0$		ABE 02	BELL	Repl. by ISHIKAWA 03
¹ Assumes equal production of B^+ and B^0 at the $\Upsilon(4S)$.				
² The second error is a total of systematic uncertainties including model dependence.				

$\Gamma(K \mu^+ \mu^-)/\Gamma(K e^+ e^-)$ ($\Gamma_{115}/\Gamma_{113}$)

VALUE	DOCUMENT ID	TECN	COMMENT
$1.06 \pm 0.48 \pm 0.08$	AUBERT,B 06j	BABR	$e^+ e^- \rightarrow \Upsilon(4S)$

$\Gamma(K^*(892) \mu^+ \mu^-)/\Gamma_{\text{total}}$ (Γ_{116})/ Γ
 Test for $\Delta B = 1$ weak neutral current. Allowed by higher-order electroweak interactions.

VALUE (units 10^{-7})	CL%	DOCUMENT ID	TECN	COMMENT
$10.3^{+2.6}_{-2.3}$		OUR AVERAGE		
$8.8^{+3.5}_{-3.0} \pm 1.2$		¹ AUBERT,B 06j	BABR	$e^+ e^- \rightarrow \Upsilon(4S)$
$11.7^{+3.6}_{-3.1} \pm 1.0$		² ISHIKAWA 03	BELL	$e^+ e^- \rightarrow \Upsilon(4S)$
••• We do not use the following data for averages, fits, limits, etc. •••				
$12.7^{+7.6}_{-6.1} \pm 1.6$		¹ AUBERT 03u	BABR	Repl. by AUBERT,B 06j
<31	90	ABE 02	BELL	Repl. by ISHIKAWA 03
¹ Assumes equal production of B^+ and B^0 at the $\Upsilon(4S)$.				
² Assumes equal production of B^0 and B^+ at $\Upsilon(4S)$. The second error is a total of systematic uncertainties including model dependence.				

$\Gamma(K^*(892) \mu^+ \mu^-)/\Gamma(K^*(892) e^+ e^-)$ ($\Gamma_{116}/\Gamma_{114}$)

VALUE	DOCUMENT ID	TECN	COMMENT
$0.91 \pm 0.45 \pm 0.06$	AUBERT,B 06j	BABR	$e^+ e^- \rightarrow \Upsilon(4S)$

$\Gamma(K \ell^+ \ell^-)/\Gamma_{\text{total}}$ (Γ_{117})/ Γ
 Test for $\Delta B = 1$ weak neutral current. Allowed by higher-order electroweak interactions.

VALUE (units 10^{-7})	CL%	DOCUMENT ID	TECN	COMMENT
3.9 ± 0.7		OUR AVERAGE		
$3.4 \pm 0.7 \pm 0.2$		¹ AUBERT,B 06j	BABR	$e^+ e^- \rightarrow \Upsilon(4S)$
$4.8^{+1.0}_{-0.9} \pm 0.3$		² ISHIKAWA 03	BELL	$e^+ e^- \rightarrow \Upsilon(4S)$
••• We do not use the following data for averages, fits, limits, etc. •••				
$6.5^{+1.4}_{-1.3} \pm 0.4$		³ AUBERT 03u	BABR	Repl. by AUBERT,B 06j
$7.5^{+2.5}_{-2.1} \pm 0.6$		⁴ ABE 02	BELL	Repl. by ISHIKAWA 03
<5.1	90	¹ AUBERT 02L	BABR	$e^+ e^- \rightarrow \Upsilon(4S)$
<17	90	⁵ ANDERSON 01B	CLE2	$e^+ e^- \rightarrow \Upsilon(4S)$
¹ Assumes equal production of B^+ and B^0 at the $\Upsilon(4S)$.				
² Assumes equal production rate for charge and neutral B meson pairs, isospin invariance, lepton universality for $B \rightarrow K \ell^+ \ell^-$, and $B(B \rightarrow K^*(892) \mu^+ \mu^-) = 1.33$. The second error is total systematic uncertainties including model dependence.				
³ Assumes all four $B \rightarrow K \ell^+ \ell^-$ modes having equal partial widths in the fit.				
⁴ Assumes lepton universality.				
⁵ The result is for di-lepton masses above 0.5 GeV.				

$\Gamma(K^*(892) \ell^+ \ell^-)/\Gamma_{\text{total}}$ (Γ_{118})/ Γ
 Test for $\Delta B = 1$ weak neutral current. Allowed by higher-order electroweak interactions.

VALUE (units 10^{-7})	CL%	DOCUMENT ID	TECN	COMMENT
9.4 ± 1.8		OUR AVERAGE		
$7.8^{+1.9}_{-1.7} \pm 1.1$		¹ AUBERT,B 06j	BABR	$e^+ e^- \rightarrow \Upsilon(4S)$
$11.5^{+2.6}_{-2.4} \pm 0.8$		² ISHIKAWA 03	BELL	$e^+ e^- \rightarrow \Upsilon(4S)$
••• We do not use the following data for averages, fits, limits, etc. •••				
$8.8^{+3.3}_{-2.9} \pm 1.0$		³ AUBERT 03u	BABR	Repl. by AUBERT,B 06j
<31	90	^{1,4} AUBERT 02L	BABR	Repl. by AUBERT 03u
<33	90	⁵ ANDERSON 01B	CLE2	$e^+ e^- \rightarrow \Upsilon(4S)$
¹ Assumes equal production of B^+ and B^0 at the $\Upsilon(4S)$.				
² Assumes equal production rate for charge and neutral B meson pairs, isospin invariance, lepton universality for $B \rightarrow K \ell^+ \ell^-$, and $B(B \rightarrow K^*(892) \mu^+ \mu^-) = 1.33$. The second error is total systematic uncertainties including model dependence.				
³ Assumes the partial width ratio of electron and muon modes to be $\Gamma(B \rightarrow K^*(892) e^+ e^-)/\Gamma(B \rightarrow K^*(892) \mu^+ \mu^-) = 1.33$.				
⁴ For averaging $K^*(892) \mu^+ \mu^-$ and $K^*(892) e^+ e^-$ modes, AUBERT 02L assumed $B(B \rightarrow K^*(892) e^+ e^-)/B(B \rightarrow K^*(892) \mu^+ \mu^-) = 1.2$.				
⁵ The result is for di-lepton masses above 0.5 GeV.				

$\Gamma(s e^\pm \mu^\mp)/\Gamma_{\text{total}}$ (Γ_{119})/ Γ
 Test for lepton family number conservation. Allowed by higher-order electroweak interactions.

VALUE	CL%	DOCUMENT ID	TECN	COMMENT
$<2.2 \times 10^{-5}$	90	GLENN 98	CLEO	$e^+ e^- \rightarrow \Upsilon(4S)$

$\Gamma(\pi e^\pm \mu^\mp)/\Gamma_{\text{total}}$ (Γ_{120})/ Γ
 Test for lepton family number conservation.

VALUE	CL%	DOCUMENT ID	TECN	COMMENT
$<9.2 \times 10^{-8}$	90	¹ AUBERT 07AG	BABR	$e^+ e^- \rightarrow \Upsilon(4S)$
••• We do not use the following data for averages, fits, limits, etc. •••				
$<1.6 \times 10^{-6}$	90	¹ EDWARDS 02B	CLE2	$e^+ e^- \rightarrow \Upsilon(4S)$
¹ Assumes equal production of B^+ and B^0 at the $\Upsilon(4S)$.				

$\Gamma(\rho e^\pm \mu^\mp)/\Gamma_{\text{total}}$ (Γ_{121})/ Γ
 Test for lepton family number conservation.

VALUE	CL%	DOCUMENT ID	TECN	COMMENT
$<3.2 \times 10^{-6}$	90	¹ EDWARDS 02B	CLE2	$e^+ e^- \rightarrow \Upsilon(4S)$
¹ Assumes equal production of B^+ and B^0 at the $\Upsilon(4S)$.				

$\Gamma(K e^\pm \mu^\mp)/\Gamma_{\text{total}}$ Γ_{122}/Γ

Test of lepton family number conservation.

VALUE (units 10^{-7})	CL%	DOCUMENT ID	TECN	COMMENT
< 0.38	90	¹ AUBERT,B 06J	BABR	$e^+e^- \rightarrow \Upsilon(4S)$

••• We do not use the following data for averages, fits, limits, etc. •••

<16	90	¹ EDWARDS 02B	CLE2	$e^+e^- \rightarrow \Upsilon(4S)$
-----	----	--------------------------	------	-----------------------------------

¹ Assumes equal production of B^+ and B^0 at the $\Upsilon(4S)$. $\Gamma(K^*(892) e^\pm \mu^\mp)/\Gamma_{\text{total}}$ Γ_{123}/Γ

Test of lepton family number conservation.

VALUE (units 10^{-7})	CL%	DOCUMENT ID	TECN	COMMENT
< 5.1	90	¹ AUBERT,B 06J	BABR	$e^+e^- \rightarrow \Upsilon(4S)$

••• We do not use the following data for averages, fits, limits, etc. •••

<62	90	¹ EDWARDS 02B	CLE2	$e^+e^- \rightarrow \Upsilon(4S)$
-----	----	--------------------------	------	-----------------------------------

¹ Assumes equal production of B^+ and B^0 at the $\Upsilon(4S)$.

CP VIOLATION

 A_{CP} is defined as

$$\frac{B(B \rightarrow \bar{f}) - B(\bar{B} \rightarrow f)}{B(B \rightarrow \bar{f}) + B(\bar{B} \rightarrow f)},$$

the CP-violation charge asymmetry of inclusive B^\pm and B^0 decay. $A_{CP}(B \rightarrow K^*(892)\gamma)$

VALUE	DOCUMENT ID	TECN	COMMENT
-0.010 ± 0.028 OUR AVERAGE			

-0.013 ± 0.036 ± 0.010	¹ AUBERT,BE 04A	BABR	$e^+e^- \rightarrow \Upsilon(4S)$
------------------------	----------------------------	------	-----------------------------------

-0.015 ± 0.044 ± 0.012	² NAKAO 04	BELL	$e^+e^- \rightarrow \Upsilon(4S)$
------------------------	-----------------------	------	-----------------------------------

+0.08 ± 0.13 ± 0.03	² COAN 00	CLE2	$e^+e^- \rightarrow \Upsilon(4S)$
---------------------	----------------------	------	-----------------------------------

••• We do not use the following data for averages, fits, limits, etc. •••

-0.044 ± 0.076 ± 0.012	³ AUBERT 02c	BABR	Repl. by AUBERT,BE 04A
------------------------	-------------------------	------	------------------------

¹ Corresponds to a 90% CL allowed region, $-0.074 < A_{CP} < 0.049$.² Assumes equal production of B^+ and B^0 at the $\Upsilon(4S)$.³ A 90% CL range is $-0.170 < A_{CP} < 0.082$. $A_{CP}(B \rightarrow s\gamma)$

VALUE	DOCUMENT ID	TECN	COMMENT
0.01 ± 0.04 OUR AVERAGE			

0.10 ± 0.18 ± 0.05	^{1,2} AUBERT 08o	BABR	$e^+e^- \rightarrow \Upsilon(4S)$
--------------------	---------------------------	------	-----------------------------------

0.025 ± 0.056 ± 0.015	³ AUBERT,B 04E	BABR	$e^+e^- \rightarrow \Upsilon(4S)$
-----------------------	---------------------------	------	-----------------------------------

0.002 ± 0.050 ± 0.030	⁴ NISHIDA 04	BELL	$e^+e^- \rightarrow \Upsilon(4S)$
-----------------------	-------------------------	------	-----------------------------------

-0.079 ± 0.108 ± 0.022	⁵ COAN 01	CLE2	$e^+e^- \rightarrow \Upsilon(4S)$
------------------------	----------------------	------	-----------------------------------

¹ The result is for $E_\gamma > 2.2$ GeV.² Uses a fully reconstructed B meson as a tag on the recoil side.³ Corresponds to $-0.06 < A_{CP} < +0.11$ at 90% CL.⁴ This measurement is performed inclusively for recoil mass X_s less than 2.1 GeV, which corresponds to $-0.093 < A_{CP} < 0.096$ at 90% CL.⁵ Corresponds to $-0.27 < A_{CP} < 0.10$ at 90% CL. $A_{CP}(b \rightarrow (s+d)\gamma)$

VALUE	DOCUMENT ID	TECN	COMMENT
-0.110 ± 0.115 ± 0.017	AUBERT,BE 06b	BABR	$e^+e^- \rightarrow \Upsilon(4S)$

 $A_{CP}(B \rightarrow X_s \ell^+ \ell^-)$

VALUE	DOCUMENT ID	TECN	COMMENT
-0.22 ± 0.26 ± 0.02	¹ AUBERT,B 04i	BABR	$e^+e^- \rightarrow \Upsilon(4S)$

¹ The final state flavor is determined by the kaon and pion charges where modes with $X_S = K_S^0, K_S^0 \pi^0$ or $K_S^0 \pi^+ \pi^-$ are not used.LEPTON FORWARD-BACKWARD ASYMMETRY
IN $B \rightarrow K^{(*)} \ell^+ \ell^-$ DECAYThe forward-backward angular asymmetry of the lepton pair in $B \rightarrow K^{(*)} \ell^+ \ell^-$ decay is defined as

$$A_{FB}(s) = \frac{N(\cos\theta > 0) - N(\cos\theta < 0)}{N(\cos\theta > 0) + N(\cos\theta < 0)},$$

where $s = q^2/m_B^2$, and θ is the angle of the lepton with respect to the flight direction of the B meson, measured in the dilepton rest frame. In addition, the fraction of longitudinal polarization F_L of the K^* and F_S , the relative contribution from scalar and pseudoscalar penguin amplitudes in $B \rightarrow K \ell^+ \ell^-$, can be measured from the angular distribution of its decay products. $A_{FB}(B \rightarrow K^* \ell^+ \ell^-) (q^2 > 0.1 \text{ GeV}^2/c^4)$

VALUE	CL%	DOCUMENT ID	TECN	COMMENT
0.50 ± 0.15 ± 0.02		¹ ISHIKAWA 06	BELL	$e^+e^- \rightarrow \Upsilon(4S)$

••• We do not use the following data for averages, fits, limits, etc. •••

>0.55	95	² AUBERT,B 06j	BABR	$e^+e^- \rightarrow \Upsilon(4S)$
-------	----	---------------------------	------	-----------------------------------

¹ Using an unbinned max. likelihood fits to the M_{bc} distribution in five q^2 bins for $\cos\theta > 0$ and $\cos\theta < 0$.² Results with different q^2 cuts are also reported. $F_L(B \rightarrow K^* \ell^+ \ell^-) (q^2 > 0.1 \text{ GeV}^2/c^4)$

VALUE	DOCUMENT ID	TECN	COMMENT
0.63^{+0.18}_{-0.19} ± 0.05	¹ AUBERT,B 06j	BABR	$e^+e^- \rightarrow \Upsilon(4S)$

¹ Results with different q^2 cuts are also reported. $A_{FB}(B \rightarrow K \ell^+ \ell^-) (q^2 > 0.1 \text{ GeV}^2/c^4)$

VALUE	DOCUMENT ID	TECN	COMMENT
0.11 ± 0.12 OUR AVERAGE			

0.15 ^{+0.21} _{-0.23} ± 0.08	¹ AUBERT,B 06j	BABR	$e^+e^- \rightarrow \Upsilon(4S)$
---	---------------------------	------	-----------------------------------

0.10 ± 0.14 ± 0.01	² ISHIKAWA 06	BELL	$e^+e^- \rightarrow \Upsilon(4S)$
--------------------	--------------------------	------	-----------------------------------

¹ Results with different q^2 cuts are also reported.² Using an unbinned max. likelihood fits to the M_{bc} distribution in five q^2 bins for $\cos\theta > 0$ and $\cos\theta < 0$. $F_S(B \rightarrow K \ell^+ \ell^-) (q^2 > 0.1 \text{ GeV}^2/c^4)$

VALUE	DOCUMENT ID	TECN	COMMENT
0.81^{+0.58}_{-0.61} ± 0.46	¹ AUBERT,B 06j	BABR	$e^+e^- \rightarrow \Upsilon(4S)$

¹ Results with different q^2 cuts are also reported.

ISOSPIN ASYMMETRY

 Δ_0 is defined as

$$\frac{\Gamma(B^0 \rightarrow f_0) - \Gamma(B^+ \rightarrow f_0)}{\Gamma(B^0 \rightarrow f_0) + \Gamma(B^+ \rightarrow f_0)},$$

the isospin asymmetry of inclusive neutral and charged B decay.

 $\Delta_0(B \rightarrow X_S \gamma)$

VALUE	DOCUMENT ID	TECN	COMMENT
-0.01 ± 0.06 OUR AVERAGE			

-0.06 ± 0.15 ± 0.07	^{1,2} AUBERT 08o	BABR	$e^+e^- \rightarrow \Upsilon(4S)$
---------------------	---------------------------	------	-----------------------------------

-0.006 ± 0.058 ± 0.026	AUBERT,B 05R	BABR	$e^+e^- \rightarrow \Upsilon(4S)$
------------------------	--------------	------	-----------------------------------

¹ The result is for $E_\gamma > 2.2$ GeV.² Uses a fully reconstructed B meson as a tag on the recoil side. $B \rightarrow X_c \ell \nu$ HADRONIC MASS MOMENTS $\langle M_X^2 - \overline{M}_D^2 \rangle$ (First Moments)

VALUE (GeV ²)	DOCUMENT ID	TECN	COMMENT
0.36 ± 0.08 OUR AVERAGE			Error includes scale factor of 1.8.

0.467 ± 0.038 ± 0.068	¹ ACOSTA 05F	CDF	$p\bar{p}$ at 1.96 TeV
-----------------------	-------------------------	-----	------------------------

0.293 ± 0.012 ± 0.058	² CSORNA 04	CLE2	$e^+e^- \rightarrow \Upsilon(4S)$
-----------------------	------------------------	------	-----------------------------------

••• We do not use the following data for averages, fits, limits, etc. •••

0.251 ± 0.023 ± 0.062	³ CRONIN-HEN..01B	CLE2	$e^+e^- \rightarrow \Upsilon(4S)$
-----------------------	------------------------------	------	-----------------------------------

¹ Moments are measured with a minimum lepton momentum of 0.7 GeV/c in the B rest frame;² Uses minimum lepton energy of 1.5 GeV and also reports moments with $E_\ell > 1.0$ GeV.³ The leptons are required to have $P_\ell > 1.5$ GeV/c. $\langle M_X^2 \rangle$ (First Moments)

VALUE (GeV ²)	DOCUMENT ID	TECN	COMMENT
4.156 ± 0.029 OUR AVERAGE			

4.144 ± 0.028 ± 0.022	¹ SCHWANDA 07	BELL	$e^+e^- \rightarrow \Upsilon(4S)$
-----------------------	--------------------------	------	-----------------------------------

4.18 ± 0.04 ± 0.03	¹ AUBERT,B 04	BABR	$e^+e^- \rightarrow \Upsilon(4S)$
--------------------	--------------------------	------	-----------------------------------

¹ The leptons are required to have $E_\ell > 1.5$ GeV/c. $\langle (M_X^2 - \overline{M}_X^2)^2 \rangle$ (Second Moments)

VALUE (GeV ⁴)	DOCUMENT ID	TECN	COMMENT
0.55 ± 0.08 OUR AVERAGE			

0.515 ± 0.061 ± 0.064	¹ SCHWANDA 07	BELL	$e^+e^- \rightarrow \Upsilon(4S)$
-----------------------	--------------------------	------	-----------------------------------

0.629 ± 0.031 ± 0.143	² CSORNA 04	CLE2	$e^+e^- \rightarrow \Upsilon(4S)$
-----------------------	------------------------	------	-----------------------------------

••• We do not use the following data for averages, fits, limits, etc. •••

1.05 ± 0.26 ± 0.13	³ ACOSTA 05F	CDF	$p\bar{p}$ at 1.96 TeV
--------------------	-------------------------	-----	------------------------

0.576 ± 0.048 ± 0.168	¹ CRONIN-HEN..01B	CLE2	$e^+e^- \rightarrow \Upsilon(4S)$
-----------------------	------------------------------	------	-----------------------------------

¹ The leptons are required to have $E_\ell > 1.5$ GeV/c.² Uses minimum lepton energy of 1.5 GeV and also reports moments with $E_\ell > 1.0$ GeV.³ Moments are measured with a minimum lepton momentum of 0.7 GeV/c in the B rest frame; $\langle (M_X^2 - \overline{M}_D^2)^2 \rangle$ (Second Moments)

VALUE (GeV ⁴)	DOCUMENT ID	TECN	COMMENT
0.639 ± 0.056 ± 0.178	¹ CRONIN-HEN..01B	CLE2	$e^+e^- \rightarrow \Upsilon(4S)$

¹ The leptons are required to have $E_\ell > 1.5$ GeV/c. $B \rightarrow X_c \ell \nu$ LEPTON MOMENTUM MOMENTS $R_0 (\Gamma_{E_1 > 1.7 \text{ GeV}} / \Gamma_{E_1 > 1.5 \text{ GeV}})$

VALUE	DOCUMENT ID	TECN	COMMENT
0.6187 ± 0.0014 ± 0.0016	¹ MAHMOOD 03	CLE2	$e^+e^- \rightarrow \Upsilon(4S)$

¹ The leptons are required to have $E_\ell > 1.5$ GeV in the B rest frame.

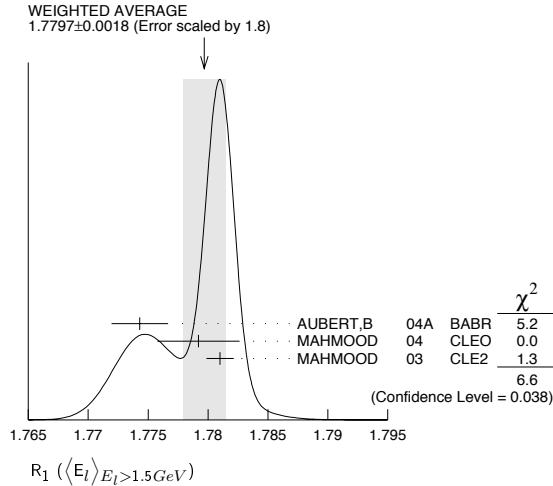
Meson Particle Listings

B^\pm/B^0 ADMIXTURE

$R_1 (\langle E_l \rangle_{E_l > 1.5 \text{ GeV}})$

VALUE	DOCUMENT ID	TECN	COMMENT
1.7797 ± 0.0018 OUR AVERAGE	Error includes scale factor of 1.8. See the ideogram below.		
1.7743 ± 0.0019 ± 0.0014	1 AUBERT,B	04A	BABR $e^+e^- \rightarrow \Upsilon(4S)$
1.7792 ± 0.0021 ± 0.0027	2 MAHMOOD	04	CLEO $e^+e^- \rightarrow \Upsilon(4S)$
1.7810 ± 0.0007 ± 0.0009	3 MAHMOOD	03	CLE2 $e^+e^- \rightarrow \Upsilon(4S)$

- ¹ The leptons are required to have $E_l > 1.5$ GeV in the B rest frame. The result with $E_l > 0.6$ GeV is also given.
- ² Uses $E_e > 1.5$ GeV and also reports moments with other minimum minimum E_e conditions, as low as $E_e > 0.6$ GeV.
- ³ The leptons are required to have $E_l > 1.5$ GeV in the B rest frame.



$R_2 (\langle E_l^2 - \bar{E}_l^2 \rangle_{E_l > 1.5 \text{ GeV}})$

VALUE (10^{-3} GeV^2)	DOCUMENT ID	TECN	COMMENT
30.8 ± 0.8 OUR AVERAGE			
30.3 ± 0.9 ± 0.5	1 AUBERT,B	04A	BABR $e^+e^- \rightarrow \Upsilon(4S)$
31.6 ± 0.8 ± 1.0	2 MAHMOOD	04	CLEO $e^+e^- \rightarrow \Upsilon(4S)$

- ¹ The leptons are required to have $E_l > 1.5$ GeV in the B rest frame. The result with $E_l > 0.6$ GeV is also given.
- ² Uses $E_e > 1.5$ GeV and also reports moments with other minimum minimum E_e conditions, as low as $E_e > 0.6$ GeV.

$R_3 (\langle E_l^3 - \bar{E}_l^3 \rangle_{E_l > 1.5 \text{ GeV}})$

VALUE (10^{-3} GeV^3)	DOCUMENT ID	TECN	COMMENT
2.12 ± 0.47 ± 0.20	1 AUBERT,B	04A	BABR $e^+e^- \rightarrow \Upsilon(4S)$

- ¹ The leptons are required to have $E_l > 1.5$ GeV in the B rest frame. The result with $E_l > 0.6$ GeV is also given.

$B \rightarrow X_s \gamma$ PHOTON ENERGY MOMENTS

$\langle E_\gamma \rangle$

VALUE (GeV)	DOCUMENT ID	TECN	COMMENT
2.288 ± 0.030 OUR AVERAGE			
2.289 ± 0.058 ± 0.027	1,2 AUBERT	08o	BABR $e^+e^- \rightarrow \Upsilon(4S)$
2.288 ± 0.025 ± 0.023	1 AUBERT,BE	06B	BABR $e^+e^- \rightarrow \Upsilon(4S)$

- ¹ The result is for $E_\gamma > 1.9$ GeV.
- ² Uses a fully reconstructed B meson as a tag on the recoil side.

$\langle E_\gamma^2 \rangle - \langle E_\gamma \rangle^2$

VALUE (GeV^2)	DOCUMENT ID	TECN	COMMENT
0.033 ± 0.005 OUR AVERAGE			
0.0334 ± 0.0124 ± 0.0062	1,2 AUBERT	08o	BABR $e^+e^- \rightarrow \Upsilon(4S)$
0.0328 ± 0.0040 ± 0.0043	1 AUBERT,BE	06B	BABR $e^+e^- \rightarrow \Upsilon(4S)$

- ¹ The result is for $E_\gamma > 1.9$ GeV.
- ² Uses a fully reconstructed B meson as a tag on the recoil side.

B^\pm/B^0 ADMIXTURE REFERENCES

AUBERT 08N	PRL 100 021801	B. Aubert et al.	(BABAR Collab.)
AUBERT 08O	PR D77 051103	B. Aubert et al.	(BABAR Collab.)
AUBERT 07AC	PRL 99 051801	B. Aubert et al.	(BABAR Collab.)
AUBERT 07C	PR D75 012003	B. Aubert et al.	(BABAR Collab.)
AUBERT 07E	PRL 98 051802	B. Aubert et al.	(BABAR Collab.)
AUBERT 07L	PRL 98 151802	B. Aubert et al.	(BABAR Collab.)
HUANG 07	PR D75 012002	G.S. Huang et al.	(CLEO Collab.)
SCHWANDA 07	PR D75 032005	C. Schwanda et al.	(BELLE Collab.)
URQUIJO 07	PR D75 032001	P. Urquijo et al.	(BELLE Collab.)
AUBERT 06H	PR D73 012006	B. Aubert et al.	(BABAR Collab.)
AUBERT,B 06J	PR D73 092001	B. Aubert et al.	(BABAR Collab.)
AUBERT,B 06Y	PR D74 091105R	B. Aubert et al.	(BABAR Collab.)
AUBERT,BE 06B	PRL 97 171803	B. Aubert et al.	(BABAR Collab.)
GOKHROO 06	PRL 97 162002	G. Gokhroo et al.	(BELLE Collab.)

ISHIKAWA 06	PRL 96 251801	A. Ishikawa et al.	(BELLE Collab.)
MOHAPATRA 06	PRL 96 221601	D. Mohapatra et al.	(BELLE Collab.)
ABAZOV 05O	PRL 95 171803	V.M. Abazov et al.	(DO Collab.)
ACOSTA 05F	PR D71 051103R	D. Acosta et al.	(CDF Collab.)
ARTUSO 05B	PRL 95 261801	M. Artuso et al.	(CLEO Collab.)
AUBERT 05	PRL 94 011801	B. Aubert et al.	(BABAR Collab.)
AUBERT,B 05M	PRL 95 142003	B. Aubert et al.	(BABAR Collab.)
AUBERT,B 05X	PR D72 052004	B. Aubert et al.	(BABAR Collab.)
AUBERT,B 05R	PRL 95 111801	B. Aubert et al.	(BABAR Collab.)
Also	PRL 97 019003 (errata)	B. Aubert et al.	(BABAR Collab.)
CHOI 05	PRL 94 182002	S.-K. Choi et al.	(BELLE Collab.)
IWASAKI 05	PR D72 092005	M. Iwasaki et al.	(BELLE Collab.)
LIMOSANI 05	PL B621 28	A. Limosani et al.	(BELLE Collab.)
MOHAPATRA 05	PR D72 011101R	D. Mohapatra et al.	(BELLE Collab.)
NISHIDA 05	PL B610 23	S. Nishida et al.	(BELLE Collab.)
OKABE 05	PL B614 27	T. Okabe et al.	(BELLE Collab.)
ABDALLAH 04D	EPJ C33 213	J. Abdallah et al.	(DELPHI Collab.)
AUBERT 04C	PRL 92 111801	B. Aubert et al.	(BaBar Collab.)
AUBERT 04I	PRL 92 071802	B. Aubert et al.	(BABAR Collab.)
AUBERT 04J	PR D69 052005	B. Aubert et al.	(BABAR Collab.)
AUBERT 04X	PRL 93 011803	B. Aubert et al.	(BABAR Collab.)
AUBERT,B 04	PR D69 111103R	B. Aubert et al.	(BABAR Collab.)
AUBERT,B 04A	PR D69 111104R	B. Aubert et al.	(BABAR Collab.)
AUBERT,B 04E	PRL 93 021804	B. Aubert et al.	(BABAR Collab.)
AUBERT,B 04F	PRL 93 061801	B. Aubert et al.	(BABAR Collab.)
AUBERT,B 04I	PRL 93 081802	B. Aubert et al.	(BABAR Collab.)
AUBERT,BE 04A	PR D70 112006	B. Aubert et al.	(BABAR Collab.)
CSORNA 04	PR D70 032002	S.E. Csorna et al.	(CLEO Collab.)
KOPPENBURG 04	PRL 93 061803	P. Koppenburg et al.	(BELLE Collab.)
MAHMOOD 04	PR D70 032003	A.H. Mahmod et al.	(CLEO Collab.)
NAKAO 04	PR D69 112001	M. Nakao et al.	(BELLE Collab.)
NISHIDA 04	PRL 93 031803	S. Nishida et al.	(BELLE Collab.)
ADAM 03B	PR D68 012004	N.E. Adam et al.	(CLEO Collab.)
AUBERT 03	PR D67 031101R	B. Aubert et al.	(BaBar Collab.)
AUBERT 03F	PR D67 032002	B. Aubert et al.	(BaBar Collab.)
AUBERT 03U	PRL 91 221802	B. Aubert et al.	(BaBar Collab.)
BONVICINI 03	PR D68 011101R	G. Bonvicini et al.	(CLEO Collab.)
HUANG 03	PRL 91 241802	H.-C. Huang et al.	(BELLE Collab.)
ISHIKAWA 03	PRL 91 261601	A. Ishikawa et al.	(BELLE Collab.)
KANEKO 03	PRL 90 021801	J. Kaneko et al.	(BELLE Collab.)
KROKOVNY 03B	PRL 91 262002	P. Krokovny et al.	(BELLE Collab.)
MAHMOOD 03	PR D67 072001	A.H. Mahmod et al.	(CLEO Collab.)
ABE 02	PRL 88 021801	K. Abe et al.	(CLEO Collab.)
ABE 02Y	PRL 89 011803	K. Abe et al.	(BELLE Collab.)
ABE 02Y	PL B547 181	K. Abe et al.	(BELLE Collab.)
ANDERSON 02	PRL 89 282001	S. Anderson et al.	(CLEO Collab.)
AUBERT 02C	PRL 88 101805	B. Aubert et al.	(BaBar Collab.)
AUBERT 02G	PR D65 091104R	B. Aubert et al.	(BaBar Collab.)
AUBERT 02L	PRL 88 241801	B. Aubert et al.	(BaBar Collab.)
BORNHEIM 02	PRL 88 231803	A. Bornheim et al.	(CLEO Collab.)
EDWARDS 02B	PR D65 111102R	K.W. Edwards et al.	(CLEO Collab.)
ABE 01F	PL B511 151	K. Abe et al.	(BELLE Collab.)
ANDERSON 01B	PR D64 072001	K. Abe et al.	(BELLE Collab.)
ANDERSON 01B	PRL 87 031803	S. Anderson et al.	(CLEO Collab.)
CHEN 01	PR D63 031102	S. Chen et al.	(CLEO Collab.)
CHEN 01C	PRL 87 251807	S. Chen et al.	(CLEO Collab.)
COAN 01	PRL 86 5661	T.E. Coan et al.	(CLEO Collab.)
CRONIN-HENNESSY 01B	PRL 87 251808	D. Cronin-Hennessy et al.	(CLEO Collab.)
PDG 01	Unofficial 2001 WWW edition		
ABREU 00R	PL B475 407	P. Abreu et al.	(DELPHI Collab.)
COAN 00	PRL 84 5283	T.E. Coan et al.	(CLEO Collab.)
RICHICHI 00	PRL 85 520	S.J. Richichi et al.	(CLEO Collab.)
BARATE 98Q	EPJ C4 387	R. Barate et al.	(ALEPH Collab.)
BERGFELD 98	PRL 81 272	T. Bergfeld et al.	(CLEO Collab.)
BISHAI 98	PR D57 2847	M. Bishai et al.	(CLEO Collab.)
BONVICINI 98	PR D57 6004	G. Bonvicini et al.	(CLEO Collab.)
BROWDER 98	PRL 81 1786	T.E. Browder et al.	(CLEO Collab.)
COAN 98	PRL 80 1150	T.E. Coan et al.	(CLEO Collab.)
GLENN 98	PRL 80 2289	S. Glenn et al.	(CLEO Collab.)
ACKERSTAFF 97N	ZPHY C74 423	K. Ackerstaff et al.	(OPAL Collab.)
AMMAR 97	PR D55 13	R. Ammar et al.	(CLEO Collab.)
BARISH 97	PRL 79 3599	B. Barish et al.	(CLEO Collab.)
BUSKULIC 97B	ZPHY C73 601	D. Buskulic et al.	(ALEPH Collab.)
GIBBONS 97B	PR D56 3783	L. Gibbons et al.	(CLEO Collab.)
ALBRECHT 96D	PL B374 256	H. Albrecht et al.	(ARGUS Collab.)
BARISH 96B	PRL 76 15710	B.C. Barish et al.	(CLEO Collab.)
GIBAUT 96	PR D53 4734	D. Gibaut et al.	(CLEO Collab.)
KUBOTA 96	PR D53 6033	Y. Kubota et al.	(CLEO Collab.)
PDG 96	PR D54 1	R. M. Barnett et al.	
ALAM 95	PRL 74 2885	M.S. Alam et al.	(CLEO Collab.)
ALBRECHT 95D	PL B353 554	H. Albrecht et al.	(ARGUS Collab.)
BALEST 95B	PR D52 2661	R. Balest et al.	(CLEO Collab.)
BARISH 95	PR D51 1014	B.C. Barish et al.	(CLEO Collab.)
BUSKULIC 95B	PL B345 103	D. Buskulic et al.	(ALEPH Collab.)
ALBRECHT 94C	ZPHY C62 371	H. Albrecht et al.	(ARGUS Collab.)
ALBRECHT 94J	ZPHY C61 1	H. Albrecht et al.	(ARGUS Collab.)
PROCARIO 94	PRL 73 1472	M. Procaro et al.	(CLEO Collab.)
ALBRECHT 93	ZPHY C57 533	H. Albrecht et al.	(ARGUS Collab.)
ALBRECHT 93E	ZPHY C60 11	H. Albrecht et al.	(ARGUS Collab.)
ALBRECHT 93H	PL B318 397	H. Albrecht et al.	(ARGUS Collab.)
ALBRECHT 93I	ZPHY C58 191	H. Albrecht et al.	(ARGUS Collab.)
ALEXANDER 93B	PL B319 365	J. Alexander et al.	(CLEO Collab.)
ARTUSO 93	PL B311 307	M. Artuso	(SYRA)
BARTELT 93B	PRL 71 4111	J.E. Bartelt et al.	(CLEO Collab.)
ALBRECHT 92E	PL B277 209	H. Albrecht et al.	(ARGUS Collab.)
ALBRECHT 92G	ZPHY C54 1	H. Albrecht et al.	(ARGUS Collab.)
ALBRECHT 92O	ZPHY C56 1	H. Albrecht et al.	(ARGUS Collab.)
BORTOLETTO 92	PR D45 21	D. Bortolotto et al.	(CLEO Collab.)
CRAWFORD 92	PR D45 752	G. Crawford et al.	(CLEO Collab.)
HENDERSON 92	PR D45 2212	S. Henderson et al.	(CLEO Collab.)
LESIAK 92	ZPHY C55 33	T. Lesiak et al.	(Crystal Ball Collab.)
ALBRECHT 91C	PL B255 297	H. Albrecht et al.	(ARGUS Collab.)
ALBRECHT 91H	ZPHY C52 353	H. Albrecht et al.	(ARGUS Collab.)
FULTON 91	PR D43 651	R. Fulton et al.	(CLEO Collab.)
YANAGISAWA 91	PRL 66 2436	C. Yanagisawa et al.	(CUSB II Collab.)
ALBRECHT 90	PL B234 409	H. Albrecht et al.	(ARGUS Collab.)
ALBRECHT 90H	PL B249 359	H. Albrecht et al.	(ARGUS Collab.)
BORTOLETTO 90	PRL 64 2117	D. Bortolotto et al.	(CLEO Collab.)
Also	PR D45 21	D. Bortolotto et al.	(CLEO Collab.)
FULTON 90	PRL 64 16	R. Fulton et al.	(CLEO Collab.)
MASCHMANN 90	ZPHY C46 555	W.S. Maschmann et al.	(Crystal Ball Collab.)
PDG 90	PL B239 1	J.J. Hernandez et al.	(IFIC, BOST, CIT+)
ALBRECHT 89K	ZPHY C42 519	H. Albrecht et al.	(ARGUS Collab.)
ISGUR 89B	PR D39 799	N. Isgur et al.	(TNT0, CIT)
WACHS 89	ZPHY C42 33	K. Wachs et al.	(Crystal Ball Collab.)
ALBRECHT 88E	PL B210 263	H. Albrecht et al.	(ARGUS Collab.)
ALBRECHT 88H	PL B210 258	H. Albrecht et al.	(ARGUS Collab.)
KOERNER 88	ZPHY C38 511	J.G. Korner, G.A. Schuler	(MANZ, DESY)
ALAM 87	PRL 59 22	M.S. Alam et al.	(CLEO Collab.)
ALAM 87B	PRL 58 1814	M.S. Alam et al.	(CLEO Collab.)
ALBRECHT 87D	PL B199 451	H. Albrecht et al.	(ARGUS Collab.)

See key on page 373

Meson Particle Listings

 B^\pm/B^0 ADMIXTURE, $B^\pm/B^0/B_s^0/b$ -baryon ADMIXTURE

ALBRECHT	87H	PL B187 425	H. Albrecht et al.	(ARGUS Collab.)
BEAN	87	PR D35 3533	A. Bean et al.	(CLEO Collab.)
BEHRENDIS	87	PRL 59 407	S. Behrendis et al.	(CLEO Collab.)
BORTOLETTO	87	PR D35 19	D. Bortoletto et al.	(CLEO Collab.)
ALAM	86	PR D34 3279	M.S. Alam et al.	(CLEO Collab.)
BALTRUSAITIS...	86E	PRL 56 2140	R.M. Baltrusaitis et al.	(Mark III Collab.)
BORTOLETTO	86	PRL 56 800	D. Bortoletto et al.	(CLEO Collab.)
HAAS	86	PRL 56 2781	J. Haas et al.	(CLEO Collab.)
ALBRECHT	85H	PL 162B 395	H. Albrecht et al.	(ARGUS Collab.)
CSORNA	85	PRL 54 1894	S.E. Csorna et al.	(CLEO Collab.)
HAAS	85	PRL 55 1248	J. Haas et al.	(CLEO Collab.)
AVERY	84	PRL 53 1309	P. Avery et al.	(CLEO Collab.)
CHEN	84	PRL 52 1084	A. Chen et al.	(CLEO Collab.)
LEVMAN	84	PL 141B 271	G.M. Levman et al.	(CLEO Collab.)
ALAM	83B	PRL 51 1143	M.S. Alam et al.	(CLEO Collab.)
GREEN	83	PRL 51 347	J. Green et al.	(CLEO Collab.)
KLOPFEN...	83B	PL 130B 444	C. Klopffenstein et al.	(CUSB Collab.)
ALTARELLI	82	NP B208 365	G. Altarelli et al.	(ROMA, INFN, FRAS)
BRODY	82	PRL 48 1070	A.D. Brody et al.	(CLEO Collab.)
GIANNINI	82	NP B206 1	G. Giannini et al.	(CUSB Collab.)
BEBEK	81	PRL 46 84	C. Bebek et al.	(CLEO Collab.)
CHADWICK	81	PRL 46 88	K. Chadwick et al.	(CLEO Collab.)
ABRAMS	80	PRL 44 10	G.S. Abrams et al.	(SLAC, LBL)

- ⁹BUSKULIC 93o analyzed using dipole method.
- ¹⁰Combines ABREU 96E secondary vertex result with ABREU 94L impact parameter result.
- ¹¹From proper time distribution of $b \rightarrow J/\psi(1S)$ anything.
- ¹²ABE 93j analyzed using $J/\psi(1S) \rightarrow \mu\mu$ vertices.
- ¹³ABREU 93d data analyzed using $D/D^*\ell$ anything event vertices.
- ¹⁴ABREU 93g data analyzed using charged and neutral vertices.
- ¹⁵ACTON 93c analysed using $D/D^*\ell$ anything event vertices.
- ¹⁶ABREU 92 is combined result of muon and hadron impact parameter analyses. Hadron tracks gave $(12.7 \pm 0.4 \pm 1.2) \times 10^{-13}$ s for an admixture of B species weighted by production fraction and mean charge multiplicity, while muon tracks gave $(13.0 \pm 1.0 \pm 0.8) \times 10^{-13}$ s for an admixture weighted by production fraction and semileptonic branching fraction.
- ¹⁷ACTON 92 is combined result of muon and electron impact parameter analyses.
- ¹⁸BUSKULIC 92f uses the lepton impact parameter distribution for data from the 1991 run.
- ¹⁹BUSKULIC 92g use $J/\psi(1S)$ tags to measure the average b lifetime. This is comparable to other methods only if the $J/\psi(1S)$ branching fractions of the different b -flavored hadrons are in the same ratio.
- ²⁰Using $Z \rightarrow e^+X$ or μ^+X , ADEVA 91H determined the average lifetime for an admixture of B hadrons from the impact parameter distribution of the lepton.
- ²¹Using $Z \rightarrow J/\psi(1S)X$, $J/\psi(1S) \rightarrow \ell^+\ell^-$, ALEXANDER 91G determined the average lifetime for an admixture of B hadrons from the decay point of the $J/\psi(1S)$.
- ²²Using $Z \rightarrow eX$ or μX , DECAMP 91c determines the average lifetime for an admixture of B hadrons from the signed impact parameter distribution of the lepton.
- ²³HAGEMANN 90 uses electrons and muons in an impact parameter analysis.
- ²⁴LYONS 90 combine the results of the B lifetime measurements of ONG 89, BRAUN-SCHWEIG 89b, KLEM 88, and ASH 87, and JADE data by private communication. They use statistical techniques which include variation of the error with the mean life, and possible correlations between the systematic errors. This result is not independent of the measured results used in our average.
- ²⁵We have combined an overall scale error of 15% in quadrature with the systematic error of ± 0.7 to obtain ± 2.1 systematic error.
- ²⁶Statistical and systematic errors were combined by BROM 87.

 $B^\pm/B^0/B_s^0/b$ -baryon ADMIXTURE $B^\pm/B^0/B_s^0/b$ -baryon ADMIXTURE MEAN LIFE

Each measurement of the B mean life is an average over an admixture of various bottom mesons and baryons which decay weakly. Different techniques emphasize different admixtures of produced particles, which could result in a different B mean life.

"OUR EVALUATION" is an average using rescaled values of the data listed below. The average and rescaling were performed by the Heavy Flavor Averaging Group (HFAG) and are described at <http://www.slac.stanford.edu/xorg/hfag/>. The averaging/rescaling procedure takes into account correlations between the measurements and asymmetric lifetime errors, but ignores the small differences due to different techniques.

VALUE (10^{-12} s)	EVTS	DOCUMENT ID	TECN	COMMENT
1.568 ± 0.009 OUR EVALUATION				
1.570 ± 0.005 ± 0.008		¹ ABDALLAH 04E	DLPH	$e^+e^- \rightarrow Z$
1.533 ± 0.015 $\pm^{+0.035}_{-0.031}$		² ABE 98b	CDF	$p\bar{p}$ at 1.8 TeV
1.549 ± 0.009 ± 0.015		³ ACCIARRI 98	L3	$e^+e^- \rightarrow Z$
1.611 ± 0.010 ± 0.027		⁴ ACKERSTAFF 97f	OPAL	$e^+e^- \rightarrow Z$
1.582 ± 0.011 ± 0.027		⁴ ABREU 96E	DLPH	$e^+e^- \rightarrow Z$
1.533 ± 0.013 ± 0.022	19.8k	⁵ BUSKULIC 96f	ALEP	$e^+e^- \rightarrow Z$
1.564 ± 0.030 ± 0.036		⁶ ABE,K 95b	SLD	$e^+e^- \rightarrow Z$
1.542 ± 0.021 ± 0.045		⁷ ABREU 94L	DLPH	$e^+e^- \rightarrow Z$
1.523 ± 0.034 ± 0.038	5372	⁸ ACTON 93L	OPAL	$e^+e^- \rightarrow Z$
1.511 ± 0.022 ± 0.078		⁹ BUSKULIC 93o	ALEP	$e^+e^- \rightarrow Z$
• • • Data do not use the following data for averages, fits, limits, etc. • • •				
1.575 ± 0.010 ± 0.026		¹⁰ ABREU 96E	DLPH	$e^+e^- \rightarrow Z$
1.50 $\pm^{+0.24}_{-0.21}$ ± 0.03		¹¹ ABREU 94p	DLPH	$e^+e^- \rightarrow Z$
1.46 ± 0.06 ± 0.06	5344	¹² ABE 93j	CDF	Repl. by ABE 98b
1.23 $\pm^{+0.14}_{-0.13}$ ± 0.15	188	¹³ ABREU 93d	DLPH	Sup. by ABREU 94L
1.49 ± 0.11 ± 0.12	253	¹⁴ ABREU 93g	DLPH	Sup. by ABREU 94L
1.51 $\pm^{+0.16}_{-0.14}$ ± 0.11	130	¹⁵ ACTON 93c	OPAL	$e^+e^- \rightarrow Z$
1.535 ± 0.035 ± 0.028	7357	⁸ ADRIANI 93k	L3	Repl. by ACCIARRI 98
1.28 ± 0.10		¹⁶ ABREU 92	DLPH	Sup. by ABREU 94L
1.37 ± 0.07 ± 0.06	1354	¹⁷ ACTON 92	OPAL	Sup. by ACTON 93L
1.49 ± 0.03 ± 0.06		¹⁸ BUSKULIC 92f	ALEP	Sup. by BUSKULIC 96f
1.35 $\pm^{+0.19}_{-0.17}$ ± 0.05		¹⁹ BUSKULIC 92g	ALEP	$e^+e^- \rightarrow Z$
1.32 ± 0.08 ± 0.09	1386	²⁰ ADEVA 91h	L3	Sup. by ADRIANI 93k
1.32 $\pm^{+0.31}_{-0.25}$ ± 0.15	37	²¹ ALEXANDER 91g	OPAL	$e^+e^- \rightarrow Z$
1.29 ± 0.06 ± 0.10	2973	²² DECAMP 91c	ALEP	Sup. by BUSKULIC 92f
1.36 $\pm^{+0.25}_{-0.23}$		²³ HAGEMANN 90	JADE	$E_{cm}^{ee} = 35$ GeV
1.13 ± 0.15		²⁴ LYONS 90	RVUE	
1.35 ± 0.10 ± 0.24		BRAUNSCH... 89b	TASS	$E_{cm}^{ee} = 35$ GeV
0.98 ± 0.12 ± 0.13		ONG 89	MRK2	$E_{cm}^{ee} = 29$ GeV
1.17 $\pm^{+0.27}_{-0.22}$ $\pm^{+0.17}_{-0.16}$		KLEM 88	DLCO	$E_{cm}^{ee} = 29$ GeV
1.29 ± 0.20 ± 0.21		²⁵ ASH 87	MAC	$E_{cm}^{ee} = 29$ GeV
1.02 $\pm^{+0.42}_{-0.39}$	301	²⁶ BROM 87	HRS	$E_{cm}^{ee} = 29$ GeV

- ¹ Measurement performed using an inclusive reconstruction and B flavor identification technique.
- ² Measured using inclusive $J/\psi(1S) \rightarrow \mu^+\mu^-$ vertex.
- ³ ACCIARRI 98 uses inclusively reconstructed secondary vertex and lepton impact parameter.
- ⁴ ACKERSTAFF 97f uses inclusively reconstructed secondary vertices.
- ⁵ BUSKULIC 96f analyzed using 3D impact parameter.
- ⁶ ABE,K 95b uses an inclusive topological technique.
- ⁷ ABREU 94L uses charged particle impact parameters. Their result from inclusively reconstructed secondary vertices is superseded by ABREU 96E.
- ⁸ ACTON 93L and ADRIANI 93k analyzed using lepton (e and μ) impact parameter at Z .

CHARGED b -HADRON ADMIXTURE MEAN LIFE

VALUE (10^{-12} s)	DOCUMENT ID	TECN	COMMENT
1.72 ± 0.08 ± 0.06	²⁷ ADAM 95	DLPH	$e^+e^- \rightarrow Z$
²⁷ ADAM 95 data analyzed using vertex-charge technique to tag b -hadron charge.			

NEUTRAL b -HADRON ADMIXTURE MEAN LIFE

VALUE (10^{-12} s)	DOCUMENT ID	TECN	COMMENT
1.58 ± 0.11 ± 0.09	²⁸ ADAM 95	DLPH	$e^+e^- \rightarrow Z$
²⁸ ADAM 95 data analyzed using vertex-charge technique to tag b -hadron charge.			

MEAN LIFE RATIO $\tau_{\text{charged } b\text{-hadron}}/\tau_{\text{neutral } b\text{-hadron}}$

VALUE	DOCUMENT ID	TECN	COMMENT
1.09 $\pm^{+0.11}_{-0.10}$ ± 0.08	²⁹ ADAM 95	DLPH	$e^+e^- \rightarrow Z$
²⁹ ADAM 95 data analyzed using vertex-charge technique to tag b -hadron charge.			

$$|\Delta\tau_b|/\tau_{b,\bar{b}}$$

$\tau_{b,\bar{b}}$ and $|\Delta\tau_b|$ are the mean life average and difference between b and \bar{b} hadrons.

VALUE	DOCUMENT ID	TECN	COMMENT
-0.001 ± 0.012 ± 0.008	³⁰ ABBIENDI 99j	OPAL	$e^+e^- \rightarrow Z$

³⁰Data analyzed using both the jet charge and the charge of secondary vertex in the opposite hemisphere.

 \bar{b} PRODUCTION FRACTIONS AND DECAY MODES

The branching fraction measurements are for an admixture of B mesons and baryons at energies above the $T(4S)$. Only the highest energy results (LEP, Tevatron, $S\bar{p}\bar{p}S$) are used in the branching fraction averages. In the following, we assume that the production fractions are the same at the LEP and at the Tevatron.

For inclusive branching fractions, e.g., $B \rightarrow D^\pm$ anything, the values usually are multiplicities, not branching fractions. They can be greater than one.

The modes below are listed for a \bar{b} initial state. b modes are their charge conjugates. Reactions indicate the weak decay vertex and do not include mixing.

Meson Particle Listings

$B^\pm/B^0/B_s^0/b$ -baryon ADMIXTURE

Mode	Fraction (Γ_i/Γ)	Scale factor/ Confidence level
------	--------------------------------	-----------------------------------

PRODUCTION FRACTIONS

The production fractions for weakly decaying b -hadrons at high energy have been calculated from the best values of mean lives, mixing parameters, and branching fractions in this edition by the Heavy Flavor Averaging Group (HFAG) as described in the note “ B^0/\bar{B}^0 Mixing” in the B^0 Particle Listings. The production fractions in b -hadronic Z decay are also listed at the end of the section. Values assume

$$B(\bar{b} \rightarrow B^+) = B(\bar{b} \rightarrow B^0) \\ B(\bar{b} \rightarrow B^+) + B(\bar{b} \rightarrow B^0) + B(\bar{b} \rightarrow B_s^0) + B(b \rightarrow b\text{-baryon}) = 100\%.$$

The notation for production fractions varies in the literature (f_d , d_{B^0} , $f(b \rightarrow \bar{B}^0)$, $Br(b \rightarrow \bar{B}^0)$). We use our own branching fraction notation here, $B(\bar{b} \rightarrow B^0)$.

Γ_1	B^+	(39.9 ± 1.1) %
Γ_2	B^0	(39.9 ± 1.1) %
Γ_3	B_s^0	(11.0 ± 1.2) %
Γ_4	b -baryon	(9.2 ± 1.9) %
Γ_5	B_c	—

DECAY MODES

Semileptonic and leptonic modes

Γ_6	ν anything	(23.1 ± 1.5) %	
Γ_7	$\ell^+ \nu_\ell$ anything	[a] (10.69 ± 0.22) %	
Γ_8	$e^+ \nu_e$ anything	(10.86 ± 0.35) %	
Γ_9	$\mu^+ \nu_\mu$ anything	(10.95 ± 0.29) %	
Γ_{10}	$D^- \ell^+ \nu_\ell$ anything	[a] (2.3 ± 0.4) %	S=1.8
Γ_{11}	$D^- \pi^+ \ell^+ \nu_\ell$ anything	(4.9 ± 1.9) × 10 ⁻³	
Γ_{12}	$D^- \pi^- \ell^+ \nu_\ell$ anything	(2.6 ± 1.6) × 10 ⁻³	
Γ_{13}	$\bar{D}^0 \ell^+ \nu_\ell$ anything	[a] (6.84 ± 0.35) %	
Γ_{14}	$\bar{D}^0 \pi^- \ell^+ \nu_\ell$ anything	(1.07 ± 0.27) %	
Γ_{15}	$\bar{D}^0 \pi^+ \ell^+ \nu_\ell$ anything	(2.3 ± 1.6) × 10 ⁻³	
Γ_{16}	$D^{*-} \ell^+ \nu_\ell$ anything	[a] (2.75 ± 0.19) %	
Γ_{17}	$D^{*-} \pi^- \ell^+ \nu_\ell$ anything	(6 ± 7) × 10 ⁻⁴	
Γ_{18}	$D^{*-} \pi^+ \ell^+ \nu_\ell$ anything	(4.8 ± 1.0) × 10 ⁻³	
Γ_{19}	$\bar{D}_j^0 \ell^+ \nu_\ell$ anything × $B(\bar{D}_j^0 \rightarrow D^{*+} \pi^-)$	[a,b] (2.6 ± 0.9) × 10 ⁻³	
Γ_{20}	$D_j^- \ell^+ \nu_\ell$ anything × $B(D_j^- \rightarrow D^0 \pi^-)$	[a,b] (7.0 ± 2.3) × 10 ⁻³	
Γ_{21}	$\bar{D}_2^*(2460)^0 \ell^+ \nu_\ell$ anything × $B(\bar{D}_2^*(2460)^0 \rightarrow D^{*-} \pi^+)$	< 1.4 × 10 ⁻³	CL=90%
Γ_{22}	$D_2^*(2460)^- \ell^+ \nu_\ell$ anything × $B(D_2^*(2460)^- \rightarrow D^0 \pi^-)$	(4.2 ± 1.5) × 10 ⁻³	
Γ_{23}	$\bar{D}_2^*(2460)^0 \ell^+ \nu_\ell$ anything × $B(\bar{D}_2^*(2460)^0 \rightarrow D^- \pi^+)$	(1.6 ± 0.8) × 10 ⁻³	
Γ_{24}	charmless $\ell \bar{\nu}_\ell$	[a] (1.7 ± 0.5) × 10 ⁻³	
Γ_{25}	$\tau^+ \nu_\tau$ anything	(2.41 ± 0.23) %	
Γ_{26}	$D^{*-} \tau \nu_\tau$ anything	(9 ± 4) × 10 ⁻³	
Γ_{27}	$\bar{c} \rightarrow \ell^- \bar{\nu}_\ell$ anything	[a] (8.02 ± 0.19) %	
Γ_{28}	$c \rightarrow \ell^+ \nu$ anything	(1.6 ± 0.4) %	

Charmed meson and baryon modes

Γ_{29}	\bar{D}^0 anything	(59.6 ± 2.9) %	
Γ_{30}	$D^0 D_s^\pm$ anything	[c] (9.1 ± 3.9) %	
Γ_{31}	$D^\mp D_s^\pm$ anything	[c] (4.0 ± 2.3) %	
Γ_{32}	$\bar{D}^0 D^0$ anything	[c] (5.1 ± 2.0) %	
Γ_{33}	$D^0 D^\pm$ anything	[c] (2.7 ± 1.8) %	
Γ_{34}	$D^\pm D^\mp$ anything	[c] < 9 × 10 ⁻³	CL=90%
Γ_{35}	D^0 anything		
Γ_{36}	D^+ anything		
Γ_{37}	D^- anything	(23.1 ± 1.7) %	
Γ_{38}	$D^*(2010)^\pm$ anything	(17.3 ± 2.0) %	
Γ_{39}	$D_1(2420)^0$ anything	(5.0 ± 1.5) %	
Γ_{40}	$D^*(2010)^\mp D_s^\pm$ anything	[c] (3.3 ± 1.6) %	

Γ_{41}	$D^0 D^*(2010)^\pm$ anything	[c] (3.0 ± 1.1) %
Γ_{42}	$D^*(2010)^\pm D^\mp$ anything	[c] (2.5 ± 1.2) %
Γ_{43}	$D^*(2010)^\pm D^*(2010)^\mp$ anything	[c] (1.2 ± 0.4) %
Γ_{44}	$\bar{D} D$ anything	(10 ± 11) %
Γ_{45}	$D_2^*(2460)^0$ anything	(4.7 ± 2.7) %
Γ_{46}	D_s^- anything	(15.0 ± 2.1) %
Γ_{47}	D_s^+ anything	(10.1 ± 3.1) %
Γ_{48}	A_c^+ anything	(9.7 ± 2.9) %
Γ_{49}	\bar{c}/c anything	[d] (116.2 ± 3.2) %

Charmonium modes

Γ_{50}	$J/\psi(1S)$ anything	(1.16 ± 0.10) %
Γ_{51}	$\psi(2S)$ anything	(4.8 ± 2.4) × 10 ⁻³
Γ_{52}	$\chi_{c1}(1P)$ anything	(1.3 ± 0.4) %

K or K* modes

Γ_{53}	$\bar{S}\gamma$	(3.1 ± 1.1) × 10 ⁻⁴	
Γ_{54}	$\bar{S}\mathcal{P}\nu$	< 6.4 × 10 ⁻⁴	CL=90%
Γ_{55}	K^\pm anything	(74 ± 6) %	
Γ_{56}	K_S^0 anything	(29.0 ± 2.9) %	

Pion modes

Γ_{57}	π^\pm anything	(397 ± 21) %
Γ_{58}	π^0 anything	[d] (278 ± 60) %
Γ_{59}	ϕ anything	(2.82 ± 0.23) %

Baryon modes

Γ_{60}	$\rho/\bar{\rho}$ anything	(13.1 ± 1.1) %
---------------	----------------------------	------------------

Other modes

Γ_{61}	charged anything	[d] (497 ± 7) %
Γ_{62}	hadron ⁺ hadron ⁻	(1.7 ± 1.0) × 10 ⁻⁵
Γ_{63}	charmless	(7 ± 21) × 10 ⁻³

Baryon modes

Γ_{64}	$\Lambda/\bar{\Lambda}$ anything	(5.9 ± 0.6) %
Γ_{65}	b -baryon anything	(10.2 ± 2.8) %

$\Delta B = 1$ weak neutral current ($B1$) modes

Γ_{66}	$e^+ e^-$ anything		
Γ_{67}	$\mu^+ \mu^-$ anything	$B1$	< 3.2 × 10 ⁻⁴
Γ_{68}	$\nu \bar{\nu}$ anything		CL=90%

[a] An ℓ indicates an e or a μ mode, not a sum over these modes.

[b] D_j represents an unresolved mixture of pseudoscalar and tensor D^{**} (P -wave) states.

[c] The value is for the sum of the charge states or particle/antiparticle states indicated.

[d] Inclusive branching fractions have a multiplicity definition and can be greater than 100%.

$B^\pm/B^0/B_s^0/b$ -baryon ADMIXTURE BRANCHING RATIOS

$\Gamma(B^+)/\Gamma_{\text{total}}$	Γ_1/Γ
“OUR EVALUATION” is an average using rescaled values of the data listed below and from the best values of mean lives, mixing parameters, and branching fractions in this edition by the Heavy Flavor Averaging Group (HFAG) as described at http://www.slac.stanford.edu/xorg/hfag/ .	

VALUE	DOCUMENT ID	TECN	COMMENT
0.398 ± 0.012 OUR EVALUATION			
0.4099 ± 0.0082 ± 0.0111	³¹ ABDALLAH	03k	DLPH $e^+ e^- \rightarrow Z$

³¹ The analysis is based on a neural network, to estimate the charge of the weakly-decaying b hadron by distinguishing its decay products from particles produced at the primary vertex.

$\Gamma(B_s^0)/[\Gamma(B^+) + \Gamma(B^0)]$	$\Gamma_3/(\Gamma_1 + \Gamma_2)$
“OUR EVALUATION” is an average using rescaled values of the data listed below and from the best values of mean lives, mixing parameters, and branching fractions in this edition by the Heavy Flavor Averaging Group (HFAG) as described at http://www.slac.stanford.edu/xorg/hfag/ .	

VALUE	DOCUMENT ID	TECN	COMMENT
0.138 ± 0.017 OUR EVALUATION			
0.21 ± 0.04 OUR AVERAGE			

0.213 ± 0.068	³² AFFOLDER	00e	CDF $p\bar{p}$ at 1.8 TeV
0.21 ± 0.036 +0.038 -0.030	³³ ABE	99P	CDF $p\bar{p}$ at 1.8 TeV

³² AFFOLDER 00e uses several electron-charm final states in $b \rightarrow c e^- X$.

³³ ABE 99P uses the numbers of $K^*(892)^0$, $K^*(892)^+$, and $\phi(1020)$ events produced in association with the double semileptonic decays $b \rightarrow c \mu^- X$ with $c \rightarrow s \mu^+ X$.

See key on page 373

Meson Particle Listings

 $B^\pm/B^0/B_s^0/b$ -baryon ADMIXTURE $\Gamma(b\text{-baryon})/[\Gamma(B^\pm) + \Gamma(B^0)]$ $\Gamma_4/(\Gamma_1 + \Gamma_2)$

VALUE	DOCUMENT ID	TECN	COMMENT
0.115 ± 0.026 OUR EVALUATION			
0.118 ± 0.042	34 AFFOLDER	00E CDF	$p\bar{p}$ at 1.8 TeV

 $\Gamma(\nu\text{ anything})/\Gamma_{\text{total}}$ Γ_6/Γ

VALUE	DOCUMENT ID	TECN	COMMENT
0.2308 ± 0.0077 ± 0.0124	35,36 ACCIARRI	96c L3	$e^+e^- \rightarrow Z$

³⁴ AFFOLDER 00E uses several electron-charm final states in $b \rightarrow ce^-X$.

³⁵ ACCIARRI 96c assumes relative b semileptonic decay rates $e:\mu:\tau$ of 1:1:0.25. Based on missing-energy spectrum.

³⁶ Assumes Standard Model value for R_B .

 $\Gamma(\ell^+ \nu_\ell \text{ anything})/\Gamma_{\text{total}}$ Γ_7/Γ

"OUR EVALUATION" is an average of the data listed below, excluding all asymmetry measurements, performed by the LEP Electroweak Working Group as described in the "Note on the Z boson" in the Z Particle Listings.

VALUE	DOCUMENT ID	TECN	COMMENT
0.1069 ± 0.0022 OUR EVALUATION			
0.1064 ± 0.0016 OUR AVERAGE			
0.1070 ± 0.0010 ± 0.0035	37 HEISTER	02G ALEP	$e^+e^- \rightarrow Z$
0.1070 ± 0.0008 ± 0.0037	38 ABREU	01L DLPH	$e^+e^- \rightarrow Z$
0.1083 ± 0.0010 ± 0.0028	39 ABBIENDI	00E OPAL	$e^+e^- \rightarrow Z$
0.1016 ± 0.0013 ± 0.0030	40 ACCIARRI	00 L3	$e^+e^- \rightarrow Z$
0.1085 ± 0.0012 ± 0.0047	41,42 ACCIARRI	96c L3	$e^+e^- \rightarrow Z$
• • • We do not use the following data for averages, fits, limits, etc. • • •			
0.1106 ± 0.0039 ± 0.0022	43 ABREU	95D DLPH	$e^+e^- \rightarrow Z$
0.114 ± 0.003 ± 0.004	44 BUSKULIC	94G ALEP	$e^+e^- \rightarrow Z$
0.100 ± 0.007 ± 0.007	45 ABREU	93c DLPH	$e^+e^- \rightarrow Z$
0.105 ± 0.006 ± 0.005	46 AKERS	93B OPAL	Repl. by ABBI- ENDI 00E

³⁷ Uses the combination of lepton transverse momentum spectrum and the correlation between the charge of the lepton and opposite jet charge. The first error is statistic and the second error is the total systematic error including the modeling.

³⁸ The experimental systematic and model uncertainties are combined in quadrature.

³⁹ ABBIENDI 00E result is determined by comparing the distribution of several kinematic variables of leptonic events in a lifetime tagged $Z \rightarrow b\bar{b}$ sample using artificial neural network techniques. The first error is statistic; the second error is the total systematic error.

⁴⁰ ACCIARRI 00 result obtained from a combined fit of $R_b = \Gamma(Z \rightarrow b\bar{b})/\Gamma(Z \rightarrow \text{hadrons})$ and $B(b \rightarrow \ell\nu X)$, using double-tagging method.

⁴¹ ACCIARRI 96c result obtained by a fit to the single lepton spectrum.

⁴² Assumes Standard Model value for R_B .

⁴³ ABREU 95D give systematic errors ± 0.0019 (model) and 0.0012 (R_c). We combine these in quadrature.

⁴⁴ BUSKULIC 94G uses e and μ events. This value is from a global fit to the lepton p_T (relative to jet) spectra which also determines the b and c production fractions, the fragmentation functions, and the forward-backward asymmetries. This branching ratio depends primarily on the ratio of dileptons to single leptons at high p_T , but the lower p_T portion of the lepton spectrum is included in the global fit to reduce the model dependence. The model dependence is ± 0.0026 and is included in the systematic error.

⁴⁵ ABREU 93c event count includes ee events. Combining ee , $\mu\mu$, and $e\mu$ events, they obtain $0.100 \pm 0.007 \pm 0.007$.

⁴⁶ AKERS 93B analysis performed using single and dilepton events.

 $\Gamma(e^+ \nu_e \text{ anything})/\Gamma_{\text{total}}$ Γ_8/Γ

VALUE	DOCUMENT ID	TECN	COMMENT
0.1086 ± 0.0035 OUR AVERAGE			
0.1078 ± 0.0008 ± 0.0050	47 ABBIENDI	00E OPAL	$e^+e^- \rightarrow Z$
0.1089 ± 0.0020 ± 0.0051	48,49 ACCIARRI	96c L3	$e^+e^- \rightarrow Z$
0.107 ± 0.015 ± 0.007	50 ABREU	93c DLPH	$e^+e^- \rightarrow Z$
0.138 ± 0.032 ± 0.008	51 ADEVA	91c L3	$e^+e^- \rightarrow Z$
• • • We do not use the following data for averages, fits, limits, etc. • • •			
0.086 ± 0.027 ± 0.008	52 ABE	93E VNS	$E_{\text{cm}}^e = 58$ GeV
0.109 ± 0.014 ± 0.0055	2719 53 AKERS	93B OPAL	Repl. by ABBI- ENDI 00E
0.111 ± 0.028 ± 0.026	BEHREND	90D CELL	$E_{\text{cm}}^e = 43$ GeV
0.150 ± 0.011 ± 0.022	BEHREND	90D CELL	$E_{\text{cm}}^e = 35$ GeV
0.112 ± 0.009 ± 0.011	ONG	88 MRK2	$E_{\text{cm}}^e = 29$ GeV
0.149 ± 0.022 ± 0.019	PAL	86 DLCO	$E_{\text{cm}}^e = 29$ GeV
0.110 ± 0.018 ± 0.010	AIHARA	85 TPC	$E_{\text{cm}}^e = 29$ GeV
0.111 ± 0.034 ± 0.040	ALTHOFF	84J TASS	$E_{\text{cm}}^e = 34.6$ GeV
0.146 ± 0.028	KOOP	84 DLCO	Repl. by PAL 86
0.116 ± 0.021 ± 0.017	NELSON	83 MRK2	$E_{\text{cm}}^e = 29$ GeV

⁴⁷ ABBIENDI 00E result is determined by comparing the distribution of several kinematic variables of leptonic events in a lifetime tagged $Z \rightarrow b\bar{b}$ sample using artificial neural network techniques. The first error is statistic; the second error is the total systematic error.

⁴⁸ ACCIARRI 96c result obtained by a fit to the single lepton spectrum.

⁴⁹ Assumes Standard Model value for R_B .

⁵⁰ ABREU 93c event count includes ee events. Combining ee , $\mu\mu$, and $e\mu$ events, they obtain $0.100 \pm 0.007 \pm 0.007$.

⁵¹ ADEVA 91c measure the average $B(b \rightarrow eX)$ branching ratio using single and double tagged b enhanced Z events. Combining e and μ results, they obtain $0.113 \pm 0.010 \pm 0.006$. Constraining the initial number of b quarks by the Standard Model prediction

(378 ± 3 MeV) for the decay of the Z into $b\bar{b}$, the electron result gives $0.112 \pm 0.004 \pm 0.008$. They obtain $0.119 \pm 0.003 \pm 0.006$ when e and μ results are combined. Used to measure the $b\bar{b}$ width itself, this electron result gives $370 \pm 12 \pm 24$ MeV and combined with the muon result gives $385 \pm 7 \pm 22$ MeV.

⁵² ABE 93E experiment also measures forward-backward asymmetries and fragmentation functions for b and c .

⁵³ AKERS 93B analysis performed using single and dilepton events.

 $\Gamma(\mu^+ \nu_\mu \text{ anything})/\Gamma_{\text{total}}$ Γ_9/Γ

VALUE	EVTs	DOCUMENT ID	TECN	COMMENT
0.1095 ± 0.0029 OUR AVERAGE				
-0.0025				
0.1096 ± 0.0008 ± 0.0034		54 ABBIENDI	00E OPAL	$e^+e^- \rightarrow Z$
-0.0027				
0.1082 ± 0.0015 ± 0.0059	55,56	ACCIARRI	96c L3	$e^+e^- \rightarrow Z$
0.110 ± 0.012 ± 0.007	656	57 ABREU	93c DLPH	$e^+e^- \rightarrow Z$
0.113 ± 0.012 ± 0.006		58 ADEVA	91c L3	$e^+e^- \rightarrow Z$
• • • We do not use the following data for averages, fits, limits, etc. • • •				
0.122 ± 0.006 ± 0.007		56 UENO	96 AMY	e^+e^- at 57.9 GeV
0.101 ± 0.010 ± 0.0055	4248	59 AKERS	93B OPAL	Repl. by ABBI- ENDI 00E
-0.009				
0.104 ± 0.023 ± 0.016		BEHREND	90D CELL	$E_{\text{cm}}^e = 43$ GeV
0.148 ± 0.010 ± 0.016		BEHREND	90D CELL	$E_{\text{cm}}^e = 35$ GeV
0.118 ± 0.012 ± 0.010		ONG	88 MRK2	$E_{\text{cm}}^e = 29$ GeV
0.117 ± 0.016 ± 0.015		BARTEL	87 JADE	$E_{\text{cm}}^e = 34.6$ GeV
0.114 ± 0.018 ± 0.025		BARTEL	85J JADE	Repl. by BARTEL 87
0.117 ± 0.028 ± 0.010		ALTHOFF	84G TASS	$E_{\text{cm}}^e = 34.5$ GeV
0.105 ± 0.015 ± 0.013		ADEVA	83B MRKJ	$E_{\text{cm}}^e = 33-38.5$ GeV
0.155 ± 0.054 ± 0.029		FERNANDEZ	83D MAC	$E_{\text{cm}}^e = 29$ GeV

⁵⁴ ABBIENDI 00E result is determined by comparing the distribution of several kinematic variables of leptonic events in a lifetime tagged $Z \rightarrow b\bar{b}$ sample using artificial neural network techniques. The first error is statistic; the second error is the total systematic error.

⁵⁵ ACCIARRI 96c result obtained by a fit to the single lepton spectrum.

⁵⁶ Assumes Standard Model value for R_B .

⁵⁷ ABREU 93c event count includes $\mu\mu$ events. Combining ee , $\mu\mu$, and $e\mu$ events, they obtain $0.100 \pm 0.007 \pm 0.007$.

⁵⁸ ADEVA 91c measure the average $B(b \rightarrow eX)$ branching ratio using single and double tagged b enhanced Z events. Combining e and μ results, they obtain $0.113 \pm 0.010 \pm 0.006$. Constraining the initial number of b quarks by the Standard Model prediction (378 ± 3 MeV) for the decay of the Z into $b\bar{b}$, the muon result gives $0.123 \pm 0.003 \pm 0.006$. They obtain $0.119 \pm 0.003 \pm 0.006$ when e and μ results are combined. Used to measure the $b\bar{b}$ width itself, this muon result gives $394 \pm 9 \pm 22$ MeV and combined with the electron result gives $385 \pm 7 \pm 22$ MeV.

⁵⁹ AKERS 93B analysis performed using single and dilepton events.

 $\Gamma(D^- \ell^+ \nu_\ell \text{ anything})/\Gamma_{\text{total}}$ Γ_{10}/Γ

VALUE	DOCUMENT ID	TECN	COMMENT
0.023 ± 0.004 OUR AVERAGE			Error includes scale factor of 1.8.
0.0272 ± 0.0028 ± 0.0018	60 ABREU	00R DLPH	$e^+e^- \rightarrow Z$
0.0197 ± 0.0025 ± 0.0005	61 AKERS	95Q OPAL	$e^+e^- \rightarrow Z$

⁶⁰ ABREU 00R reports their experiment's uncertainties $\pm 0.0019 \pm 0.0016 \pm 0.0018$, where the first error is statistical, the second is systematic, and the third is the uncertainty due to the D branching fraction. We combine first two in quadrature.

⁶¹ AKERS 95Q reports $[B(\bar{D}^- \rightarrow D^- \ell^+ \nu_\ell \text{ anything})] \times [B(D^+ \rightarrow K^- \pi^+ \pi^+)] = (1.82 \pm 0.20 \pm 0.12) \times 10^{-3}$. We divide by our best value $B(D^+ \rightarrow K^- \pi^+ \pi^+) = (9.22 \pm 0.21) \times 10^{-2}$. Our first error is their experiment's error and our second error is the systematic error from using our best value.

 $\Gamma(D^- \pi^+ \ell^+ \nu_\ell \text{ anything})/\Gamma_{\text{total}}$ Γ_{11}/Γ

VALUE	DOCUMENT ID	TECN	COMMENT
0.0049 ± 0.0018 ± 0.0007			
0.0049 ± 0.0018 ± 0.0007	ABREU	00R DLPH	$e^+e^- \rightarrow Z$

 $\Gamma(D^- \pi^- \ell^+ \nu_\ell \text{ anything})/\Gamma_{\text{total}}$ Γ_{12}/Γ

VALUE	DOCUMENT ID	TECN	COMMENT
0.0026 ± 0.0015 ± 0.0004			
0.0026 ± 0.0015 ± 0.0004	ABREU	00R DLPH	$e^+e^- \rightarrow Z$

 $\Gamma(\bar{D}^0 \ell^+ \nu_\ell \text{ anything})/\Gamma_{\text{total}}$ Γ_{13}/Γ

VALUE	DOCUMENT ID	TECN	COMMENT
0.0684 ± 0.0035 OUR AVERAGE			
0.0704 ± 0.0040 ± 0.0017	62 ABREU	00R DLPH	$e^+e^- \rightarrow Z$
0.065 ± 0.006 ± 0.001	63 AKERS	95Q OPAL	$e^+e^- \rightarrow Z$

⁶² ABREU 00R reports their experiment's uncertainties $\pm 0.0034 \pm 0.0036 \pm 0.0017$, where the first error is statistical, the second is systematic, and the third is the uncertainty due to the D branching fraction. We combine first two in quadrature.

⁶³ AKERS 95Q reports $[B(\bar{D}^0 \rightarrow \bar{D}^0 \ell^+ \nu_\ell \text{ anything})] \times [B(D^0 \rightarrow K^- \pi^+)] = (2.52 \pm 0.14 \pm 0.17) \times 10^{-3}$. We divide by our best value $B(D^0 \rightarrow K^- \pi^+) = (3.89 \pm 0.05) \times 10^{-2}$. Our first error is their experiment's error and our second error is the systematic error from using our best value.

 $\Gamma(\bar{D}^0 \pi^- \ell^+ \nu_\ell \text{ anything})/\Gamma_{\text{total}}$ Γ_{14}/Γ

VALUE	DOCUMENT ID	TECN	COMMENT
0.0107 ± 0.0025 ± 0.0011			
0.0107 ± 0.0025 ± 0.0011	ABREU	00R DLPH	$e^+e^- \rightarrow Z$

 $\Gamma(\bar{D}^0 \pi^+ \ell^+ \nu_\ell \text{ anything})/\Gamma_{\text{total}}$ Γ_{15}/Γ

VALUE	DOCUMENT ID	TECN	COMMENT
0.0023 ± 0.0015 ± 0.0004			
0.0023 ± 0.0015 ± 0.0004	ABREU	00R DLPH	$e^+e^- \rightarrow Z$

Meson Particle Listings

 $B^\pm/B^0/B_s^0/b$ -baryon ADMIXTURE $\Gamma(D^{*-} \ell^+ \nu_\ell \text{ anything})/\Gamma_{\text{total}}$ Γ_{16}/Γ

VALUE	DOCUMENT ID	TECN	COMMENT
0.0275 ± 0.0019 OUR AVERAGE			
0.0275 ± 0.0021 ± 0.0009	64 ABREU	00R	DLPH $e^+ e^- \rightarrow Z$
0.0276 ± 0.0027 ± 0.0011	65 AKERS	95Q	OPAL $e^+ e^- \rightarrow Z$

64 ABREU 00R reports their experiment's uncertainties $\pm 0.0017 \pm 0.0013 \pm 0.0009$, where the first error is statistical, the second is systematic, and the third is the uncertainty due to the D branching fraction. We combine first two in quadrature.

65 AKERS 95Q reports $[B(\bar{D} \rightarrow D^* \ell^+ \nu_\ell X) \times B(D^{*+} \rightarrow D^0 \pi^+) \times B(D^0 \rightarrow K^- \pi^+)] = ((7.53 \pm 0.47 \pm 0.56) \times 10^{-4})$ and uses $B(D^{*+} \rightarrow D^0 \pi^+) = 0.681 \pm 0.013$ and $B(D^0 \rightarrow K^- \pi^+) = 0.0401 \pm 0.0014$ to obtain the above result. The first error is the experiments error and the second error is the systematic error from the D^{*+} and D^0 branching ratios.

 $\Gamma(D^{*-} \pi^+ \ell^+ \nu_\ell \text{ anything})/\Gamma_{\text{total}}$ Γ_{18}/Γ

VALUE	DOCUMENT ID	TECN	COMMENT
0.0048 ± 0.0009 ± 0.0005	ABREU	00R	DLPH $e^+ e^- \rightarrow Z$

 $\Gamma(D^{*-} \pi^- \ell^+ \nu_\ell \text{ anything})/\Gamma_{\text{total}}$ Γ_{17}/Γ

VALUE	DOCUMENT ID	TECN	COMMENT
0.0006 ± 0.0007 ± 0.0002	ABREU	00R	DLPH $e^+ e^- \rightarrow Z$

 $\Gamma(D_j^0 \ell^+ \nu_\ell \text{ anything} \times B(D_j^0 \rightarrow D^{*+} \pi^-))/\Gamma_{\text{total}}$ Γ_{19}/Γ

D_j represents an unresolved mixture of pseudoscalar and tensor D^{**} (P -wave) states.

VALUE (units 10^{-3})	DOCUMENT ID	TECN	COMMENT
2.6 ± 0.79 ± 0.39	ABBIENDI	03M	OPAL $e^+ e^- \rightarrow Z$
• • • We do not use the following data for averages, fits, limits, etc. • • •			
6.1 ± 1.3 ± 1.3	AKERS	95Q	OPAL Repl. by ABBI- ENDI 03M

 $\Gamma(D_j^- \ell^+ \nu_\ell \text{ anything} \times B(D_j^- \rightarrow D^0 \pi^-))/\Gamma_{\text{total}}$ Γ_{20}/Γ

D_j represents an unresolved mixture of pseudoscalar and tensor D^{**} (P -wave) states.

VALUE (units 10^{-3})	DOCUMENT ID	TECN	COMMENT
7.0 ± 1.9 ± 1.2	AKERS	95Q	OPAL $e^+ e^- \rightarrow Z$

 $\Gamma(D_2^+(2460)^0 \ell^+ \nu_\ell \text{ anything} \times B(D_2^+(2460)^0 \rightarrow D^{*+} \pi^+))/\Gamma_{\text{total}}$ Γ_{21}/Γ

VALUE (units 10^{-3})	CL%	DOCUMENT ID	TECN	COMMENT
<1.4	90	ABBIENDI	03M	OPAL $e^+ e^- \rightarrow Z$

 $\Gamma(D_2^+(2460)^- \ell^+ \nu_\ell \text{ anything} \times B(D_2^+(2460)^- \rightarrow D^0 \pi^-))/\Gamma_{\text{total}}$ Γ_{22}/Γ

VALUE (units 10^{-3})	DOCUMENT ID	TECN	COMMENT
4.2 ± 1.3 ± 0.7	AKERS	95Q	OPAL $e^+ e^- \rightarrow Z$

 $\Gamma(D_2^+(2460)^0 \ell^+ \nu_\ell \text{ anything} \times B(D_2^+(2460)^0 \rightarrow D^- \pi^+))/\Gamma_{\text{total}}$ Γ_{23}/Γ

VALUE (units 10^{-3})	DOCUMENT ID	TECN	COMMENT
1.6 ± 0.7 ± 0.3	AKERS	95Q	OPAL $e^+ e^- \rightarrow Z$

 $\Gamma(\text{charmless } \ell \nu_\ell)/\Gamma_{\text{total}}$ Γ_{24}/Γ

"OUR EVALUATION" is an average of the data listed below performed by the LEP Heavy Flavour Steering Group. The averaging procedure takes into account correlations between the measurements.

VALUE	DOCUMENT ID	TECN	COMMENT
0.00171 ± 0.00052 OUR EVALUATION			
0.0017 ± 0.0004 OUR AVERAGE			

0.00163 ± 0.00053 ± 0.00055	66 ABBIENDI	01R	OPAL $e^+ e^- \rightarrow Z$
0.00157 ± 0.00035 ± 0.00055	67 ABREU	00D	DLPH $e^+ e^- \rightarrow Z$
0.00173 ± 0.00055 ± 0.00055	68 BARATE	99G	ALEP $e^+ e^- \rightarrow Z$
0.0033 ± 0.0010 ± 0.0017	69 ACCIARRI	98K	L3 $e^+ e^- \rightarrow Z$

66 Obtained from the best fit of the MC simulated events to the data based on the $b \rightarrow X_{\ell} \ell \nu$ neutral network output distributions.

67 ABREU 00D result obtained from a fit to the numbers of decays in $b \rightarrow u$ enriched and depleted samples and their lepton spectra, and assuming $|V_{cb}| = 0.0384 \pm 0.0033$ and $\tau_b = 1.564 \pm 0.014$ ps.

68 Uses lifetime tagged $b\bar{b}$ sample.

69 ACCIARRI 98K assumes $R_b = 0.2174 \pm 0.0009$ at Z decay.

 $\Gamma(\tau^+ \nu_\tau \text{ anything})/\Gamma_{\text{total}}$ Γ_{25}/Γ

VALUE (units 10^{-2})	EVTS	DOCUMENT ID	TECN	COMMENT
2.41 ± 0.23 OUR AVERAGE				

2.78 ± 0.18 ± 0.51		70 ABBIENDI	01Q	OPAL $e^+ e^- \rightarrow Z$
2.43 ± 0.20 ± 0.25		71 BARATE	01E	ALEP $e^+ e^- \rightarrow Z$
2.19 ± 0.24 ± 0.39		72 ABREU	00C	DLPH $e^+ e^- \rightarrow Z$
1.7 ± 0.5 ± 1.1		73,74 ACCIARRI	96C	L3 $e^+ e^- \rightarrow Z$
2.4 ± 0.7 ± 0.8	1032	75 ACCIARRI	94C	L3 $e^+ e^- \rightarrow Z$
• • • We do not use the following data for averages, fits, limits, etc. • • •				
2.75 ± 0.30 ± 0.37	405	76 BUSKULIC	95	ALEP Repl. by BARATE 01E
4.08 ± 0.76 ± 0.62		BUSKULIC	93B	ALEP Repl. by BUSKULIC 95

70 ABBIENDI 01Q uses a missing energy technique.

71 The energy-flow and b -tagging algorithms were used.

72 Uses the missing energy in $Z \rightarrow b\bar{b}$ decays without identifying leptons.

73 ACCIARRI 96C result obtained from missing energy spectrum.

74 Assumes Standard Model value for R_B .

75 This is a direct result using tagged $b\bar{b}$ events at the Z , but species are not separated.

76 BUSKULIC 95 uses missing-energy technique.

 $\Gamma(D^{*-} \tau \nu_\tau \text{ anything})/\Gamma_{\text{total}}$ Γ_{26}/Γ

VALUE	DOCUMENT ID	TECN	COMMENT
(0.88 ± 0.31 ± 0.28) × 10⁻²	77 BARATE	01E	ALEP $e^+ e^- \rightarrow Z$

77 The energy-flow and b -tagging algorithms were used.

 $\Gamma(\bar{D} \rightarrow \tau^- \ell^+ \nu_\ell \text{ anything})/\Gamma_{\text{total}}$ Γ_{27}/Γ

"OUR EVALUATION" is an average of the data listed below, excluding all asymmetry measurements, performed by the LEP Electroweak Working Group as described in the "Note on the Z boson" in the Z Particle Listings.

VALUE	DOCUMENT ID	TECN	COMMENT
0.0802 ± 0.0019 OUR EVALUATION			
0.0817 ± 0.0020 OUR AVERAGE			

0.0818 ± 0.0015 ± 0.0024	78 HEISTER	02G	ALEP $e^+ e^- \rightarrow Z$
0.0798 ± 0.0022 ± 0.0025	79 ABREU	01L	DLPH $e^+ e^- \rightarrow Z$
0.0840 ± 0.0016 ± 0.0039	80 ABBIENDI	00E	OPAL $e^+ e^- \rightarrow Z$

• • • We do not use the following data for averages, fits, limits, etc. • • •

0.0770 ± 0.0097 ± 0.0046	81 ABREU	95D	DLPH $e^+ e^- \rightarrow Z$
0.082 ± 0.003 ± 0.012	82 BUSKULIC	94G	ALEP $e^+ e^- \rightarrow Z$
0.077 ± 0.004 ± 0.007	83 AKERS	93B	OPAL Repl. by ABBI- ENDI 00E

78 Uses the combination of lepton transverse momentum spectrum and the correlation between the charge of the lepton and opposite jet charge. The first error is statistic and the second error is the total systematic error including the modeling.

79 The experimental systematic and model uncertainties are combined in quadrature.

80 ABBIENDI 00E result is determined by comparing the distribution of several kinematic variables of leptonic events in a lifetime tagged $Z \rightarrow b\bar{b}$ sample using artificial neural network techniques. The first error is statistic; the second error is the total systematic error.

81 ABREU 95D give systematic errors ± 0.0033 (model) and 0.0032 (R_c). We combine these in quadrature. This result is from the same global fit as their $\Gamma(\bar{D} \rightarrow \ell^+ \nu_\ell X)$ data.

82 BUSKULIC 94G uses e and μ events. This value is from the same global fit as their $\Gamma(\bar{D} \rightarrow \ell^+ \nu_\ell \text{ anything})/\Gamma_{\text{total}}$ data.

83 AKERS 93B analysis performed using single and dilepton events.

 $\Gamma(c \rightarrow \ell^+ \nu \text{ anything})/\Gamma_{\text{total}}$ Γ_{28}/Γ

VALUE	DOCUMENT ID	TECN	COMMENT
0.0161 ± 0.0020 ± 0.0034	84 ABREU	01L	DLPH $e^+ e^- \rightarrow Z$

84 The experimental systematic and model uncertainties are combined in quadrature.

 $\Gamma(D^0 \text{ anything})/\Gamma_{\text{total}}$ Γ_{29}/Γ

VALUE	DOCUMENT ID	TECN	COMMENT
0.596 ± 0.028 ± 0.007	85 BUSKULIC	96Y	ALEP $e^+ e^- \rightarrow Z$

85 BUSKULIC 96Y reports $0.605 \pm 0.024 \pm 0.016$ for $B(D^0 \rightarrow K^- \pi^+) = 0.0383$. We rescale to our best value $B(D^0 \rightarrow K^- \pi^+) = (3.89 \pm 0.05) \times 10^{-2}$. Our first error is their experiment's error and our second error is the systematic error from using our best value.

 $\Gamma(D^0 D_s^\pm \text{ anything})/\Gamma_{\text{total}}$ Γ_{30}/Γ

VALUE	DOCUMENT ID	TECN	COMMENT
0.091 + 0.020 + 0.034	86 BARATE	98Q	ALEP $e^+ e^- \rightarrow Z$
- 0.018 - 0.022			

86 The systematic error includes the uncertainties due to the charm branching ratios.

 $\Gamma(D^\mp D_s^\pm \text{ anything})/\Gamma_{\text{total}}$ Γ_{31}/Γ

VALUE	DOCUMENT ID	TECN	COMMENT
0.040 + 0.017 + 0.016	87 BARATE	98Q	ALEP $e^+ e^- \rightarrow Z$
- 0.014 - 0.011			

87 The systematic error includes the uncertainties due to the charm branching ratios.

 $[\Gamma(D^0 D_s^\pm \text{ anything}) + \Gamma(D^\mp D_s^\pm \text{ anything})]/\Gamma_{\text{total}}$ $(\Gamma_{30} + \Gamma_{31})/\Gamma$

VALUE	DOCUMENT ID	TECN	COMMENT
0.131 + 0.025 + 0.048	88 BARATE	98Q	ALEP $e^+ e^- \rightarrow Z$
- 0.022 - 0.031			

88 The systematic error includes the uncertainties due to the charm branching ratios.

 $\Gamma(D^0 D^0 \text{ anything})/\Gamma_{\text{total}}$ Γ_{32}/Γ

VALUE	DOCUMENT ID	TECN	COMMENT
0.051 + 0.016 + 0.012	89 BARATE	98Q	ALEP $e^+ e^- \rightarrow Z$
- 0.014 - 0.011			

89 The systematic error includes the uncertainties due to the charm branching ratios.

 $\Gamma(D^0 D^\pm \text{ anything})/\Gamma_{\text{total}}$ Γ_{33}/Γ

VALUE	DOCUMENT ID	TECN	COMMENT
0.027 + 0.015 + 0.010	90 BARATE	98Q	ALEP $e^+ e^- \rightarrow Z$
- 0.013 - 0.009			

90 The systematic error includes the uncertainties due to the charm branching ratios.

 $[\Gamma(D^0 D^0 \text{ anything}) + \Gamma(D^0 D^\pm \text{ anything})]/\Gamma_{\text{total}}$ $(\Gamma_{32} + \Gamma_{33})/\Gamma$

VALUE	DOCUMENT ID	TECN	COMMENT
0.078 + 0.020 + 0.018	91 BARATE	98Q	ALEP $e^+ e^- \rightarrow Z$
- 0.018 - 0.016			

91 The systematic error includes the uncertainties due to the charm branching ratios.

See key on page 373

Meson Particle Listings

$B^\pm/B^0/B_s^0/b$ -baryon ADMIXTURE

$\Gamma(D^\pm D^\mp \text{ anything})/\Gamma_{\text{total}}$					Γ_{34}/Γ
VALUE	CL%	DOCUMENT ID	TECN	COMMENT	
<0.009	90	BARATE	98Q	ALEP	$e^+e^- \rightarrow Z$

$[\Gamma(D^0 \text{ anything}) + \Gamma(D^+ \text{ anything})]/\Gamma_{\text{total}}$					$(\Gamma_{35} + \Gamma_{36})/\Gamma$
VALUE	CL%	DOCUMENT ID	TECN	COMMENT	
$0.093 \pm 0.017 \pm 0.014$		92	ABDALLAH	03E	DLPH $e^+e^- \rightarrow Z$

⁹²The second error is the total of systematic uncertainties including the branching fractions used in the measurement.

$\Gamma(D^- \text{ anything})/\Gamma_{\text{total}}$					Γ_{37}/Γ
VALUE	CL%	DOCUMENT ID	TECN	COMMENT	
$0.231 \pm 0.016 \pm 0.005$		93	BUSKULIC	96Y	ALEP $e^+e^- \rightarrow Z$

⁹³BUSKULIC 96Y reports $0.234 \pm 0.013 \pm 0.010$ for $B(D^+ \rightarrow K^- \pi^+ \pi^+) = 0.091$. We rescale to our best value $B(D^+ \rightarrow K^- \pi^+ \pi^+) = (9.22 \pm 0.21) \times 10^{-2}$. Our first error is their experiment's error and our second error is the systematic error from using our best value.

$\Gamma(D^*(2010)^+ \text{ anything})/\Gamma_{\text{total}}$					Γ_{38}/Γ
VALUE	CL%	DOCUMENT ID	TECN	COMMENT	
$0.173 \pm 0.016 \pm 0.012$		94	ACKERSTAFF	98E	OPAL $e^+e^- \rightarrow Z$

⁹⁴Uses lepton tags to select $Z \rightarrow b\bar{b}$ events.

$\Gamma(D_1(2420)^0 \text{ anything})/\Gamma_{\text{total}}$					Γ_{39}/Γ
VALUE	CL%	DOCUMENT ID	TECN	COMMENT	
$0.050 \pm 0.014 \pm 0.006$		95	ACKERSTAFF	97W	OPAL $e^+e^- \rightarrow Z$

⁹⁵ACKERSTAFF 97W assumes $B(D_1^0(2460) \rightarrow D^* + \pi^-) = 0.21 \pm 0.04$ and $\Gamma_{b\bar{b}}/\Gamma_{\text{hadrons}} = 0.216$ at Z decay.

$\Gamma(D^*(2010)^\mp D_s^\pm \text{ anything})/\Gamma_{\text{total}}$					Γ_{40}/Γ
VALUE	CL%	DOCUMENT ID	TECN	COMMENT	
$0.033 \pm 0.010 + 0.012$ $-0.009 - 0.009$		96	BARATE	98Q	ALEP $e^+e^- \rightarrow Z$

⁹⁶The systematic error includes the uncertainties due to the charm branching ratios.

$\Gamma(D^0 D^*(2010)^\pm \text{ anything})/\Gamma_{\text{total}}$					Γ_{41}/Γ
VALUE	CL%	DOCUMENT ID	TECN	COMMENT	
$0.030 \pm 0.009 + 0.007$ $-0.008 - 0.005$		97	BARATE	98Q	ALEP $e^+e^- \rightarrow Z$

⁹⁷The systematic error includes the uncertainties due to the charm branching ratios.

$\Gamma(D^*(2010)^\pm D^\mp \text{ anything})/\Gamma_{\text{total}}$					Γ_{42}/Γ
VALUE	CL%	DOCUMENT ID	TECN	COMMENT	
$0.025 \pm 0.010 + 0.006$ $-0.009 - 0.005$		98	BARATE	98Q	ALEP $e^+e^- \rightarrow Z$

⁹⁸The systematic error includes the uncertainties due to the charm branching ratios.

$\Gamma(D^*(2010)^\pm D^*(2010)^\mp \text{ anything})/\Gamma_{\text{total}}$					Γ_{43}/Γ
VALUE	CL%	DOCUMENT ID	TECN	COMMENT	
$0.012 \pm 0.004 \pm 0.002$ $-0.003 - 0.002$		99	BARATE	98Q	ALEP $e^+e^- \rightarrow Z$

⁹⁹The systematic error includes the uncertainties due to the charm branching ratios.

$\Gamma(\bar{D} D \text{ anything})/\Gamma_{\text{total}}$					Γ_{44}/Γ
VALUE	CL%	DOCUMENT ID	TECN	COMMENT	
$0.10 \pm 0.032 \pm 0.107$ -0.095		100	ABBIENDI	04I	OPAL $e^+e^- \rightarrow Z$

¹⁰⁰Measurement performed using an inclusive identification of B mesons and the D candidates.

$\Gamma(D_s^*(2460)^0 \text{ anything})/\Gamma_{\text{total}}$					Γ_{45}/Γ
VALUE	CL%	DOCUMENT ID	TECN	COMMENT	
$0.047 \pm 0.024 \pm 0.013$		101	ACKERSTAFF	97W	OPAL $e^+e^- \rightarrow Z$

¹⁰¹ACKERSTAFF 97W assumes $B(D_s^*(2460) \rightarrow D^* + \pi^-) = 0.21 \pm 0.04$ and $\Gamma_{b\bar{b}}/\Gamma_{\text{hadrons}} = 0.216$ at Z decay.

$\Gamma(D_s^- \text{ anything})/\Gamma_{\text{total}}$					Γ_{46}/Γ
VALUE	CL%	DOCUMENT ID	TECN	COMMENT	
$0.150 \pm 0.017 \pm 0.012$		102	BUSKULIC	96Y	ALEP $e^+e^- \rightarrow Z$

¹⁰²BUSKULIC 96Y reports $0.183 \pm 0.019 \pm 0.009$ for $B(D_s^+ \rightarrow \phi \pi^+) = 0.036$. We rescale to our best value $B(D_s^+ \rightarrow \phi \pi^+) = (4.38 \pm 0.35) \times 10^{-2}$. Our first error is their experiment's error and our second error is the systematic error from using our best value.

$\Gamma(D_s^+ \text{ anything})/\Gamma_{\text{total}}$					Γ_{47}/Γ
VALUE	CL%	DOCUMENT ID	TECN	COMMENT	
$0.101 \pm 0.010 \pm 0.029$		103	ABDALLAH	03E	DLPH $e^+e^- \rightarrow Z$

¹⁰³The second error is the total of systematic uncertainties including the branching fractions used in the measurement.

$\Gamma(b \rightarrow \Lambda_c^+ \text{ anything})/\Gamma_{\text{total}}$					Γ_{48}/Γ
VALUE	CL%	DOCUMENT ID	TECN	COMMENT	
$0.097 \pm 0.013 \pm 0.025$		104	BUSKULIC	96Y	ALEP $e^+e^- \rightarrow Z$

¹⁰⁴BUSKULIC 96Y reports $0.110 \pm 0.014 \pm 0.006$ for $B(\Lambda_c^+ \rightarrow p K^- \pi^+) = 0.044$. We rescale to our best value $B(\Lambda_c^+ \rightarrow p K^- \pi^+) = (5.0 \pm 1.3) \times 10^{-2}$. Our first error is their experiment's error and our second error is the systematic error from using our best value.

$\Gamma(\bar{c}/c \text{ anything})/\Gamma_{\text{total}}$					Γ_{49}/Γ
VALUE	CL%	DOCUMENT ID	TECN	COMMENT	
1.162 ± 0.032		OUR AVERAGE			

VALUE	CL%	DOCUMENT ID	TECN	COMMENT	
1.12 ± 0.11 -0.10		105	ABBIENDI	04I	OPAL $e^+e^- \rightarrow Z$
$1.166 \pm 0.031 \pm 0.080$		106	ABREU	00	DLPH $e^+e^- \rightarrow Z$
1.147 ± 0.041		107	ABREU	98D	DLPH $e^+e^- \rightarrow Z$
$1.230 \pm 0.036 \pm 0.065$		108	BUSKULIC	96Y	ALEP $e^+e^- \rightarrow Z$

¹⁰⁵Measurement performed using an inclusive identification of B mesons and the D candidates.

¹⁰⁶Evaluated via summation of exclusive and inclusive channels.

¹⁰⁷ABREU 98D results are extracted from a fit to the b -tagging probability distribution based on the impact parameter.

¹⁰⁸BUSKULIC 96Y assumes PDG 96 production fractions for B^0, B^+, B_s, b baryons, and PDG 96 branching ratios for charm decays. This is sum of their inclusive $\bar{D}^0, D^-, \bar{D}_s,$ and Λ_c branching ratios, corrected to include inclusive Ξ_c and charmonium.

$\Gamma(J/\psi(1S) \text{ anything})/\Gamma_{\text{total}}$					Γ_{50}/Γ
VALUE (units 10^{-2})	CL%	EVTS	DOCUMENT ID	TECN	COMMENT
1.16 ± 0.10		OUR AVERAGE			

VALUE (units 10^{-2})	CL%	EVTS	DOCUMENT ID	TECN	COMMENT		
$1.12 \pm 0.12 \pm 0.10$			109	ABREU	94P	DLPH $e^+e^- \rightarrow Z$	
$1.16 \pm 0.16 \pm 0.14$			121	110	ADRIANI	93J	L3 $e^+e^- \rightarrow Z$
$1.21 \pm 0.13 \pm 0.08$					BUSKULIC	92G	ALEP $e^+e^- \rightarrow Z$

• • • We do not use the following data for averages, fits, limits, etc. • • •
 $1.3 \pm 0.2 \pm 0.2$ 111 ADRIANI 92 L3 $e^+e^- \rightarrow Z$
 <4.9 90 MATTEUZZI 83 MRK2 $E_{\text{cm}}^e = 29$ GeV

¹⁰⁹ABREU 94P is an inclusive measurement from b decays at the Z . Uses $J/\psi(1S) \rightarrow e^+e^-$ and $\mu^+\mu^-$ channels. Assumes $\Gamma(Z \rightarrow b\bar{b})/\Gamma_{\text{hadron}} = 0.22$.

¹¹⁰ADRIANI 93J is an inclusive measurement from b decays at the Z . Uses $J/\psi(1S) \rightarrow \mu^+\mu^-$ and $J/\psi(1S) \rightarrow e^+e^-$ channels.

¹¹¹ADRIANI 92 measurement is an inclusive result for $B(Z \rightarrow J/\psi(1S) X) = (4.1 \pm 0.7 \pm 0.3) \times 10^{-3}$ which is used to extract the b -hadron contribution to $J/\psi(1S)$ production.

$\Gamma(\psi(2S) \text{ anything})/\Gamma_{\text{total}}$					Γ_{51}/Γ
VALUE	CL%	DOCUMENT ID	TECN	COMMENT	
$0.0048 \pm 0.0022 \pm 0.0010$		112	ABREU	94P	DLPH $e^+e^- \rightarrow Z$

¹¹²ABREU 94P is an inclusive measurement from b decays at the Z . Uses $\psi(2S) \rightarrow J/\psi(1S) \pi^+ \pi^-, J/\psi(1S) \rightarrow \mu^+ \mu^-$ channels. Assumes $\Gamma(Z \rightarrow b\bar{b})/\Gamma_{\text{hadron}} = 0.22$.

$\Gamma(\chi_{c1}(1P) \text{ anything})/\Gamma_{\text{total}}$					Γ_{52}/Γ
VALUE	CL%	EVTS	DOCUMENT ID	TECN	COMMENT
0.013 ± 0.004		OUR AVERAGE			

VALUE	CL%	EVTS	DOCUMENT ID	TECN	COMMENT		
$0.011 \pm 0.005 \pm 0.001$			113	ABREU	94P	DLPH $e^+e^- \rightarrow Z$	
$0.018 \pm 0.007 \pm 0.001$			19	114	ADRIANI	93J	L3 $e^+e^- \rightarrow Z$

¹¹³ABREU 94P reports $0.014 \pm 0.006 \pm 0.004$ for $B(\chi_{c1}(1P) \rightarrow \gamma J/\psi(1S)) = 0.273 \pm 0.016$. We rescale to our best value $B(\chi_{c1}(1P) \rightarrow \gamma J/\psi(1S)) = (36.0 \pm 1.9) \times 10^{-2}$. Our first error is their experiment's error and our second error is the systematic error from using our best value. Assumes $\chi_{c2}(1P)$ and $\Gamma(Z \rightarrow b\bar{b})/\Gamma_{\text{hadron}} = 0.22$.

¹¹⁴ADRIANI 93J reports $0.024 \pm 0.009 \pm 0.002$ for $B(\chi_{c1}(1P) \rightarrow \gamma J/\psi(1S)) = 0.273 \pm 0.016$. We rescale to our best value $B(\chi_{c1}(1P) \rightarrow \gamma J/\psi(1S)) = (36.0 \pm 1.9) \times 10^{-2}$. Our first error is their experiment's error and our second error is the systematic error from using our best value.

$\Gamma(\chi_{c1}(1P) \text{ anything})/\Gamma(J/\psi(1S) \text{ anything})$					Γ_{52}/Γ_{50}		
VALUE	CL%	EVTS	DOCUMENT ID	TECN	COMMENT		
1.92 ± 0.82			121	115	ADRIANI	93J	L3 $e^+e^- \rightarrow Z$

• • • We do not use the following data for averages, fits, limits, etc. • • •

¹¹⁵ADRIANI 93J is a ratio of inclusive measurements from b decays at the Z using only the $J/\psi(1S) \rightarrow \mu^+ \mu^-$ channel since some systematics cancel.

$\Gamma(\bar{\Sigma}\gamma)/\Gamma_{\text{total}}$					Γ_{53}/Γ
VALUE (units 10^{-4})	CL%	DOCUMENT ID	TECN	COMMENT	
$3.11 \pm 0.80 \pm 0.72$		116	BARATE	98I	ALEP $e^+e^- \rightarrow Z$

• • • We do not use the following data for averages, fits, limits, etc. • • •

VALUE	CL%	DOCUMENT ID	TECN	COMMENT		
<5.4		90	117	ADAM	96D	DLPH $e^+e^- \rightarrow Z$
<12		90	118	ADRIANI	93L	L3 $e^+e^- \rightarrow Z$

¹¹⁶BARATE 98I uses lifetime tagged $Z \rightarrow b\bar{b}$ sample.

¹¹⁷ADAM 96D assumes $f_{B^0} = f_{B^-} = 0.39$ and $f_{B_s} = 0.12$.

¹¹⁸ADRIANI 93L result is for $\bar{D} \rightarrow \bar{\Sigma}\gamma$ is performed inclusively.

$\Gamma(\bar{\Sigma}\nu)/\Gamma_{\text{total}}$					Γ_{54}/Γ	
VALUE	CL%	DOCUMENT ID	TECN	COMMENT		
$<6.4 \times 10^{-4}$		90	119	BARATE	01E	ALEP $e^+e^- \rightarrow Z$

¹¹⁹The energy-flow and b -tagging algorithms were used.

Meson Particle Listings

$B^\pm/B^0/B_s^0/b$ -baryon ADMIXTURE

$\Gamma(K^\pm \text{ anything})/\Gamma_{\text{total}}$ Γ_{55}/Γ

VALUE	DOCUMENT ID	TECN	COMMENT
0.74 ± 0.06 OUR AVERAGE			
0.72 ± 0.02 ± 0.06	BARATE	98v	ALEP $e^+e^- \rightarrow Z$
0.88 ± 0.05 ± 0.18	ABREU	95c	DLPH $e^+e^- \rightarrow Z$

$\Gamma(K_S^0 \text{ anything})/\Gamma_{\text{total}}$ Γ_{56}/Γ

VALUE	DOCUMENT ID	TECN	COMMENT
0.290 ± 0.011 ± 0.027			
	ABREU	95c	DLPH $e^+e^- \rightarrow Z$

$\Gamma(\pi^\pm \text{ anything})/\Gamma_{\text{total}}$ Γ_{57}/Γ

VALUE	DOCUMENT ID	TECN	COMMENT
3.97 ± 0.02 ± 0.21			
	BARATE	98v	ALEP $e^+e^- \rightarrow Z$

$\Gamma(\pi^0 \text{ anything})/\Gamma_{\text{total}}$ Γ_{58}/Γ

VALUE	DOCUMENT ID	TECN	COMMENT
2.78 ± 0.15 ± 0.60			
	120 ADAM	96	DLPH $e^+e^- \rightarrow Z$

120 ADA M 96 measurement obtained from a fit to the rapidity distribution of $\pi^{0/s}$ in $Z \rightarrow b\bar{b}$ events.

$\Gamma(\phi \text{ anything})/\Gamma_{\text{total}}$ Γ_{59}/Γ

VALUE	DOCUMENT ID	TECN	COMMENT
0.0282 ± 0.0013 ± 0.0019			
	ABBIENDI	00z	OPAL $e^+e^- \rightarrow Z$

$\Gamma(p/\bar{p} \text{ anything})/\Gamma_{\text{total}}$ Γ_{60}/Γ

VALUE	DOCUMENT ID	TECN	COMMENT
0.131 ± 0.011 OUR AVERAGE			
0.131 ± 0.004 ± 0.011	BARATE	98v	ALEP $e^+e^- \rightarrow Z$
0.141 ± 0.018 ± 0.056	ABREU	95c	DLPH $e^+e^- \rightarrow Z$

$\Gamma(\text{charged anything})/\Gamma_{\text{total}}$ Γ_{61}/Γ

VALUE	DOCUMENT ID	TECN	COMMENT
4.97 ± 0.03 ± 0.06			
	121 ABREU	98H	DLPH $e^+e^- \rightarrow Z$

• • • We do not use the following data for averages, fits, limits, etc. • • •

5.84 ± 0.04 ± 0.38 ABREU 95c DLPH Repl. by ABREU 98H

121 ABREU 98H measurement excludes the contribution from K^0 and Λ decay.

$\Gamma(\text{hadron}^+ \text{ hadron}^-)/\Gamma_{\text{total}}$ Γ_{62}/Γ

VALUE (units 10^{-5})	DOCUMENT ID	TECN	COMMENT
1.7^{+1.0}_{-0.7} ± 0.2			
	122,123 BUSKULIC	96v	ALEP $e^+e^- \rightarrow Z$

122 BUSKULIC 96v assumes PDG 96 production fractions for B^0, B^+, B_s, b baryons.

123 Average branching fraction of weakly decaying B hadrons into two long-lived charged hadrons, weighted by their production cross section and lifetimes.

$\Gamma(\text{charmless})/\Gamma_{\text{total}}$ Γ_{63}/Γ

VALUE	DOCUMENT ID	TECN	COMMENT
0.007 ± 0.021			
	124 ABREU	98D	DLPH $e^+e^- \rightarrow Z$

124 ABREU 98D results are extracted from a fit to the b -tagging probability distribution based on the impact parameter. The expected hidden charm contribution of 0.026 ± 0.004 has been subtracted.

$\Gamma(\Lambda/\bar{\Lambda} \text{ anything})/\Gamma_{\text{total}}$ Γ_{64}/Γ

VALUE	DOCUMENT ID	TECN	COMMENT
0.059 ± 0.006 OUR AVERAGE			
0.0587 ± 0.0046 ± 0.0048	ACKERSTAFF	97N	OPAL $e^+e^- \rightarrow Z$
0.059 ± 0.007 ± 0.009	ABREU	95c	DLPH $e^+e^- \rightarrow Z$

$\Gamma(b\text{-baryon anything})/\Gamma_{\text{total}}$ Γ_{65}/Γ

VALUE	DOCUMENT ID	TECN	COMMENT
0.102 ± 0.007 ± 0.027			
	125 BARATE	98v	ALEP $e^+e^- \rightarrow Z$

125 BARATE 98v assumes $B(B_{S^*} \rightarrow pX) = 8 \pm 4\%$ and $B(b\text{-baryon} \rightarrow pX) = 58 \pm 6\%$.

$\Gamma(\mu^+ \mu^- \text{ anything})/\Gamma_{\text{total}}$ Γ_{67}/Γ

VALUE	CL%	DOCUMENT ID	TECN	COMMENT
< 3.2 × 10⁻⁴				
		90	ABBOTT	98B D0 $p\bar{p}$ 1.8 TeV

• • • We do not use the following data for averages, fits, limits, etc. • • •

< 5.0 × 10 ⁻⁵	90	126	ALBAJAR	91c UA1 $E_{\text{cm}}^{e^+e^-} = 630$ GeV
< 0.02	95		ALTHOFF	84G TASS $E_{\text{cm}}^{e^+e^-} = 34.5$ GeV
< 0.007	95		ADEVA	83 MRKJ $E_{\text{cm}}^{e^+e^-} = 30\text{--}38$ GeV
< 0.007	95		BARTEL	83B JADE $E_{\text{cm}}^{e^+e^-} = 33\text{--}37$ GeV

126 Both ABBOTT 98B and GLENN 98 claim that the efficiency quoted in ALBAJAR 91c was overestimated by a large factor.

$[\Gamma(e^+e^- \text{ anything}) + \Gamma(\mu^+ \mu^- \text{ anything})]/\Gamma_{\text{total}}$ $(\Gamma_{66} + \Gamma_{67})/\Gamma$

VALUE	CL%	DOCUMENT ID	TECN	COMMENT
< 0.008				
	90		MATTEUZZI	83 MRK2 $E_{\text{cm}}^{e^+e^-} = 29$ GeV

• • • We do not use the following data for averages, fits, limits, etc. • • •

$\Gamma(\nu\bar{\nu} \text{ anything})/\Gamma_{\text{total}}$ Γ_{68}/Γ

VALUE	DOCUMENT ID	TECN	COMMENT
• • • We do not use the following data for averages, fits, limits, etc. • • •			
< 3.9 × 10 ⁻⁴	127 GROSSMAN	96	RVUE $e^+e^- \rightarrow Z$

127 GROSSMAN 96 limit is derived from the ALEPH BUSKULIC 95 limit $B(B^+ \rightarrow \tau^+ \nu_\tau) < 1.8 \times 10^{-3}$ at CL=90% using conservative simplifying assumptions.

χ_b AT HIGH ENERGY

For a discussion of $B\text{--}\bar{B}$ mixing, see the note on " $B^0\text{--}\bar{B}^0$ Mixing" in the B^0 Particle Listings.

χ_b is the average $B\text{--}\bar{B}$ mixing parameter at high-energy $\chi_b = f'_d \chi_d + f'_s \chi_s$ where f'_d and f'_s are the fractions of B^0 and B_s^0 hadrons in an unbiased sample of semileptonic b -hadron decays.

"OUR EVALUATION" is an average using rescaled values of the data listed below. The average and rescaling were performed by the Heavy Flavor Averaging Group (HFAG) and are described at <http://www.slac.stanford.edu/xorg/hfag/>. The averaging/rescaling procedure takes into account correlations between the measurements.

Γ_{total} Γ_{69}/Γ

VALUE	EVTS	DOCUMENT ID	TECN	COMMENT
0.1284 ± 0.0069 OUR EVALUATION				
0.129 ± 0.004 OUR AVERAGE				
0.132 ± 0.001 ± 0.024	128	ABAZOV	06s D0	$p\bar{p}$ at 1.96 TeV
0.152 ± 0.007 ± 0.011	129	ACOSTA	04A CDF	$p\bar{p}$ at 1.8 TeV
0.1312 ± 0.0049 ± 0.0042	130	ABBIENDI	03P OPAL	$e^+e^- \rightarrow Z$
0.127 ± 0.013 ± 0.006	131	ABREU	01L DLPH	$e^+e^- \rightarrow Z$
0.1192 ± 0.0068 ± 0.0051	132	ACCIARRI	99D L3	$e^+e^- \rightarrow Z$
0.121 ± 0.016 ± 0.006	133	ABREU	94J DLPH	$e^+e^- \rightarrow Z$
0.114 ± 0.014 ± 0.008	134	BUSKULIC	94G ALEP	$e^+e^- \rightarrow Z$
0.129 ± 0.022	135	BUSKULIC	92B ALEP	$e^+e^- \rightarrow Z$
0.176 ± 0.031 ± 0.032	1112	136	ABE	91G CDF $p\bar{p}$ 1.8 TeV
0.148 ± 0.029 ± 0.017	137	ALBAJAR	91D UA1	$p\bar{p}$ 630 GeV

• • • We do not use the following data for averages, fits, limits, etc. • • •

0.131 ± 0.020 ± 0.016 138 ABE 97I CDF Repl. by ACOSTA 04A

0.1107 ± 0.0062 ± 0.0055 139 ALEXANDER 96 OPAL Repl. by ABBIENDI 03P

0.136 ± 0.037 ± 0.040	140	UENO	96 AMY	e^+e^- at 57.9 GeV
0.144 ± 0.014 ± 0.017 ± 0.011	141	ABREU	94F DLPH	Sup. by ABREU 94J
0.131 ± 0.014	142	ABREU	94J DLPH	$e^+e^- \rightarrow Z$
0.123 ± 0.012 ± 0.008		ACCIARRI	94D L3	Repl. by ACCIARRI 99D
0.157 ± 0.020 ± 0.032	143	ALBAJAR	94 UA1	$\sqrt{s} = 630$ GeV
0.121 ± 0.044 ± 0.017	1665	144	ABREU	93C DLPH Sup. by ABREU 94J
0.143 ± 0.022 ± 0.007	145	AKERS	93B OPAL	Sup. by ALEXANDER 96
0.145 ± 0.041 ± 0.035 ± 0.018	146	ACTON	92c OPAL	$e^+e^- \rightarrow Z$
0.121 ± 0.017 ± 0.006	147	ADEVA	92c L3	Sup. by ACCIARRI 94D
0.132 ± 0.22 ± 0.015 ± 0.012	823	148	DECAMP	91 ALEP $e^+e^- \rightarrow Z$
0.178 ± 0.049 ± 0.040 ± 0.020	149	ADEVA	90P L3	$e^+e^- \rightarrow Z$
0.17 ± 0.15 ± 0.08	150,151	WEIR	90 MRK2	e^+e^- 29 GeV
0.21 ± 0.29 ± 0.15	150	BAND	88 MAC	$E_{\text{cm}}^{e^+e^-} = 29$ GeV
> 0.02 at 90% CL	150	BAND	88 MAC	$E_{\text{cm}}^{e^+e^-} = 29$ GeV
0.121 ± 0.047	150,152	ALBAJAR	87c UA1	Repl. by ALBAJAR 91D
< 0.12 at 90% CL	150,153	SCHAAD	85 MRK2	$E_{\text{cm}}^{e^+e^-} = 29$ GeV

128 Uses the dimuon charge asymmetry. Averaged over the mix of b -flavored hadrons.

129 Measurement performed using events containing a dimuon or an e/μ pair.

130 The average B mixing parameter is determined simultaneously with b and c forward-backward asymmetries in the fit.

131 The experimental systematic and model uncertainties are combined in quadrature.

132 ACCIARRI 99D uses maximum-likelihood fits to extract χ_b as well as the A_{FB}^b in $Z \rightarrow b\bar{b}$ events containing prompt leptons.

133 This ABREU 94J result is from 5182 $\ell\ell$ and 279 $\Lambda\ell$ events. The systematic error includes 0.004 for model dependence.

134 BUSKULIC 94G data analyzed using $ee, e\mu, \mu\mu$ events.

135 BUSKULIC 92B uses a jet charge technique combined with electrons and muons.

136 ABE 91G measurement of χ is done with $e\mu$ and ee events.

137 ALBAJAR 91D measurement of χ is done with dimuons.

138 Uses di-muon events.

139 ALEXANDER 96 uses a maximum likelihood fit to simultaneously extract χ as well as the forward-backward asymmetries in $e^+e^- \rightarrow Z \rightarrow b\bar{b}$ and $c\bar{c}$.

140 UENO 96 extracted χ from the energy dependence of the forward-backward asymmetry.

141 ABREU 94F uses the average electric charge sum of the jets recoiling against a b -quark jet tagged by a high p_T muon. The result is for $\bar{\chi} = f_d \chi_d + 0.9 f_s \chi_s$.

142 This ABREU 94J result combines $\ell\ell, A\ell$, and jet-charge ℓ (ABREU 94F) analyses. It is for $\bar{\chi} = f_d \chi_d + 0.96 f_s \chi_s$.

143 ALBAJAR 94 uses dimuon events. Not independent of ALBAJAR 91D.

144 ABREU 93c data analyzed using $ee, e\mu, \mu\mu$ events.

See key on page 373

Meson Particle Listings

 $B^\pm/B^0/B_s^0/b$ -baryon ADMIXTURE, V_{cb} and V_{ub} CKM Matrix Elements

- 145 AKERS 93B analysis performed using dilepton events.
 146 ACTON 92c uses electrons and muons. Superseded by AKERS 93B.
 147 ADEVA 92c uses electrons and muons.
 148 DECAmp 91 done with opposite and like-sign dileptons. Superseded by BUSKULIC 92B.
 149 ADEVA 90P measurement uses $e\bar{e}$, $\mu\mu$, and $e\mu$ events from 118k events at the Z. Superseded by ADEVA 92C.
 150 These experiments are not in the average because the combination of B_s and B_d mesons which they see could differ from those at higher energy.
 151 The WEIR 90 measurement supersedes the limit obtained in SCHAAD 85. The 90% CL are 0.06 and 0.38.
 152 ALBAJAR 87C measured $\chi = (\overline{B}^0 \rightarrow B^0 \rightarrow \mu^+ X)$ divided by the average production weighted semileptonic branching fraction for B hadrons at 546 and 630 GeV.
 153 Limit is average probability for hadron containing B quark to produce a positive lepton.

B-HADRON FRACTIONS IN HADRONIC Z DECAY

The production fractions for b -hadrons in hadronic Z decays have been calculated from the best values of mean lives, mixing parameters and branching fractions in this edition by the Heavy Flavor Averaging Group (HFAG) (see <http://www.slac.stanford.edu/xorg/hfag/>).

The values reported below assume:

$$f(\overline{b} \rightarrow B^+) = f(\overline{b} \rightarrow B^0) \\ f(\overline{b} \rightarrow B^+) + f(\overline{b} \rightarrow B^0) + f(\overline{b} \rightarrow B_s^0) + f(b \rightarrow b\text{-baryon}) = 1$$

The values are:

$$f(\overline{b} \rightarrow B^+) = f(\overline{b} \rightarrow B^0) = 0.402 \pm 0.009$$

$$f(\overline{b} \rightarrow B_s^0) = 0.104 \pm 0.009$$

$$f(b \rightarrow b\text{-baryon}) = 0.091 \pm 0.015$$

as obtained using a time-integrated mixing parameter $\overline{\chi} = 0.1259 \pm 0.0042$ given by a fit to heavy quark quantities with asymmetries removed (see the note "The Z boson").

 $B^\pm/B^0/B_s^0/b$ -baryon ADMIXTURE REFERENCES

ABAZOV	06S	PR D74 092001	V.M. Abazov et al.	(D0 Collab.)
ABBIENDI	04I	EPJ C35 149	G. Abbiendi et al.	(OPAL Collab.)
ABDALLAH	04E	EPJ C33 307	J. Abdallah et al.	(DELPHI Collab.)
ACOSTA	04A	PR D69 012002	D. Acosta et al.	(CDF Collab.)
ABBIENDI	03M	EPJ C30 467	G. Abbiendi et al.	(OPAL Collab.)
ABBIENDI	03P	PL B577 18	G. Abbiendi et al.	(OPAL Collab.)
ABDALLAH	03E	PL B561 26	J. Abdallah et al.	(DELPHI Collab.)
ABDALLAH	03K	PL B576 29	J. Abdallah et al.	(DELPHI Collab.)
HEISTER	02G	EPJ C22 613	A. Heister et al.	(ALEPH Collab.)
ABBIENDI	01Q	PL B520 1	G. Abbiendi et al.	(OPAL Collab.)
ABBIENDI	01R	EPJ C21 399	G. Abbiendi et al.	(OPAL Collab.)
ABREU	01L	EPJ C20 455	P. Abreu et al.	(DELPHI Collab.)
BARATE	01E	EPJ C19 213	R. Barate et al.	(ALEPH Collab.)
ABBIENDI	00E	EPJ C13 225	G. Abbiendi et al.	(OPAL Collab.)
ABBIENDI	00Z	PL B492 13	G. Abbiendi et al.	(OPAL Collab.)
ABREU	00	EPJ C12 225	P. Abreu et al.	(DELPHI Collab.)
ABREU	00C	PL B496 43	P. Abreu et al.	(DELPHI Collab.)
ABREU	00D	PL B478 14	P. Abreu et al.	(DELPHI Collab.)
ABREU	00R	PL B475 407	P. Abreu et al.	(DELPHI Collab.)
ACCIARRI	00	EPJ C13 47	M. Acciari et al.	(L3 Collab.)
AFFOLDER	00E	PRL 84 1663	T. Affolder et al.	(CDF Collab.)
ABBIENDI	99J	EPJ C12 609	G. Abbiendi et al.	(OPAL Collab.)
ABE	99P	PR D60 092005	F. Abe et al.	(CDF Collab.)
ACCIARRI	99D	PL B448 152	M. Acciari et al.	(L3 Collab.)
BARATE	99G	EPJ C6 555	R. Barate et al.	(ALEPH Collab.)
ABBOTT	98B	PL B423 419	B. Abbott et al.	(D0 Collab.)
ABE	98B	PR D57 5382	F. Abe et al.	(CDF Collab.)
ABREU	98D	PL B426 193	P. Abreu et al.	(DELPHI Collab.)
ABREU	98H	PL B425 399	P. Abreu et al.	(DELPHI Collab.)
ACCIARRI	98K	PL B416 220	M. Acciari et al.	(L3 Collab.)
ACCIARRI	98K	PL B436 174	M. Acciari et al.	(L3 Collab.)
ACKERSTAFF	98E	EPJ C1 439	K. Ackerstaff et al.	(OPAL Collab.)
BARATE	98I	PL B429 169	R. Barate et al.	(ALEPH Collab.)
BARATE	98Q	EPJ C4 387	R. Barate et al.	(ALEPH Collab.)
BARATE	98V	EPJ C5 205	R. Barate et al.	(ALEPH Collab.)
GLENN	98	PRL 80 2289	S. Glenn et al.	(CLEO Collab.)
ABE	97I	PR D55 2546	F. Abe et al.	(CDF Collab.)
ACKERSTAFF	97F	ZPHY C73 397	K. Ackerstaff et al.	(OPAL Collab.)
ACKERSTAFF	97N	ZPHY C74 423	K. Ackerstaff et al.	(OPAL Collab.)
ACKERSTAFF	97W	ZPHY C76 425	K. Ackerstaff et al.	(OPAL Collab.)
ABREU	96E	PL B377 195	P. Abreu et al.	(DELPHI Collab.)
ACCIARRI	96C	ZPHY C71 379	M. Acciari et al.	(L3 Collab.)
ADAM	96	ZPHY C69 561	W. Adam et al.	(DELPHI Collab.)
ADAM	96D	ZPHY C72 207	W. Adam et al.	(DELPHI Collab.)
ALEXANDER	96	ZPHY C70 357	G. Alexander et al.	(OPAL Collab.)
BUSKULIC	96F	PL B369 151	D. Buskulić et al.	(ALEPH Collab.)
BUSKULIC	96V	PL B384 471	D. Buskulić et al.	(ALEPH Collab.)
BUSKULIC	96Y	PL B388 648	D. Buskulić et al.	(ALEPH Collab.)
GROSSMAN	96	NP B465 369	Y. Grossman, Z. Ligeti, E. Nardi	(REHO, CIT)
Also		NP B480 753 (erratum)	Y. Grossman, Z. Ligeti, E. Nardi	
PDG	96	PR D54 1	R. M. Barnett et al.	(AMY Collab.)
UENO	96	PL B381 365	K. Ueno et al.	(SLD Collab.)
ABE,K	95B	PRL 75 3624	K. Abe et al.	(SLD Collab.)
ABREU	95C	PL B347 447	P. Abreu et al.	(DELPHI Collab.)
ABREU	95D	ZPHY C66 323	P. Abreu et al.	(DELPHI Collab.)
ADAM	95	ZPHY C68 363	W. Adam et al.	(DELPHI Collab.)
AKERS	95Q	ZPHY C67 57	R. Akers et al.	(OPAL Collab.)
BUSKULIC	95	PL B343 444	D. Buskulić et al.	(ALEPH Collab.)
ABREU	94F	PL B322 459	P. Abreu et al.	(DELPHI Collab.)
ABREU	94J	PL B332 488	P. Abreu et al.	(DELPHI Collab.)
ABREU	94L	ZPHY C63 3	P. Abreu et al.	(DELPHI Collab.)
ABREU	94P	PL B341 109	P. Abreu et al.	(DELPHI Collab.)
ACCIARRI	94C	PL B332 201	M. Acciari et al.	(L3 Collab.)
ACCIARRI	94D	PL B335 542	M. Acciari et al.	(L3 Collab.)
ALBAJAR	94	ZPHY C61 41	C. Albajar et al.	(UA1 Collab.)
BUSKULIC	94G	ZPHY C62 179	D. Buskulić et al.	(ALEPH Collab.)
ABE	93E	PL B313 288	K. Abe et al.	(VENUS Collab.)
ABE	93J	PRL 71 3421	F. Abe et al.	(CDF Collab.)
ABREU	93C	PL B301 145	P. Abreu et al.	(DELPHI Collab.)
ABREU	93D	ZPHY C57 181	P. Abreu et al.	(DELPHI Collab.)
ABREU	93G	PL B312 253	P. Abreu et al.	(DELPHI Collab.)
ACTON	93C	PL B307 247	P.D. Acton et al.	(OPAL Collab.)
ACTON	93L	ZPHY C60 217	P.D. Acton et al.	(OPAL Collab.)
ADRIANI	93J	PL B317 467	O. Adriani et al.	(L3 Collab.)
ADRIANI	93K	PL B317 474	O. Adriani et al.	(L3 Collab.)
ADRIANI	93L	PL B317 637	O. Adriani et al.	(L3 Collab.)

AKERS	93B	ZPHY C60 199	R. Akers et al.	(OPAL Collab.)
BUSKULIC	93B	PL B298 479	D. Buskulić et al.	(ALEPH Collab.)
BUSKULIC	93O	PL B314 459	D. Buskulić et al.	(ALEPH Collab.)
ABREU	92	ZPHY C53 567	P. Abreu et al.	(DELPHI Collab.)
ACTON	92	PL B274 513	D.P. Acton et al.	(OPAL Collab.)
ACTON	92C	PL B276 379	D.P. Acton et al.	(OPAL Collab.)
ADEVA	92C	PL B288 395	B. Adeva et al.	(L3 Collab.)
ADRIANI	92	PL B288 412	O. Adriani et al.	(L3 Collab.)
BUSKULIC	92B	PL B284 177	D. Buskulić et al.	(ALEPH Collab.)
BUSKULIC	92F	PL B295 174	D. Buskulić et al.	(ALEPH Collab.)
BUSKULIC	92G	PL B295 396	D. Buskulić et al.	(ALEPH Collab.)
ABE	91G	PRL 67 3351	F. Abe et al.	(CDF Collab.)
ADEVA	91C	PL B261 177	B. Adeva et al.	(L3 Collab.)
ADEVA	91H	PL B270 111	B. Adeva et al.	(L3 Collab.)
ALBAJAR	91C	PL B262 163	C. Albajar et al.	(UA1 Collab.)
ALBAJAR	91D	PL B262 171	C. Albajar et al.	(UA1 Collab.)
ALEXANDER	91G	PL B266 485	G. Alexander et al.	(OPAL Collab.)
DECAmp	91	PL B258 236	D. Decamp et al.	(ALEPH Collab.)
DECAmp	91C	PL B257 492	D. Decamp et al.	(ALEPH Collab.)
ADEVA	90P	PL B252 703	B. Adeva et al.	(L3 Collab.)
BEHREND	90D	ZPHY C47 333	H.J. Behrend et al.	(CELLO Collab.)
HAGEMANN	90	ZPHY C48 401	J. Hagemann et al.	(JADE Collab.)
LYONS	90	PR D41 982	L. Lyons, A.J. Martin, D.H. Saxon	(OXF, BRIS+)
WEIR	90	PL B240 289	A.J. Weir et al.	(Mark II Collab.)
BRAUNSCHE...	89B	ZPHY C44 1	R. Braunschweig et al.	(TASSO Collab.)
ONG	89	PRL 62 1236	R.A. Ong et al.	(Mark II Collab.)
BAND	88	PL B200 221	H.R. Band et al.	(MAC Collab.)
KLEM	88	PR D37 41	D.E. Klem et al.	(DELCO Collab.)
ONG	88	PRL 60 2587	R.A. Ong et al.	(Mark II Collab.)
ALBAJAR	87C	PL B186 247	C. Albajar et al.	(UA1 Collab.)
ASH	87	PRL 58 640	W.W. Ash et al.	(MAC Collab.)
BARTEL	87	ZPHY C33 339	W. Bartel et al.	(JADE Collab.)
BROM	87	PL B195 301	J.M. Brom et al.	(HRS Collab.)
PAL	86	PR D33 2708	T. Pal et al.	(DELCO Collab.)
AIHARA	85	ZPHY C27 39	H. Aihara et al.	(TPC Collab.)
BARTEL	85J	PL 163B 277	W. Bartel et al.	(JADE Collab.)
SCHAAD	85	PL 160B 188	T. Schaad et al.	(Mark II Collab.)
ALTHOFF	84G	ZPHY C22 219	M. Althoff et al.	(TASSO Collab.)
ALTHOFF	84J	PL 146B 443	M. Althoff et al.	(TASSO Collab.)
KOOP	84	PRL 52 970	D.E. Koop et al.	(DELCO Collab.)
ADEVA	83B	PRL 50 799	B. Adeva et al.	(Mark-J Collab.)
ADEVA	83B	PRL 51 443	B. Adeva et al.	(Mark-J Collab.)
BARTEL	83B	PL 132B 2411	W. Bartel et al.	(JADE Collab.)
FERNANDEZ	83D	PL 50 2054	E. Fernandez et al.	(MAC Collab.)
MATTEUZZI	83	PL 129B 141	C. Matteuzzi et al.	(Mark II Collab.)
NELSON	83	PRL 50 1542	M.E. Nelson et al.	(Mark II Collab.)

 V_{cb} and V_{ub} CKM Matrix Elements

OMITTED FROM SUMMARY TABLE

DETERMINATION OF V_{cb} AND V_{ub}

Revised March 2008 by R. Kowalewski (Univ. of Victoria, Canada) and T. Mannel (Univ. of Siegen, Germany).

INTRODUCTION

Precision determinations of $|V_{ub}|$ and $|V_{cb}|$ are central to testing the CKM sector of the Standard Model, and complement the measurements of CP asymmetries in B decays. The length of the side of the unitarity triangle opposite the well-measured angle β is proportional to the ratio $|V_{ub}|/|V_{cb}|$, making its determination a high priority of the heavy-flavor physics program.

The semileptonic transitions $b \rightarrow c\ell\nu_\ell$ and $b \rightarrow u\ell\nu_\ell$ provide two avenues for determining these CKM matrix elements, namely through inclusive and exclusive final states. The experimental and theoretical techniques underlying these two avenues are independent, providing a crucial cross-check on our understanding. Significant progress has been made in both approaches since the previous review [1].

The theory underlying the determination of $|V_{qb}|$ is mature. The theoretical approaches all use the fact that the mass m_b of the b quark is large compared to the scale Λ_{QCD} that determines low-energy hadronic physics. The basis for precise calculations is a systematic expansion in powers of Λ_{QCD}/m_b , where effective-field-theory methods are used to separate non-perturbative from perturbative contributions. The expansion in Λ_{QCD}/m_b and α_s works well enough to enable a precision determination of $|V_{cb}|$ and $|V_{ub}|$ in semileptonic decays.

Meson Particle Listings

V_{cb} and V_{ub} CKM Matrix Elements

The large data samples available at the B factories have opened up new possibilities experimentally. Analyses where one B meson from an $\mathcal{R}(4S)$ decay is fully reconstructed allow a recoiling semileptonic B decay to be studied with higher purity than was previously possible. Improved knowledge of $\bar{B} \rightarrow X_c \ell \bar{\nu}_\ell$ decays allows partial rates for $\bar{B} \rightarrow X_u \ell \bar{\nu}_\ell$ transitions to be measured in regions previously considered inaccessible, increasing the acceptance for $\bar{B} \rightarrow X_u \ell \bar{\nu}_\ell$ transitions and reducing theoretical uncertainties.

At present, the inclusive determinations of both $|V_{cb}|$ and $|V_{ub}|$ are more precise than the corresponding exclusive determinations. Improvement of the exclusive determinations remains an important goal, and future progress, in particular in lattice QCD, may provide this.

Throughout this review the numerical results quoted are based on the methods of the Heavy Flavor Averaging Group [2].

DETERMINATION OF V_{cb}

Summary: The determination of $|V_{cb}|$ from $\bar{B} \rightarrow D^* \ell \bar{\nu}_\ell$ decays is currently at a relative precision of about 3%. The main limitation is the knowledge of the form factor near the maximum momentum transfer to the leptons. Further progress from lattice calculations of the form factors is needed to improve the precision. For the $\bar{B} \rightarrow D \ell \bar{\nu}_\ell$ channel, experimental measurements must also be improved.

Determinations of $|V_{cb}|$ from inclusive decays are currently below 2% relative uncertainty. The limitations arise mainly from our ignorance of higher order perturbative and non-perturbative corrections.

The values obtained from inclusive and exclusive determinations are currently only marginally consistent with each other:

$$|V_{cb}| = (41.6 \pm 0.6) \times 10^{-3} \text{ (inclusive)} \quad (1)$$

$$|V_{cb}| = (38.6 \pm 1.3) \times 10^{-3} \text{ (exclusive)}. \quad (2)$$

An average of the above gives $|V_{cb}| = (41.2 \pm 0.5) \times 10^{-3}$, with $P(\chi^2) = 0.03$. Scaling the error by $\sqrt{\chi^2/\text{ndf}} = 2.1$ we quote

$$|V_{cb}| = (41.2 \pm 1.1) \times 10^{-3}. \quad (3)$$

$|V_{cb}|$ from exclusive decays

Exclusive determinations of $|V_{cb}|$ are based on a study of semileptonic B decays into the ground-state charmed mesons D and D^* . The main uncertainties in this approach stem from our ignorance of the form factors describing the $B \rightarrow D$ and $B \rightarrow D^*$ transitions. However, in the limit of infinite bottom- and charm-quark masses, only a single form factor appears, the Isgur-Wise function [3], which depends on the product of the four-velocities v and v' of the initial- and final-state hadrons.

The extraction of $|V_{cb}|$ is based on the distribution of the variable $w \equiv v \cdot v'$, which corresponds to the energy of the final-state $D^{(*)}$ meson in the rest frame of the decay. Heavy Quark Symmetry (HQS) [3,4] predicts the normalization of the

rate at $w = 1$, the point of maximum momentum transfer to the leptons, and $|V_{cb}|$ is obtained from an extrapolation of the measured spectrum to $w = 1$.

A precise determination requires corrections to the HQS prediction for the normalization, as well as some information on the slope of the form factors near the point $w = 1$, since the phase space vanishes there. The corrections to the HQS prediction due to finite quark masses are given in terms of the symmetry-breaking parameter

$$\frac{1}{\mu} = \frac{1}{m_c} - \frac{1}{m_b},$$

which is essentially $1/m_c$ for realistic quark masses. HQS ensures that those matrix elements that correspond to the currents that generate the HQS are normalized at $w = 1$; as a result, some of the form factors either vanish or are normalized at $w = 1$. Due to Luke's Theorem [5] (which is an application of the Ademollo-Gatto theorem [6] to heavy quarks), the leading correction to those form factors normalized due to HQS is quadratic in $1/\mu$, while for the form factors that vanish in the infinite mass limit, the corrections are in general linear in $1/m_c$ and $1/m_b$. Thus we have, using the definitions as in Eq. (2.84) of Ref. 7,

$$\begin{aligned} h_i(1) &= 1 + \mathcal{O}(1/\mu^2) & \text{for } i = +, V, A_1, A_3, \\ h_i(1) &= \mathcal{O}(1/m_c, 1/m_b) & \text{for } i = -, A_2. \end{aligned} \quad (4)$$

In addition to these corrections, there are perturbatively calculable radiative corrections from QCD and QED, which will be discussed in the relevant sections. Both - radiative corrections as well as $1/m$ corrections - are considered in the framework of Heavy Quark Effective Theory (HQET) [8], which provides for a systematic expansion.

$\bar{B} \rightarrow D^* \ell \bar{\nu}_\ell$

The decay rate for $\bar{B} \rightarrow D^* \ell \bar{\nu}_\ell$ is given by

$$\frac{d\Gamma}{dw}(\bar{B} \rightarrow D^* \ell \bar{\nu}_\ell) = \frac{G_F^2}{48\pi^3} |V_{cb}|^2 m_{D^*}^3 (w^2 - 1)^{1/2} P(w) (\mathcal{F}(w))^2, \quad (5)$$

where $P(w)$ is a phase-space factor with $P(1) = 12(m_B - m_{D^*})^2$, and $\mathcal{F}(w)$ is dominated by the axial vector form factor h_{A_1} as $w \rightarrow 1$. In the infinite-mass limit, the HQS normalization gives $\mathcal{F}(1) = 1$.

The form factor $\mathcal{F}(w)$ must be parametrized to perform an extrapolation to the zero-recoil point. A frequently used one-parameter form motivated by analyticity and unitarity is [9,10]

$$\begin{aligned} \mathcal{F}(w) &= \eta_{\text{QED}} \eta_A \left[1 + \delta_{1/m^2} + \dots \right] \\ &= [1 - 8\rho_{A_1}^2 z + (53\rho_{A_1}^2 - 15)z^2 - (231\rho_{A_1}^2 - 91)z^3], \end{aligned} \quad (6)$$

with $z = (\sqrt{w+1} - \sqrt{2})/(\sqrt{w+1} + \sqrt{2})$ originating from a conformal transformation. The parameter $\rho_{A_1}^2$ is the slope of the form factor at $w = 1$. The η_{QED} and η_A factors are the QED [11] and QCD [12] short-distance radiative corrections

$$\eta_{\text{QED}} = 1.007, \quad \eta_A = 0.960 \pm 0.007, \quad (7)$$

and δ_{1/m^2} comes from non-perturbative $1/m^2$ corrections.

Recently, lattice simulations which include effects from finite quark masses have been used to calculate the deviation of $\mathcal{F}(1)$ from unity. The value quoted from these calculations, multiplied by η_{QED} , is

$$\mathcal{F}(1) = 0.930 \pm 0.023, \quad (8)$$

where the errors quoted in Ref. 13 have been added in quadrature. This value is compatible with estimates based on non-lattice methods.

Many experiments [14–21] have measured the differential rate as a function of w . Fig. 1 shows corresponding values of $|V_{cb}|\mathcal{F}(1)$ and $\rho_{A_1}^2$ (as defined in Ref. 10). These measurements have been updated using more precise values [20] for the form factor ratios $R_1 \propto A_2/A_1$ and $R_2 \propto V/A_1$. The leading sources of uncertainty on $|V_{cb}|\mathcal{F}(1)$ are due to detection efficiencies and $D^{(*)}$ decay branching fractions, while for ρ^2 the uncertainties in R_1 and R_2 still dominate. Related measurements [22,23] of $\Gamma(\overline{B} \rightarrow D^*\ell\overline{\nu}_\ell)$ using samples at the $\Upsilon(4S)$, in which the opposite B is fully reconstructed, have recently been made. These use the measured missing mass squared to isolate signal decays, and have very little sensitivity to the form factor slope. The curves corresponding to constant total rate are shown in Fig. 1.

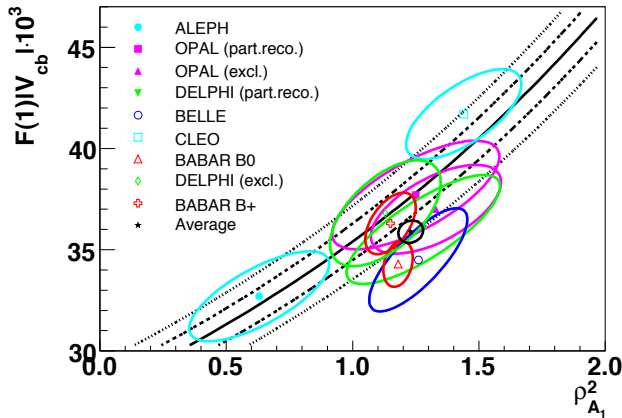


Figure 1: Measurements of $|V_{cb}|\mathcal{F}(1)$ vs. $\rho_{A_1}^2$ are shown as $\Delta\chi^2 = 1$ ellipses. The curves (central value, $\pm 1\sigma$ and $\pm 2\sigma$) correspond to the measurement of the total rate $\Gamma(\overline{B} \rightarrow D^*\ell\overline{\nu}_\ell)$ from Ref. 22. Color version at end of book.

The confidence level of the average[†] based on the measurements in Fig. 1 is $\sim 2.6\%$. In light of the marginal consistency, we choose to rescale the errors by $\sqrt{\chi^2/\text{ndf}} = 1.5$ to find

[†] Note that the average does not include the BaBar B^+ measurement, nor the measurement of $\Gamma(\overline{B} \rightarrow D^*\ell\overline{\nu}_\ell)$ shown in the figure, pending a full treatment of their correlations with the BaBar B^0 measurement.

$|V_{cb}|\mathcal{F}(1) = (35.9 \pm 0.8) \times 10^{-3}$. Along with the value given above for $\mathcal{F}(1)$ this yields

$$|V_{cb}| = (38.6 \pm 0.9_{\text{exp}} \pm 1.0_{\text{theo}}) \times 10^{-3}. \quad (9)$$

$\overline{B} \rightarrow D\ell\overline{\nu}_\ell$

The differential rate for $\overline{B} \rightarrow D\ell\overline{\nu}_\ell$ is given by

$$\frac{d\Gamma}{dw}(\overline{B} \rightarrow D\ell\overline{\nu}_\ell) = \frac{G_F^2}{48\pi^3} |V_{cb}|^2 (m_B + m_D)^2 m_D^3 (w^2 - 1)^{3/2} (\mathcal{G}(w))^2. \quad (10)$$

The form factor is

$$\mathcal{G}(w) = h_+(w) - \frac{m_B - m_D}{m_B + m_D} h_-(w), \quad (11)$$

where h_+ is normalized due to HQS and h_- vanishes in the heavy mass limit. Thus,

$$\mathcal{G}(1) = 1 + \mathcal{O}\left(\frac{m_B - m_D}{m_B + m_D} \frac{1}{m_c}\right), \quad (12)$$

and the corrections to the HQET predictions are parametrically larger than was the case for $\overline{B} \rightarrow D^*\ell\overline{\nu}_\ell$.

In order to get a more precise prediction for the form factor $\mathcal{G}(1)$, the heavy quark limit can be supplemented by additional assumptions. It has been argued in Ref. 24 that in a limit in which the kinetic energy μ_π^2 is equal to the chromomagnetic moment μ_G^2 (these quantities are discussed below in more detail), one may obtain the value

$$\mathcal{G}(1) = 1.04 \pm 0.01_{\text{power}} \pm 0.01_{\text{pert}}. \quad (13)$$

Recently, lattice calculations including effects beyond the heavy mass limit have become available, and hence the fact that deviations from the HQET predictions are parametrically larger than in the case $\overline{B} \rightarrow D^*\ell\overline{\nu}_\ell$ is irrelevant. These unquenched calculations quote a (preliminary) value [25]

$$\mathcal{G}(1) = 1.074 \pm 0.018 \pm 0.016, \quad (14)$$

which has an error comparable to the one quoted for $\mathcal{F}(1)$, although some uncertainties have not been taken into account.

The measurements [14,26,27] of $|V_{cb}|\mathcal{G}(1)$ result in an average value $|V_{cb}|\mathcal{G}(1) = (42.3 \pm 4.5) \times 10^{-3}$. Using the value given in Eq. (14) for $\mathcal{G}(1)$, accounting for the QED correction and conservatively adding the theory uncertainties linearly results in

$$|V_{cb}| = (39.4 \pm 4.2 \pm 1.3) \times 10^{-3}, \quad (15)$$

where the first uncertainty is from experiment and the second from theory.

Measuring the differential rate at $w = 1$ is more difficult in $\overline{B} \rightarrow D\ell\overline{\nu}_\ell$ decays than in $\overline{B} \rightarrow D^*\ell\overline{\nu}_\ell$ decays, since the rate is smaller and the background from mis-reconstructed $\overline{B} \rightarrow D^*\ell\overline{\nu}_\ell$ decays is significant; this is reflected in the larger experimental uncertainty. The B factories can address these limitations by studying decays recoiling against fully reconstructed B mesons, or doing a global fit to $\overline{B} \rightarrow X_c\ell\overline{\nu}_\ell$ decays. Theoretical input

Meson Particle Listings

V_{cb} and V_{ub} CKM Matrix Elements

on the shape of the w spectrum in $\overline{B} \rightarrow D\ell\overline{\nu}_\ell$ is valuable, as precise measurements of the total rate are easier; a recent measurement [22] of $\mathcal{B}(\overline{B} \rightarrow D\ell\overline{\nu}_\ell)$ has an uncertainty of $\sim 5\%$.

Prospects for Lattice determinations of the $B \rightarrow D^{(*)}$ form factors

Lattice determinations of the $B \rightarrow D^{(*)}$ form factors have improved significantly over the last few years. The key for the improvements [13,28] is a set of double-ratios, constructed so that all uncertainties scale with the deviation of the form factor from unity. In combination with the possibility to perform unquenched calculations, *i.e.*, calculations with realistic sea quarks, these double ratios yield quite precise predictions for form factors.

The remaining uncertainties are due to the chiral extrapolation from the light quark masses used in the numerical lattice computation to realistic up and down quark masses, and to discretization errors. These sources of uncertainty will be reduced with larger lattice sizes and smaller lattice spacings. The total uncertainty in the lattice values of $\mathcal{F}(1)$ and $\mathcal{G}(1)$ obtained from this method will be 2-3%. However, in the light of the current $> 2\sigma$ tension between inclusive and exclusive $|V_{cb}|$, a revision of the systematic uncertainties becomes important.

In addition to the lattice calculations of form factor normalizations, first results for the w dependence of the form factors are available [29]. While these first results are still in the quenched approximation, one can expect further calculations of form factor shapes in the near future, which will allow comparisons with the experimentally measured shapes.

Decays to Excited D Meson States

Above the ground state D and D^* mesons lie four positive-parity states with one unit of orbital angular momentum, generically denoted as D^{**} . In the heavy mass limit, they form two spin-symmetry doublets with $j_\ell = 1/2$ and $j_\ell = 3/2$, where j_ℓ is the total angular momentum of the light degrees of freedom. The doublet with $j_\ell = 3/2$ is expected to be narrow, while the states with $j_\ell = 1/2$ should be broad, consistent with experimental measurements. Furthermore, one expects that in the heavy mass limit $\Gamma(B \rightarrow D^{**}(j_\ell = 3/2)\ell\overline{\nu}) \gg \Gamma(B \rightarrow D^{**}(j_\ell = 1/2)\ell\overline{\nu})$. A recent measurement indicates this expectation may be violated [23]. If this result is confirmed, it may indicate substantial mixing between the two spin-symmetry doublets, which can occur due to terms of order $1/m_c$. However, the impact on the exclusive V_{cb} determination is expected to be small, since the zero-recoil point is protected against corrections of order $1/m_c$ by Luke's theorem.

$|V_{cb}|$ from inclusive decays

At present, the most precise determinations of $|V_{cb}|$ come from inclusive decays. The method is based on a measurement of the total semileptonic decay rate, together with the leptonic energy and the hadronic invariant mass spectra of inclusive semileptonic decays. The total decay rate can be calculated

quite reliably in terms of non-perturbative parameters that can be extracted from the information contained in the spectra.

Inclusive semileptonic rate

The theoretical foundation for the calculation of the total semileptonic rate is the Operator Product Expansion (OPE), which yields the Heavy Quark Expansion (HQE), a systematic expansion in inverse powers of the b -quark mass [30,31]. The validity of the OPE is proven in the deep euclidean region for the momenta (which is satisfied, *e.g.*, in deep inelastic scattering), but its application to heavy quark decays requires a continuation to time-like momenta $p_B^2 = M_B^2$, where possible contributions which are exponentially damped in the euclidean region could become oscillatory. The validity of the OPE for inclusive decays is equivalent to the assumption of parton-hadron duality, hereafter referred to simply as duality, and possible oscillatory contributions would be an indication of duality violation.

Duality-violating effects are hard to quantify. In practice, they would appear as unnaturally large coefficients of higher order terms in the $1/m$ expansion [32]. The description of ~ 60 measurements in terms of ~ 6 free parameters in global fits to $\overline{B} \rightarrow X_c\ell\overline{\nu}_\ell$ decays provides a non-trivial testing ground for the HQE predictions. Present fits include terms up to order $1/m_b^3$, the coefficients of which have sizes as expected *a priori* by theory. The consistency of the data with these OPE fits will be discussed later; no indication is found that terms of order $1/m_b^4$ or higher are large, and there is no evidence for duality violations in the data. Thus duality or, likewise, the validity of the OPE, is assumed in the analysis, and no further uncertainty is assigned to potential duality violations.

The OPE result for the total rate can be written schematically (the details of the expression can be found, *e.g.*, in Ref. 33) as

$$\Gamma = |V_{cb}|^2 \hat{\Gamma}_0 m_b^5(\mu) (1 + A_{ew}) A^{\text{pert}}(r, \mu) \times \left[z_0(r) + z_2(r) \left(\frac{\mu_\pi^2}{m_b^2}, \frac{\mu_G^2}{m_b^2} \right) + z_3(r) \left(\frac{\rho_D^3}{m_b^3}, \frac{\rho_{LS}^3}{m_b^3} \right) + z_4(r) \left(\frac{s_i}{m_b^4} \right) + \dots \right], \quad (16)$$

where A_{ew} denotes the electroweak, and $A^{\text{pert}}(r, \mu)$ the QCD radiative corrections, r is the ratio m_c/m_b , and the z_i are known phase-space functions.

This expression is known up to order $1/m_b^4$, where the terms of order $1/m_b^3$ and $1/m_b^4$ have been computed only at tree level [34-36]. The leading term is the parton model, which is known completely to order α_s , and the terms of order $\alpha_s^2\beta_0$ (where β_0 is the first coefficient of the QCD β function, $\beta_0 = (33 - 2n_f)/3$) have been included by the usual BLM procedure [33,37]. Furthermore, the corrections of order $\alpha_s\mu_\pi^2/m_b^2$ have been computed recently [38].

The HQE parameters are given in terms of forward matrix elements by

$$\begin{aligned}\bar{A} &= M_B - m_b \\ \mu_\pi^2 &= -\langle B|\bar{b}(iD_\perp)^2b|B\rangle \\ \mu_G^2 &= \langle B|\bar{b}(iD_\perp^\mu)(iD_\perp^\nu)\sigma_{\mu\nu}b|B\rangle \\ \rho_D^3 &= \langle B|\bar{b}(iD_{\perp\mu})(ivD)(iD_\perp^\nu)b|B\rangle \\ \rho_{LS}^3 &= \langle B|\bar{b}(iD_\perp^\mu)(ivD)(iD_\perp^\nu)\sigma_{\mu\nu}b|B\rangle,\end{aligned}\quad (17)$$

while the five hadronic parameters s_i of the order $1/m_b^4$ can be found in Ref. 35; these have not yet been included in the fits. The non-perturbative matrix elements depend on the renormalization scale μ , on the chosen renormalization scheme, and on the quark mass m_b . The rates and the spectra depend strongly on m_b (or equivalently on \bar{A}), which makes the discussion of renormalization issues mandatory.

Using the pole-mass definition for the heavy quark masses, it is well known that the corresponding perturbative series of decay rates does not converge very well, making a precision determination of $|V_{cb}|$ in such a scheme impossible. The solution to this problem is to choose an appropriate “short-distance” mass definition. Frequently used mass definitions are the kinetic scheme [39,40], or the 1S scheme [41]. Both of these schemes have been applied to semi-leptonic $b \rightarrow c$ transitions, yielding comparable results and uncertainties.

The 1S scheme eliminates the b quark pole mass by relating it to the perturbative expression for the mass of the 1S state of the Υ system. The physical mass of the $\Upsilon(1S)$ contains non-perturbative contributions, which have been estimated in Ref. 42. These non-perturbative contributions are small; nevertheless, the best determination of the b quark mass in the 1S scheme is obtained from sum rules for $e^+e^- \rightarrow b\bar{b}$.

Alternatively one may use a short-distance mass definition such as the $\overline{\text{MS}}$ mass $m_b^{\overline{\text{MS}}}(m_b)$. However, it has been argued that the scale m_b is unnaturally high for B decays, while for smaller scales $\mu \sim 1 \text{ GeV}$ $m_b^{\overline{\text{MS}}}(\mu)$ is under poor control. For this reason, the so-called “kinetic mass” $m_b^{\text{kin}}(\mu)$ has been proposed. It is the mass entering the non-relativistic expression for the kinetic energy of a heavy quark, and is defined using heavy quark sum rules [40].

The HQE parameters also depend on the renormalization scale and scheme. The matrix elements given in Eq. (17) are defined with the full QCD fields and states, which is the definition frequently used in the kinetic scheme. Sometimes slightly different parameters λ_1 and λ_2 are used, which are defined in the infinite mass limit. The relation between these parameters is

$$\begin{aligned}\bar{A}_{\text{HQET}} &= \lim_{m_b \rightarrow \infty} \bar{A}, \quad -\lambda_1 = \lim_{m_b \rightarrow \infty} \mu_\pi^2 \\ \lambda_2 &= \lim_{m_b \rightarrow \infty} \mu_G^2, \quad \rho_1 = \lim_{m_b \rightarrow \infty} \rho_D^3 \\ \rho_2 &= \lim_{m_b \rightarrow \infty} \rho_{LS}^3.\end{aligned}$$

Defining the kinetic energy and the chromomagnetic moment in the infinite-mass limit (as, *e.g.*, in the 1S scheme)

requires that $1/m_b$ corrections to the matrix elements defined in Eq. (17) be taken into account once one goes beyond order $1/m_b^2$. As a result, additional quantities $\mathcal{T}_1 \cdots \mathcal{T}_4$ appear at order $1/m_b^3$. However, these quantities are correlated such that the total number of non-perturbative parameters to order $1/m_b^3$ is the same as in the scheme where m_b is kept finite in the matrix elements which define the non-perturbative parameters. A detailed discussion of these issues can be found in Ref. 43.

In order to define the HQE parameters properly, one must adopt a renormalization scheme, as was done for the heavy quark mass. Since all these parameters can again be determined by heavy quark sum rules, one may adopt a scheme similar to the kinetic scheme for the quark mass. The HQE parameters in the kinetic scheme depend on powers of the renormalization scale μ , and the above relations are valid in the limit $\mu \rightarrow 0$, leaving only logarithms of μ .

Some of these parameters also appear in the relation for the heavy hadron masses. The quantity \bar{A} is determined once a definition is specified for the quark mass. The parameter μ_G^2 can be extracted from the mass splitting in the lowest spin-symmetry doublet of heavy mesons

$$\mu_G^2(\mu) = \frac{3}{4}C_G(\mu, m_b)(M_{B^*}^2 - M_B^2), \quad (18)$$

where $C_G(\mu, m_b)$ is a perturbatively-computable coefficient which depends on the scheme. In the kinetic scheme we have

$$\mu_G^2(1 \text{ GeV}) = 0.35_{-0.02}^{+0.03} \text{ GeV}^2. \quad (19)$$

Determination of HQE Parameters and $|V_{cb}|$

Several experiments have measured moments in $\bar{B} \rightarrow X_c \ell \bar{\nu}_\ell$ decays [44–51] as a function of the minimum lepton momentum. The measurements of the moments of the electron-energy spectrum ($0^{\text{th}}\text{--}3^{\text{rd}}$), and of the squared-hadronic mass spectrum ($0^{\text{th}}\text{--}2^{\text{nd}}$), have statistical uncertainties that are roughly equal to their systematic uncertainties. They can be improved with more data and significant effort. Measurements of photon energy moments ($0^{\text{th}}\text{--}2^{\text{nd}}$) in $B \rightarrow X_s \gamma$ decays [52–55] as a function of the minimum accepted photon energy are still primarily statistics-limited. Global fits to these moments [56–61] have been performed in the 1S and kinetic schemes. A global fit to a large set of hadronic-mass and electron-energy moments in $\bar{B} \rightarrow X_c \ell \bar{\nu}_\ell$ decays in the 1S scheme gives [61]

$$|V_{cb}| = (41.56 \pm 0.39 \pm 0.08) \times 10^{-3} \quad (20)$$

$$m_b^{\text{1S}} = 4.751 \pm 0.058 \text{ GeV} \quad (21)$$

$$\lambda_1^{\text{1S}} = -0.274 \pm 0.047 \text{ GeV}, \quad (22)$$

where the first error includes experimental and theoretical uncertainties, and the second error on $|V_{cb}|$ comes from the B lifetime. The mass value can be compared with a determination based on the $e^+e^- \rightarrow b\bar{b}$ cross-section near threshold [62] of

Meson Particle Listings

V_{cb} and V_{ub} CKM Matrix Elements

$m_b^{1S} = 4.69 \pm 0.03$ GeV. The same data have been fitted in the kinetic scheme, resulting in [58]

$$|V_{cb}| = (41.68 \pm 0.39 \pm 0.58) \times 10^{-3} \quad (23)$$

$$m_b^{\text{kin}} = 4.677 \pm 0.053 \text{ GeV} \quad (24)$$

$$\mu_\pi^2(\text{kin}) = 0.387 \pm 0.039 \text{ GeV} , \quad (25)$$

where the first error includes experimental and theoretical uncertainties, and the second error on $|V_{cb}|$ is from the estimated accuracy of the HQE for the total semileptonic rate. The mass value may be compared with $m_b^{\text{kin}} = 4.56 \pm 0.06$ GeV, extracted from the threshold region of $e^+e^- \rightarrow b\bar{b}$ [63].

In each scheme, theoretical uncertainties are estimated and included in performing the fits. Similar values for the parameters are obtained when only experimental uncertainties are used in the fits, and when photon-energy-spectrum moments from $\bar{B} \rightarrow X_s\gamma$ are included. The χ^2/dof is substantially below unity in all fits, suggesting that the theoretical uncertainties may be overestimated, and showing no evidence for duality violations at a significant level.

The fits in the two schemes agree well on $|V_{cb}|$. We take the arithmetic averages of the values and of the errors to quote an inclusive $|V_{cb}|$ determination:

$$|V_{cb}| = (41.6 \pm 0.6) \times 10^{-3} . \quad (26)$$

The m_b values must be quoted in the same scheme to be directly compared. A translation at NNLO [64] of $m_b^{\text{kin}} = 4.68$ GeV gives

$$m_b^{1S} = 4.80 \pm 0.01 \text{ GeV} , \quad (27)$$

(the estimated uncertainty comes from varying the scale μ from $m_b/2$ to $2m_b$) to be compared with Eq. (21). The translation of m_b from one scheme to another yields an estimate of the size of the residual uncertainties. While the comparison given above is sensitive to issues beyond scheme translation, the 50 MeV difference serves as an indicator of the size of potential effects. The uncertainties on m_b are further discussed in the section on the determination of $|V_{ub}|$.

The precision of these results can be further improved. The prospects for more precise moments measurements were discussed above. Improvements can be made in the theory by calculating higher-order perturbative corrections [65] and, more importantly, by calculating perturbative corrections to the matrix elements defining the HQE parameters. The inclusion of still-higher-order moments may improve the sensitivity of the fits to higher-order terms in the HQE.

Determination of $|V_{ub}|$

Summary: The determination of $|V_{ub}|$ is the focus of significant experimental and theoretical work. The determinations based on inclusive semileptonic decays using different calculational ansätze are consistent. The total uncertainty is 10%, of which the dominant uncertainty (7%) comes from a 60 MeV error used for m_b . Significant progress has been made in measurements of $\bar{B} \rightarrow \pi\ell\bar{\nu}_\ell$ decays; the branching fraction is now

known to 6%, and the q^2 shape is reasonably well constrained experimentally. Further improvements in the form-factor normalization are needed to take full advantage of this precision.

The values obtained from inclusive and exclusive determinations are

$$|V_{ub}| = (4.12 \pm 0.43) \times 10^{-3} \quad (\text{inclusive}), \quad (28)$$

$$|V_{ub}| = (3.5 \pm_{0.5}^{0.6}) \times 10^{-3} \quad (\text{exclusive}). \quad (29)$$

The two determinations are independent, and the dominant uncertainties are on multiplicative factors. We weight the two values by their relative errors and treat the uncertainties as Gaussian distributed to find

$$|V_{ub}| = (3.95 \pm 0.35) \times 10^{-3} , \quad (30)$$

with $P(\chi^2) = 0.4$.

$|V_{ub}|$ from inclusive decays

The theoretical description of inclusive $\bar{B} \rightarrow X_u\ell\bar{\nu}_\ell$ decays is based on the Heavy Quark Expansion, as for $\bar{B} \rightarrow X_c\ell\bar{\nu}_\ell$ decays, and leads to a predicted total decay rate with uncertainties below 5% [66,67]. Unfortunately, the total decay rate is hard to measure due to the large background from CKM-favored $\bar{B} \rightarrow X_c\ell\bar{\nu}_\ell$ transitions. Calculating the partial decay rate in regions of phase space where $\bar{B} \rightarrow X_c\ell\bar{\nu}_\ell$ decays are suppressed is more challenging, as the HQE convergence in these regions is spoiled, requiring the introduction of a non-perturbative distribution function, the ‘‘shape function’’ (SF) [68,69], whose form is unknown. The shape function becomes important when the light-cone momentum component $P_+ \equiv E_X - |P_X|$ is not large compared to Λ_{QCD} . This additional difficulty can be addressed in two complementary ways. The leading-shape function can either be measured in the radiative decay $\bar{B} \rightarrow X_s\gamma$, or be modeled with constraints on the 0th-2nd moments, and the results applied to the calculation of the $\bar{B} \rightarrow X_u\ell\bar{\nu}_\ell$ partial decay rate [70–72]; in such an approach, the largest challenges are for the theory. Alternatively, measurements of $\bar{B} \rightarrow X_u\ell\bar{\nu}_\ell$ partial decay rates can be extended further into the $\bar{B} \rightarrow X_c\ell\bar{\nu}_\ell$ -allowed region, enabling a simplified theoretical (pure HQE) treatment [73], but requiring precise experimental knowledge of the $\bar{B} \rightarrow X_c\ell\bar{\nu}_\ell$ background.

The shape function is a universal property of B mesons at leading order. It has been recognized for over a decade [68,69] that the leading SF can be measured in $\bar{B} \rightarrow X_s\gamma$ decays. However, sub-leading shape functions [74–79] arise at each order in $1/m_b$, and differ in semileptonic and radiative B decays. The form of the shape functions cannot be calculated from first principles. Prescriptions that relate directly the partial rates for $\bar{B} \rightarrow X_s\gamma$ and $\bar{B} \rightarrow X_u\ell\bar{\nu}_\ell$ decays, and thereby avoid any parameterization of the leading shape function, are available [80–83]; uncertainties due to sub-leading SF remain in these approaches. Existing measurements, however, have tended to use parameterizations of the leading SF that respect constraints on the zeroth, first, and second moments. At leading order, the first and second moments are equal to

$\bar{\Lambda} = M_B - m_b$ and μ_π^2 , respectively. The relations between SF moments and the non-perturbative parameters of the HQE are known to second order in α_s [84]. As a result, measurements of HQE parameters from global fits to $\bar{B} \rightarrow X_c \ell \bar{\nu}_\ell$ and $\bar{B} \rightarrow X_s \gamma$ moments can be used to constrain the SF moments, as well as provide accurate values of m_b and other parameters for use in determining $|V_{ub}|$. The possibility of measuring these HQE parameters directly from moments in $\bar{B} \rightarrow X_u \ell \bar{\nu}_\ell$ decays has been explored [85], but the experimental precision achievable there is not competitive with other approaches.

The calculations which are used for the fits performed by HFAG are documented in Refs. [70] (BLNP), [86] (GGOU), [87] (DGE), and [73] (BLL).

The calculations start from the triple differential rate using the variables

$$P_l = M_B - 2E_l, \quad P_- = E_X + |\vec{P}_X|, \quad P_+ = E_X - |\vec{P}_X| \quad (31)$$

for which the differential rate becomes

$$\frac{d^3\Gamma}{dP_+ dP_- dP_l} = \frac{G_F^2 |V_{ub}|^2}{16\pi^2} (M_B - P_+) \left\{ (P_- - P_l)(M_B - P_- + P_l - P_+) \mathcal{F}_1 + (M_B - P_-)(P_- - P_+) \mathcal{F}_2 + (P_- - P_l)(P_l - P_+) \mathcal{F}_3 \right\}. \quad (32)$$

The “structure functions” \mathcal{F}_i can be calculated using factorization theorems that have been proven to subleading order in the $1/m_b$ expansion.

The BLNP [70] calculation uses these factorization theorems to write the \mathcal{F}_i in terms of perturbatively-calculable hard coefficients H and jet functions J , which are convolved with the (soft) light-cone distribution functions S , the shape functions of the B meson.

The leading order term in the $1/m_b$ expansion of the \mathcal{F}_i contains a single non-perturbative function, and is calculated to subleading order in α_s , while at subleading order in the $1/m_b$ expansion, there are several independent non-perturbative functions which have been calculated only at tree level in the α_s expansion.

To extract the non-perturbative input, one can study the photon-energy spectrum in $B \rightarrow X_s \gamma$ [72]. This spectrum is known at a similar accuracy as the P_+ spectrum in $B \rightarrow X_u \ell \bar{\nu}_\ell$. Going to subleading order in the $1/m_b$ expansion requires the modeling of subleading SFs, a large variety of which were studied in Ref. 70.

A recent calculation (GGOU) [86] uses a hard, Wilsonian cut-off that matches the definition of the kinetic mass. The non-perturbative input is similar to what is used in BLNP, but the shape functions are defined differently. In particular, they are defined at finite m_b , and depend on the light-cone component k_+ of the b quark momentum, and on the momentum transfer q^2 to the leptons. These functions include sub-leading effects to all orders; as a result, they are non-universal, with one shape function corresponding to each structure function in

Eq. (32). Their k_+ moments can be computed in the OPE, and related to observables and to the shape functions defined in Ref. 70.

Going to subleading order in α_s requires the definition of a renormalization scheme for the HQE parameters and for the shape function. It has been noted that the relation between the moments of the shape function and the forward matrix elements of local operators is plagued by ultraviolet problems which require additional renormalization. A possible scheme for improving this behavior has been suggested in Refs. [70,72], which introduce a particular definition of the quark mass (the so-called shape-function scheme) based on the first moment of the measured spectrum. Likewise, the HQE parameters can be defined from measured moments of spectra, corresponding to moments of the shape function.

One can also attempt to calculate the SF by using additional assumptions. One possible approach (DGE) is the so-called “dressed gluon approximation” [87], where the perturbative result is continued into the infrared regime using the renormalon structure obtained in the large β_0 limit, where β_0 has been defined following Eq. (16). Alternatively, one may assume an analytic behaviour for the strong coupling in the infrared to perform an extrapolation of perturbation theory [88].

While attempts to quantify the shape function are important, the impact of uncertainties in the shape function is significantly reduced in some recent measurements that cover a larger portion of the $\bar{B} \rightarrow X_u \ell \bar{\nu}_\ell$ phase space. Several measurements using a combination of cuts on the leptonic momentum transfer q^2 and the hadronic invariant mass M_X , as suggested in Ref. 89, have been made. Measurements of the electron spectrum in $\bar{B} \rightarrow X_u \ell \bar{\nu}_\ell$ decays have been made down to 1.9 GeV, at which point shape-function uncertainties are not dominant. The measurements quoted below have used a variety of functional forms to parameterize the leading shape function; in no case does this lead to more than a 2% uncertainty on $|V_{ub}|$.

Weak Annihilation [86,90,91] (WA) can in principle contribute significantly in the restricted region (at high q^2) accepted by measurements of $\bar{B} \rightarrow X_u \ell \bar{\nu}_\ell$ decays. An estimate [73] based on leptonic D_s decays [91] leads to a $\sim 3\%$ uncertainty on the total $\bar{B} \rightarrow X_u \ell \bar{\nu}_\ell$ rate from the $\Upsilon(4S)$. The differential spectrum from WA decays is not known, but they are expected to contribute predominantly at high q^2 , and may be a significant source of uncertainty for $|V_{ub}|$ measurements that only accept a small fraction, f_u , of the full $\bar{B} \rightarrow X_u \ell \bar{\nu}_\ell$ phase space. Model-dependent limits on WA were determined in Ref. 92, where the CLEO data were fitted to combinations of WA models and a spectator $\bar{B} \rightarrow X_u \ell \bar{\nu}_\ell$ component and background. More direct experimental constraints [93] on WA have recently been made by comparing the $\bar{B} \rightarrow X_u \ell \bar{\nu}_\ell$ decay rates of charged and neutral B mesons. The sensitivity of $|V_{ub}|$ determinations to WA can also be reduced by removing the region at high q^2 in those measurements where q^2 is determined.

Meson Particle Listings

V_{cb} and V_{ub} CKM Matrix Elements

Measurements

We summarize the measurements used in the determination of $|V_{ub}|$ below. Given the improved precision and more rigorous theoretical interpretation of the recent measurements, earlier determinations [94–97] will not be further considered in this review.

Electron momentum “endpoint” measurements [98–100] reconstruct a single charged electron to determine a partial decay rate for $\overline{B} \rightarrow X_u \ell \overline{\nu}_\ell$. This results in a high $\mathcal{O}(50\%)$ selection efficiency and only modest sensitivity to the modeling of detector response. The decay rate can be cleanly extracted for $E_e > 2.3 \text{ GeV}$, but this is deep in the SF region, where theoretical uncertainties are large. Measurements down to 2.0 or 1.9 GeV exist, but have low ($< 1/10$) signal-to-background (S/B) ratio, making the control of the $\overline{B} \rightarrow X_c \ell \overline{\nu}_\ell$ background a crucial point. In these analyses, the inclusive electron momentum spectrum from $B\overline{B}$ events is determined by subtracting the $e^+e^- \rightarrow q\overline{q}$ continuum background using data samples collected just below $B\overline{B}$ threshold. The continuum-subtracted spectrum is fitted to a combination of a model $\overline{B} \rightarrow X_u \ell \overline{\nu}_\ell$ spectrum and several components ($D\ell\overline{\nu}_\ell$, $D^*\ell\overline{\nu}_\ell$, ...) of the $\overline{B} \rightarrow X_c \ell \overline{\nu}_\ell$ background. The resulting partial branching fractions for various E_e cuts are given in Table 1. The leading uncertainty at the lower lepton momentum cuts comes from the $\overline{B} \rightarrow X_c \ell \overline{\nu}_\ell$ background. Prospects for further reducing the lepton momentum cut are improving in light of better knowledge of the semileptonic decays to higher mass $X_c \ell \overline{\nu}$ states [22,23]. The determination of $|V_{ub}|$ from these measurements is discussed below.

An untagged “neutrino reconstruction” measurement [101] from BaBar uses a combination [102] of a high-energy electron, with a measurement of the missing momentum vector. This allows a much higher S/B ~ 0.7 at the same E_e cut and a $\mathcal{O}(5\%)$ selection efficiency, but at the cost of a smaller accepted phase space for $\overline{B} \rightarrow X_u \ell \overline{\nu}_\ell$ decays and uncertainties associated with the determination of the missing momentum. A control sample of $\Upsilon(4S) \rightarrow B\overline{B}$ decays where one B is reconstructed as $\overline{B} \rightarrow D^0(X)e\overline{\nu}$ with $D^0 \rightarrow K^-\pi^+$ is used to reduce uncertainties from detector and background modeling. The partial branching fraction and $|V_{ub}|$ are given in Table 1.

The large samples accumulated at the B factories allow studies in which one B meson is fully reconstructed and the recoiling B decays semileptonically [103–105]. The experiments can fully reconstruct a “tag” B candidate in about 0.5% (0.3%) of B^+B^- ($B^0\overline{B}^0$) events. An electron or muon with center-of-mass momentum above 1.0 GeV is required amongst the charged tracks not assigned to the tag B , and the remaining particles are assigned to the X_u system. The full set of kinematic properties (E_ℓ , M_X , q^2 , etc.) are available for studying the semileptonically decaying B , making possible selections that accept up to 70% of the full $\overline{B} \rightarrow X_u \ell \overline{\nu}_\ell$ rate. Despite requirements (e.g., on the square of the missing mass) aimed at rejecting events with additional missing particles, undetected or mis-measured particles from $\overline{B} \rightarrow X_c \ell \overline{\nu}_\ell$ decay

(e.g., K_L^0 and additional neutrinos) remain an important source of uncertainty.

BaBar [103] and Belle [104] have measured partial rates with cuts on M_X , M_X , and q^2 , and P_+ based on large samples of $B\overline{B}$ events. As these are highly correlated measurements, only one from each experiment (namely based on M_X) is used in the average given in Table 1. In each case, the experimental systematics have significant contributions from the modeling of $\overline{B} \rightarrow X_u \ell \overline{\nu}_\ell$ and $\overline{B} \rightarrow X_c \ell \overline{\nu}_\ell$ decays, and from the detector response to charged particles, photons, and neutral hadrons.

An analysis [105] on 80 fb^{-1} that integrates the $\overline{B} \rightarrow X_u \ell \overline{\nu}_\ell$ rate for $M_X < 2.5 \text{ GeV}$, capturing $\sim 96\%$ of the total rate, is noteworthy for the smallness ($< 3\%$) of the theoretical error; however, the statistical uncertainty on $|V_{ub}|$ is 18%, so it would have no impact if included in the current average. More precise measurements of this type would be valuable.

Determination of $|V_{ub}|$

The determination of $|V_{ub}|$ from the measured partial rates requires input from theory. The BLNP, GGOU, and DGE calculations described previously are used to determine $|V_{ub}|$ from all measured partial $\overline{B} \rightarrow X_u \ell \overline{\nu}_\ell$ rates; the values are given in Table 1. The m_b input values used [106] are $m_b^{SF} = 4.71 \pm 0.06 \text{ GeV}$ for BLNP, based on global fits to $\overline{B} \rightarrow X_c \ell \overline{\nu}_\ell$ moments; $m_b^{\text{kin}} = 4.61 \pm 0.03 \text{ GeV}$ for GGOU, based on global fits to $\overline{B} \rightarrow X_c \ell \overline{\nu}_\ell$ and $\overline{B} \rightarrow X_s \gamma$ moments; and $m_b^{MS} = 4.20 \pm 0.07 \text{ GeV}$ for DGE, based on an average of m_b determinations. While these values are compatible within errors, they do not correspond to a unique value when translated to a common scheme; this is further discussed below. An additional error contribution for WA has been added to the DGE error budget.

As an illustration of the relative sizes of the uncertainties entering $|V_{ub}|$, we give the error breakdown for the BLNP average: statistical—2.0%; experimental—2.5%; $\overline{B} \rightarrow X_c \ell \overline{\nu}_\ell$ modeling—1.8%; $\overline{B} \rightarrow X_u \ell \overline{\nu}_\ell$ modeling—1.1%; HQE parameters (including m_b)—6.3%; shape-function parameterization—0.4%; subleading SFs—0.7%; scale matching—3.6%; Weak Annihilation—1.4%. The uncertainty on m_b dominates the uncertainty on $|V_{ub}|$ from HQE parameters.

The statistical correlations amongst the measurements used in the average are tiny (due to small overlaps among signal events and large differences in S/B ratios), and have been ignored in performing the average. Correlated systematic and theoretical errors are taken into account, both within an experiment and between experiments.

The $|V_{ub}|$ values do not show a marked trend versus f_u . The P-values of the averages are around 0.4, suggesting that the ratios of calculated partial widths in the different phase space regions are in reasonable agreement with ratios of measured widths. However, the measured values [103,104] of the ratio $\Gamma(\overline{B} \rightarrow X_u \ell \overline{\nu}_\ell, P_+ < 0.66 \text{ GeV}) / \Gamma(\overline{B} \rightarrow X_u \ell \overline{\nu}_\ell, M_X < 1.7 \text{ GeV}, q^2 > 8 \text{ GeV}^2)$ average† to

† This assumes that the correlation coefficient between the P_+ and M_X - q^2 partial branching fractions found by BaBar, 0.38, also applies to the Belle measurements.

Table 1: $|V_{ub}|$ (in units of 10^{-5}) from inclusive $\bar{B} \rightarrow X_u \ell \bar{\nu}_\ell$ measurements. The first uncertainty on $|V_{ub}|$ is experimental, while the second includes both theoretical ($\sim 4\%$) and HQE parameter uncertainties (the remainder). The values are listed in order of increasing f_u (0.19 to 0.66).

Ref.	BLNP	GGOU	DGE
[98]	$353 \pm 41 \pm 35$	$371 \pm 43 \pm 32$	$386 \pm 45 \pm 28$
[101]	$395 \pm 27 \pm 39$	not avail.	$443 \pm 30 \pm 37$
[100]	$390 \pm 22 \pm 33$	$408 \pm 23 \pm 27$	$430 \pm 29 \pm 25$
[99]	$437 \pm 40 \pm 33$	$456 \pm 42 \pm 26$	$481 \pm 45 \pm 22$
[107]	$398 \pm 42 \pm 32$	$416 \pm 44 \pm 29$	$444 \pm 47 \pm 22$
[103]	$374 \pm 18 \pm 31$	$402 \pm 19 \pm 28$	$456 \pm 22 \pm 30$
[104]	$366 \pm 24 \pm 27$	$389 \pm 26 \pm 22$	$429 \pm 28 \pm 26$
	$399 \pm 14 \pm 30$	$395 \pm 15 \pm 21$	$443 \pm 17 \pm 25$

1.22 ± 0.12 . The theoretical predictions for this ratio are 1.63 [70], 1.18 [86], and 1.58 [87]. This comparison may indicate an underestimate of some theoretical uncertainties.

The BLNP and GGOU averages appear to agree well. However, if the same m_b input is used for BLNP and GGOU, the BLNP average is $\sim 9\%$ higher than the GGOU average. This difference is large compared to the theoretical uncertainties assigned to the calculations, which are 3-4% in each case. Based on this comparison, we choose to add in quadrature an additional uncertainty of 7% to the inclusive $|V_{ub}|$ average.

To quote an inclusive $|V_{ub}|$ value, we take the arithmetic mean of the values in Table 1. The uncertainty is calculated by summing in quadrature the arithmetic mean of the errors in Table 1 (after adjusting them to correspond to $\sigma_{m_b} = 0.06$ GeV), and the aforementioned 7% additional uncertainty. We find

$$|V_{ub}| = (4.12 \pm 0.15_{\text{exp}} \pm 0.40_{\text{th}}) \times 10^{-3}. \quad (33)$$

As was the case with $|V_{cb}|$, it is hard to assign an uncertainty to $|V_{ub}|$ for possible duality violations. However, theoretical arguments suggest that duality should hold even better in $b \rightarrow u \ell \bar{\nu}_\ell$ than in $b \rightarrow c \ell \bar{\nu}_\ell$ [32]. On the other hand, unless duality violations are much larger in $\bar{B} \rightarrow X_u \ell \bar{\nu}_\ell$ decays than in $\bar{B} \rightarrow X_c \ell \bar{\nu}_\ell$ decays, the precision of the $|V_{ub}|$ determination is not yet at the level where duality violations are likely to be significant.

There is another aspect of duality which affects the quoted results. The theoretical expressions are valid at the parton level, and do not incorporate any resonant structure (e.g. $\bar{B} \rightarrow \pi \ell \bar{\nu}_\ell$); this must be added “by hand” to the simulated $\bar{B} \rightarrow X_u \ell \bar{\nu}_\ell$ event samples used to calculate acceptances and efficiencies. The uncertainties corresponding to this procedure have been estimated by the experiments to be at the level of 1-2% on $|V_{ub}|$.

A separate class of analyses follows the strategy discussed in Refs. [80–83], where integrals of differential distributions in

$\bar{B} \rightarrow X_u \ell \bar{\nu}_\ell$ decays are compared with corresponding integrals in $\bar{B} \rightarrow X_s \gamma$ decays to extract $|V_{ub}|$, thereby eliminating the need to model the leading-shape function. A study [108] using the measured BaBar electron spectrum in $\bar{B} \rightarrow X_u \ell \bar{\nu}_\ell$ decays provides $|V_{ub}|$ determinations using all available “SF-free” calculations; the resulting $|V_{ub}|$ values have total uncertainties of $\sim 12\%$, and are fully compatible with the average quoted above.

The BLL [89] calculation can be used for measurements with cuts on M_X and q^2 . Using the HQE parameter input determined from the global fit in the 1S scheme [61] yields a $|V_{ub}|$ value of $(4.83 \pm 0.24 \pm 0.37) \times 10^{-3}$, which is 7–17% higher than the corresponding values obtained from the other calculations.

HQE parameters and shape function input

The global fits to $\bar{B} \rightarrow X_c \ell \bar{\nu}_\ell$ moments discussed earlier provide input values for the heavy quark parameters needed in calculating $\bar{B} \rightarrow X_u \ell \bar{\nu}_\ell$ partial rates. These HQE parameters are also used to constrain the first and second moments of the shape function.

Fig. 2 shows the results of separate fits to moments from semileptonic decays, and those from the $\bar{B} \rightarrow X_s \gamma$ photon energy spectrum. The ellipses correspond to $\Delta\chi^2 = 1$ contours (CL=39%); the probability of having the two ellipses separated by as much or more than the fit results is about 20%. The $\bar{B} \rightarrow X_s \gamma$ moments have some dependence [109] on the model chosen for the shape function, since the experiments require photon energies to exceed cuts in the range 1.8-2.0 GeV. The global fit assumes an uncertainty of 30% on the difference between the calculated moments with a realistic shape function model and those based on the pure OPE calculation.

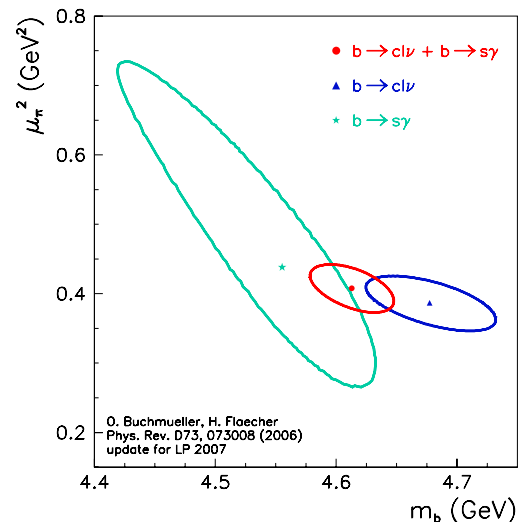


Figure 2: Fit results from global moment fits in the kinetic scheme [58]. The $\Delta\chi^2 = 1$ curves for separate fits to $\bar{B} \rightarrow X_s \gamma$ moments and $\bar{B} \rightarrow X_c \ell \bar{\nu}_\ell$ moments are shown along with the combined fit. Color version at end of book.

Meson Particle Listings

V_{cb} and V_{ub} CKM Matrix Elements

The uncertainty on m_b will continue to be a leading contribution to the uncertainty in $|V_{ub}|$. The determinations of m_b using $\overline{B} \rightarrow X_c \ell \overline{\nu}_\ell$ moments are on solid theoretical ground and are performed using order α_S^2 calculations. Concern has been expressed about the theoretical control of $\mathcal{O}(1/m_b)$ corrections to the $\overline{B} \rightarrow X_s \gamma$ moments. Furthermore, the $|V_{ub}|$ calculations are currently done at $\mathcal{O}(\alpha_S)$, calling into question the use of a very small uncertainty on m_b in the $|V_{ub}|$ determination. Fixed-order translations of m_b from one scheme to another bring in an additional source of uncertainty (see Eq. (27)). In light of these considerations, the m_b used in the $|V_{ub}|$ determination given here has had its error increased to 0.06 GeV.

Status and outlook

At present, as indicated by the average given above, the uncertainty on $|V_{ub}|$ from inclusive decays is at the 10% level. The uncertainty on m_b taken here is 60 MeV, contributing an uncertainty of 7% on $|V_{ub}|$. Prospects are good for reducing this to the 30 MeV level by extending the $|V_{ub}|$ calculations to $\mathcal{O}(\alpha_S^2)$. Further progress can also be expected on some of the other leading sources of uncertainty. The Weak Annihilation contribution is now being addressed with data; further improvement can be expected with the full B factory dataset. The uncertainties on $|V_{ub}|$ quoted in the calculations are at the 4% level, and there is some indication that these may be underestimated. Improving our confidence in, and eventually reducing, these theory uncertainties will require improvements in the calculations. For the approaches making use of the shape function, this amounts to improvements in relating the spectra from $\overline{B} \rightarrow X_u \ell \overline{\nu}_\ell$ and $\overline{B} \rightarrow X_s \gamma$ decays by calculating radiative corrections and the effects of subleading shape functions, while approaches less sensitive to shape functions require calculations of higher-order radiative corrections. Experimental uncertainties will be reduced through higher statistics, a better understanding of $\overline{B} \rightarrow X_c \ell \overline{\nu}_\ell$ decays, and the incorporation of improved measurements on D decays. The two approaches stated earlier, namely determining the shape function from the $\overline{B} \rightarrow X_s \gamma$ photon spectrum, and applying it to $\overline{B} \rightarrow X_u \ell \overline{\nu}_\ell$ decays, and pushing the measurements into regions where shape function and duality uncertainties become negligible, are complementary and should both be pursued.

$|V_{ub}|$ from exclusive decays

Exclusive charmless semileptonic decays offer a complementary means of determining $|V_{ub}|$. For the experiments, the specification of the final state provides better background rejection, but the lower branching fraction reflects itself in lower yields compared with inclusive decays. For theory, the calculation of the form factors for $\overline{B} \rightarrow X_u \ell \overline{\nu}_\ell$ decays is challenging, but brings in a different set of uncertainties from those encountered in inclusive decays. In this review, we focus on $\overline{B} \rightarrow \pi \ell \overline{\nu}_\ell$, as it is the most promising mode for both experiment and theory, and recent improvements have been made in both areas. Measurements of other exclusive states can be found in Refs. [110–113].

$\overline{B} \rightarrow \pi \ell \overline{\nu}_\ell$ form factor calculations

The relevant form factors for the decay $\overline{B} \rightarrow \pi \ell \overline{\nu}_\ell$ are usually defined as

$$\langle \pi(p_\pi) | V^\mu | B(p_B) \rangle = \quad (34)$$

$$f_+(q^2) \left[p_B^\mu + p_\pi^\mu - \frac{m_B^2 - m_\pi^2}{q^2} q^\mu \right] + f_0(q^2) \frac{m_B^2 - m_\pi^2}{q^2} q^\mu,$$

in terms of which the rate becomes (in the limit $m_\ell \rightarrow 0$)

$$\frac{d\Gamma}{dq^2} = \frac{G_F^2 |V_{ub}|^2}{24\pi^3} |p_\pi|^3 |f_+(q^2)|^2, \quad (35)$$

where p_π is the momentum of pion in the B meson rest frame.

Currently-available non-perturbative methods for the calculation of the form factors include lattice QCD and light-cone sum rules. The two methods are complementary in phase space, since the lattice calculation is restricted to the kinematical range of high momentum transfer q^2 to the leptons, due to large discretization errors, while light-cone sum rules provide information near $q^2 = 0$. Interpolations between these two regions may be constrained by unitarity and analyticity.

Unquenched simulations, for which quark loop effects in the QCD vacuum are fully incorporated, have become quite common, and the first results based on these simulations for the $\overline{B} \rightarrow \pi \ell \overline{\nu}_\ell$ form factors have been obtained recently by the Fermilab/MILC collaboration [25] and the HPQCD collaboration [114].

The two calculations differ in the way the b quark is simulated, with HPQCD using nonrelativistic QCD, and Fermilab/MILC the so-called Fermilab heavy quark method; they agree within the quoted errors.

In order to obtain the partially-integrated differential rate, the BK parameterization [115]

$$f_+(q^2) = \frac{c_B(1 - \alpha_B)}{(1 - \tilde{q}^2)(1 - \alpha_B \tilde{q}^2)}, \quad (36)$$

$$f_0(q^2) = \frac{c_B(1 - \alpha_B)}{(1 - \tilde{q}^2/\beta_B)}, \quad (37)$$

with $\tilde{q}^2 \equiv q^2/m_{B^*}^2$ is used to extrapolate to small values of q^2 . It includes the leading pole contribution from B^* , and higher poles are modeled by a single pole. The heavy-quark scaling is satisfied if the parameters c_B , α_B , and β_B scale appropriately. However, the BK parameterization should be used with some caution, since it is not consistent with SCET [116]. Alternatively, one may use analyticity and unitarity bounds to constrain the form factors. Making use of the heavy quark limit, stringent constraints on the shape of the form factor can be derived [117], and the conformal mapping of the kinematical variables onto the complex unit disc yields a rapidly converging series in this variable. The use of lattice data in combination with a data point at small q^2 from SCET or sum rules provides a stringent constraint on the shape of the form factor [118].

The results for the integrated rate with $q^2 > q_{\text{cut}}^2 = 16\text{GeV}^2$ are

$$\begin{aligned} \Gamma &= |V_{ub}|^2 \times (2.07 \pm 0.57) \text{ ps}^{-1}, & \text{HPQCD;} \\ &= |V_{ub}|^2 \times (1.83 \pm 0.50) \text{ ps}^{-1}, & \text{Fermilab/MILC.} \end{aligned}$$

Here the statistical and systematic errors are added in quadrature.

Much work remains to be done, since the current combined statistical plus systematic errors in the lattice results are still at the 10-14% level on $|V_{ub}|$, and need to be reduced. Reduction of errors to the 5 ~ 6% level for $|V_{ub}|$ may be feasible within the next few years, although that could involve carrying out a two-loop (or fully non-perturbative) matching between lattice and continuum QCD heavy-to-light current operators, and/or going to smaller lattice spacing.

Another established non-perturbative approach to obtain the form factors is through Light-Cone QCD Sum Rules (LCSR), where the heavy mass limit has been discussed from the point of view of SCET in [119]. The sum-rule approach provides an approximation for the product $f_B f_+(q^2)$, valid in the region $0 < q^2 < \sim 14 \text{ GeV}^2$. The determination of $f_+(q^2)$ itself requires knowledge of the decay constant f_B , which usually is obtained by replacing f_B by its two-point QCD (SVZ) sum rule [120] in terms of perturbative and condensate contributions. The advantage of this procedure is the approximate cancellation of various theoretical uncertainties in the ratio $(f_B f_+)/f_B$. The LCSR for $f_B f_+$ is based on the light-cone OPE of the relevant vacuum-to-pion correlation function, calculated in full QCD at finite b -quark mass. The resulting expressions actually comprise a triple expansion: in the twist t of the operators near the light-cone, in α_s , and in the deviation of the pion distribution amplitudes from their asymptotic form, which is fixed from conformal symmetry.

There are multiple sources of uncertainties in the LCQCD calculation, which are discussed in Refs. [121,122]. The total uncertainty adds up to about 15%, resulting in the LCQCD prediction

$$f_+(0) = 0.26 \pm 0.04, \quad (38)$$

which is consistent with the values quoted in Refs. [121] and [122]. It is interesting to note that the results from the LQCD and LCSR are consistent with each other when the BK parameterization is used to relate them. This increases confidence in the theoretical predictions for the rate of $\overline{B} \rightarrow \pi \ell \overline{\nu}_\ell$.

LC-sum rules are valid in the kinematic region of small q^2 , and thus can be used to obtain an estimate of the q^2 dependence in a region $q^2 \leq 14 \text{ GeV}^2$ [123]. This is complementary to the lattice results at large values of q^2 , and the results from LCQCD smoothly extrapolate the lattice data to small values of q^2 .

An alternative determination of $|V_{ub}|$ has been proposed by several authors [124–125]. It is based on a model-independent relation between rare decays such as $\overline{B} \rightarrow K^* \ell^+ \ell^-$ and $\overline{B} \rightarrow \rho \ell \overline{\nu}_\ell$, which can be obtained at large momentum transfer q to the leptons. This method is based on the HQET relations between the matrix elements of the $B \rightarrow K^*$ and the $B \rightarrow \rho$ transitions, and a systematic, OPE-based expansion in powers of m_c^2/q^2 and Λ_{QCD}/q . The theoretical uncertainty is claimed

to be of the order of 5% for $|V_{ub}|$; however, it requires a precise measurement of the exclusive rare decay $\overline{B} \rightarrow K^* \ell^+ \ell^-$, which is a task for future ultra-high-rate experiments.

$\overline{B} \rightarrow \pi \ell \overline{\nu}_\ell$ measurements

The $\overline{B} \rightarrow \pi \ell \overline{\nu}_\ell$ measurements fall into two broad classes: untagged, in which case the reconstruction of the missing momentum of the event serves as an estimator for the unseen neutrino, and tagged, in which the second B meson in the event is fully reconstructed in either a hadronic or semileptonic decay mode. The tagged measurements have high and uniform acceptance, S/B as high as 10, but low statistics. The untagged measurements have somewhat higher background levels (S/B \leq 1) and make slightly more restrictive kinematic cuts, but have adequate statistics to measure the q^2 dependence of the form factor.

Table 2: Total and partial branching fractions for $\overline{B}^0 \rightarrow \pi^+ \ell^- \overline{\nu}_\ell$. The uncertainties are from statistics and systematics. Measurements of $\mathcal{B}(B^- \rightarrow \pi^0 \ell^- \overline{\nu}_\ell)$ have been multiplied by a factor $2\tau_{B^0}/\tau_{B^+}$ to obtain the values below.

	$\mathcal{B} \times 10^4$	$\mathcal{B}(q^2 > 16) \times 10^4$
CLEO π^+, π^0 [112]	$1.37 \pm 0.15 \pm 0.11$	$0.41 \pm 0.08 \pm 0.04$
BaBar π^+, π^0 [126]	$1.46 \pm 0.07 \pm 0.08$	$0.38 \pm 0.04 \pm 0.03$
Belle SL π^+ [127]	$1.38 \pm 0.19 \pm 0.14$	$0.36 \pm 0.10 \pm 0.04$
Belle SL π^0 [127]	$1.43 \pm 0.26 \pm 0.16$	$0.37 \pm 0.15 \pm 0.04$
Belle had π^+ [128]	$1.49 \pm 0.26 \pm 0.06$	NA
Belle had π^0 [128]	$1.60 \pm 0.32 \pm 0.11$	NA
BaBar SL π^+ [129]	$1.12 \pm 0.25 \pm 0.10$	$0.29 \pm 0.15 \pm 0.04$
BaBar SL π^0 [129]	$1.36 \pm 0.33 \pm 0.15$	$0.19 \pm 0.22 \pm 0.07$
BaBar had π^+ [129]	$1.07 \pm 0.27 \pm 0.15$	$0.65 \pm 0.20 \pm 0.13$
BaBar had π^0 [129]	$1.52 \pm 0.41 \pm 0.20$	$0.48 \pm 0.22 \pm 0.11$
Average	$1.39 \pm 0.06 \pm 0.06$	$0.35 \pm 0.03 \pm 0.03$

CLEO has analyzed $\overline{B} \rightarrow \pi \ell \overline{\nu}_\ell$ and $\overline{B} \rightarrow \rho \ell \overline{\nu}_\ell$ using an untagged analysis [112]. Similar analyses have been done by BaBar [113,126]. The leading systematic uncertainties in the untagged $\overline{B} \rightarrow \pi \ell \overline{\nu}_\ell$ analyses are associated with modeling the missing momentum reconstruction, with backgrounds from $\overline{B} \rightarrow X_c \ell \overline{\nu}_\ell$ and $\overline{B} \rightarrow X_u \ell \overline{\nu}_\ell$ decays, and with varying the form factor for the $\overline{B} \rightarrow \rho \ell \overline{\nu}_\ell$ decay. The values obtained for the full and partial branching fractions are listed in Table 2 above the horizontal line.

BaBar has recently measured the differential $\overline{B} \rightarrow \pi \ell \overline{\nu}_\ell$ rate versus q^2 with good accuracy [126]. A fit using the BK parameterization [115] gives $\alpha = 0.52 \pm 0.05 \pm 0.03$ with $P(\chi^2) = 65\%$. The q^2 spectrum, shown in Fig. 3, is compatible with the shapes expected from both LCSR and LQCD calculations, but is incompatible ($P(\chi^2) = 0.06\%$) with the ISGW2 [130] model.

Meson Particle Listings

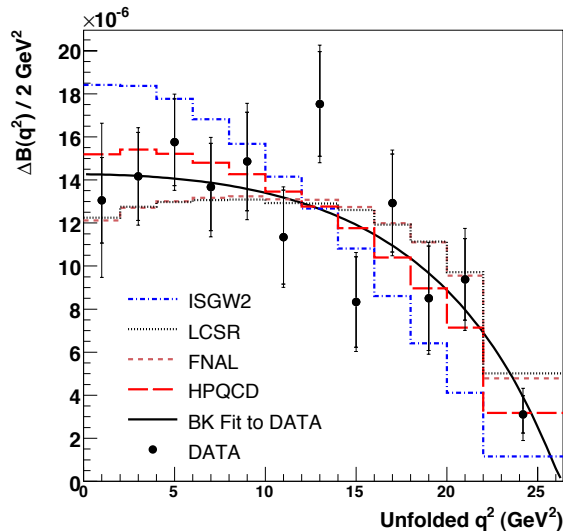
 V_{cb} and V_{ub} CKM Matrix Elements

Figure 3: The differential branching fraction versus q^2 from BaBar [126] with several theoretical predictions overlaid. Color version at end of book.

Belle [127] and BaBar [129] have performed analyses based on reconstructing a B in the $\overline{D}^{(*)}\ell^+\nu_\ell$ decay mode, and looking for a $\overline{B} \rightarrow \pi\ell\overline{\nu}_\ell$ or $\overline{B} \rightarrow \rho\ell\overline{\nu}_\ell$ decay amongst the remaining particles in the event. The fact that the B and \overline{B} are back-to-back in the $\Upsilon(4S)$ frame is used to construct a discriminating variable and obtain a signal-to-noise ratio above unity for all q^2 bins. A related technique was discussed in Ref. 131. BaBar [129] and Belle [128] have also used their samples of B mesons reconstructed in hadronic decay modes to measure exclusive charmless semileptonic decays giving very clean but low-yield samples. The resulting full and partial branching fractions are given in Table 2. The average of the tagged analyses provides an accuracy on the $\overline{B} \rightarrow \pi\ell\overline{\nu}_\ell$ branching fraction comparable to that obtained with untagged analyses.

The outlook for further improvements in these measurements with larger B-factory data samples is good. The tagged measurements in particular will improve; the current estimates of systematic uncertainties in these measurements have a significant statistical component, so the total experimental uncertainty should fall as $1/\sqrt{N}$.

$|V_{ub}|$ can be obtained from the average $\overline{B} \rightarrow \pi\ell\overline{\nu}_\ell$ branching fraction and the measured q^2 spectrum. Fits to the measured q^2 spectrum from Ref. 126 using a theoretically motivated parameterization (*e.g.*, from Ref. 9) remove most of the model dependence from theoretical uncertainties in the shape of the spectrum. This allows a good determination [132] of the product

$$|V_{ub}|f_+(0) = (9.1 \pm 0.3 \pm 0.6) \times 10^{-4}, \quad (39)$$

where the first error is from the uncertainty on $\mathcal{B}(\overline{B} \rightarrow \pi\ell\overline{\nu}_\ell)$, and the second from the parameterization of shape versus q^2 . Having the shape of the form factor versus q^2 allows

determinations of the normalization at any q^2 value to be used. Several determinations of $|V_{ub}|$ are given in Table 3, where the LQCD results have been expressed as $f_+(0)$ using the aforementioned fit to the measured q^2 spectrum. Based on these values we pick

$$|V_{ub}| = (3.5^{+0.6}_{-0.5}) \times 10^{-3}. \quad (40)$$

The uncertainty is dominated by the form factor normalization, the calculations of which were discussed previously.

Table 3: Determinations of $|V_{ub}|$ based on $\overline{B} \rightarrow \pi\ell\overline{\nu}_\ell$ decays. The first error on $|V_{ub}|$ is due to the uncertainty on $|V_{ub}|f_+(0)$ and the second error comes from uncertainty on $f_+(0)$.

Method	$f_+(0)$	$ V_{ub} \times (10^{-3})$
LCSR (Eq. (38))	0.26 ± 0.04	$3.5 \pm 0.3^{+0.6}_{-0.5}$
LQCD(FNAL) [25]	0.25 ± 0.03	$3.6 \pm 0.3^{+0.5}_{-0.4}$
LQCD(HPQCD) [114]	0.27 ± 0.03	$3.3 \pm 0.3^{+0.4}_{-0.3}$

Conclusion

The study of semileptonic B meson decays continues to be an active area for both theory and experiment. Substantial progress has been made in the application of HQE calculations to inclusive decays, with fits to moments of $\overline{B} \rightarrow X_c\ell\overline{\nu}_\ell$ and $B \rightarrow X_s\gamma$ decays providing precise values for $|V_{cb}|$ and m_b . However, the tension between the inclusive and exclusive $|V_{cb}|$ values highlights the need for further work.

Measurements of inclusive $\overline{B} \rightarrow X_u\ell\overline{\nu}_\ell$ decays have improved, and additional theoretical treatments and improved knowledge of m_b have strengthened our determination of $|V_{ub}|$. Further progress in these areas is possible, but will require higher-order radiative corrections from the theory and, in the case of $|V_{ub}|$, improved experimental knowledge of the $\overline{B} \rightarrow X_c\ell\overline{\nu}_\ell$ background. While there has been impressive progress in the past few years, new challenges will need to be overcome to achieve a precision below 5% on $|V_{ub}|$ from inclusive decays.

Progress in both $b \rightarrow u$ and $b \rightarrow c$ exclusive channels depends crucially on progress in lattice calculations. Here the prospects are good (*see, e.g.*, Ref. 133), since unquenched lattice simulations are now possible, although the ultimate attainable precision is hard to estimate.

The measurements of $\overline{B} \rightarrow \pi\ell\overline{\nu}_\ell$ have improved significantly, including the first reasonably precise determination of the q^2 dependence. The experimental input will continue to improve as B-factory data sets increase. Reducing the theoretical uncertainties to a comparable level will require significant effort, but is clearly vital in order to compare the extracted $|V_{ub}|$ with the one obtained from inclusive decays.

Both $|V_{cb}|$ and $|V_{ub}|$ are indispensable inputs into unitarity triangle fits. In particular, knowing $|V_{ub}|$ with a precision of better than 10% allows a test of CKM unitarity in the most

direct way, by comparing the length of the $|V_{ub}|$ side of the unitarity triangle with the measurement of $\sin(2\beta)$. This comparison of a “tree” process ($b \rightarrow u$) with a “loop-induced” process ($B^0 - \bar{B}^0$ mixing) provides sensitivity to possible contributions from new physics. While the effort required to further improve our knowledge of these CKM matrix elements is large, it is well motivated.

The authors would like to acknowledge helpful discussions with C. Schwanda, E. Barberio, F. Di Lodovico, V. Luth, A. Hoang, and I. I. Bigi.

References

1. R. Kowalewski and T. Mannel, *J. Phys.* **G33**, 1 (2006).
2. E. Barberio *et al.*, [arXiv:0704.3575](#).
3. N. Isgur and M.B. Wise, *Phys. Lett.* **B232**, 113 (1989); *ibid.*, **B237**, 527 (1990).
4. M.A. Shifman and M.B. Voloshin, *Sov. J. Nucl. Phys.* **47**, 511 (1988) [*Yad. Fiz.* **47**, 801 (1988)].
5. M.E. Luke, *Phys. Lett.* **B252**, 447 (1990).
6. M. Ademollo and R. Gatto, *Phys. Rev. Lett.* **13**, 264 (1964).
7. A.V. Manohar and M.B. Wise, *Camb. Monogr. Part. Phys. Nucl. Phys. Cosmol.* **10**, 1 (2000).
8. B. Grinstein, *Nucl. Phys.* **B339**, 253 (1990); H. Georgi, *Phys. Lett.* **B240**, 447 (1990); A.F. Falk *et al.*, *Nucl. Phys.* **B343**, 1 (1990); E. Eichten and B. Hill, *Phys. Lett.* **B234**, 511 (1990).
9. C.G. Boyd, B. Grinstein, and R.F. Lebed, *Phys. Rev.* **D56**, 6895 (1997); *ibid.*, *Phys. Rev. Lett.* **74**, 4603 (1995); C.G. Boyd and M.J. Savage, *Phys. Rev.* **D56**, 303 (1997).
10. I. Caprini *et al.*, *Nucl. Phys.* **B530**, 153 (1998).
11. A. Sirlin, *Nucl. Phys.* **B196**, 83 (1982).
12. A. Czarnecki and K. Melnikov, *Nucl. Phys.* **B505**, 65 (1997).
13. J. Laiho *et al.*, [arXiv:0710.1111](#); S. Hashimoto *et al.*, *Phys. Rev.* **D66**, 014503 (2002).
14. D. Buskulic *et al.* (ALEPH Collab.), *Phys. Lett.* **B395**, 373 (1997).
15. G. Abbiendi *et al.* (OPAL Collab.), *Phys. Lett.* **B482**, 15 (2000).
16. P. Abreu *et al.* (DELPHI Collab.), *Phys. Lett.* **B510**, 55 (2001).
17. J. Abdallah *et al.* (DELPHI Collab.), *Eur. Phys. J.* **C33**, 213 (2004).
18. N.E. Adam *et al.* (CLEO Collab.), *Phys. Rev.* **D67**, 032001 (2003).
19. B. Aubert *et al.* (BaBar Collab.), *Phys. Rev.* **D71**, 051502 (2005); updated in [arXiv:0705.4008](#).
20. B. Aubert *et al.* (BaBar Collab.), *Phys. Rev.* **D74**, 092004 (2006); updated in [arXiv:0705.4008](#).
21. B. Aubert *et al.* (BaBar Collab.), [arXiv:0707.2655](#).
22. B. Aubert *et al.* (BaBar Collab.), *Phys. Rev.* **D76**, 051101 (2007); updated in [arXiv:0708.1738](#).
23. D. Liventsev *et al.* (Belle Collab.), *Phys. Rev.* **D72**, 051109 (2005); updated in [arXiv:0711.3252](#).
24. N. Uraltsev, *Phys. Lett.* **B585**, 253 (2004).
25. M. Okamoto *et al.* *Nucl. Phys. (Proc. Supp.)* **B140**, 461 (2005). A. Kronfeld, talk presented at the workshop CKM05, San Diego, CA - Workshop on the Unitarity Triangle, 15-18 March 2005.
26. J.E. Bartelt *et al.* (CLEO Collab.), *Phys. Rev. Lett.* **82**, 3746 (1999).
27. K. Abe *et al.* (Belle Collab.), *Phys. Lett.* **B526**, 247 (2002).
28. S. Hashimoto *et al.*, *Phys. Rev.* **D61**, 014502 (2000).
29. G.M. de Divitiis, R. Petronzio, and N. Tantalo, *JHEP* **0710**, 062 (2007).
30. A.V. Manohar and M.B. Wise, *Phys. Rev.* **D49**, 1310 (1994).
31. I.I.Y. Bigi *et al.*, *Phys. Rev. Lett.* **71**, 496 (1993), *Phys. Lett.* **B323**, 408 (1994).
32. M.A. Shifman, [hep-ph/0009131](#), I.I.Y. Bigi and N. Uraltsev, *Int. J. Mod. Phys.* **A16**, 5201 (2001).
33. D. Benson *et al.*, *Nucl. Phys.* **B665**, 367 (2003).
34. M. Gremm and A. Kapustin, *Phys. Rev.* **D55**, 6924 (1997).
35. B.M. Dassingier, T. Mannel, and S. Turczyk, *JHEP* **0703**, 087 (2007).
36. I.I. Bigi, N. Uraltsev, and R. Zwicky, *Eur. Phys. J.* **C50**, 539 (2007).
37. P. Gambino and N. Uraltsev, *Eur. Phys. J.* **C34**, 181 (2004).
38. T. Becher, H. Boos, and E. Lunghi, [arXiv:0708.0855](#).
39. I.I.Y. Bigi *et al.*, *Phys. Rev.* **D56**, 4017 (1997).
40. I.I.Y. Bigi *et al.*, *Phys. Rev.* **D52**, 196 (1995).
41. A.H. Hoang *et al.*, *Phys. Rev.* **D59**, 074017 (1999).
42. H. Jautwyler, *Phys. Lett.* **B98**, 447 (1981); M.B. Voloshin, *Sov. J. Nucl. Phys.* **36**, 143 (1982).
43. C.W. Bauer *et al.*, *Phys. Rev.* **D70**, 094017 (2004).
44. S.E. Csorna *et al.* (CLEO Collab.), *Phys. Rev.* **D70**, 032002 (2004).
45. A.H. Mahmood *et al.* (CLEO Collab.), *Phys. Rev.* **D70**, 032003 (2004).
46. B. Aubert *et al.* (BaBar Collab.), *Phys. Rev.* **D69**, 111103 (2004); updated in [arXiv:0707.2670](#).
47. B. Aubert *et al.* (BaBar Collab.), *Phys. Rev.* **D69**, 111104 (2004).
48. C. Schwanda *et al.* (Belle Collab.), *Phys. Rev.* **D75**, 032005 (2007).
49. P. Urquijo *et al.* (Belle Collab.), *Phys. Rev.* **D75**, 032001 (2007).
50. J. Abdallah *et al.* (DELPHI Collab.), *Eur. Phys. J.* **C45**, 35 (2006).
51. D. Acosta *et al.* (CDF Collab.), *Phys. Rev.* **D71**, 051103 (2005).
52. P. Koppenburg *et al.* (Belle Collab.), *Phys. Rev. Lett.* **93**, 061803 (2004); K. Abe *et al.* (Belle Collab.), [hep-ex/0508005](#).
53. B. Aubert *et al.* (BaBar Collab.), *Phys. Rev.* **D72**, 052004 (2005).
54. B. Aubert *et al.* (BaBar Collab.), [hep-ex/0507001](#).
55. S. Chen *et al.* (CLEO Collab.), *Phys. Rev. Lett.* **87**, 251807 (2001).
56. M. Battaglia *et al.*, *Phys. Lett.* **B556**, 41 (2003).
57. B. Aubert *et al.* (BaBar Collab.), *Phys. Rev. Lett.* **93**, 011803 (2004).

Meson Particle Listings

 V_{cb} and V_{ub} CKM Matrix Elements

58. O. Buchmüller and H. Flächer, [hep-ph/0507253](http://www.slac.stanford.edu/xorg/hfag/semi/LP07/gbl_fits/kinetic/lp07-update.pdf); updated in http://www.slac.stanford.edu/xorg/hfag/semi/LP07/gbl_fits/kinetic/lp07-update.pdf.
59. C.W. Bauer *et al.*, Phys. Rev. **D70**, 094017 (2004).
60. K. Abe *et al.* (Belle Collab.), [hep-ex/0611047](http://arxiv.org/abs/hep-ex/0611047).
61. See http://www.slac.stanford.edu/xorg/hfag2/semi/LP07gbl_fits/1S/index.html.
62. A. H. Hoang, Phys. Rev. **D61**, 034005 (2000), updated in [hep-ph/0008102](http://arxiv.org/abs/hep-ph/0008102).
63. K. Melnikov and A. Yelkhovsky, Phys. Rev. **D59**, 114009 (1999).
64. M. Neubert, [arXiv:0801.0675](http://arxiv.org/abs/0801.0675).
65. M. Neubert, [hep-ph/0506245](http://arxiv.org/abs/hep-ph/0506245).
66. A. H. Hoang *et al.*, Phys. Rev. **D59**, 074017 (1999).
67. N. Uraltsev, Int. J. Mod. Phys. **A14**, 4641 (1999).
68. M. Neubert, Phys. Rev. **D49**, 4623 (1994); *ibid.*, **D49**, 3392 (1994).
69. I. Bigi *et al.*, Int. J. Mod. Phys. **A9**, 2467 (1994).
70. B.O. Lange, M. Neubert, and G. Paz, Phys. Rev. **D72**, 073006 (2005).
71. C. W. Bauer *et al.*, Phys. Lett. **B543**, 261 (2002).
72. T. Mannel and S. Recksiegel, Phys. Rev. **D60**, 114040 (1999).
73. C.W. Bauer, Z. Ligeti, and M. E. Luke, Phys. Rev. **D64**, 113004 (2001).
74. C.W. Bauer *et al.*, Phys. Rev. **D68**, 094001 (2003).
75. S.W. Bosch *et al.*, JHEP **0411**, 073 (2004).
76. A.W. Leibovich *et al.*, Phys. Lett. **B539**, 242 (2002).
77. M. Neubert, Phys. Lett. **B543**, 269 (2002).
78. K.S.M. Lee and I.W. Stewart, Nucl. Phys. **B721**, 325 (2005).
79. M. Beneke *et al.*, JHEP **0506**, 071 (2005).
80. M. Neubert, Phys. Lett. **B513**, 88 (2001); Phys. Lett. **B543**, 269 (2002).
81. A.K. Leibovich *et al.*, Phys. Rev. **D61**, 053006 (2000); **D62**, 014010 (2000); Phys. Lett. **B486**, 86 (2000); **B513**, 83 (2001).
82. A.H. Hoang *et al.*, Phys. Rev. **D71**, 093007 (2005).
83. B. Lange *et al.*, JHEP **0510**, 084 (2005); B. Lange, JHEP **0601**, 104 (2006).
84. M. Neubert, Phys. Lett. **B612**, 13 (2005).
85. P. Gambino *et al.*, [hep-ph/0505091](http://arxiv.org/abs/hep-ph/0505091).
86. P. Gambino *et al.*, JHEP **0710**, 058 (2007).
87. J.R.Andersen and E. Gardi, JHEP **0601**, 097 (2006).
88. U. Aglietti *et al.*, [arXiv:0711.0860](http://arxiv.org/abs/0711.0860).
89. C.W. Bauer *et al.*, Phys. Rev. **D64**, 113004 (2001); Phys. Lett. **B479**, 395 (2000).
90. I.I.Y. Bigi and N.G. Uraltsev, Nucl. Phys. **B423**, 33 (1994).
91. M.B. Voloshin, Phys. Lett. **B515**, 74 (2001).
92. J.L. Rosner *et al.* (CLEO Collab.), Phys. Rev. Lett. **96**, 121801 (2006).
93. B. Aubert *et al.* (BaBar Collab.), [arXiv:0708.1753](http://arxiv.org/abs/0708.1753).
94. R. Barate *et al.* (ALEPH Collab.), Eur. Phys. J. **C6**, 555 (1999).
95. M. Acciarri *et al.* (L3 Collab.), Phys. Lett. **B436**, 174 (1998).
96. G. Abbiendi *et al.* (OPAL Collab.), Eur. Phys. J. **C21**, 399 (2001).
97. P. Abreu *et al.* (DELPHI Collab.), Phys. Lett. **B478**, 14 (2000).
98. A. Bornheim *et al.* (CLEO Collab.), Phys. Rev. Lett. **88**, 231803 (2002).
99. A. Limosani *et al.* (Belle Collab.), Phys. Lett. **B621**, 28 (2005).
100. B. Aubert *et al.* (BaBar Collab.), Phys. Rev. **D73**, 012006 (2006).
101. B. Aubert *et al.* (BaBar Collab.), Phys. Rev. Lett. **95**, 111801 (2005), Erratum-*ibid.* **97**, 019903(E) (2006).
102. R. Kowalewski and S. Menke, Phys. Lett. **B541**, 29 (2002).
103. B. Aubert *et al.* (BaBar Collab.), Phys. Rev. Lett. **92**, 071802 (2004), updated in [arXiv:0708.3702](http://arxiv.org/abs/0708.3702).
104. I. Bizjak *et al.* (Belle Collab.), Phys. Rev. Lett. **95**, 241801 (2005).
105. B. Aubert *et al.* (BaBar Collab.), Phys. Rev. Lett. **96**, 221801 (2006).
106. See <http://www.slac.stanford.edu/xorg/hfag2/semi/LP07/home.shtml>.
107. H. Kakuno *et al.* (Belle Collab.), Phys. Rev. Lett. **92**, 101801 (2004).
108. V. Golubev, Y. Skovpen, and V. Luth, Phys. Rev. **D76**, 114003 (2007).
109. D. Benson *et al.*, Nucl. Phys. **B710**, 371 (2005).
110. B. Aubert *et al.* (BaBar Collab.), Phys. Rev. Lett. **90**, 181801 (2003).
111. C. Schwanda *et al.* (Belle Collab.), Phys. Rev. Lett. **93**, 131803 (2004).
112. N.E. Adam *et al.* (CLEO Collab.), Phys. Rev. Lett. **99**, 041802 (2007); Phys. Rev. **D76**, 012007 (2007); supercedes Phys. Rev. **D68**, 072003 (2003).
113. B. Aubert *et al.* (BaBar Collab.), Phys. Rev. **D72**, 051102 (2005).
114. E. Dalgic *et al.* (HPQCD), Phys. Rev. **D73**, 074502 (2006), Erratum-*ibid.*, **D75** 119906, 2007.
115. D. Becirevic and A.B. Kaidalov, Phys. Lett. **B478**, 417 (2000).
116. T. Becher and R.J. Hill, [hep-ph/0509090](http://arxiv.org/abs/hep-ph/0509090).
117. T. Becher and R.J. Hill, Phys. Lett. **B633**, 61 (2006).
118. M.C. Arnesen *et al.*, Phys. Rev. Lett. **95**, 071802 (2005).
119. T. Hurth *et al.*, [hep-ph/0509167](http://arxiv.org/abs/hep-ph/0509167).
120. M.A. Shifman, A.I. Vainshtein, and V.I. Zakharov, Nucl. Phys. **B147**, 385 (1979); *ibid.*, **B147**, 448 (1979).
121. P. Ball and R. Zwicky, Phys. Rev. **D71**, 014015 (2005).
122. G. Duplancic *et al.*, SI-HEP2007-17.
123. P. Ball and R. Zwicky, Phys. Rev. **D71**, 014015 (2005).
124. N. Isgur and M.B. Wise, Phys. Rev. **D42**, 2388 (1990).
125. B. Grinstein and D. Pirjol, Phys. Rev. **D70**, 114005 (2004).
126. B. Aubert *et al.* (BaBar Collab.), Phys. Rev. Lett. **98**, 091801 (2007).
127. K. Abe *et al.* (Belle Collab.), Phys. Lett. **B648**, 139 (2007).
128. K. Abe *et al.* (Belle Collab.), [hep-ex/0610054](http://arxiv.org/abs/hep-ex/0610054).
129. B. Aubert *et al.* (BaBar Collab.), Phys. Rev. Lett. **97**, 211801 (2006).

130. D. Scora and N. Isgur, Phys. Rev. **D52**, 2783 (1995).
 131. W. Brower and H. Paar, Nucl. Instrum. Methods **A421**, 411 (1999).
 132. P. Ball, arXiv:0705.2290; J.M. Flynn and J. Nieves, Phys. Lett. **B649**, 269 (2007); T. Becher and R.J. Hill, Phys. Lett. **B633**, 61 (2006); M. Arnesen *et al.*, Phys. Rev. Lett. **95**, 071802 (2005).
 133. C.T.H. Davies *et al.* (HPQCD, MILC, and Fermilab Lattice Collab.), Phys. Rev. Lett. **92**, 022001 (2004).

 V_{cb} MEASUREMENTS

For the discussion of V_{cb} measurements, which is not repeated here, see the review on "Determination of $|V_{cb}|$ and $|V_{ub}|$."

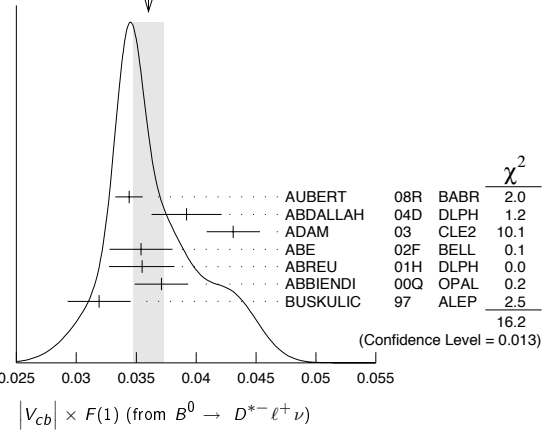
The CKM matrix element $|V_{cb}|$ can be determined by studying the rate of the semileptonic decay $B \rightarrow D^{(*)} \ell \nu$ as a function of the recoil kinematics of $D^{(*)}$ mesons. Taking advantage of theoretical constraints on the normalization and a linear ω dependence of the form factors provided by Heavy Quark Effective Theory (HQET), the $|V_{cb}| \times F(\omega)$ and ρ^2 (a^2) can be simultaneously extracted from data, where ω is the scalar product of the two-meson four velocities, $F(1)$ is the form factor at zero recoil ($\omega=1$) and ρ^2 is the slope, sometimes denoted as a^2 . Using the theoretical input of $F(1)$, a value of $|V_{cb}|$ can be obtained.

"OUR EVALUATION" is an average using rescaled values of the data listed below. The average and rescaling were performed by the Heavy Flavor Averaging Group (HFAG) and are described at <http://www.slac.stanford.edu/xorg/hfag/>. The averaging/rescaling procedure takes into account correlations between the measurements.

 $|V_{cb}| \times F(1)$ (from $B^0 \rightarrow D^{*-} \ell^+ \nu$)

VALUE	DOCUMENT ID	TECN	COMMENT
0.03618 ± 0.00055 OUR EVALUATION	with $\rho^2=1.17 \pm 0.05$ and a correlation 0.24. The fitted χ^2 is 33.9 for 17 degrees of freedom.		
0.0360 ± 0.0013 OUR AVERAGE	Error includes scale factor of 1.6. See the ideogram below.		
0.0344 ± 0.0003 ± 0.0011	1 AUBERT	08R BABR	$e^+ e^- \rightarrow \Upsilon(4S)$
0.0392 ± 0.0018 ± 0.0023	2 ABDALLAH	04D DLPH	$e^+ e^- \rightarrow Z^0$
0.0431 ± 0.0013 ± 0.0018	3 ADAM	03 CLE2	$e^+ e^- \rightarrow \Upsilon(4S)$
0.0354 ± 0.0019 ± 0.0018	4 ABE	02F BELL	$e^+ e^- \rightarrow \Upsilon(4S)$
0.0355 ± 0.0014 $^{+0.0023}_{-0.0024}$	5 ABREU	01H DLPH	$e^+ e^- \rightarrow Z$
0.0371 ± 0.0010 ± 0.0020	6 ABBIENDI	00Q OPAL	$e^+ e^- \rightarrow Z$
0.0319 ± 0.0018 ± 0.0019	7 BUSKULIC	97 ALEP	$e^+ e^- \rightarrow Z$
• • • We do not use the following data for averages, fits, limits, etc. • • •			
0.0355 ± 0.0003 ± 0.0016	8 AUBERT	05E BABR	Repl. by AUBERT 08R
0.0377 ± 0.0011 ± 0.0019	9 ABDALLAH	04D DLPH	$e^+ e^- \rightarrow Z^0$
0.0431 ± 0.0013 ± 0.0018	10 BRIERE	02 CLE2	$e^+ e^- \rightarrow \Upsilon(4S)$
0.0328 ± 0.0019 ± 0.0022	ACKERSTAFF	97G OPAL	Repl. by ABBIENDI 00Q
0.0350 ± 0.0019 ± 0.0023	11 ABREU	96P DLPH	Repl. by ABREU 01H
0.0351 ± 0.0019 ± 0.0020	12 BARISH	95 CLE2	Repl. by ADAM 03
0.0314 ± 0.0023 ± 0.0025	BUSKULIC	95N ALEP	Repl. by BUSKULIC 97

- ¹ Measured using fully reconstructed D^* sample and a simultaneous fit to the Caprini-Lellouch-Neubert form factor parameters: $\rho^2 = 1.191 \pm 0.048 \pm 0.028$, $R_1(1) = 1.429 \pm 0.061 \pm 0.044$, and $R_2(1) = 0.827 \pm 0.038 \pm 0.022$.
² Measurement using fully reconstructed D^* sample with a $\rho^2 = 1.32 \pm 0.15 \pm 0.33$.
³ Average of the $B^0 \rightarrow D^*(2010)^- \ell^+ \nu$ and $B^+ \rightarrow \bar{D}^*(2007)^0 \ell^+ \nu$ modes with $\rho^2 = 1.61 \pm 0.09 \pm 0.21$ and $f_{\pm} = 0.521 \pm 0.012$.
⁴ Measured using exclusive $B^0 \rightarrow D^*(892)^- e^+ \nu$ decays with $\rho^2 = 1.35 \pm 0.17 \pm 0.19$ and a correlation of 0.91.
⁵ ABREU 01H measured using about 5000 partial reconstructed D^* sample with a $\rho^2 = 1.34 \pm 0.14^{+0.24}_{-0.22}$.
⁶ ABBIENDI 00Q: measured using both inclusively and exclusively reconstructed $D^{*\pm}$ samples with a $\rho^2 = 1.21 \pm 0.12 \pm 0.20$. The statistical and systematic correlations between $|V_{cb}| \times F(1)$ and ρ^2 are 0.90 and 0.54 respectively.
⁷ BUSKULIC 97: measured using exclusively reconstructed $D^{*\pm}$ with a $a^2 = 0.31 \pm 0.17 \pm 0.08$. The statistical correlation is 0.92.
⁸ Measurement using fully reconstructed D^* sample with a $\rho^2 = 1.29 \pm 0.03 \pm 0.27$.
⁹ Combines with previous partial reconstructed D^* measurement with a $\rho^2 = 1.39 \pm 0.10 \pm 0.33$.
¹⁰ BRIERE 02 result is based on the same analysis and data sample reported in ADAM 03.
¹¹ ABREU 96P: measured using both inclusively and exclusively reconstructed $D^{*\pm}$ samples.
¹² BARISH 95: measured using both exclusive reconstructed $B^0 \rightarrow D^{*-} \ell^+ \nu$ and $B^+ \rightarrow D^{*0} \ell^+ \nu$ samples. They report their experiment's uncertainties $\pm 0.0019 \pm 0.0018 \pm 0.0008$, where the first error is statistical, the second is systematic, and the third is the uncertainty in the lifetimes. We combine the last two in quadrature.

WEIGHTED AVERAGE
0.0360 ± 0.0013 (Error scaled by 1.6) **$|V_{cb}| \times F(1)$ (from $B \rightarrow D^- \ell^+ \nu$)**

VALUE	DOCUMENT ID	TECN	COMMENT
0.0423 ± 0.0045 OUR EVALUATION	with $\rho^2=1.17 \pm 0.18$ and a correlation of 0.93. The fitted χ^2 is 0.3 for 4 degrees of freedom.		
0.039 ± 0.004 OUR AVERAGE			
0.0411 ± 0.0044 ± 0.0052	13 ABE	02E BELL	$e^+ e^- \rightarrow \Upsilon(4S)$
0.0416 ± 0.0047 ± 0.0037	14 BARTELT	99 CLE2	$e^+ e^- \rightarrow \Upsilon(4S)$
0.0278 ± 0.0068 ± 0.0065	15 BUSKULIC	97 ALEP	$e^+ e^- \rightarrow Z$
• • • We do not use the following data for averages, fits, limits, etc. • • •			
0.0337 ± 0.0044 $^{+0.0072}_{-0.0049}$	16 ATHANAS	97 CLE2	Repl. by BARTELT 99

- ¹³ Using the missing energy and momentum to extract kinematic information about the undetected neutrino in the $B^0 \rightarrow D^- \ell^+ \nu$ decay.
¹⁴ BARTELT 99: measured using both exclusive reconstructed $B^0 \rightarrow D^- \ell^+ \nu$ and $B^+ \rightarrow D^0 \ell^+ \nu$ samples.
¹⁵ BUSKULIC 97: measured using exclusively reconstructed D^{\pm} with a $a^2 = -0.05 \pm 0.53 \pm 0.38$. The statistical correlation is 0.99.
¹⁶ ATHANAS 97: measured using both exclusive reconstructed $B^0 \rightarrow D^- \ell^+ \nu$ and $B^+ \rightarrow D^0 \ell^+ \nu$ samples with a $\rho^2 = 0.59 \pm 0.22 \pm 0.12^{+0.59}_{-0}$. They report their experiment's uncertainties $\pm 0.0044 \pm 0.0048^{+0.0053}_{-0.0012}$, where the first error is statistical, the second is systematic, and the third is the uncertainty due to the form factor model variations. We combine the last two in quadrature.

 V_{ub} MEASUREMENTS

For the discussion of V_{ub} measurements, which is not repeated here, see the review on "Determination of $|V_{cb}|$ and $|V_{ub}|$."

The CKM matrix element $|V_{ub}|$ can be determined by studying the rate of the charmless semileptonic decay $b \rightarrow u \ell \nu$. The relevant branching ratio measurements based on exclusive and inclusive decays can be found in the B Listings, and are not repeated here.

 V_{cb} and V_{ub} CKM Matrix Elements REFERENCES

AUBERT	08R	PR D77 032002	B. Aubert <i>et al.</i>	(BABAR Collab.)
AUBERT	05E	PR D71 051502R	B. Aubert <i>et al.</i>	(BABAR Collab.)
ABDALLAH	04D	EPJ C33 213	J. Abdallah <i>et al.</i>	(DELPHI Collab.)
ADAM	03	PR D67 032001	N.E. Adam <i>et al.</i>	(CLEO Collab.)
ABE	02E	PL B526 258	K. Abe <i>et al.</i>	(BELLE Collab.)
ABE	02F	PL B526 247	K. Abe <i>et al.</i>	(BELLE Collab.)
BRIERE	02	PRL 89 081803	R. Briere <i>et al.</i>	(CLEO Collab.)
ABREU	01H	PL B510 55	P. Abreu <i>et al.</i>	(DELPHI Collab.)
ABBIENDI	00Q	PL B482 15	G. Abbiendi <i>et al.</i>	(OPAL Collab.)
BARTELT	99	PRL 82 3746	J. Bartelt <i>et al.</i>	(CLEO Collab.)
ACKERSTAFF	97G	PL B395 328	K. Ackerstaff <i>et al.</i>	(OPAL Collab.)
ATHANAS	97	PRL 79 2208	M. Athanas <i>et al.</i>	(CLEO Collab.)
BUSKULIC	97	PL B395 373	D. Buskulic <i>et al.</i>	(ALEPH Collab.)
ABREU	96P	ZPHY C71 539	P. Abreu <i>et al.</i>	(DELPHI Collab.)
BARISH	95	PR D51 1014	B.C. Barish <i>et al.</i>	(CLEO Collab.)
BUSKULIC	95N	PL B359 236	D. Buskulic <i>et al.</i>	(ALEPH Collab.)

Meson Particle Listings

$B^*, B_s^*(5732), B_1(5721)^0$

B^*

$$I(J^P) = \frac{1}{2}(1^-)$$

I, J, P need confirmation. Quantum numbers shown are quark-model predictions.

B^* MASS

From mass difference below and the average of our B masses $(m_{B^\pm} + m_{B^0})/2$.

VALUE (MeV)	DOCUMENT ID
5325.1 ± 0.5 OUR FIT	

$m_{B^*} - m_B$

VALUE (MeV)	EVTS	DOCUMENT ID	TECN	COMMENT
45.78 ± 0.35 OUR FIT				
45.78 ± 0.35 OUR AVERAGE				
46.2 ± 0.3 ± 0.8		¹ ACKERSTAFF 97M	OPAL	$e^+e^- \rightarrow Z$
45.3 ± 0.35 ± 0.87	4227	¹ BUSKULIC 96D	ALEP	$E_{cm}^{ee} = 88-94$ GeV
45.5 ± 0.3 ± 0.8		¹ ABREU 95R	DLPH	$E_{cm}^{ee} = 88-94$ GeV
46.3 ± 1.9	1378	¹ ACCIARRI 95B	L3	$E_{cm}^{ee} = 88-94$ GeV
46.4 ± 0.3 ± 0.8		² AKERIB 91	CLE2	$e^+e^- \rightarrow \gamma X$
45.6 ± 0.8		² WU 91	CSB2	$e^+e^- \rightarrow \gamma X, \gamma \ell X$
45.4 ± 1.0		³ LEE-FRANZINI 90	CSB2	$e^+e^- \rightarrow \Upsilon(5S)$
• • • We do not use the following data for averages, fits, limits, etc. • • •				
52 ± 2 ± 4	1400	⁴ HAN 85	CUSB	$e^+e^- \rightarrow \gamma eX$

- ¹ u, d, s flavor averaged.
- ² These papers report E_γ in the B^* center of mass. The $m_{B^*} - m_B$ is 0.2 MeV higher. $E_{cm} = 10.61-10.7$ GeV. Admixture of B^0 and B^+ mesons, but not B_s .
- ³ LEE-FRANZINI 90 value is for an admixture of B^0 and B^+ . They measure $46.7 \pm 0.4 \pm 0.2$ MeV for an admixture of $B^0, B^+,$ and B_s , and use the shape of the photon line to separate the above value.
- ⁴ HAN 85 is for $E_{cm} = 10.6-11.2$ GeV, giving an admixture of $B^0, B^+,$ and B_s .

$$|(m_{B^{*+}} - m_{B^+}) - (m_{B^{*0}} - m_{B^0})|$$

VALUE (MeV)	CL%	DOCUMENT ID	TECN	COMMENT
< 6	95	ABREU 95R	DLPH	$E_{cm}^{ee} = 88-94$ GeV

B^* DECAY MODES

Mode	Fraction (Γ_i/Γ)
$\Gamma_1 B\gamma$	dominant

B^* REFERENCES

ACKERSTAFF 97M	ZPHY C74 413	K. Ackerstaff et al.	(OPAL Collab.)
BUSKULIC 96D	ZPHY C69 393	D. Buskulic et al.	(ALEPH Collab.)
ABREU 95R	ZPHY C68 353	P. Abreu et al.	(DELPHI Collab.)
ACCIARRI 95B	PL B345 589	M. Acciari et al.	(L3 Collab.)
AKERIB 91	PRL 67 1692	D.S. Akerib et al.	(CLEO Collab.)
WU 91	PL B273 177	Q.W. Wu et al.	(CUSB II Collab.)
LEE-FRANZINI 90	PRL 65 2947	J. Lee-Franzini et al.	(CUSB II Collab.)
HAN 85	PRL 55 36	K. Han et al.	(COLU, LSU, MPIM, STON)

$B_s^*(5732)$
or B^{**}

$$I(J^P) = ?(??)$$

I, J, P need confirmation.

OMITTED FROM SUMMARY TABLE

Signal can be interpreted as stemming from several narrow and broad resonances. Needs confirmation.

$B_s^*(5732)$ MASS

VALUE (MeV)	EVTS	DOCUMENT ID	TECN	COMMENT
5698 ± 8 OUR AVERAGE	Error includes scale factor of 1.2.			
5710 ± 20		¹ AFFOLDER 01F	CDF	$p\bar{p}$ at 1.8 TeV
5695 ⁺¹⁷ ₋₁₉		² BARATE 98L	ALEP	$e^+e^- \rightarrow Z$
5704 ± 4 ± 10	1944	³ BUSKULIC 96D	ALEP	$E_{cm}^{ee} = 88-94$ GeV
5732 ± 5 ± 20	2157	ABREU 95B	DLPH	$E_{cm}^{ee} = 88-94$ GeV
5681 ± 11	1738	AKERS 95E	OPAL	$E_{cm}^{ee} = 88-94$ GeV
• • • We do not use the following data for averages, fits, limits, etc. • • •				
5713 ± 2		⁴ ACCIARRI 99N	L3	$e^+e^- \rightarrow Z$

- ¹ AFFOLDER 01F uses the reconstructed B meson through semileptonic decay channels. The fraction of light B mesons that are produced at $L=1 B^{**}$ states is measured to be $0.28 \pm 0.06 \pm 0.03$.
- ² BARATE 98L uses fully reconstructed B mesons to search for B^{**} production in the $B\pi^\pm$ system. In the framework of heavy quark symmetry (HQSS), they also measured the mass of B_2^* to be 5739^{+8+6}_{-11-4} MeV/ c^2 and the relative production rate of $B(b \rightarrow B_2^* \rightarrow B^{(*)}\pi)/B(b \rightarrow B_{u,d}) = (31 \pm 9^{+6}_{-5})\%$.
- ³ Using $m_{B\pi^-} - m_B = 424 \pm 4 \pm 10$ MeV.
- ⁴ ACCIARRI 99N uses inclusive reconstructed B mesons to search for B^{**} production in the $B^{(*)}\pi^\pm$ system. In the framework of HQET, they measured the mass of B_1^* and B_2^* to be $5670 \pm 10 \pm 13$ MeV and $5768 \pm 5 \pm 6$ with the $B(b \rightarrow B^{**}) = (32 \pm 3 \pm 6) \times 10^{-2}$. They also reported the evidence for the existence of an excited B -meson state or mixture of states in the region 5.9–6.0 GeV.

$B_s^*(5732)$ WIDTH

VALUE (MeV)	EVTS	DOCUMENT ID	TECN	COMMENT
128 ± 18 OUR AVERAGE				
145 ± 28	2157	ABREU 95B	DLPH	$E_{cm}^{ee} = 88-94$ GeV
116 ± 24	1738	AKERS 95E	OPAL	$E_{cm}^{ee} = 88-94$ GeV

$B_s^*(5732)$ DECAY MODES

Mode	Fraction (Γ_i/Γ)
$\Gamma_1 B^*\pi + B\pi$	dominant
$\Gamma_2 B^*\pi(X)$	[a] (85 ± 29) %

[a] X refers to decay modes with or without additional accompanying decay particles.

$B_s^*(5732)$ BRANCHING RATIOS

X refers to decay modes with or without additional accompanying decay particles.

$\Gamma(B^*\pi(X))/\Gamma_{total}$	DOCUMENT ID	TECN	COMMENT	Γ_2/Γ
0.85^{+0.26}_{-0.27} ± 0.12	ABBIENDI 02E	OPAL	$e^+e^- \rightarrow Z$	

$B_s^*(5732)$ REFERENCES

ABBIENDI 02E	EPJ C23 437	G. Abbiendi et al.	(OPAL Collab.)
AFFOLDER 01F	PR D64 072002	T. Affolder et al.	(CDF Collab.)
ACCIARRI 99N	PL B465 323	M. Acciari et al.	(L3 Collab.)
BARATE 98L	PL B425 215	R. Barate et al.	(ALEPH Collab.)
BUSKULIC 96D	ZPHY C69 393	D. Buskulic et al.	(ALEPH Collab.)
ABREU 95B	PL B345 598	P. Abreu et al.	(DELPHI Collab.)
AKERS 95E	ZPHY C66 19	R. Akers et al.	(OPAL Collab.)

$B_1(5721)^0$

$$I(J^P) = \frac{1}{2}(1^+) \text{ Status: } ***$$

I, J, P need confirmation.

Quantum numbers shown are quark-model predictions.

$B_1(5721)^0$ MASS

OUR FIT uses m_{B^+} and $m_{B_1^0} - m_{B^+}$ to determine $m_{B_1(5721)^0}$.

VALUE (MeV)	DOCUMENT ID
5720.7 ± 2.7 OUR FIT	

$m_{B_1^0} - m_{B^+}$

VALUE (MeV)	DOCUMENT ID	TECN	COMMENT
441.5 ± 2.7 OUR FIT			
441.5 ± 2.4 ± 1.3	ABAZOV 07T	D0	$p\bar{p}$ at 1.96 TeV

$B_1(5721)^0$ DECAY MODES

Mode	Fraction (Γ_i/Γ)
$\Gamma_1 B^{*+}\pi^-$	dominant

$B_1(5721)^0$ BRANCHING RATIOS

$\Gamma(B^{*+}\pi^-)/\Gamma_{total}$	DOCUMENT ID	TECN	COMMENT	Γ_1/Γ
dominant	¹ ABAZOV 07T	D0	$p\bar{p}$ at 1.96 TeV	
¹ Observed in $B_1^0 \rightarrow B^{*+}\pi^-$ with $B^{*+} \rightarrow B^+\gamma$ and $B^+ \rightarrow J/\psi\pi^+$.				

$B_1(5721)^0$ REFERENCES

ABAZOV 07T	PRL 99 172001	V.M. Abazov et al.	(D0 Collab.)
------------	---------------	--------------------	--------------

See key on page 373

Meson Particle Listings

 $B_1(5721)^0, B_2^*(5747)^0$ $B_2^*(5747)^0$ $I(J^P) = \frac{1}{2}(2^+)$ Status: ***
 I, J, P need confirmation.

Quantum numbers shown are quark-model predictions.

 $B_2^*(5747)^0$ MASS

OUR FIT uses $m_{B^+}, m_{B_1^0} - m_{B^+}$, and $m_{B_2^0} - m_{B_1^0}$ to determine $m_{B_2^*(5747)^0}$.
The -0.659 correlation between statistical uncertainties of $m_{B_1^0} - m_{B^+}$ and $m_{B_2^0} - m_{B_1^0}$ measurements reported by ABAZOV 07T is taken into account.

VALUE (MeV)	DOCUMENT ID
5746.9 ± 2.9 OUR FIT	

 $m_{B_2^0} - m_{B_1^0}$

VALUE (MeV)	DOCUMENT ID	TECN	COMMENT
26.2 ± 3.2 OUR FIT			

26.2 ± 3.1 ± 0.9	¹ ABAZOV	07T	D0	$p\bar{p}$ at 1.96 TeV
-------------------------	---------------------	-----	----	------------------------

¹ Observed in $B_2^{*0} \rightarrow B^{*+}\pi^-$ and $B_2^{*0} \rightarrow B^+\pi^-$ with $B^{*+} \rightarrow B^+\gamma$ and $B^+ \rightarrow J/\psi\pi^+$.

 $B_2^*(5747)^0$ DECAY MODES

Mode	Fraction (Γ_i/Γ)
Γ_1 $B^+\pi^-$	dominant
Γ_2 $B^{*+}\pi^-$	dominant

 $B_2^*(5747)^0$ BRANCHING RATIOS

$\Gamma(B^+\pi^-)/\Gamma_{\text{total}}$	VALUE	DOCUMENT ID	TECN	COMMENT	Γ_1/Γ
dominant		ABAZOV	07T	D0	$p\bar{p}$ at 1.96 TeV

$\Gamma(B^{*+}\pi^-)/\Gamma_{\text{total}}$	VALUE	DOCUMENT ID	TECN	COMMENT	Γ_2/Γ
dominant		ABAZOV	07T	D0	$p\bar{p}$ at 1.96 TeV

$\Gamma(B^{*+}\pi^-)/\Gamma(B^+\pi^-)$	VALUE	DOCUMENT ID	TECN	COMMENT	Γ_2/Γ_1
1.10 ± 0.42 ± 0.31		² ABAZOV	07T	D0	$p\bar{p}$ at 1.96 TeV

² Converted from measured ratio of $R = B(B_2^{*0} \rightarrow B^{*+}\pi^-) / B(B_2^{*0} \rightarrow B^{*+}\pi^-)$
 $= 0.475 \pm 0.095 \pm 0.069$.

 $B_2^*(5747)^0$ REFERENCES

ABAZOV	07T	PRL 99 172001	V.M. Abazov <i>et al.</i>	(D0 Collab.)
--------	-----	---------------	---------------------------	--------------

Meson Particle Listings

B_s^0

BOTTOM, STRANGE MESONS

$(B = \pm 1, S = \mp 1)$

$B_s^0 = s\bar{b}, \bar{B}_s^0 = \bar{s}b$, similarly for $B_s^{*\prime}$ s

B_s^0

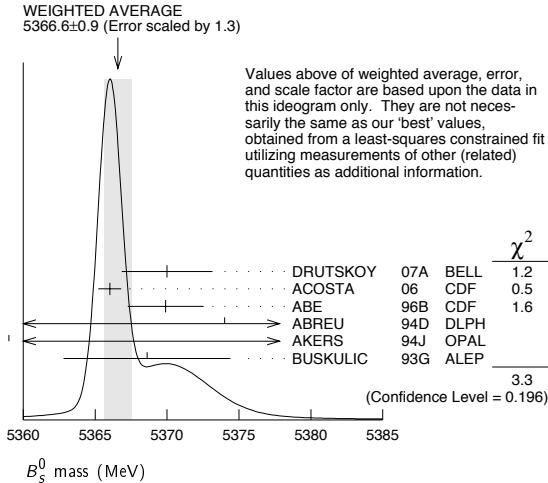
$$I(J^P) = 0(0^-)$$

I, J, P need confirmation. Quantum numbers shown are quark-model predictions.

B_s^0 MASS

VALUE (MeV)	EVTS	DOCUMENT ID	TECN	COMMENT
5366.3 ± 0.6 OUR FIT				
5366.6 ± 0.9 OUR AVERAGE				Error includes scale factor of 1.3. See the ideogram below.
5370 ± 1 ± 3		DRUTSKOY 07A	BELL	$e^+e^- \rightarrow \Upsilon(5S)$
5366.01 ± 0.73 ± 0.33		1 ACOSTA 06	CDF	$p\bar{p}$ at 1.96 TeV
5369.9 ± 2.3 ± 1.3	32	2 ABE 96B	CDF	$p\bar{p}$ at 1.8 TeV
5374 ± 16 ± 2	3	ABREU 94D	DLPH	$e^+e^- \rightarrow Z$
5359 ± 19 ± 7	1	2 AKERS 94J	OPAL	$e^+e^- \rightarrow Z$
5368.6 ± 5.6 ± 1.5	2	BUSKULIC 93G	ALEP	$e^+e^- \rightarrow Z$
• • • We do not use the following data for averages, fits, limits, etc. • • •				
5370 ± 40	6	3 AKERS 94J	OPAL	$e^+e^- \rightarrow Z$
5383.3 ± 4.5 ± 5.0	14	ABE 93F	CDF	Repl by ABE 96B

- 1 Uses exclusively reconstructed final states containing a $J/\psi \rightarrow \mu^+\mu^-$ decays.
- 2 From the decay $B_s \rightarrow J/\psi(1S)\phi$.
- 3 From the decay $B_s \rightarrow D_s^-\pi^+$.



$$m_{B_s^0} - m_B$$

m_B is the average of our B masses $(m_{B^\pm} + m_{B^0})/2$.

VALUE (MeV)	CL%	DOCUMENT ID	TECN	COMMENT
87.0 ± 0.6 OUR FIT				
86.9 ± 0.8 OUR AVERAGE				
86.64 ± 0.80 ± 0.08		4 ACOSTA 06	CDF	$p\bar{p}$ at 1.96 TeV
89.7 ± 2.7 ± 1.2		ABE 96B	CDF	$p\bar{p}$ at 1.8 TeV
• • • We do not use the following data for averages, fits, limits, etc. • • •				
80 to 130	68	LEE-FRANZINI 90	CSB2	$e^+e^- \rightarrow \Upsilon(5S)$

- 4 The reported result is $m_{B_s^0} - m_{B^0} = 86.38 \pm 0.90 \pm 0.06$ MeV. We convert it to the mass difference with respect to the average of $(m_{B^\pm} + m_{B^0})/2$.

$$m_{B_s^0 H} - m_{B_s^0 L}$$

See the $B_s^0 \bar{B}_s^0$ MIXING section near the end of these B_s^0 Listings.

B_s^0 MEAN LIFE

"OUR EVALUATION" is an average using rescaled values of the data listed below. The average and rescaling were performed by the Heavy Flavor Averaging Group (HFAG) and are described at <http://www.slac.stanford.edu/xorg/hfag/>. The averaging/rescaling procedure takes into account correlations between the measurements and asymmetric lifetime errors.

The First "OUR EVALUATION" is an average of $1 / [\Gamma_{B_s^0 L} + \Gamma_{B_s^0 H}]$.
The Second "OUR EVALUATION" is the average of $B_s \rightarrow D_s X$ data listed below.

VALUE (10^{-12} s)	EVTS	DOCUMENT ID	TECN	COMMENT
1.470 ± 0.026 OUR EVALUATION				First
1.425 ± 0.041 OUR EVALUATION				Second
1.398 ± 0.044 ± 0.028		5 ABAZOV 06v	D0	$p\bar{p}$ at 1.96 TeV
1.42 ± 0.14 ± 0.03		6 ABREU 00Y	DLPH	$e^+e^- \rightarrow Z$
1.53 ± 0.16 ± 0.07		7 ABREU,P 00G	DLPH	$e^+e^- \rightarrow Z$
1.36 ± 0.09 ± 0.06		8 ABE 99D	CDF	$p\bar{p}$ at 1.8 TeV
1.72 ± 0.20 ± 0.18		9 ACKERSTAFF 98F	OPAL	$e^+e^- \rightarrow Z$
1.50 ± 0.16 ± 0.04		8 ACKERSTAFF 98G	OPAL	$e^+e^- \rightarrow Z$
1.47 ± 0.14 ± 0.08		7 BARATE 98c	ALEP	$e^+e^- \rightarrow Z$
1.54 ± 0.14 ± 0.04		8 BUSKULIC 96M	ALEP	$e^+e^- \rightarrow Z$
• • • We do not use the following data for averages, fits, limits, etc. • • •				
1.51 ± 0.11		10 BARATE 98c	ALEP	$e^+e^- \rightarrow Z$
1.56 ± 0.29 ± 0.08		8 ABREU 96F	DLPH	Repl. by ABREU 00Y
1.65 ± 0.34 ± 0.12		7 ABREU 96F	DLPH	Repl. by ABREU 00Y
1.76 ± 0.20 ± 0.15		11 ABREU 96F	DLPH	Repl. by ABREU 00Y
1.60 ± 0.26 ± 0.13		12 ABREU 96F	DLPH	Repl. by ABREU,P 00G
1.67 ± 0.14		13 ABREU 96F	DLPH	$e^+e^- \rightarrow Z$
1.61 ± 0.30 ± 0.18		90 7 BUSKULIC 96E	ALEP	Repl. by BARATE 98c
1.42 ± 0.27 ± 0.11		76 8 ABE 95R	CDF	Repl. by ABE 99D
1.74 ± 1.08 ± 0.07		8 14 ABE 95R	CDF	Sup. by ABE 96N
1.54 ± 0.25 ± 0.06		79 8 AKERS 95G	OPAL	Repl. by ACKERSTAFF 98G
1.59 ± 0.17 ± 0.03		134 8 BUSKULIC 95O	ALEP	Sup. by BUSKULIC 96M
0.96 ± 0.37		41 15 ABREU 94E	DLPH	Sup. by ABREU 96F
1.92 ± 0.45 ± 0.04		31 8 BUSKULIC 94C	ALEP	Sup. by BUSKULIC 95O
1.13 ± 0.35 ± 0.09		22 8 ACTON 93H	OPAL	Sup. by AKERS 95G

- 5 Measured using $D_s \mu^+$ vertices.
- 6 Uses $D_s^- \ell^+$, and $\phi \ell^+$ vertices.
- 7 Measured using D_s hadron vertices.
- 8 Measured using $D_s^- \ell^+$ vertices.
- 9 ACKERSTAFF 98F use fully reconstructed $D_s^- \rightarrow \phi\pi^-$ and $D_s^- \rightarrow K^{*0}K^-$ in the inclusive B_s^0 decay.
- 10 Combined results from $D_s^- \ell^+$ and D_s hadron.
- 11 Measured using $\phi \ell$ vertices.
- 12 Measured using inclusive D_s vertices.
- 13 Combined result for the four ABREU 96F methods.
- 14 Exclusive reconstruction of $B_s \rightarrow \psi\phi$.
- 15 ABREU 94E uses the flight-distance distribution of D_s vertices, ϕ -lepton vertices, and $D_s \mu$ vertices.

B_s^0 MEAN LIFE (Flavor specific)

VALUE (10^{-12} s)	DOCUMENT ID	TECN	COMMENT
1.417 ± 0.042 OUR EVALUATION			
1.41 ± 0.04 OUR AVERAGE			
1.398 ± 0.044 ± 0.028	16 ABAZOV 06v	D0	$p\bar{p}$ at 1.96 TeV
1.42 ± 0.14 ± 0.03	17 ABREU 00Y	DLPH	$e^+e^- \rightarrow Z$
1.36 ± 0.09 ± 0.06	18 ABE 99D	CDF	$p\bar{p}$ at 1.8 TeV
1.50 ± 0.16 ± 0.04	19 ACKERSTAFF 98G	OPAL	$e^+e^- \rightarrow Z$
1.54 ± 0.14 ± 0.04	18 BUSKULIC 96M	ALEP	$e^+e^- \rightarrow Z$
16 Measured using $D_s^- \mu^+$ vertices.			
17 Uses $D_s^- \ell^+$, and $\phi \ell^+$ vertices.			
18 Measured using $D_s^- \ell^+$ vertices.			
19 ACKERSTAFF 98F use fully reconstructed $D_s^- \rightarrow \phi\pi^-$ and $D_s^- \rightarrow K^{*0}K^-$ in the inclusive B_s^0 decay.			

B_S^0 MEAN LIFE ($B_S \rightarrow J/\psi\phi$)

VALUE (10^{-12} s)	DOCUMENT ID	TECN	COMMENT
1.429 ± 0.088	OUR EVALUATION		
1.43 ± 0.09	OUR AVERAGE		
$1.444^{+0.098}_{-0.090} \pm 0.020$	20	ABAZOV 05B D0	$p\bar{p}$ at 1.96 TeV
$1.34^{+0.23}_{-0.19} \pm 0.05$	20	ABE 98B CDF	$p\bar{p}$ at 1.8 TeV
• • • We do not use the following data for averages, fits, limits, etc. • • •			
$1.39^{+0.13}_{-0.16} +0.01_{-0.02}$	21	ABAZOV 05W D0	$p\bar{p}$ at 1.96 TeV
$1.40^{+0.15}_{-0.13} \pm 0.02$	21	ACOSTA 05 CDF	Repl. by AALTONEN 2008J
$1.34^{+0.23}_{-0.19} \pm 0.05$	22	ABE 96N CDF	Repl. by ABE 98B
20 Measured using fully reconstructed $B_S \rightarrow J/\psi(1S)\phi$ decay.			
21 Measured using the time-dependent angular analysis of $B_S^0 \rightarrow J/\psi\phi$ decays.			
22 ABE 96N uses 58 ± 12 exclusive $B_S \rightarrow J/\psi(1S)\phi$ events.			

 $\tau_{B_S^0}/\tau_{B^0}$ MEAN LIFE RATIO $\tau_{B_S^0}/\tau_{B^0}$ (direct measurements)

VALUE	DOCUMENT ID	TECN	COMMENT
$0.91 \pm 0.09 \pm 0.003$	23	ABAZOV 05W D0	$p\bar{p}$ at 1.96 TeV
• • • We do not use the following data for averages, fits, limits, etc. • • •			
$0.980^{+0.076}_{-0.071} \pm 0.003$	24	ABAZOV 05B D0	Repl. by ABAZOV 05W
23 Measured using the time-dependent angular analysis of $B_S^0 \rightarrow J/\psi\phi$ decays.			
24 Measured mean life ratio using fully reconstructed decays.			

 B_{SH}^0 MEAN LIFE

B_{SH}^0 is the heavy mass state of two B_S^0 CP eigenstates.

"OUR EVALUATION" is an average using rescaled values of the data listed below. The average and rescaling were performed by the Heavy Flavor Averaging Group (HFAG) and are described at <http://www.slac.stanford.edu/xorg/hfag/>. The averaging/rescaling procedure takes into account correlations between the measurements.

VALUE (10^{-12} s)	DOCUMENT ID	TECN	COMMENT
$1.525^{+0.062}_{-0.063}$	OUR EVALUATION		
1.44 ± 0.05	OUR AVERAGE		
$1.437^{+0.054}_{-0.047}$	25,26	AALTONEN 08J CDF	$p\bar{p}$ at 1.96 TeV
$1.58^{+0.39}_{-0.42} +0.01_{-0.02}$	26	ABAZOV 05W D0	$p\bar{p}$ at 1.96 TeV
• • • We do not use the following data for averages, fits, limits, etc. • • •			
$2.07^{+0.58}_{-0.46} \pm 0.03$	26	ACOSTA 05 CDF	Repl. by AALTONEN 08J
25 Obtained from $\Delta\Gamma_S$ and Γ_S fit with a correlation of 0.6.			
26 Measured using the time-dependent angular analysis of $B_S^0 \rightarrow J/\psi\phi$ decays.			

 B_{SL}^0 MEAN LIFE

B_{SL}^0 is the light state of two B_S^0 CP eigenstates.

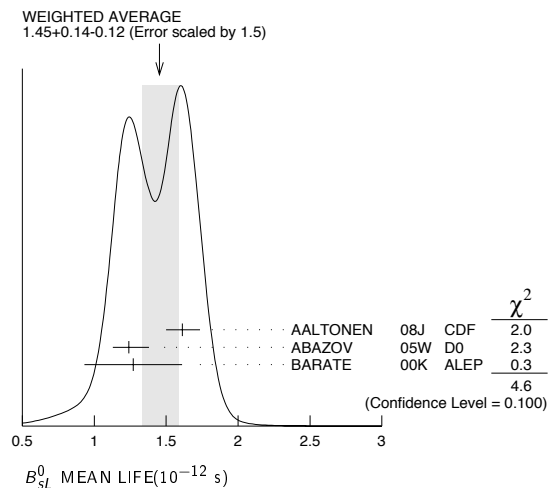
"OUR EVALUATION" is an average using rescaled values of the data listed below. The average and rescaling were performed by the Heavy Flavor Averaging Group (HFAG) and are described at <http://www.slac.stanford.edu/xorg/hfag/>. The averaging/rescaling procedure takes into account correlations between the measurements.

VALUE (10^{-12} s)	DOCUMENT ID	TECN	COMMENT
$1.419^{+0.039}_{-0.038}$	OUR EVALUATION		
$1.45^{+0.14}_{-0.12}$	OUR AVERAGE Error includes scale factor of 1.5. See the ideogram below.		
$1.613^{+0.123}_{-0.113}$	27,28	AALTONEN 08J CDF	$p\bar{p}$ at 1.96 TeV
$1.24^{+0.14}_{-0.11} +0.01_{-0.02}$	28	ABAZOV 05W D0	$p\bar{p}$ at 1.96 TeV
$1.27 \pm 0.33 \pm 0.08$	29	BARATE 00K ALEP	$e^+e^- \rightarrow Z$
• • • We do not use the following data for averages, fits, limits, etc. • • •			
$1.05^{+0.16}_{-0.13} \pm 0.02$	28	ACOSTA 05 CDF	Repl. by AALTONEN 08J

27 Obtained from $\Delta\Gamma_S$ and Γ_S fit with a correlation of 0.6.

28 Measured using the time-dependent angular analysis of $B_S^0 \rightarrow J/\psi\phi$ decays.

29 Uses $\phi\phi$ correlations from $B_S^0 \rightarrow D_S^{(*)+} D_S^{(*)-}$.

 $\Delta\Gamma_{B_S^0}/\Gamma_{B_S^0}$

$\Gamma_{B_S^0}$ and $\Delta\Gamma_{B_S^0}$ are the decay rate average and difference between two B_S^0 CP eigenstates (light – heavy).

"OUR EVALUATION" is an average of all available B_S semi-leptonic lifetime measurements with the $\Delta\Gamma_{B_S^0}/\Gamma_S$ analyses performed by the Heavy

Flavor Averaging Group (HFAG) as described in our "Review on $B-\bar{B}$ Mixing" in the B^0 Section of these Listings. The corresponding 95% CL is $-0.052 < \Delta\Gamma_{B_S^0}/\Gamma_{B_S^0} < 0.18$.

VALUE	CL%	DOCUMENT ID	TECN	COMMENT
$0.069^{+0.058}_{-0.062}$	OUR EVALUATION			
$0.116^{+0.09}_{-0.10} \pm 0.010$	30	AALTONEN 08J CDF		$p\bar{p}$ at 1.96 TeV
$0.24^{+0.28}_{-0.38} +0.03_{-0.04}$	30,31	ABAZOV 05W D0		$p\bar{p}$ at 1.96 TeV
• • • We do not use the following data for averages, fits, limits, etc. • • •				
$0.65^{+0.25}_{-0.33} \pm 0.01$	30	ACOSTA 05 CDF		Repl. by AALTONEN 08J
<0.46	95	32 ABREU 00Y	DLPH	$e^+e^- \rightarrow Z$
<0.69	95	33 ABREU,P 00G	DLPH	$e^+e^- \rightarrow Z$
<0.83	95	34 ABE 99D	CDF	$p\bar{p}$ at 1.8 TeV
<0.67	95	35 ACCIARRI 98S	L3	$e^+e^- \rightarrow Z$
30 Measured using the time-dependent angular analysis of $B_S^0 \rightarrow J/\psi\phi$ decays.				
31 Uses $ A_0 ^2 - A_{\parallel} ^2 = 0.355 \pm 0.066$ from ACOSTA 05.				
32 Uses $D_S^- \ell^+$, and $\phi\ell^+$ vertices.				
33 Measured using D_S hadron vertices.				
34 ABE 99D assumes $\tau_{B_S^0} = 1.55 \pm 0.05$ ps.				
35 ACCIARRI 98S assumes $\tau_{B_S^0} = 1.49 \pm 0.06$ ps and PDG 98 values of b production fraction.				

 $\Delta\Gamma_{B_S^0}$

"OUR EVALUATION" is an average using rescaled values of the data listed below. The average and rescaling were performed by the Heavy Flavor Averaging Group (HFAG) and are described at <http://www.slac.stanford.edu/xorg/hfag/>. The averaging/rescaling procedure takes into account correlations between the measurements.

VALUE (10^{12} s $^{-1}$)	DOCUMENT ID	TECN	COMMENT
$0.049^{+0.040}_{-0.043}$	OUR EVALUATION		
0.09 ± 0.05	OUR AVERAGE		
$0.076^{+0.059}_{-0.063} \pm 0.006$	36	AALTONEN 08J CDF	$p\bar{p}$ at 1.96 TeV
0.13 ± 0.09	37	ABAZOV 07N D0	$p\bar{p}$ at 1.96 TeV
• • • We do not use the following data for averages, fits, limits, etc. • • •			
$0.12^{+0.08}_{-0.10} \pm 0.02$	36,38	ABAZOV 07 D0	Repl. by ABAZOV 07N
$0.47^{+0.19}_{-0.24} \pm 0.01$	36	ACOSTA 05 CDF	Repl. by AALTONEN 08J

Meson Particle Listings

 B_s^0

³⁶ Measured using the time-dependent angular analysis of $B_s^0 \rightarrow J/\psi\phi$ decays and assuming CP -violating phase $\phi_s = 0$.

³⁷ Combines D^0 measurements of time-dependent angular distributions in $B_s^0 \rightarrow J/\psi\phi$ and charge asymmetry in semileptonic decays. There is a 4-fold ambiguity in the solution.

³⁸ ABAZOV 07 reports $0.17 \pm 0.09 \pm 0.02$ with CP -violating phase ϕ_s as a free parameter.

 $\Delta\Gamma_s^{CP} / \Gamma_s$

Γ_s and $\Delta\Gamma_s^{CP}$ are the decay rate average and difference between even, $\Gamma_s^{CP=even}$, and odd, $\Gamma_s^{CP=odd}$, CP eigenstates.

VALUE	CL%	DOCUMENT ID	TECN	COMMENT
0.10 ± 0.05 OUR AVERAGE				Error includes scale factor of 1.2.
0.079 ^{+0.038+0.031} _{-0.035-0.030}		³⁹ ABAZOV	07Y D0	$p\bar{p}$ at 1.96 TeV
0.25 ^{+0.21} _{-0.14}		⁴⁰ BARATE	00K ALEP	$e^+e^- \rightarrow Z$
• • • We do not use the following data for averages, fits, limits, etc. • • •				
>0.012	95	³⁹ AALTONEN	08F CDF	$p\bar{p}$ at 1.96 TeV
³⁹ Assumes $2\text{B}(B_s^0 \rightarrow D_s^{(*)}D_s^{(*)}) \simeq \Delta\Gamma_s^{CP} / \Gamma_s$.				
⁴⁰ Uses $\phi\phi$ correlations from $B_s^0 \rightarrow D_s^{(*)+}D_s^{(*)-}$.				

 $1 / \Gamma_{B_s^0}$

"OUR EVALUATION" is an average using rescaled values of the data listed below. The average and rescaling were performed by the Heavy Flavor Averaging Group (HFAG) and are described at <http://www.slac.stanford.edu/xorg/hfag/>. The averaging/rescaling procedure takes into account correlations between the measurements.

VALUE (10^{-12} s)	DOCUMENT ID	TECN	COMMENT
1.47^{+0.026}_{-0.027} OUR EVALUATION			
1.52 ± 0.04 ± 0.02	⁴¹ AALTONEN	08J CDF	$p\bar{p}$ at 1.96 TeV
⁴¹ Measured using the time-dependent angular analysis of $B_s^0 \rightarrow J/\psi\phi$ decays.			

 B_s^0 DECAY MODES

These branching fractions all scale with $\text{B}(\bar{b} \rightarrow B_s^0)$, the LEP B_s^0 production fraction. The first four were evaluated using $\text{B}(\bar{b} \rightarrow B_s^0) = (10.7 \pm 1.2)\%$ and the rest assume $\text{B}(\bar{b} \rightarrow B_s^0) = 12\%$.

The branching fraction $\text{B}(B_s^0 \rightarrow D_s^- \ell^+ \nu_\ell \text{ anything})$ is not a pure measurement since the measured product branching fraction $\text{B}(\bar{b} \rightarrow B_s^0) \times \text{B}(B_s^0 \rightarrow D_s^- \ell^+ \nu_\ell \text{ anything})$ was used to determine $\text{B}(\bar{b} \rightarrow B_s^0)$, as described in the note on " B^0 - \bar{B}^0 Mixing"

For inclusive branching fractions, e.g., $B \rightarrow D^{\pm} \text{ anything}$, the values usually are multiplicities, not branching fractions. They can be greater than one.

Mode	Fraction (Γ_i/Γ)	Scale factor/ Confidence level
Γ_1 D_s^- anything	(93 ± 25) %	
Γ_2 $D_s^- \ell^+ \nu_\ell$ anything	[a] (7.9 ± 2.4) %	
Γ_3 $D_s^- \pi^+$	(3.2 ± 0.9) × 10 ⁻³	S=1.3
Γ_4 $D_s^- \pi^+ \pi^+ \pi^-$	(8.4 ± 3.3) × 10 ⁻³	
Γ_5 $D_s^{(*)+} D_s^{(*)-}$	(4.9 ± $\frac{2.9}{2.5}$) %	S=1.2
Γ_6 $D_s^+ D_s^-$	(1.1 ± 0.4) %	
Γ_7 $D_s^{*+} D_s^{*-}$	< 12.1 %	CL=90%
Γ_8 $D_s^{*+} D_s^{*-}$	< 25.7 %	CL=90%
Γ_9 $J/\psi(1S)\phi$	(9.3 ± 3.3) × 10 ⁻⁴	
Γ_{10} $J/\psi(1S)\pi^0$	< 1.2 × 10 ⁻³	CL=90%
Γ_{11} $J/\psi(1S)\eta$	< 3.8 × 10 ⁻³	CL=90%
Γ_{12} $\psi(2S)\phi$	(4.8 ± 2.2) × 10 ⁻⁴	
Γ_{13} $\pi^+ \pi^-$	< 1.7 × 10 ⁻⁶	CL=90%
Γ_{14} $\pi^0 \pi^0$	< 2.1 × 10 ⁻⁴	CL=90%
Γ_{15} $\eta \pi^0$	< 1.0 × 10 ⁻³	CL=90%
Γ_{16} $\eta \eta$	< 1.5 × 10 ⁻³	CL=90%
Γ_{17} $\rho^0 \rho^0$	< 3.20 × 10 ⁻⁴	CL=90%
Γ_{18} $\phi \rho^0$	< 6.17 × 10 ⁻⁴	CL=90%
Γ_{19} $\phi \phi$	(1.4 ± 0.8) × 10 ⁻⁵	
Γ_{20} $\pi^+ K^-$	< 5.6 × 10 ⁻⁶	CL=90%
Γ_{21} $K^+ K^-$	(3.3 ± 0.9) × 10 ⁻⁵	
Γ_{22} $\bar{K}^*(892)^0 \rho^0$	< 7.67 × 10 ⁻⁴	CL=90%

Γ_{23} $\bar{K}^*(892)^0 K^*(892)^0$		< 1.681	× 10 ⁻³	CL=90%
Γ_{24} $\phi K^*(892)^0$		< 1.013	× 10 ⁻³	CL=90%
Γ_{25} $p\bar{p}$		< 5.9	× 10 ⁻⁵	CL=90%
Γ_{26} $\gamma\gamma$	B1	< 5.3	× 10 ⁻⁵	CL=90%
Γ_{27} $\phi\gamma$		< 1.2	× 10 ⁻⁴	CL=90%

Lepton Family number (LF) violating modes or $\Delta B = 1$ weak neutral current (B1) modes

Γ_{28} $\mu^+ \mu^-$	B1	< 4.7	× 10 ⁻⁸	CL=90%
Γ_{29} $e^+ e^-$	B1	< 5.4	× 10 ⁻⁵	CL=90%
Γ_{30} $e^\pm \mu^\mp$	LF [b]	< 6.1	× 10 ⁻⁶	CL=90%
Γ_{31} $\phi(1020)\mu^+ \mu^-$	B1	< 3.2	× 10 ⁻⁶	CL=90%
Γ_{32} $\phi\nu\bar{\nu}$	B1	< 5.4	× 10 ⁻³	CL=90%

[a] Not a pure measurement. See note at head of B_s^0 Decay Modes.

[b] The value is for the sum of the charge states or particle/antiparticle states indicated.

 B_s^0 BRANCHING RATIOS

$\Gamma(D_s^- \text{ anything})/\Gamma_{\text{total}}$	Γ_1/Γ
0.93 ± 0.25 OUR AVERAGE	
0.91 ± 0.18 ± 0.41	⁴² DRUTSKOY 07 BELL $e^+e^- \rightarrow \Upsilon(4S)$
0.81 ± 0.24 ± 0.22	90 ⁴³ BUSKULIC 96E ALEP $e^+e^- \rightarrow Z$
1.56 ± 0.58 ± 0.44	147 ⁴⁴ ACTON 92N OPAL $e^+e^- \rightarrow Z$

⁴² The extraction of this result takes into account the correlation between the measurements of $\text{B}(\Upsilon(5S) \rightarrow D_s X)$ and $\text{B}(\Upsilon(5S) \rightarrow D^0 X)$.

⁴³ BUSKULIC 96E separate $c\bar{c}$ and $b\bar{b}$ sources of D_s^+ mesons using a lifetime tag, subtract generic $\bar{b} \rightarrow W^+ \rightarrow D_s^+$ events, and obtain $\text{B}(\bar{b} \rightarrow B_s^0) \times \text{B}(B_s^0 \rightarrow D_s^- \text{ anything}) = 0.088 \pm 0.020 \pm 0.020$ assuming $\text{B}(D_s^- \rightarrow \phi\pi^-) = (3.5 \pm 0.4) \times 10^{-2}$ and PDG 1994 values for the relative partial widths to other D_s channels. We evaluate using our current values $\text{B}(\bar{b} \rightarrow B_s^0) = 0.107 \pm 0.014$ and $\text{B}(D_s^- \rightarrow \phi\pi^-) = 0.036 \pm 0.009$. Our first error is their experiment's and our second error is that due to $\text{B}(\bar{b} \rightarrow B_s^0)$ and $\text{B}(D_s^- \rightarrow \phi\pi^-)$.

⁴⁴ ACTON 92N assume that excess of $147 \pm 48 D_s^0$ events over that expected from B^0 , B^+ , and $c\bar{c}$ is all from B_s^0 decay. The product branching fraction is measured to be $\text{B}(\bar{b} \rightarrow B_s^0)\text{B}(B_s^0 \rightarrow D_s^- \text{ anything}) \times \text{B}(D_s^- \rightarrow \phi\pi^-) = (5.9 \pm 1.9 \pm 1.1) \times 10^{-3}$. We evaluate using our current values $\text{B}(\bar{b} \rightarrow B_s^0) = 0.107 \pm 0.014$ and $\text{B}(D_s^- \rightarrow \phi\pi^-) = 0.036 \pm 0.009$. Our first error is their experiment's and our second error is that due to $\text{B}(\bar{b} \rightarrow B_s^0)$ and $\text{B}(D_s^- \rightarrow \phi\pi^-)$.

 $\Gamma(D_s^- \ell^+ \nu_\ell \text{ anything})/\Gamma_{\text{total}}$

The values and averages in this section serve only to show what values result if one assumes our $\text{B}(\bar{b} \rightarrow B_s^0)$. They cannot be thought of as measurements since the underlying product branching fractions were also used to determine $\text{B}(\bar{b} \rightarrow B_s^0)$ as described in the note on "Production and Decay of b -Flavored Hadrons."

VALUE	EVTS	DOCUMENT ID	TECN	COMMENT
0.079 ± 0.024 OUR AVERAGE				
0.076 ± 0.012 ± 0.021	134	⁴⁵ BUSKULIC 95O ALEP	$e^+e^- \rightarrow Z$	
0.107 ± 0.043 ± 0.029		⁴⁶ ABREU 92M DLPH	$e^+e^- \rightarrow Z$	
0.103 ± 0.036 ± 0.028	18	⁴⁷ ACTON 92N OPAL	$e^+e^- \rightarrow Z$	
• • • We do not use the following data for averages, fits, limits, etc. • • •				
0.13 ± 0.04 ± 0.04	27	⁴⁸ BUSKULIC 92E ALEP	$e^+e^- \rightarrow Z$	

⁴⁵ BUSKULIC 95O use $D_s \ell$ correlations. The measured product branching ratio is $\text{B}(\bar{b} \rightarrow B_s) \times \text{B}(B_s \rightarrow D_s^- \ell^+ \nu_\ell \text{ anything}) = (0.82 \pm 0.09^{+0.13}_{-0.14})\%$ assuming $\text{B}(D_s^- \rightarrow \phi\pi^-) = (3.5 \pm 0.4) \times 10^{-2}$ and PDG 1994 values for the relative partial widths to the six other D_s channels used in this analysis. Combined with results from $\Upsilon(4S)$ experiments this can be used to extract $\text{B}(\bar{b} \rightarrow B_s) = (11.0 \pm 1.2^{+2.5}_{-2.6})\%$. We evaluate using our current values $\text{B}(\bar{b} \rightarrow B_s^0) = 0.107 \pm 0.014$ and $\text{B}(D_s^- \rightarrow \phi\pi^-) = 0.036 \pm 0.009$. Our first error is their experiment's and our second error is that due to $\text{B}(\bar{b} \rightarrow B_s^0)$ and $\text{B}(D_s^- \rightarrow \phi\pi^-)$.

⁴⁶ ABREU 92M measured muons only and obtained product branching ratio $\text{B}(Z \rightarrow b\bar{b}) \times \text{B}(\bar{b} \rightarrow B_s) \times \text{B}(B_s \rightarrow D_s^- \mu^+ \nu_\mu \text{ anything}) \times \text{B}(D_s^- \rightarrow \phi\pi^-) = (18 \pm 8) \times 10^{-5}$. We evaluate using our current values $\text{B}(\bar{b} \rightarrow B_s^0) = 0.107 \pm 0.014$ and $\text{B}(D_s^- \rightarrow \phi\pi^-) = 0.036 \pm 0.009$. Our first error is their experiment's and our second error is that due to $\text{B}(\bar{b} \rightarrow B_s^0)$ and $\text{B}(D_s^- \rightarrow \phi\pi^-)$. We use $\text{B}(Z \rightarrow b\bar{b}) = 2\text{B}(Z \rightarrow b\bar{b}) = 2 \times (0.2212 \pm 0.0019)$.

⁴⁷ ACTON 92N is measured using $D_s^- \rightarrow \phi\pi^-$ and $K^*(892)^0 K^+$ events. The product branching fraction measured is measured to be $\text{B}(\bar{b} \rightarrow B_s^0)\text{B}(B_s^0 \rightarrow D_s^- \ell^+ \nu_\ell \text{ anything}) \times \text{B}(D_s^- \rightarrow \phi\pi^-) = (3.9 \pm 1.1 \pm 0.8) \times 10^{-4}$. We evaluate using our current values $\text{B}(\bar{b} \rightarrow B_s^0) = 0.107 \pm 0.014$ and $\text{B}(D_s^- \rightarrow \phi\pi^-) = 0.036 \pm 0.009$. Our first error is their experiment's and our second error is that due to $\text{B}(\bar{b} \rightarrow B_s^0)$ and $\text{B}(D_s^- \rightarrow \phi\pi^-)$.

⁴⁸ BUSKULIC 92E is measured using $D_s^- \rightarrow \phi\pi^-$ and $K^*(892)^0 K^+$ events. They use $2.7 \pm 0.7\%$ for the π^+ branching fraction. The average product branching fraction is measured to be $\text{B}(\bar{b} \rightarrow B_s^0)\text{B}(B_s^0 \rightarrow D_s^- \ell^+ \nu_\ell \text{ anything}) = 0.020 \pm 0.0055^{+0.005}_{-0.006}$. We evaluate using our current values $\text{B}(\bar{b} \rightarrow B_s^0) = 0.107 \pm 0.014$ and $\text{B}(D_s^- \rightarrow \phi\pi^-) = 0.036 \pm 0.009$. Our first error is their experiment's and our second error is that due to $\text{B}(\bar{b} \rightarrow B_s^0)$ and $\text{B}(D_s^- \rightarrow \phi\pi^-)$. Superseded by BUSKULIC 95O.

See key on page 373

Meson Particle Listings

 B_s^0 $\Gamma(D_s^- \pi^+)/\Gamma_{\text{total}}$ Γ_3/Γ

VALUE (units 10^{-3})	EVTS	DOCUMENT ID	TECN	COMMENT
3.2 ± 0.9 OUR AVERAGE				Error includes scale factor of 1.3.
$3.0 \pm 0.7 \pm 0.1$		49 ABULENCIA	07c CDF	$p\bar{p}$ at 1.96 TeV
$6.8 \pm 2.2 \pm 1.6$		DRUTSKOY	07A BELL	$e^+e^- \rightarrow \Upsilon(5S)$
$3.5 \pm 1.1 \pm 0.2$		50 ABULENCIA	06j CDF	Repl. by ABULENCIA 07c
<130	6	51 AKERS	94j OPAL	$e^+e^- \rightarrow Z$
seen	1	BUSKULIC	93g ALEP	$e^+e^- \rightarrow Z$

49 ABULENCIA 07c reports $[B(B_s^0 \rightarrow D_s^- \pi^+)] / [B(B^0 \rightarrow D^- \pi^+)] = 1.13 \pm 0.08 \pm 0.23$. We multiply by our best value $B(B^0 \rightarrow D^- \pi^+) = (2.68 \pm 0.13) \times 10^{-3}$. Our first error is their experiment's error and our second error is the systematic error from using our best value.

50 ABULENCIA 06j reports $[B(B_s^0 \rightarrow D_s^- \pi^+)] / [B(B^0 \rightarrow D^- \pi^+)] = 1.32 \pm 0.18 \pm 0.38$. We multiply by our best value $B(B^0 \rightarrow D^- \pi^+) = (2.68 \pm 0.13) \times 10^{-3}$. Our first error is their experiment's error and our second error is the systematic error from using our best value.

51 AKERS 94j sees ≤ 6 events and measures the limit on the product branching fraction $f(\bar{b} \rightarrow B_s^0) \cdot B(B_s^0 \rightarrow D_s^- \pi^+) < 1.3\%$ at CL = 90%. We divide by our current value $B(\bar{b} \rightarrow B_s^0) = 0.105$.

 $\Gamma(D_s^- \pi^+ \pi^+ \pi^-)/\Gamma_{\text{total}}$ Γ_4/Γ

VALUE (units 10^{-3})	DOCUMENT ID	TECN	COMMENT
$8.4 \pm 1.9 \pm 2.7$	52 ABULENCIA	07c CDF	$p\bar{p}$ at 1.96 TeV
52 ABULENCIA 07c reports $[B(B_s^0 \rightarrow D_s^- \pi^+ \pi^+ \pi^-)] / [B(B^0 \rightarrow D^- \pi^+ \pi^+ \pi^-)] = 1.05 \pm 0.10 \pm 0.22$. We multiply by our best value $B(B^0 \rightarrow D^- \pi^+ \pi^+ \pi^-) = (8.0 \pm 2.5) \times 10^{-3}$. Our first error is their experiment's error and our second error is the systematic error from using our best value.			

 $\Gamma(D_s^+ D_s^-)/\Gamma_{\text{total}}$ Γ_6/Γ

VALUE (units 10^{-3})	CL%	DOCUMENT ID	TECN	COMMENT
$10.7^{+3.6}_{-3.3} \pm 1.1$		53 AALTONEN	08f CDF	$p\bar{p}$ at 1.96 TeV
<67	90	DRUTSKOY	07A BELL	$e^+e^- \rightarrow \Upsilon(5S)$

53 AALTONEN 08f reports $[B(B_s^0 \rightarrow D_s^+ D_s^-)] / [B(B^0 \rightarrow D^- D_s^+)] = 1.44^{+0.48}_{-0.44}$. We multiply by our best value $B(B^0 \rightarrow D^- D_s^+) = (7.4 \pm 0.7) \times 10^{-3}$. Our first error is their experiment's error and our second error is the systematic error from using our best value.

 $\Gamma(D_s^{*+} D_s^-)/\Gamma_{\text{total}}$ Γ_7/Γ

VALUE	CL%	DOCUMENT ID	TECN	COMMENT
<0.121	90	DRUTSKOY	07A BELL	$e^+e^- \rightarrow \Upsilon(5S)$

 $\Gamma(D_s^{*+} D_s^{*-})/\Gamma_{\text{total}}$ Γ_8/Γ

VALUE	CL%	DOCUMENT ID	TECN	COMMENT
<0.257	90	DRUTSKOY	07A BELL	$e^+e^- \rightarrow \Upsilon(5S)$

 $\Gamma(D_s^{(*)+} D_s^{(*)-})/\Gamma_{\text{total}}$ Γ_5/Γ

VALUE	CL%	DOCUMENT ID	TECN	COMMENT
$0.049^{+0.029}_{-0.025}$ OUR AVERAGE				Error includes scale factor of 1.2.
$0.039^{+0.019}_{-0.017} \pm 0.016$		54 ABAZOV	07Y D0	$p\bar{p}$ at 1.96 TeV
$0.12 \pm 0.05 \pm 0.10$		55 BARATE	00k ALEP	$e^+e^- \rightarrow Z$

54 Uses the final states where $D_s^+ \rightarrow \phi \pi^+$ and $D_s^- \rightarrow \phi \mu^- \bar{\nu}_\mu$.

55 Uses $\phi \phi$ correlations from $B_s^0(\text{short}) \rightarrow D_s^{(*)+} D_s^{(*)-}$.

 $\Gamma(J/\psi(1S)\phi)/\Gamma_{\text{total}}$ Γ_9/Γ

VALUE (units 10^{-3})	EVTS	DOCUMENT ID	TECN	COMMENT
$0.93 \pm 0.28 \pm 0.17$		56 ABE	96q CDF	$p\bar{p}$
• • • We do not use the following data for averages, fits, limits, etc. • • •				
<6	1	57 AKERS	94j OPAL	$e^+e^- \rightarrow Z$
seen	14	58 ABE	93f CDF	$p\bar{p}$ at 1.8 TeV
seen	1	59 ACTON	92n OPAL	Sup. by AKERS 94j

56 ABE 96q assumes $f_u = f_d$ and $f_s/f_u = 0.40 \pm 0.06$. Uses $B \rightarrow J/\psi(1S) K$ and $B \rightarrow J/\psi(1S) K^*$ branching fractions from PDG 94. They quote two systematic errors, ± 0.10 and ± 0.14 where the latter is the uncertainty in f_s . We combine in quadrature.

57 AKERS 94j sees one event and measures the limit on the product branching fraction $f(\bar{b} \rightarrow B_s^0) \cdot B(B_s^0 \rightarrow J/\psi(1S)\phi) < 7 \times 10^{-4}$ at CL = 90%. We divide by $B(\bar{b} \rightarrow B_s^0) = 0.112$.

58 ABE 93f measured using $J/\psi(1S) \rightarrow \mu^+ \mu^-$ and $\phi \rightarrow K^+ K^-$.

59 In ACTON 92n a limit on the product branching fraction is measured to be $f(\bar{b} \rightarrow B_s^0) \cdot B(B_s^0 \rightarrow J/\psi(1S)\phi) \leq 0.22 \times 10^{-2}$.

 $\Gamma(J/\psi(1S)\pi^0)/\Gamma_{\text{total}}$ Γ_{10}/Γ

VALUE	CL%	DOCUMENT ID	TECN
<1.2 $\times 10^{-3}$	90	60 ACCIARRI	97c L3
60 ACCIARRI 97c assumes B^0 production fraction $(39.5 \pm 4.0\%)$ and B_s $(12.0 \pm 3.0\%)$.			

 $\Gamma(J/\psi(1S)\eta)/\Gamma_{\text{total}}$ Γ_{11}/Γ

VALUE	CL%	DOCUMENT ID	TECN
<3.8 $\times 10^{-3}$	90	61 ACCIARRI	97c L3
61 ACCIARRI 97c assumes B^0 production fraction $(39.5 \pm 4.0\%)$ and B_s $(12.0 \pm 3.0\%)$.			

 $\Gamma(\psi(2S)\phi)/\Gamma_{\text{total}}$ Γ_{12}/Γ

VALUE (units 10^{-4})	EVTS	DOCUMENT ID	TECN	COMMENT
$4.8 \pm 1.4 \pm 1.7$		62 ABULENCIA	06n CDF	$p\bar{p}$ at 1.96 TeV
• • • We do not use the following data for averages, fits, limits, etc. • • •				
seen	1	BUSKULIC	93g ALEP	$e^+e^- \rightarrow Z$

62 ABULENCIA 06n reports $[B(B_s^0 \rightarrow \psi(2S)\phi)] / [B(B_s^0 \rightarrow J/\psi(1S)\phi)] = 0.52 \pm 0.13 \pm 0.07$. We multiply by our best value $B(B_s^0 \rightarrow J/\psi(1S)\phi) = (9.3 \pm 3.3) \times 10^{-4}$. Our first error is their experiment's error and our second error is the systematic error from using our best value.

 $\Gamma(\pi^+ \pi^-)/\Gamma_{\text{total}}$ Γ_{13}/Γ

VALUE (units 10^{-6})	CL%	DOCUMENT ID	TECN	COMMENT
< 1.7	90	63 ABULENCIA,A	06d CDF	$p\bar{p}$ at 1.96 TeV
<232	90	64 ABE	00c SLD	$e^+e^- \rightarrow Z$
<170	90	65 BUSKULIC	96v ALEP	$e^+e^- \rightarrow Z$

63 ABULENCIA,A 06d obtains this from $B(B_s \rightarrow \pi^+ \pi^-) / B(B_s \rightarrow K^+ K^-) < 0.05$ at 90% CL, assuming $B(B_s \rightarrow K^+ K^-) = (33 \pm 6 \pm 7) \times 10^{-6}$.

64 ABE 00c assumes $B(Z \rightarrow b\bar{b}) = (21.7 \pm 0.1)\%$ and the B fractions $f_{B^0} = f_{B^+} = (39.7^{+1.8}_{-2.2})\%$ and $f_{B_s} = (10.5^{+1.8}_{-2.2})\%$.

65 BUSKULIC 96v assumes PDG 96 production fractions for B^0 , B^+ , B_s , b baryons.

 $\Gamma(\pi^0 \pi^0)/\Gamma_{\text{total}}$ Γ_{14}/Γ

VALUE	CL%	DOCUMENT ID	TECN	COMMENT
<2.1 $\times 10^{-4}$	90	66 ACCIARRI	95h L3	$e^+e^- \rightarrow Z$
66 ACCIARRI 95h assumes $f_{B^0} = 39.5 \pm 4.0$ and $f_{B_s} = 12.0 \pm 3.0\%$.				

 $\Gamma(\eta \pi^0)/\Gamma_{\text{total}}$ Γ_{15}/Γ

VALUE	CL%	DOCUMENT ID	TECN	COMMENT
<1.0 $\times 10^{-3}$	90	67 ACCIARRI	95h L3	$e^+e^- \rightarrow Z$
67 ACCIARRI 95h assumes $f_{B^0} = 39.5 \pm 4.0$ and $f_{B_s} = 12.0 \pm 3.0\%$.				

 $\Gamma(\eta \eta)/\Gamma_{\text{total}}$ Γ_{16}/Γ

VALUE	CL%	DOCUMENT ID	TECN	COMMENT
<1.5 $\times 10^{-3}$	90	68 ACCIARRI	95h L3	$e^+e^- \rightarrow Z$
68 ACCIARRI 95h assumes $f_{B^0} = 39.5 \pm 4.0$ and $f_{B_s} = 12.0 \pm 3.0\%$.				

 $\Gamma(\rho^0 \rho^0)/\Gamma_{\text{total}}$ Γ_{17}/Γ

VALUE	CL%	DOCUMENT ID	TECN	COMMENT
<3.20 $\times 10^{-4}$	90	69 ABE	00c SLD	$e^+e^- \rightarrow Z$
69 ABE 00c assumes $B(Z \rightarrow b\bar{b}) = (21.7 \pm 0.1)\%$ and the B fractions $f_{B^0} = f_{B^+} = (39.7^{+1.8}_{-2.2})\%$ and $f_{B_s} = (10.5^{+1.8}_{-2.2})\%$.				

 $\Gamma(\phi \rho^0)/\Gamma_{\text{total}}$ Γ_{18}/Γ

VALUE	CL%	DOCUMENT ID	TECN	COMMENT
<6.17 $\times 10^{-4}$	90	70 ABE	00c SLD	$e^+e^- \rightarrow Z$
70 ABE 00c assumes $B(Z \rightarrow b\bar{b}) = (21.7 \pm 0.1)\%$ and the B fractions $f_{B^0} = f_{B^+} = (39.7^{+1.8}_{-2.2})\%$ and $f_{B_s} = (10.5^{+1.8}_{-2.2})\%$.				

 $\Gamma(\phi \phi)/\Gamma_{\text{total}}$ Γ_{19}/Γ

VALUE (units 10^{-6})	CL%	DOCUMENT ID	TECN	COMMENT
$14^{+6}_{-5} \pm 6$		71 ACOSTA	05j CDF	$p\bar{p}$ at 1.96 TeV
• • • We do not use the following data for averages, fits, limits, etc. • • •				
<1183	90	72 ABE	00c SLD	$e^+e^- \rightarrow Z$

71 Uses $B(B^0 \rightarrow J/\psi\phi) = (1.38 \pm 0.49) \times 10^{-3}$ and production cross-section ratio of $\sigma(B_s)/\sigma(B^0) = 0.26 \pm 0.04$.

72 ABE 00c assumes $B(Z \rightarrow b\bar{b}) = (21.7 \pm 0.1)\%$ and the B fractions $f_{B^0} = f_{B^+} = (39.7^{+1.8}_{-2.2})\%$ and $f_{B_s} = (10.5^{+1.8}_{-2.2})\%$.

Meson Particle Listings

 B_S^0 $\Gamma(\pi^+ K^-)/\Gamma_{\text{total}}$ Γ_{20}/Γ

VALUE (units 10^{-6})	CL%	DOCUMENT ID	TECN	COMMENT
< 5.6	90	73 ABULENCIA,A 06D	CDF	$p\bar{p}$ at 1.96 TeV
••• We do not use the following data for averages, fits, limits, etc. •••				
<261	90	74 ABE	00c SLD	$e^+e^- \rightarrow Z$
<210	90	75 BUSKULIC	96v ALEP	$e^+e^- \rightarrow Z$
<260	90	76 AKERS	94L OPAL	$e^+e^- \rightarrow Z$
73 ABULENCIA,A 06D obtains this from $(f_S/f_d)(B(B_S \rightarrow \pi^+ K^-)/B(B^0 \rightarrow K^+ \pi^-)) < 0.08$ at 90% CL, assuming $f_S/f_d = 0.260 \pm 0.039$ and $B(B^0 \rightarrow K^+ \pi^-) = (18.9 \pm 0.7) \times 10^{-6}$.				
74 ABE 00c assumes $B(Z \rightarrow b\bar{b}) = (21.7 \pm 0.1)\%$ and the B fractions $f_{B^0} = f_{B^+} = (39.7_{-2.2}^{+1.8})\%$ and $f_{B_S} = (10.5_{-2.2}^{+1.8})\%$.				
75 BUSKULIC 96v assumes PDG 96 production fractions for B^0, B^+, B_S, b baryons.				
76 Assumes $B(Z \rightarrow b\bar{b}) = 0.217$ and $B_d^0(B_S^0)$ fraction 39.5% (12%).				

 $\Gamma(K^+ K^-)/\Gamma_{\text{total}}$ Γ_{21}/Γ

VALUE (units 10^{-5})	CL%	DOCUMENT ID	TECN	COMMENT
$3.3 \pm 0.6 \pm 0.7$		77 ABULENCIA,A 06D	CDF	$p\bar{p}$ at 1.96 TeV
••• We do not use the following data for averages, fits, limits, etc. •••				
<31	90	DRUTSKOY 07A	BELL	$e^+e^- \rightarrow \Upsilon(5S)$
<28.3	90	78 ABE	00c SLD	$e^+e^- \rightarrow Z$
< 5.9	90	79 BUSKULIC	96v ALEP	$e^+e^- \rightarrow Z$
<14	90	80 AKERS	94L OPAL	$e^+e^- \rightarrow Z$
77 ABULENCIA,A 06D obtains this from $(f_S/f_d)(B(B_S \rightarrow K^+ K^-)/B(B^0 \rightarrow K^+ \pi^-)) = 0.46 \pm 0.08 \pm 0.07$, assuming $f_S/f_d = 0.260 \pm 0.039$ and $B(B^0 \rightarrow K^+ \pi^-) = (18.9 \pm 0.7) \times 10^{-6}$.				
78 ABE 00c assumes $B(Z \rightarrow b\bar{b}) = (21.7 \pm 0.1)\%$ and the B fractions $f_{B^0} = f_{B^+} = (39.7_{-2.2}^{+1.8})\%$ and $f_{B_S} = (10.5_{-2.2}^{+1.8})\%$.				
79 BUSKULIC 96v assumes PDG 96 production fractions for B^0, B^+, B_S, b baryons.				
80 Assumes $B(Z \rightarrow b\bar{b}) = 0.217$ and $B_d^0(B_S^0)$ fraction 39.5% (12%).				

 $\Gamma(\bar{K}^*(892)^0 \rho^0)/\Gamma_{\text{total}}$ Γ_{22}/Γ

VALUE	CL%	DOCUMENT ID	TECN	COMMENT
$< 7.67 \times 10^{-4}$	90	81 ABE	00c SLD	$e^+e^- \rightarrow Z$
81 ABE 00c assumes $B(Z \rightarrow b\bar{b}) = (21.7 \pm 0.1)\%$ and the B fractions $f_{B^0} = f_{B^+} = (39.7_{-2.2}^{+1.8})\%$ and $f_{B_S} = (10.5_{-2.2}^{+1.8})\%$.				

 $\Gamma(\bar{K}^*(892)^0 K^*(892)^0)/\Gamma_{\text{total}}$ Γ_{23}/Γ

VALUE	CL%	DOCUMENT ID	TECN	COMMENT
$< 16.81 \times 10^{-4}$	90	82 ABE	00c SLD	$e^+e^- \rightarrow Z$
82 ABE 00c assumes $B(Z \rightarrow b\bar{b}) = (21.7 \pm 0.1)\%$ and the B fractions $f_{B^0} = f_{B^+} = (39.7_{-2.2}^{+1.8})\%$ and $f_{B_S} = (10.5_{-2.2}^{+1.8})\%$.				

 $\Gamma(\phi K^*(892)^0)/\Gamma_{\text{total}}$ Γ_{24}/Γ

VALUE	CL%	DOCUMENT ID	TECN	COMMENT
$< 10.13 \times 10^{-4}$	90	83 ABE	00c SLD	$e^+e^- \rightarrow Z$
83 ABE 00c assumes $B(Z \rightarrow b\bar{b}) = (21.7 \pm 0.1)\%$ and the B fractions $f_{B^0} = f_{B^+} = (39.7_{-2.2}^{+1.8})\%$ and $f_{B_S} = (10.5_{-2.2}^{+1.8})\%$.				

 $\Gamma(\rho\bar{\rho})/\Gamma_{\text{total}}$ Γ_{25}/Γ

VALUE	CL%	DOCUMENT ID	TECN	COMMENT
$< 5.9 \times 10^{-5}$	90	84 BUSKULIC	96v ALEP	$e^+e^- \rightarrow Z$
84 BUSKULIC 96v assumes PDG 96 production fractions for B^0, B^+, B_S, b baryons.				

 $\Gamma(\gamma\gamma)/\Gamma_{\text{total}}$ Γ_{26}/Γ

VALUE	CL%	DOCUMENT ID	TECN	COMMENT
$< 5.3 \times 10^{-5}$	90	DRUTSKOY 07A	BELL	$e^+e^- \rightarrow \Upsilon(5S)$
••• We do not use the following data for averages, fits, limits, etc. •••				
<14.8 $\times 10^{-5}$	90	85 ACCIARRI	95i L3	$e^+e^- \rightarrow Z$
85 ACCIARRI 95i assumes $f_{B^0} = 39.5 \pm 4.0$ and $f_{B_S} = 12.0 \pm 3.0\%$.				

 $\Gamma(\phi\gamma)/\Gamma_{\text{total}}$ Γ_{27}/Γ

VALUE	CL%	DOCUMENT ID	TECN	COMMENT
$< 1.2 \times 10^{-4}$	90	ACOSTA 02G	CDF	$p\bar{p}$ at 1.8 TeV
••• We do not use the following data for averages, fits, limits, etc. •••				
<3.9 $\times 10^{-4}$	90	DRUTSKOY 07A	BELL	$e^+e^- \rightarrow \Upsilon(5S)$
<7 $\times 10^{-4}$	90	86 ADAM	96D DLPH	$e^+e^- \rightarrow Z$
86 ADAM 96D assumes $f_{B^0} = f_{B^-} = 0.39$ and $f_{B_S} = 0.12$.				

 $\Gamma(\mu^+ \mu^-)/\Gamma_{\text{total}}$ Γ_{28}/Γ

VALUE	CL%	DOCUMENT ID	TECN	COMMENT
$< 4.7 \times 10^{-8}$	90	87 AALTONEN	08i CDF	$p\bar{p}$ at 1.96 TeV
••• We do not use the following data for averages, fits, limits, etc. •••				
<4.4 $\times 10^{-8}$	90	88 ABAZOV	07Q D0	$p\bar{p}$ at 1.96 TeV
<4.1 $\times 10^{-7}$	90	89 ABAZOV	05E D0	$p\bar{p}$ at 1.96 TeV
<1.5 $\times 10^{-7}$	90	90 ABULENCIA	05 CDF	$p\bar{p}$ at 1.96 TeV
<5.8 $\times 10^{-7}$	90	91 ACOSTA	04D CDF	$p\bar{p}$ at 1.96 TeV
<2.0 $\times 10^{-6}$	90	92 ABE	98 CDF	$p\bar{p}$ at 1.8 TeV
<3.8 $\times 10^{-5}$	90	93 ACCIARRI	97B L3	$e^+e^- \rightarrow Z$
<8.4 $\times 10^{-6}$	90	94 ABE	96L CDF	Repl. by ABE 98
87 Uses B production ratio $f(\bar{b} \rightarrow B^+)/f(\bar{b} \rightarrow B_S^0) = 3.86 \pm 0.59$, and the number of $B^+ \rightarrow J/\psi K^+$ decays.				
88 Uses B production ratio $f(\bar{b} \rightarrow B^+)/f(\bar{b} \rightarrow B_S^0) = 3.86 \pm 0.54$ and the number of $B^+ \rightarrow J/\psi K^+$ decays.				
89 Assumes production cross-section $\sigma(B_S)/\sigma(B^+) = 0.270 \pm 0.034$.				
90 Assumes production cross section $\sigma(B^+)/\sigma(B_S) = 3.71 \pm 0.41$ and $B(B^+ \rightarrow J/\psi K^+ \rightarrow \mu^+ \mu^- K^+) = (5.88 \pm 0.26) \times 10^{-5}$.				
91 Assumes production cross-section $\sigma(B_S)/\sigma(B^+) = 0.100/0.391$ and the CDF measured value of $\sigma(B^+) = 3.6 \pm 0.6 \mu\text{b}$.				
92 ABE 98 assumes production of $\sigma(B^0) = \sigma(B^+)$ and $\sigma(B_S)/\sigma(B^0) = 1/3$. They normalize to their measured $\sigma(B^0, p_T(B) > 6, y < 1.0) = 2.39 \pm 0.32 \pm 0.44 \mu\text{b}$.				
93 ACCIARRI 97B assume PDG 96 production fractions for B^+, B^0, B_S , and Λ_b .				
94 ABE 96L assumes B^+/B_S production ratio 3/1. They normalize to their measured $\sigma(B^+, p_T(B) > 6 \text{ GeV}/c, y < 1) = 2.39 \pm 0.54 \mu\text{b}$.				

 $\Gamma(e^+ e^-)/\Gamma_{\text{total}}$ Γ_{29}/Γ

VALUE	CL%	DOCUMENT ID	TECN	COMMENT
$< 5.4 \times 10^{-5}$	90	95 ACCIARRI	97B L3	$e^+e^- \rightarrow Z$
95 ACCIARRI 97B assume PDG 96 production fractions for B^+, B^0, B_S , and Λ_b .				

 $\Gamma(e^\pm \mu^\mp)/\Gamma_{\text{total}}$ Γ_{30}/Γ

VALUE	CL%	DOCUMENT ID	TECN	COMMENT
$< 6.1 \times 10^{-6}$	90	ABE	98V CDF	$p\bar{p}$ at 1.8 TeV
••• We do not use the following data for averages, fits, limits, etc. •••				
<4.1 $\times 10^{-5}$	90	96 ACCIARRI	97B L3	$e^+e^- \rightarrow Z$
96 ACCIARRI 97B assume PDG 96 production fractions for B^+, B^0, B_S , and Λ_b .				

 $\Gamma(\phi(1020) \mu^+ \mu^-)/\Gamma_{\text{total}}$ Γ_{31}/Γ

VALUE	CL%	DOCUMENT ID	TECN	COMMENT
$< 3.2 \times 10^{-6}$	90	97 ABAZOV	06G D0	$p\bar{p}$ at 1.96 TeV
••• We do not use the following data for averages, fits, limits, etc. •••				
<4.7 $\times 10^{-5}$	90	ACOSTA 02D	CDF	$p\bar{p}$ at 1.8 TeV
97 Uses $B(B_S^0 \rightarrow J/\psi \phi) = 9.3 \times 10^{-4}$.				

 $\Gamma(\phi\nu\bar{\nu})/\Gamma_{\text{total}}$ Γ_{32}/Γ

VALUE	CL%	DOCUMENT ID	TECN	COMMENT
$< 5.4 \times 10^{-3}$	90	98 ADAM	96D DLPH	$e^+e^- \rightarrow Z$
98 ADAM 96D assumes $f_{B^0} = f_{B^-} = 0.39$ and $f_{B_S} = 0.12$.				

POLARIZATION IN B_S^0 DECAY Γ_L/Γ in $B_S^0 \rightarrow J/\psi(1S)\phi$

VALUE	EVTS	DOCUMENT ID	TECN	COMMENT
0.533 ± 0.021 OUR AVERAGE				
0.531 $\pm 0.020 \pm 0.007$	99	AALTONEN 08j	CDF	$p\bar{p}$ at 1.96 TeV
0.61 $\pm 0.14 \pm 0.02$	100	AFFOLDER 00N	CDF	$p\bar{p}$ at 1.8 TeV
0.56 $\pm 0.21_{-0.04}^{+0.02}$	19	ABE 95Z	CDF	$p\bar{p}$ at 1.8 TeV
99 Measured using the time-dependent angular analysis of $B_S^0 \rightarrow J/\psi \phi$ decays.				
100 AFFOLDER 00N measurements are based on 40 B_S^0 candidates obtained from a data sample of 89 pb $^{-1}$. The P -wave fraction is found to be 0.23 $\pm 0.19 \pm 0.04$.				

 Γ_{\perp}/Γ in $B_S^0 \rightarrow J/\psi(1S)\phi$

VALUE	DOCUMENT ID	TECN	COMMENT
$0.239 \pm 0.029 \pm 0.011$	101	AALTONEN 08j	CDF $p\bar{p}$ at 1.96 TeV
101 Measured using the time-dependent angular analysis of $B_S^0 \rightarrow J/\psi \phi$ decays.			

$B_s^0\text{-}\bar{B}_s^0$ MIXING

For a discussion of $B_s^0\text{-}\bar{B}_s^0$ mixing see the note on " $B^0\text{-}\bar{B}^0$ Mixing" in the B^0 Particle Listings above.

χ_s is a measure of the time-integrated $B_s^0\text{-}\bar{B}_s^0$ mixing probability that produced $B_s^0(\bar{B}_s^0)$ decays as a $\bar{B}_s^0(B_s^0)$. Mixing violates $\Delta B \neq 2$ rule.

$$\chi_s = \frac{x_s^2}{2(1+x_s^2)}$$

$$x_s = \frac{\Delta m_{B_s^0}}{\Gamma_{B_s^0}} = (m_{B_{sH}^0} - m_{B_{sL}^0}) \tau_{B_s^0},$$

where H, L stand for heavy and light states of two B_s^0 CP eigenstates and

$$\tau_{B_s^0} = \frac{1}{0.5(\Gamma_{B_{sH}^0} + \Gamma_{B_{sL}^0})}.$$

$$\Delta m_{B_s^0} = m_{B_{sH}^0} - m_{B_{sL}^0}$$

$\Delta m_{B_s^0}$ is a measure of 2π times the $B_s^0\text{-}\bar{B}_s^0$ oscillation frequency in time-dependent mixing experiments.

VALUE (10^{12} h s^{-1})	CL%	DOCUMENT ID	TECN	COMMENT
17.77 ± 0.10 ± 0.07		102 ABULENCIA,A 06G	CDF	$p\bar{p}$ at 1.96 TeV
• • • We do not use the following data for averages, fits, limits, etc. • • •				
17-21	90	103 ABAZOV 06B	D0	$p\bar{p}$ at 1.96 TeV
17.31 ^{+0.33} _{-0.18} ± 0.07		104 ABULENCIA 06Q	CDF	Repl. by ABULENCIA,A 06G
> 8.0	95	105 ABDALLAH 04J	DLPH	$e^+e^- \rightarrow Z^0$
> 4.9	95	106 ABDALLAH 04J	DLPH	$e^+e^- \rightarrow Z^0$
> 8.5	95	107 ABDALLAH 04J	DLPH	$e^+e^- \rightarrow Z^0$
> 5.0	95	108 ABDALLAH 03B	DLPH	$e^+e^- \rightarrow Z$
>10.3	95	109 ABE 03	SLD	$e^+e^- \rightarrow Z$
>10.9	95	110 HEISTER 03E	ALEP	$e^+e^- \rightarrow Z$
> 5.3	95	111 ABE 02V	SLD	$e^+e^- \rightarrow Z$
> 1.0	95	112 ABBIENDI 01D	OPAL	$e^+e^- \rightarrow Z$
> 7.4	95	113 ABREU 00Y	DLPH	Repl. by ABDALLAH 04J
> 4.0	95	114 ABREU,P 00G	DLPH	$e^+e^- \rightarrow Z$
> 5.2	95	115 ABBIENDI 99S	OPAL	$e^+e^- \rightarrow Z$
<96	95	116 ABE 99D	CDF	$p\bar{p}$ at 1.8 TeV
> 5.8	95	117 ABE 99J	CDF	$p\bar{p}$ at 1.8 TeV
> 9.6	95	118 BARATE 99J	ALEP	$e^+e^- \rightarrow Z$
> 7.9	95	119 BARATE 98C	ALEP	Repl. by BARATE 99J
> 3.1	95	120 ACKERSTAFF 97U	OPAL	Repl. by ABBIENDI 99S
> 2.2	95	121 ACKERSTAFF 97V	OPAL	Repl. by ABBIENDI 99S
> 6.5	95	122 ADAM 97	DLPH	Repl. by ABREU 00Y
> 6.6	95	123 BUSKULIC 96M	ALEP	Repl. by BARATE 98C
> 2.2	95	121 AKERS 95J	OPAL	Sup. by ACKERSTAFF 97V
> 5.7	95	124 BUSKULIC 95J	ALEP	$e^+e^- \rightarrow Z$
> 1.8	95	121 BUSKULIC 94B	ALEP	$e^+e^- \rightarrow Z$

102 Significance of oscillation signal is 5.4 σ . Also reports $|V_{td} / V_{ts}| = 0.2060 \pm 0.0007 + 0.0081$ _{-0.0060}.

103 A likelihood scan over the oscillation frequency, Δm_s , gives a most probable value of 19 ps^{-1} and a range of $17 < \Delta m_s < 21 (\text{ps}^{-1})$ at 90% C.L. assuming Gaussian uncertainties. Also excludes $\Delta m_s < 14.8 \text{ ps}^{-1}$ at 95% C.L.

104 Significance of oscillation signal is 0.2%. Also reported the value $|V_{td} / V_{ts}| = 0.208 \pm 0.001 + 0.008$ _{-0.002 - 0.006}.

105 Uses leptons emitted with large momentum transverse to a jet and improved techniques for vertexing and flavor-tagging.

106 Updates of D_s -lepton analysis.

107 Combined results from all Delphi analyses.

108 Events with a high transverse momentum lepton were removed and an inclusively reconstructed vertex was required.

109 ABE 03 uses the novel "charge dipole" technique to reconstruct separate secondary and tertiary vertices originating from the $B \rightarrow D$ decay chain. The analysis excludes $\Delta m_s < 4.9 \text{ ps}^{-1}$ and $7.9 < \Delta m_s < 10.3 \text{ ps}^{-1}$.

110 Three analyses based on complementary event selections: (1) fully-reconstructed hadronic decays; (2) semileptonic decays with D_s exclusively reconstructed; (3) inclusive semileptonic decays.

111 ABE 02v uses exclusively reconstructed D_s^- mesons and excludes $\Delta m_s < 1.4 \text{ ps}^{-1}$ and $2.4 < \Delta m_s < 5.3 \text{ ps}^{-1}$ at 95% C.L.

112 Uses fully or partially reconstructed $D_s \ell$ vertices and a mixing tag as a flavor tagging.

113 Replaced by ABDALLAH 04A. Uses $D_s^- \ell^+$, and $\phi \ell^+$ vertices, and a multi-variable discriminant as a flavor tagging.

114 Uses inclusive D_s vertices and fully reconstructed B_s decays and a multi-variable discriminant as a flavor tagging.

115 Uses $\ell\text{-}Q_{\text{hem}}$ and $\ell\text{-}\ell$.

116 ABE 99D assumes $\tau_{B_s^0} = 1.55 \pm 0.05 \text{ ps}$ and $\Delta\Gamma/\Delta m = (5.6 \pm 2.6) \times 10^{-3}$.

117 ABE 99J uses $\phi\text{-}\ell\text{-}\ell$ correlation.

118 BARATE 99J uses combination of an inclusive lepton and D_s^- -based analyses.

119 BARATE 98C combines results from $D_s h\text{-}\ell/Q_{\text{hem}}$, $D_s h\text{-}K$ in the same side, $D_s \ell\text{-}\ell/Q_{\text{hem}}$ and $D_s \ell\text{-}K$ in the same side.

120 Uses $\ell\text{-}Q_{\text{hem}}$.

121 Uses $\ell\text{-}\ell$.

122 ADAM 97 combines results from $D_s \ell\text{-}Q_{\text{hem}}$, $\ell\text{-}Q_{\text{hem}}$, and $\ell\text{-}\ell$.

123 BUSKULIC 96M uses D_s lepton correlations and lepton, kaon, and jet charge tags.

124 BUSKULIC 95J uses $\ell\text{-}Q_{\text{hem}}$. They find $\Delta m_s > 5.6 [> 6.1]$ for $f_s = 10\% [12\%]$. We interpolate to our central value $f_s = 10.5\%$.

$$x_s = \Delta m_{B_s^0} / \Gamma_{B_s^0}$$

This is derived by the Heavy Flavor Averaging Group (HFAG) from the results on $\Delta m_{B_s^0}$ and "OUR EVALUATION" of the B_s^0 mean lifetime.

VALUE DOCUMENT ID

26.1 ± 0.5 OUR EVALUATION

χ_s

This $B_s^0\text{-}\bar{B}_s^0$ integrated mixing parameter is derived from x_s above.

VALUE DOCUMENT ID

0.49927 ± 0.00003 OUR EVALUATION

CP VIOLATION PARAMETERS in B_s^0

$\text{Re}(\epsilon_{B_s^0}) / (1 + |\epsilon_{B_s^0}|^2)$

CP impurity in B_s^0 system.

"OUR EVALUATION" is an average using rescaled values of the data listed below. The average and rescaling were performed by the Heavy Flavor Averaging Group (HFAG) and are described at <http://www.slac.stanford.edu/xorg/hfag/>. The averaging/scaling procedure takes into account correlation between the measurements.

VALUE (units 10^{-3}) DOCUMENT ID TECN COMMENT

-0.75 ± 2.52 OUR EVALUATION

6.1 ± 4.8 ± 0.9 125 ABAZOV 07A D0 $p\bar{p}$ at 1.96 TeV

125 The first direct measurement of the time integrated flavor untagged charge asymmetry in semileptonic B_s^0 decays is reported as $2\alpha_{SL}^S(\text{untagged}) = A_{SL}^S = (2.45 \pm 1.93 \pm 0.35) \times 10^{-2}$.

CP Violation phase β_s in the B_s^0 System

β_s is the CP-violating phase, defined as $\beta_s = \arg(-\frac{V_{ts}V_{td}^*}{V_{cs}V_{cb}^*})$.

VALUE DOCUMENT ID TECN COMMENT

0.35 +0.20 126,127 ABAZOV 07N D0 $p\bar{p}$ at 1.96 TeV

-0.24

• • • We do not use the following data for averages, fits, limits, etc. • • •

128 AALTONEN 08G CDF $p\bar{p}$ at 1.96 GeV

0.395 ± 0.280 +0.005
-0.070 126,129 ABAZOV 07 D0 Repl. by ABAZOV 07N

126 Reports ϕ_s which equals to $-2\beta_s$.

127 Combines D^0 measurements of time-dependent angular distributions in $B^0 \rightarrow J/\psi\phi$ and charge asymmetry in semileptonic decays. There is a 4-fold ambiguity in the solution.

128 Reports $0.32 < 2\beta_s < 2.82$ at 68% C.L. and confidence regions in the two-dimensional space of $2\beta_s$ and $\Delta\Gamma$ from the first measurement of $B_s^0 \rightarrow J/\psi\phi$ decays using flavor tagging. The probability of a deviation from SM prediction as large as the level of observed data is 15%.

129 The first direct measurement of the CP-violating mixing phase is reported from the time-dependent analysis of flavor untagged $B_s^0 \rightarrow J/\psi\phi$ decays.

 B_s^0 REFERENCES

AALTONEN 08F	PRL 100 021803	T. Aaltonen et al.	(CDF Collab.)
AALTONEN 08G	PRL 100 161802	T. Aaltonen et al.	(CDF Collab.)
AALTONEN 08I	PRL 100 101802	T. Aaltonen et al.	(CDF Collab.)
AALTONEN 08J	PRL 100 121803	T. Aaltonen et al.	(CDF Collab.)
ABAZOV 07	PRL 98 121801	V.M. Abazov et al.	(D0 Collab.)
ABAZOV 07A	PRL 98 151801	V.M. Abazov et al.	(D0 Collab.)
ABAZOV 07N	PR D76 057101	V.M. Abazov et al.	(D0 Collab.)
ABAZOV 07Q	PR D76 092001	V.M. Abazov et al.	(D0 Collab.)
ABAZOV 07Y	PRL 99 241801	V.M. Abazov et al.	(D0 Collab.)
ABULENCIA 07C	PRL 98 061802	A. Abulencia et al.	(FNAL CDF Collab.)
DRUTSKOY 07	PRL 98 052001	A. Drutskoy et al.	(BELLE Collab.)
DRUTSKOY 07A	PR D76 012002	A. Drutskoy et al.	(BELLE Collab.)
ABAZOV 06B	PRL 97 021802	V.M. Abazov et al.	(D0 Collab.)
ABAZOV 06G	PR D74 031107R	V.M. Abazov et al.	(D0 Collab.)
ABAZOV 06V	PRL 97 241801	V.M. Abazov et al.	(D0 Collab.)
ABULENCIA 06J	PRL 96 191801	A. Abulencia et al.	(CDF Collab.)
ABULENCIA 06N	PRL 96 231801	A. Abulencia et al.	(CDF Collab.)
ABULENCIA 06Q	PRL 97 052003	A. Abulencia et al.	(CDF Collab.)
ABULENCIA,A 06D	PRL 97 211802	A. Abulencia et al.	(CDF Collab.)
ABULENCIA,A 06G	PRL 97 242003	A. Abulencia et al.	(CDF Collab.)
ACOSTA 06	PRL 96 202001	D. Acosta et al.	(CDF Collab.)
ABAZOV 05B	PRL 94 042001	V.M. Abazov et al.	(D0 Collab.)
ABAZOV 05E	PRL 94 071802	V.M. Abazov et al.	(D0 Collab.)
ABAZOV 05W	PRL 95 171801	V.M. Abazov et al.	(D0 Collab.)
ABULENCIA 05	PRL 95 221805	A. Abulencia et al.	(CDF Collab.)
Also	PRL 95 241905 (erratum)	A. Abulencia et al.	(CDF Collab.)
ACOSTA 05	PRL 94 101803	D. Acosta et al.	(CDF Collab.)
ACOSTA 05J	PRL 95 031801	D. Acosta et al.	(CDF Collab.)
ABDALLAH 04A	PL B585 63	J. Abdallah et al.	(DELPHI Collab.)
ABDALLAH 04J	EPJ C35 35	J. Abdallah et al.	(DELPHI Collab.)
ACOSTA 04D	PRL 93 032001	D. Acosta et al.	(CDF Collab.)
ABDALLAH 03B	EPJ C28 155	J. Abdallah et al.	(DELPHI Collab.)
ABE 03	PR D67 012006	K. Abe et al.	(SLD Collab.)
HEISTER 03E	EPJ C29 143	A. Heister et al.	(ALEPH Collab.)
ABE 02V	PR D66 032009	K. Abe et al.	(SLD Collab.)
ACOSTA 02D	PR D65 111101R	D. Acosta et al.	(CDF Collab.)

Meson Particle Listings

$B_s^0, B_s^*, B_{s1}(5830)^0, B_{s2}^*(5840)^0$

ACOSTA	02G	PR D66 112002	D. Acosta et al.	(CDF Collab.)
ABBIENDI	01D	EPJ C19 241	G. Abbiendi et al.	(OPAL Collab.)
ABE	00C	PR D62 071101R	K. Abe et al.	(SLD Collab.)
ABREU	00Y	EPJ C16 555	P. Abreu et al.	(DELPHI Collab.)
ABREU,P	00G	EPJ C18 229	P. Abreu et al.	(DELPHI Collab.)
AFFOLDER	00N	PRL 85 4668	T. Affolder et al.	(CDF Collab.)
BARATE	00K	PL B486 286	R. Barate et al.	(ALEPH Collab.)
ABBIENDI	99S	EPJ C11 587	G. Abbiendi et al.	(OPAL Collab.)
ABE	99D	PR D59 032004	F. Abe et al.	(CDF Collab.)
ABE	99J	PRL 82 3576	F. Abe et al.	(CDF Collab.)
BARATE	99J	EPJ C7 553	R. Barate et al.	(ALEPH Collab.)
Also		EPJ C12 181 (erratum)	R. Barate et al.	(ALEPH Collab.)
ABE	98	PR D57 R3811	F. Abe et al.	(CDF Collab.)
ABE	98B	PR D57 5382	F. Abe et al.	(CDF Collab.)
ABE	98V	PRL 81 5742	F. Abe et al.	(CDF Collab.)
ACCIARRI	98S	PL B438 417	M. Acciari et al.	(L3 Collab.)
ACKERSTAFF	98F	EPJ C2 407	K. Ackerstaff et al.	(OPAL Collab.)
ACKERSTAFF	98G	PL B426 161	K. Ackerstaff et al.	(OPAL Collab.)
BARATE	98C	EPJ C4 367	R. Barate et al.	(ALEPH Collab.)
BARATE	98Q	EPJ C4 387	R. Barate et al.	(ALEPH Collab.)
PDG	98	EPJ C3 1	C. Caso et al.	(CDF Collab.)
ACCIARRI	97B	PL B391 474	M. Acciari et al.	(L3 Collab.)
ACCIARRI	97C	PL B391 481	M. Acciari et al.	(L3 Collab.)
ACKERSTAFF	97U	ZPHY C76 401	K. Ackerstaff et al.	(OPAL Collab.)
ACKERSTAFF	97V	ZPHY C76 417	K. Ackerstaff et al.	(OPAL Collab.)
ADAM	97	PL B414 382	W. Adam et al.	(DELPHI Collab.)
ABE	96B	PR D53 3496	F. Abe et al.	(CDF Collab.)
ABE	96L	PRL 76 4675	F. Abe et al.	(CDF Collab.)
ABE	96N	PRL 77 1945	F. Abe et al.	(CDF Collab.)
ABE	96Q	PR D54 6596	F. Abe et al.	(CDF Collab.)
ABREU	96F	ZPHY C71 11	P. Abreu et al.	(DELPHI Collab.)
ADAM	90D	ZPHY C72 207	W. Adam et al.	(DELPHI Collab.)
BUSKULIC	96E	ZPHY C69 585	D. Buskulic et al.	(ALEPH Collab.)
BUSKULIC	96M	PL B377 205	D. Buskulic et al.	(ALEPH Collab.)
BUSKULIC	96V	PL B384 471	D. Buskulic et al.	(ALEPH Collab.)
PDG	96	PR D54 1	R. M. Barnett et al.	(CDF Collab.)
ABE	95R	PRL 74 4988	F. Abe et al.	(CDF Collab.)
ABE	95Z	PRL 75 3068	F. Abe et al.	(CDF Collab.)
ACCIARRI	95H	PL B363 127	M. Acciari et al.	(L3 Collab.)
ACCIARRI	95I	PL B363 137	M. Acciari et al.	(L3 Collab.)
AKERS	95G	PL B350 273	R. Akers et al.	(OPAL Collab.)
AKERS	95J	ZPHY C66 555	R. Akers et al.	(OPAL Collab.)
BUSKULIC	95I	PL B356 409	D. Buskulic et al.	(ALEPH Collab.)
BUSKULIC	95O	PL B361 221	D. Buskulic et al.	(ALEPH Collab.)
ABREU	94D	PL B324 500	P. Abreu et al.	(DELPHI Collab.)
ABREU	94E	ZPHY C61 407	P. Abreu et al.	(DELPHI Collab.)
Also		PL B289 199	P. Abreu et al.	(DELPHI Collab.)
AKERS	94J	PL B337 196	R. Akers et al.	(OPAL Collab.)
AKERS	94L	PL B337 393	R. Akers et al.	(OPAL Collab.)
BUSKULIC	94B	PL B322 441	D. Buskulic et al.	(ALEPH Collab.)
BUSKULIC	94C	PL B322 275	D. Buskulic et al.	(ALEPH Collab.)
PDG	94	PR D50 1173	L. Montanet et al.	(CERN, LBL, BOST+)
ABE	93F	PRL 71 1685	F. Abe et al.	(CDF Collab.)
ACTON	93H	PL B312 501	P.D. Acton et al.	(OPAL Collab.)
BUSKULIC	93G	PL B311 425	D. Buskulic et al.	(ALEPH Collab.)
ABREU	92M	PL B289 199	P. Abreu et al.	(DELPHI Collab.)
ACTON	92N	PL B295 357	P.D. Acton et al.	(OPAL Collab.)
BUSKULIC	92E	PL B294 145	D. Buskulic et al.	(ALEPH Collab.)
LEE-FRANZINI	90	PRL 65 2947	J. Lee-Franzini et al.	(CUSB II Collab.)

B_s^*

 $I(J^P) = 0(1^-)$

I, J, P need confirmation. Quantum numbers shown are quark-model predictions.

B_s^* MASS

From mass difference below and the B_s^0 mass.

VALUE (MeV)	DOCUMENT ID	TECN	COMMENT
5412.8 ± 1.3 OUR FIT	Error includes scale factor of 1.2.		
5413.1 ± 2.6 OUR AVERAGE	Error includes scale factor of 1.8.		
5418 ± 1 ± 3	DRUTSKOY 07A BELL	e ⁺ e ⁻ → $\Upsilon(5S)$	
5411.7 ± 1.6 ± 0.6	¹ AQUINES 06 CLEO	e ⁺ e ⁻ → $\Upsilon(5S)$	
• • • We do not use the following data for averages, fits, limits, etc. • • •			
5414 ± 1 ± 3	² BONVICINI 06 CLEO	e ⁺ e ⁻ → $\Upsilon(5S)$	
¹ Utilized the beam constrained invariant mass peak positions for B_s^* and B_s^* to extract the measurement.			
² Uses 14 candidates consistent with B_s decays into final states with a J/ψ and a $D_s^{(*)-}$.			

$m_{B_s^*} - m_{B_s}$

VALUE (MeV)	DOCUMENT ID	TECN	COMMENT
46.5 ± 1.2 OUR FIT	Error includes scale factor of 1.1.		
46.1 ± 1.5 OUR AVERAGE			
45.7 ± 1.7 ± 0.7	³ AQUINES 06 CLEO	e ⁺ e ⁻ → $\Upsilon(5S)$	
47.0 ± 2.6	⁴ LEE-FRANZINI 90 CSB2	e ⁺ e ⁻ → $\Upsilon(5S)$	
• • • We do not use the following data for averages, fits, limits, etc. • • •			
48 ± 1 ± 3	⁵ BONVICINI 06 CLEO	Repl. by AQUINES 06	
³ Utilized the beam constrained invariant mass peak positions for B_s^* and B_s^* to extract the measurement.			
⁴ LEE-FRANZINI 90 measure 46.7 ± 0.4 ± 0.2 MeV for an admixture of $B_s^0, B_s^+,$ and B_s^- . They use the shape of the photon line to separate the above value for B_s^- .			
⁵ Uses 14 candidates consistent with B_s decays into final states with a J/ψ and a $D_s^{(*)-}$.			

$$|(m_{B_s^*} - m_{B_s}) - (m_{B^*} - m_B)|$$

VALUE (MeV)	CL%	DOCUMENT ID	TECN	COMMENT
<6	95	ABREU 95R	DLPH	$E_{cm}^e = 88-94$ GeV

B_s^* DECAY MODES

Mode	Fraction (Γ_i/Γ)
$\Gamma_1 B_s \gamma$	dominant

B_s^* REFERENCES

DRUTSKOY 07A	PR D76 012002	A. Drutskoy et al.	(BELLE Collab.)
AQUINES 06	PRL 96 152001	O. Aquines et al.	(CLEO Collab.)
BONVICINI 06	PRL 96 022002	G. Bonvicini et al.	(CLEO Collab.)
ABREU 95R	ZPHY C68 353	P. Abreu et al.	(DELPHI Collab.)
LEE-FRANZINI 90	PRL 65 2947	J. Lee-Franzini et al.	(CUSB II Collab.)

$B_{s1}(5830)^0$

$I(J^P) = \frac{1}{2}(1^+)$ Status: * * *
I, J, P need confirmation.

Quantum numbers shown are quark-model predictions.

$B_{s1}(5830)^0$ MASS

VALUE (MeV)	DOCUMENT ID	TECN	COMMENT
5829.4 ± 0.7	¹ AALTONEN 08k	CDF	$p\bar{p}$ at 1.96 TeV
¹ Uses two-body decays into K^- and B^+ mesons reconstructed as $B^+ \rightarrow J/\psi K^+, J/\psi \rightarrow \mu^+ \mu^-$ or $B^+ \rightarrow \bar{D}^0 \pi^+, \bar{D}^0 \rightarrow K^+ \pi^-$.			

$m_{B_{s1}^0} - m_{B^{*+}}$

VALUE (MeV)	DOCUMENT ID	TECN	COMMENT
504.41 ± 0.21 ± 0.14	² AALTONEN 08k	CDF	$p\bar{p}$ at 1.96 TeV
² Uses two-body decays into K^- and B^+ mesons reconstructed as $B^+ \rightarrow J/\psi K^+, J/\psi \rightarrow \mu^+ \mu^-$ or $B^+ \rightarrow \bar{D}^0 \pi^+, \bar{D}^0 \rightarrow K^+ \pi^-$.			

$B_{s1}(5830)^0$ DECAY MODES

Mode	Fraction (Γ_i/Γ)
$\Gamma_1 B^{*+} K^-$	dominant

$B_{s1}(5830)^0$ BRANCHING RATIOS

$\Gamma(B^{*+} K^-)/\Gamma_{total}$	Γ_1/Γ		
dominant	dominant		
VALUE	DOCUMENT ID	TECN	COMMENT
dominant	AALTONEN 08k	CDF	$p\bar{p}$ at 1.96 TeV

$B_{s1}(5830)^0$ REFERENCES

AALTONEN 08k	PRL 100 082001	T. Aaltonen et al.	(CDF Collab.)
--------------	----------------	--------------------	---------------

$B_{s2}^*(5840)^0$

$I(J^P) = \frac{1}{2}(2^+)$ Status: * * *
I, J, P need confirmation.

Quantum numbers shown are quark-model predictions.

$B_{s2}^*(5840)^0$ MASS

VALUE (MeV)	DOCUMENT ID	TECN	COMMENT
5839.7 ± 0.6 OUR AVERAGE			
5839.7 ± 0.7	¹ AALTONEN 08k	CDF	$p\bar{p}$ at 1.96 TeV
5839.6 ± 1.1 ± 0.7	² ABAZOV 08E	D0	$p\bar{p}$ at 1.96 TeV
¹ Uses two-body decays into K^- and B^+ mesons reconstructed as $B^+ \rightarrow J/\psi K^+, J/\psi \rightarrow \mu^+ \mu^-$ or $B^+ \rightarrow \bar{D}^0 \pi^+, \bar{D}^0 \rightarrow K^+ \pi^-$.			
² Observed in $B_{s2}^0 \rightarrow B^+ K^-$. Measured production rate of B_{s2}^0 relative to B^+ to be $(1.15 \pm 0.23 \pm 0.13)\%$.			

$m_{B_{s2}^0} - m_{B_{s1}^0}$

VALUE (MeV)	DOCUMENT ID	TECN	COMMENT
10.5 ± 0.6	³ AALTONEN 08k	CDF	$p\bar{p}$ at 1.96 TeV
³ Uses two-body decays into K^- and B^+ mesons reconstructed as $B^+ \rightarrow J/\psi K^+, J/\psi \rightarrow \mu^+ \mu^-$ or $B^+ \rightarrow \bar{D}^0 \pi^+, \bar{D}^0 \rightarrow K^+ \pi^-$.			

$B_{s2}^*(5840)^0$ DECAY MODES

Mode	Fraction (Γ_i/Γ)
$\Gamma_1 B^+ K^-$	dominant

Meson Particle Listings

 $B_{s2}^*(5840)^0, B_{sJ}^*(5850)$ $B_{s2}^*(5840)^0$ BRANCHING RATIOS

$\Gamma(B^+ K^-)/\Gamma_{\text{total}}$	DOCUMENT ID	TECN	COMMENT	Γ_1/Γ
dominant	AALTONEN	08K CDF	$p\bar{p}$ at 1.96 TeV	
dominant	⁴ ABAZOV	08E D0	$p\bar{p}$ at 1.96 TeV	

⁴ Measured production rate of B_{s2}^{*0} relative to B^+ to be $(1.15 \pm 0.23 \pm 0.13)\%$.

 $B_{s2}^*(5840)^0$ REFERENCES

AALTONEN	08K	PRL 100 082001	T. Aaltonen et al.	(CDF Collab.)
ABAZOV	08E	PRL 100 082002	V.M. Abazov et al.	(D0 Collab.)

 $B_{sJ}^*(5850)$

$I(J^P) = ?(??)$
 I, J, P need confirmation.

OMITTED FROM SUMMARY TABLE

Signal can be interpreted as coming from $\bar{b}s$ states. Needs confirmation.

 $B_{sJ}^*(5850)$ MASS

VALUE (MeV)	EVTS	DOCUMENT ID	TECN	COMMENT
5853 ± 15	141	AKERS	95E OPAL	$E_{\text{cm}}^{\text{e}^+e^-} = 88-94$ GeV

 $B_{sJ}^*(5850)$ WIDTH

VALUE (MeV)	EVTS	DOCUMENT ID	TECN	COMMENT
47 ± 22	141	AKERS	95E OPAL	$E_{\text{cm}}^{\text{e}^+e^-} = 88-94$ GeV

 $B_{sJ}^*(5850)$ REFERENCES

AKERS	95E	ZPHY C66 19	R. Akers et al.	(OPAL Collab.)
-------	-----	-------------	-----------------	----------------

Meson Particle Listings

B_c^\pm

BOTTOM, CHARMED MESONS

($B = C = \pm 1$)

$B_c^+ = c\bar{b}, B_c^- = \bar{c}b$, similarly for B_c^* 's

B_c^\pm

$I(J^P) = 0(0^-)$
I, J, P need confirmation.

Quantum numbers shown are quark-model predictions.

B_c^\pm MASS

VALUE (GeV)	DOCUMENT ID	TECN	COMMENT
6.276 ± 0.004 OUR AVERAGE			
6.2756 ± 0.0029 ± 0.0025	¹ AALTONEN 08M	CDF	$p\bar{p}$ at 1.96 TeV
6.4 ± 0.39 ± 0.13	² ABE 98M	CDF	$p\bar{p}$ at 1.8 TeV
• • • We do not use the following data for averages, fits, limits, etc. • • •			
6.2857 ± 0.0053 ± 0.0012	¹ ABULENCIA 06C	CDF	Repl. by AALTONEN 08M
6.32 ± 0.06	³ ACKERSTAFF 98O	OPAL	$e^+e^- \rightarrow Z$

- ¹ Measured using a fully reconstructed decay mode of $B_c \rightarrow J/\psi\pi$.
- ² ABE 98M observed $20.4^{+6.2}_{-5.5}$ events in the $B_c^+ \rightarrow J/\psi(1S)\ell\nu\ell$ with a significance of > 4.8 standard deviations. The mass value is estimated from $m(J/\psi(1S)\ell)$.
- ³ ACKERSTAFF 98O observed 2 candidate events in the $B_c \rightarrow J/\psi(1S)\pi^+$ channel with an estimated background of 0.63 ± 0.20 events.

B_c^\pm MEAN LIFE

VALUE (10^{-12} s)	DOCUMENT ID	TECN	COMMENT
0.46 ± 0.07 OUR AVERAGE			
$0.463^{+0.073}_{-0.065} \pm 0.036$	⁴ ABULENCIA 06O	CDF	$p\bar{p}$ at 1.96 TeV
$0.46^{+0.18}_{-0.16} \pm 0.03$	⁴ ABE 98M	CDF	$p\bar{p}$ 1.8 TeV

⁴ The lifetime is measured from the $J/\psi(1S)e$ decay vertices.

B_c^\pm DECAY MODES × $B(\bar{b} \rightarrow B_c)$

B_c^- modes are charge conjugates of the modes below.

Mode	Fraction (Γ_i/Γ)	Confidence level
The following quantities are not pure branching ratios; rather the fraction $\Gamma_i/\Gamma \times B(\bar{b} \rightarrow B_c)$.		
Γ_1 $J/\psi(1S)\ell^+\nu_\ell$ anything	$(5.2^{+2.4}_{-2.1}) \times 10^{-5}$	
Γ_2 $J/\psi(1S)\pi^+$	$< 8.2 \times 10^{-5}$	90%
Γ_3 $J/\psi(1S)\pi^+\pi^+\pi^-$	$< 5.7 \times 10^{-4}$	90%
Γ_4 $J/\psi(1S)a_1(1260)$	$< 1.2 \times 10^{-3}$	90%
Γ_5 $D^*(2010)^+\bar{D}^0$	$< 6.2 \times 10^{-3}$	90%

B_c^\pm BRANCHING RATIOS

VALUE	CL%	DOCUMENT ID	TECN	COMMENT
$(5.2^{+2.4}_{-2.1}) \times 10^{-5}$		⁵ ABE 98M	CDF	$p\bar{p}$ 1.8 TeV
• • • We do not use the following data for averages, fits, limits, etc. • • •				
$< 1.6 \times 10^{-4}$	90	⁶ ACKERSTAFF 98O	OPAL	$e^+e^- \rightarrow Z$
$< 1.9 \times 10^{-4}$	90	⁷ ABREU 97E	DLPH	$e^+e^- \rightarrow Z$
$< 1.2 \times 10^{-4}$	90	⁸ BARATE 97H	ALEP	$e^+e^- \rightarrow Z$

- ⁵ ABE 98M result is derived from the measurement of $[\sigma(B_c) \times B(B_c \rightarrow J/\psi(1S)\ell\nu\ell)] / [\sigma(B^+) \times B(B^+ \rightarrow J/\psi(1S)K^+)] = 0.132^{+0.041}_{-0.037}(\text{stat}) \pm 0.031(\text{sys}) \pm 0.032(\text{lifetime})$ by using PDG 98 values of $B(b \rightarrow B^+)$ and $B(B^+ \rightarrow J/\psi(1S)K^+)$.
- ⁶ ACKERSTAFF 98O reports $B(Z \rightarrow B_c X)/B(Z \rightarrow qq) \times B(B_c \rightarrow J/\psi(1S)\ell\nu\ell) < 6.95 \times 10^{-5}$ at 90%CL. We rescale to our PDG 98 values of $B(Z \rightarrow b\bar{b})$.
- ⁷ ABREU 97E value listed is for an assumed $\tau_{B_c} = 0.4$ ps and improves to 1.6×10^{-4} for $\tau_{B_c} = 1.4$ ps.
- ⁸ BARATE 97H reports $B(Z \rightarrow B_c X)/B(Z \rightarrow qq) \times B(B_c \rightarrow J/\psi(1S)\ell\nu\ell) < 5.2 \times 10^{-5}$ at 90%CL. We rescale to our PDG 96 values of $B(Z \rightarrow b\bar{b})$. A $B_c^+ \rightarrow J/\psi(1S)\mu^+\nu_\mu$ candidate event is found, compared to all the known background sources 2×10^{-3} , which gives $m_{B_c} = 5.96^{+0.25}_{-0.19}$ GeV and $\tau_{B_c} = 1.77 \pm 0.17$ ps.

$\Gamma(J/\psi(1S)\pi^+)/\Gamma_{\text{total}} \times B(\bar{b} \rightarrow B_c)$ $\Gamma_2/\Gamma \times B$

VALUE	CL%	DOCUMENT ID	TECN	COMMENT
$< 8.2 \times 10^{-5}$	90	⁹ BARATE 97H	ALEP	$e^+e^- \rightarrow Z$
• • • We do not use the following data for averages, fits, limits, etc. • • •				
$< 2.4 \times 10^{-4}$	90	¹⁰ ACKERSTAFF 98O	OPAL	$e^+e^- \rightarrow Z$
$< 3.4 \times 10^{-4}$	90	¹¹ ABREU 97E	DLPH	$e^+e^- \rightarrow Z$
$< 2.0 \times 10^{-5}$	95	¹² ABE 96R	CDF	$p\bar{p}$ 1.8 TeV

- ⁹ BARATE 97H reports $B(Z \rightarrow B_c X)/B(Z \rightarrow qq) \times B(B_c \rightarrow J/\psi(1S)\pi) < 3.6 \times 10^{-5}$ at 90%CL. We rescale to our PDG 96 values of $B(Z \rightarrow b\bar{b})$.
- ¹⁰ ACKERSTAFF 98O reports $B(Z \rightarrow B_c X)/B(Z \rightarrow qq) \times B(B_c \rightarrow J/\psi(1S)\pi^+) < 1.06 \times 10^{-4}$ at 90%CL. We rescale to our PDG 98 values of $B(Z \rightarrow b\bar{b})$.
- ¹¹ ABREU 97E value listed is for an assumed $\tau_{B_c} = 0.4$ ps and improves to 2.7×10^{-4} for $\tau_{B_c} = 1.4$ ps.
- ¹² ABE 96R reports $B(b \rightarrow B_c X)/B(b \rightarrow B^+ X) \times B(B_c^+ \rightarrow J/\psi(1S)\pi^+)/B(B^+ \rightarrow J/\psi(1S)K^+) < 0.053$ at 95%CL for $\tau_{B_c} = 0.8$ ps. It changes from 0.15 to 0.04 for $0.17 \text{ ps} < \tau_{B_c} < 1.6$ ps. We rescale to our PDG 96 values of $B(b \rightarrow B^+) = 0.378 \pm 0.022$ and $B(B^+ \rightarrow J/\psi(1S)K^+) = 0.00101 \pm 0.00014$.

$\Gamma(J/\psi(1S)\pi^+\pi^+\pi^-)/\Gamma_{\text{total}} \times B(\bar{b} \rightarrow B_c)$ $\Gamma_3/\Gamma \times B$

VALUE	CL%	DOCUMENT ID	TECN	COMMENT
$< 5.7 \times 10^{-4}$	90	¹³ ABREU 97E	DLPH	$e^+e^- \rightarrow Z$
¹³ ABREU 97E value listed is independent of $0.4 \text{ ps} < \tau_{B_c} < 1.4$ ps.				

$\Gamma(J/\psi(1S)a_1(1260))/\Gamma_{\text{total}} \times B(\bar{b} \rightarrow B_c)$ $\Gamma_4/\Gamma \times B$

VALUE	CL%	DOCUMENT ID	TECN	COMMENT
$< 1.2 \times 10^{-3}$	90	¹⁴ ACKERSTAFF 98O	OPAL	$e^+e^- \rightarrow Z$
¹⁴ ACKERSTAFF 98O reports $B(Z \rightarrow B_c X)/B(Z \rightarrow qq) \times B(B_c \rightarrow J/\psi(1S)a_1(1260)) < 5.29 \times 10^{-4}$ at 90%CL. We rescale to our PDG 98 values of $B(Z \rightarrow b\bar{b})$.				

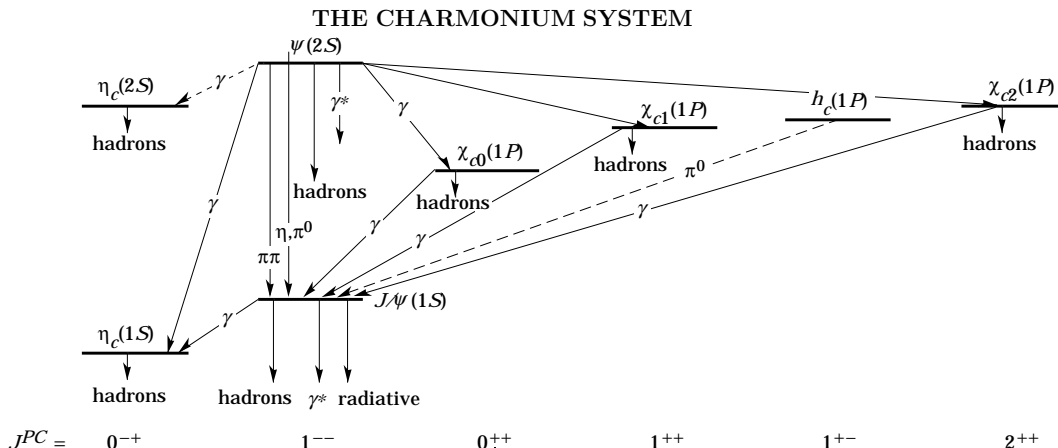
$\Gamma(D^*(2010)^+\bar{D}^0)/\Gamma_{\text{total}} \times B(\bar{b} \rightarrow B_c)$ $\Gamma_5/\Gamma \times B$

VALUE	CL%	DOCUMENT ID	TECN	COMMENT
$< 6.2 \times 10^{-3}$	90	¹⁵ BARATE 98Q	ALEP	$e^+e^- \rightarrow Z$
¹⁵ BARATE 98Q reports $B(Z \rightarrow B_c X) \times B(B_c \rightarrow D^*(2010)^+\bar{D}^0) < 1.9 \times 10^{-3}$ at 90%CL. We rescale to our PDG 98 values of $B(Z \rightarrow b\bar{b})$.				

B_c^\pm REFERENCES

AALTONEN 08M	PRL 100 182002	T. Aaltonen et al.	(CDF Collab.)
ABULENCIA 06C	PRL 96 082002	A. Abulencia et al.	(CDF Collab.)
ABULENCIA 06O	PRL 97 012002	A. Abulencia et al.	(CDF Collab.)
ABE 98M	PRL 81 2432	F. Abe et al.	(CDF Collab.)
Also	PR D58 112004	F. Abe et al.	(CDF Collab.)
ACKERSTAFF 98O	PL B420 157	K. Ackersstaff et al.	(OPAL Collab.)
BARATE 98Q	EPJ C4 387	R. Barate et al.	(ALEPH Collab.)
PDG 98	EPJ C3 1	C. Caso et al.	(ALEPH Collab.)
ABREU 97E	PL B398 207	P. Abreu et al.	(DELPHI Collab.)
BARATE 97H	PL B402 213	R. Barate et al.	(ALEPH Collab.)
ABE 96R	PRL 77 5176	F. Abe et al.	(CDF Collab.)
PDG 96	PR D54 1	R. M. Barnett et al.	(CDF Collab.)

$c\bar{c}$ MESONS



The current state of knowledge of the charmonium system and transitions, as interpreted by the charmonium model. Uncertain states and transitions are indicated by dashed lines. The notation γ^* refers to decay processes involving intermediate virtual photons, including decays to e^+e^- and $\mu^+\mu^-$.

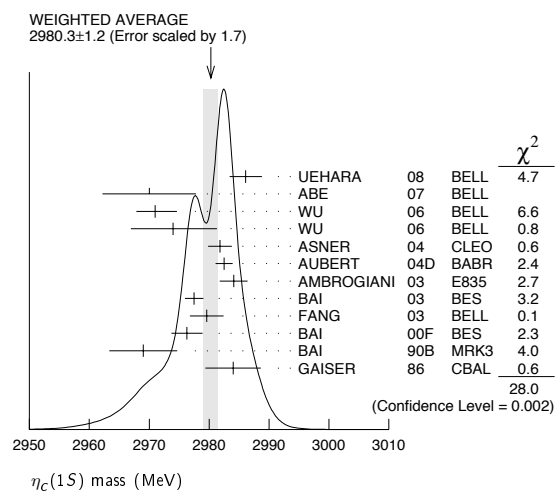
$\eta_c(1S)$

$I^G(J^{PC}) = 0^+(0^{-+})$

$\eta_c(1S)$ MASS

VALUE (MeV)	EVTS	DOCUMENT ID	TECN	COMMENT
2980.3 ± 1.2 OUR AVERAGE		Error includes scale factor of 1.7. See the ideogram below.		
2986.1 ± 1.0 ± 2.5	7.5k	UEHARA	08 BELL	$\gamma\gamma \rightarrow \eta_c \rightarrow \text{hadrons}$
2970 ± 5 ± 6	501	¹ ABE	07 BELL	$e^+e^- \rightarrow J/\psi(c\bar{c})$
2971 ± 3 ± $\frac{2}{1}$	195	WU	06 BELL	$B^+ \rightarrow p\bar{p}K^+$
2974 ± 7 ± $\frac{2}{1}$	20	WU	06 BELL	$B^+ \rightarrow \Lambda\bar{\Lambda}K^+$
2981.8 ± 1.3 ± 1.5	592	ASNER	04 CLEO	$\gamma\gamma \rightarrow \eta_c \rightarrow K_S^0 K^\pm \pi^\mp$
2982.5 ± 1.1 ± 0.9	2547 ± 90	AUBERT	04D BABR	$\gamma\gamma \rightarrow \eta_c(1S) \rightarrow K\bar{K}\pi$
2984.1 ± 2.1 ± 1.0	190	² AMBROGIANI	03 E835	$\bar{p}p \rightarrow \eta_c \rightarrow \gamma\gamma$
2977.5 ± 1.0 ± 1.2		³ BAI	03 BES	$J/\psi \rightarrow \eta_c$
2979.6 ± 2.3 ± 1.6	182 ± 25	FANG	03 BELL	$B \rightarrow \eta_c K$
2976.3 ± 2.3 ± 1.2	4,5,6 BAI	00F BES		$J/\psi \rightarrow \gamma\eta_c$ and $\psi(2S) \rightarrow \gamma\eta_c$
2969 ± 4 ± 4	80	BAI	90B MRK3	$J/\psi \rightarrow \gamma K^+ K^- K^+ K^-$
2984 ± 2.3 ± 4.0		GAISER	86 CBAL	$J/\psi \rightarrow \gamma X, \psi(2S) \rightarrow \gamma X$
• • • We do not use the following data for averages, fits, limits, etc. • • •				
2982 ± 5	273 ± 43	⁷ AUBERT	06E BABR	$B^\pm \rightarrow K^\pm X_{c\bar{c}}$
2976.6 ± 2.9 ± 1.3	140	4,5 BAI	00F BES	$J/\psi \rightarrow \gamma\eta_c$
2980.4 ± 2.3 ± 0.6		⁸ BRANDENB...	00B CLE2	$\gamma\gamma \rightarrow \eta_c \rightarrow K^\pm K_S^0 \pi^\mp$
2975.8 ± 3.9 ± 1.2		4,5 BAI	99B BES	Sup. by BAI 00F
2999 ± 8	25	ABREU	98o DLPH	$e^+e^- \rightarrow e^+e^- + \text{hadrons}$
2988.3 ± $\frac{3.3}{3.1}$		ARMSTRONG	95F E760	$\bar{p}p \rightarrow \gamma\gamma$
2974.4 ± 1.9		⁴ BISELLO	91 DM2	$J/\psi \rightarrow \eta_c \gamma$
2956 ± 12 ± 12		BAI	90B MRK3	$J/\psi \rightarrow \gamma K^+ K^- K_S^0 K_L^0$
2982.6 ± $\frac{2.7}{2.3}$	12	BAGLIN	87B SPEC	$\bar{p}p \rightarrow \gamma\gamma$
2980.2 ± 1.6		⁴ BALTRUSAIT...86	MRK3	$J/\psi \rightarrow \eta_c \gamma$
2976 ± 8		⁹ BALTRUSAIT...84	MRK3	$J/\psi \rightarrow 2\phi\gamma$
2982 ± 8	18	¹⁰ HIMEL	80B MRK2	e^+e^-
2980 ± 9		¹⁰ PARTRIDGE	80B CBAL	e^+e^-

- 1 From a fit of the J/ψ recoil mass spectrum. Supersedes ABE,K 02 and ABE 04c.
- 2 Using mass of $\psi(2S) = 3686.00$ MeV.
- 3 From a simultaneous fit of five decay modes of the η_c .
- 4 Average of several decay modes.
- 5 Using an η_c width of 13.2 MeV.
- 6 Weighted average of the $\psi(2S)$ and $J/\psi(1S)$ samples.
- 7 From the fit of the kaon momentum spectrum. Systematic errors not evaluated.
- 8 Superseded by ASNER 04.
- 9 $\eta_c \rightarrow \phi\phi$.
- 10 Mass adjusted by us to correspond to $J/\psi(1S)$ mass = 3097 MeV.



$\eta_c(1S)$ WIDTH

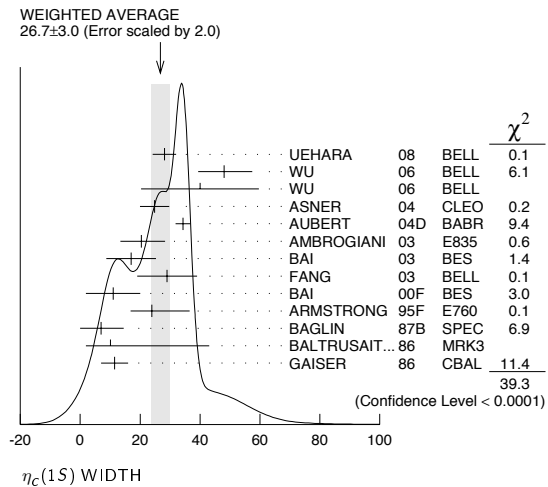
VALUE (MeV)	CL%	EVTS	DOCUMENT ID	TECN	COMMENT
26.7 ± 3.0 OUR AVERAGE			Error includes scale factor of 2.0. See the ideogram below.		
28.1 ± 3.2 ± 2.2		7.5k	UEHARA	08 BELL	$\gamma\gamma \rightarrow \eta_c \rightarrow \text{hadrons}$
48 ± $\frac{8}{7}$ ± 5		195	WU	06 BELL	$B^+ \rightarrow p\bar{p}K^+$
40 ± 19 ± 5		20	WU	06 BELL	$B^+ \rightarrow \Lambda\bar{\Lambda}K^+$
24.8 ± 3.4 ± 3.5		592	ASNER	04 CLEO	$\gamma\gamma \rightarrow \eta_c \rightarrow K_S^0 K^\pm \pi^\mp$
34.3 ± 2.3 ± 0.9		2547 ± 90	AUBERT	04D BABR	$\gamma\gamma \rightarrow \eta_c(1S) \rightarrow K\bar{K}\pi$
20.4 ± $\frac{7.7}{6.7}$ ± 2.0		190	AMBROGIANI	03 E835	$\bar{p}p \rightarrow \eta_c \rightarrow \gamma\gamma$
17.0 ± 3.7 ± 7.4			¹¹ BAI	03 BES	$J/\psi \rightarrow \eta_c$

Meson Particle Listings

$\eta_c(1S)$

$29 \pm 8 \pm 6$	182 ± 25	FANG	03 BELL	$B \rightarrow \eta_c K$
$11.0 \pm 8.1 \pm 4.1$	12 BAI	00F BES	$J/\psi \rightarrow \gamma \eta_c$ and $\psi(2S) \rightarrow \gamma \eta_c$	
23.9 ± 12.6		ARMSTRONG	95F E760	$\bar{p}p \rightarrow \gamma \gamma$
7.0 ± 7.5	12	BAGLIN	87B SPEC	$\bar{p}p \rightarrow \gamma \gamma$
10.1 ± 33.0	23	13 BALTRUSAIT...86	MRK3	$J/\psi \rightarrow \gamma \rho \bar{p}$
11.5 ± 4.5		GAISER	86 CBAL	$J/\psi \rightarrow \gamma X$, $\psi(2S) \rightarrow \gamma X$
$27.0 \pm 5.8 \pm 1.4$	14	BRANDENB...	00B CLE2	$\gamma \gamma \rightarrow \eta_c \rightarrow K^\pm K_S^0 \pi^\mp$
< 40	90	18 HIMEL	80B MRK2	$e^+ e^-$
< 20	90	PARTRIDGE	80B CBAL	$e^+ e^-$

• • • We do not use the following data for averages, fits, limits, etc. • • •
 11 From a simultaneous fit of five decay modes of the η_c .
 12 From a fit to the 4-prong invariant mass in $\psi(2S) \rightarrow \gamma \eta_c$ and $J/\psi(1S) \rightarrow \gamma \eta_c$ decays.
 13 Positive and negative errors correspond to 90% confidence level.
 14 Superseded by ASNER 04.



$\eta_c(1S)$ DECAY MODES

Mode	Fraction (Γ_i/Γ)	Confidence level
Decays involving hadronic resonances		
Γ_1 $\eta'(958) \pi \pi$	$(4.1 \pm 1.7) \%$	
Γ_2 $\rho \rho$	$(2.0 \pm 0.7) \%$	
Γ_3 $K^*(892)^0 K^- \pi^+ + c.c.$	$(2.0 \pm 0.7) \%$	
Γ_4 $K^*(892) \bar{K}^*(892)$	$(9.2 \pm 3.4) \times 10^{-3}$	
Γ_5 $K^{*0} \bar{K}^{*0} \pi^+ \pi^-$	$(1.5 \pm 0.8) \%$	
Γ_6 $\phi K^+ K^-$	$(2.9 \pm 1.4) \times 10^{-3}$	
Γ_7 $\phi \phi$	$(2.7 \pm 0.9) \times 10^{-3}$	
Γ_8 $\phi 2(\pi^+ \pi^-)$	$< 4.7 \times 10^{-3}$	90%
Γ_9 $a_0(980) \pi$	$< 2 \%$	90%
Γ_{10} $a_2(1320) \pi$	$< 2 \%$	90%
Γ_{11} $K^*(892) \bar{K} + c.c.$	$< 1.28 \%$	90%
Γ_{12} $f_2(1270) \eta$	$< 1.1 \%$	90%
Γ_{13} $\omega \omega$	$< 3.1 \times 10^{-3}$	90%
Γ_{14} $\omega \phi$	$< 1.7 \times 10^{-3}$	90%
Γ_{15} $f_2(1270) f_2(1270)$	$(1.0 \pm 0.4) \%$	
Γ_{16} $f_2(1270) f_2'(1525)$	$(8 \pm 4) \times 10^{-3}$	
Decays into stable hadrons		
Γ_{17} $K \bar{K} \pi$	$(7.0 \pm 1.2) \%$	
Γ_{18} $\eta \pi \pi$	$(4.9 \pm 1.8) \%$	
Γ_{19} $\pi^+ \pi^- K^+ K^-$	$(1.5 \pm 0.6) \%$	
Γ_{20} $K^+ K^- 2(\pi^+ \pi^-)$	$(10 \pm 4) \times 10^{-3}$	
Γ_{21} $2(K^+ K^-)$	$(1.5 \pm 0.7) \times 10^{-3}$	
Γ_{22} $2(\pi^+ \pi^-)$	$(1.20 \pm 0.30) \%$	
Γ_{23} $3(\pi^+ \pi^-)$	$(2.0 \pm 0.7) \%$	
Γ_{24} $\rho \bar{\rho}$	$(1.3 \pm 0.4) \times 10^{-3}$	
Γ_{25} $\Lambda \bar{\Lambda}$	$(1.04 \pm 0.31) \times 10^{-3}$	
Γ_{26} $K \bar{K} \eta$	$< 3.1 \%$	90%
Γ_{27} $\pi^+ \pi^- \rho \bar{\rho}$	$< 1.2 \%$	90%

Radiative decays

$$\Gamma_{28} \gamma \gamma \quad (2.4 \pm 1.1 \pm 0.9) \times 10^{-4}$$

Charge conjugation (C), Parity (P), Lepton family number (LF) violating modes

Γ_{29} $\pi^+ \pi^-$	$P, CP < 8.7$	$\times 10^{-4}$	90%
Γ_{30} $\pi^0 \pi^0$	$P, CP < 5.6$	$\times 10^{-4}$	90%
Γ_{31} $K^+ K^-$	$P, CP < 7.6$	$\times 10^{-4}$	90%
Γ_{32} $K_S^0 K_S^0$	$P, CP < 4.2$	$\times 10^{-4}$	90%

$\eta_c(1S)$ PARTIAL WIDTHS

$\Gamma(\gamma \gamma)$	VALUE (keV)	EVTS	DOCUMENT ID	TECN	COMMENT	Γ_{28}
-------------------------	-------------	------	-------------	------	---------	---------------

$7.2 \pm 0.7 \pm 2.0$ OUR AVERAGE Error includes scale factor of 1.3. Treating systematic errors as correlated.

6.7 ± 0.9 OUR AVERAGE

$5.5 \pm 1.2 \pm 1.8$	157 ± 33	15 KUO	05 BELL	$\gamma \gamma \rightarrow \rho \bar{p}$
$7.4 \pm 0.4 \pm 2.3$		16 ASNER	04 CLEO	$\gamma \gamma \rightarrow \eta_c \rightarrow K_S^0 K^\pm \pi^\mp$
$13.9 \pm 2.0 \pm 3.0$	41	17 ABDALLAH	03J DLPH	$\gamma \gamma \rightarrow \eta_c$
$3.8 \pm 1.1 \pm 1.9$	190	18 AMBROGIANI	03 E835	$\bar{p}p \rightarrow \eta_c \rightarrow \gamma \gamma$
$6.9 \pm 1.7 \pm 2.1$	76	19 ACCIARRI	99T L3	$e^+ e^- \rightarrow e^+ e^- \eta_c$
$27 \pm 16 \pm 10$	5	16 SHIRAI	98 AMY	$58 e^+ e^-$
$6.7 \pm 2.4 \pm 1.7 \pm 2.3$		15 ARMSTRONG	95F E760	$\bar{p}p \rightarrow \gamma \gamma$
11.3 ± 4.2		20 ALBRECHT	94H ARG	$e^+ e^- \rightarrow e^+ e^- \eta_c$
$5.9 \pm 2.1 \pm 1.9$		18 CHEN	90B CLEO	$e^+ e^- \rightarrow e^+ e^- \eta_c$
$6.4 \pm 5.0 \pm 3.4$		21 AIHARA	88D TPC	$e^+ e^- \rightarrow e^+ e^- X$
$4.3 \pm 3.4 \pm 2.4$		15 BAGLIN	87B SPEC	$\bar{p}p \rightarrow \gamma \gamma$
28 ± 15	16,22	BERGER	86 PLUT	$\gamma \gamma \rightarrow K \bar{K} \pi$

• • • We do not use the following data for averages, fits, limits, etc. • • •
 5.2 \pm 1.2 273 \pm 43 23,24 AUBERT 06E BABR $B^\pm \rightarrow K^\pm X_{c\bar{c}}$
 7.6 \pm 0.8 \pm 2.3 16,25 BRANDENB... 00B CLE2 $\gamma \gamma \rightarrow \eta_c \rightarrow K^\pm K_S^0 \pi^\mp$
 8.0 \pm 2.3 \pm 2.4 17 26 ADRIANI 93N L3 $e^+ e^- \rightarrow e^+ e^- \eta_c$
 15 Normalized to $B(\eta_c \rightarrow \rho \bar{p}) = (1.3 \pm 0.4) \times 10^{-3}$.
 16 Normalized to $B(\eta_c \rightarrow K^\pm K_S^0 \pi^\mp)$.
 17 Average of $K_S^0 K^\pm \pi^\mp$, $\pi^+ \pi^- K^+ K^-$, and $2(K^+ K^-)$ decay modes.
 18 Normalized to the sum of $B(\eta_c \rightarrow K^\pm K_S^0 \pi^\mp)$, $B(\eta_c \rightarrow K^+ K^- \pi^+ \pi^-)$, and $B(\eta_c \rightarrow 2\pi^+ 2\pi^-)$.
 19 Normalized to the sum of 9 branching ratios.
 20 Normalized to the sum of $B(\eta_c \rightarrow K^\pm K_S^0 \pi^\mp)$, $B(\eta_c \rightarrow \phi \phi)$, $B(\eta_c \rightarrow K^+ K^- \pi^+ \pi^-)$, and $B(\eta_c \rightarrow 2\pi^+ 2\pi^-)$.
 21 Normalized to the sum of $B(\eta_c \rightarrow K^\pm K_S^0 \pi^\mp)$, $B(\eta_c \rightarrow 2K^+ 2K^-)$, $B(\eta_c \rightarrow K^+ K^- \pi^+ \pi^-)$, and $B(\eta_c \rightarrow 2\pi^+ 2\pi^-)$.
 22 Re-evaluated by AIHARA 88D.
 23 Calculated by us using $\Gamma(\eta_c \rightarrow K \bar{K} \pi) \times \Gamma(\eta_c \rightarrow \gamma \gamma) / \Gamma = 0.44 \pm 0.05$ keV from PDG 06 and $B(\eta_c \rightarrow K \bar{K} \pi) = (8.5 \pm 1.8) \%$ from AUBERT 06E.
 24 Systematic errors not evaluated.
 25 Superseded by ASNER 04.
 26 Superseded by ACCIARRI 99T.

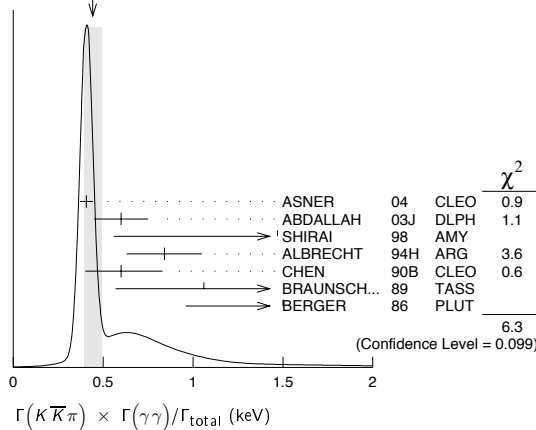
$\eta_c(1S) \Gamma(i)\Gamma(\gamma \gamma)/\Gamma(\text{total})$

$\Gamma(K \bar{K} \pi) \times \Gamma(\gamma \gamma)/\Gamma_{\text{total}}$	VALUE (keV)	CL% EVTS	DOCUMENT ID	TECN	COMMENT	$\Gamma_{17} \Gamma_{28}/\Gamma$
--	-------------	----------	-------------	------	---------	----------------------------------

0.44 ± 0.05 OUR AVERAGE Error includes scale factor of 1.4. See the ideogram below.

$0.407 \pm 0.022 \pm 0.028$		27,28	ASNER	04 CLEO	$\gamma \gamma \rightarrow \eta_c \rightarrow K_S^0 K^\pm \pi^\mp$	
$0.60 \pm 0.12 \pm 0.09$		41	28,29 ABDALLAH	03J DLPH	$\gamma \gamma \rightarrow K_S^0 K^\pm \pi^\mp$	
$1.47 \pm 0.87 \pm 0.27$			28 SHIRAI	98 AMY	$\gamma \gamma \rightarrow \eta_c \rightarrow K^\pm K_S^0 \pi^\mp$	
0.84 ± 0.21			28 ALBRECHT	94H ARG	$\gamma \gamma \rightarrow K^\pm K_S^0 \pi^\mp$	
$0.60 \pm 0.23 \pm 0.20$			28 CHEN	90B CLEO	$\gamma \gamma \rightarrow \eta_c K^\pm K_S^0 \pi^\mp$	
$1.06 \pm 0.41 \pm 0.27$		11	28 BRAUNSCH...	89 TASS	$\gamma \gamma \rightarrow K \bar{K} \pi$	
$1.5 \pm 0.60 \pm 0.3 \pm 0.45$		7	28 BERGER	86 PLUT	$\gamma \gamma \rightarrow K \bar{K} \pi$	

• • • We do not use the following data for averages, fits, limits, etc. • • •
 $0.418 \pm 0.044 \pm 0.022$ 28,30 BRANDENB... 00B CLE2 $\gamma \gamma \rightarrow \eta_c \rightarrow K^\pm K_S^0 \pi^\mp$
 < 0.63 95 28 BEHREND 89 CELL $\gamma \gamma \rightarrow K_S^0 K^\pm \pi^\mp$
 < 4.4 95 ALTHOFF 85B TASS $\gamma \gamma \rightarrow K \bar{K} \pi$

WEIGHTED AVERAGE
0.44±0.05 (Error scaled by 1.4) $\eta_c(1S)$ BRANCHING RATIOS

HADRONIC DECAYS

$\Gamma(\eta'(958)\pi\pi)/\Gamma_{total}$		Γ_1/Γ	
VALUE	EVTS	DOCUMENT ID	TECN COMMENT
0.041±0.017	14	35 BALTRUSAIT...86	MRK3 $J/\psi \rightarrow \eta_c \gamma$

$\Gamma(\rho\rho)/\Gamma_{total}$		Γ_2/Γ	
VALUE (units 10^{-3})	CL% EVTS	DOCUMENT ID	TECN COMMENT
20 ± 7 OUR EVALUATION		(Treating systematic errors as correlated.)	
18 ± 5 OUR AVERAGE			

12.6 ± 3.8 ± 5.1	72	35 ABLIKIM	05L BES2 $J/\psi \rightarrow \pi^+ \pi^- \pi^+ \pi^- \gamma$
26.0 ± 2.4 ± 8.8	113	35 BISELLO	91 DM2 $J/\psi \rightarrow \gamma \rho^0 \rho^0$
23.6 ± 10.6 ± 8.2	32	35 BISELLO	91 DM2 $J/\psi \rightarrow \gamma \rho^+ \rho^-$
• • • We do not use the following data for averages, fits, limits, etc. • • •			
<14	90	35 BALTRUSAIT...86	MRK3 $J/\psi \rightarrow \eta_c \gamma$

$\Gamma(K^*(892)^0 K^- \pi^+ + c.c.)/\Gamma_{total}$		Γ_3/Γ	
VALUE	EVTS	DOCUMENT ID	TECN COMMENT
0.02±0.007	63	35 BALTRUSAIT...86	MRK3 $J/\psi \rightarrow \eta_c \gamma$

$\Gamma(K^*(892)\bar{K}^*(892))/\Gamma_{total}$		Γ_4/Γ	
VALUE (units 10^{-4})	EVTS	DOCUMENT ID	TECN COMMENT
92±34 OUR EVALUATION		(Treating systematic errors as correlated.)	
91±26 OUR AVERAGE			

108±25±44	60	35 ABLIKIM	05L BES2 $J/\psi \rightarrow K^+ K^- \pi^+ \pi^- \gamma$
82±28±27	14	35 BISELLO	91 DM2 $e^+ e^- \rightarrow \gamma K^+ K^- \pi^+ \pi^-$
90±5.0	9	35 BALTRUSAIT...86	MRK3 $J/\psi \rightarrow \eta_c \gamma$

$\Gamma(K^{*0}\bar{K}^{*0}\pi^+\pi^-)/\Gamma_{total}$		Γ_5/Γ	
VALUE (units 10^{-4})	EVTS	DOCUMENT ID	TECN COMMENT
150±63±43	45	36 ABLIKIM	06A BES2 $J/\psi \rightarrow K^{*0}\bar{K}^{*0}\pi^+\pi^- \gamma$

$\Gamma(\phi K^+ K^-)/\Gamma_{total}$		Γ_6/Γ	
VALUE (units 10^{-3})	EVTS	DOCUMENT ID	TECN COMMENT
2.9±0.9±1.1	14.1±4.4 -0.8±3.7	37 HUANG	03 BELL $B^+ \rightarrow (\phi K^+ K^-) K^+$

$\Gamma(\phi\phi)/\Gamma_{total}$		Γ_7/Γ	
VALUE (units 10^{-4})	EVTS	DOCUMENT ID	TECN COMMENT
27 ± 9 OUR EVALUATION		(Treating systematic errors as correlated.)	
27 ± 5 OUR AVERAGE			

25.3 ± 5.1 ± 9.1	72	35 ABLIKIM	05L BES2 $J/\psi \rightarrow K^+ K^- K^+ K^- \gamma$
26 ± 9	357 ± 64	35 BAI	04 BES $J/\psi \rightarrow \gamma K^+ K^- K^+ K^-$
18 ± 8 ± 7	7.0±3.0 -2.3	37 HUANG	03 BELL $B^+ \rightarrow (\phi\phi) K^+$
31 ± 7 ± 10	19	35 BISELLO	91 DM2 $J/\psi \rightarrow \gamma K^+ K^- K^+ K^-$
30 ± 18 -12 ± 10	5	35 BISELLO	91 DM2 $J/\psi \rightarrow \gamma K^+ K^- K_S^0 K_L^0$
74 ± 18 ± 24	80	35 BAI	90B MRK3 $J/\psi \rightarrow \gamma K^+ K^- K^+ K^-$
67 ± 21 ± 24		35 BAI	90B MRK3 $J/\psi \rightarrow \gamma K^+ K^- K_S^0 K_L^0$

$\Gamma(\phi 2(\pi^+ \pi^-))/\Gamma_{total}$		Γ_8/Γ	
VALUE (units 10^{-4})	CL%	DOCUMENT ID	TECN COMMENT
<50	90	38 ABLIKIM	06A BES2 $J/\psi \rightarrow \phi 2(\pi^+ \pi^-) \gamma$

$\Gamma(a_0(980)\pi)/\Gamma_{total}$		Γ_9/Γ	
VALUE	CL%	DOCUMENT ID	TECN COMMENT
<0.02	90	35,39 BALTRUSAIT...86	MRK3 $J/\psi \rightarrow \eta_c \gamma$

$\Gamma(a_2(1320)\pi)/\Gamma_{total}$		Γ_{10}/Γ	
VALUE	CL%	DOCUMENT ID	TECN COMMENT
<0.02	90	35 BALTRUSAIT...86	MRK3 $J/\psi \rightarrow \eta_c \gamma$

$\Gamma(K^*(892)\bar{K} + c.c.)/\Gamma_{total}$		Γ_{11}/Γ	
VALUE	CL%	DOCUMENT ID	TECN COMMENT
<0.0128	90	BISELLO	91 DM2 $J/\psi \rightarrow \gamma K_S^0 K_{\pm}^{\pm} \pi^{\mp}$
<0.0132	90	35 BISELLO	91 DM2 $J/\psi \rightarrow \gamma K^+ K^- \pi^0$

$\Gamma(f_2(1270)\eta)/\Gamma_{total}$		Γ_{12}/Γ	
VALUE	CL%	DOCUMENT ID	TECN COMMENT
<0.011	90	35 BALTRUSAIT...86	MRK3 $J/\psi \rightarrow \eta_c \gamma$

$\Gamma(\omega\omega)/\Gamma_{total}$		Γ_{13}/Γ	
VALUE	CL%	DOCUMENT ID	TECN COMMENT
<0.0031	90	35 BALTRUSAIT...86	MRK3 $J/\psi \rightarrow \eta_c \gamma$

<0.0063	90	35 ABLIKIM	05L BES2 $J/\psi \rightarrow \pi^+ \pi^- \pi^0 \pi^+ \pi^- \pi^0 \gamma$
<0.0063		35 BISELLO	91 DM2 $J/\psi \rightarrow \gamma \omega \omega$

 $\Gamma(\pi^+ \pi^- K^+ K^-) \times \Gamma(\gamma\gamma)/\Gamma_{total}$

VALUE (eV)	EVTS	DOCUMENT ID	TECN	COMMENT
27 ± 6 OUR AVERAGE				
25.7 ± 3.2 ± 4.9	2019 ± 248	UEHARA	08 BELL	$\gamma\gamma \rightarrow \pi^+ \pi^- K^+ K^-$
280 ± 100 ± 60	42	31 ABDALLAH	03J DLPH	$\gamma\gamma \rightarrow \pi^+ \pi^- K^+ K^-$
170 ± 80 ± 20	13.9 ± 6.6	ALBRECHT	94H ARG	$\gamma\gamma \rightarrow \pi^+ \pi^- K^+ K^-$

 $\Gamma(K^*(892)\bar{K}^*(892)) \times \Gamma(\gamma\gamma)/\Gamma_{total}$

VALUE (eV)	EVTS	DOCUMENT ID	TECN	COMMENT
32.4±4.2±5.8	882 ± 115	UEHARA	08 BELL	$\gamma\gamma \rightarrow \pi^+ \pi^- K^+ K^-$

 $\Gamma(f_2(1270)f_2'(1525)) \times \Gamma(\gamma\gamma)/\Gamma_{total}$

VALUE (eV)	EVTS	DOCUMENT ID	TECN	COMMENT
49 ± 9 ± 13	1128 ± 206	UEHARA	08 BELL	$\gamma\gamma \rightarrow \pi^+ \pi^- K^+ K^-$

 $\Gamma(2(K^+ K^-)) \times \Gamma(\gamma\gamma)/\Gamma_{total}$

VALUE (eV)	EVTS	DOCUMENT ID	TECN	COMMENT
5.8 ± 1.9 OUR AVERAGE				
5.6 ± 1.1 ± 1.6	216 ± 42	UEHARA	08 BELL	$\gamma\gamma \rightarrow 2(K^+ K^-)$
350 ± 90 ± 60	46	32 ABDALLAH	03J DLPH	$\gamma\gamma \rightarrow 2(K^+ K^-)$
231 ± 90 ± 23	9.1 ± 3.3	33 ALBRECHT	94H ARG	$\gamma\gamma \rightarrow 2(K^+ K^-)$

 $\Gamma(\phi\phi) \times \Gamma(\gamma\gamma)/\Gamma_{total}$

VALUE (eV)	EVTS	DOCUMENT ID	TECN	COMMENT
6.8±1.2±1.3	132 ± 23	UEHARA	08 BELL	$\gamma\gamma \rightarrow 2(K^+ K^-)$

 $\Gamma(2(\pi^+ \pi^-)) \times \Gamma(\gamma\gamma)/\Gamma_{total}$

VALUE (eV)	EVTS	DOCUMENT ID	TECN	COMMENT
42 ± 6 OUR AVERAGE				
40.7 ± 3.7 ± 5.3	5381 ± 492	UEHARA	08 BELL	$\gamma\gamma \rightarrow 2(\pi^+ \pi^-)$
180 ± 70 ± 20	21.4 ± 8.6	ALBRECHT	94H ARG	$\gamma\gamma \rightarrow 2(\pi^+ \pi^-)$

 $\Gamma(\rho\rho) \times \Gamma(\gamma\gamma)/\Gamma_{total}$

VALUE (eV)	CL%	EVTS	DOCUMENT ID	TECN	COMMENT
• • • We do not use the following data for averages, fits, limits, etc. • • •					
<39	90	< 1556	UEHARA	08 BELL	$\gamma\gamma \rightarrow 2(\pi^+ \pi^-)$

 $\Gamma(f_2(1270)f_2(1270)) \times \Gamma(\gamma\gamma)/\Gamma_{total}$

VALUE (eV)	EVTS	DOCUMENT ID	TECN	COMMENT
69±17±12	3182 ± 766	UEHARA	08 BELL	$\gamma\gamma \rightarrow 2(\pi^+ \pi^-)$

 $\Gamma(\rho\bar{\rho}) \times \Gamma(\gamma\gamma)/\Gamma_{total}$

VALUE (eV)	EVTS	DOCUMENT ID	TECN	COMMENT
6.2 ± 1.1 ± 1.0 OUR AVERAGE				Error includes scale factor of 1.1.
7.20 ± 1.53 ± 0.67 -0.75	157 ± 33	34 KUO	05 BELL	$\gamma\gamma \rightarrow \rho\bar{\rho}$
4.6 ± 1.3 ± 0.4 -1.1	190	34 AMBROGIANI	03 E835	$\bar{p}p \rightarrow \gamma\gamma$
8.1 ± 2.9 -2.0		34 ARMSTRONG	95F E760	$\bar{p}p \rightarrow \gamma\gamma$

27 Calculated by us from the value reported in ASNER 04 that assumes $B(\eta_c \rightarrow K\bar{K}\pi) = 5.5 \pm 1.7\%$

28 We have multiplied $K^{\pm} K_S^0 \pi^{\mp}$ measurement by 3 to obtain $K\bar{K}\pi$.

29 Calculated by us from the value reported in ABDALLAH 03J, which uses $B(\eta_c \rightarrow K_S^0 K^{\pm} \pi^{\mp}) = (1.5 \pm 0.4)\%$.

30 Superseded by ASNER 04.

31 Calculated by us from the value reported in ABDALLAH 03J, which uses $B(\eta_c \rightarrow \pi^+ \pi^- K^+ K^-) = (2.0 \pm 0.7)\%$.

32 Calculated by us from the value reported in ABDALLAH 03J, which uses $B(\eta_c \rightarrow 2(K^+ K^-)) = (2.1 \pm 1.2)\%$.

33 Includes all topological modes except $\eta_c \rightarrow \phi\phi$.

34 Not independent from the $\Gamma_{\gamma\gamma}$ reported by the same experiment.

Meson Particle Listings

 $\eta_c(1S)$

$\Gamma(\omega\phi)/\Gamma_{\text{total}}$					Γ_{14}/Γ
VALUE	CL%	DOCUMENT ID	TECN	COMMENT	
<0.0017	90	35 ABLIKIM	05L BES2	$J/\psi \rightarrow \pi^+ \pi^- \pi^0 K^+ K^- \gamma$	

$\Gamma(f_2(1270) f_2'(1270))/\Gamma_{\text{total}}$					Γ_{15}/Γ
VALUE (units 10^{-2})	EVTS	DOCUMENT ID	TECN	COMMENT	
$1.02^{+0.33}_{-0.39} \pm 0.29$	91.2 ± 19.8	40 ABLIKIM	04M BES	$J/\psi \rightarrow \gamma 2\pi^+ 2\pi^-$	

$\Gamma(K\bar{K}\pi)/\Gamma_{\text{total}}$					Γ_{17}/Γ
VALUE (units 10^{-2})	CL%	EVTS	DOCUMENT ID	TECN	COMMENT
7.0 ± 1.2 OUR EVALUATION					(Treating systematic errors as correlated.)
6.1 ± 0.8 OUR AVERAGE					
8.5 ± 1.8			41 AUBERT	06E BABR	$B^\pm \rightarrow K^\pm X_{C\bar{C}}$
5.1 ± 2.1	609 ± 71		35 BAI	04 BES	$J/\psi \rightarrow \gamma K^\pm \pi^\mp K_S^0$
$6.90 \pm 1.42 \pm 1.32$		33	35 BISELLO	91 DM2	$J/\psi \rightarrow \gamma K^+ K^- \pi^0$
$5.43 \pm 0.94 \pm 0.94$		68	35 BISELLO	91 DM2	$J/\psi \rightarrow \gamma K^\pm \pi^\mp K_S^0$
4.8 ± 1.7		95	35,42 BALTRUSAIT..86	MRK3	$J/\psi \rightarrow \eta_c \gamma$
$16.1^{+9.2}_{-7.3}$			43 HIMEL	80B MRK2	$\psi(2S) \rightarrow \eta_c \gamma$
• • • We do not use the following data for averages, fits, limits, etc. • • •					
< 10.7	90		35 PARTRIDGE	80B CBAL	$J/\psi \rightarrow \eta_c \gamma$

$\Gamma(\phi\phi)/\Gamma(K\bar{K}\pi)$					Γ_{7}/Γ_{17}
VALUE	DOCUMENT ID	TECN	COMMENT		
$0.055 \pm 0.014 \pm 0.005$	AUBERT,B	04B BABR	$B^\pm \rightarrow K^\pm \eta_c$		

$\Gamma(\eta\pi\pi)/\Gamma_{\text{total}}$					Γ_{18}/Γ
VALUE	EVTS	DOCUMENT ID	TECN	COMMENT	
0.049 ± 0.018 OUR EVALUATION					
0.047 ± 0.015 OUR AVERAGE					
0.054 ± 0.020	75	35 BALTRUSAIT..86	MRK3	$J/\psi \rightarrow \eta_c \gamma$	
$0.037 \pm 0.013 \pm 0.020$	18	35 PARTRIDGE	80B CBAL	$J/\psi \rightarrow \eta\pi^+ \pi^- \gamma$	

$\Gamma(\pi^+ \pi^- K^+ K^-)/\Gamma_{\text{total}}$					Γ_{19}/Γ
VALUE	EVTS	DOCUMENT ID	TECN	COMMENT	
0.015 ± 0.006 OUR EVALUATION					
0.0142 ± 0.0033 OUR AVERAGE					
0.012 ± 0.004	413 ± 54	35 BAI	04 BES	$J/\psi \rightarrow \gamma K^+ K^- \pi^+ \pi^-$	
0.021 ± 0.007	110	35 BALTRUSAIT..86	MRK3	$J/\psi \rightarrow \eta_c \gamma$	
$0.014^{+0.022}_{-0.009}$		43 HIMEL	80B MRK2	$\psi(2S) \rightarrow \eta_c \gamma$	

$\Gamma(K^+ K^- 2(\pi^+ \pi^-))/\Gamma_{\text{total}}$					Γ_{20}/Γ
VALUE (units 10^{-4})	EVTS	DOCUMENT ID	TECN	COMMENT	
$95 \pm 31 \pm 27$	100	44 ABLIKIM	06A BES2	$J/\psi \rightarrow K^+ K^- 2(\pi^+ \pi^-) \gamma$	

$\Gamma(2(K^+ K^-))/\Gamma_{\text{total}}$					Γ_{21}/Γ
VALUE	EVTS	DOCUMENT ID	TECN	COMMENT	
0.0015 ± 0.0007 OUR EVALUATION					
$0.0014^{+0.0005}_{-0.0004} \pm 0.0006$	$14.5^{+4.6}_{-3.0}$	37 HUANG	03 BELL	$B^+ \rightarrow 2(K^+ K^-)$	
$0.021 \pm 0.010 \pm 0.006$		45 ALBRECHT	94H ARG	$\gamma\gamma \rightarrow K^+ K^- K^+ K^-$	

$\Gamma(2(K^+ K^-))/\Gamma(K\bar{K}\pi)$					Γ_{21}/Γ_{17}
VALUE	DOCUMENT ID	TECN	COMMENT		
$0.023 \pm 0.007 \pm 0.006$	AUBERT,B	04B BABR	$B^\pm \rightarrow K^\pm \eta_c$		

$\Gamma(2(\pi^+ \pi^-))/\Gamma_{\text{total}}$					Γ_{22}/Γ
VALUE (units 10^{-2})	EVTS	DOCUMENT ID	TECN	COMMENT	
1.2 ± 0.3 OUR EVALUATION					
1.15 ± 0.26 OUR AVERAGE					
1.0 ± 0.5	542 ± 75	35 BAI	04 BES	$J/\psi \rightarrow \gamma 2(\pi^+ \pi^-)$	
$1.05 \pm 0.17 \pm 0.34$	137	35 BISELLO	91 DM2	$J/\psi \rightarrow \gamma 2\pi^+ 2\pi^-$	
1.3 ± 0.6	25	35 BALTRUSAIT..86	MRK3	$J/\psi \rightarrow \eta_c \gamma$	
$2.0^{+1.5}_{-1.0}$		43 HIMEL	80B MRK2	$\psi(2S) \rightarrow \eta_c \gamma$	

$\Gamma(3(\pi^+ \pi^-))/\Gamma_{\text{total}}$					Γ_{23}/Γ
VALUE (units 10^{-4})	EVTS	DOCUMENT ID	TECN	COMMENT	
$204 \pm 45 \pm 58$	479	46 ABLIKIM	06A BES2	$J/\psi \rightarrow 3(\pi^+ \pi^-) \gamma$	

$\Gamma(p\bar{p})/\Gamma_{\text{total}}$					Γ_{24}/Γ
VALUE (units 10^{-4})	EVTS	DOCUMENT ID	TECN	COMMENT	
13 ± 4 OUR EVALUATION					(Treating systematic errors as correlated.)
14.0 ± 2.2 OUR AVERAGE					
$15.5^{+2.1}_{-2.5} \pm 2.1$	195	47 WU	06 BELL	$B^+ \rightarrow p\bar{p} K^+$	
15 ± 6	213 ± 33	35 BAI	04 BES	$J/\psi \rightarrow \gamma p\bar{p}$	
$10 \pm 3 \pm 4$	18	35 BISELLO	91 DM2	$J/\psi \rightarrow \gamma p\bar{p}$	
11 ± 6	23	35 BALTRUSAIT..86	MRK3	$J/\psi \rightarrow \eta_c \gamma$	
29^{+29}_{-15}		43 HIMEL	80B MRK2	$\psi(2S) \rightarrow \eta_c \gamma$	

$\Gamma(p\bar{p}) \times \Gamma(\phi\phi)/\Gamma_{\text{total}}^2$			Γ_{24}/Γ^2
VALUE (units 10^{-9})	DOCUMENT ID	TECN	COMMENT
$4.0^{+3.5}_{-3.2}$	BAGLIN	89 SPEC	$\bar{p}p \rightarrow K^+ K^- K^+ K^-$

$\Gamma(\Lambda\bar{\Lambda})/\Gamma_{\text{total}}$					Γ_{25}/Γ
VALUE (units 10^{-4})	CL%	EVTS	DOCUMENT ID	TECN	COMMENT
$10.4^{+2.9}_{-2.7} \pm 1.4$		20	48 WU	06 BELL	$B^+ \rightarrow \Lambda\bar{\Lambda} K^+$
• • • We do not use the following data for averages, fits, limits, etc. • • •					
< 20	90		35 BISELLO	91 DM2	$e^+ e^- \rightarrow \gamma \Lambda\bar{\Lambda}$

$\Gamma(\Lambda\bar{\Lambda})/\Gamma(p\bar{p})$			Γ_{25}/Γ_{24}
VALUE	DOCUMENT ID	TECN	COMMENT
$0.67^{+0.19}_{-0.16} \pm 0.12$	49 WU	06 BELL	$B^+ \rightarrow p\bar{p} K^+, \Lambda\bar{\Lambda} K^+$

$\Gamma(K\bar{K}\eta)/\Gamma_{\text{total}}$					Γ_{26}/Γ
VALUE	CL%	DOCUMENT ID	TECN	COMMENT	
<0.031	90	35 BALTRUSAIT..86	MRK3	$J/\psi \rightarrow \eta_c \gamma$	

$\Gamma(\pi^+ \pi^- \rho\bar{\rho})/\Gamma_{\text{total}}$					Γ_{27}/Γ
VALUE	CL%	DOCUMENT ID	TECN	COMMENT	
<0.012	90	HIMEL	80B MRK2	$\psi(2S) \rightarrow \eta_c \gamma$	

35 The quoted branching ratios use $B(J/\psi(1S) \rightarrow \gamma \eta_c(1S)) = 0.0127 \pm 0.0036$. Where relevant, the error in this branching ratio is treated as a common systematic in computing averages.

36 ABLIKIM 06A reports $[B(\eta_c(1S) \rightarrow K^*0 \bar{K}^*0 \pi^+ \pi^-)] \times [B(J/\psi(1S) \rightarrow \gamma \eta_c(1S))] = (1.91 \pm 0.64 \pm 0.48) \times 10^{-4}$. We divide by our best value $B(J/\psi(1S) \rightarrow \gamma \eta_c(1S)) = (1.3 \pm 0.4) \times 10^{-2}$. Our first error is their experiment's error and our second error is the systematic error from using our best value.

37 Using $B(B^+ \rightarrow \eta_c K^+) = (1.25 \pm 0.12^{+0.10}_{-0.12}) \times 10^{-3}$ from FANG 03 and $B(\eta_c \rightarrow K\bar{K}\pi) = (5.5 \pm 1.7) \times 10^{-2}$.

38 ABLIKIM 06A reports $[B(\eta_c(1S) \rightarrow \phi 2(\pi^+ \pi^-))] \times [B(J/\psi(1S) \rightarrow \gamma \eta_c(1S))] < 0.603 \times 10^{-4}$. We divide by our best value $B(J/\psi(1S) \rightarrow \gamma \eta_c(1S)) = 0.013$.

39 We are assuming $B(\rho(980) \rightarrow \eta\pi) > 0.5$.

40 ABLIKIM 04M reports $[B(\eta_c(1S) \rightarrow f_2(1270) f_2'(1270))] \times [B(J/\psi(1S) \rightarrow \gamma \eta_c(1S))] = (1.3 \pm 0.3^{+0.3}_{-0.4}) \times 10^{-4}$. We divide by our best value $B(J/\psi(1S) \rightarrow \gamma \eta_c(1S)) = (1.3 \pm 0.4) \times 10^{-2}$. Our first error is their experiment's error and our second error is the systematic error from using our best value.

41 Determined from the ratio of $B(B^\pm \rightarrow K^\pm \eta_c) B(\eta_c \rightarrow K\bar{K}\pi) = (7.4 \pm 0.5 \pm 0.7) \times 10^{-5}$ reported in AUBERT,B 04B and $B(B^\pm \rightarrow K^\pm \eta_c) = (8.7 \pm 1.5) \times 10^{-3}$ reported in AUBERT 06E.

42 Average from $K^+ K^- \pi^0$ and $K^\pm K_S^0 \pi^\mp$ decay channels.

43 Estimated using $B(\psi(2S) \rightarrow \gamma \eta_c(1S)) = 0.0028 \pm 0.0006$.

44 ABLIKIM 06A reports $[B(\eta_c(1S) \rightarrow K^+ K^- 2(\pi^+ \pi^-))] \times [B(J/\psi(1S) \rightarrow \gamma \eta_c(1S))] = (1.21 \pm 0.32 \pm 0.24) \times 10^{-4}$. We divide by our best value $B(J/\psi(1S) \rightarrow \gamma \eta_c(1S)) = (1.3 \pm 0.4) \times 10^{-2}$. Our first error is their experiment's error and our second error is the systematic error from using our best value.

45 Normalized to the sum of $B(\eta_c \rightarrow K^\pm K_S^0 \pi^\mp)$, $B(\eta_c \rightarrow \phi\phi)$, $B(\eta_c \rightarrow K^+ K^- \pi^+ \pi^-)$, and $B(\eta_c \rightarrow 2\pi^+ 2\pi^-)$.

46 ABLIKIM 06A reports $[B(\eta_c(1S) \rightarrow 3(\pi^+ \pi^-))] \times [B(J/\psi(1S) \rightarrow \gamma \eta_c(1S))] = (2.59 \pm 0.32 \pm 0.47) \times 10^{-4}$. We divide by our best value $B(J/\psi(1S) \rightarrow \gamma \eta_c(1S)) = (1.3 \pm 0.4) \times 10^{-2}$. Our first error is their experiment's error and our second error is the systematic error from using our best value.

47 WU 06 reports $[B(\eta_c(1S) \rightarrow p\bar{p})] \times [B(B^+ \rightarrow \eta_c K^+)] = (1.42 \pm 0.11^{+0.16}_{-0.20}) \times 10^{-6}$. We divide by our best value $B(B^+ \rightarrow \eta_c K^+) = (9.1 \pm 1.3) \times 10^{-4}$. Our first error is their experiment's error and our second error is the systematic error from using our best value.

48 WU 06 reports $[B(\eta_c(1S) \rightarrow \Lambda\bar{\Lambda})] \times [B(B^+ \rightarrow \eta_c K^+)] = (0.95^{+0.25+0.08}_{-0.22-0.11}) \times 10^{-6}$. We divide by our best value $B(B^+ \rightarrow \eta_c K^+) = (9.1 \pm 1.3) \times 10^{-4}$. Our first error is their experiment's error and our second error is the systematic error from using our best value.

49 Not independent from other $\eta_c \rightarrow \Lambda\bar{\Lambda}, p\bar{p}$ branching ratios reported by WU 06.

RADIATIVE DECAYS

$\Gamma(\gamma\gamma)/\Gamma_{\text{total}}$					Γ_{28}/Γ
VALUE (units 10^{-4})	CL%	EVTS	DOCUMENT ID	TECN	COMMENT
$2.4^{+1.1}_{-0.8} \pm 0.3$		13	50 WICHT	08 BELL	$B^\pm \rightarrow K^\pm \gamma \gamma$

• • • We do not use the following data for averages, fits, limits, etc. • • •

$2.80^{+0.67}_{-0.58} \pm 1.0$			51 ARMSTRONG	95 F E760	$\bar{p}p \rightarrow \gamma\gamma$
< 9	90		52 BISELLO	91 DM2	$J/\psi \rightarrow \gamma\gamma\gamma$
$6^{+4}_{-3} \pm 4$			51 BAGLIN	87B SPEC	$\bar{p}p \rightarrow \gamma\gamma$
< 18	90		53 BLOOM	83 CBAL	$J/\psi \rightarrow \eta_c \gamma$

See key on page 373

Meson Particle Listings

$\eta_c(1S), J/\psi(1S)$

⁵⁰ WICHT 08 reports $[B(\eta_c(1S) \rightarrow \gamma\gamma)] \times [B(B^+ \rightarrow \eta_c K^+)] = (2.2^{+0.9+0.4}_{-0.7-0.2}) \times 10^{-7}$.

We divide by our best value $B(B^+ \rightarrow \eta_c K^+) = (9.1 \pm 1.3) \times 10^{-4}$. Our first error is their experiment's error and our second error is the systematic error from using our best value.

⁵¹ Not independent from the values of the total and two-photon width quoted by the same experiment.

⁵² The quoted branching ratios use $B(J/\psi(1S) \rightarrow \gamma\eta_c(1S)) = 0.0127 \pm 0.0036$. Where relevant, the error in this branching ratio is treated as a common systematic in computing averages.

⁵³ Using $B(J/\psi(1S) \rightarrow \gamma\eta_c(1S)) = 0.0127 \pm 0.0036$.

$\Gamma(\rho\bar{\rho}) \times \Gamma(\gamma\gamma)/\Gamma_{\text{total}}^2$	$\Gamma_{24}\Gamma_{28}/\Gamma^2$			
VALUE (units 10^{-5})	EVTS	DOCUMENT ID	TECN	COMMENT
0.26 ± 0.05 OUR AVERAGE		Error includes scale factor of 1.4.		
0.224 ^{+0.038} _{-0.037}	190	AMBROGIANI 03	E835	$\bar{p}p \rightarrow \eta_c \rightarrow \gamma\gamma$
0.336 ^{+0.080} _{-0.070}		ARMSTRONG 95F	E760	$\bar{p}p \rightarrow \gamma\gamma$
0.68 ^{+0.42} _{-0.31}	12	BAGLIN 87B	SPEC	$\bar{p}p \rightarrow \gamma\gamma$

Charge conjugation (C), Parity (P),

Lepton family number (LF) violating modes

$\Gamma(\pi^+\pi^-)/\Gamma_{\text{total}}$	Γ_{29}/Γ			
VALUE (units 10^{-5})	CL%	DOCUMENT ID	TECN	COMMENT
<90		54 ABLIKIM 06B	BES2	$J/\psi \rightarrow \pi^+\pi^-\gamma$

⁵⁴ ABLIKIM 06B reports $[B(\eta_c(1S) \rightarrow \pi^+\pi^-)] \times [B(J/\psi(1S) \rightarrow \gamma\eta_c(1S))] < 1.1 \times 10^{-5}$. We divide by our best value $B(J/\psi(1S) \rightarrow \gamma\eta_c(1S)) = 0.013$.

$\Gamma(\pi^0\pi^0)/\Gamma_{\text{total}}$	Γ_{30}/Γ			
VALUE (units 10^{-5})	CL%	DOCUMENT ID	TECN	COMMENT
<60		55 ABLIKIM 06B	BES2	$J/\psi \rightarrow \pi^0\pi^0\gamma$

⁵⁵ ABLIKIM 06B reports $[B(\eta_c(1S) \rightarrow \pi^0\pi^0)] \times [B(J/\psi(1S) \rightarrow \gamma\eta_c(1S))] < 0.71 \times 10^{-5}$. We divide by our best value $B(J/\psi(1S) \rightarrow \gamma\eta_c(1S)) = 0.013$.

$\Gamma(K^+K^-)/\Gamma_{\text{total}}$	Γ_{31}/Γ			
VALUE (units 10^{-5})	CL%	DOCUMENT ID	TECN	COMMENT
<80		56 ABLIKIM 06B	BES2	$J/\psi \rightarrow K^+K^-\gamma$

⁵⁶ ABLIKIM 06B reports $[B(\eta_c(1S) \rightarrow K^+K^-)] \times [B(J/\psi(1S) \rightarrow \gamma\eta_c(1S))] < 0.96 \times 10^{-5}$. We divide by our best value $B(J/\psi(1S) \rightarrow \gamma\eta_c(1S)) = 0.013$.

$\Gamma(K_S^0 K_S^0)/\Gamma_{\text{total}}$	Γ_{32}/Γ			
VALUE (units 10^{-5})	CL%	DOCUMENT ID	TECN	COMMENT
<40		57 ABLIKIM 06B	BES2	$J/\psi \rightarrow K_S^0 K_S^0 \gamma$

⁵⁷ ABLIKIM 06B reports $[B(\eta_c(1S) \rightarrow K_S^0 K_S^0)] \times [B(J/\psi(1S) \rightarrow \gamma\eta_c(1S))] < 0.53 \times 10^{-5}$. We divide by our best value $B(J/\psi(1S) \rightarrow \gamma\eta_c(1S)) = 0.013$.

$\eta_c(1S)$ REFERENCES

UEHARA 08 EPJ C53 1	S. Uehara et al.	(BELLE Collab.)
WICHT 08 PL B662 323	J. Wicht et al.	(BELLE Collab.)
ABE 07 PRL 98 082001	K. Abe et al.	(BELLE Collab.)
ABLIKIM 06A PL B633 15	M. Ablikim et al.	(BES Collab.)
ABLIKIM 06B EPJ C45 337	M. Ablikim et al.	(BES Collab.)
AUBERT 06E PRL 96 052002	B. Aubert et al.	(BABAR Collab.)
PDG 06 JPG 33 1	W.-M. Yao et al.	(PDG Collab.)
WU 06 PRL 97 162003	C.-H. Wu et al.	(BELLE Collab.)
ABLIKIM 05L PR D72 072005	M. Ablikim et al.	(BES Collab.)
KUO 05 PL B621 41	C.C. Kuo et al.	(BELLE Collab.)
ABE 04G PR D70 071102	K. Abe et al.	(BELLE Collab.)
ABLIKIM 04M PR D70 112008	M. Ablikim et al.	(BES Collab.)
ASNER 04 PRL 92 142001	D.M. Asner et al.	(CLEO Collab.)
AUBERT 04D PRL 92 142002	B. Aubert et al.	(BABAR Collab.)
AUBERT,B 04B PR D70 011101R	B. Aubert et al.	(BABAR Collab.)
BAI 04 PL B578 16	J.Z. Bai et al.	(BES Collab.)
ABDALLAH 03J EPJ C31 481	J. Abdallah et al.	(DELPHI Collab.)
AMBROGIANI 03 PL B566 45	M. Ambrogiani et al.	(FNAL E835 Collab.)
BAI 03 PL B595 174	J.Z. Bai et al.	(BES Collab.)
FANG 03 PRL 90 071801	F. Fang et al.	(BELLE Collab.)
HUANG 03 PRL 91 241802	H.-C. Huang et al.	(BELLE Collab.)
ABE,K 02 PRL 89 142001	K. Abe et al.	(BELLE Collab.)
BAI 00F PR D62 072001	J.Z. Bai et al.	(BES Collab.)
BRANDENB... 00B PRL 85 3095	G. Brandenburg et al.	(CLEO Collab.)
ACCIARRI 93T PL B461 155	M. Acciari et al.	(L3 Collab.)
BAI 93B PR D60 072001	J.Z. Bai et al.	(BES Collab.)
ABREU 95O PL B441 479	P. Abreu et al.	(DELPHI Collab.)
SHIRAI 98 PL B424 405	M. Shirai et al.	(AMY Collab.)
ARMSTRONG 95F PR D52 4839	T.A. Armstrong et al.	(FNAL, FERR, GENO+)
ALBRECHT 94H PL B338 390	H. Albrecht et al.	(ARGUS Collab.)
ADRIANI 93N PL B318 575	O. Adriani et al.	(L3 Collab.)
BISELLO 91 NP B350 1	D. Bisello et al.	(DM2 Collab.)
BAI 90B PRL 65 1309	Z. Bai et al.	(Mark III Collab.)
CHEN 90B PL B243 169	W.Y. Chen et al.	(CLEO Collab.)
BAGLIN 89 PL B231 557	C. Baglin, S. Baird, G. Bassompierre	(R704 Collab.)
BEHREND 89 ZPHY C42 367	H.J. Behrend et al.	(CELLO Collab.)
BRUNSCH... 89 ZPHY C41 533	W. Brunschweig et al.	(TASSO Collab.)
AIHARA 85D PRL 60 2355	H. Aihara et al.	(TPC Collab.)
BAGLIN 87B PL B187 191	C. Baglin et al.	(R704 Collab.)
BALTRUSAIT... 86 PR D33 629	R.M. Baltrusaitis et al.	(Mark III Collab.)
BERGER 86 PL 167B 120	C. Berger et al.	(PLUTO Collab.)
GAISER 86 PR D34 711	J. Gaiser et al.	(Crystal Ball Collab.)
ALTHOFF 85B ZPHY C29 189	M. Althoff et al.	(TASSO Collab.)
BALTRUSAIT... 84 PRL 52 2126	R.M. Baltrusaitis et al.	(CIT, USAC, J)P
BLOOM 83 ARNS 33 143	E.D. Bloom, C. Peck	(SLAC, CIT)
HIMEL 80B PRL 45 1146	T.M. Himel et al.	(SLAC, LBL, UC)
PARTRIDGE 80B PRL 45 1150	R. Partridge et al.	(CIT, HARV, PRIN+)

OTHER RELATED PAPERS

ARMSTRONG 89 PL B221 216 T.A. Armstrong et al. (CERN, CDF, BIRM+)

J/ψ(1S)

$$I^G(J^{PC}) = 0^-(1^{--})$$

J/ψ(1S) MASS

VALUE (MeV)	EVTS	DOCUMENT ID	TECN	COMMENT
3096.916 ± 0.011 OUR AVERAGE				
3096.917 ± 0.010 ± 0.007		AULCHENKO 03	KEDR	$e^+e^- \rightarrow$ hadrons
3096.89 ± 0.09	502	¹ ARTAMONOV 00	OLYA	$e^+e^- \rightarrow$ hadrons
3096.91 ± 0.03 ± 0.01		² ARMSTRONG 93B	E760	$\bar{p}p \rightarrow e^+e^-$
3096.95 ± 0.1 ± 0.3	193	BAGLIN 87	SPEC	$\bar{p}p \rightarrow e^+e^-X$
••• We do not use the following data for averages, fits, limits, etc. •••				
3097.5 ± 0.3		GRIBUSHIN 96	FMP5	515 $\pi^-Be \rightarrow 2\mu X$
3098.4 ± 2.0	38k	LEMOIGNE 82	GOLI	185 $\pi^-Be \rightarrow \gamma\mu^+\mu^-A$
3096.93 ± 0.09	502	³ ZHOLENTZ 80	REDE	e^+e^-
3097.0 ± 1		⁴ BRANDELIK 79c	DASP	e^+e^-

¹ Reanalysis of ZHOLENTZ 80 using new electron mass (COHEN 87) and radiative corrections (KURAEV 85).

² Mass central value and systematic error recalculated by us according to Eq. (16) in ARMSTRONG 93B, using the value for the $\psi(2S)$ mass from AULCHENKO 03.

³ Superseded by ARTAMONOV 00.

⁴ From a simultaneous fit to e^+e^- , $\mu^+\mu^-$ and hadronic channels assuming $\Gamma(e^+e^-) = \Gamma(\mu^+\mu^-)$.

J/ψ(1S) WIDTH

VALUE (keV)	EVTS	DOCUMENT ID	TECN	COMMENT
93.2 ± 2.1 OUR AVERAGE				
96.1 ± 3.2	13k	⁵ ADAMS 06A	CLEO	$e^+e^- \rightarrow \mu^+\mu^-\gamma$
93.7 ± 3.5	7.8k	⁵ AUBERT 04	BABR	$e^+e^- \rightarrow \mu^+\mu^-\gamma$
84.4 ± 8.9		BAI 95B	BES	e^+e^-
91 ± 11 ± 6		⁶ ARMSTRONG 93B	E760	$\bar{p}p \rightarrow e^+e^-$
85.5 ^{+6.1} _{-5.8}		⁷ HSUEH 92	RVUE	See T mini-review

⁵ Calculated by us from the reported values of $\Gamma(e^+e^-) \times B(\mu^+\mu^-)$ using $B(e^+e^-) = (5.94 \pm 0.06)\%$ and $B(\mu^+\mu^-) = (5.93 \pm 0.06)\%$.

⁶ The initial-state radiation correction reevaluated by ANDREOTTI 07 in its Ref. [4].

⁷ Using data from COFFMAN 92, BALDINI-CELIO 75, BOYARSKI 75, ESPOSITO 75B, BRANDELIK 79c.

J/ψ(1S) DECAY MODES

Mode	Fraction (Γ_i/Γ)	Scale factor/ Confidence level
Γ_1 hadrons	(87.7 ± 0.5) %	
Γ_2 virtual $\gamma \rightarrow$ hadrons	(13.50 ± 0.30) %	
Γ_3 e^+e^-	(5.94 ± 0.06) %	
Γ_4 $\mu^+\mu^-$	(5.93 ± 0.06) %	
Decays involving hadronic resonances		
Γ_5 $\rho\pi$	(1.69 ± 0.15) %	S=2.4
Γ_6 $\rho^0\pi^0$	(5.6 ± 0.7) × 10 ⁻³	
Γ_7 $a_2(1320)\rho$	(1.09 ± 0.22) %	
Γ_8 $\omega\pi^+\pi^-\pi^-\pi^-$	(8.5 ± 3.4) × 10 ⁻³	
Γ_9 $\omega\pi^+\pi^-\pi^0$	(4.0 ± 0.7) × 10 ⁻³	
Γ_{10} $\omega\pi^+\pi^-$	(8.6 ± 0.7) × 10 ⁻³	S=1.1
Γ_{11} $\omega f_2(1270)$	(4.3 ± 0.6) × 10 ⁻³	
Γ_{12} $K^*(892)^0 K_S^0(1430)^0 + c.c.$	(6.0 ± 0.6) × 10 ⁻³	
Γ_{13} $K^*(892)^0 K_S^0(1770)^0 + c.c. \rightarrow K^*(892)^0 K^-\pi^+ + c.c.$	(6.9 ± 0.9) × 10 ⁻⁴	
Γ_{14} $\omega K^*(892) K + c.c.$	(6.1 ± 0.9) × 10 ⁻³	
Γ_{15} $K^+ K^*(892)^- + c.c.$	(5.12 ± 0.30) × 10 ⁻³	
Γ_{16} $K^+ K^*(892)^- + c.c. \rightarrow K^+ K^-\pi^0 + c.c.$	(1.97 ± 0.20) × 10 ⁻³	
Γ_{17} $K^+ K^*(892)^- + c.c. \rightarrow K^0 K^+ \pi^- + c.c.$	(3.0 ± 0.4) × 10 ⁻³	
Γ_{18} $K^0 K^*(892)^0 + c.c.$	(4.39 ± 0.31) × 10 ⁻³	
Γ_{19} $K^0 K^*(892)^0 + c.c. \rightarrow K^0 K^+ \pi^- + c.c.$	(3.2 ± 0.4) × 10 ⁻³	
Γ_{20} $K_1(1400)^\pm K^\mp$	(3.8 ± 1.4) × 10 ⁻³	
Γ_{21} $K^*(892)^0 K^+ \pi^- + c.c.$	seen	
Γ_{22} $\omega\pi^0\pi^0$	(3.4 ± 0.8) × 10 ⁻³	
Γ_{23} $b_1(1235)^\pm \pi^\mp$	[a] (3.0 ± 0.5) × 10 ⁻³	
Γ_{24} $\omega K^\pm K_S^0 \pi^\mp$	[a] (3.4 ± 0.5) × 10 ⁻³	
Γ_{25} $b_1(1235)^0 \pi^0$	(2.3 ± 0.6) × 10 ⁻³	
Γ_{26} $\eta K^\pm K_S^0 \pi^\mp$	[a] (2.2 ± 0.4) × 10 ⁻³	

Γ_{168}	$\gamma f_J(2220) \rightarrow \gamma p \bar{p}$	$(1.5 \pm 0.8) \times 10^{-5}$
Γ_{169}	$\gamma f_0(1500)$	$> (5.7 \pm 0.8) \times 10^{-4}$
Γ_{170}	$\gamma e^+ e^-$	$(8.8 \pm 1.4) \times 10^{-3}$

Weak decays

Γ_{171}	$D^- e^+ \nu_e + c.c.$	< 1.2	$\times 10^{-5}$	CL=90%
Γ_{172}	$\bar{D}^0 e^+ e^- + c.c.$	< 1.1	$\times 10^{-5}$	CL=90%
Γ_{173}	$D_s^- e^+ \nu_e + c.c.$	< 3.6	$\times 10^{-5}$	CL=90%

**Charge conjugation (C), Parity (P),
Lepton Family number (LF) violating modes**

Γ_{174}	$\gamma \gamma$	C	< 2.2	$\times 10^{-5}$	CL=90%
Γ_{175}	$e^\pm \mu^\mp$	LF	< 1.1	$\times 10^{-6}$	CL=90%
Γ_{176}	$e^\pm \tau^\mp$	LF	< 8.3	$\times 10^{-6}$	CL=90%
Γ_{177}	$\mu^\pm \tau^\mp$	LF	< 2.0	$\times 10^{-6}$	CL=90%

[a] The value is for the sum of the charge states or particle/antiparticle states indicated.

[b] Includes $p \bar{p} \pi^+ \pi^- \gamma$ and excludes $p \bar{p} \eta, p \bar{p} \omega, p \bar{p} \eta'$.

[c] See the "Note on the $\eta(1405)$ " in the $\eta(1405)$ Particle Listings.

$J/\psi(1S)$ PARTIAL WIDTHS

$\Gamma(\text{hadrons})$

VALUE (keV)	DOCUMENT ID	TECN	COMMENT
••• We do not use the following data for averages, fits, limits, etc. •••			
74.1 ± 8.1	BAI	95B	BES $e^+ e^-$
59 ± 24	BALDINI...	75	FRAG $e^+ e^-$
59 ± 14	BOYARSKI	75	MRK1 $e^+ e^-$
50 ± 25	ESPOSITO	75B	FRAM $e^+ e^-$

$\Gamma(e^+ e^-)$

VALUE (keV)	EVTs	DOCUMENT ID	TECN	COMMENT
$5.55 \pm 0.14 \pm 0.02$ OUR EVALUATION				
••• We do not use the following data for averages, fits, limits, etc. •••				
5.71 ± 0.16	13k	⁸ ADAMS	06A	CLEO $e^+ e^- \rightarrow \mu^+ \mu^- \gamma$
5.57 ± 0.19	7.8k	⁸ AUBERT	04	BABR $e^+ e^- \rightarrow \mu^+ \mu^- \gamma$
5.14 ± 0.39		BAI	95B	BES $e^+ e^-$
$5.36^{+0.29}_{-0.28}$		⁹ HSUEH	92	RVUE See γ mini-review
4.72 ± 0.35		ALEXANDER	89	RVUE See γ mini-review
4.4 ± 0.6		⁹ BRANDELIK	79C	DASP $e^+ e^-$
4.6 ± 0.8		¹⁰ BALDINI...	75	FRAG $e^+ e^-$
4.8 ± 0.6		BOYARSKI	75	MRK1 $e^+ e^-$
4.6 ± 1.0		ESPOSITO	75B	FRAM $e^+ e^-$
⁸ Calculated by us from the reported values of $\Gamma(e^+ e^-) \times B(\mu^+ \mu^-)$ using $B(\mu^+ \mu^-) = (5.93 \pm 0.06)\%$.				
⁹ From a simultaneous fit to $e^+ e^-$, $\mu^+ \mu^-$, and hadronic channels assuming $\Gamma(e^+ e^-) = \Gamma(\mu^+ \mu^-)$.				
¹⁰ Assuming equal partial widths for $e^+ e^-$ and $\mu^+ \mu^-$.				

$\Gamma(\mu^+ \mu^-)$

VALUE (keV)	DOCUMENT ID	TECN	COMMENT
••• We do not use the following data for averages, fits, limits, etc. •••			
5.13 ± 0.52	BAI	95B	BES $e^+ e^-$
4.8 ± 0.6	BOYARSKI	75	MRK1 $e^+ e^-$
5 ± 1	ESPOSITO	75B	FRAM $e^+ e^-$

$\Gamma(\gamma \gamma)$

VALUE (eV)	CL%	DOCUMENT ID	TECN	COMMENT
< 5.4	90	BRANDELIK	79C	DASP $e^+ e^-$

$J/\psi(1S) \Gamma(i) \Gamma(e^+ e^-) / \Gamma(\text{total})$

This combination of a partial width with the partial width into $e^+ e^-$ and with the total width is obtained from the integrated cross section into channel i in the $e^+ e^-$ annihilation.

$\Gamma(\text{hadrons}) \times \Gamma(e^+ e^-) / \Gamma_{\text{total}}$

VALUE (keV)	DOCUMENT ID	TECN	COMMENT
••• We do not use the following data for averages, fits, limits, etc. •••			
4 ± 0.8	¹¹ BALDINI...	75	FRAG $e^+ e^-$
3.9 ± 0.8	¹¹ ESPOSITO	75B	FRAM $e^+ e^-$
¹¹ Data redundant with branching ratios or partial widths above.			

$\Gamma(e^+ e^-) \times \Gamma(e^+ e^-) / \Gamma_{\text{total}}$

VALUE (keV)	DOCUMENT ID	TECN	COMMENT
••• We do not use the following data for averages, fits, limits, etc. •••			
0.35 ± 0.02	BRANDELIK	79C	DASP $e^+ e^-$
0.32 ± 0.07	¹² BALDINI...	75	FRAG $e^+ e^-$
0.34 ± 0.09	¹² ESPOSITO	75B	FRAM $e^+ e^-$
0.36 ± 0.10	¹² FORD	75	SPEC $e^+ e^-$
¹² Data redundant with branching ratios or partial widths above.			

$\Gamma(\mu^+ \mu^-) \times \Gamma(e^+ e^-) / \Gamma_{\text{total}}$

VALUE (keV)	EVTs	DOCUMENT ID	TECN	COMMENT
0.335 ± 0.007 OUR AVERAGE				
$0.3384 \pm 0.0058 \pm 0.0071$	13k	ADAMS	06A	CLEO $e^+ e^- \rightarrow \mu^+ \mu^- \gamma$
$0.3301 \pm 0.0077 \pm 0.0073$	7.8k	AUBERT	04	BABR $e^+ e^- \rightarrow \mu^+ \mu^- \gamma$
••• We do not use the following data for averages, fits, limits, etc. •••				
0.51 ± 0.09		DASP	75	DASP $e^+ e^-$
0.38 ± 0.05		¹³ ESPOSITO	75B	FRAM $e^+ e^-$
¹³ Data redundant with branching ratios or partial widths above.				

$\Gamma(\omega \pi^+ \pi^- \pi^0) \times \Gamma(e^+ e^-) / \Gamma_{\text{total}}$

VALUE (10^{-2} keV)	EVTs	DOCUMENT ID	TECN	COMMENT
$2.2 \pm 0.3 \pm 0.2$	170	AUBERT	06D	BABR $10.6 e^+ e^- \rightarrow \omega \pi^+ \pi^- \pi^0 \gamma$

$\Gamma(\phi(2\pi^+ \pi^-)) \times \Gamma(e^+ e^-) / \Gamma_{\text{total}}$

VALUE (10^{-2} keV)	EVTs	DOCUMENT ID	TECN	COMMENT
$0.96 \pm 0.19 \pm 0.01$				
$0.96 \pm 0.19 \pm 0.01$	35	¹⁴ AUBERT	06D	BABR $10.6 e^+ e^- \rightarrow \phi(2\pi^+ \pi^-) \gamma$
¹⁴ AUBERT 06D reports $[\Gamma(J/\psi(1S) \rightarrow \phi(2\pi^+ \pi^-)) \times \Gamma(J/\psi(1S) \rightarrow e^+ e^-) / \Gamma_{\text{total}}] \times [B(\phi(1020) \rightarrow K^+ K^-)] = (0.47 \pm 0.09 \pm 0.03) \times 10^{-2}$ keV. We divide by our best value $B(\phi(1020) \rightarrow K^+ K^-) = (49.2 \pm 0.6) \times 10^{-2}$. Our first error is their experiment's error and our second error is the systematic error from using our best value.				

$\Gamma(\phi \pi^+ \pi^-) \times \Gamma(e^+ e^-) / \Gamma_{\text{total}}$

VALUE (eV)	EVTs	DOCUMENT ID	TECN	COMMENT
$5.3 \pm 0.7 \pm 0.1$				
$5.3 \pm 0.7 \pm 0.1$	103	¹⁵ AUBERT, BE	06D	BABR $10.6 e^+ e^- \rightarrow K^+ K^- \pi^+ \pi^- \gamma$
¹⁵ AUBERT, BE 06D reports $[\Gamma(J/\psi(1S) \rightarrow \phi \pi^+ \pi^-) \times \Gamma(J/\psi(1S) \rightarrow e^+ e^-) / \Gamma_{\text{total}}] \times [B(\phi(1020) \rightarrow K^+ K^-)] = 2.61 \pm 0.30 \pm 0.18$ eV. We divide by our best value $B(\phi(1020) \rightarrow K^+ K^-) = (49.2 \pm 0.6) \times 10^{-2}$. Our first error is their experiment's error and our second error is the systematic error from using our best value.				

$\Gamma(\phi_0(980) \rightarrow \phi \pi^+ \pi^-) \times \Gamma(e^+ e^-) / \Gamma_{\text{total}}$

VALUE (keV)	EVTs	DOCUMENT ID	TECN	COMMENT
$1.02 \pm 0.24 \pm 0.01$				
$1.02 \pm 0.24 \pm 0.01$	20 ± 5	¹⁶ AUBERT	07AK	BABR $10.6 e^+ e^- \rightarrow \pi^+ \pi^- K^+ K^- \gamma$
¹⁶ AUBERT 07AK reports $[\Gamma(J/\psi(1S) \rightarrow \phi_0(980) \rightarrow \phi \pi^+ \pi^-) \times \Gamma(J/\psi(1S) \rightarrow e^+ e^-) / \Gamma_{\text{total}}] \times [B(\phi(1020) \rightarrow K^+ K^-)] = 0.50 \pm 0.11 \pm 0.04$ eV. We divide by our best value $B(\phi(1020) \rightarrow K^+ K^-) = (49.2 \pm 0.6) \times 10^{-2}$. Our first error is their experiment's error and our second error is the systematic error from using our best value.				

$\Gamma(\phi^0 \pi^0) \times \Gamma(e^+ e^-) / \Gamma_{\text{total}}$

VALUE (eV)	EVTs	DOCUMENT ID	TECN	COMMENT
$3.13 \pm 0.88 \pm 0.04$				
$3.13 \pm 0.88 \pm 0.04$	23	¹⁷ AUBERT, BE	06D	BABR $10.6 e^+ e^- \rightarrow K^+ K^- \pi^0 \pi^0 \gamma$
¹⁷ AUBERT, BE 06D reports $[\Gamma(J/\psi(1S) \rightarrow \phi^0 \pi^0) \times \Gamma(J/\psi(1S) \rightarrow e^+ e^-) / \Gamma_{\text{total}}] \times [B(\phi(1020) \rightarrow K^+ K^-)] = 1.54 \pm 0.40 \pm 0.16$ eV. We divide by our best value $B(\phi(1020) \rightarrow K^+ K^-) = (49.2 \pm 0.6) \times 10^{-2}$. Our first error is their experiment's error and our second error is the systematic error from using our best value.				

$\Gamma(\phi_0(980) \rightarrow \phi \pi^0 \pi^0) \times \Gamma(e^+ e^-) / \Gamma_{\text{total}}$

VALUE (eV)	EVTs	DOCUMENT ID	TECN	COMMENT
$0.96 \pm 0.40 \pm 0.01$				
$0.96 \pm 0.40 \pm 0.01$	7.0 ± 2.8	¹⁸ AUBERT	07AK	BABR $10.6 e^+ e^- \rightarrow \pi^0 \pi^0 K^+ K^- \gamma$
¹⁸ AUBERT 07AK reports $[\Gamma(J/\psi(1S) \rightarrow \phi_0(980) \rightarrow \phi \pi^0 \pi^0) \times \Gamma(J/\psi(1S) \rightarrow e^+ e^-) / \Gamma_{\text{total}}] \times [B(\phi(1020) \rightarrow K^+ K^-)] = 0.47 \pm 0.19 \pm 0.05$ eV. We divide by our best value $B(\phi(1020) \rightarrow K^+ K^-) = (49.2 \pm 0.6) \times 10^{-2}$. Our first error is their experiment's error and our second error is the systematic error from using our best value.				

$\Gamma(\phi_2(1270)) \times \Gamma(e^+ e^-) / \Gamma_{\text{total}}$

VALUE (eV)	EVTs	DOCUMENT ID	TECN	COMMENT
$4.0 \pm 0.7 \pm 0.1$				
$4.0 \pm 0.7 \pm 0.1$	44 ± 7	^{19,20} AUBERT	07AK	BABR $10.6 e^+ e^- \rightarrow \pi^+ \pi^- K^+ K^- \gamma$
¹⁹ Using $B(\phi \rightarrow (K^+ K^-)) = (49.3 \pm 0.6)\%$.				
²⁰ AUBERT 07AK reports $[\Gamma(J/\psi(1S) \rightarrow \phi_2(1270)) \times \Gamma(J/\psi(1S) \rightarrow e^+ e^-) / \Gamma_{\text{total}}] \times [B(\phi_2(1270) \rightarrow \pi \pi)] = 3.41 \pm 0.55 \pm 0.28$ eV. We divide by our best value $B(\phi_2(1270) \rightarrow \pi \pi) = (84.8^{+2.4}_{-1.2}) \times 10^{-2}$. Our first error is their experiment's error and our second error is the systematic error from using our best value.				

$\Gamma(\pi^+ \pi^- \pi^0) \times \Gamma(e^+ e^-) / \Gamma_{\text{total}}$

VALUE (keV)	DOCUMENT ID	TECN	COMMENT
$0.122 \pm 0.005 \pm 0.008$			
	AUBERT, B	04N	BABR $10.6 e^+ e^- \rightarrow \pi^+ \pi^- \pi^0 \gamma$

$\Gamma(K^+ \bar{K}^*(892)^- + c.c.) \times \Gamma(e^+ e^-) / \Gamma_{\text{total}}$

VALUE (eV)	DOCUMENT ID	TECN	COMMENT
$29.0 \pm 1.7 \pm 1.3$			
	AUBERT	08s	BABR $10.6 e^+ e^- \rightarrow K^+ \bar{K}^*(892)^- \gamma$

Meson Particle Listings

 $J/\psi(1S)$

$\Gamma(K^0\bar{K}^*(892)^0 + c.c.) \times \Gamma(e^+e^-)/\Gamma_{total}$					$\Gamma_{18}\Gamma_3/\Gamma$
VALUE (eV)	DOCUMENT ID	TECN	COMMENT		
$26.6 \pm 2.5 \pm 1.5$	AUBERT	08s	BABR	$10.6 e^+e^- \rightarrow K^0\bar{K}^*(892)^0\gamma$	

$\Gamma(K^+\bar{K}^*(892)^- + c.c. \rightarrow K^+K^-\pi^0) \times \Gamma(e^+e^-)/\Gamma_{total}$					$\Gamma_{16}\Gamma_3/\Gamma$
VALUE (eV)	EVTS	DOCUMENT ID	TECN	COMMENT	
$10.96 \pm 0.85 \pm 0.70$	155	AUBERT	08s	BABR	$10.6 e^+e^- \rightarrow K^+K^-\pi^0\gamma$

$\Gamma(K^+\bar{K}^*(892)^- + c.c. \rightarrow K^0K^\pm\pi^\mp) \times \Gamma(e^+e^-)/\Gamma_{total}$					$\Gamma_{17}\Gamma_3/\Gamma$
VALUE (eV)	EVTS	DOCUMENT ID	TECN	COMMENT	
$16.76 \pm 1.70 \pm 1.00$	89	AUBERT	08s	BABR	$10.6 e^+e^- \rightarrow K_S^0K^\pm\pi^\mp\gamma$

$\Gamma(K^0\bar{K}^*(892)^0 + c.c. \rightarrow K^0K^\pm\pi^\mp) \times \Gamma(e^+e^-)/\Gamma_{total}$					$\Gamma_{19}\Gamma_3/\Gamma$
VALUE (eV)	EVTS	DOCUMENT ID	TECN	COMMENT	
$17.70 \pm 1.70 \pm 1.00$	94	AUBERT	08s	BABR	$10.6 e^+e^- \rightarrow K_S^0K^\pm\pi^\mp\gamma$

$\Gamma(\pi^+\pi^-K^+K^-) \times \Gamma(e^+e^-)/\Gamma_{total}$					$\Gamma_{80}\Gamma_3/\Gamma$
VALUE (eV)	EVTS	DOCUMENT ID	TECN	COMMENT	
$36.3 \pm 1.3 \pm 2.1$	1586 \pm 58	AUBERT	07AK	BABR	$10.6 e^+e^- \rightarrow \pi^+\pi^-K^+K^-\gamma$
• • • We do not use the following data for averages, fits, limits, etc. • • •					
$33.6 \pm 2.7 \pm 2.7$	233	²¹ AUBERT	05D	BABR	$10.6 e^+e^- \rightarrow K^+K^-\pi^+\pi^-\gamma$
²¹ Superseded by AUBERT 07AK.					

$\Gamma(K^*(892)^0\bar{K}^*(892)^0) \times \Gamma(e^+e^-)/\Gamma_{total}$					$\Gamma_{62}\Gamma_3/\Gamma$
VALUE (eV)	EVTS	DOCUMENT ID	TECN	COMMENT	
$1.28 \pm 0.40 \pm 0.11$	25 \pm 8	²² AUBERT	07AK	BABR	$10.6 e^+e^- \rightarrow \pi^+\pi^-K^+K^-\gamma$
²² Dividing by $(2/3)^2$ to take twice into account that $B(K^{*0} \rightarrow K^+\pi^-) = 2/3$.					

$\Gamma(K^*(892)^0\bar{K}_2^*(1430)^0 + c.c.) \times \Gamma(e^+e^-)/\Gamma_{total}$					$\Gamma_{12}\Gamma_3/\Gamma$
VALUE (eV)	EVTS	DOCUMENT ID	TECN	COMMENT	
$33 \pm 4 \pm 1$	317 \pm 23	^{23,24} AUBERT	07AK	BABR	$10.6 e^+e^- \rightarrow \pi^+\pi^-K^+K^-\gamma$
²³ Dividing by 2/3 to take into account that $B(K^{*0} \rightarrow K^+\pi^-) = 2/3$.					
²⁴ AUBERT 07AK reports $[\Gamma(J/\psi(1S) \rightarrow K^*(892)^0\bar{K}_2^*(1430)^0 + c.c.) \times \Gamma(J/\psi(1S) \rightarrow e^+e^-)/\Gamma_{total}] \times [B(K_2^*(1430) \rightarrow K\pi)] = 16.4 \pm 1.1 \pm 1.4$ eV. We divide by our best value $B(K_2^*(1430) \rightarrow K\pi) = (49.9 \pm 1.2) \times 10^{-2}$. Our first error is their experiment's error and our second error is the systematic error from using our best value.					

$\Gamma(K^*(892)^0\bar{K}_2^*(1770)^0 + c.c. \rightarrow K^*(892)^0K^-\pi^+ + c.c.) \times \Gamma(e^+e^-)/\Gamma_{total}$					$\Gamma_{13}\Gamma_3/\Gamma$
VALUE (eV)	EVTS	DOCUMENT ID	TECN	COMMENT	
$3.8 \pm 0.4 \pm 0.3$	110 \pm 14	²⁵ AUBERT	07AK	BABR	$10.6 e^+e^- \rightarrow \pi^+\pi^-K^+K^-\gamma$
²⁵ Dividing by 2/3 to take into account that $B(K^{*0} \rightarrow K^+\pi^-) = 2/3$.					

$\Gamma(\pi^0\pi^0K^+K^-) \times \Gamma(e^+e^-)/\Gamma_{total}$					$\Gamma_{82}\Gamma_3/\Gamma$
VALUE (eV)	EVTS	DOCUMENT ID	TECN	COMMENT	
$13.6 \pm 1.1 \pm 1.3$	203 \pm 16	AUBERT	07AK	BABR	$10.6 e^+e^- \rightarrow \pi^0\pi^0K^+K^-\gamma$

$\Gamma(2(\pi^+\pi^-)) \times \Gamma(e^+e^-)/\Gamma_{total}$					$\Gamma_{85}\Gamma_3/\Gamma$
VALUE (eV)	EVTS	DOCUMENT ID	TECN	COMMENT	
$19.5 \pm 1.4 \pm 1.3$	270	AUBERT	05D	BABR	$10.6 e^+e^- \rightarrow 2(\pi^+\pi^-)\gamma$

$\Gamma(3(\pi^+\pi^-)) \times \Gamma(e^+e^-)/\Gamma_{total}$					$\Gamma_{86}\Gamma_3/\Gamma$
VALUE (10^{-2} keV)	EVTS	DOCUMENT ID	TECN	COMMENT	
$2.37 \pm 0.16 \pm 0.14$	496	AUBERT	06D	BABR	$10.6 e^+e^- \rightarrow 3(\pi^+\pi^-)\gamma$

$\Gamma(2(\pi^+\pi^-\pi^0)) \times \Gamma(e^+e^-)/\Gamma_{total}$					$\Gamma_{87}\Gamma_3/\Gamma$
VALUE (10^{-2} keV)	EVTS	DOCUMENT ID	TECN	COMMENT	
$8.9 \pm 0.5 \pm 1.0$	761	AUBERT	06D	BABR	$10.6 e^+e^- \rightarrow 2(\pi^+\pi^-\pi^0)\gamma$

$\Gamma(2(\pi^+\pi^-)K^+K^-) \times \Gamma(e^+e^-)/\Gamma_{total}$					$\Gamma_{102}\Gamma_3/\Gamma$
VALUE (10^{-2} keV)	EVTS	DOCUMENT ID	TECN	COMMENT	
$2.75 \pm 0.23 \pm 0.17$	205	AUBERT	06D	BABR	$10.6 e^+e^- \rightarrow K^+K^-2(\pi^+\pi^-)\gamma$

$\Gamma(2(K^+K^-)) \times \Gamma(e^+e^-)/\Gamma_{total}$					$\Gamma_{111}\Gamma_3/\Gamma$
VALUE (eV)	EVTS	DOCUMENT ID	TECN	COMMENT	
$4.11 \pm 0.39 \pm 0.30$	156 \pm 15	AUBERT	07AK	BABR	$10.6 e^+e^- \rightarrow 2(K^+K^-)\gamma$
• • • We do not use the following data for averages, fits, limits, etc. • • •					
$4.0 \pm 0.7 \pm 0.6$	38	²⁶ AUBERT	05D	BABR	$10.6 e^+e^- \rightarrow 2(K^+K^-)\gamma$
²⁶ Superseded by AUBERT 07AK.					

$\Gamma(2(\pi^+\pi^-\pi^0)) \times \Gamma(e^+e^-)/\Gamma_{total}$					$\Gamma_{75}\Gamma_3/\Gamma$
VALUE (eV)	EVTS	DOCUMENT ID	TECN	COMMENT	
$303 \pm 5 \pm 18$	4990	AUBERT	07AU	BABR	$10.6 e^+e^- \rightarrow 2(\pi^+\pi^-\pi^0)\gamma$

$\Gamma(\omega\pi^+\pi^-) \times \Gamma(e^+e^-)/\Gamma_{total}$					$\Gamma_{10}\Gamma_3/\Gamma$
VALUE (eV)	EVTS	DOCUMENT ID	TECN	COMMENT	
$53.6 \pm 5.0 \pm 0.4$	788	²⁷ AUBERT	07AU	BABR	$10.6 e^+e^- \rightarrow \omega\pi^+\pi^-\gamma$

²⁷ AUBERT 07AU reports $[\Gamma(J/\psi(1S) \rightarrow \omega\pi^+\pi^-) \times \Gamma(J/\psi(1S) \rightarrow e^+e^-)/\Gamma_{total}] \times [B(\omega(782) \rightarrow \pi^+\pi^-\pi^0)] = 47.8 \pm 3.1 \pm 3.2$ eV. We divide by our best value $B(\omega(782) \rightarrow \pi^+\pi^-\pi^0) = (89.2 \pm 0.7) \times 10^{-2}$. Our first error is their experiment's error and our second error is the systematic error from using our best value.

$\Gamma(\eta\pi^+\pi^-) \times \Gamma(e^+e^-)/\Gamma_{total}$					$\Gamma_{53}\Gamma_3/\Gamma$
VALUE (eV)	EVTS	DOCUMENT ID	TECN	COMMENT	
$2.24 \pm 0.98 \pm 0.03$	9	²⁸ AUBERT	07AU	BABR	$10.6 e^+e^- \rightarrow \eta\pi^+\pi^-\gamma$

²⁸ AUBERT 07AU reports $[\Gamma(J/\psi(1S) \rightarrow \eta\pi^+\pi^-) \times \Gamma(J/\psi(1S) \rightarrow e^+e^-)/\Gamma_{total}] \times [B(\eta \rightarrow \pi^+\pi^-\pi^0)] = 0.51 \pm 0.22 \pm 0.03$ eV. We divide by our best value $B(\eta \rightarrow \pi^+\pi^-\pi^0) = (22.73 \pm 0.28) \times 10^{-2}$. Our first error is their experiment's error and our second error is the systematic error from using our best value.

$\Gamma(2(\pi^+\pi^-\eta)) \times \Gamma(e^+e^-)/\Gamma_{total}$					$\Gamma_{88}\Gamma_3/\Gamma$
VALUE (eV)	EVTS	DOCUMENT ID	TECN	COMMENT	
$13.1 \pm 2.4 \pm 0.1$	85	²⁹ AUBERT	07AU	BABR	$10.6 e^+e^- \rightarrow 2(\pi^+\pi^-\eta)\gamma$

²⁹ AUBERT 07AU reports $[\Gamma(J/\psi(1S) \rightarrow 2(\pi^+\pi^-\eta)) \times \Gamma(J/\psi(1S) \rightarrow e^+e^-)/\Gamma_{total}] \times [B(\eta \rightarrow 2\gamma)] = 5.16 \pm 0.85 \pm 0.39$ eV. We divide by our best value $B(\eta \rightarrow 2\gamma) = (39.31 \pm 0.20) \times 10^{-2}$. Our first error is their experiment's error and our second error is the systematic error from using our best value.

$\Gamma(\pi^+\pi^-\pi^0K^+K^-) \times \Gamma(e^+e^-)/\Gamma_{total}$					$\Gamma_{78}\Gamma_3/\Gamma$
VALUE (eV)	EVTS	DOCUMENT ID	TECN	COMMENT	
$107.0 \pm 4.3 \pm 6.4$	768	AUBERT	07AU	BABR	$10.6 e^+e^- \rightarrow K^+K^-\pi^+\pi^-\pi^0\gamma$

$\Gamma(\phi\eta) \times \Gamma(e^+e^-)/\Gamma_{total}$					$\Gamma_{42}\Gamma_3/\Gamma$
VALUE (eV)	EVTS	DOCUMENT ID	TECN	COMMENT	
$6.1 \pm 2.7 \pm 0.4$	6	³⁰ AUBERT	07AU	BABR	$10.6 e^+e^- \rightarrow \phi\eta\gamma$

³⁰ AUBERT 07AU quotes $\Gamma_{ee}^{J/\psi} \cdot B(J/\psi \rightarrow \phi\eta) \cdot B(\phi \rightarrow K^+K^-) \cdot B(\eta \rightarrow 3\pi) = 0.84 \pm 0.37 \pm 0.05$ eV.

$\Gamma(\omega K\bar{K}) \times \Gamma(e^+e^-)/\Gamma_{total}$					$\Gamma_{28}\Gamma_3/\Gamma$
VALUE (eV)	EVTS	DOCUMENT ID	TECN	COMMENT	
$3.70 \pm 1.98 \pm 0.03$	24	³¹ AUBERT	07AU	BABR	$10.6 e^+e^- \rightarrow \omega K^+K^-\gamma$

³¹ AUBERT 07AU reports $[\Gamma(J/\psi(1S) \rightarrow \omega K\bar{K}) \times \Gamma(J/\psi(1S) \rightarrow e^+e^-)/\Gamma_{total}] \times [B(\omega(782) \rightarrow \pi^+\pi^-\pi^0)] = 3.3 \pm 1.3 \pm 1.2$ eV. We divide by our best value $B(\omega(782) \rightarrow \pi^+\pi^-\pi^0) = (89.2 \pm 0.7) \times 10^{-2}$. Our first error is their experiment's error and our second error is the systematic error from using our best value.

$\Gamma(\pi^+\pi^-K^+K^-\eta) \times \Gamma(e^+e^-)/\Gamma_{total}$					$\Gamma_{81}\Gamma_3/\Gamma$
VALUE (eV)	EVTS	DOCUMENT ID	TECN	COMMENT	
$26.0 \pm 3.9 \pm 0.1$	73	³² AUBERT	07AU	BABR	$10.6 e^+e^- \rightarrow K^+K^-\pi^+\pi^-\eta\gamma$

³² AUBERT 07AU reports $[\Gamma(J/\psi(1S) \rightarrow \pi^+\pi^-K^+K^-\eta) \times \Gamma(J/\psi(1S) \rightarrow e^+e^-)/\Gamma_{total}] \times [B(\eta \rightarrow 2\gamma)] = 10.2 \pm 1.3 \pm 0.8$ eV. We divide by our best value $B(\eta \rightarrow 2\gamma) = (39.31 \pm 0.20) \times 10^{-2}$. Our first error is their experiment's error and our second error is the systematic error from using our best value.

$\Gamma(p\bar{p}) \times \Gamma(e^+e^-)/\Gamma_{total}$					$\Gamma_{90}\Gamma_3/\Gamma$
VALUE (eV)	EVTS	DOCUMENT ID	TECN	COMMENT	
11.6 ± 0.9 OUR AVERAGE	Error includes scale factor of 1.2.				

$12.0 \pm 0.6 \pm 0.5$ 438 AUBERT 06b $e^+e^- \rightarrow p\bar{p}\gamma$
 9.7 ± 1.7 33 ARMSTRONG 93B E760 $\bar{p}p \rightarrow e^+e^-$
³³ Using $\Gamma_{total} = 85.5^{+6.1}_{-5.8}$ MeV.

$\Gamma(\Sigma^0\bar{\Sigma}^0) \times \Gamma(e^+e^-)/\Gamma_{total}$					$\Gamma_{101}\Gamma_3/\Gamma$
VALUE (eV)	DOCUMENT ID	TECN	COMMENT		
$6.4 \pm 1.2 \pm 0.6$	AUBERT	07BD	BABR	$10.6 e^+e^- \rightarrow \Sigma^0\bar{\Sigma}^0\gamma$	

$\Gamma(\Lambda\bar{\Lambda}) \times \Gamma(e^+e^-)/\Gamma_{total}$					$\Gamma_{108}\Gamma_3/\Gamma$
VALUE (eV)	DOCUMENT ID	TECN	COMMENT		
$10.7 \pm 0.9 \pm 0.7$	AUBERT	07BD	BABR	$10.6 e^+e^- \rightarrow \Lambda\bar{\Lambda}\gamma$	

 $J/\psi(1S)$ BRANCHING RATIOS

For the first four branching ratios, see also the partial widths, and (partial widths) $\times \Gamma(e^+e^-)/\Gamma_{total}$ above.

$\Gamma(\text{hadrons})/\Gamma_{total}$				Γ_1/Γ
VALUE	DOCUMENT ID	TECN	COMMENT	
0.877 ± 0.005 OUR AVERAGE				
0.878 \pm 0.005	BAI	95B	BES	e^+e^-
0.86 \pm 0.02	BOYARSKI	75	MRK1	e^+e^-

See key on page 373

Meson Particle Listings

$J/\psi(1S)$

$\Gamma(\text{virtual } \gamma \rightarrow \text{hadrons})/\Gamma_{\text{total}}$ Γ_2/Γ

VALUE	DOCUMENT ID	TECN	COMMENT
0.135 ± 0.003	34,35 SETH	04	RVUE e^+e^-
••• We do not use the following data for averages, fits, limits, etc. •••			
0.17 ± 0.02	34 BOYARSKI	75	MRK1 e^+e^-

³⁴Included in $\Gamma(\text{hadrons})/\Gamma_{\text{total}}$.

³⁵Using $B(J/\psi \rightarrow \ell^+\ell^-) = (5.90 \pm 0.09)\%$ from RPP-2002 and $R = 2.28 \pm 0.04$ determined by a fit to data from BAI 00 and BAI 02c.

$\Gamma(e^+e^-)/\Gamma_{\text{total}}$ Γ_3/Γ

VALUE (units 10^{-2})	EVTS	DOCUMENT ID	TECN	COMMENT
5.94 ± 0.06 OUR AVERAGE				
5.945 ± 0.067 ± 0.042	15k	LI	05c	CLEO $\psi(2S) \rightarrow J/\psi \pi^+ \pi^-$
5.90 ± 0.05 ± 0.10		BAI	98D	BES $\psi(2S) \rightarrow J/\psi \pi^+ \pi^-$
6.09 ± 0.33		BAI	95B	BES e^+e^-
5.92 ± 0.15 ± 0.20		COFFMAN	92	MRK3 $\psi(2S) \rightarrow J/\psi \pi^+ \pi^-$
6.9 ± 0.9		BOYARSKI	75	MRK1 e^+e^-

$\Gamma(\mu^+\mu^-)/\Gamma_{\text{total}}$ Γ_4/Γ

VALUE (units 10^{-2})	EVTS	DOCUMENT ID	TECN	COMMENT
5.93 ± 0.06 OUR AVERAGE				
5.960 ± 0.065 ± 0.050	17k	LI	05c	CLEO $\psi(2S) \rightarrow J/\psi \pi^+ \pi^-$
5.84 ± 0.06 ± 0.10		BAI	98D	BES $\psi(2S) \rightarrow J/\psi \pi^+ \pi^-$
6.08 ± 0.33		BAI	95B	BES e^+e^-
5.90 ± 0.15 ± 0.19		COFFMAN	92	MRK3 $\psi(2S) \rightarrow J/\psi \pi^+ \pi^-$
6.9 ± 0.9		BOYARSKI	75	MRK1 e^+e^-

$\Gamma(e^+e^-)/\Gamma(\mu^+\mu^-)$ Γ_3/Γ_4

VALUE	DOCUMENT ID	TECN	COMMENT
0.997 ± 0.012 ± 0.006	LI	05c	CLEO $\psi(2S) \rightarrow J/\psi \pi^+ \pi^-$
••• We do not use the following data for averages, fits, limits, etc. •••			
1.00 ± 0.07	BAI	95B	BES e^+e^-
1.00 ± 0.05	BOYARSKI	75	MRK1 e^+e^-
0.91 ± 0.15	ESPOSITO	75B	FRAM e^+e^-
0.93 ± 0.10	FORD	75	SPEC e^+e^-

HADRONIC DECAYS

$\Gamma(\rho\pi)/\Gamma_{\text{total}}$ Γ_5/Γ

VALUE (units 10^{-2})	EVTS	DOCUMENT ID	TECN	COMMENT
1.69 ± 0.15 OUR AVERAGE				Error includes scale factor of 2.4. See the ideogram below.
2.18 ± 0.19	36,37	AUBERT,B	04N	BABR $10.6 e^+e^- \rightarrow \pi^+\pi^-\pi^0\gamma$
2.184 ± 0.005 ± 0.201	220k	37,38	BAI	04H BES $e^+e^- \rightarrow J/\psi \rightarrow \pi^+\pi^-\pi^0$
2.091 ± 0.021 ± 0.116		37,39	BAI	04H BES $\psi(2S) \rightarrow \pi^+\pi^- J/\psi$
1.21 ± 0.20		BAI	96D	BES $e^+e^- \rightarrow \rho\pi$
1.42 ± 0.01 ± 0.19		COFFMAN	88	MRK3 e^+e^-
1.3 ± 0.3	150	FRANKLIN	83	MRK2 e^+e^-
1.6 ± 0.4	183	ALEXANDER	78	PLUT e^+e^-
1.33 ± 0.21		BRANDELIK	78B	DASP e^+e^-
1.0 ± 0.2	543	BARTEL	76	CNTR e^+e^-
1.3 ± 0.3	153	JEAN-MARIE	76	MRK1 e^+e^-

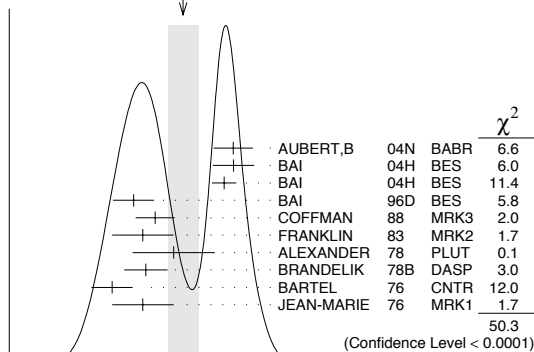
³⁶From the ratio of $\Gamma(e^+e^-) B(\pi^+\pi^-\pi^0)$ and $\Gamma(e^+e^-) B(\mu^+\mu^-)$ (AUBERT 04).

³⁷Not independent of their $B(\pi^+\pi^-\pi^0)$.

³⁸From $J/\psi \rightarrow \pi^+\pi^-\pi^0$ events directly.

³⁹Obtained comparing the rates for $\pi^+\pi^-\pi^0$ and $\mu^+\mu^-$, using J/ψ events produced via $\psi(2S) \rightarrow \pi^+\pi^- J/\psi$ and with $B(J/\psi \rightarrow \mu^+\mu^-) = 5.88 \pm 0.10\%$.

WEIGHTED AVERAGE
1.69 ± 0.15 (Error scaled by 2.4)



$\Gamma(\rho\pi)/\Gamma_{\text{total}}$ (units 10^{-2})

$\Gamma(\rho^0\pi^0)/\Gamma(\rho\pi)$ Γ_6/Γ_5

VALUE	DOCUMENT ID	TECN	COMMENT
0.328 ± 0.005 ± 0.027	COFFMAN	88	MRK3 e^+e^-
••• We do not use the following data for averages, fits, limits, etc. •••			
0.35 ± 0.08	ALEXANDER	78	PLUT e^+e^-
0.32 ± 0.08	BRANDELIK	78B	DASP e^+e^-
0.39 ± 0.11	BARTEL	76	CNTR e^+e^-
0.37 ± 0.09	JEAN-MARIE	76	MRK1 e^+e^-

$\Gamma(a_2(1320)\rho)/\Gamma_{\text{total}}$ Γ_7/Γ

VALUE (units 10^{-3})	EVTS	DOCUMENT ID	TECN	COMMENT
10.9 ± 2.2 OUR AVERAGE				
11.7 ± 0.7 ± 2.5	7584	AUGUSTIN	89	DM2 $J/\psi \rightarrow \rho^0 \rho^+ \pi^-$
8.4 ± 4.5	36	VANNUCCI	77	MRK1 $e^+e^- \rightarrow 2(\pi^+\pi^-)\pi^0$

$\Gamma(\omega\pi^+\pi^-\pi^0)/\Gamma_{\text{total}}$ Γ_8/Γ

VALUE (units 10^{-4})	EVTS	DOCUMENT ID	TECN	COMMENT
85 ± 34	140	VANNUCCI	77	MRK1 $e^+e^- \rightarrow 3(\pi^+\pi^-)\pi^0$

$\Gamma(\omega\pi^+\pi^0)/\Gamma_{\text{total}}$ Γ_9/Γ

VALUE (units 10^{-2})	EVTS	DOCUMENT ID	TECN	COMMENT
0.40 ± 0.06 ± 0.04	170	40 AUBERT	06D	BABR $10.6 e^+e^- \rightarrow \omega\pi^+\pi^-\pi^0\gamma$
⁴⁰ Using $\Gamma(J/\psi \rightarrow e^+e^-) = 5.52 \pm 0.14 \pm 0.04$ keV.				

$\Gamma(\omega\pi^+\pi^-)/\Gamma_{\text{total}}$ Γ_{10}/Γ

VALUE (units 10^{-3})	EVTS	DOCUMENT ID	TECN	COMMENT
8.6 ± 0.7 OUR AVERAGE				Error includes scale factor of 1.1.
9.7 ± 0.6 ± 0.6	788	41 AUBERT	07AU	BABR $10.6 e^+e^- \rightarrow \omega\pi^+\pi^-\gamma$
7.0 ± 1.6	18058	AUGUSTIN	89	DM2 $J/\psi \rightarrow 2(\pi^+\pi^-)\pi^0$
7.8 ± 1.6	215	BURMESTER	77D	PLUT e^+e^-
6.8 ± 1.9	348	VANNUCCI	77	MRK1 $e^+e^- \rightarrow 2(\pi^+\pi^-)\pi^0$
⁴¹ AUBERT 07AU quotes $\Gamma_{ee}^{J/\psi} \cdot B(J/\psi \rightarrow \omega\pi^+\pi^-) \cdot B(\omega \rightarrow 3\pi) = 47.8 \pm 3.1 \pm 3.2$ eV.				

$\Gamma(\omega f_2(1270))/\Gamma_{\text{total}}$ Γ_{11}/Γ

VALUE (units 10^{-3})	EVTS	DOCUMENT ID	TECN	COMMENT
4.3 ± 0.6 OUR AVERAGE				
4.3 ± 0.2 ± 0.6	5860	AUGUSTIN	89	DM2 e^+e^-
4.0 ± 1.6	70	BURMESTER	77D	PLUT e^+e^-
••• We do not use the following data for averages, fits, limits, etc. •••				
1.9 ± 0.8	81	VANNUCCI	77	MRK1 $e^+e^- \rightarrow 2(\pi^+\pi^-)\pi^0$

$\Gamma(K^*(892)^0 \bar{K}_2^0(1430)^0 + c.c.)/\Gamma_{\text{total}}$ Γ_{12}/Γ

VALUE (units 10^{-3})	EVTS	DOCUMENT ID	TECN	COMMENT
6.0 ± 0.6 OUR AVERAGE				
5.9 ± 0.6 ± 0.2	317 ± 23	42,43 AUBERT	07AK	BABR $10.6 e^+e^- \rightarrow \pi^+\pi^-\pi^0 K^+ K^-$
6.7 ± 2.6	40	VANNUCCI	77	MRK1 $e^+e^- \rightarrow \pi^+\pi^- K^+ K^-$

⁴²Using $B(K_2^0(1430)^0 \rightarrow K\pi) = (49.9 \pm 1.2)\%$.

⁴³AUBERT 07AK reports $[B(J/\psi(1S) \rightarrow K^*(892)^0 \bar{K}_2^0(1430)^0 + c.c.) \times [\Gamma(J/\psi(1S) \rightarrow e^+e^-)]] = (32.9 \pm 2.3 \pm 2.7) \times 10^{-3}$ keV. We divide by our best value $\Gamma(J/\psi(1S) \rightarrow e^+e^-) = 5.55 \pm 0.14 \pm 0.02$ keV. Our first error is their experiment's error and our second error is the systematic error from using our best value.

$\Gamma(\omega K^*(892) \bar{K} + c.c.)/\Gamma_{\text{total}}$ Γ_{14}/Γ

VALUE (units 10^{-4})	EVTS	DOCUMENT ID	TECN	COMMENT
61 ± 9 OUR AVERAGE				
62.0 ± 6.8 ± 10.6	899 ± 98	ABLIKIM	08E	BES2 $J/\psi \rightarrow \omega K_S^0 K^\pm \pi^\mp$
65.3 ± 10.2 ± 13.5	176 ± 28	ABLIKIM	08E	BES2 $J/\psi \rightarrow \omega K^+ K^- \pi^0$
53 ± 14 ± 14	530 ± 140	BECKER	87	MRK3 $e^+e^- \rightarrow \text{hadrons}$

$\Gamma(K^+ \bar{K}^*(892)^- + c.c.)/\Gamma_{\text{total}}$ Γ_{15}/Γ

VALUE (units 10^{-3})	EVTS	DOCUMENT ID	TECN	COMMENT
5.12 ± 0.30 OUR AVERAGE				
5.2 ± 0.4 ± 0.1		44 AUBERT	08s	BABR $10.6 e^+e^- \rightarrow K^+ K^*(892)^- \gamma$
4.57 ± 0.17 ± 0.70	2285	JOUSSET	90	DM2 $J/\psi \rightarrow \text{hadrons}$
5.26 ± 0.13 ± 0.53		COFFMAN	88	MRK3 $J/\psi \rightarrow K^\pm K_S^0 \pi^\mp, K^+ K^- \pi^0$

••• We do not use the following data for averages, fits, limits, etc. •••

2.6 ± 0.6 24 FRANKLIN 83 MRK2 $J/\psi \rightarrow K^+ K^- \pi^0$

3.2 ± 0.6 48 VANNUCCI 77 MRK1 $J/\psi \rightarrow K^\pm K_S^0 \pi^\mp$

4.1 ± 1.2 39 BRAUNSCH... 76 DASP $J/\psi \rightarrow K^\pm X$

⁴⁴AUBERT 08s reports $[B(J/\psi(1S) \rightarrow K^+ \bar{K}^*(892)^- + c.c.) \times [\Gamma(J/\psi(1S) \rightarrow e^+e^-)]] = (29.0 \pm 1.7 \pm 1.3) \times 10^{-3}$ keV. We divide by our best value $\Gamma(J/\psi(1S) \rightarrow e^+e^-) = 5.55 \pm 0.14 \pm 0.02$ keV. Our first error is their experiment's error and our second error is the systematic error from using our best value.

Meson Particle Listings

$J/\psi(1S)$

$\Gamma(K^+\bar{K}^*(892)^- + c.c. \rightarrow K^+K^-\pi^0)/\Gamma_{total}$ Γ_{16}/Γ

VALUE (units 10^{-3})	EVTS	DOCUMENT ID	TECN	COMMENT
1.97 ± 0.20 ± 0.05	155	45 AUBERT	08s BABR	10.6 $e^+e^- \rightarrow K^+K^-\pi^0\gamma$
⁴⁵ AUBERT 08s reports $[B(J/\psi(1S) \rightarrow K^+\bar{K}^*(892)^- + c.c. \rightarrow K^+K^-\pi^0)] \times [\Gamma(J/\psi(1S) \rightarrow e^+e^-)] = (10.96 \pm 0.85 \pm 0.70) \times 10^{-3}$ keV. We divide by our best value $\Gamma(J/\psi(1S) \rightarrow e^+e^-) = 5.55 \pm 0.14 \pm 0.02$ keV. Our first error is their experiment's error and our second error is the systematic error from using our best value.				

$\Gamma(K^+\bar{K}^*(892)^- + c.c. \rightarrow K^0K^\pm\pi^\mp)/\Gamma_{total}$ Γ_{17}/Γ

VALUE (units 10^{-3})	EVTS	DOCUMENT ID	TECN	COMMENT
3.0 ± 0.4 ± 0.1	89	46 AUBERT	08s BABR	10.6 $e^+e^- \rightarrow K_S^0K^\pm\pi^\mp\gamma$
⁴⁶ AUBERT 08s reports $[B(J/\psi(1S) \rightarrow K^+\bar{K}^*(892)^- + c.c. \rightarrow K^0K^\pm\pi^\mp)] \times [\Gamma(J/\psi(1S) \rightarrow e^+e^-)] = (16.76 \pm 1.70 \pm 1.00) \times 10^{-3}$ keV. We divide by our best value $\Gamma(J/\psi(1S) \rightarrow e^+e^-) = 5.55 \pm 0.14 \pm 0.02$ keV. Our first error is their experiment's error and our second error is the systematic error from using our best value.				

$\Gamma(K^0\bar{K}^*(892)^0 + c.c.)/\Gamma_{total}$ Γ_{18}/Γ

VALUE (units 10^{-3})	EVTS	DOCUMENT ID	TECN	COMMENT
4.39 ± 0.31 OUR AVERAGE				
4.8 ± 0.5 ± 0.1		47 AUBERT	08s BABR	10.6 $e^+e^- \rightarrow K^0\bar{K}^*(892)^0\gamma$
3.96 ± 0.15 ± 0.60	1192	JOUSSET	90 DM2	$J/\psi \rightarrow$ hadrons
4.33 ± 0.12 ± 0.45		COFFMAN	88 MRK3	$J/\psi \rightarrow K^\pm K_S^0\pi^\mp$

• • • We do not use the following data for averages, fits, limits, etc. • • •
 2.7 ± 0.6 ⁴⁵ VANNUCCI 77 MRK1 $J/\psi \rightarrow K^\pm K_S^0\pi^\mp$
⁴⁷AUBERT 08s reports $[B(J/\psi(1S) \rightarrow K^0\bar{K}^*(892)^0 + c.c.)] \times [\Gamma(J/\psi(1S) \rightarrow e^+e^-)] = (26.6 \pm 2.5 \pm 1.5) \times 10^{-3}$ keV. We divide by our best value $\Gamma(J/\psi(1S) \rightarrow e^+e^-) = 5.55 \pm 0.14 \pm 0.02$ keV. Our first error is their experiment's error and our second error is the systematic error from using our best value.

$\Gamma(K^0\bar{K}^*(892)^0 + c.c. \rightarrow K^0K^\pm\pi^\mp)/\Gamma_{total}$ Γ_{19}/Γ

VALUE (units 10^{-3})	EVTS	DOCUMENT ID	TECN	COMMENT
3.2 ± 0.4 ± 0.1	94	48 AUBERT	08s BABR	10.6 $e^+e^- \rightarrow K_S^0K^\pm\pi^\mp\gamma$
⁴⁸ AUBERT 08s reports $[B(J/\psi(1S) \rightarrow K^0\bar{K}^*(892)^0 + c.c. \rightarrow K^0K^\pm\pi^\mp)] \times [\Gamma(J/\psi(1S) \rightarrow e^+e^-)] = (17.70 \pm 1.70 \pm 1.00) \times 10^{-3}$ keV. We divide by our best value $\Gamma(J/\psi(1S) \rightarrow e^+e^-) = 5.55 \pm 0.14 \pm 0.02$ keV. Our first error is their experiment's error and our second error is the systematic error from using our best value.				

$\Gamma(K^0\bar{K}^*(892)^0 + c.c.)/\Gamma(K^+\bar{K}^*(892)^- + c.c.)$ Γ_{18}/Γ_{15}

VALUE	DOCUMENT ID	TECN	COMMENT
0.82 ± 0.05 ± 0.09	COFFMAN 88	MRK3	$J/\psi \rightarrow K\bar{K}^*(892) + c.c.$

$\Gamma(K_1(1400)^\pm K^\mp)/\Gamma_{total}$ Γ_{20}/Γ

VALUE (units 10^{-3})	DOCUMENT ID	TECN	COMMENT
3.8 ± 0.8 ± 1.2	49 BAI	99c BES	e^+e^-
⁴⁹ Assuming $B(K_1(1400) \rightarrow K^*\pi) = 0.94 \pm 0.06$			

$\Gamma(\bar{K}^*(892)^0 K^+\pi^- + c.c.)/\Gamma_{total}$ Γ_{21}/Γ

VALUE	DOCUMENT ID	TECN	COMMENT
seen	50 ABLIKIM	06c BES2	$J/\psi \rightarrow \bar{K}^*(892)^0 K^+\pi^-$
⁵⁰ A $K_0^*(800)$ is observed by ABLIKIM 06c in the $K^+\pi^-$ mass spectrum of the $\bar{K}^*(892)^0 K^+\pi^-$ final state against the $\bar{K}^*(892)$. A corresponding branching fraction of the $J/\psi(1S)$ is not presented.			

$\Gamma(\omega\pi^0\pi^0)/\Gamma_{total}$ Γ_{22}/Γ

VALUE (units 10^{-3})	EVTS	DOCUMENT ID	TECN	COMMENT
3.4 ± 0.3 ± 0.7	509	AUGUSTIN	89 DM2	$J/\psi \rightarrow \pi^+\pi^-\pi^0$

$\Gamma(b_1(1235)^\pm\pi^\mp)/\Gamma_{total}$ Γ_{23}/Γ

VALUE (units 10^{-4})	EVTS	DOCUMENT ID	TECN	COMMENT
30 ± 5 OUR AVERAGE				
31 ± 6	4600	AUGUSTIN	89 DM2	$J/\psi \rightarrow 2(\pi^+\pi^-)\pi^0$
29 ± 7	87	BURMESTER	77D PLUT	e^+e^-

$\Gamma(\omega K^\pm K_S^0\pi^\mp)/\Gamma_{total}$ Γ_{24}/Γ

VALUE (units 10^{-4})	EVTS	DOCUMENT ID	TECN	COMMENT
34 ± 5 OUR AVERAGE				
37.7 ± 0.8 ± 5.8	1972 ± 41	ABLIKIM	08E BES2	$e^+e^- \rightarrow J/\psi$
29.5 ± 1.4 ± 7.0	879 ± 41	BECKER	87 MRK3	$e^+e^- \rightarrow$ hadrons

$\Gamma(b_1(1235)^0\pi^0)/\Gamma_{total}$ Γ_{25}/Γ

VALUE (units 10^{-4})	EVTS	DOCUMENT ID	TECN	COMMENT
23 ± 3 ± 5	229	AUGUSTIN	89 DM2	e^+e^-

$\Gamma(\eta K^\pm K_S^0\pi^\mp)/\Gamma_{total}$ Γ_{26}/Γ

VALUE (units 10^{-4})	EVTS	DOCUMENT ID	TECN	COMMENT
21.8 ± 2.2 ± 3.4	232 ± 23	ABLIKIM	08E BES2	$e^+e^- \rightarrow J/\psi$

$\Gamma(\phi K^*(892)\bar{K} + c.c.)/\Gamma_{total}$ Γ_{27}/Γ

VALUE (units 10^{-4})	EVTS	DOCUMENT ID	TECN	COMMENT
21.8 ± 2.3 OUR AVERAGE				
20.8 ± 2.7 ± 3.9	195 ± 25	ABLIKIM	08E BES2	$J/\psi \rightarrow \phi K_S^0 K^\pm\pi^\mp$
29.6 ± 3.7 ± 4.7	238 ± 30	ABLIKIM	08E BES2	$J/\psi \rightarrow \phi K^+K^-\pi^0$
20.7 ± 2.4 ± 3.0		FALVARD	88 DM2	$J/\psi \rightarrow$ hadrons
20 ± 3 ± 3	155 ± 20	BECKER	87 MRK3	$e^+e^- \rightarrow$ hadrons

$\Gamma(\omega K\bar{K})/\Gamma_{total}$ Γ_{28}/Γ

VALUE (units 10^{-4})	EVTS	DOCUMENT ID	TECN	COMMENT
1.6 ± 0.5 OUR AVERAGE				
1.36 ± 0.50 ± 0.10	24	⁵¹ AUBERT	07AU BABR	10.6 $e^+e^- \rightarrow \omega K^+K^-\gamma$
19.8 ± 2.1 ± 3.9		⁵² FALVARD	88 DM2	$J/\psi \rightarrow$ hadrons
16 ± 10	22	FELDMAN	77 MRK1	e^+e^-
⁵¹ AUBERT 07AU quotes $\Gamma_{ee}^{J/\psi} \cdot B(J/\psi \rightarrow \omega K^+K^-) \cdot B(\eta \rightarrow 3\pi) = 3.3 \pm 1.3 \pm 0.2$ eV. ⁵² Addition of ωK^+K^- and $\omega K^0\bar{K}^0$ branching ratios.				

$\Gamma(\omega f_0(1710) \rightarrow \omega K\bar{K})/\Gamma_{total}$ Γ_{29}/Γ

VALUE (units 10^{-4})	DOCUMENT ID	TECN	COMMENT
4.8 ± 1.1 ± 0.3	53,54 FALVARD	88 DM2	$J/\psi \rightarrow$ hadrons
⁵³ Includes unknown branching fraction $f_0(1710) \rightarrow K\bar{K}$. ⁵⁴ Addition of $f_0(1710) \rightarrow K^+K^-$ and $f_0(1710) \rightarrow K^0\bar{K}^0$ branching ratios.			

$\Gamma(\phi 2(\pi^+\pi^-))/\Gamma_{total}$ Γ_{30}/Γ

VALUE (units 10^{-4})	EVTS	DOCUMENT ID	TECN	COMMENT
16.6 ± 2.3 OUR AVERAGE				
17.3 ± 3.3 ± 1.2	35	⁵⁵ AUBERT	06D BABR	10.6 $e^+e^- \rightarrow \phi 2(\pi^+\pi^-)\gamma$
16.0 ± 1.0 ± 3.0		FALVARD	88 DM2	$J/\psi \rightarrow$ hadrons
⁵⁵ Using $\Gamma(J/\psi \rightarrow e^+e^-) = 5.52 \pm 0.14 \pm 0.04$ keV.				

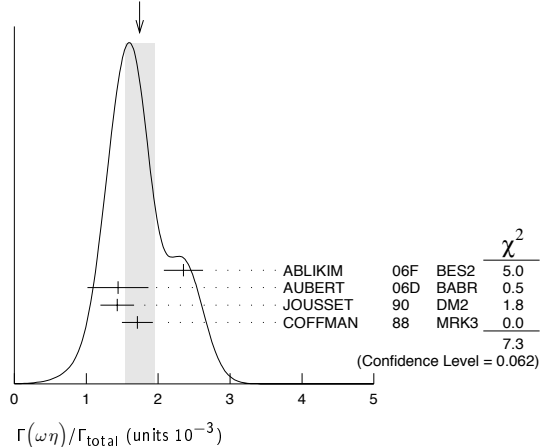
$\Gamma(\Delta(1232)^{++}\bar{p}\pi^-)/\Gamma_{total}$ Γ_{31}/Γ

VALUE (units 10^{-3})	EVTS	DOCUMENT ID	TECN	COMMENT
1.58 ± 0.23 ± 0.40	332	EATON	84 MRK2	e^+e^-

$\Gamma(\omega\eta)/\Gamma_{total}$ Γ_{32}/Γ

VALUE (units 10^{-3})	EVTS	DOCUMENT ID	TECN	COMMENT
1.74 ± 0.20 OUR AVERAGE				Error includes scale factor of 1.6. See the ideogram below.
2.352 ± 0.273	5k	⁵⁶ ABLIKIM	06F BES2	$J/\psi \rightarrow \omega\eta$
1.44 ± 0.40 ± 0.14	13	⁵⁷ AUBERT	06D BABR	10.6 $e^+e^- \rightarrow \omega\eta\gamma$
1.43 ± 0.10 ± 0.21	378	JOUSSET	90 DM2	$J/\psi \rightarrow$ hadrons
1.71 ± 0.08 ± 0.20		COFFMAN	88 MRK3	$e^+e^- \rightarrow 3\pi\eta$
⁵⁶ Using $B(\eta \rightarrow 2\gamma) = (39.43 \pm 0.26)\%$, $B(\eta \rightarrow \pi^+\pi^-\pi^0) = 22.6 \pm 0.4\%$, $B(\eta \rightarrow \pi^+\pi^-\gamma) = 4.68 \pm 0.11\%$, and $B(\omega \rightarrow \pi^+\pi^-\pi^0) = (89.1 \pm 0.7)\%$. ⁵⁷ Using $\Gamma(J/\psi \rightarrow e^+e^-) = 5.52 \pm 0.14 \pm 0.04$ keV.				

WEIGHTED AVERAGE
1.74 ± 0.20 (Error scaled by 1.6)



$\Gamma(\phi K\bar{K})/\Gamma_{total}$ Γ_{33}/Γ

VALUE (units 10^{-4})	EVTS	DOCUMENT ID	TECN	COMMENT
18.3 ± 2.4 OUR AVERAGE				Error includes scale factor of 1.5. See the ideogram below.
21.4 ± 0.4 ± 2.2		ABLIKIM	05 BES2	$J/\psi \rightarrow \phi\pi^+\pi^-$
48 $\begin{smallmatrix} +20 \\ -16 \end{smallmatrix}$ ± 6	9.0 $\begin{smallmatrix} +3.7 \\ -3.0 \end{smallmatrix}$	^{58,59} HUANG	03 BELL	$B^+ \rightarrow (\phi K^+K^-) K^+$
14.6 ± 0.8 ± 2.1		⁶⁰ FALVARD	88 DM2	$J/\psi \rightarrow$ hadrons
18 ± 8	14	FELDMAN	77 MRK1	e^+e^-

See key on page 373

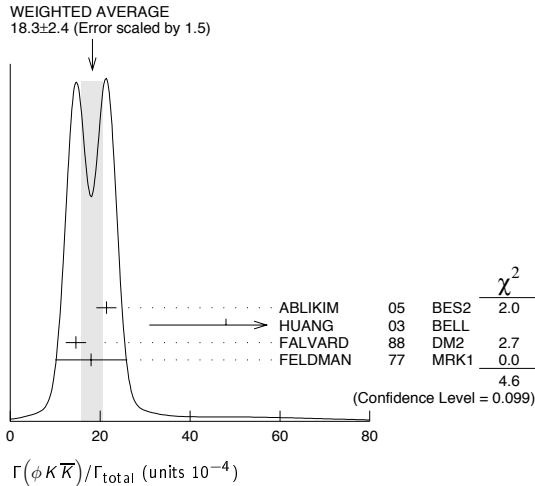
Meson Particle Listings

$J/\psi(1S)$

⁵⁸We have multiplied K^+K^- measurement by 2 to obtain $K\bar{K}$.

⁵⁹Using $B(B^+ \rightarrow J/\psi K^+) = (1.01 \pm 0.05) \times 10^{-3}$.

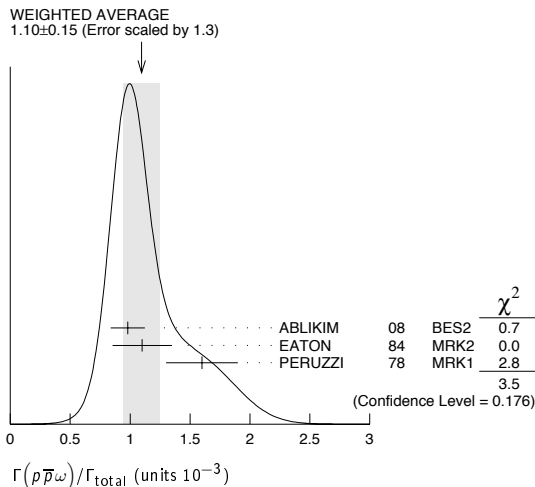
⁶⁰Addition of ϕK^+K^- and $\phi K^0\bar{K}^0$ branching ratios.



VALUE (units 10^{-4})	DOCUMENT ID	TECN	COMMENT
$3.6 \pm 0.2 \pm 0.6$	61,62	FALVARD	88 DM2 $J/\psi \rightarrow$ hadrons

⁶¹Including interference with $f_2'(1525)$.
⁶²Includes unknown branching fraction $f_0(1710) \rightarrow K\bar{K}$.

VALUE (units 10^{-3})	EVTS	DOCUMENT ID	TECN	COMMENT
1.10 ± 0.15 OUR AVERAGE				Error includes scale factor of 1.3. See the ideogram below.
$0.98 \pm 0.03 \pm 0.14$	2449	ABLIKIM	08	BES2 e^+e^-
$1.10 \pm 0.17 \pm 0.18$	486	EATON	84	MRK2 e^+e^-
1.6 ± 0.3	77	PERUZZI	78	MRK1 e^+e^-



VALUE (units 10^{-3})	EVTS	DOCUMENT ID	TECN	COMMENT
$1.10 \pm 0.09 \pm 0.28$	233	EATON	84	MRK2 e^+e^-

VALUE (units 10^{-3})	EVTS	DOCUMENT ID	TECN	COMMENT
1.03 ± 0.13 OUR AVERAGE				
$1.00 \pm 0.04 \pm 0.21$	631 ± 25	HENRARD	87	DM2 $e^+e^- \rightarrow \Sigma^{*-}$
$1.19 \pm 0.04 \pm 0.25$	754 ± 27	HENRARD	87	DM2 $e^+e^- \rightarrow \Sigma^{*+}$
$0.86 \pm 0.18 \pm 0.22$	56	EATON	84	MRK2 $e^+e^- \rightarrow \Sigma^{*-}$
$1.03 \pm 0.24 \pm 0.25$	68	EATON	84	MRK2 $e^+e^- \rightarrow \Sigma^{*+}$

VALUE (units 10^{-3})	EVTS	DOCUMENT ID	TECN	COMMENT
0.9 ± 0.4 OUR AVERAGE				Error includes scale factor of 1.7.
$0.68 \pm 0.23 \pm 0.17$	19	EATON	84	MRK2 e^+e^-
1.8 ± 0.6	19	PERUZZI	78	MRK1 e^+e^-

VALUE (units 10^{-4})	EVTS	DOCUMENT ID	TECN	COMMENT
8 ± 4 OUR AVERAGE				Error includes scale factor of 2.7.
$12.3 \pm 0.6 \pm 2.0$	63,64	FALVARD	88	DM2 $J/\psi \rightarrow$ hadrons
4.8 ± 1.8	46	GIDAL	81	MRK2 $J/\psi \rightarrow K^+K^-K^+K^-$

⁶³Re-evaluated using $B(f_2'(1525) \rightarrow K\bar{K}) = 0.713$.

⁶⁴Including interference with $f_0(1710)$.

VALUE (units 10^{-3})	EVTS	DOCUMENT ID	TECN	COMMENT
0.94 ± 0.09 OUR AVERAGE				Error includes scale factor of 1.2.
0.96 ± 0.13	103	AUBERT, BE	06D	BABR $10.6 e^+e^- \rightarrow K^+K^-\pi^+\pi^-\gamma$
$1.09 \pm 0.02 \pm 0.13$		ABLIKIM	05	BES2 $J/\psi \rightarrow \phi\pi^+\pi^-$
$0.78 \pm 0.03 \pm 0.12$		FALVARD	88	DM2 $J/\psi \rightarrow$ hadrons
2.1 ± 0.9	23	FELDMAN	77	MRK1 e^+e^-

⁶⁵Derived by us. AUBERT, BE 06D measures $\Gamma(J/\psi \rightarrow e^+e^-) \times B(J/\psi \rightarrow \phi\pi^+\pi^-) \times B(\phi \rightarrow K^+K^-) = (2.61 \pm 0.30 \pm 0.18)$ eV

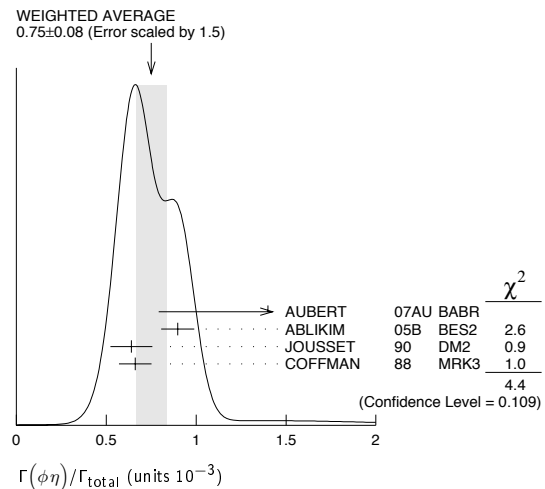
VALUE (units 10^{-3})	EVTS	DOCUMENT ID	TECN	COMMENT
0.56 ± 0.16	23	AUBERT, BE	06D	BABR $10.6 e^+e^- \rightarrow K^+K^-\pi^0\pi^0\gamma$
		AUBERT, BE	06D	BABR measures $\Gamma(J/\psi \rightarrow e^+e^-) \times B(J/\psi \rightarrow \phi\pi^0\pi^0) \times B(\phi \rightarrow K^+K^-) = (1.54 \pm 0.40 \pm 0.16)$ eV

VALUE (units 10^{-4})	EVTS	DOCUMENT ID	TECN	COMMENT
7.2 ± 0.8 OUR AVERAGE				
$7.4 \pm 0.6 \pm 1.4$	227 ± 19	ABLIKIM	08E	BES2 $e^+e^- \rightarrow J/\psi$
$7.4 \pm 0.9 \pm 1.1$		FALVARD	88	DM2 $J/\psi \rightarrow$ hadrons
$7 \pm 0.6 \pm 1.0$	163 ± 15	BECKER	87	MRK3 $e^+e^- \rightarrow$ hadrons

VALUE (units 10^{-4})	EVTS	DOCUMENT ID	TECN	COMMENT
$6.8 \pm 1.9 \pm 1.7$	111 ± 31 -26	BECKER	87	MRK3 $e^+e^- \rightarrow$ hadrons

VALUE (units 10^{-3})	EVTS	DOCUMENT ID	TECN	COMMENT
0.75 ± 0.08 OUR AVERAGE				Error includes scale factor of 1.5. See the ideogram below.
$1.4 \pm 0.6 \pm 0.1$	6	AUBERT	07AU	BABR $10.6 e^+e^- \rightarrow \phi\eta\gamma$
$0.898 \pm 0.024 \pm 0.089$		ABLIKIM	05B	BES2 $e^+e^- \rightarrow J/\psi \rightarrow$ hadr
$0.64 \pm 0.04 \pm 0.11$	346	JOUSSET	90	DM2 $J/\psi \rightarrow$ hadrons
$0.661 \pm 0.045 \pm 0.078$		COFFMAN	88	MRK3 $e^+e^- \rightarrow K^+K^-\eta$

⁶⁷AUBERT 07AU quotes $\Gamma_{ee}^{J/\psi} \cdot B(J/\psi \rightarrow \phi\eta) \cdot B(\phi \rightarrow K^+K^-) \cdot B(\eta \rightarrow \gamma\gamma) = 0.84 \pm 0.37 \pm 0.05$ eV.



VALUE (units 10^{-3})	EVTS	DOCUMENT ID	TECN	COMMENT
$0.59 \pm 0.09 \pm 0.12$	75 ± 11	HENRARD	87	DM2 e^+e^-

VALUE (units 10^{-3})	EVTS	DOCUMENT ID	TECN	COMMENT
$0.51 \pm 0.26 \pm 0.18$	89	EATON	84	MRK2 e^+e^-

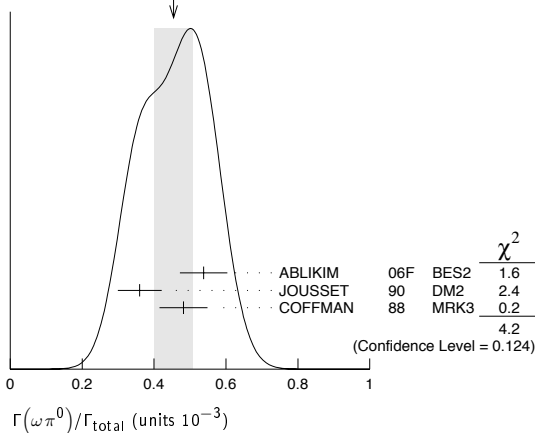
Meson Particle Listings

 $J/\psi(1S)$ $\Gamma(\omega\pi^0)/\Gamma_{\text{total}}$ Γ_{45}/Γ

VALUE (units 10^{-3})	EVTS	DOCUMENT ID	TECN	COMMENT
0.45 ± 0.05 OUR AVERAGE		Error includes scale factor of 1.4. See the ideogram below.		
0.538 ± 0.012 ± 0.065	2090	⁶⁸ ABLIKIM	06F BES2	$J/\psi \rightarrow \omega\pi^0$
0.360 ± 0.028 ± 0.054	222	JOUSSET	90 DM2	$J/\psi \rightarrow \text{hadrons}$
0.482 ± 0.019 ± 0.064		COFFMAN	88 MRK3	$e^+e^- \rightarrow \pi^0\pi^+\pi^-\pi^0$

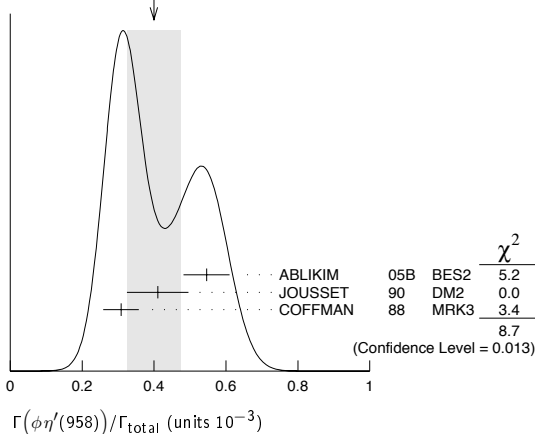
⁶⁸ Using $B(\omega \rightarrow \pi^+\pi^-\pi^0) = (89.1 \pm 0.7)\%$.

WEIGHTED AVERAGE
0.45±0.05 (Error scaled by 1.4)

 $\Gamma(\phi\eta'(958))/\Gamma_{\text{total}}$ Γ_{46}/Γ

VALUE (units 10^{-3})	CL%	EVTS	DOCUMENT ID	TECN	COMMENT
0.40 ± 0.07 OUR AVERAGE			Error includes scale factor of 2.1. See the ideogram below.		
0.546 ± 0.031 ± 0.056			ABLIKIM	05B BES2	$e^+e^- \rightarrow J/\psi \rightarrow \text{hadr}$
0.41 ± 0.03 ± 0.08		167	JOUSSET	90 DM2	$J/\psi \rightarrow \text{hadrons}$
0.308 ± 0.034 ± 0.036			COFFMAN	88 MRK3	$e^+e^- \rightarrow K^+K^-\eta'$
< 1.3		90	VANNUCCI	77 MRK1	e^+e^-

WEIGHTED AVERAGE
0.40±0.07 (Error scaled by 2.1)

 $\Gamma(\phi f_0(980))/\Gamma_{\text{total}}$ Γ_{47}/Γ

VALUE (units 10^{-4})	EVTS	DOCUMENT ID	TECN	COMMENT
3.2 ± 0.9 OUR AVERAGE		Error includes scale factor of 1.9.		
4.6 ± 0.4 ± 0.8		⁶⁹ FALVARD	88 DM2	$J/\psi \rightarrow \text{hadrons}$
2.6 ± 0.6	50	⁶⁹ GIDAL	81 MRK2	$J/\psi \rightarrow K^+K^-K^+K^-$

⁶⁹ Assuming $B(f_0(980) \rightarrow \pi\pi) = 0.78$.

 $\Gamma(\phi f_0(980) \rightarrow \phi\pi^+\pi^-)/\Gamma_{\text{total}}$ Γ_{48}/Γ

VALUE (units 10^{-3})	EVTS	DOCUMENT ID	TECN	COMMENT
0.182 ± 0.042 ± 0.005	19.5 ± 4.5	^{70,71} AUBERT	07AK BABR	$10.6 e^+e^- \rightarrow \pi^+\pi^-K^+K^-$

⁷⁰ Using $B(\phi \rightarrow K^+K^-) = (49.3 \pm 0.6)\%$.

⁷¹ AUBERT 07AK reports $[B(J/\psi(1S) \rightarrow \phi f_0(980) \rightarrow \phi\pi^+\pi^-)] \times [\Gamma(J/\psi(1S) \rightarrow e^+e^-)] = (1.01 \pm 0.22 \pm 0.08) \times 10^{-3}$ keV. We divide by our best value $\Gamma(J/\psi(1S) \rightarrow e^+e^-) = 5.55 \pm 0.14 \pm 0.02$ keV. Our first error is their experiment's error and our second error is the systematic error from using our best value.

 $\Gamma(\phi f_0(980) \rightarrow \phi\pi^0\pi^0)/\Gamma_{\text{total}}$ Γ_{49}/Γ

VALUE (units 10^{-3})	EVTS	DOCUMENT ID	TECN	COMMENT
0.171 ± 0.073 ± 0.004	7.0 ± 2.8	^{72,73} AUBERT	07AK BABR	$10.6 e^+e^- \rightarrow \pi^0\pi^0K^+K^-$

⁷² Using $B(\phi \rightarrow K^+K^-) = (49.3 \pm 0.6)\%$.

⁷³ AUBERT 07AK reports $[B(J/\psi(1S) \rightarrow \phi f_0(980) \rightarrow \phi\pi^0\pi^0)] \times [\Gamma(J/\psi(1S) \rightarrow e^+e^-)] = (0.95 \pm 0.39 \pm 0.10) \times 10^{-3}$ keV. We divide by our best value $\Gamma(J/\psi(1S) \rightarrow e^+e^-) = 5.55 \pm 0.14 \pm 0.02$ keV. Our first error is their experiment's error and our second error is the systematic error from using our best value.

 $\Gamma(\Xi(1530)^-\Xi^0)/\Gamma_{\text{total}}$ Γ_{50}/Γ

VALUE (units 10^{-3})	EVTS	DOCUMENT ID	TECN	COMMENT
0.32 ± 0.12 ± 0.07	24 ± 9	HENRARD	87 DM2	e^+e^-

 $\Gamma(\Sigma(1385)^-\Sigma^+(or\ c.c.))/\Gamma_{\text{total}}$ Γ_{51}/Γ

VALUE (units 10^{-3})	EVTS	DOCUMENT ID	TECN	COMMENT
0.31 ± 0.05 OUR AVERAGE				
0.30 ± 0.03 ± 0.07	74 ± 8	HENRARD	87 DM2	$e^+e^- \rightarrow \Sigma^{*-}$
0.34 ± 0.04 ± 0.07	77 ± 9	HENRARD	87 DM2	$e^+e^- \rightarrow \Sigma^{*+}$
0.29 ± 0.11 ± 0.10	26	EATON	84 MRK2	$e^+e^- \rightarrow \Sigma^{*-}$
0.31 ± 0.11 ± 0.11	28	EATON	84 MRK2	$e^+e^- \rightarrow \Sigma^{*+}$

 $\Gamma(\phi f_1(1285))/\Gamma_{\text{total}}$ Γ_{52}/Γ

VALUE (units 10^{-4})	EVTS	DOCUMENT ID	TECN	COMMENT
2.6 ± 0.5 OUR AVERAGE		Error includes scale factor of 1.1.		
3.2 ± 0.6 ± 0.4		JOUSSET	90 DM2	$J/\psi \rightarrow \phi 2(\pi^+\pi^-)$
2.1 ± 0.5 ± 0.4	25	⁷⁴ JOUSSET	90 DM2	$J/\psi \rightarrow \phi\eta\pi^+\pi^-$
• • • We do not use the following data for averages, fits, limits, etc. • • •				
0.6 ± 0.2 ± 0.1	16 ± 6	BECKER	87 MRK3	$J/\psi \rightarrow \phi K\bar{K}\pi$

⁷⁴ We attribute to the $f_1(1285)$ the signal observed in the $\pi^+\pi^-\eta$ invariant mass distribution at 1297 MeV.

 $\Gamma(\rho\eta)/\Gamma_{\text{total}}$ Γ_{54}/Γ

VALUE (units 10^{-3})	EVTS	DOCUMENT ID	TECN	COMMENT
0.193 ± 0.023 OUR AVERAGE				
0.194 ± 0.017 ± 0.029	299	JOUSSET	90 DM2	$J/\psi \rightarrow \text{hadrons}$
0.193 ± 0.013 ± 0.029		COFFMAN	88 MRK3	$e^+e^- \rightarrow \pi^+\pi^-\eta$

 $\Gamma(\eta\pi^+\pi^-)/\Gamma_{\text{total}}$ Γ_{53}/Γ

VALUE (units 10^{-3})	EVTS	DOCUMENT ID	TECN	COMMENT
0.40 ± 0.17 ± 0.03	9	⁷⁵ AUBERT	07AU BABR	$10.6 e^+e^- \rightarrow \eta\pi^+\pi^-\gamma$

⁷⁵ AUBERT 07AU quotes $\Gamma_{ee}^{J/\psi} \cdot B(J/\psi \rightarrow \eta\pi^+\pi^-) \cdot B(\eta \rightarrow 3\pi) = 0.51 \pm 0.22 \pm 0.03$ eV.

 $\Gamma(\omega\eta'(958))/\Gamma_{\text{total}}$ Γ_{55}/Γ

VALUE (units 10^{-3})	EVTS	DOCUMENT ID	TECN	COMMENT
0.182 ± 0.021 OUR AVERAGE				
0.226 ± 0.043	218	⁷⁶ ABLIKIM	06F BES2	$J/\psi \rightarrow \omega\eta'$
0.18 $^{+0.10}_{-0.08}$ ± 0.03	6	JOUSSET	90 DM2	$J/\psi \rightarrow \text{hadrons}$
0.166 ± 0.017 ± 0.019		COFFMAN	88 MRK3	$e^+e^- \rightarrow 3\pi\eta'$

⁷⁶ Using $B(\eta' \rightarrow \pi^+\pi^-\eta) = (44.3 \pm 1.5)\%$, $B(\eta' \rightarrow \pi^+\pi^-\gamma) = 29.5 \pm 1.0\%$, $B(\eta \rightarrow 2\gamma) = 39.43 \pm 0.26\%$, and $B(\omega \rightarrow \pi^+\pi^-\pi^0) = (89.1 \pm 0.7)\%$.

 $\Gamma(\omega f_0(980))/\Gamma_{\text{total}}$ Γ_{56}/Γ

VALUE (units 10^{-4})	EVTS	DOCUMENT ID	TECN	COMMENT
1.41 ± 0.27 ± 0.47		⁷⁷ AUGUSTIN	89 DM2	$J/\psi \rightarrow 2(\pi^+\pi^-)\pi^0$

⁷⁷ Assuming $B(f_0(980) \rightarrow \pi\pi) = 0.78$.

 $\Gamma(\rho\eta'(958))/\Gamma_{\text{total}}$ Γ_{57}/Γ

VALUE (units 10^{-3})	EVTS	DOCUMENT ID	TECN	COMMENT
0.105 ± 0.018 OUR AVERAGE				
0.083 ± 0.030 ± 0.012	19	JOUSSET	90 DM2	$J/\psi \rightarrow \text{hadrons}$
0.114 ± 0.014 ± 0.016		COFFMAN	88 MRK3	$J/\psi \rightarrow \pi^+\pi^-\eta'$

 $\Gamma(\rho\bar{\rho}\phi)/\Gamma_{\text{total}}$ Γ_{98}/Γ

VALUE (units 10^{-4})	EVTS	DOCUMENT ID	TECN	COMMENT
0.45 ± 0.13 ± 0.07		FALVARD	88 DM2	$J/\psi \rightarrow \text{hadrons}$

 $\Gamma(a_2(1320)^\pm\pi^\mp)/\Gamma_{\text{total}}$ Γ_{58}/Γ

VALUE (units 10^{-4})	CL%	DOCUMENT ID	TECN	COMMENT
< 43	90	BRAUNSCH...	76 DASP	e^+e^-

 $\Gamma(K\bar{K}_2^*(1430) + c.c.)/\Gamma_{\text{total}}$ Γ_{59}/Γ

VALUE (units 10^{-4})	CL%	DOCUMENT ID	TECN	COMMENT
< 40	90	VANNUCCI	77 MRK1	$e^+e^- \rightarrow K^0\bar{K}_2^{*0}$
• • • We do not use the following data for averages, fits, limits, etc. • • •				
< 66	90	BRAUNSCH...	76 DASP	$e^+e^- \rightarrow K^\pm\bar{K}_2^{*\mp}$

See key on page 373

Meson Particle Listings

$J/\psi(1S)$

$\Gamma(K_1(1270)^\pm K^\mp)/\Gamma_{total}$					Γ_{60}/Γ
VALUE (units 10^{-3})	CL%	DOCUMENT ID	TECN	COMMENT	
<3.0	90	⁷⁸ BAI	99c	BES e^+e^-	
⁷⁸ Assuming $B(K_1(1270) \rightarrow K\rho)=0.42 \pm 0.06$					

$\Gamma(K_2^*(1430)^0 \bar{K}_2^*(1430)^0)/\Gamma_{total}$					Γ_{61}/Γ
VALUE (units 10^{-4})	CL%	DOCUMENT ID	TECN	COMMENT	
<29	90	VANNUCCI	77	MRK1 $e^+e^- \rightarrow \pi^+\pi^-K^+K^-$	

$\Gamma(K^*(892)^0 \bar{K}^*(892)^0)/\Gamma_{total}$					Γ_{62}/Γ
VALUE (units 10^{-4})	CL%	EVTS	DOCUMENT ID	TECN	COMMENT
2.3 ± 0.7 ± 0.1		25 ± 8	⁷⁹ AUBERT	07AK BABR	10.6 $e^+e^- \rightarrow \pi^+\pi^-K^+K^- \gamma$

• • • We do not use the following data for averages, fits, limits, etc. • • •

VALUE (units 10^{-4})	CL%	DOCUMENT ID	TECN	COMMENT
<5	90	VANNUCCI	77	MRK1 $e^+e^- \rightarrow \pi^+\pi^-K^+K^-$
⁷⁹ AUBERT	07AK	reports $[B(J/\psi(1S) \rightarrow K^*(892)^0 \bar{K}^*(892)^0)] \times [\Gamma(J/\psi(1S) \rightarrow e^+e^-)] = (1.28 \pm 0.40 \pm 0.11) \times 10^{-3}$ keV. We divide by our best value $\Gamma(J/\psi(1S) \rightarrow e^+e^-) = 5.55 \pm 0.14 \pm 0.02$ keV. Our first error is their experiment's error and our second error is the systematic error from using our best value.		

$\Gamma(\phi f_2(1270))/\Gamma_{total}$					Γ_{63}/Γ
VALUE (units 10^{-3})	CL%	EVTS	DOCUMENT ID	TECN	COMMENT
0.72 ± 0.13 ± 0.02		44 ± 7	^{80,81} AUBERT	07AK BABR	10.6 $e^+e^- \rightarrow \pi^+\pi^-K^+K^- \gamma$

• • • We do not use the following data for averages, fits, limits, etc. • • •

VALUE (units 10^{-3})	CL%	DOCUMENT ID	TECN	COMMENT
< 0.45	90	FALVARD	88	DM2 $J/\psi \rightarrow$ hadrons
< 0.37	90	VANNUCCI	77	MRK1 $e^+e^- \rightarrow \pi^+\pi^-K^+K^-$

⁸⁰ Using $B(f_2(1270) \rightarrow \pi\pi) = (84.8^{+2.4}_{-1.2})\%$

⁸¹ AUBERT 07AK reports $[B(J/\psi(1S) \rightarrow \phi f_2(1270))] \times [\Gamma(J/\psi(1S) \rightarrow e^+e^-)] = (4.02 \pm 0.65 \pm 0.33) \times 10^{-3}$ keV. We divide by our best value $\Gamma(J/\psi(1S) \rightarrow e^+e^-) = 5.55 \pm 0.14 \pm 0.02$ keV. Our first error is their experiment's error and our second error is the systematic error from using our best value.

$\Gamma(\rho\bar{\rho})/\Gamma_{total}$					Γ_{95}/Γ
VALUE (units 10^{-3})	CL%	DOCUMENT ID	TECN	COMMENT	
<0.31	90	EATON	84	MRK2 $e^+e^- \rightarrow$ hadrons γ	

$\Gamma(\phi\eta(1405) \rightarrow \phi\eta\pi\pi)/\Gamma_{total}$					Γ_{64}/Γ
VALUE (units 10^{-4})	CL%	DOCUMENT ID	TECN	COMMENT	
<2.5	90	⁸² FALVARD	88	DM2 $J/\psi \rightarrow$ hadrons	

⁸² Includes unknown branching fraction $\eta(1405) \rightarrow \eta\pi\pi$.

$\Gamma(\omega f_2(1525))/\Gamma_{total}$					Γ_{65}/Γ
VALUE (units 10^{-4})	CL%	DOCUMENT ID	TECN	COMMENT	
<2.2	90	⁸³ VANNUCCI	77	MRK1 $e^+e^- \rightarrow \pi^+\pi^-\pi^0 K^+K^-$	

• • • We do not use the following data for averages, fits, limits, etc. • • •

VALUE (units 10^{-4})	CL%	DOCUMENT ID	TECN	COMMENT
<2.8	90	⁸³ FALVARD	88	DM2 $J/\psi \rightarrow$ hadrons

⁸³ Re-evaluated assuming $B(f_2(1525) \rightarrow K\bar{K}) = 0.713$.

$\Gamma(\Sigma(1385)^0 \bar{\Lambda})/\Gamma_{total}$					Γ_{66}/Γ
VALUE (units 10^{-3})	CL%	DOCUMENT ID	TECN	COMMENT	
<0.2	90	HENRARD	87	DM2 e^+e^-	

$\Gamma(\Delta(1232)^+ \bar{p})/\Gamma_{total}$					Γ_{67}/Γ
VALUE (units 10^{-3})	CL%	DOCUMENT ID	TECN	COMMENT	
<0.1	90	HENRARD	87	DM2 e^+e^-	

$\Gamma(\Theta(1540)\bar{\Theta}(1540) \rightarrow K_S^0 \rho K^- \bar{n} + c.c.)/\Gamma_{total}$					Γ_{68}/Γ
VALUE (units 10^{-5})	CL%	DOCUMENT ID	TECN	COMMENT	
<1.1	90	BAI	04G	BES2 e^+e^-	

$\Gamma(\Theta(1540)K^- \bar{n} \rightarrow K_S^0 \rho K^- \bar{n})/\Gamma_{total}$					Γ_{69}/Γ
VALUE (units 10^{-5})	CL%	DOCUMENT ID	TECN	COMMENT	
<2.1	90	BAI	04G	BES2 e^+e^-	

$\Gamma(\Theta(1540)K_S^0 \bar{p} \rightarrow K_S^0 \bar{p} K^+ n)/\Gamma_{total}$					Γ_{70}/Γ
VALUE (units 10^{-5})	CL%	DOCUMENT ID	TECN	COMMENT	
<1.6	90	BAI	04G	BES2 e^+e^-	

$\Gamma(\bar{\Theta}(1540)K^+ n \rightarrow K_S^0 \bar{p} K^+ n)/\Gamma_{total}$					Γ_{71}/Γ
VALUE (units 10^{-5})	CL%	DOCUMENT ID	TECN	COMMENT	
<5.6	90	BAI	04G	BES2 e^+e^-	

$\Gamma(\bar{\Theta}(1540)K_S^0 \rho \rightarrow K_S^0 \rho K^- \bar{n})/\Gamma_{total}$					Γ_{72}/Γ
VALUE (units 10^{-5})	CL%	DOCUMENT ID	TECN	COMMENT	
<1.1	90	BAI	04G	BES2 e^+e^-	

$\Gamma(\Sigma^0 \bar{\Lambda})/\Gamma_{total}$					Γ_{73}/Γ
VALUE (units 10^{-4})	CL%	DOCUMENT ID	TECN	COMMENT	
<0.9	90	HENRARD	87	DM2 e^+e^-	

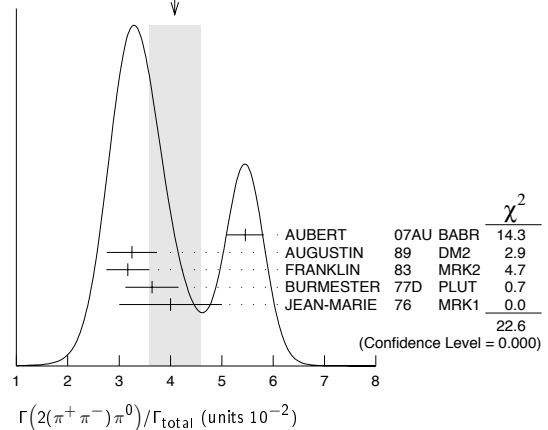
$\Gamma(\phi\pi^0)/\Gamma_{total}$					Γ_{74}/Γ
VALUE (units 10^{-6})	CL%	DOCUMENT ID	TECN	COMMENT	
<6.4	90	ABLIKIM	05B	BES2 $e^+e^- \rightarrow J/\psi \rightarrow \phi\gamma\gamma$	
• • • We do not use the following data for averages, fits, limits, etc. • • •					
<6.8	90	COFFMAN	88	MRK3 $e^+e^- \rightarrow K^+K^-\pi^0$	

STABLE HADRONS

$\Gamma(2(\pi^+\pi^-\pi^0))/\Gamma_{total}$					Γ_{75}/Γ
VALUE (units 10^{-2})	CL%	EVTS	DOCUMENT ID	TECN	COMMENT
4.1 ± 0.5 OUR AVERAGE			Error includes scale factor of 2.4. See the ideogram below.		
5.46 ± 0.34 ± 0.14	4990	⁸⁴ AUBERT	07AU	BABR	10.6 $e^+e^- \rightarrow 2(\pi^+\pi^-)\pi^0 \gamma$
3.25 ± 0.49	46055	AUGUSTIN	89	DM2	$J/\psi \rightarrow 2(\pi^+\pi^-)\pi^0$
3.17 ± 0.42	147	FRANKLIN	83	MRK2	$e^+e^- \rightarrow$ hadrons
3.64 ± 0.52	1500	BURMESTER	77D	PLUT	e^+e^-
4 ± 1	675	JEAN-MARIE	76	MRK1	e^+e^-

⁸⁴ AUBERT 07AU reports $[B(J/\psi(1S) \rightarrow 2(\pi^+\pi^-)\pi^0)] \times [\Gamma(J/\psi(1S) \rightarrow e^+e^-)] = 0.303 \pm 0.005 \pm 0.018$ keV. We divide by our best value $\Gamma(J/\psi(1S) \rightarrow e^+e^-) = 5.55 \pm 0.14 \pm 0.02$ keV. Our first error is their experiment's error and our second error is the systematic error from using our best value.

WEIGHTED AVERAGE
4.1 ± 0.5 (Error scaled by 2.4)



$\Gamma(\omega\pi^+\pi^-)/\Gamma(2(\pi^+\pi^-)\pi^0)$					Γ_{10}/Γ_{75}
VALUE	CL%	DOCUMENT ID	TECN	COMMENT	
• • • We do not use the following data for averages, fits, limits, etc. • • •					
0.3		⁸⁵ JEAN-MARIE	76	MRK1	e^+e^-

⁸⁵ Final state $(\pi^+\pi^-)\pi^0$ under the assumption that $\pi\pi$ is isospin 0.

$\Gamma(3(\pi^+\pi^-\pi^0))/\Gamma_{total}$					Γ_{76}/Γ
VALUE	CL%	EVTS	DOCUMENT ID	TECN	COMMENT
0.029 ± 0.006 OUR AVERAGE					
0.028 ± 0.009	11		FRANKLIN	83	MRK2 $e^+e^- \rightarrow$ hadrons
0.029 ± 0.007	181		JEAN-MARIE	76	MRK1 e^+e^-

$\Gamma(\pi^+\pi^-\pi^0)/\Gamma_{total}$					Γ_{77}/Γ
VALUE (units 10^{-3})	CL%	EVTS	DOCUMENT ID	TECN	COMMENT
20.7 ± 1.3 OUR AVERAGE			Error includes scale factor of 1.7. See the ideogram below.		
23.9 ± 2.1 ± 0.5	256	⁸⁶ AUBERT	07AU	BABR	10.6 $e^+e^- \rightarrow J/\psi\pi^+\pi^-\gamma$
21.8 ± 1.9		^{87,88} AUBERT,B	04N	BABR	10.6 $e^+e^- \rightarrow \pi^+\pi^-\pi^0\gamma$
21.84 ± 0.05 ± 2.01	220k	^{88,89} BAI	04H	BES	e^+e^-
20.91 ± 0.21 ± 1.16		^{88,90} BAI	04H	BES	e^+e^-
15 ± 2	168	FRANKLIN	83	MRK2	e^+e^-

⁸⁶ AUBERT 07AU reports $[B(J/\psi(1S) \rightarrow \pi^+\pi^-\pi^0)] \times [\Gamma(\psi(2S) \rightarrow J/\psi(1S)\pi^+\pi^-) \times \Gamma(\psi(2S) \rightarrow e^+e^-)]/\Gamma_{total} = (18.6 \pm 1.2 \pm 1.1) \times 10^{-3}$ keV. We divide by our best value $\Gamma(\psi(2S) \rightarrow J/\psi(1S)\pi^+\pi^-) \times \Gamma(\psi(2S) \rightarrow e^+e^-)/\Gamma_{total} = 0.777 \pm 0.016$ keV. Our first error is their experiment's error and our second error is the systematic error from using our best value.

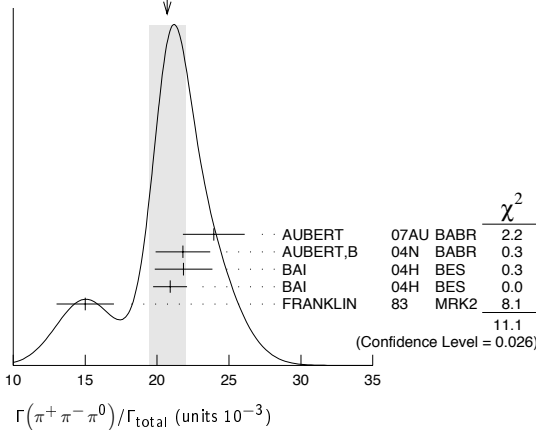
⁸⁷ From the ratio of $\Gamma(e^+e^-)B(\pi^+\pi^-\pi^0)$ and $\Gamma(e^+e^-)B(\mu^+\mu^-)$ (AUBERT 04).

⁸⁸ Mostly $\rho\pi$, see also $\rho\pi$ subsection.

⁸⁹ From $J/\psi \rightarrow \pi^+\pi^-\pi^0$ events directly.

⁹⁰ Obtained comparing the rates for $\pi^+\pi^-\pi^0$ and $\mu^+\mu^-$, using J/ψ events produced via $\psi(2S) \rightarrow \pi^+\pi^-J/\psi$ and with $B(J/\psi \rightarrow \mu^+\mu^-) = 5.88 \pm 0.10\%$.

Meson Particle Listings

 $J/\psi(1S)$ WEIGHTED AVERAGE
20.7±1.3 (Error scaled by 1.7) $\Gamma(\pi^+\pi^-\pi^0 K^+K^-)/\Gamma_{total}$ Γ_{78}/Γ

VALUE (units 10^{-2})	EVTS	DOCUMENT ID	TECN	COMMENT
1.79±0.29 OUR AVERAGE		Error includes scale factor of 2.2.		
1.93±0.14±0.05	768	⁹¹ AUBERT	07AU	BABR 10.6 $e^+e^- \rightarrow K^+K^-\pi^+\pi^-\pi^0\gamma$
1.2 ± 0.3	309	VANNUCCI	77	MRK1 e^+e^-

⁹¹AUBERT 07AU reports $[B(J/\psi(1S) \rightarrow \pi^+\pi^-\pi^0 K^+K^-)] \times [\Gamma(J/\psi(1S) \rightarrow e^+e^-)] = 0.1070 \pm 0.0043 \pm 0.0064$ keV. We divide by our best value $\Gamma(J/\psi(1S) \rightarrow e^+e^-) = 5.55 \pm 0.14 \pm 0.02$ keV. Our first error is their experiment's error and our second error is the systematic error from using our best value.

 $\Gamma(4(\pi^+\pi^-\pi^0))/\Gamma_{total}$ Γ_{79}/Γ

VALUE (units 10^{-4})	EVTS	DOCUMENT ID	TECN	COMMENT
90±30	13	JEAN-MARIE	76	MRK1 e^+e^-

 $\Gamma(\pi^+\pi^-K^+K^-)/\Gamma_{total}$ Γ_{80}/Γ

VALUE (units 10^{-3})	EVTS	DOCUMENT ID	TECN	COMMENT
6.6±0.5 OUR AVERAGE				
6.5±0.4±0.2	1.6k	⁹² AUBERT	07AK	BABR 10.6 $e^+e^- \rightarrow \pi^+\pi^-K^+K^- \gamma$
7.2±2.3	205	VANNUCCI	77	MRK1 e^+e^-

• • • We do not use the following data for averages, fits, limits, etc. • • •

⁹²AUBERT 07AK reports $[B(J/\psi(1S) \rightarrow \pi^+\pi^-K^+K^-)] \times [\Gamma(J/\psi(1S) \rightarrow e^+e^-)] = (36.3 \pm 1.3 \pm 2.1) \times 10^{-3}$ keV. We divide by our best value $\Gamma(J/\psi(1S) \rightarrow e^+e^-) = 5.55 \pm 0.14 \pm 0.02$ keV. Our first error is their experiment's error and our second error is the systematic error from using our best value.

⁹³Superseded by AUBERT 07AK. AUBERT 05D reports $[B(J/\psi(1S) \rightarrow \pi^+\pi^-K^+K^-)] \times [\Gamma(J/\psi(1S) \rightarrow e^+e^-)] = (33.6 \pm 2.7 \pm 2.7) \times 10^{-3}$ keV. We divide by our best value $\Gamma(J/\psi(1S) \rightarrow e^+e^-) = 5.55 \pm 0.14 \pm 0.02$ keV. Our first error is their experiment's error and our second error is the systematic error from using our best value.

 $\Gamma(\pi^+\pi^-K^+K^-\eta)/\Gamma_{total}$ Γ_{81}/Γ

VALUE (units 10^{-3})	EVTS	DOCUMENT ID	TECN	COMMENT
1.84±0.28±0.05	73	⁹⁴ AUBERT	07AU	BABR 10.6 $e^+e^- \rightarrow K^+K^-\pi^+\pi^-\eta \gamma$

⁹⁴AUBERT 07AU reports $[B(J/\psi(1S) \rightarrow \pi^+\pi^-K^+K^-\eta)] \times [\Gamma(J/\psi(1S) \rightarrow e^+e^-)] = (10.2 \pm 1.3 \pm 0.8) \times 10^{-3}$ keV. We divide by our best value $\Gamma(J/\psi(1S) \rightarrow e^+e^-) = 5.55 \pm 0.14 \pm 0.02$ keV. Our first error is their experiment's error and our second error is the systematic error from using our best value.

 $\Gamma(\pi^0\pi^0 K^+K^-)/\Gamma_{total}$ Γ_{82}/Γ

VALUE (units 10^{-3})	EVTS	DOCUMENT ID	TECN	COMMENT
2.45±0.31±0.06	203 ± 16	⁹⁵ AUBERT	07AK	BABR 10.6 $e^+e^- \rightarrow \pi^0\pi^0 K^+K^- \gamma$

⁹⁵AUBERT 07AK reports $[B(J/\psi(1S) \rightarrow \pi^0\pi^0 K^+K^-)] \times [\Gamma(J/\psi(1S) \rightarrow e^+e^-)] = (13.6 \pm 1.1 \pm 1.3) \times 10^{-3}$ keV. We divide by our best value $\Gamma(J/\psi(1S) \rightarrow e^+e^-) = 5.55 \pm 0.14 \pm 0.02$ keV. Our first error is their experiment's error and our second error is the systematic error from using our best value.

 $\Gamma(\eta\phi f_0(980) \rightarrow \eta\phi\pi^+\pi^-)/\Gamma_{total}$ Γ_{83}/Γ

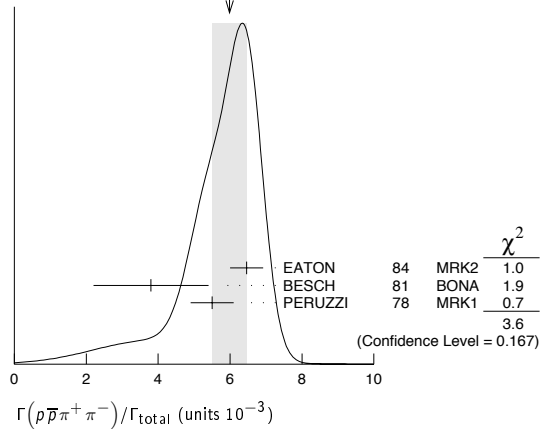
VALUE (units 10^{-4})	EVTS	DOCUMENT ID	TECN	COMMENT
3.23±0.75±0.73	52	ABLIKIM	08F	BES $J/\psi \rightarrow \eta\phi f_0(980)$

 $\Gamma(K\bar{K}\pi)/\Gamma_{total}$ Γ_{84}/Γ

VALUE (units 10^{-4})	EVTS	DOCUMENT ID	TECN	COMMENT
61 ± 10 OUR AVERAGE				
55.2±12.0	25	FRANKLIN	83	MRK2 $e^+e^- \rightarrow K^+K^-\pi^0$
78.0±21.0	126	VANNUCCI	77	MRK1 $e^+e^- \rightarrow K_S^0 K^\pm \pi^\mp$

 $\Gamma(\rho\bar{\rho}\pi^+\pi^-)/\Gamma_{total}$ Γ_{92}/Γ

VALUE (units 10^{-3})	EVTS	DOCUMENT ID	TECN	COMMENT
6.0 ± 0.5 OUR AVERAGE		Error includes scale factor of 1.3. See the ideogram below.		
6.46±0.17±0.43	1435	EATON	84	MRK2 e^+e^-
3.8 ± 1.6	48	BESCH	81	BONA e^+e^-
5.5 ± 0.6	533	PERUZZI	78	MRK1 e^+e^-

WEIGHTED AVERAGE
6.0±0.5 (Error scaled by 1.3) $\Gamma(2(\pi^+\pi^-))/\Gamma_{total}$ Γ_{85}/Γ

VALUE (units 10^{-3})	EVTS	DOCUMENT ID	TECN	COMMENT
3.55±0.23 OUR AVERAGE				
3.53±0.12±0.29	1107	⁹⁶ ABLIKIM	05H	BES2 $e^+e^- \rightarrow \psi(2S) \rightarrow J/\psi\pi^+\pi^-, J/\psi \rightarrow 2(\pi^+\pi^-)$
3.51±0.34±0.09	270	⁹⁷ AUBERT	05D	BABR 10.6 $e^+e^- \rightarrow 2(\pi^+\pi^-)\gamma$
4.0 ± 1.0	76	JEAN-MARIE	76	MRK1 e^+e^-

⁹⁶Computed using $B(J/\psi \rightarrow \mu^+\mu^-) = 0.0588 \pm 0.0010$.

⁹⁷AUBERT 05D reports $[B(J/\psi(1S) \rightarrow 2(\pi^+\pi^-))] \times [\Gamma(J/\psi(1S) \rightarrow e^+e^-)] = (19.5 \pm 1.4 \pm 1.3) \times 10^{-3}$ keV. We divide by our best value $\Gamma(J/\psi(1S) \rightarrow e^+e^-) = 5.55 \pm 0.14 \pm 0.02$ keV. Our first error is their experiment's error and our second error is the systematic error from using our best value.

 $\Gamma(3(\pi^+\pi^-))/\Gamma_{total}$ Γ_{86}/Γ

VALUE (units 10^{-4})	EVTS	DOCUMENT ID	TECN	COMMENT
43 ± 4 OUR AVERAGE				
43.0± 2.9±2.8	496	⁹⁸ AUBERT	06D	BABR 10.6 $e^+e^- \rightarrow 3(\pi^+\pi^-)\gamma$
40 ± 20	32	JEAN-MARIE	76	MRK1 e^+e^-

⁹⁸Using $\Gamma(J/\psi \rightarrow e^+e^-) = 5.52 \pm 0.14 \pm 0.04$ keV.

 $\Gamma(2(\pi^+\pi^-\pi^0))/\Gamma_{total}$ Γ_{87}/Γ

VALUE (units 10^{-2})	EVTS	DOCUMENT ID	TECN	COMMENT
1.62±0.09±0.19	761	⁹⁹ AUBERT	06D	BABR 10.6 $e^+e^- \rightarrow 2(\pi^+\pi^-\pi^0)\gamma$
		⁹⁹ Using $\Gamma(J/\psi \rightarrow e^+e^-) = 5.52 \pm 0.14 \pm 0.04$ keV.		

 $\Gamma(2(\pi^+\pi^-\eta))/\Gamma_{total}$ Γ_{88}/Γ

VALUE (units 10^{-3})	EVTS	DOCUMENT ID	TECN	COMMENT
2.29±0.24 OUR AVERAGE				
2.35±0.39±0.20	85	¹⁰⁰ AUBERT	07AU	BABR 10.6 $e^+e^- \rightarrow 2(\pi^+\pi^-\eta)\gamma$
2.26±0.08±0.27	4839	ABLIKIM	05c	BES2 $e^+e^- \rightarrow 2(\pi^+\pi^-\eta)$

¹⁰⁰AUBERT 07AU quotes $\Gamma_{ee}^{J/\psi} \cdot B(J/\psi \rightarrow 2(\pi^+\pi^-\eta)) \cdot B(\eta \rightarrow \gamma\gamma) = 5.16 \pm 0.85 \pm 0.39$ eV.

 $\Gamma(3(\pi^+\pi^-\eta))/\Gamma_{total}$ Γ_{89}/Γ

VALUE (units 10^{-4})	EVTS	DOCUMENT ID	TECN	COMMENT
7.24±0.96±1.11	616	ABLIKIM	05c	BES2 $e^+e^- \rightarrow 3(\pi^+\pi^-\eta)$

 $\Gamma(\eta\pi^+\pi^-)/\Gamma_{total}$ Γ_{100}/Γ

VALUE (units 10^{-3})	EVTS	DOCUMENT ID	TECN	COMMENT
3.8±3.6	5	BESCH	81	BONA e^+e^-

 $\Gamma(\Sigma^0\bar{\Sigma}^0)/\Gamma_{total}$ Γ_{101}/Γ

VALUE (units 10^{-3})	EVTS	DOCUMENT ID	TECN	COMMENT
1.29±0.09 OUR AVERAGE				
1.15±0.24±0.03		¹⁰¹ AUBERT	07BD	BABR 10.6 $e^+e^- \rightarrow \Sigma^0\bar{\Sigma}^0\gamma$
1.33±0.04±0.11	1779	ABLIKIM	06	BES2 $J/\psi \rightarrow \Sigma^0\bar{\Sigma}^0$
1.06±0.04±0.23	884 ± 30	PALLIN	87	DM2 $e^+e^- \rightarrow \Sigma^0\bar{\Sigma}^0$
1.58±0.16±0.25	90	EATON	84	MRK2 $e^+e^- \rightarrow \Sigma^0\bar{\Sigma}^0$
1.3 ± 0.4	52	PERUZZI	78	MRK1 $e^+e^- \rightarrow \Sigma^0\bar{\Sigma}^0$

• • • We do not use the following data for averages, fits, limits, etc. • • •

2.4 ± 2.6

3

BESCH 81 BONA $e^+e^- \rightarrow \Sigma^+\bar{\Sigma}^-$

¹⁰¹ AUBERT 07BD reports $[B(J/\psi(1S) \rightarrow \Sigma^0 \Sigma^0)] \times [\Gamma(J/\psi(1S) \rightarrow e^+ e^-)] = (6.4 \pm 1.2 \pm 0.6) \times 10^{-3}$ keV. We divide by our best value $\Gamma(J/\psi(1S) \rightarrow e^+ e^-) = 5.55 \pm 0.14 \pm 0.02$ keV. Our first error is their experiment's error and our second error is the systematic error from using our best value.

$\Gamma(2(\pi^+ \pi^-) K^+ K^-) / \Gamma_{total}$ Γ_{102} / Γ

VALUE (units 10^{-3})	EVTS	DOCUMENT ID	TECN	COMMENT
47 ± 7 OUR AVERAGE				Error includes scale factor of 1.3.
49.8 ± 4.2 ± 3.4	205	¹⁰² AUBERT	06D BABR	10.6 $e^+ e^- \rightarrow \omega K^+ K^- 2(\pi^+ \pi^-) \gamma$
31 ± 13	30	VANNUCCI	77 MRK1	$e^+ e^-$

¹⁰² Using $\Gamma(J/\psi \rightarrow e^+ e^-) = 5.52 \pm 0.14 \pm 0.04$ keV.

$\Gamma(\rho \bar{\rho} \pi^+ \pi^- \pi^0) / \Gamma_{total}$ Γ_{93} / Γ

Including $\rho \bar{\rho} \pi^+ \pi^- \gamma$ and excluding ω, η, η'

VALUE (units 10^{-3})	EVTS	DOCUMENT ID	TECN	COMMENT
2.3 ± 0.9 OUR AVERAGE				Error includes scale factor of 1.9.
3.36 ± 0.65 ± 0.28	364	EATON	84 MRK2	$e^+ e^-$
1.6 ± 0.6	39	PERUZZI	78 MRK1	$e^+ e^-$

$\Gamma(\rho \bar{\rho}) / \Gamma_{total}$ Γ_{90} / Γ

VALUE (units 10^{-3})	EVTS	DOCUMENT ID	TECN	COMMENT
2.17 ± 0.07 OUR AVERAGE				
2.19 ± 0.16 ± 0.08	317	¹⁰³ WU	06 BELL	$B^+ \rightarrow \rho \bar{\rho} K^+$
2.26 ± 0.01 ± 0.14	63316	BAI	04E BES2	$e^+ e^- \rightarrow J/\psi$
1.97 ± 0.22	99	BALDINI	98 FENI	$e^+ e^-$
1.91 ± 0.04 ± 0.30		PALLIN	87 DM2	$e^+ e^-$
2.16 ± 0.07 ± 0.15	1420	EATON	84 MRK2	$e^+ e^-$
2.5 ± 0.4	133	BRANDELIK	79C DASP	$e^+ e^-$
2.0 ± 0.5		BESCH	78 BONA	$e^+ e^-$
2.2 ± 0.2	331	¹⁰⁴ PERUZZI	78 MRK1	$e^+ e^-$
• • • We do not use the following data for averages, fits, limits, etc. • • •				
2.0 ± 0.3	48	ANTONELLI	93 SPEC	$e^+ e^-$

¹⁰³ WU 06 reports $[B(J/\psi(1S) \rightarrow \rho \bar{\rho})] \times [B(B^+ \rightarrow J/\psi(1S) K^+)] = (2.21 \pm 0.13 \pm 0.10) \times 10^{-6}$. We divide by our best value $B(B^+ \rightarrow J/\psi(1S) K^+) = (1.007 \pm 0.035) \times 10^{-3}$. Our first error is their experiment's error and our second error is the systematic error from using our best value.

¹⁰⁴ Assuming angular distribution $(1 + \cos^2 \theta)$.

$\Gamma(\rho \bar{\rho} \eta) / \Gamma_{total}$ Γ_{94} / Γ

VALUE (units 10^{-3})	EVTS	DOCUMENT ID	TECN	COMMENT
2.09 ± 0.18 OUR AVERAGE				
2.03 ± 0.13 ± 0.15	826	EATON	84 MRK2	$e^+ e^-$
2.5 ± 1.2		BRANDELIK	79C DASP	$e^+ e^-$
2.3 ± 0.4	197	PERUZZI	78 MRK1	$e^+ e^-$

$\Gamma(\rho \bar{\rho} \pi^-) / \Gamma_{total}$ Γ_{103} / Γ

VALUE (units 10^{-3})	EVTS	DOCUMENT ID	TECN	COMMENT
2.12 ± 0.09 OUR AVERAGE				
2.36 ± 0.02 ± 0.21	59k	ABLIKIM	06K BES2	$J/\psi \rightarrow \rho \pi^- \bar{\pi}$
2.47 ± 0.02 ± 0.24	55k	ABLIKIM	06K BES2	$J/\psi \rightarrow \bar{\rho} \pi^+ n$
2.02 ± 0.07 ± 0.16	1288	EATON	84 MRK2	$e^+ e^- \rightarrow \rho \pi^-$
1.93 ± 0.07 ± 0.16	1191	EATON	84 MRK2	$e^+ e^- \rightarrow \bar{\rho} \pi^+$
1.7 ± 0.7	32	BESCH	81 BONA	$e^+ e^- \rightarrow \rho \pi^-$
1.6 ± 1.2	5	BESCH	81 BONA	$e^+ e^- \rightarrow \bar{\rho} \pi^+$
2.16 ± 0.29	194	PERUZZI	78 MRK1	$e^+ e^- \rightarrow \rho \pi^-$
2.04 ± 0.27	204	PERUZZI	78 MRK1	$e^+ e^- \rightarrow \bar{\rho} \pi^+$

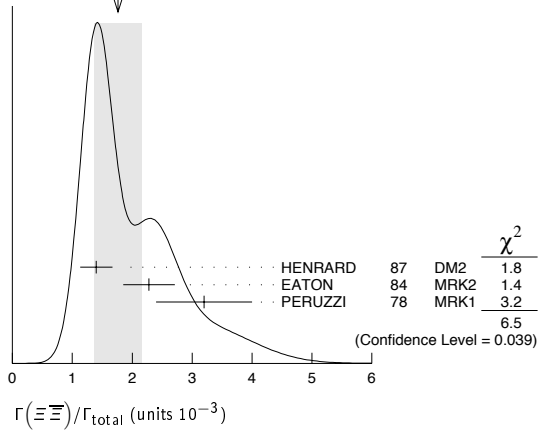
$\Gamma(n \bar{n}) / \Gamma_{total}$ Γ_{99} / Γ

VALUE (units 10^{-2})	EVTS	DOCUMENT ID	TECN	COMMENT
0.22 ± 0.04 OUR AVERAGE				
0.231 ± 0.049	79	BALDINI	98 FENI	$e^+ e^-$
0.18 ± 0.09		BESCH	78 BONA	$e^+ e^-$
• • • We do not use the following data for averages, fits, limits, etc. • • •				
0.190 ± 0.055	40	ANTONELLI	93 SPEC	$e^+ e^-$

$\Gamma(\Xi \Xi) / \Gamma_{total}$ Γ_{107} / Γ

VALUE (units 10^{-3})	EVTS	DOCUMENT ID	TECN	COMMENT
1.8 ± 0.4 OUR AVERAGE				Error includes scale factor of 1.8. See the ideogram below.
1.40 ± 0.12 ± 0.24	132 ± 11	HENRARD	87 DM2	$e^+ e^- \rightarrow \Xi^- \Xi^+$
2.28 ± 0.16 ± 0.40	194	EATON	84 MRK2	$e^+ e^- \rightarrow \Xi^- \Xi^+$
3.2 ± 0.8	71	PERUZZI	78 MRK1	$e^+ e^-$

WEIGHTED AVERAGE
1.8 ± 0.4 (Error scaled by 1.8)



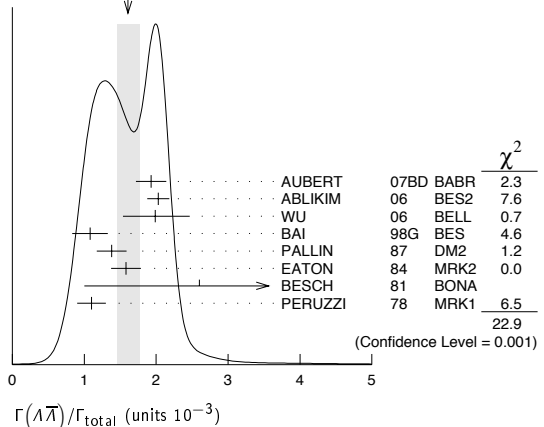
$\Gamma(\Lambda \bar{\Lambda}) / \Gamma_{total}$ Γ_{108} / Γ

VALUE (units 10^{-3})	EVTS	DOCUMENT ID	TECN	COMMENT
1.61 ± 0.15 OUR AVERAGE				Error includes scale factor of 2.0. See the ideogram below.
1.93 ± 0.21 ± 0.05		¹⁰⁵ AUBERT	07BD BABR	10.6 $e^+ e^- \rightarrow \Lambda \bar{\Lambda} \gamma$
2.03 ± 0.03 ± 0.15	8887	ABLIKIM	06 BES2	$J/\psi \rightarrow \Lambda \bar{\Lambda}$
2.0 ± 0.5 ± 0.1	46	¹⁰⁶ WU	06 BELL	$B^+ \rightarrow \Lambda \bar{\Lambda} K^+$
1.08 ± 0.06 ± 0.24	631	BAI	98G BES	$e^+ e^-$
1.38 ± 0.05 ± 0.20	1847	PALLIN	87 DM2	$e^+ e^-$
1.58 ± 0.08 ± 0.19	365	EATON	84 MRK2	$e^+ e^-$
2.6 ± 1.6	5	BESCH	81 BONA	$e^+ e^-$
1.1 ± 0.2	196	PERUZZI	78 MRK1	$e^+ e^-$

¹⁰⁵ AUBERT 07BD reports $[B(J/\psi(1S) \rightarrow \Lambda \bar{\Lambda})] \times [\Gamma(J/\psi(1S) \rightarrow e^+ e^-)] = (10.7 \pm 0.9 \pm 0.7) \times 10^{-3}$ keV. We divide by our best value $\Gamma(J/\psi(1S) \rightarrow e^+ e^-) = 5.55 \pm 0.14 \pm 0.02$ keV. Our first error is their experiment's error and our second error is the systematic error from using our best value.

¹⁰⁶ WU 06 reports $[B(J/\psi(1S) \rightarrow \Lambda \bar{\Lambda})] \times [B(B^+ \rightarrow J/\psi(1S) K^+)] = (2.00^{+0.34} \pm 0.34) \times 10^{-6}$. We divide by our best value $B(B^+ \rightarrow J/\psi(1S) K^+) = (1.007 \pm 0.035) \times 10^{-3}$. Our first error is their experiment's error and our second error is the systematic error from using our best value.

WEIGHTED AVERAGE
1.61 ± 0.15 (Error scaled by 2.0)



$\Gamma(\Lambda \bar{\Lambda}) / \Gamma(\rho \bar{\rho})$ $\Gamma_{108} / \Gamma_{90}$

VALUE	DOCUMENT ID	TECN	COMMENT
0.90^{+0.15} ± 0.10	¹⁰⁷ WU	06 BELL	$B^+ \rightarrow \rho \bar{\rho} K^+, \Lambda \bar{\Lambda} K^+$

¹⁰⁷ Not independent of other $J/\psi \rightarrow \Lambda \bar{\Lambda}, \rho \bar{\rho}$ branching ratios reported by WU 06.

$\Gamma(\rho \bar{\rho} \pi^0) / \Gamma_{total}$ Γ_{91} / Γ

VALUE (units 10^{-3})	EVTS	DOCUMENT ID	TECN	COMMENT
1.09 ± 0.09 OUR AVERAGE				
1.13 ± 0.09 ± 0.09	685	EATON	84 MRK2	$e^+ e^-$
1.4 ± 0.4		BRANDELIK	79C DASP	$e^+ e^-$
1.00 ± 0.15	109	PERUZZI	78 MRK1	$e^+ e^-$

Meson Particle Listings

$J/\psi(1S)$

$\Gamma(\Lambda\bar{\Sigma}^- \pi^+ \text{ (or c.c.)})/\Gamma_{\text{total}}$					Γ_{109}/Γ
VALUE (units 10^{-3})	EVTS	DOCUMENT ID	TECN	COMMENT	
0.83 ± 0.07 OUR AVERAGE	Error	includes scale factor of 1.2.			
0.770 ± 0.051 ± 0.083	335	108 ABLIKIM	07H BES2	$e^+e^- \rightarrow \Lambda\bar{\Sigma}^+\pi^-$	
0.747 ± 0.056 ± 0.076	254	108 ABLIKIM	07H BES2	$e^+e^- \rightarrow \Lambda\bar{\Sigma}^-\pi^+$	
0.90 ± 0.06 ± 0.16	225 ± 15	HENRRARD	87 DM2	$e^+e^- \rightarrow \Lambda\bar{\Sigma}^+\pi^-$	
1.11 ± 0.06 ± 0.20	342 ± 18	HENRRARD	87 DM2	$e^+e^- \rightarrow \Lambda\bar{\Sigma}^-\pi^+$	
1.53 ± 0.17 ± 0.38	135	EATON	84 MRK2	$e^+e^- \rightarrow \Lambda\bar{\Sigma}^+\pi^-$	
1.38 ± 0.21 ± 0.35	118	EATON	84 MRK2	$e^+e^- \rightarrow \Lambda\bar{\Sigma}^-\pi^+$	
108 Using $B(\Lambda \rightarrow \pi^- p) = 63.9\%$ and $B(\Sigma^+ \rightarrow \pi^0 p) = 51.6\%$.					

$\Gamma(\rho K^- \bar{\Lambda})/\Gamma_{\text{total}}$					Γ_{110}/Γ
VALUE (units 10^{-3})	EVTS	DOCUMENT ID	TECN	COMMENT	
0.89 ± 0.07 ± 0.14	307	EATON	84 MRK2	e^+e^-	

$\Gamma(2(K^+ K^-))/\Gamma_{\text{total}}$					Γ_{111}/Γ
VALUE (units 10^{-3})	EVTS	DOCUMENT ID	TECN	COMMENT	
0.76 ± 0.09 OUR AVERAGE					
0.74 ± 0.09 ± 0.02	156 ± 15	109 AUBERT	07AK BABR	$10.6 e^+e^- \rightarrow 2(K^+ K^-)\gamma$	
1.4 $^{+0.5}_{-0.4}$ ± 0.2	11.0 $^{+4.3}_{-3.5}$	110 HUANG	03 BELL	$B^+ \rightarrow 2(K^+ K^-) K^+$	
0.7 ± 0.3		VANNUCCI	77 MRK1	e^+e^-	

• • • We do not use the following data for averages, fits, limits, etc. • • •

0.72 ± 0.17 ± 0.02 38 111 AUBERT 05D BABR 10.6 $e^+e^- \rightarrow 2(K^+ K^-)\gamma$

109 AUBERT 07AK reports $[B(J/\psi(1S) \rightarrow 2(K^+ K^-))] \times [\Gamma(J/\psi(1S) \rightarrow e^+e^-)] = (4.11 \pm 0.39 \pm 0.30) \times 10^{-3}$ keV. We divide by our best value $\Gamma(J/\psi(1S) \rightarrow e^+e^-) = 5.55 \pm 0.14 \pm 0.02$ keV. Our first error is their experiment's error and our second error is the systematic error from using our best value.

110 Using $B(B^+ \rightarrow J/\psi K^+) = (1.01 \pm 0.05) \times 10^{-3}$.

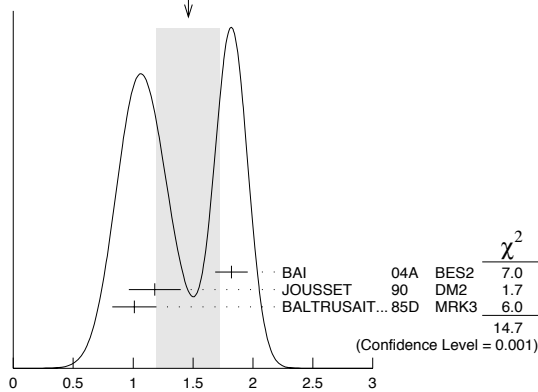
111 Superseded by AUBERT 07AK. AUBERT 05D reports $[B(J/\psi(1S) \rightarrow 2(K^+ K^-))] \times [\Gamma(J/\psi(1S) \rightarrow e^+e^-)] = (4.0 \pm 0.7 \pm 0.6) \times 10^{-3}$ keV. We divide by our best value $\Gamma(J/\psi(1S) \rightarrow e^+e^-) = 5.55 \pm 0.14 \pm 0.02$ keV. Our first error is their experiment's error and our second error is the systematic error from using our best value.

$\Gamma(\rho K^- \bar{\Sigma}^0)/\Gamma_{\text{total}}$					Γ_{112}/Γ
VALUE (units 10^{-3})	EVTS	DOCUMENT ID	TECN	COMMENT	
0.29 ± 0.06 ± 0.05	90	EATON	84 MRK2	e^+e^-	

$\Gamma(K^+ K^-)/\Gamma_{\text{total}}$					Γ_{113}/Γ
VALUE (units 10^{-4})	EVTS	DOCUMENT ID	TECN	COMMENT	
2.37 ± 0.31 OUR AVERAGE					
2.39 ± 0.24 ± 0.22	107	BALTRUSAIT...85D	MRK3	e^+e^-	
2.2 ± 0.9	6	BRANDELIK	79C DASP	e^+e^-	

$\Gamma(K_S^0 K_L^0)/\Gamma_{\text{total}}$					Γ_{114}/Γ
VALUE (units 10^{-4})	EVTS	DOCUMENT ID	TECN	COMMENT	
1.46 ± 0.26 OUR AVERAGE	Error	includes scale factor of 2.7. See the ideogram below.			
1.82 ± 0.04 ± 0.13	2155 ± 45	112 BAI	04A BES2	$J/\psi \rightarrow K_S^0 K_L^0 \rightarrow \pi^+\pi^- X$	
1.18 ± 0.12 ± 0.18		JOUSSET	90 DM2	$J/\psi \rightarrow \text{hadrons}$	
1.01 ± 0.16 ± 0.09	74	BALTRUSAIT...85D	MRK3	e^+e^-	
112 Using $B(K_S^0 \rightarrow \pi^+\pi^-) = 0.6868 \pm 0.0027$.					

WEIGHTED AVERAGE
1.46 ± 0.26 (Error scaled by 2.7)



$\Gamma(\Lambda\bar{\Lambda})/\Gamma_{\text{total}}$					Γ_{114}/Γ
VALUE (units 10^{-4})	EVTS	DOCUMENT ID	TECN	COMMENT	
2.62 ± 0.60 ± 0.44	44	113 ABLIKIM	07H BES2	$e^+e^- \rightarrow \psi(2S)$	

$\Gamma(\Lambda\bar{\Lambda}\eta)/\Gamma_{\text{total}}$					Γ_{115}/Γ
VALUE (units 10^{-4})	EVTS	DOCUMENT ID	TECN	COMMENT	
2.62 ± 0.60 ± 0.44	44	113 ABLIKIM	07H BES2	$e^+e^- \rightarrow \psi(2S)$	
113 Using $B(\Lambda \rightarrow \pi^- p) = 63.9\%$ and $B(\eta \rightarrow \gamma\gamma) = 39.4\%$.					

$\Gamma(\Lambda\bar{\Lambda}\pi^0)/\Gamma_{\text{total}}$					Γ_{116}/Γ
VALUE (units 10^{-4})	CL%	EVTS	DOCUMENT ID	TECN	COMMENT
<0.64	90		114 ABLIKIM	07H BES2	$e^+e^- \rightarrow \psi(2S)$
• • • We do not use the following data for averages, fits, limits, etc. • • •					
2.3 ± 0.7 ± 0.8		11	BAI	98G BES	e^+e^-
2.2 ± 0.5 ± 0.5		19 ± 4	HENRRARD	87 DM2	e^+e^-
114 Using $B(\Lambda \rightarrow \pi^- p) = 63.9\%$.					

$\Gamma(\Lambda\bar{\Lambda}K_S^0 + \text{c.c.})/\Gamma_{\text{total}}$					Γ_{117}/Γ
VALUE (units 10^{-4})	EVTS	DOCUMENT ID	TECN	COMMENT	
6.46 ± 0.20 ± 1.07	1058	115 ABLIKIM	08C BES2	$e^+e^- \rightarrow J/\psi$	
115 Using $B(\bar{\Lambda} \rightarrow \bar{p}\pi^+) = 63.9\%$ and $B(K_S^0 \rightarrow \pi^+\pi^-) = 69.2\%$.					

$\Gamma(\pi^+\pi^-)/\Gamma_{\text{total}}$					Γ_{118}/Γ
VALUE (units 10^{-4})	EVTS	DOCUMENT ID	TECN	COMMENT	
1.47 ± 0.23 OUR AVERAGE					
1.58 ± 0.20 ± 0.15	84	BALTRUSAIT...85D	MRK3	e^+e^-	
1.0 ± 0.5	5	BRANDELIK	78B DASP	e^+e^-	
1.6 ± 1.6	1	VANNUCCI	77 MRK1	e^+e^-	

$\Gamma(\Lambda\bar{\Sigma}^+ + \text{c.c.})/\Gamma_{\text{total}}$					Γ_{119}/Γ
VALUE (units 10^{-3})	CL%	DOCUMENT ID	TECN	COMMENT	
<0.15	90	PERUZZI	78 MRK1	$e^+e^- \rightarrow \Lambda X$	

$\Gamma(K_S^0 K_L^0)/\Gamma_{\text{total}}$					Γ_{120}/Γ
VALUE (units 10^{-4})	CL%	DOCUMENT ID	TECN	COMMENT	
<0.01	95	116 BAI	04D BES	e^+e^-	
• • • We do not use the following data for averages, fits, limits, etc. • • •					
<0.052	90	116 BALTRUSAIT...85C	MRK3	e^+e^-	
116 Forbidden by CP.					

RADIATIVE DECAYS

$\Gamma(\gamma\eta_c(1S))/\Gamma_{\text{total}}$					Γ_{121}/Γ
VALUE	EVTS	DOCUMENT ID	TECN	COMMENT	
0.0127 ± 0.0036					
• • • We do not use the following data for averages, fits, limits, etc. • • •					
0.0079 ± 0.0020	273 ± 43	117 AUBERT	06E BABR	$B^{\pm} \rightarrow K^{\pm} X_c \bar{c}$	
seen	16	BALTRUSAIT...84	MRK3	$J/\psi \rightarrow 2\phi\gamma$	
117 Calculated by the authors using an average of $B(J/\psi \rightarrow \gamma\eta_c) \times B(\eta_c \rightarrow K\bar{K}\pi)$ from BALTRUSAITIS 86, BISELLO 91, BAI 04 and $B(\eta_c \rightarrow K\bar{K}\pi) = (8.5 \pm 1.8)\%$ from AUBERT 06E.					

$\Gamma(\gamma\pi^+\pi^-2\pi^0)/\Gamma_{\text{total}}$					Γ_{122}/Γ
VALUE (units 10^{-3})	EVTS	DOCUMENT ID	TECN	COMMENT	
8.3 ± 0.2 ± 3.1					
8.3 ± 0.2 ± 3.1		118 BALTRUSAIT...86B	MRK3	$J/\psi \rightarrow 4\pi\gamma$	
118 4π mass less than 2.0 GeV.					

$\Gamma(\gamma\eta\pi\pi)/\Gamma_{\text{total}}$					Γ_{123}/Γ
VALUE (units 10^{-3})	EVTS	DOCUMENT ID	TECN	COMMENT	
6.1 ± 1.0 OUR AVERAGE					
5.85 ± 0.3 ± 1.05		119 EDWARDS	83B CBAL	$J/\psi \rightarrow \eta\pi^+\pi^-$	
7.8 ± 1.2 ± 2.4		119 EDWARDS	83B CBAL	$J/\psi \rightarrow \eta 2\pi^0$	
119 Broad enhancement at 1700 MeV.					

$\Gamma(\gamma\eta(1405/1475) \rightarrow \gamma K\bar{K}\pi)/\Gamma_{\text{total}}$					Γ_{125}/Γ
VALUE (units 10^{-3})	EVTS	DOCUMENT ID	TECN	COMMENT	
2.8 ± 0.6 OUR AVERAGE	Error	includes scale factor of 1.6. See the ideogram below.			
1.66 ± 0.1 ± 0.58		120,121 BAI	00D BES	$J/\psi \rightarrow \gamma K^{\pm} K_S^0 \pi^{\mp}$	
3.8 ± 0.3 ± 0.6		122 AUGUSTIN	90 DM2	$J/\psi \rightarrow \gamma K\bar{K}\pi$	
4.0 ± 0.7 ± 1.0		122 EDWARDS	82E CBAL	$J/\psi \rightarrow K^+ K^- \pi^0 \gamma$	
4.3 ± 1.7		122,123 SCHARRE	80 MRK2	e^+e^-	
• • • We do not use the following data for averages, fits, limits, etc. • • •					
1.78 ± 0.21 ± 0.33		122,124,125 AUGUSTIN	92 DM2	$J/\psi \rightarrow \gamma K\bar{K}\pi$	
0.83 ± 0.13 ± 0.18		122,126,127 AUGUSTIN	92 DM2	$J/\psi \rightarrow \gamma K\bar{K}\pi$	
0.66 $^{+0.17}_{-0.16}$ ± 0.24		122,125,128 BAI	90C MRK3	$J/\psi \rightarrow \gamma K_S^0 K^{\pm} \pi^{\mp}$	
1.03 $^{+0.21}_{-0.18}$ ± 0.26		122,127,129 BAI	90C MRK3	$J/\psi \rightarrow \gamma K_S^0 K^{\pm} \pi^{\mp}$	

120 Interference with the $J/\psi(1S)$ radiative transition to the broad $K\bar{K}\pi$ pseudoscalar state around 1800 is $(0.15 \pm 0.01 \pm 0.05) \times 10^{-3}$.

121 Interference with $J/\psi \rightarrow \gamma f_1(1420)$ is $(-0.03 \pm 0.01 \pm 0.01) \times 10^{-3}$.

122 Includes unknown branching fraction $\eta(1405) \rightarrow K\bar{K}\pi$.

123 Corrected for spin-zero hypothesis for $\eta(1405)$.

124 From fit to the $a_0(980)\pi 0^-$ partial wave.

125 $a_0(980)\pi$ mode.

126 From fit to the $K^*(892)K 0^-$ partial wave.

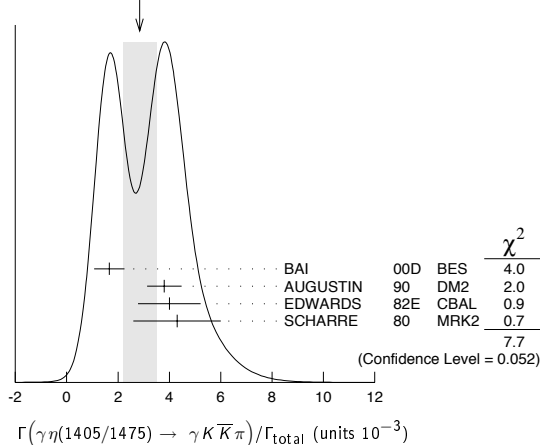
127 K^*K mode.

128 From $a_0(980)\pi$ final state.

129 From $K^*(890)K$ final state.

See key on page 373

Meson Particle Listings

 $J/\psi(1S)$ WEIGHTED AVERAGE
2.8±0.6 (Error scaled by 1.6) $\Gamma(\gamma\eta(1405/1475) \rightarrow \gamma\gamma\rho^0)/\Gamma_{\text{total}}$ Γ_{126}/Γ

VALUE (units 10^{-4})	DOCUMENT ID	TECN	COMMENT
0.78 ± 0.20 OUR AVERAGE	Error includes scale factor of 1.8.		
1.07 ± 0.17 ± 0.11	130 BAI	04J	BES2 $J/\psi \rightarrow \gamma\gamma\pi^+\pi^-$
0.64 ± 0.12 ± 0.07	130 COFFMAN	90	MRK3 $J/\psi \rightarrow \gamma\gamma\pi^+\pi^-$

130 Includes unknown branching fraction $\eta(1405) \rightarrow \gamma\rho^0$.

 $\Gamma(\gamma\eta(1405/1475) \rightarrow \gamma\eta\pi^+\pi^-)/\Gamma_{\text{total}}$ Γ_{127}/Γ

VALUE (units 10^{-4})	EVTS	DOCUMENT ID	TECN	COMMENT
3.0 ± 0.5 OUR AVERAGE				
2.6 ± 0.7 ± 0.4		BAI	99	BES $J/\psi \rightarrow \gamma\eta\pi^+\pi^-$
3.38 ± 0.33 ± 0.64		131 BOLTON	92B	MRK3 $J/\psi \rightarrow \gamma\eta\pi^+\pi^-$
••• We do not use the following data for averages, fits, limits, etc. •••				
7.0 ± 0.6 ± 1.1	261	132 AUGUSTIN	90	DM2 $J/\psi \rightarrow \gamma\eta\pi^+\pi^-$

131 Via $a_0(980)\pi$.
132 Includes unknown branching fraction to $\eta\pi^+\pi^-$.

 $\Gamma(\gamma\eta(1405/1475) \rightarrow \gamma\gamma\phi)/\Gamma_{\text{total}}$ Γ_{128}/Γ

VALUE (units 10^{-4})	CL%	DOCUMENT ID	TECN	COMMENT
<0.82	95	BAI	04J	BES2 $J/\psi \rightarrow \gamma\gamma K^+K^-$

 $\Gamma(\gamma\rho\rho)/\Gamma_{\text{total}}$ Γ_{129}/Γ

VALUE (units 10^{-3})	CL%	DOCUMENT ID	TECN	COMMENT
4.5 ± 0.8 OUR AVERAGE				
4.7 ± 0.3 ± 0.9		133 BALTRUSAIT..86B	MRK3	$J/\psi \rightarrow 4\pi\gamma$
3.75 ± 1.05 ± 1.20		134 BURKE	82	MRK2 $J/\psi \rightarrow 4\pi\gamma$
••• We do not use the following data for averages, fits, limits, etc. •••				
<0.09	90	135 BISELLO	89B	$J/\psi \rightarrow 4\pi\gamma$

133 4π mass less than 2.0 GeV.
134 4π mass less than 2.0 GeV. We have multiplied $2\rho^0$ measurement by 3 to obtain 2ρ .
135 4π mass in the range 2.0–25 GeV.

 $\Gamma(\gamma\rho\omega)/\Gamma_{\text{total}}$ Γ_{130}/Γ

VALUE (units 10^{-4})	CL%	DOCUMENT ID	TECN	COMMENT
<5.4	90	ABLIKIM	08A	BES2 $e^+e^- \rightarrow J/\psi$

 $\Gamma(\gamma\rho\phi)/\Gamma_{\text{total}}$ Γ_{131}/Γ

VALUE (units 10^{-5})	CL%	DOCUMENT ID	TECN	COMMENT
<8.8	90	ABLIKIM	08A	BES2 $e^+e^- \rightarrow J/\psi$

 $\Gamma(\gamma\eta_2(1870) \rightarrow \gamma\eta\pi^+\pi^-)/\Gamma_{\text{total}}$ Γ_{124}/Γ

VALUE (units 10^{-4})	DOCUMENT ID	TECN	COMMENT
6.2 ± 2.2 ± 0.9	BAI	99	BES $J/\psi \rightarrow \gamma\eta\pi^+\pi^-$

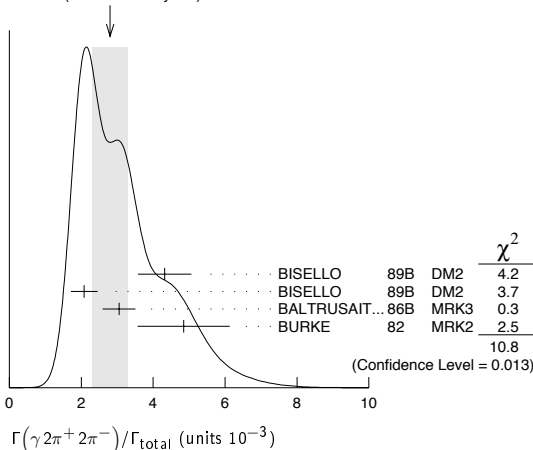
 $\Gamma(\gamma\eta'(958))/\Gamma_{\text{total}}$ Γ_{132}/Γ

VALUE (units 10^{-3})	EVTS	DOCUMENT ID	TECN	COMMENT
4.71 ± 0.27 OUR AVERAGE		Error includes scale factor of 1.1.		
5.55 ± 0.44	35k	ABLIKIM	06E	BES2 $J/\psi \rightarrow \eta'\gamma$
4.50 ± 0.14 ± 0.53		BOLTON	92B	MRK3 $J/\psi \rightarrow \gamma\pi^+\pi^-\eta$, $\eta \rightarrow \gamma\gamma$
4.30 ± 0.31 ± 0.71		BOLTON	92B	MRK3 $J/\psi \rightarrow \gamma\pi^+\pi^-\eta$, $\eta \rightarrow \pi^+\pi^-\pi^0$
4.04 ± 0.16 ± 0.85	622	AUGUSTIN	90	DM2 $J/\psi \rightarrow \gamma\eta\pi^+\pi^-$
4.39 ± 0.09 ± 0.66	2420	AUGUSTIN	90	DM2 $J/\psi \rightarrow \gamma\gamma\pi^+\pi^-$
4.1 ± 0.3 ± 0.6		BLOOM	83	CBAL $e^+e^- \rightarrow 3\gamma +$ hadrons
••• We do not use the following data for averages, fits, limits, etc. •••				
2.9 ± 1.1	6	BRANDELIK	79C	DASP $e^+e^- \rightarrow 3\gamma$
2.4 ± 0.7	57	BARTEL	76	CNTR $e^+e^- \rightarrow 2\gamma\rho$

 $\Gamma(\gamma 2\pi^+ 2\pi^-)/\Gamma_{\text{total}}$ Γ_{133}/Γ

VALUE (units 10^{-3})	DOCUMENT ID	TECN	COMMENT
2.8 ± 0.5 OUR AVERAGE	Error includes scale factor of 1.9. See the ideogram below.		
4.32 ± 0.14 ± 0.73	136 BISELLO	89B	DM2 $J/\psi \rightarrow 4\pi\gamma$
2.08 ± 0.13 ± 0.35	137 BISELLO	89B	DM2 $J/\psi \rightarrow 4\pi\gamma$
3.05 ± 0.08 ± 0.45	137 BALTRUSAIT..86B	MRK3	$J/\psi \rightarrow 4\pi\gamma$
4.85 ± 0.45 ± 1.20	138 BURKE	82	MRK2 e^+e^-

136 4π mass less than 3.0 GeV.
137 4π mass less than 2.0 GeV.
138 4π mass less than 2.5 GeV.

WEIGHTED AVERAGE
2.8±0.5 (Error scaled by 1.9) $\Gamma(\gamma f_2(1270) f_2(1270))/\Gamma_{\text{total}}$ Γ_{134}/Γ

VALUE (units 10^{-4})	EVTS	DOCUMENT ID	TECN	COMMENT
9.5 ± 0.7 ± 1.6	646 ± 45	ABLIKIM	04M	BES $J/\psi \rightarrow \gamma 2\pi^+ 2\pi^-$

 $\Gamma(\gamma f_2(1270) f_2(1270) (\text{non resonant}))/\Gamma_{\text{total}}$ Γ_{135}/Γ

VALUE (units 10^{-4})	DOCUMENT ID	TECN	COMMENT	
8.2 ± 0.8 ± 1.7	139	ABLIKIM	04M	BES $J/\psi \rightarrow \gamma 2\pi^+ 2\pi^-$

139 Subtracting contribution from intermediate $\eta_c(1S)$ decays.

 $\Gamma(\gamma K^+ K^- \pi^+ \pi^-)/\Gamma_{\text{total}}$ Γ_{136}/Γ

VALUE (units 10^{-3})	EVTS	DOCUMENT ID	TECN	COMMENT
2.1 ± 0.1 ± 0.6	1516	BAI	00B	BES $J/\psi \rightarrow \gamma K^+ K^0 \pi^+ \pi^-$

 $\Gamma(\gamma f_4(2050))/\Gamma_{\text{total}}$ Γ_{137}/Γ

VALUE (units 10^{-3})	DOCUMENT ID	TECN	COMMENT	
2.7 ± 0.5 ± 0.5	140	BALTRUSAIT..87	MRK3	$J/\psi \rightarrow \gamma\pi^+\pi^-$

140 Assuming branching fraction $f_4(2050) \rightarrow \pi\pi/\text{total} = 0.167$.

 $\Gamma(\gamma\omega\omega)/\Gamma_{\text{total}}$ Γ_{138}/Γ

VALUE (units 10^{-3})	EVTS	DOCUMENT ID	TECN	COMMENT
1.61 ± 0.33 OUR AVERAGE				
6.0 ± 4.8 ± 1.8		ABLIKIM	08A	BES2 $J/\psi \rightarrow \gamma\omega\pi^+\pi^-$
1.41 ± 0.2 ± 0.42	120 ± 17	BISELLO	87	SPEC e^+e^- , hadrons γ
1.76 ± 0.09 ± 0.45		BALTRUSAIT..85C	MRK3	$e^+e^- \rightarrow$ hadrons γ

 $\Gamma(\gamma\eta(1405/1475) \rightarrow \gamma\rho^0\rho^0)/\Gamma_{\text{total}}$ Γ_{139}/Γ

VALUE (units 10^{-3})	DOCUMENT ID	TECN	COMMENT	
1.7 ± 0.4 OUR AVERAGE	Error includes scale factor of 1.3.			
2.1 ± 0.4	BUGG	95	MRK3 $J/\psi \rightarrow \gamma\pi^+\pi^-\pi^+\pi^-$	
1.36 ± 0.38	141,142	BISELLO	89B	DM2 $J/\psi \rightarrow 4\pi\gamma$

141 Estimated by us from various fits.
142 Includes unknown branching fraction to $\rho^0\rho^0$.

 $\Gamma(\gamma f_2(1270))/\Gamma_{\text{total}}$ Γ_{140}/Γ

VALUE (units 10^{-3})	EVTS	DOCUMENT ID	TECN	COMMENT	
1.43 ± 0.11 OUR AVERAGE					
1.62 ± 0.26 ± 0.02 -0.05		143	ABLIKIM	06V	BES2 $e^+e^- \rightarrow J/\psi \rightarrow \gamma\pi^+\pi^-$
1.42 ± 0.21 ± 0.02 -0.04		144	ABLIKIM	06V	BES2 $e^+e^- \rightarrow J/\psi \rightarrow \gamma\pi^0\pi^0$
1.33 ± 0.05 ± 0.20		145	AUGUSTIN	87	DM2 $J/\psi \rightarrow \gamma\pi^+\pi^-$
1.36 ± 0.09 ± 0.23		145	BALTRUSAIT..87	MRK3	$J/\psi \rightarrow \gamma\pi^+\pi^-$
1.48 ± 0.25 ± 0.30	178	EDWARDS	82B	CBAL $e^+e^- \rightarrow 2\pi^0\gamma$	
2.0 ± 0.7	35	ALEXANDER	78	PLUT e^+e^-	
1.2 ± 0.6	30	146	BRA NDELIK	78B	DASP $e^+e^- \rightarrow \pi^+\pi^-\gamma$

Meson Particle Listings

 $J/\psi(1S)$

¹⁴³ ABLIKIM 06v reports $[B(J/\psi(1S) \rightarrow \gamma f_2(1270))] \times [B(f_2(1270) \rightarrow \pi\pi)] = (1.371 \pm 0.010 \pm 0.222) \times 10^{-3}$. We divide by our best value $B(f_2(1270) \rightarrow \pi\pi) = (84.8^{+2.4}_{-1.2}) \times 10^{-2}$. Our first error is their experiment's error and our second error is the systematic error from using our best value.

¹⁴⁴ ABLIKIM 06v reports $[B(J/\psi(1S) \rightarrow \gamma f_2(1270))] \times [B(f_2(1270) \rightarrow \pi\pi)] = (1.200 \pm 0.027 \pm 0.174) \times 10^{-3}$. We divide by our best value $B(f_2(1270) \rightarrow \pi\pi) = (84.8^{+2.4}_{-1.2}) \times 10^{-2}$. Our first error is their experiment's error and our second error is the systematic error from using our best value.

¹⁴⁵ Estimated using $B(f_2(1270) \rightarrow \pi\pi) = 0.843 \pm 0.012$. The errors do not contain the uncertainty in the $f_2(1270)$ decay.

¹⁴⁶ Restated by us to take account of spread of E1, M2, E3 transitions.

$\Gamma(\gamma f_0(1710) \rightarrow \gamma K\bar{K})/\Gamma_{\text{total}}$ Γ_{141}/Γ

VALUE (units 10^{-4})	CL%	DOCUMENT ID	TECN	COMMENT
0.9 ± 1.2 OUR AVERAGE		Error includes scale factor of 1.2.		
9.62 ± 0.29	$+3.51$ -1.86	147 BAI	03G BES	$J/\psi \rightarrow \gamma K\bar{K}$
5.0 ± 0.8	$+1.8$ -0.4	148,149 BAI	96C BES	$J/\psi \rightarrow \gamma K^+ K^-$
9.2 ± 1.4	± 1.4	149 AUGUSTIN	88 DM2	$J/\psi \rightarrow \gamma K^+ K^-$
10.4 ± 1.2	± 1.6	149 AUGUSTIN	88 DM2	$J/\psi \rightarrow \gamma K_S^0 K_S^0$
9.6 ± 1.2	± 1.8	149 BALTRUSAIT..87	MRK3	$J/\psi \rightarrow \gamma K^+ K^-$
• • • We do not use the following data for averages, fits, limits, etc. • • •				
1.6 ± 0.2	$+0.6$ -0.2	149,150 BAI	96C BES	$J/\psi \rightarrow \gamma K^+ K^-$
< 0.8		90 151 BISELLO	89B	$J/\psi \rightarrow 4\pi\gamma$
1.6 ± 0.4	± 0.3	152 BALTRUSAIT..87	MRK3	$J/\psi \rightarrow \gamma\pi^+\pi^-$
3.8 ± 1.6		153 EDWARDS	82D CBAL	$e^+e^- \rightarrow \eta\eta\gamma$

¹⁴⁷ Includes unknown branching ratio to K^+K^- or $K_S^0K_S^0$.

¹⁴⁸ Assuming $J^P = 2^+$ for $f_0(1710)$.

¹⁴⁹ Includes unknown branching fraction to K^+K^- or $K_S^0K_S^0$. We have multiplied K^+K^- measurement by 2, and $K_S^0K_S^0$ by 4 to obtain $K\bar{K}$ result.

¹⁵⁰ Assuming $J^P = 0^+$ for $f_0(1710)$.

¹⁵¹ Includes unknown branching fraction to $\rho^0\rho^0$.

¹⁵² Includes unknown branching fraction to $\pi^+\pi^-$.

¹⁵³ Includes unknown branching fraction to $\eta\eta$.

$\Gamma(\gamma f_0(1710) \rightarrow \gamma\pi\pi)/\Gamma_{\text{total}}$ Γ_{142}/Γ

VALUE (units 10^{-4})	DOCUMENT ID	TECN	COMMENT
4.0 ± 1.0 OUR AVERAGE	Error includes scale factor of 1.7. See the ideogram below.		
$3.96 \pm 0.06 \pm 1.12$	154 ABLIKIM	06V BES2	$e^+e^- \rightarrow J/\psi \rightarrow \gamma\pi^+\pi^-$
$3.99 \pm 0.15 \pm 2.64$	154 ABLIKIM	06V BES2	$e^+e^- \rightarrow J/\psi \rightarrow \gamma\pi^0\pi^0$
• • • We do not use the following data for averages, fits, limits, etc. • • •			
$2.5 \pm 1.6 \pm 0.8$	BAI	98H BES	$J/\psi \rightarrow \gamma\pi^0\pi^0$

¹⁵⁴ Including unknown branching fraction to $\pi\pi$.

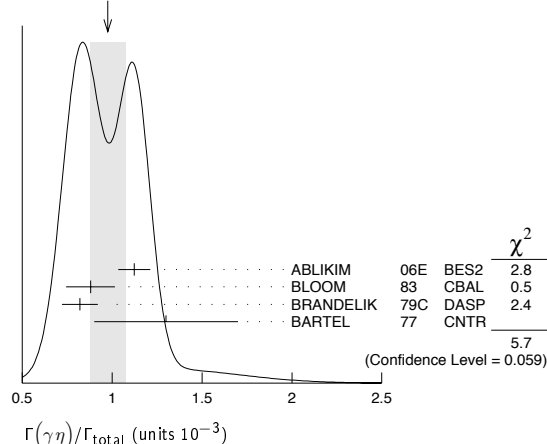
$\Gamma(\gamma f_0(1710) \rightarrow \gamma\omega\omega)/\Gamma_{\text{total}}$ Γ_{143}/Γ

VALUE (units 10^{-3})	EVTS	DOCUMENT ID	TECN	COMMENT
$0.31 \pm 0.06 \pm 0.08$	180	ABLIKIM	06H BES	$J/\psi \rightarrow \gamma\omega\omega$

$\Gamma(\gamma\eta)/\Gamma_{\text{total}}$ Γ_{144}/Γ

VALUE (units 10^{-3})	EVTS	DOCUMENT ID	TECN	COMMENT
0.98 ± 0.10 OUR AVERAGE	Error includes scale factor of 1.7. See the ideogram below.			
1.123 ± 0.089	11k	ABLIKIM	06E BES2	$J/\psi \rightarrow \gamma\eta$
$0.88 \pm 0.08 \pm 0.11$		BLOOM	83 CBAL	e^+e^-
0.82 ± 0.10		BRANDELIK	79C DASP	e^+e^-
1.3 ± 0.4	21	BARTEL	77 CNTR	e^+e^-

WEIGHTED AVERAGE
 0.98 ± 0.10 (Error scaled by 1.7)



$\Gamma(\gamma f_1(1420) \rightarrow \gamma K\bar{K}\pi)/\Gamma_{\text{total}}$ Γ_{145}/Γ

VALUE (units 10^{-3})	DOCUMENT ID	TECN	COMMENT
0.79 ± 0.13 OUR AVERAGE			
$0.68 \pm 0.04 \pm 0.24$	BAI	00D BES	$J/\psi \rightarrow \gamma K^{\pm} K_S^0 \pi^{\mp}$
$0.76 \pm 0.15 \pm 0.21$	155,156 AUGUSTIN	92 DM2	$J/\psi \rightarrow \gamma K\bar{K}\pi$
$0.87 \pm 0.14 \pm 0.14$	155 BAI	90C MRK3	$J/\psi \rightarrow \gamma K_S^0 K^{\pm} \pi^{\mp}$

¹⁵⁵ Included unknown branching fraction $f_1(1420) \rightarrow K\bar{K}\pi$.

¹⁵⁶ From fit to the $K^*(892)K1^{++}$ partial wave.

$\Gamma(\gamma f_1(1285))/\Gamma_{\text{total}}$ Γ_{146}/Γ

VALUE (units 10^{-3})	DOCUMENT ID	TECN	COMMENT
0.61 ± 0.08 OUR AVERAGE			
$0.69 \pm 0.16 \pm 0.20$	157 BAI	04J BES2	$J/\psi \rightarrow \gamma\gamma\rho^0$
$0.61 \pm 0.04 \pm 0.21$	158 BAI	00D BES	$J/\psi \rightarrow \gamma K^{\pm} K_S^0 \pi^{\mp}$
$0.45 \pm 0.09 \pm 0.17$	159 BAI	99 BES	$J/\psi \rightarrow \gamma\eta\pi^+\pi^-$
$0.625 \pm 0.063 \pm 0.103$	160 BOLTON	92 MRK3	$J/\psi \rightarrow \gamma f_1(1285)$
$0.70 \pm 0.08 \pm 0.16$	161 BOLTON	92B MRK3	$J/\psi \rightarrow \gamma\eta\pi^+\pi^-$

¹⁵⁷ Assuming $B(f_1(1285) \rightarrow \rho^0\gamma) = 0.055 \pm 0.013$.

¹⁵⁸ Assuming $\Gamma(f_1(1285) \rightarrow K\bar{K}\pi)/\Gamma_{\text{total}} = 0.090 \pm 0.004$.

¹⁵⁹ Assuming $\Gamma(f_1(1285) \rightarrow \eta\pi\pi)/\Gamma_{\text{total}} = 0.5 \pm 0.18$.

¹⁶⁰ Obtained summing the sequential decay channels

$B(J/\psi \rightarrow \gamma f_1(1285), f_1(1285) \rightarrow \pi\pi\pi) = (1.44 \pm 0.39 \pm 0.27) \times 10^{-4}$;
 $B(J/\psi \rightarrow \gamma f_1(1285), f_1(1285) \rightarrow a_0(980)\pi, a_0(980) \rightarrow \eta\pi) = (3.90 \pm 0.42 \pm 0.87) \times 10^{-4}$;

$B(J/\psi \rightarrow \gamma f_1(1285), f_1(1285) \rightarrow a_0(980)\pi, a_0(980) \rightarrow K\bar{K}) = (0.66 \pm 0.26 \pm 0.29) \times 10^{-4}$;

$B(J/\psi \rightarrow \gamma f_1(1285), f_1(1285) \rightarrow \gamma\rho^0) = (0.25 \pm 0.07 \pm 0.03) \times 10^{-4}$.

¹⁶¹ Using $B(f_1(1285) \rightarrow a_0(980)\pi) = 0.37$, and including unknown branching ratio for $a_0(980) \rightarrow \eta\pi$.

$\Gamma(\gamma f_1(1510) \rightarrow \gamma\eta\pi^+\pi^-)/\Gamma_{\text{total}}$ Γ_{147}/Γ

VALUE (units 10^{-4})	DOCUMENT ID	TECN	COMMENT
$4.5 \pm 1.0 \pm 0.7$	BAI	99 BES	$J/\psi \rightarrow \gamma\eta\pi^+\pi^-$

$\Gamma(\gamma f_2'(1525))/\Gamma_{\text{total}}$ Γ_{148}/Γ

VALUE (units 10^{-4})	CL%	EVTS	DOCUMENT ID	TECN	COMMENT
4.5 ± 0.7 OUR AVERAGE					
$3.85 \pm 0.17 \pm 1.91$			162 BAI	03G BES	$J/\psi \rightarrow \gamma K\bar{K}$
3.6 ± 0.4	$+1.4$ -0.4		162 BAI	96C BES	$J/\psi \rightarrow \gamma K^+ K^-$
5.6 ± 1.4	± 0.9		162 AUGUSTIN	88 DM2	$J/\psi \rightarrow \gamma K^+ K^-$
4.5 ± 0.4	± 0.9		162 AUGUSTIN	88 DM2	$J/\psi \rightarrow \gamma K_S^0 K_S^0$
$6.8 \pm 1.6 \pm 1.4$			162 BALTRUSAIT..87	MRK3	$J/\psi \rightarrow \gamma K^+ K^-$

• • • We do not use the following data for averages, fits, limits, etc. • • •

< 3.4 90 4 ¹⁶³ BRANDELIK 79C DASP $e^+e^- \rightarrow \pi^+\pi^-\gamma$

< 2.3 90 3 ALEXANDER 78 PLUT $e^+e^- \rightarrow K^+K^-\gamma$

¹⁶² Using $B(f_2'(1525) \rightarrow K\bar{K}) = 0.888$.

¹⁶³ Assuming isotropic production and decay of the $f_2'(1525)$ and isospin.

$\Gamma(\gamma f_2(1640) \rightarrow \gamma\omega\omega)/\Gamma_{\text{total}}$ Γ_{149}/Γ

VALUE (units 10^{-3})	EVTS	DOCUMENT ID	TECN	COMMENT
$0.28 \pm 0.05 \pm 0.17$	141	ABLIKIM	06H BES	$J/\psi \rightarrow \gamma\omega\omega$

$\Gamma(\gamma f_2(1910) \rightarrow \gamma\omega\omega)/\Gamma_{\text{total}}$ Γ_{150}/Γ

VALUE (units 10^{-3})	EVTS	DOCUMENT ID	TECN	COMMENT
$0.20 \pm 0.04 \pm 0.13$	151	ABLIKIM	06H BES	$J/\psi \rightarrow \gamma\omega\omega$

$\Gamma(\gamma f_2(1950) \rightarrow \gamma K^*(892)\bar{K}^*(892))/\Gamma_{\text{total}}$ Γ_{151}/Γ

VALUE (units 10^{-3})	DOCUMENT ID	TECN	COMMENT
$0.7 \pm 0.1 \pm 0.2$	BAI	00B BES	$J/\psi \rightarrow \gamma K^+ K^0 \pi^+ \pi^-$

$\Gamma(\gamma K^*(892)\bar{K}^*(892))/\Gamma_{\text{total}}$ Γ_{152}/Γ

VALUE (units 10^{-3})	EVTS	DOCUMENT ID	TECN	COMMENT
$4.0 \pm 0.3 \pm 1.3$	320	164 BAI	00B BES	$J/\psi \rightarrow \gamma K^+ K^0 \pi^+ \pi^-$

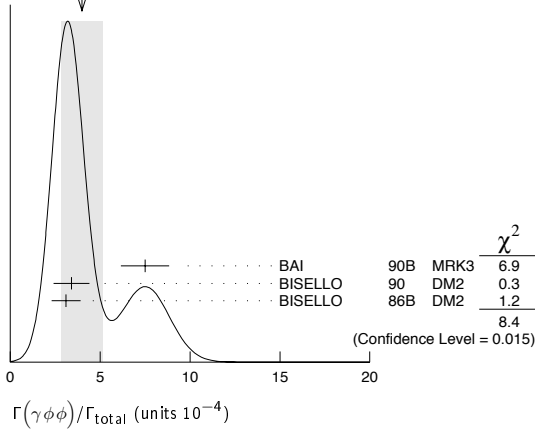
¹⁶⁴ Summed over all charges.

$\Gamma(\gamma\phi\phi)/\Gamma_{\text{total}}$ Γ_{153}/Γ

VALUE (units 10^{-4})	EVTS	DOCUMENT ID	TECN	COMMENT
4.0 ± 1.2 OUR AVERAGE	Error includes scale factor of 2.1. See the ideogram below.			
$7.5 \pm 0.6 \pm 1.2$	168	BAI	90B MRK3	$J/\psi \rightarrow \gamma 4K$
$3.4 \pm 0.8 \pm 0.6$	33 ± 7	165 BISELLO	90 DM2	$J/\psi \rightarrow \gamma K^+ K^- K_S^0 K_L^0$
$3.1 \pm 0.7 \pm 0.4$		165 BISELLO	86B DM2	$J/\psi \rightarrow \gamma K^+ K^- K^+ K^-$

¹⁶⁵ $\phi\phi$ mass less than 2.9 GeV, η_c excluded.

WEIGHTED AVERAGE
4.0±1.2 (Error scaled by 2.1)



$\Gamma(\gamma\rho\bar{\rho})/\Gamma_{\text{total}}$		Γ_{154}/Γ		
VALUE (units 10^{-3})	CL%	EVTS	DOCUMENT ID	TECN COMMENT
0.38±0.07±0.07		49	EATON	84 MRK2 e^+e^-
••• We do not use the following data for averages, fits, limits, etc. •••				
<0.11	90		PERUZZI	78 MRK1 e^+e^-

$\Gamma(\gamma\eta(2225))/\Gamma_{\text{total}}$		Γ_{155}/Γ		
VALUE (units 10^{-3})	CL%	EVTS	DOCUMENT ID	TECN COMMENT
0.29±0.06 OUR AVERAGE				
0.33±0.08±0.05		166	BAI	90B MRK3 $J/\psi \rightarrow \gamma K^+ K^- K^+ K^-$
0.27±0.06±0.06		166	BAI	90B MRK3 $J/\psi \rightarrow \gamma K^+ K^- K_S^0 K_L^0$
0.24 ^{+0.15} _{-0.10}		167,168	BISELLO	89B DM2 $J/\psi \rightarrow 4\pi\gamma$

¹⁶⁶ Includes unknown branching fraction to $\phi\phi$.

¹⁶⁷ Estimated by us from various fits.

¹⁶⁸ Includes unknown branching fraction to $\rho^0\rho^0$.

$\Gamma(\gamma\eta(1760) \rightarrow \gamma\rho^0\rho^0)/\Gamma_{\text{total}}$		Γ_{156}/Γ		
VALUE (units 10^{-3})	CL%	EVTS	DOCUMENT ID	TECN COMMENT
0.13±0.09		169,170	BISELLO	89B DM2 $J/\psi \rightarrow 4\pi\gamma$

¹⁶⁹ Estimated by us from various fits.

¹⁷⁰ Includes unknown branching fraction to $\rho^0\rho^0$.

$\Gamma(\gamma\eta(1760) \rightarrow \gamma\omega\omega)/\Gamma_{\text{total}}$		Γ_{157}/Γ		
VALUE (units 10^{-3})	CL%	EVTS	DOCUMENT ID	TECN COMMENT
1.98±0.08±0.32		1045	ABLIKIM	06H BES $J/\psi \rightarrow \gamma\omega\omega$

$\Gamma(\gamma X(1835))/\Gamma_{\text{total}}$		Γ_{158}/Γ		
VALUE (units 10^{-5})	CL%	EVTS	DOCUMENT ID	TECN COMMENT
22.0±4.0±4.0		264	171	ABLIKIM 05R BES2 $J/\psi \rightarrow \gamma\pi^+\pi^-\eta'$
••• We do not use the following data for averages, fits, limits, etc. •••				
26.1±2.7±6.5		95	172	ABLIKIM 06J BES2 $J/\psi \rightarrow \gamma\omega\phi$
7.0±0.4 ^{+1.9} _{-0.8}			173	BAI 03F BES2 $J/\psi \rightarrow \gamma\rho\bar{\rho}$

¹⁷¹ Including the unknown branching fraction to $\pi^+\pi^-\eta'$.

¹⁷² Including the unknown branching ratio to $\omega\phi$.

¹⁷³ Including the unknown branching fraction to $\rho\bar{\rho}$. The fit including final state interaction effects according to SIBIRTEV 05A gives close results.

$\Gamma(\gamma(K\bar{K}\pi) [J^{PC} = 0^- +])/ \Gamma_{\text{total}}$		Γ_{159}/Γ		
VALUE (units 10^{-3})	CL%	EVTS	DOCUMENT ID	TECN COMMENT
0.7 ± 0.4 OUR AVERAGE				Error includes scale factor of 2.1.
0.58±0.03±0.20			174	BAI 00D BES $J/\psi \rightarrow \gamma K^\pm K_S^0 \pi^\mp$
2.1 ± 0.1 ± 0.7			175	BAI 00D BES $J/\psi \rightarrow \gamma K^\pm K_S^0 \pi^\mp$

¹⁷⁴ For a broad structure around 1800 MeV.

¹⁷⁵ For a broad structure around 2040 MeV.

$\Gamma(\gamma\pi^0)/\Gamma_{\text{total}}$		Γ_{160}/Γ		
VALUE (units 10^{-5})	CL%	EVTS	DOCUMENT ID	TECN COMMENT
3.3^{+0.6}_{-0.4} OUR AVERAGE				
3.13 ^{+0.65} _{-0.47}		586	ABLIKIM	06E BES2 $J/\psi \rightarrow \pi^0\gamma$
3.6 ± 1.1 ± 0.7			BLOOM	83 CBAL e^+e^-
7.3 ± 4.7		10	BRANDELIK	79C DASP e^+e^-

$\Gamma(\gamma\rho\bar{\rho}\pi^+\pi^-)/\Gamma_{\text{total}}$		Γ_{161}/Γ		
VALUE (units 10^{-3})	CL%	DOCUMENT ID	TECN	COMMENT
<0.79	90	EATON	84	MRK2 e^+e^-

$\Gamma(\gamma\gamma)/\Gamma_{\text{total}}$		Γ_{174}/Γ		
VALUE (units 10^{-5})	CL%	DOCUMENT ID	TECN	COMMENT
< 2.2	90	ABLIKIM	07J	BES2 $\psi(2S) \rightarrow J/\psi\pi^+\pi^-$
••• We do not use the following data for averages, fits, limits, etc. •••				
<16	90	176	WICHT	08 BELL $B^\pm \rightarrow K^\pm\gamma\gamma$
<50	90		BARTEL	77 CNTR e^+e^-

¹⁷⁶ WICHT 08 reports $[B(J/\psi(1S) \rightarrow \gamma\gamma)] \times [B(B^+ \rightarrow J/\psi(1S) K^+)] < 0.16 \times 10^{-6}$. We divide by our best value $B(B^+ \rightarrow J/\psi(1S) K^+) = 0.001007$.

$\Gamma(\gamma A\bar{A})/\Gamma_{\text{total}}$		Γ_{162}/Γ		
VALUE (units 10^{-3})	CL%	DOCUMENT ID	TECN	COMMENT
<0.13	90	HENRARD	87	DM2 e^+e^-
••• We do not use the following data for averages, fits, limits, etc. •••				
<0.16	90	BAI	98G	BES e^+e^-

$\Gamma(3\gamma)/\Gamma_{\text{total}}$		Γ_{163}/Γ		
VALUE (units 10^{-3})	CL%	DOCUMENT ID	TECN	COMMENT
<0.055	90	PARTRIDGE	80	CBAL e^+e^-

$\Gamma(\gamma f_0(2200))/\Gamma_{\text{total}}$		Γ_{164}/Γ		
VALUE (units 10^{-4})	CL%	DOCUMENT ID	TECN	COMMENT
••• We do not use the following data for averages, fits, limits, etc. •••				
1.5		177	AUGUSTIN	88 DM2 $J/\psi \rightarrow \gamma K_S^0 K_S^0$
¹⁷⁷ Includes unknown branching fraction to $K_S^0 K_S^0$.				

$\Gamma(\gamma f_J(2220))/\Gamma_{\text{total}}$		Γ_{165}/Γ		
VALUE (units 10^{-5})	CL%	EVTS	DOCUMENT ID	TECN COMMENT
>250	99.9		178	HASAN 96 SPEC $\bar{p}p \rightarrow \pi^+\pi^-$
••• We do not use the following data for averages, fits, limits, etc. •••				
>300			179	BAI 96B BES $e^+e^- \rightarrow \gamma\bar{p}p$,
				$K\bar{K}$
< 2.3	95		180	AUGUSTIN 88 DM2 $J/\psi \rightarrow \gamma K^+ K^-$
< 1.6	95		180	AUGUSTIN 88 DM2 $J/\psi \rightarrow \gamma K_S^0 K_S^0$
12.4 ^{+6.4} _{-5.2} ±2.8		23	180	BALTRUSAIT...86D MRK3 $J/\psi \rightarrow \gamma K_S^0 K_S^0$
8.4 ^{+3.4} _{-2.8} ±1.6		93	180	BALTRUSAIT...86D MRK3 $J/\psi \rightarrow \gamma K^+ K^-$

¹⁷⁸ Using BAI 96B.

¹⁷⁹ Using BARNES 93.

¹⁸⁰ Includes unknown branching fraction to K^+K^- or $K_S^0 K_S^0$.

$\Gamma(\gamma f_J(2220) \rightarrow \gamma\pi\pi)/\Gamma_{\text{total}}$		Γ_{166}/Γ		
VALUE (units 10^{-4})	CL%	EVTS	DOCUMENT ID	TECN COMMENT
0.84±0.26±0.30			BAI	96B BES $e^+e^- \rightarrow J/\psi \rightarrow \gamma\pi^+\pi^-$
••• We do not use the following data for averages, fits, limits, etc. •••				
1.4 ± 0.8 ± 0.4			BAI	98H BES $J/\psi \rightarrow \gamma\pi^0\pi^0$

$\Gamma(\gamma f_J(2220) \rightarrow \gamma K\bar{K})/\Gamma_{\text{total}}$		Γ_{167}/Γ		
VALUE (units 10^{-5})	CL%	EVTS	DOCUMENT ID	TECN COMMENT
8.1±3.0 OUR AVERAGE				
6.6±2.9±2.4			BAI	96B BES $e^+e^- \rightarrow J/\psi \rightarrow \gamma K^+ K^-$
10.8±4.0±3.2			BAI	96B BES $e^+e^- \rightarrow J/\psi \rightarrow \gamma K_S^0 K_S^0$

$\Gamma(\gamma f_J(2220) \rightarrow \gamma\rho\bar{\rho})/\Gamma_{\text{total}}$		Γ_{168}/Γ		
VALUE (units 10^{-5})	CL%	EVTS	DOCUMENT ID	TECN COMMENT
1.5 ± 0.6 ± 0.5			BAI	96B BES $e^+e^- \rightarrow J/\psi \rightarrow \gamma\rho\bar{\rho}$

$\Gamma(\gamma f_0(1500))/\Gamma_{\text{total}}$		Γ_{169}/Γ		
VALUE (units 10^{-4})	CL%	EVTS	DOCUMENT ID	TECN COMMENT
1.01±0.32 OUR AVERAGE				
1.00±0.03±0.45			181	ABLIKIM 06V BES2 $e^+e^- \rightarrow J/\psi \rightarrow \gamma\pi^+\pi^-$
1.02±0.09±0.45			181	ABLIKIM 06V BES2 $e^+e^- \rightarrow J/\psi \rightarrow \gamma\pi^0\pi^0$
••• We do not use the following data for averages, fits, limits, etc. •••				
>5.7 ± 0.8			182,183	BUGG 95 MRK3 $J/\psi \rightarrow \gamma\pi^+\pi^-\pi^+\pi^-$

¹⁸¹ Including unknown branching fraction to $\pi\pi$.

¹⁸² Including unknown branching ratio for $f_0(1500) \rightarrow \pi^+\pi^-\pi^+\pi^-$.

¹⁸³ Assuming that $f_0(1500)$ decays only to two S-wave dipions.

$\Gamma(\gamma e^+e^-)/\Gamma_{\text{total}}$		Γ_{170}/Γ		
VALUE (units 10^{-3})	CL%	EVTS	DOCUMENT ID	TECN COMMENT
8.8±1.3±0.4			184	ARMSTRONG 96 E760 $\bar{p}p \rightarrow e^+e^-\gamma$
¹⁸⁴ For $E_\gamma > 100$ MeV.				

Meson Particle Listings

 $J/\psi(1S)$

WEAK DECAYS

$\Gamma(D^- e^+ \nu_e + c.c.)/\Gamma_{\text{total}}$				Γ_{171}/Γ
VALUE (units 10^{-5})	CL%	DOCUMENT ID	TECN	COMMENT
<1.2	90	ABLIKIM	06M BES2	$e^+ e^- \rightarrow J/\psi$

$\Gamma(D^0 e^+ e^- + c.c.)/\Gamma_{\text{total}}$				Γ_{172}/Γ
VALUE (units 10^{-5})	CL%	DOCUMENT ID	TECN	COMMENT
<1.1	90	ABLIKIM	06M BES2	$e^+ e^- \rightarrow J/\psi$

$\Gamma(D_s^- e^+ \nu_e + c.c.)/\Gamma_{\text{total}}$				Γ_{173}/Γ
VALUE (units 10^{-5})	CL%	DOCUMENT ID	TECN	COMMENT
<3.6	90	185 ABLIKIM	06M BES2	$e^+ e^- \rightarrow J/\psi$

185 Using $B(D_s^- \rightarrow \phi \pi^-) = 4.4 \pm 0.5\%$.

LEPTON FAMILY NUMBER (LF) VIOLATING MODES

$\Gamma(e^\pm \mu^\mp)/\Gamma_{\text{total}}$				Γ_{175}/Γ
VALUE (units 10^{-6})	CL%	DOCUMENT ID	TECN	COMMENT
<1.1	90	BAI	03D BES	$e^+ e^- \rightarrow J/\psi$

$\Gamma(e^\pm \tau^\mp)/\Gamma_{\text{total}}$				Γ_{176}/Γ
VALUE (units 10^{-6})	CL%	DOCUMENT ID	TECN	COMMENT
<8.3	90	ABLIKIM	04 BES	$e^+ e^- \rightarrow J/\psi$

$\Gamma(\mu^\pm \tau^\mp)/\Gamma_{\text{total}}$				Γ_{177}/Γ
VALUE (units 10^{-6})	CL%	DOCUMENT ID	TECN	COMMENT
<2.0	90	ABLIKIM	04 BES	$e^+ e^- \rightarrow J/\psi$

 $J/\psi(1S)$ REFERENCES

ABLIKIM	08	EPJ C53 15	M. Ablikim et al.	(BES Collab.)
ABLIKIM	08A	PR D77 012001	M. Ablikim et al.	(BES Collab.)
ABLIKIM	08C	PL B659 789	M. Ablikim et al.	(BES Collab.)
ABLIKIM	08E	PR D77 032005	M. Ablikim et al.	(BES Collab.)
ABLIKIM	08F	PRL 100 102003	M. Ablikim et al.	(BES Collab.)
AUBERT	08S	PR D77 092002	B. Aubert et al.	(BABAR Collab.)
WICHT	08	PL B662 323	J. Wicht et al.	(BELLE Collab.)
ABLIKIM	07H	PR D76 092003	M. Ablikim et al.	(BES Collab.)
ABLIKIM	07J	PR D76 117101	M. Ablikim et al.	(BES Collab.)
ANDREOTTI	07	PL B654 74	M. Andreotti et al.	(Femlab E335 Collab.)
AUBERT	07AK	PR D76 012008	B. Aubert et al.	(BABAR Collab.)
AUBERT	07AU	PR D76 092005	B. Aubert et al.	(BABAR Collab.)
AUBERT	07BD	PR D76 092006	B. Aubert et al.	(BABAR Collab.)
ABLIKIM	06	PL B632 181	M. Ablikim et al.	(BES Collab.)
ABLIKIM	06C	PL B633 681	M. Ablikim et al.	(BES Collab.)
ABLIKIM	06E	PR D73 052008	M. Ablikim et al.	(BES Collab.)
ABLIKIM	06F	PR D73 052007	M. Ablikim et al.	(BES Collab.)
ABLIKIM	06H	PR D73 112007	M. Ablikim et al.	(BES Collab.)
ABLIKIM	06J	PRL 96 162002	M. Ablikim et al.	(BES Collab.)
ABLIKIM	06K	PRL 97 062001	M. Ablikim et al.	(BES Collab.)
ABLIKIM	06M	PL B639 418	M. Ablikim et al.	(BES Collab.)
ABLIKIM	06V	PL B642 441	M. Ablikim et al.	(BES Collab.)
ADAMS	06A	PR D73 051103R	G.S. Adams et al.	(CLEO Collab.)
AUBERT	06B	PR D73 012005	B. Aubert et al.	(BABAR Collab.)
AUBERT	06D	PR D73 052003	B. Aubert et al.	(BABAR Collab.)
AUBERT	06E	PRL 96 052002	B. Aubert et al.	(BABAR Collab.)
AUBERT_BE	06D	PR D74 091103R	B. Aubert et al.	(BABAR Collab.)
WU	06	PRL 97 162003	C.-H. Wu et al.	(BELLE Collab.)
ABLIKIM	05	PL B607 243	M. Ablikim et al.	(BES Collab.)
ABLIKIM	05B	PR D71 032003	M. Ablikim et al.	(BES Collab.)
ABLIKIM	05C	PL B610 192	M. Ablikim et al.	(BES Collab.)
ABLIKIM	05H	PR D72 012002	M. Ablikim et al.	(BES Collab.)
ABLIKIM	05R	PRL 95 262001	M. Ablikim et al.	(BES Collab.)
AUBERT	05D	PR D71 052001	B. Aubert et al.	(BABAR Collab.)
LI	05C	PR D71 111103	Z. Li et al.	(CLEO Collab.)
SIBIRITSEV	05A	PR D71 054010	A. Sibiritshev, J. Haidenbauer	
ABLIKIM	04	PL B598 172	M. Ablikim et al.	(BES Collab.)
ABLIKIM	04M	PR D70 112008	M. Ablikim et al.	(BES Collab.)
AUBERT	04	PR D69 011103	B. Aubert et al.	(BABAR Collab.)
AUBERT_B	04N	PR D70 072004	B. Aubert et al.	(BABAR Collab.)
BAI	04	PL B578 16	J.Z. Bai et al.	(BES Collab.)
BAI	04A	PR D69 012003	J.Z. Bai et al.	(BES Collab.)
BAI	04D	PL B589 71	J.Z. Bai et al.	(BES Collab.)
BAI	04E	PL B591 42	J.Z. Bai et al.	(BES Collab.)
BAI	04G	PR D70 012004	J.Z. Bai et al.	(BES Collab.)
BAI	04H	PR D70 012005	J.Z. Bai et al.	(BES Collab.)
BAI	04J	PL B594 47	J.Z. Bai et al.	(BES Collab.)
SETH	04	PR D69 097503	K.K. Seth	
AULCHENKO	03	PL B573 63	V.M. Aulchenko et al.	(KEDR Collab.)
BAI	03D	PL B561 49	J.Z. Bai et al.	(BES Collab.)
BAI	03F	PRL 91 022001	J.Z. Bai et al.	(BES Collab.)
BAI	03G	PR D68 052003	J.Z. Bai et al.	(BES Collab.)
HUANG	03	PRL 91 241802	H.-C. Huang et al.	(BELLE Collab.)
BAI	02C	PRL 88 101802	J.Z. Bai et al.	(BES Collab.)
ARTAMONOV	00	PL B474 427	A.S. Artamonov et al.	(BES Collab.)
BAI	00	PRL 84 594	J.Z. Bai et al.	(BES Collab.)
BAI	00B	PL B472 200	J.Z. Bai et al.	(BES Collab.)
BAI	00D	PL B476 25	J.Z. Bai et al.	(BES Collab.)
BAI	99	PL B446 356	J.Z. Bai et al.	(BES Collab.)
BAI	99C	PRL 83 1918	J.Z. Bai et al.	(BES Collab.)
BAI	98D	PR D58 092006	J.Z. Bai et al.	(BES Collab.)
BAI	98G	PL B424 213	J.Z. Bai et al.	(BES Collab.)
BAI	98H	PRL 81 1179	J.Z. Bai et al.	(BES Collab.)
BALDINI	98	PL B444 111	R. Baldini et al.	(FENICE Collab.)
ARMSTRONG	96	PR D54 7067	T.A. Armstrong et al.	(E760 Collab.)
BAI	96B	PRL 76 3502	J.Z. Bai et al.	(BES Collab.)
BAI	96C	PRL 77 3959	J.Z. Bai et al.	(BES Collab.)
BAI	96D	PR D54 1221	J.Z. Bai et al.	(BES Collab.)
GRIBUSHIN	96	PR D53 4723	A. Gribushin et al.	(E672 Collab., E706 Collab.)
HASAN	96	PL B388 376	A. Hasan, D.V. Bugg	(BRUN, LOQM)
BAI	95B	PL B355 374	J.Z. Bai et al.	(BES Collab.)
BUGG	95	PL B353 378	D.V. Bugg et al.	(LOQM, PNPI, WASH)

ANTONELLI	93	PL B301 317	A. Antonelli et al.	(FENICE Collab.)
ARMSTRONG	93B	PR D47 772	T.A. Armstrong et al.	(FNAL E760 Collab.)
BARNES	93	PL B309 469	P.D. Barnes, P. Birfen, W.H. Breunlich	
AUGUSTIN	92	PR D46 1951	J.E. Augustin, G. Cosme	(DM2 Collab.)
BOLTON	92	PL B278 495	T. Bolton et al.	(Mark III Collab.)
BOLTON	92B	PRL 69 1328	T. Bolton et al.	(Mark III Collab.)
COFFMAN	92	PRL 68 282	D.M. Coffman et al.	(Mark III Collab.)
HSUEH	92	PR D45 R2181	S. Hsueh, S. Palestini	(FNAL, TORI)
BISELLO	91	NP B350 1	D. Bisello et al.	(DM2 Collab.)
AUGUSTIN	90	PR D42 10	J.E. Augustin et al.	(DM2 Collab.)
BAI	90C	PRL 65 1309	Z. Bai et al.	(Mark III Collab.)
BAI	90B	PRL 65 2507	Z. Bai et al.	(Mark III Collab.)
BISELLO	90	PL B241 617	D. Bisello et al.	(DM2 Collab.)
COFFMAN	90	PR D41 1410	D.M. Coffman et al.	(Mark III Collab.)
JOUSSET	90	PR D41 1389	J. Jousset et al.	(DM2 Collab.)
ALEXANDER	89	NP B320 45	J.P. Alexander et al.	(LBL, MICH, SLAC)
AUGUSTIN	89	NP B320 1	J.E. Augustin, G. Cosme	(DM2 Collab.)
BISELLO	89B	PR D39 701	G. Busetto et al.	(DM2 Collab.)
AUGUSTIN	88	PRL 60 2238	J.E. Augustin et al.	(DM2 Collab.)
COFFMAN	88	PR D38 2695	D.M. Coffman et al.	(Mark III Collab.)
FALVARD	88	PR D38 2706	A. Falvard et al.	(CLER, FRAS, LALO+)
AUGUSTIN	87	ZPHY C36 369	J.E. Augustin et al.	(LALO, CLER, FRAS+)
BAGLIN	87	NP B286 592	C. Baglin et al.	(LAPP, CERN, GENO, LYON+)
BALTRUSAITIS...	87	PR D35 2077	R.M. Baltrusaitis et al.	(Mark III Collab.)
BECKER	87	PRL 59 186	J.J. Becker et al.	(Mark III Collab.)
BISELLO	87	PL B192 239	D. Bisello et al.	(PADO, CLER, FRAS+)
COHEN	87	RMP 59 1121	E.R. Cohen, B.N. Taylor	(RIS C, NBS)
HENNRAD	87	NP B292 670	P. Henrard et al.	(CLER, FRAS, LALO+)
PALLIN	87	NP B292 653	D. Pallin et al.	(CLER, FRAS, LALO, PADO)
BALTRUSAITIS...	86	PR D33 629	R.M. Baltrusaitis et al.	(Mark III Collab.)
BALTRUSAITIS...	86B	PR D33 1222	R.M. Baltrusaitis et al.	(Mark III Collab.)
BALTRUSAITIS...	86D	PRL 56 107	R.M. Baltrusaitis et al.	(CIT, UCSC, ILL, SLAC+)
BISELLO	86B	PL B179 294	D. Bisello et al.	(DM2 Collab.)
GAISER	86	PR D34 711	J. Gaiser et al.	(Crystal Ball Collab.)
BALTRUSAITIS...	85C	PRL 55 1723	R.M. Baltrusaitis et al.	(CIT, UCSC+)
BALTRUSAITIS...	85D	PR D32 566	R.M. Baltrusaitis et al.	(CIT, UCSC+)
KURAEV	85	SJNP 41 466	E.A. Kuraev, V.S. Fadin	(NOVO)
BALTRUSAITIS...	84	PRL 52 2126	Translated from YAF 41 733.	
EATON	84	PR D29 804	R.M. Baltrusaitis et al.	(CIT, UCSC+)
BLOOM	83	ARNS 33 143	M.W. Eaton et al.	(LBL, SLAC)
EDWARDS	83B	PRL 51 259	E.D. Bloom, C. Peck	(SLAC, CIT)
FRANKLIN	83	PRL 51 963	C. Edwards et al.	(CIT, HARV, PRIN+)
BURKE	82	PRL 49 632	M.E.B. Franklin et al.	(LBL, SLAC)
EDWARDS	82B	PR D25 3065	D.L. Burke et al.	(LBL, SLAC)
EDWARDS	82D	PR D25 3065	C. Edwards et al.	(CIT, HARV, PRIN+)
EDWARDS	82D	PR D25 3065	C. Edwards et al.	(CIT, HARV, PRIN+)
EDWARDS	82E	ARNS 33 143	E.D. Bloom, C. Peck	(SLAC, CIT)
EDWARDS	82E	PRL 49 259	C. Edwards et al.	(CIT, HARV, PRIN+)
LEMOIGNE	82	PL 113B 509	Y. Lemoigne et al.	(SACL, LOIC, SHMP+)
BESCH	81	ZPHY C8 1	H.J. Besch et al.	(BONN, DESY, MANZ)
GIDAL	81	PL 107B 153	G. Gidal et al.	(SLAC, LBL)
PARTRIDGE	80	PRL 44 712	R. Partridge et al.	(CIT, HARV, PRIN+)
SCHARRE	80	PL 97B 329	D.L. Scharre et al.	(SLAC, LBL)
ZHOLENTZ	80	PL 96B 214	A.A. Zholents et al.	(NOVO)
ZHOLENTZ	80	SJNP 34 814	A.A. Zholents et al.	(NOVO)
BRANDELIK	79C	ZPHY C1 233	R. Brandelik et al.	(DASP Collab.)
ALEXANDER	78	PL 72B 493	G. Alexander et al.	(DESY, HAMB, SIEG+)
BESCH	78	PL 78B 347	H.J. Besch et al.	(BONN, DESY, MANZ)
BRANDELIK	78B	PL 74B 232	R. Brandelik et al.	(DASP Collab.)
PERUZZI	78	PR D17 2901	I. Peruzzi et al.	(SLAC, LBL)
BARTEL	77	PL 64B 493	W. Bartel et al.	(DESY, HEIDP)
BURMESTER	77D	PL 72B 135	J. Burmester et al.	(DESY, HAMB, SIEG+)
FELDMAN	77	PRPL 33C 285	G.J. Feldman, M.L. Perl	(LBL, SLAC)
VANNUCCI	77	PR D15 1814	F. Vannucci et al.	(SLAC, LBL)
BARTEL	76	PL 64B 483	W. Bartel et al.	(DESY, HEIDP)
BRAUNSCHEW...	76	PL 63B 487	W. Braunschweig et al.	(DASP Collab.)
JEAN-MARIE	76	PRL 36 291	B. Jean-Marie et al.	(SLAC, LBL) IG
BALDINI...	75	PL 58B 471	R. Baldini-Celio et al.	(FRAS, ROMA)
BOYARSKI	75	PRL 34 1357	A.M. Boyarski et al.	(SLAC, LBL) JPC
DASP	75	PL 56B 491	W. Braunschweig et al.	(DASP Collab.)
ESPOSITO	75B	LNC 14 73	B. Esposito et al.	(FRAS, NAPL, PADO+)
FORD	75	PRL 34 604	R.L. Ford et al.	(SLAC, PENN)

OTHER RELATED PAPERS

LI	07A	PR D76 094016	B.A. Li	
LIU	07B	PR D75 074017	X. Liu et al.	
ABLIKIM	06A	PL B633 191	M. Ablikim et al.	(BES Collab.)
ABLIKIM	06B	EPJ C45 337	M. Ablikim et al.	(BES Collab.)
ABLIKIM	06Q	PRL 97 202002	M. Ablikim et al.	(BES Collab.)
ABLIKIM	06S	PRL 97 142002	M. Ablikim et al.	(BES Collab.)
GLOZMAN	06	PR D73 017503	L.Ya. Gvozman	
ABLIKIM	04J	PRL 93 112002	M. Ablikim et al.	(BES Collab.)
DATTA	03C	PL B567 273	A. Datta, P.J. O'Donnell	
LI	03B	EPJ C28 335	D.M. Li et al.	
LI	03D	JMP A18 3335	D.M. Li et al.	
BAI	01B	PL B510 75	J.Z. Bai et al.	(BES Collab.)
CHEN	98	PRL 80 5060	Y.Q. Chen, E. Braaten	
SUZUKI	98	PR D57 5717	M. Suzuki	
BARATE	93	PL 121B 449	R. Barate et al.	(SACL, LOIC, SHMP, IND)
ABRAMS	74	PRL 33 1453	G.S. Abrams et al.	(LBL, SLAC)
ASH	74	LNC 11 705	W.W. Ash et al.	(FRAS, UMD, NAPL, PADO+)
AUBERT	74	PRL 33 1404	J.J. Aubert et al.	(MIT, BNL)
AUGUSTIN	74	PRL 33 1406	J.E. Augustin et al.	(SLAC, LBL)
BACCI	74	PRL 33 1408	C. Bacci et al.	(FRAS)
BACCI	74	PRL 33 1649 (erratum)	C. Bacci	
BALDINI...	74	LNC 11 711	R. Baldini-Celio et al.	(FRAS, ROMA)
BARBIELLINI	74	LNC 11 718	G. Barbiellini et al.	(FRAS, NAPL, PISA+)
BRAUNSCHEW...	74	PL 53B 393	W. Braunschweig et al.	(DASP Collab.)
CHRISTENS...	70	PRL 25 1523	J.C. Christenson et al.	(COLU, BNL, CERN)

BRANCHING RATIOS OF $\psi(2S)$ AND $\chi_{c0,1,2}$

Updated May 2008 by J.J. Hernández-Rey (IFIC, Valencia), S. Navas (University of Granada), and C. Patrignani (INFN, Genova).

Since 2002, the treatment of the branching ratios of the $\psi(2S)$ and $\chi_{c0,1,2}$ has undergone an important restructuring.

When measuring a branching ratio experimentally, it is not always possible to normalize the number of events observed in the corresponding decay mode to the total number of particles produced. Therefore, the experimenters sometimes report the number of observed decays with respect to another decay mode of the same, or another particle in the relevant decay chain. This is actually equivalent to measuring combinations of branching fractions of several decay modes.

To extract the branching ratio of a given decay mode, the collaborations use some previously reported measurements of the required branching ratios. However, the values are frequently taken from the *Review of Particle Physics* (RPP), which in turn uses the branching ratio reported by the experiment in the following edition, giving rise either to correlations or to plain vicious circles.

One of these inconsistencies within the $\psi(2S)$ decays was reported in Ref. 10. To obtain the branching ratios of the decay modes $\psi(2S) \rightarrow J/\psi(1S) \pi^+ \pi^-$, $\psi(2S) \rightarrow J/\psi(1S) \pi^0 \pi^0$, and $\psi(2S) \rightarrow J/\psi(1S) \eta$, E760 Collaboration [2] used the value of $B(\psi(2S) \rightarrow J/\psi(1S) \text{ anything})$ given in Ref. 6, obtained with a fit that included the above decays. The values obtained in this way in Ref. 2 were subsequently used in the 1998 edition of RPP [7] as new entries in the same fit.

A more subtle correlation, among others, was pointed out in Ref. 5. The BES Collaboration [3] obtained the value of $B(\chi_{c0} \rightarrow p\bar{p})$ in e^+e^- collisions from the number of observed decays $\psi(2S) \rightarrow \gamma \chi_{c0} \rightarrow \gamma p\bar{p}$, and the total number of $\psi(2S)$ produced, which was estimated in turn from the observed number of decays of the type $\psi(2S) \rightarrow J/\psi(1S) \pi^+ \pi^-$ [4]. To this end, they used the values of the branching ratios of $\psi(2S) \rightarrow J/\psi(1S) \pi^+ \pi^-$ and $\psi(2S) \rightarrow \gamma \chi_{c0}$ given in the 1996 edition of RPP [6]. On the other hand, in $p\bar{p}$ collision experiments (*e.g.*, E835 Collaboration [1]), the value of $B(\psi(2S) \rightarrow \gamma \chi_{c0})$ was entered inversely in the determination of $B(\chi_{c0} \rightarrow p\bar{p})$ from a measurement of $\Gamma(\chi_{c0} \rightarrow p\bar{p}) \times B(\chi_{c0} \rightarrow \gamma J/\psi(1S))$, since it was used to derive $B(\chi_{c0} \rightarrow \gamma J/\psi(1S))$. Therefore, a hidden correlation was introduced in RPP when quoting the values of the corresponding unfolded magnitudes for both types of experiments.

The way to avoid these dependencies and correlations is to extract the branching ratios through a fit that uses the truly measured combinations of branching fractions and partial widths. This fit, in fact, should involve decays from the four concerned particles, $\psi(2S)$, χ_{c0} , χ_{c1} , and χ_{c2} , and occasionally some combinations of branching ratios of more than one of them. This is what is done since the 2002 edition [9].

The PDG policy is to quote the results of the collaborations in a manner as close as possible to what appears in their original

publications. However, in order to avoid the problems mentioned above, we had in some cases to work out the values originally measured, using the number of events and detection efficiencies given by the collaborations, or rescaling back the published results. The information was sometimes spread over several articles, and some articles referred to papers still unpublished, which in turn contained the relevant numbers in footnotes.

Even though the experimental collaborations are entitled to extract whatever branching ratios they consider appropriate by using other published results, we would like to encourage them to also quote explicitly in their articles the actual quantities measured, so that they can be used directly in averages and fits of different experimental determinations.

To inform the reader how we computed some of the values used in this edition of RPP, we use footnotes to indicate the branching ratios actually given by the experiments, and the quantities they use to derive them from the true combination of branching ratios actually measured.

None of the branching ratios of the $\chi_{c0,1,2}$ are measured independently of the $\psi(2S)$ radiative decays. We tried to identify those branching ratios which can be correlated in a non-trivial way, and although we cannot preclude the existence of other cases, we are confident that the most relevant correlations have already been removed. Nevertheless, correlations in the errors of different quantities measured by the same experiment have not been taken into account.

FIT INFORMATION

This is an overall fit to 4 total widths, 1 partial width, 24 combinations of partial widths, 8 branching ratios, and 66 combinations of branching ratios. Of the latter, 44 involve decays of more than one particle.

The overall fit uses 190 measurements to determine 44 parameters and has a χ^2 of 268.6 for 146 degrees of freedom

The relatively high χ^2 of the fit, 1.9 per d.o.f., can be traced back to a few specific discrepancies in the data. No rescaling of errors has been applied.

Meson Particle Listings

 $\chi_{c0}(1P)$ $\chi_{c0}(1P)$ WIDTH

VALUE (MeV)	EVTS	DOCUMENT ID	TECN	COMMENT
10.2±0.7 OUR FIT				
10.5±0.8 OUR AVERAGE Error includes scale factor of 1.1.				
10.6±1.9±2.6	5.4k	UEHARA 08	BELL	$\gamma\gamma \rightarrow \chi_{c0} \rightarrow \text{hadrons}$
12.6 ^{+1.5+0.9} _{-1.6-1.1}		ABLIKIM 05	BES2	$\psi(2S) \rightarrow \gamma\chi_{c0}$
8.6 ^{+1.7} _{-1.3±0.1}		ANDREOTTI 03	E835	$\bar{p}p \rightarrow \chi_{c0} \rightarrow \pi^0\pi^0$
9.7±1.0	392	⁵ BAGNASCO 02	E835	$\bar{p}p \rightarrow \chi_{c0} \rightarrow J/\psi\gamma$
16.6 ^{+5.2} _{-3.7±0.1}		AMBROGIANI 99B	E835	$\bar{p}p \rightarrow e^+e^-\gamma$
14.3±2.0±3.0		BAI 98I	BES	$\psi(2S) \rightarrow \gamma\pi^+\pi^-$
13.5±3.3±4.2		GAISER 86	CBAL	$\psi(2S) \rightarrow \gamma X, \gamma\pi^0\pi^0$

⁵ Recalculated by ANDREOTTI 05A.

 $\chi_{c0}(1P)$ DECAY MODES

Mode	Fraction (Γ_i/Γ)	Scale factor/ Confidence level
Hadronic decays		
Γ_1 $2(\pi^+\pi^-)$	(2.23±0.20) %	
Γ_2 $\rho\rho$		
Γ_3 $f_0(980)f_0(980)$	(6.9 ± 2.2) × 10 ⁻⁴	
Γ_4 $\pi^+\pi^-K^+K^-$	(1.79±0.16) %	
Γ_5 $f_0(980)f_0(980)$	(1.7 ^{+1.1} _{-0.9}) × 10 ⁻⁴	
Γ_6 $f_0(980)f_0(2200)$	(8.3 ^{+2.1} _{-2.6}) × 10 ⁻⁴	
Γ_7 $f_0(1370)f_0(1370)$	< 2.8 × 10 ⁻⁴	CL=90%
Γ_8 $f_0(1370)f_0(1500)$	< 1.8 × 10 ⁻⁴	CL=90%
Γ_9 $f_0(1370)f_0(1710)$	(7.0 ^{+3.7} _{-2.4}) × 10 ⁻⁴	
Γ_{10} $f_0(1500)f_0(1370)$	< 1.4 × 10 ⁻⁴	CL=90%
Γ_{11} $f_0(1500)f_0(1500)$	< 5 × 10 ⁻⁵	CL=90%
Γ_{12} $f_0(1500)f_0(1710)$	< 7 × 10 ⁻⁵	CL=90%
Γ_{13} $\rho^0\pi^+\pi^-$	(8.7 ± 2.8) × 10 ⁻³	
Γ_{14} $3(\pi^+\pi^-)$	(1.20±0.18) %	
Γ_{15} $K^+\bar{K}^*(892)^0\pi^- + \text{c.c.}$	(7.2 ± 1.6) × 10 ⁻³	
Γ_{16} $K_1(1270)^+K^- + \text{c.c.} \rightarrow$ $\pi^+\pi^-K^+K^-$	(6.5 ± 2.0) × 10 ⁻³	
Γ_{17} $K_1(1400)^+K^- + \text{c.c.} \rightarrow$ $\pi^+\pi^-K^+K^-$	< 2.8 × 10 ⁻³	CL=90%
Γ_{18} $K^*(892)^0K^*(892)^0$	(1.8 ± 0.6) × 10 ⁻³	
Γ_{19} $K_0^*(1430)^0\bar{K}_0^*(1430)^0 \rightarrow$ $\pi^+\pi^-K^+K^-$	(1.02 ^{+0.38} _{-0.30}) × 10 ⁻³	
Γ_{20} $K_0^*(1430)^0\bar{K}_2^*(1430)^0 + \text{c.c.} \rightarrow$ $\pi^+\pi^-K^+K^-$	(8.3 ^{+2.1} _{-2.5}) × 10 ⁻⁴	
Γ_{21} $\pi\pi$	(7.3 ± 0.6) × 10 ⁻³	
Γ_{22} $\pi^0\eta$		
Γ_{23} $\pi^0\eta'$		
Γ_{24} $\eta\eta$	(2.4 ± 0.4) × 10 ⁻³	
Γ_{25} $\eta\pi^+\pi^-$	< 1.1 × 10 ⁻³	CL=90%
Γ_{26} $\eta\eta'$	< 5 × 10 ⁻⁴	CL=90%
Γ_{27} $\eta'\eta'$	(1.7 ± 0.4) × 10 ⁻³	
Γ_{28} $\omega\omega$	(2.3 ± 0.7) × 10 ⁻³	
Γ_{29} K^+K^-	(5.7 ± 0.6) × 10 ⁻³	
Γ_{30} $K_S^0K_S^0$	(2.82±0.28) × 10 ⁻³	
Γ_{31} $\pi^+\pi^-\eta$	< 2.1 × 10 ⁻⁴	
Γ_{32} $\pi^+\pi^-\eta'$	< 4 × 10 ⁻⁴	
Γ_{33} $\bar{K}^0K^+\pi^- + \text{c.c.}$	< 9.8 × 10 ⁻⁵	
Γ_{34} $K^+K^-\pi^0$	< 6 × 10 ⁻⁵	
Γ_{35} $K^+K^-\eta$	< 2.4 × 10 ⁻⁴	
Γ_{36} $K^+K^-\bar{K}_S^0K_S^0$	(1.5 ± 0.5) × 10 ⁻³	
Γ_{37} $K^+K^-\bar{K}^+K^-$	(2.81±0.30) × 10 ⁻³	
Γ_{38} $K^+K^-\phi$	(1.01±0.26) × 10 ⁻³	
Γ_{39} $K_S^0K_S^0\pi^+\pi^-$	(5.9 ± 1.1) × 10 ⁻³	
Γ_{40} $\phi\phi$	(9.3 ± 2.0) × 10 ⁻⁴	
Γ_{41} $p\bar{p}$	(2.15±0.19) × 10 ⁻⁴	
Γ_{42} $p\bar{p}\pi^0$	(5.8 ± 1.2) × 10 ⁻⁴	
Γ_{43} $p\bar{p}\eta$	(3.8 ± 1.1) × 10 ⁻⁴	
Γ_{44} $\pi^+\pi^-p\bar{p}$	(2.1 ± 0.7) × 10 ⁻³	S=1.4
Γ_{45} $K_S^0K_S^0p\bar{p}$	< 8.8 × 10 ⁻⁴	CL=90%
Γ_{46} $p\bar{p}\pi^-$	(1.17±0.32) × 10 ⁻³	
Γ_{47} $\Lambda\bar{\Lambda}$	(4.4 ± 1.5) × 10 ⁻⁴	
Γ_{48} $\Lambda\bar{\Lambda}\pi^+\pi^-$	< 4.0 × 10 ⁻³	CL=90%
Γ_{49} $K^+\bar{p}\Lambda + \text{c.c.}$	(1.05±0.20) × 10 ⁻³	
Γ_{50} $\Xi^-\bar{\Xi}^+$	< 1.03 × 10 ⁻³	CL=90%

Radiative decays

Γ_{51} $\gamma J/\psi(1S)$	(1.28±0.11) %
Γ_{52} $\gamma\gamma$	(2.35±0.23) × 10 ⁻⁴

 $\chi_{c0}(1P)$ PARTIAL WIDTHS $\chi_{c0}(1P) \Gamma(i)\Gamma(\gamma J/\psi(1S))/\Gamma(\text{total})$

$\Gamma(p\bar{p}) \times \Gamma(\gamma J/\psi(1S))/\Gamma_{\text{total}}$	VALUE (eV)	EVTS	DOCUMENT ID	TECN	COMMENT	$\Gamma_{41}\Gamma_{51}/\Gamma$
28.0± 2.7 OUR FIT						
• • • We do not use the following data for averages, fits, limits, etc. • • •						
26.6± 2.6±1.4	392	^{6,7} BAGNASCO 02	E835		$\bar{p}p \rightarrow \chi_{c0} \rightarrow J/\psi\gamma$	
48.7 ^{+11.3} _{-8.9±2.4}		^{6,7} AMBROGIANI 99B	E835		$\bar{p}p \rightarrow \gamma J/\psi$	

⁶ Calculated by us using $B(J/\psi(1S) \rightarrow e^+e^-) = 0.0593 \pm 0.0010$.

⁷ Values in $(\Gamma(p\bar{p}) \times \Gamma(\gamma J/\psi(1S))/\Gamma_{\text{total}})$ and $(\Gamma(p\bar{p}) \times \Gamma(\gamma J/\psi(1S))/\Gamma_{\text{total}})^2$ are not independent. The latter is used in the fit since it is less correlated to the total width.

 $\chi_{c0}(1P) \Gamma(i)\Gamma(\gamma\gamma)/\Gamma(\text{total})$

$\Gamma(\pi\pi) \times \Gamma(\gamma\gamma)/\Gamma_{\text{total}}$	VALUE (eV)	EVTS	DOCUMENT ID	TECN	COMMENT	$\Gamma_{21}\Gamma_{52}/\Gamma$
17.6±2.0 OUR FIT						
22.7±3.2±3.5	129 ± 18		⁸ NAKAZAWA 05	BELL	$e^+e^- \rightarrow e^+e^-\chi_{c0}$	
$\Gamma(K^+K^-) \times \Gamma(\gamma\gamma)/\Gamma_{\text{total}}$						
13.8±1.5 OUR FIT						
14.3±1.6±2.3	153 ± 17		NAKAZAWA 05	BELL	$e^+e^- \rightarrow e^+e^-\chi_{c0}$	
$\Gamma(K_S^0K_S^0) \times \Gamma(\gamma\gamma)/\Gamma_{\text{total}}$						
6.8 ± 0.8 OUR FIT						
7.00±0.65±0.71	134 ± 12		CHEN 07b	BELL	$e^+e^- \rightarrow e^+e^-\chi_{c0}$	

$\Gamma(2(\pi^+\pi^-)) \times \Gamma(\gamma\gamma)/\Gamma_{\text{total}}$	VALUE (eV)	EVTS	DOCUMENT ID	TECN	COMMENT	$\Gamma_1\Gamma_{52}/\Gamma$
53 ± 4 OUR FIT						
49 ± 10 OUR AVERAGE Error includes scale factor of 1.8.						
44.7± 3.6±4.9	3.6k		UEHARA 08	BELL	$\gamma\gamma \rightarrow \chi_{c0} \rightarrow 2(\pi^+\pi^-)$	
75 ± 13 ± 8			EISENSTEIN 01	CLE2	$e^+e^- \rightarrow e^+e^-\chi_{c0}$	

$\Gamma(\rho\rho) \times \Gamma(\gamma\gamma)/\Gamma_{\text{total}}$	VALUE (eV)	CL%	EVTS	DOCUMENT ID	TECN	COMMENT	$\Gamma_2\Gamma_{52}/\Gamma$
• • • We do not use the following data for averages, fits, limits, etc. • • •							
<12	90	<252		UEHARA 08	BELL	$\gamma\gamma \rightarrow \chi_{c0} \rightarrow 2(\pi^+\pi^-)$	

$\Gamma(\pi^+\pi^-K^+K^-) \times \Gamma(\gamma\gamma)/\Gamma_{\text{total}}$	VALUE (eV)	EVTS	DOCUMENT ID	TECN	COMMENT	$\Gamma_4\Gamma_{52}/\Gamma$
43 ± 4 OUR FIT						
38.8±3.7±4.7	1.7k		UEHARA 08	BELL	$\gamma\gamma \rightarrow \chi_{c0} \rightarrow K^+K^-\pi^+\pi^-$	

$\Gamma(K^+\bar{K}^*(892)^0\pi^- + \text{c.c.}) \times \Gamma(\gamma\gamma)/\Gamma_{\text{total}}$	VALUE (eV)	EVTS	DOCUMENT ID	TECN	COMMENT	$\Gamma_{15}\Gamma_{52}/\Gamma$
17 ± 4 OUR FIT						
16.7±6.1±3.0	495 ± 182		UEHARA 08	BELL	$\gamma\gamma \rightarrow \chi_{c0} \rightarrow K^+K^-\pi^+\pi^-$	

$\Gamma(K^*(892)^0\bar{K}^*(892)^0) \times \Gamma(\gamma\gamma)/\Gamma_{\text{total}}$	VALUE (eV)	CL%	EVTS	DOCUMENT ID	TECN	COMMENT	$\Gamma_{18}\Gamma_{52}/\Gamma$
• • • We do not use the following data for averages, fits, limits, etc. • • •							
<6	90	<148		UEHARA 08	BELL	$\gamma\gamma \rightarrow \chi_{c0} \rightarrow K^+K^-\pi^+\pi^-$	

$\Gamma(K^+K^-K^+K^-) \times \Gamma(\gamma\gamma)/\Gamma_{\text{total}}$	VALUE (eV)	EVTS	DOCUMENT ID	TECN	COMMENT	$\Gamma_{37}\Gamma_{52}/\Gamma$
6.7±0.8 OUR FIT						
7.9±1.3±1.1	215 ± 36		UEHARA 08	BELL	$\gamma\gamma \rightarrow \chi_{c0} \rightarrow 2(K^+K^-)$	

$\Gamma(\phi\phi) \times \Gamma(\gamma\gamma)/\Gamma_{\text{total}}$	VALUE (eV)	EVTS	DOCUMENT ID	TECN	COMMENT	$\Gamma_{40}\Gamma_{52}/\Gamma$
2.2±0.5 OUR FIT						
2.3±0.9±0.4	23.6 ± 9.6		UEHARA 08	BELL	$\gamma\gamma \rightarrow \chi_{c0} \rightarrow 2(K^+K^-)$	

⁸ We have multiplied $\pi^+\pi^-$ measurement by 3/2 to obtain $\pi\pi$.

 $\chi_{c0}(1P)$ BRANCHING RATIOS

HADRONIC DECAYS

$\Gamma(2(\pi^+\pi^-))/\Gamma_{\text{total}}$	VALUE	DOCUMENT ID	Γ_1/Γ
0.0223±0.0020 OUR FIT			

$\Gamma(\rho^0 \pi^+ \pi^-) / \Gamma(2(\pi^+ \pi^-))$					$\Gamma(K_S^0(1430)^0 \bar{K}_S^0(1430)^0 \rightarrow \pi^+ \pi^- K^+ K^-) / \Gamma_{\text{total}}$					
VALUE	DOCUMENT ID	TECN	COMMENT		VALUE (units 10^{-4})	EVTS	DOCUMENT ID	TECN	COMMENT	
0.39 ± 0.14 OUR FIT	TANENBAUM 78	MRK1	$\psi(2S) \rightarrow \gamma \chi_{c0}$	Γ_{13}/Γ_1	10.2 ± 3.8 - 2.9 ± 0.4	83	24	ABLIKIM	05Q BES2 $\psi(2S) \rightarrow \gamma \pi^+ \pi^- K^+ K^-$	
0.39 ± 0.12										
$\Gamma(\rho^0 \pi^+ \pi^-) / \Gamma_{\text{total}}$					$\Gamma(K_S^0(1430)^0 \bar{K}_S^0(1430)^0 + \text{c.c.} \rightarrow \pi^+ \pi^- K^+ K^-) / \Gamma_{\text{total}}$					
VALUE	DOCUMENT ID	TECN	COMMENT		VALUE (units 10^{-4})	EVTS	DOCUMENT ID	TECN	COMMENT	
0.0087 ± 0.0028 OUR FIT				Γ_{13}/Γ	8.3 ± 2.0 - 2.5 ± 0.4	62	25	ABLIKIM	05Q BES2 $\psi(2S) \rightarrow \gamma \pi^+ \pi^- K^+ K^-$	
$\Gamma(f_0(980) \bar{f}_0(980)) / \Gamma_{\text{total}}$					$\Gamma(\pi \pi) / \Gamma_{\text{total}}$					
VALUE (units 10^{-4})	EVTS	DOCUMENT ID	TECN	COMMENT	VALUE (units 10^{-3})	DOCUMENT ID	TECN	COMMENT		
6.9 ± 2.2 ± 0.3	36 ± 9	9	ABLIKIM	04G BES $\psi(2S) \rightarrow \gamma 2\pi^+ 2\pi^-$	7.3 ± 0.6 OUR FIT				Γ_{21}/Γ	
$\Gamma(\pi^+ \pi^- K^+ K^-) / \Gamma_{\text{total}}$					$\Gamma(\eta \eta) / \Gamma_{\text{total}}$					
VALUE (units 10^{-3})	DOCUMENT ID	TECN	COMMENT		VALUE (units 10^{-3})	DOCUMENT ID	TECN	COMMENT		
17.9 ± 1.6 OUR FIT				Γ_{4}/Γ	2.4 ± 0.4 OUR FIT				Γ_{24}/Γ	
$\Gamma(K^+ \bar{K}^*(892)^0 \pi^- + \text{c.c.}) / \Gamma(\pi^+ \pi^- K^+ K^-)$					$\Gamma(\eta \eta) / \Gamma(\pi \pi)$					
VALUE	DOCUMENT ID	TECN	COMMENT		VALUE	DOCUMENT ID	TECN	COMMENT		
0.40 ± 0.11 OUR FIT	TANENBAUM 78	MRK1	$\psi(2S) \rightarrow \gamma \chi_{c0}$	Γ_{15}/Γ_4	0.32 ± 0.07 OUR FIT				Γ_{24}/Γ_{21}	
0.41 ± 0.10					• • • We do not use the following data for averages, fits, limits, etc. • • •					
					0.26 ± 0.09 ± 0.03	26	ANDREOTTI	05C E835 $\bar{p}p \rightarrow 2 \text{ mesons}$		
					0.24 ± 0.10 ± 0.08	26	BAI	03C BES $\psi(2S) \rightarrow 5\gamma$		
$\Gamma(K^+ \bar{K}^*(892)^0 \pi^- + \text{c.c.}) / \Gamma_{\text{total}}$					$\Gamma(\eta \pi^+ \pi^-) / \Gamma_{\text{total}}$					
VALUE	DOCUMENT ID	TECN	COMMENT		VALUE (units 10^{-3})	CL%	DOCUMENT ID	TECN	COMMENT	
0.0072 ± 0.0016 OUR FIT				Γ_{15}/Γ	<1.1	90	27	ABLIKIM	06R BES2 $\psi(2S) \rightarrow \gamma \chi_{c0}$	
$\Gamma(f_0(980) \bar{f}_0(980)) / \Gamma_{\text{total}}$					$\Gamma(\eta \eta') / \Gamma_{\text{total}}$					
VALUE (units 10^{-5})	EVTS	DOCUMENT ID	TECN	COMMENT	VALUE (units 10^{-3})	CL%	DOCUMENT ID	TECN	COMMENT	
17 ± 11 - 9 ± 1	28	10	ABLIKIM	05Q BES2 $\psi(2S) \rightarrow \gamma \pi^+ \pi^- K^+ K^-$	<0.5	90	28	ADAMS	07 CLEO $\psi(2S) \rightarrow \gamma \chi_{c0}$	
$\Gamma(f_0(980) \bar{f}_0(2200)) / \Gamma_{\text{total}}$					$\Gamma(\omega \omega) / \Gamma_{\text{total}}$					
VALUE (units 10^{-4})	EVTS	DOCUMENT ID	TECN	COMMENT	VALUE (units 10^{-3})	EVTS	DOCUMENT ID	TECN	COMMENT	
8.3 ± 2.6 ± 0.4	77	11	ABLIKIM	05Q BES2 $\psi(2S) \rightarrow \gamma \pi^+ \pi^- K^+ K^-$	2.3 ± 0.7 ± 0.1	38.1 ± 9.6	30	ABLIKIM	05N BES2 $\psi(2S) \rightarrow \gamma \chi_{c0} \rightarrow \gamma 6\pi$	
$\Gamma(f_0(1370) \bar{f}_0(1370)) / \Gamma_{\text{total}}$					$\Gamma(K^+ K^-) / \Gamma_{\text{total}}$					
VALUE (units 10^{-4})	CL%	DOCUMENT ID	TECN	COMMENT	VALUE (units 10^{-3})	DOCUMENT ID	TECN	COMMENT		
<2.8	90	12	ABLIKIM	05Q BES2 $\psi(2S) \rightarrow \gamma \pi^+ \pi^- K^+ K^-$	5.7 ± 0.6 OUR FIT				Γ_{29}/Γ	
$\Gamma(f_0(1370) \bar{f}_0(1500)) / \Gamma_{\text{total}}$					$\Gamma(K_S^0 K_S^0) / \Gamma_{\text{total}}$					
VALUE (units 10^{-4})	CL%	DOCUMENT ID	TECN	COMMENT	VALUE (units 10^{-3})	DOCUMENT ID	TECN	COMMENT		
<1.8	90	13	ABLIKIM	05Q BES2 $\psi(2S) \rightarrow \gamma \pi^+ \pi^- K^+ K^-$	2.82 ± 0.28 OUR FIT				Γ_{30}/Γ	
$\Gamma(f_0(1370) \bar{f}_0(1710)) / \Gamma_{\text{total}}$					$\Gamma(K_S^0 K_S^0) / \Gamma(\pi \pi)$					
VALUE (units 10^{-4})	EVTS	DOCUMENT ID	TECN	COMMENT	VALUE	DOCUMENT ID	TECN	COMMENT		
7.0 ± 3.7 ± 0.3	61	14	ABLIKIM	05Q BES2 $\psi(2S) \rightarrow \gamma \pi^+ \pi^- K^+ K^-$	0.38 ± 0.05 OUR FIT				Γ_{30}/Γ_{21}	
					• • • We do not use the following data for averages, fits, limits, etc. • • •					
					0.31 ± 0.05 ± 0.05	31,32	CHEN	07B BELL $e^+ e^- \rightarrow e^+ e^- \chi_{c0}$		
$\Gamma(f_0(1500) \bar{f}_0(1370)) / \Gamma_{\text{total}}$					$\Gamma(K_S^0 K_S^0) / \Gamma(K^+ K^-)$					
VALUE (units 10^{-4})	CL%	DOCUMENT ID	TECN	COMMENT	VALUE	DOCUMENT ID	TECN	COMMENT		
<1.4	90	15	ABLIKIM	05Q BES2 $\psi(2S) \rightarrow \gamma \pi^+ \pi^- K^+ K^-$	0.49 ± 0.08 OUR FIT				Γ_{30}/Γ_{29}	
					• • • We do not use the following data for averages, fits, limits, etc. • • •					
					0.49 ± 0.07 ± 0.08	32,33	CHEN	07B BELL $e^+ e^- \rightarrow e^+ e^- \chi_{c0}$		
$\Gamma(f_0(1500) \bar{f}_0(1500)) / \Gamma_{\text{total}}$					$\Gamma(\pi^+ \pi^- \eta) / \Gamma_{\text{total}}$					
VALUE (units 10^{-4})	CL%	DOCUMENT ID	TECN	COMMENT	VALUE (units 10^{-3})	EVTS	DOCUMENT ID	TECN	COMMENT	
<0.5	90	16	ABLIKIM	05Q BES2 $\psi(2S) \rightarrow \gamma \pi^+ \pi^- K^+ K^-$	<0.21	90	34	ATHAR	07 CLEO $\psi(2S) \rightarrow \gamma h^+ h^- h^0$	
$\Gamma(f_0(1500) \bar{f}_0(1710)) / \Gamma_{\text{total}}$					$\Gamma(\pi^+ \pi^- \eta') / \Gamma_{\text{total}}$					
VALUE (units 10^{-4})	CL%	DOCUMENT ID	TECN	COMMENT	VALUE (units 10^{-3})	EVTS	DOCUMENT ID	TECN	COMMENT	
<0.7	90	17	ABLIKIM	05Q BES2 $\psi(2S) \rightarrow \gamma \pi^+ \pi^- K^+ K^-$	<0.4	90	35	ATHAR	07 CLEO $\psi(2S) \rightarrow \gamma h^+ h^- h^0$	
$\Gamma(3(\pi^+ \pi^-)) / \Gamma_{\text{total}}$					$\Gamma(\bar{K}^0 K^+ \pi^- + \text{c.c.}) / \Gamma_{\text{total}}$					
VALUE (units 10^{-3})	DOCUMENT ID	TECN	COMMENT		VALUE (units 10^{-3})	CL%	EVTS	DOCUMENT ID	TECN	COMMENT
12.0 ± 1.8 OUR EVALUATION	Treating systematic error as correlated.			Γ_{14}/Γ	<0.10	90	36	ATHAR	07 CLEO $\psi(2S) \rightarrow \gamma h^+ h^- h^0$	
12.0 ± 1.7 OUR AVERAGE					• • • We do not use the following data for averages, fits, limits, etc. • • •					
11.7 ± 1.0 ± 1.9	18	BAI	99B BES $\psi(2S) \rightarrow \gamma \chi_{c0}$		<0.7	90	37,38	ABLIKIM	06R BES2 $\psi(2S) \rightarrow \gamma \chi_{c0}$	
12.5 ± 2.9 ± 0.5	18	TANENBAUM 78	MRK1 $\psi(2S) \rightarrow \gamma \chi_{c0}$		<0.7	90	18,38	BAI	99B BES $\psi(2S) \rightarrow \gamma \chi_{c0}$	
$\Gamma(K_1(1270)^+ K^- + \text{c.c.} \rightarrow \pi^+ \pi^- K^+ K^-) / \Gamma_{\text{total}}$					$\Gamma(K^+ K^- \pi^0) / \Gamma_{\text{total}}$					
VALUE (units 10^{-3})	EVTS	DOCUMENT ID	TECN	COMMENT	VALUE (units 10^{-3})	EVTS	DOCUMENT ID	TECN	COMMENT	
6.5 ± 2.9 ± 0.3	68	19	ABLIKIM	05Q BES2 $\psi(2S) \rightarrow \gamma \pi^+ \pi^- K^+ K^-$	<0.06	90	39	ATHAR	07 CLEO $\psi(2S) \rightarrow \gamma h^+ h^- h^0$	
$\Gamma(K_1(1400)^+ K^- + \text{c.c.} \rightarrow \pi^+ \pi^- K^+ K^-) / \Gamma_{\text{total}}$					$\Gamma(K^+ K^- \pi^0) / \Gamma_{\text{total}}$					
VALUE (units 10^{-3})	CL%	DOCUMENT ID	TECN	COMMENT	VALUE (units 10^{-3})	EVTS	DOCUMENT ID	TECN	COMMENT	
<2.8	90	20	ABLIKIM	05Q BES2 $\psi(2S) \rightarrow \gamma \pi^+ \pi^- K^+ K^-$						
$\Gamma(K^*(892)^0 \bar{K}^*(892)^0) / \Gamma_{\text{total}}$					$\Gamma(K^+ K^- \pi^0) / \Gamma_{\text{total}}$					
VALUE (units 10^{-3})	EVTS	DOCUMENT ID	TECN	COMMENT	VALUE (units 10^{-3})	EVTS	DOCUMENT ID	TECN	COMMENT	
1.8 ± 0.6 ± 0.1	64	21	ABLIKIM	05Q BES2 $\psi(2S) \rightarrow \gamma \pi^+ \pi^- K^+ K^-$						
• • • We do not use the following data for averages, fits, limits, etc. • • •										
1.6 ± 0.4 ± 0.1	30.1 ± 5.7	22,23	ABLIKIM	04H BES Repl. by ABLIKIM 05Q						

Meson Particle Listings

 $\chi_{c0}(1P)$ $\Gamma(K^+ K^- \eta)/\Gamma_{\text{total}}$ Γ_{35}/Γ

VALUE (units 10^{-3})	EVTS	DOCUMENT ID	TECN	COMMENT
<0.24	90	40 ATHAR	07 CLEO	$\psi(2S) \rightarrow \gamma h^+ h^- h^0$

 $\Gamma(K^+ K^- K_S^0 K_S^0)/\Gamma_{\text{total}}$ Γ_{36}/Γ

VALUE (units 10^{-3})	EVTS	DOCUMENT ID	TECN	COMMENT
$1.5 \pm 0.5 \pm 0.1$	16.8 ± 4.8	41 ABLIKIM	05o BES2	$\psi(2S) \rightarrow \gamma \chi_{c0}$

 $\Gamma(K^+ K^- K^+ K^-)/\Gamma_{\text{total}}$ Γ_{37}/Γ

VALUE (units 10^{-3})	DOCUMENT ID
2.81 ± 0.30 OUR FIT	

 $\Gamma(K^+ K^- \phi)/\Gamma_{\text{total}}$ Γ_{38}/Γ

VALUE (units 10^{-3})	EVTS	DOCUMENT ID	TECN	COMMENT
$1.01 \pm 0.26 \pm 0.04$	38	42 ABLIKIM	06T BES2	$\psi(2S) \rightarrow \gamma 2K^+ 2K^-$

 $\Gamma(K_S^0 K_S^0 \pi^+ \pi^-)/\Gamma_{\text{total}}$ Γ_{39}/Γ

VALUE (units 10^{-3})	EVTS	DOCUMENT ID	TECN	COMMENT
$5.9 \pm 1.1 \pm 0.3$	152 ± 14	43 ABLIKIM	05o BES2	$\psi(2S) \rightarrow \gamma \chi_{c0}$

 $\Gamma(\phi\phi)/\Gamma_{\text{total}}$ Γ_{40}/Γ

VALUE (units 10^{-3})	DOCUMENT ID
0.93 ± 0.20 OUR FIT	

 $\Gamma(\rho\bar{\rho})/\Gamma_{\text{total}}$ Γ_{41}/Γ

VALUE (units 10^{-4})	DOCUMENT ID
2.15 ± 0.19 OUR FIT	

 $\Gamma(\rho\bar{\rho}\pi^0)/\Gamma_{\text{total}}$ Γ_{42}/Γ

VALUE (units 10^{-3})	DOCUMENT ID	TECN	COMMENT
$0.58 \pm 0.12 \pm 0.02$	44 ATHAR	07 CLEO	$\psi(2S) \rightarrow \gamma h^+ h^- h^0$

 $\Gamma(\rho\bar{\rho}\eta)/\Gamma_{\text{total}}$ Γ_{43}/Γ

VALUE (units 10^{-3})	DOCUMENT ID	TECN	COMMENT
$0.38 \pm 0.11 \pm 0.02$	45 ATHAR	07 CLEO	$\psi(2S) \rightarrow \gamma h^+ h^- h^0$

 $\Gamma(\pi^+ \pi^- \rho\bar{\rho})/\Gamma_{\text{total}}$ Γ_{44}/Γ

VALUE (units 10^{-3})	DOCUMENT ID	TECN	COMMENT
2.1 ± 0.7 OUR EVALUATION	Error includes scale factor of 1.4. Treating systematic error as correlated.		
2.1 ± 1.0 OUR AVERAGE	Error includes scale factor of 2.0.		
$1.57 \pm 0.21 \pm 0.53$	18 BAI	99B BES	$\psi(2S) \rightarrow \gamma \chi_{c0}$
$4.20 \pm 1.15 \pm 0.18$	18 TANENBAUM	78 MRK1	$\psi(2S) \rightarrow \gamma \chi_{c0}$

 $\Gamma(K_S^0 K_S^0 \rho\bar{\rho})/\Gamma_{\text{total}}$ Γ_{45}/Γ

VALUE (units 10^{-4})	CL%	DOCUMENT ID	TECN	COMMENT
<8.8	90	46 ABLIKIM	06D BES2	$\psi(2S) \rightarrow \chi_{c0} \gamma$

 $\Gamma(\rho\bar{\rho}\pi^-)/\Gamma_{\text{total}}$ Γ_{46}/Γ

VALUE (units 10^{-4})	DOCUMENT ID	TECN	COMMENT
$11.7 \pm 3.2 \pm 0.5$	47 ABLIKIM	06I BES2	$\psi(2S) \rightarrow \gamma \rho \pi^- X$

 $\Gamma(\Lambda\bar{\Lambda})/\Gamma_{\text{total}}$ Γ_{47}/Γ

VALUE (units 10^{-4})	EVTS	DOCUMENT ID	TECN	COMMENT
$4.4 \pm 1.2 \pm 0.9$	$15.2^{+4.2}_{-4.0}$	18 BAI	03E BES	$\psi(2S) \rightarrow \gamma \chi_{c0} \rightarrow \gamma \Lambda\bar{\Lambda}$

 $\Gamma(\Lambda\bar{\Lambda}\pi^+ \pi^-)/\Gamma_{\text{total}}$ Γ_{48}/Γ

VALUE (units 10^{-3})	CL%	DOCUMENT ID	TECN	COMMENT
<4.0	90	46 ABLIKIM	06D BES2	$\psi(2S) \rightarrow \chi_{c0} \gamma$

 $\Gamma(K^+ \bar{p} \Lambda + \text{c.c.})/\Gamma_{\text{total}}$ Γ_{49}/Γ

VALUE (units 10^{-3})	DOCUMENT ID	TECN	COMMENT
$1.05 \pm 0.20 \pm 0.04$	48 ATHAR	07 CLEO	$\psi(2S) \rightarrow \gamma h^+ h^- h^0$

 $\Gamma(\Xi^- \bar{\Xi}^+)/\Gamma_{\text{total}}$ Γ_{50}/Γ

VALUE (units 10^{-4})	CL%	DOCUMENT ID	TECN	COMMENT
<10.3	90	46 ABLIKIM	06D BES2	$\psi(2S) \rightarrow \chi_{c0} \gamma$

 $\Gamma(\rho\bar{\rho}) \times \Gamma(\pi\pi)/\Gamma_{\text{total}}^2$ $\Gamma_{41}\Gamma_{21}/\Gamma^2$

VALUE (units 10^{-7})	DOCUMENT ID	TECN	COMMENT
15.8 ± 1.6 OUR FIT			
$15.3 \pm 2.4 \pm 0.8$	49 ANDREOTTI	03 E835	$\bar{p}p \rightarrow \chi_{c0} \rightarrow \pi^0 \pi^0$

 $\Gamma(\rho\bar{\rho}) \times \Gamma(\pi^0 \eta)/\Gamma_{\text{total}}^2$ $\Gamma_{41}\Gamma_{22}/\Gamma^2$

VALUE (units 10^{-7})	DOCUMENT ID	TECN	COMMENT
<0.4	ANDREOTTI	05c E835	$\bar{p}p \rightarrow \pi^0 \eta$

 $\Gamma(\rho\bar{\rho}) \times \Gamma(\pi^0 \eta')/\Gamma_{\text{total}}^2$ $\Gamma_{41}\Gamma_{23}/\Gamma^2$

VALUE (units 10^{-7})	DOCUMENT ID	TECN	COMMENT
<2.5	ANDREOTTI	05c E835	$\bar{p}p \rightarrow \pi^0 \eta$

 $\Gamma(\rho\bar{\rho}) \times \Gamma(\eta\eta)/\Gamma_{\text{total}}^2$ $\Gamma_{41}\Gamma_{24}/\Gamma^2$

VALUE (units 10^{-7})	DOCUMENT ID	TECN	COMMENT
5.1 ± 0.9 OUR FIT			
$4.0 \pm 1.2^{+0.5}_{-0.3}$	ANDREOTTI	05c E835	$\bar{p}p \rightarrow \eta\eta$

 $\Gamma(\rho\bar{\rho}) \times \Gamma(\eta\eta')/\Gamma_{\text{total}}^2$ $\Gamma_{41}\Gamma_{26}/\Gamma^2$

VALUE (units 10^{-6})	DOCUMENT ID	TECN	COMMENT
$2.1^{+2.3}_{-1.5}$	ANDREOTTI	05c E835	$\bar{p}p \rightarrow \pi^0 \eta$

• • • We do not use the following data for averages, fits, limits, etc. • • •

9 ABLIKIM 04G reports $[B(\chi_{c0}(1P) \rightarrow f_0(980) f_0(980))] \times [B(\psi(2S) \rightarrow \gamma \chi_{c0}(1P))]$ = $(6.5 \pm 1.6 \pm 1.3) \times 10^{-5}$. We divide by our best value $B(\psi(2S) \rightarrow \gamma \chi_{c0}(1P)) = (9.4 \pm 0.4) \times 10^{-2}$. Our first error is their experiment's error and our second error is the systematic error from using our best value.

10 ABLIKIM 05q reports $[B(\chi_{c0}(1P) \rightarrow f_0(980) f_0(980))] \times [B(\psi(2S) \rightarrow \gamma \chi_{c0}(1P))]$ = $(1.59 \pm 0.50^{+0.89}_{-0.72}) \times 10^{-5}$. We divide by our best value $B(\psi(2S) \rightarrow \gamma \chi_{c0}(1P)) = (9.4 \pm 0.4) \times 10^{-2}$. Our first error is their experiment's error and our second error is the systematic error from using our best value. One of the $f_0(980)$ mesons is identified via decay to $\pi^+ \pi^-$ while the other via $K^+ K^-$ decay.

11 ABLIKIM 05q reports $(8.42 \pm 1.42^{+1.65}_{-2.29}) \times 10^{-4}$ for $B(\psi(2S) \rightarrow \gamma \chi_{c0}(1P)) = (9.22 \pm 0.11 \pm 0.46) \times 10^{-2}$. We rescale to our best value $B(\psi(2S) \rightarrow \gamma \chi_{c0}(1P)) = (9.4 \pm 0.4) \times 10^{-2}$. Our first error is their experiment's error and our second error is the systematic error from using our best value. The f_0 mesons are identified via $f_0(980) \rightarrow \pi^+ \pi^-$ and $f_0(2200) \rightarrow K^+ K^-$ decays.
--

12 ABLIKIM 05q reports $< 2.9 \times 10^{-4}$ for $B(\psi(2S) \rightarrow \gamma \chi_{c0}(1P)) = (9.22 \pm 0.11 \pm 0.46) \times 10^{-2}$. We rescale to our best value $B(\psi(2S) \rightarrow \gamma \chi_{c0}(1P)) = 0.094$. One of the $f_0(1370)$ mesons is identified via decay to $\pi^+ \pi^-$ while the other via $K^+ K^-$ decay.
--

13 ABLIKIM 05q reports $< 1.8 \times 10^{-4}$ for $B(\psi(2S) \rightarrow \gamma \chi_{c0}(1P)) = (9.22 \pm 0.11 \pm 0.46) \times 10^{-2}$. We rescale to our best value $B(\psi(2S) \rightarrow \gamma \chi_{c0}(1P)) = 0.094$. The f_0 mesons are identified via $f_0(1370) \rightarrow \pi^+ \pi^-$ and $f_0(1500) \rightarrow K^+ K^-$ decays.
--

14 ABLIKIM 05q reports $(7.12 \pm 1.85^{+3.28}_{-1.68}) \times 10^{-4}$ for $B(\psi(2S) \rightarrow \gamma \chi_{c0}(1P)) = (9.22 \pm 0.11 \pm 0.46) \times 10^{-2}$. We rescale to our best value $B(\psi(2S) \rightarrow \gamma \chi_{c0}(1P)) = (9.4 \pm 0.4) \times 10^{-2}$. Our first error is their experiment's error and our second error is the systematic error from using our best value. The f_0 mesons are identified via $f_0(1370) \rightarrow \pi^+ \pi^-$ and $f_0(1710) \rightarrow K^+ K^-$ decays.

15 ABLIKIM 05q reports $< 1.4 \times 10^{-4}$ for $B(\psi(2S) \rightarrow \gamma \chi_{c0}(1P)) = (9.22 \pm 0.11 \pm 0.46) \times 10^{-2}$. We rescale to our best value $B(\psi(2S) \rightarrow \gamma \chi_{c0}(1P)) = 0.094$. The f_0 mesons are identified via $f_0(1500) \rightarrow \pi^+ \pi^-$ and $f_0(1370) \rightarrow K^+ K^-$ decays.
--

16 ABLIKIM 05q reports $< 0.55 \times 10^{-4}$ for $B(\psi(2S) \rightarrow \gamma \chi_{c0}(1P)) = (9.22 \pm 0.11 \pm 0.46) \times 10^{-2}$. We rescale to our best value $B(\psi(2S) \rightarrow \gamma \chi_{c0}(1P)) = 0.094$. One of the $f_0(1500)$ is identified via decay to $\pi^+ \pi^-$ while the other via $K^+ K^-$ decay.
--

17 ABLIKIM 05q reports $< 0.73 \times 10^{-4}$ for $B(\psi(2S) \rightarrow \gamma \chi_{c0}(1P)) = (9.22 \pm 0.11 \pm 0.46) \times 10^{-2}$. We rescale to our best value $B(\psi(2S) \rightarrow \gamma \chi_{c0}(1P)) = 0.094$. The f_0 mesons are identified via $f_0(1500) \rightarrow \pi^+ \pi^-$ and $f_0(1710) \rightarrow K^+ K^-$ decays.

18 Rescaled by us using $B(\psi(2S) \rightarrow \gamma \chi_{c0}) = (9.4 \pm 0.4)\%$ and $B(\psi(2S) \rightarrow J/\psi(1S) \pi^+ \pi^-) = (32.6 \pm 0.5)\%$.
--

19 ABLIKIM 05q reports $(6.66 \pm 1.31^{+1.60}_{-1.51}) \times 10^{-3}$ for $B(\psi(2S) \rightarrow \gamma \chi_{c0}(1P)) = (9.22 \pm 0.11 \pm 0.46) \times 10^{-2}$. We rescale to our best value $B(\psi(2S) \rightarrow \gamma \chi_{c0}(1P)) = (9.4 \pm 0.4) \times 10^{-2}$. Our first error is their experiment's error and our second error is the systematic error from using our best value. The measurement assumes $B(K_1(1270) \rightarrow K \rho(770)) = 42 \pm 6\%$.

20 ABLIKIM 05q reports $< 2.85 \times 10^{-3}$ for $B(\psi(2S) \rightarrow \gamma \chi_{c0}(1P)) = (9.22 \pm 0.11 \pm 0.46) \times 10^{-2}$. We rescale to our best value $B(\psi(2S) \rightarrow \gamma \chi_{c0}(1P)) = 0.094$. The measurement assumes $B(K_1(1400) \rightarrow K^*(892) \pi) = 94 \pm 6\%$.
--

21 ABLIKIM 05q reports $[B(\chi_{c0}(1P) \rightarrow K^*(892)^0 \bar{K}^*(892)^0)] \times [B(\psi(2S) \rightarrow \gamma \chi_{c0}(1P))]$ = $(0.168 \pm 0.035^{+0.047}_{-0.040}) \times 10^{-3}$. We divide by our best value $B(\psi(2S) \rightarrow \gamma \chi_{c0}(1P)) = (9.4 \pm 0.4) \times 10^{-2}$. Our first error is their experiment's error and our second error is the systematic error from using our best value.
--

22 Assumes $B(K^*(892)^0 \rightarrow K^- \pi^+) = 2/3$.
--

23 ABLIKIM 04H reports $[B(\chi_{c0}(1P) \rightarrow K^*(892)^0 \bar{K}^*(892)^0)] \times [B(\psi(2S) \rightarrow \gamma \chi_{c0}(1P))]$ = $(1.53 \pm 0.29 \pm 0.26) \times 10^{-4}$. We divide by our best value $B(\psi(2S) \rightarrow \gamma \chi_{c0}(1P)) = (9.4 \pm 0.4) \times 10^{-2}$. Our first error is their experiment's error and our second error is the systematic error from using our best value.

24 ABLIKIM 05q reports $(10.44 \pm 2.37^{+3.05}_{-1.90}) \times 10^{-4}$ for $B(\psi(2S) \rightarrow \gamma \chi_{c0}(1P)) = (9.22 \pm 0.11 \pm 0.46) \times 10^{-2}$. We rescale to our best value $B(\psi(2S) \rightarrow \gamma \chi_{c0}(1P)) = (9.4 \pm 0.4) \times 10^{-2}$. Our first error is their experiment's error and our second error is the systematic error from using our best value.
--

25 ABLIKIM 05q reports $(8.49 \pm 1.66^{+1.32}_{-1.99}) \times 10^{-4}$ for $B(\psi(2S) \rightarrow \gamma \chi_{c0}(1P)) = (9.22 \pm 0.11 \pm 0.46) \times 10^{-2}$. We rescale to our best value $B(\psi(2S) \rightarrow \gamma \chi_{c0}(1P)) = (9.4 \pm 0.4) \times 10^{-2}$. Our first error is their experiment's error and our second error is the systematic error from using our best value.

26 We have multiplied $\pi^0 \pi^0$ measurement by 3 to obtain $\pi\pi$.

27 ABLIKIM 06r reports $< 1.1 \times 10^{-3}$ for $B(\psi(2S) \rightarrow \gamma \chi_{c0}(1P)) = (9.2 \pm 0.4) \times 10^{-2}$. We rescale to our best value $B(\psi(2S) \rightarrow \gamma \chi_{c0}(1P)) = 0.094$.

28 ADAMS 07 reports $< 0.5 \times 10^{-3}$ for $B(\psi(2S) \rightarrow \gamma \chi_{c0}(1P)) = 0.0922 \pm 0.0011 \pm 0.0046$. We rescale to our best value $B(\psi(2S) \rightarrow \gamma \chi_{c0}(1P)) = 0.094$.
--

29 ADAMS 07 reports $(1.7 \pm 0.4 \pm 0.2) \times 10^{-3}$ for $B(\psi(2S) \rightarrow \gamma \chi_{c0}(1P)) = 0.0922 \pm 0.0011 \pm 0.0046$. We rescale to our best value $B(\psi(2S) \rightarrow \gamma \chi_{c0}(1P)) = (9.4 \pm 0.4) \times 10^{-2}$. Our first error is their experiment's error and our second error is the systematic error from using our best value.

- ³⁰ ABLIKIM 05N reports $[B(\chi_{c0}(1P) \rightarrow \omega\omega)] \times [B(\psi(2S) \rightarrow \gamma\chi_{c0}(1P))] = (0.212 \pm 0.053 \pm 0.037) \times 10^{-3}$. We divide by our best value $B(\psi(2S) \rightarrow \gamma\chi_{c0}(1P)) = (9.4 \pm 0.4) \times 10^{-2}$. Our first error is their experiment's error and our second error is the systematic error from using our best value.
- ³¹ Using $\Gamma(\pi\pi) \times \Gamma(\gamma\gamma)/\Gamma_{\text{total}}$ from the $\pi^+\pi^-$ measurement of NAKAZAWA 05 rescaled by 3/2 to convert to $\pi\pi$.
- ³² Not independent from other measurements.
- ³³ Using $\Gamma(K^+K^-) \times \Gamma(\gamma\gamma)/\Gamma_{\text{total}}$ from NAKAZAWA 05.
- ³⁴ ATHAR 07 reports $< 0.21 \times 10^{-3}$ for $B(\psi(2S) \rightarrow \gamma\chi_{c0}(1P)) = (9.22 \pm 0.11 \pm 0.46) \times 10^{-2}$. We rescale to our best value $B(\psi(2S) \rightarrow \gamma\chi_{c0}(1P)) = 0.094$.
- ³⁵ ATHAR 07 reports $< 0.38 \times 10^{-3}$ for $B(\psi(2S) \rightarrow \gamma\chi_{c0}(1P)) = (9.22 \pm 0.11 \pm 0.46) \times 10^{-2}$. We rescale to our best value $B(\psi(2S) \rightarrow \gamma\chi_{c0}(1P)) = 0.094$.
- ³⁶ ATHAR 07 reports $< 0.10 \times 10^{-3}$ for $B(\psi(2S) \rightarrow \gamma\chi_{c0}(1P)) = (9.22 \pm 0.11 \pm 0.46) \times 10^{-2}$. We rescale to our best value $B(\psi(2S) \rightarrow \gamma\chi_{c0}(1P)) = 0.094$.
- ³⁷ ABLIKIM 06R reports $< 0.70 \times 10^{-3}$ for $B(\psi(2S) \rightarrow \gamma\chi_{c0}(1P)) = (9.2 \pm 0.4) \times 10^{-2}$. We rescale to our best value $B(\psi(2S) \rightarrow \gamma\chi_{c0}(1P)) = 0.094$.
- ³⁸ We have multiplied the $K_S^0 K^+\pi^-$ measurement by a factor of 2 to convert to $K^0 K^+\pi^-$.
- ³⁹ ATHAR 07 reports $< 0.06 \times 10^{-3}$ for $B(\psi(2S) \rightarrow \gamma\chi_{c0}(1P)) = (9.22 \pm 0.11 \pm 0.46) \times 10^{-2}$. We rescale to our best value $B(\psi(2S) \rightarrow \gamma\chi_{c0}(1P)) = 0.094$.
- ⁴⁰ ATHAR 07 reports $< 0.24 \times 10^{-3}$ for $B(\psi(2S) \rightarrow \gamma\chi_{c0}(1P)) = (9.22 \pm 0.11 \pm 0.46) \times 10^{-2}$. We rescale to our best value $B(\psi(2S) \rightarrow \gamma\chi_{c0}(1P)) = 0.094$.
- ⁴¹ ABLIKIM 05o reports $[B(\chi_{c0}(1P) \rightarrow K^+K^-K_S^0K_S^0)] \times [B(\psi(2S) \rightarrow \gamma\chi_{c0}(1P))] = (0.138 \pm 0.039 \pm 0.025) \times 10^{-3}$. We divide by our best value $B(\psi(2S) \rightarrow \gamma\chi_{c0}(1P)) = (9.4 \pm 0.4) \times 10^{-2}$. Our first error is their experiment's error and our second error is the systematic error from using our best value.
- ⁴² ABLIKIM 06T reports $(1.03 \pm 0.22 \pm 0.15) \times 10^{-3}$ for $B(\psi(2S) \rightarrow \gamma\chi_{c0}(1P)) = (9.2 \pm 0.4) \times 10^{-2}$. We rescale to our best value $B(\psi(2S) \rightarrow \gamma\chi_{c0}(1P)) = (9.4 \pm 0.4) \times 10^{-2}$. Our first error is their experiment's error and our second error is the systematic error from using our best value.
- ⁴³ ABLIKIM 05o reports $[B(\chi_{c0}(1P) \rightarrow K_S^0K_S^0\pi^+\pi^-)] \times [B(\psi(2S) \rightarrow \gamma\chi_{c0}(1P))] = (0.558 \pm 0.051 \pm 0.089) \times 10^{-3}$. We divide by our best value $B(\psi(2S) \rightarrow \gamma\chi_{c0}(1P)) = (9.4 \pm 0.4) \times 10^{-2}$. Our first error is their experiment's error and our second error is the systematic error from using our best value.
- ⁴⁴ ATHAR 07 reports $(0.59 \pm 0.10 \pm 0.08) \times 10^{-3}$ for $B(\psi(2S) \rightarrow \gamma\chi_{c0}(1P)) = (9.22 \pm 0.11 \pm 0.46) \times 10^{-2}$. We rescale to our best value $B(\psi(2S) \rightarrow \gamma\chi_{c0}(1P)) = (9.4 \pm 0.4) \times 10^{-2}$. Our first error is their experiment's error and our second error is the systematic error from using our best value.
- ⁴⁵ ATHAR 07 reports $(0.39 \pm 0.11 \pm 0.04) \times 10^{-3}$ for $B(\psi(2S) \rightarrow \gamma\chi_{c0}(1P)) = (9.22 \pm 0.11 \pm 0.46) \times 10^{-2}$. We rescale to our best value $B(\psi(2S) \rightarrow \gamma\chi_{c0}(1P)) = (9.4 \pm 0.4) \times 10^{-2}$. Our first error is their experiment's error and our second error is the systematic error from using our best value.
- ⁴⁶ Using $B(\psi(2S) \rightarrow \chi_{c0}\gamma) = (9.2 \pm 0.5)\%$
- ⁴⁷ ABLIKIM 06i reports $[B(\chi_{c0}(1P) \rightarrow p\bar{p}\pi^-)] \times [B(\psi(2S) \rightarrow \gamma\chi_{c0}(1P))] = (1.10 \pm 0.24 \pm 0.18) \times 10^{-4}$. We divide by our best value $B(\psi(2S) \rightarrow \gamma\chi_{c0}(1P)) = (9.4 \pm 0.4) \times 10^{-2}$. Our first error is their experiment's error and our second error is the systematic error from using our best value.
- ⁴⁸ ATHAR 07 reports $(1.07 \pm 0.17 \pm 0.12) \times 10^{-3}$ for $B(\psi(2S) \rightarrow \gamma\chi_{c0}(1P)) = (9.22 \pm 0.11 \pm 0.46) \times 10^{-2}$. We rescale to our best value $B(\psi(2S) \rightarrow \gamma\chi_{c0}(1P)) = (9.4 \pm 0.4) \times 10^{-2}$. Our first error is their experiment's error and our second error is the systematic error from using our best value.
- ⁴⁹ We have multiplied $B(\rho\bar{\rho})\cdot B(\pi^0\pi^0)$ measurement by 3 to obtain $B(\rho\bar{\rho})\cdot B(\pi\pi)$.

RADIATIVE DECAYS

$\Gamma(\gamma J/\psi(1S))/\Gamma_{\text{total}} \quad \Gamma_{51}/\Gamma$

VALUE (units 10^{-4})	DOCUMENT ID	TECN	COMMENT
128 ± 11 OUR FIT			
••• We do not use the following data for averages, fits, limits, etc. •••			
200 ± 20 ± 20	⁵⁰ ADAM	05A	CLEO $e^+e^- \rightarrow \psi(2S) \rightarrow \gamma\chi_{c0}$

$\Gamma(\gamma\gamma)/\Gamma_{\text{total}} \quad \Gamma_{52}/\Gamma$

VALUE (units 10^{-4})	CL%	DOCUMENT ID	TECN	COMMENT
2.35 ± 0.23 OUR FIT				
••• We do not use the following data for averages, fits, limits, etc. •••				
< 8	90	⁵¹ WICHT	08	BELL $B^\pm \rightarrow K^\pm \gamma\gamma$

$\Gamma(\gamma\gamma)/\Gamma(\gamma J/\psi(1S)) \quad \Gamma_{52}/\Gamma_{51}$

VALUE (units 10^{-2})	DOCUMENT ID	TECN	COMMENT
1.83 ± 0.25 OUR FIT			
2.0 ± 0.4 OUR AVERAGE			
2.2 ± 0.4 ± 0.1	⁵² ANDREOTTI	04	E835 $p\bar{p} \rightarrow \chi_{c0} \rightarrow \gamma\gamma$
1.45 ± 0.74	⁵³ AMBROGIANI	00B	E835 $\bar{p}p \rightarrow \chi_{c2} \rightarrow \gamma\gamma, \gamma J/\psi$

$\Gamma(\rho\bar{\rho}) \times \Gamma(\gamma J/\psi(1S))/\Gamma_{\text{total}}^2 \quad \Gamma_{41}\Gamma_{51}/\Gamma^2$

VALUE (units 10^{-7})	EVTS	DOCUMENT ID	TECN	COMMENT
27.5 ± 1.9 OUR FIT				
28.2 ± 2.1 OUR AVERAGE				
28.0 ± 1.9 ± 1.3	392	^{53,54,55} BAGNASCO	02	E835 $\bar{p}p \rightarrow \chi_{c0} \rightarrow J/\psi\gamma$
29.3 ± 5.7 ± 1.5	89	^{53,54} AMBROGIANI	99B	$\bar{p}p \rightarrow \chi_{c0} \rightarrow J/\psi\gamma$

$\Gamma(\rho\bar{\rho}) \times \Gamma(\gamma\gamma)/\Gamma_{\text{total}}^2 \quad \Gamma_{41}\Gamma_{52}/\Gamma^2$

VALUE (units 10^{-8})	DOCUMENT ID	TECN	COMMENT
5.0 ± 0.7 OUR FIT			
••• We do not use the following data for averages, fits, limits, etc. •••			
6.52 ± 1.18 ± 0.48	⁵² ANDREOTTI	04	E835 $p\bar{p} \rightarrow \chi_{c0} \rightarrow \gamma\gamma$

- ⁵⁰ Uses $B(\psi(2S) \rightarrow \gamma\chi_{c0}) \rightarrow \gamma\gamma J/\psi$ from ADAM 05A and $B(\psi(2S) \rightarrow \gamma\chi_{c0})$ from ATHAR 04.
- ⁵¹ WICHT 08 reports $[B(\chi_{c0}(1P) \rightarrow \gamma\gamma)] \times [B(B^+ \rightarrow \chi_{c0}(1P) K^+)] < 0.11 \times 10^{-6}$. We divide by our best value $B(B^+ \rightarrow \chi_{c0}(1P) K^+) = 0.000140$.
- ⁵² The values of $B(\rho\bar{\rho})B(\gamma\gamma)$ and $B(\gamma\gamma)B(\gamma J/\psi)$ measured by ANDREOTTI 04 are not independent. The latter is used in the fit because of smaller systematics.
- ⁵³ Calculated by us using $B(J/\psi(1S) \rightarrow e^+e^-) = 0.0593 \pm 0.0010$.
- ⁵⁴ Values in $(\Gamma(\rho\bar{\rho}) \times \Gamma(\gamma J/\psi(1S)))/\Gamma_{\text{total}}$ and $(\Gamma(\rho\bar{\rho}) \times \Gamma(\gamma J/\psi(1S)))/\Gamma_{\text{total}}^2$ are not independent. The latter is used in the fit since it is less correlated to the total width.
- ⁵⁵ Recalculated by ANDREOTTI 05A.

$\chi_{c0}(1P)$ CROSS-PARTICLE BRANCHING RATIOS

$B(\chi_{c0}(1P) \rightarrow \rho\bar{\rho}) \times B(\psi(2S) \rightarrow \gamma\chi_{c0}(1P))$

VALUE (units 10^{-6})	EVTS	DOCUMENT ID	TECN	COMMENT
20.1 ± 2.1 OUR FIT				
23.6 ± 3.7 ± 3.4	89.5 ± 14	BAI	04F	BES $\psi(2S) \rightarrow \gamma\chi_{c0}(1P) \rightarrow \gamma\bar{p}p$

$B(\chi_{c0}(1P) \rightarrow \rho\bar{\rho}) \times \frac{\Gamma(\psi(2S) \rightarrow \gamma\chi_{c0}(1P))}{\Gamma(\psi(2S) \rightarrow J/\psi(1S)\pi^+\pi^-)}$

VALUE (units 10^{-5})	DOCUMENT ID	TECN	COMMENT
6.2 ± 0.8 OUR FIT			
4.6 ± 1.9	⁵⁶ BAI	98i	BES $\psi(2S) \rightarrow \gamma\chi_{c0} \rightarrow \gamma\bar{p}p$

- ⁵⁶ Calculated by us. The value for $B(\chi_{c0} \rightarrow \rho\bar{\rho})$ reported in BAI 98i is derived using $B(\psi(2S) \rightarrow \gamma\chi_{c0}) = (9.3 \pm 0.8)\%$ and $B(\psi(2S) \rightarrow J/\psi(1S)\pi^+\pi^-) = (32.4 \pm 2.6)\%$ [BAI 98d].

$B(\chi_{c0}(1P) \rightarrow \gamma J/\psi(1S)) \times B(\psi(2S) \rightarrow \gamma\chi_{c0}(1P))$

VALUE (units 10^{-2})	EVTS	DOCUMENT ID	TECN	COMMENT
0.120 ± 0.010 OUR FIT				
0.073 ± 0.018 OUR AVERAGE				
0.069 ± 0.018	⁵⁷ OREGLIA	82	CBAL	$\psi(2S) \rightarrow \gamma\chi_{c0}$
0.4 ± 0.3	⁵⁸ BRANDELNIK	79B	DASP	$\psi(2S) \rightarrow \gamma\chi_{c0}$
0.16 ± 0.11	⁵⁸ BARTEL	78B	CNTR	$\psi(2S) \rightarrow \gamma\chi_{c0}$
3.3 ± 1.7	⁵⁹ BIDDICK	77	CNTR	$e^+e^- \rightarrow \gamma\chi$

- We do not use the following data for averages, fits, limits, etc. •••
- 0.18 ± 0.01 ± 0.02
- 172
- ⁶⁰ ADAM
- 05A
- CLEO
- $\psi(2S) \rightarrow J/\psi\gamma\gamma$
- ⁵⁷ Recalculated by us using $B(J/\psi(1S) \rightarrow e^+e^-) = 0.1181 \pm 0.0020$.
- ⁵⁸ Recalculated by us using $B(J/\psi(1S) \rightarrow \mu^+\mu^-) = 0.0588 \pm 0.0010$.
- ⁵⁹ Assumes isotropic gamma distribution.
- ⁶⁰ Not independent from other values reported by ADAM 05A.

$B(\chi_{c0}(1P) \rightarrow \gamma J/\psi) \times \frac{\Gamma(\psi(2S) \rightarrow \gamma\chi_{c0}(1P))}{\Gamma(\psi(2S) \rightarrow J/\psi(1S)\text{anything})}$

VALUE (units 10^{-2})	EVTS	DOCUMENT ID	TECN	COMMENT
0.2091 ± 0.0032 OUR FIT				
0.31 ± 0.02 ± 0.03	172	ADAM	05A	CLEO $\psi(2S) \rightarrow J/\psi\gamma\gamma$

$B(\chi_{c0}(1P) \rightarrow \gamma J/\psi) \times \frac{\Gamma(\psi(2S) \rightarrow \gamma\chi_{c0}(1P))}{\Gamma(\psi(2S) \rightarrow J/\psi(1S)\pi^+\pi^-)}$

VALUE (units 10^{-2})	EVTS	DOCUMENT ID	TECN	COMMENT
0.368 ± 0.032 OUR FIT				
••• We do not use the following data for averages, fits, limits, etc. •••				
0.55 ± 0.04 ± 0.06	172	⁶¹ ADAM	05A	CLEO $\psi(2S) \rightarrow J/\psi\gamma\gamma$

- ⁶¹ Not independent from other values reported by ADAM 05A.

$B(\chi_{c0}(1P) \rightarrow \gamma\gamma) \times B(\psi(2S) \rightarrow \gamma\chi_{c0}(1P))$

VALUE (units 10^{-5})	DOCUMENT ID	TECN	COMMENT
2.20 ± 0.26 OUR FIT			
3.7 ± 1.8 ± 1.0	LEE	85	CBAL $\psi(2S) \rightarrow \gamma\chi_{c0}$

$B(\chi_{c0}(1P) \rightarrow \pi\pi) \times \frac{\Gamma(\psi(2S) \rightarrow \gamma\chi_{c0}(1P))}{\Gamma(\psi(2S) \rightarrow J/\psi(1S)\pi^+\pi^-)}$

VALUE (units 10^{-4})	EVTS	DOCUMENT ID	TECN	COMMENT
21.1 ± 1.7 OUR FIT				
20.7 ± 1.7 OUR AVERAGE				
23.9 ± 2.7 ± 4.1	97 ± 11	⁶² BAI	03C	BES $\psi(2S) \rightarrow \gamma\chi_{c0} \rightarrow \gamma\pi^0\pi^0$
20.2 ± 1.1 ± 1.5	720 ± 32	⁶³ BAI	98i	BES $\psi(2S) \rightarrow \gamma\chi_{c0} \rightarrow \gamma\pi^+\pi^-$

- ⁶² We have multiplied $\pi^0\pi^0$ measurement by 3 to obtain $\pi\pi$.
- ⁶³ Calculated by us. The value for $B(\chi_{c0} \rightarrow \pi^+\pi^-)$ reported in BAI 98i is derived using $B(\psi' \rightarrow \gamma\chi_{c0}) = (9.3 \pm 0.8)\%$ and $B(\psi' \rightarrow J/\psi\pi^+\pi^-) = (32.4 \pm 2.6)\%$ [BAI 98d]. We have multiplied $\pi^+\pi^-$ measurement by 3/2 to obtain $\pi\pi$.

Meson Particle Listings

 $\chi_{c0}(1P)$

$$B(\chi_{c0}(1P) \rightarrow \eta\eta) \times B(\psi(2S) \rightarrow \gamma\chi_{c0}(1P))$$

VALUE (units 10^{-4})	EVTS	DOCUMENT ID	TECN	COMMENT
2.2 ± 0.4 OUR FIT				
2.86 ± 0.46 ± 0.37	48	64 ADAMS	07 CLEO	$\psi(2S) \rightarrow \gamma\chi_{c0}$

⁶⁴ Calculated by us. The value of $B(\chi_{c0}(1P) \rightarrow \eta\eta)$ reported by ADAMS 07 was derived using $B(\psi(2S) \rightarrow \gamma\chi_{c0}(1P)) = (9.22 \pm 0.11 \pm 0.46)\%$ (ATHAR 04).

$$B(\chi_{c0}(1P) \rightarrow \eta\eta) \times \frac{\Gamma(\psi(2S) \rightarrow \gamma\chi_{c0}(1P))}{\Gamma(\psi(2S) \rightarrow J/\psi(1S)\pi^+\pi^-)}$$

VALUE (units 10^{-3})	DOCUMENT ID	TECN	COMMENT
0.68 ± 0.12 OUR FIT			
0.578 ± 0.241 ± 0.158	BAI	03c BES	$\psi(2S) \rightarrow \gamma\eta\eta$

$$B(\chi_{c0}(1P) \rightarrow K^+K^-) \times \frac{\Gamma(\psi(2S) \rightarrow \gamma\chi_{c0}(1P))}{\Gamma(\psi(2S) \rightarrow J/\psi(1S)\pi^+\pi^-)}$$

VALUE (units 10^{-3})	EVTS	DOCUMENT ID	TECN	COMMENT
1.65 ± 0.17 OUR FIT				
1.63 ± 0.10 ± 0.15	774 ± 38	65 BAI	98i BES	$\psi(2S) \rightarrow \gamma K^+K^-$

⁶⁵ Calculated by us. The value for $B(\chi_{c0} \rightarrow K^+K^-)$ reported by BAI 98i is derived using $B(\psi(2S) \rightarrow \gamma\chi_{c0}) = (9.3 \pm 0.8)\%$ and $B(\psi(2S) \rightarrow J/\psi\pi^+\pi^-) = (32.4 \pm 2.6)\%$ [BAI 98d].

$$B(\chi_{c0}(1P) \rightarrow K_S^0 K_S^0) \times B(\psi(2S) \rightarrow \gamma\chi_{c0}(1P))$$

VALUE (units 10^{-4})	EVTS	DOCUMENT ID	TECN	COMMENT
2.64 ± 0.25 OUR FIT				
3.02 ± 0.19 ± 0.33	322	ABLIKIM	05o BES2	$\psi(2S) \rightarrow \gamma K_S^0 K_S^0$

$$B(\chi_{c0}(1P) \rightarrow K_S^0 K_S^0) \times \frac{\Gamma(\psi(2S) \rightarrow \gamma\chi_{c0}(1P))}{\Gamma(\psi(2S) \rightarrow J/\psi(1S)\pi^+\pi^-)}$$

VALUE (units 10^{-4})	DOCUMENT ID	TECN	COMMENT
8.1 ± 0.8 OUR FIT			
5.6 ± 0.8 ± 1.3	66 BAI	99b BES	$\psi(2S) \rightarrow \gamma K_S^0 K_S^0$

⁶⁶ Calculated by us. The value of $B(\chi_{c0} \rightarrow K_S^0 K_S^0)$ reported by BAI 99b was derived using $B(\psi(2S) \rightarrow \gamma\chi_{c0}(1P)) = (9.3 \pm 0.8)\%$ and $B(\psi(2S) \rightarrow J/\psi\pi^+\pi^-) = (32.4 \pm 2.6)\%$ [BAI 98d].

$$B(\chi_{c0}(1P) \rightarrow 2(\pi^+\pi^-)) \times \frac{\Gamma(\psi(2S) \rightarrow \gamma\chi_{c0}(1P))}{\Gamma(\psi(2S) \rightarrow J/\psi(1S)\pi^+\pi^-)}$$

VALUE (units 10^{-3})	DOCUMENT ID	TECN	COMMENT
6.4 ± 0.6 OUR FIT			
6.9 ± 2.4 OUR AVERAGE	Error includes scale factor of 3.8.		
4.4 ± 0.1 ± 0.9	67 BAI	99b BES	$\psi(2S) \rightarrow \gamma\chi_{c0}$
9.3 ± 0.9	68 TANENBAUM	78 MRK1	$\psi(2S) \rightarrow \gamma\chi_{c0}$

⁶⁷ Calculated by us. The value for $B(\chi_{c0} \rightarrow 2\pi^+\pi^-)$ reported in BAI 99b is derived using $B(\psi(2S) \rightarrow \gamma\chi_{c0}) = (9.3 \pm 0.8)\%$ and $B(\psi(2S) \rightarrow J/\psi(1S)\pi^+\pi^-) = (32.4 \pm 2.6)\%$ [BAI 98d].

⁶⁸ The value $B(\psi(1S) \rightarrow \gamma\chi_{c0}) \times B(\chi_{c0} \rightarrow 2\pi^+\pi^-)$ reported in TANENBAUM 78 is derived using $B(\psi(2S) \rightarrow J/\psi(1S)\pi^+\pi^-) \times B(J/\psi(1S) \rightarrow \ell^+\ell^-) = (4.6 \pm 0.7)\%$. Calculated by us using $B(J/\psi(1S) \rightarrow \ell^+\ell^-) = 0.1181 \pm 0.0020$.

$$B(\chi_{c0}(1P) \rightarrow K^+K^-\pi^+\pi^-) \times B(\psi(2S) \rightarrow \gamma\chi_{c0}(1P))$$

VALUE (units 10^{-3})	DOCUMENT ID	TECN	COMMENT
1.68 ± 0.13 OUR FIT			
1.64 ± 0.05 ± 0.2	ABLIKIM	05q BES2	$\psi(2S) \rightarrow \gamma\chi_{c0}$

$$B(\chi_{c0}(1P) \rightarrow K^+K^-\pi^+\pi^-) \times \frac{\Gamma(\psi(2S) \rightarrow \gamma\chi_{c0}(1P))}{\Gamma(\psi(2S) \rightarrow J/\psi(1S)\pi^+\pi^-)}$$

VALUE (units 10^{-3})	DOCUMENT ID	TECN	COMMENT
5.1 ± 0.4 OUR FIT			
5.8 ± 1.6 OUR AVERAGE	Error includes scale factor of 2.3.		
4.22 ± 0.20 ± 0.97	BAI	99b BES	$\psi(2S) \rightarrow \gamma\chi_{c0}$
7.4 ± 1.0	69 TANENBAUM	78 MRK1	$\psi(2S) \rightarrow \gamma\chi_{c0}$

⁶⁹ The reported value is derived using $B(\psi(2S) \rightarrow \pi^+\pi^-J/\psi) \times B(J/\psi \rightarrow \ell^+\ell^-) = (4.6 \pm 0.7)\%$. Calculated by us using $B(J/\psi \rightarrow \ell^+\ell^-) = 0.1181 \pm 0.0020$.

$$B(\chi_{c0}(1P) \rightarrow K^+K^-K^+K^-) \times B(\psi(2S) \rightarrow \gamma\chi_{c0}(1P))$$

VALUE (units 10^{-4})	EVTS	DOCUMENT ID	TECN	COMMENT
2.63 ± 0.27 OUR FIT				
3.20 ± 0.11 ± 0.41	278	70 ABLIKIM	06t BES2	$\psi(2S) \rightarrow \gamma 2K^+ 2K^-$

⁷⁰ Calculated by us. The value of $B(\chi_{c0} \rightarrow 2K^+ 2K^-)$ reported by ABLIKIM 06t was derived using $B(\psi(2S) \rightarrow \gamma\chi_{c0}(1P)) = (9.2 \pm 0.4)\%$.

$$B(\chi_{c0}(1P) \rightarrow K^+K^-K^+K^-) \times \frac{\Gamma(\psi(2S) \rightarrow \gamma\chi_{c0}(1P))}{\Gamma(\psi(2S) \rightarrow J/\psi(1S)\pi^+\pi^-)}$$

VALUE (units 10^{-4})	DOCUMENT ID	TECN	COMMENT
8.1 ± 0.8 OUR FIT			
6.1 ± 0.8 ± 0.9	71 BAI	99b BES	$\psi(2S) \rightarrow \gamma 2K^+ 2K^-$

⁷¹ Calculated by us. The value of $B(\chi_{c0} \rightarrow 2K^+ 2K^-)$ reported by BAI 99b was derived using $B(\psi(2S) \rightarrow \gamma\chi_{c0}(1P)) = (9.3 \pm 0.8)\%$ and $B(\psi(2S) \rightarrow J/\psi\pi^+\pi^-) = (32.4 \pm 2.6)\%$ [BAI 98d].

$$B(\chi_{c0}(1P) \rightarrow \phi\phi) \times B(\psi(2S) \rightarrow \gamma\chi_{c0}(1P))$$

VALUE (units 10^{-4})	EVTS	DOCUMENT ID	TECN	COMMENT
0.87 ± 0.18 OUR FIT				
0.86 ± 0.19 ± 0.12	26	72 ABLIKIM	06t BES2	$\psi(2S) \rightarrow \gamma 2K^+ 2K^-$

⁷² Calculated by us. The value of $B(\chi_{c0} \rightarrow \phi\phi)$ reported by ABLIKIM 06t was derived using $B(\psi(2S) \rightarrow \gamma\chi_{c0}(1P)) = (9.2 \pm 0.4)\%$.

$$B(\chi_{c0}(1P) \rightarrow \phi\phi) \times \frac{\Gamma(\psi(2S) \rightarrow \gamma\chi_{c0}(1P))}{\Gamma(\psi(2S) \rightarrow J/\psi(1S)\pi^+\pi^-)}$$

VALUE (units 10^{-4})	DOCUMENT ID	TECN	COMMENT
2.7 ± 0.6 OUR FIT			
2.6 ± 1.0 ± 1.1	73 BAI	99b BES	$\psi(2S) \rightarrow \gamma 2K^+ 2K^-$

⁷³ Calculated by us. The value of $B(\chi_{c0} \rightarrow \phi\phi)$ reported by BAI 99b was derived using $B(\psi(2S) \rightarrow \gamma\chi_{c0}(1P)) = (9.3 \pm 0.8)\%$ and $B(\psi(2S) \rightarrow J/\psi\pi^+\pi^-) = (32.4 \pm 2.6)\%$ [BAI 98d].

$\chi_{c0}(1P)$ REFERENCES

UEHARA	08	EPJ C53 1	S. Uehara <i>et al.</i>	(BELLE Collab.)
WICHT	08	PL B662 323	J. Wicht <i>et al.</i>	(BELLE Collab.)
ABE	07	PRL 98 082001	K. ABE <i>et al.</i>	(BELLE Collab.)
ADAMS	07	PR D75 071101R	G.S. Adams <i>et al.</i>	(CLEO Collab.)
ATHAR	07	PR D75 032002	S.B. Athar <i>et al.</i>	(CLEO Collab.)
CHEN	07B	PL B651 15	W.T. Chen <i>et al.</i>	(BELLE Collab.)
ABLIKIM	06D	PR D73 052006	M. Ablikim <i>et al.</i>	(BES Collab.)
ABLIKIM	06I	PR D74 012004	M. Ablikim <i>et al.</i>	(BES Collab.)
ABLIKIM	06R	PR D74 072001	M. Ablikim <i>et al.</i>	(BES Collab.)
ABLIKIM	06T	PL B642 197	M. Ablikim <i>et al.</i>	(BES Collab.)
ABLIKIM	05G	PR D71 092002	M. Ablikim <i>et al.</i>	(BES Collab.)
ABLIKIM	05N	PL B630 7	M. Ablikim <i>et al.</i>	(BES Collab.)
ABLIKIM	05O	PL B630 21	M. Ablikim <i>et al.</i>	(BES Collab.)
ABLIKIM	05Q	PR D72 092002	M. Ablikim <i>et al.</i>	(BES Collab.)
ADAM	05A	PRL 94 232002	N.E. Adam <i>et al.</i>	(CLEO Collab.)
ANDREOTTI	05A	NP B717 34	M. Andreotti <i>et al.</i>	(FNAL E835 Collab.)
ANDREOTTI	05C	PR D72 112002	M. Andreotti <i>et al.</i>	(FNAL E835 Collab.)
NAKAZAWA	05	PL B615 39	H. Nakazawa <i>et al.</i>	(BELLE Collab.)
ABE	04G	PR D70 071102	K. ABE <i>et al.</i>	(BELLE Collab.)
ABLIKIM	04G	PR D70 092002	M. Ablikim <i>et al.</i>	(BES Collab.)
ABLIKIM	04H	PR D70 092003	M. Ablikim <i>et al.</i>	(BES Collab.)
ANDREOTTI	04	PL B584 16	M. Andreotti <i>et al.</i>	(E835 Collab.)
ATHAR	04	PR D70 112002	S.B. Athar <i>et al.</i>	(CLEO Collab.)
BAI	04F	PR D69 092001	J.Z. Bai <i>et al.</i>	(BES Collab.)
ANDREOTTI	03	PRL 91 091801	M. Andreotti <i>et al.</i>	(FNAL E835 Collab.)
AULCHENKO	03	PL B573 83	V.M. Aulchenko <i>et al.</i>	(KEDR Collab.)
BAI	03C	PR D67 032004	J.Z. Bai <i>et al.</i>	(BES Collab.)
BAI	03E	PR D67 112001	J.Z. Bai <i>et al.</i>	(BES Collab.)
ABE,K	02	PRL 89 142001	K. ABE <i>et al.</i>	(BELLE Collab.)
BAGNASCO	02	PL B533 237	S. Bagnasco <i>et al.</i>	(FNAL E835 Collab.)
EISENSTEIN	01	PRL 87 061801	B.I. Eisenstein <i>et al.</i>	(CLEO Collab.)
AMBROGIANI	00B	PR D62 052002	M. Ambrogiani <i>et al.</i>	(FNAL E835 Collab.)
AMBROGIANI	99B	PRL 83 2902	M. Ambrogiani <i>et al.</i>	(FNAL E835 Collab.)
BAI	99B	PR D60 072001	J.Z. Bai <i>et al.</i>	(BES Collab.)
BAI	98D	PR D58 092006	J.Z. Bai <i>et al.</i>	(BES Collab.)
BAI	98I	PRL 81 3091	J.Z. Bai <i>et al.</i>	(BES Collab.)
GAISSER	86	PR D34 711	J. Gaiser <i>et al.</i>	(Crystal Ball Collab.)
LEE	85	SLAC 282	R.A. Lee	(SLAC)
OREGLIA	82	PR D25 2259	M.J. Oreglia <i>et al.</i>	(SLAC, CIT, HARV+)
BRANDELIK	79B	NP B160 426	R. Brandelik <i>et al.</i>	(DASP Collab.)
BARTEL	78B	PL 79B 492	W. Bartel <i>et al.</i>	(DESY, HEIDP)
TANENBAUM	78	PR D17 1731	W.M. Tanenbaum <i>et al.</i>	(SLAC, LBL)
Also		Private Comm.	G. Trilling	(LBL, UCB)
BIDDICK	77	PRL 38 1324	C.J. Biddick <i>et al.</i>	(UCSD, UMD, PAVI+)

OTHER RELATED PAPERS

VANBEVEREN	06A	PR D74 037501	E. van Beberen <i>et al.</i>	(Omega Expt.)
BARBERIS	00G	PL B485 357	D. Barberis <i>et al.</i>	(L3 Collab.)
ACCIARRI	99T	PL B461 155	M. Acciari <i>et al.</i>	(CLEO Collab.)
CHEN	90B	PL B243 169	W.Y. Chen <i>et al.</i>	(TPC Collab.)
AIHARA	88D	PRL 60 2355	H. Aihara <i>et al.</i>	(L3 Collab.)
FELDMAN	75B	PRL 35 821	G.J. Feldman <i>et al.</i>	(LBL, SLAC)
Also		PRL 35 1184 (Errat.)	G.J. Feldman <i>et al.</i>	(LBL, SLAC)
TANENBAUM	75	PRL 35 1323	W.M. Tanenbaum <i>et al.</i>	(LBL, SLAC)

$\chi_{c1}(1P)$

$I^G(J^{PC}) = 0^+(1^{++})$

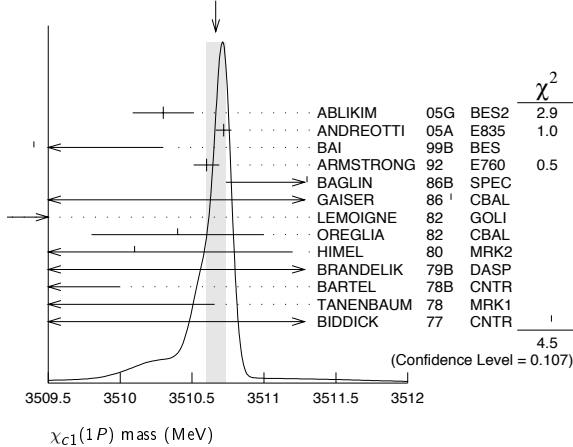
See the Review on " $\psi(2S)$ and χ_c branching ratios" before the $\chi_{c0}(1P)$ Listings.

$\chi_{c1}(1P)$ MASS

VALUE (MeV)	EVTs	DOCUMENT ID	TECN	COMMENT
3510.66 ± 0.07 OUR AVERAGE		Error includes scale factor of 1.5. See the ideogram below.		
3510.30 ± 0.14 ± 0.16		ABLIKIM 05G	BES2	$\psi(2S) \rightarrow \gamma \chi_{c1}$
3510.719 ± 0.051 ± 0.019		ANDREOTTI 05A	E835	$p\bar{p} \rightarrow e^+e^- \gamma$
3509.4 ± 0.9		BAI 99B	BES	$\psi(2S) \rightarrow \gamma X$
3510.60 ± 0.087 ± 0.019	513	¹ ARMSTRONG 92	E760	$\bar{p}p \rightarrow e^+e^- \gamma$
3511.3 ± 0.4 ± 0.4	30	BAGLIN 86B	SPEC	$\bar{p}p \rightarrow e^+e^- X$
3512.3 ± 0.3 ± 4.0		² GAISER 86	CBAL	$\psi(2S) \rightarrow \gamma X$
3507.4 ± 1.7	91	³ LEMOIGNE 82	GOLI	$185 \pi^- Be \rightarrow \gamma \mu^+ \mu^- A$
3510.4 ± 0.6		OREGLIA 82	CBAL	$e^+e^- \rightarrow J/\psi 2\gamma$
3510.1 ± 1.1	254	⁴ HIMEL 80	MRK2	$e^+e^- \rightarrow J/\psi 2\gamma$
3509 ± 11	21	BRANDELIK 79B	DASP	$e^+e^- \rightarrow J/\psi 2\gamma$
3507 ± 3		⁴ BARTEL 78B	CNTR	$e^+e^- \rightarrow J/\psi 2\gamma$
3505.0 ± 4 ± 4		^{4,5} TANENBAUM 78	MRK1	e^+e^-
3513 ± 7	367	⁴ BIDDICK 77	CNTR	$\psi(2S) \rightarrow \gamma X$
3500 ± 10	40	TANENBAUM 75	MRK1	Hadrons γ

• • • We do not use the following data for averages, fits, limits, etc. • • •
¹ Recalculated by ANDREOTTI 05A, using the value of $\psi(2S)$ mass from AULCHENKO 03.
² Using mass of $\psi(2S) = 3686.0$ MeV.
³ $J/\psi(1S)$ mass constrained to 3097 MeV.
⁴ Mass value shifted by us by amount appropriate for $\psi(2S)$ mass = 3686 MeV and $J/\psi(1S)$ mass = 3097 MeV.
⁵ From a simultaneous fit to radiative and hadronic decay channels.

WEIGHTED AVERAGE
3510.66±0.07 (Error scaled by 1.5)



$\chi_{c1}(1P)$ WIDTH

VALUE (MeV)	CL%	EVTs	DOCUMENT ID	TECN	COMMENT
0.89 ± 0.05 OUR FIT					
0.88 ± 0.05 OUR AVERAGE					
1.39 +0.40 +0.26 -0.38 -0.77			ABLIKIM 05G	BES2	$\psi(2S) \rightarrow \gamma \chi_{c1}$
0.876 ± 0.045 ± 0.026			ANDREOTTI 05A	E835	$p\bar{p} \rightarrow e^+e^- \gamma$
0.87 ± 0.11 ± 0.08	513		⁶ ARMSTRONG 92	E760	$\bar{p}p \rightarrow e^+e^- \gamma$
<1.3	95		BAGLIN 86B	SPEC	$\bar{p}p \rightarrow e^+e^- X$
<3.8	90		GAISER 86	CBAL	$\psi(2S) \rightarrow \gamma X$

• • • We do not use the following data for averages, fits, limits, etc. • • •
⁶ Recalculated by ANDREOTTI 05A.

$\chi_{c1}(1P)$ DECAY MODES

Mode	Fraction (Γ_i/Γ)	Scale factor/ Confidence level
------	--------------------------------	-----------------------------------

Hadronic decays

Γ_1	$3(\pi^+ \pi^-)$	$(5.8 \pm 1.4) \times 10^{-3}$	S=1.2
Γ_2	$2(\pi^+ \pi^-)$	$(7.6 \pm 2.6) \times 10^{-3}$	
Γ_3	$\pi^+ \pi^- K^+ K^-$	$(4.5 \pm 1.0) \times 10^{-3}$	
Γ_4	$\pi^+ \pi^- \eta$	$(5.2 \pm 0.6) \times 10^{-3}$	
Γ_5	$\pi^+ \pi^- \eta'$	$(2.5 \pm 0.5) \times 10^{-3}$	
Γ_6	$\rho^0 \pi^+ \pi^-$	$(3.9 \pm 3.5) \times 10^{-3}$	
Γ_7	$K^+ K^- \eta$	$(3.5 \pm 1.1) \times 10^{-4}$	
Γ_8	$K^0 K^+ \pi^- + c.c.$	$(7.7 \pm 0.7) \times 10^{-3}$	
Γ_9	$K^+ K^- \pi^0$	$(2.01 \pm 0.28) \times 10^{-3}$	
Γ_{10}	$\eta \pi^+ \pi^-$	$(5.8 \pm 1.1) \times 10^{-3}$	
Γ_{11}	$a_0(980)^+ \pi^- + c.c. \rightarrow \eta \pi^+ \pi^-$	$(2.0 \pm 0.7) \times 10^{-3}$	
Γ_{12}	$f_2(1270) \eta$	$(3.0 \pm 0.9) \times 10^{-3}$	
Γ_{13}	$K^+ \bar{K}^*(892)^0 \pi^- + c.c.$	$(3.2 \pm 2.1) \times 10^{-3}$	
Γ_{14}	$K^*(892)^0 \bar{K}^*(892)^0$	$(1.6 \pm 0.4) \times 10^{-3}$	
Γ_{15}	$K^*(892)^0 \bar{K}^0 + c.c.$	$(1.1 \pm 0.4) \times 10^{-3}$	
Γ_{16}	$K^*(892)^+ K^- + c.c.$	$(1.6 \pm 0.7) \times 10^{-3}$	
Γ_{17}	$K_S^*(1430)^0 \bar{K}^0 + c.c. \rightarrow K_S^0 K^+ \pi^- + c.c.$	< 9 $\times 10^{-4}$	CL=90%
Γ_{18}	$K_S^*(1430)^+ K^- + c.c. \rightarrow K_S^0 K^+ \pi^- + c.c.$	< 2.4 $\times 10^{-3}$	CL=90%
Γ_{19}	$\pi^+ \pi^- K_S^0 K_S^0$	$(7.6 \pm 3.2) \times 10^{-4}$	
Γ_{20}	$K^+ K^- K_S^0 K_S^0$	< 5 $\times 10^{-4}$	CL=90%
Γ_{21}	$K^+ K^- K^+ K^-$	$(5.8 \pm 1.2) \times 10^{-4}$	
Γ_{22}	$K^+ K^- \phi$	$(4.5 \pm 1.7) \times 10^{-4}$	
Γ_{23}	$p\bar{p}$	$(6.6 \pm 0.5) \times 10^{-5}$	
Γ_{24}	$p\bar{p} \pi^0$	$(1.2 \pm 0.5) \times 10^{-4}$	
Γ_{25}	$p\bar{p} \eta$	< 1.6 $\times 10^{-4}$	CL=90%
Γ_{26}	$\pi^+ \pi^- p\bar{p}$	$(5.0 \pm 1.9) \times 10^{-4}$	
Γ_{27}	$K_S^0 K_S^0 p\bar{p}$	< 4.5 $\times 10^{-4}$	CL=90%
Γ_{28}	$\Lambda \bar{\Lambda}$	$(2.4 \pm 1.0) \times 10^{-4}$	
Γ_{29}	$\Lambda \bar{\Lambda} \pi^+ \pi^-$	< 1.5 $\times 10^{-3}$	CL=90%
Γ_{30}	$K^+ \bar{p} \Lambda$	$(3.4 \pm 1.0) \times 10^{-4}$	
Γ_{31}	$\Xi^- \bar{\Xi}^+$	< 3.4 $\times 10^{-4}$	CL=90%
Γ_{32}	$\pi^+ \pi^- + K^+ K^-$	< 2.1 $\times 10^{-3}$	
Γ_{33}	$K_S^0 K_S^0$	< 7 $\times 10^{-5}$	CL=90%

Radiative decays

Γ_{34}	$\gamma J/\psi(1S)$	$(36.0 \pm 1.9) \%$
Γ_{35}	$\gamma \gamma$	

$\chi_{c1}(1P)$ PARTIAL WIDTHS

$\chi_{c1}(1P) \Gamma(i) \Gamma(\gamma J/\psi(1S)) / \Gamma(\text{total})$

VALUE (eV)	DOCUMENT ID	TECN	COMMENT
21.3 ± 0.9 OUR FIT			
21.4 ± 0.9 OUR AVERAGE			
21.5 ± 0.5 ± 0.8	⁷ ANDREOTTI 05A	E835	$p\bar{p} \rightarrow e^+e^- \gamma$
21.4 ± 1.5 ± 2.2	^{7,8} ARMSTRONG 92	E760	$\bar{p}p \rightarrow e^+e^- \gamma$
19.9 ± 4.4 4.0	⁷ BAGLIN 86B	SPEC	$\bar{p}p \rightarrow e^+e^- X$

⁷ Calculated by us using $B(J/\psi(1S) \rightarrow e^+e^-) = 0.0593 \pm 0.0010$.
⁸ Recalculated by ANDREOTTI 05A.

$\chi_{c1}(1P)$ BRANCHING RATIOS

HADRONIC DECAYS

$\Gamma(3(\pi^+ \pi^-)) / \Gamma_{\text{total}}$	Γ_1 / Γ		
VALUE (units 10^{-3})	DOCUMENT ID	TECN	COMMENT
5.8 ± 1.4 OUR EVALUATION	Error includes scale factor of 1.2. Treating systematic error as correlated.		
5.8 ± 1.1 OUR AVERAGE			
5.4 ± 0.7 ± 0.9	⁹ BAI	99B	BES $\psi(2S) \rightarrow \gamma \chi_{c1}$
16.0 ± 5.9 ± 0.8	⁹ TANENBAUM 78	MRK1	$\psi(2S) \rightarrow \gamma \chi_{c1}$
$\Gamma(2(\pi^+ \pi^-)) / \Gamma_{\text{total}}$	Γ_2 / Γ		
VALUE (units 10^{-3})	DOCUMENT ID	TECN	COMMENT
7.6 ± 2.6 OUR EVALUATION	Treating systematic error as correlated.		
8 ± 4 OUR AVERAGE	Error includes scale factor of 1.5.		
4.6 ± 2.1 ± 2.6	⁹ BAI	99B	BES $\psi(2S) \rightarrow \gamma \chi_{c1}$
12.5 ± 4.2 ± 0.6	⁹ TANENBAUM 78	MRK1	$\psi(2S) \rightarrow \gamma \chi_{c1}$
$\Gamma(\pi^+ \pi^- K^+ K^-) / \Gamma_{\text{total}}$	Γ_3 / Γ		
VALUE (units 10^{-3})	DOCUMENT ID	TECN	COMMENT
4.5 ± 1.0 OUR EVALUATION	Treating systematic error as correlated.		
4.5 ± 0.9 OUR AVERAGE			
4.2 ± 0.4 ± 0.9	⁹ BAI	99B	BES $\psi(2S) \rightarrow \gamma \chi_{c1}$
7.3 ± 3.0 ± 0.4	⁹ TANENBAUM 78	MRK1	$\psi(2S) \rightarrow \gamma \chi_{c1}$

Meson Particle Listings

 $\chi_{c1}(1P)$

$\Gamma(\pi^+\pi^-\eta)/\Gamma_{\text{total}}$	VALUE (units 10^{-3})	DOCUMENT ID	TECN	COMMENT	Γ_4/Γ		
$5.2 \pm 0.5 \pm 0.2$		10	ATHAR 07	CLEO $\psi(2S) \rightarrow \gamma h^+ h^- h^0$			
$\Gamma(\pi^+\pi^-\eta')/\Gamma_{\text{total}}$	VALUE (units 10^{-3})	DOCUMENT ID	TECN	COMMENT	Γ_5/Γ		
$2.5 \pm 0.5 \pm 0.1$		11	ATHAR 07	CLEO $\psi(2S) \rightarrow \gamma h^+ h^- h^0$			
$\Gamma(\rho^0\pi^+\pi^-)/\Gamma_{\text{total}}$	VALUE (units 10^{-4})	DOCUMENT ID	TECN	COMMENT	Γ_6/Γ		
39 ± 35		12	TANENBAUM 78	MRK1 $\psi(2S) \rightarrow \gamma \chi_{c1}$			
$\Gamma(K^+K^-\eta)/\Gamma_{\text{total}}$	VALUE (units 10^{-3})	DOCUMENT ID	TECN	COMMENT	Γ_7/Γ		
$0.35 \pm 0.11 \pm 0.02$		13	ATHAR 07	CLEO $\psi(2S) \rightarrow \gamma h^+ h^- h^0$			
$\Gamma(K^0K^+\pi^- + \text{c.c.})/\Gamma_{\text{total}}$	VALUE (units 10^{-3})	DOCUMENT ID	TECN	COMMENT	Γ_8/Γ		
7.7 ± 0.7 OUR FIT							
$\Gamma(K^+K^-\pi^0)/\Gamma_{\text{total}}$	VALUE (units 10^{-3})	DOCUMENT ID	TECN	COMMENT	Γ_9/Γ		
$2.01 \pm 0.26 \pm 0.09$		14	ATHAR 07	CLEO $\psi(2S) \rightarrow \gamma h^+ h^- h^0$			
$\Gamma(\eta\pi^+\pi^-)/\Gamma_{\text{total}}$	VALUE (units 10^{-3})	EVTS	DOCUMENT ID	TECN	COMMENT	Γ_{10}/Γ	
$5.8 \pm 1.0 \pm 0.3$	222		15	ABLIKIM 06R	BES2 $\psi(2S) \rightarrow \gamma \chi_{c1}$		
$\Gamma(a_0(980)^+\pi^- + \text{c.c.} \rightarrow \eta\pi^+\pi^-)/\Gamma_{\text{total}}$	VALUE (units 10^{-3})	EVTS	DOCUMENT ID	TECN	COMMENT	Γ_{11}/Γ	
$2.0 \pm 0.7 \pm 0.1$	58		16	ABLIKIM 06R	BES2 $\psi(2S) \rightarrow \gamma \chi_{c1}$		
$\Gamma(f_2(1270)\eta)/\Gamma_{\text{total}}$	VALUE (units 10^{-3})	EVTS	DOCUMENT ID	TECN	COMMENT	Γ_{12}/Γ	
$3.0 \pm 0.8 \pm 0.1$	53		17	ABLIKIM 06R	BES2 $\psi(2S) \rightarrow \gamma \chi_{c1}$		
$\Gamma(K^+\bar{K}^*(892)^0\pi^- + \text{c.c.})/\Gamma_{\text{total}}$	VALUE (units 10^{-4})	DOCUMENT ID	TECN	COMMENT	Γ_{13}/Γ		
32 ± 21		12	TANENBAUM 78	MRK1 $\psi(2S) \rightarrow \gamma \chi_{c1}$			
$\Gamma(K^*(892)^0\bar{K}^*(892)^0)/\Gamma_{\text{total}}$	VALUE (units 10^{-3})	EVTS	DOCUMENT ID	TECN	COMMENT	Γ_{14}/Γ	
$1.6 \pm 0.4 \pm 0.1$	28.4 ± 5.5	18,19	ABLIKIM 04H	BES $\psi(2S) \rightarrow \gamma K^+ K^- \pi^+ \pi^-$			
$\Gamma(K^*(892)^0\bar{K}^0 + \text{c.c.})/\Gamma_{\text{total}}$	VALUE (units 10^{-3})	EVTS	DOCUMENT ID	TECN	COMMENT	Γ_{15}/Γ	
$1.09 \pm 0.40 \pm 0.05$	22		20	ABLIKIM 06R	BES2 $\psi(2S) \rightarrow \gamma \chi_{c1}$		
$\Gamma(K^*(892)^+K^- + \text{c.c.})/\Gamma_{\text{total}}$	VALUE (units 10^{-3})	EVTS	DOCUMENT ID	TECN	COMMENT	Γ_{16}/Γ	
$1.6 \pm 0.7 \pm 0.1$	27		21	ABLIKIM 06R	BES2 $\psi(2S) \rightarrow \gamma \chi_{c1}$		
$\Gamma(K_S^*(1430)^0\bar{K}^0 + \text{c.c.} \rightarrow K_S^0K^+\pi^- + \text{c.c.})/\Gamma_{\text{total}}$	VALUE (units 10^{-3})	CL%	DOCUMENT ID	TECN	COMMENT	Γ_{17}/Γ	
<0.9	90		22	ABLIKIM 06R	BES2 $\psi(2S) \rightarrow \gamma \chi_{c1}$		
$\Gamma(K_S^*(1430)^+K^- + \text{c.c.} \rightarrow K_S^0K^+\pi^- + \text{c.c.})/\Gamma_{\text{total}}$	VALUE (units 10^{-3})	CL%	DOCUMENT ID	TECN	COMMENT	Γ_{18}/Γ	
<2.4	90		23	ABLIKIM 06R	BES2 $\psi(2S) \rightarrow \gamma \chi_{c1}$		
$\Gamma(\pi^+\pi^-\bar{K}_S^0K_S^0)/\Gamma_{\text{total}}$	VALUE (units 10^{-4})	EVTS	DOCUMENT ID	TECN	COMMENT	Γ_{19}/Γ	
$7.6 \pm 3.2 \pm 0.3$	19.8 ± 7.7		24	ABLIKIM 05o	BES2 $\psi(2S) \rightarrow \chi_{c1}\gamma$		
$\Gamma(K^+K^-K_S^0K_S^0)/\Gamma_{\text{total}}$	VALUE (units 10^{-4})	CL%	EVTS	DOCUMENT ID	TECN	COMMENT	Γ_{20}/Γ
<5	90	3.2 ± 2.4		25	ABLIKIM 05o	BES2 $\psi(2S) \rightarrow \chi_{c1}\gamma$	
$\Gamma(K^+K^-K^+K^-)/\Gamma_{\text{total}}$	VALUE (units 10^{-3})	DOCUMENT ID	TECN	COMMENT	Γ_{21}/Γ		
0.58 ± 0.12 OUR FIT							
$\Gamma(K^+K^-\phi)/\Gamma_{\text{total}}$	VALUE (units 10^{-3})	EVTS	DOCUMENT ID	TECN	COMMENT	Γ_{22}/Γ	
$0.45 \pm 0.17 \pm 0.02$	17		26	ABLIKIM 06T	BES2 $\psi(2S) \rightarrow \gamma 2K^+ 2K^-$		
$\Gamma(\rho\bar{\rho})/\Gamma_{\text{total}}$	VALUE (units 10^{-4})	DOCUMENT ID	TECN	COMMENT	Γ_{23}/Γ		
0.66 ± 0.05 OUR FIT							
$\Gamma(\rho\bar{\rho}\pi^0)/\Gamma_{\text{total}}$	VALUE (units 10^{-3})	DOCUMENT ID	TECN	COMMENT	Γ_{24}/Γ		
$0.12 \pm 0.05 \pm 0.01$		27	ATHAR 07	CLEO $\psi(2S) \rightarrow \gamma h^+ h^- h^0$			
$\Gamma(\rho\bar{\rho}\eta)/\Gamma_{\text{total}}$	VALUE (units 10^{-3})	CL%	DOCUMENT ID	TECN	COMMENT	Γ_{25}/Γ	
<0.16	90		28	ATHAR 07	CLEO $\psi(2S) \rightarrow \gamma h^+ h^- h^0$		
$\Gamma(\pi^+\pi^-\rho\bar{\rho})/\Gamma_{\text{total}}$	VALUE (units 10^{-3})	DOCUMENT ID	TECN	COMMENT	Γ_{26}/Γ		
0.50 ± 0.19 OUR EVALUATION 0.50 ± 0.19 OUR AVERAGE				Treating systematic error as correlated.			
$0.46 \pm 0.12 \pm 0.15$ $1.08 \pm 0.77 \pm 0.05$		9	BAI 99B	BES $\psi(2S) \rightarrow \gamma \chi_{c1}$			
		9	TANENBAUM 78	MRK1 $\psi(2S) \rightarrow \gamma \chi_{c1}$			
$\Gamma(K_S^0K_S^0\rho\bar{\rho})/\Gamma_{\text{total}}$	VALUE (units 10^{-4})	CL%	DOCUMENT ID	TECN	COMMENT	Γ_{27}/Γ	
<4.5	90		29	ABLIKIM 06D	BES2 $\psi(2S) \rightarrow \gamma \chi_{c1}$		
$\Gamma(\Lambda\bar{\Lambda})/\Gamma_{\text{total}}$	VALUE (units 10^{-4})	EVTS	DOCUMENT ID	TECN	COMMENT	Γ_{28}/Γ	
$2.4 \pm 0.9 \pm 0.5$	$9.0^{+3.5}_{-3.1}$		9	BAI 03E	BES $\psi(2S) \rightarrow \gamma \chi_{c1} \rightarrow \gamma \Lambda\bar{\Lambda}$		
$\Gamma(\Lambda\bar{\Lambda}\pi^+\pi^-)/\Gamma_{\text{total}}$	VALUE (units 10^{-3})	CL%	DOCUMENT ID	TECN	COMMENT	Γ_{29}/Γ	
<1.5	90		29	ABLIKIM 06D	BES2 $\psi(2S) \rightarrow \gamma \chi_{c1}$		
$\Gamma(K^+\bar{\rho}\Lambda)/\Gamma_{\text{total}}$	VALUE (units 10^{-3})	DOCUMENT ID	TECN	COMMENT	Γ_{30}/Γ		
$0.34 \pm 0.10 \pm 0.02$		30	ATHAR 07	CLEO $\psi(2S) \rightarrow \gamma h^+ h^- h^0$			
$\Gamma(\Xi^-\Xi^+)/\Gamma_{\text{total}}$	VALUE (units 10^{-4})	CL%	DOCUMENT ID	TECN	COMMENT	Γ_{31}/Γ	
<3.4	90		29	ABLIKIM 06D	BES2 $\psi(2S) \rightarrow \gamma \chi_{c1}$		
$[\Gamma(\pi^+\pi^-) + \Gamma(K^+K^-)]/\Gamma_{\text{total}}$	VALUE (units 10^{-4})	CL%	DOCUMENT ID	TECN	COMMENT	Γ_{32}/Γ	
<21			12	FELDMAN 77	MRK1 $\psi(2S) \rightarrow \gamma \chi_{c1}$		
<38	90		12	BRANDELIK 79B	DASP $\psi(2S) \rightarrow \gamma \chi_{c1}$		
$\Gamma(K_S^0K_S^0)/\Gamma_{\text{total}}$	VALUE (units 10^{-4})	CL%	DOCUMENT ID	TECN	COMMENT	Γ_{33}/Γ	
<0.7	90		31	ABLIKIM 05o	BES2 $\psi(2S) \rightarrow \chi_{c1}\gamma$		
9 Rescaled by us using $B(\psi(2S) \rightarrow \gamma \chi_{c1}) = (8.8 \pm 0.4)\%$ and $B(\psi(2S) \rightarrow J/\psi(1S)\pi^+\pi^-) = (32.6 \pm 0.5)\%$.							
10 ATHAR 07 reports $(5.0 \pm 0.3 \pm 0.5) \times 10^{-3}$ for $B(\psi(2S) \rightarrow \gamma \chi_{c1}(1P)) = 0.0907 \pm 0.0011 \pm 0.0054$. We rescale to our best value $B(\psi(2S) \rightarrow \gamma \chi_{c1}(1P)) = (8.8 \pm 0.4) \times 10^{-2}$. Our first error is their experiment's error and our second error is the systematic error from using our best value.							
11 ATHAR 07 reports $(2.4 \pm 0.4 \pm 0.3) \times 10^{-3}$ for $B(\psi(2S) \rightarrow \gamma \chi_{c1}(1P)) = 0.0907 \pm 0.0011 \pm 0.0054$. We rescale to our best value $B(\psi(2S) \rightarrow \gamma \chi_{c1}(1P)) = (8.8 \pm 0.4) \times 10^{-2}$. Our first error is their experiment's error and our second error is the systematic error from using our best value.							
12 Estimated using $B(\psi(2S) \rightarrow \gamma \chi_{c1}(1P)) = 0.087$. The errors do not contain the uncertainty in the $\psi(2S)$ decay.							
13 ATHAR 07 reports $(0.34 \pm 0.10 \pm 0.04) \times 10^{-3}$ for $B(\psi(2S) \rightarrow \gamma \chi_{c1}(1P)) = 0.0907 \pm 0.0011 \pm 0.0054$. We rescale to our best value $B(\psi(2S) \rightarrow \gamma \chi_{c1}(1P)) = (8.8 \pm 0.4) \times 10^{-2}$. Our first error is their experiment's error and our second error is the systematic error from using our best value.							
14 ATHAR 07 reports $(1.95 \pm 0.16 \pm 0.23) \times 10^{-3}$ for $B(\psi(2S) \rightarrow \gamma \chi_{c1}(1P)) = 0.0907 \pm 0.0011 \pm 0.0054$. We rescale to our best value $B(\psi(2S) \rightarrow \gamma \chi_{c1}(1P)) = (8.8 \pm 0.4) \times 10^{-2}$. Our first error is their experiment's error and our second error is the systematic error from using our best value.							
15 ABLIKIM 06R reports $(5.9 \pm 0.7 \pm 0.8) \times 10^{-3}$ for $B(\psi(2S) \rightarrow \gamma \chi_{c1}(1P)) = (8.7 \pm 0.4) \times 10^{-2}$. We rescale to our best value $B(\psi(2S) \rightarrow \gamma \chi_{c1}(1P)) = (8.8 \pm 0.4) \times 10^{-2}$. Our first error is their experiment's error and our second error is the systematic error from using our best value.							
16 ABLIKIM 06R reports $(2.0 \pm 0.5 \pm 0.5) \times 10^{-3}$ for $B(\psi(2S) \rightarrow \gamma \chi_{c1}(1P)) = (8.7 \pm 0.4) \times 10^{-2}$. We rescale to our best value $B(\psi(2S) \rightarrow \gamma \chi_{c1}(1P)) = (8.8 \pm 0.4) \times 10^{-2}$. Our first error is their experiment's error and our second error is the systematic error from using our best value.							
17 ABLIKIM 06R reports $(3.0 \pm 0.7 \pm 0.5) \times 10^{-3}$ for $B(\psi(2S) \rightarrow \gamma \chi_{c1}(1P)) = (8.7 \pm 0.4) \times 10^{-2}$. We rescale to our best value $B(\psi(2S) \rightarrow \gamma \chi_{c1}(1P)) = (8.8 \pm 0.4) \times 10^{-2}$. Our first error is their experiment's error and our second error is the systematic error from using our best value.							
18 ABLIKIM 04H reports $[B(\chi_{c1}(1P) \rightarrow K^*(892)^0\bar{K}^*(892)^0)] \times [B(\psi(2S) \rightarrow \gamma \chi_{c1}(1P))] = (1.40 \pm 0.27 \pm 0.22) \times 10^{-4}$. We divide by our best value $B(\psi(2S) \rightarrow \gamma \chi_{c1}(1P)) = (8.8 \pm 0.4) \times 10^{-2}$. Our first error is their experiment's error and our second error is the systematic error from using our best value.							
19 Assumes $B(K^*(892)^0 \rightarrow K^-\pi^+) = 2/3$.							

- 20 ABLIKIM 06R reports $(1.1 \pm 0.4 \pm 0.1) \times 10^{-3}$ for $B(\psi(2S) \rightarrow \gamma \chi_{c1}(1P)) = (8.7 \pm 0.4) \times 10^{-2}$. We rescale to our best value $B(\psi(2S) \rightarrow \gamma \chi_{c1}(1P)) = (8.8 \pm 0.4) \times 10^{-2}$. Our first error is their experiment's error and our second error is the systematic error from using our best value.
- 21 ABLIKIM 06R reports $(1.6 \pm 0.7 \pm 0.2) \times 10^{-3}$ for $B(\psi(2S) \rightarrow \gamma \chi_{c1}(1P)) = (8.7 \pm 0.4) \times 10^{-2}$. We rescale to our best value $B(\psi(2S) \rightarrow \gamma \chi_{c1}(1P)) = (8.8 \pm 0.4) \times 10^{-2}$. Our first error is their experiment's error and our second error is the systematic error from using our best value.
- 22 ABLIKIM 06R reports $< 0.9 \times 10^{-3}$ for $B(\psi(2S) \rightarrow \gamma \chi_{c1}(1P)) = (8.7 \pm 0.4) \times 10^{-2}$. We rescale to our best value $B(\psi(2S) \rightarrow \gamma \chi_{c1}(1P)) = 0.088$.
- 23 ABLIKIM 06R reports $< 2.4 \times 10^{-3}$ for $B(\psi(2S) \rightarrow \gamma \chi_{c1}(1P)) = (8.7 \pm 0.4) \times 10^{-2}$. We rescale to our best value $B(\psi(2S) \rightarrow \gamma \chi_{c1}(1P)) = 0.088$.
- 24 ABLIKIM 05o reports $[B(\chi_{c1}(1P) \rightarrow \pi^+ \pi^- K_S^0 K_S^0)] \times [B(\psi(2S) \rightarrow \gamma \chi_{c1}(1P))] = (0.67 \pm 0.26 \pm 0.11) \times 10^{-4}$. We divide by our best value $B(\psi(2S) \rightarrow \gamma \chi_{c1}(1P)) = (8.8 \pm 0.4) \times 10^{-2}$. Our first error is their experiment's error and our second error is the systematic error from using our best value.
- 25 ABLIKIM 05o reports $[B(\chi_{c1}(1P) \rightarrow K^+ K^- K_S^0 K_S^0)] \times [B(\psi(2S) \rightarrow \gamma \chi_{c1}(1P))] < 4.2 \times 10^{-5}$. We divide by our best value $B(\psi(2S) \rightarrow \gamma \chi_{c1}(1P)) = 0.088$.
- 26 ABLIKIM 06T reports $(0.46 \pm 0.16 \pm 0.06) \times 10^{-3}$ for $B(\psi(2S) \rightarrow \gamma \chi_{c1}(1P)) = (8.7 \pm 0.4) \times 10^{-2}$. We rescale to our best value $B(\psi(2S) \rightarrow \gamma \chi_{c1}(1P)) = (8.8 \pm 0.4) \times 10^{-2}$. Our first error is their experiment's error and our second error is the systematic error from using our best value.
- 27 ATHAR 07 reports $(0.12 \pm 0.05 \pm 0.01) \times 10^{-3}$ for $B(\psi(2S) \rightarrow \gamma \chi_{c1}(1P)) = 0.0907 \pm 0.0011 \pm 0.0054$. We rescale to our best value $B(\psi(2S) \rightarrow \gamma \chi_{c1}(1P)) = (8.8 \pm 0.4) \times 10^{-2}$. Our first error is their experiment's error and our second error is the systematic error from using our best value.
- 28 ATHAR 07 reports $< 0.16 \times 10^{-3}$ for $B(\psi(2S) \rightarrow \gamma \chi_{c1}(1P)) = 0.0907 \pm 0.0011 \pm 0.0054$. We rescale to our best value $B(\psi(2S) \rightarrow \gamma \chi_{c1}(1P)) = 0.088$.
- 29 Using $B(\psi(2S) \rightarrow \chi_{c1} \gamma) (9.1 \pm 0.6)\%$.
- 30 ATHAR 07 reports $(0.33 \pm 0.09 \pm 0.04) \times 10^{-3}$ for $B(\psi(2S) \rightarrow \gamma \chi_{c1}(1P)) = 0.0907 \pm 0.0011 \pm 0.0054$. We rescale to our best value $B(\psi(2S) \rightarrow \gamma \chi_{c1}(1P)) = (8.8 \pm 0.4) \times 10^{-2}$. Our first error is their experiment's error and our second error is the systematic error from using our best value.
- 31 ABLIKIM 05o reports $[B(\chi_{c1}(1P) \rightarrow K_S^0 K_S^0)] \times [B(\psi(2S) \rightarrow \gamma \chi_{c1}(1P))] < 0.6 \times 10^{-5}$. We divide by our best value $B(\psi(2S) \rightarrow \gamma \chi_{c1}(1P)) = 0.088$.

RADIATIVE DECAYS

$\Gamma(\gamma J/\psi(1S))/\Gamma_{\text{total}}$				Γ_{34}/Γ
VALUE	DOCUMENT ID	TECN	COMMENT	
0.360±0.019 OUR FIT				

• • • We do not use the following data for averages, fits, limits, etc. • • •

0.379±0.008±0.021	32 ADAM	05A	CLEO	$e^+ e^- \rightarrow \psi(2S) \rightarrow \gamma \chi_{c1}$
-------------------	---------	-----	------	---

$\Gamma(\gamma\gamma)/\Gamma_{\text{total}}$				Γ_{35}/Γ
VALUE	CL%	DOCUMENT ID	TECN	COMMENT
0.51±0.10 OUR FIT				

• • • We do not use the following data for averages, fits, limits, etc. • • •

<0.0015	90	33 YAMADA	77	DASP	$e^+ e^- \rightarrow 3\gamma$
---------	----	-----------	----	------	-------------------------------

32 Uses $B(\psi(2S) \rightarrow \gamma \chi_{c1} \rightarrow \gamma J/\psi)$ from ADAM 05A and $B(\psi(2S) \rightarrow \gamma \chi_{c1})$ from ATHAR 04.

33 Estimated using $B(\psi(2S) \rightarrow \gamma \chi_{c1}(1P)) = 0.087$. The errors do not contain the uncertainty in the $\psi(2S)$ decay.

 $\chi_{c1}(1P)$ CROSS-PARTICLE BRANCHING RATIOS

$$B(\chi_{c1}(1P) \rightarrow p\bar{p}) \times \frac{\Gamma(\psi(2S) \rightarrow \gamma \chi_{c1}(1P))}{\Gamma(\psi(2S) \rightarrow J/\psi(1S) \pi^+ \pi^-)}$$

VALUE (units 10^{-5})	DOCUMENT ID	TECN	COMMENT
1.78±0.19 OUR FIT			
1.1 ±1.0	34 BAI	98i	BES $\psi(2S) \rightarrow \gamma \chi_{c1} \rightarrow \gamma p\bar{p}$

$$B(\chi_{c1}(1P) \rightarrow \gamma J/\psi(1S)) \times B(\psi(2S) \rightarrow \gamma \chi_{c1}(1P))$$

VALUE (units 10^{-2})	EVTS	DOCUMENT ID	TECN	COMMENT
3.15±0.08 OUR FIT				
2.70±0.13 OUR AVERAGE				
2.81±0.05±0.23	13k	BAI	04i	BES2 $\psi(2S) \rightarrow J/\psi \gamma\gamma$
2.56±0.12±0.20		GAISER	86	CBAL $\psi(2S) \rightarrow \gamma X$
2.78±0.30		35 OREGLIA	82	CBAL $\psi(2S) \rightarrow \gamma \chi_{c1}$
2.2 ±0.5		36 BRANDELIK	79B	DASP $\psi(2S) \rightarrow \gamma \chi_{c1}$
2.9 ±0.5		36 BARTEL	78B	CNTR $\psi(2S) \rightarrow \gamma \chi_{c1}$
5.0 ±1.5		37 BIDDICK	77	CNTR $e^+ e^- \rightarrow \gamma X$
2.8 ±0.9		35 WHITAKER	76	MRK1 $e^+ e^-$
• • • We do not use the following data for averages, fits, limits, etc. • • •				
3.44±0.06±0.13	3.7k	38 ADAM	05A	CLEO $\psi(2S) \rightarrow J/\psi \gamma\gamma$

$$B(\chi_{c1}(1P) \rightarrow \gamma J/\psi) \times \frac{\Gamma(\psi(2S) \rightarrow \gamma \chi_{c1}(1P))}{\Gamma(\psi(2S) \rightarrow J/\psi(1S) \text{ anything})}$$

VALUE (units 10^{-2})	EVTS	DOCUMENT ID	TECN	COMMENT
5.49±0.08 OUR FIT				
5.77±0.10±0.12	3.7k	ADAM	05A	CLEO $\psi(2S) \rightarrow J/\psi \gamma\gamma$

$$B(\chi_{c1}(1P) \rightarrow \gamma J/\psi(1S)) \times \frac{\Gamma(\psi(2S) \rightarrow \gamma \chi_{c1}(1P))}{\Gamma(\psi(2S) \rightarrow J/\psi(1S) \pi^+ \pi^-)}$$

VALUE (units 10^{-2})	EVTS	DOCUMENT ID	TECN	COMMENT
9.67±0.33 OUR FIT				
9.5 ±1.8 OUR AVERAGE				
12.6 ±0.3 ±3.8	3k	39 ABLIKIM	04B	BES $\psi(2S) \rightarrow J/\psi X$
8.5 ±2.1		40 HIMEL	80	MRK2 $\psi(2S) \rightarrow \gamma \chi_{c1}$
• • • We do not use the following data for averages, fits, limits, etc. • • •				
10.24±0.17±0.23	3.7k	38 ADAM	05A	CLEO $\psi(2S) \rightarrow J/\psi \gamma\gamma$

$$B(\chi_{c1}(1P) \rightarrow K^0 K^+ \pi^- + \text{c.c.}) \times B(\psi(2S) \rightarrow \gamma \chi_{c1}(1P))$$

VALUE (units 10^{-4})	DOCUMENT ID	TECN	COMMENT
6.7±0.5 OUR FIT			
7.2±0.6 OUR AVERAGE			
7.3±0.5±0.5	41 ATHAR	07	CLEO $\psi(2S) \rightarrow \gamma K_S^0 K^+ \pi^-$
7.0±0.5±0.9	42 ABLIKIM	06R	BES2 $\psi(2S) \rightarrow \gamma \chi_{c1}$

$$B(\chi_{c1}(1P) \rightarrow K^0 K^+ \pi^- + \text{c.c.}) \times \frac{\Gamma(\psi(2S) \rightarrow \gamma \chi_{c1}(1P))}{\Gamma(\psi(2S) \rightarrow J/\psi(1S) \pi^+ \pi^-)}$$

VALUE (units 10^{-4})	DOCUMENT ID	TECN	COMMENT
20.6±1.7 OUR FIT			
13.2±2.4±3.2	43 BAI	99B	BES $\psi(2S) \rightarrow \gamma K_S^0 K^+ \pi^-$

$$B(\chi_{c1}(1P) \rightarrow K^+ K^- K^+ K^-) \times B(\psi(2S) \rightarrow \gamma \chi_{c1}(1P))$$

VALUE (units 10^{-4})	EVTS	DOCUMENT ID	TECN	COMMENT
0.51±0.10 OUR FIT				
0.61±0.11±0.08	54	44 ABLIKIM	06T	BES2 $\psi(2S) \rightarrow \gamma K^+ K^+ K^- K^-$

$$B(\chi_{c1}(1P) \rightarrow K^+ K^- K^+ K^-) \times \frac{\Gamma(\psi(2S) \rightarrow \gamma \chi_{c1}(1P))}{\Gamma(\psi(2S) \rightarrow J/\psi(1S) \pi^+ \pi^-)}$$

VALUE (units 10^{-4})	DOCUMENT ID	TECN	COMMENT
1.56±0.32 OUR FIT			
1.13±0.40±0.29	45 BAI	99B	BES $\psi(2S) \rightarrow \gamma K^+ K^+ K^- K^-$

$$B(\chi_{c1}(1P) \rightarrow p\bar{p}) \times B(\psi(2S) \rightarrow \gamma \chi_{c1}(1P))$$

VALUE (units 10^{-6})	EVTS	DOCUMENT ID	TECN	COMMENT
5.8±0.6 OUR FIT				
4.8±1.4±0.6	18.2 ^{+5.5} _{-4.9}	BAI	04F	BES $\psi(2S) \rightarrow \gamma \chi_{c1}(1P) \rightarrow \gamma p\bar{p}$

34 Calculated by us. The value for $B(\chi_{c1} \rightarrow p\bar{p})$ reported in BAI 98i is derived using $B(\psi(2S) \rightarrow \gamma \chi_{c1}) = (8.7 \pm 0.8)\%$ and $B(\psi(2S) \rightarrow J/\psi(1S) \pi^+ \pi^-) = (32.4 \pm 2.6)\%$ [BAI 98d].

35 Recalculated by us using $B(J/\psi(1S) \rightarrow \ell^+ \ell^-) = 0.1181 \pm 0.0020$.

36 Recalculated by us using $B(J/\psi(1S) \rightarrow \mu^+ \mu^-) = 0.0588 \pm 0.0010$.

37 Assumes isotropic gamma distribution.

38 Not independent from other values reported by ADAM 05A.

39 From a fit to the J/ψ recoil mass spectra.

40 The value for $B(\psi(2S) \rightarrow \gamma \chi_{c1}) \times B(\chi_{c1} \rightarrow \gamma J/\psi(1S))$ quoted in HIMEL 80 is derived using $B(\psi(2S) \rightarrow J/\psi(1S) \pi^+ \pi^-) = (33 \pm 3)\%$ and $B(J/\psi(1S) \rightarrow \ell^+ \ell^-) = 0.138 \pm 0.018$. Calculated by us using $B(J/\psi(1S) \rightarrow \ell^+ \ell^-) = 0.1181 \pm 0.0020$.

41 Calculated by us. The value of $B(\chi_{c1} \rightarrow K^0 K^+ \pi^- + \text{c.c.})$ reported by ATHAR 07 was derived using $B(\psi(2S) \rightarrow \gamma \chi_{c1}(1P)) = (9.07 \pm 0.11 \pm 0.54)\%$.

42 Calculated by us. ABLIKIM 06R reports $B(\chi_{c1} \rightarrow K_S^0 K^+ \pi^-) = (4.0 \pm 0.3 \pm 0.5) \times 10^{-3}$. We use $B(\psi(2S) \rightarrow \gamma \chi_{c1}) = (8.7 \pm 0.4) \times 10^{-2}$.

43 Calculated by us. The value of $B(\chi_{c1} \rightarrow K_S^0 K^+ \pi^-)$ reported by BAI 99B was derived using $B(\psi(2S) \rightarrow \gamma \chi_{c1}(1P)) = (8.7 \pm 0.8)\%$ and $B(\psi(2S) \rightarrow J/\psi \pi^+ \pi^-) = (32.4 \pm 2.6)\%$ [BAI 98d].

44 Calculated by us. The value of $B(\chi_{c1} \rightarrow 2K^+ 2K^-)$ reported by ABLIKIM 06T was derived using $B(\psi(2S) \rightarrow \gamma \chi_{c1}(1P)) = (8.7 \pm 0.8)\%$.

45 Calculated by us. The value of $B(\chi_{c1} \rightarrow 2K^+ 2K^-)$ reported by BAI 99B was derived using $B(\psi(2S) \rightarrow \gamma \chi_{c1}(1P)) = (8.7 \pm 0.8)\%$ and $B(\psi(2S) \rightarrow J/\psi \pi^+ \pi^-) = (32.4 \pm 2.6)\%$ [BAI 98d].

MULTIPOLE AMPLITUDES IN $\chi_{c1}(1P) \rightarrow \gamma J/\psi(1S)$

$$a_2 = M_2/\sqrt{E_1^2 + M_2^2} \text{ Magnetic quadrupole fractional transition amplitude}$$

VALUE	EVTS	DOCUMENT ID	TECN	COMMENT
-0.002±0.008				
-0.017 OUR AVERAGE				
0.002±0.032±0.004	2090	AMBROGIANI	02	E835 $p\bar{p} \rightarrow \chi_{c1} \rightarrow J/\psi \gamma$
-0.002±0.008	921	OREGLIA	82	CBAL $\psi(2S) \rightarrow \chi_{c1} \gamma \rightarrow J/\psi \gamma\gamma$

Meson Particle Listings

$\chi_{c1}(1P)$, $h_c(1P)$, $\chi_{c2}(1P)$

$\chi_{c1}(1P)$ REFERENCES

Author	Year	PR	Doc ID	TECN	Comment
ATHAR	07	PR	D75 032002		S.B. Athar et al. (CLEO Collab.)
ABLIKIM	06D	PR	D73 052006		M. Ablikim et al. (BES Collab.)
ABLIKIM	06R	PR	D74 072001		M. Ablikim et al. (BES Collab.)
ABLIKIM	06T	PL	B642 197		M. Ablikim et al. (BES Collab.)
ABLIKIM	05G	PR	D71 092002		M. Ablikim et al. (BES Collab.)
ABLIKIM	05O	PL	B630 21		M. Ablikim et al. (BES Collab.)
ADAM	05A	PRL	94 232002		N.E. Adam et al. (CLEO Collab.)
ANDREOTTI	05A	NP	B717 34		M. Andreotti et al. (FNAL E835 Collab.)
ABLIKIM	04B	PR	D70 012003		M. Ablikim et al. (BES Collab.)
ABLIKIM	04H	PR	D70 092003		M. Ablikim et al. (BES Collab.)
ATHAR	04	PR	D70 112002		S.B. Athar et al. (CLEO Collab.)
BAI	04F	PR	D59 092001		J.Z. Bai et al. (BES Collab.)
BAI	04I	PR	D70 012006		J.Z. Bai et al. (BES Collab.)
AULCHENKO	03	PL	B573 63		V.M. Aulchenko et al. (KEDR Collab.)
BAI	03E	PR	D67 112001		J.Z. Bai et al. (BES Collab.)
AMBROGIANI	02	PR	D65 052002		M. Ambrogiani et al. (FNAL E835 Collab.)
BAI	99B	PR	D60 072001		J.Z. Bai et al. (BES Collab.)
BAI	98D	PR	D58 092006		J.Z. Bai et al. (BES Collab.)
BAI	98I	PRL	81 3091		J.Z. Bai et al. (BES Collab.)
ARMSTRONG	92	NP	B373 35		T.A. Armstrong et al. (FNAL, FERR, GENO+)
Also		PRL	68 1468		T.A. Armstrong et al. (FNAL, FERR, GENO+)
BAGLIN	86B	PL	B172 455		C. Baglin (LAPP, CERN, GENO, LYON, OSLO+)
GAISER	86	PR	D34 711		J. Gaiser et al. (Crystal Ball Collab.)
LEMOIGNE	82	PL	113B 509		Y. Lemoigne et al. (SACL, LOIC, SHMP+)
OREGLIA	82	PR	D25 2259		M.J. Oreglia et al. (SLAC, CIT, HARV+)
Also		Private Comm.			M.J. Oreglia (SLAC, CIT, HARV+)
HIMEL	80	PRL	44 920		T. Himel et al. (LBL, SLAC)
Also		Private Comm.			G. Trilling (LBL, SLAC)
BRANDELIK	79B	NP	B160 426		R. Brandelik et al. (DASP Collab.)
BARTEL	78B	PL	79B 492		W. Bartel et al. (DESY, HEIDP)
TANENBAUM	78	PR	D17 1731		W.M. Tanenbaum et al. (SLAC, LBL)
Also		Private Comm.			G. Trilling (LBL, UCB)
BIDDICK	77	PRL	38 1324		C.J. Biddick et al. (UCSD, UMD, PAVI+)
FELDMAN	77	PRPL	33C 285		G.J. Feldman, M.L. Perl (LBL, SLAC)
YAMADA	77	Hamburg Conf.	69		S. Yamada (DASP Collab.)
WHITAKER	76	PRL	37 1596		J.S. Whitaker et al. (SLAC, LBL)
TANENBAUM	75	PRL	35 1323		W.M. Tanenbaum et al. (LBL, SLAC)

OTHER RELATED PAPERS

Author	Year	PL	Doc ID	TECN	Comment
BARBERIS	00G	PL	B485 357		D. Barberis et al. (Omega Expt.)
BARATE	93	PL	121B 449		R. Barate et al. (SACL, LOIC, SHMP, IND)
BRAUNSCH...	75B	PL	57B 407		W. Braunschweig et al. (DASP Collab.)
SIMPSON	75	PRL	35 699		J.W. Simpson et al. (STAN, PENN)

$h_c(1P)$

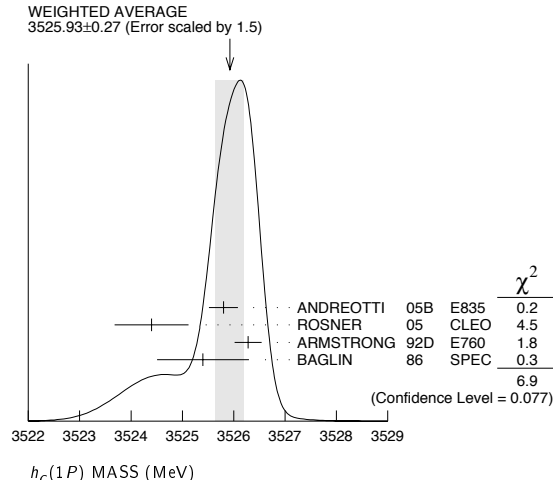
$$I^G(J^{PC}) = ?^2(1^{+-})$$

Quantum numbers are quark model prediction, $C = -$ established by $\eta_c\gamma$ decay.

$h_c(1P)$ MASS

VALUE (MeV)	EVTS	DOCUMENT ID	TECN	COMMENT
3525.93 ± 0.27 OUR AVERAGE				Error includes scale factor of 1.5. See the ideogram below.
3525.8 ± 0.2 ± 0.2	13	ANDREOTTI 05B E835		$\bar{p}p \rightarrow \eta_c\gamma$
3524.4 ± 0.6 ± 0.4	168 ± 40	ROSNER 05 CLEO		$\psi(2S) \rightarrow \pi^0 \eta_c\gamma$
3526.28 ± 0.18 ± 0.19	59	¹ ARMSTRONG 92D E760		$\bar{p}p \rightarrow J/\psi\pi^0$
3525.4 ± 0.8 ± 0.4	5	BAGLIN 86 SPEC		$\bar{p}p \rightarrow J/\psi X$
••• We do not use the following data for averages, fits, limits, etc. •••				
3527 ± 8	42	ANTONIAZZI 94 E705		300 $\pi^\pm, pLi \rightarrow J/\psi\pi^0 X$

¹ Mass central value and systematic error recalculated by us according to Eq. (16) in ARMSTRONG 93B, using the value for the $\psi(2S)$ mass from AULCHENKO 03.



$h_c(1P)$ WIDTH

VALUE (MeV)	CL%	EVTS	DOCUMENT ID	TECN	COMMENT
<1		13	ANDREOTTI 05B E835		$\bar{p}p \rightarrow \eta_c\gamma$
••• We do not use the following data for averages, fits, limits, etc. •••					
<1.1	90	59	ARMSTRONG 92D E760		$\bar{p}p \rightarrow J/\psi\pi^0$

$h_c(1P)$ DECAY MODES

Mode	Fraction (Γ_i/Γ)
Γ_1 $J/\psi(1S)\pi^0$	
Γ_2 $J/\psi(1S)\pi\pi$	not seen
Γ_3 $p\bar{p}$	
Γ_4 $\eta_c\gamma$	seen

$h_c(1P)$ PARTIAL WIDTHS

$h_c(1P) \Gamma(i)\Gamma(\bar{p}p)/\Gamma(\text{total})$

$\Gamma(\eta_c\gamma) \times \Gamma(p\bar{p})/\Gamma_{\text{total}}$	Γ_4/Γ_3			
VALUE (eV)	EVTS	DOCUMENT ID	TECN	COMMENT
12.0 ± 4.5	13	² ANDREOTTI 05B E835		$\bar{p}p \rightarrow \eta_c\gamma$
² Assuming $\Gamma = 1$ MeV.				

$h_c(1P)$ BRANCHING RATIOS

$\Gamma(J/\psi(1S)\pi\pi)/\Gamma(J/\psi(1S)\pi^0)$	Γ_2/Γ_1			
VALUE	CL%	DOCUMENT ID	TECN	COMMENT
<0.18	90	ARMSTRONG 92D E760		$\bar{p}p \rightarrow J/\psi\pi^0$

$\Gamma(\eta_c\gamma)/\Gamma_{\text{total}}$	Γ_4/Γ			
VALUE	EVTS	DOCUMENT ID	TECN	COMMENT
seen	168 ± 40	³ ROSNER 05 CLEO		$\psi(2S) \rightarrow \pi^0 \eta_c\gamma$
³ CLEO measures the product $B(\psi(2S) \rightarrow \pi^0 h_c) \times B(h_c \rightarrow \eta_c\gamma)$ to be $(4.0 \pm 0.8 \pm 0.7) \times 10^{-4}$.				

$h_c(1P)$ REFERENCES

Author	Year	PR	Doc ID	TECN	Comment
ANDREOTTI	05B	PR	D72 032001		M. Andreotti et al. (FNAL E835 Collab.)
ROSNER	05	PRL	95 102003		J.L. Rosner et al. (CLEO Collab.)
AULCHENKO	03	PL	B573 63		V.M. Aulchenko et al. (KEDR Collab.)
ANTONIAZZI	94	PR	D50 4258		L. Antoniazzi et al. (E705 Collab.)
ARMSTRONG	93B	PR	D47 772		T.A. Armstrong et al. (FNAL E760 Collab.)
ARMSTRONG	92D	PRL	69 2337		T.A. Armstrong et al. (FNAL, FERR, GENO+)
BAGLIN	86	PL	B171 135		C. Baglin et al. (LAPP, CERN, TORI, STRB+)

OTHER RELATED PAPERS

Author	Year	PR	Doc ID	TECN	Comment
FANG	06	PR	D74 012007		F. Fang et al. (BELLE Collab.)
HAIDENBAU...	06	PR	D74 017501		J. Haidenbauer et al.
SWANSON	06	PRPL	429 243		E.S. Swanson (PITT)
AUBERT	05R	PR	D71 07103R		B. Aubert et al. (BABAR Collab.)
RUBIN	05	PR	D72 092004		P. Rubin et al. (CLEO Collab.)
EICHTEN	02	PRL	89 162002		E.J. Eichten, K. Lane, C. Quigg

$\chi_{c2}(1P)$

$$I^G(J^{PC}) = 0^+(2^{++})$$

See the Review on " $\psi(2S)$ and χ_c branching ratios" before the $\chi_{c0}(1P)$ Listings.

$\chi_{c2}(1P)$ MASS

VALUE (MeV)	EVTS	DOCUMENT ID	TECN	COMMENT
3556.20 ± 0.09 OUR AVERAGE				
3555.3 ± 0.6 ± 2.2	2.5k	UEHARA 08 BELL		$\gamma\gamma \rightarrow$ hadrons
3555.70 ± 0.59 ± 0.39		ABLIKIM 05G BES2		$\psi(2S) \rightarrow \gamma\chi_{c2}$
3556.173 ± 0.123 ± 0.020		ANDREOTTI 05A E835		$p\bar{p} \rightarrow e^+e^-\gamma$
3559.9 ± 2.9		EISENSTEIN 01 CLE2		$e^+e^- \rightarrow e^+e^-\chi_{c2}$
3556.4 ± 0.7		BAI 99B BES		$\psi(2S) \rightarrow \gamma X$
3556.22 ± 0.131 ± 0.020	585	¹ ARMSTRONG 92 E760		$\bar{p}p \rightarrow e^+e^-\gamma$
3556.9 ± 0.4 ± 0.5	50	BAGLIN 86B SPEC		$\bar{p}p \rightarrow e^+e^- X$
3557.8 ± 0.2 ± 4		² GAISER 86 CBAL		$\psi(2S) \rightarrow \gamma X$
3553.4 ± 2.2	66	³ LEMOIGNE 82 GOLI		185 $\pi^-Be \rightarrow \gamma\mu^+\mu^-A$
3555.9 ± 0.7		⁴ OREGLIA 82 CBAL		$e^+e^- \rightarrow J/\psi 2\gamma$
3557 ± 1.5	69	HIMEL 80 MRK2		$e^+e^- \rightarrow J/\psi 2\gamma$
3551 ± 11	15	BRANDELIK 79B DASP		$e^+e^- \rightarrow J/\psi 2\gamma$
3553 ± 4		⁵ BARTEL 78B CNTR		$e^+e^- \rightarrow J/\psi 2\gamma$
3553 ± 4 ± 4		^{5,6} TANENBAUM 78 MRK1		e^+e^-
3563 ± 7	360	⁵ BIDDICK 77 CNTR		$e^+e^- \rightarrow \gamma X$
••• We do not use the following data for averages, fits, limits, etc. •••				
3543 ± 10	4	WHITAKER 76 MRK1		$e^+e^- \rightarrow J/\psi 2\gamma$

¹ Recalculated by ANDREOTTI 05A, using the value of $\psi(2S)$ mass from AULCHENKO 03.
² Using mass of $\psi(2S) = 3686.0$ MeV.
³ $J/\psi(1S)$ mass constrained to 3097 MeV.
⁴ Assuming $\psi(2S)$ mass = 3686 MeV and $J/\psi(1S)$ mass = 3097 MeV.
⁵ Mass value shifted by us by amount appropriate for $\psi(2S)$ mass = 3686 MeV and $J/\psi(1S)$ mass = 3097 MeV.
⁶ From a simultaneous fit to radiative and hadronic decay channels.

$\chi_{c2}(1P)$ WIDTH

VALUE (MeV)	EVTs	DOCUMENT ID	TECN	COMMENT
2.03 ± 0.12 OUR FIT				
1.95 ± 0.13 OUR AVERAGE				
1.915 ± 0.188 ± 0.013		ANDREOTTI 05A	E835	$p\bar{p} \rightarrow e^+e^-\gamma$
1.96 ± 0.17 ± 0.07	585	⁷ ARMSTRONG 92	E760	$\bar{p}p \rightarrow e^+e^-\gamma$
2.6 ^{+1.4} _{-1.0}	50	BAGLIN 86B	SPEC	$\bar{p}p \rightarrow e^+e^-X$
2.8 ^{+2.1} _{-2.0}		⁸ GAISER 86	CBAL	$\psi(2S) \rightarrow \gamma X$

⁷ Recalculated by ANDREOTTI 05A.
⁸ Errors correspond to 90% confidence level; authors give only width range.

$\chi_{c2}(1P)$ DECAY MODES

Mode	Fraction (Γ_i/Γ)	Confidence level
Hadronic decays		
Γ_1 $2(\pi^+\pi^-)$	(1.14 ± 0.12) %	
Γ_2 $\rho\rho$		
Γ_3 $\pi^+\pi^-K^+K^-$	(9.4 ± 1.1) × 10 ⁻³	
Γ_4 $3(\pi^+\pi^-)$	(8.6 ± 1.8) × 10 ⁻³	
Γ_5 $K^+\bar{K}^*(892)^0\pi^- + c.c.$	(2.3 ± 1.3) × 10 ⁻³	
Γ_6 $K^*(892)^0\bar{K}^*(892)^0$	(2.6 ± 0.5) × 10 ⁻³	
Γ_7 $\phi\phi$	(1.54 ± 0.30) × 10 ⁻³	
Γ_8 $\omega\omega$	(2.0 ± 0.7) × 10 ⁻³	
Γ_9 $\pi\pi$	(2.17 ± 0.25) × 10 ⁻³	
Γ_{10} $\rho^0\pi^+\pi^-$	(4.1 ± 1.8) × 10 ⁻³	
Γ_{11} $\pi^+\pi^-\eta$	(5.5 ± 1.5) × 10 ⁻⁴	
Γ_{12} $\pi^+\pi^-\eta'$	(5.7 ± 2.1) × 10 ⁻⁴	
Γ_{13} $\eta\eta$	< 5 × 10 ⁻⁴	90%
Γ_{14} K^+K^-	(7.9 ± 1.4) × 10 ⁻⁴	
Γ_{15} $K_S^0 K_S^0$	(6.5 ± 0.8) × 10 ⁻⁴	
Γ_{16} $\bar{K}^0 K^+\pi^- + c.c.$	(1.40 ± 0.21) × 10 ⁻³	
Γ_{17} $K^+K^-\pi^0$	(3.5 ± 0.9) × 10 ⁻⁴	
Γ_{18} $K^+K^-\eta$	< 4 × 10 ⁻⁴	90%
Γ_{19} $\eta\pi^+\pi^-$	< 1.7 × 10 ⁻³	90%
Γ_{20} $\eta\eta'$	< 2.6 × 10 ⁻⁴	90%
Γ_{21} $\eta'\eta'$	< 3.5 × 10 ⁻⁴	90%
Γ_{22} $\pi^+\pi^-K_S^0 K_S^0$	(2.5 ± 0.6) × 10 ⁻³	
Γ_{23} $K^+K^-K_S^0 K_S^0$	< 4 × 10 ⁻⁴	90%
Γ_{24} $K^+K^-K^+K^-$	(1.84 ± 0.24) × 10 ⁻³	
Γ_{25} $K^+K^-\phi$	(1.63 ± 0.34) × 10 ⁻³	
Γ_{26} $K_S^0 K_S^0 p\bar{p}$	< 7.9 × 10 ⁻⁴	90%
Γ_{27} $p\bar{p}$	(6.7 ± 0.5) × 10 ⁻⁵	
Γ_{28} $p\bar{p}\pi^0$	(4.9 ± 1.0) × 10 ⁻⁴	
Γ_{29} $p\bar{p}\eta$	(2.1 ± 0.8) × 10 ⁻⁴	
Γ_{30} $\pi^+\pi^-p\bar{p}$	(1.32 ± 0.34) × 10 ⁻³	
Γ_{31} $p\bar{p}\pi^-$	(1.2 ± 0.4) × 10 ⁻³	
Γ_{32} $\Lambda\bar{\Lambda}$	(2.7 ± 1.3) × 10 ⁻⁴	
Γ_{33} $\Lambda\bar{\Lambda}\pi^+\pi^-$	< 3.5 × 10 ⁻³	90%
Γ_{34} $K^+\bar{p}\Lambda + c.c.$	(9.6 ± 1.9) × 10 ⁻⁴	
Γ_{35} $\Xi^-\bar{\Xi}^+$	< 3.7 × 10 ⁻⁴	90%
Γ_{36} $J/\psi(1S)\pi^+\pi^-\pi^0$	< 1.5 %	90%
Radiative decays		
Γ_{37} $\gamma J/\psi(1S)$	(20.0 ± 1.0) %	
Γ_{38} $\gamma\gamma$	(2.43 ± 0.18) × 10 ⁻⁴	

$\chi_{c2}(1P)$ PARTIAL WIDTHS

$\chi_{c2}(1P) \Gamma(i)\Gamma(J/\psi(1S))/\Gamma(\text{total})$

$\Gamma(p\bar{p}) \times \Gamma(\gamma J/\psi(1S))/\Gamma(\text{total})$	DOCUMENT ID	TECN	COMMENT	$\Gamma_{27}\Gamma_{37}/\Gamma$
27.3 ± 1.4 OUR FIT				
27.5 ± 1.5 OUR AVERAGE				
27.0 ± 1.5 ± 1.1	⁹ ANDREOTTI 05A	E835	$p\bar{p} \rightarrow e^+e^-\gamma$	
27.7 ± 1.5 ± 2.0	^{9,10} ARMSTRONG 92	E760	$\bar{p}p \rightarrow e^+e^-\gamma$	
36 ± 8	⁹ BAGLIN 86B	SPEC	$\bar{p}p \rightarrow e^+e^-X$	

$\Gamma(\gamma\gamma) \times \Gamma(\gamma J/\psi(1S))/\Gamma(\text{total})$ $\Gamma_{38}\Gamma_{37}/\Gamma$

VALUE (eV)	EVTs	DOCUMENT ID	TECN	COMMENT
99 ± 7 OUR FIT				
117 ± 10 OUR AVERAGE				
111 ± 12 ± 9	147 ± 15	¹¹ DOBBS 06	CLE3	10.4 $e^+e^- \rightarrow e^+e^-\chi_{c2}$
114 ± 11 ± 9	136 ± 13.3	^{11,12} ABE 02T	BELL	$e^+e^- \rightarrow e^+e^-\chi_{c2}$
139 ± 55 ± 21		^{11,13} ACCIARRI 99E	L3	$e^+e^- \rightarrow e^+e^-\chi_{c2}$
242 ± 65 ± 51		^{11,14} ACKER.,K... 98	OPAL	$e^+e^- \rightarrow e^+e^-\chi_{c2}$
150 ± 42 ± 36		^{11,15} DOMINICK 94	CLE2	$e^+e^- \rightarrow e^+e^-\chi_{c2}$
470 ± 240 ± 120		^{11,16} BAUER 93	TPC	$e^+e^- \rightarrow e^+e^-\chi_{c2}$

⁹ Calculated by us using $B(J/\psi(1S) \rightarrow e^+e^-) = 0.0593 \pm 0.0010$.
¹⁰ Recalculated by ANDREOTTI 05A.
¹¹ Calculated by us using $B(J/\psi \rightarrow \ell^+\ell^-) = 0.1187 \pm 0.0008$.
¹² All systematic errors added in quadrature.
¹³ The value for $\Gamma(\chi_{c2} \rightarrow \gamma\gamma)$ reported in ACCIARRI 99E is derived using $B(\chi_{c2} \rightarrow \gamma J/\psi(1S)) \times B(J/\psi(1S) \rightarrow \ell^+\ell^-) = 0.0162 \pm 0.0014$.
¹⁴ The value for $\Gamma(\chi_{c2} \rightarrow \gamma\gamma)$ reported in ACKERSTAFF, K 98 is derived using $B(\chi_{c2} \rightarrow \gamma J/\psi(1S)) = 0.135 \pm 0.011$ and $B(J/\psi(1S) \rightarrow \ell^+\ell^-) = 0.1203 \pm 0.0038$.
¹⁵ The value for $\Gamma(\chi_{c2} \rightarrow \gamma\gamma)$ reported in DOMINICK 94 is derived using $B(\chi_{c2} \rightarrow \gamma J/\psi(1S)) = 0.135 \pm 0.011$, $B(J/\psi(1S) \rightarrow e^+e^-) = 0.0627 \pm 0.0020$, and $B(J/\psi(1S) \rightarrow \mu^+\mu^-) = 0.0597 \pm 0.0025$.
¹⁶ The value for $\Gamma(\chi_{c2} \rightarrow \gamma\gamma)$ reported in BAUER 93 is derived using $B(\chi_{c2} \rightarrow \gamma J/\psi(1S)) = 0.135 \pm 0.011$, $B(J/\psi(1S) \rightarrow e^+e^-) = 0.0627 \pm 0.0020$, and $B(J/\psi(1S) \rightarrow \mu^+\mu^-) = 0.0597 \pm 0.0025$.

$\chi_{c2}(1P) \Gamma(i)\Gamma(\gamma\gamma)/\Gamma(\text{total})$

$\Gamma(2(\pi^+\pi^-)) \times \Gamma(\gamma\gamma)/\Gamma(\text{total})$ $\Gamma_1\Gamma_{38}/\Gamma$

VALUE (eV)	EVTs	DOCUMENT ID	TECN	COMMENT
5.6 ± 0.5 OUR FIT				
5.2 ± 0.7 OUR AVERAGE				
5.01 ± 0.44 ± 0.55	1597 ± 138	UEHARA 08	BELL	$\gamma\gamma \rightarrow \chi_{c2} \rightarrow 2(\pi^+\pi^-)$
6.4 ± 1.8 ± 0.8		EISENSTEIN 01	CLE2	$e^+e^- \rightarrow e^+e^-\chi_{c2}$

$\Gamma(\rho^0\pi^+\pi^-) \times \Gamma(\gamma\gamma)/\Gamma(\text{total})$ $\Gamma_{10}\Gamma_{38}/\Gamma$

VALUE (eV)	EVTs	DOCUMENT ID	TECN	COMMENT
2.0 ± 0.9 OUR FIT				
3.2 ± 1.9 ± 0.5	986 ± 578	UEHARA 08	BELL	$\gamma\gamma \rightarrow \chi_{c2} \rightarrow 2(\pi^+\pi^-)$

$\Gamma(\rho\rho) \times \Gamma(\gamma\gamma)/\Gamma(\text{total})$ $\Gamma_2\Gamma_{38}/\Gamma$

VALUE (eV)	CL%	EVTs	DOCUMENT ID	TECN	COMMENT
• • •					We do not use the following data for averages, fits, limits, etc. • • •
< 7.8	90	< 598	UEHARA 08	BELL	$\gamma\gamma \rightarrow \chi_{c2} \rightarrow 2(\pi^+\pi^-)$

$\Gamma(\pi^+\pi^-K^+K^-) \times \Gamma(\gamma\gamma)/\Gamma(\text{total})$ $\Gamma_3\Gamma_{38}/\Gamma$

VALUE (eV)	EVTs	DOCUMENT ID	TECN	COMMENT
4.6 ± 0.5 OUR FIT				
4.42 ± 0.42 ± 0.53	780 ± 74	UEHARA 08	BELL	$\gamma\gamma \rightarrow \chi_{c2} \rightarrow K^+K^-\pi^+\pi^-$

$\Gamma(K^*(892)^0\bar{K}^*(892)^0) \times \Gamma(\gamma\gamma)/\Gamma(\text{total})$ $\Gamma_6\Gamma_{38}/\Gamma$

VALUE (eV)	EVTs	DOCUMENT ID	TECN	COMMENT
1.27 ± 0.24 OUR FIT				
0.8 ± 0.17 ± 0.27	151 ± 30	UEHARA 08	BELL	$\gamma\gamma \rightarrow \chi_{c2} \rightarrow K^+K^-\pi^+\pi^-$

$\Gamma(K^+K^-K^+K^-) \times \Gamma(\gamma\gamma)/\Gamma(\text{total})$ $\Gamma_{24}\Gamma_{38}/\Gamma$

VALUE (eV)	EVTs	DOCUMENT ID	TECN	COMMENT
0.91 ± 0.12 OUR FIT				
1.10 ± 0.21 ± 0.15	126 ± 24	UEHARA 08	BELL	$\gamma\gamma \rightarrow \chi_{c2} \rightarrow 2(K^+K^-)$

$\Gamma(\phi\phi) \times \Gamma(\gamma\gamma)/\Gamma(\text{total})$ $\Gamma_7\Gamma_{38}/\Gamma$

VALUE (eV)	EVTs	DOCUMENT ID	TECN	COMMENT
0.76 ± 0.14 OUR FIT				
0.58 ± 0.18 ± 0.16	26.5 ± 8.1	UEHARA 08	BELL	$\gamma\gamma \rightarrow \chi_{c2} \rightarrow 2(K^+K^-)$

$\Gamma(\pi\pi) \times \Gamma(\gamma\gamma)/\Gamma(\text{total})$ $\Gamma_9\Gamma_{38}/\Gamma$

VALUE (eV)	EVTs	DOCUMENT ID	TECN	COMMENT
1.07 ± 0.11 OUR FIT				
1.14 ± 0.21 ± 0.17	54 ± 10	¹⁷ NAKAZAWA 05	BELL	$e^+e^- \rightarrow e^+e^-\chi_{c2}$

$\Gamma(K^+K^-) \times \Gamma(\gamma\gamma)/\Gamma(\text{total})$ $\Gamma_{14}\Gamma_{38}/\Gamma$

VALUE (eV)	EVTs	DOCUMENT ID	TECN	COMMENT
0.39 ± 0.04 OUR FIT				
0.44 ± 0.11 ± 0.07	33 ± 8	NAKAZAWA 05	BELL	$e^+e^- \rightarrow e^+e^-\chi_{c2}$

$\Gamma(K_S^0 K_S^0) \times \Gamma(\gamma\gamma)/\Gamma(\text{total})$ $\Gamma_{15}\Gamma_{38}/\Gamma$

VALUE (eV)	EVTs	DOCUMENT ID	TECN	COMMENT
0.320 ± 0.032 OUR FIT				
0.31 ± 0.05 ± 0.03	38 ± 7	CHEN 07B	BELL	$e^+e^- \rightarrow e^+e^-\chi_{c2}$

¹⁷ We have multiplied $\pi^+\pi^-$ measurement by 3/2 to obtain $\pi\pi$.

Meson Particle Listings

 $\chi_{c2}(1P)$ $\chi_{c2}(1P)$ BRANCHING RATIOS

HADRONIC DECAYS

$\Gamma(2(\pi^+\pi^-))/\Gamma_{\text{total}}$	DOCUMENT ID	TECN	COMMENT	Γ_1/Γ
0.0114 ± 0.0012 OUR FIT				
$\Gamma(\rho^0\pi^+\pi^-)/\Gamma(2(\pi^+\pi^-))$	DOCUMENT ID	TECN	COMMENT	Γ_{10}/Γ_1
0.36 ± 0.17 OUR FIT 0.31 ± 0.17	TANENBAUM 78	MRK1	$\psi(2S) \rightarrow \gamma\chi_{c2}$	
$\Gamma(\rho^0\pi^+\pi^-)/\Gamma_{\text{total}}$	DOCUMENT ID	TECN	COMMENT	Γ_{10}/Γ
41 ± 18 OUR FIT				
$\Gamma(\pi^+\pi^-K^+K^-)/\Gamma_{\text{total}}$	DOCUMENT ID	TECN	COMMENT	Γ_3/Γ
9.4 ± 1.1 OUR FIT				
$\Gamma(K^+\bar{K}^*(892)^0\pi^- + \text{c.c.})/\Gamma(\pi^+\pi^-K^+K^-)$	DOCUMENT ID	TECN	COMMENT	Γ_5/Γ_3
0.25 ± 0.14 OUR FIT 0.25 ± 0.13	TANENBAUM 78	MRK1	$\psi(2S) \rightarrow \gamma\chi_{c2}$	
$\Gamma(K^+\bar{K}^*(892)^0\pi^- + \text{c.c.})/\Gamma_{\text{total}}$	DOCUMENT ID	TECN	COMMENT	Γ_5/Γ
23 ± 13 OUR FIT				
$\Gamma(3(\pi^+\pi^-))/\Gamma_{\text{total}}$	DOCUMENT ID	TECN	COMMENT	Γ_4/Γ
8.6 ± 1.8 OUR EVALUATION 8.6 ± 1.8 OUR AVERAGE 8.6 ± 0.9 ± 1.6 8.7 ± 5.9 ± 0.4	18 BAI 18 TANENBAUM 78	99B MRK1	$\psi(2S) \rightarrow \gamma\chi_{c2}$ $\psi(2S) \rightarrow \gamma\chi_{c2}$	
$\Gamma(K^*(892)^0\bar{K}^*(892)^0)/\Gamma_{\text{total}}$	DOCUMENT ID	TECN	COMMENT	Γ_6/Γ
2.6 ± 0.5 OUR FIT				
$\Gamma(\phi\phi)/\Gamma_{\text{total}}$	DOCUMENT ID	TECN	COMMENT	Γ_7/Γ
1.54 ± 0.30 OUR FIT				
$\Gamma(\omega\omega)/\Gamma_{\text{total}}$	DOCUMENT ID	TECN	COMMENT	Γ_8/Γ
2.0 ± 0.7 ± 0.1	27.7 ± 7.4	19 ABLIKIM	05N BES2 $\psi(2S) \rightarrow \gamma\chi_{c2} \rightarrow \gamma^6\pi$	
$\Gamma(\pi\pi)/\Gamma_{\text{total}}$	DOCUMENT ID	TECN	COMMENT	Γ_9/Γ
2.17 ± 0.25 OUR FIT				
$\Gamma(\pi^+\pi^-\eta)/\Gamma_{\text{total}}$	DOCUMENT ID	TECN	COMMENT	Γ_{11}/Γ
0.55 ± 0.15 ± 0.03	20 ATHAR	07 CLEO	$\psi(2S) \rightarrow \gamma h^+ h^- h^0$	
$\Gamma(\pi^+\pi^-\eta')/\Gamma_{\text{total}}$	DOCUMENT ID	TECN	COMMENT	Γ_{12}/Γ
0.57 ± 0.21 ± 0.03	21 ATHAR	07 CLEO	$\psi(2S) \rightarrow \gamma h^+ h^- h^0$	
$\Gamma(\eta\eta)/\Gamma_{\text{total}}$	DOCUMENT ID	TECN	COMMENT	Γ_{13}/Γ
< 5	90	22 ADAMS	07 CLEO $\psi(2S) \rightarrow \gamma\chi_{c2}$	
• • • We do not use the following data for averages, fits, limits, etc. • • •				
<12	90	18 BAI	03C BES $\psi(2S) \rightarrow \gamma\eta\eta \rightarrow 5\gamma$	
7.9 ± 4.1 ± 2.4		23 LEE	85 CBAL $\psi' \rightarrow \text{photons}$	
$\Gamma(K^+K^-)/\Gamma_{\text{total}}$	DOCUMENT ID	TECN	COMMENT	Γ_{14}/Γ
0.79 ± 0.14 OUR FIT				
$\Gamma(K_S^0 K_S^0)/\Gamma_{\text{total}}$	DOCUMENT ID	TECN	COMMENT	Γ_{15}/Γ
0.65 ± 0.08 OUR FIT				
$\Gamma(K_S^0 K_S^0)/\Gamma(\pi\pi)$	DOCUMENT ID	TECN	COMMENT	Γ_{15}/Γ_9
0.30 ± 0.06 OUR FIT • • • We do not use the following data for averages, fits, limits, etc. • • • 0.27 ± 0.07 ± 0.04	24,25 CHEN	07B BELL	$e^+e^- \rightarrow e^+e^-\chi_{c2}$	

 $\Gamma(K_S^0 K_S^0)/\Gamma(K^+K^-)$

VALUE	DOCUMENT ID	TECN	COMMENT	Γ_{15}/Γ_{14}
0.83 ± 0.19 OUR FIT • • • We do not use the following data for averages, fits, limits, etc. • • • 0.70 ± 0.21 ± 0.12	25,26 CHEN	07B BELL	$e^+e^- \rightarrow e^+e^-\chi_{c2}$	
$\Gamma(\bar{K}^0 K^+ \pi^- + \text{c.c.})/\Gamma_{\text{total}}$	DOCUMENT ID	TECN	COMMENT	Γ_{16}/Γ
1.40 ± 0.21 OUR AVERAGE 1.46 ± 0.23 ± 0.07 1.2 ± 0.4 ± 0.1	27 ATHAR 28 ABLIKIM	07 CLEO 06R BES2	$\psi(2S) \rightarrow \gamma h^+ h^- h^0$ $\psi(2S) \rightarrow \gamma\chi_{c2}$	
• • • We do not use the following data for averages, fits, limits, etc. • • • <2.0	90	18 BAI	99B BES $\psi(2S) \rightarrow \gamma\chi_{c2}$	
$\Gamma(K^+K^-\pi^0)/\Gamma_{\text{total}}$	DOCUMENT ID	TECN	COMMENT	Γ_{17}/Γ
0.35 ± 0.09 ± 0.02	29 ATHAR	07 CLEO	$\psi(2S) \rightarrow \gamma h^+ h^- h^0$	
$\Gamma(K^+K^-\eta)/\Gamma_{\text{total}}$	DOCUMENT ID	TECN	COMMENT	Γ_{18}/Γ
< 0.4	90	30 ATHAR	07 CLEO $\psi(2S) \rightarrow \gamma h^+ h^- h^0$	
$\Gamma(\eta\pi^+\pi^-)/\Gamma_{\text{total}}$	DOCUMENT ID	TECN	COMMENT	Γ_{19}/Γ
< 1.7	90	31 ABLIKIM	06R BES2 $\psi(2S) \rightarrow \gamma\chi_{c2}$	
$\Gamma(\eta\eta)/\Gamma_{\text{total}}$	DOCUMENT ID	TECN	COMMENT	Γ_{20}/Γ
< 2.6	90	32 ADAMS	07 CLEO $\psi(2S) \rightarrow \gamma\chi_{c2}$	
$\Gamma(\eta'\eta)/\Gamma_{\text{total}}$	DOCUMENT ID	TECN	COMMENT	Γ_{21}/Γ
< 3.5	90	33 ADAMS	07 CLEO $\psi(2S) \rightarrow \gamma\chi_{c2}$	
$\Gamma(\pi^+\pi^-K_S^0 K_S^0)/\Gamma_{\text{total}}$	DOCUMENT ID	TECN	COMMENT	Γ_{22}/Γ
2.5 ± 0.6 ± 0.1	57 ± 11	34 ABLIKIM	05o BES2 $\psi(2S) \rightarrow \gamma\chi_{c2}$	
$\Gamma(K^+K^-K_S^0 K_S^0)/\Gamma_{\text{total}}$	DOCUMENT ID	TECN	COMMENT	Γ_{23}/Γ
< 4	90	2.3 ± 2.2	35 ABLIKIM 05o BES2 $e^+e^- \rightarrow \chi_{c2}\gamma$	
$\Gamma(K^+K^-K^+K^-)/\Gamma_{\text{total}}$	DOCUMENT ID	TECN	COMMENT	Γ_{24}/Γ
1.84 ± 0.24 OUR FIT				
$\Gamma(K^+K^-\phi)/\Gamma_{\text{total}}$	DOCUMENT ID	TECN	COMMENT	Γ_{25}/Γ
1.63 ± 0.34 ± 0.08	52	36 ABLIKIM	06T BES2 $\psi(2S) \rightarrow \gamma 2K^+ 2K^-$	
$\Gamma(K_S^0 K_S^0 \rho\bar{\rho})/\Gamma_{\text{total}}$	DOCUMENT ID	TECN	COMMENT	Γ_{26}/Γ
< 7.9	90	37 ABLIKIM	06D BES2 $\psi(2S) \rightarrow \chi_{c2}\gamma$	
$\Gamma(\rho\bar{\rho})/\Gamma_{\text{total}}$	DOCUMENT ID	TECN	COMMENT	Γ_{27}/Γ
0.67 ± 0.05 OUR FIT				
$\Gamma(\rho\bar{\rho}\pi^0)/\Gamma_{\text{total}}$	DOCUMENT ID	TECN	COMMENT	Γ_{28}/Γ
0.49 ± 0.10 ± 0.02	38 ATHAR	07 CLEO	$\psi(2S) \rightarrow \gamma h^+ h^- h^0$	
$\Gamma(\rho\bar{\rho}\eta)/\Gamma_{\text{total}}$	DOCUMENT ID	TECN	COMMENT	Γ_{29}/Γ
0.21 ± 0.08 ± 0.01	39 ATHAR	07 CLEO	$\psi(2S) \rightarrow \gamma h^+ h^- h^0$	
$\Gamma(\pi^+\pi^-\rho\bar{\rho})/\Gamma_{\text{total}}$	DOCUMENT ID	TECN	COMMENT	Γ_{30}/Γ
1.32 ± 0.34 OUR EVALUATION 1.3 ± 0.4 OUR AVERAGE 1.17 ± 0.19 ± 0.30 2.64 ± 1.03 ± 0.14	18 BAI 18 TANENBAUM 78	99B MRK1	BES $\psi(2S) \rightarrow \gamma\chi_{c2}$ MRK1 $\psi(2S) \rightarrow \gamma\chi_{c2}$	
• • • We do not use the following data for averages, fits, limits, etc. • • • Error includes scale factor of 1.3.				
$\Gamma(\rho\bar{\rho}\pi^-)/\Gamma_{\text{total}}$	DOCUMENT ID	TECN	COMMENT	Γ_{31}/Γ
12 ± 4 ± 1	40 ABLIKIM	06I BES2	$\psi(2S) \rightarrow \gamma\rho\pi^- X$	
$\Gamma(\Lambda\bar{\Lambda})/\Gamma_{\text{total}}$	DOCUMENT ID	TECN	COMMENT	Γ_{32}/Γ
2.7 ± 1.2 ± 0.5	8.3 ± 3.7 3.4	18 BAI	03E BES $\psi(2S) \rightarrow \gamma\chi_{c2} \rightarrow \gamma\Lambda\bar{\Lambda}$	

$\Gamma(\overline{A}\pi^+\pi^-)/\Gamma_{\text{total}}$		Γ_{33}/Γ	
VALUE (units 10^{-3})	CL%	DOCUMENT ID	TECN COMMENT
<3.5	90	37 ABLIKIM	06D BES2 $\psi(2S) \rightarrow \chi_{c2}\gamma$

$\Gamma(K^+\overline{p}A + \text{c.c.})/\Gamma_{\text{total}}$		Γ_{34}/Γ	
VALUE (units 10^{-3})	CL%	DOCUMENT ID	TECN COMMENT
0.96 ± 0.18 ± 0.05		41 ATHAR	07 CLEO $\psi(2S) \rightarrow \gamma h^+ h^- h^0$

$\Gamma(\Xi^-\overline{\Xi}^+)/\Gamma_{\text{total}}$		Γ_{35}/Γ	
VALUE (units 10^{-4})	CL%	DOCUMENT ID	TECN COMMENT
<3.7	90	37 ABLIKIM	06D BES2 $\psi(2S) \rightarrow \chi_{c2}\gamma$

$\Gamma(J/\psi(1S)\pi^+\pi^-\pi^0)/\Gamma_{\text{total}}$		Γ_{36}/Γ	
VALUE	CL%	DOCUMENT ID	TECN COMMENT
<0.015	90	BARATE	81 SPEC 190 GeV $\pi^- \text{Be} \rightarrow 2\pi 2\mu$

¹⁸Rescaled by us using $B(\psi(2S) \rightarrow \gamma\chi_{c2}) = (8.3 \pm 0.4)\%$ and $B(\psi(2S) \rightarrow J/\psi(1S)\pi^+\pi^-) = (32.6 \pm 0.5)\%$. Multiplied by a factor of 2 to convert from $K_S^0 K^+\pi^-$ to $K^0 K^+\pi^-$ decay.

¹⁹ABLIKIM 05N reports $[B(\chi_{c2}(1P) \rightarrow \omega\omega)] \times [B(\psi(2S) \rightarrow \gamma\chi_{c2}(1P))] = (0.165 \pm 0.044 \pm 0.032) \times 10^{-3}$. We divide by our best value $B(\psi(2S) \rightarrow \gamma\chi_{c2}(1P)) = (8.3 \pm 0.4) \times 10^{-2}$. Our first error is their experiment's error and our second error is the systematic error from using our best value.

²⁰ATHAR 07 reports $(0.49 \pm 0.12 \pm 0.06) \times 10^{-3}$ for $B(\psi(2S) \rightarrow \gamma\chi_{c2}(1P)) = (9.33 \pm 0.14 \pm 0.61) \times 10^{-2}$. We rescale to our best value $B(\psi(2S) \rightarrow \gamma\chi_{c2}(1P)) = (8.3 \pm 0.4) \times 10^{-2}$. Our first error is their experiment's error and our second error is the systematic error from using our best value.

²¹ATHAR 07 reports $(0.51 \pm 0.18 \pm 0.06) \times 10^{-3}$ for $B(\psi(2S) \rightarrow \gamma\chi_{c2}(1P)) = (9.33 \pm 0.14 \pm 0.61) \times 10^{-2}$. We rescale to our best value $B(\psi(2S) \rightarrow \gamma\chi_{c2}(1P)) = (8.3 \pm 0.4) \times 10^{-2}$. Our first error is their experiment's error and our second error is the systematic error from using our best value.

²²ADAMS 07 reports $< 4.7 \times 10^{-4}$ for $B(\psi(2S) \rightarrow \gamma\chi_{c2}(1P)) = 0.0933 \pm 0.0014 \pm 0.0061$. We rescale to our best value $B(\psi(2S) \rightarrow \gamma\chi_{c2}(1P)) = 0.083$.

²³Calculated using $B(\psi(2S) \rightarrow \gamma\chi_{c2}(1P)) = 0.078 \pm 0.008$.

²⁴Using $\Gamma(\pi\pi) \times \Gamma(\gamma\gamma)/\Gamma_{\text{total}}$ from the $\pi^+\pi^-$ measurement of NAKAZAWA 05 rescaled by 3/2 to convert to $\pi\pi$.

²⁵Not independent from other measurements.

²⁶Using $\Gamma(K^+K^-) \times \Gamma(\gamma\gamma)/\Gamma_{\text{total}}$ from NAKAZAWA 05.

²⁷ATHAR 07 reports $(1.3 \pm 0.2 \pm 0.1) \times 10^{-3}$ for $B(\psi(2S) \rightarrow \gamma\chi_{c2}(1P)) = (9.33 \pm 0.14 \pm 0.61) \times 10^{-2}$. We rescale to our best value $B(\psi(2S) \rightarrow \gamma\chi_{c2}(1P)) = (8.3 \pm 0.4) \times 10^{-2}$. Our first error is their experiment's error and our second error is the systematic error from using our best value.

²⁸We have multiplied the $K_S^0 K^+\pi^-$ measurement by a factor of 2 to convert to $K^0 K^+\pi^-$. ABLIKIM 06R reports $(1.2 \pm 0.4 \pm 0.2) \times 10^{-3}$ for $B(\psi(2S) \rightarrow \gamma\chi_{c2}(1P)) = (8.1 \pm 0.6) \times 10^{-2}$. We rescale to our best value $B(\psi(2S) \rightarrow \gamma\chi_{c2}(1P)) = (8.3 \pm 0.4) \times 10^{-2}$. Our first error is their experiment's error and our second error is the systematic error from using our best value.

²⁹ATHAR 07 reports $(0.31 \pm 0.07 \pm 0.04) \times 10^{-3}$ for $B(\psi(2S) \rightarrow \gamma\chi_{c2}(1P)) = (9.33 \pm 0.14 \pm 0.61) \times 10^{-2}$. We rescale to our best value $B(\psi(2S) \rightarrow \gamma\chi_{c2}(1P)) = (8.3 \pm 0.4) \times 10^{-2}$. Our first error is their experiment's error and our second error is the systematic error from using our best value.

³⁰ATHAR 07 reports $< 0.33 \times 10^{-3}$ for $B(\psi(2S) \rightarrow \gamma\chi_{c2}(1P)) = (9.33 \pm 0.14 \pm 0.61) \times 10^{-2}$. We rescale to our best value $B(\psi(2S) \rightarrow \gamma\chi_{c2}(1P)) = 0.083$.

³¹ABLIKIM 06R reports $< 1.7 \times 10^{-3}$ for $B(\psi(2S) \rightarrow \gamma\chi_{c2}(1P)) = (8.1 \pm 0.4) \times 10^{-2}$. We rescale to our best value $B(\psi(2S) \rightarrow \gamma\chi_{c2}(1P)) = 0.083$.

³²ADAMS 07 reports $< 2.3 \times 10^{-4}$ for $B(\psi(2S) \rightarrow \gamma\chi_{c2}(1P)) = 0.0933 \pm 0.0014 \pm 0.0061$. We rescale to our best value $B(\psi(2S) \rightarrow \gamma\chi_{c2}(1P)) = 0.083$.

³³ADAMS 07 reports $< 3.1 \times 10^{-4}$ for $B(\psi(2S) \rightarrow \gamma\chi_{c2}(1P)) = 0.0933 \pm 0.0014 \pm 0.0061$. We rescale to our best value $B(\psi(2S) \rightarrow \gamma\chi_{c2}(1P)) = 0.083$.

³⁴ABLIKIM 05o reports $[B(\chi_{c2}(1P) \rightarrow \pi^+\pi^-K_S^0K_S^0)] \times [B(\psi(2S) \rightarrow \gamma\chi_{c2}(1P))] = (0.207 \pm 0.039 \pm 0.033) \times 10^{-3}$. We divide by our best value $B(\psi(2S) \rightarrow \gamma\chi_{c2}(1P)) = (8.3 \pm 0.4) \times 10^{-2}$. Our first error is their experiment's error and our second error is the systematic error from using our best value.

³⁵ABLIKIM 05o reports $[B(\chi_{c2}(1P) \rightarrow K^+K^-K_S^0K_S^0)] \times [B(\psi(2S) \rightarrow \gamma\chi_{c2}(1P))] < 3.5 \times 10^{-5}$. We divide by our best value $B(\psi(2S) \rightarrow \gamma\chi_{c2}(1P)) = 0.083$.

³⁶ABLIKIM 06T reports $(1.67 \pm 0.26 \pm 0.24) \times 10^{-3}$ for $B(\psi(2S) \rightarrow \gamma\chi_{c2}(1P)) = (8.1 \pm 0.4) \times 10^{-2}$. We rescale to our best value $B(\psi(2S) \rightarrow \gamma\chi_{c2}(1P)) = (8.3 \pm 0.4) \times 10^{-2}$. Our first error is their experiment's error and our second error is the systematic error from using our best value.

³⁷Using $B(\psi(2S) \rightarrow \chi_{c2}\gamma) = (9.3 \pm 0.6)\%$.

³⁸ATHAR 07 reports $(0.44 \pm 0.08 \pm 0.05) \times 10^{-3}$ for $B(\psi(2S) \rightarrow \gamma\chi_{c2}(1P)) = (9.33 \pm 0.14 \pm 0.61) \times 10^{-2}$. We rescale to our best value $B(\psi(2S) \rightarrow \gamma\chi_{c2}(1P)) = (8.3 \pm 0.4) \times 10^{-2}$. Our first error is their experiment's error and our second error is the systematic error from using our best value.

³⁹ATHAR 07 reports $(0.19 \pm 0.07 \pm 0.02) \times 10^{-3}$ for $B(\psi(2S) \rightarrow \gamma\chi_{c2}(1P)) = (9.33 \pm 0.14 \pm 0.61) \times 10^{-2}$. We rescale to our best value $B(\psi(2S) \rightarrow \gamma\chi_{c2}(1P)) = (8.3 \pm 0.4) \times 10^{-2}$. Our first error is their experiment's error and our second error is the systematic error from using our best value.

⁴⁰ABLIKIM 06i reports $[B(\chi_{c2}(1P) \rightarrow p\overline{p}\pi^-)] \times [B(\psi(2S) \rightarrow \gamma\chi_{c2}(1P))] = (0.97 \pm 0.20 \pm 0.26) \times 10^{-4}$. We divide by our best value $B(\psi(2S) \rightarrow \gamma\chi_{c2}(1P)) = (8.3 \pm 0.4) \times 10^{-2}$. Our first error is their experiment's error and our second error is the systematic error from using our best value.

⁴¹ATHAR 07 reports $(0.85 \pm 0.14 \pm 0.10) \times 10^{-3}$ for $B(\psi(2S) \rightarrow \gamma\chi_{c2}(1P)) = (9.33 \pm 0.14 \pm 0.61) \times 10^{-2}$. We rescale to our best value $B(\psi(2S) \rightarrow \gamma\chi_{c2}(1P)) = (8.3 \pm 0.4) \times 10^{-2}$. Our first error is their experiment's error and our second error is the systematic error from using our best value.

RADIATIVE DECAYS

$\Gamma(\gamma J/\psi(1S))/\Gamma_{\text{total}}$		Γ_{37}/Γ	
VALUE	CL%	DOCUMENT ID	TECN COMMENT
0.200 ± 0.010 OUR FIT			

• • • We do not use the following data for averages, fits, limits, etc. • • •

0.199 ± 0.005 ± 0.012 ⁴²ADAM 05A CLEO $e^+e^- \rightarrow \psi(2S) \rightarrow \gamma\chi_{c2}$

$\Gamma(\gamma\gamma)/\Gamma_{\text{total}}$		Γ_{38}/Γ	
VALUE (units 10^{-4})	CL%	DOCUMENT ID	TECN COMMENT
2.43 ± 0.18 OUR FIT			

$\Gamma(\gamma\gamma)/\Gamma(\gamma J/\psi(1S))$		Γ_{38}/Γ_{37}	
VALUE (units 10^{-3})	CL%	DOCUMENT ID	TECN COMMENT
1.21 ± 0.10 OUR FIT			

0.99 ± 0.18 ⁴³AMBROGIANI 00B E835 $\overline{p}p \rightarrow \chi_{c2} \rightarrow \gamma\gamma, \gamma J/\psi$

$\Gamma(\gamma\gamma) \times \Gamma(\overline{p}p)/\Gamma_{\text{total}}^2$		$\Gamma_{38}\Gamma_{27}/\Gamma^2$	
VALUE (units 10^{-8})	CL%	DOCUMENT ID	TECN COMMENT
1.64 ± 0.20 OUR FIT			

1.7 ± 0.4 OUR AVERAGE

1.60 ± 0.42 ARMSTRONG 93 E760 $\overline{p}p \rightarrow \gamma\gamma X$

9.9 ± 4.5 BAGLIN 87B SPEC $\overline{p}p \rightarrow \gamma\gamma X$

⁴²Uses $B(\psi(2S) \rightarrow \gamma\chi_{c2} \rightarrow \gamma J/\psi)$ from ADAM 05A and $B(\psi(2S) \rightarrow \gamma\chi_{c2})$ from ATHAR 04.

⁴³Calculated by us using $B(J/\psi(1S) \rightarrow e^+e^-) = 0.0593 \pm 0.0010$.

 $\chi_{c2}(1P)$ CROSS-PARTICLE BRANCHING RATIOS

$$B(\chi_{c2}(1P) \rightarrow K^+K^-\pi^+\pi^-) \times \frac{\Gamma(\psi(2S) \rightarrow \gamma\chi_{c2}(1P))}{\Gamma(\psi(2S) \rightarrow J/\psi(1S)\pi^+\pi^-)}$$

VALUE (units 10^{-3})	CL%	DOCUMENT ID	TECN COMMENT
2.38 ± 0.28 OUR FIT			

2.5 ± 0.9 OUR AVERAGE Error includes scale factor of 2.3.

1.90 ± 0.14 ± 0.44 BAI 99B BES $\psi(2S) \rightarrow \gamma\chi_{c2}$

3.8 ± 0.67 ⁴⁴TANENBAUM 78 MRK1 $\psi(2S) \rightarrow \gamma\chi_{c2}$

$$B(\chi_{c2}(1P) \rightarrow K^*(892)^0\overline{K}^*(892)^0) \times B(\psi(2S) \rightarrow \gamma\chi_{c2}(1P))$$

VALUE (units 10^{-4})	CL%	DOCUMENT ID	TECN COMMENT
2.1 ± 0.4 OUR FIT			

3.11 ± 0.36 ± 0.48 ABLIKIM 04H BES2 $\psi(2S) \rightarrow \gamma\chi_{c2}$

$$B(\chi_{c2}(1P) \rightarrow \overline{p}p) \times \frac{\Gamma(\psi(2S) \rightarrow \gamma\chi_{c2}(1P))}{\Gamma(\psi(2S) \rightarrow J/\psi(1S)\pi^+\pi^-)}$$

VALUE (units 10^{-5})	CL%	DOCUMENT ID	TECN COMMENT
1.70 ± 0.17 OUR FIT			

1.4 ± 1.1 ⁴⁵BAI 98I BES $\psi(2S) \rightarrow \gamma\chi_{c2} \rightarrow \gamma\overline{p}p$

$$B(\chi_{c2}(1P) \rightarrow \overline{p}p) \times B(\psi(2S) \rightarrow \gamma\chi_{c2}(1P))$$

VALUE (units 10^{-6})	CL%	EVTS	DOCUMENT ID	TECN COMMENT
5.6 ± 0.6 OUR FIT				

4.4 ± 1.6 ± 0.6 14.3 ± 5.2 _{-4.7} BAI 04F BES $\psi(2S) \rightarrow \gamma\chi_{c2}(1P) \rightarrow \gamma\overline{p}p$

$$B(\chi_{c2}(1P) \rightarrow K^+K^-) \times \frac{\Gamma(\psi(2S) \rightarrow \gamma\chi_{c2}(1P))}{\Gamma(\psi(2S) \rightarrow J/\psi(1S)\pi^+\pi^-)}$$

VALUE (units 10^{-3})	CL%	EVTS	DOCUMENT ID	TECN COMMENT
0.199 ± 0.017 OUR FIT				

0.190 ± 0.034 ± 0.019 115 ± 13 ⁴⁶BAI 98I BES $\psi(2S) \rightarrow \gamma K^+K^-$

$$B(\chi_{c2}(1P) \rightarrow K_S^0 K_S^0) \times B(\psi(2S) \rightarrow \gamma\chi_{c2}(1P))$$

VALUE (units 10^{-5})	CL%	EVTS	DOCUMENT ID	TECN COMMENT
5.4 ± 0.7 OUR FIT				

5.72 ± 0.76 ± 0.63 65 ABLIKIM 05o BES2 $\psi(2S) \rightarrow \gamma K_S^0 K_S^0$

$$B(\chi_{c2}(1P) \rightarrow K_S^0 K_S^0) \times \frac{\Gamma(\psi(2S) \rightarrow \gamma\chi_{c2}(1P))}{\Gamma(\psi(2S) \rightarrow J/\psi(1S)\pi^+\pi^-)}$$

VALUE (units 10^{-5})	CL%	DOCUMENT ID	TECN COMMENT
16.4 ± 1.4 OUR FIT			

14.7 ± 4.1 ± 3.3 ⁴⁷BAI 99B BES $\psi(2S) \rightarrow \gamma K_S^0 K_S^0$

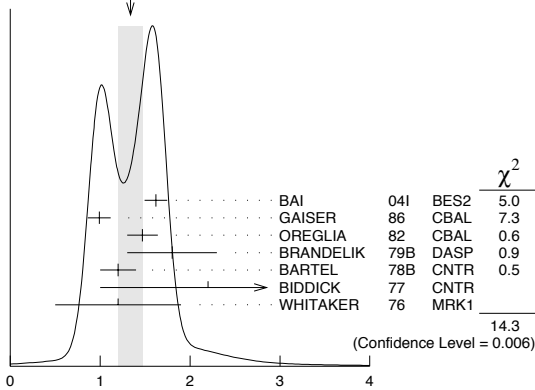
Meson Particle Listings

 $\chi_{c2}(1P)$

$$B(\chi_{c2}(1P) \rightarrow \gamma J/\psi(1S)) \times B(\psi(2S) \rightarrow \gamma \chi_{c2}(1P))$$

VALUE (units 10^{-2})	EVTS	DOCUMENT ID	TECN	COMMENT
1.66 ± 0.04 OUR FIT				
1.34 ± 0.14 OUR AVERAGE				Error includes scale factor of 1.9. See the ideogram below.
1.62 ± 0.04 ± 0.12	5.8k	BAI	04I	BES2 $\psi(2S) \rightarrow J/\psi \gamma \gamma$
0.99 ± 0.10 ± 0.08		GAISER	86	CBAL $\psi(2S) \rightarrow \gamma X$
1.47 ± 0.17	48	OREGLIA	82	CBAL $\psi(2S) \rightarrow \gamma \chi_{c2}$
1.8 ± 0.5	49	BRANDELIK	79B	DASP $\psi(2S) \rightarrow \gamma \chi_{c2}$
1.2 ± 0.2	49	BARTEL	78B	CNTR $\psi(2S) \rightarrow \gamma \chi_{c2}$
2.2 ± 1.2	50	BIDDICK	77	CNTR $e^+ e^- \rightarrow \gamma X$
1.2 ± 0.7	48	WHITAKER	76	MRK1 $e^+ e^-$
• • • We do not use the following data for averages, fits, limits, etc. • • •				
1.85 ± 0.04 ± 0.07	1.9k	51 ADAM	05A	CLEO $\psi(2S) \rightarrow J/\psi \gamma \gamma$

WEIGHTED AVERAGE
1.34 ± 0.14 (Error scaled by 1.9)



$$B(\chi_{c2}(1P) \rightarrow \gamma J/\psi(1S)) \times B(\psi(2S) \rightarrow \gamma \chi_{c2}(1P))$$

$$B(\chi_{c2}(1P) \rightarrow \gamma J/\psi) \times \frac{\Gamma(\psi(2S) \rightarrow \gamma \chi_{c2}(1P))}{\Gamma(\psi(2S) \rightarrow J/\psi(1S) \text{ anything})}$$

VALUE (units 10^{-2})	EVTS	DOCUMENT ID	TECN	COMMENT
2.88 ± 0.04 OUR FIT				
3.11 ± 0.07 ± 0.07	1.9k	ADAM	05A	CLEO $\psi(2S) \rightarrow J/\psi \gamma \gamma$

$$B(\chi_{c2}(1P) \rightarrow \gamma J/\psi(1S)) \times \frac{\Gamma(\psi(2S) \rightarrow \gamma \chi_{c2}(1P))}{\Gamma(\psi(2S) \rightarrow J/\psi(1S) \pi^+ \pi^-)}$$

VALUE (units 10^{-2})	EVTS	DOCUMENT ID	TECN	COMMENT
5.08 ± 0.18 OUR FIT				
4.2 ± 1.1 OUR AVERAGE				
6.0 ± 2.8	1.3k	52 ABLIKIM	04B	BES $\psi(2S) \rightarrow J/\psi X$
3.9 ± 1.2	53	HIMEL	80	MRK2 $\psi(2S) \rightarrow \gamma \chi_{c2}$
• • • We do not use the following data for averages, fits, limits, etc. • • •				
5.52 ± 0.13 ± 0.13	1.9k	51 ADAM	05A	CLEO $\psi(2S) \rightarrow J/\psi \gamma \gamma$

$$B(\chi_{c2}(1P) \rightarrow \gamma \gamma) \times B(\psi(2S) \rightarrow \gamma \chi_{c2}(1P))$$

VALUE (units 10^{-5})	DOCUMENT ID	TECN	COMMENT
2.01 ± 0.19 OUR FIT			
7.0 ± 2.1 ± 2.0	LEE	85	CBAL $\psi(2S) \rightarrow \gamma \chi_{c2}$

$$B(\chi_{c2}(1P) \rightarrow \pi \pi) \times \frac{\Gamma(\psi(2S) \rightarrow \gamma \chi_{c2}(1P))}{\Gamma(\psi(2S) \rightarrow J/\psi(1S) \pi^+ \pi^-)}$$

VALUE (units 10^{-3})	EVTS	DOCUMENT ID	TECN	COMMENT
0.55 ± 0.05 OUR FIT				
0.54 ± 0.06 OUR AVERAGE				
0.66 ± 0.18 ± 0.37	21 ± 6	54 BAI	03c	BES $\psi(2S) \rightarrow \gamma \pi^0 \pi^0$
0.54 ± 0.05 ± 0.04	185 ± 16	55 BAI	98i	BES $\psi(2S) \rightarrow \gamma \pi^+ \pi^-$

$$B(\chi_{c2}(1P) \rightarrow 2(\pi^+ \pi^-)) \times \frac{\Gamma(\psi(2S) \rightarrow \gamma \chi_{c2}(1P))}{\Gamma(\psi(2S) \rightarrow J/\psi(1S) \pi^+ \pi^-)}$$

VALUE (units 10^{-3})	DOCUMENT ID	TECN	COMMENT	
2.88 ± 0.29 OUR FIT				
3.1 ± 1.0 OUR AVERAGE			Error includes scale factor of 2.5.	
2.3 ± 0.1 ± 0.5	56	BAI	99B	BES $\psi(2S) \rightarrow \gamma \chi_{c2}$
4.3 ± 0.6	57	TANENBAUM	78	MRK1 $\psi(2S) \rightarrow \gamma \chi_{c2}$

$$B(\chi_{c2}(1P) \rightarrow K^+ K^- K^+ K^-) \times B(\psi(2S) \rightarrow \gamma \chi_{c2}(1P))$$

VALUE (units 10^{-4})	EVTS	DOCUMENT ID	TECN	COMMENT
1.52 ± 0.18 OUR FIT				
1.76 ± 0.16 ± 0.24	160	58 ABLIKIM	06T	BES2 $\psi(2S) \rightarrow \gamma 2K^+ 2K^-$

$$B(\chi_{c2}(1P) \rightarrow K^+ K^- K^+ K^-) \times \frac{\Gamma(\psi(2S) \rightarrow \gamma \chi_{c2}(1P))}{\Gamma(\psi(2S) \rightarrow J/\psi(1S) \pi^+ \pi^-)}$$

VALUE (units 10^{-4})	DOCUMENT ID	TECN	COMMENT	
4.7 ± 0.4 OUR FIT				
3.6 ± 0.6 ± 0.6	59	BAI	99B	BES $\psi(2S) \rightarrow \gamma 2K^+ 2K^-$

$$B(\chi_{c2}(1P) \rightarrow \phi \phi) \times B(\psi(2S) \rightarrow \gamma \chi_{c2}(1P))$$

VALUE (units 10^{-4})	EVTS	DOCUMENT ID	TECN	COMMENT
1.27 ± 0.24 OUR FIT				
1.38 ± 0.24 ± 0.23	41	60 ABLIKIM	06T	BES2 $\psi(2S) \rightarrow \gamma 2K^+ 2K^-$

$$B(\chi_{c2}(1P) \rightarrow \phi \phi) \times \frac{\Gamma(\psi(2S) \rightarrow \gamma \chi_{c2}(1P))}{\Gamma(\psi(2S) \rightarrow J/\psi(1S) \pi^+ \pi^-)}$$

VALUE (units 10^{-4})	DOCUMENT ID	TECN	COMMENT	
3.89 ± 0.33 OUR FIT				
4.8 ± 1.3 ± 1.3	61	BAI	99B	BES $\psi(2S) \rightarrow \gamma 2K^+ 2K^-$

44 The reported value is derived using $B(\psi(2S) \rightarrow \pi^+ \pi^- J/\psi) \times B(J/\psi \rightarrow \ell^+ \ell^-) = (4.6 \pm 0.7)\%$. Calculated by us using $B(J/\psi \rightarrow \ell^+ \ell^-) = 0.1181 \pm 0.0020$.

45 Calculated by us. The value for $B(\chi_{c2} \rightarrow p\bar{p})$ reported in BAI 98i is derived using $B(\psi(2S) \rightarrow \gamma \chi_{c2}) = (7.8 \pm 0.8)\%$ and $B(\psi(2S) \rightarrow J/\psi(1S) \pi^+ \pi^-) = (32.4 \pm 2.6)\%$ [BAI 98d].

46 Calculated by us. The value for $B(\chi_{c2} \rightarrow K^+ K^-)$ reported by BAI 98i is derived using $B(\psi(2S) \rightarrow \gamma \chi_{c2}) = (7.8 \pm 0.8)\%$ and $B(\psi(2S) \rightarrow J/\psi \pi^+ \pi^-) = (32.4 \pm 2.6)\%$ [BAI 98d].

47 Calculated by us. The value of $B(\chi_{c2} \rightarrow K_S^0 K_S^0)$ reported by BAI 99b was derived using $B(\psi(2S) \rightarrow \gamma \chi_{c2}(1P)) = (7.8 \pm 0.8)\%$ and $B(\psi(2S) \rightarrow J/\psi \pi^+ \pi^-) = (32.4 \pm 2.6)\%$ [BAI 98d].

48 Recalculated by us using $B(J/\psi(1S) \rightarrow \ell^+ \ell^-) = 0.1181 \pm 0.0020$.

49 Recalculated by us using $B(J/\psi(1S) \rightarrow \mu^+ \mu^-) = 0.0588 \pm 0.0010$.

50 Assumes isotropic gamma distribution.

51 Not independent from other values reported by ADAM 05A.

52 From a fit to the J/ψ recoil mass spectra.

53 The value for $B(\psi(2S) \rightarrow \gamma \chi_{c2}) \times B(\chi_{c2} \rightarrow \gamma J/\psi(1S))$ reported in HIMEL 80 is derived using $B(\psi(2S) \rightarrow J/\psi(1S) \pi^+ \pi^-) = (33 \pm 3)\%$ and $B(J/\psi(1S) \rightarrow \ell^+ \ell^-) = 0.138 \pm 0.018$. Calculated by us using $B(J/\psi(1S) \rightarrow \ell^+ \ell^-) = (0.1181 \pm 0.0020)$.

54 We have multiplied $\pi^0 \pi^0$ measurement by 3 to obtain $\pi \pi$.

55 Calculated by us. The value for $B(\chi_{c2} \rightarrow \pi^+ \pi^-)$ reported by BAI 98i is derived using $B(\psi(2S) \rightarrow \gamma \chi_{c2}) = (7.8 \pm 0.8)\%$ and $B(\psi(2S) \rightarrow J/\psi \pi^+ \pi^-) = (32.4 \pm 2.6)\%$ [BAI 98d]. We have multiplied $\pi^+ \pi^-$ measurement by 3/2 to obtain $\pi \pi$.

56 Calculated by us. The value for $B(\chi_{c2} \rightarrow 2\pi^+ 2\pi^-)$ reported in BAI 99b is derived using $B(\psi(2S) \rightarrow \gamma \chi_{c2}) = (7.8 \pm 0.8)\%$ and $B(\psi(2S) \rightarrow J/\psi(1S) \pi^+ \pi^-) = (32.4 \pm 2.6)\%$ [BAI 98d].

57 The value for $B(\psi(2S) \rightarrow \gamma \chi_{c2}) \times B(\chi_{c2} \rightarrow 2\pi^+ \pi^-)$ reported in TANENBAUM 78 is derived using $B(\psi(2S) \rightarrow J/\psi(1S) \pi^+ \pi^-) \times B(J/\psi(1S) \rightarrow \ell^+ \ell^-) = (4.6 \pm 0.7)\%$. Calculated by us using $B(J/\psi(1S) \rightarrow \ell^+ \ell^-) = 0.1181 \pm 0.0020$.

58 Calculated by us. The value of $B(\chi_{c2} \rightarrow 2K^+ 2K^-)$ reported by ABLIKIM 06t was derived using $B(\psi(2S) \rightarrow \gamma \chi_{c2}(1P)) = (8.1 \pm 0.4)\%$.

59 Calculated by us. The value of $B(\chi_{c2} \rightarrow 2K^+ 2K^-)$ reported by BAI 99b was derived using $B(\psi(2S) \rightarrow \gamma \chi_{c2}(1P)) = (7.8 \pm 0.8)\%$ and $B(\psi(2S) \rightarrow J/\psi \pi^+ \pi^-) = (32.4 \pm 2.6)\%$ [BAI 98d].

60 Calculated by us. The value of $B(\chi_{c2} \rightarrow \phi \phi)$ reported by ABLIKIM 06t was derived using $B(\psi(2S) \rightarrow \gamma \chi_{c2}(1P)) = (8.1 \pm 0.4)\%$.

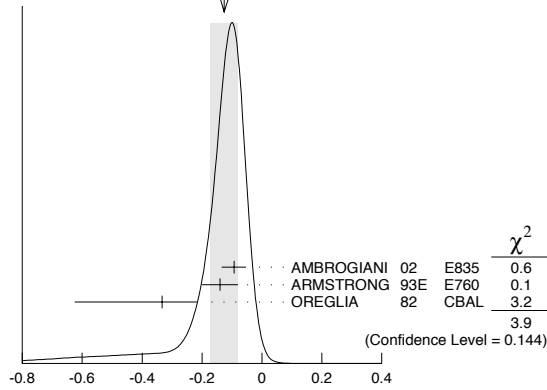
61 Calculated by us. The value of $B(\chi_{c2} \rightarrow \phi \phi)$ reported by BAI 99b was derived using $B(\psi(2S) \rightarrow \gamma \chi_{c2}(1P)) = (7.8 \pm 0.8)\%$ and $B(\psi(2S) \rightarrow J/\psi \pi^+ \pi^-) = (32.4 \pm 2.6)\%$ [BAI 98d].

MULTIPOLE AMPLITUDES IN $\chi_{c2}(1P) \rightarrow \gamma J/\psi(1S)$ RADIATIVE DECAY

$a_2 = M_2/\sqrt{E_1^2 + M_2^2 + E_3^2}$ Magnetic quadrupole fractional transition amplitude

VALUE	EVTS	DOCUMENT ID	TECN	COMMENT
-0.13 ± 0.05 OUR AVERAGE				Error includes scale factor of 1.4. See the ideogram below.
-0.093 ± 0.039	5908	62 AMBROGIANI	02	E835 $p\bar{p} \rightarrow \chi_{c2} \rightarrow J/\psi \gamma$
-0.041 ± 0.006	1904	62 ARMSTRONG	93E	E760 $p\bar{p} \rightarrow \chi_{c2} \rightarrow J/\psi \gamma$
-0.14 ± 0.06	441	62 OREGLIA	82	CBAL $\psi(2S) \rightarrow \chi_{c1} \gamma \rightarrow J/\psi \gamma \gamma$
-0.333 ± 0.116				
-0.292				

WEIGHTED AVERAGE
-0.13±0.05 (Error scaled by 1.4)



$$a_2 = M_2/\sqrt{E_1^2 + M_2^2 + E_3^2}$$

$a_3 = E_3/\sqrt{E_1^2 + M_2^2 + E_3^2}$ Electric octupole fractional transition amplitude

VALUE	EVTS	DOCUMENT ID	TECN	COMMENT
0.011^{+0.041}_{-0.033} OUR AVERAGE				
0.020 ^{+0.055} _{-0.044} ± 0.009	5908	AMBROGIANI 02	E835	$p\bar{p} \rightarrow \chi_{c2} \rightarrow J/\psi\gamma$
0.00 ^{+0.06} _{-0.05}	1904	ARMSTRONG 93E	E760	$p\bar{p} \rightarrow \chi_{c2} \rightarrow J/\psi\gamma$

⁶² Assuming $a_3=0$.

$\chi_{c2}(1P)$ REFERENCES

UEHARA 08 EPJ C53 1 S. Uehara et al. (BELLE Collab.)
ADAMS 07 PR D75 071101R G.S. Adams et al. (CLEO Collab.)
ATHAR 07 PR D75 032002 S.B. Athar et al. (CLEO Collab.)
CHEN 07B PL B651 15 W.T. Chen et al. (BELLE Collab.)
ABLIKIM 06D PR D73 052006 M. Ablikim et al. (BES Collab.)
ABLIKIM 06I PR D74 012004 M. Ablikim et al. (BES Collab.)
ABLIKIM 06R PR D74 072001 M. Ablikim et al. (BES Collab.)
ABLIKIM 06T PL B642 197 M. Ablikim et al. (BES Collab.)
DOBBS 06 PR D73 071101R S. Dobbs et al. (CLEO Collab.)
ABLIKIM 05G PR D71 092002 M. Ablikim et al. (BES Collab.)
ABLIKIM 05N PL B630 7 M. Ablikim et al. (BES Collab.)
ABLIKIM 05O PL B630 21 M. Ablikim et al. (BES Collab.)
ADAM 05A PRL 94 232002 N.E. Adam et al. (CLEO Collab.)
ANDREOTTI 05A NP B717 34 M. Andreotti et al. (FNAL E835 Collab.)
NAKAZAWA 05 PL B615 39 H. Nakazawa et al. (BELLE Collab.)
ABLIKIM 04B PR D70 012003 M. Ablikim et al. (BES Collab.)
ABLIKIM 04H PR D70 092003 M. Ablikim et al. (BES Collab.)
ATHAR 04 PR D70 112002 S.B. Athar et al. (CLEO Collab.)
BAI 04F PR D69 092001 J.Z. Bai et al. (BES Collab.)
BAI 04I PR D70 012006 J.Z. Bai et al. (BES Collab.)
AULCHENKO 03 PL B573 63 V.M. Aulchenko et al. (KEDR Collab.)
BAI 03C PR D67 032004 J.Z. Bai et al. (BES Collab.)
BAI 03E PR D67 112001 J.Z. Bai et al. (BES Collab.)
ABE 02T PL B540 33 K. Abe et al. (BELLE Collab.)
AMBROGIANI 02 PR D65 052002 M. Ambrogiani et al. (FNAL E835 Collab.)
EISENSTEIN 01 PRL 87 061801 B.I. Eisenstein et al. (CLEO Collab.)
AMBROGIANI 00B PR D62 052002 M. Ambrogiani et al. (FNAL E835 Collab.)
ACCIARRI 99B PL B453 73 M. Acciari et al. (L3 Collab.)
BAI 99B PR D60 072001 J.Z. Bai et al. (BES Collab.)
ACKER.,K... 98 PL B439 197 K. Ackerstaff et al. (OPAL Collab.)
BAI 98D PR D58 092006 J.Z. Bai et al. (BES Collab.)
BAI 98I PRL 81 3091 J.Z. Bai et al. (BES Collab.)
DOMINICK 94 PR D50 4265 J. Dominick et al. (CLEO Collab.)
ARMSTRONG 93 PRL 70 2988 T.A. Armstrong et al. (FNAL E760 Collab.)
ARMSTRONG 93E PR D48 3037 T.A. Armstrong et al. (FNAL E760 Collab.)
BAUER 93 PL B302 345 D.A. Bauer et al. (TPC Collab.)
ARMSTRONG 92 NP B373 35 T.A. Armstrong et al. (FNAL, FERR, GENO+)
Also PRL 68 1468 T.A. Armstrong et al. (FNAL, FERR, GENO+)
BAGLIN 87B PL B187 191 C. Baglin et al. (R704 Collab.)
BAGLIN 85B PL B172 455 C. Baglin et al. (BES Collab.)
GAISER 86 PR D34 711 J. Gaiser et al. (LAPP, CERN, GENO, OSLO+)
LEE 85 SLAC 282 R.A. Lee et al. (Crystal Ball Collab.)
LEMOIGNE 82 PL 113B 509 Y. Lemoigne et al. (SACL, LOIC, SHMP+)
OREGLIA 82 PR D25 2259 M.J. Oreglia et al. (SLAC, CIT, HARV+)
Also Private Comm. M.J. Oreglia (EFI)
BARATE 81 PR D24 2994 R. Barate et al. (SACL, LOIC, SHMP, CERN+)
HIMEL 80 PRL 44 920 T. Himel et al. (LBL, SLAC)
Also Private Comm. G. Trilling (LBL, UCB)
BRANDELIC 79B NP B160 426 R. Brandelik et al. (DASP Collab.)
BARTEL 78B PL 79B 492 W. Bartel et al. (DESY, HEIDP)
TANENBAUM 78 PR D17 1731 W.M. Tanenbaum et al. (SLAC, LBL)
Also Private Comm. G. Trilling (LBL, UCB)
BIDDICK 77 PRL 38 1324 C.J. Biddick et al. (UCSD, UMD, PAVI+)
WHITAKER 76 PRL 37 1596 J.S. Whitaker et al. (SLAC, LBL)

OTHER RELATED PAPERS

ABLIKIM 04I PR D70 092004 M. Ablikim et al. (BES Collab.)
BARBERIS 00G PL B485 357 D. Barberis et al. (Omega Exptl.)
ACCIARRI 99T PL B461 155 M. Acciari et al. (L3 Collab.)
CHEN 90B PL B243 169 W.Y. Chen et al. (CLEO Collab.)
AIHARA 88D PRL 60 2355 H. Aihara et al. (TPC Collab.)
BARATE 83 PL 121B 449 R. Barate et al. (SACL, LOIC, SHMP, IND)
FELDMAN 75B PRL 35 821 G.J. Feldman et al. (LBL, SLAC)
Also PRL 35 1184 (Errat.) G.J. Feldman et al. (LBL, SLAC)
TANENBAUM 75 PRL 35 1323 W.M. Tanenbaum et al. (LBL, SLAC)

$\eta_c(2S)$

$$I^G(J^{PC}) = 0^+(0^{-+})$$

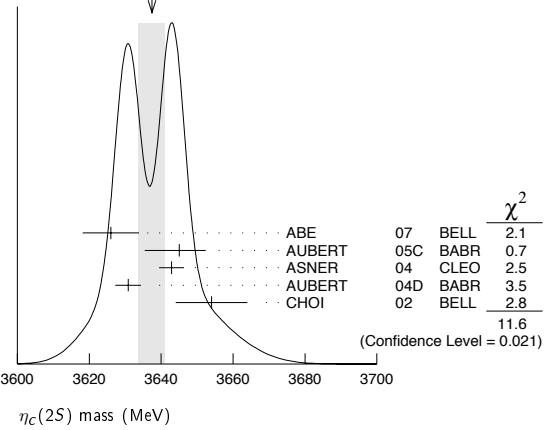
Quantum numbers are quark model predictions.

$\eta_c(2S)$ MASS

VALUE (MeV)	EVTS	DOCUMENT ID	TECN	COMMENT
3637 ± 4 OUR AVERAGE				Error includes scale factor of 1.7. See the ideogram below.
3626 ± 5 ± 6	311	¹ ABE	07 BELL	$e^+e^- \rightarrow J/\psi(c\bar{c})$
3645.0 ± 5.5 ^{+4.9} _{-7.8}	121 ± 27	AUBERT	05c BABR	$e^+e^- \rightarrow J/\psi c\bar{c}$
3642.9 ± 3.1 ± 1.5	61	ASNER	04 CLEO	$\gamma\gamma \rightarrow \eta_c \rightarrow K_S^0 K^\pm \pi^\mp$
3630.8 ± 3.4 ± 1.0	112 ± 24	AUBERT	04d BABR	$\gamma\gamma \rightarrow \eta_c(2S) \rightarrow K\bar{K}\pi$
3654 ± 6 ± 8	39 ± 11	CHOI	02 BELL	$B \rightarrow K K_S K^- \pi^+$
••• We do not use the following data for averages, fits, limits, etc. •••				
3639 ± 7	98 ± 52	² AUBERT	06E BABR	$B^\pm \rightarrow K^\pm \chi_{c2} \bar{c}$
3594 ± 5		³ EDWARDS	82c CBAL	$e^+e^- \rightarrow \gamma X$

¹ From a fit of the J/ψ recoil mass spectrum. Supersedes ABE,K 02 and ABE 04G.
² From the fit of the kaon momentum spectrum. Systematic errors not evaluated.
³ Assuming mass of $\psi(2S) = 3686$ MeV.

WEIGHTED AVERAGE
3637±4 (Error scaled by 1.7)



$\eta_c(2S)$ WIDTH

VALUE (MeV)	CL%	EVTS	DOCUMENT ID	TECN	COMMENT
14 ± 7 OUR AVERAGE					
6.3 ± 12.4 ± 4.0		61	ASNER	04 CLEO	$\gamma\gamma \rightarrow \eta_c \rightarrow K_S^0 K^\pm \pi^\mp$
17.0 ± 8.3 ± 2.5		112 ± 24	AUBERT	04d BABR	$\gamma\gamma \rightarrow \eta_c(2S) \rightarrow K\bar{K}\pi$
••• We do not use the following data for averages, fits, limits, etc. •••					
<23	90	98 ± 52	⁴ AUBERT	06E BABR	$B^\pm \rightarrow K^\pm \chi_{c2} \bar{c}$
22 ± 14		121 ± 27	AUBERT	05c BABR	$e^+e^- \rightarrow J/\psi c\bar{c}$
<55	90	39 ± 11	⁵ CHOI	02 BELL	$B \rightarrow K K_S K^- \pi^+$
<8.0	95		⁶ EDWARDS	82c CBAL	$e^+e^- \rightarrow \gamma X$

⁴ From the fit of the kaon momentum spectrum. Systematic errors not evaluated.
⁵ For a mass value of 3654 ± 6 MeV
⁶ For a mass value of 3594 ± 5 MeV

$\eta_c(2S)$ DECAY MODES

Mode	Fraction (Γ_i/Γ)	Confidence level
Γ_1 hadrons	not seen	
Γ_2 $K\bar{K}\pi$	seen	
Γ_3 $2\pi^+2\pi^-$	not seen	
Γ_4 $K^+K^-\pi^+\pi^-$	not seen	
Γ_5 $2K^+2K^-$	not seen	
Γ_6 $p\bar{p}$	not seen	
Γ_7 $\gamma\gamma$	<5 × 10 ⁻⁴	90%

$\eta_c(2S)$ PARTIAL WIDTHS

$\Gamma(\gamma\gamma)$	DOCUMENT ID	TECN	COMMENT
1.3 ± 0.6	⁷ ASNER	04 CLEO	$\gamma\gamma \rightarrow \eta_c \rightarrow K_S^0 K^\pm \pi^\mp$

Meson Particle Listings

$\eta_c(2S), \psi(2S)$

⁷ They measure $\Gamma(\eta_c(2S) \rightarrow \gamma\gamma) B(\eta_c(2S) \rightarrow K\bar{K}\pi) = (0.18 \pm 0.05 \pm 0.02) \Gamma(\eta_c(1S) \rightarrow \gamma\gamma) B(\eta_c(1S) \rightarrow K\bar{K}\pi)$. The value for $\Gamma(\eta_c(2S) \rightarrow \gamma\gamma)$ is derived assuming that the branching fractions for $\eta_c(2S)$ and $\eta_c(1S)$ decays to $K_S K \pi$ are equal and using $\Gamma(\eta_c(1S) \rightarrow \gamma\gamma) = 7.4 \pm 0.4 \pm 2.3$ keV.

$\eta_c(2S) \Gamma(i)\Gamma(\gamma\gamma)/\Gamma(\text{total})$

VALUE (eV)	CL%	DOCUMENT ID	TECN	COMMENT	$\Gamma_3\Gamma_7/\Gamma$
<6.5	90	UEHARA 08	BELL	$\gamma\gamma \rightarrow \eta_c(2S) \rightarrow 2(\pi^+\pi^-)$	

VALUE (eV)	CL%	DOCUMENT ID	TECN	COMMENT	$\Gamma_4\Gamma_7/\Gamma$
<5.0	90	UEHARA 08	BELL	$\gamma\gamma \rightarrow \eta_c(2S) \rightarrow K^+K^-\pi^+\pi^-$	

VALUE (eV)	CL%	DOCUMENT ID	TECN	COMMENT	$\Gamma_5\Gamma_7/\Gamma$
<2.9	90	UEHARA 08	BELL	$\gamma\gamma \rightarrow \eta_c(2S) \rightarrow 2(K^+K^-)$	

$\eta_c(2S) \Gamma(i)\Gamma(\gamma\gamma)/\Gamma^2(\text{total})$

VALUE (units 10^{-8})	CL%	DOCUMENT ID	TECN	COMMENT	$\Gamma_6\Gamma_7/\Gamma^2$
< 5.6	90	8,9,10 AMBROGIANI 01	E835	$\bar{p}p \rightarrow \gamma\gamma$	
< 8.0	90	8,9,11 AMBROGIANI 01	E835	$\bar{p}p \rightarrow \gamma\gamma$	
<12.0	90	9,11 AMBROGIANI 01	E835	$\bar{p}p \rightarrow \gamma\gamma$	

• • • We do not use the following data for averages, fits, limits, etc. • • •
⁸ Including the measurements of ARMSTRONG 95F in the AMBROGIANI 01 analysis.
⁹ For a total width $\Gamma=5$ MeV.
¹⁰ For the resonance mass region 3589–3599 MeV/ c^2 .
¹¹ For the resonance mass region 3575–3660 MeV/ c^2 .

$\eta_c(2S)$ BRANCHING RATIOS

$\Gamma(\text{hadrons})/\Gamma_{\text{total}}$	DOCUMENT ID	TECN	COMMENT	Γ_1/Γ
not seen	ABREU 98a	DLPH	$e^+e^- \rightarrow e^+e^- + \text{hadrons}$	
seen	12 EDWARDS 82c	CBAL	$e^+e^- \rightarrow \gamma X$	

¹² For a mass value of 3594 ± 5 MeV

$\Gamma(K\bar{K}\pi)/\Gamma_{\text{total}}$	EVTS	DOCUMENT ID	TECN	COMMENT	Γ_2/Γ
seen	39 ± 11	13 CHOI 02	BELL	$B \rightarrow K K_S K^-\pi^+$	

¹³ For a mass value of 3654 ± 6 MeV

$\Gamma(2\pi^+2\pi^-)/\Gamma_{\text{total}}$	DOCUMENT ID	TECN	COMMENT	Γ_3/Γ
not seen	UEHARA 08	BELL	$\gamma\gamma \rightarrow \eta_c(2S)$	

$\Gamma(K^+K^-\pi^+\pi^-)/\Gamma_{\text{total}}$	DOCUMENT ID	TECN	COMMENT	Γ_4/Γ
not seen	UEHARA 08	BELL	$\gamma\gamma \rightarrow \eta_c(2S)$	

$\Gamma(2K^+2K^-)/\Gamma_{\text{total}}$	DOCUMENT ID	TECN	COMMENT	Γ_5/Γ
not seen	UEHARA 08	BELL	$\gamma\gamma \rightarrow \eta_c(2S)$	

VALUE	DOCUMENT ID	TECN	COMMENT
not seen	AMBROGIANI 01	E835	$\bar{p}p \rightarrow \gamma\gamma$

$\Gamma(\gamma\gamma)/\Gamma_{\text{total}}$	CL%	DOCUMENT ID	TECN	COMMENT	Γ_7/Γ
<0.0005	90	14 WICHT 08	BELL	$B^\pm \rightarrow K^\pm \gamma\gamma$	
<0.01	90	LEE 85	CBAL	$\psi' \rightarrow \text{photons}$	

¹⁴ WICHT 08 reports $[B(\eta_c(2S) \rightarrow \gamma\gamma)] \times [B(B^+ \rightarrow \eta_c(2S) K^+)] < 0.18 \times 10^{-6}$. We divide by our best value $B(B^+ \rightarrow \eta_c(2S) K^+) = 0.00034$.

$\eta_c(2S)$ REFERENCES

UEHARA 08	EPJ C53 1	S. Uehara et al.	(BELLE Collab.)
WICHT 08	PL B662 323	J. Wicht et al.	(BELLE Collab.)
ABE 07	PRL 98 082001	K. Abe et al.	(BELLE Collab.)
AUBERT 06	PRL 96 052002	B. Aubert et al.	(BABAR Collab.)
AUBERT 05C	PR D72 031101R	B. Aubert et al.	(BABAR Collab.)
ABE 04G	PR D70 071102	K. Abe et al.	(BELLE Collab.)
ASNER 04	PRL 92 142001	D.M. Asner et al.	(CLEO Collab.)
AUBERT 04D	PRL 92 142002	B. Aubert et al.	(BABAR Collab.)
ABE,K 02	PRL 89 142001	K. Abe et al.	(BELLE Collab.)
CHOI 02	PRL 89 102001	S.-K. Choi et al.	(BELLE Collab.)
AMBROGIANI 01	PR D64 052003	M. Ambrogiani et al.	(FNAL E835 Collab.)
ABREU 98O	PL B441 479	P. Abreu et al.	(DELPHI Collab.)
ARMSTRONG 95F	PR D52 4839	T.A. Armstrong et al.	(FNAL FERR, GENO+)
LEE 85	SLAC 282	R.A. Lee	(SLAC)
EDWARDS 82C	PRL 48 70	C. Edwards et al.	(CIT, HARV, PRIN+)

OTHER RELATED PAPERS

PENNINGTON 07A	PR D76 077502	M.R. Pennington, DJ. Wilson	(PITT)
SWANSON 06	PRPL 429 243	E.S. Swanson	
BADALIAN 03	PR D67 071901	A.M. Badalian, B.L.G. Bakker	
EICHTEN 02	PRL 89 162002	E.J. Eichten, K. Lane, C. Quigg	
ACCIARRI 99T	PL B461 155	M. Acciarri et al.	(L3 Collab.)
OREGLIA 82	PR D25 2259	M.J. Oreglia et al.	(SLAC, CIT, HARV+)
PORTER 81	SLAC Summer Inst. 355	F.C. Porter et al.	(CIT, HARV, PRIN+)
BARTEL 78B	PL 79B 492	W. Bartel et al.	(DESY, HEIDP)

$\psi(2S)$

$$J^G(J^PC) = 0^-(1^{--})$$

See the Review on " $\psi(2S)$ and χ_C branching ratios" before the $\chi_{c0}(1P)$ Listings.

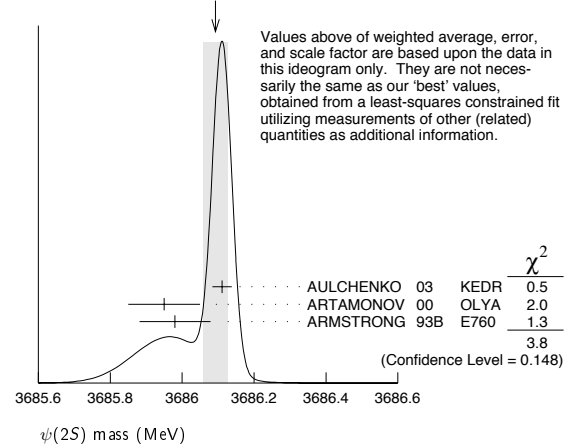
$\psi(2S)$ MASS

OUR FIT includes measurements of $m_{\psi(2S)}, m_{\psi(3770)}$, and $m_{\psi(3770)} - m_{\psi(2S)}$.

VALUE (MeV)	EVTS	DOCUMENT ID	TECN	COMMENT
3686.09 ± 0.04 OUR FIT				Error includes scale factor of 1.6.
3686.093 ± 0.034 OUR AVERAGE				Error includes scale factor of 1.4. See the ideogram below.
3686.111 ± 0.025 ± 0.009		AULCHENKO 03	KEDR	$e^+e^- \rightarrow \text{hadrons}$
3685.95 ± 0.10	413	1 ARTAMONOV 00	OLYA	$e^+e^- \rightarrow \text{hadrons}$
3685.98 ± 0.09 ± 0.04		2 ARMSTRONG 93B	E760	$\bar{p}p \rightarrow e^+e^-$
3686.00 ± 0.10	413	3 ZHOLENTZ 80	OLYA	e^+e^-

• • • We do not use the following data for averages, fits, limits, etc. • • •
¹ Reanalysis of ZHOLENTZ 80 using new electron mass (COHEN 87) and radiative corrections (KURAEV 85).
² Mass central value and systematic error recalculated by us according to Eq.(16) in ARMSTRONG 93B, using the value for the $J/\psi(1S)$ mass from AULCHENKO 03.
³ Superseded by ARTAMONOV 00.

WEIGHTED AVERAGE
 3686.093±0.034 (Error scaled by 1.4)



$m_{\psi(2S)} - m_{J/\psi(1S)}$

VALUE (MeV)	DOCUMENT ID	TECN	COMMENT
589.194 ± 0.027 ± 0.011 OUR AVERAGE			
589.194 ± 0.027 ± 0.011	4 AULCHENKO 03	KEDR	$e^+e^- \rightarrow \text{hadrons}$
589.7 ± 1.2	LEMOIGNE 82	GOLI	$185 \pi^- \text{Be} \rightarrow \gamma \mu^+ \mu^- A$
589.07 ± 0.13	4 ZHOLENTZ 80	OLYA	e^+e^-
588.7 ± 0.8	LUTH 75	MRK1	
588 ± 1	5 BAI 98E	BES	e^+e^-

• • • We do not use the following data for averages, fits, limits, etc. • • •
⁴ Redundant with data in mass above.
⁵ Systematic errors not evaluated.

$\psi(2S)$ WIDTH

VALUE (keV)	EVTS	DOCUMENT ID	TECN	COMMENT
317 ± 9 OUR FIT				
286 ± 16 OUR AVERAGE				
358 ± 88 ± 4		ABLIKIM 08B	BES2	$e^+e^- \rightarrow \text{hadrons}$
290 ± 25 ± 4	2.7k	ANDREOTTI 07	E835	$p\bar{p} \rightarrow e^+e^-, J/\psi X$
331 ± 58 ± 2		ABLIKIM 06L	BES2	$e^+e^- \rightarrow \text{hadrons}$
264 ± 27		6 BAI 02B	BES2	e^+e^-
287 ± 37 ± 16		7 ARMSTRONG 93B	E760	$\bar{p}p \rightarrow e^+e^-$

⁶ From a simultaneous fit to the hadronic and $\mu^+\mu^-$ cross section, assuming $\Gamma = \Gamma_h + \Gamma_e + \Gamma_\mu + \Gamma_\tau$ and lepton universality. Does not include vacuum polarization correction.
⁷ The initial-state radiation correction reevaluated by ANDREOTTI 07 in its Ref. [4].

$\psi(2S)$ DECAY MODES

Mode	Fraction (Γ_i/Γ)	Scale factor/ Confidence level
Γ_1 hadrons	(97.85±0.13) %	
Γ_2 virtual $\gamma \rightarrow$ hadrons	(1.73±0.14) %	S=1.5
Γ_3 light hadrons		
Γ_4 e^+e^-	(7.52±0.17) × 10 ⁻³	
Γ_5 $\mu^+\mu^-$	(7.5 ± 0.8) × 10 ⁻³	
Γ_6 $\tau^+\tau^-$	(3.0 ± 0.4) × 10 ⁻³	
Decays into $J/\psi(1S)$ and anything		
Γ_7 $J/\psi(1S)$ anything	(57.4 ± 0.9) %	
Γ_8 $J/\psi(1S)$ neutrals	(23.5 ± 0.4) %	
Γ_9 $J/\psi(1S)\pi^+\pi^-$	(32.6 ± 0.5) %	
Γ_{10} $J/\psi(1S)\pi^0\pi^0$	(16.84±0.33) %	
Γ_{11} $J/\psi(1S)\eta$	(3.16±0.07) %	
Γ_{12} $J/\psi(1S)\pi^0$	(1.26±0.13) × 10 ⁻³	S=1.3
Hadronic decays		
Γ_{13} $3(\pi^+\pi^-)\pi^0$	(3.5 ± 1.6) × 10 ⁻³	
Γ_{14} $2(\pi^+\pi^-)\pi^0$	(2.9 ± 1.0) × 10 ⁻³	S=4.6
Γ_{15} $\rho\pi(1320)$	(2.6 ± 0.9) × 10 ⁻⁴	
Γ_{16} $\rho\bar{p}$	(2.74±0.12) × 10 ⁻⁴	
Γ_{17} $\Delta^{++}\bar{\Delta}^{--}$	(1.28±0.35) × 10 ⁻⁴	
Γ_{18} $\Lambda\bar{\Lambda}\pi^0$	< 1.2 × 10 ⁻⁴	CL=90%
Γ_{19} $\Lambda\bar{\Lambda}\eta$	< 4.9 × 10 ⁻⁵	CL=90%
Γ_{20} $\Lambda\bar{p}K^+$	(1.00±0.14) × 10 ⁻⁴	
Γ_{21} $\Lambda\bar{p}K^+\pi^+\pi^-$	(1.8 ± 0.4) × 10 ⁻⁴	
Γ_{22} $\Lambda\bar{\Lambda}\pi^+\pi^-$	(2.8 ± 0.6) × 10 ⁻⁴	
Γ_{23} $\Lambda\bar{\Lambda}$	(2.8 ± 0.5) × 10 ⁻⁴	S=2.6
Γ_{24} $\Sigma^+\bar{\Sigma}^-$	(2.6 ± 0.8) × 10 ⁻⁴	
Γ_{25} $\Sigma^0\bar{\Sigma}^0$	(2.2 ± 0.4) × 10 ⁻⁴	S=1.5
Γ_{26} $\Sigma(1385)^+\bar{\Sigma}(1385)^-$	(1.1 ± 0.4) × 10 ⁻⁴	
Γ_{27} $\Xi^-\bar{\Xi}^+$	(1.8 ± 0.6) × 10 ⁻⁴	S=2.8
Γ_{28} $\Xi^0\bar{\Xi}^0$	(2.8 ± 0.9) × 10 ⁻⁴	
Γ_{29} $\Xi(1530)^0\bar{\Xi}(1530)^0$	< 8.1 × 10 ⁻⁵	CL=90%
Γ_{30} $\Omega^-\bar{\Omega}^+$	< 7.3 × 10 ⁻⁵	CL=90%
Γ_{31} $\pi^0\rho\bar{p}$	(1.33±0.17) × 10 ⁻⁴	
Γ_{32} $\eta\rho\bar{p}$	(6.0 ± 1.2) × 10 ⁻⁵	
Γ_{33} $\omega\rho\bar{p}$	(6.9 ± 2.1) × 10 ⁻⁵	
Γ_{34} $\phi\rho\bar{p}$	< 2.4 × 10 ⁻⁵	CL=90%
Γ_{35} $\pi^+\pi^-\rho\bar{p}$	(6.0 ± 0.4) × 10 ⁻⁴	
Γ_{36} $\rho\bar{p}\pi^-$ or c.c.	(2.48±0.17) × 10 ⁻⁴	
Γ_{37} $\rho\bar{p}\pi^-\pi^0$	(3.2 ± 0.7) × 10 ⁻⁴	
Γ_{38} $2(\pi^+\pi^-\pi^0)$	(4.7 ± 1.5) × 10 ⁻³	
Γ_{39} $\eta\pi^+\pi^-$	< 1.6 × 10 ⁻⁴	CL=90%
Γ_{40} $\eta\pi^+\pi^-\pi^0$	(9.5 ± 1.7) × 10 ⁻⁴	
Γ_{41} $2(\pi^+\pi^-)\eta$	(1.2 ± 0.6) × 10 ⁻³	
Γ_{42} $\eta'\pi^+\pi^-\pi^0$	(4.5 ± 2.1) × 10 ⁻⁴	
Γ_{43} $\omega\pi^+\pi^-$	(7.3 ± 1.2) × 10 ⁻⁴	S=2.1
Γ_{44} $b_1^+\pi^\mp$	(4.0 ± 0.6) × 10 ⁻⁴	S=1.1
Γ_{45} $b_1^0\pi^0$	(2.4 ± 0.6) × 10 ⁻⁴	
Γ_{46} $\omega f_2(1270)$	(2.2 ± 0.4) × 10 ⁻⁴	
Γ_{47} $\pi^+\pi^-K^+K^-$	(7.5 ± 0.9) × 10 ⁻⁴	S=1.9
Γ_{48} $\rho^0K^+K^-$	(2.2 ± 0.4) × 10 ⁻⁴	
Γ_{49} $K^*(892)^0\bar{K}_2^*(1430)^0$	(1.9 ± 0.5) × 10 ⁻⁴	
Γ_{50} $K^+K^-\pi^+\pi^-\eta$	(1.3 ± 0.7) × 10 ⁻³	
Γ_{51} $K^+K^-2(\pi^+\pi^-)\pi^0$	(1.00±0.31) × 10 ⁻³	
Γ_{52} $K^+K^-2(\pi^+\pi^-)$	(1.8 ± 0.9) × 10 ⁻³	
Γ_{53} $K_1(1270)^\pm K^\mp$	(1.00±0.28) × 10 ⁻³	
Γ_{54} $K_S^0 K_S^0 \pi^+\pi^-$	(2.2 ± 0.4) × 10 ⁻⁴	
Γ_{55} $\rho^0\rho\bar{p}$	(5.0 ± 2.2) × 10 ⁻⁵	
Γ_{56} $K^+\bar{K}^*(892)^0\pi^- + c.c.$	(6.7 ± 2.5) × 10 ⁻⁴	
Γ_{57} $2(\pi^+\pi^-)$	(2.4 ± 0.6) × 10 ⁻⁴	S=2.2
Γ_{58} $\rho^0\pi^+\pi^-$	(2.2 ± 0.6) × 10 ⁻⁴	S=1.4
Γ_{59} $K^+K^-\pi^+\pi^-\pi^0$	(1.26±0.09) × 10 ⁻³	
Γ_{60} $\omega f_0(1710) \rightarrow \omega K^+K^-$	(5.9 ± 2.2) × 10 ⁻⁵	
Γ_{61} $K^*(892)^0 K^-\pi^+\pi^0 + c.c.$	(8.6 ± 2.2) × 10 ⁻⁴	
Γ_{62} $K^*(892)^+ K^-\pi^+\pi^- + c.c.$	(9.6 ± 2.8) × 10 ⁻⁴	
Γ_{63} $K^*(892)^+ K^-\rho^0 + c.c.$	(7.3 ± 2.6) × 10 ⁻⁴	
Γ_{64} $K^*(892)^0 K^-\rho^+ + c.c.$	(6.1 ± 1.8) × 10 ⁻⁴	
Γ_{65} ηK^+K^-	< 1.3 × 10 ⁻⁴	CL=90%
Γ_{66} ωK^+K^-	(1.85±0.25) × 10 ⁻⁴	S=1.1
Γ_{67} $3(\pi^+\pi^-)$	(3.5 ± 2.0) × 10 ⁻⁴	S=2.8
Γ_{68} $\rho\bar{p}\pi^+\pi^-\pi^0$	(7.3 ± 0.7) × 10 ⁻⁴	

Γ_{69} K^+K^-	(6.3 ± 0.7) × 10 ⁻⁵	
Γ_{70} $K_S^0 K_L^0$	(5.4 ± 0.5) × 10 ⁻⁵	
Γ_{71} $\pi^+\pi^-\pi^0$	(1.68±0.26) × 10 ⁻⁴	S=1.4
Γ_{72} $\rho(2150)\pi \rightarrow \pi^+\pi^-\pi^0$	(1.9 ^{+1.2} _{-0.4}) × 10 ⁻⁴	
Γ_{73} $\rho(770)\pi \rightarrow \pi^+\pi^-\pi^0$	(3.2 ± 1.2) × 10 ⁻⁵	S=1.8
Γ_{74} $\pi^+\pi^-$	(8 ± 5) × 10 ⁻⁵	
Γ_{75} $K_1(1400)^\pm K^\mp$	< 3.1 × 10 ⁻⁴	CL=90%
Γ_{76} $K^+K^-\pi^0$	< 2.96 × 10 ⁻⁵	CL=90%
Γ_{77} $K^+\bar{K}^*(892)^- + c.c.$	(1.7 ^{+0.8} _{-0.7}) × 10 ⁻⁵	
Γ_{78} $K^*(892)^0\bar{K}^0 + c.c.$	(1.09±0.20) × 10 ⁻⁴	
Γ_{79} $\phi\pi^+\pi^-$	(1.17±0.29) × 10 ⁻⁴	S=1.7
Γ_{80} $\phi f_0(980) \rightarrow \pi^+\pi^-$	(6.8 ± 2.4) × 10 ⁻⁵	S=1.1
Γ_{81} $2(K^+K^-)$	(6.0 ± 1.4) × 10 ⁻⁵	
Γ_{82} ϕK^+K^-	(7.0 ± 1.6) × 10 ⁻⁵	
Γ_{83} $2(K^+K^-)\pi^0$	(1.10±0.28) × 10 ⁻⁴	
Γ_{84} $\phi\eta$	(2.8 ^{+1.0} _{-0.8}) × 10 ⁻⁵	
Γ_{85} $\phi\eta'$	(3.1 ± 1.6) × 10 ⁻⁵	
Γ_{86} $\omega\eta'$	(3.2 ^{+2.5} _{-2.1}) × 10 ⁻⁵	
Γ_{87} $\omega\pi^0$	(2.1 ± 0.6) × 10 ⁻⁵	
Γ_{88} $\rho\eta'$	(1.9 ^{+1.7} _{-1.2}) × 10 ⁻⁵	
Γ_{89} $\rho\eta$	(2.2 ± 0.6) × 10 ⁻⁵	S=1.1
Γ_{90} $\omega\eta$	< 1.1 × 10 ⁻⁵	CL=90%
Γ_{91} $\phi\pi^0$	< 4 × 10 ⁻⁶	CL=90%
Γ_{92} $\eta_c\pi^+\pi^-\pi^0$	< 1.0 × 10 ⁻³	CL=90%
Γ_{93} $\rho\bar{p}K^+K^-$	(2.7 ± 0.7) × 10 ⁻⁵	
Γ_{94} $\Lambda n K_S^0 + c.c.$	(8.1 ± 1.8) × 10 ⁻⁵	
Γ_{95} $\phi f_2'(1525)$	(4.4 ± 1.6) × 10 ⁻⁵	
Γ_{96} $\Theta(1540)\bar{\Theta}(1540) \rightarrow K_S^0 p K^-\bar{n} + c.c.$	< 8.8 × 10 ⁻⁶	CL=90%
Γ_{97} $\Theta(1540)K^-\bar{n} \rightarrow K_S^0 p K^-\bar{n}$	< 1.0 × 10 ⁻⁵	CL=90%
Γ_{98} $\Theta(1540)K_S^0\bar{p} \rightarrow K_S^0\bar{p}K^+n$	< 7.0 × 10 ⁻⁶	CL=90%
Γ_{99} $\bar{\Theta}(1540)K^+n \rightarrow K_S^0\bar{p}K^+n$	< 2.6 × 10 ⁻⁵	CL=90%
Γ_{100} $\bar{\Theta}(1540)K_S^0 p \rightarrow K_S^0 p K^-\bar{n}$	< 6.0 × 10 ⁻⁶	CL=90%
Γ_{101} $K_S^0 K_S^0$	< 4.6 × 10 ⁻⁶	
Radiative decays		
Γ_{102} $\gamma\chi_{c0}(1P)$	(9.4 ± 0.4) %	
Γ_{103} $\gamma\chi_{c1}(1P)$	(8.8 ± 0.4) %	
Γ_{104} $\gamma\chi_{c2}(1P)$	(8.3 ± 0.4) %	
Γ_{105} $\gamma\eta_c(1S)$	(3.0 ± 0.5) × 10 ⁻³	
Γ_{106} $\gamma\eta_c(2S)$	< 2.0 × 10 ⁻³	CL=90%
Γ_{107} $\gamma\pi^0$	< 5.4 × 10 ⁻³	CL=95%
Γ_{108} $\gamma\eta'(958)$	(1.36±0.24) × 10 ⁻⁴	
Γ_{109} $\gamma f_2(1270)$	(2.1 ± 0.4) × 10 ⁻⁴	
Γ_{110} $\gamma f_0(1710)$		
Γ_{111} $\gamma f_0(1710) \rightarrow \gamma\pi\pi$	(3.0 ± 1.3) × 10 ⁻⁵	
Γ_{112} $\gamma f_0(1710) \rightarrow \gamma K\bar{K}$	(6.0 ± 1.6) × 10 ⁻⁵	
Γ_{113} $\gamma\gamma$	< 1.4 × 10 ⁻⁴	CL=90%
Γ_{114} $\gamma\eta$	< 9 × 10 ⁻⁵	CL=90%
Γ_{115} $\gamma\eta\pi^+\pi^-$	(8.7 ± 2.1) × 10 ⁻⁴	
Γ_{116} $\gamma\eta(1405)$		
Γ_{117} $\gamma\eta(1405) \rightarrow \gamma K\bar{K}\pi$	< 9 × 10 ⁻⁵	CL=90%
Γ_{118} $\gamma\eta(1405) \rightarrow \eta\pi^+\pi^-$	(3.6 ± 2.5) × 10 ⁻⁵	
Γ_{119} $\gamma\eta(1475)$		
Γ_{120} $\gamma\eta(1475) \rightarrow K\bar{K}\pi$	< 1.4 × 10 ⁻⁴	CL=90%
Γ_{121} $\gamma\eta(1475) \rightarrow \eta\pi^+\pi^-$	< 8.8 × 10 ⁻⁵	CL=90%
Γ_{122} $\gamma 2(\pi^+\pi^-)$	(4.0 ± 0.6) × 10 ⁻⁴	
Γ_{123} $\gamma K^{*0}K^+\pi^- + c.c.$	(3.7 ± 0.9) × 10 ⁻⁴	
Γ_{124} $\gamma K^{*0}\bar{K}^{*0}$	(2.4 ± 0.7) × 10 ⁻⁴	
Γ_{125} $\gamma K_S^0 K^+\pi^- + c.c.$	(2.6 ± 0.5) × 10 ⁻⁴	
Γ_{126} $\gamma K^+K^-\pi^+\pi^-$	(1.9 ± 0.5) × 10 ⁻⁴	
Γ_{127} $\gamma\rho\bar{p}$	(2.9 ± 0.6) × 10 ⁻⁵	
Γ_{128} $\gamma\pi^+\pi^-\rho\bar{p}$	(2.8 ± 1.4) × 10 ⁻⁵	
Γ_{129} $\gamma 2(\pi^+\pi^-)K^+K^-$	< 2.2 × 10 ⁻⁴	CL=90%
Γ_{130} $\gamma 3(\pi^+\pi^-)$	< 1.7 × 10 ⁻⁴	CL=90%
Γ_{131} $\gamma K^+K^-K^+K^-$	< 4 × 10 ⁻⁵	CL=90%

Meson Particle Listings

$\psi(2S)$

$\psi(2S)$ PARTIAL WIDTHS

$\Gamma(\text{hadrons})$

VALUE (keV)	DOCUMENT ID	TECN	COMMENT	Γ_1
• • • We do not use the following data for averages, fits, limits, etc. • • •				
258 ± 26	BAI	02B	BES2 e^+e^-	
224 ± 56	LUTH	75	MRK1 e^+e^-	

$\Gamma(e^+e^-)$

VALUE (keV)	DOCUMENT ID	TECN	COMMENT	Γ_4
2.38 ± 0.04 OUR FIT				
2.33 ± 0.07 OUR AVERAGE				
2.338 ± 0.037 ± 0.096	ABLIKIM	08B	BES2 $e^+e^- \rightarrow \text{hadrons}$	
2.330 ± 0.036 ± 0.110	ABLIKIM	06L	BES2 $e^+e^- \rightarrow \text{hadrons}$	
2.44 ± 0.21	⁸ BAI	02B	BES2 e^+e^-	
2.14 ± 0.21	ALEXANDER	89	RVUE See γ mini-review	
• • • We do not use the following data for averages, fits, limits, etc. • • •				
2.0 ± 0.3	BRANDELIK	79c	DASP e^+e^-	
2.1 ± 0.3	⁹ LUTH	75	MRK1 e^+e^-	

⁸ From a simultaneous fit to e^+e^- , $\mu^+\mu^-$, and hadronic channel, assuming $\Gamma_e = \Gamma_\mu = \Gamma_\tau/0.38847$.

⁹ From a simultaneous fit to e^+e^- , $\mu^+\mu^-$, and hadronic channels assuming $\Gamma(e^+e^-) = \Gamma(\mu^+\mu^-)$.

$\Gamma(\gamma\gamma)$

VALUE (eV)	CL%	DOCUMENT ID	TECN	COMMENT	Γ_{113}
<43	90	BRANDELIK	79c	DASP e^+e^-	

$\psi(2S) \Gamma(i)\Gamma(e^+e^-)/\Gamma(\text{total})$

This combination of a partial width with the partial width into e^+e^- and with the total width is obtained from the integrated cross section into channel(i) in the e^+e^- annihilation. We list only data that have not been used to determine the partial width $\Gamma(i)$ or the branching ratio $\Gamma(i)/\text{total}$.

$\Gamma(\text{hadrons}) \times \Gamma(e^+e^-)/\Gamma_{\text{total}}$

VALUE (keV)	DOCUMENT ID	TECN	COMMENT	$\Gamma_1\Gamma_4/\Gamma$
• • • We do not use the following data for averages, fits, limits, etc. • • •				
2.2 ± 0.4	ABRAMS	75	MRK1 e^+e^-	

$\Gamma(\tau^+\tau^-) \times \Gamma(e^+e^-)/\Gamma_{\text{total}}$

VALUE (eV)	EVTs	DOCUMENT ID	TECN	COMMENT	$\Gamma_6\Gamma_4/\Gamma$
• • • We do not use the following data for averages, fits, limits, etc. • • •					
9.0 ± 2.6	79	¹⁰ ANASHIN	07	KEDR $e^+e^- \rightarrow \psi(2S) \rightarrow \tau^+\tau^-$	

$\Gamma(J/\psi(1S)\pi^+\pi^-) \times \Gamma(e^+e^-)/\Gamma_{\text{total}}$

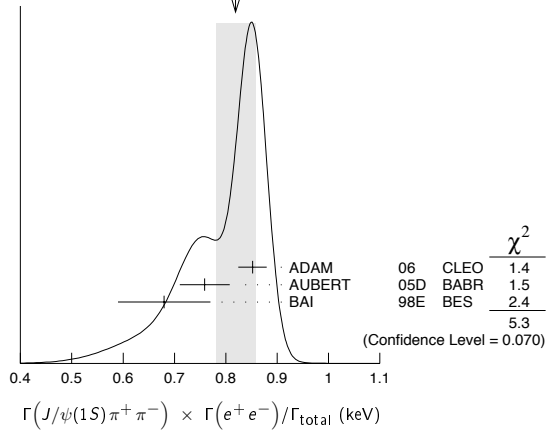
VALUE (keV)	EVTs	DOCUMENT ID	TECN	COMMENT	$\Gamma_9\Gamma_4/\Gamma$
0.777 ± 0.016 OUR FIT					
0.82 ± 0.04 OUR AVERAGE Error includes scale factor of 1.6. See the ideogram below.					
0.852 ± 0.010 ± 0.026	19.5k ± 243	ADAM	06	CLEO 3.773 $e^+e^- \rightarrow \gamma\psi(2S)$	
0.76 ± 0.05 ± 0.01	544	¹¹ AUBERT	05D	BABR 10.6 $e^+e^- \rightarrow \pi^+\pi^-\mu^+\mu^- \gamma$	
0.68 ± 0.09		¹² BAI	98E	BES e^+e^-	
• • • We do not use the following data for averages, fits, limits, etc. • • •					
0.90 ± 0.08 ± 0.06	256	¹³ AUBERT	07AU	BABR 10.6 $e^+e^- \rightarrow J/\psi\pi^+\pi^-\gamma$	

¹¹ AUBERT 05D reports $[\Gamma(\psi(2S) \rightarrow J/\psi(1S)\pi^+\pi^-) \times \Gamma(\psi(2S) \rightarrow e^+e^-)/\Gamma_{\text{total}}] \times [B(J/\psi(1S) \rightarrow \mu^+\mu^-)] = 0.0450 \pm 0.0018 \pm 0.0022$ keV. We divide by our best value $B(J/\psi(1S) \rightarrow \mu^+\mu^-) = (5.93 \pm 0.06) \times 10^{-2}$. Our first error is their experiment's error and our second error is the systematic error from using our best value.

¹² The value of $\Gamma(e^+e^-)$ quoted in BAI 98E is derived using $B(\psi(2S) \rightarrow J/\psi(1S)\pi^+\pi^-) = (32.4 \pm 2.6) \times 10^{-2}$ and $B(J/\psi(1S) \rightarrow \ell^+\ell^-) = 0.1203 \pm 0.0038$. Recalculated by us using $B(J/\psi(1S) \rightarrow \ell^+\ell^-) = 0.1181 \pm 0.0020$.

¹³ AUBERT 07AU reports $[\Gamma(\psi(2S) \rightarrow J/\psi(1S)\pi^+\pi^-) \times \Gamma(\psi(2S) \rightarrow e^+e^-)/\Gamma_{\text{total}}] \times [B(J/\psi(1S) \rightarrow \pi^+\pi^-\pi^0)] = 0.0186 \pm 0.0012 \pm 0.0011$ keV. We divide by our best value $B(J/\psi(1S) \rightarrow \pi^+\pi^-\pi^0) = (2.07 \pm 0.13) \times 10^{-2}$. Our first error is their experiment's error and our second error is the systematic error from using our best value.

WEIGHTED AVERAGE
0.82 ± 0.04 (Error scaled by 1.6)



$\Gamma(J/\psi(1S)\pi^0\pi^0) \times \Gamma(e^+e^-)/\Gamma_{\text{total}}$

VALUE (keV)	EVTs	DOCUMENT ID	TECN	COMMENT	$\Gamma_{10}\Gamma_4/\Gamma$
0.401 ± 0.009 OUR FIT					
0.411 ± 0.008 ± 0.018 3.6k ± 96 ADAM 06 CLEO 3.773 $e^+e^- \rightarrow \gamma\psi(2S)$					

$\Gamma(J/\psi(1S)\eta) \times \Gamma(e^+e^-)/\Gamma_{\text{total}}$

VALUE (eV)	EVTs	DOCUMENT ID	TECN	COMMENT	$\Gamma_{11}\Gamma_4/\Gamma$
75.2 ± 2.1 OUR FIT					
87 ± 9 OUR AVERAGE					
83 ± 25 ± 5	14	¹⁴ AUBERT	07AU	BABR 10.6 $e^+e^- \rightarrow J/\psi\pi^+\pi^-\pi^0\gamma$	
88 ± 6 ± 7	291 ± 24	ADAM	06	CLEO 3.773 $e^+e^- \rightarrow \gamma\psi(2S)$	
¹⁴ AUBERT 07AU quotes $\Gamma_{ee}^{\psi(2S)} \cdot B(\psi(2S) \rightarrow J/\psi\eta) \cdot B(J/\psi \rightarrow \mu^+\mu^-) \cdot B(\eta \rightarrow \pi^+\pi^-\pi^0) = 1.11 \pm 0.33 \pm 0.07$ eV.					

$\Gamma(J/\psi(1S)\pi^0) \times \Gamma(e^+e^-)/\Gamma_{\text{total}}$

VALUE (eV)	CL%	EVTs	DOCUMENT ID	TECN	COMMENT	$\Gamma_{12}\Gamma_4/\Gamma$
<8 90 <37 ADAM 06 CLEO 3.773 $e^+e^- \rightarrow \gamma\psi(2S)$						

$\Gamma(p\bar{p}) \times \Gamma(e^+e^-)/\Gamma_{\text{total}}$

VALUE (eV)	EVTs	DOCUMENT ID	TECN	COMMENT	$\Gamma_{16}\Gamma_4/\Gamma$
0.651 ± 0.029 OUR FIT					
0.59 ± 0.05 OUR AVERAGE					
0.579 ± 0.038 ± 0.036	2.7k	ANDREOTTI	07	E835 $p\bar{p} \rightarrow e^+e^-, J/\psi X$	
0.70 ± 0.17 ± 0.03	22	AUBERT	06B	$e^+e^- \rightarrow p\bar{p}\gamma$	

$\Gamma(\Lambda\bar{\Lambda}) \times \Gamma(e^+e^-)/\Gamma_{\text{total}}$

VALUE (eV)	DOCUMENT ID	TECN	COMMENT	$\Gamma_{23}\Gamma_4/\Gamma$
1.5 ± 0.4 ± 0.1				
	AUBERT	07BD	BABR	10.6 $e^+e^- \rightarrow \Lambda\bar{\Lambda}\gamma$

$\Gamma(2\pi^+\pi^-\pi^0) \times \Gamma(e^+e^-)/\Gamma_{\text{total}}$

VALUE (eV)	EVTs	DOCUMENT ID	TECN	COMMENT	$\Gamma_{38}\Gamma_4/\Gamma$
11.2 ± 3.3 ± 1.3 43 AUBERT 06D BABR 10.6 $e^+e^- \rightarrow 2(\pi^+\pi^-\pi^0)\gamma$					

$\Gamma(K^+K^-2\pi^+\pi^-) \times \Gamma(e^+e^-)/\Gamma_{\text{total}}$

VALUE (eV)	EVTs	DOCUMENT ID	TECN	COMMENT	$\Gamma_{52}\Gamma_4/\Gamma$
4.4 ± 2.1 ± 0.3 26 AUBERT 06D BABR 10.6 $e^+e^- \rightarrow K^+K^-2(\pi^+\pi^-)\gamma$					

$\Gamma(\pi^+\pi^-K^+K^-) \times \Gamma(e^+e^-)/\Gamma_{\text{total}}$

VALUE (eV)	EVTs	DOCUMENT ID	TECN	COMMENT	$\Gamma_{47}\Gamma_4/\Gamma$
2.56 ± 0.42 ± 0.16 85 AUBERT 07AK BABR 10.6 $e^+e^- \rightarrow \pi^+\pi^-K^+K^- \gamma$					

$\Gamma(\phi\phi_0(980) \rightarrow \pi^+\pi^-) \times \Gamma(e^+e^-)/\Gamma_{\text{total}}$

VALUE (eV)	EVTs	DOCUMENT ID	TECN	COMMENT	$\Gamma_{80}\Gamma_4/\Gamma$
0.346 ± 0.168 ± 0.004 6 ± 3 ¹⁵ AUBERT 07AK BABR 10.6 $e^+e^- \rightarrow \pi^+\pi^-K^+K^- \gamma$					

¹⁵ AUBERT 07AK reports $[\Gamma(\psi(2S) \rightarrow \phi\phi_0(980) \rightarrow \pi^+\pi^-) \times \Gamma(\psi(2S) \rightarrow e^+e^-)/\Gamma_{\text{total}}] \times [B(\phi(1020) \rightarrow K^+K^-)] = 0.17 \pm 0.08 \pm 0.02$ eV. We divide by our best value $B(\phi(1020) \rightarrow K^+K^-) = (49.2 \pm 0.6) \times 10^{-2}$. Our first error is their experiment's error and our second error is the systematic error from using our best value.

$\Gamma(\phi\pi^+\pi^-) \times \Gamma(e^+e^-)/\Gamma_{\text{total}}$

VALUE (eV)	EVTs	DOCUMENT ID	TECN	COMMENT	$\Gamma_{79}\Gamma_4/\Gamma$
0.57 ± 0.23 ± 0.01 10 ¹⁶ AUBERT, BE 06D BABR 10.6 $e^+e^- \rightarrow K^+K^-\pi^+\pi^- \gamma$					

¹⁶ AUBERT, BE 06D reports $[\Gamma(\psi(2S) \rightarrow \phi\pi^+\pi^-) \times \Gamma(\psi(2S) \rightarrow e^+e^-)/\Gamma_{\text{total}}] \times [B(\phi(1020) \rightarrow K^+K^-)] = 0.28 \pm 0.11 \pm 0.02$ eV. We divide by our best value $B(\phi(1020) \rightarrow K^+K^-) = (49.2 \pm 0.6) \times 10^{-2}$. Our first error is their experiment's error and our second error is the systematic error from using our best value.

$\Gamma(2(\pi^+\pi^-\pi^0) \times \Gamma(e^+e^-))/\Gamma_{total}$					$\Gamma_{14}\Gamma_4/\Gamma$
VALUE (eV)	EVTS	DOCUMENT ID	TECN	COMMENT	
29.7±2.2±1.8	410	AUBERT	07AU BABR	10.6 e ⁺ e ⁻ → 2(π ⁺ π ⁻)π ⁰ γ	

$\Gamma(\omega\pi^+\pi^-) \times \Gamma(e^+e^-)/\Gamma_{total}$					$\Gamma_{43}\Gamma_4/\Gamma$
VALUE (eV)	EVTS	DOCUMENT ID	TECN	COMMENT	
3.01±0.84±0.02	37	17 AUBERT	07AU BABR	10.6 e ⁺ e ⁻ → ωπ ⁺ π ⁻ γ	

¹⁷AUBERT 07AU reports [$\Gamma(\psi(2S) \rightarrow \omega\pi^+\pi^-) \times \Gamma(\psi(2S) \rightarrow e^+e^-)/\Gamma_{total}$] × [B(ω(782) → π⁺π⁻π⁰)] = 2.69 ± 0.73 ± 0.16 eV. We divide by our best value B(ω(782) → π⁺π⁻π⁰) = (89.2 ± 0.7) × 10⁻². Our first error is their experiment's error and our second error is the systematic error from using our best value.

$\Gamma(2(\pi^+\pi^-\eta) \times \Gamma(e^+e^-))/\Gamma_{total}$					$\Gamma_{41}\Gamma_4/\Gamma$
VALUE (eV)	EVTS	DOCUMENT ID	TECN	COMMENT	
2.87±1.41±0.01	16	18 AUBERT	07AU BABR	10.6 e ⁺ e ⁻ → 2(π ⁺ π ⁻)ηγ	

¹⁸AUBERT 07AU reports [$\Gamma(\psi(2S) \rightarrow 2(\pi^+\pi^-\eta) \times \Gamma(\psi(2S) \rightarrow e^+e^-)/\Gamma_{total}$] × [B(η → 2γ)] = 1.13 ± 0.55 ± 0.08 eV. We divide by our best value B(η → 2γ) = (39.31 ± 0.20) × 10⁻². Our first error is their experiment's error and our second error is the systematic error from using our best value.

$\Gamma(K^+K^-\pi^+\pi^-\pi^0) \times \Gamma(e^+e^-)/\Gamma_{total}$					$\Gamma_{59}\Gamma_4/\Gamma$
VALUE (eV)	EVTS	DOCUMENT ID	TECN	COMMENT	
4.4±1.3±0.3	32	AUBERT	07AU BABR	10.6 e ⁺ e ⁻ → K ⁺ K ⁻ π ⁺ π ⁻ π ⁰ γ	

$\Gamma(K^+K^-\pi^+\pi^-\eta) \times \Gamma(e^+e^-)/\Gamma_{total}$					$\Gamma_{50}\Gamma_4/\Gamma$
VALUE (eV)	EVTS	DOCUMENT ID	TECN	COMMENT	
3.05±1.80±0.02	7	19 AUBERT	07AU BABR	10.6 e ⁺ e ⁻ → K ⁺ K ⁻ π ⁺ π ⁻ ηγ	

¹⁹AUBERT 07AU reports [$\Gamma(\psi(2S) \rightarrow K^+K^-\pi^+\pi^-\eta) \times \Gamma(\psi(2S) \rightarrow e^+e^-)/\Gamma_{total}$] × [B(η → 2γ)] = 1.2 ± 0.7 ± 0.1 eV. We divide by our best value B(η → 2γ) = (39.31 ± 0.20) × 10⁻². Our first error is their experiment's error and our second error is the systematic error from using our best value.

ψ(2S) BRANCHING RATIOS

$\Gamma(\text{hadrons})/\Gamma_{total}$					Γ_1/Γ
VALUE	DOCUMENT ID	TECN	COMMENT		
0.9785±0.0013 OUR AVERAGE					
0.9779±0.0015	20 BAI	02B	BES2	e ⁺ e ⁻	
0.981 ± 0.003	20 LUTH	75	MRK1	e ⁺ e ⁻	

²⁰Includes cascade decay into J/ψ(1S).

$\Gamma(\text{virtual } \gamma \rightarrow \text{hadrons})/\Gamma_{total}$					Γ_2/Γ
VALUE	DOCUMENT ID	TECN	COMMENT		
0.0173±0.0014 OUR AVERAGE				Error includes scale factor of 1.5.	
0.0166±0.0010	21,22 SETH	04	RVUE	e ⁺ e ⁻	
0.0199±0.0019	21 BAI	02B	BES2	e ⁺ e ⁻	
0.029 ± 0.004	21 LUTH	75	MRK1	e ⁺ e ⁻	

²¹Included in Γ(hadrons)/Γ_{total}.
²²Using B(ψ(2S) → ℓ⁺ℓ⁻) = (0.73 ± 0.04)% from RPP-2002 and R = 2.28 ± 0.04 determined by a fit to data from BAI 00 and BAI 02c.

$\Gamma(\text{light hadrons})/\Gamma_{total}$					Γ_3/Γ
VALUE	DOCUMENT ID	TECN	COMMENT		
0.169±0.026	23 ADAM	05A	CLEO	e ⁺ e ⁻ → ψ(2S)	

²³Uses B(J/ψX) from ADAM 05A, B(χ_{cJ}γ), B(η_cγ) from ATHAR 04 and B(ℓ⁺ℓ⁻γ) from PDG 04.

$\Gamma(e^+e^-)/\Gamma_{total}$					Γ_4/Γ
VALUE (units 10 ⁻⁴)	DOCUMENT ID	TECN	COMMENT		
75.2± 1.7 OUR FIT					

²⁴From an overall fit assuming equal partial widths for e⁺e⁻ and μ⁺μ⁻. For a measurement of the ratio see the entry Γ(μ⁺μ⁻)/Γ(e⁺e⁻) below. Includes LUTH 75, HILGER 75, BURMESTER 77.

$\Gamma(\mu^+\mu^-)/\Gamma_{total}$					Γ_5/Γ
VALUE (units 10 ⁻⁴)	DOCUMENT ID	TECN	COMMENT		
75±8 OUR FIT					

$\Gamma(\mu^+\mu^-)/\Gamma(e^+e^-)$					Γ_5/Γ_4
VALUE	DOCUMENT ID	TECN	COMMENT		
0.99±0.11 OUR FIT					

²⁴From an overall fit assuming equal partial widths for e⁺e⁻ and μ⁺μ⁻. For a measurement of the ratio see the entry Γ(μ⁺μ⁻)/Γ(e⁺e⁻) below. Includes LUTH 75, HILGER 75, BURMESTER 77.

$\Gamma(\mu^+\mu^-)/\Gamma(e^+e^-)$					Γ_5/Γ_4
VALUE	DOCUMENT ID	TECN	COMMENT		
0.89±0.16	BOYARSKI	75c	MRK1	e ⁺ e ⁻	

$\Gamma(\tau^+\tau^-)/\Gamma_{total}$					Γ_6/Γ
VALUE (units 10 ⁻⁴)	DOCUMENT ID	TECN	COMMENT		
30 ± 4 OUR FIT					
30.8±2.1±3.8	25 ABLIKIM	06W	BES	e ⁺ e ⁻ → ψ(2S)	

²⁵Computed using PDG 02 value of B(ψ(2S) → hadrons) = 0.9810 ± 0.0030 to estimate the total number of ψ(2S) events.

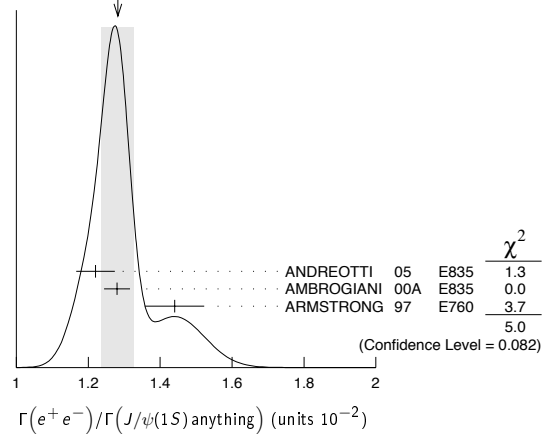
DECAYS INTO J/ψ(1S) AND ANYTHING

$\Gamma(J/\psi(1S) \text{ anything})/\Gamma_{total}$					Γ_7/Γ
VALUE	EVTS	DOCUMENT ID	TECN	COMMENT	
0.574 ± 0.009 OUR FIT					
0.592 ± 0.018 OUR AVERAGE					
0.5950±0.0015±0.0190	151k	ADAM	05A	CLEO	e ⁺ e ⁻ → ψ(2S)
0.51 ± 0.12		BRANDELIK	79c	DASP	e ⁺ e ⁻ → μ ⁺ μ ⁻ X
0.57 ± 0.08		ABRAMS	75B	MRK1	e ⁺ e ⁻ → μ ⁺ μ ⁻ X

$\Gamma(e^+e^-)/\Gamma(J/\psi(1S) \text{ anything})$					Γ_4/Γ_7
VALUE (units 10 ⁻²)	EVTS	DOCUMENT ID	TECN	COMMENT	
1.309±0.026 OUR FIT					
1.28 ± 0.04 OUR AVERAGE				Error includes scale factor of 1.6. See the ideogram below.	
1.22 ± 0.02 ± 0.05	5097 ± 73	26 ANDREOTTI	05	E835	ρ ⁺ ρ ⁻ → ψ(2S) → e ⁺ e ⁻
1.28 ± 0.03 ± 0.02		26 AMBROGIANI	00A	E835	ρ ⁺ ρ ⁻ → ψ(2S)
1.44 ± 0.08 ± 0.02		26 ARMSTRONG	97	E760	ρ ⁺ ρ ⁻ → ψ(2S)

²⁶Using B(J/ψ(1S) → e⁺e⁻) = 0.0593 ± 0.0010.

WEIGHTED AVERAGE
1.28±0.04 (Error scaled by 1.6)



$\Gamma(\mu^+\mu^-)/\Gamma(J/\psi(1S) \text{ anything})$					Γ_5/Γ_7
VALUE	DOCUMENT ID	TECN	COMMENT		
0.0130±0.0014 OUR FIT					
0.014 ± 0.003	HILGER	75	SPEC	e ⁺ e ⁻	

$\Gamma(J/\psi(1S) \text{ neutrals})/\Gamma_{total}$					Γ_8/Γ
VALUE	DOCUMENT ID	TECN	COMMENT		
0.235±0.004 OUR FIT					

$\Gamma(J/\psi(1S) \pi^+\pi^-)/\Gamma_{total}$					Γ_9/Γ
VALUE	EVTS	DOCUMENT ID	TECN	COMMENT	
0.326 ± 0.005 OUR FIT					
0.323 ± 0.013 OUR AVERAGE					
0.323 ± 0.014		BAI	02B	BES2	e ⁺ e ⁻
0.32 ± 0.04		ABRAMS	75B	MRK1	e ⁺ e ⁻ → J/ψπ ⁺ π ⁻

²⁷Not independent from other values reported by ADAM 05A.

$\Gamma(e^+e^-)/\Gamma(J/\psi(1S) \pi^+\pi^-)$					Γ_4/Γ_9
VALUE	DOCUMENT ID	TECN	COMMENT		
0.0230±0.0008 OUR FIT					
0.0252±0.0028±0.0011	28 AUBERT	02B	BABR	e ⁺ e ⁻	

²⁸Using B(J/ψ(1S) → e⁺e⁻) = 0.0593 ± 0.0010.

$\Gamma(\mu^+\mu^-)/\Gamma(J/\psi(1S) \pi^+\pi^-)$					Γ_5/Γ_9
VALUE	DOCUMENT ID	TECN	COMMENT		
0.0229±0.0026 OUR FIT					
0.0224±0.0029 OUR AVERAGE					
0.0216±0.0026±0.0014	29 AUBERT	02B	BABR	e ⁺ e ⁻	
0.0327±0.0077±0.0072	29 GRIBUSHIN	96	FMPS	515 π ⁻ Be → 2μX	

²⁹Using B(J/ψ(1S) → μ⁺μ⁻) = 0.0588 ± 0.0010.

Meson Particle Listings

 $\psi(2S)$ $\Gamma(\tau^+\tau^-)/\Gamma(J/\psi(1S)\pi^+\pi^-)$ Γ_6/Γ_9

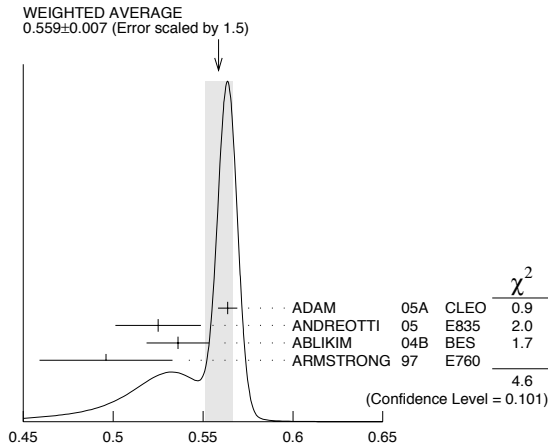
VALUE (units 10^{-3})	DOCUMENT ID	TECN	COMMENT
9.2 ± 1.1 OUR FIT			
8.73 ± 1.39 ± 1.57	BAI	02	BES e^+e^-

 $\Gamma(J/\psi(1S)\pi^+\pi^-)/\Gamma(J/\psi(1S)\text{anything})$ Γ_9/Γ_7

VALUE	EVTS	DOCUMENT ID	TECN	COMMENT
0.5680 ± 0.0031 OUR FIT				
0.559 ± 0.007 OUR AVERAGE				Error includes scale factor of 1.5. See the ideogram below.
0.5637 ± 0.0027 ± 0.0046	60k	ADAM	05A	CLEO $e^+e^- \rightarrow \psi(2S)$
0.525 ± 0.009 ± 0.022	4090 ± 67	ANDREOTTI	05	E835 $\psi(2S) \rightarrow J/\psi X$
0.536 ± 0.007 ± 0.016	20k	30,31	ABLIKIM	04B BES $\psi(2S) \rightarrow J/\psi X$
0.496 ± 0.037		ARMSTRONG	97	E760 $\bar{p}p \rightarrow \psi(2S)$

³⁰ From a fit to the J/ψ recoil mass spectra.

³¹ ABLIKIM 04B quotes $B(\psi(2S) \rightarrow J/\psi X) / B(\psi(2S) \rightarrow J/\psi\pi^+\pi^-)$.

 $\Gamma(J/\psi(1S)\pi^+\pi^-)/\Gamma(J/\psi(1S)\text{anything})$ Γ_9/Γ_7 $\Gamma(J/\psi(1S)\text{neutrals})/\Gamma(J/\psi(1S)\pi^+\pi^-)$ Γ_8/Γ_9

VALUE	DOCUMENT ID	TECN	COMMENT
0.721 ± 0.008 OUR FIT			
0.73 ± 0.09	TANENBAUM	76	MRK1 e^+e^-

 $\Gamma(J/\psi(1S)\pi^0\pi^0)/\Gamma_{\text{total}}$ Γ_{10}/Γ

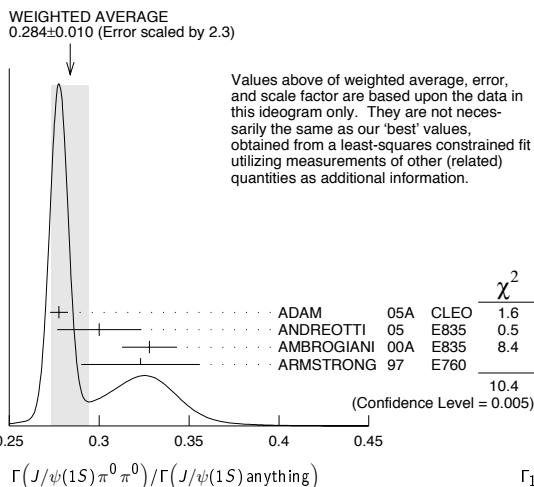
VALUE	EVTS	DOCUMENT ID	TECN	COMMENT
0.1684 ± 0.0033 OUR FIT				
0.1652 ± 0.0014 ± 0.0058	13.4k	32	ADAM	05A CLEO $e^+e^- \rightarrow \psi(2S)$

• • • We do not use the following data for averages, fits, limits, etc. • • •

³² Not independent from other values reported by ADAM 05A.

 $\Gamma(J/\psi(1S)\pi^0\pi^0)/\Gamma(J/\psi(1S)\text{anything})$ Γ_{10}/Γ_7

VALUE	EVTS	DOCUMENT ID	TECN	COMMENT
0.2933 ± 0.0032 OUR FIT				
0.284 ± 0.010 OUR AVERAGE				Error includes scale factor of 2.3. See the ideogram below.
0.2776 ± 0.0025 ± 0.0043	13.4k	ADAM	05A	CLEO $e^+e^- \rightarrow \psi(2S)$
0.300 ± 0.008 ± 0.022	1655 ± 44	ANDREOTTI	05	E835 $\psi(2S) \rightarrow J/\psi X$
0.328 ± 0.013 ± 0.008		AMBROGIANI	00A	E835 $\bar{p}\bar{p} \rightarrow \psi(2S)$
0.323 ± 0.033		ARMSTRONG	97	E760 $\bar{p}p \rightarrow \psi(2S)$

 $\Gamma(J/\psi(1S)\pi^0\pi^0)/\Gamma(J/\psi(1S)\text{anything})$ Γ_{10}/Γ_7 $\Gamma(J/\psi(1S)\pi^0\pi^0)/\Gamma(J/\psi(1S)\pi^+\pi^-)$ Γ_{10}/Γ_9

VALUE	EVTS	DOCUMENT ID	TECN	COMMENT
0.516 ± 0.017 OUR FIT				
0.570 ± 0.009 ± 0.026	14k	33	ABLIKIM	04B BES $\psi(2S) \rightarrow J/\psi X$
• • • We do not use the following data for averages, fits, limits, etc. • • •				
0.4924 ± 0.0047 ± 0.0086	73k	34,35	ADAM	05A CLEO $e^+e^- \rightarrow \psi(2S)$
0.571 ± 0.018 ± 0.044		36	ANDREOTTI	05 E835 $\psi(2S) \rightarrow J/\psi X$
0.53 ± 0.06			TANENBAUM	76 MRK1 e^+e^-
0.64 ± 0.15		37	HILGER	75 SPEC e^+e^-

³³ From a fit to the J/ψ recoil mass spectra.

³⁴ Not independent from other values reported by ADAM 05A.

³⁵ Using 13,217 $J/\psi\pi^0\pi^0$ and 60,010 $J/\psi\pi^+\pi^-$ events.

³⁶ Not independent from other values reported by ANDREOTTI 05.

³⁷ Ignoring the $J/\psi(1S)\eta$ and $J/\psi(1S)\gamma\gamma$ decays.

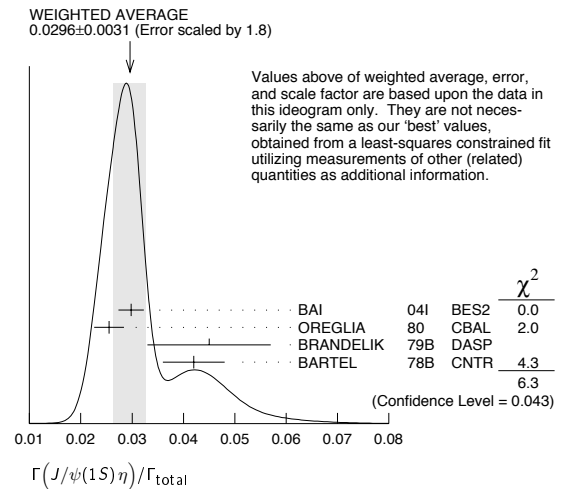
 $\Gamma(J/\psi(1S)\eta)/\Gamma_{\text{total}}$ Γ_{11}/Γ

VALUE	EVTS	DOCUMENT ID	TECN	COMMENT
0.0316 ± 0.0007 OUR FIT				
0.0296 ± 0.0031 OUR AVERAGE				Error includes scale factor of 1.8. See the ideogram below.
0.0298 ± 0.0009 ± 0.0023	5.7k	BAI	04i	BES2 $\psi(2S) \rightarrow J/\psi\gamma\gamma$
0.0255 ± 0.0029	386	38	OREGLIA	80 CBAL $e^+e^- \rightarrow J/\psi 2\gamma$
0.045 ± 0.012	17	39	BRANDELK	79B DASP $e^+e^- \rightarrow J/\psi 2\gamma$
0.042 ± 0.006	164	39	BARTEL	78B CNTR e^+e^-
• • • We do not use the following data for averages, fits, limits, etc. • • •				
0.0325 ± 0.0006 ± 0.0011	2.8k	40	ADAM	05A CLEO $e^+e^- \rightarrow \psi(2S)$
0.043 ± 0.008	44		TANENBAUM	76 MRK1 e^+e^-

³⁸ Recalculated by us using $B(J/\psi(1S) \rightarrow \ell^+\ell^-) = 0.1181 \pm 0.0020$.

³⁹ Recalculated by us using $B(J/\psi(1S) \rightarrow \mu^+\mu^-) = 0.0588 \pm 0.0010$.

⁴⁰ Not independent from other values reported by ADAM 05A.

 $\Gamma(J/\psi(1S)\eta)/\Gamma(J/\psi(1S)\text{anything})$ Γ_{11}/Γ_7

VALUE	EVTS	DOCUMENT ID	TECN	COMMENT
0.0550 ± 0.0011 OUR FIT				
0.0548 ± 0.0012 OUR AVERAGE				
0.0546 ± 0.0010 ± 0.0007	2.8k	ADAM	05A	CLEO $e^+e^- \rightarrow \psi(2S)$
0.050 ± 0.006 ± 0.003	298 ± 20	ANDREOTTI	05	E835 $\psi(2S) \rightarrow J/\psi X$
0.072 ± 0.009		AMBROGIANI	00A	E835 $\bar{p}\bar{p} \rightarrow \psi(2S)$
0.061 ± 0.015		ARMSTRONG	97	E760 $\bar{p}p \rightarrow \psi(2S)$

 $\Gamma(J/\psi(1S)\eta)/\Gamma(J/\psi(1S)\pi^+\pi^-)$ Γ_{11}/Γ_9

VALUE	EVTS	DOCUMENT ID	TECN	COMMENT
0.0968 ± 0.0033 OUR FIT				
0.096 ± 0.010 OUR AVERAGE				
0.098 ± 0.005 ± 0.010	2k	41	ABLIKIM	04B BES $\psi(2S) \rightarrow J/\psi X$
0.091 ± 0.021		42	HIMEL	80 MRK2 $e^+e^- \rightarrow \psi(2S) X$
• • • We do not use the following data for averages, fits, limits, etc. • • •				
0.0968 ± 0.0019 ± 0.0013	2.8k	43	ADAM	05A CLEO $e^+e^- \rightarrow \psi(2S)$
0.095 ± 0.007 ± 0.007		44	ANDREOTTI	05 E835 $\psi(2S) \rightarrow J/\psi X$

⁴¹ From a fit to the J/ψ recoil mass spectra.

⁴² The value for $B(\psi(2S) \rightarrow J/\psi(1S)\eta)$ reported in HIMEL 80 is derived using $B(\psi(2S) \rightarrow J/\psi(1S)\pi^+\pi^-) = (33 \pm 3)\%$ and $B(J/\psi(1S) \rightarrow \ell^+\ell^-) = 0.138 \pm 0.018$. Calculated by us using $B(J/\psi(1S) \rightarrow \ell^+\ell^-) = (0.1181 \pm 0.0020)$.

⁴³ Not independent from other values reported by ADAM 05A.

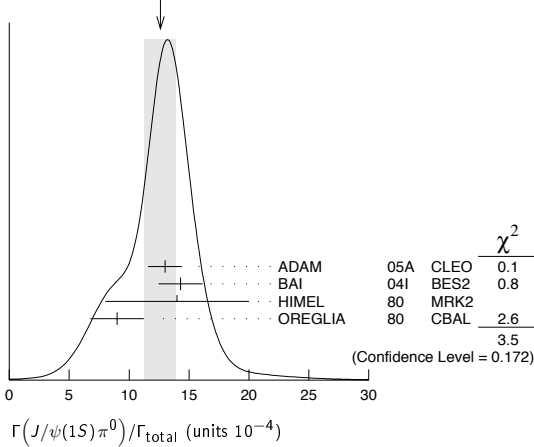
⁴⁴ Not independent from other values reported by ANDREOTTI 05.

$\Gamma(J/\psi(1S)\pi^0)/\Gamma_{total}$ Γ_{12}/Γ

VALUE (units 10^{-4})	EVTS	DOCUMENT ID	TECN	COMMENT
12.6 ± 1.3 OUR AVERAGE	Error includes scale factor of 1.3. See the ideogram below.			
13 ± 1 ± 1	88	ADAM	05A	CLEO $e^+e^- \rightarrow \psi(2S)$
14.3 ± 1.4 ± 1.2	280	BAI	04i	BES2 $\psi(2S) \rightarrow J/\psi\gamma\gamma$
14 ± 6	7	HIMEL	80	MRK2 e^+e^-
9 ± 2 ± 1	23	45 OREGLIA	80	CBAL $\psi(2S) \rightarrow J/\psi 2\gamma$

⁴⁵ Recalculated by us using $B(J/\psi(1S) \rightarrow \ell^+\ell^-) = 0.1181 \pm 0.0020$.

WEIGHTED AVERAGE
12.6 ± 1.3 (Error scaled by 1.3)



$\Gamma(J/\psi(1S)\pi^0)/\Gamma(J/\psi(1S)\text{anything})$ Γ_{12}/Γ_7

VALUE (units 10^{-2})	DOCUMENT ID	TECN	COMMENT
0.22 ± 0.02 ± 0.01	46 ADAM	05A	CLEO $e^+e^- \rightarrow \psi(2S) \rightarrow J/\psi\gamma\gamma$

⁴⁶ Not independent from other values reported by ADAM 05A.

$\Gamma(J/\psi(1S)\pi^0)/\Gamma(J/\psi(1S)\pi^+\pi^-)$ Γ_{12}/Γ_9

VALUE (units 10^{-2})	DOCUMENT ID	TECN	COMMENT
0.39 ± 0.04 ± 0.01	47 ADAM	05A	CLEO $e^+e^- \rightarrow \psi(2S) \rightarrow J/\psi\gamma\gamma$

⁴⁷ Not independent from other values reported by ADAM 05A.

HADRONIC DECAYS

$\Gamma(3(\pi^+\pi^-)\pi^0)/\Gamma_{total}$ Γ_{13}/Γ

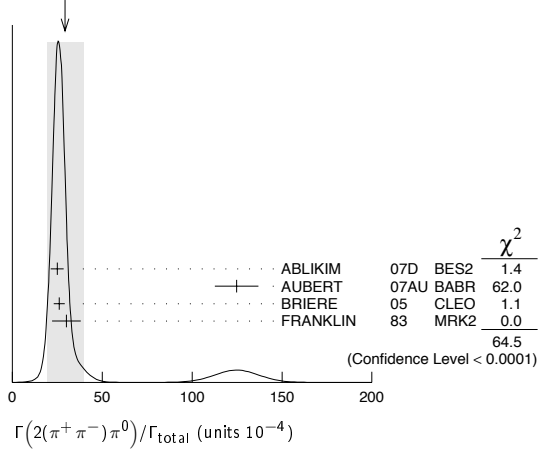
VALUE (units 10^{-4})	EVTS	DOCUMENT ID	TECN	COMMENT
35 ± 16	6	FRANKLIN	83	MRK2 $e^+e^- \rightarrow \text{hadrons}$

$\Gamma(2(\pi^+\pi^-)\pi^0)/\Gamma_{total}$ Γ_{14}/Γ

VALUE (units 10^{-4})	EVTS	DOCUMENT ID	TECN	COMMENT
29 ± 10 OUR AVERAGE	Error includes scale factor of 4.6. See the ideogram below.			
24.9 ± 0.7 ± 3.6	2173	ABLIKIM	07D	BES2 $e^+e^- \rightarrow \psi(2S)$
125 ± 12 ± 2	410	48 AUBERT	07AU	BABR 10.6 $e^+e^- \rightarrow 2(\pi^+\pi^-)\pi^0\gamma$
26.1 ± 0.7 ± 3.0	1703	BRIERE	05	CLEO $e^+e^- \rightarrow \psi(2S) \rightarrow 2(\pi^+\pi^-)\pi^0$
30 ± 8	42	FRANKLIN	83	MRK2 e^+e^-

⁴⁸ AUBERT 07AU reports $[B(\psi(2S) \rightarrow 2(\pi^+\pi^-)\pi^0)] \times [\Gamma(\psi(2S) \rightarrow e^+e^-)] = (297 \pm 22 \pm 18) \times 10^{-4}$ keV. We divide by our best value $\Gamma(\psi(2S) \rightarrow e^+e^-) = 2.38 \pm 0.04$ keV. Our first error is their experiment's error and our second error is the systematic error from using our best value.

WEIGHTED AVERAGE
29 ± 10 (Error scaled by 4.6)



$\Gamma(\rho_{22}(1320))/\Gamma_{total}$ Γ_{15}/Γ

VALUE (units 10^{-4})	CL%	EVTS	DOCUMENT ID	TECN	COMMENT
2.55 ± 0.73 ± 0.47		112 ± 31	BAI	04c	BES2 $\psi(2S) \rightarrow 2(\pi^+\pi^-)\pi^0$

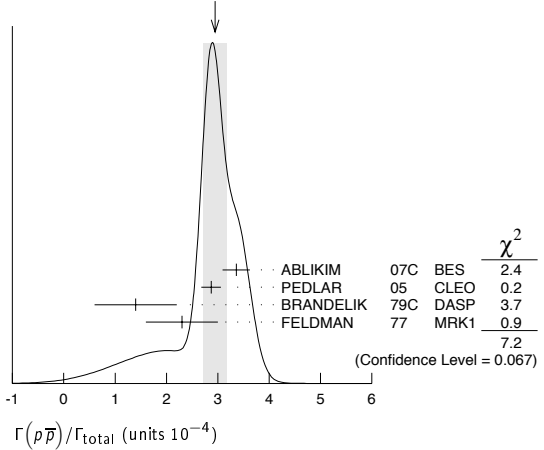
••• We do not use the following data for averages, fits, limits, etc. •••

< 2.3	90		BAI	98J	BES e^+e^-
-------	----	--	-----	-----	--------------

$\Gamma(\rho\bar{p})/\Gamma_{total}$ Γ_{16}/Γ

VALUE (units 10^{-4})	EVTS	DOCUMENT ID	TECN	COMMENT
2.74 ± 0.12 OUR FIT				
2.95 ± 0.23 OUR AVERAGE	Error includes scale factor of 1.5. See the ideogram below.			
3.36 ± 0.09 ± 0.25	1618	ABLIKIM	07c	BES $e^+e^- \rightarrow \psi(2S) \rightarrow \rho\bar{p}$
2.87 ± 0.12 ± 0.15	557	PEDLAR	05	CLEO $e^+e^- \rightarrow \psi(2S) \rightarrow \rho\bar{p}$
1.4 ± 0.8	4	BRANDELIK	79c	DASP $e^+e^- \rightarrow \psi(2S) \rightarrow \rho\bar{p}$
2.3 ± 0.7		FELDMAN	77	MRK1 $e^+e^- \rightarrow \psi(2S) \rightarrow \rho\bar{p}$

WEIGHTED AVERAGE
2.95 ± 0.23 (Error scaled by 1.5)



$\Gamma(\rho\bar{p})/\Gamma(J/\psi(1S)\pi^+\pi^-)$ Γ_{16}/Γ_9

VALUE (units 10^{-4})	DOCUMENT ID	TECN	COMMENT
8.4 ± 0.4 OUR FIT			
6.98 ± 0.49 ± 0.97	BAI	01	BES $e^+e^- \rightarrow \psi(2S) \rightarrow \rho\bar{p}$

$\Gamma(\Delta^{++}\bar{\Delta}^{--})/\Gamma_{total}$ Γ_{17}/Γ

VALUE (units 10^{-5})	EVTS	DOCUMENT ID	TECN	COMMENT
12.8 ± 1.0 ± 3.4	157	49 BAI	01	BES $e^+e^- \rightarrow \psi(2S) \rightarrow \text{hadrons}$

⁴⁹ Estimated using $B(\psi(2S) \rightarrow J/\psi\pi^+\pi^-) = 0.310 \pm 0.028$.

$\Gamma(\Lambda\bar{\Lambda}\pi^0)/\Gamma_{total}$ Γ_{18}/Γ

VALUE (units 10^{-4})	CL%	DOCUMENT ID	TECN	COMMENT
< 1.2	90	50 ABLIKIM	07H	BES2 $e^+e^- \rightarrow \psi(2S)$

⁵⁰ Using $B(\Lambda \rightarrow \pi^-p) = 63.9\%$ and $B(\eta \rightarrow \gamma\gamma) = 39.4\%$.

$\Gamma(\Lambda\bar{\Lambda}\eta)/\Gamma_{total}$ Γ_{19}/Γ

VALUE (units 10^{-4})	CL%	DOCUMENT ID	TECN	COMMENT
< 0.49	90	51 ABLIKIM	07H	BES2 $e^+e^- \rightarrow \psi(2S)$

⁵¹ Using $B(\Lambda \rightarrow \pi^-p) = 63.9\%$.

Meson Particle Listings

$\psi(2S)$

$\Gamma(\Lambda\bar{p}K^+)/\Gamma_{total}$					Γ_{20}/Γ
VALUE (units 10^{-4})	EVTS	DOCUMENT ID	TECN	COMMENT	
1.0 ± 0.1 ± 0.1	74.0	BRIERE	05	CLEO $e^+e^- \rightarrow \psi(2S) \rightarrow p\bar{p}K^+\pi^-$	

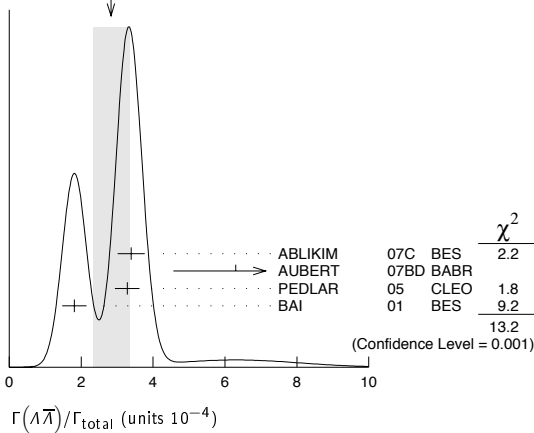
$\Gamma(\Lambda\bar{p}K^+\pi^+\pi^-)/\Gamma_{total}$					Γ_{21}/Γ
VALUE (units 10^{-4})	EVTS	DOCUMENT ID	TECN	COMMENT	
1.8 ± 0.3 ± 0.3	45.8	BRIERE	05	CLEO $e^+e^- \rightarrow \psi(2S) \rightarrow p\bar{p}K^+\pi^+\pi^-$	

$\Gamma(\Lambda\bar{\Lambda}\pi^+\pi^-)/\Gamma_{total}$					Γ_{22}/Γ
VALUE (units 10^{-4})	EVTS	DOCUMENT ID	TECN	COMMENT	
2.8 ± 0.4 ± 0.5	73.4	BRIERE	05	CLEO $e^+e^- \rightarrow \psi(2S) \rightarrow p\bar{p}2(\pi^+\pi^-)$	

$\Gamma(\Lambda\bar{\Lambda})/\Gamma_{total}$					Γ_{23}/Γ	
VALUE (units 10^{-4})	CL%	EVTS	DOCUMENT ID	TECN	COMMENT	
2.8 ± 0.5 OUR AVERAGE			Error includes scale factor of 2.6. See the ideogram below.			
3.39 ± 0.20 ± 0.32		337	ABLIKIM	07c	BES $e^+e^- \rightarrow \psi(2S) \rightarrow$ hadrons	
6.3 ± 1.7 ± 0.1		52	AUBERT	07BD	BABR $10.6 e^+e^- \rightarrow \Lambda\bar{\Lambda}\gamma$	
3.28 ± 0.23 ± 0.25		208	PEDLAR	05	CLEO $e^+e^- \rightarrow \psi(2S) \rightarrow$ hadrons	
1.81 ± 0.20 ± 0.27		80	53	BAI	01	BES $e^+e^- \rightarrow \psi(2S) \rightarrow$ hadrons

• • • We do not use the following data for averages, fits, limits, etc. • • •
 < 4 90 FELDMAN 77 MRK1 $e^+e^- \rightarrow \psi(2S) \rightarrow$ hadrons
 52 AUBERT 07BD reports $[B(\psi(2S) \rightarrow \Lambda\bar{\Lambda})] \times [\Gamma(\psi(2S) \rightarrow e^+e^-)] = (15 \pm 4 \pm 1) \times 10^{-4}$ keV. We divide by our best value $\Gamma(\psi(2S) \rightarrow e^+e^-) = 2.38 \pm 0.04$ keV. Our first error is their experiment's error and our second error is the systematic error from using our best value.
 53 Estimated using $B(\psi(2S) \rightarrow J/\psi\pi^+\pi^-) = 0.310 \pm 0.028$.

WEIGHTED AVERAGE
2.8±0.5 (Error scaled by 2.6)

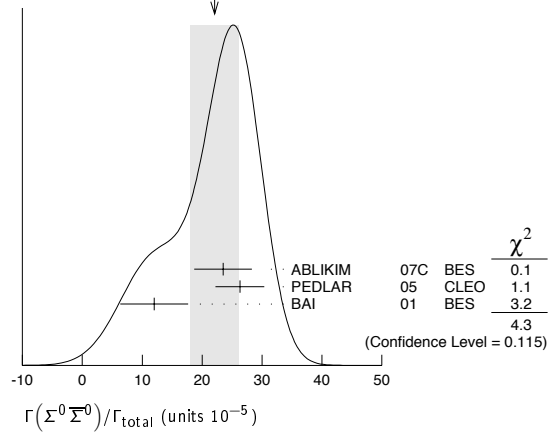


$\Gamma(\Sigma^+\bar{\Sigma}^-)/\Gamma_{total}$					Γ_{24}/Γ
VALUE (units 10^{-5})	EVTS	DOCUMENT ID	TECN	COMMENT	
25.7 ± 4.4 ± 6.8	35	PEDLAR	05	CLEO $e^+e^- \rightarrow \psi(2S) \rightarrow$ hadrons	

$\Gamma(\Sigma^0\bar{\Sigma}^0)/\Gamma_{total}$					Γ_{25}/Γ	
VALUE (units 10^{-5})	CL%	EVTS	DOCUMENT ID	TECN	COMMENT	
22 ± 4 OUR AVERAGE			Error includes scale factor of 1.5. See the ideogram below.			
23.5 ± 3.6 ± 3.2		59	ABLIKIM	07c	BES $e^+e^- \rightarrow \psi(2S) \rightarrow$ hadrons	
26.3 ± 3.5 ± 2.1		58	PEDLAR	05	CLEO $e^+e^- \rightarrow \psi(2S) \rightarrow$ hadrons	
12 ± 4 ± 4		8	54	BAI	01	BES $e^+e^- \rightarrow \psi(2S) \rightarrow$ hadrons

54 Estimated using $B(\psi(2S) \rightarrow J/\psi\pi^+\pi^-) = 0.310 \pm 0.028$.

WEIGHTED AVERAGE
22±4 (Error scaled by 1.5)



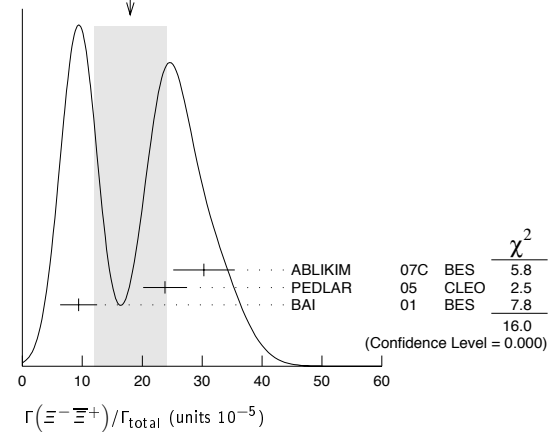
$\Gamma(\Sigma(1385)^+\bar{\Sigma}(1385)^-)/\Gamma_{total}$					Γ_{26}/Γ
VALUE (units 10^{-5})	EVTS	DOCUMENT ID	TECN	COMMENT	
11 ± 3 ± 3	14	55	BAI	01	BES $e^+e^- \rightarrow \psi(2S) \rightarrow$ hadrons

55 Estimated using $B(\psi(2S) \rightarrow J/\psi\pi^+\pi^-) = 0.310 \pm 0.028$.

$\Gamma(\Xi^-\bar{\Xi}^+)/\Gamma_{total}$					Γ_{27}/Γ	
VALUE (units 10^{-5})	CL%	EVTS	DOCUMENT ID	TECN	COMMENT	
18 ± 6 OUR AVERAGE			Error includes scale factor of 2.8. See the ideogram below.			
30.3 ± 4.0 ± 3.2		67	ABLIKIM	07c	BES $e^+e^- \rightarrow \psi(2S) \rightarrow$ hadrons	
23.8 ± 3.0 ± 2.1		63	PEDLAR	05	CLEO $e^+e^- \rightarrow \psi(2S) \rightarrow$ hadrons	
9.4 ± 2.7 ± 1.5		12	56	BAI	01	BES $e^+e^- \rightarrow \psi(2S) \rightarrow$ hadrons

• • • We do not use the following data for averages, fits, limits, etc. • • •
 < 20 90 FELDMAN 77 MRK1 $e^+e^- \rightarrow \psi(2S) \rightarrow$ hadrons
 56 Estimated using $B(\psi(2S) \rightarrow J/\psi\pi^+\pi^-) = 0.310 \pm 0.028$.

WEIGHTED AVERAGE
18±6 (Error scaled by 2.8)



$\Gamma(\Xi^0\bar{\Xi}^0)/\Gamma_{total}$					Γ_{28}/Γ
VALUE (units 10^{-5})	EVTS	DOCUMENT ID	TECN	COMMENT	
27.5 ± 6.4 ± 6.1	19	PEDLAR	05	CLEO $e^+e^- \rightarrow \psi(2S) \rightarrow$ hadrons	

$\Gamma(\Xi(1530)^0\bar{\Xi}(1530)^0)/\Gamma_{total}$					Γ_{29}/Γ	
VALUE (units 10^{-5})	CL%	EVTS	DOCUMENT ID	TECN	COMMENT	
< 8.1		90	57	BAI	01	BES $e^+e^- \rightarrow \psi(2S) \rightarrow$ hadrons

• • • We do not use the following data for averages, fits, limits, etc. • • •
 < 32 90 PEDLAR 05 CLEO $e^+e^- \rightarrow \psi(2S) \rightarrow$ hadrons
 57 Estimated using $B(\psi(2S) \rightarrow J/\psi\pi^+\pi^-) = 0.310 \pm 0.028$.

$\Gamma(\Omega^-\bar{\Omega}^+)/\Gamma_{total}$					Γ_{30}/Γ	
VALUE (units 10^{-5})	CL%	EVTS	DOCUMENT ID	TECN	COMMENT	
< 7.3		90	58	BAI	01	BES $e^+e^- \rightarrow \psi(2S) \rightarrow$ hadrons

• • • We do not use the following data for averages, fits, limits, etc. • • •
 < 16 90 PEDLAR 05 CLEO $e^+e^- \rightarrow \psi(2S) \rightarrow$ hadrons
 58 Estimated using $B(\psi(2S) \rightarrow J/\psi\pi^+\pi^-) = 0.310 \pm 0.028$.

$\Gamma(\pi^0 p\bar{p})/\Gamma_{total}$ Γ_{31}/Γ

VALUE (units 10^{-4})	EVTS	DOCUMENT ID	TECN	COMMENT
1.33±0.17 OUR AVERAGE				
1.32±0.10±0.15	256 ± 18	⁵⁹ ABLIKIM	05E BES2	$e^+e^- \rightarrow \psi(2S) \rightarrow p\bar{p}\gamma\gamma$
1.4 ± 0.5	9	FRANKLIN	83 MRK2	$e^+e^- \rightarrow \psi(2S) \rightarrow p\bar{p}\gamma\gamma$

⁵⁹ Computed using $B(\pi^0 \rightarrow \gamma\gamma) = (98.80 \pm 0.03)\%$.

$\Gamma(\eta p\bar{p})/\Gamma_{total}$ Γ_{32}/Γ

VALUE (units 10^{-4})	EVTS	DOCUMENT ID	TECN	COMMENT
0.60±0.12 OUR AVERAGE				
0.58±0.11±0.07	44.8 ± 8.5	⁶⁰ ABLIKIM	05E BES2	$e^+e^- \rightarrow \psi(2S) \rightarrow p\bar{p}\eta\gamma\gamma$
0.8 ± 0.3 ± 0.3	9.8	BRIERE	05 CLEO	$e^+e^- \rightarrow \psi(2S) \rightarrow p\bar{p}\pi^+\pi^-\pi^0$

⁶⁰ Computed using $B(\eta \rightarrow \gamma\gamma) = (39.43 \pm 0.26)\%$.

$\Gamma(\omega p\bar{p})/\Gamma_{total}$ Γ_{33}/Γ

VALUE (units 10^{-4})	EVTS	DOCUMENT ID	TECN	COMMENT
0.69±0.21 OUR AVERAGE				
0.6 ± 0.2 ± 0.2	21.2	BRIERE	05 CLEO	$e^+e^- \rightarrow \psi(2S) \rightarrow p\bar{p}\pi^+\pi^-\pi^0$
0.8 ± 0.3 ± 0.1	14.9 ± 0.1	⁶¹ BAI	03B BES	$\psi(2S) \rightarrow p\bar{p}\pi^+\pi^-\pi^0$

⁶¹ Normalized to $B(\psi(2S) \rightarrow J/\psi\pi^+\pi^-) = 0.305 \pm 0.016$.

$\Gamma(\phi p\bar{p})/\Gamma_{total}$ Γ_{34}/Γ

VALUE (units 10^{-4})	CL%	DOCUMENT ID	TECN	COMMENT
<0.24	90	BRIERE	05 CLEO	$e^+e^- \rightarrow \psi(2S) \rightarrow p\bar{p}K^+K^-$
<0.26	90	⁶² BAI	03B BES	$\psi(2S) \rightarrow K^+K^-p\bar{p}$

• • • We do not use the following data for averages, fits, limits, etc. • • •

⁶² Normalized to $B(\psi(2S) \rightarrow J/\psi\pi^+\pi^-) = 0.305 \pm 0.016$.

$\Gamma(\pi^+\pi^-p\bar{p})/\Gamma_{total}$ Γ_{35}/Γ

VALUE (units 10^{-4})	EVTS	DOCUMENT ID	TECN	COMMENT
6.0±0.4 OUR AVERAGE				
5.9±0.2±0.4	904.5	BRIERE	05 CLEO	$e^+e^- \rightarrow \psi(2S) \rightarrow p\bar{p}\pi^+\pi^-$
8 ± 2		⁶³ TANENBAUM	78 MRK1	e^+e^-

⁶³ Assuming entirely strong decay.

$\Gamma(p\bar{p}\pi^- \text{ or c.c.})/\Gamma_{total}$ Γ_{36}/Γ

VALUE (units 10^{-4})	EVTS	DOCUMENT ID	TECN	COMMENT
2.48±0.17 OUR AVERAGE				
2.45±0.11±0.21	851	ABLIKIM	06i BES2	$e^+e^- \rightarrow p\pi^-X$
2.52±0.12±0.22	849	ABLIKIM	06i BES2	$e^+e^- \rightarrow \bar{p}\pi^+X$

$\Gamma(p\bar{p}\pi^-\pi^0)/\Gamma_{total}$ Γ_{37}/Γ

VALUE (units 10^{-4})	EVTS	DOCUMENT ID	TECN	COMMENT
3.18±0.50±0.50	135 ± 21	ABLIKIM	06i BES2	$e^+e^- \rightarrow p\pi^-\pi^0X$

$\Gamma(\eta\pi^+\pi^-)/\Gamma_{total}$ Γ_{39}/Γ

VALUE (units 10^{-4})	CL%	DOCUMENT ID	TECN	COMMENT
<1.6	90	BRIERE	05 CLEO	$e^+e^- \rightarrow \psi(2S) \rightarrow 2(\pi^+\pi^-)\pi^0$

$\Gamma(\eta\pi^+\pi^-\pi^0)/\Gamma_{total}$ Γ_{40}/Γ

VALUE (units 10^{-4})	EVTS	DOCUMENT ID	TECN	COMMENT
9.5±0.7±1.5				
10.3±0.8±1.4	201.7	⁶⁴ BRIERE	05 CLEO	$e^+e^- \rightarrow \psi(2S) \rightarrow \text{hadr}$
8.1±1.4±1.6	50.0	⁶⁵ BRIERE	05 CLEO	$e^+e^- \rightarrow \psi(2S) \rightarrow \eta 3\pi(\eta \rightarrow \gamma\gamma)$
		⁶⁵ BRIERE	05 CLEO	$e^+e^- \rightarrow \psi(2S) \rightarrow \eta 3\pi(\eta \rightarrow 3\pi)$

• • • We do not use the following data for averages, fits, limits, etc. • • •

⁶⁴ Average of $\eta \rightarrow \gamma\gamma$ and $\eta \rightarrow 3\pi$.
⁶⁵ Not independent from other values reported by BRIERE 05.

$\Gamma(2(\pi^+\pi^-)\eta)/\Gamma_{total}$ Γ_{41}/Γ

VALUE (units 10^{-3})	EVTS	DOCUMENT ID	TECN	COMMENT
1.2±0.6±0.1	16	⁶⁶ AUBERT	07AU BABR	$10.6 e^+e^- \rightarrow 2(\pi^+\pi^-)\eta\gamma$

⁶⁶ AUBERT 07AU quotes $\Gamma_{ee}^{\psi(2S)} \cdot B(\psi(2S) \rightarrow 2(\pi^+\pi^-)\eta) \cdot B(\eta \rightarrow \gamma\gamma) = 1.2 \pm 0.7 \pm 0.1 \text{ eV}$.

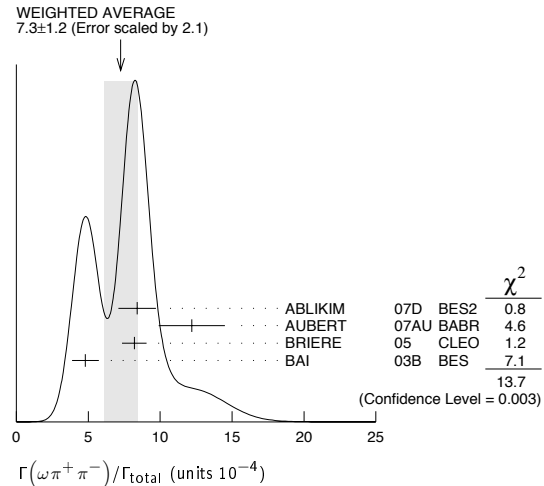
$\Gamma(\eta'\pi^+\pi^-\pi^0)/\Gamma_{total}$ Γ_{42}/Γ

VALUE (units 10^{-4})	EVTS	DOCUMENT ID	TECN	COMMENT
4.5±1.6±1.3	12.8	BRIERE	05 CLEO	$e^+e^- \rightarrow \psi(2S) \rightarrow \text{hadr}$

$\Gamma(\omega\pi^+\pi^-)/\Gamma_{total}$ Γ_{43}/Γ

VALUE (units 10^{-4})	EVTS	DOCUMENT ID	TECN	COMMENT
7.3±1.2 OUR AVERAGE				Error includes scale factor of 2.1. See the ideogram below.
8.4±0.5±1.2	386	ABLIKIM	07D BES2	$e^+e^- \rightarrow \psi(2S)$
12.2±2.2±0.7	37	⁶⁷ AUBERT	07AU BABR	$10.6 e^+e^- \rightarrow \omega\pi^+\pi^-\gamma$
8.2±0.5±0.7	391	BRIERE	05 CLEO	$e^+e^- \rightarrow \psi(2S) \rightarrow 2(\pi^+\pi^-)\pi^0$
4.8±0.6±0.7	100 ± 22	⁶⁸ BAI	03B BES	$\psi(2S) \rightarrow 2(\pi^+\pi^-)\pi^0$

⁶⁷ AUBERT 07AU quotes $\Gamma_{ee}^{\psi(2S)} \cdot B(\psi(2S) \rightarrow \omega\pi^+\pi^-) \cdot B(\omega \rightarrow 3\pi) = 2.69 \pm 0.73 \pm 0.16 \text{ eV}$.
⁶⁸ Normalized to $B(\psi(2S) \rightarrow J/\psi\pi^+\pi^-) = 0.305 \pm 0.016$.



$\Gamma(b_1^+\pi^-\pi^0)/\Gamma_{total}$ Γ_{44}/Γ

VALUE (units 10^{-4})	EVTS	DOCUMENT ID	TECN	COMMENT
4.0 ± 0.6 OUR AVERAGE				Error includes scale factor of 1.1.
5.1 ± 0.6 ± 0.8	202	ABLIKIM	07D BES2	$e^+e^- \rightarrow \psi(2S)$
4.18±0.43±0.92	170	ADAM	05 CLEO	$e^+e^- \rightarrow \psi(2S)$
3.2 ± 0.6 ± 0.5	61 ± 11	^{69,70} BAI	03B BES	$\psi(2S) \rightarrow 2(\pi^+\pi^-)\pi^0$
5.2 ± 0.8 ± 1.0		⁶⁹ BAI	99c BES	Repl. by BAI 03b

• • • We do not use the following data for averages, fits, limits, etc. • • •

⁶⁹ Assuming $B(b_1 \rightarrow \omega\pi) = 1$.
⁷⁰ Normalized to $B(\psi(2S) \rightarrow J/\psi\pi^+\pi^-) = 0.305 \pm 0.016$.

$\Gamma(b_1^0\pi^0)/\Gamma_{total}$ Γ_{45}/Γ

VALUE (units 10^{-4})	EVTS	DOCUMENT ID	TECN	COMMENT
2.35^{+0.47}_{-0.42} ± 0.40	45	ADAM	05 CLEO	$e^+e^- \rightarrow \psi(2S)$

$\Gamma(\omega f_2(1270))/\Gamma_{total}$ Γ_{46}/Γ

VALUE (units 10^{-4})	CL%	EVTS	DOCUMENT ID	TECN	COMMENT
2.2 ± 0.4 OUR AVERAGE					
2.3 ± 0.5 ± 0.4		57	ABLIKIM	07D BES2	$e^+e^- \rightarrow \psi(2S)$
2.05±0.41±0.38		62±12	BAI	04c BES2	$\psi(2S) \rightarrow 2(\pi^+\pi^-)\pi^0$

• • • We do not use the following data for averages, fits, limits, etc. • • •

VALUE	CL%	EVTS	DOCUMENT ID	TECN	COMMENT
<1.5	90		⁷¹ BAI	03B BES	$\psi(2S) \rightarrow 2(\pi^+\pi^-)\pi^0$
<1.7	90		BAI	98J BES	Repl. by BAI 03b

⁷¹ Normalized to $B(\psi(2S) \rightarrow J/\psi\pi^+\pi^-) = 0.305 \pm 0.016$.

$\Gamma(\pi^+\pi^-K^+K^-)/\Gamma_{total}$ Γ_{47}/Γ

VALUE (units 10^{-4})	EVTS	DOCUMENT ID	TECN	COMMENT
7.5±0.9 OUR AVERAGE				Error includes scale factor of 1.9.
10.8±1.9±0.2	85	⁷² AUBERT	07AK BABR	$10.6 e^+e^- \rightarrow \pi^+\pi^-K^+K^-\gamma$
7.1±0.3±0.4	817.2	BRIERE	05 CLEO	$e^+e^- \rightarrow \psi(2S) \rightarrow K^+K^-\pi^+\pi^-$
16 ± 4		⁷³ TANENBAUM	78 MRK1	e^+e^-

⁷² AUBERT 07AK reports $[B(\psi(2S) \rightarrow \pi^+\pi^-K^+K^-)] \times [\Gamma(\psi(2S) \rightarrow e^+e^-)] = (2.56 \pm 0.42 \pm 0.16) \times 10^{-3} \text{ keV}$. We divide by our best value $\Gamma(\psi(2S) \rightarrow e^+e^-) = 2.38 \pm 0.04 \text{ keV}$. Our first error is their experiment's error and our second error is the systematic error from using our best value.
⁷³ Assuming entirely strong decay.

$\Gamma(\rho^0K^+K^-)/\Gamma_{total}$ Γ_{48}/Γ

VALUE (units 10^{-4})	EVTS	DOCUMENT ID	TECN	COMMENT
2.2±0.2±0.4	223.8	BRIERE	05 CLEO	$e^+e^- \rightarrow \psi(2S) \rightarrow K^+K^-\pi^+\pi^-$

Meson Particle Listings

$\psi(2S)$

$\Gamma(K^*(892)^0 \bar{K}_S^0(1430)^0)/\Gamma_{total}$ Γ_{49}/Γ

VALUE (units 10^{-4})	CL%	EVTS	DOCUMENT ID	TECN	COMMENT
1.86 ± 0.32 ± 0.43		93 ± 16	BAI	04c	$\psi(2S) \rightarrow K^+ K^- \pi^+ \pi^-$

• • • We do not use the following data for averages, fits, limits, etc. • • •
 <1.2 90 BAI 98J BES $e^+ e^-$

$\Gamma(K^+ K^- \pi^+ \pi^- \eta)/\Gamma_{total}$ Γ_{50}/Γ

VALUE (units 10^{-3})	EVTS	DOCUMENT ID	TECN	COMMENT
1.3 ± 0.7 ± 0.1	7	⁷⁴ AUBERT	07AU BABR	10.6 $e^+ e^- \rightarrow K^+ K^- \pi^+ \pi^- \eta \gamma$
		⁷⁴ AUBERT	07AU quotes $\Gamma_{ee}^{\psi(2S)} \cdot B(\psi(2S) \rightarrow 2(\pi^+ \pi^-) \eta) \cdot B(\eta \rightarrow \gamma \gamma) = 1.2 \pm 0.7 \pm 0.1$ eV.	

$\Gamma(K_1(1270)^\pm K^\mp)/\Gamma_{total}$ Γ_{53}/Γ

VALUE (units 10^{-4})	DOCUMENT ID	TECN	COMMENT
10.0 ± 1.8 ± 2.1	⁷⁵ BAI	99c BES	$e^+ e^-$
			⁷⁵ Assuming $B(K_1(1270) \rightarrow K \rho) = 0.42 \pm 0.06$

$\Gamma(K_S^0 K_L^0 \pi^+ \pi^-)/\Gamma_{total}$ Γ_{54}/Γ

VALUE (units 10^{-4})	EVTS	DOCUMENT ID	TECN	COMMENT
2.20 ± 0.25 ± 0.37	83 ± 9	ABLIKIM	050 BES2	$e^+ e^- \rightarrow \psi(2S)$

$\Gamma(\rho^0 \rho \bar{\rho})/\Gamma_{total}$ Γ_{55}/Γ

VALUE (units 10^{-4})	EVTS	DOCUMENT ID	TECN	COMMENT
0.5 ± 0.1 ± 0.2	61.1	BRIERE	05 CLEO	$e^+ e^- \rightarrow \psi(2S) \rightarrow \rho \bar{\rho} \pi^+ \pi^-$

$\Gamma(K^+ \bar{K}^*(892)^0 \pi^- + c.c.)/\Gamma_{total}$ Γ_{56}/Γ

VALUE (units 10^{-4})	DOCUMENT ID	TECN	COMMENT
6.7 ± 2.5	TANENBAUM	78 MRK1	$e^+ e^-$

$\Gamma(2(\pi^+ \pi^-))/\Gamma_{total}$ Γ_{57}/Γ

VALUE (units 10^{-4})	EVTS	DOCUMENT ID	TECN	COMMENT
2.4 ± 0.6 OUR AVERAGE				Error includes scale factor of 2.2.
2.2 ± 0.2 ± 0.2	308	BRIERE	05 CLEO	$e^+ e^- \rightarrow \psi(2S) \rightarrow 2(\pi^+ \pi^-)$
4.5 ± 1.0		TANENBAUM	78 MRK1	$e^+ e^-$

$\Gamma(\rho^0 \pi^+ \pi^-)/\Gamma_{total}$ Γ_{58}/Γ

VALUE (units 10^{-4})	EVTS	DOCUMENT ID	TECN	COMMENT
2.2 ± 0.6 OUR AVERAGE				Error includes scale factor of 1.4.
2.0 ± 0.2 ± 0.4	285.5	BRIERE	05 CLEO	$e^+ e^- \rightarrow \psi(2S) \rightarrow 2(\pi^+ \pi^-)$
4.2 ± 1.5		TANENBAUM	78 MRK1	$e^+ e^-$

$\Gamma(K^+ K^- \pi^+ \pi^- \pi^0)/\Gamma_{total}$ Γ_{59}/Γ

VALUE (units 10^{-4})	EVTS	DOCUMENT ID	TECN	COMMENT
12.6 ± 0.9 OUR AVERAGE				
18.5 ± 5.6 ± 0.3	32	⁷⁶ AUBERT	07AU BABR	10.6 $e^+ e^- \rightarrow K^+ K^- \pi^+ \pi^- \pi^0 \gamma$
11.7 ± 1.0 ± 1.5	597	ABLIKIM	06G BES2	$\psi(2S) \rightarrow K^+ K^- \pi^+ \pi^- \pi^0$
12.7 ± 0.5 ± 1.0	711.6	BRIERE	05 CLEO	$e^+ e^- \rightarrow \psi(2S) \rightarrow K^+ K^- \pi^+ \pi^- \pi^0$

⁷⁶AUBERT 07AU reports $[B(\psi(2S) \rightarrow K^+ K^- \pi^+ \pi^- \pi^0)] \times [\Gamma(\psi(2S) \rightarrow e^+ e^-)] = (44 \pm 13 \pm 3) \times 10^{-4}$ keV. We divide by our best value $\Gamma(\psi(2S) \rightarrow e^+ e^-) = 2.38 \pm 0.04$ keV. Our first error is their experiment's error and our second error is the systematic error from using our best value.

$\Gamma(K^+ K^- 2(\pi^+ \pi^-) \pi^0)/\Gamma_{total}$ Γ_{51}/Γ

VALUE (units 10^{-4})	EVTS	DOCUMENT ID	TECN	COMMENT
10.0 ± 2.5 ± 1.8	65	ABLIKIM	07D BES2	$e^+ e^- \rightarrow \psi(2S)$

$\Gamma(\omega f_0(1710) \rightarrow \omega K^+ K^-)/\Gamma_{total}$ Γ_{60}/Γ

VALUE (units 10^{-5})	EVTS	DOCUMENT ID	TECN	COMMENT
5.9 ± 2.0 ± 0.9	19	ABLIKIM	06G BES2	$\psi(2S) \rightarrow K^+ K^- \pi^+ \pi^- \pi^0$

$\Gamma(K^*(892)^0 K^- \pi^+ \pi^0 + c.c.)/\Gamma_{total}$ Γ_{61}/Γ

VALUE (units 10^{-4})	EVTS	DOCUMENT ID	TECN	COMMENT
8.6 ± 1.3 ± 1.8	238	ABLIKIM	06G BES2	$\psi(2S) \rightarrow K^+ K^- \pi^+ \pi^- \pi^0$

$\Gamma(K^*(892)^+ K^- \pi^+ \pi^- + c.c.)/\Gamma_{total}$ Γ_{62}/Γ

VALUE (units 10^{-4})	EVTS	DOCUMENT ID	TECN	COMMENT
9.6 ± 2.2 ± 1.7	133	ABLIKIM	06G BES2	$\psi(2S) \rightarrow K^+ K^- \pi^+ \pi^- \pi^0$

$\Gamma(K^*(892)^+ K^- \rho^0 + c.c.)/\Gamma_{total}$ Γ_{63}/Γ

VALUE (units 10^{-4})	EVTS	DOCUMENT ID	TECN	COMMENT
7.3 ± 2.2 ± 1.4	78	ABLIKIM	06G BES2	$\psi(2S) \rightarrow K^+ K^- \pi^+ \pi^- \pi^0$

$\Gamma(K^*(892)^0 K^- \rho^+ + c.c.)/\Gamma_{total}$ Γ_{64}/Γ

VALUE (units 10^{-4})	EVTS	DOCUMENT ID	TECN	COMMENT
6.1 ± 1.3 ± 1.2	125	ABLIKIM	06G BES2	$\psi(2S) \rightarrow K^+ K^- \pi^+ \pi^- \pi^0$

$\Gamma(\eta K^+ K^-)/\Gamma_{total}$ Γ_{65}/Γ

VALUE (units 10^{-4})	CL%	DOCUMENT ID	TECN	COMMENT
<1.3	90	BRIERE	05 CLEO	$e^+ e^- \rightarrow \psi(2S) \rightarrow K^+ K^- \pi^+ \pi^- \pi^0$

$\Gamma(\omega K^+ K^-)/\Gamma_{total}$ Γ_{66}/Γ

VALUE (units 10^{-4})	EVTS	DOCUMENT ID	TECN	COMMENT
1.85 ± 0.25 OUR AVERAGE				Error includes scale factor of 1.1.
2.38 ± 0.37 ± 0.29	78	ABLIKIM	06G BES2	$\psi(2S) \rightarrow K^+ K^- \pi^+ \pi^- \pi^0$
1.9 ± 0.3 ± 0.3	76.8	BRIERE	05 CLEO	$e^+ e^- \rightarrow \psi(2S) \rightarrow K^+ K^- \pi^+ \pi^- \pi^0$
1.5 ± 0.3 ± 0.2	23.0 ± 5.2	⁷⁷ BAI	03B BES	$\psi(2S) \rightarrow K^+ K^- \pi^+ \pi^- \pi^0$

⁷⁷ Normalized to $B(\psi(2S) \rightarrow J/\psi \pi^+ \pi^-) = 0.305 \pm 0.016$.

$\Gamma(3(\pi^+ \pi^-))/\Gamma_{total}$ Γ_{67}/Γ

VALUE (units 10^{-4})	EVTS	DOCUMENT ID	TECN	COMMENT
3.5 ± 2.0 OUR AVERAGE				Error includes scale factor of 2.8.
5.45 ± 0.42 ± 0.87	671	ABLIKIM	05H BES2	$e^+ e^- \rightarrow \psi(2S) \rightarrow 3(\pi^+ \pi^-)$
1.5 ± 1.0		⁷⁸ TANENBAUM	78 MRK1	$e^+ e^-$

⁷⁸ Assuming entirely strong decay.

$\Gamma(\rho \bar{\rho} \pi^+ \pi^- \pi^0)/\Gamma_{total}$ Γ_{68}/Γ

VALUE (units 10^{-4})	EVTS	DOCUMENT ID	TECN	COMMENT
7.3 ± 0.4 ± 0.6	434.9	BRIERE	05 CLEO	$e^+ e^- \rightarrow \psi(2S) \rightarrow \rho \bar{\rho} \pi^+ \pi^- \pi^0$

$\Gamma(K^+ K^-)/\Gamma_{total}$ Γ_{69}/Γ

VALUE (units 10^{-5})	CL%	DOCUMENT ID	TECN	COMMENT
6.3 ± 0.7 OUR AVERAGE				
6.3 ± 0.6 ± 0.3		DOBBS	06A CLEO	$e^+ e^-$
10 ± 7		BRANDELK	79c DASP	$e^+ e^-$

• • • We do not use the following data for averages, fits, limits, etc. • • •
 < 5 90 FELDMAN 77 MRK1 $e^+ e^-$

$\Gamma(K_S^0 K_L^0)/\Gamma_{total}$ Γ_{70}/Γ

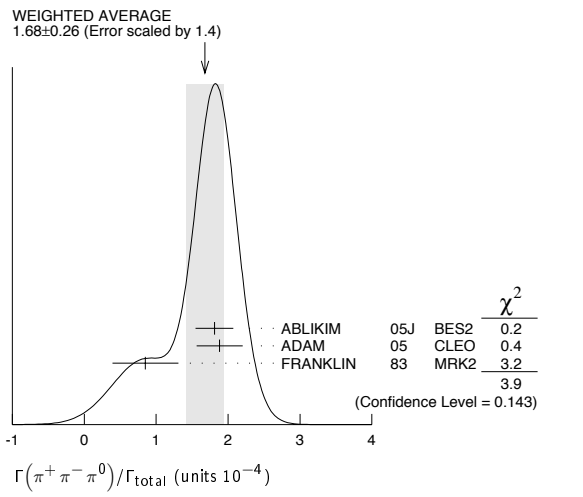
VALUE (units 10^{-5})	EVTS	DOCUMENT ID	TECN	COMMENT
5.4 ± 0.5 OUR AVERAGE				
5.8 ± 0.8 ± 0.4		DOBBS	06A CLEO	$e^+ e^-$
5.24 ± 0.47 ± 0.48	156 ± 14	⁷⁹ BAI	04B BES2	$\psi(2S) \rightarrow K_S^0 K_L^0 \rightarrow \pi^+ \pi^- X$

⁷⁹ Using $B(K_S^0 \rightarrow \pi^+ \pi^-) = 0.6860 \pm 0.0027$.

$\Gamma(\pi^+ \pi^- \pi^0)/\Gamma_{total}$ Γ_{71}/Γ

VALUE (units 10^{-4})	EVTS	DOCUMENT ID	TECN	COMMENT
1.68 ± 0.26 OUR AVERAGE				Error includes scale factor of 1.4. See the ideogram below.
1.81 ± 0.18 ± 0.19	260 ± 19	⁸⁰ ABLIKIM	05J BES2	$e^+ e^- \rightarrow \psi(2S)$
1.88 ^{+0.16} _{-0.15} ± 0.28	194	ADAM	05 CLEO	$e^+ e^- \rightarrow \psi(2S)$
0.85 ± 0.46	4	FRANKLIN	83 MRK2	$e^+ e^- \rightarrow$ hadrons

⁸⁰ From a PW analysis of $\psi(2S) \rightarrow \pi^+ \pi^- \pi^0$.



$\Gamma(\rho(2150)\pi \rightarrow \pi^+\pi^-\pi^0)/\Gamma_{\text{total}}$ Γ_{72}/Γ

VALUE (units 10^{-4})	DOCUMENT ID	TECN	COMMENT
$1.94 \pm 0.25 \pm 1.15$ -0.34	81 ABLIKIM	05J BES2	$\psi(2S) \rightarrow \rho(2150)\pi \rightarrow \pi^+\pi^-\pi^0$

⁸¹ From a PW analysis of $\psi(2S) \rightarrow \pi^+\pi^-\pi^0$.

 $\Gamma(\rho(770)\pi \rightarrow \pi^+\pi^-\pi^0)/\Gamma_{\text{total}}$ Γ_{73}/Γ

VALUE (units 10^{-4})	CL%	EVTS	DOCUMENT ID	TECN	COMMENT
0.32 ± 0.12 OUR AVERAGE					Error includes scale factor of 1.8.
$0.51 \pm 0.07 \pm 0.11$			82 ABLIKIM	05J BES2	$\psi(2S) \rightarrow \rho(770)\pi \rightarrow \pi^+\pi^-\pi^0$
$0.24 \pm 0.08 \pm 0.02$			22 ADAM	05 CLEO	$e^+e^- \rightarrow \psi(2S)$

• • • We do not use the following data for averages, fits, limits, etc. • • •

<0.83	90	1	FRANKLIN	83 MRK2	e^+e^-
<10	90		BARTEL	76 CNTR	e^+e^-
<10	90		83 ABRAMS	75 MRK1	e^+e^-

⁸² From a PW analysis of $\psi(2S) \rightarrow \pi^+\pi^-\pi^0$.

⁸³ Final state $\rho^0\pi^0$.

 $\Gamma(\pi^+\pi^-)/\Gamma_{\text{total}}$ Γ_{74}/Γ

VALUE (units 10^{-5})	CL%	DOCUMENT ID	TECN	COMMENT
8 ± 5		BRANDELIK	79C DASP	e^+e^-
<2.1	90	DOBBS	06A CLEO	$e^+e^- \rightarrow \psi(2S)$
<5	90	FELDMAN	77 MRK1	e^+e^-

• • • We do not use the following data for averages, fits, limits, etc. • • •

 $\Gamma(K_1(1400)^\pm K^\mp)/\Gamma_{\text{total}}$ Γ_{75}/Γ

VALUE (units 10^{-4})	CL%	DOCUMENT ID	TECN	COMMENT
<3.1		84 BAI	99C BES	e^+e^-

⁸⁴ Assuming $B(K_1(1400) \rightarrow K^*\pi) = 0.94 \pm 0.06$

 $\Gamma(K^+K^-\pi^0)/\Gamma_{\text{total}}$ Γ_{76}/Γ

VALUE (units 10^{-5})	CL%	EVTS	DOCUMENT ID	TECN	COMMENT
<2.96			FRANKLIN	83 MRK2	$e^+e^- \rightarrow \text{hadrons}$

 $\Gamma(K^+\bar{K}^*(892)^- + \text{c.c.})/\Gamma_{\text{total}}$ Γ_{77}/Γ

VALUE (units 10^{-5})	CL%	EVTS	DOCUMENT ID	TECN	COMMENT
1.7 ± 0.8 OUR AVERAGE					
$2.9 \pm 1.3 \pm 0.4$			9.6 \pm 4.2	ABLIKIM	05i BES2 $e^+e^- \rightarrow \psi(2S)$
$1.3 \pm 1.0 \pm 0.3$			7	ADAM	05 CLEO $e^+e^- \rightarrow \psi(2S)$

• • • We do not use the following data for averages, fits, limits, etc. • • •

<5.4	90		FRANKLIN	83 MRK2	$e^+e^- \rightarrow \text{hadrons}$
------	----	--	----------	---------	-------------------------------------

 $\Gamma(K^*(892)^0\bar{K}^0 + \text{c.c.})/\Gamma_{\text{total}}$ Γ_{78}/Γ

VALUE (units 10^{-5})	EVTS	DOCUMENT ID	TECN	COMMENT	
10.9 ± 2.0 OUR AVERAGE					
$13.3 \pm 2.4 \pm 1.7$			65.6 \pm 9.0	ABLIKIM	05i BES2 $e^+e^- \rightarrow \psi(2S)$
$9.2 \pm 2.7 \pm 0.9$			25	ADAM	05 CLEO $e^+e^- \rightarrow \psi(2S)$

 $\Gamma(K^+\bar{K}^*(892)^- + \text{c.c.})/\Gamma(K^*(892)^0\bar{K}^0 + \text{c.c.})$ Γ_{77}/Γ_{78}

VALUE	DOCUMENT ID	TECN	COMMENT
0.16 ± 0.06 OUR AVERAGE			
$0.22 \pm 0.10 \pm 0.14$	ABLIKIM	05i BES2	$e^+e^- \rightarrow \psi(2S)$
$0.14 \pm 0.08 \pm 0.06$	ADAM	05 CLEO	$e^+e^- \rightarrow \psi(2S)$

 $\Gamma(\phi\pi^+\pi^-)/\Gamma_{\text{total}}$ Γ_{79}/Γ

VALUE (units 10^{-4})	EVTS	DOCUMENT ID	TECN	COMMENT	
1.17 ± 0.29 OUR AVERAGE				Error includes scale factor of 1.7.	
$2.39 \pm 0.94 \pm 0.04$			10 \pm 4	85,86 AUBERT	07AK BABR $10.6 e^+e^- \rightarrow \pi^+\pi^-\pi^0 K^+K^-\gamma$
$0.9 \pm 0.2 \pm 0.1$			47.6	BRIERE	05 CLEO $e^+e^- \rightarrow \psi(2S) \rightarrow K^+K^-\pi^+\pi^-$
$1.5 \pm 0.2 \pm 0.2$			51.5 \pm 8.3	87 BAI	03B BES $\psi(2S) \rightarrow K^+K^-\pi^+\pi^-$

⁸⁵ AUBERT 07AK reports $[B(\psi(2S) \rightarrow \phi\pi^+\pi^-)] \times [\Gamma(\psi(2S) \rightarrow e^+e^-)] = (0.57 \pm 0.22 \pm 0.04) \times 10^{-3}$ keV. We divide by our best value $\Gamma(\psi(2S) \rightarrow e^+e^-) = 2.38 \pm 0.04$ keV. Our first error is their experiment's error and our second error is the systematic error from using our best value.

⁸⁶ Using $B(\phi \rightarrow K^+K^-) = (49.3 \pm 0.6)\%$.

⁸⁷ Normalized to $B(\psi(2S) \rightarrow J/\psi\pi^+\pi^-) = 0.305 \pm 0.016$.

 $\Gamma(\phi f_0(980) \rightarrow \pi^+\pi^-)/\Gamma_{\text{total}}$ Γ_{80}/Γ

VALUE (units 10^{-4})	EVTS	DOCUMENT ID	TECN	COMMENT	
0.68 ± 0.24 OUR AVERAGE				Error includes scale factor of 1.1.	
$1.43 \pm 0.69 \pm 0.02$			6 \pm 3	88,89 AUBERT	07AK BABR $10.6 e^+e^- \rightarrow \pi^+\pi^-\pi^0 K^+K^-\gamma$
$0.6 \pm 0.2 \pm 0.1$			18.4 \pm 6.4	90 BAI	03B BES $\psi(2S) \rightarrow K^+K^-\pi^+\pi^-$
$0.6 \pm 0.2 \pm 0.1$			18.4 \pm 6.4	90 BAI	03B BES $\psi(2S) \rightarrow K^+K^-\pi^+\pi^-$

⁸⁸ AUBERT 07AK reports $[B(\psi(2S) \rightarrow \phi f_0(980) \rightarrow \pi^+\pi^-)] \times [\Gamma(\psi(2S) \rightarrow e^+e^-)] = (0.34 \pm 0.16 \pm 0.04) \times 10^{-3}$ keV. We divide by our best value $\Gamma(\psi(2S) \rightarrow e^+e^-) = 2.38 \pm 0.04$ keV. Our first error is their experiment's error and our second error is the systematic error from using our best value.

⁸⁹ Using $B(\phi \rightarrow K^+K^-) = (49.3 \pm 0.6)\%$.

⁹⁰ Normalized to $B(\psi(2S) \rightarrow J/\psi\pi^+\pi^-) = 0.305 \pm 0.016$.

 $\Gamma(2(K^+K^-))/\Gamma_{\text{total}}$ Γ_{81}/Γ

VALUE (units 10^{-4})	EVTS	DOCUMENT ID	TECN	COMMENT
$0.6 \pm 0.1 \pm 0.1$				
	59.2	BRIERE	05 CLEO	$e^+e^- \rightarrow \psi(2S) \rightarrow 2(K^+K^-)$

 $\Gamma(\phi K^+K^-)/\Gamma_{\text{total}}$ Γ_{82}/Γ

VALUE (units 10^{-4})	EVTS	DOCUMENT ID	TECN	COMMENT	
0.70 ± 0.16 OUR AVERAGE					
$0.8 \pm 0.2 \pm 0.1$			36.8	BRIERE	05 CLEO $e^+e^- \rightarrow \psi(2S) \rightarrow 2(K^+K^-)$
$0.6 \pm 0.2 \pm 0.1$			16.1 \pm 5.0	91 BAI	03B BES $\psi(2S) \rightarrow 2(K^+K^-)$

⁹¹ Normalized to $B(\psi(2S) \rightarrow J/\psi\pi^+\pi^-) = 0.305 \pm 0.016$.

 $\Gamma(2(K^+K^-)\pi^0)/\Gamma_{\text{total}}$ Γ_{83}/Γ

VALUE (units 10^{-4})	EVTS	DOCUMENT ID	TECN	COMMENT
$1.1 \pm 0.2 \pm 0.2$				
	44.7	BRIERE	05 CLEO	$e^+e^- \rightarrow \psi(2S) \rightarrow 2(K^+K^-)\pi^0$

 $\Gamma(\phi\eta)/\Gamma_{\text{total}}$ Γ_{84}/Γ

VALUE (units 10^{-5})	EVTS	DOCUMENT ID	TECN	COMMENT	
2.8 ± 1.0 OUR AVERAGE					
$2.0 \pm 1.5 \pm 0.4$			6	ADAM	05 CLEO $e^+e^- \rightarrow \psi(2S)$
$3.3 \pm 1.1 \pm 0.5$			17	ABLIKIM	04K BES $e^+e^- \rightarrow \psi(2S)$

 $\Gamma(\phi\eta')/\Gamma_{\text{total}}$ Γ_{85}/Γ

VALUE (units 10^{-5})	EVTS	DOCUMENT ID	TECN	COMMENT
$3.1 \pm 1.4 \pm 0.7$				
	8	92 ABLIKIM	04K BES	$e^+e^- \rightarrow \psi(2S)$

⁹² Calculated combining $\eta' \rightarrow \gamma\rho$ and $\eta\pi^+\pi^-$ channels.

 $\Gamma(\omega\eta)/\Gamma_{\text{total}}$ Γ_{86}/Γ

VALUE (units 10^{-5})	EVTS	DOCUMENT ID	TECN	COMMENT
$3.2 \pm 2.4 \pm 0.7$				
	4	93 ABLIKIM	04K BES	$e^+e^- \rightarrow \psi(2S)$

⁹³ Calculated combining $\eta' \rightarrow \gamma\rho$ and $\eta\pi^+\pi^-$ channels.

 $\Gamma(\omega\pi^0)/\Gamma_{\text{total}}$ Γ_{87}/Γ

VALUE (units 10^{-5})	EVTS	DOCUMENT ID	TECN	COMMENT	
2.1 ± 0.6 OUR AVERAGE					
$2.5 \pm 1.2 \pm 0.2$			14	ADAM	05 CLEO $e^+e^- \rightarrow \psi(2S)$
$1.87 \pm 0.68 \pm 0.28$			14	ABLIKIM	04L BES $e^+e^- \rightarrow \psi(2S)$

 $\Gamma(\rho\eta')/\Gamma_{\text{total}}$ Γ_{88}/Γ

VALUE (units 10^{-5})	EVTS	DOCUMENT ID	TECN	COMMENT
$1.87 \pm 1.64 \pm 0.33$				
	2	ABLIKIM	04L BES	$e^+e^- \rightarrow \psi(2S)$

 $\Gamma(\rho\eta)/\Gamma_{\text{total}}$ Γ_{89}/Γ

VALUE (units 10^{-5})	EVTS	DOCUMENT ID	TECN	COMMENT	
2.2 ± 0.6 OUR AVERAGE				Error includes scale factor of 1.1.	
$3.0 \pm 1.1 \pm 0.9$			18	ADAM	05 CLEO $e^+e^- \rightarrow \psi(2S)$
$1.78 \pm 0.67 \pm 0.17$			13	ABLIKIM	04L BES $e^+e^- \rightarrow \psi(2S)$

 $\Gamma(\omega\eta)/\Gamma_{\text{total}}$ Γ_{90}/Γ

VALUE (units 10^{-5})	CL%	DOCUMENT ID	TECN	COMMENT
<1.1				
	90	ADAM	05 CLEO	$e^+e^- \rightarrow \psi(2S)$
<3.1	90	ABLIKIM	04K BES	$e^+e^- \rightarrow \psi(2S)$

• • • We do not use the following data for averages, fits, limits, etc. • • •

 $\Gamma(\phi\pi^0)/\Gamma_{\text{total}}$ Γ_{91}/Γ

VALUE (units 10^{-5})	CL%	DOCUMENT ID	TECN	COMMENT
<0.4				
	90	ABLIKIM	04K BES	$e^+e^- \rightarrow \psi(2S)$
<0.7	90	ADAM	05 CLEO	$e^+e^- \rightarrow \psi(2S)$

• • • We do not use the following data for averages, fits, limits, etc. • • •

Meson Particle Listings

 $\psi(2S)$

$\Gamma(\eta_c \pi^+ \pi^- \pi^0)/\Gamma_{\text{total}}$					Γ_{92}/Γ
VALUE (units 10^{-3})	CL%	DOCUMENT ID	TECN	COMMENT	
<1.0	90	PEDLAR	07	CLEO $e^+ e^- \rightarrow \psi(2S)$	

$\Gamma(p\bar{p}K^+K^-)/\Gamma_{\text{total}}$					Γ_{93}/Γ
VALUE (units 10^{-5})	EVTS	DOCUMENT ID	TECN	COMMENT	
$2.7 \pm 0.6 \pm 0.4$	30.1	BRIERE	05	CLEO $e^+ e^- \rightarrow \psi(2S) \rightarrow p\bar{p}K^+K^-$	

$\Gamma(\bar{\Lambda}nK_S^0 + \text{c.c.})/\Gamma_{\text{total}}$					Γ_{94}/Γ
VALUE (units 10^{-4})	EVTS	DOCUMENT ID	TECN	COMMENT	
$0.81 \pm 0.11 \pm 0.14$	50	⁹⁴ ABLIKIM	08c	BES2 $e^+ e^- \rightarrow J/\psi$	
⁹⁴ Using $B(\bar{\Lambda} \rightarrow \bar{p}\pi^+) = 63.9\%$ and $B(K_S^0 \rightarrow \pi^+\pi^-) = 69.2\%$.					

$\Gamma(\phi f_2'(1525))/\Gamma_{\text{total}}$					Γ_{95}/Γ
VALUE (units 10^{-4})	CL%	EVTS	DOCUMENT ID	TECN	COMMENT
$0.44 \pm 0.12 \pm 0.11$		20 ± 6	BAI	04c	$\psi(2S) \rightarrow 2(K^+K^-)$
• • • We do not use the following data for averages, fits, limits, etc. • • •					
<0.45	90		BAI	98J	BES $e^+ e^- \rightarrow 2(K^+K^-)$

$\Gamma(\Theta(1540)\bar{\Theta}(1540) \rightarrow K_S^0 p K^- \bar{\pi} + \text{c.c.})/\Gamma_{\text{total}}$					Γ_{96}/Γ
VALUE (units 10^{-5})	CL%	DOCUMENT ID	TECN	COMMENT	
<0.88	90	BAI	04G	BES2 $e^+ e^-$	

$\Gamma(\Theta(1540)K^- \bar{\pi} \rightarrow K_S^0 p K^- \bar{\pi})/\Gamma_{\text{total}}$					Γ_{97}/Γ
VALUE (units 10^{-5})	CL%	DOCUMENT ID	TECN	COMMENT	
<1.0	90	BAI	04G	BES2 $e^+ e^-$	

$\Gamma(\Theta(1540)K_S^0 \bar{p} \rightarrow K_S^0 \bar{p} K^+ n)/\Gamma_{\text{total}}$					Γ_{98}/Γ
VALUE (units 10^{-5})	CL%	DOCUMENT ID	TECN	COMMENT	
<0.70	90	BAI	04G	BES2 $e^+ e^-$	

$\Gamma(\bar{\Theta}(1540)K^+ n \rightarrow K_S^0 \bar{p} K^+ n)/\Gamma_{\text{total}}$					Γ_{99}/Γ
VALUE (units 10^{-5})	CL%	DOCUMENT ID	TECN	COMMENT	
<2.6	90	BAI	04G	BES2 $e^+ e^-$	

$\Gamma(\bar{\Theta}(1540)K_S^0 p \rightarrow K_S^0 p K^- \bar{\pi})/\Gamma_{\text{total}}$					Γ_{100}/Γ
VALUE (units 10^{-5})	CL%	DOCUMENT ID	TECN	COMMENT	
<0.60	90	BAI	04G	BES2 $e^+ e^-$	

$\Gamma(K_S^0 K_S^0)/\Gamma_{\text{total}}$					Γ_{101}/Γ
VALUE (units 10^{-4})	CL%	DOCUMENT ID	TECN	COMMENT	
<0.046		⁹⁵ BAI	04D	BES $e^+ e^-$	
⁹⁵ Forbidden by CP.					

RADIATIVE DECAYS

$\Gamma(\gamma\chi_{c0}(1P))/\Gamma_{\text{total}}$					Γ_{102}/Γ
VALUE (units 10^{-2})	EVTS	DOCUMENT ID	TECN	COMMENT	
9.4 ± 0.4 OUR FIT					
9.2 ± 0.4 OUR AVERAGE					
9.22 ± 0.11 ± 0.46	72600	ATHAR	04	CLEO $e^+ e^- \rightarrow \gamma X$	
9.9 ± 0.5 ± 0.8		⁹⁶ GAISER	86	CBAL $e^+ e^- \rightarrow \gamma X$	
7.2 ± 2.3		⁹⁶ BIDDICK	77	CNTR $e^+ e^- \rightarrow \gamma X$	
7.5 ± 2.6		⁹⁶ WHITAKER	76	MRK1 $e^+ e^-$	
⁹⁶ Angular distribution $(1+\cos^2\theta)$ assumed.					

$\Gamma(\gamma\chi_{c1}(1P))/\Gamma_{\text{total}}$					Γ_{103}/Γ
VALUE (units 10^{-2})	EVTS	DOCUMENT ID	TECN	COMMENT	
8.8 ± 0.4 OUR FIT					
8.9 ± 0.5 OUR AVERAGE					
9.07 ± 0.11 ± 0.54	76700	ATHAR	04	CLEO $e^+ e^- \rightarrow \gamma X$	
9.0 ± 0.5 ± 0.7		⁹⁷ GAISER	86	CBAL $e^+ e^- \rightarrow \gamma X$	
7.1 ± 1.9		⁹⁸ BIDDICK	77	CNTR $e^+ e^- \rightarrow \gamma X$	
⁹⁷ Angular distribution $(1-0.189 \cos^2\theta)$ assumed.					
⁹⁸ Valid for isotropic distribution of the photon.					

$\Gamma(\gamma\chi_{c2}(1P))/\Gamma_{\text{total}}$					Γ_{104}/Γ
VALUE (units 10^{-2})	EVTS	DOCUMENT ID	TECN	COMMENT	
8.3 ± 0.4 OUR FIT					
8.8 ± 0.5 OUR AVERAGE					
9.33 ± 0.14 ± 0.61	79300	ATHAR	04	CLEO $e^+ e^- \rightarrow \gamma X$	
8.0 ± 0.5 ± 0.7		⁹⁹ GAISER	86	CBAL $e^+ e^- \rightarrow \gamma X$	
7.0 ± 2.0		¹⁰⁰ BIDDICK	77	CNTR $e^+ e^- \rightarrow \gamma X$	
⁹⁹ Angular distribution $(1-0.052 \cos^2\theta)$ assumed.					
¹⁰⁰ Valid for isotropic distribution of the photon.					

$[\Gamma(\gamma\chi_{c0}(1P)) + \Gamma(\gamma\chi_{c1}(1P)) + \Gamma(\gamma\chi_{c2}(1P))]/\Gamma_{\text{total}}$					$(\Gamma_{102} + \Gamma_{103} + \Gamma_{104})/\Gamma$
VALUE	CL%	DOCUMENT ID	TECN	COMMENT	
• • • We do not use the following data for averages, fits, limits, etc. • • •					
27.6 ± 0.3 ± 2.0		¹⁰¹ ATHAR	04	CLEO $e^+ e^- \rightarrow \gamma X$	
¹⁰¹ Not independent from ATHAR 04 measurements of $B(\gamma\chi_{cJ})$.					

$\Gamma(\gamma\chi_{c0}(1P))/\Gamma(\gamma\chi_{c1}(1P))$					$\Gamma_{102}/\Gamma_{103}$
VALUE	CL%	DOCUMENT ID	TECN	COMMENT	
• • • We do not use the following data for averages, fits, limits, etc. • • •					
1.02 ± 0.01 ± 0.07		¹⁰² ATHAR	04	CLEO $e^+ e^- \rightarrow \gamma X$	
¹⁰² Not independent from ATHAR 04 measurements of $B(\gamma\chi_{cJ})$.					

$\Gamma(\gamma\chi_{c2}(1P))/\Gamma(\gamma\chi_{c1}(1P))$					$\Gamma_{104}/\Gamma_{103}$
VALUE	CL%	DOCUMENT ID	TECN	COMMENT	
• • • We do not use the following data for averages, fits, limits, etc. • • •					
1.03 ± 0.02 ± 0.03		¹⁰³ ATHAR	04	CLEO $e^+ e^- \rightarrow \gamma X$	
¹⁰³ Not independent from ATHAR 04 measurements of $B(\gamma\chi_{cJ})$.					

$\Gamma(\gamma\chi_{c0}(1P))/\Gamma(\gamma\chi_{c2}(1P))$					$\Gamma_{102}/\Gamma_{104}$
VALUE	CL%	DOCUMENT ID	TECN	COMMENT	
• • • We do not use the following data for averages, fits, limits, etc. • • •					
0.99 ± 0.02 ± 0.08		¹⁰⁴ ATHAR	04	CLEO $e^+ e^- \rightarrow \gamma X$	
¹⁰⁴ Not independent from ATHAR 04 measurements of $B(\gamma\chi_{cJ})$.					

$\Gamma(\gamma\eta_c(1S))/\Gamma_{\text{total}}$					Γ_{105}/Γ
VALUE (units 10^{-2})	EVTS	DOCUMENT ID	TECN	COMMENT	
0.30 ± 0.05 OUR AVERAGE					
0.32 ± 0.04 ± 0.06	2560	¹⁰⁵ ATHAR	04	CLEO $e^+ e^- \rightarrow \gamma X$	
0.28 ± 0.06		¹⁰⁶ GAISER	86	CBAL $e^+ e^- \rightarrow \gamma X$	
¹⁰⁵ ATHAR 04 used $\Gamma_{\eta_c(1S)} = 24.8 \pm 4.9$ MeV to obtain this result.					
¹⁰⁶ GAISER 86 used $\Gamma_{\eta_c(1S)} = 11.5 \pm 4.5$ MeV to obtain this result.					

$\Gamma(\gamma\eta_c(2S))/\Gamma_{\text{total}}$					Γ_{106}/Γ
VALUE (units 10^{-2})	CL%	DOCUMENT ID	TECN	COMMENT	
<0.20	90	ATHAR	04	CLEO $e^+ e^- \rightarrow \gamma X$	
• • • We do not use the following data for averages, fits, limits, etc. • • •					
0.2 to 1.3	95	EDWARDS	82c	CBAL $e^+ e^- \rightarrow \gamma X$	

$\Gamma(\gamma\pi^0)/\Gamma_{\text{total}}$					Γ_{107}/Γ
VALUE (units 10^{-4})	CL%	DOCUMENT ID	TECN	COMMENT	
< 54	95	¹⁰⁷ LIBERMAN	75	SPEC $e^+ e^-$	
• • • We do not use the following data for averages, fits, limits, etc. • • •					
<100	90	WIJK	75	DASP $e^+ e^-$	
¹⁰⁷ Restated by us using $B(\psi(2S) \rightarrow \mu^+ \mu^-) = 0.0077$.					

$\Gamma(\gamma\eta'(958))/\Gamma_{\text{total}}$					Γ_{108}/Γ
VALUE (units 10^{-4})	CL%	EVTS	DOCUMENT ID	TECN	COMMENT
1.36 ± 0.24 OUR AVERAGE					
1.24 ± 0.27 ± 0.15		23	ABLIKIM	06R	BES2 $e^+ e^- \rightarrow \psi(2S)$
1.54 ± 0.31 ± 0.20		~ 43	BAI	98F	BES $\psi(2S) \rightarrow \pi^+ \pi^- 2\gamma, \pi^+ \pi^- 3\gamma$
• • • We do not use the following data for averages, fits, limits, etc. • • •					
< 60	90	¹⁰⁸ BRAUNSCH...	77	DASP $e^+ e^-$	
< 11	90	¹⁰⁹ BARTEL	76	CNTR $e^+ e^-$	
¹⁰⁸ Restated by us using total decay width 228 keV.					
¹⁰⁹ The value is normalized to the branching ratio for $\Gamma(J/\psi(1S)\eta)/\Gamma_{\text{total}}$.					

$\Gamma(\gamma f_2(1270))/\Gamma_{\text{total}}$					Γ_{109}/Γ
VALUE (units 10^{-4})	EVTS	DOCUMENT ID	TECN	COMMENT	
2.12 ± 0.19 ± 0.32		110,111	BAI	03c	BES $\psi(2S) \rightarrow \gamma \pi \pi$
• • • We do not use the following data for averages, fits, limits, etc. • • •					
2.08 ± 0.19 ± 0.33	200.6 ± 18.8	¹¹⁰ BAI		03c	BES $\psi(2S) \rightarrow \gamma \pi^+ \pi^-$
2.90 ± 1.08 ± 1.07	29.9 ± 11.1	¹¹⁰ BAI		03c	BES $\psi(2S) \rightarrow \gamma \pi^0 \pi^0$
¹¹⁰ Normalized to $B(\psi(2S) \rightarrow J/\psi \pi^+ \pi^-) = 0.305 \pm 0.016$.					
¹¹¹ Combining the results from $\pi^+ \pi^-$ and $\pi^0 \pi^0$ decay modes.					

$\Gamma(\gamma f_0(1710) \rightarrow \gamma \pi \pi)/\Gamma_{\text{total}}$					Γ_{111}/Γ
VALUE (units 10^{-4})	EVTS	DOCUMENT ID	TECN	COMMENT	
0.301 ± 0.041 ± 0.124		35.6 ± 4.8	¹¹² BAI	03c	BES $\psi(2S) \rightarrow \gamma \pi^+ \pi^-$
¹¹² Normalized to $B(\psi(2S) \rightarrow J/\psi \pi^+ \pi^-) = 0.305 \pm 0.016$.					

See key on page 373

Meson Particle Listings

$\psi(2S)$

$\Gamma(\gamma f_0(1710) \rightarrow \gamma K \bar{K})/\Gamma_{total}$ Γ_{112}/Γ

Table with columns: VALUE (units 10^-4), CL%, EVTS, DOCUMENT ID, TECN, COMMENT. Row 1: 0.604 ± 0.090 ± 0.132, 39.6 ± 5.9, 13,114, BAI, 03c, BES, ψ(2S) → γ K+ K-

• • • We do not use the following data for averages, fits, limits, etc. • • •

< 1.56 90 6.8 ± 3.1, 13,114 BAI 03c BES ψ(2S) → γ K_S^0 K_S^0

113 Includes unknown branching fractions to K+ K- or K_S^0 K_S^0. We have multiplied the K+ K- result by a factor of 2 and the K_S^0 K_S^0 result by a factor of 4 to obtain the K K-bar result.

114 Normalized to B(ψ(2S) → J/ψ π+ π-) = 0.305 ± 0.016.

$\Gamma(\gamma \eta)/\Gamma_{total}$ Γ_{114}/Γ

Table with columns: VALUE (units 10^-4), CL%, DOCUMENT ID, TECN, COMMENT. Row 1: <0.9, 90, BAI, 98F, BES, ψ(2S) → π+ π- 3γ

• • • We do not use the following data for averages, fits, limits, etc. • • •

<2 90 YAMADA 77 DASP e+ e- → 3γ

$\Gamma(\gamma \eta \pi^+ \pi^-)/\Gamma_{total}$ Γ_{115}/Γ

Table with columns: VALUE (units 10^-4), EVTS, DOCUMENT ID, TECN, COMMENT. Row 1: 8.71 ± 1.25 ± 1.64, 418, ABLIKIM, 06R, BES2, ψ(2S) → γ η π+ π-

$\Gamma(\gamma \eta(1405) \rightarrow \gamma K \bar{K} \pi)/\Gamma_{total}$ Γ_{117}/Γ

Table with columns: VALUE (units 10^-4), CL%, DOCUMENT ID, TECN, COMMENT. Row 1: <0.9, 90, ABLIKIM, 06R, BES2, ψ(2S) → γ K_S^0 K+ π- + c.c.

• • • We do not use the following data for averages, fits, limits, etc. • • •

<1.3 90 ABLIKIM 06R BES2 ψ(2S) → γ K+ K- π^0

<1.2 90 115 SCHARRE 80 MRK1 e+ e-

115 Includes unknown branching fraction η(1405) → K K-bar π.

$\Gamma(\gamma \eta(1405) \rightarrow \eta \pi^+ \pi^-)/\Gamma_{total}$ Γ_{118}/Γ

Table with columns: VALUE (units 10^-4), EVTS, DOCUMENT ID, TECN, COMMENT. Row 1: 0.36 ± 0.25 ± 0.05, 10, ABLIKIM, 06R, BES2, ψ(2S) → γ η π+ π-

$\Gamma(\gamma \eta(1475) \rightarrow K \bar{K} \pi)/\Gamma_{total}$ Γ_{120}/Γ

Table with columns: VALUE (units 10^-4), CL%, DOCUMENT ID, TECN, COMMENT. Row 1: <1.4, 90, ABLIKIM, 06R, BES2, ψ(2S) → γ K+ K- π^0

• • • We do not use the following data for averages, fits, limits, etc. • • •

<1.5 90 ABLIKIM 06R BES2 ψ(2S) → γ K_S^0 K+ π- + c.c.

$\Gamma(\gamma \eta(1475) \rightarrow \eta \pi^+ \pi^-)/\Gamma_{total}$ Γ_{121}/Γ

Table with columns: VALUE (units 10^-4), CL%, DOCUMENT ID, TECN, COMMENT. Row 1: <0.88, 90, ABLIKIM, 06R, BES2, ψ(2S) → γ η π+ π-

$\Gamma(\gamma 2(\pi^+ \pi^-))/\Gamma_{total}$ Γ_{122}/Γ

Table with columns: VALUE (units 10^-5), EVTS, DOCUMENT ID, TECN, COMMENT. Row 1: 39.6 ± 2.8 ± 5.0, 583, ABLIKIM, 07D, BES2, e+ e- → ψ(2S)

$\Gamma(\gamma K^0 K^+ \pi^- + c.c.)/\Gamma_{total}$ Γ_{123}/Γ

Table with columns: VALUE (units 10^-5), EVTS, DOCUMENT ID, TECN, COMMENT. Row 1: 37.0 ± 6.1 ± 7.2, 237, ABLIKIM, 07D, BES2, e+ e- → ψ(2S)

$\Gamma(\gamma K^0 \bar{K}^0)/\Gamma_{total}$ Γ_{124}/Γ

Table with columns: VALUE (units 10^-5), EVTS, DOCUMENT ID, TECN, COMMENT. Row 1: 24.0 ± 4.5 ± 5.0, 41, ABLIKIM, 07D, BES2, e+ e- → ψ(2S)

$\Gamma(\gamma K_S^0 K^+ \pi^- + c.c.)/\Gamma_{total}$ Γ_{125}/Γ

Table with columns: VALUE (units 10^-5), EVTS, DOCUMENT ID, TECN, COMMENT. Row 1: 25.6 ± 3.6 ± 3.6, 115, ABLIKIM, 07D, BES2, e+ e- → ψ(2S)

$\Gamma(\gamma K^+ K^- \pi^+ \pi^-)/\Gamma_{total}$ Γ_{126}/Γ

Table with columns: VALUE (units 10^-5), EVTS, DOCUMENT ID, TECN, COMMENT. Row 1: 19.1 ± 2.7 ± 4.3, 132, ABLIKIM, 07D, BES2, e+ e- → ψ(2S)

$\Gamma(\gamma \rho \bar{\rho})/\Gamma_{total}$ Γ_{127}/Γ

Table with columns: VALUE (units 10^-5), EVTS, DOCUMENT ID, TECN, COMMENT. Row 1: 2.9 ± 0.4 ± 0.4, 142, ABLIKIM, 07D, BES2, e+ e- → ψ(2S)

$\Gamma(\gamma \pi^+ \pi^- \rho \bar{\rho})/\Gamma_{total}$ Γ_{128}/Γ

Table with columns: VALUE (units 10^-5), EVTS, DOCUMENT ID, TECN, COMMENT. Row 1: 2.8 ± 1.2 ± 0.7, 17, ABLIKIM, 07D, BES2, e+ e- → ψ(2S)

$\Gamma(\gamma 2(\pi^+ \pi^-) K^+ K^-)/\Gamma_{total}$ Γ_{129}/Γ

Table with columns: VALUE (units 10^-5), CL%, DOCUMENT ID, TECN, COMMENT. Row 1: <22, 90, ABLIKIM, 07D, BES2, e+ e- → ψ(2S)

$\Gamma(\gamma 3(\pi^+ \pi^-))/\Gamma_{total}$ Γ_{130}/Γ

Table with columns: VALUE (units 10^-5), CL%, DOCUMENT ID, TECN, COMMENT. Row 1: <17, 90, ABLIKIM, 07D, BES2, e+ e- → ψ(2S)

$\Gamma(\gamma K^+ K^- K^+ K^-)/\Gamma_{total}$ Γ_{131}/Γ

Table with columns: VALUE (units 10^-5), CL%, DOCUMENT ID, TECN, COMMENT. Row 1: <4, 90, ABLIKIM, 07D, BES2, e+ e- → ψ(2S)

ψ(2S) CROSS-PARTICLE BRANCHING RATIOS

For measurements involving B(ψ(2S) → γ χ_{c,J}(1P)) × B(χ_{c,J}(1P) → X) see the corresponding entries in the χ_{c,J}(1P) sections.

ψ(2S) REFERENCES

Table listing references for ψ(2S) with columns: ABLIKIM, 08B, PL, B659, 74, M. Ablikim et al., (BES Collab.)

Meson Particle Listings

$\psi(2S)$, $\psi(3770)$

OTHER RELATED PAPERS

AUBERT, BE	06F	PR D74 111103R	B. Aubert et al.	(BABAR Collab.)
AMBROGIANI	05	PL B610 177	M. Ambrogiani et al.	(FNAL E853 Collab.)
GUO	05	NP A761 269	F.-K. Guo et al.	
VOLOSHIN	05	PR D71 114003	M.B. Voloshin	
ABLIKIM	04I	PR D70 092004	M. Ablikim et al.	(BES Collab.)
ABLIKIM	04J	PRL 93 112002	M. Ablikim et al.	(BES Collab.)
LIU	04B	PR D70 094001	K.-Y. Liu, K.-T. Chao	
WANG	04C	PR D70 077505	P. Wang, X.H. Mo, C.Z. Yuan	
BAI	00E	PR D62 032002	J. Bai et al.	(BES Collab.)
CHEN	98	PRL 80 5060	Y.Q. Chen, E. Braaten	
SUZUKI	98	PR D57 5717	M. Suzuki	
BARATE	83	PL 121B 449	R. Barate et al.	(SACL, LOIC, SHMP, IND)
AUBERT	75B	PRL 33 1624	J.J. Aubert et al.	(MIT, BNL)
BRAUNSCH...	75B	PL 57B 407	W. Braunschweig et al.	(DASP Collab.)
CAMERINI	75	PRL 35 483	U. Camerini et al.	(WISC, SLAC)
FELDMAN	75B	PRL 35 821	G.J. Feldman et al.	(LBL, SLAC)
GRECO	75	PL 56B 367	M. Greco, G. Pancheri-Srivastava, Y. Srivastava	
JACKSON	75	NIM 128 13	J.D. Jackson, D.L. Scharre	(LBL)
SIMPSON	75	PRL 35 699	J.W. Simpson et al.	(STAN, PENN)
ABRAMS	74	PRL 33 1453	G.S. Abrams et al.	(LBL, SLAC)

$\psi(3770)$

$$I^G(J^{PC}) = 0^-(1^{--})$$

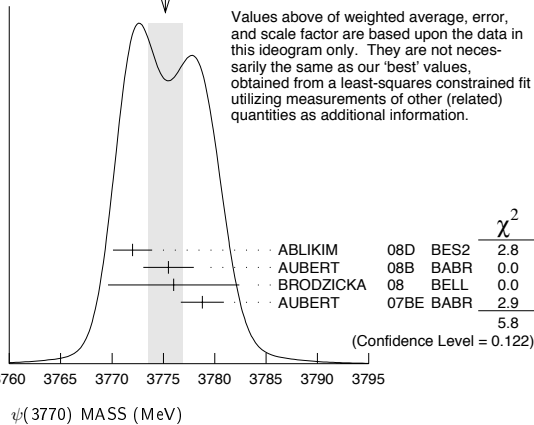
$\psi(3770)$ MASS

OUR FIT includes measurements of $m_{\psi(2S)}$, $m_{\psi(3770)}$, and $m_{\psi(3770)} - m_{\psi(2S)}$.

VALUE (MeV)	EVTS	DOCUMENT ID	TECN	COMMENT
3772.92 ± 0.35 OUR FIT				Error includes scale factor of 1.1.
3775.2 ± 1.7 OUR AVERAGE				Error includes scale factor of 1.4. See the ideogram below.
3772.0 ± 1.9		¹ ABLIKIM	08D BES2	$e^+e^- \rightarrow$ hadrons
3775.5 ± 2.4 ± 0.5	57	AUBERT	08B BABR	$B \rightarrow D\bar{D}K$
3776 ± 5 ± 4	68	BRODZICKA	08 BELL	$B^+ \rightarrow D^0\bar{D}^0 K^+$
3778.8 ± 1.9 ± 0.9		AUBERT	07BE BABR	$e^+e^- \rightarrow D\bar{D}\gamma$
• • • We do not use the following data for averages, fits, limits, etc. • • •				
3778.4 ± 3.0 ± 1.3	34	CHISTOV	04 BELL	Sup. by BRODZICKA 08

¹ Reanalysis of data presented in BAI 02c. From a global fit over the center-of-mass energy region 3.7–5.0 GeV covering the $\psi(3770)$, $\psi(4040)$, $\psi(4160)$, and $\psi(4415)$ resonances. Phase angle fixed in the fit to $\delta = 0^\circ$.

WEIGHTED AVERAGE
3775.2 ± 1.7 (Error scaled by 1.4)



$m_{\psi(3770)} - m_{\psi(2S)}$

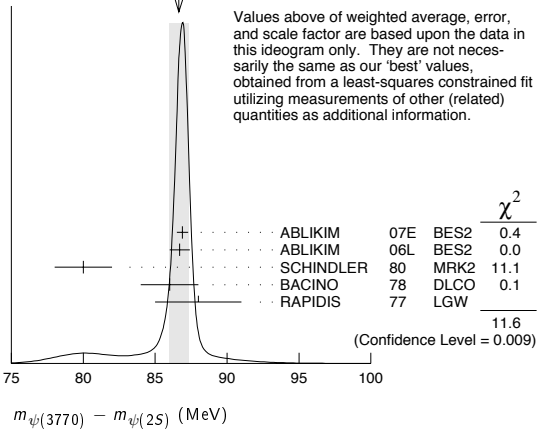
OUR FIT includes measurements of $m_{\psi(2S)}$, $m_{\psi(3770)}$, and $m_{\psi(3770)} - m_{\psi(2S)}$.

VALUE (MeV)	DOCUMENT ID	TECN	COMMENT
86.83 ± 0.35 OUR FIT			Error includes scale factor of 1.1.
86.6 ± 0.7 OUR AVERAGE			Error includes scale factor of 2.0. See the ideogram below.
86.9 ± 0.4	² ABLIKIM	07E BES2	$e^+e^- \rightarrow$ hadrons
86.7 ± 0.7	ABLIKIM	06L BES2	$e^+e^- \rightarrow$ hadrons
80 ± 2	SCHINDLER	80 MRK2	e^+e^-
86 ± 2	³ BACINO	78 DLCO	e^+e^-
88 ± 3	RAPIDIS	77 LGW	e^+e^-

² BES-II $\psi(2S)$ mass subtracted (see ABLIKIM 06L).

³ SPEAR $\psi(2S)$ mass subtracted (see SCHINDLER 80).

WEIGHTED AVERAGE
86.6 ± 0.7 (Error scaled by 2.0)



$\psi(3770)$ WIDTH

VALUE (MeV)	EVTS	DOCUMENT ID	TECN	COMMENT
27.3 ± 1.0 OUR FIT				
27.6 ± 1.0 OUR AVERAGE				
30.4 ± 8.5		⁴ ABLIKIM	08D BES2	$e^+e^- \rightarrow$ hadrons
27 ± 10 ± 5	68	BRODZICKA	08 BELL	$B^+ \rightarrow D^0\bar{D}^0 K^+$
28.5 ± 1.2 ± 0.2		ABLIKIM	07E BES2	$e^+e^- \rightarrow$ hadrons
23.5 ± 3.7 ± 0.9		AUBERT	07BE BABR	$e^+e^- \rightarrow D\bar{D}\gamma$
26.9 ± 2.4 ± 0.3		ABLIKIM	06L BES2	$e^+e^- \rightarrow$ hadrons
24 ± 5		SCHINDLER	80 MRK2	e^+e^-
24 ± 5		BACINO	78 DLCO	e^+e^-
28 ± 5		RAPIDIS	77 LGW	e^+e^-

⁴ Reanalysis of data presented in BAI 02c. From a global fit over the center-of-mass energy region 3.7–5.0 GeV covering the $\psi(3770)$, $\psi(4040)$, $\psi(4160)$, and $\psi(4415)$ resonances. Phase angle fixed in the fit to $\delta = 0^\circ$.

$\psi(3770)$ DECAY MODES

In addition to the dominant decay mode to $D\bar{D}$, $\psi(3770)$ was found to decay into the final states containing the J/ψ (BAI 05, ADAM 06). ADAMS 06 and HUANG 06A searched for various decay modes with light hadrons and found a statistically significant signal for the decay to $\phi\eta$ only (ADAMS 06).

Mode	Fraction (Γ_i/Γ)	Scale factor / Confidence level
Γ_1 $D\bar{D}$	(85.3 ± 3.2) %	
Γ_2 $D^0\bar{D}^0$	(48.7 ± 3.2) %	
Γ_3 D^+D^-	(36.1 ± 2.8) %	
Γ_4 $J/\psi\pi^+\pi^-$	(1.93 ± 0.28) × 10 ⁻³	
Γ_5 $J/\psi\pi^0\pi^0$	(8.0 ± 3.0) × 10 ⁻⁴	
Γ_6 $J/\psi\eta$	(9 ± 4) × 10 ⁻⁴	
Γ_7 $J/\psi\pi^0$	< 2.8 × 10 ⁻⁴	CL=90%
Γ_8 $\gamma\chi_{c0}$	(7.3 ± 0.9) × 10 ⁻³	
Γ_9 $\gamma\chi_{c1}$	(2.9 ± 0.6) × 10 ⁻³	
Γ_{10} $\gamma\chi_{c2}$	< 9 × 10 ⁻⁴	CL=90%
Γ_{11} e^+e^-	(9.7 ± 0.7) × 10 ⁻⁶	S=1.2
Γ_{12} $K_S^0 K_L^0$	< 1.2 × 10 ⁻⁵	CL=90%
Γ_{13} $2(\pi^+\pi^-)$	< 1.12 × 10 ⁻³	CL=90%
Γ_{14} $2(\pi^+\pi^-)\pi^0$	< 1.06 × 10 ⁻³	CL=90%
Γ_{15} $\omega\pi^+\pi^-$	< 6.0 × 10 ⁻⁴	CL=90%
Γ_{16} $3(\pi^+\pi^-)$	< 9.1 × 10 ⁻³	
Γ_{17} $3(\pi^+\pi^-)\pi^0$	< 1.37 %	
Γ_{18} $\eta\pi^+\pi^-$	< 1.24 × 10 ⁻³	CL=90%
Γ_{19} $\rho^0\pi^+\pi^-$	< 6.9 × 10 ⁻³	CL=90%
Γ_{20} $\eta 3\pi$	< 1.34 × 10 ⁻³	CL=90%
Γ_{21} $\eta 2(\pi^+\pi^-)$	< 2.43 %	
Γ_{22} $\eta' 3\pi$	< 2.44 × 10 ⁻³	CL=90%
Γ_{23} $K^+K^-\pi^+\pi^-$	< 9.0 × 10 ⁻⁴	CL=90%
Γ_{24} $\phi\pi^+\pi^-$	< 4.1 × 10 ⁻⁴	CL=90%
Γ_{25} $\phi\pi^0$	not seen	
Γ_{26} $\phi\eta$	(3.1 ± 0.7) × 10 ⁻⁴	
Γ_{27} $4(\pi^+\pi^-)$	< 1.67 %	CL=90%
Γ_{28} $4(\pi^+\pi^-)\pi^0$	< 3.06 %	CL=90%
Γ_{29} $\phi f_0(980)$	< 4.5 × 10 ⁻⁴	CL=90%
Γ_{30} $K^+K^-\pi^+\pi^-\pi^0$	< 2.36 × 10 ⁻³	CL=90%
Γ_{31} $K^+K^-\rho^0\pi^0$	< 8 × 10 ⁻⁴	CL=90%

Γ_{32}	$K^+ K^- \rho^+ \pi^-$	< 1.46	%	CL=90%
Γ_{33}	$\omega K^+ K^-$	< 3.4	$\times 10^{-4}$	CL=90%
Γ_{34}	$\phi \pi^+ \pi^- \pi^0$	< 3.8	$\times 10^{-3}$	CL=90%
Γ_{35}	$K^{*0} K^- \pi^+ \pi^0 + c.c.$	< 1.62	%	CL=90%
Γ_{36}	$K^{*+} K^- \pi^+ \pi^- + c.c.$	< 3.23	%	CL=90%
Γ_{37}	$K^+ K^- 2(\pi^+ \pi^-)$	< 1.03	%	CL=90%
Γ_{38}	$K^+ K^- 2(\pi^+ \pi^-) \pi^0$	< 3.60	%	CL=90%
Γ_{39}	$\eta K^+ K^-$	< 4.1	$\times 10^{-4}$	CL=90%
Γ_{40}	$\rho^0 K^+ K^-$	< 5.0	$\times 10^{-3}$	CL=90%
Γ_{41}	$2(K^+ K^-)$	< 6.0	$\times 10^{-4}$	CL=90%
Γ_{42}	$\phi K^+ K^-$	< 7.5	$\times 10^{-4}$	CL=90%
Γ_{43}	$2(K^+ K^-) \pi^0$	< 2.9	$\times 10^{-4}$	CL=90%
Γ_{44}	$2(K^+ K^-) \pi^+ \pi^-$	< 3.2	$\times 10^{-3}$	CL=90%
Γ_{45}	$K^{*0} K^- \pi^+ + c.c.$	< 9.7	$\times 10^{-3}$	CL=90%
Γ_{46}	$\rho \bar{p} \pi^0$	< 1.2	$\times 10^{-3}$	CL=90%
Γ_{47}	$\rho \bar{p} \pi^+ \pi^-$	< 5.8	$\times 10^{-4}$	CL=90%
Γ_{48}	$\Lambda \bar{\Lambda}$	< 1.2	$\times 10^{-4}$	CL=90%
Γ_{49}	$\rho \bar{p} \pi^+ \pi^- \pi^0$	< 1.85	$\times 10^{-3}$	CL=90%
Γ_{50}	$\omega \rho \bar{p}$	< 2.9	$\times 10^{-4}$	CL=90%
Γ_{51}	$\Lambda \bar{\Lambda} \pi^0$	< 1.2	$\times 10^{-3}$	CL=90%
Γ_{52}	$\rho \bar{p} 2(\pi^+ \pi^-)$	< 2.6	$\times 10^{-3}$	CL=90%
Γ_{53}	$\eta \rho \bar{p}$	< 5.4	$\times 10^{-4}$	CL=90%
Γ_{54}	$\rho^0 \rho \bar{p}$	< 1.7	$\times 10^{-3}$	CL=90%
Γ_{55}	$\rho \bar{p} K^+ K^-$	< 3.2	$\times 10^{-4}$	CL=90%
Γ_{56}	$\phi \rho \bar{p}$	< 1.3	$\times 10^{-4}$	CL=90%
Γ_{57}	$\Lambda \bar{\Lambda} \pi^+ \pi^-$	< 2.5	$\times 10^{-4}$	CL=90%
Γ_{58}	$\Lambda \bar{p} K^+$	< 2.8	$\times 10^{-4}$	CL=90%
Γ_{59}	$\Lambda \bar{p} K^+ \pi^+ \pi^-$	< 6.3	$\times 10^{-4}$	CL=90%
Γ_{60}	$\pi^+ \pi^- \pi^0$	not seen		
Γ_{61}	$\rho \pi$	not seen		
Γ_{62}	$\omega \pi^0$	not seen		
Γ_{63}	$\rho \eta$	not seen		
Γ_{64}	$\omega \eta$	not seen		
Γ_{65}	$\rho \eta'$	not seen		
Γ_{66}	$\omega \eta'$	not seen		
Γ_{67}	$\phi \eta'$	not seen		
Γ_{68}	$K^{*0} \bar{K}^0$	not seen		
Γ_{69}	$K^{*+} K^-$	not seen		
Γ_{70}	$b_1 \pi$	not seen		

$\psi(3770)$ PARTIAL WIDTHS

$\Gamma(e^+ e^-)$	Γ_{11}			
VALUE (keV)	EVTS	DOCUMENT ID	TECN	COMMENT
0.265 ± 0.018 OUR FIT		Error includes scale factor of 1.3.		
0.259 ± 0.016 OUR AVERAGE		Error includes scale factor of 1.2.		
0.22 ± 0.05	5	ABLIKIM	08D BES2	$e^+ e^- \rightarrow$ hadrons
0.277 ± 0.011 ± 0.013		ABLIKIM	07E BES2	$e^+ e^- \rightarrow$ hadrons
0.204 ± 0.003 ± $\frac{0.041}{0.027}$	1.427M	6 BESSON	06 CLEO	$e^+ e^- \rightarrow$ hadrons
0.276 ± 0.050		SCHINDLER	80 MRK2	$e^+ e^-$
0.18 ± 0.06		BACINO	78 DLCO	$e^+ e^-$
• • • We do not use the following data for averages, fits, limits, etc. • • •				
0.37 ± 0.09	7	RAPIDIS	77 LGW	$e^+ e^-$
5 Reanalysis of data presented in BAI 02c. From a global fit over the center-of-mass energy region 3.7–5.0 GeV covering the $\psi(3770)$, $\psi(4040)$, $\psi(4160)$, and $\psi(4415)$ resonances. Phase angle fixed in the fit to $\delta = 0^\circ$.				
6 BESSON 06 measure $\sigma(e^+ e^- \rightarrow \psi(3770) \rightarrow \text{hadrons}) = 6.38 \pm 0.08^{+0.41}_{-0.30}$ nb at $\sqrt{s} = 3773 \pm 1$ MeV, and obtain $\Gamma_{e^+ e^-}$ from the Born-level cross section calculated using $\psi(3770)$ mass and width from our 2004 edition.				
7 See also $\Gamma(e^+ e^-)/\Gamma_{\text{total}}$ below.				

$\psi(3770)$ BRANCHING RATIOS

$\Gamma(D\bar{D})/\Gamma_{\text{total}}$	Γ_1/Γ		
VALUE	DOCUMENT ID	TECN	COMMENT
0.853 ± 0.032 OUR AVERAGE			
0.849 ± 0.056 ± 0.018	8	ABLIKIM	08B BES2 $e^+ e^- \rightarrow$ non- $D\bar{D}$
0.866 ± 0.050 ± 0.036	9	ABLIKIM	07K BES2 $e^+ e^- \rightarrow$ non- $D\bar{D}$
0.836 ± 0.073 ± 0.042		ABLIKIM	06L BES2 $e^+ e^- \rightarrow D\bar{D}$
0.855 ± 0.017 ± 0.058	10	ABLIKIM	06N BES2 $e^+ e^- \rightarrow D\bar{D}$
$\Gamma(D^0 \bar{D}^0)/\Gamma_{\text{total}}$	Γ_2/Γ		
VALUE	DOCUMENT ID	TECN	COMMENT
0.487 ± 0.032 OUR AVERAGE			
0.467 ± 0.047 ± 0.023		ABLIKIM	06L BES2 $e^+ e^- \rightarrow D^0 \bar{D}^0$
0.499 ± 0.013 ± 0.038	10	ABLIKIM	06N BES2 $e^+ e^- \rightarrow D^0 \bar{D}^0$

$\Gamma(D^+ D^-)/\Gamma_{\text{total}}$	Γ_3/Γ		
VALUE	DOCUMENT ID	TECN	COMMENT
0.361 ± 0.028 OUR AVERAGE			
0.369 ± 0.037 ± 0.028		ABLIKIM	06L BES2 $e^+ e^- \rightarrow D^+ D^-$
0.357 ± 0.011 ± 0.034	10	ABLIKIM	06N BES2 $e^+ e^- \rightarrow D^+ D^-$

$\Gamma(D^0 \bar{D}^0)/\Gamma(D^+ D^-)$	Γ_2/Γ_3			
VALUE	EVTS	DOCUMENT ID	TECN	COMMENT
1.260 ± 0.021 OUR AVERAGE				
1.39 ± 0.31 ± 0.12		PAKHOVA	08 BELL	$10.6 e^+ e^- \rightarrow D\bar{D}\gamma$
1.78 ± 0.33 ± 0.24		AUBERT	078E BABR	$e^+ e^- \rightarrow D\bar{D}\gamma$
1.258 ± 0.016 ± 0.014		DOBBS	07 CLEO	$e^+ e^- \rightarrow D\bar{D}$
1.27 ± 0.12 ± 0.08		ABLIKIM	06L BES2	$e^+ e^- \rightarrow D\bar{D}$
2.43 ± 1.50 ± 0.43	34	11 CHISTOV	04 BELL	$B^+ \rightarrow \psi(3770) K^+$

$\Gamma(J/\psi \pi^+ \pi^-)/\Gamma_{\text{total}}$	Γ_4/Γ			
VALUE (units 10^{-3})	EVTS	DOCUMENT ID	TECN	COMMENT
1.93 ± 0.28 OUR AVERAGE				
1.89 ± 0.20 ± 0.20	231 ± 33	ADAM	06 CLEO	$e^+ e^- \rightarrow \psi(3770)$
3.4 ± 1.4 ± 0.9	17.8 ± 4.8	BAI	05 BES2	$e^+ e^- \rightarrow \psi(3770)$

$\Gamma(J/\psi \pi^0 \pi^0)/\Gamma_{\text{total}}$	Γ_5/Γ			
VALUE (units 10^{-2})	EVTS	DOCUMENT ID	TECN	COMMENT
0.080 ± 0.025 ± 0.016	39 ± 14	ADAM	06 CLEO	$e^+ e^- \rightarrow \psi(3770)$

$\Gamma(J/\psi \eta)/\Gamma_{\text{total}}$	Γ_6/Γ			
VALUE (units 10^{-5})	EVTS	DOCUMENT ID	TECN	COMMENT
87 ± 33 ± 22	22 ± 10	ADAM	06 CLEO	$e^+ e^- \rightarrow \psi(3770)$

$\Gamma(J/\psi \pi^0)/\Gamma_{\text{total}}$	Γ_7/Γ				
VALUE (units 10^{-5})	CL%	EVTS	DOCUMENT ID	TECN	COMMENT
< 28	90	< 10	ADAM	06 CLEO	$e^+ e^- \rightarrow \psi(3770)$

$\Gamma(\gamma \chi_{c0})/\Gamma_{\text{total}}$	Γ_8/Γ				
VALUE (units 10^{-3})	CL%	EVTS	DOCUMENT ID	TECN	COMMENT
7.3 ± 0.7 ± 0.6	274 ± 27	12	BRIERE	06 CLEO	$e^+ e^- \rightarrow \psi(3770) \rightarrow \gamma + \text{hadrons}$
• • • We do not use the following data for averages, fits, limits, etc. • • •					
< 44	90	13	COAN	06A CLEO	$e^+ e^- \rightarrow \psi(3770) \rightarrow \gamma \gamma J/\psi$

$\Gamma(\gamma \chi_{c1})/\Gamma_{\text{total}}$	Γ_9/Γ				
VALUE (units 10^{-3})	EVTS	DOCUMENT ID	TECN	COMMENT	
2.9 ± 0.5 ± 0.4		14	BRIERE	06 CLEO	$e^+ e^- \rightarrow \psi(3770) \rightarrow \gamma + \text{hadrons}, \gamma \gamma J/\psi$
• • • We do not use the following data for averages, fits, limits, etc. • • •					
3.9 ± 1.4 ± 0.6	54 ± 17	15	BRIERE	06 CLEO	$e^+ e^- \rightarrow \psi(3770) \rightarrow \gamma + \text{hadrons}$
2.8 ± 0.5 ± 0.4	53 ± 10	13	COAN	06A CLEO	$e^+ e^- \rightarrow \psi(3770) \rightarrow \gamma \gamma J/\psi$

$\Gamma(\gamma \chi_{c1})/\Gamma(J/\psi \pi^+ \pi^-)$	Γ_9/Γ_4				
VALUE	EVTS	DOCUMENT ID	TECN	COMMENT	
1.49 ± 0.31 ± 0.26	53 ± 10	16	COAN	06A CLEO	$e^+ e^- \rightarrow \psi(3770) \rightarrow \gamma \gamma J/\psi$

$\Gamma(\gamma \chi_{c0})/\Gamma(\gamma \chi_{c1})$	Γ_8/Γ_9		
VALUE	DOCUMENT ID	TECN	COMMENT
2.5 ± 0.6	17	BRIERE	06 CLEO $e^+ e^- \rightarrow \psi(3770)$

$\Gamma(\gamma \chi_{c2})/\Gamma_{\text{total}}$	Γ_{10}/Γ			
VALUE (units 10^{-3})	CL%	DOCUMENT ID	TECN	COMMENT
< 0.9	90	13	COAN	06A CLEO $e^+ e^- \rightarrow \psi(3770) \rightarrow \gamma \gamma J/\psi$
• • • We do not use the following data for averages, fits, limits, etc. • • •				
< 2.0	90	18	BRIERE	06 CLEO $e^+ e^- \rightarrow \psi(3770) \rightarrow \gamma + \text{hadrons}$

$\Gamma(\gamma \chi_{c0})/\Gamma(\gamma \chi_{c2})$	Γ_8/Γ_{10}			
VALUE	CL%	DOCUMENT ID	TECN	COMMENT
> 8	90	17	BRIERE	06 CLEO $e^+ e^- \rightarrow \psi(3770)$

$\Gamma(e^+ e^-)/\Gamma_{\text{total}}$	Γ_{11}/Γ		
VALUE (units 10^{-5})	DOCUMENT ID	TECN	COMMENT
0.97 ± 0.07 OUR FIT	Error includes scale factor of 1.2.		
1.3 ± 0.2	RAPIDIS	77 LGW	$e^+ e^-$

$\Gamma(K_S^0 K_L^0)/\Gamma_{\text{total}}$	Γ_{12}/Γ			
VALUE (units 10^{-5})	CL%	DOCUMENT ID	TECN	COMMENT
< 1.2	90	19	CRONIN-HEN..06	CLEO $e^+ e^- \rightarrow \psi(3770)$
• • • We do not use the following data for averages, fits, limits, etc. • • •				
< 21	90	20	ABLIKIM	04F BES $e^+ e^- \rightarrow \psi(3770)$

Meson Particle Listings

 $\psi(3770)$ $\Gamma(2(\pi^+\pi^-))/\Gamma_{\text{total}}$ Γ_{13}/Γ

VALUE (units 10^{-4})	CL%	DOCUMENT ID	TECN	COMMENT
<11.2	90	21 HUANG	06A CLEO	$e^+e^- \rightarrow \psi(3770)$
••• We do not use the following data for averages, fits, limits, etc. •••				
<48		22,23 ABLIKIM	07B BES2	$e^+e^- \rightarrow \psi(3770)$

 $\Gamma(2(\pi^+\pi^-\pi^0))/\Gamma_{\text{total}}$ Γ_{14}/Γ

VALUE (units 10^{-4})	CL%	DOCUMENT ID	TECN	COMMENT
<10.6	90	21 HUANG	06A CLEO	$e^+e^- \rightarrow \psi(3770)$
••• We do not use the following data for averages, fits, limits, etc. •••				
<62		22,23 ABLIKIM	07B BES2	$e^+e^- \rightarrow \psi(3770)$

 $\Gamma(\omega\pi^+\pi^-)/\Gamma_{\text{total}}$ Γ_{15}/Γ

VALUE (units 10^{-4})	CL%	DOCUMENT ID	TECN	COMMENT
< 6.0	90	21 HUANG	06A CLEO	$e^+e^- \rightarrow \psi(3770)$
••• We do not use the following data for averages, fits, limits, etc. •••				
<55	90	24 ABLIKIM	07I BES2	$3.77 e^+e^-$

 $\Gamma(3(\pi^+\pi^-))/\Gamma_{\text{total}}$ Γ_{16}/Γ

VALUE (units 10^{-4})	CL%	DOCUMENT ID	TECN	COMMENT
<91		22,23 ABLIKIM	07B BES2	$e^+e^- \rightarrow \psi(3770)$

 $\Gamma(3(\pi^+\pi^-\pi^0))/\Gamma_{\text{total}}$ Γ_{17}/Γ

VALUE (units 10^{-4})	CL%	DOCUMENT ID	TECN	COMMENT
<137		22,23 ABLIKIM	07B BES2	$e^+e^- \rightarrow \psi(3770)$

 $\Gamma(\eta\pi^+\pi^-)/\Gamma_{\text{total}}$ Γ_{18}/Γ

VALUE (units 10^{-4})	CL%	DOCUMENT ID	TECN	COMMENT
<12.4	90	21 HUANG	06A CLEO	$e^+e^- \rightarrow \psi(3770)$

 $\Gamma(\rho^0\pi^+\pi^-)/\Gamma_{\text{total}}$ Γ_{19}/Γ

VALUE (units 10^{-3})	CL%	DOCUMENT ID	TECN	COMMENT
<6.9	90	22,23 ABLIKIM	07F BES2	$e^+e^- \rightarrow \psi(3770)$

 $\Gamma(\eta3\pi)/\Gamma_{\text{total}}$ Γ_{20}/Γ

VALUE (units 10^{-4})	CL%	DOCUMENT ID	TECN	COMMENT
<13.4	90	21 HUANG	06A CLEO	$e^+e^- \rightarrow \psi(3770)$

 $\Gamma(\eta2(\pi^+\pi^-))/\Gamma_{\text{total}}$ Γ_{21}/Γ

VALUE (units 10^{-4})	CL%	DOCUMENT ID	TECN	COMMENT
<243		22,23 ABLIKIM	07B BES2	$e^+e^- \rightarrow \psi(3770)$

 $\Gamma(\eta'3\pi)/\Gamma_{\text{total}}$ Γ_{22}/Γ

VALUE (units 10^{-4})	CL%	DOCUMENT ID	TECN	COMMENT
<24.4	90	21 HUANG	06A CLEO	$e^+e^- \rightarrow \psi(3770)$

 $\Gamma(K^+K^-\pi^+\pi^-)/\Gamma_{\text{total}}$ Γ_{23}/Γ

VALUE (units 10^{-4})	CL%	DOCUMENT ID	TECN	COMMENT
< 9.0	90	21 HUANG	06A CLEO	$e^+e^- \rightarrow \psi(3770)$
••• We do not use the following data for averages, fits, limits, etc. •••				
<48		22,23 ABLIKIM	07B BES2	$e^+e^- \rightarrow \psi(3770)$

 $\Gamma(\phi\pi^+\pi^-)/\Gamma_{\text{total}}$ Γ_{24}/Γ

VALUE (units 10^{-4})	CL%	DOCUMENT ID	TECN	COMMENT
< 4.1	90	21 HUANG	06A CLEO	$e^+e^- \rightarrow \psi(3770)$
••• We do not use the following data for averages, fits, limits, etc. •••				
<16		22,23 ABLIKIM	07B BES2	$e^+e^- \rightarrow \psi(3770)$

 $\Gamma(\phi\pi^0)/\Gamma_{\text{total}}$ Γ_{25}/Γ

VALUE (units 10^{-4})	CL%	DOCUMENT ID	TECN	COMMENT
<5		22,23 ABLIKIM	07B BES2	$e^+e^- \rightarrow \psi(3770)$

 $\Gamma(\phi\eta)/\Gamma_{\text{total}}$ Γ_{26}/Γ

VALUE (units 10^{-4})	CL%	DOCUMENT ID	TECN	COMMENT
$3.1 \pm 0.6 \pm 0.3$		25 ADAMS	06 CLEO	$3.773 e^+e^- \rightarrow \phi\eta$
••• We do not use the following data for averages, fits, limits, etc. •••				
<19		22,23 ABLIKIM	07B BES2	$e^+e^- \rightarrow \psi(3770)$

 $\Gamma(4(\pi^+\pi^-))/\Gamma_{\text{total}}$ Γ_{27}/Γ

VALUE (units 10^{-3})	CL%	DOCUMENT ID	TECN	COMMENT
<16.7	90	22,23 ABLIKIM	07F BES2	$e^+e^- \rightarrow \psi(3770)$

 $\Gamma(4(\pi^+\pi^-\pi^0))/\Gamma_{\text{total}}$ Γ_{28}/Γ

VALUE (units 10^{-3})	CL%	DOCUMENT ID	TECN	COMMENT
<30.6	90	22,23 ABLIKIM	07F BES2	$e^+e^- \rightarrow \psi(3770)$

 $\Gamma(\phi\eta(980))/\Gamma_{\text{total}}$ Γ_{29}/Γ

VALUE (units 10^{-4})	CL%	DOCUMENT ID	TECN	COMMENT
<4.5	90	21 HUANG	06A CLEO	$e^+e^- \rightarrow \psi(3770)$

 $\Gamma(K^+K^-\pi^+\pi^-)/\Gamma_{\text{total}}$ Γ_{30}/Γ

VALUE (units 10^{-4})	CL%	DOCUMENT ID	TECN	COMMENT
< 23.6	90	21 HUANG	06A CLEO	$e^+e^- \rightarrow \psi(3770)$
••• We do not use the following data for averages, fits, limits, etc. •••				
<111		22,23 ABLIKIM	07B BES2	$e^+e^- \rightarrow \psi(3770)$

 $\Gamma(K^+K^-\rho^0\pi^0)/\Gamma_{\text{total}}$ Γ_{31}/Γ

VALUE (units 10^{-4})	CL%	DOCUMENT ID	TECN	COMMENT
<8	90	24 ABLIKIM	07I BES2	$3.77 e^+e^-$

 $\Gamma(K^+K^-\rho^+\pi^-)/\Gamma_{\text{total}}$ Γ_{32}/Γ

VALUE (units 10^{-4})	CL%	DOCUMENT ID	TECN	COMMENT
<146	90	24 ABLIKIM	07I BES2	$3.77 e^+e^-$

 $\Gamma(\omega K^+K^-)/\Gamma_{\text{total}}$ Γ_{33}/Γ

VALUE (units 10^{-4})	CL%	DOCUMENT ID	TECN	COMMENT
< 3.4	90	21 HUANG	06A CLEO	$e^+e^- \rightarrow \psi(3770)$
••• We do not use the following data for averages, fits, limits, etc. •••				
<66	90	24 ABLIKIM	07I BES2	$3.77 e^+e^-$

 $\Gamma(\phi\pi^+\pi^-\pi^0)/\Gamma_{\text{total}}$ Γ_{34}/Γ

VALUE (units 10^{-4})	CL%	DOCUMENT ID	TECN	COMMENT
<38	90	24 ABLIKIM	07I BES2	$3.77 e^+e^-$

 $\Gamma(K^*0K^-\pi^+\pi^0 + \text{c.c.})/\Gamma_{\text{total}}$ Γ_{35}/Γ

VALUE (units 10^{-4})	CL%	DOCUMENT ID	TECN	COMMENT
<162	90	24 ABLIKIM	07I BES2	$3.77 e^+e^-$

 $\Gamma(K^*+K^-\pi^+\pi^- + \text{c.c.})/\Gamma_{\text{total}}$ Γ_{36}/Γ

VALUE (units 10^{-4})	CL%	DOCUMENT ID	TECN	COMMENT
<323	90	24 ABLIKIM	07I BES2	$3.77 e^+e^-$

 $\Gamma(K^+K^-\pi^+\pi^-)/\Gamma_{\text{total}}$ Γ_{37}/Γ

VALUE (units 10^{-3})	CL%	DOCUMENT ID	TECN	COMMENT
<10.3	90	22,23 ABLIKIM	07F BES2	$e^+e^- \rightarrow \psi(3770)$

 $\Gamma(K^+K^-\pi^+\pi^-\pi^0)/\Gamma_{\text{total}}$ Γ_{38}/Γ

VALUE (units 10^{-3})	CL%	DOCUMENT ID	TECN	COMMENT
<36.0	90	22,23 ABLIKIM	07F BES2	$e^+e^- \rightarrow \psi(3770)$

 $\Gamma(\eta K^+K^-)/\Gamma_{\text{total}}$ Γ_{39}/Γ

VALUE (units 10^{-4})	CL%	DOCUMENT ID	TECN	COMMENT
<4.1	90	21 HUANG	06A CLEO	$e^+e^- \rightarrow \psi(3770)$

 $\Gamma(\rho^0 K^+K^-)/\Gamma_{\text{total}}$ Γ_{40}/Γ

VALUE (units 10^{-3})	CL%	DOCUMENT ID	TECN	COMMENT
<5.0	90	22,23 ABLIKIM	07F BES2	$e^+e^- \rightarrow \psi(3770)$

 $\Gamma(2(K^+K^-))/\Gamma_{\text{total}}$ Γ_{41}/Γ

VALUE (units 10^{-4})	CL%	DOCUMENT ID	TECN	COMMENT
< 6.0	90	21 HUANG	06A CLEO	$e^+e^- \rightarrow \psi(3770)$
••• We do not use the following data for averages, fits, limits, etc. •••				
<17		22,23 ABLIKIM	07B BES2	$e^+e^- \rightarrow \psi(3770)$

 $\Gamma(\phi K^+K^-)/\Gamma_{\text{total}}$ Γ_{42}/Γ

VALUE (units 10^{-4})	CL%	DOCUMENT ID	TECN	COMMENT
< 7.5	90	21 HUANG	06A CLEO	$e^+e^- \rightarrow \psi(3770)$
••• We do not use the following data for averages, fits, limits, etc. •••				
<24		22,23 ABLIKIM	07B BES2	$e^+e^- \rightarrow \psi(3770)$

 $\Gamma(2(K^+K^-)\pi^0)/\Gamma_{\text{total}}$ Γ_{43}/Γ

VALUE (units 10^{-4})	CL%	DOCUMENT ID	TECN	COMMENT
< 2.9	90	21 HUANG	06A CLEO	$e^+e^- \rightarrow \psi(3770)$
••• We do not use the following data for averages, fits, limits, etc. •••				
<46		22,23 ABLIKIM	07B BES2	$e^+e^- \rightarrow \psi(3770)$

 $\Gamma(2(K^+K^-)\pi^+\pi^-)/\Gamma_{\text{total}}$ Γ_{44}/Γ

VALUE (units 10^{-3})	CL%	DOCUMENT ID	TECN	COMMENT
<3.2	90	22,23 ABLIKIM	07F BES2	$e^+e^- \rightarrow \psi(3770)$

 $\Gamma(K^*0K^-\pi^+ + \text{c.c.})/\Gamma_{\text{total}}$ Γ_{45}/Γ

VALUE (units 10^{-3})	CL%	DOCUMENT ID	TECN	COMMENT
<9.7	90	22,23 ABLIKIM	07F BES2	$e^+e^- \rightarrow \psi(3770)$

Meson Particle Listings

$\psi(3770)$, New charmonium-like states

$\Gamma(\rho\bar{\rho}\pi^0)/\Gamma_{\text{total}}$					Γ_{46}/Γ
VALUE (units 10^{-4})	CL%	DOCUMENT ID	TECN	COMMENT	
<12		22,23	ABLIKIM 07B	BES2 $e^+e^- \rightarrow \psi(3770)$	

$\Gamma(\rho\bar{\rho}\pi^+\pi^-)/\Gamma_{\text{total}}$					Γ_{47}/Γ
VALUE (units 10^{-4})	CL%	DOCUMENT ID	TECN	COMMENT	
< 5.8	90	21	HUANG 06A	CLEO $e^+e^- \rightarrow \psi(3770)$	
••• We do not use the following data for averages, fits, limits, etc. •••					
<16		22,23	ABLIKIM 07B	BES2 $e^+e^- \rightarrow \psi(3770)$	

$\Gamma(\Lambda\bar{\Lambda})/\Gamma_{\text{total}}$					Γ_{48}/Γ
VALUE (units 10^{-4})	CL%	DOCUMENT ID	TECN	COMMENT	
<1.2	90	21	HUANG 06A	CLEO $e^+e^- \rightarrow \psi(3770)$	
••• We do not use the following data for averages, fits, limits, etc. •••					
<4	90	22,23	ABLIKIM 07F	BES2 $e^+e^- \rightarrow \psi(3770)$	

$\Gamma(\rho\bar{\rho}\pi^+\pi^-\pi^0)/\Gamma_{\text{total}}$					Γ_{49}/Γ
VALUE (units 10^{-4})	CL%	DOCUMENT ID	TECN	COMMENT	
<18.5	90	21	HUANG 06A	CLEO $e^+e^- \rightarrow \psi(3770)$	
••• We do not use the following data for averages, fits, limits, etc. •••					
<73		22,23	ABLIKIM 07B	BES2 $e^+e^- \rightarrow \psi(3770)$	

$\Gamma(\omega\rho\bar{\rho})/\Gamma_{\text{total}}$					Γ_{50}/Γ
VALUE (units 10^{-4})	CL%	DOCUMENT ID	TECN	COMMENT	
< 2.9	90	21	HUANG 06A	CLEO $e^+e^- \rightarrow \psi(3770)$	
••• We do not use the following data for averages, fits, limits, etc. •••					
<30	90	24	ABLIKIM 07I	BES2 $3.77 e^+e^-$	

$\Gamma(\Lambda\bar{\Lambda}\pi^0)/\Gamma_{\text{total}}$					Γ_{51}/Γ
VALUE (units 10^{-4})	CL%	DOCUMENT ID	TECN	COMMENT	
<12	90	24	ABLIKIM 07I	BES2 $3.77 e^+e^-$	

$\Gamma(\rho\bar{\rho}2(\pi^+\pi^-))/\Gamma_{\text{total}}$					Γ_{52}/Γ
VALUE (units 10^{-3})	CL%	DOCUMENT ID	TECN	COMMENT	
<2.6	90	22,23	ABLIKIM 07F	BES2 $e^+e^- \rightarrow \psi(3770)$	

$\Gamma(\eta\rho\bar{\rho})/\Gamma_{\text{total}}$					Γ_{53}/Γ
VALUE (units 10^{-4})	CL%	DOCUMENT ID	TECN	COMMENT	
<5.4	90	21	HUANG 06A	CLEO $e^+e^- \rightarrow \psi(3770)$	

$\Gamma(\rho^0\rho\bar{\rho})/\Gamma_{\text{total}}$					Γ_{54}/Γ
VALUE (units 10^{-3})	CL%	DOCUMENT ID	TECN	COMMENT	
<1.7	90	22,23	ABLIKIM 07F	BES2 $e^+e^- \rightarrow \psi(3770)$	

$\Gamma(\rho\bar{\rho}K^+K^-)/\Gamma_{\text{total}}$					Γ_{55}/Γ
VALUE (units 10^{-4})	CL%	DOCUMENT ID	TECN	COMMENT	
< 3.2	90	21	HUANG 06A	CLEO $e^+e^- \rightarrow \psi(3770)$	
••• We do not use the following data for averages, fits, limits, etc. •••					
<11		22,23	ABLIKIM 07B	BES2 $e^+e^- \rightarrow \psi(3770)$	

$\Gamma(\phi\rho\bar{\rho})/\Gamma_{\text{total}}$					Γ_{56}/Γ
VALUE (units 10^{-4})	CL%	DOCUMENT ID	TECN	COMMENT	
<1.3	90	21	HUANG 06A	CLEO $e^+e^- \rightarrow \psi(3770)$	
••• We do not use the following data for averages, fits, limits, etc. •••					
<9		22,23	ABLIKIM 07B	BES2 $e^+e^- \rightarrow \psi(3770)$	

$\Gamma(\Lambda\bar{\Lambda}\pi^+\pi^-)/\Gamma_{\text{total}}$					Γ_{57}/Γ
VALUE (units 10^{-4})	CL%	DOCUMENT ID	TECN	COMMENT	
< 2.5	90	21	HUANG 06A	CLEO $e^+e^- \rightarrow \psi(3770)$	
••• We do not use the following data for averages, fits, limits, etc. •••					
<39	90	22,23	ABLIKIM 07F	BES2 $e^+e^- \rightarrow \psi(3770)$	

$\Gamma(\Lambda\bar{\rho}K^+)/\Gamma_{\text{total}}$					Γ_{58}/Γ
VALUE (units 10^{-4})	CL%	DOCUMENT ID	TECN	COMMENT	
<2.8	90	21	HUANG 06A	CLEO $e^+e^- \rightarrow \psi(3770)$	

$\Gamma(\Lambda\bar{\rho}K^+\pi^+\pi^-)/\Gamma_{\text{total}}$					Γ_{59}/Γ
VALUE (units 10^{-4})	CL%	DOCUMENT ID	TECN	COMMENT	
<6.3	90	21	HUANG 06A	CLEO $e^+e^- \rightarrow \psi(3770)$	

⁸ Neglecting interference.

⁹ Using $\sigma^{\text{obs}} = 7.07 \pm 0.58$ nb and neglecting interference.

¹⁰ From a measurement of $\sigma(e^+e^- \rightarrow D\bar{D})$ at $\sqrt{s} = 3773$ MeV, using the $\psi(3770)$ resonance parameters measured by ABLIKIM 06L.

¹¹ See ADLER 88C for older measurements of this quantity.

¹² Uses $B(\psi(2S) \rightarrow \gamma\chi_{c0}) = 9.33 \pm 0.14 \pm 0.61\%$ from ATHAR 04, $\psi(2S)$ mass and width from PDG 04, and $\Gamma_{ee}(\psi(2S)) = 2.54 \pm 0.03 \pm 0.11$ keV from ADAM 06.

¹³ Using $\Gamma_{ee}(\psi(2S)) = (2.54 \pm 0.03 \pm 0.11)$ keV from ADAM 06 and taking $\sigma(e^+e^- \rightarrow D\bar{D})$ from HE 05 for $\sigma(e^+e^- \rightarrow \psi(3770))$.

¹⁴ Averages the two measurements from COAN 06A and BRIERE 06.

¹⁵ Uses $B(\psi(2S) \rightarrow \gamma\chi_{c1}) = 9.07 \pm 0.11 \pm 0.54\%$ from ATHAR 04, $\psi(2S)$ mass and width from PDG 04, and $\Gamma_{ee}(\psi(2S)) = 2.54 \pm 0.03$ keV from ADAM 06.

¹⁶ Using $B(\psi(3770) \rightarrow J/\psi\pi^+\pi^-) = (1.89 \pm 0.20 \pm 0.20) \times 10^{-3}$ from ADAM 06.

¹⁷ Not independent of other results in BRIERE 06.

¹⁸ Uses $B(\psi(2S) \rightarrow \gamma\chi_{c2}) = 9.22 \pm 0.11 \pm 0.46\%$ from ATHAR 04, $\psi(2S)$ mass and width from PDG 04, and $\Gamma_{ee}(\psi(2S)) = 2.54 \pm 0.03 \pm 0.11$ keV from ADAM 06.

¹⁹ Using $\sigma(e^+e^- \rightarrow \psi(3770) \rightarrow \text{hadrons}) = (6.38 \pm 0.08^{+0.41}_{-0.30})$ nb from BESSON 06 and $B(K_S^0 \rightarrow \pi^+\pi^-) = 0.6895 \pm 0.0014$.

²⁰ Using $B(K_S^0 \rightarrow \pi^+\pi^-) = 0.6860 \pm 0.0027$.

²¹ Using $\sigma_{\text{tot}}(e^+e^- \rightarrow \psi(3770)) = 7.9 \pm 0.6$ nb at the resonance.

²² Assuming that interference effects between resonance and continuum can be neglected.

²³ Using $\sigma^{\text{obs}}(e^+e^- \rightarrow \psi(3770)) = 7.15 \pm 0.38$ nb.

²⁴ Using $\sigma^{\text{obs}} = 7.15 \pm 0.27 \pm 0.27$ nb and neglecting interference.

²⁵ Comparing $\sigma(e^+e^- \rightarrow \phi\eta)$ at $\sqrt{s} = 3.773$ GeV and $\sqrt{s} = 3.671$ GeV, and using $\sigma(\psi(3770) \rightarrow D\bar{D}) = 6.39 \pm 0.20$ nb.

$\psi(3770)$ REFERENCES

ABLIKIM 08B	PL B659 74	M. Ablikim <i>et al.</i>	(BES Collab.)
ABLIKIM 08D	PL B660 315	M. Ablikim <i>et al.</i>	(BES Collab.)
AUBERT 08B	PR D77 011102R	B. Aubert <i>et al.</i>	(BABAR Collab.)
BRODZICKA 08	PRL 100 092001	J. Brodzicka <i>et al.</i>	(BELLE Collab.)
PAKHOVA 08	PR D77 011103R	G. Pakhlova <i>et al.</i>	(BELLE Collab.)
ABLIKIM 07B	PL B650 111	M. Ablikim <i>et al.</i>	(BES Collab.)
ABLIKIM 07E	PL B652 238	M. Ablikim <i>et al.</i>	(BES Collab.)
ABLIKIM 07F	PL B656 30	M. Ablikim <i>et al.</i>	(BES Collab.)
ABLIKIM 07I	EPJ C52 805	M. Ablikim <i>et al.</i>	(BES Collab.)
ABLIKIM 07K	PR D76 122002	M. Ablikim <i>et al.</i>	(BES Collab.)
AUBERT 07BE	PR D76 111105R	B. Aubert <i>et al.</i>	(BABAR Collab.)
DOBBS 07	PR D76 112001	S. Dobbs <i>et al.</i>	(CLEO Collab.)
ABLIKIM 06L	PRL 97 121801	M. Ablikim <i>et al.</i>	(BES Collab.)
ABLIKIM 06N	PL B641 145	M. Ablikim <i>et al.</i>	(BES Collab.)
ADAM 06	PRL 96 082004	N.E. Adam <i>et al.</i>	(CLEO Collab.)
ADAMS 06	PR D73 012002	G.S. Adams <i>et al.</i>	(CLEO Collab.)
BESSON 06	PRL 96 092002	D. Besson <i>et al.</i>	(CLEO Collab.)
BRIERE 06	PR D74 031106R	R.A. Briere <i>et al.</i>	(CLEO Collab.)
COAN 06A	PRL 96 182002	T.E. Coan <i>et al.</i>	(CLEO Collab.)
CRONIN-HENNESSY...	06 PR D74 012005	D. Cronin-Hennessy <i>et al.</i>	(CLEO Collab.)
HUANG 06A	PRL 96 032003	G.S. Huang <i>et al.</i>	(CLEO Collab.)
BAI 05	PL B605 63	J.Z. Bai <i>et al.</i>	(BES Collab.)
HE 05	PRL 95 121801	Q. He <i>et al.</i>	(CLEO Collab.)
Also	PRL 96 199903 (errata.)	Q. He <i>et al.</i>	(CLEO Collab.)
ABLIKIM 04F	PR D70 077101	M. Ablikim <i>et al.</i>	(BES Collab.)
ATHAR 04	PR D70 112002	S.B. Athar <i>et al.</i>	(CLEO Collab.)
CHISTOV 04	PRL 93 051803	R. Chistov <i>et al.</i>	(BELLE Collab.)
PDG 04	PL B592 1	S. Eidelman <i>et al.</i>	
BAI 02C	PRL 88 101802	J.Z. Bai <i>et al.</i>	(BES Collab.)
ADLER 88C	PRL 60 89	J. Adler <i>et al.</i>	(Mark III Collab.)
SCHINDLER 80	PR D21 2716	R.H. Schindler <i>et al.</i>	(Mark II Collab.)
BACINO 78	PRL 40 671	W.J. Bacino <i>et al.</i>	(SLAC, UCLA, UCI)
RAPIDIS 77	PRL 39 526	P.A. Rapidis <i>et al.</i>	(LGW Collab.)

OTHER RELATED PAPERS

ABLIKIM 06X	PRL 97 262001	M. Ablikim <i>et al.</i>	(BES Collab.)
AUBERT_BE 06F	PR D74 111103R	B. Aubert <i>et al.</i>	(BABAR Collab.)
ABLIKIM 05K	NP B727 395	M. Ablikim <i>et al.</i>	(BES Collab.)
ABLIKIM 05M	PR D72 072007	M. Ablikim <i>et al.</i>	(BES Collab.)
BARNES 05	PR D72 054026	T. Barnes, S. Godfrey, E.S. Swanson	(CLEO Collab.)
HE 05	PRL 95 121801	Q. He <i>et al.</i>	(CLEO Collab.)
Also	PRL 96 199903 (errata.)	Q. He <i>et al.</i>	(CLEO Collab.)
VOLOSHIN 05A	PR D71 114003	M.B. Voloshin	
VOLOSHIN 05B	PAN 68 771	M.B. Voloshin	
Translated from YAF 68 804.			
ABLIKIM 04D	PL B603 130	M. Ablikim <i>et al.</i>	(BES Collab.)
LIU 04B	PR D70 094001	K.-Y. Liu, K.-T. Chao	
WANG 04C	PR D70 077505	P. Wang, X.H. Mo, C.Z. Yuan	
WANG 04D	PR D70 114014	P. Wang, C.Z. Yuan, X.H. Mo	

NEW CHARMONIUM-LIKE STATES

Excerpted with permission of Rev. Mod. Phys. from Eichten *et al.* (RMP, to be published) with updates in May 2008 by S. Eidelman (Novosibirsk), H. Mahlke-Krüger (Cornell U.), and C. Patrignani (INFN, Genova).

Many new charmonium states above $D\bar{D}$ threshold have recently been observed. While some of these states appear to be consistent with conventional $c\bar{c}$ states, others do not. Here we give a brief survey of the new states and their possible interpretations. In many cases, the picture is not entirely clear. This situation could be remedied by a coherent search of the decay pattern to $D\bar{D}^*$, search for production in two-photon

Meson Particle Listings

New charmonium-like states

collisions and initial state radiation (ISR), the study of radiative decays of charmonia, analysis of angular distributions to determine quantum numbers, and of course, by improved statistical precision of the current measurements. The uncertainty in the interpretation for these states is reflected in the arbitrariness of the nomenclature used in the literature. In this review, we refer to them as to $X(m)$, following the standard naming convention for states of uncertain assignment. Note that some of the states discussed below are not yet in the regular listings because they are observed by a single experiment only.

1. $X(3872)$

The $X(3872)$, discovered by Belle in B decays [1] and confirmed by BaBar [2] and in hadronic production by CDF [3] and D0 [4], is a narrow state of mass $3872 \text{ MeV}/c^2$ that was first seen decaying to $J/\psi\pi^+\pi^-$. No signal at this mass was seen in $B \rightarrow X^- K$, $X^- \rightarrow \pi^-\pi^0 J/\psi$ [5], which would have implied a charged partner of $X(3872)$. It was not observed in two-photon production or initial state radiation [6]. Subsequent studies focused on determining the mass, width, and decay properties in order to establish its quantum numbers and possible position in the charmonium system of states. To date, decays to $\pi^+\pi^- J/\psi$, $\gamma J/\psi$, $D^0\bar{D}^0\pi^0$, and possibly $\pi^+\pi^-\pi^0 J/\psi$ have been reported.

The averaged mass of this state is $M = 3872.2 \pm 0.8 \text{ MeV}/c^2$ [7]; the width is determined to be below detector resolution, $\Gamma < 2.3 \text{ MeV}$ (90% C.L.) [1] in $J/\psi\pi^+\pi^-$ decays and $3.0_{-1.4}^{+1.9} \pm 0.9 \text{ MeV}$ [8] in $\bar{D}^{*0}D^0$ decays.

The combined branching fraction product from Belle and BaBar is $\mathcal{B}[B^+ \rightarrow K^+ X(3872)] \times \mathcal{B}[X(3872) \rightarrow \pi^+\pi^- J/\psi] = (11.4 \pm 2.0) \times 10^{-6}$ [9]. After setting a limit of $\mathcal{B}[B^+ \rightarrow K^+ X(3872)] < 3.2 \times 10^{-4}$ (90% C.L.), BaBar [10] derives $\mathcal{B}[X(3872) \rightarrow \pi^+\pi^- J/\psi] > 4.2\%$ (90% C.L.). We can compare this with other states above open flavor threshold: $\mathcal{B}[\psi(3770) \rightarrow \pi^+\pi^- J/\psi] = (1.93 \pm 0.28) \times 10^{-3}$ [9] (partial width 46 keV) and limits $\mathcal{B}[\psi(4040, 4160) \rightarrow \pi^+\pi^- J/\psi]$ of order 10^{-3} [7] (partial widths $\sim 100 \text{ keV}$).

Regular charmonium states that cannot decay to D pairs are also expected to have a narrow width; however, in these cases, E1 transitions to the χ_{cJ} states are preferred. This behavior is not seen in the data for $X(3872)$ [1]. This result also disfavors its interpretation as a $1^{1,3}D_2$ state.

Decay into a pair of D mesons has not been observed, and upper limits on the rate are in the range of a few times that for $\pi^+\pi^- J/\psi$ [11]. A signal in $B \rightarrow (D^0\bar{D}^0\pi^0)K$ with $m(D^0\bar{D}^0\pi^0)$ observed by Belle in the right range is the first candidate for open-charm decays of $X(3872)$ [12], confirmed by BaBar in Ref. 8. BaBar also observes $X(3872) \rightarrow D^0\bar{D}^0\gamma$. The relative rate of $D^0\bar{D}^0\pi^0$ and $D^0\bar{D}^0\gamma$ supports the hypothesis that the $X(3872)$ predominantly decays to $D^0\bar{D}^{*0}$. The observed rate is an order of magnitude above that for $\pi^+\pi^- J/\psi$.

The dipion mass distribution favors high $m(\pi^+\pi^-)$ values. This is not untypical for charmonium states (*cf.* $\psi(2S) \rightarrow \pi^+\pi^- J/\psi$), but could be an indication that the pion pair might

even be produced in a ρ configuration; if that were indeed the case the $X(3872)$ could not be a charmonium state. A search for $X(3872) \rightarrow \pi^0\pi^0 J/\psi$ would be most helpful to clarify this aspect (as well as to determine the $\pi^0\pi^0 J/\psi : \pi^+\pi^- J/\psi$ ratio) because the decay chain $X(3872) \rightarrow \rho^0 J/\psi \rightarrow \pi^0\pi^0 J/\psi$ would be forbidden. Observation of $X(3872) \rightarrow \pi^0\pi^0 J/\psi$ would therefore rule out the hypothesis of an intermediate ρ state. The decay $X(3872) \rightarrow \pi^+\pi^-\pi^0 J/\psi$ was observed at a rate comparable to that of $\pi^+\pi^- J/\psi$ [13]. The $m(\pi^+\pi^-\pi^0)$ distribution is concentrated at the highest values, coinciding with the kinematic limit, which prompted speculations that the decay might proceed through (the low-side tail of) an ω .

Since the $X(3872)$ lies well above $D\bar{D}$ threshold but is narrower than experimental resolution, unnatural $J^P = 0^-, 1^+, 2^-$ is favored. An angular distribution analysis by the Belle collaboration, utilizing in part suggestions in Ref. 14, favors $J^{PC} = 1^{++}$ [15], although a higher-statistics analysis by CDF cannot distinguish between $J^{PC} = 1^{++}$ or 2^{-+} [16] (see also [17–19]). $J^{PC} = 2^{-+}$ is disfavored by the observation of the $D^0\bar{D}^0\pi^0$ decay mode [8,12], which would require at least two units of relative orbital angular momentum in the three-body state, very near threshold. On the other hand, it has been argued [20] that $J^{PC} = 2^{-+}$ could more naturally explain the observed mass shift between the $\pi^+\pi^- J/\psi$ and the $D^0\bar{D}^{*0}$ modes.

Of conventional $c\bar{c}$ states, only the $1D$ and $2P$ multiplets are nearby in mass. Taking into account the angular distribution analysis, only the $J^{PC} = 1^{++} 2^3P_1$ and $2^{-+} 1^1D_2$ assignments are possible. The decay $X(3872) \rightarrow \gamma J/\psi$ is observed at a rate about a quarter or less of that for the $X(3872) \rightarrow \pi^+\pi^- J/\psi$ [13,21], and implies $C = +$. This would be an E1 transition for 2^3P_1 , but a more suppressed higher multipole for 2^{-+} , and therefore the $J^{PC} = 1^{++}$ interpretation, appears more likely assuming $c\bar{c}$ content. For a 1^{++} state, the only surviving candidate is the 2^3P_1 . However, an identification of the $Z(3931)$ with the 2^3P_2 implies a 2^3P_2 mass of $\sim 3930 \text{ MeV}/c^2$, which is inconsistent with the 2^3P_1 interpretation of the $X(3872)$ if the $2^3P_2 - 2^3P_1$ mass splittings are decidedly lower than $50 \text{ MeV}/c^2$ [22,23]. This favors the conclusion that the $X(3872)$ may be a $D^0\bar{D}^{*0}$ molecule or “tetraquark” [24] state. It has many features in common with an S -wave bound state of $(D^0\bar{D}^{*0} + \bar{D}^0 D^{*0})/\sqrt{2} \sim c\bar{c}u\bar{u}$ with $J^{PC} = 1^{++}$ [25]. Its simultaneous decay to $\rho J/\psi$ and $\omega J/\psi$ with roughly equal branching ratios is a consequence of this “molecular” assignment. The upper limit on $X(3872) \rightarrow \eta J/\psi$ [26] is consistent with expectations for a charmonium state, as well as a hybrid. A new measurement of $M(D^0) = 1864.847 \pm 0.150 \pm 0.095 \text{ MeV}/c^2$ [27] implies $M(D^0\bar{D}^{*0}) = 3871.81 \pm 0.36 \text{ MeV}/c^2$, and hence a binding energy consistent with zero.

2. $X(3930)$ (or $Z(3930)$) : a $\chi_{c2}(2P)$ candidate

Belle has reported a candidate for a $2^3P_2(\chi_{c2}(2P))$ state in $\gamma\gamma$ collisions [28], decaying to $D\bar{D}$. The state appears as an enhancement in the $m(D\bar{D})$ distribution at a statistical significance of 5.3σ . The relative D^+D^- and $D^0\bar{D}^0$ rates are consistent with expectations based on isospin invariance and the $D^+ - D^0$ mass difference. A fit combining charged and neutral modes yields mass and width $M = 3929 \pm 5 \pm 2$ MeV/ c^2 and $\Gamma = 29 \pm 10 \pm 2$ MeV. Although in principle the D -pair could be produced from $D^*\bar{D}$, the observed transverse momentum spectrum of the $D\bar{D}$ pair is consistent with no contribution from $D^*\bar{D}$.

The $X(3930)$ interpretation as $\eta_c(3S)$ is ruled out by the observation of its decay to $D\bar{D}$. Both $\chi_{c0}(2P)$ and $\chi_{c2}(2P)$ are expected to decay to $D\bar{D}$ (however, $\chi_{c1}(2P)$ only decays to $D^*\bar{D}$). To distinguish between the two remaining hypotheses, the distribution in θ^* , which is the angle of the D -meson relative to the beam axis in the $\gamma\gamma$ center-of-mass frame, is examined. This distribution is consistent with $\sin^4\theta^*$ as expected for a state with $J = 2, \lambda = \pm 2$. The two-photon width is, under the assumption of a tensor state, measured to be $\Gamma_{\gamma\gamma} \cdot \mathcal{B}_{D\bar{D}} = 0.18 \pm 0.05 \pm 0.03$ keV.

BaBar has searched for $X(3930)$ decay into $\gamma J/\psi$ [21], and set an upper limit $\mathcal{B}(B \rightarrow X(3930) + K) \times \mathcal{B}(X(3930) \rightarrow \gamma J/\psi) < 2.5 \times 10^{-6}$.

The predicted mass of the $\chi_{c2}(2P)$ is 3972 MeV/ c^2 and the predicted partial widths and total width assuming $M[2^3P_2(c\bar{c})] = 3930$ MeV/ c^2 are [22,29]

$$\Gamma(\chi_{c2}(2P) \rightarrow D\bar{D}) = 21.5 \text{ MeV},$$

$$\Gamma(\chi_{c2}(2P) \rightarrow D\bar{D}^*) = 7.1 \text{ MeV and}$$

$$\Gamma_{\text{total}}(\chi_{c2}(2P)) = 28.6 \text{ MeV},$$

in good agreement with the experimental measurement. Furthermore, using $\Gamma(\chi_{c2}(2P) \rightarrow \gamma\gamma) = 0.67$ keV [30] $\times \mathcal{B}(\chi_{c2}(2P) \rightarrow D\bar{D}) = 70\%$ implies $\Gamma_{\gamma\gamma} \cdot \mathcal{B}_{D\bar{D}} = 0.47$ keV, which is within a factor of 2 of the observed number, fairly good agreement considering the typical reliability of two-photon partial width predictions.

The observed $X(3930)$ properties are consistent with those predicted for the $\chi_{c2}(2P)$ $2^3P_2(c\bar{c})$ state. So far, the only mild surprise is the observed mass, which is 40 – 50 MeV/ c^2 below expectations. Adjusting that, all other properties observed so far can probably be accommodated within the framework of [22,29]. The $\chi_{c2}(2P)$ interpretation could be confirmed by observation of the $D\bar{D}^*$ final state. We also note that the $\chi_{c2}(2P)$ is predicted to undergo radiative transitions to $\psi(2S)$ with a partial width of $\mathcal{O}(100$ keV) [22,23]. Needs confirmation.

3. $X(3940)$

Belle studied double-charmonium production and $e^+e^- \rightarrow J/\psi + X$ near the $\Upsilon(4S)$ [31], and observed enhancements for the well-known charmonium states η_c , χ_{c0} , and $\eta_c(2S)$ at rates and masses consistent with other determinations. In addition, a peak at a higher energy was found. The mass and width were measured to be $M = 3936 \pm 14 \pm 6$ MeV/ c^2 and $\Gamma = 39 \pm 26$ (stat) MeV.

To further examine the properties of this enhancement, Belle searched for exclusive decays $J/\psi \rightarrow D\bar{D}^{(*)}$, given that these decays are kinematically accessible. An enhancement at the $X(3940)$ mass is seen for $D\bar{D}^*$, but not for $D\bar{D}$. The mass and width determined in this study are $M = (3943 \pm 6 \pm 6)$ MeV/ c^2 , $\Gamma < 52$ MeV (90% C.L.). Note that the inclusive and exclusive samples have some overlap, and thus the two mass measurements are not statistically independent. The overlap has been eliminated for the branching fraction determination. A signal of 5.0σ significance was seen for $D\bar{D}^*$, but none for $D\bar{D}$. In addition, the $X(3940)$ did not show a signal for a decay to $\omega J/\psi$, unlike the $Y(3940)$.

If confirmed, the decay to $D\bar{D}^*$ but not $D\bar{D}$ suggests the $X(3940)$ has unnatural parity. The lower masses η_c and η'_c are also produced in double-charm production. One is therefore led to try an η'_c assignment, although this state is expected to have a somewhat higher mass [23]. The predicted width for a 3^1S_0 state with a mass of 3943 MeV/ c^2 is ~ 50 MeV [22], which is in not in conflict with the obtained upper limit for the $X(3940)$ width.

Another possibility due to the dominant $D\bar{D}^*$ final states is that the $X(3940)$ is the $2^3P_1(c\bar{c})$ χ'_1 state. It is natural to consider the $2P(c\bar{c})$, since the 2^3P_J states are predicted to lie in the 3920–3980 MeV/ c^2 mass region, and the widths are predicted to be in the range $\Gamma(2^3P_J) = 30$ –165 MeV [23]. The dominant $D\bar{D}^*$ mode would then suggest that the $X(3940)$ is the $2^3P_1(c\bar{c})$ state. The problems with this interpretation are (1) there is no evidence for the $1^3P_1(c\bar{c})$ state in the same data, (2) the predicted width of the $2^3P_1(c\bar{c})$ is 140 MeV (assuming $M(2^3P_1(c\bar{c})) = 3943$ MeV/ c^2) [32], and (3) there is another candidate for the $1^3P_1(c\bar{c})$ state, the $X(3945)$ (or $Y(3940)$).

A possible interpretation of the $X(3940)$ is that it is the $3^1S_0(c\bar{c})$ η''_c state. Tests of this assignment are to study the angular distribution of the $D\bar{D}^*$ final state and to observe it in $\gamma\gamma \rightarrow D\bar{D}^*$.

Further analysis of Belle confirms the $X(3940)$ and reports a new state $X(4160)$ [33].

Meson Particle Listings

New charmonium-like states

4. $X(3945)$ (or $Y(3940)$)

The $X(3945)$ is seen by Belle in the $\omega J/\psi$ subsystem in the decay $B \rightarrow K\omega(\rightarrow \pi^+\pi^-\pi^0)J/\psi$ [34]. The final state is selected by kinematic constraints that incorporate the parent particle mass $m(B)$ and the fact that the B -meson pair is produced with no additional particles. Background from decays such as $K_1(1270) \rightarrow \omega K$ is reduced by requiring $m(\omega J/\psi) > 1.6 \text{ GeV}$. The $K\omega J/\psi$ final state yield is then further examined in bins of $m(\omega J/\psi)$. A threshold enhancement is observed, which is fit with a threshold function suitable for phase-space production of this final state and an S -wave Breit-Wigner shape. The reported mass and width of the enhancement are $M = 3943 \pm 11 \pm 13 \text{ MeV}/c^2$ and $\Gamma = 87 \pm 22 \pm 26 \text{ MeV}$. A fit without a resonance contribution gives no good description of the data. The state has been recently confirmed in the same process by BaBar [35]: the mass and width, $M = 3914.6_{-3.4}^{+3.8} \pm 1.9 \text{ MeV}/c^2$ and $\Gamma = 34_{-8}^{+12} \pm 5 \text{ MeV}$, are somewhat smaller than the values reported by Belle, but are not incompatible with them. The average mass and width values are $M = 3916 \pm 7 \text{ MeV}/c^2$ ($s=1.6$) and $\Gamma = 41 \pm 18 \text{ MeV}$ ($s=1.5$).

The mass and width of the $X(3945)$ suggest a radially excited P -wave charmonium state. Belle has measured a combined branching ratio of $\mathcal{B}(B \rightarrow KX) \cdot \mathcal{B}(X \rightarrow \omega J/\psi) = (7.1 \pm 1.3 \pm 3.1) \times 10^{-5}$. BaBar measures $\mathcal{B}(B^+ \rightarrow K^+X) \cdot \mathcal{B}(X \rightarrow \omega J/\psi) = (4.9_{-0.9}^{+1.0} \pm 0.5) \times 10^{-5}$, $\mathcal{B}(B^0 \rightarrow K^0X) \cdot \mathcal{B}(X \rightarrow \omega J/\psi) = (1.3_{-1.1}^{+1.3} \pm 0.2) \times 10^{-5}$, with a ratio $\mathcal{B}(B^0 \rightarrow K^0X) : \mathcal{B}(B^+ \rightarrow K^+X) = 0.27_{-0.23}^{+0.28} {}_{-0.01}^{+0.04}$. One expects that $\mathcal{B}(B \rightarrow K\chi_{cJ}(2P)) < \mathcal{B}(B \rightarrow K\chi_{cJ}) = 4 \times 10^{-4}$. This implies that $\mathcal{B}(X(3945) \rightarrow \omega J/\psi) > 12\%$, which is unusual for a $c\bar{c}$ state above open-charm threshold.

For the $\chi_{c1}(2P) 2^3P_1(c\bar{c})$, we expect $D\bar{D}^*$ to be the dominant decay mode with a predicted width of 140 MeV [32], which is not inconsistent with that of the $X(3945)$ within the theoretical and experimental uncertainties. The mass of the $\chi_{c1}(2P)$ state is expected to be smaller than the mass of the $\chi_{c2}(2P)$. If we identify the $\chi_{c2}(2P)$ with the state observed by Belle in $\gamma\gamma \rightarrow D\bar{D}$, the smaller mass value measured by BaBar would be consistent with the assignment of the $X(3945)$ as the $\chi_{c1}(2P)$ state. Furthermore, the χ_{c1} is also seen in B -decays. Although the decay $1^{++} \rightarrow \omega J/\psi$ is unusual, the corresponding decay $\chi_{b1}(2P) \rightarrow \omega\Upsilon(1S)$ has also been seen [36]. One possible explanation for this unusual decay mode is that rescattering through $D\bar{D}^*$ is responsible: $1^{++} \rightarrow D\bar{D}^* \rightarrow \omega J/\psi$. Another contributing factor might be mixing with the possible molecular state tentatively identified with the $X(3872)$.

BaBar has searched for the $X(3945)$ decay into $\gamma J/\psi$ [21], and set an upper limit $\mathcal{B}(B \rightarrow X(3945) + K) \times \mathcal{B}(X(3945) \rightarrow \gamma J/\psi) < 1.4 \times 10^{-5}$.

The $\chi_{c1}(2P)$ assignment can be tested by searching for the $D\bar{D}$ and $D\bar{D}^*$ final states, and by studying their angular distributions. With the present experimental data, a $\chi_{c1}(2P)$ assignment cannot be ruled out.

5. $X(4260)$ (or $Y(4260)$) and further states in $\pi^+\pi^-J/\psi$

Perhaps the most intriguing of the recently discovered states is the $X(4260)$ reported by BaBar as an enhancement in the $\pi^+\pi^-J/\psi$ subsystem in the radiative return reaction $e^+e^- \rightarrow \gamma_{\text{ISR}}J/\psi\pi^+\pi^-$ [37]. This state was subsequently confirmed in radiative return by CLEO [38] and Belle [39]. Further evidence was seen by BaBar in $B \rightarrow K(\pi^+\pi^-J/\psi)$ [40].

The CLEO Collaboration has also confirmed the $X(4260)$ in a direct scan [41]. There are also weak signals for $\psi(4160) \rightarrow \pi^+\pi^-J/\psi$ (3.6σ) and $\pi^0\pi^0J/\psi$ (2.6σ), consistent with the $X(4260)$ tail, and for $\psi(4040) \rightarrow \pi^+\pi^-J/\psi$ (3.3σ). In addition to a clear enhancement around $4.25 \text{ GeV}/c^2$, the $\pi^+\pi^-J/\psi$ invariant mass distribution observed by Belle also exhibits a clustering of events around $4.05 \text{ GeV}/c^2$, which is significantly above the background level. If they use the same functional form as BaBar (a single Breit-Wigner resonance plus an incoherent second-order polynomial background), they find parameters of the $X(4260)$ consistent with BaBar. If a second resonance is added, the quality of the fit improves significantly. Assuming that there are two resonances described by Breit-Wigner amplitudes, Belle performs another fit and obtains parameters of these structures [39]. Both structures are significant: for example, the one at $4.05 \text{ GeV}/c^2$ has a significance of 7.4σ . In a case of relatively low statistics and constant width (no energy dependence), such a fit has two equally good solutions (exactly the same fit quality) with equal mass and width, but notably different partial widths to e^+e^- , and the relative phase between the two structures. The masses and widths are reported as $M(R1) = 4008 \pm 40_{-28}^{+114} \text{ MeV}/c^2$, $\Gamma(R1) = 226 \pm 44 \pm 87 \text{ MeV}$, $M(R2) = 4247 \pm 12_{-32}^{+17} \text{ MeV}/c^2$, $\Gamma(R2) = 108 \pm 19 \pm 10 \text{ MeV}$. The coupling is consistent with the other measurements for solution I for the partial width. Solution II, though equally valid, leads to a value $B(X \rightarrow \pi^+\pi^-J/\psi) \times \Gamma_{e^+e^-}$ substantially higher.

The overall pattern is not similar to BaBar [37], where a two-resonance fit gave a lower structure with mass close to $4260 \text{ MeV}/c^2$, and a width of 50 MeV along with a narrow one at $4330 \text{ MeV}/c^2$, with no significant improvement of the fit quality. (The single-resonance baseline fit resulted in $M = 4259 \pm 8_{-6}^{+2} \text{ MeV}/c^2$, $\Gamma = 88 \pm 23_{-4}^{+6} \text{ MeV}$; adding the $\psi(4040)$, $\psi(4160)$, or $\psi(4415)$ did not help.)

Mass and width of the higher structure measured by Belle are consistent with those of the $X(4260)$ observed by BaBar [37] and CLEO [38]. Although the mass of the first resonance is close to that of the $\psi(4040)$, the fitted width is much higher than the world average one ($80 \pm 10 \text{ MeV}$). The mass of the second resonance is higher than that of the $\psi(4160)$. Therefore, these structures should be considered as new states rather than confirmation of the existing ψ' states. Of course, interpretation of these enhancements as new resonances is not at all unambiguous; they are close to $D^{(*)}\bar{D}^{(*)}$ thresholds, where coupled-channel effects and rescattering may strongly affect the cross section.

A variety of channels have been searched for now [41–45], of which $\pi^0\pi^0 J/\psi$ and $K^+K^- J/\psi$ only have been observed [41,46]. The ratios between the branching fractions of different channels should help narrow down the possible explanations of $X(4260)$. For example, the upper limit for the ratio of $D\bar{D}$ to $\pi^+\pi^- J/\psi$ of 1.0 at 90% C.L. [43] may not seem particularly tight at first glance, but is to be compared, for example, with the same ratio for the $\psi(3770)$, where it is about 500.

A number of explanations have appeared in the literature: $\psi(4S)$ [47], $c\bar{s}\bar{c}s$ tetraquark [48], and $c\bar{c}$ hybrid [49–52]. In some models, the mass of the $X(4260)$ is consistent with the $4S(c\bar{c})$ level [47]. Indeed, a $4S$ charmonium level at 4260 MeV/ c^2 was anticipated on exactly this basis [53]. With this assignment, the nS levels of charmonium and bottomonium are remarkably congruent to one another. However, other calculations using a linear plus Coulomb potential identify the $4^3S_1(c\bar{c})$ level with the $\psi(4415)$ state (*e.g.*, Ref. 23). If this is the case the first unaccounted-for $1^{--}(c\bar{c})$ state is the $\psi(3^3D_1)$. Quark models estimate its mass to be $M(3^3D_1) \simeq 4500$ MeV/ c^2 , which is much too heavy to be the $X(4260)$. The $X(4260)$ therefore represents an overpopulation of the expected 1^{--} states. The absence of open-charm production also argues against it being a conventional $c\bar{c}$ state.

The hybrid interpretation of $X(4260)$ is appealing. The flux-tube model predicts that the lowest $c\bar{c}$ hybrid mass is ~ 4200 MeV/ c^2 [54] with lattice-gauge theory having similar expectations [55]. Models of hybrids typically expect the wave function at the origin to vanish, implying a small e^+e^- width in agreement with the observed value. Lattice-gauge theory found that the $b\bar{b}$ hybrids have large couplings to closed-flavor channels [56]. The proposed scenario resembles the situation in charmonium, where the hybrid candidate $X(4260)$ shows a surprisingly large partial width $\Gamma(\pi^+\pi^- J/\psi)$ compared to its other decay modes. Moreover, $J/\psi\pi^+\pi^-$ production is much more prominent at the $X(4260)$ than at the conventional states $\psi(4040)$, $\psi(4160)$, and $\psi(4415)$.

One predicted consequence of the hybrid hypothesis is that the dominant hybrid charmonium open-charm decay modes are expected to be a meson pair with an S -wave (D , D^* , D_s , D_s^*) and a P -wave (D_J , D_{sJ}) in the final state [50]. The dominant decay mode is expected to be $D\bar{D}_1 + \text{c.c.}$. Evidence for a large $D\bar{D}_1$ signal would be strong evidence for the hybrid interpretation. A complication is that $D\bar{D}_1$ threshold is 4287 MeV/ c^2 , if we consider the lightest D_1 to be the narrow state noted in Ref. 9 at 2422 MeV/ c^2 . The possibility also exists that the $Y(4260)$ could be a $D\bar{D}_1$ bound state. It would decay to $D\pi\bar{D}^*$, where the D and π are not in a D^* . Note that the dip in $R_{e^+e^-}$ occurs just below $D\bar{D}_1$ threshold, which may be the first S -wave meson pair accessible in $c\bar{c}$ fragmentation [50,57]. In addition to the hybrid decay modes given above, lattice-gauge theory suggests that we search for other closed-charm modes with $J^{PC} = 1^{--}$: $J/\psi\eta$, $J/\psi\eta'$, $\chi_{cJ}\omega$, and more. Distinguishing

among the interpretations of the $X(4260)$ will likely require careful measurement of several decay modes.

If the $X(4260)$ is a hybrid, it is expected to be a member of a multiplet consisting of eight states with masses in the 4.0 to 4.5 GeV/ c^2 mass range, with lattice-gauge theory preferring the higher end of the range [58]. It would be most convincing if some of these partners were found, especially the J^{PC} exotics. In the flux-tube model, the exotic states have $J^{PC} = 0^{+-}$, 1^{-+} , and 2^{+-} , while the non-exotic, low-lying hybrids have 0^{-+} , 1^{+-} , 2^{-+} , 1^{++} , and 1^{--} .

6. $X(4360)$ (or $Y(4360)$) and further states in $\pi^+\pi^-\psi(2S)$

In the radiative return process $e^+e^- \rightarrow \gamma + X$, BaBar [59] reports a broad structure decaying to $\pi^+\pi^-\psi(2S)$, where $\psi(2S) \rightarrow \pi^+\pi^- J/\psi$. A single-resonance hypothesis with $M(X) = (4324 \pm 24)$ MeV/ c^2 and $\Gamma(X) = (172 \pm 33)$ MeV (errors are statistical only) is adequate to fit the observed mass spectrum. However, they cannot exclude that the structure observed is a manifestation of a new decay mode of the $X(4260)$.

Belle also studies this final state with a 2.2 times bigger statistics, and observes two distinct peaks in the $\pi^+\pi^-\psi(2S)$ invariant mass distribution, at 4.36 GeV/ c^2 and 4.66 GeV/ c^2 [60]. Assuming that there are two Breit-Wigner resonances, they obtain the parameters of the structures: $M(X1) = 4361 \pm 9 \pm 9$ MeV/ c^2 , $\Gamma(X1) = 74 \pm 15 \pm 10$ MeV, $M(X2) = 4664 \pm 11 \pm 5$ MeV/ c^2 , $\Gamma(X2) = 48 \pm 15 \pm 3$ MeV. The lighter structure is approximately at the same mass as that of BaBar, but its width is significantly smaller. Belle concludes that their states are distinct from those observed in $e^+e^- \rightarrow \pi^+\pi^- J/\psi$ by BaBar [37] and Belle [39]. A combined fit to the $\pi^+\pi^-\psi(2S)$ cross section measured by Belle and BaBar [61] yields $M(X1) = 4355_{-10}^{+9} \pm 9$ MeV/ c^2 , $\Gamma(X1) = 103_{-15}^{+17} \pm 11$ MeV for the $X(4360)$, and $M(X2) = 4661_{-8}^{+9} \pm 6$ MeV/ c^2 , $\Gamma(X2) = 42_{-12}^{+17} \pm 6$ MeV for the $X(4660)$.

Ref. 52 employs the QCD string model to calculate the properties of various hybrids, and finds that the lowest vector hybrid has a mass of 4397 MeV/ c^2 . It also argues that strong coupling of the vector hybrid to the DD_1 and D^*D_0 modes can cause considerable threshold attraction, so that the vector hybrid state is responsible for formation of the near-threshold $X(4260)$ and $X(4360)$.

Ref. 62 considers the canonical charmonium assignments for the $X(4360)$ and $X(4660)$, and concludes that the latter is a good candidate for a 5^3S_1 $c\bar{c}$ state. The $X(4360)$ can be a 3^3D_1 $c\bar{c}$ state, but a charmonium hybrid interpretation cannot be excluded.

Although the width of the state observed by BaBar is larger than that of Belle, systematic uncertainties are not estimated by BaBar. We place both observations under one state $X(4360)$.

Meson Particle Listings

New charmonium-like states

7. $X^+(4330)$ (or $Z^+(4330)$): a state in $\pi^\pm\psi(2S)$

The Belle Collaboration reports a distinct peak in the $\pi^\pm\psi(2S)$ invariant mass distribution in $B \rightarrow K\pi^\pm\psi(2S)$ decays [63]. The peak is too narrow to be caused by interference effects in the $K\pi$ channel. When fitted with a Breit-Wigner function, the mass and width of the state are $(4433 \pm 4 \pm 2)$ MeV/ c^2 and (45_{-13}^{+18+30}) MeV, respectively.

The structure is unique in that it is the first charmonium-like candidate to have a non-zero electric charge. This could be the first observation of the tetraquark charmonium configuration. Ref. 64 notes that the mass of this structure is not far from the threshold for production of $D^*\bar{D}_1(2420)$, and suggests a production mechanism in which an anticharmed meson $\bar{c}\bar{q}$ and a charmed meson $c\bar{q}$ are produced, and rescatter to a $c\bar{c} = \psi(2S)$ and $q\bar{q} = \pi$. To explain why the J/ψ is not produced by the same mechanism, it is assumed that rescattering may favor close values of the Q value for both sides. Ref. 65 studies whether this state could be a loosely bound molecular state of $D_1 - D^*$, or $D'_1 - D^*$ arising from the one-pion-exchange potential, and concludes that such interaction alone is not sufficiently strong. At the same time, the authors of Ref. 66 claim that using QCD sum rules to describe a $D^* - D_1$ molecule with $J^P = 1^-$, they can reproduce the mass of the new state.

8. Conclusions

Note that interpretation of most of these enhancements as new resonances is not at all unambiguous; they are close to $D^{(*)}\bar{D}^{(*)}$ thresholds, where coupled-channel effects and rescattering may strongly affect the cross section. This is particularly important in such cases as the $X(3872)$, which lies right at the $D^0\bar{D}^{*0}$ threshold. Systematic searches for these states in various processes and independent confirmation are highly desirable.

References

1. S.K. Choi *et al.* [Belle Collaboration], Phys. Rev. Lett. **91**, 262001 (2003).
2. B. Aubert *et al.* [BaBar Collaboration], Phys. Rev. **D71**, 071103 (2005).
3. D. Acosta *et al.* [CDF II Collaboration], Phys. Rev. Lett. **93**, 072001 (2004).
4. V.M. Abazov *et al.* [D0 Collaboration], Phys. Rev. Lett. **93**, 162002 (2004).
5. B. Aubert *et al.* [BaBar Collaboration], Phys. Rev. **D71**, 031501 (2005).
6. S. Dobbs *et al.* [CLEO Collaboration], Phys. Rev. Lett. **94**, 032004 (2005).
7. *Review of Particle Physics*, 2008.
8. B. Aubert *et al.* [BaBar Collaboration], Phys. Rev. **D77**, 011102R (2008).
9. W.M. Yao *et al.*, [Particle Data Group], J. Phys. **G33**, 1 (2006).
10. B. Aubert *et al.* [BaBar Collaboration], Phys. Rev. Lett. **96**, 052002 (2006).
11. R. Chistov *et al.* [Belle Collaboration], Phys. Rev. Lett. **93**, 052803 (2004).
12. G. Gokhroo *et al.* [Belle Collaboration], Phys. Rev. Lett. **97**, 162002 (2006).
13. K. Abe *et al.* [Belle Collaboration], Belle report BELLE-CONF-0540, arXiv:hep-ex/0505037, paper no. LP-2005-175, contributed to the *XXII International Symposium on Lepton-Photon Interactions at High Energy*, Uppsala, Sweden, June 30 – July 5, 2005.
14. J.L. Rosner, Phys. Rev. **D70**, 094023 (2004).
15. K. Abe *et al.* [Belle Collaboration], Belle report BELLE-CONF-0541, arXiv:hep-ex/0505038, paper no. LP-2005-176, contributed to the *XXII International Symposium on Lepton-Photon Interactions at High Energy*, Uppsala, Sweden, June 30 – July 5, 2005.
16. A. Abulencia *et al.* [CDF Collaboration], Phys. Rev. Lett. **98**, 132002 (2007).
17. E.S. Swanson, presented at the *Conference on the Intersections of Particle and Nuclear Physics (CIPANP 2006)*, Rio Grande, Puerto Rico, May 30 – June 3, 2006, AIP Conf. Proc. **870**, edited by T. M. Liss, p. 349.
18. H. Marsiske, in *Proceedings of the Fourth International Conference on Flavor Physics and CP Violation (FPCP 2006)*, April 9 - 12, 2006 Vancouver, B.C., Canada, eConf **C060409**, 211 (2006) [arXiv:hep-ex/0605117].
19. I. Kravchenko, in *Proceedings of the Fourth International Conference on Flavor Physics and CP Violation (FPCP 2006)*, April 9 - 12, 2006 Vancouver, B.C., Canada, eConf **C060409**, 222 (2006) [arXiv:hep-ex/0605076].
20. W. Dunwoodie and V. Ziegler, Phys. Rev. Lett. **100**, 062006 (2008) [arXiv:0710.5191 [hep-ex]].
21. B. Aubert *et al.* [BaBar Collaboration], Phys. Rev. **D74**, 071101 (2006).
22. E.J. Eichten, K. Lane, and C. Quigg, Phys. Rev. **D73**, 014014 (2006) [Erratum-*ibid.* **D 73**, 079903 (2006)].
23. T. Barnes, S. Godfrey, and E.S. Swanson, Phys. Rev. **D72**, 054026 (2005).
24. D. Ebert, R.N. Faustov, and V.O. Galkin, Phys. Lett. **B634**, 214 (2006).
25. F.E. Close and P.R. Page, Phys. Lett. **B578**, 119 (2004); N.A. Tornqvist, Phys. Lett. **B590**, 209 (2004); E.S. Swanson, Phys. Lett. **B588**, 189 (2004); *ibid.* **598**, 197 (2004).
26. B. Aubert *et al.* [BABAR Collaboration], Phys. Rev. Lett. **93**, 041801 (2004).
27. C. Cawlfeld *et al.* [CLEO Collaboration], Phys. Rev. Lett. **98**, 092002 (2007).
28. S. Uehara *et al.* [Belle Collaboration], Phys. Rev. Lett. **96**, 082003 (2006).
29. T. Barnes, S. Godfrey, and E.S. Swanson [23] obtain similar results when the 2^3P_2 mass is rescaled to 3930 MeV. See E. Swanson, AIP Conf. Proc. **814**, 203 (2006) [Int. J. Mod. Phys. A **21**, 733 (2006)].
30. T. Barnes, Oak Ridge National Laboratory Report No. ORNL-CCIP-92-05; Invited paper at *Int. Workshop on Photon-Photon Collisions*, La Jolla, CA, March 22 – 26, 1992.
31. K. Abe *et al.* [Belle Collaboration], Phys. Rev. Lett. **98**, 082001 (2007).
32. T. Barnes, Int. J. Mod. Phys. **A21**, 5583 (2006).
33. P. Pakhlov *et al.* [Belle Collaboration], Phys. Rev. Lett. **100**, 202001 (2008).
34. S.-K. Choi *et al.* [Belle Collaboration], Phys. Rev. Lett. **94**, 182002 (2005).

See key on page 373

Meson Particle Listings

New charmonium-like states, X(3872)

35. B. Aubert *et al.* [BaBar Collaboration], arXiv:0711.2047 [hep-ex].

36. H. Severini *et al.* [CLEO Collaboration], Phys. Rev. Lett. **92**, 222002 (2004).

37. B. Aubert *et al.* [BaBar Collaboration], Phys. Rev. Lett. **95**, 142001 (2005).

38. Q. He *et al.* [CLEO Collaboration], Phys. Rev. **D74**, 091104 (2006).

39. C.-Z. Yuan *et al.* [Belle Collaboration], Phys. Rev. Lett. **99**, 182004 (2007).

40. B. Aubert *et al.* [BABAR Collaboration], Phys. Rev. **D73**, 011101 (2006).

41. T.E. Coan *et al.* [CLEO Collaboration], Phys. Rev. Lett. **96**, 162003 (2006).

42. B. Aubert *et al.* [BABAR Collaboration], Phys. Rev. **D73**, 012005 (2006).

43. B. Aubert *et al.* [BABAR Collaboration], Phys. Rev. **D76**, 111105 (2007).

44. B. Aubert *et al.* [BABAR Collaboration], Phys. Rev. **D76**, 012008 (2007).

45. B. Aubert *et al.* [BABAR Collaboration], Phys. Rev. **D77**, 092002 (2008).

46. C.-Z. Yuan *et al.* [Belle Collaboration], Phys. Rev. **D77**, 011105 (2008).

47. F.J. Llanes-Estrada, Phys. Rev. **D72**, 031503 (2005).

48. L. Maiani *et al.*, Phys. Rev. **D72**, 031502 (2005).

49. S.L. Zhu, Phys. Lett. **B625**, 212 (2005).

50. F.E. Close and P.R. Page, Phys. Lett. **B628**, 215 (2005).

51. E. Kou and O. Pène, Phys. Lett. **B631**, 164 (2005).

52. Yu.S. Kalashnikova and A.V. Nefediev, Phys. Rev. **D77**, 054025 (2008).

53. C. Quigg and J.L. Rosner, Phys. Lett. **B71**, 153 (1977).

54. See, for example, T. Barnes, F.E. Close, and E.S. Swanson, Phys. Rev. **D52**, 5242 (1995).

55. P. Lacock *et al.* [UKQCD Collaboration], Phys. Lett. **B401**, 308 (1997).

56. C. McNeile, C. Michael, and P. Penanen [UKQCD Collaboration], Phys. Rev. **D65**, 094505 (2002).

57. J.L. Rosner, Phys. Rev. **D74**, 076006 (2006).

58. X. Liao and T. Manke, Columbia University Report No. CU-TP-1063, arXiv:hep-lat/0210030.

59. B. Aubert *et al.* [BaBar Collaboration], Phys. Rev. Lett. **98**, 212001 (2007).

60. X.-L. Wang *et al.* [Belle Collaboration], Phys. Rev. Lett. **99**, 142002 (2007).

61. Z. Q. Liu, X.S. Qin, and C.Z. Yuan, arXiv:0805.3560 [hep-ex].

62. G.-J. Ding, J.-J. Zhu, and M.-L. Yan, Phys. Rev. **D77**, 014022 (2008).

63. S.-K. Choi *et al.* [Belle Collaboration], Phys. Rev. Lett. **100**, 142001 (2008).

64. J.L. Rosner, Phys. Rev. **D76**, 114002 (2007).

65. X. Liu *et al.*, Phys. Rev. **D77**, 034003 (2008).

66. S.-H. Lee *et al.*, Phys. Lett. **B661**, 28 (2008).

X(3872)

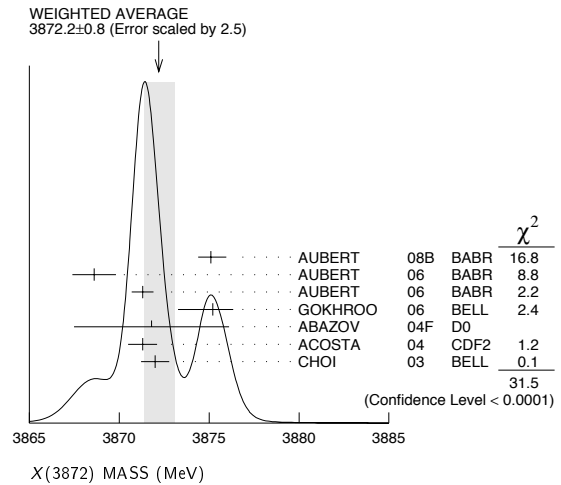
$$J^G(J^{PC}) = 0^?(?^{?+})$$

Seen by CHOI 03 in $B \rightarrow K \pi^+ \pi^- J/\psi(1S)$ decays as a narrow peak in the invariant mass distribution of the $\pi^+ \pi^- J/\psi(1S)$ final state, but not seen in the $\gamma \chi_{c1}$ final state of these decays. Possibly absent in the invariant mass spectrum of the final state $\pi^+ \pi^- J/\psi(1S)$ in $e^+ e^-$ collisions. Interpretation as a 1^{--} charmonium state not favored. Isovector hypothesis excluded by AUBERT 05B. A helicity amplitude analysis of the $X(3872) \rightarrow J/\psi \pi^+ \pi^-$ decay gives two possible J^{PC} assignments: $J^{PC} = 1^{++}$ and 2^{--} (ABULENCIA 07E).

X(3872) MASS

VALUE (MeV)	EVTs	DOCUMENT ID	TECN	COMMENT
3872.2 ± 0.8 OUR AVERAGE		Error includes scale factor of 2.5. See the ideogram below.		
3875.1 ^{+0.7} _{-0.5} ± 0.5	33 ± 6	¹ AUBERT	08B BABR	$B \rightarrow \bar{D}^{*0} D^0 K$
3868.6 ± 1.2 ± 0.2	8	² AUBERT	06 BABR	$B^0 \rightarrow K_S^0 J/\psi \pi^+ \pi^-$
3871.3 ± 0.6 ± 0.1	61	² AUBERT	06 BABR	$B^- \rightarrow K^- J/\psi \pi^+ \pi^-$
3875.2 ± 0.7 ^{+0.9} _{-1.8}	24 ± 6	¹ GOKHROO	06 BELL	$B \rightarrow D^0 \bar{D}^0 \pi^0 K$
3871.8 ± 3.1 ± 3.0	522	^{3,4} ABAZOV	04F D0	$\rho \bar{p} \rightarrow J/\psi \pi^+ \pi^- X$
3871.3 ± 0.7 ± 0.4	730	⁴ ACOSTA	04 CDF2	$\rho \bar{p} \rightarrow J/\psi \pi^+ \pi^- X$
3872.0 ± 0.6 ± 0.5	36	CHOI	03 BELL	$B \rightarrow K \pi^+ \pi^- J/\psi$
••• We do not use the following data for averages, fits, limits, etc. •••				
3873.4 ± 1.4	25	⁵ AUBERT	05R BABR	$B^+ \rightarrow K^+ J/\psi \pi^+ \pi^-$
3836 ± 13	58	^{4,6} ANTONIAZZI	94 E705	$300 \pi^+ \pi^- \text{Li}^- \rightarrow J/\psi \pi^+ \pi^- X$

¹ May not necessarily be the same state as that observed in the $J/\psi \pi^+ \pi^-$ mode.
² Calculated from the corresponding $m_{X(3872)} - m_{\psi(2S)}$ using $m_{\psi(2S)} = 3686.093$ MeV.
³ Calculated from the corresponding $m_{X(3872)} - m_{J/\psi}$ using $m_{J/\psi} = 3096.916$ MeV.
⁴ Width consistent with detector resolution.
⁵ Calculated from the corresponding $m_{X(3872)\pm} - m_{\psi(2S)}$ using $m_{\psi(2S)} = 3685.96$ MeV. Superseded by AUBERT 06.
⁶ A lower mass value can be due to an incorrect momentum scale for soft pions.



$m_{X(3872)\pm} - m_{J/\psi}$

VALUE (MeV)	EVTs	DOCUMENT ID	TECN	COMMENT
774.9 ± 3.1 ± 3.0	522	ABAZOV	04F D0	$\rho \bar{p} \rightarrow J/\psi \pi^+ \pi^- X$

$m_{X(3872)\pm} - m_{\psi(2S)}$

VALUE (MeV)	EVTs	DOCUMENT ID	TECN	COMMENT
••• We do not use the following data for averages, fits, limits, etc. •••				
187.4 ± 1.4	25	⁷ AUBERT	05R BABR	$B^+ \rightarrow K^+ J/\psi \pi^+ \pi^-$
⁷ Superseded by AUBERT 06.				

X(3872) WIDTH

VALUE (MeV)	CL%	EVTs	DOCUMENT ID	TECN	COMMENT
3.0^{+1.9}_{-1.4} ± 0.9		33 ± 6	⁸ AUBERT	08B BABR	$B \rightarrow \bar{D}^{*0} D^0 K$
••• We do not use the following data for averages, fits, limits, etc. •••					
<4.1	90	69	AUBERT	06 BABR	$B \rightarrow K \pi^+ \pi^- J/\psi$
<2.3	90	36	CHOI	03 BELL	$B \rightarrow K \pi^+ \pi^- J/\psi$

Meson Particle Listings

X(3872)

⁸ May not necessarily be the same state as that observed in the $J/\psi\pi^+\pi^-$ mode.

X(3872) DECAY MODES

Mode	Fraction (Γ_i/Γ)
Γ_1 e^+e^-	
Γ_2 $\pi^+\pi^- J/\psi(1S)$	seen
Γ_3 $\rho^0 J/\psi(1S)$	seen
Γ_4 $\gamma\gamma$	
Γ_5 $D^0\bar{D}^0$	not seen
Γ_6 D^+D^-	not seen
Γ_7 $D^0\bar{D}^0\pi^0$	seen
Γ_8 γX_{c1}	
Γ_9 $\eta J/\psi$	
Γ_{10} $\gamma J/\psi$	

X(3872) PARTIAL WIDTHS

$\Gamma(e^+e^-)$		Γ_1	
VALUE (keV)	CL%	DOCUMENT ID	TECN COMMENT
<0.28	90	⁹ YUAN	04 RVUE $e^+e^- \rightarrow \pi^+\pi^- J/\psi$

• • • We do not use the following data for averages, fits, limits, etc. • • •

⁹ Using BAI 98E data on $e^+e^- \rightarrow \pi^+\pi^-\ell^+\ell^-$. Assuming that $\Gamma(\pi^+\pi^- J/\psi)$ of X(3872) is the same as that of $\psi(2S)$ (85.4 keV).

X(3872) $\Gamma(i)\Gamma(e^+e^-)/\Gamma(\text{total})$

$\Gamma(\pi^+\pi^- J/\psi(1S)) \times \Gamma(e^+e^-)/\Gamma_{\text{total}}$		$\Gamma_2\Gamma_1/\Gamma$	
VALUE (eV)	CL%	DOCUMENT ID	TECN COMMENT
<6.2	90	^{10,11} AUBERT	05D BABR $10.6 e^+e^- \rightarrow K^+K^-\pi^+\pi^-\gamma$

• • • We do not use the following data for averages, fits, limits, etc. • • •

VALUE	CL%	DOCUMENT ID	TECN COMMENT
<8.3	90	¹¹ DOBBS	05 CLE3 $e^+e^- \rightarrow \pi^+\pi^- J/\psi$
<10	90	¹² YUAN	04 RVUE $e^+e^- \rightarrow \pi^+\pi^- J/\psi$

¹⁰ Using $B(X(3872) \rightarrow J/\psi\pi^+\pi^-) \cdot B(J/\psi \rightarrow \mu^+\mu^-) \cdot \Gamma(X(3872) \rightarrow e^+e^-) < 3.7$ eV from AUBERT 05D and $B(J/\psi \rightarrow \mu^+\mu^-) = 0.0588 \pm 0.0010$ from the PDG 04.

¹¹ Assuming X(3872) has $J^{PC} = 1^{--}$.

¹² Using BAI 98E data on $e^+e^- \rightarrow \pi^+\pi^-\ell^+\ell^-$. From theoretical calculation of the production cross section and using $B(J/\psi \rightarrow \mu^+\mu^-) = (5.88 \pm 0.10)\%$.

X(3872) $\Gamma(i)\Gamma(\gamma\gamma)/\Gamma(\text{total})$

$\Gamma(\gamma\gamma) \times \Gamma(\pi^+\pi^- J/\psi(1S))/\Gamma_{\text{total}}$		$\Gamma_4\Gamma_2/\Gamma$	
VALUE (eV)	CL%	DOCUMENT ID	TECN COMMENT
<12.9	90	¹³ DOBBS	05 CLE3 $e^+e^- \rightarrow \pi^+\pi^- J/\psi\gamma$

¹³ Assuming X(3872) has positive C parity and spin 0.

X(3872) BRANCHING RATIOS

$\Gamma(\pi^+\pi^- J/\psi(1S))/\Gamma_{\text{total}}$		Γ_2/Γ	
VALUE	CL%	DOCUMENT ID	TECN COMMENT
>0.042	90	^{14,15} AUBERT	06E BABR $B^{\pm} \rightarrow K^{\pm} X_{c\bar{c}}$

¹⁴ Calculated by us using $B(B^{\pm} \rightarrow K^{\pm} X(3872)) < 3.2 \times 10^{-4}$ from AUBERT 06E and $B(B^{\pm} \rightarrow K^{\pm} X(3872)) \times B(X(3872) \rightarrow J/\psi\pi^+\pi^-) = (11.4 \pm 2.0) \times 10^{-6}$ from the 2006 Edition of this Review (PDG 06).

¹⁵ Decay proceeds via the $\rho^0 J/\psi$ (ABULENCIA 06B).

$\Gamma(D^0\bar{D}^0)/\Gamma(\pi^+\pi^- J/\psi(1S))$		Γ_5/Γ_2	
VALUE	CL%	DOCUMENT ID	TECN COMMENT
not seen		CHISTOV	04 BELL $B \rightarrow K D^0\bar{D}^0$

• • • We do not use the following data for averages, fits, limits, etc. • • •

$\Gamma(D^+D^-)/\Gamma(\pi^+\pi^- J/\psi(1S))$		Γ_6/Γ_2	
VALUE	CL%	DOCUMENT ID	TECN COMMENT
not seen		CHISTOV	04 BELL $B \rightarrow K D^+D^-$

• • • We do not use the following data for averages, fits, limits, etc. • • •

$\Gamma(D^0\bar{D}^0\pi^0)/\Gamma(\pi^+\pi^- J/\psi(1S))$		Γ_7/Γ_2	
VALUE	CL%	DOCUMENT ID	TECN COMMENT
seen		¹⁶ GOKHROO	06 BELL $B \rightarrow D^0\bar{D}^0\pi^0 K$

¹⁶ May not necessarily be the same state as that observed in the $J/\psi\pi^+\pi^-$ mode. Supersedes CHISTOV 04.

$\Gamma(\gamma X_{c1})/\Gamma(\pi^+\pi^- J/\psi(1S))$		Γ_8/Γ_2	
VALUE	CL%	DOCUMENT ID	TECN COMMENT
<0.89	90	CHOI	03 BELL $B \rightarrow K\pi^+\pi^- J/\psi$

$\Gamma(\eta J/\psi)/\Gamma(\pi^+\pi^- J/\psi(1S))$

VALUE	CL%	DOCUMENT ID	TECN COMMENT	Γ_9/Γ_2
<0.6	90	AUBERT	04Y BABR $B \rightarrow K\eta J/\psi$	

• • • We do not use the following data for averages, fits, limits, etc. • • •

$\Gamma(\gamma J/\psi)/\Gamma_{\text{total}}$

VALUE	CL%	DOCUMENT ID	TECN COMMENT	Γ_{10}/Γ
>0.010	19	¹⁷ AUBERT, BE	06M BABR $B^+ \rightarrow K^+ J/\psi\gamma$	

¹⁷ AUBERT, BE 06M reports $[B(X(3872) \rightarrow \gamma J/\psi)] \times [B(B^+ \rightarrow X(3872) K^+)] = (3.3 \pm 1.0 \pm 0.3) \times 10^{-6}$. We divide by our best value $B(B^+ \rightarrow X(3872) K^+) < 3.2 \times 10^{-4}$.

X(3872) REFERENCES

AUBERT	08B	PR D77 011102R	B. Aubert et al.	(BABAR Collab.)
ABULENCIA	07E	PRL 98 132002	A. Abulencia et al.	(CDF Collab.)
ABULENCIA	06B	PRL 96 102002	A. Abulencia et al.	(CDF Collab.)
AUBERT	06	PR D73 011101R	B. Aubert et al.	(BABAR Collab.)
AUBERT	06E	PRL 96 052002	B. Aubert et al.	(BABAR Collab.)
AUBERT, BE	06M	PR D74 071101R	B. Aubert et al.	(BABAR Collab.)
GOKHROO	06	PRL 97 162002	G. Gokhroo et al.	(BELLE Collab.)
PDG	06	JPG 33 1	W.-M. Yao et al.	(PDG Collab.)
AUBERT	05B	PR D71 031501R	B. Aubert et al.	(BABAR Collab.)
AUBERT	05D	PR D71 052001	B. Aubert et al.	(BABAR Collab.)
AUBERT	05R	PR D71 071103R	B. Aubert et al.	(BABAR Collab.)
DOBBS	05	PRL 94 032004	S. Dobbs et al.	(CLEO Collab.)
ABAZOV	04F	PRL 93 162002	V.M. Abazov et al.	(DO Collab.)
ACOSTA	04	PRL 93 072001	D. Acosta et al.	(CDF Collab.)
AUBERT	04Y	PRL 93 041801	B. Aubert et al.	(BABAR Collab.)
CHISTOV	04	PRL 93 051803	R. Chistov et al.	(BELLE Collab.)
PDG	04	PL B592 1	S. Eidelman et al.	
YUAN	04	PL B579 74	C.Z. Yuan et al.	
CHOI	03	PRL 91 262001	S.-K. Choi et al.	(BELLE Collab.)
BAI	98E	PR D57 3854	J.Z. Bai et al.	(BES Collab.)
ANTONIAZZI	94	PR D50 4258	L. Antoniazzi et al.	(E705 Collab.)

OTHER RELATED PAPERS

BRAATEN	08	PR D77 014029	E. Braaten, M. Lu	
CHAO	08	PL B661 348	K.-T. Chao	(BELLE Collab.)
CHOI	08	PRL 100 142001	S.-K. Choi et al.	
DING	08	PR D77 014033	G.-J. Ding, J.-J. Zhu, M.-L. Yan	
DUBYNSKIY	08	PR D77 014013	S. Dubynskiy, M.B. Voloshin	
DUNWOODIE	08	PRL 100 062006	W. Dunwoodie, V. Ziegler	
KALASHNIK...	08	PR D77 054025	Yu.S. Kalashnikova, A.V. Nefediev	
LEE	08	PL B661 28	S.H. Lee et al.	
LI	08	PR D77 054001	Y. Li, C.-D. Lu, W. Wang	
LIU	08A	PR D77 034003	X. Liu et al.	
YUAN	08	PR D77 011105R	C.Z. Yuan et al.	(BELLE Collab.)
BRAATEN	07	PR D76 054010	E. Braaten et al.	
BRAATEN	07A	PR D76 094028	E. Braaten, M. Lu	
CHIU	07	PL B646 95	T.-W. Chiu, T.-H. Hsieh	
COLANGELO	07	PL B650 166	P. Colangelo et al.	
FLEMING	07	PR D76 034006	S. Fleming et al.	
GAMERMANN	07	EPJ A33 119	D. Gamermann, E. Oset	
HANHART	07A	PR D76 034007	C. Hanhart et al.	
KONG	07	PL B657 192	Y. Kong, A. Zhang	
MAIANI	07B	PRL 99 182003	L. Maiani, A. Polosa	
MATHEUS	07	PR D75 014005	R. Matheus et al.	
MATHEUS	07A	PR D76 056005	R.D. Matheus	
MENG	07	PR D75 114002	C. Meng, K.-T. Chao	
ROSNER	07	PR D76 114002	J. Rosner	
VIJANDE	07	PR D76 094022	J. Vijande et al.	
VOLOSHIN	07	PR D76 014007	M.B. Voloshin	
ABD-EL-HADY	06	PR D73 073010	A. Abd-El-Hady	
ALFIKY	06	PL B640 238	M. Alfiky, F. Gabbiani, A.A. Petrov	(WAYN)
BRAATEN	06	PR D73 011501	E. Braaten	
BRIERE	06	PR D74 031106R	R.A. Briere et al.	(CLEO Collab.)
COAN	06A	PRL 96 182002	T.E. Coan et al.	(CLEO Collab.)
DUBYNSKIY	06	PR D74 094017	S. Dubynskiy, M. Voloshin	
EICHTEN	06	PR D73 014014	E.J. Eichten, K. Lane, C. Quigg	
HOGAASEN	06	PR D73 054013	H. Hogaasen et al.	
HOU	06	PR D74 017504	W.-S. Hou	
KARLINER	06	PL B638 221	M. Karliner, H.J. Lipkin	
NAVARRA	06	PL B639 272	F.S. Navarra, M. Nielsen	
ROSNER	06C	PR D74 076006	J.L. Rosner	
SWANSON	06	PRL 97 243	E.S. Swanson	(PITT)
VOLOSHIN	06	JMP A21 1239	M. Voloshin	
YUAN	06	PL B634 399	C.Z. Yuan, P. Wang, X.H. Mo	
BIGI	05	PR D72 114016	I. Bigi et al.	
BRAATEN	05	PR D72 014012	E. Braaten, M. Kusunoki	
BRAATEN	05A	PR D72 054022	E. Braaten, M. Kusunoki	
BRAATEN	05B	PR D71 074005	E. Braaten, M. Kusunoki	
BUGG	05	PR D71 016006	D. Bugg	
KALASHNIK...	05A	PR D72 034010	Yu.S. Kalashnikova	
KIM	05	PR D71 034025	T. Kim, P. Ko	
LI	05	PL B605 306	B.A. Li	
MAIANI	05	PR D71 014028	L. Maiani et al.	
SETH	05	PL B612 1	K.K. Seth	
SUZUKI	05	PR D72 114013	M. Suzuki	
BARNES	04	PR D69 054008	T. Barnes, S. Godfrey	
BRAATEN	04	PR D69 074005	E. Braaten et al.	
BRAATEN	04A	PR D69 114012	E. Braaten, M. Kusunoki	
BRAATEN	04B	PRL 93 162001	E. Braaten, M. Kusunoki, S. Nussinov	
BUGG	04B	PL B598 8	D.V. Bugg	
CLOSE	04	PL B578 119	F.E. Close, P.R. Page	
EICHTEN	04	PR D69 094019	E. Eichten, K. Lane, C. Quigg	
PAKVASA	04	PL B579 67	S. Pakvasa, M. Suzuki	
ROSNER	04	PR D70 094023	J.L. Rosner	
SWANSON	04A	PL B588 189	E. Swanson	
SWANSON	04B	PL B598 197	E. Swanson	
TORNQVIST	04	PL B590 209	N. Tornqvist	
VOLOSHIN	04	PL B579 316	M.B. Voloshin	
VOLOSHIN	04A	PL B604 69	M.B. Voloshin	
WONG	04	PR C69 055202	C. Wong	
BAI	98E	PR D57 3854	J.Z. Bai et al.	(BES Collab.)

See key on page 373

Meson Particle Listings

 $\chi_{c2}(2P)$, $X(3940)$, $X(3945)$ **$\chi_{c2}(2P)$**

$$I^G(J^{PC}) = 0^+(2^{++})$$

OMITTED FROM SUMMARY TABLE

 $\chi_{c2}(2P)$ MASS

VALUE (MeV)	EVTS	DOCUMENT ID	TECN	COMMENT
3929 ± 5 ± 2	64	UEHARA 06	BELL	10.6 $e^+e^- \rightarrow e^+e^-D\bar{D}$

 $\chi_{c2}(2P)$ WIDTH

VALUE (MeV)	EVTS	DOCUMENT ID	TECN	COMMENT
29 ± 10 ± 2	64	UEHARA 06	BELL	10.6 $e^+e^- \rightarrow e^+e^-D\bar{D}$

 $\chi_{c2}(2P)$ DECAY MODES

Mode	Fraction (Γ_i/Γ)
Γ_1 $\gamma\gamma$	
Γ_2 $D\bar{D}$	
Γ_3 D^+D^-	
Γ_4 $D^0\bar{D}^0$	

 $\chi_{c2}(2P)$ PARTIAL WIDTHS $\chi_{c2}(2P)$ $\Gamma(\gamma\gamma)\Gamma(i)/\Gamma(\text{total})$

$\Gamma(\gamma\gamma) \times \Gamma(D\bar{D})/\Gamma_{\text{total}}$	VALUE (keV)	EVTS	DOCUMENT ID	TECN	COMMENT	$\Gamma_1\Gamma_2/\Gamma$
0.18 ± 0.05 ± 0.03	64	¹ UEHARA 06	BELL	10.6 $e^+e^- \rightarrow e^+e^-D\bar{D}$		

¹ Assuming $B(D^+D^-) = 0.89 B(D^0\bar{D}^0)$. $\chi_{c2}(2P)$ BRANCHING RATIOS

$\Gamma(D^+D^-)/\Gamma(D^0\bar{D}^0)$	VALUE	EVTS	DOCUMENT ID	TECN	COMMENT	Γ_3/Γ_4
0.74 ± 0.43 ± 0.16	64	UEHARA 06	BELL	10.6 $e^+e^- \rightarrow e^+e^-D\bar{D}$		

 $\chi_{c2}(2P)$ REFERENCES

UEHARA 06 PRL 96 082003 S. Uehara et al. (BELLE Collab.)

OTHER RELATED PAPERS

BUISSERET 07 PR C76 025206 F. Buisseret
 EICHTEN 06 PR D73 014014 E.J. Eichten, K. Lane, C. Quigg
 SWANSON 06 PRPL 429 243 E.S. Swanson (PITT)

 $X(3940)$

$$I^G(J^{PC}) = ?^?(?^{??})$$

OMITTED FROM SUMMARY TABLE

Reported by ABE 07, observed in $e^+e^- \rightarrow J/\psi X$. $X(3940)$ MASS

VALUE (MeV)	EVTS	DOCUMENT ID	TECN	COMMENT
3943 ± 6 ± 6	25	¹ ABE 07	BELL	$e^+e^- \rightarrow J/\psi X$
3936 ± 14	266	² ABE 07	BELL	$e^+e^- \rightarrow J/\psi(c\bar{c})$

¹ From a fit to $D^{*+}D^-$ and $D^{*0}\bar{D}^0$ events.² From the inclusive fit. Not independent of the exclusive measurement by ABE 07. $X(3940)$ WIDTH

VALUE (MeV)	CL%	EVTS	DOCUMENT ID	TECN	COMMENT
<52	90	25	ABE 07	BELL	$e^+e^- \rightarrow J/\psi X$

 $X(3940)$ DECAY MODES

Mode	Fraction (Γ_i/Γ)	Confidence level
Γ_1 $D\bar{D}^*$	>45 %	90%
Γ_2 $D\bar{D}$	<41 %	90%
Γ_3 $J/\psi\omega$	<26 %	90%

 $X(3940)$ BRANCHING RATIOS

$\Gamma(D\bar{D}^*)/\Gamma_{\text{total}}$	VALUE	CL%	EVTS	DOCUMENT ID	TECN	COMMENT	Γ_1/Γ
>0.45	90	25	³ ABE 07	BELL	$e^+e^- \rightarrow J/\psi X$		

³ For $X(3940)$ decaying to final states with more than two tracks.

$\Gamma(D\bar{D})/\Gamma_{\text{total}}$	VALUE	CL%	EVTS	DOCUMENT ID	TECN	COMMENT	Γ_2/Γ
<0.41	90	⁴ ABE 07	BELL	$e^+e^- \rightarrow J/\psi X$			

⁴ For $X(3940)$ decaying to final states with more than two tracks.

$\Gamma(J/\psi\omega)/\Gamma_{\text{total}}$	VALUE	CL%	EVTS	DOCUMENT ID	TECN	COMMENT	Γ_3/Γ
<0.26	90	⁵ ABE 07	BELL	$e^+e^- \rightarrow J/\psi X$			

⁵ For $X(3940)$ decaying to final states with more than two tracks. $X(3940)$ REFERENCES

ABE 07 PRL 98 082001 K. Abe et al. (BELLE Collab.)

OTHER RELATED PAPERS

BUISSERET 07 PR C76 025206 F. Buisseret

 $X(3945)$

$$I^G(J^{PC}) = ?^?(?^{??})$$

OMITTED FROM SUMMARY TABLE

Quantum numbers are not established. Seen by CHOI 05 in $B \rightarrow K\omega J/\psi$ decays as a threshold enhancement in the invariant mass distribution of the $\omega J/\psi$. $X(3945)$ MASS

VALUE (MeV)	EVTS	DOCUMENT ID	TECN	COMMENT
3943 ± 11 ± 13	58 ± 11	¹ CHOI 05	BELL	$B \rightarrow K\omega J/\psi$

¹ $\omega J/\psi$ threshold enhancement fitted as an S-wave Breit-Wigner resonance. $X(3945)$ WIDTH

VALUE (MeV)	EVTS	DOCUMENT ID	TECN	COMMENT
87 ± 22 ± 26	58 ± 11	² CHOI 05	BELL	$B \rightarrow K\omega J/\psi$

² $\omega J/\psi$ threshold enhancement fitted as an S-wave Breit-Wigner resonance. $X(3945)$ DECAY MODES

Mode	Fraction (Γ_i/Γ)
Γ_1 $\omega J/\psi$	seen

 $X(3945)$ REFERENCES

CHOI 05 PRL 94 182002 S.-K. Choi et al. (BELLE Collab.)

OTHER RELATED PAPERS

BUISSERET 07 PR C76 025206 F. Buisseret
 SWANSON 06 PRPL 429 243 E.S. Swanson (PITT)
 VANBEVEREN 06A PR D74 037501 E. van Beberen et al.

Meson Particle Listings

 $\psi(4040)$ $\psi(4040)$

$$J^G(J^{PC}) = 0^-(1^{--})$$

 $\psi(4040)$ MASS

VALUE (MeV)	DOCUMENT ID	TECN	COMMENT
4039 ± 1 OUR ESTIMATE			
4039.6 ± 4.3	¹ ABLIKIM	08D	BES2 $e^+e^- \rightarrow$ hadrons
••• We do not use the following data for averages, fits, limits, etc. •••			
4037 ± 2	² SETH	05A	RVUE $e^+e^- \rightarrow$ hadrons
4040 ± 1	³ SETH	05A	RVUE $e^+e^- \rightarrow$ hadrons
4040 ± 10	BRANDELIK	78C	DASP e^+e^-

¹ Reanalysis of data presented in BAI 02c. From a global fit over the center-of-mass energy region 3.7–5.0 GeV covering the $\psi(3770)$, $\psi(4040)$, $\psi(4160)$, and $\psi(4415)$ resonances. Phase angle fixed in the fit to $\delta = (130 \pm 46)^\circ$.

² From a fit to Crystal Ball (OSTERHELD 86) data.

³ From a fit to BES (BAI 02c) data.

 $\psi(4040)$ WIDTH

VALUE (MeV)	DOCUMENT ID	TECN	COMMENT
80 ± 10 OUR ESTIMATE			
84.5 ± 12.3	⁴ ABLIKIM	08D	BES2 $e^+e^- \rightarrow$ hadrons
••• We do not use the following data for averages, fits, limits, etc. •••			
85 ± 10	⁵ SETH	05A	RVUE $e^+e^- \rightarrow$ hadrons
89 ± 6	⁶ SETH	05A	RVUE $e^+e^- \rightarrow$ hadrons
52 ± 10	BRANDELIK	78C	DASP e^+e^-

⁴ Reanalysis of data presented in BAI 02c. From a global fit over the center-of-mass energy region 3.7–5.0 GeV covering the $\psi(3770)$, $\psi(4040)$, $\psi(4160)$, and $\psi(4415)$ resonances. Phase angle fixed in the fit to $\delta = (130 \pm 46)^\circ$.

⁵ From a fit to Crystal Ball (OSTERHELD 86) data.

⁶ From a fit to BES (BAI 02c) data.

 $\psi(4040)$ DECAY MODES

Mode	Fraction (Γ_i/Γ)	Confidence level
Γ_1 e^+e^-	$(1.07 \pm 0.16) \times 10^{-5}$	
Γ_2 $D^0\bar{D}^0$	seen	
Γ_3 $D^*(2007)^0\bar{D}^0 + c.c.$	seen	
Γ_4 $D^*(2007)^0\bar{D}^*(2007)^0$	seen	
Γ_5 $J/\psi(1S)$ hadrons		
Γ_6 $J/\psi\pi^+\pi^-$	< 4	$\times 10^{-3}$ 90%
Γ_7 $J/\psi\pi^0\pi^0$	< 2	$\times 10^{-3}$ 90%
Γ_8 $J/\psi\eta$	< 7	$\times 10^{-3}$ 90%
Γ_9 $J/\psi\pi^0$	< 2	$\times 10^{-3}$ 90%
Γ_{10} $J/\psi\pi^+\pi^-\pi^0$	< 2	$\times 10^{-3}$ 90%
Γ_{11} $\chi_{c1}\gamma$	< 1.1	% 90%
Γ_{12} $\chi_{c2}\gamma$	< 1.7	% 90%
Γ_{13} $\chi_{c1}\pi^+\pi^-\pi^0$	< 1.1	% 90%
Γ_{14} $\chi_{c2}\pi^+\pi^-\pi^0$	< 3.2	% 90%
Γ_{15} $\phi\pi^+\pi^-$	< 3	$\times 10^{-3}$ 90%
Γ_{16} $\mu^+\mu^-$		

 $\psi(4040)$ PARTIAL WIDTHS

$\Gamma(e^+e^-)$	DOCUMENT ID	TECN	COMMENT	Γ_1
0.83 ± 0.07 OUR ESTIMATE				
0.83 ± 0.20	⁷ ABLIKIM	08D	BES2 $e^+e^- \rightarrow$ hadrons	
••• We do not use the following data for averages, fits, limits, etc. •••				
0.88 ± 0.11	⁸ SETH	05A	RVUE $e^+e^- \rightarrow$ hadrons	
0.91 ± 0.13	⁹ SETH	05A	RVUE $e^+e^- \rightarrow$ hadrons	
0.75 ± 0.15	BRANDELIK	78C	DASP e^+e^-	

⁷ Reanalysis of data presented in BAI 02c. From a global fit over the center-of-mass energy region 3.7–5.0 GeV covering the $\psi(3770)$, $\psi(4040)$, $\psi(4160)$, and $\psi(4415)$ resonances. Phase angle fixed in the fit to $\delta = (130 \pm 46)^\circ$.

⁸ From a fit to Crystal Ball (OSTERHELD 86) data.

⁹ From a fit to BES (BAI 02c) data.

 $\psi(4040)$ BRANCHING RATIOS

$\Gamma(e^+e^-)/\Gamma_{\text{total}}$	DOCUMENT ID	TECN	COMMENT	Γ_1/Γ
0.83 ± 0.07				
••• We do not use the following data for averages, fits, limits, etc. •••				
~ 1.0	FELDMAN	77	MRK1 e^+e^-	

$\Gamma(D^0\bar{D}^0)/\Gamma(D^*(2007)^0\bar{D}^0 + c.c.)$	DOCUMENT ID	TECN	COMMENT	Γ_2/Γ_3
0.05 ± 0.03	¹⁰ GOLDHABER	77	MRK1 e^+e^-	

$\Gamma(D^*(2007)^0\bar{D}^*(2007)^0)/\Gamma(D^*(2007)^0\bar{D}^0 + c.c.)$	DOCUMENT ID	TECN	COMMENT	Γ_4/Γ_3
32.0 ± 12.0	¹⁰ GOLDHABER	77	MRK1 e^+e^-	

$\Gamma(J/\psi\pi^+\pi^-)/\Gamma_{\text{total}}$	DOCUMENT ID	TECN	COMMENT	Γ_6/Γ
< 4	COAN	06	CLEO 3.97–4.06 $e^+e^- \rightarrow$ hadrons	

$\Gamma(J/\psi\pi^0\pi^0)/\Gamma_{\text{total}}$	DOCUMENT ID	TECN	COMMENT	Γ_7/Γ
< 2	COAN	06	CLEO 3.97–4.06 $e^+e^- \rightarrow$ hadrons	

$\Gamma(J/\psi\eta)/\Gamma_{\text{total}}$	DOCUMENT ID	TECN	COMMENT	Γ_8/Γ
< 7	COAN	06	CLEO 3.97–4.06 $e^+e^- \rightarrow$ hadrons	

$\Gamma(J/\psi\pi^0)/\Gamma_{\text{total}}$	DOCUMENT ID	TECN	COMMENT	Γ_9/Γ
< 2	COAN	06	CLEO 3.97–4.06 $e^+e^- \rightarrow$ hadrons	

$\Gamma(J/\psi\pi^+\pi^-\pi^0)/\Gamma_{\text{total}}$	DOCUMENT ID	TECN	COMMENT	Γ_{10}/Γ
< 2	COAN	06	CLEO 3.97–4.06 $e^+e^- \rightarrow$ hadrons	

$\Gamma(\chi_{c1}\gamma)/\Gamma_{\text{total}}$	DOCUMENT ID	TECN	COMMENT	Γ_{11}/Γ
< 11	COAN	06	CLEO 3.97–4.06 $e^+e^- \rightarrow$ hadrons	

$\Gamma(\chi_{c2}\gamma)/\Gamma_{\text{total}}$	DOCUMENT ID	TECN	COMMENT	Γ_{12}/Γ
< 17	COAN	06	CLEO 3.97–4.06 $e^+e^- \rightarrow$ hadrons	

$\Gamma(\chi_{c1}\pi^+\pi^-\pi^0)/\Gamma_{\text{total}}$	DOCUMENT ID	TECN	COMMENT	Γ_{13}/Γ
< 11	COAN	06	CLEO 3.97–4.06 $e^+e^- \rightarrow$ hadrons	

$\Gamma(\chi_{c2}\pi^+\pi^-\pi^0)/\Gamma_{\text{total}}$	DOCUMENT ID	TECN	COMMENT	Γ_{14}/Γ
< 32	COAN	06	CLEO 3.97–4.06 $e^+e^- \rightarrow$ hadrons	

$\Gamma(\phi\pi^+\pi^-)/\Gamma_{\text{total}}$	DOCUMENT ID	TECN	COMMENT	Γ_{15}/Γ
< 3	COAN	06	CLEO 3.97–4.06 $e^+e^- \rightarrow$ hadrons	

¹⁰ Phase-space factor (p^3) explicitly removed.

 $\psi(4040)$ REFERENCES

ABLIKIM	08D	PL B660 315	M. Ablikim <i>et al.</i>	(BES Collab.)
COAN	06	PRL 96 162003	T.E. Coan <i>et al.</i>	(CLEO Collab.)
SETH	05A	PR D72 017501	K.K. Seth	
BAI	02C	PRL 88 101802	J.Z. Bai <i>et al.</i>	(BES Collab.)
OSTERHELD	86	SLAC-PUB-4160	A. Osterheld <i>et al.</i>	(SLAC Crystal Ball Collab.)
BRANDELIK	78C	PL 76B 361	R. Brandelik <i>et al.</i>	(DASP Collab.)
		Also	R. Brandelik <i>et al.</i>	(DASP Collab.)
FELDMAN	77	PRPL 33C 285	G.J. Feldman, M.L. Perl	(LBL, SLAC)
GOLDHABER	77	PL 69B 503	G. Goldhaber <i>et al.</i>	(Mark I Collab.)

OTHER RELATED PAPERS

PAKHOVA	08	PR D77 011103R	G. Pakhlova <i>et al.</i>	(BELLE Collab.)
PAKHOVA	07	PRL 98 092001	G. Pakhlova <i>et al.</i>	(BELLE Collab.)
DUBYSNKIY	06A	MPL A21 2779	S. Dubynskiy, M.B. Voloshin	
HEIKKILA	84	PR D29 110	K. Heikkilä, N.A. Tornqvist, S. Ono	(HELS, AACHT)
ONO	84	ZPHY C26 307	S. Ono	(ORSAY)
SIEGRIST	82	PR D26 969	J.L. Siegrist <i>et al.</i>	(SLAC, LBL)
AUGUSTIN	75	PRL 34 764	J.E. Augustin <i>et al.</i>	(SLAC, LBL)
BACCI	75	PL 58B 481	C. Bacci <i>et al.</i>	(ROMA, FRAS)
BOYARSKI	75B	PRL 34 762	A.M. Boyarski <i>et al.</i>	(SLAC, LBL)
ESPOSITO	75	PL 58B 478	B. Esposito <i>et al.</i>	(FRAS, NAPL, PADO+)

See key on page 373

Meson Particle Listings

$\psi(4160)$, $X(4260)$

$\psi(4160)$

$I^G(J^{PC}) = 0^-(1^{--})$

$\psi(4160)$ MASS

VALUE (MeV)	DOCUMENT ID	TECN	COMMENT
4191.7 ± 3 OUR ESTIMATE			
4191.7 ± 6.5	1 ABLIKIM	08D	BES2 $e^+e^- \rightarrow$ hadrons
4151 ± 4	2 SETH	05A	RVUE $e^+e^- \rightarrow$ hadrons
4155 ± 5	3 SETH	05A	RVUE $e^+e^- \rightarrow$ hadrons
4159 ± 20	BRANDELIK	78C	DASP e^+e^-

¹ Reanalysis of data presented in BAI 02c. From a global fit over the center-of-mass energy region 3.7–5.0 GeV covering the $\psi(3770)$, $\psi(4040)$, $\psi(4160)$, and $\psi(4415)$ resonances. Phase angle fixed in the fit to $\delta = (293 \pm 57)^\circ$.

² From a fit to Crystal Ball (OSTERHELD 86) data.

³ From a fit to BES (BAI 02c) data.

$\psi(4160)$ WIDTH

VALUE (MeV)	DOCUMENT ID	TECN	COMMENT
103 ± 8 OUR ESTIMATE			
71.8 ± 12.3	4 ABLIKIM	08D	BES2 $e^+e^- \rightarrow$ hadrons
107 ± 10	5 SETH	05A	RVUE $e^+e^- \rightarrow$ hadrons
107 ± 16	6 SETH	05A	RVUE $e^+e^- \rightarrow$ hadrons
78 ± 20	BRANDELIK	78C	DASP e^+e^-

⁴ Reanalysis of data presented in BAI 02c. From a global fit over the center-of-mass energy region 3.7–5.0 GeV covering the $\psi(3770)$, $\psi(4040)$, $\psi(4160)$, and $\psi(4415)$ resonances. Phase angle fixed in the fit to $\delta = (293 \pm 57)^\circ$.

⁵ From a fit to Crystal Ball (OSTERHELD 86) data.

⁶ From a fit to BES (BAI 02c) data.

$\psi(4160)$ DECAY MODES

Mode	Fraction (Γ_i/Γ)	Confidence level
Γ_1 e^+e^-	$(8.1 \pm 0.9) \times 10^{-6}$	
Γ_2 $J/\psi \pi^+ \pi^-$	$< 3 \times 10^{-3}$	90%
Γ_3 $J/\psi \pi^0 \pi^0$	$< 3 \times 10^{-3}$	90%
Γ_4 $J/\psi K^+ K^-$	$< 2 \times 10^{-3}$	90%
Γ_5 $J/\psi \eta$	$< 8 \times 10^{-3}$	90%
Γ_6 $J/\psi \pi^0$	$< 1 \times 10^{-3}$	90%
Γ_7 $J/\psi \eta'$	$< 5 \times 10^{-3}$	90%
Γ_8 $J/\psi \pi^+ \pi^- \pi^0$	$< 1 \times 10^{-3}$	90%
Γ_9 $\psi(2S) \pi^+ \pi^-$	$< 4 \times 10^{-3}$	90%
Γ_{10} $\chi_{c1} \gamma$	$< 7 \times 10^{-3}$	90%
Γ_{11} $\chi_{c2} \gamma$	< 1.3 %	90%
Γ_{12} $\chi_{c1} \pi^+ \pi^- \pi^0$	$< 2 \times 10^{-3}$	90%
Γ_{13} $\chi_{c2} \pi^+ \pi^- \pi^0$	$< 8 \times 10^{-3}$	90%
Γ_{14} $\phi \pi^+ \pi^-$	$< 2 \times 10^{-3}$	90%

$\psi(4160)$ PARTIAL WIDTHS

$\Gamma(e^+e^-)$	DOCUMENT ID	TECN	COMMENT	Γ_1
0.83 ± 0.07 OUR ESTIMATE				
0.48 ± 0.22	7 ABLIKIM	08D	BES2 $e^+e^- \rightarrow$ hadrons	
0.83 ± 0.08	8 SETH	05A	RVUE $e^+e^- \rightarrow$ hadrons	
0.84 ± 0.13	9 SETH	05A	RVUE $e^+e^- \rightarrow$ hadrons	
0.77 ± 0.23	BRANDELIK	78C	DASP e^+e^-	

⁷ Reanalysis of data presented in BAI 02c. From a global fit over the center-of-mass energy region 3.7–5.0 GeV covering the $\psi(3770)$, $\psi(4040)$, $\psi(4160)$, and $\psi(4415)$ resonances. Phase angle fixed in the fit to $\delta = (293 \pm 57)^\circ$.

⁸ From a fit to Crystal Ball (OSTERHELD 86) data.

⁹ From a fit to BES (BAI 02c) data.

$\psi(4160)$ BRANCHING RATIOS

$\Gamma(J/\psi \pi^+ \pi^-)/\Gamma_{total}$	DOCUMENT ID	TECN	COMMENT	Γ_2/Γ
< 3				
< 3	COAN	06	CLEO 4.12–4.2 $e^+e^- \rightarrow$ hadrons	
$\Gamma(J/\psi \pi^0 \pi^0)/\Gamma_{total}$	DOCUMENT ID	TECN	COMMENT	Γ_3/Γ
< 3				
< 3	COAN	06	CLEO 4.12–4.2 $e^+e^- \rightarrow$ hadrons	
$\Gamma(J/\psi K^+ K^-)/\Gamma_{total}$	DOCUMENT ID	TECN	COMMENT	Γ_4/Γ
< 2				
< 2	COAN	06	CLEO 4.12–4.2 $e^+e^- \rightarrow$ hadrons	

$\Gamma(J/\psi \eta)/\Gamma_{total}$	DOCUMENT ID	TECN	COMMENT	Γ_5/Γ
< 8				
< 8	COAN	06	CLEO 4.12–4.2 $e^+e^- \rightarrow$ hadrons	

$\Gamma(J/\psi \pi^0)/\Gamma_{total}$	DOCUMENT ID	TECN	COMMENT	Γ_6/Γ
< 1				
< 1	COAN	06	CLEO 4.12–4.2 $e^+e^- \rightarrow$ hadrons	

$\Gamma(J/\psi \eta')/\Gamma_{total}$	DOCUMENT ID	TECN	COMMENT	Γ_7/Γ
< 5				
< 5	COAN	06	CLEO 4.12–4.2 $e^+e^- \rightarrow$ hadrons	

$\Gamma(J/\psi \pi^+ \pi^- \pi^0)/\Gamma_{total}$	DOCUMENT ID	TECN	COMMENT	Γ_8/Γ
< 1				
< 1	COAN	06	CLEO 4.12–4.2 $e^+e^- \rightarrow$ hadrons	

$\Gamma(\psi(2S) \pi^+ \pi^-)/\Gamma_{total}$	DOCUMENT ID	TECN	COMMENT	Γ_9/Γ
< 4				
< 4	COAN	06	CLEO 4.12–4.2 $e^+e^- \rightarrow$ hadrons	

$\Gamma(\chi_{c1} \gamma)/\Gamma_{total}$	DOCUMENT ID	TECN	COMMENT	Γ_{10}/Γ
< 7				
< 7	COAN	06	CLEO 4.12–4.2 $e^+e^- \rightarrow$ hadrons	

$\Gamma(\chi_{c2} \gamma)/\Gamma_{total}$	DOCUMENT ID	TECN	COMMENT	Γ_{11}/Γ
< 13				
< 13	COAN	06	CLEO 4.12–4.2 $e^+e^- \rightarrow$ hadrons	

$\Gamma(\chi_{c1} \pi^+ \pi^- \pi^0)/\Gamma_{total}$	DOCUMENT ID	TECN	COMMENT	Γ_{12}/Γ
< 2				
< 2	COAN	06	CLEO 4.12–4.2 $e^+e^- \rightarrow$ hadrons	

$\Gamma(\chi_{c2} \pi^+ \pi^- \pi^0)/\Gamma_{total}$	DOCUMENT ID	TECN	COMMENT	Γ_{13}/Γ
< 8				
< 8	COAN	06	CLEO 4.12–4.2 $e^+e^- \rightarrow$ hadrons	

$\Gamma(\phi \pi^+ \pi^-)/\Gamma_{total}$	DOCUMENT ID	TECN	COMMENT	Γ_{14}/Γ
< 2				
< 2	COAN	06	CLEO 4.12–4.2 $e^+e^- \rightarrow$ hadrons	

$\psi(4160)$ REFERENCES

ABLIKIM	08D	PL B660 315	M. Ablikim <i>et al.</i>	(BES Collab.)
COAN	06	PRL 96 162003	T.E. Coan <i>et al.</i>	(CLEO Collab.)
SETH	05A	PR D72 017501	K.K. Seth	
BAI	02C	PRL 88 101802	J.Z. Bai <i>et al.</i>	(BES Collab.)
OSTERHELD	86	SLAC-PUB-4160	A. Osterheld <i>et al.</i>	(SLAC Crystal Ball Collab.)
BRANDELIK	78C	PL 76B 361	R. Brandelik <i>et al.</i>	(DASP Collab.)

OTHER RELATED PAPERS

PAKHLOVA	08	PR D77 011103R	G. Pakhlova <i>et al.</i>	(BELLE Collab.)
PAKHLOVA	07	PRL 98 092001	G. Pakhlova <i>et al.</i>	(BELLE Collab.)
IDDIR	98	PL B433 125	F. Ididir <i>et al.</i>	
ONO	84	ZPHY C26 307	S. Ono	(ORSAY)
BURMESTER	77	PL 66B 395	J. Burmester <i>et al.</i>	(DESY, HAMB, SIEG+)

$X(4260)$

$I^G(J^{PC}) = ?^?(1^{--})$

Seen in radiative return from e^+e^- collisions at $\sqrt{s} = 9.54\text{--}10.58$ GeV by AUBERT, B 05i, HE 06B, and YUAN 07, and in e^+e^- collisions at $\sqrt{s} \approx 4.26$ GeV by COAN 06. Possibly seen by AUBERT 06 in $B^- \rightarrow K^- \pi^+ \pi^- J/\psi$. See also the mini-review under the $X(3872)$. (See the index for the page number.)

$X(4260)$ MASS

VALUE (MeV)	EVTS	DOCUMENT ID	TECN	COMMENT
4263 ± 9 OUR AVERAGE				Error includes scale factor of 1.1.
4247 ± 12 ± 17/32		1 YUAN	07	BELL 10.58 $e^+e^- \rightarrow \gamma \pi^+ \pi^- J/\psi$
4284 ± 17 ± 4	13.6	HE	06B	CLEO 9.4–10.6 $e^+e^- \rightarrow \gamma \pi^+ \pi^- J/\psi$
4259 ± 8 ± 2/6	125	2 AUBERT, B	05i	BABR 10.58 $e^+e^- \rightarrow \gamma \pi^+ \pi^- J/\psi$

¹ From a two-resonance fit.

² From a single-resonance fit. Two interfering resonances are not excluded.

Meson Particle Listings

X(4260), X(4360)

X(4260) WIDTH

VALUE (MeV)	EVTS	DOCUMENT ID	TECN	COMMENT
95 ± 14 OUR AVERAGE				
108 ± 19 ± 10		³ YUAN	07 BELL	10.58 e ⁺ e ⁻ → γπ ⁺ π ⁻ J/ψ
73 ⁺³⁹ ₋₂₅ ± 5	13.6	HE	06B CLEO	9.4–10.6 e ⁺ e ⁻ → γπ ⁺ π ⁻ J/ψ
88 ± 23 ⁺⁶ ₋₄	125	⁴ AUBERT,B	05i BABR	10.58 e ⁺ e ⁻ → γπ ⁺ π ⁻ J/ψ
³ From a two-resonance fit. ⁴ From a single-resonance fit. Two interfering resonances are not excluded.				

X(4260) DECAY MODES

Mode	Fraction (Γ _i /Γ)
Γ ₁ e ⁺ e ⁻	
Γ ₂ J/ψπ ⁺ π ⁻	seen
Γ ₃ J/ψπ ⁰ π ⁰	[a] seen
Γ ₄ J/ψK ⁺ K ⁻	[a] seen
Γ ₅ J/ψη	[a] not seen
Γ ₆ J/ψπ ⁰	[a] not seen
Γ ₇ J/ψη'	[a] not seen
Γ ₈ J/ψπ ⁺ π ⁻ π ⁰	[a] not seen
Γ ₉ J/ψηη	[a] not seen
Γ ₁₀ ψ(2S)π ⁺ π ⁻	[a] not seen
Γ ₁₁ ψ(2S)η	[a] not seen
Γ ₁₂ χ _{c0} ω	[a] not seen
Γ ₁₃ χ _{c1} γ	[a] not seen
Γ ₁₄ χ _{c2} γ	[a] not seen
Γ ₁₅ χ _{c1} π ⁺ π ⁻ π ⁰	[a] not seen
Γ ₁₆ χ _{c2} π ⁺ π ⁻ π ⁰	[a] not seen
Γ ₁₇ φπ ⁺ π ⁻	[a] not seen
Γ ₁₈ φ ₀ (980) → φπ ⁺ π ⁻	
Γ ₁₉ D [±]	not seen
Γ ₂₀ p \bar{p}	
Γ ₂₁ K _S ⁰ K [±] π [∓]	
Γ ₂₂ K ⁺ K ⁻ π ⁰	

[a] See COAN 06 for details.

X(4260) Γ(i)Γ(e⁺e⁻)/Γ(total)

VALUE (eV)	EVTS	DOCUMENT ID	TECN	COMMENT
5.9^{+1.2}_{-0.9} OUR AVERAGE				
6.0 ± 1.2 ^{+4.7} _{-0.5}		⁵ YUAN	07 BELL	10.58 e ⁺ e ⁻ → γπ ⁺ π ⁻ J/ψ
8.9 ^{+3.9} _{-3.1} ± 1.8	8.1	HE	06B CLEO	9.4–10.6 e ⁺ e ⁻ → γπ ⁺ π ⁻ J/ψ
5.5 ± 1.0 ^{+0.8} _{-0.7}	125	⁶ AUBERT,B	05i BABR	10.58 e ⁺ e ⁻ → γπ ⁺ π ⁻ J/ψ
• • • We do not use the following data for averages, fits, limits, etc. • • •				
20.6 ± 2.3 ^{+9.1} _{-1.7}		⁷ YUAN	07 BELL	10.58 e ⁺ e ⁻ → γπ ⁺ π ⁻ J/ψ
⁵ Solution I of two equivalent solutions in a fit using two interfering resonances. ⁶ From a single-resonance fit. Two interfering resonances are not excluded. ⁷ Solution II of two equivalent solutions in a fit using two interfering resonances.				

Γ(J/ψK⁺K⁻) × Γ(e⁺e⁻)/Γ_{total}

VALUE (eV)	CL%	DOCUMENT ID	TECN	COMMENT
<1.2	90	⁸ YUAN	08 BELL	e ⁺ e ⁻ → γK ⁺ K ⁻ J/ψ
⁸ From a fit of the broad K ⁺ K ⁻ J/ψ enhancement including a coherent X(4260) amplitude with mass and width from YUAN 07.				

Γ(φπ⁺π⁻) × Γ(e⁺e⁻)/Γ_{total}

VALUE (eV)	CL%	DOCUMENT ID	TECN	COMMENT
<0.4	90	AUBERT,BE	06D BABR	10.6 e ⁺ e ⁻ → K ⁺ K ⁻ π ⁺ π ⁻ γ

Γ(φ₀(980) → φπ⁺π⁻) × Γ(e⁺e⁻)/Γ_{total}

VALUE (eV)	CL%	DOCUMENT ID	TECN	COMMENT
<0.28	90	⁹ AUBERT	07AK BABR	10.6 e ⁺ e ⁻ → π ⁺ π ⁻ K ⁺ K ⁻ γ
⁹ AUBERT 07AK reports [Γ(X(4260) → φ ₀ (980) → φπ ⁺ π ⁻) × Γ(X(4260) → e ⁺ e ⁻)/Γ _{total}] × [B(φ(1020) → K ⁺ K ⁻)] < 0.14 eV. We divide by our best value B(φ(1020) → K ⁺ K ⁻) = 0.492.				

Γ(K_S⁰ K[±]π[∓]) × Γ(e⁺e⁻)/Γ_{total}

VALUE (eV)	CL%	DOCUMENT ID	TECN	COMMENT
<0.5	90	AUBERT	08s BABR	10.6 e ⁺ e ⁻ → K _S ⁰ K [±] π [∓] γ

Γ(K⁺K⁻π⁰) × Γ(e⁺e⁻)/Γ_{total}

VALUE (eV)	CL%	DOCUMENT ID	TECN	COMMENT
<0.6	90	AUBERT	08s BABR	10.6 e ⁺ e ⁻ → K ⁺ K ⁻ π ⁰ γ

X(4260) BRANCHING RATIOS

Γ(p \bar{p})/Γ(J/ψπ⁺π⁻)

VALUE	CL%	DOCUMENT ID	COMMENT
<1.13	90	¹⁰ AUBERT	06B e ⁺ e ⁻ → p \bar{p} γ

Γ(D \bar{D})/Γ(J/ψπ⁺π⁻)

VALUE	CL%	DOCUMENT ID	TECN	COMMENT
<1.0	90	¹⁰ AUBERT	07BE BABR	e ⁺ e ⁻ → D \bar{D} γ
¹⁰ Using 4259 ± 10 MeV for the mass and 88 ± 24 MeV for the width of X(4260).				

X(4260) REFERENCES

AUBERT	08S	PR D77 092002	B. Aubert <i>et al.</i>	(BABAR Collab.)
YUAN	08	PR D77 011105R	C.Z. Yuan <i>et al.</i>	(BELLE Collab.)
AUBERT	07AK	PR D76 012008	B. Aubert <i>et al.</i>	(BABAR Collab.)
AUBERT	07BE	PR D76 111105R	B. Aubert <i>et al.</i>	(BABAR Collab.)
YUAN	07	PRL 99 182004	C.Z. Yuan <i>et al.</i>	(BELLE Collab.)
AUBERT	06	PR D73 011101R	B. Aubert <i>et al.</i>	(BABAR Collab.)
AUBERT	06B	PR D73 012005	B. Aubert <i>et al.</i>	(BABAR Collab.)
AUBERT,BE	06D	PR D74 091103R	B. Aubert <i>et al.</i>	(BABAR Collab.)
COAN	06	PRL 96 162003	T.E. Coan <i>et al.</i>	(CLEO Collab.)
HE	06B	PR D74 091104R	Q. He <i>et al.</i>	(CLEO Collab.)
AUBERT,B	05i	PRL 95 142001	B. Aubert <i>et al.</i>	(BABAR Collab.)

OTHER RELATED PAPERS

KALASHNIK...	08	PR D77 054025	Yu.S. Kalashnikova, A.V. Nefediev	
PAKHLOVA	08	PR D77 011103R	G. Pakhlova <i>et al.</i>	(BELLE Collab.)
PAKHLOVA	07	PRL 98 092001	G. Pakhlova <i>et al.</i>	(BELLE Collab.)
CHIU	06	PR D73 094510	T.-W. Chiu, T.-H. Hsieh	
HOU	06	PR D74 017504	W.-S. Hou	
MAO	06	PL B640 182	X.H. Mo <i>et al.</i>	
QIAO	06	PL B639 263	C. Qiao	
ROSNER	06C	PR D74 076006	J.L. Rosner	
SWANSON	06	PRPL 429 243	E.S. Swanson	(PITT)
YUAN	06	PL B634 399	C.Z. Yuan, P. Wang, X.H. Mo	
BIGI	05	PR D72 114016	I. Bigi <i>et al.</i>	
CLOSE	05A	PL B628 215	F.E. Close, P.R. Page	
KOU	05	PL B631 164	E. Kou	
LIU	05	PR D72 054023	X. Liu, X.Q. Zeng, X.Q. Li	
LLANES-EST...	05	PR D72 031503	F. Llanes-Estrada	
MAIANI	05A	PR D72 031502R	L. Maiani <i>et al.</i>	
ZHU	05	PL B625 212	S.-L. Zhu	

X(4360)

$$J^G(J^{PC}) = ?^?(1^- -)$$

OMITTED FROM SUMMARY TABLE

Seen in radiative return from e⁺e⁻ collisions at √s = 9.54–10.58 GeV by AUBERT 07S and WANG 07D. See also the review under the X(3872) particle listings. (See the index for the page number.)

X(4360) MASS

VALUE (MeV)	DOCUMENT ID	TECN	COMMENT
4361 ± 9 ± 9	¹ WANG	07D BELL	10.58 e ⁺ e ⁻ → γπ ⁺ π ⁻ ψ(2S)
• • • We do not use the following data for averages, fits, limits, etc. • • •			
4324 ± 24	² AUBERT	07s BABR	10.58 e ⁺ e ⁻ → γπ ⁺ π ⁻ ψ(2S)
¹ From a two-resonance fit. ² From a single-resonance fit. Systematic errors not estimated.			

X(4360) WIDTH

VALUE (MeV)	DOCUMENT ID	TECN	COMMENT
74 ± 15 ± 10	³ WANG	07D BELL	10.58 e ⁺ e ⁻ → γπ ⁺ π ⁻ ψ(2S)
• • • We do not use the following data for averages, fits, limits, etc. • • •			
172 ± 33	⁴ AUBERT	07s BABR	10.58 e ⁺ e ⁻ → γπ ⁺ π ⁻ ψ(2S)
³ From a two-resonance fit. ⁴ From a single-resonance fit. Systematic errors not estimated.			

X(4360) DECAY MODES

Mode	Fraction (Γ _i /Γ)
Γ ₁ e ⁺ e ⁻	
Γ ₂ ψ(2S)π ⁺ π ⁻	seen

Meson Particle Listings

X(4360), $\psi(4415)$

X(4360) $\Gamma(I)\Gamma(e^+e^-)/\Gamma(\text{total})$

$\Gamma(\psi(2S)\pi^+\pi^-) \times \Gamma(e^+e^-)/\Gamma_{\text{total}}$	DOCUMENT ID	TECN	COMMENT	$\Gamma_2\Gamma_1/\Gamma$
••• We do not use the following data for averages, fits, limits, etc. •••				
$10.4 \pm 1.7 \pm 1.5$	⁵ WANG	07D	BELL 10.58 $e^+e^- \rightarrow \gamma\pi^+\pi^-\psi(2S)$	
$11.8 \pm 1.8 \pm 1.4$	⁶ WANG	07D	BELL 10.58 $e^+e^- \rightarrow \gamma\pi^+\pi^-\psi(2S)$	

⁵ Solution I of two equivalent solutions in a fit using two interfering resonances.
⁶ Solution II of two equivalent solutions in a fit using two interfering resonances.

X(4360) REFERENCES

AUBERT	07S	PRL 98 212001	B. Aubert <i>et al.</i>	(BABAR Collab.)
WANG	07D	PRL 99 142002	X.-L. Wang <i>et al.</i>	(BELLE Collab.)

OTHER RELATED PAPERS

DING	08	PR D77 014033	G.-J. Ding, J.-J. Zhu, M.-L. Yan
KALASHNIK...	08	PR D77 054025	Yu.S. Kalashnikova, A.V. Nefediev

$\psi(4415)$

$$I^G(J^{PC}) = 0^-(1^{--})$$

$\psi(4415)$ MASS

VALUE (MeV)	DOCUMENT ID	TECN	COMMENT
4421 ± 4 OUR ESTIMATE			
4415.1 ± 7.9	¹ ABLIKIM	08D	BES2 $e^+e^- \rightarrow$ hadrons
••• We do not use the following data for averages, fits, limits, etc. •••			
4411 ± 7	² PAKHLOVA	08A	BELL 10.6 $e^+e^- \rightarrow D^0D^-\pi^+\gamma$
4425 ± 6	³ SETH	05A	RVUE $e^+e^- \rightarrow$ hadrons
4429 ± 9	⁴ SETH	05A	RVUE $e^+e^- \rightarrow$ hadrons
4417 ± 10	BRANDELIK	78C	DASP e^+e^-
4414 ± 7	SIEGRIST	76	MRK1 e^+e^-

¹ Reanalysis of data presented in BAI 02c. From a global fit over the center-of-mass energy region 3.7–5.0 GeV covering the $\psi(3770)$, $\psi(4040)$, $\psi(4160)$, and $\psi(4415)$ resonances. Phase angle fixed in the fit to $\delta = (234 \pm 88)^\circ$.
² Systematic uncertainties not estimated.
³ From a fit to Crystal Ball (OSTERHELD 86) data.
⁴ From a fit to BES (BAI 02c) data.

$\psi(4415)$ WIDTH

VALUE (MeV)	DOCUMENT ID	TECN	COMMENT
62 ± 20 OUR ESTIMATE			
71.5 ± 19.0	⁵ ABLIKIM	08D	BES2 $e^+e^- \rightarrow$ hadrons
••• We do not use the following data for averages, fits, limits, etc. •••			
77 ± 20	⁶ PAKHLOVA	08A	BELL 10.6 $e^+e^- \rightarrow D^0D^-\pi^+\gamma$
119 ± 16	⁷ SETH	05A	RVUE $e^+e^- \rightarrow$ hadrons
118 ± 35	⁸ SETH	05A	RVUE $e^+e^- \rightarrow$ hadrons
66 ± 15	BRANDELIK	78C	DASP e^+e^-
33 ± 10	SIEGRIST	76	MRK1 e^+e^-

⁵ Reanalysis of data presented in BAI 02c. From a global fit over the center-of-mass energy region 3.7–5.0 GeV covering the $\psi(3770)$, $\psi(4040)$, $\psi(4160)$, and $\psi(4415)$ resonances. Phase angle fixed in the fit to $\delta = (234 \pm 88)^\circ$.
⁶ Systematic uncertainties not estimated.
⁷ From a fit to Crystal Ball (OSTERHELD 86) data.
⁸ From a fit to BES (BAI 02c) data.

$\psi(4415)$ DECAY MODES

Mode	Fraction (Γ_i/Γ)	Confidence level
Γ_1 hadrons	dominant	
Γ_2 $D^0D^-\pi^+$		
Γ_3 $(D^0D^-\pi^+)_{non-res}$	< 2.3 %	90%
Γ_4 $D\bar{D}_2^*(2460) \rightarrow D^0D^-\pi^+$	(10 ± 4) %	
Γ_5 e^+e^-	(9.4 ± 3.2) × 10 ⁻⁶	

$\psi(4415)$ PARTIAL WIDTHS

$\Gamma(e^+e^-)$	DOCUMENT ID	TECN	COMMENT	Γ_5
0.58 ± 0.07 OUR ESTIMATE				
0.35 ± 0.12	⁹ ABLIKIM	08D	BES2 $e^+e^- \rightarrow$ hadrons	
••• We do not use the following data for averages, fits, limits, etc. •••				
0.72 ± 0.11	¹⁰ SETH	05A	RVUE $e^+e^- \rightarrow$ hadrons	
0.64 ± 0.23	¹¹ SETH	05A	RVUE $e^+e^- \rightarrow$ hadrons	
0.49 ± 0.13	BRANDELIK	78C	DASP e^+e^-	
0.44 ± 0.14	SIEGRIST	76	MRK1 e^+e^-	

⁹ Reanalysis of data presented in BAI 02c. From a global fit over the center-of-mass energy region 3.7–5.0 GeV covering the $\psi(3770)$, $\psi(4040)$, $\psi(4160)$, and $\psi(4415)$ resonances. Phase angle fixed in the fit to $\delta = (234 \pm 88)^\circ$.
¹⁰ From a fit to Crystal Ball (OSTERHELD 86) data.
¹¹ From a fit to BES (BAI 02c) data.

$\psi(4415)$ BRANCHING RATIOS

$\Gamma(\text{hadrons})/\Gamma_{\text{total}}$	DOCUMENT ID	TECN	COMMENT	Γ_1/Γ
dominant	SIEGRIST	76	MRK1 e^+e^-	

$\Gamma(D\bar{D}_2^*(2460) \rightarrow D^0D^-\pi^+)/\Gamma_{\text{total}}$	DOCUMENT ID	TECN	COMMENT	Γ_4/Γ
10.5 ± 2.4 ± 3.8	¹² PAKHLOVA	08A	BELL 10.6 $e^+e^- \rightarrow D^0D^-\pi^+\gamma$	

¹² Using 4421 ± 4 MeV for the mass and 62 ± 20 MeV for the width of $\psi(4415)$.

$\Gamma((D^0D^-\pi^+)_{non-res})/\Gamma(D\bar{D}_2^*(2460) \rightarrow D^0D^-\pi^+)$	DOCUMENT ID	TECN	COMMENT	Γ_3/Γ_4
< 0.22	¹³ PAKHLOVA	08A	BELL 10.6 $e^+e^- \rightarrow D^0D^-\pi^+\gamma$	

¹³ Using 4421 ± 4 MeV for the mass and 62 ± 20 MeV for the width of $\psi(4415)$.

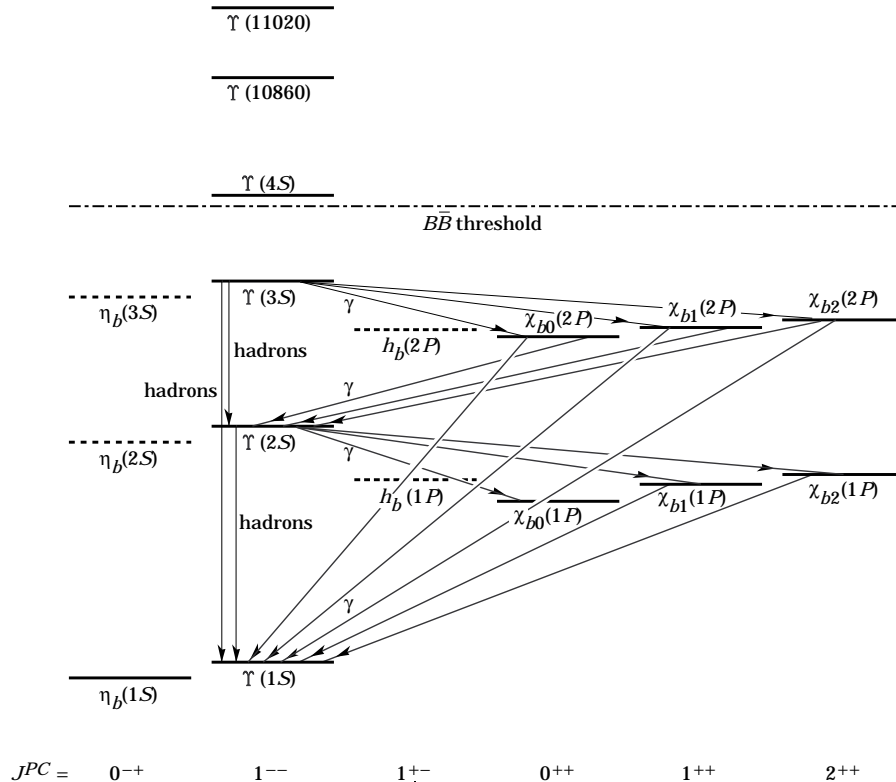
$\psi(4415)$ REFERENCES

ABLIKIM	08D	PL B660 315	M. Ablikim <i>et al.</i>	(BES Collab.)
PAKHOVA	08A	PRL 100 062001	G. Pakhlova <i>et al.</i>	(BELLE Collab.)
SETH	05A	PR D72 017501	K.K. Seth	
BAI	02C	PRL 88 101802	J.Z. Bai <i>et al.</i>	(BES Collab.)
OSTERHELD	86	SLAC-PUB-4160	A. Osterheld <i>et al.</i>	(SLAC Crystal Ball Collab.)
BRANDELIK	78C	PL 76B 361	R. Brandelik <i>et al.</i>	(DASP Collab.)
SIEGRIST	76	PRL 36 700	J.L. Siegrist <i>et al.</i>	(LBL, SLAC)

OTHER RELATED PAPERS

PAKHOVA	08	PR D77 011103R	G. Pakhlova <i>et al.</i>	(BELLE Collab.)
PAKHOVA	07	PRL 98 092001	G. Pakhlova <i>et al.</i>	(BELLE Collab.)
BURMESTER	77	PL 66B 395	J. Burmester <i>et al.</i>	(DESY, HAMB, SIEG+)
LUTH	77	PL 70B 120	V. Luth <i>et al.</i>	(LBL, SLAC)

$b\bar{b}$ MESONS

THE BOTTOMONIUM SYSTEM


The level scheme of the $b\bar{b}$ states showing experimentally established states with solid lines. Singlet states are called η_b and h_b , triplet states Υ and χ_{bJ} . In parentheses it is sufficient to give the radial quantum number and the orbital angular momentum to specify the states with all their quantum numbers. *E.g.*, $h_b(2P)$ means 2^1P_1 with $n = 2$, $L = 1$, $S = 0$, $J = 1$, $PC = +- -$. If found, D -wave states would be called $\eta_b(nD)$ and $\Upsilon_J(nD)$, with $J = 1, 2, 3$ and $n = 1, 2, 3, 4, \dots$. For the χ_b states, the spins of only the $\chi_{b2}(1P)$ and $\chi_{b1}(1P)$ have been experimentally established. The spins of the other χ_b are given as the preferred values, based on the quarkonium models. The figure also shows the observed hadronic and radiative transitions.

WIDTH DETERMINATIONS OF THE Υ STATES

As is the case for the $J/\psi(1S)$ and $\psi(2S)$, the full widths of the $b\bar{b}$ states $\Upsilon(1S)$, $\Upsilon(2S)$, and $\Upsilon(3S)$ are not directly measurable, since they are much narrower than the energy resolution of the e^+e^- storage rings where these states are produced. The common indirect method to determine Γ starts from

$$\Gamma = \Gamma_{\ell\ell} / B_{\ell\ell}, \quad (1)$$

where $\Gamma_{\ell\ell}$ is one leptonic partial width and $B_{\ell\ell}$ is the corresponding branching fraction ($\ell = e, \mu$, or τ). One then assumes $e\text{-}\mu\text{-}\tau$ universality and uses

$$\begin{aligned} \Gamma_{\ell\ell} &= \Gamma_{ee} \\ B_{\ell\ell} &= \text{average of } B_{ee}, B_{\mu\mu}, \text{ and } B_{\tau\tau}. \end{aligned} \quad (2)$$

The electronic partial width Γ_{ee} is also not directly measurable at e^+e^- storage rings, only in the combination $\Gamma_{ee}\Gamma_{\text{had}}/\Gamma$, where Γ_{had} is the hadronic partial width and

$$\Gamma_{\text{had}} + 3\Gamma_{ee} = \Gamma. \quad (3)$$

This combination is obtained experimentally from the energy-integrated hadronic cross section

$$\begin{aligned} &\int_{\text{resonance}} \sigma(e^+e^- \rightarrow \Upsilon \rightarrow \text{hadrons}) dE \\ &= \frac{6\pi^2 \Gamma_{ee} \Gamma_{\text{had}}}{M^2 \Gamma} C_r = \frac{6\pi^2 \Gamma_{ee}^{(0)} \Gamma_{\text{had}}}{M^2 \Gamma} C_r^{(0)}, \end{aligned} \quad (4)$$

where M is the Υ mass, and C_r and $C_r^{(0)}$ are radiative correction factors. C_r is used for obtaining Γ_{ee} as defined in Eq. (1), and contains corrections from all orders of QED for describing $(b\bar{b}) \rightarrow e^+e^-$. The lowest order QED value $\Gamma_{ee}^{(0)}$, relevant for comparison with potential-model calculations, is defined by the

See key on page 373

Meson Particle Listings

Bottomonium, $\eta_b(1S)$, $\Upsilon(1S)$

lowest order QED graph (Born term) alone, and is about 7% lower than Γ_{ee} .

The Listings give experimental results on B_{ee} , $B_{\mu\mu}$, $B_{\tau\tau}$, and $\Gamma_{ee}\Gamma_{had}/\Gamma$. The entries of the last quantity have been re-evaluated consistently using the correction procedure of KU-RAEV 85. The partial width Γ_{ee} is obtained from the average values for $\Gamma_{ee}\Gamma_{had}/\Gamma$ and $B_{\ell\ell}$ using

$$\Gamma_{ee} = \frac{\Gamma_{ee}\Gamma_{had}}{\Gamma(1-3B_{\ell\ell})}. \quad (5)$$

The total width Γ is then obtained from Eq. (1). We do not list Γ_{ee} and Γ values of individual experiments. The Γ_{ee} values in the Meson Summary Table are also those defined in Eq. (1).

$\eta_b(1S)$

$$J^{PC} = 0^+(0^{-+})$$

OMITTED FROM SUMMARY TABLE

Quantum numbers shown are quark-model predictions. One event is observed with the expected background of one. Needs confirmation.

$\eta_b(1S)$ MASS

VALUE (MeV)	DOCUMENT ID	TECN	COMMENT
9300 ± 20 ± 20	HEISTER	02D ALEP	181-209 e^+e^-

$\eta_b(1S)$ DECAY MODES

Mode	Fraction (Γ_i/Γ)
Γ_1 $3h^+3h^-$	seen
Γ_2 $2h^+2h^-$	not seen
Γ_3 $4h^+4h^-$	
Γ_4 $\gamma\gamma$	seen

$\eta_b(1S)$ $\Gamma(i)\Gamma(\gamma\gamma)/\Gamma(\text{total})$

$\Gamma(3h^+3h^-) \times \Gamma(\gamma\gamma)/\Gamma_{\text{total}}$	CL%	DOCUMENT ID	TECN	COMMENT	$\Gamma_1\Gamma_4/\Gamma$
<470	95	ABDALLAH	06 DLPH	161-209 e^+e^-	
<132	95	HEISTER	02D ALEP	181-209 e^+e^-	

• • • We do not use the following data for averages, fits, limits, etc. • • •

$\Gamma(2h^+2h^-) \times \Gamma(\gamma\gamma)/\Gamma_{\text{total}}$	CL%	DOCUMENT ID	TECN	COMMENT	$\Gamma_2\Gamma_4/\Gamma$
<190	95	ABDALLAH	06 DLPH	161-209 e^+e^-	
<48	95	HEISTER	02D ALEP	181-209 e^+e^-	

• • • We do not use the following data for averages, fits, limits, etc. • • •

$\Gamma(4h^+4h^-) \times \Gamma(\gamma\gamma)/\Gamma_{\text{total}}$	CL%	DOCUMENT ID	TECN	COMMENT	$\Gamma_3\Gamma_4/\Gamma$
<660	95	ABDALLAH	06 DLPH	161-209 e^+e^-	

• • • We do not use the following data for averages, fits, limits, etc. • • •

$\eta_b(1S)$ REFERENCES

ABDALLAH	06	PL B634 340	J.M. Abdallah et al.	(DELPHI Collab.)
HEISTER	02D	PL B530 56	A. Heister et al.	(ALEPH Collab.)

$\Upsilon(1S)$

$$J^{PC} = 0^-(1^{--})$$

$\Upsilon(1S)$ MASS

VALUE (MeV)	DOCUMENT ID	TECN	COMMENT
9460.30 ± 0.26 OUR AVERAGE	Error includes scale factor of 3.3.		
9460.51 ± 0.09 ± 0.05	¹ ARTAMONOV 00	MD1	$e^+e^- \rightarrow$ hadrons
9459.97 ± 0.11 ± 0.07	MACKAY 84	REDE	$e^+e^- \rightarrow$ hadrons
• • • We do not use the following data for averages, fits, limits, etc. • • •			
9460.60 ± 0.09 ± 0.05	^{2,3} BARU	92B REDE	$e^+e^- \rightarrow$ hadrons
9460.59 ± 0.12	BARU	86 REDE	$e^+e^- \rightarrow$ hadrons
9460.6 ± 0.4	^{3,4} ARTAMONOV 84	REDE	$e^+e^- \rightarrow$ hadrons

¹ Reanalysis of BARU 92B and ARTAMONOV 84 using new electron mass (COHEN 87).

² Superseding BARU 86.

³ Superseded by ARTAMONOV 00.

⁴ Value includes data of ARTAMONOV 82.

$\Upsilon(1S)$ WIDTH

VALUE (keV)	DOCUMENT ID
54.02 ± 1.25 OUR EVALUATION	See the Note on "Width Determinations of the Υ States"

$\Upsilon(1S)$ DECAY MODES

Mode	Fraction (Γ_i/Γ)	Confidence level
Γ_1 $\tau^+\tau^-$	(2.60 ± 0.10) %	
Γ_2 e^+e^-	(2.38 ± 0.11) %	
Γ_3 $\mu^+\mu^-$	(2.48 ± 0.05) %	

Hadronic decays

Γ_4 $\eta'(958)$ anything	(2.94 ± 0.24) %	
Γ_5 $J/\psi(1S)$ anything	(6.5 ± 0.7) × 10 ⁻⁴	
Γ_6 χ_{c0} anything	< 5 × 10 ⁻³	90%
Γ_7 χ_{c1} anything	(2.3 ± 0.7) × 10 ⁻⁴	
Γ_8 χ_{c2} anything	(3.4 ± 1.0) × 10 ⁻⁴	
Γ_9 $\psi(2S)$ anything	(2.7 ± 0.9) × 10 ⁻⁴	
Γ_{10} $\rho\pi$	< 2 × 10 ⁻⁴	90%
Γ_{11} $\pi^+\pi^-$	< 5 × 10 ⁻⁴	90%
Γ_{12} K^+K^-	< 5 × 10 ⁻⁴	90%
Γ_{13} $p\bar{p}$	< 5 × 10 ⁻⁴	90%
Γ_{14} $\pi_0^0\pi^+\pi^-$	< 1.84 × 10 ⁻⁵	90%
Γ_{15} $D^*(2010)^\pm$ anything		
Γ_{16} \bar{d} anything	(2.86 ± 0.28) × 10 ⁻⁵	

Radiative decays

Γ_{17} $\gamma\pi^+\pi^-$	(6.3 ± 1.8) × 10 ⁻⁵	
Γ_{18} $\gamma\pi^0\pi^0$	(1.7 ± 0.7) × 10 ⁻⁵	
Γ_{19} $\gamma\pi^0\eta$	< 2.4 × 10 ⁻⁶	90%
Γ_{20} K^+K^- with $2 < m_{K^+K^-} < 3$ GeV	(1.14 ± 0.13) × 10 ⁻⁵	
Γ_{21} $\gamma p\bar{p}$ with $2 < m_{p\bar{p}} < 3$ GeV	< 6 × 10 ⁻⁶	90%
Γ_{22} $\gamma 2h^+2h^-$	(7.0 ± 1.5) × 10 ⁻⁴	
Γ_{23} $\gamma 3h^+3h^-$	(5.4 ± 2.0) × 10 ⁻⁴	
Γ_{24} $\gamma 4h^+4h^-$	(7.4 ± 3.5) × 10 ⁻⁴	
Γ_{25} $\gamma\pi^+\pi^-K^+K^-$	(2.9 ± 0.9) × 10 ⁻⁴	
Γ_{26} $\gamma 2\pi^+2\pi^-$	(2.5 ± 0.9) × 10 ⁻⁴	
Γ_{27} $\gamma 3\pi^+3\pi^-$	(2.5 ± 1.2) × 10 ⁻⁴	
Γ_{28} $\gamma 2\pi^+2\pi^-K^+K^-$	(2.4 ± 1.2) × 10 ⁻⁴	
Γ_{29} $\gamma\pi^+\pi^-p\bar{p}$	(1.5 ± 0.6) × 10 ⁻⁴	
Γ_{30} $\gamma 2\pi^+2\pi^-p\bar{p}$	(4 ± 6) × 10 ⁻⁵	
Γ_{31} $\gamma 2K^+2K^-$	(2.0 ± 2.0) × 10 ⁻⁵	
Γ_{32} $\gamma\eta'(958)$	< 1.9 × 10 ⁻⁶	90%
Γ_{33} $\gamma\eta$	< 1.0 × 10 ⁻⁶	90%
Γ_{34} $\gamma f_0(980)$	< 3 × 10 ⁻⁵	90%
Γ_{35} $\gamma f_2'(1525)$	(3.7 $^{+1.2}_{-1.1}$) × 10 ⁻⁵	
Γ_{36} $\gamma f_2(1270)$	(1.01 ± 0.09) × 10 ⁻⁴	
Γ_{37} $\gamma\eta(1405)$	< 8.2 × 10 ⁻⁵	90%
Γ_{38} $\gamma f_0(1500)$	< 1.5 × 10 ⁻⁵	90%
Γ_{39} $\gamma f_0(1710)$	< 2.6 × 10 ⁻⁴	90%
Γ_{40} $\gamma f_0(1710) \rightarrow \gamma K^+K^-$	< 7 × 10 ⁻⁶	90%
Γ_{41} $\gamma f_0(1710) \rightarrow \gamma\pi^0\pi^0$	< 1.4 × 10 ⁻⁶	90%
Γ_{42} $\gamma f_0(1710) \rightarrow \gamma\eta\eta$	< 1.8 × 10 ⁻⁶	90%
Γ_{43} $\gamma f_4(2050)$	< 5.3 × 10 ⁻⁵	90%

Meson Particle Listings

$\Upsilon(1S)$

Γ_{44}	$\gamma f_0(2200) \rightarrow \gamma K^+ K^-$	< 2	$\times 10^{-4}$	90%
Γ_{45}	$\gamma f_J(2220) \rightarrow \gamma K^+ K^-$	< 8	$\times 10^{-7}$	90%
Γ_{46}	$\gamma f_J(2220) \rightarrow \gamma \pi^+ \pi^-$	< 6	$\times 10^{-7}$	90%
Γ_{47}	$\gamma f_J(2220) \rightarrow \gamma p \bar{p}$	< 1.1	$\times 10^{-6}$	90%
Γ_{48}	$\gamma \eta(2225) \rightarrow \gamma \phi \phi$	< 3	$\times 10^{-3}$	90%
Γ_{49}	γX	[a] < 3	$\times 10^{-5}$	90%
Γ_{50}	$\gamma X \bar{X}$	[b] < 1	$\times 10^{-3}$	90%
Γ_{51}	$\gamma X \rightarrow \gamma + \geq 4$ prongs	[c] < 1.78	$\times 10^{-4}$	95%

Other decays

Γ_{52}	invisible	< 2.5	$\times 10^{-3}$	90%
---------------	-----------	-------	------------------	-----

[a] X = pseudoscalar with $m < 7.2$ GeV

[b] $X \bar{X}$ = vectors with $m < 3.1$ GeV

[c] $1.5 \text{ GeV} < m_X < 5.0 \text{ GeV}$

$\Upsilon(1S) \Gamma(i) \Gamma(e^+ e^-) / \Gamma(\text{total})$

$\Gamma(e^+ e^-) \times \Gamma(\mu^+ \mu^-) / \Gamma_{\text{total}}$	DOCUMENT ID	TECN	COMMENT	$\Gamma_2 \Gamma_3 / \Gamma$
31.2 ± 1.6 ± 1.7	KOBEL	92	CBAL	$e^+ e^- \rightarrow \mu^+ \mu^-$

$\Gamma(\text{hadrons}) \times \Gamma(e^+ e^-) / \Gamma_{\text{total}}$	DOCUMENT ID	TECN	COMMENT	$\Gamma_0 \Gamma_2 / \Gamma$
1.240 ± 0.016 OUR AVERAGE				
1.252 ± 0.004 ± 0.019	5 ROSNER	06	CLEO	9.5 $e^+ e^- \rightarrow$ hadrons
1.187 ± 0.023 ± 0.031	5 BARU	92B	MD1	$e^+ e^- \rightarrow$ hadrons
1.23 ± 0.02 ± 0.05	5 JAKUBOWSKI	88	CBAL	$e^+ e^- \rightarrow$ hadrons
1.37 ± 0.06 ± 0.09	6 GILES	84B	CLEO	$e^+ e^- \rightarrow$ hadrons
1.23 ± 0.08 ± 0.04	6 ALBRECHT	82	DASP	$e^+ e^- \rightarrow$ hadrons
1.13 ± 0.07 ± 0.11	6 NICZYPORUK	82	LENA	$e^+ e^- \rightarrow$ hadrons
1.09 ± 0.25	6 BOCK	80	CNTR	$e^+ e^- \rightarrow$ hadrons
1.35 ± 0.14	7 BERGER	79	PLUT	$e^+ e^- \rightarrow$ hadrons

⁵ Radiative corrections evaluated following KURAEV 85.

⁶ Radiative corrections reevaluated by BUCHMUELLER 88 following KURAEV 85.

⁷ Radiative corrections reevaluated by ALEXANDER 89 using $B(\mu\mu) = 0.026$.

$\Upsilon(1S)$ PARTIAL WIDTHS

$\Gamma(e^+ e^-)$	DOCUMENT ID	Γ_2
1.340 ± 0.018 OUR EVALUATION		

$\Upsilon(1S)$ BRANCHING RATIOS

$\Gamma(\tau^+ \tau^-) / \Gamma_{\text{total}}$	DOCUMENT ID	TECN	COMMENT	Γ_1 / Γ
2.60 ± 0.10 OUR AVERAGE				
2.53 ± 0.13 ± 0.05	8 BESSON	07	CLEO	$e^+ e^- \rightarrow \Upsilon(1S) \rightarrow \tau^+ \tau^-$
2.61 ± 0.12 ^{+0.09} _{-0.13}	25k CINABRO	94B	CLE2	$e^+ e^- \rightarrow \tau^+ \tau^-$
2.7 ± 0.4 ± 0.2	9 ALBRECHT	85c	ARG	$\Upsilon(2S) \rightarrow \pi^+ \pi^- \tau^+ \tau^-$
3.4 ± 0.4 ± 0.4	GILES	83	CLEO	$e^+ e^- \rightarrow \tau^+ \tau^-$

⁸ BESSON 07 reports $[B(\Upsilon(1S) \rightarrow \tau^+ \tau^-)] / [B(\Upsilon(1S) \rightarrow \mu^+ \mu^-)] = 1.02 \pm 0.02 \pm 0.05$. We multiply by our best value $B(\Upsilon(1S) \rightarrow \mu^+ \mu^-) = (2.48 \pm 0.05) \times 10^{-2}$. Our first error is their experiment's error and our second error is the systematic error from using our best value.

⁹ Using $B(\Upsilon(1S) \rightarrow ee) = B(\Upsilon(1S) \rightarrow \mu\mu) = 0.0256$; not used for width evaluations.

$\Gamma(e^+ e^-) / \Gamma_{\text{total}}$	DOCUMENT ID	TECN	COMMENT	Γ_2 / Γ
2.38 ± 0.11 OUR AVERAGE				
2.29 ± 0.08 ± 0.11	ALEXANDER	98	CLE2	$\Upsilon(2S) \rightarrow \pi^+ \pi^- e^+ e^-$
2.42 ± 0.14 ± 0.14	307 ALBRECHT	87	ARG	$\Upsilon(2S) \rightarrow \pi^+ \pi^- e^+ e^-$
2.8 ± 0.3 ± 0.2	826 BESSON	84	CLEO	$\Upsilon(2S) \rightarrow \pi^+ \pi^- e^+ e^-$
5.1 ± 3.0	BERGER	80c	PLUT	$e^+ e^- \rightarrow e^+ e^-$

$\Gamma(\mu^+ \mu^-) / \Gamma_{\text{total}}$	DOCUMENT ID	TECN	COMMENT	Γ_3 / Γ
0.0248 ± 0.0005 OUR AVERAGE				
0.0249 ± 0.0002 ± 0.0007	345k ADAMS	05	CLEO	$e^+ e^- \rightarrow \mu^+ \mu^-$
0.0249 ± 0.0008 ± 0.0013	ALEXANDER	98	CLE2	$\Upsilon(2S) \rightarrow \pi^+ \pi^- \mu^+ \mu^-$
0.0212 ± 0.0020 ± 0.0010	10 BARU	92	MD1	$e^+ e^- \rightarrow \mu^+ \mu^-$
0.0231 ± 0.0012 ± 0.0010	10 KOBEL	92	CBAL	$e^+ e^- \rightarrow \mu^+ \mu^-$
0.0252 ± 0.0007 ± 0.0007	CHEN	89B	CLEO	$e^+ e^- \rightarrow \mu^+ \mu^-$
0.0261 ± 0.0009 ± 0.0011	KAARSBERG	89	CSB2	$e^+ e^- \rightarrow \mu^+ \mu^-$
0.0230 ± 0.0025 ± 0.0013	86 ALBRECHT	87	ARG	$\Upsilon(2S) \rightarrow \pi^+ \pi^- \mu^+ \mu^-$

0.029 ± 0.003 ± 0.002	864	BESSON	84	CLEO	$\Upsilon(2S) \rightarrow \pi^+ \pi^- \mu^+ \mu^-$
0.027 ± 0.003 ± 0.003	ANDREWS	83	CLEO	$e^+ e^- \rightarrow \mu^+ \mu^-$	
0.032 ± 0.013 ± 0.003	ALBRECHT	82	DASP	$e^+ e^- \rightarrow \mu^+ \mu^-$	
0.038 ± 0.015 ± 0.002	NICZYPORUK	82	LENA	$e^+ e^- \rightarrow \mu^+ \mu^-$	
0.014 ^{+0.034} _{-0.014}	BOCK	80	CNTR	$e^+ e^- \rightarrow \mu^+ \mu^-$	
0.022 ± 0.020	BERGER	79	PLUT	$e^+ e^- \rightarrow \mu^+ \mu^-$	

¹⁰ Taking into account interference between the resonance and continuum.

$\Gamma(\tau^+ \tau^-) / \Gamma(\mu^+ \mu^-)$	DOCUMENT ID	TECN	COMMENT	Γ_1 / Γ_3
1.02 ± 0.02 ± 0.05	60k			
	BESSON	07	CLEO	$e^+ e^- \rightarrow \Upsilon(1S)$

$\Gamma(\eta'(958) \text{ anything}) / \Gamma_{\text{total}}$	DOCUMENT ID	TECN	COMMENT	Γ_4 / Γ
0.0294 ± 0.0024 OUR AVERAGE				
0.030 ± 0.002 ± 0.002	AQUINES	06A	CLE3	$\Upsilon(1S) \rightarrow \eta' \text{ anything}$
0.028 ± 0.004 ± 0.002	ARTUSO	03	CLE2	$\Upsilon(1S) \rightarrow \eta' \text{ anything}$

$\Gamma(J/\psi(1S) \text{ anything}) / \Gamma_{\text{total}}$	DOCUMENT ID	TECN	COMMENT	Γ_5 / Γ	
0.65 ± 0.07 OUR AVERAGE					
0.64 ± 0.04 ± 0.06	730 ± 40	BRIERE	04	CLEO	$e^+ e^- \rightarrow J/\psi X$
1.1 ± 0.4 ± 0.2	11 FULTON	89	CLEO	$e^+ e^- \rightarrow \mu^+ \mu^- X$	
< 0.68	90	ALBRECHT	92J	ARG	$e^+ e^- \rightarrow e^+ e^- X, \mu^+ \mu^- X$
< 1.7	90	MASCHMANN	90	CBAL	$e^+ e^- \rightarrow$ hadrons
< 20	90	NICZYPORUK	83	LENA	

¹¹ Using $B((J/\psi) \rightarrow \mu^+ \mu^-) = (6.9 \pm 0.9)\%$.

$\Gamma(\chi_{c0} \text{ anything}) / \Gamma(J/\psi(1S) \text{ anything})$	DOCUMENT ID	TECN	COMMENT	Γ_6 / Γ_5	
< 7.4	90	BRIERE	04	CLEO	$e^+ e^- \rightarrow J/\psi X$

$\Gamma(\chi_{c1} \text{ anything}) / \Gamma(J/\psi(1S) \text{ anything})$	DOCUMENT ID	TECN	COMMENT	Γ_7 / Γ_5	
0.35 ± 0.08 ± 0.06	52 ± 12	BRIERE	04	CLEO	$e^+ e^- \rightarrow J/\psi X$

$\Gamma(\chi_{c2} \text{ anything}) / \Gamma(J/\psi(1S) \text{ anything})$	DOCUMENT ID	TECN	COMMENT	Γ_8 / Γ_5	
0.52 ± 0.12 ± 0.09	47 ± 11	BRIERE	04	CLEO	$e^+ e^- \rightarrow J/\psi X$

$\Gamma(\psi(2S) \text{ anything}) / \Gamma(J/\psi(1S) \text{ anything})$	DOCUMENT ID	TECN	COMMENT	Γ_9 / Γ_5	
0.41 ± 0.11 ± 0.08	42 ± 11	BRIERE	04	CLEO	$e^+ e^- \rightarrow J/\psi \pi^+ \pi^- X$

$\Gamma(\rho\pi) / \Gamma_{\text{total}}$	DOCUMENT ID	TECN	COMMENT	Γ_{10} / Γ	
< 2	90	FULTON	90B	$\Upsilon(1S) \rightarrow \rho^0 \pi^0$	
< 10	90	BLINOV	90	MD1	$\Upsilon(1S) \rightarrow \rho^0 \pi^0$
< 21	90	NICZYPORUK	83	LENA	$\Upsilon(1S) \rightarrow \rho^0 \pi^0$

$\Gamma(\pi^+ \pi^-) / \Gamma_{\text{total}}$	DOCUMENT ID	TECN	COMMENT	Γ_{11} / Γ	
< 5	90	BARU	92	MD1	$\Upsilon(1S) \rightarrow \pi^+ \pi^-$

$\Gamma(K^+ K^-) / \Gamma_{\text{total}}$	DOCUMENT ID	TECN	COMMENT	Γ_{12} / Γ	
< 5	90	BARU	92	MD1	$\Upsilon(1S) \rightarrow K^+ K^-$

$\Gamma(p\bar{p}) / \Gamma_{\text{total}}$	DOCUMENT ID	TECN	COMMENT	Γ_{13} / Γ	
< 5	90	12 BARU	96	MD1	$\Upsilon(1S) \rightarrow p\bar{p}$

¹² Supersedes BARU 92 in this node.

$\Gamma(\pi^0 \pi^+ \pi^-) / \Gamma_{\text{total}}$	DOCUMENT ID	TECN	COMMENT	Γ_{14} / Γ	
< 1.84	90	ANASTASSOV	99	CLE2	$e^+ e^- \rightarrow$ hadrons

$\Gamma(D^*(2010)^\pm \text{ anything}) / \Gamma_{\text{total}}$	DOCUMENT ID	TECN	COMMENT	Γ_{15} / Γ	
< 19	90	13 ALBRECHT	92J	ARG	$e^+ e^- \rightarrow D^0 \pi^\pm X$

¹³ For $x_p > 0.2$.

$\Gamma(\bar{d} \text{ anything}) / \Gamma_{\text{total}}$	DOCUMENT ID	TECN	COMMENT	Γ_{16} / Γ	
2.86 ± 0.19 ± 0.21	455	ASNER	07	CLEO	$e^+ e^- \rightarrow \bar{d} X$

Meson Particle Listings
 $\Upsilon(1S)$ $\Gamma(ggg, gg\gamma \rightarrow \bar{d} \text{ anything})/\Gamma(ggg, gg\gamma \rightarrow \text{anything})$

VALUE (units 10^{-5})	EVTS	DOCUMENT ID	TECN	COMMENT
$3.36 \pm 0.23 \pm 0.25$	455	ASNER	07 CLEO	$e^+e^- \rightarrow \bar{d}X$

 $\Gamma(\gamma\pi^+\pi^-)/\Gamma_{\text{total}}$ Γ_{17}/Γ

VALUE (units 10^{-5})	DOCUMENT ID	TECN	COMMENT
$6.3 \pm 1.2 \pm 1.3$	14 ANASTASSOV 99	CLE2	$e^+e^- \rightarrow \text{hadrons}$

¹⁴ For $m_{\pi\pi} > 1$ GeV.

 $\Gamma(\gamma\pi^0\pi^0)/\Gamma_{\text{total}}$ Γ_{18}/Γ

VALUE (units 10^{-5})	DOCUMENT ID	TECN	COMMENT
$1.7 \pm 0.6 \pm 0.3$	15 ANASTASSOV 99	CLE2	$e^+e^- \rightarrow \text{hadrons}$

¹⁵ For $m_{\pi\pi} > 1$ GeV.

 $\Gamma(\gamma\pi^0\eta)/\Gamma_{\text{total}}$ Γ_{19}/Γ

VALUE (units 10^{-6})	CL%	DOCUMENT ID	TECN	COMMENT
< 2.4	90	16 BESSON 07A	CLEO	$e^+e^- \rightarrow \Upsilon(1S)$

¹⁶ BESSON 07A obtained this limit for $0.7 < m_{\pi^0\eta} < 3$ GeV.

 $\Gamma(K^+K^- \text{ with } 2 < m_{K^+K^-} < 3 \text{ GeV})/\Gamma_{\text{total}}$ Γ_{20}/Γ

VALUE (units 10^{-5})	CL%	DOCUMENT ID	TECN	COMMENT
$1.14 \pm 0.08 \pm 0.10$	90	ATHAR	06 CLE3	$\Upsilon(1S) \rightarrow \gamma K^+K^-$

 $\Gamma(\gamma\rho\bar{\rho} \text{ with } 2 < m_{\rho\bar{\rho}} < 3 \text{ GeV})/\Gamma_{\text{total}}$ Γ_{21}/Γ

VALUE (units 10^{-5})	CL%	DOCUMENT ID	TECN	COMMENT
< 0.6	90	ATHAR	06 CLE3	$\Upsilon(1S) \rightarrow \gamma\rho\bar{\rho}$

 $\Gamma(\gamma 2h^+2h^-)/\Gamma_{\text{total}}$ Γ_{22}/Γ

VALUE (units 10^{-4})	EVTS	DOCUMENT ID	TECN	COMMENT
$7.0 \pm 1.1 \pm 1.0$	80 \pm 12	FULTON	90B CLEO	$e^+e^- \rightarrow \text{hadrons}$

 $\Gamma(\gamma 3h^+3h^-)/\Gamma_{\text{total}}$ Γ_{23}/Γ

VALUE (units 10^{-4})	EVTS	DOCUMENT ID	TECN	COMMENT
$5.4 \pm 1.5 \pm 1.3$	39 \pm 11	FULTON	90B CLEO	$e^+e^- \rightarrow \text{hadrons}$

 $\Gamma(\gamma 4h^+4h^-)/\Gamma_{\text{total}}$ Γ_{24}/Γ

VALUE (units 10^{-4})	EVTS	DOCUMENT ID	TECN	COMMENT
$7.4 \pm 2.5 \pm 2.5$	36 \pm 12	FULTON	90B CLEO	$e^+e^- \rightarrow \text{hadrons}$

 $\Gamma(\gamma\pi^+\pi^-K^+K^-)/\Gamma_{\text{total}}$ Γ_{25}/Γ

VALUE (units 10^{-4})	EVTS	DOCUMENT ID	TECN	COMMENT
$2.9 \pm 0.7 \pm 0.6$	29 \pm 8	FULTON	90B CLEO	$e^+e^- \rightarrow \text{hadrons}$

 $\Gamma(\gamma 2\pi^+2\pi^-)/\Gamma_{\text{total}}$ Γ_{26}/Γ

VALUE (units 10^{-4})	EVTS	DOCUMENT ID	TECN	COMMENT
$2.5 \pm 0.7 \pm 0.5$	26 \pm 7	FULTON	90B CLEO	$e^+e^- \rightarrow \text{hadrons}$

 $\Gamma(\gamma 3\pi^+3\pi^-)/\Gamma_{\text{total}}$ Γ_{27}/Γ

VALUE (units 10^{-4})	EVTS	DOCUMENT ID	TECN	COMMENT
$2.5 \pm 0.9 \pm 0.8$	17 \pm 5	FULTON	90B CLEO	$e^+e^- \rightarrow \text{hadrons}$

 $\Gamma(\gamma 2\pi^+2\pi^-K^+K^-)/\Gamma_{\text{total}}$ Γ_{28}/Γ

VALUE (units 10^{-4})	EVTS	DOCUMENT ID	TECN	COMMENT
$2.4 \pm 0.9 \pm 0.8$	18 \pm 7	FULTON	90B CLEO	$e^+e^- \rightarrow \text{hadrons}$

 $\Gamma(\gamma\pi^+\pi^-\rho\bar{\rho})/\Gamma_{\text{total}}$ Γ_{29}/Γ

VALUE (units 10^{-4})	EVTS	DOCUMENT ID	TECN	COMMENT
$1.5 \pm 0.5 \pm 0.3$	22 \pm 6	FULTON	90B CLEO	$e^+e^- \rightarrow \text{hadrons}$

 $\Gamma(\gamma 2\pi^+2\pi^-\rho\bar{\rho})/\Gamma_{\text{total}}$ Γ_{30}/Γ

VALUE (units 10^{-4})	EVTS	DOCUMENT ID	TECN	COMMENT
$0.4 \pm 0.4 \pm 0.4$	7 \pm 6	FULTON	90B CLEO	$e^+e^- \rightarrow \text{hadrons}$

 $\Gamma(\gamma 2K^+2K^-)/\Gamma_{\text{total}}$ Γ_{31}/Γ

VALUE (units 10^{-4})	EVTS	DOCUMENT ID	TECN	COMMENT
0.2 ± 0.2	2 \pm 2	FULTON	90B CLEO	$e^+e^- \rightarrow \text{hadrons}$

 $\Gamma(\gamma\eta(958))/\Gamma_{\text{total}}$ Γ_{32}/Γ

VALUE (units 10^{-6})	CL%	DOCUMENT ID	TECN	COMMENT
< 1.9	90	ATHAR	07A CLEO	$\Upsilon(1S) \rightarrow \gamma\eta' \rightarrow \gamma\pi^+\pi^-\eta, \gamma\rho$
< 16	90	RICHICHI	01B CLE2	$\Upsilon(1S) \rightarrow \gamma\eta' \rightarrow \gamma\eta\pi^+\pi^-$

• • • We do not use the following data for averages, fits, limits, etc. • • •

 $\Gamma(\gamma\eta)/\Gamma_{\text{total}}$ Γ_{33}/Γ

VALUE (units 10^{-6})	CL%	DOCUMENT ID	TECN	COMMENT
< 1.0	90	ATHAR	07A CLEO	$\Upsilon(1S) \rightarrow \gamma\eta \rightarrow \gamma\gamma\gamma, \gamma\pi^+\pi^-\pi^0, \gamma 3\pi^0$

• • • We do not use the following data for averages, fits, limits, etc. • • •

< 21 90 MASEK 02 CLEO $\Upsilon(1S) \rightarrow \gamma\eta$

 $\Gamma(\gamma f_0(980))/\Gamma_{\text{total}}$ Γ_{34}/Γ

VALUE (units 10^{-5})	CL%	DOCUMENT ID	TECN	COMMENT
< 3	90	17 ATHAR	06 CLE3	$\Upsilon(1S) \rightarrow \gamma\pi^+\pi^-$

¹⁷ Assuming $B(f_0(980) \rightarrow \pi\pi) = 1$.

 $\Gamma(\gamma f_2'(1525))/\Gamma_{\text{total}}$ Γ_{35}/Γ

VALUE (units 10^{-5})	CL%	DOCUMENT ID	TECN	COMMENT
$3.7 \pm 0.9 \pm 0.8$		ATHAR	06 CLE3	$\Upsilon(1S) \rightarrow \gamma K^+K^-$

• • • We do not use the following data for averages, fits, limits, etc. • • •

VALUE (units 10^{-5})	CL%	DOCUMENT ID	TECN	COMMENT
< 14	90	18 FULTON	90B CLEO	$\Upsilon(1S) \rightarrow \gamma K^+K^-$
< 19.4	90	18 ALBRECHT	89 ARG	$\Upsilon(1S) \rightarrow \gamma K^+K^-$

¹⁸ Assuming $B(f_2'(1525) \rightarrow K\bar{K}) = 0.71$.

 $\Gamma(\gamma f_2(1270))/\Gamma_{\text{total}}$ Γ_{36}/Γ

VALUE (units 10^{-5})	CL%	DOCUMENT ID	TECN	COMMENT
10.1 ± 0.9 OUR AVERAGE				
$10.5 \pm 1.6 \pm 1.9$		19 BESSON	07A CLE3	$\Upsilon(1S) \rightarrow \gamma\pi^0\pi^0$
$10.2 \pm 0.8 \pm 0.7$		ATHAR	06 CLE3	$\Upsilon(1S) \rightarrow \gamma\pi^+\pi^-$
$8.1 \pm 2.3 \pm 2.9$		20 ANASTASSOV	99 CLE2	$e^+e^- \rightarrow \text{hadrons}$

• • • We do not use the following data for averages, fits, limits, etc. • • •

VALUE (units 10^{-5})	CL%	DOCUMENT ID	TECN	COMMENT
< 21	90	20 FULTON	90B CLEO	$\Upsilon(1S) \rightarrow \gamma\pi^+\pi^-$
< 13	90	20 ALBRECHT	89 ARG	$\Upsilon(1S) \rightarrow \gamma\pi^+\pi^-$
< 81	90	SCHMITT	88 CBAL	$\Upsilon(1S) \rightarrow \gamma X$

¹⁹ Using $B(f_2(1270) \rightarrow \pi^0\pi^0) = B(f_2(1270) \rightarrow \pi\pi)/3$ and $B(f_2(1270) \rightarrow \pi\pi) = (0.845 \pm 0.025 \pm 0.012)\%$.

²⁰ Using $B(f_2(1270) \rightarrow \pi\pi) = 0.84$.

 $\Gamma(\gamma\eta(1405))/\Gamma_{\text{total}}$ Γ_{37}/Γ

VALUE (units 10^{-5})	CL%	DOCUMENT ID	TECN	COMMENT
< 8.2	90	21 FULTON	90B CLEO	$\Upsilon(1S) \rightarrow \gamma K^\pm\pi^\mp K_S^0$

²¹ Includes unknown branching ratio of $\eta(1405) \rightarrow K^\pm\pi^\mp K_S^0$.

 $\Gamma(\gamma f_0(1500))/\Gamma_{\text{total}}$ Γ_{38}/Γ

VALUE (units 10^{-5})	CL%	DOCUMENT ID	TECN	COMMENT
< 1.5	90	22 BESSON	07A CLEO	$e^+e^- \rightarrow \Upsilon(1S) \rightarrow \gamma\pi^0\pi^0$

• • • We do not use the following data for averages, fits, limits, etc. • • •

VALUE (units 10^{-5})	CL%	DOCUMENT ID	TECN	COMMENT
< 6.1	90	23 BESSON	07A CLEO	$e^+e^- \rightarrow \Upsilon(1S) \rightarrow \gamma\eta\eta$

²² Using $B(f_0(1500) \rightarrow \pi^0\pi^0) = B(f_0(1500) \rightarrow \pi\pi)/3$ and $B(f_0(1500) \rightarrow \pi\pi) = (0.349 \pm 0.023)\%$.

²³ Calculated by us using $B(f_0(1500) \rightarrow \eta\eta) = (5.1 \pm 0.9)\%$.

 $\Gamma(\gamma f_0(1710))/\Gamma_{\text{total}}$ Γ_{39}/Γ

VALUE (units 10^{-4})	CL%	DOCUMENT ID	TECN	COMMENT
< 2.6	90	24 ALBRECHT	89 ARG	$\Upsilon(1S) \rightarrow \gamma K^+K^-$

• • • We do not use the following data for averages, fits, limits, etc. • • •

VALUE (units 10^{-4})	CL%	DOCUMENT ID	TECN	COMMENT
< 6.3	90	24 FULTON	90B CLEO	$\Upsilon(1S) \rightarrow \gamma K^+K^-$
< 19	90	24 FULTON	90B CLEO	$\Upsilon(1S) \rightarrow \gamma K_S^0 K_S^0$
< 8	90	25 ALBRECHT	89 ARG	$\Upsilon(1S) \rightarrow \gamma\pi^+\pi^-$
< 24	90	26 SCHMITT	88 CBAL	$\Upsilon(1S) \rightarrow \gamma X$

²⁴ Assuming $B(f_0(1710) \rightarrow K\bar{K}) = 0.38$.

²⁵ Assuming $B(f_0(1710) \rightarrow \pi\pi) = 0.04$.

²⁶ Assuming $B(f_0(1710) \rightarrow \eta\eta) = 0.18$.

 $\Gamma(\gamma f_0(1710) \rightarrow \gamma K^+K^-)/\Gamma_{\text{total}}$ Γ_{40}/Γ

VALUE (units 10^{-5})	CL%	DOCUMENT ID	TECN	COMMENT
< 0.7	90	ATHAR	06 CLEO	$e^+e^- \rightarrow \Upsilon(1S) \rightarrow \gamma K^+K^-$

 $\Gamma(\gamma f_0(1710) \rightarrow \gamma\pi^0\pi^0)/\Gamma_{\text{total}}$ Γ_{41}/Γ

VALUE (units 10^{-6})	CL%	DOCUMENT ID	TECN	COMMENT
< 1.4	90	BESSON	07A CLEO	$e^+e^- \rightarrow \Upsilon(1S) \rightarrow \gamma\pi^0\pi^0$

 $\Gamma(\gamma f_0(1710) \rightarrow \gamma\eta\eta)/\Gamma_{\text{total}}$ Γ_{42}/Γ

VALUE (units 10^{-6})	CL%	DOCUMENT ID	TECN	COMMENT
< 1.8	90	BESSON	07A CLEO	$e^+e^- \rightarrow \Upsilon(1S) \rightarrow \gamma\eta\eta$

 $\Gamma(\gamma f_4(2050))/\Gamma_{\text{total}}$ Γ_{43}/Γ

VALUE (units 10^{-5})	CL%	DOCUMENT ID	TECN	COMMENT
< 5.3	90	27 ATHAR	06 CLE3	$\Upsilon(1S) \rightarrow \gamma\pi^+\pi^-$

²⁷ Assuming $B(f_4(2050) \rightarrow \pi\pi) = 0.17$.

 $\Gamma(\gamma f_0(2200) \rightarrow \gamma K^+K^-)/\Gamma_{\text{total}}$ Γ_{44}/Γ

VALUE (units 10^{-5})	CL%	DOCUMENT ID	TECN	COMMENT
< 0.0002	90	BARU	89 MD1	$\Upsilon(1S) \rightarrow \gamma K^+K^-$

Meson Particle Listings

$\Upsilon(1S), \chi_{b0}(1P)$

$\Gamma(\gamma f_J(2220) \rightarrow \gamma K^+ K^-) / \Gamma_{\text{total}}$ Γ_{45} / Γ

VALUE (units 10^{-7})	CL%	DOCUMENT ID	TECN	COMMENT
< 8	90	ATHAR 06	CLE3	$\Upsilon(1S) \rightarrow \gamma K^+ K^-$
••• We do not use the following data for averages, fits, limits, etc. •••				
< 160	90	MASEK 02	CLEO	$\Upsilon(1S) \rightarrow \gamma K^+ K^-$
< 150	90	FULTON 90B	CLEO	$\Upsilon(1S) \rightarrow \gamma K^+ K^-$
< 290	90	ALBRECHT 89	ARG	$\Upsilon(1S) \rightarrow \gamma K^+ K^-$
< 2000	90	BARU 89	MD1	$\Upsilon(1S) \rightarrow \gamma K^+ K^-$

$\Gamma(\gamma f_J(2220) \rightarrow \gamma \pi^+ \pi^-) / \Gamma_{\text{total}}$ Γ_{46} / Γ

VALUE (units 10^{-7})	CL%	DOCUMENT ID	TECN	COMMENT
< 6	90	ATHAR 06	CLE3	$\Upsilon(1S) \rightarrow \gamma \pi^+ \pi^-$
••• We do not use the following data for averages, fits, limits, etc. •••				
< 120	90	MASEK 02	CLEO	$\Upsilon(1S) \rightarrow \gamma \pi^+ \pi^-$

$\Gamma(\gamma f_J(2220) \rightarrow \gamma \rho^0) / \Gamma_{\text{total}}$ Γ_{47} / Γ

VALUE (units 10^{-7})	CL%	DOCUMENT ID	TECN	COMMENT
< 11	90	ATHAR 06	CLE3	$\Upsilon(1S) \rightarrow \gamma \rho^0$
••• We do not use the following data for averages, fits, limits, etc. •••				
< 160	90	MASEK 02	CLEO	$\Upsilon(1S) \rightarrow \gamma \rho^0$

$\Gamma(\gamma \eta(2225) \rightarrow \gamma \phi) / \Gamma_{\text{total}}$ Γ_{48} / Γ

VALUE	CL%	DOCUMENT ID	TECN	COMMENT
< 0.003	90	BARU 89	MD1	$\Upsilon(1S) \rightarrow \gamma K^+ K^- K^+ K^-$

$\Gamma(\gamma X) / \Gamma_{\text{total}}$ Γ_{49} / Γ

(X = pseudoscalar with $m < 7.2$ GeV)

VALUE (units 10^{-5})	CL%	DOCUMENT ID	TECN	COMMENT
< 3	90	²⁸ BALEST 95	CLEO	$e^+ e^- \rightarrow \gamma + X$

²⁸ For a noninteracting pseudoscalar X with mass < 7.2 GeV.

$\Gamma(\gamma X \bar{X}) / \Gamma_{\text{total}}$ Γ_{50} / Γ

(X \bar{X} = vectors with $m < 3.1$ GeV)

VALUE (units 10^{-3})	CL%	DOCUMENT ID	TECN	COMMENT
< 1	90	²⁹ BALEST 95	CLEO	$e^+ e^- \rightarrow \gamma + X \bar{X}$

²⁹ For a noninteracting vector X with mass < 3.1 GeV.

$\Gamma(\gamma X \rightarrow \gamma + \geq 4 \text{ prongs}) / \Gamma_{\text{total}}$ Γ_{51} / Γ

(1.5 GeV < $m_X < 5.0$ GeV)

VALUE (units 10^{-4})	CL%	DOCUMENT ID	TECN	COMMENT
< 1.78	95	ROSNER 07A	CLEO	$e^+ e^- \rightarrow \gamma X$

$\Gamma(\text{invisible}) / \Gamma_{\text{total}}$ Γ_{52} / Γ

VALUE (units 10^{-2})	CL%	DOCUMENT ID	TECN	COMMENT
< 0.25	90	TAJIMA 07	BELL	$\Upsilon(3S) \rightarrow \pi^+ \pi^- \Upsilon(1S)$
••• We do not use the following data for averages, fits, limits, etc. •••				
< 0.39	90	RUBIN 07	CLEO	$\Upsilon(2S) \rightarrow \pi^+ \pi^- \Upsilon(1S)$

$\Upsilon(1S)$ REFERENCES

ASNER 07	PR D75 012009	D.M. Asner et al.	(CLEO Collab.)
ATHAR 07A	PR D76 072003	S.B. Athar et al.	(CLEO Collab.)
BESSON 07	PRL 98 052002	D. Besson et al.	(CLEO Collab.)
BESSON 07A	PR D75 072001	D. Besson et al.	(CLEO Collab.)
ROSNER 07A	PR D76 117102	J.L. Rosner et al.	(CLEO Collab.)
RUBIN 07	PR D75 031104	P. Rubin et al.	(CLEO Collab.)
TAJIMA 07	PRL 98 132001	O. Tajima et al.	(BELLE Collab.)
AQUINES 06A	PR D74 092006	O. Aquines et al.	(CLEO Collab.)
ATHAR 06	PR D73 032001	S.B. Athar et al.	(CLEO Collab.)
ROSNER 06	PRL 96 092003	J.L. Rosner et al.	(CLEO Collab.)
ADAMS 05	PRL 94 012001	G.S. Adams et al.	(CLEO Collab.)
BRIERE 04	PR D70 072001	R.A. Briere et al.	(CLEO Collab.)
ARTUSO 03	PR D67 052003	M. Artuso et al.	(CLEO Collab.)
MASEK 02	PR D65 072002	G. Masek et al.	(CLEO Collab.)
RICHICHI 01B	PRL 87 141801	S.J. Richichi et al.	(CLEO Collab.)
ARTAMONOV 00	PL B474 427	A.S. Artamonov et al.	(CLEO Collab.)
ANASTASSOV 99	PRL 82 286	A. Anastassov et al.	(CLEO Collab.)
ALEXANDER 98	PR D58 052004	J.P. Alexander et al.	(CLEO Collab.)
BARU 96	PRPL 267 71	S.E. Baru et al.	(NOVO)
BALEST 95	PR D51 2053	R. Balest et al.	(CLEO Collab.)
CINABRO 94B	PL B340 129	D. Cinabro et al.	(CLEO Collab.)
ALBRECHT 92J	ZPHY C55 25	H. Albrecht et al.	(ARGUS Collab.)
BARU 92	ZPHY C54 229	S.E. Baru et al.	(NOVO)
BARU 92B	ZPHY C56 547	S.E. Baru et al.	(NOVO)
KOBEL 92	ZPHY C53 193	M. Kobel et al.	(Crystal Ball Collab.)
BLINOV 90	PL B245 311	A.E. Blinov et al.	(NOVO)
FULTON 90B	PR D41 1401	R. Fulton et al.	(CLEO Collab.)
MASCHMANN 90	ZPHY C46 555	W.S. Maschmann et al.	(Crystal Ball Collab.)
ALBRECHT 89	ZPHY C42 349	H. Albrecht et al.	(ARGUS Collab.)
ALEXANDER 89	NP B320 45	J.P. Alexander et al.	(LBL, MICH, SLAC)
BARU 89	ZPHY C42 505	S.E. Baru et al.	(NOVO)
CHEN 89B	PR D39 3528	W.Y. Chen et al.	(CLEO Collab.)
FULTON 89	PL B224 445	R. Fulton et al.	(CLEO Collab.)
KAARSBERG 89	PRL 62 2077	T.M. Kaarsberg et al.	(CUSB Collab.)
BUCHMUEL... 88	HE $e^+ e^-$ Physics 412	W. Buchmueller, S. Cooper	(HANN, DESY, MIT)

Editors: A. Ali and P. Soeding, World Scientific, Singapore

JAKUBOWSKI 88	ZPHY C40 49	Z. Jakubowski et al.	(Crystal Ball Collab.)
SCHMITT 88	ZPHY C40 199	P. Schmitt et al.	(Crystal Ball Collab.)
ALBRECHT 87	ZPHY C35 283	H. Albrecht et al.	(ARGUS Collab.)
COHEN 87	RMP 59 1121	E.R. Cohen, B.N. Taylor	(RIS C, NBS)
BARU 86	ZPHY C30 551	S.E. Baru et al.	(NOVO)
ALBRECHT 85C	PL 154B 452	H. Albrecht et al.	(ARGUS Collab.)
KURAEV 85	SJNP 41 466	E.A. Kurayev, V.S. Fadin	(NOVO)

Translated from YAF 41 73A.

ARTAMONOV 84	PL 137B 272	A.S. Artamonov et al.	(NOVO)
BESSON 84B	PR D30 1433	D. Besson et al.	(CLEO Collab.)
GILES 84B	PR D29 1285	R. Giles et al.	(CLEO Collab.)
MACKAY 84	PR D29 2483	W.W. MacKay et al.	(CUSB Collab.)
ANDREWS 83	PRL 50 807	D.E. Andrews et al.	(CLEO Collab.)
GILES 83	PRL 50 877	R. Giles et al.	(HARV, OSU, ROCH, RUTG+)
NICZYPORUK 83	ZPHY C17 197	B. Niczyporuk et al.	(LENA Collab.)
ALBRECHT 82	PL 116B 383	H. Albrecht et al.	(DESY, DORT, HEIDH+)
ARTAMONOV 82	PL 118B 225	A.S. Artamonov et al.	(NOVO)
NICZYPORUK 82	ZPHY C15 299	B. Niczyporuk et al.	(LENA Collab.)
BERGER 80C	PL 93B 497	C. Berger et al.	(PLUTO Collab.)
BOCK 80	ZPHY C6 125	P. Bock et al.	(HEIDP, MPIM, DESY, HAMB)
BERGER 79	ZPHY C1 343	C. Berger et al.	(PLUTO Collab.)

OTHER RELATED PAPERS

BRIERE 07	PR D76 012005	R.A. Briere et al.	(CLEO Collab.)
CRONIN-HEN... 07	PR D76 072001	D. Cronin-Hennessy et al.	(CLEO Collab.)
BESSON 06A	PR D74 012003	D. Besson et al.	(CLEO Collab.)
KOENIGS... 86	DESY 86/136	K. Koenigsman	(DESY)
ALBRECHT 84	PL 134B 137	H. Albrecht et al.	(ARGUS Collab.)
ARTAMONOV 84	PL 137B 272	A.S. Artamonov et al.	(NOVO)
ARTAMONOV 82	PL 118B 225	A.S. Artamonov et al.	(NOVO)
BERGER 78	PL 76B 243	C. Berger et al.	(PLUTO Collab.)
BIENLEIN 78	PL 78B 360	J.K. Bienlein et al.	(DESY, HAMB, HEIDH+)
DARDEN 78	PL 76B 246	C.W. Darden et al.	(DESY, DORT, HEIDH+)
GARELICK 78	PR D18 945	D.A. Garelick et al.	(NEAS, WASH, TUFTS)
KAPLAN 78	PRL 40 435	D.M. Kaplan et al.	(STON, FNAL, COLU)
YOH 78	PRL 41 684	J.K. Yoh et al.	(COLU, FNAL, STON)
COBB 77	PL 72B 273	J.H. Cobb et al.	(BNL, CERN, SYRA, YALE)
HERB 77	PRL 39 252	S.W. Herb et al.	(COLU, FNAL, STON)
INNES 77	PRL 39 1240	W.R. Innes et al.	(COLU, FNAL, STON)

$\chi_{b0}(1P)$

$$I^G(J^{PC}) = 0^+(0^{++})$$

J needs confirmation.

Observed in radiative decay of the $\Upsilon(2S)$, therefore $C = +$. Branching ratio requires E1 transition, M1 is strongly disfavored, therefore $P = +$.

$\chi_{b0}(1P)$ MASS

VALUE (MeV)	DOCUMENT ID
9859.44 ± 0.42 ± 0.31 OUR EVALUATION	From average γ energy below, using $\Upsilon(2S)$ mass = 10023.26 ± 0.31 MeV

γ ENERGY IN $\Upsilon(2S)$ DECAY

VALUE (MeV)	DOCUMENT ID	TECN	COMMENT
162.5 ± 0.4 OUR AVERAGE			
162.56 ± 0.19 ± 0.42	ARTUSO 05	CLEO	$\Upsilon(2S) \rightarrow \gamma X$
162.0 ± 0.8 ± 1.2	EDWARDS 99	CLE2	$\Upsilon(2S) \rightarrow \gamma \chi(1P)$
162.1 ± 0.5 ± 1.4	ALBRECHT 85E	ARG	$\Upsilon(2S) \rightarrow \text{conv. } \gamma X$
163.8 ± 1.6 ± 2.7	NERNST 85	CBAL	$\Upsilon(2S) \rightarrow \gamma X$
158.0 ± 7 ± 1	HAAS 84	CLEO	$\Upsilon(2S) \rightarrow \text{conv. } \gamma X$
••• We do not use the following data for averages, fits, limits, etc. •••			
149.4 ± 0.7 ± 5.0	KLOPFEN... 83	CUSB	$\Upsilon(2S) \rightarrow \gamma X$

$\chi_{b0}(1P)$ DECAY MODES

Mode	Fraction (Γ_i / Γ)	Confidence level
$\Gamma_1 \quad \gamma \Upsilon(1S)$	< 6 %	90%

$\chi_{b0}(1P)$ BRANCHING RATIOS

$\Gamma(\gamma \Upsilon(1S)) / \Gamma_{\text{total}}$	Γ_1 / Γ			
VALUE	CL%	DOCUMENT ID	TECN	COMMENT
< 0.06	90	WALK 86	CBAL	$\Upsilon(2S) \rightarrow \gamma \gamma \ell^+ \ell^-$
••• We do not use the following data for averages, fits, limits, etc. •••				
< 0.11	90	PAUSS 83	CUSB	$\Upsilon(2S) \rightarrow \gamma \gamma \ell^+ \ell^-$

$\chi_{b0}(1P)$ REFERENCES

ARTUSO 05	PRL 94 032001	M. Artuso et al.	(CLEO Collab.)
EDWARDS 99	PR D59 032003	K.W. Edwards et al.	(CLEO Collab.)
WALK 86	PR D34 2611	W.S. Walk et al.	(Crystal Ball Collab.)
ALBRECHT 85E	PL 160B 331	H. Albrecht et al.	(ARGUS Collab.)
NERNST 85	PRL 54 2195	R. Nernst et al.	(Crystal Ball Collab.)
HAAS 84	PRL 52 799	J. Haas et al.	(CLEO Collab.)
KLOPFEN... 83	PRL 51 160	C. Klopfenstein et al.	(CUSB Collab.)
PAUSS 83	PL 130B 439	F. Pauss et al.	(MPIM, COLU, CORN, LSU+)

See key on page 373

Meson Particle Listings

$\chi_{b1}(1P), \chi_{b2}(1P), \Upsilon(2S)$

$\chi_{b1}(1P)$ $I^G(J^{PC}) = 0^+(1^{++})$
 J needs confirmation.
 Observed in radiative decay of the $\Upsilon(2S)$, therefore $C = +$. Branching ratio requires E1 transition, M1 is strongly disfavored, therefore $P = +$. $J = 1$ from SKWARNICKI 87.

$\chi_{b2}(1P)$ $I^G(J^{PC}) = 0^+(2^{++})$
 J needs confirmation.
 Observed in radiative decay of the $\Upsilon(2S)$, therefore $C = +$. Branching ratio requires E1 transition, M1 is strongly disfavored, therefore $P = +$. $J = 2$ from SKWARNICKI 87.

$\chi_{b1}(1P)$ MASS

VALUE (MeV)	DOCUMENT ID
9892.78 ± 0.26 ± 0.31 OUR EVALUATION	From average γ energy below, using $\Upsilon(2S)$ mass = 10023.26 ± 0.31 MeV

$\chi_{b2}(1P)$ MASS

VALUE (MeV)	DOCUMENT ID
9912.21 ± 0.26 ± 0.31 OUR EVALUATION	From average γ energy below, using $\Upsilon(2S)$ mass = 10023.26 ± 0.31 MeV

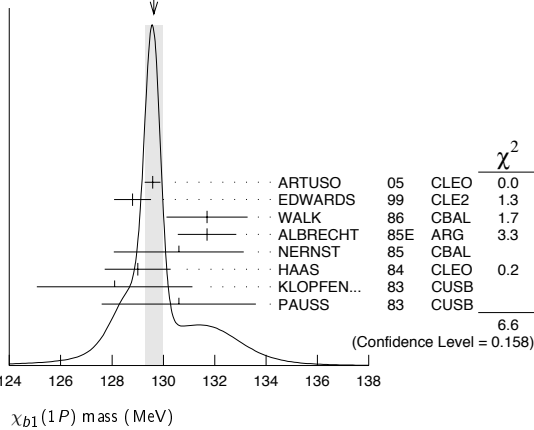
γ ENERGY IN $\Upsilon(2S)$ DECAY

VALUE (MeV)	DOCUMENT ID	TECN	COMMENT
129.63 ± 0.33 OUR AVERAGE	Error includes scale factor of 1.3.		See the ideogram below.
129.58 ± 0.09 ± 0.29	ARTUSO 05	CLEO	$\Upsilon(2S) \rightarrow \gamma X$
128.8 ± 0.4 ± 0.6	EDWARDS 99	CLE2	$\Upsilon(2S) \rightarrow \gamma \chi(1P)$
131.7 ± 0.9 ± 1.3	WALK 86	CBAL	$\Upsilon(2S) \rightarrow \gamma \gamma \ell^+ \ell^-$
131.7 ± 0.3 ± 1.1	ALBRECHT 85E	ARG	$\Upsilon(2S) \rightarrow \text{conv.} \gamma X$
130.6 ± 0.8 ± 2.4	NERNST 85	CBAL	$\Upsilon(2S) \rightarrow \gamma X$
129 ± 0.8 ± 1	HAAS 84	CLEO	$\Upsilon(2S) \rightarrow \text{conv.} \gamma X$
128.1 ± 0.4 ± 3.0	KLOPFEN... 83	CUSB	$\Upsilon(2S) \rightarrow \gamma X$
130.6 ± 3.0	PAUSS 83	CUSB	$\Upsilon(2S) \rightarrow \gamma \gamma \ell^+ \ell^-$

γ ENERGY IN $\Upsilon(2S)$ DECAY

VALUE (MeV)	DOCUMENT ID	TECN	COMMENT
110.44 ± 0.29 OUR AVERAGE	Error includes scale factor of 1.1.		
110.58 ± 0.08 ± 0.30	ARTUSO 05	CLEO	$\Upsilon(2S) \rightarrow \gamma X$
110.8 ± 0.3 ± 0.6	EDWARDS 99	CLE2	$\Upsilon(2S) \rightarrow \gamma \chi(1P)$
107.0 ± 1.1 ± 1.3	WALK 86	CBAL	$\Upsilon(2S) \rightarrow \gamma \gamma \ell^+ \ell^-$
110.6 ± 0.3 ± 0.9	ALBRECHT 85E	ARG	$\Upsilon(2S) \rightarrow \text{conv.} \gamma X$
110.4 ± 0.8 ± 2.2	NERNST 85	CBAL	$\Upsilon(2S) \rightarrow \gamma X$
109.5 ± 0.7 ± 1.0	HAAS 84	CLEO	$\Upsilon(2S) \rightarrow \text{conv.} \gamma X$
108.2 ± 0.3 ± 2.0	KLOPFEN... 83	CUSB	$\Upsilon(2S) \rightarrow \gamma X$
108.8 ± 4.0	PAUSS 83	CUSB	$\Upsilon(2S) \rightarrow \gamma \gamma \ell^+ \ell^-$

WEIGHTED AVERAGE
 129.63±0.33 (Error scaled by 1.3)



$\chi_{b2}(1P)$ DECAY MODES

Mode	Fraction (Γ_i/Γ)
$\Gamma_1 \gamma \Upsilon(1S)$	(22 ± 4) %

$\chi_{b2}(1P)$ BRANCHING RATIOS

$\Gamma(\gamma \Upsilon(1S))/\Gamma_{\text{total}}$	DOCUMENT ID	TECN	COMMENT	Γ_1/Γ
0.22 ± 0.04 OUR AVERAGE				
0.27 ± 0.06 ± 0.06	WALK 86	CBAL	$\Upsilon(2S) \rightarrow \gamma \gamma \ell^+ \ell^-$	
0.20 ± 0.05	KLOPFEN... 83	CUSB	$\Upsilon(2S) \rightarrow \gamma \gamma \ell^+ \ell^-$	

$\chi_{b2}(1P)$ REFERENCES

ARTUSO 05	PRL 94 032001	M. Artuso et al.	(CLEO Collab.)
EDWARDS 99	PR D59 032003	K.W. Edwards et al.	(CLEO Collab.)
SKWARNICKI 87	PRL 58 972	T. Skwarnicki et al.	(Crystal Ball Collab.)
WALK 86	PR D34 2611	W.S. Walk et al.	(Crystal Ball Collab.)
ALBRECHT 85E	PL 160B 331	H. Albrecht et al.	(ARGUS Collab.)
NERNST 85	PRL 54 2195	R. Nernst et al.	(Crystal Ball Collab.)
HAAS 84	PRL 52 799	J. Haas et al.	(CLEO Collab.)
KLOPFEN... 83	PRL 51 160	C. Klopffenstein et al.	(CUSB Collab.)
PAUSS 83	PL 130B 439	F. Pauss et al.	(MPIM, COLU, CORN, LSU+)

$\Upsilon(2S)$ $I^G(J^{PC}) = 0^-(1^{--})$

$\Upsilon(2S)$ MASS

VALUE (GeV)	DOCUMENT ID	TECN	COMMENT
10.02326 ± 0.00031 OUR AVERAGE			
10.0235 ± 0.0005	¹ ARTAMONOV 00	MD1	$e^+ e^- \rightarrow \text{hadrons}$
10.0231 ± 0.0004	BARBER 84	REDE	$e^+ e^- \rightarrow \text{hadrons}$
••• We do not use the following data for averages, fits, limits, etc. •••			
10.0236 ± 0.0005	^{2,3} BARU	86B	$e^+ e^- \rightarrow \text{hadrons}$
			¹ Reanalysis of BARU 86B using new electron mass (COHEN 87).
			² Reanalysis of ARTAMONOV 84.
			³ Superseded by ARTAMONOV 00.

$\Upsilon(2S)$ WIDTH

VALUE (keV)	DOCUMENT ID
31.98 ± 2.63 OUR EVALUATION	See the Note on "Width Determinations of the Υ States"

$\Upsilon(2S)$ DECAY MODES

Mode	Fraction (Γ_i/Γ)	Scale factor/Confidence level
$\Gamma_1 \Upsilon(1S) \pi^+ \pi^-$	(18.8 ± 0.6) %	
$\Gamma_2 \Upsilon(1S) \pi^0 \pi^0$	(9.0 ± 0.8) %	
$\Gamma_3 \tau^+ \tau^-$	(2.00 ± 0.21) %	
$\Gamma_4 \mu^+ \mu^-$	(1.93 ± 0.17) %	S=2.2
$\Gamma_5 e^+ e^-$	(1.91 ± 0.16) %	
$\Gamma_6 \Upsilon(1S) \pi^0$	< 1.1	× 10 ⁻³ CL=90%
$\Gamma_7 \Upsilon(1S) \eta$	< 2	× 10 ⁻³ CL=90%
$\Gamma_8 J/\psi(1S)$ anything	< 6	× 10 ⁻³ CL=90%
$\Gamma_9 \bar{d}$ anything	(3.4 ± 0.6) × 10 ⁻⁵	
Γ_{10} hadrons	(94 ± 11) %	

$\chi_{b1}(1P)$ DECAY MODES

Mode	Fraction (Γ_i/Γ)
$\Gamma_1 \gamma \Upsilon(1S)$	(35 ± 8) %

$\chi_{b1}(1P)$ BRANCHING RATIOS

$\Gamma(\gamma \Upsilon(1S))/\Gamma_{\text{total}}$	DOCUMENT ID	TECN	COMMENT	Γ_1/Γ
0.35 ± 0.08 OUR AVERAGE				
0.32 ± 0.06 ± 0.07	WALK 86	CBAL	$\Upsilon(2S) \rightarrow \gamma \gamma \ell^+ \ell^-$	
0.47 ± 0.18	KLOPFEN... 83	CUSB	$\Upsilon(2S) \rightarrow \gamma \gamma \ell^+ \ell^-$	

$\chi_{b1}(1P)$ Cross-Particle Branching Ratios

$B(\chi_{b2}(1P) \rightarrow pX + \bar{p}X)/B(\chi_{b1}(1P) \rightarrow pX + \bar{p}X)$	DOCUMENT ID	TECN	COMMENT
1.068 ± 0.010 ± 0.040	BRIERE 07	CLEO	$\Upsilon(2S) \rightarrow \gamma \chi_{b,J}(1P)$

$B(\chi_{b0}(1P) \rightarrow pX + \bar{p}X)/B(\chi_{b1}(1P) \rightarrow pX + \bar{p}X)$	DOCUMENT ID	TECN	COMMENT
1.11 ± 0.15 ± 0.20	BRIERE 07	CLEO	$\Upsilon(2S) \rightarrow \gamma \chi_{b,J}(1P)$

$\chi_{b1}(1P)$ REFERENCES

BRIERE 07	PR D76 012005	R.A. Briere et al.	(CLEO Collab.)
ARTUSO 05	PRL 94 032001	M. Artuso et al.	(CLEO Collab.)
EDWARDS 99	PR D59 032003	K.W. Edwards et al.	(CLEO Collab.)
SKWARNICKI 87	PRL 58 972	T. Skwarnicki et al.	(Crystal Ball Collab.)
WALK 86	PR D34 2611	W.S. Walk et al.	(Crystal Ball Collab.)
ALBRECHT 85E	PL 160B 331	H. Albrecht et al.	(ARGUS Collab.)
NERNST 85	PRL 54 2195	R. Nernst et al.	(Crystal Ball Collab.)
HAAS 84	PRL 52 799	J. Haas et al.	(CLEO Collab.)
KLOPFEN... 83	PRL 51 160	C. Klopffenstein et al.	(CUSB Collab.)
PAUSS 83	PL 130B 439	F. Pauss et al.	(MPIM, COLU, CORN, LSU+)

Meson Particle Listings

$\Upsilon(2S)$

Radiative decays

Γ	Decay	Value	CL	EVTS	CL=90%
Γ_{11}	$\gamma \chi_{b1}(1P)$	$(6.9 \pm 0.4) \%$			
Γ_{12}	$\gamma \chi_{b2}(1P)$	$(7.15 \pm 0.35) \%$			
Γ_{13}	$\gamma \chi_{b0}(1P)$	$(3.8 \pm 0.4) \%$			
Γ_{14}	$\gamma f_0(1710)$	< 5.9	$\times 10^{-4}$		CL=90%
Γ_{15}	$\gamma f_2'(1525)$	< 5.3	$\times 10^{-4}$		CL=90%
Γ_{16}	$\gamma f_2(1270)$	< 2.41	$\times 10^{-4}$		CL=90%
Γ_{17}	$\gamma f_J(2220)$				
Γ_{18}	$\gamma \eta_b(1S)$	< 5.1	$\times 10^{-4}$		CL=90%
Γ_{19}	$\gamma X \rightarrow \gamma + \geq 4$ prongs	$[a] < 1.95$	$\times 10^{-4}$		CL=95%

[a] 1.5 GeV < m_X < 5.0 GeV

$\Upsilon(2S) \Gamma(I)\Gamma(e^+e^-)/\Gamma(\text{total})$

$\Gamma(e^+e^-) \times \Gamma(\mu^+\mu^-)/\Gamma(\text{total})$	DOCUMENT ID	TECN	COMMENT	Γ_5/Γ
0.65 ± 0.15 ± 1.0	KOBEL	92	CBAL $e^+e^- \rightarrow \mu^+\mu^-$	

$\Gamma(\text{hadrons}) \times \Gamma(e^+e^-)/\Gamma(\text{total})$	DOCUMENT ID	TECN	COMMENT	$\Gamma_{10}\Gamma_5/\Gamma$
0.577 ± 0.009 OUR AVERAGE				
0.581 ± 0.004 ± 0.009	4 ROSNER	06	CLEO $10.0 e^+e^- \rightarrow$ hadrons	
0.552 ± 0.031 ± 0.017	4 BARU	96	MD1 $e^+e^- \rightarrow$ hadrons	
0.54 ± 0.04 ± 0.02	4 JAKUBOWSKI	88	CBAL $e^+e^- \rightarrow$ hadrons	
0.58 ± 0.03 ± 0.04	5 GILES	84B	CLEO $e^+e^- \rightarrow$ hadrons	
0.60 ± 0.12 ± 0.07	5 ALBRECHT	82	DASP $e^+e^- \rightarrow$ hadrons	
0.54 ± 0.07 ^{+0.09} / _{-0.05}	5 NICZYPORUK	81c	LENA $e^+e^- \rightarrow$ hadrons	
0.41 ± 0.18	5 BOCK	80	CNTR $e^+e^- \rightarrow$ hadrons	

⁴Radiative corrections evaluated following KURAEV 85.
⁵Radiative corrections reevaluated by BUCHMUELLER 88 following KURAEV 85.

$\Upsilon(2S)$ PARTIAL WIDTHS

$\Gamma(e^+e^-)$	DOCUMENT ID	Γ_5
0.612 ± 0.011 OUR EVALUATION		

$\Upsilon(2S)$ BRANCHING RATIOS

$\Gamma(\Upsilon(1S)\pi^+\pi^-)/\Gamma(\text{total})$	EVTS	DOCUMENT ID	TECN	COMMENT	Γ_1/Γ
0.188 ± 0.006 OUR AVERAGE					
0.192 ± 0.002 ± 0.010	52.6k	6 ALEXANDER	98	CLE2 $\pi^+\pi^-\ell^+\ell^-$, $\pi^+\pi^-\text{MM}$	
0.181 ± 0.005 ± 0.010	11.6k	ALBRECHT	87	ARG $e^+e^- \rightarrow$ $\pi^+\pi^-\text{MM}$	
0.169 ± 0.040		GELPHMAN	85	CBAL $e^+e^- \rightarrow$ $e^+e^-\pi^+\pi^-$	
0.191 ± 0.012 ± 0.006		BESSION	84	CLEO $\pi^+\pi^-\text{MM}$	
0.189 ± 0.026		FONSECA	84	CUSB $e^+e^- \rightarrow$ $\ell^+\ell^-\pi^+\pi^-$	
0.21 ± 0.07	7	NICZYPORUK	81B	LENA $e^+e^- \rightarrow$ $\ell^+\ell^-\pi^+\pi^-$	

⁶Using $B(\Upsilon(1S) \rightarrow e^+e^-) = (2.52 \pm 0.17)\%$ and $B(\Upsilon(1S) \rightarrow \mu^+\mu^-) = (2.48 \pm 0.07)\%$.

$\Gamma(\Upsilon(1S)\pi^0\pi^0)/\Gamma(\text{total})$	EVTS	DOCUMENT ID	TECN	COMMENT	Γ_2/Γ
0.090 ± 0.008 OUR AVERAGE					
0.092 ± 0.006 ± 0.008	275	7 ALEXANDER	98	CLE2 $e^+e^- \rightarrow \ell^+\ell^-\pi^0\pi^0$	
0.095 ± 0.019 ± 0.019	25	ALBRECHT	87	ARG $e^+e^- \rightarrow \pi^0\pi^0\ell^+\ell^-$	
0.080 ± 0.015		GELPHMAN	85	CBAL $e^+e^- \rightarrow \ell^+\ell^-\pi^0\pi^0$	
0.103 ± 0.023		FONSECA	84	CUSB $e^+e^- \rightarrow \ell^+\ell^-\pi^0\pi^0$	

⁷Using $B(\Upsilon(1S) \rightarrow e^+e^-) = (2.52 \pm 0.17)\%$ and $B(\Upsilon(1S) \rightarrow \mu^+\mu^-) = (2.48 \pm 0.07)\%$.

$\Gamma(\tau^+\tau^-)/\Gamma(\text{total})$	EVTS	DOCUMENT ID	TECN	COMMENT	Γ_3/Γ
2.00 ± 0.21 OUR AVERAGE					
2.00 ± 0.12 ± 0.18	22k	8 BESSION	07	CLEO $e^+e^- \rightarrow \Upsilon(2S) \rightarrow \tau^+\tau^-$	
1.7 ± 1.5 ± 0.6		HAAS	84B	CLEO $e^+e^- \rightarrow \tau^+\tau^-$	

⁸BESSION 07 reports $[B(\Upsilon(2S) \rightarrow \tau^+\tau^-)] / [B(\Upsilon(2S) \rightarrow \mu^+\mu^-)] = 1.04 \pm 0.04 \pm 0.05$. We multiply by our best value $B(\Upsilon(2S) \rightarrow \mu^+\mu^-) = (1.93 \pm 0.17) \times 10^{-2}$. Our first error is their experiment's error and our second error is the systematic error from using our best value.

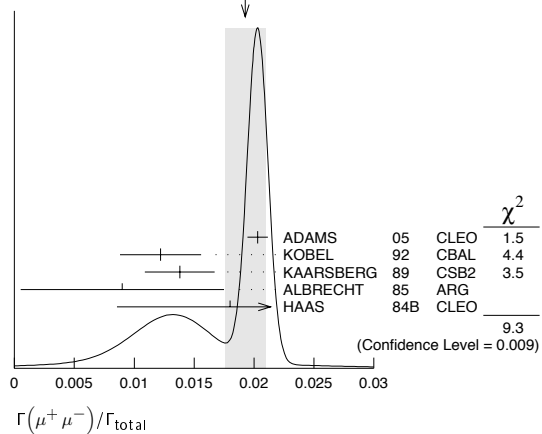
$\Gamma(\mu^+\mu^-)/\Gamma(\text{total})$

VALUE	CL%	EVTS	DOCUMENT ID	TECN	COMMENT	Γ_4/Γ
0.0193 ± 0.0017 OUR AVERAGE					Error includes scale factor of 2.2. See the ideogram below.	
0.0203 ± 0.0003 ± 0.0008		120k	ADAMS	05	CLEO $e^+e^- \rightarrow$ $\mu^+\mu^-$	
0.0122 ± 0.0028 ± 0.0019			9 KOBEL	92	CBAL $e^+e^- \rightarrow$ $\mu^+\mu^-$	
0.0138 ± 0.0025 ± 0.0015			KAARSBERG	89	CSB2 $e^+e^- \rightarrow$ $\mu^+\mu^-$	
0.009 ± 0.006 ± 0.006			10 ALBRECHT	85	ARG $e^+e^- \rightarrow$ $\mu^+\mu^-$	
0.018 ± 0.008 ± 0.005			HAAS	84B	CLEO $e^+e^- \rightarrow$ $\mu^+\mu^-$	
< 0.038		90	NICZYPORUK	81c	LENA $e^+e^- \rightarrow$ $\mu^+\mu^-$	

••• We do not use the following data for averages, fits, limits, etc. •••

⁹Taking into account interference between the resonance and continuum.
¹⁰Re-evaluated using $B(\Upsilon(1S) \rightarrow \mu^+\mu^-) = 0.026$.

WEIGHTED AVERAGE
 0.0193 ± 0.0017 (Error scaled by 2.2)



$\Gamma(\tau^+\tau^-)/\Gamma(\mu^+\mu^-)$	EVTS	DOCUMENT ID	TECN	COMMENT	Γ_3/Γ_4
1.04 ± 0.04 ± 0.05	22k	BESSION	07	CLEO $e^+e^- \rightarrow \Upsilon(2S)$	

$\Gamma(\Upsilon(1S)\pi^0)/\Gamma(\text{total})$	CL%	DOCUMENT ID	TECN	COMMENT	Γ_6/Γ
< 0.0011		ALEXANDER	98	CLE2 $e^+e^- \rightarrow \ell^+\ell^-\gamma\gamma$	
< 0.008		LURZ	87	CBAL $e^+e^- \rightarrow \ell^+\ell^-\gamma\gamma$	

$\Gamma(\Upsilon(1S)\eta)/\Gamma(\text{total})$	CL%	DOCUMENT ID	TECN	COMMENT	Γ_7/Γ
< 0.002		FONSECA	84	CUSB	
< 0.0028		ALEXANDER	98	CLE2 $e^+e^- \rightarrow \ell^+\ell^-\eta$	
< 0.005		ALBRECHT	87	ARG $e^+e^- \rightarrow$ $\pi^+\pi^-\ell^+\ell^-$	
< 0.007		LURZ	87	CBAL $e^+e^- \rightarrow \ell^+\ell^-\text{MM}$ $3\pi^0$	
< 0.010		BESSION	84	CLEO	

$\Gamma(J/\psi(1S) \text{ anything})/\Gamma(\text{total})$	CL%	DOCUMENT ID	TECN	COMMENT	Γ_8/Γ
< 0.006		MASCHMANN	90	CBAL $e^+e^- \rightarrow$ hadrons	

$\Gamma(\bar{d} \text{ anything})/\Gamma(\text{total})$	EVTS	DOCUMENT ID	TECN	COMMENT	Γ_9/Γ
3.37 ± 0.50 ± 0.25	58	ASNER	07	CLEO $e^+e^- \rightarrow \bar{d}X$	

$\Gamma(\gamma\chi_{b1}(1P))/\Gamma(\text{total})$	EVTS	DOCUMENT ID	TECN	COMMENT	Γ_{11}/Γ
0.069 ± 0.004 OUR AVERAGE					
0.0693 ± 0.0012 ± 0.0041	407k	ARTUSO	05	CLEO $e^+e^- \rightarrow \gamma X$	
0.069 ± 0.005 ± 0.009		EDWARDS	99	CLE2 $\Upsilon(2S) \rightarrow \gamma\chi(1P)$	
0.091 ± 0.018 ± 0.022		ALBRECHT	85E	ARG $e^+e^- \rightarrow \gamma\text{conv. } X$	
0.065 ± 0.007 ± 0.012		NERNST	85	CBAL $e^+e^- \rightarrow \gamma X$	
0.080 ± 0.017 ± 0.016		HAAS	84	CLEO $e^+e^- \rightarrow \gamma\text{conv. } X$	
0.059 ± 0.014		KLOPFEN...	83	CUSB $e^+e^- \rightarrow \gamma X$	

See key on page 373

Meson Particle Listings

$\Upsilon(2S)$, $\Upsilon(1D)$, $\chi_{b0}(2P)$

$\Gamma(\gamma\chi_{b2}(1P))/\Gamma_{total}$ Γ_{12}/Γ

VALUE	EVTS	DOCUMENT ID	TECN	COMMENT
0.0715 ± 0.0035 OUR AVERAGE				
0.0724 ± 0.0011 ± 0.0040	410k	ARTUSO 05	CLEO	$e^+e^- \rightarrow \gamma X$
0.074 ± 0.005 ± 0.008		EDWARDS 99	CLE2	$\Upsilon(2S) \rightarrow \gamma\chi(1P)$
0.098 ± 0.021 ± 0.024		ALBRECHT 85E	ARG	$e^+e^- \rightarrow \gamma conv. X$
0.058 ± 0.007 ± 0.010		NERNST 85	CBAL	$e^+e^- \rightarrow \gamma X$
0.102 ± 0.018 ± 0.021		HAAS 84	CLEO	$e^+e^- \rightarrow \gamma conv. X$
0.061 ± 0.014		KLOPFEN... 83	CUSB	$e^+e^- \rightarrow \gamma X$

$\Gamma(\gamma\chi_{b0}(1P))/\Gamma_{total}$ Γ_{13}/Γ

VALUE	EVTS	DOCUMENT ID	TECN	COMMENT
0.038 ± 0.004 OUR AVERAGE				
0.0375 ± 0.0012 ± 0.0047	198k	ARTUSO 05	CLEO	$e^+e^- \rightarrow \gamma X$
0.034 ± 0.005 ± 0.006		EDWARDS 99	CLE2	$\Upsilon(2S) \rightarrow \gamma\chi(1P)$
0.064 ± 0.014 ± 0.016		ALBRECHT 85E	ARG	$e^+e^- \rightarrow \gamma conv. X$
0.036 ± 0.008 ± 0.009		NERNST 85	CBAL	$e^+e^- \rightarrow \gamma X$
0.044 ± 0.023 ± 0.009		HAAS 84	CLEO	$e^+e^- \rightarrow \gamma conv. X$
••• We do not use the following data for averages, fits, limits, etc. •••				
0.035 ± 0.014		KLOPFEN... 83	CUSB	$e^+e^- \rightarrow \gamma X$

$\Gamma(\gamma f_0(1710))/\Gamma_{total}$ Γ_{14}/Γ

VALUE (units 10^{-5})	CL%	DOCUMENT ID	TECN	COMMENT
<5.9		11 ALBRECHT 89	ARG	$\Upsilon(2S) \rightarrow \gamma K^+ K^-$
••• We do not use the following data for averages, fits, limits, etc. •••				
< 5.9		12 ALBRECHT 89	ARG	$\Upsilon(2S) \rightarrow \gamma\pi^+\pi^-$
11 Re-evaluated assuming $B(f_0(1710) \rightarrow K^+K^-) = 0.19$.				
12 Includes unknown branching ratio of $f_0(1710) \rightarrow \pi^+\pi^-$.				

$\Gamma(\gamma f'_2(1525))/\Gamma_{total}$ Γ_{15}/Γ

VALUE (units 10^{-5})	CL%	DOCUMENT ID	TECN	COMMENT
<5.3		13 ALBRECHT 89	ARG	$\Upsilon(2S) \rightarrow \gamma K^+ K^-$
13 Re-evaluated assuming $B(f'_2(1525) \rightarrow K\bar{K}) = 0.71$.				

$\Gamma(\gamma f_2(1270))/\Gamma_{total}$ Γ_{16}/Γ

VALUE (units 10^{-5})	CL%	DOCUMENT ID	TECN	COMMENT
<24.1		14 ALBRECHT 89	ARG	$\Upsilon(2S) \rightarrow \gamma\pi^+\pi^-$
14 Using $B(f_2(1270) \rightarrow \pi\pi) = 0.84$.				

$\Gamma(\gamma f_J(2220))/\Gamma_{total}$ Γ_{17}/Γ

VALUE (units 10^{-5})	CL%	DOCUMENT ID	TECN	COMMENT
••• We do not use the following data for averages, fits, limits, etc. •••				
<6.8		15 ALBRECHT 89	ARG	$\Upsilon(2S) \rightarrow \gamma K^+ K^-$
15 Includes unknown branching ratio of $f_J(2220) \rightarrow K^+K^-$.				

$\Gamma(\gamma\eta_b(1S))/\Gamma_{total}$ Γ_{18}/Γ

VALUE (units 10^{-4})	CL%	DOCUMENT ID	TECN	COMMENT
<5.1		90 ARTUSO 05	CLEO	$e^+e^- \rightarrow \gamma X$

$\Gamma(\gamma X \rightarrow \gamma + \geq 4 \text{ prongs})/\Gamma_{total}$ Γ_{19}/Γ

(1.5 GeV < m_X < 5.0 GeV)

VALUE (units 10^{-4})	CL%	DOCUMENT ID	TECN	COMMENT
<1.95		95 ROSNER 07A	CLEO	$e^+e^- \rightarrow \gamma X$

$\Upsilon(2S)$ REFERENCES

ASNER 07 PR D75 012009	D.M. Asner et al.	(CLEO Collab.)
BESSON 07 PRL 98 052002	D. Besson et al.	(CLEO Collab.)
ROSNER 07A PR D76 117102	J.L. Rosner et al.	(CLEO Collab.)
ROSNER 06 PRL 96 092003	J.L. Rosner et al.	(CLEO Collab.)
ADAMS 05 PRL 94 012001	G.S. Adams et al.	(CLEO Collab.)
ARTUSO 05 PRL 94 032001	M. Artuso et al.	(CLEO Collab.)
ARTAMONOV 00 PL B474 427	A.S. Artamonov et al.	(NOVO)
EDWARDS 99 PR D59 032003	K.W. Edwards et al.	(CLEO Collab.)
ALEXANDER 98 PR D58 052004	J.P. Alexander et al.	(CLEO Collab.)
BARU 96 PRPL 267 71	S.E. Baru et al.	(NOVO)
KOBEL 92 ZPHY C53 193	M. Kobel et al.	(Crystal Ball Collab.)
MASCHMANN 90 ZPHY C46 555	W.S. Maschmann et al.	(Crystal Ball Collab.)
ALBRECHT 89 ZPHY C42 349	H. Albrecht et al.	(ARGUS Collab.)
KAARSBERG 89 PRL 62 2077	T.M. Kaarsberg et al.	(CUSB Collab.)
BUCHMUEL... 88 HE e^+e^- Physics 412	W. Buchmueller, S. Cooper	(HANN, DESY, MIT)
Editors: A. Ali and P. Soeding, World Scientific, Singapore		
JAKUBOWSKI 88 ZPHY C40 49	Z. Jakubowski et al.	(Crystal Ball Collab.)
ALBRECHT 87 ZPHY C35 283	H. Albrecht et al.	(ARGUS Collab.)
COHEN 87 RMP 59 1121	E.R. Cohen, B.N. Taylor	(RIS-C, NBS)
LURZ 87 ZPHY C36 383	B. Lurz et al.	(Crystal Ball Collab.)
BARU 86B ZPHY C22 622 (erratum)	S.E. Baru et al.	(NOVO)
ALBRECHT 85 ZPHY C28 45	H. Albrecht et al.	(ARGUS Collab.)
ALBRECHT 85E PL 160B 331	H. Albrecht et al.	(ARGUS Collab.)
GELPHMAN 85 PR D32 2893	D. Gelpman et al.	(Crystal Ball Collab.)
KURAEV 85 SJNP 41 466	E.A. Kurayev, V.S. Fadin	(NOVO)
Translated from YAF 41 733.		
NERNST 85 PRL 54 2195	R. Nernst et al.	(Crystal Ball Collab.)
ARTAMONOV 84 PL 137B 272	A.S. Artamonov et al.	(NOVO)
BARBER 84 PL 135B 498	D.P. Barber et al.	(NOVO)
BESSON 84 PR D30 1433	D. Besson et al.	(CLEO Collab.)
FONSECA 84 NP B242 31	V. Fonseca et al.	(CUSB Collab.)
GILES 84B PR D29 1285	R. Giles et al.	(CLEO Collab.)
HAAS 84 PRL 52 799	J. Haas et al.	(CLEO Collab.)
HAAS 84B PR D30 1996	J. Haas et al.	(CLEO Collab.)
KLOPFEN... 83 PRL 51 160	C. Klopstein et al.	(CUSB Collab.)
ALBRECHT 82 PL 116B 383	H. Albrecht et al.	(DESY, DORT, HEIDH+)
NICZYPORUK 81B PL 100B 95	B. Niczyporuk et al.	(LENA Collab.)
NICZYPORUK 81C PL 99B 169	B. Niczyporuk et al.	(LENA Collab.)
BOCK 80 ZPHY C6 125	P. Bock et al.	(HEIDP, MPIM, DESY, HAMB)

OTHER RELATED PAPERS

BRIERE 07 PR D76 012005	R.A. Briere et al.	(CLEO Collab.)
CRONIN-HEN... 07 PR D76 072001	D. Cronin-Hennessy et al.	(CLEO Collab.)
BESSON 06A PR D74 012003	D. Besson et al.	(CLEO Collab.)
GUO 05 NP A761 269	F.-K. Guo et al.	(CLEO Collab.)
ALEXANDER 89 NP B320 45	J.P. Alexander et al.	(LBL, MICH, SLAC)
WALK 86 PR D34 2611	W.S. Walk et al.	(Crystal Ball Collab.)
ALBRECHT 84 PL 134B 137	H. Albrecht et al.	(ARGUS Collab.)
ARTAMONOV 84 PL 137B 272	A.S. Artamonov et al.	(NOVO)
ANDREWS 83 PRL 50 807	D.E. Andrews et al.	(CLEO Collab.)
GREEN 82 PRL 49 617	J. Green et al.	(CLEO Collab.)
BIENLEIN 78 PL 78B 360	J.K. Bienlein et al.	(DESY, HAMB, HEIDP+)
DARDEN 78 PL 76B 246	C.W. Darden et al.	(DESY, DORT, HEIDH+)
KAPLAN 78 PRL 40 435	D.M. Kaplan et al.	(STON, FNAL, COLU)
YOH 78 PRL 41 684	J.K. Yoh et al.	(COLU, FNAL, STON)
COBB 77 PL 72B 273	J.H. Cobb et al.	(BNL, CERN, SYRA, YALE)
HERB 77 PRL 39 252	S.W. Herb et al.	(COLU, FNAL, STON)
INNES 77 PRL 39 1240	W.R. Innes et al.	(COLU, FNAL, STON)

$\Upsilon(1D)$

$$I^G(J^{PC}) = 0^-(2^{--})$$

OMITTED FROM SUMMARY TABLE
J needs confirmation.

$\Upsilon(1D)$ MASS

VALUE (MeV)	EVTS	DOCUMENT ID	TECN	COMMENT
10161.1 ± 0.6 ± 1.6	38	BONVICINI 04	CLE3	$\Upsilon(3S) \rightarrow \gamma X$

$\Upsilon(1D)$ DECAY MODES

Mode	Fraction (Γ_i/Γ)
$\Gamma_1 \gamma\gamma \Upsilon(1S)$	seen
$\Gamma_2 \gamma\chi_{bJ}(1P)$	
$\Gamma_3 \eta \Upsilon(1S)$	
$\Gamma_4 \pi^+\pi^- \Upsilon(1S)$	

$\Upsilon(1D)$ BRANCHING RATIOS

$\Gamma(\eta \Upsilon(1S))/\Gamma(\gamma\gamma \Upsilon(1S))$	Γ_3/Γ_1
<0.25	
90	BONVICINI 04 CLE3 $\Upsilon(3S) \rightarrow \gamma X$

$\Gamma(\pi^+\pi^- \Upsilon(1S))/\Gamma(\gamma\gamma \Upsilon(1S))$	Γ_4/Γ_1
<1.2	
90	1 BONVICINI 04 CLE3 $\Upsilon(3S) \rightarrow \gamma X$

1 Assuming $J = 2$.

$\Upsilon(1D)$ REFERENCES

BONVICINI 04 PR D70 032001	G. Bonvicini et al.	(CLEO Collab.)
----------------------------	---------------------	----------------

$\chi_{b0}(2P)$

$$I^G(J^{PC}) = 0^+(0^{++})$$

Observed in radiative decay of the $\Upsilon(3S)$, therefore $C = +$. Branching ratio requires E1 transition, M1 is strongly disfavored, therefore $P = +$.

$\chi_{b0}(2P)$ MASS

VALUE (GeV)	DOCUMENT ID
10.2325 ± 0.0004 ± 0.0005 OUR EVALUATION	From γ energy below, using $\Upsilon(3S)$ mass = 10355.2 ± 0.5 MeV

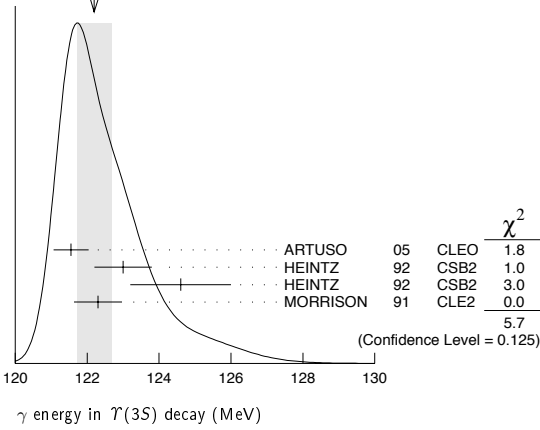
γ ENERGY IN $\Upsilon(3S)$ DECAY

VALUE (MeV)	EVTS	DOCUMENT ID	TECN	COMMENT
121.9 ± 0.4 OUR EVALUATION				Treating systematic errors as correlated
122.2 ± 0.5 OUR AVERAGE				Error includes scale factor of 1.4. See the ideogram below.
121.55 ± 0.16 ± 0.46		ARTUSO 05	CLEO	$\Upsilon(3S) \rightarrow \gamma X$
123.0 ± 0.8	4959	1 HEINTZ 92	CSB2	$e^+e^- \rightarrow \gamma X$
124.6 ± 1.4	17	2 HEINTZ 92	CSB2	$e^+e^- \rightarrow \ell^+\ell^-\gamma\gamma$
122.3 ± 0.3 ± 0.6	9903	MORRISON 91	CLE2	$e^+e^- \rightarrow \gamma X$
1 A systematic uncertainty on the energy scale of 0.9% not included. Supersedes NARAIN 91.				
2 A systematic uncertainty on the energy scale of 0.9% not included. Supersedes HEINTZ 91.				

Meson Particle Listings

$\chi_{b0}(2P), \chi_{b1}(2P)$

WEIGHTED AVERAGE
122.2±0.5 (Error scaled by 1.4)

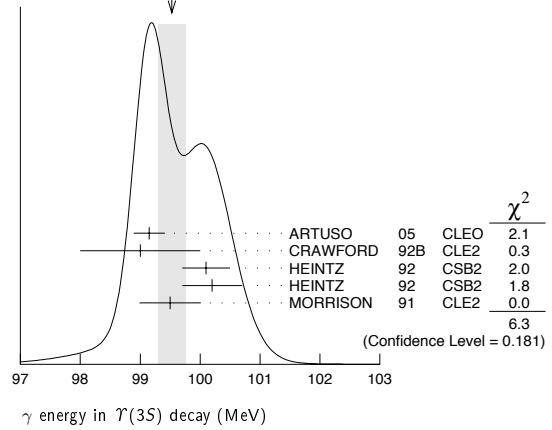


γ ENERGY IN $T(3S)$ DECAY

VALUE (MeV)	EVTS	DOCUMENT ID	TECN	COMMENT
99.26 ± 0.22 OUR EVALUATION		Treating systematic errors as correlated		
99.53 ± 0.23 OUR AVERAGE		Error includes scale factor of 1.3. See the ideogram below.		
99.15 ± 0.07 ± 0.25		ARTUSO 05	CLEO	$T(3S) \rightarrow \gamma X$
99 ± 1	169	CRAWFORD 92B	CLE2	$e^+e^- \rightarrow \ell^+\ell^-\gamma\gamma$
100.1 ± 0.4	11147	² HEINTZ 92	CSB2	$e^+e^- \rightarrow \gamma X$
100.2 ± 0.5	223	³ HEINTZ 92	CSB2	$e^+e^- \rightarrow \ell^+\ell^-\gamma\gamma$
99.5 ± 0.1 ± 0.5	25759	MORRISON 91	CLE2	$e^+e^- \rightarrow \gamma X$

²A systematic uncertainty on the energy scale of 0.9% not included. Supersedes NARAIN 91.
³A systematic uncertainty on the energy scale of 0.9% not included. Supersedes HEINTZ 91.

WEIGHTED AVERAGE
99.53±0.23 (Error scaled by 1.3)



$\chi_{b0}(2P)$ DECAY MODES

Mode	Fraction (Γ_i/Γ)
$\Gamma_1 \quad \gamma T(2S)$	(4.6 ± 2.1) %
$\Gamma_2 \quad \gamma T(1S)$	(9 ± 6) × 10 ⁻³

$\chi_{b0}(2P)$ BRANCHING RATIOS

$\Gamma(\gamma T(2S))/\Gamma_{total}$	CL%	DOCUMENT ID	TECN	COMMENT	Γ_1/Γ
<0.089	90	³ CRAWFORD 92B	CLE2	$e^+e^- \rightarrow \ell^+\ell^-\gamma\gamma$	
0.046 ± 0.020 ± 0.007		⁴ HEINTZ 92	CSB2	$e^+e^- \rightarrow \ell^+\ell^-\gamma\gamma$	

³Using $B(T(2S) \rightarrow \mu^+\mu^-) = (1.37 \pm 0.26)\%$, $B(T(3S) \rightarrow \gamma\gamma T(2S)) \times 2 B(T(2S) \rightarrow \mu^+\mu^-) < 1.19 \times 10^{-4}$, and $B(T(3S) \rightarrow \chi_{b0}(2P)\gamma) = 0.049$.
⁴Using $B(T(2S) \rightarrow \mu^+\mu^-) = (1.44 \pm 0.10)\%$, $B(T(3S) \rightarrow \gamma\chi_{b0}(2P)) = (6.0 \pm 0.4 \pm 0.6)\%$ and assuming $e\mu$ universality. Supersedes HEINTZ 91.

$\Gamma(\gamma T(1S))/\Gamma_{total}$	CL%	DOCUMENT ID	TECN	COMMENT	Γ_2/Γ
<0.025	90	⁵ CRAWFORD 92B	CLE2	$e^+e^- \rightarrow \ell^+\ell^-\gamma\gamma$	
0.009 ± 0.006 ± 0.001		⁶ HEINTZ 92	CSB2	$e^+e^- \rightarrow \ell^+\ell^-\gamma\gamma$	

⁵Using $B(T(1S) \rightarrow \mu^+\mu^-) = (2.57 \pm 0.07)\%$, $B(T(3S) \rightarrow \gamma\gamma T(1S)) \times 2 B(T(1S) \rightarrow \mu^+\mu^-) < 0.63 \times 10^{-4}$, and $B(T(3S) \rightarrow \chi_{b0}(2P)\gamma) = 0.049$.
⁶Using $B(T(1S) \rightarrow \mu^+\mu^-) = (2.57 \pm 0.07)\%$, $B(T(3S) \rightarrow \gamma\chi_{b0}(2P)) = (6.0 \pm 0.4 \pm 0.6)\%$ and assuming $e\mu$ universality. Supersedes HEINTZ 91.

$\chi_{b0}(2P)$ REFERENCES

ARTUSO 05	PRL 94 032001	M. Artuso et al.	(CLEO Collab.)
CRAWFORD 92B	PL B294 139	G. Crawford, R. Fulton	(CLEO Collab.)
HEINTZ 92	PR D46 1928	U. Heintz et al.	(CUSB II Collab.)
HEINTZ 91	PRL 66 1563	U. Heintz et al.	(CUSB Collab.)
MORRISON 91	PRL 67 1696	R.J. Morrison et al.	(CLEO Collab.)
NARAIN 91	PRL 66 3113	M. Narain et al.	(CUSB Collab.)

OTHER RELATED PAPERS

EIGEN 82	PRL 49 1616	G. Eigen et al.	(CUSB Collab.)
HAN 82	PRL 49 1612	K. Han et al.	(CUSB Collab.)

$\chi_{b1}(2P)$

$$I^G(JPC) = 0^+(1^{++})$$

J needs confirmation.

Observed in radiative decay of the $T(3S)$, therefore $C = +$. Branching ratio requires E1 transition, M1 is strongly disfavored, therefore $P = +$.

$\chi_{b1}(2P)$ MASS

VALUE (GeV)	DOCUMENT ID
10.25546 ± 0.00022 ± 0.00050 OUR EVALUATION	From γ energy below, using $T(3S)$ mass = 10355.2 ± 0.5 MeV

$m_{\chi_{b1}(2P)} - m_{\chi_{b0}(2P)}$

VALUE (MeV)	DOCUMENT ID	TECN	COMMENT
23.5 ± 0.7 ± 0.7	¹ HEINTZ 92	CSB2	$e^+e^- \rightarrow \gamma X, \ell^+\ell^-\gamma\gamma$

¹From the average photon energy for inclusive and exclusive events. Supersedes NARAIN 91.

$\chi_{b1}(2P)$ DECAY MODES

Mode	Fraction (Γ_i/Γ)	Scale factor
$\Gamma_1 \quad \omega T(1S)$	(1.63 ^{+0.38} _{-0.34}) %	
$\Gamma_2 \quad \gamma T(2S)$	(21 ± 4) %	1.5
$\Gamma_3 \quad \gamma T(1S)$	(8.5 ± 1.3) %	1.3
$\Gamma_4 \quad \pi\pi\chi_{b1}(1P)$	(8.6 ± 3.1) × 10 ⁻³	

$\chi_{b1}(2P)$ BRANCHING RATIOS

$\Gamma(\omega T(1S))/\Gamma_{total}$	CL%	DOCUMENT ID	TECN	COMMENT	Γ_1/Γ
1.63^{+0.35}_{-0.31} ± 0.16 ± 0.15		32.6 ^{+6.9} _{-6.1}	⁴ CRONIN-HEN..04	CLE3	$T(3S) \rightarrow \gamma\omega T(1S)$

⁴Using $B(T(3S) \rightarrow \gamma\chi_{b1}(2P)) = (11.3 \pm 0.6)\%$ and $B(T(1S) \rightarrow \ell^+\ell^-) = 2 B(T(1S) \rightarrow \mu^+\mu^-) = 2(2.48 \pm 0.06)\%$.

$\Gamma(\gamma T(2S))/\Gamma_{total}$	CL%	DOCUMENT ID	TECN	COMMENT	Γ_2/Γ
0.21 ± 0.04 OUR AVERAGE		Error includes scale factor of 1.5.			
0.356 ± 0.042 ± 0.092		⁵ CRAWFORD 92B	CLE2	$e^+e^- \rightarrow \ell^+\ell^-\gamma\gamma$	
0.199 ± 0.020 ± 0.022		⁶ HEINTZ 92	CSB2	$e^+e^- \rightarrow \ell^+\ell^-\gamma\gamma$	

⁵Using $B(T(2S) \rightarrow \mu^+\mu^-) = (1.37 \pm 0.26)\%$, $B(T(3S) \rightarrow \gamma\gamma T(2S)) \times 2 B(T(2S) \rightarrow \mu^+\mu^-) = (10.23 \pm 1.20 \pm 1.26) \times 10^{-4}$, and $B(T(3S) \rightarrow \gamma\chi_{b1}(2P)) = 0.105 \pm 0.003 \pm 0.013$.
⁶Using $B(T(2S) \rightarrow \mu^+\mu^-) = (1.44 \pm 0.10)\%$, $B(T(3S) \rightarrow \gamma\chi_{b1}(2P)) = (11.5 \pm 0.5 \pm 0.5)\%$ and assuming $e\mu$ universality. Supersedes HEINTZ 91.

$\Gamma(\gamma T(1S))/\Gamma_{total}$	CL%	DOCUMENT ID	TECN	COMMENT	Γ_3/Γ
0.085 ± 0.013 OUR AVERAGE		Error includes scale factor of 1.3.			
0.120 ± 0.021 ± 0.021		⁷ CRAWFORD 92B	CLE2	$e^+e^- \rightarrow \ell^+\ell^-\gamma\gamma$	
0.080 ± 0.009 ± 0.007		⁸ HEINTZ 92	CSB2	$e^+e^- \rightarrow \ell^+\ell^-\gamma\gamma$	

⁷Using $B(T(1S) \rightarrow \mu^+\mu^-) = (2.57 \pm 0.07)\%$, $B(T(3S) \rightarrow \gamma\gamma T(1S)) \times 2 B(T(1S) \rightarrow \mu^+\mu^-) = (6.47 \pm 1.12 \pm 0.82) \times 10^{-4}$ and $B(T(3S) \rightarrow \gamma\chi_{b1}(2P)) = 0.105 \pm 0.003 \pm 0.013$.
⁸Using $B(T(1S) \rightarrow \mu^+\mu^-) = (2.57 \pm 0.07)\%$, $B(T(3S) \rightarrow \gamma\chi_{b1}(2P)) = (11.5 \pm 0.5 \pm 0.5)\%$ and assuming $e\mu$ universality. Supersedes HEINTZ 91.

See key on page 373

Meson Particle Listings

$\chi_{b1}(2P), \chi_{b2}(2P), \Upsilon(3S)$

$\Gamma(\pi\pi\chi_{b1}(1P))/\Gamma_{total}$	Γ_4/Γ		
VALUE (units 10^{-3})	DOCUMENT ID	TECN	COMMENT
$8.6 \pm 2.3 \pm 2.1$	9 CRAWFIELD 06	CLE3	$\Upsilon(3S) \rightarrow 2(\gamma\pi\ell)$
9 CRAWFIELD 06 quote $\Gamma(\chi_b(2P) \rightarrow \pi\pi\chi_b(1P)) = 0.83 \pm 0.22 \pm 0.08 \pm 0.19$ keV assuming l-spin conservation, no D-wave contribution, $\Gamma(\chi_{b1}(2P)) = 96 \pm 16$ keV, and $\Gamma(\chi_{b2}(2P)) = 138 \pm 19$ keV.			

$\chi_{b1}(2P)$ Cross-Particle Branching Ratios

$B(\chi_{b2}(2P) \rightarrow \rho X + \bar{\rho} X)/B(\chi_{b1}(2P) \rightarrow \rho X + \bar{\rho} X)$	Γ_3/Γ		
VALUE	DOCUMENT ID	TECN	COMMENT
$1.109 \pm 0.007 \pm 0.040$	BRIERE 07	CLEO	$\Upsilon(3S) \rightarrow \gamma\chi_{bJ}(2P)$

$B(\chi_{b0}(2P) \rightarrow \rho X + \bar{\rho} X)/B(\chi_{b1}(2P) \rightarrow \rho X + \bar{\rho} X)$	Γ_3/Γ		
VALUE	DOCUMENT ID	TECN	COMMENT
$1.082 \pm 0.025 \pm 0.060$	BRIERE 07	CLEO	$\Upsilon(3S) \rightarrow \gamma\chi_{bJ}(2P)$

$\chi_{b1}(2P)$ REFERENCES

BRIERE 07	PR D76 012005	R.A. Briere et al.	(CLEO Collab.)
CRAWFIELD 06	PR D73 012003	C. Cawfield et al.	(CLEO Collab.)
ARTUSO 05	PRL 94 032001	M. Artuso et al.	(CLEO Collab.)
CRONIN-HEN... 04	PRL 92 222002	D. Cronin-Hennessy et al.	(CLEO3 Collab.)
CRAWFORD 92B	PL B294 139	G. Crawford, R. Fulton	(CLEO Collab.)
HEINTZ 92	PR D46 1928	U. Heintz et al.	(CUSB II Collab.)
HEINTZ 91	PRL 66 1563	U. Heintz et al.	(CUSB Collab.)
MORRISON 91	PRL 67 1696	R.J. Morrison et al.	(CLEO Collab.)
NARAIN 91	PRL 66 3113	M. Narain et al.	(CUSB Collab.)

OTHER RELATED PAPERS

EIGEN 82	PRL 49 1616	G. Eigen et al.	(CUSB Collab.)
HAN 82	PRL 49 1612	K. Han et al.	(CUSB Collab.)

$\chi_{b2}(2P)$

$J^G(J^{PC}) = 0^+(2^{++})$
J needs confirmation.

Observed in radiative decay of the $\Upsilon(3S)$, therefore $C = +$. Branching ratio requires E1 transition, M1 is strongly disfavored, therefore $P = +$.

$\chi_{b2}(2P)$ MASS

VALUE (GeV)	DOCUMENT ID
$10.26865 \pm 0.00022 \pm 0.00050$ OUR EVALUATION	From γ energy below, using $\Upsilon(3S)$ mass = 10355.2 ± 0.5 MeV

$m_{\chi_{b2}(2P)} - m_{\chi_{b1}(2P)}$

VALUE (MeV)	DOCUMENT ID	TECN	COMMENT
$13.5 \pm 0.4 \pm 0.5$	1 HEINTZ 92	CSB2	$e^+e^- \rightarrow \gamma\chi, \ell^+\ell^-\gamma\gamma$
1 From the average photon energy for inclusive and exclusive events. Supersedes NARAIN 91.			

γ ENERGY IN $\Upsilon(3S)$ DECAY

VALUE (MeV)	EVTS	DOCUMENT ID	TECN	COMMENT
86.19 ± 0.22 OUR EVALUATION	Treating systematic errors as correlated			
86.40 ± 0.18 OUR AVERAGE				
$86.04 \pm 0.06 \pm 0.27$		ARTUSO 05	CLEO	$\Upsilon(3S) \rightarrow \gamma X$
86 ± 1	101	CRAWFORD 92B	CLE2	$e^+e^- \rightarrow \ell^+\ell^-\gamma\gamma$
86.7 ± 0.4	10319	2 HEINTZ 92	CSB2	$e^+e^- \rightarrow \gamma X$
86.9 ± 0.4	157	3 HEINTZ 92	CSB2	$e^+e^- \rightarrow \ell^+\ell^-\gamma\gamma$
$86.4 \pm 0.1 \pm 0.4$	30741	MORRISON 91	CLE2	$e^+e^- \rightarrow \gamma X$
2 A systematic uncertainty on the energy scale of 0.9% not included. Supersedes NARAIN 91.				
3 A systematic uncertainty on the energy scale of 0.9% not included. Supersedes HEINTZ 91.				

$\chi_{b2}(2P)$ DECAY MODES

Mode	Fraction (Γ_i/Γ)
$\Gamma_1 \omega \Upsilon(1S)$	$(1.10^{+0.34}_{-0.30})\%$
$\Gamma_2 \gamma \Upsilon(2S)$	$(16.2 \pm 2.4)\%$
$\Gamma_3 \gamma \Upsilon(1S)$	$(7.1 \pm 1.0)\%$
$\Gamma_4 \pi\pi\chi_{b2}(1P)$	$(6.0 \pm 2.1) \times 10^{-3}$

$\chi_{b2}(2P)$ BRANCHING RATIOS

$\Gamma(\omega \Upsilon(1S))/\Gamma_{total}$	Γ_1/Γ			
VALUE (units 10^{-2})	EVTS	DOCUMENT ID	TECN	COMMENT
$1.10^{+0.32+0.11}_{-0.28-0.10}$	$20.1^{+5.8}_{-5.1}$	4 CRONIN-HEN..04	CLE3	$\Upsilon(3S) \rightarrow \gamma\omega \Upsilon(1S)$
4 Using $B(\Upsilon(3S) \rightarrow \gamma\chi_{b2}(2P)) = (11.4 \pm 0.8)\%$ and $B(\Upsilon(1S) \rightarrow \ell^+\ell^-) = 2 B(\Upsilon(1S) \rightarrow \mu^+\mu^-) = 2(2.48 \pm 0.06)\%$.				

$\Gamma(\gamma \Upsilon(2S))/\Gamma_{total}$	Γ_2/Γ		
VALUE	DOCUMENT ID	TECN	COMMENT
0.162 ± 0.024 OUR AVERAGE			
$0.135 \pm 0.025 \pm 0.035$	5 CRAWFORD 92B	CLE2	$e^+e^- \rightarrow \ell^+\ell^-\gamma\gamma$
$0.173 \pm 0.021 \pm 0.019$	6 HEINTZ 92	CSB2	$e^+e^- \rightarrow \ell^+\ell^-\gamma\gamma$
5 Using $B(\Upsilon(2S) \rightarrow \mu^+\mu^-) = (1.37 \pm 0.26)\%$, $B(\Upsilon(3S) \rightarrow \gamma\gamma \Upsilon(2S)) \times 2 B(\Upsilon(2S) \rightarrow \mu^+\mu^-) = (4.98 \pm 0.94 \pm 0.62) \times 10^{-4}$, and $B(\Upsilon(3S) \rightarrow \gamma\chi_{b2}(2P)) = 0.135 \pm 0.003 \pm 0.017$.			
6 Using $B(\Upsilon(2S) \rightarrow \mu^+\mu^-) = (1.44 \pm 0.10)\%$, $B(\Upsilon(3S) \rightarrow \gamma\chi_{b2}(2P)) = (11.1 \pm 0.5 \pm 0.4)\%$ and assuming $e\mu$ universality. Supersedes HEINTZ 91.			

$\Gamma(\gamma \Upsilon(1S))/\Gamma_{total}$	Γ_3/Γ		
VALUE	DOCUMENT ID	TECN	COMMENT
0.071 ± 0.010 OUR AVERAGE			
$0.072 \pm 0.014 \pm 0.013$	7 CRAWFORD 92B	CLE2	$e^+e^- \rightarrow \ell^+\ell^-\gamma\gamma$
$0.070 \pm 0.010 \pm 0.006$	8 HEINTZ 92	CSB2	$e^+e^- \rightarrow \ell^+\ell^-\gamma\gamma$
7 Using $B(\Upsilon(1S) \rightarrow \mu^+\mu^-) = (2.57 \pm 0.07)\%$, $B(\Upsilon(3S) \rightarrow \gamma\gamma \Upsilon(2S)) \times 2 B(\Upsilon(1S) \rightarrow \mu^+\mu^-) = (5.03 \pm 0.94 \pm 0.63) \times 10^{-4}$, and $B(\Upsilon(3S) \rightarrow \gamma\chi_{b2}(2P)) = 0.135 \pm 0.003 \pm 0.017$.			
8 Using $B(\Upsilon(1S) \rightarrow \mu^+\mu^-) = (2.57 \pm 0.07)\%$, $B(\Upsilon(3S) \rightarrow \gamma\chi_{b2}(2P)) = (11.1 \pm 0.5 \pm 0.4)\%$ and assuming $e\mu$ universality. Supersedes HEINTZ 91.			

$\Gamma(\pi\pi\chi_{b2}(1P))/\Gamma_{total}$	Γ_4/Γ		
VALUE (units 10^{-3})	DOCUMENT ID	TECN	COMMENT
$6.0 \pm 1.6 \pm 1.4$	9 CRAWFIELD 06	CLE3	$\Upsilon(3S) \rightarrow 2(\gamma\pi\ell)$
9 CRAWFIELD 06 quote $\Gamma(\chi_b(2P) \rightarrow \pi\pi\chi_b(1P)) = 0.83 \pm 0.22 \pm 0.08 \pm 0.19$ keV assuming l-spin conservation, no D-wave contribution, $\Gamma(\chi_{b1}(2P)) = 96 \pm 16$ keV, and $\Gamma(\chi_{b2}(2P)) = 138 \pm 19$ keV.			

$\chi_{b2}(2P)$ REFERENCES

CRAWFIELD 06	PR D73 012003	C. Cawfield et al.	(CLEO Collab.)
ARTUSO 05	PRL 94 032001	M. Artuso et al.	(CLEO Collab.)
CRONIN-HEN... 04	PRL 92 222002	D. Cronin-Hennessy et al.	(CLEO3 Collab.)
CRAWFORD 92B	PL B294 139	G. Crawford, R. Fulton	(CLEO Collab.)
HEINTZ 92	PR D46 1928	U. Heintz et al.	(CUSB II Collab.)
HEINTZ 91	PRL 66 1563	U. Heintz et al.	(CUSB Collab.)
MORRISON 91	PRL 67 1696	R.J. Morrison et al.	(CLEO Collab.)
NARAIN 91	PRL 66 3113	M. Narain et al.	(CUSB Collab.)

OTHER RELATED PAPERS

EIGEN 82	PRL 49 1616	G. Eigen et al.	(CUSB Collab.)
HAN 82	PRL 49 1612	K. Han et al.	(CUSB Collab.)

$\Upsilon(3S)$

$J^G(J^{PC}) = 0^-(1^{--})$

$\Upsilon(3S)$ MASS

VALUE (GeV)	DOCUMENT ID	TECN	COMMENT
10.3552 ± 0.0005	1 ARTAMONOV 00	MD1	$e^+e^- \rightarrow$ hadrons
••• We do not use the following data for averages, fits, limits, etc. •••			
10.3553 ± 0.0005	2,3 BARU	86B	$e^+e^- \rightarrow$ hadrons
1 Reanalysis of BARU 86B using new electron mass (COHEN 87).			
2 Reanalysis of ARTAMONOV 84.			
3 Superseded by ARTAMONOV 00.			

$\Upsilon(3S)$ WIDTH

VALUE (keV)	DOCUMENT ID
20.32 ± 1.85 OUR EVALUATION	See the Note on "Width Determinations of the Υ States"

$\Upsilon(3S)$ DECAY MODES

Mode	Fraction (Γ_i/Γ)	Scale factor/Confidence level
$\Gamma_1 \Upsilon(2S)$ anything	$(10.6 \pm 0.8)\%$	
$\Gamma_2 \Upsilon(2S)\pi^+\pi^-$	$(2.8 \pm 0.6)\%$	S=2.2
$\Gamma_3 \Upsilon(2S)\pi^0\pi^0$	$(2.00 \pm 0.32)\%$	
$\Gamma_4 \Upsilon(2S)\gamma\gamma$	$(5.0 \pm 0.7)\%$	
$\Gamma_5 \Upsilon(1S)\pi^+\pi^-$	$(4.48 \pm 0.21)\%$	
$\Gamma_6 \Upsilon(1S)\pi^0\pi^0$	$(2.06 \pm 0.28)\%$	
$\Gamma_7 \Upsilon(1S)\eta$	$< 2.2 \times 10^{-3}$	CL=90%
$\Gamma_8 \tau^+\tau^-$	$(2.29 \pm 0.30)\%$	
$\Gamma_9 \mu^+\mu^-$	$(2.18 \pm 0.21)\%$	S=2.1
$\Gamma_{10} e^+e^-$	seen	

Meson Particle Listings

$\Upsilon(3S)$

Radiative decays

Γ	Decay	Value	Units	Source
Γ_{11}	$\gamma\chi_{b2}(2P)$	$(13.1 \pm 1.6) \%$		S=3.4
Γ_{12}	$\gamma\chi_{b1}(2P)$	$(12.6 \pm 1.2) \%$		S=2.4
Γ_{13}	$\gamma\chi_{b0}(2P)$	$(5.9 \pm 0.6) \%$		S=1.4
Γ_{14}	$\gamma\chi_{b0}(1P)$	$(3.0 \pm 1.1) \times 10^{-3}$		
Γ_{15}	$\gamma\eta_b(2S)$	< 6.2	$\times 10^{-4}$	CL=90%
Γ_{16}	$\gamma\eta_b(1S)$	< 4.3	$\times 10^{-4}$	CL=90%
Γ_{17}	$\gamma X \rightarrow \gamma + \geq 4$ prongs	$[a] < 2.2$	$\times 10^{-4}$	CL=95%

[a] 1.5 GeV < m_X < 5.0 GeV

$\Upsilon(3S) \Gamma(\ell^+ \ell^-) / \Gamma(\text{total})$

VALUE (keV)	DOCUMENT ID	TECN	COMMENT	$\Gamma_0 \Gamma_{10} / \Gamma$
0.414 ± 0.007 OUR AVERAGE				
0.413 ± 0.004 ± 0.006	ROSNER	06	CLEO 10.4 $e^+ e^- \rightarrow$ hadrons	
0.45 ± 0.03 ± 0.03	⁴ GILES	84B	CLEO $e^+ e^- \rightarrow$ hadrons	

⁴Radiative corrections reevaluated by BUCHMUELLER 88 following KURAEV 85.

$\Upsilon(3S)$ PARTIAL WIDTHS

VALUE (keV)	DOCUMENT ID	Γ_{10}
0.443 ± 0.008 OUR EVALUATION		

$\Upsilon(3S)$ BRANCHING RATIOS

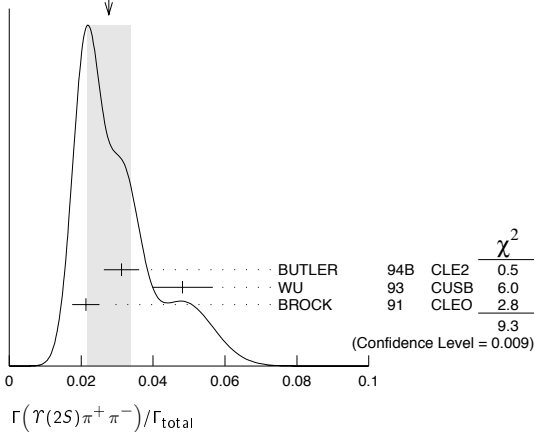
VALUE	EVTS	DOCUMENT ID	TECN	COMMENT	Γ_1 / Γ
0.106 ± 0.008 OUR AVERAGE					
0.1023 ± 0.0105	4625	^{5,6,7} BUTLER	94B	CLE2 $e^+ e^- \rightarrow \ell^+ \ell^- X$	
0.111 ± 0.012	4891	^{6,7,8} BROCK	91	CLEO $e^+ e^- \rightarrow \pi^+ \pi^- X, \pi^+ \pi^- \ell^+ \ell^-$	

VALUE	EVTS	DOCUMENT ID	TECN	COMMENT	Γ_2 / Γ
0.028 ± 0.006 OUR AVERAGE				Error includes scale factor of 2.2. See the ideogram below.	
0.0312 ± 0.0049	980	^{5,9} BUTLER	94B	CLE2 $e^+ e^- \rightarrow \pi^+ \pi^- \ell^+ \ell^-$	
0.0482 ± 0.0065 ± 0.0053	138	⁸ WU	93	CUSB $\Upsilon(3S) \rightarrow \pi^+ \pi^- \ell^+ \ell^-$	
0.0213 ± 0.0038	974	⁸ BROCK	91	CLEO $e^+ e^- \rightarrow \pi^+ \pi^- X, \pi^+ \pi^- \ell^+ \ell^-$	

• • • We do not use the following data for averages, fits, limits, etc. • • •

0.031 ± 0.020	5	MAGERAS	82	CUSB $\Upsilon(3S) \rightarrow \pi^+ \pi^- \ell^+ \ell^-$	
---------------	---	---------	----	---	--

WEIGHTED AVERAGE
0.028 ± 0.006 (Error scaled by 2.2)



$\Upsilon(3S) \Gamma(\pi^+ \pi^-) / \Gamma(\text{total})$

VALUE	EVTS	DOCUMENT ID	TECN	COMMENT	Γ_5 / Γ
0.0448 ± 0.0021 OUR AVERAGE					
0.0452 ± 0.0035	11830	⁶ BUTLER	94B	CLE2 $e^+ e^- \rightarrow \pi^+ \pi^- X,$	
0.0446 ± 0.0034 ± 0.0050	451	⁶ WU	93	CUSB $\Upsilon(3S) \rightarrow \pi^+ \pi^- \ell^+ \ell^-$	
0.0446 ± 0.0030	11221	⁶ BROCK	91	CLEO $e^+ e^- \rightarrow \pi^+ \pi^- X,$	

• • • We do not use the following data for averages, fits, limits, etc. • • •

0.049 ± 0.010	22	GREEN	82	CLEO $\Upsilon(3S) \rightarrow \pi^+ \pi^- \ell^+ \ell^-$	
0.039 ± 0.013	26	MAGERAS	82	CUSB $\Upsilon(3S) \rightarrow \pi^+ \pi^- \ell^+ \ell^-$	

$\Upsilon(3S) \Gamma(\pi^0 \pi^0) / \Gamma(\text{total})$

VALUE	EVTS	DOCUMENT ID	TECN	COMMENT	Γ_6 / Γ
0.0206 ± 0.0028 OUR AVERAGE					
0.0199 ± 0.0034	56	⁶ BUTLER	94B	CLE2 $e^+ e^- \rightarrow \ell^+ \ell^- \pi^0 \pi^0$	
0.022 ± 0.004 ± 0.003	33	¹² HEINTZ	92	CSB2 $e^+ e^- \rightarrow \ell^+ \ell^- \pi^0 \pi^0$	

$\Upsilon(3S) \Gamma(\eta) / \Gamma(\text{total})$

VALUE	CL%	DOCUMENT ID	TECN	COMMENT	Γ_7 / Γ
< 0.0022	90	BROCK	91	CLEO $e^+ e^- \rightarrow \pi^+ \pi^- \pi^0 \ell^+ \ell^-$	

$\Upsilon(3S) \Gamma(\tau^+ \tau^-) / \Gamma(\text{total})$

VALUE (units 10 ⁻²)	EVTS	DOCUMENT ID	TECN	COMMENT	Γ_8 / Γ
2.29 ± 0.21 ± 0.22	15k	¹³ BESSON	07	CLEO $e^+ e^- \rightarrow \Upsilon(3S) \rightarrow \tau^+ \tau^-$	

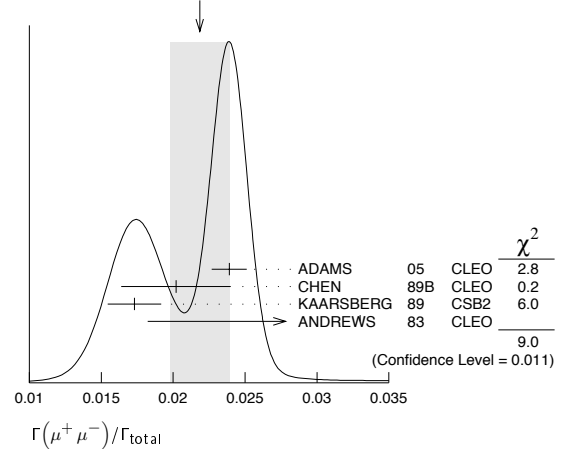
$\Upsilon(3S) \Gamma(\tau^+ \tau^-) / \Gamma(\mu^+ \mu^-)$

VALUE	EVTS	DOCUMENT ID	TECN	COMMENT	Γ_8 / Γ_9
1.05 ± 0.08 ± 0.05	15k	BESSON	07	CLEO $e^+ e^- \rightarrow \Upsilon(3S)$	

$\Upsilon(3S) \Gamma(\mu^+ \mu^-) / \Gamma(\text{total})$

VALUE	EVTS	DOCUMENT ID	TECN	COMMENT	Γ_9 / Γ
0.0218 ± 0.0021 OUR AVERAGE				Error includes scale factor of 2.1. See the ideogram below.	
0.0239 ± 0.0007 ± 0.0010	81k	ADAMS	05	CLEO $e^+ e^- \rightarrow \mu^+ \mu^-$	
0.0202 ± 0.0019 ± 0.0033		CHEN	89B	CLEO $e^+ e^- \rightarrow \mu^+ \mu^-$	
0.0173 ± 0.0015 ± 0.0011		KAARSBERG	89	CSB2 $e^+ e^- \rightarrow \mu^+ \mu^-$	
0.033 ± 0.013 ± 0.007	1096	ANDREWS	83	CLEO $e^+ e^- \rightarrow \mu^+ \mu^-$	

WEIGHTED AVERAGE
0.0218 ± 0.0021 (Error scaled by 2.1)



$\Upsilon(3S) \Gamma(\gamma\chi_{b2}(2P)) / \Gamma(\text{total})$

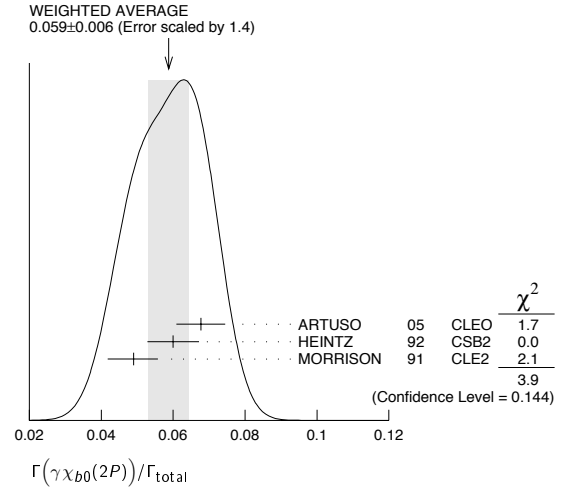
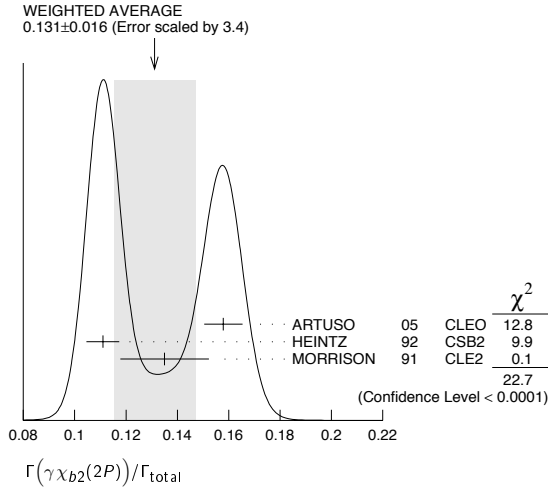
VALUE	EVTS	DOCUMENT ID	TECN	COMMENT	Γ_{11} / Γ
0.131 ± 0.016 OUR AVERAGE				Error includes scale factor of 3.4. See the ideogram below.	
0.1579 ± 0.0017 ± 0.0073	568k	ARTUSO	05	CLEO $e^+ e^- \rightarrow \gamma X$	
0.111 ± 0.005 ± 0.004	10319	¹⁴ HEINTZ	92	CSB2 $e^+ e^- \rightarrow \gamma X$	
0.135 ± 0.003 ± 0.017	30741	MORRISON	91	CLE2 $e^+ e^- \rightarrow \gamma X$	

$\Upsilon(3S) \Gamma(\pi^0 \pi^0) / \Gamma(\text{total})$

VALUE	EVTS	DOCUMENT ID	TECN	COMMENT	Γ_3 / Γ
0.0200 ± 0.0032 OUR AVERAGE					
0.0216 ± 0.0039	9,10	BUTLER	94B	CLE2 $e^+ e^- \rightarrow \ell^+ \ell^- \pi^0 \pi^0$	
0.017 ± 0.005 ± 0.002	10	¹¹ HEINTZ	92	CSB2 $e^+ e^- \rightarrow \ell^+ \ell^- \pi^0 \pi^0$	

$\Upsilon(3S) \Gamma(\gamma\gamma) / \Gamma(\text{total})$

VALUE	DOCUMENT ID	TECN	COMMENT	Γ_4 / Γ
0.0502 ± 0.0069	⁹ BUTLER	94B	CLE2 $e^+ e^- \rightarrow \ell^+ \ell^- 2\gamma$	



$\Gamma(\gamma\chi_{b1}(2P))/\Gamma_{total}$ Γ_{12}/Γ

VALUE	EVTS	DOCUMENT ID	TECN	COMMENT
0.126 ± 0.012 OUR AVERAGE				Error includes scale factor of 2.4. See the ideogram below.
0.1454 ± 0.0018 ± 0.0073	537k	ARTUSO 05	CLEO	$e^+e^- \rightarrow \gamma X$
0.115 ± 0.005 ± 0.005	11147	¹⁴ HEINTZ 92	CSB2	$e^+e^- \rightarrow \gamma X$
0.105 ± 0.003 ± 0.013	25759	MORRISON 91	CLE2	$e^+e^- \rightarrow \gamma X$

$\Gamma(\gamma\chi_{b0}(1P))/\Gamma_{total}$ Γ_{14}/Γ

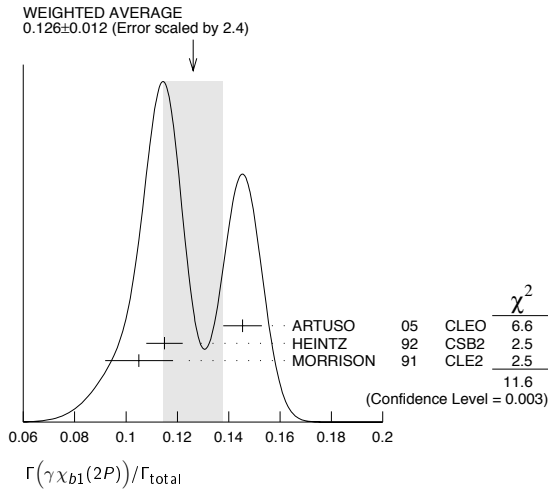
VALUE (units 10^{-2})	EVTS	DOCUMENT ID	TECN	COMMENT
0.30 ± 0.04 ± 0.10	8.7k	ARTUSO 05	CLEO	$e^+e^- \rightarrow \gamma X$

$\Gamma(\gamma\eta_b(2S))/\Gamma_{total}$ Γ_{15}/Γ

VALUE (units 10^{-4})	CL%	DOCUMENT ID	TECN	COMMENT
<6.2	90	ARTUSO 05	CLEO	$e^+e^- \rightarrow \gamma X$

$\Gamma(\gamma\eta_b(1S))/\Gamma_{total}$ Γ_{16}/Γ

VALUE (units 10^{-4})	CL%	DOCUMENT ID	TECN	COMMENT
<4.3	90	ARTUSO 05	CLEO	$e^+e^- \rightarrow \gamma X$



$\Gamma(\gamma X \rightarrow \gamma + \geq 4 \text{ prongs})/\Gamma_{total}$ Γ_{17}/Γ
(1.5 GeV < m_X < 5.0 GeV)

VALUE (units 10^{-4})	CL%	DOCUMENT ID	TECN	COMMENT
<2.2	95	ROSNER 07A	CLEO	$e^+e^- \rightarrow \gamma X$
⁵ Using $B(\Upsilon(2S) \rightarrow \Upsilon(1S)\gamma\gamma) = (0.038 \pm 0.007)\%$, and $B(\Upsilon(2S) \rightarrow \Upsilon(1S)\pi^0\pi^0) = (1/2)B(\Upsilon(2S) \rightarrow \Upsilon(1S)\pi^+\pi^-)$. ⁶ Using $B(\Upsilon(1S) \rightarrow \mu^+\mu^-) = (2.48 \pm 0.06)\%$. With the assumption of $e\mu$ universality. ⁷ Using $B(\Upsilon(2S) \rightarrow \Upsilon(1S)\pi^+\pi^-) = (18.5 \pm 0.8)\%$. ⁸ Using $B(\Upsilon(2S) \rightarrow \mu^+\mu^-) = (1.31 \pm 0.21)\%$, $B(\Upsilon(2S) \rightarrow \Upsilon(1S)\gamma\gamma) \times 2B(\Upsilon(1S) \rightarrow \mu^+\mu^-) = (0.188 \pm 0.035)\%$, and $B(\Upsilon(2S) \rightarrow \Upsilon(1S)\pi^0\pi^0) \times 2B(\Upsilon(1S) \rightarrow \mu^+\mu^-) = (0.436 \pm 0.056)\%$. With the assumption of $e\mu$ universality. ⁹ From the exclusive mode. ¹⁰ $B(\Upsilon(2S) \rightarrow \mu^+\mu^-) = (1.31 \pm 0.21)\%$ and assuming $e\mu$ universality. ¹¹ $B(\Upsilon(2S) \rightarrow \mu^+\mu^-) = (1.44 \pm 0.10)\%$ and assuming $e\mu$ universality. Supersedes HEINTZ 91. ¹² Using $B(\Upsilon(1S) \rightarrow \mu^+\mu^-) = (2.57 \pm 0.07)\%$ and assuming $e\mu$ universality. Supersedes HEINTZ 91. ¹³ BESSON 07 reports $[B(\Upsilon(3S) \rightarrow \tau^+\tau^-)] / [B(\Upsilon(3S) \rightarrow \mu^+\mu^-)] = 1.05 \pm 0.08 \pm 0.05$. We multiply by our best value $B(\Upsilon(3S) \rightarrow \mu^+\mu^-) = (2.18 \pm 0.21) \times 10^{-2}$. Our first error is their experiment's error and our second error is the systematic error from using our best value. ¹⁴ Supersedes NARAIN 91.				

$\Gamma(\gamma\chi_{b0}(2P))/\Gamma_{total}$ Γ_{13}/Γ

VALUE	EVTS	DOCUMENT ID	TECN	COMMENT
0.059 ± 0.006 OUR AVERAGE				Error includes scale factor of 1.4. See the ideogram below.
0.0677 ± 0.0020 ± 0.0065	225k	ARTUSO 05	CLEO	$e^+e^- \rightarrow \gamma X$
0.060 ± 0.004 ± 0.006	4959	¹⁴ HEINTZ 92	CSB2	$e^+e^- \rightarrow \gamma X$
0.049 ± 0.003 ± 0.006	9903	MORRISON 91	CLE2	$e^+e^- \rightarrow \gamma X$

$\Upsilon(3S)$ REFERENCES

BESSON 07	PRL 98 052002	D. Besson <i>et al.</i>	(CLEO Collab.)
ROSNER 07A	PR D76 137102	J.L. Rosner <i>et al.</i>	(CLEO Collab.)
ROSNER 06	PRL 96 092003	J.L. Rosner <i>et al.</i>	(CLEO Collab.)
ADAMS 05	PRL 94 012001	G.S. Adams <i>et al.</i>	(CLEO Collab.)
ARTUSO 05	PRL 94 032001	M. Artuso <i>et al.</i>	(CLEO Collab.)
ARTAMONOV 00	PL B474 427	A.S. Artamonov <i>et al.</i>	
BUTLER 94B	PR D49 40	F. Butler <i>et al.</i>	(CLEO Collab.)
WU 93	PL B301 307	Q.W. Wu <i>et al.</i>	(CSUB Collab.)
HEINTZ 92	PR D46 1928	U. Heintz <i>et al.</i>	(CSUB II Collab.)
BROCK 91	PR D43 1448	I.C. Brock <i>et al.</i>	(CLEO Collab.)
HEINTZ 91	PRL 66 1563	U. Heintz <i>et al.</i>	(CSUB Collab.)
MORRISON 91	PRL 67 1696	R.J. Morrison <i>et al.</i>	(CLEO Collab.)
NARAIN 91	PRL 66 3113	M. Narain <i>et al.</i>	(CSUB Collab.)
CHEN 89B	PR D39 3528	W.Y. Chen <i>et al.</i>	(CLEO Collab.)
KAARSBERG 89	PRL 62 2077	T.M. Kaarsberg <i>et al.</i>	(CSUB Collab.)
BUCHMUELLER 88	HE e^+e^- Physics 412	W. Buchmuller, S. Cooper	(HANN, DESY, MIT)
Editors: A. Ali and P. Soeding, World Scientific, Singapore			
COHEN 87	RMP 59 1121	E.R. Cohen, B.N. Taylor	(RIS C, NBS)
BARU 86B	ZPHY C32 622 (erratum)	S.E. Baru <i>et al.</i>	(NOVO)
KURAEV 85	SJNP 41 466	E.A. Kurayev, V.S. Fadin	(NOVO)
Translated from YAF 41 733.			
ARTAMONOV 84	PL 137B 272	A.S. Artamonov <i>et al.</i>	(NOVO)
GILES 84B	PR D29 1285	R. Giles <i>et al.</i>	(CLEO Collab.)
ANDREWS 83	PRL 50 807	D.E. Andrews <i>et al.</i>	(CLEO Collab.)
GREEN 82	PRL 49 617	J. Green <i>et al.</i>	(CLEO Collab.)
MAGERAS 82	PL 118B 453	G. Mageras <i>et al.</i>	(COLU, CORN, LSU+)

Meson Particle Listings

 $\Upsilon(3S)$, $\Upsilon(4S)$

OTHER RELATED PAPERS

BRIERE	07	PR D76 012005	R.A. Briere et al.	(CLEO Collab.)
CRONIN-HEN.	07	PR D76 072001	D. Cronin-Hennessy et al.	(CLEO Collab.)
BESSION	06A	PR D74 012003	D. Besson et al.	(CLEO Collab.)
GUO	05	NP A761 269	F.-K. Guo et al.	
ROSNER	03	PR D67 097504	J.L. Rosner	
ALEXANDER	89	NP B320 45	J.P. Alexander et al.	(LBL, MICH, SLAC)
ARTAMONOV	84	PL 137B 272	A.S. Artamonov et al.	(NOVO)
GILES	84B	PR D29 1285	R. Giles et al.	(CLEO Collab.)
HAN	82	PRL 49 1612	K. Han et al.	(CUSB Collab.)
PETERSON	82	PL 114B 277	D. Peterson et al.	(CUSB Collab.)
KAPLAN	78	PRL 40 435	D.M. Kaplan et al.	(STON, FNAL, COLU)
YOH	78	PRL 41 684	J.K. Yoh et al.	(COLU, FNAL, STON)
COBB	77	PL 72B 273	J.H. Cobb et al.	(BNL, CERN, SYRA, YALE)
HERB	77	PRL 39 252	S.W. Herb et al.	(COLU, FNAL, STON)
INNES	77	PRL 39 1240	W.R. Innes et al.	(COLU, FNAL, STON)

$\Upsilon(4S)$
or $\Upsilon(10580)$

$$J^{PC} = 0^{-}(1^{-})^{-}$$

 $\Upsilon(4S)$ MASS

VALUE (GeV)	DOCUMENT ID	TECN	COMMENT
10.5794 ± 0.0012 OUR AVERAGE			
10.5793 ± 0.0004 ± 0.0012	AUBERT	05Q	BABR $e^+e^- \rightarrow$ hadrons
10.5800 ± 0.0035	¹ BEBEK	87	CLEO $e^+e^- \rightarrow$ hadrons
• • • We do not use the following data for averages, fits, limits, etc. • • •			
10.5774 ± 0.0010	² LOVELOCK	85	CUSB $e^+e^- \rightarrow$ hadrons
¹ Reanalysis of BESSION 85.			
² No systematic error given.			

 $\Upsilon(4S)$ WIDTH

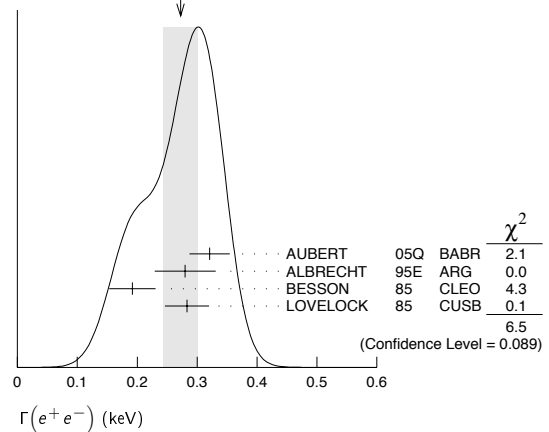
VALUE (MeV)	DOCUMENT ID	TECN	COMMENT
20.5 ± 2.5 OUR AVERAGE			
20.7 ± 1.6 ± 2.5	AUBERT	05Q	BABR $e^+e^- \rightarrow$ hadrons
20 ± 2 ± 4	BESSION	85	CLEO $e^+e^- \rightarrow$ hadrons
• • • We do not use the following data for averages, fits, limits, etc. • • •			
25 ± 2.5	LOVELOCK	85	CUSB $e^+e^- \rightarrow$ hadrons

 $\Upsilon(4S)$ DECAY MODES

Mode	Fraction (Γ_i/Γ)	Confidence level
Γ_1 $B\bar{B}$	> 96 %	95%
Γ_2 B^+B^-	(51.6 ± 0.6) %	
Γ_3 D_s^+ anything + c.c.	(18.3 ± 2.6) %	
Γ_4 $B^0\bar{B}^0$	(48.4 ± 0.6) %	
Γ_5 $J/\psi K_S^0(J/\psi, \eta_c) K_S^0$	< 4 × 10 ⁻⁷	90%
Γ_6 non- $B\bar{B}$	< 4 %	95%
Γ_7 e^+e^-	(1.57 ± 0.08) × 10 ⁻⁵	
Γ_8 $J/\psi(1S)$ anything	< 1.9 × 10 ⁻⁴	95%
Γ_9 D^{*+} anything + c.c.	< 7.4 %	90%
Γ_{10} ϕ anything	(7.1 ± 0.6) %	
Γ_{11} $\phi\eta$	< 2.5 × 10 ⁻⁶	90%
Γ_{12} $\Upsilon(1S)$ anything	< 4 × 10 ⁻³	90%
Γ_{13} $\Upsilon(1S)\pi^+\pi^-$	(9.0 ± 1.5) × 10 ⁻⁵	
Γ_{14} $\Upsilon(2S)\pi^+\pi^-$	(8.8 ± 1.9) × 10 ⁻⁵	
Γ_{15} \bar{d} anything	< 1.3 × 10 ⁻⁵	90%

 $\Upsilon(4S)$ PARTIAL WIDTHS

$\Gamma(e^+e^-)$	DOCUMENT ID	TECN	COMMENT
0.272 ± 0.029 OUR AVERAGE			Error includes scale factor of 1.5. See the ideogram below.
0.321 ± 0.017 ± 0.029	AUBERT	05Q	BABR $e^+e^- \rightarrow$ hadrons
0.28 ± 0.05 ± 0.01	³ ALBRECHT	95E	ARG $e^+e^- \rightarrow$ hadrons
0.192 ± 0.007 ± 0.038	BESSION	85	CLEO $e^+e^- \rightarrow$ hadrons
0.283 ± 0.037	LOVELOCK	85	CUSB $e^+e^- \rightarrow$ hadrons
³ Using LEYAOUANC 77 parametrization of $\Gamma(s)$.			

WEIGHTED AVERAGE
0.272 ± 0.029 (Error scaled by 1.5) $\Upsilon(4S)$ BRANCHING RATIOS $B\bar{B}$ DECAYS

The ratio of branching fraction to charged and neutral B mesons is often derived assuming isospin invariance in the decays, and relies on the knowledge of the B^+/B^0 lifetime ratio. "OUR EVALUATION" is obtained based on averages of rescaled data listed below. The average and rescaling were performed by the Heavy Flavor Averaging Group (HFAG) and are described at <http://www.slac.stanford.edu/xorg/hfag/>. The averaging/rescaling procedure takes into account the common dependence of the measurement on the value of the lifetime ratio.

$\Gamma(B^+B^-)/\Gamma_{\text{total}}$	DOCUMENT ID	TECN	COMMENT
0.516 ± 0.006 OUR EVALUATION			Assuming $B(\Upsilon(4S) \rightarrow B\bar{B}) = 1$
0.516 ± 0.006	ARTUSO	05B	CLE3 $e^+e^- \rightarrow D_X X$

$\Gamma(D_s^+ \text{ anything} + \text{c.c.})/\Gamma_{\text{total}}$	DOCUMENT ID	TECN	COMMENT
0.183 ± 0.021 ± 0.015			
0.183 ± 0.021 ± 0.015	⁴ ARTUSO	05B	CLE3 $e^+e^- \rightarrow D_X X$

⁴ ARTUSO 05B reports $B(\Upsilon(4S) \rightarrow D_s^+ \text{ anything} + \text{c.c.}) \times [B(D_s^+ \rightarrow \phi\pi^+)] = (8.0 \pm 0.2 \pm 0.9) \times 10^{-3}$. We divide by our best value $B(D_s^+ \rightarrow \phi\pi^+) = (4.38 \pm 0.35) \times 10^{-2}$. Our first error is their experiment's error and our second error is the systematic error from using our best value.

$\Gamma(B^0\bar{B}^0)/\Gamma_{\text{total}}$	DOCUMENT ID	TECN	COMMENT
0.484 ± 0.006 OUR EVALUATION			Assuming $B(\Upsilon(4S) \rightarrow B\bar{B}) = 1$
0.487 ± 0.010 ± 0.008	⁵ AUBERT, B	05H	BABR $\Upsilon(4S) \rightarrow \bar{B}B \rightarrow D^* \ell \nu_\ell$

⁵ Direct measurement. This value is averaged with the value extracted from the $\Gamma(B^+B^-) / \Gamma(B^0\bar{B}^0)$ measurements.

$\Gamma(B^+B^-)/\Gamma(B^0\bar{B}^0)$	DOCUMENT ID	TECN	COMMENT
1.065 ± 0.026 OUR EVALUATION			
1.006 ± 0.036 ± 0.031	⁶ AUBERT	04F	BABR $\Upsilon(4S) \rightarrow B\bar{B} \rightarrow J/\psi K$
1.01 ± 0.03 ± 0.09	⁶ HASTINGS	03	BELL $\Upsilon(4S) \rightarrow B\bar{B} \rightarrow$ dileptons
1.058 ± 0.084 ± 0.136	⁷ ATHAR	02	CLEO $\Upsilon(4S) \rightarrow B\bar{B} \rightarrow D^* \ell \nu$
1.10 ± 0.06 ± 0.05	⁸ AUBERT	02	BABR $\Upsilon(4S) \rightarrow B\bar{B} \rightarrow (c\bar{c}) K^* K^*$
1.04 ± 0.07 ± 0.04	⁹ ALEXANDER	01	CLEO $\Upsilon(4S) \rightarrow B\bar{B} \rightarrow J/\psi K^* K^*$

⁶ HASTINGS 03 and AUBERT 04F assume $\tau(B^+) / \tau(B^0) = 1.083 \pm 0.017$.
⁷ ATHAR 02 assumes $\tau(B^+) / \tau(B^0) = 1.074 \pm 0.028$. Supersedes BARISH 95.
⁸ AUBERT 02 assumes $\tau(B^+) / \tau(B^0) = 1.062 \pm 0.029$.
⁹ ALEXANDER 01 assumes $\tau(B^+) / \tau(B^0) = 1.066 \pm 0.024$.

$\Gamma(J/\psi K_S^0(J/\psi, \eta_c) K_S^0)/\Gamma_{\text{total}}$	DOCUMENT ID	TECN	COMMENT
< 4			Forbidden by CP invariance.
< 4	90	¹⁰ TAJIMA	07A BELL $\Upsilon(4S) \rightarrow B^0\bar{B}^0$

¹⁰ $\Upsilon(4S)$ with $CP = +1$ decays to the final state with $CP = -1$.

non- $B\bar{B}$ DECAYS

$\Gamma(\text{non-}B\bar{B})/\Gamma_{\text{total}}$	DOCUMENT ID	TECN	COMMENT
< 0.04			
< 0.04	95	BARISH	96B CLEO e^+e^-

See key on page 373

Meson Particle Listings

$\Upsilon(4S), \Upsilon(10860)$

$\Gamma(e^+e^-)/\Gamma_{total}$ Γ_7/Γ

VALUE (units 10^{-9})	DOCUMENT ID	TECN	COMMENT
1.57 ± 0.08 OUR AVERAGE			
$1.55 \pm 0.04 \pm 0.07$	AUBERT	05Q	BABR $e^+e^- \rightarrow$ hadrons
$2.77 \pm 0.50 \pm 0.49$	11 ALBRECHT	95E	ARG $e^+e^- \rightarrow$ hadrons

¹¹ Using LEYAOUANC 77 parametrization of $\Gamma(s)$.

$\Gamma(J/\psi(1S) \text{ anything})/\Gamma_{total}$ Γ_8/Γ

VALUE (units 10^{-4})	CL%	DOCUMENT ID	TECN	COMMENT
<1.9	95	12 ABE	02D	BELL $e^+e^- \rightarrow J/\psi X \rightarrow \ell^+ \ell^- X$
••• We do not use the following data for averages, fits, limits, etc. •••				
<4.7	90	12 AUBERT	01C	BABR $e^+e^- \rightarrow J/\psi X \rightarrow \ell^+ \ell^- X$

¹² Uses $B(J/\psi \rightarrow e^+e^-) = 0.0593 \pm 0.0010$ and $B(J/\psi \rightarrow \mu^+\mu^-) = 0.0588 \pm 0.0010$.

$\Gamma(D^{*+} \text{ anything} + c.c.)/\Gamma_{total}$ Γ_9/Γ

VALUE	CL%	DOCUMENT ID	TECN	COMMENT
<0.074	90	13 ALEXANDER	90C	CLEO e^+e^-

¹³ For $x > 0.473$.

$\Gamma(\phi \text{ anything})/\Gamma_{total}$ Γ_{10}/Γ

VALUE (units 10^{-2})	CL%	DOCUMENT ID	TECN	COMMENT
$7.1 \pm 0.1 \pm 0.6$		HUANG	07	CLEO $\Upsilon(4S) \rightarrow \phi X$
••• We do not use the following data for averages, fits, limits, etc. •••				
<0.23	90	14 ALEXANDER	90C	CLEO e^+e^-

¹⁴ For $x > 0.52$.

$\Gamma(\phi\eta)/\Gamma_{total}$ Γ_{11}/Γ

VALUE (units 10^{-6})	CL%	DOCUMENT ID	TECN	COMMENT
<2.5	90	AUBERT, BE	06F	BABR $e^+e^- \rightarrow \phi\eta$

$\Gamma(\Upsilon(1S) \text{ anything})/\Gamma_{total}$ Γ_{12}/Γ

VALUE	CL%	DOCUMENT ID	TECN	COMMENT
<0.004	90	ALEXANDER	90C	CLEO e^+e^-

$\Gamma(\Upsilon(1S)\pi^+\pi^-)/\Gamma_{total}$ Γ_{13}/Γ

VALUE (units 10^{-4})	CL%	EVTS	DOCUMENT ID	TECN	COMMENT
$0.90 \pm 0.15 \pm 0.02$		167 ± 19	15 AUBERT	06R	BABR $e^+e^- \rightarrow \pi^+\pi^-\mu^+\mu^-$
••• We do not use the following data for averages, fits, limits, etc. •••					
$1.78 \pm 0.40 \pm 0.03$			16,17 SOKOLOV	07	BELL $e^+e^- \rightarrow \pi^+\pi^-\mu^+\mu^-$
<1.2	90		GLENN	99	CLE2 e^+e^-

¹⁵ AUBERT 06R reports $[B(\Upsilon(4S) \rightarrow \Upsilon(1S)\pi^+\pi^-)] \times [B(\Upsilon(1S) \rightarrow \mu^+\mu^-)] = (2.23 \pm 0.25 \pm 0.27) \times 10^{-6}$. We divide by our best value $B(\Upsilon(1S) \rightarrow \mu^+\mu^-) = (2.48 \pm 0.05) \times 10^{-2}$. Our first error is their experiment's error and our second error is the systematic error from using our best value.

¹⁶ SOKOLOV 07 reports $[B(\Upsilon(4S) \rightarrow \Upsilon(1S)\pi^+\pi^-)] \times [B(\Upsilon(1S) \rightarrow \mu^+\mu^-)] = (4.42 \pm 0.81 \pm 0.56) \times 10^{-6}$. We divide by our best value $B(\Upsilon(1S) \rightarrow \mu^+\mu^-) = (2.48 \pm 0.05) \times 10^{-2}$. Our first error is their experiment's error and our second error is the systematic error from using our best value.

¹⁷ According to the authors, systematic errors were underestimated.

$\Gamma(\Upsilon(2S)\pi^+\pi^-)/\Gamma_{total}$ Γ_{14}/Γ

VALUE (units 10^{-4})	CL%	EVTS	DOCUMENT ID	TECN	COMMENT
$0.88 \pm 0.17 \pm 0.08$		97 ± 15	18 AUBERT	06R	BABR $e^+e^- \rightarrow \pi^+\pi^-\mu^+\mu^-$
••• We do not use the following data for averages, fits, limits, etc. •••					
<3.9	90		GLENN	99	CLE2 e^+e^-

¹⁸ AUBERT 06R reports $[B(\Upsilon(4S) \rightarrow \Upsilon(2S)\pi^+\pi^-)] \times [B(\Upsilon(2S) \rightarrow \mu^+\mu^-)] = (1.69 \pm 0.26 \pm 0.20) \times 10^{-6}$. We divide by our best value $B(\Upsilon(2S) \rightarrow \mu^+\mu^-) = (1.93 \pm 0.17) \times 10^{-2}$. Our first error is their experiment's error and our second error is the systematic error from using our best value.

$\Gamma(\bar{d} \text{ anything})/\Gamma_{total}$ Γ_{15}/Γ

VALUE (units 10^{-5})	CL%	DOCUMENT ID	TECN	COMMENT
<1.3	90	ASNER	07	CLEO $e^+e^- \rightarrow \bar{d}X$

$\Upsilon(4S)$ REFERENCES

ASNER	07	PR D75 012009	D.M. Asner et al.	(CLEO Collab.)
HUANG	07	PR D75 012002	G.S. Huang et al.	(CLEO Collab.)
SOKOLOV	07	PR D75 071303R	A. Sokolov et al.	(BELLE Collab.)
TAJIMA	07A	PRL 99 211601	O. Tajima et al.	(BELLE Collab.)
AUBERT	06R	PRL 96 232001	B. Aubert et al.	(BABAR Collab.)
AUBERT, BE	06F	PR D74 111103R	B. Aubert et al.	(BABAR Collab.)
ARTUSO	05B	PRL 95 261801	M. Artuso et al.	(CLEO Collab.)
AUBERT	05Q	PR D72 032005	B. Aubert et al.	(BABAR Collab.)
AUBERT, B	05H	PRL 95 042001	B. Aubert et al.	(BABAR Collab.)
AUBERT	04F	PR D69 071101	B. Aubert et al.	(BABAR Collab.)
HASTINGS	03	PR D67 052004	N.C. Hastings et al.	(BELLE Collab.)
ABE	02D	PRL 88 052001	K. Abe et al.	(BELLE Collab.)
ATHAR	02	PR D66 052003	S.B. Athar et al.	(CLEO Collab.)
AUBERT	02	PR D65 032001	B. Aubert et al.	(BABAR Collab.)
ALEXANDER	01	PRL 86 2737	J.P. Alexander et al.	(CLEO Collab.)
AUBERT	01C	PRL 87 162002	B. Aubert et al.	(BABAR Collab.)
GLENN	99	PR D59 052003	S. Glenn et al.	(CLEO Collab.)
BARISH	96B	PRL 76 1570	B.C. Barish et al.	(CLEO Collab.)
ALBRECHT	95E	ZPHY C65 619	H. Albrecht et al.	(ARGUS Collab.)
BARISH	95	PR D51 1014	B.C. Barish et al.	(CLEO Collab.)
ALEXANDER	90C	PRL 64 2226	J. Alexander et al.	(CLEO Collab.)
BEBEK	87	PR D36 1289	C. Bebek et al.	(CLEO Collab.)
BESSON	85	PRL 54 381	D. Besson et al.	(CLEO Collab.)
LOVELOCK	85	PRL 54 377	D.M.J. Lovelock et al.	(CUSB Collab.)
LEYAOUANC	77	PL B71 397	A. Le Yaouanc et al.	(ORSAY)

OTHER RELATED PAPERS

GO	07	PRL 99 131802	A. Go et al.	(BELLE Collab.)
VOLOSHIN	05A	PAN 68 771	M.B. Voloshin	
		Translated from YAF 68 804.		
ABE	01J	PR D64 072001	K. Abe et al.	(BELLE Collab.)
HENDERS-ON	92	PR D45 2212	S. Henderson et al.	(CLEO Collab.)
ANDREWS	80B	PRL 45 219	D. Andrews et al.	(CLEO Collab.)
FINOCCHI...	80	PRL 45 222	G. Finocchiaro et al.	(CUSB Collab.)

$\Upsilon(10860)$

$$I^G(J^{PC}) = 0^-(1^{--})$$

$\Upsilon(10860)$ MASS

VALUE (GeV)	DOCUMENT ID	TECN	COMMENT
10.865 ± 0.008 OUR AVERAGE			Error includes scale factor of 1.1.
$10.868 \pm 0.006 \pm 0.005$	BESSION	85	CLEO $e^+e^- \rightarrow$ hadrons
10.845 ± 0.020	LOVELOCK	85	CUSB $e^+e^- \rightarrow$ hadrons

$\Upsilon(10860)$ WIDTH

VALUE (MeV)	DOCUMENT ID	TECN	COMMENT
110 ± 13 OUR AVERAGE			
$112 \pm 17 \pm 23$	BESSION	85	CLEO $e^+e^- \rightarrow$ hadrons
110 ± 15	LOVELOCK	85	CUSB $e^+e^- \rightarrow$ hadrons

$\Upsilon(10860)$ DECAY MODES

Mode	Fraction (Γ_i/Γ)	Confidence level
Γ_1 e^+e^-	$(2.8 \pm 0.7) \times 10^{-6}$	
Γ_2 $B\bar{B}X$	$(5.9 \pm 14) \%$	
Γ_3 $B\bar{B}$	$< 13.8 \%$	90%
Γ_4 $B\bar{B}^* + c.c.$	$(14 \pm 6) \%$	
Γ_5 $B^*\bar{B}^*$	$(44 \pm 11) \%$	
Γ_6 $B\bar{B}^*(*)\pi$	$< 19.7 \%$	90%
Γ_7 $B\bar{B}\pi\pi$	$< 8.9 \%$	90%
Γ_8 $B_s^{(*)}\bar{B}_s^{(*)}(X)$	$(19.3 \pm 2.9) \%$	
Γ_9 $B_s^{(*)}\bar{B}_s^{(*)}$		
Γ_{10} $B_s\bar{B}_s$		
Γ_{11} $B_s\bar{B}_s^* + c.c.$		
Γ_{12} $B_s^*\bar{B}_s^*$		
Γ_{13} $\Upsilon(1S)\pi^+\pi^-$	$(5.3 \pm 0.6) \times 10^{-3}$	
Γ_{14} $\Upsilon(2S)\pi^+\pi^-$	$(7.8 \pm 1.3) \times 10^{-3}$	
Γ_{15} $\Upsilon(3S)\pi^+\pi^-$	$(4.8 \pm 1.9) \times 10^{-3}$	
Γ_{16} $\Upsilon(1S)K^+K^-$	$(6.1 \pm 1.8) \times 10^{-4}$	

Inclusive Decays.

These decay modes are submodes of one or more of the decay modes above.

Γ_{17} ϕ anything	$(13.8 \pm 2.4) \%$
Γ_{18} D^0 anything + c.c.	$(108 \pm 8) \%$
Γ_{19} D_s anything + c.c.	$(47 \pm 6) \%$
Γ_{20} J/ψ anything	$(2.06 \pm 0.21) \%$

$\Upsilon(10860)$ PARTIAL WIDTHS

$\Gamma(e^+e^-)$	VALUE (keV)	DOCUMENT ID	TECN	COMMENT
	0.31 ± 0.07 OUR AVERAGE			Error includes scale factor of 1.3.
	$0.22 \pm 0.05 \pm 0.07$	BESSION	85	CLEO $e^+e^- \rightarrow$ hadrons
	0.365 ± 0.070	LOVELOCK	85	CUSB $e^+e^- \rightarrow$ hadrons

$\Upsilon(10860)$ BRANCHING RATIOS

$\Gamma(B\bar{B}X)/\Gamma_{total}$	VALUE	DOCUMENT ID	TECN	COMMENT
	$0.589 \pm 0.100 \pm 0.092$	1 HUANG	07	CLEO $\Upsilon(5S) \rightarrow$ hadrons

$\Gamma(B\bar{B})/\Gamma_{total}$	VALUE	CL%	DOCUMENT ID	TECN	COMMENT
	<0.138	90	1 HUANG	07	CLEO $\Upsilon(5S) \rightarrow$ hadrons

$\Gamma(B\bar{B}^*)/\Gamma(B\bar{B}X)$	VALUE	CL%	DOCUMENT ID	TECN	COMMENT
	<0.22	90	AQUINES	06	CLE3 $\Upsilon(5S) \rightarrow$ hadrons

$\Gamma(B\bar{B}^* + c.c.)/\Gamma_{total}$	VALUE	DOCUMENT ID	TECN	COMMENT
	$0.143 \pm 0.053 \pm 0.027$	1 HUANG	07	CLEO $\Upsilon(5S) \rightarrow$ hadrons

Meson Particle Listings

 $\Upsilon(10860), \Upsilon(11020)$

$\Gamma(B\bar{B}^* + c.c.)/\Gamma(B\bar{B}X)$		Γ_4/Γ_2	
VALUE	EVTS	DOCUMENT ID	TECN COMMENT
$0.24 \pm 0.09 \pm 0.03$	10	AQUINES 06	CLE3 $\Upsilon(5S) \rightarrow$ hadrons

$\Gamma(B^*\bar{B}^*)/\Gamma_{\text{total}}$		Γ_5/Γ	
VALUE	EVTS	DOCUMENT ID	TECN COMMENT
$0.436 \pm 0.083 \pm 0.072$		1 HUANG 07	CLEO $\Upsilon(5S) \rightarrow$ hadrons

$\Gamma(B^*\bar{B}^*)/\Gamma(B\bar{B}X)$		Γ_5/Γ_2	
VALUE	EVTS	DOCUMENT ID	TECN COMMENT
$0.74 \pm 0.15 \pm 0.08$	31	AQUINES 06	CLE3 $\Upsilon(5S) \rightarrow$ hadrons

$\Gamma(B\bar{B}^{(*)}\pi)/\Gamma_{\text{total}}$		Γ_6/Γ	
VALUE	CL%	DOCUMENT ID	TECN COMMENT
<0.197	90	1 HUANG 07	CLEO $\Upsilon(5S) \rightarrow$ hadrons

$\Gamma(B\bar{B}^{(*)}\pi)/\Gamma(B\bar{B}X)$		Γ_6/Γ_2	
VALUE	CL%	DOCUMENT ID	TECN COMMENT
<0.32	90	AQUINES 06	CLE3 $\Upsilon(5S) \rightarrow$ hadrons

$\Gamma(B\bar{B}\pi\pi)/\Gamma_{\text{total}}$		Γ_7/Γ	
VALUE	CL%	DOCUMENT ID	TECN COMMENT
<0.089	90	1 HUANG 07	CLEO $\Upsilon(5S) \rightarrow$ hadrons

$\Gamma(B\bar{B}\pi\pi)/\Gamma(B\bar{B}X)$		Γ_7/Γ_2	
VALUE	CL%	DOCUMENT ID	TECN COMMENT
<0.14	90	AQUINES 06	CLE3 $\Upsilon(5S) \rightarrow$ hadrons

$\Gamma(B_s^{(*)}\bar{B}_s^{(*)}(X))/\Gamma_{\text{total}}$		Γ_8/Γ	
VALUE	EVTS	DOCUMENT ID	TECN COMMENT
0.193 ± 0.029 OUR EVALUATION			Taking into account common systematics.

0.195 ± 0.030 OUR AVERAGE
 -0.023

$0.180 \pm 0.013 \pm 0.032$

0.21 ± 0.06
 -0.03

• • • We do not use the following data for averages, fits, limits, etc. • • •

$0.160 \pm 0.026 \pm 0.058$

$\Gamma(B_s^*\bar{B}_s^*)/\Gamma(B_s^{(*)}\bar{B}_s^{(*)})$		$\Gamma_{12}/\Gamma_9 = \Gamma_{12}/(\Gamma_{10} + \Gamma_{11} + \Gamma_{12})$	
VALUE (units 10^{-2})	EVTS	DOCUMENT ID	TECN COMMENT
$93 \pm 7 \pm 1$		5 DRUTSKOY 07A	BELL $10.86 e^+e^- \rightarrow B_s^{(*)}\bar{B}_s^{(*)}$

$\Gamma(B_s\bar{B}_s)/\Gamma(B_s^*\bar{B}_s^*)$		Γ_{10}/Γ_{12}	
VALUE	CL%	DOCUMENT ID	TECN COMMENT
<0.16	90	BONVICINI 06	CLE3 e^+e^-

$\Gamma(B_s\bar{B}_s^* + c.c.)/\Gamma(B_s^*\bar{B}_s^*)$		Γ_{11}/Γ_{12}	
VALUE	CL%	DOCUMENT ID	TECN COMMENT
<0.16	90	BONVICINI 06	CLE3 e^+e^-

$\Gamma(\Upsilon(1S)\pi^+\pi^-)/\Gamma_{\text{total}}$		Γ_{13}/Γ	
VALUE (units 10^{-3})	EVTS	DOCUMENT ID	TECN COMMENT
$5.3 \pm 0.3 \pm 0.5$	325	6 CHEN 08	BELL $10.87 e^+e^- \rightarrow \Upsilon(1S)\pi^+\pi^-$

$\Gamma(\Upsilon(2S)\pi^+\pi^-)/\Gamma_{\text{total}}$		Γ_{14}/Γ	
VALUE (units 10^{-3})	EVTS	DOCUMENT ID	TECN COMMENT
$7.8 \pm 0.6 \pm 1.1$	186	6 CHEN 08	BELL $10.87 e^+e^- \rightarrow \Upsilon(2S)\pi^+\pi^-$

$\Gamma(\Upsilon(3S)\pi^+\pi^-)/\Gamma_{\text{total}}$		Γ_{15}/Γ	
VALUE (units 10^{-3})	EVTS	DOCUMENT ID	TECN COMMENT
$4.8 \pm 1.9 \pm 0.7$	10	6 CHEN 08	BELL $10.87 e^+e^- \rightarrow \Upsilon(3S)\pi^+\pi^-$

$\Gamma(\Upsilon(1S)K^+K^-)/\Gamma_{\text{total}}$		Γ_{16}/Γ	
VALUE (units 10^{-4})	EVTS	DOCUMENT ID	TECN COMMENT
$6.1 \pm 1.6 \pm 1.0$	20	6 CHEN 08	BELL $10.87 e^+e^- \rightarrow \Upsilon(1S)K^+K^-$

$\Gamma(\phi \text{ anything})/\Gamma_{\text{total}}$		Γ_{17}/Γ	
VALUE	EVTS	DOCUMENT ID	TECN COMMENT
$0.138 \pm 0.007 \pm 0.023$ -0.015		HUANG 07	CLEO $\Upsilon(5S) \rightarrow \phi X$

$\Gamma(D^0 \text{ anything} + c.c.)/\Gamma_{\text{total}}$		Γ_{18}/Γ	
VALUE	EVTS	DOCUMENT ID	TECN COMMENT
$1.076 \pm 0.040 \pm 0.068$		DRUTSKOY 07	BELL $\Upsilon(5S) \rightarrow D^0 X$

$\Gamma(D_s \text{ anything} + c.c.)/\Gamma_{\text{total}}$		Γ_{19}/Γ	
VALUE	EVTS	DOCUMENT ID	TECN COMMENT
0.47 ± 0.06 OUR AVERAGE			

$0.472 \pm 0.024 \pm 0.072$		2 DRUTSKOY 07	BELL $\Upsilon(5S) \rightarrow D_s X$
$0.45 \pm 0.10 \pm 0.04$		7 ARTUSO 05B	CLE3 $e^+e^- \rightarrow D_s X$

$\Gamma(J/\psi \text{ anything})/\Gamma_{\text{total}}$		Γ_{20}/Γ	
VALUE (units 10^{-2})	EVTS	DOCUMENT ID	TECN COMMENT
$2.060 \pm 0.160 \pm 0.134$		DRUTSKOY 07	BELL $\Upsilon(5S) \rightarrow J/\psi X$

¹ Using measurements or limits from AQUINES 06.

² Using $B(D_s^+ \rightarrow \phi\pi^+) = (4.4 \pm 0.6)\%$ from PDG 06.

³ Supersedes ARTUSO 05B. Combining inclusive ϕ , D_s , and B measurements. Using $B(D_s^+ \rightarrow \phi\pi^+) = 4.4 \pm 0.6\%$ from PDG 06.

⁴ Uses a model-dependent estimate $B(B_s \rightarrow D_s X) = (92 \pm 11)\%$.

⁵ From a measurement of $\sigma(e^+e^- \rightarrow B_s^*\bar{B}_s^*) / \sigma(e^+e^- \rightarrow B_s^{(*)}\bar{B}_s^{(*)})$ at $\sqrt{s} = 10.86$ GeV.

⁶ Assuming that the observed events are solely due to the $\Upsilon(5S)$ resonance.

⁷ ARTUSO 05B reports $[B(\Upsilon(10860) \rightarrow D_s \text{ anything} + c.c.)] \times [B(D_s^+ \rightarrow \phi\pi^+)] = 0.0198 \pm 0.0019 \pm 0.0038$. We divide by our best value $B(D_s^+ \rightarrow \phi\pi^+) = (4.38 \pm 0.35) \times 10^{-2}$. Our first error is their experiment's error and our second error is the systematic error from using our best value.

 $\Upsilon(10860)$ REFERENCES

CHEN 08	PRL 100 112001	K.-F. Chen <i>et al.</i>	(BELLE Collab.)
DRUTSKOY 07	PRL 98 052001	A. Drutskoy <i>et al.</i>	(BELLE Collab.)
DRUTSKOY 07A	PR D76 012002	A. Drutskoy <i>et al.</i>	(BELLE Collab.)
HUANG 07	PR D75 012002	G.S. Huang <i>et al.</i>	(CLEO Collab.)
AQUINES 06	PRL 96 152001	O. Aquines <i>et al.</i>	(CLEO Collab.)
BONVICINI 06	PRL 96 022002	G. Bonvicini <i>et al.</i>	(CLEO Collab.)
PDG 06	JPG 33 1	W.-M. Yao <i>et al.</i>	(PDG Collab.)
ARTUSO 05B	PRL 95 261801	M. Artuso <i>et al.</i>	(CLEO Collab.)
BESSION 85	PRL 54 381	D. Besson <i>et al.</i>	(CLEO Collab.)
LOVELOCK 85	PRL 54 377	D.M.J. Lovelock <i>et al.</i>	(CUSB Collab.)

 $\Upsilon(11020)$

$$J^G(J^{PC}) = 0^-(1^{--})$$

 $\Upsilon(11020)$ MASS

VALUE (GeV)	DOCUMENT ID	TECN	COMMENT
11.019 ± 0.008 OUR AVERAGE			
$11.019 \pm 0.005 \pm 0.007$	BESSION 85	CLEO	$e^+e^- \rightarrow$ hadrons
11.020 ± 0.030	LOVELOCK 85	CUSB	$e^+e^- \rightarrow$ hadrons

 $\Upsilon(11020)$ WIDTH

VALUE (MeV)	DOCUMENT ID	TECN	COMMENT
79 ± 16 OUR AVERAGE			
$61 \pm 13 \pm 22$	BESSION 85	CLEO	$e^+e^- \rightarrow$ hadrons
90 ± 20	LOVELOCK 85	CUSB	$e^+e^- \rightarrow$ hadrons

 $\Upsilon(11020)$ DECAY MODES

Mode	Fraction (Γ_i/Γ)
$\Gamma_1 e^+e^-$	$(1.6 \pm 0.5) \times 10^{-6}$

 $\Upsilon(11020)$ PARTIAL WIDTHS

$\Gamma(e^+e^-)$		Γ_1	
VALUE (keV)	EVTS	DOCUMENT ID	TECN COMMENT
0.130 ± 0.030 OUR AVERAGE			
$0.095 \pm 0.03 \pm 0.035$		BESSION 85	CLEO $e^+e^- \rightarrow$ hadrons
0.156 ± 0.040		LOVELOCK 85	CUSB $e^+e^- \rightarrow$ hadrons

 $\Upsilon(11020)$ REFERENCES

BESSION 85	PRL 54 381	D. Besson <i>et al.</i>	(CLEO Collab.)
LOVELOCK 85	PRL 54 377	D.M.J. Lovelock <i>et al.</i>	(CUSB Collab.)

See key on page 373

Meson Particle Listings
Non- $q\bar{q}$ Candidates,

NON- $q\bar{q}$ CANDIDATES

We include here reference lists on gluonium and other non- $q\bar{q}$ candidates. For a review see PDG 06, Journal of Physics, G 33 1 (2006). See also the "Note on scalar mesons" in the $f_0(600)$ Particle Listings and the review on "New charmonium-like states" in $c\bar{c}$ listings. Other possible states are listed in the section on Further States.

Non- $q\bar{q}$ Candidates

OMITTED FROM SUMMARY TABLE

NON- $q\bar{q}$ CANDIDATES REFERENCES

CHOI	08	PRL 100 142001	S.-K. Choi <i>et al.</i>	(BELLE Collab.)
LEE	08	PL B661 28	S.H. Lee <i>et al.</i>	
LI	08	PR D77 054001	Y. Li, C.-D. Lu, W. Wang	
LIU	08A	PR D77 034003	X. Liu <i>et al.</i>	
AMBROSINO	07A	PL B648 267	F. Ambrosino <i>et al.</i>	(KLOE Collab.)
BUISSERET	07	PR C76 025206	F. Buisseret	
CHEN	07E	PR D76 094025	H.-X. Chen, A. Hosaka, S.L. Zhu	
CHIU	07	PL B646 95	T.-W. Chiu, T.-H. Hsieh	
DING	07A	PL B657 49	G.-J. Ding, M.-L. Yan	
FAESSLER	07B	PR D76 114008	A. Faessler <i>et al.</i>	
GENERAL	07	EPJ C51 347	I.J. General, S.R. Contanch, F.J. Llanes-Estrada	
GENERAL	07A	PL B653 216	L.J. General <i>et al.</i>	
GLOZMAN	07	PRPL 444 1	L.Ya. Glozman	
GUO	07	PL B647 133	F.-K. Guo <i>et al.</i>	
HANHART	07	PR D75 074015	C. Hanhart <i>et al.</i>	
LEMMER	07	PL B650 152	R.H. Lemmer	
MAIANI	07	EPJ C50 609	L. Maiani <i>et al.</i>	
MATHEUS	07	PR D75 014005	R. Matheus <i>et al.</i>	
MATHUR	07	PR D76 114505	N. Mathur	
ROSENBER	07	PR D76 114002	J. Rosenberg	
SANTOPINTO	07	PR C75 045206	E. Santopinto, G. Galata	
YANG	07	PR D76 094001	K.-C. Yang	
ABD-EL-HADY	06	PR D73 073010	A. Abd-El-Hady	
ACHARD	06A	PL B638 128	P. Achard <i>et al.</i>	(L3 Collab.)
ALFIKY	06	PL B640 238	M. Alfiky, F. Gabbiani, A.A. Petrov	(WAYN)
ANISOVICH	06A	PAN 69 520	V.V. Anisovich <i>et al.</i>	
AUBERT	06	PR D73 011101R	B. Aubert <i>et al.</i>	(BABAR Collab.)
BRAATEN	06	PR D73 011501	E. Braaten	
BUISSERET	06	EPJ A29 343	F. Buisseret, V. Mathieu	(UMH)
BURNS	06	PR D74 034003	T.J. Burns, F.E. Close	
CHEN	06	PR D73 014516	Y. Chen, A. Alexandru, S.J. Dong	
CHENG	06	PR D73 014017	H.-Y. Cheng, C.-K. Chua, K.-C. Yang	
CHENG	06A	PR D74 094005	H.-Y. Cheng, C.-K. Chua, K.-F. Liu	
CHIU	06	PR D73 094510	T.-W. Chiu, T.-H. Hsieh	
COOK	06	PR D74 094501	M.S. Cook, H.R. Fiebig	
CUI	06	PR D73 014018	Y. Cui <i>et al.</i>	
DING	06	PL B643 33	G.-J. Ding, M.-L. Yan	(CST)
DMITRASINO...	06	MPL A21 533	V. Dmitrasinovic	
DUBYNYSKIY	06	PR D74 094017	S. Dubynskiy, M. Voloshin	
FARIBORZ	06	PR D74 054030	A.H. Fariborz	
GIACOSA	06	PR D74 014028	F. Giacosa	
GUO	06A	PR D74 097503	F.-K. Guo, P.-N. Shen	
HE	06	PR D73 051502R	X.-G. He, X.-Q. Li, X.-Q. Zeng	
HOGAASEN	06	PR D73 054013	H. Hogaasen <i>et al.</i>	
KARLINER	06	PL B638 221	M. Karliner, H.J. Lipkin	
KOCHELEV	06	PL B633 283	N. Kochelev, D.-P. Min	(SEOUL, JINR)
LEE	06A	EPJ A30 423	H.-J. Lee	
LI	06	PR D74 034019	B.A. Li	
LI	06A	PR D74 054017	B.A. Li	
LI	06B	MPL A21 743	D.M. Li <i>et al.</i>	
LOAN	06	JMP A21 2905	M. Loan <i>et al.</i>	
NAVARRA	06	PL B639 272	F.S. Navarra, M. Nielsen	
NIELSEN	06	PL B634 35	M. Nielsen	
PELAEZ	06	PRL 97 242002	J.R. Pelaez, G. Rios	
QIAO	06	PL B639 263	C. Qiao	
SWANSON	06	PRPL 429 243	E.S. Swanson	(PITT)
UEHARA	06	PRL 96 082003	S. Uehara <i>et al.</i>	(BELLE Collab.)
VENTO	06	PR D73 054006	V. Vento	
VIJANDE	06	PR D73 034002	J. Vijande, F. Fernandez, A. Valcarce	
VOLOSHIN	06	JMP A21 1239	M. Voloshin	
WANG	06	PR D73 094020	Z.-G. Wang, S.-L. Wan	
YUAN	06	PL B634 399	C.-Z. Yuan, P. Wang, X.H. Mo	
ZHAO	06	PR D74 114025	Q. Zhao, B.S. Zhou	(BES Collab.)
ABLIKIM	05	PL B607 243	M. Ablikim <i>et al.</i>	(BES Collab.)
ABLIKIM	05R	PRL 95 262001	M. Ablikim <i>et al.</i>	(L3 Collab.)
ACHARD	05B	PL B615 19	P. Achard <i>et al.</i>	
ANIKIN	05	PL B626 86	I.V. Anikin, B. Pire, O.V. Teryaev	
ANISOVICH	05	JETPL 80 715	V.V. Anisovich	
ANISOVICH	05A	JETPL 81 417	V.V. Anisovich, A.V. Sarantsev	
ANISOVICH	05C	JMP A20 6307	V.V. Anisovich, M.A. Matveev, A.V. Sarantsev	
AUBERT	05B	PR D71 031501R	B. Aubert <i>et al.</i>	(BABAR Collab.)
AUBERT	05R	PR D71 071103R	B. Aubert <i>et al.</i>	(BABAR Collab.)
AUBERT.B	05I	PRL 95 142001	B. Aubert <i>et al.</i>	(BABAR Collab.)
BICUDO	05	NP A748 537	P. Bicudo	
BIGI	05	PR D72 114016	I. Bigi <i>et al.</i>	
BRAATEN	05	PR D72 014012	E. Braaten, M. Kusunoki	
BRAATEN	05A	PR D72 054022	E. Braaten, M. Kusunoki	
BRAATEN	05B	PR D71 074005	E. Braaten, M. Kusunoki	
BRACCO	05	PL B624 217	M.E. Bracco, A. Lozae, R.D. Matheus	
BRITO	05	PL B608 69	T.V. Brito <i>et al.</i>	
CHANG	05B	PL B623 218	C.-H. Chang, C.S. Kim, G. Wang	
CHANOWITZ	05	PRL 95 172001	M. Chanowitz	
CHOI	05	PRL 94 182002	S.-K. Choi <i>et al.</i>	(BELLE Collab.)
CLOSE	05	PR D71 094022	F.E. Close, Q. Zhao	
CLOSE	05A	PL B628 215	F.E. Close, P.R. Page	
DING	05	PR C72 015208	G.-J. Ding, M.-L. Yan	(CST)
GIACOSA	05	PR C71 025202	F. Giacosa <i>et al.</i>	
GIACOSA	05A	PL B622 277	F. Giacosa <i>et al.</i>	
GUO	05	NP A761 269	F.-K. Guo <i>et al.</i>	
HEDDITCH	05	PR D72 114507	J.N. Hedditch <i>et al.</i>	
HUANG	05A	PR D71 034015	M.Q. Huang, D.W. Wang	
INWASAKI	05A	PR D72 094016	M. Inasaki, T. Fukutome	
JAFFE	05	PRPL 409 1	R.L. Jaffe	
KALASHNIK...	05	EPJ A24 437	Yu.S. Kalashnikova, A.E. Kudryavtsev, A.V. Nefediev	

KANADA-EN...	05	PR D71 094005	Y. Kanada-Enyo, O. Morimatsu, T. Nishikawa
KIM	05	PR D71 034025	T. Kim, P. Ko
KIM	05A	PR D72 074012	H. Kim, Y. Oh
KOU	05	PL B631 164	E. Kou
LI	05	PL B605 306	B.A. Li
LI	05E	MPL A20 2497	D.-M. Li <i>et al.</i>
LIU	05	PR D72 054023	X. Liu, X.Q. Zeng, X.Q. Li
LOISEAU	05	PR C72 011001	B. Loiseau, S. Wycech
LU	05	PRL 94 032002	M. Lu <i>et al.</i>
MAIANI	05	PR D71 014028	L. Maiani <i>et al.</i>
MAIANI	05A	PR D72 031502R	L. Maiani <i>et al.</i>
POPLAWSKI	05	PR D71 056003	N.J. Poplawski, A.P. Szczepaniak, J.T. Londergan
SETH	05	PL B612 1	K.K. Seth
SUZUKI	05	PR D72 114013	M. Suzuki
VIJANDE	05	PR D72 034025	J. Vijande, A. Valcarce, F. Fernandez
VOLOSHIN	05	PR D71 114003	M.B. Voloshin
WANG	05A	PL B617 141	M.-Z. Wang <i>et al.</i>
WANG	05C	EPJ C42 89	Z.-G. Wang, W.-M. Yang
ZHANG	05	PR D71 011502R	Z.F. Zhang, H.Y. Jin
ZHAO	05	PR D72 074001	Q. Zhao
ZHAO	05A	PL B631 22	Q. Zhao, B.-S. Zou, Z.-B. Ma
ZHU	05	PL B625 212	S.-L. Zhu
ABAZOV	04F	PRL 93 162002	V.M. Abazov <i>et al.</i>
ABE	04	EPJ C32 323	K. Abe <i>et al.</i>
ABLIKIM	04E	PL B603 138	M. Ablikim <i>et al.</i>
ACOSTA	04	PRL 93 072001	D. Acosta <i>et al.</i>
AMSLER	04	PRPL 389 61	C. Amisler, N.A. Tornqvist
AMSLER	04A	NP A740 130	C. Amisler <i>et al.</i>
BARNES	04	PR D69 054008	T. Barnes, S. Godfrey
BARNES	04A	PL B600 223	T. Barnes <i>et al.</i>
BARU	04	PL B506 53	V. Baru <i>et al.</i>
BRAATEN	04	PR D69 074005	E. Braaten <i>et al.</i>
BRAATEN	04B	PRL 93 162001	E. Braaten, M. Kusunoki, S. Nussinov
BUGG	04C	PRPL 397 257	D.V. Bugg
CHAO	04A	PL B599 43	K.-T. Chao
CHEN	04	PR D69 076003	J.-X. Chen, J.-C. Su
CHEN	04A	PR D69 054002	C.-H. Chen
CHEN	04C	PRL 93 232001	Y.-Q. Chen, X.-Q. Li
CLOSE	04B	PR D70 094015	F.E. Close, J.J. Dudek
CLOSE	04B	PR D69 034010	F.E. Close, J.J. Dudek
COHEN	04	PL B578 359	T.D. Cohen <i>et al.</i>
DAI	04	JHEP 0411 043	N.-B. Dai <i>et al.</i>
DMITRASINO...	04	PR D70 096011	V. Dmitrasinovic
EICHTEN	04	PR D69 094019	E. Eichten, K. Lane, C. Quigg
FADDEEV	04	PR D70 114033	L. Faddeev <i>et al.</i>
FARIBORZ	04	JMP A19 2095	A.H. Fariborz
GLOZMAN	04	PL B587 69	L.Ya. Glozman
KREWALD	04	PR D69 016003	S. Krewald, R.H. Lemmer, F.P. Sassen
KUHN	04	PL B595 109	J. Kuhn <i>et al.</i>
LIPKIN	04	PL B580 50	H.J. Lipkin
LIU	04A	PR D70 094009	Y.-R. Liu
LONGACRE	04	PR D70 094041	R.S. Longacre, S.J. Lindenbaum
MAIANI	04	PR D70 054009	L. Maiani <i>et al.</i>
NAPSUCIALE	04A	PR D70 094043	N.M. Napsuciale, S. Rodriguez
PELAEZ	04	PRL 92 102001	J.R. Pelaez
PELAEZ	04A	MPL A19 2879	J.R. Pelaez
SWANSON	04	PL B582 167	E. Swanson
SWANSON	04A	PL B588 189	E. Swanson
SWANSON	04B	PL B598 197	E. Swanson
TESHIMA	04	JPG 30 663	T. Teshima <i>et al.</i>
TORNQVIST	04	PL B590 209	N. Tornqvist
VANBEVEREN	04	MPL A19 1949	E. van Beveren, G. Rupp
VOLOSHIN	04A	PL B604 69	M.B. Voloshin
WONG	04	PR C69 055202	C. Wong
ZOU	04	PR D69 034004	B.S. Zou, H.C. Chiang
AUBERT	03G	PRL 90 242001	B. Aubert <i>et al.</i>
BARNES	03	PR D68 054006	T. Barnes <i>et al.</i>
BESSON	03	PR D68 032002	D. Besson <i>et al.</i>
CHENG	03B	PR D67 054021	H.Y. Cheng
CHENG	03C	PL B566 193	H.-Y. Cheng, W.-S. Hou
CHOI	03	PRL 91 262001	S.-K. Choi <i>et al.</i>
TERASAKI	03	PR D68 011501	K. Terasaki
ABE	02K	PRL 88 181803	K. Abe <i>et al.</i>
ALOSIO	02C	PL B536 209	A. Aloisio <i>et al.</i>
ALOSIO	02D	PL B537 21	A. Aloisio <i>et al.</i>
AMSLER	02	EPJ C23 29	C. Amisler <i>et al.</i>
AMSLER	02B	PL B541 22	C. Amisler
CHUNG	02C	EPJ A15 539	S.U. Chung, E. Klempt, J.G. Korener
CLOSE	02B	JPG 28 R249	F.E. Close, N. Tornqvist
ABELE	01	EPJ C19 667	A. Abele <i>et al.</i>
ABELE	01B	EPJ C21 261	A. Abele <i>et al.</i>
ACCARIARI	01H	PL B501 173	M. Acciarri <i>et al.</i>
AITALA	01A	PRL 86 765	E.M. Aitala <i>et al.</i>
AMSLER	01	PL B520 175	C. Amisler <i>et al.</i>
AMSLER	01B	EPJ C21 531	F.E. Close, A. Kirk
IDDIR	01	PL B507 183	F. Idir, A.S. Safir
IVANOV	01	PRL 86 3977	E.I. Ivanov <i>et al.</i>
ACHASOV	00F	PL B479 53	M.N. Achasov <i>et al.</i>
ALFORD	00	NP B578 367	M. Alford, R.L. Jaffe
BARATE	00E	PL B472 189	R. Barate <i>et al.</i>
BARBERIS	00C	PL B471 440	D. Barberis <i>et al.</i>
KIRK	00	PL B489 29	A. Kirk
LEE	00	PR D61 014015	W. Lee, D. Weingarten
ABELE	99	PL B446 349	A. Abele <i>et al.</i>
AKHMETSHIN	99B	PL B462 371	R.R. Akhmetshin <i>et al.</i>
BAKER	99	PL B449 114	C.A. Baker <i>et al.</i>
BARBERIS	99D	PL B462 462	D. Barberis <i>et al.</i>
CHUNG	99	PR D69 092001	Z. Chung <i>et al.</i>
DELBOURGO	99	PR B446 332	R. Delbourgo, D. Liu, M. Scadron
DONNACHIE	99	PR D60 114011	A. Donnachie, Yu.S. Kalashnikova
DUENNWEBER	99	NP A 663 + 664, 592C	W. Duennweber
MINKOWSKI	99	EPJ C9 283	P. Minkowski, W. Ochs
MORNINGSTAR	99	PR D60 034509	C.J. Morningstar, M. Peardon
PAGE	99	PR D59 034016	P.R. Page, E.S. Swanson, A.P. Szczepaniak
ABELE	98	PR D57 3860	A. Abele <i>et al.</i>
ABELE	98B	PL B423 175	A. Abele <i>et al.</i>
ADAMS	98B	PRL 81 5760	G.S. Adams <i>et al.</i>
AMSLER	98	RMP 70 1293	C. Amisler
BARBERIS	98	PL B432 436	D. Barberis <i>et al.</i>
BERTIN	98	PR D57 55	A. Bertin <i>et al.</i>
CLOSE	98B	PL B419 387	F.E. Close

Meson Particle Listings

FRABETTI	97	PL B391 235	P.L. Frabetti <i>et al.</i>	(FNAL E687 Collab.)	LEE	94	PL B323 227	J.H. Lee <i>et al.</i>	(BNL, IND, KYUN, MASD+)
LACOCK	97	PL B401 308	P. Lacock <i>et al.</i>	(EDIN, LIVP)	BALI	93	PL B309 378	G.S. Bali <i>et al.</i>	(LIVP)
MICHAEL	97	Hadron 97 Conf.	C. Michael		BELADIDZE	93	PL B313 276	G.M. Beladidze <i>et al.</i>	(VES Collab.)
AIP Conf.	Proc.	432 657			ADAMO	92	PL B287 368	A. Adamo <i>et al.</i>	(OBELIX Collab.)
OLLER	97B	Hadron 97 Conf.	J.A. Oller, E. Oset		GOUZ	92	Dallas HEP 92, p. 572	Yu.P. Gouz <i>et al.</i>	(VES Collab.)
AIP Conf.	Proc.	432 413			Proceedings XXVI Int. Conf. on High Energy Physics				
THOMPSON	97	PRL 79 1630	D.R. Thompson <i>et al.</i>	(BNL E852 Collab.)	KARCH	92	ZPHY C54 33	K. Karch <i>et al.</i>	(Crystal Ball Collab.)
WEINGARTEN	97	NPPS 53 232	D. Weingarten		ALDE	90	PL B241 600	D.M. Alde <i>et al.</i>	(SERP, BELG, LANL, LAPP+)
ABELE	96B	PL B385 425	A. Abele <i>et al.</i>	(Crystal Barrel Collab.)	MAY	90	ZPHY C46 203	B. May <i>et al.</i>	(ASTERIX Collab.)
ADOMEIT	96	ZPHY C71 227	J. Adomeit <i>et al.</i>	(Crystal Barrel Collab.)	WEINSTEIN	90	PR D41 2236	J. Weinstein, N. Isgur	(TNTO)
AMSLER	96	PR D53 295	C. Amstler, F.E. Close	(ZURI, RAL)	ALDE	88B	PL B205 397	D.M. Alde <i>et al.</i>	(SERP, BELG, LANL, LAPP)
BAI	96B	PRL 76 3502	J.Z. Bai <i>et al.</i>	(BES Collab.)	ASTON	88D	NP B301 525	D. Aston <i>et al.</i>	(SLAC, NAGO, CINC, INUS)
TORNQVIST	96	PRL 76 1575	N.A. Tornqvist, M. Roos	(HELS)	ETKIN	88	PL B201 568	A. Etkin <i>et al.</i>	(BNL, CUNY)
AMELIN	95B	PL B356 595	D.V. Amelin <i>et al.</i>	(SERP, TBIL)	CLOSE	87B	PL B196 245	F.E. Close, H.J. Lipkin	
CLOSE	95	NP B443 233	F.E. Close, P.R. Page	(RAL)	BOOTH	86	NP B273 677	P.S.L. Booth <i>et al.</i>	(LIVP, GLAS, CERN)
PROKOSHKIN	95B	PAN 58 606	Y.D. Prokoshkin, S.A. Sadovsky	(SERP)	BARNES	85	PL B165 434	T. Barnes	
		Translated from YAF 58 662			ISGUR	85	PRL 54 869	N. Isgur, R. Kokoski, J. Paton	(TNTO)
PROKOSHKIN	95C	PAN 58 853	Y.D. Prokoshkin, S.A. Sadovsky	(SERP)	JAFFE	77	PR D15 267,281	R. Jaffe	(MIT)
		Translated from YAF 58 921							
SEXTON	95	PRL 75 4563	J. Sexton <i>et al.</i>	(IBM)					

<i>N</i> BARYONS (<i>S</i> = 0, <i>I</i> = 1/2)	
<i>p</i>	1061
<i>n</i>	1069
<i>N</i> resonances	1076

Δ BARYONS (<i>S</i> = 0, <i>I</i> = 3/2)	
Δ resonances	1104

EXOTIC BARYONS	
Pentaquarks	1124

Λ BARYONS (<i>S</i> = -1, <i>I</i> = 0)	
Λ	1126
Λ resonances	1130

Σ BARYONS (<i>S</i> = -1, <i>I</i> = 1)	
Σ^+	1142
Σ^0	1144
Σ^-	1145
Σ resonances	1147

Ξ BARYONS (<i>S</i> = -2, <i>I</i> = 1/2)	
Ξ^0	1166
Ξ^-	1168
Ξ resonances	1171

Ω BARYONS (<i>S</i> = -3, <i>I</i> = 0)	
Ω^-	1179
Ω resonances	1180

CHARMED BARYONS (<i>C</i> = +1)	
Λ_c^+	1184
$\Lambda_c(2595)^+$	1190
$\Lambda_c(2625)^+$	1191
$\Lambda_c(2765)^+$	1191
$\Lambda_c(2880)^+$	1192
$\Lambda_c(2940)^+$	1192
$\Sigma_c(2455)$	1192
$\Sigma_c(2520)$	1193
$\Sigma_c(2800)$	1194
Ξ_c^+	1194
Ξ_c^0	1196
$\Xi_c^{'+}$	1197
$\Xi_c^{'0}$	1197
$\Xi_c(2645)$	1197
$\Xi_c(2790)$	1198
$\Xi_c(2815)$	1198
$\Xi_c(2930)$	1198
$\Xi_c(2980)$	1199
$\Xi_c(3055)$	1199
$\Xi_c(3080)$	1199
$\Xi_c(3123)$	1199
Ω_c^0	1200
$\Omega_c(2770)^0$	1200

DOUBLY-CHARMED BARYONS (<i>C</i> = +2)	
Ξ_{cc}^+	1201

BOTTOM (BEAUTY) BARYONS (<i>B</i> = -1)	
Λ_b^0	1202
Σ_b	1203
Σ_b^*	1204
Ξ_b^0, Ξ_b^-	1204
<i>b</i> -baryon ADMIXTURE ($\Lambda_b, \Xi_b, \Sigma_b, \Omega_b$)	1204

Notes in the Baryon Listings

Baryon Decay Parameters	1071
<i>N</i> and Δ Resonances	1075
Pentaquarks (new)	1124
Baryon Magnetic Moments	1126
Λ and Σ Resonances	1128
The $\Sigma(1670)$ Region	1152
Radiative Hyperon Decays	1167
Ξ Resonances	1171
Charmed Baryons (rev.)	1182
Λ_c^+ Branching Fractions	1185



N BARYONS

(S = 0, I = 1/2)

$p, N^+ = uud; \quad n, N^0 = udd$



$$I(J^P) = \frac{1}{2}(\frac{1}{2}^+) \text{ Status: } ****$$

p MASS (atomic mass units u)

The mass is known much more precisely in u (atomic mass units) than in MeV. See the next data block.

VALUE (u)	DOCUMENT ID	TECN	COMMENT
1.00727646688 ± 0.00000000013	MOHR	05	RVUE 2002 CODATA value
••• We do not use the following data for averages, fits, limits, etc. •••			
1.00727646688 ± 0.00000000013	MOHR	99	RVUE 1998 CODATA value
1.007276470 ± 0.000000012	COHEN	87	RVUE 1986 CODATA value

p MASS (MeV)

The mass is known much more precisely in u (atomic mass units) than in MeV. The conversion from u to MeV, $1 u = 931.494043 \pm 0.000080 \text{ MeV}/c^2$ (MOHR 05, the 2002 CODATA value), involves the relatively poorly known electronic charge.

VALUE (MeV)	DOCUMENT ID	TECN	COMMENT
938.272029 ± 0.000080	MOHR	05	RVUE 2002 CODATA value
••• We do not use the following data for averages, fits, limits, etc. •••			
938.271998 ± 0.000038	MOHR	99	RVUE 1998 CODATA value
938.27231 ± 0.00028	COHEN	87	RVUE 1986 CODATA value
938.2796 ± 0.0027	COHEN	73	RVUE 1973 CODATA value

$|m_p - m_{\bar{p}}|/m_p$

A test of CPT invariance. Note that the comparison of the \bar{p} and p charge-to-mass ratio, given in the next data block, is much better determined.

VALUE	CL%	DOCUMENT ID	TECN	COMMENT
< 2 × 10⁻⁹	90	¹ HORI	06	SPEC $\bar{p}e^-$ He atom
••• We do not use the following data for averages, fits, limits, etc. •••				
< 1.0 × 10 ⁻⁸	90	¹ HORI	03	SPEC $\bar{p}e^-$ ⁴ He, $\bar{p}e^-$ ³ He
< 6 × 10 ⁻⁸	90	¹ HORI	01	SPEC $\bar{p}e^-$ He atom
< 5 × 10 ⁻⁷		² TORII	99	SPEC $\bar{p}e^-$ He atom

- ¹HORI 01, HORI 03, and HORI 06 use the more-precisely-known constraint on the \bar{p} charge-to-mass ratio of GABRIELSE 99 (see below) to get their results. Their results are not independent of the HORI 01, HORI 03, and HORI 06 values for $|q_p + q_{\bar{p}}|/e$, below.
- ²TORII 99 uses the more-precisely-known constraint on the \bar{p} charge-to-mass ratio of GABRIELSE 95 (see below) to get this result. This is not independent of the TORII 99 value for $|q_p + q_{\bar{p}}|/e$, below.

\bar{p}/p CHARGE-TO-MASS RATIO, $|q_{\bar{p}}/m_{\bar{p}}|/(q_p/m_p)$

A test of CPT invariance. Listed here are measurements involving the inertial masses. For a discussion of what may be inferred about the ratio of \bar{p} and p gravitational masses, see ERICSON 90; they obtain an upper bound of 10^{-6} – 10^{-7} for violation of the equivalence principle for \bar{p} 's.

VALUE	DOCUMENT ID	TECN	COMMENT
0.9999999991 ± 0.0000000009	GABRIELSE	99	TRAP Penning trap
••• We do not use the following data for averages, fits, limits, etc. •••			
1.0000000015 ± 0.0000000011	³ GABRIELSE	95	TRAP Penning trap
1.000000023 ± 0.0000000042	⁴ GABRIELSE	90	TRAP Penning trap

- ³Equation (2) of GABRIELSE 95 should read $M(\bar{p})/M(p) = 0.9999999985$ (11) (G. Gabrielse, private communication).
- ⁴GABRIELSE 90 also measures $m_{\bar{p}}/m_{e^-} = 1836.152660 \pm 0.000083$ and $m_p/m_{e^-} = 1836.152680 \pm 0.000088$. Both are completely consistent with the 1986 CODATA (COHEN 87) value for m_p/m_{e^-} of 1836.152701 ± 0.000037 .

$$\left(\frac{q_{\bar{p}}}{m_{\bar{p}}} - \frac{q_p}{m_p} \right) / \frac{q_p}{m_p}$$

A test of CPT invariance. Taken from the \bar{p}/p charge-to-mass ratio, above.

VALUE	DOCUMENT ID
(-9 ± 9) × 10⁻¹¹ OUR EVALUATION	

$|q_p + q_{\bar{p}}|/e$

A test of CPT invariance. Note that the comparison of the \bar{p} and p charge-to-mass ratios given above is much better determined. See also a similar test involving the electron.

VALUE	CL%	DOCUMENT ID	TECN	COMMENT
< 2 × 10⁻⁹	90	⁵ HORI	06	SPEC $\bar{p}e^-$ He atom
••• We do not use the following data for averages, fits, limits, etc. •••				
< 1.0 × 10 ⁻⁸	90	⁵ HORI	03	SPEC $\bar{p}e^-$ ⁴ He, $\bar{p}e^-$ ³ He
< 6 × 10 ⁻⁸	90	⁵ HORI	01	SPEC $\bar{p}e^-$ He atom
< 5 × 10 ⁻⁷		⁶ TORII	99	SPEC $\bar{p}e^-$ He atom
< 2 × 10 ⁻⁵		⁷ HUGHES	92	RVUE

- ⁵HORI 01, HORI 03, and HORI 06 use the more-precisely-known constraint on the \bar{p} charge-to-mass ratio of GABRIELSE 99 (see above) to get their results. Their results are not independent of the HORI 01, HORI 03, and HORI 06 values for $|m_p - m_{\bar{p}}|/m_p$, above.
- ⁶TORII 99 uses the more-precisely-known constraint on the \bar{p} charge-to-mass ratio of GABRIELSE 95 (see above) to get this result. This is not independent of the TORII 99 value for $|m_p - m_{\bar{p}}|/m_p$, above.
- ⁷HUGHES 92 uses recent measurements of Rydberg-energy and cyclotron-frequency ratios.

$|q_p + q_e|/e$

See DYLLA 73 for a summary of experiments on the neutrality of matter. See also "n CHARGE" in the neutron Listings.

VALUE	DOCUMENT ID	COMMENT
< 1.0 × 10⁻²¹	⁸ DYLLA	73 Neutrality of SF ₆
••• We do not use the following data for averages, fits, limits, etc. •••		
< 3.2 × 10 ⁻²⁰	⁹ SENGUPTA	00 binary pulsar
< 0.8 × 10 ⁻²¹	MARINELLI	84 Magnetic levitation

- ⁸Assumes that $q_n = q_p + q_e$.
- ⁹SENGUPTA 00 uses the difference between the observed rate of rotational energy loss by the binary pulsar PSR B1913+16 and the rate predicted by general relativity to set this limit. See the paper for assumptions.

p MAGNETIC MOMENT

See the "Note on Baryon Magnetic Moments" in the A Listings.

VALUE (μ _N)	DOCUMENT ID	TECN	COMMENT
2.792847351 ± 0.000000028	MOHR	05	RVUE 2002 CODATA value
••• We do not use the following data for averages, fits, limits, etc. •••			
2.792847337 ± 0.000000029	MOHR	99	RVUE 1998 CODATA value
2.792847386 ± 0.000000063	COHEN	87	RVUE 1986 CODATA value
2.7928456 ± 0.0000011	COHEN	73	RVUE 1973 CODATA value

\bar{p} MAGNETIC MOMENT

A few early results have been omitted.

VALUE (μ _N)	DOCUMENT ID	TECN	COMMENT
-2.800 ± 0.008 OUR AVERAGE			
-2.8005 ± 0.0090	KREISSL	88	CNTR \bar{p} ²⁰⁸ Pb ¹¹ → ¹⁰ X-ray
-2.817 ± 0.048	ROBERTS	78	CNTR
-2.791 ± 0.021	HU	75	CNTR Exotic atoms

$(\mu_p + \mu_{\bar{p}}) / \mu_p$

A test of CPT invariance. Calculated from the p and \bar{p} magnetic moments, above.

VALUE	DOCUMENT ID
(-2.6 ± 2.9) × 10⁻³ OUR EVALUATION	

p ELECTRIC DIPOLE MOMENT

A nonzero value is forbidden by both T invariance and P invariance.

VALUE (10 ⁻²³ e cm)	EVTS	DOCUMENT ID	TECN	COMMENT
< 0.54	10	DMITRIEV	03	Uses ¹⁹⁹ Hg atom EDM
••• We do not use the following data for averages, fits, limits, etc. •••				
- 3.7 ± 6.3		CHO	89	NMR TI F molecules
< 400		DZUBA	85	THEO Uses ¹²⁹ Xe moment
130 ± 200		¹¹ WILKENING	84	
900 ± 1400		¹² WILKENING	84	
700 ± 900	1G	HARRISON	69	MBR Molecular beam

- ¹⁰DMITRIEV 03 calculates this limit from the limit on the electric dipole moment of the ¹⁹⁹Hg atom.
- ¹¹This WILKENING 84 value includes a finite-size effect and a magnetic effect.
- ¹²This WILKENING 84 value is more cautious than the other and excludes the finite-size effect, which relies on uncertain nuclear integrals.

Baryon Particle Listings

p

p ELECTRIC POLARIZABILITY α_p

For a very complete review of the "polarizability of the nucleon and Compton scattering," see SCHUMACHER 05. His recommended values for the proton are $\alpha_p = (12.0 \pm 0.6) \times 10^{-4} \text{ fm}^3$ and $\beta_p = (1.9 \mp 0.6) \times 10^{-4} \text{ fm}^3$, almost exactly our averages.

VALUE (10^{-4} fm^3)	DOCUMENT ID	TECN	COMMENT
12.0 \pm 0.6 OUR AVERAGE			
12.1 \pm 1.1 \pm 0.5	13 BEANE	03	EFT + γp
11.82 \pm 0.98 \pm 0.52 \pm 0.98	14 BLANPIED	01	LEGS $p(\vec{\gamma}, \gamma), p(\vec{\gamma}, \pi^0), p(\vec{\gamma}, \pi^+)$
11.9 \pm 0.5 \pm 1.3	15 OLMOSDEL...	01	CNTR γp Compton scattering
12.1 \pm 0.8 \pm 0.5	16 MACGIBBON	95	RVUE global average
11.7 \pm 0.8 \pm 0.7	17 BARANOV	01	RVUE Global average
12.5 \pm 0.6 \pm 0.9	MACGIBBON	95	CNTR γp Compton scattering
9.8 \pm 0.4 \pm 1.1	HALLIN	93	CNTR γp Compton scattering
10.62 \pm 1.25 \pm 1.07 \pm 1.19 \pm 1.03	ZIEGER	92	CNTR γp Compton scattering
10.9 \pm 2.2 \pm 1.3	18 FEDERSPIEL	91	CNTR γp Compton scattering

- 13 BEANE 03 uses effective field theory and low-energy γp and γd Compton-scattering data. It also gets for the isoscalar polarizabilities (see the erratum) $\alpha_N = (13.0 \pm 1.9 \pm 3.9) \times 10^{-4} \text{ fm}^3$ and $\beta_N = (-1.8 \pm 1.9 \pm 2.1) \times 10^{-4} \text{ fm}^3$.
- 14 BLANPIED 01 gives $\alpha_p + \beta_p$ and $\alpha_p - \beta_p$. The separate α_p and β_p are provided to us by A. Sandorfi. The first error above is statistics plus systematics; the second is from the model.
- 15 This OLMOSDELEON 01 result uses the TAPS data alone, and does not use the (re-evaluated) sum-rule constraint that $\alpha + \beta = (13.8 \pm 0.4) \times 10^{-4} \text{ fm}^3$. See the paper for a discussion.
- 16 MACGIBBON 95 combine the results of ZIEGER 92, FEDERSPIEL 91, and their own experiment to get a "global average" in which model errors and systematic errors are treated in a consistent way. See MACGIBBON 95 for a discussion.
- 17 BARANOV 01 combines the results of 10 experiments from 1958 through 1995 to get a global average that takes into account both systematic and model errors and does not use the theoretical constraint on the sum $\alpha_p + \beta_p$.
- 18 FEDERSPIEL 91 obtains for the (static) electric polarizability α_p , defined in terms of the induced electric dipole moment by $\mathbf{D} = 4\pi\epsilon_0\alpha_p\mathbf{E}$, the value $(7.0 \pm 2.2 \pm 1.3) \times 10^{-4} \text{ fm}^3$.

p MAGNETIC POLARIZABILITY β_p

The electric and magnetic polarizabilities are subject to a dispersion sum-rule constraint $\bar{\alpha} + \bar{\beta} = (14.2 \pm 0.5) \times 10^{-4} \text{ fm}^3$. Errors here are anticorrelated with those on $\bar{\alpha}_p$ due to this constraint.

VALUE (10^{-4} fm^3)	DOCUMENT ID	TECN	COMMENT
1.9 \pm 0.5 OUR AVERAGE			
3.4 \pm 1.1 \pm 0.1	19 BEANE	03	EFT + γp
1.43 \pm 0.98 \pm 0.52 \pm 0.98	20 BLANPIED	01	LEGS $p(\vec{\gamma}, \gamma), p(\vec{\gamma}, \pi^0), p(\vec{\gamma}, \pi^+)$
1.2 \pm 0.7 \pm 0.5	21 OLMOSDEL...	01	CNTR γp Compton scattering
2.1 \pm 0.8 \pm 0.5	22 MACGIBBON	95	RVUE global average
2.3 \pm 0.9 \pm 0.7	23 BARANOV	01	RVUE Global average
1.7 \pm 0.6 \pm 0.9	MACGIBBON	95	CNTR γp Compton scattering
4.4 \pm 0.4 \pm 1.1	HALLIN	93	CNTR γp Compton scattering
3.58 \pm 1.19 \pm 1.03 \pm 1.25 \pm 1.07	ZIEGER	92	CNTR γp Compton scattering
3.3 \pm 2.2 \pm 1.3	FEDERSPIEL	91	CNTR γp Compton scattering

- 19 BEANE 03 uses effective field theory and low-energy γp and γd Compton-scattering data. It also gets for the isoscalar polarizabilities (see the erratum) $\alpha_N = (13.0 \pm 1.9 \pm 3.9) \times 10^{-4} \text{ fm}^3$ and $\beta_N = (-1.8 \pm 1.9 \pm 2.1) \times 10^{-4} \text{ fm}^3$.
- 20 BLANPIED 01 gives $\alpha_p + \beta_p$ and $\alpha_p - \beta_p$. The separate α_p and β_p are provided to us by A. Sandorfi. The first error above is statistics plus systematics; the second is from the model.
- 21 This OLMOSDELEON 01 result uses the TAPS data alone, and does not use the (re-evaluated) sum-rule constraint that $\alpha + \beta = (13.8 \pm 0.4) \times 10^{-4} \text{ fm}^3$. See the paper for a discussion.
- 22 MACGIBBON 95 combine the results of ZIEGER 92, FEDERSPIEL 91, and their own experiment to get a "global average" in which model errors and systematic errors are treated in a consistent way. See MACGIBBON 95 for a discussion.
- 23 BARANOV 01 combines the results of 10 experiments from 1958 through 1995 to get a global average that takes into account both systematic and model errors and does not use the theoretical constraint on the sum $\alpha_p + \beta_p$.

p CHARGE RADIUS

This is the rms charge radius, $\sqrt{\langle r^2 \rangle}$.

VALUE (fm)	DOCUMENT ID	COMMENT
0.8750 \pm 0.0068	MOHR	05 2002 CODATA value

• • • We do not use the following data for averages, fits, limits, etc. • • •

0.897 \pm 0.018	BLUNDEN	05	SICK 03 + 2γ correction
0.895 \pm 0.010 \pm 0.013	SICK	03	$ep \rightarrow ep$ reanalysis
0.830 \pm 0.040 \pm 0.040	24 ESCHRICH	01	$ep \rightarrow ep$
0.883 \pm 0.014	MELNIKOV	00	1S Lamb Shift in H
0.880 \pm 0.015	ROSENFELDR.	00	ep + Coul. corrections
0.847 \pm 0.008	MERGELL	96	ep + disp. relations
0.877 \pm 0.024	WONG	94	reanalysis of Mainz ep data
0.865 \pm 0.020	MCCORD	91	$ep \rightarrow ep$
0.862 \pm 0.012	SIMON	80	$ep \rightarrow ep$
0.880 \pm 0.030	BORKOWSKI	74	$ep \rightarrow ep$
0.810 \pm 0.020	AKIMOV	72	$ep \rightarrow ep$
0.800 \pm 0.025	FREREJACQ...	66	$ep \rightarrow ep$ (CH_2 tgt.)
0.805 \pm 0.011	HAND	63	$ep \rightarrow ep$

24 ESCHRICH 01 actually gives $\langle r^2 \rangle = (0.69 \pm 0.06 \pm 0.06) \text{ fm}^2$.

p MEAN LIFE

A test of baryon conservation. See the "p Partial Mean Lives" section below for limits for identified final states. The limits here are to "anything" or are for "disappearance" modes of a bound proton (p) or (n). See also the 3ν modes in the "Partial Mean Lives" section. Table 1 of BACK 03 is a nice summary.

LIMIT (years)	PARTICLE	CL%	DOCUMENT ID	TECN	COMMENT
>5.8 \times 10²⁹	n	90	25 ARAKI	06	KLND $n \rightarrow$ invisible
>2.1 \times 10²⁹	p	90	26 AHMED	04	SNO $p \rightarrow$ invisible
• • • We do not use the following data for averages, fits, limits, etc. • • •					
>1.9 \times 10 ²⁹	n	90	26 AHMED	04	SNO $n \rightarrow$ invisible
>1.8 \times 10 ²⁵	n	90	27 BACK	03	BORX
>1.1 \times 10 ²⁶	p	90	27 BACK	03	BORX
>3.5 \times 10 ²⁸	p	90	28 ZDESENKO	03	$p \rightarrow$ invisible
>1 \times 10 ²⁸	p	90	29 AHMAD	02	SNO $p \rightarrow$ invisible
>4 \times 10 ²³	p	95	TRETYAK	01	$d \rightarrow n + ?$
>1.9 \times 10 ²⁴	p	90	30 BERNABEI	00B	DAMA
>1.6 \times 10 ²⁵	p, n	31,32	EVANS	77	
>3 \times 10 ²³	p	32	DIX	70	CNTR
>3 \times 10 ²³	p, n	32,33	FLEROV	58	

25 ARAKI 06 looks for signs of de-excitation of the residual nucleus after disappearance of a neutron from the s shell of ^{12}C .

26 AHMED 04 looks for the de-excitation of a residual $^{15}\text{O}^*$ or $^{15}\text{N}^*$ following the disappearance of a neutron or proton in ^{16}O .

27 BACK 03 looks for decays of unstable nuclides left after N decays of parent ^{12}C , ^{13}C , ^{16}O nuclei. These are "invisible channel" limits.

28 ZDESENKO 03 gets this limit on proton disappearance in deuterium by analyzing SNO data in AHMAD 02.

29 AHMAD 02 (see its footnote 7) looks for neutrons left behind after the disappearance of the proton in deuterons.

30 BERNABEI 00B looks for the decay of a ^{128}I nucleus following the disappearance of a proton in the otherwise-stable ^{129}Xe nucleus.

31 EVANS 77 looks for the daughter nuclide ^{129}Xe from possible ^{130}Te decays in ancient Te ore samples.

32 This mean-life limit has been obtained from a half-life limit by dividing the latter by $\ln(2) = 0.693$.

33 FLEROV 58 looks for the spontaneous fission of a ^{232}Th nucleus after the disappearance of one of its nucleons.

\bar{p} MEAN LIFE

Of the two astrophysical limits here, that of GEER 00b involves considerably more refinements in its modeling. The other limits come from direct observations of stored antiprotons. See also " \bar{p} Partial Mean Lives" after "p Partial Mean Lives," below, for exclusive-mode limits. The (lifetime/branching fraction) limit there is 7×10^5 years, for $\bar{p} \rightarrow e^- \gamma$. We advance only the exclusive-mode limits to our Summary Tables.

LIMIT (years)	CL%	EVTS	DOCUMENT ID	TECN	COMMENT
• • • We do not use the following data for averages, fits, limits, etc. • • •					
>8 \times 10 ⁵	90		34 GEER	00b	\bar{p}/p ratio, cosmic rays
>0.28			GABRIELSE	90	TRAP Penning trap
>0.08	90	1	BELL	79	CNTR Storage ring
>1 \times 10 ⁷			GOLDEN	79	SPEC \bar{p}/p ratio, cosmic rays
>3.7 \times 10 ⁻³			BREGMAN	78	CNTR Storage ring

34 GEER 00b uses agreement between a model of galactic \bar{p} production and propagation and the observed \bar{p}/p cosmic-ray spectrum to set this limit.

p DECAY MODES

See the "Note on Nucleon Decay" in our 1994 edition (Phys. Rev. **D50**, 1173) for a short review.

The "partial mean life" limits tabulated here are the limits on τ/B_j , where τ is the total mean life and B_j is the branching fraction for the mode in question. For N decays, p and n indicate proton and neutron partial lifetimes.

Mode	Partial mean life (10^{30} years)	Confidence level
------	--------------------------------------	------------------

Antilepton + meson

τ_1	$N \rightarrow e^+ \pi$	> 158 (n), > 1600 (p)	90%
τ_2	$N \rightarrow \mu^+ \pi$	> 100 (n), > 473 (p)	90%
τ_3	$N \rightarrow \nu \pi$	> 112 (n), > 25 (p)	90%
τ_4	$p \rightarrow e^+ \eta$	> 313	90%
τ_5	$p \rightarrow \mu^+ \eta$	> 126	90%
τ_6	$n \rightarrow \nu \eta$	> 158	90%
τ_7	$N \rightarrow e^+ \rho$	> 217 (n), > 75 (p)	90%
τ_8	$N \rightarrow \mu^+ \rho$	> 228 (n), > 110 (p)	90%
τ_9	$N \rightarrow \nu \rho$	> 19 (n), > 162 (p)	90%
τ_{10}	$p \rightarrow e^+ \omega$	> 107	90%
τ_{11}	$p \rightarrow \mu^+ \omega$	> 117	90%
τ_{12}	$n \rightarrow \nu \omega$	> 108	90%
τ_{13}	$N \rightarrow e^+ K$	> 17 (n), > 150 (p)	90%
τ_{14}	$p \rightarrow e^+ K_S^0$	> 120	90%
τ_{15}	$p \rightarrow e^+ K_L^0$	> 51	90%
τ_{16}	$N \rightarrow \mu^+ K$	> 26 (n), > 120 (p)	90%
τ_{17}	$p \rightarrow \mu^+ K_S^0$	> 150	90%
τ_{18}	$p \rightarrow \mu^+ K_L^0$	> 83	90%
τ_{19}	$N \rightarrow \nu K$	> 86 (n), > 670 (p)	90%
τ_{20}	$n \rightarrow \nu K_S^0$	> 51	90%
τ_{21}	$p \rightarrow e^+ K^*(892)^0$	> 84	90%
τ_{22}	$N \rightarrow \nu K^*(892)$	> 78 (n), > 51 (p)	90%

Antilepton + mesons

τ_{23}	$p \rightarrow e^+ \pi^+ \pi^-$	> 82	90%
τ_{24}	$p \rightarrow e^+ \pi^0 \pi^0$	> 147	90%
τ_{25}	$n \rightarrow e^+ \pi^- \pi^0$	> 52	90%
τ_{26}	$p \rightarrow \mu^+ \pi^+ \pi^-$	> 133	90%
τ_{27}	$p \rightarrow \mu^+ \pi^0 \pi^0$	> 101	90%
τ_{28}	$n \rightarrow \mu^+ \pi^- \pi^0$	> 74	90%
τ_{29}	$n \rightarrow e^+ K^0 \pi^-$	> 18	90%

Lepton + meson

τ_{30}	$n \rightarrow e^- \pi^+$	> 65	90%
τ_{31}	$n \rightarrow \mu^- \pi^+$	> 49	90%
τ_{32}	$n \rightarrow e^- \rho^+$	> 62	90%
τ_{33}	$n \rightarrow \mu^- \rho^+$	> 7	90%
τ_{34}	$n \rightarrow e^- K^+$	> 32	90%
τ_{35}	$n \rightarrow \mu^- K^+$	> 57	90%

Lepton + mesons

τ_{36}	$p \rightarrow e^- \pi^+ \pi^+$	> 30	90%
τ_{37}	$n \rightarrow e^- \pi^+ \pi^0$	> 29	90%
τ_{38}	$p \rightarrow \mu^- \pi^+ \pi^+$	> 17	90%
τ_{39}	$n \rightarrow \mu^- \pi^+ \pi^0$	> 34	90%
τ_{40}	$p \rightarrow e^- \pi^+ K^+$	> 75	90%
τ_{41}	$p \rightarrow \mu^- \pi^+ K^+$	> 245	90%

Antilepton + photon(s)

τ_{42}	$p \rightarrow e^+ \gamma$	> 670	90%
τ_{43}	$p \rightarrow \mu^+ \gamma$	> 478	90%
τ_{44}	$n \rightarrow \nu \gamma$	> 28	90%
τ_{45}	$p \rightarrow e^+ \gamma \gamma$	> 100	90%
τ_{46}	$n \rightarrow \nu \gamma \gamma$	> 219	90%

Three (or more) leptons

τ_{47}	$p \rightarrow e^+ e^+ e^-$	> 793	90%
τ_{48}	$p \rightarrow e^+ \mu^+ \mu^-$	> 359	90%
τ_{49}	$p \rightarrow e^+ \nu \nu$	> 17	90%
τ_{50}	$n \rightarrow e^+ e^- \nu$	> 257	90%
τ_{51}	$n \rightarrow \mu^+ e^- \nu$	> 83	90%
τ_{52}	$n \rightarrow \mu^+ \mu^- \nu$	> 79	90%
τ_{53}	$p \rightarrow \mu^+ e^+ e^-$	> 529	90%
τ_{54}	$p \rightarrow \mu^+ \mu^+ \mu^-$	> 675	90%
τ_{55}	$p \rightarrow \mu^+ \nu \nu$	> 21	90%
τ_{56}	$p \rightarrow e^- \mu^+ \mu^+$	> 6	90%
τ_{57}	$n \rightarrow 3\nu$	> 0.0005	90%
τ_{58}	$n \rightarrow 5\nu$		

Inclusive modes

τ_{59}	$N \rightarrow e^+$ anything	> 0.6 (n, p)	90%
τ_{60}	$N \rightarrow \mu^+$ anything	> 12 (n, p)	90%
τ_{61}	$N \rightarrow \nu$ anything		
τ_{62}	$N \rightarrow e^+ \pi^0$ anything	> 0.6 (n, p)	90%
τ_{63}	$N \rightarrow 2$ bodies, ν -free		

$\Delta B = 2$ dinucleon modes

The following are lifetime limits per iron nucleus.

τ_{64}	$pp \rightarrow \pi^+ \pi^+$	> 0.7	90%
τ_{65}	$p n \rightarrow \pi^+ \pi^0$	> 2	90%
τ_{66}	$n n \rightarrow \pi^+ \pi^-$	> 0.7	90%
τ_{67}	$n n \rightarrow \pi^0 \pi^0$	> 3.4	90%
τ_{68}	$pp \rightarrow e^+ e^+$	> 5.8	90%
τ_{69}	$pp \rightarrow e^+ \mu^+$	> 3.6	90%
τ_{70}	$pp \rightarrow \mu^+ \mu^+$	> 1.7	90%
τ_{71}	$p n \rightarrow e^+ \bar{\nu}$	> 2.8	90%
τ_{72}	$p n \rightarrow \mu^+ \bar{\nu}$	> 1.6	90%
τ_{73}	$n n \rightarrow \nu_e \bar{\nu}_e$	> 0.000049	90%
τ_{74}	$n n \rightarrow \nu_\mu \bar{\nu}_\mu$		
τ_{75}	$p n \rightarrow$ invisible	> 2.1×10^{-5}	90%
τ_{76}	$pp \rightarrow$ invisible	> 0.00005	90%

\bar{p} DECAY MODES

Mode	Partial mean life (years)	Confidence level	
τ_{77}	$\bar{p} \rightarrow e^- \gamma$	> 7×10^5 90%	
τ_{78}	$\bar{p} \rightarrow \mu^- \gamma$	> 5×10^4 90%	
τ_{79}	$\bar{p} \rightarrow e^- \pi^0$	> 4×10^5 90%	
τ_{80}	$\bar{p} \rightarrow \mu^- \pi^0$	> 5×10^4 90%	
τ_{81}	$\bar{p} \rightarrow e^- \eta$	> 2×10^4 90%	
τ_{82}	$\bar{p} \rightarrow \mu^- \eta$	> 8×10^3 90%	
τ_{83}	$\bar{p} \rightarrow e^- K_S^0$	> 900 90%	
τ_{84}	$\bar{p} \rightarrow \mu^- K_S^0$	> 4×10^3 90%	
τ_{85}	$\bar{p} \rightarrow e^- K_L^0$	> 9×10^3 90%	
τ_{86}	$\bar{p} \rightarrow \mu^- K_L^0$	> 7×10^3 90%	
τ_{87}	$\bar{p} \rightarrow e^- \gamma \gamma$	> 2×10^4 90%	
τ_{88}	$\bar{p} \rightarrow \mu^- \gamma \gamma$	> 2×10^4 90%	
τ_{89}	$\bar{p} \rightarrow e^- \rho$		
τ_{90}	$\bar{p} \rightarrow e^- \omega$	> 200 90%	
τ_{91}	$\bar{p} \rightarrow e^- K^*(892)^0$		

p PARTIAL MEAN LIVES

The "partial mean life" limits tabulated here are the limits on τ/B_j , where τ is the total mean life for the proton and B_j is the branching fraction for the mode in question.

Decaying particle: p = proton, n = bound neutron. The same event may appear under more than one partial decay mode. Background estimates may be accurate to a factor of two.

Antilepton + meson

$\tau(N \rightarrow e^+ \pi)$	τ_1				
$LIMIT$ (10^{10} years)					
PARTICLE	CL%	EVTs	BKGD EST	DOCUMENT ID	TECN
> 158	n	90	3 5	MCGREW 99	IMB3
> 1600	p	90	0 0.1	SHIOZAWA 98	SKAM
• • • We do not use the following data for averages, fits, limits, etc. • • •					
> 540	p	90	0 0.2	MCGREW 99	IMB3
> 70	p	90	0 0.5	BERGER 91	FREJ
> 70	n	90	0 \leq 0.1	BERGER 91	FREJ
> 550	p	90	0 0.7	35 BECKER-SZ...	90 IMB3
> 260	p	90	0 < 0.04	HIRATA 89c	KAMI
> 130	n	90	0 < 0.2	HIRATA 89c	KAMI
> 310	p	90	0 0.6	SEIDEL 88	IMB
> 100	n	90	0 1.6	SEIDEL 88	IMB
> 1.3	n	90	0	BARTELT 87	SOUND
> 1.3	p	90	0	BARTELT 87	SOUND
> 250	p	90	0 0.3	HAINES 86	IMB
> 31	n	90	8 9	HAINES 86	IMB
> 64	p	90	0 < 0.4	ARISAKA 85	KAMI
> 26	n	90	0 < 0.7	ARISAKA 85	KAMI
> 82	p (free)	90	0 0.2	BLEWITT 85	IMB
> 250	p	90	0 0.2	BLEWITT 85	IMB
> 25	n	90	4 4	PARK 85	IMB
> 15	p, n	90	0	BATTISTONI 84	NUSX
> 0.5	p	90	1 0.3	36 BARTELT 83	SOUND
> 0.5	n	90	1 0.3	36 BARTELT 83	SOUND
> 5.8	p	90	2	37 KRISHNA...	82 KOLR
> 5.8	n	90	2	37 KRISHNA...	82 KOLR
> 0.1	n	90		38 GURR 67	CNTR

35 This BECKER-SZENDY 90 result includes data from SEIDEL 88.

36 Limit based on zero events.

37 We have calculated 90% CL limit from 1 confined event.

38 We have converted half-life to 90% CL mean life.

Baryon Particle Listings

 p $\tau(N \rightarrow \mu^+ \pi)$ τ_2

LIMIT (10^{30} years)	PARTICLE	CL%	EVTs	BKGD EST	DOCUMENT ID	TECN
>473	p	90	0	0.6	MCGREW 99	IMB3
>100	n	90	0	<0.2	HIRATA 89c	KAMI
••• We do not use the following data for averages, fits, limits, etc. •••						
> 90	n	90	1	1.9	MCGREW 99	IMB3
> 81	p	90	0	0.2	BERGER 91	FREJ
> 35	n	90	1	1.0	BERGER 91	FREJ
>230	p	90	0	<0.07	HIRATA 89c	KAMI
>270	p	90	0	0.5	SEIDEL 88	IMB
> 63	n	90	0	0.5	SEIDEL 88	IMB
> 76	p	90	2	1	HAINES 86	IMB
> 23	n	90	8	7	HAINES 86	IMB
> 46	p	90	0	<0.7	ARISAKA 85	KAMI
> 20	n	90	0	<0.4	ARISAKA 85	KAMI
> 59	p (free)	90	0	0.2	BLEWITT 85	IMB
>100	p	90	1	0.4	BLEWITT 85	IMB
> 38	n	90	1	4	PARK 85	IMB
> 10	p, n	90	0		BATTISTONI 84	NUSX
> 1.3	p, n	90	0		ALEKSEEV 81	BAKS

 $\tau(N \rightarrow \nu \pi)$ τ_3

LIMIT (10^{30} years)	PARTICLE	CL%	EVTs	BKGD EST	DOCUMENT ID	TECN
> 16	p	90	6	6.7	WALL 00b	SOU2
>112	n	90	6	6.6	MCGREW 99	IMB3
••• We do not use the following data for averages, fits, limits, etc. •••						
> 39	n	90	4	3.8	WALL 00b	SOU2
> 10	p	90	15	20.3	MCGREW 99	IMB3
> 13	n	90	1	1.2	BERGER 89	FREJ
> 10	p	90	11	14	BERGER 89	FREJ
> 25	p	90	32	32.8	39 HIRATA 89c	KAMI
>100	n	90	1	3	HIRATA 89c	KAMI
> 6	n	90	73	60	HAINES 86	IMB
> 2	p	90	16	13	KAJITA 86	KAMI
> 40	n	90	0	1	KAJITA 86	KAMI
> 7	n	90	28	19	PARK 85	IMB
> 7	n	90	0		BATTISTONI 84	NUSX
> 2	p	90	≤ 3		BATTISTONI 84	NUSX
> 5.8	p	90	1		40 KRISHNA... 82	KOLR
> 0.3	p	90	2		41 CHERRY 81	HOME
> 0.1	p	90			42 GURR 67	CNTR

39 In estimating the background, this HIRATA 89c limit (as opposed to the later limits of WALL 00b and MCGREW 99) does not take into account present understanding that the flux of ν_{μ} originating in the upper atmosphere is depleted. Doing so would reduce the background and thus also would reduce the limit here.

40 We have calculated 90% CL limit from 1 confined event.

41 We have converted 2 possible events to 90% CL limit.

42 We have converted half-life to 90% CL mean life.

 $\tau(p \rightarrow e^+ \eta)$ τ_4

LIMIT (10^{30} years)	PARTICLE	CL%	EVTs	BKGD EST	DOCUMENT ID	TECN
>313	p	90	0	0.2	MCGREW 99	IMB3
••• We do not use the following data for averages, fits, limits, etc. •••						
> 81	p	90	1	1.7	WALL 00b	SOU2
> 44	p	90	0	0.1	BERGER 91	FREJ
>140	p	90	0	<0.04	HIRATA 89c	KAMI
>100	p	90	0	0.6	SEIDEL 88	IMB
>200	p	90	5	3.3	HAINES 86	IMB
> 64	p	90	0	<0.8	ARISAKA 85	KAMI
> 64	p (free)	90	5	6.5	BLEWITT 85	IMB
>200	p	90	5	4.7	BLEWITT 85	IMB
> 1.2	p	90	2		43 CHERRY 81	HOME

43 We have converted 2 possible events to 90% CL limit.

 $\tau(p \rightarrow \mu^+ \eta)$ τ_5

LIMIT (10^{30} years)	PARTICLE	CL%	EVTs	BKGD EST	DOCUMENT ID	TECN
>126	p	90	3	2.8	MCGREW 99	IMB3
••• We do not use the following data for averages, fits, limits, etc. •••						
> 89	p	90	0	1.6	WALL 00b	SOU2
> 26	p	90	1	0.8	BERGER 91	FREJ
> 69	p	90	1	<0.08	HIRATA 89c	KAMI
> 1.3	p	90	0	0.7	PHILLIPS 89	HPW
> 34	p	90	1	1.5	SEIDEL 88	IMB
> 46	p	90	7	6	HAINES 86	IMB
> 26	p	90	1	<0.8	ARISAKA 85	KAMI
> 17	p (free)	90	6	6	BLEWITT 85	IMB
> 46	p	90	7	8	BLEWITT 85	IMB

 $\tau(n \rightarrow \nu \eta)$ τ_6

LIMIT (10^{30} years)	PARTICLE	CL%	EVTs	BKGD EST	DOCUMENT ID	TECN
>158	n	90	0	1.2	MCGREW 99	IMB3
••• We do not use the following data for averages, fits, limits, etc. •••						
> 71	n	90	2	3.7	WALL 00b	SOU2
> 29	n	90	0	0.9	BERGER 89	FREJ
> 54	n	90	2	0.9	HIRATA 89c	KAMI
> 16	n	90	3	2.1	SEIDEL 88	IMB
> 25	n	90	7	6	HAINES 86	IMB
> 30	n	90	0	0.4	KAJITA 86	KAMI
> 18	n	90	4	3	PARK 85	IMB
> 0.6	n	90	2		44 CHERRY 81	HOME

44 We have converted 2 possible events to 90% CL limit.

 $\tau(N \rightarrow e^+ \rho)$ τ_7

LIMIT (10^{30} years)	PARTICLE	CL%	EVTs	BKGD EST	DOCUMENT ID	TECN
>217	n	90	4	4.8	MCGREW 99	IMB3
> 75	p	90	2	2.7	HIRATA 89c	KAMI
••• We do not use the following data for averages, fits, limits, etc. •••						
> 29	p	90	0	2.2	BERGER 91	FREJ
> 41	n	90	0	1.4	BERGER 91	FREJ
> 58	n	90	0	1.9	HIRATA 89c	KAMI
> 38	n	90	2	4.1	SEIDEL 88	IMB
> 1.2	p	90	0		BARTELT 87	SOU2
> 1.5	n	90	0		BARTELT 87	SOU2
> 17	p	90	7	7	HAINES 86	IMB
> 14	n	90	9	4	HAINES 86	IMB
> 12	p	90	0	<1.2	ARISAKA 85	KAMI
> 6	n	90	2	<1	ARISAKA 85	KAMI
> 6.7	p (free)	90	6	6	BLEWITT 85	IMB
> 17	p	90	7	7	BLEWITT 85	IMB
> 12	n	90	4	2	PARK 85	IMB
> 0.6	n	90	1	0.3	45 BARTELT 83	SOU2
> 0.5	p	90	1	0.3	45 BARTELT 83	SOU2
> 9.8	p	90	1		46 KRISHNA... 82	KOLR
> 0.8	p	90	2		47 CHERRY 81	HOME

45 Limit based on zero events.

46 We have calculated 90% CL limit from 0 confined events.

47 We have converted 2 possible events to 90% CL limit.

 $\tau(N \rightarrow \mu^+ \rho)$ τ_8

LIMIT (10^{30} years)	PARTICLE	CL%	EVTs	BKGD EST	DOCUMENT ID	TECN
>228	n	90	3	9.5	MCGREW 99	IMB3
>110	p	90	0	1.7	HIRATA 89c	KAMI
••• We do not use the following data for averages, fits, limits, etc. •••						
> 12	p	90	0	0.5	BERGER 91	FREJ
> 22	n	90	0	1.1	BERGER 91	FREJ
> 23	n	90	1	1.8	HIRATA 89c	KAMI
> 4.3	p	90	0	0.7	PHILLIPS 89	HPW
> 30	p	90	0	0.5	SEIDEL 88	IMB
> 11	n	90	1	1.1	SEIDEL 88	IMB
> 16	p	90	4	4.5	HAINES 86	IMB
> 7	n	90	6	5	HAINES 86	IMB
> 12	p	90	0	<0.7	ARISAKA 85	KAMI
> 5	n	90	1	<1.2	ARISAKA 85	KAMI
> 5.5	p (free)	90	4	5	BLEWITT 85	IMB
> 16	p	90	4	5	BLEWITT 85	IMB
> 9	n	90	1	2	PARK 85	IMB

 $\tau(N \rightarrow \nu \rho)$ τ_9

LIMIT (10^{30} years)	PARTICLE	CL%	EVTs	BKGD EST	DOCUMENT ID	TECN
>162	p	90	18	21.7	MCGREW 99	IMB3
> 19	n	90	0	0.5	SEIDEL 88	IMB
••• We do not use the following data for averages, fits, limits, etc. •••						
> 9	n	90	4	2.4	BERGER 89	FREJ
> 24	p	90	0	0.9	BERGER 89	FREJ
> 27	p	90	5	1.5	HIRATA 89c	KAMI
> 13	n	90	4	3.6	HIRATA 89c	KAMI
> 13	p	90	1	1.1	SEIDEL 88	IMB
> 8	p	90	6	5	HAINES 86	IMB
> 2	n	90	15	10	HAINES 86	IMB
> 11	p	90	2	1	KAJITA 86	KAMI
> 4	n	90	2	2	KAJITA 86	KAMI
> 4.1	p (free)	90	6	7	BLEWITT 85	IMB
> 8.4	p	90	6	5	BLEWITT 85	IMB
> 2	n	90	7	3	PARK 85	IMB
> 0.9	p	90	2		48 CHERRY 81	HOME
> 0.6	n	90	2		48 CHERRY 81	HOME

48 We have converted 2 possible events to 90% CL limit.

$\tau(p \rightarrow e^+ \omega)$ τ_{10}

LIMIT (10^{30} years)	PARTICLE	CL%	EVTs	BKGD EST	DOCUMENT ID	TECN
>107	p	90	7	10.8	MCGREW 99	IMB3
••• We do not use the following data for averages, fits, limits, etc. •••						
> 17	p	90	0	1.1	BERGER 91	FREJ
> 45	p	90	2	1.45	HIRATA 89c	KAMI
> 26	p	90	1	1.0	SEIDEL 88	IMB
> 1.5	p	90	0		BARTELT 87	SOUND
> 37	p	90	6	5.3	HAINES 86	IMB
> 25	p	90	1	<1.4	ARISAKA 85	KAMI
> 12	p (free)	90	6	7.5	BLEWITT 85	IMB
> 37	p	90	6	5.7	BLEWITT 85	IMB
> 0.6	p	90	1	0.3	49 BARTELT 83	SOUND
> 9.8	p	90	1		50 KRISHNA... 82	KOLR
> 2.8	p	90	2		51 CHERRY 81	HOME

49 Limit based on zero events.
50 We have calculated 90% CL limit from 0 confined events.
51 We have converted 2 possible events to 90% CL limit.

$\tau(p \rightarrow \mu^+ \omega)$ τ_{11}

LIMIT (10^{30} years)	PARTICLE	CL%	EVTs	BKGD EST	DOCUMENT ID	TECN
>117	p	90	11	12.1	MCGREW 99	IMB3
••• We do not use the following data for averages, fits, limits, etc. •••						
> 11	p	90	0	1.0	BERGER 91	FREJ
> 57	p	90	2	1.9	HIRATA 89c	KAMI
> 4.4	p	90	0	0.7	PHILLIPS 89	HPW
> 10	p	90	2	1.3	SEIDEL 88	IMB
> 23	p	90	2	1	HAINES 86	IMB
> 6.5	p (free)	90	9	8.7	BLEWITT 85	IMB
> 23	p	90	8	7	BLEWITT 85	IMB

$\tau(n \rightarrow \nu \omega)$ τ_{12}

LIMIT (10^{30} years)	PARTICLE	CL%	EVTs	BKGD EST	DOCUMENT ID	TECN
>108	n	90	12	22.5	MCGREW 99	IMB3
••• We do not use the following data for averages, fits, limits, etc. •••						
> 17	n	90	1	0.7	BERGER 89	FREJ
> 43	n	90	3	2.7	HIRATA 89c	KAMI
> 6	n	90	2	1.3	SEIDEL 88	IMB
> 12	n	90	6	6	HAINES 86	IMB
> 18	n	90	2	2	KAJITA 86	KAMI
> 16	n	90	1	2	PARK 85	IMB
> 2.0	n	90	2		52 CHERRY 81	HOME

52 We have converted 2 possible events to 90% CL limit.

$\tau(N \rightarrow e^+ K)$ τ_{13}

LIMIT (10^{30} years)	PARTICLE	CL%	EVTs	BKGD EST	DOCUMENT ID	TECN
> 17	n	90	35	29.4	MCGREW 99	IMB3
>150	p	90	0	<0.27	HIRATA 89c	KAMI
••• We do not use the following data for averages, fits, limits, etc. •••						
> 85	p	90	3	4.9	WALL 00	SOU2
> 31	p	90	23	25.2	MCGREW 99	IMB3
> 60	p	90	0		BERGER 91	FREJ
> 70	p	90	0	1.8	SEIDEL 88	IMB
> 77	p	90	5	4.5	HAINES 86	IMB
> 38	p	90	0	<0.8	ARISAKA 85	KAMI
> 24	p (free)	90	7	8.5	BLEWITT 85	IMB
> 77	p	90	5	4	BLEWITT 85	IMB
> 1.3	p	90	0		ALEKSEEV 81	BAKS
> 1.3	n	90	0		ALEKSEEV 81	BAKS

$\tau(p \rightarrow e^+ K_S^0)$ τ_{14}

LIMIT (10^{30} years)	PARTICLE	CL%	EVTs	BKGD EST	DOCUMENT ID	TECN
>2000	p	90	6	4.7	53 KOBAYASHI 05	SKAM
••• We do not use the following data for averages, fits, limits, etc. •••						
> 120	p	90	1	1.3	WALL 00	SOU2
> 76	p	90	0	0.5	BERGER 91	FREJ

53 We have doubled the $p \rightarrow e^+ K^0$ limit given in KOBAYASHI 05 to obtain this $p \rightarrow e^+ K_S^0$ limit.

$\tau(p \rightarrow e^+ K_L^0)$ τ_{15}

LIMIT (10^{30} years)	PARTICLE	CL%	EVTs	BKGD EST	DOCUMENT ID	TECN
>51	p	90	2	3.5	WALL 00	SOU2
••• We do not use the following data for averages, fits, limits, etc. •••						
>44	p	90	0	≤ 0.1	BERGER 91	FREJ

$\tau(N \rightarrow \mu^+ K)$ τ_{16}

LIMIT (10^{30} years)	PARTICLE	CL%	EVTs	BKGD EST	DOCUMENT ID	TECN
>120	p	90	0	<1.2	WALL 00	SOU2
>120	p	90	4	7.2	MCGREW 99	IMB3
> 26	n	90	20	28.4	MCGREW 99	IMB3
>120	p	90	1	0.4	HIRATA 89c	KAMI
••• We do not use the following data for averages, fits, limits, etc. •••						
> 54	p	90	0		BERGER 91	FREJ
> 3.0	p	90	0	0.7	PHILLIPS 89	HPW
> 19	p	90	3	2.5	SEIDEL 88	IMB
> 1.5	p	90	0		54 BARTELT 87	SOUND
> 1.1	n	90	0		BARTELT 87	SOUND
> 40	p	90	7	6	HAINES 86	IMB
> 19	p	90	1	<1.1	ARISAKA 85	KAMI
> 6.7	p (free)	90	11	13	BLEWITT 85	IMB
> 40	p	90	7	8	BLEWITT 85	IMB
> 6	p	90	1		BATTISTONI 84	NUSX
> 0.6	p	90	0		55 BARTELT 83	SOUND
> 0.4	n	90	0		55 BARTELT 83	SOUND
> 5.8	p	90	2		56 KRISHNA... 82	KOLR
> 2.0	p	90	0		CHERRY 81	HOME
> 0.2	n	90			57 GURR 67	CNTR

54 BARTELT 87 limit applies to $p \rightarrow \mu^+ K_S^0$.
55 Limit based on zero events.
56 We have calculated 90% CL limit from 1 confined event.
57 We have converted half-life to 90% CL mean life.

$\tau(p \rightarrow \mu^+ K_S^0)$ τ_{17}

LIMIT (10^{30} years)	PARTICLE	CL%	EVTs	BKGD EST	DOCUMENT ID	TECN
>2600	p	90	3	3.9	58 KOBAYASHI 05	SKAM
••• We do not use the following data for averages, fits, limits, etc. •••						
> 150	p	90	0	<0.8	WALL 00	SOU2
> 64	p	90	0	1.2	BERGER 91	FREJ

58 We have doubled the $p \rightarrow \mu^+ K^0$ limit given in KOBAYASHI 05 to obtain this $p \rightarrow \mu^+ K_S^0$ limit.

$\tau(p \rightarrow \mu^+ K_L^0)$ τ_{18}

LIMIT (10^{30} years)	PARTICLE	CL%	EVTs	BKGD EST	DOCUMENT ID	TECN
>83	p	90	0	0.4	WALL 00	SOU2
••• We do not use the following data for averages, fits, limits, etc. •••						
>44	p	90	0	≤ 0.1	BERGER 91	FREJ

$\tau(N \rightarrow \nu K)$ τ_{19}

LIMIT (10^{30} years)	PARTICLE	CL%	EVTs	BKGD EST	DOCUMENT ID	TECN
>2300	n	90	0	1.3	KOBAYASHI 05	SKAM
> 86	p	90	0	2.4	HIRATA 89c	KAMI
••• We do not use the following data for averages, fits, limits, etc. •••						
> 26	n	90	16	9.1	WALL 00	SOU2
> 670	p	90			HAYATO 99	SKAM
> 151	p	90	15	21.4	MCGREW 99	IMB3
> 30	n	90	34	34.1	MCGREW 99	IMB3
> 43	p	90	1	1.54	59 ALLISON 98	SOU2
> 15	n	90	1	1.8	BERGER 89	FREJ
> 15	p	90	1	1.8	BERGER 89	FREJ
> 100	p	90	9	7.3	HIRATA 89c	KAMI
> 0.28	p	90	0	0.7	PHILLIPS 89	HPW
> 0.3	p	90	0		BARTELT 87	SOUND
> 0.75	n	90	0		60 BARTELT 87	SOUND
> 10	p	90	6	5	HAINES 86	IMB
> 15	n	90	3	5	HAINES 86	IMB
> 28	p	90	3	3	KAJITA 86	KAMI
> 32	n	90	0	1.4	KAJITA 86	KAMI
> 1.8	p (free)	90	6	11	BLEWITT 85	IMB
> 9.6	p	90	6	5	BLEWITT 85	IMB
> 10	n	90	2	2	PARK 85	IMB
> 5	n	90	0		BATTISTONI 84	NUSX
> 2	p	90	0		BATTISTONI 84	NUSX
> 0.3	n	90	0		61 BARTELT 83	SOUND
> 0.1	p	90	0		61 BARTELT 83	SOUND
> 5.8	p	90	1		62 KRISHNA... 82	KOLR
> 0.3	n	90	2		63 CHERRY 81	HOME

59 This ALLISON 98 limit is with no background subtraction; with subtraction the limit becomes $> 46 \times 10^{30}$ years.
60 BARTELT 87 limit applies to $n \rightarrow \nu K_S^0$.
61 Limit based on zero events.
62 We have calculated 90% CL limit from 1 confined event.
63 We have converted 2 possible events to 90% CL limit.

Baryon Particle Listings

 p $\tau(n \rightarrow \nu K_S^0)$ 720

LIMIT (10^{30} years)	PARTICLE	CL%	EVTs	BKGD EST	DOCUMENT ID	TECN
>260	n	90	34	30	⁶⁴ KOBAYASHI 05	SKAM

••• We do not use the following data for averages, fits, limits, etc. •••

> 51	n	90	16	9.1	WALL 00	SOU2
------	---	----	----	-----	---------	------

⁶⁴ We have doubled the $n \rightarrow \nu K^0$ limit given in KOBAYASHI 05 to obtain this $n \rightarrow \nu K_S^0$ limit.

 $\tau(p \rightarrow e^+ K^*(892)^0)$ 721

LIMIT (10^{30} years)	PARTICLE	CL%	EVTs	BKGD EST	DOCUMENT ID	TECN
>84	p	90	38	52.0	MCGREW 99	IMB3

••• We do not use the following data for averages, fits, limits, etc. •••

>10	p	90	0	0.8	BERGER 91	FREJ
>52	p	90	2	1.55	HIRATA 89c	KAMI
>10	p	90	1	<1	ARISAKA 85	KAMI

 $\tau(N \rightarrow \nu K^*(892))$ 722

LIMIT (10^{30} years)	PARTICLE	CL%	EVTs	BKGD EST	DOCUMENT ID	TECN
>51	p	90	7	9.1	MCGREW 99	IMB3
>78	n	90	40	50	MCGREW 99	IMB3

••• We do not use the following data for averages, fits, limits, etc. •••

>22	n	90	0	2.1	BERGER 89	FREJ
>17	p	90	0	2.4	BERGER 89	FREJ
>20	p	90	5	2.1	HIRATA 89c	KAMI
>21	n	90	4	2.4	HIRATA 89c	KAMI
>10	p	90	7	6	HAINES 86	IMB
> 5	n	90	8	7	HAINES 86	IMB
> 8	p	90	3	2	KAJITA 86	KAMI
> 6	n	90	2	1.6	KAJITA 86	KAMI
> 5.8	p (free)	90	10	1.6	BLEWITT 85	IMB
> 9.6	p	90	7	6	BLEWITT 85	IMB
> 7	n	90	1	4	PARK 85	IMB
> 2.1	p	90	1		⁶⁵ BATTISTONI 82	NUSX

⁶⁵ We have converted 1 possible event to 90% CL limit.

Antilepton + mesons

 $\tau(p \rightarrow e^+ \pi^+ \pi^-)$ 723

LIMIT (10^{30} years)	PARTICLE	CL%	EVTs	BKGD EST	DOCUMENT ID	TECN
>82	p	90	16	23.1	MCGREW 99	IMB3

••• We do not use the following data for averages, fits, limits, etc. •••

>21	p	90	0	2.2	BERGER 91	FREJ
-----	---	----	---	-----	-----------	------

 $\tau(p \rightarrow e^+ \pi^0 \pi^0)$ 724

LIMIT (10^{30} years)	PARTICLE	CL%	EVTs	BKGD EST	DOCUMENT ID	TECN
>147	p	90	2	0.8	MCGREW 99	IMB3

••• We do not use the following data for averages, fits, limits, etc. •••

> 38	p	90	1	0.5	BERGER 91	FREJ
------	---	----	---	-----	-----------	------

 $\tau(n \rightarrow e^+ \pi^- \pi^0)$ 725

LIMIT (10^{30} years)	PARTICLE	CL%	EVTs	BKGD EST	DOCUMENT ID	TECN
>52	n	90	38	34.2	MCGREW 99	IMB3

••• We do not use the following data for averages, fits, limits, etc. •••

>32	n	90	1	0.8	BERGER 91	FREJ
-----	---	----	---	-----	-----------	------

 $\tau(p \rightarrow \mu^+ \pi^+ \pi^-)$ 726

LIMIT (10^{30} years)	PARTICLE	CL%	EVTs	BKGD EST	DOCUMENT ID	TECN
>133	p	90	25	38.0	MCGREW 99	IMB3

••• We do not use the following data for averages, fits, limits, etc. •••

> 17	p	90	1	2.6	BERGER 91	FREJ
> 3.3	p	90	0	0.7	PHILLIPS 89	HPW

 $\tau(p \rightarrow \mu^+ \pi^0 \pi^0)$ 727

LIMIT (10^{30} years)	PARTICLE	CL%	EVTs	BKGD EST	DOCUMENT ID	TECN
>101	p	90	3	1.6	MCGREW 99	IMB3

••• We do not use the following data for averages, fits, limits, etc. •••

> 33	p	90	1	0.9	BERGER 91	FREJ
------	---	----	---	-----	-----------	------

 $\tau(n \rightarrow \mu^+ \pi^- \pi^0)$ 728

LIMIT (10^{30} years)	PARTICLE	CL%	EVTs	BKGD EST	DOCUMENT ID	TECN
>74	n	90	17	20.8	MCGREW 99	IMB3

••• We do not use the following data for averages, fits, limits, etc. •••

>33	n	90	0	1.1	BERGER 91	FREJ
-----	---	----	---	-----	-----------	------

 $\tau(n \rightarrow e^+ K^0 \pi^-)$ 729

LIMIT (10^{30} years)	PARTICLE	CL%	EVTs	BKGD EST	DOCUMENT ID	TECN
>18	n	90	1	0.2	BERGER 91	FREJ

Lepton + meson

 $\tau(n \rightarrow e^- \pi^+)$ 730

LIMIT (10^{30} years)	PARTICLE	CL%	EVTs	BKGD EST	DOCUMENT ID	TECN
>65	n	90	0	1.6	SEIDEL 88	IMB

••• We do not use the following data for averages, fits, limits, etc. •••

>55	n	90	0	1.09	BERGER 91B	FREJ
>16	n	90	9	7	HAINES 86	IMB
>25	n	90	2	4	PARK 85	IMB

 $\tau(n \rightarrow \mu^- \pi^+)$ 731

LIMIT (10^{30} years)	PARTICLE	CL%	EVTs	BKGD EST	DOCUMENT ID	TECN
>49	n	90	0	0.5	SEIDEL 88	IMB

••• We do not use the following data for averages, fits, limits, etc. •••

>33	n	90	0	1.40	BERGER 91B	FREJ
> 2.7	n	90	0	0.7	PHILLIPS 89	HPW
>25	n	90	7	6	HAINES 86	IMB
>27	n	90	2	3	PARK 85	IMB

 $\tau(n \rightarrow e^- \rho^+)$ 732

LIMIT (10^{30} years)	PARTICLE	CL%	EVTs	BKGD EST	DOCUMENT ID	TECN
>62	n	90	2	4.1	SEIDEL 88	IMB

••• We do not use the following data for averages, fits, limits, etc. •••

>12	n	90	13	6	HAINES 86	IMB
>12	n	90	5	3	PARK 85	IMB

 $\tau(n \rightarrow \mu^- \rho^+)$ 733

LIMIT (10^{30} years)	PARTICLE	CL%	EVTs	BKGD EST	DOCUMENT ID	TECN
>7	n	90	1	1.1	SEIDEL 88	IMB

••• We do not use the following data for averages, fits, limits, etc. •••

>2.6	n	90	0	0.7	PHILLIPS 89	HPW
>9	n	90	7	5	HAINES 86	IMB
>9	n	90	2	2	PARK 85	IMB

 $\tau(n \rightarrow e^- K^+)$ 734

LIMIT (10^{30} years)	PARTICLE	CL%	EVTs	BKGD EST	DOCUMENT ID	TECN
>32	n	90	3	2.96	BERGER 91B	FREJ

••• We do not use the following data for averages, fits, limits, etc. •••

> 0.23	n	90	0	0.7	PHILLIPS 89	HPW
--------	---	----	---	-----	-------------	-----

 $\tau(n \rightarrow \mu^- K^+)$ 735

LIMIT (10^{30} years)	PARTICLE	CL%	EVTs	BKGD EST	DOCUMENT ID	TECN
>57	n	90	0	2.18	BERGER 91B	FREJ

••• We do not use the following data for averages, fits, limits, etc. •••

> 4.7	n	90	0	0.7	PHILLIPS 89	HPW
-------	---	----	---	-----	-------------	-----

Lepton + mesons

 $\tau(p \rightarrow e^- \pi^+ \pi^+)$ 736

LIMIT (10^{30} years)	PARTICLE	CL%	EVTs	BKGD EST	DOCUMENT ID	TECN
>30	p	90	1	2.50	BERGER 91B	FREJ

••• We do not use the following data for averages, fits, limits, etc. •••

> 2.0	p	90	0	0.7	PHILLIPS 89	HPW
-------	---	----	---	-----	-------------	-----

 $\tau(n \rightarrow e^- \pi^+ \pi^0)$ 737

LIMIT (10^{30} years)	PARTICLE	CL%	EVTs	BKGD EST	DOCUMENT ID	TECN
>29	n	90	1	0.78	BERGER 91B	FREJ

 $\tau(p \rightarrow \mu^- \pi^+ \pi^+)$ 738

LIMIT (10^{30} years)	PARTICLE	CL%	EVTs	BKGD EST	DOCUMENT ID	TECN
>17	p	90	1	1.72	BERGER 91B	FREJ

••• We do not use the following data for averages, fits, limits, etc. •••

> 7.8	p	90	0	0.7	PHILLIPS 89	HPW
-------	---	----	---	-----	-------------	-----

 $\tau(n \rightarrow \mu^- \pi^+ \pi^0)$ 739

LIMIT (10^{30} years)	PARTICLE	CL%	EVTs	BKGD EST	DOCUMENT ID	TECN
>34	n	90	0	0.78	BERGER 91B	FREJ

$\tau(p \rightarrow e^- \pi^+ K^+)$ **T40**

LIMIT (10^{30} years)	PARTICLE	CL%	EVTs	BKGD EST	DOCUMENT ID	TECN
>75	p	90	81	127.2	MCGREW 99	IMB3
>20	p	90	3	2.50	BERGER 91B	FREJ

$\tau(p \rightarrow \mu^- \pi^+ K^+)$ **T41**

LIMIT (10^{30} years)	PARTICLE	CL%	EVTs	BKGD EST	DOCUMENT ID	TECN
>245	p	90	3	4.0	MCGREW 99	IMB3
> 5	p	90	2	0.78	BERGER 91B	FREJ

Antilepton + photon(s)

$\tau(p \rightarrow e^+ \gamma)$ **T42**

LIMIT (10^{30} years)	PARTICLE	CL%	EVTs	BKGD EST	DOCUMENT ID	TECN
>670	p	90	0	0.1	MCGREW 99	IMB3
>133	p	90	0	0.3	BERGER 91	FREJ
>460	p	90	0	0.6	SEIDEL 88	IMB
>360	p	90	0	0.3	HAINES 86	IMB
> 87	p (free)	90	0	0.2	BLEWITT 85	IMB
>360	p	90	0	0.2	BLEWITT 85	IMB
> 0.1	p	90			66 GURR 67	CNTR

$\tau(p \rightarrow \mu^+ \gamma)$ **T43**

LIMIT (10^{30} years)	PARTICLE	CL%	EVTs	BKGD EST	DOCUMENT ID	TECN
>478	p	90	0	0.1	MCGREW 99	IMB3
>155	p	90	0	0.1	BERGER 91	FREJ
>380	p	90	0	0.5	SEIDEL 88	IMB
> 97	p	90	3	2	HAINES 86	IMB
> 61	p (free)	90	0	0.2	BLEWITT 85	IMB
>280	p	90	0	0.6	BLEWITT 85	IMB
> 0.3	p	90			67 GURR 67	CNTR

$\tau(n \rightarrow \nu \gamma)$ **T44**

LIMIT (10^{30} years)	PARTICLE	CL%	EVTs	BKGD EST	DOCUMENT ID	TECN
>28	n	90	163	144.7	MCGREW 99	IMB3
>24	n	90	10	6.86	BERGER 91B	FREJ
> 9	n	90	73	60	HAINES 86	IMB
>11	n	90	28	19	PARK 85	IMB

$\tau(p \rightarrow e^+ \gamma \gamma)$ **T45**

LIMIT (10^{30} years)	PARTICLE	CL%	EVTs	BKGD EST	DOCUMENT ID	TECN
>100	p	90	1	0.8	BERGER 91	FREJ

$\tau(n \rightarrow \nu \gamma \gamma)$ **T46**

LIMIT (10^{30} years)	PARTICLE	CL%	EVTs	BKGD EST	DOCUMENT ID	TECN
>219	n	90	5	7.5	MCGREW 99	IMB3

Three (or more) leptons

$\tau(p \rightarrow e^+ e^+ e^-)$ **T47**

LIMIT (10^{30} years)	PARTICLE	CL%	EVTs	BKGD EST	DOCUMENT ID	TECN
>793	p	90	0	0.5	MCGREW 99	IMB3
>147	p	90	0	0.1	BERGER 91	FREJ
>510	p	90	0	0.3	HAINES 86	IMB
> 89	p (free)	90	0	0.5	BLEWITT 85	IMB
>510	p	90	0	0.7	BLEWITT 85	IMB

$\tau(p \rightarrow e^+ \mu^+ \mu^-)$ **T48**

LIMIT (10^{30} years)	PARTICLE	CL%	EVTs	BKGD EST	DOCUMENT ID	TECN
>359	p	90	1	0.9	MCGREW 99	IMB3
> 81	p	90	0	0.16	BERGER 91	FREJ
> 5.0	p	90	0	0.7	PHILLIPS 89	HPW

$\tau(p \rightarrow e^+ \nu \nu)$ **T49**

LIMIT (10^{30} years)	PARTICLE	CL%	EVTs	BKGD EST	DOCUMENT ID	TECN
>17	p	90	152	153.7	MCGREW 99	IMB3
>11	p	90	11	6.08	BERGER 91B	FREJ

$\tau(n \rightarrow e^+ e^- \nu)$ **T50**

LIMIT (10^{30} years)	PARTICLE	CL%	EVTs	BKGD EST	DOCUMENT ID	TECN
>257	n	90	5	7.5	MCGREW 99	IMB3
> 74	n	90	0	< 0.1	BERGER 91B	FREJ
> 45	n	90	5	5	HAINES 86	IMB
> 26	n	90	4	3	PARK 85	IMB

$\tau(n \rightarrow \mu^+ e^- \nu)$ **T51**

LIMIT (10^{30} years)	PARTICLE	CL%	EVTs	BKGD EST	DOCUMENT ID	TECN
>83	n	90	25	29.4	MCGREW 99	IMB3
>47	n	90	0	< 0.1	BERGER 91B	FREJ

$\tau(n \rightarrow \mu^+ \mu^- \nu)$ **T52**

LIMIT (10^{30} years)	PARTICLE	CL%	EVTs	BKGD EST	DOCUMENT ID	TECN
>79	n	90	100	145	MCGREW 99	IMB3
>42	n	90	0	1.4	BERGER 91B	FREJ
> 5.1	n	90	0	0.7	PHILLIPS 89	HPW
>16	n	90	14	7	HAINES 86	IMB
>19	n	90	4	7	PARK 85	IMB

$\tau(p \rightarrow \mu^+ e^+ e^-)$ **T53**

LIMIT (10^{30} years)	PARTICLE	CL%	EVTs	BKGD EST	DOCUMENT ID	TECN
>529	p	90	0	1.0	MCGREW 99	IMB3
> 91	p	90	0	≤ 0.1	BERGER 91	FREJ

$\tau(p \rightarrow \mu^+ \mu^+ \mu^-)$ **T54**

LIMIT (10^{30} years)	PARTICLE	CL%	EVTs	BKGD EST	DOCUMENT ID	TECN
>675	p	90	0	0.3	MCGREW 99	IMB3
>119	p	90	0	0.2	BERGER 91	FREJ
> 10.5	p	90	0	0.7	PHILLIPS 89	HPW
>190	p	90	1	0.1	HAINES 86	IMB
> 44	p (free)	90	1	0.7	BLEWITT 85	IMB
>190	p	90	1	0.9	BLEWITT 85	IMB
> 2.1	p	90	1		68 BATTISTONI 82	NUSX

68 We have converted 1 possible event to 90% CL limit.

$\tau(p \rightarrow \mu^+ \nu \nu)$ **T55**

LIMIT (10^{30} years)	PARTICLE	CL%	EVTs	BKGD EST	DOCUMENT ID	TECN
>21	p	90	7	11.23	BERGER 91B	FREJ

$\tau(p \rightarrow e^- \mu^+ \mu^+)$ **T56**

LIMIT (10^{30} years)	PARTICLE	CL%	EVTs	BKGD EST	DOCUMENT ID	TECN
>6.0	p	90	0	0.7	PHILLIPS 89	HPW

$\tau(n \rightarrow 3\nu)$ **T57**

See also the "to anything" and "disappearance" limits for bound nucleons in the "p Mean Life" data block just in front of the list of possible p decay modes. Such modes could of course be to three (or five) neutrinos, and the limits are stronger, but we do not repeat them here.

LIMIT (10^{30} years)	PARTICLE	CL%	EVTs	BKGD EST	DOCUMENT ID	TECN
>0.00049	n	90	2	2	69 SUZUKI 93B	KAMI

69 We do not use the following data for averages, fits, limits, etc. ...
>0.0023 n 90
>0.00003 n 90 11 6.1
>0.00012 n 90 7 11.2
>0.0005 n 90 0

70 The SUZUKI 93B limit applies to any of $\nu_e \nu_e \bar{\nu}_e$, $\nu_\mu \nu_\mu \bar{\nu}_\mu$, or $\nu_\tau \nu_\tau \bar{\nu}_\tau$.

71 GLICENSTEIN 97 uses Kamioka data and the idea that the disappearance of the neutron's magnetic moment should produce radiation.

72 The first BERGER 91B limit is for $n \rightarrow \nu_e \nu_e \bar{\nu}_e$, the second is for $n \rightarrow \nu_\mu \nu_\mu \bar{\nu}_\mu$.

$\tau(n \rightarrow 5\nu)$ **T58**

See the note on $\tau(n \rightarrow 3\nu)$ on the previous data block.

LIMIT (10^{30} years)	PARTICLE	CL%	EVTs	BKGD EST	DOCUMENT ID	TECN
>0.0017	n	90			72 GLICENSTEIN 97	KAMI

72 GLICENSTEIN 97 uses Kamioka data and the idea that the disappearance of the neutron's magnetic moment should produce radiation.

Baryon Particle Listings

p

———— Inclusive modes ————

$\tau(N \rightarrow e^+ \text{ anything})$ 759

LIMIT (10^{30} years)	PARTICLE	CL%	EVTs	BKGD EST	DOCUMENT ID	TECN	COMMENT
>0.6	p, n	90			73 LEARNED	79 RVUE	

⁷³The electron may be primary or secondary.

$\tau(N \rightarrow \mu^+ \text{ anything})$ 760

LIMIT (10^{30} years)	PARTICLE	CL%	EVTs	BKGD EST	DOCUMENT ID	TECN	COMMENT
>12	p, n	90	2		74,75 CHERRY	81 HOME	
> 1.8	p, n	90			75 COWSIK	80 CNTR	
> 6	p, n	90			75 LEARNED	79 RVUE	

⁷⁴We have converted 2 possible events to 90% CL limit.

⁷⁵The muon may be primary or secondary.

$\tau(N \rightarrow \nu \text{ anything})$ 761

Anything = $\pi, \rho, K, \text{ etc.}$

LIMIT (10^{30} years)	PARTICLE	CL%	EVTs	BKGD EST	DOCUMENT ID	TECN	COMMENT
>0.0002	p, n	90	0		LEARNED	79 RVUE	

$\tau(N \rightarrow e^+ \pi^0 \text{ anything})$ 762

LIMIT (10^{30} years)	PARTICLE	CL%	EVTs	BKGD EST	DOCUMENT ID	TECN	COMMENT
>0.6	p, n	90	0		LEARNED	79 RVUE	

$\tau(N \rightarrow 2 \text{ bodies, } \nu\text{-free})$ 763

LIMIT (10^{30} years)	PARTICLE	CL%	EVTs	BKGD EST	DOCUMENT ID	TECN	COMMENT
>1.3	p, n	90	0		ALEKSEEV	81 BAKS	

———— $\Delta B = 2$ dinucleon modes ————

$\tau(pp \rightarrow \pi^+ \pi^+)$ 764

LIMIT (10^{30} years)	CL%	EVTs	BKGD EST	DOCUMENT ID	TECN	COMMENT
>0.7	90	4	2.34	BERGER	91B FREJ	τ per iron nucleus

$\tau(pp \rightarrow \pi^+ \pi^0)$ 765

LIMIT (10^{30} years)	CL%	EVTs	BKGD EST	DOCUMENT ID	TECN	COMMENT
>2.0	90	0	0.31	BERGER	91B FREJ	τ per iron nucleus

$\tau(nn \rightarrow \pi^+ \pi^-)$ 766

LIMIT (10^{30} years)	CL%	EVTs	BKGD EST	DOCUMENT ID	TECN	COMMENT
>0.7	90	4	2.18	BERGER	91B FREJ	τ per iron nucleus

$\tau(nn \rightarrow \pi^0 \pi^0)$ 767

LIMIT (10^{30} years)	CL%	EVTs	BKGD EST	DOCUMENT ID	TECN	COMMENT
>3.4	90	0	0.78	BERGER	91B FREJ	τ per iron nucleus

$\tau(pp \rightarrow e^+ e^+)$ 768

LIMIT (10^{30} years)	CL%	EVTs	BKGD EST	DOCUMENT ID	TECN	COMMENT
>5.8	90	0	<0.1	BERGER	91B FREJ	τ per iron nucleus

$\tau(pp \rightarrow e^+ \mu^+)$ 769

LIMIT (10^{30} years)	CL%	EVTs	BKGD EST	DOCUMENT ID	TECN	COMMENT
>3.6	90	0	<0.1	BERGER	91B FREJ	τ per iron nucleus

$\tau(pp \rightarrow \mu^+ \mu^+)$ 770

LIMIT (10^{30} years)	CL%	EVTs	BKGD EST	DOCUMENT ID	TECN	COMMENT
>1.7	90	0	0.62	BERGER	91B FREJ	τ per iron nucleus

$\tau(pp \rightarrow e^+ \bar{\nu})$ 771

LIMIT (10^{30} years)	CL%	EVTs	BKGD EST	DOCUMENT ID	TECN	COMMENT
>2.8	90	5	9.67	BERGER	91B FREJ	τ per iron nucleus

$\tau(pp \rightarrow \mu^+ \bar{\nu})$ 772

LIMIT (10^{30} years)	CL%	EVTs	BKGD EST	DOCUMENT ID	TECN	COMMENT
>1.6	90	4	4.37	BERGER	91B FREJ	τ per iron nucleus

$\tau(nn \rightarrow \nu_e \bar{\nu}_e)$ 773

We include "invisible" modes here.

LIMIT (10^{30} years)	CL%	EVTs	BKGD EST	DOCUMENT ID	TECN	COMMENT
>1.4	90			76 ARAKI	06 KLND	$nn \rightarrow$ invisible
>0.000042	90			77 TRETAK	04 CNTR	
>0.000049	90			78 BACK	03 BORX	
>0.000012	90			79 BERNABEI	00B DAMA	
>0.000012	90	5	9.7	BERGER	91B FREJ	τ per iron nucleus

⁷⁶ARAKI 06 looks for signs of de-excitation of the residual nucleus after disappearance of two neutrons from the s shell of ^{12}C .

⁷⁷TRETAK 04 uses data from an old Homestake-mine radiochemical experiment on limits for invisible decays of ^{39}K to ^{37}Ar .

⁷⁸BACK 03 looks for decays of unstable nuclides left after NN decays of parent ^{12}C , ^{13}C , ^{16}O nuclei. These are "invisible channel" limits.

⁷⁹BERNABEI 00B looks for the decay of a $^{127}_{54}\text{Xe}$ nucleus following the disappearance of an nn pair in the otherwise-stable $^{129}_{54}\text{Xe}$ nucleus. The limit here applies as well to $nn \rightarrow \nu_e \bar{\nu}_e, nn \rightarrow \nu_\tau \bar{\nu}_\tau$, or any "disappearance" mode.

$\tau(nn \rightarrow \nu_\mu \bar{\nu}_\mu)$ 774

LIMIT (10^{30} years)	CL%	EVTs	BKGD EST	DOCUMENT ID	TECN	COMMENT
>0.000006	90	4	4.4	BERGER	91B FREJ	τ per iron nucleus

$\tau(pn \rightarrow \text{invisible})$ 775

This violates charge conservation as well as baryon number conservation.

VALUE (years)	CL%	DOCUMENT ID	TECN
>0.000021	90	80 TRETAK	04 CNTR

⁸⁰TRETAK 04 uses data from an old Homestake-mine radiochemical experiment on limits for invisible decays of ^{39}K to ^{37}Ar .

$\tau(pp \rightarrow \text{invisible})$ 776

This violates charge conservation as well as baryon number conservation.

LIMIT (10^{30} years)	CL%	EVTs	BKGD EST	DOCUMENT ID	TECN	COMMENT
>0.00005	90			81 BACK	03 BORX	
>0.0000055	90			82 BERNABEI	00B DAMA	

⁸¹BACK 03 looks for decays of unstable nuclides left after NN decays of parent ^{12}C , ^{13}C , ^{16}O nuclei. These are "invisible channel" limits.

⁸²BERNABEI 00B looks for the decay of a $^{127}_{54}\text{Te}$ nucleus following the disappearance of a pp pair in the otherwise-stable $^{129}_{54}\text{Xe}$ nucleus.

\bar{p} PARTIAL MEAN LIVES

The "partial mean life" limits tabulated here are the limits on $\bar{\tau}/B_j$, where $\bar{\tau}$ is the total mean life for the antiproton and B_j is the branching fraction for the mode in question.

$\tau(\bar{p} \rightarrow e^- \gamma)$ 777

VALUE (years)	CL%	DOCUMENT ID	TECN	COMMENT
> 7×10^5	90	GEER	00 APEX	8.9 GeV/c \bar{p} beam
>1848	95	GEER	94 CALO	8.9 GeV/c \bar{p} beam

$\tau(\bar{p} \rightarrow \mu^- \gamma)$ 778

VALUE (years)	CL%	DOCUMENT ID	TECN	COMMENT
> 5×10^4	90	GEER	00 APEX	8.9 GeV/c \bar{p} beam
> 5.0×10^4	90	HU	98B APEX	8.9 GeV/c \bar{p} beam

$\tau(\bar{p} \rightarrow e^- \pi^0)$ 779

VALUE (years)	CL%	DOCUMENT ID	TECN	COMMENT
> 4×10^5	90	GEER	00 APEX	8.9 GeV/c \bar{p} beam
>554	95	GEER	94 CALO	8.9 GeV/c \bar{p} beam

$\tau(\bar{p} \rightarrow \mu^- \pi^0)$ 780

VALUE (years)	CL%	DOCUMENT ID	TECN	COMMENT
> 5×10^4	90	GEER	00 APEX	8.9 GeV/c \bar{p} beam
> 4.8×10^4	90	HU	98B APEX	8.9 GeV/c \bar{p} beam

$\tau(\bar{p} \rightarrow e^- \eta)$ 781

VALUE (years)	CL%	DOCUMENT ID	TECN	COMMENT
> 2×10^4	90	GEER	00 APEX	8.9 GeV/c \bar{p} beam
>171	95	GEER	94 CALO	8.9 GeV/c \bar{p} beam

See key on page 373

Baryon Particle Listings

p, n

$\tau(\bar{p} \rightarrow \mu^- \eta)$ 782

VALUE (years)	CL%	DOCUMENT ID	TECN	COMMENT
$> 8 \times 10^3$	90	GEER 00	APEX	8.9 GeV/c \bar{p} beam
••• We do not use the following data for averages, fits, limits, etc. •••				
$> 7.9 \times 10^3$	90	HU 98B	APEX	8.9 GeV/c \bar{p} beam

$\tau(\bar{p} \rightarrow e^- K_S^0)$ 783

VALUE (years)	CL%	DOCUMENT ID	TECN	COMMENT
> 900	90	GEER 00	APEX	8.9 GeV/c \bar{p} beam
••• We do not use the following data for averages, fits, limits, etc. •••				
> 29	95	GEER 94	CALO	8.9 GeV/c \bar{p} beam

$\tau(\bar{p} \rightarrow \mu^- K_S^0)$ 784

VALUE (years)	CL%	DOCUMENT ID	TECN	COMMENT
$> 4 \times 10^3$	90	GEER 00	APEX	8.9 GeV/c \bar{p} beam
••• We do not use the following data for averages, fits, limits, etc. •••				
$> 4.3 \times 10^3$	90	HU 98B	APEX	8.9 GeV/c \bar{p} beam

$\tau(\bar{p} \rightarrow e^- K_L^0)$ 785

VALUE (years)	CL%	DOCUMENT ID	TECN	COMMENT
$> 9 \times 10^3$	90	GEER 00	APEX	8.9 GeV/c \bar{p} beam
••• We do not use the following data for averages, fits, limits, etc. •••				
> 9	95	GEER 94	CALO	8.9 GeV/c \bar{p} beam

$\tau(\bar{p} \rightarrow \mu^- K_L^0)$ 786

VALUE (years)	CL%	DOCUMENT ID	TECN	COMMENT
$> 7 \times 10^3$	90	GEER 00	APEX	8.9 GeV/c \bar{p} beam
••• We do not use the following data for averages, fits, limits, etc. •••				
$> 6.5 \times 10^3$	90	HU 98B	APEX	8.9 GeV/c \bar{p} beam

$\tau(\bar{p} \rightarrow e^- \gamma)$ 787

VALUE (years)	CL%	DOCUMENT ID	TECN	COMMENT
$> 2 \times 10^4$	90	GEER 00	APEX	8.9 GeV/c \bar{p} beam

$\tau(\bar{p} \rightarrow \mu^- \gamma)$ 788

VALUE (years)	CL%	DOCUMENT ID	TECN	COMMENT
$> 2 \times 10^4$	90	GEER 00	APEX	8.9 GeV/c \bar{p} beam
••• We do not use the following data for averages, fits, limits, etc. •••				
$> 2.3 \times 10^4$	90	HU 98B	APEX	8.9 GeV/c \bar{p} beam

$\tau(\bar{p} \rightarrow e^- \rho)$ 789

VALUE (years)	CL%	DOCUMENT ID	TECN	COMMENT
> 200	90	⁸³ GEER 00	APEX	8.9 GeV/c \bar{p} beam
••• We do not use the following data for averages, fits, limits, etc. •••				
⁸³ This GEER 00 measurement has been withdrawn; see GEER 00c.				

$\tau(\bar{p} \rightarrow e^- \omega)$ 790

VALUE (years)	CL%	DOCUMENT ID	TECN	COMMENT
> 200	90	GEER 00	APEX	8.9 GeV/c \bar{p} beam

$\tau(\bar{p} \rightarrow e^- K^*(892)^0)$ 791

VALUE (years)	CL%	DOCUMENT ID	TECN	COMMENT
$> 1 \times 10^3$	90	⁸⁴ GEER 00	APEX	8.9 GeV/c \bar{p} beam
••• We do not use the following data for averages, fits, limits, etc. •••				
⁸⁴ This GEER 00 measurement has been withdrawn; see GEER 00c.				

WALL	00B	PR D62 092003		D. Wall <i>et al.</i> (Soudan-2 Collab.)
GABRIELSE	99	PRL 82 3198		G. Gabrielse <i>et al.</i>
HAYATO	99	PRL 83 1529		Y. Hayato <i>et al.</i> (Super-Kamiokande Collab.)
MCGREW	99	PR D59 052004		C. McGrew <i>et al.</i> (IMB-3 Collab.)
MOHR	99	JPCRD 28 1713		P.J. Mohr, B.N. Taylor (NIST)
	Also	RMP 72 351		P.J. Mohr, B.N. Taylor (NIST)
TORII	99	PR A59 2237		H.A. Torii <i>et al.</i> (CERN PS-205 Collab.)
ALLISON	98	PL B47 217		V.W.M. Allison <i>et al.</i> (Soudan-2 Collab.)
HU	98B	PR D58 111101		M. Hu <i>et al.</i> (FNAL APEX Collab.)
SHIOZAWA	98	PRL 81 3319		M. Shiozawa <i>et al.</i> (Super-Kamiokande Collab.)
GLICENSTEIN	97	PL B411 326		J.F. Glischenstein (SACL)
MERGELL	96	NP A596 367		P. Merpell <i>et al.</i> (MANZ, BONN)
GABRIELSE	95	PRL 74 3544		G. Gabrielse <i>et al.</i> (HARV, MANZ, SEOUL)
MACGIBBON	95	PR C52 2097		B.E. MacGibbon <i>et al.</i> (ILL, SASK, INRM)
GEER	94	PRL 72 1596		S. Geer <i>et al.</i> (FNAL, UCLA, PSU)
WONG	94	IJMP E3 821		C.W. Wong (UCLA)
HALLIN	93	PR C48 1497		E.L. Hallin <i>et al.</i> (SASK, BOST, ILL)
SUZUKI	93B	PL B311 357		Y. Suzuki <i>et al.</i> (KAMIOKANDE Collab.)
HUGHES	92	PRL 69 578		R.J. Hughes, B.I. Deutch (LANL, AARH)
ZIEGER	92	PL B276 34		A. Zieger <i>et al.</i> (MPCM)
	Also	PL B281 417 (erratum)		A. Zieger <i>et al.</i> (MPCM)
BERGER	91	ZPHY C50 385		C. Berger <i>et al.</i> (FREJUS Collab.)
BERGER	91B	PL B269 227		C. Berger <i>et al.</i> (FREJUS Collab.)
FEDERSPIEL	91	PRL 67 1511		F.J. Federspiel <i>et al.</i> (ILL)
MCCORD	91	NIM B56/57 496		M. McCord <i>et al.</i>
BECKER-SZ...	90	PR D42 2974		R.A. Becker-Szendy <i>et al.</i> (IMB-3 Collab.)
ERICSON	90	EPL 11 295		T.E.O. Ericson, A. Richter (CERN, DARM)
GABRIELSE	90	PRL 65 1317		G. Gabrielse <i>et al.</i> (HARV, MANZ, WASH+)
BERGER	89	NP B313 509		C. Berger <i>et al.</i> (FREJUS Collab.)
CHO	89	PRL 63 2859		D. Cho, K. Sangster, E.A. Hinds (YALE)
HIRATA	89C	PRL 63 3008		K. Hirata <i>et al.</i> (Kamioikande Collab.)
PHILLIPS	89	PL B224 348		T.J. Phillips <i>et al.</i> (HPW Collab.)
KREISSL	88	ZPHY C37 557		A. Kreissl <i>et al.</i> (CERN PS176 Collab.)
SEIDEL	88	PRL 61 2522		S. Seidel <i>et al.</i> (IMB Collab.)
BARTELT	87	PR D36 1990		J.E. Bartelt <i>et al.</i> (Soudan Collab.)
	Also	PR D40 1701 (erratum)		J.E. Bartelt <i>et al.</i> (Soudan Collab.)
COHEN	87	RMP 59 1121		E.R. Cohen, B.N. Taylor (RIS, NBS)
HAINES	86	PRL 57 1986		T.J. Haines <i>et al.</i> (IMB Collab.)
KAJITA	86	JPSJ 55 711		T. Kajita <i>et al.</i> (Kamioikande Collab.)
ARISAKA	85	JPSJ 54 3213		K. Arisaka <i>et al.</i> (Kamioikande Collab.)
BLEWITT	85	PRL 55 2114		G.B. Blewitt <i>et al.</i> (IMB Collab.)
DZUBA	85	PL B54B 93		V.A. Dzuba, V.V. Flambaum, P.G. Silvestrov (NOVO)
PARK	85	PRL 54 22		H.S. Park <i>et al.</i> (IMB Collab.)
BATTISTONI	84	PL 133B 454		G. Battistoni <i>et al.</i> (NUSEX Collab.)
MARINELLI	84	PL 137B 439		M. Marinelli, G. Morpurgo (GENO)
WILKENING	84	PR A29 425		D.A. Wilkening, N.F. Ramsey, D.J. Larson (HARV+)
BARTELT	83	PRL 50 651		J.E. Bartelt <i>et al.</i> (MINN, ANL)
BATTISTONI	82	PL 118B 461		G. Battistoni <i>et al.</i> (NUSEX Collab.)
KRISHNA...	82	PL 115B 349		M.R. Krishnaswamy <i>et al.</i> (TATA, OSKC+)
ALEKSEEV	81	JETPL 33 651		E.N. Alekseev <i>et al.</i> (PNPI)
CHERRY	81	Translated from ZETFP 33 664		M.L. Cherry <i>et al.</i> (PENN, BNL)
COWSIK	80	PR D22 2204		R. Cowsik, V.S. Narasimham (TATA)
SIMON	80	NP A333 381		G.G. Simon <i>et al.</i>
BELL	79	PL 86B 215		M. Bell <i>et al.</i> (CERN)
GOLDEN	79	PRL 43 1196		R.L. Golden <i>et al.</i> (NASA, PSSL)
LEARNED	79	PRL 43 907		J.G. Learned, F. Reines, A. Soni (UCI)
BREGMAN	78	PL 78B 174		M. Bregman <i>et al.</i> (CERN)
ROBERTS	78	PR D17 358		B.L. Roberts (WILL, RHEL)
EVANS	77	SCI 197 989		J.C. Evans Jr., R.I. Steinberg (BNL, PENN)
HU	75	NP A254 403		E. Hu <i>et al.</i> (COLU, YALE)
BORKOWSKI	74	NP A222 269		F. Borkowski <i>et al.</i>
COHEN	73	JPCRD 2 664		E.R. Cohen, B.N. Taylor (RIS, NBS)
DYLLA	73	PR A7 1224		H.F. Dylla, J.G. King (MIT)
AKIMOV	72	JETP 35 651		Yu.K. Akimov <i>et al.</i> (YERE)
		Translated from ZETF 62 1231		
DIX	70	Thesis Case		F.W. Dix (CASE)
HARRISON	69	PRL 22 1263		G.E. Harrison, P.G.H. Sanders, S.J. Wright (OXF)
GURR	67	PR 158 1321		H.S. Gurr <i>et al.</i> (CASE, WITP)
FREREJACQ...	66	PR 141 1308		D. Frerejacque <i>et al.</i>
HAND	63	RMP 35 335		L.N. Hand <i>et al.</i>
FLEROV	58	DOKL 3 79		G.N. Flerov <i>et al.</i> (ASCI)

n

$$I(J^P) = \frac{1}{2}(\frac{1}{2}^+) \text{ Status: } ***$$

We have omitted some results that have been superseded by later experiments. See our earlier editions.

n MASS (atomic mass units u)

The mass is known much more precisely in u (atomic mass units) than in MeV. See the next data block.

VALUE (u)	DOCUMENT ID	TECN	COMMENT
1.00866491560 ± 0.0000000055	MOHR 05	RVUE	2002 CODATA value
••• We do not use the following data for averages, fits, limits, etc. •••			
1.00866491578 ± 0.0000000055	MOHR 99	RVUE	1998 CODATA value
1.008665904 ± 0.000000014	COHEN 87	RVUE	1986 CODATA value

n MASS (MeV)

The mass is known much more precisely in u (atomic mass units) than in MeV. The conversion from u to MeV, $1 u = 931.494043 \pm 0.000080 \text{ MeV}/c^2$ (MOHR 05, the 2002 CODATA value), involves the relatively poorly known electronic charge.

VALUE (MeV)	DOCUMENT ID	TECN	COMMENT
939.565360 ± 0.000081	MOHR 05	RVUE	2002 CODATA value
••• We do not use the following data for averages, fits, limits, etc. •••			
939.565331 ± 0.000037	¹ KESSLER 99	SPEC	$np \rightarrow d\gamma$
939.565330 ± 0.000038	MOHR 99	RVUE	1998 CODATA value
939.56565 ± 0.00028	^{2,3} DIFILIPPO 94	TRAP	Penning trap
939.56563 ± 0.00028	COHEN 87	RVUE	1986 CODATA value
939.56564 ± 0.00028	^{3,4} GREENE 86	SPEC	$np \rightarrow d\gamma$
939.5731 ± 0.0027	³ COHEN 73	RVUE	1973 CODATA value

p REFERENCES

ARAKI	06	PRL 96 101802	T. Araki <i>et al.</i> (KamLAND Collab.)
HORI	06	PRL 96 243401	M. Hori <i>et al.</i>
BLUNDEN	05	PR C72 057601	P.G. Blunden, I. Sick (MANI, BASL)
KOBAYASHI	05	PR D72 052007	K. Kobayashi <i>et al.</i> (Super-Kamiokande Collab.)
MOHR	05	RMP 77 1	P.J. Mohr, B.N. Taylor (NIST)
SCHUMACHER	05	PPNP 55 567	M. Schumacher (GOET)
AHMED	04	PRL 92 102004	S.N. Ahmed <i>et al.</i> (SNO Collab.)
TRETYAK	04	JETPL 79 106	V.I. Tretyak, V.Yu. Denisov, Yu.G. Zdesenko (KIEV)
		Translated from ZETFP 79 136	
BACK	03	PL B563 23	H.O. Back <i>et al.</i> (BOREXINO Collab.)
BEANE	03	PL B567 200	S.R. Beane <i>et al.</i>
	Also	PL B607 320 (erratum)	S.R. Beane <i>et al.</i>
DMITRIEV	03	PRL 91 212303	V.F. Dmitriev, R.A. Senkov (NOVO)
HORI	03	PRL 91 123401	M. Hori <i>et al.</i> (CERN ASACUSA Collab.)
SICK	03	PL B576 62	I. Sick (BASL)
ZDESENKO	03	PL B553 135	Yu.G. Zdesenko, V.I. Tretyak (KIEV)
AHMAD	02	PRL 89 011301	Q.R. Ahmad <i>et al.</i> (SNO Collab.)
BARANOV	01	PPN 32 376	P.S. Baranov <i>et al.</i>
		Translated from FECAV 32 699	
BLANPIED	01	PR C64 025203	G. Blanpied <i>et al.</i> (BNL LEGS Collab.)
ESCHRICH	01	PL B522 233	I. Eschrich <i>et al.</i> (FNAL SELEX Collab.)
HORI	01	PRL 87 093401	M. Hori <i>et al.</i> (CERN ASACUSA Collab.)
OLMOSDEL...	01	EPJ A10 207	V. Omos de Leon <i>et al.</i> (MANI TAPS Collab.)
TRETYAK	01	PL B505 59	V.I. Tretyak, Yu.G. Zdesenko (KIEV)
BERNABEI	00B	PL B493 12	R. Bernabei <i>et al.</i> (Gran Sasso DAMA Collab.)
GEER	00	PRL 84 590	S. Geer <i>et al.</i> (FNAL APEX Collab.)
	Also	PR D62 052004	S. Geer <i>et al.</i> (FNAL APEX Collab.)
	Also	PRL 85 3546 (erratum)	S. Geer <i>et al.</i> (FNAL APEX Collab.)
GEER	00C	APJ 532 648	S. Geer <i>et al.</i> (FNAL APEX Collab.)
GEER	00D	PRL 84 1673	K.H. Geer, D.C. Kennedy (SLAC, KARL)
MELNIKOV	00	PRL 84 1673	K. Melnikov <i>et al.</i>
ROSENFELDR...	00	PL B479 381	R. Rosenfelder
SENGUPTA	00	PL B484 275	S. Sengupta
WALL	00	PR D61 072004	D. Wall <i>et al.</i> (Soudan-2 Collab.)

Baryon Particle Listings

n

- ¹ We use the 1998 CODATA u-to-MeV conversion factor (see the heading above) to get this mass in MeV from the much more precisely measured KESSLER 99 value of $1.00866491637 \pm 0.0000000082$ u.
- ² The mass is known much more precisely in u: $m = 1.0086649235 \pm 0.0000000023$ u. We use the 1986 CODATA conversion factor to get the mass in MeV.
- ³ These determinations are not independent of the $m_n - m_p$ measurements below.
- ⁴ The mass is known much more precisely in u: $m = 1.008664919 \pm 0.000000014$ u.

\bar{n} MASS

VALUE (MeV)	EVTS	DOCUMENT ID	TECN	COMMENT
939.485 ± 0.051	59	⁵ CRESTI	86	HBC $\bar{p}p \rightarrow \bar{n}n$

⁵ This is a corrected result (see the erratum). The error is statistical. The maximum systematic error is 0.029 MeV.

$(m_n - m_{\bar{n}}) / m_n$

A test of *CPT* invariance. Calculated from the *n* and \bar{n} masses, above.

VALUE	DOCUMENT ID
$(9 \pm 5) \times 10^{-5}$ OUR EVALUATION	

$m_n - m_p$

VALUE (MeV)	DOCUMENT ID	TECN	COMMENT
1.2933317 ± 0.0000005	⁶ MOHR	05	RVUE 2002 CODATA value
• • • We do not use the following data for averages, fits, limits, etc. • • •			
1.2933318 ± 0.0000005	⁷ MOHR	99	RVUE 1998 CODATA value
1.293318 ± 0.0000009	⁸ COHEN	87	RVUE 1986 CODATA value
1.2933328 ± 0.0000072	GREENE	86	SPEC $np \rightarrow d\gamma$
1.293429 ± 0.0000036	COHEN	73	RVUE 1973 CODATA value

⁶ Calculated by us from the MOHR 05 ratio $m_n/m_p = 1.00137841870 \pm 0.00000000058$. In u, $m_n - m_p = (1.3884487 \pm 0.00000006) \times 10^{-3}$ u.

⁷ Calculated by us from the MOHR 99 ratio $m_n/m_p = 1.00137841887 \pm 0.00000000058$. In u, $m_n - m_p = (1.3884489 \pm 0.00000006) \times 10^{-3}$ u.

⁸ Calculated by us from the COHEN 87 ratio $m_n/m_p = 1.001378404 \pm 0.000000009$. In u, $m_n - m_p = 0.001388434 \pm 0.000000009$ u.

n MEAN LIFE

We now compile only direct measurements of the lifetime, not those inferred from decay correlation measurements. For the average, we only use measurements with an error less than 10 s.

The most recent result, that of SEREBROV 05, is so far from other results that it makes no sense to include it in the average. It is up to workers in this field to resolve this issue. Until this major disagreement is understood our present average of 885.7 ± 0.8 s must be suspect.

For recent reviews of neutron physics, see NICO 05a and SEVERIJNS 06.

Limits on lifetimes for *bound* neutrons are given in the section "*p* PARTIAL MEAN LIVES."

VALUE (s)	DOCUMENT ID	TECN	COMMENT
885.7 ± 0.8 OUR AVERAGE			
886.3 ± 1.2 ± 3.2	NICO	05	CNTR In-beam <i>n</i> , trapped <i>p</i>
885.4 ± 0.9 ± 0.4	ARZUMANOV	00	CNTR UCN double bottle
889.2 ± 3.0 ± 3.8	BYRNE	96	CNTR Penning trap
882.6 ± 2.7	⁹ MAMPE	93	CNTR Gravitational trap
888.4 ± 3.1 ± 1.1	NESVIZHEV...	92	CNTR Gravitational trap
887.6 ± 3.0	MAMPE	89	CNTR Gravitational trap
891 ± 9	SPIVAK	88	CNTR Beam
• • • We do not use the following data for averages, fits, limits, etc. • • •			
878.5 ± 0.7 ± 0.3	¹⁰ SEREBROV	05	CNTR Gravitational trap
886.8 ± 1.2 ± 3.2	DEWEY	03	CNTR See NICO 05
888.4 ± 2.9	ALFIMENKOV	90	CNTR See NESVIZHEVSKII 92
893.6 ± 3.8 ± 3.7	BYRNE	90	CNTR See BYRNE 96
878 ± 27 ± 14	KOSSAKOW...	89	TPC Pulsed beam
877 ± 10	PAUL	89	CNTR Storage ring
876 ± 10 ± 19	LAST	88	SPEC Pulsed beam
903 ± 13	KOSVINTSEV	86	CNTR Gravitational trap
937 ± 18	¹¹ BYRNE	80	CNTR
875 ± 95	KOSVINTSEV	80	CNTR
881 ± 8	BONDAREN...	78	CNTR See SPIVAK 88
918 ± 14	CHRISTENSEN72	CNTR	

⁹IGNATOVICH 95 calls into question some of the corrections and averaging procedures used by MAMPE 93. The response, BONDARENKO 96, denies the validity of the criticisms.

¹⁰This SEREBROV 05 result is 6.5 standard deviations from our average of previous results and 5.6 standard deviations from the previous most precise result (that of ARZUMANOV 00).

¹¹This measurement has been withdrawn (J. Byrne, private communication, 1990).

n MAGNETIC MOMENT

See the "Note on Baryon Magnetic Moments" in the *A* Listings.

VALUE (μ_N)	DOCUMENT ID	TECN	COMMENT
-1.91304273 ± 0.00000045	MOHR	05	RVUE 2002 CODATA value
• • • We do not use the following data for averages, fits, limits, etc. • • •			
-1.91304272 ± 0.00000045	MOHR	99	RVUE 1998 CODATA value
-1.91304275 ± 0.00000045	COHEN	87	RVUE 1986 CODATA value
-1.91304277 ± 0.00000048	¹² GREENE	82	MRS

¹²GREENE 82 measures the moment to be $(1.04187564 \pm 0.00000026) \times 10^{-3}$ Bohr magnetons. The value above is obtained by multiplying this by $m_p/m_e = 1836.152701 \pm 0.000037$ (the 1986 CODATA value from COHEN 87).

n ELECTRIC DIPOLE MOMENT

A nonzero value is forbidden by both *T* invariance and *P* invariance. A number of early results have been omitted. See RAMSEY 90 and GOLUB 94 for reviews.

VALUE (10^{-25} ecm)	CL%	DOCUMENT ID	TECN	COMMENT
< 0.29	90	¹³ BAKER	06	MRS UCN's, $h\nu = 2\mu_n B \pm 2d_n E$
• • • We do not use the following data for averages, fits, limits, etc. • • •				
< 0.63	90	¹⁴ HARRIS	99	MRS $d = (-0.1 \pm 0.36) \times 10^{-25}$
< 0.97	90	ALTAREV	96	MRS $(+0.26 \pm 0.40 \pm 0.16) \times 10^{-25}$
< 1.1	95	ALTAREV	92	MRS See ALTAREV 96
< 1.2	95	SMITH	90	MRS See HARRIS 99
< 2.6	95	ALTAREV	86	MRS $d = (-1.4 \pm 0.6) \times 10^{-25}$
0.3 ± 4.8		PENDLEBURY	84	MRS Ultracold neutrons
< 6	90	ALTAREV	81	MRS $d = (2.1 \pm 2.4) \times 10^{-25}$
< 16	90	ALTAREV	79	MRS $d = (4.0 \pm 7.5) \times 10^{-25}$

¹³LAMOREAUX 07 faults BAKER 06 for not including in the estimate of systematic error an effect due to the Earth's rotation. BAKER 07 replies (1) that the effect was included implicitly in the analysis and (2) that further analysis confirms that the BAKER 06 limit is correct as is. See also SILENKO 07.

¹⁴This HARRIS 99 result includes the result of SMITH 90. However, the averaging of the results of these two experiments has been criticized by LAMOREAUX 00.

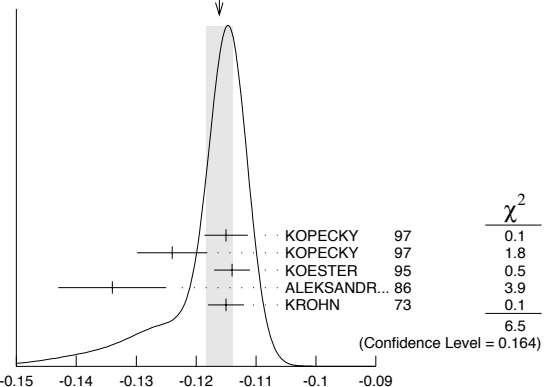
n MEAN-SQUARE CHARGE RADIUS

The mean-square charge radius of the neutron, $\langle r_n^2 \rangle$, is related to the neutron-electron scattering length b_{ne} by $\langle r_n^2 \rangle = 3(m_e a_0 / m_n) b_{ne}$, where m_e and m_n are the masses of the electron and neutron, and a_0 is the Bohr radius. Numerically, $\langle r_n^2 \rangle = 86.34 b_{ne}$, if we use a_0 for a nucleus with infinite mass.

VALUE (fm^2)	DOCUMENT ID	COMMENT
-0.1161 ± 0.0022 OUR AVERAGE		Error includes scale factor of 1.3. See the ideogram below.
-0.115 ± 0.002 ± 0.003	KOPECKY	97 <i>ne</i> scattering (Pb)
-0.124 ± 0.003 ± 0.005	KOPECKY	97 <i>ne</i> scattering (Bi)
-0.114 ± 0.003	KOESTER	95 <i>ne</i> scattering (Pb, Bi)
-0.134 ± 0.009	ALEKSANDR...	86 <i>ne</i> scattering (Bi)
-0.115 ± 0.003	¹⁵ KROHN	73 <i>ne</i> scattering (Ne, Ar, Kr, Xe)
• • • We do not use the following data for averages, fits, limits, etc. • • •		
-0.113 ± 0.003 ± 0.004	KOPECKY	95 <i>ne</i> scattering (Pb)
-0.114 ± 0.003	KOESTER	86 <i>ne</i> scattering (Pb, Bi)
-0.118 ± 0.002	KOESTER	76 <i>ne</i> scattering (Pb)
-0.120 ± 0.002	KOESTER	76 <i>ne</i> scattering (Bi)
-0.116 ± 0.003	KROHN	66 <i>ne</i> scattering (Ne, Ar, Kr, Xe)

¹⁵This value is as corrected by KOESTER 76.

WEIGHTED AVERAGE
-0.1161 ± 0.0022 (Error scaled by 1.3)



n mean-square charge radius

***n* ELECTRIC POLARIZABILITY α_n**

Following is the electric polarizability α_n defined in terms of the induced electric dipole moment by $\mathbf{D} = 4\pi\epsilon_0\alpha_n\mathbf{E}$. For a review, see SCHMIEDMAYER 89.

For a very complete review of the "polarizability of the nucleon and Compton scattering," see SCHUMACHER 05. His recommended values for the neutron are $\alpha_n = (12.5 \pm 1.7) \times 10^{-4} \text{ fm}^3$ and $\beta_n = (2.7 \pm 1.8) \times 10^{-4} \text{ fm}^3$, which agree with our averages within errors.

VALUE (10^{-4} fm^3)	DOCUMENT ID	TECN	COMMENT
----------------------------------	-------------	------	---------

VALUE (10^{-4} fm^3)	DOCUMENT ID	TECN	COMMENT
11.6 ± 1.5 OUR AVERAGE			
12.5 ± 1.8 ^{+1.6} _{-1.3}	16 KOSSERT	03 CNTR	$\gamma d \rightarrow \gamma p n$
8.8 ± 2.4 ± 3.0	17 LUNDIN	03 CNTR	$\gamma d \rightarrow \gamma d$
12.0 ± 1.5 ± 2.0	SCHMIEDM...	91 CNTR	<i>n</i> Pb transmission
10.7 ^{+3.3} _{-10.7}	ROSE	90B CNTR	$\gamma d \rightarrow \gamma n p$

• • • We do not use the following data for averages, fits, limits, etc. • • •

VALUE	DOCUMENT ID	TECN	COMMENT
13.6	18 KOLB	00 CNTR	$\gamma d \rightarrow \gamma n p$
0.0 ± 5.0	19 KOESTER	95 CNTR	<i>n</i> Pb, <i>n</i> Bi transmission
11.7 ^{+4.3} _{-11.7}	ROSE	90 CNTR	See ROSE 90b
8 ± 10	KOESTER	88 CNTR	<i>n</i> Pb, <i>n</i> Bi transmission
12 ± 10	SCHMIEDM...	88 CNTR	<i>n</i> Pb, <i>n</i> C transmission

16 KOSSERT 03 gets $\alpha_n - \beta_n = (9.8 \pm 3.6^{+2.1}_{-1.1} \pm 2.2) \times 10^{-4} \text{ fm}^3$, and uses $\alpha_n + \beta_n = (15.2 \pm 0.5) \times 10^{-4} \text{ fm}^3$ from LEVCHUK 00. Thus the errors on α_n and β_n are anti-correlated.

17 LUNDIN 03 measures $\alpha_n - \beta_n = (6.4 \pm 2.4) \times 10^{-4} \text{ fm}^3$ and uses accurate values for α_p and α_d and a precise sum-rule result for $\alpha_n + \beta_n$. The second error is a model uncertainty, and errors on α_n and β_n are anticorrelated.

18 KOLB 00 obtains this value with a lower limit of $7.6 \times 10^{-4} \text{ fm}^3$ but no upper limit from this experiment alone. Combined with results of ROSE 90, the 1- σ range is (7.6-14.0) $\times 10^{-4} \text{ fm}^3$.

19 KOESTER 95 uses natural Pb and the isotopes 208, 207, and 206. See this paper for a discussion of methods used by various groups to extract α_n from data.

***n* MAGNETIC POLARIZABILITY β_n**

VALUE (10^{-4} fm^3)	DOCUMENT ID	TECN	COMMENT
----------------------------------	-------------	------	---------

VALUE (10^{-4} fm^3)	DOCUMENT ID	TECN	COMMENT
3.7 ± 2.0 OUR AVERAGE			
2.7 ± 1.8 ^{+1.3} _{-1.6}	20 KOSSERT	03 CNTR	$\gamma d \rightarrow \gamma p n$
6.5 ± 2.4 ± 3.0	21 LUNDIN	03 CNTR	$\gamma d \rightarrow \gamma d$

• • • We do not use the following data for averages, fits, limits, etc. • • •

VALUE	DOCUMENT ID	TECN	COMMENT
1.6	22 KOLB	00 CNTR	$\gamma d \rightarrow \gamma n p$

20 KOSSERT 03 gets $\alpha_n - \beta_n = (9.8 \pm 3.6^{+2.1}_{-1.1} \pm 2.2) \times 10^{-4} \text{ fm}^3$, and uses $\alpha_n + \beta_n = (15.2 \pm 0.5) \times 10^{-4} \text{ fm}^3$ from LEVCHUK 00. Thus the errors on α_n and β_n are anti-correlated.

21 LUNDIN 03 measures $\alpha_n - \beta_n = (6.4 \pm 2.4) \times 10^{-4} \text{ fm}^3$ and uses accurate values for α_p and α_d and a precise sum-rule result for $\alpha_n + \beta_n$. The second error is a model uncertainty, and errors on α_n and β_n are anticorrelated.

22 KOLB 00 obtains this value with an upper limit of $7.6 \times 10^{-4} \text{ fm}^3$ but no lower limit from this experiment alone. Combined with results of ROSE 90, the 1- σ range is (1.2-7.6) $\times 10^{-4} \text{ fm}^3$.

***n* CHARGE**

See also " $|q_p + q_e|/e$ " in the proton Listings.

VALUE ($10^{-21} e$)	DOCUMENT ID	TECN	COMMENT
------------------------	-------------	------	---------

VALUE ($10^{-21} e$)	DOCUMENT ID	TECN	COMMENT
- 0.4 ± 1.1	23 BAUMANN	88	Cold <i>n</i> deflection
-15 ± 22	24 GAEHLER	82 CNTR	Cold <i>n</i> deflection

23 The BAUMANN 88 error ±1.1 gives the 68% CL limits about the the value -0.4.

24 The GAEHLER 82 error ±22 gives the 90% CL limits about the the value -15.

LIMIT ON $n\bar{n}$ OSCILLATIONS

Mean Time for $n\bar{n}$ Transition in Vacuum

A test of $\Delta B=2$ baryon number nonconservation. MOHAPATRA 80 and MOHAPATRA 89 discuss the theoretical motivations for looking for $n\bar{n}$ oscillations. DOVER 83 and DOVER 85 give phenomenological analyses. The best limits come from looking for the decay of neutrons bound in nuclei. However, these analyses require model-dependent corrections for nuclear effects. See KABIR 83, DOVER 89, ALBERICO 91, and GAL 00 for discussions. Direct searches for $n \rightarrow \bar{n}$ transitions using reactor neutrons are cleaner but give somewhat poorer limits. We include limits for both free and bound neutrons in the Summary Table.

VALUE (s)	CL%	DOCUMENT ID	TECN	COMMENT
-----------	-----	-------------	------	---------

VALUE (s)	CL%	DOCUMENT ID	TECN	COMMENT
>1.3 × 10⁸	90	CHUNG	02B SOU2	<i>n</i> bound in iron
>8.6 × 10⁷	90	BALDO-...	94 CNTR	Reactor (free) neutrons

• • • We do not use the following data for averages, fits, limits, etc. • • •

VALUE	DOCUMENT ID	TECN	COMMENT
>1 × 10 ⁷	90 BALDO-...	90 CNTR	See BALDO-CEOLIN 94
>1.2 × 10 ⁸	90 BERGER	90 FREJ	<i>n</i> bound in iron
>4.9 × 10 ⁵	90 BRESSI	90 CNTR	Reactor neutrons
>4.7 × 10 ⁵	90 BRESSI	89 CNTR	See BRESSI 90
>1.2 × 10 ⁸	90 TAKITA	86 CNTR	<i>n</i> bound in oxygen
>1 × 10 ⁶	90 FIDECARO	85 CNTR	Reactor neutrons
>8.8 × 10 ⁷	90 PARK	85B CNTR	
>3 × 10 ⁷	BATTISTONI	84 NUSX	
>2.7 × 10 ⁷ -1.1 × 10 ⁸	JONES	84 CNTR	
>2 × 10 ⁷	CHERRY	83 CNTR	

LIMIT ON $n n'$ OSCILLATIONS

Lee and Yang (LEE 56) proposed the existence of mirror world in an attempt to restore global parity symmetry. See BEREZHIANI 06 for a recent discussions.

VALUE (s)	CL%	DOCUMENT ID	TECN	COMMENT
-----------	-----	-------------	------	---------

VALUE (s)	CL%	DOCUMENT ID	TECN	COMMENT
>103	95	BAN	07 CNTR	UCN, B field on & off

***n* DECAY MODES**

Mode	Fraction (Γ_i/Γ)	Confidence level
Γ_1 $p e^- \bar{\nu}_e$	100	%
Γ_2 hydrogen-atom $\bar{\nu}_e$		
Γ_3 $p e^- \bar{\nu}_e \gamma$	[a] (3.13 ± 0.35) × 10 ⁻³	

Charge conservation (Q) violating mode

Mode	Fraction (Γ_i/Γ)	Confidence level
Γ_4 $p \nu_e \bar{\nu}_e$	Q < 8	× 10 ⁻²⁷ 68%

[a] This limit is for γ energies between 35 and 100 keV.

***n* BRANCHING RATIOS**

$\Gamma(\text{hydrogen-atom } \bar{\nu}_e)/\Gamma_{\text{total}}$	Γ_2/Γ
---	-------------------

VALUE	CL%	DOCUMENT ID	TECN
-------	-----	-------------	------

• • • We do not use the following data for averages, fits, limits, etc. • • •

VALUE	CL%	DOCUMENT ID	TECN
<3 × 10 ⁻²	95	25 GREEN	90 RVUE

25 GREEN 90 infers that $\tau(\text{hydrogen-atom } \bar{\nu}_e) > 3 \times 10^4 \text{ s}$ by comparing neutron lifetime measurements made in storage experiments with those made in β -decay experiments. However, the result depends sensitively on the lifetime measurements, and does not of course take into account more recent measurements of same.

$\Gamma(p e^- \bar{\nu}_e \gamma)/\Gamma_{\text{total}}$	Γ_3/Γ
--	-------------------

VALUE (units 10 ⁻³)	CL%	DOCUMENT ID	TECN	COMMENT
---------------------------------	-----	-------------	------	---------

• • • We do not use the following data for averages, fits, limits, etc. • • •

VALUE (units 10 ⁻³)	CL%	DOCUMENT ID	TECN	COMMENT
3.13 ± 0.11 ± 0.33		26 NICO	06 CNTR	γ, p, e^- coincidence
<6.9	90	27 BECK	02 CNTR	γ, p, e^- coincidence

26 This NICO 06 result is for γ energies between 15 and 340 keV.

27 This BECK 02 limit is for γ energies between 35 and 100 keV.

$\Gamma(p \nu_e \bar{\nu}_e)/\Gamma_{\text{total}}$	Γ_4/Γ
---	-------------------

Forbidden by charge conservation.

VALUE	CL%	DOCUMENT ID	TECN	COMMENT
<8 × 10⁻²⁷	68	28 NORMAN	96 RVUE	⁷¹ Ga → ⁷¹ Ge neutrals
<9.7 × 10 ⁻¹⁸	90	ROY	83 CNTR	¹¹³ Cd → ^{113m} In neut.
<7.9 × 10 ⁻²¹		VAIDYA	83 CNTR	⁸⁷ Rb → ^{87m} Sr neut.
<9 × 10 ⁻²⁴	90	BARABANOV	80 CNTR	⁷¹ Ga → ⁷¹ GeX
<3 × 10 ⁻¹⁹		NORMAN	79 CNTR	⁸⁷ Rb → ^{87m} Sr neut.

28 NORMAN 96 gets this limit by attributing SAGE and GALLEX counting rates to the charge-nonconserving transition ⁷¹Ga → ⁷¹Ge+neutrals rather than to solar-neutrino reactions.

BARYON DECAY PARAMETERS

Written 1996 by E.D. Commins (University of California, Berkeley).

Baryon semileptonic decays

The typical spin-1/2 baryon semileptonic decay is described by a matrix element, the hadronic part of which may be written as:

$$\bar{B}_f [f_1(q^2)\gamma_\lambda + i f_2(q^2)\sigma_{\lambda\mu}q^\mu + g_1(q^2)\gamma_\lambda\gamma_5 + g_3(q^2)\gamma_5q_\lambda] B_i . \tag{1}$$

Baryon Particle Listings

n

Here B_i and \overline{B}_f are spinors describing the initial and final baryons, and $q = p_i - p_f$, while the terms in f_1 , f_2 , g_1 , and g_3 account for vector, induced tensor (“weak magnetism”), axial vector, and induced pseudoscalar contributions [1]. Second-class current contributions are ignored here. In the limit of zero momentum transfer, f_1 reduces to the vector coupling constant g_V , and g_1 reduces to the axial-vector coupling constant g_A . The latter coefficients are related by Cabibbo’s theory [2], generalized to six quarks (and three mixing angles) by Kobayashi and Maskawa [3]. The g_3 term is negligible for transitions in which an e^\pm is emitted, and gives a very small correction, which can be estimated by PCAC [4], for μ^\pm modes. Recoil effects include weak magnetism, and are taken into account adequately by considering terms of first order in

$$\delta = \frac{m_i - m_f}{m_i + m_f}, \quad (2)$$

where m_i and m_f are the masses of the initial and final baryons.

The experimental quantities of interest are the total decay rate, the lepton-neutrino angular correlation, the asymmetry coefficients in the decay of a polarized initial baryon, and the polarization of the decay baryon in its own rest frame for an unpolarized initial baryon. Formulae for these quantities are derived by standard means [5] and are analogous to formulae for nuclear beta decay [6]. We use the notation of Ref. 6 in the Listings for neutron beta decay. For comparison with experiments at higher q^2 , it is necessary to modify the form factors at $q^2 = 0$ by a “dipole” q^2 dependence, and for high-precision comparisons to apply appropriate radiative corrections [7].

The ratio g_A/g_V may be written as

$$g_A/g_V = |g_A/g_V| e^{i\phi_{AV}}. \quad (3)$$

The presence of a “triple correlation” term in the transition probability, proportional to $\text{Im}(g_A/g_V)$ and of the form

$$\sigma_i \cdot (\mathbf{p}_\ell \times \mathbf{p}_\nu) \quad (4)$$

for initial baryon polarization or

$$\sigma_f \cdot (\mathbf{p}_\ell \times \mathbf{p}_\nu) \quad (5)$$

for final baryon polarization, would indicate failure of time-reversal invariance. The phase angle ϕ has been measured precisely only in neutron decay (and in ^{19}Ne nuclear beta decay), and the results are consistent with T invariance.

Hyperon nonleptonic decays

The amplitude for a spin-1/2 hyperon decaying into a spin-1/2 baryon and a spin-0 meson may be written in the form

$$M = G_F m_\pi^2 \cdot \overline{B}_f (A - B\gamma_5) B_i, \quad (6)$$

where A and B are constants [1]. The transition rate is proportional to

$$R = 1 + \gamma \hat{\omega}_f \cdot \hat{\omega}_i + (1 - \gamma)(\hat{\omega}_f \cdot \hat{\mathbf{n}})(\hat{\omega}_i \cdot \hat{\mathbf{n}}) + \alpha(\hat{\omega}_f \cdot \hat{\mathbf{n}} + \hat{\omega}_i \cdot \hat{\mathbf{n}}) + \beta \hat{\mathbf{n}} \cdot (\hat{\omega}_f \times \hat{\omega}_i), \quad (7)$$

where $\hat{\mathbf{n}}$ is a unit vector in the direction of the final baryon momentum, and $\hat{\omega}_i$ and $\hat{\omega}_f$ are unit vectors in the directions of the initial and final baryon spins. (The sign of the last term in the above equation was incorrect in our 1988 and 1990 editions.) The parameters α , β , and γ are defined as

$$\begin{aligned} \alpha &= 2 \text{Re}(s^*p) / (|s|^2 + |p|^2), \\ \beta &= 2 \text{Im}(s^*p) / (|s|^2 + |p|^2), \\ \gamma &= (|s|^2 - |p|^2) / (|s|^2 + |p|^2), \end{aligned} \quad (8)$$

where $s = A$ and $p = |\mathbf{p}_f| B / (E_f + m_f)$; here E_f and \mathbf{p}_f are the energy and momentum of the final baryon. The parameters α , β , and γ satisfy

$$\alpha^2 + \beta^2 + \gamma^2 = 1. \quad (9)$$

If the hyperon polarization is \mathbf{P}_Y , the polarization \mathbf{P}_B of the decay baryons is

$$\mathbf{P}_B = \frac{(\alpha + \mathbf{P}_Y \cdot \hat{\mathbf{n}})\hat{\mathbf{n}} + \beta(\mathbf{P}_Y \times \hat{\mathbf{n}}) + \gamma\hat{\mathbf{n}} \times (\mathbf{P}_Y \times \hat{\mathbf{n}})}{1 + \alpha\mathbf{P}_Y \cdot \hat{\mathbf{n}}}. \quad (10)$$

Here \mathbf{P}_B is defined in the rest system of the baryon, obtained by a Lorentz transformation along $\hat{\mathbf{n}}$ from the hyperon rest frame, in which $\hat{\mathbf{n}}$ and \mathbf{P}_Y are defined.

An additional useful parameter ϕ is defined by

$$\beta = (1 - \alpha^2)^{1/2} \sin\phi. \quad (11)$$

In the Listings, we compile α and ϕ for each decay, since these quantities are most closely related to experiment and are essentially uncorrelated. When necessary, we have changed the signs of reported values to agree with our sign conventions. In the Baryon Summary Table, we give α , ϕ , and Δ (defined below) with errors, and also give the value of γ without error.

Time-reversal invariance requires, in the absence of final-state interactions, that s and p be relatively real, and therefore that $\beta = 0$. However, for the decays discussed here, the final-state interaction is strong. Thus

$$s = |s| e^{i\delta_s} \text{ and } p = |p| e^{i\delta_p}, \quad (12)$$

where δ_s and δ_p are the pion-baryon s - and p -wave strong interaction phase shifts. We then have

$$\beta = \frac{-2|s||p|}{|s|^2 + |p|^2} \sin(\delta_s - \delta_p). \quad (13)$$

One also defines $\Delta = -\tan^{-1}(\beta/\alpha)$. If T invariance holds, $\Delta = \delta_s - \delta_p$. For $\Lambda \rightarrow p\pi^-$ decay, the value of Δ may be compared with the s - and p -wave phase shifts in low-energy π^-p scattering, and the results are consistent with T invariance.

See also the note on “Radiative Hyperon Decays” in the Ξ^0 Listings in this *Review*.

References

1. E.D. Commins and P.H. Bucksbaum, *Weak Interactions of Leptons and Quarks* (Cambridge University Press, Cambridge, England, 1983).

2. N. Cabibbo, Phys. Rev. Lett. **10**, 531 (1963).
3. M. Kobayashi and T. Maskawa, Prog. Theor. Phys. **49**, 652 (1973).
4. M.L. Goldberger and S.B. Treiman, Phys. Rev. **111**, 354 (1958).
5. P.H. Frampton and W.K. Tung, Phys. Rev. **D3**, 1114 (1971).
6. J.D. Jackson, S.B. Treiman, and H.W. Wyld, Jr., Phys. Rev. **106**, 517 (1957), and Nucl. Phys. **4**, 206 (1957).
7. Y. Yokoo, S. Suzuki, and M. Morita, Prog. Theor. Phys. **50**, 1894 (1973).

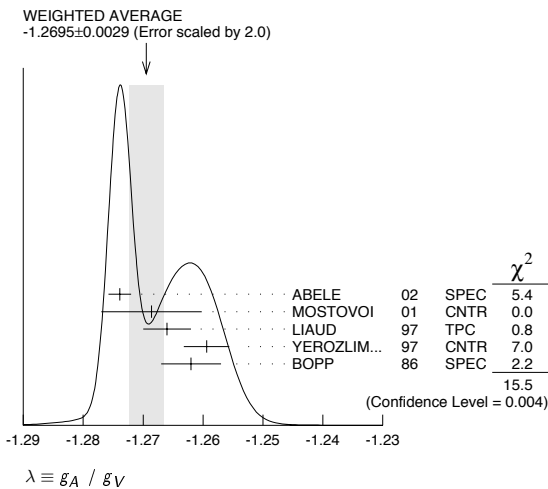
$n \rightarrow p e^- \bar{\nu}_e$ DECAY PARAMETERS

See the above "Note on Baryon Decay Parameters." For discussions of recent results, see the references cited at the beginning of the section on the neutron mean life. For discussions of the values of the weak coupling constants g_A and g_V obtained using the neutron lifetime and asymmetry parameter A , comparisons with other methods of obtaining these constants, and implications for particle physics and for astrophysics, see DUBBERS 91 and WOOLCOCK 91. For tests of the $V-A$ theory of neutron decay, see EROZOLIMSKII 91b, MOSTOVOI 96, NICO 05, and SEVERIJNS 06.

$\lambda \equiv g_A / g_V$

VALUE	DOCUMENT ID	TECN	COMMENT
-1.2695 ± 0.0029 OUR AVERAGE	Error includes scale factor of 2.0. See the ideogram below.		
-1.2739 ± 0.0019	29 ABELE	02 SPEC	Cold <i>n</i> , polarized, A
-1.2686 ± 0.0046 ± 0.007	30 MOSTOVOI	01 CNTR	A and B × polarizations
-1.266 ± 0.004	LIAUD	97 TPC	Cold <i>n</i> , polarized, A
-1.2594 ± 0.0038	31 YEROZLIM...	97 CNTR	Cold <i>n</i> , polarized, A
-1.262 ± 0.005	BOPP	86 SPEC	Cold <i>n</i> , polarized, A
• • • We do not use the following data for averages, fits, limits, etc. • • •			
-1.275 ± 0.006 ± 0.015	SCHUMANN	08 CNTR	Cold <i>n</i> , polarized
-1.274 ± 0.003	ABELE	97D SPEC	Cold <i>n</i> , polarized, A
-1.266 ± 0.004	SCHRECK...	95 TPC	See LIAUD 97
-1.2544 ± 0.0036	EROZOLIM...	91 CNTR	See YEROZOLIMSKY 97
-1.226 ± 0.042	MOSTOVOY	83 RVUE	
-1.261 ± 0.012	EROZOLIM...	79 CNTR	Cold <i>n</i> , polarized, A
-1.259 ± 0.017	32 STRATOWA	78 CNTR	<i>p</i> recoil spectrum, <i>a</i>
-1.263 ± 0.015	EROZOLIM...	77 CNTR	See EROZOLIMSKII 79
-1.250 ± 0.036	32 DOBROZE...	75 CNTR	See STRATOWA 78
-1.258 ± 0.015	33 KROHN	75 CNTR	Cold <i>n</i> , polarized, A
-1.263 ± 0.016	34 KROPF	74 RVUE	<i>n</i> decay alone
-1.250 ± 0.009	34 KROPF	74 RVUE	<i>n</i> decay + nuclear ft

- 29 This is the combined result of ABELE 02 and ABELE 97D.
 30 MOSTOVOI 01 measures the two *P*-odd correlations *A* and *B*, or rather *SA* and *SB*, where *S* is the *n* polarization, in free neutron decay.
 31 YEROZOLIMSKY 97 makes a correction to the EROZOLIMSKII 91 value.
 32 These experiments measure the absolute value of g_A/g_V only.
 33 KROHN 75 includes events of CHRISTENSEN 70.
 34 KROPF 74 reviews all data through 1972.

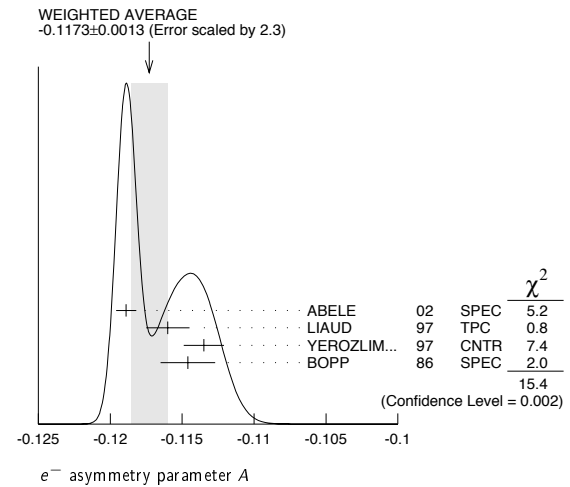


e^- ASYMMETRY PARAMETER *A*

This is the neutron-spin electron-momentum correlation coefficient. Unless otherwise noted, the values are corrected for radiative effects and weak magnetism. In the Standard Model, *A* is related to $\lambda \equiv g_A/g_V$ by $A = -2\lambda(\lambda - 1) / (1 + 3\lambda^2)$; this assumes that g_A and g_V are real.

VALUE	DOCUMENT ID	TECN	COMMENT
-0.1173 ± 0.0013 OUR AVERAGE	Error includes scale factor of 2.3. See the ideogram below.		
-0.1189 ± 0.0007	35 ABELE	02 SPEC	Cold <i>n</i> , polarized
-0.1160 ± 0.0009 ± 0.0012	LIAUD	97 TPC	Cold <i>n</i> , polarized
-0.1135 ± 0.0014	36 YEROZLIM...	97 CNTR	Cold <i>n</i> , polarized
-0.1146 ± 0.0019	BOPP	86 SPEC	Cold <i>n</i> , polarized
• • • We do not use the following data for averages, fits, limits, etc. • • •			
-0.1168 ± 0.0017	37 MOSTOVOI	01 CNTR	Inferred
-0.1189 ± 0.0012	ABELE	97D SPEC	Cold <i>n</i> , polarized
-0.1160 ± 0.0009 ± 0.0011	SCHRECK...	95 TPC	See LIAUD 97
-0.1116 ± 0.0014	EROZOLIM...	91 CNTR	See YEROZOLIMSKY 97
-0.114 ± 0.005	38 EROZOLIM...	79 CNTR	Cold <i>n</i> , polarized
-0.113 ± 0.006	38 KROHN	75 CNTR	Cold <i>n</i> , polarized

- 35 This is the combined result of ABELE 02 and ABELE 97D.
 36 YEROZOLIMSKY 97 makes a correction to the EROZOLIMSKII 91 value.
 37 MOSTOVOI 01 calculates this from its measurement of $\lambda = g_A/g_V$ above.
 38 These results are not corrected for radiative effects and weak magnetism, but the corrections are small compared to the errors.



$\bar{\nu}_e$ ASYMMETRY PARAMETER *B*

This is the neutron-spin antineutrino-momentum correlation coefficient. In the Standard Model, *B* is related to $\lambda \equiv g_A/g_V$ by $B = 2\lambda(\lambda + 1) / (1 + 3\lambda^2)$; this assumes that g_A and g_V are real.

VALUE	DOCUMENT ID	TECN	COMMENT
0.9807 ± 0.0030 OUR AVERAGE			
0.9802 ± 0.0034 ± 0.0036	SCHUMANN	07 CNTR	Cold <i>n</i> , polarized
0.967 ± 0.006 ± 0.010	KREUZ	05 CNTR	Cold <i>n</i> , polarized
0.9801 ± 0.0046	SEREBROV	98 CNTR	Cold <i>n</i> , polarized
0.9894 ± 0.0083	KUZNETSOV	95 CNTR	Cold <i>n</i> , polarized
1.00 ± 0.05	CHRISTENSEN70	CNTR	Cold <i>n</i> , polarized
0.995 ± 0.034	EROZOLIM...	70C CNTR	Cold <i>n</i> , polarized
• • • We do not use the following data for averages, fits, limits, etc. • • •			
0.9876 ± 0.0004	39 MOSTOVOI	01 CNTR	Inferred

- 39 MOSTOVOI 01 calculates this from its measurement of $\lambda = g_A/g_V$ above.

PROTON ASYMMETRY PARAMETER *C*

Describes the correlation between the neutron spin and the proton momentum. In the Standard Model, *C* is related to $\lambda \equiv g_A/g_V$ by $C = -x_c(A + B) = x_c 4\lambda / (1 + 3\lambda^2)$, where $x_c = 0.27484$ is a kinematic factor; this assumes that g_A and g_V are real.

VALUE	DOCUMENT ID	TECN	COMMENT
-0.2377 ± 0.0010 ± 0.0024	SCHUMANN	08 CNTR	Cold <i>n</i> , polarized

$e^- \bar{\nu}_e$ ANGULAR CORRELATION COEFFICIENT *a*

For a review of past experiments and plans for future measurements of the *a* parameter, see WIETFELDT 05. In the Standard Model, *a* is related to $\lambda \equiv g_A/g_V$ by $a = (1 - \lambda^2) / (1 + 3\lambda^2)$; this assumes that g_A and g_V are real.

VALUE	DOCUMENT ID	TECN	COMMENT
-0.103 ± 0.004 OUR AVERAGE			
-0.1054 ± 0.0055	BYRNE	02 SPEC	Proton recoil spectrum
-0.1017 ± 0.0051	STRATOWA	78 CNTR	Proton recoil spectrum
-0.091 ± 0.039	GRIGOREV	68 SPEC	Proton recoil spectrum
• • • We do not use the following data for averages, fits, limits, etc. • • •			
-0.1045 ± 0.0014	40 MOSTOVOI	01 CNTR	Inferred

- 40 MOSTOVOI 01 calculates this from its measurement of $\lambda = g_A/g_V$ above.

Baryon Particle Listings

n

 ϕ_{AV} , PHASE OF g_A RELATIVE TO g_V

Time reversal invariance requires this to be 0 or 180°. This is related to D given in the next data block and $\lambda \equiv g_A/g_V$ by $\sin(\phi_{AV}) = D(1+3\lambda^2)/2\lambda$; this assumes that g_A and g_V are real.

VALUE (°)	DOCUMENT ID	TECN	COMMENT
180.06 ± 0.07 OUR AVERAGE			
180.04 ± 0.09	SOLDNER 04	CNTR	Cold n , polarized
180.08 ± 0.13	LISING 00	CNTR	Polarized >93%
179.71 ± 0.39	EROZOLIM... 78	CNTR	Cold n , polarized
180.35 ± 0.43	EROZOLIM... 74	CNTR	Cold n , polarized
180.14 ± 0.22	STEINBERG 74	CNTR	Cold n , polarized

• • • We do not use the following data for averages, fits, limits, etc. • • •

181.1 ± 1.3	⁴¹ KROPP 74	RVUE	n decay
-------------	------------------------	------	-----------

⁴¹KROPP 74 reviews all data through 1972.

TRIPLE CORRELATION COEFFICIENT D

These are measurements of the component of n spin perpendicular to the decay plane in β decay. Should be zero if T invariance is not violated.

VALUE (units 10^{-4})	DOCUMENT ID	TECN	COMMENT
-4 ± 6 OUR AVERAGE			
-2.8 ± 6.4 ± 3.0	SOLDNER 04	CNTR	Cold n , polarized
-6 ± 12 ± 5	LISING 00	CNTR	Polarized >93%
+22 ± 30	EROZOLIM... 78	CNTR	Cold n , polarized
-27 ± 50	⁴² EROZOLIM... 74	CNTR	Cold n , polarized
-11 ± 17	STEINBERG 74	CNTR	Cold n , polarized

⁴²EROZOLIMSKII 78 says asymmetric proton losses and nonuniform beam polarization may give a systematic error up to 30×10^{-4} , thus increasing the EROZOLIMSKII 74 error to 50×10^{-4} . STEINBERG 74 and STEINBERG 76 estimate these systematic errors to be insignificant in their experiment.

n REFERENCES

We have omitted some papers that have been superseded by later experiments. See our earlier editions.

SCHUMANN 08	PRL 100 151801	M. Schumann <i>et al.</i>	(HEID, ILLG, KARL+)
BAKER 07	PRL 98 149102	C.A. Baker <i>et al.</i>	(RAL, SUSS, ILLG)
BAN 07	PRL 99 161603	G. Ban <i>et al.</i>	(CAEN, JAGL, PSI, JINR+)
LAMOREAUX 07	PRL 98 149101	S.K. Lamoreaux, R. Golub	(YALE, NCAR)
SCHUMANN 07	PRL 99 191803	M. Schumann <i>et al.</i>	(HEID, ILLG, KARL+)
SILENKO 07	PPNL 4 468	A.Ya. Silenko	(Belarussian U.)
BAKER 06	PRL 97 131801	C.A. Baker <i>et al.</i>	(RAL, SUSS, ILLG)
BEREZHIANI 06	PRL 96 081801	Z. Berzhiani, L. Bento	(Aguila U., LISB)
NICO 06	NAT 444 1059	J.S. Nico <i>et al.</i>	(NIST, TULN, MICH, UMD+)
SEVERJINS 06	RMP 78 991	N. Severjins, M. Beck, O. Navilat-Cuncic	(LEUV+)
KREUZ 05	PL B619 263	M. Kreuz <i>et al.</i>	(HEID, ILLG, MANZ, KARL+)
MOHR 05	RMP 77 1	P.J. Mohr, B.N. Taylor	(NIST)
NICO 05	PR C71 055502	J.S. Nico <i>et al.</i>	(NIST, TULN, IND, TENN+)
NICO 05A	ARNPS 55 27	J.S. Nico, W.M. Snow	(NIST)
SCHUMACHER 05	PPNP 55 567	M. Schumacher	(GOET)
SEREBROV 05	PL B605 72	A. Serebrov <i>et al.</i>	(PNPI, JINR, ILLG)
Also	JPG 20 1225	A.P. Serebrov <i>et al.</i>	(PPNP, JINR, ILLG)
WIETFIELDT 05	MPL A20 1783	F.E. Wietfeldt	(TULN)
SOLDNER 04	PL B581 49	T. Soldner <i>et al.</i>	(ILLG, MUNT)
DEWEY 03	PRL 91 152302	M.S. Dewey <i>et al.</i>	(NIST, TULN, IND+)
KOSSERT 03	EPJ A16 259	K. Kossert <i>et al.</i>	(Mainz MAMI Collab.)
Also	PRL 88 162301	K. Kossert <i>et al.</i>	(Mainz MAMI Collab.)
LUNDIN 03	PRL 90 192501	M. Lundin <i>et al.</i>	(NIST)
ABELE 02	PRL 88 211801	H. Abele <i>et al.</i>	(PERKEO-II Collab.)
BECK 02	JETPL 76 332	M. Beck <i>et al.</i>	(LEUV, SUSS, KIAE, PNPI)
Byrne 02	JPG 20 1225	J. Byrne <i>et al.</i>	(TULN)
CHUNG 02B	PR D66 032004	J. Chung <i>et al.</i>	(SOUDAN-2 Collab.)
MOSTOVOI 01	PAN 64 1955	Yu.A. Mostovoi <i>et al.</i>	(KIAE)
Also	Translated from YAF 64 2040		
ARZUMANOV 00	PL B483 15	S. Arzumanov <i>et al.</i>	(KIAE)
GAL 00	PR C61 028201	A. Gal	(KIAE)
KOLB 00	PRL 85 1388	N.R. Kolb <i>et al.</i>	(KIAE)
LAMOREAUX 00	PR D61 051301R	S.K. Lamoreaux, R. Golub	(KIAE)
LEVCHUK 00	NP A674 449	M.I. Levchuk, A.I. L'vov	(BELA, LEBD)
LISING 00	PR C62 055501	L. Lising <i>et al.</i>	(NIST emit Collab.)
HARRIS 99	PRL 82 904	P.G. Harris <i>et al.</i>	(KIAE)
KESSLER 99	PL A255 221	E.G. Kessler Jr <i>et al.</i>	(KIAE)
MOHR 99	JPCRD 28 1713	P.J. Mohr, B.N. Taylor	(NIST)
Also	RMP 72 351	P.J. Mohr, B.N. Taylor	(NIST)
SEREBROV 98	JETP 86 1074	A.P. Serebrov <i>et al.</i>	(KIAE)
Also	Translated from ZETF 113 1963		
ABELE 97D	PL B407 212	H. Abele <i>et al.</i>	(HEIDP, ILLG)
KOPECKY 97	PR C56 2229	S. Kopecky <i>et al.</i>	(KIAE)
LIAUD 97	NP A612 52	P. Liaud <i>et al.</i>	(ILLG, LAPP)
YEROZOLIM... 97	PL B412 240	B.G. Eroozolimsky <i>et al.</i>	(HARV, PNPI, KIAE)
ALTAREV 96	PAN 59 1152	I.S. Altarev <i>et al.</i>	(PNPI)
Also	Translated from YAF 59 1204		
BONDAREN... 96	JETPL 64 416	L.N. Bondarenko <i>et al.</i>	(KIAE)
Also	Translated from ZETFP 64 382		
BYRNE 96	EPL 33 187	J. Byrne <i>et al.</i>	(SUSS, ILLG)
MOSTOVOI 96	PAN 59 968	Yu.A. Mostovoy	(KIAE)
Also	Translated from YAF 59 1013		
NORMAN 96	PR D53 4086	E.B. Norman, J.N. Bahcall, M. Goldhaber	(LBL+)
IGNATOVICH 95	JETPL 62 1	V.K. Ignatovich	(JINR)
Also	Translated from ZETFP 62 3		
KOESTER 95	PR C51 3363	L. Koester <i>et al.</i>	(+)
KOPECKY 95	PR 74 2427	S. Kopecky <i>et al.</i>	(+)
KUZNETSOV 95	PRL 75 794	I.A. Kuznetsov <i>et al.</i>	(PNPI, KIAE, HARV+)
SCHRECK... 95	PL B349 427	K. Schreckenbach <i>et al.</i>	(MUNT, ILLG, LAPP)
BALDO... 94	ZPHY C63 409	M. Baldo-Ceolin <i>et al.</i>	(HEID, ILLG, PADO+)
DIFILIPPO 94	PRL 73 1481	F. Difilippo <i>et al.</i>	(MIT)
Also	PRL 71 1998	V. Natarajan <i>et al.</i>	(MIT)
GOLUB 94	PRPL 237C 1	R. Golub, K. Lamoreaux	(HAHN, WASH)
MAMPE 93	JETPL 57 82	B. Mampe <i>et al.</i>	(KIAE)
Also	Translated from ZETFP 57 77		
ALTAREV 92	PL B276 242	I.S. Altarev <i>et al.</i>	(PNPI)
NEVIZHEV... 92	JETP 75 405	V.V. Nesvizhevsky <i>et al.</i>	(PNPI, JINR)
Also	Translated from ZETF 102 740		
ALBERICO 91	NP A523 488	W.M. Alberico, A. de Pace, M. Pignone	(TORI)
DUBBERS 91	NP A527 239c	D. Dubbers	(ILLG)
Also	EPL 11 195	D. Dubbers, W. Mampe, J. Dohner	(ILLG, HEID)
EROZOLIM... 91	PL B263 33	B.G. Eroozolimsky <i>et al.</i>	(PNPI, KIAE)
Also	SJNP 52 999	B.G. Eroozolimsky <i>et al.</i>	(PNPI, KIAE)
Also	Translated from YAF 52 1583		

EROZOLIM... 91B	SJNP 53 260	B.G. Eroozolimsky, Y.A. Mostovoy	(KIAE)
Also	Translated from YAF 53 418		
SCHMIEDM... 91	PRL 66 1015	J. Schriedmayer <i>et al.</i>	(TUW, ORNL)
WOOLCOCK 91	MPL A6 2579	W.S. Woolcock	(CANB)
ALFIMENKOV 90	JETPL 52 373	V.P. Alfimenkov <i>et al.</i>	(PNPI, JINR)
Also	Translated from ZETFP 52 984		
BALDO... 90	PL B236 95	M. Baldo-Ceolin <i>et al.</i>	(PADO, PAVI, HEIDP+)
BERGER 90	PL B240 237	C. Berger <i>et al.</i>	(FREJUS Collab.)
BRESSI 90	NC 103A 731	G. Bressi <i>et al.</i>	(PAVI, ROMA, MILA)
BYRNE 90	PRL 65 289	J. Byrne <i>et al.</i>	(SUSS, NBS, SCOT, CBNM)
GREEN 90	JPG 16 175	K. Green, D. Thompson	(RAL)
RAMSEY 90	ARNPS 40 1	N.F. Ramsey	(HARV)
ROSE 90	PL B234 460	K.W. Rose <i>et al.</i>	(GOET, MPCM, MANZ)
ROSE 90B	NP A514 621	K.W. Rose <i>et al.</i>	(GOET, MPCM)
SMITH 90	PL B234 191	K.F. Smith <i>et al.</i>	(SUSS, RAL, HARV+)
BRESSI 89	ZPHY C49 175	G. Bressi <i>et al.</i>	(INFN, MILA, PAVI, ROMA)
DOVER 89	NIM A284 13	C.B. Dover, A. Gal, J.M. Richard	(BNL, HEBR+)
KOSSAKOV... 89	NP A503 473	R. Kossakowski <i>et al.</i>	(LAPP, SAVO, ISNG+)
MAMPE 89	PRL 63 593	W. Mampe <i>et al.</i>	(ILLG, RISL, SUSS, URI)
MOHAPATRA 89	NIM A284 1	R.N. Mohapatra	(UMD)
PAUL 89	ZPHY C45 25	W. Paul <i>et al.</i>	(BONN, WUPP, MPH, ILLG)
SCHMIEDM... 89	NIM A284 137	J. Schriedmayer, H. Rauch, P. Rieths	(WIEN)
BAUMANN 88	PR D37 3107	J. Baumann <i>et al.</i>	(BAYR, MUNI, ILLG)
KOESTER 88	ZPHY A329 229	L. Koester, W. Waschowski, J. Meier	(MUNI, MUNT)
LAST 88	PRL 60 995	I. Last <i>et al.</i>	(HEIDP, ILLG, ANL)
SCHMIEDM... 88	PRL 61 1065	J. Schriedmayer, H. Rauch, P. Rieths	(TUW)
Also	PRL 61 2509 (erratum)	J. Schriedmayer, H. Rauch, P. Rieths	(TUW)
SPIVAK 88	JETP 67 1735	P.E. Spivak	(KIAE)
Also	Translated from ZETF 94 1		
COHEN 87	RMP 59 1121	E.R. Cohen, B.N. Taylor	(RIS C, NBS)
ALEKSANDR... 86	SJNP 44 900	Yu.A. Aleksandrov <i>et al.</i>	(KIAE)
Also	Translated from YAF 44 1384		
ALTAREV 86	JETPL 44 460	I.S. Altarev <i>et al.</i>	(PNPI)
Also	Translated from ZETFP 44 364		
BOPP 86	PRL 56 919	P. Bopp <i>et al.</i>	(HEIDP, ANL, ILLG)
Also	ZPHY C37 179	E. Klempf <i>et al.</i>	(HEIDP, ANL, ILLG)
CRESTI 86	PL B177 206	M. Cresti <i>et al.</i>	(PADO)
Also	PL B200 587 (erratum)	M. Cresti <i>et al.</i>	(PADO)
GREENE 86	PRL 56 819	G.L. Greene <i>et al.</i>	(NBS, ILLG)
KOESTER 86	Physica B137 282	L. Koester <i>et al.</i>	(KIAE)
KOSVINTSEV 86	JETPL 44 571	Y.Y. Kosvintsev, V.I. Morozov, G.I. Terekhov	(KIAE)
Also	Translated from ZETFP 44 444		
TAKITA 86	PR D34 902	M. Takita <i>et al.</i>	(KEK, TOKY+)
DOVER 85	PR C31 1423	C.B. Dover, A. Gal, J.M. Richard	(BNL)
FIDECARO 85	PL 156B 122	G. Fidecaro <i>et al.</i>	(CERN, ILLG, PADO+)
PARK 85B	NP B252 261	H.S. Park <i>et al.</i>	(IMB Collab.)
BATTISTONI 84	PL 133B 454	G. Battistoni <i>et al.</i>	(NUSSEX Collab.)
JONES 84	PRL 52 720	T.W. Jones <i>et al.</i>	(IMB Collab.)
PENDLEBURY 84	PL 136B 327	J.M. Pendlebury <i>et al.</i>	(SUSS, HARV, RAL+)
CHERRY 83	PRL 50 1354	M.L. Cherry <i>et al.</i>	(PENN, BNL)
DOVER 83	PR D27 1090	C.B. Dover, A. Gal, J.M. Richard	(BNL)
KABIR 83	PRL 51 231	P.K. Kabir	(HARV)
MOSTOVOY 83	JETPL 37 196	Yu.A. Mostovoy	(KIAE)
Also	Translated from ZETFP 37 162		
ROY 83	PR D28 1770	A. Roy <i>et al.</i>	(TATA)
VAIDYA 83	PR D27 486	S.C. Vaidya <i>et al.</i>	(TATA)
GAEHLER 82	PR D25 2887	R. Gahler, J. Kalus, W. Mampe	(BAYR, ILLG)
GREENE 82	Metrologia 18 93	G.L. Greene <i>et al.</i>	(YALE, HARV, ILLG+)
ALTAREV 81	PL 102B 13	I.S. Altarev <i>et al.</i>	(PNPI)
BARABANOV 80	JETPL 32 359	I.R. Barabanov <i>et al.</i>	(PNPI)
Also	Translated from ZETFP 32 284		
BYRNE 80	PL 92B 274	J. Byrne <i>et al.</i>	(SUSS, RL)
KOSVINTSEV 80	JETPL 31 236	Y.Y. Kosvintsev <i>et al.</i>	(JINR)
Also	Translated from ZETFP 31 257		
MOHAPATRA 80	PRL 44 1316	R.N. Mohapatra, R.E. Marshak	(CUNY, VPI)
ALTAREV 79	JETPL 29 730	I.S. Altarev <i>et al.</i>	(PNPI)
Also	Translated from ZETFP 29 794		
EROZOLIM... 79	SJNP 30 356	B.G. Eroozolimsky <i>et al.</i>	(KIAE)
Also	Translated from YAF 30 692		
NORMAN 79	PRL 43 1226	E.B. Norman, A.G. Seamster	(WASH)
BONDAREN... 78	JETPL 28 303	L.N. Bondarenko <i>et al.</i>	(KIAE)
Also	Translated from ZETFP 28 328		
Also	Smolenice Conf.	P.G. Bondarenko	(KIAE)
EROZOLIM... 78	SJNP 28 48	B.G. Eroozolimsky <i>et al.</i>	(KIAE)
STRATOWA 78	PR D18 3970	C. Stratowa, R. Dobrozemsky, P. Weinzler	(SEIB)
EROZOLIM... 77	JETPL 23 663	B.G. Eroozolimsky <i>et al.</i>	(KIAE)
Also	Translated from ZETFP 23 720		
KOESTER 76	PRL 36 1021	L. Koester <i>et al.</i>	(KIAE)
STEINBERG 76	PR D13 2469	R.I. Steinberg <i>et al.</i>	(YALE, ISNG)
DOBROZE... 75	PR D11 510	R. Dobrozemsky <i>et al.</i>	(SEIB)
KROHN 75	PL 55B 175	V.E. Krohn, G.R. Ringo	(ANL)
EROZOLIM... 74	JETPL 20 345	B.G. Eroozolimsky <i>et al.</i>	(KIAE)
Also	Translated from ZETFP 20 745		
KROPP 74	ZPHY 267 129	H. Kropf, E. Paul	(LINZ)
Also	NP A154 160	H. Paul	(VIEN)
STEINBERG 74	PRL 33 41	R.I. Steinberg <i>et al.</i>	(YALE, ISNG)
COHEN 73	JPCRD 2 664	E.R. Cohen, B.N. Taylor	(RIS C, NBS)
KROHN 73	PR D8 1305	V.E. Krohn, G.R. Ringo	(KIAE)
CHRISTENSEN 72	PR D5 1628	C.J. Christensen <i>et al.</i>	(RISO)
CHRISTENSEN 70	PR C1 1693	C.J. Christensen, V.E. Krohn, G.R. Ringo	(ANL)
EROZOLIM... 70C	PL 35B 351	B.G. Eroozolimsky <i>et al.</i>	(KIAE)
GRIGOREV 68	SJNP 6 239	V.K. Grigoriev <i>et al.</i>	(ITEP)
Also	Translated from YAF 6 329		
KROHN 66	PR 148 1303	V.E. Krohn, G.R. Ringo	(KIAE)
LEE 56	PR 104 254	T.D. Lee, C.N. Yang	(COLU, BNL)

N* AND Δ RESONANCES*I. Introduction**

The excited states of the nucleon have been studied in a large number of formation and production experiments. The conventional (*i.e.*, Breit-Wigner) masses, pole positions, widths,

Table 1. The status of the *N* and Δ resonances. Only those with an overall status of *** or **** are included in the main Baryon Summary Table.

Particle	$L_{2I,2J}$	Overall status	Status as seen in —						
			$N\pi$	$N\eta$	ΛK	ΣK	$\Delta\pi$	$N\rho$	$N\gamma$
<i>N</i> (939) P_{11}	****								
<i>N</i> (1440) P_{11}	****	****	*				***	*	***
<i>N</i> (1520) D_{13}	****	****	***				****	****	****
<i>N</i> (1535) S_{11}	****	****	****	****			*	**	***
<i>N</i> (1650) S_{11}	****	****	*	***	**		***	**	***
<i>N</i> (1675) D_{15}	****	****	*	*			****	*	****
<i>N</i> (1680) F_{15}	****	****	*				****	****	****
<i>N</i> (1700) D_{13}	***	***	*	**	*		**	*	**
<i>N</i> (1710) P_{11}	***	***	**	**	*		**	*	***
<i>N</i> (1720) P_{13}	****	****	*	**	*		*	**	**
<i>N</i> (1900) P_{13}	**	**						*	
<i>N</i> (1990) F_{17}	**	**	*	*	*				*
<i>N</i> (2000) F_{15}	**	**	*	*	*		*	**	
<i>N</i> (2080) D_{13}	**	**	*	*					*
<i>N</i> (2090) S_{11}	*	*							
<i>N</i> (2100) P_{11}	*	*	*						
<i>N</i> (2190) G_{17}	****	****	*	*	*		*	*	
<i>N</i> (2200) D_{15}	**	**	*	*					
<i>N</i> (2220) H_{19}	****	****	*						
<i>N</i> (2250) G_{19}	****	****	*						
<i>N</i> (2600) I_{11}	***	***							
<i>N</i> (2700) K_{113}	**	**							
Δ (1232) P_{33}	****	****	F						****
Δ (1600) P_{33}	***	***	o				***	*	**
Δ (1620) S_{31}	****	****	r				****	****	***
Δ (1700) D_{33}	****	****	b		*		***	**	***
Δ (1750) P_{31}	*	*	i						
Δ (1900) S_{31}	**	**	d		*	*	**	**	*
Δ (1905) F_{35}	****	****	d		*	**	**	**	***
Δ (1910) P_{31}	****	****	e		*	*	*	*	*
Δ (1920) P_{33}	***	***	n		*	**	*	*	*
Δ (1930) D_{35}	***	***			*				**
Δ (1940) D_{33}	*	*	F						
Δ (1950) F_{37}	****	****	o		*	****	*	****	****
Δ (2000) F_{35}	**	**	r			**			
Δ (2150) S_{31}	*	*	b						
Δ (2200) G_{37}	*	*	i						
Δ (2300) H_{39}	**	**	d						
Δ (2350) D_{35}	*	*	d						
Δ (2390) F_{37}	*	*	e						
Δ (2400) G_{39}	**	**	n						
Δ (2420) H_{311}	****	****							*
Δ (2750) I_{313}	**	**							
Δ (2950) K_{315}	**	**							

**** Existence is certain, and properties are at least fairly well explored.
 *** Existence ranges from very likely to certain, but further confirmation is desirable and/or quantum numbers, branching fractions, *etc.* are not well determined.
 ** Evidence of existence is only fair.
 * Evidence of existence is poor.

and elasticities of the *N* and Δ resonances in the Baryon Summary Table come largely from partial-wave analyses of πN total, elastic, and charge-exchange scattering data. Partial-wave analyses have also been performed on much smaller data sets to get $N\eta$, ΛK , and ΣK branching fractions. Other branching

fractions come from isobar-model analyses of $\pi N \rightarrow N\pi\pi$ data. Finally, many $N\gamma$ branching fractions have been determined from photoproduction experiments (see Sec. III).

Table 1 lists all the *N* and Δ entries in the Baryon Listings and gives our evaluation of the status of each, both overall and channel by channel. Only the “established” resonances (overall status 3 or 4 stars) appear in the Baryon Summary Table. We generally consider a resonance to be established only if it has been seen in at least two independent analyses of elastic scattering and if the relevant partial-wave amplitudes do not behave erratically or have large errors.

We have, in this 2006 *Review*, made slight adjustments to our estimates of *N* and Δ masses, widths, and elasticities.

II. Using the *N* and Δ listings

Written 2002 by G. Höhler (University of Karlsruhe) and R.L. Workman, (George Washington University)

In the inelastic region, a resonance is associated with a cluster of poles on different Riemann sheets. If one of these poles is located near the real axis and far enough from branch points, it will be strongly dominant. If one of the final-state particles itself has a strong decay, it is also necessary to consider branch points in the lower half plane that belong to thresholds for two-particle final states; see for example Refs. 3 and 4.

Our Particle Listings and Summary Tables include pole parameters for the *N* and Δ resonances. However, the Breit-Wigner parameters are most often quoted and are used in model-based studies of the baryons and associated reaction dynamics. Problems associated with this choice were discussed in our 2000 edition [5]. Here we just point out that the use of Breit-Wigner parameters for complicated structures, such as the *N*(1440), should be avoided. In this case, the method used in Ref. 4 is suitable for the analysis.

In the search for “missing” quark-model states, indications of new structures occasionally are found. Often these are associated (if possible) with the one- and two-star states listed in Table 1. We caution against this: The status of the one- and two-star states found in the Karlsruhe-Helsinki (KH80) [2] and Carnegie-Mellon/Berkeley (CMB80) [6] fits is now doubtful. Predictions for π^+p spin-rotation parameters from those fits are in significant disagreement with recent ITEP/PNPI measurements [7], whereas the predictions of Ref. 8 are good. This discrepancy has been associated in Ref. 7 with the behavior of a zero trajectory at a “critical point” (see Sec. 2.1.1 of Ref. 2) near a pion lab momentum of 0.8 GeV/c. According to Ref. 7, the effect on the 4-star resonances Δ (1905) and Δ (1950) is small, but the effect on the 3-star resonances Δ (1920) and Δ (1930) is large. For a study of the approximation made in Ref. 7 and of problems with some higher resonances, the detailed treatment of zero trajectories in Ref. 9 is relevant. This problem should also be considered in any multi-channel analysis that uses the KH80 and CMB80 amplitudes as input.

Baryon Particle Listings

N 's and Δ 's, $N(1440)$

III. Electromagnetic interactions

Revised 2003 by R.L. Workman (George Washington University)

Nearly all the entries in the Listings concerning electromagnetic properties of the N and Δ resonances are $N\gamma$ couplings. These couplings, the helicity amplitudes $A_{1/2}$ and $A_{3/2}$, have been obtained in partial-wave analyses of single-pion photoproduction, η photoproduction, and Compton scattering. Most photoproduction analyses have taken the existence, masses, and widths of the resonances from the $\pi N \rightarrow \pi N$ analyses, and have only determined the $N\gamma$ couplings. This approach is only applicable to resonances with a significant $N\pi$ coupling. A brief description of the various methods of analysis of photoproduction data may be found in our 1992 edition [10].

Our Listings omit a number of analyses that are now obsolete. Most of the older results may be found in our 1982 edition [11]. The errors quoted for the couplings in the Listings are calculated in different ways in different analyses and therefore should be used with care. In general, the systematic differences between the analyses caused by using different parameterization schemes are probably more indicative of the true uncertainties than are the quoted errors.

Probably the most reliable analyses, for most resonances, are ARAI 80, CRAWFORD 80, AWAJI 81, FUJII 81, CRAWFORD 83, and ARNDT 96. There is an update to the Crawford analysis [1]. The errors we give on $N\gamma$ couplings are a combination of the stated statistical errors on the analyses and the systematic differences between them. The analyses are given equal weight, except ARNDT 96 is weighted, rather arbitrarily, by a factor of two because its data set is at least 50% larger than those of the other analyses and contains many new high-quality measurements. The $\Delta(1232)$ and $N(1535)$ are special cases and are discussed in the 2002 *Review* [12].

The Baryon Summary Table gives $N\gamma$ branching fractions for those resonances whose couplings are considered to be reasonably well established. The $N\gamma$ partial width Γ_γ is given in terms of the helicity amplitudes $A_{1/2}$ and $A_{3/2}$ by

$$\Gamma_\gamma = \frac{k^2}{\pi} \frac{2M_N}{(2J+1)M_R} [|A_{1/2}|^2 + |A_{3/2}|^2] .$$

Here M_N and M_R are the nucleon and resonance masses, J is the resonance spin, and k is the photon c.m. decay momentum.

See our 2002 *Review* for some further discussion [12].

See our 2004 *Review* for a brief discussion of non- qqq baryon candidates [13], and this *Review* for a note, "Pentaquarks."

References

1. Proceedings of the Workshop on the Physics of Excited Nucleons (NSTAR2001), eds. D. Drechsel and L. Tiator (World Scientific, Singapore, 2001).
2. G. Höhler, Pion-Nucleon Scattering, Landolt-Börnstein Vol. I/9b2 (1983), ed. H. Schopper, Springer Verlag.

3. W.R. Frazier and A.W. Hendry, Phys. Rev. **134**, B1307 (1964).
4. R.E. Cutkosky and S. Wang, Phys. Rev. **D42**, 235 (1990).
5. D.E. Groom *et al.*, Eur. Phys. J. **C15**, 1 (2000).
6. R.E. Cutkosky *et al.*, Baryon 1980, *IV International Conference on Baryon Resonances*, Toronto, ed. N. Isgur, p. 19.
7. I.G. Alekseev *et al.*, Phys. Rev. **C55**, 2049 (1997); Phys. Lett. **B485**, 32 (2000); Eur. Phys. J. **A12**, 117 (2001).
8. R.A. Arndt *et al.*, Phys. Rev. **C52**, 2120 (1995).
9. I. Sabba-Stefanescu, Progress of Physics **35**, 573 (1987).
10. K. Hikasa *et al.*, Phys. Rev. **D45**, S1 (1992).
11. M. Roos *et al.*, Phys. Lett. **B111**, 1 (1982).
12. K. Hagiwara *et al.*, Phys. Rev. **D66**, 010001 (2002).
13. S. Eidelman *et al.*, Phys. Lett. **B592**, 1 (2004).

$N(1440) P_{11}$

$$I(J^P) = \frac{1}{2}(\frac{1}{2}^+) \text{ Status: } ***$$

Most of the results published before 1975 were last included in our 1982 edition, Physics Letters **111B** 1 (1982). Some further obsolete results published before 1984 were last included in our 2006 edition, Journal of Physics, G **33** 1 (2006).

$N(1440)$ BREIT-WIGNER MASS

VALUE (MeV)	DOCUMENT ID	TECN	COMMENT
1420 to 1470 (≈ 1440) OUR ESTIMATE			
1485.0 \pm 1.2	ARNDT	06	DPWA $\pi N \rightarrow \pi N, \eta N$
1462 \pm 10	MANLEY	92	IPWA $\pi N \rightarrow \pi N \& N\pi\pi$
1440 \pm 30	CUTKOSKY	80	IPWA $\pi N \rightarrow \pi N$
1410 \pm 12	HOEHLER	79	IPWA $\pi N \rightarrow \pi N$
••• We do not use the following data for averages, fits, limits, etc. •••			
1436 \pm 15	SARANTSEV	08	DPWA Multichannel
1468.0 \pm 4.5	ARNDT	04	DPWA $\pi N \rightarrow \pi N, \eta N$
1518 \pm 5	PENNER	02c	DPWA Multichannel
1479 \pm 80	VRANA	00	DPWA Multichannel
1463 \pm 7	ARNDT	96	IPWA $\gamma N \rightarrow \pi N$
1467	ARNDT	95	DPWA $\pi N \rightarrow N\pi$
1421 \pm 18	BATINIC	95	DPWA $\pi N \rightarrow N\pi, N\eta$
1465	LI	93	IPWA $\gamma N \rightarrow \pi N$
1471	CUTKOSKY	90	IPWA $\pi N \rightarrow \pi N$
1380	¹ LONGACRE	77	IPWA $\pi N \rightarrow N\pi\pi$
1390	² LONGACRE	75	IPWA $\pi N \rightarrow N\pi\pi$

$N(1440)$ BREIT-WIGNER WIDTH

VALUE (MeV)	DOCUMENT ID	TECN	COMMENT
200 to 450 (≈ 300) OUR ESTIMATE			
284 \pm 18	ARNDT	06	DPWA $\pi N \rightarrow \pi N, \eta N$
391 \pm 34	MANLEY	92	IPWA $\pi N \rightarrow \pi N \& N\pi\pi$
340 \pm 70	CUTKOSKY	80	IPWA $\pi N \rightarrow \pi N$
135 \pm 10	HOEHLER	79	IPWA $\pi N \rightarrow \pi N$
••• We do not use the following data for averages, fits, limits, etc. •••			
335 \pm 40	SARANTSEV	08	DPWA Multichannel
360 \pm 26	ARNDT	04	DPWA $\pi N \rightarrow \pi N, \eta N$
668 \pm 41	PENNER	02c	DPWA Multichannel
490 \pm 120	VRANA	00	DPWA Multichannel
360 \pm 20	ARNDT	96	IPWA $\gamma N \rightarrow \pi N$
440	ARNDT	95	DPWA $\pi N \rightarrow N\pi$
250 \pm 63	BATINIC	95	DPWA $\pi N \rightarrow N\pi, N\eta$
315	LI	93	IPWA $\gamma N \rightarrow \pi N$
545 \pm 170	CUTKOSKY	90	IPWA $\pi N \rightarrow \pi N$
200	¹ LONGACRE	77	IPWA $\pi N \rightarrow N\pi\pi$
200	² LONGACRE	75	IPWA $\pi N \rightarrow N\pi\pi$

$N(1440)$ POLE POSITION

REAL PART	DOCUMENT ID	TECN	COMMENT
VALUE (MeV)			
1350 to 1380 (≈ 1365) OUR ESTIMATE			
1359	³ ARNDT	06	DPWA $\pi N \rightarrow \pi N, \eta N$
1385	⁴ HOEHLER	93	SPED $\pi N \rightarrow \pi N$
1375 \pm 30	CUTKOSKY	80	IPWA $\pi N \rightarrow \pi N$

See key on page 373

Baryon Particle Listings

N(1440)

••• We do not use the following data for averages, fits, limits, etc. •••

1371 ± 7	SARANTSEV	08	DPWA	Multichannel
1357	5 ARNDT	04	DPWA	$\pi N \rightarrow \pi N, \eta N$
1383	VRANA	00	DPWA	Multichannel
1346	6 ARNDT	95	DPWA	$\pi N \rightarrow N\pi$
1360	7 ARNDT	91	DPWA	$\pi N \rightarrow \pi N$ Soln SM90
1370	CUTKOSKY	90	IPWA	$\pi N \rightarrow \pi N$
1381 or 1379	8 LONGACRE	78	IPWA	$\pi N \rightarrow N\pi\pi$
1360 or 1333	1 LONGACRE	77	IPWA	$\pi N \rightarrow N\pi\pi$

-2xIMAGINARY PART

VALUE (MeV)	DOCUMENT ID	TECN	COMMENT
160 to 220 (≈ 190) OUR ESTIMATE			
162	3 ARNDT	06	DPWA $\pi N \rightarrow \pi N, \eta N$
164	4 HOEHLER	93	SPED $\pi N \rightarrow \pi N$
180 ± 40	CUTKOSKY	80	IPWA $\pi N \rightarrow \pi N$
••• We do not use the following data for averages, fits, limits, etc. •••			
192 ± 20	SARANTSEV	08	DPWA Multichannel
160	5 ARNDT	04	DPWA $\pi N \rightarrow \pi N, \eta N$
316	VRANA	00	DPWA Multichannel
176	6 ARNDT	95	DPWA $\pi N \rightarrow N\pi$
252	7 ARNDT	91	DPWA $\pi N \rightarrow \pi N$ Soln SM90
228	CUTKOSKY	90	IPWA $\pi N \rightarrow \pi N$
209 or 210	8 LONGACRE	78	IPWA $\pi N \rightarrow N\pi\pi$
167 or 234	1 LONGACRE	77	IPWA $\pi N \rightarrow N\pi\pi$

N(1440) ELASTIC POLE RESIDUE

MODULUS |r|

VALUE (MeV)	DOCUMENT ID	TECN	COMMENT
38	3 ARNDT	06	DPWA $\pi N \rightarrow \pi N, \eta N$
40	HOEHLER	93	SPED $\pi N \rightarrow \pi N$
52 ± 5	CUTKOSKY	80	IPWA $\pi N \rightarrow \pi N$
••• We do not use the following data for averages, fits, limits, etc. •••			
36	5 ARNDT	04	DPWA $\pi N \rightarrow \pi N, \eta N$
42	6 ARNDT	95	DPWA $\pi N \rightarrow N\pi$
109	7 ARNDT	91	DPWA $\pi N \rightarrow \pi N$ Soln SM90
74	CUTKOSKY	90	IPWA $\pi N \rightarrow \pi N$

PHASE θ

VALUE (°)	DOCUMENT ID	TECN	COMMENT
-98	3 ARNDT	06	DPWA $\pi N \rightarrow \pi N, \eta N$
-100 ± 35	CUTKOSKY	80	IPWA $\pi N \rightarrow \pi N$
••• We do not use the following data for averages, fits, limits, etc. •••			
-102	5 ARNDT	04	DPWA $\pi N \rightarrow \pi N, \eta N$
-101	6 ARNDT	95	DPWA $\pi N \rightarrow N\pi$
-93	7 ARNDT	91	DPWA $\pi N \rightarrow \pi N$ Soln SM90
-84	CUTKOSKY	90	IPWA $\pi N \rightarrow \pi N$

N(1440) DECAY MODES

The following branching fractions are our estimates, not fits or averages.

Mode	Fraction (Γ_i/Γ)
Γ_1 $N\pi$	0.55 to 0.75
Γ_2 $N\eta$	
Γ_3 $N\pi\pi$	30-40 %
Γ_4 $\Delta\pi$	20-30 %
Γ_5 $\Delta(1232)\pi, P\text{-wave}$	
Γ_6 $N\rho$	<8 %
Γ_7 $N\rho, S=1/2, P\text{-wave}$	
Γ_8 $N\rho, S=3/2, P\text{-wave}$	
Γ_9 $N(\pi\pi)_{S\text{-wave}}^{J=0}$	5-10 %
Γ_{10} $p\gamma$	0.035-0.048 %
Γ_{11} $p\gamma, \text{helicity}=1/2$	0.035-0.048 %
Γ_{12} $n\gamma$	0.009-0.032 %
Γ_{13} $n\gamma, \text{helicity}=1/2$	0.009-0.032 %

N(1440) BRANCHING RATIOS

$\Gamma(N\pi)/\Gamma_{\text{total}}$	DOCUMENT ID	TECN	COMMENT
0.55 to 0.75 OUR ESTIMATE			
0.787 ± 0.016	ARNDT	06	DPWA $\pi N \rightarrow \pi N, \eta N$
0.69 ± 0.03	MANLEY	92	IPWA $\pi N \rightarrow \pi N \& N\pi\pi$
0.68 ± 0.04	CUTKOSKY	80	IPWA $\pi N \rightarrow \pi N$
0.51 ± 0.05	HOEHLER	79	IPWA $\pi N \rightarrow \pi N$
••• We do not use the following data for averages, fits, limits, etc. •••			
0.750 ± 0.024	ARNDT	04	DPWA $\pi N \rightarrow \pi N, \eta N$
0.57 ± 0.01	PENNER	02c	DPWA Multichannel
0.72 ± 0.05	VRANA	00	DPWA Multichannel
0.68	ARNDT	95	DPWA $\pi N \rightarrow N\pi$
0.56 ± 0.08	BATINIC	95	DPWA $\pi N \rightarrow N\pi, N\eta$

$\Gamma(N\eta)/\Gamma_{\text{total}}$	DOCUMENT ID	TECN	COMMENT
0.00 ± 0.01	VRANA	00	DPWA Multichannel

Note: Signs of couplings from $\pi N \rightarrow N\pi\pi$ analyses were changed in the 1986 edition to agree with the baryon-first convention; the overall phase ambiguity is resolved by choosing a negative sign for the $\Delta(1620) S_{31}$ coupling to $\Delta(1232)\pi$.

$(\Gamma_i\Gamma_f)^{1/2}/\Gamma_{\text{total}}$ in $N\pi \rightarrow N(1440) \rightarrow \Delta(1232)\pi, P\text{-wave}$	DOCUMENT ID	TECN	COMMENT
+0.37 to +0.41 OUR ESTIMATE			
+0.39 ± 0.02	MANLEY	92	IPWA $\pi N \rightarrow \pi N \& N\pi\pi$
+0.41	1,9 LONGACRE	77	IPWA $\pi N \rightarrow N\pi\pi$
+0.37	2 LONGACRE	75	IPWA $\pi N \rightarrow N\pi\pi$

$\Gamma(\Delta(1232)\pi, P\text{-wave})/\Gamma_{\text{total}}$	DOCUMENT ID	TECN	COMMENT
0.16 ± 0.01	VRANA	00	DPWA Multichannel

$(\Gamma_i\Gamma_f)^{1/2}/\Gamma_{\text{total}}$ in $N\pi \rightarrow N(1440) \rightarrow N\rho, S=1/2, P\text{-wave}$	DOCUMENT ID	TECN	COMMENT
±0.07 to ±0.25 OUR ESTIMATE			
-0.11	1,9 LONGACRE	77	IPWA $\pi N \rightarrow N\pi\pi$
+0.23	2 LONGACRE	75	IPWA $\pi N \rightarrow N\pi\pi$

$\Gamma(N\rho, S=1/2, P\text{-wave})/\Gamma_{\text{total}}$	DOCUMENT ID	TECN	COMMENT
0.00 ± 0.01	VRANA	00	DPWA Multichannel

$(\Gamma_i\Gamma_f)^{1/2}/\Gamma_{\text{total}}$ in $N\pi \rightarrow N(1440) \rightarrow N\rho, S=3/2, P\text{-wave}$	DOCUMENT ID	TECN	COMMENT
+0.18	1,9 LONGACRE	77	IPWA $\pi N \rightarrow N\pi\pi$

$(\Gamma_i\Gamma_f)^{1/2}/\Gamma_{\text{total}}$ in $N\pi \rightarrow N(1440) \rightarrow N(\pi\pi)_{S\text{-wave}}^{J=0}$	DOCUMENT ID	TECN	COMMENT
±0.17 to ±0.25 OUR ESTIMATE			
+0.24 ± 0.03	MANLEY	92	IPWA $\pi N \rightarrow \pi N \& N\pi\pi$
-0.18	1,9 LONGACRE	77	IPWA $\pi N \rightarrow N\pi\pi$
-0.23	2 LONGACRE	75	IPWA $\pi N \rightarrow N\pi\pi$

$\Gamma(N(\pi\pi)_{S\text{-wave}}^{J=0})/\Gamma_{\text{total}}$	DOCUMENT ID	TECN	COMMENT
0.12 ± 0.01	VRANA	00	DPWA Multichannel

N(1440) PHOTON DECAY AMPLITUDES

Papers on γN amplitudes predating 1981 may be found in our 2006 edition, Journal of Physics, G 33 1 (2006).

N(1440) → p γ , helicity-1/2 amplitude A_{1/2}

VALUE (GeV ^{-1/2})	DOCUMENT ID	TECN	COMMENT
-0.065 ± 0.004 OUR ESTIMATE			
-0.051 ± 0.002	DUGGER	07	DPWA $\gamma N \rightarrow \pi N$
-0.063 ± 0.005	ARNDT	96	IPWA $\gamma N \rightarrow \pi N$
-0.069 ± 0.018	CRAWFORD	83	IPWA $\gamma N \rightarrow \pi N$
-0.063 ± 0.008	AWAJI	81	DPWA $\gamma N \rightarrow \pi N$
••• We do not use the following data for averages, fits, limits, etc. •••			
-0.061	DRECHSEL	07	DPWA $\gamma N \rightarrow \pi N$
-0.087	PENNER	02d	DPWA Multichannel
-0.085 ± 0.003	LI	93	IPWA $\gamma N \rightarrow \pi N$
-0.129	10 WADA	84	DPWA Compton scattering

N(1440) → n γ , helicity-1/2 amplitude A_{1/2}

VALUE (GeV ^{-1/2})	DOCUMENT ID	TECN	COMMENT
+0.040 ± 0.010 OUR ESTIMATE			
0.045 ± 0.015	ARNDT	96	IPWA $\gamma N \rightarrow \pi N$
0.037 ± 0.010	AWAJI	81	DPWA $\gamma N \rightarrow \pi N$
0.030 ± 0.003	FUJII	81	DPWA $\gamma N \rightarrow \pi N$
••• We do not use the following data for averages, fits, limits, etc. •••			
0.054	DRECHSEL	07	DPWA $\gamma N \rightarrow \pi N$
0.121	PENNER	02d	DPWA Multichannel
0.085 ± 0.006	LI	93	IPWA $\gamma N \rightarrow \pi N$

Baryon Particle Listings

 $N(1440)$, $N(1520)$ $N(1440)$ FOOTNOTES

- ¹ LONGACRE 77 pole positions are from a search for poles in the unitarized T-matrix; the first (second) value uses, in addition to $\pi N \rightarrow N\pi\pi$ data, elastic amplitudes from a Saclay (CERN) partial-wave analysis. The other LONGACRE 77 values are from eyeball fits with Breit-Wigner circles to the T-matrix amplitudes.
- ² From method II of LONGACRE 75: eyeball fits with Breit-Wigner circles to the T-matrix amplitudes.
- ³ ARNDT 06 also finds a second-sheet pole with real part = 1388 MeV, $-2 \times$ imaginary part = 165 MeV, and residue with modulus 86 MeV and phase = -46 degrees.
- ⁴ See HOEHLER 93 for a detailed discussion of the evidence for and the pole parameters of N and Δ resonances as determined from Argand diagrams of πN elastic partial-wave amplitudes and from plots of the speeds with which the amplitudes traverse the diagrams.
- ⁵ ARNDT 04 also finds a second-sheet pole with real part = 1385 MeV, $-2 \times$ imaginary part = 166 MeV, and residue with modulus 82 MeV and phase = -51° .
- ⁶ ARNDT 95 also finds a second-sheet pole with real part = 1383 MeV, $-2 \times$ imaginary part = 210 MeV, and residue with modulus 92 MeV and phase = -54° .
- ⁷ ARNDT 91 (Soln SM90) also finds a second-sheet pole with real part = 1413 MeV, $-2 \times$ imaginary part = 256 MeV, and residue = $(78-153i)$ MeV.
- ⁸ LONGACRE 78 values are from a search for poles in the unitarized T-matrix. The first (second) value uses, in addition to $\pi N \rightarrow N\pi\pi$ data, elastic amplitudes from a Saclay (CERN) partial-wave analysis.
- ⁹ LONGACRE 77 considers this coupling to be well determined.
- ¹⁰ WADA 84 is inconsistent with other analyses; see the Note on N and Δ Resonances.

 $N(1440)$ REFERENCES

For early references, see Physics Letters **111B** 1 (1982).

Author	Year	Reference	Author	Year	Reference
SARANTSEV	08	PL B659 94	A.V. Sarantsev et al.	(CB-ELSA/A2-TAPS Collab.)	
DRECHSEL	07	EPJ A34 69	D. Drechsel, S.S. Kamalov, L. Tiator	(MAIN Z, JINR)	
DUGGER	07	PR C76 025211	M. Dugger et al.	(Jefferson Lab CLAS Collab.)	
ARNDT	06	PR C74 045205	R.A. Arndt et al.	(GWU)	
PDG	06	JPG 33 1	W.-M. Yao et al.	(PDG Collab.)	
ARNDT	04	PR C69 035213	R.A. Arndt et al.	(GWU, TRIU)	
PENNER	02C	PR C66 055211	G. Penner, U. Mosel	(GIES)	
PENNER	02D	PR C66 055212	G. Penner, U. Mosel	(GIES)	
VRANA	00	PRPL 328 181	T.P. Vrana, S.A. Dytman, T.-S.H. Lee	(PITT-)	
ARNDT	96	PR C53 430	R.A. Arndt, I.I. Strakovsky, R.L. Workman	(VPI)	
ARNDT	95	PR C52 2120	R.A. Arndt et al.	(VPI, BRCO)	
BATINIC	95	PR C51 2310	M. Batinic et al.	(BOSK, UCLA)	
Also		PR C57 1004 (erratum)	M. Batinic et al.		
HOEHLER	93	πN Newsletter 9 1	G. Hohlner	(KARL)	
LI	93	PR C47 2759	Z.J. Li et al.	(VPI)	
MANLEY	92	PR D45 4002	D.M. Manley, E.M. Saleski	(KENT) IJP	
Also		PR D30 904	D.M. Manley et al.	(VPI)	
ARNDT	91	PR D43 2131	R.A. Arndt et al.	(VPI, TELE) IJP	
CUTKOSKY	90	PR D42 235	R.E. Cutkosky et al.	(CMU)	
WADA	84	NP B247 313	Y. Wada et al.	(INUS)	
CRAWFORD	83	NP B211 1	R.L. Crawford, W.T. Morton	(GLAS)	
PDG	82	PL 111B 1	M. Roos et al.	(HELS, CIT, CERN)	
AWAJI	81	Bonn Conf. 352	N. Awaji, R. Kajikawa	(NAGO)	
Also		NP B197 365	K. Fujii et al.	(NAGO)	
FUJII	81	NP B187 53	K. Fujii et al.	(NAGO, OSAK)	
CUTKOSKY	80	Toronto Conf. 19	R.E. Cutkosky et al.	(CMU, LBL) IJP	
Also		PR D20 2839	R.E. Cutkosky et al.	(KARL) IJP	
HOEHLER	79	PDAT 12-1	G. Hohlner et al.	(KARL) IJP	
Also		Toronto Conf. 3	R. Koch	(KARL) IJP	
LONGACRE	78	PR D17 1795	R.S. Longacre et al.	(LBL, SLAC)	
LONGACRE	77	NP B122 483	J. Dolbeau et al.	(SACL) IJP	
Also		NP B108 365	J. Dolbeau et al.	(SACL) IJP	
LONGACRE	75	PL 55B 415	R.S. Longacre et al.	(LBL, SLAC) IJP	

 $N(1520) D_{13}$

$$I(J^P) = \frac{1}{2}(\frac{3}{2}^-) \text{ Status: } ***$$

Most of the results published before 1975 were last included in our 1982 edition, Physics Letters **111B** 1 (1982). Some further obsolete results published before 1984 were last included in our 2006 edition, Journal of Physics, G **33** 1 (2006).

 $N(1520)$ BREIT-WIGNER MASS

VALUE (MeV)	DOCUMENT ID	TECN	COMMENT
1515 to 1525 (≈ 1520) OUR ESTIMATE			
1514.5 \pm 0.2	ARNDT 06	DPWA	$\pi N \rightarrow \pi N, \eta N$
1524 \pm 4	MANLEY 92	IPWA	$\pi N \rightarrow \pi N \& N\pi\pi$
1525 \pm 10	CUTKOSKY 80	IPWA	$\pi N \rightarrow \pi N$
1519 \pm 4	HOEHLER 79	IPWA	$\pi N \rightarrow \pi N$
• • • We do not use the following data for averages, fits, limits, etc. • • •			
1520 \pm 10	THOMA 08	DPWA	Multichannel
1516.3 \pm 0.8	ARNDT 04	DPWA	$\pi N \rightarrow \pi N, \eta N$
1509 \pm 1	PENNER 02C	DPWA	Multichannel
1518 \pm 3	VRANA 00	DPWA	Multichannel
1516 \pm 10	ARNDT 96	IPWA	$\gamma N \rightarrow \pi N$
1515	ARNDT 95	DPWA	$\pi N \rightarrow N\pi$
1526 \pm 18	BATINIC 95	DPWA	$\pi N \rightarrow N\pi, N\eta$
1510	LI 93	IPWA	$\gamma N \rightarrow \pi N$
1510	¹ LONGACRE 77	IPWA	$\pi N \rightarrow N\pi\pi$
1520	² LONGACRE 75	IPWA	$\pi N \rightarrow N\pi\pi$

 $N(1520)$ BREIT-WIGNER WIDTH

VALUE (MeV)	DOCUMENT ID	TECN	COMMENT
100 to 125 (≈ 115) OUR ESTIMATE			
103.6 \pm 0.4	ARNDT 06	DPWA	$\pi N \rightarrow \pi N, \eta N$
124 \pm 8	MANLEY 92	IPWA	$\pi N \rightarrow \pi N \& N\pi\pi$
120 \pm 15	CUTKOSKY 80	IPWA	$\pi N \rightarrow \pi N$
114 \pm 7	HOEHLER 79	IPWA	$\pi N \rightarrow \pi N$
• • • We do not use the following data for averages, fits, limits, etc. • • •			
125 \pm 15	THOMA 08	DPWA	Multichannel
98.6 \pm 2.6	ARNDT 04	DPWA	$\pi N \rightarrow \pi N, \eta N$
100 \pm 2	PENNER 02C	DPWA	Multichannel
124 \pm 4	VRANA 00	DPWA	Multichannel
106 \pm 4	ARNDT 96	IPWA	$\gamma N \rightarrow \pi N$
106	ARNDT 95	DPWA	$\pi N \rightarrow N\pi$
143 \pm 32	BATINIC 95	DPWA	$\pi N \rightarrow N\pi, N\eta$
120	LI 93	IPWA	$\gamma N \rightarrow \pi N$
110	¹ LONGACRE 77	IPWA	$\pi N \rightarrow N\pi\pi$
150	² LONGACRE 75	IPWA	$\pi N \rightarrow N\pi\pi$

 $N(1520)$ POLE POSITION

REAL PART

VALUE (MeV)	DOCUMENT ID	TECN	COMMENT
1505 to 1515 (≈ 1510) OUR ESTIMATE			
1515	ARNDT 06	DPWA	$\pi N \rightarrow \pi N, \eta N$
1510	³ HOEHLER 93	ARGD	$\pi N \rightarrow \pi N$
1510 \pm 5	CUTKOSKY 80	IPWA	$\pi N \rightarrow \pi N$
• • • We do not use the following data for averages, fits, limits, etc. • • •			
1509 \pm 7	THOMA 08	DPWA	Multichannel
1514	ARNDT 04	DPWA	$\pi N \rightarrow \pi N, \eta N$
1504	VRANA 00	DPWA	Multichannel
1515	ARNDT 95	DPWA	$\pi N \rightarrow N\pi$
1511	ARNDT 91	DPWA	$\pi N \rightarrow \pi N$ Soln SM90
1514 or 1511	⁴ LONGACRE 78	IPWA	$\pi N \rightarrow N\pi\pi$
1508 or 1505	¹ LONGACRE 77	IPWA	$\pi N \rightarrow N\pi\pi$

 $-2 \times$ IMAGINARY PART

VALUE (MeV)	DOCUMENT ID	TECN	COMMENT
105 to 120 (≈ 110) OUR ESTIMATE			
113	ARNDT 06	DPWA	$\pi N \rightarrow \pi N, \eta N$
120	³ HOEHLER 93	ARGD	$\pi N \rightarrow \pi N$
114 \pm 10	CUTKOSKY 80	IPWA	$\pi N \rightarrow \pi N$
• • • We do not use the following data for averages, fits, limits, etc. • • •			
113 \pm 12	THOMA 08	DPWA	Multichannel
102	ARNDT 04	DPWA	$\pi N \rightarrow \pi N, \eta N$
112	VRANA 00	DPWA	Multichannel
110	ARNDT 95	DPWA	$\pi N \rightarrow N\pi$
108	ARNDT 91	DPWA	$\pi N \rightarrow \pi N$ Soln SM90
146 or 137	⁴ LONGACRE 78	IPWA	$\pi N \rightarrow N\pi\pi$
109 or 107	¹ LONGACRE 77	IPWA	$\pi N \rightarrow N\pi\pi$

 $N(1520)$ ELASTIC POLE RESIDUEMODULUS $|r|$

VALUE (MeV)	DOCUMENT ID	TECN	COMMENT
38	ARNDT 06	DPWA	$\pi N \rightarrow \pi N, \eta N$
32	HOEHLER 93	ARGD	$\pi N \rightarrow \pi N$
35 \pm 2	CUTKOSKY 80	IPWA	$\pi N \rightarrow \pi N$
• • • We do not use the following data for averages, fits, limits, etc. • • •			
35	ARNDT 04	DPWA	$\pi N \rightarrow \pi N, \eta N$
34	ARNDT 95	DPWA	$\pi N \rightarrow N\pi$
33	ARNDT 91	DPWA	$\pi N \rightarrow \pi N$ Soln SM90

PHASE θ

VALUE ($^\circ$)	DOCUMENT ID	TECN	COMMENT
-5	ARNDT 06	DPWA	$\pi N \rightarrow \pi N, \eta N$
-8	HOEHLER 93	ARGD	$\pi N \rightarrow \pi N$
-12 \pm 5	CUTKOSKY 80	IPWA	$\pi N \rightarrow \pi N$
• • • We do not use the following data for averages, fits, limits, etc. • • •			
-6	ARNDT 04	DPWA	$\pi N \rightarrow \pi N, \eta N$
7	ARNDT 95	DPWA	$\pi N \rightarrow N\pi$
-10	ARNDT 91	DPWA	$\pi N \rightarrow \pi N$ Soln SM90

 $N(1520)$ DECAY MODES

The following branching fractions are our estimates, not fits or averages.

Mode	Fraction (Γ_i/Γ)
Γ_1 $N\pi$	0.55 to 0.65
Γ_2 $N\eta$	$(2.3 \pm 0.4) \times 10^{-3}$
Γ_3 $N\pi\pi$	40-50 %
Γ_4 $\Delta\pi$	15-25 %
Γ_5 $\Delta(1232)\pi$, S-wave	5-12 %
Γ_6 $\Delta(1232)\pi$, D-wave	10-14 %

See key on page 373

Baryon Particle Listings

$N(1520)$

Γ_7	$N\rho$	15–25 %
Γ_8	$N\rho, S=1/2, D\text{-wave}$	
Γ_9	$N\rho, S=3/2, S\text{-wave}$	
Γ_{10}	$N\rho, S=3/2, D\text{-wave}$	
Γ_{11}	$N(\pi\pi)_{S=0}^{J=0}$	<8 %
Γ_{12}	$p\gamma$	0.46–0.56 %
Γ_{13}	$p\gamma, \text{helicity}=1/2$	0.001–0.034 %
Γ_{14}	$p\gamma, \text{helicity}=3/2$	0.44–0.53 %
Γ_{15}	$n\gamma$	0.30–0.53 %
Γ_{16}	$n\gamma, \text{helicity}=1/2$	0.04–0.10 %
Γ_{17}	$n\gamma, \text{helicity}=3/2$	0.25–0.45 %

$N(1520)$ BRANCHING RATIOS

$\Gamma(N\pi)/\Gamma_{\text{total}}$	DOCUMENT ID	TECN	COMMENT	Γ_1/Γ
0.55 to 0.65 OUR ESTIMATE				
0.632 ± 0.001	ARNDT 06	DPWA	$\pi N \rightarrow \pi N, \eta N$	
0.59 ± 0.03	MANLEY 92	IPWA	$\pi N \rightarrow \pi N \& N\pi\pi$	
0.58 ± 0.03	CUTKOSKY 80	IPWA	$\pi N \rightarrow \pi N$	
0.54 ± 0.03	HOEHLER 79	IPWA	$\pi N \rightarrow \pi N$	
• • • We do not use the following data for averages, fits, limits, etc. • • •				
0.58 ± 0.08	THOMA 08	DPWA	Multichannel	
0.640 ± 0.005	ARNDT 04	DPWA	$\pi N \rightarrow \pi N, \eta N$	
0.56 ± 0.01	PENNER 02c	DPWA	Multichannel	
0.63 ± 0.02	VRANA 00	DPWA	Multichannel	
0.61	ARNDT 95	DPWA	$\pi N \rightarrow N\pi$	
0.46 ± 0.06	BATINIC 95	DPWA	$\pi N \rightarrow N\pi, N\eta$	

$\Gamma(N\eta)/\Gamma_{\text{total}}$	DOCUMENT ID	TECN	COMMENT	Γ_2/Γ
0.0023 ± 0.0004 OUR AVERAGE				
0.0023 ± 0.0004	PENNER 02c	DPWA	Multichannel	
0.00 ± 0.01	VRANA 00	DPWA	Multichannel	
• • • We do not use the following data for averages, fits, limits, etc. • • •				
0.002 ± 0.001	THOMA 08	DPWA	Multichannel	
0.0008 to 0.0012	ARNDT 05	DPWA	Multichannel	
0.0008 ± 0.0001	TIATOR 99	DPWA	$\gamma p \rightarrow p\eta$	
0.001 ± 0.002	BATINIC 95	DPWA	$\pi N \rightarrow N\pi, N\eta$	

Note: Signs of couplings from $\pi N \rightarrow N\pi\pi$ analyses were changed in the 1986 edition to agree with the baryon-first convention; the overall phase ambiguity is resolved by choosing a negative sign for the $\Delta(1620) S_{31}$ coupling to $\Delta(1232)\pi$.

$(\Gamma_1\Gamma_7)^{1/2}/\Gamma_{\text{total}}$ in $N\pi \rightarrow N(1520) \rightarrow \Delta(1232)\pi, S\text{-wave}$	DOCUMENT ID	TECN	COMMENT	$(\Gamma_1\Gamma_5)^{1/2}/\Gamma$
-0.26 to -0.20 OUR ESTIMATE				
-0.18 ± 0.05	MANLEY 92	IPWA	$\pi N \rightarrow \pi N \& N\pi\pi$	
-0.26	^{1,5} LONGACRE 77	IPWA	$\pi N \rightarrow N\pi\pi$	
-0.24	² LONGACRE 75	IPWA	$\pi N \rightarrow N\pi\pi$	

$\Gamma(\Delta(1232)\pi, S\text{-wave})/\Gamma_{\text{total}}$	DOCUMENT ID	TECN	COMMENT	Γ_5/Γ
0.15 ± 0.02	VRANA 00	DPWA	Multichannel	
• • • We do not use the following data for averages, fits, limits, etc. • • •				
0.12 ± 0.04	THOMA 08	DPWA	Multichannel	

$(\Gamma_1\Gamma_7)^{1/2}/\Gamma_{\text{total}}$ in $N\pi \rightarrow N(1520) \rightarrow \Delta(1232)\pi, D\text{-wave}$	DOCUMENT ID	TECN	COMMENT	$(\Gamma_1\Gamma_6)^{1/2}/\Gamma$
-0.28 to -0.24 OUR ESTIMATE				
-0.29 ± 0.03	MANLEY 92	IPWA	$\pi N \rightarrow \pi N \& N\pi\pi$	
-0.21	^{1,5} LONGACRE 77	IPWA	$\pi N \rightarrow N\pi\pi$	
-0.30	² LONGACRE 75	IPWA	$\pi N \rightarrow N\pi\pi$	

$\Gamma(\Delta(1232)\pi, D\text{-wave})/\Gamma_{\text{total}}$	DOCUMENT ID	TECN	COMMENT	Γ_6/Γ
0.11 ± 0.02	VRANA 00	DPWA	Multichannel	
• • • We do not use the following data for averages, fits, limits, etc. • • •				
0.14 ± 0.05	THOMA 08	DPWA	Multichannel	

$(\Gamma_1\Gamma_7)^{1/2}/\Gamma_{\text{total}}$ in $N\pi \rightarrow N(1520) \rightarrow N\rho, S=3/2, S\text{-wave}$	DOCUMENT ID	TECN	COMMENT	$(\Gamma_1\Gamma_9)^{1/2}/\Gamma$
-0.35 to -0.31 OUR ESTIMATE				
-0.35 ± 0.03	MANLEY 92	IPWA	$\pi N \rightarrow \pi N \& N\pi\pi$	
-0.35	^{1,5} LONGACRE 77	IPWA	$\pi N \rightarrow N\pi\pi$	
-0.24	² LONGACRE 75	IPWA	$\pi N \rightarrow N\pi\pi$	

$\Gamma(N\rho, S=3/2, S\text{-wave})/\Gamma_{\text{total}}$	DOCUMENT ID	TECN	COMMENT	Γ_9/Γ
0.09 ± 0.01	VRANA 00	DPWA	Multichannel	

$(\Gamma_1\Gamma_7)^{1/2}/\Gamma_{\text{total}}$ in $N\pi \rightarrow N(1520) \rightarrow N(\pi\pi)_{S=0}^{J=0}$	DOCUMENT ID	TECN	COMMENT	$(\Gamma_1\Gamma_{11})^{1/2}/\Gamma$
-0.22 to -0.06 OUR ESTIMATE				
-0.13	^{1,5} LONGACRE 77	IPWA	$\pi N \rightarrow N\pi\pi$	
-0.17	² LONGACRE 75	IPWA	$\pi N \rightarrow N\pi\pi$	

$\Gamma(N(\pi\pi)_{S=0}^{J=0})/\Gamma_{\text{total}}$	DOCUMENT ID	TECN	COMMENT	Γ_{11}/Γ
0.01 ± 0.01	VRANA 00	DPWA	Multichannel	
• • • We do not use the following data for averages, fits, limits, etc. • • •				
<0.04	THOMA 08	DPWA	Multichannel	

$N(1520)$ PHOTON DECAY AMPLITUDES

Papers on γN amplitudes predating 1981 may be found in our 2006 edition, Journal of Physics, G **33** 1 (2006).

$N(1520) \rightarrow p\gamma, \text{helicity-1/2 amplitude } A_{1/2}$	DOCUMENT ID	TECN	COMMENT
-0.024 ± 0.009 OUR ESTIMATE			
-0.028 ± 0.002	DUGGER 07	DPWA	$\gamma N \rightarrow \pi N$
-0.038 ± 0.003	AHRENS 02	DPWA	$\gamma N \rightarrow \pi N$
-0.020 ± 0.007	ARNDT 96	IPWA	$\gamma N \rightarrow \pi N$
-0.028 ± 0.014	CRAWFORD 83	IPWA	$\gamma N \rightarrow \pi N$
-0.007 ± 0.004	AWAJI 81	DPWA	$\gamma N \rightarrow \pi N$
• • • We do not use the following data for averages, fits, limits, etc. • • •			
-0.027	DRECHSEL 07	DPWA	$\gamma N \rightarrow \pi N$
-0.003	PENNER 02d	DPWA	Multichannel
-0.052 ± 0.010 ± 0.007	⁶ MUKHOPAD... 98		$\gamma p \rightarrow \eta p$
-0.020 ± 0.002	LI 93	IPWA	$\gamma N \rightarrow \pi N$
-0.012	WADA 84	DPWA	Compton scattering

$N(1520) \rightarrow p\gamma, \text{helicity-3/2 amplitude } A_{3/2}$	DOCUMENT ID	TECN	COMMENT
+0.166 ± 0.005 OUR ESTIMATE			
0.143 ± 0.002	DUGGER 07	DPWA	$\gamma N \rightarrow \pi N$
0.147 ± 0.010	AHRENS 02	DPWA	$\gamma N \rightarrow \pi N$
0.167 ± 0.005	ARNDT 96	IPWA	$\gamma N \rightarrow \pi N$
0.156 ± 0.022	CRAWFORD 83	IPWA	$\gamma N \rightarrow \pi N$
0.168 ± 0.013	AWAJI 81	DPWA	$\gamma N \rightarrow \pi N$
• • • We do not use the following data for averages, fits, limits, etc. • • •			
0.161	DRECHSEL 07	DPWA	$\gamma N \rightarrow \pi N$
0.151	PENNER 02d	DPWA	Multichannel
0.130 ± 0.020 ± 0.015	⁶ MUKHOPAD... 98		$\gamma p \rightarrow \eta p$
0.167 ± 0.002	LI 93	IPWA	$\gamma N \rightarrow \pi N$
0.168	WADA 84	DPWA	Compton scattering

$N(1520) \rightarrow n\gamma, \text{helicity-1/2 amplitude } A_{1/2}$	DOCUMENT ID	TECN	COMMENT
-0.059 ± 0.009 OUR ESTIMATE			
-0.048 ± 0.008	ARNDT 96	IPWA	$\gamma N \rightarrow \pi N$
-0.066 ± 0.013	AWAJI 81	DPWA	$\gamma N \rightarrow \pi N$
-0.067 ± 0.004	FUJII 81	DPWA	$\gamma N \rightarrow \pi N$
• • • We do not use the following data for averages, fits, limits, etc. • • •			
-0.077	DRECHSEL 07	DPWA	$\gamma N \rightarrow \pi N$
-0.084	PENNER 02d	DPWA	Multichannel
-0.058 ± 0.003	LI 93	IPWA	$\gamma N \rightarrow \pi N$

$N(1520) \rightarrow n\gamma, \text{helicity-3/2 amplitude } A_{3/2}$	DOCUMENT ID	TECN	COMMENT
-0.139 ± 0.011 OUR ESTIMATE			
-0.140 ± 0.010	ARNDT 96	IPWA	$\gamma N \rightarrow \pi N$
-0.124 ± 0.009	AWAJI 81	DPWA	$\gamma N \rightarrow \pi N$
-0.158 ± 0.003	FUJII 81	DPWA	$\gamma N \rightarrow \pi N$
• • • We do not use the following data for averages, fits, limits, etc. • • •			
-0.154	DRECHSEL 07	DPWA	$\gamma N \rightarrow \pi N$
-0.159	PENNER 02d	DPWA	Multichannel
-0.131 ± 0.003	LI 93	IPWA	$\gamma N \rightarrow \pi N$

$N(1520)$ FOOTNOTES

- LONGACRE 77 pole positions are from a search for poles in the unitarized T-matrix; the first (second) value uses, in addition to $\pi N \rightarrow N\pi\pi$ data, elastic amplitudes from a Saclay (CERN) partial-wave analysis. The other LONGACRE 77 values are from eyeball fits with Breit-Wigner circles to the T-matrix amplitudes.
- From method II of LONGACRE 75: eyeball fits with Breit-Wigner circles to the T-matrix amplitudes.
- See HOEHLER 93 for a detailed discussion of the evidence for and the pole parameters of N and Δ resonances as determined from Argand diagrams of πN elastic partial-wave amplitudes and from plots of the speeds with which the amplitudes traverse the diagrams.
- LONGACRE 78 values are from a search for poles in the unitarized T-matrix. The first (second) value uses, in addition to $\pi N \rightarrow N\pi\pi$ data, elastic amplitudes from a Saclay (CERN) partial-wave analysis.
- LONGACRE 77 considers this coupling to be well determined.
- MUKHOPADHYAY 98 uses an effective Lagrangian approach to analyze η photoproduction data. The ratio of the $A_{3/2}$ and $A_{1/2}$ amplitudes is determined, with less model dependence than the amplitudes themselves, to be $A_{3/2}/A_{1/2} = -2.5 \pm 0.5 \pm 0.4$.

Baryon Particle Listings

$N(1520)$, $N(1535)$

$N(1520)$ REFERENCES

For early references, see Physics Letters **111B** 1 (1982). For very early references, see Reviews of Modern Physics **37** 633 (1965).

THOMA	08	PL B659 87	U. Thoma <i>et al.</i>	(CB-ELSA Collab.)
DRECHSEL	07	EPJ A34 69	D. Drechsel, S.S. Kamalov, L. Tiator	(MAINZ, JINR)
DUGGER	07	PR C76 025211	M. Dugger <i>et al.</i>	(Jefferson Lab CLAS Collab.)
ARNDT	06	PR C74 045205	R.A. Arndt <i>et al.</i>	(GWU)
PDG	06	JPG 33 1	W.-M. Yao <i>et al.</i>	(PDG Collab.)
ARNDT	05	PR C72 045202	R.A. Arndt <i>et al.</i>	(GWU, PHPI)
ARNDT	04	PR C69 035213	R.A. Arndt <i>et al.</i>	(GWU, TRIU)
AHRENS	02	PRL 88 232002	J. Ahrens <i>et al.</i>	(Mainz MAMI GDH/A2 Collab.)
PENNER	02C	PR C66 055211	G. Penner, U. Mosel	(GIES)
PENNER	02D	PR C66 055212	G. Penner, U. Mosel	(GIES)
VRANA	00	PRPL 328 181	T.P. Vrana, S.A. Dytman., T.-S.H. Lee	(PITT+)
TIATOR	99	PR C60 035210	L. Tiator <i>et al.</i>	
MUKHOPAD...	98	PL B444 7	N.C. Mukhopadhyay, N. Mathur	
ARNDT	96	PR C53 430	R.A. Arndt, I.I. Strakovsky, R.L. Workman	(VPI)
ARNDT	95	PR C52 2120	R.A. Arndt <i>et al.</i>	(VPI, BRCO)
BATINIC	95	PR C51 2310	M. Batinic <i>et al.</i>	(BOSK, UCLA)
Also		PR C57 1004 (erratum)	M. Batinic <i>et al.</i>	
HOEHLER	93	πN Newsletter 9 1	G. Hoehler	(KARL)
LI	93	PR C47 2759	Z.J. Li <i>et al.</i>	(VPI)
MANLEY	92	PR D45 4002	D.M. Manley, E.M. Saleski	(KENT) IJP
Also		PR D30 904	D.M. Manley <i>et al.</i>	(VPI)
ARNDT	91	PR D43 2131	R.A. Arndt <i>et al.</i>	(VPI, TELE) IJP
WADA	84	NP B247 313	Y. Wada <i>et al.</i>	(INUS)
CRAWFORD	83	NP B211 1	R.L. Crawford, W.T. Morton	(GLAS)
PDG	82	PL 111B 1	M. Roos <i>et al.</i>	(HELS, CIT, CERN)
AWAJI	81	Bonn Conf. 352	N. Awaji, R. Kajikawa	(NAGO)
Also		NP B197 365	K. Fujii <i>et al.</i>	(NAGO, OSAK)
FUJII	81	NP B187 53	K. Fujii <i>et al.</i>	(CMU, LBL) IJP
CUTKOSKY	80	Toronto Conf. 19	R.E. Cutkosky <i>et al.</i>	(CMU, LBL) IJP
Also		PR D20 2839	R.E. Cutkosky <i>et al.</i>	
HOEHLER	79	PDAT 12-1	G. Hoehler <i>et al.</i>	(KARLT) IJP
Also		Toronto Conf. 3	R. Koch	(KARLT) IJP
LONGACRE	78	PR D17 1795	R.S. Longacre <i>et al.</i>	(LBL, SLAC)
LONGACRE	77	NP B122 493	R.S. Longacre, J. Dolbeau	(SACL) IJP
Also		NP B108 365	J. Dolbeau <i>et al.</i>	(SACL) IJP
LONGACRE	75	PL 55B 415	R.S. Longacre <i>et al.</i>	(LBL, SLAC) IJP

$N(1535) S_{11}$

$$I(J^P) = \frac{1}{2}(\frac{1}{2}^-) \text{ Status: } ***$$

Most of the results published before 1975 were last included in our 1982 edition, Physics Letters **111B** 1 (1982). Some further obsolete results published before 1984 were last included in our 2006 edition, Journal of Physics, G **33** 1 (2006).

$N(1535)$ BREIT-WIGNER MASS

VALUE (MeV)	DOCUMENT ID	TECN	COMMENT
1525 to 1545 (≈ 1535) OUR ESTIMATE			
1547.0 \pm 0.7	ARNDT 06	DPWA	$\pi N \rightarrow \pi N, \eta N$
1534 \pm 7	MANLEY 92	IPWA	$\pi N \rightarrow \pi N$ & $N\pi\pi$
1550 \pm 40	CUTKOSKY 80	IPWA	$\pi N \rightarrow \pi N$
1526 \pm 7	HOEHLER 79	IPWA	$\pi N \rightarrow \pi N$
••• We do not use the following data for averages, fits, limits, etc. •••			
1548 \pm 15	THOMA 08	DPWA	Multichannel
1546.7 \pm 2.2	ARNDT 04	DPWA	$\pi N \rightarrow \pi N, \eta N$
1526 \pm 2	PENNER 02C	DPWA	Multichannel
1530 \pm 10	BAI 01B	BES	$J/\psi \rightarrow \rho\bar{p}\eta$
1522 \pm 11	THOMPSON 01	CLAS	$\gamma^*p \rightarrow \rho\eta$
1542 \pm 3	VRANA 00	DPWA	Multichannel
1532 \pm 5	ARMSTRONG 99B	DPWA	$\gamma^*p \rightarrow \rho\eta$
1549.0 \pm 2.1	ABAEV 96	DPWA	$\pi^-p \rightarrow \eta n$
1525 \pm 10	ARNDT 96	IPWA	$\gamma N \rightarrow \pi N$
1535	ARNDT 95	DPWA	$\pi N \rightarrow N\pi$
1542 \pm 6	BATINIC 95	DPWA	$\pi N \rightarrow N\pi, N\eta$
1537	BATINIC 95B	DPWA	$\pi N \rightarrow N\pi, N\eta$
1544 \pm 13	KRUSCHE 95	DPWA	$\gamma p \rightarrow \rho\eta$
1518	LI 93	IPWA	$\gamma N \rightarrow \pi N$
1520	¹ LONGACRE 77	IPWA	$\pi N \rightarrow N\pi\pi$
1510	² LONGACRE 75	IPWA	$\pi N \rightarrow N\pi\pi$

$N(1535)$ BREIT-WIGNER WIDTH

VALUE (MeV)	DOCUMENT ID	TECN	COMMENT
125 to 175 (≈ 150) OUR ESTIMATE			
188.4 \pm 3.8	ARNDT 06	DPWA	$\pi N \rightarrow \pi N, \eta N$
148.2 \pm 8.1	GREEN 97	DPWA	$\pi N \rightarrow \pi N, \eta N$
151 \pm 27	MANLEY 92	IPWA	$\pi N \rightarrow \pi N$ & $N\pi\pi$
240 \pm 80	CUTKOSKY 80	IPWA	$\pi N \rightarrow \pi N$
120 \pm 20	HOEHLER 79	IPWA	$\pi N \rightarrow \pi N$
••• We do not use the following data for averages, fits, limits, etc. •••			
170 \pm 20	THOMA 08	DPWA	Multichannel
178.0 \pm 11.6	ARNDT 04	DPWA	$\pi N \rightarrow \pi N, \eta N$
129 \pm 8	PENNER 02C	DPWA	Multichannel
95 \pm 25	BAI 01B	BES	$J/\psi \rightarrow \rho\bar{p}\eta$
143 \pm 18	THOMPSON 01	CLAS	$\gamma^*p \rightarrow \rho\eta$
112 \pm 19	VRANA 00	DPWA	Multichannel
154 \pm 20	ARMSTRONG 99B	DPWA	$\gamma^*p \rightarrow \rho\eta$
212 \pm 20	³ KRUSCHE 97	DPWA	$\gamma N \rightarrow \eta N$
168.8 \pm 11.6	ABAEV 96	DPWA	$\pi^-p \rightarrow \eta n$

103 \pm 5	ARNDT 96	IPWA	$\gamma N \rightarrow \pi N$
66	ARNDT 95	DPWA	$\pi N \rightarrow N\pi$
150 \pm 15	BATINIC 95	DPWA	$\pi N \rightarrow N\pi, N\eta$
145	BATINIC 95B	DPWA	$\pi N \rightarrow N\pi, N\eta$
200 \pm 40	KRUSCHE 95	DPWA	$\gamma p \rightarrow \rho\eta$
84	LI 93	IPWA	$\gamma N \rightarrow \pi N$
135	¹ LONGACRE 77	IPWA	$\pi N \rightarrow N\pi\pi$
100	² LONGACRE 75	IPWA	$\pi N \rightarrow N\pi\pi$

$N(1535)$ POLE POSITION

REAL PART

VALUE (MeV)	DOCUMENT ID	TECN	COMMENT
1490 to 1530 (≈ 1510) OUR ESTIMATE			
1502	ARNDT 06	DPWA	$\pi N \rightarrow \pi N, \eta N$
1487	⁴ HOEHLER 93	SPED	$\pi N \rightarrow \pi N$
	CUTKOSKY 80	IPWA	$\pi N \rightarrow \pi N$
1510 \pm 50			
••• We do not use the following data for averages, fits, limits, etc. •••			
1508 \pm $\frac{10}{-30}$	THOMA 08	DPWA	Multichannel
1526	ARNDT 04	DPWA	$\pi N \rightarrow \pi N, \eta N$
1525	VRANA 00	DPWA	Multichannel
1510 \pm 10	⁵ ARNDT 98	DPWA	$\pi N \rightarrow \pi N, \eta N$
1501	ARNDT 95	DPWA	$\pi N \rightarrow N\pi$
1499	ARNDT 91	DPWA	$\pi N \rightarrow \pi N$ Soln SM90
1496 or 1499	⁶ LONGACRE 78	IPWA	$\pi N \rightarrow N\pi\pi$
1525 or 1527	¹ LONGACRE 77	IPWA	$\pi N \rightarrow N\pi\pi$

-2xIMAGINARY PART

VALUE (MeV)	DOCUMENT ID	TECN	COMMENT
90 to 250 (≈ 170) OUR ESTIMATE			
95	ARNDT 06	DPWA	$\pi N \rightarrow \pi N, \eta N$
260 \pm 80	CUTKOSKY 80	IPWA	$\pi N \rightarrow \pi N$
••• We do not use the following data for averages, fits, limits, etc. •••			
165 \pm 15	THOMA 08	DPWA	Multichannel
130	ARNDT 04	DPWA	$\pi N \rightarrow \pi N, \eta N$
102	VRANA 00	DPWA	Multichannel
170 \pm 30	⁵ ARNDT 98	DPWA	$\pi N \rightarrow \pi N, \eta N$
124	ARNDT 95	DPWA	$\pi N \rightarrow N\pi$
110	ARNDT 91	DPWA	$\pi N \rightarrow \pi N$ Soln SM90
103 or 105	⁶ LONGACRE 78	IPWA	$\pi N \rightarrow N\pi\pi$
135 or 123	¹ LONGACRE 77	IPWA	$\pi N \rightarrow N\pi\pi$

$N(1535)$ ELASTIC POLE RESIDUE

MODULUS $|r|$

VALUE (MeV)	DOCUMENT ID	TECN	COMMENT
16	ARNDT 06	DPWA	$\pi N \rightarrow \pi N, \eta N$
120 \pm 40	CUTKOSKY 80	IPWA	$\pi N \rightarrow \pi N$
••• We do not use the following data for averages, fits, limits, etc. •••			
33	ARNDT 04	DPWA	$\pi N \rightarrow \pi N, \eta N$
31	ARNDT 95	DPWA	$\pi N \rightarrow N\pi$
23	ARNDT 91	DPWA	$\pi N \rightarrow \pi N$ Soln SM90

PHASE θ

VALUE ($^\circ$)	DOCUMENT ID	TECN	COMMENT
-16	ARNDT 06	DPWA	$\pi N \rightarrow \pi N, \eta N$
+15 \pm 45	CUTKOSKY 80	IPWA	$\pi N \rightarrow \pi N$
••• We do not use the following data for averages, fits, limits, etc. •••			
14	ARNDT 04	DPWA	$\pi N \rightarrow \pi N, \eta N$
-12	ARNDT 95	DPWA	$\pi N \rightarrow N\pi$
-13	ARNDT 91	DPWA	$\pi N \rightarrow \pi N$ Soln SM90

$N(1535)$ DECAY MODES

The following branching fractions are our estimates, not fits or averages.

Mode	Fraction (Γ_i/Γ)
Γ_1 $N\pi$	35-55 %
Γ_2 $N\eta$	45-60 %
Γ_3 $N\pi\pi$	1-10 %
Γ_4 $\Delta\pi$	<1 %
Γ_5 $\Delta(1232)\pi, D\text{-wave}$	
Γ_6 $N\rho$	<4 %
Γ_7 $N\rho, S=1/2, S\text{-wave}$	
Γ_8 $N\rho, S=3/2, D\text{-wave}$	
Γ_9 $N(\pi\pi)_{S=0}^{\zeta=0}$	<3 %
Γ_{10} $N(1440)\pi$	<7 %
Γ_{11} $p\gamma$	0.15-0.35 %
Γ_{12} $p\gamma, \text{helicity}=1/2$	0.15-0.35 %
Γ_{13} $n\gamma$	0.004-0.29 %
Γ_{14} $n\gamma, \text{helicity}=1/2$	0.004-0.29 %

See key on page 373

Baryon Particle Listings
N(1535)

N(1535) BRANCHING RATIOS

$\Gamma(N\pi)/\Gamma_{\text{total}}$				Γ_1/Γ
VALUE	DOCUMENT ID	TECN	COMMENT	
0.35 to 0.55 OUR ESTIMATE				
0.355 ± 0.002	ARNDT	06	DPWA	$\pi N \rightarrow \pi N, \eta N$
0.394 ± 0.009	GREEN	97	DPWA	$\pi N \rightarrow \pi N, \eta N$
0.51 ± 0.05	MANLEY	92	IPWA	$\pi N \rightarrow \pi N \& N\pi\pi$
0.50 ± 0.10	CUTKOSKY	80	IPWA	$\pi N \rightarrow \pi N$
0.38 ± 0.04	HOEHLER	79	IPWA	$\pi N \rightarrow \pi N$
• • • We do not use the following data for averages, fits, limits, etc. • • •				
0.37 ± 0.09	THOMA	08	DPWA	Multichannel
0.360 ± 0.009	ARNDT	04	DPWA	$\pi N \rightarrow \pi N, \eta N$
0.36 ± 0.01	PENNER	02c	DPWA	Multichannel
0.35 ± 0.08	VRANA	00	DPWA	Multichannel
0.330 ± 0.011	ABAEV	96	DPWA	$\pi^- p \rightarrow \eta n$
0.31	ARNDT	95	DPWA	$\pi N \rightarrow N\pi$
0.34 ± 0.09	BATINIC	95	DPWA	$\pi N \rightarrow N\pi, N\eta$

$\Gamma(N\eta)/\Gamma_{\text{total}}$				Γ_2/Γ
VALUE	DOCUMENT ID	TECN	COMMENT	
+0.45-0.60 OUR ESTIMATE				
0.529 ± 0.010 OUR AVERAGE				
0.53 ± 0.01	PENNER	02c	DPWA	Multichannel
0.51 ± 0.05	VRANA	00	DPWA	Multichannel
• • • We do not use the following data for averages, fits, limits, etc. • • •				
0.40 ± 0.10	THOMA	08	DPWA	Multichannel
>0.45	95	7	ARMSTRONG	99b DPWA $p(e, e'p)\eta$
0.568 ± 0.011	GREEN	97	DPWA	$\pi N \rightarrow \pi N, \eta N$
0.591 ± 0.017	ABAEV	96	DPWA	$\pi^- p \rightarrow \eta n$
0.63 ± 0.07	BATINIC	95	DPWA	$\pi N \rightarrow N\pi, N\eta$

$(\Gamma_1\Gamma_2)^{1/2}/\Gamma_{\text{total}}$ in $N\pi \rightarrow N(1535) \rightarrow N\eta$				$(\Gamma_1\Gamma_2)^{1/2}/\Gamma$
VALUE	DOCUMENT ID	TECN	COMMENT	
+0.44 to +0.50 OUR ESTIMATE				
+0.47 ± 0.02	MANLEY	92	IPWA	$\pi N \rightarrow \pi N \& N\pi\pi$

Note: Signs of couplings from $\pi N \rightarrow N\pi\pi$ analyses were changed in the 1986 edition to agree with the baryon-first convention; the overall phase ambiguity is resolved by choosing a negative sign for the $\Delta(1620) S_{31}$ coupling to $\Delta(1232)\pi$.

$(\Gamma_1\Gamma_2)^{1/2}/\Gamma_{\text{total}}$ in $N\pi \rightarrow N(1535) \rightarrow \Delta(1232)\pi, D\text{-wave}$				$(\Gamma_1\Gamma_2)^{1/2}/\Gamma$
VALUE	DOCUMENT ID	TECN	COMMENT	
-0.04 to +0.06 OUR ESTIMATE				
+0.00 ± 0.04	MANLEY	92	IPWA	$\pi N \rightarrow \pi N \& N\pi\pi$
0.00	1	LONGACRE	77	IPWA $\pi N \rightarrow N\pi\pi$
+0.06	2	LONGACRE	75	IPWA $\pi N \rightarrow N\pi\pi$

$\Gamma(\Delta(1232)\pi, D\text{-wave})/\Gamma_{\text{total}}$				Γ_5/Γ
VALUE	DOCUMENT ID	TECN	COMMENT	
0.01 ± 0.01	VRANA	00	DPWA	Multichannel
• • • We do not use the following data for averages, fits, limits, etc. • • •				
0.23 ± 0.08	THOMA	08	DPWA	Multichannel

$(\Gamma_1\Gamma_2)^{1/2}/\Gamma_{\text{total}}$ in $N\pi \rightarrow N(1535) \rightarrow N\rho, S=1/2, S\text{-wave}$				$(\Gamma_1\Gamma_2)^{1/2}/\Gamma$
VALUE	DOCUMENT ID	TECN	COMMENT	
-0.14 to -0.06 OUR ESTIMATE				
-0.10 ± 0.03	MANLEY	92	IPWA	$\pi N \rightarrow \pi N \& N\pi\pi$
-0.10	1	LONGACRE	77	IPWA $\pi N \rightarrow N\pi\pi$
-0.09	2	LONGACRE	75	IPWA $\pi N \rightarrow N\pi\pi$

$\Gamma(N\rho, S=1/2, S\text{-wave})/\Gamma_{\text{total}}$				Γ_7/Γ
VALUE	DOCUMENT ID	TECN	COMMENT	
0.02 ± 0.01	VRANA	00	DPWA	Multichannel

$\Gamma(N\rho, S=3/2, D\text{-wave})/\Gamma_{\text{total}}$				Γ_8/Γ
VALUE	DOCUMENT ID	TECN	COMMENT	
0.00 ± 0.01	VRANA	00	DPWA	Multichannel

$(\Gamma_1\Gamma_2)^{1/2}/\Gamma_{\text{total}}$ in $N\pi \rightarrow N(1535) \rightarrow N(\pi\pi)_{S=0}^{I=0}$				$(\Gamma_1\Gamma_2)^{1/2}/\Gamma$
VALUE	DOCUMENT ID	TECN	COMMENT	
+0.03 to +0.13 OUR ESTIMATE				
+0.07 ± 0.04	MANLEY	92	IPWA	$\pi N \rightarrow \pi N \& N\pi\pi$
+0.08	1	LONGACRE	77	IPWA $\pi N \rightarrow N\pi\pi$
+0.09	2	LONGACRE	75	IPWA $\pi N \rightarrow N\pi\pi$

$\Gamma(N(\pi\pi)_{S=0}^{I=0})/\Gamma_{\text{total}}$				Γ_9/Γ
VALUE	DOCUMENT ID	TECN	COMMENT	
0.02 ± 0.01	VRANA	00	DPWA	Multichannel

$(\Gamma_1\Gamma_2)^{1/2}/\Gamma_{\text{total}}$ in $N\pi \rightarrow N(1535) \rightarrow N(1440)\pi$				$(\Gamma_1\Gamma_2)^{1/2}/\Gamma$
VALUE	DOCUMENT ID	TECN	COMMENT	
+0.10 ± 0.05	MANLEY	92	IPWA	$\pi N \rightarrow \pi N \& N\pi\pi$

$\Gamma(N(1440)\pi)/\Gamma_{\text{total}}$				Γ_{10}/Γ
VALUE	DOCUMENT ID	TECN	COMMENT	
0.08 ± 0.02	8	STAROSTIN	03	$\pi^- p \rightarrow n3\pi^0$
0.10 ± 0.09		VRANA	00	DPWA Multichannel

N(1535) PHOTON DECAY AMPLITUDES

Papers on γN amplitudes predating 1981 may be found in our 2006 edition, Journal of Physics, G **33** 1 (2006).

N(1535) $\rightarrow p\gamma$, helicity-1/2 amplitude $A_{1/2}$

VALUE (GeV ^{-1/2})	DOCUMENT ID	TECN	COMMENT
+0.090 ± 0.030 OUR ESTIMATE			
0.091 ± 0.002	DUGGER	07	DPWA $\gamma N \rightarrow \pi N$
0.120 ± 0.011 ± 0.015	3	KRUSCHE	97 DPWA $\gamma N \rightarrow \eta N$
0.060 ± 0.015	ARNDT	96	IPWA $\gamma N \rightarrow \pi N$
0.097 ± 0.006	BENMERROU..95	DPWA	$\gamma N \rightarrow N\eta$
0.095 ± 0.011	9	BENMERROU..91	$\gamma p \rightarrow p\eta$
0.053 ± 0.015	CRAWFORD	83	IPWA $\gamma N \rightarrow \pi N$
0.077 ± 0.021	AWAJI	81	DPWA $\gamma N \rightarrow \pi N$
• • • We do not use the following data for averages, fits, limits, etc. • • •			
0.066	DRECHSEL	07	DPWA $\gamma N \rightarrow \pi N$
0.090	PENNER	02D	DPWA Multichannel
0.110 to 0.140	KRUSCHE	95	DPWA $\gamma p \rightarrow p\eta$
0.125 ± 0.025	KRUSCHE	95c	IPWA $\gamma d \rightarrow \eta N(N)$
0.061 ± 0.003	LI	93	IPWA $\gamma N \rightarrow \pi N$
0.055	WADA	84	DPWA Compton scattering

N(1535) $\rightarrow n\gamma$, helicity-1/2 amplitude $A_{1/2}$

VALUE (GeV ^{-1/2})	DOCUMENT ID	TECN	COMMENT
-0.046 ± 0.027 OUR ESTIMATE			
-0.020 ± 0.035	ARNDT	96	IPWA $\gamma N \rightarrow \pi N$
0.035 ± 0.014	AWAJI	81	DPWA $\gamma N \rightarrow \pi N$
-0.062 ± 0.003	FUJII	81	DPWA $\gamma N \rightarrow \pi N$
• • • We do not use the following data for averages, fits, limits, etc. • • •			
-0.051	DRECHSEL	07	DPWA $\gamma N \rightarrow \pi N$
-0.024	PENNER	02D	DPWA Multichannel
-0.100 ± 0.030	KRUSCHE	95c	IPWA $\gamma d \rightarrow \eta N(N)$
-0.046 ± 0.005	LI	93	IPWA $\gamma N \rightarrow \pi N$

N(1535) $\rightarrow N\gamma$, ratio $A_{1/2}^n/A_{1/2}^p$

VALUE (GeV ^{-1/2})	DOCUMENT ID	TECN	
• • • We do not use the following data for averages, fits, limits, etc. • • •			
-0.84 ± 0.15	MUKHOPAD...	95B	IPWA

N(1535) FOOTNOTES

- LONGACRE 77 pole positions are from a search for poles in the unitarized T-matrix; the first (second) value uses, in addition to $\pi N \rightarrow N\pi\pi$ data, elastic amplitudes from a Saclay (CERN) partial-wave analysis. The other LONGACRE 77 values are from eyeball fits with Breit-Wigner circles to the T-matrix amplitudes.
- From method II of LONGACRE 75: eyeball fits with Breit-Wigner circles to the T-matrix amplitudes.
- KRUSCHE 97 fits with the mass fixed at 1544 MeV.
- See HOEHLER 93 for a detailed discussion of the evidence for and the pole parameters of N and Δ resonances as determined from Argand diagrams of πN elastic partial-wave amplitudes and from plots of the speeds with which the amplitudes traverse the diagrams.
- ARNDT 98 also lists pole residues, which display more model dependence than do the associated pole positions.
- LONGACRE 78 values are from a search for poles in the unitarized T-matrix. The first (second) value uses, in addition to $\pi N \rightarrow N\pi\pi$ data, elastic amplitudes from a Saclay (CERN) partial-wave analysis.
- The best value ARMSTRONG 99b obtains is $\simeq 0.55$; this assumes S_{11} dominance in the reaction $p(e, e'p)\eta$ at $Q^2=4$ (GeV/c)².
- This STAROSTIN 03 value is an estimate made using simplest assumptions.
- BENMERROUCHE 91 uses an effective Lagrangian approach to analyze η photoproduction data.

N(1535) REFERENCES

For early references, see Physics Letters **111B** 1 (1982).

THOMA	08	PL B659 87	U. Thoma et al.	(CB-ELSA Collab.)
DRECHSEL	07	EPL A34 69	D. Drechsel, S.S. Kamalov, L. Tiator	(MAINZ, JINR)
DUGGER	07	PR C76 025211	M. Dugger et al.	(Jefferson Lab CLAS Collab.)
ARNDT	06	PR C74 045205	R.A. Arndt et al.	(GWU)
PDG	06	JPG 33 1	W.-M. Yao et al.	(PDG Collab.)
ARNDT	04	PR C69 035213	R.A. Arndt et al.	(GWU, TRIU)
STAROSTIN	03	PR C67 068201	A. Starostin et al.	(BNL Crystal Ball Collab.)
PENNER	02C	PR C66 055211	G. Penner, U. Mosel	(GIES)
PENNER	02D	PR C66 055212	G. Penner, U. Mosel	(GIES)
BAI	01B	PL B810 75	J.Z. Bai et al.	(BES Collab.)
THOMPSON	01	PRL 86 1702	R. Thompson et al.	(Jefferson CLAS Collab.)
VRANA	00	PRPL 328 181	T.P. Vrana, S.A. Dytman, T.-S.H. Lee	(PITT+)
ARMSTRONG	99B	PR D60 052004	C.S. Armstrong et al.	
ARNDT	98	PR C58 3636	R.A. Arndt et al.	
GREEN	97	PR C55 R2167	A.M. Green, S. Wycech	(HELS, WINR)
KRUSCHE	97	PL B397 171	B. Krusche et al.	(GIES, RPI, SASK)
ABAEV	96	PR C53 385	V.V. Abaev, B.M.K. Nefkens	(UCLA)
ARNDT	96	PR C53 430	R.A. Arndt, I.I. Strakovsky, R.L. Workman	(VPI)
ARNDT	95	PR C52 2120	R.A. Arndt et al.	(VPI, BRCC)
BATINIC	95	PR C51 2310	M. Batinic et al.	(BOSK, UCLA)
Also		PR C57 1004 (erratum)	M. Batinic et al.	

Baryon Particle Listings

$N(1535), N(1650)$

BATINIC	95B	PR C52 2188	M. Batinic, I. Slaus, A. Svarc	(BOSK)
BENMERROU...	95	PR D51 3237	M. Benmerrouche, N.C. Mukhopadhyay, J.F. Zhang	
KRUSCHE	95	PRL 74 3736	B. Krusche <i>et al.</i>	(GIES, MANZ, GLAS+)
KRUSCHE	95C	PL B358 40	B. Krusche <i>et al.</i>	(GIES, MANZ, GLAS+)
MUKHOPAD...	95B	PL B364 1	N.C. Mukhopadhyay, J.F. Zhang, M. Benmerrouche	
HOEHLER	93	πN Newsletter 9 1	G. Hohler	(KARL)
LI	92	PR C47 2759	Z.J. Li <i>et al.</i>	(VPI)
MANLEY	92	PR D45 4002	D.M. Manley, E.M. Saleski	(KENT) IJP
Also		PR D30 304	D.M. Manley <i>et al.</i>	(VPI)
ARNDT	91	PR D43 2131	R.A. Arndt <i>et al.</i>	(VPI, TELE) IJP
BENMERROU...	91	PRL 67 1070	M. Benmerrouche, N.C. Mukhopadhyay	(RPI)
WADA	84	NP B247 313	Y. Wada <i>et al.</i>	(INUS)
CRAWFORD	83	NP B211 1	R.L. Crawford, W.T. Morton	(GLAS)
PDG	82	PL 111B 1	M. Roos <i>et al.</i>	(HELS, CIT, CERN)
AWAJI	81	Bonn Conf. 352	N. Awaji, R. Kajikawa	(NAGO)
Also		NP B197 365	K. Fujii <i>et al.</i>	(NAGO)
FUJII	81	NP B187 53	K. Fujii <i>et al.</i>	(NAGO, OSAK)
CUTKOSKY	80	Toronto Conf. 19	R.E. Cutkosky <i>et al.</i>	(CMU, LBL) IJP
Also		PR D20 2839	R.E. Cutkosky <i>et al.</i>	(CMU, LBL) IJP
HOEHLER	79	PDAT 12-1	G. Hohler <i>et al.</i>	(KARL) IJP
Also		Toronto Conf. 3	R. Koch	(KARL) IJP
LONGACRE	78	PR D17 1795	R.S. Longacre <i>et al.</i>	(LBL, SLAC)
LONGACRE	77	NP B122 493	R.S. Longacre, J. Dolbeau	(SACL)
Also		NP B108 365	J. Dolbeau <i>et al.</i>	(SACL) IJP
LONGACRE	75	PL 55B 415	R.S. Longacre <i>et al.</i>	(LBL, SLAC) IJP

$N(1650)$ POLE POSITION

REAL PART

VALUE (MeV)	DOCUMENT ID	TECN	COMMENT
1640 to 1670 (≈ 1655) OUR ESTIMATE			
1648	ARNDT	06	DPWA $\pi N \rightarrow \pi N, \eta N$
1670	⁵ HOEHLER	93	ARGD $\pi N \rightarrow \pi N$
1640 \pm 20	CUTKOSKY	80	IPWA $\pi N \rightarrow \pi N$
• • • We do not use the following data for averages, fits, limits, etc. • • •			
1645 \pm 15	THOMA	08	DPWA Multichannel
1653	ARNDT	04	DPWA $\pi N \rightarrow \pi N, \eta N$
1663	VRANA	00	DPWA Multichannel
1660 \pm 10	⁶ ARNDT	98	DPWA $\pi N \rightarrow \pi N, \eta N$
1673	ARNDT	95	DPWA $\pi N \rightarrow N\pi$
1689	¹ ARNDT	95	DPWA $\pi N \rightarrow N\pi$
1657	ARNDT	91	DPWA $\pi N \rightarrow \pi N$ Soln SM90
1648 or 1651	⁷ LONGACRE	78	IPWA $\pi N \rightarrow N\pi\pi$
1699 or 1698	³ LONGACRE	77	IPWA $\pi N \rightarrow N\pi\pi$

-2xIMAGINARY PART

VALUE (MeV)	DOCUMENT ID	TECN	COMMENT
150 to 180 (≈ 165) OUR ESTIMATE			
80	ARNDT	06	DPWA $\pi N \rightarrow \pi N, \eta N$
163	⁵ HOEHLER	93	ARGD $\pi N \rightarrow \pi N$
150 \pm 30	CUTKOSKY	80	IPWA $\pi N \rightarrow \pi N$
• • • We do not use the following data for averages, fits, limits, etc. • • •			
187 \pm 20	THOMA	08	DPWA Multichannel
182	ARNDT	04	DPWA $\pi N \rightarrow \pi N, \eta N$
240	VRANA	00	DPWA Multichannel
140 \pm 20	⁶ ARNDT	98	DPWA $\pi N \rightarrow \pi N, \eta N$
82	ARNDT	95	DPWA $\pi N \rightarrow N\pi$
192	¹ ARNDT	95	DPWA $\pi N \rightarrow N\pi$
160	ARNDT	91	DPWA $\pi N \rightarrow \pi N$ Soln SM90
117 or 119	⁷ LONGACRE	78	IPWA $\pi N \rightarrow N\pi\pi$
174 or 173	³ LONGACRE	77	IPWA $\pi N \rightarrow N\pi\pi$

$N(1650)$ ELASTIC POLE RESIDUE

MODULUS $|r|$

VALUE (MeV)	DOCUMENT ID	TECN	COMMENT
14	ARNDT	06	DPWA $\pi N \rightarrow \pi N, \eta N$
39	HOEHLER	93	ARGD $\pi N \rightarrow \pi N$
60 \pm 10	CUTKOSKY	80	IPWA $\pi N \rightarrow \pi N$
• • • We do not use the following data for averages, fits, limits, etc. • • •			
69	ARNDT	04	DPWA $\pi N \rightarrow \pi N, \eta N$
22	ARNDT	95	DPWA $\pi N \rightarrow N\pi$
72	¹ ARNDT	95	DPWA $\pi N \rightarrow N\pi$
54	ARNDT	91	DPWA $\pi N \rightarrow \pi N$ Soln SM90

PHASE θ

VALUE ($^\circ$)	DOCUMENT ID	TECN	COMMENT
-69	ARNDT	06	DPWA $\pi N \rightarrow \pi N, \eta N$
-37	HOEHLER	93	ARGD $\pi N \rightarrow \pi N$
-75 \pm 25	CUTKOSKY	80	IPWA $\pi N \rightarrow \pi N$
• • • We do not use the following data for averages, fits, limits, etc. • • •			
-55	ARNDT	04	DPWA $\pi N \rightarrow \pi N, \eta N$
29	ARNDT	95	DPWA $\pi N \rightarrow N\pi$
-85	¹ ARNDT	95	DPWA $\pi N \rightarrow N\pi$
-38	ARNDT	91	DPWA $\pi N \rightarrow \pi N$ Soln SM90

$N(1650)$ DECAY MODES

The following branching fractions are our estimates, not fits or averages.

Mode	Fraction (Γ_i/Γ)
Γ_1 $N\pi$	0.60 to 0.95
Γ_2 $N\eta$	3-10 %
Γ_3 ΛK	3-11 %
Γ_4 ΣK	
Γ_5 $N\pi\pi$	10-20 %
Γ_6 $\Delta\pi$	1-7 %
Γ_7 $\Delta(1232)\pi, D\text{-wave}$	
Γ_8 $N\rho$	4-12 %
Γ_9 $N\rho, S=1/2, S\text{-wave}$	
Γ_{10} $N\rho, S=3/2, D\text{-wave}$	
Γ_{11} $N(\pi\pi)_{S\text{-wave}}^{\ell=0}$	< 4 %
Γ_{12} $N(1440)\pi$	< 5 %
Γ_{13} $p\gamma$	0.04-0.18 %
Γ_{14} $p\gamma, \text{helicity}=1/2$	0.04-0.18 %
Γ_{15} $n\gamma$	0.003-0.17 %
Γ_{16} $n\gamma, \text{helicity}=1/2$	0.003-0.17 %

$N(1650) S_{11}$

$$I(J^P) = \frac{1}{2}(\frac{1}{2}^-) \text{ Status: } ***$$

Most of the results published before 1975 were last included in our 1982 edition, Physics Letters **111B** 1 (1982). Some further obsolete results published before 1984 were last included in our 2006 edition, Journal of Physics, G **33** 1 (2006).

$N(1650)$ BREIT-WIGNER MASS

VALUE (MeV)	DOCUMENT ID	TECN	COMMENT
1645 to 1670 (≈ 1655) OUR ESTIMATE			
1634.7 \pm 1.1	ARNDT	06	DPWA $\pi N \rightarrow \pi N, \eta N$
1659 \pm 9	MANLEY	92	IPWA $\pi N \rightarrow \pi N \& N\pi\pi$
1650 \pm 30	CUTKOSKY	80	IPWA $\pi N \rightarrow \pi N$
1670 \pm 8	HOEHLER	79	IPWA $\pi N \rightarrow \pi N$
• • • We do not use the following data for averages, fits, limits, etc. • • •			
1655 \pm 15	THOMA	08	DPWA Multichannel
1651.2 \pm 4.7	ARNDT	04	DPWA $\pi N \rightarrow \pi N, \eta N$
1665 \pm 2	PENNER	02c	DPWA Multichannel
1647 \pm 20	BAI	01B	BES $J/\psi \rightarrow p\bar{p}\eta$
1689 \pm 12	VRANA	00	DPWA Multichannel
1677 \pm 8	ARNDT	96	IPWA $\gamma N \rightarrow \pi N$
1667	ARNDT	95	DPWA $\pi N \rightarrow N\pi$
1712	¹ ARNDT	95	DPWA $\pi N \rightarrow N\pi$
1669 \pm 17	BATINIC	95	DPWA $\pi N \rightarrow N\pi, N\eta$
1713 \pm 27	² BATINIC	95	DPWA $\pi N \rightarrow N\pi, N\eta$
1674	LI	93	IPWA $\gamma N \rightarrow \pi N$
1672	MUSETTE	80	IPWA $\pi^- \rho \rightarrow \Lambda K^0$
1680	SAXON	80	DPWA $\pi^- \rho \rightarrow \Lambda K^0$
1700	³ LONGACRE	77	IPWA $\pi N \rightarrow N\pi\pi$
1660	⁴ LONGACRE	75	IPWA $\pi N \rightarrow N\pi\pi$

$N(1650)$ BREIT-WIGNER WIDTH

VALUE (MeV)	DOCUMENT ID	TECN	COMMENT
145 to 185 (≈ 165) OUR ESTIMATE			
115.4 \pm 2.8	ARNDT	06	DPWA $\pi N \rightarrow \pi N, \eta N$
167.9 \pm 9.4	GREEN	97	DPWA $\pi N \rightarrow \pi N, \eta N$
173 \pm 12	MANLEY	92	IPWA $\pi N \rightarrow \pi N \& N\pi\pi$
150 \pm 40	CUTKOSKY	80	IPWA $\pi N \rightarrow \pi N$
180 \pm 20	HOEHLER	79	IPWA $\pi N \rightarrow \pi N$
• • • We do not use the following data for averages, fits, limits, etc. • • •			
180 \pm 20	THOMA	08	DPWA Multichannel
130.6 \pm 7.0	ARNDT	04	DPWA $\pi N \rightarrow \pi N, \eta N$
138 \pm 7	PENNER	02c	DPWA Multichannel
145 \pm 80	BAI	01B	BES $J/\psi \rightarrow p\bar{p}\eta$
-45			
202 \pm 40	VRANA	00	DPWA Multichannel
160 \pm 12	ARNDT	96	IPWA $\gamma N \rightarrow \pi N$
90	ARNDT	95	DPWA $\pi N \rightarrow N\pi$
184	¹ ARNDT	95	DPWA $\pi N \rightarrow N\pi$
215 \pm 32	BATINIC	95	DPWA $\pi N \rightarrow N\pi, N\eta$
279 \pm 54	² BATINIC	95	DPWA $\pi N \rightarrow N\pi, N\eta$
225	LI	93	IPWA $\gamma N \rightarrow \pi N$
179	MUSETTE	80	IPWA $\pi^- \rho \rightarrow \Lambda K^0$
120	SAXON	80	DPWA $\pi^- \rho \rightarrow \Lambda K^0$
170	³ LONGACRE	77	IPWA $\pi N \rightarrow N\pi\pi$
130	⁴ LONGACRE	75	IPWA $\pi N \rightarrow N\pi\pi$

See key on page 373

Baryon Particle Listings

 $N(1650)$ $N(1650)$ BRANCHING RATIOS

$\Gamma(N\pi)/\Gamma_{\text{total}}$		Γ_1/Γ	
VALUE	DOCUMENT ID	TECN	COMMENT
0.60 to 0.95 OUR ESTIMATE			
1.0	ARNDT 06	DPWA	$\pi N \rightarrow \pi N, \eta N$
0.735 ± 0.011	GREEN 97	DPWA	$\pi N \rightarrow \pi N, \eta N$
0.89 ± 0.07	MANLEY 92	IPWA	$\pi N \rightarrow \pi N \& N\pi\pi$
0.65 ± 0.10	CUTKOSKY 80	IPWA	$\pi N \rightarrow \pi N$
0.61 ± 0.04	HOEHLER 79	IPWA	$\pi N \rightarrow \pi N$
• • • We do not use the following data for averages, fits, limits, etc. • • •			
0.70 ± 0.15	THOMA 08	DPWA	Multichannel
1.000	ARNDT 04	DPWA	$\pi N \rightarrow \pi N, \eta N$
0.65 ± 0.04	PENNER 02c	DPWA	Multichannel
0.74 ± 0.02	VRANA 00	DPWA	Multichannel
0.99	ARNDT 95	DPWA	$\pi N \rightarrow N\pi$
0.27	¹ ARNDT 95	DPWA	$\pi N \rightarrow N\pi$
0.94 ± 0.07	BATINIC 95	DPWA	$\pi N \rightarrow N\pi, N\eta$
0.49 ± 0.21	² BATINIC 95	DPWA	$\pi N \rightarrow N\pi, N\eta$

$\Gamma(N\eta)/\Gamma_{\text{total}}$		Γ_2/Γ	
VALUE	DOCUMENT ID	TECN	COMMENT
0.023 ± 0.022 OUR AVERAGE Error includes scale factor of 4.3.			
0.010 ± 0.006	PENNER 02c	DPWA	Multichannel
0.06 ± 0.01	VRANA 00	DPWA	Multichannel
• • • We do not use the following data for averages, fits, limits, etc. • • •			
0.15 ± 0.06	THOMA 08	DPWA	Multichannel
0.06 ± 0.05	BATINIC 95	DPWA	$\pi N \rightarrow N\pi, N\eta$
0.02 ± 0.03	² BATINIC 95	DPWA	$\pi N \rightarrow N\pi, N\eta$

$\Gamma(\Lambda K)/\Gamma_{\text{total}}$		Γ_3/Γ	
VALUE	DOCUMENT ID	TECN	COMMENT
0.029 ± 0.004 OUR AVERAGE Error includes scale factor of 1.2.			
0.04 ± 0.01	SHKLYAR 05	DPWA	Multichannel
0.027 ± 0.004	PENNER 02c	DPWA	Multichannel

$(\Gamma_1\Gamma_7)^{1/2}/\Gamma_{\text{total}}$ in $N\pi \rightarrow N(1650) \rightarrow \Lambda K$		$(\Gamma_1\Gamma_3)^{1/2}/\Gamma$	
VALUE	DOCUMENT ID	TECN	COMMENT
-0.27 to -0.17 OUR ESTIMATE			
-0.22	BELL 83	DPWA	$\pi^- p \rightarrow \Lambda K^0$
-0.22	SAXON 80	DPWA	$\pi^- p \rightarrow \Lambda K^0$

$(\Gamma_1\Gamma_7)^{1/2}/\Gamma_{\text{total}}$ in $N\pi \rightarrow N(1650) \rightarrow \Sigma K$		$(\Gamma_1\Gamma_4)^{1/2}/\Gamma$	
VALUE	DOCUMENT ID	TECN	COMMENT
• • • We do not use the following data for averages, fits, limits, etc. • • •			
-0.254	LIVANOS 80	DPWA	$\pi p \rightarrow \Sigma K$

Note: Signs of couplings from $\pi N \rightarrow N\pi\pi$ analyses were changed in the 1986 edition to agree with the baryon-first convention; the overall phase ambiguity is resolved by choosing a negative sign for the $\Delta(1620) S_{31}$ coupling to $\Delta(1232)\pi$.

$(\Gamma_1\Gamma_7)^{1/2}/\Gamma_{\text{total}}$ in $N\pi \rightarrow N(1650) \rightarrow \Delta(1232)\pi, D\text{-wave}$		$(\Gamma_1\Gamma_7)^{1/2}/\Gamma$	
VALUE	DOCUMENT ID	TECN	COMMENT
+0.15 to 0.23 OUR ESTIMATE			
+0.12 ± 0.04	MANLEY 92	IPWA	$\pi N \rightarrow \pi N \& N\pi\pi$
+0.29	^{3,8} LONGACRE 77	IPWA	$\pi N \rightarrow N\pi\pi$
+0.15	⁴ LONGACRE 75	IPWA	$\pi N \rightarrow N\pi\pi$
• • • We do not use the following data for averages, fits, limits, etc. • • •			
+0.26 ± 0.14	THOMA 08	DPWA	Multichannel

$\Gamma(\Delta(1232)\pi, D\text{-wave})/\Gamma_{\text{total}}$		Γ_7/Γ	
VALUE	DOCUMENT ID	TECN	COMMENT
0.02 ± 0.01	VRANA 00	DPWA	Multichannel
• • • We do not use the following data for averages, fits, limits, etc. • • •			
0.10 ± 0.05	THOMA 08	DPWA	Multichannel

$(\Gamma_1\Gamma_7)^{1/2}/\Gamma_{\text{total}}$ in $N\pi \rightarrow N(1650) \rightarrow N\rho, S=1/2, S\text{-wave}$		$(\Gamma_1\Gamma_9)^{1/2}/\Gamma$	
VALUE	DOCUMENT ID	TECN	COMMENT
±0.03 to ±0.19 OUR ESTIMATE			
-0.01 ± 0.09	MANLEY 92	IPWA	$\pi N \rightarrow \pi N \& N\pi\pi$
+0.17	^{3,8} LONGACRE 77	IPWA	$\pi N \rightarrow N\pi\pi$
-0.16	⁴ LONGACRE 75	IPWA	$\pi N \rightarrow N\pi\pi$

$\Gamma(N\rho, S=1/2, S\text{-wave})/\Gamma_{\text{total}}$		Γ_9/Γ	
VALUE	DOCUMENT ID	TECN	COMMENT
0.01 ± 0.01	VRANA 00	DPWA	Multichannel

$(\Gamma_1\Gamma_7)^{1/2}/\Gamma_{\text{total}}$ in $N\pi \rightarrow N(1650) \rightarrow N\rho, S=3/2, D\text{-wave}$		$(\Gamma_1\Gamma_{10})^{1/2}/\Gamma$	
VALUE	DOCUMENT ID	TECN	COMMENT
+0.17 to +0.29 OUR ESTIMATE			
+0.16 ± 0.06	MANLEY 92	IPWA	$\pi N \rightarrow \pi N \& N\pi\pi$
+0.29	^{3,8} LONGACRE 77	IPWA	$\pi N \rightarrow N\pi\pi$

$\Gamma(N\rho, S=3/2, D\text{-wave})/\Gamma_{\text{total}}$		Γ_{10}/Γ	
VALUE	DOCUMENT ID	TECN	COMMENT
0.13 ± 0.03	VRANA 00	DPWA	Multichannel

$(\Gamma_1\Gamma_7)^{1/2}/\Gamma_{\text{total}}$ in $N\pi \rightarrow N(1650) \rightarrow N(\pi\pi)_{S\text{-wave}}^{I=0}$		$(\Gamma_1\Gamma_{11})^{1/2}/\Gamma$	
VALUE	DOCUMENT ID	TECN	COMMENT
+0.04 to +0.18 OUR ESTIMATE			
+0.12 ± 0.08	MANLEY 92	IPWA	$\pi N \rightarrow \pi N \& N\pi\pi$
0.00	^{3,8} LONGACRE 77	IPWA	$\pi N \rightarrow N\pi\pi$
+0.25	⁴ LONGACRE 75	IPWA	$\pi N \rightarrow N\pi\pi$

$\Gamma(N(\pi\pi)_{S\text{-wave}}^{I=0})/\Gamma_{\text{total}}$		Γ_{11}/Γ	
VALUE	DOCUMENT ID	TECN	COMMENT
0.01 ± 0.01	VRANA 00	DPWA	Multichannel

$(\Gamma_1\Gamma_7)^{1/2}/\Gamma_{\text{total}}$ in $N\pi \rightarrow N(1650) \rightarrow N(1440)\pi$		$(\Gamma_1\Gamma_{12})^{1/2}/\Gamma$	
VALUE	DOCUMENT ID	TECN	COMMENT
+0.11 ± 0.06	MANLEY 92	IPWA	$\pi N \rightarrow \pi N \& N\pi\pi$

$\Gamma(N(1440)\pi)/\Gamma_{\text{total}}$		Γ_{12}/Γ	
VALUE	DOCUMENT ID	TECN	COMMENT
0.03 ± 0.01	VRANA 00	DPWA	Multichannel

 $N(1650)$ PHOTON DECAY AMPLITUDES

Papers on γN amplitudes predating 1981 may be found in our 2006 edition, Journal of Physics, G **33** 1 (2006).

 $N(1650) \rightarrow \gamma N$, helicity-1/2 amplitude $A_{1/2}$

VALUE (GeV ^{-1/2})	DOCUMENT ID	TECN	COMMENT
+0.053 ± 0.016 OUR ESTIMATE			
0.022 ± 0.007	DUGGER 07	DPWA	$\gamma N \rightarrow \pi N$
0.069 ± 0.005	ARNDT 96	IPWA	$\gamma N \rightarrow \pi N$
0.033 ± 0.015	CRAWFORD 83	IPWA	$\gamma N \rightarrow \pi N$
0.050 ± 0.010	AWAJI 81	DPWA	$\gamma N \rightarrow \pi N$
• • • We do not use the following data for averages, fits, limits, etc. • • •			
0.033	DRECHSEL 07	DPWA	$\gamma N \rightarrow \pi N$
0.049	PENNER 02D	DPWA	Multichannel
0.068 ± 0.003	LI 93	IPWA	$\gamma N \rightarrow \pi N$
0.091	WADA 84	DPWA	Compton scattering

 $N(1650) \rightarrow n\gamma$, helicity-1/2 amplitude $A_{1/2}$

VALUE (GeV ^{-1/2})	DOCUMENT ID	TECN	COMMENT
-0.015 ± 0.021 OUR ESTIMATE			
-0.015 ± 0.005	ARNDT 96	IPWA	$\gamma N \rightarrow \pi N$
-0.008 ± 0.004	AWAJI 81	DPWA	$\gamma N \rightarrow \pi N$
0.004 ± 0.004	FUJII 81	DPWA	$\gamma N \rightarrow \pi N$
• • • We do not use the following data for averages, fits, limits, etc. • • •			
0.009	DRECHSEL 07	DPWA	$\gamma N \rightarrow \pi N$
-0.011	PENNER 02D	DPWA	Multichannel
-0.002 ± 0.002	LI 93	IPWA	$\gamma N \rightarrow \pi N$

 $N(1650) \gamma p \rightarrow \Lambda K^+$ AMPLITUDES

$(\Gamma_1\Gamma_7)^{1/2}/\Gamma_{\text{total}}$ in $p\gamma \rightarrow N(1650) \rightarrow \Lambda K^+$		$(E_{0+} \text{ amplitude})$	
VALUE (units 10 ⁻³)	DOCUMENT ID	TECN	COMMENT
• • • We do not use the following data for averages, fits, limits, etc. • • •			
7.8 ± 0.3	WORKMAN 90	DPWA	
8.13	TANABE 89	DPWA	

$p\gamma \rightarrow N(1650) \rightarrow \Lambda K^+$ phase angle θ		$(E_{0+} \text{ amplitude})$	
VALUE (degrees)	DOCUMENT ID	TECN	COMMENT
• • • We do not use the following data for averages, fits, limits, etc. • • •			
-107 ± 3	WORKMAN 90	DPWA	
-107.8	TANABE 89	DPWA	

 $N(1650)$ FOOTNOTES

- ARNDT 95 finds two distinct states.
- BATINIC 95 finds two distinct states. This second resonance was associated with the $N(2090) S_{11}$.
- LONGACRE 77 pole positions are from a search for poles in the unitarized T-matrix; the first (second) value uses, in addition to $\pi N \rightarrow N\pi\pi$ data, elastic amplitudes from a Saclay (CERN) partial-wave analysis. The other LONGACRE 77 values are from eyeball fits with Breit-Wigner circles to the T-matrix amplitudes.
- From method II of LONGACRE 75: eyeball fits with Breit-Wigner circles to the T-matrix amplitudes.
- See HOEHLER 93 for a detailed discussion of the evidence for and the pole parameters of N and Δ resonances as determined from Argand diagrams of πN elastic partial-wave amplitudes and from plots of the speeds with which the amplitudes traverse the diagrams.
- ARNDT 98 also lists pole residues, which display more model dependence than do the associated pole positions.
- LONGACRE 78 values are from a search for poles in the unitarized T-matrix. The first (second) value uses, in addition to $\pi N \rightarrow N\pi\pi$ data, elastic amplitudes from a Saclay (CERN) partial-wave analysis.
- LONGACRE 77 considers this coupling to be well determined.

Baryon Particle Listings

$N(1650)$, $N(1675)$

$N(1650)$ REFERENCES

For early references, see Physics Letters **111B** 1 (1982).

THOMA	08	PL B659 87	U. Thoma et al.	(CB-ELSA Collab.)
DRECHSEL	07	EPJ A34 69	D. Drechsel, S.S. Kamalov, L. Tiator	(MAINZ, JINR)
DUGGER	07	PR C76 025211	M. Dugger et al.	(Jefferson Lab CLAS Collab.)
ARNDT	06	PR C74 045205	R.A. Arndt et al.	(GVU)
PDG		JPG 33 1	W.-M. Yao et al.	(PDG Collab.)
SHKLYAR	05	PR C72 015210	V. Shklyar, H. Lenske, U. Mosel	(GIES)
ARNDT	04	PR C69 035213	R.A. Arndt et al.	(GWU, TRIU)
PENNER	02C	PR C66 055211	G. Penner, U. Mosel	(GIES)
PENNER	02D	PR C66 055212	G. Penner, U. Mosel	(GIES)
BAI	01B	PL B510 75	J.Z. Bai et al.	(BES Collab.)
VRANA	00	PRPL 326 181	T.P. Vrana, S.A. Dytman, T.-S.H. Lee	(PITT+)
ARNDT	98	PR C58 3636	R.A. Arndt et al.	
GREEN	97	PR C55 R2167	A.M. Green, S. Wycech	(HELS, WINR)
ARNDT	96	PR C53 430	R.A. Arndt, I.I. Strakovsky, R.L. Workman	(VPI)
ARNDT	95	PR C52 2120	R.A. Arndt et al.	(VPI, BRCO)
BATINIC	95	PR C51 2310	M. Batinic et al.	(BOSK, UCLA)
Also		PR C57 1004 (erratum)	M. Batinic et al.	
HOEHLER	93	πN Newsletter 9 1	G. Hohler	(KARL)
LI	93	PR C47 2759	Z.J. Li et al.	(VPI)
MANLEY	92	PR D45 4002	D.M. Manley, E.M. Saleski	(KENT) IJP
Also		PR D30 904	D.M. Manley et al.	(VPI)
ARNDT	91	PR D43 2131	R.A. Arndt et al.	(VPI, TELE) IJP
WORKMAN	90	PR C42 781	R.L. Workman	(VPI)
TANABE	89	PR C39 741	H. Tanabe, M. Kohno, C. Bennhold	(MANZ)
Also		NC 102A 193	M. Kohno, H. Tanabe, C. Bennhold	(MANZ)
WADA	84	NP B247 313	Y. Wada et al.	(INUS)
BELL	83	NP B222 389	K.W. Bell et al.	(RL) IJP
CRAWFORD	83	NP B211 1	R.L. Crawford, W.T. Morton	(GLAS)
PDG	82	PL 111B 1	M. Roos et al.	(HELS, CIT, CERN)
AWAJI	81	Bonn Conf. 352	N. Awaji, R. Kajikawa	(NAGO)
Also		NP B197 365	K. Fujii et al.	(NAGO)
FUJII	81	NP B187 53	K. Fujii et al.	(NAGO, OSAK)
CUTKOSKY	80	Toronto Conf. 19	R.E. Cutkosky et al.	(CMU, LBL) IJP
Also		PR D20 2839	R.E. Cutkosky et al.	(CMU, LBL) IJP
LIVANOS	80	Toronto Conf. 35	P. Livanos et al.	(SACL) IJP
MUSETTE	80	NC 57A 37	M. Musette	(BRUX) IJP
SAXON	80	NP B162 522	D.H. Saxon et al.	(RHEL, BRIS) IJP
HOEHLER	79	PDAT 12-1	G. Hor et al.	(KARL) IJP
Also		Toronto Conf. 3	R. Koch	(KARL) IJP
LONGACRE	78	PR D17 1795	R.S. Longacre et al.	(LBL, SLAC) IJP
LONGACRE	77	NP B122 493	R.S. Longacre, J. Dolbeau	(SACL) IJP
Also		NP B108 365	J. Dolbeau et al.	(SACL) IJP
LONGACRE	75	PL 55B 415	R.S. Longacre et al.	(LBL, SLAC) IJP

$N(1675) D_{15}$

 $I(J^P) = \frac{1}{2}(\frac{5}{2}^-)$ Status: * * * *

Most of the results published before 1975 were last included in our 1982 edition, Physics Letters **111B** 1 (1982). Some further obsolete results published before 1984 were last included in our 2006 edition, Journal of Physics, G **33** 1 (2006).

$N(1675)$ BREIT-WIGNER MASS

VALUE (MeV)	DOCUMENT ID	TECN	COMMENT
1670 to 1680 (≈ 1675) OUR ESTIMATE			
1674.1 \pm 0.2	ARNDT	06	DPWA $\pi N \rightarrow \pi N, \eta N$
1676 \pm 2	MANLEY	92	IPWA $\pi N \rightarrow \pi N \& N\pi\pi$
1675 \pm 10	CUTKOSKY	80	IPWA $\pi N \rightarrow \pi N$
1679 \pm 8	HOEHLER	79	IPWA $\pi N \rightarrow \pi N$
• • • We do not use the following data for averages, fits, limits, etc. • • •			
1678 \pm 15	THOMA	08	DPWA Multichannel
1676.2 \pm 0.6	ARNDT	04	DPWA $\pi N \rightarrow \pi N, \eta N$
1685 \pm 4	VRANA	00	DPWA Multichannel
1673 \pm 5	ARNDT	96	IPWA $\gamma N \rightarrow \pi N$
1673	ARNDT	95	DPWA $\pi N \rightarrow N\pi$
1683 \pm 19	BATINIC	95	DPWA $\pi N \rightarrow N\pi, N\eta$
1666	LI	93	IPWA $\gamma N \rightarrow \pi N$
1670	SAXON	80	DPWA $\pi^- \rho \rightarrow \Lambda K^0$
1650	¹ LONGACRE	77	IPWA $\pi N \rightarrow N\pi\pi$
1660	² LONGACRE	75	IPWA $\pi N \rightarrow N\pi\pi$

$N(1675)$ BREIT-WIGNER WIDTH

VALUE (MeV)	DOCUMENT ID	TECN	COMMENT
130 to 165 (≈ 150) OUR ESTIMATE			
146.5 \pm 1.0	ARNDT	06	DPWA $\pi N \rightarrow \pi N, \eta N$
159 \pm 7	MANLEY	92	IPWA $\pi N \rightarrow \pi N \& N\pi\pi$
160 \pm 20	CUTKOSKY	80	IPWA $\pi N \rightarrow \pi N$
120 \pm 15	HOEHLER	79	IPWA $\pi N \rightarrow \pi N$
• • • We do not use the following data for averages, fits, limits, etc. • • •			
220 \pm 25	THOMA	08	DPWA Multichannel
151.8 \pm 3.0	ARNDT	04	DPWA $\pi N \rightarrow \pi N, \eta N$
131 \pm 10	VRANA	00	DPWA Multichannel
154 \pm 7	ARNDT	96	IPWA $\gamma N \rightarrow \pi N$
154	ARNDT	95	DPWA $\pi N \rightarrow N\pi$
142 \pm 23	BATINIC	95	DPWA $\pi N \rightarrow N\pi, N\eta$
136	LI	93	IPWA $\gamma N \rightarrow \pi N$
40	SAXON	80	DPWA $\pi^- \rho \rightarrow \Lambda K^0$
130	¹ LONGACRE	77	IPWA $\pi N \rightarrow N\pi\pi$
150	² LONGACRE	75	IPWA $\pi N \rightarrow N\pi\pi$

$N(1675)$ POLE POSITION

REAL PART

VALUE (MeV)	DOCUMENT ID	TECN	COMMENT
1655 to 1665 (≈ 1660) OUR ESTIMATE			
1657	ARNDT	06	DPWA $\pi N \rightarrow \pi N, \eta N$
1656	³ HOEHLER	93	ARGD $\pi N \rightarrow \pi N$
1660 \pm 10	CUTKOSKY	80	IPWA $\pi N \rightarrow \pi N$
• • • We do not use the following data for averages, fits, limits, etc. • • •			
1639 \pm 10	THOMA	08	DPWA Multichannel
1659	ARNDT	04	DPWA $\pi N \rightarrow \pi N, \eta N$
1674	VRANA	00	DPWA Multichannel
1663	ARNDT	95	DPWA $\pi N \rightarrow N\pi$
1655	ARNDT	91	DPWA $\pi N \rightarrow \pi N$ Soln SM90
1663 or 1668	⁴ LONGACRE	78	IPWA $\pi N \rightarrow N\pi\pi$
1649 or 1650	¹ LONGACRE	77	IPWA $\pi N \rightarrow N\pi\pi$

-2xIMAGINARY PART

VALUE (MeV)	DOCUMENT ID	TECN	COMMENT
125 to 150 (≈ 135) OUR ESTIMATE			
139	ARNDT	06	DPWA $\pi N \rightarrow \pi N, \eta N$
126	³ HOEHLER	93	ARGD $\pi N \rightarrow \pi N$
140 \pm 10	CUTKOSKY	80	IPWA $\pi N \rightarrow \pi N$
• • • We do not use the following data for averages, fits, limits, etc. • • •			
180 \pm 20	THOMA	08	DPWA Multichannel
146	ARNDT	04	DPWA $\pi N \rightarrow \pi N, \eta N$
120	VRANA	00	DPWA Multichannel
152	ARNDT	95	DPWA $\pi N \rightarrow N\pi$
124	ARNDT	91	DPWA $\pi N \rightarrow \pi N$ Soln SM90
146 or 171	⁴ LONGACRE	78	IPWA $\pi N \rightarrow N\pi\pi$
127 or 127	¹ LONGACRE	77	IPWA $\pi N \rightarrow N\pi\pi$

$N(1675)$ ELASTIC POLE RESIDUE

MODULUS $|r|$

VALUE (MeV)	DOCUMENT ID	TECN	COMMENT
27	ARNDT	06	DPWA $\pi N \rightarrow \pi N, \eta N$
23	HOEHLER	93	ARGD $\pi N \rightarrow \pi N$
31 \pm 5	CUTKOSKY	80	IPWA $\pi N \rightarrow \pi N$
• • • We do not use the following data for averages, fits, limits, etc. • • •			
29	ARNDT	04	DPWA $\pi N \rightarrow \pi N, \eta N$
29	ARNDT	95	DPWA $\pi N \rightarrow N\pi$
28	ARNDT	91	DPWA $\pi N \rightarrow \pi N$ Soln SM90

PHASE θ

VALUE ($^\circ$)	DOCUMENT ID	TECN	COMMENT
-21	ARNDT	06	DPWA $\pi N \rightarrow \pi N, \eta N$
-22	HOEHLER	93	ARGD $\pi N \rightarrow \pi N$
-30 \pm 10	CUTKOSKY	80	IPWA $\pi N \rightarrow \pi N$
• • • We do not use the following data for averages, fits, limits, etc. • • •			
-22	ARNDT	04	DPWA $\pi N \rightarrow \pi N, \eta N$
-6	ARNDT	95	DPWA $\pi N \rightarrow N\pi$
-17	ARNDT	91	DPWA $\pi N \rightarrow \pi N$ Soln SM90

$N(1675)$ DECAY MODES

The following branching fractions are our estimates, not fits or averages.

Mode	Fraction (Γ_i/Γ)
Γ_1 $N\pi$	0.35 to 0.45
Γ_2 $N\eta$	(0.0 \pm 1.0) %
Γ_3 ΛK	<1 %
Γ_4 ΣK	
Γ_5 $N\pi\pi$	50-60 %
Γ_6 $\Delta\pi$	50-60 %
Γ_7 $\Delta(1232)\pi$, D-wave	
Γ_8 $\Delta(1232)\pi$, G-wave	
Γ_9 $N\rho$	<1-3 %
Γ_{10} $N\rho$, S=1/2, D-wave	
Γ_{11} $N\rho$, S=3/2, D-wave	
Γ_{12} $N\rho$, S=3/2, G-wave	
Γ_{13} $N(\pi\pi)_{S=0}^0$	
Γ_{14} $p\gamma$	0.004-0.023 %
Γ_{15} $p\gamma$, helicity=1/2	0.0-0.015 %
Γ_{16} $p\gamma$, helicity=3/2	0.0-0.011 %
Γ_{17} $n\gamma$	0.02-0.12 %
Γ_{18} $n\gamma$, helicity=1/2	0.006-0.046 %
Γ_{19} $n\gamma$, helicity=3/2	0.01-0.08 %

N(1675) BRANCHING RATIOS

$\Gamma(N\pi)/\Gamma_{\text{total}}$	DOCUMENT ID	TECN	COMMENT	Γ_1/Γ
0.35 to 0.45 OUR ESTIMATE				
0.393 ± 0.001	ARNDT 06	DPWA	$\pi N \rightarrow \pi N, \eta N$	
0.47 ± 0.02	MANLEY 92	IPWA	$\pi N \rightarrow \pi N \& N\pi\pi$	
0.38 ± 0.05	CUTKOSKY 80	IPWA	$\pi N \rightarrow \pi N$	
0.38 ± 0.03	HOEHLER 79	IPWA	$\pi N \rightarrow \pi N$	
• • • We do not use the following data for averages, fits, limits, etc. • • •				
0.30 ± 0.08	THOMA 08	DPWA	Multichannel	
0.400 ± 0.002	ARNDT 04	DPWA	$\pi N \rightarrow \pi N, \eta N$	
0.35 ± 0.01	VRANA 00	DPWA	Multichannel	
0.38	ARNDT 95	DPWA	$\pi N \rightarrow N\pi$	
0.31 ± 0.06	BATINIC 95	DPWA	$\pi N \rightarrow N\pi, N\eta$	

$\Gamma(N\eta)/\Gamma_{\text{total}}$	DOCUMENT ID	TECN	COMMENT	Γ_2/Γ
0.00 ± 0.01				
• • • We do not use the following data for averages, fits, limits, etc. • • •				
0.03 ± 0.03	THOMA 08	DPWA	Multichannel	
0.001 ± 0.001	BATINIC 95	DPWA	$\pi N \rightarrow N\pi, N\eta$	

$(\Gamma_1\Gamma_2)^{1/2}/\Gamma_{\text{total}}$ in $N\pi \rightarrow N(1675) \rightarrow \Lambda K$	DOCUMENT ID	TECN	COMMENT	$(\Gamma_1\Gamma_3)^{1/2}/\Gamma$
±0.04 to ±0.08 OUR ESTIMATE				
-0.01	BELL 83	DPWA	$\pi^- p \rightarrow \Lambda K^0$	
+0.036	5 SAXON 80	DPWA	$\pi^- p \rightarrow \Lambda K^0$	

Note: Signs of couplings from $\pi N \rightarrow N\pi\pi$ analyses were changed in the 1986 edition to agree with the baryon-first convention; the overall phase ambiguity is resolved by choosing a negative sign for the $\Delta(1620) S_{31}$ coupling to $\Delta(1232)\pi$.

$(\Gamma_1\Gamma_2)^{1/2}/\Gamma_{\text{total}}$ in $N\pi \rightarrow N(1675) \rightarrow \Delta(1232)\pi, D\text{-wave}$	DOCUMENT ID	TECN	COMMENT	$(\Gamma_1\Gamma_7)^{1/2}/\Gamma$
+0.46 to +0.50 OUR ESTIMATE				
+0.496 ± 0.003	MANLEY 92	IPWA	$\pi N \rightarrow \pi N \& N\pi\pi$	
+0.46	1,6 LONGACRE 77	IPWA	$\pi N \rightarrow N\pi\pi$	
+0.50	2 LONGACRE 75	IPWA	$\pi N \rightarrow N\pi\pi$	

$\Gamma(\Delta(1232)\pi, D\text{-wave})/\Gamma_{\text{total}}$	DOCUMENT ID	TECN	COMMENT	Γ_7/Γ
0.63 ± 0.02	VRANA 00	DPWA	Multichannel	
• • • We do not use the following data for averages, fits, limits, etc. • • •				
0.24 ± 0.08	THOMA 08	DPWA	Multichannel	

$(\Gamma_1\Gamma_7)^{1/2}/\Gamma_{\text{total}}$ in $N\pi \rightarrow N(1675) \rightarrow N\rho, S=1/2, D\text{-wave}$	DOCUMENT ID	TECN	COMMENT	$(\Gamma_1\Gamma_{10})^{1/2}/\Gamma$
+0.04 ± 0.02	MANLEY 92	IPWA	$\pi N \rightarrow \pi N \& N\pi\pi$	

$\Gamma(N\rho, S=1/2, D\text{-wave})/\Gamma_{\text{total}}$	DOCUMENT ID	TECN	COMMENT	Γ_{10}/Γ
0.00 ± 0.01	VRANA 00	DPWA	Multichannel	

$(\Gamma_1\Gamma_7)^{1/2}/\Gamma_{\text{total}}$ in $N\pi \rightarrow N(1675) \rightarrow N\rho, S=3/2, D\text{-wave}$	DOCUMENT ID	TECN	COMMENT	$(\Gamma_1\Gamma_{11})^{1/2}/\Gamma$
-0.12 to -0.06 OUR ESTIMATE				
-0.03 ± 0.02	MANLEY 92	IPWA	$\pi N \rightarrow \pi N \& N\pi\pi$	
-0.15	1,6 LONGACRE 77	IPWA	$\pi N \rightarrow N\pi\pi$	

$\Gamma(N\rho, S=3/2, D\text{-wave})/\Gamma_{\text{total}}$	DOCUMENT ID	TECN	COMMENT	Γ_{11}/Γ
0.01 ± 0.01	VRANA 00	DPWA	Multichannel	

$(\Gamma_1\Gamma_7)^{1/2}/\Gamma_{\text{total}}$ in $N\pi \rightarrow N(1675) \rightarrow N(\pi\pi)_{S=0}^0$	DOCUMENT ID	TECN	COMMENT	$(\Gamma_1\Gamma_{13})^{1/2}/\Gamma$
+0.03	1,6 LONGACRE 77	IPWA	$\pi N \rightarrow N\pi\pi$	

N(1675) PHOTON DECAY AMPLITUDES

Papers on γN amplitudes predating 1981 may be found in our 2006 edition, Journal of Physics, G 33 1 (2006).

N(1675) $\rightarrow \rho\gamma$, helicity-1/2 amplitude $A_{1/2}$

VALUE (GeV ^{-1/2})	DOCUMENT ID	TECN	COMMENT
+0.019 ± 0.008 OUR ESTIMATE			
0.018 ± 0.002	DUGGER 07	DPWA	$\gamma N \rightarrow \pi N$
0.015 ± 0.010	ARNDT 96	IPWA	$\gamma N \rightarrow \pi N$
0.021 ± 0.011	CRAWFORD 83	IPWA	$\gamma N \rightarrow \pi N$
0.034 ± 0.005	AWAJI 81	DPWA	$\gamma N \rightarrow \pi N$
• • • We do not use the following data for averages, fits, limits, etc. • • •			
0.015	DRECHSEL 07	DPWA	$\gamma N \rightarrow \pi N$
0.012 ± 0.002	LI 93	IPWA	$\gamma N \rightarrow \pi N$

N(1675) $\rightarrow \rho\gamma$, helicity-3/2 amplitude $A_{3/2}$

VALUE (GeV ^{-1/2})	DOCUMENT ID	TECN	COMMENT
+0.015 ± 0.009 OUR ESTIMATE			
0.021 ± 0.001	DUGGER 07	DPWA	$\gamma N \rightarrow \pi N$
0.010 ± 0.007	ARNDT 96	IPWA	$\gamma N \rightarrow \pi N$
0.015 ± 0.009	CRAWFORD 83	IPWA	$\gamma N \rightarrow \pi N$
0.024 ± 0.008	AWAJI 81	DPWA	$\gamma N \rightarrow \pi N$
• • • We do not use the following data for averages, fits, limits, etc. • • •			
0.022	DRECHSEL 07	DPWA	$\gamma N \rightarrow \pi N$
0.021 ± 0.002	LI 93	IPWA	$\gamma N \rightarrow \pi N$

N(1675) $\rightarrow n\gamma$, helicity-1/2 amplitude $A_{1/2}$

VALUE (GeV ^{-1/2})	DOCUMENT ID	TECN	COMMENT
-0.043 ± 0.012 OUR ESTIMATE			
-0.049 ± 0.010	ARNDT 96	IPWA	$\gamma N \rightarrow \pi N$
-0.057 ± 0.024	AWAJI 81	DPWA	$\gamma N \rightarrow \pi N$
-0.033 ± 0.004	FUJII 81	DPWA	$\gamma N \rightarrow \pi N$
• • • We do not use the following data for averages, fits, limits, etc. • • •			
-0.062	DRECHSEL 07	DPWA	$\gamma N \rightarrow \pi N$
-0.060 ± 0.003	LI 93	IPWA	$\gamma N \rightarrow \pi N$

N(1675) $\rightarrow n\gamma$, helicity-3/2 amplitude $A_{3/2}$

VALUE (GeV ^{-1/2})	DOCUMENT ID	TECN	COMMENT
-0.058 ± 0.013 OUR ESTIMATE			
-0.051 ± 0.010	ARNDT 96	IPWA	$\gamma N \rightarrow \pi N$
-0.077 ± 0.018	AWAJI 81	DPWA	$\gamma N \rightarrow \pi N$
-0.069 ± 0.004	FUJII 81	DPWA	$\gamma N \rightarrow \pi N$
• • • We do not use the following data for averages, fits, limits, etc. • • •			
-0.084	DRECHSEL 07	DPWA	$\gamma N \rightarrow \pi N$
-0.074 ± 0.003	LI 93	IPWA	$\gamma N \rightarrow \pi N$

N(1675) FOOTNOTES

- LONGACRE 77 pole positions are from a search for poles in the unitarized T-matrix; the first (second) value uses, in addition to $\pi N \rightarrow N\pi\pi$ data, elastic amplitudes from a Saclay (CERN) partial-wave analysis. The other LONGACRE 77 values are from eyeball fits with Breit-Wigner circles to the T-matrix amplitudes.
- From method II of LONGACRE 75: eyeball fits with Breit-Wigner circles to the T-matrix amplitudes.
- See HOEHLER 93 for a detailed discussion of the evidence for and the pole parameters of N and Δ resonances as determined from Argand diagrams of πN elastic partial-wave amplitudes and from plots of the speeds with which the amplitudes traverse the diagrams.
- LONGACRE 78 values are from a search for poles in the unitarized T-matrix. The first (second) value uses, in addition to $\pi N \rightarrow N\pi\pi$ data, elastic amplitudes from a Saclay (CERN) partial-wave analysis.
- SAXON 80 finds the coupling phase is near 90°.
- LONGACRE 77 considers this coupling to be well determined.

N(1675) REFERENCES

For early references, see Physics Letters 111B 1 (1982).

THOMA 08	PL B659 87	U. Thoma <i>et al.</i>	(CB-ELSA Collab.)
DRECHSEL 07	EPJ A34 69	D. Drechsel, S.S. Kamalov, L. Tiator	(MAINZ, JINR)
DUGGER 07	PR C76 025211	M. Dugger <i>et al.</i>	(Jefferson Lab CLAS Collab.)
ARNDT 06	PR C74 045205	R.A. Arndt <i>et al.</i>	(GWU)
PDG 06	JPG 33 1	W.-M. Yao <i>et al.</i>	(PDG Collab.)
ARNDT 04	PR C69 035213	R.A. Arndt <i>et al.</i>	(GWU, TRIU)
VRANA 00	PRPL 328 181	T.P. Vrana, S.A. Dytman, T.-S.H. Lee	(PITT+)
ARNDT 96	PR C53 430	R.A. Arndt, I.I. Strakovsky, R.L. Workman	(VPI)
ARNDT 95	PR C52 2120	R.A. Arndt <i>et al.</i>	(VPI, BRCC)
BATINIC 95	PR C51 2310	M. Batinic <i>et al.</i>	(BOSK, UCLA)
Also	PR C57 1004 (erratum)	M. Batinic <i>et al.</i>	
HOEHLER 93	πN Newsletter 9 1	G. Hohler	(KARL)
LI 93	PR C47 2759	Z.J. Li <i>et al.</i>	(VPI)
MANLEY 92	PR D45 4002	D.M. Manley, E.M. Saleski	(KENT, IJP)
Also	PR D30 904	D.M. Manley <i>et al.</i>	(VPI)
ARNDT 91	PR D43 2131	R.A. Arndt <i>et al.</i>	(VPI, TELE IJP)
BELL 83	NP B222 389	K.W. Bell <i>et al.</i>	(RL IJP)
CRAWFORD 83	NP B211 1	R.L. Crawford, W.T. Morton	(GLAS)
PDG 82	PL 111B 1	M. Roos <i>et al.</i>	(HEL, CIT, CERN)
AWAJI 81	Bonn Conf. 352	N. Awaji, R. Kajikawa	(NAGO)
Also	NP B197 365	K. Fujii <i>et al.</i>	(NAGO)
FUJII 81	NP B187 53	K. Fujii <i>et al.</i>	(NAGO, OSAK)
CUTKOSKY 80	Toronto Conf. 19	R.E. Cutkosky <i>et al.</i>	(CMU, LBL) IJP
Also	PR D20 2839	R.E. Cutkosky <i>et al.</i>	(CMU, LBL) IJP
SAXON 80	NP B162 522	D.H. Saxon <i>et al.</i>	(RHEL, BRIS) IJP
HOEHLER 79	PDAT 12-1	G. Hohler <i>et al.</i>	(KARL) IJP
Also	Toronto Conf. 3	R. Koch	(KARL) IJP
LONGACRE 78	PR D17 1795	R.S. Longacre <i>et al.</i>	(LBL, SLAC)
LONGACRE 77	NP B122 493	R.S. Longacre, J. Dolbeau	(SACL) IJP
Also	NP B108 365	J. Dolbeau <i>et al.</i>	(SACL) IJP
LONGACRE 75	PL 55B 415	R.S. Longacre <i>et al.</i>	(LBL, SLAC) IJP

N(1675) $\rightarrow \rho\gamma$, helicity-1/2 amplitude $A_{1/2}$

Baryon Particle Listings

N(1680)

N(1680) F₁₅

$$I(J^P) = \frac{1}{2}(\frac{5}{2}^+) \text{ Status: } ****$$

Most of the results published before 1975 were last included in our 1982 edition, Physics Letters **111B** 1 (1982). Some further obsolete results published before 1984 were last included in our 2006 edition, Journal of Physics, G **33** 1 (2006).

N(1680) BREIT-WIGNER MASS

VALUE (MeV)	DOCUMENT ID	TECN	COMMENT
1680 to 1690 (≈ 1685) OUR ESTIMATE			
1680.1 ± 0.2	ARNDT 06	DPWA	$\pi N \rightarrow \pi N, \eta N$
1684 ± 4	MANLEY 92	IPWA	$\pi N \rightarrow \pi N \& N\pi\pi$
1680 ± 10	CUTKOSKY 80	IPWA	$\pi N \rightarrow \pi N$
1684 ± 3	HOEHLER 79	IPWA	$\pi N \rightarrow \pi N$
••• We do not use the following data for averages, fits, limits, etc. •••			
1684 ± 8	THOMA 08	DPWA	Multichannel
1683.2 ± 0.7	ARNDT 04	DPWA	$\pi N \rightarrow \pi N, \eta N$
1679 ± 3	VRANA 00	DPWA	Multichannel
1679 ± 5	ARNDT 96	IPWA	$\gamma N \rightarrow \pi N$
1678	ARNDT 95	DPWA	$\pi N \rightarrow N\pi$
1674 ± 12	BATINIC 95	DPWA	$\pi N \rightarrow N\pi, N\eta$
1660	¹ LONGACRE 77	IPWA	$\pi N \rightarrow N\pi\pi$
1670	² LONGACRE 75	IPWA	$\pi N \rightarrow N\pi\pi$

N(1680) BREIT-WIGNER WIDTH

VALUE (MeV)	DOCUMENT ID	TECN	COMMENT
120 to 140 (≈ 130) OUR ESTIMATE			
128.0 ± 1.1	ARNDT 06	DPWA	$\pi N \rightarrow \pi N, \eta N$
139 ± 8	MANLEY 92	IPWA	$\pi N \rightarrow \pi N \& N\pi\pi$
120 ± 10	CUTKOSKY 80	IPWA	$\pi N \rightarrow \pi N$
128 ± 8	HOEHLER 79	IPWA	$\pi N \rightarrow \pi N$
••• We do not use the following data for averages, fits, limits, etc. •••			
105 ± 8	THOMA 08	DPWA	Multichannel
134.4 ± 3.8	ARNDT 04	DPWA	$\pi N \rightarrow \pi N, \eta N$
128 ± 9	VRANA 00	DPWA	Multichannel
124 ± 4	ARNDT 96	IPWA	$\gamma N \rightarrow \pi N$
126	ARNDT 95	DPWA	$\pi N \rightarrow N\pi$
126 ± 20	BATINIC 95	DPWA	$\pi N \rightarrow N\pi, N\eta$
150	¹ LONGACRE 77	IPWA	$\pi N \rightarrow N\pi\pi$
130	² LONGACRE 75	IPWA	$\pi N \rightarrow N\pi\pi$

N(1680) POLE POSITION

REAL PART

VALUE (MeV)	DOCUMENT ID	TECN	COMMENT
1665 to 1680 (≈ 1675) OUR ESTIMATE			
1674	ARNDT 06	DPWA	$\pi N \rightarrow \pi N, \eta N$
1673	³ HOEHLER 93	ARGD	$\pi N \rightarrow \pi N$
1667 ± 5	CUTKOSKY 80	IPWA	$\pi N \rightarrow \pi N$
••• We do not use the following data for averages, fits, limits, etc. •••			
1674 ± 5	THOMA 08	DPWA	Multichannel
1678	ARNDT 04	DPWA	$\pi N \rightarrow \pi N, \eta N$
1667	VRANA 00	DPWA	Multichannel
1670	ARNDT 95	DPWA	$\pi N \rightarrow N\pi$
1670	ARNDT 91	DPWA	$\pi N \rightarrow \pi N$ Soln SM90
1668 or 1674	⁴ LONGACRE 78	IPWA	$\pi N \rightarrow N\pi\pi$
1656 or 1653	¹ LONGACRE 77	IPWA	$\pi N \rightarrow N\pi\pi$

-2xIMAGINARY PART

VALUE (MeV)	DOCUMENT ID	TECN	COMMENT
110 to 135 (≈ 120) OUR ESTIMATE			
115	ARNDT 06	DPWA	$\pi N \rightarrow \pi N, \eta N$
135	³ HOEHLER 93	ARGD	$\pi N \rightarrow \pi N$
110 ± 10	CUTKOSKY 80	IPWA	$\pi N \rightarrow \pi N$
••• We do not use the following data for averages, fits, limits, etc. •••			
95 ± 10	THOMA 08	DPWA	Multichannel
120	ARNDT 04	DPWA	$\pi N \rightarrow \pi N, \eta N$
122	VRANA 00	DPWA	Multichannel
120	ARNDT 95	DPWA	$\pi N \rightarrow N\pi$
116	ARNDT 91	DPWA	$\pi N \rightarrow \pi N$ Soln SM90
132 or 137	⁴ LONGACRE 78	IPWA	$\pi N \rightarrow N\pi\pi$
145 or 143	¹ LONGACRE 77	IPWA	$\pi N \rightarrow N\pi\pi$

N(1680) ELASTIC POLE RESIDUE

MODULUS |r|

VALUE (MeV)	DOCUMENT ID	TECN	COMMENT
42	ARNDT 06	DPWA	$\pi N \rightarrow \pi N, \eta N$
44	HOEHLER 93	ARGD	$\pi N \rightarrow \pi N$
34 ± 2	CUTKOSKY 80	IPWA	$\pi N \rightarrow \pi N$
••• We do not use the following data for averages, fits, limits, etc. •••			
43	ARNDT 04	DPWA	$\pi N \rightarrow \pi N, \eta N$
40	ARNDT 95	DPWA	$\pi N \rightarrow N\pi$
37	ARNDT 91	DPWA	$\pi N \rightarrow \pi N$ Soln SM90

PHASE θ

VALUE (°)	DOCUMENT ID	TECN	COMMENT
-4	ARNDT 06	DPWA	$\pi N \rightarrow \pi N, \eta N$
-17	HOEHLER 93	ARGD	$\pi N \rightarrow \pi N$
-25 ± 5	CUTKOSKY 80	IPWA	$\pi N \rightarrow \pi N$
••• We do not use the following data for averages, fits, limits, etc. •••			
1	ARNDT 04	DPWA	$\pi N \rightarrow \pi N, \eta N$
+1	ARNDT 95	DPWA	$\pi N \rightarrow N\pi$
-14	ARNDT 91	DPWA	$\pi N \rightarrow \pi N$ Soln SM90

N(1680) DECAY MODES

The following branching fractions are our estimates, not fits or averages.

Mode	Fraction (Γ_i/Γ)
Γ_1 $N\pi$	0.65 to 0.70
Γ_2 $N\eta$	(0.0 ± 1.0) %
Γ_3 ΛK	
Γ_4 ΣK	
Γ_5 $N\pi\pi$	30-40 %
Γ_6 $\Delta\pi$	5-15 %
Γ_7 $\Delta(1232)\pi, P\text{-wave}$	6-14 %
Γ_8 $\Delta(1232)\pi, F\text{-wave}$	<2 %
Γ_9 $N\rho$	3-15 %
Γ_{10} $N\rho, S=1/2, F\text{-wave}$	
Γ_{11} $N\rho, S=3/2, P\text{-wave}$	<12 %
Γ_{12} $N\rho, S=3/2, F\text{-wave}$	1-5 %
Γ_{13} $N(\pi\pi)_{S\text{-wave}}^{I=0}$	5-20 %
Γ_{14} $p\gamma$	0.21-0.32 %
Γ_{15} $p\gamma, \text{helicity}=1/2$	0.001-0.011 %
Γ_{16} $p\gamma, \text{helicity}=3/2$	0.20-0.32 %
Γ_{17} $n\gamma$	0.021-0.046 %
Γ_{18} $n\gamma, \text{helicity}=1/2$	0.004-0.029 %
Γ_{19} $n\gamma, \text{helicity}=3/2$	0.01-0.024 %

N(1680) BRANCHING RATIOS

$\Gamma(N\pi)/\Gamma_{\text{total}}$	DOCUMENT ID	TECN	COMMENT	Γ_1/Γ
0.65 to 0.70 OUR ESTIMATE				
0.701 ± 0.001	ARNDT 06	DPWA	$\pi N \rightarrow \pi N, \eta N$	
0.70 ± 0.03	MANLEY 92	IPWA	$\pi N \rightarrow \pi N \& N\pi\pi$	
0.62 ± 0.05	CUTKOSKY 80	IPWA	$\pi N \rightarrow \pi N$	
0.65 ± 0.02	HOEHLER 79	IPWA	$\pi N \rightarrow \pi N$	
••• We do not use the following data for averages, fits, limits, etc. •••				
0.72 ± 0.15	THOMA 08	DPWA	Multichannel	
0.670 ± 0.004	ARNDT 04	DPWA	$\pi N \rightarrow \pi N, \eta N$	
0.69 ± 0.02	VRANA 00	DPWA	Multichannel	
0.68	ARNDT 95	DPWA	$\pi N \rightarrow N\pi$	
0.69 ± 0.04	BATINIC 95	DPWA	$\pi N \rightarrow N\pi, N\eta$	

 $(\Gamma_1\Gamma_7)^{1/2}/\Gamma_{\text{total}}$ in $N\pi \rightarrow N(1680) \rightarrow N\eta$ $(\Gamma_1\Gamma_2)^{1/2}/\Gamma$

VALUE	DOCUMENT ID	TECN	COMMENT
••• We do not use the following data for averages, fits, limits, etc. •••			
not seen	BAKER 79	DPWA	$\pi^- p \rightarrow n\eta$

 $\Gamma(N\eta)/\Gamma_{\text{total}}$ Γ_2/Γ

VALUE	DOCUMENT ID	TECN	COMMENT
0.00 ± 0.01	VRANA 00	DPWA	Multichannel
••• We do not use the following data for averages, fits, limits, etc. •••			
<0.01	THOMA 08	DPWA	Multichannel
0.0015 ^{+0.0035} _{-0.0010}	TIATOR 99	DPWA	$\gamma p \rightarrow p\eta$
0.01 ± 0.004	BATINIC 95	DPWA	$\pi N \rightarrow N\pi, N\eta$

 $(\Gamma_1\Gamma_7)^{1/2}/\Gamma_{\text{total}}$ in $N\pi \rightarrow N(1680) \rightarrow \Lambda K$ $(\Gamma_1\Gamma_3)^{1/2}/\Gamma$

Coupling to ΛK not required in the analyses of SAXON 80 or BELL 83.

Note: Signs of couplings from $\pi N \rightarrow N\pi\pi$ analyses were changed in the 1986 edition to agree with the baryon-first convention; the overall phase ambiguity is resolved by choosing a negative sign for the $\Delta(1620)$ S_{31} coupling to $\Delta(1232)\pi$.

 $(\Gamma_1\Gamma_7)^{1/2}/\Gamma_{\text{total}}$ in $N\pi \rightarrow N(1680) \rightarrow \Delta(1232)\pi, P\text{-wave}$ $(\Gamma_1\Gamma_7)^{1/2}/\Gamma$

VALUE	DOCUMENT ID	TECN	COMMENT
-0.31 to -0.21 OUR ESTIMATE			
-0.26 ± 0.04	MANLEY 92	IPWA	$\pi N \rightarrow \pi N \& N\pi\pi$
-0.27	^{1,5} LONGACRE 77	IPWA	$\pi N \rightarrow N\pi\pi$
-0.25	² LONGACRE 75	IPWA	$\pi N \rightarrow N\pi\pi$

See key on page 373

Baryon Particle Listings

N(1680)

$\Gamma(\Delta(1232)\pi, P\text{-wave})/\Gamma_{\text{total}}$ **Γ_7/Γ**

VALUE	DOCUMENT ID	TECN	COMMENT
0.14±0.03	VRANA 00	DPWA	Multichannel
0.08±0.03	THOMA 08	DPWA	Multichannel

••• We do not use the following data for averages, fits, limits, etc. •••

$(\Gamma_7/\Gamma)^{1/2}/\Gamma_{\text{total}}$ in $N\pi \rightarrow N(1680) \rightarrow \Delta(1232)\pi, F\text{-wave}$ **$(\Gamma_7\Gamma_8)^{1/2}/\Gamma$**

VALUE	DOCUMENT ID	TECN	COMMENT
+0.03 to +0.11 OUR ESTIMATE			
+0.07±0.03	MANLEY 92	IPWA	$\pi N \rightarrow \pi N \& N\pi\pi$
+0.07	1.5 LONGACRE 77	IPWA	$\pi N \rightarrow N\pi\pi$
+0.08	2 LONGACRE 75	IPWA	$\pi N \rightarrow N\pi\pi$

$\Gamma(\Delta(1232)\pi, F\text{-wave})/\Gamma_{\text{total}}$ **Γ_8/Γ**

VALUE	DOCUMENT ID	TECN	COMMENT
0.01±0.01	VRANA 00	DPWA	Multichannel
0.04±0.03	THOMA 08	DPWA	Multichannel

••• We do not use the following data for averages, fits, limits, etc. •••

$(\Gamma_7/\Gamma)^{1/2}/\Gamma_{\text{total}}$ in $N\pi \rightarrow N(1680) \rightarrow N\rho, S=3/2, P\text{-wave}$ **$(\Gamma_7\Gamma_{11})^{1/2}/\Gamma$**

VALUE	DOCUMENT ID	TECN	COMMENT
-0.30 to -0.10 OUR ESTIMATE			
-0.20±0.05	MANLEY 92	IPWA	$\pi N \rightarrow \pi N \& N\pi\pi$
-0.23	1.5 LONGACRE 77	IPWA	$\pi N \rightarrow N\pi\pi$
-0.30	2 LONGACRE 75	IPWA	$\pi N \rightarrow N\pi\pi$

$\Gamma(N\rho, S=3/2, P\text{-wave})/\Gamma_{\text{total}}$ **Γ_{11}/Γ**

VALUE	DOCUMENT ID	TECN	COMMENT
0.05±0.01	VRANA 00	DPWA	Multichannel

$(\Gamma_7/\Gamma)^{1/2}/\Gamma_{\text{total}}$ in $N\pi \rightarrow N(1680) \rightarrow N\rho, S=3/2, F\text{-wave}$ **$(\Gamma_7\Gamma_{12})^{1/2}/\Gamma$**

VALUE	DOCUMENT ID	TECN	COMMENT
-0.18 to -0.10 OUR ESTIMATE			
-0.13±0.03	MANLEY 92	IPWA	$\pi N \rightarrow \pi N \& N\pi\pi$
-0.15	1.5 LONGACRE 77	IPWA	$\pi N \rightarrow N\pi\pi$

$\Gamma(N\rho, S=3/2, F\text{-wave})/\Gamma_{\text{total}}$ **Γ_{12}/Γ**

VALUE	DOCUMENT ID	TECN	COMMENT
0.03±0.01	VRANA 00	DPWA	Multichannel

$(\Gamma_7/\Gamma)^{1/2}/\Gamma_{\text{total}}$ in $N\pi \rightarrow N(1680) \rightarrow N(\pi\pi)_{S=0}^0$ **$(\Gamma_7\Gamma_{13})^{1/2}/\Gamma$**

VALUE	DOCUMENT ID	TECN	COMMENT
+0.25 to +0.35 OUR ESTIMATE			
+0.29±0.04	MANLEY 92	IPWA	$\pi N \rightarrow \pi N \& N\pi\pi$
+0.31	1.5 LONGACRE 77	IPWA	$\pi N \rightarrow N\pi\pi$
+0.30	2 LONGACRE 75	IPWA	$\pi N \rightarrow N\pi\pi$

$\Gamma(N(\pi\pi)_{S=0}^0)/\Gamma_{\text{total}}$ **Γ_{13}/Γ**

VALUE	DOCUMENT ID	TECN	COMMENT
0.09±0.01	VRANA 00	DPWA	Multichannel
0.11±0.05	THOMA 08	DPWA	Multichannel

••• We do not use the following data for averages, fits, limits, etc. •••

N(1680) PHOTON DECAY AMPLITUDES

Papers on γN amplitudes predating 1981 may be found in our 2006 edition, Journal of Physics, G **33** 1 (2006).

$N(1680) \rightarrow p\gamma, \text{ helicity-1/2 amplitude } A_{1/2}$

VALUE (GeV ^{-1/2})	DOCUMENT ID	TECN	COMMENT
-0.015 ± 0.006 OUR ESTIMATE			
-0.017 ± 0.001	DUGGER 07	DPWA	$\gamma N \rightarrow \pi N$
-0.010 ± 0.004	ARNDT 96	IPWA	$\gamma N \rightarrow \pi N$
-0.017 ± 0.018	CRAWFORD 83	IPWA	$\gamma N \rightarrow \pi N$
-0.009 ± 0.006	AWAJI 81	DPWA	$\gamma N \rightarrow \pi N$
••• We do not use the following data for averages, fits, limits, etc. •••			
-0.025	DRECHSEL 07	DPWA	$\gamma N \rightarrow \pi N$
-0.006 ± 0.002	LI 93	IPWA	$\gamma N \rightarrow \pi N$

$N(1680) \rightarrow p\gamma, \text{ helicity-3/2 amplitude } A_{3/2}$

VALUE (GeV ^{-1/2})	DOCUMENT ID	TECN	COMMENT
+0.133 ± 0.012 OUR ESTIMATE			
0.134 ± 0.002	DUGGER 07	DPWA	$\gamma N \rightarrow \pi N$
0.145 ± 0.005	ARNDT 96	IPWA	$\gamma N \rightarrow \pi N$
0.132 ± 0.010	CRAWFORD 83	IPWA	$\gamma N \rightarrow \pi N$
0.115 ± 0.008	AWAJI 81	DPWA	$\gamma N \rightarrow \pi N$
••• We do not use the following data for averages, fits, limits, etc. •••			
0.134	DRECHSEL 07	DPWA	$\gamma N \rightarrow \pi N$
0.154 ± 0.002	LI 93	IPWA	$\gamma N \rightarrow \pi N$

$N(1680) \rightarrow n\gamma, \text{ helicity-1/2 amplitude } A_{1/2}$

VALUE (GeV ^{-1/2})	DOCUMENT ID	TECN	COMMENT
+0.029 ± 0.010 OUR ESTIMATE			
0.030 ± 0.005	ARNDT 96	IPWA	$\gamma N \rightarrow \pi N$
0.017 ± 0.014	AWAJI 81	DPWA	$\gamma N \rightarrow \pi N$
0.032 ± 0.003	FUJII 81	DPWA	$\gamma N \rightarrow \pi N$
••• We do not use the following data for averages, fits, limits, etc. •••			
0.028	DRECHSEL 07	DPWA	$\gamma N \rightarrow \pi N$
0.022 ± 0.002	LI 93	IPWA	$\gamma N \rightarrow \pi N$

$N(1680) \rightarrow n\gamma, \text{ helicity-3/2 amplitude } A_{3/2}$

VALUE (GeV ^{-1/2})	DOCUMENT ID	TECN	COMMENT
-0.033 ± 0.009 OUR ESTIMATE			
-0.040 ± 0.015	ARNDT 96	IPWA	$\gamma N \rightarrow \pi N$
-0.033 ± 0.013	AWAJI 81	DPWA	$\gamma N \rightarrow \pi N$
-0.023 ± 0.005	FUJII 81	DPWA	$\gamma N \rightarrow \pi N$
••• We do not use the following data for averages, fits, limits, etc. •••			
-0.038	DRECHSEL 07	DPWA	$\gamma N \rightarrow \pi N$
-0.048 ± 0.002	LI 93	IPWA	$\gamma N \rightarrow \pi N$

N(1680) FOOTNOTES

- LONGACRE 77 pole positions are from a search for poles in the unitarized T-matrix; the first (second) value uses, in addition to $\pi N \rightarrow N\pi\pi$ data, elastic amplitudes from a Saclay (CERN) partial-wave analysis. The other LONGACRE 77 values are from eyeball fits with Breit-Wigner circles to the T-matrix amplitudes.
- From method II of LONGACRE 75: eyeball fits with Breit-Wigner circles to the T-matrix amplitudes.
- See HOEHLER 93 for a detailed discussion of the evidence for and the pole parameters of N and Δ resonances as determined from Argand diagrams of πN elastic partial-wave amplitudes and from plots of the speeds with which the amplitudes traverse the diagrams.
- LONGACRE 78 values are from a search for poles in the unitarized T-matrix. The first (second) value uses, in addition to $\pi N \rightarrow N\pi\pi$ data, elastic amplitudes from a Saclay (CERN) partial-wave analysis.
- LONGACRE 77 considers this coupling to be well determined.

N(1680) REFERENCES

For early references, see Physics Letters **111B** 1 (1982). For very early references, see Reviews of Modern Physics **37** 633 (1965).

THOMA 08	PL B659 87	U. Thoma <i>et al.</i>	(CB-ELSA Collab.)
DRECHSEL 07	EPJ A34 69	D. Drechsel, S.S. Kamalov, L. Tiator	(MAINZ, JINR)
DUGGER 07	PR C76 025211	M. Dugger <i>et al.</i>	(Jefferson Lab CLAS Collab.)
ARNDT 06	PR C74 045205	R.A. Arndt <i>et al.</i>	(GWU)
PDG 06	JPG 33 1	W.-M. Yao <i>et al.</i>	(PDG Collab.)
ARNDT 04	PR C69 035213	R.A. Arndt <i>et al.</i>	(GWU, TRIU)
VRANA 00	PRPL 320 181	T.P. Vrana, S.A. Dytman, T.-S.H. Lee	(PITT+)
TIATOR 99	PR C60 035210	L. Tiator <i>et al.</i>	
ARNDT 96	PR C53 430	R.A. Arndt, I.I. Strakovsky, R.L. Workman	(VPI)
ARNDT 95	PR C52 2120	R.A. Arndt <i>et al.</i>	(VPI, BRCC)
BATINIC 95	PR C51 2310	M. Batinic <i>et al.</i>	(BOSK, UCLA)
Also	PR C57 1004 (erratum)	M. Batinic <i>et al.</i>	
HOEHLER 93	<i>n</i> N Newsletter 9 1	G. Hohler	(KARL)
LI 93	PR C47 2759	Z.J. Li <i>et al.</i>	(VPI)
MANLEY 92	PR D45 4002	D.M. Manley, E.M. Saleski	(KENT) IJP
Also	PR D30 904	D.M. Manley <i>et al.</i>	(VPI)
ARNDT 91	PR D43 2131	R.A. Arndt <i>et al.</i>	(VPI, TELE) IJP
BELL 83	NP B222 389	K.W. Bell <i>et al.</i>	(RL) IJP
CRAWFORD 83	NP B211 1	R.L. Crawford, W.T. Morton	(GLAS)
PDG 82	PL 111B 1	M. Roos <i>et al.</i>	(HELS, CIT, CERN)
AWAJI 81	Bonn Conf. 352	N. Awaji, R. Kajikawa	(NAGO)
Also	NP B197 365	K. Fujii <i>et al.</i>	(NAGO)
FUJII 81	NP B187 53	K. Fujii <i>et al.</i>	(NAGO, OSAK)
CUTKOSKY 80	Toronto Conf. 19	R.E. Cutkosky <i>et al.</i>	(CMU, LBL) IJP
Also	PR D20 2839	R.E. Cutkosky <i>et al.</i>	(RHEL, BRIS) IJP
SAXON 80	NP B162 522	D.H. Saxon <i>et al.</i>	(RHEL) IJP
BAKER 79	NP B156 93	R.D. Baker <i>et al.</i>	(RHL) IJP
HOEHLER 79	PDAT 12-1	G. Hohler <i>et al.</i>	(KARL) IJP
Also	Toronto Conf. 3	R. Koch	(KARL) IJP
LONGACRE 78	PR D17 1795	R.S. Longacre <i>et al.</i>	(LBL, SLAC)
LONGACRE 77	NP B122 433	R.S. Longacre, J. Dolbeau	(SACL) IJP
Also	NP B108 365	J. Dolbeau <i>et al.</i>	(SACL) IJP
LONGACRE 75	PL 55B 415	R.S. Longacre <i>et al.</i>	(LBL, SLAC) IJP

Baryon Particle Listings

 $N(1700)$ $N(1700) D_{13}$

$$I(J^P) = \frac{1}{2}(\frac{3}{2}^-) \text{ Status: } ***$$

Most of the results published before 1975 are now obsolete and have been omitted. They may be found in our 1982 edition, Physics Letters **111B** 1 (1982). Some further obsolete results published before 1984 were last included in our 2006 edition, Journal of Physics, G **33** 1 (2006).

The various partial-wave analyses do not agree very well.

The latest GWU analysis (ARNDT 06) finds no evidence for this resonance.

 $N(1700)$ BREIT-WIGNER MASS

VALUE (MeV)	DOCUMENT ID	TECN	COMMENT
1650 to 1750 (≈ 1700) OUR ESTIMATE			
1737 \pm 44	MANLEY 92	IPWA	$\pi N \rightarrow \pi N$ & $N\pi\pi$
1675 \pm 25	CUTKOSKY 80	IPWA	$\pi N \rightarrow \pi N$
1731 \pm 15	HOEHLER 79	IPWA	$\pi N \rightarrow \pi N$
• • • We do not use the following data for averages, fits, limits, etc. • • •			
1740 \pm 20	THOMA 08	DPWA	Multichannel
1736 \pm 33	VRANA 00	DPWA	Multichannel
1791 \pm 46	BATINIC 95	DPWA	$\pi N \rightarrow N\pi, N\eta$
1650	SAXON 80	DPWA	$\pi^- \rho \rightarrow \Lambda K^0$
1690 to 1710	BAKER 78	DPWA	$\pi^- \rho \rightarrow \Lambda K^0$
1719	BARBOUR 78	DPWA	$\gamma N \rightarrow \pi N$
1670 \pm 10	¹ BAKER 77	IPWA	$\pi^- \rho \rightarrow \Lambda K^0$
1690	¹ BAKER 77	DPWA	$\pi^- \rho \rightarrow \Lambda K^0$
1660	² LONGACRE 77	IPWA	$\pi N \rightarrow N\pi\pi$
1710	³ LONGACRE 75	IPWA	$\pi N \rightarrow N\pi\pi$

 $N(1700)$ BREIT-WIGNER WIDTH

VALUE (MeV)	DOCUMENT ID	TECN	COMMENT
50 to 150 (≈ 100) OUR ESTIMATE			
250 \pm 220	MANLEY 92	IPWA	$\pi N \rightarrow \pi N$ & $N\pi\pi$
90 \pm 40	CUTKOSKY 80	IPWA	$\pi N \rightarrow \pi N$
110 \pm 30	HOEHLER 79	IPWA	$\pi N \rightarrow \pi N$
• • • We do not use the following data for averages, fits, limits, etc. • • •			
180 \pm 30	THOMA 08	DPWA	Multichannel
175 \pm 133	VRANA 00	DPWA	Multichannel
215 \pm 60	BATINIC 95	DPWA	$\pi N \rightarrow N\pi, N\eta$
70	SAXON 80	DPWA	$\pi^- \rho \rightarrow \Lambda K^0$
70 to 100	BAKER 78	DPWA	$\pi^- \rho \rightarrow \Lambda K^0$
126	BARBOUR 78	DPWA	$\gamma N \rightarrow \pi N$
90 \pm 25	¹ BAKER 77	IPWA	$\pi^- \rho \rightarrow \Lambda K^0$
100	¹ BAKER 77	DPWA	$\pi^- \rho \rightarrow \Lambda K^0$
600	² LONGACRE 77	IPWA	$\pi N \rightarrow N\pi\pi$
300	³ LONGACRE 75	IPWA	$\pi N \rightarrow N\pi\pi$

 $N(1700)$ POLE POSITION

VALUE (MeV)	DOCUMENT ID	TECN	COMMENT
REAL PART			
1630 to 1730 (≈ 1680) OUR ESTIMATE			
1700	⁴ HOEHLER 93	SPED	$\pi N \rightarrow \pi N$
1660 \pm 30	CUTKOSKY 80	IPWA	$\pi N \rightarrow \pi N$
• • • We do not use the following data for averages, fits, limits, etc. • • •			
1710 \pm 15	THOMA 08	DPWA	Multichannel
1704	VRANA 00	DPWA	Multichannel
not seen	ARNDT 91	DPWA	$\pi N \rightarrow \pi N$ Soln SM90
1710 or 1678	⁵ LONGACRE 78	IPWA	$\pi N \rightarrow N\pi\pi$
1616 or 1613	² LONGACRE 77	IPWA	$\pi N \rightarrow N\pi\pi$

-2xIMAGINARY PART

VALUE (MeV)	DOCUMENT ID	TECN	COMMENT
50 to 150 (≈ 100) OUR ESTIMATE			
120	⁴ HOEHLER 93	SPED	$\pi N \rightarrow \pi N$
90 \pm 40	CUTKOSKY 80	IPWA	$\pi N \rightarrow \pi N$
• • • We do not use the following data for averages, fits, limits, etc. • • •			
155 \pm 25	THOMA 08	DPWA	Multichannel
156	VRANA 00	DPWA	Multichannel
not seen	ARNDT 91	DPWA	$\pi N \rightarrow \pi N$ Soln SM90
607 or 567	⁵ LONGACRE 78	IPWA	$\pi N \rightarrow N\pi\pi$
577 or 575	² LONGACRE 77	IPWA	$\pi N \rightarrow N\pi\pi$

 $N(1700)$ ELASTIC POLE RESIDUE

VALUE (MeV)	DOCUMENT ID	TECN	COMMENT
5	HOEHLER 93	SPED	$\pi N \rightarrow \pi N$
6 \pm 3	CUTKOSKY 80	IPWA	$\pi N \rightarrow \pi N$

PHASE θ

VALUE ($^\circ$)	DOCUMENT ID	TECN	COMMENT
0 \pm 50	CUTKOSKY 80	IPWA	$\pi N \rightarrow \pi N$

 $N(1700)$ DECAY MODES

The following branching fractions are our estimates, not fits or averages.

Mode	Fraction (Γ_i/Γ)
Γ_1 $N\pi$	5–15 %
Γ_2 $N\eta$	(0.0 \pm 1.0) %
Γ_3 ΛK	< 3 %
Γ_4 ΣK	
Γ_5 $N\pi\pi$	85–95 %
Γ_6 $\Delta\pi$	
Γ_7 $\Delta(1232)\pi, S\text{-wave}$	
Γ_8 $\Delta(1232)\pi, D\text{-wave}$	
Γ_9 $N\rho$	< 35 %
Γ_{10} $N\rho, S=1/2, D\text{-wave}$	
Γ_{11} $N\rho, S=3/2, S\text{-wave}$	
Γ_{12} $N\rho, S=3/2, D\text{-wave}$	
Γ_{13} $N(\pi\pi)_{S\text{-wave}}^{I=0}$	
Γ_{14} $p\gamma$	0.01–0.05 %
Γ_{15} $p\gamma, \text{helicity}=1/2$	0.0–0.024 %
Γ_{16} $p\gamma, \text{helicity}=3/2$	0.002–0.026 %
Γ_{17} $n\gamma$	0.01–0.13 %
Γ_{18} $n\gamma, \text{helicity}=1/2$	0.0–0.09 %
Γ_{19} $n\gamma, \text{helicity}=3/2$	0.01–0.05 %

 $N(1700)$ BRANCHING RATIOS

$\Gamma(N\pi)/\Gamma_{\text{total}}$	DOCUMENT ID	TECN	COMMENT	Γ_1/Γ
0.05 to 0.15 OUR ESTIMATE				
0.01 \pm 0.02	MANLEY 92	IPWA	$\pi N \rightarrow \pi N$ & $N\pi\pi$	
0.11 \pm 0.05	CUTKOSKY 80	IPWA	$\pi N \rightarrow \pi N$	
0.08 \pm 0.03	HOEHLER 79	IPWA	$\pi N \rightarrow \pi N$	
• • • We do not use the following data for averages, fits, limits, etc. • • •				
0.08 $^{+0.08}_{-0.04}$	THOMA 08	DPWA	Multichannel	
0.04 \pm 0.02	VRANA 00	DPWA	Multichannel	
0.04 \pm 0.05	BATINIC 95	DPWA	$\pi N \rightarrow N\pi, N\eta$	

$\Gamma(N\eta)/\Gamma_{\text{total}}$	DOCUMENT ID	TECN	COMMENT	Γ_2/Γ
0.00 \pm 0.01				
0.10 \pm 0.05	THOMA 08	DPWA	Multichannel	
0.10 \pm 0.06	BATINIC 95	DPWA	$\pi N \rightarrow N\pi, N\eta$	

$(\Gamma_i\Gamma_f)^{1/2}/\Gamma_{\text{total}}$ in $N\pi \rightarrow N(1700) \rightarrow \Lambda K$	DOCUMENT ID	TECN	COMMENT	$(\Gamma_1\Gamma_3)^{1/2}/\Gamma$
-0.06 to +0.04 OUR ESTIMATE				
-0.012	BELL 83	DPWA	$\pi^- \rho \rightarrow \Lambda K^0$	
-0.012	SAXON 80	DPWA	$\pi^- \rho \rightarrow \Lambda K^0$	
• • • We do not use the following data for averages, fits, limits, etc. • • •				
-0.04	⁶ BAKER 78	DPWA	See SAXON 80	
-0.03 \pm 0.004	¹ BAKER 77	IPWA	$\pi^- \rho \rightarrow \Lambda K^0$	
-0.03	¹ BAKER 77	DPWA	$\pi^- \rho \rightarrow \Lambda K^0$	
+0.026 \pm 0.019	DEVENISH 74B		Fixed- t dispersion rel.	

$(\Gamma_i\Gamma_f)^{1/2}/\Gamma_{\text{total}}$ in $N\pi \rightarrow N(1700) \rightarrow \Sigma K$	DOCUMENT ID	TECN	COMMENT	$(\Gamma_1\Gamma_4)^{1/2}/\Gamma$
0.00 \pm 0.08 OUR ESTIMATE				
not seen	LIVANOS 80	DPWA	$\pi p \rightarrow \Sigma K$	
< 0.017	⁷ DEANS 75	DPWA	$\pi N \rightarrow \Sigma K$	

Note: Signs of couplings from $\pi N \rightarrow N\pi\pi$ analyses were changed in the 1986 edition to agree with the baryon-first convention; the overall phase ambiguity is resolved by choosing a negative sign for the $\Delta(1620) S_{31}$ coupling to $\Delta(1232)\pi$.

$(\Gamma_i\Gamma_f)^{1/2}/\Gamma_{\text{total}}$ in $N\pi \rightarrow N(1700) \rightarrow \Delta(1232)\pi, S\text{-wave}$	DOCUMENT ID	TECN	COMMENT	$(\Gamma_1\Gamma_7)^{1/2}/\Gamma$
0.00 to \pm 0.08 OUR ESTIMATE				
+0.02 \pm 0.03	MANLEY 92	IPWA	$\pi N \rightarrow \pi N$ & $N\pi\pi$	
0.00	² LONGACRE 77	IPWA	$\pi N \rightarrow N\pi\pi$	
-0.16	³ LONGACRE 75	IPWA	$\pi N \rightarrow N\pi\pi$	

See key on page 373

Baryon Particle Listings
N(1700) $\Gamma(\Delta(1232)\pi, S\text{-wave})/\Gamma_{\text{total}}$ Γ_7/Γ

VALUE	DOCUMENT ID	TECN	COMMENT
0.11 ± 0.01	VRANA	00	DPWA Multichannel
••• We do not use the following data for averages, fits, limits, etc. •••			
0.10 ± 0.05	THOMA	08	DPWA Multichannel

 $(\Gamma_7/\Gamma)^{1/2}/\Gamma_{\text{total}}$ in $N\pi \rightarrow N(1700) \rightarrow \Delta(1232)\pi, D\text{-wave}$ $(\Gamma_7/\Gamma)^{1/2}/\Gamma$

VALUE	DOCUMENT ID	TECN	COMMENT
±0.04 to ±0.20 OUR ESTIMATE			
+0.10 ± 0.09	MANLEY	92	IPWA $\pi N \rightarrow \pi N$ & $N\pi\pi$
-0.12	2 LONGACRE	77	IPWA $\pi N \rightarrow N\pi\pi$
+0.14	3 LONGACRE	75	IPWA $\pi N \rightarrow N\pi\pi$

 $\Gamma(\Delta(1232)\pi, D\text{-wave})/\Gamma_{\text{total}}$ Γ_8/Γ

VALUE	DOCUMENT ID	TECN	COMMENT
0.79 ± 0.56	VRANA	00	DPWA Multichannel
••• We do not use the following data for averages, fits, limits, etc. •••			
0.20 ± 0.11	THOMA	08	DPWA Multichannel

 $(\Gamma_8/\Gamma)^{1/2}/\Gamma_{\text{total}}$ in $N\pi \rightarrow N(1700) \rightarrow N\rho, S=3/2, S\text{-wave}$ $(\Gamma_8/\Gamma)^{1/2}/\Gamma$

VALUE	DOCUMENT ID	TECN	COMMENT
±0.01 to ±0.13 OUR ESTIMATE			
-0.04 ± 0.06	MANLEY	92	IPWA $\pi N \rightarrow \pi N$ & $N\pi\pi$
-0.07	2 LONGACRE	77	IPWA $\pi N \rightarrow N\pi\pi$
+0.07	3 LONGACRE	75	IPWA $\pi N \rightarrow N\pi\pi$

 $\Gamma(N\rho, S=3/2, S\text{-wave})/\Gamma_{\text{total}}$ Γ_{11}/Γ

VALUE	DOCUMENT ID	TECN	COMMENT
0.07 ± 0.01	VRANA	00	DPWA Multichannel

 $(\Gamma_{11}/\Gamma)^{1/2}/\Gamma_{\text{total}}$ in $N\pi \rightarrow N(1700) \rightarrow N(\pi\pi)_{S=0}^0$ $(\Gamma_{11}/\Gamma)^{1/2}/\Gamma$

VALUE	DOCUMENT ID	TECN	COMMENT
±0.02 to ±0.28 OUR ESTIMATE			
+0.02 ± 0.02	MANLEY	92	IPWA $\pi N \rightarrow \pi N$ & $N\pi\pi$
0.00	2 LONGACRE	77	IPWA $\pi N \rightarrow N\pi\pi$
+0.2	3 LONGACRE	75	IPWA $\pi N \rightarrow N\pi\pi$

 $\Gamma(N(\pi\pi)_{S=0}^0)/\Gamma_{\text{total}}$ Γ_{13}/Γ

VALUE	DOCUMENT ID	TECN	COMMENT
0.00 ± 0.01	VRANA	00	DPWA Multichannel
••• We do not use the following data for averages, fits, limits, etc. •••			
0.18 ± 0.12	THOMA	08	DPWA Multichannel

N(1700) PHOTON DECAY AMPLITUDES

Papers on γN amplitudes predating 1981 may be found in our 2006 edition, Journal of Physics, G **33** 1 (2006).

N(1700) $\rightarrow \rho\gamma$, helicity-1/2 amplitude $A_{1/2}$

VALUE (GeV ^{-1/2})	DOCUMENT ID	TECN	COMMENT
-0.018 ± 0.013 OUR ESTIMATE			
-0.016 ± 0.014	CRAWFORD	83	IPWA $\gamma N \rightarrow \pi N$
-0.002 ± 0.013	AWAJI	81	DPWA $\gamma N \rightarrow \pi N$
••• We do not use the following data for averages, fits, limits, etc. •••			
-0.033 ± 0.021	BARBOUR	78	DPWA $\gamma N \rightarrow \pi N$

N(1700) $\rightarrow \rho\gamma$, helicity-3/2 amplitude $A_{3/2}$

VALUE (GeV ^{-1/2})	DOCUMENT ID	TECN	COMMENT
-0.002 ± 0.024 OUR ESTIMATE			
-0.009 ± 0.012	CRAWFORD	83	IPWA $\gamma N \rightarrow \pi N$
0.029 ± 0.014	AWAJI	81	DPWA $\gamma N \rightarrow \pi N$
••• We do not use the following data for averages, fits, limits, etc. •••			
-0.014 ± 0.025	BARBOUR	78	DPWA $\gamma N \rightarrow \pi N$

N(1700) $\rightarrow n\gamma$, helicity-1/2 amplitude $A_{1/2}$

VALUE (GeV ^{-1/2})	DOCUMENT ID	TECN	COMMENT
0.000 ± 0.050 OUR ESTIMATE			
0.006 ± 0.024	AWAJI	81	DPWA $\gamma N \rightarrow \pi N$
-0.002 ± 0.013	FUJII	81	DPWA $\gamma N \rightarrow \pi N$
••• We do not use the following data for averages, fits, limits, etc. •••			
+0.050 ± 0.042	BARBOUR	78	DPWA $\gamma N \rightarrow \pi N$

N(1700) $\rightarrow n\gamma$, helicity-3/2 amplitude $A_{3/2}$

VALUE (GeV ^{-1/2})	DOCUMENT ID	TECN	COMMENT
-0.003 ± 0.044 OUR ESTIMATE			
-0.033 ± 0.017	AWAJI	81	DPWA $\gamma N \rightarrow \pi N$
0.018 ± 0.018	FUJII	81	DPWA $\gamma N \rightarrow \pi N$
••• We do not use the following data for averages, fits, limits, etc. •••			
+0.035 ± 0.030	BARBOUR	78	DPWA $\gamma N \rightarrow \pi N$

N(1700) $\gamma p \rightarrow \Lambda K^+$ AMPLITUDES $(\Gamma_7/\Gamma)^{1/2}/\Gamma_{\text{total}}$ in $p\gamma \rightarrow N(1700) \rightarrow \Lambda K^+$ (E_{2-} amplitude)

VALUE (units 10 ⁻³)	DOCUMENT ID	TECN	
••• We do not use the following data for averages, fits, limits, etc. •••			
4.09	TANABE	89	DPWA

 $(\Gamma_8/\Gamma)^{1/2}/\Gamma_{\text{total}}$ in $p\gamma \rightarrow N(1700) \rightarrow \Lambda K^+$ (M_{2-} amplitude)

VALUE (units 10 ⁻³)	DOCUMENT ID	TECN	
••• We do not use the following data for averages, fits, limits, etc. •••			
-7.09	TANABE	89	DPWA

 $p\gamma \rightarrow N(1700) \rightarrow \Lambda K^+$ phase angle θ (E_{2-} amplitude)

VALUE (degrees)	DOCUMENT ID	TECN	
••• We do not use the following data for averages, fits, limits, etc. •••			
-35.9	TANABE	89	DPWA

N(1700) FOOTNOTES

- The two BAKER 77 entries are from an IPWA using the Barrelet-zero method and from a conventional energy-dependent analysis.
- LONGACRE 77 pole positions are from a search for poles in the unitarized T-matrix; the first (second) value uses, in addition to $\pi N \rightarrow N\pi\pi$ data, elastic amplitudes from a Saclay (CERN) partial-wave analysis. The other LONGACRE 77 values are from eyeball fits with Breit-Wigner circles to the T-matrix amplitudes.
- From method II of LONGACRE 75: eyeball fits with Breit-Wigner circles to the T-matrix amplitudes.
- See HOEHLER 93 for a detailed discussion of the evidence for and the pole parameters of N and Δ resonances as determined from Argand diagrams of πN elastic partial-wave amplitudes and from plots of the speeds with which the amplitudes traverse the diagrams.
- LONGACRE 78 values are from a search for poles in the unitarized T-matrix. The first (second) value uses, in addition to $\pi N \rightarrow N\pi\pi$ data, elastic amplitudes from a Saclay (CERN) partial-wave analysis.
- The overall phase of BAKER 78 couplings has been changed to agree with previous conventions.
- The range given is from the four best solutions.

N(1700) REFERENCES

For early references, see Physics Letters **111B** 1 (1982).

THOMA	08	PL B659 87	U. Thoma <i>et al.</i>	(CB-ELSA Collab.)
ARNDT	06	PR C74 045205	R.A. Arndt <i>et al.</i>	(GWU)
PDG	06	JPG 33 1	W.-M. Yao <i>et al.</i>	(PDG Collab.)
VRANA	00	PRPL 328 181	T.P. Vrana, S.A. Dytman, T.-S.H. Lee	(PITT+)
BATINIC	95	PR C51 2310	M. Batinic <i>et al.</i>	(BOSK, UCLA)
		Also	PR C57 1004 (erratum)	M. Batinic <i>et al.</i>
HOEHLER	93	πN Newsletter 9 1	G. Hohler	(KARL)
MANLEY	92	PR D45 4002	D.M. Manley, E.M. Saleski	(KENT) IJP
		Also	PR D30 904	D.M. Manley <i>et al.</i>
ARNDT	91	PR D43 2131	R.A. Arndt <i>et al.</i>	(VPI)
TANABE	89	PR C39 741	H. Tanabe, M. Kohno, C. Bennhold	(VPI, TELE) IJP
		Also	NC 102A 193	M. Kohno, H. Tanabe, C. Bennhold
BELL	83	NP B222 389	K.W. Bell <i>et al.</i>	(RL) IJP
CRAWFORD	83	NP B211 1	R.L. Crawford, W.T. Morton	(GLAS)
PDG	82	PL 111B 1	M. Roos <i>et al.</i>	(HELS, CIT, CERN)
AWAJI	81	Bonn Conf. 352	N. Awaji, R. Kajikawa	(NAGO)
		Also	NP B197 365	K. Fujii <i>et al.</i>
FUJII	81	NP B187 53	K. Fujii <i>et al.</i>	(NAGO, OSAK)
CUTKOSKY	80	Toronto Conf. 19	R.E. Cutkosky <i>et al.</i>	(CMU, LBL) IJP
		Also	PR D20 2839	R.E. Cutkosky <i>et al.</i>
LIVANOS	80	Toronto Conf. 35	P. Livanos <i>et al.</i>	(SACL) IJP
SAXON	80	NP B162 522	D.H. Saxon <i>et al.</i>	(RHEL, BRIS) IJP
HOEHLER	79	PDAT 12-1	G. Hohler <i>et al.</i>	(KARL) IJP
		Also	Toronto Conf. 3	R. Koch
BAKER	78	NP B141 29	R.D. Baker <i>et al.</i>	(RL, CAVE) IJP
BARBOUR	78	NP B141 253	I.M. Barbour, R.L. Crawford, N.H. Parsons	(GLAS)
LONGACRE	78	PR D17 1795	R.S. Longacre <i>et al.</i>	(LBL, SLAC)
BAKER	77	NP B126 365	R.D. Baker <i>et al.</i>	(RHEL) IJP
LONGACRE	77	NP B122 493	R.S. Longacre, J. Dolbeau	(SACL) IJP
		Also	NP B108 365	J. Dolbeau <i>et al.</i>
DEANS	75	NP B96 90	S.R. Deans <i>et al.</i>	(SFLA, ALAH) IJP
LONGACRE	75	PL 55B 415	R.S. Longacre <i>et al.</i>	(LBL, SLAC) IJP
DEVENISH	74B	NP B81 330	R.C.E. Devenish, C.D. Froggatt, B.R. Martin	(DESY+)

Baryon Particle Listings

 $N(1710)$ $N(1710) P_{11}$

$$I(J^P) = \frac{1}{2}(\frac{1}{2}^+) \text{ Status: } ***$$

Most of the results published before 1975 were last included in our 1982 edition, Physics Letters **111B** 1 (1982). Some further obsolete results published before 1984 were last included in our 2006 edition, Journal of Physics, G **33** 1 (2006).

The latest GWU analysis (ARNDT 06) finds no evidence for this resonance.

 $N(1710)$ BREIT-WIGNER MASS

VALUE (MeV)	DOCUMENT ID	TECN	COMMENT
1680 to 1740 (≈ 1710) OUR ESTIMATE			
1717 \pm 28	MANLEY 92	IPWA	$\pi N \rightarrow \pi N & N\pi\pi$
1700 \pm 50	CUTKOSKY 80	IPWA	$\pi N \rightarrow \pi N$
1723 \pm 9	HOEHLER 79	IPWA	$\pi N \rightarrow \pi N$
• • • We do not use the following data for averages, fits, limits, etc. • • •			
1752 \pm 3	PENNER 02c	DPWA	Multichannel
1699 \pm 65	VRANA 00	DPWA	Multichannel
1720 \pm 10	ARNDT 96	IPWA	$\gamma N \rightarrow \pi N$
1766 \pm 34	¹ BATINIC 95	DPWA	$\pi N \rightarrow N\pi, N\eta$
1706	CUTKOSKY 90	IPWA	$\pi N \rightarrow \pi N$
1730	SAXON 80	DPWA	$\pi^- p \rightarrow \Lambda K^0$
1720	² LONGACRE 77	IPWA	$\pi N \rightarrow N\pi\pi$
1710	³ LONGACRE 75	IPWA	$\pi N \rightarrow N\pi\pi$

 $N(1710)$ BREIT-WIGNER WIDTH

VALUE (MeV)	DOCUMENT ID	TECN	COMMENT
50 to 250 (≈ 100) OUR ESTIMATE			
480 \pm 230	MANLEY 92	IPWA	$\pi N \rightarrow \pi N & N\pi\pi$
93 \pm 30	CUTKOSKY 90	IPWA	$\pi N \rightarrow \pi N$
90 \pm 30	CUTKOSKY 80	IPWA	$\pi N \rightarrow \pi N$
120 \pm 15	HOEHLER 79	IPWA	$\pi N \rightarrow \pi N$
• • • We do not use the following data for averages, fits, limits, etc. • • •			
386 \pm 59	PENNER 02c	DPWA	Multichannel
143 \pm 100	VRANA 00	DPWA	Multichannel
105 \pm 10	ARNDT 96	IPWA	$\gamma N \rightarrow \pi N$
185 \pm 61	BATINIC 95	DPWA	$\pi N \rightarrow N\pi, N\eta$
540	BELL 83	DPWA	$\pi^- p \rightarrow \Lambda K^0$
550	SAXON 80	DPWA	$\pi^- p \rightarrow \Lambda K^0$
120	² LONGACRE 77	IPWA	$\pi N \rightarrow N\pi\pi$
75	³ LONGACRE 75	IPWA	$\pi N \rightarrow N\pi\pi$

 $N(1710)$ POLE POSITION

REAL PART

VALUE (MeV)	DOCUMENT ID	TECN	COMMENT
1670 to 1770 (≈ 1720) OUR ESTIMATE			
1690	⁴ HOEHLER 93	SPED	$\pi N \rightarrow \pi N$
1698	CUTKOSKY 90	IPWA	$\pi N \rightarrow \pi N$
1690 \pm 20	CUTKOSKY 80	IPWA	$\pi N \rightarrow \pi N$
• • • We do not use the following data for averages, fits, limits, etc. • • •			
1679	VRANA 00	DPWA	Multichannel
1770	ARNDT 95	DPWA	$\pi N \rightarrow N\pi$
1636	ARNDT 91	DPWA	$\pi N \rightarrow \pi N$ Soln SM90
1708 or 1712	⁵ LONGACRE 78	IPWA	$\pi N \rightarrow N\pi\pi$
1720 or 1711	² LONGACRE 77	IPWA	$\pi N \rightarrow N\pi\pi$

-2*x*IMAGINARY PART

VALUE (MeV)	DOCUMENT ID	TECN	COMMENT
80 to 380 (≈ 230) OUR ESTIMATE			
200	⁴ HOEHLER 93	SPED	$\pi N \rightarrow \pi N$
88	CUTKOSKY 90	IPWA	$\pi N \rightarrow \pi N$
80 \pm 20	CUTKOSKY 80	IPWA	$\pi N \rightarrow \pi N$
• • • We do not use the following data for averages, fits, limits, etc. • • •			
132	VRANA 00	DPWA	Multichannel
378	ARNDT 95	DPWA	$\pi N \rightarrow N\pi$
544	ARNDT 91	DPWA	$\pi N \rightarrow \pi N$ Soln SM90
17 or 22	⁵ LONGACRE 78	IPWA	$\pi N \rightarrow N\pi\pi$
123 or 115	² LONGACRE 77	IPWA	$\pi N \rightarrow N\pi\pi$

 $N(1710)$ ELASTIC POLE RESIDUEMODULUS $|r|$

VALUE (MeV)	DOCUMENT ID	TECN	COMMENT
15	HOEHLER 93	SPED	$\pi N \rightarrow \pi N$
9	CUTKOSKY 90	IPWA	$\pi N \rightarrow \pi N$
8 \pm 2	CUTKOSKY 80	IPWA	$\pi N \rightarrow \pi N$
• • • We do not use the following data for averages, fits, limits, etc. • • •			
37	ARNDT 95	DPWA	$\pi N \rightarrow N\pi$
149	ARNDT 91	DPWA	$\pi N \rightarrow \pi N$ Soln SM90

PHASE θ

VALUE ($^\circ$)	DOCUMENT ID	TECN	COMMENT
-167	CUTKOSKY 90	IPWA	$\pi N \rightarrow \pi N$
175 \pm 35	CUTKOSKY 80	IPWA	$\pi N \rightarrow \pi N$
• • • We do not use the following data for averages, fits, limits, etc. • • •			
-167	ARNDT 95	DPWA	$\pi N \rightarrow N\pi$
149	ARNDT 91	DPWA	$\pi N \rightarrow \pi N$ Soln SM90

 $N(1710)$ DECAY MODES

The following branching fractions are our estimates, not fits or averages.

Mode	Fraction (Γ_i/Γ)
Γ_1 $N\pi$	10-20 %
Γ_2 $N\eta$	(6.2 \pm 1.0) %
Γ_3 $N\omega$	(13.0 \pm 2.0) %
Γ_4 ΛK	5-25 %
Γ_5 ΣK	
Γ_6 $N\pi\pi$	40-90 %
Γ_7 $\Delta\pi$	15-40 %
Γ_8 $\Delta(1232)\pi, P\text{-wave}$	
Γ_9 $N\rho$	5-25 %
Γ_{10} $N\rho, S=1/2, P\text{-wave}$	
Γ_{11} $N\rho, S=3/2, P\text{-wave}$	
Γ_{12} $N(\pi\pi)_{S\text{-wave}}^L=0$	10-40 %
Γ_{13} $p\gamma$	0.002-0.05%
Γ_{14} $p\gamma, \text{ helicity}=1/2$	0.002-0.05%
Γ_{15} $n\gamma$	0.0-0.02%
Γ_{16} $n\gamma, \text{ helicity}=1/2$	0.0-0.02%

 $N(1710)$ BRANCHING RATIOS

$\Gamma(N\pi)/\Gamma_{\text{total}}$	Γ_1/Γ		
VALUE	DOCUMENT ID	TECN	COMMENT
0.10 to 0.20 OUR ESTIMATE			
0.09 \pm 0.04	MANLEY 92	IPWA	$\pi N \rightarrow \pi N & N\pi\pi$
0.20 \pm 0.04	CUTKOSKY 80	IPWA	$\pi N \rightarrow \pi N$
0.12 \pm 0.04	HOEHLER 79	IPWA	$\pi N \rightarrow \pi N$
• • • We do not use the following data for averages, fits, limits, etc. • • •			
0.14 \pm 0.08	PENNER 02c	DPWA	Multichannel
0.27 \pm 0.13	VRANA 00	DPWA	Multichannel
0.08 \pm 0.14	BATINIC 95	DPWA	$\pi N \rightarrow N\pi, N\eta$

 $\Gamma(N\eta)/\Gamma_{\text{total}}$

VALUE	DOCUMENT ID	TECN	COMMENT
0.062 \pm 0.010 OUR AVERAGE			
0.36 \pm 0.11	PENNER 02c	DPWA	Multichannel
0.06 \pm 0.01	VRANA 00	DPWA	Multichannel
• • • We do not use the following data for averages, fits, limits, etc. • • •			
0.16 \pm 0.10	BATINIC 95	DPWA	$\pi N \rightarrow N\pi, N\eta$

 $\Gamma(N\omega)/\Gamma_{\text{total}}$

VALUE	DOCUMENT ID	TECN	COMMENT
0.13 \pm 0.02			
	PENNER 02c	DPWA	Multichannel

 $(\Gamma_i\Gamma_f)^{1/2}/\Gamma_{\text{total}}$ in $N\pi \rightarrow N(1710) \rightarrow \Lambda K$

VALUE	DOCUMENT ID	TECN	COMMENT
+0.12 to +0.18 OUR ESTIMATE			
+0.16	BELL 83	DPWA	$\pi^- p \rightarrow \Lambda K^0$
+0.14	SAXON 80	DPWA	$\pi^- p \rightarrow \Lambda K^0$

 $\Gamma(\Lambda K)/\Gamma_{\text{total}}$

VALUE	DOCUMENT ID	TECN	COMMENT
0.05 \pm 0.03	SHKLYAR 05	DPWA	Multichannel
0.05 \pm 0.02	PENNER 02c	DPWA	Multichannel
0.1 \pm 0.1	VRANA 00	DPWA	Multichannel

 $\Gamma(\Sigma K)/\Gamma_{\text{total}}$

VALUE	DOCUMENT ID	TECN	COMMENT
• • • We do not use the following data for averages, fits, limits, etc. • • •			
0.07 \pm 0.07	PENNER 02c	DPWA	Multichannel

 $(\Gamma_i\Gamma_f)^{1/2}/\Gamma_{\text{total}}$ in $N\pi \rightarrow N(1710) \rightarrow \Sigma K$

VALUE	DOCUMENT ID	TECN	COMMENT
• • • We do not use the following data for averages, fits, limits, etc. • • •			
-0.034	LIVANOS 80	DPWA	$\pi p \rightarrow \Sigma K$

Note: Signs of couplings from $\pi N \rightarrow N\pi\pi$ analyses were changed in the 1986 edition to agree with the baryon-first convention; the overall phase

ambiguity is resolved by choosing a negative sign for the $\Delta(1620) S_{31}$ coupling to $\Delta(1232) \pi$.

$(\Gamma_1 \Gamma_f)^{1/2} / \Gamma_{\text{total}}$ in $N\pi \rightarrow N(1710) \rightarrow \Delta(1232) \pi, P\text{-wave}$ $(\Gamma_1 \Gamma_8)^{1/2} / \Gamma$

VALUE	DOCUMENT ID	TECN	COMMENT
± 0.16 to ± 0.22 OUR ESTIMATE			
-0.21 ± 0.04	MANLEY 92	IPWA	$\pi N \rightarrow \pi N \& N\pi\pi$
-0.17	2 LONGACRE 77	IPWA	$\pi N \rightarrow N\pi\pi$
+0.20	3 LONGACRE 75	IPWA	$\pi N \rightarrow N\pi\pi$

$\Gamma(\Delta(1232) \pi, P\text{-wave}) / \Gamma_{\text{total}}$ Γ_8 / Γ

VALUE	DOCUMENT ID	TECN	COMMENT
0.39 ± 0.08	VRANA 00	DPWA	Multichannel

$(\Gamma_1 \Gamma_f)^{1/2} / \Gamma_{\text{total}}$ in $N\pi \rightarrow N(1710) \rightarrow N\rho, S=1/2, P\text{-wave}$ $(\Gamma_1 \Gamma_{10})^{1/2} / \Gamma$

VALUE	DOCUMENT ID	TECN	COMMENT
± 0.09 to ± 0.19 OUR ESTIMATE			
+0.05 ± 0.06	MANLEY 92	IPWA	$\pi N \rightarrow \pi N \& N\pi\pi$
+0.19	2 LONGACRE 77	IPWA	$\pi N \rightarrow N\pi\pi$
-0.20	3 LONGACRE 75	IPWA	$\pi N \rightarrow N\pi\pi$

$\Gamma(N\rho, S=1/2, P\text{-wave}) / \Gamma_{\text{total}}$ Γ_{10} / Γ

VALUE	DOCUMENT ID	TECN	COMMENT
0.17 ± 0.01	VRANA 00	DPWA	Multichannel

$(\Gamma_1 \Gamma_f)^{1/2} / \Gamma_{\text{total}}$ in $N\pi \rightarrow N(1710) \rightarrow N\rho, S=3/2, P\text{-wave}$ $(\Gamma_1 \Gamma_{11})^{1/2} / \Gamma$

VALUE	DOCUMENT ID	TECN	COMMENT
+0.31	2 LONGACRE 77	IPWA	$\pi N \rightarrow N\pi\pi$

$(\Gamma_1 \Gamma_f)^{1/2} / \Gamma_{\text{total}}$ in $N\pi \rightarrow N(1710) \rightarrow N(\pi\pi)_{S=0}^{J=0}$ $(\Gamma_1 \Gamma_{12})^{1/2} / \Gamma$

VALUE	DOCUMENT ID	TECN	COMMENT
± 0.14 to ± 0.22 OUR ESTIMATE			
+0.04 ± 0.05	MANLEY 92	IPWA	$\pi N \rightarrow \pi N \& N\pi\pi$
-0.26	2 LONGACRE 77	IPWA	$\pi N \rightarrow N\pi\pi$
-0.28	3 LONGACRE 75	IPWA	$\pi N \rightarrow N\pi\pi$

$\Gamma(N(\pi\pi)_{S=0}^{J=0}) / \Gamma_{\text{total}}$ Γ_{12} / Γ

VALUE	DOCUMENT ID	TECN	COMMENT
0.01 ± 0.01	VRANA 00	DPWA	Multichannel

N(1710) PHOTON DECAY AMPLITUDES

Papers on γN amplitudes predating 1981 may be found in our 2006 edition, Journal of Physics, G **33** 1 (2006).

N(1710) $\rightarrow \rho\gamma$, helicity-1/2 amplitude $A_{1/2}$

VALUE (GeV ^{-1/2})	DOCUMENT ID	TECN	COMMENT
± 0.009 to ± 0.022 OUR ESTIMATE			
0.007 ± 0.015	ARNDT 96	IPWA	$\gamma N \rightarrow \pi N$
0.006 ± 0.018	CRAWFORD 83	IPWA	$\gamma N \rightarrow \pi N$
0.028 ± 0.009	AWAJI 81	DPWA	$\gamma N \rightarrow \pi N$
• • • We do not use the following data for averages, fits, limits, etc. • • •			
0.044	PENNER 02D	DPWA	Multichannel
-0.037 ± 0.002	LI 93	IPWA	$\gamma N \rightarrow \pi N$

N(1710) $\rightarrow n\gamma$, helicity-1/2 amplitude $A_{1/2}$

VALUE (GeV ^{-1/2})	DOCUMENT ID	TECN	COMMENT
-0.002 to ± 0.014 OUR ESTIMATE			
-0.002 ± 0.015	ARNDT 96	IPWA	$\gamma N \rightarrow \pi N$
0.000 ± 0.018	AWAJI 81	DPWA	$\gamma N \rightarrow \pi N$
-0.001 ± 0.003	FUJII 81	DPWA	$\gamma N \rightarrow \pi N$
• • • We do not use the following data for averages, fits, limits, etc. • • •			
-0.024	PENNER 02D	DPWA	Multichannel
0.052 ± 0.003	LI 93	IPWA	$\gamma N \rightarrow \pi N$

N(1710) $\gamma\rho \rightarrow \Lambda K^+$ AMPLITUDES

$(\Gamma_1 \Gamma_f)^{1/2} / \Gamma_{\text{total}}$ in $\rho\gamma \rightarrow N(1710) \rightarrow \Lambda K^+$ $(M_{1-} \text{ amplitude})$

VALUE (units 10 ⁻³)	DOCUMENT ID	TECN	COMMENT
• • • We do not use the following data for averages, fits, limits, etc. • • •			
-10.6 ± 0.4	WORKMAN 90	DPWA	
-7.21	TANABE 89	DPWA	

$\rho\gamma \rightarrow N(1710) \rightarrow \Lambda K^+$ phase angle θ $(M_{1-} \text{ amplitude})$

VALUE (degrees)	DOCUMENT ID	TECN	COMMENT
• • • We do not use the following data for averages, fits, limits, etc. • • •			
215 ± 3	WORKMAN 90	DPWA	
176.3	TANABE 89	DPWA	

N(1710) FOOTNOTES

- BATINIC 95 finds a second state with a 6 MeV mass difference.
- LONGACRE 77 pole positions are from a search for poles in the unitarized T-matrix; the first (second) value uses, in addition to $\pi N \rightarrow N\pi\pi$ data, elastic amplitudes from a Saclay (CERN) partial-wave analysis. The other LONGACRE 77 values are from eyeball fits with Breit-Wigner circles to the T-matrix amplitudes.
- From method II of LONGACRE 75: eyeball fits with Breit-Wigner circles to the T-matrix amplitudes.
- See HOEHLER 93 for a detailed discussion of the evidence for and the pole parameters of N and Δ resonances as determined from Argand diagrams of πN elastic partial-wave amplitudes and from plots of the speeds with which the amplitudes traverse the diagrams.
- LONGACRE 78 values are from a search for poles in the unitarized T-matrix. The first (second) value uses, in addition to $\pi N \rightarrow N\pi\pi$ data, elastic amplitudes from a Saclay (CERN) partial-wave analysis.

N(1710) REFERENCES

For early references, see Physics Letters **111B** 1 (1982).

ARNDT 06	PR C74 045205	R.A. Arndt <i>et al.</i>	(GWU)
PDG 06	JPG 33 1	W.-M. Yao <i>et al.</i>	(PDG Collab.)
SHKLYAR 05	PR C72 015210	V. Shklyar, H. Lenske, U. Mosel	(GIES)
PENNER 02C	PR C66 055211	G. Penner, U. Mosel	(GIES)
PENNER 02D	PR C66 055212	G. Penner, U. Mosel	(GIES)
VRANA 00	PRPL 328 181	T.P. Vrana, S.A. Dytman, T.-S.H. Lee	(PITT+)
ARNDT 96	PR C53 430	R.A. Arndt, I.I. Strakovsky, R.L. Workman	(VPI)
ARNDT 95	PR C52 2120	R.A. Arndt <i>et al.</i>	(VPI, BRCO)
BATINIC 95	PR C51 2310	M. Batinic <i>et al.</i>	(BOSK, UCLA)
	Also	PR C57 1004 (erratum)	M. Batinic <i>et al.</i>
HOEHLER 93	πN Newsletter 9 1	G. Höhler	(KARL)
LI 93	PR C47 2759	Z.J. Li <i>et al.</i>	(VPI)
MANLEY 92	PR D45 4002	D.M. Manley, E.M. Saleski	(KENT) IJP
	Also	PR D30 904	D.M. Manley <i>et al.</i>
ARNDT 91	PR D43 2131	R.A. Arndt <i>et al.</i>	(VPI, TELE) IJP
CUTKOSKY 90	PR D42 235	R.E. Cutkosky, S. Wang	(CMU)
WORKMAN 90	PR C42 781	R.L. Workman	(VPI)
TANABE 89	PR C39 741	H. Tanabe, M. Kohno, C. Bennhold	(MANZ)
	Also	NC 102A 193	M. Kohno, H. Tanabe, C. Bennhold
BELL 83	NP B222 389	K.W. Bell <i>et al.</i>	(RL) IJP
CRAWFORD 83	NP B211 1	R.L. Crawford, W.T. Morton	(GLAS)
PDG 82	PL 111B 1	M. Roos <i>et al.</i>	(HELS, CIT, CERN)
AWAJI 81	Bonn Conf. 352	N. Awaji, R. Kajikawa	(NAGO)
	Also	NP B197 365	K. Fujii <i>et al.</i>
FUJII 81	NP B187 53	K. Fujii <i>et al.</i>	(NAGO, OSAK)
CUTKOSKY 80	Toronto Conf. 19	R.E. Cutkosky <i>et al.</i>	(CMU, LBL) IJP
	Also	PR D20 2839	R.E. Cutkosky <i>et al.</i>
LIVANOS 80	Toronto Conf. 35	P. Livanos <i>et al.</i>	(SACL) IJP
SAXON 80	NP B162 522	D.H. Saxon <i>et al.</i>	(RHEL, BRIS) IJP
HOEHLER 79	PDAT 12-1	G. Höhler <i>et al.</i>	(KARL) IJP
	Also	Toronto Conf. 3	R. Koch <i>et al.</i>
LONGACRE 78	PR D17 1795	R.S. Longacre <i>et al.</i>	(LBL, SLAC)
LONGACRE 77	NP B122 493	R.S. Longacre, J. Dolbeau	(SACL) IJP
	Also	NP B108 365	J. Dolbeau <i>et al.</i>
LONGACRE 75	PL 55B 415	R.S. Longacre <i>et al.</i>	(LBL, SLAC) IJP

N(1720) P_{13}

$I(J^P) = \frac{1}{2}(\frac{3}{2}^+)$ Status: * * * *

Most of the results published before 1975 were last included in our 1982 edition, Physics Letters **111B** 1 (1982). Some further obsolete results published before 1984 were last included in our 2006 edition, Journal of Physics, G **33** 1 (2006).

N(1720) BREIT-WIGNER MASS

VALUE (MeV)	DOCUMENT ID	TECN	COMMENT
1700 to 1750 (≈ 1720) OUR ESTIMATE			
1763.8 ± 4.6	ARNDT 06	DPWA	$\pi N \rightarrow \pi N, \eta N$
1717 ± 31	MANLEY 92	IPWA	$\pi N \rightarrow \pi N \& N\pi\pi$
1700 ± 50	CUTKOSKY 80	IPWA	$\pi N \rightarrow \pi N$
1710 ± 20	HOEHLER 79	IPWA	$\pi N \rightarrow \pi N$
• • • We do not use the following data for averages, fits, limits, etc. • • •			
1790 ± 100	THOMA 08	DPWA	Multichannel
1749.6 ± 4.5	ARNDT 04	DPWA	$\pi N \rightarrow \pi N, \eta N$
1705 ± 10	PENNER 02C	DPWA	Multichannel
1716 ± 112	VRANA 00	DPWA	Multichannel
1713 ± 10	ARNDT 96	IPWA	$\gamma N \rightarrow \pi N$
1820	ARNDT 95	DPWA	$\pi N \rightarrow N\pi$
1711 ± 26	BATINIC 95	DPWA	$\pi N \rightarrow N\pi, N\eta$
1720	LI 93	IPWA	$\gamma N \rightarrow \pi N$
1690	SAXON 80	DPWA	$\pi^- p \rightarrow \Lambda K^0$
1750	1 LONGACRE 77	IPWA	$\pi N \rightarrow N\pi\pi$
1720	2 LONGACRE 75	IPWA	$\pi N \rightarrow N\pi\pi$

N(1720) BREIT-WIGNER WIDTH

VALUE (MeV)	DOCUMENT ID	TECN	COMMENT
150 to 300 (≈ 200) OUR ESTIMATE			
210 ± 22	ARNDT 06	DPWA	$\pi N \rightarrow \pi N, \eta N$
380 ± 180	MANLEY 92	IPWA	$\pi N \rightarrow \pi N \& N\pi\pi$
125 ± 70	CUTKOSKY 80	IPWA	$\pi N \rightarrow \pi N$
190 ± 30	HOEHLER 79	IPWA	$\pi N \rightarrow \pi N$

Baryon Particle Listings

 $N(1720)$

••• We do not use the following data for averages, fits, limits, etc. •••

690±100	THOMA	08	DPWA	Multichannel
256± 22	ARNDT	04	DPWA	$\pi N \rightarrow \pi N, \eta N$
237± 73	PENNER	02c	DPWA	Multichannel
121± 39	VRANA	00	DPWA	Multichannel
153± 15	ARNDT	96	IPWA	$\gamma N \rightarrow \pi N$
354	ARNDT	95	DPWA	$\pi N \rightarrow N\pi$
235± 51	BATINIC	95	DPWA	$\pi N \rightarrow N\pi, N\eta$
200	LI	93	IPWA	$\gamma N \rightarrow \pi N$
120	SAXON	80	DPWA	$\pi^- p \rightarrow \Lambda K^0$
130	¹ LONGACRE	77	IPWA	$\pi N \rightarrow N\pi\pi$
150	² LONGACRE	75	IPWA	$\pi N \rightarrow N\pi\pi$

 $N(1720)$ POLE POSITION

REAL PART

VALUE (MeV)	DOCUMENT ID	TECN	COMMENT
1660 to 1690 (≈ 1675) OUR ESTIMATE			
1666	ARNDT	06	DPWA $\pi N \rightarrow \pi N, \eta N$
1686	³ HOEHLER	93	SPED $\pi N \rightarrow \pi N$
1680±30	CUTKOSKY	80	IPWA $\pi N \rightarrow \pi N$
••• We do not use the following data for averages, fits, limits, etc. •••			
1630±90	THOMA	08	DPWA Multichannel
1655	ARNDT	04	DPWA $\pi N \rightarrow \pi N, \eta N$
1692	VRANA	00	DPWA Multichannel
1717	ARNDT	95	DPWA $\pi N \rightarrow N\pi$
1675	ARNDT	91	DPWA $\pi N \rightarrow \pi N$ Soln SM90
1716 or 1716	⁴ LONGACRE	78	IPWA $\pi N \rightarrow N\pi\pi$
1745 or 1748	¹ LONGACRE	77	IPWA $\pi N \rightarrow N\pi\pi$

-2xIMAGINARY PART

VALUE (MeV)	DOCUMENT ID	TECN	COMMENT
115 to 275 OUR ESTIMATE			
355	ARNDT	06	DPWA $\pi N \rightarrow \pi N, \eta N$
187	³ HOEHLER	93	SPED $\pi N \rightarrow \pi N$
120±40	CUTKOSKY	80	IPWA $\pi N \rightarrow \pi N$
••• We do not use the following data for averages, fits, limits, etc. •••			
460±80	THOMA	08	DPWA Multichannel
278	ARNDT	04	DPWA $\pi N \rightarrow \pi N, \eta N$
94	VRANA	00	DPWA Multichannel
388	ARNDT	95	DPWA $\pi N \rightarrow N\pi$
114	ARNDT	91	DPWA $\pi N \rightarrow \pi N$ Soln SM90
124 or 126	⁴ LONGACRE	78	IPWA $\pi N \rightarrow N\pi\pi$
135 or 123	¹ LONGACRE	77	IPWA $\pi N \rightarrow N\pi\pi$

 $N(1720)$ ELASTIC POLE RESIDUEMODULUS $|r|$

VALUE (MeV)	DOCUMENT ID	TECN	COMMENT
25	ARNDT	06	DPWA $\pi N \rightarrow \pi N, \eta N$
15	HOEHLER	93	SPED $\pi N \rightarrow \pi N$
8±2	CUTKOSKY	80	IPWA $\pi N \rightarrow \pi N$
••• We do not use the following data for averages, fits, limits, etc. •••			
20	ARNDT	04	DPWA $\pi N \rightarrow \pi N, \eta N$
39	ARNDT	95	DPWA $\pi N \rightarrow N\pi$
11	ARNDT	91	DPWA $\pi N \rightarrow \pi N$ Soln SM90

PHASE θ

VALUE (°)	DOCUMENT ID	TECN	COMMENT
-94	ARNDT	06	DPWA $\pi N \rightarrow \pi N, \eta N$
-160±30	CUTKOSKY	80	IPWA $\pi N \rightarrow \pi N$
••• We do not use the following data for averages, fits, limits, etc. •••			
-88	ARNDT	04	DPWA $\pi N \rightarrow \pi N, \eta N$
-70	ARNDT	95	DPWA $\pi N \rightarrow N\pi$
-130	ARNDT	91	DPWA $\pi N \rightarrow \pi N$ Soln SM90

 $N(1720)$ DECAY MODES

The following branching fractions are our estimates, not fits or averages.

Mode	Fraction (Γ_i/Γ)
Γ_1 $N\pi$	10–20 %
Γ_2 $N\eta$	(4.0±1.0) %
Γ_3 ΛK	1–15 %
Γ_4 ΣK	
Γ_5 $N\pi\pi$	>70 %
Γ_6 $\Delta\pi$	
Γ_7 $\Delta(1232)\pi, P\text{-wave}$	
Γ_8 $N\rho$	70–85 %
Γ_9 $N\rho, S=1/2, P\text{-wave}$	

Γ_{10} $N\rho, S=3/2, P\text{-wave}$	
Γ_{11} $N(\pi\pi)_{S\text{-wave}}^{J=0}$	
Γ_{12} $p\gamma$	0.003–0.10 %
Γ_{13} $p\gamma, \text{helicity}=1/2$	0.003–0.08 %
Γ_{14} $p\gamma, \text{helicity}=3/2$	0.001–0.03 %
Γ_{15} $n\gamma$	0.002–0.39 %
Γ_{16} $n\gamma, \text{helicity}=1/2$	0.0–0.002 %
Γ_{17} $n\gamma, \text{helicity}=3/2$	0.001–0.39 %

 $N(1720)$ BRANCHING RATIOS

$\Gamma(N\pi)/\Gamma_{\text{total}}$	VALUE	DOCUMENT ID	TECN	COMMENT	Γ_1/Γ
0.10 to 0.20 OUR ESTIMATE					
	0.094±0.005	ARNDT	06	DPWA $\pi N \rightarrow \pi N, \eta N$	
	0.13 ±0.05	MANLEY	92	IPWA $\pi N \rightarrow \pi N \& N\pi\pi$	
	0.10 ±0.04	CUTKOSKY	80	IPWA $\pi N \rightarrow \pi N$	
	0.14 ±0.03	HOEHLER	79	IPWA $\pi N \rightarrow \pi N$	
••• We do not use the following data for averages, fits, limits, etc. •••					
	0.09 ±0.06	THOMA	08	DPWA Multichannel	
	0.190±0.004	ARNDT	04	DPWA $\pi N \rightarrow \pi N, \eta N$	
	0.17 ±0.02	PENNER	02c	DPWA Multichannel	
	0.05 ±0.05	VRANA	00	DPWA Multichannel	
	0.16	ARNDT	95	DPWA $\pi N \rightarrow N\pi$	
	0.18 ±0.04	BATINIC	95	DPWA $\pi N \rightarrow N\pi, N\eta$	

$\Gamma(N\eta)/\Gamma_{\text{total}}$	VALUE	DOCUMENT ID	TECN	COMMENT	Γ_2/Γ
0.04 ±0.01					
••• We do not use the following data for averages, fits, limits, etc. •••					
	0.10 ±0.07	THOMA	08	DPWA Multichannel	
	0.002±0.002	PENNER	02c	DPWA Multichannel	
	0.002±0.01	BATINIC	95	DPWA $\pi N \rightarrow N\pi, N\eta$	

$\Gamma(\Lambda K)/\Gamma_{\text{total}}$	VALUE	DOCUMENT ID	TECN	COMMENT	Γ_3/Γ
0.044±0.004 OUR AVERAGE					
	0.043±0.004	SHKLYAR	05	DPWA Multichannel	
	0.09 ±0.03	PENNER	02c	DPWA Multichannel	
••• We do not use the following data for averages, fits, limits, etc. •••					
	0.12 ±0.09	THOMA	08	DPWA Multichannel	

$(\Gamma_i\Gamma_f)^{1/2}/\Gamma_{\text{total}}$ in $N\pi \rightarrow N(1720) \rightarrow \Lambda K$	VALUE	DOCUMENT ID	TECN	COMMENT	$(\Gamma_1\Gamma_3)^{1/2}/\Gamma$
-0.14 to -0.06 OUR ESTIMATE					
	-0.09	BELL	83	DPWA $\pi^- p \rightarrow \Lambda K^0$	
	-0.11	SAXON	80	DPWA $\pi^- p \rightarrow \Lambda K^0$	

Note: Signs of couplings from $\pi N \rightarrow N\pi\pi$ analyses were changed in the 1986 edition to agree with the baryon-first convention; the overall phase ambiguity is resolved by choosing a negative sign for the $\Delta(1620) S_{31}$ coupling to $\Delta(1232)\pi$.

$(\Gamma_i\Gamma_f)^{1/2}/\Gamma_{\text{total}}$ in $N\pi \rightarrow N(1720) \rightarrow \Delta(1232)\pi, P\text{-wave}$	VALUE	DOCUMENT ID	TECN	COMMENT	$(\Gamma_1\Gamma_7)^{1/2}/\Gamma$
±0.27 to ±0.37 OUR ESTIMATE					
	-0.17	¹ LONGACRE	77	IPWA $\pi N \rightarrow N\pi\pi$	

$(\Gamma_i\Gamma_f)^{1/2}/\Gamma_{\text{total}}$ in $N\pi \rightarrow N(1720) \rightarrow N\rho, S=1/2, P\text{-wave}$	VALUE	DOCUMENT ID	TECN	COMMENT	$(\Gamma_1\Gamma_9)^{1/2}/\Gamma$
	+0.34±0.05	MANLEY	92	IPWA $\pi N \rightarrow \pi N \& N\pi\pi$	
	-0.26	¹ LONGACRE	77	IPWA $\pi N \rightarrow N\pi\pi$	
	+0.40	² LONGACRE	75	IPWA $\pi N \rightarrow N\pi\pi$	

$\Gamma(N\rho, S=1/2, P\text{-wave})/\Gamma_{\text{total}}$	VALUE	DOCUMENT ID	TECN	COMMENT	Γ_9/Γ
	0.91±0.01	VRANA	00	DPWA Multichannel	

$(\Gamma_i\Gamma_f)^{1/2}/\Gamma_{\text{total}}$ in $N\pi \rightarrow N(1720) \rightarrow N\rho, S=3/2, P\text{-wave}$	VALUE	DOCUMENT ID	TECN	COMMENT	$(\Gamma_1\Gamma_{10})^{1/2}/\Gamma$
	+0.15	¹ LONGACRE	77	IPWA $\pi N \rightarrow N\pi\pi$	

$(\Gamma_i\Gamma_f)^{1/2}/\Gamma_{\text{total}}$ in $N\pi \rightarrow N(1720) \rightarrow N(\pi\pi)_{S\text{-wave}}^{J=0}$	VALUE	DOCUMENT ID	TECN	COMMENT	$(\Gamma_1\Gamma_{11})^{1/2}/\Gamma$
	-0.19	¹ LONGACRE	77	IPWA $\pi N \rightarrow N\pi\pi$	

N(1720) PHOTON DECAY AMPLITUDES

Papers on γN amplitudes predating 1981 may be found in our 2006 edition, Journal of Physics, G **33** 1 (2006).

N(1720) $\rightarrow p\gamma$, helicity-1/2 amplitude $A_{1/2}$

VALUE (GeV ^{-1/2})	DOCUMENT ID	TECN	COMMENT
+0.018 ± 0.030 OUR ESTIMATE			
0.097 ± 0.003	DUGGER 07	DPWA	$\gamma N \rightarrow \pi N$
-0.015 ± 0.015	ARNDT 96	IPWA	$\gamma N \rightarrow \pi N$
0.044 ± 0.066	CRAWFORD 83	IPWA	$\gamma N \rightarrow \pi N$
-0.004 ± 0.007	AWAJI 81	DPWA	$\gamma N \rightarrow \pi N$
• • • We do not use the following data for averages, fits, limits, etc. • • •			
0.073	DRECHSEL 07	DPWA	$\gamma N \rightarrow \pi N$
-0.053	PENNER 02D	DPWA	Multichannel
0.012 ± 0.003	LI 93	IPWA	$\gamma N \rightarrow \pi N$

N(1720) $\rightarrow p\gamma$, helicity-3/2 amplitude $A_{3/2}$

VALUE (GeV ^{-1/2})	DOCUMENT ID	TECN	COMMENT
-0.019 ± 0.020 OUR ESTIMATE			
-0.007 ± 0.010	ARNDT 96	IPWA	$\gamma N \rightarrow \pi N$
-0.024 ± 0.006	CRAWFORD 83	IPWA	$\gamma N \rightarrow \pi N$
-0.040 ± 0.016	AWAJI 81	DPWA	$\gamma N \rightarrow \pi N$
• • • We do not use the following data for averages, fits, limits, etc. • • •			
-0.011	DRECHSEL 07	DPWA	$\gamma N \rightarrow \pi N$
0.027	PENNER 02D	DPWA	Multichannel
-0.022 ± 0.003	LI 93	IPWA	$\gamma N \rightarrow \pi N$

N(1720) $\rightarrow n\gamma$, helicity-1/2 amplitude $A_{1/2}$

VALUE (GeV ^{-1/2})	DOCUMENT ID	TECN	COMMENT
+0.001 ± 0.015 OUR ESTIMATE			
-0.039 ± 0.003	DUGGER 07	DPWA	$\gamma N \rightarrow \pi N$
0.007 ± 0.015	ARNDT 96	IPWA	$\gamma N \rightarrow \pi N$
0.002 ± 0.005	AWAJI 81	DPWA	$\gamma N \rightarrow \pi N$
• • • We do not use the following data for averages, fits, limits, etc. • • •			
-0.003	DRECHSEL 07	DPWA	$\gamma N \rightarrow \pi N$
-0.004	PENNER 02D	DPWA	Multichannel
0.050 ± 0.004	LI 93	IPWA	$\gamma N \rightarrow \pi N$

N(1720) $\rightarrow n\gamma$, helicity-3/2 amplitude $A_{3/2}$

VALUE (GeV ^{-1/2})	DOCUMENT ID	TECN	COMMENT
-0.029 ± 0.061 OUR ESTIMATE			
-0.005 ± 0.025	ARNDT 96	IPWA	$\gamma N \rightarrow \pi N$
-0.015 ± 0.019	AWAJI 81	DPWA	$\gamma N \rightarrow \pi N$
• • • We do not use the following data for averages, fits, limits, etc. • • •			
-0.031	DRECHSEL 07	DPWA	$\gamma N \rightarrow \pi N$
0.003	PENNER 02D	DPWA	Multichannel
-0.017 ± 0.004	LI 93	IPWA	$\gamma N \rightarrow \pi N$

N(1720) $\gamma p \rightarrow \Lambda K^+$ AMPLITUDES

$(\Gamma_1 \Gamma_1)^{1/2} / \Gamma_{\text{total}}$ in $p\gamma \rightarrow N(1720) \rightarrow \Lambda K^+$ (E_{1+} amplitude)

VALUE (units 10 ⁻³)	DOCUMENT ID	TECN	COMMENT
• • • We do not use the following data for averages, fits, limits, etc. • • •			
10.2 ± 0.2	WORKMAN 90	DPWA	
9.52	TANABE 89	DPWA	

$p\gamma \rightarrow N(1720) \rightarrow \Lambda K^+$ phase angle θ (E_{1+} amplitude)

VALUE (degrees)	DOCUMENT ID	TECN	COMMENT
• • • We do not use the following data for averages, fits, limits, etc. • • •			
-124 ± 2	WORKMAN 90	DPWA	
-103.4	TANABE 89	DPWA	

$(\Gamma_1 \Gamma_1)^{1/2} / \Gamma_{\text{total}}$ in $p\gamma \rightarrow N(1720) \rightarrow \Lambda K^+$ (M_{1+} amplitude)

VALUE (units 10 ⁻³)	DOCUMENT ID	TECN	COMMENT
• • • We do not use the following data for averages, fits, limits, etc. • • •			
-4.5 ± 0.2	WORKMAN 90	DPWA	
3.18	TANABE 89	DPWA	

N(1720) FOOTNOTES

- LONGACRE 77 pole positions are from a search for poles in the unitarized T-matrix; the first (second) value uses, in addition to $\pi N \rightarrow N\pi\pi$ data, elastic amplitudes from a Saclay (CERN) partial-wave analysis. The other LONGACRE 77 values are from eyeball fits with Breit-Wigner circles to the T-matrix amplitudes.
- From method II of LONGACRE 75: eyeball fits with Breit-Wigner circles to the T-matrix amplitudes.
- See HOEHLER 93 for a detailed discussion of the evidence for and the pole parameters of N and Δ resonances as determined from Argand diagrams of πN elastic partial-wave amplitudes and from plots of the speeds with which the amplitudes traverse the diagrams.
- LONGACRE 78 values are from a search for poles in the unitarized T-matrix. The first (second) value uses, in addition to $\pi N \rightarrow N\pi\pi$ data, elastic amplitudes from a Saclay (CERN) partial-wave analysis.

N(1720) REFERENCES

For early references, see Physics Letters **111B** 1 (1982).

THOMA 08	PL B659 87	U. Thoma et al.	(CB-ELSA Collab.)
DRECHSEL 07	EPJ A34 69	D. Drechsel, S.S. Kamalov, L. Tiator	(MAINZ, JINR)
DUGGER 07	PR C76 025211	M. Dugger et al.	(Jefferson Lab CLAS Collab.)
ARNDT 06	PR C74 045205	R.A. Arndt et al.	(GWU)
PDG 06	JPG 33 1	W.-M. Yao et al.	(PDG Collab.)
SHKLYAR 05	PR C72 015210	V. Shklyar, H. Lenske, U. Mosel	(GIES)
ARNDT 04	PR C69 035213	R.A. Arndt et al.	(GWU, TRIU)
PENNER 02C	PR C66 055211	G. Penner, U. Mosel	(GIES)
PENNER 02D	PR C66 055212	G. Penner, U. Mosel	(GIES)
VRANA 00	PRPL 328 181	T.P. Vrana, S.A. Dytman, T.-S.H. Lee	(PITT+)
ARNDT 96	PR C53 430	R.A. Arndt, I.I. Strakovsky, R.L. Workman	(VPI)
ARNDT 95	PR C52 2120	R.A. Arndt et al.	(VPI, BRCO)
BATINIC 95	PR C51 2310	M. Batinic et al.	(BOSK, UCLA)
Also	PR C57 1004 (erratum)	M. Batinic et al.	
HOEHLER 93	πN Newsletter 9 1	G. Hoehler	(KARL)
LI 93	PR C47 2759	Z.J. Li et al.	(VPI)
MANLEY 92	PR D45 4002	D.M. Manley, E.M. Saleski	(KENT) IJP
Also	PR D30 904	D.M. Manley et al.	(VPI)
ARNDT 91	PR D43 2131	R.A. Arndt et al.	(VPI, TELE) IJP
WORKMAN 90	PR C42 781	R.L. Workman	(VPI)
TANABE 89	PR C39 741	H. Tanabe, M. Kohno, C. Bennhold	(MANZ)
Also	NC 102A 193	M. Kohno, H. Tanabe, C. Bennhold	(MANZ)
BELL 83	NP B222 389	K.W. Bell et al.	(RL) IJP
CRAWFORD 83	NP B211 1	R.L. Crawford, W.T. Morton	(GLAS)
PDG 82	PL I11B 1	M. Roos et al.	(HELS, CIT, CERN)
AWAJI 81	Bonn Conf. 352	N. Awaji, R. Kajikawa	(NAGO)
Also	NP B197 365	K. Fujii et al.	(NAGO)
CUTKOSKY 80	Toronto Conf. 19	R.E. Cutkosky et al.	(CMU, LBL) IJP
Also	PR D20 2839	R.E. Cutkosky et al.	(CMU, BRIS) IJP
SAXON 80	NP B162 522	D.H. Saxon et al.	(RHEL, BRIS) IJP
HOEHLER 79	PDAT 12-1	G. Hoehler et al.	(KARLT) IJP
Also	Toronto Conf. 3	R. Koch	(KARLT) IJP
LONGACRE 78	PR D17 1795	R.S. Longacre et al.	(LBL, SLAC)
LONGACRE 77	NP B122 493	R.S. Longacre, J. Dolbeau	(SACL) IJP
Also	NP B108 365	J. Dolbeau et al.	(SACL) IJP
LONGACRE 75	PL 55B 415	R.S. Longacre et al.	(LBL, SLAC) IJP

N(1900) P_{13}

$I(J^P) = \frac{1}{2}(\frac{3}{2}^+)$ Status: **

OMITTED FROM SUMMARY TABLE

The latest GWU analysis (ARNDT 06) finds no evidence for this resonance.

N(1900) BREIT-WIGNER MASS

VALUE (MeV)	DOCUMENT ID	TECN	COMMENT
≈ 1900 OUR ESTIMATE			
1915 ± 60	NIKONOV 08	DPWA	Multichannel
1879 ± 17	MANLEY 92	IPWA	$\pi N \rightarrow \pi N$ & $N\pi\pi$
• • • We do not use the following data for averages, fits, limits, etc. • • •			
1951 ± 53	PENNER 02C	DPWA	Multichannel

N(1900) BREIT-WIGNER WIDTH

VALUE (MeV)	DOCUMENT ID	TECN	COMMENT
180 ± 40	NIKONOV 08	DPWA	Multichannel
498 ± 78	MANLEY 92	IPWA	$\pi N \rightarrow \pi N$ & $N\pi\pi$
• • • We do not use the following data for averages, fits, limits, etc. • • •			
622 ± 42	PENNER 02C	DPWA	Multichannel

N(1900) DECAY MODES

Mode	Fraction (Γ_i / Γ)
Γ_1 $N\pi$	
Γ_2 $N\pi\pi$	
Γ_3 $N\rho, S=1/2, P$ -wave	
Γ_4 $N\eta$	(14 ± 5) %
Γ_5 $N\omega$	(39 ± 9) %
Γ_6 ΛK	(2.40 ± 0.30) %
Γ_7 ΣK	

N(1900) BRANCHING RATIOS

$\Gamma(N\pi) / \Gamma_{\text{total}}$	DOCUMENT ID	TECN	COMMENT	Γ_1 / Γ
VALUE				
0.26 ± 0.06	MANLEY 92	IPWA	$\pi N \rightarrow \pi N$ & $N\pi\pi$	
• • • We do not use the following data for averages, fits, limits, etc. • • •				
0.02 - 0.09	NIKONOV 08	DPWA	Multichannel	
0.16 ± 0.02	PENNER 02C	DPWA	Multichannel	
$\Gamma(N\eta) / \Gamma_{\text{total}}$				
VALUE				
0.14 ± 0.05	PENNER 02C	DPWA	Multichannel	
$\Gamma(N\omega) / \Gamma_{\text{total}}$				
VALUE				
0.39 ± 0.09	PENNER 02C	DPWA	Multichannel	

Baryon Particle Listings

$N(1900)$, $N(1990)$

$(\Gamma_1 \Gamma_7)^{1/2} / \Gamma_{\text{total}}$ in $N\pi \rightarrow N(1900) \rightarrow N\rho, S=1/2, P\text{-wave}$				$(\Gamma_1 \Gamma_3)^{1/2} / \Gamma$
VALUE	DOCUMENT ID	TECN	COMMENT	
-0.34 ± 0.03	MANLEY	92	IPWA	$\pi N \rightarrow \pi N \& N\pi\pi$
$\Gamma(\Lambda K) / \Gamma_{\text{total}}$				Γ_6 / Γ
VALUE	DOCUMENT ID	TECN	COMMENT	
0.024 ± 0.003	SHKLYAR	05	DPWA	Multichannel
••• We do not use the following data for averages, fits, limits, etc. •••				
0.05 - 0.15	NIKONOV	08	DPWA	Multichannel
0.001 ± 0.001	PENNER	02c	DPWA	Multichannel
$\Gamma(\Sigma K) / \Gamma_{\text{total}}$				Γ_7 / Γ
VALUE	DOCUMENT ID	TECN	COMMENT	
••• We do not use the following data for averages, fits, limits, etc. •••				
0.01 ± 0.01	PENNER	02c	DPWA	Multichannel

$N(1900)$ PHOTON DECAY AMPLITUDES

Papers on γN amplitudes predating 1981 may be found in our 2006 edition, Journal of Physics, G **33** 1 (2006).

$N(1900) \rightarrow p\gamma$, helicity-1/2 amplitude $A_{1/2}$			
VALUE (GeV ^{-1/2})	DOCUMENT ID	TECN	COMMENT
••• We do not use the following data for averages, fits, limits, etc. •••			
-0.017	PENNER	02D	DPWA Multichannel
$N(1900) \rightarrow p\gamma$, helicity-3/2 amplitude $A_{3/2}$			
VALUE (GeV ^{-1/2})	DOCUMENT ID	TECN	COMMENT
••• We do not use the following data for averages, fits, limits, etc. •••			
0.031	PENNER	02D	DPWA Multichannel
$N(1900) \rightarrow n\gamma$, helicity-1/2 amplitude $A_{1/2}$			
VALUE (GeV ^{-1/2})	DOCUMENT ID	TECN	COMMENT
••• We do not use the following data for averages, fits, limits, etc. •••			
-0.016	PENNER	02D	DPWA Multichannel
$N(1900) \rightarrow n\gamma$, helicity-3/2 amplitude $A_{3/2}$			
VALUE (GeV ^{-1/2})	DOCUMENT ID	TECN	COMMENT
••• We do not use the following data for averages, fits, limits, etc. •••			
-0.002	PENNER	02D	DPWA Multichannel

$N(1900)$ REFERENCES

NIKONOV	08	PL B662 245	V.A. Nikonov <i>et al.</i>	(Bonn, Gatchina)
ARNDT	06	PR C74 045205	R.A. Arndt <i>et al.</i>	(GWU)
PDG	06	JPG 33 1	W.-M. Yao <i>et al.</i>	(PDG Collab.)
SHKLYAR	05	PR C72 015210	V. Shklyar, H. Lenske, U. Mosel	(GIES)
PENNER	02c	PR C66 055211	G. Penner, U. Mosel	(GIES)
PENNER	02D	PR C66 055212	G. Penner, U. Mosel	(GIES)
MANLEY	92	PR D45 4002	D.M. Manley, E.M. Saleski	(KENT)
Also		PR D30 904	D.M. Manley <i>et al.</i>	(VPI)

$N(1990) F_{17}$ $I(J^P) = \frac{1}{2}(7^+)$ Status: **

OMITTED FROM SUMMARY TABLE

Most of the results published before 1975 are now obsolete and have been omitted. They may be found in our 1982 edition, Physics Letters **111B** 1 (1982). Some further obsolete results published before 1984 were last included in our 2006 edition, Journal of Physics, G **33** 1 (2006).

The various analyses do not agree very well with one another.

The latest GWU analysis (ARNDT 06) finds no evidence for this resonance.

$N(1990)$ BREIT-WIGNER MASS

VALUE (MeV)	DOCUMENT ID	TECN	COMMENT
≈ 1990 OUR ESTIMATE			
2086 ± 28	MANLEY	92	IPWA $\pi N \rightarrow \pi N \& N\pi\pi$
1970 ± 50	CUTKOSKY	80	IPWA $\pi N \rightarrow \pi N$
2005 ± 150	HOEHLER	79	IPWA $\pi N \rightarrow \pi N$
1999	BARBOUR	78	DPWA $\gamma N \rightarrow \pi N$
••• We do not use the following data for averages, fits, limits, etc. •••			
2311 ± 16	VRANA	00	DPWA Multichannel

$N(1990)$ BREIT-WIGNER WIDTH

VALUE (MeV)	DOCUMENT ID	TECN	COMMENT
535 ± 120	MANLEY	92	IPWA $\pi N \rightarrow \pi N \& N\pi\pi$
350 ± 120	CUTKOSKY	80	IPWA $\pi N \rightarrow \pi N$
350 ± 100	HOEHLER	79	IPWA $\pi N \rightarrow \pi N$
216	BARBOUR	78	DPWA $\gamma N \rightarrow \pi N$
••• We do not use the following data for averages, fits, limits, etc. •••			
205 ± 72	VRANA	00	DPWA Multichannel

$N(1990)$ POLE POSITION

REAL PART

VALUE (MeV)	DOCUMENT ID	TECN	COMMENT
1900 ± 30	CUTKOSKY	80	IPWA $\pi N \rightarrow \pi N$
••• We do not use the following data for averages, fits, limits, etc. •••			
2301	VRANA	00	DPWA Multichannel
not seen	ARNDT	91	DPWA $\pi N \rightarrow \pi N$ Soln SM90

-2xIMAGINARY PART

VALUE (MeV)	DOCUMENT ID	TECN	COMMENT
260 ± 60	CUTKOSKY	80	IPWA $\pi N \rightarrow \pi N$
••• We do not use the following data for averages, fits, limits, etc. •••			
202	VRANA	00	DPWA Multichannel
not seen	ARNDT	91	DPWA $\pi N \rightarrow \pi N$ Soln SM90

$N(1990)$ ELASTIC POLE RESIDUE

MODULUS $|r|$

VALUE (MeV)	DOCUMENT ID	TECN	COMMENT
9 ± 3	CUTKOSKY	80	IPWA $\pi N \rightarrow \pi N$

PHASE θ

VALUE (°)	DOCUMENT ID	TECN	COMMENT
-60 ± 30	CUTKOSKY	80	IPWA $\pi N \rightarrow \pi N$

$N(1990)$ DECAY MODES

Mode
Γ_1 $N\pi$
Γ_2 $N\eta$
Γ_3 ΛK
Γ_4 ΣK
Γ_5 $N\pi\pi$
Γ_6 $p\gamma$, helicity=1/2
Γ_7 $p\gamma$, helicity=3/2
Γ_8 $n\gamma$, helicity=1/2
Γ_9 $n\gamma$, helicity=3/2

$N(1990)$ BRANCHING RATIOS

$\Gamma(N\pi) / \Gamma_{\text{total}}$	DOCUMENT ID	TECN	COMMENT	Γ_1 / Γ
0.06 ± 0.02	MANLEY	92	IPWA	$\pi N \rightarrow \pi N \& N\pi\pi$
0.06 ± 0.02	CUTKOSKY	80	IPWA	$\pi N \rightarrow \pi N$
0.04 ± 0.02	HOEHLER	79	IPWA	$\pi N \rightarrow \pi N$
••• We do not use the following data for averages, fits, limits, etc. •••				
0.22 ± 0.11	VRANA	00	DPWA	Multichannel

$(\Gamma_1 \Gamma_7)^{1/2} / \Gamma_{\text{total}}$ in $N\pi \rightarrow N(1990) \rightarrow N\eta$	DOCUMENT ID	TECN	COMMENT	$(\Gamma_1 \Gamma_2)^{1/2} / \Gamma$
-0.043	BAKER	79	DPWA	$\pi^- p \rightarrow n\eta$

$\Gamma(N\eta) / \Gamma_{\text{total}}$	DOCUMENT ID	TECN	COMMENT	Γ_2 / Γ
0.00 ± 0.01	VRANA	00	DPWA	Multichannel

$(\Gamma_1 \Gamma_7)^{1/2} / \Gamma_{\text{total}}$ in $N\pi \rightarrow N(1990) \rightarrow \Lambda K$	DOCUMENT ID	TECN	COMMENT	$(\Gamma_1 \Gamma_3)^{1/2} / \Gamma$
+0.01	BELL	83	DPWA	$\pi^- p \rightarrow \Lambda K^0$
not seen	SAXON	80	DPWA	$\pi^- p \rightarrow \Lambda K^0$
-0.021 ± 0.033	DEVENISH	74B		Fixed-t dispersion rel.

$(\Gamma_1 \Gamma_7)^{1/2} / \Gamma_{\text{total}}$ in $N\pi \rightarrow N(1990) \rightarrow \Sigma K$	DOCUMENT ID	TECN	COMMENT	$(\Gamma_1 \Gamma_4)^{1/2} / \Gamma$
0.010 to 0.023	DEANS	75	DPWA	$\pi N \rightarrow \Sigma K$
0.06	LANGBEIN	73	IPWA	$\pi N \rightarrow \Sigma K$ (sol. 1)

$(\Gamma_1 \Gamma_7)^{1/2} / \Gamma_{\text{total}}$ in $N\pi \rightarrow N(1990) \rightarrow N\pi\pi$	DOCUMENT ID	TECN	COMMENT	$(\Gamma_1 \Gamma_5)^{1/2} / \Gamma$
not seen	LONGACRE	75	IPWA	$\pi N \rightarrow N\pi\pi$

See key on page 373

Baryon Particle Listings

$N(1990)$, $N(2000)$

$N(1990)$ PHOTON DECAY AMPLITUDES

Papers on γN amplitudes predating 1981 may be found in our 2006 edition, Journal of Physics, G 33 1 (2006).

$N(1990) \rightarrow p\gamma$, helicity-1/2 amplitude $A_{1/2}$

VALUE (GeV ^{-1/2})	DOCUMENT ID	TECN	COMMENT
0.030 ± 0.029	AWAJI 81	DPWA	$\gamma N \rightarrow \pi N$
••• We do not use the following data for averages, fits, limits, etc. •••			
0.040	BARBOUR 78	DPWA	$\gamma N \rightarrow \pi N$

$N(1990) \rightarrow p\gamma$, helicity-3/2 amplitude $A_{3/2}$

VALUE (GeV ^{-1/2})	DOCUMENT ID	TECN	COMMENT
0.086 ± 0.060	AWAJI 81	DPWA	$\gamma N \rightarrow \pi N$
••• We do not use the following data for averages, fits, limits, etc. •••			
+0.004	BARBOUR 78	DPWA	$\gamma N \rightarrow \pi N$

$N(1990) \rightarrow n\gamma$, helicity-1/2 amplitude $A_{1/2}$

VALUE (GeV ^{-1/2})	DOCUMENT ID	TECN	COMMENT
-0.001	AWAJI 81	DPWA	$\gamma N \rightarrow \pi N$
••• We do not use the following data for averages, fits, limits, etc. •••			
-0.069	BARBOUR 78	DPWA	$\gamma N \rightarrow \pi N$

$N(1990) \rightarrow n\gamma$, helicity-3/2 amplitude $A_{3/2}$

VALUE (GeV ^{-1/2})	DOCUMENT ID	TECN	COMMENT
-0.178	AWAJI 81	DPWA	$\gamma N \rightarrow \pi N$
••• We do not use the following data for averages, fits, limits, etc. •••			
-0.072	BARBOUR 78	DPWA	$\gamma N \rightarrow \pi N$

$N(1990)$ FOOTNOTES

¹ The range given for DEANS 75 is from the four best solutions.

$N(1990)$ REFERENCES

For early references, see Physics Letters 111B 1 (1982).

ARNDT 06	PR C74 045205	R.A. Arndt <i>et al.</i>	(GWU)
PDG 06	JPG 33 1	W.-M. Yao <i>et al.</i>	(PDG Collab.)
VRANA 00	PRPL 328 181	T.P. Vrana, S.A. Dytman, T.-S.H. Lee	(PITT+)
MANLEY 92	PR D45 4002	D.M. Manley, E.M. Saleksi	(KENT) IJP
Also	PR D30 904	D.M. Manley <i>et al.</i>	(VPI)
ARNDT 91	PR D43 2131	R.A. Arndt <i>et al.</i>	(VPI, TELE) IJP
BELL 83	NP B222 389	K.W. Bell <i>et al.</i>	(RL) IJP
PDG 82	PL 111B 1	M. Roos <i>et al.</i>	(HELS, CIT, CERN)
AWAJI 81	Bonn Conf. 352	N. Awaji, R. Kajikawa	(NAGO)
Also	NP B197 345	K. Fujii <i>et al.</i>	(NAGO)
CUTKOSKY 80	Toronto Conf. 19	R.E. Cutkosky <i>et al.</i>	(CMU, LBL) IJP
Also	PR D20 2839	R.E. Cutkosky <i>et al.</i>	(CMU, LBL) IJP
SAXON 80	NP B162 522	D.H. Saxon <i>et al.</i>	(RHEL, BRIS) IJP
BAKER 79	NP B156 93	R.D. Baker <i>et al.</i>	(RHEL) IJP
HOEHLER 79	PDAT 12-1	G. Hohler <i>et al.</i>	(KARLT) IJP
Also	Toronto Conf. 3	R. Koch	(KARLT) IJP
BARBOUR 78	NP B141 253	I.M. Barbour, R.L. Crawford, N.H. Parsons	(GLAS)
DEANS 75	NP B96 90	S.R. Deans <i>et al.</i>	(SFLA, ALAH) IJP
LONGACRE 75	PL 55B 415	R.S. Longacre <i>et al.</i>	(LBL, SLAC) IJP
DEVENISH 74B	NP B81 330	R.C.E. Devenish, C.D. Froggatt, B.R. Martin	(DESY+) IJP
LANGBEIN 73	NP B53 251	W. Langbein, F. Wagner	(MUNI) IJP

$N(2000) F_{15}$

$$I(J^P) = \frac{1}{2}(\frac{5}{2}^+) \text{ Status: } * *$$

OMITTED FROM SUMMARY TABLE

Older results have been retained simply because there is little information at all about this possible state.

$N(2000)$ BREIT-WIGNER MASS

VALUE (MeV)	DOCUMENT ID	TECN	COMMENT
≈ 2000 OUR ESTIMATE			
1817.7	ARNDT 06	DPWA	$\pi N \rightarrow \pi N, \eta N$
1903 ± 87	MANLEY 92	IPWA	$\pi N \rightarrow \pi N \& N\pi\pi$
1882 ± 10	HOEHLER 79	IPWA	$\pi N \rightarrow \pi N$
2025	AYED 76	IPWA	$\pi N \rightarrow \pi N$
1970	¹ LANGBEIN 73	IPWA	$\pi N \rightarrow \Sigma K$ (sol. 2)
2175	ALMEHED 72	IPWA	$\pi N \rightarrow \pi N$
1930	DEANS 72	MPWA	$\gamma p \rightarrow \Lambda K$ (sol. D)
••• We do not use the following data for averages, fits, limits, etc. •••			
1814	ARNDT 95	DPWA	$\pi N \rightarrow \pi N$

$N(2000)$ BREIT-WIGNER WIDTH

VALUE (MeV)	DOCUMENT ID	TECN	COMMENT
117.6	ARNDT 06	DPWA	$\pi N \rightarrow \pi N, \eta N$
490 ± 310	MANLEY 92	IPWA	$\pi N \rightarrow \pi N \& N\pi\pi$
95 ± 20	HOEHLER 79	IPWA	$\pi N \rightarrow \pi N$
157	AYED 76	IPWA	$\pi N \rightarrow \pi N$
170	¹ LANGBEIN 73	IPWA	$\pi N \rightarrow \Sigma K$ (sol. 2)
150	ALMEHED 72	IPWA	$\pi N \rightarrow \pi N$
112	DEANS 72	MPWA	$\gamma p \rightarrow \Lambda K$ (sol. D)
••• We do not use the following data for averages, fits, limits, etc. •••			
176	ARNDT 95	DPWA	$\pi N \rightarrow \pi N$

$N(2000)$ POLE POSITION

REAL PART

VALUE (MeV)	DOCUMENT ID	TECN	COMMENT
1807	ARNDT 06	DPWA	$\pi N \rightarrow \pi N, \eta N$
••• We do not use the following data for averages, fits, limits, etc. •••			
1779	ARNDT 04	DPWA	$\pi N \rightarrow \pi N, \eta N$

-2xIMAGINARY PART

VALUE (MeV)	DOCUMENT ID	TECN	COMMENT
109	ARNDT 06	DPWA	$\pi N \rightarrow \pi N, \eta N$
••• We do not use the following data for averages, fits, limits, etc. •••			
248	ARNDT 04	DPWA	$\pi N \rightarrow \pi N, \eta N$

$N(2000)$ ELASTIC POLE RESIDUE

MODULUS $|r|$

VALUE (MeV)	DOCUMENT ID	TECN	COMMENT
60	ARNDT 06	DPWA	$\pi N \rightarrow \pi N, \eta N$
••• We do not use the following data for averages, fits, limits, etc. •••			
47	ARNDT 04	DPWA	$\pi N \rightarrow \pi N, \eta N$

PHASE θ

VALUE (°)	DOCUMENT ID	TECN	COMMENT
-67	ARNDT 06	DPWA	$\pi N \rightarrow \pi N, \eta N$
••• We do not use the following data for averages, fits, limits, etc. •••			
-61	ARNDT 04	DPWA	$\pi N \rightarrow \pi N, \eta N$

$N(2000)$ DECAY MODES

Mode	DOCUMENT ID	TECN	COMMENT
$\Gamma_1 N\pi$			
$\Gamma_2 N\eta$			
$\Gamma_3 \Lambda K$			
$\Gamma_4 \Sigma K$			
$\Gamma_5 N\pi\pi$			
$\Gamma_6 \Delta(1232)\pi, P\text{-wave}$			
$\Gamma_7 N\rho, S=3/2, P\text{-wave}$			
$\Gamma_8 N\rho, S=3/2, F\text{-wave}$			
$\Gamma_9 p\gamma$			

$N(2000)$ BRANCHING RATIOS

$\Gamma(N\pi)/\Gamma_{\text{total}}$	DOCUMENT ID	TECN	COMMENT	Γ_1/Γ
0.127	ARNDT 06	DPWA	$\pi N \rightarrow \pi N, \eta N$	
0.08 ± 0.05	MANLEY 92	IPWA	$\pi N \rightarrow \pi N \& N\pi\pi$	
0.04 ± 0.02	HOEHLER 79	IPWA	$\pi N \rightarrow \pi N$	
0.08	AYED 76	IPWA	$\pi N \rightarrow \pi N$	
0.25	ALMEHED 72	IPWA	$\pi N \rightarrow \pi N$	
••• We do not use the following data for averages, fits, limits, etc. •••				
0.10	ARNDT 95	DPWA	$\pi N \rightarrow N\pi$	

$(\Gamma_1\Gamma_2)^{1/2}/\Gamma_{\text{total}}$ in $N\pi \rightarrow N(2000) \rightarrow N\eta$	DOCUMENT ID	TECN	COMMENT	$(\Gamma_1\Gamma_2)^{1/2}/\Gamma$
+0.03	BAKER 79	DPWA	$\pi^- p \rightarrow n\eta$	

$(\Gamma_1\Gamma_3)^{1/2}/\Gamma_{\text{total}}$ in $N\pi \rightarrow N(2000) \rightarrow \Lambda K$	DOCUMENT ID	TECN	COMMENT	$(\Gamma_1\Gamma_3)^{1/2}/\Gamma$
not seen	SAXON 80	DPWA	$\pi^- p \rightarrow \Lambda K^0$	

$(\Gamma_1\Gamma_4)^{1/2}/\Gamma_{\text{total}}$ in $N\pi \rightarrow N(2000) \rightarrow \Sigma K$	DOCUMENT ID	TECN	COMMENT	$(\Gamma_1\Gamma_4)^{1/2}/\Gamma$
0.022	² DEANS 75	DPWA	$\pi N \rightarrow \Sigma K$	
0.05	¹ LANGBEIN 73	IPWA	$\pi N \rightarrow \Sigma K$ (sol. 2)	

$(\Gamma_1\Gamma_6)^{1/2}/\Gamma_{\text{total}}$ in $N\pi \rightarrow N(2000) \rightarrow \Delta(1232)\pi, P\text{-wave}$	DOCUMENT ID	TECN	COMMENT	$(\Gamma_1\Gamma_6)^{1/2}/\Gamma$
+0.10 ± 0.06	MANLEY 92	IPWA	$\pi N \rightarrow \pi N \& N\pi\pi$	

$(\Gamma_1\Gamma_7)^{1/2}/\Gamma_{\text{total}}$ in $N\pi \rightarrow N(2000) \rightarrow N\rho, S=3/2, P\text{-wave}$	DOCUMENT ID	TECN	COMMENT	$(\Gamma_1\Gamma_7)^{1/2}/\Gamma$
-0.22 ± 0.08	MANLEY 92	IPWA	$\pi N \rightarrow \pi N \& N\pi\pi$	

$(\Gamma_1\Gamma_8)^{1/2}/\Gamma_{\text{total}}$ in $N\pi \rightarrow N(2000) \rightarrow N\rho, S=3/2, F\text{-wave}$	DOCUMENT ID	TECN	COMMENT	$(\Gamma_1\Gamma_8)^{1/2}/\Gamma$
+0.11 ± 0.06	MANLEY 92	IPWA	$\pi N \rightarrow \pi N \& N\pi\pi$	

Baryon Particle Listings

 $N(2000)$, $N(2080)$

$(\Gamma_1 \Gamma_2)^{1/2} / \Gamma_{\text{total}}$ in $p\gamma \rightarrow N(2000) \rightarrow \Lambda K$	$(\Gamma_3 \Gamma_4)^{1/2} / \Gamma$		
VALUE	DOCUMENT ID	TECN	COMMENT
0.0022	DEANS	72	MPWA $\gamma p \rightarrow \Lambda K$ (sol. D)

 $N(2000)$ FOOTNOTES

- ¹ Not seen in solution 1 of LANGBEIN 73.
² Value given is from solution 1 of DEANS 75; not present in solutions 2, 3, or 4.

 $N(2000)$ REFERENCES

ARNDT	06	PR C74 045205	R.A. Arndt et al.	(GWU)
ARNDT	04	PR C59 035213	R.A. Arndt et al.	(GWU, TRIU)
ARNDT	95	PR C52 2120	R.A. Arndt et al.	(VPI, BRCO)
MANLEY	92	PR D45 4002	D.M. Manley, E.M. Saleski	(KENT) IJP
Also		PR D30 904	D.M. Manley et al.	(VPI)
SAXON	80	NP B162 522	D.H. Saxon et al.	(RHEL, BRIS) IJP
BAKER	79	NP B156 93	R.D. Baker et al.	(RHEL) IJP
HOEHLER	79	PDAT 12-1	G. Hoehler et al.	(KARLT) IJP
Also		Toronto Conf. 3	R. Koch	(KARLT) IJP
AYED	76	Thesis CEA-N-1921	R. Ayed	(SACL) IJP
DEANS	75	NP B36 90	S.R. Deans et al.	(SFLA, ALAH) IJP
LANGBEIN	73	NP B53 251	W. Langbein, F. Wagner	(MUNI) IJP
ALMEHED	72	NP B40 157	S. Almeded, C. Lovelace	(LUND, RUTG) IJP
DEANS	72	PR D6 1906	S.R. Deans et al.	(SFLA) IJP

 $N(2080) D_{13}$

$$I(J^P) = \frac{1}{2}(\frac{3}{2}^-) \text{ Status: } **$$

OMITTED FROM SUMMARY TABLE

There is some evidence for two resonances in this wave between 1800 and 2200 MeV (see CUTKOSKY 80). However, the solution of HOEHLER 79 is quite different.

Most of the results published before 1975 are now obsolete and have been omitted. They may be found in our 1982 edition, Physics Letters **111B** 1 (1982). Some further obsolete results published before 1984 were last included in our 2006 edition, Journal of Physics, G **33** 1 (2006).

The latest GWU analysis (ARNDT 06) finds no evidence for this resonance.

 $N(2080)$ BREIT-WIGNER MASS

VALUE (MeV)	DOCUMENT ID	TECN	COMMENT
≈ 2080 OUR ESTIMATE			
1804 \pm 55	MANLEY 92	IPWA	$\pi N \rightarrow \pi N$ & $N\pi\pi$
1920	BELL 83	DPWA	$\pi^- p \rightarrow \Lambda K^0$
1880 \pm 100	¹ CUTKOSKY 80	IPWA	$\pi N \rightarrow \pi N$
2060 \pm 80	¹ CUTKOSKY 80	IPWA	$\pi N \rightarrow \pi N$
1900	SAXON 80	DPWA	$\pi^- p \rightarrow \Lambda K^0$
2081 \pm 20	HOEHLER 79	IPWA	$\pi N \rightarrow \pi N$
• • • We do not use the following data for averages, fits, limits, etc. • • •			
1946 \pm 1	PENNER 02c	DPWA	Multichannel
1895	MART 00	DPWA	$\gamma p \rightarrow \Lambda K^+$
2003 \pm 18	VRANA 00	DPWA	Multichannel
1986 \pm 75	BATINIC 95	DPWA	$\pi N \rightarrow N\pi, N\eta$
1880	BAKER 79	DPWA	$\pi^- p \rightarrow n\eta$

 $N(2080)$ BREIT-WIGNER WIDTH

VALUE (MeV)	DOCUMENT ID	TECN	COMMENT
450 \pm 185	MANLEY 92	IPWA	$\pi N \rightarrow \pi N$ & $N\pi\pi$
320	BELL 83	DPWA	$\pi^- p \rightarrow \Lambda K^0$
180 \pm 60	¹ CUTKOSKY 80	IPWA	$\pi N \rightarrow \pi N$ (lower m)
300 \pm 100	¹ CUTKOSKY 80	IPWA	$\pi N \rightarrow \pi N$ (higher m)
240	SAXON 80	DPWA	$\pi^- p \rightarrow \Lambda K^0$
265 \pm 40	HOEHLER 79	IPWA	$\pi N \rightarrow \pi N$
• • • We do not use the following data for averages, fits, limits, etc. • • •			
859 \pm 7	PENNER 02c	DPWA	Multichannel
372	MART 00	DPWA	$\gamma p \rightarrow \Lambda K^+$
1070 \pm 858	VRANA 00	DPWA	Multichannel
1050 \pm 225	BATINIC 95	DPWA	$\pi N \rightarrow N\pi, N\eta$
87	BAKER 79	DPWA	$\pi^- p \rightarrow n\eta$

 $N(2080)$ POLE POSITION**REAL PART**

VALUE (MeV)	DOCUMENT ID	TECN	COMMENT
1880 \pm 100	¹ CUTKOSKY 80	IPWA	$\pi N \rightarrow \pi N$ (lower m)
2050 \pm 70	¹ CUTKOSKY 80	IPWA	$\pi N \rightarrow \pi N$ (higher m)
• • • We do not use the following data for averages, fits, limits, etc. • • •			
1824	VRANA 00	DPWA	Multichannel
not seen	ARNDT 91	DPWA	$\pi N \rightarrow \pi N$ Soln SM90

–2xIMAGINARY PART

VALUE (MeV)	DOCUMENT ID	TECN	COMMENT
160 \pm 80	¹ CUTKOSKY 80	IPWA	$\pi N \rightarrow \pi N$ (lower m)
200 \pm 80	¹ CUTKOSKY 80	IPWA	$\pi N \rightarrow \pi N$ (higher m)
• • • We do not use the following data for averages, fits, limits, etc. • • •			
614	VRANA 00	DPWA	Multichannel
not seen	ARNDT 91	DPWA	$\pi N \rightarrow \pi N$ Soln SM90

 $N(2080)$ ELASTIC POLE RESIDUE**MODULUS $|r|$**

VALUE (MeV)	DOCUMENT ID	TECN	COMMENT
10 \pm 5	¹ CUTKOSKY 80	IPWA	$\pi N \rightarrow \pi N$ (lower m)
30 \pm 20	¹ CUTKOSKY 80	IPWA	$\pi N \rightarrow \pi N$ (higher m)

PHASE θ

VALUE ($^\circ$)	DOCUMENT ID	TECN	COMMENT
100 \pm 80	¹ CUTKOSKY 80	IPWA	$\pi N \rightarrow \pi N$ (lower m)
0 \pm 100	¹ CUTKOSKY 80	IPWA	$\pi N \rightarrow \pi N$ (higher m)

 $N(2080)$ DECAY MODES

Mode	Fraction (Γ_i/Γ)	Scale factor
Γ_1 $N\pi$		
Γ_2 $N\eta$	(3.5 \pm 3.5) %	2.5
Γ_3 $N\omega$	(21 \pm 7) %	
Γ_4 ΛK		
Γ_5 ΣK	(7 \pm 4) $\times 10^{-3}$	
Γ_6 $N\pi\pi$		
Γ_7 $\Delta(1232)\pi$, S-wave		
Γ_8 $\Delta(1232)\pi$, D-wave		
Γ_9 $N\rho$, S=3/2, S-wave		
Γ_{10} $N(\pi\pi)_{S=0}^1$		
Γ_{11} $p\gamma$, helicity=1/2		
Γ_{12} $p\gamma$, helicity=3/2		
Γ_{13} $n\gamma$, helicity=1/2		
Γ_{14} $n\gamma$, helicity=3/2		
Γ_{15} $p\gamma$		

 $N(2080)$ BRANCHING RATIOS

$\Gamma(N\pi)/\Gamma_{\text{total}}$	DOCUMENT ID	TECN	COMMENT	Γ_1/Γ
0.23 \pm 0.03	MANLEY 92	IPWA	$\pi N \rightarrow \pi N$ & $N\pi\pi$	
0.10 \pm 0.04	¹ CUTKOSKY 80	IPWA	$\pi N \rightarrow \pi N$ (lower m)	
0.14 \pm 0.07	¹ CUTKOSKY 80	IPWA	$\pi N \rightarrow \pi N$ (higher m)	
0.06 \pm 0.02	HOEHLER 79	IPWA	$\pi N \rightarrow \pi N$	
• • • We do not use the following data for averages, fits, limits, etc. • • •				
0.12 \pm 0.02	PENNER 02c	DPWA	Multichannel	
0.13 \pm 0.03	VRANA 00	DPWA	Multichannel	
0.09 \pm 0.02	BATINIC 95	DPWA	$\pi N \rightarrow N\pi, N\eta$	

 $\Gamma(N\eta)/\Gamma_{\text{total}}$

VALUE	DOCUMENT ID	TECN	COMMENT	Γ_2/Γ
0.035 \pm 0.035 OUR AVERAGE	Error includes scale factor of 2.5.			
0.07 \pm 0.02	PENNER 02c	DPWA	Multichannel	
0.00 \pm 0.02	VRANA 00	DPWA	Multichannel	
• • • We do not use the following data for averages, fits, limits, etc. • • •				
0.07 \pm 0.04	BATINIC 95	DPWA	$\pi N \rightarrow N\pi, N\eta$	

 $(\Gamma_1 \Gamma_2)^{1/2} / \Gamma_{\text{total}}$ in $N\pi \rightarrow N(2080) \rightarrow N\eta$

VALUE	DOCUMENT ID	TECN	COMMENT	$(\Gamma_1 \Gamma_2)^{1/2} / \Gamma$
0.065	BAKER 79	DPWA	$\pi^- p \rightarrow n\eta$	

 $\Gamma(N\omega)/\Gamma_{\text{total}}$

VALUE	DOCUMENT ID	TECN	COMMENT	Γ_3/Γ
0.21 \pm 0.07	PENNER 02c	DPWA	Multichannel	

 $\Gamma(\Lambda K)/\Gamma_{\text{total}}$

VALUE	DOCUMENT ID	TECN	COMMENT	Γ_4/Γ
• • • We do not use the following data for averages, fits, limits, etc. • • •				
0.002 \pm 0.002	PENNER 02c	DPWA	Multichannel	

 $(\Gamma_1 \Gamma_3)^{1/2} / \Gamma_{\text{total}}$ in $N\pi \rightarrow N(2080) \rightarrow \Lambda K$

VALUE	DOCUMENT ID	TECN	COMMENT	$(\Gamma_1 \Gamma_3)^{1/2} / \Gamma$
+0.04	BELL 83	DPWA	$\pi^- p \rightarrow \Lambda K^0$	
+0.03	SAXON 80	DPWA	$\pi^- p \rightarrow \Lambda K^0$	

 $\Gamma(\Sigma K)/\Gamma_{\text{total}}$

VALUE	DOCUMENT ID	TECN	COMMENT	Γ_5/Γ
0.007 \pm 0.004	PENNER 02c	DPWA	Multichannel	

See key on page 373

Baryon Particle Listings

$N(2080)$, $N(2090)$

$(\Gamma_1 \Gamma_f)^{1/2} / \Gamma_{\text{total}}$ in $N\pi \rightarrow N(2080) \rightarrow \Sigma K$	$(\Gamma_1 \Gamma_5)^{1/2} / \Gamma$		
VALUE	DOCUMENT ID	TECN	COMMENT
0.014 to 0.037	2 DEANS	75	DPWA $\pi N \rightarrow \Sigma K$

$(\Gamma_1 \Gamma_f)^{1/2} / \Gamma_{\text{total}}$ in $N\pi \rightarrow N(2080) \rightarrow \Delta(1232)\pi$, S-wave	$(\Gamma_1 \Gamma_7)^{1/2} / \Gamma$		
VALUE	DOCUMENT ID	TECN	COMMENT
-0.09 ± 0.09	MANLEY	92	IPWA $\pi N \rightarrow \pi N$ & $N\pi\pi$

$\Gamma(\Delta(1232)\pi, \text{S-wave}) / \Gamma_{\text{total}}$	Γ_7 / Γ		
VALUE	DOCUMENT ID	TECN	COMMENT
0.40 ± 0.10	VRANA	00	DPWA Multichannel

$(\Gamma_1 \Gamma_f)^{1/2} / \Gamma_{\text{total}}$ in $N\pi \rightarrow N(2080) \rightarrow \Delta(1232)\pi$, D-wave	$(\Gamma_1 \Gamma_8)^{1/2} / \Gamma$		
VALUE	DOCUMENT ID	TECN	COMMENT
+0.22 ± 0.07	MANLEY	92	IPWA $\pi N \rightarrow \pi N$ & $N\pi\pi$

$\Gamma(\Delta(1232)\pi, \text{D-wave}) / \Gamma_{\text{total}}$	Γ_8 / Γ		
VALUE	DOCUMENT ID	TECN	COMMENT
0.17 ± 0.10	VRANA	00	DPWA Multichannel

$(\Gamma_1 \Gamma_f)^{1/2} / \Gamma_{\text{total}}$ in $N\pi \rightarrow N(2080) \rightarrow N\rho, S=3/2$, S-wave	$(\Gamma_1 \Gamma_9)^{1/2} / \Gamma$		
VALUE	DOCUMENT ID	TECN	COMMENT
-0.24 ± 0.06	MANLEY	92	IPWA $\pi N \rightarrow \pi N$ & $N\pi\pi$

$\Gamma(N\rho, S=3/2, \text{S-wave}) / \Gamma_{\text{total}}$	Γ_9 / Γ		
VALUE	DOCUMENT ID	TECN	COMMENT
0.06 ± 0.06	VRANA	00	DPWA Multichannel

$(\Gamma_1 \Gamma_f)^{1/2} / \Gamma_{\text{total}}$ in $N\pi \rightarrow N(2080) \rightarrow N(\pi\pi)_{S=0}^0$	$(\Gamma_1 \Gamma_{10})^{1/2} / \Gamma$		
VALUE	DOCUMENT ID	TECN	COMMENT
+0.25 ± 0.06	MANLEY	92	IPWA $\pi N \rightarrow \pi N$ & $N\pi\pi$

$\Gamma(N(\pi\pi)_{S=0}^0) / \Gamma_{\text{total}}$	Γ_{10} / Γ		
VALUE	DOCUMENT ID	TECN	COMMENT
0.24 ± 0.24	VRANA	00	DPWA Multichannel

$(\Gamma_1 \Gamma_f)^{1/2} / \Gamma_{\text{total}}$ in $p\gamma \rightarrow N(2080) \rightarrow N\eta$	$(\Gamma_{15} \Gamma_2)^{1/2} / \Gamma$		
VALUE	DOCUMENT ID	TECN	COMMENT
0.0037	HICKS	73	MPWA $\gamma p \rightarrow p\eta$

$N(2080)$ PHOTON DECAY AMPLITUDES

Papers on γN amplitudes predating 1981 may be found in our 2006 edition, Journal of Physics, G **33** 1 (2006).

$N(2080) \rightarrow p\gamma$, helicity-1/2 amplitude $A_{1/2}$

VALUE (GeV ^{-1/2})	DOCUMENT ID	TECN	COMMENT
-0.020 ± 0.008	AWAJI	81	DPWA $\gamma N \rightarrow \pi N$
• • • We do not use the following data for averages, fits, limits, etc. • • •			
0.012	PENNER	02D	DPWA Multichannel
0.026 ± 0.052	DEVENISH	74	DPWA $\gamma N \rightarrow \pi N$

$N(2080) \rightarrow p\gamma$, helicity-3/2 amplitude $A_{3/2}$

VALUE (GeV ^{-1/2})	DOCUMENT ID	TECN	COMMENT
0.017 ± 0.011	AWAJI	81	DPWA $\gamma N \rightarrow \pi N$
• • • We do not use the following data for averages, fits, limits, etc. • • •			
-0.010	PENNER	02D	DPWA Multichannel
0.128 ± 0.057	DEVENISH	74	DPWA $\gamma N \rightarrow \pi N$

$N(2080) \rightarrow n\gamma$, helicity-1/2 amplitude $A_{1/2}$

VALUE (GeV ^{-1/2})	DOCUMENT ID	TECN	COMMENT
0.007 ± 0.013	AWAJI	81	DPWA $\gamma N \rightarrow \pi N$
• • • We do not use the following data for averages, fits, limits, etc. • • •			
0.023	PENNER	02D	DPWA Multichannel
0.053 ± 0.083	DEVENISH	74	DPWA $\gamma N \rightarrow \pi N$

$N(2080) \rightarrow n\gamma$, helicity-3/2 amplitude $A_{3/2}$

VALUE (GeV ^{-1/2})	DOCUMENT ID	TECN	COMMENT
-0.053 ± 0.034	AWAJI	81	DPWA $\gamma N \rightarrow \pi N$
• • • We do not use the following data for averages, fits, limits, etc. • • •			
-0.009	PENNER	02D	DPWA Multichannel
0.100 ± 0.141	DEVENISH	74	DPWA $\gamma N \rightarrow \pi N$

$N(2080) \gamma p \rightarrow \Lambda K^+$ AMPLITUDES

$(\Gamma_1 \Gamma_f)^{1/2} / \Gamma_{\text{total}}$ in $p\gamma \rightarrow N(2080) \rightarrow \Lambda K^+$	$(E_{2-} \text{ amplitude})$		
VALUE (units 10 ⁻³)	DOCUMENT ID	TECN	COMMENT
• • • We do not use the following data for averages, fits, limits, etc. • • •			
2.29 ^{+0.7} _{-0.2}	MART	00	DPWA $\gamma p \rightarrow \Lambda K^+$
5.5 ± 0.3	WORKMAN	90	DPWA
4.09	TANABE	89	DPWA

$p\gamma \rightarrow N(2080) \rightarrow \Lambda K^+$ phase angle θ	$(E_{2-} \text{ amplitude})$		
VALUE (degrees)	DOCUMENT ID	TECN	
• • • We do not use the following data for averages, fits, limits, etc. • • •			
-48 ± 5	WORKMAN	90	DPWA
-35.9	TANABE	89	DPWA

$(\Gamma_1 \Gamma_f)^{1/2} / \Gamma_{\text{total}}$ in $p\gamma \rightarrow N(2080) \rightarrow \Lambda K^+$	$(M_{2-} \text{ amplitude})$		
VALUE (units 10 ⁻³)	DOCUMENT ID	TECN	
• • • We do not use the following data for averages, fits, limits, etc. • • •			
-6.7 ± 0.2	WORKMAN	90	DPWA
-4.09	TANABE	89	DPWA

$N(2080)$ FOOTNOTES

- CUTKOSKY 80 finds a lower mass D_{13} resonance, as well as one in this region. Both are listed here.
- The range given for DEANS 75 is from the four best solutions. Disagrees with $\pi^+ p \rightarrow \Sigma^+ K^+$ data of WINNIK 77 around 1920 MeV.

$N(2080)$ REFERENCES

For early references, see Physics Letters **111B** 1 (1982).

ARNDT 06	PR C74 045205	R.A. Arndt <i>et al.</i>	(GWU)
PDG 06	JPG 33 1	W.-M. Yao <i>et al.</i>	(PDG Collab.)
PENNER 02C	PR C66 055211	G. Penner, U. Mosel	(GIES)
PENNER 02D	PR C66 055212	G. Penner, U. Mosel	(GIES)
MART 00	PR C61 012201	T. Mart, C. Bennhold	
VRANA 00	PRPL 328 181	T.P. Vrana, S.A. Dytman, T.-S.H. Lee	(PITT+)
BATINIC 95	PR C51 2310	M. Batinić <i>et al.</i>	(BOSK, UCLA)
Also	PR C57 1004 (erratum)	M. Batinić <i>et al.</i>	
MANLEY 92	PR D45 4002	D.M. Manley, E.M. Saleski	(KENT) IJP
Also	PR D30 904	D.M. Manley <i>et al.</i>	(VPI)
ARNDT 91	PR D43 2131	R.A. Arndt <i>et al.</i>	(VPI, TELE) IJP
WORKMAN 90	PR C42 701	R.L. Workman	(VPI)
TANABE 89	PR C39 741	H. Tanabe, M. Kohno, C. Bennhold	(MANZ)
Also	NC 102A 193	M. Kohno, H. Tanabe, C. Bennhold	(MANZ)
BELL 83	NP B222 389	K.W. Bell <i>et al.</i>	(RL) IJP
PDG 82	PL 111B 1	M. Roos <i>et al.</i>	(HELS, CIT, CERN)
AWAJI 81	Bonn Conf. 352	N. Awaji, R. Kajikawa	(NAGO)
Also	NP B197 365	K. Fujii <i>et al.</i>	(NAGO)
CUTKOSKY 80	Toronto Conf. 19	R.E. Cutkosky <i>et al.</i>	(CMU, LBL) IJP
Also	PR D20 2839	R.E. Cutkosky <i>et al.</i>	(CMU, LBL) IJP
SAXON 80	NP B162 522	D.H. Saxon <i>et al.</i>	(RHEL, BRIS) IJP
BAKER 79	NP B156 93	R.D. Baker <i>et al.</i>	(RHEL) IJP
HOEHLER 79	PDAT 12-1	G. Hoehler <i>et al.</i>	(KARLT) IJP
Also	Toronto Conf. 3	R. Koch	(KARLT) IJP
WINNIK 77	NP B128 66	M. Winnik <i>et al.</i>	(HAIF) I
DEANS 75	NP B96 90	S.R. Deans <i>et al.</i>	(SFLA, LAH) IJP
DEVENISH 74	PL 52B 227	R.C.E. Devenish, D.H. Lyth, W.A. Rankin	(DESY+) IJP
HICKS 73	PR D7 2614	H.R. Hicks <i>et al.</i>	(CMU, ORNL, SFLA) IJP

$N(2090) S_{11}$

$$I(J^P) = \frac{1}{2}(\frac{1}{2}^-) \text{ Status: } *$$

OMITTED FROM SUMMARY TABLE

Any structure in the S_{11} wave above 1800 MeV is listed here. A few early results that are now obsolete have been omitted.

The latest GWU analysis (ARNDT 06) finds no evidence for this resonance.

$N(2090)$ BREIT-WIGNER MASS

VALUE (MeV)	DOCUMENT ID	TECN	COMMENT
≈ 2090 OUR ESTIMATE			
1928 ± 59	MANLEY	92	IPWA $\pi N \rightarrow \pi N$ & $N\pi\pi$
2180 ± 80	CUTKOSKY	80	IPWA $\pi N \rightarrow \pi N$
1880 ± 20	HOEHLER	79	IPWA $\pi N \rightarrow \pi N$
• • • We do not use the following data for averages, fits, limits, etc. • • •			
1822 ± 43	VRANA	00	DPWA Multichannel
1897 ± 50 ⁺³⁰ ₋₂	PLOETZKE	98	SPEC $\gamma p \rightarrow p\eta$ (958)

$N(2090)$ BREIT-WIGNER WIDTH

VALUE (MeV)	DOCUMENT ID	TECN	COMMENT
414 ± 157	MANLEY	92	IPWA $\pi N \rightarrow \pi N$ & $N\pi\pi$
350 ± 100	CUTKOSKY	80	IPWA $\pi N \rightarrow \pi N$
95 ± 30	HOEHLER	79	IPWA $\pi N \rightarrow \pi N$
• • • We do not use the following data for averages, fits, limits, etc. • • •			
248 ± 185	VRANA	00	DPWA Multichannel
396 ± 155 ⁺³⁵ ₋₄₅	PLOETZKE	98	SPEC $\gamma p \rightarrow p\eta$ (958)

$N(2090)$ POLE POSITION

REAL PART	DOCUMENT ID	TECN	COMMENT
VALUE (MeV)			
2150 ± 70	CUTKOSKY	80	IPWA $\pi N \rightarrow \pi N$
1937 or 1949	¹ LONGACRE	78	IPWA $\pi N \rightarrow N\pi\pi$
• • • We do not use the following data for averages, fits, limits, etc. • • •			
1795	VRANA	00	DPWA Multichannel

Baryon Particle Listings

 $N(2090)$, $N(2100)$

-2xIMAGINARY PART

VALUE (MeV)	DOCUMENT ID	TECN	COMMENT
350±100	CUTKOSKY 80	IPWA	$\pi N \rightarrow \pi N$
139 or 131	¹ LONGACRE 78	IPWA	$\pi N \rightarrow N\pi\pi$
••• We do not use the following data for averages, fits, limits, etc. •••			
220	VRANA 00	DPWA	Multichannel

 $N(2090)$ ELASTIC POLE RESIDUEMODULUS $|r|$

VALUE (MeV)	DOCUMENT ID	TECN	COMMENT
40±20	CUTKOSKY 80	IPWA	$\pi N \rightarrow \pi N$

PHASE θ

VALUE (°)	DOCUMENT ID	TECN	COMMENT
0±90	CUTKOSKY 80	IPWA	$\pi N \rightarrow \pi N$

 $N(2090)$ DECAY MODES

Mode	
Γ_1	$N\pi$
Γ_2	$N\eta$
Γ_3	ΛK
Γ_4	$N\pi\pi$
Γ_5	$\Delta\pi$
Γ_6	$\Delta(1232)\pi$, D-wave
Γ_7	$N\rho$
Γ_8	$N\rho$, $S=1/2$, S-wave
Γ_9	$N\rho$, $S=3/2$, D-wave
Γ_{10}	$N(\pi\pi)_{S=0}^{I=0}$
Γ_{11}	$N(1440)\pi$

 $N(2090)$ BRANCHING RATIOS

$\Gamma(N\pi)/\Gamma_{\text{total}}$	DOCUMENT ID	TECN	COMMENT	Γ_1/Γ
0.10±0.10	MANLEY 92	IPWA	$\pi N \rightarrow \pi N$ & $N\pi\pi$	
0.18±0.08	CUTKOSKY 80	IPWA	$\pi N \rightarrow \pi N$	
0.09±0.05	HOEHLER 79	IPWA	$\pi N \rightarrow \pi N$	
••• We do not use the following data for averages, fits, limits, etc. •••				
0.17±0.03	VRANA 00	DPWA	Multichannel	

$\Gamma(N\eta)/\Gamma_{\text{total}}$	DOCUMENT ID	TECN	COMMENT	Γ_2/Γ
0.41±0.04	VRANA 00	DPWA	Multichannel	

$(\Gamma_1\Gamma_7)^{1/2}/\Gamma_{\text{total}}$ in $N\pi \rightarrow N(2090) \rightarrow \Lambda K$	DOCUMENT ID	TECN	COMMENT	$(\Gamma_1\Gamma_3)^{1/2}/\Gamma$
not seen	SAXON 80	DPWA	$\pi^- \rho \rightarrow \Lambda K^0$	

$\Gamma(\Delta(1232)\pi, D\text{-wave})/\Gamma_{\text{total}}$	DOCUMENT ID	TECN	COMMENT	Γ_6/Γ
0.01±0.01	VRANA 00	DPWA	Multichannel	

$\Gamma(N\rho, S=1/2, S\text{-wave})/\Gamma_{\text{total}}$	DOCUMENT ID	TECN	COMMENT	Γ_8/Γ
0.36±0.01	VRANA 00	DPWA	Multichannel	

$\Gamma(N\rho, S=3/2, D\text{-wave})/\Gamma_{\text{total}}$	DOCUMENT ID	TECN	COMMENT	Γ_9/Γ
0.01±0.01	VRANA 00	DPWA	Multichannel	

$\Gamma(N(\pi\pi)_{S=0}^{I=0})/\Gamma_{\text{total}}$	DOCUMENT ID	TECN	COMMENT	Γ_{10}/Γ
0.02±0.01	VRANA 00	DPWA	Multichannel	

$\Gamma(N(1440)\pi)/\Gamma_{\text{total}}$	DOCUMENT ID	TECN	COMMENT	Γ_{11}/Γ
0.02±0.01	VRANA 00	DPWA	Multichannel	

 $N(2090)$ FOOTNOTES

¹ LONGACRE 78 values are from a search for poles in the unitarized T-matrix. The first (second) value uses, in addition to $\pi N \rightarrow N\pi\pi$ data, elastic amplitudes from a Saclay (CERN) partial-wave analysis.

 $N(2090)$ REFERENCES

ARNDT 06	PR C74 045205	R.A. Arndt et al.	(GWU)
VRANA 00	PRPL 329 181	T.P. Vrana, S.A. Dytman., T.-S.H. Lee	(PITT+)
PLOETZKE 98	PL B444 555	R. Ploetzke et al.	(Bonn SAPHIR Collab.)
MANLEY 92	PR D45 4002	D.M. Manley, E.M. Saleski	(KENT) IJP
Also	PR D30 904	D.M. Manley et al.	(VPI)
CUTKOSKY 80	Toronto Conf. 19	R.E. Cutkosky et al.	(CMU, LBL) IJP
Also	PR D20 2839	R.E. Cutkosky et al.	(CMU, LBL)
SAXON 80	NP B162 522	D.H. Saxon et al.	(RHEL, BRIS) IJP
HOEHLER 79	PDAT 12-1	G. Hohler et al.	(KARLT) IJP
Also	Toronto Conf. 3	R. Koch	(KARLT) IJP
LONGACRE 78	PR D17 1795	R.S. Longacre et al.	(LBL, SLAC)

 $N(2100) P_{11}$

$$I(J^P) = \frac{1}{2}(\frac{1}{2}^+) \text{ Status: } *$$

OMITTED FROM SUMMARY TABLE

The latest GWU analysis (ARNDT 06) finds no evidence for this resonance.

 $N(2100)$ BREIT-WIGNER MASS

VALUE (MeV)	DOCUMENT ID	TECN	COMMENT
≈ 2100 OUR ESTIMATE			
1885±30	MANLEY 92	IPWA	$\pi N \rightarrow \pi N$ & $N\pi\pi$
2125±75	CUTKOSKY 80	IPWA	$\pi N \rightarrow \pi N$
2050±20	HOEHLER 79	IPWA	$\pi N \rightarrow \pi N$
••• We do not use the following data for averages, fits, limits, etc. •••			
2068±3 ⁺¹⁵ ₋₄₀	ABLIKIM 06k	BES	$J/\psi \rightarrow (p\pi^-)\bar{\pi}$
2084±93	VRANA 00	DPWA	Multichannel
1986±26 ⁺¹⁰ ₋₃₀	PLOETZKE 98	SPEC	$\gamma p \rightarrow p\eta'(958)$
2203±70	BATINIC 95	DPWA	$\pi N \rightarrow N\pi, N\eta$

 $N(2100)$ BREIT-WIGNER WIDTH

VALUE (MeV)	DOCUMENT ID	TECN	COMMENT
113±44	MANLEY 92	IPWA	$\pi N \rightarrow \pi N$ & $N\pi\pi$
260±100	CUTKOSKY 80	IPWA	$\pi N \rightarrow \pi N$
200±30	HOEHLER 79	IPWA	$\pi N \rightarrow \pi N$
••• We do not use the following data for averages, fits, limits, etc. •••			
165±14±40	ABLIKIM 06k	BES	$J/\psi \rightarrow (p\pi^-)\bar{\pi}$
1077±643	VRANA 00	DPWA	Multichannel
296±100 ⁺⁶⁰ ₋₁₀	PLOETZKE 98	SPEC	$\gamma p \rightarrow p\eta'(958)$
418±171	BATINIC 95	DPWA	$\pi N \rightarrow N\pi, N\eta$

 $N(2100)$ POLE POSITION

REAL PART	DOCUMENT ID	TECN	COMMENT
2120±40	CUTKOSKY 80	IPWA	$\pi N \rightarrow \pi N$
••• We do not use the following data for averages, fits, limits, etc. •••			
1810	VRANA 00	DPWA	Multichannel
not seen	ARNDT 91	DPWA	$\pi N \rightarrow \pi N$ Soln SM90

-2xIMAGINARY PART

VALUE (MeV)	DOCUMENT ID	TECN	COMMENT
240±80	CUTKOSKY 80	IPWA	$\pi N \rightarrow \pi N$
••• We do not use the following data for averages, fits, limits, etc. •••			
622	VRANA 00	DPWA	Multichannel
not seen	ARNDT 91	DPWA	$\pi N \rightarrow \pi N$ Soln SM90

 $N(2100)$ ELASTIC POLE RESIDUE

MODULUS $ r $	DOCUMENT ID	TECN	COMMENT
14±7	CUTKOSKY 80	IPWA	$\pi N \rightarrow \pi N$

PHASE θ

VALUE (°)	DOCUMENT ID	TECN	COMMENT
35±25	CUTKOSKY 80	IPWA	$\pi N \rightarrow \pi N$

 $N(2100)$ DECAY MODES

Mode	Fraction (Γ_j/Γ)	
Γ_1	$N\pi$	
Γ_2	$N\eta$	(61±60) %
Γ_3	ΛK	
Γ_4	$N\pi\pi$	
Γ_5	$\Delta(1232)\pi$, P-wave	
Γ_6	$N\rho$, $S=1/2$, P-wave	
Γ_7	$N(\pi\pi)_{S=0}^{I=0}$	

N(2100) BRANCHING RATIOS

$\Gamma(N\pi)/\Gamma_{total}$	DOCUMENT ID	TECN	COMMENT	Γ_1/Γ
0.15±0.06	MANLEY 92	IPWA	$\pi N \rightarrow \pi N & N\pi\pi$	
0.12±0.03	CUTKOSKY 80	IPWA	$\pi N \rightarrow \pi N$	
0.10±0.04	HOEHLER 79	IPWA	$\pi N \rightarrow \pi N$	
••• We do not use the following data for averages, fits, limits, etc. •••				
0.02±0.05	VRANA 00	DPWA	Multichannel	
0.11±0.07	BATINIC 95	DPWA	$\pi N \rightarrow N\pi, N\eta$	
$\Gamma(N\eta)/\Gamma_{total}$	DOCUMENT ID	TECN	COMMENT	Γ_2/Γ
0.61±0.61	VRANA 00	DPWA	Multichannel	
••• We do not use the following data for averages, fits, limits, etc. •••				
0.86±0.07	BATINIC 95	DPWA	$\pi N \rightarrow N\pi, N\eta$	
$\Gamma(\Lambda K)/\Gamma_{total}$	DOCUMENT ID	TECN	COMMENT	Γ_3/Γ
0.21±0.20	VRANA 00	DPWA	Multichannel	
$(\Gamma_i \Gamma_j)^{1/2}/\Gamma_{total}$ in $N\pi \rightarrow N(2100) \rightarrow \Delta(1232)\pi, P\text{-wave}$	DOCUMENT ID	TECN	COMMENT	$(\Gamma_1 \Gamma_5)^{1/2}/\Gamma$
-0.19±0.08	MANLEY 92	IPWA	$\pi N \rightarrow \pi N & N\pi\pi$	
$\Gamma(\Delta(1232)\pi, P\text{-wave})/\Gamma_{total}$	DOCUMENT ID	TECN	COMMENT	Γ_5/Γ
0.02±0.01	VRANA 00	DPWA	Multichannel	
$\Gamma(N\rho, S=1/2, P\text{-wave})/\Gamma_{total}$	DOCUMENT ID	TECN	COMMENT	Γ_6/Γ
0.04±0.01	VRANA 00	DPWA	Multichannel	
$\Gamma(N(\pi\pi)_{S=0}^0)/\Gamma_{total}$	DOCUMENT ID	TECN	COMMENT	Γ_7/Γ
0.10±0.01	VRANA 00	DPWA	Multichannel	

N(2100) REFERENCES

ABLIKIM 06K	PRL 97 062001	M. Ablikim et al.	(BES Collab.)
ARNDT 06	PR C74 045205	R.A. Arndt et al.	(GWU)
VRANA 00	PRPL 328 181	T.P. Vrana, S.A. Dytman., T.-S.H. Lee	(PITT+)
PLOETZKE 98	PL B444 555	R. Ploetzke et al.	(Bonn SAPHIR Collab.)
BATINIC 95	PR C51 2310	M. Batinic et al.	(BOSK, UCLA)
Also	PR C57 1004 (erratum)	M. Batinic et al.	
MANLEY 92	PR D45 4002	D.M. Manley, E.M. Saleski	(KENT) IJP
Also	PR D30 904	D.M. Manley et al.	(VPI)
ARNDT 91	PR D43 2131	R.A. Arndt et al.	(VPI, TELE) IJP
CUTKOSKY 80	Toronto Conf. 19	R.E. Cutkosky et al.	(CMU, LBL) IJP
Also	PR D20 2839	R.E. Cutkosky et al.	(CMU, LBL)
HOEHLER 79	PDAT 12-1	G. Hohlner et al.	(KARLT) IJP
Also	Toronto Conf. 3	R. Koch	(KARLT) IJP

N(2190) G_{17}

$I(J^P) = \frac{1}{2}(\frac{7}{2}^-)$ Status: ***

Most of the results published before 1975 were last included in our 1982 edition, Physics Letters **111B** 1 (1982). Some further obsolete results published before 1984 were last included in our 2006 edition, Journal of Physics, G **33** 1 (2006).

N(2190) BREIT-WIGNER MASS

VALUE (MeV)	DOCUMENT ID	TECN	COMMENT
2100 to 2200 (≈ 2190) OUR ESTIMATE			
2152.4±1.4	ARNDT 06	DPWA	$\pi N \rightarrow \pi N, \eta N$
2127 ± 9	MANLEY 92	IPWA	$\pi N \rightarrow \pi N & N\pi\pi$
2200 ± 70	CUTKOSKY 80	IPWA	$\pi N \rightarrow \pi N$
2140 ± 12	HOEHLER 79	IPWA	$\pi N \rightarrow \pi N$
2140 ± 40	HENDRY 78	MPWA	$\pi N \rightarrow \pi N$
••• We do not use the following data for averages, fits, limits, etc. •••			
2192.1±1.7	ARNDT 04	DPWA	$\pi N \rightarrow \pi N, \eta N$
2168 ± 18	VRANA 00	DPWA	Multichannel
2131	ARNDT 95	DPWA	$\pi N \rightarrow N\pi$
2198 ± 68	BATINIC 95	DPWA	$\pi N \rightarrow N\pi, N\eta$
2180	SAXON 80	DPWA	$\pi^- p \rightarrow \Lambda K^0$

N(2190) BREIT-WIGNER WIDTH

VALUE (MeV)	DOCUMENT ID	TECN	COMMENT
300 to 700 (≈ 500) OUR ESTIMATE			
484±13	ARNDT 06	DPWA	$\pi N \rightarrow \pi N, \eta N$
550±50	MANLEY 92	IPWA	$\pi N \rightarrow \pi N & N\pi\pi$
500±150	CUTKOSKY 80	IPWA	$\pi N \rightarrow \pi N$
390±30	HOEHLER 79	IPWA	$\pi N \rightarrow \pi N$
270±50	HENDRY 78	MPWA	$\pi N \rightarrow \pi N$

••• We do not use the following data for averages, fits, limits, etc. •••

726±62	ARNDT 04	DPWA	$\pi N \rightarrow \pi N, \eta N$
453±101	VRANA 00	DPWA	Multichannel
476	ARNDT 95	DPWA	$\pi N \rightarrow \pi N$
805±140	BATINIC 95	DPWA	$\pi N \rightarrow N\pi, N\eta$
80	SAXON 80	DPWA	$\pi^- p \rightarrow \Lambda K^0$

N(2190) POLE POSITION

REAL PART

VALUE (MeV)	DOCUMENT ID	TECN	COMMENT
2050 to 2100 (≈ 2075) OUR ESTIMATE			
2070	ARNDT 06	DPWA	$\pi N \rightarrow \pi N, \eta N$
2042	¹ HOEHLER 93	SPED	$\pi N \rightarrow \pi N$
2100±50	CUTKOSKY 80	IPWA	$\pi N \rightarrow \pi N$
••• We do not use the following data for averages, fits, limits, etc. •••			
2076	ARNDT 04	DPWA	$\pi N \rightarrow \pi N, \eta N$
2107	VRANA 00	DPWA	Multichannel
2030	ARNDT 95	DPWA	$\pi N \rightarrow N\pi$
2060	ARNDT 91	DPWA	$\pi N \rightarrow \pi N$ Soln SM90

-2xIMAGINARY PART

VALUE (MeV)	DOCUMENT ID	TECN	COMMENT
400 to 520 (≈ 450) OUR ESTIMATE			
520	ARNDT 06	DPWA	$\pi N \rightarrow \pi N, \eta N$
482	¹ HOEHLER 93	SPED	$\pi N \rightarrow \pi N$
400±160	CUTKOSKY 80	IPWA	$\pi N \rightarrow \pi N$
••• We do not use the following data for averages, fits, limits, etc. •••			
502	ARNDT 04	DPWA	$\pi N \rightarrow \pi N, \eta N$
380	VRANA 00	DPWA	Multichannel
460	ARNDT 95	DPWA	$\pi N \rightarrow N\pi$
464	ARNDT 91	DPWA	$\pi N \rightarrow \pi N$ Soln SM90

N(2190) ELASTIC POLE RESIDUE

MODULUS $|r|$

VALUE (MeV)	DOCUMENT ID	TECN	COMMENT
72	ARNDT 06	DPWA	$\pi N \rightarrow \pi N, \eta N$
45	HOEHLER 93	SPED	$\pi N \rightarrow \pi N$
25±10	CUTKOSKY 80	IPWA	$\pi N \rightarrow \pi N$
••• We do not use the following data for averages, fits, limits, etc. •••			
68	ARNDT 04	DPWA	$\pi N \rightarrow \pi N, \eta N$
46	ARNDT 95	DPWA	$\pi N \rightarrow N\pi$
54	ARNDT 91	DPWA	$\pi N \rightarrow \pi N$ Soln SM90

PHASE θ

VALUE (°)	DOCUMENT ID	TECN	COMMENT
-32	ARNDT 06	DPWA	$\pi N \rightarrow \pi N, \eta N$
-30±50	CUTKOSKY 80	IPWA	$\pi N \rightarrow \pi N$
••• We do not use the following data for averages, fits, limits, etc. •••			
-32	ARNDT 04	DPWA	$\pi N \rightarrow \pi N, \eta N$
-23	ARNDT 95	DPWA	$\pi N \rightarrow N\pi$
-44	ARNDT 91	DPWA	$\pi N \rightarrow \pi N$ Soln SM90

N(2190) DECAY MODES

The following branching fractions are our estimates, not fits or averages.

Mode	Fraction (Γ_i/Γ)
Γ_1 $N\pi$	10-20 %
Γ_2 $N\eta$	(0.0±1.0) %
Γ_3 ΛK	
Γ_4 ΣK	
Γ_5 $N\pi\pi$	
Γ_6 $N\rho$	
Γ_7 $N\rho, S=3/2, D\text{-wave}$	
Γ_8 $p\gamma, \text{ helicity}=1/2$	
Γ_9 $p\gamma, \text{ helicity}=3/2$	
Γ_{10} $n\gamma, \text{ helicity}=1/2$	
Γ_{11} $n\gamma, \text{ helicity}=3/2$	

N(2190) BRANCHING RATIOS

$\Gamma(N\pi)/\Gamma_{total}$	DOCUMENT ID	TECN	COMMENT	Γ_1/Γ
0.1 to 0.2 OUR ESTIMATE				
0.238±0.001	ARNDT 06	DPWA	$\pi N \rightarrow \pi N, \eta N$	
0.22±0.01	MANLEY 92	IPWA	$\pi N \rightarrow \pi N & N\pi\pi$	
0.12 ± 0.06	CUTKOSKY 80	IPWA	$\pi N \rightarrow \pi N$	
0.14 ± 0.02	HOEHLER 79	IPWA	$\pi N \rightarrow \pi N$	
0.16 ± 0.04	HENDRY 78	MPWA	$\pi N \rightarrow \pi N$	
••• We do not use the following data for averages, fits, limits, etc. •••				
0.230±0.002	ARNDT 04	DPWA	$\pi N \rightarrow \pi N, \eta N$	
0.20 ± 0.04	VRANA 00	DPWA	Multichannel	
0.23	ARNDT 95	DPWA	$\pi N \rightarrow N\pi$	
0.19 ± 0.05	BATINIC 95	DPWA	$\pi N \rightarrow N\pi, N\eta$	

Baryon Particle Listings

 $N(2190)$, $N(2200)$

$\Gamma(N\eta)/\Gamma_{\text{total}}$	DOCUMENT ID	TECN	COMMENT	Γ_2/Γ
VALUE				
0.00 ± 0.01	VRANA	00	DPWA Multichannel	
••• We do not use the following data for averages, fits, limits, etc. •••				
0.001 ± 0.003	BATINIC	95	DPWA $\pi N \rightarrow N\pi, N\eta$	

$(\Gamma_1\Gamma_2)^{1/2}/\Gamma_{\text{total}}$ in $N\pi \rightarrow N(2190) \rightarrow \Lambda K$	DOCUMENT ID	TECN	COMMENT	$(\Gamma_1\Gamma_3)^{1/2}/\Gamma$
VALUE				
-0.02	BELL	83	DPWA $\pi^- p \rightarrow \Lambda K^0$	
-0.02	SAXON	80	DPWA $\pi^- p \rightarrow \Lambda K^0$	

$(\Gamma_1\Gamma_2)^{1/2}/\Gamma_{\text{total}}$ in $N\pi \rightarrow N(2190) \rightarrow N\rho, S=3/2, D\text{-wave}$	DOCUMENT ID	TECN	COMMENT	$(\Gamma_1\Gamma_2)^{1/2}/\Gamma$
VALUE				
-0.25 ± 0.03	MANLEY	92	IPWA $\pi N \rightarrow \pi N \& N\pi\pi$	

$\Gamma(N\rho, S=3/2, D\text{-wave})/\Gamma_{\text{total}}$	DOCUMENT ID	TECN	COMMENT	Γ_7/Γ
VALUE				
0.29 ± 0.28	VRANA	00	DPWA Multichannel	

 $N(2190)$ PHOTON DECAY AMPLITUDES

Papers on γN amplitudes predating 1981 may be found in our 2006 edition, Journal of Physics, G **33** 1 (2006).

$N(2190) \rightarrow \rho\gamma$, helicity-1/2 amplitude $A_{1/2}$

$N(2190) \rightarrow \rho\gamma$, helicity-3/2 amplitude $A_{3/2}$

$N(2190) \rightarrow n\gamma$, helicity-1/2 amplitude $A_{1/2}$

$N(2190) \rightarrow n\gamma$, helicity-3/2 amplitude $A_{3/2}$

 $N(2190) \gamma\rho \rightarrow \Lambda K^+$ AMPLITUDES

$(\Gamma_1\Gamma_2)^{1/2}/\Gamma_{\text{total}}$ in $\rho\gamma \rightarrow N(2190) \rightarrow \Lambda K^+$	DOCUMENT ID	TECN	COMMENT	(E_{4-} amplitude)
VALUE (units 10^{-3})				
••• We do not use the following data for averages, fits, limits, etc. •••				
2.5 ± 1.0	WORKMAN	90	DPWA	
2.04	TANABE	89	DPWA	

$\rho\gamma \rightarrow N(2190) \rightarrow \Lambda K^+$ phase angle θ	DOCUMENT ID	TECN	COMMENT	(E_{4-} amplitude)
VALUE (degrees)				
••• We do not use the following data for averages, fits, limits, etc. •••				
-4 ± 9	WORKMAN	90	DPWA	
-27.5	TANABE	89	DPWA	

$(\Gamma_1\Gamma_2)^{1/2}/\Gamma_{\text{total}}$ in $\rho\gamma \rightarrow N(2190) \rightarrow \Lambda K^+$	DOCUMENT ID	TECN	COMMENT	(M_{4-} amplitude)
VALUE (units 10^{-3})				
••• We do not use the following data for averages, fits, limits, etc. •••				
-7.0 ± 0.7	WORKMAN	90	DPWA	
-5.78	TANABE	89	DPWA	

 $N(2190)$ FOOTNOTES

¹ See HOEHLER 93 for a detailed discussion of the evidence for and the pole parameters of N and Δ resonances as determined from Argand diagrams of πN elastic partial-wave amplitudes and from plots of the speeds with which the amplitudes traverse the diagrams.

 $N(2190)$ REFERENCES

For early references, see Physics Letters **111B** 1 (1982).

ARNDT	06	PR C74 045205	R.A. Arndt et al.	(GWU)
PDG	06	JPG 33 1	W.-M. Yao et al.	(PDG Collab.)
ARNDT	04	PR C69 035213	R.A. Arndt et al.	(GWU, TRIU)
VRANA	00	PRPL 328 181	T.P. Vrana, S.A. Dytman, T.-S.H. Lee	(PITT+)
ARNDT	95	PR C52 2120	R.A. Arndt et al.	(VPI, BRCO)
BATINIC	95	PR C51 2310	M. Batinic et al.	(BOSK, UCLA)
Also		PR C57 1004 (erratum)	M. Batinic et al.	
HOEHLER	93	πN Newsletter 9 1	G. Hoehler	(KARL)
MANLEY	92	PR D45 4002	D.M. Manley, E.M. Saleski	(KENT) IJP
Also		PR D30 304	D.M. Manley et al.	(VPI)
ARNDT	91	PR D43 2131	R.A. Arndt et al.	(VPI, TELE) IJP
WORKMAN	90	PR C42 781	R.L. Workman	(VPI)
TANABE	89	PR C39 741	H. Tanabe, M. Kohno, C. Bennhold	(MANZ)
Also		NC 102A 193	M. Kohno, H. Tanabe, C. Bennhold	(MANZ)
BELL	83	NP B222 389	K.W. Bell et al.	(RL) IJP
PDG	82	PL 111B 1	M. Roos et al.	(HELS, CIT, CERN)
CUTKOSKY	80	Toronto Conf. 19	R.E. Cutkosky et al.	(CMU, LBL) IJP
Also		PR D20 2839	R.E. Cutkosky et al.	(CMU, LBL) IJP
SAXON	80	NP B162 522	D.H. Saxon et al.	(RHEL, BRIS) IJP
HOEHLER	79	PDAT 12-1	G. Hoehler et al.	(KARLT) IJP
Also		Toronto Conf. 3	R. Koch	(KARLT) IJP
HENDRY	78	PRL 41 222	A.W. Hendry	(IND, LBL) IJP
Also		ANP 136 1	A.W. Hendry	(IND)

 $N(2200) D_{15}$

$$I(J^P) = \frac{1}{2}(\frac{5}{2}^-) \text{ Status: } **$$

OMITTED FROM SUMMARY TABLE

The mass is not well determined. A few early results have been omitted.

The latest GWU analysis (ARNDT 06) finds no evidence for this resonance.

 $N(2200)$ BREIT-WIGNER MASS

VALUE (MeV)	DOCUMENT ID	TECN	COMMENT
≈ 2200 OUR ESTIMATE			
1900	BELL	83	DPWA $\pi^- p \rightarrow \Lambda K^0$
2180 ± 80	CUTKOSKY	80	IPWA $\pi N \rightarrow \pi N$
1920	SAXON	80	DPWA $\pi^- p \rightarrow \Lambda K^0$
2228 ± 30	HOEHLER	79	IPWA $\pi N \rightarrow \pi N$
••• We do not use the following data for averages, fits, limits, etc. •••			
2240 ± 65	BATINIC	95	DPWA $\pi N \rightarrow N\pi, N\eta$

 $N(2200)$ BREIT-WIGNER WIDTH

VALUE (MeV)	DOCUMENT ID	TECN	COMMENT
130	BELL	83	DPWA $\pi^- p \rightarrow \Lambda K^0$
400 ± 100	CUTKOSKY	80	IPWA $\pi N \rightarrow \pi N$
220	SAXON	80	DPWA $\pi^- p \rightarrow \Lambda K^0$
310 ± 50	HOEHLER	79	IPWA $\pi N \rightarrow \pi N$
••• We do not use the following data for averages, fits, limits, etc. •••			
761 ± 139	BATINIC	95	DPWA $\pi N \rightarrow N\pi, N\eta$

 $N(2200)$ POLE POSITION

REAL PART

VALUE (MeV)	DOCUMENT ID	TECN	COMMENT
2100 ± 60	CUTKOSKY	80	IPWA $\pi N \rightarrow \pi N$

-2xIMAGINARY PART

VALUE (MeV)	DOCUMENT ID	TECN	COMMENT
360 ± 80	CUTKOSKY	80	IPWA $\pi N \rightarrow \pi N$

 $N(2200)$ ELASTIC POLE RESIDUEMODULUS $|r|$

VALUE (MeV)	DOCUMENT ID	TECN	COMMENT
20 ± 10	CUTKOSKY	80	IPWA $\pi N \rightarrow \pi N$

PHASE θ

VALUE ($^\circ$)	DOCUMENT ID	TECN	COMMENT
-90 ± 50	CUTKOSKY	80	IPWA $\pi N \rightarrow \pi N$

 $N(2200)$ DECAY MODES

Mode
Γ_1 $N\pi$
Γ_2 $N\eta$
Γ_3 ΛK

 $N(2200)$ BRANCHING RATIOS

$\Gamma(N\pi)/\Gamma_{\text{total}}$	DOCUMENT ID	TECN	COMMENT	Γ_1/Γ
VALUE				
0.10 ± 0.03	CUTKOSKY	80	IPWA $\pi N \rightarrow \pi N$	
0.07 ± 0.02	HOEHLER	79	IPWA $\pi N \rightarrow \pi N$	
••• We do not use the following data for averages, fits, limits, etc. •••				
0.08 ± 0.04	BATINIC	95	DPWA $\pi N \rightarrow N\pi, N\eta$	

$\Gamma(N\eta)/\Gamma_{\text{total}}$	DOCUMENT ID	TECN	COMMENT	Γ_2/Γ
VALUE				
••• We do not use the following data for averages, fits, limits, etc. •••				
0.001 ± 0.01	BATINIC	95	DPWA $\pi N \rightarrow N\pi, N\eta$	

$(\Gamma_1\Gamma_2)^{1/2}/\Gamma_{\text{total}}$ in $N\pi \rightarrow N(2200) \rightarrow N\eta$	DOCUMENT ID	TECN	COMMENT	$(\Gamma_1\Gamma_2)^{1/2}/\Gamma$
VALUE				
0.066	BAKER	79	DPWA $\pi^- p \rightarrow n\eta$	

$(\Gamma_1\Gamma_2)^{1/2}/\Gamma_{\text{total}}$ in $N\pi \rightarrow N(2200) \rightarrow \Lambda K$	DOCUMENT ID	TECN	COMMENT	$(\Gamma_1\Gamma_3)^{1/2}/\Gamma$
VALUE				
-0.03	BELL	83	DPWA $\pi^- p \rightarrow \Lambda K^0$	
-0.05	SAXON	80	DPWA $\pi^- p \rightarrow \Lambda K^0$	

See key on page 373

Baryon Particle Listings

$N(2200)$, $N(2220)$, $N(2250)$

$N(2200)$ REFERENCES

ARNDT	06	PR C74 045205	R.A. Arndt <i>et al.</i>	(GWU)
BATINIC	95	PR C51 2310	M. Batinic <i>et al.</i>	(BOSK, UCLA)
Also		PR C57 1004 (erratum)	M. Batinic <i>et al.</i>	
BELL	83	NP B222 389	K.W. Bell <i>et al.</i>	(RL) IJP
CUTKOSKY	80	Toronto Conf. 19	R.E. Cutkosky <i>et al.</i>	(CMU, LBL) IJP
Also		PR D20 2839	R.E. Cutkosky <i>et al.</i>	(CMU, LBL)
SAXON	80	NP B162 522	D.H. Saxon <i>et al.</i>	(RHEL, BRIS) IJP
BAKER	79	NP B156 93	R.D. Baker <i>et al.</i>	(RHEL) IJP
HOEHLER	79	PDAT 12-1	G. Hoehler <i>et al.</i>	(KARLT) IJP
Also		Toronto Conf. 3	R. Koch	(KARLT) IJP

$N(2220) H_{19}$

$$I(J^P) = \frac{1}{2}(\frac{9}{2}^+) \text{ Status: } ****$$

Most of the results published before 1975 were last included in our 1982 edition, Physics Letters **111B** 1 (1982). Some further obsolete results published before 1980 were last included in our 2006 edition, Journal of Physics, **G 33** 1 (2006).

$N(2220)$ BREIT-WIGNER MASS

VALUE (MeV)	DOCUMENT ID	TECN	COMMENT
2200 to 2300 (≈ 2250) OUR ESTIMATE			
2316.3 \pm 2.9	ARNDT 06	DPWA	$\pi N \rightarrow \pi N, \eta N$
2230 \pm 80	CUTKOSKY 80	IPWA	$\pi N \rightarrow \pi N$
2205 \pm 10	HOEHLER 79	IPWA	$\pi N \rightarrow \pi N$
2300 \pm 100	HENDRY 78	MPWA	$\pi N \rightarrow \pi N$
••• We do not use the following data for averages, fits, limits, etc. •••			
2270 \pm 11	ARNDT 04	DPWA	$\pi N \rightarrow \pi N, \eta N$
2258	ARNDT 95	DPWA	$\pi N \rightarrow N\pi$

$N(2220)$ BREIT-WIGNER WIDTH

VALUE (MeV)	DOCUMENT ID	TECN	COMMENT
350 to 500 (≈ 400) OUR ESTIMATE			
633 \pm 17	ARNDT 06	DPWA	$\pi N \rightarrow \pi N, \eta N$
500 \pm 150	CUTKOSKY 80	IPWA	$\pi N \rightarrow \pi N$
365 \pm 30	HOEHLER 79	IPWA	$\pi N \rightarrow \pi N$
450 \pm 150	HENDRY 78	MPWA	$\pi N \rightarrow \pi N$
••• We do not use the following data for averages, fits, limits, etc. •••			
366 \pm 42	ARNDT 04	DPWA	$\pi N \rightarrow \pi N, \eta N$
334	ARNDT 95	DPWA	$\pi N \rightarrow N\pi$

$N(2220)$ POLE POSITION

REAL PART

VALUE (MeV)	DOCUMENT ID	TECN	COMMENT
2130 to 2200 (≈ 2170) OUR ESTIMATE			
2199	ARNDT 06	DPWA	$\pi N \rightarrow \pi N, \eta N$
2135	¹ HOEHLER 93	ARGD	$\pi N \rightarrow \pi N$
2160 \pm 80	CUTKOSKY 80	IPWA	$\pi N \rightarrow \pi N$
••• We do not use the following data for averages, fits, limits, etc. •••			
2209	ARNDT 04	DPWA	$\pi N \rightarrow \pi N, \eta N$
2203	ARNDT 95	DPWA	$\pi N \rightarrow N\pi$
2253	ARNDT 91	DPWA	$\pi N \rightarrow \pi N$ Soln SM90

-2xIMAGINARY PART

VALUE (MeV)	DOCUMENT ID	TECN	COMMENT
400 to 560 (≈ 480) OUR ESTIMATE			
372	ARNDT 06	DPWA	$\pi N \rightarrow \pi N, \eta N$
400	¹ HOEHLER 93	ARGD	$\pi N \rightarrow \pi N$
480 \pm 100	CUTKOSKY 80	IPWA	$\pi N \rightarrow \pi N$
••• We do not use the following data for averages, fits, limits, etc. •••			
564	ARNDT 04	DPWA	$\pi N \rightarrow \pi N, \eta N$
536	ARNDT 95	DPWA	$\pi N \rightarrow N\pi$
640	ARNDT 91	DPWA	$\pi N \rightarrow \pi N$ Soln SM90

$N(2220)$ ELASTIC POLE RESIDUE

MODULUS $|r|$

VALUE (MeV)	DOCUMENT ID	TECN	COMMENT
33	ARNDT 06	DPWA	$\pi N \rightarrow \pi N, \eta N$
40	HOEHLER 93	ARGD	$\pi N \rightarrow \pi N$
45 \pm 20	CUTKOSKY 80	IPWA	$\pi N \rightarrow \pi N$
••• We do not use the following data for averages, fits, limits, etc. •••			
96	ARNDT 04	DPWA	$\pi N \rightarrow \pi N, \eta N$
68	ARNDT 95	DPWA	$\pi N \rightarrow N\pi$
85	ARNDT 91	DPWA	$\pi N \rightarrow \pi N$ Soln SM90

PHASE θ

VALUE ($^\circ$)	DOCUMENT ID	TECN	COMMENT
-33	ARNDT 06	DPWA	$\pi N \rightarrow \pi N, \eta N$
-50	HOEHLER 93	ARGD	$\pi N \rightarrow \pi N$
-45 \pm 25	CUTKOSKY 80	IPWA	$\pi N \rightarrow \pi N$
••• We do not use the following data for averages, fits, limits, etc. •••			
-71	ARNDT 04	DPWA	$\pi N \rightarrow \pi N, \eta N$
-43	ARNDT 95	DPWA	$\pi N \rightarrow N\pi$
-62	ARNDT 91	DPWA	$\pi N \rightarrow \pi N$ Soln SM90

$N(2220)$ DECAY MODES

The following branching fractions are our estimates, not fits or averages.

Mode	Fraction (Γ_i/Γ)
Γ_1 $N\pi$	10-20 %
Γ_2 $N\eta$	
Γ_3 ΛK	

$N(2220)$ BRANCHING RATIOS

$\Gamma(N\pi)/\Gamma_{\text{total}}$	DOCUMENT ID	TECN	COMMENT	Γ_1/Γ
0.1 to 0.2 OUR ESTIMATE				
0.246 \pm 0.001	ARNDT 06	DPWA	$\pi N \rightarrow \pi N, \eta N$	
0.15 \pm 0.03	CUTKOSKY 80	IPWA	$\pi N \rightarrow \pi N$	
0.18 \pm 0.015	HOEHLER 79	IPWA	$\pi N \rightarrow \pi N$	
0.12 \pm 0.04	HENDRY 78	MPWA	$\pi N \rightarrow \pi N$	
••• We do not use the following data for averages, fits, limits, etc. •••				
0.200 \pm 0.006	ARNDT 04	DPWA	$\pi N \rightarrow \pi N, \eta N$	
0.26	ARNDT 95	DPWA	$\pi N \rightarrow N\pi$	

$(\Gamma_1\Gamma_2)^{1/2}/\Gamma_{\text{total}}$ in $N\pi \rightarrow N(2220) \rightarrow \Lambda K$

VALUE	DOCUMENT ID	TECN	COMMENT	$(\Gamma_1\Gamma_3)^{1/2}/\Gamma$
not required	BELL 83	DPWA	$\pi^- p \rightarrow \Lambda K^0$	
not seen	SAXON 80	DPWA	$\pi^- p \rightarrow \Lambda K^0$	

$N(2220)$ FOOTNOTES

¹ See HOEHLER 93 for a detailed discussion of the evidence for and the pole parameters of N and Δ resonances as determined from Argand diagrams of πN elastic partial-wave amplitudes and from plots of the speeds with which the amplitudes traverse the diagrams.

$N(2220)$ REFERENCES

For early references, see Physics Letters **111B** 1 (1982).

ARNDT	06	PR C74 045205	R.A. Arndt <i>et al.</i>	(GWU)
PDG	06	JPG 33 1	W.-M. Yao <i>et al.</i>	(PDG Collab.)
ARNDT	04	PR C69 035213	R.A. Arndt <i>et al.</i>	(GWU, TRIU)
ARNDT	95	PR C52 2120	R.A. Arndt <i>et al.</i>	(VPI, BRCO)
HOEHLER	93	πN Newsletter 9 1	G. Hoehler	(KARL)
ARNDT	91	PR D43 2131	R.A. Arndt <i>et al.</i>	(VPI, TELE) IJP
BELL	83	NP B222 389	K.W. Bell <i>et al.</i>	(RL) IJP
PDG	82	PL 111B 1	M. Roos <i>et al.</i>	(HELS, CIT, CERN)
CUTKOSKY	80	Toronto Conf. 19	R.E. Cutkosky <i>et al.</i>	(CMU, LBL) IJP
Also		PR D20 2839	R.E. Cutkosky <i>et al.</i>	(CMU, LBL) IJP
SAXON	80	NP B162 522	D.H. Saxon <i>et al.</i>	(RHEL, BRIS) IJP
HOEHLER	79	PDAT 12-1	G. Hoehler <i>et al.</i>	(KARLT) IJP
Also		Toronto Conf. 3	R. Koch	(KARLT) IJP
HENDRY	78	PRL 41 222	A.W. Hendry	(IND, LBL) IJP
Also		ANP 136 1	A.W. Hendry	(IND)

$N(2250) G_{19}$

$$I(J^P) = \frac{1}{2}(\frac{9}{2}^-) \text{ Status: } ****$$

Some obsolete results published before 1980 were last included in our 2006 edition, Journal of Physics, **G 33** 1 (2006).

$N(2250)$ BREIT-WIGNER MASS

VALUE (MeV)	DOCUMENT ID	TECN	COMMENT
2200 to 2350 (≈ 2275) OUR ESTIMATE			
2302 \pm 6	ARNDT 06	DPWA	$\pi N \rightarrow \pi N, \eta N$
2250 \pm 80	CUTKOSKY 80	IPWA	$\pi N \rightarrow \pi N$
2268 \pm 15	HOEHLER 79	IPWA	$\pi N \rightarrow \pi N$
2200 \pm 100	HENDRY 78	MPWA	$\pi N \rightarrow \pi N$
••• We do not use the following data for averages, fits, limits, etc. •••			
2376 \pm 43	ARNDT 04	DPWA	$\pi N \rightarrow \pi N, \eta N$
2291	ARNDT 95	DPWA	$\pi N \rightarrow N\pi$

Baryon Particle Listings

 $N(2250)$, $N(2600)$ $N(2250)$ BREIT-WIGNER WIDTH

VALUE (MeV)	DOCUMENT ID	TECN	COMMENT
230 to 800 (≈ 500) OUR ESTIMATE			
628 \pm 28	ARNDT 06	DPWA	$\pi N \rightarrow \pi N, \eta N$
480 \pm 120	CUTKOSKY 80	IPWA	$\pi N \rightarrow \pi N$
300 \pm 40	HOEHLER 79	IPWA	$\pi N \rightarrow \pi N$
350 \pm 100	HENDRY 78	MPWA	$\pi N \rightarrow \pi N$
••• We do not use the following data for averages, fits, limits, etc. •••			
924 \pm 178	ARNDT 04	DPWA	$\pi N \rightarrow \pi N, \eta N$
772	ARNDT 95	DPWA	$\pi N \rightarrow \pi N$

 $N(2250)$ POLE POSITION

REAL PART

VALUE (MeV)	DOCUMENT ID	TECN	COMMENT
2150 to 2250 (≈ 2200) OUR ESTIMATE			
2217	ARNDT 06	DPWA	$\pi N \rightarrow \pi N, \eta N$
2187	¹ HOEHLER 93	SPED	$\pi N \rightarrow \pi N$
2150 \pm 50	CUTKOSKY 80	IPWA	$\pi N \rightarrow \pi N$
••• We do not use the following data for averages, fits, limits, etc. •••			
2238	ARNDT 04	DPWA	$\pi N \rightarrow \pi N, \eta N$
2087	ARNDT 95	DPWA	$\pi N \rightarrow \pi N$
2243	ARNDT 91	DPWA	$\pi N \rightarrow \pi N$ Soln SM90

-2xIMAGINARY PART

VALUE (MeV)	DOCUMENT ID	TECN	COMMENT
350 to 550 (≈ 450) OUR ESTIMATE			
431	ARNDT 06	DPWA	$\pi N \rightarrow \pi N, \eta N$
388	¹ HOEHLER 93	SPED	$\pi N \rightarrow \pi N$
360 \pm 100	CUTKOSKY 80	IPWA	$\pi N \rightarrow \pi N$
••• We do not use the following data for averages, fits, limits, etc. •••			
536	ARNDT 04	DPWA	$\pi N \rightarrow \pi N, \eta N$
680	ARNDT 95	DPWA	$\pi N \rightarrow \pi N$
650	ARNDT 91	DPWA	$\pi N \rightarrow \pi N$ Soln SM90

 $N(2250)$ ELASTIC POLE RESIDUEMODULUS $|r|$

VALUE (MeV)	DOCUMENT ID	TECN	COMMENT
21	ARNDT 06	DPWA	$\pi N \rightarrow \pi N, \eta N$
21	HOEHLER 93	SPED	$\pi N \rightarrow \pi N$
20 \pm 6	CUTKOSKY 80	IPWA	$\pi N \rightarrow \pi N$
••• We do not use the following data for averages, fits, limits, etc. •••			
33	ARNDT 04	DPWA	$\pi N \rightarrow \pi N, \eta N$
24	ARNDT 95	DPWA	$\pi N \rightarrow \pi N$
47	ARNDT 91	DPWA	$\pi N \rightarrow \pi N$ Soln SM90

PHASE θ

VALUE ($^\circ$)	DOCUMENT ID	TECN	COMMENT
-20	ARNDT 06	DPWA	$\pi N \rightarrow \pi N, \eta N$
-50 \pm 20	CUTKOSKY 80	IPWA	$\pi N \rightarrow \pi N$
••• We do not use the following data for averages, fits, limits, etc. •••			
-25	ARNDT 04	DPWA	$\pi N \rightarrow \pi N, \eta N$
-44	ARNDT 95	DPWA	$\pi N \rightarrow \pi N$
-37	ARNDT 91	DPWA	$\pi N \rightarrow \pi N$ Soln SM90

 $N(2250)$ DECAY MODES

The following branching fractions are our estimates, not fits or averages.

Mode	Fraction (Γ_i/Γ)
Γ_1 $N\pi$	5-15 %
Γ_2 $N\eta$	
Γ_3 ΛK	

 $N(2250)$ BRANCHING RATIOS

$\Gamma(N\pi)/\Gamma_{\text{total}}$	DOCUMENT ID	TECN	COMMENT	Γ_1/Γ
0.05 to 0.15 OUR ESTIMATE				
0.089 \pm 0.001	ARNDT 06	DPWA	$\pi N \rightarrow \pi N, \eta N$	
0.10 \pm 0.02	CUTKOSKY 80	IPWA	$\pi N \rightarrow \pi N$	
0.10 \pm 0.02	HOEHLER 79	IPWA	$\pi N \rightarrow \pi N$	
0.09 \pm 0.02	HENDRY 78	MPWA	$\pi N \rightarrow \pi N$	
••• We do not use the following data for averages, fits, limits, etc. •••				
0.110 \pm 0.004	ARNDT 04	DPWA	$\pi N \rightarrow \pi N, \eta N$	
0.10	ARNDT 95	DPWA	$\pi N \rightarrow \pi N$	

$(\Gamma_i\Gamma_j)^{1/2}/\Gamma_{\text{total}}$ in $N\pi \rightarrow N(2250) \rightarrow \Lambda K$	DOCUMENT ID	TECN	COMMENT	$(\Gamma_1\Gamma_3)^{1/2}/\Gamma$
-0.02	BELL 83	DPWA	$\pi^- p \rightarrow \Lambda K^0$	
not seen	SAXON 80	DPWA	$\pi^- p \rightarrow \Lambda K^0$	

 $N(2250)$ FOOTNOTES

¹ See HOEHLER 93 for a detailed discussion of the evidence for and the pole parameters of N and Δ resonances as determined from Argand diagrams of πN elastic partial-wave amplitudes and from plots of the speeds with which the amplitudes traverse the diagrams.

 $N(2250)$ REFERENCES

ARNDT 06	PR C74 045205	R.A. Arndt et al.	(GWU)
PDG 06	JPG 33 1	W.-M. Yao et al.	(PDG Collab.)
ARNDT 04	PR C69 035213	R.A. Arndt et al.	(GWU, TRIU)
ARNDT 95	PR C52 2120	R.A. Arndt et al.	(VPI, BRCO)
HOEHLER 93	πN Newsletter 9 1	G. Hohlner	(KARL)
ARNDT 91	PR D43 2131	R.A. Arndt et al.	(VPI, TELE) IJP
BELL 83	NP B222 389	K.W. Bell et al.	(RL) IJP
CUTKOSKY 80	Toronto Conf. 19	R.E. Cutkosky et al.	(CMU, LBL) IJP
Also	PR D20 2839	R.E. Cutkosky et al.	(CMU, LBL) IJP
SAXON 80	NP B162 522	D.H. Saxon et al.	(RHEL, BRIS) IJP
HOEHLER 79	PDAT 12-1	G. Hohlner et al.	(KARL) IJP
Also	Toronto Conf. 3	R. Koch	(KARL) IJP
HENDRY 78	PRL 41 222	A.W. Hendry	(IND, LBL) IJP
Also	ANP 136 1	A.W. Hendry	(IND)

$$N(2600) I_{1,11}$$

$$I(J^P) = \frac{1}{2}(\frac{1}{2}^-) \text{Status: } ** *$$

 $N(2600)$ BREIT-WIGNER MASS

VALUE (MeV)	DOCUMENT ID	TECN	COMMENT
2550 to 2750 (≈ 2600) OUR ESTIMATE			
2623 \pm 197	ARNDT 06	DPWA	$\pi N \rightarrow \pi N, \eta N$
2577 \pm 50	HOEHLER 79	IPWA	$\pi N \rightarrow \pi N$
2700 \pm 100	HENDRY 78	MPWA	$\pi N \rightarrow \pi N$

 $N(2600)$ BREIT-WIGNER WIDTH

VALUE (MeV)	DOCUMENT ID	TECN	COMMENT
500 to 800 (≈ 650) OUR ESTIMATE			
1311 \pm 996	ARNDT 06	DPWA	$\pi N \rightarrow \pi N, \eta N$
400 \pm 100	HOEHLER 79	IPWA	$\pi N \rightarrow \pi N$
900 \pm 100	HENDRY 78	MPWA	$\pi N \rightarrow \pi N$

 $N(2600)$ DECAY MODES

Mode	Fraction (Γ_i/Γ)
Γ_1 $N\pi$	5-10 %

 $N(2600)$ BRANCHING RATIOS

$\Gamma(N\pi)/\Gamma_{\text{total}}$	DOCUMENT ID	TECN	COMMENT	Γ_1/Γ
0.05 to 0.1 OUR ESTIMATE				
0.050 \pm 0.018	ARNDT 06	DPWA	$\pi N \rightarrow \pi N, \eta N$	
0.05 \pm 0.01	HOEHLER 79	IPWA	$\pi N \rightarrow \pi N$	
0.08 \pm 0.02	HENDRY 78	MPWA	$\pi N \rightarrow \pi N$	

 $N(2600)$ REFERENCES

ARNDT 06	PR C74 045205	R.A. Arndt et al.	(GWU)
HOEHLER 79	PDAT 12-1	G. Hohlner et al.	(KARL) IJP
Also	Toronto Conf. 3	R. Koch	(KARL) IJP
HENDRY 78	PRL 41 222	A.W. Hendry	(IND, LBL) IJP
Also	ANP 136 1	A.W. Hendry	(IND)

See key on page 373

Baryon Particle Listings
 $N(2700)$, $N(\sim 3000)$

$N(2700) K_{1,13}$

$I(J^P) = \frac{1}{2}(1\frac{3}{2}^+)$ Status: **

OMITTED FROM SUMMARY TABLE
 The latest GWU analysis (ARNDT 06) finds no evidence for this resonance.

$N(2700)$ BREIT-WIGNER MASS

VALUE (MeV)	DOCUMENT ID	TECN	COMMENT
≈ 2700 OUR ESTIMATE			
2612 \pm 45	HOEHLER 79	IPWA	$\pi N \rightarrow \pi N$
3000 \pm 100	HENDRY 78	MPWA	$\pi N \rightarrow \pi N$

$N(2700)$ BREIT-WIGNER WIDTH

VALUE (MeV)	DOCUMENT ID	TECN	COMMENT
350 \pm 50	HOEHLER 79	IPWA	$\pi N \rightarrow \pi N$
900 \pm 150	HENDRY 78	MPWA	$\pi N \rightarrow \pi N$

$N(2700)$ DECAY MODES

Mode	Γ_1	$N\pi$

$N(2700)$ BRANCHING RATIOS

$\Gamma(N\pi)/\Gamma_{total}$	DOCUMENT ID	TECN	COMMENT	Γ_1/Γ
0.04 \pm 0.01	HOEHLER 79	IPWA	$\pi N \rightarrow \pi N$	
0.07 \pm 0.02	HENDRY 78	MPWA	$\pi N \rightarrow \pi N$	

$N(2700)$ REFERENCES

ARNDT 06	PR C74 045205	R.A. Arndt et al.	(GWU)
HOEHLER 79	PDAT 12-1	G. Hoehler et al.	(KARLT) IJP
Also	Toronto Conf. 3	R. Koch	(KARLT) IJP
HENDRY 78	PRL 41 222	A.W. Hendry	(IND, LBL) IJP
Also	ANP 136 1	A.W. Hendry	(IND)

**$N(\sim 3000)$ Region
 Partial-Wave Analyses**

OMITTED FROM SUMMARY TABLE
 We list here miscellaneous high-mass candidates for isospin-1/2 resonances found in partial-wave analyses.

Our 1982 edition had an $N(3245)$, an $N(3690)$, and an $N(3755)$, each a narrow peak seen in a production experiment. Since nothing has been heard from them since the 1960's, we declare them to be dead. There was also an $N(3030)$, deduced from total cross-section and 180° elastic cross-section measurements; it is the KOCH 80 $L_{1,15}$ state below.

$N(\sim 3000)$ BREIT-WIGNER MASS

VALUE (MeV)	DOCUMENT ID	TECN	COMMENT
≈ 3000 OUR ESTIMATE			
2600	KOCH 80	IPWA	$\pi N \rightarrow \pi N D_{13}$
3100	KOCH 80	IPWA	$\pi N \rightarrow \pi N L_{1,15}$ wave
3500	KOCH 80	IPWA	$\pi N \rightarrow \pi N M_{1,17}$ wave
3500 to 4000	KOCH 80	IPWA	$\pi N \rightarrow \pi N N_{1,19}$ wave
3500 \pm 200	HENDRY 78	MPWA	$\pi N \rightarrow \pi N L_{1,15}$ wave
3800 \pm 200	HENDRY 78	MPWA	$\pi N \rightarrow \pi N M_{1,17}$ wave
4100 \pm 200	HENDRY 78	MPWA	$\pi N \rightarrow \pi N N_{1,19}$ wave

$N(\sim 3000)$ BREIT-WIGNER WIDTH

VALUE (MeV)	DOCUMENT ID	TECN	COMMENT
1300 \pm 200	HENDRY 78	MPWA	$\pi N \rightarrow \pi N L_{1,15}$ wave
1600 \pm 200	HENDRY 78	MPWA	$\pi N \rightarrow \pi N M_{1,17}$ wave
1900 \pm 300	HENDRY 78	MPWA	$\pi N \rightarrow \pi N N_{1,19}$ wave

$N(\sim 3000)$ DECAY MODES

Mode	Γ_1	$N\pi$

$N(\sim 3000)$ BRANCHING RATIOS

$\Gamma(N\pi)/\Gamma_{total}$	DOCUMENT ID	TECN	COMMENT	Γ_1/Γ
0.055 \pm 0.02	HENDRY 78	MPWA	$\pi N \rightarrow \pi N L_{1,15}$ wave	
0.040 \pm 0.015	HENDRY 78	MPWA	$\pi N \rightarrow \pi N M_{1,17}$ wave	
0.030 \pm 0.015	HENDRY 78	MPWA	$\pi N \rightarrow \pi N N_{1,19}$ wave	

$N(\sim 3000)$ REFERENCES

KOCH 80	Toronto Conf. 3	R. Koch	(KARLT) IJP
HENDRY 78	PRL 41 222	A.W. Hendry	(IND, LBL) IJP
Also	ANP 136 1	A.W. Hendry	(IND) IJP

Baryon Particle Listings

 $\Delta(1232)$ **Δ BARYONS**
($S = 0, I = 3/2$)

$$\Delta^{++} = uuu, \Delta^+ = uud, \Delta^0 = udd, \Delta^- = ddd$$

 $\Delta(1232) P_{33}$

$$I(J^P) = \frac{3}{2}(\frac{3}{2}^+) \text{ Status: } ****$$

Most of the results published before 1975 were last included in our 1982 edition, Physics Letters **111B** 1 (1982). Some further obsolete results published before 1984 were last included in our 2006 edition, Journal of Physics, G **33** 1 (2006).

 $\Delta(1232)$ BREIT-WIGNER MASSES**MIXED CHARGES**

VALUE (MeV)	DOCUMENT ID	TECN	COMMENT
1231 to 1233 (≈ 1232) OUR ESTIMATE			
1233.4 \pm 0.4	ARNDT 06	DPWA	$\pi N \rightarrow \pi N, \eta N$
1231 \pm 1	MANLEY 92	IPWA	$\pi N \rightarrow \pi N \& N\pi\pi$
1232 \pm 3	CUTKOSKY 80	IPWA	$\pi N \rightarrow \pi N$
1233 \pm 2	HOEHLER 79	IPWA	$\pi N \rightarrow \pi N$
••• We do not use the following data for averages, fits, limits, etc. •••			
1232.9 \pm 1.2	ARNDT 04	DPWA	$\pi N \rightarrow \pi N, \eta N$
1228 \pm 1	PENNER 02c	DPWA	Multichannel
1234 \pm 5	VRANA 00	DPWA	Multichannel
1233	ARNDT 95	DPWA	$\pi N \rightarrow N\pi$

 $\Delta(1232)^{++}$ MASS

VALUE (MeV)	DOCUMENT ID	TECN	COMMENT
••• We do not use the following data for averages, fits, limits, etc. •••			
1230.55 \pm 0.20	GRIDNEV 06	DPWA	$\pi N \rightarrow \pi N$
1231.88 \pm 0.29	BERNICHIA 96		Fit to PEDRONI 78
1230.5 \pm 0.2	ABAEV 95	IPWA	$\pi N \rightarrow \pi N$
1230.9 \pm 0.3	KOCH 80b	IPWA	$\pi N \rightarrow \pi N$
1231.1 \pm 0.2	PEDRONI 78		$\pi N \rightarrow \pi N$ 70–370 MeV

 $\Delta(1232)^+$ MASS

VALUE (MeV)	DOCUMENT ID	COMMENT
••• We do not use the following data for averages, fits, limits, etc. •••		
1234.9 \pm 1.4	MIROSHNIC... 79	Fit photoproduction

 $\Delta(1232)^0$ MASS

VALUE (MeV)	DOCUMENT ID	TECN	COMMENT
••• We do not use the following data for averages, fits, limits, etc. •••			
1233.40 \pm 0.22	GRIDNEV 06	DPWA	$\pi N \rightarrow \pi N$
1234.35 \pm 0.75	BERNICHIA 96		Fit to PEDRONI 78
1233.1 \pm 0.3	ABAEV 95	IPWA	$\pi N \rightarrow \pi N$
1233.6 \pm 0.5	KOCH 80b	IPWA	$\pi N \rightarrow \pi N$
1233.8 \pm 0.2	PEDRONI 78		$\pi N \rightarrow \pi N$ 70–370 MeV

 $m_{\Delta^0} - m_{\Delta^{++}}$

VALUE (MeV)	DOCUMENT ID	TECN	COMMENT
••• We do not use the following data for averages, fits, limits, etc. •••			
2.86 \pm 0.30	GRIDNEV 06	DPWA	$\pi N \rightarrow \pi N$
2.25 \pm 0.68	BERNICHIA 96		Fit to PEDRONI 78
2.6 \pm 0.4	ABAEV 95	IPWA	$\pi N \rightarrow \pi N$
2.7 \pm 0.3	³ PEDRONI 78		See the masses

 $\Delta(1232)$ BREIT-WIGNER WIDTHS**MIXED CHARGES**

VALUE (MeV)	DOCUMENT ID	TECN	COMMENT
116 to 120 (≈ 118) OUR ESTIMATE			
118.7 \pm 0.6	ARNDT 06	DPWA	$\pi N \rightarrow \pi N, \eta N$
118 \pm 4	MANLEY 92	IPWA	$\pi N \rightarrow \pi N \& N\pi\pi$
120 \pm 5	CUTKOSKY 80	IPWA	$\pi N \rightarrow \pi N$
116 \pm 5	HOEHLER 79	IPWA	$\pi N \rightarrow \pi N$
••• We do not use the following data for averages, fits, limits, etc. •••			
118.0 \pm 2.2	ARNDT 04	DPWA	$\pi N \rightarrow \pi N, \eta N$
106 \pm 1	PENNER 02c	DPWA	Multichannel
112 \pm 18	VRANA 00	DPWA	Multichannel
114	ARNDT 95	DPWA	$\pi N \rightarrow N\pi$

 $\Delta(1232)^{++}$ WIDTH

VALUE (MeV)	DOCUMENT ID	TECN	COMMENT
••• We do not use the following data for averages, fits, limits, etc. •••			
112.2 \pm 0.7	GRIDNEV 06	DPWA	$\pi N \rightarrow \pi N$
109.07 \pm 0.48	BERNICHIA 96		Fit to PEDRONI 78
111.0 \pm 1.0	KOCH 80b	IPWA	$\pi N \rightarrow \pi N$
111.3 \pm 0.5	PEDRONI 78		$\pi N \rightarrow \pi N$ 70–370 MeV

 $\Delta(1232)^+$ WIDTH

VALUE (MeV)	DOCUMENT ID	COMMENT
••• We do not use the following data for averages, fits, limits, etc. •••		
131.1 \pm 2.4	MIROSHNIC... 79	Fit photoproduction

 $\Delta(1232)^0$ WIDTH

VALUE (MeV)	DOCUMENT ID	TECN	COMMENT
••• We do not use the following data for averages, fits, limits, etc. •••			
116.9 \pm 0.7	GRIDNEV 06	DPWA	$\pi N \rightarrow \pi N$
117.58 \pm 1.16	BERNICHIA 96		Fit to PEDRONI 78
113.0 \pm 1.5	KOCH 80b	IPWA	$\pi N \rightarrow \pi N$
117.9 \pm 0.9	PEDRONI 78		$\pi N \rightarrow \pi N$ 70–370 MeV

 $\Delta^0 - \Delta^{++}$ WIDTH DIFFERENCE

VALUE (MeV)	DOCUMENT ID	TECN	COMMENT
••• We do not use the following data for averages, fits, limits, etc. •••			
4.66 \pm 1.0	GRIDNEV 06	DPWA	$\pi N \rightarrow \pi N$
8.45 \pm 1.11	BERNICHIA 96		Fit to PEDRONI 78
5.1 \pm 1.0	ABAEV 95	IPWA	$\pi N \rightarrow \pi N$
6.6 \pm 1.0	PEDRONI 78		See the widths

 $\Delta(1232)$ POLE POSITIONS**REAL PART, MIXED CHARGES**

VALUE (MeV)	DOCUMENT ID	TECN	COMMENT
1209 to 1211 (≈ 1210) OUR ESTIMATE			
1211	ARNDT 06	DPWA	$\pi N \rightarrow \pi N, \eta N$
1209	⁴ HOEHLER 93	ARGD	$\pi N \rightarrow \pi N$
1210 \pm 1	CUTKOSKY 80	IPWA	$\pi N \rightarrow \pi N$
••• We do not use the following data for averages, fits, limits, etc. •••			
1210	ARNDT 04	DPWA	$\pi N \rightarrow \pi N, \eta N$
1217	VRANA 00	DPWA	Multichannel
1211	ARNDT 95	DPWA	$\pi N \rightarrow N\pi$
1210	ARNDT 91	DPWA	$\pi N \rightarrow \pi N$ Soln SM90

–2xIMAGINARY PART, MIXED CHARGES

VALUE (MeV)	DOCUMENT ID	TECN	COMMENT
98 to 102 (≈ 100) OUR ESTIMATE			
99	ARNDT 06	DPWA	$\pi N \rightarrow \pi N, \eta N$
100	⁴ HOEHLER 93	ARGD	$\pi N \rightarrow \pi N$
100 \pm 2	CUTKOSKY 80	IPWA	$\pi N \rightarrow \pi N$
••• We do not use the following data for averages, fits, limits, etc. •••			
100	ARNDT 04	DPWA	$\pi N \rightarrow \pi N, \eta N$
96	VRANA 00	DPWA	Multichannel
100	ARNDT 95	DPWA	$\pi N \rightarrow N\pi$
100	ARNDT 91	DPWA	$\pi N \rightarrow \pi N$ Soln SM90

REAL PART, $\Delta(1232)^{++}$

VALUE (MeV)	DOCUMENT ID	COMMENT
••• We do not use the following data for averages, fits, limits, etc. •••		
1212.50 \pm 0.24	BERNICHIA 96	Fit to PEDRONI 78

–2xIMAGINARY PART, $\Delta(1232)^{++}$

VALUE (MeV)	DOCUMENT ID	COMMENT
••• We do not use the following data for averages, fits, limits, etc. •••		
97.37 \pm 0.42	BERNICHIA 96	Fit to PEDRONI 78

REAL PART, $\Delta(1232)^+$

VALUE (MeV)	DOCUMENT ID	TECN	COMMENT
••• We do not use the following data for averages, fits, limits, etc. •••			
1211 \pm 1 to 1212 \pm 1	HANSTEIN 96	DPWA	$\gamma N \rightarrow \pi N$
1206.9 \pm 0.9 to 1210.5 \pm 1.8	MIROSHNIC... 79		Fit photoproduction

–2xIMAGINARY PART, $\Delta(1232)^+$

VALUE (MeV)	DOCUMENT ID	TECN	COMMENT
••• We do not use the following data for averages, fits, limits, etc. •••			
102 \pm 2 to 99 \pm 2	¹ HANSTEIN 96	DPWA	$\gamma N \rightarrow \pi N$
111.2 \pm 2.0 to 116.6 \pm 2.2	MIROSHNIC... 79		Fit photoproduction

¹ The second (lower) value of HANSTEIN 96 here goes with the second (higher) value of the real part in the preceding data block.

REAL PART, $\Delta(1232)^0$

VALUE (MeV)	DOCUMENT ID	COMMENT
••• We do not use the following data for averages, fits, limits, etc. •••		
1213.20 \pm 0.66	BERNICHIA 96	Fit to PEDRONI 78

–2xIMAGINARY PART, $\Delta(1232)^0$

VALUE (MeV)	DOCUMENT ID	COMMENT
••• We do not use the following data for averages, fits, limits, etc. •••		
104.10 \pm 1.01	BERNICHIA 96	Fit to PEDRONI 78

$\Delta(1232)$ ELASTIC POLE RESIDUES

ABSOLUTE VALUE, MIXED CHARGES

VALUE (MeV)	DOCUMENT ID	TECN	COMMENT
52	ARNDT 06	DPWA	$\pi N \rightarrow \pi N, \eta N$
50	HOEHLER 93	ARGD	$\pi N \rightarrow \pi N$
53±2	CUTKOSKY 80	IPWA	$\pi N \rightarrow \pi N$
••• We do not use the following data for averages, fits, limits, etc. •••			
53	ARNDT 04	DPWA	$\pi N \rightarrow \pi N, \eta N$
38	⁵ ARNDT 95	DPWA	$\pi N \rightarrow N\pi$
52	ARNDT 91	DPWA	$\pi N \rightarrow \pi N$ Soln SM90

PHASE, MIXED CHARGES

VALUE (°)	DOCUMENT ID	TECN	COMMENT
-47	ARNDT 06	DPWA	$\pi N \rightarrow \pi N, \eta N$
-48	HOEHLER 93	ARGD	$\pi N \rightarrow \pi N$
-47±1	CUTKOSKY 80	IPWA	$\pi N \rightarrow \pi N$
••• We do not use the following data for averages, fits, limits, etc. •••			
-47	ARNDT 04	DPWA	$\pi N \rightarrow \pi N, \eta N$
-22	⁵ ARNDT 95	DPWA	$\pi N \rightarrow N\pi$
-31	ARNDT 91	DPWA	$\pi N \rightarrow \pi N$ Soln SM90

 $\Delta(1232)$ DECAY MODES

The following branching fractions are our estimates, not fits or averages.

Mode	Fraction (Γ_i/Γ)
Γ_1 $N\pi$	100 %
Γ_2 $N\gamma$	0.52-0.60 %
Γ_3 $N\gamma$, helicity=1/2	0.11-0.13 %
Γ_4 $N\gamma$, helicity=3/2	0.41-0.47 %

 $\Delta(1232)$ BRANCHING RATIOS

$\Gamma(N\pi)/\Gamma_{\text{total}}$	DOCUMENT ID	TECN	COMMENT	Γ_1/Γ
1.0 OUR ESTIMATE				
1.00	ARNDT 06	DPWA	$\pi N \rightarrow \pi N, \eta N$	
1.0	MANLEY 92	IPWA	$\pi N \rightarrow \pi N \& N\pi\pi$	
1.0	CUTKOSKY 80	IPWA	$\pi N \rightarrow \pi N$	
1.0	HOEHLER 79	IPWA	$\pi N \rightarrow \pi N$	
••• We do not use the following data for averages, fits, limits, etc. •••				
1.000	ARNDT 04	DPWA	$\pi N \rightarrow \pi N, \eta N$	
1.00	PENNER 02c	DPWA	Multichannel	
1.00 ± 0.01	VRANA 00	DPWA	Multichannel	
1.0	ARNDT 95	DPWA	$\pi N \rightarrow N\pi$	

 $\Delta(1232)$ PHOTON DECAY AMPLITUDES

Papers on γN amplitudes predating 1981 may be found in our 2006 edition, Journal of Physics, G **33** 1 (2006).

 $\Delta(1232) \rightarrow N\gamma$, helicity-1/2 amplitude $A_{1/2}$

VALUE (GeV ^{-1/2})	DOCUMENT ID	TECN	COMMENT
-0.135 ± 0.006 OUR ESTIMATE			
-0.139 ± 0.004	DUGGER 07	DPWA	$\gamma N \rightarrow \pi N$
-0.137 ± 0.005	AHRENS 04A	DPWA	$\tilde{\gamma}p \rightarrow N\pi$
-0.129 ± 0.001	ARNDT 02	DPWA	$\gamma p \rightarrow N\pi$
-0.1357 ± 0.0013 ± 0.0037	BLANPIED 01	LEGS	$\gamma p \rightarrow p\gamma, p\pi^0, n\pi^+$
-0.131 ± 0.001	BECK 00	IPWA	$\tilde{\gamma}p \rightarrow p\pi^0, n\pi^+$
-0.140 ± 0.005	KAMALOV 99	DPWA	$\gamma N \rightarrow \pi N$
-0.1294 ± 0.0013	HANSTEIN 98	IPWA	$\gamma N \rightarrow \pi N$
-0.135 ± 0.005	ARNDT 97	IPWA	$\gamma N \rightarrow \pi N$
-0.1278 ± 0.0012	DAVIDSON 97	DPWA	$\gamma N \rightarrow \pi N$
-0.141 ± 0.005	ARNDT 96	IPWA	$\gamma N \rightarrow \pi N$
-0.135 ± 0.016	DAVIDSON 91B	FIT	$\gamma N \rightarrow \pi N$
-0.145 ± 0.015	CRAWFORD 83	IPWA	$\gamma N \rightarrow \pi N$
-0.138 ± 0.004	AWAJI 81	DPWA	$\gamma N \rightarrow \pi N$
••• We do not use the following data for averages, fits, limits, etc. •••			
-0.140	DRECHSEL 07	DPWA	$\gamma N \rightarrow \pi N$
-0.128	PENNER 02D	DPWA	Multichannel
-0.1312	HANSTEIN 98	DPWA	$\gamma N \rightarrow \pi N$
-0.143 ± 0.004	LI 93	IPWA	$\gamma N \rightarrow \pi N$
-0.140 ± 0.007	DAVIDSON 90	FIT	See DAVIDSON 91B

 $\Delta(1232) \rightarrow N\gamma$, helicity-3/2 amplitude $A_{3/2}$

VALUE (GeV ^{-1/2})	DOCUMENT ID	TECN	COMMENT
-0.250 ± 0.008 OUR ESTIMATE			
-0.258 ± 0.005	DUGGER 07	DPWA	$\gamma N \rightarrow \pi N$
-0.256 ± 0.003	AHRENS 04A	DPWA	$\tilde{\gamma}p \rightarrow N\pi$
-0.243 ± 0.001	ARNDT 02	DPWA	$\gamma p \rightarrow N\pi$
-0.2669 ± 0.0016 ± 0.0078	BLANPIED 01	LEGS	$\gamma p \rightarrow p\gamma, p\pi^0, n\pi^+$
-0.251 ± 0.001	BECK 00	IPWA	$\tilde{\gamma}p \rightarrow p\pi^0, n\pi^+$

-0.258 ± 0.006	KAMALOV 99	DPWA	$\gamma N \rightarrow \pi N$
-0.2466 ± 0.0013	HANSTEIN 98	IPWA	$\gamma N \rightarrow \pi N$
-0.250 ± 0.008	ARNDT 97	IPWA	$\gamma N \rightarrow \pi N$
-0.2524 ± 0.0013	DAVIDSON 97	DPWA	$\gamma N \rightarrow \pi N$
-0.261 ± 0.005	ARNDT 96	IPWA	$\gamma N \rightarrow \pi N$
-0.251 ± 0.033	DAVIDSON 91B	FIT	$\gamma N \rightarrow \pi N$
-0.263 ± 0.026	CRAWFORD 83	IPWA	$\gamma N \rightarrow \pi N$
-0.259 ± 0.006	AWAJI 81	DPWA	$\gamma N \rightarrow \pi N$
••• We do not use the following data for averages, fits, limits, etc. •••			
-0.265	DRECHSEL 07	DPWA	$\gamma N \rightarrow \pi N$
-0.247	PENNER 02D	DPWA	Multichannel
-0.2522	HANSTEIN 98	DPWA	$\gamma N \rightarrow \pi N$
-0.262 ± 0.004	LI 93	IPWA	$\gamma N \rightarrow \pi N$
-0.254 ± 0.011	DAVIDSON 90	FIT	See DAVIDSON 91B

 $\Delta(1232) \rightarrow N\gamma, E_2/M_1$ ratio

VALUE	DOCUMENT ID	TECN	COMMENT
-0.025 ± 0.005 OUR ESTIMATE			
-0.0274 ± 0.0003 ± 0.0030	AHRENS 04A	DPWA	$\tilde{\gamma}p \rightarrow N\pi$
-0.020 ± 0.002	ARNDT 02	DPWA	$\gamma p \rightarrow N\pi$
-0.0307 ± 0.0026 ± 0.0024	BLANPIED 01	LEGS	$\gamma p \rightarrow p\gamma, p\pi^0, n\pi^+$
-0.016 ± 0.004 ± 0.002	GALLER 01	DPWA	$\gamma p \rightarrow \gamma p$
-0.025 ± 0.001 ± 0.002	BECK 00	IPWA	$\tilde{\gamma}p \rightarrow p\pi^0, n\pi^+$
-0.0233 ± 0.0017	HANSTEIN 98	IPWA	$\gamma N \rightarrow \pi N$
-0.015 ± 0.005	⁶ ARNDT 97	IPWA	$\gamma N \rightarrow \pi N$
-0.0319 ± 0.0024	DAVIDSON 97	DPWA	$\gamma N \rightarrow \pi N$
••• We do not use the following data for averages, fits, limits, etc. •••			
-0.022	DRECHSEL 07	DPWA	$\gamma N \rightarrow \pi N$
-0.026	PENNER 02D	DPWA	Multichannel
-0.0254 ± 0.0010	HANSTEIN 98	DPWA	$\gamma N \rightarrow \pi N$
-0.025 ± 0.002 ± 0.002	BECK 97	IPWA	$\gamma N \rightarrow \pi N$
-0.030 ± 0.003 ± 0.002	BLANPIED 97	DPWA	$\gamma N \rightarrow \pi N, \gamma N$
-0.027 ± 0.003 ± 0.001	KHANDAKER 95	DPWA	$\gamma N \rightarrow \pi N$
-0.015 ± 0.005	WORKMAN 92	IPWA	$\gamma N \rightarrow \pi N$
-0.0157 ± 0.0072	DAVIDSON 91B	FIT	$\gamma N \rightarrow \pi N$
-0.0107 ± 0.0037	DAVIDSON 90	FIT	$\gamma N \rightarrow \pi N$
-0.015 ± 0.002	DAVIDSON 86	FIT	$\gamma N \rightarrow \pi N$
+0.037 ± 0.004	TANABE 85	FIT	$\gamma N \rightarrow \pi N$

 $\Delta(1232) \rightarrow N\gamma$, absolute value of E_2/M_1 ratio at pole

VALUE	DOCUMENT ID	TECN	COMMENT
••• We do not use the following data for averages, fits, limits, etc. •••			
0.065 ± 0.007	ARNDT 97	DPWA	$\gamma N \rightarrow \pi N$
0.058	HANSTEIN 96	DPWA	$\gamma N \rightarrow \pi N$

 $\Delta(1232) \rightarrow N\gamma$, phase of E_2/M_1 ratio at pole

VALUE	DOCUMENT ID	TECN	COMMENT
••• We do not use the following data for averages, fits, limits, etc. •••			
-122 ± 5	ARNDT 97	DPWA	$\gamma N \rightarrow \pi N$
-127.2	HANSTEIN 96	DPWA	$\gamma N \rightarrow \pi N$

 $\Delta(1232)$ MAGNETIC MOMENTS $\Delta(1232)^{++}$ MAGNETIC MOMENT

The values are extracted from UCLA and SIN data on π^+p bremsstrahlung using a variety of different theoretical approximations and methods. Our estimate is *only* a rough guess of the range we expect the moment to lie within.

VALUE (μ_N)	DOCUMENT ID	TECN	COMMENT
3.7 to 7.5 OUR ESTIMATE			
••• We do not use the following data for averages, fits, limits, etc. •••			
6.14 ± 0.51	LOPEZCAST... 01	DPWA	$\pi^+p \rightarrow \pi^+p\gamma$
4.52 ± 0.50 ± 0.45	BOSSHARD 91		$\pi^+p \rightarrow \pi^+p\gamma$ (SIN data)
3.7 to 4.2	LIN 91B		$\pi^+p \rightarrow \pi^+p\gamma$ (from UCLA data)
4.6 to 4.9	LIN 91B		$\pi^+p \rightarrow \pi^+p\gamma$ (from SIN data)
5.6 to 7.5	WITTMAN 88		$\pi^+p \rightarrow \pi^+p\gamma$ (from UCLA data)
6.9 to 9.8	HELLER 87		$\pi^+p \rightarrow \pi^+p\gamma$ (from UCLA data)
4.7 to 6.7	NEFKENS 78		$\pi^+p \rightarrow \pi^+p\gamma$ (UCLA data)

 $\Delta(1232)^+$ MAGNETIC MOMENT

VALUE (μ_N)	DOCUMENT ID	COMMENT
••• We do not use the following data for averages, fits, limits, etc. •••		
2.7 ^{+1.0} _{-1.3} ± 1.5 ± 3	² KOTULLA 02	$\gamma p \rightarrow p\pi^0\gamma'$
²		The second error is systematic, the third is an estimate of theoretical uncertainties.

 $\Delta(1232)$ FOOTNOTES

- Using $\pi^\pm d$ as well, PEDRONI 78 determine $(M^- - M^{++}) + (M^0 - M^+)/3 = 4.6 \pm 0.2$ MeV.
- See HOEHLER 93 for a detailed discussion of the evidence for and the pole parameters of N and Δ resonances as determined from Argand diagrams of πN elastic partial-wave amplitudes and from plots of the speeds with which the amplitudes traverse the diagrams.
- This ARNDT 95 value is in error, as pointed out by HOEHLER 01. The corrected value is in line with the ARNDT 91 value (R.A. Arndt, private communication).
- This ARNDT 97 value is very sensitive to the database being fitted. The result is from a fit to the full pion photoproduction database, apart from the BLANPIED 97 cross-section measurements.

Baryon Particle Listings

$\Delta(1232), \Delta(1600)$

$\Delta(1232)$ REFERENCES

For early references, see Physics Letters **111B** 1 (1982).

DRECHSEL 07	EPJ A34 69	D. Drechsel, S.S. Kamalov, L. Tiator (MANZ, JINR)
DUGGER 07	PR C76 025211	M. Dugger <i>et al.</i> (Jefferson Lab CLAS Collab.)
ARNDT 06	PR C74 045205	R.A. Arndt <i>et al.</i> (GWU)
GRIDNEV 06	PAN 69 1542	A.B. Gridnev <i>et al.</i> (PNPI, BONN, GWU)
PDG 06	JPG 33 1	W.-M. Yao <i>et al.</i> (PDG Collab.)
AHRENS 04A	EPJ A21 323	J. Ahrens <i>et al.</i> (Mainz GDH, A2 Collab.)
ARNDT 04	PR C69 035213	R.A. Arndt <i>et al.</i> (GWU, TRIU)
ARNDT 02	PR C66 055213	R.A. Arndt <i>et al.</i> (GWU)
KOTULLA 02	PRL 89 272001	M. Kotulla <i>et al.</i> (MAMI TAPS Collab.)
PENNER 02C	PR C66 055211	G. Penner, U. Mosel (GIES)
PENNER 02D	PR C66 055212	G. Penner, U. Mosel (GIES)
BLANPIED 01	PR C64 025203	G. Blanpied <i>et al.</i> (BNL LEGS Collab.)
GALLER 01	PL B503 245	G. Galler <i>et al.</i> (Mainz LARA Collab.)
HOHLER 01	NSTAR 2001 185	G. Höhler (KARL)
LOPEZCAST... 01	PL B517 339	G. Lopez Castro, A. Mariano
Also	NP A697 440	G. Lopez Castro, A. Mariano
BECK 00	PR C61 035204	R. Beck <i>et al.</i> (Mainz Microtron DAPHNE Col.)
VRANA 00	PRPL 328 181	T.P. Vrana, S.A. Dytman, T.-S.H. Lee (PITT+)
KAMALOV 99	PRL 83 4494	S.S. Kamalov, S.N. Yang (Taiwan U.)
HANSTEIN 98	NP A632 561	O. Hanstein, D. Drechsel, L. Tiator
ARNDT 97	PR C56 577	R.A. Arndt, I.I. Strakovsky, R.L. Workman (VPI)
BECK 97	PRL 78 606	R. Beck <i>et al.</i> (MANZ, SACL, PAVI, GLAS)
Also	PRL 79 4510	R.L. Beck, H.P. Krahn (MANZ)
Also	PRL 79 4512	R.L. Beck, H.P. Krahn (MANZ)
Also	PRL 79 4515 (erratum)	R.L. Beck <i>et al.</i> (MANZ, SACL, PAVI, GLAS)
BLANPIED 97	PRL 79 4337	G.S. Blanpied <i>et al.</i> (LEGS Collab.)
DAVIDSON 97	PRL 79 4509	R.M. Davidson, N.C.A. Mukhopadhyay (RPI)
ARNDT 96	PR C53 430	R.A. Arndt, I.I. Strakovsky, R.L. Workman (VPI)
BERNICHIA 96	NP A597 623	A. Bernichia, G. Lopez Castro, J. Pestieau (LOUV+)
HANSTEIN 96	PL B385 45	O. Hanstein, D. Drechsel, L. Tiator (MANZ)
ABAEV 95	ZPHY A352 85	V.V. Abaev, S.P. Kruglov (PNPI)
ARNDT 95	PR C52 2120	R.A. Arndt <i>et al.</i> (VPI, BRCO)
KHANDAKER 95	PR D51 3966	M. Khandaker, A.M. Sandomi (BNL, VPI)
HOEHLER 93	π N Newsletter 9 1	G. Höhler (KARL)
LI 93	PR C47 2759	Z.J. Li <i>et al.</i> (VPI)
MANLEY 92	PR D45 4002	D.M. Manley, E.M. Saleski (KENT) IJP
Also	PR D30 304	D.M. Manley <i>et al.</i> (VPI)
WORKMAN 92	PR C46 1546	R.L. Workman, R.A. Arndt, Z.J. Li (VPI)
ARNDT 91	PR D43 2131	R.A. Arndt <i>et al.</i> (VPI, TELE) IJP
BOSSHARD 91	PR D44 1962	A. Bosshard <i>et al.</i> (ZURI, LBL, VILL+)
Also	PRL 64 2619	A. Bosshard <i>et al.</i> (CATH, LAUS, LBL+)
DAVIDSON 91B	PR D43 71	R.M. Davidson, N.C. Mukhopadhyay, R.S. Wittman (RPI)
LIN 91B	PR C44 1819	D.H. Lin, M.K. Liou, Z.M. Ding (CUNY, CSOK)
Also	PR C43 R930	D. Lin, M.K. Liou (CUNY)
DAVIDSON 90	PR D42 20	R.M. Davidson, N.C. Mukhopadhyay (RPI)
WITTMAN 88	PR C37 2075	R. Wittman (TRIU)
HELLER 87	PR C35 718	L. Heller <i>et al.</i> (LANL, MIT, ILL)
DAVIDSON 86	PRL 56 804	R.M. Davidson, N.C. Mukhopadhyay, R. Wittman (RPI)
TANABE 85	PR C31 1876	H. Tanabe, K. Ohta (KOMAB)
CRAWFORD 83	NP B211 1	R.L. Crawford, W.T. Morton (GLAS)
PDG 82	PL 111B 1	M. Roos <i>et al.</i> (HELS, CIT, CERN)
AWAJI 81	Bonn Conf. 352	N. Awaji, R. Kajikawa (NAGO)
Also	NP B197 365	K. Fujii <i>et al.</i> (NAGO)
CUTKOSKY 80	Toronto Conf. 19	R.E. Cutkosky <i>et al.</i> (CMU, LBL) IJP
Also	PR D20 2839	R.E. Cutkosky <i>et al.</i> (CMU, LBL)
KOCH 80B	NP A336 331	R. Koch, E. Pietarinen (KARLT) IJP
HOEHLER 79	PDAT 12-1	G. Höhler <i>et al.</i> (KARLT) IJP
Also	Toronto Conf. 3	R. Koch (KARLT) IJP
MIROSHNIC... 79	SJNP 29 94	I.I. Miroshnichenko <i>et al.</i> (KFTI) IJP
Also	Translated from YAF 29 188	
NEFKENS 78	PR D18 3911	B.M.K. Nefkens <i>et al.</i> (UCLA, CATH) IJP
PEDRONI 78	NP A300 321	E. Pedroni <i>et al.</i> (SIN, ISNG, KARLE+) IJP

$\Delta(1600) P_{33}$

$$I(J^P) = \frac{3}{2}(\frac{3}{2}^+) \text{ Status: } ***$$

Most of the results published before 1975 are now obsolete and have been omitted. They may be found in our 1982 edition, Physics Letters **111B** 1 (1982). Some further obsolete results published before 1984 were last included in our 2006 edition, Journal of Physics, G **33** 1 (2006).

The various analyses are not in good agreement.

$\Delta(1600)$ BREIT-WIGNER MASS

VALUE (MeV)	DOCUMENT ID	TECN	COMMENT
1550 to 1700 (\approx 1600) OUR ESTIMATE			
1706 \pm 10	MANLEY 92	IPWA	$\pi N \rightarrow \pi N & N\pi\pi$
1600 \pm 50	CUTKOSKY 80	IPWA	$\pi N \rightarrow \pi N$
1522 \pm 13	HOEHLER 79	IPWA	$\pi N \rightarrow \pi N$
••• We do not use the following data for averages, fits, limits, etc. •••			
1667 \pm 1	PENNER 02c	DPWA	Multichannel
1687 \pm 44	VRANA 00	DPWA	Multichannel
1672 \pm 15	ARNDT 96	IPWA	$\gamma N \rightarrow \pi N$
1706	LI 93	IPWA	$\gamma N \rightarrow \pi N$
1690	BARNHAM 80	IPWA	$\pi N \rightarrow N\pi\pi$
1560	¹ LONGACRE 77	IPWA	$\pi N \rightarrow N\pi\pi$
1640	² LONGACRE 75	IPWA	$\pi N \rightarrow N\pi\pi$

$\Delta(1600)$ BREIT-WIGNER WIDTH

VALUE (MeV)	DOCUMENT ID	TECN	COMMENT
250 to 450 (\approx 350) OUR ESTIMATE			
430 \pm 73	MANLEY 92	IPWA	$\pi N \rightarrow \pi N & N\pi\pi$
300 \pm 100	CUTKOSKY 80	IPWA	$\pi N \rightarrow \pi N$
220 \pm 40	HOEHLER 79	IPWA	$\pi N \rightarrow \pi N$

••• We do not use the following data for averages, fits, limits, etc. •••

397 \pm 10	PENNER 02c	DPWA	Multichannel
493 \pm 75	VRANA 00	DPWA	Multichannel
315 \pm 20	ARNDT 96	IPWA	$\gamma N \rightarrow \pi N$
215	LI 93	IPWA	$\gamma N \rightarrow \pi N$
250	BARNHAM 80	IPWA	$\pi N \rightarrow N\pi\pi$
180	¹ LONGACRE 77	IPWA	$\pi N \rightarrow N\pi\pi$
300	² LONGACRE 75	IPWA	$\pi N \rightarrow N\pi\pi$

$\Delta(1600)$ POLE POSITION

REAL PART

VALUE (MeV)	DOCUMENT ID	TECN	COMMENT
1500 to 1700 (\approx 1600) OUR ESTIMATE			
1457	ARNDT 06	DPWA	$\pi N \rightarrow \pi N, \eta N$
1550	³ HOEHLER 93	SPED	$\pi N \rightarrow \pi N$
1550 \pm 40	CUTKOSKY 80	IPWA	$\pi N \rightarrow \pi N$
••• We do not use the following data for averages, fits, limits, etc. •••			
1599	VRANA 00	DPWA	Multichannel
1675	ARNDT 95	DPWA	$\pi N \rightarrow \pi N$
1612	ARNDT 91	DPWA	$\pi N \rightarrow \pi N$ Soln SM90
1609 or 1610	⁴ LONGACRE 78	IPWA	$\pi N \rightarrow N\pi\pi$
1541 or 1542	¹ LONGACRE 77	IPWA	$\pi N \rightarrow N\pi\pi$

-2xIMAGINARY PART

VALUE (MeV)	DOCUMENT ID	TECN	COMMENT
200 to 400 (\approx 300) OUR ESTIMATE			
400	ARNDT 06	DPWA	$\pi N \rightarrow \pi N, \eta N$
200 \pm 60	CUTKOSKY 80	IPWA	$\pi N \rightarrow \pi N$
••• We do not use the following data for averages, fits, limits, etc. •••			
312	VRANA 00	DPWA	Multichannel
386	ARNDT 95	DPWA	$\pi N \rightarrow \pi N$
230	ARNDT 91	DPWA	$\pi N \rightarrow \pi N$ Soln SM90
323 or 325	⁴ LONGACRE 78	IPWA	$\pi N \rightarrow N\pi\pi$
178 or 178	¹ LONGACRE 77	IPWA	$\pi N \rightarrow N\pi\pi$

$\Delta(1600)$ ELASTIC POLE RESIDUE

MODULUS $|r|$

VALUE (MeV)	DOCUMENT ID	TECN	COMMENT
44	ARNDT 06	DPWA	$\pi N \rightarrow \pi N, \eta N$
17 \pm 4	CUTKOSKY 80	IPWA	$\pi N \rightarrow \pi N$
••• We do not use the following data for averages, fits, limits, etc. •••			
52	ARNDT 95	DPWA	$\pi N \rightarrow \pi N$
16	ARNDT 91	DPWA	$\pi N \rightarrow \pi N$ Soln SM90

PHASE θ

VALUE ($^\circ$)	DOCUMENT ID	TECN	COMMENT
+147	ARNDT 06	DPWA	$\pi N \rightarrow \pi N, \eta N$
-150 \pm 30	CUTKOSKY 80	IPWA	$\pi N \rightarrow \pi N$
••• We do not use the following data for averages, fits, limits, etc. •••			
+ 14	ARNDT 95	DPWA	$\pi N \rightarrow \pi N$
- 73	ARNDT 91	DPWA	$\pi N \rightarrow \pi N$ Soln SM90

$\Delta(1600)$ DECAY MODES

The following branching fractions are our estimates, not fits or averages.

Mode	Fraction (Γ_i/Γ)
Γ_1 $N\pi$	10-25 %
Γ_2 ΣK	
Γ_3 $N\pi\pi$	75-90 %
Γ_4 $\Delta\pi$	40-70 %
Γ_5 $\Delta(1232)\pi, P$ -wave	
Γ_6 $\Delta(1232)\pi, F$ -wave	
Γ_7 $N\rho$	<25 %
Γ_8 $N\rho, S=1/2, P$ -wave	
Γ_9 $N\rho, S=3/2, P$ -wave	
Γ_{10} $N\rho, S=3/2, F$ -wave	
Γ_{11} $N(1440)\pi$	10-35 %
Γ_{12} $N(1440)\pi, P$ -wave	
Γ_{13} $N\gamma$	0.001-0.02 %
Γ_{14} $N\gamma, \text{helicity}=1/2$	0.0-0.02 %
Γ_{15} $N\gamma, \text{helicity}=3/2$	0.001-0.005 %

$\Delta(1600)$ BRANCHING RATIOS

$\Gamma(N\pi)/\Gamma_{\text{total}}$	VALUE	DOCUMENT ID	TECN	COMMENT	Γ_1/Γ
0.10 to 0.25 OUR ESTIMATE					
0.12±0.02		MANLEY	92	IPWA $\pi N \rightarrow \pi N$ & $N\pi\pi$	
0.18±0.04		CUTKOSKY	80	IPWA $\pi N \rightarrow \pi N$	
0.21±0.06		HOEHLER	79	IPWA $\pi N \rightarrow \pi N$	
••• We do not use the following data for averages, fits, limits, etc. •••					
0.13±0.01		PENNER	02c	DPWA Multichannel	
0.28±0.05		VRANA	00	DPWA Multichannel	

$(\Gamma_1/\Gamma)^{1/2}/\Gamma_{\text{total}}$ in $N\pi \rightarrow \Delta(1600) \rightarrow \Sigma K$	VALUE	DOCUMENT ID	TECN	COMMENT	$(\Gamma_1/\Gamma)^{1/2}/\Gamma$
-0.36 to -0.28 OUR ESTIMATE					
••• We do not use the following data for averages, fits, limits, etc. •••					
0.006 to 0.042		5 DEANS	75	DPWA $\pi N \rightarrow \Sigma K$	

Note: Signs of couplings from $\pi N \rightarrow N\pi\pi$ analyses were changed in the 1986 edition to agree with the baryon-first convention; the overall phase ambiguity is resolved by choosing a negative sign for the $\Delta(1620)$ S_{31} coupling to $\Delta(1232)\pi$.

$(\Gamma_1/\Gamma)^{1/2}/\Gamma_{\text{total}}$ in $N\pi \rightarrow \Delta(1600) \rightarrow \Delta(1232)\pi, P\text{-wave}$	VALUE	DOCUMENT ID	TECN	COMMENT	$(\Gamma_1/\Gamma)^{1/2}/\Gamma$
+0.27 to +0.33 OUR ESTIMATE					
+0.29±0.02		MANLEY	92	IPWA $\pi N \rightarrow \pi N$ & $N\pi\pi$	
+0.24±0.05		BARNHAM	80	IPWA $\pi N \rightarrow N\pi\pi$	
+0.34		1,6 LONGACRE	77	IPWA $\pi N \rightarrow N\pi\pi$	
+0.30		2 LONGACRE	75	IPWA $\pi N \rightarrow N\pi\pi$	

$\Gamma(\Delta(1232)\pi, P\text{-wave})/\Gamma_{\text{total}}$	VALUE	DOCUMENT ID	TECN	COMMENT	Γ_5/Γ
0.59±0.10		VRANA	00	DPWA Multichannel	

$(\Gamma_1/\Gamma)^{1/2}/\Gamma_{\text{total}}$ in $N\pi \rightarrow \Delta(1600) \rightarrow \Delta(1232)\pi, F\text{-wave}$	VALUE	DOCUMENT ID	TECN	COMMENT	$(\Gamma_1/\Gamma)^{1/2}/\Gamma$
-0.15 to -0.03 OUR ESTIMATE					
-0.07		1,6 LONGACRE	77	IPWA $\pi N \rightarrow N\pi\pi$	

$(\Gamma_1/\Gamma)^{1/2}/\Gamma_{\text{total}}$ in $N\pi \rightarrow \Delta(1600) \rightarrow N\rho, S=1/2, P\text{-wave}$	VALUE	DOCUMENT ID	TECN	COMMENT	$(\Gamma_1/\Gamma)^{1/2}/\Gamma$
+0.10		1,6 LONGACRE	77	IPWA $\pi N \rightarrow N\pi\pi$	

$(\Gamma_1/\Gamma)^{1/2}/\Gamma_{\text{total}}$ in $N\pi \rightarrow \Delta(1600) \rightarrow N\rho, S=3/2, P\text{-wave}$	VALUE	DOCUMENT ID	TECN	COMMENT	$(\Gamma_1/\Gamma)^{1/2}/\Gamma$
+0.10		1,6 LONGACRE	77	IPWA $\pi N \rightarrow N\pi\pi$	

$(\Gamma_1/\Gamma)^{1/2}/\Gamma_{\text{total}}$ in $N\pi \rightarrow \Delta(1600) \rightarrow N(1440)\pi, P\text{-wave}$	VALUE	DOCUMENT ID	TECN	COMMENT	$(\Gamma_1/\Gamma)^{1/2}/\Gamma$
+0.15 to +0.23 OUR ESTIMATE					
+0.16±0.02		MANLEY	92	IPWA $\pi N \rightarrow \pi N$ & $N\pi\pi$	
+0.23±0.04		BARNHAM	80	IPWA $\pi N \rightarrow N\pi\pi$	

$\Gamma(N(1440)\pi)/\Gamma_{\text{total}}$	VALUE	DOCUMENT ID	TECN	COMMENT	Γ_{11}/Γ
0.13±0.04		VRANA	00	DPWA Multichannel	

 $\Delta(1600)$ PHOTON DECAY AMPLITUDES

Papers on γN amplitudes predating 1981 may be found in our 2006 edition, Journal of Physics, G **33** 1 (2006).

$\Delta(1600) \rightarrow N\gamma, \text{helicity-1/2 amplitude } A_{1/2}$	VALUE (GeV ^{-1/2})	DOCUMENT ID	TECN	COMMENT
-0.023±0.020 OUR ESTIMATE				
-0.018±0.015		ARNDT	96	IPWA $\gamma N \rightarrow \pi N$
-0.039±0.030		CRAWFORD	83	IPWA $\gamma N \rightarrow \pi N$
-0.046±0.013		AWAJI	81	DPWA $\gamma N \rightarrow \pi N$
••• We do not use the following data for averages, fits, limits, etc. •••				
0.0		PENNER	02d	DPWA Multichannel
-0.026±0.002		LI	93	IPWA $\gamma N \rightarrow \pi N$
-0.200		7 WADA	84	DPWA Compton scattering
0.000±0.030		BARBOUR	78	DPWA $\gamma N \rightarrow \pi N$

$\Delta(1600) \rightarrow N\gamma, \text{helicity-3/2 amplitude } A_{3/2}$	VALUE (GeV ^{-1/2})	DOCUMENT ID	TECN	COMMENT
-0.009±0.021 OUR ESTIMATE				
-0.025±0.015		ARNDT	96	IPWA $\gamma N \rightarrow \pi N$
-0.013±0.014		CRAWFORD	83	IPWA $\gamma N \rightarrow \pi N$
0.025±0.031		AWAJI	81	DPWA $\gamma N \rightarrow \pi N$
••• We do not use the following data for averages, fits, limits, etc. •••				
-0.024		PENNER	02d	DPWA Multichannel
-0.016±0.002		LI	93	IPWA $\gamma N \rightarrow \pi N$
0.023		WADA	84	DPWA Compton scattering
0.000±0.045		BARBOUR	78	DPWA $\gamma N \rightarrow \pi N$

 $\Delta(1600)$ FOOTNOTES

- LONGACRE 77 pole positions are from a search for poles in the unitarized T-matrix; the first (second) value uses, in addition to $\pi N \rightarrow N\pi\pi$ data, elastic amplitudes from a Saclay (CERN) partial-wave analysis. The other LONGACRE 77 values are from eyeball fits with Breit-Wigner circles to the T-matrix amplitudes.
- From method II of LONGACRE 75: eyeball fits with Breit-Wigner circles to the T-matrix amplitudes.
- See HOEHLER 93 for a detailed discussion of the evidence for and the pole parameters of N and Δ resonances as determined from Argand diagrams of πN elastic partial-wave amplitudes and from plots of the speeds with which the amplitudes traverse the diagrams.
- LONGACRE 78 values are from a search for poles in the unitarized T-matrix. The first (second) value uses, in addition to $\pi N \rightarrow N\pi\pi$ data, elastic amplitudes from a Saclay (CERN) partial-wave analysis.
- The range given is from the four best solutions. DEANS 75 disagrees with $\pi^+ p \rightarrow \Sigma^+ K^+$ data of WINNIK 77 around 1920 MeV.
- LONGACRE 77 considers this coupling to be well determined.
- WADA 84 is inconsistent with other analyses — see the Note on N and Δ Resonances.

 $\Delta(1600)$ REFERENCES

For early references, see Physics Letters **111B** 1 (1982).

ARNDT 06	PR C74 045205	R.A. Arndt et al.	(GWU)
PDG 06	JPG 33 1	W.-M. Yao et al.	(PDG Collab.)
PENNER 02c	PR C66 055211	G. Penner, U. Mosel	(GIES)
PENNER 02d	PR C66 055212	G. Penner, U. Mosel	(GIES)
VRANA 00	PRPL 328 181	T.P. Vrana, S.A. Dytman, T.-S.H. Lee	(PIIT+)
ARNDT 96	PR C53 430	R.A. Arndt, I.I. Strakovsky, R.L. Workman	(VPI)
ARNDT 95	PR C52 2120	R.A. Arndt et al.	(VPI, BRCO)
HOEHLER 93	πN Newsletter 9 1	G. H\"ohler	(KARL)
LI 93	PR C47 2759	Z.J. Li et al.	(VPI)
MANLEY 92	PR D45 4002	D.M. Manley, E.M. Saleski	(KENT) IUP
Also	PR D30 904	D.M. Manley et al.	(VPI)
ARNDT 91	PR D43 2131	R.A. Arndt et al.	(VPI, TELE) IUP
WADA 84	NP B247 313	Y. Wada et al.	(INUS)
CRAWFORD 83	NP B211 1	R.L. Crawford, W.T. Morton	(GLAS)
PDG 82	PL 111B 1	M. Roos et al.	(HELS, CIT, CERN)
AWAJI 81	Bonn Conf. 352	N. Awaji, R. Kajikawa	(NAGO)
Also	NP B197 365	K. Fujii et al.	(NAGO)
BARNHAM 80	NP B168 243	K.W.J. Barnham et al.	(LOIC)
CUTKOSKY 80	Toronto Conf. 19	R.E. Cutkosky et al.	(CMU, LBL) IUP
Also	PR D20 2839	R.E. Cutkosky et al.	(CMU, LBL) IUP
HOEHLER 79	PDAT 12-1	G. H\"ohler et al.	(KARLT) IUP
Also	Toronto Conf. 3	R. Koch	(KARLT) IUP
BARBOUR 78	NP B141 253	I.M. Barbour, R.L. Crawford, N.H. Parsons	(GLAS)
LONGACRE 78	PR D17 1795	R.S. Longacre et al.	(LBL, SLAC)
LONGACRE 77	NP B122 493	R.S. Longacre, J. Dolbeau	(SACL) IUP
Also	NP B108 365	J. Dolbeau et al.	(SACL) IUP
WINNIK 77	NP B128 66	M. Winnik et al.	(HAIF) I
DEANS 75	NP B96 90	S.R. Deans et al.	(SFLA, ALAH) IUP
LONGACRE 75	PL 55B 415	R.S. Longacre et al.	(LBL, SLAC) IUP

 $\Delta(1620) S_{31}$

$$I(J^P) = \frac{3}{2}(\frac{1}{2}^-) \text{ Status: } ***$$

Most of the results published before 1975 were last included in our 1982 edition, Physics Letters **111B** 1 (1982). Some further obsolete results published before 1984 were last included in our 2006 edition, Journal of Physics, G **33** 1 (2006).

 $\Delta(1620)$ BREIT-WIGNER MASS

VALUE (MeV)	DOCUMENT ID	TECN	COMMENT
1600 to 1660 (\approx 1630) OUR ESTIMATE			
1615.2± 0.4	ARNDT	06	DPWA $\pi N \rightarrow \pi N, \eta N$
1672 ± 7	MANLEY	92	IPWA $\pi N \rightarrow \pi N$ & $N\pi\pi$
1620 ± 20	CUTKOSKY	80	IPWA $\pi N \rightarrow \pi N$
1610 ± 7	HOEHLER	79	IPWA $\pi N \rightarrow \pi N$
••• We do not use the following data for averages, fits, limits, etc. •••			
1650 ± 25	THOMA	08	DPWA Multichannel
1614.1 ± 1.1	ARNDT	04	DPWA $\pi N \rightarrow \pi N, \eta N$
1612 ± 2	PENNER	02c	DPWA Multichannel
1617 ± 15	VRANA	00	DPWA Multichannel
1672 ± 5	ARNDT	96	IPWA $\gamma N \rightarrow \pi N$
1617	ARNDT	95	DPWA $\pi N \rightarrow \pi N$
1669	LI	93	IPWA $\gamma N \rightarrow \pi N$
1620	BARNHAM	80	IPWA $\pi N \rightarrow N\pi\pi$
1712.8± 6.0	1 CHEW	80	BPWA $\pi^+ p \rightarrow \pi^+ p$
1786.7± 2.0	1 CHEW	80	BPWA $\pi^+ p \rightarrow \pi^+ p$
1580	2 LONGACRE	77	IPWA $\pi N \rightarrow N\pi\pi$
1600	3 LONGACRE	75	IPWA $\pi N \rightarrow N\pi\pi$

 $\Delta(1620)$ BREIT-WIGNER WIDTH

VALUE (MeV)	DOCUMENT ID	TECN	COMMENT
135 to 150 (\approx 145) OUR ESTIMATE			
146.9± 1.9	ARNDT	06	DPWA $\pi N \rightarrow \pi N, \eta N$
154 ± 37	MANLEY	92	IPWA $\pi N \rightarrow \pi N$ & $N\pi\pi$
140 ± 20	CUTKOSKY	80	IPWA $\pi N \rightarrow \pi N$
139 ± 18	HOEHLER	79	IPWA $\pi N \rightarrow \pi N$

Baryon Particle Listings

 $\Delta(1620)$

• • • We do not use the following data for averages, fits, limits, etc. • • •

250 ± 60	THOMA	08	DPWA	Multichannel
141.0 ± 6.0	ARNDT	04	DPWA	$\pi N \rightarrow \pi N, \eta N$
202 ± 7	PENNER	02c	DPWA	Multichannel
143 ± 4.2	VRANA	00	DPWA	Multichannel
147 ± 8	ARNDT	96	IPWA	$\gamma N \rightarrow \pi N$
108	ARNDT	95	DPWA	$\pi N \rightarrow N\pi$
184	LI	93	IPWA	$\gamma N \rightarrow \pi N$
120	BARNHAM	80	IPWA	$\pi N \rightarrow N\pi\pi$
228.3 ± 18.0	¹ CHEW	80	BPWA	$\pi^+ p \rightarrow \pi^+ p$ (lower mass)
30.0 ± 6.4	¹ CHEW	80	BPWA	$\pi^+ p \rightarrow \pi^+ p$ (higher mass)
120	² LONGACRE	77	IPWA	$\pi N \rightarrow N\pi\pi$
150	³ LONGACRE	75	IPWA	$\pi N \rightarrow N\pi\pi$

 $\Delta(1620)$ POLE POSITION

REAL PART

VALUE (MeV)	DOCUMENT ID	TECN	COMMENT
1590 to 1610 (≈ 1600) OUR ESTIMATE			
1595	ARNDT	06	DPWA $\pi N \rightarrow \pi N, \eta N$
1608	⁴ HOEHLER	93	SPED $\pi N \rightarrow \pi N$
1600 ± 15	CUTKOSKY	80	IPWA $\pi N \rightarrow \pi N$
• • • We do not use the following data for averages, fits, limits, etc. • • •			
1615 ± 25	THOMA	08	DPWA Multichannel
1594	ARNDT	04	DPWA $\pi N \rightarrow \pi N, \eta N$
1607	VRANA	00	DPWA Multichannel
1585	ARNDT	95	DPWA $\pi N \rightarrow N\pi$
1587	ARNDT	91	DPWA $\pi N \rightarrow \pi N$ Soln SM90
1583 or 1583	⁵ LONGACRE	78	IPWA $\pi N \rightarrow N\pi\pi$
1575 or 1572	² LONGACRE	77	IPWA $\pi N \rightarrow N\pi\pi$

-2xIMAGINARY PART

VALUE (MeV)	DOCUMENT ID	TECN	COMMENT
115 to 120 (≈ 118) OUR ESTIMATE			
135	ARNDT	06	DPWA $\pi N \rightarrow \pi N, \eta N$
116	⁴ HOEHLER	93	SPED $\pi N \rightarrow \pi N$
120 ± 20	CUTKOSKY	80	IPWA $\pi N \rightarrow \pi N$
• • • We do not use the following data for averages, fits, limits, etc. • • •			
180 ± 35	THOMA	08	DPWA Multichannel
118	ARNDT	04	DPWA $\pi N \rightarrow \pi N, \eta N$
148	VRANA	00	DPWA Multichannel
104	ARNDT	95	DPWA $\pi N \rightarrow N\pi$
120	ARNDT	91	DPWA $\pi N \rightarrow \pi N$ Soln SM90
143 or 149	⁵ LONGACRE	78	IPWA $\pi N \rightarrow N\pi\pi$
119 or 128	² LONGACRE	77	IPWA $\pi N \rightarrow N\pi\pi$

 $\Delta(1620)$ ELASTIC POLE RESIDUEMODULUS $|r|$

VALUE (MeV)	DOCUMENT ID	TECN	COMMENT
15	ARNDT	06	DPWA $\pi N \rightarrow \pi N, \eta N$
19	HOEHLER	93	SPED $\pi N \rightarrow \pi N$
15 ± 2	CUTKOSKY	80	IPWA $\pi N \rightarrow \pi N$
• • • We do not use the following data for averages, fits, limits, etc. • • •			
17	ARNDT	04	DPWA $\pi N \rightarrow \pi N, \eta N$
14	ARNDT	95	DPWA $\pi N \rightarrow N\pi$
15	ARNDT	91	DPWA $\pi N \rightarrow \pi N$ Soln SM90

PHASE θ

VALUE (°)	DOCUMENT ID	TECN	COMMENT
- 92	ARNDT	06	DPWA $\pi N \rightarrow \pi N, \eta N$
- 95	HOEHLER	93	SPED $\pi N \rightarrow \pi N$
-110 ± 20	CUTKOSKY	80	IPWA $\pi N \rightarrow \pi N$
• • • We do not use the following data for averages, fits, limits, etc. • • •			
-104	ARNDT	04	DPWA $\pi N \rightarrow \pi N, \eta N$
-121	ARNDT	95	DPWA $\pi N \rightarrow N\pi$
-125	ARNDT	91	DPWA $\pi N \rightarrow \pi N$ Soln SM90

 $\Delta(1620)$ DECAY MODES

The following branching fractions are our estimates, not fits or averages.

Mode	Fraction (Γ_j/Γ)
Γ_1 $N\pi$	20–30 %
Γ_2 $N\pi\pi$	70–80 %
Γ_3 $\Delta\pi$	30–60 %
Γ_4 $\Delta(1232)\pi, D\text{-wave}$	
Γ_5 $N\rho$	7–25 %
Γ_6 $N\rho, S=1/2, S\text{-wave}$	
Γ_7 $N\rho, S=3/2, D\text{-wave}$	
Γ_8 $N(1440)\pi$	
Γ_9 $N\gamma$	0.004–0.044 %
Γ_{10} $N\gamma, \text{ helicity}=1/2$	0.004–0.044 %

 $\Delta(1620)$ BRANCHING RATIOS

$\Gamma(N\pi)/\Gamma_{\text{total}}$	DOCUMENT ID	TECN	COMMENT	Γ_1/Γ
0.2 to 0.3 OUR ESTIMATE				
0.315 ± 0.001	ARNDT	06	DPWA $\pi N \rightarrow \pi N, \eta N$	
0.09 ± 0.02	MANLEY	92	IPWA $\pi N \rightarrow \pi N \& N\pi\pi$	
0.25 ± 0.03	CUTKOSKY	80	IPWA $\pi N \rightarrow \pi N$	
0.35 ± 0.06	HOEHLER	79	IPWA $\pi N \rightarrow \pi N$	
• • • We do not use the following data for averages, fits, limits, etc. • • •				
0.22 ± 0.12	THOMA	08	DPWA Multichannel	
0.310 ± 0.004	ARNDT	04	DPWA $\pi N \rightarrow \pi N, \eta N$	
0.34 ± 0.01	PENNER	02c	DPWA Multichannel	
0.45 ± 0.05	VRANA	00	DPWA Multichannel	
0.29	ARNDT	95	DPWA $\pi N \rightarrow N\pi$	
0.60	¹ CHEW	80	BPWA $\pi^+ p \rightarrow \pi^+ p$ (lower mass)	
0.36	¹ CHEW	80	BPWA $\pi^+ p \rightarrow \pi^+ p$ (higher mass)	

Note: Signs of couplings from $\pi N \rightarrow N\pi\pi$ analyses were changed in the 1986 edition to agree with the baryon-first convention; the overall phase ambiguity is resolved by choosing a negative sign for the $\Delta(1620) S_{31}$ coupling to $\Delta(1232)\pi$.

$(\Gamma_1\Gamma_7)^{1/2}/\Gamma_{\text{total}}$ in $N\pi \rightarrow \Delta(1620) \rightarrow \Delta(1232)\pi, D\text{-wave}$	DOCUMENT ID	TECN	COMMENT	$(\Gamma_1\Gamma_4)^{1/2}/\Gamma$
-0.36 to -0.28 OUR ESTIMATE				
-0.24 ± 0.03	MANLEY	92	IPWA $\pi N \rightarrow \pi N \& N\pi\pi$	
-0.33 ± 0.06	BARNHAM	80	IPWA $\pi N \rightarrow N\pi\pi$	
-0.39	^{2,6} LONGACRE	77	IPWA $\pi N \rightarrow N\pi\pi$	
-0.40	³ LONGACRE	75	IPWA $\pi N \rightarrow N\pi\pi$	

$\Gamma(\Delta(1232)\pi, D\text{-wave})/\Gamma_{\text{total}}$	DOCUMENT ID	TECN	COMMENT	Γ_4/Γ
0.39 ± 0.02				
0.39 ± 0.02	VRANA	00	DPWA Multichannel	
• • • We do not use the following data for averages, fits, limits, etc. • • •				
0.48 ± 0.25	THOMA	08	DPWA Multichannel	

$(\Gamma_1\Gamma_7)^{1/2}/\Gamma_{\text{total}}$ in $N\pi \rightarrow \Delta(1620) \rightarrow N\rho, S=1/2, S\text{-wave}$	DOCUMENT ID	TECN	COMMENT	$(\Gamma_1\Gamma_6)^{1/2}/\Gamma$
+0.12 to +0.22 OUR ESTIMATE				
+0.15 ± 0.02	MANLEY	92	IPWA $\pi N \rightarrow \pi N \& N\pi\pi$	
+0.40 ± 0.10	BARNHAM	80	IPWA $\pi N \rightarrow N\pi\pi$	
+0.08	^{2,6} LONGACRE	77	IPWA $\pi N \rightarrow N\pi\pi$	
+0.28	³ LONGACRE	75	IPWA $\pi N \rightarrow N\pi\pi$	

$\Gamma(N\rho, S=1/2, S\text{-wave})/\Gamma_{\text{total}}$	DOCUMENT ID	TECN	COMMENT	Γ_6/Γ
0.14 ± 0.03				
0.14 ± 0.03	VRANA	00	DPWA Multichannel	

$(\Gamma_1\Gamma_7)^{1/2}/\Gamma_{\text{total}}$ in $N\pi \rightarrow \Delta(1620) \rightarrow N\rho, S=3/2, D\text{-wave}$	DOCUMENT ID	TECN	COMMENT	$(\Gamma_1\Gamma_7)^{1/2}/\Gamma$
-0.15 to -0.03 OUR ESTIMATE				
-0.06 ± 0.02	MANLEY	92	IPWA $\pi N \rightarrow \pi N \& N\pi\pi$	
-0.13	^{2,6} LONGACRE	77	IPWA $\pi N \rightarrow N\pi\pi$	

$\Gamma(N\rho, S=3/2, D\text{-wave})/\Gamma_{\text{total}}$	DOCUMENT ID	TECN	COMMENT	Γ_7/Γ
0.02 ± 0.01				
0.02 ± 0.01	VRANA	00	DPWA Multichannel	

$(\Gamma_1\Gamma_7)^{1/2}/\Gamma_{\text{total}}$ in $N\pi \rightarrow \Delta(1620) \rightarrow N(1440)\pi$	DOCUMENT ID	TECN	COMMENT	$(\Gamma_1\Gamma_8)^{1/2}/\Gamma$
0.11 ± 0.05				
0.11 ± 0.05	BARNHAM	80	IPWA $\pi N \rightarrow N\pi\pi$	

$\Gamma(N(1440)\pi)/\Gamma_{\text{total}}$	DOCUMENT ID	TECN	COMMENT	Γ_8/Γ
0.00 ± 0.01				
0.00 ± 0.01	VRANA	00	DPWA Multichannel	
• • • We do not use the following data for averages, fits, limits, etc. • • •				
0.19 ± 0.12	THOMA	08	DPWA Multichannel	

 $\Delta(1620)$ PHOTON DECAY AMPLITUDES

Papers on γN amplitudes predating 1981 may be found in our 2006 edition, Journal of Physics, G 33 1 (2006).

 $\Delta(1620) \rightarrow N\gamma, \text{ helicity}=1/2$ amplitude $A_{1/2}$

VALUE (GeV ^{-1/2})	DOCUMENT ID	TECN	COMMENT
+0.027 ± 0.011 OUR ESTIMATE			
0.050 ± 0.002	DUGGER	07	DPWA $\gamma N \rightarrow \pi N$
0.035 ± 0.020	ARNDT	96	IPWA $\gamma N \rightarrow \pi N$
0.035 ± 0.010	CRAWFORD	83	IPWA $\gamma N \rightarrow \pi N$
0.010 ± 0.015	AWAJI	81	DPWA $\gamma N \rightarrow \pi N$

See key on page 373

Baryon Particle Listings

$\Delta(1620)$, $\Delta(1700)$

••• We do not use the following data for averages, fits, limits, etc. •••

0.066	DRECHSEL	07	DPWA	$\gamma N \rightarrow \pi N$
-0.050	PENNER	02D	DPWA	Multichannel
0.042 ± 0.003	LI	93	IPWA	$\gamma N \rightarrow \pi N$
0.066	WADA	84	DPWA	Compton scattering

$\Delta(1620)$ FOOTNOTES

- ¹ CHEW 80 reports two S_{31} resonances at somewhat higher masses than other analyses. Problems with this analysis are discussed in section 2.1.11 of HOEHLER 83.
- ² LONGACRE 77 pole positions are from a search for poles in the unitarized T-matrix; the first (second) value uses, in addition to $\pi N \rightarrow N\pi\pi$ data, elastic amplitudes from a Saclay (CERN) partial-wave analysis. The other LONGACRE 77 values are from eyeball fits with Breit-Wigner circles to the T-matrix amplitudes.
- ³ From method II of LONGACRE 75: eyeball fits with Breit-Wigner circles to the T-matrix amplitudes.
- ⁴ See HOEHLER 93 for a detailed discussion of the evidence for and the pole parameters of N and Δ resonances as determined from Argand diagrams of πN elastic partial-wave amplitudes and from plots of the speeds with which the amplitudes traverse the diagrams.
- ⁵ LONGACRE 78 values are from a search for poles in the unitarized T-matrix. The first (second) value uses, in addition to $\pi N \rightarrow N\pi\pi$ data, elastic amplitudes from a Saclay (CERN) partial-wave analysis.
- ⁶ LONGACRE 77 considers this coupling to be well determined.

$\Delta(1620)$ REFERENCES

For early references, see Physics Letters **111B** 1 (1982).

THOMA	08	PL B659 87	U. Thoma <i>et al.</i>	(CB-ELSA Collab.)
DRECHSEL	07	EPJ A34 69	D. Drechsel, S.S. Kamalov, L. Tiator	(MAIN Z, JINR)
DUGGER	07	PR C76 025211	M. Dugger <i>et al.</i>	(Jefferson Lab CLAS Collab.)
ARNDT	06	PR C74 045205	R.A. Arndt <i>et al.</i>	(GWU)
PDG	06	JPG 33 1	W.-M. Yao <i>et al.</i>	(PDG Collab.)
ARNDT	04	PR C69 035213	R.A. Arndt <i>et al.</i>	(GWU, TRIU)
PENNER	02C	PR C66 055211	G. Penner, U. Mosel	(GIES)
PENNER	02D	PR C66 055212	G. Penner, U. Mosel	(GIES)
VRANA	00	PRPL 328 181	T.P. Vrana, S.A. Dytman, T.-S.H. Lee	(PITT+)
ARNDT	96	PR C53 430	R.A. Arndt, I.I. Strakovsky, R.L. Workman	(VPI)
ARNDT	95	PR C52 2120	R.A. Arndt <i>et al.</i>	(VPI, BRCO)
HOEHLER	93	πN Newsletter 9 1	G. Hohler	(KARL)
LI	93	PR C47 2759	Z.J. Li <i>et al.</i>	(VPI)
MANLEY	92	PR D45 4002	D.M. Manley, E.M. Saleski	(KENT) IJP
Also		PR D30 904	D.M. Manley <i>et al.</i>	(VPI)
ARNDT	91	PR D43 2131	R.A. Arndt <i>et al.</i>	(VPI, TELE) IJP
WADA	84	NP B247 313	Y. Wada <i>et al.</i>	(INUS)
CRAWFORD	83	NP B211 1	R.L. Crawford, W.T. Morton	(GLAS)
HOEHLER	83	Landolt-Boernstein 1/9B2	G. Hohler	(KARL)
PDG	82	PL 111B 1	M. Roos <i>et al.</i>	(HELS, CIT, CERN)
AWAJI	81	Bonn Conf. 352	N. Awaji, R. Kajikawa	(NAGO)
Also		NP B197 365	K. Fujii <i>et al.</i>	(NAGO)
BARNHAM	80	NP B168 243	K.W.J. Barnham <i>et al.</i>	(LOIC)
CHEW	80	Toronto Conf. 123	D.M. Chew	(LBL) IJP
CUTKOSKY	80	Toronto Conf. 19	R.E. Cutkosky <i>et al.</i>	(CMU, LBL) IJP
Also		PR D20 2839	R.E. Cutkosky <i>et al.</i>	(CMU, LBL) IJP
HOEHLER	79	PDAT 12-1	G. Hohler <i>et al.</i>	(KARL) IJP
Also		Toronto Conf. 3	R. Koch	(KARL) IJP
LONGACRE	78	PR D17 1795	R.S. Longacre <i>et al.</i>	(LBL, SLAC) IJP
LONGACRE	77	NP B122 493	R.S. Longacre, J. Dolbeau	(SACL) IJP
Also		NP B108 345	J. Dolbeau <i>et al.</i>	(SACL) IJP
LONGACRE	75	PL 55B 415	R.S. Longacre <i>et al.</i>	(LBL, SLAC) IJP

$\Delta(1700) D_{33}$

$$I(J^P) = \frac{3}{2}(\frac{3}{2}^-) \text{ Status: } ***$$

Most of the results published before 1975 were last included in our 1982 edition, Physics Letters **111B** 1 (1982). Some further obsolete results published before 1984 were last included in our 2006 edition, Journal of Physics, G **33** 1 (2006).

$\Delta(1700)$ BREIT-WIGNER MASS

VALUE (MeV)	DOCUMENT ID	TECN	COMMENT
1670 to 1750 (≈ 1700) OUR ESTIMATE			
1695.0 ± 1.3	ARNDT	06	DPWA $\pi N \rightarrow \pi N, \eta N$
1762 ± 44	MANLEY	92	IPWA $\pi N \rightarrow \pi N \& N\pi\pi$
1710 ± 30	CUTKOSKY	80	IPWA $\pi N \rightarrow \pi N$
1680 ± 70	HOEHLER	79	IPWA $\pi N \rightarrow \pi N$
••• We do not use the following data for averages, fits, limits, etc. •••			
1770 ± 40	THOMA	08	DPWA Multichannel
1687.9 ± 2.5	ARNDT	04	DPWA $\pi N \rightarrow \pi N, \eta N$
1678 ± 1	PENNER	02C	DPWA Multichannel
1732 ± 23	VRANA	00	DPWA Multichannel
1690 ± 15	ARNDT	96	IPWA $\gamma N \rightarrow \pi N$
1680	ARNDT	95	DPWA $\pi N \rightarrow N\pi$
1655	LI	93	IPWA $\gamma N \rightarrow \pi N$
1650	BARNHAM	80	IPWA $\pi N \rightarrow N\pi\pi$
1718.4 $^{+13.1}_{-13.0}$	¹ CHEW	80	BPWA $\pi^+ p \rightarrow \pi^+ p$
1600	² LONGACRE	77	IPWA $\pi N \rightarrow N\pi\pi$
1680	³ LONGACRE	75	IPWA $\pi N \rightarrow N\pi\pi$

$\Delta(1700)$ BREIT-WIGNER WIDTH

VALUE (MeV)	DOCUMENT ID	TECN	COMMENT
200 to 400 (≈ 300) OUR ESTIMATE			
375.5 ± 7.0	ARNDT	06	DPWA $\pi N \rightarrow \pi N, \eta N$
600 ± 250	MANLEY	92	IPWA $\pi N \rightarrow \pi N \& N\pi\pi$
280 ± 80	CUTKOSKY	80	IPWA $\pi N \rightarrow \pi N$
230 ± 80	HOEHLER	79	IPWA $\pi N \rightarrow \pi N$
••• We do not use the following data for averages, fits, limits, etc. •••			
630 ± 150	THOMA	08	DPWA Multichannel
364.8 ± 16.6	ARNDT	04	DPWA $\pi N \rightarrow \pi N, \eta N$
606 ± 15	PENNER	02C	DPWA Multichannel
119 ± 70	VRANA	00	DPWA Multichannel
285 ± 20	ARNDT	96	IPWA $\gamma N \rightarrow \pi N$
272	ARNDT	95	DPWA $\pi N \rightarrow N\pi$
348	LI	93	IPWA $\gamma N \rightarrow \pi N$
160	BARNHAM	80	IPWA $\pi N \rightarrow N\pi\pi$
193.3 ± 26.0	¹ CHEW	80	BPWA $\pi^+ p \rightarrow \pi^+ p$
200	² LONGACRE	77	IPWA $\pi N \rightarrow N\pi\pi$
240	³ LONGACRE	75	IPWA $\pi N \rightarrow N\pi\pi$

$\Delta(1700)$ POLE POSITION

REAL PART

VALUE (MeV)	DOCUMENT ID	TECN	COMMENT
1620 to 1680 (≈ 1650) OUR ESTIMATE			
1632	ARNDT	06	DPWA $\pi N \rightarrow \pi N, \eta N$
1651	⁴ HOEHLER	93	SPED $\pi N \rightarrow \pi N$
1675 ± 25	CUTKOSKY	80	IPWA $\pi N \rightarrow \pi N$
••• We do not use the following data for averages, fits, limits, etc. •••			
1610 ± 35	THOMA	08	DPWA Multichannel
1617	ARNDT	04	DPWA $\pi N \rightarrow \pi N, \eta N$
1726	VRANA	00	DPWA Multichannel
1655	ARNDT	95	DPWA $\pi N \rightarrow N\pi$
1646	ARNDT	91	DPWA $\pi N \rightarrow \pi N$ Soln SM90
1681 or 1672	⁵ LONGACRE	78	IPWA $\pi N \rightarrow N\pi\pi$
1600 or 1594	² LONGACRE	77	IPWA $\pi N \rightarrow N\pi\pi$

-2xIMAGINARY PART

VALUE (MeV)	DOCUMENT ID	TECN	COMMENT
160 to 240 (≈ 200) OUR ESTIMATE			
253	ARNDT	06	DPWA $\pi N \rightarrow \pi N, \eta N$
159	⁴ HOEHLER	93	SPED $\pi N \rightarrow \pi N$
220 ± 40	CUTKOSKY	80	IPWA $\pi N \rightarrow \pi N$
••• We do not use the following data for averages, fits, limits, etc. •••			
320 ± 60	THOMA	08	DPWA Multichannel
226	ARNDT	04	DPWA $\pi N \rightarrow \pi N, \eta N$
118	VRANA	00	DPWA Multichannel
242	ARNDT	95	DPWA $\pi N \rightarrow N\pi$
208	ARNDT	91	DPWA $\pi N \rightarrow \pi N$ Soln SM90
245 or 241	⁵ LONGACRE	78	IPWA $\pi N \rightarrow N\pi\pi$
208 or 201	² LONGACRE	77	IPWA $\pi N \rightarrow N\pi\pi$

$\Delta(1700)$ ELASTIC POLE RESIDUE

MODULUS |r|

VALUE (MeV)	DOCUMENT ID	TECN	COMMENT
18	ARNDT	06	DPWA $\pi N \rightarrow \pi N, \eta N$
10	HOEHLER	93	SPED $\pi N \rightarrow \pi N$
13 ± 3	CUTKOSKY	80	IPWA $\pi N \rightarrow \pi N$
••• We do not use the following data for averages, fits, limits, etc. •••			
16	ARNDT	04	DPWA $\pi N \rightarrow \pi N, \eta N$
16	ARNDT	95	DPWA $\pi N \rightarrow N\pi$
13	ARNDT	91	DPWA $\pi N \rightarrow \pi N$ Soln SM90

PHASE θ

VALUE (°)	DOCUMENT ID	TECN	COMMENT
-40	ARNDT	06	DPWA $\pi N \rightarrow \pi N, \eta N$
-20 ± 25	CUTKOSKY	80	IPWA $\pi N \rightarrow \pi N$
••• We do not use the following data for averages, fits, limits, etc. •••			
-47	ARNDT	04	DPWA $\pi N \rightarrow \pi N, \eta N$
-12	ARNDT	95	DPWA $\pi N \rightarrow N\pi$
-22	ARNDT	91	DPWA $\pi N \rightarrow \pi N$ Soln SM90

$\Delta(1700)$ DECAY MODES

The following branching fractions are our estimates, not fits or averages.

Mode	Fraction (Γ_i/Γ)
Γ_1 $N\pi$	10-20 %
Γ_2 ΣK	
Γ_3 $N\pi\pi$	80-90 %
Γ_4 $\Delta\pi$	30-60 %
Γ_5 $\Delta(1232)\pi$, S-wave	25-50 %
Γ_6 $\Delta(1232)\pi$, D-wave	1-7 %

Baryon Particle Listings

 $\Delta(1700), \Delta(1750)$

Γ_7	$N\rho$	30–55 %
Γ_8	$N\rho, S=1/2, D\text{-wave}$	
Γ_9	$N\rho, S=3/2, S\text{-wave}$	5–20 %
Γ_{10}	$N\rho, S=3/2, D\text{-wave}$	
Γ_{11}	$N\gamma$	0.12–0.26 %
Γ_{12}	$N\gamma, \text{helicity}=1/2$	0.08–0.16 %
Γ_{13}	$N\gamma, \text{helicity}=3/2$	0.025–0.12 %

 $\Delta(1700)$ BRANCHING RATIOS

$\Gamma(N\pi)/\Gamma_{\text{total}}$	DOCUMENT ID	TECN	COMMENT	Γ_1/Γ
0.10 to 0.20 OUR ESTIMATE				
0.156 ± 0.001	ARNDT	06	DPWA $\pi N \rightarrow \pi N, \eta N$	
0.14 ± 0.06	MANLEY	92	IPWA $\pi N \rightarrow \pi N \& N\pi\pi$	
0.12 ± 0.03	CUTKOSKY	80	IPWA $\pi N \rightarrow \pi N$	
0.20 ± 0.03	HOEHLER	79	IPWA $\pi N \rightarrow \pi N$	
• • • We do not use the following data for averages, fits, limits, etc. • • •				
0.15 ± 0.08	THOMA	08	DPWA Multichannel	
0.150 ± 0.001	ARNDT	04	DPWA $\pi N \rightarrow \pi N, \eta N$	
0.14 ± 0.01	PENNER	02c	DPWA Multichannel	
0.05 ± 0.01	VRANA	00	DPWA Multichannel	
0.16	ARNDT	95	DPWA $\pi N \rightarrow \pi N$	
0.16	¹ CHEW	80	BPWA $\pi^+ p \rightarrow \pi^+ p$	

Note: Signs of couplings from $\pi N \rightarrow N\pi\pi$ analyses were changed in the 1986 edition to agree with the baryon-first convention; the overall phase ambiguity is resolved by choosing a negative sign for the $\Delta(1620)$ S_{31} coupling to $\Delta(1232)\pi$.

$(\Gamma_1\Gamma_2)^{1/2}/\Gamma_{\text{total}}$ in $N\pi \rightarrow \Delta(1700) \rightarrow \Delta(1232)\pi, S\text{-wave}$	DOCUMENT ID	TECN	COMMENT	$(\Gamma_1\Gamma_5)^{1/2}/\Gamma$
+0.21 to +0.29 OUR ESTIMATE				
+0.32 ± 0.06	MANLEY	92	IPWA $\pi N \rightarrow \pi N \& N\pi\pi$	
+0.18 ± 0.04	^{2,6} BARNHAM	80	IPWA $\pi N \rightarrow N\pi\pi$	
+0.30	^{2,6} LONGACRE	77	IPWA $\pi N \rightarrow N\pi\pi$	
+0.24	³ LONGACRE	75	IPWA $\pi N \rightarrow N\pi\pi$	

$\Gamma(\Delta(1232)\pi, S\text{-wave})/\Gamma_{\text{total}}$	DOCUMENT ID	TECN	COMMENT	Γ_5/Γ
0.90 ± 0.02	VRANA	00	DPWA Multichannel	

$(\Gamma_1\Gamma_2)^{1/2}/\Gamma_{\text{total}}$ in $N\pi \rightarrow \Delta(1700) \rightarrow \Delta(1232)\pi, D\text{-wave}$	DOCUMENT ID	TECN	COMMENT	$(\Gamma_1\Gamma_6)^{1/2}/\Gamma$
+0.05 to +0.11 OUR ESTIMATE				
+0.08 ± 0.03	MANLEY	92	IPWA $\pi N \rightarrow \pi N \& N\pi\pi$	
0.14 ± 0.04	BARNHAM	80	IPWA $\pi N \rightarrow N\pi\pi$	
+0.05	^{2,6} LONGACRE	77	IPWA $\pi N \rightarrow N\pi\pi$	
+0.10	³ LONGACRE	75	IPWA $\pi N \rightarrow N\pi\pi$	

$\Gamma(\Delta(1232)\pi, D\text{-wave})/\Gamma_{\text{total}}$	DOCUMENT ID	TECN	COMMENT	Γ_6/Γ
0.04 ± 0.01	VRANA	00	DPWA Multichannel	

$(\Gamma_1\Gamma_2)^{1/2}/\Gamma_{\text{total}}$ in $N\pi \rightarrow \Delta(1700) \rightarrow N\rho, S=1/2, D\text{-wave}$	DOCUMENT ID	TECN	COMMENT	$(\Gamma_1\Gamma_8)^{1/2}/\Gamma$
+0.17 ± 0.05	BARNHAM	80	IPWA $\pi N \rightarrow N\pi\pi$	

$(\Gamma_1\Gamma_2)^{1/2}/\Gamma_{\text{total}}$ in $N\pi \rightarrow \Delta(1700) \rightarrow N\rho, S=3/2, S\text{-wave}$	DOCUMENT ID	TECN	COMMENT	$(\Gamma_1\Gamma_9)^{1/2}/\Gamma$
±0.11 to ±0.19 OUR ESTIMATE				
+0.10 ± 0.03	MANLEY	92	IPWA $\pi N \rightarrow \pi N \& N\pi\pi$	
+0.04	^{2,6} LONGACRE	77	IPWA $\pi N \rightarrow N\pi\pi$	
−0.30	³ LONGACRE	75	IPWA $\pi N \rightarrow N\pi\pi$	

$\Gamma(N\rho, S=3/2, S\text{-wave})/\Gamma_{\text{total}}$	DOCUMENT ID	TECN	COMMENT	Γ_9/Γ
0.01 ± 0.01	VRANA	00	DPWA Multichannel	

$(\Gamma_1\Gamma_2)^{1/2}/\Gamma_{\text{total}}$ in $N\pi \rightarrow \Delta(1700) \rightarrow N\rho, S=3/2, D\text{-wave}$	DOCUMENT ID	TECN	COMMENT	$(\Gamma_1\Gamma_{10})^{1/2}/\Gamma$
0.18 ± 0.07	BARNHAM	80	IPWA $\pi N \rightarrow N\pi\pi$	

 $\Delta(1700)$ PHOTON DECAY AMPLITUDES

Papers on γN amplitudes predating 1981 may be found in our 2006 edition, Journal of Physics, G **33** 1 (2006).

$\Delta(1700) \rightarrow N\gamma, \text{helicity}=1/2$ amplitude $A_{1/2}$	DOCUMENT ID	TECN	COMMENT
+0.104 ± 0.015 OUR ESTIMATE			
0.125 ± 0.003	DUGGER	07	DPWA $\gamma N \rightarrow \pi N$
0.090 ± 0.025	ARNDT	96	IPWA $\gamma N \rightarrow \pi N$
0.111 ± 0.017	CRAWFORD	83	IPWA $\gamma N \rightarrow \pi N$
0.089 ± 0.033	AWAJI	81	DPWA $\gamma N \rightarrow \pi N$

- • • We do not use the following data for averages, fits, limits, etc. • • •
- 0.226 DRECHSEL 07 DPWA $\gamma N \rightarrow \pi N$
- 0.096 PENNER 02d DPWA Multichannel
- 0.121 ± 0.004 LI 93 IPWA $\gamma N \rightarrow \pi N$

 $\Delta(1700) \rightarrow N\gamma, \text{helicity}=3/2$ amplitude $A_{3/2}$

VALUE (GeV ^{-1/2})	DOCUMENT ID	TECN	COMMENT								
+0.085 ± 0.022 OUR ESTIMATE											
0.105 ± 0.003	DUGGER	07	DPWA $\gamma N \rightarrow \pi N$								
0.097 ± 0.020	ARNDT	96	IPWA $\gamma N \rightarrow \pi N$								
0.107 ± 0.015	CRAWFORD	83	IPWA $\gamma N \rightarrow \pi N$								
0.060 ± 0.015	AWAJI	81	DPWA $\gamma N \rightarrow \pi N$								
0.210	DRECHSEL	07	DPWA $\gamma N \rightarrow \pi N$	0.154	PENNER	02d	DPWA Multichannel	0.115 ± 0.004	LI	93	IPWA $\gamma N \rightarrow \pi N$
0.210	DRECHSEL	07	DPWA $\gamma N \rightarrow \pi N$								
0.154	PENNER	02d	DPWA Multichannel								
0.115 ± 0.004	LI	93	IPWA $\gamma N \rightarrow \pi N$								

 $\Delta(1700)$ FOOTNOTES

- Problems with CHEW 80 are discussed in section 2.1.11 of HOEHLER 83.
- LONGACRE 77 pole positions are from a search for poles in the unitarized T-matrix; the first (second) value uses, in addition to $\pi N \rightarrow N\pi\pi$ data, elastic amplitudes from a Saclay (CERN) partial-wave analysis. The other LONGACRE 77 values are from eyeball fits with Breit-Wigner circles to the T-matrix amplitudes.
- From method II of LONGACRE 75: eyeball fits with Breit-Wigner circles to the T-matrix amplitudes.
- See HOEHLER 93 for a detailed discussion of the evidence for and the pole parameters of N and Δ resonances as determined from Argand diagrams of πN elastic partial-wave amplitudes and from plots of the speeds with which the amplitudes traverse the diagrams.
- LONGACRE 78 values are from a search for poles in the unitarized T-matrix. The first (second) value uses, in addition to $\pi N \rightarrow N\pi\pi$ data, elastic amplitudes from a Saclay (CERN) partial-wave analysis.
- LONGACRE 77 considers this coupling to be well determined.

 $\Delta(1700)$ REFERENCES

For early references, see Physics Letters **111B** 1 (1982).

THOMA 08	PL B659 87	U. Thoma et al.	(CB-ELSA Collab.)
DRECHSEL 07	EJ A34 69	D. Drechsel, S.S. Kamalov, L. Tiator	(MAINZ, JINR)
DUGGER 07	PR C76 025211	M. Dugger et al.	(Jefferson Lab CLAS Collab.)
ARNDT 06	PR C74 045205	R.A. Arndt et al.	(GWU)
PDG 06	JPG 33 1	W.-M. Yao et al.	(PDG Collab.)
ARNDT 04	PR C69 035213	R.A. Arndt et al.	(GWU, TRIU)
PENNER 02c	PR C66 055211	G. Penner, U. Mosel	(GIES)
PENNER 02d	PR C66 055212	G. Penner, U. Mosel	(GIES)
VRANA 00	PRPL 328 181	T.P. Vrana, S.A. Dytman, T.-S.H. Lee	(PITT+)
ARNDT 96	PR C53 430	R.A. Arndt, I.I. Strakovsky, R.L. Workman	(VPI)
ARNDT 95	PR C52 2120	R.A. Arndt et al.	(VPI, BRCO)
HOEHLER 93	πN Newsletter 9 1	G. Hohlner	(KARL)
LI 93	PR C47 2759	Z.J. Li et al.	(VPI)
MANLEY 92	PR D45 4002	D.M. Manley, E.M. Saleski	(KENT) IJP
Also	PR D30 904	D.M. Manley et al.	(VPI)
ARNDT 91	PR D43 2131	R.A. Arndt et al.	(VPI, TELE) IJP
CRAWFORD 83	NP B211 1	R.L. Crawford, W.T. Morton	(GLAS)
HOEHLER 83	Landolt-Boernstein 1/9B2	G. Hohlner	(KARL)
PDG 82	PL 111B 1	M. Roos et al.	(HELS, CIT, CERN)
AWAJI 81	Bonn Conf. 352	N. Awaji, R. Kajikawa	(NAGO)
Also	NP B197 365	K. Fujii et al.	(NAGO)
BARNHAM 80	NP B168 243	K.W.J. Barnham et al.	(LOIC)
CHEW 80	Toronto Conf. 123	D.M. Chew	(LBL) IJP
CUTKOSKY 80	Toronto Conf. 19	R.E. Cutkosky et al.	(CMU, LBL) IJP
Also	PR D20 2839	R.E. Cutkosky et al.	(CMU, LBL) IJP
HOEHLER 79	PDAT 12-1	G. Hohlner et al.	(KARL) IJP
Also	Toronto Conf. 3	R. Koch	(KARL) IJP
LONGACRE 78	PR D17 1795	R.S. Longacre et al.	(LBL, SLAC)
LONGACRE 77	NP B122 493	R.S. Longacre, J. Dolbeau	(SACL) IJP
Also	NP B108 365	J. Dolbeau et al.	(SACL) IJP
LONGACRE 75	PL 55B 415	R.S. Longacre et al.	(LBL, SLAC) IJP

 $\Delta(1750) P_{31}$

$$I(J^P) = \frac{3}{2}(\frac{1}{2}^+) \text{ Status: } *$$

OMITTED FROM SUMMARY TABLE

The latest GWU analysis (ARNDT 06) finds no evidence for this resonance.

 $\Delta(1750)$ BREIT-WIGNER MASS

VALUE (MeV)	DOCUMENT ID	TECN	COMMENT												
≈ 1750 OUR ESTIMATE															
1744 ± 36	MANLEY	92	IPWA $\pi N \rightarrow \pi N \& N\pi\pi$												
1712 ± 1	PENNER	02c	DPWA Multichannel	1721 ± 61	VRANA	00	DPWA Multichannel	1715.2 ± 21.0	¹ CHEW	80	BPWA $\pi^+ p \rightarrow \pi^+ p$	1778.4 ± 9.0	¹ CHEW	80	BPWA $\pi^+ p \rightarrow \pi^+ p$
1712 ± 1	PENNER	02c	DPWA Multichannel												
1721 ± 61	VRANA	00	DPWA Multichannel												
1715.2 ± 21.0	¹ CHEW	80	BPWA $\pi^+ p \rightarrow \pi^+ p$												
1778.4 ± 9.0	¹ CHEW	80	BPWA $\pi^+ p \rightarrow \pi^+ p$												

 $\Delta(1750)$ BREIT-WIGNER WIDTH

VALUE (MeV)	DOCUMENT ID	TECN	COMMENT												
300 ± 120	MANLEY	92	IPWA $\pi N \rightarrow \pi N \& N\pi\pi$												
643 ± 17	PENNER	02c	DPWA Multichannel	70 ± 50	VRANA	00	DPWA Multichannel	93.3 ± 55.0	¹ CHEW	80	BPWA $\pi^+ p \rightarrow \pi^+ p$	23.0 ± 29.0	¹ CHEW	80	BPWA $\pi^+ p \rightarrow \pi^+ p$
643 ± 17	PENNER	02c	DPWA Multichannel												
70 ± 50	VRANA	00	DPWA Multichannel												
93.3 ± 55.0	¹ CHEW	80	BPWA $\pi^+ p \rightarrow \pi^+ p$												
23.0 ± 29.0	¹ CHEW	80	BPWA $\pi^+ p \rightarrow \pi^+ p$												

$\Delta(1750)$ POLE POSITION

REAL PART

VALUE (MeV)	DOCUMENT ID	TECN	COMMENT
1748	² ARNDT	04	DPWA $\pi N \rightarrow \pi N, \eta N$
•••	We do not use the following data for averages, fits, limits, etc. •••		
1714	VRANA	00	DPWA Multichannel

–2xIMAGINARY PART

VALUE (MeV)	DOCUMENT ID	TECN	COMMENT
524	² ARNDT	04	DPWA $\pi N \rightarrow \pi N, \eta N$
•••	We do not use the following data for averages, fits, limits, etc. •••		
68	VRANA	00	DPWA Multichannel

$\Delta(1750)$ ELASTIC POLE RESIDUE

MODULUS $|r|$

VALUE (MeV)	DOCUMENT ID	TECN	COMMENT
48	² ARNDT	04	DPWA $\pi N \rightarrow \pi N, \eta N$

PHASE θ

VALUE (°)	DOCUMENT ID	TECN	COMMENT
158	² ARNDT	04	DPWA $\pi N \rightarrow \pi N, \eta N$

$\Delta(1750)$ DECAY MODES

Mode	Fraction (Γ_i/Γ)
Γ_1 $N\pi$	
Γ_2 $N\pi\pi$	
Γ_3 $N(1440)\pi$	
Γ_4 ΣK	

$\Delta(1750)$ BRANCHING RATIOS

$\Gamma(N\pi)/\Gamma_{total}$	VALUE	DOCUMENT ID	TECN	COMMENT	Γ_1/Γ
0.08±0.03	MANLEY	92	IPWA	$\pi N \rightarrow \pi N \& N\pi\pi$	
•••	We do not use the following data for averages, fits, limits, etc. •••				
0.01±0.01	PENNER	02c	DPWA	Multichannel	
0.06±0.09	VRANA	00	DPWA	Multichannel	
0.18	¹ CHEW	80	BPWA	$\pi^+ p \rightarrow \pi^+ p$	
0.20	¹ CHEW	80	BPWA	$\pi^+ p \rightarrow \pi^+ p$	

$(\Gamma_1\Gamma_2)^{1/2}/\Gamma_{total}$ in $N\pi \rightarrow \Delta(1700) \rightarrow N(1440)\pi$	VALUE	DOCUMENT ID	TECN	COMMENT	$(\Gamma_1\Gamma_3)^{1/2}/\Gamma$
+0.15±0.03	MANLEY	92	IPWA	$\pi N \rightarrow \pi N \& N\pi\pi$	

$\Gamma(N(1440)\pi)/\Gamma_{total}$	VALUE	DOCUMENT ID	TECN	COMMENT	Γ_3/Γ
0.83±0.01	VRANA	00	DPWA	Multichannel	

$\Gamma(\Sigma K)/\Gamma_{total}$	VALUE	DOCUMENT ID	TECN	COMMENT	Γ_4/Γ
0.001±0.001	PENNER	02c	DPWA	Multichannel	

$\Delta(1750)$ PHOTON DECAY AMPLITUDES

Papers on γN amplitudes predating 1981 may be found in our 2006 edition, Journal of Physics, G **33** 1 (2006).

$\Delta(1750) \rightarrow N\gamma$, helicity-1/2 amplitude $A_{1/2}$

VALUE (GeV ^{-1/2})	DOCUMENT ID	TECN	COMMENT
0.053	PENNER	02d	DPWA Multichannel

$\Delta(1750)$ FOOTNOTES

- ¹ CHEW 80 reports four resonances in the P_{31} wave — see also the $\Delta(1910)$. Problems with this analysis are discussed in section 2.1.11 of HOEHLER 83.
- ² ARNDT 04 gives no corresponding Breit-Wigner parameters for this state, because the mass so obtained is about 500 MeV higher than that suggested by the position of the pole.

$\Delta(1750)$ REFERENCES

ARNDT 06	PR C74 045205	R.A. Arndt et al.	(GWU)
PDG 06	JPG 33 1	W.-M. Yao et al.	(PDG Collab.)
ARNDT 04	PR C69 035213	R.A. Arndt et al.	(GWU, TRIU)
PENNER 02c	PR C66 055211	G. Penner, U. Mosel	(GIES)
PENNER 02d	PR C66 055212	G. Penner, U. Mosel	(GIES)
VRANA 00	PRPL 328 181	T.P. Vrana, S.A. Dytman et al., T.-S.H. Lee	(PITT+)
MANLEY 92	PR D45 4002	D.M. Manley, E.M. Salski	(KENT)
Also	PR D30 904	D.M. Manley et al.	(VPI)
HOEHLER 83	Landolt-Boernstein 1/9B2	G. Hohler	(KARLT)
CHEW 80	Toronto Conf. 123	D.M. Chew	(LBL)

$\Delta(1900) S_{31}$

$I(J^P) = \frac{3}{2}(\frac{1}{2}^-)$ Status: **

OMITTED FROM SUMMARY TABLE

Some obsolete results published before 1980 were last included in our 2006 edition, Journal of Physics, G **33** 1 (2006). Some further obsolete results published before 1984 were last included in our 2006 edition, Journal of Physics, G **33** 1 (2006).

The latest GWU analysis (ARNDT 06) finds no evidence for this resonance.

$\Delta(1900)$ BREIT-WIGNER MASS

VALUE (MeV)	DOCUMENT ID	TECN	COMMENT
1850 to 1950 (≈ 1900) OUR ESTIMATE			
1920 ± 24	MANLEY	92	IPWA $\pi N \rightarrow \pi N \& N\pi\pi$
1890 ± 50	CUTKOSKY	80	IPWA $\pi N \rightarrow \pi N$
1908 ± 30	HOEHLER	79	IPWA $\pi N \rightarrow \pi N$
•••	We do not use the following data for averages, fits, limits, etc. •••		
1802 ± 87	VRANA	00	DPWA Multichannel
1918.5 ± 23.0	CHEW	80	BPWA $\pi^+ p \rightarrow \pi^+ p$

$\Delta(1900)$ BREIT-WIGNER WIDTH

VALUE (MeV)	DOCUMENT ID	TECN	COMMENT
140 to 240 (≈ 200) OUR ESTIMATE			
263 ± 39	MANLEY	92	IPWA $\pi N \rightarrow \pi N \& N\pi\pi$
170 ± 50	CUTKOSKY	80	IPWA $\pi N \rightarrow \pi N$
140 ± 40	HOEHLER	79	IPWA $\pi N \rightarrow \pi N$
•••	We do not use the following data for averages, fits, limits, etc. •••		
48 ± 45	VRANA	00	DPWA Multichannel
93.5 ± 54.0	CHEW	80	BPWA $\pi^+ p \rightarrow \pi^+ p$

$\Delta(1900)$ POLE POSITION

REAL PART

VALUE (MeV)	DOCUMENT ID	TECN	COMMENT
1780	¹ HOEHLER	93	SPED $\pi N \rightarrow \pi N$
1870 ± 40	CUTKOSKY	80	IPWA $\pi N \rightarrow \pi N$
•••	We do not use the following data for averages, fits, limits, etc. •••		
1795	VRANA	00	DPWA Multichannel
not seen	ARNDT	91	DPWA $\pi N \rightarrow \pi N$ Soln SM90
2029 or 2025	² LONGACRE	78	IPWA $\pi N \rightarrow N\pi\pi$

–2xIMAGINARY PART

VALUE (MeV)	DOCUMENT ID	TECN	COMMENT
180 ± 50	CUTKOSKY	80	IPWA $\pi N \rightarrow \pi N$
•••	We do not use the following data for averages, fits, limits, etc. •••		
58	VRANA	00	DPWA Multichannel
not seen	ARNDT	91	DPWA $\pi N \rightarrow \pi N$ Soln SM90
164 or 163	² LONGACRE	78	IPWA $\pi N \rightarrow N\pi\pi$

$\Delta(1900)$ ELASTIC POLE RESIDUE

MODULUS $|r|$

VALUE (MeV)	DOCUMENT ID	TECN	COMMENT
10 ± 3	CUTKOSKY	80	IPWA $\pi N \rightarrow \pi N$

PHASE θ

VALUE (°)	DOCUMENT ID	TECN	COMMENT
+20 ± 40	CUTKOSKY	80	IPWA $\pi N \rightarrow \pi N$

$\Delta(1900)$ DECAY MODES

The following branching fractions are our estimates, not fits or averages.

Mode	Fraction (Γ_i/Γ)
Γ_1 $N\pi$	10–30 %
Γ_2 ΣK	
Γ_3 $N\pi\pi$	
Γ_4 $\Delta\pi$	
Γ_5 $\Delta(1232)\pi$, D-wave	
Γ_6 $N\rho$	
Γ_7 $N\rho$, S=1/2, S-wave	
Γ_8 $N\rho$, S=3/2, D-wave	
Γ_9 $N(1440)\pi$, S-wave	
Γ_{10} $N\gamma$, helicity=1/2	

Baryon Particle Listings

 $\Delta(1900)$, $\Delta(1905)$ $\Delta(1900)$ BRANCHING RATIOS

$\Gamma(N\pi)/\Gamma_{\text{total}}$	DOCUMENT ID	TECN	COMMENT	Γ_1/Γ
0.1 to 0.3 OUR ESTIMATE				
0.41±0.04	MANLEY	92	IPWA $\pi N \rightarrow \pi N$ & $N\pi\pi$	
0.10±0.03	CUTKOSKY	80	IPWA $\pi N \rightarrow \pi N$	
0.08±0.04	HOEHLER	79	IPWA $\pi N \rightarrow \pi N$	
• • • We do not use the following data for averages, fits, limits, etc. • • •				
0.33±0.10	VRANA	00	DPWA Multichannel	
0.28	CHEW	80	BPWA $\pi^+ p \rightarrow \pi^+ p$	

$(\Gamma_1\Gamma_2)^{1/2}/\Gamma_{\text{total}}$ in $N\pi \rightarrow \Delta(1900) \rightarrow \Sigma K$	DOCUMENT ID	TECN	COMMENT	$(\Gamma_1\Gamma_2)^{1/2}/\Gamma$
VALUE				
<0.03	CANDLIN	84	DPWA $\pi^+ p \rightarrow \Sigma^+ K^+$	

$(\Gamma_1\Gamma_2)^{1/2}/\Gamma_{\text{total}}$ in $N\pi \rightarrow \Delta(1900) \rightarrow \Delta(1232)\pi$, D-wave	DOCUMENT ID	TECN	COMMENT	$(\Gamma_1\Gamma_5)^{1/2}/\Gamma$
VALUE				
+0.25±0.07	MANLEY	92	IPWA $\pi N \rightarrow \pi N$ & $N\pi\pi$	

$\Gamma(\Delta(1232)\pi, D\text{-wave})/\Gamma_{\text{total}}$	DOCUMENT ID	TECN	COMMENT	Γ_5/Γ
VALUE				
0.28±0.01	VRANA	00	DPWA Multichannel	

$(\Gamma_1\Gamma_7)^{1/2}/\Gamma_{\text{total}}$ in $N\pi \rightarrow \Delta(1900) \rightarrow N\rho, S=1/2$, S-wave	DOCUMENT ID	TECN	COMMENT	$(\Gamma_1\Gamma_7)^{1/2}/\Gamma$
VALUE				
-0.14±0.11	MANLEY	92	IPWA $\pi N \rightarrow \pi N$ & $N\pi\pi$	

$\Gamma(N\rho, S=1/2, S\text{-wave})/\Gamma_{\text{total}}$	DOCUMENT ID	TECN	COMMENT	Γ_7/Γ
VALUE				
0.30±0.02	VRANA	00	DPWA Multichannel	

$(\Gamma_1\Gamma_8)^{1/2}/\Gamma_{\text{total}}$ in $N\pi \rightarrow \Delta(1900) \rightarrow N\rho, S=3/2$, D-wave	DOCUMENT ID	TECN	COMMENT	$(\Gamma_1\Gamma_8)^{1/2}/\Gamma$
VALUE				
-0.37±0.07	MANLEY	92	IPWA $\pi N \rightarrow \pi N$ & $N\pi\pi$	

$\Gamma(N\rho, S=3/2, D\text{-wave})/\Gamma_{\text{total}}$	DOCUMENT ID	TECN	COMMENT	Γ_8/Γ
VALUE				
0.05±0.01	VRANA	00	DPWA Multichannel	

$(\Gamma_1\Gamma_9)^{1/2}/\Gamma_{\text{total}}$ in $N\pi \rightarrow \Delta(1900) \rightarrow N(1440)\pi$, S-wave	DOCUMENT ID	TECN	COMMENT	$(\Gamma_1\Gamma_9)^{1/2}/\Gamma$
VALUE				
-0.16±0.11	MANLEY	92	IPWA $\pi N \rightarrow \pi N$ & $N\pi\pi$	

$\Gamma(N(1440)\pi, S\text{-wave})/\Gamma_{\text{total}}$	DOCUMENT ID	TECN	COMMENT	Γ_9/Γ
VALUE				
0.04±0.01	VRANA	00	DPWA Multichannel	

 $\Delta(1900)$ PHOTON DECAY AMPLITUDES

Papers on γN amplitudes predating 1981 may be found in our 2006 edition, Journal of Physics, G **33** 1 (2006).

 $\Delta(1900) \rightarrow N\gamma$, helicity-1/2 amplitude $A_{1/2}$

VALUE (GeV ^{-1/2})	DOCUMENT ID	TECN	COMMENT
-0.004±0.016	CRAWFORD	83	IPWA $\gamma N \rightarrow \pi N$
0.029±0.008	AWAJI	81	DPWA $\gamma N \rightarrow \pi N$

 $\Delta(1900)$ FOOTNOTES

- ¹ See HOEHLER 93 for a detailed discussion of the evidence for and the pole parameters of N and Δ resonances as determined from Argand diagrams of πN elastic partial-wave amplitudes and from plots of the speeds with which the amplitudes traverse the diagrams.
- ² LONGACRE 78 values are from a search for poles in the unitarized T-matrix. The first (second) value uses, in addition to $\pi N \rightarrow N\pi\pi$ data, elastic amplitudes from a Saclay (CERN) partial-wave analysis.

 $\Delta(1900)$ REFERENCES

For early references, see Physics Letters **111B** 1 (1982).

ARNDT	06	PR C74 045205	R.A. Arndt et al.	(GWU)
PDG	06	JPG 33 1	W.-M. Yao et al.	(PDG Collab.)
VRANA	00	PRPL 329 181	T.P. Vrana, S.A. Dytman, T.-S.H. Lee	(PITT+)
HOEHLER	93	πN Newsletter 9 1	G. Hoehler	(KARL)
MANLEY	92	PR D45 4002	D.M. Manley, E.M. Saleski	(KENT) IJP
Also		PR D30 904	D.M. Manley et al.	(VPI)
ARNDT	91	PR D43 2131	R.A. Arndt et al.	(VPI, TELE) IJP
CANDLIN	84	NP B238 477	D.J. Candlin et al.	(EDIN, RAL, LOWC)
CRAWFORD	83	NP B211 1	R.L. Crawford, W.T. Morton	(GLAS)
AWAJI	81	Bonn Conf. 352	N. Awaji, R. Kajikawa	(NAGO)
Also		NP B197 365	K. Fujii et al.	(NAGO)
CHEW	80	Toronto Conf. 123	D.M. Chew	(LBL) IJP
CUTKOSKY	80	Toronto Conf. 19	R.E. Cutkosky et al.	(CMU, LBL) IJP
Also		PR D20 2839	R.E. Cutkosky et al.	(CMU, LBL) IJP
HOEHLER	79	PDAT 12-1	G. Hoehler et al.	(KARLT) IJP
Also		Toronto Conf. 3	R. Koch	(KARLT) IJP
LONGACRE	78	PR D17 1795	R.S. Longacre et al.	(LBL, SLAC)

 $\Delta(1905) F_{35}$

$$I(J^P) = \frac{3}{2}(\frac{5}{2}^+) \text{ Status: } ***$$

Most of the results published before 1975 were last included in our 1982 edition, Physics Letters **111B** 1 (1982). Some further obsolete results published before 1984 were last included in our 2006 edition, Journal of Physics, G **33** 1 (2006).

 $\Delta(1905)$ BREIT-WIGNER MASS

VALUE (MeV)	DOCUMENT ID	TECN	COMMENT
1865 to 1915 (\approx 1890) OUR ESTIMATE			
1857.8±1.6	ARNDT	06	DPWA $\pi N \rightarrow \pi N, \eta N$
1881 ±18	MANLEY	92	IPWA $\pi N \rightarrow \pi N$ & $N\pi\pi$
1910 ±30	CUTKOSKY	80	IPWA $\pi N \rightarrow \pi N$
1905 ±20	HOEHLER	79	IPWA $\pi N \rightarrow \pi N$
• • • We do not use the following data for averages, fits, limits, etc. • • •			
1855.7±4.2	ARNDT	04	DPWA $\pi N \rightarrow \pi N, \eta N$
1873 ±77	VRANA	00	DPWA Multichannel
1895 ±8	ARNDT	96	IPWA $\gamma N \rightarrow \pi N$
1850	ARNDT	95	DPWA $\pi N \rightarrow N\pi$
1960 ±40	CANDLIN	84	DPWA $\pi^+ p \rightarrow \Sigma^+ K^+$
1787.0 ^{+6.0} _{-5.7}	CHEW	80	BPWA $\pi^+ p \rightarrow \pi^+ p$
1830	¹ LONGACRE	75	IPWA $\pi N \rightarrow N\pi\pi$

 $\Delta(1905)$ BREIT-WIGNER WIDTH

VALUE (MeV)	DOCUMENT ID	TECN	COMMENT
270 to 400 (\approx 330) OUR ESTIMATE			
320.6±8.6	ARNDT	06	DPWA $\pi N \rightarrow \pi N, \eta N$
327 ±51	MANLEY	92	IPWA $\pi N \rightarrow \pi N$ & $N\pi\pi$
400 ±100	CUTKOSKY	80	IPWA $\pi N \rightarrow \pi N$
260 ±20	HOEHLER	79	IPWA $\pi N \rightarrow \pi N$
• • • We do not use the following data for averages, fits, limits, etc. • • •			
334 ±22	ARNDT	04	DPWA $\pi N \rightarrow \pi N, \eta N$
461 ±111	VRANA	00	DPWA Multichannel
354 ±10	ARNDT	96	IPWA $\gamma N \rightarrow \pi N$
294	ARNDT	95	DPWA $\pi N \rightarrow N\pi$
270 ±40	CANDLIN	84	DPWA $\pi^+ p \rightarrow \Sigma^+ K^+$
66.0 ^{+24.0} _{-16.0}	CHEW	80	BPWA $\pi^+ p \rightarrow \pi^+ p$
220	¹ LONGACRE	75	IPWA $\pi N \rightarrow N\pi\pi$

 $\Delta(1905)$ POLE POSITION

REAL PART

VALUE (MeV)	DOCUMENT ID	TECN	COMMENT
1825 to 1835 (\approx 1830) OUR ESTIMATE			
1819	ARNDT	06	DPWA $\pi N \rightarrow \pi N, \eta N$
1829	² HOEHLER	93	SPED $\pi N \rightarrow \pi N$
1830±40	CUTKOSKY	80	IPWA $\pi N \rightarrow \pi N$
• • • We do not use the following data for averages, fits, limits, etc. • • •			
1825	ARNDT	04	DPWA $\pi N \rightarrow \pi N, \eta N$
1793	VRANA	00	DPWA Multichannel
1832	ARNDT	95	DPWA $\pi N \rightarrow N\pi$
1794	ARNDT	91	DPWA $\pi N \rightarrow \pi N$ Soln SM90
1813 or 1808	³ LONGACRE	78	IPWA $\pi N \rightarrow N\pi\pi$

-2xIMAGINARY PART

VALUE (MeV)	DOCUMENT ID	TECN	COMMENT
265 to 300 (\approx 280) OUR ESTIMATE			
247	ARNDT	06	DPWA $\pi N \rightarrow \pi N, \eta N$
303	² HOEHLER	93	SPED $\pi N \rightarrow \pi N$
280±60	CUTKOSKY	80	IPWA $\pi N \rightarrow \pi N$
• • • We do not use the following data for averages, fits, limits, etc. • • •			
270	ARNDT	04	DPWA $\pi N \rightarrow \pi N, \eta N$
302	VRANA	00	DPWA Multichannel
254	ARNDT	95	DPWA $\pi N \rightarrow N\pi$
230	ARNDT	91	DPWA $\pi N \rightarrow \pi N$ Soln SM90
193 or 187	³ LONGACRE	78	IPWA $\pi N \rightarrow N\pi\pi$

 $\Delta(1905)$ ELASTIC POLE RESIDUE

MODULUS $ r $	DOCUMENT ID	TECN	COMMENT
VALUE (MeV)			
15	ARNDT	06	DPWA $\pi N \rightarrow \pi N, \eta N$
25	HOEHLER	93	SPED $\pi N \rightarrow \pi N$
25±8	CUTKOSKY	80	IPWA $\pi N \rightarrow \pi N$
• • • We do not use the following data for averages, fits, limits, etc. • • •			
16	ARNDT	04	DPWA $\pi N \rightarrow \pi N, \eta N$
12	ARNDT	95	DPWA $\pi N \rightarrow N\pi$
14	ARNDT	91	DPWA $\pi N \rightarrow \pi N$ Soln SM90

PHASE θ

VALUE ($^\circ$)	DOCUMENT ID	TECN	COMMENT
-30	ARNDT 06	DPWA	$\pi N \rightarrow \pi N, \eta N$
-50 \pm 20	CUTKOSKY 80	IPWA	$\pi N \rightarrow \pi N$
• • • We do not use the following data for averages, fits, limits, etc. • • •			
-25	ARNDT 04	DPWA	$\pi N \rightarrow \pi N, \eta N$
-4	ARNDT 95	DPWA	$\pi N \rightarrow N\pi$
-40	ARNDT 91	DPWA	$\pi N \rightarrow \pi N$ Soln SM90

$\Delta(1905)$ DECAY MODES

The following branching fractions are our estimates, not fits or averages.

Mode	Fraction (Γ_i/Γ)
Γ_1 $N\pi$	0.09 to 0.15
Γ_2 ΣK	
Γ_3 $N\pi\pi$	85-95 %
Γ_4 $\Delta\pi$	<25 %
Γ_5 $\Delta(1232)\pi$, P-wave	
Γ_6 $\Delta(1232)\pi$, F-wave	
Γ_7 $N\rho$	>60 %
Γ_8 $N\rho$, S=3/2, P-wave	
Γ_9 $N\rho$, S=3/2, F-wave	
Γ_{10} $N\rho$, S=1/2, F-wave	
Γ_{11} $N\gamma$	0.01-0.03 %
Γ_{12} $N\gamma$, helicity=1/2	0.0-0.1 %
Γ_{13} $N\gamma$, helicity=3/2	0.004-0.03 %

$\Delta(1905)$ BRANCHING RATIOS

$\Gamma(N\pi)/\Gamma_{total}$	DOCUMENT ID	TECN	COMMENT	Γ_1/Γ
0.09 to 0.15 OUR ESTIMATE				
0.122 \pm 0.001	ARNDT 06	DPWA	$\pi N \rightarrow \pi N, \eta N$	
0.12 \pm 0.03	MANLEY 92	IPWA	$\pi N \rightarrow \pi N$ & $N\pi\pi$	
0.08 \pm 0.03	CUTKOSKY 80	IPWA	$\pi N \rightarrow \pi N$	
0.15 \pm 0.02	HOEHLER 79	IPWA	$\pi N \rightarrow \pi N$	
• • • We do not use the following data for averages, fits, limits, etc. • • •				
0.120 \pm 0.002	ARNDT 04	DPWA	$\pi N \rightarrow \pi N, \eta N$	
0.09 \pm 0.01	VRANA 00	DPWA	Multichannel	
0.12	ARNDT 95	DPWA	$\pi N \rightarrow N\pi$	
0.11	CHEW 80	BPWA	$\pi^+ p \rightarrow \pi^+ p$	

$(\Gamma_1\Gamma_2)^{1/2}/\Gamma_{total}$ in $N\pi \rightarrow \Delta(1905) \rightarrow \Sigma K$	DOCUMENT ID	TECN	COMMENT	$(\Gamma_1\Gamma_2)^{1/2}/\Gamma$
VALUE				
-0.015 \pm 0.003	CANDLIN 84	DPWA	$\pi^+ p \rightarrow \Sigma^+ K^+$	

Note: Signs of couplings from $\pi N \rightarrow N\pi\pi$ analyses were changed in the 1986 edition to agree with the baryon-first convention; the overall phase ambiguity is resolved by choosing a negative sign for the $\Delta(1620) S_{31}$ coupling to $\Delta(1232)\pi$.

$(\Gamma_1\Gamma_7)^{1/2}/\Gamma_{total}$ in $N\pi \rightarrow \Delta(1905) \rightarrow \Delta(1232)\pi$, P-wave	DOCUMENT ID	TECN	COMMENT	$(\Gamma_1\Gamma_7)^{1/2}/\Gamma$
VALUE				
-0.04 \pm 0.05	MANLEY 92	IPWA	$\pi N \rightarrow \pi N$ & $N\pi\pi$	

$\Gamma(\Delta(1232)\pi, P\text{-wave})/\Gamma_{total}$	DOCUMENT ID	TECN	COMMENT	Γ_5/Γ
VALUE				
0.23 \pm 0.01	VRANA 00	DPWA	Multichannel	

$(\Gamma_1\Gamma_7)^{1/2}/\Gamma_{total}$ in $N\pi \rightarrow \Delta(1905) \rightarrow \Delta(1232)\pi$, F-wave	DOCUMENT ID	TECN	COMMENT	$(\Gamma_1\Gamma_7)^{1/2}/\Gamma$
VALUE				
+0.02 \pm 0.03	MANLEY 92	IPWA	$\pi N \rightarrow \pi N$ & $N\pi\pi$	
+0.20	¹ LONGACRE 75	IPWA	$\pi N \rightarrow N\pi\pi$	

$\Gamma(\Delta(1232)\pi, F\text{-wave})/\Gamma_{total}$	DOCUMENT ID	TECN	COMMENT	Γ_6/Γ
VALUE				
0.44 \pm 0.01	VRANA 00	DPWA	Multichannel	

$(\Gamma_1\Gamma_8)^{1/2}/\Gamma_{total}$ in $N\pi \rightarrow \Delta(1905) \rightarrow N\rho$, S=3/2, P-wave	DOCUMENT ID	TECN	COMMENT	$(\Gamma_1\Gamma_8)^{1/2}/\Gamma$
VALUE				
+0.030 to +0.36 OUR ESTIMATE				
+0.33 \pm 0.03	MANLEY 92	IPWA	$\pi N \rightarrow \pi N$ & $N\pi\pi$	
+0.33	¹ LONGACRE 75	IPWA	$\pi N \rightarrow N\pi\pi$	

$\Gamma(N\rho, S=3/2, P\text{-wave})/\Gamma_{total}$	DOCUMENT ID	TECN	COMMENT	Γ_8/Γ
VALUE				
0.24 \pm 0.01	VRANA 00	DPWA	Multichannel	

$\Delta(1905)$ PHOTON DECAY AMPLITUDES

Papers on γN amplitudes predating 1981 may be found in our 2006 edition, Journal of Physics, G **33** 1 (2006).

$\Delta(1905) \rightarrow N\gamma$, helicity-1/2 amplitude $A_{1/2}$

VALUE ($\text{GeV}^{-1/2}$)	DOCUMENT ID	TECN	COMMENT
+0.026 \pm 0.011 OUR ESTIMATE			
0.021 \pm 0.004	DUGGER 07	DPWA	$\gamma N \rightarrow \pi N$
0.022 \pm 0.005	ARNDT 96	IPWA	$\gamma N \rightarrow \pi N$
0.021 \pm 0.010	CRAWFORD 83	IPWA	$\gamma N \rightarrow \pi N$
0.043 \pm 0.020	AWAJI 81	DPWA	$\gamma N \rightarrow \pi N$
• • • We do not use the following data for averages, fits, limits, etc. • • •			
0.018	DRECHSEL 07	DPWA	$\gamma N \rightarrow \pi N$
0.055 \pm 0.004	LI 93	IPWA	$\gamma N \rightarrow \pi N$

$\Delta(1905) \rightarrow N\gamma$, helicity-3/2 amplitude $A_{3/2}$

VALUE ($\text{GeV}^{-1/2}$)	DOCUMENT ID	TECN	COMMENT
-0.045 \pm 0.020 OUR ESTIMATE			
-0.046 \pm 0.005	DUGGER 07	DPWA	$\gamma N \rightarrow \pi N$
-0.045 \pm 0.005	ARNDT 96	IPWA	$\gamma N \rightarrow \pi N$
-0.056 \pm 0.028	CRAWFORD 83	IPWA	$\gamma N \rightarrow \pi N$
-0.025 \pm 0.023	AWAJI 81	DPWA	$\gamma N \rightarrow \pi N$
• • • We do not use the following data for averages, fits, limits, etc. • • •			
-0.028	DRECHSEL 07	DPWA	$\gamma N \rightarrow \pi N$
0.002 \pm 0.003	LI 93	IPWA	$\gamma N \rightarrow \pi N$

$\Delta(1905)$ FOOTNOTES

- From method II of LONGACRE 75: eyeball fits with Breit-Wigner circles to the T-matrix amplitudes.
- See HOEHLER 93 for a detailed discussion of the evidence for and the pole parameters of N and Δ resonances as determined from Argand diagrams of πN elastic partial-wave amplitudes and from plots of the speeds with which the amplitudes traverse the diagrams.
- LONGACRE 78 values are from a search for poles in the unitarized T-matrix. The first (second) value uses, in addition to $\pi N \rightarrow N\pi\pi$ data, elastic amplitudes from a Saclay (CERN) partial-wave analysis.

$\Delta(1905)$ REFERENCES

For early references, see Physics Letters **111B** 1 (1982).

DRECHSEL 07	EPJ A34 69	D. Drechsel, S.S. Kamalov, L. Tiator (MAINZ, JINR)
DUGGER 07	PR C76 025211	M. Dugger et al. (Jefferson Lab CLAS Collab.)
ARNDT 06	PR C74 045205	R.A. Arndt et al. (GWU)
PDG 06	JPG 33 1	W.-M. Yao et al. (PDG Collab.)
ARNDT 04	PR C69 035213	R.A. Arndt et al. (GWU, TRIU)
VRANA 00	PRPL 328 181	T.P. Vrana, S.A. Dytman, T.-S.H. Lee (PITT+)
ARNDT 96	PR C53 430	R.A. Arndt, I.I. Strakovsky, R.L. Workman (VPI)
ARNDT 95	PR C52 2120	R.A. Arndt et al. (VPI, BRCC)
HOEHLER 93	πN Newsletter 9 1	G. Hohlner (KARL)
LI 93	PR C47 2759	Z.J. Li et al. (VPI)
MANLEY 92	PR D45 4002	D.M. Manley, E.M. Saleski (KENT) IJP
Also	PR D30 304	D.M. Manley et al. (VPI)
ARNDT 91	PR D43 2131	R.A. Arndt et al. (VPI, TELE) IJP
CANDLIN 84	NP B238 477	D.J. Candlin et al. (EDIN, RAL, LOWC)
CRAWFORD 83	NP B211 1	R.L. Crawford, W.T. Morton (GLAS)
PDG 82	PL 111B 1	M. Roos et al. (HELS, CIT, CERN)
AWAJI 81	Bonn Conf. 352	N. Awaji, R. Kajikawa (NAGO)
Also	NP B197 365	K. Fujii et al. (NAGO)
CHEW 80	Toronto Conf. 123	D.M. Chew (LBL) IJP
CUTKOSKY 80	Toronto Conf. 19	R.E. Cutkosky et al. (CMU, LBL) IJP
Also	PR D20 2839	R.E. Cutkosky et al. (CMU, LBL) IJP
HOEHLER 79	PDAT 12-1	G. Hohlner et al. (KARL) IJP
Also	Toronto Conf. 3	R. Koch (KARL) IJP
LONGACRE 78	PR D17 1795	R.S. Longacre et al. (LBL, SLAC)
LONGACRE 75	PL 55B 415	R.S. Longacre et al. (LBL, SLAC) IJP

$\Delta(1910) P_{31}$

$I(J^P) = \frac{3}{2}(\frac{1}{2}^+)$ Status: * * * *

Most of the results published before 1975 were last included in our 1982 edition, Physics Letters **111B** 1 (1982). Some further obsolete results published before 1984 were last included in our 2006 edition, Journal of Physics, G **33** 1 (2006).

$\Delta(1910)$ BREIT-WIGNER MASS

VALUE (MeV)	DOCUMENT ID	TECN	COMMENT
1870 to 1920 (\approx 1910) OUR ESTIMATE			
2067.9 \pm 1.7	ARNDT 06	DPWA	$\pi N \rightarrow \pi N, \eta N$
1882 \pm 10	MANLEY 92	IPWA	$\pi N \rightarrow \pi N$ & $N\pi\pi$
1910 \pm 40	CUTKOSKY 80	IPWA	$\pi N \rightarrow \pi N$
1888 \pm 20	HOEHLER 79	IPWA	$\pi N \rightarrow \pi N$
• • • We do not use the following data for averages, fits, limits, etc. • • •			
1995 \pm 12	VRANA 00	DPWA	Multichannel
2152	ARNDT 95	DPWA	$\pi N \rightarrow N\pi$
1960.1 \pm 21.0	¹ CHEW 80	BPWA	$\pi^+ p \rightarrow \pi^+ p$
2121.4 $^{+13.0}_{-14.3}$	¹ CHEW 80	BPWA	$\pi^+ p \rightarrow \pi^+ p$
1790	² LONGACRE 77	IPWA	$\pi N \rightarrow N\pi\pi$

Baryon Particle Listings

 $\Delta(1910)$ $\Delta(1910)$ BREIT-WIGNER WIDTH

VALUE (MeV)	DOCUMENT ID	TECN	COMMENT
190 to 270 (≈ 250) OUR ESTIMATE			
543 \pm 10	ARNDT 06	DPWA	$\pi N \rightarrow \pi N, \eta N$
239 \pm 25	MANLEY 92	IPWA	$\pi N \rightarrow \pi N \& N\pi\pi$
225 \pm 50	CUTKOSKY 80	IPWA	$\pi N \rightarrow \pi N$
280 \pm 50	HOEHLER 79	IPWA	$\pi N \rightarrow \pi N$
••• We do not use the following data for averages, fits, limits, etc. •••			
713 \pm 465	VRANA 00	DPWA	Multichannel
760	ARNDT 95	DPWA	$\pi N \rightarrow N\pi$
152.9 \pm 60.0	¹ CHEW 80	BPWA	$\pi^+ p \rightarrow \pi^+ p$
172.2 \pm 37.0	¹ CHEW 80	BPWA	$\pi^+ p \rightarrow \pi^+ p$
170	² LONGACRE 77	IPWA	$\pi N \rightarrow N\pi\pi$

 $\Delta(1910)$ POLE POSITION

REAL PART

VALUE (MeV)	DOCUMENT ID	TECN	COMMENT
1830 to 1880 (≈ 1855) OUR ESTIMATE			
1771	ARNDT 06	DPWA	$\pi N \rightarrow \pi N, \eta N$
1874	³ HOEHLER 93	SPED	$\pi N \rightarrow \pi N$
1880 \pm 30	CUTKOSKY 80	IPWA	$\pi N \rightarrow \pi N$
••• We do not use the following data for averages, fits, limits, etc. •••			
1880	VRANA 00	DPWA	Multichannel
1810	ARNDT 95	DPWA	$\pi N \rightarrow N\pi$
1950	ARNDT 91	DPWA	$\pi N \rightarrow \pi N$ Soln SM90
1792 or 1801	² LONGACRE 77	IPWA	$\pi N \rightarrow N\pi\pi$

-2xIMAGINARY PART

VALUE (MeV)	DOCUMENT ID	TECN	COMMENT
200 to 500 (≈ 350) OUR ESTIMATE			
479	ARNDT 06	DPWA	$\pi N \rightarrow \pi N, \eta N$
283	³ HOEHLER 93	SPED	$\pi N \rightarrow \pi N$
200 \pm 40	CUTKOSKY 80	IPWA	$\pi N \rightarrow \pi N$
••• We do not use the following data for averages, fits, limits, etc. •••			
496	VRANA 00	DPWA	Multichannel
494	ARNDT 95	DPWA	$\pi N \rightarrow N\pi$
398	ARNDT 91	DPWA	$\pi N \rightarrow \pi N$ Soln SM90
172 or 165	² LONGACRE 77	IPWA	$\pi N \rightarrow N\pi\pi$

 $\Delta(1910)$ ELASTIC POLE RESIDUEMODULUS $|r|$

VALUE (MeV)	DOCUMENT ID	TECN	COMMENT
45	ARNDT 06	DPWA	$\pi N \rightarrow \pi N, \eta N$
38	HOEHLER 93	SPED	$\pi N \rightarrow \pi N$
20 \pm 4	CUTKOSKY 80	IPWA	$\pi N \rightarrow \pi N$
••• We do not use the following data for averages, fits, limits, etc. •••			
53	ARNDT 95	DPWA	$\pi N \rightarrow N\pi$
37	ARNDT 91	DPWA	$\pi N \rightarrow \pi N$ Soln SM90

PHASE θ

VALUE ($^\circ$)	DOCUMENT ID	TECN	COMMENT
+172	ARNDT 06	DPWA	$\pi N \rightarrow \pi N, \eta N$
- 90 \pm 30	CUTKOSKY 80	IPWA	$\pi N \rightarrow \pi N$
••• We do not use the following data for averages, fits, limits, etc. •••			
-176	ARNDT 95	DPWA	$\pi N \rightarrow N\pi$
- 91	ARNDT 91	DPWA	$\pi N \rightarrow \pi N$ Soln SM90

 $\Delta(1910)$ DECAY MODES

The following branching fractions are our estimates, not fits or averages.

Mode	Fraction (Γ_i/Γ)
Γ_1 $N\pi$	15-30 %
Γ_2 ΣK	
Γ_3 $N\pi\pi$	
Γ_4 $\Delta\pi$	
Γ_5 $\Delta(1232)\pi, P$ -wave	
Γ_6 $N\rho$	
Γ_7 $N\rho, S=3/2, P$ -wave	
Γ_8 $N(1440)\pi$	
Γ_9 $N(1440)\pi, P$ -wave	
Γ_{10} $N\gamma$	0.0-0.2 %
Γ_{11} $N\gamma, \text{helicity}=1/2$	0.0-0.2 %

 $\Delta(1910)$ BRANCHING RATIOS $\Gamma(N\pi)/\Gamma_{\text{total}}$

VALUE	DOCUMENT ID	TECN	COMMENT	Γ_1/Γ
0.15 to 0.3 OUR ESTIMATE				
0.239 \pm 0.001	ARNDT 06	DPWA	$\pi N \rightarrow \pi N, \eta N$	
0.23 \pm 0.08	MANLEY 92	IPWA	$\pi N \rightarrow \pi N \& N\pi\pi$	
0.19 \pm 0.03	CUTKOSKY 80	IPWA	$\pi N \rightarrow \pi N$	
0.24 \pm 0.06	HOEHLER 79	IPWA	$\pi N \rightarrow \pi N$	
••• We do not use the following data for averages, fits, limits, etc. •••				
0.29 \pm 0.21	VRANA 00	DPWA	Multichannel	
0.26	ARNDT 95	DPWA	$\pi N \rightarrow N\pi$	
0.17	¹ CHEW 80	BPWA	$\pi^+ p \rightarrow \pi^+ p$	
0.40	¹ CHEW 80	BPWA	$\pi^+ p \rightarrow \pi^+ p$	

 $(\Gamma_i\Gamma_f)^{1/2}/\Gamma_{\text{total}}$ in $N\pi \rightarrow \Delta(1910) \rightarrow \Sigma K$

VALUE	DOCUMENT ID	TECN	COMMENT	$(\Gamma_1\Gamma_2)^{1/2}/\Gamma$
< 0.03	CANDLIN 84	DPWA	$\pi^+ p \rightarrow \Sigma^+ K^+$	
••• We do not use the following data for averages, fits, limits, etc. •••				
-0.019	LIVANOS 80	DPWA	$\pi p \rightarrow \Sigma K$	

Note: Signs of couplings from $\pi N \rightarrow N\pi\pi$ analyses were changed in the 1986 edition to agree with the baryon-first convention; the overall phase ambiguity is resolved by choosing a negative sign for the $\Delta(1620)$ S_{31} coupling to $\Delta(1232)\pi$.

 $(\Gamma_i\Gamma_f)^{1/2}/\Gamma_{\text{total}}$ in $N\pi \rightarrow \Delta(1910) \rightarrow \Delta(1232)\pi, P$ -wave

VALUE	DOCUMENT ID	TECN	COMMENT	$(\Gamma_1\Gamma_5)^{1/2}/\Gamma$
+0.06	² LONGACRE 77	IPWA	$\pi N \rightarrow N\pi\pi$	

 $(\Gamma_i\Gamma_f)^{1/2}/\Gamma_{\text{total}}$ in $N\pi \rightarrow \Delta(1910) \rightarrow N\rho, S=3/2, P$ -wave

VALUE	DOCUMENT ID	TECN	COMMENT	$(\Gamma_1\Gamma_7)^{1/2}/\Gamma$
+0.29	² LONGACRE 77	IPWA	$\pi N \rightarrow N\pi\pi$	

 $(\Gamma_i\Gamma_f)^{1/2}/\Gamma_{\text{total}}$ in $N\pi \rightarrow \Delta(1910) \rightarrow N(1440)\pi, P$ -wave

VALUE	DOCUMENT ID	TECN	COMMENT	$(\Gamma_1\Gamma_9)^{1/2}/\Gamma$
-0.39 \pm 0.04	MANLEY 92	IPWA	$\pi N \rightarrow \pi N \& N\pi\pi$	

 $\Gamma(N(1440)\pi)/\Gamma_{\text{total}}$

VALUE	DOCUMENT ID	TECN	COMMENT	Γ_8/Γ
0.56 \pm 0.07	VRANA 00	DPWA	Multichannel	

 $\Delta(1910)$ PHOTON DECAY AMPLITUDES

Papers on γN amplitudes predating 1981 may be found in our 2006 edition, Journal of Physics, G **33** 1 (2006).

 $\Delta(1910) \rightarrow N\gamma, \text{helicity-1/2 amplitude } A_{1/2}$

VALUE ($\text{GeV}^{-1/2}$)	DOCUMENT ID	TECN	COMMENT
+0.003 \pm 0.014 OUR ESTIMATE			
-0.002 \pm 0.008	ARNDT 96	IPWA	$\gamma N \rightarrow \pi N$
0.014 \pm 0.030	CRAWFORD 83	IPWA	$\gamma N \rightarrow \pi N$
0.025 \pm 0.011	AWAJI 81	DPWA	$\gamma N \rightarrow \pi N$
••• We do not use the following data for averages, fits, limits, etc. •••			
0.032 \pm 0.003	LI 93	IPWA	$\gamma N \rightarrow \pi N$

 $\Delta(1910)$ FOOTNOTES

- ¹ CHEW 80 reports four resonances in the P_{31} wave — see also the $\Delta(1750)$. Problems with this analysis are discussed in section 2.I.11 of HOEHLER 83.
- ² LONGACRE 77 pole positions are from a search for poles in the unitarized T-matrix; the first (second) value uses, in addition to $\pi N \rightarrow N\pi\pi$ data, elastic amplitudes from a Saclay (CERN) partial-wave analysis. The other LONGACRE 77 values are from eyeball fits with Breit-Wigner circles to the T-matrix amplitudes.
- ³ See HOEHLER 93 for a detailed discussion of the evidence for and the pole parameters of N and Δ resonances as determined from Argand diagrams of πN elastic partial-wave amplitudes and from plots of the speeds with which the amplitudes traverse the diagrams.

 $\Delta(1910)$ REFERENCES

For early references, see Physics Letters **111B** 1 (1982).

ARNDT 06	PR C74 045205	R.A. Arndt <i>et al.</i>	(GWU)
PDG 06	JPG 33 1	W.-M. Yao <i>et al.</i>	(PDG Collab.)
VRANA 00	PRPL 328 181	T.P. Vrana, S.A. Dytman, T.-S.H. Lee	(PIIT+)
ARNDT 96	PR C53 430	R.A. Arndt, I.I. Strakovsky, R.L. Workman	(VPI)
ARNDT 95	PR C52 2120	R.A. Arndt <i>et al.</i>	(VPI, BRCC)
HOEHLER 93	πN Newsletter 9 1	G. Hohlner	(KARL)
LI 93	PR C47 2759	Z.J. Li <i>et al.</i>	(VPI)
MANLEY 92	PR D45 4002	D.M. Manley, E.M. Saleski	(KENT) IJP
Also	PR D30 904	D.M. Manley <i>et al.</i>	(VPI)
ARNDT 91	PR D43 2131	R.A. Arndt <i>et al.</i>	(VPI, TELE) IJP
CANDLIN 84	NP B238 477	D.J. Candlin <i>et al.</i>	(EDIN, RAL, LOWC)

See key on page 373

Baryon Particle Listings

$\Delta(1910)$, $\Delta(1920)$

CRAWFORD	83	NP B211 1	R.L. Crawford, W.T. Morton	(GLAS)
HOEHLER	83	Landolt-Boernstein 1/9B2	G. Hohler	(KARLT)
PDG	82	PL 111B 1	M. Roos <i>et al.</i>	(HELS, CIT, CERN)
AWAJI	81	Bonn Conf. 352	N. Awaji, R. Kajikawa	(NAGO)
Also		NP B197 365	K. Fujii <i>et al.</i>	(NAGO)
CHEW	80	Toronto Conf. 123	D.M. Chew	(LBL) IJP
CUTKOSKY	80	Toronto Conf. 19	R.E. Cutkosky <i>et al.</i>	(CMU, LBL) IJP
Also		PR D20 2839	P. Livanos <i>et al.</i>	(SACL) IJP
LIVANOS	80	Toronto Conf. 35	G. Hohler <i>et al.</i>	(KARLT) IJP
HOEHLER	79	PDAT 12-1	R. Koch	(KARLT) IJP
Also		Toronto Conf. 3	R.S. Longacre, J. Dolbeau	(SACL) IJP
LONGACRE	77	NP B122 493	J. Dolbeau <i>et al.</i>	(SACL) IJP
Also		NP B108 365		

 $\Delta(1920)$ DECAY MODES

The following branching fractions are our estimates, not fits or averages.

Mode	Fraction (Γ_i/Γ)
Γ_1 $N\pi$	5–20 %
Γ_2 ΣK	(2.10 ± 0.30) %
Γ_3 $N\pi\pi$	
Γ_4 $\Delta(1232)\pi$, P -wave	
Γ_5 $N(1440)\pi$, P -wave	
Γ_6 $N\gamma$, helicity=1/2	
Γ_7 $N\gamma$, helicity=3/2	

 $\Delta(1920)$ BRANCHING RATIOS

$\Gamma(N\pi)/\Gamma_{\text{total}}$				Γ_1/Γ
VALUE	DOCUMENT ID	TECN	COMMENT	
0.05 to 0.2 OUR ESTIMATE				
0.02 ± 0.02	MANLEY	92	IPWA $\pi N \rightarrow \pi N$ & $N\pi\pi$	
0.20 ± 0.05	CUTKOSKY	80	IPWA $\pi N \rightarrow \pi N$	
0.14 ± 0.04	HOEHLER	79	IPWA $\pi N \rightarrow \pi N$	
• • • We do not use the following data for averages, fits, limits, etc. • • •				
0.15 ± 0.01	PENNER	02c	DPWA Multichannel	
0.05 ± 0.04	VRANA	00	DPWA Multichannel	
0.24	¹ CHEW	80	BPWA $\pi^+ p \rightarrow \pi^+ p$	
0.18	¹ CHEW	80	BPWA $\pi^+ p \rightarrow \pi^+ p$	

$(\Gamma_1 \Gamma_7)^{1/2}/\Gamma_{\text{total}}$ in $N\pi \rightarrow \Delta(1920) \rightarrow \Sigma K$				$(\Gamma_1 \Gamma_2)^{1/2}/\Gamma$
VALUE	DOCUMENT ID	TECN	COMMENT	
−0.05 ± 0.015	CANDLIN	84	DPWA $\pi^+ p \rightarrow \Sigma^+ K^+$	
• • • We do not use the following data for averages, fits, limits, etc. • • •				
−0.049	LIVANOS	80	DPWA $\pi p \rightarrow \Sigma K$	

$\Gamma(\Sigma K)/\Gamma_{\text{total}}$				Γ_2/Γ
VALUE	DOCUMENT ID	TECN	COMMENT	
0.021 ± 0.003	PENNER	02c	DPWA Multichannel	

$(\Gamma_1 \Gamma_7)^{1/2}/\Gamma_{\text{total}}$ in $N\pi \rightarrow \Delta(1920) \rightarrow \Delta(1232)\pi$, P -wave				$(\Gamma_1 \Gamma_4)^{1/2}/\Gamma$
VALUE	DOCUMENT ID	TECN	COMMENT	
−0.13 ± 0.04	MANLEY	92	IPWA $\pi N \rightarrow \pi N$ & $N\pi\pi$	

$\Gamma(\Delta(1232)\pi, P\text{-wave})/\Gamma_{\text{total}}$				Γ_4/Γ
VALUE	DOCUMENT ID	TECN	COMMENT	
0.41 ± 0.03	VRANA	00	DPWA Multichannel	

$(\Gamma_1 \Gamma_7)^{1/2}/\Gamma_{\text{total}}$ in $N\pi \rightarrow \Delta(1920) \rightarrow N(1440)\pi$, P -wave				$(\Gamma_1 \Gamma_5)^{1/2}/\Gamma$
VALUE	DOCUMENT ID	TECN	COMMENT	
+0.06 ± 0.07	MANLEY	92	IPWA $\pi N \rightarrow \pi N$ & $N\pi\pi$	

$\Gamma(N(1440)\pi, P\text{-wave})/\Gamma_{\text{total}}$				Γ_5/Γ
VALUE	DOCUMENT ID	TECN	COMMENT	
0.53 ± 0.08	VRANA	00	DPWA Multichannel	

 $\Delta(1920)$ PHOTON DECAY AMPLITUDESPapers on γN amplitudes predating 1981 may be found in our 2006 edition, Journal of Physics, G **33** 1 (2006). **$\Delta(1920) \rightarrow N\gamma$, helicity-1/2 amplitude $A_{1/2}$**

VALUE ($\text{GeV}^{-1/2}$)	DOCUMENT ID	TECN	COMMENT
0.040 ± 0.014	AWAJI	81	DPWA $\gamma N \rightarrow \pi N$
• • • We do not use the following data for averages, fits, limits, etc. • • •			
−0.007	PENNER	02D	DPWA Multichannel

 $\Delta(1920) \rightarrow N\gamma$, helicity-3/2 amplitude $A_{3/2}$

VALUE ($\text{GeV}^{-1/2}$)	DOCUMENT ID	TECN	COMMENT
0.023 ± 0.017	AWAJI	81	DPWA $\gamma N \rightarrow \pi N$
• • • We do not use the following data for averages, fits, limits, etc. • • •			
−0.001	PENNER	02D	DPWA Multichannel

 $\Delta(1920)$ FOOTNOTES

- ¹ CHEW 80 reports two P_{33} resonances in this mass region. Problems with this analysis are discussed in section 2.1.11 of HOEHLER 83.
- ² See HOEHLER 93 for a detailed discussion of the evidence for and the pole parameters of N and Δ resonances as determined from Argand diagrams of πN elastic partial-wave amplitudes and from plots of the speeds with which the amplitudes traverse the diagrams.

 $\Delta(1920) P_{33}$

$$I(J^P) = \frac{3}{2}(\frac{3}{2}^+) \text{ Status: } ***$$

Most of the results published before 1975 were last included in our 1982 edition, Physics Letters **111B** 1 (1982). Some further obsolete results published before 1984 were last included in our 2006 edition, Journal of Physics, G **33** 1 (2006).

The latest GWU analysis (ARNDT 06) finds no evidence for this resonance.

 $\Delta(1920)$ BREIT-WIGNER MASS

VALUE (MeV)	DOCUMENT ID	TECN	COMMENT
1900 to 1970 (≈ 1920) OUR ESTIMATE			
2014 ± 16	MANLEY	92	IPWA $\pi N \rightarrow \pi N$ & $N\pi\pi$
1920 ± 80	CUTKOSKY	80	IPWA $\pi N \rightarrow \pi N$
1868 ± 10	HOEHLER	79	IPWA $\pi N \rightarrow \pi N$
• • • We do not use the following data for averages, fits, limits, etc. • • •			
2057 ± 1	PENNER	02c	DPWA Multichannel
1889 ± 100	VRANA	00	DPWA Multichannel
1840 ± 40	CANDLIN	84	DPWA $\pi^+ p \rightarrow \Sigma^+ K^+$
1955.0 ± 13.0	¹ CHEW	80	BPWA $\pi^+ p \rightarrow \pi^+ p$
2065.0 ± 13.6 12.9	¹ CHEW	80	BPWA $\pi^+ p \rightarrow \pi^+ p$

 $\Delta(1920)$ BREIT-WIGNER WIDTH

VALUE (MeV)	DOCUMENT ID	TECN	COMMENT
150 to 300 (≈ 200) OUR ESTIMATE			
152 ± 55	MANLEY	92	IPWA $\pi N \rightarrow \pi N$ & $N\pi\pi$
300 ± 100	CUTKOSKY	80	IPWA $\pi N \rightarrow \pi N$
220 ± 80	HOEHLER	79	IPWA $\pi N \rightarrow \pi N$
• • • We do not use the following data for averages, fits, limits, etc. • • •			
525 ± 32	PENNER	02c	DPWA Multichannel
123 ± 53	VRANA	00	DPWA Multichannel
200 ± 40	CANDLIN	84	DPWA $\pi^+ p \rightarrow \Sigma^+ K^+$
88.3 ± 35.0	¹ CHEW	80	BPWA $\pi^+ p \rightarrow \pi^+ p$
62.0 ± 44.0	¹ CHEW	80	BPWA $\pi^+ p \rightarrow \pi^+ p$

 $\Delta(1920)$ POLE POSITION**REAL PART**

VALUE (MeV)	DOCUMENT ID	TECN	COMMENT
1850 to 1950 (≈ 1900) OUR ESTIMATE			
1900	² HOEHLER	93	SPED $\pi N \rightarrow \pi N$
1900 ± 80	CUTKOSKY	80	IPWA $\pi N \rightarrow \pi N$
• • • We do not use the following data for averages, fits, limits, etc. • • •			
1880	VRANA	00	DPWA Multichannel
not seen	ARNDT	91	DPWA $\pi N \rightarrow \pi N$ Soln SM90

−2×IMAGINARY PART

VALUE (MeV)	DOCUMENT ID	TECN	COMMENT
200 to 400 (≈ 300) OUR ESTIMATE			
300 ± 100	CUTKOSKY	80	IPWA $\pi N \rightarrow \pi N$
• • • We do not use the following data for averages, fits, limits, etc. • • •			
120	VRANA	00	DPWA Multichannel
not seen	ARNDT	91	DPWA $\pi N \rightarrow \pi N$ Soln SM90

 $\Delta(1920)$ ELASTIC POLE RESIDUE**MODULUS $|r|$**

VALUE (MeV)	DOCUMENT ID	TECN	COMMENT
24 ± 4	CUTKOSKY	80	IPWA $\pi N \rightarrow \pi N$

PHASE θ

VALUE (°)	DOCUMENT ID	TECN	COMMENT
−15.0 ± 3.0	CUTKOSKY	80	IPWA $\pi N \rightarrow \pi N$

Baryon Particle Listings

 $\Delta(1920)$, $\Delta(1930)$ $\Delta(1920)$ REFERENCESFor early references, see Physics Letters **111B** 1 (1982).

ARNDT	06	PR C74 045205	R.A. Arndt et al.	(GWU)
PDG	06	JPG 33 1	W.-M. Yao et al.	(PDG Collab.)
PENNER	02C	PR C66 055211	G. Penner, U. Mosel	(GIES)
PENNER	02D	PR C66 055212	G. Penner, U. Mosel	(GIES)
VRANA	00	PRPL 328 181	T.P. Vrana, S.A. Dytman, T.-S.H. Lee	(PITT+)
HOEHLER	93	πN Newsletter 9 1	G. Höhler	(KARL)
MANLEY	92	PR D45 4002	D.M. Manley, E.M. Saleski	(KENT) IJP
Also		PR D30 904	D.M. Manley et al.	(VPI)
ARNDT	91	PR D43 2131	R.A. Arndt et al.	(VPI, TELE) IJP
CANDLIN	84	NP B238 477	D.J. Candlin et al.	(EDIN, RAL, LOWC)
HOEHLER	83	Landolt-Boernstein 1/9B2	G. Höhler	(KARLT)
PDG	82	PL 111B 1	M. Roos et al.	(HEL5, CIT, CERN)
AWAJI	81	Bonn Conf. 352	N. Awaji, R. Kajikawa	(NAGO)
Also		NP B197 365	K. Fujii et al.	(LBL) IJP
CHEW	80	Toronto Conf. 123	D.M. Chew	(LBL) IJP
CUTKOSKY	80	Toronto Conf. 19	R.E. Cutkosky et al.	(CMU, LBL) IJP
Also		PR D20 2839	R.E. Cutkosky et al.	(CMU, LBL) IJP
LIVANOS	80	Toronto Conf. 35	P. Livanos et al.	(SACL) IJP
HOEHLER	79	PDAT 12-1	G. Höhler et al.	(KARLT) IJP
Also		Toronto Conf. 3	R. Koch	(KARLT) IJP

 $\Delta(1930) D_{35}$

$$I(J^P) = \frac{3}{2}(\frac{5}{2}^-) \text{ Status: } ***$$

Most of the results published before 1975 were last included in our 1982 edition, Physics Letters **111B** 1 (1982). Some further obsolete results published before 1984 were last included in our 2006 edition, Journal of Physics, G **33** 1 (2006).

 $\Delta(1930)$ BREIT-WIGNER MASS

VALUE (MeV)	DOCUMENT ID	TECN	COMMENT
1900 to 2020 (\approx 1960) OUR ESTIMATE			
2233 \pm 53	ARNDT 06	DPWA	$\pi N \rightarrow \pi N, \eta N$
1956 \pm 22	MANLEY 92	IPWA	$\pi N \rightarrow \pi N \& N\pi\pi$
1940 \pm 30	CUTKOSKY 80	IPWA	$\pi N \rightarrow \pi N$
1901 \pm 15	HOEHLER 79	IPWA	$\pi N \rightarrow \pi N$
••• We do not use the following data for averages, fits, limits, etc. •••			
2046 \pm 45	ARNDT 04	DPWA	$\pi N \rightarrow \pi N, \eta N$
1932 \pm 100	VRANA 00	DPWA	Multichannel
1955 \pm 15	ARNDT 96	IPWA	$\gamma N \rightarrow \pi N$
2056	ARNDT 95	DPWA	$\pi N \rightarrow N\pi$
1963	LI 93	IPWA	$\gamma N \rightarrow \pi N$
1910.0 $^{+15.0}_{-17.2}$	CHEW 80	BPWA	$\pi^+ p \rightarrow \pi^+ p$

 $\Delta(1930)$ BREIT-WIGNER WIDTH

VALUE (MeV)	DOCUMENT ID	TECN	COMMENT
220 to 500 (\approx 360) OUR ESTIMATE			
773 \pm 187	ARNDT 06	DPWA	$\pi N \rightarrow \pi N, \eta N$
530 \pm 140	MANLEY 92	IPWA	$\pi N \rightarrow \pi N \& N\pi\pi$
320 \pm 60	CUTKOSKY 80	IPWA	$\pi N \rightarrow \pi N$
195 \pm 60	HOEHLER 79	IPWA	$\pi N \rightarrow \pi N$
••• We do not use the following data for averages, fits, limits, etc. •••			
402 \pm 198	ARNDT 04	DPWA	$\pi N \rightarrow \pi N, \eta N$
316 \pm 237	VRANA 00	DPWA	Multichannel
350 \pm 20	ARNDT 96	IPWA	$\gamma N \rightarrow \pi N$
590	ARNDT 95	DPWA	$\pi N \rightarrow N\pi$
260	LI 93	IPWA	$\gamma N \rightarrow \pi N$
74.8 $^{+17.0}_{-16.0}$	CHEW 80	BPWA	$\pi^+ p \rightarrow \pi^+ p$

 $\Delta(1930)$ POLE POSITION

REAL PART

VALUE (MeV)	DOCUMENT ID	TECN	COMMENT
1840 to 1960 (\approx 1900) OUR ESTIMATE			
2001	ARNDT 06	DPWA	$\pi N \rightarrow \pi N, \eta N$
1850	¹ HOEHLER 93	SPED	$\pi N \rightarrow \pi N$
1890 \pm 50	CUTKOSKY 80	IPWA	$\pi N \rightarrow \pi N$
••• We do not use the following data for averages, fits, limits, etc. •••			
1966	ARNDT 04	DPWA	$\pi N \rightarrow \pi N, \eta N$
1883	VRANA 00	DPWA	Multichannel
1913	ARNDT 95	DPWA	$\pi N \rightarrow N\pi$
2018	ARNDT 91	DPWA	$\pi N \rightarrow \pi N$ Soln SM90

-2xIMAGINARY PART

VALUE (MeV)	DOCUMENT ID	TECN	COMMENT
175 to 360 (\approx 270) OUR ESTIMATE			
387	ARNDT 06	DPWA	$\pi N \rightarrow \pi N, \eta N$
180	¹ HOEHLER 93	SPED	$\pi N \rightarrow \pi N$
260 \pm 60	CUTKOSKY 80	IPWA	$\pi N \rightarrow \pi N$
••• We do not use the following data for averages, fits, limits, etc. •••			
364	ARNDT 04	DPWA	$\pi N \rightarrow \pi N, \eta N$
250	VRANA 00	DPWA	Multichannel
246	ARNDT 95	DPWA	$\pi N \rightarrow N\pi$
398	ARNDT 91	DPWA	$\pi N \rightarrow \pi N$ Soln SM90

 $\Delta(1930)$ ELASTIC POLE RESIDUEMODULUS $|r|$

VALUE (MeV)	DOCUMENT ID	TECN	COMMENT
7	ARNDT 06	DPWA	$\pi N \rightarrow \pi N, \eta N$
20	HOEHLER 93	SPED	$\pi N \rightarrow \pi N$
18 \pm 6	CUTKOSKY 80	IPWA	$\pi N \rightarrow \pi N$
••• We do not use the following data for averages, fits, limits, etc. •••			
16	ARNDT 04	DPWA	$\pi N \rightarrow \pi N, \eta N$
8	ARNDT 95	DPWA	$\pi N \rightarrow N\pi$
15	ARNDT 91	DPWA	$\pi N \rightarrow \pi N$ Soln SM90

PHASE θ

VALUE ($^\circ$)	DOCUMENT ID	TECN	COMMENT
-12	ARNDT 06	DPWA	$\pi N \rightarrow \pi N, \eta N$
-20 \pm 40	CUTKOSKY 80	IPWA	$\pi N \rightarrow \pi N$
••• We do not use the following data for averages, fits, limits, etc. •••			
-21	ARNDT 04	DPWA	$\pi N \rightarrow \pi N, \eta N$
-47	ARNDT 95	DPWA	$\pi N \rightarrow N\pi$
-24	ARNDT 91	DPWA	$\pi N \rightarrow \pi N$ Soln SM90

 $\Delta(1930)$ DECAY MODES

The following branching fractions are our estimates, not fits or averages.

Mode	Fraction (Γ_i/Γ)
Γ_1 $N\pi$	0.05 to 0.15
Γ_2 ΣK	
Γ_3 $N\pi\pi$	
Γ_4 $N\gamma$	0.0-0.02 %
Γ_5 $N\gamma$, helicity=1/2	0.0-0.01 %
Γ_6 $N\gamma$, helicity=3/2	0.0-0.01 %

 $\Delta(1930)$ BRANCHING RATIOS

$\Gamma(N\pi)/\Gamma_{\text{total}}$	DOCUMENT ID	TECN	COMMENT	Γ_1/Γ
0.05 to 0.15 OUR ESTIMATE				
0.081 \pm 0.012	ARNDT 06	DPWA	$\pi N \rightarrow \pi N, \eta N$	
0.18 \pm 0.02	MANLEY 92	IPWA	$\pi N \rightarrow \pi N \& N\pi\pi$	
0.14 \pm 0.04	CUTKOSKY 80	IPWA	$\pi N \rightarrow \pi N$	
0.04 \pm 0.03	HOEHLER 79	IPWA	$\pi N \rightarrow \pi N$	
••• We do not use the following data for averages, fits, limits, etc. •••				
0.040 \pm 0.014	ARNDT 04	DPWA	$\pi N \rightarrow \pi N, \eta N$	
0.09 \pm 0.08	VRANA 00	DPWA	Multichannel	
0.11	ARNDT 95	DPWA	$\pi N \rightarrow N\pi$	
0.11	CHEW 80	BPWA	$\pi^+ p \rightarrow \pi^+ p$	

 $(\Gamma_1\Gamma_f)^{1/2}/\Gamma_{\text{total}}$ in $N\pi \rightarrow \Delta(1930) \rightarrow \Sigma K$

VALUE	DOCUMENT ID	TECN	COMMENT
< 0.015	CANDLIN 84	DPWA	$\pi^+ p \rightarrow \Sigma^+ K^+$
••• We do not use the following data for averages, fits, limits, etc. •••			
-0.031	LIVANOS 80	DPWA	$\pi p \rightarrow \Sigma K$

 $(\Gamma_1\Gamma_f)^{1/2}/\Gamma_{\text{total}}$ in $N\pi \rightarrow \Delta(1930) \rightarrow N\pi\pi$

VALUE	DOCUMENT ID	TECN	COMMENT
not seen	LONGACRE 75	IPWA	$\pi N \rightarrow N\pi\pi$

 $\Delta(1930)$ PHOTON DECAY AMPLITUDESPapers on γN amplitudes predating 1981 may be found in our 2006 edition, Journal of Physics, G **33** 1 (2006). $\Delta(1930) \rightarrow N\gamma$, helicity-1/2 amplitude $A_{1/2}$

VALUE ($\text{GeV}^{-1/2}$)	DOCUMENT ID	TECN	COMMENT
-0.009 \pm 0.028 OUR ESTIMATE			
-0.007 \pm 0.010	ARNDT 96	IPWA	$\gamma N \rightarrow \pi N$
0.009 \pm 0.009	AWAJI 81	DPWA	$\gamma N \rightarrow \pi N$
••• We do not use the following data for averages, fits, limits, etc. •••			
-0.019 \pm 0.001	LI 93	IPWA	$\gamma N \rightarrow \pi N$

 $\Delta(1930) \rightarrow N\gamma$, helicity-3/2 amplitude $A_{3/2}$

VALUE ($\text{GeV}^{-1/2}$)	DOCUMENT ID	TECN	COMMENT
-0.018 \pm 0.028 OUR ESTIMATE			
0.005 \pm 0.010	ARNDT 96	IPWA	$\gamma N \rightarrow \pi N$
-0.025 \pm 0.011	AWAJI 81	DPWA	$\gamma N \rightarrow \pi N$
••• We do not use the following data for averages, fits, limits, etc. •••			
0.009 \pm 0.001	LI 93	IPWA	$\gamma N \rightarrow \pi N$

See key on page 373

Baryon Particle Listings

$\Delta(1930)$, $\Delta(1940)$, $\Delta(1950)$

$\Delta(1930)$ FOOTNOTES

¹ See HOEHLER 93 for a detailed discussion of the evidence for and the pole parameters of N and Δ resonances as determined from Argand diagrams of πN elastic partial-wave amplitudes and from plots of the speeds with which the amplitudes traverse the diagrams.

$\Delta(1930)$ REFERENCES

For early references, see Physics Letters **111B** 1 (1982).

Author	Year	Document ID	TECN	COMMENT
ARNDT	06	PR C74 045205		R.A. Arndt et al. (GWU)
PDG	06	JPG 33 1		W.-M. Yao et al. (PDG Collab.)
ARNDT	04	PR C69 035213		R.A. Arndt et al. (GWU, TRIU)
VRANA	00	PRPL 328 181		T.P. Vrana, S.A. Dytman, T.-S.H. Lee (PITT+)
ARNDT	96	PR C53 430		R.A. Arndt, I.I. Strakovsky, R.L. Workman (VPI)
ARNDT	95	PR C52 2120		R.A. Arndt et al. (VPI, BRCO)
HOEHLER	93	πN Newsletter 9 1		G. Hohler (KARL)
LI	93	PR C47 2759		Z.J. Li et al. (VPI)
MANLEY	92	PR D45 4002		D.M. Manley, E.M. Saleski (KENT) IJP
Also		PR D30 904		D.M. Manley et al. (VPI)
ARNDT	91	PR D43 2131		R.A. Arndt et al. (VPI, TELE) IJP
CANDLIN	84	NP B238 477		D.J. Candlin et al. (EDIN, RAL, LOWC)
PDG	82	PL 111B 1		M. Roos et al. (HELS, CIT, CERN)
AWAJI	81	Bonn Conf. 352		N. Awaji, R. Kajikawa (NAGO)
Also		NP B197 365		K. Fujii et al. (NAGO)
CHEW	80	Toronto Conf. 123		D.M. Chew (LBL) IJP
CUTKOSKY	80	Toronto Conf. 19		R.E. Cutkosky et al. (CMU, LBL) IJP
Also		PR D20 2839		R.E. Cutkosky et al. (CMU, LBL) IJP
LIVANOS	80	Toronto Conf. 35		P. Livanos et al. (SACL)
HOEHLER	79	PDAT 12-1		G. Hohler et al. (KARL) IJP
Also		Toronto Conf. 3		R. Koch (KARL) IJP
LONGACRE	75	PL 55B 415		R.S. Longacre et al. (LBL, SLAC) IJP

$\Delta(1940)$ BRANCHING RATIOS

$\Gamma(N\pi)/\Gamma_{\text{total}}$	DOCUMENT ID	TECN	COMMENT	Γ_1/Γ
0.18 ± 0.12	MANLEY 92	IPWA	$\pi N \rightarrow \pi N \& N\pi\pi$	
0.18	CHEW 80	BPWA	$\pi^+ p \rightarrow \pi^+ p$	
0.05 ± 0.02	CUTKOSKY 80	IPWA	$\pi N \rightarrow \pi N$	

$(\Gamma_1\Gamma_2)^{1/2}/\Gamma_{\text{total}}$ in $N\pi \rightarrow \Delta(1940) \rightarrow \Sigma K$	DOCUMENT ID	TECN	COMMENT	$(\Gamma_1\Gamma_2)^{1/2}/\Gamma$
<0.015	CANDLIN 84	DPWA	$\pi^+ p \rightarrow \Sigma^+ K^+$	

$(\Gamma_1\Gamma_2)^{1/2}/\Gamma_{\text{total}}$ in $N\pi \rightarrow \Delta(1940) \rightarrow \Delta(1232)\pi, S\text{-wave}$	DOCUMENT ID	TECN	COMMENT	$(\Gamma_1\Gamma_2)^{1/2}/\Gamma$
+0.11 ± 0.10	MANLEY 92	IPWA	$\pi N \rightarrow \pi N \& N\pi\pi$	

$(\Gamma_1\Gamma_2)^{1/2}/\Gamma_{\text{total}}$ in $N\pi \rightarrow \Delta(1940) \rightarrow \Delta(1232)\pi, D\text{-wave}$	DOCUMENT ID	TECN	COMMENT	$(\Gamma_1\Gamma_2)^{1/2}/\Gamma$
+0.27 ± 0.16	MANLEY 92	IPWA	$\pi N \rightarrow \pi N \& N\pi\pi$	

$(\Gamma_1\Gamma_2)^{1/2}/\Gamma_{\text{total}}$ in $N\pi \rightarrow \Delta(1940) \rightarrow N\rho, S=3/2, S\text{-wave}$	DOCUMENT ID	TECN	COMMENT	$(\Gamma_1\Gamma_2)^{1/2}/\Gamma$
+0.25 ± 0.10	MANLEY 92	IPWA	$\pi N \rightarrow \pi N \& N\pi\pi$	

$\Delta(1940)$ PHOTON DECAY AMPLITUDES

Papers on γN amplitudes predating 1981 may be found in our 2006 edition, Journal of Physics, G **33** 1 (2006).

$\Delta(1940) \rightarrow N\gamma, \text{ helicity-1/2 amplitude } A_{1/2}$

VALUE (GeV ^{-1/2})	DOCUMENT ID	TECN	COMMENT
-0.036 ± 0.058	AWAJI 81	DPWA	$\gamma N \rightarrow \pi N$

$\Delta(1940) \rightarrow N\gamma, \text{ helicity-3/2 amplitude } A_{3/2}$

VALUE (GeV ^{-1/2})	DOCUMENT ID	TECN	COMMENT
-0.031 ± 0.012	AWAJI 81	DPWA	$\gamma N \rightarrow \pi N$

$\Delta(1940)$ FOOTNOTES

¹ LONGACRE 78 values are from a search for poles in the unitarized T-matrix. The first (second) value uses, in addition to $\pi N \rightarrow N\pi\pi$ data, elastic amplitudes from a Saclay (CERN) partial-wave analysis.

$\Delta(1940)$ REFERENCES

Author	Year	Document ID	TECN	COMMENT
ARNDT	06	PR C74 045205		R.A. Arndt et al. (GWU)
PDG	06	JPG 33 1		W.-M. Yao et al. (PDG Collab.)
MANLEY	92	PR D45 4002		D.M. Manley, E.M. Saleski (KENT) IJP
Also		PR D30 904		D.M. Manley et al. (VPI)
CANDLIN	84	NP B238 477		D.J. Candlin et al. (EDIN, RAL, LOWC)
AWAJI	81	Bonn Conf. 352		N. Awaji, R. Kajikawa (NAGO)
Also		NP B197 365		K. Fujii et al. (NAGO)
CHEW	80	Toronto Conf. 123		D.M. Chew (LBL) IJP
CUTKOSKY	80	Toronto Conf. 19		R.E. Cutkosky et al. (CMU, LBL) IJP
Also		PR D20 2839		R.E. Cutkosky et al. (CMU, LBL) IJP
LONGACRE	78	PR D17 1795		R.S. Longacre et al. (LBL, SLAC)

$\Delta(1950) F_{37}$

$$I(J^P) = \frac{3}{2}(\frac{7}{2}^+) \text{ Status: } ***$$

Most of the results published before 1975 were last included in our 1982 edition, Physics Letters **111B** 1 (1982). Some further obsolete results published before 1984 were last included in our 2006 edition, Journal of Physics, G **33** 1 (2006).

$\Delta(1950)$ BREIT-WIGNER MASS

VALUE (MeV)	DOCUMENT ID	TECN	COMMENT
1915 to 1950 (≈ 1930) OUR ESTIMATE			
1921.3 ± 0.2	ARNDT 06	DPWA	$\pi N \rightarrow \pi N, \eta N$
1945 ± 2	MANLEY 92	IPWA	$\pi N \rightarrow \pi N \& N\pi\pi$
1950 ± 15	CUTKOSKY 80	IPWA	$\pi N \rightarrow \pi N$
1913 ± 8	HOEHLER 79	IPWA	$\pi N \rightarrow \pi N$
• • • We do not use the following data for averages, fits, limits, etc. • • •			
1923.3 ± 0.5	ARNDT 04	DPWA	$\pi N \rightarrow \pi N, \eta N$
1936 ± 5	VRANA 00	DPWA	Multichannel
1947 ± 9	ARNDT 96	IPWA	$\gamma N \rightarrow \pi N$
1921	ARNDT 95	DPWA	$\pi N \rightarrow \pi N$
1940	LI 93	IPWA	$\gamma N \rightarrow \pi N$
1925 ± 20	CANDLIN 84	DPWA	$\pi^+ p \rightarrow \Sigma^+ K^+$
1855.0 ^{+11.0} _{-10.0}	CHEW 80	BPWA	$\pi^+ p \rightarrow \pi^+ p$
1925	¹ LONGACRE 75	IPWA	$\pi N \rightarrow N\pi\pi$

$\Delta(1940)$ BREIT-WIGNER MASS

VALUE (MeV)	DOCUMENT ID	TECN	COMMENT
≈ 1940 OUR ESTIMATE			
2057 ± 110	MANLEY 92	IPWA	$\pi N \rightarrow \pi N \& N\pi\pi$
2058.1 ± 34.5	CHEW 80	BPWA	$\pi^+ p \rightarrow \pi^+ p$
1940 ± 100	CUTKOSKY 80	IPWA	$\pi N \rightarrow \pi N$

$\Delta(1940)$ BREIT-WIGNER WIDTH

VALUE (MeV)	DOCUMENT ID	TECN	COMMENT
460 ± 320	MANLEY 92	IPWA	$\pi N \rightarrow \pi N \& N\pi\pi$
198.4 ± 45.5	CHEW 80	BPWA	$\pi^+ p \rightarrow \pi^+ p$
200 ± 100	CUTKOSKY 80	IPWA	$\pi N \rightarrow \pi N$

$\Delta(1940)$ POLE POSITION

REAL PART	DOCUMENT ID	TECN	COMMENT
1900 ± 100	CUTKOSKY 80	IPWA	$\pi N \rightarrow \pi N$
1915 or 1926	¹ LONGACRE 78	IPWA	$\pi N \rightarrow N\pi\pi$

-2xIMAGINARY PART

VALUE (MeV)	DOCUMENT ID	TECN	COMMENT
200 ± 60	CUTKOSKY 80	IPWA	$\pi N \rightarrow \pi N$
190 or 186	¹ LONGACRE 78	IPWA	$\pi N \rightarrow N\pi\pi$

$\Delta(1940)$ ELASTIC POLE RESIDUE

MODULUS |r|

VALUE (MeV)	DOCUMENT ID	TECN	COMMENT
8 ± 3	CUTKOSKY 80	IPWA	$\pi N \rightarrow \pi N$

PHASE θ

VALUE (°)	DOCUMENT ID	TECN	COMMENT
135 ± 45	CUTKOSKY 80	IPWA	$\pi N \rightarrow \pi N$

$\Delta(1940)$ DECAY MODES

Mode
Γ_1 $N\pi$
Γ_2 ΣK
Γ_3 $N\pi\pi$
Γ_4 $\Delta(1232)\pi, S\text{-wave}$
Γ_5 $\Delta(1232)\pi, D\text{-wave}$
Γ_6 $N\rho, S=3/2, S\text{-wave}$
Γ_7 $N\gamma, \text{ helicity}=1/2$
Γ_8 $N\gamma, \text{ helicity}=3/2$

Baryon Particle Listings

 $\Delta(1950)$ $\Delta(1950)$ BREIT-WIGNER WIDTH

VALUE (MeV)	DOCUMENT ID	TECN	COMMENT
235 to 335 (≈ 285) OUR ESTIMATE			
271.1 \pm 1.1	ARNDT 06	DPWA	$\pi N \rightarrow \pi N, \eta N$
300 \pm 7	MANLEY 92	IPWA	$\pi N \rightarrow \pi N \& N\pi\pi$
340 \pm 5.0	CUTKOSKY 80	IPWA	$\pi N \rightarrow \pi N$
224 \pm 10	HOEHLER 79	IPWA	$\pi N \rightarrow \pi N$
••• We do not use the following data for averages, fits, limits, etc. •••			
278.2 \pm 3.0	ARNDT 04	DPWA	$\pi N \rightarrow \pi N, \eta N$
245 \pm 12	VRANA 00	DPWA	Multichannel
302 \pm 9	ARNDT 96	IPWA	$\gamma N \rightarrow \pi N$
232	ARNDT 95	DPWA	$\pi N \rightarrow N\pi$
306	LI 93	IPWA	$\gamma N \rightarrow \pi N$
330 \pm 4.0	CANDLIN 84	DPWA	$\pi^+ p \rightarrow \Sigma^+ K^+$
157.2 $^{+22.0}_{-19.0}$	CHEW 80	BPWA	$\pi^+ p \rightarrow \pi^+ p$
240	¹ LONGACRE 75	IPWA	$\pi N \rightarrow N\pi\pi$

 $\Delta(1950)$ POLE POSITION

REAL PART

VALUE (MeV)	DOCUMENT ID	TECN	COMMENT
1870 to 1890 (≈ 1880) OUR ESTIMATE			
1876	ARNDT 06	DPWA	$\pi N \rightarrow \pi N, \eta N$
1878	² HOEHLER 93	ARGD	$\pi N \rightarrow \pi N$
1890 \pm 15	CUTKOSKY 80	IPWA	$\pi N \rightarrow \pi N$
••• We do not use the following data for averages, fits, limits, etc. •••			
1874	ARNDT 04	DPWA	$\pi N \rightarrow \pi N, \eta N$
1910	VRANA 00	DPWA	Multichannel
1880	ARNDT 95	DPWA	$\pi N \rightarrow N\pi$
1884	ARNDT 91	DPWA	$\pi N \rightarrow \pi N$ Soln SM90
1924 or 1924	³ LONGACRE 78	IPWA	$\pi N \rightarrow N\pi\pi$

-2xIMAGINARY PART

VALUE (MeV)	DOCUMENT ID	TECN	COMMENT
220 to 260 (≈ 240) OUR ESTIMATE			
227	ARNDT 06	DPWA	$\pi N \rightarrow \pi N, \eta N$
230	² HOEHLER 93	ARGD	$\pi N \rightarrow \pi N$
260 \pm 4.0	CUTKOSKY 80	IPWA	$\pi N \rightarrow \pi N$
••• We do not use the following data for averages, fits, limits, etc. •••			
236	ARNDT 04	DPWA	$\pi N \rightarrow \pi N, \eta N$
230	VRANA 00	DPWA	Multichannel
236	ARNDT 95	DPWA	$\pi N \rightarrow N\pi$
238	ARNDT 91	DPWA	$\pi N \rightarrow \pi N$ Soln SM90
258 or 258	³ LONGACRE 78	IPWA	$\pi N \rightarrow N\pi\pi$

 $\Delta(1950)$ ELASTIC POLE RESIDUEMODULUS $|r|$

VALUE (MeV)	DOCUMENT ID	TECN	COMMENT
53	ARNDT 06	DPWA	$\pi N \rightarrow \pi N, \eta N$
47	HOEHLER 93	ARGD	$\pi N \rightarrow \pi N$
50 \pm 7	CUTKOSKY 80	IPWA	$\pi N \rightarrow \pi N$
••• We do not use the following data for averages, fits, limits, etc. •••			
57	ARNDT 04	DPWA	$\pi N \rightarrow \pi N, \eta N$
54	ARNDT 95	DPWA	$\pi N \rightarrow N\pi$
61	ARNDT 91	DPWA	$\pi N \rightarrow \pi N$ Soln SM90

PHASE θ

VALUE ($^\circ$)	DOCUMENT ID	TECN	COMMENT
-31	ARNDT 06	DPWA	$\pi N \rightarrow \pi N, \eta N$
-32	HOEHLER 93	ARGD	$\pi N \rightarrow \pi N$
-33 \pm 8	CUTKOSKY 80	IPWA	$\pi N \rightarrow \pi N$
••• We do not use the following data for averages, fits, limits, etc. •••			
-34	ARNDT 04	DPWA	$\pi N \rightarrow \pi N, \eta N$
-17	ARNDT 95	DPWA	$\pi N \rightarrow N\pi$
-23	ARNDT 91	DPWA	$\pi N \rightarrow \pi N$ Soln SM90

 $\Delta(1950)$ DECAY MODES

The following branching fractions are our estimates, not fits or averages.

Mode	Fraction (Γ_i/Γ)
Γ_1 $N\pi$	0.35 to 0.45
Γ_2 ΣK	
Γ_3 $N\pi\pi$	
Γ_4 $\Delta\pi$	20-30 %
Γ_5 $\Delta(1232)\pi$, F-wave	
Γ_6 $\Delta(1232)\pi$, H-wave	
Γ_7 $N\rho$	<10 %
Γ_8 $N\rho$, $S=1/2$, F-wave	
Γ_9 $N\rho$, $S=3/2$, F-wave	
Γ_{10} $N\gamma$	0.08-0.13 %
Γ_{11} $N\gamma$, helicity=1/2	0.03-0.055 %
Γ_{12} $N\gamma$, helicity=3/2	0.05-0.075 %

 $\Delta(1950)$ BRANCHING RATIOS $\Gamma(N\pi)/\Gamma_{\text{total}}$

VALUE	DOCUMENT ID	TECN	COMMENT	Γ_1/Γ
0.35 to 0.45 OUR ESTIMATE				
0.471 \pm 0.001	ARNDT 06	DPWA	$\pi N \rightarrow \pi N, \eta N$	
0.38 \pm 0.01	MANLEY 92	IPWA	$\pi N \rightarrow \pi N \& N\pi\pi$	
0.39 \pm 0.04	CUTKOSKY 80	IPWA	$\pi N \rightarrow \pi N$	
0.38 \pm 0.02	HOEHLER 79	IPWA	$\pi N \rightarrow \pi N$	
••• We do not use the following data for averages, fits, limits, etc. •••				
0.480 \pm 0.002	ARNDT 04	DPWA	$\pi N \rightarrow \pi N, \eta N$	
0.44 \pm 0.01	VRANA 00	DPWA	Multichannel	
0.49	ARNDT 95	DPWA	$\pi N \rightarrow N\pi$	
0.44	CHEW 80	BPWA	$\pi^+ p \rightarrow \pi^+ p$	

 $(\Gamma_i\Gamma_f)^{1/2}/\Gamma_{\text{total}}$ in $N\pi \rightarrow \Delta(1950) \rightarrow \Sigma K$

VALUE	DOCUMENT ID	TECN	COMMENT	$(\Gamma_1\Gamma_2)^{1/2}/\Gamma$
-0.053 \pm 0.005	CANDLIN 84	DPWA	$\pi^+ p \rightarrow \Sigma^+ K^+$	

Note: Signs of couplings from $\pi N \rightarrow N\pi\pi$ analyses were changed in the 1986 edition to agree with the baryon-first convention; the overall phase ambiguity is resolved by choosing a negative sign for the $\Delta(1620) S_{31}$ coupling to $\Delta(1232)\pi$.

 $(\Gamma_i\Gamma_f)^{1/2}/\Gamma_{\text{total}}$ in $N\pi \rightarrow \Delta(1950) \rightarrow \Delta(1232)\pi$, F-wave

VALUE	DOCUMENT ID	TECN	COMMENT	$(\Gamma_1\Gamma_5)^{1/2}/\Gamma$
+0.28 to +0.32 OUR ESTIMATE				
+0.27 \pm 0.02	MANLEY 92	IPWA	$\pi N \rightarrow \pi N \& N\pi\pi$	
+0.32	¹ LONGACRE 75	IPWA	$\pi N \rightarrow N\pi\pi$	

 $\Gamma(\Delta(1232)\pi, F\text{-wave})/\Gamma_{\text{total}}$

VALUE	DOCUMENT ID	TECN	COMMENT	Γ_5/Γ
0.36 \pm 0.01	VRANA 00	DPWA	Multichannel	

 $(\Gamma_i\Gamma_f)^{1/2}/\Gamma_{\text{total}}$ in $N\pi \rightarrow \Delta(1950) \rightarrow N\rho$, $S=3/2$, F-wave

VALUE	DOCUMENT ID	TECN	COMMENT	$(\Gamma_1\Gamma_9)^{1/2}/\Gamma$
+0.24	¹ LONGACRE 75	IPWA	$\pi N \rightarrow N\pi\pi$	

 $\Delta(1950)$ PHOTON DECAY AMPLITUDES

Papers on γN amplitudes predating 1981 may be found in our 2006 edition, Journal of Physics, G **33** 1 (2006).

 $\Delta(1950) \rightarrow N\gamma$, helicity-1/2 amplitude $A_{1/2}$

VALUE ($\text{GeV}^{-1/2}$)	DOCUMENT ID	TECN	COMMENT
-0.076 \pm 0.012 OUR ESTIMATE			
-0.079 \pm 0.006	ARNDT 96	IPWA	$\gamma N \rightarrow \pi N$
-0.068 \pm 0.007	AWAJI 81	DPWA	$\gamma N \rightarrow \pi N$
••• We do not use the following data for averages, fits, limits, etc. •••			
-0.094	DRECHSEL 07	DPWA	$\gamma N \rightarrow \pi N$
-0.102 \pm 0.003	LI 93	IPWA	$\gamma N \rightarrow \pi N$

 $\Delta(1950) \rightarrow N\gamma$, helicity-3/2 amplitude $A_{3/2}$

VALUE ($\text{GeV}^{-1/2}$)	DOCUMENT ID	TECN	COMMENT
-0.097 \pm 0.010 OUR ESTIMATE			
-0.103 \pm 0.006	ARNDT 96	IPWA	$\gamma N \rightarrow \pi N$
-0.094 \pm 0.016	AWAJI 81	DPWA	$\gamma N \rightarrow \pi N$
••• We do not use the following data for averages, fits, limits, etc. •••			
-0.121	DRECHSEL 07	DPWA	$\gamma N \rightarrow \pi N$
-0.115 \pm 0.003	LI 93	IPWA	$\gamma N \rightarrow \pi N$

 $\Delta(1950)$ FOOTNOTES

¹ From method II of LONGACRE 75: eyeball fits with Breit-Wigner circles to the T-matrix amplitudes.

² See HOEHLER 93 for a detailed discussion of the evidence for and the pole parameters of N and Δ resonances as determined from Argand diagrams of πN elastic partial-wave amplitudes and from plots of the speeds with which the amplitudes traverse the diagrams.

³ LONGACRE 78 values are from a search for poles in the unitarized T-matrix. The first (second) value uses, in addition to $\pi N \rightarrow N\pi\pi$ data, elastic amplitudes from a Saclay (CERN) partial-wave analysis.

 $\Delta(1950)$ REFERENCES

DRECHSEL 07	EPJ A34 69	D. Drechsel, S.S. Kamalov, L. Tiator	(MAINZ, JINR)
ARNDT 06	PR C74 045205	R.A. Arndt et al.	(GWU)
PDG 06	JPG 33 1	W.-M. Yao et al.	(PDG Collab.)
ARNDT 04	PR C69 035213	R.A. Arndt et al.	(GWU, TRIUMF)
VRANA 00	PRPL 328 181	T.P. Vrana, S.A. Dytman, T.-S.H. Lee	(PITT+)
ARNDT 96	PR C53 430	R.A. Arndt, I.I. Strakovsky, R.L. Workman	(VPI)
ARNDT 95	PR C52 2120	R.A. Arndt et al.	(BRCC)
HOEHLER 93	πN Newsletter 9 1	G. Hoehler	(KARL)
LI 93	PR C47 2759	Z.J. Li et al.	(VPI)
MANLEY 92	PR D45 4002	D.M. Manley, E.M. Saleski	(KENT) IUP
Also	PR D30 904	D.M. Manley et al.	(VPI)

See key on page 373

Baryon Particle Listings
 $\Delta(1950)$, $\Delta(2000)$, $\Delta(2150)$

ARNDT	91	PR D43 2131	R.A. Arndt et al.	(VPI, TELE) IJP
CANDLIN	84	NP B238 477	D.J. Candlin et al.	(EDIN, RAL, LOWC)
PDG	82	PL 111B 1	M. Roos et al.	(HELS, CIT, CERN)
AWAJI	81	Bonn Conf. 352	N. Awaji, R. Kajikawa	(NAGO)
	Also	NP B197 365	K. Fujii et al.	(NAGO)
CHEW	80	Toronto Conf. 123	D.M. Chew	(LBL) IJP
CUTKOSKY	80	Toronto Conf. 19	R.E. Cutkosky et al.	(CMU, LBL) IJP
	Also	PR D20 2839	R.E. Cutkosky et al.	(CMU, LBL) IJP
HOEHLER	79	PDAT 12-1	G. Hoehler et al.	(KARLT) IJP
	Also	Toronto Conf. 3	R. Koch	(KARLT) IJP
LONGACRE	78	PR D17 1795	R.S. Longacre et al.	(LBL, SLAC) IJP
LONGACRE	75	PL 55B 415	R.S. Longacre et al.	(LBL, SLAC) IJP

 $\Delta(2000) F_{35}$

$$I(J^P) = \frac{3}{2}(\frac{5}{2}^+) \text{ Status: } **$$

OMITTED FROM SUMMARY TABLE

The latest GWU analysis (ARNDT 06) finds no evidence for this resonance.

 $\Delta(2000)$ BREIT-WIGNER MASS

VALUE (MeV)	DOCUMENT ID	TECN	COMMENT
≈ 2000 OUR ESTIMATE			
1724 \pm 61	VRANA 00	DPWA	Multichannel
1752 \pm 32	MANLEY 92	IPWA	$\pi N \rightarrow \pi N$ & $N\pi\pi$
2200 \pm 125	CUTKOSKY 80	IPWA	$\pi N \rightarrow \pi N$

 $\Delta(2000)$ BREIT-WIGNER WIDTH

VALUE (MeV)	DOCUMENT ID	TECN	COMMENT
138 \pm 68	VRANA 00	DPWA	Multichannel
251 \pm 93	MANLEY 92	IPWA	$\pi N \rightarrow \pi N$ & $N\pi\pi$
400 \pm 125	CUTKOSKY 80	IPWA	$\pi N \rightarrow \pi N$

 $\Delta(2000)$ POLE POSITION

REAL PART

VALUE (MeV)	DOCUMENT ID	TECN	COMMENT
1697	VRANA 00	DPWA	Multichannel
2150 \pm 100	CUTKOSKY 80	IPWA	$\pi N \rightarrow \pi N$

-2xIMAGINARY PART

VALUE (MeV)	DOCUMENT ID	TECN	COMMENT
112	VRANA 00	DPWA	Multichannel
350 \pm 100	CUTKOSKY 80	IPWA	$\pi N \rightarrow \pi N$

 $\Delta(2000)$ ELASTIC POLE RESIDUEMODULUS $|r|$

VALUE (MeV)	DOCUMENT ID	TECN	COMMENT
16 \pm 5	CUTKOSKY 80	IPWA	$\pi N \rightarrow \pi N$

PHASE θ

VALUE ($^\circ$)	DOCUMENT ID	TECN	COMMENT
150 \pm 90	CUTKOSKY 80	IPWA	$\pi N \rightarrow \pi N$

 $\Delta(2000)$ DECAY MODES

Mode	
Γ_1	$N\pi$
Γ_2	$N\pi\pi$
Γ_3	$\Delta(1232)\pi, P\text{-wave}$
Γ_4	$\Delta(1232)\pi, F\text{-wave}$
Γ_5	$N\rho, S=3/2, P\text{-wave}$

 $\Delta(2000)$ BRANCHING RATIOS

$\Gamma(N\pi)/\Gamma_{\text{total}}$	DOCUMENT ID	TECN	COMMENT	Γ_1/Γ
0.00 \pm 0.01	VRANA 00	DPWA	Multichannel	
0.02 \pm 0.01	MANLEY 92	IPWA	$\pi N \rightarrow \pi N$ & $N\pi\pi$	
0.07 \pm 0.04	CUTKOSKY 80	IPWA	$\pi N \rightarrow \pi N$	

$(\Gamma_1\Gamma_2)^{1/2}/\Gamma_{\text{total}}$ in $N\pi \rightarrow \Delta(2000) \rightarrow \Delta(1232)\pi, P\text{-wave}$	DOCUMENT ID	TECN	COMMENT	$(\Gamma_1\Gamma_3)^{1/2}/\Gamma$
+0.07 \pm 0.03	MANLEY 92	IPWA	$\pi N \rightarrow \pi N$ & $N\pi\pi$	

$\Gamma(\Delta(1232)\pi, P\text{-wave})/\Gamma_{\text{total}}$	DOCUMENT ID	TECN	COMMENT	Γ_3/Γ
0.00 \pm 0.01	VRANA 00	DPWA	Multichannel	

$(\Gamma_1\Gamma_2)^{1/2}/\Gamma_{\text{total}}$ in $N\pi \rightarrow \Delta(2000) \rightarrow \Delta(1232)\pi, F\text{-wave}$	DOCUMENT ID	TECN	COMMENT	$(\Gamma_1\Gamma_4)^{1/2}/\Gamma$
+0.09 \pm 0.04	MANLEY 92	IPWA	$\pi N \rightarrow \pi N$ & $N\pi\pi$	

$\Gamma(\Delta(1232)\pi, F\text{-wave})/\Gamma_{\text{total}}$	DOCUMENT ID	TECN	COMMENT	Γ_4/Γ
0.40 \pm 0.01	VRANA 00	DPWA	Multichannel	

$(\Gamma_1\Gamma_2)^{1/2}/\Gamma_{\text{total}}$ in $N\pi \rightarrow \Delta(2000) \rightarrow N\rho, S=3/2, P\text{-wave}$	DOCUMENT ID	TECN	COMMENT	$(\Gamma_1\Gamma_5)^{1/2}/\Gamma$
-0.06 \pm 0.01	MANLEY 92	IPWA	$\pi N \rightarrow \pi N$ & $N\pi\pi$	

$\Gamma(N\rho, S=3/2, P\text{-wave})/\Gamma_{\text{total}}$	DOCUMENT ID	TECN	COMMENT	Γ_5/Γ
0.60 \pm 0.60	VRANA 00	DPWA	Multichannel	

 $\Delta(2000)$ REFERENCES

ARNDT 06	PR C74 045205	R.A. Arndt et al.	(GWU)	
VRANA 00	PRPL 328 181	T.P. Vrana, S.A. Dytman., T.-S.H. Lee	(PITT+)	
MANLEY 92	PR D45 4002	D.M. Manley, E.M. Saleski	(KENT) IJP	
	Also	PR D30 904	D.M. Manley et al.	(VPI)
CUTKOSKY 80	Toronto Conf. 19	R.E. Cutkosky et al.	(CMU, LBL)	
	Also	PR D20 2839	R.E. Cutkosky et al.	(CMU, LBL)

 $\Delta(2150) S_{31}$

$$I(J^P) = \frac{3}{2}(\frac{1}{2}^-) \text{ Status: } *$$

OMITTED FROM SUMMARY TABLE

The latest GWU analysis (ARNDT 06) finds no evidence for this resonance.

 $\Delta(2150)$ BREIT-WIGNER MASS

VALUE (MeV)	DOCUMENT ID	TECN	COMMENT
≈ 2150 OUR ESTIMATE			
2047.4 \pm 27.0	¹ CHEW 80	BPWA	$\pi^+ p \rightarrow \pi^+ p$
2203.2 \pm 8.4	¹ CHEW 80	BPWA	$\pi^+ p \rightarrow \pi^+ p$
2150 \pm 100	CUTKOSKY 80	IPWA	$\pi N \rightarrow \pi N$

 $\Delta(2150)$ BREIT-WIGNER WIDTH

VALUE (MeV)	DOCUMENT ID	TECN	COMMENT
121.6 \pm 62.0	¹ CHEW 80	BPWA	$\pi^+ p \rightarrow \pi^+ p$
120.5 \pm 45.0	¹ CHEW 80	BPWA	$\pi^+ p \rightarrow \pi^+ p$
200 \pm 100	CUTKOSKY 80	IPWA	$\pi N \rightarrow \pi N$

 $\Delta(2150)$ POLE POSITION

REAL PART

VALUE (MeV)	DOCUMENT ID	TECN	COMMENT
2140 \pm 80	CUTKOSKY 80	IPWA	$\pi N \rightarrow \pi N$

-2xIMAGINARY PART

VALUE (MeV)	DOCUMENT ID	TECN	COMMENT
200 \pm 80	CUTKOSKY 80	IPWA	$\pi N \rightarrow \pi N$

 $\Delta(2150)$ ELASTIC POLE RESIDUEMODULUS $|r|$

VALUE (MeV)	DOCUMENT ID	TECN	COMMENT
7 \pm 2	CUTKOSKY 80	IPWA	$\pi N \rightarrow \pi N$

PHASE θ

VALUE ($^\circ$)	DOCUMENT ID	TECN	COMMENT
-60 \pm 90	CUTKOSKY 80	IPWA	$\pi N \rightarrow \pi N$

 $\Delta(2150)$ DECAY MODES

Mode	
Γ_1	$N\pi$
Γ_2	ΣK

 $\Delta(2150)$ BRANCHING RATIOS

$\Gamma(N\pi)/\Gamma_{\text{total}}$	DOCUMENT ID	TECN	COMMENT	Γ_1/Γ
0.41	¹ CHEW 80	BPWA	$\pi^+ p \rightarrow \pi^+ p$	
0.37	¹ CHEW 80	BPWA	$\pi^+ p \rightarrow \pi^+ p$	
0.08 \pm 0.02	CUTKOSKY 80	IPWA	$\pi N \rightarrow \pi N$	

$(\Gamma_1\Gamma_2)^{1/2}/\Gamma_{\text{total}}$ in $N\pi \rightarrow \Delta(2150) \rightarrow \Sigma K$	DOCUMENT ID	TECN	COMMENT	$(\Gamma_1\Gamma_2)^{1/2}/\Gamma$
<0.03	CANDLIN 84	DPWA	$\pi^+ p \rightarrow \Sigma^+ K^+$	

Baryon Particle Listings

 $\Delta(2150)$, $\Delta(2200)$, $\Delta(2300)$ $\Delta(2150)$ FOOTNOTES

¹ CHEW 80 reports two S_{31} resonances in this mass region. Problems with this analysis are discussed in section 2.1.11 of HOEHLER 83.

 $\Delta(2150)$ REFERENCES

ARNDT	06	PR C74 045205	R.A. Arndt et al.	(GWU)
CANDLIN	84	NP B238 477	D.J. Candlin et al.	(EDIN, RAL, LOWC)
HOEHLER	83	Landolt-Boernstein 1/9B2 6	G. Hoehler et al.	(KARLT)
CHEW	80	Toronto Conf. 123	D.M. Chew	(LBL) IJP
CUTKOSKY	80	Toronto Conf. 19	R.E. Cutkosky et al.	(CMU, LBL) IJP
Also		PR D20 2839	R.E. Cutkosky et al.	(CMU, LBL)

 $\Delta(2200)$ G_{37}

$$I(J^P) = \frac{3}{2}(\frac{7}{2}^-) \text{ Status: } *$$

OMITTED FROM SUMMARY TABLE

The various analyses are not in good agreement.

The latest GWU analysis (ARNDT 06) finds no evidence for this resonance.

 $\Delta(2200)$ BREIT-WIGNER MASS

VALUE (MeV)	DOCUMENT ID	TECN	COMMENT
≈ 2200 OUR ESTIMATE			
2200 \pm 80	CUTKOSKY 80	IPWA	$\pi N \rightarrow \pi N$
2215 \pm 60	HOEHLER 79	IPWA	$\pi N \rightarrow \pi N$
2280 \pm 80	HENDRY 78	MPWA	$\pi N \rightarrow \pi N$
• • • We do not use the following data for averages, fits, limits, etc. • • •			
2280 \pm 40	CANDLIN 84	DPWA	$\pi^+ p \rightarrow \Sigma^+ K^+$

 $\Delta(2200)$ BREIT-WIGNER WIDTH

VALUE (MeV)	DOCUMENT ID	TECN	COMMENT
450 \pm 100	CUTKOSKY 80	IPWA	$\pi N \rightarrow \pi N$
400 \pm 100	HOEHLER 79	IPWA	$\pi N \rightarrow \pi N$
400 \pm 150	HENDRY 78	MPWA	$\pi N \rightarrow \pi N$
• • • We do not use the following data for averages, fits, limits, etc. • • •			
400 \pm 50	CANDLIN 84	DPWA	$\pi^+ p \rightarrow \Sigma^+ K^+$

 $\Delta(2200)$ POLE POSITION

VALUE (MeV)	DOCUMENT ID	TECN	COMMENT
2100 \pm 50	CUTKOSKY 80	IPWA	$\pi N \rightarrow \pi N$
$-2 \times$ IMAGINARY PART			
340 \pm 80	CUTKOSKY 80	IPWA	$\pi N \rightarrow \pi N$

 $\Delta(2200)$ ELASTIC POLE RESIDUE

MODE	VALUE (MeV)	DOCUMENT ID	TECN	COMMENT
Γ_1	$N \pi$			
Γ_2	ΣK			

MODE	VALUE (MeV)	DOCUMENT ID	TECN	COMMENT
Γ_1	$N \pi$			
Γ_2	ΣK			

 $\Delta(2200)$ DECAY MODES

MODE	VALUE (MeV)	DOCUMENT ID	TECN	COMMENT
Γ_1	$N \pi$			
Γ_2	ΣK			

 $\Delta(2200)$ BRANCHING RATIOS

$\Gamma(N\pi)/\Gamma_{\text{total}}$	VALUE	DOCUMENT ID	TECN	COMMENT	Γ_1/Γ
Γ_1	$N \pi$				
Γ_2	ΣK				

$(\Gamma_1 \Gamma_2)^{1/2}/\Gamma_{\text{total}}$ in $N\pi \rightarrow \Delta(2200) \rightarrow \Sigma K$	VALUE	DOCUMENT ID	TECN	COMMENT	$(\Gamma_1 \Gamma_2)^{1/2}/\Gamma$
Γ_1	$N \pi$				
Γ_2	ΣK				

 $\Delta(2200)$ REFERENCES

ARNDT	06	PR C74 045205	R.A. Arndt et al.	(GWU)
CANDLIN	84	NP B238 477	D.J. Candlin et al.	(EDIN, RAL, LOWC)
CUTKOSKY	80	Toronto Conf. 19	R.E. Cutkosky et al.	(CMU, LBL) IJP
Also		PR D20 2839	R.E. Cutkosky et al.	(CMU, LBL) IJP
HOEHLER	79	PDAT 12-1	G. Hoehler et al.	(KARLT) IJP
Also		Toronto Conf. 3	R. Koch	(KARLT) IJP
HENDRY	78	PRL 41 222	A.W. Hendry	(IND, LBL) IJP
Also		ANP 136 1	A.W. Hendry	(IND)

 $\Delta(2300)$ H_{39}

$$I(J^P) = \frac{3}{2}(\frac{9}{2}^+) \text{ Status: } **$$

OMITTED FROM SUMMARY TABLE

The latest GWU analysis (ARNDT 06) finds no evidence for this resonance.

 $\Delta(2300)$ BREIT-WIGNER MASS

VALUE (MeV)	DOCUMENT ID	TECN	COMMENT
≈ 2300 OUR ESTIMATE			
2204.5 \pm 3.4	CHEW 80	BPWA	$\pi^+ p \rightarrow \pi^+ p$
2400 \pm 125	CUTKOSKY 80	IPWA	$\pi N \rightarrow \pi N$
2217 \pm 80	HOEHLER 79	IPWA	$\pi N \rightarrow \pi N$
2450 \pm 100	HENDRY 78	MPWA	$\pi N \rightarrow \pi N$
• • • We do not use the following data for averages, fits, limits, etc. • • •			
2400	CANDLIN 84	DPWA	$\pi^+ p \rightarrow \Sigma^+ K^+$

 $\Delta(2300)$ BREIT-WIGNER WIDTH

VALUE (MeV)	DOCUMENT ID	TECN	COMMENT
32.3 \pm 1.0	CHEW 80	BPWA	$\pi^+ p \rightarrow \pi^+ p$
425 \pm 150	CUTKOSKY 80	IPWA	$\pi N \rightarrow \pi N$
300 \pm 100	HOEHLER 79	IPWA	$\pi N \rightarrow \pi N$
500 \pm 200	HENDRY 78	MPWA	$\pi N \rightarrow \pi N$
• • • We do not use the following data for averages, fits, limits, etc. • • •			
200	CANDLIN 84	DPWA	$\pi^+ p \rightarrow \Sigma^+ K^+$

 $\Delta(2300)$ POLE POSITION

REAL PART	VALUE (MeV)	DOCUMENT ID	TECN	COMMENT
Γ_1	$N \pi$			
Γ_2	ΣK			

 $-2 \times$ IMAGINARY PART

VALUE (MeV)	DOCUMENT ID	TECN	COMMENT
420 \pm 160	CUTKOSKY 80	IPWA	$\pi N \rightarrow \pi N$

 $\Delta(2300)$ ELASTIC POLE RESIDUE

MODE	VALUE (MeV)	DOCUMENT ID	TECN	COMMENT
Γ_1	$N \pi$			
Γ_2	ΣK			

MODE	VALUE (MeV)	DOCUMENT ID	TECN	COMMENT
Γ_1	$N \pi$			
Γ_2	ΣK			

 $\Delta(2300)$ DECAY MODES

MODE	VALUE (MeV)	DOCUMENT ID	TECN	COMMENT
Γ_1	$N \pi$			
Γ_2	ΣK			

 $\Delta(2300)$ BRANCHING RATIOS

$\Gamma(N\pi)/\Gamma_{\text{total}}$	VALUE	DOCUMENT ID	TECN	COMMENT	Γ_1/Γ
Γ_1	$N \pi$				
Γ_2	ΣK				

$(\Gamma_1 \Gamma_2)^{1/2}/\Gamma_{\text{total}}$ in $N\pi \rightarrow \Delta(2300) \rightarrow \Sigma K$	VALUE	DOCUMENT ID	TECN	COMMENT	$(\Gamma_1 \Gamma_2)^{1/2}/\Gamma$
Γ_1	$N \pi$				
Γ_2	ΣK				

 $\Delta(2300)$ REFERENCES

ARNDT	06	PR C74 045205	R.A. Arndt et al.	(GWU)
CANDLIN	84	NP B238 477	D.J. Candlin et al.	(EDIN, RAL, LOWC)
CHEW	80	Toronto Conf. 123	D.M. Chew	(LBL) IJP
CUTKOSKY	80	Toronto Conf. 19	R.E. Cutkosky et al.	(CMU, LBL) IJP
Also		PR D20 2839	R.E. Cutkosky et al.	(CMU, LBL)
HOEHLER	79	PDAT 12-1	G. Hoehler et al.	(KARLT) IJP
Also		Toronto Conf. 3	R. Koch	(KARLT) IJP
HENDRY	78	PRL 41 222	A.W. Hendry	(IND, LBL) IJP
Also		ANP 136 1	A.W. Hendry	(IND)

See key on page 373

Baryon Particle Listings
 $\Delta(2350)$, $\Delta(2390)$ $\Delta(2350) D_{35}$

$$I(J^P) = \frac{3}{2}(\frac{5}{2}^-) \text{ Status: } *$$

OMITTED FROM SUMMARY TABLE

The latest GWU analysis (ARNDT 06) finds no evidence for this resonance.

 $\Delta(2350)$ BREIT-WIGNER MASS

VALUE (MeV)	DOCUMENT ID	TECN	COMMENT
≈ 2350 OUR ESTIMATE			
2171 \pm 18	MANLEY 92	IPWA	$\pi N \rightarrow \pi N$ & $N\pi\pi$
2400 \pm 125	CUTKOSKY 80	IPWA	$\pi N \rightarrow \pi N$
2305 \pm 26	HOEHLER 79	IPWA	$\pi N \rightarrow \pi N$
••• We do not use the following data for averages, fits, limits, etc. •••			
2459 \pm 100	VRANA 00	DPWA	Multichannel

 $\Delta(2350)$ BREIT-WIGNER WIDTH

VALUE (MeV)	DOCUMENT ID	TECN	COMMENT
264 \pm 51	MANLEY 92	IPWA	$\pi N \rightarrow \pi N$ & $N\pi\pi$
400 \pm 150	CUTKOSKY 80	IPWA	$\pi N \rightarrow \pi N$
300 \pm 70	HOEHLER 79	IPWA	$\pi N \rightarrow \pi N$
••• We do not use the following data for averages, fits, limits, etc. •••			
480 \pm 360	VRANA 00	DPWA	Multichannel

 $\Delta(2350)$ POLE POSITION

REAL PART

VALUE (MeV)	DOCUMENT ID	TECN	COMMENT
2400 \pm 125	CUTKOSKY 80	IPWA	$\pi N \rightarrow \pi N$
••• We do not use the following data for averages, fits, limits, etc. •••			
2427	VRANA 00	DPWA	Multichannel

-2xIMAGINARY PART

VALUE (MeV)	DOCUMENT ID	TECN	COMMENT
400 \pm 150	CUTKOSKY 80	IPWA	$\pi N \rightarrow \pi N$
••• We do not use the following data for averages, fits, limits, etc. •••			
458	VRANA 00	DPWA	Multichannel

 $\Delta(2350)$ ELASTIC POLE RESIDUEMODULUS $|r|$

VALUE (MeV)	DOCUMENT ID	TECN	COMMENT
15 \pm 8	CUTKOSKY 80	IPWA	$\pi N \rightarrow \pi N$

PHASE θ

VALUE ($^\circ$)	DOCUMENT ID	TECN	COMMENT
-70 \pm 70	CUTKOSKY 80	IPWA	$\pi N \rightarrow \pi N$

 $\Delta(2350)$ DECAY MODES

Mode	Γ_1	Γ_2
$N\pi$		
ΣK		

 $\Delta(2350)$ BRANCHING RATIOS

$\Gamma(N\pi)/\Gamma_{\text{total}}$	DOCUMENT ID	TECN	COMMENT	Γ_1/Γ
0.020 \pm 0.003	MANLEY 92	IPWA	$\pi N \rightarrow \pi N$ & $N\pi\pi$	
0.20 \pm 0.10	CUTKOSKY 80	IPWA	$\pi N \rightarrow \pi N$	
0.04 \pm 0.02	HOEHLER 79	IPWA	$\pi N \rightarrow \pi N$	
••• We do not use the following data for averages, fits, limits, etc. •••				
0.07 \pm 0.14	VRANA 00	DPWA	Multichannel	

$(\Gamma_1 \Gamma_2)^{1/2}/\Gamma_{\text{total}}$ in $N\pi \rightarrow \Delta(2350) \rightarrow \Sigma K$	DOCUMENT ID	TECN	COMMENT	$(\Gamma_1 \Gamma_2)^{1/2}/\Gamma$
<0.015	CANDLIN 84	DPWA	$\pi^+ p \rightarrow \Sigma^+ K^+$	

 $\Delta(2350)$ REFERENCES

ARNDT 06	PR C74 045205	R.A. Arndt et al.	(GWU)
VRANA 00	PRPL 328 181	T.P. Vrana, S.A. Dymman., T.-S.H. Lee	(PITT+)
MANLEY 92	PR D45 4002	D.M. Manley, E.M. Saleski	(KENT) IJP
Also	PR D30 904	D.M. Manley et al.	(VPI)
CANDLIN 84	NP B238 477	D.J. Candlin et al.	(EDIN, RAL, LOWC)
CUTKOSKY 80	Toronto Conf. 19	R.E. Cutkosky et al.	(CMU, LBL) IJP
Also	PR D20 2839	R.E. Cutkosky et al.	(CMU, LBL)
HOEHLER 79	PDAT 12-1	G. Hoehler et al.	(KARLT) IJP
Also	Toronto Conf. 3	R. Koch	(KARLT) IJP

 $\Delta(2390) F_{37}$

$$I(J^P) = \frac{3}{2}(\frac{7}{2}^+) \text{ Status: } *$$

OMITTED FROM SUMMARY TABLE

The latest GWU analysis (ARNDT 06) finds no evidence for this resonance.

 $\Delta(2390)$ BREIT-WIGNER MASS

VALUE (MeV)	DOCUMENT ID	TECN	COMMENT
≈ 2390 OUR ESTIMATE			
2350 \pm 100	CUTKOSKY 80	IPWA	$\pi N \rightarrow \pi N$
2425 \pm 60	HOEHLER 79	IPWA	$\pi N \rightarrow \pi N$

 $\Delta(2390)$ BREIT-WIGNER WIDTH

VALUE (MeV)	DOCUMENT ID	TECN	COMMENT
300 \pm 100	CUTKOSKY 80	IPWA	$\pi N \rightarrow \pi N$
300 \pm 80	HOEHLER 79	IPWA	$\pi N \rightarrow \pi N$

 $\Delta(2390)$ POLE POSITION

REAL PART

VALUE (MeV)	DOCUMENT ID	TECN	COMMENT
2350 \pm 100	CUTKOSKY 80	IPWA	$\pi N \rightarrow \pi N$

-2xIMAGINARY PART

VALUE (MeV)	DOCUMENT ID	TECN	COMMENT
260 \pm 100	CUTKOSKY 80	IPWA	$\pi N \rightarrow \pi N$

 $\Delta(2390)$ ELASTIC POLE RESIDUE

MODE	MODE	MODE
MODULUS $ r $		
12 \pm 6	CUTKOSKY 80	IPWA
		$\pi N \rightarrow \pi N$

PHASE θ

VALUE ($^\circ$)	DOCUMENT ID	TECN	COMMENT
-90 \pm 60	CUTKOSKY 80	IPWA	$\pi N \rightarrow \pi N$

 $\Delta(2390)$ DECAY MODES

Mode	Γ_1	Γ_2
$N\pi$		
ΣK		

 $\Delta(2390)$ BRANCHING RATIOS

$\Gamma(N\pi)/\Gamma_{\text{total}}$	DOCUMENT ID	TECN	COMMENT	Γ_1/Γ
0.08 \pm 0.04	CUTKOSKY 80	IPWA	$\pi N \rightarrow \pi N$	
0.07 \pm 0.04	HOEHLER 79	IPWA	$\pi N \rightarrow \pi N$	

$(\Gamma_1 \Gamma_2)^{1/2}/\Gamma_{\text{total}}$ in $N\pi \rightarrow \Delta(2390) \rightarrow \Sigma K$	DOCUMENT ID	TECN	COMMENT	$(\Gamma_1 \Gamma_2)^{1/2}/\Gamma$
<0.015	CANDLIN 84	DPWA	$\pi^+ p \rightarrow \Sigma^+ K^+$	

 $\Delta(2390)$ REFERENCES

ARNDT 06	PR C74 045205	R.A. Arndt et al.	(GWU)
CANDLIN 84	NP B238 477	D.J. Candlin et al.	(EDIN, RAL, LOWC)
CUTKOSKY 80	Toronto Conf. 19	R.E. Cutkosky et al.	(CMU, LBL) IJP
Also	PR D20 2839	R.E. Cutkosky et al.	(CMU, LBL)
HOEHLER 79	PDAT 12-1	G. Hoehler et al.	(KARLT) IJP
Also	Toronto Conf. 3	R. Koch	(KARLT) IJP

Baryon Particle Listings

 $\Delta(2400)$, $\Delta(2420)$ $\Delta(2400) G_{39}$

$I(J^P) = \frac{3}{2}(\frac{9}{2}^-)$ Status: **

OMITTED FROM SUMMARY TABLE

 $\Delta(2400)$ BREIT-WIGNER MASS

VALUE (MeV)	DOCUMENT ID	TECN	COMMENT
≈ 2400 OUR ESTIMATE			
2643 \pm 141	ARNDT 06	DPWA	$\pi N \rightarrow \pi N, \eta N$
2300 \pm 100	CUTKOSKY 80	IPWA	$\pi N \rightarrow \pi N$
2468 \pm 50	HOEHLER 79	IPWA	$\pi N \rightarrow \pi N$
2200 \pm 100	HENDRY 78	MPWA	$\pi N \rightarrow \pi N$

 $\Delta(2400)$ BREIT-WIGNER WIDTH

VALUE (MeV)	DOCUMENT ID	TECN	COMMENT
895 \pm 432	ARNDT 06	DPWA	$\pi N \rightarrow \pi N, \eta N$
330 \pm 100	CUTKOSKY 80	IPWA	$\pi N \rightarrow \pi N$
480 \pm 100	HOEHLER 79	IPWA	$\pi N \rightarrow \pi N$
450 \pm 200	HENDRY 78	MPWA	$\pi N \rightarrow \pi N$

 $\Delta(2400)$ POLE POSITION

REAL PART

VALUE (MeV)	DOCUMENT ID	TECN	COMMENT
1983	ARNDT 06	DPWA	$\pi N \rightarrow \pi N, \eta N$
2260 \pm 60	CUTKOSKY 80	IPWA	$\pi N \rightarrow \pi N$

-2xIMAGINARY PART

VALUE (MeV)	DOCUMENT ID	TECN	COMMENT
878	ARNDT 06	DPWA	$\pi N \rightarrow \pi N, \eta N$
320 \pm 160	CUTKOSKY 80	IPWA	$\pi N \rightarrow \pi N$

 $\Delta(2400)$ ELASTIC POLE RESIDUEMODULUS $|r|$

VALUE (MeV)	DOCUMENT ID	TECN	COMMENT
24	ARNDT 06	DPWA	$\pi N \rightarrow \pi N, \eta N$
8 \pm 4	CUTKOSKY 80	IPWA	$\pi N \rightarrow \pi N$

PHASE θ

VALUE ($^\circ$)	DOCUMENT ID	TECN	COMMENT
-139	ARNDT 06	DPWA	$\pi N \rightarrow \pi N, \eta N$
-25 \pm 15	CUTKOSKY 80	IPWA	$\pi N \rightarrow \pi N$

 $\Delta(2400)$ DECAY MODES

Mode	Fraction (Γ_i/Γ)
Γ_1 $N\pi$	
Γ_2 ΣK	

 $\Delta(2400)$ BRANCHING RATIOS

$\Gamma(N\pi)/\Gamma_{\text{total}}$	DOCUMENT ID	TECN	COMMENT	Γ_1/Γ
0.064 \pm 0.022	ARNDT 06	DPWA	$\pi N \rightarrow \pi N, \eta N$	
0.05 \pm 0.02	CUTKOSKY 80	IPWA	$\pi N \rightarrow \pi N$	
0.06 \pm 0.03	HOEHLER 79	IPWA	$\pi N \rightarrow \pi N$	
0.10 \pm 0.03	HENDRY 78	MPWA	$\pi N \rightarrow \pi N$	

$(\Gamma_1\Gamma_2)^{1/2}/\Gamma_{\text{total}}$ in $N\pi \rightarrow \Delta(2400) \rightarrow \Sigma K$	DOCUMENT ID	TECN	COMMENT	$(\Gamma_1\Gamma_2)^{1/2}/\Gamma$
<0.015	CANDLIN 84	DPWA	$\pi^+ p \rightarrow \Sigma^+ K^+$	

 $\Delta(2400)$ REFERENCES

ARNDT 06	PR C74 045205	R.A. Arndt et al.	(GWU)
CANDLIN 84	NP B238 477	D.J. Candlin et al.	(EDIN, RAL, LOWC)
CUTKOSKY 80	Toronto Conf. 19	R.E. Cutkosky et al.	(CMU, LBL) IJP
Also	PR D20 2839	R.E. Cutkosky et al.	(CMU, LBL)
HOEHLER 79	PDAT 12-1	G. Hoehler et al.	(KARLT) IJP
Also	Toronto Conf. 3	R. Koch	(KARLT) IJP
HENDRY 78	PRL 41 222	A.W. Hendry	(IND, LBL) IJP
Also	ANP 136 1	A.W. Hendry	(IND)

 $\Delta(2420) H_{3,11}$

$I(J^P) = \frac{3}{2}(\frac{11}{2}^+)$ Status: ***

Most of the results published before 1975 are now obsolete and have been omitted. They may be found in our 1982 edition, Physics Letters **111B** 1 (1982). $\Delta(2420)$ BREIT-WIGNER MASS

VALUE (MeV)	DOCUMENT ID	TECN	COMMENT
2300 to 2500 (≈ 2420) OUR ESTIMATE			
2633 \pm 29	ARNDT 06	DPWA	$\pi N \rightarrow \pi N, \eta N$
2400 \pm 125	CUTKOSKY 80	IPWA	$\pi N \rightarrow \pi N$
2416 \pm 17	HOEHLER 79	IPWA	$\pi N \rightarrow \pi N$
2400 \pm 60	HENDRY 78	MPWA	$\pi N \rightarrow \pi N$
••• We do not use the following data for averages, fits, limits, etc. •••			
2400	CANDLIN 84	DPWA	$\pi^+ p \rightarrow \Sigma^+ K^+$
2358.0 \pm 9.0	CHEW 80	BPWA	$\pi^+ p \rightarrow \pi^+ p$

 $\Delta(2420)$ BREIT-WIGNER WIDTH

VALUE (MeV)	DOCUMENT ID	TECN	COMMENT
300 to 500 (≈ 400) OUR ESTIMATE			
692 \pm 47	ARNDT 06	DPWA	$\pi N \rightarrow \pi N, \eta N$
450 \pm 150	CUTKOSKY 80	IPWA	$\pi N \rightarrow \pi N$
340 \pm 28	HOEHLER 79	IPWA	$\pi N \rightarrow \pi N$
460 \pm 100	HENDRY 78	MPWA	$\pi N \rightarrow \pi N$
••• We do not use the following data for averages, fits, limits, etc. •••			
400	CANDLIN 84	DPWA	$\pi^+ p \rightarrow \Sigma^+ K^+$
202.2 \pm 45.0	CHEW 80	BPWA	$\pi^+ p \rightarrow \pi^+ p$

 $\Delta(2420)$ POLE POSITION

REAL PART

VALUE (MeV)	DOCUMENT ID	TECN	COMMENT
2260 to 2400 (≈ 2330) OUR ESTIMATE			
2529	ARNDT 06	DPWA	$\pi N \rightarrow \pi N, \eta N$
2300	¹ HOEHLER 93	ARGD	$\pi N \rightarrow \pi N$
2360 \pm 100	CUTKOSKY 80	IPWA	$\pi N \rightarrow \pi N$

-2xIMAGINARY PART

VALUE (MeV)	DOCUMENT ID	TECN	COMMENT
350 to 750 (≈ 550) OUR ESTIMATE			
621	ARNDT 06	DPWA	$\pi N \rightarrow \pi N, \eta N$
620	¹ HOEHLER 93	ARGD	$\pi N \rightarrow \pi N$
420 \pm 100	CUTKOSKY 80	IPWA	$\pi N \rightarrow \pi N$

 $\Delta(2420)$ ELASTIC POLE RESIDUEMODULUS $|r|$

VALUE (MeV)	DOCUMENT ID	TECN	COMMENT
33	ARNDT 06	DPWA	$\pi N \rightarrow \pi N, \eta N$
39	HOEHLER 93	ARGD	$\pi N \rightarrow \pi N$
18 \pm 6	CUTKOSKY 80	IPWA	$\pi N \rightarrow \pi N$

PHASE θ

VALUE ($^\circ$)	DOCUMENT ID	TECN	COMMENT
-45	ARNDT 06	DPWA	$\pi N \rightarrow \pi N, \eta N$
-60	HOEHLER 93	ARGD	$\pi N \rightarrow \pi N$
-30 \pm 40	CUTKOSKY 80	IPWA	$\pi N \rightarrow \pi N$

 $\Delta(2420)$ DECAY MODES

The following branching fractions are our estimates, not fits or averages.

Mode	Fraction (Γ_i/Γ)
Γ_1 $N\pi$	5-15 %
Γ_2 ΣK	

 $\Delta(2420)$ BRANCHING RATIOS

$\Gamma(N\pi)/\Gamma_{\text{total}}$	DOCUMENT ID	TECN	COMMENT	Γ_1/Γ
0.05 to 0.15 OUR ESTIMATE				
0.085 \pm 0.008	ARNDT 06	DPWA	$\pi N \rightarrow \pi N, \eta N$	
0.08 \pm 0.03	CUTKOSKY 80	IPWA	$\pi N \rightarrow \pi N$	
0.08 \pm 0.015	HOEHLER 79	IPWA	$\pi N \rightarrow \pi N$	
0.11 \pm 0.02	HENDRY 78	MPWA	$\pi N \rightarrow \pi N$	
••• We do not use the following data for averages, fits, limits, etc. •••				
0.22	CHEW 80	BPWA	$\pi^+ p \rightarrow \pi^+ p$	

See key on page 373

Baryon Particle Listings

$\Delta(2420)$, $\Delta(2750)$, $\Delta(2950)$, $\Delta(\sim 3000)$

$(\Gamma_1 \Gamma_2)^{1/2} / \Gamma_{\text{total}}$ in $N\pi \rightarrow \Delta(2420) \rightarrow \Sigma K$	$(\Gamma_1 \Gamma_2)^{1/2} / \Gamma$		
VALUE	DOCUMENT ID	TECN	COMMENT
-0.016	CANDLIN	84	DPWA $\pi^+ p \rightarrow \Sigma^+ K^+$

$\Delta(2420)$ FOOTNOTES

¹ See HOEHLER 93 for a detailed discussion of the evidence for and the pole parameters of N and Δ resonances as determined from Argand diagrams of πN elastic partial-wave amplitudes and from plots of the speeds with which the amplitudes traverse the diagrams.

$\Delta(2420)$ REFERENCES

ARNDT 06	PR C74 045205	R.A. Arndt <i>et al.</i>	(GWU)
HOEHLER 93	πN Newsletter 9 1	G. Hohler	(KARL)
CANDLIN 84	NP B238 477	D.J. Candlin <i>et al.</i>	(EDIN, RAL, LOWC)
PDG 82	PL 111B 1	M. Roos <i>et al.</i>	(HELS, CIT, CERN)
CHEW 80	Toronto Conf. 123	D.M. Chew	(LBL) IJP
CUTKOSKY 80	Toronto Conf. 19	R.E. Cutkosky <i>et al.</i>	(CMU, LBL) IJP
Also	PR D20 2839	R.E. Cutkosky <i>et al.</i>	(CMU, LBL)
HOEHLER 79	PDAT 12-1	G. Hohler <i>et al.</i>	(KARLT) IJP
Also	Toronto Conf. 3	R. Koch	(KARLT) IJP
HENDRY 78	PRL 41 222	A.W. Hendry	(IND, LBL) IJP
Also	ANP 136 1	A.W. Hendry	(IND)

$\Delta(2750) I_{3,13}$

$$I(J^P) = \frac{3}{2}(1\frac{3}{2}^-) \text{Status: } **$$

OMITTED FROM SUMMARY TABLE
 The latest GWU analysis (ARNDT 06) finds no evidence for this resonance.

$\Delta(2750)$ BREIT-WIGNER MASS

VALUE (MeV)	DOCUMENT ID	TECN	COMMENT
≈ 2750 OUR ESTIMATE			
2794 \pm 80	HOEHLER	79	IPWA $\pi N \rightarrow \pi N$
2650 \pm 100	HENDRY	78	MPWA $\pi N \rightarrow \pi N$

$\Delta(2750)$ BREIT-WIGNER WIDTH

VALUE (MeV)	DOCUMENT ID	TECN	COMMENT
350 \pm 100	HOEHLER	79	IPWA $\pi N \rightarrow \pi N$
500 \pm 100	HENDRY	78	MPWA $\pi N \rightarrow \pi N$

$\Delta(2750)$ DECAY MODES

Mode
$\Gamma_1 N \pi$

$\Delta(2750)$ BRANCHING RATIOS

$\Gamma(N\pi) / \Gamma_{\text{total}}$	Γ_1 / Γ		
VALUE	DOCUMENT ID	TECN	COMMENT
0.04 \pm 0.015	HOEHLER	79	IPWA $\pi N \rightarrow \pi N$
0.05 \pm 0.01	HENDRY	78	MPWA $\pi N \rightarrow \pi N$

$\Delta(2750)$ REFERENCES

ARNDT 06	PR C74 045205	R.A. Arndt <i>et al.</i>	(GWU)
HOEHLER 79	PDAT 12-1	G. Hohler <i>et al.</i>	(KARLT) IJP
Also	Toronto Conf. 3	R. Koch	(KARLT) IJP
HENDRY 78	PRL 41 222	A.W. Hendry	(IND, LBL) IJP
Also	ANP 136 1	A.W. Hendry	(IND)

$\Delta(2950) K_{3,15}$

$$I(J^P) = \frac{3}{2}(1\frac{5}{2}^+) \text{Status: } **$$

OMITTED FROM SUMMARY TABLE

$\Delta(2950)$ BREIT-WIGNER MASS

VALUE (MeV)	DOCUMENT ID	TECN	COMMENT
≈ 2950 OUR ESTIMATE			
2990 \pm 100	HOEHLER	79	IPWA $\pi N \rightarrow \pi N$
2850 \pm 100	HENDRY	78	MPWA $\pi N \rightarrow \pi N$

$\Delta(2950)$ BREIT-WIGNER WIDTH

VALUE (MeV)	DOCUMENT ID	TECN	COMMENT
330 \pm 100	HOEHLER	79	IPWA $\pi N \rightarrow \pi N$
700 \pm 200	HENDRY	78	MPWA $\pi N \rightarrow \pi N$

$\Delta(2950)$ DECAY MODES

Mode
$\Gamma_1 N \pi$

$\Delta(2950)$ BRANCHING RATIOS

$\Gamma(N\pi) / \Gamma_{\text{total}}$	Γ_1 / Γ		
VALUE	DOCUMENT ID	TECN	COMMENT
0.04 \pm 0.02	HOEHLER	79	IPWA $\pi N \rightarrow \pi N$
0.03 \pm 0.01	HENDRY	78	MPWA $\pi N \rightarrow \pi N$

$\Delta(2950)$ REFERENCES

HOEHLER 79	PDAT 12-1	G. Hohler <i>et al.</i>	(KARLT) IJP
Also	Toronto Conf. 3	R. Koch	(KARLT) IJP
HENDRY 78	PRL 41 222	A.W. Hendry	(IND, LBL) IJP
Also	ANP 136 1	A.W. Hendry	(IND)

$\Delta(\sim 3000)$ Region
 Partial-Wave Analyses

OMITTED FROM SUMMARY TABLE

We list here miscellaneous high-mass candidates for isospin-3/2 resonances found in partial-wave analyses.

Our 1982 edition also had a $\Delta(2850)$ and a $\Delta(3230)$. The evidence for them was deduced from total cross-section and 180° elastic cross-section measurements. The $\Delta(2850)$ has been resolved into the $\Delta(2750) I_{3,13}$ and $\Delta(2950) K_{3,15}$. The $\Delta(3230)$ is perhaps related to the $K_{3,13}$ of HENDRY 78 and to the $L_{3,17}$ of KOCH 80.

$\Delta(\sim 3000)$ BREIT-WIGNER MASS

VALUE (MeV)	DOCUMENT ID	TECN	COMMENT
≈ 3000 OUR ESTIMATE			
3300	¹ KOCH	80	IPWA $\pi N \rightarrow \pi N L_{3,17}$ wave
3500	¹ KOCH	80	IPWA $\pi N \rightarrow \pi N M_{3,19}$ wave
2850 \pm 150	HENDRY	78	MPWA $\pi N \rightarrow \pi N I_{3,11}$ wave
3200 \pm 200	HENDRY	78	MPWA $\pi N \rightarrow \pi N K_{3,13}$ wave
3300 \pm 200	HENDRY	78	MPWA $\pi N \rightarrow \pi N L_{3,17}$ wave
3700 \pm 200	HENDRY	78	MPWA $\pi N \rightarrow \pi N M_{3,19}$ wave
4100 \pm 300	HENDRY	78	MPWA $\pi N \rightarrow \pi N N_{3,21}$ wave

$\Delta(\sim 3000)$ BREIT-WIGNER WIDTH

VALUE (MeV)	DOCUMENT ID	TECN	COMMENT
700 \pm 200	HENDRY	78	MPWA $\pi N \rightarrow \pi N I_{3,11}$ wave
1000 \pm 300	HENDRY	78	MPWA $\pi N \rightarrow \pi N K_{3,13}$ wave
1100 \pm 300	HENDRY	78	MPWA $\pi N \rightarrow \pi N L_{3,17}$ wave
1300 \pm 400	HENDRY	78	MPWA $\pi N \rightarrow \pi N M_{3,19}$ wave
1600 \pm 500	HENDRY	78	MPWA $\pi N \rightarrow \pi N N_{3,21}$ wave

$\Delta(\sim 3000)$ DECAY MODES

Mode
$\Gamma_1 N \pi$

$\Delta(\sim 3000)$ BRANCHING RATIOS

$\Gamma(N\pi) / \Gamma_{\text{total}}$	Γ_1 / Γ		
VALUE	DOCUMENT ID	TECN	COMMENT
0.06 \pm 0.02	HENDRY	78	MPWA $\pi N \rightarrow \pi N I_{3,11}$ wave
0.045 \pm 0.02	HENDRY	78	MPWA $\pi N \rightarrow \pi N K_{3,13}$ wave
0.03 \pm 0.01	HENDRY	78	MPWA $\pi N \rightarrow \pi N L_{3,17}$ wave
0.025 \pm 0.01	HENDRY	78	MPWA $\pi N \rightarrow \pi N M_{3,19}$ wave
0.018 \pm 0.01	HENDRY	78	MPWA $\pi N \rightarrow \pi N N_{3,21}$ wave

$\Delta(\sim 3000)$ FOOTNOTES

¹ In addition, KOCH 80 reports some evidence for an $S_{31} \Delta(2700)$ and a $P_{33} \Delta(2800)$.

$\Delta(\sim 3000)$ REFERENCES

KOCH 80	Toronto Conf. 3	R. Koch	(KARLT) IJP
HENDRY 78	PRL 41 222	A.W. Hendry	(IND, LBL) IJP
Also	ANP 136 1	A.W. Hendry	(IND)

EXOTIC BARYONS

PENTAQUARKS

Written May 2008 by C.G. Wohl (LBNL).

See pp. 1019–1022 of the 2006 *Review* [1] for the evidence for the $\Theta(1540)$, $\Phi(1860)$, and $\Theta_c(3100)$, and for the early unsuccessful attempts to confirm them. The table below lists papers published since then giving results of further unsuccessful searches. There are experiments at high energies and low; in new reactions and old; there are experiments—some by the same groups that claimed the original discoveries—with orders-of-magnitude greater statistics than before; there are experiments that find 100,000 $\Lambda(1520)$ s in $\bar{K}N$, but no hint of a $\Theta(1540)$ in KN . Many of the experiments search over large ranges of mass. The limits on production of a pentaquark given in the

last column of the table are at 90 or 95% confidence level; the cross-section limits are in some cases now fractions of a nanobarn. The limits often involve assumptions about the width of the pentaquark, its production angular distribution, or other matters. There is not room (or reason) to give here all the details—for which, see the papers.

There are two or three recent experiments that find weak evidence for signals near the nominal masses, but there is simply no point in tabulating them in view of the overwhelming evidence that the claimed pentaquarks do not exist. The only advance in particle physics thought worthy of mention in the American Institute of Physics “Physics News in 2003” was a false alarm. The whole story—the discoveries themselves, the tidal wave of papers by theorists and phenomenologists that followed, and the eventual “undiscovery”—is a curious episode in the history of science.

Table 1: Unsuccessful searches for pentaquarks. There are ten more unsuccessful searches for the $\Theta(1540)$, nine for the $\Phi(1860)$, and three for the $\Theta_c(3100)$ listed in our 2006 edition [1].

Experiment	Reaction	Energy, etc.	Limits, etc.
<u>Searches for the $\Theta(1540)^+$</u>			
BABAR [2]	$B^0 \rightarrow (pK_S^0)\bar{p}$	\sqrt{s} 10.58 GeV	$< 2 \times 10^{-7}$ per B^0
CLAS [3]	$\gamma p \rightarrow (nK^+/pK_S^0)K^0$	E_γ 1.6–3.8 GeV	$\sigma < 0.7$ nb, 100k $\Lambda(1520)$
CLAS [4]	$\gamma d \rightarrow (nK^+)pK^-$	E_γ 0.8–3.6 GeV	$\sigma < 0.3$ nb
CLAS [5]	$\gamma d \rightarrow (nK^+)\Lambda$	E_γ 0.8–3.6 GeV	$\sigma < 5$ –25 nb
COSY-ANKE [6]	$pp \rightarrow (pK_S^0)\Lambda\pi^+$	p_p 3.65 GeV/c	$\sigma < 58$ nb
COSY-TOF [7]	$pp \rightarrow (pK_S^0)\Sigma^+$	p_p 3.059 GeV/c	$\sigma < 150$ nb
DELPHI [8]	$Z \rightarrow (pK_S^0)X$	\sqrt{s} 91.2 GeV	$< 5.1 \times 10^{-4}$ per Z
FOCUS [9]	$\gamma A \rightarrow (pK_S^0)X$	\bar{E}_γ 180 GeV	400k $\Sigma(1385)^+$
HERA-H1 [10]	$ep \rightarrow (p/\bar{p}K_S^0)eX$	$5 < Q^2 < 100$ GeV ²	$\sigma < 30$ –90 pb
KEK-E522 [11]	$\pi^- p \rightarrow K^-(X)$	p_π 1.9 GeV/c	$\sigma < 3.9$ nb
L3 [12]	$\gamma^*\gamma^* \rightarrow (p/\bar{p}K_S^0)X$	$E_{\gamma\gamma} > 5$ GeV	$\sigma < 1.8$ nb
NOMAD [13]	$\nu_\mu N \rightarrow (pK_S^0)X$		$< 2.13 \times 10^{-3}$ per evt
<u>Searches for a pK^+ state</u>			
CLAS [14]	$\gamma p \rightarrow (pK^+)K^-$	E_γ 1.8–3.8 GeV	$\sigma < 0.15$ nb
DELPHI [8]	$Z \rightarrow (pK^+)X$	\sqrt{s} 91.2 GeV	$< 1.6 \times 10^{-3}$ per Z
JLAB-HALL-A [15]	$ep \rightarrow eK^-(X)$	E_e 5 GeV	$< 5\%$ of $\Lambda(1520)$
<u>Searches for the $\Phi(1860)$</u>			
CDF [16]	$\bar{p}p \rightarrow (\Xi^-\pi^\pm)X$	\sqrt{s} 1.96 TeV	1.9k $\Xi(1530)^0$
DELPHI [8]	$Z \rightarrow (\Xi^-\pi^-)X$	\sqrt{s} 91.2 GeV	$< 2.9 \times 10^{-4}$ per Z
FOCUS [17]	$\gamma N \rightarrow (\Xi^-\pi^-)X$	\bar{E}_γ 180 GeV	65k $\Xi(1530)^0$
HERA-H1 [18]	$ep \rightarrow (\Xi^-\pi^\pm)eX$	$2 < Q^2 < 100$ GeV ²	163 $\Xi(1530)^0$
SERP-EXCHARM [19]	$nC \rightarrow (\Xi^-\pi^\pm)X$	\bar{E}_n 51 GeV	1.5k $\Xi(1530)^0$
<u>Searches for the $\Theta_c(3100)$</u>			
BABAR [20]	$e^+e^- \rightarrow (pD^{*-})X$	\sqrt{s} 10.58 GeV	125k evts
CHORUS [21]	$\bar{\nu}_\mu A \rightarrow \mu^+X$	\bar{E}_ν 18 GeV	2262 evts
DELPHI [8]	$Z \rightarrow (pD^{*-})X$	\sqrt{s} 91.2 GeV	$< 8.8 \times 10^{-4}$ per Z

References

1. W.-M Yao *et al.*, J. Phys. **G33**, 1 (2006).
 2. B. Aubert *et al.*, Phys. Rev. **D76**, 092004 (2007).
 3. R. De Vita *et al.*, Phys. Rev. **D74**, 032001 (2006).
 4. B. McKinnon *et al.*, Phys. Rev. Lett. **96**, 212001 (2006).
 5. S. Niccolai *et al.*, Phys. Rev. Lett. **97**, 032001 (2006).
 6. M. Nekipelov *et al.*, J. Phys. **G34**, 627 (2007).
 7. M. Abdel-Bary *et al.*, Phys. Lett. **B649**, 252 (2007).
 8. J. Abdallah *et al.*, Phys. Lett. **B653**, 151 (2007).
 9. J.M. Link *et al.*, Phys. Lett. **B639**, 604 (2006).
 10. A. Aktas *et al.*, Phys. Lett. **B639**, 202 (2006).
 11. K. Miwa *et al.*, Phys. Lett. **B635**, 72 (2006).
 12. P. Achard *et al.*, Eur. Phys. J. **C49**, 395 (2007).
 13. O. Samoylov *et al.*, Eur. Phys. J. **C49**, 499 (2007).
 14. V. Kubarovsky *et al.*, Phys. Rev. Lett. **97**, 102001 (2006).
 15. Y. Qiang *et al.*, Phys. Rev. **C75**, 055208 (2007).
 16. A. Abulencia *et al.*, Phys. Rev. **D75**, 032003 (2007).
 17. J.M. Link *et al.*, Phys. Lett. **B661**, 14 (2008).
 18. A. Aktas *et al.*, Eur. Phys. J. **C52**, 507 (2007).
 19. A.N. Aleev *et al.*, Sov. J. Nucl. Phys. **70**, 1527 (2007).
 20. B. Aubert *et al.*, Phys. Rev. **D73**, 091101 (2006).
 21. G. De Lellis *et al.*, Nucl. Phys. **B763**, 268 (2007).
-

Baryon Particle Listings

Λ

Λ BARYONS

$(S = -1, I = 0)$

$\Lambda^0 = uds$

$I(J^P) = 0(\frac{1}{2}^+)$ Status: * * * *

We have omitted some results that have been superseded by later experiments. See our earlier editions.

Λ MASS

The fit uses Λ , Σ^+ , Σ^0 , Σ^- mass and mass-difference measurements.

VALUE (MeV)	EVTS	DOCUMENT ID	TECN	COMMENT
1115.683 ± 0.006 OUR FIT				
1115.683 ± 0.006 OUR AVERAGE				
1115.678 ± 0.006 ± 0.006	20k	HARTOUNI	94	SPEC pp 27.5 GeV/c
1115.690 ± 0.008 ± 0.006	18k	¹ HARTOUNI	94	SPEC pp 27.5 GeV/c
• • • We do not use the following data for averages, fits, limits, etc. • • •				
1115.59 ± 0.08	935	HYMAN	72	HEBC
1115.39 ± 0.12	195	MAYEUR	67	EMUL
1115.6 ± 0.4		LONDON	66	HBC
1115.65 ± 0.07	488	² SCHMIDT	65	HBC
1115.44 ± 0.12		³ BHOWMIK	63	RVUE

¹We assume *CPT* invariance: this is the $\bar{\Lambda}$ mass as measured by HARTOUNI 94. See below for the fractional mass difference, testing *CPT*.
²The SCHMIDT 65 masses have been reevaluated using our April 1973 proton and K^\pm and π^\pm masses. P. Schmidt, private communication (1974).
³The mass has been raised 35 keV to take into account a 46 keV increase in the proton mass and an 11 keV decrease in the π^\pm mass (note added Reviews of Modern Physics **39** 1 (1967)).

$$(m_\Lambda - m_{\bar{\Lambda}}) / m_\Lambda$$

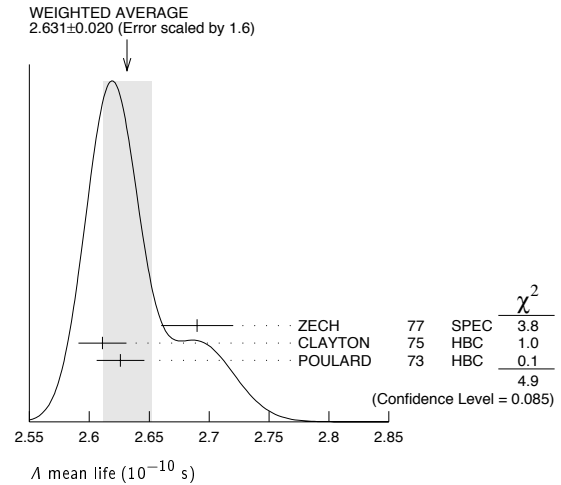
A test of *CPT* invariance.

VALUE (units 10^{-5})	EVTS	DOCUMENT ID	TECN	COMMENT
- 0.1 ± 1.1 OUR AVERAGE				Error includes scale factor of 1.6.
+ 1.3 ± 1.2	31k	⁴ RYBICKI	96	NA32 π^- Cu, 230 GeV
- 1.08 ± 0.90		HARTOUNI	94	SPEC pp 27.5 GeV/c
4.5 ± 5.4		CHIEN	66	HBC 6.9 GeV/c $\bar{p}p$
• • • We do not use the following data for averages, fits, limits, etc. • • •				
-26 ± 13		BADIER	67	HBC 2.4 GeV/c $\bar{p}p$
⁴ RYBICKI 96 is an analysis of old ACCMOR (NA32) data.				

Λ MEAN LIFE

Measurements with an error $\geq 0.1 \times 10^{-10}$ s have been omitted altogether, and only the latest high-statistics measurements are used for the average.

VALUE (10^{-10} s)	EVTS	DOCUMENT ID	TECN	COMMENT
2.631 ± 0.020 OUR AVERAGE				Error includes scale factor of 1.6. See the ideogram below.
2.69 ± 0.03	53k	ZECH	77	SPEC Neutral hyperon beam
2.611 ± 0.020	34k	CLAYTON	75	HBC 0.96-1.4 GeV/c $K^- p$
2.626 ± 0.020	36k	POULARD	73	HBC 0.4-2.3 GeV/c $K^- p$
• • • We do not use the following data for averages, fits, limits, etc. • • •				
2.69 ± 0.05	6582	ALTHOFF	73B	OSPK $\pi^+ n \rightarrow \Lambda K^+$
2.54 ± 0.04	4572	BALTAY	71B	HBC $K^- p$ at rest
2.535 ± 0.035	8342	GRIMM	68	HBC
2.47 ± 0.08	2600	HEPP	68	HBC
2.35 ± 0.09	916	BURAN	66	HLBC
2.452 ^{+0.056} _{-0.054}	2213	ENGELMANN	66	HBC
2.59 ± 0.09	794	HUBBARD	64	HBC
2.59 ± 0.07	1378	SCHWARTZ	64	HBC
2.36 ± 0.06	2239	BLOCK	63	HEBC



$$(\tau_\Lambda - \tau_{\bar{\Lambda}}) / \tau_\Lambda$$

A test of *CPT* invariance.

VALUE	DOCUMENT ID	TECN	COMMENT
-0.001 ± 0.009 OUR AVERAGE			
-0.0018 ± 0.0066 ± 0.0056	BARNES	96	CNTR LEAR $\bar{p}p \rightarrow \bar{\Lambda}\Lambda$
0.04 ± 0.085	BADIER	67	HBC 2.4 GeV/c $\bar{p}p$

BARYON MAGNETIC MOMENTS

Written 1994 by C.G. Wohl (LBNL).

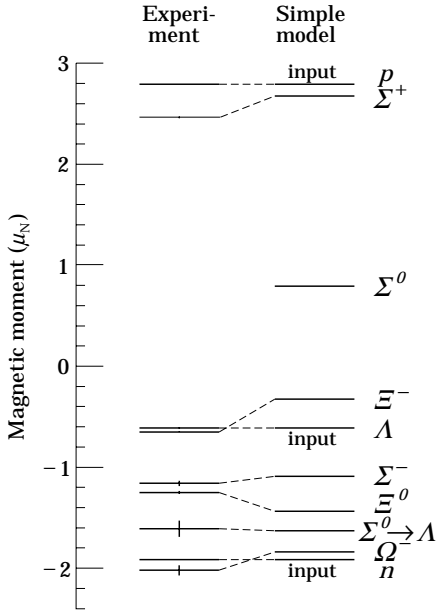
The figure below shows the measured magnetic moments of the stable baryons. It also shows the predictions of the simplest quark model, using the measured p , n , and Λ moments as input. In this model, the moments are [1]

$$\begin{aligned} \mu_p &= (4\mu_u - \mu_d)/3 & \mu_n &= (4\mu_d - \mu_u)/3 \\ \mu_{\Sigma^+} &= (4\mu_u - \mu_s)/3 & \mu_{\Sigma^-} &= (4\mu_d - \mu_s)/3 \\ \mu_{\Xi^0} &= (4\mu_s - \mu_u)/3 & \mu_{\Xi^-} &= (4\mu_s - \mu_d)/3 \\ \mu_\Lambda &= \mu_s & \mu_{\Sigma^0} &= (2\mu_u + 2\mu_d - \mu_s)/3 \\ & & \mu_{\Omega^-} &= 3\mu_s \end{aligned}$$

and the $\Sigma^0 \rightarrow \Lambda$ transition moment is

$$\mu_{\Sigma^0\Lambda} = (\mu_d - \mu_u)/\sqrt{3}.$$

The quark moments that result from this model are $\mu_u = +1.852 \mu_N$, $\mu_d = -0.972 \mu_N$, and $\mu_s = -0.613 \mu_N$. The corresponding effective quark masses, taking the quarks to be Dirac point particles, where $\mu = q\hbar/2m$, are 338, 322, and 510 MeV. As the figure shows, the model gives a good first approximation to the experimental moments. For efforts to make a better model, we refer to the literature [2].



Λ DECAY MODES

Mode	Fraction (Γ_i/Γ)
Γ_1 $p\pi^-$	$(63.9 \pm 0.5) \%$
Γ_2 $n\pi^0$	$(35.8 \pm 0.5) \%$
Γ_3 $n\gamma$	$(1.75 \pm 0.15) \times 10^{-3}$
Γ_4 $p\pi^-\gamma$	[a] $(8.4 \pm 1.4) \times 10^{-4}$
Γ_5 $p e^- \bar{\nu}_e$	$(8.32 \pm 0.14) \times 10^{-4}$
Γ_6 $p\mu^- \bar{\nu}_\mu$	$(1.57 \pm 0.35) \times 10^{-4}$

[a] See the Listings below for the pion momentum range used in this measurement.

CONSTRAINED FIT INFORMATION

An overall fit to 5 branching ratios uses 20 measurements and one constraint to determine 5 parameters. The overall fit has a $\chi^2 = 10.5$ for 16 degrees of freedom.

The following *off-diagonal* array elements are the correlation coefficients $\langle \delta x_i \delta x_j \rangle / (\delta x_i \delta x_j)$, in percent, from the fit to the branching fractions, $x_i \equiv \Gamma_i/\Gamma_{\text{total}}$. The fit constrains the x_i whose labels appear in this array to sum to one.

x_2	-100			
x_3	-2	-1		
x_5	46	-46	-1	
x_6	0	0	0	0
	x_1	x_2	x_3	x_5

Λ BRANCHING RATIOS

$\Gamma(p\pi^-)/\Gamma(N\pi)$				$\Gamma_1/(\Gamma_1+\Gamma_2)$
VALUE	EVTS	DOCUMENT ID	TECN	COMMENT
0.641 ± 0.005 OUR FIT				
0.640 ± 0.005 OUR AVERAGE				
0.646 ± 0.008	4572	BALTAY	71B HBC	$K^- p$ at rest
0.635 ± 0.007	6736	DOYLE	69 HBC	$\pi^- p \rightarrow \Lambda K^0$
0.643 ± 0.016	903	HUMPHREY	62 HBC	
0.624 ± 0.030		CRAWFORD	59B HBC	$\pi^- p \rightarrow \Lambda K^0$

$\Gamma(n\pi^0)/\Gamma(N\pi)$				$\Gamma_2/(\Gamma_1+\Gamma_2)$
VALUE	EVTS	DOCUMENT ID	TECN	COMMENT
0.359 ± 0.005 OUR FIT				
0.310 ± 0.028 OUR AVERAGE				
0.35 ± 0.05		BROWN	63 HLBC	
0.291 ± 0.034	75	CHRETIEN	63 HLBC	

$\Gamma(n\gamma)/\Gamma_{\text{total}}$				Γ_3/Γ
VALUE (units 10^{-3})	EVTS	DOCUMENT ID	TECN	COMMENT
1.75 ± 0.15 OUR FIT				
1.75 ± 0.15	1816	LARSON	93 SPEC	$K^- p$ at rest
• • • We do not use the following data for averages, fits, limits, etc. • • •				
$1.78 \pm 0.24^{+0.14}_{-0.16}$	287	NOBLE	92 SPEC	See LARSON 93

$\Gamma(n\gamma)/\Gamma(n\pi^0)$				Γ_3/Γ_2
VALUE (units 10^{-3})	EVTS	DOCUMENT ID	TECN	COMMENT
2.86 ± 0.74 ± 0.57	24	BIAGI	86 SPEC	SPS hyperon beam
• • • We do not use the following data for averages, fits, limits, etc. • • •				

$\Gamma(p\pi^-\gamma)/\Gamma(p\pi^-)$				Γ_4/Γ_1
VALUE (units 10^{-3})	EVTS	DOCUMENT ID	TECN	COMMENT
1.32 ± 0.22	72	BAGGETT	72C HBC	$\pi^- < 95$ MeV/c

$\Gamma(p e^- \bar{\nu}_e)/\Gamma(p\pi^-)$				Γ_5/Γ_1
VALUE (units 10^{-3})	EVTS	DOCUMENT ID	TECN	COMMENT
1.301 ± 0.019 OUR FIT				
1.301 ± 0.019 OUR AVERAGE				
1.335 ± 0.056	7111	BOURQUIN	83 SPEC	SPS hyperon beam
1.313 ± 0.024	10k	WISE	80 SPEC	
1.23 ± 0.11	544	LINDQUIST	77 SPEC	$\pi^- p \rightarrow K^0 \Lambda$
1.27 ± 0.07	1089	KATZ	73 HBC	
1.31 ± 0.06	1078	ALTHOFF	71 OSPK	
1.17 ± 0.13	86	CANTER	71 HBC	$K^- p$ at rest
1.20 ± 0.12	143	MALONEY	69 HBC	
1.17 ± 0.18	120	BAGLIN	64 FBC	K^- freon 1.45 GeV/c
1.23 ± 0.20	150	ELY	63 FBC	
• • • We do not use the following data for averages, fits, limits, etc. • • •				
1.32 ± 0.15	218	LINDQUIST	71 OSPK	See LINDQUIST 77

⁷ Changed by us from $\Gamma(p e^- \bar{\nu}_e)/\Gamma(N\pi)$ assuming the authors used $\Gamma(p\pi^-)/\Gamma_{\text{total}} = 2/3$.

⁸ Changed by us from $\Gamma(p e^- \bar{\nu}_e)/\Gamma(N\pi)$ because $\Gamma(p e^- \nu)/\Gamma(p\pi^-)$ is the directly measured quantity.

References

- See, for example, D.H. Perkins, *Introduction to High Energy Physics* (Addison-Wesley, Reading, MA, 1987), or D. Griffiths, *Introduction to Elementary Particles* (Harper & Row, New York, 1987).
- See, for example, J. Franklin, Phys. Rev. **D29**, 2648 (1984); H.J. Lipkin, Nucl. Phys. **B241**, 477 (1984); K. Suzuki, H. Kumagai, and Y. Tanaka, Europhys. Lett. **2**, 109 (1986); S.K. Gupta and S.B. Khadkikar, Phys. Rev. **D36**, 307 (1987); M.I. Krivoruchenko, Sov. J. Nucl. Phys. **45**, 109 (1987); L. Brekke and J.L. Rosner, Comm. Nucl. Part. Phys. **18**, 83 (1988); K.-T. Chao, Phys. Rev. **D41**, 920 (1990) and references cited therein Also, see references cited in discussions of results in the experimental papers..

Λ MAGNETIC MOMENT

See the "Note on Baryon Magnetic Moments" above. Measurements with an error $\geq 0.15 \mu_N$ have been omitted.

VALUE (μ_N)	EVTS	DOCUMENT ID	TECN	COMMENT
-0.613 ± 0.004 OUR AVERAGE				
-0.606 ± 0.015	200k	COX	81 SPEC	
-0.6138 ± 0.0047	3M	SCHACHIN...	78 SPEC	
-0.59 ± 0.07	350k	HELLER	77 SPEC	
-0.57 ± 0.05	1.2M	BUNCE	76 SPEC	
-0.66 ± 0.07	1300	DAHL-JENSEN71	EMUL	200 KG field

Λ ELECTRIC DIPOLE MOMENT

A nonzero value is forbidden by both *T* invariance and *P* invariance.

VALUE (10^{-16} e cm)	CL%	DOCUMENT ID	TECN	COMMENT
< 1.5	95	⁵ PONDROM	81 SPEC	
• • • We do not use the following data for averages, fits, limits, etc. • • •				
<100	95	⁶ BARONI	71 EMUL	
<500	95	GIBSON	66 EMUL	

⁵ PONDROM 81 measures $(-3.0 \pm 7.4) \times 10^{-17}$ e-cm.

⁶ BARONI 71 measures $(-5.9 \pm 2.9) \times 10^{-15}$ e-cm.

Baryon Particle Listings

 Λ , Λ' s and Σ' 's $\Gamma(\rho\mu^- \bar{\nu}_\mu)/\Gamma(N\pi)$

VALUE (units 10^{-4})	EVTS	DOCUMENT ID	TECN	COMMENT
1.57 ± 0.35				OUR FIT
1.57 ± 0.35				OUR AVERAGE
1.4 ± 0.5	14	BAGGETT	72B	HBC $K^- p$ at rest
2.4 ± 0.8	9	CANTER	71B	HBC $K^- p$ at rest
1.3 ± 0.7	3	LIND	64	RVUE
1.5 ± 1.2	2	RONNE	64	FBC

 Λ DECAY PARAMETERS

See the "Note on Baryon Decay Parameters" in the neutron Listings. Some early results have been omitted.

 α_- FOR $\Lambda \rightarrow p\pi^-$

VALUE	EVTS	DOCUMENT ID	TECN	COMMENT
0.642 ± 0.013				OUR AVERAGE
0.584 ± 0.046	8500	ASTBURY	75	SPEC
0.649 ± 0.023	10325	CLELAND	72	OSPK
0.67 ± 0.06	3520	DAUBER	69	HBC From Ξ decay
0.645 ± 0.017	10130	OVERSETH	67	OSPK Λ from $\pi^- p$
0.62 ± 0.07	1156	CRONIN	63	CNTR Λ from $\pi^- p$

 ϕ ANGLE FOR $\Lambda \rightarrow p\pi^-$

VALUE ($^\circ$)	EVTS	DOCUMENT ID	TECN	COMMENT
-6.5 ± 3.5				OUR AVERAGE
-7.0 ± 4.5	10325	CLELAND	72	OSPK Λ from $\pi^- p$
-8.0 ± 6.0	10130	OVERSETH	67	OSPK Λ from $\pi^- p$
13.0 ± 17.0	1156	CRONIN	63	OSPK Λ from $\pi^- p$

 $\alpha_0 / \alpha_- = \alpha(\Lambda \rightarrow n\pi^0) / \alpha(\Lambda \rightarrow p\pi^-)$

VALUE	EVTS	DOCUMENT ID	TECN	COMMENT
1.01 ± 0.07				OUR AVERAGE
1.000 ± 0.068	4760	⁹ OLSEN	70	OSPK $\pi^+ n \rightarrow \Lambda K^+$
1.10 ± 0.27		CORK	60	CNTR

⁹ OLSEN 70 compares proton and neutron distributions from Λ decay.

 $[\alpha_-(\Lambda) + \alpha_+(\bar{\Lambda})] / [\alpha_-(\Lambda) - \alpha_+(\bar{\Lambda})]$

Zero if CP is conserved; α_- and α_+ are the asymmetry parameters for $\Lambda \rightarrow p\pi^-$ and $\bar{\Lambda} \rightarrow \bar{p}\pi^+$ decay. See also the Ξ^- for a similar test involving the decay chain $\Xi^- \rightarrow \Lambda\pi^-, \Lambda \rightarrow p\pi^-$ and the corresponding antiparticle chain.

VALUE	EVTS	DOCUMENT ID	TECN	COMMENT
0.012 ± 0.021				OUR AVERAGE
$+0.013 \pm 0.022$	96k	BARNES	96	CNTR LEAR $\bar{p}p \rightarrow \bar{\Lambda}\Lambda$
$+0.01 \pm 0.10$	770	TIXIER	88	DM2 $J/\psi \rightarrow \Lambda\bar{\Lambda}$
-0.02 ± 0.14	10k	¹⁰ CHAUVAT	85	CNTR $pp, \bar{p}p$ ISR
-0.07 ± 0.09	4063	BARNES	87	CNTR See BARNES 96

 g_A / g_V FOR $\Lambda \rightarrow p e^- \bar{\nu}_e$

Measurements with fewer than 500 events have been omitted. Where necessary, signs have been changed to agree with our conventions, which are given in the "Note on Baryon Decay Parameters" in the neutron Listings. The measurements all assume that the form factor $g_2 = 0$. See also the footnote on DWORKIN 90.

VALUE	EVTS	DOCUMENT ID	TECN	COMMENT
-0.718 ± 0.015				OUR AVERAGE
$-0.719 \pm 0.016 \pm 0.012$	37k	¹¹ DWORKIN	90	SPEC $e\nu$ angular corr.
-0.70 ± 0.03	7111	BOURQUIN	83	SPEC $\Xi \rightarrow \Lambda\pi^-$
-0.734 ± 0.031	10k	¹² WISE	81	SPEC $e\nu$ angular correl.
-0.63 ± 0.06	817	ALTHOFF	73	OSPK Polarized Λ

¹¹ The tabulated result assumes the weak-magnetism coupling $w \equiv g_w(0)/g_V(0)$ to be 0.97, as given by the CVC hypothesis and as assumed by the other listed measurements. However, DWORKIN 90 measures w to be 0.15 ± 0.30 , and then $g_A/g_V = -0.731 \pm 0.016$.

¹² This experiment measures only the absolute value of g_A/g_V .

 $\Gamma_6/(\Gamma_1+\Gamma_2)$ Λ REFERENCES

We have omitted some papers that have been superseded by later experiments. See our earlier editions.

BARNES	96	PR C54 1877	P.D. Barnes <i>et al.</i>	(CERN PS-185 Collab.)
RYBIK	96	APP B27 2155	K. Rybicki	
HARTOUNI	94	PRL 72 1322	E.P. Hartouni <i>et al.</i>	(BNL E766 Collab.)
Also		PRL 72 2821 (erratum)	E.P. Hartouni <i>et al.</i>	(BNL E766 Collab.)
LARSON	93	PR D47 799	K.D. Larson <i>et al.</i>	(BNL-811 Collab.)
NOBLE	92	PRL 69 414	A.J. Noble <i>et al.</i>	(BIRM, BOST, BRCO+)
DWORKIN	90	PR D41 780	J. Dworkin <i>et al.</i>	(MICH, WIS C, RUTG+)
TIXIER	88	PL B212 523	M.H. Tixier <i>et al.</i>	(DM2 Collab.)
BARNES	87	PL B199 147	P.D. Barnes <i>et al.</i>	(CMU, SA CL, LANL+)
BIAGI	86	ZPHY C30 201	S.F. Biagi <i>et al.</i>	(BRIS, CERN, GEVA+)
CHAUVAT	85	PL 163B 273	P. Chauvat <i>et al.</i>	(CERN, CLER, UCLA+)
BOURQUIN	83	ZPHY C21 1	M.H. Bourquin <i>et al.</i>	(BRIS, GEVA, HEIDP+)
COX	81	PRL 46 877	P.T. Cox <i>et al.</i>	(MICH, WIS C, RUTG, MINN+)
PONDROM	81	PR D23 814	L. Pondrom <i>et al.</i>	(WISC, MICH, RUTG+)
WISE	81	PL 98B 123	J.E. Wise <i>et al.</i>	(MASA, BNL)
WISE	80	PL 91B 165	J.E. Wise <i>et al.</i>	(MASA, BNL)
SCHACHIN...	78	PRL 41 1348	L. Schachinger <i>et al.</i>	(MICH, RUTG, WIS C)
HELLER	77	PL 68B 480	K. Heller <i>et al.</i>	(MICH, WIS C, HEIDH)
LINDQUIST	77	PR D16 2104	J. Lindquist <i>et al.</i>	(EFI, OSU, ANL)
Also		JPG 2 L211	J. Lindquist <i>et al.</i>	(EFI, WUSL, OSU+)
ZECH	77	NP B124 413	G. Zech <i>et al.</i>	(SIEG, CERN, DORT, HEIDH)
BUNCE	76	PRL 36 1113	G.R.M. Bunce <i>et al.</i>	(WISC, MICH, RUTG)
ASTBURY	75	NP B39 30	P. Astbury <i>et al.</i>	(LOIC, CERN, ETH+)
CLAYTON	75	NP B95 130	E.F. Clayton <i>et al.</i>	(LOIC, RHEL)
ALTHOFF	73	PL 43B 237	K.H. Althoff <i>et al.</i>	(CERN, HEID)
ALTHOFF	73B	NP B66 29	K.H. Althoff <i>et al.</i>	(CERN, HEID)
KATZ	73	Thesis MDDP-TR-74-044	C.M. Katz	(UMD)
POULARD	73	PL 46B 135	G. Poulard, A. Givernaud, A.C. Borg	(SA CL)
BAGGETT	72B	ZPHY 252 362	M.J. Baggett <i>et al.</i>	(HEID)
BAGGETT	72C	PL 42B 379	M.J. Baggett <i>et al.</i>	(HEID)
CLELAND	72	NP B40 221	W.E. Cleland <i>et al.</i>	(CERN, GEVA, LUND)
HYMAN	72	PR D5 1063	L.G. Hyman <i>et al.</i>	(ANL, CMU)
ALTHOFF	71	PL 37B 531	K.H. Althoff <i>et al.</i>	(CERN, HEID)
BALTAY	71B	PR D4 670	C. Baltay <i>et al.</i>	(COLU, BING)
BARONI	71	LNC 2 1256	G. Baroni, S. Petrer, G. Romano	(ROMA)
CANTER	71	PRL 25 868	J. Canter <i>et al.</i>	(STON, COLU)
CANTER	71B	PRL 27 59	J. Canter <i>et al.</i>	(STON, COLU)
DAHL-JENSEN	71	NC 3A 1	E. Dahl-Jensen <i>et al.</i>	(CERN, ANKA, LAUS+)
LINDQUIST	71	PRL 27 612	J. Lindquist <i>et al.</i>	(EFI, WUSL, OSU+)
OLSEN	70	PRL 24 843	S.L. Olsen <i>et al.</i>	(WISC, MICH)
DAUBER	69	PR 179 1262	P.M. Dauber <i>et al.</i>	(LRL)
DOYLE	69	Thesis UCRL 18139	J.C. Doyle	(LRL)
MALONEY	69	PRL 23 425	J.E. Maloney, B. Sechi-Zorn	(UMD)
GRIMM	68	NC 54A 187	H.J. Grimm	(HEID)
HEPP	68	ZPHY 214 71	V. Hepp, H. Schleich	(HEID)
BADIER	67	PL 25B 152	J. Badier <i>et al.</i>	(EPOL)
MAYEUR	67	ULibr.BruX.Bul. 32	C. Mayeur, E. Tompa, J.H. Wickens	(BELG, LOUC)
OVERSETH	67	PRL 19 391	O.E. Overseth, R.F. Roth	(MICH, PRIN)
PDG	67	RMP 39 1	A.H. Rosenfeld <i>et al.</i>	(LRL, CERN, YALE)
BURAN	66	PL 20 318	T. Buran <i>et al.</i>	(OSLO)
CHIEN	66	PR 152 1171	C.Y. Chien <i>et al.</i>	(YALE, BNL)
ENGELMANN	66	NC 45A 1038	R. Engelmann <i>et al.</i>	(HEID, REHO)
GIBSON	66	NC 45A 882	W.M. Gibson, K. Green	(BRIS)
LONDON	66	PR 143 1034	G.W. London <i>et al.</i>	(BNL, SYRA)
SCHMIDT	65	PR 140B 1328	P. Schmidt	(COLU)
BAGLIN	64	NC 35 977	C. Baglin <i>et al.</i>	(EPOL, CERN, LOUC, RHEL+)
HUBBARD	64	PR 135 B183	J.R. Hubbard <i>et al.</i>	(LRL)
LIND	64	PR 135 B1483	V.G. Lind <i>et al.</i>	(WIS C)
RONNE	64	PL 11 357	B.E. Ronne <i>et al.</i>	(CERN, EPOL, LOUC+)
SCHWARTZ	64	Thesis UCRL 11360	J.A. Schwartz	(LRL)
BHOWMIK	63	NC 28 1494	B. Bhowmik, D.P. Goyal	(DELH)
BLOCK	63	PR 130 766	M.M. Block <i>et al.</i>	(NWES, BGNA, SYRA+)
BROWN	63	PR 130 769	J.L. Brown <i>et al.</i>	(LRL, MICH)
CHRETIEN	63	PR 131 2208	M. Chretien <i>et al.</i>	(BRAN, BROW, HARV+)
CRONIN	63	PR 129 1795	J.W. Cronin, O.E. Overseth	(PRIN)
ELY	63	PR 131 868	R.P. Ely <i>et al.</i>	(LRL)
HUMPHREY	62	PR 127 1305	W.E. Humphrey, R.R. Ross	(LRL)
CORK	60	PR 120 1000	B. Cork <i>et al.</i>	(LRL, PRIN, BNL)
CRAWFORD	59B	PRL 2 266	F.S. Crawford <i>et al.</i>	(LRL)

Λ AND Σ RESONANCES

Introduction: The only new data entries in this 2006 Review are two measurements of the $\Lambda(1520) \rightarrow \Lambda\gamma$ branching fraction and measurements of the $\Sigma(1385) \rightarrow \Lambda\gamma$ and $\Sigma^- \rightarrow \gamma$ branching fractions. The field remains at a standstill. What follows is a much abbreviated version of the note on Λ and Σ Resonances from our 1990 edition [1]. In particular, see that edition for some representative Argand plots from partial-wave analyses.

Table 1 is an attempt to evaluate the status, both overall and channel by channel, of each Λ and Σ resonance in the Particle Listings. The evaluations are of course partly subjective. A blank indicates there is no evidence at all: either the relevant couplings are small or the resonance does not really exist. The main Baryon Summary Table includes only the established resonances (overall status 3 or 4 stars). A number of the 1- and 2-star entries may eventually disappear, but there are certainly many resonances yet to be discovered underlying the established ones.

Sign conventions for resonance couplings: In terms of the isospin-0 and -1 elastic scattering amplitudes A_0 and A_1 , the amplitude for $K^- p \rightarrow \bar{K}^0 n$ scattering is $\pm(A_1 - A_0)/2$, where the sign depends on conventions used in conjunction with the Clebsch-Gordan coefficients (such as, is the baryon or the meson the “first” particle). If this reaction is partial-wave analyzed and if the overall phase is chosen so that, say, the $\Sigma(1775)D_{15}$ amplitude at resonance points along the positive imaginary axis (points “up”), then any Σ at resonance will point “up” and any Λ at resonance will point “down” (along the negative imaginary axis). Thus the phase at resonance determines the isospin. The above ignores background amplitudes in the resonating partial waves.

That is the basic idea. In a similar but somewhat more complicated way, the phases of the $\bar{K}N \rightarrow \Lambda\pi$ and $\bar{K}N \rightarrow \Sigma\pi$ amplitudes for a resonating wave help determine the SU(3) multiplet to which the resonance belongs. Again, a convention has to be adopted for some overall arbitrary phases: which way is “up”? Our convention is that of Levi-Setti [2] and is shown in Fig. 1, which also compares experimental results with theoretical predictions for the signs of several resonances. In the Listings, a + or - sign in front of a measurement of an inelastic resonance coupling indicates the sign (the *absence* of a sign means that the sign is not determined, *not* that it is positive). For more details, see Appendix II of our 1982 edition [3].

Errors on masses and widths: The errors quoted on resonance parameters from partial-wave analyses are often only statistical, and the parameters can change by more than these errors when a different parametrization of the waves is used. Furthermore, the different analyses use more or less the same data, so it is not really appropriate to treat the different determinations of the resonance parameters as independent or to average them together. In any case, the spread of the masses, widths, and branching fractions from the different analyses is certainly a better indication of the uncertainties than are the quoted errors. In the Baryon Summary Table, we usually give a range reflecting the spread of the values rather than a particular value with error.

For three states, the $\Lambda(1520)$, the $\Lambda(1820)$, and the $\Sigma(1775)$, there is enough information to make an overall fit to the various branching fractions. It is then necessary to use the quoted errors, but the errors obtained from the fit should not be taken seriously.

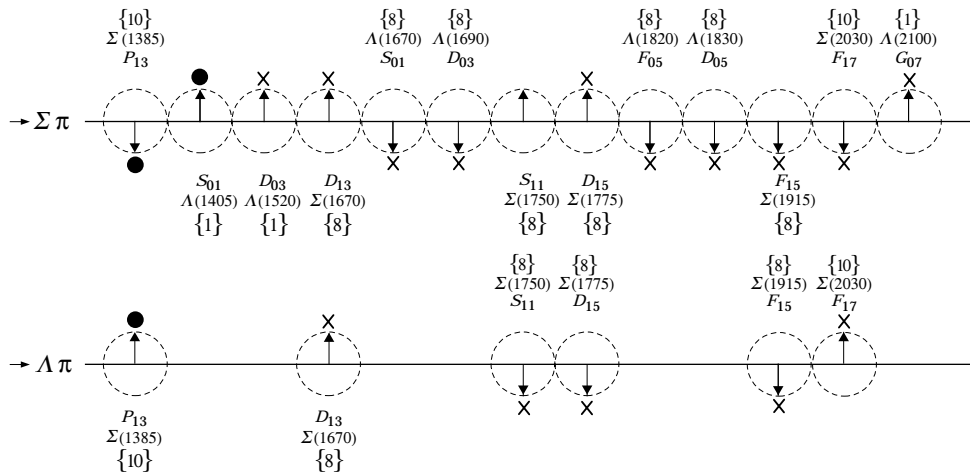


Figure 1. The signs of the imaginary parts of resonating amplitudes in the $\bar{K}N \rightarrow \Lambda\pi$ and $\Sigma\pi$ channels. The signs of the $\Sigma(1385)$ and $\Lambda(1405)$, marked with a \bullet , are set by convention, and then the others are determined relative to them. The signs required by the SU(3) assignments of the resonances are shown with an arrow, and the experimentally determined signs are shown with an \times .

Baryon Particle Listings

 Λ 's and Σ 's, $\Lambda(1405)$ Table 1. The status of the Λ and Σ resonances. Only those with an overall status of *** or **** are included in the main Baryon Summary Table.

Particle	$L_{I,2J}$	Overall status	Status as seen in —			
			$N\bar{K}$	$\Lambda\pi$	$\Sigma\pi$	Other channels
$\Lambda(1116)$	P_{01}	****		F		$N\pi$ (weakly)
$\Lambda(1405)$	S_{01}	****	****	o	****	
$\Lambda(1520)$	D_{03}	****	****	r	****	$\Lambda\pi\pi, \Lambda\gamma$
$\Lambda(1600)$	P_{01}	***	***	b	**	
$\Lambda(1670)$	S_{01}	****	****	i	****	$\Lambda\eta$
$\Lambda(1690)$	D_{03}	****	****	d	****	$\Lambda\pi\pi, \Sigma\pi\pi$
$\Lambda(1800)$	S_{01}	***	***	d	**	$N\bar{K}^*, \Sigma(1385)\pi$
$\Lambda(1810)$	P_{01}	***	***	e	**	$N\bar{K}^*$
$\Lambda(1820)$	F_{05}	****	****	n	****	$\Sigma(1385)\pi$
$\Lambda(1830)$	D_{05}	****	***	F	****	$\Sigma(1385)\pi$
$\Lambda(1890)$	P_{03}	****	****	o	**	$N\bar{K}^*, \Sigma(1385)\pi$
$\Lambda(2000)$	*	*	*	r	*	$\Lambda\omega, N\bar{K}^*$
$\Lambda(2020)$	F_{07}	*	*	b	*	
$\Lambda(2100)$	G_{07}	****	****	i	***	$\Lambda\omega, N\bar{K}^*$
$\Lambda(2110)$	F_{05}	***	**	d	*	$\Lambda\omega, N\bar{K}^*$
$\Lambda(2325)$	D_{03}	*	*	d	*	$\Lambda\omega$
$\Lambda(2350)$		***	***	e	*	
$\Lambda(2585)$		**	**	n		
$\Sigma(1193)$	P_{11}	****				$N\pi$ (weakly)
$\Sigma(1385)$	P_{13}	****		****	****	
$\Sigma(1480)$	*	*	*	*	*	
$\Sigma(1560)$		**	**	**	**	
$\Sigma(1580)$	D_{13}	*	*	*	*	
$\Sigma(1620)$	S_{11}	**	**	*	*	
$\Sigma(1660)$	P_{11}	***	***	*	**	
$\Sigma(1670)$	D_{13}	****	****	****	****	several others
$\Sigma(1690)$		**	*	**	*	$\Lambda\pi\pi$
$\Sigma(1750)$	S_{11}	***	***	**	*	$\Sigma\eta$
$\Sigma(1770)$	P_{11}	*				
$\Sigma(1775)$	D_{15}	****	****	****	***	several others
$\Sigma(1840)$	P_{13}	*	*	**	*	
$\Sigma(1880)$	P_{11}	**	**	**	**	$N\bar{K}^*$
$\Sigma(1915)$	F_{15}	****	***	****	***	$\Sigma(1385)\pi$
$\Sigma(1940)$	D_{13}	***	*	***	**	quasi-2-body
$\Sigma(2000)$	S_{11}	*	*	*	*	$N\bar{K}^*, \Lambda(1520)\pi$
$\Sigma(2030)$	F_{17}	****	****	****	**	several others
$\Sigma(2070)$	F_{15}	*	*	*	*	
$\Sigma(2080)$	P_{13}	**	*	**	*	
$\Sigma(2100)$	G_{17}	*	*	*	*	
$\Sigma(2250)$		***	***	*	*	
$\Sigma(2455)$		**	*	*	*	
$\Sigma(2620)$		**	*	*	*	
$\Sigma(3000)$		*	*	*	*	
$\Sigma(3170)$		*	*	*	*	multi-body

**** Existence is certain, and properties are at least fairly well explored.
 *** Existence ranges from very likely to certain, but further confirmation is desirable and/or quantum numbers, branching fractions, etc. are not well determined.
 ** Evidence of existence is only fair.
 * Evidence of existence is poor.

Production experiments: Partial-wave analyses of course separate partial waves, whereas a peak in a cross section or an invariant mass distribution usually cannot be disentangled from background and analyzed for its quantum numbers; and more than one resonance may be contributing to the peak. Results from partial-wave analyses and from production experiments are generally kept separate in the Listings, and in the Baryon Summary Table results from production experiments are used only for the low-mass states. The $\Sigma(1385)$ and $\Lambda(1405)$ of course lie below the $\bar{K}N$ threshold and nearly everything about them is learned from production experiments; and

production and formation experiments agree quite well in the case of $\Lambda(1520)$ and results have been combined. There is some disagreement between production and formation experiments in the 1600–1700 MeV region: see the note on the $\Sigma(1670)$.

References

1. Particle Data Group, Phys. Lett. **B239**, VIII.64 (1990).
2. R. Levi-Setti, in *Proceedings of the Lund International Conference on Elementary Particles* (Lund, 1969), p. 339.
3. Particle Data Group, Phys. Lett. **111B** (1982).

 $\Lambda(1405) S_{01}$

$$I(J^P) = 0(\frac{1}{2}^-) \text{ Status: } ***$$

See the “Note on the $\Lambda(1405)$ ” in our 2000 edition, Eur. Phys. J. **C15**, p. 748 (2000).

For a recent discussion and earlier references on evidence for a 2-pole structure of the $\Lambda(1405)$, see MAGAS 05. For a recent experiment that gives no support to the 2-pole model, see ZYCHOR 08. The $\Lambda(1405)$ presumably belongs to a $J^P = 1/2^+$ SU(4) $\bar{4}$ multiplet, whose other members are the $\Lambda_C(2595)^+$, $\Xi_C(2790)^+$, and $\Xi_C(2790)^0$; see Fig. 1 of our note on “Charmed Baryons.” Each of these charmed particles is followed by one of slightly higher mass: the $\Lambda_c(2625)^+$, $\Xi_c(2815)^+$, and $\Xi_c(2815)^0$. Although the evidence for their J^P assignments is not strong, they presumably belong to a $J^P = 3/2^+$ SU(4) $\bar{4}$ multiplet with the $\Lambda(1520)$. The charmed baryons have clear, narrow signals, with no complications of threshold behavior. The conclusion here is that there is no room for two ordinary 3-quark states near 1405 MeV.

 $\Lambda(1405)$ MASS

PRODUCTION EXPERIMENTS

VALUE (MeV)	EVTS	DOCUMENT ID	TECN	COMMENT
1406.5 ± 4.0		¹ DALITZ	91	M-matrix fit
••• We do not use the following data for averages, fits, limits, etc. •••				
1391 ± 1	700	¹ HEMINGWAY	85	HBC K^-p 4.2 GeV/c
~ 1405	400	² THOMAS	73	HBC π^-p 1.69 GeV/c
1405	120	BARBARO...	68B	DBC K^-d 2.1–2.7 GeV/c
1400 ± 5	67	BIRMINGHAM	66	HBC K^-p 3.5 GeV/c
1382 ± 8		ENGLER	65	HDBC π^-p, π^+d 1.68 GeV/c
1400 ± 24		MUSGRAVE	65	HBC $\bar{p}p$ 3–4 GeV/c
1410		ALEXANDER	62	HBC π^-p 2.1 GeV/c
1405		ALSTON	62	HBC K^-p 1.2–0.5 GeV/c
1405		ALSTON	61B	HBC K^-p 1.15 GeV/c

EXTRAPOLATIONS BELOW $N\bar{K}$ THRESHOLD

VALUE (MeV)	DOCUMENT ID	TECN	COMMENT
••• We do not use the following data for averages, fits, limits, etc. •••			
1407.56 or 1407.50	³ KIMURA	00	potential model
1411	⁴ MARTIN	81	K-matrix fit
1406	⁵ CHAO	73	DPWA 0-range fit (sol. B)
1421	MARTIN	70	RVUE Constant K-matrix
1416 ± 4	MARTIN	69	HBC Constant K-matrix
1403 ± 3	KIM	67	HBC K-matrix fit
1407.5 ± 1.2	⁶ KITTEL	66	HBC 0-effective-range fit
1410.7 ± 1.0	KIM	65	HBC 0-effective-range fit
1409.6 ± 1.7	⁶ SAKITT	65	HBC 0-effective-range fit

 $\Lambda(1405)$ WIDTH

PRODUCTION EXPERIMENTS

VALUE (MeV)	EVTS	DOCUMENT ID	TECN	COMMENT
50 ± 2		¹ DALITZ	91	M-matrix fit
••• We do not use the following data for averages, fits, limits, etc. •••				
32 ± 1	700	¹ HEMINGWAY	85	HBC K^-p 4.2 GeV/c
45 to 55	400	² THOMAS	73	HBC π^-p 1.69 GeV/c
35	120	BARBARO...	68B	DBC K^-d 2.1–2.7 GeV/c
50 ± 10	67	BIRMINGHAM	66	HBC K^-p 3.5 GeV/c
89 ± 20		ENGLER	65	HDBC
60 ± 20		MUSGRAVE	65	HBC
35 ± 5		ALEXANDER	62	HBC
50		ALSTON	62	HBC
20		ALSTON	61B	HBC

See key on page 373

Baryon Particle Listings

$\Lambda(1405)$, $\Lambda(1520)$

EXTRAPOLATIONS BELOW $N\bar{K}$ THRESHOLD

VALUE (MeV)	DOCUMENT ID	TECN	COMMENT
••• We do not use the following data for averages, fits, limits, etc. •••			
50.24 or 50.26	3 KIMURA	00	potential model
30	4 MARTIN	81	K-matrix fit
55	5,7 CHAO	73	DPWA 0-range fit (sol. B)
20	MARTIN	70	RVUE Constant K-matrix
29 ± 6	MARTIN	69	HBC Constant K-matrix
50 ± 5	KIM	67	HBC K-matrix fit
34.1 ± 4.1	6 KITTEL	66	HBC
37.0 ± 3.2	KIM	65	HBC
28.2 ± 4.1	6 SAKITT	65	HBC

$\Lambda(1405)$ DECAY MODES

Mode	Fraction (Γ_i/Γ)
Γ_1 $\Sigma \pi$	100 %
Γ_2 $\Lambda \gamma$	
Γ_3 $\Sigma^0 \gamma$	
Γ_4 $N\bar{K}$	

$\Lambda(1405)$ PARTIAL WIDTHS

$\Gamma(\Lambda\gamma)$	Γ_2	
VALUE (keV)	DOCUMENT ID	COMMENT
••• We do not use the following data for averages, fits, limits, etc. •••		
27 ± 8	BURKHARDT 91	Isobar model fit
$\Gamma(\Sigma^0 \gamma)$	Γ_3	
VALUE (keV)	DOCUMENT ID	COMMENT
••• We do not use the following data for averages, fits, limits, etc. •••		
10 ± 4 or 23 ± 7	BURKHARDT 91	Isobar model fit

$\Lambda(1405)$ BRANCHING RATIOS

$\Gamma(N\bar{K})/\Gamma(\Sigma \pi)$	Γ_4/Γ_1			
VALUE	CL%	DOCUMENT ID	TECN	COMMENT
••• We do not use the following data for averages, fits, limits, etc. •••				
<3	95	HEMINGWAY 85	HBC	$K^- p$ 4.2 GeV/c

$\Lambda(1405)$ FOOTNOTES

- DALITZ 91 fits the HEMINGWAY 85 data.
- THOMAS 73 data is fit by CHAO 73 (see next section).
- The KIMURA 00 values are from fits A and B from a coupled-channel potential model using low-energy $\bar{K}N$ and $\Sigma \pi$ data, kaonic-hydrogen x-ray measurements, and our $\Lambda(1405)$ mass and width. The results bear mainly on the nature of the $\Lambda(1405)$: three-quark state or $\bar{K}N$ bound state.
- The MARTIN 81 fit includes the $K^\pm p$ forward scattering amplitudes and the dispersion relations they must satisfy.
- See also the accompanying paper of THOMAS 73.
- Data of SAKITT 65 are used in the fit by KITTEL 66.
- An asymmetric shape, with $\Gamma/2 = 41$ MeV below resonance, 14 MeV above.

$\Lambda(1405)$ REFERENCES

ZYCHOR 08	PL B660 167	I. Zychor et al.	(COSY ANKE Collab.)
MAGAS 05	PRL 95 052301	V.K. Magas, E. Oset, A. Ramos	(BARC, VALE)
KIMURA 00	PR C52 015206	M. Kimura et al.	
BURKHARDT 91	PR C44 607	H. Burkhardt, J. Lowe	(NOTT, UNM, BIRM)
DALITZ 91	JPG 17 289	R.H. Dalitz, A. Deloff	(OXFTP, WINR)
HEMINGWAY 85	NP B253 742	R.J. Hemingway	(CERN) J
MARTIN 81	NP B179 33	A.D. Martin	(DURH)
CHAO 73	NP B56 46	Y.A. Chao et al.	(RHEL, CMU, LOUC)
THOMAS 73	NP B56 15	D.W. Thomas et al.	(CMU) J
MARTIN 70	NP B16 479	A.D. Martin, G.G. Ross	(DURH)
MARTIN 69	PR 183 1352	B.R. Martin, M. Sakitt	(LOUC, BNL)
Also	PR 183 1345	B.R. Martin, M. Sakitt	(LOUC, BNL)
BARBARO-... 68B	PRL 21 573	A. Barbaro-Galieri et al.	(LRL, SLAC)
KIM 67	PRL 19 1074	J.K. Kim	(YALE)
BIRMINGHAM 66	PR 152 1148	M. Haque et al.	(BIRM, GLAS, LOIC, OXF+)
KITTEL 66	PL 21 349	W. Kittel, G. Otter, I. Wacek	(VIER)
ENGLER 65	PRL 15 224	A. Engler et al.	(CMU, BNL) J
KIM 65	PRL 14 29	J.K. Kim	(COLU)
MUSGRAVE 65	NC 35 735	B. Musgrave et al.	(BIRM, CERN, EPOL+)
SAKITT 65	PR 139 B719	M. Sakitt et al.	(UMD, LRL)
ALEXANDER 62	PRL 8 447	G. Alexander et al.	(LRL) I
ALSTON 62	CERN Conf. 311	M.H. Alston et al.	(LRL) I
ALSTON 61B	PRL 6 698	M.H. Alston et al.	(LRL) I

OTHER RELATED PAPERS

IWASAKI 97	PRL 78 3067	M. Iwasaki et al.	(KEK 228 Collab.)
FINK 90	PR C41 2720	P.J. Fink et al.	(IBMY, ORST, ANSM)
LEINWEBER 90	ANP 198 203	D.B. Leinweber	(MCMS)
MUELLER-GR... 90	NP A513 557	A. Mueller-Groeling	(JULI)
BARRETT 89	NC 102A 179	R.C. Barrett	(SURR)
BATTY 89	NC 102A 255	C.J. Batty, A. Gal	(RAL, HEBR)
CAPSTICK 89	Excited Baryons 88, p.32	S. Capstick	(GUEL)
LOWE 89	NC 102A 167	J. Lowe	(BIRM)
WHITEHOUSE 89	PRL 63 1352	D.A. Whitehouse et al.	(BIRM, BOST, BRCO+)
SIEGEL 88	PR C38 2221	P.B. Siegel, W. Weise	(REGE)
WORKMAN 88	PR D37 3117	R.L. Workman, H.W. Fearing	(TRIU)
SCHNICK 87	PRL 58 1719	J. Schnick, R.H. Landau	(ORST)
CAPSTICK 86	PR D34 2809	S. Capstick, N. Isgur	(TNT0)
JENNINGS 86	PL B176 229	B.K. Jennings	(TRIU)

MALTMAN 86	PR D34 1372	K. Maltman, N. Isgur	(LANL, TNT0)
ZHONG 86	PL B171 471	Y.S. Zhong et al.	(ADLD, TRIU, SURR)
BURKHARDT 85	NP A440 653	H. Burkhardt, J. Lowe, A.S. Rosenthal	(NOTT+)
DAREWYCH 85	PR D32 1765	J.W. Darewych, R. Koniuk, N. Isgur	(YORKC, TNT0)
VEIT 85	PR D31 1033	E.A. Veit et al.	(TRIU, ADLD, SURR)
KIANG 84	PR C30 1638	D. Kiang et al.	(DALH, MCMS)
MILLER 84	Conference paper	D.J. Miller	(LOUC)
Conf. Intersections between Particle and Nuclear Physics, p. 783			
VANDIJK 84	PR D30 937	W. van Dijk	(MCMS)
VEIT 84	PL 137B 415	E.A. Veit et al.	(TRIU, SURR, CERN)
DALITZ 82	Heid. Conf.	R.H. Dalitz et al.	(OXFTP)
Heidelberg Conf., p. 201			
DALITZ 81	Kaon Conf.	R.H. Dalitz, J.G. McGinley	(OXFTP)
Low and Intermediate Energy Kaon-Nucleon Physics, p.381			
MARTIN 81B	Kaon Conf.	A.D. Martin	(DURH)
Low and Intermediate Energy Kaon-Nucleon Physics, p. 97			
OADES 77	NC 42A 462	G.C. Oades, G. Rasche	(AARH, ZURI)
SHAW 73	Purdue Conf. 417	G.L. Shaw	(UCI)
BARBARO-... 72	LBL-555	A. Barbaro-Galieri	(LBL)
DOBSON 72	PR D6 3256	P.N. Dobson, R. McElhaney	(HAWA)
RAJASEKA... 72	PR D5 610	G. Rajasekaran	(TATA)
Earlier papers also cited in RAJASEKARAN 72.			
CLINE 71	PRL 26 1194	D. Cline, R. Laumann, J. Mapp	(WISC)
MARTIN 71	PL 35B 62	A.D. Martin, A.D. Martin, G.G. Ross	(DURH, LOUC+)
DALITZ 67	PR 153 1617	R.H. Dalitz, T.C. Wong, G. Rajasekaran	(OXFTP+)
DONALD 66	PL 22 711	R.A. Donald et al.	(LIVP)
KADYK 66	PRL 17 539	J.A. Kadyk et al.	(LRL)
ABRAMS 65	PR 139 B454	G.S. Abrams, B. Sechi-Zorn	(UMD)

$\Lambda(1520) D_{03}$

$$I(J^P) = 0(\frac{3}{2}^-) \text{ Status: } ***$$

Discovered by FERRO-LUZZI 62; the elaboration in WATSON 63 is the classic paper on the Breit-Wigner analysis of a multichannel resonance.

The measurements of the mass, width, and elasticity published before 1975 are now obsolete and have been omitted. They were last listed in our 1982 edition Physics Letters **111B** 1 (1982).

Production and formation experiments agree quite well, so they are listed together here.

$\Lambda(1520)$ MASS

VALUE (MeV)	EVTS	DOCUMENT ID	TECN	COMMENT
1519.5 ± 1.0 OUR ESTIMATE				
1519.50 ± 0.18 OUR AVERAGE				
1517.3 ± 1.5	300	BARBER 80D	SPEC	$\gamma p \rightarrow \Lambda(1520) K^+$
1519 ± 1		GOPAL 80	DPWA	$\bar{K}N \rightarrow \bar{K}N$
1517.8 ± 1.2	5k	BARLAG 79	HBC	$K^- p$ 4.2 GeV/c
1520.0 ± 0.5		ALSTON-... 78	DPWA	$\bar{K}N \rightarrow \bar{K}N$
1519.7 ± 0.3	4k	CAMERON 77	HBC	$K^- p$ 0.96-1.36 GeV/c
1519 ± 1		GOPAL 77	DPWA	$\bar{K}N$ multichannel
1519.4 ± 0.3	2000	CORDEN 75	DBC	$K^- d$ 1.4-1.8 GeV/c

$\Lambda(1520)$ WIDTH

VALUE (MeV)	EVTS	DOCUMENT ID	TECN	COMMENT
15.6 ± 1.0 OUR ESTIMATE				
15.59 ± 0.27 OUR AVERAGE				
16.3 ± 3.3	300	BARBER 80D	SPEC	$\gamma p \rightarrow \Lambda(1520) K^+$
16 ± 1		GOPAL 80	DPWA	$\bar{K}N \rightarrow \bar{K}N$
14 ± 3	677	1 BARLAG 79	HBC	$K^- p$ 4.2 GeV/c
15.4 ± 0.5		ALSTON-... 78	DPWA	$\bar{K}N \rightarrow \bar{K}N$
16.3 ± 0.5	4k	CAMERON 77	HBC	$K^- p$ 0.96-1.36 GeV/c
15.0 ± 0.5		GOPAL 77	DPWA	$\bar{K}N$ multichannel
15.5 ± 1.6	2000	CORDEN 75	DBC	$K^- d$ 1.4-1.8 GeV/c

$\Lambda(1520)$ DECAY MODES

Mode	Fraction (Γ_i/Γ)
Γ_1 $N\bar{K}$	45 ± 1%
Γ_2 $\Sigma \pi$	42 ± 1%
Γ_3 $\Lambda \pi \pi$	10 ± 1%
Γ_4 $\Sigma(1385)\pi$	
Γ_5 $\Sigma(1385)\pi(\rightarrow \Lambda \pi \pi)$	
Γ_6 $\Lambda(\pi \pi) s$ -wave	
Γ_7 $\Sigma \pi \pi$	0.9 ± 0.1%
Γ_8 $\Lambda \gamma$	0.85 ± 0.15%
Γ_9 $\Sigma^0 \gamma$	

Baryon Particle Listings

 $\Lambda(1520)$

CONSTRAINED FIT INFORMATION

An overall fit to 9 branching ratios uses 26 measurements and one constraint to determine 6 parameters. The overall fit has a $\chi^2 = 17.6$ for 21 degrees of freedom.

The following *off-diagonal* array elements are the correlation coefficients $\langle \delta x_i \delta x_j \rangle / (\delta x_i \delta x_j)$, in percent, from the fit to the branching fractions, $x_i \equiv \Gamma_i / \Gamma_{\text{total}}$. The fit constrains the x_i whose labels appear in this array to sum to one.

x_2	-64				
x_3	-32	-34			
x_7	-4	-3	-1		
x_8	-8	-7	-3	0	
x_9	-24	-21	-10	-1	-1
	x_1	x_2	x_3	x_7	x_8

 $\Lambda(1520)$ BRANCHING RATIOS

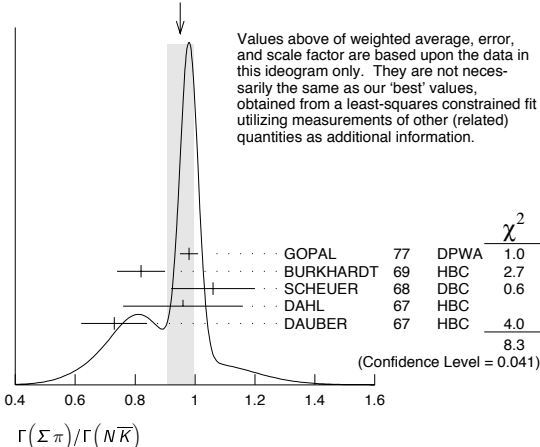
See "Sign conventions for resonance couplings" in the Note on Λ and Σ Resonances.

$\Gamma(N\bar{K})/\Gamma_{\text{total}}$		Γ_1/Γ		
VALUE	DOCUMENT ID	TECN	COMMENT	
0.45 ± 0.01 OUR ESTIMATE				
0.447 ± 0.007 OUR FIT				Error includes scale factor of 1.2.
0.455 ± 0.011 OUR AVERAGE				
0.47 ± 0.02	GOPAL	80	DPWA $\bar{K}N \rightarrow \bar{K}N$	
0.45 ± 0.03	ALSTON-...	78	DPWA $\bar{K}N \rightarrow \bar{K}N$	
0.448 ± 0.014	CORDEN	75	DBC $K^- d$ 1.4–1.8 GeV/c	
• • • We do not use the following data for averages, fits, limits, etc. • • •				
0.47 ± 0.01	GOPAL	77	DPWA See GOPAL 80	
0.42	MAST	76	HBC $K^- p \rightarrow \bar{K}^0 n$	

$\Gamma(\Sigma\pi)/\Gamma_{\text{total}}$		Γ_2/Γ		
VALUE	DOCUMENT ID	TECN	COMMENT	
0.42 ± 0.01 OUR ESTIMATE				
0.420 ± 0.007 OUR FIT				Error includes scale factor of 1.2.
0.423 ± 0.011 OUR AVERAGE				
0.426 ± 0.014	CORDEN	75	DBC $K^- d$ 1.4–1.8 GeV/c	
0.418 ± 0.017	BARBARO-...	69B	HBC $K^- p$ 0.28–0.45 GeV/c	
• • • We do not use the following data for averages, fits, limits, etc. • • •				
0.46	KIM	71	DPWA K-matrix analysis	

$\Gamma(\Sigma\pi)/\Gamma(N\bar{K})$		Γ_2/Γ_1		
VALUE	DOCUMENT ID	TECN	COMMENT	
0.940 ± 0.026 OUR FIT				Error includes scale factor of 1.3.
0.95 ± 0.04 OUR AVERAGE				Error includes scale factor of 1.7. See the ideogram below.
0.98 ± 0.03	² GOPAL	77	DPWA $\bar{K}N$ multichannel	
0.82 ± 0.08	BURKHARDT	69	HBC $K^- p$ 0.8–1.2 GeV/c	
1.06 ± 0.14	SCHUEER	68	DBC $K^- N$ 3 GeV/c	
0.96 ± 0.20	DAHL	67	HBC $\pi^- p$ 1.6–4 GeV/c	
0.73 ± 0.11	DAUBER	67	HBC $K^- p$ 2 GeV/c	
• • • We do not use the following data for averages, fits, limits, etc. • • •				
1.06 ± 0.12	BERTHON	74	HBC Quasi-2-body σ	
1.72 ± 0.78	MUSGRAVE	65	HBC	

WEIGHTED AVERAGE
0.95 ± 0.04 (Error scaled by 1.7)



$\Gamma(\Lambda\pi\pi)/\Gamma_{\text{total}}$		Γ_3/Γ		
VALUE	DOCUMENT ID	TECN	COMMENT	
0.10 ± 0.01 OUR ESTIMATE				
0.095 ± 0.005 OUR FIT				Error includes scale factor of 1.2.
0.096 ± 0.008 OUR AVERAGE				Error includes scale factor of 1.6.
0.091 ± 0.006	CORDEN	75	DBC $K^- d$ 1.4–1.8 GeV/c	
0.11 ± 0.01	³ MAST	73B	IPWA $K^- p \rightarrow \Lambda\pi\pi$	

$\Gamma(\Lambda\pi\pi)/\Gamma(N\bar{K})$		Γ_3/Γ_1		
VALUE	DOCUMENT ID	TECN	COMMENT	
0.213 ± 0.012 OUR FIT				Error includes scale factor of 1.2.
0.202 ± 0.021 OUR AVERAGE				
0.22 ± 0.03	BURKHARDT	69	HBC $K^- p$ 0.8–1.2 GeV/c	
0.19 ± 0.04	SCHEUER	68	DBC $K^- N$ 3 GeV/c	
0.17 ± 0.05	DAHL	67	HBC $\pi^- p$ 1.6–4 GeV/c	
0.21 ± 0.18	DAUBER	67	HBC $K^- p$ 2 GeV/c	
• • • We do not use the following data for averages, fits, limits, etc. • • •				
0.27 ± 0.13	BERTHON	74	HBC Quasi-2-body σ	
0.2	KIM	71	DPWA K-matrix analysis	

$\Gamma(\Sigma\pi)/\Gamma(\Lambda\pi\pi)$		Γ_2/Γ_3		
VALUE	DOCUMENT ID	TECN	COMMENT	
4.42 ± 0.25 OUR FIT				Error includes scale factor of 1.2.
3.9 ± 0.6 OUR AVERAGE				
3.9 ± 1.0	UHLIG	67	HBC $K^- p$ 0.9–1.0 GeV/c	
3.3 ± 1.1	BIRMINGHAM	66	HBC $K^- p$ 3.5 GeV/c	
4.5 ± 1.0	ARMENTEROS65c		HBC	

$\Gamma(\Sigma(1385)\pi)/\Gamma_{\text{total}}$		Γ_4/Γ		
VALUE	DOCUMENT ID	TECN	COMMENT	
0.041 ± 0.005				
	CHAN	72	HBC $K^- p \rightarrow \Lambda\pi\pi$	

$\Gamma(\Sigma(1385)\pi(\rightarrow\Lambda\pi\pi))/\Gamma(\Lambda\pi\pi)$		Γ_5/Γ_3		
VALUE	DOCUMENT ID	TECN	COMMENT	
0.58 ± 0.22				The $\Lambda\pi\pi$ mode is largely due to $\Sigma(1385)\pi$. Only the values of $(\Sigma(1385)\pi) / (\Lambda 2\pi)$ given by MAST 73B and CORDEN 75 are based on real 3-body partial-wave analyses. The discrepancy between the two results is essentially due to the different hypotheses made concerning the shape of the $(\pi\pi)_{S\text{-wave}}$ state.
0.82 ± 0.10	⁴ MAST	73B	IPWA $K^- p \rightarrow \Lambda\pi\pi$	
• • • We do not use the following data for averages, fits, limits, etc. • • •				
0.39 ± 0.10	⁵ BURKHARDT	71	HBC $K^- p \rightarrow (\Lambda\pi\pi)\pi$	

$\Gamma(\Lambda(\pi\pi)_{S\text{-wave}})/\Gamma(\Lambda\pi\pi)$		Γ_6/Γ_3		
VALUE	DOCUMENT ID	TECN	COMMENT	
0.20 ± 0.08				
	CORDEN	75	DBC $K^- d$ 1.4–1.8 GeV/c	

$\Gamma(\Sigma\pi\pi)/\Gamma_{\text{total}}$		Γ_7/Γ		
VALUE	DOCUMENT ID	TECN	COMMENT	
0.009 ± 0.001 OUR ESTIMATE				
0.0086 ± 0.0005 OUR FIT				
0.0086 ± 0.0005 OUR AVERAGE				
0.007 ± 0.002	⁶ CORDEN	75	DBC $K^- d$ 1.4–1.8 GeV/c	
0.0085 ± 0.0006	⁷ MAST	73	MPWA $K^- p \rightarrow \Sigma\pi\pi$	
0.010 ± 0.0015	BARBARO-...	69B	HBC $K^- p$ 0.28–0.45 GeV/c	

$\Gamma(\Lambda\gamma)/\Gamma_{\text{total}}$		Γ_8/Γ		
VALUE (units 10^{-3})	EVT S	DOCUMENT ID	TECN	COMMENT
8.5 ± 1.5 OUR ESTIMATE				
8.8 ± 1.1 OUR FIT				
8.8 ± 1.1 OUR AVERAGE				
10.7 ± 2.9 ^{+1.5} _{-0.4}	32	TAYLOR	05	CLAS $\gamma p \rightarrow K^+ \Lambda\gamma$
10.2 ± 2.1 ± 1.5	290	ANTIPOV	04A	SPNX $pN(C) \rightarrow \Lambda(1520)K^+N(C)$
8.0 ± 1.4	238	MAST	68B	HBC Using $\Gamma(N\bar{K})/\Gamma_{\text{total}} = 0.45$

$\Gamma(\Sigma^0\gamma)/\Gamma_{\text{total}}$		Γ_9/Γ		
VALUE	DOCUMENT ID	TECN	COMMENT	
0.0195 ± 0.0034 OUR FIT				
0.02 ± 0.0035	⁸ MAST	68B	HBC	Not measured; see note

 $\Lambda(1520)$ FOOTNOTES

- From the best-resolution sample of $\Lambda\pi\pi$ events only.
- The $\bar{K}N \rightarrow \Sigma\pi$ amplitude at resonance is $+0.46 \pm 0.01$.
- Assumes $\Gamma(N\bar{K})/\Gamma_{\text{total}} = 0.46 \pm 0.02$.
- Both $\Sigma(1385)\pi$ DS_{03} and $\Sigma(\pi\pi)$ DP_{03} contribute.
- The central bin (1514–1524 MeV) gives 0.74 ± 0.10 ; other bins are lower by 2-to-5 standard deviations.
- Much of the $\Sigma\pi\pi$ decay proceeds via $\Sigma(1385)\pi$.
- Assumes $\Gamma(N\bar{K})/\Gamma_{\text{total}} = 0.46$.
- Calculated from $\Gamma(\Lambda\gamma)/\Gamma_{\text{total}}$, assuming SU(3). Needed to constrain the sum of all the branching ratios to be unity.

Baryon Particle Listings

$\Lambda(1520), \Lambda(1600), \Lambda(1670)$

$\Lambda(1520)$ REFERENCES

Author	Year	Ref	Technique	Comment
TAYLOR	05	PR C71 054609	S. Taylor et al.	(JLab CLAS Collab.)
Also		PR C72 039902 (errat.)	S. Taylor et al.	(JLab CLAS Collab.)
ANTIPOV	04A	PL B604 22	Yu.M. Antipov et al.	(IHEP SPHINX Collab.)
PDG	82	PL 111B 1	M. Roos et al.	(HELS, CIT, CERN)
BARBER	80D	ZPHY C7 17	D.P. Barber et al.	(DARE, LANC, SHEF)
GOPAL	80	Toronto Conf. 159	G.P. Gopal	(RHEL) IJP
BARLAG	79	NP B149 220	S.J.M. Barlag et al.	(AMST, CERN, NIJM+)
ALSTON-...	78	PR D18 182	M. Alston-Garnjost et al.	(LBL, MTHO+) IJP
Also		PRL 38 1007	M. Alston-Garnjost et al.	(LBL, MTHO+) IJP
CAMERON	77	NP B131 399	W. Cameron et al.	(RHEL, LOIC) IJP
GOPAL	77	NP B119 362	G.P. Gopal et al.	(LOIC, RHEL) IJP
MAST	76	PR D14 13	T.S. Mast et al.	(LBL)
CORDEN	75	NP B84 306	M.J. Corden et al.	(BIRM)
BERTHON	74	NC 21A 146	A. Berthon et al.	(CDEF, RHEL, SAACL+)
MAST	73	PR D7 3212	T.S. Mast et al.	(LBL) IJP
MAST	73B	PR D7 5	T.S. Mast et al.	(LBL) IJP
CHAN	72	PRL 28 256	S.B. Chan et al.	(MASA, YALE)
BURKHARDT	71	NP B27 64	E. Burkhardt et al.	(HEID, CERN, SACL)
KIM	71	PRL 27 356	J.K. Kim	(HARV) IJP
Also		Duke Conf. 161	J.K. Kim	(HARV) IJP
Hyperon Resonances, 1970				
BARBARO-...	69B	Lund Conf. 352	A. Barbaro-Galiferi et al.	(LRL)
Also		Duke Conf. 95	R.D. Tripp	(LRL)
Hyperon Resonances 1970				
BURKHARDT	69	NP B14 106	E. Burkhardt et al.	(HEID, EFI, CERN+)
MAST	68B	PRL 21 1715	T.S. Mast et al.	(LRL)
SCHUEER	68	NP B8 503	J.C. Schueer et al.	(SABRE Collab.)
DAHL	67	PR 163 1377	O.I. Dahl et al.	(LRL)
DAUBER	67	PL 24B 525	P.M. Dauber et al.	(UCLA)
UHLIG	67	PR 155 1448	R.P. Uhlig et al.	(UMD, NRL)
BIRMINGHAM	66	PR 152 1148	M. Haque et al.	(BIRM, GLAS, LOIC, OXF+)
ARMENTEROS	65C	PL 19 338	R. Armenteros et al.	(CERN, HEID, SACL)
MUSGRAVE	65	NC 35 735	B. Musgrave et al.	(BIRM, CERN, EPOL+)
WATSON	63	PR 131 2248	M.B. Watson, M. Ferro-Luzzi, R.D. Tripp	(LRL) IJP
FERRO-LUZZI	62	PRL 8 28	M. Ferro-Luzzi, R.D. Tripp, M.B. Watson	(LRL) IJP

$\Lambda(1600) P_{01}$

$$I(J^P) = 0(\frac{1}{2}^+) \text{ Status: } ***$$

See also the $\Lambda(1810) P_{01}$. There are quite possibly two P_{01} states in this region.

$\Lambda(1600)$ MASS

VALUE (MeV)	DOCUMENT ID	TECN	COMMENT
1560 to 1700 (≈ 1600) OUR ESTIMATE			
1568 \pm 20	GOPAL 80	DPWA	$\bar{K}N \rightarrow \bar{K}N$
1703 \pm 100	ALSTON-... 78	DPWA	$\bar{K}N \rightarrow \bar{K}N$
1573 \pm 25	GOPAL 77	DPWA	$\bar{K}N$ multichannel
1596 \pm 6	KANE 74	DPWA	$K^-p \rightarrow \Sigma\pi$
1620 \pm 10	LANGBEIN 72	IPWA	$\bar{K}N$ multichannel
••• We do not use the following data for averages, fits, limits, etc. •••			
1572 or 1617	¹ MARTIN 77	DPWA	$\bar{K}N$ multichannel
1646 \pm 7	² CARROLL 76	DPWA	Isospin-0 total σ
1570	KIM 71	DPWA	K-matrix analysis

$\Lambda(1600)$ WIDTH

VALUE (MeV)	DOCUMENT ID	TECN	COMMENT
50 to 250 (≈ 150) OUR ESTIMATE			
116 \pm 20	GOPAL 80	DPWA	$\bar{K}N \rightarrow \bar{K}N$
593 \pm 200	ALSTON-... 78	DPWA	$\bar{K}N \rightarrow \bar{K}N$
147 \pm 50	GOPAL 77	DPWA	$\bar{K}N$ multichannel
175 \pm 20	KANE 74	DPWA	$K^-p \rightarrow \Sigma\pi$
60 \pm 10	LANGBEIN 72	IPWA	$\bar{K}N$ multichannel
••• We do not use the following data for averages, fits, limits, etc. •••			
247 or 271	¹ MARTIN 77	DPWA	$\bar{K}N$ multichannel
20	² CARROLL 76	DPWA	Isospin-0 total σ
50	KIM 71	DPWA	K-matrix analysis

$\Lambda(1600)$ DECAY MODES

Mode	Fraction (Γ_i/Γ)
Γ_1 $N\bar{K}$	15-30 %
Γ_2 $\Sigma\pi$	10-60 %

The above branching fractions are our estimates, not fits or averages.

$\Lambda(1600)$ BRANCHING RATIOS

See "Sign conventions for resonance couplings" in the Note on Λ and Σ Resonances.

$\Gamma(N\bar{K})/\Gamma_{\text{total}}$	DOCUMENT ID	TECN	COMMENT
0.15 to 0.30 OUR ESTIMATE			
0.23 \pm 0.04	GOPAL 80	DPWA	$\bar{K}N \rightarrow \bar{K}N$
0.14 \pm 0.05	ALSTON-... 78	DPWA	$\bar{K}N \rightarrow \bar{K}N$
0.25 \pm 0.15	LANGBEIN 72	IPWA	$\bar{K}N$ multichannel
••• We do not use the following data for averages, fits, limits, etc. •••			
0.24 \pm 0.04	GOPAL 77	DPWA	See GOPAL 80
0.30 or 0.29	¹ MARTIN 77	DPWA	$\bar{K}N$ multichannel

$(\Gamma_1\Gamma_2)^{1/2}/\Gamma_{\text{total}}$ in $N\bar{K} \rightarrow \Lambda(1600) \rightarrow \Sigma\pi$

VALUE	DOCUMENT ID	TECN	COMMENT
-0.16 \pm 0.04	GOPAL 77	DPWA	$\bar{K}N$ multichannel
-0.33 \pm 0.11	KANE 74	DPWA	$K^-p \rightarrow \Sigma\pi$
0.28 \pm 0.09	LANGBEIN 72	IPWA	$\bar{K}N$ multichannel
••• We do not use the following data for averages, fits, limits, etc. •••			
-0.39 or -0.39	¹ MARTIN 77	DPWA	$\bar{K}N$ multichannel
not seen	HEPP 76B	DPWA	$K^-N \rightarrow \Sigma\pi$

$\Lambda(1600)$ FOOTNOTES

- ¹ The two MARTIN 77 values are from a T-matrix pole and from a Breit-Wigner fit.
- ² A total cross-section bump with $(J+1/2)\Gamma_{\text{el}}/\Gamma_{\text{total}} = 0.04$.

$\Lambda(1600)$ REFERENCES

Author	Year	Ref	Technique	Comment
GOPAL	80	Toronto Conf. 159	G.P. Gopal	(RHEL) IJP
ALSTON-...	78	PR D18 182	M. Alston-Garnjost et al.	(LBL, MTHO+) IJP
Also		PRL 38 1007	M. Alston-Garnjost et al.	(LBL, MTHO+) IJP
GOPAL	77	NP B119 362	G.P. Gopal et al.	(LOIC, RHEL) IJP
MARTIN	77	NP B127 349	B.R. Martin, M.K. Pidcock, R.G. Moorhouse	(LOUC+) IJP
Also		NP B126 266	B.R. Martin, M.K. Pidcock	(LOUC) IJP
Also		NP B126 285	B.R. Martin, M.K. Pidcock	(LOUC) IJP
CARROLL	76	PRL 37 806	A.S. Carroll et al.	(BNL) I
HEPP	76B	PL 65B 487	V. Hepp et al.	(CERN, HEIDH, MPIM) IJP
KANE	74	LBL-2452	D.F. Kane	(LBL) IJP
LANGBEIN	72	NP B47 477	W. Langbein, F. Wagner	(MPIM) IJP
KIM	71	PRL 27 356	J.K. Kim	(HARV) IJP

$\Lambda(1670) S_{01}$

$$I(J^P) = 0(\frac{1}{2}^-) \text{ Status: } ***$$

The measurements of the mass, width, and elasticity published before 1974 are now obsolete and have been omitted. They were last listed in our 1982 edition Physics Letters **111B** 1 (1982).

$\Lambda(1670)$ MASS

VALUE (MeV)	DOCUMENT ID	TECN	COMMENT
1660 to 1680 (≈ 1670) OUR ESTIMATE			
1677.5 \pm 0.8	¹ GARCIA-REC...03	DPWA	$\bar{K}N$ multichannel
1673 \pm 2	MANLEY 02	DPWA	$\bar{K}N$ multichannel
1670.8 \pm 1.7	KOISO 85	DPWA	$K^-p \rightarrow \Sigma\pi$
1667 \pm 5	GOPAL 80	DPWA	$\bar{K}N \rightarrow \bar{K}N$
1671 \pm 3	ALSTON-... 78	DPWA	$\bar{K}N \rightarrow \bar{K}N$
1670 \pm 5	GOPAL 77	DPWA	$\bar{K}N$ multichannel
1675 \pm 2	HEPP 76B	DPWA	$K^-N \rightarrow \Sigma\pi$
1679 \pm 1	KANE 74	DPWA	$K^-p \rightarrow \Sigma\pi$
1665 \pm 5	PREVOST 74	DPWA	$K^-N \rightarrow \Sigma(1385)\pi$
••• We do not use the following data for averages, fits, limits, etc. •••			
1668.9 \pm 2.0	ABAEV 96	DPWA	$K^-p \rightarrow \Lambda\eta$
1664	² MARTIN 77	DPWA	$\bar{K}N$ multichannel

$\Lambda(1670)$ WIDTH

VALUE (MeV)	DOCUMENT ID	TECN	COMMENT
25 to 50 (≈ 35) OUR ESTIMATE			
29.2 \pm 1.4	¹ GARCIA-REC...03	DPWA	$\bar{K}N$ multichannel
23 \pm 6	MANLEY 02	DPWA	$\bar{K}N$ multichannel
34.1 \pm 3.7	KOISO 85	DPWA	$K^-p \rightarrow \Sigma\pi$
29 \pm 5	GOPAL 80	DPWA	$\bar{K}N \rightarrow \bar{K}N$
29 \pm 5	ALSTON-... 78	DPWA	$\bar{K}N \rightarrow \bar{K}N$
45 \pm 10	GOPAL 77	DPWA	$\bar{K}N$ multichannel
46 \pm 5	HEPP 76B	DPWA	$K^-N \rightarrow \Sigma\pi$
40 \pm 3	KANE 74	DPWA	$K^-p \rightarrow \Sigma\pi$
19 \pm 5	PREVOST 74	DPWA	$K^-N \rightarrow \Sigma(1385)\pi$
••• We do not use the following data for averages, fits, limits, etc. •••			
21.1 \pm 3.6	ABAEV 96	DPWA	$K^-p \rightarrow \Lambda\eta$
12	² MARTIN 77	DPWA	$\bar{K}N$ multichannel

$\Lambda(1670)$ DECAY MODES

Mode	Fraction (Γ_i/Γ)
Γ_1 $N\bar{K}$	20-30 %
Γ_2 $\Sigma\pi$	25-55 %
Γ_3 $\Lambda\eta$	10-25 %
Γ_4 $\Sigma(1385)\pi$	

The above branching fractions are our estimates, not fits or averages.

Baryon Particle Listings

 $\Lambda(1670), \Lambda(1690)$ $\Lambda(1670)$ BRANCHING RATIOS

See "Sign conventions for resonance couplings" in the Note on Λ and Σ Resonances.

$\Gamma(N\bar{K})/\Gamma_{\text{total}}$	DOCUMENT ID	TECN	COMMENT	Γ_1/Γ
0.20 to 0.30 OUR ESTIMATE				
0.37±0.07	MANLEY 02	DPWA	$\bar{K}N$ multichannel	
0.18±0.03	GOPAL 80	DPWA	$\bar{K}N \rightarrow \bar{K}N$	
0.17±0.03	ALSTON... 78	DPWA	$\bar{K}N \rightarrow \bar{K}N$	
••• We do not use the following data for averages, fits, limits, etc. •••				
0.20±0.03	GOPAL 77	DPWA	See GOPAL 80	
0.15	² MARTIN 77	DPWA	$\bar{K}N$ multichannel	

$\Gamma(\Lambda\eta)/\Gamma_{\text{total}}$	DOCUMENT ID	TECN	COMMENT	Γ_3/Γ
0.30±0.08	ABAEV 96	DPWA	$K^-p \rightarrow \Lambda\eta$	
••• We do not use the following data for averages, fits, limits, etc. •••				

$(\Gamma_1\Gamma_2)^{1/2}/\Gamma_{\text{total}}$ in $N\bar{K} \rightarrow \Lambda(1670) \rightarrow \Sigma\pi$	DOCUMENT ID	TECN	COMMENT	$(\Gamma_1\Gamma_2)^{1/2}/\Gamma$
0.38±0.03	MANLEY 02	DPWA	$\bar{K}N$ multichannel	
0.26±0.02	KOISO 85	DPWA	$K^-p \rightarrow \Sigma\pi$	
0.31±0.03	GOPAL 77	DPWA	$\bar{K}N$ multichannel	
0.29±0.03	HEPP 76B	DPWA	$K^-N \rightarrow \Sigma\pi$	
0.23±0.03	LONDON 75	HLBC	$K^-p \rightarrow \Sigma^0\pi^0$	
0.27±0.02	KANE 74	DPWA	$K^-p \rightarrow \Sigma\pi$	
••• We do not use the following data for averages, fits, limits, etc. •••				
0.13	² MARTIN 77	DPWA	$\bar{K}N$ multichannel	

$(\Gamma_1\Gamma_3)^{1/2}/\Gamma_{\text{total}}$ in $N\bar{K} \rightarrow \Lambda(1670) \rightarrow \Lambda\eta$	DOCUMENT ID	TECN	COMMENT	$(\Gamma_1\Gamma_3)^{1/2}/\Gamma$
0.24±0.04	MANLEY 02	DPWA	$\bar{K}N$ multichannel	
0.20±0.05	BAXTER 73	DPWA	$K^-p \rightarrow$ neutrals	
••• We do not use the following data for averages, fits, limits, etc. •••				
0.24	KIM 71	DPWA	K-matrix analysis	
0.26	ARMENTEROS69C	HBC		
0.20 or 0.23	BERLEY 65	HBC		

$(\Gamma_1\Gamma_4)^{1/2}/\Gamma_{\text{total}}$ in $N\bar{K} \rightarrow \Lambda(1670) \rightarrow \Sigma(1385)\pi$	DOCUMENT ID	TECN	COMMENT	$(\Gamma_1\Gamma_4)^{1/2}/\Gamma$
0.17±0.06	MANLEY 02	DPWA	$\bar{K}N$ multichannel	
0.18±0.05	PREVOST 74	DPWA	$K^-N \rightarrow \Sigma(1385)\pi$	

 $\Lambda(1670)$ FOOTNOTES

- ¹ GARCIA-RECIO 03 gives pole, not Breit-Wigner, parameters, but the narrow width of the $\Lambda(1670)$ means there will be little difference.
² MARTIN 77 obtains identical resonance parameters from a T-matrix pole and from a Breit-Wigner fit.

 $\Lambda(1670)$ REFERENCES

GARCIA-RECIO 03	PR D67 076009	C. Garcia-Recio et al.	(GRAN, VALE)
MANLEY 02	PRL 88 012002	D.M. Manley et al.	(BNL Crystal Ball Collab.)
ABAEV 96	PR C53 385	V.V. Abaev, B.M.K. Nefkens	(UCLA)
KOISO 85	NP A433 619	H. Koiso et al.	(TOKY, MASA)
PDG 82	PL 111B 1	M. Roos et al.	(HELSE, CIT, CERN)
GOPAL 80	Toronto Conf. 159	G.P. Gopal	(RHEL) IJP
ALSTON... 78	PR D18 182	M. Alston-Garnjost et al.	(LBL, MTHO+) IJP
Also	PRL 38 1007	M. Alston-Garnjost et al.	(LBL, MTHO+) IJP
GOPAL 77	NP B119 362	G.P. Gopal et al.	(LOIC, RHEL) IJP
MARTIN 77	NP B127 349	B.R. Martin, M.K. Piddcock, R.G. Moorhouse	(LOUC+) IJP
Also	NP B126 266	B.R. Martin, M.K. Piddcock	(LOUC) IJP
Also	NP B126 285	B.R. Martin, M.K. Piddcock	(LOUC) IJP
HEPP 76B	PL 65B 487	V. Hepp et al.	(CERN, HEIDH, MPIM) IJP
LONDON 75	NP B95 289	G.W. London et al.	(BNL, CERN, EPOL+) IJP
KANE 74	LBL-2452	D.F. Kane	(LBL) IJP
PREVOST 74	NP B69 246	J. Prevost et al.	(SACL, CERN, HEID)
BAXTER 73	NP B67 125	D.F. Baxter et al.	(OXF) IJP
KIM 71	PRL 27 356	J.K. Kim	(HARV) IJP
Also	Duke Conf. 161	J.K. Kim	(HARV) IJP
ARMENTEROS 69C	Lund Paper 229	R. Armenteros et al.	(CERN, HEID, SACL) IJP
Values are quoted in LEVI-SETTI 69.			
BERLEY 65	PRL 15 641	D. Berley et al.	(BNL) IJP

 $\Lambda(1690) D_{03}$

$$I(J^P) = 0(\frac{3}{2}^-) \text{ Status: } ***$$

The measurements of the mass, width, and elasticity published before 1974 are now obsolete and have been omitted. They were last listed in our 1982 edition Physics Letters **111B** 1 (1982).

 $\Lambda(1690)$ MASS

VALUE (MeV)	DOCUMENT ID	TECN	COMMENT
1685 to 1695 (≈ 1690) OUR ESTIMATE			
1695.7±2.6	KOISO 85	DPWA	$K^-p \rightarrow \Sigma\pi$
1690 ±5	GOPAL 80	DPWA	$\bar{K}N \rightarrow \bar{K}N$
1692 ±5	ALSTON... 78	DPWA	$\bar{K}N \rightarrow \bar{K}N$
1690 ±5	GOPAL 77	DPWA	$\bar{K}N$ multichannel
1690 ±3	HEPP 76B	DPWA	$K^-N \rightarrow \Sigma\pi$
1689 ±1	KANE 74	DPWA	$K^-p \rightarrow \Sigma\pi$
••• We do not use the following data for averages, fits, limits, etc. •••			
1687 or 1689	¹ MARTIN 77	DPWA	$\bar{K}N$ multichannel
1692 ±4	CARROLL 76	DPWA	Isospin-0 total σ

 $\Lambda(1690)$ WIDTH

VALUE (MeV)	DOCUMENT ID	TECN	COMMENT
50 to 70 (≈ 60) OUR ESTIMATE			
67.2±5.6	KOISO 85	DPWA	$K^-p \rightarrow \Sigma\pi$
61 ±5	GOPAL 80	DPWA	$\bar{K}N \rightarrow \bar{K}N$
64 ±10	ALSTON... 78	DPWA	$\bar{K}N \rightarrow \bar{K}N$
60 ±5	GOPAL 77	DPWA	$\bar{K}N$ multichannel
82 ±8	HEPP 76B	DPWA	$K^-N \rightarrow \Sigma\pi$
60 ±4	KANE 74	DPWA	$K^-p \rightarrow \Sigma\pi$
••• We do not use the following data for averages, fits, limits, etc. •••			
62 or 62	¹ MARTIN 77	DPWA	$\bar{K}N$ multichannel
38	CARROLL 76	DPWA	Isospin-0 total σ

 $\Lambda(1690)$ DECAY MODES

Mode	Fraction (Γ_i/Γ)
Γ_1 $N\bar{K}$	20–30 %
Γ_2 $\Sigma\pi$	20–40 %
Γ_3 $\Lambda\pi\pi$	~ 25 %
Γ_4 $\Sigma\pi\pi$	~ 20 %
Γ_5 $\Lambda\eta$	
Γ_6 $\Sigma(1385)\pi, S$ -wave	

The above branching fractions are our estimates, not fits or averages.

 $\Lambda(1690)$ BRANCHING RATIOS

The sum of all the quoted branching ratios is more than 1.0. The two-body ratios are from partial-wave analyses, and thus probably are more reliable than the three-body ratios, which are determined from bumps in cross sections. Of the latter, the $\Sigma\pi\pi$ bump looks more significant. (The error given for the $\Lambda\pi\pi$ ratio looks unreasonably small.) Hardly any of the $\Sigma\pi\pi$ decay can be via $\Sigma(1385)$, for then seven times as much $\Lambda\pi\pi$ decay would be required. See "Sign conventions for resonance couplings" in the Note on Λ and Σ Resonances.

$\Gamma(N\bar{K})/\Gamma_{\text{total}}$	DOCUMENT ID	TECN	COMMENT	Γ_1/Γ
0.2 to 0.3 OUR ESTIMATE				
0.23±0.03	GOPAL 80	DPWA	$\bar{K}N \rightarrow \bar{K}N$	
0.22±0.03	ALSTON... 78	DPWA	$\bar{K}N \rightarrow \bar{K}N$	
••• We do not use the following data for averages, fits, limits, etc. •••				
0.24±0.03	GOPAL 77	DPWA	See GOPAL 80	
0.28 or 0.26	¹ MARTIN 77	DPWA	$\bar{K}N$ multichannel	

$(\Gamma_1\Gamma_2)^{1/2}/\Gamma_{\text{total}}$ in $N\bar{K} \rightarrow \Lambda(1690) \rightarrow \Sigma\pi$	DOCUMENT ID	TECN	COMMENT	$(\Gamma_1\Gamma_2)^{1/2}/\Gamma$
0.34±0.02	KOISO 85	DPWA	$K^-p \rightarrow \Sigma\pi$	
0.25±0.03	GOPAL 77	DPWA	$\bar{K}N$ multichannel	
0.29±0.03	HEPP 76B	DPWA	$K^-N \rightarrow \Sigma\pi$	
0.28±0.03	LONDON 75	HLBC	$K^-p \rightarrow \Sigma^0\pi^0$	
0.28±0.02	KANE 74	DPWA	$K^-p \rightarrow \Sigma\pi$	
••• We do not use the following data for averages, fits, limits, etc. •••				
0.30 or 0.28	¹ MARTIN 77	DPWA	$\bar{K}N$ multichannel	

$(\Gamma_1\Gamma_3)^{1/2}/\Gamma_{\text{total}}$ in $N\bar{K} \rightarrow \Lambda(1690) \rightarrow \Lambda\eta$	DOCUMENT ID	TECN	COMMENT	$(\Gamma_1\Gamma_3)^{1/2}/\Gamma$
0.00±0.03	BAXTER 73	DPWA	$K^-p \rightarrow$ neutrals	

See key on page 373

Baryon Particle Listings

$\Lambda(1690)$, $\Lambda(1800)$, $\Lambda(1810)$

$(\Gamma_1\Gamma_7)/\Gamma_{\text{total}}$ in $N\bar{K} \rightarrow \Lambda(1690) \rightarrow \Lambda\pi\pi$ $(\Gamma_1\Gamma_3)/\Gamma$
 VALUE DOCUMENT ID TECN COMMENT

••• We do not use the following data for averages, fits, limits, etc. •••
 0.25±0.02 ² BARTLEY 68 HDBC $K^-p \rightarrow \Lambda\pi\pi$

$(\Gamma_1\Gamma_7)/\Gamma_{\text{total}}$ in $N\bar{K} \rightarrow \Lambda(1690) \rightarrow \Sigma\pi\pi$ $(\Gamma_1\Gamma_4)/\Gamma$
 VALUE DOCUMENT ID TECN COMMENT

0.21 ARMENTEROS68C HDBC $K^-N \rightarrow \Sigma\pi\pi$

$(\Gamma_1\Gamma_7)/\Gamma_{\text{total}}$ in $N\bar{K} \rightarrow \Lambda(1690) \rightarrow \Sigma(1385)\pi$, S-wave $(\Gamma_1\Gamma_6)/\Gamma$
 VALUE DOCUMENT ID TECN COMMENT

+0.27±0.04 PREVOST 74 DPWA $K^-N \rightarrow \Sigma(1385)\pi$

$\Lambda(1690)$ FOOTNOTES

- The two MARTIN 77 values are from a T-matrix pole and from a Breit-Wigner fit. Another D_{03} Λ at 1966 MeV is also suggested by MARTIN 77, but is very uncertain.
- BARTLEY 68 uses only cross-section data. The enhancement is not seen by PREVOST 71.

$\Lambda(1690)$ REFERENCES

KOISO 85 NP A433 619 H. Koiso et al. (TOKY, MASA)	PL 111B 1 M. Roos et al. (HELZ, CIT, CERN)
PDG 82 Toronto Conf. 159 G.P. Gopal (RHEL) IJP	
ALSTON-... 78 PR D18 182 M. Alston-Garnjost et al. (LBL, MTHO+) IJP	
Also PRL 38 1007 M. Alston-Garnjost et al. (LBL, MTHO+) IJP	
GOPAL 77 NP B119 362 G.P. Gopal et al. (LOIC, RHEL) IJP	
MARTIN 77 NP B127 349 B.R. Martin, M.K. Pidcock, R.G. Moorhouse (LOUC+) IJP	
Also NP B126 266 B.R. Martin, M.K. Pidcock (LOUC) IJP	
Also NP B126 285 B.R. Martin, M.K. Pidcock (LOUC) IJP	
CARROLL 76 PRL 37 806 A.S. Carroll et al. (BNL) I	
HEPP 76B PL 65B 487 V. Hepp et al. (CERN, HEIDH, MPIM) IJP	
LONDON 75 NP B85 289 G.W. London et al. (BNL, CERN, EPOL+) I	
KANE 74 LBL-2452 D.F. Kane (LBL) IJP	
PREVOST 74 NP B69 246 J. Prevost et al. (SACL, CERN, HEID) I	
BAXTER 73 NP B67 125 D.F. Baxter et al. (OXF) IJP	
PREVOST 71 Amsterdam Conf. J. Prevost (CERN, HEID, SACL) I	
ARMENTEROS 68C NP B8 216 R. Armenteros et al. (CERN, HEID, SACL) I	
BARTLEY 68 PRL 21 1111 J.H. Bartley et al. (TUFTS, FSU, BRAN) I	

$\Lambda(1800) S_{01}$ $I(J^P) = 0(\frac{1}{2}^-)$ Status: ***

This is the second resonance in the S_{01} wave, the first being the $\Lambda(1670)$.

$\Lambda(1800)$ MASS

VALUE (MeV)	DOCUMENT ID	TECN	COMMENT
1720 to 1850 (≈ 1800) OUR ESTIMATE			
1845±10	MANLEY 02	DPWA	$\bar{K}N$ multichannel
1841±10	GOPAL 80	DPWA	$\bar{K}N \rightarrow \bar{K}N$
1725±20	ALSTON-... 78	DPWA	$\bar{K}N \rightarrow \bar{K}N$
1825±20	GOPAL 77	DPWA	$\bar{K}N$ multichannel
1830±20	LANGBEIN 72	IPWA	$\bar{K}N$ multichannel
••• We do not use the following data for averages, fits, limits, etc. •••			
1767 or 1842	¹ MARTIN 77	DPWA	$\bar{K}N$ multichannel
1780	KIM 71	DPWA	K-matrix analysis
1872±10	BRICMAN 70B	DPWA	$\bar{K}N \rightarrow \bar{K}N$

$\Lambda(1800)$ WIDTH

VALUE (MeV)	DOCUMENT ID	TECN	COMMENT
200 to 400 (≈ 300) OUR ESTIMATE			
518±84	MANLEY 02	DPWA	$\bar{K}N$ multichannel
228±20	GOPAL 80	DPWA	$\bar{K}N \rightarrow \bar{K}N$
185±20	ALSTON-... 78	DPWA	$\bar{K}N \rightarrow \bar{K}N$
230±20	GOPAL 77	DPWA	$\bar{K}N$ multichannel
70±15	LANGBEIN 72	IPWA	$\bar{K}N$ multichannel
••• We do not use the following data for averages, fits, limits, etc. •••			
435 or 473	¹ MARTIN 77	DPWA	$\bar{K}N$ multichannel
40	KIM 71	DPWA	K-matrix analysis
100±20	BRICMAN 70B	DPWA	$\bar{K}N \rightarrow \bar{K}N$

$\Lambda(1800)$ DECAY MODES

Mode	Fraction (Γ_i/Γ)
Γ_1 $N\bar{K}$	25–40 %
Γ_2 $\Sigma\pi$	seen
Γ_3 $\Sigma(1385)\pi$	seen
Γ_4 $N\bar{K}^*(892)$	seen
Γ_5 $N\bar{K}^*(892)$, S=1/2, S-wave	
Γ_6 $N\bar{K}^*(892)$, S=3/2, D-wave	

The above branching fractions are our estimates, not fits or averages.

$\Lambda(1800)$ BRANCHING RATIOS

See "Sign conventions for resonance couplings" in the Note on Λ and Σ Resonances.

$\Gamma(N\bar{K})/\Gamma_{\text{total}}$ Γ_1/Γ
 VALUE DOCUMENT ID TECN COMMENT

0.25 to 0.40 OUR ESTIMATE

0.24±0.10	MANLEY 02	DPWA	$\bar{K}N$ multichannel
0.36±0.04	GOPAL 80	DPWA	$\bar{K}N \rightarrow \bar{K}N$
0.28±0.05	ALSTON-... 78	DPWA	$\bar{K}N \rightarrow \bar{K}N$
0.35±0.15	LANGBEIN 72	IPWA	$\bar{K}N$ multichannel
••• We do not use the following data for averages, fits, limits, etc. •••			
0.37±0.05	GOPAL 77	DPWA	See GOPAL 80
1.21 or 0.70	¹ MARTIN 77	DPWA	$\bar{K}N$ multichannel
0.80	KIM 71	DPWA	K-matrix analysis
0.18±0.02	BRICMAN 70B	DPWA	$\bar{K}N \rightarrow \bar{K}N$

$(\Gamma_1\Gamma_7)/\Gamma_{\text{total}}$ in $N\bar{K} \rightarrow \Lambda(1800) \rightarrow \Sigma\pi$ $(\Gamma_1\Gamma_2)/\Gamma$
 VALUE DOCUMENT ID TECN COMMENT

-0.08±0.05	GOPAL 77	DPWA	$\bar{K}N$ multichannel
••• We do not use the following data for averages, fits, limits, etc. •••			
-0.74 or -0.43	¹ MARTIN 77	DPWA	$\bar{K}N$ multichannel
0.24	KIM 71	DPWA	K-matrix analysis

$(\Gamma_1\Gamma_7)/\Gamma_{\text{total}}$ in $N\bar{K} \rightarrow \Lambda(1800) \rightarrow \Sigma(1385)\pi$ $(\Gamma_1\Gamma_3)/\Gamma$
 VALUE DOCUMENT ID TECN COMMENT

+0.056±0.028 ² CAMERON 78 DPWA $K^-p \rightarrow \Sigma(1385)\pi$

$(\Gamma_1\Gamma_7)/\Gamma_{\text{total}}$ in $N\bar{K} \rightarrow \Lambda(1800) \rightarrow N\bar{K}^*(892)$, S=1/2, S-wave $(\Gamma_1\Gamma_5)/\Gamma$
 VALUE DOCUMENT ID TECN COMMENT

-0.17±0.03 ² CAMERON 78B DPWA $K^-p \rightarrow N\bar{K}^*$

$(\Gamma_1\Gamma_7)/\Gamma_{\text{total}}$ in $N\bar{K} \rightarrow \Lambda(1800) \rightarrow N\bar{K}^*(892)$, S=3/2, D-wave $(\Gamma_1\Gamma_6)/\Gamma$
 VALUE DOCUMENT ID TECN COMMENT

-0.13±0.04 CAMERON 78B DPWA $K^-p \rightarrow N\bar{K}^*$

$\Lambda(1800)$ FOOTNOTES

- The two MARTIN 77 values are from a T-matrix pole and from a Breit-Wigner fit.
- The published sign has been changed to be in accord with the baryon-first convention.

$\Lambda(1800)$ REFERENCES

MANLEY 02 PRL 88 012002 D.M. Manley et al. (BNL Crystal Ball Collab.)	
GOPAL 80 Toronto Conf. 159 G.P. Gopal (RHEL) IJP	
ALSTON-... 78 PR D18 182 M. Alston-Garnjost et al. (LBL, MTHO+) IJP	
Also PRL 38 1007 M. Alston-Garnjost et al. (LBL, MTHO+) IJP	
CAMERON 78 NP B143 189 W. Cameron et al. (RHEL, LOIC) IJP	
CAMERON 78B NP B146 327 W. Cameron et al. (RHEL, LOIC) IJP	
GOPAL 77 NP B119 362 G.P. Gopal et al. (LOIC, RHEL) IJP	
MARTIN 77 NP B127 349 B.R. Martin, M.K. Pidcock, R.G. Moorhouse (LOUC+) IJP	
Also NP B126 266 B.R. Martin, M.K. Pidcock (LOUC) IJP	
Also NP B126 285 B.R. Martin, M.K. Pidcock (LOUC) IJP	
LANGBEIN 72 NP B47 477 W. Langbein, F. Wagner (MPIM) IJP	
KIM 71 PRL 27 356 J.K. Kim (HARV) IJP	
Also Duke Conf. 161 J.K. Kim (HARV) IJP	
BRICMAN 70B PL 33B 511 Hyperon Resonances, 1970 C. Bricman, M. Ferro-Luzzi, J.P. Lagnaux (CERN) IJP	

$\Lambda(1810) P_{01}$ $I(J^P) = 0(\frac{1}{2}^+)$ Status: ***

Almost all the recent analyses contain a P_{01} state, and sometimes two of them, but the masses, widths, and branching ratios vary greatly. See also the $\Lambda(1600) P_{01}$.

$\Lambda(1810)$ MASS

VALUE (MeV)	DOCUMENT ID	TECN	COMMENT
1750 to 1850 (≈ 1810) OUR ESTIMATE			
1841±20	GOPAL 80	DPWA	$\bar{K}N \rightarrow \bar{K}N$
1853±20	GOPAL 77	DPWA	$\bar{K}N$ multichannel
1735±5	CARROLL 76	DPWA	Isospin-0 total σ
1746±10	PREVOST 74	DPWA	$K^-N \rightarrow \Sigma(1385)\pi$
1780±20	LANGBEIN 72	IPWA	$\bar{K}N$ multichannel
••• We do not use the following data for averages, fits, limits, etc. •••			
1861 or 1953	¹ MARTIN 77	DPWA	$\bar{K}N$ multichannel
1755	KIM 71	DPWA	K-matrix analysis
1800	ARMENTEROS70	HBC	$\bar{K}N \rightarrow \bar{K}N$
1750	ARMENTEROS70	HBC	$\bar{K}N \rightarrow \Sigma\pi$
1690±10	BARBARO-... 70	HBC	$\bar{K}N \rightarrow \Sigma\pi$
1740	BAILEY 69	DPWA	$\bar{K}N \rightarrow \bar{K}N$
1745	ARMENTEROS68B	HBC	$\bar{K}N \rightarrow \bar{K}N$

Baryon Particle Listings

 $\Lambda(1810), \Lambda(1820)$ $\Lambda(1810)$ WIDTH

VALUE (MeV)	DOCUMENT ID	TECN	COMMENT
50 to 250 (≈ 150) OUR ESTIMATE			
164 \pm 20	GOPAL 80	DPWA	$\bar{K}N \rightarrow \bar{K}N$
90 \pm 20	CAMERON 78B	DPWA	$K^-p \rightarrow N\bar{K}^*$
166 \pm 20	GOPAL 77	DPWA	$\bar{K}N$ multichannel
46 \pm 20	PREVOST 74	DPWA	$K^-N \rightarrow \Sigma(1385)\pi$
120 \pm 10	LANGBEIN 72	IPWA	$\bar{K}N$ multichannel
••• We do not use the following data for averages, fits, limits, etc. •••			
535 or 585	¹ MARTIN 77	DPWA	$\bar{K}N$ multichannel
28	CARROLL 76	DPWA	Isospin-0 total σ
35	KIM 71	DPWA	K-matrix analysis
30	ARMENTEROS70	HBC	$\bar{K}N \rightarrow \bar{K}N$
70	ARMENTEROS70	HBC	$\bar{K}N \rightarrow \Sigma\pi$
22	BARBARO... 70	HBC	$\bar{K}N \rightarrow \Sigma\pi$
300	BAILEY 69	DPWA	$\bar{K}N \rightarrow \bar{K}N$
147	ARMENTEROS68B	HBC	

 $\Lambda(1810)$ DECAY MODES

Mode	Fraction (Γ_i/Γ)
Γ_1 $N\bar{K}$	20–50 %
Γ_2 $\Sigma\pi$	10–40 %
Γ_3 $\Sigma(1385)\pi$	seen
Γ_4 $N\bar{K}^*(892)$	30–60 %
Γ_5 $N\bar{K}^*(892), S=1/2, P$ -wave	
Γ_6 $N\bar{K}^*(892), S=3/2, P$ -wave	

The above branching fractions are our estimates, not fits or averages.

 $\Lambda(1810)$ BRANCHING RATIOS

See "Sign conventions for resonance couplings" in the Note on Λ and Σ Resonances.

$\Gamma(N\bar{K})/\Gamma_{\text{total}}$	DOCUMENT ID	TECN	COMMENT	Γ_1/Γ
0.2 to 0.5 OUR ESTIMATE				
0.24 \pm 0.04	GOPAL 80	DPWA	$\bar{K}N \rightarrow \bar{K}N$	
0.36 \pm 0.05	LANGBEIN 72	IPWA	$\bar{K}N$ multichannel	
••• We do not use the following data for averages, fits, limits, etc. •••				
0.21 \pm 0.04	GOPAL 77	DPWA	See GOPAL 80	
0.52 or 0.49	¹ MARTIN 77	DPWA	$\bar{K}N$ multichannel	
0.30	KIM 71	DPWA	K-matrix analysis	
0.15	ARMENTEROS70	DPWA	$\bar{K}N \rightarrow \bar{K}N$	
0.55	BAILEY 69	DPWA	$\bar{K}N \rightarrow \bar{K}N$	
0.4	ARMENTEROS68B	DPWA	$\bar{K}N \rightarrow \bar{K}N$	

$(\Gamma_1\Gamma_2)^{1/2}/\Gamma_{\text{total}}$ in $N\bar{K} \rightarrow \Lambda(1810) \rightarrow \Sigma\pi$	DOCUMENT ID	TECN	COMMENT	$(\Gamma_1\Gamma_2)^{1/2}/\Gamma$
VALUE				
-0.24 \pm 0.04	GOPAL 77	DPWA	$\bar{K}N$ multichannel	
••• We do not use the following data for averages, fits, limits, etc. •••				
+0.25 or +0.23	¹ MARTIN 77	DPWA	$\bar{K}N$ multichannel	
< 0.01	LANGBEIN 72	IPWA	$\bar{K}N$ multichannel	
0.17	KIM 71	DPWA	K-matrix analysis	
+0.20	² ARMENTEROS70	DPWA	$\bar{K}N \rightarrow \Sigma\pi$	
-0.13 \pm 0.03	BARBARO... 70	DPWA	$\bar{K}N \rightarrow \Sigma\pi$	

$(\Gamma_1\Gamma_3)^{1/2}/\Gamma_{\text{total}}$ in $N\bar{K} \rightarrow \Lambda(1810) \rightarrow \Sigma(1385)\pi$	DOCUMENT ID	TECN	COMMENT	$(\Gamma_1\Gamma_3)^{1/2}/\Gamma$
VALUE				
+0.18 \pm 0.10	PREVOST 74	DPWA	$K^-N \rightarrow \Sigma(1385)\pi$	

$(\Gamma_1\Gamma_5)^{1/2}/\Gamma_{\text{total}}$ in $N\bar{K} \rightarrow \Lambda(1810) \rightarrow N\bar{K}^*(892), S=1/2, P$ -wave	DOCUMENT ID	TECN	COMMENT	$(\Gamma_1\Gamma_5)^{1/2}/\Gamma$
VALUE				
-0.14 \pm 0.03	² CAMERON 78B	DPWA	$K^-p \rightarrow N\bar{K}^*$	

$(\Gamma_1\Gamma_6)^{1/2}/\Gamma_{\text{total}}$ in $N\bar{K} \rightarrow \Lambda(1810) \rightarrow N\bar{K}^*(892), S=3/2, P$ -wave	DOCUMENT ID	TECN	COMMENT	$(\Gamma_1\Gamma_6)^{1/2}/\Gamma$
VALUE				
+0.35 \pm 0.06	CAMERON 78B	DPWA	$K^-p \rightarrow N\bar{K}^*$	

 $\Lambda(1810)$ FOOTNOTES

- ¹ The two MARTIN 77 values are from a T-matrix pole and from a Breit-Wigner fit.
² The published sign has been changed to be in accord with the baryon-first convention.

 $\Lambda(1810)$ REFERENCES

GOPAL 80	Toronto Conf. 159	G.P. Gopal	(RHEL) IJP
CAMERON 78B	NP B146 327	W. Cameron et al.	(RHEL, LOIC) IJP
GOPAL 77	NP B119 362	G.P. Gopal et al.	(LOIC, RHEL) IJP
MARTIN 77	NP B127 349	B.R. Martin, M.K. Pidcock, R.G. Moorhouse	(LOUC+) IJP
Also	NP B126 266	B.R. Martin, M.K. Pidcock	(LOUC)
Also	NP B126 285	B.R. Martin, M.K. Pidcock	(LOUC) IJP
CARROLL 76	PRL 37 806	A.S. Carroll et al.	(BNL) I
PREVOST 74	NP B69 246	J. Prevost et al.	(SACL, CERN, HEID)
LANGBEIN 72	NP B47 477	W. Langbein, F. Wagner	(MPIM) IJP
KIM 71	PRL 27 356	J.K. Kim	(HARV) IJP
Also	Duke Conf. 161	J.K. Kim	(HARV) IJP
Hyperon Resonances, 1970			
ARMENTEROS 70	Duke Conf. 123	R. Armenteros et al.	(CERN, HEID, SACL) IJP
Hyperon Resonances, 1970			
BARBARO... 70	Duke Conf. 173	A. Barbaro-Galtieri	(LRL) IJP
Hyperon Resonances, 1970			
BAILEY 69	Thesis UCL 50617	J.M. Bailey	(LLL) IJP
ARMENTEROS 68B	NP B8 195	R. Armenteros et al.	(CERN, HEID, SACL) IJP

 $\Lambda(1820) F_{05}$

$$I(J^P) = 0(\frac{5}{2}^+) \text{ Status: } ***$$

This resonance is the cornerstone for all partial-wave analyses in this region. Most of the results published before 1973 are now obsolete and have been omitted. They may be found in our 1982 edition Physics Letters **111B** 1 (1982).

Most of the quoted errors are statistical only; the systematic errors due to the particular parametrizations used in the partial-wave analyses are not included. For this reason we do not calculate weighted averages for the mass and width.

 $\Lambda(1820)$ MASS

VALUE (MeV)	DOCUMENT ID	TECN	COMMENT
1815 to 1825 (≈ 1820) OUR ESTIMATE			
1823 \pm 3	GOPAL 80	DPWA	$\bar{K}N \rightarrow \bar{K}N$
1819 \pm 2	ALSTON... 78	DPWA	$\bar{K}N \rightarrow \bar{K}N$
1822 \pm 2	GOPAL 77	DPWA	$\bar{K}N$ multichannel
1821 \pm 2	KANE 74	DPWA	$K^-p \rightarrow \Sigma\pi$
••• We do not use the following data for averages, fits, limits, etc. •••			
1830	DECLAIS 77	DPWA	$\bar{K}N \rightarrow \bar{K}N$
1817 or 1819	¹ MARTIN 77	DPWA	$\bar{K}N$ multichannel

 $\Lambda(1820)$ WIDTH

VALUE (MeV)	DOCUMENT ID	TECN	COMMENT
70 to 90 (≈ 80) OUR ESTIMATE			
77 \pm 5	GOPAL 80	DPWA	$\bar{K}N \rightarrow \bar{K}N$
72 \pm 5	ALSTON... 78	DPWA	$\bar{K}N \rightarrow \bar{K}N$
81 \pm 5	GOPAL 77	DPWA	$\bar{K}N$ multichannel
87 \pm 3	KANE 74	DPWA	$K^-p \rightarrow \Sigma\pi$
••• We do not use the following data for averages, fits, limits, etc. •••			
82	DECLAIS 77	DPWA	$\bar{K}N \rightarrow \bar{K}N$
76 or 76	¹ MARTIN 77	DPWA	$\bar{K}N$ multichannel

 $\Lambda(1820)$ DECAY MODES

Mode	Fraction (Γ_i/Γ)
Γ_1 $N\bar{K}$	55–65 %
Γ_2 $\Sigma\pi$	8–14 %
Γ_3 $\Sigma(1385)\pi$	5–10 %
Γ_4 $\Sigma(1385)\pi, P$ -wave	
Γ_5 $\Sigma(1385)\pi, F$ -wave	
Γ_6 $\Lambda\eta$	
Γ_7 $\Sigma\pi\pi$	

The above branching fractions are our estimates, not fits or averages.

 $\Lambda(1820)$ BRANCHING RATIOS

Errors quoted do not include uncertainties in the parametrizations used in the partial-wave analyses and are thus too small. See also "Sign conventions for resonance couplings" in the Note on Λ and Σ Resonances.

$\Gamma(N\bar{K})/\Gamma_{\text{total}}$	DOCUMENT ID	TECN	COMMENT	Γ_1/Γ
0.55 to 0.65 OUR ESTIMATE				
0.58 \pm 0.02	GOPAL 80	DPWA	$\bar{K}N \rightarrow \bar{K}N$	
0.60 \pm 0.03	ALSTON... 78	DPWA	$\bar{K}N \rightarrow \bar{K}N$	
••• We do not use the following data for averages, fits, limits, etc. •••				
0.51	DECLAIS 77	DPWA	$\bar{K}N \rightarrow \bar{K}N$	
0.57 \pm 0.02	GOPAL 77	DPWA	See GOPAL 80	
0.59 or 0.58	¹ MARTIN 77	DPWA	$\bar{K}N$ multichannel	

Baryon Particle Listings

$\Lambda(1820)$, $\Lambda(1830)$, $\Lambda(1890)$

$(\Gamma_1 \Gamma_f)^{1/2} / \Gamma_{\text{total}}$ in $N\bar{K} \rightarrow \Lambda(1820) \rightarrow \Sigma\pi$	DOCUMENT ID	TECN	COMMENT
VALUE			
-0.28 ± 0.03	GOPAL	77	DPWA $\bar{K}N$ multichannel
-0.28 ± 0.01	KANE	74	DPWA $K^-p \rightarrow \Sigma\pi$
••• We do not use the following data for averages, fits, limits, etc. •••			
-0.25 or -0.25	¹ MARTIN	77	DPWA $\bar{K}N$ multichannel

$(\Gamma_1 \Gamma_f)^{1/2} / \Gamma_{\text{total}}$ in $N\bar{K} \rightarrow \Lambda(1820) \rightarrow \Lambda\eta$	DOCUMENT ID	TECN	COMMENT
VALUE			
$-0.096^{+0.040}_{-0.020}$	RADER	73	MPWA

$\Gamma(\Sigma\pi\pi) / \Gamma_{\text{total}}$	DOCUMENT ID	TECN	COMMENT
VALUE			
no clear signal	² ARMENTEROS68c	HDBC	$K^-N \rightarrow \Sigma\pi\pi$

$(\Gamma_1 \Gamma_f)^{1/2} / \Gamma_{\text{total}}$ in $N\bar{K} \rightarrow \Lambda(1820) \rightarrow \Sigma(1385)\pi$, P-wave	DOCUMENT ID	TECN	COMMENT
VALUE			
-0.167 ± 0.054	³ CAMERON	78	DPWA $K^-p \rightarrow \Sigma(1385)\pi$
$+0.27 \pm 0.03$	PREVOST	74	DPWA $K^-N \rightarrow \Sigma(1385)\pi$

$(\Gamma_1 \Gamma_f)^{1/2} / \Gamma_{\text{total}}$ in $N\bar{K} \rightarrow \Lambda(1820) \rightarrow \Sigma(1385)\pi$, F-wave	DOCUMENT ID	TECN	COMMENT
VALUE			
$+0.065 \pm 0.029$	³ CAMERON	78	DPWA $K^-p \rightarrow \Sigma(1385)\pi$

$\Lambda(1820)$ FOOTNOTES

- The two MARTIN 77 values are from a T-matrix pole and from a Breit-Wigner fit.
- There is a suggestion of a bump, enough to be consistent with what is expected from $\Sigma(1385) \rightarrow \Sigma\pi$ decay.
- The published sign has been changed to be in accord with the baryon-first convention.

$\Lambda(1820)$ REFERENCES

PDG	82	PL 111B 1	M. Roos <i>et al.</i>	(HEL5, CIT, CERN)
GOPAL	80	Toronto Conf. 159	G.P. Gopal	(RHEL) IJP
ALSTON-...	78	PR D18 182	M. Alston-Garnjost <i>et al.</i>	(LBL, MTHO+) IJP
Also		PRL 38 1007	M. Alston-Garnjost <i>et al.</i>	(LBL, MTHO+) IJP
CAMERON	78	NP B143 189	W. Cameron <i>et al.</i>	(RHEL, LOIC) IJP
DECLAIS	77	CERN 77-16	Y. Declais <i>et al.</i>	(CAEN, CERN) IJP
GOPAL	77	NP B119 362	G.P. Gopal <i>et al.</i>	(LOIC, RHEL) IJP
MARTIN	77	NP B127 349	B.R. Martin, M.K. Pidcock, R.G. Moorhouse	(LOUC+) IJP
Also		NP B126 266	B.R. Martin, M.K. Pidcock	(LOUC) IJP
Also		NP B126 285	B.R. Martin, M.K. Pidcock	(LOUC) IJP
KANE	74	LBL-2452	D.F. Kane	(LBL) IJP
PREVOST	74	NP B69 246	J. Prevost <i>et al.</i>	(SACL, CERN, HEID)
RADER	73	NC 16A 178	R.K. Rader <i>et al.</i>	(SACL, HEID, CERN+)
ARMENTEROS 68c		NP B8 216	R. Armenteros <i>et al.</i>	(CERN, HEID, SACL) I

$\Lambda(1830) D_{05}$

 $I(J^P) = 0(\frac{5}{2}^-)$ Status: * * * *

For results published before 1973 (they are now obsolete), see our 1982 edition Physics Letters **111B** 1 (1982).

The best evidence for this resonance is in the $\Sigma\pi$ channel.

$\Lambda(1830)$ MASS

VALUE (MeV)	DOCUMENT ID	TECN	COMMENT
1810 to 1830 (≈ 1830) OUR ESTIMATE			
1831 ± 10	GOPAL	80	DPWA $\bar{K}N \rightarrow \bar{K}N$
1825 ± 10	GOPAL	77	DPWA $\bar{K}N$ multichannel
1825 ± 1	KANE	74	DPWA $K^-p \rightarrow \Sigma\pi$
••• We do not use the following data for averages, fits, limits, etc. •••			
1817 or 1818	¹ MARTIN	77	DPWA $\bar{K}N$ multichannel

$\Lambda(1830)$ WIDTH

VALUE (MeV)	DOCUMENT ID	TECN	COMMENT
60 to 110 (≈ 95) OUR ESTIMATE			
100 ± 10	GOPAL	80	DPWA $\bar{K}N \rightarrow \bar{K}N$
94 ± 10	GOPAL	77	DPWA $\bar{K}N$ multichannel
119 ± 3	KANE	74	DPWA $K^-p \rightarrow \Sigma\pi$
••• We do not use the following data for averages, fits, limits, etc. •••			
56 or 56	¹ MARTIN	77	DPWA $\bar{K}N$ multichannel

$\Lambda(1830)$ DECAY MODES

Mode	Fraction (Γ_i / Γ)
Γ_1 $N\bar{K}$	3–10 %
Γ_2 $\Sigma\pi$	35–75 %
Γ_3 $\Sigma(1385)\pi$	>15 %
Γ_4 $\Sigma(1385)\pi$, D-wave	
Γ_5 $\Lambda\eta$	

The above branching fractions are our estimates, not fits or averages.

$\Lambda(1830)$ BRANCHING RATIOS

See "Sign conventions for resonance couplings" in the Note on Λ and Σ Resonances.

$\Gamma(N\bar{K}) / \Gamma_{\text{total}}$	DOCUMENT ID	TECN	COMMENT	Γ_1 / Γ
VALUE				
0.03 to 0.10 OUR ESTIMATE				
0.08 ± 0.03	GOPAL	80	DPWA $\bar{K}N \rightarrow \bar{K}N$	
0.02 ± 0.02	ALSTON-...	78	DPWA $\bar{K}N \rightarrow \bar{K}N$	
••• We do not use the following data for averages, fits, limits, etc. •••				
0.04 ± 0.03	GOPAL	77	DPWA See GOPAL 80	
0.04 or 0.04	¹ MARTIN	77	DPWA $\bar{K}N$ multichannel	

$(\Gamma_1 \Gamma_f)^{1/2} / \Gamma_{\text{total}}$ in $N\bar{K} \rightarrow \Lambda(1830) \rightarrow \Sigma\pi$	DOCUMENT ID	TECN	COMMENT	$(\Gamma_1 \Gamma_2)^{1/2} / \Gamma$
VALUE				
-0.17 ± 0.03	GOPAL	77	DPWA $\bar{K}N$ multichannel	
-0.15 ± 0.01	KANE	74	DPWA $K^-p \rightarrow \Sigma\pi$	
••• We do not use the following data for averages, fits, limits, etc. •••				
-0.17 or -0.17	¹ MARTIN	77	DPWA $\bar{K}N$ multichannel	

$(\Gamma_1 \Gamma_f)^{1/2} / \Gamma_{\text{total}}$ in $N\bar{K} \rightarrow \Lambda(1830) \rightarrow \Lambda\eta$	DOCUMENT ID	TECN	COMMENT	$(\Gamma_1 \Gamma_5)^{1/2} / \Gamma$
VALUE				
-0.044 ± 0.020	RADER	73	MPWA	

$(\Gamma_1 \Gamma_f)^{1/2} / \Gamma_{\text{total}}$ in $N\bar{K} \rightarrow \Lambda(1830) \rightarrow \Sigma(1385)\pi$	DOCUMENT ID	TECN	COMMENT	$(\Gamma_1 \Gamma_3)^{1/2} / \Gamma$
VALUE				
$+0.141 \pm 0.014$	² CAMERON	78	DPWA $K^-p \rightarrow \Sigma(1385)\pi$	
$+0.13 \pm 0.03$	PREVOST	74	DPWA $K^-N \rightarrow \Sigma(1385)\pi$	

$\Lambda(1830)$ FOOTNOTES

- The two MARTIN 77 values are from a T-matrix pole and from a Breit-Wigner fit.
- The CAMERON 78 upper limit on G-wave decay is 0.03. The published sign has been changed to be in accord with the baryon-first convention.

$\Lambda(1830)$ REFERENCES

PDG	82	PL 111B 1	M. Roos <i>et al.</i>	(HEL5, CIT, CERN)
GOPAL	80	Toronto Conf. 159	G.P. Gopal	(RHEL) IJP
ALSTON-...	78	PR D18 182	M. Alston-Garnjost <i>et al.</i>	(LBL, MTHO+) IJP
Also		PRL 38 1007	M. Alston-Garnjost <i>et al.</i>	(LBL, MTHO+) IJP
CAMERON	78	NP B143 189	W. Cameron <i>et al.</i>	(RHEL, LOIC) IJP
GOPAL	77	NP B119 362	G.P. Gopal <i>et al.</i>	(LOIC, RHEL) IJP
MARTIN	77	NP B127 349	B.R. Martin, M.K. Pidcock, R.G. Moorhouse	(LOUC+) IJP
Also		NP B126 266	B.R. Martin, M.K. Pidcock	(LOUC) IJP
Also		NP B126 285	B.R. Martin, M.K. Pidcock	(LOUC) IJP
KANE	74	LBL-2452	D.F. Kane	(LBL) IJP
PREVOST	74	NP B69 246	J. Prevost <i>et al.</i>	(SACL, CERN, HEID)
RADER	73	NC 16A 178	R.K. Rader <i>et al.</i>	(SACL, HEID, CERN+)

$\Lambda(1890) P_{03}$

 $I(J^P) = 0(\frac{3}{2}^+)$ Status: * * * *

For results published before 1974 (they are now obsolete), see our 1982 edition Physics Letters **111B** 1 (1982).

The $J^P = 3/2^+$ assignment is consistent with all available data (including polarization) and recent partial-wave analyses. The dominant inelastic modes remain unknown.

$\Lambda(1890)$ MASS

VALUE (MeV)	DOCUMENT ID	TECN	COMMENT
1850 to 1910 (≈ 1890) OUR ESTIMATE			
1897 ± 5	GOPAL	80	DPWA $\bar{K}N \rightarrow \bar{K}N$
1908 ± 10	ALSTON-...	78	DPWA $\bar{K}N \rightarrow \bar{K}N$
1900 ± 5	GOPAL	77	DPWA $\bar{K}N$ multichannel
1894 ± 10	HEMINGWAY	75	DPWA $K^-p \rightarrow \bar{K}N$
••• We do not use the following data for averages, fits, limits, etc. •••			
1856 or 1868	¹ MARTIN	77	DPWA $\bar{K}N$ multichannel
1900	² NAKKASYAN	75	DPWA $K^-p \rightarrow \Lambda\omega$

$\Lambda(1890)$ WIDTH

VALUE (MeV)	DOCUMENT ID	TECN	COMMENT
60 to 200 (≈ 100) OUR ESTIMATE			
74 ± 10	GOPAL	80	DPWA $\bar{K}N \rightarrow \bar{K}N$
119 ± 20	ALSTON-...	78	DPWA $\bar{K}N \rightarrow \bar{K}N$
72 ± 10	GOPAL	77	DPWA $\bar{K}N$ multichannel
107 ± 10	HEMINGWAY	75	DPWA $K^-p \rightarrow \bar{K}N$
••• We do not use the following data for averages, fits, limits, etc. •••			
191 or 193	¹ MARTIN	77	DPWA $\bar{K}N$ multichannel
100	² NAKKASYAN	75	DPWA $K^-p \rightarrow \Lambda\omega$

Baryon Particle Listings

 $\Lambda(1890)$, $\Lambda(2000)$ $\Lambda(1890)$ DECAY MODES

Mode	Fraction (Γ_i/Γ)
Γ_1 $N\bar{K}$	20–35 %
Γ_2 $\Sigma\pi$	3–10 %
Γ_3 $\Sigma(1385)\pi$	seen
Γ_4 $\Sigma(1385)\pi$, P -wave	
Γ_5 $\Sigma(1385)\pi$, F -wave	
Γ_6 $N\bar{K}^*(892)$	seen
Γ_7 $N\bar{K}^*(892)$, $S=1/2$, P -wave	
Γ_8 $\Lambda\omega$	

The above branching fractions are our estimates, not fits or averages.

 $\Lambda(1890)$ BRANCHING RATIOS

See "Sign conventions for resonance couplings" in the Note on Λ and Σ Resonances.

$\Gamma(N\bar{K})/\Gamma_{\text{total}}$	DOCUMENT ID	TECN	COMMENT	Γ_1/Γ
0.20 to 0.35 OUR ESTIMATE				
0.20±0.02	GOPAL	80	DPWA $\bar{K}N \rightarrow \bar{K}N$	
0.34±0.05	ALSTON-...	78	DPWA $\bar{K}N \rightarrow \bar{K}N$	
0.24±0.04	HEMINGWAY	75	DPWA $K^-p \rightarrow \bar{K}N$	
••• We do not use the following data for averages, fits, limits, etc. •••				
0.18±0.02	GOPAL	77	DPWA See GOPAL 80	
0.36 or 0.34	1 MARTIN	77	DPWA $\bar{K}N$ multichannel	

$(\Gamma_i\Gamma_f)^{1/2}/\Gamma_{\text{total}}$ in $N\bar{K} \rightarrow \Lambda(1890) \rightarrow \Sigma\pi$	DOCUMENT ID	TECN	COMMENT	$(\Gamma_1\Gamma_2)^{1/2}/\Gamma$
VALUE				
-0.09±0.03	GOPAL	77	DPWA $\bar{K}N$ multichannel	
••• We do not use the following data for averages, fits, limits, etc. •••				
+0.15 or +0.14	1 MARTIN	77	DPWA $\bar{K}N$ multichannel	

$(\Gamma_i\Gamma_f)^{1/2}/\Gamma_{\text{total}}$ in $N\bar{K} \rightarrow \Lambda(1890) \rightarrow \Lambda\omega$	DOCUMENT ID	TECN	COMMENT	$(\Gamma_1\Gamma_8)^{1/2}/\Gamma$
VALUE				
seen	BACCARI	77	IPWA $K^-p \rightarrow \Lambda\omega$	
0.032	2 NAKKASYAN	75	DPWA $K^-p \rightarrow \Lambda\omega$	

$(\Gamma_i\Gamma_f)^{1/2}/\Gamma_{\text{total}}$ in $N\bar{K} \rightarrow \Lambda(1890) \rightarrow \Sigma(1385)\pi$, P -wave	DOCUMENT ID	TECN	COMMENT	$(\Gamma_1\Gamma_4)^{1/2}/\Gamma$
VALUE				
<0.03	CAMERON	78	DPWA $K^-p \rightarrow \Sigma(1385)\pi$	

$(\Gamma_i\Gamma_f)^{1/2}/\Gamma_{\text{total}}$ in $N\bar{K} \rightarrow \Lambda(1890) \rightarrow \Sigma(1385)\pi$, F -wave	DOCUMENT ID	TECN	COMMENT	$(\Gamma_1\Gamma_5)^{1/2}/\Gamma$
VALUE				
-0.126±0.055	3 CAMERON	78	DPWA $K^-p \rightarrow \Sigma(1385)\pi$	

$(\Gamma_i\Gamma_f)^{1/2}/\Gamma_{\text{total}}$ in $N\bar{K} \rightarrow \Lambda(1890) \rightarrow N\bar{K}^*(892)$	DOCUMENT ID	TECN	COMMENT	$(\Gamma_1\Gamma_6)^{1/2}/\Gamma$
VALUE				
-0.07±0.03	3,4 CAMERON	78B	DPWA $K^-p \rightarrow N\bar{K}^*$	

 $\Lambda(1890)$ FOOTNOTES

- The two MARTIN 77 values are from a T-matrix pole and from a Breit-Wigner fit.
- Found in one of two best solutions.
- The published sign has been changed to be in accord with the baryon-first convention.
- Upper limits on the P_3 and F_3 waves are each 0.03.

 $\Lambda(1890)$ REFERENCES

PDG	82	PL 111B 1	M. Roos <i>et al.</i>	(HEL5, CIT, CERN)
GOPAL	80	Toronto Conf. 159	G.P. Gopal	(RHEL) IJP
ALSTON-...	78	PR D18 182	M. Alston-Garnjost <i>et al.</i>	(LBL, MTHO+) IJP
Also		PRL 38 1007	M. Alston-Garnjost <i>et al.</i>	(LBL, MTHO+) IJP
CAMERON	78	NP B143 189	W. Cameron <i>et al.</i>	(RHEL, LOIC) IJP
CAMERON	78B	NP B146 327	W. Cameron <i>et al.</i>	(RHEL, LOIC) IJP
BACCARI	77	NC 41A 96	B. Baccari <i>et al.</i>	(SACL, CDEF) IJP
GOPAL	77	NP B119 362	G.P. Gopal <i>et al.</i>	(LOIC, RHEL) IJP
MARTIN	77	NP B127 349	B.R. Martin, M.K. Pidcock, R.G. Moorhouse	(LOIC+) IJP
Also		NP B126 266	B.R. Martin, M.K. Pidcock	(LOIC) IJP
Also		NP B126 285	B.R. Martin, M.K. Pidcock	(LOIC) IJP
HEMINGWAY	75	NP B91 12	R.J. Hemingway <i>et al.</i>	(CERN, HEIDH, MPIM) IJP
NAKKASYAN	75	NP B93 85	A. Nakkasyan	(CERN) IJP

 $\Lambda(2000)$

$$I(J^P) = 0(?)^? \quad \text{Status: } *$$

OMITTED FROM SUMMARY TABLE

We list here all the ambiguous resonance possibilities with a mass around 2 GeV. The proposed quantum numbers are D_3 (BARBARO-GALTIERI 70 in $\Sigma\pi$), D_3+F_5 , P_3+D_5 , or P_1+D_3 (BRANDSTETTER 72 in $\Lambda\omega$), and S_1 (CAMERON 78B in $N\bar{K}^*$). The first two of the above analyses should now be considered obsolete. See also NAKKASYAN 75.

 $\Lambda(2000)$ MASS

VALUE (MeV)	DOCUMENT ID	TECN	COMMENT
≈ 2000 OUR ESTIMATE			
2030±30	CAMERON 78B	DPWA	$K^-p \rightarrow N\bar{K}^*$
1935 to 1971	1 BRANDSTET...72	DPWA	$K^-p \rightarrow \Lambda\omega$
1951 to 2034	1 BRANDSTET...72	DPWA	$K^-p \rightarrow \Lambda\omega$
2010±30	BARBARO-... 70	DPWA	$K^-p \rightarrow \Sigma\pi$

 $\Lambda(2000)$ WIDTH

VALUE (MeV)	DOCUMENT ID	TECN	COMMENT
125±25	CAMERON 78B	DPWA	$K^-p \rightarrow N\bar{K}^*$
180 to 240	1 BRANDSTET...72	DPWA	(lower mass)
73 to 154	1 BRANDSTET...72	DPWA	(higher mass)
130±50	BARBARO-... 70	DPWA	$K^-p \rightarrow \Sigma\pi$

 $\Lambda(2000)$ DECAY MODES

Mode
Γ_1 $N\bar{K}$
Γ_2 $\Sigma\pi$
Γ_3 $\Lambda\omega$
Γ_4 $N\bar{K}^*(892)$, $S=1/2$, S -wave
Γ_5 $N\bar{K}^*(892)$, $S=3/2$, D -wave

 $\Lambda(2000)$ BRANCHING RATIOS

See "Sign conventions for resonance couplings" in the Note on Λ and Σ Resonances.

$(\Gamma_i\Gamma_f)^{1/2}/\Gamma_{\text{total}}$ in $N\bar{K} \rightarrow \Lambda(2000) \rightarrow \Sigma\pi$	DOCUMENT ID	TECN	COMMENT	$(\Gamma_1\Gamma_2)^{1/2}/\Gamma$
VALUE				
-0.20±0.04	BARBARO-... 70	DPWA	$K^-p \rightarrow \Sigma\pi$	

$(\Gamma_i\Gamma_f)^{1/2}/\Gamma_{\text{total}}$ in $N\bar{K} \rightarrow \Lambda(2000) \rightarrow \Lambda\omega$	DOCUMENT ID	TECN	COMMENT	$(\Gamma_1\Gamma_3)^{1/2}/\Gamma$
VALUE				
0.17 to 0.25	1 BRANDSTET...72	DPWA	(lower mass)	
0.04 to 0.15	1 BRANDSTET...72	DPWA	(higher mass)	

$(\Gamma_i\Gamma_f)^{1/2}/\Gamma_{\text{total}}$ in $N\bar{K} \rightarrow \Lambda(2000) \rightarrow N\bar{K}^*(892)$, $S=1/2$, S -wave	DOCUMENT ID	TECN	COMMENT	$(\Gamma_1\Gamma_4)^{1/2}/\Gamma$
VALUE				
-0.12±0.03	2 CAMERON 78B	DPWA	$K^-p \rightarrow N\bar{K}^*$	

$(\Gamma_i\Gamma_f)^{1/2}/\Gamma_{\text{total}}$ in $N\bar{K} \rightarrow \Lambda(2000) \rightarrow N\bar{K}^*(892)$, $S=3/2$, D -wave	DOCUMENT ID	TECN	COMMENT	$(\Gamma_1\Gamma_5)^{1/2}/\Gamma$
VALUE				
+0.09±0.03	CAMERON 78B	DPWA	$K^-p \rightarrow N\bar{K}^*$	

 $\Lambda(2000)$ FOOTNOTES

- The parameters quoted here are ranges from the three best fits; the lower state probably has $J \leq 3/2$, and the higher one probably has $J \leq 5/2$.
- The published sign has been changed to be in accord with the baryon-first convention.

 $\Lambda(2000)$ REFERENCES

CAMERON 78B	NP B146 327	W. Cameron <i>et al.</i>	(RHEL, LOIC) IJP
NAKKASYAN 75	NP B93 85	A. Nakkasyan	(CERN) IJP
BRANDSTET... 72	NP B39 13	A.A. Brandstetter <i>et al.</i>	(RHEL, CDEF+) IJP
BARBARO-... 70	Duke Conf. 173	A. Barbaro-Galieri	(LRL) IJP
Hyperon Resonances, 1970			

$\Lambda(2020) F_{07}$ $I(J^P) = 0(\frac{7}{2}^+)$ Status: *

OMITTED FROM SUMMARY TABLE

In LITCHFIELD 71, need for the state rests solely on a possibly inconsistent polarization measurement at 1.784 GeV/c. HEMINGWAY 75 does not require this state. GOPAL 77 does not need it in either $N\bar{K}$ or $\Sigma\pi$. With new K^-n angular distributions included, DECLAIS 77 sees it. However, this and other new data are included in GOPAL 80 and the state is not required. BACCARI 77 weakly supports it.

$\Lambda(2020)$ MASS

VALUE (MeV)	DOCUMENT ID	TECN	COMMENT
≈ 2020 OUR ESTIMATE			
2140	BACCARI 77	DPWA	$K^-p \rightarrow \Lambda\omega$
2117	DECLAIS 77	DPWA	$\bar{K}N \rightarrow \bar{K}N$
2100±30	LITCHFIELD 71	DPWA	$K^-p \rightarrow \bar{K}N$
2020±20	BARBARO... 70	DPWA	$K^-p \rightarrow \Sigma\pi$

$\Lambda(2020)$ WIDTH

VALUE (MeV)	DOCUMENT ID	TECN	COMMENT
128	BACCARI 77	DPWA	$K^-p \rightarrow \Lambda\omega$
167	DECLAIS 77	DPWA	$\bar{K}N \rightarrow \bar{K}N$
120±30	LITCHFIELD 71	DPWA	$K^-p \rightarrow \bar{K}N$
160±30	BARBARO... 70	DPWA	$K^-p \rightarrow \Sigma\pi$

$\Lambda(2020)$ DECAY MODES

Mode	Fraction (Γ_i/Γ)
Γ_1 $N\bar{K}$	25-35 %
Γ_2 $\Sigma\pi$	~ 5 %
Γ_3 $\Lambda\eta$	<3 %
Γ_4 ΞK	<3 %
Γ_5 $\Lambda\omega$	<8 %
Γ_6 $N\bar{K}^*(892)$	10-20 %
Γ_7 $N\bar{K}^*(892), S=1/2, G\text{-wave}$	
Γ_8 $N\bar{K}^*(892), S=3/2, D\text{-wave}$	

$\Lambda(2020)$ BRANCHING RATIOS

See "Sign conventions for resonance couplings" in the Note on Λ and Σ Resonances.

$\Gamma(N\bar{K})/\Gamma_{\text{total}}$	DOCUMENT ID	TECN	COMMENT	Γ_1/Γ
0.05	DECLAIS 77	DPWA	$\bar{K}N \rightarrow \bar{K}N$	
0.05±0.02	LITCHFIELD 71	DPWA	$K^-p \rightarrow \bar{K}N$	

$(\Gamma_1\Gamma_2)^{1/2}/\Gamma_{\text{total}}$ in $N\bar{K} \rightarrow \Lambda(2020) \rightarrow \Sigma\pi$	DOCUMENT ID	TECN	COMMENT	$(\Gamma_1\Gamma_2)^{1/2}/\Gamma$
-0.15±0.02	BARBARO... 70	DPWA	$K^-p \rightarrow \Sigma\pi$	

$(\Gamma_1\Gamma_3)^{1/2}/\Gamma_{\text{total}}$ in $N\bar{K} \rightarrow \Lambda(2020) \rightarrow \Lambda\omega$	DOCUMENT ID	TECN	COMMENT	$(\Gamma_1\Gamma_3)^{1/2}/\Gamma$
<0.05	BACCARI 77	DPWA	$K^-p \rightarrow \Lambda\omega$	

$\Lambda(2020)$ REFERENCES

GOPAL 80	Toronto Conf. 159	G.P. Gopal	(RHEL)
BACCARI 77	NC 41A 96	B. Baccari et al.	(SAEL, CDEF) IJP
DECLAIS 77	CERN 77-16	Y. Declais et al.	(CAEN, CERN) IJP
GOPAL 77	NP B119 362	G.P. Gopal et al.	(LOIC, RHEL)
HEMINGWAY 75	NP B91 12	R.J. Hemingway et al.	(CERN, HEIDH, MPIM) IJP
LITCHFIELD 71	NP B30 125	P.J. Litchfield et al.	(RHEL, CDEF, SAEL) IJP
BARBARO... 70	Duke Conf. 173	A. Barbaro-Galteri	(LRL) IJP

Hyperon Resonances, 1970

$\Lambda(2100) G_{07}$ $I(J^P) = 0(\frac{7}{2}^-)$ Status: ****

Discovered by COOL 66 and by WOHL 66. Most of the results published before 1973 are now obsolete and have been omitted. They may be found in our 1982 edition Physics Letters **111B** 1 (1982).

This entry only includes results from partial-wave analyses. Parameters of peaks seen in cross sections and in invariant-mass distributions around 2100 MeV used to be listed in a separate entry immediately following. It may be found in our 1986 edition Physics Letters **170B** 1 (1986).

$\Lambda(2100)$ MASS

VALUE (MeV)	DOCUMENT ID	TECN	COMMENT
2090 to 2110 (≈ 2100) OUR ESTIMATE			
2104±10	GOPAL 80	DPWA	$\bar{K}N \rightarrow \bar{K}N$
2106±30	DEBELLEFON 78	DPWA	$\bar{K}N \rightarrow \bar{K}N$
2110±10	GOPAL 77	DPWA	$\bar{K}N$ multichannel
2105±10	HEMINGWAY 75	DPWA	$K^-p \rightarrow \bar{K}N$
2115±10	KANE 74	DPWA	$K^-p \rightarrow \Sigma\pi$
••• We do not use the following data for averages, fits, limits, etc. •••			
2094	BACCARI 77	DPWA	$K^-p \rightarrow \Lambda\omega$
2094	DECLAIS 77	DPWA	$\bar{K}N \rightarrow \bar{K}N$
2110 or 2089	¹ NAKKASYAN 75	DPWA	$K^-p \rightarrow \Lambda\omega$

$\Lambda(2100)$ WIDTH

VALUE (MeV)	DOCUMENT ID	TECN	COMMENT
100 to 250 (≈ 200) OUR ESTIMATE			
157±40	DEBELLEFON 78	DPWA	$\bar{K}N \rightarrow \bar{K}N$
250±30	GOPAL 77	DPWA	$\bar{K}N$ multichannel
241±30	HEMINGWAY 75	DPWA	$K^-p \rightarrow \bar{K}N$
152±15	KANE 74	DPWA	$K^-p \rightarrow \Sigma\pi$
••• We do not use the following data for averages, fits, limits, etc. •••			
98	BACCARI 77	DPWA	$K^-p \rightarrow \Lambda\omega$
250	DECLAIS 77	DPWA	$\bar{K}N \rightarrow \bar{K}N$
244 or 302	¹ NAKKASYAN 75	DPWA	$K^-p \rightarrow \Lambda\omega$

$\Lambda(2100)$ DECAY MODES

Mode	Fraction (Γ_i/Γ)
Γ_1 $N\bar{K}$	25-35 %
Γ_2 $\Sigma\pi$	~ 5 %
Γ_3 $\Lambda\eta$	<3 %
Γ_4 ΞK	<3 %
Γ_5 $\Lambda\omega$	<8 %
Γ_6 $N\bar{K}^*(892)$	10-20 %
Γ_7 $N\bar{K}^*(892), S=1/2, G\text{-wave}$	
Γ_8 $N\bar{K}^*(892), S=3/2, D\text{-wave}$	

The above branching fractions are our estimates, not fits or averages.

$\Lambda(2100)$ BRANCHING RATIOS

See "Sign conventions for resonance couplings" in the Note on Λ and Σ Resonances.

$\Gamma(N\bar{K})/\Gamma_{\text{total}}$	DOCUMENT ID	TECN	COMMENT	Γ_1/Γ
0.25 to 0.35 OUR ESTIMATE				
0.34±0.03	GOPAL 80	DPWA	$\bar{K}N \rightarrow \bar{K}N$	
0.24±0.06	DEBELLEFON 78	DPWA	$\bar{K}N \rightarrow \bar{K}N$	
0.31±0.03	HEMINGWAY 75	DPWA	$K^-p \rightarrow \bar{K}N$	
••• We do not use the following data for averages, fits, limits, etc. •••				
0.29	DECLAIS 77	DPWA	$\bar{K}N \rightarrow \bar{K}N$	
0.30±0.03	GOPAL 77	DPWA	See GOPAL 80	

$(\Gamma_1\Gamma_2)^{1/2}/\Gamma_{\text{total}}$ in $N\bar{K} \rightarrow \Lambda(2100) \rightarrow \Sigma\pi$	DOCUMENT ID	TECN	COMMENT	$(\Gamma_1\Gamma_2)^{1/2}/\Gamma$
+0.12±0.04	GOPAL 77	DPWA	$\bar{K}N$ multichannel	
+0.11±0.01	KANE 74	DPWA	$K^-p \rightarrow \Sigma\pi$	

$(\Gamma_1\Gamma_3)^{1/2}/\Gamma_{\text{total}}$ in $N\bar{K} \rightarrow \Lambda(2100) \rightarrow \Lambda\eta$	DOCUMENT ID	TECN	COMMENT	$(\Gamma_1\Gamma_3)^{1/2}/\Gamma$
-0.050±0.020	RADER 73	MPWA	$K^-p \rightarrow \Lambda\eta$	

$(\Gamma_1\Gamma_4)^{1/2}/\Gamma_{\text{total}}$ in $N\bar{K} \rightarrow \Lambda(2100) \rightarrow \Xi K$	DOCUMENT ID	TECN	COMMENT	$(\Gamma_1\Gamma_4)^{1/2}/\Gamma$
0.035±0.018	LITCHFIELD 71	DPWA	$K^-p \rightarrow \Xi K$	
••• We do not use the following data for averages, fits, limits, etc. •••				
0.003	MULLER 69B	DPWA	$K^-p \rightarrow \Xi K$	
0.05	TRIPP 67	RVUE	$K^-p \rightarrow \Xi K$	

$(\Gamma_1\Gamma_5)^{1/2}/\Gamma_{\text{total}}$ in $N\bar{K} \rightarrow \Lambda(2100) \rightarrow \Lambda\omega$	DOCUMENT ID	TECN	COMMENT	$(\Gamma_1\Gamma_5)^{1/2}/\Gamma$
-0.070	² BACCARI 77	DPWA	GD_{37} wave	
+0.011	² BACCARI 77	DPWA	GG_{17} wave	
+0.008	² BACCARI 77	DPWA	GG_{37} wave	
0.122 or 0.154	¹ NAKKASYAN 75	DPWA	$K^-p \rightarrow \Lambda\omega$	

$(\Gamma_1\Gamma_6)^{1/2}/\Gamma_{\text{total}}$ in $N\bar{K} \rightarrow \Lambda(2100) \rightarrow N\bar{K}^*(892), S=3/2, D\text{-wave}$	DOCUMENT ID	TECN	COMMENT	$(\Gamma_1\Gamma_6)^{1/2}/\Gamma$
+0.21±0.04	CAMERON 78B	DPWA	$K^-p \rightarrow N\bar{K}^*$	

Baryon Particle Listings

 $\Lambda(2100)$, $\Lambda(2110)$, $\Lambda(2325)$

$(\Gamma_i \Gamma_f)^{J^P} / \Gamma_{\text{total}}$ in $N\bar{K} \rightarrow \Lambda(2100) \rightarrow N\bar{K}^*(892)$, $S=1/2$, G -wave $(\Gamma_1 \Gamma_7)^{J^P} / \Gamma$	VALUE	DOCUMENT ID	TECN	COMMENT
	-0.04 ± 0.03	³ CAMERON	78B	DPWA $K^- p \rightarrow N\bar{K}^*$

 $\Lambda(2100)$ FOOTNOTES

- ¹ The NAKKASYAN 75 values are from the two best solutions found. Each has the $\Lambda(2100)$ and one additional resonance (P_3 or F_5).
- ² Note that the three for BACCARI 77 entries are for three different waves.
- ³ The published sign has been changed to be in accord with the baryon-first convention. The upper limit on the G_3 wave is 0.03.

 $\Lambda(2100)$ REFERENCES

PDG	86	PL 170B 1	M. Aguilar-Benitez <i>et al.</i>	(CERN, CIT+)
PDG	82	PL 111B 1	M. Roos <i>et al.</i>	(HELSE, CIT, CERN)
GOPAL	80	Toronto Conf. 159	G.P. Gopal	(RHEL) IJP
CAMERON	78B	NP B146 327	W. Cameron <i>et al.</i>	(RHEL, LOIC) IJP
DEBELLEFON	78	NC 42A 403	A. de Bellefon <i>et al.</i>	(CDEF, SAEL) IJP
BACCARI	77	NC 41A 96	B. Baccari <i>et al.</i>	(SAEL, CDEF) IJP
DECLAIS	77	CERN 77-16	Y. Declais <i>et al.</i>	(CAEN, CERN) IJP
GOPAL	77	NP B119 362	G.P. Gopal <i>et al.</i>	(LOIC, RHEL) IJP
HENNINGWAY	75	NP B91 12	R.J. Henningway <i>et al.</i>	(CERN, HEIDH, MPIM) IJP
NAKKASYAN	75	NP B93 85	A. Nakkasyan	(CERN) IJP
KANE	74	LBL-2452	D.F. Kane	(LBL) IJP
RADER	73	NC 16A 178	R.K. Rader <i>et al.</i>	(SAEL, HEID, CERN+) IJP
LITCHFIELD	71	NP B30 125	P.J. Litchfield <i>et al.</i>	(RHEL, CDEF, SAEL) IJP
MULLER	69B	Thesis UCL 19372	R.A. Muller	(LRL)
TRIPP	67	NP B3 10	R.D. Tripp <i>et al.</i>	(LRL, SLAC, CERN+) IJP
COOL	66	PRL 16 1228	R.L. Cool <i>et al.</i>	(BNL)
WOHL	66	PRL 17 107	C.G. Wohl, F.T. Solmitz, M.L. Stevenson	(LRL) IJP

 $\Lambda(2110)$ F_{05}

$$I(J^P) = 0(\frac{5}{2}^+) \text{ Status: } ***$$

For results published before 1974 (they are now obsolete), see our 1982 edition Physics Letters **111B** 1 (1982). All the references have been retained.

This resonance is in the Baryon Summary Table, but the evidence for it could be better.

 $\Lambda(2110)$ MASS

VALUE (MeV)	DOCUMENT ID	TECN	COMMENT
2090 to 2140 (≈ 2110) OUR ESTIMATE			
2092 \pm 25	GOPAL	80	DPWA $\bar{K} N \rightarrow \bar{K} N$
2125 \pm 25	CAMERON	78B	DPWA $K^- p \rightarrow N\bar{K}^*$
2106 \pm 50	DEBELLEFON	78	DPWA $\bar{K} N \rightarrow \bar{K} N$
2140 \pm 20	DEBELLEFON	77	DPWA $K^- p \rightarrow \Sigma\pi$
2100 \pm 50	GOPAL	77	DPWA $\bar{K} N$ multichannel
2112 \pm 7	KANE	74	DPWA $K^- p \rightarrow \Sigma\pi$
••• We do not use the following data for averages, fits, limits, etc. •••			
2137	BACCARI	77	DPWA $K^- p \rightarrow \Lambda\omega$
2103	¹ NAKKASYAN	75	DPWA $K^- p \rightarrow \Lambda\omega$

 $\Lambda(2110)$ WIDTH

VALUE (MeV)	DOCUMENT ID	TECN	COMMENT
150 to 250 (≈ 200) OUR ESTIMATE			
245 \pm 25	GOPAL	80	DPWA $\bar{K} N \rightarrow \bar{K} N$
160 \pm 30	CAMERON	78B	DPWA $K^- p \rightarrow N\bar{K}^*$
251 \pm 50	DEBELLEFON	78	DPWA $\bar{K} N \rightarrow \bar{K} N$
140 \pm 20	DEBELLEFON	77	DPWA $K^- p \rightarrow \Sigma\pi$
200 \pm 50	GOPAL	77	DPWA $\bar{K} N$ multichannel
190 \pm 30	KANE	74	DPWA $K^- p \rightarrow \Sigma\pi$
••• We do not use the following data for averages, fits, limits, etc. •••			
132	BACCARI	77	DPWA $K^- p \rightarrow \Lambda\omega$
391	¹ NAKKASYAN	75	DPWA $K^- p \rightarrow \Lambda\omega$

 $\Lambda(2110)$ DECAY MODES

Mode	Fraction (Γ_i/Γ)
Γ_1 $N\bar{K}$	5–25 %
Γ_2 $\Sigma\pi$	10–40 %
Γ_3 $\Lambda\omega$	seen
Γ_4 $\Sigma(1385)\pi$	seen
Γ_5 $\Sigma(1385)\pi$, P -wave	
Γ_6 $N\bar{K}^*(892)$	10–60 %
Γ_7 $N\bar{K}^*(892)$, $S=1/2$, F -wave	

The above branching fractions are our estimates, not fits or averages.

 $\Lambda(2110)$ BRANCHING RATIOS

See "Sign conventions for resonance couplings" in the Note on Λ and Σ Resonances.

$\Gamma(N\bar{K})/\Gamma_{\text{total}}$	VALUE	DOCUMENT ID	TECN	COMMENT	Γ_1/Γ
	0.05 to 0.25 OUR ESTIMATE				
	0.07 \pm 0.03	GOPAL	80	DPWA $\bar{K} N \rightarrow \bar{K} N$	
	0.27 \pm 0.06	² DEBELLEFON	78	DPWA $\bar{K} N \rightarrow \bar{K} N$	
••• We do not use the following data for averages, fits, limits, etc. •••					
	0.07 \pm 0.03	GOPAL	77	DPWA	See GOPAL 80

$(\Gamma_i \Gamma_f)^{J^P} / \Gamma_{\text{total}}$ in $N\bar{K} \rightarrow \Lambda(2110) \rightarrow \Sigma\pi$	VALUE	DOCUMENT ID	TECN	COMMENT	$(\Gamma_1 \Gamma_2)^{J^P} / \Gamma$
	+0.14 \pm 0.01	DEBELLEFON	77	DPWA $K^- p \rightarrow \Sigma\pi$	
	+0.20 \pm 0.03	KANE	74	DPWA $K^- p \rightarrow \Sigma\pi$	
••• We do not use the following data for averages, fits, limits, etc. •••					
	+0.10 \pm 0.03	GOPAL	77	DPWA	$\bar{K} N$ multichannel

$(\Gamma_i \Gamma_f)^{J^P} / \Gamma_{\text{total}}$ in $N\bar{K} \rightarrow \Lambda(2110) \rightarrow \Lambda\omega$	VALUE	DOCUMENT ID	TECN	COMMENT	$(\Gamma_1 \Gamma_3)^{J^P} / \Gamma$
	< 0.05	BACCARI	77	DPWA $K^- p \rightarrow \Lambda\omega$	
	0.112	¹ NAKKASYAN	75	DPWA $K^- p \rightarrow \Lambda\omega$	

$(\Gamma_i \Gamma_f)^{J^P} / \Gamma_{\text{total}}$ in $N\bar{K} \rightarrow \Lambda(2110) \rightarrow \Sigma(1385)\pi$	VALUE	DOCUMENT ID	TECN	COMMENT	$(\Gamma_1 \Gamma_4)^{J^P} / \Gamma$
	+0.071 \pm 0.025	³ CAMERON	78	DPWA $K^- p \rightarrow \Sigma(1385)\pi$	

$(\Gamma_i \Gamma_f)^{J^P} / \Gamma_{\text{total}}$ in $N\bar{K} \rightarrow \Lambda(2110) \rightarrow N\bar{K}^*(892)$	VALUE	DOCUMENT ID	TECN	COMMENT	$(\Gamma_1 \Gamma_6)^{J^P} / \Gamma$
	-0.17 \pm 0.04	⁴ CAMERON	78B	DPWA $K^- p \rightarrow N\bar{K}^*$	

 $\Lambda(2110)$ FOOTNOTES

- ¹ Found in one of two best solutions.
- ² The published error of 0.6 was a misprint.
- ³ The CAMERON 78 upper limit on F -wave decay is 0.03. The sign here has been changed to be in accord with the baryon-first convention.
- ⁴ The published sign has been changed to be in accord with the baryon-first convention. The CAMERON 78B upper limits on the P_3 and F_3 waves are each 0.03.

 $\Lambda(2110)$ REFERENCES

PDG	82	PL 111B 1	M. Roos <i>et al.</i>	(HELSE, CIT, CERN)
GOPAL	80	Toronto Conf. 159	G.P. Gopal	(RHEL) IJP
CAMERON	78	NP B143 189	W. Cameron <i>et al.</i>	(RHEL, LOIC) IJP
CAMERON	78B	NP B146 327	W. Cameron <i>et al.</i>	(RHEL, LOIC) IJP
DEBELLEFON	78	NC 42A 403	A. de Bellefon <i>et al.</i>	(CDEF, SAEL) IJP
BACCARI	77	NC 41A 96	B. Baccari <i>et al.</i>	(SAEL, CDEF) IJP
DEBELLEFON	77	NC 37A 175	A. de Bellefon <i>et al.</i>	(CDEF, SAEL) IJP
GOPAL	77	NP B119 362	G.P. Gopal <i>et al.</i>	(LOIC, RHEL) IJP
NAKKASYAN	75	NP B93 85	A. Nakkasyan	(CERN) IJP
KANE	74	LBL-2452	D.F. Kane	(LBL) IJP

 $\Lambda(2325)$ D_{03}

$$I(J^P) = 0(\frac{3}{2}^-) \text{ Status: } *$$

OMITTED FROM SUMMARY TABLE

BACCARI 77 finds this state with either $J^P = 3/2^-$ or $3/2^+$ in a energy-dependent partial-wave analyses of $K^- p \rightarrow \Lambda\omega$ from 2070 to 2436 MeV. A subsequent semi-energy-independent analysis from threshold to 2436 MeV selects $3/2^-$. DEBELLEFON 78 (same group) also sees this state in an energy-dependent partial-wave analysis of $K^- p \rightarrow \bar{K} N$ data, and finds $J^P = 3/2^-$ or $3/2^+$. They again prefer $J^P = 3/2^-$, but only on the basis of model-dependent considerations.

 $\Lambda(2325)$ MASS

VALUE (MeV)	DOCUMENT ID	TECN	COMMENT
≈ 2325 OUR ESTIMATE			
2342 \pm 30	DEBELLEFON	78	DPWA $\bar{K} N \rightarrow \bar{K} N$
2327 \pm 20	BACCARI	77	DPWA $K^- p \rightarrow \Lambda\omega$

 $\Lambda(2325)$ WIDTH

VALUE (MeV)	DOCUMENT ID	TECN	COMMENT
177 \pm 40	DEBELLEFON	78	DPWA $\bar{K} N \rightarrow \bar{K} N$
160 \pm 40	BACCARI	77	IPWA $K^- p \rightarrow \Lambda\omega$

See key on page 373

Baryon Particle Listings
 $\Lambda(2325)$, $\Lambda(2350)$, $\Lambda(2585)$ Bumps

$\Lambda(2325)$ DECAY MODES

Mode	
Γ_1	$N\bar{K}$
Γ_2	$\Lambda\omega$

$\Lambda(2325)$ BRANCHING RATIOS

$\Gamma(N\bar{K})/\Gamma_{total}$	DOCUMENT ID	TECN	COMMENT	Γ_1/Γ
0.19 ± 0.06	DEBELLEFON 78	DPWA	$\bar{K}N \rightarrow \bar{K}N$	

$(\Gamma_1\Gamma_2)^{1/2}/\Gamma_{total}$ in $N\bar{K} \rightarrow \Lambda(2325) \rightarrow \Lambda\omega$	DOCUMENT ID	TECN	COMMENT	$(\Gamma_1\Gamma_2)^{1/2}/\Gamma$
0.06 ± 0.02	¹ BACCARI 77	IPWA	DS_{33} wave	
0.05 ± 0.02	¹ BACCARI 77	DPWA	DD_{13} wave	
0.08 ± 0.03	¹ BACCARI 77	DPWA	DD_{33} wave	

$\Lambda(2325)$ FOOTNOTES

¹ Note that the three BACCARI 77 entries are for three different waves.

$\Lambda(2325)$ REFERENCES

DEBELLEFON 78	NC 42A 403	A. de Bellefon et al.	(CDEF, SACL) IJP
BACCARI 77	NC 41A 96	B. Baccari et al.	(SACL, CDEF) IJP

$\Lambda(2350) H_{09}$ $I(J^P) = 0(\frac{9}{2}^+)$ Status: * * *

DAUM 68 favors $J^P = 7/2^-$ or $9/2^+$. BRICMAN 70 favors $9/2^+$. LASINSKI 71 suggests three states in this region using a Pomeron + resonances model. There are now also three formation experiments from the College de France-Saclay group, DEBELLEFON 77, BACCARI 77, and DEBELLEFON 78, which find $9/2^+$ in energy-dependent partial-wave analyses of $\bar{K}N \rightarrow \Sigma\pi$, $\Lambda\omega$, and $N\bar{K}$.

$\Lambda(2350)$ MASS

VALUE (MeV)	DOCUMENT ID	TECN	COMMENT
2340 to 2370 (≈ 2350) OUR ESTIMATE			
2370 ± 50	DEBELLEFON 78	DPWA	$\bar{K}N \rightarrow \bar{K}N$
2365 ± 20	DEBELLEFON 77	DPWA	$K^-p \rightarrow \Sigma\pi$
2358 ± 6	BRICMAN 70	CNTR	Total, charge exchange
• • • We do not use the following data for averages, fits, limits, etc. • • •			
2372	BACCARI 77	DPWA	$K^-p \rightarrow \Lambda\omega$
2344 ± 15	COOL 70	CNTR	K^-p, K^-d total
2360 ± 20	LU 70	CNTR	$\gamma p \rightarrow K^+Y^*$
2340 ± 7	BUGG 68	CNTR	K^-p, K^-d total

$\Lambda(2350)$ WIDTH

VALUE (MeV)	DOCUMENT ID	TECN	COMMENT
100 to 250 (≈ 150) OUR ESTIMATE			
204 ± 50	DEBELLEFON 78	DPWA	$\bar{K}N \rightarrow \bar{K}N$
110 ± 20	DEBELLEFON 77	DPWA	$K^-p \rightarrow \Sigma\pi$
324 ± 30	BRICMAN 70	CNTR	Total, charge exchange
• • • We do not use the following data for averages, fits, limits, etc. • • •			
257	BACCARI 77	DPWA	$K^-p \rightarrow \Lambda\omega$
190	COOL 70	CNTR	K^-p, K^-d total
55	LU 70	CNTR	$\gamma p \rightarrow K^+Y^*$
140 ± 20	BUGG 68	CNTR	K^-p, K^-d total

$\Lambda(2350)$ DECAY MODES

Mode	Fraction (Γ_i/Γ)
Γ_1	$N\bar{K}$ ~ 12 %
Γ_2	$\Sigma\pi$ ~ 10 %
Γ_3	$\Lambda\omega$

The above branching fractions are our estimates, not fits or averages.

$\Lambda(2350)$ BRANCHING RATIOS

See "Sign conventions for resonance couplings" in the Note on Λ and Σ Resonances.

$\Gamma(N\bar{K})/\Gamma_{total}$	DOCUMENT ID	TECN	COMMENT	Γ_1/Γ
≈ 0.12 OUR ESTIMATE				
0.12 ± 0.04	DEBELLEFON 78	DPWA	$\bar{K}N \rightarrow \bar{K}N$	

$(\Gamma_1\Gamma_2)^{1/2}/\Gamma_{total}$ in $N\bar{K} \rightarrow \Lambda(2350) \rightarrow \Sigma\pi$	DOCUMENT ID	TECN	COMMENT	$(\Gamma_1\Gamma_2)^{1/2}/\Gamma$
−0.11 ± 0.02	DEBELLEFON 77	DPWA	$K^-p \rightarrow \Sigma\pi$	

$(\Gamma_1\Gamma_2)^{1/2}/\Gamma_{total}$ in $N\bar{K} \rightarrow \Lambda(2350) \rightarrow \Lambda\omega$	DOCUMENT ID	TECN	COMMENT	$(\Gamma_1\Gamma_2)^{1/2}/\Gamma$
<0.05	BACCARI 77	DPWA	$K^-p \rightarrow \Lambda\omega$	

$\Lambda(2350)$ REFERENCES

DEBELLEFON 78	NC 42A 403	A. de Bellefon et al.	(CDEF, SACL) IJP
BACCARI 77	NC 41A 96	B. Baccari et al.	(SACL, CDEF) IJP
DEBELLEFON 77	NC 37A 175	A. de Bellefon et al.	(CDEF, SACL) IJP
LASINSKI 71	NP B29 125	T.A. Lasinski	(EF) IJP
BRICMAN 70	PL 31B 152	C. Bricman et al.	(CERN, CAEN, SACL)
COOL 70	PR D1 1887	R.L. Cool et al.	(BNL) I
Also	PRL 16 1228	R.L. Cool et al.	(BNL) I
LU 70	PR D2 1846	D.C. Lu et al.	(YALE)
BUGG 68	PR 168 1466	D.V. Bugg et al.	(RHEL, BIRM, CAVE) I
DAUM 68	NP B7 19	C. Daum et al.	(CERN) JP

$\Lambda(2585)$ Bumps

$I(J^P) = 0(?^?)$ Status: * *

OMITTED FROM SUMMARY TABLE

$\Lambda(2585)$ MASS (BUMPS)

VALUE (MeV)	DOCUMENT ID	TECN	COMMENT
≈ 2585 OUR ESTIMATE			
2585 ± 45	ABRAMS 70	CNTR	K^-p, K^-d total
2530 ± 25	LU 70	CNTR	$\gamma p \rightarrow K^+Y^*$

$\Lambda(2585)$ WIDTH (BUMPS)

VALUE (MeV)	DOCUMENT ID	TECN	COMMENT
300	ABRAMS 70	CNTR	K^-p, K^-d total
150	LU 70	CNTR	$\gamma p \rightarrow K^+Y^*$

$\Lambda(2585)$ DECAY MODES (BUMPS)

Mode	
Γ_1	$N\bar{K}$

$\Lambda(2585)$ BRANCHING RATIOS (BUMPS)

$(J+\frac{1}{2}) \times \Gamma(N\bar{K})/\Gamma_{total}$	DOCUMENT ID	TECN	COMMENT	Γ_1/Γ
J is not known, so only $(J+\frac{1}{2}) \times \Gamma(N\bar{K})/\Gamma_{total}$ can be given.				
1	ABRAMS 70	CNTR	K^-p, K^-d total	
0.12 ± 0.12	¹ BRICMAN 70	CNTR	Total, charge exchange	

$\Lambda(2585)$ FOOTNOTES (BUMPS)

¹ The resonance is at the end of the region analyzed — no clear signal.

$\Lambda(2585)$ REFERENCES (BUMPS)

ABRAMS 70	PR D1 1917	R.J. Abrams et al.	(BNL) I
Also	PRL 16 1228	R.L. Cool et al.	(BNL) I
BRICMAN 70	PL 31B 152	C. Bricman et al.	(CERN, CAEN, SACL)
LU 70	PR D2 1846	D.C. Lu et al.	(YALE)

Baryon Particle Listings

Σ^+

Σ BARYONS

($S = -1, I = 1$)

$\Sigma^+ = uus, \Sigma^0 = uds, \Sigma^- = dds$

Σ^+

$I(J^P) = 1(\frac{1}{2}^+)$ Status: ****

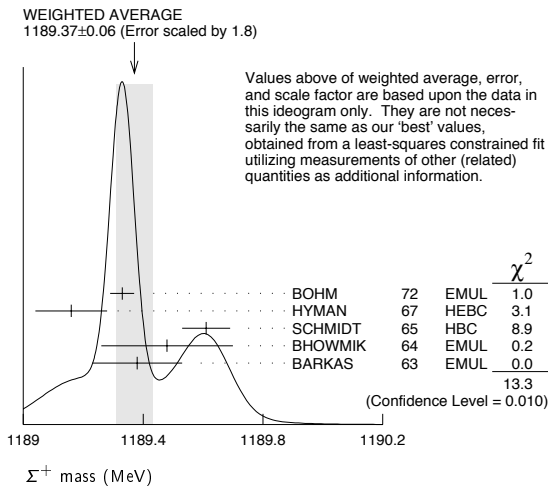
We have omitted some results that have been superseded by later experiments. See our earlier editions.

Σ^+ MASS

The fit uses $\Sigma^+, \Sigma^0, \Sigma^-$, and Λ mass and mass-difference measurements.

VALUE (MeV)	EVTS	DOCUMENT ID	TECN	COMMENT
1189.37 ± 0.07 OUR FIT				Error includes scale factor of 2.2.
1189.37 ± 0.06 OUR AVERAGE				Error includes scale factor of 1.8. See the ideogram below.
1189.33 ± 0.04	607	¹ BOHM 72	EMUL	
1189.16 ± 0.12		HYMAN 67	HEBC	
1189.61 ± 0.08	4205	SCHMIDT 65	HBC	See note with Λ mass
1189.48 ± 0.22	58	² BHOWMIK 64	EMUL	
1189.38 ± 0.15	144	² BARKAS 63	EMUL	

¹BOHM 72 is updated with our 1973 $K^-, \pi^-,$ and π^0 masses (Reviews of Modern Physics **45** S1 (1973)).
²These masses have been raised 30 keV to take into account a 46 keV increase in the proton mass and a 21 keV decrease in the π^0 mass (note added 1967 edition, Reviews of Modern Physics **39** 1 (1967)).



Σ^+ MEAN LIFE

Measurements with fewer than 1000 events have been omitted.

VALUE (10^{-10} s)	EVTS	DOCUMENT ID	TECN	COMMENT
0.8018 ± 0.0026 OUR AVERAGE				
0.8038 ± 0.0040 ± 0.0014		BARBOSA 00	E761	hyperons, 375 GeV
0.8043 ± 0.0080 ± 0.0014		³ BARBOSA 00	E761	hyperons, 375 GeV
0.798 ± 0.005	30k	MARRAFFINO 80	HBC	$K^- p$ 0.42-0.5 GeV/c
0.807 ± 0.013	5719	CONFORTO 76	HBC	$K^- p$ 1-1.4 GeV/c
0.795 ± 0.010	20k	EISELE 70	HBC	$K^- p$ at rest
0.803 ± 0.008	10664	BARLOUTAUD 69	HBC	$K^- p$ 0.4-1.2 GeV/c
0.83 ± 0.032	1300	⁴ CHANG 66	HBC	

³This is a measurement of the Σ^- lifetime. Here we assume CPT invariance; see below for the fractional $\Sigma^+ - \Sigma^-$ lifetime difference obtained by BARBOSA 00.
⁴We have increased the CHANG 66 error of 0.018; see our 1970 edition, Reviews of Modern Physics **42** 87 (1970).

$$(\tau_{\Sigma^+} - \tau_{\Sigma^-}) / \tau_{\Sigma^+}$$

A test of CPT invariance.

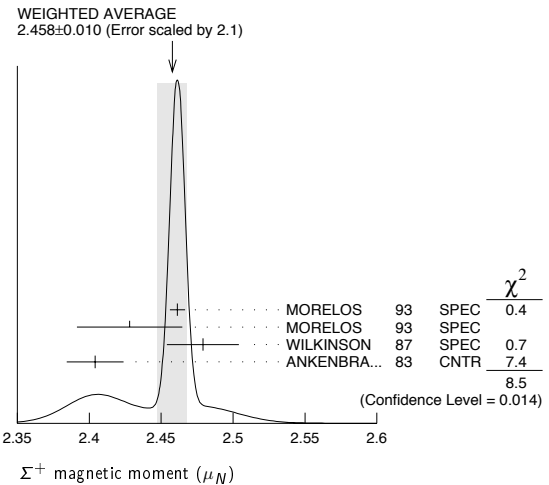
VALUE	DOCUMENT ID	TECN	COMMENT
(-6 ± 12) × 10⁻⁴	BARBOSA 00	E761	hyperons, 375 GeV

Σ^+ MAGNETIC MOMENT

See the "Note on Baryon Magnetic Moments" in the Λ Listings. Measurements with an error $\geq 0.1 \mu_N$ have been omitted.

VALUE (μ_N)	EVTS	DOCUMENT ID	TECN	COMMENT
2.458 ± 0.010 OUR AVERAGE				Error includes scale factor of 2.1. See the ideogram below.
2.4613 ± 0.0034 ± 0.0040	250k	MORELOS 93	SPEC	p Cu 800 GeV
2.428 ± 0.036 ± 0.007	12k	⁵ MORELOS 93	SPEC	p Cu 800 GeV
2.479 ± 0.012 ± 0.022	137k	WILKINSON 87	SPEC	p Be 400 GeV
2.4040 ± 0.0198	44k	⁶ ANKENBRA... 83	CNTR	p Cu 400 GeV

⁵We assume CPT invariance: this is (minus) the Σ^- magnetic moment as measured by MORELOS 93. See below for the moment difference testing CPT .
⁶ANKENBRANDT 83 gives the value $2.38 \pm 0.02 \mu_N$. MORELOS 93 uses the same hyperon magnet and claims to determine the field integral better, leading to the revised value given here.



$$(\mu_{\Sigma^+} + \mu_{\Sigma^-}) / \mu_{\Sigma^+}$$

A test of CPT invariance.

VALUE	DOCUMENT ID	TECN	COMMENT
0.014 ± 0.015	⁷ MORELOS 93	SPEC	p Cu 800 GeV

⁷This is our calculation from the MORELOS 93 measurements of the Σ^+ and Σ^- magnetic moments given above. The statistical error on μ_{Σ^-} dominates the error here.

Σ^+ DECAY MODES

Mode	Fraction (Γ_i/Γ)	Confidence level
Γ_1 $p\pi^0$	(51.57 ± 0.30) %	
Γ_2 $n\pi^+$	(48.31 ± 0.30) %	
Γ_3 $p\gamma$	(1.23 ± 0.05) × 10 ⁻³	
Γ_4 $n\pi^+\gamma$	[a] (4.5 ± 0.5) × 10 ⁻⁴	
Γ_5 $\Lambda e^+\nu_e$	(2.0 ± 0.5) × 10 ⁻⁵	

$\Delta S = \Delta Q$ (SQ) violating modes or $\Delta S = 1$ weak neutral current (S1) modes

Γ_i	Mode	Fraction	Confidence level	90%
Γ_6	$n e^+\nu_e$	SQ < 5	× 10 ⁻⁶	90%
Γ_7	$n\mu^+\nu_\mu$	SQ < 3.0	× 10 ⁻⁵	90%
Γ_8	$p e^+ e^-$	S1 < 7	× 10 ⁻⁶	
Γ_9	$p\mu^+\mu^-$	S1 (9 ± 9 / -8)	× 10 ⁻⁸	

[a] See the Listings below for the pion momentum range used in this measurement.

CONSTRAINED FIT INFORMATION

An overall fit to 2 branching ratios uses 14 measurements and one constraint to determine 3 parameters. The overall fit has a $\chi^2 = 7.7$ for 12 degrees of freedom.

The following *off-diagonal* array elements are the correlation coefficients $\langle \delta x_i \delta x_j \rangle / (\delta x_i \delta x_j)$, in percent, from the fit to the branching fractions, $x_i \equiv \Gamma_i/\Gamma_{\text{total}}$. The fit constrains the x_i whose labels appear in this array to sum to one.

x_2	-100
x_3	12 -14
	x_1 x_2

See key on page 373

Baryon Particle Listings

Σ^+

Σ^+ BRANCHING RATIOS

$\Gamma(n\pi^+)/\Gamma(N\pi)$ $\Gamma_2/(\Gamma_1+\Gamma_2)$

VALUE	EVTS	DOCUMENT ID	TECN	COMMENT
0.4836 ± 0.0030 OUR FIT				
0.4836 ± 0.0030 OUR AVERAGE				
0.4828 ± 0.0036	10k	8 MARRAFFINO 80	HBC	$K^- p$ 0.42–0.5 GeV/c
0.488 ± 0.008	1861	NOWAK 78	HBC	
0.484 ± 0.015	537	TOVEE 71	EMUL	
0.488 ± 0.010	1331	BARLOUTAUD 69	HBC	$K^- p$ 0.4–1.2 GeV/c
0.46 ± 0.02	534	CHANG 66	HBC	
0.490 ± 0.024	308	HUMPHREY 62	HBC	

⁸ MARRAFFINO 80 actually gives $\Gamma(p\pi^0)/\Gamma(\text{total}) = 0.5172 \pm 0.0036$.

$\Gamma(p\gamma)/\Gamma(p\pi^0)$ Γ_3/Γ_1

VALUE (units 10^{-3})	EVTS	DOCUMENT ID	TECN	COMMENT
2.38 ± 0.10 OUR FIT				
2.38 ± 0.10 OUR AVERAGE				
2.32 ± 0.11 ± 0.10	32k	TIMM 95	E761	Σ^+ 375 GeV
2.81 ± 0.39 +0.21 -0.43	408	HESSEY 89	CNTR	$K^- p \rightarrow \Sigma^+ \pi^-$ at rest
2.52 ± 0.28	190	⁹ KOBAYASHI 87	CNTR	$\pi^+ p \rightarrow \Sigma^+ K^+$
2.46 +0.30 -0.35	155	BIAGI 85	CNTR	CERN hyperon beam
2.11 ± 0.38	46	MANZ 80	HBC	$K^- p \rightarrow \Sigma^+ \pi^-$
2.1 ± 0.3	45	ANG 69B	HBC	$K^- p$ at rest
2.76 ± 0.51	31	GERSHWIN 69B	HBC	$K^- p \rightarrow \Sigma^+ \pi^-$
3.7 ± 0.8	24	BAZIN 65	HBC	$K^- p$ at rest

⁹ KOBAYASHI 87 actually gives $\Gamma(p\gamma)/\Gamma(\text{total}) = (1.30 \pm 0.15) \times 10^{-3}$.

$\Gamma(n\pi^+ \gamma)/\Gamma(n\pi^+)$ Γ_4/Γ_2

The π^+ momentum cuts differ, so we do not average the results but simply use the latest value in the Summary Table.

VALUE (units 10^{-3})	EVTS	DOCUMENT ID	TECN	COMMENT
0.93 ± 0.10				
0.93 ± 0.10	180	EBENHOH 73	HBC	$\pi^+ < 150$ MeV/c
••• We do not use the following data for averages, fits, limits, etc. •••				
0.27 ± 0.05	29	ANG 69B	HBC	$\pi^+ < 110$ MeV/c
~ 1.8		BAZIN 65B	HBC	$\pi^+ < 116$ MeV/c

$\Gamma(\Lambda e^+ \nu_e)/\Gamma_{\text{total}}$ Γ_5/Γ

VALUE (units 10^{-5})	EVTS	DOCUMENT ID	TECN	COMMENT
2.0 ± 0.5 OUR AVERAGE				
1.6 ± 0.7	5	BALTAY 69	HBC	$K^- p$ at rest
2.9 ± 1.0	10	EISELE 69	HBC	$K^- p$ at rest
2.0 ± 0.8	6	BARASH 67	HBC	$K^- p$ at rest

$\Gamma(n e^+ \nu_e)/\Gamma(n\pi^+)$ Γ_6/Γ_2

Test of $\Delta S = \Delta Q$ rule. Experiments with an effective denominator less than 100,000 have been omitted.

EFFECTIVE DENOM.	EVTS	DOCUMENT ID	TECN	COMMENT
< 1.1 × 10⁻⁵ OUR LIMIT Our 90% CL limit = (2.3 events)/(effective denominator sum). [Number of events increased to 2.3 for a 90% confidence level.]				
111000	0	¹⁰ EBENHOH 74	HBC	$K^- p$ at rest
105000	0	¹⁰ SECHI-ZORN 73	HBC	$K^- p$ at rest

¹⁰ Effective denominator calculated by us.

$\Gamma(n\mu^+ \nu_\mu)/\Gamma(n\pi^+)$ Γ_7/Γ_2

Test of $\Delta S = \Delta Q$ rule.

EFFECTIVE DENOM.	EVTS	DOCUMENT ID	TECN	COMMENT
< 6.2 × 10⁻⁵ OUR LIMIT Our 90% CL limit = (6.7 events)/(effective denominator sum). [Number of events increased to 6.7 for a 90% confidence level.]				
33800	0	BAGGETT 69B	HBC	
62000	2	¹¹ EISELE 69B	HBC	
10150	0	¹² COURANT 64	HBC	
1710	0	¹² NAUENBERG 64	HBC	
120	1	GALTIERI 62	EMUL	

¹¹ Effective denominator calculated by us.
¹² Effective denominator taken from EISELE 67.

$\Gamma(p e^+ e^-)/\Gamma_{\text{total}}$ Γ_8/Γ

VALUE (units 10^{-6})	DOCUMENT ID	TECN	COMMENT
< 7			
	¹³ ANG 69B	69B	HBC $K^- p$ at rest

¹³ ANG 69B found three $p e^+ e^-$ events in agreement with $\gamma \rightarrow e^+ e^-$ conversion from $\Sigma^+ \rightarrow p\gamma$. The limit given here is for neutral currents.

$\Gamma(p\mu^+ \mu^-)/\Gamma_{\text{total}}$ Γ_9/Γ

A test for a $\Delta S = 1$ weak neutral current, but also allowed by higher-order electroweak interactions.

VALUE (units 10^{-8})	EVTS	DOCUMENT ID	TECN	COMMENT
8.6 +6.6 -5.4 ± 5.5				
	3	¹⁴ PARK 05	HYCP	p Cu, 800 GeV

¹⁴ The masses of the three dimuons of PARK 05 are within 1 MeV of one another, perhaps indicating the existence of a new state P^0 with mass 214.3 ± 0.5 MeV. In that case, the decay is $\Sigma^+ \rightarrow p P^0$, $P^0 \rightarrow \mu^+ \mu^-$, with a branching fraction of $(3.1 +2.4 -1.9 \pm 1.5) \times 10^{-8}$.

$\Gamma(\Sigma^+ \rightarrow n e^+ \nu_e)/\Gamma(\Sigma^- \rightarrow n e^- \bar{\nu}_e)$

VALUE	CL%	EVTS	DOCUMENT ID	TECN	COMMENT
< 0.009 OUR LIMIT Our 90% CL limit, using $\Gamma(n e^+ \nu_e)/\Gamma(n\pi^+)$ above.					
••• We do not use the following data for averages, fits, limits, etc. •••					
< 0.019	90	0	EBENHOH 74	HBC	$K^- p$ at rest
< 0.018	90	0	SECHI-ZORN 73	HBC	$K^- p$ at rest
< 0.12	95	0	COLE 71	HBC	$K^- p$ at rest
< 0.03	90	0	EISELE 69B	HBC	See EBENHOH 74

$\Gamma(\Sigma^+ \rightarrow n\mu^+ \nu_\mu)/\Gamma(\Sigma^- \rightarrow n\mu^- \bar{\nu}_\mu)$

VALUE	EVTS	DOCUMENT ID	TECN	COMMENT
< 0.12 OUR LIMIT Our 90% CL limit, using $\Gamma(n\mu^+ \nu_\mu)/\Gamma(n\pi^+)$ above.				
••• We do not use the following data for averages, fits, limits, etc. •••				
0.06 +0.045 -0.03	2	EISELE 69B	HBC	$K^- p$ at rest

$\Gamma(\Sigma^+ \rightarrow n\ell^+ \nu)/\Gamma(\Sigma^- \rightarrow n\ell^- \bar{\nu})$ Test of $\Delta S = \Delta Q$ rule.

VALUE	EVTS	DOCUMENT ID	TECN	COMMENT
< 0.043 OUR LIMIT Our 90% CL limit, using $[\Gamma(n e^+ \nu_e) + \Gamma(n\mu^+ \nu_\mu)]/\Gamma(n\pi^+)$.				
••• We do not use the following data for averages, fits, limits, etc. •••				
< 0.08	1	NORTON 69	HBC	
< 0.034	0	BAGGETT 67	HBC	

Σ^+ DECAY PARAMETERS

See the "Note on Baryon Decay Parameters" in the neutron Listings. A few early results have been omitted.

α_0 FOR $\Sigma^+ \rightarrow p\pi^0$

VALUE	EVTS	DOCUMENT ID	TECN	COMMENT
-0.980 +0.017 -0.015 OUR FIT				
-0.980 +0.017 -0.013 OUR AVERAGE				
-0.945 +0.055 -0.042	1259	¹⁵ LIPMAN 73	OSPK	$\pi^+ p \rightarrow \Sigma^+$
-0.940 ± 0.045	16k	BELLAAMY 72	ASPK	$\pi^+ p \rightarrow \Sigma^+ K^+$
-0.98 +0.05 -0.02	1335	¹⁶ HARRIS 70	OSPK	$\pi^+ p \rightarrow \Sigma^+ K^+$
-0.999 ± 0.022	32k	BANGERTER 69	HBC	$K^- p$ 0.4 GeV/c

¹⁵ Decay protons scattered off aluminum.
¹⁶ Decay protons scattered off carbon.

ϕ_0 ANGLE FOR $\Sigma^+ \rightarrow p\pi^0$ (tan $\phi_0 = \beta/\gamma$)

VALUE (°)	EVTS	DOCUMENT ID	TECN	COMMENT
36 ± 34 OUR AVERAGE				
38.1 +35.7 -37.1	1259	¹⁷ LIPMAN 73	OSPK	$\pi^+ p \rightarrow \Sigma^+ K^+$
22 ± 90		¹⁸ HARRIS 70	OSPK	$\pi^+ p \rightarrow \Sigma^+ K^+$

¹⁷ Decay proton scattered off aluminum.
¹⁸ Decay protons scattered off carbon.

α_+ / α_0 Older results have been omitted.

VALUE	EVTS	DOCUMENT ID	TECN	COMMENT
-0.069 ± 0.013 OUR FIT				
-0.073 ± 0.021				
	23k	MARRAFFINO 80	HBC	$K^- p$ 0.42–0.5 GeV/c
α_+ FOR $\Sigma^+ \rightarrow n\pi^+$				
0.068 ± 0.013 OUR FIT				
0.066 ± 0.016 OUR AVERAGE				
0.037 ± 0.049	4101	BERLEY 70B	HBC	
0.069 ± 0.017	35k	BANGERTER 69	HBC	$K^- p$ 0.4 GeV/c

ϕ_+ ANGLE FOR $\Sigma^+ \rightarrow n\pi^+$ (tan $\phi_+ = \beta/\gamma$)

VALUE (°)	EVTS	DOCUMENT ID	TECN	COMMENT
167 ± 20 OUR AVERAGE Error includes scale factor of 1.1.				
184 ± 24	1054	¹⁹ BERLEY 70B	HBC	
143 ± 29	560	BANGERTER 69B	HBC	$K^- p$ 0.4 GeV/c

¹⁹ Changed from 176 to 184° to agree with our sign convention.

α_γ FOR $\Sigma^+ \rightarrow p\gamma$

VALUE	EVTS	DOCUMENT ID	TECN	COMMENT
-0.76 ± 0.08 OUR AVERAGE				
-0.720 ± 0.086 ± 0.045	35k	²⁰ FOUCHER 92	SPEC	Σ^+ 375 GeV
-0.86 ± 0.13 ± 0.04	190	KOBAYASHI 87	CNTR	$\pi^+ p \rightarrow \Sigma^+ K^+$
-0.53 +0.38 -0.36	46	MANZ 80	HBC	$K^- p \rightarrow \Sigma^+ \pi^-$
-1.03 +0.52 -0.42	61	GERSHWIN 69B	HBC	$K^- p \rightarrow \Sigma^+ \pi^-$

²⁰ See TIMM 95 for a detailed description of the analysis.

Baryon Particle Listings

Σ^+, Σ^0

Σ^+ REFERENCES

We have omitted some papers that have been superseded by later experiments. See our earlier editions.

Author	Year	Ref	Collab.
PARK	05	PRL 94 021801	H.K. Park <i>et al.</i> (FNAL HyperCP Collab.)
BARBOSA	00	PR D61 031101R	R.F. Barbosa <i>et al.</i> (FNAL E761 Collab.)
TIMM	95	PR D51 04630	S. Timm <i>et al.</i> (FNAL E761 Collab.)
MORELOS	93	PRL 71 3417	A. Morelos <i>et al.</i> (FNAL E761 Collab.)
FOUCHER	92	PRL 68 3004	M. Foucher <i>et al.</i> (FNAL E761 Collab.)
HESSEY	89	ZPHY C42 175	N.P. Hessey <i>et al.</i> (BNL-811 Collab.)
KOBAYASHI	87	PRL 59 868	N. Kobayashi <i>et al.</i> (KYOT)
WILKINSON	87	PRL 58 855	C.A. Wilkinson <i>et al.</i> (WISC, MICH, RUTG+) (CERN WA62 Collab.)
BIAGI	85	ZPHY C28 495	S.F. Biagi <i>et al.</i> (FNAL IOWA, ISU+)
ANKENBRANDT	83	PRL 51 863	C.M. Ankenbrandt <i>et al.</i> (MPIM, VAND)
MANZ	80	PL 96B 217	A. Manz <i>et al.</i> (VAND, MPIM)
MARRAFFINO	80	PR D21 2501	J. Marraffino <i>et al.</i> (VAND, MPIM)
NOWAK	78	NP B139 61	R.J. Nowak <i>et al.</i> (LOUC, BELG, DURH+)
CONFORTO	76	NP B105 189	B. Conforto <i>et al.</i> (RHEL, LOIC)
EBENHOF	74	ZPHY 264 367	H. Ebenhof <i>et al.</i> (HEIDT)
EBENHOF	73	ZPHY 264 413	W. Ebenhof <i>et al.</i> (HEIDT)
LIPMAN	73	PL 43B 89	N.H. Lipman <i>et al.</i> (RHEL, SUSS, LOWC)
PDG	73	RMP 45 51	T.A. Lasinski <i>et al.</i> (LBL, BRAN, CERN+)
SECHI-ZORN	73	PR D8 12	B. Sechi-Zorn, G.A. Snow (UMD)
BELLAMY	72	PL 39B 299	E.H. Bellamy <i>et al.</i> (LOWC, RHEL, SUSS)
BOHM	72	NP B48 1	G. Bohm (BERL, KIDR, BRUX, IASD, DUUC+)
Also		IIHE-73.2 Nov	G. Bohm
COLE	71	PR D4 631	J. Cole <i>et al.</i> (STON, COLU)
TOWEE	71	NP B33 493	D.W. Towe <i>et al.</i> (LOUC, KIDR, BERL+)
BERLEY	70B	PR D1 2015	D. Berley <i>et al.</i> (BNL, MASA, YALE)
EISELE	70	ZPHY 238 372	F. Eisele <i>et al.</i> (HEID)
HARRIS	70	PRL 24 165	F. Harris <i>et al.</i> (MICH, WISC)
PDG	70	RMP 42 87	A. Barbaro-Galtieri <i>et al.</i> (LRL, BRAN+)
ANG	69B	ZPHY 228 151	G. Ang <i>et al.</i> (HEID)
BAGGETT	69B	Thesis MDDP-TR-973	N.V. Baggett (UMD)
BALTAY	69	PRL 22 615	C. Baltay <i>et al.</i> (COLU, STON)
BANGERTER	69	Thesis UCRL 19244	R.O. Bangenter (LRL)
BANGERTER	69B	PR 187 1821	R.O. Bangenter <i>et al.</i> (LRL)
BARLOUTAUD	69	NP B14 153	R. Barloutaud <i>et al.</i> (SACL, CERN, HEID)
EISELE	69	ZPHY 221 1	F. Eisele <i>et al.</i> (HEID)
Also			W. Willis <i>et al.</i> (BNL, CERN, HEID, UMD)
EISELE	69B	ZPHY 221 401	F. Eisele <i>et al.</i> (HEID)
GERSHWIN	69B	PR 188 2077	L.K. Gershwin <i>et al.</i> (LRL)
Also		Thesis UCRL 19246	L.K. Gershwin (LRL)
NORTON	69	Thesis Nevis 175	H. Norton (COLU)
BAGGETT	67	PRL 19 1458	N. Baggett <i>et al.</i> (UMD)
Also		Vienna Abs. 374	N.V. Baggett, B. Kehoe (UMD)
Also		Private Comm.	N.V. Baggett (UMD)
BARASH	67	PRL 19 181	N. Barash <i>et al.</i> (UMD)
EISELE	67	ZPHY 205 409	F. Eisele <i>et al.</i> (HEID)
HYMAN	67	PL 25B 376	L.G. Hyman <i>et al.</i> (ANL, CMU, WUES)
PDG	67	RMP 39 1	A.H. Rosenfeld <i>et al.</i> (LRL, CERN, YALE)
CHANG	66	PR 151 1081	C.Y. Chang (COLU)
Also		Thesis Nevis 145	C.Y. Chang (COLU)
BAZIN	65	PRL 14 154	M. Bazin <i>et al.</i> (PRIN, COLU)
BAZIN	65B	PR 140B 1358	M. Bazin <i>et al.</i> (PRIN, RUTG, COLU)
SCHMIDT	65	PR 140B 1328	P. Schmidt (COLU)
BHOWMIK	64	NP 53 22	B. Bhowmik <i>et al.</i> (DELH)
COURANT	64	PR 136 B1791	H. Courant <i>et al.</i> (CERN, HEID, UMD+)
NAUENBERG	64	PRL 12 679	U. Nauenberg <i>et al.</i> (COLU, RUTG, PRIN)
BARKAS	63	PRL 11 26	W.H. Barkas, J.N. Dyer, H.H. Heckman (LRL)
Also		Thesis UCRL 9450	J.N. Dyer (LRL)
GALTIERI	62	PRL 9 24	A. Barbaro-Galtieri <i>et al.</i> (LRL)
HUMPHREY	62	PR 127 1305	W.E. Humphrey, R.R. Ross (LRL)



$$I(J^P) = 1(\frac{1}{2}^+) \text{ Status: } ****$$

COURANT 63 and ALFF-STEINBERGER 65, using $\Sigma^0 \rightarrow \Lambda e^+ e^-$ decays (Dalitz decays), determined the Σ^0 parity to be positive, given that $J = 1/2$ and that certain very reasonable assumptions about form factors are true. The results of experiments involving the Primakoff effect, from which the Σ^0 mean life and $\Sigma^0 \rightarrow \Lambda$ transition magnetic moment come (see below), strongly support $J = 1/2$.

Σ^0 MASS

The fit uses $\Sigma^+, \Sigma^0, \Sigma^-$, and Λ mass and mass-difference measurements.

VALUE (MeV)	EVTS	DOCUMENT ID	TECN	COMMENT
1192.642 ± 0.024 OUR FIT				
••• We do not use the following data for averages, fits, limits, etc. •••				
1192.65 ± 0.020 ± 0.014	3327	¹ WANG	97 SPEC	$\Sigma^0 \rightarrow \Lambda \gamma \rightarrow (\rho \pi^-)(e^+ e^-)$

¹ This WANG 97 result is redundant with the Σ^0 - Λ mass-difference measurement below.

$m_{\Sigma^-} - m_{\Sigma^0}$

VALUE (MeV)	EVTS	DOCUMENT ID	TECN	COMMENT
4.807 ± 0.035 OUR FIT				Error includes scale factor of 1.1.
4.86 ± 0.08 OUR AVERAGE				Error includes scale factor of 1.2.
4.87 ± 0.12	37	DOSCH	65 HBC	
5.01 ± 0.12	12	SCHMIDT	65 HBC	See note with Λ mass
4.75 ± 0.1	18	BURNSTEIN	64 HBC	

$m_{\Sigma^0} - m_{\Lambda}$

VALUE (MeV)	EVTS	DOCUMENT ID	TECN	COMMENT
76.959 ± 0.023 OUR FIT				
76.966 ± 0.020 ± 0.013	3327	WANG	97 SPEC	$\Sigma^0 \rightarrow \Lambda \gamma \rightarrow (\rho \pi^-)(e^+ e^-)$
••• We do not use the following data for averages, fits, limits, etc. •••				
76.23 ± 0.55	109	COLAS	75 HLBC	$\Sigma^0 \rightarrow \Lambda \gamma$
76.63 ± 0.28	208	SCHMIDT	65 HBC	See note with Λ mass

Σ^0 MEAN LIFE

These lifetimes are deduced from measurements of the cross sections for the Primakoff process $\Lambda \rightarrow \Sigma^0$ in nuclear Coulomb fields. An alternative expression of the same information is the Σ^0 - Λ transition magnetic moment given in the following section. The relation is $(\mu_{\Sigma \Lambda} / \mu_N)^2 \tau = 1.92951 \times 10^{-19}$ s (see DEVLIN 86).

VALUE (10^{-20} s)	DOCUMENT ID	TECN	COMMENT
7.4 ± 0.7 OUR EVALUATION			Using $\mu_{\Sigma \Lambda}$ (see the above note).
6.5 ^{+1.7} _{-1.1}	² DEVLIN	86 SPEC	Primakoff effect
7.6 ± 0.5 ± 0.7	³ PETERSEN	86 SPEC	Primakoff effect
••• We do not use the following data for averages, fits, limits, etc. •••			
5.8 ± 1.3	² DYDAK	77 SPEC	See DEVLIN 86

² DEVLIN 86 is a recalculation of the results of DYDAK 77 removing a numerical approximation made in that work.
³ An additional uncertainty of the Primakoff formalism is estimated to be < 5%.

$|\mu(\Sigma^0 \rightarrow \Lambda)|$ TRANSITION MAGNETIC MOMENT

See the note in the Σ^0 mean-life section above. Also, see the "Note on Baryon Magnetic Moments" in the Λ Listings.

VALUE (μ_N)	DOCUMENT ID	TECN	COMMENT
1.61 ± 0.08 OUR AVERAGE			
1.72 ^{+0.17} _{-0.19}	⁴ DEVLIN	86 SPEC	Primakoff effect
1.59 ± 0.05 ± 0.07	⁵ PETERSEN	86 SPEC	Primakoff effect
••• We do not use the following data for averages, fits, limits, etc. •••			
1.82 ^{+0.25} _{-0.18}	⁴ DYDAK	77 SPEC	See DEVLIN 86

⁴ DEVLIN 86 is a recalculation of the results of DYDAK 77 removing a numerical approximation made in that work.
⁵ An additional uncertainty of the Primakoff formalism is estimated to be < 2.5%.

Σ^0 DECAY MODES

Mode	Fraction (Γ_i/Γ)	Confidence level
$\Gamma_1 \Lambda \gamma$	100 %	
$\Gamma_2 \Lambda \gamma \gamma$	< 3 %	90%
$\Gamma_3 \Lambda e^+ e^-$	[a] 5×10^{-3}	

[a] A theoretical value using QED.

Σ^0 BRANCHING RATIOS

$\Gamma(\Lambda \gamma \gamma)/\Gamma_{total}$	CL%	DOCUMENT ID	TECN	Γ_2/Γ
< 0.03	90	COLAS	75 HLBC	

$\Gamma(\Lambda e^+ e^-)/\Gamma_{total}$	DOCUMENT ID	COMMENT	Γ_3/Γ
See COURANT 63 and ALFF-STEINBERGER 65 for measurements of the invariant-mass spectrum of the Dalitz pairs.			
0.00545	FEINBERG	58 Theoretical QED calculation	

Σ^0 REFERENCES

WANG	97	PR D56 2544	M.H.L.S. Wang <i>et al.</i> (BNL-E766 Collab.)
DEVLIN	86	PR D34 1626	T. Devlin, P.C. Petersen, A. Berevas (RUTG)
PETERSEN	86	PRL 57 949	P.C. Petersen <i>et al.</i> (RUTG, WISC, MICH+)
DYDAK	77	NP B118 1	F. Dydak <i>et al.</i> (CERN, DORT, HEID)
COLAS	75	NP B91 253	J. Colas <i>et al.</i> (ORSAY)
ALFF-...	65	PR 137 B1105	C. Alff-Steinberger <i>et al.</i> (COLU, RUTG+)
DOSCH	65	PL 14 239	H.C. Dosch <i>et al.</i> (HEID)
SCHMIDT	65	PR 140B 1328	P. Schmidt (COLU)
BURNSTEIN	64	PRL 13 66	R.A. Burnstein <i>et al.</i> (UMD)
COURANT	63	PRL 10 409	H. Courant <i>et al.</i> (CERN, UMD)
FEINBERG	58	PR 109 1019	G. Feinberg (BNL)



$I(J^P) = 1(\frac{1}{2}^+)$ Status: * * * *

We have omitted some results that have been superseded by later experiments. See our earlier editions.

Σ^- MASS

The fit uses Σ^+ , Σ^0 , Σ^- , and Λ mass and mass-difference measurements.

VALUE (MeV)	EVTS	DOCUMENT ID	TECN	COMMENT
1197.449 ± 0.030 OUR FIT				Error includes scale factor of 1.2.
1197.45 ± 0.04 OUR AVERAGE				Error includes scale factor of 1.2.
1197.417 ± 0.040		GUREV 93	SPEC	Σ^- C atom, crystal diff.
1197.532 ± 0.057		GALL 88	CNTR	Σ^- Pb, Σ^- W atoms
1197.43 ± 0.08	3000	SCHMIDT 65	HBC	See note with Λ mass
• • • We do not use the following data for averages, fits, limits, etc. • • •				
1197.24 ± 0.15		¹ DUGAN 75	CNTR	Exotic atoms
¹ GALL 88 concludes that the DUGAN 75 mass needs to be reevaluated.				

$m_{\Sigma^-} - m_{\Sigma^+}$

VALUE (MeV)	EVTS	DOCUMENT ID	TECN	COMMENT
8.08 ± 0.08 OUR FIT				Error includes scale factor of 1.9.
8.09 ± 0.16 OUR AVERAGE				
7.91 ± 0.23	86	BOHM 72	EMUL	
8.25 ± 0.25	2500	DOSCH 65	HBC	
8.25 ± 0.40	87	BARKAS 63	EMUL	

$m_{\Sigma^-} - m_{\Lambda}$

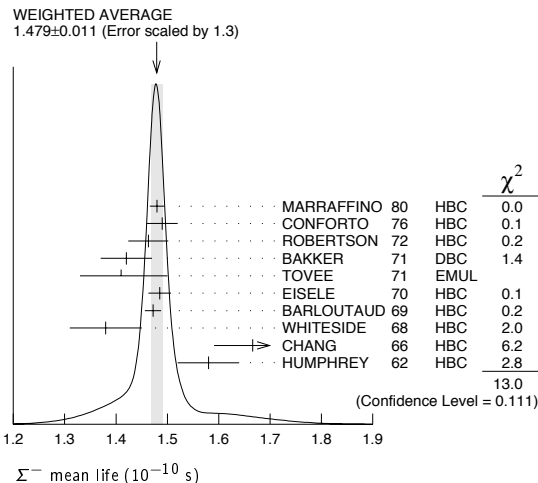
VALUE (MeV)	EVTS	DOCUMENT ID	TECN	COMMENT
81.766 ± 0.030 OUR FIT				Error includes scale factor of 1.2.
81.69 ± 0.07 OUR AVERAGE				
81.64 ± 0.09	2279	HEPP 68	HBC	
81.80 ± 0.13	85	SCHMIDT 65	HBC	See note with Λ mass
81.70 ± 0.19		BURNSTEIN 64	HBC	

Σ^- MEAN LIFE

Measurements with an error $\geq 0.2 \times 10^{-10}$ s have been omitted.

VALUE (10^{-10} s)	EVTS	DOCUMENT ID	TECN	COMMENT
1.479 ± 0.011 OUR AVERAGE				Error includes scale factor of 1.3. See the ideogram below.
1.480 ± 0.014	16k	MARRAFFINO 80	HBC	$K^- p$ 0.42–0.5 GeV/c
1.49 ± 0.03	8437	CONFORTO 76	HBC	$K^- p$ 1–1.4 GeV/c
1.463 ± 0.039	2400	ROBERTSON 72	HBC	$K^- p$ 0.25 GeV/c
1.42 ± 0.05	1383	BAKKER 71	DBC	$K^- N \rightarrow \Sigma^- \pi \pi$
1.41 ± 0.09		TOVEE 71	EMUL	
1.485 ± 0.022	100k	EISELE 70	HBC	$K^- p$ at rest
1.472 ± 0.016	10k	BARLOUTAUD 69	HBC	$K^- p$ 0.4–1.2 GeV/c
1.38 ± 0.07	506	WHITESIDE 68	HBC	$K^- p$ at rest
1.666 ± 0.075	3267	² CHANG 66	HBC	$K^- p$ at rest
1.58 ± 0.06	1208	HUMPHREY 62	HBC	$K^- p$ at rest

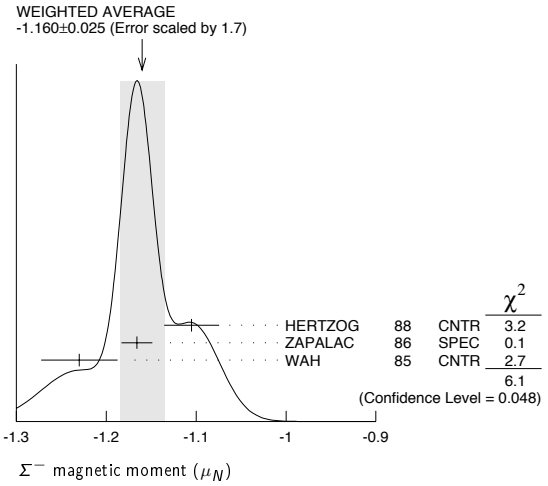
²We have increased the CHANG 66 error of 0.026; see our 1970 edition, Reviews of Modern Physics **42** 87 (1970).



Σ^- MAGNETIC MOMENT

See the "Note on Baryon Magnetic Moments" in the Λ Listings. Measurements with an error $\geq 0.3 \mu_N$ have been omitted.

VALUE (μ_N)	EVTS	DOCUMENT ID	TECN	COMMENT
-1.160 ± 0.025 OUR AVERAGE				Error includes scale factor of 1.7. See the ideogram below.
-1.105 ± 0.029 ± 0.010		HERTZOG 88	CNTR	Σ^- Pb, Σ^- W atoms
-1.166 ± 0.014 ± 0.010	671k	ZAPALAC 86	SPEC	$n e^- \nu, n \pi^-$ decays
-1.23 ± 0.03 ± 0.03		WAH 85	CNTR	ρ Cu $\rightarrow \Sigma^- X$
• • • We do not use the following data for averages, fits, limits, etc. • • •				
-0.89 ± 0.14	516k	DECK 83	SPEC	ρ Be $\rightarrow \Sigma^- X$



Σ^- CHARGE RADIUS

VALUE (fm)	DOCUMENT ID	TECN	COMMENT
0.780 ± 0.080 ± 0.060	³ ESCHRICH 01	SELX	$\Sigma^- e \rightarrow \Sigma^- e$
³ ESCHRICH 01 actually gives $\langle r^2 \rangle = (0.61 \pm 0.12 \pm 0.09) \text{ fm}^2$.			

Σ^- DECAY MODES

Mode	Fraction (Γ_i/Γ)
Γ_1 $n \pi^-$	(99.848 ± 0.005) %
Γ_2 $n \pi^- \gamma$	[a] (4.6 ± 0.6) × 10 ⁻⁴
Γ_3 $n e^- \bar{\nu}_e$	(1.017 ± 0.034) × 10 ⁻³
Γ_4 $n \mu^- \bar{\nu}_\mu$	(4.5 ± 0.4) × 10 ⁻⁴
Γ_5 $\Lambda e^- \bar{\nu}_e$	(5.73 ± 0.27) × 10 ⁻⁵

[a] See the Listings below for the pion momentum range used in this measurement.

CONSTRAINED FIT INFORMATION

An overall fit to 3 branching ratios uses 16 measurements and one constraint to determine 4 parameters. The overall fit has a $\chi^2 = 8.7$ for 13 degrees of freedom.

The following off-diagonal array elements are the correlation coefficients $\langle \delta x_i \delta x_j \rangle / (\delta x_i \delta x_j)$, in percent, from the fit to the branching fractions, $x_i \equiv \Gamma_i/\Gamma_{\text{total}}$. The fit constrains the x_i whose labels appear in this array to sum to one.

x_3	-64		
x_4	-77	0	
x_5	-5	0	0
	x_1	x_3	x_4

Σ^- BRANCHING RATIOS

$\Gamma(n\pi^- \gamma)/\Gamma(n\pi^-)$	Γ_2/Γ_1		
The π^+ momentum cuts differ, so we do not average the results but simply use the latest value for the Summary Table.			
VALUE (units 10 ⁻³)	DOCUMENT ID	TECN	COMMENT
0.46 ± 0.06	292	EBENHOH 73	HBC $\pi^+ < 150$ MeV/c
• • • We do not use the following data for averages, fits, limits, etc. • • •			
0.10 ± 0.02	23	ANG 69B	HBC $\pi^- < 110$ MeV/c
~ 1.1		BAZIN 65B	HBC $\pi^- < 166$ MeV/c

Baryon Particle Listings

Σ^-

$\Gamma(n e^- \bar{\nu}_e) / \Gamma(n \pi^-)$

Measurements with an error $\geq 0.2 \times 10^{-3}$ have been omitted.

VALUE (units 10^{-3})	EVTS	DOCUMENT ID	TECN	COMMENT
1.019 ± 0.031				OUR AVERAGE
0.96 ± 0.05	2847	BOURQUIN	83c	SPEC SPS hyperon beam
1.09 $\begin{smallmatrix} +0.06 \\ -0.08 \end{smallmatrix}$	601	⁴ EBENHOH	74	HBC $K^- p$ at rest
1.05 $\begin{smallmatrix} +0.07 \\ -0.13 \end{smallmatrix}$	455	⁴ SECHI-ZORN	73	HBC $K^- p$ at rest
0.97 ± 0.15	57	COLE	71	HBC $K^- p$ at rest
1.11 ± 0.09	180	BIERMAN	68	HBC

⁴ An additional negative systematic error is included for internal radiative corrections and latest form factors; see BOURQUIN 83c.

$\Gamma(n \mu^- \bar{\nu}_\mu) / \Gamma(n \pi^-)$

VALUE (units 10^{-3})	EVTS	DOCUMENT ID	TECN	COMMENT
0.45 ± 0.04				OUR FIT
0.45 ± 0.04				OUR AVERAGE
0.38 ± 0.11	13	COLE	71	HBC $K^- p$ at rest
0.43 ± 0.06	72	ANG	69	HBC $K^- p$ at rest
0.43 ± 0.09	56	BAGGETT	69	HBC $K^- p$ at rest
0.56 ± 0.20	11	BAZIN	65B	HBC $K^- p$ at rest
0.66 ± 0.15	22	COURANT	64	HBC

$\Gamma(\Lambda e^- \bar{\nu}_e) / \Gamma(n \pi^-)$

VALUE (units 10^{-4})	EVTS	DOCUMENT ID	TECN	COMMENT
0.574 ± 0.027				OUR FIT
0.574 ± 0.027				OUR AVERAGE
0.561 ± 0.031	1620	⁵ BOURQUIN	82	SPEC SPS hyperon beam
0.63 ± 0.11	114	THOMPSON	80	ASPK Hyperon beam
0.52 ± 0.09	31	BALTAY	69	HBC $K^- p$ at rest
0.69 ± 0.12	31	EISELE	69	HBC $K^- p$ at rest
0.64 ± 0.12	35	BARASH	67	HBC $K^- p$ at rest
0.75 ± 0.28	11	COURANT	64	HBC $K^- p$ at rest

⁵ The value is from BOURQUIN 83b, and includes radiation corrections and new acceptance.

Σ^- DECAY PARAMETERS

See the "Note on Baryon Decay Parameters" in the neutron Listings. Older, outdated results have been omitted.

α_- FOR $\Sigma^- \rightarrow n \pi^-$

VALUE	EVTS	DOCUMENT ID	TECN	COMMENT
-0.068 ± 0.008				OUR AVERAGE
-0.062 ± 0.024	28k	HANSL	78	HBC $K^- p \rightarrow \Sigma^- \pi^+$
-0.067 ± 0.011	60k	BOGERT	70	HBC $K^- p$ 0.4 GeV/c
-0.071 ± 0.012	51k	BANGERTER	69	HBC $K^- p$ 0.4 GeV/c

ϕ ANGLE FOR $\Sigma^- \rightarrow n \pi^-$

($\tan \phi = \beta / \gamma$)

VALUE (°)	EVTS	DOCUMENT ID	TECN	COMMENT
10 ± 15				OUR AVERAGE
+ 5 ± 23	1092	⁶ BERLEY	70B	HBC n rescattering
14 ± 19	1385	BANGERTER	69B	HBC $K^- p$ 0.4 GeV/c

⁶ BERLEY 70b changed from -5 to +5° to agree with our sign convention.

g_A/g_V FOR $\Sigma^- \rightarrow n e^- \bar{\nu}_e$

Measurements with fewer than 500 events have been omitted. Where necessary, signs have been changed to agree with our conventions, which are given in the "Note on Baryon Decay Parameters" in the neutron Listings. What is actually listed is $|g_1/f_1 - 0.237g_2/f_1|$. This reduces to $g_A/g_V \equiv g_1(0)/f_1(0)$ on making the usual assumption that $g_2 = 0$. See also the note on HSUEH 88.

VALUE	EVTS	DOCUMENT ID	TECN	COMMENT
0.340 ± 0.017				OUR AVERAGE
+0.327 ± 0.007 ± 0.019	50k	⁷ HSUEH	88	SPEC Σ^- 250 GeV
+0.34 ± 0.05	4456	⁸ BOURQUIN	83c	SPEC SPS hyperon beam
0.385 ± 0.037	3507	⁹ TANENBAUM	74	ASPK

• • • We do not use the following data for averages, fits, limits, etc. • • •

0.29 ± 0.07	25k	HSUEH	85	SPEC See HSUEH 88
0.17 $\begin{smallmatrix} +0.07 \\ -0.09 \end{smallmatrix}$	519	DECAMP	77	ELEC Hyperon beam

⁷ The sign is, with our conventions, unambiguously positive. The value assumes, as usual, that $g_2 = 0$. If g_2 is included in the fit, than (with our sign convention) $g_2 = -0.56 \pm 0.37$, with a corresponding reduction of g_A/g_V to $+0.20 \pm 0.08$.

⁸ BOURQUIN 83c favors the positive sign by at least 2.6 standard deviations.

⁹ TANENBAUM 74 gives 0.435 ± 0.035 , assuming no q^2 dependence in g_A and g_V . The listed result allows q^2 dependence, and is taken from HSUEH 88.

$f_2(0)/f_1(0)$ FOR $\Sigma^- \rightarrow n e^- \bar{\nu}_e$

The signs have been changed to be in accord with our conventions, given in the "Note on Baryon Decay Parameters" in the neutron Listings.

VALUE	EVTS	DOCUMENT ID	TECN	COMMENT
0.97 ± 0.14				OUR AVERAGE
+0.96 ± 0.07 ± 0.13	50k	HSUEH	88	SPEC Σ^- 250 GeV
+1.02 ± 0.34	4456	BOURQUIN	83c	SPEC SPS hyperon beam

TRIPLE CORRELATION COEFFICIENT D for $\Sigma^- \rightarrow n e^- \bar{\nu}_e$

The coefficient D of the term $D \mathbf{P}(\hat{p}_e \times \hat{p}_\nu)$ in the $\Sigma^- \rightarrow n e^- \bar{\nu}$ decay angular distribution. A nonzero value would indicate a violation of time-reversal invariance.

VALUE	EVTS	DOCUMENT ID	TECN	COMMENT
0.11 ± 0.10	50k	HSUEH	88	SPEC Σ^- 250 GeV

g_V/g_A FOR $\Sigma^- \rightarrow \Lambda e^- \bar{\nu}_e$

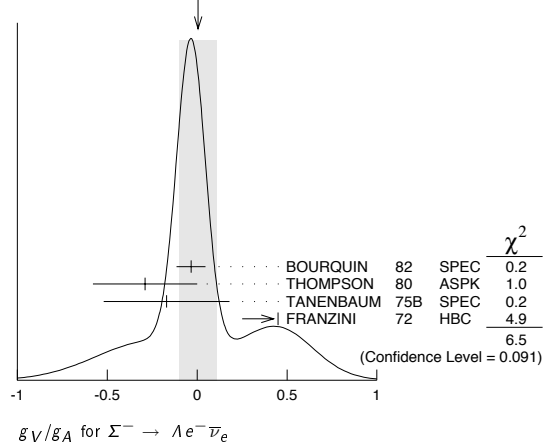
For the sign convention, see the "Note on Baryon Decay Parameters" in the neutron Listings. The value is predicted to be zero by conserved vector current theory. The values averaged assume CVC-SU(3) weak magnetism term.

VALUE	EVTS	DOCUMENT ID	TECN	COMMENT
0.01 ± 0.10				OUR AVERAGE
-0.034 ± 0.080	1620	¹⁰ BOURQUIN	82	SPEC SPS hyperon beam
-0.29 ± 0.29	114	THOMPSON	80	ASPK BNL hyperon beam
-0.17 ± 0.35	55	TANENBAUM	75B	SPEC BNL hyperon beam
+0.45 ± 0.20	186	^{10,11} FRANZINI	72	HBC

¹⁰ The sign has been changed to agree with our convention.

¹¹ The FRANZINI 72 value includes the events of earlier papers.

WEIGHTED AVERAGE
0.01 ± 0.10 (Error scaled by 1.5)



g_{WM}/g_A FOR $\Sigma^- \rightarrow \Lambda e^- \bar{\nu}_e$

The values quoted assume the CVC prediction $g_V = 0$.

VALUE	EVTS	DOCUMENT ID	TECN	COMMENT
2.4 ± 1.7				OUR AVERAGE
1.75 ± 3.5	114	THOMPSON	80	ASPK BNL hyperon beam
3.5 ± 4.5	55	TANENBAUM	75B	SPEC BNL hyperon beam
2.4 ± 2.1	186	FRANZINI	72	HBC

Σ^- REFERENCES

We have omitted some papers that have been superseded by later experiments. See our earlier editions.

ESCHRICH	01	PL B522 233	I. Eschrich <i>et al.</i>	(FNAL SELEX Collab.)
GUREV	93	JETPL 57 400	M.P. Gurev <i>et al.</i>	(PNPI)
			Translated from ZETFP 57 383.	
GALL	88	PRL 60 186	K.P. Gall <i>et al.</i>	(BOST, MIT, WILL, CIT+)
HERTZOG	88	PR D37 1142	D.W. Hertzog <i>et al.</i>	(WILL, BOST, MIT+)
HSUEH	88	PR D38 2056	S.Y. Hsueh <i>et al.</i>	(CHIC, ELMT, FNAL+)
ZAPALAC	86	PRL 57 1526	G. Zapalac <i>et al.</i>	(EFI, ELMT, FNAL+)
HSUEH	85	PRL 54 2399	S.Y. Hsueh <i>et al.</i>	(CHIC, ELMT, FNAL+)
WAH	85	PRL 55 2551	Y.W. Wah <i>et al.</i>	(FNAL, IOWA, ISU)
BOURQUIN	83B	ZPHY C21 27	M.H. Bourquin <i>et al.</i>	(BRIS, GEVA, HEIDP+)
BOURQUIN	83C	ZPHY C21 17	M.H. Bourquin <i>et al.</i>	(BRIS, GEVA, HEIDP+)
DECK	83	PR D28 1	L. Deck <i>et al.</i>	(RUTG, WBS C, MICH, MINN)
BOURQUIN	82	ZPHY C12 307	M.H. Bourquin <i>et al.</i>	(BRIS, GEVA, HEIDP+)
MARRAFFINO	80	PR D21 2501	J. Marraffino <i>et al.</i>	(VAND, MFM)
THOMPSON	80	PR D21 25	J.A. Thompson <i>et al.</i>	(PITT, BNL)
HANSL	78	NP B132 45	T. Hansl <i>et al.</i>	(MPIM, VAND)
DECAMP	77	PL 66B 295	D. Decamp <i>et al.</i>	(LALO, EPOL)
CONFORTO	76	NP B105 189	B. Conforto <i>et al.</i>	(RHEL, LOIC)
DUGAN	75	NP A254 396	G. Dugan <i>et al.</i>	(COLU, YALE)
TANENBAUM	75B	PR D12 1871	W. Tanenbaum <i>et al.</i>	(YALE, FNAL, BNL)
EBENHOH	74	ZPHY 266 367	H. Ebenhoeh <i>et al.</i>	(HEIDT)
TANENBAUM	74	PRL 33 175	W. Tanenbaum <i>et al.</i>	(YALE, FNAL, BNL)
EBENHOH	73	ZPHY 264 413	W. Ebenhoeh <i>et al.</i>	(HEIDT)
SECHI-ZORN	73	PR D8 12	B. Sechi-Zorn, G.A. Snow	(UMD)
BOHM	72	NP B48 1	G. Bohm <i>et al.</i>	(BERL, KIDR, BRUX, IASD+)
FRANZINI	72	PR D6 2417	P. Franzini <i>et al.</i>	(COLU, HEID, UMD+)
ROBERTSON	72	Thesis UMI 78-00877	R.M. Robertson	(IIT)
BAKKER	71	LNC 1 37	A.M. Bakker <i>et al.</i>	(SABRE Collab.)
COLE	71	PR D4 631	J. Cole <i>et al.</i>	(STON, COLU)
			Also Thesis Nevis 175	
TOVEE	71	NP B33 493	D.N. Tovee <i>et al.</i>	(LOUC, KIDR, BERL+)
BERLEY	70B	PR D1 2015	D. Berley <i>et al.</i>	(BNL, MASA, YALE)
BOGERT	70	PR D2 6	D.V. Bogert <i>et al.</i>	(BNL, MASA, YALE)
EISELE	70	ZPHY 238 372	F. Eisele <i>et al.</i>	(HEID)
PDG	70	RMP 42 87	A. Barbaro-Gatti <i>et al.</i>	(LRL, BRAN+)
ANG	69	ZPHY 223 103	G. Ang <i>et al.</i>	(HEID)
ANG	69B	ZPHY 228 151	G. Ang <i>et al.</i>	(HEID)

BAGGETT 69	PRL 23 249	N.V. Baggett, B. Kehoe, G.A. Snow	(UMD)
BALTY 69	PRL 22 615	C. Balty <i>et al.</i>	(COLU, STON)
BANGERTER 69	Thesis UCRL 19244	R.O. Bangener	(LRL)
BANGERTER 69B	PR 187 1821	R.O. Bangener <i>et al.</i>	(LRL)
BARLOUTAUD 69	NP B14 153	R. Barloutaud <i>et al.</i>	(SACL, CERN, HEID)
EISELE 69	ZPHY 221 1	F. Eisele <i>et al.</i>	(HEID)
BIERMAN 68	PRL 20 1459	E. Bierman <i>et al.</i>	(PRIN)
HEPP 68	ZPHY 214 71	V. Hepp, H. Schleich	(HEID)
WHITESIDE 68	NC 54A 537	H. Whiteside, J. Gollub	(OBER)
BARASH 67	PRL 19 181	N. Barash <i>et al.</i>	(UMD)
CHANG 66	PR 151 1081	C.Y. Chang	(COLU)
BAZIN 65B	PR 140B 1358	M. Bazin <i>et al.</i>	(PRIN, RUTG, COLU)
DOSCH 65	PL 14 239	H.C. Dosch <i>et al.</i>	(HEID)
Also	PR 151 1081	C.Y. Chang	(COLU)
SCHMIDT 65	PR 140B 1328	P. Schmidt	(COLU)
BURNSTEIN 64	PRL 13 66	R.A. Burnstein <i>et al.</i>	(UMD)
COURANT 64	PR 136 B1791	H. Courant <i>et al.</i>	(CERN, HEID, UMD+)
BARKAS 63	PRL 11 26	W.H. Barkas, J.N. Dyer, H.H. Heckman	(LRL)
HUMPHREY 62	PR 127 1305	W.E. Humphrey, R.R. Ross	(LRL)

$\Sigma(1385) P_{13}$ $I(J^P) = 1(\frac{3}{2}^+)$ Status: * * * *

Discovered by ALSTON 60. Early measurements of the mass and width for combined charge states have been omitted. They may be found in our 1984 edition Reviews of Modern Physics 56 S1 (1984).

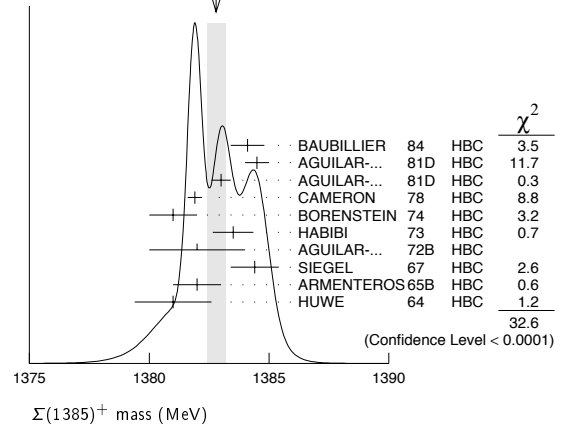
We average only the most significant determinations. We do not average results from inclusive experiments with large backgrounds or results which are not accompanied by some discussion of experimental resolution. Nevertheless systematic differences between experiments remain. (See the ideograms in the Listings below.) These differences could arise from interference effects that change with production mechanism and/or beam momentum. They can also be accounted for in part by differences in the parametrizations employed. (See BORENSTEIN 74 for a discussion on this point.) Thus BORENSTEIN 74 uses a Breit-Wigner with energy-independent width, since a P -wave was found to give unsatisfactory fits. CAMERON 78 uses the same form. On the other hand HOLMGREN 77 obtains a good fit to their $\Lambda\pi$ spectrum with a P -wave Breit-Wigner, but includes the partial width for the $\Sigma\pi$ decay mode in the parametrization. AGUILAR-BENITEZ 81D gives masses and widths for five different Breit-Wigner shapes. The results vary considerably. Only the best-fit S -wave results are given here.

$\Sigma(1385)$ MASSES

$\Sigma(1385)^+$ MASS

VALUE (MeV)	EVTS	DOCUMENT ID	TECN	COMMENT
1382.8 ± 0.4 OUR AVERAGE				Error includes scale factor of 2.0. See the ideogram below.
1384.1 ± 0.7	1897	BAUBILLIER 84	HBC	K^-p 8.25 GeV/c
1384.5 ± 0.5	5256	AGUILAR-... 81D	HBC	$K^-p \rightarrow \Lambda\pi\pi$ 4.2 GeV/c
1383.0 ± 0.4	9361	AGUILAR-... 81D	HBC	$K^-p \rightarrow \Lambda 3\pi$ 4.2 GeV/c
1381.9 ± 0.3	6900	CAMERON 78	HBC	K^-p 0.96-1.36 GeV/c
1381 ± 1	6846	BORENSTEIN 74	HBC	K^-p 2.18 GeV/c
1383.5 ± 0.85	2300	HABIBI 73	HBC	$K^-p \rightarrow \Lambda\pi\pi$
1382 ± 2	400	AGUILAR-... 72B	HBC	$K^-p \rightarrow \Lambda\pi$'s
1384.4 ± 1.0	1260	SIEGEL 67	HBC	K^-p 2.1 GeV/c
1382 ± 1	750	ARMENTEROS65B	HBC	K^-p 0.9-1.2 GeV/c
1381.0 ± 1.6	859	HUWE 64	HBC	K^-p 1.22 GeV/c
• • • We do not use the following data for averages, fits, limits, etc. • • •				
1385.1 ± 1.2	600	BAKER 80	HYBR	π^+p 7 GeV/c
1383.2 ± 1.0	750	BAKER 80	HYBR	K^-p 7 GeV/c
1381 ± 2	7k	1 BAUBILLIER 79B	HBC	K^-p 8.25 GeV/c
1391 ± 2	2k	CAUTIS 79	HYBR	π^+p/K^-p 11.5 GeV
1390 ± 2	100	1 SUGAHARA 79B	HBC	π^-p 6 GeV/c
1385 ± 3	22k	1,2 BARREIRO 77B	HBC	K^-p 4.2 GeV/c
1385 ± 1	2594	HOLMGREN 77	HBC	See AGUILAR-BENITEZ 81D
1380 ± 2		1 BARDADIN-... 75	HBC	K^-p 14.3 GeV/c
1382 ± 1	3740	3 BERTHON 74	HBC	K^-p 1263-1843 MeV/c
1390 ± 6	46	AGUILAR-... 70B	HBC	$K^-p \rightarrow \Sigma\pi$'s 4 GeV/c
1383 ± 8	62	4 BIRMINGHAM 66	HBC	K^-p 3.5 GeV/c
1378 ± 5	135	LONDON 66	HBC	K^-p 2.24 GeV/c
1384.3 ± 1.9	250	4 SMITH 65	HBC	K^-p 1.8 GeV/c
1382.6 ± 2.1	250	4 SMITH 65	HBC	K^-p 1.95 GeV/c
1375.0 ± 3.9	170	COOPER 64	HBC	K^-p 1.45 GeV/c
1376.0 ± 3.9	154	4 ELY 61	HLBC	K^-p 1.11 GeV/c

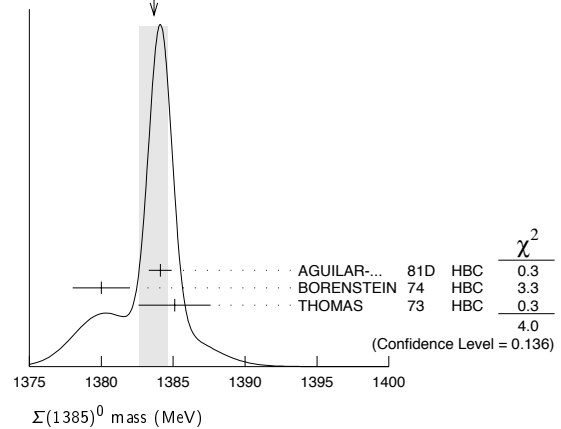
WEIGHTED AVERAGE
1382.8 ± 0.4 (Error scaled by 2.0)



$\Sigma(1385)^0$ MASS

VALUE (MeV)	EVTS	DOCUMENT ID	TECN	COMMENT
1383.7 ± 1.0 OUR AVERAGE				Error includes scale factor of 1.4. See the ideogram below.
1384.1 ± 0.8	5722	AGUILAR-... 81D	HBC	$K^-p \rightarrow \Lambda 3\pi$ 4.2 GeV/c
1380 ± 2	3100	5 BORENSTEIN 74	HBC	$K^-p \rightarrow \Lambda 3\pi$ 2.18 GeV/c
1385.1 ± 2.5	240	4 THOMAS 73	HBC	$\pi^-p \rightarrow \Lambda\pi^0 K^0$
• • • We do not use the following data for averages, fits, limits, etc. • • •				
1389 ± 3	500	6 BAUBILLIER 79B	HBC	K^-p 8.25 GeV/c

WEIGHTED AVERAGE
1383.7 ± 1.0 (Error scaled by 1.4)



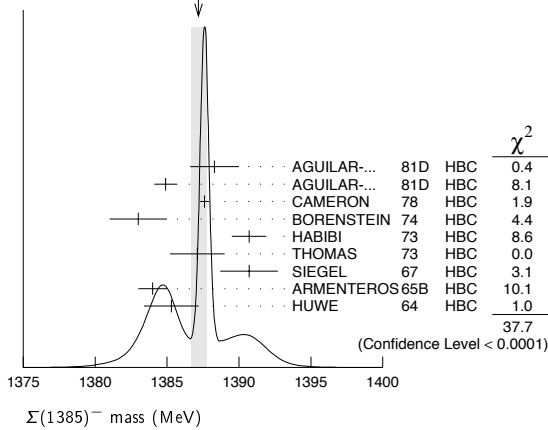
$\Sigma(1385)^-$ MASS

VALUE (MeV)	EVTS	DOCUMENT ID	TECN	COMMENT
1387.2 ± 0.5 OUR AVERAGE				Error includes scale factor of 2.2. See the ideogram below.
1388.3 ± 1.7	620	AGUILAR-... 81D	HBC	$K^-p \rightarrow \Lambda\pi\pi$ 4.2 GeV/c
1384.9 ± 0.8	3346	AGUILAR-... 81D	HBC	$K^-p \rightarrow \Lambda 3\pi$ 4.2 GeV/c
1387.6 ± 0.3	9720	CAMERON 78	HBC	K^-p 0.96-1.36 GeV/c
1383 ± 2	2303	BORENSTEIN 74	HBC	K^-p 2.18 GeV/c
1390.7 ± 1.2	1900	HABIBI 73	HBC	$K^-p \rightarrow \Lambda\pi\pi$
1387.1 ± 1.9	630	4 THOMAS 73	HBC	$\pi^-p \rightarrow \Lambda\pi^- K^+$
1390.7 ± 2.0	370	SIEGEL 67	HBC	K^-p 2.1 GeV/c
1384 ± 1	1380	ARMENTEROS65B	HBC	K^-p 0.9-1.2 GeV/c
1385.3 ± 1.9	1086	4 HUWE 64	HBC	K^-p 1.15-1.30 GeV/c
• • • We do not use the following data for averages, fits, limits, etc. • • •				
1383 ± 1	4.5k	1 BAUBILLIER 79B	HBC	K^-p 8.25 GeV/c
1380 ± 6	150	1 SUGAHARA 79B	HBC	π^-p 6 GeV/c
1387 ± 3	12k	1,2 BARREIRO 77B	HBC	K^-p 4.2 GeV/c
1391 ± 3	193	HOLMGREN 77	HBC	See AGUILAR-BENITEZ 81D
1383 ± 2		1 BARDADIN-... 75	HBC	K^-p 14.3 GeV/c
1389 ± 1	3060	3 BERTHON 74	HBC	K^-p 1263-1843 MeV/c
1389 ± 9	15	LONDON 66	HBC	K^-p 2.24 GeV/c
1391.5 ± 2.6	120	4 SMITH 65	HBC	K^-p 1.8 GeV/c
1399.8 ± 2.2	58	4 SMITH 65	HBC	K^-p 1.95 GeV/c
1392.0 ± 6.2	200	COOPER 64	HBC	K^-p 1.45 GeV/c
1382 ± 3	93	DAHL 61	DBC	K^-d 0.45 GeV/c
1376.0 ± 4.4	224	4 ELY 61	HLBC	K^-p 1.11 GeV/c

Baryon Particle Listings

$\Sigma(1385)$

WEIGHTED AVERAGE
1387.2±0.5 (Error scaled by 2.2)



$m_{\Sigma(1385)^-} - m_{\Sigma(1385)^+}$

VALUE (MeV)	CL%	DOCUMENT ID	TECN	COMMENT
••• We do not use the following data for averages, fits, limits, etc. •••				
- 2 to +6	95	7 BORENSTEIN 74	HBC	$K^- p$ 2.18 GeV/c
7.2±1.4		7 HABIBI 73	HBC	$K^- p \rightarrow \Lambda \pi \pi$
6.3±2.0		7 SIEGEL 67	HBC	$K^- p$ 2.1 GeV/c
11 ±9		7 LONDON 66	HBC	$K^- p$ 2.24 GeV/c
9 ±6		7 LONDON 66	HBC	$\Lambda 3\pi$ events
2.0±1.5		7 ARMENTEROS65B	HBC	$K^- p$ 0.9-1.2 GeV/c
7.2±2.1		7 SMITH 65	HBC	$K^- p$ 1.8 GeV/c
17.2±2.0		7 SMITH 65	HBC	$K^- p$ 1.95 GeV/c
17 ±7		7 COOPER 64	HBC	$K^- p$ 1.45 GeV/c
4.3±2.2		7 HUWE 64	HBC	$K^- p$ 1.22 GeV/c
0.0±4.2		7 ELY 61	HLBC	$K^- p$ 1.11 GeV/c

$m_{\Sigma(1385)^0} - m_{\Sigma(1385)^+}$

VALUE (MeV)	CL%	DOCUMENT ID	TECN	COMMENT
••• We do not use the following data for averages, fits, limits, etc. •••				
-4 to +4	95	7 BORENSTEIN 74	HBC	$K^- p$ 2.18 GeV/c

$m_{\Sigma(1385)^-} - m_{\Sigma(1385)^0}$

VALUE (MeV)	DOCUMENT ID	TECN	COMMENT
••• We do not use the following data for averages, fits, limits, etc. •••			
2.0±2.4	7 THOMAS 73	HBC	$\pi^- p \rightarrow \Lambda \pi^- K^+$

$\Sigma(1385)$ WIDTHS

$\Sigma(1385)^+$ WIDTH

VALUE (MeV)	EVTS	DOCUMENT ID	TECN	COMMENT
35.8± 0.8 OUR AVERAGE				
37.2± 2.0	1897	BAUBILLIER 84	HBC	$K^- p$ 8.25 GeV/c
35.1± 1.7	5256	AGUILAR-... 81D	HBC	$K^- p \rightarrow \Lambda \pi \pi$ 4.2 GeV/c
37.5± 2.0	9361	AGUILAR-... 81D	HBC	$K^- p \rightarrow \Lambda 3\pi$ 4.2 GeV/c
35.5± 1.9	6900	CAMERON 78	HBC	$K^- p$ 0.96-1.36 GeV/c
34.0± 1.6	6846	8 BORENSTEIN 74	HBC	$K^- p$ 2.18 GeV/c
38.3± 3.2	2300	9 HABIBI 73	HBC	$K^- p \rightarrow \Lambda \pi \pi$
32.5± 6.0	400	AGUILAR-... 72B	HBC	$K^- p \rightarrow \pi$'s
36 ± 4	1260	9 SIEGEL 67	HBC	$K^- p$ 2.1 GeV/c
32.0± 4.7	750	9 ARMENTEROS65B	HBC	$K^- p$ 0.95-1.20 GeV/c
46.5± 6.4	859	9 HUWE 64	HBC	$K^- p$ 1.15-1.30 GeV/c
••• We do not use the following data for averages, fits, limits, etc. •••				
40 ± 3	600	BAKER 80	HYBR	$\pi^+ p$ 7 GeV/c
37 ± 2	750	BAKER 80	HYBR	$K^- p$ 7 GeV/c
37 ± 2	7k	1 BAUBILLIER 79B	HBC	$K^- p$ 8.25 GeV/c
30 ± 4	2k	CAUTIS 79	HYBR	$\pi^+ p / K^- p$ 11.5 GeV
30 ± 6	100	1 SUGAHARA 79B	HBC	$\pi^- p$ 6 GeV/c
43 ± 5	22k	1,2 BARREIRO 77B	HBC	$K^- p$ 4.2 GeV/c
34 ± 2	2594	HOLMGREN 77	HBC	See AGUILAR-BENITEZ 81D
40.0± 3.2		1 BARDADIN-... 75	HBC	$K^- p$ 14.3 GeV/c
48 ± 3	3740	3 BERTHON 74	HBC	$K^- p$ 1263-1843 MeV/c
33 ± 20	46	9 AGUILAR-... 70B	HBC	$K^- p \rightarrow \Sigma \pi$'s 4 GeV/c
25 ± 32	62	9 BIRMINGHAM 66	HBC	$K^- p$ 3.5 GeV/c
30.3± 7.5	250	9 SMITH 65	HBC	$K^- p$ 1.8 GeV/c
33.1± 8.3	250	9 SMITH 65	HBC	$K^- p$ 1.95 GeV/c
51 ± 16	170	9 COOPER 64	HBC	$K^- p$ 1.45 GeV/c
48 ± 16	154	9 ELY 61	HLBC	$K^- p$ 1.11 GeV/c

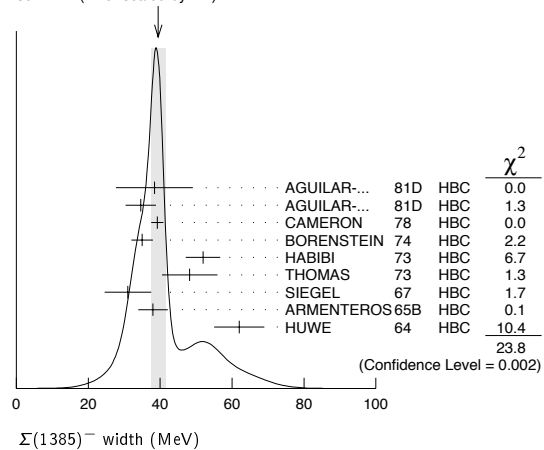
$\Sigma(1385)^0$ WIDTH

VALUE (MeV)	EVTS	DOCUMENT ID	TECN	COMMENT
36 ± 5 OUR AVERAGE				
34.8± 5.6	5722	AGUILAR-... 81D	HBC	$K^- p \rightarrow \Lambda 3\pi$ 4.2 GeV/c
39.3± 10.2	240	9 THOMAS 73	HBC	$\pi^- p \rightarrow \Lambda \pi^0 K^0$
••• We do not use the following data for averages, fits, limits, etc. •••				
53 ± 8	3100	10 BORENSTEIN 74	HBC	$K^- p \rightarrow \Lambda 3\pi$ 2.18 GeV/c
30 ± 9	106	CURTIS 63	OSPK	$\pi^- p$ 1.5 GeV/c

$\Sigma(1385)^-$ WIDTH

VALUE (MeV)	EVTS	DOCUMENT ID	TECN	COMMENT
39.4± 2.1 OUR AVERAGE				
Error includes scale factor of 1.7. See the ideogram below.				
38.4± 10.7	620	AGUILAR-... 81D	HBC	$K^- p \rightarrow \Lambda \pi \pi$ 4.2 GeV/c
34.6± 4.2	3346	AGUILAR-... 81D	HBC	$K^- p \rightarrow \Lambda 3\pi$ 4.2 GeV/c
39.2± 1.7	9720	CAMERON 78	HBC	$K^- p$ 0.96-1.36 GeV/c
35 ± 3	2303	8 BORENSTEIN 74	HBC	$K^- p$ 2.18 GeV/c
51.9± 4.8	1900	9 HABIBI 73	HBC	$K^- p \rightarrow \Lambda \pi \pi$
48.2± 7.7	630	9 THOMAS 73	HBC	$\pi^- p \rightarrow \Lambda \pi^- K^0$
31.0± 6.5	370	9 SIEGEL 67	HBC	$K^- p$ 2.1 GeV/c
38.0± 4.1	1382	9 ARMENTEROS65B	HBC	$K^- p$ 0.95-1.20 GeV/c
62 ± 7	1086	HUWE 64	HBC	$K^- p$ 1.15-1.30 GeV/c
••• We do not use the following data for averages, fits, limits, etc. •••				
44 ± 4	4.5k	1 BAUBILLIER 79B	HBC	$K^- p$ 8.25 GeV/c
58 ± 4	150	1 SUGAHARA 79B	HBC	$\pi^- p$ 6 GeV/c
45 ± 5	12k	1,2 BARREIRO 77B	HBC	$K^- p$ 4.2 GeV/c
35 ± 10	193	HOLMGREN 77	HBC	See AGUILAR-BENITEZ 81D
47 ± 6		1 BARDADIN-... 75	HBC	$K^- p$ 14.3 GeV/c
40 ± 3	3060	3 BERTHON 74	HBC	$K^- p$ 1263-1843 MeV/c
29.2± 10.6	120	9 SMITH 65	HBC	$K^- p$ 1.80 GeV/c
17.1± 8.9	58	9 SMITH 65	HBC	$K^- p$ 1.95 GeV/c
88 ± 24	200	9 COOPER 64	HBC	$K^- p$ 1.45 GeV/c
40		DAHL 61	DBC	$K^- d$ 0.45 GeV/c
66 ± 18	224	9 ELY 61	HLBC	$K^- p$ 1.11 GeV/c

WEIGHTED AVERAGE
39.4±2.1 (Error scaled by 1.7)



$\Sigma(1385)$ POLE POSITIONS

$\Sigma(1385)^+$ REAL PART

VALUE	DOCUMENT ID	COMMENT
1379±1	LICHTENBERG74	Extrapolates HABIBI 73

$\Sigma(1385)^+$ -IMAGINARY PART

VALUE	DOCUMENT ID	COMMENT
17.5±1.5	LICHTENBERG74	Extrapolates HABIBI 73

$\Sigma(1385)^-$ REAL PART

VALUE	DOCUMENT ID	COMMENT
1383±1	LICHTENBERG74	Extrapolates HABIBI 73

$\Sigma(1385)^-$ -IMAGINARY PART

VALUE	DOCUMENT ID	COMMENT
22.5±1.5	LICHTENBERG74	Extrapolates HABIBI 73

Baryon Particle Listings
 $\Sigma(1385), \Sigma(1480)$ Bumps

$\Sigma(1385)$ DECAY MODES

Mode	Fraction (Γ_i/Γ)	Confidence level
$\Gamma_1 \Lambda\pi$	(87.0±1.5) %	
$\Gamma_2 \Sigma\pi$	(11.7±1.5) %	
$\Gamma_3 \Lambda\gamma$	(1.3±0.4) %	
$\Gamma_4 \Sigma^-\gamma$	< 2.4 × 10 ⁻⁴	90%
$\Gamma_5 N\bar{K}$		

The above branching fractions are our estimates, not fits or averages.

$\Sigma(1385)$ BRANCHING RATIOS

$\Gamma(\Sigma\pi)/\Gamma(\Lambda\pi)$	DOCUMENT ID	TECN	CHG	COMMENT	Γ_2/Γ_1
0.135 ± 0.011 OUR AVERAGE					
0.20 ± 0.06	DIONISI 78B	HBC	±	$K^-p \rightarrow Y^* K\bar{K}$	
0.16 ± 0.03	BERTHON 74	HBC	+	K^-p 1.26–1.84 GeV/c	
0.11 ± 0.02	BERTHON 74	HBC	-	K^-p 1.26–1.84 GeV/c	
0.21 ± 0.05	BORENSTEIN 74	HBC	+	$K^-p \rightarrow \Lambda\pi^+\pi^-$, $\Sigma^0\pi^+\pi^-$	
0.18 ± 0.04	MAST 73	MPWA	±	$K^-p \rightarrow \Lambda\pi^+\pi^-$, $\Sigma^0\pi^+\pi^-$	
0.10 ± 0.05	THOMAS 73	HBC	-	$\pi^-p \rightarrow \Lambda K\pi, \Sigma K\pi$	
0.16 ± 0.07	AGUILAR... 72B	HBC	+	K^-p 3.9, 4.6 GeV/c	
0.13 ± 0.04	COLLEY 71B	DBC	-0	K^-N 1.5 GeV/c	
0.13 ± 0.04	PAN 69	HBC	+	$\pi^+p \rightarrow \Lambda K\pi, \Sigma K\pi$	
0.08 ± 0.06	LONDON 66	HBC	+	K^-p 2.24 GeV/c	
0.163 ± 0.041	ARMENTEROS65B	HBC	±	K^-p 0.95–1.20 GeV/c	
0.09 ± 0.04	HUWE 64	HBC	±	K^-p 1.2–1.7 GeV	
••• We do not use the following data for averages, fits, limits, etc. •••					
<0.04	ALSTON 62	HBC	±0	K^-p 1.15 GeV/c	
0.04 ± 0.04	BASTIEN 61	HBC	±		

$\Gamma(\Lambda\gamma)/\Gamma(\Lambda\pi)$	CL%	EVTS	DOCUMENT ID	TECN	COMMENT	Γ_3/Γ_1
1.53 ± 0.39^{+0.15}_{-0.24}		61	TAYLOR	05	CLAS $\gamma p \rightarrow K^+\Lambda\gamma$	
••• We do not use the following data for averages, fits, limits, etc. •••						
<6	90		COLAS	75	HLBC K^-p , 575–970 MeV	

$\Gamma(\Sigma^-\gamma)/\Gamma_{total}$	CL%	DOCUMENT ID	TECN	CHG	COMMENT	Γ_4/Γ
<2.4 × 10⁻⁴	90	11 MOLCHANOV 04	SELX	-	$\Sigma^-p \rightarrow \Sigma(1385)^-p$, 600 GeV	
••• We do not use the following data for averages, fits, limits, etc. •••						
<6.1 × 10 ⁻⁴	90	12 ARIK	77	SPEC	$\Sigma^-p \rightarrow \Sigma(1385)^-p$, 23 GeV	

$(\Gamma_i/\Gamma_f)^{1/2}/\Gamma_{total}$ in $N\bar{K} \rightarrow \Sigma(1385) \rightarrow \Lambda\pi$	DOCUMENT ID	CHG	COMMENT	$(\Gamma_5/\Gamma_1)^{1/2}/\Gamma$
+0.586 ± 0.319	13 DEVENISH	74B	0	Fixed-t dispersion rel.

$\Sigma(1385)$ FOOTNOTES

- From fit to inclusive $\Lambda\pi$ spectrum.
- Includes data of HOLMGREN 77.
- The errors are statistical only. The resolution is not unfolded.
- The error is enlarged to Γ/\sqrt{N} . See the note on the $K^*(892)$ mass in the 1984 edition.
- From a fit to $\Lambda\pi^0$ with the width fixed at 34 MeV.
- From fit to inclusive $\Lambda\pi^0$ spectrum with the width fixed at 40 MeV.
- Redundant with data in the mass Listings.
- Results from $\Lambda\pi^+\pi^-$ and $\Lambda\pi^+\pi^-\pi^0$ combined by us.
- The error is enlarged to $4\Gamma/\sqrt{N}$. See the note on the $K^*(892)$ mass in the 1984 edition.
- Consistent with +, 0, and - widths equal.
- We calculate this from the MOLCHANOV 04 upper limit of 9.5 keV on the $\Sigma^-\gamma$ width.
- We calculate this from the ARIK 77 upper limit of 24 keV on the $\Sigma^-\gamma$ width.
- An extrapolation of the parametrized amplitude below threshold.

$\Sigma(1385)$ REFERENCES

TAYLOR 05	PR C71 054609	S. Taylor et al.	(JLab CLAS Collab.)
Also	PR C72 039902 (errata.)	S. Taylor et al.	(JLab CLAS Collab.)
MOLCHANOV 04	PL B590 161	V.V. Molchanov et al.	(FNAL SELEX Collab.)
BAUBILLIER 84	ZPHY C23 213	M. Baubillier et al.	(BIRM, CERN, GLAS+)
PDG 84	RMP 56 51	C.G. Wohl et al.	(LBL, CIT, CERN)
AGUILAR... 81D	AFIS A77 144	M. Aguilar-Benitez, J. Salicio	(MADR)
BAKER 80	NP B166 207	P.A. Baker et al.	(LOIC)
BAUBILLIER 79B	NP B148 18	M. Baubillier et al.	(BIRM, CERN, GLAS+)
CAUTIS 75	NP B156 507	C.V. Cautis et al.	(SLAC)
SUGAHARA 79B	NP B156 237	R. Sugahara et al.	(KEK, OSKC, KIBK)
CAMERON 78	NP B143 189	W. Cameron et al.	(RHEL, LOIC)
DIONISI 78B	PL 78B 154	C. Dionisi, R. Armenteros, J. Diaz	(CERN, AMST+)
ARIK 77	PRL 38 1000	E. Arik et al.	(PITT, BNL, MASA)
BARREIRO 77B	NP B126 319	F. Barreiro et al.	(CERN, AMST, NIUM)
HOLMGREN 77	NP B119 261	S.O. Holmgren et al.	(CERN, AMST, NIUM)
BARDADIN... 75	NP B98 418	M. Bardadin-Otwinowska et al.	(SACL, EPOL+)
COLAS 75	NP B91 253	J. Colas et al.	(ORSAY)
BERTHON 74	NC 21A 146	A. Berthon et al.	(CDEF, RHEL, SACL+)
BORENSTEIN 74	PR D9 3006	S.R. Borenstein et al.	(BNL, MICH)
DEVENISH 74B	NP B81 330	R.C.E. Devenish, C.D. Froggatt, B.R. Martin	(DESY+)

LICHTENBERG 74	PR D10 3865	D.B. Lichtenberg	(IND)
Also	Private Comm.	D.B. Lichtenberg	(IND)
HABIBI 73	Thesis Nevis 199	M. Habibi	(COLU)
Also	Purdue Conf. 387	C. Baltay et al.	(COLU, BING)
MAST 73	PR D7 3212	T.S. Mast et al.	(LBL)JJP
Also	PR D7 5	T.S. Mast et al.	(LBL)JJP
THOMAS 73	NP B56 15	D.W. Thomas et al.	(CMU)JP
AGUILAR... 72B	PR D6 29	M. Aguilar-Benitez et al.	(BNL)
COLLEY 71B	NP B31 61	D.C. Colley et al.	(BIRM, EDIN, GLAS+)
AGUILAR... 70B	PRL 25 58	M. Aguilar-Benitez et al.	(BNL, SYRA)
PAN 69	PRL 23 808	Y.L. Pan, F.L. Forman	(PENN)I
SIEGEL 67	Thesis UCRL 18041	D.M. Siegel	(LRL)
BIRMINGHAM 66	PR 152 1148	M. Haque et al.	(BIRM, GLAS, LOIC, OXF+)
LONDON 66	PR 143 1034	G.W. London et al.	(BNL, SYRA)J
ARMENTEROS 65B	PL 19 75	R. Armenteros et al.	(CERN, HEID, SACL)
SMITH 65	Thesis UCLA	L.T. Smith	(UCLA)
COOPER 64	PL 8 365	W.A. Cooper et al.	(CERN, AMST)
HUWE 64	Thesis UCRL 11291	D.O. Huwe	(LRL)JP
Also	PR 181 1824	D.O. Huwe	(LRL)J
CURTIS 63	PR 132 1771	L.J. Curtis et al.	(MICH)J
ALSTON 62	CERN Conf. 311	M.H. Alston et al.	(LRL)
BASTIEN 61	PRL 6 702	P.L. Bastien, M. Ferro-Luzzi, A.H. Rosenfeld	(LRL)
DAHL 61	PRL 6 142	O.I. Dahl et al.	(LRL)
ELY 61	PRL 7 461	R.P. Ely et al.	(LRL)J
ALSTON 60	PRL 5 520	M.H. Alston et al.	(LRL)I

$\Sigma(1480)$ Bumps

$I(J^P) = 1(?^?)$ Status: *

OMITTED FROM SUMMARY TABLE

These are peaks seen in $\Lambda\pi$ and $\Sigma\pi$ spectra in the reaction $\pi^+p \rightarrow (Y\pi)K^+$ at 1.7 GeV/c. Also, the Y polarization oscillates in the same region.

MILLER 70 suggests a possible alternate explanation in terms of a reflection of $N(1675) \rightarrow \Lambda K$ decay. However, such an explanation for the $(\Sigma^+\pi^0)K^+$ channel in terms of $\Delta(1650) \rightarrow \Sigma K$ decay seems unlikely (see PAN 70). In addition such reflections would also have to account for the oscillation of the Y polarization in the 1480 MeV region.

HANSON 71, with less data than PAN 70, can neither confirm nor deny the existence of this state. MAST 75 sees no structure in this region in $K^-p \rightarrow \Lambda\pi^0$.

ENGELEN 80 performs a multichannel analysis of $K^-p \rightarrow p\bar{K}^0\pi^-$ at 4.2 GeV/c. They observe a 3.5 standard-deviation signal at 1480 MeV in $p\bar{K}^0$ which cannot be explained as a reflection of any competing channel.

PRAKHOV 04 sees no evidence for this or other light Σ resonances, aside from the $\Sigma(1385)$, in $K^-p \rightarrow \Lambda\pi^0\pi^0$.

ZYCHOR 06 finds peaks in $pp \rightarrow pK^+(\pi^\pm X^\mp)$ at $p_{beam} = 3.65$ GeV/c.

$\Sigma(1480)$ MASS
(PRODUCTION EXPERIMENTS)

VALUE (MeV)	EVTS	DOCUMENT ID	TECN	COMMENT
≈ 1480 OUR ESTIMATE				
1480 ± 15	365 ± 60	ZYCHOR 06	SPEC	$pp \rightarrow pK^+(\pi^\pm X^\mp)$
1480	120	ENGELEN 80	HBC	$K^-p \rightarrow (p\bar{K}^0)\pi^-$
1485 ± 10		CLINE 73	MPWA	$K^-d \rightarrow (\Lambda\pi^-)p$
1479 ± 10		PAN 70	HBC	$\pi^+p \rightarrow (\Lambda\pi^+)K^+$
1465 ± 15		PAN 70	HBC	$\pi^+p \rightarrow (\Sigma\pi)K^+$

$\Sigma(1480)$ WIDTH
(PRODUCTION EXPERIMENTS)

VALUE (MeV)	EVTS	DOCUMENT ID	TECN	COMMENT
60 ± 15	365 ± 60	ZYCHOR 06	SPEC	$pp \rightarrow pK^+(\pi^\pm X^\mp)$
80 ± 20	120	ENGELEN 80	HBC	$K^-p \rightarrow (p\bar{K}^0)\pi^-$
40 ± 20		CLINE 73	MPWA	$K^-d \rightarrow (\Lambda\pi^-)p$
31 ± 15		PAN 70	HBC	$\pi^+p \rightarrow (\Lambda\pi^+)K^+$
30 ± 20		PAN 70	HBC	$\pi^+p \rightarrow (\Sigma\pi)K^+$

$\Sigma(1480)$ DECAY MODES
(PRODUCTION EXPERIMENTS)

Mode	Γ_3/Γ_2
$\Gamma_1 N\bar{K}$	
$\Gamma_2 \Lambda\pi$	
$\Gamma_3 \Sigma\pi$	

$\Sigma(1480)$ BRANCHING RATIOS
(PRODUCTION EXPERIMENTS)

$\Gamma(\Sigma\pi)/\Gamma(\Lambda\pi)$	DOCUMENT ID	TECN	CHG	Γ_3/Γ_2
0.82 ± 0.51	PAN 70	HBC	+	

Baryon Particle Listings

 $\Sigma(1480)$ Bumps, $\Sigma(1560)$ Bumps, $\Sigma(1580)$

$\Gamma(N\bar{K})/\Gamma(\Lambda\pi)$	Γ_1/Γ_2			
VALUE	DOCUMENT ID	TECN	CHG	
0.72±0.50	PAN	70	HBC	+

$\Gamma(N\bar{K})/\Gamma_{\text{total}}$	Γ_1/Γ			
VALUE	DOCUMENT ID	TECN	COMMENT	
small	CLINE	73	MPWA	$K^-d \rightarrow (\Lambda\pi^-)p$

 **$\Sigma(1480)$ REFERENCES
(PRODUCTION EXPERIMENTS)**

ZYCHOR	06	PRL 96 012002	I. Zychor <i>et al.</i>	(ANKE Collab.)
PRAKHOV	04	PR C69 042202R	S. Prakhov <i>et al.</i>	(BNL Crystal Ball Collab.)
ENGELN	80	NP B167 61	J.J. Engelen <i>et al.</i>	(NIJM, AMST, CERN+)
MAST	75	PR D11 3078	T.S. Mast <i>et al.</i>	(LBL)
CLINE	73	LNC 6 205	D. Cline, R. Laumann, J. Mapp	(WISC) IJP
HANSON	71	PR D4 1296	P. Hanson, G.E. Kalmus, J. Louie	(LBL) I
MILLER	70	Duke Conf. 229	D.H. Miller	(PURD)
PAN	70	PR D2 449	Y.L. Pan <i>et al.</i>	(PENN)
Also		PRL 23 808	Y.L. Pan, F.L. Forman	(PENN) I
Also		PRL 23 806	Y.L. Pan, F.L. Forman	(PENN) I

 $\Sigma(1560)$ Bumps $I(J^P) = 1(?)^?$ Status: **

OMITTED FROM SUMMARY TABLE

This entry lists peaks reported in mass spectra around 1560 MeV without implying that they are necessarily related.

DIONISI 78B observes a 6 standard-deviation enhancement at 1553 MeV in the charged $\Lambda/\Sigma\pi$ mass spectra from $K^-p \rightarrow (\Lambda/\Sigma)\pi K\bar{K}$ at 4.2 GeV/c. In a CERN ISR experiment, LOCKMAN 78 reports a narrow 6 standard-deviation enhancement at 1572 MeV in $\Lambda\pi^\pm$ from the reaction $pp \rightarrow \Lambda\pi^+\pi^-X$. These enhancements are unlikely to be associated with the $\Sigma(1580)$ (which has not been confirmed by several recent experiments – see the next entry in the Listings).

CARROLL 76 observes a bump at 1550 MeV (as well as one at 1580 MeV) in the isospin-1 $\bar{K}N$ total cross section, but uncertainties in cross section measurements outside the mass range of the experiment preclude estimating its significance.

See also MEADOWS 80 for a review of this state.

 **$\Sigma(1560)$ MASS
(PRODUCTION EXPERIMENTS)**

VALUE (MeV)	EVTS	DOCUMENT ID	TECN	CHG	COMMENT
≈ 1560 OUR ESTIMATE					
1553±7	121	DIONISI	78B	HBC	$K^-p \rightarrow (Y\pi)K\bar{K}$
1572±4	40	LOCKMAN	78	SPEC	$pp \rightarrow \Lambda\pi^+\pi^-X$

 **$\Sigma(1560)$ WIDTH
(PRODUCTION EXPERIMENTS)**

VALUE (MeV)	EVTS	DOCUMENT ID	TECN	CHG	COMMENT
79±30	121	DIONISI	78B	HBC	$K^-p \rightarrow (Y\pi)K\bar{K}$
15±6	40	¹ LOCKMAN	78	SPEC	$pp \rightarrow \Lambda\pi^+\pi^-X$

 **$\Sigma(1560)$ DECAY MODES
(PRODUCTION EXPERIMENTS)**

Mode	Fraction (Γ_i/Γ)
Γ_1 $\Lambda\pi$	seen
Γ_2 $\Sigma\pi$	

 **$\Sigma(1560)$ BRANCHING RATIOS
(PRODUCTION EXPERIMENTS)**

$\Gamma(\Sigma\pi)/[\Gamma(\Lambda\pi) + \Gamma(\Sigma\pi)]$	$\Gamma_2/(\Gamma_1+\Gamma_2)$			
VALUE	DOCUMENT ID	TECN	CHG	COMMENT
0.35±0.12	DIONISI	78B	HBC	$K^-p \rightarrow (Y\pi)K\bar{K}$

$\Gamma(\Lambda\pi)/\Gamma_{\text{total}}$	Γ_1/Γ			
VALUE	DOCUMENT ID	TECN	CHG	COMMENT
seen	LOCKMAN	78	SPEC	$pp \rightarrow \Lambda\pi^+\pi^-X$

 **$\Sigma(1560)$ FOOTNOTES
(PRODUCTION EXPERIMENTS)**

¹ The width observed by LOCKMAN 78 is consistent with experimental resolution.

 **$\Sigma(1560)$ REFERENCES
(PRODUCTION EXPERIMENTS)**

MEADOWS	80	Toronto Conf. 283	B.T. Meadows	(CINC)
DIONISI	78B	PL 78B 154	C. Dionisi, R. Armenteros, J. Diaz	(CERN, AMST+)
LOCKMAN	78	Saclay DPHPE 78-01	W. Lockman <i>et al.</i>	(UCLA, SACL)
CARROLL	76	PRL 37 806	A.S. Carroll <i>et al.</i>	(BNL) I

 $\Sigma(1580) D_{13}$

$$I(J^P) = 1(\frac{3}{2}^-) \text{ Status: } *$$

OMITTED FROM SUMMARY TABLE

Seen in the isospin-1 $\bar{K}N$ cross section at BNL (LI 73, CARROLL 76) and in a partial-wave analysis of $K^-p \rightarrow \Lambda\pi^0$ for c.m. energies 1560–1600 MeV by LITCHFIELD 74. LITCHFIELD 74 finds $J^P = 3/2^-$. Not seen by ENGLER 78 or by CAMERON 78C (with larger statistics in $K_L^0 p \rightarrow \Lambda\pi^+$ and $\Sigma^0\pi^+$).

Neither OLMSTED 04 (in $K^-p \rightarrow \Lambda\pi^0$) nor PRAKHOV 04 (in $K^-p \rightarrow \Lambda\pi^0\pi^0$) see any evidence for this state.

 $\Sigma(1580)$ MASS

VALUE (MeV)	DOCUMENT ID	TECN	COMMENT
≈ 1580 OUR ESTIMATE			
1583±4	¹ CARROLL	76	DPWA Isospin-1 total σ
1582±4	² LITCHFIELD	74	DPWA $K^-p \rightarrow \Lambda\pi^0$

 $\Sigma(1580)$ WIDTH

VALUE (MeV)	DOCUMENT ID	TECN	COMMENT
15	¹ CARROLL	76	DPWA Isospin-1 total σ
11±4	² LITCHFIELD	74	DPWA $K^-p \rightarrow \Lambda\pi^0$

 $\Sigma(1580)$ DECAY MODES

Mode
Γ_1 $N\bar{K}$
Γ_2 $\Lambda\pi$
Γ_3 $\Sigma\pi$

 $\Sigma(1580)$ BRANCHING RATIOS

See "Sign conventions for resonance couplings" in the Note on Λ and Σ Resonances.

$\Gamma(N\bar{K})/\Gamma_{\text{total}}$	Γ_1/Γ			
VALUE	DOCUMENT ID	TECN	COMMENT	
+0.03±0.01	² LITCHFIELD	74	DPWA	$\bar{K}N$ multichannel

$(\Gamma_1\Gamma_f)^{1/2}/\Gamma_{\text{total}}$ in $N\bar{K} \rightarrow \Sigma(1580) \rightarrow \Lambda\pi$	$(\Gamma_1\Gamma_2)^{1/2}/\Gamma$			
VALUE	DOCUMENT ID	TECN	COMMENT	
not seen	CAMERON	78C	HBC	$K_L^0 p \rightarrow \Lambda\pi^+$
not seen	ENGLER	78	HBC	$K_L^0 p \rightarrow \Lambda\pi^+$
+0.10±0.02	² LITCHFIELD	74	DPWA	$K^-p \rightarrow \Lambda\pi^0$

$(\Gamma_1\Gamma_f)^{1/2}/\Gamma_{\text{total}}$ in $N\bar{K} \rightarrow \Sigma(1580) \rightarrow \Sigma\pi$	$(\Gamma_1\Gamma_3)^{1/2}/\Gamma$			
VALUE	DOCUMENT ID	TECN	COMMENT	
not seen	CAMERON	78C	HBC	$K_L^0 p \rightarrow \Sigma^0\pi^+$
not seen	ENGLER	78	HBC	$K_L^0 p \rightarrow \Sigma^0\pi^+$
+0.03±0.04	² LITCHFIELD	74	DPWA	$\bar{K}N$ multichannel

 $\Sigma(1580)$ FOOTNOTES

¹ CARROLL 76 sees a total-cross-section bump with $(J+1/2) \Gamma_{\text{el}} / \Gamma_{\text{total}} = 0.06$.

² The main effect observed by LITCHFIELD 74 is in the $\Lambda\pi$ final state; the $\bar{K}N$ and $\Sigma\pi$ couplings are estimated from a multichannel fit including total-cross-section data of LI 73.

 $\Sigma(1580)$ REFERENCES

OLMSTED	04	PL B588 29	J. Olmsted <i>et al.</i>	(BNL Crystal Ball Collab.)
PRAKHOV	04	PR C69 042202R	S. Prakhov <i>et al.</i>	(BNL Crystal Ball Collab.)
CAMERON	78C	NP B132 189	W. Cameron <i>et al.</i>	(BGNA, EDIN, GLAS+)
ENGLER	78	PR D18 3061	A. Engler <i>et al.</i>	(CMU, ANL)
CARROLL	76	PRL 37 806	A.S. Carroll <i>et al.</i>	(BNL) I
LITCHFIELD	74	PL 51B 509	P.J. Litchfield	(CERN) IJP
LI	73	Purdue Conf. 283	K.K. Li	(BNL) I

See key on page 373

Baryon Particle Listings

 $\Sigma(1620)$, $\Sigma(1620)$ Production Experiments $\Sigma(1620) S_{11}$

$$I(J^P) = 1(\frac{1}{2}^-) \text{ Status: } **$$

OMITTED FROM SUMMARY TABLE

The S_{11} state at 1697 MeV reported by VANHORN 75 is tentatively listed under the $\Sigma(1750)$. CARROLL 76 sees two bumps in the isospin-1 total cross section near this mass.

Production experiments are listed separately in the next entry.

 $\Sigma(1620)$ MASS

VALUE (MeV)	DOCUMENT ID	TECN	COMMENT
≈ 1620 OUR ESTIMATE			
1600 \pm 6	1 MORRIS	78 DPWA	$K^- n \rightarrow \Lambda \pi^-$
1608 \pm 5	2 CARROLL	76 DPWA	Isospin-1 total σ
1633 \pm 10	3 CARROLL	76 DPWA	Isospin-1 total σ
1630 \pm 10	LANGBEIN	72 IPWA	$\bar{K} N$ multichannel
1620	KIM	71 DPWA	K-matrix analysis

 $\Sigma(1620)$ WIDTH

VALUE (MeV)	DOCUMENT ID	TECN	COMMENT
87 \pm 19	1 MORRIS	78 DPWA	$K^- n \rightarrow \Lambda \pi^-$
15	2 CARROLL	76 DPWA	Isospin-1 total σ
10	3 CARROLL	76 DPWA	Isospin-1 total σ
65 \pm 20	LANGBEIN	72 IPWA	$\bar{K} N$ multichannel
40	KIM	71 DPWA	K-matrix analysis

 $\Sigma(1620)$ DECAY MODES

Mode	Γ
Γ_1 $N\bar{K}$	
Γ_2 $\Lambda\pi$	
Γ_3 $\Sigma\pi$	

 $\Sigma(1620)$ BRANCHING RATIOS

$\Gamma(N\bar{K})/\Gamma_{\text{total}}$	DOCUMENT ID	TECN	COMMENT	Γ_1/Γ
0.22 \pm 0.02	LANGBEIN	72 IPWA	$\bar{K} N$ multichannel	
0.05	KIM	71 DPWA	K-matrix analysis	

$(\Gamma_1\Gamma_2)^{1/2}/\Gamma_{\text{total}}$ in $N\bar{K} \rightarrow \Sigma(1620) \rightarrow \Lambda\pi$	DOCUMENT ID	TECN	COMMENT	$(\Gamma_1\Gamma_2)^{1/2}/\Gamma$
0.12 \pm 0.02	1 MORRIS	78 DPWA	$K^- n \rightarrow \Lambda \pi^-$	
not seen	BAILLON	75 IPWA	$\bar{K} N \rightarrow \Lambda \pi$	
0.15	KIM	71 DPWA	K-matrix analysis	

$(\Gamma_1\Gamma_3)^{1/2}/\Gamma_{\text{total}}$ in $N\bar{K} \rightarrow \Sigma(1620) \rightarrow \Sigma\pi$	DOCUMENT ID	TECN	COMMENT	$(\Gamma_1\Gamma_3)^{1/2}/\Gamma$
not seen	HEPP	76B DPWA	$K^- N \rightarrow \Sigma\pi$	
0.40 \pm 0.06	LANGBEIN	72 IPWA	$\bar{K} N$ multichannel	
0.08	KIM	71 DPWA	K-matrix analysis	

 $\Sigma(1620)$ FOOTNOTES

- ¹ MORRIS 78 obtains an equally good fit without including this resonance.
² Total cross-section bump with $(J+1/2)$ $\Gamma_{\text{el}}/\Gamma_{\text{total}}$ is 0.06 seen by CARROLL 76.
³ Total cross-section bump with $(J+1/2)$ $\Gamma_{\text{el}}/\Gamma_{\text{total}}$ is 0.04 seen by CARROLL 76.

 $\Sigma(1620)$ REFERENCES

MORRIS	78	PR D17 55	W.A. Morris et al.	(FSU) IJP
CARROLL	76	PRL 37 806	A.S. Carroll et al.	(BNL) I
HEPP	76B	PL 65B 487	V. Hepp et al.	(CERN, HEIDH, MPIM) IJP
BAILLON	75	NP B94 39	P.H. Baillon, P.J. Litchfield	(CERN, RHEL) IJP
VANHORN	75	NP B87 145	A.J. van Horn	(LBL) IJP
Also		NP B87 157	A.J. van Horn	(LBL) IJP
LANGBEIN	72	NP B47 477	W. Langbein, F. Wagner	(MPIM) IJP
KIM	71	PRL 27 356	J.K. Kim	(HARV) IJP
Also		Duke Conf. 161	J.K. Kim	(HARV) IJP
Hyperon Resonances, 1970				

 $\Sigma(1620)$ Production Experiments

$$I(J^P) = 1(?^?)$$

OMITTED FROM SUMMARY TABLE

Formation experiments are listed separately in the previous entry.

The results of CRENNELL 69B at 3.9 GeV/c are not confirmed by SABRE 70 at 3.0 GeV/c. However, at 4.5 GeV/c, AMMANN 70 sees a peak at 1642 MeV which on the basis of branching ratios they do not associate with the $\Sigma(1670)$. See MILLER 70 for a review of these conflicts.

 $\Sigma(1620)$ MASS (PRODUCTION EXPERIMENTS)

VALUE (MeV)	EVTS	DOCUMENT ID	TECN	CHG	COMMENT
≈ 1620 OUR ESTIMATE					
1642 \pm 12		AMMANN	70 DBC		$K^- N$ 4.5 GeV/c
1618 \pm 3	20	BLUMENFELD	69 HBC	+	$K_L^0 p$
1619 \pm 8		CRENNELL	69B DBC	±	$K^- N \rightarrow \Lambda \pi \pi$
••• We do not use the following data for averages, fits, limits, etc. •••					
1616 \pm 8		CRENNELL	68 DBC	±	See CRENNELL 69B

 $\Sigma(1620)$ WIDTH (PRODUCTION EXPERIMENTS)

VALUE (MeV)	EVTS	DOCUMENT ID	TECN	CHG	COMMENT
55 \pm 24		AMMANN	70 DBC		$K^- N$ 4.5 GeV/c
30 \pm 10	20	BLUMENFELD	69 HBC	+	
72 \pm $\frac{22}{15}$		CRENNELL	69B DBC	±	
••• We do not use the following data for averages, fits, limits, etc. •••					
66 \pm 16		CRENNELL	68 DBC	±	See CRENNELL 69B

 $\Sigma(1620)$ DECAY MODES (PRODUCTION EXPERIMENTS)

Mode	Γ
Γ_1 $N\bar{K}$	
Γ_2 $\Lambda\pi$	
Γ_3 $\Sigma\pi$	
Γ_4 $\Lambda\pi\pi$	
Γ_5 $\Sigma(1385)\pi$	
Γ_6 $\Lambda(1405)\pi$	

 $\Sigma(1620)$ BRANCHING RATIOS (PRODUCTION EXPERIMENTS)

$\Gamma(\Lambda\pi\pi)/\Gamma(\Lambda\pi)$	DOCUMENT ID	TECN	CHG	Γ_4/Γ_2
~ 2.5	BLUMENFELD	69 HBC	+	

$\Gamma(N\bar{K})/\Gamma(\Lambda\pi)$	DOCUMENT ID	TECN	CHG	COMMENT	Γ_1/Γ_2
0.4 \pm 0.4	AMMANN	70 DBC		$K^- p$ 4.5 GeV/c	
0.0 \pm 0.1	CRENNELL	68 DBC	+	See CRENNELL 69B	

$\Gamma(\Lambda\pi)/\Gamma_{\text{total}}$	DOCUMENT ID	TECN	CHG	Γ_2/Γ
large	CRENNELL	68 DBC	±	

$\Gamma(\Sigma(1385)\pi)/\Gamma(\Lambda\pi)$	DOCUMENT ID	TECN	CHG	COMMENT	Γ_5/Γ_2
< 0.3	AMMANN	70 DBC		$K^- p$ 4.5 GeV/c	
0.2 \pm 0.1	CRENNELL	68 DBC	±		

$\Gamma(\Sigma\pi)/\Gamma(\Lambda\pi)$	DOCUMENT ID	TECN	COMMENT	Γ_3/Γ_2
< 1.1	AMMANN	70 DBC	$K^- N$ 4.5 GeV/c	

$\Gamma(\Lambda(1405)\pi)/\Gamma(\Lambda\pi)$	DOCUMENT ID	TECN	COMMENT	Γ_6/Γ_2
0.7 \pm 0.4	AMMANN	70 DBC	$K^- p$ 4.5 GeV/c	

Baryon Particle Listings

 $\Sigma(1620)$ Production Experiments, $\Sigma(1660)$, $\Sigma(1670)$ $\Sigma(1620)$ REFERENCES
(PRODUCTION EXPERIMENTS)

NAME	REF	DOC ID	TECN	COMMENT
AMMANN	70	PRL 24 327		A.C. Ammann <i>et al.</i> (PURD, IND)
Also		PR D7 1345		A.C. Ammann <i>et al.</i> (PURD, IUPU)
MILLER	70	Duke Conf. 229		D.H. Miller (PURD)
Hyperon Resonances, 1970				
SABRE	70	NP B16 201		R. Barloutaud <i>et al.</i> (SABRE Collab.)
BLUMENFELD	69	PL 29B 58		B.J. Blumenfeld, G.R. Kalbfleisch (BNL)1
CRENNELL	69B	Lund Paper 183		D.J. Crennell <i>et al.</i> (BNL, CUNY)1
Results are quoted in LEVI-SETTI 69C.				
Also		Lund Conf.		R. Levi-Setti (EFI)
CRENNELL	68	PRL 21 648		D.J. Crennell <i>et al.</i> (BNL, CUNY)1

 $\Sigma(1660) P_{11}$

$$I(J^P) = 1(\frac{1}{2}^+) \text{ Status: } ***$$

For results published before 1974 (they are now obsolete), see our 1982 edition Physics Letters **111B** 1 (1982).

 $\Sigma(1660)$ MASS

VALUE (MeV)	DOCUMENT ID	TECN	COMMENT
1630 to 1690 (≈ 1660) OUR ESTIMATE			
1665.1 \pm 11.2	1 KOISO	85	DPWA $K^-p \rightarrow \Sigma\pi$
1670 \pm 10	GOPAL	80	DPWA $\bar{K}N \rightarrow \bar{K}N$
1679 \pm 10	ALSTON-...	78	DPWA $\bar{K}N \rightarrow \bar{K}N$
1676 \pm 15	GOPAL	77	DPWA $\bar{K}N$ multichannel
1668 \pm 25	VANHORN	75	DPWA $K^-p \rightarrow \Lambda\pi^0$
1670 \pm 20	KANE	74	DPWA $K^-p \rightarrow \Sigma\pi$
••• We do not use the following data for averages, fits, limits, etc. •••			
1565 or 1597	2 MARTIN	77	DPWA $\bar{K}N$ multichannel
1660 \pm 30	3 BAILLON	75	IPWA $\bar{K}N \rightarrow \Lambda\pi$
1671 \pm 2	4 PONTE	75	DPWA $K^-p \rightarrow \Lambda\pi^0$

 $\Sigma(1660)$ WIDTH

VALUE (MeV)	DOCUMENT ID	TECN	COMMENT
40 to 200 (≈ 100) OUR ESTIMATE			
81.5 \pm 22.2	1 KOISO	85	DPWA $K^-p \rightarrow \Sigma\pi$
152 \pm 20	GOPAL	80	DPWA $\bar{K}N \rightarrow \bar{K}N$
38 \pm 10	ALSTON-...	78	DPWA $\bar{K}N \rightarrow \bar{K}N$
120 \pm 20	GOPAL	77	DPWA $\bar{K}N$ multichannel
230 $+165$ -60	VANHORN	75	DPWA $K^-p \rightarrow \Lambda\pi^0$
250 \pm 110	KANE	74	DPWA $K^-p \rightarrow \Sigma\pi$
••• We do not use the following data for averages, fits, limits, etc. •••			
202 or 217	2 MARTIN	77	DPWA $\bar{K}N$ multichannel
80 \pm 40	3 BAILLON	75	IPWA $\bar{K}N \rightarrow \Lambda\pi$
81 \pm 10	4 PONTE	75	DPWA $K^-p \rightarrow \Lambda\pi^0$

 $\Sigma(1660)$ DECAY MODES

Mode	Fraction (Γ_i/Γ)
Γ_1 $N\bar{K}$	10–30 %
Γ_2 $\Lambda\pi$	seen
Γ_3 $\Sigma\pi$	seen

 $\Sigma(1660)$ BRANCHING RATIOS

See "Sign conventions for resonance couplings" in the Note on Λ and Σ Resonances.

$\Gamma(N\bar{K})/\Gamma_{\text{total}}$	DOCUMENT ID	TECN	COMMENT	Γ_1/Γ
0.1 to 0.3 OUR ESTIMATE				
0.12 \pm 0.03	GOPAL	80	DPWA $\bar{K}N \rightarrow \bar{K}N$	
0.10 \pm 0.05	ALSTON-...	78	DPWA $\bar{K}N \rightarrow \bar{K}N$	
••• We do not use the following data for averages, fits, limits, etc. •••				
< 0.04	GOPAL	77	DPWA See GOPAL 80	
0.27 or 0.29	2 MARTIN	77	DPWA $\bar{K}N$ multichannel	

$(\Gamma_1\Gamma_2)^{1/2}/\Gamma_{\text{total}}$ in $N\bar{K} \rightarrow \Sigma(1660) \rightarrow \Lambda\pi$	DOCUMENT ID	TECN	COMMENT	$(\Gamma_1\Gamma_2)^{1/2}/\Gamma$
0.1 to 0.3 OUR ESTIMATE				
< 0.04	GOPAL	77	DPWA $\bar{K}N$ multichannel	
0.12 $+0.12$ -0.04	VANHORN	75	DPWA $K^-p \rightarrow \Lambda\pi^0$	
••• We do not use the following data for averages, fits, limits, etc. •••				
– 0.10 or – 0.11	2 MARTIN	77	DPWA $\bar{K}N$ multichannel	
– 0.04 \pm 0.02	3 BAILLON	75	IPWA $\bar{K}N \rightarrow \Lambda\pi$	
+ 0.16 \pm 0.01	4 PONTE	75	DPWA $K^-p \rightarrow \Lambda\pi^0$	

$(\Gamma_1\Gamma_2)^{1/2}/\Gamma_{\text{total}}$ in $N\bar{K} \rightarrow \Sigma(1660) \rightarrow \Sigma\pi$	DOCUMENT ID	TECN	COMMENT	$(\Gamma_1\Gamma_3)^{1/2}/\Gamma$
– 0.13 \pm 0.04	1 KOISO	85	DPWA $K^-p \rightarrow \Sigma\pi$	
– 0.16 \pm 0.03	GOPAL	77	DPWA $\bar{K}N$ multichannel	
– 0.11 \pm 0.01	KANE	74	DPWA $K^-p \rightarrow \Sigma\pi$	
••• We do not use the following data for averages, fits, limits, etc. •••				
– 0.34 or – 0.37	2 MARTIN	77	DPWA $\bar{K}N$ multichannel	
not seen	HEPP	76B	DPWA $K^-N \rightarrow \Sigma\pi$	

 $\Sigma(1660)$ FOOTNOTES

- The evidence of KOISO 85 is weak.
- The two MARTIN 77 values are from a T-matrix pole and from a Breit-Wigner fit.
- From solution 1 of BAILLON 75; not present in solution 2.
- From solution 2 of PONTE 75; not present in solution 1.

 $\Sigma(1660)$ REFERENCES

KOISO	85	NP A433 619	H. Koiso <i>et al.</i>	(TOKY, MASA)
PDG	82	PL 111B 1	M. Roos <i>et al.</i>	(HELSE, CIT, CERN)
GOPAL	80	Toronto Conf. 159	G.P. Gopal	(RHEL) IJP
ALSTON-...	78	PR D18 182	M. Alston-Garnjost <i>et al.</i>	(LBL, MTHO+) IJP
Also		PRL 38 1007	M. Alston-Garnjost <i>et al.</i>	(LBL, MTHO+) IJP
GOPAL	77	NP B119 352	G.P. Gopal <i>et al.</i>	(LOIC, RHEL) IJP
MARTIN	77	NP B127 349	B.R. Martin, M.K. Pidcock, R.G. Moorhouse	(LOUC+) IJP
Also		NP B126 266	B.R. Martin, M.K. Pidcock	(LOUC) IJP
Also		NP B126 285	B.R. Martin, M.K. Pidcock	(LOUC) IJP
HEPP	76B	PL 65B 487	V. Hepp <i>et al.</i>	(CERN, HEIDH, MPIM) IJP
BAILLON	75	NP B94 39	P.H. Baillon, P.J. Lichfield	(CERN, RHEL) IJP
PONTE	75	NP D12 2597	R.A. Ponte <i>et al.</i>	(MASA, TENN, UCR) IJP
VANHORN	75	NP B87 145	A.J. van Horn	(LBL) IJP
Also		NP B87 157	A.J. van Horn	(LBL) IJP
KANE	74	LBL-2452	D.F. Kane	(LBL) IJP

THE $\Sigma(1670)$ REGION

Production experiments: The measured $\Sigma\pi/\Sigma\pi\pi$ branching ratio for the $\Sigma(1670)$ produced in the reaction $K^-p \rightarrow \pi^-\Sigma(1670)^+$ is strongly dependent on momentum transfer. This was first discovered by EBERHARD 69, who suggested that there exist two Σ resonances with the same mass and quantum numbers: one with a large $\Sigma\pi\pi$ (mainly $\Lambda(1405)\pi$) branching fraction produced peripherally, and the other with a large $\Sigma\pi$ branching fraction produced at larger angles. The experimental results have been confirmed by AGUILAR-BENITEZ 70, ASPELL 74, ESTES 74, and TIMMERMANS 76. If, in fact, there are two resonances, the most likely quantum numbers for both the $\Sigma\pi$ and the $\Lambda(1405)\pi$ states are D_{13} . There is also possibly a third Σ in this region, the $\Sigma(1690)$ in the Listings, the main evidence for which is a large $\Lambda\pi/\Sigma\pi$ branching ratio. These topics have been reviewed by EBERHARD 73 and by MILLER 70.

Formation experiments: Two states are also observed near this mass in formation experiments. One of these, the $\Sigma(1670)D_{13}$, has the same quantum numbers as those observed in production and has a large $\Sigma\pi/\Sigma\pi\pi$ branching ratio; it may well be the $\Sigma(1670)$ produced at larger angles (see TIMMERMANS 76). The other state, the $\Sigma(1660)P_{11}$, has different quantum numbers, its $\Sigma\pi/\Sigma\pi\pi$ branching ratio is unknown, and its relation to the produced $\Sigma(1670)$ states is obscure.

See key on page 373

Baryon Particle Listings

$\Sigma(1670)$

$\Sigma(1670) D_{13}$

$$I(J^P) = 1(\frac{3}{2}^-) \text{ Status: } ****$$

For most results published before 1974 (they are now obsolete), see our 1982 edition Physics Letters **111B** 1 (1982).

Results from production experiments are listed separately in the next entry.

$\Sigma(1670)$ MASS

VALUE (MeV)	DOCUMENT ID	TECN	COMMENT
1665 to 1685 (≈ 1670) OUR ESTIMATE			
1665.1 \pm 4.1	KOISO 85	DPWA	$K^- p \rightarrow \Sigma \pi$
1682 \pm 5	GOPAL 80	DPWA	$\bar{K} N \rightarrow \bar{K} N$
1679 \pm 10	ALSTON-... 78	DPWA	$\bar{K} N \rightarrow \bar{K} N$
1670 \pm 5	GOPAL 77	DPWA	$\bar{K} N$ multichannel
1670 \pm 6	HEPP 76B	DPWA	$K^- N \rightarrow \Sigma \pi$
1685 \pm 20	BAILLON 75	IPWA	$\bar{K} N \rightarrow \Lambda \pi$
1659 \pm $^{+12}_{-5}$	VANHORN 75	DPWA	$K^- p \rightarrow \Lambda \pi^0$
1670 \pm 2	KANE 74	DPWA	$K^- p \rightarrow \Sigma \pi$
••• We do not use the following data for averages, fits, limits, etc. •••			
1667 or 1668	¹ MARTIN 77	DPWA	$\bar{K} N$ multichannel
1650	DEBELLEFON 76	IPWA	$K^- p \rightarrow \Lambda \pi^0$
1671 \pm 3	PONTE 75	DPWA	$K^- p \rightarrow \Lambda \pi^0$ (sol. 1)
1655 \pm 2	PONTE 75	DPWA	$K^- p \rightarrow \Lambda \pi^0$ (sol. 2)

$\Sigma(1670)$ WIDTH

VALUE (MeV)	DOCUMENT ID	TECN	COMMENT
40 to 80 (≈ 60) OUR ESTIMATE			
65.0 \pm 7.3	KOISO 85	DPWA	$K^- p \rightarrow \Sigma \pi$
79 \pm 10	GOPAL 80	DPWA	$\bar{K} N \rightarrow \bar{K} N$
56 \pm 20	ALSTON-... 78	DPWA	$\bar{K} N \rightarrow \bar{K} N$
50 \pm 5	GOPAL 77	DPWA	$\bar{K} N$ multichannel
56 \pm 3	HEPP 76B	DPWA	$K^- N \rightarrow \Sigma \pi$
85 \pm 25	BAILLON 75	IPWA	$\bar{K} N \rightarrow \Lambda \pi$
32 \pm 11	VANHORN 75	DPWA	$K^- p \rightarrow \Lambda \pi^0$
79 \pm 6	KANE 74	DPWA	$K^- p \rightarrow \Sigma \pi$
••• We do not use the following data for averages, fits, limits, etc. •••			
46 or 46	¹ MARTIN 77	DPWA	$\bar{K} N$ multichannel
80	DEBELLEFON 76	IPWA	$K^- p \rightarrow \Lambda \pi^0$
44 \pm 11	PONTE 75	DPWA	$K^- p \rightarrow \Lambda \pi^0$ (sol. 1)
76 \pm 5	PONTE 75	DPWA	$K^- p \rightarrow \Lambda \pi^0$ (sol. 2)

$\Sigma(1670)$ DECAY MODES

Mode	Fraction (Γ_i/Γ)
Γ_1 $N\bar{K}$	7-13 %
Γ_2 $\Lambda\pi$	5-15 %
Γ_3 $\Sigma\pi$	30-60 %
Γ_4 $\Lambda\pi\pi$	
Γ_5 $\Sigma\pi\pi$	
Γ_6 $\Sigma(1385)\pi$	
Γ_7 $\Sigma(1385)\pi, S$ -wave	
Γ_8 $\Lambda(1405)\pi$	
Γ_9 $\Lambda(1520)\pi$	

The above branching fractions are our estimates, not fits or averages.

$\Sigma(1670)$ BRANCHING RATIOS

See "Sign conventions for resonance couplings" in the Note on Λ and Σ Resonances.

$\Gamma(N\bar{K})/\Gamma_{total}$	DOCUMENT ID	TECN	COMMENT	Γ_1/Γ
0.07 to 0.13 OUR ESTIMATE				
0.10 \pm 0.03	GOPAL 80	DPWA	$\bar{K} N \rightarrow \bar{K} N$	
0.11 \pm 0.03	ALSTON-... 78	DPWA	$\bar{K} N \rightarrow \bar{K} N$	
••• We do not use the following data for averages, fits, limits, etc. •••				
0.08 \pm 0.03	GOPAL 77	DPWA	See GOPAL 80	
0.07 or 0.07	¹ MARTIN 77	DPWA	$\bar{K} N$ multichannel	
$(\Gamma_1\Gamma_f)^{1/2}/\Gamma_{total}$ in $N\bar{K} \rightarrow \Sigma(1670) \rightarrow \Lambda\pi$				
VALUE	DOCUMENT ID	TECN	COMMENT	$(\Gamma_1\Gamma_2)^{1/2}/\Gamma$
0.17 \pm 0.03	² MORRIS 78	DPWA	$K^- n \rightarrow \Lambda \pi^-$	
0.13 \pm 0.02	² MORRIS 78	DPWA	$K^- n \rightarrow \Lambda \pi^-$	
+0.10 \pm 0.02	GOPAL 77	DPWA	$\bar{K} N$ multichannel	
+0.06 \pm 0.02	BAILLON 75	IPWA	$\bar{K} N \rightarrow \Lambda \pi$	
+0.09 \pm 0.02	VANHORN 75	DPWA	$K^- p \rightarrow \Lambda \pi^0$	
+0.018 \pm 0.060	DEVENISH 74B		Fixed-t dispersion rel.	

••• We do not use the following data for averages, fits, limits, etc. •••

+0.08 or +0.08	¹ MARTIN 77	DPWA	$\bar{K} N$ multichannel
+0.05	DEBELLEFON 76	IPWA	$K^- p \rightarrow \Lambda \pi^0$
0.08 \pm 0.01	PONTE 75	DPWA	$K^- p \rightarrow \Lambda \pi^0$ (sol. 1)
0.17 \pm 0.01	PONTE 75	DPWA	$K^- p \rightarrow \Lambda \pi^0$ (sol. 2)

$(\Gamma_1\Gamma_f)^{1/2}/\Gamma_{total}$ in $N\bar{K} \rightarrow \Sigma(1670) \rightarrow \Sigma\pi$	DOCUMENT ID	TECN	COMMENT	$(\Gamma_1\Gamma_3)^{1/2}/\Gamma$
+0.20 \pm 0.02	KOISO 85	DPWA	$K^- p \rightarrow \Sigma \pi$	
+0.21 \pm 0.02	GOPAL 77	DPWA	$\bar{K} N$ multichannel	
+0.20 \pm 0.01	HEPP 76B	DPWA	$K^- N \rightarrow \Sigma \pi$	
+0.21 \pm 0.03	KANE 74	DPWA	$K^- p \rightarrow \Sigma \pi$	
••• We do not use the following data for averages, fits, limits, etc. •••				
+0.18 or +0.17	¹ MARTIN 77	DPWA	$\bar{K} N$ multichannel	

$\Gamma(\Lambda\pi\pi)/\Gamma_{total}$	DOCUMENT ID	TECN	COMMENT	Γ_4/Γ
<0.11	ARMENTEROS68E	HBC	$K^- p (\Gamma_1=0.09)$	

$(\Gamma_1\Gamma_f)^{1/2}/\Gamma_{total}$ in $N\bar{K} \rightarrow \Sigma(1670) \rightarrow \Sigma(1385)\pi, S$ -wave	DOCUMENT ID	TECN	COMMENT	$(\Gamma_1\Gamma_7)^{1/2}/\Gamma$
+0.11 \pm 0.03	PREVOST 74	DPWA	$K^- N \rightarrow \Sigma(1385)\pi$	
••• We do not use the following data for averages, fits, limits, etc. •••				
0.17 \pm 0.02	³ SIMS 68	DBC	$K^- N \rightarrow \Lambda\pi\pi$	

$\Gamma(\Sigma\pi\pi)/\Gamma_{total}$	DOCUMENT ID	TECN	COMMENT	Γ_5/Γ
<0.14	⁴ ARMENTEROS68E	HBC	$K^- p, K^- d (\Gamma_1=0.09)$	

$\Gamma(\Lambda(1405)\pi)/\Gamma_{total}$	DOCUMENT ID	TECN	COMMENT	Γ_8/Γ
<0.06	ARMENTEROS68E	HBC	$K^- p, K^- d (\Gamma_1=0.09)$	

$\Gamma_i\Gamma_f/\Gamma_{total}^2$ in $N\bar{K} \rightarrow \Sigma(1670) \rightarrow \Lambda(1405)\pi$	DOCUMENT ID	TECN	COMMENT	$\Gamma_1\Gamma_8/\Gamma^2$
0.007 \pm 0.002	⁵ BRUCKER 70	DBC	$K^- N \rightarrow \Sigma\pi\pi$	
••• We do not use the following data for averages, fits, limits, etc. •••				
<0.03	BERLEY 69	HBC	$K^- p$ 0.6-0.82 GeV/c	

$\Gamma(\Lambda(1405)\pi)/\Gamma(\Sigma(1385)\pi)$	DOCUMENT ID	TECN	COMMENT	Γ_8/Γ_6
0.23 \pm 0.08	BRUCKER 70	DBC	$K^- N \rightarrow \Sigma\pi\pi$	

$(\Gamma_1\Gamma_f)^{1/2}/\Gamma_{total}$ in $N\bar{K} \rightarrow \Sigma(1670) \rightarrow \Lambda(1520)\pi$	DOCUMENT ID	TECN	COMMENT	$(\Gamma_1\Gamma_9)^{1/2}/\Gamma$
0.081 \pm 0.016	⁶ CAMERON 77	DPWA	P -wave decay	

$\Sigma(1670)$ FOOTNOTES

- The two MARTIN 77 values are from a T-matrix pole and from a Breit-Wigner fit.
- Results are with and without an S_{11} $\Sigma(1620)$ in the fit.
- SIMS 68 uses only cross-section data. Result used as upper limit only.
- Ratio only for $\Sigma\pi\pi$ system in $l = 1$, which cannot be $\Sigma(1385)$.
- Assuming the $\Lambda(1405)\pi$ cross-section bump is due only to $3/2^-$ resonance.
- The CAMERON 77 upper limit on F -wave decay is 0.03.

$\Sigma(1670)$ REFERENCES

KOISO 85	NP A433 619	H. Koiso et al.	(TOKY, MASA)
PDG 82	PL 111B 1	M. Roos et al.	(HELS, CIT, CERN)
GOPAL 80	Toronto Conf. 159	G.P. Gopal	(RHEL) IJP
ALSTON-... 78	PR D18 182	M. Alston-Garnjost et al.	(LBL, MTHO+) IJP
	Also	M. Alston-Garnjost et al.	(LBL, MTHO+) IJP
MORRIS 78	PR D17 55	W.A. Morris et al.	(FSU) IJP
CAMERON 77	NP B131 399	W. Cameron et al.	(RHEL, LOIC) IJP
GOPAL 77	NP B119 362	G.P. Gopal et al.	(LOIC, RHEL) IJP
MARTIN 77	NP B127 349	B.R. Martin, M.K. Pidcock, R.G. Moorhouse	(LOUC+) IJP
	Also	B.R. Martin, M.K. Pidcock	(LOUC) IJP
	Also	B.R. Martin, M.K. Pidcock	(LOUC) IJP
DEBELLEFON 76	NP B109 129	A. de Bellefon, A. Berthon	(CDF) IJP
HEPP 76B	PL 65B 487	V. Hepp et al.	(CERN, HEIDH, MFIM) IJP
BAILLON 75	NP B94 39	P.H. Baillon, P.J. Litchfield	(CERN, RHEL) IJP
PONTE 75	PR D12 2597	R.A. Ponte et al.	(MASA, TENN, UCR) IJP
VANHORN 75	NP B87 145	A.J. van Horn	(LBL) IJP
	Also	A.J. van Horn	(LBL) IJP
DEVENISH 74B	NP B81 330	R.C.E. Devenish, C.D. Froggatt, B.R. Martin	(DESY+) IJP
KANE 74	LBL-2452	D.F. Kane	(LBL) IJP
PREVOST 74	NP B69 246	J. Prevost et al.	(SACL, CERN, HEID)
BRUCKER 70	Duke Conf. 155	E.B. Brucker et al.	(FSU) I
	Hyperon Resonances, 1970		
	Berley 69	PL 30B 430	(BNL)
ARMENTEROS 68E	PL 28B 521	R. Armenteros et al.	(CERN, HEID, SACL) I
SIMS 68	PRL 21 1413	W.H. Sims et al.	(FSU, TUFTS, BRAN)

Baryon Particle Listings

 $\Sigma(1670)$ Bumps $\Sigma(1670)$ Bumps

$I(J^P) = 1(?)^2$

OMITTED FROM SUMMARY TABLE

Formation experiments are listed separately in the preceding entry.

Probably there are two states at the same mass with the same quantum numbers, one decaying to $\Sigma\pi$ and $\Lambda\pi$, the other to $\Lambda(1405)\pi$. See the note in front of the preceding entry.

 $\Sigma(1670)$ MASS
(PRODUCTION EXPERIMENTS)

VALUE (MeV)	EVTS	DOCUMENT ID	TECN	CHG	COMMENT
≈ 1670 OUR ESTIMATE					
1670 \pm 4		¹ CARROLL 76	DPWA		Isospin-1 total σ
1675 \pm 10		² HEPP 76	DBC	-	$K^- N$ 1.6-1.75 GeV/c
1665 \pm 1		APSELL 74	HBC		$K^- p$ 2.87 GeV/c
1688 \pm 2 or 1683 \pm 5	1.2k	BERTHON 74	HBC	0	Quasi-2-body σ
1670 \pm 6		AGUILAR-... 70B	HBC		$K^- p \rightarrow \Sigma\pi\pi$ 4 GeV
1668 \pm 10		AGUILAR-... 70B	HBC		$K^- p \rightarrow \Sigma 3\pi$ 4 GeV
1660 \pm 10		ALVAREZ 63	HBC	+	$K^- p$ 1.51 GeV/c
• • • We do not use the following data for averages, fits, limits, etc. • • •					
1668 \pm 10	150	³ FERRERSORIA 81	OMEG	-	$\pi^- p$ 9,12 GeV/c
1655 to 1677		TIMMERMANS76	HBC	+	$K^- p$ 4.2 GeV/c
1665 \pm 5		BUGG 68	CNTR		$K^- p$, d total σ
1661 \pm 9	70	PRIMER 68	HBC	+	See BARNES 69E
1685		ALEXANDER 62C	HBC	-0	$\pi^- p$ 2-2.2 GeV/c

 $\Sigma(1670)$ WIDTH
(PRODUCTION EXPERIMENTS)

VALUE (MeV)	EVTS	DOCUMENT ID	TECN	CHG	COMMENT
67.0 \pm 2.4		APSELL 74	HBC		$K^- p$ 2.87 GeV/c
110 \pm 12		AGUILAR-... 70B	HBC		$K^- p \rightarrow \Sigma\pi\pi$ 4 GeV
135 $\begin{smallmatrix} +40 \\ -30 \end{smallmatrix}$		AGUILAR-... 70B	HBC		$K^- p \rightarrow \Sigma 3\pi$ 4 GeV
40 \pm 10		ALVAREZ 63	HBC	+	
• • • We do not use the following data for averages, fits, limits, etc. • • •					
90 \pm 20	150	³ FERRERSORIA 81	OMEG	-	$\pi^- p$ 9,12 GeV/c
52		¹ CARROLL 76	DPWA		Isospin-1 total σ
48 to 63		TIMMERMANS76	HBC	+	$K^- p$ 4.2 GeV/c
30 \pm 15		BUGG 68	CNTR		
60 \pm 20	70	PRIMER 68	HBC	+	See BARNES 69E
45		ALEXANDER 62C	HBC	-0	

 $\Sigma(1670)$ DECAY MODES
(PRODUCTION EXPERIMENTS)

Mode	
Γ_1	$N\bar{K}$
Γ_2	$\Lambda\pi$
Γ_3	$\Sigma\pi$
Γ_4	$\Lambda\pi\pi$
Γ_5	$\Sigma\pi\pi$
Γ_6	$\Sigma(1385)\pi$
Γ_7	$\Lambda(1405)\pi$

 $\Sigma(1670)$ BRANCHING RATIOS
(PRODUCTION EXPERIMENTS)

$\Gamma(N\bar{K})/\Gamma(\Sigma\pi)$	Γ_1/Γ_3				
VALUE	EVTS	DOCUMENT ID	TECN	CHG	COMMENT
<0.03		TIMMERMANS76	HBC	+	$K^- p$ 4.2 GeV/c
<0.10		BERTHON 74	HBC	0	Quasi-2-body σ
<0.2		AGUILAR-... 70B	HBC		
<0.26		BARNES 69E	HBC	+	$K^- p$ 3.9-5 GeV/c
0.025		BUGG 68	CNTR	0	Assuming $J = 3/2$
<0.24	0	PRIMER 68	HBC	+	$K^- p$ 4.6-5 GeV/c
<0.6		LONDON 66	HBC	+	$K^- p$ 2.25 GeV/c
<0.19	0	ALVAREZ 63	HBC	+	$K^- p$ 1.15 GeV/c
≥ 0.5 ± 0.25		SMITH 63	HBC	-0	

 $\Gamma(\Lambda\pi)/\Gamma(\Sigma\pi)$

VALUE	EVTS	DOCUMENT ID	TECN	CHG	COMMENT	Γ_2/Γ_3
0.76 \pm 0.09		ESTES 74	HBC	0	$K^- p$ 2.1, 2.6 GeV/c	
0.45 \pm 0.15		BARNES 69E	HBC	+	$K^- p$ 3.9-5 GeV/c	
0.15 \pm 0.07		HUWE 69	HBC	+		
0.11 \pm 0.06	33	BUTTON-...	68	HBC	+	$K^- p$ 1.7 GeV/c
• • • We do not use the following data for averages, fits, limits, etc. • • •						
$\leq 0.45 \pm 0.07$		TIMMERMANS76	HBC	+	$K^- p$ 4.2 GeV/c	
0.55 \pm 0.11		BERTHON 74	HBC	0	Quasi-2-body σ	
0	0	PRIMER 68	HBC	+	See BARNES 69E	
<0.6		LONDON 66	HBC	+	$K^- p$ 2.25 GeV/c	
1.2	130	ALVAREZ 63	HBC	+	$K^- p$ 1.15 GeV/c	
1.2		SMITH 63	HBC	-0		

 $\Gamma(\Lambda\pi\pi)/\Gamma(\Sigma\pi)$

VALUE	EVTS	DOCUMENT ID	TECN	CHG	COMMENT	Γ_4/Γ_3
<0.6		LONDON 66	HBC	+	$K^- p$ 2.25 GeV/c	
0.56	90	ALVAREZ 63	HBC	+	$K^- p$ 1.15 GeV/c	
0.17		SMITH 63	HBC	-0		

 $\Gamma(\Sigma\pi\pi)/\Gamma(\Sigma\pi)$

VALUE	EVTS	DOCUMENT ID	TECN	CHG	COMMENT	Γ_5/Γ_3
largest at small angles		ESTES 74	HBC	0	$K^- p$ 2.1, 2.6 GeV/c	
• • • We do not use the following data for averages, fits, limits, etc. • • •						
<0.2	²	HEPP 76	DBC	-	$K^- N$ 1.6-1.75 GeV/c	
0.56	180	ALVAREZ 63	HBC	+	$K^- p$ 1.15 GeV/c	

 $\Gamma(\Lambda(1405)\pi)/\Gamma(\Sigma\pi)$

VALUE	EVTS	DOCUMENT ID	TECN	CHG	COMMENT	Γ_7/Γ_3
1.8 \pm 0.3 to 0.02 \pm 0.07		^{3,4} TIMMERMANS76	HBC	+	$K^- p$ 4.2 GeV/c	
largest at small angles		ESTES 74	HBC	\pm	$K^- p$ 2.1, 2.6 GeV/c	
3.0 \pm 1.6	50	LONDON 66	HBC	+	$K^- p$ 2.25 GeV/c	
• • • We do not use the following data for averages, fits, limits, etc. • • •						
0.58 \pm 0.20	17	PRIMER 68	HBC	+	See BARNES 69E	

 $\Gamma(\Sigma\pi)/\Gamma(\Sigma\pi\pi)$

VALUE	EVTS	DOCUMENT ID	TECN	CHG	COMMENT	Γ_3/Γ_5
varies with prod. angle		⁵ APSELL 74	HBC	+	$K^- p$ 2.87 GeV/c	
1.39 \pm 0.16		BERTHON 74	HBC	0	Quasi-2-body σ	
2.5 to 0.24		⁴ EBERHARD 69	HBC		$K^- p$ 2.6 GeV/c	
<0.4		BIRMINGHAM 66	HBC	+	$K^- p$ 3.5 GeV/c	
0.30 \pm 0.15		LONDON 66	HBC	+	$K^- p$ 2.25 GeV/c	

 $\Gamma(\Lambda(1405)\pi)/\Gamma(\Sigma\pi\pi)$

VALUE	EVTS	DOCUMENT ID	TECN	CHG	COMMENT	Γ_7/Γ_5
0.97 \pm 0.08		TIMMERMANS76	HBC		$K^- p$ 4.2 GeV/c	
1.00 \pm 0.02		APSELL 74	HBC		$K^- p$ 2.87 GeV/c	
0.90 $\begin{smallmatrix} +0.10 \\ -0.16 \end{smallmatrix}$		EBERHARD 65	HBC	+	$K^- p$ 2.45 GeV/c	

 $\Gamma(\Lambda(1405)\pi)/\Gamma(\Sigma(1385)\pi)$

VALUE	EVTS	DOCUMENT ID	TECN	CHG	COMMENT	Γ_7/Γ_6
<0.8		EBERHARD 65	HBC	+	$K^- p$ 2.45 GeV/c	

 $\Gamma(\Lambda\pi\pi)/\Gamma(\Sigma\pi\pi)$

VALUE	EVTS	DOCUMENT ID	TECN	CHG	COMMENT	Γ_4/Γ_5
0.35 \pm 0.2		BIRMINGHAM 66	HBC	+	$K^- p$ 3.5 GeV/c	

 $\Gamma(\Lambda\pi)/\Gamma(\Sigma\pi\pi)$

VALUE	EVTS	DOCUMENT ID	TECN	CHG	COMMENT	Γ_2/Γ_5
<0.2		BIRMINGHAM 66	HBC	+	$K^- p$ 3.5 GeV/c	

 $\Gamma(\Lambda\pi)/[\Gamma(\Lambda\pi) + \Gamma(\Sigma\pi)]$

VALUE	EVTS	DOCUMENT ID	TECN	CHG	COMMENT	$\Gamma_2/(\Gamma_2 + \Gamma_3)$
<0.6		AGUILAR-... 70B	HBC			

 $\Gamma(\Sigma(1385)\pi)/\Gamma(\Sigma\pi)$

VALUE	EVTS	DOCUMENT ID	TECN	CHG	COMMENT	Γ_6/Γ_3
$\leq 0.21 \pm 0.05$		TIMMERMANS76	HBC		$K^- p$ 4.2 GeV/c	

See key on page 373

Baryon Particle Listings

$\Sigma(1670)$ Bumps, $\Sigma(1690)$ Bumps, $\Sigma(1750)$

$\Sigma(1670)$ QUANTUM NUMBERS
(PRODUCTION EXPERIMENTS)

VALUE	EVTS	DOCUMENT ID	TECN	CHG	COMMENT
$J^P = 3/2^-$	400	BUTTON-...	68	HBC	$\pm \Sigma^0 \pi$
$J^P = 3/2^-$		EBERHARD	67	HBC	$+$ $\Lambda(1405) \pi$
$J^P = 3/2^+$		LEVEQUE	65	HBC	$\Lambda(1405) \pi$

$\Sigma(1670)$ FOOTNOTES

- Total cross-section bump with $(J+1/2) \Gamma_{el} / \Gamma_{total} = 0.23$.
- Enhancements in $\Sigma \pi$ and $\Sigma \pi \pi$ cross sections.
- Backward production in the $\Lambda \pi^- K^+$ final state.
- Depending on production angle.
- APSELL 74, ESTES 74, and TIMMERMANS 76 find strong branching ratio dependence on production angle, as in earlier production experiments.

$\Sigma(1670)$ REFERENCES
(PRODUCTION EXPERIMENTS)

FERRERSORIA 81	NP B178 373	A. Ferrer Soria et al.	(CERN, CDEF, EPOL+)
CARROLL 76	PRL 37 806	A.S. Carroll et al.	(BNL) I
HEPP 76	NP B115 82	V. Hepp et al.	(CERN, HEID, MPIM) I
TIMMERMANS 76	NP B112 77	J.J.M. Timmermans et al.	(NIJM, CERN+JP)
APSELL 74	PR D10 1419	S.P. Apsell et al.	(BRAN, UMD, SYRA+) I
BERTHON 74	NC 21A 146	A. Berthon et al.	(CDEF, RHEL, SACL+)
ESTES 74	Thesis LBL-3827	R.D. Estes	(LBL)
AGUILAR-... 70B	PRL 25 58	M. Aguilar-Benitez et al.	(BNL, SYRA)
BARNES 69E	BNL 13823	V.E. Barnes et al.	(BNL, SYRA)
EBERHARD 69	PRL 22 200	P.H. Eberhard et al.	(LRL)
HUWE 69	PR 181 1824	D.O. Huwe	(LRL)
BUGG 68	PR 168 1466	D.V. Bugg et al.	(RHEL, BIRM, CAVE) I
BUTTON-... 68	PRL 21 1123	J. Button-Shafer	(MASA, LRL) JP
PRIMER 68	PRL 20 610	M. Primer et al.	(SYRA, BNL)
EBERHARD 67	PR 163 1446	P. Eberhard et al.	(LRL, ILL) JP
BIRMINGHAM 66	PR 152 1148	M. Haque et al.	(BIRM, GLAS, LOIC, OXF+)
LONDON 66	PR 143 1034	G.W. London et al.	(BNL, SYRA) IJ
EBERHARD 65	PRL 14 466	P.H. Eberhard et al.	(LRL, ILL) I
LEVEQUE 65	PL 18 69	A. Leveque et al.	(SACL, EPOL, GLAS+JP)
ALVAREZ 63	PRL 10 184	L.W. Alvarez et al.	(LRL) I
SMITH 63	Athens Conf. 67	G.A. Smith	(LRL)
ALEXANDER 62C	CERN Conf. 320	G. Alexander et al.	(LRL) I

$\Sigma(1690)$ BRANCHING RATIOS
(PRODUCTION EXPERIMENTS)

$\Gamma(N\bar{K})/\Gamma(\Lambda\pi)$		Γ_1/Γ_2			
VALUE	EVTS	DOCUMENT ID	TECN	CHG	COMMENT
small		GODDARD	79	HBC	$+$ $\pi^+ p$ 10.2 GeV/c
<0.2		MOTT	69	HBC	$+$ $K^- p$ 5.5 GeV/c
0.4 ± 0.25	18	COLLEY	67	HBC	$+$ 6/30 events

$\Gamma(\Sigma\pi)/\Gamma(\Lambda\pi)$		Γ_3/Γ_2			
VALUE	CL%	DOCUMENT ID	TECN	CHG	COMMENT
small		GODDARD	79	HBC	$+$ $\pi^+ p$ 10.2 GeV/c
<0.4	90	MOTT	69	HBC	$+$ $K^- p$ 5.5 GeV/c
0.3 ± 0.3		COLLEY	67	HBC	$+$ 4/30 events

$\Gamma(\Sigma(1385)\pi)/\Gamma(\Lambda\pi)$		Γ_4/Γ_2			
VALUE		DOCUMENT ID	TECN	CHG	COMMENT
<0.5		MOTT	69	HBC	$+$ $K^- p$ 5.5 GeV/c

$\Gamma(\Lambda\pi \text{ (including } \Sigma(1385)\pi)/\Gamma(\Lambda\pi)$		Γ_5/Γ_2			
VALUE		DOCUMENT ID	TECN	CHG	COMMENT
2.0 ± 0.6		BLUMENFELD	69	HBC	$+$ 31/15 events
0.5 ± 0.25		COLLEY	67	HBC	$+$ 15/30 events

$\Gamma(\Sigma(1385)\pi)/\Gamma(\Lambda\pi \text{ (including } \Sigma(1385)\pi)$		Γ_4/Γ_5			
VALUE		DOCUMENT ID	TECN	CHG	COMMENT
large		SIMS	68	HBC	$-$ $K^- N \rightarrow \Lambda \pi \pi$
small		COLLEY	67	HBC	$+$ $K^- p$ 6 GeV/c

$\Sigma(1690)$ FOOTNOTES
(PRODUCTION EXPERIMENTS)

- From $\pi^+ p \rightarrow (\Lambda \pi^+) K^+$, $J > 1/2$ is not required by the data.
- From $\pi^+ p \rightarrow (\Lambda \pi^+) (K \pi)^+$, $J > 1/2$ is indicated, but large background precludes a definite conclusion.
- See the $\Sigma(1670)$ Listings. AGUILAR-BENITEZ 70B with three times the data of PRIMER 68 find no evidence for the $\Sigma(1690)$.
- This analysis, which is difficult and requires several assumptions and shows no unambiguous $\Sigma(1690)$ signal, suggests $J^P = 5/2^+$. Such a state would lead all previously known Y^* trajectories.

$\Sigma(1690)$ REFERENCES
(PRODUCTION EXPERIMENTS)

GODDARD 79	PR D19 1350	M.C. Goddard et al.	(TNTO, BNL) IJ
AGUILAR-... 70B	PRL 25 58	M. Aguilar-Benitez et al.	(BNL, SYRA)
ADERHOLZ 69	NP B11 259	M. Aderholz et al.	(AACH3, BERL, CERN+) I
BLUMENFELD 69	PL 29B 58	B.J. Blumenfeld, G.R. Kabbleisch	(BNL) I
MOTT 69	PR 177 1966	J. Mott et al.	(NWES, ANL) I
Also	PRL 18 266	M. Derrick et al.	(ANL, NWES) I
PRIMER 68	PRL 20 610	M. Primer et al.	(SYRA, BNL) I
SIMS 68	PRL 21 1413	W.H. Sims et al.	(FSU, TUFTS, BRAN) I
COLLEY 67	PL 24B 489	D.C. Colley	(BIRM, GLAS, LOIC, MUNI, OXF+) I

$\Sigma(1690)$ Bumps

$I(J^P) = 1(?)^?$ Status: **

OMITTED FROM SUMMARY TABLE

See the note preceding the $\Sigma(1670)$ Listings. Seen in production experiments only, mainly in $\Lambda \pi$.

$\Sigma(1690)$ MASS
(PRODUCTION EXPERIMENTS)

VALUE (MeV)	EVTS	DOCUMENT ID	TECN	CHG	COMMENT
≈ 1690 OUR ESTIMATE					
1698 ± 20	70	¹ GODDARD	79	HBC	$+$ $\pi^+ p$ 10.3 GeV/c
1707 ± 20	40	² GODDARD	79	HBC	$+$ $\pi^+ p$ 10.3 GeV/c
1698 ± 20	15	ADERHOLZ	69	HBC	$+$ $\pi^+ p$ 8 GeV/c
1682 ± 2	46	BLUMENFELD	69	HBC	$+$ K_{Lp}^0
1700 ± 20		MOTT	69	HBC	$+$ $K^- p$ 5.5 GeV/c
1694 ± 24	60	³ PRIMER	68	HBC	$+$ $K^- p$ 4.6-5 GeV/c
1700 ± 6		⁴ SIMS	68	HBC	$-$ $K^- N \rightarrow \Lambda \pi \pi$
1715 ± 12	30	COLLEY	67	HBC	$+$ $K^- p$ 6 GeV/c

$\Sigma(1690)$ WIDTH
(PRODUCTION EXPERIMENTS)

VALUE (MeV)	EVTS	DOCUMENT ID	TECN	CHG	COMMENT
240 ± 60	70	¹ GODDARD	79	HBC	$+$ $\pi^+ p$ 10.3 GeV/c
130_{-60}^{+100}	40	² GODDARD	79	HBC	$+$ $\pi^+ p$ 10.3 GeV/c
142 ± 40	15	ADERHOLZ	69	HBC	$+$ $\pi^+ p$ 8 GeV/c
25 ± 10	46	BLUMENFELD	69	HBC	$+$ K_{Lp}^0
130 ± 25		MOTT	69	HBC	$+$ $K^- p$ 5.5 GeV/c
105 ± 35	60	³ PRIMER	68	HBC	$+$ $K^- p$ 4.6-5 GeV/c
62 ± 14		⁴ SIMS	68	HBC	$-$ $K^- N \rightarrow \Lambda \pi \pi$
100 ± 35	30	COLLEY	67	HBC	$+$ $K^- p$ 6 GeV/c

$\Sigma(1690)$ DECAY MODES
(PRODUCTION EXPERIMENTS)

Mode	
Γ_1	$N\bar{K}$
Γ_2	$\Lambda \pi$
Γ_3	$\Sigma \pi$
Γ_4	$\Sigma(1385)\pi$
Γ_5	$\Lambda \pi \pi$ (including $\Sigma(1385)\pi$)

$\Sigma(1750) S_{11}$

$I(J^P) = 1(\frac{1}{2}^-)$ Status: ***

For most results published before 1974 (they are now obsolete), see our 1982 edition Physics Letters **111B** 1 (1982).

There is evidence for this state in many partial-wave analyses, but with wide variations in the mass, width, and couplings. The latest analyses indicated significant couplings to $N\bar{K}$ and $\Lambda \pi$, as well as to $\Sigma \eta$ whose threshold is at 1746 MeV (JONES 74).

$\Sigma(1750)$ MASS

VALUE (MeV)	DOCUMENT ID	TECN	COMMENT
≈ 1750 OUR ESTIMATE			
1756 ± 10	GOPAL	80	DPWA $\bar{K} N \rightarrow \bar{K} N$
1770 ± 10	ALSTON-...	78	DPWA $\bar{K} N \rightarrow \bar{K} N$
1770 ± 15	GOPAL	77	DPWA $\bar{K} N$ multichannel
••• We do not use the following data for averages, fits, limits, etc. •••			
1800 or 1813	¹ MARTIN	77	DPWA $\bar{K} N$ multichannel
1715 ± 10	² CARROLL	76	DPWA Isospin-1 total σ
1730	DEBELLEFON	76	IPWA $K^- p \rightarrow \Lambda \pi^0$
1780 ± 30	BAILLON	75	IPWA $\bar{K} N \rightarrow \Lambda \pi$ (sol. 1)
1700 ± 30	BAILLON	75	IPWA $\bar{K} N \rightarrow \Lambda \pi$ (sol. 2)
1697_{-10}^{+20}	VANHORN	75	DPWA $K^- p \rightarrow \Lambda \pi^0$
1785 ± 12	CHU	74	DBC Fits $\sigma(K^- n \rightarrow \Sigma^- \eta)$
1760 ± 5	³ JONES	74	HBC Fits $\sigma(K^- p \rightarrow \Sigma^0 \eta)$
1739 ± 10	PREVOST	74	DPWA $K^- N \rightarrow \Sigma(1385)\pi$

Baryon Particle Listings

 $\Sigma(1750)$, $\Sigma(1770)$ $\Sigma(1750)$ WIDTH

VALUE (MeV)	DOCUMENT ID	TECN	COMMENT
60 to 160 (≈ 90) OUR ESTIMATE			
64 \pm 10	GOPAL	80	DPWA $\bar{K}N \rightarrow \bar{K}N$
161 \pm 20	ALSTON-...	78	DPWA $\bar{K}N \rightarrow \bar{K}N$
60 \pm 10	GOPAL	77	DPWA $\bar{K}N$ multichannel
••• We do not use the following data for averages, fits, limits, etc. •••			
117 or 119	¹ MARTIN	77	DPWA $\bar{K}N$ multichannel
10	² CARROLL	76	DPWA Isospin-1 total σ
110	DEBELLEFON	76	IPWA $K^-p \rightarrow \Lambda\pi^0$
140 \pm 30	BAILLON	75	IPWA $\bar{K}N \rightarrow \Lambda\pi$ (sol. 1)
160 \pm 50	BAILLON	75	IPWA $\bar{K}N \rightarrow \Lambda\pi$ (sol. 2)
66 $^{+14}_{-12}$	VANHORN	75	DPWA $K^-p \rightarrow \Lambda\pi^0$
89 \pm 33	CHU	74	DBC Fits $\sigma(K^-n \rightarrow \Sigma^-\eta)$
92 \pm 7	³ JONES	74	HBC Fits $\sigma(K^-p \rightarrow \Sigma^0\eta)$
108 \pm 20	PREVOST	74	DPWA $K^-N \rightarrow \Sigma(1385)\pi$

 $\Sigma(1750)$ DECAY MODES

Mode	Fraction (Γ_i/Γ)
Γ_1 $N\bar{K}$	10–40 %
Γ_2 $\Lambda\pi$	seen
Γ_3 $\Sigma\pi$	<8 %
Γ_4 $\Sigma\eta$	15–55 %
Γ_5 $\Sigma(1385)\pi$	
Γ_6 $\Lambda(1520)\pi$	

The above branching fractions are our estimates, not fits or averages.

 $\Sigma(1750)$ BRANCHING RATIOS

See "Sign conventions for resonance couplings" in the Note on Λ and Σ Resonances.

$\Gamma(N\bar{K})/\Gamma_{\text{total}}$	DOCUMENT ID	TECN	COMMENT	Γ_1/Γ
0.1 to 0.4 OUR ESTIMATE				
0.14 \pm 0.03	GOPAL	80	DPWA $\bar{K}N \rightarrow \bar{K}N$	
0.33 \pm 0.05	ALSTON-...	78	DPWA $\bar{K}N \rightarrow \bar{K}N$	
••• We do not use the following data for averages, fits, limits, etc. •••				
0.15 \pm 0.03	GOPAL	77	DPWA See GOPAL 80	
0.06 or 0.05	¹ MARTIN	77	DPWA $\bar{K}N$ multichannel	

$(\Gamma_1\Gamma_2)^{1/2}/\Gamma_{\text{total}}$ in $N\bar{K} \rightarrow \Sigma(1750) \rightarrow \Lambda\pi$	DOCUMENT ID	TECN	COMMENT	$(\Gamma_1\Gamma_2)^{1/2}/\Gamma$
0.04 \pm 0.03				
0.04 \pm 0.03	GOPAL	77	DPWA $\bar{K}N$ multichannel	
••• We do not use the following data for averages, fits, limits, etc. •••				
-0.10 or -0.09	¹ MARTIN	77	DPWA $\bar{K}N$ multichannel	
-0.12	DEBELLEFON	76	IPWA $K^-p \rightarrow \Lambda\pi^0$	
-0.12 \pm 0.02	BAILLON	75	IPWA $\bar{K}N \rightarrow \Lambda\pi$ (sol. 1)	
-0.13 \pm 0.03	BAILLON	75	IPWA $\bar{K}N \rightarrow \Lambda\pi$ (sol. 2)	
-0.13 \pm 0.04	VANHORN	75	DPWA $K^-p \rightarrow \Lambda\pi^0$	
-0.120 \pm 0.077	DEVENISH	74B	Fixed- t dispersion rel.	

$(\Gamma_1\Gamma_3)^{1/2}/\Gamma_{\text{total}}$ in $N\bar{K} \rightarrow \Sigma(1750) \rightarrow \Sigma\pi$	DOCUMENT ID	TECN	COMMENT	$(\Gamma_1\Gamma_3)^{1/2}/\Gamma$
-0.09 \pm 0.05				
-0.09 \pm 0.05	GOPAL	77	DPWA $\bar{K}N$ multichannel	
••• We do not use the following data for averages, fits, limits, etc. •••				
+0.06 or +0.06	¹ MARTIN	77	DPWA $\bar{K}N$ multichannel	
0.13 \pm 0.02	LANGBEIN	72	IPWA $\bar{K}N$ multichannel	

$(\Gamma_1\Gamma_4)^{1/2}/\Gamma_{\text{total}}$ in $N\bar{K} \rightarrow \Sigma(1750) \rightarrow \Sigma\eta$	DOCUMENT ID	TECN	COMMENT	$(\Gamma_1\Gamma_4)^{1/2}/\Gamma$
0.23 \pm 0.01				
0.23 \pm 0.01	³ JONES	74	HBC Fits $\sigma(K^-p \rightarrow \Sigma^0\eta)$	
••• We do not use the following data for averages, fits, limits, etc. •••				
seen	CLINE	69	DBC Threshold bump	

$(\Gamma_1\Gamma_5)^{1/2}/\Gamma_{\text{total}}$ in $N\bar{K} \rightarrow \Sigma(1750) \rightarrow \Sigma(1385)\pi$	DOCUMENT ID	TECN	COMMENT	$(\Gamma_1\Gamma_5)^{1/2}/\Gamma$
+0.18 \pm 0.15				
+0.18 \pm 0.15	PREVOST	74	DPWA $K^-N \rightarrow \Sigma(1385)\pi$	

$(\Gamma_1\Gamma_6)^{1/2}/\Gamma_{\text{total}}$ in $N\bar{K} \rightarrow \Sigma(1750) \rightarrow \Lambda(1520)\pi$	DOCUMENT ID	TECN	COMMENT	$(\Gamma_1\Gamma_6)^{1/2}/\Gamma$
0.032 \pm 0.021				
0.032 \pm 0.021	CAMERON	77	DPWA P -wave decay	

 $\Sigma(1750)$ FOOTNOTES

- The two MARTIN 77 values are from a T-matrix pole and from a Breit-Wigner fit.
- A total cross-section bump with $(J+1/2)\Gamma_{\text{el}}/\Gamma_{\text{total}} = 0.30$.
- An S-wave Breit-Wigner fit to the threshold cross section with no background and errors statistical only.

 $\Sigma(1750)$ REFERENCES

PDG	82	PL 111B 1	M. Roos <i>et al.</i>	(HEL5, CIT, CERN)
GOPAL	80	Toronto Conf. 159	G.P. Gopal	(RHEL) IJP
ALSTON-...	78	PR D18 182	M. Alston-Garnjost <i>et al.</i>	(LBL, MTHO+) IJP
			M. Alston-Garnjost <i>et al.</i>	(LBL, MTHO+) IJP
			W. Cameron <i>et al.</i>	(RHEL, LOIC) IJP
CAMERON	77	NP B131 399	G.P. Gopal <i>et al.</i>	(LOIC, RHEL) IJP
GOPAL	77	NP B119 362	B.R. Martin, M.K. Pidcock, R.G. Moorhouse	(LOUC+) IJP
MARTIN	77	NP B127 349	B.R. Martin, M.K. Pidcock	(LOUC) IJP
			B.R. Martin, M.K. Pidcock	(LOUC) IJP
			A.S. Carroll <i>et al.</i>	(BNL) I
CARROLL	76	PRL 37 806	A. de Bellefon, A. Berthon	(CDEF) IJP
DEBELLEFON	76	NP B109 129	P.H. Baillon, P.J. Litchfield	(CERN, RHEL) IJP
BAILLON	75	NP B94 39	A.J. van Horn	(LBL) IJP
VANHORN	75	NP B87 145	A.J. van Horn	(LBL) IJP
			R.Y.L. Chu <i>et al.</i>	(PLAT, TUFTS, BRAN) IJP
CHU	74	NC 20A 35	R.C.E. Devenish, C.D. Froggatt, B.R. Martin	(DESY+) IJP
DEVENISH	74B	NP B81 330	M.D. Jones	(CHIC) IJP
JONES	74	NP B73 141	J. Prevost <i>et al.</i>	(SACL, CERN, HEID) IJP
PREVOST	74	NP B69 246	W. Langbein, F. Wagner	(MFIM) IJP
LANGBEIN	72	NP B47 477	D. Cline, R. Laumann, J. Mapp	(WIS C)
CLINE	69	LCN 2 407		

 $\Sigma(1770) P_{11}$

$$I(J^P) = 1(\frac{1}{2}^+) \text{ Status: } *$$

OMITTED FROM SUMMARY TABLE

Evidence for this state now rests solely on solution 1 of BAILLON 75, (see the footnotes) but the $\Lambda\pi$ partial-wave amplitudes of this solution are in disagreement with amplitudes from most other $\Lambda\pi$ analyses.

 $\Sigma(1770)$ MASS

VALUE (MeV)	DOCUMENT ID	TECN	COMMENT
≈ 1770 OUR ESTIMATE			
1738 \pm 10	¹ GOPAL	77	DPWA $\bar{K}N$ multichannel
1770 \pm 20	² BAILLON	75	IPWA $\bar{K}N \rightarrow \Lambda\pi$
1772	³ KANE	72	DPWA $K^-p \rightarrow \Sigma\pi$

 $\Sigma(1770)$ WIDTH

VALUE (MeV)	DOCUMENT ID	TECN	COMMENT
72 \pm 10	¹ GOPAL	77	DPWA $\bar{K}N$ multichannel
80 \pm 30	² BAILLON	75	IPWA $\bar{K}N \rightarrow \Lambda\pi$
80	³ KANE	72	DPWA $K^-p \rightarrow \Sigma\pi$

 $\Sigma(1770)$ DECAY MODES

Mode
Γ_1 $N\bar{K}$
Γ_2 $\Lambda\pi$
Γ_3 $\Sigma\pi$

 $\Sigma(1770)$ BRANCHING RATIOS

See "Sign conventions for resonance couplings" in the Note on Λ and Σ Resonances.

$\Gamma(N\bar{K})/\Gamma_{\text{total}}$	DOCUMENT ID	TECN	COMMENT	Γ_1/Γ
0.14 \pm 0.04				
0.14 \pm 0.04	¹ GOPAL	77	DPWA $\bar{K}N$ multichannel	
$(\Gamma_1\Gamma_2)^{1/2}/\Gamma_{\text{total}}$ in $N\bar{K} \rightarrow \Sigma(1770) \rightarrow \Lambda\pi$	DOCUMENT ID	TECN	COMMENT	$(\Gamma_1\Gamma_2)^{1/2}/\Gamma$
< 0.04				
< 0.04	GOPAL	77	DPWA $\bar{K}N$ multichannel	
-0.08 \pm 0.02	² BAILLON	75	IPWA $\bar{K}N \rightarrow \Lambda\pi$	
$(\Gamma_1\Gamma_3)^{1/2}/\Gamma_{\text{total}}$ in $N\bar{K} \rightarrow \Sigma(1770) \rightarrow \Sigma\pi$	DOCUMENT ID	TECN	COMMENT	$(\Gamma_1\Gamma_3)^{1/2}/\Gamma$
< 0.04				
< 0.04	GOPAL	77	DPWA $\bar{K}N$ multichannel	
-0.108	³ KANE	72	DPWA $K^-p \rightarrow \Sigma\pi$	

 $\Sigma(1770)$ FOOTNOTES

- Required to fit the isospin-1 total cross section of CARROLL 76 in the $\bar{K}N$ channel. The addition of new K^-p polarization and K^-n differential cross-section data in GOPAL 80 find it to be more consistent with the $\Sigma(1660) P_{11}$.
- From solution 1 of BAILLON 75; not present in solution 2.
- Not required in KANE 74, which supersedes KANE 72.

$\Sigma(1770)$ REFERENCES

GOPAL	80	Tomato Conf. 159	G.P. Gopal	(RHEL)
GOPAL	77	NP B119 362	G.P. Gopal et al.	(LOIC, RHEL) IJP
CARROLL	76	PRL 37 806	A.S. Carroll et al.	(BNL) I
BAILLON	75	NP B94 39	P.H. Baillon, P.J. Litchfield	(CERN, RHEL) IJP
KANE	74	LBL-2452	D.F. Kane	(LBL) IJP
KANE	72	PR D5 1583	D.F.J. Kane	(LBL)

 $\Sigma(1775) D_{15}$

$$I(J^P) = 1(\frac{5}{2}^-) \text{ Status: } ****$$

Discovered by GALTIERI 63, this resonance plays the same role as cornerstone for isospin-1 analyses in this region as the $\Lambda(1820)F_{05}$ does in the isospin-0 channel.

For most results published before 1974 (they are now obsolete), see our 1982 edition Physics Letters **111B** 1 (1982).

 $\Sigma(1775)$ MASS

VALUE (MeV)	DOCUMENT ID	TECN	COMMENT
1770 to 1780 (≈ 1775) OUR ESTIMATE			
1778 \pm 5	GOPAL 80	DPWA	$\bar{K}N \rightarrow \bar{K}N$
1777 \pm 5	ALSTON... 78	DPWA	$\bar{K}N \rightarrow \bar{K}N$
1774 \pm 5	GOPAL 77	DPWA	$\bar{K}N$ multichannel
1775 \pm 10	BAILLON 75	IPWA	$\bar{K}N \rightarrow \Lambda\pi$
1774 \pm 10	VANHORN 75	DPWA	$K^-p \rightarrow \Lambda\pi^0$
1772 \pm 6	KANE 74	DPWA	$K^-p \rightarrow \Sigma\pi$
••• We do not use the following data for averages, fits, limits, etc. •••			
1772 or 1777	¹ MARTIN 77	DPWA	$\bar{K}N$ multichannel
1765	DEBELLEFON 76	IPWA	$K^-p \rightarrow \Lambda\pi^0$

 $\Sigma(1775)$ WIDTH

VALUE (MeV)	DOCUMENT ID	TECN	COMMENT
105 to 135 (≈ 120) OUR ESTIMATE			
137 \pm 10	GOPAL 80	DPWA	$\bar{K}N \rightarrow \bar{K}N$
116 \pm 10	ALSTON... 78	DPWA	$\bar{K}N \rightarrow \bar{K}N$
130 \pm 10	GOPAL 77	DPWA	$\bar{K}N$ multichannel
125 \pm 15	BAILLON 75	IPWA	$\bar{K}N \rightarrow \Lambda\pi$
146 \pm 18	VANHORN 75	DPWA	$K^-p \rightarrow \Lambda\pi^0$
154 \pm 10	KANE 74	DPWA	$K^-p \rightarrow \Sigma\pi$
••• We do not use the following data for averages, fits, limits, etc. •••			
102 or 103	¹ MARTIN 77	DPWA	$\bar{K}N$ multichannel
120	DEBELLEFON 76	IPWA	$K^-p \rightarrow \Lambda\pi^0$

 $\Sigma(1775)$ DECAY MODES

Mode	Fraction (Γ_i/Γ)
Γ_1 $N\bar{K}$	37-43%
Γ_2 $\Lambda\pi$	14-20%
Γ_3 $\Sigma\pi$	2-5%
Γ_4 $\Sigma(1385)\pi$	8-12%
Γ_5 $\Sigma(1385)\pi, D\text{-wave}$	
Γ_6 $\Lambda(1520)\pi$	17-23%
Γ_7 $\Sigma\pi\pi$	

The above branching fractions are our estimates, not fits or averages.

CONSTRAINED FIT INFORMATION

An overall fit to 8 branching ratios uses 16 measurements and one constraint to determine 5 parameters. The overall fit has a $\chi^2 = 63.9$ for 12 degrees of freedom.

The following *off-diagonal* array elements are the correlation coefficients $\langle \delta x_i \delta x_j \rangle / (\delta x_i \delta x_j)$, in percent, from the fit to the branching fractions, $x_i \equiv \Gamma_i/\Gamma_{\text{total}}$. The fit constrains the x_i whose labels appear in this array to sum to one.

x_2	-30			
x_3	-17	-21		
x_4	-37	-49	-14	
x_6	-81	6	8	16
	x_1	x_2	x_3	x_4

 $\Sigma(1775)$ BRANCHING RATIOS

See "Sign conventions for resonance couplings" in the Note on Λ and Σ Resonances. Also, the errors quoted do not include uncertainties due to the parametrization used in the partial-wave analyses and are thus too small.

 $\Gamma(N\bar{K})/\Gamma_{\text{total}}$ Γ_1/Γ

VALUE	DOCUMENT ID	TECN	COMMENT
0.37 to 0.43 OUR ESTIMATE			
0.45 \pm 0.04 OUR FIT	Error includes scale factor of 3.1.		
0.391 \pm 0.017 OUR AVERAGE			
0.40 \pm 0.02	GOPAL 80	DPWA	$\bar{K}N \rightarrow \bar{K}N$
0.37 \pm 0.03	ALSTON... 78	DPWA	$\bar{K}N \rightarrow \bar{K}N$
••• We do not use the following data for averages, fits, limits, etc. •••			
0.41 \pm 0.03	GOPAL 77	DPWA	See GOPAL 80
0.37 or 0.36	¹ MARTIN 77	DPWA	$\bar{K}N$ multichannel

 $(\Gamma_1\Gamma_2)^{1/2}/\Gamma_{\text{total}}$ in $N\bar{K} \rightarrow \Sigma(1775) \rightarrow \Lambda\pi$ $(\Gamma_1\Gamma_2)^{1/2}/\Gamma$

VALUE	DOCUMENT ID	TECN	COMMENT
0.305 \pm 0.018 OUR FIT Error includes scale factor of 2.4.			
-0.262 \pm 0.015 OUR AVERAGE			
-0.28 \pm 0.03	GOPAL 77	DPWA	$\bar{K}N$ multichannel
-0.25 \pm 0.02	BAILLON 75	IPWA	$\bar{K}N \rightarrow \Lambda\pi$
-0.28 \pm 0.04	VANHORN 75	DPWA	$K^-p \rightarrow \Lambda\pi^0$
-0.25 \pm 0.048	DEVENISH 74B		Fixed- t dispersion rel.
••• We do not use the following data for averages, fits, limits, etc. •••			
-0.29 or -0.28	¹ MARTIN 77	DPWA	$\bar{K}N$ multichannel
-0.30	DEBELLEFON 76	IPWA	$K^-p \rightarrow \Lambda\pi^0$

 $(\Gamma_1\Gamma_3)^{1/2}/\Gamma_{\text{total}}$ in $N\bar{K} \rightarrow \Sigma(1775) \rightarrow \Sigma\pi$ $(\Gamma_1\Gamma_3)^{1/2}/\Gamma$

VALUE	DOCUMENT ID	TECN	COMMENT
0.105 \pm 0.025 OUR FIT Error includes scale factor of 3.1.			
0.098 \pm 0.016 OUR AVERAGE Error includes scale factor of 1.8.			
+0.13 \pm 0.02	GOPAL 77	DPWA	$\bar{K}N$ multichannel
0.09 \pm 0.01	KANE 74	DPWA	$K^-p \rightarrow \Sigma\pi$
••• We do not use the following data for averages, fits, limits, etc. •••			
+0.08 or +0.08	¹ MARTIN 77	DPWA	$\bar{K}N$ multichannel

 $(\Gamma_1\Gamma_6)^{1/2}/\Gamma_{\text{total}}$ in $N\bar{K} \rightarrow \Sigma(1775) \rightarrow \Lambda(1520)\pi$ $(\Gamma_1\Gamma_6)^{1/2}/\Gamma$

VALUE	DOCUMENT ID	TECN	COMMENT
0.315 \pm 0.010 OUR FIT Error includes scale factor of 1.5.			
0.303 \pm 0.009 OUR AVERAGE Signs on measurements were ignored.			
-0.305 \pm 0.010	² CAMERON 77	DPWA	$K^-p \rightarrow \Lambda(1520)\pi^0$
0.31 \pm 0.02	BARLETTA 72	DPWA	$K^-p \rightarrow \Lambda(1520)\pi^0$
0.27 \pm 0.03	ARMENTEROS65c	HBC	$K^-p \rightarrow \Lambda(1520)\pi^0$

 $(\Gamma_1\Gamma_7)^{1/2}/\Gamma_{\text{total}}$ in $N\bar{K} \rightarrow \Sigma(1775) \rightarrow \Sigma(1385)\pi$ $(\Gamma_1\Gamma_7)^{1/2}/\Gamma$

VALUE	DOCUMENT ID	TECN	COMMENT
0.211 \pm 0.022 OUR FIT Error includes scale factor of 2.8.			
0.188 \pm 0.010 OUR AVERAGE Signs on measurements were ignored.			
-0.184 \pm 0.011	³ CAMERON 78	DPWA	$K^-p \rightarrow \Sigma(1385)\pi$
+0.20 \pm 0.02	PREVOST 74	DPWA	$K^-N \rightarrow \Sigma(1385)\pi$
••• We do not use the following data for averages, fits, limits, etc. •••			
0.32 \pm 0.06	SIMS 68	DBC	$K^-N \rightarrow \Lambda\pi\pi$
0.24 \pm 0.03	ARMENTEROS67c	HBC	$K^-p \rightarrow \Lambda\pi\pi$

 $\Gamma(\Lambda\pi)/\Gamma(N\bar{K})$ Γ_2/Γ_1

VALUE	DOCUMENT ID	TECN	COMMENT
0.46 \pm 0.09 OUR FIT Error includes scale factor of 2.9.			
0.33 \pm 0.05	UHLIG 67	HBC	K^-p 0.9 GeV/c

 $\Gamma(\Sigma\pi\pi)/\Gamma_{\text{total}}$ Γ_7/Γ

VALUE	DOCUMENT ID	TECN	COMMENT
••• We do not use the following data for averages, fits, limits, etc. •••			
0.12	⁴ ARMENTEROS68c	HDBC	$K^-N \rightarrow \Sigma\pi\pi$

 $\Gamma(\Sigma(1385)\pi)/\Gamma(N\bar{K})$ Γ_4/Γ_1

VALUE	DOCUMENT ID	TECN	COMMENT
0.22 \pm 0.07 OUR FIT Error includes scale factor of 3.6.			
0.25 \pm 0.09	UHLIG 67	HBC	K^-p 0.9 GeV/c

 $\Gamma(\Lambda(1520)\pi)/\Gamma(N\bar{K})$ Γ_6/Γ_1

VALUE	DOCUMENT ID	TECN	COMMENT
0.49 \pm 0.11 OUR FIT Error includes scale factor of 3.5.			
0.28 \pm 0.05	UHLIG 67	HBC	K^-p 0.9 GeV/c

Baryon Particle Listings

 $\Sigma(1775)$, $\Sigma(1840)$, $\Sigma(1880)$ $\Sigma(1775)$ FOOTNOTES

- ¹ The two MARTIN 77 values are from a T-matrix pole and from a Breit-Wigner fit.
² This rate combines P -wave- and F -wave decays. The CAMERON 77 results for the separate P -wave- and F -wave decays are -0.303 ± 0.010 and -0.037 ± 0.014 . The published signs have been changed here to be in accord with the baryon-first convention.
³ The CAMERON 78 upper limit on G -wave decay is 0.03.
⁴ For about 3/4 of this, the $\Sigma\pi$ system has $l = 0$ and is almost entirely $\Lambda(1520)$. For the rest, the $\Sigma\pi$ has $l = 1$, which is about what is expected from the known $\Sigma(1775) \rightarrow \Sigma(1385)\pi$ rate, as seen in $\Lambda\pi\pi$.

 $\Sigma(1775)$ REFERENCES

PDG	82	PL 111B 1	M. Roos et al.	(HEL5, CIT, CERN)
GOPAL	80	Tomoto Conf. 159	G.P. Gopal	(RHEL) IJP
ALSTON-...	78	PR D18 182	M. Alston-Garnjost et al.	(LBL, MTHO+) IJP
		PRL 38 1007	M. Alston-Garnjost et al.	(LBL, MTHO+) IJP
CAMERON	78	NP B143 189	W. Cameron et al.	(RHEL, LOIC) IJP
CAMERON	77	NP B131 399	W. Cameron et al.	(RHEL, LOIC) IJP
GOPAL	77	NP B119 362	G.P. Gopal et al.	(LOIC, RHEL) IJP
MARTIN	77	NP B127 349	B.R. Martin, M.K. Pidcock, R.G. Moorhouse	(LOUC+) IJP
		Also NP B126 266	B.R. Martin, M.K. Pidcock	(LOUC) IJP
		Also NP B126 285	B.R. Martin, M.K. Pidcock	(LOUC) IJP
DEBELLEFON	76	NP B109 129	A. de Bellefon, A. Berthom	(CDEF) IJP
BAILLON	75	NP B94 39	P.H. Baillon, P.J. Litchfield	(CERN, RHEL) IJP
VANHORN	75	NP B87 145	A.J. van Horn	(LBL) IJP
		Also NP B87 157	A.J. van Horn	(LBL) IJP
DEVENISH	74B	NP B81 330	R.C.E. Devenish, C.D. Froggatt, B.R. Martin	(DESY+) IJP
KANE	74	LBL-2452	D.F. Kane	(LBL) IJP
PREVOST	74	NP B69 246	J. Prevost et al.	(SACL, CERN, HEID) IJP
BARLETTA	72	NP B40 45	W.A. Barletta	(EFI) IJP
		Also PRL 17 841	S. Fenster et al.	(CHIC, ANL, CERN) IJP
ARMENTEROS	68C	NP B8 216	R. Armenteros et al.	(CERN, HEID, SACL) I
SIMS	68	PRL 21 1413	W.H. Sims et al.	(FSU, TUFTS, BRAN)
ARMENTEROS	67C	ZPHY 202 466	R. Armenteros et al.	(CERN, HEID, SACL)
UHLIG	67	PR 155 1446	R.P. Uhlig et al.	(UMD, NRL)
ARMENTEROS	65C	PL 19 338	R. Armenteros et al.	(CERN, HEID, SACL) IJP
GALTIERI	63	PL 6 296	A. Galtieri, A. Hussain, R. Tripp	(LRL) IJ

 $\Sigma(1840) P_{13}$

$$I(J^P) = 1(\frac{3}{2}^+) \text{ Status: } *$$

OMITTED FROM SUMMARY TABLE

For the time being, we list together here all resonance claims in the P_{13} wave between 1700 and 1900 MeV.

 $\Sigma(1840)$ MASS

VALUE (MeV)	DOCUMENT ID	TECN	COMMENT
≈ 1840 OUR ESTIMATE			
1798 or 1802	¹ MARTIN 77	DPWA	$\bar{K}N$ multichannel
1720 \pm 30	² BAILLON 75	IPWA	$\bar{K}N \rightarrow \Lambda\pi$
1925 \pm 200	VANHORN 75	DPWA	$K^-p \rightarrow \Lambda\pi^0$
1840 \pm 10	LANGBEIN 72	IPWA	$\bar{K}N$ multichannel

 $\Sigma(1840)$ WIDTH

VALUE (MeV)	DOCUMENT ID	TECN	COMMENT
93 or 93	¹ MARTIN 77	DPWA	$\bar{K}N$ multichannel
120 \pm 30	² BAILLON 75	IPWA	$\bar{K}N \rightarrow \Lambda\pi$
65 $^{+50}_{-20}$	VANHORN 75	DPWA	$K^-p \rightarrow \Lambda\pi^0$
120 \pm 10	LANGBEIN 72	IPWA	$\bar{K}N$ multichannel

 $\Sigma(1840)$ DECAY MODES

Mode
Γ_1 $N\bar{K}$
Γ_2 $\Lambda\pi$
Γ_3 $\Sigma\pi$

 $\Sigma(1840)$ BRANCHING RATIOS

See "Sign conventions for resonance couplings" in the Note on Λ and Σ Resonances.

$\Gamma(N\bar{K})/\Gamma_{\text{total}}$	DOCUMENT ID	TECN	COMMENT	Γ_1/Γ
0 or 0	¹ MARTIN 77	DPWA	$\bar{K}N$ multichannel	
0.37 \pm 0.13	LANGBEIN 72	IPWA	$\bar{K}N$ multichannel	

$(\Gamma_1\Gamma_2)^{1/2}/\Gamma_{\text{total}}$ in $N\bar{K} \rightarrow \Sigma(1840) \rightarrow \Lambda\pi$	DOCUMENT ID	TECN	COMMENT	$(\Gamma_1\Gamma_2)^{1/2}/\Gamma$
+0.03 or +0.03	¹ MARTIN 77	DPWA	$\bar{K}N$ multichannel	
+0.11 \pm 0.02	² BAILLON 75	IPWA	$\bar{K}N \rightarrow \Lambda\pi$	
+0.06 \pm 0.04	VANHORN 75	DPWA	$K^-p \rightarrow \Lambda\pi^0$	
+0.122 \pm 0.078	DEVENISH 74B		Fixed- t dispersion rel.	
0.20 \pm 0.04	LANGBEIN 72	IPWA	$\bar{K}N$ multichannel	

$(\Gamma_1\Gamma_2)^{1/2}/\Gamma_{\text{total}}$ in $N\bar{K} \rightarrow \Sigma(1840) \rightarrow \Sigma\pi$	DOCUMENT ID	TECN	COMMENT	$(\Gamma_1\Gamma_2)^{1/2}/\Gamma$
-0.04 or -0.04	¹ MARTIN 77	DPWA	$\bar{K}N$ multichannel	
0.15 \pm 0.04	LANGBEIN 72	IPWA	$\bar{K}N$ multichannel	

 $\Sigma(1840)$ FOOTNOTES

- ¹ The two MARTIN 77 values are from a T-matrix pole and from a Breit-Wigner fit.
² From solution 1 of BAILLON 75; not present in solution 2.

 $\Sigma(1840)$ REFERENCES

MARTIN	77	NP B127 349	B.R. Martin, M.K. Pidcock, R.G. Moorhouse	(LOUC+) IJP
		Also NP B126 266	B.R. Martin, M.K. Pidcock	(LOUC) IJP
		Also NP B126 285	B.R. Martin, M.K. Pidcock	(LOUC) IJP
BAILLON	75	NP B94 39	P.H. Baillon, P.J. Litchfield	(CERN, RHEL) IJP
VANHORN	75	NP B87 145	A.J. van Horn	(LBL) IJP
		Also NP B87 157	A.J. van Horn	(LBL) IJP
DEVENISH	74B	NP B81 330	R.C.E. Devenish, C.D. Froggatt, B.R. Martin	(DESY+) IJP
LANGBEIN	72	NP B47 477	W. Langbein, F. Wagner	(MPIM) IJP

 $\Sigma(1880) P_{11}$

$$I(J^P) = 1(\frac{1}{2}^+) \text{ Status: } **$$

OMITTED FROM SUMMARY TABLE

A P_{11} resonance is suggested by several partial-wave analyses, but with wide variations in the mass and other parameters. We list here all claims which lie well above the $P_{11} \Sigma(1770)$.

 $\Sigma(1880)$ MASS

VALUE (MeV)	DOCUMENT ID	TECN	COMMENT
≈ 1880 OUR ESTIMATE			
1826 \pm 20	GOPAL 80	DPWA	$\bar{K}N \rightarrow \bar{K}N$
1870 \pm 10	CAMERON 78B	DPWA	$K^-p \rightarrow N\bar{K}^*$
1847 or 1863	¹ MARTIN 77	DPWA	$\bar{K}N$ multichannel
1960 \pm 30	² BAILLON 75	IPWA	$\bar{K}N \rightarrow \Lambda\pi$
1985 \pm 50	VANHORN 75	DPWA	$K^-p \rightarrow \Lambda\pi^0$
1898	³ LEA 73	DPWA	Multichannel K-matrix
~ 1850	ARMENTEROS70	IPWA	$\bar{K}N \rightarrow \bar{K}N$
1950 \pm 50	BARBARO-... 70	DPWA	$K^-N \rightarrow \Lambda\pi$
1920 \pm 30	LITCHFIELD 70	DPWA	$K^-N \rightarrow \Lambda\pi$
1850	BAILEY 69	DPWA	$\bar{K}N \rightarrow \bar{K}N$
1882 \pm 40	SMART 68	DPWA	$K^-N \rightarrow \Lambda\pi$

 $\Sigma(1880)$ WIDTH

VALUE (MeV)	DOCUMENT ID	TECN	COMMENT
86 \pm 15	GOPAL 80	DPWA	$\bar{K}N \rightarrow \bar{K}N$
80 \pm 10	CAMERON 78B	DPWA	$K^-p \rightarrow N\bar{K}^*$
216 or 220	¹ MARTIN 77	DPWA	$\bar{K}N$ multichannel
260 \pm 40	² BAILLON 75	IPWA	$\bar{K}N \rightarrow \Lambda\pi$
220 \pm 140	VANHORN 75	DPWA	$K^-p \rightarrow \Lambda\pi^0$
222	³ LEA 73	DPWA	Multichannel K-matrix
~ 30	ARMENTEROS70	IPWA	$\bar{K}N \rightarrow \bar{K}N$
200 \pm 50	BARBARO-... 70	DPWA	$K^-N \rightarrow \Lambda\pi$
170 \pm 40	LITCHFIELD 70	DPWA	$K^-N \rightarrow \Lambda\pi$
200	BAILEY 69	DPWA	$\bar{K}N \rightarrow \bar{K}N$
222 \pm 150	SMART 68	DPWA	$K^-N \rightarrow \Lambda\pi$

 $\Sigma(1880)$ DECAY MODES

Mode
Γ_1 $N\bar{K}$
Γ_2 $\Lambda\pi$
Γ_3 $\Sigma\pi$
Γ_4 $N\bar{K}^*(892)$, $S=1/2$, P -wave
Γ_5 $N\bar{K}^*(892)$, $S=3/2$, P -wave

 $\Sigma(1880)$ BRANCHING RATIOS

See "Sign conventions for resonance couplings" in the Note on Λ and Σ Resonances.

$\Gamma(N\bar{K})/\Gamma_{\text{total}}$	DOCUMENT ID	TECN	COMMENT	Γ_1/Γ
0.06 \pm 0.02	GOPAL 80	DPWA	$\bar{K}N \rightarrow \bar{K}N$	
0.27 or 0.27	¹ MARTIN 77	DPWA	$\bar{K}N$ multichannel	
0.31	³ LEA 73	DPWA	Multichannel K-matrix	
0.20	ARMENTEROS70	IPWA	$\bar{K}N \rightarrow \bar{K}N$	
0.22	BAILEY 69	DPWA	$\bar{K}N \rightarrow \bar{K}N$	

Baryon Particle Listings
 $\Sigma(1880), \Sigma(1915)$

$(\Gamma_i \Gamma_f)^{1/2} / \Gamma_{\text{total}}$ in $N\bar{K} \rightarrow \Sigma(1880) \rightarrow \Lambda\pi$ $(\Gamma_1 \Gamma_2)^{1/2} / \Gamma$

VALUE	DOCUMENT ID	TECN	COMMENT
-0.24 or -0.24	1 MARTIN 77	DPWA	$\bar{K}N$ multichannel
-0.12 \pm 0.02	2 BAILLON 75	IPWA	$\bar{K}N \rightarrow \Lambda\pi$
+0.05 \pm 0.07 -0.02	VANHORN 75	DPWA	$K^- p \rightarrow \Lambda\pi^0$
-0.169 \pm 0.119	DEVENISH 74B	DPWA	Fixed- t dispersion rel.
-0.30	3 LEA 73	DPWA	Multichannel K-matrix
-0.09 \pm 0.04	BARBARO... 70	DPWA	$K^- N \rightarrow \Lambda\pi$
-0.14 \pm 0.03	LITCHFIELD 70	DPWA	$K^- N \rightarrow \Lambda\pi$
-0.11 \pm 0.03	SMART 68	DPWA	$K^- N \rightarrow \Lambda\pi$

$(\Gamma_i \Gamma_f)^{1/2} / \Gamma_{\text{total}}$ in $N\bar{K} \rightarrow \Sigma(1880) \rightarrow \Sigma\pi$ $(\Gamma_1 \Gamma_3)^{1/2} / \Gamma$

VALUE	DOCUMENT ID	TECN	COMMENT
+0.30 or +0.29 not seen	1 MARTIN 77	DPWA	$\bar{K}N$ multichannel
	3 LEA 73	DPWA	Multichannel K-matrix

$(\Gamma_i \Gamma_f)^{1/2} / \Gamma_{\text{total}}$ in $N\bar{K} \rightarrow \Sigma(1880) \rightarrow N\bar{K}^*(892), S=1/2, P\text{-wave}$ $(\Gamma_1 \Gamma_4)^{1/2} / \Gamma$

VALUE	DOCUMENT ID	TECN	COMMENT
-0.05 \pm 0.03	4 CAMERON 78B	DPWA	$K^- p \rightarrow N\bar{K}^*$

$(\Gamma_i \Gamma_f)^{1/2} / \Gamma_{\text{total}}$ in $N\bar{K} \rightarrow \Sigma(1880) \rightarrow N\bar{K}^*(892), S=3/2, P\text{-wave}$ $(\Gamma_1 \Gamma_5)^{1/2} / \Gamma$

VALUE	DOCUMENT ID	TECN	COMMENT
+0.11 \pm 0.03	CAMERON 78B	DPWA	$K^- p \rightarrow N\bar{K}^*$

$\Sigma(1880)$ FOOTNOTES

- The two MARTIN 77 values are from a T-matrix pole and from a Breit-Wigner fit.
- From solution 1 of BAILLON 75; not present in solution 2.
- Only unconstrained states from table 1 of LEA 73 are listed.
- The published sign has been changed to be in accord with the baryon-first convention.

$\Sigma(1880)$ REFERENCES

GOPAL 80	Toronto Conf. 159	G.P. Gopal	(RHEL) IJP
CAMERON 78B	NP B146 327	W. Cameron et al.	(RHEL, LOIC) IJP
MARTIN 77	NP B127 349	B.R. Martin, M.K. Pidcock, R.G. Moorhouse	(LOUC+) IJP
Also	NP B126 266	B.R. Martin, M.K. Pidcock	(LOUC) IJP
Also	NP B126 285	B.R. Martin, M.K. Pidcock	(LOUC) IJP
BAILLON 75	NP B94 39	P.H. Baillon, P.J. Litchfield	(CERN, RHEL) IJP
VANHORN 75	NP B87 145	A.J. van Horn	(LBL) IJP
Also	NP B87 157	A.J. van Horn	(LBL) IJP
DEVENISH 74B	NP B81 330	R.C.E. Devenish, C.D. Froggatt, B.R. Martin	(DESY+) IJP
LEA 73	NP B56 77	A.T. Lea et al.	(RHEL, LOUC, GLAS, AARH) IJP
ARMENTEROS 70	Duke Conf. 123	R. Armenteros et al.	(CERN, HEID, SACL) IJP
Hyperon Resonances, 1970			
BARBARO... 70	Duke Conf. 173	A. Barbaro-Galsteri	(LRL) IJP
Hyperon Resonances, 1970			
LITCHFIELD 70	NP B22 269	P.J. Litchfield	(RHEL) IJP
BAILEY 69	Thesis UCLR 50617	J.M. Bailey	(LLL) IJP
SMART 68	PR 169 1330	W.M. Smart	(LRL) IJP

$\Sigma(1915) F_{15} \quad I(J^P) = 1(\frac{5}{2}^+)$ Status: * * * *

Discovered by COOL 66. For results published before 1974 (they are now obsolete), see our 1982 edition Physics Letters **111B** 1 (1982).

This entry only includes results from partial-wave analyses. Parameters of peaks seen in cross sections and invariant-mass distributions in this region used to be listed in a separate entry immediately following. They may be found in our 1986 edition Physics Letters **170B** 1 (1986).

$\Sigma(1915)$ MASS

VALUE (MeV)	DOCUMENT ID	TECN	COMMENT
1900 to 1935 (\approx 1915) OUR ESTIMATE			
1937 \pm 20	ALSTON... 78	DPWA	$\bar{K}N \rightarrow \bar{K}N$
1894 \pm 5	1 CORDEN 77c	DPWA	$K^- n \rightarrow \Sigma\pi$
1909 \pm 5	1 CORDEN 77c	DPWA	$K^- n \rightarrow \Sigma\pi$
1920 \pm 10	GOPAL 77	DPWA	$\bar{K}N$ multichannel
1900 \pm 4	2 CORDEN 76	DPWA	$K^- n \rightarrow \Lambda\pi^-$
1920 \pm 30	BAILLON 75	IPWA	$\bar{K}N \rightarrow \Lambda\pi$
1914 \pm 10	HEMINGWAY 75	DPWA	$K^- p \rightarrow \bar{K}N$
1920 \pm 15 -20	VANHORN 75	DPWA	$K^- p \rightarrow \Lambda\pi^0$
1920 \pm 5	KANE 74	DPWA	$K^- p \rightarrow \Sigma\pi$
• • • We do not use the following data for averages, fits, limits, etc. • • •			
not seen	DECLAIS 77	DPWA	$\bar{K}N \rightarrow \bar{K}N$
1925 or 1933	3 MARTIN 77	DPWA	$\bar{K}N$ multichannel
1915	DEBELLEFON 76	IPWA	$K^- p \rightarrow \Lambda\pi^0$

$\Sigma(1915)$ WIDTH

VALUE (MeV)	DOCUMENT ID	TECN	COMMENT
80 to 160 (\approx 120) OUR ESTIMATE			
161 \pm 20	ALSTON... 78	DPWA	$\bar{K}N \rightarrow \bar{K}N$
107 \pm 14	1 CORDEN 77c	DPWA	$K^- n \rightarrow \Sigma\pi$
85 \pm 13	1 CORDEN 77c	DPWA	$K^- n \rightarrow \Sigma\pi$
130 \pm 10	GOPAL 77	DPWA	$\bar{K}N$ multichannel
75 \pm 14	2 CORDEN 76	DPWA	$K^- n \rightarrow \Lambda\pi^-$
70 \pm 20	BAILLON 75	IPWA	$\bar{K}N \rightarrow \Lambda\pi$
85 \pm 15	HEMINGWAY 75	DPWA	$K^- p \rightarrow \bar{K}N$
102 \pm 18	VANHORN 75	DPWA	$K^- p \rightarrow \Lambda\pi^0$
162 \pm 25	KANE 74	DPWA	$K^- p \rightarrow \Sigma\pi$
• • • We do not use the following data for averages, fits, limits, etc. • • •			
171 or 173	3 MARTIN 77	DPWA	$\bar{K}N$ multichannel
60	DEBELLEFON 76	IPWA	$K^- p \rightarrow \Lambda\pi^0$

$\Sigma(1915)$ DECAY MODES

Mode	Fraction (Γ_i/Γ)
Γ_1 $N\bar{K}$	5-15 %
Γ_2 $\Lambda\pi$	seen
Γ_3 $\Sigma\pi$	seen
Γ_4 $\Sigma(1385)\pi$	<5 %
Γ_5 $\Sigma(1385)\pi, P\text{-wave}$	
Γ_6 $\Sigma(1385)\pi, F\text{-wave}$	

The above branching fractions are our estimates, not fits or averages.

$\Sigma(1915)$ BRANCHING RATIOS

See "Sign conventions for resonance couplings" in the Note on Λ and Σ Resonances.

$\Gamma(N\bar{K})/\Gamma_{\text{total}}$	DOCUMENT ID	TECN	COMMENT	Γ_1/Γ
0.05 to 0.15 OUR ESTIMATE				
0.03 \pm 0.02	4 GOPAL 80	DPWA	$\bar{K}N \rightarrow \bar{K}N$	
0.14 \pm 0.05	ALSTON... 78	DPWA	$\bar{K}N \rightarrow \bar{K}N$	
0.11 \pm 0.04	HEMINGWAY 75	DPWA	$K^- p \rightarrow \bar{K}N$	
• • • We do not use the following data for averages, fits, limits, etc. • • •				
0.05 \pm 0.03	GOPAL 77	DPWA	See GOPAL 80	
0.08 or 0.08	3 MARTIN 77	DPWA	$\bar{K}N$ multichannel	

$(\Gamma_i \Gamma_f)^{1/2} / \Gamma_{\text{total}}$ in $N\bar{K} \rightarrow \Sigma(1915) \rightarrow \Lambda\pi$ $(\Gamma_1 \Gamma_2)^{1/2} / \Gamma$

VALUE	DOCUMENT ID	TECN	COMMENT
-0.09 \pm 0.03	GOPAL 77	DPWA	$\bar{K}N$ multichannel
-0.10 \pm 0.01	2 CORDEN 76	DPWA	$K^- n \rightarrow \Lambda\pi^-$
-0.06 \pm 0.02	BAILLON 75	IPWA	$\bar{K}N \rightarrow \Lambda\pi$
-0.09 \pm 0.02	VANHORN 75	DPWA	$K^- p \rightarrow \Lambda\pi^0$
-0.087 \pm 0.056	DEVENISH 74B	DPWA	Fixed- t dispersion rel.
• • • We do not use the following data for averages, fits, limits, etc. • • •			
-0.09 or -0.09	3 MARTIN 77	DPWA	$\bar{K}N$ multichannel
-0.10	DEBELLEFON 76	IPWA	$K^- p \rightarrow \Lambda\pi^0$

$(\Gamma_i \Gamma_f)^{1/2} / \Gamma_{\text{total}}$ in $N\bar{K} \rightarrow \Sigma(1915) \rightarrow \Sigma\pi$ $(\Gamma_1 \Gamma_3)^{1/2} / \Gamma$

VALUE	DOCUMENT ID	TECN	COMMENT
-0.17 \pm 0.01	1 CORDEN 77c	DPWA	$K^- n \rightarrow \Sigma\pi$
-0.15 \pm 0.02	1 CORDEN 77c	DPWA	$K^- n \rightarrow \Sigma\pi$
-0.19 \pm 0.03	GOPAL 77	DPWA	$\bar{K}N$ multichannel
-0.16 \pm 0.03	KANE 74	DPWA	$K^- p \rightarrow \Sigma\pi$
• • • We do not use the following data for averages, fits, limits, etc. • • •			
-0.05 or -0.05	3 MARTIN 77	DPWA	$\bar{K}N$ multichannel

$(\Gamma_i \Gamma_f)^{1/2} / \Gamma_{\text{total}}$ in $N\bar{K} \rightarrow \Sigma(1915) \rightarrow \Sigma(1385)\pi, P\text{-wave}$ $(\Gamma_1 \Gamma_5)^{1/2} / \Gamma$

VALUE	DOCUMENT ID	TECN	COMMENT
<0.01	CAMERON 78	DPWA	$K^- p \rightarrow \Sigma(1385)\pi$

$(\Gamma_i \Gamma_f)^{1/2} / \Gamma_{\text{total}}$ in $N\bar{K} \rightarrow \Sigma(1915) \rightarrow \Sigma(1385)\pi, F\text{-wave}$ $(\Gamma_1 \Gamma_6)^{1/2} / \Gamma$

VALUE	DOCUMENT ID	TECN	COMMENT
+0.039 \pm 0.009	5 CAMERON 78	DPWA	$K^- p \rightarrow \Sigma(1385)\pi$

$\Sigma(1915)$ FOOTNOTES

- The two entries for CORDEN 77c are from two different acceptable solutions.
- Preferred solution 3; see CORDEN 76 for other possibilities.
- The two MARTIN 77 values are from a T-matrix pole and from a Breit-Wigner fit.
- The mass and width are fixed to the GOPAL 77 values due to the low elasticity.
- The published sign has been changed to be in accord with the baryon-first convention.

Baryon Particle Listings

$\Sigma(1915), \Sigma(1940)$

$\Sigma(1915)$ REFERENCES

PDG	86	PL 170B 1	M. Aguilar-Benitez <i>et al.</i>	(CERN, CIT+)
PDG	82	PL 111B 1	M. Roos <i>et al.</i>	(HEL5, CIT, CERN)
GOPAL	80	Toronto Conf. 159	G.P. Gopal	(RHEL) IJP
ALSTON-...	78	PR D18 182	M. Alston-Garnjost <i>et al.</i>	(LBL, MTHO+) IJP
Also		PRL 38 1007	M. Alston-Garnjost <i>et al.</i>	(LBL, MTHO+) IJP
CAMERON	78	NP B143 189	W. Cameron <i>et al.</i>	(RHEL, LOIC) IJP
CORDEN	77C	NP B125 61	M.J. Corden <i>et al.</i>	(BIRM) IJP
DECLAIS	77	CERN 77-16	Y. Declais <i>et al.</i>	(CAEN, CERN) IJP
GOPAL	77	NP B119 362	G.P. Gopal <i>et al.</i>	(LOIC, RHEL) IJP
MARTIN	77	NP B127 349	B.R. Martin, M.K. Pidcock, R.G. Moorhouse	(LOUC+) IJP
Also		NP B126 266	B.R. Martin, M.K. Pidcock	(LOUC) IJP
Also		NP B126 285	B.R. Martin, M.K. Pidcock	(LOUC) IJP
CORDEN	76	NP B104 382	M.J. Corden <i>et al.</i>	(BIRM) IJP
DEBELLEFON	76	NP B109 129	A. de Bellefon, A. Berthon	(CDEF) IJP
BAILLON	75	NP B94 39	P.H. Baillon, P.J. Litchfield	(CERN, RHEL) IJP
HEMINGWAY	75	NP B91 12	R.J. Hemingway <i>et al.</i>	(CERN, HEIDH, MPIM) IJP
VANHORN	75	NP B87 145	A.J. van Horn	(LBL) IJP
Also		NP B87 157	A.J. van Horn	(LBL) IJP
DEVENISH	74B	NP B81 330	R.C.E. Devenish, C.D. Froggatt, B.R. Martin	(DESY+) IJP
KANE	74	LBL-2452	D.F. Kane	(LBL) IJP
COOL	66	PRL 16 1228	R.L. Cool <i>et al.</i>	(BNL)

$\Sigma(1940)$ BRANCHING RATIOS

See "Sign conventions for resonance couplings" in the Note on Λ and Σ Resonances.

$\Gamma(N\bar{K})/\Gamma_{\text{total}}$	DOCUMENT ID	TECN	COMMENT	Γ_1/Γ
VALUE				
<0.2 OUR ESTIMATE				
<0.04	GOPAL	77	DPWA $\bar{K}N$ multichannel	
0.14 or 0.13	¹ MARTIN	77	DPWA $\bar{K}N$ multichannel	

$(\Gamma_1\Gamma_f)^{1/2}/\Gamma_{\text{total}}$ in $N\bar{K} \rightarrow \Sigma(1940) \rightarrow \Lambda\pi$	DOCUMENT ID	TECN	COMMENT	$(\Gamma_1\Gamma_2)^{1/2}/\Gamma$
VALUE				
-0.06 ± 0.03	GOPAL	77	DPWA $\bar{K}N$ multichannel	
-0.04 ± 0.02	BAILLON	75	IPWA $\bar{K}N \rightarrow \Lambda\pi$	
-0.05 ± 0.03	VANHORN	75	DPWA $K^-p \rightarrow \Lambda\pi^0$	
-0.153 ± 0.070	DEVENISH	74B	Fixed-t dispersion rel.	
••• We do not use the following data for averages, fits, limits, etc. •••				
-0.15 or -0.14	¹ MARTIN	77	DPWA $\bar{K}N$ multichannel	

$(\Gamma_1\Gamma_f)^{1/2}/\Gamma_{\text{total}}$ in $N\bar{K} \rightarrow \Sigma(1940) \rightarrow \Sigma\pi$	DOCUMENT ID	TECN	COMMENT	$(\Gamma_1\Gamma_3)^{1/2}/\Gamma$
VALUE				
-0.08 ± 0.04	GOPAL	77	DPWA $\bar{K}N$ multichannel	
-0.14 ± 0.04	KANE	74	DPWA $K^-p \rightarrow \Sigma\pi$	
••• We do not use the following data for averages, fits, limits, etc. •••				
+0.16 or +0.16	¹ MARTIN	77	DPWA $\bar{K}N$ multichannel	

$(\Gamma_1\Gamma_f)^{1/2}/\Gamma_{\text{total}}$ in $N\bar{K} \rightarrow \Sigma(1940) \rightarrow \Lambda(1520)\pi, P\text{-wave}$	DOCUMENT ID	TECN	COMMENT	$(\Gamma_1\Gamma_7)^{1/2}/\Gamma$
VALUE				
< 0.03	CAMERON	77	DPWA $K^-p \rightarrow \Lambda(1520)\pi^0$	
-0.11 ± 0.04	LITCHFIELD	74B	DPWA $K^-p \rightarrow \Lambda(1520)\pi^0$	

$(\Gamma_1\Gamma_f)^{1/2}/\Gamma_{\text{total}}$ in $N\bar{K} \rightarrow \Sigma(1940) \rightarrow \Lambda(1520)\pi, F\text{-wave}$	DOCUMENT ID	TECN	COMMENT	$(\Gamma_1\Gamma_8)^{1/2}/\Gamma$
VALUE				
0.062 ± 0.021	CAMERON	77	DPWA $K^-p \rightarrow \Lambda(1520)\pi^0$	
-0.08 ± 0.04	LITCHFIELD	74B	DPWA $K^-p \rightarrow \Lambda(1520)\pi^0$	

$(\Gamma_1\Gamma_f)^{1/2}/\Gamma_{\text{total}}$ in $N\bar{K} \rightarrow \Sigma(1940) \rightarrow \Delta(1232)\bar{K}, S\text{-wave}$	DOCUMENT ID	TECN	COMMENT	$(\Gamma_1\Gamma_{10})^{1/2}/\Gamma$
VALUE				
-0.16 ± 0.05	LITCHFIELD	74C	DPWA $K^-p \rightarrow \Delta(1232)\bar{K}$	

$(\Gamma_1\Gamma_f)^{1/2}/\Gamma_{\text{total}}$ in $N\bar{K} \rightarrow \Sigma(1940) \rightarrow \Delta(1232)\bar{K}, D\text{-wave}$	DOCUMENT ID	TECN	COMMENT	$(\Gamma_1\Gamma_{11})^{1/2}/\Gamma$
VALUE				
-0.14 ± 0.05	LITCHFIELD	74C	DPWA $K^-p \rightarrow \Delta(1232)\bar{K}$	

$(\Gamma_1\Gamma_f)^{1/2}/\Gamma_{\text{total}}$ in $N\bar{K} \rightarrow \Sigma(1940) \rightarrow \Sigma(1385)\pi$	DOCUMENT ID	TECN	COMMENT	$(\Gamma_1\Gamma_4)^{1/2}/\Gamma$
VALUE				
+0.066 ± 0.025	² CAMERON	78	DPWA $K^-p \rightarrow \Sigma(1385)\pi$	

$(\Gamma_1\Gamma_f)^{1/2}/\Gamma_{\text{total}}$ in $N\bar{K} \rightarrow \Sigma(1940) \rightarrow N\bar{K}^*(892)$	DOCUMENT ID	TECN	COMMENT	$(\Gamma_1\Gamma_{12})^{1/2}/\Gamma$
VALUE				
-0.09 ± 0.02	³ CAMERON	78B	DPWA $K^-p \rightarrow N\bar{K}^*$	

$\Sigma(1940)$ FOOTNOTES

- The two MARTIN 77 values are from a T-matrix pole and from a Breit-Wigner fit.
- The published sign has been changed to be in accord with the baryon-first convention.
- Upper limits on the D_1 and D_3 waves are each 0.03.

$\Sigma(1940)$ REFERENCES

PDG	82	PL 111B 1	M. Roos <i>et al.</i>	(HEL5, CIT, CERN)
GOPAL	80	Toronto Conf. 159	G.P. Gopal	(RHEL)
CAMERON	78	NP B143 189	W. Cameron <i>et al.</i>	(RHEL, LOIC) IJP
CAMERON	78B	NP B146 327	W. Cameron <i>et al.</i>	(RHEL, LOIC) IJP
CAMERON	77	NP B131 399	W. Cameron <i>et al.</i>	(RHEL, LOIC) IJP
GOPAL	77	NP B119 362	G.P. Gopal <i>et al.</i>	(LOIC, RHEL) IJP
GOYAL	77	PR D16 2746	D.P. Goyal, A.V. Sodhi	(DELH)
MARTIN	77	NP B127 349	B.R. Martin, M.K. Pidcock, R.G. Moorhouse	(LOUC+) IJP
Also		NP B126 266	B.R. Martin, M.K. Pidcock	(LOUC) IJP
Also		NP B126 285	B.R. Martin, M.K. Pidcock	(LOUC) IJP
DEBELLEFON	76	NP B109 129	A. de Bellefon, A. Berthon	(CDEF) IJP
BAILLON	75	NP B94 39	P.H. Baillon, P.J. Litchfield	(CERN, RHEL) IJP
HEMINGWAY	75	NP B91 12	R.J. Hemingway <i>et al.</i>	(CERN, HEIDH, MPIM) IJP
VANHORN	75	NP B87 145	A.J. van Horn	(LBL) IJP
Also		NP B87 157	A.J. van Horn	(LBL) IJP
DEVENISH	74B	NP B81 330	R.C.E. Devenish, C.D. Froggatt, B.R. Martin	(DESY+) IJP
KANE	74	LBL-2452	D.F. Kane	(LBL) IJP
LITCHFIELD	74B	NP B74 19	P.J. Litchfield <i>et al.</i>	(CERN, HEIDH) IJP
LITCHFIELD	74C	NP B74 39	P.J. Litchfield <i>et al.</i>	(CERN, HEIDH) IJP

$\Sigma(1940) D_{13}$ $I(J^P) = 1(\frac{3}{2}^-)$ Status: ***

For results published before 1974 (they are now obsolete), see our 1982 edition Physics Letters **111B** 1 (1982).

Not all analyses require this state. It is not required by the GOPAL 77 analysis of $K^-n \rightarrow (\Sigma\pi)^-$ nor by the GOPAL 80 analysis of $K^-n \rightarrow K^-n$. See also HEMINGWAY 75.

$\Sigma(1940)$ MASS

VALUE (MeV)	DOCUMENT ID	TECN	COMMENT
1900 to 1950 (≈ 1940) OUR ESTIMATE			
1920 ± 50	GOPAL	77	DPWA $\bar{K}N$ multichannel
1950 ± 30	BAILLON	75	IPWA $\bar{K}N \rightarrow \Lambda\pi$
1949 +40 -60	VANHORN	75	DPWA $K^-p \rightarrow \Lambda\pi^0$
1935 ± 80	KANE	74	DPWA $K^-p \rightarrow \Sigma\pi$
1940 ± 20	LITCHFIELD	74B	DPWA $K^-p \rightarrow \Lambda(1520)\pi^0$
1950 ± 20	LITCHFIELD	74C	DPWA $K^-p \rightarrow \Delta(1232)\bar{K}$
••• We do not use the following data for averages, fits, limits, etc. •••			
1886 or 1893	¹ MARTIN	77	DPWA $\bar{K}N$ multichannel
1940	DEBELLEFON	76	IPWA $K^-p \rightarrow \Lambda\pi^0, F_{17}$ wave

$\Sigma(1940)$ WIDTH

VALUE (MeV)	DOCUMENT ID	TECN	COMMENT
150 to 300 (≈ 220) OUR ESTIMATE			
170 ± 25	CAMERON	78B	DPWA $K^-p \rightarrow N\bar{K}^*$
300 ± 80	GOPAL	77	DPWA $\bar{K}N$ multichannel
150 ± 75	BAILLON	75	IPWA $\bar{K}N \rightarrow \Lambda\pi$
160 +70 -40	VANHORN	75	DPWA $K^-p \rightarrow \Lambda\pi^0$
330 ± 80	KANE	74	DPWA $K^-p \rightarrow \Sigma\pi$
60 ± 20	LITCHFIELD	74B	DPWA $K^-p \rightarrow \Lambda(1520)\pi^0$
70 +30 -20	LITCHFIELD	74C	DPWA $K^-p \rightarrow \Delta(1232)\bar{K}$
••• We do not use the following data for averages, fits, limits, etc. •••			
157 or 159	¹ MARTIN	77	DPWA $\bar{K}N$ multichannel

$\Sigma(1940)$ DECAY MODES

Mode	Fraction (Γ_i/Γ)
Γ_1 $N\bar{K}$	<20 %
Γ_2 $\Lambda\pi$	seen
Γ_3 $\Sigma\pi$	seen
Γ_4 $\Sigma(1385)\pi$	seen
Γ_5 $\Sigma(1385)\pi, S\text{-wave}$	
Γ_6 $\Lambda(1520)\pi$	seen
Γ_7 $\Lambda(1520)\pi, P\text{-wave}$	
Γ_8 $\Lambda(1520)\pi, F\text{-wave}$	
Γ_9 $\Delta(1232)\bar{K}$	seen
Γ_{10} $\Delta(1232)\bar{K}, S\text{-wave}$	
Γ_{11} $\Delta(1232)\bar{K}, D\text{-wave}$	
Γ_{12} $N\bar{K}^*(892)$	seen
Γ_{13} $N\bar{K}^*(892), S=3/2, S\text{-wave}$	

See key on page 373

Baryon Particle Listings

 $\Sigma(2000), \Sigma(2030)$ $\Sigma(2000) S_{11}$ $I(J^P) = 1(\frac{1}{2}^-)$ Status: *

OMITTED FROM SUMMARY TABLE

We list here all reported S_{11} states lying above the $\Sigma(1750) S_{11}$. $\Sigma(2000)$ MASS

VALUE (MeV)	DOCUMENT ID	TECN	COMMENT
≈ 2000 OUR ESTIMATE			
1944 ± 15	GOPAL	80	DPWA $\bar{K}N \rightarrow \bar{K}N$
1955 ± 15	GOPAL	77	DPWA $\bar{K}N$ multichannel
1755 or 1834	¹ MARTIN	77	DPWA $\bar{K}N$ multichannel
2004 ± 40	VANHORN	75	DPWA $K^-p \rightarrow \Lambda\pi^0$

 $\Sigma(2000)$ WIDTH

VALUE (MeV)	DOCUMENT ID	TECN	COMMENT
215 ± 25	GOPAL	80	DPWA $\bar{K}N \rightarrow \bar{K}N$
170 ± 40	GOPAL	77	DPWA $\bar{K}N$ multichannel
413 or 450	¹ MARTIN	77	DPWA $\bar{K}N$ multichannel
116 ± 40	VANHORN	75	DPWA $K^-p \rightarrow \Lambda\pi^0$

 $\Sigma(2000)$ DECAY MODES

Mode	Fraction (Γ_i/Γ)
Γ_1 $N\bar{K}$	17–23 %
Γ_2 $\Lambda\pi$	17–23 %
Γ_3 $\Sigma\pi$	5–10 %
Γ_4 $\Lambda(1520)\pi$	<2 %
Γ_5 $N\bar{K}^*(892)$, $S=1/2$, S -wave	5–15 %
Γ_6 $N\bar{K}^*(892)$, $S=3/2$, D -wave	10–20 %

 $\Sigma(2000)$ BRANCHING RATIOSSee "Sign conventions for resonance couplings" in the Note on Λ and Σ Resonances.

$\Gamma(N\bar{K})/\Gamma_{\text{total}}$	DOCUMENT ID	TECN	COMMENT	Γ_1/Γ
VALUE				
0.51 ± 0.05	GOPAL	80	DPWA $\bar{K}N \rightarrow \bar{K}N$	
0.44 ± 0.05	GOPAL	77	DPWA See GOPAL 80	
0.62 or 0.57	¹ MARTIN	77	DPWA $\bar{K}N$ multichannel	

$(\Gamma_1\Gamma_2)^{1/2}/\Gamma_{\text{total}}$ in $N\bar{K} \rightarrow \Sigma(2000) \rightarrow \Lambda\pi$	DOCUMENT ID	TECN	COMMENT	$(\Gamma_1\Gamma_2)^{1/2}/\Gamma$
VALUE				
0.08 ± 0.03	GOPAL	77	DPWA $\bar{K}N$ multichannel	
−0.19 or −0.18	¹ MARTIN	77	DPWA $\bar{K}N$ multichannel	
not seen	BAILLON	75	IPWA $\bar{K}N \rightarrow \Lambda\pi$	
+0.07 + 0.02 −0.01	VANHORN	75	DPWA $K^-p \rightarrow \Lambda\pi^0$	

$(\Gamma_1\Gamma_3)^{1/2}/\Gamma_{\text{total}}$ in $N\bar{K} \rightarrow \Sigma(2000) \rightarrow \Sigma\pi$	DOCUMENT ID	TECN	COMMENT	$(\Gamma_1\Gamma_3)^{1/2}/\Gamma$
VALUE				
+0.20 ± 0.04	GOPAL	77	DPWA $\bar{K}N$ multichannel	
+0.26 or +0.24	¹ MARTIN	77	DPWA $\bar{K}N$ multichannel	

$(\Gamma_1\Gamma_4)^{1/2}/\Gamma_{\text{total}}$ in $N\bar{K} \rightarrow \Sigma(2000) \rightarrow \Lambda(1520)\pi$	DOCUMENT ID	TECN	COMMENT	$(\Gamma_1\Gamma_4)^{1/2}/\Gamma$
VALUE				
+0.081 ± 0.021	² CAMERON	77	DPWA P -wave decay	

$(\Gamma_1\Gamma_5)^{1/2}/\Gamma_{\text{total}}$ in $N\bar{K} \rightarrow \Sigma(2000) \rightarrow N\bar{K}^*(892)$, $S=1/2$, S -wave	DOCUMENT ID	TECN	COMMENT	$(\Gamma_1\Gamma_5)^{1/2}/\Gamma$
VALUE				
+0.10 ± 0.02	² CAMERON	78B	DPWA $K^-p \rightarrow N\bar{K}^*$	

$(\Gamma_1\Gamma_6)^{1/2}/\Gamma_{\text{total}}$ in $N\bar{K} \rightarrow \Sigma(2000) \rightarrow N\bar{K}^*(892)$, $S=3/2$, D -wave	DOCUMENT ID	TECN	COMMENT	$(\Gamma_1\Gamma_6)^{1/2}/\Gamma$
VALUE				
−0.07 ± 0.03	CAMERON	78B	DPWA $K^-p \rightarrow N\bar{K}^*$	

 $\Sigma(2000)$ FOOTNOTES

- ¹ The two MARTIN 77 values are from a T-matrix pole and from a Breit-Wigner fit.
² The published sign has been changed to be in accord with the baryon-first convention.

 $\Sigma(2000)$ REFERENCES

GOPAL	80	Toronto Conf.	159	G.P. Gopal	(RHEL) IJP
CAMERON	78B	NP B146	327	W. Cameron et al.	(RHEL, LOIC) IJP
CAMERON	77	NP B131	399	W. Cameron et al.	(RHEL, LOIC) IJP
GOPAL	77	NP B119	362	G.P. Gopal et al.	(LOIC, RHEL) IJP
MARTIN	77	NP B127	349	B.R. Martin, M.K. Pidcock, R.G. Moorhouse	(LOUC+) IJP
Also		NP B126	266	B.R. Martin, M.K. Pidcock	(LOUC)
Also		NP B126	285	B.R. Martin, M.K. Pidcock	(LOUC) IJP
BAILLON	75	NP B94	39	P.H. Baillon, P.J. Litchfield	(CERN, RHEL) IJP
VANHORN	75	NP B87	145	A.J. van Horn	(LBL) IJP
Also		NP B87	157	A.J. van Horn	(LBL) IJP

 $\Sigma(2030) F_{17}$ $I(J^P) = 1(\frac{7}{2}^+)$ Status: ***Discovered by COOL 66 and by WOHL 66. For most results published before 1974 (they are now obsolete), see our 1982 edition Physics Letters **111B** 1 (1982).This entry only includes results from partial-wave analyses. Parameters of peaks seen in cross sections and invariant-mass distributions around 2030 MeV may be found in our 1984 edition, Reviews of Modern Physics **56** S1 (1984). $\Sigma(2030)$ MASS

VALUE (MeV)	DOCUMENT ID	TECN	COMMENT
2025 to 2040 (≈ 2030) OUR ESTIMATE			
2036 ± 5	GOPAL	80	DPWA $\bar{K}N \rightarrow \bar{K}N$
2038 ± 10	CORDEN	77B	$K^-N \rightarrow N\bar{K}^*$
2040 ± 5	GOPAL	77	DPWA $\bar{K}N$ multichannel
2030 ± 3	¹ CORDEN	76	DPWA $K^-n \rightarrow \Lambda\pi^-$
2035 ± 15	BAILLON	75	IPWA $\bar{K}N \rightarrow \Lambda\pi$
2038 ± 10	HEMINGWAY	75	DPWA $K^-p \rightarrow \bar{K}N$
2042 ± 11	VANHORN	75	DPWA $K^-p \rightarrow \Lambda\pi^0$
2020 ± 6	KANE	74	DPWA $K^-p \rightarrow \Sigma\pi$
2035 ± 10	LITCHFIELD	74B	DPWA $K^-p \rightarrow \Lambda(1520)\pi^0$
2020 ± 30	LITCHFIELD	74C	DPWA $K^-p \rightarrow \Delta(1232)\bar{K}$
2025 ± 10	LITCHFIELD	74D	DPWA $K^-p \rightarrow \Lambda(1820)\pi^0$
• • • We do not use the following data for averages, fits, limits, etc. • • •			
2027 to 2057	GOYAL	77	DPWA $K^-N \rightarrow \Sigma\pi$
2030	DEBELLEFON	76	IPWA $K^-p \rightarrow \Lambda\pi^0$

 $\Sigma(2030)$ WIDTH

VALUE (MeV)	DOCUMENT ID	TECN	COMMENT
150 to 200 (≈ 180) OUR ESTIMATE			
172 ± 10	GOPAL	80	DPWA $\bar{K}N \rightarrow \bar{K}N$
137 ± 40	CORDEN	77B	$K^-N \rightarrow N\bar{K}^*$
190 ± 10	GOPAL	77	DPWA $\bar{K}N$ multichannel
201 ± 9	¹ CORDEN	76	DPWA $K^-n \rightarrow \Lambda\pi^-$
180 ± 20	BAILLON	75	IPWA $\bar{K}N \rightarrow \Lambda\pi$
172 ± 15	HEMINGWAY	75	DPWA $K^-p \rightarrow \bar{K}N$
178 ± 13	VANHORN	75	DPWA $K^-p \rightarrow \Lambda\pi^0$
111 ± 5	KANE	74	DPWA $K^-p \rightarrow \Sigma\pi$
160 ± 20	LITCHFIELD	74B	DPWA $K^-p \rightarrow \Lambda(1520)\pi^0$
200 ± 30	LITCHFIELD	74C	DPWA $K^-p \rightarrow \Delta(1232)\bar{K}$
• • • We do not use the following data for averages, fits, limits, etc. • • •			
260	DECLAIS	77	DPWA $\bar{K}N \rightarrow \bar{K}N$
126 to 195	GOYAL	77	DPWA $K^-N \rightarrow \Sigma\pi$
160	DEBELLEFON	76	IPWA $K^-p \rightarrow \Lambda\pi^0$
70 to 125	LITCHFIELD	74D	DPWA $K^-p \rightarrow \Lambda(1820)\pi^0$

 $\Sigma(2030)$ DECAY MODES

Mode	Fraction (Γ_i/Γ)
Γ_1 $N\bar{K}$	17–23 %
Γ_2 $\Lambda\pi$	17–23 %
Γ_3 $\Sigma\pi$	5–10 %
Γ_4 ΞK	<2 %
Γ_5 $\Sigma(1385)\pi$	5–15 %
Γ_6 $\Sigma(1385)\pi$, F -wave	
Γ_7 $\Lambda(1520)\pi$	10–20 %
Γ_8 $\Lambda(1520)\pi$, D -wave	
Γ_9 $\Lambda(1520)\pi$, G -wave	
Γ_{10} $\Delta(1232)\bar{K}$	10–20 %
Γ_{11} $\Delta(1232)\bar{K}$, F -wave	
Γ_{12} $\Delta(1232)\bar{K}$, H -wave	
Γ_{13} $N\bar{K}^*(892)$	<5 %
Γ_{14} $N\bar{K}^*(892)$, $S=1/2$, F -wave	
Γ_{15} $N\bar{K}^*(892)$, $S=3/2$, F -wave	
Γ_{16} $\Lambda(1820)\pi$, P -wave	

The above branching fractions are our estimates, not fits or averages.

Baryon Particle Listings

 $\Sigma(2030)$, $\Sigma(2070)$ $\Sigma(2030)$ BRANCHING RATIOS

See "Sign conventions for resonance couplings" in the Note on Λ and Σ Resonances.

$\Gamma(N\bar{K})/\Gamma_{\text{total}}$	DOCUMENT ID	TECN	COMMENT	Γ_1/Γ
0.17 to 0.23 OUR ESTIMATE				
0.19 ± 0.03	GOPAL 80	DPWA	$\bar{K}N \rightarrow \bar{K}N$	
0.18 ± 0.03	HEMINGWAY 75	DPWA	$K^-p \rightarrow \bar{K}N$	
• • • We do not use the following data for averages, fits, limits, etc. • • •				
0.15	DECLAIS 77	DPWA	$\bar{K}N \rightarrow \bar{K}N$	
0.24 ± 0.02	GOPAL 77	DPWA	See GOPAL 80	

$(\Gamma_1\Gamma_f)^{1/2}/\Gamma_{\text{total}}$ in $N\bar{K} \rightarrow \Sigma(2030) \rightarrow \Lambda\pi$	DOCUMENT ID	TECN	COMMENT	$(\Gamma_1\Gamma_2)^{1/2}/\Gamma$
VALUE				
+0.18 ± 0.02	GOPAL 77	DPWA	$\bar{K}N$ multichannel	
+0.20 ± 0.01	¹ CORDEN 76	DPWA	$K^-n \rightarrow \Lambda\pi^-$	
+0.18 ± 0.02	BAILLON 75	IPWA	$\bar{K}N \rightarrow \Lambda\pi$	
+0.20 ± 0.01	VANHORN 75	DPWA	$K^-p \rightarrow \Lambda\pi^0$	
+0.195 ± 0.053	DEVENISH 74B		Fixed- t dispersion rel.	
• • • We do not use the following data for averages, fits, limits, etc. • • •				
0.20	DEBELLEFON 76	IPWA	$K^-p \rightarrow \Lambda\pi^0$	

$(\Gamma_1\Gamma_f)^{1/2}/\Gamma_{\text{total}}$ in $N\bar{K} \rightarrow \Sigma(2030) \rightarrow \Sigma\pi$	DOCUMENT ID	TECN	COMMENT	$(\Gamma_1\Gamma_3)^{1/2}/\Gamma$
VALUE				
-0.09 ± 0.01	² CORDEN 77C		$K^-n \rightarrow \Sigma\pi$	
-0.06 ± 0.01	² CORDEN 77C		$K^-n \rightarrow \Sigma\pi$	
-0.15 ± 0.03	GOPAL 77	DPWA	$\bar{K}N$ multichannel	
-0.10 ± 0.01	KANE 74	DPWA	$K^-p \rightarrow \Sigma\pi$	
• • • We do not use the following data for averages, fits, limits, etc. • • •				
-0.085 ± 0.02	³ GOYAL 77	DPWA	$K^-N \rightarrow \Sigma\pi$	

$(\Gamma_1\Gamma_f)^{1/2}/\Gamma_{\text{total}}$ in $N\bar{K} \rightarrow \Sigma(2030) \rightarrow \Xi K$	DOCUMENT ID	TECN	COMMENT	$(\Gamma_1\Gamma_4)^{1/2}/\Gamma$
VALUE				
0.023	MULLER 69B	DPWA	$K^-p \rightarrow \Xi K$	
<0.05	BURGUN 68	DPWA	$K^-p \rightarrow \Xi K$	
<0.05	TRIPP 67	RVUE	$K^-p \rightarrow \Xi K$	

$(\Gamma_1\Gamma_f)^{1/2}/\Gamma_{\text{total}}$ in $N\bar{K} \rightarrow \Sigma(2030) \rightarrow \Lambda(1820)\pi$, P -wave	DOCUMENT ID	TECN	COMMENT	$(\Gamma_1\Gamma_{16})^{1/2}/\Gamma$
VALUE				
0.14 ± 0.02	CORDEN 75B	DBC	$K^-n \rightarrow N\bar{K}\pi^-$	
0.18 ± 0.04	LITCHFIELD 74D	DPWA	$K^-p \rightarrow \Lambda(1820)\pi^0$	

$(\Gamma_1\Gamma_f)^{1/2}/\Gamma_{\text{total}}$ in $N\bar{K} \rightarrow \Sigma(2030) \rightarrow \Lambda(1520)\pi$, D -wave	DOCUMENT ID	TECN	COMMENT	$(\Gamma_1\Gamma_8)^{1/2}/\Gamma$
VALUE				
+0.114 ± 0.010	⁴ CAMERON 77	DPWA	$K^-p \rightarrow \Lambda(1520)\pi^0$	
0.14 ± 0.03	LITCHFIELD 74B	DPWA	$K^-p \rightarrow \Lambda(1520)\pi^0$	
• • • We do not use the following data for averages, fits, limits, etc. • • •				
0.10 ± 0.03	⁵ CORDEN 75B	DBC	$K^-n \rightarrow N\bar{K}\pi^-$	

$(\Gamma_1\Gamma_f)^{1/2}/\Gamma_{\text{total}}$ in $N\bar{K} \rightarrow \Sigma(2030) \rightarrow \Lambda(1520)\pi$, G -wave	DOCUMENT ID	TECN	COMMENT	$(\Gamma_1\Gamma_9)^{1/2}/\Gamma$
VALUE				
+0.146 ± 0.010	⁴ CAMERON 77	DPWA	$K^-p \rightarrow \Lambda(1520)\pi^0$	
0.02 ± 0.02	LITCHFIELD 74B	DPWA	$K^-p \rightarrow \Lambda(1520)\pi^0$	

$(\Gamma_1\Gamma_f)^{1/2}/\Gamma_{\text{total}}$ in $N\bar{K} \rightarrow \Sigma(2030) \rightarrow \Delta(1232)\bar{K}$, F -wave	DOCUMENT ID	TECN	COMMENT	$(\Gamma_1\Gamma_{11})^{1/2}/\Gamma$
VALUE				
0.16 ± 0.03	LITCHFIELD 74C	DPWA	$K^-p \rightarrow \Delta(1232)\bar{K}$	
• • • We do not use the following data for averages, fits, limits, etc. • • •				
0.17 ± 0.03	⁵ CORDEN 75B	DBC	$K^-n \rightarrow N\bar{K}\pi^-$	

$(\Gamma_1\Gamma_f)^{1/2}/\Gamma_{\text{total}}$ in $N\bar{K} \rightarrow \Sigma(2030) \rightarrow \Delta(1232)\bar{K}$, H -wave	DOCUMENT ID	TECN	COMMENT	$(\Gamma_1\Gamma_{12})^{1/2}/\Gamma$
VALUE				
0.00 ± 0.02	LITCHFIELD 74C	DPWA	$K^-p \rightarrow \Delta(1232)\bar{K}$	

$(\Gamma_1\Gamma_f)^{1/2}/\Gamma_{\text{total}}$ in $N\bar{K} \rightarrow \Sigma(2030) \rightarrow \Sigma(1385)\pi$	DOCUMENT ID	TECN	COMMENT	$(\Gamma_1\Gamma_5)^{1/2}/\Gamma$
VALUE				
+0.153 ± 0.026	⁴ CAMERON 78	DPWA	$K^-p \rightarrow \Sigma(1385)\pi$	

$(\Gamma_1\Gamma_f)^{1/2}/\Gamma_{\text{total}}$ in $N\bar{K} \rightarrow \Sigma(2030) \rightarrow N\bar{K}^*(892)$, $S=1/2$, F -wave	DOCUMENT ID	TECN	COMMENT	$(\Gamma_1\Gamma_{14})^{1/2}/\Gamma$
VALUE				
+0.06 ± 0.03	⁴ CAMERON 78B	DPWA	$K^-p \rightarrow N\bar{K}^*$	
-0.02 ± 0.01	CORDEN 77B		$K^-d \rightarrow NN\bar{K}^*$	

 $(\Gamma_1\Gamma_f)^{1/2}/\Gamma_{\text{total}}$ in $N\bar{K} \rightarrow \Sigma(2030) \rightarrow N\bar{K}^*(892)$, $S=3/2$, F -wave

VALUE	DOCUMENT ID	TECN	COMMENT	$(\Gamma_1\Gamma_{15})^{1/2}/\Gamma$
+0.04 ± 0.03	⁶ CAMERON 78B	DPWA	$K^-p \rightarrow N\bar{K}^*$	
-0.12 ± 0.02	CORDEN 77B		$K^-d \rightarrow NN\bar{K}^*$	

 $\Sigma(2030)$ FOOTNOTES

- Preferred solution 3; see CORDEN 76 for other possibilities.
- The two entries for CORDEN 77c are from two different acceptable solutions.
- This coupling is extracted from unnormalized data.
- The published sign has been changed to be in accord with the baryon-first convention.
- An upper limit.
- The upper limit on the G_3 wave is 0.03.

 $\Sigma(2030)$ REFERENCES

PDG 84	RMP 56 51	C.G. Wohl <i>et al.</i>	(LBL, CIT, CERN)
PDG 82	PL 111B 1	M. Roos <i>et al.</i>	(HELS, CIT, CERN)
GOPAL 80	Toronto Conf. 159	G.P. Gopal	(RHEL) IJP
CAMERON 78	NP B143 189	W. Cameron <i>et al.</i>	(RHEL, LOIC) IJP
CAMERON 78B	NP B146 327	W. Cameron <i>et al.</i>	(RHEL, LOIC) IJP
CAMERON 77	NP B131 399	W. Cameron <i>et al.</i>	(RHEL, LOIC) IJP
CORDEN 77B	NP B121 365	M.J. Corden <i>et al.</i>	(BIRM) IJP
CORDEN 77C	NP B125 61	M.J. Corden <i>et al.</i>	(BIRM) IJP
DECLAIS 77	CERN 77-16	Y. Declais <i>et al.</i>	(CAEN, CERN) IJP
GOPAL 77	NP B119 362	G.P. Gopal <i>et al.</i>	(LOIC, RHEL) IJP
GOYAL 77	PR D16 2746	D.P. Goyal, A.V. Sodhi	(DELH) IJP
CORDEN 76	NP B104 382	M.J. Corden <i>et al.</i>	(BIRM) IJP
DEBELLEFON 76	NP B109 129	A. de Bellefon, A. Berthon	(CDEF) IJP
BAILLON 75	NP B94 39	P.H. Baillon, P.J. Litchfield	(CERN, RHEL) IJP
CORDEN 75B	NP B92 365	M.J. Corden <i>et al.</i>	(BIRM) IJP
HEMINGWAY 75	NP B91 12	R.J. Hemingway <i>et al.</i>	(CERN, HEIDH, MPIM) IJP
VANHORN 75	NP B87 145	A.J. van Horn	(LBL) IJP
Also	NP B87 157	A.J. van Horn	(LBL) IJP
DEVENISH 74B	NP B81 330	R.C.E. Devenish, C.D. Froggatt, B.R. Martin	(DESY+) IJP
KANE 74	LBL-2452	D.F. Kane	(LBL) IJP
LITCHFIELD 74B	NP B74 19	P.J. Litchfield <i>et al.</i>	(CERN, HEIDH) IJP
LITCHFIELD 74C	NP B74 39	P.J. Litchfield <i>et al.</i>	(CERN, HEIDH) IJP
LITCHFIELD 74D	NP B74 12	P.J. Litchfield <i>et al.</i>	(CERN, HEIDH) IJP
MULLER 69B	Thesis UCRL 19372	R.A. Muller	(LRL) IJP
BURGUN 68	NP B8 447	G. Burgun <i>et al.</i>	(SACL, CDEF, RHEL)
TRIPP 67	NP B3 10	R.D. Tripp <i>et al.</i>	(LRL, SLAC, CERN+)
COOL 66	PRL 16 1228	R.L. Cool <i>et al.</i>	(BNL)
WOHL 66	PRL 17 107	C.G. Wohl, F.T. Solmitz, M.L. Stevenson	(LRL) IJP

 $\Sigma(2070)$ F_{15}

$$I(J^P) = 1(\frac{5}{2}^+) \text{ Status: } *$$

OMITTED FROM SUMMARY TABLE

This state suggested by BERTHON 70B finds support in GOPAL 80 with new K^-p polarization and K^-n angular distributions. The very broad state seen in KANE 72 is not required in the later (KANE 74) analysis of $\bar{K}N \rightarrow \Sigma\pi$.

 $\Sigma(2070)$ MASS

VALUE (MeV)	DOCUMENT ID	TECN	COMMENT
≈ 2070 OUR ESTIMATE			
2051 ± 25	GOPAL 80	DPWA	$\bar{K}N \rightarrow \bar{K}N$
2057	KANE 72	DPWA	$K^-p \rightarrow \Sigma\pi$
2070 ± 10	BERTHON 70B	DPWA	$K^-p \rightarrow \Sigma\pi$

 $\Sigma(2070)$ WIDTH

VALUE (MeV)	DOCUMENT ID	TECN	COMMENT
300 ± 30	GOPAL 80	DPWA	$\bar{K}N \rightarrow \bar{K}N$
906	KANE 72	DPWA	$K^-p \rightarrow \Sigma\pi$
140 ± 20	BERTHON 70B	DPWA	$K^-p \rightarrow \Sigma\pi$

 $\Sigma(2070)$ DECAY MODES

Mode
Γ_1 $N\bar{K}$
Γ_2 $\Sigma\pi$

 $\Sigma(2070)$ BRANCHING RATIOS

See "Sign conventions for resonance couplings" in the Note on Λ and Σ Resonances.

$\Gamma(N\bar{K})/\Gamma_{\text{total}}$	DOCUMENT ID	TECN	COMMENT	Γ_1/Γ
VALUE				
0.08 ± 0.03	GOPAL 80	DPWA	$\bar{K}N \rightarrow \bar{K}N$	

$(\Gamma_1\Gamma_f)^{1/2}/\Gamma_{\text{total}}$ in $N\bar{K} \rightarrow \Sigma(2070) \rightarrow \Sigma\pi$	DOCUMENT ID	TECN	COMMENT	$(\Gamma_1\Gamma_2)^{1/2}/\Gamma$
VALUE				
+0.104	KANE 72	DPWA	$K^-p \rightarrow \Sigma\pi$	
+0.12 ± 0.02	BERTHON 70B	DPWA	$K^-p \rightarrow \Sigma\pi$	

See key on page 373

Baryon Particle Listings

$\Sigma(2070)$, $\Sigma(2080)$, $\Sigma(2100)$, $\Sigma(2250)$

 $\Sigma(2070)$ REFERENCES

GOPAL	80	Toronto Conf. 159	G.P. Gopal	(RHEL) IJP
KANE	74	LBL-2452	D.F. Kane	(LBL)
KANE	72	PR D5 1583	D.F.J. Kane	(LBL)
BERTHON	70B	NP B24 417	A. Berthon et al.	(CDEF, RHEL, SACL) IJP

 $\Sigma(2080) P_{13}$

$$I(J^P) = 1(\frac{3}{2}^+) \text{ Status: } **$$

OMITTED FROM SUMMARY TABLE

Suggested by some but not all partial-wave analyses across this region.

 $\Sigma(2080)$ MASS

VALUE (MeV)	DOCUMENT ID	TECN	COMMENT
≈ 2080 OUR ESTIMATE			
2091 \pm 7	¹ CORDEN 76	DPWA	$K^- n \rightarrow \Lambda \pi^-$
2070 to 2120	DEBELLEFON 76	IPWA	$K^- p \rightarrow \Lambda \pi^0$
2120 \pm 40	BAILLON 75	IPWA	$\bar{K} N \rightarrow \Lambda \pi$ (sol. 1)
2140 \pm 40	BAILLON 75	IPWA	$\bar{K} N \rightarrow \Lambda \pi$ (sol. 2)
2082 \pm 4	COX 70	DPWA	See CORDEN 76
2070 \pm 30	LITCHFIELD 70	DPWA	$K^- N \rightarrow \Lambda \pi$

 $\Sigma(2080)$ WIDTH

VALUE (MeV)	DOCUMENT ID	TECN	COMMENT
186 \pm 48	¹ CORDEN 76	DPWA	$K^- n \rightarrow \Lambda \pi^-$
100	DEBELLEFON 76	IPWA	$K^- p \rightarrow \Lambda \pi^0$
240 \pm 50	BAILLON 75	IPWA	$\bar{K} N \rightarrow \Lambda \pi$ (sol. 1)
200 \pm 50	BAILLON 75	IPWA	$\bar{K} N \rightarrow \Lambda \pi$ (sol. 2)
87 \pm 20	COX 70	DPWA	See CORDEN 76
250 \pm 40	LITCHFIELD 70	DPWA	$K^- N \rightarrow \Lambda \pi$

 $\Sigma(2080)$ DECAY MODES

Mode
Γ_1 $N\bar{K}$
Γ_2 $\Lambda\pi$

 $\Sigma(2080)$ BRANCHING RATIOSSee "Sign conventions for resonance couplings" in the Note on Λ and Σ Resonances.

$(\Gamma_i \Gamma_f)^{1/2} / \Gamma_{\text{total}}$ in $N\bar{K} \rightarrow \Sigma(2080) \rightarrow \Lambda\pi$	DOCUMENT ID	TECN	COMMENT	$(\Gamma_1 \Gamma_2)^{1/2} / \Gamma$
-0.10 \pm 0.03	¹ CORDEN 76	DPWA	$K^- n \rightarrow \Lambda \pi^-$	
-0.10	DEBELLEFON 76	IPWA	$K^- p \rightarrow \Lambda \pi^0$	
-0.13 \pm 0.04	BAILLON 75	IPWA	$\bar{K} N \rightarrow \Lambda \pi$ (sol. 1 and 2)	
-0.16 \pm 0.03	COX 70	DPWA	See CORDEN 76	
-0.09 \pm 0.03	LITCHFIELD 70	DPWA	$K^- N \rightarrow \Lambda \pi$	

 $\Sigma(2080)$ FOOTNOTES¹ Preferred solution 3; see CORDEN 76 for other possibilities, including a D_{15} at this mass. **$\Sigma(2080)$ REFERENCES**

CORDEN	76	NP B104 382	M.J. Corden et al.	(BIRM) IJP
DEBELLEFON	76	NP B109 129	A. de Bellefon, A. Berthon	(CDEF) IJP
Also		NP B90 1	A. de Bellefon et al.	(CDEF, SACL) IJP
BAILLON	75	NP B94 39	P.H. Baillon, P.J. Litchfield	(CERN, RHEL) IJP
COX	70	NP B19 61	G.F. Cox et al.	(BIRM, EDIN, GLAS, LOIC) IJP
LITCHFIELD	70	NP B22 269	P.J. Litchfield	(RHEL) IJP

 $\Sigma(2100) G_{17}$

$$I(J^P) = 1(\frac{7}{2}^-) \text{ Status: } *$$

OMITTED FROM SUMMARY TABLE

 $\Sigma(2100)$ MASS

VALUE (MeV)	DOCUMENT ID	TECN	COMMENT
≈ 2100 OUR ESTIMATE			
2060 \pm 20	BARBARO... 70	DPWA	$K^- p \rightarrow \Lambda \pi^0$
2120 \pm 30	BARBARO... 70	DPWA	$K^- p \rightarrow \Sigma \pi$

 $\Sigma(2100)$ WIDTH

VALUE (MeV)	DOCUMENT ID	TECN	COMMENT
70 \pm 30	BARBARO... 70	DPWA	$K^- p \rightarrow \Lambda \pi^0$
135 \pm 30	BARBARO... 70	DPWA	$K^- p \rightarrow \Sigma \pi$

 $\Sigma(2100)$ DECAY MODES

Mode
Γ_1 $N\bar{K}$
Γ_2 $\Lambda\pi$
Γ_3 $\Sigma\pi$

 $\Sigma(2100)$ BRANCHING RATIOSSee "Sign conventions for resonance couplings" in the Note on Λ and Σ Resonances.

$(\Gamma_i \Gamma_f)^{1/2} / \Gamma_{\text{total}}$ in $N\bar{K} \rightarrow \Sigma(2100) \rightarrow \Lambda\pi$	DOCUMENT ID	TECN	COMMENT	$(\Gamma_1 \Gamma_2)^{1/2} / \Gamma$
-0.07 \pm 0.02	BARBARO... 70	DPWA	$K^- p \rightarrow \Lambda \pi^0$	
$(\Gamma_i \Gamma_f)^{1/2} / \Gamma_{\text{total}}$ in $N\bar{K} \rightarrow \Sigma(2100) \rightarrow \Sigma\pi$	DOCUMENT ID	TECN	COMMENT	$(\Gamma_1 \Gamma_3)^{1/2} / \Gamma$
+0.13 \pm 0.02	BARBARO... 70	DPWA	$K^- p \rightarrow \Sigma \pi$	

 $\Sigma(2100)$ REFERENCES

BARBARO...	70	Duke Conf. 173	A. Barbaro-Galileri	(LRL) IJP
		Hyperon Resonances, 1970		

 $\Sigma(2250)$

$$I(J^P) = 1(?) \text{ Status: } ***$$

Results from partial-wave analyses are too weak to warrant separating them from the production and cross-section experiments. LASINSKI 71 in $\bar{K}N$ using a Pomeron + resonances model, and DEBELLEFON 76, DEBELLEFON 77, and DEBELLEFON 78 in energy-dependent partial-wave analyses of $\bar{K}N \rightarrow \Lambda\pi$, $\Sigma\pi$, and $N\bar{K}$, respectively, suggest two resonances around this mass.

 $\Sigma(2250)$ MASS

VALUE (MeV)	DOCUMENT ID	TECN	COMMENT
2210 to 2280 (≈ 2250) OUR ESTIMATE			
2270 \pm 50	DEBELLEFON 78	DPWA	D_5 wave
2210 \pm 30	DEBELLEFON 78	DPWA	G_9 wave
2275 \pm 20	DEBELLEFON 77	DPWA	D_5 wave
2215 \pm 20	DEBELLEFON 77	DPWA	G_9 wave
2300 \pm 30	¹ DEBELLEFON 75B	HBC	$K^- p \rightarrow \Xi^{*0} K^0$
2251 \pm 30	VANHORN 75	DPWA	$K^- p \rightarrow \Lambda \pi^0, F_5$
-20			wave
2280 \pm 14	AGUILAR... 70B	HBC	$K^- p$ 3.9, 4.6 GeV/c
2237 \pm 11	BRICMAN 70	CNTR	Total, charge exchange
2255 \pm 10	COOL 70	CNTR	$K^- p, K^- d$ total
2250 \pm 7	BUGG 68	CNTR	$K^- p, K^- d$ total
••• We do not use the following data for averages, fits, limits, etc. •••			
2260	DEBELLEFON 76	IPWA	D_5 wave
2215	DEBELLEFON 76	IPWA	G_9 wave
2250 \pm 20	LU 70	CNTR	$\gamma p \rightarrow K^+ Y^*$
2245	BLANPIED 65	CNTR	$\gamma p \rightarrow K^+ Y^*$
2299 \pm 6	BOCK 65	HBC	$\bar{p} p$ 5.7 GeV/c

Baryon Particle Listings

 $\Sigma(2250)$, $\Sigma(2455)$ Bumps $\Sigma(2250)$ WIDTH

VALUE (MeV)	DOCUMENT ID	TECN	COMMENT
60 to 150 (≈ 100) OUR ESTIMATE			
120 \pm 40	DEBELLEFON 78	DPWA	D_5 wave
80 \pm 20	DEBELLEFON 78	DPWA	G_9 wave
70 \pm 20	DEBELLEFON 77	DPWA	D_5 wave
60 \pm 20	DEBELLEFON 77	DPWA	G_9 wave
130 \pm 20	¹ DEBELLEFON 75B	HBC	$K^- p \rightarrow \Xi^{*0} K^0$
192 \pm 30	VANHORN 75	DPWA	$K^- p \rightarrow \Lambda \pi^0, F_5$ wave
100 \pm 20	AGUILAR-... 70B	HBC	$K^- p$ 3.9, 4.6 GeV/c
164 \pm 50	BRICMAN 70	CNTR	Total, charge exchange
230 \pm 20	BUGG 68	CNTR	$K^- p, K^- d$ total
• • • We do not use the following data for averages, fits, limits, etc. • • •			
100	DEBELLEFON 76	IPWA	D_5 wave
140	DEBELLEFON 76	IPWA	G_9 wave
170	COOL 70	CNTR	$K^- p, K^- d$ total
125	LU 70	CNTR	$\gamma p \rightarrow K^+ Y^*$
150	BLANPIED 65	CNTR	$\gamma p \rightarrow K^+ Y^*$
21 ⁺¹⁷ ₋₂₁	BOCK 65	HBC	$\bar{p} p$ 5.7 GeV/c

 $\Sigma(2250)$ DECAY MODES

Mode	Fraction (Γ_i/Γ)
Γ_1 $N\bar{K}$	<10 %
Γ_2 $\Lambda\pi$	seen
Γ_3 $\Sigma\pi$	seen
Γ_4 $N\bar{K}\pi$	
Γ_5 $\Xi(1530)K$	

The above branching fractions are our estimates, not fits or averages.

 $\Sigma(2250)$ BRANCHING RATIOS

See "Sign conventions for resonance couplings" in the Note on Λ and Σ Resonances.

$\Gamma(N\bar{K})/\Gamma_{\text{total}}$	DOCUMENT ID	TECN	COMMENT	Γ_1/Γ
<0.1 OUR ESTIMATE				
0.08 \pm 0.02	DEBELLEFON 78	DPWA	D_5 wave	
0.02 \pm 0.01	DEBELLEFON 78	DPWA	G_9 wave	

$(J+\frac{1}{2})\times\Gamma(N\bar{K})/\Gamma_{\text{total}}$	DOCUMENT ID	TECN	COMMENT	Γ_1/Γ
• • • We do not use the following data for averages, fits, limits, etc. • • •				
0.16 \pm 0.12	BRICMAN 70	CNTR	Total, charge exchange	
0.42	COOL 70	CNTR	$K^- p, K^- d$ total	
0.47	BUGG 68	CNTR		

$(\Gamma_1\Gamma_f)^{1/2}/\Gamma_{\text{total}}$ in $N\bar{K} \rightarrow \Sigma(2250) \rightarrow \Lambda\pi$	DOCUMENT ID	TECN	COMMENT	$(\Gamma_1\Gamma_2)^{1/2}/\Gamma$
• • • We do not use the following data for averages, fits, limits, etc. • • •				
-0.16 \pm 0.03	VANHORN 75	DPWA	$K^- p \rightarrow \Lambda \pi^0, F_5$ wave	

$(\Gamma_1\Gamma_f)^{1/2}/\Gamma_{\text{total}}$ in $N\bar{K} \rightarrow \Sigma(2250) \rightarrow \Sigma\pi$	DOCUMENT ID	TECN	COMMENT	$(\Gamma_1\Gamma_3)^{1/2}/\Gamma$
• • • We do not use the following data for averages, fits, limits, etc. • • •				
+0.11	DEBELLEFON 76	IPWA	D_5 wave	
-0.10	DEBELLEFON 76	IPWA	G_9 wave	
-0.18	BARBARO-... 70	DPWA	$K^- p \rightarrow \Lambda \pi^0, G_9$ wave	

$(\Gamma_1\Gamma_f)^{1/2}/\Gamma_{\text{total}}$ in $N\bar{K} \rightarrow \Sigma(2250) \rightarrow \Sigma\pi$	DOCUMENT ID	TECN	COMMENT	$(\Gamma_1\Gamma_3)^{1/2}/\Gamma$
+0.06 \pm 0.02	DEBELLEFON 77	DPWA	D_5 wave	
-0.03 \pm 0.02	DEBELLEFON 77	DPWA	G_9 wave	
+0.07	BARBARO-... 70	DPWA	$K^- p \rightarrow \Sigma\pi, G_9$ wave	

$\Gamma(N\bar{K})/\Gamma(\Sigma\pi)$	DOCUMENT ID	TECN	COMMENT	Γ_1/Γ_3
• • • We do not use the following data for averages, fits, limits, etc. • • •				
<0.18	BARNES 69	HBC	1 standard dev. limit	

$\Gamma(\Lambda\pi)/\Gamma(\Sigma\pi)$	DOCUMENT ID	TECN	COMMENT	Γ_2/Γ_3
• • • We do not use the following data for averages, fits, limits, etc. • • •				
<0.18	BARNES 69	HBC	1 standard dev. limit	

$(\Gamma_1\Gamma_f)^{1/2}/\Gamma_{\text{total}}$ in $N\bar{K} \rightarrow \Sigma(2250) \rightarrow \Xi(1530)K$	DOCUMENT ID	TECN	COMMENT	$(\Gamma_1\Gamma_5)^{1/2}/\Gamma$
0.18 \pm 0.04	¹ DEBELLEFON 75B	HBC	$K^- p \rightarrow \Xi^{*0} K^0$	

 $\Sigma(2250)$ FOOTNOTES

¹ Seen in the (initial and final state) D_5 wave. Isospin not determined.

 $\Sigma(2250)$ REFERENCES

DEBELLEFON 78	NC 42A 403	A. de Bellefon et al.	(CDEF, SACL) IJP
DEBELLEFON 77	NC 37A 175	A. de Bellefon et al.	(CDEF, SACL) IJP
DEBELLEFON 76	NP B109 129	A. de Bellefon, A. Berthon	(CDEF) IJP
Also	NP B90 1	A. de Bellefon et al.	(CDEF, SACL) IJP
DEBELLEFON 75B	NC 28A 289	A. de Bellefon et al.	(CDEF, SACL) IJP
VANHORN 75	NP B87 145	A.J. van Horn	(LBL) IJP
Also	NP B87 157	A.J. van Horn	(LBL) IJP
LASINSKI 71	NP B29 125	T.A. Lasinski	(EFI) IJP
AGUILAR-... 70B	PRL 25 58	M. Aguilar-Benitez et al.	(BNL, SYR) IJP
BARBARO-... 70	Duke Conf. 173	A. Barbaro-Galieri	(LRL) IJP
Hyperon Resonances, 1970			
BRICMAN 70	PL 31B 152	C. Bricman et al.	(CERN, CAEN, SACL)
COOL 70	PR D1 1887	R.L. Cool et al.	(BNL) I
Also	PRL 16 1228	R.L. Cool et al.	(BNL) I
LU 70	PR D2 1846	D.C. Lu et al.	(YALE)
BARNES 69	PRL 22 479	V.E. Barnes et al.	(BNL, SYR) I
BUGG 68	PR 168 1466	D.V. Bugg et al.	(RHEL, BIRM, CAVE) I
BLANPIED 65	PRL 14 741	W.A. Blanpied et al.	(YALE, CEA)
BOCK 65	PL 17 166	R.K. Bock et al.	(CERN, SACL)

 $\Sigma(2455)$ Bumps

$$I(J^P) = 1(?)^? \quad \text{Status: **}$$

OMITTED FROM SUMMARY TABLE

There is also some slight evidence for Y^* states in this mass region from the reaction $\gamma p \rightarrow K^+ X$ — see GREENBERG 68.

 $\Sigma(2455)$ MASS

VALUE (MeV)	DOCUMENT ID	TECN	COMMENT
≈ 2455 OUR ESTIMATE			
2455 \pm 10	ABRAMS 70	CNTR	$K^- p, K^- d$ total
2455 \pm 7	BUGG 68	CNTR	$K^- p, K^- d$ total

 $\Sigma(2455)$ WIDTH

VALUE (MeV)	DOCUMENT ID	TECN	COMMENT
140	ABRAMS 70	CNTR	$K^- p, K^- d$ total
100 \pm 20	BUGG 68	CNTR	

 $\Sigma(2455)$ DECAY MODES

Mode
Γ_1 $N\bar{K}$

 $\Sigma(2455)$ BRANCHING RATIOS

$(J+\frac{1}{2})\times\Gamma(N\bar{K})/\Gamma_{\text{total}}$	DOCUMENT ID	TECN	COMMENT	Γ_1/Γ
0.39	ABRAMS 70	CNTR	$K^- p, K^- d$ total	
0.05 \pm 0.05	¹ BRICMAN 70	CNTR	Total, charge exchange	
0.3	BUGG 68	CNTR		

 $\Sigma(2455)$ FOOTNOTES

¹ Fit of total cross section given by BRICMAN 70 is poor in this region.

 $\Sigma(2455)$ REFERENCES

ABRAMS 70	PR D1 1917	R.J. Abrams et al.	(BNL) I
Also	PRL 19 678	R.J. Abrams et al.	(BNL)
BRICMAN 70	PL 31B 152	C. Bricman et al.	(CERN, CAEN, SACL)
BUGG 68	PR 168 1466	D.V. Bugg et al.	(RHEL, BIRM, CAVE) I
GREENBERG 68	PRL 20 221	J.S. Greenberg et al.	(YALE)

See key on page 373

Baryon Particle Listings

$\Sigma(2620)$ Bumps, $\Sigma(3000)$ Bumps, $\Sigma(3170)$ Bumps

$\Sigma(2620)$ Bumps $I(J^P) = 1(?^?)$ Status: **

OMITTED FROM SUMMARY TABLE

$\Sigma(2620)$ MASS

VALUE (MeV)	DOCUMENT ID	TECN	COMMENT
≈ 2620 OUR ESTIMATE			
2542 ± 22	DIBIANCA	75	DBC $K^- N \rightarrow \Xi K \pi$
2620 ± 15	ABRAMS	70	CNTR $K^- p, K^- d$ total

$\Sigma(2620)$ WIDTH

VALUE (MeV)	DOCUMENT ID	TECN	COMMENT
221 ± 81	DIBIANCA	75	DBC $K^- N \rightarrow \Xi K \pi$
175	ABRAMS	70	CNTR $K^- p, K^- d$ total

$\Sigma(2620)$ DECAY MODES

Mode	Fraction (Γ_i/Γ)
Γ_1 $N\bar{K}$	

$\Sigma(2620)$ BRANCHING RATIOS

$(J+\frac{1}{2}) \times \Gamma(N\bar{K})/\Gamma_{total}$	DOCUMENT ID	TECN	COMMENT	Γ_1/Γ
0.32	ABRAMS	70	CNTR $K^- p, K^- d$ total	
0.36 ± 0.12	BRICMAN	70	CNTR Total, charge exchange	

$\Sigma(2620)$ REFERENCES

DIBIANCA	75	NP B98 137	F.A. Dibianca, R.J. Endorf	(CMU)
ABRAMS	70	PR D1 1917	R.J. Abrams et al.	(BNL) ¹
Also		PRL 19 678	R.J. Abrams et al.	(BNL)
BRICMAN	70	PL 31B 152	C. Bricman et al.	(CERN, CAEN, SACL)

$\Sigma(3000)$ Bumps $I(J^P) = 1(?^?)$ Status: *

OMITTED FROM SUMMARY TABLE

Seen as an enhancement in $\Lambda\pi$ and $\bar{K}N$ invariant mass spectra and in the missing mass of neutrals recoiling against a K^0 .

$\Sigma(3000)$ MASS

VALUE (MeV)	DOCUMENT ID	TECN	CHG	COMMENT
≈ 3000 OUR ESTIMATE				
3000	EHRlich	66	HBC 0	$\pi^- p$ 7.91 GeV/c

$\Sigma(3000)$ DECAY MODES

Mode	Fraction (Γ_i/Γ)
Γ_1 $N\bar{K}$	
Γ_2 $\Lambda\pi$	

$\Sigma(3000)$ REFERENCES

EHRlich	66	PR 152 1194	R. Ehrlich, W. Selove, H. Yuta	(PENN) ¹
---------	----	-------------	--------------------------------	---------------------

$\Sigma(3170)$ Bumps $I(J^P) = 1(?^?)$ Status: *

OMITTED FROM SUMMARY TABLE

Seen by AMIRZADEH 79 as a narrow 6.5-standard-deviation enhancement in the reaction $K^- p \rightarrow Y^{*+} \pi^-$ using data from independent high statistics bubble chamber experiments at 8.25 and 6.5 GeV/c. The dominant decay modes are multibody, multistrange final states and the production is via isospin-3/2 baryon exchange. Isospin 1 is favored.

Not seen in a $K^- p$ experiment in LASS at 11 GeV/c (ASTON 85B).

$\Sigma(3170)$ MASS (PRODUCTION EXPERIMENTS)

VALUE (MeV)	EVTS	DOCUMENT ID	TECN	COMMENT
≈ 3170 OUR ESTIMATE				
3170 ± 5	35	AMIRZADEH 79	HBC	$K^- p \rightarrow Y^{*+} \pi^-$

$\Sigma(3170)$ WIDTH (PRODUCTION EXPERIMENTS)

VALUE (MeV)	EVTS	DOCUMENT ID	TECN	COMMENT
<20	35	¹ AMIRZADEH 79	HBC	$K^- p \rightarrow Y^{*+} \pi^-$

$\Sigma(3170)$ DECAY MODES (PRODUCTION EXPERIMENTS)

Mode	Fraction (Γ_i/Γ)
Γ_1 $\Lambda K \bar{K} \pi$'s	seen
Γ_2 $\Sigma K \bar{K} \pi$'s	seen
Γ_3 $\Xi K \pi$'s	seen

$\Sigma(3170)$ BRANCHING RATIOS (PRODUCTION EXPERIMENTS)

$\Gamma(\Lambda K \bar{K} \pi$'s)/ Γ_{total}	DOCUMENT ID	TECN	COMMENT	Γ_1/Γ
seen	AMIRZADEH 79	HBC	$K^- p \rightarrow Y^{*+} \pi^-$	

$\Gamma(\Sigma K \bar{K} \pi$'s)/ Γ_{total}	DOCUMENT ID	TECN	COMMENT	Γ_2/Γ
seen	AMIRZADEH 79	HBC	$K^- p \rightarrow Y^{*+} \pi^-$	

$\Gamma(\Xi K \pi$'s)/ Γ_{total}	DOCUMENT ID	TECN	COMMENT	Γ_3/Γ
seen	AMIRZADEH 79	HBC	$K^- p \rightarrow Y^{*+} \pi^-$	

$\Sigma(3170)$ FOOTNOTES (PRODUCTION EXPERIMENTS)

¹ Observed width consistent with experimental resolution.

$\Sigma(3170)$ REFERENCES (PRODUCTION EXPERIMENTS)

ASTON	85B	PR D32 2270	D. Aston et al.	(SLAC, CARL, CNRC, CINC)
AMIRZADEH	79	PL 89B 125	J. Amirzadeh et al.	(BIRM, CERN, GLAS+) ¹
Also		Toronto Conf. 263	J.B. Kinson et al.	(BIRM, CERN, GLAS+) ¹

Baryon Particle Listings

 Ξ^0

Ξ BARYONS

($S = -2, I = 1/2$)

$$\Xi^0 = uss, \Xi^- = dss$$

 Ξ^0

$$I(J^P) = \frac{1}{2}(\frac{1}{2}^+) \text{ Status: } ****$$

The parity has not actually been measured, but + is of course expected.

 Ξ^0 MASS

The fit uses the Ξ^0 , Ξ^- , and Ξ^+ masses and the $\Xi^- - \Xi^0$ mass difference. It assumes that the Ξ^- and Ξ^+ masses are the same.

VALUE (MeV)	EVTS	DOCUMENT ID	TECN	COMMENT
1314.86 ± 0.20 OUR FIT				
1314.82 ± 0.06 ± 0.20	3120	FANTI	00 NA48	p Be, 450 GeV
••• We do not use the following data for averages, fits, limits, etc. •••				
1315.2 ± 0.92	49	WILQUET	72 HLBC	
1313.4 ± 1.8	1	PALMER	68 HBC	

$$m_{\Xi^-} - m_{\Xi^0}$$

The fit uses the Ξ^0 , Ξ^- , and Ξ^+ masses and the $\Xi^- - \Xi^0$ mass difference. It assumes that the Ξ^- and Ξ^+ masses are the same.

VALUE (MeV)	EVTS	DOCUMENT ID	TECN	COMMENT
6.85 ± 0.21 OUR FIT				
6.3 ± 0.7 OUR AVERAGE				
6.9 ± 2.2	29	LONDON	66 HBC	
6.1 ± 0.9	88	PJERROU	65B HBC	
6.8 ± 1.6	23	JAUNEAU	63 FBC	
••• We do not use the following data for averages, fits, limits, etc. •••				
6.1 ± 1.6	45	CARMONY	64B HBC	See PJERROU 65B

 Ξ^0 MEAN LIFE

VALUE (10^{-10} s)	EVTS	DOCUMENT ID	TECN	COMMENT
2.90 ± 0.09 OUR AVERAGE				
2.83 ± 0.16	6300	1 ZECH	77 SPEC	Neutral hyperon beam
2.88 ^{+0.21} _{-0.19}	652	BALTAY	74 HBC	1.75 GeV/c $K^- p$
2.90 ^{+0.32} _{-0.27}	157	2 MAYEUR	72 HLBC	2.1 GeV/c K^-
3.07 ^{+0.22} _{-0.20}	340	DAUBER	69 HBC	
3.0 ± 0.5	80	PJERROU	65B HBC	
2.5 ^{+0.4} _{-0.3}	101	HUBBARD	64 HBC	
3.9 ^{+1.4} _{-0.8}	24	JAUNEAU	63 FBC	
••• We do not use the following data for averages, fits, limits, etc. •••				
3.5 ^{+1.0} _{-0.8}	45	CARMONY	64B HBC	See PJERROU 65B

¹The ZECH 77 result is $\tau_{\Xi^0} = [2.77 - (\tau_A - 2.69)] \times 10^{-10}$ s, in which we use $\tau_A = 2.63 \times 10^{-10}$ s.

²The MAYEUR 72 value is modified by the erratum.

 Ξ^0 MAGNETIC MOMENT

See the "Note on Baryon Magnetic Moments" in the Λ Listings.

VALUE (μ_N)	EVTS	DOCUMENT ID	TECN	COMMENT
-1.250 ± 0.014 OUR AVERAGE				
-1.253 ± 0.014	270k	COX	81 SPEC	
-1.20 ± 0.06	42k	BUNCE	79 SPEC	

 Ξ^0 DECAY MODES

Mode	Fraction (Γ_i/Γ)	Confidence level
$\Gamma_1 \Lambda\pi^0$	(99.525 ± 0.012) %	
$\Gamma_2 \Lambda\gamma$	(1.17 ± 0.07) × 10 ⁻³	
$\Gamma_3 \Lambda e^+ e^-$	(7.6 ± 0.6) × 10 ⁻⁶	
$\Gamma_4 \Sigma^0 \gamma$	(3.33 ± 0.10) × 10 ⁻³	
$\Gamma_5 \Sigma^+ e^- \bar{\nu}_e$	(2.53 ± 0.08) × 10 ⁻⁴	
$\Gamma_6 \Sigma^+ \mu^- \bar{\nu}_\mu$	(4.6 ^{+1.8} _{-1.4}) × 10 ⁻⁶	

 $\Delta S = \Delta Q$ (SQ) violating modes or
 $\Delta S = 2$ forbidden ($S2$) modes

$\Gamma_7 \Sigma^- e^+ \nu_e$	$SQ < 9$	× 10 ⁻⁴	90%
$\Gamma_8 \Sigma^- \mu^+ \nu_\mu$	$SQ < 9$	× 10 ⁻⁴	90%
$\Gamma_9 p \pi^-$	$S2 < 8$	× 10 ⁻⁶	90%
$\Gamma_{10} p e^- \bar{\nu}_e$	$S2 < 1.3$	× 10 ⁻³	
$\Gamma_{11} p \mu^- \bar{\nu}_\mu$	$S2 < 1.3$	× 10 ⁻³	

CONSTRAINED FIT INFORMATION

An overall fit to 3 branching ratios uses 9 measurements and one constraint to determine 4 parameters. The overall fit has a $\chi^2 = 4.6$ for 6 degrees of freedom.

The following *off-diagonal* array elements are the correlation coefficients $\langle \delta x_i \delta x_j \rangle / (\delta x_i \delta x_j)$, in percent, from the fit to the branching fractions, $x_i \equiv \Gamma_i/\Gamma_{\text{total}}$. The fit constrains the x_i whose labels appear in this array to sum to one.

x_2	-57		
x_4	-82	0	
x_5	-7	0	0
	x_1	x_2	x_4

 Ξ^0 BRANCHING RATIOS

$$\Gamma(\Lambda\gamma)/\Gamma(\Lambda\pi^0) \quad \Gamma_2/\Gamma_1$$

VALUE (units 10 ⁻³)	EVTS	DOCUMENT ID	TECN	COMMENT
1.17 ± 0.07 OUR FIT				
1.17 ± 0.07 OUR AVERAGE				
1.17 ± 0.05 ± 0.06	672	³ LAI	04A NA48	p Be, 450 GeV
1.91 ± 0.34 ± 0.19	31	⁴ FANTI	00 NA48	p Be, 450 GeV
1.06 ± 0.12 ± 0.11	116	JAMES	90 SPEC	FNAL hyperons

³LAI 04A used our 2002 value of 99.5% for the $\Xi^0 \rightarrow \Lambda\pi^0$ branching fraction to get $\Gamma(\Xi^0 \rightarrow \Lambda\gamma)/\Gamma_{\text{total}} = (1.16 \pm 0.05 \pm 0.06) \times 10^{-3}$. We adjust slightly to go back to what was directly measured.

⁴FANTI 00 used our 1998 value of 99.5% for the $\Xi^0 \rightarrow \Lambda\pi^0$ branching fraction to get $\Gamma(\Xi^0 \rightarrow \Lambda\gamma)/\Gamma_{\text{total}} = (1.90 \pm 0.34 \pm 0.19) \times 10^{-3}$. We adjust slightly to go back to what was directly measured.

$$\Gamma(\Lambda e^+ e^-)/\Gamma_{\text{total}} \quad \Gamma_3/\Gamma$$

VALUE (units 10 ⁻⁶)	EVTS	DOCUMENT ID	TECN	COMMENT
7.6 ± 0.4 ± 0.5	397 ± 21	⁵ BATLEY	07c NA48	p Be, 400 GeV

⁵This BATLEY 07c result is consistent with internal bremsstrahlung.

$$\Gamma(\Sigma^0 \gamma)/\Gamma(\Lambda\pi^0) \quad \Gamma_4/\Gamma_1$$

VALUE (units 10 ⁻³)	EVTS	DOCUMENT ID	TECN	COMMENT
3.35 ± 0.10 OUR FIT				
3.35 ± 0.10 OUR AVERAGE				
3.34 ± 0.05 ± 0.09	4045	ALAVI-HARATI	01c KTEV	p nucleus, 800 GeV
3.16 ± 0.76 ± 0.32	17	⁶ FANTI	00 NA48	p Be, 450 GeV
3.56 ± 0.42 ± 0.10	85	TEIGE	89 SPEC	FNAL hyperons

⁶FANTI 00 used our 1998 value of 99.5% for the $\Xi^0 \rightarrow \Lambda\pi^0$ branching fraction to get $\Gamma(\Xi^0 \rightarrow \Sigma^0 \gamma)/\Gamma_{\text{total}} = (3.14 \pm 0.76 \pm 0.32) \times 10^{-3}$. We adjust slightly to go back to what was directly measured.

$$\Gamma(\Sigma^+ e^- \bar{\nu}_e)/\Gamma_{\text{total}} \quad \Gamma_5/\Gamma$$

VALUE (units 10 ⁻⁴)	EVTS	DOCUMENT ID	TECN	COMMENT
2.53 ± 0.08 OUR FIT				
2.53 ± 0.08 OUR AVERAGE				
2.51 ± 0.03 ± 0.09	6101	BATLEY	07 NA48	p Be, 400 GeV
2.55 ± 0.14 ± 0.10	419	⁷ BATLEY	07 NA48	p Be, 400 GeV
2.71 ± 0.22 ± 0.31	176	AFFOLDER	99 KTEV	p nucleus, 800 GeV

⁷This BATLEY 07 result is for $\Xi^0 \rightarrow \Sigma^- e^+ \nu_e$ events.

$$\Gamma(\Sigma^+ \mu^- \bar{\nu}_\mu)/\Gamma(\Sigma^+ e^- \bar{\nu}_e) \quad \Gamma_6/\Gamma_5$$

VALUE	EVTS	DOCUMENT ID	TECN	COMMENT
0.018^{+0.007}_{-0.005} ± 0.002	9	ABOUZAID	05 KTEV	p nucleus 800 GeV

$$\Gamma(\Sigma^+ \mu^- \bar{\nu}_\mu)/\Gamma(\Lambda\pi^0) \quad \Gamma_6/\Gamma_1$$

VALUE (units 10 ⁻³)	CL% EVTS	DOCUMENT ID	TECN	COMMENT
••• We do not use the following data for averages, fits, limits, etc. •••				
<1.1	90 0	YEH	74 HBC	Effective denom.=2100
<1.5		DAUBER	69 HBC	
<7		HUBBARD	66 HBC	

$$\Gamma(\Sigma^- e^+ \nu_e)/\Gamma(\Lambda\pi^0) \quad \Gamma_7/\Gamma_1$$

VALUE (units 10 ⁻³)	CL% EVTS	DOCUMENT ID	TECN	COMMENT
<0.9	90 0	YEH	74 HBC	Effective denom.=2500
••• We do not use the following data for averages, fits, limits, etc. •••				
<1.5		DAUBER	69 HBC	
<6		HUBBARD	66 HBC	

$\Gamma(\Sigma^- \mu^+ \nu_\mu)/\Gamma(\Lambda\pi^0)$ Γ_8/Γ_1 Test of $\Delta S = \Delta Q$ rule.

VALUE (units 10^{-3})	CL%	EVTS	DOCUMENT ID	TECN	COMMENT
<0.9	90	0	YEH	74	HBC Effective denom.=2500
••• We do not use the following data for averages, fits, limits, etc. •••					
<1.5			DAUBER	69	HBC
<6			HUBBARD	66	HBC

 $\Gamma(p\pi^-)/\Gamma(\Lambda\pi^0)$ Γ_9/Γ_1 $\Delta S=2$. Forbidden in first-order weak interaction.

VALUE (units 10^{-6})	CL%	EVTS	DOCUMENT ID	TECN	COMMENT
< 8.2	90		WHITE	05	HYCP p Cu, 800 GeV
••• We do not use the following data for averages, fits, limits, etc. •••					
< 36	90		GEWENIGER	75	SPEC
<1800	90	0	YEH	74	HBC Effective denom.=1300
< 900			DAUBER	69	HBC
<5000			HUBBARD	66	HBC

 $\Gamma(p e^- \bar{\nu}_e)/\Gamma(\Lambda\pi^0)$ Γ_{10}/Γ_1 $\Delta S=2$. Forbidden in first-order weak interaction.

VALUE (units 10^{-3})	CL%	EVTS	DOCUMENT ID	TECN	COMMENT
<1.3			DAUBER	69	HBC
••• We do not use the following data for averages, fits, limits, etc. •••					
<3.4	90	0	YEH	74	HBC Effective denom.=670
<6			HUBBARD	66	HBC

 $\Gamma(p\mu^- \bar{\nu}_\mu)/\Gamma(\Lambda\pi^0)$ Γ_{11}/Γ_1 $\Delta S=2$. Forbidden in first-order weak interaction.

VALUE (units 10^{-3})	CL%	EVTS	DOCUMENT ID	TECN	COMMENT
<1.3			DAUBER	69	HBC
••• We do not use the following data for averages, fits, limits, etc. •••					
<3.5	90	0	YEH	74	HBC Effective denom.=664
<6			HUBBARD	66	HBC

≡ DECAY PARAMETERS

See the "Note on Baryon Decay Parameters" in the neutron Listings.

 $\alpha(\Xi^0) \alpha_-(\Lambda)$

VALUE	EVTS	DOCUMENT ID	TECN	COMMENT
-0.264 ± 0.013 OUR AVERAGE				Error includes scale factor of 2.1.
-0.260 ± 0.004 ± 0.005	300k	HANDLER	82	SPEC FNAL hyperons
-0.317 ± 0.027	6075	BUNCE	78	SPEC FNAL hyperons
-0.35 ± 0.06	505	BALTAY	74	HBC $K^- p$ 1.75 GeV/c
-0.28 ± 0.06	739	DAUBER	69	HBC $K^- p$ 1.7-2.6 GeV/c

 α FOR $\Xi^0 \rightarrow \Lambda\pi^0$ The above average, $\alpha(\Xi^0)\alpha_-(\Lambda) = -0.264 \pm 0.013$, where the error includes a scale factor of 2.1, divided by our current average $\alpha_-(\Lambda) = 0.642 \pm 0.013$, gives the following value for $\alpha(\Xi^0)$.

VALUE	DOCUMENT ID
-0.411 ± 0.022 OUR EVALUATION	Error includes scale factor of 2.1.

 ϕ ANGLE FOR $\Xi^0 \rightarrow \Lambda\pi^0$ ($\tan\phi = \beta/\gamma$)

VALUE (°)	EVTS	DOCUMENT ID	TECN	COMMENT
21 ± 12 OUR AVERAGE				
16 ± 17	652	BALTAY	74	HBC 1.75 GeV/c $K^- p$
38 ± 19	739	⁸ DAUBER	69	HBC
- 8 ± 30	146	⁹ BERGE	66	HBC

⁸ DAUBER 69 uses $\alpha_\Lambda = 0.647 \pm 0.020$.⁹ The errors have been multiplied by 1.2 due to approximations used for the Ξ polarization; see DAUBER 69 for a discussion.

RADIATIVE HYPERON DECAYS

Written September 2003 by J.D. Jackson (LBNL).

The weak radiative decays of spin-1/2 hyperons, $B_i \rightarrow B_f \gamma$, yield information about matrix elements (form factors) similar to that gained from weak hadronic decays. For a polarized spin-1/2 hyperon decaying radiatively via a $\Delta Q = 0$, $\Delta S = 1$ transition, the angular distribution of the direction $\hat{\mathbf{p}}$ of the final spin-1/2 baryon in the hyperon rest frame is

$$\frac{dN}{d\Omega} = \frac{N}{4\pi} (1 + \alpha_\gamma \mathbf{P}_i \cdot \hat{\mathbf{p}}). \quad (1)$$

Here \mathbf{P}_i is the polarization of the decaying hyperon, and α_γ is the asymmetry parameter. In terms of the form factors $F_1(q^2)$,

$F_2(q^2)$, and $G(q^2)$ of the effective hadronic weak electromagnetic vertex,

$$F_1(q^2)\gamma_\lambda + iF_2(q^2)\sigma_{\lambda\mu}q^\mu + G(q^2)\gamma_\lambda\gamma_5,$$

 α_γ is

$$\alpha_\gamma = \frac{2\text{Re}[G(0)F_M^*(0)]}{|G(0)|^2 + |F_M(0)|^2}, \quad (2)$$

where $F_M = (m_i - m_f)[F_2 - F_1/(m_i + m_f)]$. If the decaying hyperon is unpolarized, the decay baryon has a longitudinal polarization given by $P_f = -\alpha_\gamma$ [1].

The angular distribution for the weak hadronic decay, $B_i \rightarrow B_f \pi$, has the same form as Eq. (1), but of course with a different asymmetry parameter, α_π . Now, however, if the decaying hyperon is unpolarized, the decay baryon has a longitudinal polarization given by $P_f = +\alpha_\pi$ [2,3]. The difference of sign is because the spins of the pion and photon are different.

$\Xi^0 \rightarrow \Lambda\gamma$ decay—The radiative decay $\Xi^0 \rightarrow \Lambda\gamma$ of an unpolarized Ξ^0 uses the hadronic decay $\Lambda \rightarrow p\pi^-$ as the analyzer. As noted above, the longitudinal polarization of the Λ will be $P_\Lambda = -\alpha_{\Xi\Lambda\gamma}$. Let α_- be the $\Lambda \rightarrow p\pi^-$ asymmetry parameter and $\theta_{\Lambda p}$ be the angle, as seen in the Λ rest frame, between the Λ line of flight and the proton momentum. Then the hadronic version of Eq. (1) applied to the $\Lambda \rightarrow p\pi^-$ decay gives

$$\frac{dN}{d\cos\theta_{\Lambda p}} = \frac{N}{2} (1 - \alpha_{\Xi\Lambda\gamma} \alpha_- \cos\theta_{\Lambda p}) \quad (3)$$

for the angular distribution of the proton in the Λ frame. The only published measurement of $\alpha_{\Xi\Lambda\gamma}$ [4] got the sign wrong, as explained in an erratum 12 years later [5]. The corrected result is $\alpha_{\Xi\Lambda\gamma} = -0.43 \pm 0.44$.

$\Xi^0 \rightarrow \Sigma^0\gamma$ decay—The asymmetry parameter here, $\alpha_{\Xi\Sigma\gamma}$, is measured by following the decay chain $\Xi^0 \rightarrow \Sigma^0\gamma$, $\Sigma^0 \rightarrow \Lambda\gamma$, $\Lambda \rightarrow p\pi^-$. Again, for an unpolarized Ξ^0 , the longitudinal polarization of the Σ^0 will be $P_\Sigma = -\alpha_{\Xi\Sigma\gamma}$. In the $\Sigma^0 \rightarrow \Lambda\gamma$ decay, a parity-conserving magnetic-dipole transition, the polarization of the Σ^0 is transferred to the Λ , as may be seen as follows. Let $\theta_{\Sigma\Lambda}$ be the angle seen in the Σ^0 rest frame between the Σ^0 line of flight and the Λ momentum. For Σ^0 helicity +1/2, the probability amplitudes for positive and negative spin states of the Σ^0 along the Λ momentum are $\cos(\theta_{\Sigma\Lambda}/2)$ and $\sin(\theta_{\Sigma\Lambda}/2)$. Then the amplitude for a negative helicity photon and a negative helicity Λ is $\cos(\theta_{\Sigma\Lambda}/2)$, while the amplitude for positive helicities for the photon and Λ is $\sin(\theta_{\Sigma\Lambda}/2)$. For Σ^0 helicity -1/2, the amplitudes are interchanged. If the Σ^0 has longitudinal polarization P_Σ , the probabilities for Λ helicities $\pm 1/2$ are therefore

$$p(\pm 1/2) = \frac{1}{2}(1 \mp P_\Sigma) \cos^2(\theta_{\Sigma\Lambda}/2) + \frac{1}{2}(1 \pm P_\Sigma) \sin^2(\theta_{\Sigma\Lambda}/2), \quad (4)$$

and the longitudinal polarization of the Λ is

$$P_\Lambda = -P_\Sigma \cos\theta_{\Sigma\Lambda} = +\alpha_{\Xi\Sigma\gamma} \cos\theta_{\Sigma\Lambda}. \quad (5)$$

Baryon Particle Listings

 Ξ^0, Ξ^-

Using Eq. (1) for the $\Lambda \rightarrow p\pi^-$ decay again, we get for the joint angular distribution of the $\Sigma^0 \rightarrow \Lambda\gamma, \Lambda \rightarrow p\pi^-$ chain,

$$\frac{d^2N}{d\cos\theta_{\Sigma\Lambda}d\cos\theta_{\Lambda p}} = \frac{N}{4} (1 + \alpha_{\Xi\Sigma\gamma} \cos\theta_{\Sigma\Lambda} \alpha_- \cos\theta_{\Lambda p}). \quad (6)$$

The KTeV collaboration recently measured $\alpha_{\Xi\Sigma\gamma}$ to be -0.63 ± 0.09 [6]. The only other measurement has been withdrawn [7].

References

1. R.E. Behrends, Phys. Rev. **111**, 1691 (1958); see Eq. (7) or (8).
2. In ancient times, the signs of the asymmetry term in the angular distributions of radiative and hadronic decays of polarized hyperons were sometimes opposite. For roughly 40 years, however, the overwhelming convention has been to make them the same. The aim, not always achieved, is to remove ambiguities.
3. For the definition of α_{π} , see the note on “Baryon Decay Parameters,” in the Neutron Listings in this Review..
4. C. James *et al.*, Phys. Rev. Lett. **64**, 843 (1990).
5. C. James *et al.*, Phys. Rev. Lett. **89**, 169901 (2002) (erratum). The various sign conventions spelled out here are discussed.
6. A. Alavi-Harati *et al.*, Phys. Rev. Lett. **86**, 3239 (2001).
7. S. Teige *et al.*, Phys. Rev. Lett. **63**, 2717 (1989); erratum, Phys. Rev. Lett. **89**, 169902 (2002).

 α FOR $\Xi^0 \rightarrow \Lambda\gamma$

See the note above on “Radiative Hyperon Decays.”

VALUE	EVTS	DOCUMENT ID	TECN	COMMENT
-0.73 ± 0.17 OUR AVERAGE				
$-0.78 \pm 0.18 \pm 0.06$	672	LAI 04A	NA48	p Be, 450 GeV
-0.43 ± 0.44	87	¹⁰ JAMES 90	SPEC	FNAL hyperons

¹⁰The sign has been changed; see the erratum, JAMES 02.

 α FOR $\Xi^0 \rightarrow \Lambda e^+ e^-$

VALUE	EVTS	DOCUMENT ID	TECN	COMMENT
-0.8 ± 0.2	397 ± 21	¹¹ BATLEY 07c	NA48	p Be, 400 GeV

¹¹This BATLEY 07c result is consistent with the asymmetry α for $\Xi^0 \rightarrow \Lambda\gamma$, as expected if the mechanism is internal bremsstrahlung.

 α FOR $\Xi^0 \rightarrow \Sigma^0\gamma$

See the note above on “Radiative Hyperon Decays.”

VALUE	EVTS	DOCUMENT ID	TECN	COMMENT
$-0.63 \pm 0.08 \pm 0.05$	4045	ALAVI-HARATI01c	KTEV	p nucleus, 800 GeV
$+0.20 \pm 0.32 \pm 0.05$	85	¹² TEIGE 89	SPEC	FNAL hyperons

¹²This result has been withdrawn, due to an error. See the erratum, TEIGE 02.

 $g_1(0)/f_1(0)$ FOR $\Xi^0 \rightarrow \Sigma^+ e^- \bar{\nu}_e$

VALUE	EVTS	DOCUMENT ID	TECN	COMMENT
1.21 ± 0.05 OUR AVERAGE				
$+1.20 \pm 0.04 \pm 0.03$	6520	¹³ BATLEY 07	NA48	p Be, 400 GeV
$+1.32^{+0.21}_{-0.17} \pm 0.05$	487	¹⁴ ALAVI-HARATI01i	KTEV	p nucleus, 800 GeV

¹³This BATLEY 07 result uses our 2006 value of V_{US} from semileptonic kaon decays as input.

¹⁴ALAVI-HARATI 01i assumes here that the second-class current is zero and that the weak-magnetism term takes its exact SU(3) value.

 $g_2(0)/f_1(0)$ FOR $\Xi^0 \rightarrow \Sigma^+ e^- \bar{\nu}_e$

VALUE	EVTS	DOCUMENT ID	TECN	COMMENT
$-1.7^{+2.1}_{-2.0} \pm 0.5$	487	¹⁵ ALAVI-HARATI01i	KTEV	p nucleus, 800 GeV

¹⁵ALAVI-HARATI 01i thus assumes that $g_2 = 0$ in calculating g_1/f_1 , above.

 $f_2(0)/f_1(0)$ FOR $\Xi^0 \rightarrow \Sigma^+ e^- \bar{\nu}_e$

VALUE	EVTS	DOCUMENT ID	TECN	COMMENT
$2.0 \pm 1.2 \pm 0.5$	487	ALAVI-HARATI01i	KTEV	p nucleus, 800 GeV

 Ξ^0 REFERENCES

BATLEY 07	PL B645 36	J.R. Batley <i>et al.</i>	(CERN NA48/1 Collab.)
BATLEY 07C	PL B650 1	J.R. Batley <i>et al.</i>	(CERN NA48 Collab.)
ABOUZAID 05	PRL 95 081801	E. Abouzaid <i>et al.</i>	(FNAL KTeV Collab.)
WHITE 05	PRL 94 101804	C.G. White <i>et al.</i>	(FNAL HyperCP Collab.)
LAI 04A	PL B584 251	A. Lai <i>et al.</i>	(CERN NA48 Collab.)
JAMES 02	PRL 89 169901 (erratum)	C. James <i>et al.</i>	(MINN, MICH, WIS C, RUTG)
TEIGE 02	PRL 89 169902 (erratum)	S. Teige <i>et al.</i>	(RUTG, MICH, MINN)
ALAVI-HARATI 01C	PRL 86 3239	A. Alavi-Harati <i>et al.</i>	(FNAL KTeV Collab.)
ALAVI-HARATI 01i	PRL 87 132001	A. Alavi-Harati <i>et al.</i>	(FNAL KTeV Collab.)
FANTI 00	EPJ C12 69	V. Fanti <i>et al.</i>	(CERN NA48 Collab.)
AFFOLDER 99	PRL 82 3751	A. Affolder <i>et al.</i>	(FNAL KTeV Collab.)
JAMES 90	PRL 64 843	C. James <i>et al.</i>	(MINN, MICH, WIS C, RUTG)
TEIGE 89	PRL 63 2717	S. Teige <i>et al.</i>	(RUTG, MICH, MINN)
HANDLER 82	PR D25 639	R. Handler <i>et al.</i>	(WISC, MICH, MINN+)
COX 81	PRL 46 877	P.T. Cox <i>et al.</i>	(MICH, WISC, RUTG, MINN+)
BUNCE 79	PL 86B 386	G.R.M. Bunce <i>et al.</i>	(BNL, MICH, RUTG+)
BUNCE 78	PR D18 633	G.R.M. Bunce <i>et al.</i>	(WISC, MICH, RUTG)
ZECH 77	NP B124 413	G. Zech <i>et al.</i>	(SIEG, CERN, DORT, HEIDH)
GEWENIGER 75	PL 57B 193	C. Geweniger <i>et al.</i>	(CERN, HEIDH)
BALTAY 74	PR D9 49	C. Baltay <i>et al.</i>	(COLU, BING, J)
YEH 74	PR D10 3545	N. Yeh <i>et al.</i>	(BING, COLU)
MAYEUR 72	NP B47 333	C. Mayeur <i>et al.</i>	(BRUX, CERN, TUFTS, LOUC)
Also	NP B53 268 (erratum)	C. Mayeur	
WILQUET 72	PL 42B 372	G. Wilquet <i>et al.</i>	(BRUX, CERN, TUFTS+)
DAUBER 69	PR 179 1262	P.M. Dauber <i>et al.</i>	(LRL)
PALMER 68	PL 26B 323	R.B. Palmer <i>et al.</i>	(BNL, SYRA)
BERGE 66	PR 147 945	J.P. Berge <i>et al.</i>	(LRL)
HUBBARD 66	Thesis UCRL 11510	J.R. Hubbard	(LRL)
LONDON 66	PR 143 1034	G.W. London <i>et al.</i>	(BNL, SYRA)
PJERROU 65B	PR 14 275	G.M. Pjerrou <i>et al.</i>	(UCLA)
Also	Thesis	G.M. Pjerrou	(UCLA)
CARMONY 64B	PRL 12 482	D.D. Carmony <i>et al.</i>	(UCLA)
HUBBARD 64	PR 135 B183	J.R. Hubbard <i>et al.</i>	(LRL)
JAUNEAU 63	PL 4 49	L. Jauneau <i>et al.</i>	(EPOL, CERN, LOUC+)
Also	Siena Conf. 1 1	L. Jauneau <i>et al.</i>	(EPOL, CERN, LOUC+)



$$I(J^P) = \frac{1}{2}(\frac{1}{2}^+) \text{ Status: } ***$$

The parity has not actually been measured, but + is of course expected.

We have omitted some results that have been superseded by later experiments. See our earlier editions.

 Ξ^- MASS

The fit uses the Ξ^- , Ξ^+ , and Ξ^0 masses and the $\Xi^- - \Xi^+$ mass difference. It assumes that the Ξ^- and Ξ^+ masses are the same.

VALUE (MeV)	EVTS	DOCUMENT ID	TECN	COMMENT
1321.71 ± 0.07 OUR FIT				
$1321.70 \pm 0.08 \pm 0.05$	2478 ± 68	ABDALLAH 06E	DLPH	from Z decays
$\bullet \bullet \bullet$	$\bullet \bullet \bullet$	We do not use the following data for averages, fits, limits, etc. $\bullet \bullet \bullet$		
1321.46 ± 0.34	632	DIBIANCA 75	DBC	$4.9 \text{ GeV}/c \ K^- d$
1321.12 ± 0.41	268	WILQUET 72	HLBC	
1321.87 ± 0.51	195	¹ GOLDWASSER 70	HBC	$5.5 \text{ GeV}/c \ K^- p$
1321.67 ± 0.52	6	CHIEN 66	HBC	$6.9 \text{ GeV}/c \ \bar{p} p$
1321.4 ± 1.1	299	LONDON 66	HBC	
1321.3 ± 0.4	149	PJERROU 65B	HBC	
1321.1 ± 0.3	241	² BADIER 64	HBC	
1321.4 ± 0.4	517	² JAUNEAU 63D	FBC	
1321.1 ± 0.65	62	² SCHNEIDER 63	HBC	

¹GOLDWASSER 70 uses $m_{\Lambda} = 1115.58 \text{ MeV}$.

²These masses have been increased 0.09 MeV because the Λ mass increased.

 Ξ^+ MASS

The fit uses the Ξ^- , Ξ^+ , and Ξ^0 masses and the $\Xi^- - \Xi^+$ mass difference. It assumes that the Ξ^- and Ξ^+ masses are the same.

VALUE (MeV)	EVTS	DOCUMENT ID	TECN	COMMENT
1321.71 ± 0.07 OUR FIT				
$1321.73 \pm 0.08 \pm 0.05$	2256 ± 63	ABDALLAH 06E	DLPH	from Z decays
$\bullet \bullet \bullet$	$\bullet \bullet \bullet$	We do not use the following data for averages, fits, limits, etc. $\bullet \bullet \bullet$		
1321.6 ± 0.8	35	VOTRUBA 72	HBC	$10 \text{ GeV}/c \ K^+ p$
1321.2 ± 0.4	34	STONE 70	HBC	
1320.69 ± 0.93	5	CHIEN 66	HBC	$6.9 \text{ GeV}/c \ \bar{p} p$

$$(m_{\Xi^-} - m_{\Xi^+}) / m_{\Xi^-}$$

A test of CPT invariance.

VALUE	DOCUMENT ID	TECN	COMMENT
$(-2.5 \pm 8.7) \times 10^{-5}$	ABDALLAH 06E	DLPH	from Z decays

Ξ⁻ MEAN LIFE

Measurements with an error $> 0.2 \times 10^{-10}$ s or with systematic errors not included have been omitted.

VALUE (10^{-10} s)	EVTS	DOCUMENT ID	TECN	COMMENT
1.639 ± 0.015 OUR AVERAGE				
1.65 ± 0.07 ± 0.12	2478 ± 68	ABDALLAH	06E	DLPH from Z decays
1.652 ± 0.051	32k	BOURQUIN	84	SPEC Hyperon beam
1.665 ± 0.065	41k	BOURQUIN	79	SPEC Hyperon beam
1.609 ± 0.028	4286	HEMINGWAY	78	HBC 4.2 GeV/c $K^- p$
1.67 ± 0.08		DIBIANCA	75	DBC 4.9 GeV/c $K^- d$
1.63 ± 0.03	4303	BALTAY	74	HBC 1.75 GeV/c $K^- p$
1.73 ^{+0.08} _{-0.07}	680	MAYEUR	72	HLBC 2.1 GeV/c K^-
1.61 ± 0.04	2610	DAUBER	69	HBC
1.80 ± 0.16	299	LONDON	66	HBC
1.70 ± 0.12	246	PJERROU	65B	HBC
1.69 ± 0.07	794	HUBBARD	64	HBC
1.86 ^{+0.15} _{-0.14}	517	JAUNEAU	63D	FBC

Ξ⁺ MEAN LIFE

VALUE (10^{-10} s)	EVTS	DOCUMENT ID	TECN	COMMENT
1.70 ± 0.08 ± 0.12	2256 ± 63	ABDALLAH	06E	DLPH from Z decays
••• We do not use the following data for averages, fits, limits, etc. •••				
1.55 ^{+0.35} _{-0.20}	35	³ VOTRUBA	72	HBC 10 GeV/c $K^+ p$
1.6 ± 0.3	34	STONE	70	HBC
1.9 ^{+0.7} _{-0.5}	12	³ SHEN	67	HBC
1.51 ± 0.55	5	³ CHIEN	66	HBC 6.9 GeV/c $\bar{p} p$

³The error is statistical only.

$$(\tau_{\Xi^-} - \tau_{\Xi^+}) / \tau_{\Xi^-}$$

A test of CPT invariance.

VALUE	DOCUMENT ID	TECN	COMMENT
-0.01 ± 0.07	ABDALLAH	06E	DLPH from Z decays

Ξ⁻ MAGNETIC MOMENT

See the "Note on Baryon Magnetic Moments" in the Λ Listings.

VALUE (μ_N)	EVTS	DOCUMENT ID	TECN	COMMENT
-0.6507 ± 0.0025 OUR AVERAGE				
-0.6505 ± 0.0025	4.36M	DURYEA	92	SPEC 800 GeV p Be
-0.661 ± 0.036 ± 0.036	44k	TROST	89	SPEC $\Xi^- \sim 250$ GeV
-0.69 ± 0.04	218k	RAMEIKA	84	SPEC 400 GeV p Be
••• We do not use the following data for averages, fits, limits, etc. •••				
-0.674 ± 0.021 ± 0.020	122k	HO	90	SPEC See DURYEA 92
-2.1 ± 0.8	2436	COOL	74	OSPK 1.8 GeV/c $K^- p$
-0.1 ± 2.1	2724	BINGHAM	70B	OSPK 1.8 GeV/c $K^- p$

Ξ⁺ MAGNETIC MOMENT

See the "Note on Baryon Magnetic Moments" in the Λ Listings.

VALUE (μ_N)	EVTS	DOCUMENT ID	TECN	COMMENT
+0.657 ± 0.028 ± 0.020	70k	HO	90	SPEC 800 GeV p Be

$$(\mu_{\Xi^-} + \mu_{\Xi^+}) / |\mu_{\Xi^-}|$$

A test of CPT invariance. We calculate this from the Ξ^- and Ξ^+ magnetic moments above.

VALUE	DOCUMENT ID
+0.01 ± 0.05 OUR EVALUATION	

Ξ⁻ DECAY MODES

Mode	Fraction (Γ_i/Γ)	Confidence level
Γ_1 $\Lambda\pi^-$	(99.887 ± 0.035) %	
Γ_2 $\Sigma^- \gamma$	(1.27 ± 0.23) × 10 ⁻⁴	
Γ_3 $\Lambda e^- \bar{\nu}_e$	(5.63 ± 0.31) × 10 ⁻⁴	
Γ_4 $\Lambda \mu^- \bar{\nu}_\mu$	(3.5 ^{+3.5} _{-2.2}) × 10 ⁻⁴	
Γ_5 $\Sigma^0 e^- \bar{\nu}_e$	(8.7 ± 1.7) × 10 ⁻⁵	
Γ_6 $\Sigma^0 \mu^- \bar{\nu}_\mu$	< 8 × 10 ⁻⁴	90%
Γ_7 $\Xi^0 e^- \bar{\nu}_e$	< 2.3 × 10 ⁻³	90%

ΔS = 2 forbidden (S2) modes

Γ_8 $n\pi^-$	S2	< 1.9	× 10 ⁻⁵	90%
Γ_9 $n e^- \bar{\nu}_e$	S2	< 3.2	× 10 ⁻³	90%
Γ_{10} $n \mu^- \bar{\nu}_\mu$	S2	< 1.5	%	90%
Γ_{11} $p\pi^- \pi^-$	S2	< 4	× 10 ⁻⁴	90%
Γ_{12} $p\pi^- e^- \bar{\nu}_e$	S2	< 4	× 10 ⁻⁴	90%
Γ_{13} $p\pi^- \mu^- \bar{\nu}_\mu$	S2	< 4	× 10 ⁻⁴	90%
Γ_{14} $p\mu^- \mu^-$	L	< 4	× 10 ⁻⁸	90%

CONSTRAINED FIT INFORMATION

An overall fit to 4 branching ratios uses 5 measurements and one constraint to determine 5 parameters. The overall fit has a $\chi^2 = 1.0$ for 1 degrees of freedom.

The following *off-diagonal* array elements are the correlation coefficients $\langle \delta x_i \delta x_j \rangle / (\delta x_i \delta x_j)$, in percent, from the fit to the branching fractions, $x_i \equiv \Gamma_i / \Gamma_{\text{total}}$. The fit constrains the x_i whose labels appear in this array to sum to one.

x_2	-6			
x_3	-8	0		
x_4	-99	0	-1	
x_5	-5	0	0	0
	x_1	x_2	x_3	x_4

Ξ⁻ BRANCHING RATIOS

A number of early results have been omitted.

Γ(Σ⁻γ)/Γ(Λπ⁻)Γ₂/Γ₁

VALUE (units 10 ⁻⁴)	EVTS	DOCUMENT ID	TECN	COMMENT
1.27 ± 0.24 OUR FIT				
1.27 ± 0.23 OUR AVERAGE				
1.22 ± 0.23 ± 0.06	211	⁴ DUBBS	94	E761 Ξ ⁻ 375 GeV
2.27 ± 1.02	9	BIAGI	87B	SPEC SPS hyperon beam

⁴DUBBS 94 also finds weak evidence that the asymmetry parameter α_γ is positive ($\alpha_\gamma = 1.0 \pm 1.3$).

Γ(Λe⁻ν_e)/Γ(Λπ⁻)Γ₃/Γ₁

VALUE (units 10 ⁻³)	EVTS	DOCUMENT ID	TECN	COMMENT
0.564 ± 0.031 OUR FIT				
0.564 ± 0.031	2857	BOURQUIN	83	SPEC SPS hyperon beam
••• We do not use the following data for averages, fits, limits, etc. •••				
0.30 ± 0.13	11	THOMPSON	80	ASPK Hyperon beam

Γ(Λμ⁻ν_μ)/Γ(Λπ⁻)Γ₄/Γ₁

VALUE (units 10 ⁻³)	CL%	EVTS	DOCUMENT ID	TECN	COMMENT
0.35 ^{+0.35} _{-0.22} OUR FIT					
0.35 ± 0.35		1	YEH	74	HBC Effective denom.=2859
••• We do not use the following data for averages, fits, limits, etc. •••					
< 2.3	90	0	THOMPSON	80	ASPK Effective denom.=1017
< 1.3			DAUBER	69	HBC
< 1.2			BERGE	66	HBC

Γ(Σ⁰e⁻ν_e)/Γ(Λπ⁻)Γ₅/Γ₁

VALUE (units 10 ⁻³)	EVTS	DOCUMENT ID	TECN	COMMENT
0.087 ± 0.017 OUR FIT				
0.087 ± 0.017	154	BOURQUIN	83	SPEC SPS hyperon beam

[Γ(Λe⁻ν_e) + Γ(Σ⁰e⁻ν_e)]/Γ(Λπ⁻)(Γ₃+Γ₅)/Γ₁

VALUE (units 10 ⁻³)	EVTS	DOCUMENT ID	TECN	COMMENT
••• We do not use the following data for averages, fits, limits, etc. •••				
0.651 ± 0.031	3011	⁵ BOURQUIN	83	SPEC SPS hyperon beam
0.68 ± 0.22	17	⁶ DUCLOS	71	OSPK

⁵ See the separate BOURQUIN 83 values for $\Gamma(\Lambda e^- \bar{\nu}_e) / \Gamma(\Lambda \pi^-)$ and $\Gamma(\Sigma^0 e^- \bar{\nu}_e) / \Gamma(\Lambda \pi^-)$ above.

⁶ DUCLOS 71 cannot distinguish Σ^0 s from Λ 's. The Cabibbo theory predicts the Σ^0 rate is about a factor 6 smaller than the Λ rate.

Γ(Σ⁰μ⁻ν_μ)/Γ(Λπ⁻)Γ₆/Γ₁

VALUE (units 10 ⁻³)	CL%	EVTS	DOCUMENT ID	TECN	COMMENT	
< 0.76		90	0	YEH	74	HBC Effective denom.=3026
••• We do not use the following data for averages, fits, limits, etc. •••						
< 5				BERGE	66	HBC

Γ(Ξ⁰e⁻ν_e)/Γ(Λπ⁻)Γ₇/Γ₁

VALUE (units 10 ⁻³)	CL%	EVTS	DOCUMENT ID	TECN	COMMENT	
< 2.3		90	0	YEH	74	HBC Effective denom.=1000

Baryon Particle Listings

Ξ⁻

Γ(nπ⁻)/Γ(Λπ⁻) Γ₈/Γ₁
 ΔS=2. Forbidden in first-order weak interaction.

VALUE (units 10 ⁻³)	CL%	EVTS	DOCUMENT ID	TECN	COMMENT
<0.019	90		BIAGI 82B	SPEC	SPS hyperon beam
•••	We do not use the following data for averages, fits, limits, etc. •••				
<3.0	90	0	YEH 74	HBC	Effective denom.=760
<1.1			DAUBER 69	HBC	
<5.0			FERRO-LUZZI 63	HBC	

Γ(ne⁻ν_e)/Γ(Λπ⁻) Γ₉/Γ₁
 ΔS=2. Forbidden in first-order weak interaction.

VALUE (units 10 ⁻³)	CL%	EVTS	DOCUMENT ID	TECN	COMMENT
< 3.2	90	0	YEH 74	HBC	Effective denom.=715
•••	We do not use the following data for averages, fits, limits, etc. •••				
<10	90		BINGHAM 65	RVUE	

Γ(nμ⁻ν_μ)/Γ(Λπ⁻) Γ₁₀/Γ₁
 ΔS=2. Forbidden in first-order weak interaction.

VALUE (units 10 ⁻³)	CL%	EVTS	DOCUMENT ID	TECN	COMMENT
<15.3	90	0	YEH 74	HBC	Effective denom.=150

Γ(pπ⁻π⁻)/Γ(Λπ⁻) Γ₁₁/Γ₁
 ΔS=2. Forbidden in first-order weak interaction.

VALUE (units 10 ⁻⁴)	CL%	EVTS	DOCUMENT ID	TECN	COMMENT
<3.7	90	0	YEH 74	HBC	Effective denom.=6200

Γ(pπ⁻e⁻ν_e)/Γ(Λπ⁻) Γ₁₂/Γ₁
 ΔS=2. Forbidden in first-order weak interaction.

VALUE (units 10 ⁻⁴)	CL%	EVTS	DOCUMENT ID	TECN	COMMENT
<3.7	90	0	YEH 74	HBC	Effective denom.=6200

Γ(pπ⁻μ⁻ν_μ)/Γ(Λπ⁻) Γ₁₃/Γ₁
 ΔS=2. Forbidden in first-order weak interaction.

VALUE (units 10 ⁻⁴)	CL%	EVTS	DOCUMENT ID	TECN	COMMENT
<3.7	90	0	YEH 74	HBC	Effective denom.=6200

Γ(pμ⁻μ⁻)/Γ(Λπ⁻) Γ₁₄/Γ₁
 ΔL=2 decay, forbidden by total lepton number conservation.

VALUE (units 10 ⁻⁸)	CL%	DOCUMENT ID	TECN	COMMENT
<4.0	90	RAJARAM 05	HYCP	p Cu, 800 GeV
•••	We do not use the following data for averages, fits, limits, etc. •••			
<3.7 × 10 ⁴	90	7 LITTENBERG 92B	HBC	Uses YEH 74 data

⁷This LITTENBERG 92B limit and the identical YEH 74 limits for the preceding three modes all result from nonobservance of any 3-prong decays of the Ξ⁻. One could as well apply the limit to the sum of the four modes.

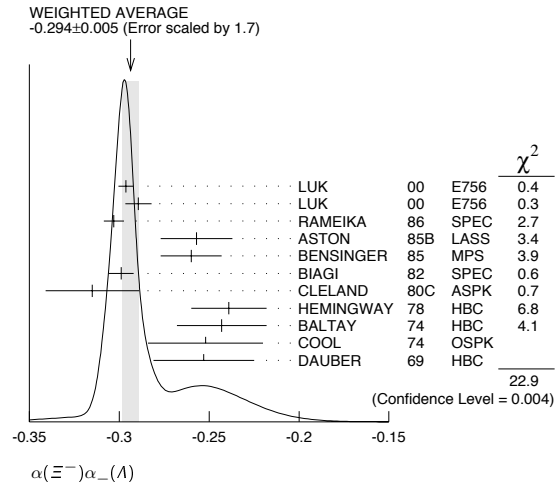
Ξ⁻ DECAY PARAMETERS

See the "Note on Baryon Decay Parameters" in the neutron Listings.

α(Ξ⁻)α₋(Λ)

VALUE	EVTS	DOCUMENT ID	TECN	COMMENT
-0.294 ± 0.005 OUR AVERAGE				Error includes scale factor of 1.7. See the ideogram below.
-0.2963 ± 0.0042	189k	LUK	00 E756	p Be, 800 GeV
-0.2894 ± 0.0073	63k	⁸ LUK	00 E756	p Be, 800 GeV
-0.303 ± 0.004 ± 0.004	192k	RAMEIKA	86 SPEC	400 GeV pBe
-0.257 ± 0.020	11k	ASTON	85B LASS	11 GeV/c K ⁻ p
-0.260 ± 0.017	21k	BENSINGER	85 MPS	5 GeV/c K ⁻ p
-0.299 ± 0.007	150k	BIAGI	82 SPEC	SPS hyperon beam
-0.315 ± 0.026	9046	CLELAND	80c ASPK	BNL hyperon beam
-0.239 ± 0.021	6599	HEMINGWAY	78 HBC	4.2 GeV/c K ⁻ p
-0.243 ± 0.025	4303	BALTAY	74 HBC	1.75 GeV/c
-0.252 ± 0.032	2436	COOL	74 OSPK	1.8 GeV/c K ⁻ p
-0.253 ± 0.028	2781	DAUBER	69 HBC	

⁸This LUK 00 value is for α(Ξ⁺)α₊(Λ̄). We assume CP conservation here by including it in the average for α(Ξ⁻)α₋(Λ). But see the second data block below for the CP test.



α FOR Ξ⁻ → Λπ⁻
 The above average, α(Ξ⁻)α₋(Λ) = -0.294 ± 0.005, where the error includes a scale factor of 1.7, divided by our current average α₋(Λ) = 0.642 ± 0.013, gives the following value for α(Ξ⁻).

-0.458 ± 0.012 OUR EVALUATION Error includes scale factor of 1.8.

α(Ξ⁻)α₋(Λ) - α(Ξ⁺)α₊(Λ̄)
 This is zero if CP is conserved. The α's are the decay-asymmetry parameters for Ξ⁻ → Λπ⁻ and Λ → pπ⁻ and for Ξ⁺ → Λ̄π⁺ and Λ̄ → p̄π⁺.

VALUE (units 10 ⁻⁴)	EVTS	DOCUMENT ID	TECN	COMMENT
0.0 ± 5.1 ± 4.4	158M	HOLMSTROM 04	HYCP	p Cu, 800 GeV
•••	We do not use the following data for averages, fits, limits, etc. •••			
+120 ± 140	252k	LUK 00	E756	p Be, 800 GeV

φ ANGLE FOR Ξ⁻ → Λπ⁻ (tanφ = β/γ)

VALUE (°)	EVTS	DOCUMENT ID	TECN	COMMENT
-2.1 ± 0.8 OUR AVERAGE				
-2.39 ± 0.64 ± 0.64	144M	⁹ HUANG	04 HYCP	p Cu, 800 GeV
-1.61 ± 2.66 ± 0.37	1.35M	¹⁰ CHAKRAVO...	03 E756	p Be, 800 GeV
5 ± 10	11k	ASTON	85B LASS	K ⁻ p
14.7 ± 16.0	21k	¹¹ BENSINGER	85 MPS	5 GeV/c K ⁻ p
11 ± 9	4303	BALTAY	74 HBC	1.75 GeV/c K ⁻ p
5 ± 16	2436	COOL	74 OSPK	1.8 GeV/c K ⁻ p
-14 ± 11	2781	DAUBER	69 HBC	Uses α _Λ = 0.647 ± 0.020
0 ± 12	1004	¹² BERGE	66 HBC	
•••	We do not use the following data for averages, fits, limits, etc. •••			
-26 ± 30	2724	BINGHAM	70B OSPK	
0 ± 20.4	364	¹² LONDON	66 HBC	Using α _Λ = 0.62
54 ± 30	356	¹² CARMONY	64B HBC	

⁹From this result and α_Ξ, HUANG 04 gets β_Ξ = -0.037 ± 0.011 ± 0.010 and γ_Ξ = 0.888 ± 0.0004 ± 0.006. And the strong p-s phase difference for Λπ⁻ scattering is (4.6 ± 1.4 ± 1.2)°.

¹⁰From this result and α_Ξ, CHAKRAVORTY 03 obtains β_Ξ = -0.025 ± 0.042 ± 0.006 and γ_Ξ = 0.889 ± 0.001 ± 0.007. And the strong p-s phase difference for Λπ⁻ scattering is (3.17 ± 5.28 ± 0.73)°.

¹¹BENSINGER 85 used α_Λ = 0.642 ± 0.013.

¹²The errors have been multiplied by 1.2 due to approximations used for the Ξ polarization; see DAUBER 69 for a discussion.

g_A / g_V FOR Ξ⁻ → Λe⁻ν_e

VALUE	EVTS	DOCUMENT ID	TECN	COMMENT
-0.25 ± 0.05	1992	¹³ BOURQUIN	83 SPEC	SPS hyperon beam

¹³BOURQUIN 83 assumes that g₂ = 0. Also, the sign has been changed to agree with our conventions, given in the "Note on Baryon Decay Parameters" in the neutron Listings.

Ξ⁻ REFERENCES

We have omitted some papers that have been superseded by later experiments. See our earlier editions.

ABDALLAH 06E	PL B639 179	J. Abdallah et al.	(DELPHI Collab.)
RAJARAM 05	PRL 94 181801	D. Rajaram et al.	(FNAL HyperCP Collab.)
HOLMSTROM 04	PRL 93 262001	T. Holmstrom et al.	(FNAL HyperCP Collab.)
HUANG 04	PRL 93 011802	M. Huang et al.	(FNAL HyperCP Collab.)
CHAKRAVO... 03	PRL 91 031601	A. Chakravorty et al.	(FNAL E756 Collab.)
LUK 00	PRL 85 4860	K.B. Luk et al.	(FNAL E756 Collab.)
DUBBS 94	PRL 72 808	T. Dubbs et al.	(FNAL E761 Collab.)
DURYEA 92	PRL 68 768	J. Duryea et al.	(MINN, FNAL, MICH, RUTG)
LITTENBERG 92B	PR D46 R892	L.S. Littenberg, R.E. Shrock	(BNL, STON)
HO 90	PRL 65 1713	P.M. Ho et al.	(MICH, FNAL, MINN, RUTG)
Also	PR D44 3402	P.M. Ho et al.	(MICH, FNAL, MINN, RUTG)
TROST 89	PR D40 1703	L.H. Trost et al.	(FNAL-715 Collab.)
BIAGI 87B	ZPHY C35 143	S.F. Biagi et al.	(BRIS, CERN, GEVA+)
RAMEIKA 86	PR D33 3172	R. Rameika et al.	(RUTG, MICH, WISC+)

ASTON	85B	PR D32 2270	D. Aston <i>et al.</i>	(SLAC, CARL, CNRC, CINC)
BENSINGER	85	NP B252 561	J.R. Bensing <i>et al.</i>	(CHIC, ELMT, FNAL+)
BOURQUIN	84	NP B241 1	M.H. Bourquin <i>et al.</i>	(BRIS, GEVA, HEIDP+)
RAMEIKA	84	PRL 52 581	R. Rameika <i>et al.</i>	(RUTG, MICH, WISC+)
BOURQUIN	83	ZPHY C21 1	M.H. Bourquin <i>et al.</i>	(BRIS, GEVA, HEIDP+)
BIAGI	82	PL 112B 265	S.F. Biagi <i>et al.</i>	(BRIS, CAVE, GEVA+)
BIAGI	82B	PL 112B 277	S.F. Biagi <i>et al.</i>	(LOQM, GEVA, RL+)
CLELAND	80C	PR D21 12	W.E. Cleland <i>et al.</i>	(PITT, BNL)
THOMPSON	80	PR D21 25	J.A. Thompson <i>et al.</i>	(PITT, BNL)
BOURQUIN	79	PL 87B 297	M.H. Bourquin <i>et al.</i>	(BRIS, GEVA, HEIDP+)
HEMINGWAY	78	NP B142 205	R.J. Hemingway <i>et al.</i>	(CERN, ZEEM, NIJM+)
DIBIANCA	75	NP B98 137	F.A. Dibianna, R.J. Endorf	(CMU)
BALTAY	74	PR D9 49	C. Baltay <i>et al.</i>	(COLU, BING) J
COOL	74	PR D10 792	R.L. Cool <i>et al.</i>	(BNL)
Also		PRL 29 1630	R.L. Cool <i>et al.</i>	(BNL)
YEH	74	PR D10 3545	N. Yeh <i>et al.</i>	(BING, COLU)
MAYEUR	72	NP B47 333	C. Mayeur <i>et al.</i>	(BRUX, CERN, TUFTS, LOUC)
VOTRUBA	72	NP B45 77	M.F. Votruba, T.M. Ratcliffe	(BIRM+)
WILQUET	72	PL 42B 372	G. Wilquet <i>et al.</i>	(BRUX, CERN, TUFTS+)
DUCLOS	71	NP B32 493	J. Duclos <i>et al.</i>	(CERN)
BINGHAM	70B	PR D1 3010	G.M. Bingham <i>et al.</i>	(UCSD, WASH)
GOLDWASSER	70	PR D1 1960	E.L. Goldwasser, P.F. Schultz	(ILL)
STONE	70	PL 32B 515	S.L. Stone <i>et al.</i>	(ROCH)
DAUBER	69	PR 179 1262	P.M. Dauber <i>et al.</i>	(LRL) J
SHEN	67	PL 25B 443	B.C. Shen, A. Firestone, G. Goldhaber	(UCB+)
BERGE	66	PR 147 945	J.P. Berge <i>et al.</i>	(LRL)
CHIEN	66	PR 152 1171	C.Y. Chien <i>et al.</i>	(YALE, BNL)
LONDON	66	PR 143 1034	G.W. London <i>et al.</i>	(BNL, SYRA)
BINGHAM	65	PRSL 285 202	H.H. Bingham	(CERN)
PJERROU	65B	PRL 14 275	G.M. Pjerrou <i>et al.</i>	(UCLA)
Also		Thesis	G.M. Pjerrou	(UCLA)
BADIER	64	Dubna Conf. 1 593	J. Badier <i>et al.</i>	(EPOL, SACL, ZEEM)
CARMONY	64B	PRL 12 482	D.D. Carmony <i>et al.</i>	(UCLA) J
HUBBARD	64	PR 135 B183	J.R. Hubbard <i>et al.</i>	(LRL)
FERRU-LUZZI	63	PR 130 1568	M. Ferro-Luzzi <i>et al.</i>	(LRL)
JAUNEAU	63D	Siena Conf. 4	L. Jauneau <i>et al.</i>	(EPOL, CERN, LOUC+)
Also		PL 5 261	L. Jauneau <i>et al.</i>	(EPOL, CERN, LOUC+)
SCHNEIDER	63	PL 4 360	J. Schneider	(CERN)

Ξ RESONANCES

The accompanying table gives our evaluation of the present status of the Ξ resonances. Not much is known about Ξ resonances. This is because (1) they can only be produced as a part of a final state, and so the analysis is more complicated than if direct formation were possible, (2) the production cross sections are small (typically a few μb), and (3) the final states are topologically complicated and difficult to study with electronic techniques. Thus early information about Ξ resonances came entirely from bubble chamber experiments, where the numbers of events are small, and only in the 1980's did electronic experiments make any significant contributions. However, nothing of significance on Ξ resonances has been added since our 1988 edition.

For a detailed earlier review, see Meadows [1].

Table 1. The status of the Ξ resonances. Only those with an overall status of *** or **** are included in the Baryon Summary Table.

Particle	$L_{2I,2J}$	Overall status	Status as seen in —				
			$\Xi\pi$	ΛK	ΣK	$\Xi(1530)\pi$	Other channels
$\Xi(1318)$	P_{11}	****					Decays weakly
$\Xi(1530)$	P_{13}	****	****				
$\Xi(1620)$		*	*				
$\Xi(1690)$		***		***	**		
$\Xi(1820)$	D_{13}	***	**	***	**	**	
$\Xi(1950)$		***	**	**		*	
$\Xi(2030)$	1	***		**	***		
$\Xi(2120)$		*		*			
$\Xi(2250)$		**					3-body decays
$\Xi(2370)$	1	**					3-body decays
$\Xi(2500)$		*		*			3-body decays

**** Existence is certain, and properties are at least fairly well explored.
 *** Existence ranges from very likely to certain, but further confirmation is desirable and/or quantum numbers, branching fractions, etc. are not well determined.
 ** Evidence of existence is only fair.
 * Evidence of existence is poor.

Reference

1. B.T. Meadows, in *Proceedings of the IVth International Conference on Baryon Resonances* (Toronto, 1980), ed. N. Isgur, p. 283.

$\Xi(1530) P_{13}$

$I(J^P) = \frac{1}{2}(\frac{3}{2}^+)$ Status: ***

This is the only Ξ resonance whose properties are all reasonably well known. Spin-parity $3/2^+$ is favored by the data.

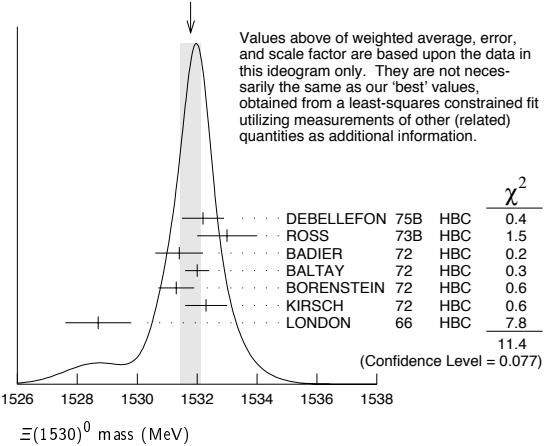
We use only those determinations of the mass and width that are accompanied by some discussion of systematics and resolution.

$\Xi(1530)$ MASSES

$\Xi(1530)^0$ MASS

VALUE (MeV)	EVTS	DOCUMENT ID	TECN	COMMENT
1531.80 ± 0.32 OUR FIT				Error includes scale factor of 1.3.
1531.78 ± 0.34 OUR AVERAGE				Error includes scale factor of 1.4. See the ideogram below.
1532.2 ± 0.7		DEBELLEFON 75B	HBC	$K^- p \rightarrow \Xi^- \bar{K} \pi$
1533 ± 1		ROSS 73B	HBC	$K^- p \rightarrow \Xi \bar{K} \pi(\pi)$
1531.4 ± 0.8	59	BADIER 72	HBC	$K^- p$ 3.95 GeV/c
1532.0 ± 0.4	1262	BALTAY 72	HBC	$K^- p$ 1.75 GeV/c
1531.3 ± 0.6	324	BORENSTEIN 72	HBC	$K^- p$ 2.2 GeV/c
1532.3 ± 0.7	286	KIRSCH 72	HBC	$K^- p$ 2.87 GeV/c
1528.7 ± 1.1	76	LONDON 66	HBC	$K^- p$ 2.24 GeV/c
••• We do not use the following data for averages, fits, limits, etc. •••				
1532.1 ± 0.4	1244	ASTON 85B	LASS	$K^- p$ 11 GeV/c
1532.1 ± 0.6	2700	1 BAUBILLIER 81B	HBC	$K^- p$ 8.25 GeV/c
1530 ± 1	450	BIAGI 81	SPEC	SPS hyperon beam
1527 ± 0.6	80	SIXEL 79	HBC	$K^- p$ 10 GeV/c
1535 ± 0.4	100	SIXEL 79	HBC	$K^- p$ 16 GeV/c
1533.6 ± 1.4	97	BERTHON 74	HBC	Quasi-2-body σ

WEIGHTED AVERAGE
 1531.78 ± 0.34 (Error scaled by 1.4)



$\Xi(1530)^-$ MASS

VALUE (MeV)	EVTS	DOCUMENT ID	TECN	COMMENT
1535.0 ± 0.6 OUR FIT				
1535.2 ± 0.8 OUR AVERAGE				
1534.5 ± 1.2		DEBELLEFON 75B	HBC	$K^- p \rightarrow \Xi^- \bar{K} \pi$
1535.3 ± 2.0		ROSS 73B	HBC	$K^- p \rightarrow \Xi \bar{K} \pi(\pi)$
1536.2 ± 1.6	185	KIRSCH 72	HBC	$K^- p$ 2.87 GeV/c
1535.7 ± 3.2	38	LONDON 66	HBC	$K^- p$ 2.24 GeV/c
••• We do not use the following data for averages, fits, limits, etc. •••				
1540 ± 3	48	BERTHON 74	HBC	Quasi-2-body σ
1534.7 ± 1.1	334	BALTAY 72	HBC	$K^- p$ 1.75 GeV/c

$m_{\Xi(1530)^-} - m_{\Xi(1530)}$

VALUE (MeV)	DOCUMENT ID	TECN	COMMENT
3.2 ± 0.6 OUR FIT			
2.9 ± 0.9 OUR AVERAGE			
2.7 ± 1.0	BALTAY 72	HBC	$K^- p$ 1.75 GeV/c
2.0 ± 3.2	MERRILL 66	HBC	$K^- p$ 1.7-2.7 GeV/c
5.7 ± 3.0	PJERROU 65B	HBC	$K^- p$ 1.8-1.95 GeV/c
••• We do not use the following data for averages, fits, limits, etc. •••			
3.9 ± 1.8	2 KIRSCH 72	HBC	$K^- p$ 2.87 GeV/c
7 ± 4	2 LONDON 66	HBC	$K^- p$ 2.24 GeV/c

Baryon Particle Listings

$\Xi(1530)$, $\Xi(1620)$, $\Xi(1690)$

$\Xi(1530)$ WIDTHS

$\Xi(1530)^0$ WIDTH

VALUE (MeV)	EVTS	DOCUMENT ID	TECN	COMMENT
9.1±0.5 OUR AVERAGE				
9.5±1.2		DEBELLEFON 75B	HBC	$K^- p \rightarrow \Xi^- \bar{K} \pi$
9.1±2.4		ROSS 73B	HBC	$K^- p \rightarrow \Xi^- \bar{K} \pi(\pi)$
11 ± 2		BADIER 72	HBC	$K^- p$ 3.95 GeV/c
9.0±0.7		BALTAY 72	HBC	$K^- p$ 1.75 GeV/c
8.4±1.4		BORENSTEIN 72	HBC	$\Xi^- \pi^+$
11.0±1.8		KIRSCH 72	HBC	$\Xi^- \pi^+$
7 ± 7		BERGE 66	HBC	$K^- p$ 1.5-1.7 GeV/c
8.5±3.5		LONDON 66	HBC	$K^- p$ 2.24 GeV/c
7 ± 2		SCHLEIN 63B	HBC	$K^- p$ 1.8, 1.95 GeV/c
12.8±1.0	2700	¹ BAUBILLIER 81B	HBC	$K^- p$ 8.25 GeV/c
19 ± 6	80	³ SIXEL 79	HBC	$K^- p$ 10 GeV/c
14 ± 5	100	³ SIXEL 79	HBC	$K^- p$ 16 GeV/c

$\Xi(1530)^-$ WIDTH

VALUE (MeV)	DOCUMENT ID	TECN	COMMENT
9.9^{+1.7}_{-1.9} OUR AVERAGE			
9.6±2.8	DEBELLEFON 75B	HBC	$K^- p \rightarrow \Xi^- \bar{K} \pi$
8.3±3.6	ROSS 73B	HBC	$K^- p \rightarrow \Xi^- \bar{K} \pi(\pi)$
7.8 ^{+3.5} _{-7.8}	BALTAY 72	HBC	$K^- p$ 1.75 GeV/c
16.2±4.6	KIRSCH 72	HBC	$\Xi^- \pi^0, \Xi^0 \pi^-$

$\Xi(1530)$ POLE POSITIONS

$\Xi(1530)^0$ REAL PART

VALUE	DOCUMENT ID	COMMENT
1531.6±0.4	LICHTENBERG74	Using HABIBI 73

$\Xi(1530)^0$ IMAGINARY PART

VALUE	DOCUMENT ID	COMMENT
4.45±0.35	LICHTENBERG74	Using HABIBI 73

$\Xi(1530)^-$ REAL PART

VALUE	DOCUMENT ID	COMMENT
1534.4±1.1	LICHTENBERG74	Using HABIBI 73

$\Xi(1530)^-$ IMAGINARY PART

VALUE	DOCUMENT ID	COMMENT
3.9 ^{+1.75} _{-3.9}	LICHTENBERG74	Using HABIBI 73

$\Xi(1530)$ DECAY MODES

Mode	Fraction (Γ_i/Γ)	Confidence level
$\Gamma_1 \Xi \pi$	100 %	
$\Gamma_2 \Xi \gamma$	< 4 %	90%

$\Xi(1530)$ BRANCHING RATIOS

$\Gamma(\Xi \gamma)/\Gamma_{\text{total}}$	CL%	DOCUMENT ID	TECN	COMMENT	Γ_2/Γ
<0.04	90	KALBFLEISCH 75	HBC	$K^- p$ 2.18 GeV/c	

$\Xi(1530)$ FOOTNOTES

- ¹BAUBILLIER 81B is a fit to the inclusive spectrum. The resolution (5 MeV) is not unfolded.
²Redundant with data in the mass Listings.
³SIXEL 79 doesn't unfold the experimental resolution of 15 MeV.

$\Xi(1530)$ REFERENCES

ASTON 85B	PR D32 2270	D. Aston et al.	(SLAC, CARL, CNRC, CINC)
BAUBILLIER 81B	NP B192 1	M. Baubillier et al.	(BIRM, CERN, GLAS+)
BIAGI 81	ZPHY C9 305	S.F. Biagi et al.	(BRIS, CAVE, GEVA+)
SIXEL 79	NP B159 125	P. Sixel et al.	(AACH3, BERL, CERN, LOIC+)
DEBELLEFON 75B	NC 28A 289	A. de Bellefon et al.	(CDEF, SACL)
KALBFLEISCH 75	PR D11 987	G.R. Kalbfleisch, R.C. Strand, J.W. Chapman	(BNL+)
BERTHON 74	NC 21A 146	A. Berthon et al.	(CDEF, RHEL, SACL+)
LICHTENBERG 74	PR D10 3865	D.B. Lichtenberg	(IND)
	Private Comm.	D.B. Lichtenberg	(IND)
HABIBI 73	Thesis Nevis 199	M. Habibi	(COLU)
ROSS 73B	Purdue Conf. 355	R.T. Ross, J.L. Lloyd, D. Radojicic	(OXF)
BADIER 72	NP B37 429	J. Badier et al.	(EPOL)
BALTAY 72	PL 42B 129	C. Baltay et al.	(COLU, BING)
BORENSTEIN 72	PR D5 1559	S.R. Borenstein et al.	(BNL, MICH) I
KIRSCH 72	NP B40 349	L.E. Kirsch et al.	(BRAN, UMD, SYRA+) I
BERGE 66	PR 147 945	J.P. Berge et al.	(LRL) I
LONDON 66	PR 143 1034	G.W. London et al.	(BNL, SYRA) IJ
MERRILL 66	Thesis UCRL 16455	D.W. Merrill	(LRL) JP
PJERROU 65B	PRL 14 275	G.M. Pjerrou et al.	(UCLA)
SCHLEIN 63B	PRL 11 167	P.E. Schlein et al.	(UCLA) IJP

OTHER RELATED PAPERS

MAZZUCATO 81	NP B178 1	M. Mazzucato et al.	(AMST, CERN, NIIM+)
BRIEFEL 77	PR D16 2706	E. Briefel et al.	(BRAN, UMD, SYRA+)
BRIEFEL 75	PR D12 1859	E. Briefel et al.	(BRAN, UMD, SYRA+)
HUNGERBU... 74	PR D10 2051	V. Hungerbuehler et al.	(YALE, FNAL, BNL+)
BUTTON... 66	PR 142 883	J. Button-Shafer et al.	(LRL) JP

$\Xi(1620)$

$I(J^P) = \frac{1}{2}(?)^?$ Status: *
 J, P need confirmation.

OMITTED FROM SUMMARY TABLE

What little evidence there is consists of weak signals in the $\Xi \pi$ channel. A number of other experiments (e.g., BORENSTEIN 72 and HASSALL 81) have looked for but not seen any effect.

$\Xi(1620)$ MASS

VALUE (MeV)	EVTS	DOCUMENT ID	TECN	COMMENT
≈ 1620 OUR ESTIMATE				
1624 ± 3	31	BRIEFEL 77	HBC	$K^- p$ 2.87 GeV/c
1633 ± 12	34	DEBELLEFON 75B	HBC	$K^- p \rightarrow \Xi^- \bar{K} \pi$
1606 ± 6	29	ROSS 72	HBC	$K^- p$ 3.1-3.7 GeV/c

$\Xi(1620)$ WIDTH

VALUE (MeV)	EVTS	DOCUMENT ID	TECN	COMMENT
22.5	31	¹ BRIEFEL 77	HBC	$K^- p$ 2.87 GeV/c
40 ± 15	34	DEBELLEFON 75B	HBC	$K^- p \rightarrow \Xi^- \bar{K} \pi$
21 ± 7	29	ROSS 72	HBC	$K^- p \rightarrow \Xi^- \pi^+ K^*0(892)$

$\Xi(1620)$ DECAY MODES

Mode	Γ_1	$\Xi \pi$

$\Xi(1620)$ FOOTNOTES

- ¹The fit is insensitive to values between 15 and 30 MeV.

$\Xi(1620)$ REFERENCES

HASSALL 81	NP B189 397	J.K. Hassall et al.	(CAVE, MSU)
BRIEFEL 77	PR D16 2706	E. Briefel et al.	(BRAN, UMD, SYRA+)
	Duke Conf. 317	E. Briefel et al.	(BRAN, UMD, SYRA+)
	Hyperon Resonances, 1970		
	Also	PR D12 1859	E. Briefel et al.
DEBELLEFON 75B	NC 28A 289	A. de Bellefon et al.	(BRAN, UMD, SYRA+)
BORENSTEIN 72	PR D5 1559	S.R. Borenstein et al.	(CDEF, SACL)
ROSS 72	PL 38B 177	R.T. Ross et al.	(BNL, MICH) I
			(OXF) I

OTHER RELATED PAPERS

HUNGERBU... 74	PR D10 2051	V. Hungerbuehler et al.	(YALE, FNAL, BNL+)
SCHMIDT 73	Purdue Conf. 363	P.E. Schmidt	(BRAN)
KALBFLEISCH 70	Duke Conf. 331	G.R. Kalbfleisch	(BNL) I
	Hyperon Resonances 1970		
APSELL 69	PRL 23 884	S.P. Apzell et al.	(BRAN, UMD, SYRA+)
BARTSCH 69	PL 28B 439	J. Bartsch et al.	(AACH, BERL, CERN+)

$\Xi(1690)$

$I(J^P) = \frac{1}{2}(?)^?$ Status: ** *

DIONISI 78 sees a threshold enhancement in both the neutral and negatively charged $\Sigma \bar{K}$ mass spectra in $K^- p \rightarrow (\Sigma \bar{K}) K \pi$ at 4.2 GeV/c. The data from the $\Sigma \bar{K}$ channels alone cannot distinguish between a resonance and a large scattering length. Weaker evidence at the same mass is seen in the corresponding $\Lambda \bar{K}$ channels, and a coupled-channel analysis yields results consistent with a new Ξ .

BIAGI 81 sees an enhancement at 1700 MeV in the diffractively produced ΛK^- system. A peak is also observed in the $\Lambda \bar{K}^0$ mass spectrum at 1660 MeV that is consistent with a 1720 MeV resonance decaying to $\Sigma^0 \bar{K}^0$, with the γ from the Σ^0 decay not detected.

BIAGI 87 provides further confirmation of this state in diffractive dissociation of Ξ^- into ΛK^- . The significance claimed is 6.7 standard deviations.

ADAMOVIICH 98 sees a peak of 1400 ± 300 events in the $\Xi^- \pi^+$ spectrum produced by 345 GeV/c Σ^- -nucleus interactions.

$\Xi(1690)$ MASSES

MIXED CHARGES

1690±10 OUR ESTIMATE This is only an educated guess; the error given is larger than the error on the average of the published values.

Baryon Particle Listings

$\Xi(1690), \Xi(1820)$

 $\Xi(1690)^0$ MASS

VALUE (MeV)	EVTS	DOCUMENT ID	TECN	COMMENT
1686 ± 4	1400	ADAMOVICH 98	WA89	Σ^- nucleus, 345 GeV/c
1699 ± 5	175	¹ DIONISI 78	HBC	$K^- p$ 4.2 GeV/c
1684 ± 5	183	² DIONISI 78	HBC	$K^- p$ 4.2 GeV/c

 $\Xi(1690)^-$ MASS

VALUE (MeV)	EVTS	DOCUMENT ID	TECN	COMMENT
1691.1 ± 1.9 ± 2.0	104	BIAGI 87	SPEC	Ξ^- Be 116 GeV
1700 ± 10	150	³ BIAGI 81	SPEC	Ξ^- H 100, 135 GeV
1694 ± 6	45	⁴ DIONISI 78	HBC	$K^- p$ 4.2 GeV/c

 $\Xi(1690)$ WIDTHS**MIXED CHARGES**

VALUE (MeV)	DOCUMENT ID
<30 OUR ESTIMATE	

 $\Xi(1690)^0$ WIDTH

VALUE (MeV)	EVTS	DOCUMENT ID	TECN	COMMENT
10 ± 6	1400	ADAMOVICH 98	WA89	Σ^- nucleus, 345 GeV/c
44 ± 23	175	¹ DIONISI 78	HBC	$K^- p$ 4.2 GeV/c
20 ± 4	183	² DIONISI 78	HBC	$K^- p$ 4.2 GeV/c

 $\Xi(1690)^-$ WIDTH

VALUE (MeV)	CL%	EVTS	DOCUMENT ID	TECN	COMMENT
< 8	90	104	BIAGI 87	SPEC	Ξ^- Be 116 GeV
47 ± 14		150	³ BIAGI 81	SPEC	Ξ^- H 100, 135 GeV
26 ± 6		45	⁴ DIONISI 78	HBC	$K^- p$ 4.2 GeV/c

 $\Xi(1690)$ DECAY MODES

Mode	Fraction (Γ_i/Γ)
Γ_1 $\Lambda \bar{K}$	seen
Γ_2 $\Sigma \bar{K}$	seen
Γ_3 $\Xi \pi$	seen
Γ_4 $\Xi^- \pi^+ \pi^0$	
Γ_5 $\Xi^- \pi^+ \pi^-$	possibly seen
Γ_6 $\Xi(1530) \pi$	

 $\Xi(1690)$ BRANCHING RATIOS

$\Gamma(\Lambda \bar{K})/\Gamma_{\text{total}}$	Γ_1/Γ				
VALUE	EVTS	DOCUMENT ID	TECN	CHG	COMMENT
seen	104	BIAGI 87	SPEC	-	Ξ^- Be 116 GeV

$\Gamma(\Sigma \bar{K})/\Gamma(\Lambda \bar{K})$	Γ_2/Γ_1				
VALUE	EVTS	DOCUMENT ID	TECN	CHG	COMMENT
0.75 ± 0.39	75	ABE 02c	BELL		$e^+ e^- \approx \Upsilon(4S)$
2.7 ± 0.9		DIONISI 78	HBC	0	$K^- p$ 4.2 GeV/c
3.1 ± 1.4		DIONISI 78	HBC	-	$K^- p$ 4.2 GeV/c

$\Gamma(\Xi \pi)/\Gamma(\Sigma \bar{K})$	Γ_3/Γ_2			
VALUE	DOCUMENT ID	TECN	CHG	COMMENT
<0.09	DIONISI 78	HBC	0	$K^- p$ 4.2 GeV/c

$\Gamma(\Xi \pi)/\Gamma_{\text{total}}$	Γ_3/Γ		
VALUE	DOCUMENT ID	TECN	COMMENT
seen	ADAMOVICH 98	WA89	Σ^- nucleus, 345 GeV/c

$\Gamma(\Xi^- \pi^+ \pi^0)/\Gamma(\Sigma \bar{K})$	Γ_4/Γ_2			
VALUE	DOCUMENT ID	TECN	CHG	COMMENT
<0.04	DIONISI 78	HBC	0	$K^- p$ 4.2 GeV/c

$\Gamma(\Xi^- \pi^+ \pi^-)/\Gamma_{\text{total}}$	Γ_5/Γ				
VALUE	EVTS	DOCUMENT ID	TECN	CHG	COMMENT
possibly seen	4	BIAGI 87	SPEC	-	Ξ^- Be 116 GeV

$\Gamma(\Xi^- \pi^+ \pi^-)/\Gamma(\Sigma \bar{K})$	Γ_5/Γ_2			
VALUE	DOCUMENT ID	TECN	CHG	COMMENT
<0.03	DIONISI 78	HBC	-	$K^- p$ 4.2 GeV/c

$\Gamma(\Xi(1530) \pi)/\Gamma(\Sigma \bar{K})$	Γ_6/Γ_2			
VALUE	DOCUMENT ID	TECN	CHG	COMMENT
<0.06	DIONISI 78	HBC	-	$K^- p$ 4.2 GeV/c

 $\Xi(1690)$ FOOTNOTES

- From a fit to the $\Sigma^+ K^-$ spectrum.
- From a coupled-channel analysis of the $\Sigma^+ K^-$ and $\Lambda \bar{K}^0$ spectra.
- A fit to the inclusive spectrum from $\Xi^- N \rightarrow \Lambda K^- X$.
- From a coupled-channel analysis of the $\Sigma^0 K^-$ and ΛK^- spectra.

 $\Xi(1690)$ REFERENCES

ABE	02c	PL B524 33	K. Abe <i>et al.</i>	(KEK BELLE Collab.)
ADAMOVICH	98	EPJ C5 621	M.I. Adamovich <i>et al.</i>	(CERN WA89 Collab.)
BIAGI	87	ZPHY C34 15	S.F. Biagi <i>et al.</i>	(BRIS, CERN, GEVA+)
BIAGI	81	ZPHY C9 305	S.F. Biagi <i>et al.</i>	(BRIS, CAVE, GEVA+)
DIONISI	78	PL 80B 145	C. Dionisi <i>et al.</i>	(CERN, AMST, NIJM+)

 $\Xi(1820) D_{13}$

$$I(J^P) = \frac{1}{2}(\frac{3}{2}^-) \text{ Status: } ***$$

The clearest evidence is an 8-standard-deviation peak in ΛK^- seen by GAY 76C. TEODORO 78 favors $J=3/2$, but cannot make a parity discrimination. BIAGI 87C is consistent with $J=3/2$ and favors negative parity for this J value.

 $\Xi(1820)$ MASS

We only average the measurements that appear to us to be most significant and best determined.

VALUE (MeV)	EVTS	DOCUMENT ID	TECN	CHG	COMMENT
1823 ± 5 OUR ESTIMATE					
1823.4 ± 1.4 OUR AVERAGE					
1819.4 ± 3.1 ± 2.0	280	¹ BIAGI 87	SPEC	0	Ξ^- Be \rightarrow (ΛK^-) X
1826 ± 3 ± 1	54	BIAGI 87c	SPEC	0	Ξ^- Be \rightarrow ($\Lambda \bar{K}^0$) X
1822 ± 6		JENKINS 83	MPS	-	$K^- p \rightarrow K^+$ (MM)
1830 ± 6	300	BIAGI 81	SPEC	-	SPS hyperon beam
1823 ± 2	130	GAY 76c	HBC	-	$K^- p$ 4.2 GeV/c
••• We do not use the following data for averages, fits, limits, etc. •••					
1817 ± 3		ADAMOVICH 99b	WA89		Σ^- nucleus, 345 GeV
1797 ± 19	74	BRIEFEL 77	HBC	0	$K^- p$ 2.87 GeV/c
1829 ± 9	68	BRIEFEL 77	HBC	-0	$\Xi(1530) \pi$
1860 ± 14	39	BRIEFEL 77	HBC	-	$\Sigma^- \bar{K}^0$
1870 ± 9	44	BRIEFEL 77	HBC	0	$\Lambda \bar{K}^0$
1813 ± 4	57	BRIEFEL 77	HBC	-	ΛK^-
1807 ± 27		DIBIANCA 75	DBC	-0	$\Xi \pi \pi, \Xi^* \pi$
1762 ± 8	28	² BADIER 72	HBC	-0	$\Xi \pi, \Xi \pi \pi, Y K$
1838 ± 5	38	² BADIER 72	HBC	-0	$\Xi \pi, \Xi \pi \pi, Y K$
1830 ± 10	25	³ CRENNELL 70b	DBC	-0	3.6, 3.9 GeV/c
1826 ± 12		⁴ CRENNELL 70b	DBC	-0	3.6, 3.9 GeV/c
1830 ± 10	40	ALITTI 69	HBC	-	$\Lambda, \Sigma \bar{K}$
1814 ± 4	30	BADIER 65	HBC	0	$\Lambda \bar{K}^0$
1817 ± 7	29	SMITH 65c	HBC	-0	$\Lambda \bar{K}^0, \Lambda K^-$
1770		HALSTEINSLID63	FBC	-0	K^- freon 3.5 GeV/c

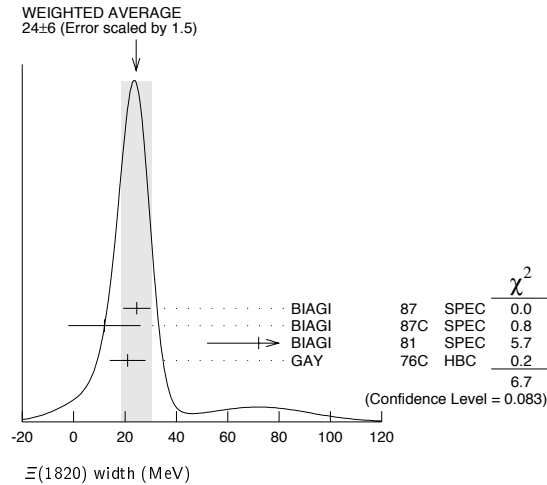
 $\Xi(1820)$ WIDTH

VALUE (MeV)	EVTS	DOCUMENT ID	TECN	CHG	COMMENT
24 +15 -10 OUR ESTIMATE					
24 ± 6 OUR AVERAGE					Error includes scale factor of 1.5. See the ideogram below.
24.6 ± 5.3	280	¹ BIAGI 87	SPEC	0	Ξ^- Be \rightarrow (ΛK^-) X
12 ± 14 ± 1.7	54	BIAGI 87c	SPEC	0	Ξ^- Be \rightarrow ($\Lambda \bar{K}^0$) X
72 ± 20	300	BIAGI 81	SPEC	-	SPS hyperon beam
21 ± 7	130	GAY 76c	HBC	-	$K^- p$ 4.2 GeV/c
••• We do not use the following data for averages, fits, limits, etc. •••					
23 ± 13		ADAMOVICH 99b	WA89		Σ^- nucleus, 345 GeV
99 ± 57	74	BRIEFEL 77	HBC	0	$K^- p$ 2.87 GeV/c
52 ± 34	68	BRIEFEL 77	HBC	-0	$\Xi(1530) \pi$
72 ± 17	39	BRIEFEL 77	HBC	-	$\Sigma^- \bar{K}^0$
44 ± 11	44	BRIEFEL 77	HBC	0	$\Lambda \bar{K}^0$
26 ± 11	57	BRIEFEL 77	HBC	-	ΛK^-
85 ± 58		DIBIANCA 75	DBC	-0	$\Xi \pi \pi, \Xi^* \pi$
51 ± 13		² BADIER 72	HBC	-0	Lower mass
58 ± 13		² BADIER 72	HBC	-0	Higher mass

Baryon Particle Listings

 $\Xi(1820)$

103	$+38$ -24	3	CRENNELL	70B	DBC	-0	3.6, 3.9 GeV/c
48	$+36$ -19	4	CRENNELL	70B	DBC	-0	3.6, 3.9 GeV/c
55	$+40$ -20		ALITTI	69	HBC	-	$\Lambda, \Sigma \bar{K}$
12	± 4		BADIER	65	HBC	0	$\Lambda \bar{K}^0$
30	± 7		SMITH	65B	HBC	-0	$\Lambda \bar{K}$
< 80			HALSTEINSLID	63	FBC	-0	K^- freon 3.5 GeV/c

 $\Xi(1820)$ DECAY MODES

Mode	Fraction (Γ_i/Γ)
Γ_1 $\Lambda \bar{K}$	large
Γ_2 $\Sigma \bar{K}$	small
Γ_3 $\Xi \pi$	small
Γ_4 $\Xi(1530)\pi$	small
Γ_5 $\Xi \pi \pi$ (not $\Xi(1530)\pi$)	

 $\Xi(1820)$ BRANCHING RATIOS

The dominant modes seem to be $\Lambda \bar{K}$ and (perhaps) $\Xi(1530)\pi$, but the branching fractions are very poorly determined.

$\Gamma(\Lambda \bar{K})/\Gamma_{\text{total}}$	VALUE	DOCUMENT ID	TECN	CHG	COMMENT	Γ_1/Γ
0.30 ± 0.15		ALITTI	69	HBC	-	$K^- p$ 3.9-5 GeV/c

$\Gamma(\Xi \pi)/\Gamma_{\text{total}}$	VALUE	DOCUMENT ID	TECN	CHG	COMMENT	Γ_3/Γ
0.10 ± 0.10		ALITTI	69	HBC	-	$K^- p$ 3.9-5 GeV/c

$\Gamma(\Xi \pi)/\Gamma(\Xi(1530)\pi)$	VALUE	CL%	DOCUMENT ID	TECN	CHG	COMMENT	Γ_3/Γ_4
< 0.36		95	GAY	76C	HBC	-	$K^- p$ 4.2 GeV/c
0.20 ± 0.20			BADIER	65	HBC	0	$K^- p$ 3 GeV/c

$\Gamma(\Xi \pi)/\Gamma(\Xi(1530)\pi)$	VALUE	DOCUMENT ID	TECN	CHG	COMMENT	Γ_3/Γ_4
1.5 ± 0.6 -0.4		APSELL	70	HBC	0	$K^- p$ 2.87 GeV/c

$\Gamma(\Sigma \bar{K})/\Gamma_{\text{total}}$	VALUE	DOCUMENT ID	TECN	CHG	COMMENT	Γ_2/Γ
0.30 ± 0.15		ALITTI	69	HBC	-	$K^- p$ 3.9-5 GeV/c

• • • We do not use the following data for averages, fits, limits, etc. • • •

< 0.02	TRIPP	67	RVUE		Use SMITH 65c
--------	-------	----	------	--	---------------

$\Gamma(\Sigma \bar{K})/\Gamma(\Lambda \bar{K})$	VALUE	DOCUMENT ID	TECN	CHG	COMMENT	Γ_2/Γ_1
0.24 ± 0.10		GAY	76C	HBC	-	$K^- p$ 4.2 GeV/c

$\Gamma(\Xi(1530)\pi)/\Gamma_{\text{total}}$	VALUE	DOCUMENT ID	TECN	CHG	COMMENT	Γ_4/Γ
0.30 ± 0.15		ALITTI	69	HBC	-	$K^- p$ 3.9-5 GeV/c

• • • We do not use the following data for averages, fits, limits, etc. • • •

seen	ASTON	85B	LASS		$K^- p$ 11 GeV/c
not seen	HASSALL	81	HBC		$K^- p$ 6.5 GeV/c
< 0.25	DAUBER	69	HBC		$K^- p$ 2.7 GeV/c

$\Gamma(\Xi(1530)\pi)/\Gamma(\Lambda \bar{K})$	VALUE	DOCUMENT ID	TECN	CHG	COMMENT	Γ_4/Γ_1
0.38 ± 0.27 OUR AVERAGE		Error includes scale factor of 2.3.				
1.0 ± 0.3		GAY	76c	HBC	-	$K^- p$ 4.2 GeV/c
0.26 ± 0.13		SMITH	65c	HBC	-0	$K^- p$ 2.45-2.7 GeV/c

$\Gamma(\Xi \pi \pi \text{ (not } \Xi(1530)\pi)/\Gamma(\Lambda \bar{K})$	VALUE	DOCUMENT ID	TECN	CHG	COMMENT	Γ_5/Γ_1
0.30 ± 0.20		BIAGI	87	SPEC	-	Ξ^- Be 116 GeV
< 0.14		BADIER	65	HBC	0	1 st. dev. limit
> 0.1		SMITH	65c	HBC	-0	$K^- p$ 2.45-2.7 GeV/c

$\Gamma(\Xi \pi \pi \text{ (not } \Xi(1530)\pi)/\Gamma(\Xi(1530)\pi)$	VALUE	DOCUMENT ID	TECN	CHG	COMMENT	Γ_5/Γ_4
consistent with zero		GAY	76c	HBC	-	$K^- p$ 4.2 GeV/c
0.3 ± 0.5		APSELL	70	HBC	0	$K^- p$ 2.87 GeV/c

 $\Xi(1820)$ FOOTNOTES

- BIAGI 87 also sees weak signals in the in the $\Xi^- \pi^+ \pi^-$ channel at 1782.6 \pm 1.4 MeV ($\Gamma = 6.0 \pm 1.5$ MeV) and 1831.9 \pm 2.8 MeV ($\Gamma = 9.6 \pm 9.9$ MeV).
- BADIER 72 adds all channels and divides the peak into lower and higher mass regions. The data can also be fitted with a single Breit-Wigner of mass 1800 MeV and width 150 MeV.
- From a fit to inclusive $\Xi \pi$, $\Xi \pi \pi$, and ΛK^- spectra.
- From a fit to inclusive $\Xi \pi$ and $\Xi \pi \pi$ spectra only.
- Including $\Xi \pi \pi$.
- DAUBER 69 uses in part the same data as SMITH 65c.
- For the decay mode $\Xi^- \pi^+ \pi^0$ only. This limit includes $\Xi(1530)\pi$.
- Or less. Upper limit for the 3-body decay.

 $\Xi(1820)$ REFERENCES

ADAMOVICH	99B	EPJ C11 271	M.I. Adamovich et al.	(CERN WA89 Collab.)
BIAGI	87	ZPHY C34 15	S.F. Biagi et al.	(BRIS, CERN, GEVA+)
BIAGI	87C	ZPHY C34 175	S.F. Biagi et al.	(BRIS, CERN, GEVA+ JP)
ASTON	85B	PR D32 2270	D. Aston et al.	(SLAC, CARL, CNRC, CINC)
JENKINS	83	PRL 51 951	C.M. Jenkins et al.	(FSU, BRAN, LBL+)
BIAGI	81	ZPHY C9 305	S.F. Biagi et al.	(BRIS, CAVE, GEVA+)
HASSALL	81	NP B189 397	J.K. Hassall et al.	(CAVE, MSU)
TEODORO	78	PL 77B 451	D. Teodoro et al.	(AMST, CERN, NIJM+ JP)
BRIEFEL	77	PR D16 2706	E. Briefel et al.	(BRAN, UMD, SYRA+)
	Also	PRL 23 884	S.P. Apse et al.	(BRAN, UMD, SYRA+)
GAY	76C	PL 62B 477	J.B. Gay et al.	(AMST, CERN, NIJM) IJ
DIBIANCA	75	NP B98 137	F.A. Dibianca, R.J. Endorf	(CNU)
BADIER	72	NP B37 429	J. Badier et al.	(EPOL)
APSELL	70	PRL 24 777	S.P. Apse et al.	(BRAN, UMD, SYRA+ I)
CRENNELL	70B	PR D1 847	D.J. Crennell et al.	(BNL)
ALITTI	69	PRL 22 79	J. Alitti et al.	(BNL, SYRA) I
DAUBER	69	PR 179 1262	P.M. Dauber et al.	(LRL)
TRIPP	67	NP B3 10	R.D. Tripp et al.	(LRL, SLAC, CERN+)
BADIER	65	PL 16 171	J. Badier et al.	(EPOL, SACL, AMST) I
SMITH	65B	Athens Conf. 251	G.A. Smith, J.S. Lindsey	(LRL)
SMITH	65C	PRL 14 25	G.A. Smith et al.	(LRL) IJP
HALSTEINSLID	63	Sienna Conf. 1 73	A. Halsteinslid et al.	(BERG, CERN, EPOL+ I)

OTHER RELATED PAPERS

TEODORO	78	PL 77B 451	D. Teodoro et al.	(AMST, CERN, NIJM+ JP)
BRIEFEL	75	PR D12 1859	E. Briefel et al.	(BRAN, UMD, SYRA+)
SCHMIDT	73	Purdue Conf. 363	P.E. Schmidt	(BRAN)
MERRILL	68	PR 167 1202	D.W. Merrill, J. Button-Shafer	(LRL)
SMITH	64	PRL 13 61	G.A. Smith et al.	(LRL) IJP

$\Xi(1950)$

$I(J^P) = \frac{1}{2}(?)^?$ Status: ***

We list here everything reported between 1875 and 2000 MeV. The accumulated evidence for a Ξ near 1950 MeV seems strong enough to include a $\Xi(1950)$ in the main Baryon Table, but not much can be said about its properties. In fact, there may be more than one Ξ near this mass.

$\Xi(1950)$ MASS

VALUE (MeV)	EVTS	DOCUMENT ID	TECN	COMMENT
1950 ± 15 OUR ESTIMATE				
1955 ± 6		ADAMOVICH 99b	WA89	Σ^- nucleus, 345 GeV
1944 ± 9	129	BIAGI 87	SPEC	$\Xi^- \text{Be} \rightarrow (\Xi^- \pi^+) \pi^- X$
1963 ± 5 ± 2	63	BIAGI 87c	SPEC	$\Xi^- \text{Be} \rightarrow (\Lambda \bar{K}^0) X$
1937 ± 7	150	BIAGI 81	SPEC	SPS hyperon beam
1961 ± 18	139	BRIEFEL 77	HBC	$2.87 K^- p \rightarrow \Xi^- \pi^+ X$
1936 ± 22	44	BRIEFEL 77	HBC	$2.87 K^- p \rightarrow \Xi^0 \pi^- X$
1964 ± 10	56	BRIEFEL 77	HBC	$\Xi(1530) \pi$
1900 ± 12		DIBIANCA 75	DBC	$\Xi \pi$
1952 ± 11	25	ROSS 73c		$(\Xi \pi)^-$
1956 ± 6	29	BADIER 72	HBC	$\Xi \pi, \Xi \pi \pi, \gamma K$
1955 ± 14	21	GOLDWASSER 70	HBC	$\Xi \pi$
1894 ± 18	66	DAUBER 69	HBC	$\Xi \pi$
1930 ± 20	27	ALITTI 68	HBC	$\Xi^- \pi^+$
1933 ± 16	35	BADIER 65	HBC	$\Xi^- \pi^+$

$\Xi(1950)$ WIDTH

VALUE (MeV)	EVTS	DOCUMENT ID	TECN	COMMENT
60 ± 20 OUR ESTIMATE				
68 ± 22		ADAMOVICH 99b	WA89	Σ^- nucleus, 345 GeV
100 ± 31	129	BIAGI 87	SPEC	$\Xi^- \text{Be} \rightarrow (\Xi^- \pi^+) \pi^- X$
25 ± 15 ± 1.2	63	BIAGI 87c	SPEC	$\Xi^- \text{Be} \rightarrow (\Lambda \bar{K}^0) X$
60 ± 8	150	BIAGI 81	SPEC	SPS hyperon beam
159 ± 5.7	139	BRIEFEL 77	HBC	$2.87 K^- p \rightarrow \Xi^- \pi^+ X$
87 ± 26	44	BRIEFEL 77	HBC	$2.87 K^- p \rightarrow \Xi^0 \pi^- X$
60 ± 39	56	BRIEFEL 77	HBC	$\Xi(1530) \pi$
63 ± 7.8		DIBIANCA 75	DBC	$\Xi \pi$
38 ± 10		ROSS 73c		$(\Xi \pi)^-$
35 ± 11	29	BADIER 72	HBC	$\Xi \pi, \Xi \pi \pi, \gamma K$
56 ± 26	21	GOLDWASSER 70	HBC	$\Xi \pi$
98 ± 23	66	DAUBER 69	HBC	$\Xi \pi$
80 ± 4.0	27	ALITTI 68	HBC	$\Xi^- \pi^+$
140 ± 35	35	BADIER 65	HBC	$\Xi^- \pi^+$

$\Xi(1950)$ DECAY MODES

Mode	Fraction (Γ_i/Γ)
$\Gamma_1 \Lambda \bar{K}$	seen
$\Gamma_2 \Sigma \bar{K}$	possibly seen
$\Gamma_3 \Xi \pi$	seen
$\Gamma_4 \Xi(1530) \pi$	
$\Gamma_5 \Xi \pi \pi$ (not $\Xi(1530) \pi$)	

$\Xi(1950)$ BRANCHING RATIOS

$\Gamma(\Sigma \bar{K})/\Gamma(\Lambda \bar{K})$					Γ_2/Γ_1
VALUE	CL%	EVTS	DOCUMENT ID	TECN	COMMENT
<2.3	90	0	BIAGI 87c	SPEC	$\Xi^- \text{Be} 116 \text{ GeV}$
$\Gamma(\Sigma \bar{K})/\Gamma_{\text{total}}$					Γ_2/Γ
VALUE	CL%	EVTS	DOCUMENT ID	TECN	COMMENT
possibly seen		17	HASSALL 81	HBC	$K^- p 6.5 \text{ GeV/c}$
$\Gamma(\Xi \pi)/\Gamma(\Xi(1530) \pi)$					Γ_3/Γ_4
VALUE	CL%	EVTS	DOCUMENT ID	TECN	COMMENT
$2.8^{+0.7}_{-0.6}$			APSELL 70	HBC	
$\Gamma(\Xi \pi \pi \text{ (not } \Xi(1530) \pi))/\Gamma(\Xi(1530) \pi)$					Γ_5/Γ_4
VALUE	CL%	EVTS	DOCUMENT ID	TECN	COMMENT
0.0 ± 0.3			APSELL 70	HBC	

$\Xi(1950)$ REFERENCES

ADAMOVICH 99b	EPJ C11 271	M.I. Adamovich et al.	(CERN WA89 Collab.)
BIAGI 87	ZPHY C34 15	S.F. Biagi et al.	(BRIS, CERN, GEVA+)
BIAGI 87c	ZPHY C34 175	S.F. Biagi et al.	(BRIS, CERN, GEVA+)
BIAGI 81	ZPHY C9 305	S.F. Biagi et al.	(BRIS, CAVE, GEVA+)
HASSALL 81	NP B189 397	J.K. Hassall et al.	(CAVE, MSU)
BRIEFEL 77	PR D16 2706	E. Briefel et al.	(BRAN, UMD, SYRA+)
Also	Duke Conf. 317	E. Briefel et al.	(BRAN, UMD, SYRA+)
Hyperon Resonances, 1970			
DIBIANCA 75	NP B98 137	F.A. Dibianna, R.J. Endorf	(CMU)
ROSS 73c	Purdue Conf. 345	R.T. Ross, J.L. Lloyd, D. Radojicic	(OXF)
BADIER 72	NP B37 429	J. Badier et al.	(EPOL)
APSELL 70	PRL 24 777	S.P. Apse et al.	(BRAN, UMD, SYRA+)
GOLDWASSER 70	PR D1 1960	E.L. Goldwasser, P.F. Schultz	(ILL)
DAUBER 69	PR 179 1262	P.M. Dauber et al.	(LRL)
ALITTI 68	PRL 21 1119	J. Alitti et al.	(BNL, SYRA)
BADIER 65	PL 16 171	J. Badier et al.	(EPOL, SACL, AMST)

$\Xi(2030)$

$I(J^P) = \frac{1}{2}(\geq \frac{5}{2})^?$ Status: ***

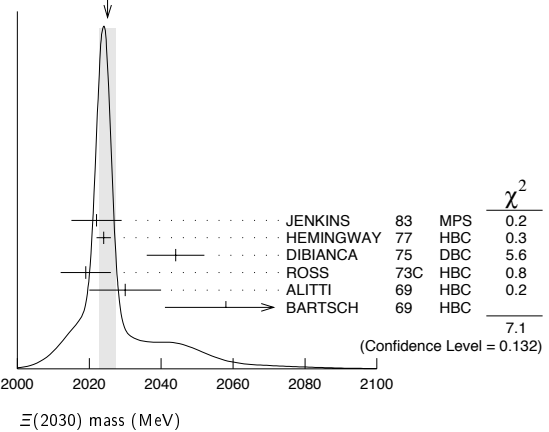
The evidence for this state has been much improved by HEMINGWAY 77, who see an eight standard deviation enhancement in $\Sigma \bar{K}$ and a weaker coupling to $\Lambda \bar{K}$. ALITTI 68 and HEMINGWAY 77 observe no signals in the $\Xi \pi \pi$ (or $\Xi(1530) \pi$) channel, in contrast to DIBIANCA 75. The decay $(\Lambda/\Sigma) \bar{K} \pi$ reported by BARTSCH 69 is also not confirmed by HEMINGWAY 77.

A moments analysis of the HEMINGWAY 77 data indicates at a level of three standard deviations that $J \geq 5/2$.

$\Xi(2030)$ MASS

VALUE (MeV)	EVTS	DOCUMENT ID	TECN	CHG	COMMENT
2025 ± 5 OUR ESTIMATE					
2025.1 ± 2.4 OUR AVERAGE Error includes scale factor of 1.3. See the ideogram below.					
2022 ± 7		JENKINS 83	MPS	-	$K^- p \rightarrow K^+$
					MM
2024 ± 2	200	HEMINGWAY 77	HBC	-	$K^- p 4.2 \text{ GeV/c}$
2044 ± 8		DIBIANCA 75	DBC	-0	$\Xi \pi \pi, \Xi^* \pi$
2019 ± 7	15	ROSS 73c	HBC	-0	$\Sigma \bar{K}$
2030 ± 10	42	ALITTI 69	HBC	-	$K^- p 3.9-5 \text{ GeV/c}$
2058 ± 17	40	BARTSCH 69	HBC	-0	$K^- p 10 \text{ GeV/c}$

WEIGHTED AVERAGE
 2025.1 ± 2.4 (Error scaled by 1.3)

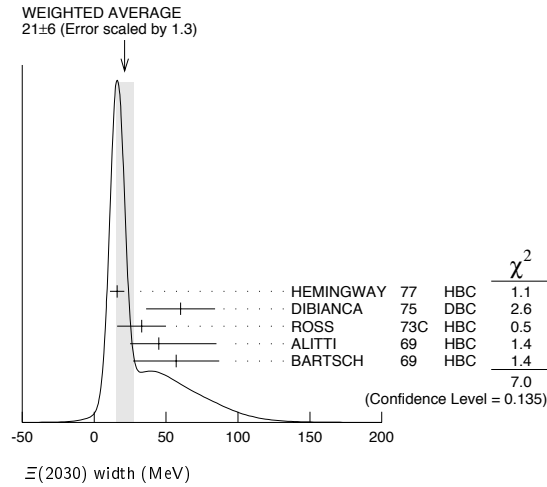


$\Xi(2030)$ WIDTH

VALUE (MeV)	EVTS	DOCUMENT ID	TECN	CHG	COMMENT
20 ± 15 OUR ESTIMATE					
21 ± 6 OUR AVERAGE Error includes scale factor of 1.3. See the ideogram below.					
16 ± 5	200	HEMINGWAY 77	HBC	-	$K^- p 4.2 \text{ GeV/c}$
60 ± 24		DIBIANCA 75	DBC	-0	$\Xi \pi \pi, \Xi^* \pi$
33 ± 17	15	ROSS 73c	HBC	-0	$\Sigma \bar{K}$
$45^{+4.0}_{-2.0}$		ALITTI 69	HBC	-	$K^- p 3.9-5 \text{ GeV/c}$
57 ± 30		BARTSCH 69	HBC	-0	$K^- p 10 \text{ GeV/c}$

Baryon Particle Listings

$\Xi(2030), \Xi(2120)$



$\Xi(2030)$ DECAY MODES

Mode	Fraction (Γ_i/Γ)
$\Gamma_1 \Lambda\bar{K}$	~ 20 %
$\Gamma_2 \Sigma\bar{K}$	~ 80 %
$\Gamma_3 \Xi\pi$	small
$\Gamma_4 \Xi(1530)\pi$	small
$\Gamma_5 \Xi\pi\pi$ (not $\Xi(1530)\pi$)	small
$\Gamma_6 \Lambda\bar{K}\pi$	small
$\Gamma_7 \Sigma\bar{K}\pi$	small

$\Xi(2030)$ BRANCHING RATIOS

$\Gamma(\Xi\pi)/[\Gamma(\Lambda\bar{K}) + \Gamma(\Sigma\bar{K}) + \Gamma(\Xi\pi) + \Gamma(\Xi(1530)\pi)]$	$\Gamma_3/(\Gamma_1+\Gamma_2+\Gamma_3+\Gamma_4)$			
VALUE	DOCUMENT ID	TECN	CHG	COMMENT

••• We do not use the following data for averages, fits, limits, etc. •••
 <0.30 ALITTI 69 HBC — 1 standard dev. limit

$\Gamma(\Xi\pi)/\Gamma(\Sigma\bar{K})$	Γ_3/Γ_2				
VALUE	CL%	DOCUMENT ID	TECN	CHG	COMMENT

<0.19 95 HEMINGWAY 77 HBC — K^-p 4.2 GeV/c

$\Gamma(\Lambda\bar{K})/[\Gamma(\Lambda\bar{K}) + \Gamma(\Sigma\bar{K}) + \Gamma(\Xi\pi) + \Gamma(\Xi(1530)\pi)]$	$\Gamma_1/(\Gamma_1+\Gamma_2+\Gamma_3+\Gamma_4)$			
VALUE	DOCUMENT ID	TECN	CHG	COMMENT

0.25±0.15 ALITTI 69 HBC — K^-p 3.9–5 GeV/c

$\Gamma(\Lambda\bar{K})/\Gamma(\Sigma\bar{K})$	Γ_1/Γ_2			
VALUE	DOCUMENT ID	TECN	CHG	COMMENT

0.22±0.09 HEMINGWAY 77 HBC — K^-p 4.2 GeV/c

$\Gamma(\Sigma\bar{K})/[\Gamma(\Lambda\bar{K}) + \Gamma(\Sigma\bar{K}) + \Gamma(\Xi\pi) + \Gamma(\Xi(1530)\pi)]$	$\Gamma_2/(\Gamma_1+\Gamma_2+\Gamma_3+\Gamma_4)$			
VALUE	DOCUMENT ID	TECN	CHG	COMMENT

0.75±0.20 ALITTI 69 HBC — K^-p 3.9–5 GeV/c

$\Gamma(\Xi(1530)\pi)/[\Gamma(\Lambda\bar{K}) + \Gamma(\Sigma\bar{K}) + \Gamma(\Xi\pi) + \Gamma(\Xi(1530)\pi)]$	$\Gamma_4/(\Gamma_1+\Gamma_2+\Gamma_3+\Gamma_4)$			
VALUE	DOCUMENT ID	TECN	CHG	COMMENT

••• We do not use the following data for averages, fits, limits, etc. •••
 <0.15 ALITTI 69 HBC — 1 standard dev. limit

$[\Gamma(\Xi(1530)\pi) + \Gamma(\Xi\pi\pi \text{ (not } \Xi(1530)\pi))]/\Gamma(\Sigma\bar{K})$	$(\Gamma_4+\Gamma_5)/\Gamma_2$				
VALUE	CL%	DOCUMENT ID	TECN	CHG	COMMENT

<0.11 95 ¹HEMINGWAY 77 HBC — K^-p 4.2 GeV/c

$\Gamma(\Lambda\bar{K}\pi)/\Gamma_{\text{total}}$	Γ_6/Γ		
VALUE	DOCUMENT ID	TECN	COMMENT

••• We do not use the following data for averages, fits, limits, etc. •••
 seen BARTSCH 69 HBC K^-p 10 GeV

$\Gamma(\Lambda\bar{K}\pi)/\Gamma(\Sigma\bar{K})$	Γ_6/Γ_2				
VALUE	CL%	DOCUMENT ID	TECN	CHG	COMMENT

<0.32 95 HEMINGWAY 77 HBC — K^-p 4.2 GeV/c

$\Gamma(\Sigma\bar{K}\pi)/\Gamma_{\text{total}}$	Γ_7/Γ		
VALUE	DOCUMENT ID	TECN	COMMENT

••• We do not use the following data for averages, fits, limits, etc. •••
 seen BARTSCH 69 HBC K^-p 10 GeV

$\Gamma(\Sigma\bar{K}\pi)/\Gamma(\Sigma\bar{K})$	Γ_7/Γ_2				
VALUE	CL%	DOCUMENT ID	TECN	CHG	COMMENT

<0.04 95 ²HEMINGWAY 77 HBC — K^-p 4.2 GeV/c

$\Xi(2030)$ FOOTNOTES

- ¹ For the decay mode $\Xi^- \pi^+ \pi^-$ only.
- ² For the decay mode $\Sigma^\pm K^- \pi^\mp$ only.

$\Xi(2030)$ REFERENCES

JENKINS 83	PRL 51 951	C.M. Jenkins et al.	(FSU, BRAN, LBL+)
HEMINGWAY 77	PL 68B 197	R.J. Hemingway et al.	(AMST, CERN, NIJM+)
Also	PL 62B 477	J.B. Gay et al.	(AMST, CERN, NIJM)
DIBIANCA 75	NP B98 137	F.A. Dibianca, R.J. Endorf	(CMU)
ROSS 73C	Purdue Conf. 345	R.T. Ross, J.L. Lloyd, D. Radojicic	(OXF)
ALITTI 69	PRL 22 79	J. Alitti et al.	(BNL, SYRA)
BARTSCH 69	PL 28B 439	J. Bartsch et al.	(AACH, BERL, CERN+)
ALITTI 68	PRL 21 1119	J. Alitti et al.	(BNL, SYRA)

$\Xi(2120)$

$I(J^P) = \frac{1}{2}(?)^?$ Status: *
 J, P need confirmation.

OMITTED FROM SUMMARY TABLE

$\Xi(2120)$ MASS

VALUE (MeV)	EVTS	DOCUMENT ID	TECN	COMMENT
-------------	------	-------------	------	---------

≈ 2120 OUR ESTIMATE
 2137±4 18 ¹CHLIAPNIK... 79 HBC K^+p 32 GeV/c
 2123±7 ²GAY 76c HBC K^-p 4.2 GeV/c

$\Xi(2120)$ WIDTH

VALUE (MeV)	EVTS	DOCUMENT ID	TECN	COMMENT
-------------	------	-------------	------	---------

<20 18 ¹CHLIAPNIK... 79 HBC K^+p 32 GeV/c
 25±12 ²GAY 76c HBC K^-p 4.2 GeV/c

$\Xi(2120)$ DECAY MODES

Mode	Fraction (Γ_i/Γ)
------	--------------------------------

$\Gamma_1 \Lambda\bar{K}$ seen

$\Xi(2120)$ BRANCHING RATIOS

$\Gamma(\Lambda\bar{K})/\Gamma_{\text{total}}$	Γ_1/Γ		
VALUE	DOCUMENT ID	TECN	COMMENT

seen ¹CHLIAPNIK... 79 HBC $K^+p \rightarrow (\bar{\Lambda} K^+) X$
 seen ²GAY 76c HBC K^-p 4.2 GeV/c

$\Xi(2120)$ FOOTNOTES

- ¹ CHLIAPNIKOV 79 does not uniquely identify the K^+ in the $(\bar{\Lambda} K^+) X$ final state. It also reports bumps with fewer events at 2240, 2540, and 2830 MeV.
- ² GAY 76c sees a 4-standard deviation signal. However, HEMINGWAY 77, with more events from the same experiment points out that the signal is greatly reduced if a cut is made on the 4-momentum u . This suggests an anomalous production mechanism if the $\Xi(2120)$ is real.

$\Xi(2120)$ REFERENCES

CHLIAPNIK... 79	NP B158 253	P.V. Chliapnikov et al.	(CERN, BELG, MONS)
HEMINGWAY 77	PL 68B 197	R.J. Hemingway et al.	(AMST, CERN, NIJM+)
GAY 76c	PL 62B 477	J.B. Gay et al.	(AMST, CERN, NIJM)

See key on page 373

Baryon Particle Listings
 $\Xi(2250)$, $\Xi(2370)$, $\Xi(2500)$ $\Xi(2250)$ $I(J^P) = \frac{1}{2}(??)$ Status: **
J, P need confirmation.

OMITTED FROM SUMMARY TABLE

The evidence for this state is mixed. BARTSCH 69 sees a bump of not much statistical significance in $\Lambda\bar{K}\pi$, $\Sigma\bar{K}\pi$, and $\Xi\pi\pi$ mass spectra. GOLDWASSER 70 sees a narrower bump in $\Xi\pi\pi$ at a higher mass. Not seen by HASSALL 81 with 45 events/ μb at 6.5 GeV/c. Seen by JENKINS 83. Perhaps seen by BIAGI 87.

 $\Xi(2250)$ MASS

VALUE (MeV)	EVTS	DOCUMENT ID	TECN	CHG	COMMENT
≈ 2250 OUR ESTIMATE					
2189 ± 7	66	BIAGI	87	SPEC	$\Xi^- \text{Be} \rightarrow (\Xi^- \pi^+ \pi^-)$ X
2214 ± 5		JENKINS	83	MPS	$K^- p \rightarrow K^+$ MM
2295 ± 15	18	GOLDWASSER 70	HBC	-	$K^- p$ 5.5 GeV/c
2244 ± 52	35	BARTSCH 69	HBC	-	$K^- p$ 10 GeV/c

 $\Xi(2250)$ WIDTH

VALUE (MeV)	EVTS	DOCUMENT ID	TECN	CHG	COMMENT
46 ± 27	66	BIAGI	87	SPEC	$\Xi^- \text{Be} \rightarrow (\Xi^- \pi^+ \pi^-)$ X
< 30		GOLDWASSER 70	HBC	-	$K^- p$ 5.5 GeV/c
130 ± 80		BARTSCH 69	HBC	-	

 $\Xi(2250)$ DECAY MODES

Mode	Fraction (Γ_i/Γ)
Γ_1 $\Xi\pi\pi$	
Γ_2 $\Lambda\bar{K}\pi$	
Γ_3 $\Sigma\bar{K}\pi$	

 $\Xi(2250)$ REFERENCES

BIAGI 87	ZPHY C34 15	S.F. Biagi <i>et al.</i>	(BRIS, CERN, GEVA+)
JENKINS 83	PRL 51 951	C.M. Jenkins <i>et al.</i>	(FSU, BRAN, LBL+)
HASSALL 81	NP B189 397	J.K. Hassall <i>et al.</i>	(CAVE, MSU)
GOLDWASSER 70	PR D1 1960	E.L. Goldwasser, P.F. Schultz	(ILL)
BARTSCH 69	PL 28B 439	J. Bartsch <i>et al.</i>	(AACH, BERL, CERN+)

 $\Xi(2370)$ $I(J^P) = \frac{1}{2}(??)$ Status: **
J, P need confirmation.

OMITTED FROM SUMMARY TABLE

 $\Xi(2370)$ MASS

VALUE (MeV)	EVTS	DOCUMENT ID	TECN	CHG	COMMENT
≈ 2370 OUR ESTIMATE					
2356 ± 10		JENKINS	83	MPS	$K^- p \rightarrow K^+$ MM
2370	50	HASSALL	81	HBC	$K^- p$ 6.5 GeV/c
2373 ± 8	94	AMIRZADEH	80	HBC	$K^- p$ 8.25 GeV/c
2392 ± 27		DIBIANCA	75	DBC	$\Xi 2\pi$

 $\Xi(2370)$ WIDTH

VALUE (MeV)	EVTS	DOCUMENT ID	TECN	CHG	COMMENT
80	50	HASSALL	81	HBC	$K^- p$ 6.5 GeV/c
80 ± 25	94	AMIRZADEH	80	HBC	$K^- p$ 8.25 GeV/c
75 ± 69		DIBIANCA	75	DBC	$\Xi 2\pi$

 $\Xi(2370)$ DECAY MODES

Mode	Fraction (Γ_i/Γ)
Γ_1 $\Lambda\bar{K}\pi$ Includes $\Gamma_4 + \Gamma_6$.	seen
Γ_2 $\Sigma\bar{K}\pi$ Includes $\Gamma_5 + \Gamma_6$.	seen
Γ_3 $\Omega^- K$	
Γ_4 $\Lambda\bar{K}^*(892)$	
Γ_5 $\Sigma\bar{K}^*(892)$	
Γ_6 $\Sigma(1385)\bar{K}$	

 $\Xi(2370)$ BRANCHING RATIOS

$\Gamma(\Lambda\bar{K}\pi)/\Gamma_{\text{total}}$	DOCUMENT ID	TECN	CHG	COMMENT	Γ_1/Γ
VALUE					
seen	AMIRZADEH 80	HBC	-0	$K^- p$ 8.25 GeV/c	
$\Gamma(\Sigma\bar{K}\pi)/\Gamma_{\text{total}}$	DOCUMENT ID	TECN	CHG	COMMENT	Γ_2/Γ
VALUE					
seen	AMIRZADEH 80	HBC	-0	$K^- p$ 8.25 GeV/c	
$[\Gamma(\Lambda\bar{K}\pi) + \Gamma(\Sigma\bar{K}\pi)]/\Gamma_{\text{total}}$	DOCUMENT ID	TECN	CHG	COMMENT	$(\Gamma_1 + \Gamma_2)/\Gamma$
VALUE					
seen	HASSALL 81	HBC	-0	$K^- p$ 6.5 GeV/c	
$\Gamma(\Omega^- K)/\Gamma_{\text{total}}$	DOCUMENT ID	TECN	CHG	COMMENT	Γ_3/Γ
VALUE					
0.09 ± 0.04	¹ KINSON 80	HBC	-	$K^- p$ 8.25 GeV/c	
$[\Gamma(\Lambda\bar{K}^*(892)) + \Gamma(\Sigma\bar{K}^*(892))]/\Gamma_{\text{total}}$	DOCUMENT ID	TECN	CHG	COMMENT	$(\Gamma_4 + \Gamma_5)/\Gamma$
VALUE					
0.22 ± 0.13	¹ KINSON 80	HBC	-	$K^- p$ 8.25 GeV/c	
$\Gamma(\Sigma(1385)\bar{K})/\Gamma_{\text{total}}$	DOCUMENT ID	TECN	CHG	COMMENT	Γ_6/Γ
VALUE					
0.12 ± 0.08	¹ KINSON 80	HBC	-	$K^- p$ 8.25 GeV/c	

 $\Xi(2370)$ FOOTNOTES¹ KINSON 80 is a reanalysis of AMIRZADEH 80 with 50% more events. $\Xi(2370)$ REFERENCES

JENKINS 83	PRL 51 951	C.M. Jenkins <i>et al.</i>	(FSU, BRAN, LBL+)
HASSALL 81	NP B189 397	J.K. Hassall <i>et al.</i>	(CAVE, MSU)
AMIRZADEH 80	PL 90B 324	J. Amirzadeh <i>et al.</i>	(BIRM, CERN, GLAS+) ¹
KINSON 80	Toronto Conf. 263	J.B. Kinson <i>et al.</i>	(BIRM, CERN, GLAS+) ¹
DIBIANCA 75	NP B98 137	F.A. Dibanca, R.J. Endorf	(CMU)

 $\Xi(2500)$ $I(J^P) = \frac{1}{2}(??)$ Status: *
J, P need confirmation.

OMITTED FROM SUMMARY TABLE

The ALITTI 69 peak might be instead the $\Xi(2370)$ or might be neither the $\Xi(2370)$ nor the $\Xi(2500)$.

 $\Xi(2500)$ MASS

VALUE (MeV)	EVTS	DOCUMENT ID	TECN	CHG	COMMENT
≈ 2500 OUR ESTIMATE					
2505 ± 10		JENKINS	83	MPS	$K^- p \rightarrow K^+$ MM
2430 ± 20	30	ALITTI 69	HBC	-	$K^- p$ 4.6-5 GeV/c
2500 ± 10	45	BARTSCH 69	HBC	-0	$K^- p$ 10 GeV/c

 $\Xi(2500)$ WIDTH

VALUE (MeV)	DOCUMENT ID	TECN	CHG
150 ± 60 -40	ALITTI 69	HBC	-
59 ± 27	BARTSCH 69	HBC	-0

 $\Xi(2500)$ DECAY MODES

Mode	Fraction (Γ_i/Γ)
Γ_1 $\Xi\pi\pi$	
Γ_2 $\Lambda\bar{K}$	
Γ_3 $\Sigma\bar{K}$	
Γ_4 $\Xi\pi\pi$	seen
Γ_5 $\Xi(1530)\pi$	
Γ_6 $\Lambda\bar{K}\pi + \Sigma\bar{K}\pi$	seen

Baryon Particle Listings

 $\Xi(2500)$ $\Xi(2500)$ BRANCHING RATIOS

$\frac{\Gamma(\Xi\pi)}{[\Gamma(\Xi\pi) + \Gamma(\Lambda\bar{K}) + \Gamma(\Sigma\bar{K}) + \Gamma(\Xi(1530)\pi)]}$	$\frac{\Gamma_1}{(\Gamma_1 + \Gamma_2 + \Gamma_3 + \Gamma_5)}$
VALUE	DOCUMENT ID TECN COMMENT
<0.5	ALITTI 69 HBC 1 standard dev. limit
$\frac{\Gamma(\Lambda\bar{K})}{[\Gamma(\Xi\pi) + \Gamma(\Lambda\bar{K}) + \Gamma(\Sigma\bar{K}) + \Gamma(\Xi(1530)\pi)]}$	$\frac{\Gamma_2}{(\Gamma_1 + \Gamma_2 + \Gamma_3 + \Gamma_5)}$
VALUE	DOCUMENT ID TECN CHG
0.5 ± 0.2	ALITTI 69 HBC -
$\frac{\Gamma(\Sigma\bar{K})}{[\Gamma(\Xi\pi) + \Gamma(\Lambda\bar{K}) + \Gamma(\Sigma\bar{K}) + \Gamma(\Xi(1530)\pi)]}$	$\frac{\Gamma_3}{(\Gamma_1 + \Gamma_2 + \Gamma_3 + \Gamma_5)}$
VALUE	DOCUMENT ID TECN CHG
0.5 ± 0.2	ALITTI 69 HBC -
$\frac{\Gamma(\Xi(1530)\pi)}{[\Gamma(\Xi\pi) + \Gamma(\Lambda\bar{K}) + \Gamma(\Sigma\bar{K}) + \Gamma(\Xi(1530)\pi)]}$	$\frac{\Gamma_5}{(\Gamma_1 + \Gamma_2 + \Gamma_3 + \Gamma_5)}$
VALUE	DOCUMENT ID TECN COMMENT
<0.2	ALITTI 69 HBC 1 standard dev. limit

$\frac{\Gamma(\Xi\pi)}{\Gamma_{\text{total}}}$	$\frac{\Gamma_4}{\Gamma}$
VALUE	DOCUMENT ID TECN CHG
seen	BARTSCH 69 HBC -0

$\frac{[\Gamma(\Lambda\bar{K}\pi) + \Gamma(\Sigma\bar{K}\pi)]}{\Gamma_{\text{total}}}$	$\frac{\Gamma_6}{\Gamma}$
VALUE	DOCUMENT ID TECN CHG
seen	BARTSCH 69 HBC -0

 $\Xi(2500)$ REFERENCES

JENKINS	83	PRL 51 951	C.M. Jenkins <i>et al.</i>	(FSU, BRAN, LBL+)
ALITTI	69	PRL 22 79	J. Alitti <i>et al.</i>	(BNL, SYRAC)
BARTSCH	69	PL 28B 439	J. Bartsch <i>et al.</i>	(AACH, BERL, CERN+)

Ω BARYONS

($S = -3, I = 0$)

$\Omega^- = sss$



$I(J^P) = 0(\frac{3}{2}^+)$ Status: * * * *

The unambiguous discovery in both production and decay was by BARNES 64. The quantum numbers follow from the assignment of the particle to the baryon decuplet. DEUTSCHMANN 78 and BAUBILLIER 78 rule out $J = 1/2$ and find consistency with $J = 3/2$. AUBERT, BE 06 finds from the decay angular distributions of $\Xi_c^0 \rightarrow \Omega^- K^+$ and $\Omega_c^0 \rightarrow \Omega^- K^+$ that $J = 3/2$; this depends on the spins of the Ξ_c^0 and Ω_c^0 being $J = 1/2$, their supposed values.

We have omitted some results that have been superseded by later experiments. See our earlier editions.

Ω^- MASS

The fit assumes the Ω^- and $\bar{\Omega}^+$ masses are the same, and averages them together.

VALUE (MeV)	EVTS	DOCUMENT ID	TECN	COMMENT
1672.45 ± 0.29 OUR FIT				
1672.43 ± 0.32 OUR AVERAGE				
1673 ± 1	100	HARTOUNI 85	SPEC	80–280 GeV $K_L^0 C$
1673.0 ± 0.8	41	BAUBILLIER 78	HBC	8.25 GeV/c $K^- p$
1671.7 ± 0.6	27	HEMINGWAY 78	HBC	4.2 GeV/c $K^- p$
1673.4 ± 1.7	4	¹ DIBIANCA 75	DBC	4.9 GeV/c $K^- d$
1673.3 ± 1.0	3	PALMER 68	HBC	$K^- p$ 4.6, 5 GeV/c
1671.8 ± 0.8	3	SCHULTZ 68	HBC	$K^- p$ 5.5 GeV/c
1674.2 ± 1.6	5	SCOTTER 68	HBC	$K^- p$ 6 GeV/c
1672.1 ± 1.0	1	² FRY 55	EMUL	
• • • We do not use the following data for averages, fits, limits, etc. • • •				
1671.43 ± 0.78	13	³ DEUTSCH... 73	HBC	$K^- p$ 10 GeV/c
1671.9 ± 1.2	6	³ SPETH 69	HBC	See DEUTSCHMANN 73
1673.0 ± 8.0	1	ABRAMS 64	HBC	$\rightarrow \Xi^- \pi^0$
1670.6 ± 1.0	1	² FRY 55B	EMUL	
1615	1	⁴ EISENBERG 54	EMUL	

- ¹DIBIANCA 75 gives a mass for each event. We quote the average.
- ²The FRY 55 and FRY 55B events were identified as Ω^- by ALVAREZ 73. The masses assume decay to ΛK^- at rest. For FRY 55B, decay from an atomic orbit could Doppler shift the K^- energy and the resulting Ω^- mass by several MeV. This shift is negligible for FRY 55 because the Ω strikes the nucleus (L.Alvarez, private communication 1973). We have calculated the error assuming that the orbital n is 4 or larger.
- ³Excluded from the average; the Ω^- lifetimes measured by the experiments differ significantly from other measurements.
- ⁴The EISENBERG 54 mass was calculated for decay in flight. ALVAREZ 73 has shown that the Ω interacted with an Ag nucleus to give $K^- \Xi Ag$.

$\bar{\Omega}^+$ MASS

The fit assumes the Ω^- and $\bar{\Omega}^+$ masses are the same, and averages them together.

VALUE (MeV)	EVTS	DOCUMENT ID	TECN	COMMENT
1672.45 ± 0.29 OUR FIT				
1672.5 ± 0.7 OUR AVERAGE				
1672 ± 1	72	HARTOUNI 85	SPEC	80–280 GeV $K_L^0 C$
1673.1 ± 1.0	1	FIRESTONE 71B	HBC	12 GeV/c $K^+ d$

$(m_{\Omega^-} - m_{\bar{\Omega}^+}) / m_{\Omega^-}$

A test of CPT invariance.

VALUE	DOCUMENT ID	TECN	COMMENT
$(-1.44 \pm 7.98) \times 10^{-5}$	CHAN 98	E756	p Be, 800 GeV

Ω^- MEAN LIFE

Measurements with an error $> 0.1 \times 10^{-10}$ s have been omitted. The fit assumes the Ω^- and $\bar{\Omega}^+$ mean lives are the same, and averages them together.

VALUE (10^{-10} s)	EVTS	DOCUMENT ID	TECN	COMMENT
0.821 ± 0.011 OUR FIT				
0.821 ± 0.011 OUR AVERAGE				
0.817 ± 0.013 ± 0.018	6934	CHAN 98	E756	p Be, 800 GeV
0.811 ± 0.037	1096	LUK 88	SPEC	p Be 400 GeV
0.823 ± 0.013	12k	BOURQUIN 84	SPEC	SPS hyperon beam
• • • We do not use the following data for averages, fits, limits, etc. • • •				
0.822 ± 0.028	2437	BOURQUIN 79B	SPEC	See BOURQUIN 84

$\bar{\Omega}^+$ MEAN LIFE

The fit assumes the Ω^- and $\bar{\Omega}^+$ mean lives are the same, and averages them together.

VALUE (10^{-10} s)	EVTS	DOCUMENT ID	TECN	COMMENT
0.821 ± 0.011 OUR FIT				
0.823 ± 0.031 ± 0.022	1801	CHAN 98	E756	p Be, 800 GeV

$(\tau_{\Omega^-} - \tau_{\bar{\Omega}^+}) / \tau_{\Omega^-}$

A test of CPT invariance. Our calculation, from the preceding two data blocks.

VALUE	DOCUMENT ID
-0.002 ± 0.040 OUR ESTIMATE	

Ω^- MAGNETIC MOMENT

VALUE (μ_N)	EVTS	DOCUMENT ID	TECN	COMMENT
-2.02 ± 0.05 OUR AVERAGE				
-2.024 ± 0.056	235k	WALLACE 95	SPEC	Ω^- 300–550 GeV
-1.94 ± 0.17 ± 0.14	25k	DIEHL 91	SPEC	Spin-transfer production

Ω^- DECAY MODES

Mode	Fraction (Γ_i/Γ)	Confidence level
$\Gamma_1 \Lambda K^-$	(67.8 ± 0.7) %	
$\Gamma_2 \Xi^0 \pi^-$	(23.6 ± 0.7) %	
$\Gamma_3 \Xi^- \pi^0$	(8.6 ± 0.4) %	
$\Gamma_4 \Xi^- \pi^+ \pi^-$	(4.3 ^{+3.4} _{-1.3}) × 10 ⁻⁴	
$\Gamma_5 \Xi(1530)^0 \pi^-$	(6.4 ^{+5.1} _{-2.0}) × 10 ⁻⁴	
$\Gamma_6 \Xi^0 e^- \bar{\nu}_e$	(5.6 ± 2.8) × 10 ⁻³	
$\Gamma_7 \Xi^- \gamma$	< 4.6 × 10 ⁻⁴	90%
$\Delta S = 2$ forbidden (S_2) modes		
$\Gamma_8 \Lambda \pi^-$	S_2 < 2.9 × 10 ⁻⁶	90%

Ω^- BRANCHING RATIOS

The BOURQUIN 84 values (which include results of BOURQUIN 79B, a separate experiment) are much more accurate than any other results, and so the other results have been omitted.

$\Gamma(\Lambda K^-)/\Gamma_{total}$	VALUE	EVTS	DOCUMENT ID	TECN	COMMENT	Γ_1/Γ
	0.678 ± 0.007	14k	BOURQUIN 84	SPEC	SPS hyperon beam	
• • • We do not use the following data for averages, fits, limits, etc. • • •						
	0.686 ± 0.013	1920	BOURQUIN 79B	SPEC	See BOURQUIN 84	

$\Gamma(\Xi^0 \pi^-)/\Gamma_{total}$	VALUE	EVTS	DOCUMENT ID	TECN	COMMENT	Γ_2/Γ
	0.236 ± 0.007	1947	BOURQUIN 84	SPEC	SPS hyperon beam	
• • • We do not use the following data for averages, fits, limits, etc. • • •						
	0.234 ± 0.013	317	BOURQUIN 79B	SPEC	See BOURQUIN 84	

$\Gamma(\Xi^- \pi^0)/\Gamma_{total}$	VALUE	EVTS	DOCUMENT ID	TECN	COMMENT	Γ_3/Γ
	0.086 ± 0.004	759	BOURQUIN 84	SPEC	SPS hyperon beam	
• • • We do not use the following data for averages, fits, limits, etc. • • •						
	0.080 ± 0.008	145	BOURQUIN 79B	SPEC	See BOURQUIN 84	

$\Gamma(\Xi^- \pi^+ \pi^-)/\Gamma_{total}$	VALUE (units 10 ⁻⁴)	EVTS	DOCUMENT ID	TECN	COMMENT	Γ_4/Γ
	4.3^{+3.4}_{-1.3}	4	BOURQUIN 84	SPEC	SPS hyperon beam	

$\Gamma(\Xi(1530)^0 \pi^-)/\Gamma_{total}$	VALUE (units 10 ⁻⁴)	EVTS	DOCUMENT ID	TECN	COMMENT	Γ_5/Γ
	6.4^{+5.1}_{-2.0}	4	⁵ BOURQUIN 84	SPEC	SPS hyperon beam	
• • • We do not use the following data for averages, fits, limits, etc. • • •						
	~ 20	1	BOURQUIN 79B	SPEC	See BOURQUIN 84	

⁵The same 4 events as in the previous mode, with the isospin factor to take into account $\Xi(1530)^0 \rightarrow \Xi^0 \pi^0$ decays included.

$\Gamma(\Xi^0 e^- \bar{\nu}_e)/\Gamma_{total}$	VALUE (units 10 ⁻³)	EVTS	DOCUMENT ID	TECN	COMMENT	Γ_6/Γ
	5.6 ± 2.8	14	BOURQUIN 84	SPEC	SPS hyperon beam	
• • • We do not use the following data for averages, fits, limits, etc. • • •						
	~ 10	3	BOURQUIN 79B	SPEC	See BOURQUIN 84	

Baryon Particle Listings

 $\Omega^-, \Omega(2250)^-, \Omega(2380)^-$ $\Gamma(\Xi^- \gamma)/\Gamma_{\text{total}}$ Γ_7/Γ

VALUE (units 10^{-4})	CL%	EVTS	DOCUMENT ID	TECN	COMMENT
< 4.6	90	0	ALBUQUERQ..94	E761	Ω^- 375 GeV
••• We do not use the following data for averages, fits, limits, etc. •••					
<22	90	9	BOURQUIN 84	SPEC	SPS hyperon beam
<31	90	0	BOURQUIN 79B	SPEC	See BOURQUIN 84

 $\Gamma(\Lambda \pi^-)/\Gamma_{\text{total}}$ Γ_8/Γ

$\Delta S=2$. Forbidden in first-order weak interaction.

VALUE (units 10^{-6})	CL%	DOCUMENT ID	TECN	COMMENT
< 2.9	90	WHITE 05	HYCP	p Cu, 800 GeV
••• We do not use the following data for averages, fits, limits, etc. •••				
< 190	90	BOURQUIN 84	SPEC	SPS hyperon beam
<1300	90	BOURQUIN 79B	SPEC	See BOURQUIN 84

 Ω^- DECAY PARAMETERS α FOR $\Omega^- \rightarrow \Lambda K^-$

Some early results have been omitted.

VALUE	EVTS	DOCUMENT ID	TECN	COMMENT
0.0180 ± 0.0024 OUR AVERAGE				
+0.0207 ± 0.0051 ± 0.0081	960k	⁶ CHEN	05 HYCP	p Cu, 800 GeV
+0.0178 ± 0.0019 ± 0.0016	4.5M	⁶ LU	05A HYCP	p Cu, 800 GeV
••• We do not use the following data for averages, fits, limits, etc. •••				
-0.028 ± 0.047	6953	CHAN	98 E756	p Be, 800 GeV
-0.034 ± 0.079	1743	LUK	88 SPEC	p Be 400 GeV
-0.025 ± 0.028	12k	BOURQUIN 84	SPEC	SPS hyperon beam

⁶The results of CHEN 05 and LU 05A are from different experimental runs. $\bar{\alpha}$ FOR $\bar{\Omega}^+ \rightarrow \bar{\Lambda} K^+$

VALUE	EVTS	DOCUMENT ID	TECN	COMMENT
-0.0181 ± 0.0028 ± 0.0026	1.89M	LU	06 HYCP	p Cu, 800 GeV
••• We do not use the following data for averages, fits, limits, etc. •••				
+0.017 ± 0.077	1823	CHAN	98 E756	p Be, 800 GeV

 $(\alpha + \bar{\alpha})/(\alpha - \bar{\alpha})$ in $\Omega^- \rightarrow \Lambda K^-, \bar{\Omega}^+ \rightarrow \bar{\Lambda} K^+$

Zero if CP is conserved.

VALUE	DOCUMENT ID	TECN	COMMENT
-0.016 ± 0.092 ± 0.089	⁷ LU	06 HYCP	p Cu, 800 GeV

⁷This value uses the results of CHEN 05, LU 05A, and LU 06. α FOR $\Omega^- \rightarrow \Xi^0 \pi^-$

VALUE	EVTS	DOCUMENT ID	TECN	COMMENT
+0.09 ± 0.14	1630	BOURQUIN 84	SPEC	SPS hyperon beam

 α FOR $\Omega^- \rightarrow \Xi^- \pi^0$

VALUE	EVTS	DOCUMENT ID	TECN	COMMENT
+0.05 ± 0.21	614	BOURQUIN 84	SPEC	SPS hyperon beam

 Ω^- REFERENCES

We have omitted some papers that have been superseded by later experiments. See our earlier editions.

AUBERT,BE 06	PRL 97 112001	B. Aubert <i>et al.</i>	(BABAR Collab.)
LU 06	PRL 96 242001	L.C. Lu <i>et al.</i>	(FNAL HyperCP Collab.)
CHEN 05	PR D71 051102R	Y.C. Chen <i>et al.</i>	(FNAL HyperCP Collab.)
LU 05A	PL B617 11	L.C. Lu <i>et al.</i>	(FNAL HyperCP Collab.)
WHITE 05	PRL 94 101804	C.G. White <i>et al.</i>	(FNAL HyperCP Collab.)
CHAN 98	PR D58 072002	A.W. Chan <i>et al.</i>	(FNAL E756 Collab.)
WALLACE 95	PRL 74 3732	N.B. Wallace <i>et al.</i>	(MINN, ARIZ, MICH+)
ALBUQUERQ.. 94	PR D50 R18	I.F. Albuquerque <i>et al.</i>	(FNAL E761 Collab.)
DIEHL 91	PRL 67 804	H.T. Diehl <i>et al.</i>	(RUTG, FNAL, MICH+)
LUK 88	PR D38 19	K.B. Luk <i>et al.</i>	(RUTG, WIS, MICH, MINN)
HARTOUNI 85	PRL 54 628	E.P. Hartouni <i>et al.</i>	(COLU, ILL, FNAL)
BOURQUIN 84	NP B241 1	M.H. Bourquin <i>et al.</i>	(BRIS, GEVA, HEIDP+)
Also	PL 87B 297	M.H. Bourquin <i>et al.</i>	(BRIS, GEVA, HEIDP+)
BOURQUIN 79B	PL 88B 192	M.H. Bourquin <i>et al.</i>	(BRIS, GEVA, HEIDP+)
BAUBILLIER 78	PL 78B 342	M. Baubillier <i>et al.</i>	(BIRM, CERN, GLAS+)
DEUTSCH.. 78	PL 78B 96	M. Deuschmann <i>et al.</i>	(AACH3, BERL, CERN+)
HEMINGWAY 78	NP B142 205	R.J. Hemingway <i>et al.</i>	(CERN, ZEEM, NJM+)
DIANCA 75	NP B59 137	F.A. Dianca, R.J. Endorf	(CMU)
ALVAREZ 73	PR D8 702	L.W. Alvarez	(LBL)
DEUTSCH.. 73	NP B61 102	M. Deuschmann <i>et al.</i>	(ABCLV Collab.)
FIRESTONE 71B	PL 26 410	I. Firestone <i>et al.</i>	(LRL)
SPETH 69	PL 29B 252	R. Speth <i>et al.</i>	(AACH, BERL, CERN, LOIC+)
PALMER 68	PL 26B 323	R.B. Palmer <i>et al.</i>	(BNL, SYRA)
SCHULTZ 68	PR 168 1509	P.F. Schultz <i>et al.</i>	(ILL, ANL, NWES+)
SCOTTER 68	PL 26B 474	D. Scotter <i>et al.</i>	(BIRM, GLAS, LOIC+)
ABRAMS 64	PRL 13 670	G.S. Abrams <i>et al.</i>	(UMD, NRL)
BARNES 64	PL 12 204	V.E. Barnes <i>et al.</i>	(BNL)
FRY 55	PR 97 1189	W.F. Fry, J. Schneps, M.S. Swami	(WIS C)
FRY 55B	NC 2 346	W.F. Fry, J. Schneps, M.S. Swami	(WIS C)
EISENBERG 54	PR 96 541	Y. Eisenberg	(CORN)

 $\Omega(2250)^-$ $I(J^P) = 0(?)^?$ Status: *** $\Omega(2250)^-$ MASS

VALUE (MeV)	EVTS	DOCUMENT ID	TECN	COMMENT
2252 ± 9 OUR AVERAGE				
2253 ± 13	44	ASTON	87B LASS	$K^- p$ 11 GeV/c
2251 ± 9 ± 8	78	BIAGI	86B SPEC	SPS Ξ^- beam

 $\Omega(2250)^-$ WIDTH

VALUE (MeV)	EVTS	DOCUMENT ID	TECN	COMMENT
55 ± 18 OUR AVERAGE				
81 ± 38	44	ASTON	87B LASS	$K^- p$ 11 GeV/c
48 ± 20	78	BIAGI	86B SPEC	SPS Ξ^- beam

 $\Omega(2250)^-$ DECAY MODES

Mode	Fraction (Γ_i/Γ)
Γ_1 $\Xi^- \pi^+ K^-$	seen
Γ_2 $\Xi(1530)^0 K^-$	seen

 $\Omega(2250)^-$ BRANCHING RATIOS

$\Gamma(\Xi(1530)^0 K^-)/\Gamma(\Xi^- \pi^+ K^-)$	Γ_2/Γ_1			
~1.0	44	ASTON	87B LASS	$K^- p$ 11 GeV/c
0.70 ± 0.20	49	BIAGI	86B SPEC	Ξ^- Be 116 GeV/c

 $\Omega(2250)^-$ REFERENCES

ASTON 87B	PL B194 579	D. Aston <i>et al.</i>	(SLAC, NAGO, CINC, INUS)
BIAGI 86B	ZPHY C31 33	S.F. Biagi <i>et al.</i>	(LOQM, GEVA, RAL+)

 $\Omega(2380)^-$

Status: **

OMITTED FROM SUMMARY TABLE

 $\Omega(2380)^-$ MASS

VALUE (MeV)	EVTS	DOCUMENT ID	TECN	COMMENT
≈ 2380 OUR ESTIMATE				
2384 ± 9 ± 8	45	BIAGI	86B SPEC	SPS Ξ^- beam

 $\Omega(2380)^-$ WIDTH

VALUE (MeV)	EVTS	DOCUMENT ID	TECN	COMMENT
26 ± 23	45	BIAGI	86B SPEC	SPS Ξ^- beam

 $\Omega(2380)^-$ DECAY MODES

Mode	Fraction (Γ_i/Γ)
Γ_1 $\Xi^- \pi^+ K^-$	
Γ_2 $\Xi(1530)^0 K^-$	seen
Γ_3 $\Xi^- \bar{K}^*(892)^0$	

 $\Omega(2380)^-$ BRANCHING RATIOS

$\Gamma(\Xi(1530)^0 K^-)/\Gamma(\Xi^- \pi^+ K^-)$	Γ_2/Γ_1				
<0.44	90	9	BIAGI	86B SPEC	Ξ^- Be 116 GeV/c

$\Gamma(\Xi^- \bar{K}^*(892)^0)/\Gamma(\Xi^- \pi^+ K^-)$	Γ_3/Γ_1			
0.5 ± 0.3	21	BIAGI	86B SPEC	Ξ^- Be 116 GeV/c

 $\Omega(2380)^-$ REFERENCES

BIAGI 86B	ZPHY C31 33	S.F. Biagi <i>et al.</i>	(LOQM, GEVA, RAL+)
-----------	-------------	--------------------------	--------------------

See key on page 373

Baryon Particle Listings

 $\Omega(2470)^-$ $\Omega(2470)^-$

Status: **

OMITTED FROM SUMMARY TABLE

A peak in the $\Omega^- \pi^+ \pi^-$ mass spectrum with a signal significance claimed to be at least 5.5 standard deviations. There is no reason to seriously doubt the existence of this state, but unless the evidence is overwhelming we usually wait for confirmation from a second experiment before elevating peaks to the Summary Table.

 $\Omega(2470)^-$ MASS

VALUE (MeV)	EVTS	DOCUMENT ID	TECN	COMMENT
2474 ± 12	59	ASTON	88G LASS	$K^- p$ 11 GeV/c

 $\Omega(2470)^-$ WIDTH

VALUE (MeV)	EVTS	DOCUMENT ID	TECN	COMMENT
72 ± 33	59	ASTON	88G LASS	$K^- p$ 11 GeV/c

 $\Omega(2470)^-$ DECAY MODES

Mode
$\Gamma_1 \quad \Omega^- \pi^+ \pi^-$

 $\Omega(2470)^-$ REFERENCES

ASTON	88G	PL B215 799	D. Aston <i>et al.</i>	(SLAC, NAGO, CINC, INUS)
-------	-----	-------------	------------------------	--------------------------

Baryon Particle Listings

Charmed Baryons

CHARMED BARYONS ($C = +1$)

$$\Lambda_c^+ = udc, \quad \Sigma_c^{++} = uuc, \quad \Sigma_c^+ = udc, \quad \Sigma_c^0 = ddc, \\ \Xi_c^+ = usc, \quad \Xi_c^0 = dsc, \quad \Omega_c^0 = ssc$$

CHARMED BARYONS

Revised March 2008 by C.G. Wohl (LBNL).

There are 17 known charmed baryons, and four other candidates not well enough established to be promoted to the Summary Tables.* Fig. 1(a) shows the mass spectrum, and for comparison Fig. 1(b) shows the spectrum of the lightest strange baryons. The Λ_c and Σ_c spectra ought to look much like the Λ and Σ spectra, since a Λ_c or a Σ_c differs from a Λ or a Σ only by the replacement of the s quark with a c quark. However, a Ξ or an Ω has more than one s quark, only *one* of which is changed to a c quark to make a Ξ_c or an Ω_c . Thus the Ξ_c and Ω_c spectra ought to be richer than the Ξ and Ω spectra.**

Before discussing the observed spectra, we review the theory of SU(4) multiplets, which tells what charmed baryons to expect; this is essential, because few of the spin-parity values given in Fig. 1(a) have been measured but have been assigned in accord with expectations of the theory. However, they are all very likely as shown (see below).

SU(4) multiplets—Baryons made from u , d , s , and c quarks belong to SU(4) multiplets. The multiplet numerology, analogous to $3 \times 3 \times 3 = 10 + 8_1 + 8_2 + 1$ for the subset of baryons made from just u , d , and s quarks, is $4 \times 4 \times 4 = 20 + 20'_1 + 20'_2 + \bar{4}$. Figure 2(a) shows the 20-plet whose bottom level is an SU(3) decuplet, such as the decuplet that includes the $\Delta(1232)$. Figure 2(b) shows the 20'-plet whose bottom level is an SU(3) octet, such as the octet that includes the nucleon. Figure 2(c) shows the $\bar{4}$ multiplet, an inverted tetrahedron. One level up from the bottom level of each multiplet are the baryons with one c quark. All the baryons in a given multiplet have the same spin and parity. Each N or Δ or SU(3)-singlet- Λ resonance calls for another 20'- or 20- or $\bar{4}$ -plet, respectively.

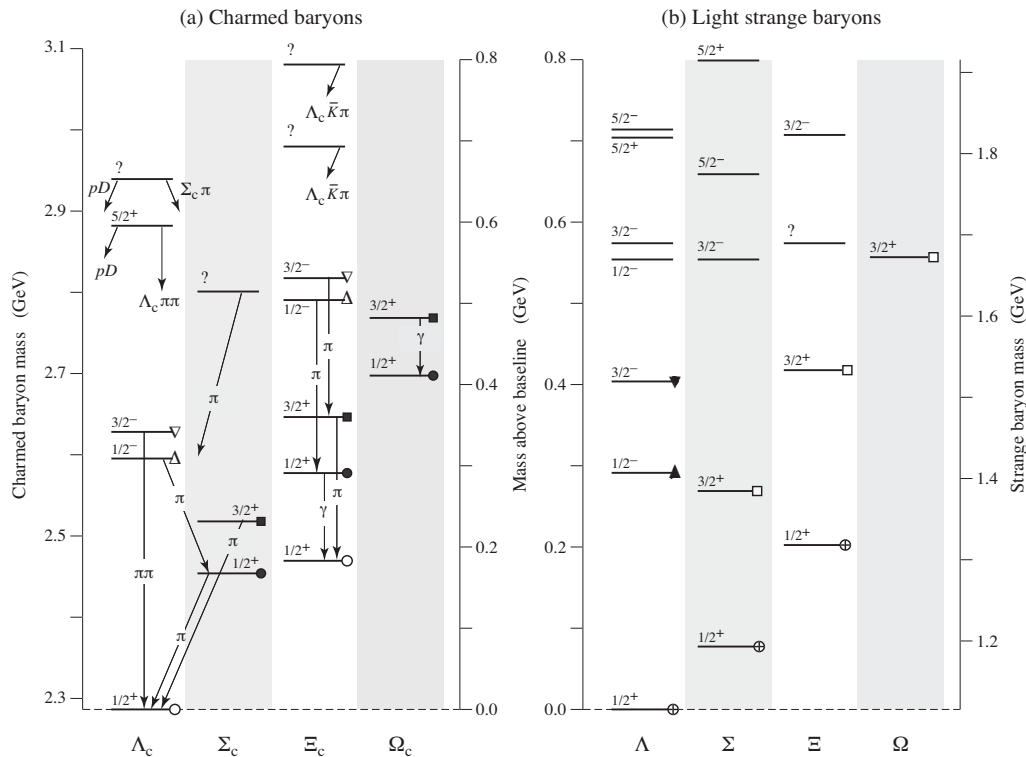


Fig. 1. (a) The known charmed baryons, and (b) the lightest “4-star” strange baryons. Note that there are two $J^P = 1/2^+$ Ξ_c states, and that the lightest Ω_c does not have $J = 3/2$. The $J^P = 1/2^+$ states, all tabbed with a circle, belong to the SU(4) multiplet that includes the nucleon; states with a circle with the same fill belong to the same SU(3) multiplet within that SU(4) multiplet. Similar remarks apply to the other states: same shape of tab, same SU(4) multiplet; same fill of that shape, same SU(3) multiplet. The $J^P = 1/2^-$ and $3/2^-$ states tabbed with triangles complete two SU(4) $\bar{4}$ multiplets.

The flavor symmetries shown in Fig. 2 are of course badly broken, but the figure is the simplest way to see what charmed baryons should exist. For example, from Fig. 2(b), we expect to find, in the same $J^P = 1/2^+$ 20'-plet as the nucleon, a Λ_c , a Σ_c , two Ξ_c 's, and an Ω_c . Note that this Ω_c has $J^P = 1/2^+$ and is not in the same SU(4) multiplet as the famous $J^P = 3/2^+$ Ω^- .

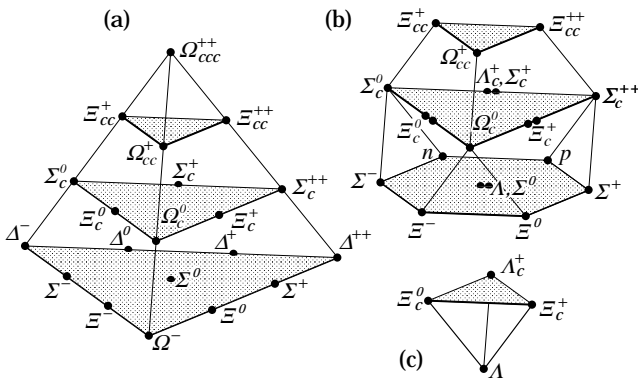


Figure 2: SU(4) multiplets of baryons made of $u, d, s,$ and c quarks. (a) The 20-plet with an SU(3) decuplet on the lowest level. (b) The 20'-plet with an SU(3) octet on the lowest level. (c) The $\bar{4}$ -plet. Note that here and in Fig. 3, but not in Fig. 1, each charge state is shown separately.

Figure 3 shows in more detail the middle level of the 20'-plet of Fig. 2(b); it splits apart into two SU(3) multiplets, a $\bar{3}$ and a 6. The states of the $\bar{3}$ are antisymmetric under the interchange of the two light quarks (the $u, d,$ and s quarks), whereas the states of the 6 are symmetric under this interchange. We use a prime to distinguish the Ξ_c in the 6 from the one in the $\bar{3}$.

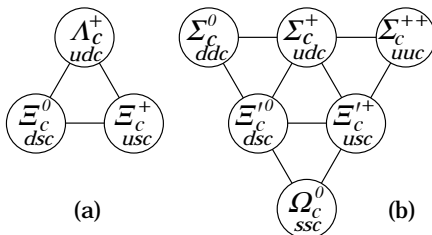


Figure 3: The SU(3) multiplets on the second level of the SU(4) multiplet of Fig. 2(b). The Λ_c and Ξ_c tabbed with open circles in Fig. 1(a) complete a $J^P = 1/2^+$ SU(3) $\bar{3}$ -plet, as in (a) here. The $\Sigma_c, \Xi_c,$ and Ω_c tabbed with closed circles in Fig. 1(a) complete a $J^P = 1/2^+$ SU(3) 6-plet, as in (b) here. Together the nine particles complete the charm = +1 level of a $J^P = 1/2^+$ SU(4) 20-plet, as in Fig. 2(a).

The observed spectra—(1) The parity of the lightest Λ_c is defined to be positive (as are the parities of the $p, n,$ and Λ); the limited evidence about its spin is consistent with $J = 1/2$. However, few of the J^P quantum numbers given in Fig. 1(a) have been measured. Models using spin-spin and spin-orbit interactions between the quarks, with parameters determined using a few of the masses as input, lead to the J^P assignments shown.[†] There are no surprises: the $J^P = 1/2^+$ states come first, then the $J^P = 3/2^+$ states . . .

(2) There is, however, evidence that many of the J^P assignments in Fig. 1(a) must be correct. As is well known, the successive mass differences between the $J^P = 3/2^+$ particles, the $\Delta(1232)^-, \Sigma(1385)^-, \Xi(1535)^-,$ and Ω^- , which lie along the lower left edge of the 20-plet in Fig. 2(a), should according to SU(3) be about equal; and indeed experimentally they nearly are. In the same way, the mass differences between the $J^P = 1/2^+$ $\Sigma_c(2455)^0, \Xi_c^0,$ and $\Omega_c^0,$ [‡] the particles along the left edge of Fig. 3(b), should be about equal—assuming, of course, that they *do* all have the same J^P . The measured differences are 124.2 ± 2.9 MeV and 119.5 ± 3.9 MeV—not perfect, but close. Similarly, the mass differences between the presumed $J^P = 3/2^+$ $\Sigma_c(2520)^0, \Xi_c(2645)^0,$ and Ω_c^0 are 128.1 ± 1.3 MeV and 122.2 ± 3.2 MeV. In Fig. 1(a), these two sets of charm particles are tabbed with solid circles and solid squares.

(3) Other evidence comes from the decay of the $\Lambda_c(2593)$. The only allowed strong decay is $\Lambda_c(2593)^+ \rightarrow \Lambda_c^+ \pi \pi$, and this appears to be dominated by the submode $\Sigma_c(2455)\pi$, despite little available phase space for the latter (the “ Q ” is about 2 MeV, the c.m. decay momentum about 20 MeV/c). Thus the decay is almost certainly s -wave, which, assuming that the $\Sigma_c(2455)$ does indeed have $J^P = 1/2^+$, makes $J^P = 1/2^-$ for the $\Lambda_c(2593)$.

(4) The heavier charmed baryons, such as the $J^P = 1/2^-$ and $3/2^-$ Λ_c 's, have much narrower widths than do their strange counterparts, such as the $\Lambda(1405)$ and $\Lambda(1520)$. The clean Λ_c spectrum has in fact been taken to settle the decades-long discussion about the nature of the $\Lambda(1405)$ —true 3-quark state or mere $\bar{K}N$ threshold effect?—unambiguously in favor of the first interpretation (which is not to say that the proximity of the $\bar{K}N$ threshold has no effect on the $\Lambda(1405)$). In fact, models of baryon-resonance spectroscopy should now *start* with the narrow charmed baryons, and work back to those broad old resonances.

Footnotes:

* The unpromoted states are a $\Lambda_c(2765)^+,$ a $\Xi_c(2930),$ a $\Xi_c(3055),$ and a $\Xi_c(3123)$. There is also weak evidence for a baryon with *two* c quarks, a Ξ_{cc}^+ at 3519 MeV. See the Particle Listings.

** For example, there are three Ω_c^0 states (properly symmetrized states of $ssc, scs,$ and css) corresponding to each Ω^- (sss) state.

† This is not the place to discuss the details of the models, nor to attempt a guide to the literature. See the discovery

Baryon Particle Listings

Charmed Baryons, Λ_c^+

papers of the various charmed baryons for references to the models that lead to the quantum-number assignments.

‡ A reminder about the Particle Data Group naming scheme: A particle has its mass as part of its name if and only if it decays strongly. Thus $\Sigma(1385)$ and $\Sigma_c(2455)$ but Ω^- and Ξ_c' .

Λ_c^+

$$I(J^P) = 0(\frac{1}{2}^+) \text{ Status: } ****$$

The parity of the Λ_c^+ is defined to be positive (as are the parities of the proton, neutron, and Λ). The quark content is udc . The spin J has not actually been measured. Results of an analysis of $pK^-\pi^+$ decays (JEZABEK 92) are consistent with the expected $J = 1/2$.

We have omitted some results that have been superseded by later experiments. The omitted results may be found in earlier editions.

 Λ_c^+ MASS

Our value in 2004, 2284.9 ± 0.6 MeV, was the average of the measurements now filed below as "not used." The BABAR measurement is so much better that we use it alone. Note that it is about 2.6 (old) standard deviations above the 2004 value.

The fit also includes $\Sigma_c^-\Lambda_c^+$ and $\Lambda_c^{*+}\Lambda_c^+$ mass-difference measurements, but this doesn't affect the Λ_c^+ mass. The new (in 2006) Λ_c^+ mass simply pushes all those other masses higher.

VALUE (MeV)	EVTS	DOCUMENT ID	TECN	COMMENT
2286.46 ± 0.14 OUR FIT				
2286.46 ± 0.14	4891	¹ AUBERT,B	05s BABR	$\Lambda_c^0 K^+$ and $\Sigma^0 K_S^0 K^+$
• • • We do not use the following data for averages, fits, limits, etc. • • •				
2284.7 ± 0.6 ± 0.7	1134	AVERY	91 CLEO	Six modes
2281.7 ± 2.7 ± 2.6	29	ALVAREZ	90b NA14	$pK^-\pi^+$
2285.8 ± 0.6 ± 1.2	101	BARLAG	89 NA32	$pK^-\pi^+$
2284.7 ± 2.3 ± 0.5	5	AGUILAR...	88b LEBC	$pK^-\pi^+$
2283.1 ± 1.7 ± 2.0	628	ALBRECHT	88c ARG	$pK^-\pi^+$, $p\bar{K}^0$, $\Lambda_3\pi$
2286.2 ± 1.7 ± 0.7	97	ANJOS	88b E691	$pK^-\pi^+$
2281 ± 3	2	JONES	87 HBC	$pK^-\pi^+$
2283 ± 3	3	BOSETTI	82 HBC	$pK^-\pi^+$
2290 ± 3	1	CALICCHIO	80 HYBR	$pK^-\pi^+$

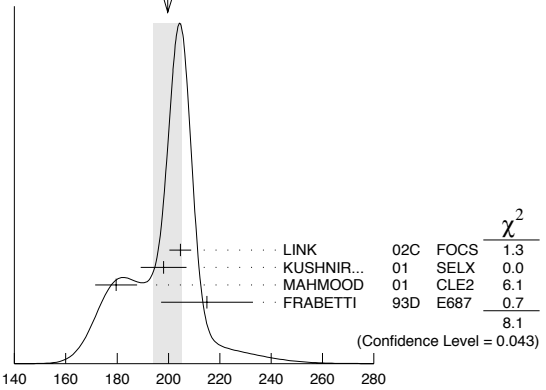
¹AUBERT,B 05s uses low-Q $\Lambda_c^0 K^+$ and $\Sigma^0 K_S^0 K^+$ decays to minimize systematic errors. The error above includes systematic as well as statistical errors. Many cross checks and adjustments to properties of the BABAR detector, as well as the large number of clean events, make this by far the best measurement of the Λ_c^+ mass.

 Λ_c^+ MEAN LIFE

Measurements with an error $\geq 100 \times 10^{-15}$ s or with fewer than 20 events have been omitted from the Listings.

VALUE (10^{-15} s)	EVTS	DOCUMENT ID	TECN	COMMENT
200 ± 6 OUR AVERAGE				
204.6 ± 3.4 ± 2.5	8034	LINK	02c FOCUS	$pK^-\pi^+$
198.1 ± 7.0 ± 5.6	1630	KUSHNIR...	01 SELX	$\Lambda_c^+ \rightarrow pK^-\pi^+$
179.6 ± 6.9 ± 4.4	4749	MAHMOOD	01 CLE2	$e^+e^- \approx \Upsilon(4S)$
215 ± 16 ± 8	1340	FRABETTI	93D E687	$\gamma\text{Be}, \Lambda_c^+ \rightarrow pK^-\pi^+$
• • • We do not use the following data for averages, fits, limits, etc. • • •				
180 ± 30 ± 30	29	ALVAREZ	90 NA14	$\gamma, \Lambda_c^+ \rightarrow pK^-\pi^+$
200 ± 30 ± 30	90	FRABETTI	90 E687	$\gamma\text{Be}, \Lambda_c^+ \rightarrow pK^-\pi^+$
196 ⁺²³ ₋₂₀	101	BARLAG	89 NA32	$pK^-\pi^+$ + c.c.
220 ± 30 ± 20	97	ANJOS	88b E691	$pK^-\pi^+$ + c.c.

WEIGHTED AVERAGE
200±6 (Error scaled by 1.6)

 Λ_c^+ DECAY MODES

Nearly all branching fractions of the Λ_c^+ are measured relative to the $pK^-\pi^+$ mode, but there are no model-independent measurements of this branching fraction. We explain how we arrive at our value of $B(\Lambda_c^+ \rightarrow pK^-\pi^+)$ in a Note at the beginning of the branching-ratio measurements, below. When this branching fraction is eventually well determined, all the other branching fractions will slide up or down proportionally as the true value differs from the value we use here.

Mode	Fraction (Γ_i/Γ)	Scale factor/ Confidence level
Hadronic modes with a p: $S = -1$ final states		
Γ_1 $p\bar{K}^0$	(2.3 ± 0.6) %	
Γ_2 $pK^-\pi^+$	[a] (5.0 ± 1.3) %	
Γ_3 $p\bar{K}^*(892)^0$	[b] (1.6 ± 0.5) %	
Γ_4 $\Delta(1232)^{++}K^-$	(8.6 ± 3.0) × 10 ⁻³	
Γ_5 $\Lambda(1520)\pi^+$	[b] (1.8 ± 0.6) %	
Γ_6 $pK^-\pi^+$ nonresonant	(2.8 ± 0.8) %	
Γ_7 $p\bar{K}^0\pi^0$	(3.3 ± 1.0) %	
Γ_8 $p\bar{K}^0\eta$	(1.2 ± 0.4) %	
Γ_9 $p\bar{K}^0\pi^+\pi^-$	(2.6 ± 0.7) %	
Γ_{10} $pK^-\pi^+\pi^0$	(3.4 ± 1.0) %	
Γ_{11} $pK^*(892)^-\pi^+$	[b] (1.1 ± 0.5) %	
Γ_{12} $p(K^-\pi^+)_{\text{nonresonant}}\pi^0$	(3.6 ± 1.2) %	
Γ_{13} $\Delta(1232)\bar{K}^*(892)$	seen	
Γ_{14} $pK^-\pi^+\pi^+\pi^-$	(1.1 ± 0.8) × 10 ⁻³	
Γ_{15} $pK^-\pi^+\pi^0\pi^0$	(8 ± 4) × 10 ⁻³	
Γ_{16} $pK^-\pi^+3\pi^0$		
Hadronic modes with a p: $S = 0$ final states		
Γ_{17} $p\pi^+\pi^-$	(3.5 ± 2.0) × 10 ⁻³	
Γ_{18} $p f_0(980)$	[b] (2.8 ± 1.9) × 10 ⁻³	
Γ_{19} $p\pi^+\pi^+\pi^-\pi^-$	(1.8 ± 1.2) × 10 ⁻³	
Γ_{20} pK^+K^-	(7.7 ± 3.5) × 10 ⁻⁴	
Γ_{21} $p\phi$	[b] (8.2 ± 2.7) × 10 ⁻⁴	
Γ_{22} $pK^+K^-\text{non-}\phi$	(3.5 ± 1.7) × 10 ⁻⁴	
Hadronic modes with a hyperon: $S = -1$ final states		
Γ_{23} $\Lambda\pi^+$	(1.07 ± 0.28) %	
Γ_{24} $\Lambda\pi^+\pi^0$	(3.6 ± 1.3) %	
Γ_{25} $\Lambda\rho^+$	< 5 %	CL=95%
Γ_{26} $\Lambda\pi^+\pi^+\pi^-$	(2.6 ± 0.7) %	
Γ_{27} $\Sigma(1385)^+\pi^+\pi^-, \Sigma^{*+} \rightarrow \Lambda\pi^+$	(7 ± 4) × 10 ⁻³	
Γ_{28} $\Sigma(1385)^-\pi^+\pi^+, \Sigma^{*-} \rightarrow \Lambda\pi^+$	(5.5 ± 1.7) × 10 ⁻³	
Γ_{29} $\Lambda\pi^+\rho^0$	(1.1 ± 0.5) %	
Γ_{30} $\Sigma(1385)^+\rho^0, \Sigma^{*+} \rightarrow \Lambda\pi^+$	(3.7 ± 3.1) × 10 ⁻³	
Γ_{31} $\Lambda\pi^+\pi^+\pi^-\text{nonresonant}$	< 8 × 10 ⁻³	CL=90%
Γ_{32} $\Lambda\pi^+\pi^+\pi^-\pi^0\text{total}$	(1.8 ± 0.8) %	
Γ_{33} $\Lambda\pi^+\eta$	[b] (1.8 ± 0.6) %	
Γ_{34} $\Sigma(1385)^+\eta$	[b] (8.5 ± 3.3) × 10 ⁻³	
Γ_{35} $\Lambda\pi^+\omega$	[b] (1.2 ± 0.5) %	
Γ_{36} $\Lambda\pi^+\pi^+\pi^-\pi^0, \text{no } \eta \text{ or } \omega$	< 7 × 10 ⁻³	CL=90%
Γ_{37} $\Lambda K^+\bar{K}^0$	(4.7 ± 1.5) × 10 ⁻³	S=1.2

Γ_{38}	$\Xi(1690)^0 K^+, \Xi^{*0} \rightarrow \Lambda \bar{K}^0$	$(1.3 \pm 0.5) \times 10^{-3}$	
Γ_{39}	$\Sigma^0 \pi^+$	$(1.05 \pm 0.28) \%$	
Γ_{40}	$\Sigma^+ \pi^0$	$(1.00 \pm 0.34) \%$	
Γ_{41}	$\Sigma^+ \eta$	$(5.5 \pm 2.3) \times 10^{-3}$	
Γ_{42}	$\Sigma^+ \pi^+ \pi^-$	$(3.6 \pm 1.0) \%$	
Γ_{43}	$\Sigma^+ \rho^0$	< 1.4	CL=95%
Γ_{44}	$\Sigma^- \pi^+ \pi^+$	$(1.9 \pm 0.8) \%$	
Γ_{45}	$\Sigma^0 \pi^+ \pi^0$	$(1.8 \pm 0.8) \%$	
Γ_{46}	$\Sigma^0 \pi^+ \pi^+ \pi^-$	$(8.3 \pm 3.1) \times 10^{-3}$	
Γ_{47}	$\Sigma^+ \pi^+ \pi^- \pi^0$	—	
Γ_{48}	$\Sigma^+ \omega$	[b] $(2.7 \pm 1.0) \%$	
Γ_{49}	$\Sigma^+ K^+ K^-$	$(2.8 \pm 0.8) \times 10^{-3}$	
Γ_{50}	$\Sigma^+ \phi$	[b] $(3.2 \pm 1.0) \times 10^{-3}$	
Γ_{51}	$\Xi(1690)^0 K^+, \Xi^{*0} \rightarrow \Sigma^+ K^-$	$(8.2 \pm 3.1) \times 10^{-4}$	
Γ_{52}	$\Sigma^+ K^+ K^-$ nonresonant	< 7	CL=90%
Γ_{53}	$\Xi^0 K^+$	$(3.9 \pm 1.4) \times 10^{-3}$	
Γ_{54}	$\Xi^- K^+ \pi^+$	$(5.1 \pm 1.4) \times 10^{-3}$	
Γ_{55}	$\Xi(1530)^0 K^+$	[b] $(2.6 \pm 1.0) \times 10^{-3}$	
Hadronic modes with a hyperon: S = 0 final states			
Γ_{56}	ΛK^+	$(5.0 \pm 1.6) \times 10^{-4}$	
Γ_{57}	$\Lambda K^+ \pi^+ \pi^-$	< 4	CL=90%
Γ_{58}	$\Sigma^0 K^+$	$(4.2 \pm 1.3) \times 10^{-4}$	
Γ_{59}	$\Sigma^0 K^+ \pi^+ \pi^-$	< 2.1	CL=90%
Γ_{60}	$\Sigma^+ K^+ \pi^-$	$(1.7 \pm 0.7) \times 10^{-3}$	
Γ_{61}	$\Sigma^+ K^*(892)^0$	[b] $(2.8 \pm 1.1) \times 10^{-3}$	
Γ_{62}	$\Sigma^- K^+ \pi^+$	< 1.0	CL=90%
Doubly Cabibbo-suppressed modes			
Γ_{63}	$p K^+ \pi^-$	< 2.3	CL=90%
Semileptonic modes			
Γ_{64}	$\Lambda \ell^+ \nu_\ell$	[c] $(2.0 \pm 0.6) \%$	
Γ_{65}	$\Lambda e^+ \nu_e$	$(2.1 \pm 0.6) \%$	
Γ_{66}	$\Lambda \mu^+ \nu_\mu$	$(2.0 \pm 0.7) \%$	
Inclusive modes			
Γ_{67}	e^+ anything	$(4.5 \pm 1.7) \%$	
Γ_{68}	$p e^+$ anything	$(1.8 \pm 0.9) \%$	
Γ_{69}	Λe^+ anything		
Γ_{70}	p anything	$(50 \pm 16) \%$	
Γ_{71}	p anything (no Λ)	$(12 \pm 19) \%$	
Γ_{72}	p hadrons		
Γ_{73}	n anything	$(50 \pm 16) \%$	
Γ_{74}	n anything (no Λ)	$(29 \pm 17) \%$	
Γ_{75}	Λ anything	$(35 \pm 11) \%$	S=1.4
Γ_{76}	Σ^\pm anything	[d] $(10 \pm 5) \%$	
Γ_{77}	3prongs	$(24 \pm 8) \%$	
$\Delta C = 1$ weak neutral current (C1) modes, or Lepton number (L) violating modes			
Γ_{78}	$p \mu^+ \mu^-$	C1 < 3.4	$\times 10^{-4}$ CL=90%
Γ_{79}	$\Sigma^- \mu^+ \mu^+$	L < 7.0	$\times 10^{-4}$ CL=90%

[a] See the note on " Λ_c^+ Branching Fractions" below.

[b] This branching fraction includes all the decay modes of the final-state resonance.

[c] An ℓ indicates an e or a μ mode, not a sum over these modes.

[d] The value is for the sum of the charge states or particle/antiparticle states indicated.

CONSTRAINED FIT INFORMATION

An overall fit to 16 branching ratios uses 30 measurements and one constraint to determine 11 parameters. The overall fit has a $\chi^2 = 15.2$ for 20 degrees of freedom.

The following *off-diagonal* array elements are the correlation coefficients $\langle \delta x_i \delta x_j \rangle / (\delta x_i \delta x_j)$, in percent, from the fit to the branching fractions, $x_i \equiv \Gamma_i / \Gamma_{\text{total}}$. The fit constrains the x_i whose labels appear in this array to sum to one.

x_{23}	96								
x_{26}	97	93							
x_{37}	82	83	80						
x_{39}	95	98	92	82					
x_{42}	91	87	89	75	86				
x_{46}	69	66	70	57	66	63			
x_{49}	87	83	85	71	82	93	60		
x_{50}	84	80	81	69	79	90	58	84	
x_{54}	93	96	90	80	94	85	64	81	78
	x_2	x_{23}	x_{26}	x_{37}	x_{39}	x_{42}	x_{46}	x_{49}	x_{50}

Λ_c^+ BRANCHING FRACTIONS

Revised 2002 by P.R. Burchat (Stanford University).

Most Λ_c^+ branching fractions are measured relative to the decay mode $\Lambda_c^+ \rightarrow p K^- \pi^+$. However, there are no completely model-independent measurements of the absolute branching fraction for $\Lambda_c^+ \rightarrow p K^- \pi^+$. Here we describe the measurements that have been used to extract $B(\Lambda_c^+ \rightarrow p K^- \pi^+)$, the model-dependence of the results, and the method we have used to average the results.

ARGUS (ALBRECHT 88C) and CLEO (CRAWFORD 92) measure $B(\bar{B} \rightarrow \Lambda_c^+ X) \cdot B(\Lambda_c^+ \rightarrow p K^- \pi^+)$ to be $(0.30 \pm 0.12 \pm 0.06) \%$ and $(0.273 \pm 0.051 \pm 0.039) \%$. Under the assumptions that decays of \bar{B} mesons to baryons are dominated by $\bar{B} \rightarrow \Lambda_c^+ X$ and that $\Lambda_c^+ X$ final states other than $\Lambda_c^+ \bar{N} X$ can be neglected, they also measure $B(\bar{B} \rightarrow \Lambda_c^+ X)$ to be $(6.8 \pm 0.5 \pm 0.3) \%$ (ALBRECHT 92O) and $(6.4 \pm 0.8 \pm 0.8) \%$ (CRAWFORD 92). Combining these results, we get $B(\Lambda_c^+ \rightarrow p K^- \pi^+) = (4.14 \pm 0.91) \%$. However, the assumption that \bar{B} decay modes to baryons other than $\Lambda_c^+ \bar{N} X$ are negligible is not on solid ground experimentally or theoretically [2]. Therefore, the branching fraction for $\Lambda_c^+ \rightarrow p K^- \pi^+$ given above may be low by some undetermined amount.

A second type of model-dependent determination of $B(\Lambda_c^+ \rightarrow p K^- \pi^+)$ is based on measurements by ARGUS (ALBRECHT 91G) and CLEO (BERGFELD 94) of $\sigma(e^+ e^- \rightarrow \Lambda_c^+ X) \cdot B(\Lambda_c^+ \rightarrow \Lambda \ell^+ \nu_\ell) = (4.15 \pm 1.03 \pm 1.18) \text{ pb}$ and $(4.77 \pm 0.25 \pm 0.66) \text{ pb}$. ARGUS (ALBRECHT 96E) and CLEO (AVERY 91) have also measured $\sigma(e^+ e^- \rightarrow \Lambda_c^+ X) \cdot B(\Lambda_c^+ \rightarrow p K^- \pi^+)$. The weighted average is $(11.2 \pm 1.3) \text{ pb}$.

From these measurements, we extract $R \equiv B(\Lambda_c^+ \rightarrow p K^- \pi^+) / B(\Lambda_c^+ \rightarrow \Lambda \ell^+ \nu_\ell) = 2.40 \pm 0.43$. We estimate the $\Lambda_c^+ \rightarrow p K^- \pi^+$ branching fraction from the equation

$$B(\Lambda_c^+ \rightarrow p K^- \pi^+) = R f F \frac{\Gamma(D \rightarrow X \ell^+ \nu_\ell)}{1 + |V_{cd}/V_{cs}|^2} \cdot \tau(\Lambda_c^+) , \quad (1)$$

where $f = B(\Lambda_c^+ \rightarrow \Lambda \ell^+ \nu_\ell) / B(\Lambda_c^+ \rightarrow X_s \ell^+ \nu_\ell)$ and $F = \Gamma(\Lambda_c^+ \rightarrow X_s \ell^+ \nu_\ell) / \Gamma(D^0 \rightarrow X_s \ell^+ \nu_\ell)$. When we use $1 + |V_{cd}/V_{cs}|^2 = 1.05$ and the world averages $\Gamma(D \rightarrow X \ell^+ \nu_\ell) =$

Baryon Particle Listings

 Λ_c^+

$(0.166 \pm 0.006) \times 10^{12} \text{ s}^{-1}$ and $\tau(\Lambda_c^+) = (0.192 \pm 0.005) \times 10^{-12} \text{ s}$, we calculate $B(\Lambda_c^+ \rightarrow pK^-\pi^+) = (7.3 \pm 1.4)\% \cdot fF$. Theoretical estimates for f and F are near 1.0 with significant uncertainties.

So, we have two results with significant model-dependence: $B(\Lambda_c^+ \rightarrow pK^-\pi^+) = (4.14 \pm 0.91)\%$ from \bar{B} decays, and $B(\Lambda_c^+ \rightarrow pK^-\pi^+) = (7.3 \pm 1.4)\% \cdot fF$ from semileptonic Λ_c^+ decays. If we set $fF = 1.0$ in the second result, and assign an uncertainty of 30% to each result to account for the unknown model-dependence, we get the consistent results $B(\Lambda_c^+ \rightarrow pK^-\pi^+) = (4.14 \pm 0.91 \pm 1.24)\%$ and $B(\Lambda_c^+ \rightarrow pK^-\pi^+) = (7.3 \pm 1.4 \pm 2.2)\%$. The weighted average of these two results is $B(\Lambda_c^+ \rightarrow pK^-\pi^+) = (5.0 \pm 1.3)\%$, where the uncertainty contains both the experimental uncertainty and the 30% estimate of model dependence in each result. We assigned the value $(5.0 \pm 1.3)\%$ to the $\Lambda_c^+ \rightarrow pK^-\pi^+$ branching fraction in our 2000 *Review* [1].

A third type of measurement of $B(\Lambda_c^+ \rightarrow pK^-\pi^+)$ has been published by CLEO (JAFPE 00). Under the assumption that a \bar{D} meson and an antiproton in opposite hemispheres is evidence for a Λ_c^+ in the hemisphere of the \bar{p} , the fraction of such $\bar{D}\bar{p}$ events with a $\Lambda_c^+ \rightarrow pK^-\pi^+$ decay can be used to determine the $\Lambda_c^+ \rightarrow pK^-\pi^+$ branching fraction. CLEO measures $B(\Lambda_c^+ \rightarrow pK^-\pi^+) = (5.0 \pm 1.3)\%$, which is coincidentally exactly the same value as our PDG 00 average given above. The quoted uncertainty includes significant contributions from model-dependent effects (*e.g.*, differences between the \bar{p} momentum spectrum in events with a Λ_c^+ and \bar{p} in the same hemisphere, and with a \bar{D} and \bar{p} in opposite hemispheres; extrapolation of the Λ_c^+ and \bar{D} momentum spectrum below the minimum value used for rejecting B decay products; and our limited understanding of backgrounds such as $DD\bar{N}\bar{p}$ events).

We have chosen to continue to assign the value $(5.0 \pm 1.3)\%$ to the $\Lambda_c^+ \rightarrow pK^-\pi^+$ branching fraction (given as PDG 02 below). As was noted earlier, most of the other Λ_c^+ decay modes are measured relative to this mode.

New methods for measuring the Λ_c^+ absolute branching fractions have been proposed [2,3].

References

1. D.E. Groom *et al.* (Particle Data Group), *Review of Particle Physics*, Eur. Phys. J. **C15**, 1 (2000).
2. I. Dunietz, Phys. Rev. **D58**, 094010 (1998).
3. P. Migliozi *et al.*, Phys. Lett. **B462**, 217 (1999).

 Λ_c^+ BRANCHING RATIOSHadronic modes with a p : $S = -1$ final states

$\Gamma(\rho\bar{K}^0)/\Gamma(\rho K^-\pi^+)$		Γ_1/Γ_2		
VALUE	EVTS	DOCUMENT ID	TECN	COMMENT
0.47 ± 0.04 OUR AVERAGE				
0.46 ± 0.02 ± 0.04	1025	ALAM	98 CLE2	$e^+e^- \approx \Upsilon(4S)$
0.44 ± 0.07 ± 0.05	133	AVERY	91 CLEO	e^+e^- 10.5 GeV
0.55 ± 0.17 ± 0.14	45	ANJOS	90 E691	γ Be 70–260 GeV
0.62 ± 0.15 ± 0.03	73	ALBRECHT	88c ARG	e^+e^- 10 GeV

$\Gamma(\rho K^-\pi^+)/\Gamma_{\text{total}}$ Γ_2/Γ

See the note on " Λ_c^+ Branching Fractions" above.

VALUE	EVTS	DOCUMENT ID	TECN	COMMENT
0.050 ± 0.013 OUR FIT				
0.050 ± 0.013		PDG	02	See note at top of ratios

••• We do not use the following data for averages, fits, limits, etc. •••

0.050 ± 0.005 ± 0.012	1205	² JAFPE	00 CLE2	e^+e^- 10.52–10.58 GeV
0.041 ± 0.010		^{3,4} ALBRECHT	92o ARG	$e^+e^- \approx \Upsilon(4S)$
0.044 ± 0.012		^{3,5} CRAWFORD	92 CLEO	e^+e^- 10.5 GeV

²JAFPE 00 assumes that a \bar{D} meson and an antiproton in opposite hemispheres tags for a Λ_c^+ in the hemisphere of the \bar{p} . The fraction of such $\bar{D}\bar{p}$ events with a $\Lambda_c^+ \rightarrow pK^-\pi^+$ decay then gives the $\rho K^-\pi^+$ branching fraction. See the paper for assumptions, caveats, etc.

³To extract $\Gamma(\rho K^-\pi^+)/\Gamma_{\text{total}}$, we use $B(\bar{B} \rightarrow \Lambda_c^+ X) \cdot B(\Lambda_c^+ \rightarrow pK^-\pi^+) = (0.28 \pm 0.06)\%$, which is the average of measurements from ARGUS (ALBRECHT 88c) and CLEO (CRAWFORD 92).

⁴ALBRECHT 92o measures $B(\bar{B} \rightarrow \Lambda_c^+ X) = (6.8 \pm 0.5 \pm 0.3)\%$.

⁵CRAWFORD 92 measures $B(\bar{B} \rightarrow \Lambda_c^+ X) = (6.4 \pm 0.8 \pm 0.8)\%$.

$\Gamma(\rho\bar{K}^*(892)^0)/\Gamma(\rho K^-\pi^+)$ Γ_3/Γ_2

Unseen decay modes of the $\bar{K}^*(892)^0$ are included.

VALUE	EVTS	DOCUMENT ID	TECN	COMMENT
0.31 ± 0.04 OUR AVERAGE				
0.29 ± 0.04 ± 0.03		⁶ AITALA	00 E791	$\pi^- N$, 500 GeV
0.35 $\pm_{-0.07}^{+0.06}$ ± 0.03	39	BOZEK	93 NA32	π^- Cu 230 GeV
0.42 ± 0.24	12	BASILE	81B CNTR	$p\bar{p} \rightarrow \Lambda_c^+ e^- X$
0.35 ± 0.11		BARLAG	90D NA32	See BOZEK 93

••• We do not use the following data for averages, fits, limits, etc. •••
⁶AITALA 00 makes a coherent 5-dimensional amplitude analysis of 946 ± 38 $\Lambda_c^+ \rightarrow pK^-\pi^+$ decays.

$\Gamma(\Delta(1232)^{++}K^-)/\Gamma(\rho K^-\pi^+)$ Γ_4/Γ_2

Unseen decay modes of the $\Lambda(1520)$ are included.

VALUE	EVTS	DOCUMENT ID	TECN	COMMENT
0.17 ± 0.04 OUR AVERAGE				Error includes scale factor of 1.1.
0.18 ± 0.03 ± 0.03		⁷ AITALA	00 E791	$\pi^- N$, 500 GeV
0.12 $\pm_{-0.05}^{+0.04}$ ± 0.05	14	BOZEK	93 NA32	π^- Cu 230 GeV
0.40 ± 0.17	17	BASILE	81B CNTR	$p\bar{p} \rightarrow \Lambda_c^+ e^- X$

⁷AITALA 00 makes a coherent 5-dimensional amplitude analysis of 946 ± 38 $\Lambda_c^+ \rightarrow pK^-\pi^+$ decays.

$\Gamma(\Lambda(1520)\pi^+)/\Gamma(\rho K^-\pi^+)$ Γ_5/Γ_2

Unseen decay modes of the $\Lambda(1520)$ are included.

VALUE	EVTS	DOCUMENT ID	TECN	COMMENT
0.35 ± 0.08 OUR AVERAGE				
0.34 ± 0.08 ± 0.05		⁸ AITALA	00 E791	$\pi^- N$, 500 GeV
0.40 $\pm_{-0.13}^{+0.18}$ ± 0.09	12	BOZEK	93 NA32	π^- Cu 230 GeV

⁸AITALA 00 makes a coherent 5-dimensional amplitude analysis of 946 ± 38 $\Lambda_c^+ \rightarrow pK^-\pi^+$ decays.

$\Gamma(\rho K^-\pi^+ \text{ nonresonant})/\Gamma(\rho K^-\pi^+)$ Γ_6/Γ_2

Unseen decay modes of the $\Lambda(1520)$ are included.

VALUE	EVTS	DOCUMENT ID	TECN	COMMENT
0.55 ± 0.06 OUR AVERAGE				
0.55 ± 0.06 ± 0.04		⁹ AITALA	00 E791	$\pi^- N$, 500 GeV
0.56 $\pm_{-0.09}^{+0.07}$ ± 0.05	71	BOZEK	93 NA32	π^- Cu 230 GeV

⁹AITALA 00 makes a coherent 5-dimensional amplitude analysis of 946 ± 38 $\Lambda_c^+ \rightarrow pK^-\pi^+$ decays.

$\Gamma(\rho\bar{K}^0\pi^0)/\Gamma(\rho K^-\pi^+)$ Γ_7/Γ_2

VALUE	EVTS	DOCUMENT ID	TECN	COMMENT
0.66 ± 0.05 ± 0.07	774	ALAM	98 CLE2	$e^+e^- \approx \Upsilon(4S)$

$\Gamma(\rho\bar{K}^0\eta)/\Gamma(\rho K^-\pi^+)$ Γ_8/Γ_2

Unseen decay modes of the η are included.

VALUE	EVTS	DOCUMENT ID	TECN	COMMENT
0.25 ± 0.04 ± 0.04	57	AMMAR	95 CLE2	$e^+e^- \approx \Upsilon(4S)$

$\Gamma(\rho\bar{K}^0\pi^+\pi^-)/\Gamma(\rho K^-\pi^+)$ Γ_9/Γ_2

VALUE	EVTS	DOCUMENT ID	TECN	COMMENT
0.51 ± 0.06 OUR AVERAGE				
0.52 ± 0.04 ± 0.05	985	ALAM	98 CLE2	$e^+e^- \approx \Upsilon(4S)$
0.43 ± 0.12 ± 0.04	83	AVERY	91 CLEO	e^+e^- 10.5 GeV
0.98 ± 0.36 ± 0.08	12	BARLAG	90D NA32	π^- 230 GeV

$\Gamma(\rho K^-\pi^+\pi^0)/\Gamma(\rho K^-\pi^+)$ Γ_{10}/Γ_2

VALUE	EVTS	DOCUMENT ID	TECN	COMMENT
0.67 ± 0.04 ± 0.11	2606	ALAM	98 CLE2	$e^+e^- \approx \Upsilon(4S)$

$\Gamma(\rho K^*(892)^-\pi^+)/\Gamma(\rho\bar{K}^0\pi^+\pi^-)$ Γ_{11}/Γ_9

Unseen decay modes of the $K^*(892)^-$ are included.

VALUE	EVTS	DOCUMENT ID	TECN	COMMENT
0.44 ± 0.14	17	ALEEVE	94 BIS2	$n N$ 20–70 GeV

$\Gamma(\rho(K^-\pi^+)_{\text{nonresonant}}\pi^0)/\Gamma(\rho K^-\pi^+)$ Γ_{12}/Γ_2

VALUE	EVTS	DOCUMENT ID	TECN	COMMENT
0.73 ± 0.12 ± 0.05	67	BOZEK	93 NA32	π^- Cu 230 GeV

$\Gamma(\Delta(1232)\bar{K}^*(892))/\Gamma_{\text{total}}$					Γ_{13}/Γ
VALUE	EVTS	DOCUMENT ID	TECN	COMMENT	
seen	35	AMENDOLIA	87	SPEC	γ Ge-Si

$\Gamma(\rho K^- \pi^+ \pi^-)/\Gamma(\rho K^- \pi^+)$					Γ_{14}/Γ_2
VALUE	DOCUMENT ID	TECN	COMMENT		
0.022 ± 0.015	BARLAG	90D	NA32	π^-	230 GeV

$\Gamma(\rho K^- \pi^+ \pi^0)/\Gamma(\rho K^- \pi^+)$					Γ_{15}/Γ_2
VALUE	EVTS	DOCUMENT ID	TECN	COMMENT	
0.16 ± 0.07 ± 0.03	15	BOZEK	93	NA32	π^- Cu 230 GeV

$\Gamma(\rho K^- \pi^+ 3\pi^0)/\Gamma(\rho K^- \pi^+)$					Γ_{16}/Γ_2
VALUE	EVTS	DOCUMENT ID	TECN	COMMENT	
• • • We do not use the following data for averages, fits, limits, etc. • • •					
0.10 ± 0.06 ± 0.02	8	BOZEK	93	NA32	π^- Cu 230 GeV

————— Hadronic modes with a ρ : $S = 0$ final states —————

$\Gamma(\rho \pi^+ \pi^-)/\Gamma(\rho K^- \pi^+)$					Γ_{17}/Γ_2
VALUE	DOCUMENT ID	TECN	COMMENT		
0.069 ± 0.036	BARLAG	90D	NA32	π^-	230 GeV

$\Gamma(\rho f_0(980))/\Gamma(\rho K^- \pi^+)$					Γ_{18}/Γ_2
VALUE	DOCUMENT ID	TECN	COMMENT		
Unseen decay modes of the $f_0(980)$ are included.					
0.055 ± 0.036	BARLAG	90D	NA32	π^-	230 GeV

$\Gamma(\rho \pi^+ \pi^+ \pi^-)/\Gamma(\rho K^- \pi^+)$					Γ_{19}/Γ_2
VALUE	DOCUMENT ID	TECN	COMMENT		
0.036 ± 0.023	BARLAG	90D	NA32	π^-	230 GeV

$\Gamma(\rho K^+ K^-)/\Gamma(\rho K^- \pi^+)$					Γ_{20}/Γ_2
VALUE	EVTS	DOCUMENT ID	TECN	COMMENT	
0.015 ± 0.006 OUR AVERAGE	Error includes scale factor of 2.1.				
0.014 ± 0.002 ± 0.002	676	ABE	02c	BELL	$e^+ e^- \approx \Upsilon(4S)$
0.039 ± 0.009 ± 0.007	214	ALEXANDER	96c	CLE2	$e^+ e^- \approx \Upsilon(4S)$
• • • We do not use the following data for averages, fits, limits, etc. • • •					
0.096 ± 0.029 ± 0.010	30	FRABETTI	93h	E687	γ Be, \bar{E}_γ 220 GeV
0.048 ± 0.027		BARLAG	90D	NA32	π^- 230 GeV

$\Gamma(\rho \phi)/\Gamma(\rho K^- \pi^+)$					Γ_{21}/Γ_2
VALUE	EVTS	DOCUMENT ID	TECN	COMMENT	
Unseen decay modes of the ϕ are included.					
0.0164 ± 0.0032 OUR AVERAGE	Error includes scale factor of 1.2.				
0.015 ± 0.002 ± 0.002	345	ABE	02c	BELL	$e^+ e^- \approx \Upsilon(4S)$
0.024 ± 0.006 ± 0.003	54	ALEXANDER	96c	CLE2	$e^+ e^- \approx \Upsilon(4S)$
• • • We do not use the following data for averages, fits, limits, etc. • • •					
0.040 ± 0.027		BARLAG	90D	NA32	π^- 230 GeV

$\Gamma(\rho K^+ K^- \text{ non-}\phi)/\Gamma(\rho K^- \pi^+)$					Γ_{22}/Γ_2
VALUE	EVTS	DOCUMENT ID	TECN	COMMENT	
0.007 ± 0.002 ± 0.002	344	ABE	02c	BELL	$e^+ e^- \approx \Upsilon(4S)$

————— Hadronic modes with a hyperon: $S = -1$ final states —————

$\Gamma(\Lambda \pi^+)/\Gamma(\rho K^- \pi^+)$					Γ_{23}/Γ_2
VALUE	CL%	EVTS	DOCUMENT ID	TECN	COMMENT
0.214 ± 0.016 OUR FIT	Error includes scale factor of 1.1.				
0.204 ± 0.019 OUR AVERAGE					
0.217 ± 0.013 ± 0.020	750	LINK	05F	FOCS	γ nucleus, $\bar{E}_\gamma \approx 180$ GeV
0.18 ± 0.03 ± 0.04		ALBRECHT	92	ARG	$e^+ e^- \approx 10.4$ GeV
0.18 ± 0.03 ± 0.03	87	VERY	91	CLEO	$e^+ e^- \approx 10.5$ GeV
• • • We do not use the following data for averages, fits, limits, etc. • • •					
<0.33	90	ANJOS	90	E691	γ Be 70–260 GeV
<0.16	90	ALBRECHT	88c	ARG	$e^+ e^- \approx 10$ GeV

$\Gamma(\Lambda \pi^+ \pi^0)/\Gamma(\rho K^- \pi^+)$					Γ_{24}/Γ_2
VALUE	EVTS	DOCUMENT ID	TECN	COMMENT	
0.73 ± 0.09 ± 0.16	464	VERY	94	CLE2	$e^+ e^- \approx \Upsilon(3S), \Upsilon(4S)$

$\Gamma(\Lambda \rho^+)/\Gamma(\rho K^- \pi^+)$					Γ_{25}/Γ_2
VALUE	CL%	DOCUMENT ID	TECN	COMMENT	
<0.95	95	VERY	94	CLE2	$e^+ e^- \approx \Upsilon(3S), \Upsilon(4S)$

$\Gamma(\Lambda \pi^+ \pi^+ \pi^-)/\Gamma(\rho K^- \pi^+)$					Γ_{26}/Γ_2
VALUE	EVTS	DOCUMENT ID	TECN	COMMENT	
0.525 ± 0.032 OUR FIT					
0.522 ± 0.032 OUR AVERAGE					
0.508 ± 0.024 ± 0.024	1356	LINK	05F	FOCS	γ nucleus, $\bar{E}_\gamma \approx 180$ GeV
0.65 ± 0.11 ± 0.12	289	VERY	91	CLEO	$e^+ e^- \approx 10.5$ GeV
0.82 ± 0.29 ± 0.27	44	ANJOS	90	E691	γ Be 70–260 GeV
0.94 ± 0.41 ± 0.13	10	BARLAG	90D	NA32	π^- 230 GeV
0.61 ± 0.16 ± 0.04	105	ALBRECHT	88c	ARG	$e^+ e^- \approx 10$ GeV

$\Gamma(\Sigma(1385)^+ \pi^+ \pi^-, \Sigma^{*+} \rightarrow \Lambda \pi^+)/\Gamma(\Lambda \pi^+ \pi^+ \pi^-)$					Γ_{27}/Γ_{26}
VALUE	DOCUMENT ID	TECN	COMMENT		
0.28 ± 0.10 ± 0.08	LINK	05F	FOCS	γ nucleus, $\bar{E}_\gamma \approx 180$ GeV	

$\Gamma(\Sigma(1385)^- \pi^+ \pi^+, \Sigma^{*-} \rightarrow \Lambda \pi^-)/\Gamma(\Lambda \pi^+ \pi^+ \pi^-)$					Γ_{28}/Γ_{26}
VALUE	DOCUMENT ID	TECN	COMMENT		
0.21 ± 0.03 ± 0.02	LINK	05F	FOCS	γ nucleus, $\bar{E}_\gamma \approx 180$ GeV	

$\Gamma(\Lambda \pi^+ \rho^0)/\Gamma(\Lambda \pi^+ \pi^+ \pi^-)$					Γ_{29}/Γ_{26}
VALUE	DOCUMENT ID	TECN	COMMENT		
0.40 ± 0.12 ± 0.12	LINK	05F	FOCS	γ nucleus, $\bar{E}_\gamma \approx 180$ GeV	

$\Gamma(\Sigma(1385)^+ \rho^0, \Sigma^{*+} \rightarrow \Lambda \pi^+)/\Gamma(\Lambda \pi^+ \pi^+ \pi^-)$					Γ_{30}/Γ_{26}
VALUE	DOCUMENT ID	TECN	COMMENT		
0.14 ± 0.09 ± 0.07	LINK	05F	FOCS	γ nucleus, $\bar{E}_\gamma \approx 180$ GeV	

$\Gamma(\Lambda \pi^+ \pi^+ \pi^- \text{ nonresonant})/\Gamma(\Lambda \pi^+ \pi^+ \pi^-)$					Γ_{31}/Γ_{26}
VALUE	CL%	DOCUMENT ID	TECN	COMMENT	
<0.3	90	LINK	05F	FOCS	γ nucleus, $\bar{E}_\gamma \approx 180$ GeV

$\Gamma(\rho \bar{K}^0 \pi^+ \pi^-)/\Gamma(\Lambda \pi^+ \pi^+ \pi^-)$					Γ_9/Γ_{26}
VALUE	EVTS	DOCUMENT ID	TECN	COMMENT	
• • • We do not use the following data for averages, fits, limits, etc. • • •					
2.6 ± 1.2		ALEEV	96	SPEC	n nucleus, 50 GeV/c
4.3 ± 1.2	130	ALEEV	84	BIS2	n C 40–70 GeV

$\Gamma(\Lambda \pi^+ \pi^+ \pi^- \pi^0 \text{ total})/\Gamma(\rho K^- \pi^+)$					Γ_{32}/Γ_2
VALUE	EVTS	DOCUMENT ID	TECN	COMMENT	
0.36 ± 0.09 ± 0.09	50	10	CRONIN-HEN..03	CLE3	$e^+ e^- \approx \Upsilon(4S)$
¹⁰ CRONIN-HENNESSY 03 finds this channel to be dominantly $\Lambda \eta \pi^+$ and $\Lambda \omega \pi^+$; see below.					

$\Gamma(\Lambda \pi^+ \eta)/\Gamma(\rho K^- \pi^+)$					Γ_{33}/Γ_2
VALUE	EVTS	DOCUMENT ID	TECN	COMMENT	
Unseen decay modes of the η are included.					
0.36 ± 0.07 OUR AVERAGE					
0.41 ± 0.17 ± 0.10	11	CRONIN-HEN..03	CLE3	$e^+ e^- \approx \Upsilon(4S)$	
0.35 ± 0.05 ± 0.06	116	AMMAR	95	CLE2	$e^+ e^- \approx \Upsilon(4S)$

$\Gamma(\Sigma(1385)^+ \eta)/\Gamma(\rho K^- \pi^+)$					Γ_{34}/Γ_2
VALUE	EVTS	DOCUMENT ID	TECN	COMMENT	
Unseen decay modes of the $\Sigma(1385)^+$ and η are included.					
0.17 ± 0.04 ± 0.03	54	AMMAR	95	CLE2	$e^+ e^- \approx \Upsilon(4S)$

$\Gamma(\Lambda \pi^+ \omega)/\Gamma(\rho K^- \pi^+)$					Γ_{35}/Γ_2
VALUE	EVTS	DOCUMENT ID	TECN	COMMENT	
Unseen decay modes of the ω are included.					
0.24 ± 0.06 ± 0.06	32	CRONIN-HEN..03	CLE3	$e^+ e^- \approx \Upsilon(4S)$	

$\Gamma(\Lambda \pi^+ \pi^+ \pi^- \pi^0, \text{ no } \eta \text{ or } \omega)/\Gamma(\rho K^- \pi^+)$					Γ_{36}/Γ_2
VALUE	CL%	DOCUMENT ID	TECN	COMMENT	
<0.13	90	CRONIN-HEN..03	CLE3	$e^+ e^- \approx \Upsilon(4S)$	

$\Gamma(\Lambda K^+ \bar{K}^0)/\Gamma(\rho K^- \pi^+)$					Γ_{37}/Γ_2
VALUE	EVTS	DOCUMENT ID	TECN	COMMENT	
0.093 ± 0.018 OUR FIT	Error includes scale factor of 1.7.				
0.131 ± 0.020 OUR AVERAGE					
0.142 ± 0.018 ± 0.022	251	LINK	05F	FOCS	γ nucleus, $\bar{E}_\gamma \approx 180$ GeV
0.12 ± 0.02 ± 0.02	59	AMMAR	95	CLE2	$e^+ e^- \approx \Upsilon(4S)$

$\Gamma(\Xi(1690)^0 K^+, \Xi^{*0} \rightarrow \Lambda \bar{K}^0)/\Gamma(\Lambda K^+ \bar{K}^0)$					Γ_{38}/Γ_{37}
VALUE	EVTS	DOCUMENT ID	TECN	COMMENT	
0.28 ± 0.07 OUR AVERAGE					
0.32 ± 0.10 ± 0.04	84 ± 24	LINK	05F	FOCS	γ nucleus, $\bar{E}_\gamma \approx 180$ GeV
0.26 ± 0.08 ± 0.03	93	ABE	02c	BELL	$e^+ e^- \approx \Upsilon(4S)$

$\Gamma(\Lambda K^+ \bar{K}^0)/\Gamma(\Lambda \pi^+)$					Γ_{37}/Γ_{23}
VALUE	EVTS	DOCUMENT ID	TECN	COMMENT	
0.43 ± 0.08 OUR FIT	Error includes scale factor of 2.0.				
0.395 ± 0.026 ± 0.036	460 ± 30	AUBERT	07u	BABR	$e^+ e^- \approx \Upsilon(4S)$

$\Gamma(\Sigma^0 \pi^+)/\Gamma(\rho K^- \pi^+)$					Γ_{39}/Γ_2
VALUE	EVTS	DOCUMENT ID	TECN	COMMENT	
0.210 ± 0.018 OUR FIT					
0.20 ± 0.04 OUR AVERAGE					
0.21 ± 0.02 ± 0.04	196	VERY	94	CLE2	$e^+ e^- \approx \Upsilon(3S), \Upsilon(4S)$
0.17 ± 0.06 ± 0.04		ALBRECHT	92	ARG	$e^+ e^- \approx 10.4$ GeV

$\Gamma(\Sigma^0 \pi^+)/\Gamma(\Lambda \pi^+)$					Γ_{39}/Γ_{23}
VALUE	EVTS	DOCUMENT ID	TECN	COMMENT	
0.98 ± 0.05 OUR FIT					
0.98 ± 0.05 OUR AVERAGE					
0.977 ± 0.015 ± 0.051	33k	AUBERT	07u	BABR	$e^+ e^- \approx \Upsilon(4S)$
1.09 ± 0.11 ± 0.19	750	LINK	05F	FOCS	γ nucleus, $\bar{E}_\gamma \approx 180$ GeV

Baryon Particle Listings

 Λ_c^+

$\Gamma(\Sigma^+\pi^0)/\Gamma(\rho K^-\pi^+)$		Γ_{40}/Γ_2	
VALUE	EVTs	DOCUMENT ID	TECN COMMENT
$0.20 \pm 0.03 \pm 0.03$	93	KUBOTA	93 CLE2 $e^+e^- \approx \Upsilon(4S)$

$\Gamma(\Sigma^+\eta)/\Gamma(\rho K^-\pi^+)$		Γ_{41}/Γ_2	
Unseen decay modes of the η are included.			
VALUE	EVTs	DOCUMENT ID	TECN COMMENT
$0.11 \pm 0.03 \pm 0.02$	26	AMMAR	95 CLE2 $e^+e^- \approx \Upsilon(4S)$

$\Gamma(\Sigma^+\pi^+\pi^-)/\Gamma(\rho K^-\pi^+)$		Γ_{42}/Γ_2	
VALUE	EVTs	DOCUMENT ID	TECN COMMENT
0.73 ± 0.08 OUR FIT			
0.68 ± 0.09 OUR AVERAGE			
$0.74 \pm 0.07 \pm 0.09$	487	KUBOTA	93 CLE2 $e^+e^- \approx \Upsilon(4S)$
$0.54^{+0.18}_{-0.15}$	11	BARLAG	92 NA32 π^- Cu 230 GeV

$\Gamma(\Sigma^+\rho^0)/\Gamma(\rho K^-\pi^+)$		Γ_{43}/Γ_2	
VALUE	CL%	DOCUMENT ID	TECN COMMENT
<0.27	95	KUBOTA	93 CLE2 $e^+e^- \approx \Upsilon(4S)$

$\Gamma(\Sigma^-\pi^+\pi^+)/\Gamma(\Sigma^+\pi^+\pi^-)$		Γ_{44}/Γ_{42}	
VALUE	EVTs	DOCUMENT ID	TECN COMMENT
$0.53 \pm 0.15 \pm 0.07$	56	FRABETTI	94E E687 γ Be, \bar{E}_γ 220 GeV

$\Gamma(\Sigma^0\pi^+\pi^0)/\Gamma(\rho K^-\pi^+)$		Γ_{45}/Γ_2	
VALUE	EVTs	DOCUMENT ID	TECN COMMENT
$0.36 \pm 0.09 \pm 0.10$	117	AVERY	94 CLE2 $e^+e^- \approx \Upsilon(3S), \Upsilon(4S)$

$\Gamma(\Sigma^0\pi^+\pi^+\pi^-)/\Gamma(\rho K^-\pi^+)$		Γ_{46}/Γ_2	
VALUE	EVTs	DOCUMENT ID	TECN COMMENT
0.17 ± 0.04 OUR FIT			
$0.21 \pm 0.05 \pm 0.05$	90	AVERY	94 CLE2 $e^+e^- \approx \Upsilon(3S), \Upsilon(4S)$

$\Gamma(\Sigma^0\pi^+\pi^+\pi^-)/\Gamma(\Lambda\pi^+\pi^+\pi^-)$		Γ_{46}/Γ_{26}	
VALUE	EVTs	DOCUMENT ID	TECN COMMENT
0.31 ± 0.08 OUR FIT			
$0.26 \pm 0.06 \pm 0.09$	480	LINK	05F FOCS γ nucleus, $\bar{E}_\gamma \approx 180$ GeV

$\Gamma(\Sigma^+\omega)/\Gamma(\rho K^-\pi^+)$		Γ_{48}/Γ_2	
Unseen decay modes of the ω are included.			
VALUE	EVTs	DOCUMENT ID	TECN COMMENT
$0.54 \pm 0.13 \pm 0.06$	107	KUBOTA	93 CLE2 $e^+e^- \approx \Upsilon(4S)$

$\Gamma(\Sigma^+K^+K^-)/\Gamma(\rho K^-\pi^+)$		Γ_{49}/Γ_2	
VALUE	EVTs	DOCUMENT ID	TECN COMMENT
0.057 ± 0.008 OUR FIT			
$0.070 \pm 0.011 \pm 0.011$	59	AVERY	93 CLE2 $e^+e^- \approx 10.5$ GeV

$\Gamma(\Sigma^+K^+K^-)/\Gamma(\Sigma^+\pi^+\pi^-)$		Γ_{49}/Γ_{42}	
VALUE	EVTs	DOCUMENT ID	TECN COMMENT
0.078 ± 0.009 OUR FIT			
0.074 ± 0.009 OUR AVERAGE			
$0.076 \pm 0.007 \pm 0.009$	246	ABE	02c BELL $e^+e^- \approx \Upsilon(4S)$
$0.071 \pm 0.011 \pm 0.011$	103	LINK	02g FOCS γ nucleus, ≈ 180 GeV

$\Gamma(\Sigma^+\phi)/\Gamma(\rho K^-\pi^+)$		Γ_{50}/Γ_2	
Unseen decay modes of the ϕ are included.			
VALUE	EVTs	DOCUMENT ID	TECN COMMENT
0.063 ± 0.011 OUR FIT			
$0.069 \pm 0.023 \pm 0.016$	26	AVERY	93 CLE2 $e^+e^- \approx 10.5$ GeV

$\Gamma(\Sigma^+\phi)/\Gamma(\Sigma^+\pi^+\pi^-)$		Γ_{50}/Γ_{42}	
Unseen decay modes of the ϕ are included.			
VALUE	EVTs	DOCUMENT ID	TECN COMMENT
0.087 ± 0.012 OUR FIT			
0.086 ± 0.012 OUR AVERAGE			
$0.085 \pm 0.012 \pm 0.012$	129	ABE	02c BELL $e^+e^- \approx \Upsilon(4S)$
$0.087 \pm 0.016 \pm 0.006$	57	LINK	02g FOCS γ nucleus, ≈ 180 GeV

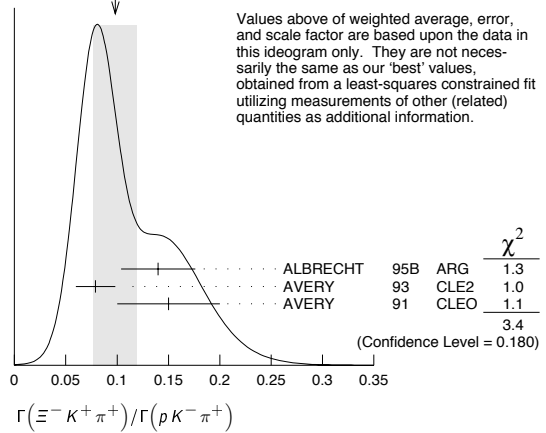
$\Gamma(\Xi(1690)^0 K^+, \Xi^{*0} \rightarrow \Sigma^+ K^-)/\Gamma(\Sigma^+\pi^+\pi^-)$		Γ_{51}/Γ_{42}	
VALUE	EVTs	DOCUMENT ID	TECN COMMENT
0.023 ± 0.005 OUR AVERAGE			
$0.023 \pm 0.005 \pm 0.005$	75	ABE	02c BELL $e^+e^- \approx \Upsilon(4S)$
$0.022 \pm 0.006 \pm 0.006$	34	LINK	02g FOCS γ nucleus, ≈ 180 GeV

$\Gamma(\Sigma^+K^+K^- \text{ nonresonant})/\Gamma(\Sigma^+\pi^+\pi^-)$		Γ_{52}/Γ_{42}	
VALUE	CL%	DOCUMENT ID	TECN COMMENT
<0.018	90	ABE	02c BELL $e^+e^- \approx \Upsilon(4S)$
<0.028	90	LINK	02g FOCS γ nucleus, ≈ 180 GeV

$\Gamma(\Xi^0 K^+)/\Gamma(\rho K^-\pi^+)$		Γ_{53}/Γ_2	
VALUE	EVTs	DOCUMENT ID	TECN COMMENT
$0.078 \pm 0.013 \pm 0.013$	56	AVERY	93 CLE2 $e^+e^- \approx 10.5$ GeV

$\Gamma(\Xi^- K^+ \pi^+)/\Gamma(\rho K^-\pi^+)$		Γ_{54}/Γ_2	
VALUE	EVTs	DOCUMENT ID	TECN COMMENT
0.102 ± 0.010 OUR FIT			Error includes scale factor of 1.1.
0.098 ± 0.021 OUR AVERAGE			Error includes scale factor of 1.3. See the ideogram below.
$0.14 \pm 0.03 \pm 0.02$	34	ALBRECHT	95B ARG $e^+e^- \approx 10.4$ GeV
$0.079 \pm 0.013 \pm 0.014$	60	AVERY	93 CLE2 $e^+e^- \approx 10.5$ GeV
$0.15 \pm 0.04 \pm 0.03$	30	AVERY	91 CLEO $e^+e^- 10.5$ GeV

WEIGHTED AVERAGE
0.098±0.021 (Error scaled by 1.3)



$\Gamma(\Xi(1530)^0 K^+)/\Gamma(\rho K^-\pi^+)$		Γ_{55}/Γ_2	
Unseen decay modes of the $\Xi(1530)^0$ are included.			
VALUE	EVTs	DOCUMENT ID	TECN COMMENT
0.052 ± 0.014 OUR AVERAGE			
$0.05 \pm 0.02 \pm 0.01$	11	ALBRECHT	95B ARG $e^+e^- \approx 10.4$ GeV
$0.053 \pm 0.016 \pm 0.010$	24	AVERY	93 CLE2 $e^+e^- \approx 10.5$ GeV

$\Gamma(\Xi^- K^+ \pi^+)/\Gamma(\Lambda\pi^+)$		Γ_{54}/Γ_{23}	
VALUE	EVTs	DOCUMENT ID	TECN COMMENT
0.47 ± 0.04 OUR FIT			
$0.480 \pm 0.016 \pm 0.039$	2665 ± 84	AUBERT	07u BABR $e^+e^- \approx \Upsilon(4S)$

Hadronic modes with a hyperon: S = 0 final states

$\Gamma(\Lambda K^+)/\Gamma(\Lambda\pi^+)$		Γ_{56}/Γ_{23}	
VALUE	EVTs	DOCUMENT ID	TECN COMMENT
0.047 ± 0.009 OUR AVERAGE			Error includes scale factor of 1.8.
$0.044 \pm 0.004 \pm 0.003$	1162 ± 101	AUBERT	07u BABR $e^+e^- \approx \Upsilon(4S)$
$0.074 \pm 0.010 \pm 0.012$	265	ABE	02c BELL $e^+e^- \approx \Upsilon(4S)$

$\Gamma(\Lambda K^+ \pi^+)/\Gamma(\Lambda\pi^+)$		Γ_{57}/Γ_{23}	
VALUE	CL%	DOCUMENT ID	TECN COMMENT
$<4.1 \times 10^{-2}$	90	AUBERT	07u BABR $e^+e^- \approx \Upsilon(4S)$

$\Gamma(\Sigma^0 K^+)/\Gamma(\Sigma^0 \pi^+)$		Γ_{58}/Γ_{39}	
VALUE	EVTs	DOCUMENT ID	TECN COMMENT
0.040 ± 0.006 OUR AVERAGE			
$0.038 \pm 0.005 \pm 0.003$	366 ± 52	AUBERT	07u BABR $e^+e^- \approx \Upsilon(4S)$
$0.056 \pm 0.014 \pm 0.008$	75	ABE	02c BELL $e^+e^- \approx \Upsilon(4S)$

$\Gamma(\Sigma^0 K^+ \pi^+)/\Gamma(\Sigma^0 \pi^+)$		Γ_{59}/Γ_{39}	
VALUE	CL%	DOCUMENT ID	TECN COMMENT
$<2.0 \times 10^{-2}$	90	AUBERT	07u BABR $e^+e^- \approx \Upsilon(4S)$

$\Gamma(\Sigma^+ K^+ \pi^-)/\Gamma(\Sigma^+\pi^+\pi^-)$		Γ_{60}/Γ_{42}	
VALUE	EVTs	DOCUMENT ID	TECN COMMENT
$0.047 \pm 0.011 \pm 0.008$	105	ABE	02c BELL $e^+e^- \approx \Upsilon(4S)$

$\Gamma(\Sigma^+ K^*(892)^0)/\Gamma(\Sigma^+\pi^+\pi^-)$		Γ_{61}/Γ_{42}	
Unseen decay modes of the $K^*(892)^0$ are included.			
VALUE	EVTs	DOCUMENT ID	TECN COMMENT
$0.078 \pm 0.018 \pm 0.013$	49	LINK	02g FOCS γ nucleus, ≈ 180 GeV

$\Gamma(\Sigma^- K^+ \pi^+)/\Gamma(\Sigma^+ K^*(892)^0)$		Γ_{62}/Γ_{61}	
VALUE	CL%	DOCUMENT ID	TECN COMMENT
<0.35	90	LINK	02g FOCS γ nucleus, ≈ 180 GeV

Doubly Cabibbo-suppressed modes

$\Gamma(\rho K^+ \pi^-)/\Gamma(\rho K^-\pi^+)$		Γ_{63}/Γ_2	
VALUE	CL%	DOCUMENT ID	TECN COMMENT
<0.0046	90	LINK	05k FOCS R = (0.05 ± 0.26 ± 0.02)%

See key on page 373

Baryon Particle Listings

Λ_C^+

Semileptonic modes

$\Gamma(\Lambda e^+ \nu_e)/\Gamma(\rho K^- \pi^+)$ Γ_{64}/Γ_2
 We average here the averages of the next two data blocks.

VALUE	DOCUMENT ID	TECN	COMMENT
0.41 ± 0.05 OUR AVERAGE			
0.42 ± 0.07	PDG	02	Our $\Gamma(\Lambda e^+ \nu_e)/\Gamma(\rho K^- \pi^+)$
0.39 ± 0.08	PDG	02	Our $\Gamma(\Lambda \mu^+ \nu_\mu)/\Gamma(\rho K^- \pi^+)$

$\Gamma(\Lambda e^+ \nu_e)/\Gamma(\rho K^- \pi^+)$ Γ_{65}/Γ_2

VALUE	DOCUMENT ID	TECN	COMMENT
0.42 ± 0.07 OUR AVERAGE			
0.43 ± 0.08	11,12 BERGFELD	94	CLE2 $e^+ e^- \approx \mathcal{T}(4S)$
0.38 ± 0.14	12,13 ALBRECHT	91G	ARG $e^+ e^- \approx 10.4$ GeV

¹¹ BERGFELD 94 measures $\sigma(e^+ e^- \rightarrow \Lambda_C^+ X) \cdot B(\Lambda_C^+ \rightarrow \Lambda e^+ \nu_e) = (4.87 \pm 0.28 \pm 0.69)$ pb.
¹² To extract $\Gamma(\Lambda_C^+ \rightarrow \Lambda e^+ \nu_e)/\Gamma(\Lambda_C^+ \rightarrow \rho K^- \pi^+)$, we use $\sigma(e^+ e^- \rightarrow \Lambda_C^+ X) \cdot B(\Lambda_C^+ \rightarrow \rho K^- \pi^+) = (11.2 \pm 1.3)$ pb, which is the weighted average of measurements from ARGUS (ALBRECHT 96E) and CLEO (AVERY 91).
¹³ ALBRECHT 91G measures $\sigma(e^+ e^- \rightarrow \Lambda_C^+ X) \cdot B(\Lambda_C^+ \rightarrow \Lambda e^+ \nu_e) = (4.20 \pm 1.28 \pm 0.71)$ pb.

$\Gamma(\Lambda \mu^+ \nu_\mu)/\Gamma(\rho K^- \pi^+)$ Γ_{66}/Γ_2

VALUE	DOCUMENT ID	TECN	COMMENT
0.39 ± 0.08 OUR AVERAGE			
0.40 ± 0.09	14,15 BERGFELD	94	CLE2 $e^+ e^- \approx \mathcal{T}(4S)$
0.35 ± 0.20	15,16 ALBRECHT	91G	ARG $e^+ e^- \approx 10.4$ GeV

¹⁴ BERGFELD 94 measures $\sigma(e^+ e^- \rightarrow \Lambda_C^+ X) \cdot B(\Lambda_C^+ \rightarrow \Lambda \mu^+ \nu_\mu) = (4.43 \pm 0.51 \pm 0.64)$ pb.
¹⁵ To extract $\Gamma(\Lambda_C^+ \rightarrow \Lambda \mu^+ \nu_\mu)/\Gamma(\Lambda_C^+ \rightarrow \rho K^- \pi^+)$, we use $\sigma(e^+ e^- \rightarrow \Lambda_C^+ X) \cdot B(\Lambda_C^+ \rightarrow \rho K^- \pi^+) = (11.2 \pm 1.3)$ pb, which is the weighted average of measurements from ARGUS (ALBRECHT 96E) and CLEO (AVERY 91).
¹⁶ ALBRECHT 91G measures $\sigma(e^+ e^- \rightarrow \Lambda_C^+ X) \cdot B(\Lambda_C^+ \rightarrow \Lambda \mu^+ \nu_\mu) = (3.91 \pm 2.02 \pm 0.90)$ pb.

Inclusive modes

$\Gamma(e^+ \text{ anything})/\Gamma_{\text{total}}$ Γ_{67}/Γ

VALUE	DOCUMENT ID	TECN	COMMENT
0.045 ± 0.017	VELLA	82	MRK2 $e^+ e^-$ 4.5–6.8 GeV

$\Gamma(\rho e^+ \text{ anything})/\Gamma_{\text{total}}$ Γ_{68}/Γ

VALUE	DOCUMENT ID	TECN	COMMENT
0.018 ± 0.009	17 VELLA	82	MRK2 $e^+ e^-$ 4.5–6.8 GeV

¹⁷ VELLA 82 includes protons from Λ decay.

$\Gamma(\Lambda e^+ \text{ anything})/\Gamma_{\text{total}}$ Γ_{69}/Γ

VALUE	DOCUMENT ID	TECN	COMMENT
• • • We do not use the following data for averages, fits, limits, etc. • • •			
0.011 ± 0.008	18 VELLA	82	MRK2 $e^+ e^-$ 4.5–6.8 GeV

¹⁸ VELLA 82 includes Λ 's from Σ^0 decay.

$\Gamma(\rho \text{ anything})/\Gamma_{\text{total}}$ Γ_{70}/Γ

VALUE	DOCUMENT ID	TECN	COMMENT
0.50 ± 0.08 ± 0.14	19 CRAWFORD	92	CLEO $e^+ e^-$ 10.5 GeV

¹⁹ This CRAWFORD 92 value includes protons from Λ decay. The value is model dependent, but account is taken of this in the systematic error.

$\Gamma(\rho \text{ anything (no } \Lambda))/\Gamma_{\text{total}}$ Γ_{71}/Γ

VALUE	DOCUMENT ID	TECN	COMMENT
0.12 ± 0.10 ± 0.16	CRAWFORD	92	CLEO $e^+ e^-$ 10.5 GeV

$\Gamma(n \text{ anything})/\Gamma_{\text{total}}$ Γ_{73}/Γ

VALUE	DOCUMENT ID	TECN	COMMENT
0.50 ± 0.08 ± 0.14	20 CRAWFORD	92	CLEO $e^+ e^-$ 10.5 GeV

²⁰ This CRAWFORD 92 value includes neutrons from Λ decay. The value is model dependent, but account is taken of this in the systematic error.

$\Gamma(n \text{ anything (no } \Lambda))/\Gamma_{\text{total}}$ Γ_{74}/Γ

VALUE	DOCUMENT ID	TECN	COMMENT
0.29 ± 0.09 ± 0.15	CRAWFORD	92	CLEO $e^+ e^-$ 10.5 GeV

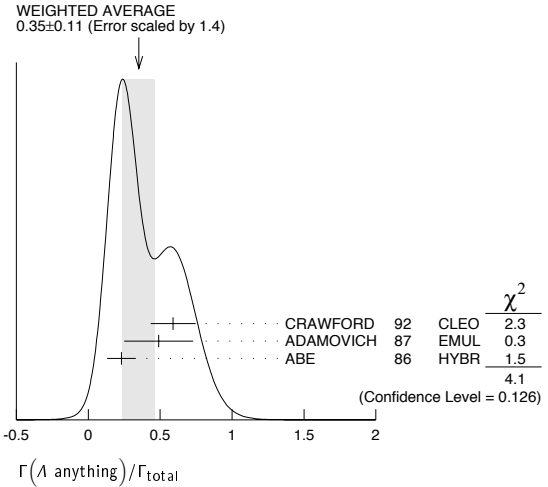
$\Gamma(\rho \text{ hadrons})/\Gamma_{\text{total}}$ Γ_{72}/Γ

VALUE	DOCUMENT ID	TECN	COMMENT
• • • We do not use the following data for averages, fits, limits, etc. • • •			
0.41 ± 0.24	ADAMOVIICH	87	EMUL γ A 20–70 GeV/c

$\Gamma(\Lambda \text{ anything})/\Gamma_{\text{total}}$ Γ_{75}/Γ

VALUE	EVTS	DOCUMENT ID	TECN	COMMENT
0.35 ± 0.11 OUR AVERAGE				Error includes scale factor of 1.4. See the ideogram below.
0.59 ± 0.10 ± 0.12		CRAWFORD	92	CLEO $e^+ e^-$ 10.5 GeV
0.49 ± 0.24		ADAMOVIICH	87	EMUL γ A 20–70 GeV/c
0.23 ± 0.10	8	²¹ ABE	86	HYBR 20 GeV γ p

²¹ ABE 86 includes Λ 's from Σ^0 decay.



$\Gamma(\Sigma^\pm \text{ anything})/\Gamma_{\text{total}}$ Γ_{76}/Γ

VALUE	EVTS	DOCUMENT ID	TECN	COMMENT
0.1 ± 0.05	5	ABE	86	HYBR 20 GeV γ p

$\Gamma(3\text{prongs})/\Gamma_{\text{total}}$ Γ_{77}/Γ

VALUE	DOCUMENT ID	TECN	COMMENT
0.24 ± 0.07 ± 0.04	KAYIS-TOPAK.03	CHRS	ν_μ emulsion, $\bar{E} = 27$ GeV

Rare or forbidden modes

$\Gamma(\rho \mu^+ \mu^-)/\Gamma_{\text{total}}$ Γ_{78}/Γ
 A test for the $\Delta C=1$ weak neutral current. Allowed by higher-order electroweak interactions.

VALUE	CL%	EVTS	DOCUMENT ID	TECN	COMMENT
< 3.4 × 10⁻⁴	90	0	KODA MA	95	E653 π^- emulsion 600 GeV

$\Gamma(\Sigma^- \mu^+ \mu^+)/\Gamma_{\text{total}}$ Γ_{79}/Γ
 A test of lepton-number conservation.

VALUE	CL%	EVTS	DOCUMENT ID	TECN	COMMENT
< 7.0 × 10⁻⁴	90	0	KODA MA	95	E653 π^- emulsion 600 GeV

Λ_C^+ DECAY PARAMETERS

See the note on "Baryon Decay Parameters" in the neutron Listings.

α FOR $\Lambda_C^+ \rightarrow \Lambda \pi^+$

VALUE	EVTS	DOCUMENT ID	TECN	COMMENT
-0.91 ± 0.15 OUR AVERAGE				
-0.78 ± 0.16 ± 0.19		LINK	06A	FOCS γ A, $\bar{E}_\gamma \approx 180$ GeV
-0.94 ± 0.21 ± 0.12	414	²² BISHAI	95	CLE2 $e^+ e^- \approx \mathcal{T}(4S)$
-0.96 ± 0.42		ALBRECHT	92	ARG $e^+ e^- \approx 10.4$ GeV
-1.1 ± 0.4	86	AVERY	90B	CLEO $e^+ e^- \approx 10.6$ GeV

²² BISHAI 95 actually gives $\alpha = -0.94 + 0.21 + 0.12$ / $-0.06 - 0.06$, chopping the errors at the physical limit -1.0 . However, for $\alpha \approx -1.0$, some experiments should get unphysical values ($\alpha < -1.0$), and for averaging with other measurements such values (or errors that extend below -1.0) should not be chopped.

α FOR $\Lambda_C^+ \rightarrow \Sigma^+ \pi^0$

VALUE	EVTS	DOCUMENT ID	TECN	COMMENT
-0.45 ± 0.31 ± 0.06	89	BISHAI	95	CLE2 $e^+ e^- \approx \mathcal{T}(4S)$

α FOR $\Lambda_C^+ \rightarrow \Lambda e^+ \nu_e$

The experiments don't cover the complete (or same incomplete) $M(\Lambda e^+)$ range, but we average them together anyway.

VALUE	EVTS	DOCUMENT ID	TECN	COMMENT
-0.86 ± 0.04 OUR AVERAGE				
-0.86 ± 0.03 ± 0.02	3201	²³ HINSON	05	CLEO $e^+ e^- \approx \mathcal{T}(4S)$
-0.91 ± 0.42 ± 0.25		²⁴ ALBRECHT	94B	ARG $e^+ e^- \approx 10$ GeV
• • • We do not use the following data for averages, fits, limits, etc. • • •				
-0.82 + 0.09 + 0.06 / -0.06 - 0.03	700	²⁵ CRAWFORD	95	CLE2 See HINSON 05
-0.89 + 0.17 + 0.09 / -0.11 - 0.05	350	²⁶ BERGFELD	94	CLE2 See CRAWFORD 95

Baryon Particle Listings

 $\Lambda_c^+, \Lambda_c(2595)^+$

²³ HINSON 05 measures the form-factor ratio $R \equiv f_2/f_1$ for $\Lambda_c^+ \rightarrow \Lambda e^+ \nu_e$ events to be $-0.31 \pm 0.05 \pm 0.04$ and the pole mass to be $2.21 \pm 0.08 \pm 0.14$ GeV/ c^2 , and from these calculates α , averaged over q^2 , where $\langle q^2 \rangle = 0.67$ (GeV/ c)².

²⁴ ALBRECHT 94b uses Λe^+ and $\Lambda \mu^+$ events in the mass range $1.85 < M(\Lambda \ell^+) < 2.20$ GeV.

²⁵ CRAWFORD 95 measures the form-factor ratio $R \equiv f_2/f_1$ for $\Lambda_c^+ \rightarrow \Lambda e^+ \nu_e$ events to be $-0.25 \pm 0.14 \pm 0.08$ and from this calculates α , averaged over q^2 , to be the above.

²⁶ BERGFELD 94 uses Λe^+ events.

 $\Lambda_c^+, \bar{\Lambda}_c^-$ CP-VIOLATING DECAY ASYMMETRIES $(\alpha + \bar{\alpha})/(\alpha - \bar{\alpha})$ in $\Lambda_c^+ \rightarrow \Lambda \pi^+, \bar{\Lambda}_c^- \rightarrow \bar{\Lambda} \pi^-$

This is zero if CP is conserved.

VALUE	DOCUMENT ID	TECN	COMMENT
$-0.07 \pm 0.19 \pm 0.24$	LINK	06A	FOCS $\gamma A, \bar{E}_\gamma \approx 180$ GeV

 $(\alpha + \bar{\alpha})/(\alpha - \bar{\alpha})$ in $\Lambda_c^+ \rightarrow \Lambda e^+ \nu_e, \bar{\Lambda}_c^- \rightarrow \bar{\Lambda} e^- \bar{\nu}_e$

This is zero if CP is conserved.

VALUE	DOCUMENT ID	TECN	COMMENT
$0.00 \pm 0.03 \pm 0.02$	HINSON	05	CLEO $e^+ e^- \approx \tau(4S)$

 Λ_c^+ REFERENCES

We have omitted some papers that have been superseded by later experiments. The omitted papers may be found in our 1992 edition (Physical Review D45, 1 June, Part II) or in earlier editions.

AUBERT	07U	PR D75 052002	B. Aubert et al.	(BABAR Collab.)
LINK	06A	PL B634 165	J.M. Link et al.	(FNAL FOCUS Collab.)
AUBERT.B	05S	PR D72 052006	B. Aubert et al.	(BABAR Collab.)
HINSON	05	PRL 94 191801	J.W. Hinson et al.	(CLEO Collab.)
LINK	05F	PL B624 22	J.M. Link et al.	(FNAL FOCUS Collab.)
LINK	05K	PL B624 166	J.M. Link et al.	(FNAL FOCUS Collab.)
CRONIN-HEN.	03	PR D67 012001	D. Cronin-Hennessy et al.	(CLEO Collab.)
KAYIS-TOPAK.	03	PL B555 156	A. Kayis-Topaksu et al.	(CERN CHORUS Collab.)
ABE	02C	PL B524 33	K. Abe et al.	(KEK BELLE Collab.)
LINK	02C	PRL 88 161801	J.M. Link et al.	(FNAL FOCUS Collab.)
LINK	02G	PL B540 25	J.M. Link et al.	(FNAL FOCUS Collab.)
PDG	02	PR D66 010001	K. Hagiwara et al.	
KUSHNIR...	01	PRL 86 5243	A. Kushnirenko et al.	(FNAL SLEX Collab.)
MAHMOOD	01	PRL 86 2232	A.H. Mahmood et al.	(CLEO Collab.)
AITALA	00	PL B471 449	E.M. Aitala et al.	(FNAL E791 Collab.)
JAFFE	00	PR D62 072005	D.E. Jaffe et al.	(CLEO Collab.)
ALAM	98	PR D57 4467	M.S. Alam et al.	(CLEO Collab.)
ALBRECHT	96E	PRL 76 2223	H. Albrecht et al.	(ARGUS Collab.)
ALEEV	96	JINRRC 3-77 31	A.N. Aleev et al.	(Serpukhov EXCHARM Collab.)
ALEXANDER	96C	PR D53 R1013	J.P. Alexander et al.	(CLEO Collab.)
ALBRECHT	95B	PL B342 397	H. Albrecht et al.	(ARGUS Collab.)
AMMAR	95	PRL 74 3534	R. Ammar et al.	(CLEO Collab.)
BISHAI	95	PL B350 256	M. Bishai et al.	(CLEO Collab.)
CRAWFORD	95	PRL 75 624	G. Crawford et al.	(CLEO Collab.)
KODAMA	95	PL B345 85	K. Kodama et al.	(FNAL E653 Collab.)
ALBRECHT	94B	PL B326 320	H. Albrecht et al.	(ARGUS Collab.)
ALEEV	94	PAN 57 1370	A.N. Aleev et al.	(Serpukhov BIS-2 Collab.)
Translated from YF 57 1443				
AVERY	94	PL B325 257	P. Avery et al.	(CLEO Collab.)
BERGFELD	94	PL B323 219	T. Bergfeld et al.	(CLEO Collab.)
FRABETTI	94E	PL B328 193	P.L. Frabetti et al.	(FNAL E687 Collab.)
AVERY	93	PRL 71 2391	P. Avery et al.	(CLEO Collab.)
BOZEK	93	PL B312 247	A. Bozek et al.	(CERN NA32 Collab.)
FRABETTI	93D	PRL 70 1755	P.L. Frabetti et al.	(FNAL E687 Collab.)
FRABETTI	93H	PL B314 477	P.L. Frabetti et al.	(FNAL E687 Collab.)
KUBOTA	93	PRL 71 3255	Y. Kubota et al.	(CLEO Collab.)
ALBRECHT	92	PL B274 239	H. Albrecht et al.	(ARGUS Collab.)
ALBRECHT	92O	ZPHY C56 1	H. Albrecht et al.	(ARGUS Collab.)
BARLAG	92	PL B283 465	S. Barlag et al.	(ACCMOR Collab.)
CRAWFORD	92	PR D45 752	G. Crawford et al.	(CLEO Collab.)
JEZABEK	92	PL B286 175	M. Jezabek, K. Rybicki, R. Rylko	(CRAC Collab.)
ALBRECHT	91G	PL B269 234	H. Albrecht et al.	(ARGUS Collab.)
AVERY	91	PR D43 3599	P. Avery et al.	(CLEO Collab.)
ALVAREZ	90	ZPHY C47 539	M.P. Alvarez et al.	(CERN NA14/2 Collab.)
ALVAREZ	90B	PL B246 256	M.P. Alvarez et al.	(CERN NA14/2 Collab.)
ANJOS	90	PR D41 801	J.C. Anjos et al.	(FNAL E691 Collab.)
AVERY	90B	PRL 65 2842	P. Avery et al.	(CLEO Collab.)
BARLAG	90D	ZPHY C40 29	S. Barlag et al.	(ACCMOR Collab.)
FRABETTI	90	PL B251 639	P.L. Frabetti et al.	(FNAL E687 Collab.)
BARLAG	89	PL B218 374	S. Barlag et al.	(ACCMOR Collab.)
AGUILAR...	88B	ZPHY C40 321	M. Aguilar-Benitez et al.	(LEBC-EHS Collab.)
Also		PL B189 254	M. Aguilar-Benitez et al.	(LEBC-EHS Collab.)
Also		PL B199 462	M. Aguilar-Benitez et al.	(LEBC-EHS Collab.)
Also		SJNP 48 833	M. Begalli et al.	(LEBC-EHS Collab.)
Translated from YAF 48 1310.				
ALBRECHT	88C	PL B207 109	H. Albrecht et al.	(ARGUS Collab.)
ANJOS	88B	PRL 60 1379	J.C. Anjos et al.	(FNAL E691 Collab.)
ADAMOVICH	87	EPL 4 887	M.I. Adamovich et al.	(Photon Emulsion Collab.)
Also		SJNP 46 447	F. Viaggi et al.	(Photon Emulsion Collab.)
Translated from YAF 46 799.				
AMENDOLIA	87	ZPHY C36 513	S.R. Amendolia et al.	(CERN NA1 Collab.)
JONES	87	ZPHY C36 593	G.T. Jones et al.	(CERN WA21 Collab.)
ABE	86	PR D33 1	K. Abe et al.	
ALEEV	84	ZPHY C23 333	A.N. Aleev et al.	(BIS-2 Collab.)
BOSETTI	82	PL 109B 234	P.C. Bosetti et al.	(AACh3, BÖNN, CERN+)
VELLA	82	PRL 48 1515	E. Vella et al.	(SLAC, LBL, UCB)
BASILE	81B	NC 62A 14	M. Basile et al.	(CERN, BÖNA, PGIA, FRAS)
CALICCHIO	80	PL 93B 521	M. Calicchio et al.	(BARI, BIRM, BRUX+)

OTHER RELATED PAPERS

MIGLIOZZI	99	PL B462 217	P. Migliozi et al.
DUNIETZ	98	PR D58 094010	I. Dunietz

 $\Lambda_c(2595)^+$

$$I(J^P) = 0(\frac{1}{2}^-) \text{ Status: } ***$$

Seen in $\Lambda_c^+ \pi^+ \pi^-$ but not in $\Lambda_c^+ \pi^0$, so this is indeed an excited Λ_c^+ rather than a Σ_c^+ . The $\Lambda_c^+ \pi^+ \pi^-$ mode is largely, and perhaps entirely, $\Sigma_c \pi$, which is just at threshold; thus (assuming, as has not yet been proven, that the Σ_c has $J^P = 1/2^+$) the J^P here is almost certainly $1/2^-$. This result is in accord with the theoretical expectation that this is the charm counterpart of the strange $\Lambda(1405)$.

 $\Lambda_c(2595)^+$ MASS

The mass is obtained from the $\Lambda_c(2595)^+ - \Lambda_c^+$ mass-difference measurements below. But the mass may be 2 or 3 MeV lower: see the footnote to BLECHMAN 03 in the next data block.

VALUE (MeV)	DOCUMENT ID
2595.4 ± 0.6 OUR FIT	Error includes scale factor of 1.1.

 $\Lambda_c(2595)^+ - \Lambda_c^+$ MASS DIFFERENCE

VALUE (MeV)	EVTS	DOCUMENT ID	TECN	COMMENT
308.9 ± 0.6 OUR FIT				Error includes scale factor of 1.1.
308.9 ± 0.6 OUR AVERAGE				Error includes scale factor of 1.1.
$309.7 \pm 0.9 \pm 0.4$	19	ALBRECHT 97	ARG	$e^+ e^- \approx 10$ GeV
$309.2 \pm 0.7 \pm 0.3$	14 ± 4.5	FRABETTI 96	E687	$\gamma Be, \bar{E}_\gamma \approx 220$ GeV
$307.5 \pm 0.4 \pm 1.0$	112 ± 17	EDWARDS 95	CLE2	$e^+ e^- \approx 10.5$ GeV
305.6 ± 0.3		¹ BLECHMAN 03		Threshold shift

• • • We do not use the following data for averages, fits, limits, etc. • • •

¹ BLECHMAN 03 finds that a more sophisticated treatment than a simple Breit-Wigner for the proximity of the threshold of the dominant decay, $\Sigma_c(2455) \pi$, lowers the $\Lambda_c(2595)^+ - \Lambda_c^+$ mass difference by 2 or 3 MeV.

 $\Lambda_c(2595)^+$ WIDTH

VALUE (MeV)	EVTS	DOCUMENT ID	TECN	COMMENT
$3.6^{+2.0}_{-1.3}$ OUR AVERAGE				
$2.9^{+2.9+1.8}_{-2.1-1.4}$	19	ALBRECHT 97	ARG	$e^+ e^- \approx 10$ GeV
$3.9^{+1.4+2.0}_{-1.2-1.0}$	112 ± 17	EDWARDS 95	CLE2	$e^+ e^- \approx 10.5$ GeV

 $\Lambda_c(2595)^+$ DECAY MODES

$\Lambda_c^+ \pi \pi$ and its submode $\Sigma_c(2455) \pi$ — the latter just barely — are the only strong decays allowed to an excited Λ_c^+ having this mass; and the submode seems to dominate.

Mode	Fraction (Γ_i/Γ)
$\Gamma_1 \Lambda_c^+ \pi^+ \pi^-$	$[a] \approx 67\%$
$\Gamma_2 \Sigma_c(2455)^+ \pi^-$	$24 \pm 7\%$
$\Gamma_3 \Sigma_c(2455)^0 \pi^+$	$24 \pm 7\%$
$\Gamma_4 \Lambda_c^+ \pi^+ \pi^- 3\text{-body}$	$18 \pm 10\%$
$\Gamma_5 \Lambda_c^+ \pi^0$	$[b]$ not seen
$\Gamma_6 \Lambda_c^+ \gamma$	not seen

[a] Assuming isospin conservation, so that the other third is $\Lambda_c^+ \pi^0 \pi^0$.

[b] A test that the isospin is indeed 0, so that the particle is indeed a Λ_c^+ .

 $\Lambda_c(2595)^+$ BRANCHING RATIOS

$\Gamma(\Sigma_c(2455)^+ \pi^-)/\Gamma(\Lambda_c^+ \pi^+ \pi^-)$	Γ_2/Γ_1
0.36 ± 0.10 OUR AVERAGE	
$0.37 \pm 0.12 \pm 0.13$	ALBRECHT 97 ARG $e^+ e^- \approx 10$ GeV
$0.36 \pm 0.09 \pm 0.09$	EDWARDS 95 CLE2 $e^+ e^- \approx 10.5$ GeV
$\Gamma(\Sigma_c(2455)^0 \pi^+)/\Gamma(\Lambda_c^+ \pi^+ \pi^-)$	Γ_3/Γ_1
0.29 ± 0.10 OUR AVERAGE	
$0.29 \pm 0.10 \pm 0.11$	ALBRECHT 97 ARG $e^+ e^- \approx 10$ GeV
$0.42 \pm 0.09 \pm 0.09$	EDWARDS 95 CLE2 $e^+ e^- \approx 10.5$ GeV

See key on page 373

Baryon Particle Listings

$\Lambda_c(2595)^+$, $\Lambda_c(2625)^+$, $\Lambda_c(2765)^+$

$$\frac{[\Gamma(\Sigma_c(2455)^{++}\pi^-) + \Gamma(\Sigma_c(2455)^0\pi^+)]}{\Gamma(\Lambda_c^+\pi^+\pi^-)} \quad (\Gamma_2+\Gamma_3)/\Gamma_1$$

VALUE	CL%	DOCUMENT ID	TECN	COMMENT
$0.66^{+0.13}_{-0.16} \pm 0.07$		ALBRECHT 97	ARG	$e^+e^- \approx 10$ GeV
>0.51	90	FRABETTI 96	E687	γ Be, $\bar{E}_\gamma \approx 220$ GeV

• • • We do not use the following data for averages, fits, limits, etc. • • •

²The results of FRABETTI 96 are consistent with this ratio being 100%.

$$\frac{\Gamma(\Lambda_c^+\pi^0)/\Gamma(\Lambda_c^+\pi^+\pi^-)}{\Lambda_c^+\pi^0 \text{ decay is forbidden by isospin conservation if this state is in fact a } \Lambda_c.} \quad \Gamma_5/\Gamma_1$$

VALUE	CL%	DOCUMENT ID	TECN	COMMENT
<3.53	90	EDWARDS 95	CLE2	$e^+e^- \approx 10.5$ GeV

$$\frac{\Gamma(\Lambda_c^+\gamma)/\Gamma(\Lambda_c^+\pi^+\pi^-)}{\Gamma_6/\Gamma_1}$$

VALUE	CL%	DOCUMENT ID	TECN	COMMENT
<0.98	90	EDWARDS 95	CLE2	$e^+e^- \approx 10.5$ GeV

$\Lambda_c(2595)^+$ REFERENCES

BLECHMAN 03	PR D67 074033	A.E. Blechman et al.	(JHU, FLOR)
ALBRECHT 97	PL B402 207	H. Albrecht et al.	(ARGUS Collab.)
FRABETTI 96	PL B365 461	P.L. Frabetti et al.	(FNAL E687 Collab.)
EDWARDS 95	PRL 74 3331	K.W. Edwards et al.	(CLEO Collab.)

$\Lambda_c(2625)^+$ $I(J^P) = 0(\frac{3}{2}^-)$ Status: * * *

Seen in $\Lambda_c^+\pi^+\pi^-$ but not in $\Lambda_c^+\pi^0$ so this is indeed an excited Λ_c^+ rather than a Σ_c^+ . The spin-parity has not been measured but is expected to be $3/2^-$: this is presumably the charm counterpart of the strange $\Lambda(1520)$.

$\Lambda_c(2625)^+$ MASS

The mass is obtained from the $\Lambda_c(2625)^+ - \Lambda_c^+$ mass-difference measurements below.

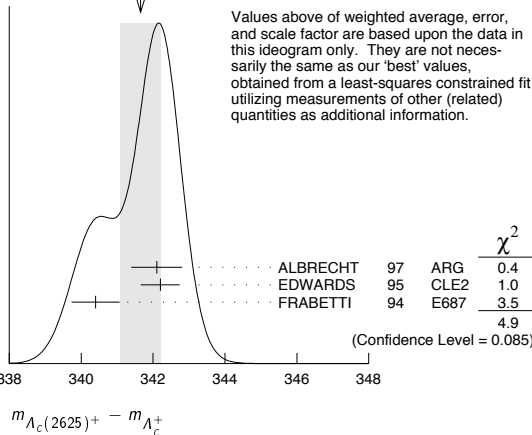
VALUE (MeV)	EVTS	DOCUMENT ID	TECN	COMMENT
2628.1 ± 0.6 OUR FIT				Error includes scale factor of 1.5.
$2626.6 \pm 0.5 \pm 1.5$	42 ± 9	ALBRECHT 93F	ARG	See ALBRECHT 97

• • • We do not use the following data for averages, fits, limits, etc. • • •

$\Lambda_c(2625)^+ - \Lambda_c^+$ MASS DIFFERENCE

VALUE (MeV)	EVTS	DOCUMENT ID	TECN	COMMENT
341.7 ± 0.6 OUR FIT				Error includes scale factor of 1.6.
341.7 ± 0.6 OUR AVERAGE				Error includes scale factor of 1.6. See the ideogram below.
$342.1 \pm 0.5 \pm 0.5$	51	ALBRECHT 97	ARG	$e^+e^- \approx 10$ GeV
$342.2 \pm 0.2 \pm 0.5$	245 ± 19	EDWARDS 95	CLE2	$e^+e^- \approx 10.5$ GeV
$340.4 \pm 0.6 \pm 0.3$	40 ± 9	FRABETTI 94	E687	γ Be, $\bar{E}_\gamma = 220$ GeV

WEIGHTED AVERAGE
 341.7 ± 0.6 (Error scaled by 1.6)



Values above of weighted average, error, and scale factor are based upon the data in this ideogram only. They are not necessarily the same as our 'best' values, obtained from a least-squares constrained fit utilizing measurements of other (related) quantities as additional information.

$\Lambda_c(2625)^+$ WIDTH

VALUE (MeV)	CL%	EVTS	DOCUMENT ID	TECN	COMMENT
<1.9	90	245 ± 19	EDWARDS 95	CLE2	$e^+e^- \approx 10.5$ GeV
<3.2	90		ALBRECHT 93F	ARG	$e^+e^- \approx \Upsilon(4S)$

• • • We do not use the following data for averages, fits, limits, etc. • • •

$\Lambda_c(2625)^+$ DECAY MODES

$\Lambda_c^+\pi\pi$ and its submode $\Sigma(2455)\pi$ are the only strong decays allowed to an excited Λ_c^+ having this mass.

Mode	Fraction (Γ_i/Γ)	Confidence level
Γ_1 $\Lambda_c^+\pi^+\pi^-$	[a] $\approx 67\%$	
Γ_2 $\Sigma_c(2455)^{++}\pi^-$	<5	90%
Γ_3 $\Sigma_c(2455)^0\pi^+$	<5	90%
Γ_4 $\Lambda_c^+\pi^+\pi^-$ 3-body	large	
Γ_5 $\Lambda_c^+\pi^0$	[b] not seen	
Γ_6 $\Lambda_c^+\gamma$	not seen	

[a] Assuming isospin conservation, so that the other third is $\Lambda_c^+\pi^0\pi^0$.

[b] A test that the isospin is indeed 0, so that the particle is indeed a Λ_c^+ .

$\Lambda_c(2625)^+$ BRANCHING RATIOS

VALUE	CL%	DOCUMENT ID	TECN	COMMENT	Γ_2/Γ_1
<0.08	90	EDWARDS 95	CLE2	$e^+e^- \approx 10.5$ GeV	

VALUE	CL%	DOCUMENT ID	TECN	COMMENT	Γ_3/Γ_1
<0.07	90	EDWARDS 95	CLE2	$e^+e^- \approx 10.5$ GeV	

$$\frac{[\Gamma(\Sigma_c(2455)^{++}\pi^-) + \Gamma(\Sigma_c(2455)^0\pi^+)]}{\Gamma(\Lambda_c^+\pi^+\pi^-)} \quad (\Gamma_2+\Gamma_3)/\Gamma_1$$

VALUE	CL%	EVTS	DOCUMENT ID	TECN	COMMENT
<0.36	90		FRABETTI 94	E687	γ Be, $\bar{E}_\gamma = 220$ GeV
0.46 ± 0.14		21	ALBRECHT 93F	ARG	$e^+e^- \approx \Upsilon(4S)$

VALUE	EVTS	DOCUMENT ID	TECN	COMMENT	Γ_4/Γ_1
0.54 ± 0.14	16	ALBRECHT 93F	ARG	$e^+e^- \approx \Upsilon(4S)$	

VALUE	CL%	DOCUMENT ID	TECN	COMMENT	Γ_5/Γ_1
<0.91	90	EDWARDS 95	CLE2	$e^+e^- \approx 10.5$ GeV	

$\Lambda_c^+\pi^0$ decay is forbidden by isospin conservation if this state is in fact a Λ_c .

VALUE	CL%	DOCUMENT ID	TECN	COMMENT	Γ_6/Γ_1
<0.52	90	EDWARDS 95	CLE2	$e^+e^- \approx 10.5$ GeV	

$\Lambda_c(2625)^+$ REFERENCES

ALBRECHT 97	PL B402 207	H. Albrecht et al.	(ARGUS Collab.)
EDWARDS 95	PRL 74 3331	K.W. Edwards et al.	(CLEO Collab.)
FRABETTI 94	PRL 72 961	P.L. Frabetti et al.	(FNAL E687 Collab.)
ALBRECHT 93F	PL B317 227	H. Albrecht et al.	(ARGUS Collab.)

$\Lambda_c(2765)^+$ or $\Sigma_c(2765)$ $I(J^P) = ?(?^?)$ Status: *

OMITTED FROM SUMMARY TABLE

A broad, statistically significant peak (997^{+141}_{-129} events) seen in $\Lambda_c^+\pi^+\pi^-$. However, nothing at all is known about its quantum numbers, including whether it is a Λ_c^+ or a Σ_c , or whether the width might be due to overlapping states.

$\Lambda_c(2765)^+$ MASS

The mass is obtained from the $\Lambda_c(2765)^+ - \Lambda_c^+$ mass-difference measurement below.

VALUE (MeV)	DOCUMENT ID
2766.6 ± 2.4 OUR FIT	

$\Lambda_c(2765)^+ - \Lambda_c^+$ MASS DIFFERENCE

VALUE (MeV)	EVTS	DOCUMENT ID	TECN	COMMENT
480.1 ± 2.4 OUR FIT				
480.1 ± 2.4	997^{+141}_{-129}	ARTUSO 01	CLE2	$e^+e^- \approx \Upsilon(4S)$

Baryon Particle Listings

 $\Lambda_c(2765)^+$, $\Lambda_c(2880)^+$, $\Lambda_c(2940)^+$, $\Sigma_c(2455)$ $\Lambda_c(2765)^+$ WIDTH

VALUE (MeV)	DOCUMENT ID	TECN	COMMENT
50	ARTUSO 01	CLE2	$e^+e^- \approx \Upsilon(4S)$

 $\Lambda_c(2765)^+$ DECAY MODES

Mode	Fraction (Γ_i/Γ)
Γ_1 $\Lambda_c^+ \pi^+ \pi^-$	seen

 $\Lambda_c(2765)^+$ REFERENCES

ARTUSO 01	PRL 86 4479	M. Artuso et al.	(CLEO Collab.)
-----------	-------------	------------------	----------------

 $\Lambda_c(2880)^+$

$$I(J^P) = 0(\frac{5}{2}^+) \text{ Status: } ***$$

A narrow peak seen in $\Lambda_c^+ \pi^+ \pi^-$ and in pD^0 . It is not seen in pD^+ , and therefore it is probably a Λ_c^+ and not a Σ_c . The evidence for spin 5/2 comes from the $\Sigma_c(2455)\pi$ decay angular distribution, and the evidence for parity + comes from agreement of the $\Sigma_c(2520)/\Sigma_c(2455)$ branching ratio with a prediction of heavy quark symmetry (see MIZUK 07).

 $\Lambda_c(2880)^+$ MASS

VALUE (MeV)	EVTS	DOCUMENT ID	TECN	COMMENT
2881.53 ± 0.35 OUR FIT				
2881.50 ± 0.35 OUR AVERAGE				
2881.9 ± 0.1 ± 0.5	2.8k ± 190	AUBERT 07	BABR	in pD^0
2881.2 ± 0.2 ± 0.4	690 ± 50	MIZUK 07	BELL	in $\Sigma_c(2455)^{0,++} \pi^\pm$

 $\Lambda_c(2880)^+ - \Lambda_c^+$ MASS DIFFERENCE

VALUE (MeV)	EVTS	DOCUMENT ID	TECN	COMMENT
595.1 ± 0.4 OUR FIT				
596 ± 1 ± 2	350 ⁺⁵⁷ ₋₅₅	ARTUSO 01	CLE2	in $\Lambda_c^+ \pi^+ \pi^-$

 $\Lambda_c(2880)^+$ WIDTH

VALUE (MeV)	CL%	EVTS	DOCUMENT ID	TECN	COMMENT
5.8 ± 1.1 OUR AVERAGE					
5.8 ± 1.5 ± 1.1		2.8k ± 190	AUBERT 07	BABR	in pD^0
5.8 ± 0.7 ± 1.1		690 ± 50	MIZUK 07	BELL	in $\Sigma_c(2455)^{0,++} \pi^\pm$
••• We do not use the following data for averages, fits, limits, etc. •••					
<8	90		ARTUSO 01	CLEO	in $\Lambda_c^+ \pi^+ \pi^-$

 $\Lambda_c(2880)^+$ DECAY MODES

Mode	Fraction (Γ_i/Γ)
Γ_1 $\Lambda_c^+ \pi^+ \pi^-$	seen
Γ_2 $\Sigma_c(2455)^{0,++} \pi^\pm$	seen
Γ_3 $\Sigma_c(2520)^{0,++} \pi^\pm$	seen
Γ_4 pD^0	seen

 $\Lambda_c(2880)^+$ BRANCHING RATIOS

$\Gamma(\Sigma_c(2455)^{0,++} \pi^\pm)/\Gamma(\Lambda_c^+ \pi^+ \pi^-)$	Γ_2/Γ_1
0.392 ± 0.031 OUR AVERAGE	Error includes scale factor of 1.3.
0.404 ± 0.021 ± 0.014	MIZUK 07 BELL in $\Sigma_c(2455)^{0,++} \pi^\pm$
0.31 ± 0.06 ± 0.03	96 ARTUSO 01 CLE2 $e^+e^- \approx \Upsilon(4S)$

$\Gamma(\Sigma_c(2520)^{0,++} \pi^\pm)/\Gamma(\Lambda_c^+ \pi^+ \pi^-)$	Γ_3/Γ_1
0.091 ± 0.025 ± 0.010	
••• We do not use the following data for averages, fits, limits, etc. •••	
<0.11	90 ARTUSO 01 CLE2 $e^+e^- \approx \Upsilon(4S)$

$\Gamma(\Sigma_c(2520)^{0,++} \pi^\pm)/\Gamma(\Sigma_c(2455)^{0,++} \pi^\pm)$	Γ_3/Γ_2
0.225 ± 0.062 ± 0.025	
••• We do not use the following data for averages, fits, limits, etc. •••	
0.225 ± 0.062 ± 0.025	¹ MIZUK 07 BELL in $\Sigma_c(2455)^{0,++} \pi^\pm$
¹ This MIZUK 07 ratio is redundant with MIZUK 07 ratios given above.	

 $\Lambda_c(2880)^+$ REFERENCES

AUBERT 07	PRL 98 012001	B. Aubert et al.	(BABAR Collab.)
MIZUK 07	PRL 98 262001	R. Mizuk et al.	(BELLE Collab.)
ARTUSO 01	PRL 86 4479	M. Artuso et al.	(CLEO Collab.)

 $\Lambda_c(2940)^+$

$$I(J^P) = 0(?^?) \text{ Status: } ***$$

A fairly narrow peak of good statistical significance first seen in the pD^0 mass spectrum. It is not seen in pD^+ , and thus it is probably a Λ_c^+ and not a Σ_c . It is also seen in $\Sigma_c(2455)^{0,++} \pi^\pm$.

 $\Lambda_c(2940)^+$ MASS

VALUE (MeV)	EVTS	DOCUMENT ID	TECN	COMMENT
2939.3^{+1.4}_{-1.5} OUR AVERAGE				
2939.8 ± 1.3 ± 1.0	2280 ± 310	AUBERT 07	BABR	in pD^0
2938.0 ± 1.3 ^{+2.0} _{-4.0}	220 ⁺⁸⁰ ₋₆₀	MIZUK 07	BELL	in $\Sigma_c(2455)^{0,++} \pi^\pm$

 $\Lambda_c(2940)^+$ WIDTH

VALUE (MeV)	EVTS	DOCUMENT ID	TECN	COMMENT
17⁺⁸₋₆ OUR AVERAGE				
17.5 ± 5.2 ± 5.9	2280 ± 310	AUBERT 07	BABR	in pD^0
13 ⁺⁸ ₋₅ ⁺²⁷ ₋₇	220 ⁺⁸⁰ ₋₆₀	MIZUK 07	BELL	in $\Sigma_c(2455)^{0,++} \pi^\pm$

 $\Lambda_c(2940)^+$ DECAY MODES

Mode	Fraction (Γ_i/Γ)
Γ_1 pD^0	seen
Γ_2 $\Sigma_c(2455)^{0,++} \pi^\pm$	seen

 $\Lambda_c(2940)^+$ REFERENCES

AUBERT 07	PRL 98 012001	B. Aubert et al.	(BABAR Collab.)
MIZUK 07	PRL 98 262001	R. Mizuk et al.	(BELLE Collab.)

 $\Sigma_c(2455)$

$$I(J^P) = 1(\frac{1}{2}^+) \text{ Status: } ***$$

Neither J nor P has been measured; $1/2^+$ is the quark model prediction.

 $\Sigma_c(2455)$ MASSES

The masses are obtained from the mass-difference measurements that follow.

 $\Sigma_c(2455)^{++}$ MASS

VALUE (MeV)	DOCUMENT ID
2454.02 ± 0.18 OUR FIT	

 $\Sigma_c(2455)^+$ MASS

VALUE (MeV)	DOCUMENT ID
2452.9 ± 0.4 OUR FIT	

 $\Sigma_c(2455)^0$ MASS

VALUE (MeV)	DOCUMENT ID
2453.76 ± 0.18 OUR FIT	

 $\Sigma_c(2455) - \Lambda_c^+$ MASS DIFFERENCES

$m_{\Sigma_c^{++}} - m_{\Lambda_c^+}$	EVTS	DOCUMENT ID	TECN	COMMENT
167.56 ± 0.11 OUR FIT				
167.57 ± 0.13 OUR AVERAGE				
167.4 ± 0.1 ± 0.2	2k	ARTUSO 02	CLE2	$e^+e^- \approx \Upsilon(4S)$
167.35 ± 0.19 ± 0.12	461	LINK 00c	FOCS	γ nucleus, \bar{E}_γ 180 GeV
167.76 ± 0.4 ± 0.15	122	AITALA 96b	E791	$\pi^- N$, 500 GeV
167.6 ± 0.6 ± 0.6	56	FRABETTI 96	E687	γ Be, $\bar{E}_\gamma \approx 220$ GeV
168.2 ± 0.3 ± 0.2	126	CRAWFORD 93	CLE2	$e^+e^- \approx \Upsilon(4S)$
167.8 ± 0.4 ± 0.3	54	BOWCOCK 89	CLEO	e^+e^- 10 GeV
168.2 ± 0.5 ± 1.6	92	ALBRECHT 88d	ARG	e^+e^- 10 GeV
167.4 ± 0.5 ± 2.0	46	DIESBURG 87	SPEC	$nA \sim 600$ GeV
••• We do not use the following data for averages, fits, limits, etc. •••				
167 ± 1	2	JONES 87	HBC	νp in BEBC
166 ± 1	1	BOSETTI 82	HBC	See JONES 87
168 ± 3	6	BALTAY 79	HLBC	ν Ne-H in 15-ft
166 ± 15	1	CAZZOLI 75	HBC	νp in BNL 7-ft

$m_{\Sigma_c^+} - m_{\Lambda_c^+}$

VALUE (MeV)	EVTS	DOCUMENT ID	TECN	COMMENT
166.4 ± 0.4 OUR FIT				
166.4 ± 0.2 ± 0.3	661	AMMAR	01	CLE2 $e^+e^- \approx \Upsilon(4S)$
• • • We do not use the following data for averages, fits, limits, etc. • • •				
168.5 ± 0.4 ± 0.2	111	CRAWFORD	93	CLE2 See AMMAR 01
168 ± 3	1	CALICCHIO	80	HBC νp in BEBC-TST

$m_{\Sigma_c^0} - m_{\Lambda_c^+}$

VALUE (MeV)	EVTS	DOCUMENT ID	TECN	COMMENT
167.30 ± 0.11 OUR FIT				
167.29 ± 0.13 OUR AVERAGE				
167.2 ± 0.1 ± 0.2	2k	ARTUSO	02	CLE2 $e^+e^- \approx \Upsilon(4S)$
167.38 ± 0.21 ± 0.13	362	LINK	00C	FOCS γ nucleus, \overline{E}_γ 180 GeV
167.38 ± 0.29 ± 0.15	143	AITALA	96B	E791 $\pi^- N$, 500 GeV
167.8 ± 0.6 ± 0.2		ALEEVE	96	SPEC n nucleus, 50 GeV/c
166.6 ± 0.5 ± 0.6	69	FRABETTI	96	E687 γ Be, $\overline{E}_\gamma \approx 220$ GeV
167.1 ± 0.3 ± 0.2	124	CRAWFORD	93	CLE2 $e^+e^- \approx \Upsilon(4S)$
168.4 ± 1.0 ± 0.3	14	ANJOS	89D	E691 γ Be 90–260 GeV
• • • We do not use the following data for averages, fits, limits, etc. • • •				
167.9 ± 0.5 ± 0.3	48	¹ BOWCOCK	89	CLEO e^+e^- 10 GeV
167.0 ± 0.5 ± 1.6	70	¹ ALBRECHT	88D	ARG e^+e^- 10 GeV
178.2 ± 0.4 ± 2.0	85	² DIESBURG	87	SPEC $nA \sim 600$ GeV
163 ± 2	1	AMMAR	86	EMUL νA

¹ This result enters the fit through $m_{\Sigma_c^{++}} - m_{\Sigma_c^0}$ given below.
² See the note on DIESBURG 87 in the $m_{\Sigma_c^{++}} - m_{\Sigma_c^0}$ section below.

$\Sigma_c(2455)$ MASS DIFFERENCES

$m_{\Sigma_c^{++}} - m_{\Sigma_c^0}$

VALUE (MeV)	DOCUMENT ID	TECN	COMMENT
0.27 ± 0.11 OUR FIT	Error includes scale factor of 1.1.		
0.26 ± 0.14 OUR AVERAGE	Error includes scale factor of 1.2.		
+ 0.2 ± 0.1 ± 0.1	ARTUSO	02	CLE2 $e^+e^- \approx \Upsilon(4S)$
- 0.03 ± 0.28 ± 0.11	LINK	00C	FOCS γ nucleus, \overline{E}_γ 180 GeV
+ 0.38 ± 0.40 ± 0.15	AITALA	96B	E791 $\pi^- N$, 500 GeV
+ 1.1 ± 0.4 ± 0.1	CRAWFORD	93	CLE2 $e^+e^- \approx \Upsilon(4S)$
- 0.1 ± 0.6 ± 0.1	BOWCOCK	89	CLEO e^+e^- 10 GeV
+ 1.2 ± 0.7 ± 0.3	ALBRECHT	88D	ARG $e^+e^- \sim 10$ GeV
• • • We do not use the following data for averages, fits, limits, etc. • • •			
-10.8 ± 2.9	³ DIESBURG	87	SPEC $nA \sim 600$ GeV

³ DIESBURG 87 is completely incompatible with the other experiments, which is surprising since it agrees with them about $m_{\Sigma_c(2455)^{++}} - m_{\Lambda_c^+}$. We go with the majority here.

$m_{\Sigma_c^+} - m_{\Sigma_c^0}$

VALUE (MeV)	DOCUMENT ID	TECN	COMMENT
-0.9 ± 0.4 OUR FIT			
• • • We do not use the following data for averages, fits, limits, etc. • • •			
1.4 ± 0.5 ± 0.3	CRAWFORD	93	CLE2 See AMMAR 01

$\Sigma_c(2455)$ WIDTHS

$\Sigma_c(2455)^{++}$ WIDTH

VALUE (MeV)	EVTS	DOCUMENT ID	TECN	COMMENT
2.23 ± 0.30 OUR AVERAGE				
2.3 ± 0.2 ± 0.3	2k	ARTUSO	02	CLE2 $e^+e^- \approx \Upsilon(4S)$
2.05 ^{+0.41} _{-0.38} ± 0.38	1110	LINK	02	FOCS γ nucleus, $\overline{E}_\gamma \approx 180$ GeV

$\Sigma_c(2455)^+$ WIDTH

VALUE (MeV)	CL%	EVTS	DOCUMENT ID	TECN	COMMENT
<4.6	90	661	AMMAR	01	CLE2 $e^+e^- \approx \Upsilon(4S)$

$\Sigma_c(2455)^0$ WIDTH

VALUE (MeV)	EVTS	DOCUMENT ID	TECN	COMMENT
2.2 ± 0.4 OUR AVERAGE	Error includes scale factor of 1.4.			
2.5 ± 0.2 ± 0.3	2k	ARTUSO	02	CLE2 $e^+e^- \approx \Upsilon(4S)$
1.55 ^{+0.41} _{-0.37} ± 0.38	913	LINK	02	FOCS γ nucleus, $\overline{E}_\gamma \approx 180$ GeV

$\Sigma_c(2455)$ DECAY MODES

$\Lambda_c^+ \pi$ is the only strong decay allowed to a Σ_c having this mass.

Mode	Fraction (Γ_i/Γ)
$\Gamma_1 \Lambda_c^+ \pi$	$\approx 100\%$

$\Sigma_c(2455)$ REFERENCES

ARTUSO	02	PR D65 071101R	M. Artuso <i>et al.</i>	(CLEO Collab.)
LINK	02	PL B525 205	J.M. Link <i>et al.</i>	(FNAL FOCUS Collab.)
AMMAR	01	PRL 86 1167	R. Ammar <i>et al.</i>	(CLEO Collab.)
LINK	00C	PL B488 218	J.M. Link <i>et al.</i>	(FNAL FOCUS Collab.)
AITALA	96B	PL B379 292	E.M. Aitala <i>et al.</i>	(FNAL E791 Collab.)
ALEEVE	96	JINRRC 3-77 31	A.N. Aleev <i>et al.</i>	(Serpukhov EXCHARM Collab.)
FRABETTI	96	PL B365 461	P.L. Frabetti <i>et al.</i>	(FNAL E687 Collab.)
CRAWFORD	93	PRL 71 3259	G. Crawford <i>et al.</i>	(CLEO Collab.)
ANJOS	89D	PRL 62 1721	J.C. Anjos <i>et al.</i>	(FNAL E691 Collab.)
BOWCOCK	89	PRL 62 1240	T.J.V. Bowcock <i>et al.</i>	(CLEO Collab.)
ALBRECHT	88D	PL B211 489	H. Albrecht <i>et al.</i>	(ARGUS Collab.)
DIESBURG	87	PRL 59 2711	M. Diesburg <i>et al.</i>	(FNAL E400 Collab.)
JONES	87	ZPHY C36 593	G.T. Jones <i>et al.</i>	(CERN WA21 Collab.)
AMMAR	86	JETPL 43 515	R. Ammar <i>et al.</i>	(ITEP)
Translated from ZETFP 43 401.				
BOSETTI	82	PL 109B 234	P.C. Bosetti <i>et al.</i>	(AACH3, BONN, CERN+)
CALICCHIO	80	PL 93B 521	M. Calicchio <i>et al.</i>	(BARI, BIRM, BRUX+)
BALTAY	79	PRL 42 1721	C. Baltay <i>et al.</i>	(COLU, BNL)
CAZZOLI	75	PRL 34 1125	E.G. Cazzoli <i>et al.</i>	(BNL)

$\Sigma_c(2520)$

$I(J^P) = 1(\frac{3}{2}^+)$ Status: ***

Seen in the $\Lambda_c^+ \pi^+$ mass spectrum. The natural assignment is that this is the $J^P = 3/2^+$ excitation of the $\Sigma_c(2455)$, the charm counterpart of the $\Sigma(1385)$, but neither J nor P has been measured.

$\Sigma_c(2520)$ MASSES

The masses are obtained from the mass-difference measurements that follow.

$\Sigma_c(2520)^{++}$ MASS

VALUE (MeV)	EVTS	DOCUMENT ID	TECN	COMMENT
2518.4 ± 0.6 OUR FIT	Error includes scale factor of 1.4.			
• • • We do not use the following data for averages, fits, limits, etc. • • •				
2530 ± 5 ± 5	6	¹ AMMOSOV	93	HLBC $\nu p \rightarrow \mu^- \Sigma_c(2530)^{++}$

¹ AMMOSOV 93 sees a cluster of 6 events and estimates the background to be 1 event.

$\Sigma_c(2520)^+$ MASS

VALUE (MeV)	DOCUMENT ID
2517.5 ± 2.3 OUR FIT	

$\Sigma_c(2520)^0$ MASS

VALUE (MeV)	DOCUMENT ID
2518.0 ± 0.5 OUR FIT	

$\Sigma_c(2520)$ MASS DIFFERENCES

$m_{\Sigma_c(2520)^{++}} - m_{\Lambda_c^+}$

VALUE (MeV)	EVTS	DOCUMENT ID	TECN	COMMENT
231.9 ± 0.6 OUR FIT	Error includes scale factor of 1.5.			
231.9 ± 1.0 OUR AVERAGE	Error includes scale factor of 2.1.			
231.5 ± 0.4 ± 0.3	1330 ± 110	ATHAR	05	CLEO e^+e^- , 9.4–11.5 GeV
234.5 ± 1.1 ± 0.8	677	BRANDENB...	97	CLE2 $e^+e^- \approx \Upsilon(4S)$

$m_{\Sigma_c(2520)^+} - m_{\Lambda_c^+}$

VALUE (MeV)	EVTS	DOCUMENT ID	TECN	COMMENT
231.0 ± 2.3 OUR FIT				
231.0 ± 1.1 ± 2.0	327	AMMAR	01	CLE2 $e^+e^- \approx \Upsilon(4S)$

$m_{\Sigma_c(2520)^0} - m_{\Lambda_c^+}$

VALUE (MeV)	EVTS	DOCUMENT ID	TECN	COMMENT
231.6 ± 0.5 OUR FIT	Error includes scale factor of 1.1.			
231.6 ± 0.5 OUR AVERAGE				
231.4 ± 0.5 ± 0.3	1350 ± 120	ATHAR	05	CLEO e^+e^- , 9.4–11.5 GeV
232.6 ± 1.0 ± 0.8	504	BRANDENB...	97	CLE2 $e^+e^- \approx \Upsilon(4S)$

$m_{\Sigma_c(2520)^{++}} - m_{\Sigma_c(2520)^0}$

VALUE (MeV)	DOCUMENT ID	TECN	COMMENT
0.3 ± 0.6 OUR FIT	Error includes scale factor of 1.2.		
0.5 ± 0.8 OUR AVERAGE			
+0.1 ± 0.8 ± 0.3	² ATHAR	05	CLEO e^+e^- , 9.4–11.5 GeV
1.9 ± 1.4 ± 1.0	³ BRANDENB...	97	CLE2 $e^+e^- \approx \Upsilon(4S)$

² This ATHAR 05 result is redundant with measurements in earlier entries.

³ This BRANDENBURG 97 result is redundant with measurements in earlier entries.

$\Sigma_c(2520)$ WIDTHS

$\Sigma_c(2520)^{++}$ WIDTH

VALUE (MeV)	EVTS	DOCUMENT ID	TECN	COMMENT
14.9 ± 1.9 OUR AVERAGE				
14.4 ^{+1.6} _{-1.5} ± 1.4	1330 ± 110	ATHAR	05	CLEO e^+e^- , 9.4–11.5 GeV
17.9 ^{+3.8} _{-3.2} ± 4.0	677	BRANDENB...	97	CLE2 $e^+e^- \approx \Upsilon(4S)$

Baryon Particle Listings

 $\Sigma_c(2520), \Sigma_c(2800), \Xi_c^+$ $\Sigma_c(2520)^+$ WIDTH

VALUE (MeV)	CL%	EVTS	DOCUMENT ID	TECN	COMMENT
<17	90	327	AMMAR	01	CLE2 $e^+e^- \approx \Upsilon(4S)$

 $\Sigma_c(2520)^0$ WIDTH

VALUE (MeV)	CL%	EVTS	DOCUMENT ID	TECN	COMMENT
16.1 ± 2.1 OUR AVERAGE					
16.6 ^{+1.9} _{-1.7} ± 1.4		1350 ± 120	ATHAR	05	CLEO e^+e^- , 9.4–11.5 GeV
13.0 ^{+3.7} _{-3.0} ± 4.0		504	BRANDENB...	97	CLE2 $e^+e^- \approx \Upsilon(4S)$

 $\Sigma_c(2520)$ DECAY MODES

$\Lambda_c^+ \pi$ is the only strong decay allowed to a Σ_c having this mass.

Mode	Fraction (Γ_i/Γ)
$\Gamma_1 \Lambda_c^+ \pi$	≈ 100 %

 $\Sigma_c(2520)$ REFERENCES

ATHAR	05	PR D71 051101R	S.B. Athar <i>et al.</i>	(CLEO Collab.)
AMMAR	01	PRL 86 1167	R. Ammar <i>et al.</i>	(CLEO Collab.)
BRANDENB...	97	PRL 78 2304	G. Brandenburg <i>et al.</i>	(CLEO Collab.)
AMMOSOV	93	JETPL 58 247	V.V. Ammosov <i>et al.</i>	(SERP)
Translated from ZETFP 58 241.				

 $\Sigma_c(2800)$

$$I(J^P) = 1(??) \quad \text{Status: } ***$$

Seen in the $\Lambda_c^+ \pi^+$, $\Lambda_c^+ \pi^0$, and $\Lambda_c^+ \pi^-$ mass spectra.

 $\Sigma_c(2800)$ MASSES

The masses are obtained from the mass-difference measurements that follow.

 $\Sigma_c(2800)^{++}$ MASS

VALUE (MeV)	DOCUMENT ID
-------------	-------------

2801⁺⁴₋₆ OUR FIT $\Sigma_c(2800)^+$ MASS

VALUE (MeV)	DOCUMENT ID
-------------	-------------

2792⁺¹⁴₋₅ OUR FIT $\Sigma_c(2800)^0$ MASS

VALUE (MeV)	DOCUMENT ID
-------------	-------------

2802⁺⁴₋₇ OUR FIT $\Sigma_c(2800)$ MASS DIFFERENCES $m_{\Sigma_c(2800)^{++}} - m_{\Lambda_c^+}$

VALUE (MeV)	EVTS	DOCUMENT ID	TECN	COMMENT
-------------	------	-------------	------	---------

514⁺⁴₋₆ OUR FIT

514.5 ^{+3.4} _{-3.1} ± 2.8 -4.9	2810 ⁺¹⁰⁹⁰ ₋₇₇₅	MIZUK	05	BELL $e^+e^- \approx \Upsilon(4S)$
---	---------------------------------------	-------	----	------------------------------------

 $m_{\Sigma_c(2800)^+} - m_{\Lambda_c^+}$

VALUE (MeV)	EVTS	DOCUMENT ID	TECN	COMMENT
-------------	------	-------------	------	---------

505⁺¹⁴₋₅ OUR FIT

505.4 ^{+5.8} _{-4.6} ± 12.4 -2.0	1540 ⁺¹⁷⁵⁰ ₋₁₀₅₀	MIZUK	05	BELL $e^+e^- \approx \Upsilon(4S)$
--	--	-------	----	------------------------------------

 $m_{\Sigma_c(2800)^0} - m_{\Lambda_c^+}$

VALUE (MeV)	EVTS	DOCUMENT ID	TECN	COMMENT
-------------	------	-------------	------	---------

515⁺⁴₋₇ OUR FIT

515.4 ^{+3.2} _{-3.1} ± 2.1 -6.0	2240 ⁺¹³⁰⁰ ₋₇₄₀	MIZUK	05	BELL $e^+e^- \approx \Upsilon(4S)$
---	---------------------------------------	-------	----	------------------------------------

 $\Sigma_c(2800)$ WIDTHS $\Sigma_c(2800)^{++}$ WIDTH

VALUE (MeV)	EVTS	DOCUMENT ID	TECN	COMMENT
-------------	------	-------------	------	---------

75 ⁺¹⁸ ₋₁₃ ± 12 -11	2810 ⁺¹⁰⁹⁰ ₋₇₇₅	MIZUK	05	BELL $e^+e^- \approx \Upsilon(4S)$
--	---------------------------------------	-------	----	------------------------------------

 $\Sigma_c(2800)^+$ WIDTH

VALUE (MeV)	EVTS	DOCUMENT ID	TECN	COMMENT
-------------	------	-------------	------	---------

62 ⁺³⁷ ₋₂₃ ± 52 -38	1540 ⁺¹⁷⁵⁰ ₋₁₀₅₀	MIZUK	05	BELL $e^+e^- \approx \Upsilon(4S)$
--	--	-------	----	------------------------------------

 $\Sigma_c(2800)^0$ WIDTH

VALUE (MeV)	EVTS	DOCUMENT ID	TECN	COMMENT
61 ⁺¹⁸ ₋₁₃ ± 22 -13	2240 ⁺¹³⁰⁰ ₋₇₄₀	MIZUK	05	BELL $e^+e^- \approx \Upsilon(4S)$

 $\Sigma_c(2800)$ DECAY MODES

Mode	Fraction (Γ_i/Γ)
$\Gamma_1 \Lambda_c^+ \pi$	seen

 $\Sigma_c(2800)$ REFERENCES

MIZUK	05	PRL 94 122002	R. Mizuk <i>et al.</i>	(BELLE Collab.)
-------	----	---------------	------------------------	-----------------



$$I(J^P) = \frac{1}{2}(\frac{1}{2}^+) \quad \text{Status: } ***$$

According to the quark model, the Ξ_c^+ (quark content usc) and Ξ_c^0 form an isospin doublet, and the spin-parity ought to be $J^P = 1/2^+$. None of I , J , or P has actually been measured.

 Ξ_c^+ MASS

The fit uses the Ξ_c^+ and Ξ_c^0 mass and mass-difference measurements.

VALUE (MeV)	EVTS	DOCUMENT ID	TECN	COMMENT
-------------	------	-------------	------	---------

2467.9 ± 0.4 OUR FIT**2467.6^{+0.4}_{-1.0}** OUR AVERAGE

2468.1 ± 0.4 ^{+0.2} _{-1.4}	4950 ± 286	¹ LESIAK	05	BELL e^+e^- , $\Upsilon(4S)$
2465.8 ± 1.9 ± 2.5	90	FRABETTI	98	E687 γ Be, $\overline{E}_\gamma = 220$ GeV
2467.0 ± 1.6 ± 2.0	147	EDWARDS	96	CLE2 $e^+e^- \approx \Upsilon(4S)$
2465.1 ± 3.6 ± 1.9	30	ALBRECHT	90F	ARG e^+e^- at $\Upsilon(4S)$
2467 ± 3 ± 4	23	ALAM	89	CLEO e^+e^- 10.6 GeV
2466.5 ± 2.7 ± 1.2	5	BARLAG	89c	ACCM π^- Cu 230 GeV
• • • We do not use the following data for averages, fits, limits, etc. • • •				
2464.4 ± 2.0 ± 1.4	30	FRABETTI	93B	E687 See FRABETTI 98
2459 ± 5 ± 30	56	² COTEUS	87	SPEC $nA \approx 600$ GeV
2460 ± 25	82	BIAGI	83	SPEC Σ^- Be 135 GeV

¹ The systematic error was (wrongly) given the other way round in LESIAK 05; see the erratum.

² Although COTEUS 87 claims to agree well with BIAGI 83 on the mass and width, there appears to be a discrepancy between the two experiments. BIAGI 83 sees a single peak (stated significance about 6 standard deviations) in the $\Lambda K^- \pi^+ \pi^+$ mass spectrum. COTEUS 87 sees *two* peaks in the same spectrum, one at the Ξ_c^+ mass, the other 75 MeV lower. The latter is attributed to $\Xi_c^+ \rightarrow \Sigma^0 K^- \pi^+ \pi^+ \rightarrow (\Lambda \gamma) K^- \pi^+ \pi^+$, with the γ unseen. The *combined* significance of the double peak is stated to be 5.5 standard deviations. But the absence of any trace of a lower peak in BIAGI 83 seems to us to throw into question the interpretation of the lower peak of COTEUS 87.

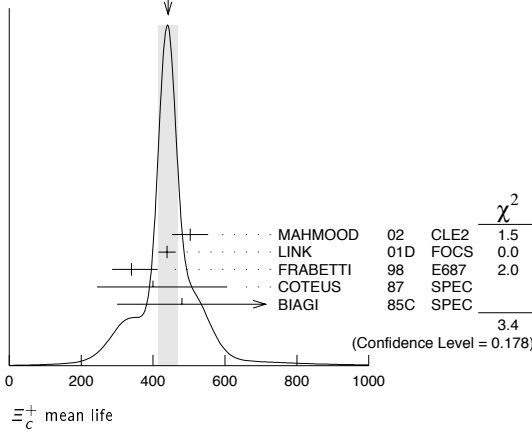
 Ξ_c^+ MEAN LIFE

VALUE (10^{-15} s)	EVTS	DOCUMENT ID	TECN	COMMENT
-----------------------	------	-------------	------	---------

442 ± 26 OUR AVERAGE Error includes scale factor of 1.3. See the ideogram below.

503 ± 47 ± 18	250	MAHMOOD	02	CLE2 $e^+e^- \approx \Upsilon(4S)$
439 ± 22 ± 9	532	LINK	01D	FOCS γ nucleus, $\overline{E}_\gamma \approx 180$ GeV
340 ⁺⁷⁰ ₋₅₀ ± 20	56	FRABETTI	98	E687 γ Be, $\overline{E}_\gamma = 220$ GeV
400 ⁺¹⁸⁰ ₋₁₂₀ ± 100	102	COTEUS	87	SPEC $nA \approx 600$ GeV
480 ⁺²¹⁰ ₋₁₅₀ ± 200 -100	53	BIAGI	85c	SPEC Σ^- Be 135 GeV
• • • We do not use the following data for averages, fits, limits, etc. • • •				
410 ⁺¹¹⁰ ₋₈₀ ± 20	30	FRABETTI	93B	E687 See FRABETTI 98
200 ⁺¹¹⁰ ₋₆₀	6	BARLAG	89c	ACCM π^- (K^-) Cu 230 GeV

WEIGHTED AVERAGE
442±26 (Error scaled by 1.3)



Ξ_c^+ DECAY MODES

Mode	Fraction (Γ_i/Γ)	Confidence level
------	--------------------------------	------------------

No absolute branching fractions have been measured.
The following are branching ratios relative to $\Xi_c^+ \pi^+ \pi^+$.

Cabibbo-favored ($S = -2$) decays

Γ_1	$p K_S^0 K_S^0$	[a]	0.087 ± 0.022	
Γ_2	$\Lambda \bar{K}^0 \pi^+$		—	
Γ_3	$\Sigma(1385)^+ \bar{K}^0$	[a,b]	1.0 ± 0.5	
Γ_4	$\Lambda K^- \pi^+ \pi^+$	[a]	0.323 ± 0.033	
Γ_5	$\Lambda \bar{K}^*(892)^0 \pi^+$	[a,b]	<0.2	90%
Γ_6	$\Sigma(1385)^+ K^- \pi^+$	[a,b]	<0.3	90%
Γ_7	$\Sigma^+ K^- \pi^+$	[a]	0.94 ± 0.11	
Γ_8	$\Sigma^+ \bar{K}^*(892)^0$	[a,b]	0.81 ± 0.15	
Γ_9	$\Sigma^0 K^- \pi^+ \pi^+$	[a]	0.29 ± 0.16	
Γ_{10}	$\Xi^0 \pi^+$	[a]	0.55 ± 0.16	
Γ_{11}	$\Xi^- \pi^+ \pi^+$	[a]	DEFINED AS 1	
Γ_{12}	$\Xi(1530)^0 \pi^+$	[a,b]	<0.1	90%
Γ_{13}	$\Xi^0 \pi^+ \pi^0$	[a]	2.34 ± 0.68	
Γ_{14}	$\Xi^0 \pi^+ \pi^+ \pi^-$	[a]	1.74 ± 0.50	
Γ_{15}	$\Xi^0 e^+ \nu_e$	[a]	2.3 ± 0.7 -0.9	
Γ_{16}	$\Omega^- K^+ \pi^+$	[a]	0.07 ± 0.04	

Cabibbo-suppressed decays

Γ_{17}	$p K^- \pi^+$	[a]	0.21 ± 0.03	
Γ_{18}	$p \bar{K}^*(892)^0$	[a,b]	0.12 ± 0.02	
Γ_{19}	$\Sigma^+ K^+ K^-$	[a]	0.15 ± 0.07	
Γ_{20}	$\Sigma^+ \phi$	[a,b]	<0.11	90%
Γ_{21}	$\Xi(1690)^0 K^+, \Xi(1690)^0 \rightarrow \Sigma^+ K^-$	[a]	<0.05	90%

[a] No absolute branching fractions have been measured. The value here is the branching ratio relative to $\Xi_c^+ \pi^+ \pi^+$.

[b] This branching fraction includes all the decay modes of the final-state resonance.

Ξ_c^+ BRANCHING RATIOS

Cabibbo-favored ($S = -2$) decays

VALUE	EVTs	DOCUMENT ID	TECN	COMMENT	Γ_1/Γ_{11}
$0.087 \pm 0.016 \pm 0.014$	168 ± 27	LESIAK	05 BELL	$e^+ e^-$, $\Upsilon(4S)$	

VALUE	EVTs	DOCUMENT ID	TECN	COMMENT	Γ_3/Γ_{11}
$1.00 \pm 0.49 \pm 0.24$	20	LINK	03E FOCS	< 1.72, 90% CL	

VALUE	EVTs	DOCUMENT ID	TECN	COMMENT	Γ_4/Γ_{11}
0.323 ± 0.033 OUR AVERAGE					
$0.32 \pm 0.03 \pm 0.02$	1177 ± 55	LESIAK	05 BELL	$e^+ e^-$, $\Upsilon(4S)$	
$0.28 \pm 0.06 \pm 0.06$	58	LINK	03E FOCS	γ nucleus, $\bar{E}_\gamma \approx 180$ GeV	
$0.58 \pm 0.16 \pm 0.07$	61	BERGFELD	96 CLE2	$e^+ e^- \approx \Upsilon(4S)$	

VALUE	EVTs	DOCUMENT ID	TECN	COMMENT	Γ_4/Γ_{11}
$0.32 \pm 0.03 \pm 0.02$	1177 ± 55	LESIAK	05 BELL	$e^+ e^-$, $\Upsilon(4S)$	
$0.28 \pm 0.06 \pm 0.06$	58	LINK	03E FOCS	γ nucleus, $\bar{E}_\gamma \approx 180$ GeV	
$0.58 \pm 0.16 \pm 0.07$	61	BERGFELD	96 CLE2	$e^+ e^- \approx \Upsilon(4S)$	

$\Gamma(\Lambda \bar{K}^*(892)^0 \pi^+)/\Gamma(\Lambda K^- \pi^+ \pi^+)$ Γ_5/Γ_4

Unseen decay modes of the $\bar{K}^*(892)^0$ are included.

VALUE	CL%	DOCUMENT ID	TECN	COMMENT
<0.5	90	BERGFELD	96 CLE2	$e^+ e^- \approx \Upsilon(4S)$

$\Gamma(\Sigma(1385)^+ K^- \pi^+)/\Gamma(\Lambda K^- \pi^+ \pi^+)$ Γ_6/Γ_4

Unseen decay modes of the $\Sigma(1385)^+$ are included.

VALUE	CL%	DOCUMENT ID	TECN	COMMENT
<0.7	90	BERGFELD	96 CLE2	$e^+ e^- \approx \Upsilon(4S)$

$\Gamma(\Sigma^+ K^- \pi^+)/\Gamma(\Xi^- \pi^+ \pi^+)$ Γ_7/Γ_{11}

VALUE	EVTs	DOCUMENT ID	TECN	COMMENT
0.94 ± 0.11 OUR AVERAGE				

$0.91 \pm 0.11 \pm 0.04$	251	LINK	03E FOCS	γ nucleus, $\bar{E}_\gamma \approx 180$ GeV
$1.18 \pm 0.26 \pm 0.17$	119	BERGFELD	96 CLE2	$e^+ e^- \approx \Upsilon(4S)$

••• We do not use the following data for averages, fits, limits, etc. •••

$0.92 \pm 0.20 \pm 0.07$	3 JUN	00 SELX	Σ^- nucleus, 600 GeV
--------------------------	----------	---------	-----------------------------

3 This JUN 00 result is redundant with other results given below.

$\Gamma(\Sigma^+ \bar{K}^*(892)^0)/\Gamma(\Xi^- \pi^+ \pi^+)$ Γ_8/Γ_{11}

Unseen decay modes of the $\bar{K}^*(892)^0$ are included.

VALUE	EVTs	DOCUMENT ID	TECN	COMMENT
0.81 ± 0.15 OUR AVERAGE				

$0.78 \pm 0.16 \pm 0.06$	119	LINK	03E FOCS	γ nucleus, $\bar{E}_\gamma \approx 180$ GeV
$0.92 \pm 0.27 \pm 0.14$	61	BERGFELD	96 CLE2	$e^+ e^- \approx \Upsilon(4S)$

••• We do not use the following data for averages, fits, limits, etc. •••

seen	59	AVERY	95 CLE2	$e^+ e^- \approx \Upsilon(4S)$
------	----	-------	---------	--------------------------------

$\Gamma(\Sigma^0 K^- \pi^+ \pi^+)/\Gamma(\Lambda K^- \pi^+ \pi^+)$ Γ_9/Γ_4

VALUE	EVTs	DOCUMENT ID	TECN	COMMENT
0.84 ± 0.36	47	4 COTEUS	87 SPEC	$nA \approx 600$ GeV

4 See, however, the note on the COTEUS 87 Ξ_c^+ mass measurement.

$\Gamma(\Xi^0 \pi^+)/\Gamma(\Xi^- \pi^+ \pi^+)$ Γ_{10}/Γ_{11}

VALUE	EVTs	DOCUMENT ID	TECN	COMMENT
0.55 ± 0.13 ± 0.09	39	EDWARDS	96 CLE2	$e^+ e^- \approx \Upsilon(4S)$

$\Gamma(\Xi^- \pi^+ \pi^+)/\Gamma_{total}$ Γ_{11}/Γ

VALUE	EVTs	DOCUMENT ID	TECN	COMMENT
••• We do not use the following data for averages, fits, limits, etc. •••				

seen	131	BERGFELD	96 CLE2	$e^+ e^- \approx \Upsilon(4S)$
seen	160	AVERY	95 CLE2	$e^+ e^- \approx \Upsilon(4S)$
seen	30	FRABETTI	93B E687	γ Be, $\bar{E}_\gamma \approx 220$ GeV
seen	30	ALBRECHT	90F ARG	$e^+ e^-$ at $\Upsilon(4S)$
seen	23	ALAM	89 CLEO	$e^+ e^-$ 10.6 GeV

$\Gamma(\Xi(1530)^0 \pi^+)/\Gamma(\Xi^- \pi^+ \pi^+)$ Γ_{12}/Γ_{11}

Unseen decay modes of the $\Xi(1530)^0$ are included.

VALUE	CL%	DOCUMENT ID	TECN	COMMENT
<0.1	90	LINK	03E FOCS	γ nucleus, $\bar{E}_\gamma \approx 180$ GeV

••• We do not use the following data for averages, fits, limits, etc. •••

<0.2	90	BERGFELD	96 CLE2	$e^+ e^- \approx \Upsilon(4S)$
------	----	----------	---------	--------------------------------

$\Gamma(\Xi^0 \pi^+ \pi^0)/\Gamma(\Xi^- \pi^+ \pi^+)$ Γ_{13}/Γ_{11}

VALUE	EVTs	DOCUMENT ID	TECN	COMMENT
2.34 ± 0.57 ± 0.37	81	EDWARDS	96 CLE2	$e^+ e^- \approx \Upsilon(4S)$

$\Gamma(\Xi(1530)^0 \pi^+)/\Gamma(\Xi^0 \pi^+ \pi^0)$ Γ_{12}/Γ_{13}

VALUE	CL%	DOCUMENT ID	TECN	COMMENT
••• We do not use the following data for averages, fits, limits, etc. •••				

<0.3	90	EDWARDS	96 CLE2	$e^+ e^- \approx \Upsilon(4S)$
------	----	---------	---------	--------------------------------

$\Gamma(\Xi^0 \pi^+ \pi^+ \pi^-)/\Gamma(\Xi^- \pi^+ \pi^+)$ Γ_{14}/Γ_{11}

VALUE	EVTs	DOCUMENT ID	TECN	COMMENT
1.74 ± 0.42 ± 0.27	57	EDWARDS	96 CLE2	$e^+ e^- \approx \Upsilon(4S)$

$\Gamma(\Xi^0 e^+ \nu_e)/\Gamma(\Xi^- \pi^+ \pi^+)$ Γ_{15}/Γ_{11}

VALUE	EVTs	DOCUMENT ID	TECN	COMMENT
2.3 ± 0.6 ± 0.3 -0.6	41	ALEXANDER	95B CLE2	$e^+ e^- \approx \Upsilon(4S)$

$\Gamma(\Omega^- K^+ \pi^+)/\Gamma(\Xi^- \pi^+ \pi^+)$ Γ_{16}/Γ_{11}

VALUE	EVTs	DOCUMENT ID	TECN	COMMENT
0.07 ± 0.03 ± 0.03	14	LINK	03E FOCS	< 0.12, 90% CL

Cabibbo-suppressed decays

$\Gamma(p K^- \pi^+)/\Gamma(\Sigma^+ K^- \pi^+)$ Γ_{17}/Γ_7

VALUE	EVTs	DOCUMENT ID	TECN	COMMENT
••• We do not use the following data for averages, fits, limits, etc. •••				

$0.22 \pm 0.06 \pm 0.03$	76	JUN	00 SELX	Σ^- nucleus, 600 GeV
--------------------------	----	-----	---------	-----------------------------

Baryon Particle Listings

$$\Xi_c^+, \Xi_c^0$$

$\Gamma(\rho K^- \pi^+)/\Gamma(\Xi^- \pi^+ \pi^+)$		Γ_{17}/Γ_{11}	
VALUE	EVTS	DOCUMENT ID	TECN COMMENT
0.214 ± 0.034 OUR AVERAGE			
0.234 ± 0.047 ± 0.022	202	LINK	01B FOCS γ nucleus
0.20 ± 0.04 ± 0.02	76	JUN	00 SELX Σ^- nucleus, 600 GeV

$\Gamma(\rho \bar{K}^*(892)^0)/\Gamma(\rho K^- \pi^+)$		Γ_{18}/Γ_{17}	
VALUE	EVTS	DOCUMENT ID	TECN COMMENT
Unseen decay modes of the $\bar{K}^*(892)^0$ are included.			
0.54 ± 0.09 ± 0.05			
		LINK	01B FOCS γ nucleus

$\Gamma(\Sigma^+ K^+ K^-)/\Gamma(\Sigma^+ K^- \pi^+)$		Γ_{19}/Γ_7	
VALUE	EVTS	DOCUMENT ID	TECN COMMENT
0.16 ± 0.06 ± 0.01			
	17	LINK	03E FOCS γ nucleus, $\bar{E}_\gamma \approx 180$ GeV

$\Gamma(\Sigma^+ \phi)/\Gamma(\Sigma^+ K^- \pi^+)$		Γ_{20}/Γ_7	
VALUE	CL%	DOCUMENT ID	TECN COMMENT
Unseen decay modes of the ϕ are included.			
<0.12			
	90	LINK	03E FOCS γ nucleus, $\bar{E}_\gamma \approx 180$ GeV

$\Gamma(\Xi(1690)^0 K^+ \times B(\Xi(1690)^0 \rightarrow \Sigma^+ K^-))/\Gamma(\Sigma^+ K^- \pi^+)$		Γ_{21}/Γ_7	
VALUE	CL%	DOCUMENT ID	TECN COMMENT
<0.05			
	90	LINK	03E FOCS γ nucleus, $\bar{E}_\gamma \approx 180$ GeV

Ξ_c^\pm REFERENCES

LESIAK	05	PL B605 237	T. Lesiak et al.	(BELLE Collab.)
Also		PL B617 198 (erratum)	T. Lesiak et al.	(BELLE Collab.)
LINK	03E	PL B571 139	J.M. Link et al.	(FNAL FOCUS Collab.)
MAHMOOD	02	PR D65 031102	A.H. Mahmood et al.	(CLEO Collab.)
LINK	01B	PL B512 277	J.M. Link et al.	(FNAL FOCUS Collab.)
LINK	01D	PL B523 53	J.M. Link et al.	(FNAL FOCUS Collab.)
JUN	00	PRL 84 1857	S.Y. Jun et al.	(FNAL SLEX Collab.)
FRABETTI	98	PL B427 211	P.L. Frabetti et al.	(FNAL E687 Collab.)
BERGFELD	96	PL B365 431	T. Bergfeld et al.	(CLEO Collab.)
EDWARDS	96	PL B373 261	K.W. Edwards et al.	(CLEO Collab.)
ALEXANDER	95B	PRL 74 3113	J. Alexander et al.	(CLEO Collab.)
Also		PRL 75 4155 (erratum)	J. Alexander et al.	(CLEO Collab.)
AVERY	95	PRL 75 4364	P. Avery et al.	(CLEO Collab.)
FRABETTI	93B	PRL 70 1381	P.L. Frabetti et al.	(FNAL E687 Collab.)
ALBRECHT	90F	PL B247 121	H. Albrecht et al.	(ARGUS Collab.)
ALAM	89	PL B226 401	M.S. Alam et al.	(CLEO Collab.)
BARLAG	89C	PL B233 522	S. Barlag et al.	(ACCMOR Collab.)
COTEUS	87	PRL 59 1530	P. Coteus et al.	(FNAL E400 Collab.)
BIAGI	85C	PL 150B 230	S.F. Biagi et al.	(CERN WA62 Collab.)
BIAGI	83	PL 122B 455	S.F. Biagi et al.	(CERN WA62 Collab.)

$$\Xi_c^0$$

$$I(J^P) = \frac{1}{2}(1/2^+)$$
 Status: ***

According to the quark model, the Ξ_c^0 (quark content dsc) and Ξ_c^\pm form an isospin doublet, and the spin-parity ought to be $J^P = 1/2^+$. None of I , J , or P has actually been measured.

Ξ_c^0 MASS

The fit uses the Ξ_c^0 and Ξ_c^\pm mass and mass-difference measurements.

VALUE (MeV)	EVTS	DOCUMENT ID	TECN	COMMENT
2471.0 ± 0.4 OUR FIT				
2471.09 ± 0.35 ± 1.00 OUR AVERAGE				
2471.0 ± 0.3 ± 0.2 ± 1.4	8620 ± 355	¹ LESIAK	05 BELL	$e^+ e^-$, $\mathcal{T}(4S)$
2470.0 ± 2.8 ± 2.6	85	FRABETTI	98B E687	γ Be, $\bar{E}_\gamma = 220$ GeV
2469 ± 2 ± 3	9	HENDERSON	92B CLEO	$\Omega^- K^+$
2472.1 ± 2.7 ± 1.6	54	ALBRECHT	90F ARG	$e^+ e^-$ at $\mathcal{T}(4S)$
2473.3 ± 1.9 ± 1.2	4	BARLAG	90 ACCM	$\pi^- (K^-)$ Cu 230
2472 ± 3 ± 4	19	ALAM	89 CLEO	$e^+ e^-$ 10.6 GeV
••• We do not use the following data for averages, fits, limits, etc. •••				
2462.1 ± 3.1 ± 1.4	42	² FRABETTI	93C E687	See FRABETTI 98B
2471 ± 3 ± 4	14	AVERY	89 CLEO	See ALAM 89

¹ The systematic error was (wrongly) given the other way round in LESIAK 05.

² The FRABETTI 93C mass is well below the other measurements.

$\Xi_c^0 - \Xi_c^\pm$ MASS DIFFERENCE

VALUE (MeV)	DOCUMENT ID	TECN	COMMENT
3.1 ± 0.5 OUR FIT			
3.1 ± 0.5 OUR AVERAGE			
+2.9 ± 0.5	LESIAK	05 BELL	$e^+ e^-$, $\mathcal{T}(4S)$
+7.0 ± 4.5 ± 2.2	ALBRECHT	90F ARG	$e^+ e^-$ at $\mathcal{T}(4S)$
+6.8 ± 3.3 ± 0.5	BARLAG	90 ACCM	$\pi^- (K^-)$ Cu 230 GeV
+5 ± 4 ± 1	ALAM	89 CLEO	$\Xi_c^0 \rightarrow \Xi^- \pi^+, \Xi_c^\pm \rightarrow \Xi^\mp \pi^+ \pi^+$

Ξ_c^0 MEAN LIFE

VALUE (10^{-15} s)	EVTS	DOCUMENT ID	TECN	COMMENT
112⁺¹³₋₁₀ OUR AVERAGE				
118 ⁺¹⁴ ₋₁₂ ± 5	110	LINK	02H FOCS	γ nucleus, ≈ 180 GeV
101 ⁺²⁵ ₋₁₇ ± 5	42	FRABETTI	93C E687	γ Be, $\bar{E}_\gamma = 220$ GeV
82 ⁺⁵⁹ ₋₃₀	4	BARLAG	90 ACCM	$\pi^- (K^-)$ Cu 230 GeV

Ξ_c^0 DECAY MODES

No absolute branching fractions have been measured. Several measurements of ratios of fractions may be found in the Listings that follow.

Mode	Fraction (Γ_i/Γ)
Γ_1 $\rho K^- K^- \pi^+$	seen
Γ_2 $\rho K^- \bar{K}^*(892)^0$	seen
Γ_3 $\rho K^- K^- \pi^+$ no $\bar{K}^*(892)^0$	seen
Γ_4 ΛK_S^0	seen
Γ_5 $\Lambda K^- \pi^+$	
Γ_6 $\Lambda \bar{K}^0 \pi^+ \pi^-$	seen
Γ_7 $\Lambda K^- \pi^+ \pi^+ \pi^-$	seen
Γ_8 $\Xi^- \pi^+$	seen
Γ_9 $\Xi^- \pi^+ \pi^+ \pi^-$	seen
Γ_{10} $\Omega^- K^+$	seen
Γ_{11} $\Xi^- e^+ \nu_e$	seen
Γ_{12} $\Xi^- \ell^+$ anything	seen

Ξ_c^0 BRANCHING RATIOS

$\Gamma(\rho K^- K^- \pi^+)/\Gamma(\Xi^- \pi^+)$		Γ_1/Γ_8	
VALUE	EVTS	DOCUMENT ID	TECN COMMENT
0.34 ± 0.04 OUR AVERAGE			
0.33 ± 0.03 ± 0.03	1908 ± 62	LESIAK	05 BELL $e^+ e^-$, $\mathcal{T}(4S)$
0.35 ± 0.06 ± 0.03	148 ± 18	DANKO	04 CLEO $e^+ e^-$

$\Gamma(\rho K^- \bar{K}^*(892)^0)/\Gamma(\Xi^- \pi^+)$		Γ_2/Γ_8	
VALUE	EVTS	DOCUMENT ID	TECN COMMENT
Unseen decay modes of the $\bar{K}^*(892)^0$ are included.			
0.210 ± 0.045 ± 0.015			
		DANKO	04 CLEO $e^+ e^-$
••• We do not use the following data for averages, fits, limits, etc. •••			
		BARLAG	90 ACCM $\pi^- (K^-)$ Cu 230 GeV

$\Gamma(\rho K^- K^- \pi^+ \text{ no } \bar{K}^*(892)^0)/\Gamma(\Xi^- \pi^+)$		Γ_3/Γ_8	
VALUE	EVTS	DOCUMENT ID	TECN COMMENT
0.21 ± 0.04 ± 0.02			
		DANKO	04 CLEO $e^+ e^-$

$\Gamma(\Lambda K_S^0)/\Gamma(\Xi^- \pi^+)$		Γ_4/Γ_8	
VALUE	EVTS	DOCUMENT ID	TECN COMMENT
0.21 ± 0.02 ± 0.02			
465 ± 37		LESIAK	05 BELL $e^+ e^-$, $\mathcal{T}(4S)$
••• We do not use the following data for averages, fits, limits, etc. •••			
	7	ALBRECHT	95B ARG $e^+ e^- \approx 10.4$ GeV

$\Gamma(\Lambda K^- \pi^+)/\Gamma(\Xi^- \pi^+)$		Γ_5/Γ_8	
VALUE	EVTS	DOCUMENT ID	TECN COMMENT
1.07 ± 0.12 ± 0.07			
2979 ± 211		LESIAK	05 BELL $e^+ e^-$, $\mathcal{T}(4S)$

$\Gamma(\Lambda \bar{K}^0 \pi^+ \pi^-)/\Gamma_{\text{total}}$		Γ_6/Γ	
VALUE	EVTS	DOCUMENT ID	TECN COMMENT
seen			
		FRABETTI	98B E687 γ Be, $\bar{E}_\gamma = 220$ GeV

$\Gamma(\Lambda K^- \pi^+ \pi^+ \pi^-)/\Gamma_{\text{total}}$		Γ_7/Γ	
VALUE	EVTS	DOCUMENT ID	TECN COMMENT
seen			
		FRABETTI	98B E687 γ Be, $\bar{E}_\gamma = 220$ GeV

$\Gamma(\Xi^- \pi^+)/\Gamma(\Xi^- \pi^+ \pi^+ \pi^-)$		Γ_8/Γ_9	
VALUE	EVTS	DOCUMENT ID	TECN COMMENT
0.30 ± 0.12 ± 0.05			
		ALBRECHT	90F ARG $e^+ e^-$ at $\mathcal{T}(4S)$

$\Gamma(\Omega^- K^+)/\Gamma(\Xi^- \pi^+)$		Γ_{10}/Γ_8	
VALUE	EVTS	DOCUMENT ID	TECN COMMENT
0.297 ± 0.024 OUR AVERAGE			
0.294 ± 0.018 ± 0.016	650	AUBERT,B	05M BABR $e^+ e^- \approx \mathcal{T}(4S)$
0.50 ± 0.21 ± 0.05	9	HENDERSON	92B CLEO $e^+ e^- \approx 10.6$ GeV

$\Gamma(\Xi^- e^+ \nu_e)/\Gamma(\Xi^- \pi^+)$		Γ_{11}/Γ_8	
VALUE	EVTS	DOCUMENT ID	TECN COMMENT
3.1 ± 1.0^{+0.3}_{-0.5}			
	54	ALEXANDER	95B CLE2 $e^+ e^- \approx \mathcal{T}(4S)$

See key on page 373

Baryon Particle Listings

$$\Xi_c^0, \Xi_c^{'+}, \Xi_c^{\prime 0}, \Xi_c(2645)$$

$\Gamma(\Xi^- \ell^+ \text{ anything})/\Gamma(\Xi^- \pi^+)$ Γ_{12}/Γ_8

The ratio is for the average (not the sum) of the $\Xi^- e^+$ anything and $\Xi^- \mu^+$ anything modes.

VALUE	EVTS	DOCUMENT ID	TECN	COMMENT
0.96 ± 0.43 ± 0.18	18	ALBRECHT 93B	ARG	$e^+ e^- \approx 10.4$ GeV

$\Gamma(\Xi^- \ell^+ \text{ anything})/\Gamma(\Xi^- \pi^+ \pi^-)$ Γ_{12}/Γ_9

The ratio is for the average (not the sum) of the $\Xi^- e^+$ anything and $\Xi^- \mu^+$ anything modes.

VALUE	EVTS	DOCUMENT ID	TECN	COMMENT
0.29 ± 0.12 ± 0.04	18	ALBRECHT 93B	ARG	$e^+ e^- \approx 10.4$ GeV

Ξ_c^0 DECAY PARAMETERS

See the note on "Baryon Decay Parameters" in the neutron Listings.

α FOR $\Xi_c^0 \rightarrow \Xi^- \pi^+$

VALUE	EVTS	DOCUMENT ID	TECN	COMMENT
-0.56 ± 0.39^{+0.10}_{-0.09}	138	CHAN	01	CLE2 $e^+ e^- \approx \Upsilon(4S)$

Ξ_c^0 REFERENCES

AUBERT,B	05M	PRL 95 142003	B. Aubert et al.	(BABAR Collab.)
LESIK	05	PL B605 237	T. Lesiak et al.	(BELLE Collab.)
Also		PL B617 198 (erratum)	T. Lesiak et al.	(BELLE Collab.)
DANKO	04	PR D69 052004	I. Danko et al.	(CLEO Collab.)
LINK	02H	PL B541 211	J.M. Link et al.	(FNAL FOCUS Collab.)
CHAN	01	PR D63 111102R	S. Chan et al.	(CLEO Collab.)
FRABETTI	98B	PL B426 403	P.L. Frabetti et al.	(FNAL E687 Collab.)
ALBRECHT	95B	PL B342 397	H. Albrecht et al.	(ARGUS Collab.)
ALEXANDER	95B	PRL 74 3113	J. Alexander et al.	(CLEO Collab.)
Also		PRL 75 4155 (erratum)	J. Alexander et al.	(CLEO Collab.)
ALBRECHT	93B	PL B303 368	H. Albrecht et al.	(ARGUS Collab.)
FRABETTI	93C	PRL 70 2058	P.L. Frabetti et al.	(FNAL E687 Collab.)
HENDERSON	92B	PL B283 161	S. Henderson et al.	(CLEO Collab.)
ALBRECHT	90F	PL B247 121	H. Albrecht et al.	(ARGUS Collab.)
BARLAG	90	PL B236 495	S. Barlag et al.	(ACCOMOR Collab.)
ALAM	89	PL B226 401	M.S. Alam et al.	(CLEO Collab.)
AVERY	89	PRL 62 863	P. Avery et al.	(CLEO Collab.)

$$\Xi_c^{'+}$$

$$I(J^P) = \frac{1}{2}(\frac{1}{2}^+) \text{ Status: } ***$$

The $\Xi_c^{'+}$ and $\Xi_c^{\prime 0}$ presumably complete the SU(3) sextet whose other members are the $\Sigma_c^{++}, \Sigma_c^+, \Sigma_c^0$, and Ω_c^0 ; see Fig. 3 in the Note on Charmed Baryons just before the A_c^+ Listings. The quantum numbers given above come from this presumption but have not been measured.

$\Xi_c^{'+}$ MASS

The mass is obtained from the mass-difference measurement that follows.

VALUE (MeV)	DOCUMENT ID
2575.7 ± 3.1 OUR FIT	

$\Xi_c^{'+} - \Xi_c^+$ MASS DIFFERENCE

VALUE (MeV)	EVTS	DOCUMENT ID	TECN	COMMENT
107.8 ± 3.0 OUR FIT				
107.8 ± 1.7 ± 2.5	25	JESSOP	99	CLE2 $e^+ e^- \approx \Upsilon(4S)$

$\Xi_c^{'+}$ DECAY MODES

The $\Xi_c^{'+} - \Xi_c^+$ mass difference is too small for any strong decay to occur.

Mode	Fraction (Γ_j/Γ)
$\Gamma_1 \Xi_c^+ \gamma$	seen

$\Xi_c^{'+}$ REFERENCES

JESSOP	99	PRL 82 492	C.P. Jessop et al.	(CLEO Collab.)
--------	----	------------	--------------------	----------------

$$\Xi_c^0$$

$$I(J^P) = \frac{1}{2}(\frac{1}{2}^+) \text{ Status: } ***$$

See the note in the Listing for the $\Xi_c^{'+}$, above.

Ξ_c^0 MASS

The mass is obtained from the mass-difference measurement that follows.

VALUE (MeV)	DOCUMENT ID
2578.0 ± 2.9 OUR FIT	

$\Xi_c^0 - \Xi_c^+$ MASS DIFFERENCE

VALUE (MeV)	EVTS	DOCUMENT ID	TECN	COMMENT
107.0 ± 2.9 OUR FIT				
107.0 ± 1.4 ± 2.5	28	JESSOP	99	CLE2 $e^+ e^- \approx \Upsilon(4S)$

Ξ_c^0 DECAY MODES

The $\Xi_c^0 - \Xi_c^+$ mass difference is too small for any strong decay to occur.

Mode	Fraction (Γ_j/Γ)
$\Gamma_1 \Xi_c^0 \gamma$	seen

Ξ_c^0 REFERENCES

JESSOP	99	PRL 82 492	C.P. Jessop et al.	(CLEO Collab.)
--------	----	------------	--------------------	----------------

$$\Xi_c(2645)$$

$$I(J^P) = \frac{1}{2}(\frac{3}{2}^+) \text{ Status: } ***$$

A narrow peak seen in the $\Xi_c \pi$ mass spectrum. The natural assignment is that this is the $J^P = 3/2^+$ excitation of the Ξ_c in the same SU(4) multiplet as the $\Delta(1232)$, but the quantum numbers have not been measured.

$\Xi_c(2645)$ MASSES

The masses are obtained from the mass-difference measurements that follow.

$\Xi_c(2645)^+$ MASS

VALUE (MeV)	DOCUMENT ID
2646.6 ± 1.4 OUR FIT	Error includes scale factor of 1.6.

$\Xi_c(2645)^0$ MASS

VALUE (MeV)	DOCUMENT ID
2646.1 ± 1.2 OUR FIT	

$\Xi_c(2645) - \Xi_c$ MASS DIFFERENCES

$m_{\Xi_c(2645)^+} - m_{\Xi_c^+}$

VALUE (MeV)	EVTS	DOCUMENT ID	TECN	COMMENT
175.6 ± 1.4 OUR FIT				Error includes scale factor of 1.7.
175.6 ± 1.4 OUR AVERAGE				Error includes scale factor of 1.7.
177.1 ± 0.5 ± 1.1	47	FRABETTI 98B	E687	γ Be, $\bar{E}_\gamma = 220$ GeV
174.3 ± 0.5 ± 1.0	34	GIBBONS 96	CLE2	$e^+ e^- \approx \Upsilon(4S)$

$m_{\Xi_c(2645)^0} - m_{\Xi_c^0}$

VALUE (MeV)	EVTS	DOCUMENT ID	TECN	COMMENT
178.2 ± 1.1 OUR FIT				
178.2 ± 0.5 ± 1.0	55	AVERY 95	CLE2	$e^+ e^- \approx \Upsilon(4S)$

$\Xi_c(2645)$ WIDTHS

$\Xi_c(2645)^+$ WIDTH

VALUE (MeV)	CL%	DOCUMENT ID	TECN	COMMENT
<3.1	90	GIBBONS 96	CLE2	$e^+ e^- \approx \Upsilon(4S)$

$\Xi_c(2645)^0$ WIDTH

VALUE (MeV)	CL%	EVTS	DOCUMENT ID	TECN	COMMENT
<5.5	90	55	AVERY 95	CLE2	$e^+ e^- \approx \Upsilon(4S)$

$\Xi_c(2645)$ DECAY MODES

$\Xi_c \pi$ is the only strong decay allowed to a Ξ_c resonance having this mass.

Mode	Fraction (Γ_j/Γ)
$\Gamma_1 \Xi_c^0 \pi^+$	seen
$\Gamma_2 \Xi_c^+ \pi^-$	seen

Baryon Particle Listings

 $\Xi_c(2645), \Xi_c(2790), \Xi_c(2815), \Xi_c(2930)$ $\Xi_c(2645)$ REFERENCES

FRABETTI	98B	PL B426 403	P.L. Frabetti <i>et al.</i>	(FNAL E607 Collab.)
GIBBONS	96	PRL 77 310	L.K. Gibbons <i>et al.</i>	(CLEO Collab.)
AVERY	95	PRL 75 4364	P. Avery <i>et al.</i>	(CLEO Collab.)

 $\Xi_c(2790)$

$$I(J^P) = \frac{1}{2}(\frac{1}{2}^-) \text{ Status: } ***$$

A peak seen in the $\Xi_c' \pi$ mass spectrum. The simplest assignment, based on the mass, width, and decay mode, is that this belongs in the same SU(4) multiplet as the $\Lambda(1405)$ and the $\Lambda_c(2595)^+$, but the spin and parity have not been measured.

 $\Xi_c(2790)$ MASSES

The masses are obtained from the mass-difference measurements that follow.

 $\Xi_c(2790)^+$ MASS

VALUE (MeV)	DOCUMENT ID
2789.2 ± 3.2 OUR FIT	

 $\Xi_c(2790)^0$ MASS

VALUE (MeV)	DOCUMENT ID
2791.9 ± 3.3 OUR FIT	

 $\Xi_c(2790) - \Xi_c$ MASS DIFFERENCES $m_{\Xi_c(2790)^+} - m_{\Xi_c^0}$

VALUE (MeV)	EVTS	DOCUMENT ID	TECN	COMMENT
318.2 ± 3.2 OUR FIT				
318.2 ± 1.3 ± 2.9	18	CSORNA	01	CLEO $e^+ e^- \approx \Upsilon(4S)$

 $m_{\Xi_c(2790)^0} - m_{\Xi_c^+}$

VALUE (MeV)	EVTS	DOCUMENT ID	TECN	COMMENT
324.0 ± 3.3 OUR FIT				
324.0 ± 1.3 ± 3.0	14	CSORNA	01	CLEO $e^+ e^- \approx \Upsilon(4S)$

 $\Xi_c(2790)$ WIDTHS $\Xi_c(2790)^+$ WIDTH

VALUE (MeV)	CL%	DOCUMENT ID	TECN	COMMENT
<15	90	CSORNA	01	CLEO $e^+ e^- \approx \Upsilon(4S)$

 $\Xi_c(2790)^0$ WIDTH

VALUE (MeV)	CL%	DOCUMENT ID	TECN	COMMENT
<12	90	CSORNA	01	CLEO $e^+ e^- \approx \Upsilon(4S)$

 $\Xi_c(2790)$ DECAY MODES

Mode	Fraction (Γ_i/Γ)
Γ_1 $\Xi_c' \pi$	seen

 $\Xi_c(2790)$ REFERENCES

CSORNA	01	PRL 86 4243	S.E. Csorna <i>et al.</i>	(CLEO Collab.)
--------	----	-------------	---------------------------	----------------

 $\Xi_c(2815)$

$$I(J^P) = \frac{1}{2}(\frac{3}{2}^-) \text{ Status: } ***$$

A narrow peak seen in the $\Xi_c \pi \pi$ mass spectrum. The simplest assignment is that this belongs to the same SU(4) multiplet as the $\Lambda(1520)$ and the $\Lambda_c(2625)$, but the spin and parity have not been measured.

 $\Xi_c(2815)$ MASSES

The masses are obtained from the mass-difference measurements that follow.

 $\Xi_c(2815)^+$ MASS

VALUE (MeV)	DOCUMENT ID
2816.5 ± 1.2 OUR FIT	

 $\Xi_c(2815)^0$ MASS

VALUE (MeV)	DOCUMENT ID
2818.2 ± 2.1 OUR FIT	

 $\Xi_c(2815) - \Xi_c$ MASS DIFFERENCES $m_{\Xi_c(2815)^+} - m_{\Xi_c^+}$

VALUE (MeV)	EVTS	DOCUMENT ID	TECN	COMMENT
348.6 ± 1.2 OUR FIT				
348.6 ± 0.6 ± 1.0	20	ALEXANDER	99B CLE2	$e^+ e^- \approx \Upsilon(4S)$

 $m_{\Xi_c(2815)^0} - m_{\Xi_c^0}$

VALUE (MeV)	EVTS	DOCUMENT ID	TECN	COMMENT
347.2 ± 2.1 OUR FIT				
347.2 ± 0.7 ± 2.0	9	ALEXANDER	99B CLE2	$e^+ e^- \approx \Upsilon(4S)$

 $\Xi_c(2815)$ WIDTHS $\Xi_c(2815)^+$ WIDTH

VALUE (MeV)	CL%	DOCUMENT ID	TECN	COMMENT
<3.5	90	ALEXANDER	99B CLE2	$e^+ e^- \approx \Upsilon(4S)$

 $\Xi_c(2815)^0$ WIDTH

VALUE (MeV)	CL%	DOCUMENT ID	TECN	COMMENT
<6.5	90	ALEXANDER	99B CLE2	$e^+ e^- \approx \Upsilon(4S)$

 $\Xi_c(2815)$ DECAY MODES

The $\Xi_c \pi \pi$ modes are consistent with being entirely via $\Xi_c(2645) \pi$.

Mode	Fraction (Γ_i/Γ)
Γ_1 $\Xi_c^+ \pi^+ \pi^-$	seen
Γ_2 $\Xi_c^0 \pi^+ \pi^-$	seen

 $\Xi_c(2815)$ REFERENCES

ALEXANDER	99B	PRL 83 3390	J.P. Alexander <i>et al.</i>	(CLEO Collab.)
-----------	-----	-------------	------------------------------	----------------

 $\Xi_c(2930)$

$$I(J^P) = ?(??) \text{ Status: } *$$

OMITTED FROM SUMMARY TABLE

A peak seen in the $\Lambda_c^+ K^-$ mass projection of $B^- \rightarrow \Lambda_c^+ \bar{\Lambda}_c^- K^-$ events.

 $\Xi_c(2930)$ MASS

VALUE (MeV)	EVTS	DOCUMENT ID	TECN	COMMENT
2931 ± 3 ± 5	≈ 34	AUBERT	08H BABR	$\Upsilon(4S) \rightarrow B \bar{B}$

 $\Xi_c(2930)$ WIDTH

VALUE (MeV)	EVTS	DOCUMENT ID	TECN	COMMENT
36 ± 7 ± 11	≈ 34	AUBERT	08H BABR	$\Upsilon(4S) \rightarrow B \bar{B}$

 $\Xi_c(2930)$ REFERENCES

AUBERT	08H	PR D77 031101R	B. Aubert <i>et al.</i>	(BABAR Collab.)
--------	-----	----------------	-------------------------	-----------------

See key on page 373

Baryon Particle Listings

$\Xi_c(2980)$, $\Xi_c(3055)$, $\Xi_c(3080)$, $\Xi_c(3123)$

 $\Xi_c(2980)$

$$I(J^P) = \frac{1}{2}(??) \quad \text{Status: } ***$$

A broad peak seen in the $\Lambda_c^+ K^- \pi^+$ mass spectrum, and possibly in the $\Lambda_c^+ K_S^0 \pi^-$ spectrum.

 $\Xi_c(2980)$ MASSES **$\Xi_c(2980)^+$ MASS**

VALUE (MeV)	EVTS	DOCUMENT ID	TECN	COMMENT
2974 ± 5 OUR AVERAGE		Error includes scale factor of 2.3.		
2969.3 ± 2.2 ± 1.7	756 ± 206	AUBERT	08J BABR	$e^+ e^- \approx 10.58$ GeV
2978.5 ± 2.1 ± 2.0	405 ± 51	CHISTOV	06 BELL	$e^+ e^- \approx \Upsilon(4S)$

 $\Xi_c(2980)^0$ MASS

The evidence is statistically much weaker for this charge state.

VALUE (MeV)	EVTS	DOCUMENT ID	TECN	COMMENT
2974 ± 4 OUR AVERAGE				
2972.9 ± 4.4 ± 1.6	67 ± 44	AUBERT	08J BABR	$e^+ e^- \approx 10.58$ GeV
2977.1 ± 8.8 ± 3.5	42 ± 21	CHISTOV	06 BELL	$e^+ e^- \approx \Upsilon(4S)$

 $\Xi_c(2980)$ WIDTHS **$\Xi_c(2980)^+$ WIDTH**

VALUE (MeV)	EVTS	DOCUMENT ID	TECN	COMMENT
33 ± 8 OUR AVERAGE		Error includes scale factor of 1.3.		
27 ± 8 ± 2	756 ± 206	AUBERT	08J BABR	$e^+ e^- \approx 10.58$ GeV
43.5 ± 7.5 ± 7.0	405 ± 51	CHISTOV	06 BELL	$e^+ e^- \approx \Upsilon(4S)$

 $\Xi_c(2980)^0$ WIDTH

VALUE (MeV)	EVTS	DOCUMENT ID	TECN	COMMENT
31 ± 7 ± 8	67 ± 44	AUBERT	08J BABR	$e^+ e^- \approx 10.58$ GeV

 $\Xi_c(2980)$ DECAY MODES

Mode	Fraction (Γ_i/Γ)
Γ_1 $\Lambda_c^+ \bar{K} \pi$	seen
Γ_2 $\Sigma_c(2455) \bar{K}$	seen
Γ_3 $\Lambda_c^+ \bar{K}$	not seen

 $\Xi_c(2980)$ BRANCHING RATIOS

$\Gamma(\Sigma_c(2455) \bar{K})/\Gamma(\Lambda_c^+ \bar{K} \pi)$	Γ_2/Γ_1
0.55 ± 0.07 ± 0.13	
AUBERT	08J BABR
CHISTOV	06 BELL
in $\Lambda_c^+ K^- \pi^+$	

 $\Xi_c(2980)$ REFERENCES

AUBERT	08J	PR D77 012002	B. Aubert et al.	(BABAR Collab.)
CHISTOV	06	PRL 97 162001	R. Chistov et al.	(BELLE Collab.)

 $\Xi_c(3055)$

$$I(J^P) = ?(??) \quad \text{Status: } ***$$

OMITTED FROM SUMMARY TABLE

A peak in the $\Sigma_c(2455)^{++} K^- \rightarrow \Lambda_c^+ K^- \pi^+$ mass spectrum with a claimed significance of 6.4 standard deviations.

 $\Xi_c(3055)$ MASSES **$\Xi_c(3055)^+$ MASS**

VALUE (MeV)	EVTS	DOCUMENT ID	TECN	COMMENT
3054.2 ± 1.2 ± 0.5	218 ± 95	AUBERT	08J BABR	$e^+ e^- \approx 10.58$ GeV

 $\Xi_c(3055)$ WIDTHS **$\Xi_c(3055)^+$ WIDTH**

VALUE (MeV)	EVTS	DOCUMENT ID	TECN	COMMENT
17 ± 6 ± 11	218 ± 95	AUBERT	08J BABR	$e^+ e^- \approx 10.58$ GeV

 $\Xi_c(3055)$ REFERENCES

AUBERT	08J	PR D77 012002	B. Aubert et al.	(BABAR Collab.)
--------	-----	---------------	------------------	-----------------

 $\Xi_c(3080)$

$$I(J^P) = \frac{1}{2}(??) \quad \text{Status: } ***$$

A narrow peak seen in the $\Lambda_c^+ K^- \pi^+$ and $\Lambda_c^+ K_S^0 \pi^-$ mass spectra.

 $\Xi_c(3080)$ MASSES **$\Xi_c(3080)^+$ MASS**

VALUE (MeV)	EVTS	DOCUMENT ID	TECN	COMMENT
3077.0 ± 0.4 ± 0.2 OUR AVERAGE				
3077.0 ± 0.4 ± 0.2	403 ± 60	AUBERT	08J BABR	$e^+ e^- \approx 10.58$ GeV
3076.7 ± 0.9 ± 0.5	326 ± 40	CHISTOV	06 BELL	$e^+ e^- \approx \Upsilon(4S)$

 $\Xi_c(3080)^0$ MASS

VALUE (MeV)	EVTS	DOCUMENT ID	TECN	COMMENT
3079.9 ± 1.4 OUR AVERAGE		Error includes scale factor of 1.3.		
3079.3 ± 1.1 ± 0.2	90 ± 27	AUBERT	08J BABR	$e^+ e^- \approx 10.58$ GeV
3082.8 ± 1.8 ± 1.5	67 ± 20	CHISTOV	06 BELL	$e^+ e^- \approx \Upsilon(4S)$

 $\Xi_c(3080)$ WIDTHS **$\Xi_c(3080)^+$ WIDTH**

VALUE (MeV)	EVTS	DOCUMENT ID	TECN	COMMENT
5.8 ± 1.0 OUR AVERAGE				
5.5 ± 1.3 ± 0.6	403 ± 60	AUBERT	08J BABR	$e^+ e^- \approx 10.58$ GeV
6.2 ± 1.2 ± 0.8	326 ± 40	CHISTOV	06 BELL	$e^+ e^- \approx \Upsilon(4S)$

 $\Xi_c(3080)^0$ WIDTH

VALUE (MeV)	EVTS	DOCUMENT ID	TECN	COMMENT
5.6 ± 2.2 OUR AVERAGE				
5.9 ± 2.3 ± 1.5	90 ± 27	AUBERT	08J BABR	$e^+ e^- \approx 10.58$ GeV
5.2 ± 3.1 ± 1.8	67 ± 20	CHISTOV	06 BELL	$e^+ e^- \approx \Upsilon(4S)$

 $\Xi_c(3080)$ DECAY MODES

Mode	Fraction (Γ_i/Γ)
Γ_1 $\Lambda_c^+ \bar{K} \pi$	seen
Γ_2 $\Sigma_c(2455) \bar{K}$	seen
Γ_3 $\Sigma_c(2455) \bar{K} + \Sigma_c(2520) \bar{K}$	seen
Γ_4 $\Lambda_c^+ \bar{K}$	not seen
Γ_5 $\Lambda_c^+ \bar{K} \pi^+ \pi^-$	not seen

 $\Xi_c(3080)$ BRANCHING RATIOS

$\Gamma(\Sigma_c(2455) \bar{K})/\Gamma(\Lambda_c^+ \bar{K} \pi)$	Γ_2/Γ_1
0.45 ± 0.06 OUR AVERAGE	
0.45 ± 0.05 ± 0.05	
0.44 ± 0.12 ± 0.07	
AUBERT	08J BABR
AUBERT	08J BABR
in $\Lambda_c^+ K^- \pi^+$	
in $\Lambda_c^+ K_S^0 \pi^-$	

$[\Gamma(\Sigma_c(2455) \bar{K}) + \Gamma(\Sigma_c(2520) \bar{K})]/\Gamma(\Lambda_c^+ \bar{K} \pi)$	Γ_3/Γ_1
0.89 ± 0.12 OUR AVERAGE	
0.95 ± 0.14 ± 0.06	
0.78 ± 0.21 ± 0.05	
AUBERT	08J BABR
AUBERT	08J BABR
in $\Lambda_c^+ K^- \pi^+$	
in $\Lambda_c^+ K_S^0 \pi^-$	

 $\Xi_c(3080)$ REFERENCES

AUBERT	08J	PR D77 012002	B. Aubert et al.	(BABAR Collab.)
CHISTOV	06	PRL 97 162001	R. Chistov et al.	(BELLE Collab.)

 $\Xi_c(3123)$

$$I(J^P) = ?(??) \quad \text{Status: } *$$

OMITTED FROM SUMMARY TABLE

A peak in the $\Sigma_c(2520)^{++} K^- \rightarrow \Lambda_c^+ K^- \pi^+$ mass spectrum with a significance of 3.6 standard deviations.

 $\Xi_c(3123)$ MASSES **$\Xi_c(3123)^+$ MASS**

VALUE (MeV)	EVTS	DOCUMENT ID	TECN	COMMENT
3122.9 ± 1.3 ± 0.3	101 ± 35	AUBERT	08J BABR	$e^+ e^- \approx 10.58$ GeV

 $\Xi_c(3123)$ WIDTHS **$\Xi_c(3123)^+$ WIDTH**

VALUE (MeV)	EVTS	DOCUMENT ID	TECN	COMMENT
4.4 ± 3.4 ± 1.7	101 ± 35	AUBERT	08J BABR	$e^+ e^- \approx 10.58$ GeV

 $\Xi_c(3123)$ REFERENCES

AUBERT	08J	PR D77 012002	B. Aubert et al.	(BABAR Collab.)
--------	-----	---------------	------------------	-----------------

Baryon Particle Listings

 $\Omega_c^0, \Omega_c(2770)^0$ 

$$I(J^P) = 0(\frac{1}{2}^+) \text{ Status: } ***$$

The quantum numbers have not been measured, but are simply assigned in accord with the quark model, in which the Ω_c^0 is the ssc ground state.

 Ω_c^0 MASS

VALUE (MeV)	EVTS	DOCUMENT ID	TECN	COMMENT
2697.5 ± 2.6 OUR FIT	Error	Error includes scale factor of 1.2.		
2697.5 ± 2.6 OUR AVERAGE	Error	Error includes scale factor of 1.2.		
2694.6 ± 2.6 ± 1.9	40	¹ CRONIN-HEN..01	CLE2	$e^+e^- \approx 10.6$ GeV
2699.9 ± 1.5 ± 2.5	42	² FRABETTI 94H	E687	γ Be, $\overline{E}_\gamma = 221$ GeV
• • • We do not use the following data for averages, fits, limits, etc. • • •				
2705.9 ± 3.3 ± 2.0	10	³ FRABETTI 93	E687	γ Be, $\overline{E}_\gamma = 221$ GeV
2719.0 ± 7.0 ± 2.5	11	⁴ ALBRECHT 92H	ARG	$e^+e^- \approx 10.6$ GeV
2740 ± 20	3	BIAGI 85B	SPEC	Σ^- Be 135 GeV/c

¹ CRONIN-HENNESSY 01 sees 40.4 ± 9.0 events in a sum over five channels.

² FRABETTI 94H claims a signal of 42.5 ± 8.8 $\Sigma^- K^- K^- \pi^+$ events. The background is about 24 events.

³ FRABETTI 93 claims a signal of 10.3 ± 3.9 $\Omega^- \pi^+$ events above a background of 5.8 events.

⁴ ALBRECHT 92H claims a signal of 11.5 ± 4.3 $\Xi^- K^- \pi^+ \pi^+$ events. The background is about 5 events.

 Ω_c^0 MEAN LIFE

VALUE (10^{-15} s)	EVTS	DOCUMENT ID	TECN	COMMENT
69 ± 12 OUR AVERAGE				
72 ± 11 ± 11	64	LINK 03C	FOCS	$\Omega^- \pi^+$, $\Xi^- K^- \pi^+ \pi^+$
55 $^{+13}_{-11} \pm 18$ $_{-23}$	86	ADAMOVICH 95B	WA89	$\Omega^- \pi^- \pi^+ \pi^+$, $\Xi^- K^- \pi^+ \pi^+$
86 $^{+27}_{-20} \pm 28$	25	FRABETTI 95D	E687	$\Sigma^+ K^- K^- \pi^+$

 Ω_c^0 DECAY MODES

No absolute branching fractions have been measured.

Mode	Fraction (Γ_i/Γ)
Γ_1 $\Sigma^+ K^- K^- \pi^+$	seen
Γ_2 $\Xi^0 K^- \pi^+$	seen
Γ_3 $\Xi^- K^- \pi^+ \pi^+$	seen
Γ_4 $\Omega^- e^+ \nu_e$	seen
Γ_5 $\Omega^- \pi^+$	seen
Γ_6 $\Omega^- \pi^+ \pi^0$	seen
Γ_7 $\Omega^- \pi^- \pi^+ \pi^+$	seen

 Ω_c^0 BRANCHING RATIOS

$\Gamma(\Sigma^+ K^- K^- \pi^+)/\Gamma_{\text{total}}$	Γ_1/Γ
VALUE EVTS	DOCUMENT ID TECN COMMENT
seen 42	FRABETTI 94H E687 γ Be, $\overline{E}_\gamma = 221$ GeV

$\Gamma(\Sigma^+ K^- K^- \pi^+)/\Gamma(\Omega^- \pi^+)$	Γ_1/Γ_5
VALUE CL%	DOCUMENT ID TECN COMMENT
<4.8 90	CRONIN-HEN..01 CLE2 $e^+e^- \approx 10.6$ GeV

$\Gamma(\Xi^0 K^- \pi^+)/\Gamma(\Omega^- \pi^+)$	Γ_2/Γ_5
VALUE EVTS	DOCUMENT ID TECN COMMENT
4.0 ± 2.5 ± 0.4 9	CRONIN-HEN..01 CLE2 $e^+e^- \approx 10.6$ GeV

$\Gamma(\Xi^- K^- \pi^+ \pi^+)/\Gamma_{\text{total}}$	Γ_3/Γ
VALUE EVTS	DOCUMENT ID TECN COMMENT
seen 11	ALBRECHT 92H ARG $e^+e^- \approx 10.6$ GeV
seen 3	BIAGI 85B SPEC Σ^- Be 135 GeV/c

$\Gamma(\Xi^- K^- \pi^+ \pi^+)/\Gamma(\Omega^- \pi^+)$	Γ_3/Γ_5
VALUE CL% EVTS	DOCUMENT ID TECN COMMENT
0.46 ± 0.13 ± 0.03 45 ± 12	AUBERT 07AH BABR $e^+e^- \approx 7(45)$
• • • We do not use the following data for averages, fits, limits, etc. • • •	
1.6 ± 1.1 ± 0.4 7	CRONIN-HEN..01 CLE2 $e^+e^- \approx 10.6$ GeV
<2.8 90	FRABETTI 93 E687 γ Be, $\overline{E}_\gamma = 221$ GeV

$\Gamma(\Omega^- \pi^+)/\Gamma(\Omega^- e^+ \nu_e)$	Γ_5/Γ_4
VALUE EVTS	DOCUMENT ID TECN COMMENT
0.41 ± 0.19 ± 0.04 11	AMMAR 02 CLE2 $e^+e^- \approx 7(45)$

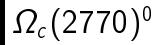
$\Gamma(\Omega^- \pi^+)/\Gamma_{\text{total}}$	Γ_5/Γ
VALUE EVTS	DOCUMENT ID TECN COMMENT
seen 13	CRONIN-HEN..01 CLE2 $e^+e^- \approx 10.6$ GeV
seen 10	FRABETTI 93 E687 γ Be, $\overline{E}_\gamma = 221$ GeV

$\Gamma(\Omega^- \pi^+ \pi^0)/\Gamma(\Omega^- \pi^+)$	Γ_6/Γ_5
VALUE EVTS	DOCUMENT ID TECN COMMENT
1.27 ± 0.31 ± 0.11 64 ± 15	AUBERT 07AH BABR $e^+e^- \approx 7(45)$
• • • We do not use the following data for averages, fits, limits, etc. • • •	
4.2 ± 2.2 ± 0.9 12	CRONIN-HEN..01 CLE2 $e^+e^- \approx 10.6$ GeV

$\Gamma(\Omega^- \pi^- \pi^+ \pi^+)/\Gamma(\Omega^- \pi^+)$	Γ_7/Γ_5
VALUE CL% EVTS	DOCUMENT ID TECN COMMENT
0.28 ± 0.09 ± 0.01 25 ± 8	AUBERT 07AH BABR $e^+e^- \approx 7(45)$
• • • We do not use the following data for averages, fits, limits, etc. • • •	
<0.56 90	CRONIN-HEN..01 CLE2 $e^+e^- \approx 10.6$ GeV
seen	ADAMOVICH 95B WA89 Σ^- 340 GeV
<1.6 90	FRABETTI 93 E687 γ Be, $\overline{E}_\gamma = 221$ GeV

 Ω_c^0 REFERENCES

AUBERT 07AH PRL 99 062001	B. Aubert <i>et al.</i>	(BABAR Collab.)
LINK 03C PL B561 41	J.M. Link <i>et al.</i>	(FNAL FOCUS Collab.)
AMMAR 02 PRL 89 171803	R. Ammar <i>et al.</i>	(CLEO Collab.)
CRONIN-HEN..01 PRL 86 3730	D. Cronin-Hennessy <i>et al.</i>	(CLEO Collab.)
ADAMOVICH 95B PL B358 151	M.I. Adamovich <i>et al.</i>	(CERN WA89 Collab.)
FRABETTI 95D PL B357 678	P.L. Frabetti <i>et al.</i>	(FNAL E687 Collab.)
FRABETTI 94H PL B338 106	P.L. Frabetti <i>et al.</i>	(FNAL E687 Collab.)
FRABETTI 93 PL B300 190	P.L. Frabetti <i>et al.</i>	(FNAL E687 Collab.)
ALBRECHT 92H PL B288 367	H. Albrecht <i>et al.</i>	(ARGUS Collab.)
BIAGI 85B ZPHY C28 175	S.F. Biagi <i>et al.</i>	(CERN WA62 Collab.)



$$I(J^P) = 0(\frac{3}{2}^+) \text{ Status: } ***$$

The natural assignment is that this goes with the $\Sigma_c(2520)$ and $\Xi_c(2645)$ to complete the lowest mass $J^P = \frac{3}{2}^+$ SU(3) sextet, part of the SU(4) 20-plet that includes the $\Delta(1232)$. But J and P have not been measured.

 $\Omega_c(2770)^0$ MASS

The mass is obtained from the mass-difference measurement that follows.

VALUE (MeV)	DOCUMENT ID
2768.3 ± 3.0 OUR FIT	Error includes scale factor of 1.2.

 $\Omega_c(2770)^0 - \Omega_c^0$ MASS DIFFERENCE

VALUE (MeV)	EVTS	DOCUMENT ID	TECN	COMMENT
70.8 ± 1.5 OUR FIT				
70.8 ± 1.0 ± 1.1	105 ± 22	AUBERT, BE 06i	BABR	$e^+e^- \approx 7(45)$

 $\Omega_c(2770)^0$ DECAY MODES

The $\Omega_c(2770)^0 - \Omega_c^0$ mass difference is too small for any strong decay to occur.

Mode	Fraction (Γ_i/Γ)
Γ_1 $\Omega_c^0 \gamma$	presumably 100%

 $\Omega_c(2770)^0$ REFERENCES

AUBERT, BE 06i PRL 97 232001	B. Aubert <i>et al.</i>	(BABAR Collab.)
------------------------------	-------------------------	-----------------

See key on page 373

Baryon Particle Listings

Ξ_{cc}^+

DOUBLY CHARMED BARYONS
(C = +2)
 $\Xi_{cc}^{++} = ucc, \Xi_{cc}^+ = dcc, \Omega_{cc}^+ = scc$

Ξ_{cc}^+

$I(J^P) = ?(??)$ Status: *

OMITTED FROM SUMMARY TABLE

This would presumably be an isospin-1/2 particle, a $ccu \Xi_{cc}^{++}$ and a $ccd \Xi_{cc}^+$. However, opposed to the evidence cited below, the BABAR experiment has found no evidence for a Ξ_{cc}^+ in a search in $\Lambda_c^+ K^- \pi^+$ and $\Xi_c^0 \pi^+$ modes, and no evidence of a Ξ_{cc}^{++} in $\Lambda_c^+ K^- \pi^+ \pi^+$ and $\Xi_c^0 \pi^+ \pi^+$ modes (AUBERT,B 06D). Nor has the BELLE experiment found any evidence for a Ξ_{cc}^+ in the $\Lambda_c^+ K^- \pi^+$ mode (CHISTOV 06).

Ξ_{cc}^+ MASS

VALUE (MeV)	EVTS	DOCUMENT ID	TECN	COMMENT
3518.9 ± 0.9 OUR AVERAGE				
3518 ± 3	6	¹ OCHERASHVI..05	SELX	Σ^- nucleus \approx 600 GeV
3519 ± 1	16	² MATTSON 02	SELX	Σ^- nucleus \approx 600 GeV

¹ OCHERASHVILI 05 claims "an excess of 5.62 events over ... 1.38 ± 0.13 events" for a significance of 4.8 σ in $pD^+ K^-$ events.

² MATTSON 02 claims "an excess of 15.9 events over an expected background of 6.1 ± 0.5 events, a statistical significance of 6.3 σ " in the $\Lambda_c^+ K^- \pi^+$ invariant-mass spectrum.

The probability that the peak is a fluctuation increases from 1.0×10^{-6} to 1.1×10^{-4} when the number of bins searched is considered.

Ξ_{cc}^+ MEAN LIFE

VALUE (10^{-15} s)	CL%	DOCUMENT ID	TECN	COMMENT
<33	90	MATTSON 02	SELX	Σ^- nucleus, \approx 600 GeV

Ξ_{cc}^+ DECAY MODES

Mode	Γ
$\Lambda_c^+ K^- \pi^+$	Γ_1
$pD^+ K^-$	Γ_2

$\Gamma(pD^+ K^-)/\Gamma(\Lambda_c^+ K^- \pi^+)$		Γ_2/Γ_1		
VALUE	EVTS	DOCUMENT ID	TECN	COMMENT
0.36 ± 0.21	6	OCHERASHVI..05	SELX	$\Sigma^- \approx$ 600 GeV

Ξ_{cc}^+ REFERENCES

AUBERT,B 06D	PR D74 011103R	B. Aubert <i>et al.</i>	(BABAR Collab.)
CHISTOV 06	PRL 97 162001	R. Chistov <i>et al.</i>	(BELLE Collab.)
OCHERASHVI..05	PL B628 18	A. Ocherashvili <i>et al.</i>	(FNAL SELEX Collab.)
MATTSON 02	PRL 89 112001	M. Mattson <i>et al.</i>	(FNAL SELEX Collab.)

Baryon Particle Listings

 Λ_b^0

BOTTOM BARYONS ($B = -1$)

$$\Lambda_b^0 = udb, \Xi_b^0 = usb, \Xi_b^- = dsb$$

 Λ_b^0

$$I(J^P) = 0(\frac{1}{2}^+) \text{ Status: } ***$$

In the quark model, a Λ_b^0 is an isospin-0 udb state. The lowest Λ_b^0 ought to have $J^P = 1/2^+$. None of I , J , or P have actually been measured.

 Λ_b^0 MASS

VALUE (MeV)	EVTS	DOCUMENT ID	TECN	COMMENT
5620.2 ± 1.6 OUR AVERAGE				
5619.7 ± 1.2 ± 1.2		1 ACOSTA	06 CDF	$p\bar{p}$ at 1.96 TeV
5621 ± 4 ± 3		2 ABE	97B CDF	$p\bar{p}$ at 1.8 TeV
5668 ± 16 ± 8	4	3 ABREU	96N DLPH	$e^+e^- \rightarrow Z$
5614 ± 21 ± 4	4	3 BUSKULIC	96L ALEP	$e^+e^- \rightarrow Z$
not seen		4 ABE	93B CDF	Sup. by ABE 97B
5640 ± 50 ± 30	16	5 ALBAJAR	91E UA1	$p\bar{p}$ 630 GeV
5640 +100 -210	52	BARI	91 SFM	$\Lambda_b^0 \rightarrow pD^0\pi^-$
5650 +150 -200	90	BARI	91 SFM	$\Lambda_b^0 \rightarrow \Lambda_c^+\pi^+\pi^-\pi^-$

- • • We do not use the following data for averages, fits, limits, etc. • • •
- 1 Uses exclusively reconstructed final states containing a $J/\psi \rightarrow \mu^+\mu^-$ decays.
- 2 ABE 97B observed 38 events with a background of 18 ± 1.6 events in the mass range 5.60–5.65 GeV/ c^2 , a significance of > 3.4 standard deviations.
- 3 Uses 4 fully reconstructed Λ_b events.
- 4 ABE 93B states that, based on the signal claimed by ALBAJAR 91E, CDF should have found $30 \pm 23 \Lambda_b^0 \rightarrow J/\psi(1S)\Lambda$ events. Instead, CDF found not more than 2 events.
- 5 ALBAJAR 91E claims 16 ± 5 events above a background of 9 ± 1 events, a significance of about 5 standard deviations.

 $m_{\Lambda_b} - m_{B^0}$

VALUE (MeV)	DOCUMENT ID	TECN	COMMENT
339.2 ± 1.4 ± 0.1	6 ACOSTA	06 CDF	$p\bar{p}$ at 1.96 TeV

- • • We do not use the following data for averages, fits, limits, etc. • • •
- 6 Uses exclusively reconstructed final states containing a $J/\psi \rightarrow \mu^+\mu^-$ decays.

 Λ_b^0 MEAN LIFE

See b -baryon Admixture section for data on b -baryon mean life average over species of b -baryon particles.

"OUR EVALUATION" is an average using rescaled values of the data listed below. The average and rescaling were performed by the Heavy Flavor Averaging Group (HFAG) and are described at <http://www.slac.stanford.edu/xorg/hfag/>. The averaging/rescaling procedure takes into account correlations between the measurements and asymmetric lifetime errors.

VALUE (10^{-12} s)	EVTS	DOCUMENT ID	TECN	COMMENT
1.383 ± 0.049 -0.048 OUR EVALUATION				
1.218 +0.130 -0.115 ± 0.042	7	ABAZOV	07s D0	$p\bar{p}$ at 1.96 TeV
1.290 +0.119+0.087 -0.110-0.091	8	ABAZOV	07u D0	$p\bar{p}$ at 1.96 TeV
1.593 +0.083 -0.078 ± 0.033	7	ABULENCIA	07A CDF	$p\bar{p}$ at 1.96 TeV
1.11 +0.19 -0.18 ± 0.05	9	ABREU	99w DLPH	$e^+e^- \rightarrow Z$
1.29 +0.24 -0.22 ± 0.06	9	ACKERSTAFF	98G OPAL	$e^+e^- \rightarrow Z$
1.21 ± 0.11	9	BARATE	98D ALEP	$e^+e^- \rightarrow Z$
1.32 ± 0.15 ± 0.07	10	ABE	96M CDF	$p\bar{p}$ at 1.8 TeV
• • • We do not use the following data for averages, fits, limits, etc. • • •				
1.22 +0.22 -0.18 ± 0.04	7	ABAZOV	05c D0	Repl. by ABAZOV 07s
1.19 +0.21 +0.07 -0.18 -0.08		ABREU	96D DLPH	Repl. by ABREU 99w
1.14 +0.22 +0.07 -0.19 ± 0.07	69	AKERS	95K OPAL	Repl. by ACKERSTAFF 98G
1.02 +0.23 -0.18 ± 0.06	44	BUSKULIC	95L ALEP	Repl. by BARATE 98D

- 7 Measured mean life using fully reconstructed $\Lambda_b^0 \rightarrow J/\psi\Lambda$ decays.
- 8 Measured using semileptonic decays $\Lambda_b^0 \rightarrow \Lambda_c^+\mu\nu X$ and $\Lambda_c^+ \rightarrow K_S^0 p$.
- 9 Averaging using $\Lambda_c \ell^-$ and $\Lambda \ell^+ \ell^-$.
- 10 Excess $\Lambda_c \ell^-$, decay lengths.

 $\tau_{\Lambda_b^0}/\tau_{B^0}$ MEAN LIFE RATIO $\tau_{\Lambda_b^0}/\tau_{B^0}$ (direct measurements)

VALUE	DOCUMENT ID	TECN	COMMENT
0.99 ± 0.10 OUR AVERAGE			Error includes scale factor of 2.0.
0.811 +0.096 -0.087 ± 0.034	11,12	ABAZOV	07s D0 $p\bar{p}$ at 1.96 TeV
1.041 ± 0.057	13	ABULENCIA	07A CDF $p\bar{p}$ at 1.96 TeV
• • • We do not use the following data for averages, fits, limits, etc. • • •			
0.87 +0.17 -0.14 ± 0.03	13	ABAZOV	05c D0 Repl. by ABAZOV 07s

- 11 Uses fully reconstructed $\Lambda_b \rightarrow J/\psi\Lambda$ decays.
- 12 Uses $B^0 \rightarrow J/\psi K_S^0$ decays for denominator.
- 13 Measured mean life ratio using fully reconstructed decays.

 Λ_b^0 DECAY MODES

These branching fractions are actually an average over weakly decaying b -baryons weighted by their production rates in Z decay (or high-energy $p\bar{p}$), branching ratios, and detection efficiencies. They scale with the LEP b -baryon production fraction $B(b \rightarrow b\text{-baryon})$ and are evaluated for our value $B(b \rightarrow b\text{-baryon}) = (9.2 \pm 1.8)\%$.

The branching fractions $B(b\text{-baryon} \rightarrow \Lambda \ell^- \bar{\nu}_\ell \text{ anything})$ and $B(\Lambda_b^0 \rightarrow \Lambda_c^+ \ell^- \bar{\nu}_\ell \text{ anything})$ are not pure measurements because the underlying measured products of these with $B(b \rightarrow b\text{-baryon})$ were used to determine $B(b \rightarrow b\text{-baryon})$, as described in the note "Production and Decay of b -Flavored Hadrons."

For inclusive branching fractions, e.g., $B \rightarrow D^\pm \text{ anything}$, the values usually are multiplicities, not branching fractions. They can be greater than one.

Mode	Fraction (Γ_i/Γ)	Confidence level
Γ_1 $J/\psi(1S)\Lambda$	$(4.7 \pm 2.8) \times 10^{-4}$	
Γ_2 $pD^0\pi^-$		
Γ_3 $\Lambda_c^+\pi^-$	$(8.8 \pm 3.2) \times 10^{-3}$	
Γ_4 $\Lambda_c^+ a_1(1260)^-$	seen	
Γ_5 $\Lambda_c^+\pi^+\pi^-\pi^-$		
Γ_6 $\Lambda K^0 2\pi^+ 2\pi^-$		
Γ_7 $\Lambda_c^+ \ell^- \bar{\nu}_\ell \text{ anything}$	[a] $(9.9 \pm 2.6)\%$	
Γ_8 $\Lambda_c^+ \ell^- \bar{\nu}_\ell$	$(5.0 +1.9-1.4)\%$	
Γ_9 $\Lambda_c^+ \pi^+ \pi^- \ell^- \bar{\nu}_\ell$	$(5.6 \pm 3.1)\%$	
Γ_{10} $p h^-$	[b] < 2.3	$\times 10^{-5}$ 90%
Γ_{11} $p\pi^-$	< 5.0	$\times 10^{-5}$ 90%
Γ_{12} pK^-	< 5.0	$\times 10^{-5}$ 90%
Γ_{13} $\Lambda\gamma$	< 1.3	$\times 10^{-3}$ 90%

[a] Not a pure measurement. See note at head of Λ_b^0 Decay Modes.

[b] Here h^- means π^- or K^- .

 Λ_b^0 BRANCHING RATIOS $\Gamma(J/\psi(1S)\Lambda)/\Gamma_{\text{total}}$

VALUE (units 10^{-4})	EVTS	DOCUMENT ID	TECN	COMMENT
4.7 ± 2.1 ± 1.9		14 ABE	97B CDF	$p\bar{p}$ at 1.8 TeV

- • • We do not use the following data for averages, fits, limits, etc. • • •
- 196 ± 120 ± 40
- 16 15 ALBAJAR 91E UA1 $J/\psi(1S) \rightarrow \mu^+\mu^-$
- 14 ABE 97B reports $(0.037 \pm 0.017(\text{stat}) \pm 0.007(\text{sys}))\%$ for $B(b \rightarrow b\text{-baryon}) = 0.1$ and for $B(B^0 \rightarrow J/\psi(1S) K_S^0) = 0.037\%$. We rescale to our PDG 98 best value $B(b \rightarrow b\text{-baryon}) = (10.1 +3.9
-3.1)\%$ and $B(B^0 \rightarrow J/\psi(1S) K_S^0) = (0.044 \pm 0.006)\%$. Our first error is their experiments's error and our second error is the systematic error from using our best value.
- 15 ALBAJAR 91E reports $(180 \pm 110) \times 10^{-4}$ for $B(\bar{b} \rightarrow b\text{-baryon}) = 0.10$. We rescale to our best value $B(\bar{b} \rightarrow b\text{-baryon}) = (9.2 \pm 1.9) \times 10^{-2}$. Our first error is their experiment's error and our second error is the systematic error from using our best value.

 $\Gamma(pD^0\pi^-)/\Gamma_{\text{total}}$

VALUE	EVTS	DOCUMENT ID	TECN	COMMENT
seen	52	BARI	91 SFM	$D^0 \rightarrow K^-\pi^+$
seen		BASILE	81 SFM	$D^0 \rightarrow K^-\pi^+$

- • • We do not use the following data for averages, fits, limits, etc. • • •

See key on page 373

Baryon Particle Listings

Λ_b^0, Σ_b

$\Gamma(\Lambda_c^+ \pi^-)/\Gamma_{total}$ Γ_3/Γ

VALUE (units 10^{-3})	EVTS	DOCUMENT ID	TECN	COMMENT
$8.8 \pm 2.8 \pm 1.5$		16 ABULENCIA	07B	CDF $p\bar{p}$ at 1.96 TeV
••• We do not use the following data for averages, fits, limits, etc. •••				
seen	3	ABREU	96N	DLPH $\Lambda_c^+ \rightarrow pK^- \pi^+$
seen	4	BUSKULIC	96L	ALEP $\Lambda_c^+ \rightarrow pK^- \pi^+, p\bar{K}^0, \Lambda\pi^+ \pi^+ \pi^-$

¹⁶The result is obtained from $(f_{baryon}/f_d) (B(\Lambda_b^0 \rightarrow \Lambda_c^+ \pi^-)/B(\bar{B}^0 \rightarrow D^+ \pi^-)) = 0.82 \pm 0.08 \pm 0.11 \pm 0.22$, assuming $f_{baryon}/f_d = 0.25 \pm 0.04$ and $B(\bar{B}^0 \rightarrow D^+ \pi^-) = (2.68 \pm 0.13) \times 10^{-3}$.

$\Gamma(\Lambda_c^+ a_1(1260)^-)/\Gamma_{total}$ Γ_4/Γ

VALUE	EVTS	DOCUMENT ID	TECN	COMMENT
seen	1	ABREU	96N	DLPH $\Lambda_c^+ \rightarrow pK^- \pi^+, a_1^- \rightarrow \rho^0 \pi^- \rightarrow \pi^+ \pi^- \pi^-$

$\Gamma(\Lambda_c^+ \pi^+ \pi^- \pi^-)/\Gamma_{total}$ Γ_5/Γ

VALUE	EVTS	DOCUMENT ID	TECN	COMMENT
••• We do not use the following data for averages, fits, limits, etc. •••				
seen	90	BARI	91	SFM $\Lambda_c^+ \rightarrow pK^- \pi^+$

$\Gamma(\Lambda K^0 2\pi^+ 2\pi^-)/\Gamma_{total}$ Γ_6/Γ

VALUE	EVTS	DOCUMENT ID	TECN	COMMENT
••• We do not use the following data for averages, fits, limits, etc. •••				
seen	4	17 ARENTON	86	FMP5 $\Lambda K_S^0 2\pi^+ 2\pi^-$

$\Gamma(\Lambda_c^+ \ell^- \bar{\nu}_\ell \text{ anything})/\Gamma_{total}$ Γ_7/Γ

The values and averages in this section serve only to show what values result if one assumes our $B(b \rightarrow b\text{-baryon})$. They cannot be thought of as measurements since the underlying product branching fractions were also used to determine $B(b \rightarrow b\text{-baryon})$ as described in the note on "Production and Decay of b -Flavored Hadrons."

VALUE	EVTS	DOCUMENT ID	TECN	COMMENT
0.099 ± 0.026 OUR AVERAGE				
$0.093 \pm 0.017 \pm 0.019$		18 BARATE	98D	ALEP $e^+ e^- \rightarrow Z$
$0.13 \pm 0.04 \pm 0.03$	29	19 ABREU	95S	DLPH $e^+ e^- \rightarrow Z$
••• We do not use the following data for averages, fits, limits, etc. •••				
$0.082 \pm 0.020 \pm 0.017$	55	20 BUSKULIC	95L	ALEP Repl. by BARATE 98D
$0.16 \pm 0.06 \pm 0.03$	21	21 BUSKULIC	92E	ALEP $\Lambda_c^+ \rightarrow pK^- \pi^+$

¹⁸BARATE 98D reports $[B(\Lambda_b^0 \rightarrow \Lambda_c^+ \ell^- \bar{\nu}_\ell \text{ anything})] \times [B(\bar{b} \rightarrow b\text{-baryon})] = 0.0086 \pm 0.0007 \pm 0.0014$. We divide by our best value $B(\bar{b} \rightarrow b\text{-baryon}) = (9.2 \pm 1.9) \times 10^{-2}$. Our first error is their experiment's error and our second error is the systematic error from using our best value. Measured using $\Lambda_c \ell^-$ and $\Lambda \ell^+ \ell^-$.

¹⁹ABREU 95S reports $[B(\Lambda_b^0 \rightarrow \Lambda_c^+ \ell^- \bar{\nu}_\ell \text{ anything})] \times [B(\bar{b} \rightarrow b\text{-baryon})] = 0.0118 \pm 0.0026 \pm 0.0031$. We divide by our best value $B(\bar{b} \rightarrow b\text{-baryon}) = (9.2 \pm 1.9) \times 10^{-2}$. Our first error is their experiment's error and our second error is the systematic error from using our best value.

²⁰BUSKULIC 95L reports $[B(\Lambda_b^0 \rightarrow \Lambda_c^+ \ell^- \bar{\nu}_\ell \text{ anything})] \times [B(\bar{b} \rightarrow b\text{-baryon})] = 0.00755 \pm 0.0014 \pm 0.0012$. We divide by our best value $B(\bar{b} \rightarrow b\text{-baryon}) = (9.2 \pm 1.9) \times 10^{-2}$. Our first error is their experiment's error and our second error is the systematic error from using our best value.

²¹BUSKULIC 92E reports $[B(\Lambda_b^0 \rightarrow \Lambda_c^+ \ell^- \bar{\nu}_\ell \text{ anything})] \times [B(\bar{b} \rightarrow b\text{-baryon})] = 0.015 \pm 0.0035 \pm 0.0045$. We divide by our best value $B(\bar{b} \rightarrow b\text{-baryon}) = (9.2 \pm 1.9) \times 10^{-2}$. Our first error is their experiment's error and our second error is the systematic error from using our best value. Superseded by BUSKULIC 95L.

$\Gamma(\Lambda_c^+ \ell^- \bar{\nu}_\ell)/\Gamma_{total}$ Γ_8/Γ

VALUE	DOCUMENT ID	TECN	COMMENT
$0.050 \pm 0.011 + 0.016$ $-0.008 - 0.012$	22 ABDALLAH	04A	DLPH $e^+ e^- \rightarrow Z^0$

²²Derived from a combined likelihood and event rate fit to the distribution of the Isgur-Wise variable and using HQET. The slope of the form factor is measured to be $\rho^2 = 2.03 \pm 0.46^{+0.72}_{-1.00}$.

$\Gamma(\Lambda_c^+ \pi^+ \pi^- \ell^- \bar{\nu}_\ell)/\Gamma_{total}$ Γ_9/Γ

VALUE	DOCUMENT ID	TECN	COMMENT
0.056 ± 0.031 -0.030	23 ABDALLAH	04A	DLPH $e^+ e^- \rightarrow Z^0$

²³Derived from the fraction of $\Gamma(\Lambda_b^0 \rightarrow \Lambda_c^+ \ell^- \bar{\nu}_\ell) / (\Gamma(\Lambda_b^0 \rightarrow \Lambda_c^+ \ell^- \bar{\nu}_\ell) + \Gamma(\Lambda_b^0 \rightarrow \Lambda_c^+ \pi^+ \pi^- \ell^- \bar{\nu}_\ell)) = 0.47^{+0.10+0.07}_{-0.08-0.06}$.

$\Gamma(\Lambda_c^+ \ell^- \bar{\nu}_\ell) / [\Gamma(\Lambda_c^+ \ell^- \bar{\nu}_\ell) + \Gamma(\Lambda_c^+ \pi^+ \pi^- \ell^- \bar{\nu}_\ell)]$ $\Gamma_8/(\Gamma_8+\Gamma_9)$

VALUE	DOCUMENT ID	TECN	COMMENT
$0.47 \pm 0.10 + 0.07$ $-0.08 - 0.06$	ABDALLAH	04A	DLPH $e^+ e^- \rightarrow Z^0$

$\Gamma(p h^-)/\Gamma_{total}$ Γ_{10}/Γ

VALUE	CL%	DOCUMENT ID	TECN	COMMENT
$<2.3 \times 10^{-5}$	90	24 ACOSTA	05o	CDF $p\bar{p}$ at 1.96 TeV

²⁴Assumes $f_\Lambda / f_d = 0.25$, and equal momentum distribution for Λ_b and B mesons.

$\Gamma(p \pi^-)/\Gamma_{total}$ Γ_{11}/Γ

VALUE	CL%	DOCUMENT ID	TECN	COMMENT
$<5.0 \times 10^{-5}$	90	25 BUSKULIC	96V	ALEP $e^+ e^- \rightarrow Z$

²⁵BUSKULIC 96V assumes PDG 96 production fractions for B^0, B^+, B_s, b baryons.

$\Gamma(p K^-)/\Gamma_{total}$ Γ_{12}/Γ

VALUE	CL%	DOCUMENT ID	TECN	COMMENT
$<5.0 \times 10^{-5}$	90	26 BUSKULIC	96V	ALEP $e^+ e^- \rightarrow Z$
$<3.6 \times 10^{-4}$	90	27 ADAM	96D	DLPH $e^+ e^- \rightarrow Z$

²⁶BUSKULIC 96V assumes PDG 96 production fractions for B^0, B^+, B_s, b baryons.
²⁷ADAM 96D assumes $f_{B^0} = f_{B^-} = 0.39$ and $f_{B_s} = 0.12$.

$\Gamma(\Lambda \gamma)/\Gamma_{total}$ Γ_{13}/Γ

VALUE	CL%	DOCUMENT ID	TECN	COMMENT
$<1.3 \times 10^{-3}$	90	ACOSTA	02G	CDF $p\bar{p}$ at 1.8 TeV

Λ_b^0 REFERENCES

ABAZOV	07S	PRL 99 142001	V.M. Abazov et al.	(D0 Collab.)
ABAZOV	07U	PRL 99 182001	V.M. Abazov et al.	(D0 Collab.)
ABULENCIA	07A	PRL 98 122001	A. Abulencia et al.	(FNAL CDF Collab.)
ABULENCIA	07B	PRL 98 122002	A. Abulencia et al.	(FNAL CDF Collab.)
ACOSTA	06	PRL 96 202001	D. Acosta et al.	(CDF Collab.)
ABAZOV	05C	PRL 94 102001	V.M. Abazov et al.	(D0 Collab.)
ACOSTA	05O	PR D72 051104R	D. Acosta et al.	(CDF Collab.)
ABDALLAH	04A	PL B585 63	J. Abdallah et al.	(DELPHI Collab.)
ACOSTA	02G	PR D66 112002	D. Acosta et al.	(CDF Collab.)
ABREU	99W	EPJ C10 185	P. Abreu et al.	(DELPHI Collab.)
ACKERS TAFF	98G	PL B426 161	K. Ackersstaff et al.	(OPAL Collab.)
BARATE	98D	EPJ C2 197	R. Barate et al.	(ALEPH Collab.)
PDG	98	EPJ C3 1	C. Caso et al.	
ABE	97B	PR D55 1142	F. Abe et al.	(CDF Collab.)
ABE	96M	PRL 77 1439	F. Abe et al.	(CDF Collab.)
ABREU	96D	ZPHY C71 149	P. Abreu et al.	(DELPHI Collab.)
ABREU	96N	PL B374 351	P. Abreu et al.	(DELPHI Collab.)
ADAM	96D	ZPHY C72 207	W. Adam et al.	(DELPHI Collab.)
BUSKULIC	96L	PL B380 442	D. Buskulic et al.	(ALEPH Collab.)
BUSKULIC	96V	PL B384 471	D. Buskulic et al.	(ALEPH Collab.)
PDG	96	PR D54 1	R. M. Barnett et al.	
ABREU	95S	ZPHY C68 375	P. Abreu et al.	(DELPHI Collab.)
AKERS	95K	PL B353 402	R. Akers et al.	(OPAL Collab.)
BUSKULIC	95L	PL B357 685	D. Buskulic et al.	(ALEPH Collab.)
ABE	93B	PR D47 R2639	F. Abe et al.	(CDF Collab.)
BUSKULIC	92E	PL B294 145	D. Buskulic et al.	(ALEPH Collab.)
ALBAJAR	91E	PL B273 540	C. Albajar et al.	(UA1 Collab.)
BARI	91	NC 104A 1787	G. Bari et al.	(CERN R422 Collab.)
ARENTON	86	NP B274 707	M.W. Arenton et al.	(ARIZ, NDAM, VAND)
BASILE	81	LCN 31 97	M. Basile et al.	(CERN R415 Collab.)

Σ_b

$I(J^P) = 1(\frac{1}{2}^+)$ Status: ** *
 I, J, P need confirmation.

In the quark model $\Sigma_b^+, \Sigma_b^0, \Sigma_b^-$ are an isotriplet (uub, udb, ddb) state. The lowest Σ_b ought to have $J^P = 1/2^+$. None of I, J, P have actually been measured.

Σ_b MASS

Σ_b^+ MASS

VALUE (MeV)	DOCUMENT ID	TECN	COMMENT
5807.8 ± 2.7 OUR FIT			
$5807.8 \pm 2.0 \pm 1.7$	1 AALTONEN	07k	CDF $p\bar{p}$ at 1.96 TeV

Σ_b^0 MASS

VALUE (MeV)	DOCUMENT ID	TECN	COMMENT
5815.2 ± 2.0 OUR FIT			
$5815.2 \pm 1.0 \pm 1.7$	1 AALTONEN	07k	CDF $p\bar{p}$ at 1.96 TeV

¹ Observed four $\Lambda_b^0 \pi^\pm$ resonances in the fully reconstructed decay mode $\Lambda_b^0 \rightarrow \Lambda_c^+ \pi^-$, where $\Lambda_c^+ \rightarrow pK^- \pi^+$.

Σ_b DECAY MODES

Mode	Fraction (Γ_i/Γ)
$\Gamma_1 \Lambda_b^0 \pi$	dominant

Σ_b BRANCHING RATIOS

$\Gamma(\Lambda_b^0 \pi)/\Gamma_{total}$	DOCUMENT ID	TECN	COMMENT
dominant	AALTONEN	07k	CDF $p\bar{p}$ at 1.96 TeV

Σ_b REFERENCES

AALTONEN	07K	PRL 99 202001	T. Aaltonen et al.	(CDF Collab.)
----------	-----	---------------	--------------------	---------------

Baryon Particle Listings

 Σ_b^* , Ξ_b^0 , Ξ_b^- , b -baryon ADMIXTURE (Λ_b , Ξ_b , Σ_b , Ω_b) Σ_b^* $I(J^P) = 1(\frac{3}{2}^+)$ Status: ***
 I, J, P need confirmation. I, J, P need confirmation. Quantum numbers shown are quark-model predictions. Σ_b^* MASSAssumes $m_{\Sigma_b^{*+}} - m_{\Sigma_b^{*0}} = m_{\Sigma_b^{*0}} - m_{\Sigma_b^{*-}}$ Σ_b^{*+} MASSVALUE (MeV) DOCUMENT ID
5829.0 ± 3.4 OUR FIT Σ_b^{*0} MASSVALUE (MeV) DOCUMENT ID
5836.4 ± 2.8 OUR FIT $m_{\Sigma_b^*} - m_{\Sigma_b}$ VALUE (MeV) DOCUMENT ID TECN COMMENT
21.2 ± 2.0 OUR FIT21.2 ± 2.0 ± 0.4
-1.9 -0.31 AALTONEN 07K CDF $p\bar{p}$ at 1.96 TeV1 Observed four $\Lambda_b^0 \pi^\pm$ resonances in the fully reconstructed decay mode $\Lambda_b^0 \rightarrow \Lambda_c^+ \pi^-$, where $\Lambda_c^+ \rightarrow p K^- \pi^+$. Assumes $m_{\Sigma_b^{*+}} - m_{\Sigma_b^{*0}} = m_{\Sigma_b^{*0}} - m_{\Sigma_b^{*-}}$ Σ_b^* DECAY MODES

Mode	Fraction (Γ_i/Γ)
Γ_1 $\Lambda_b^0 \pi$	dominant

 Σ_b^* BRANCHING RATIOS

$\Gamma(\Lambda_b^0 \pi)/\Gamma_{\text{total}}$	DOCUMENT ID	TECN	COMMENT	Γ_1/Γ
dominant	AALTONEN	07K	CDF $p\bar{p}$ at 1.96 TeV	

 Σ_b^* REFERENCES

AALTONEN 07K PRL 99 202001 T. Aaltonen et al. (CDF Collab.)

 Ξ_b^0 , Ξ_b^- $I(J^P) = \frac{1}{2}(\frac{1}{2}^+)$ Status: ***
 I, J, P need confirmation.In the quark model, Ξ_b^0 and Ξ_b^- are an isodoublet (usb , dsb) state; the lowest Ξ_b^0 and Ξ_b^- ought to have $J^P = 1/2^+$. None of I, J , or P have actually been measured. Ξ_b MASSES Ξ_b MASSVALUE (MeV) DOCUMENT ID TECN COMMENT
5792.4 ± 3.0 OUR AVERAGE

5792.9 ± 2.5 ± 1.7

1 AALTONEN 07A CDF $p\bar{p}$ at 1.96 TeV

5774 ± 11 ± 15

2 ABAZOV 07K D0 $p\bar{p}$ at 1.96 TeV1 Observed in $\Xi_b^- \rightarrow J/\psi \Xi^-$ decays with 17.5 ± 4.3 candidates, a significance of 7.7 sigma.2 Observed in $\Xi_b^- \rightarrow J/\psi \Xi^-$ decays with $15.2 \pm 4.4^{+1.9}_{-0.4}$ candidates, a significance of 5.5 sigma. Ξ_b MEAN LIFEThis is actually a measurement of the average lifetime of b -baryons that decay to a jet containing a same-sign $\Xi \mp \bar{K} \mp$ pair. Presumably the mix is mainly Ξ_b , with some Λ_b ."OUR EVALUATION" is an average using rescaled values of the data listed below. The average and rescaling were performed by the Heavy Flavor Averaging Group (HFAG) and are described at <http://www.slac.stanford.edu/xorg/hfag/>. The averaging/rescaling procedure takes into account correlations between the measurements and asymmetric lifetime errors.VALUE (10^{-12} s) EVTS DOCUMENT ID TECN COMMENT
1.42 ± 0.29 ± 0.24 OUR EVALUATION

1.40 ± 0.40 ± 0.31 ± 0.12

3 ABDALLAH 05c DLPH $e^+e^- \rightarrow Z^0$

1.35 ± 0.37 ± 0.15 ± 0.28 ± 0.17

4 BUSKULIC 96T ALEP $e^+e^- \rightarrow Z$

••• We do not use the following data for averages, fits, limits, etc. •••

1.5 ± 0.7 ± 0.4 ± 0.3

8 5 ABREU 95v DLPH Repl. by ABDALLAH 05c

3 Used the decay length of Ξ^- accompanied by a lepton of the same sign.4 Excess $\Xi^- \ell^-$, impact parameters.5 Excess $\Xi^- \ell^-$, decay lengths. Ξ_b DECAY MODES

Mode	Fraction (Γ_i/Γ)	Scale factor
Γ_1 $\Xi_b^- \rightarrow \Xi^- \ell^- \bar{\nu}_\ell \times B(\bar{b} \rightarrow \Xi_b^-)$	$(3.9 \pm 1.2) \times 10^{-4}$	1.4
Γ_2 $\Xi_b^- \rightarrow J/\psi \Xi^- \times B(\bar{b} \rightarrow \Xi_b^-)/B(\bar{b} \rightarrow \Lambda_b)$	$(1.3 \pm 1.0) \times 10^{-4}$	

 Ξ_b BRANCHING RATIOS

$\Gamma(\Xi^- \ell^- \bar{\nu}_\ell \times B(\bar{b} \rightarrow \Xi_b^-))/\Gamma_{\text{total}}$	DOCUMENT ID	TECN	COMMENT	Γ_1/Γ
3.9 ± 1.2 OUR AVERAGE			Error includes scale factor of 1.4.	
3.0 ± 1.0 ± 0.3	ABDALLAH	05c	DLPH $e^+e^- \rightarrow Z^0$	
5.4 ± 1.1 ± 0.8	BUSKULIC	96T	ALEP Excess $\Xi^- \ell^-$ over $\Xi^- \ell^+$	
•••	•••	•••	We do not use the following data for averages, fits, limits, etc. •••	
5.9 ± 2.1 ± 1.0	ABREU	95v	DLPH Repl. by ABDALLAH 05c	

 $\Gamma(J/\psi \Xi^- \times B(\bar{b} \rightarrow \Xi_b^-))/\Gamma_{\text{total}}$ Γ_2/Γ VALUE (units 10^{-4}) DOCUMENT ID TECN COMMENT
1.3 ± 0.6 ± 0.8 6 ABAZOV 07K D0 $p\bar{p}$ at 1.96 TeV6 ABAZOV 07K reports $[B(\Xi_b^- \rightarrow J/\psi \Xi^- \times B(\bar{b} \rightarrow \Xi_b^-))/B(\bar{b} \rightarrow \Lambda_b)] / [B(\Lambda_b^0 \rightarrow J/\psi(1S) \Lambda)] = 0.28 \pm 0.09^{+0.09}_{-0.08}$. We multiply by our best value $B(\Lambda_b^0 \rightarrow J/\psi(1S) \Lambda) = (4.7 \pm 2.8) \times 10^{-4}$. Our first error is their experiment's error and our second error is the systematic error from using our best value. Ξ_b REFERENCESAALTONEN 07A PRL 99 052002 T. Aaltonen et al. (CDF Collab.)
ABAZOV 07K PRL 99 052001 V.M. Abazov et al. (D0 Collab.)
ABDALLAH 05C EPJ C44 299 J. Abdallah et al. (DELPHI Collab.)
BUSKULIC 96T PL B384 449 D. Buskulic et al. (ALEPH Collab.)
ABREU 95V ZPHY C68 541 P. Abreu et al. (DELPHI Collab.) b -baryon ADMIXTURE (Λ_b , Ξ_b , Σ_b , Ω_b) b -baryon ADMIXTURE MEAN LIFEEach measurement of the b -baryon mean life is an average over an admixture of various b -baryons which decay weakly. Different techniques emphasize different admixtures of produced particles, which could result in a different b -baryon mean life. More b -baryon flavor specific channels are not included in the measurement."OUR EVALUATION" is an average using rescaled values of the data listed below. The average and rescaling were performed by the Heavy Flavor Averaging Group (HFAG) and are described at <http://www.slac.stanford.edu/xorg/hfag/>. The averaging/rescaling procedure takes into account correlations between the measurements and asymmetric lifetime errors.VALUE (10^{-12} s) EVTS DOCUMENT ID TECN COMMENT
1.319 ± 0.039 ± 0.038 OUR EVALUATION

1.218 ± 0.130 ± 0.115 ± 0.042

1 ABAZOV 07S D0 $p\bar{p}$ at 1.96 TeV

1.290 ± 0.119 ± 0.087 ± 0.110 ± 0.091

2 ABAZOV 07U D0 $p\bar{p}$ at 1.96 TeV

1.593 ± 0.083 ± 0.078 ± 0.033

1 ABULENCIA 07A CDF $p\bar{p}$ at 1.96 TeV

1.16 ± 0.20 ± 0.08

3 ABREU 99w DLPH $e^+e^- \rightarrow Z$

1.19 ± 0.14 ± 0.07

4 ABREU 99w DLPH $e^+e^- \rightarrow Z$

1.11 ± 0.19 ± 0.18 ± 0.05

5 ABREU 99w DLPH $e^+e^- \rightarrow Z$

1.29 ± 0.24 ± 0.22 ± 0.06

5 ACKERSTAFF 98G OPAL $e^+e^- \rightarrow Z$

1.20 ± 0.08 ± 0.06

6 BARATE 98D ALEP $e^+e^- \rightarrow Z$

1.21 ± 0.11

5 BARATE 98D ALEP $e^+e^- \rightarrow Z$

1.32 ± 0.15 ± 0.07

7 ABE 96M CDF $p\bar{p}$ at 1.8 TeV

1.10 ± 0.19 ± 0.17 ± 0.09

5 ABREU 96D DLPH $e^+e^- \rightarrow Z$

1.16 ± 0.11 ± 0.06

5 AKERS 96 OPAL $e^+e^- \rightarrow Z$

1.22 ± 0.22 ± 0.18 ± 0.04

1 ABAZOV 05c D0 Repl. by ABAZOV 07s

1.14 ± 0.08 ± 0.04

8 ABREU 99w DLPH $e^+e^- \rightarrow Z$

1.46 ± 0.22 ± 0.07 ± 0.21 ± 0.09

ABREU 96D DLPH Repl. by ABREU 99w

1.27 ± 0.35 ± 0.29 ± 0.09

ABREU 95S DLPH Repl. by ABREU 99w

See key on page 373

Baryon Particle Listings

b -baryon ADMIXTURE ($\Lambda_b, \Xi_b, \Sigma_b, \Omega_b$)

1.05	$\begin{smallmatrix} +0.12 \\ -0.11 \end{smallmatrix}$	± 0.09	290	BUSKULIC	95L	ALEP	Repl. by BARATE 98D
1.04	$\begin{smallmatrix} +0.48 \\ -0.38 \end{smallmatrix}$	± 0.10	11	⁹ ABREU	93F	DLPH	Excess $\Lambda\mu^-$, decay lengths
1.05	$\begin{smallmatrix} +0.23 \\ -0.20 \end{smallmatrix}$	± 0.08	157	¹⁰ AKERS	93	OPAL	Excess $\Lambda\ell^-$, decay lengths
1.12	$\begin{smallmatrix} +0.32 \\ -0.29 \end{smallmatrix}$	± 0.16	101	¹¹ BUSKULIC	92I	ALEP	Excess $\Lambda\ell^-$, impact parameters

¹ Measured mean life using fully reconstructed $\Lambda_b^0 \rightarrow J/\psi\Lambda$ decays.

² Measured using semileptonic decays $\Lambda_b(0) \rightarrow \Lambda_c^+ \mu\nu X, \Lambda_c^+ \rightarrow K_S^0 p$.

³ Measured using $\Lambda\ell^-$ decay length.

⁴ Measured using $p\ell^-$ decay length.

⁵ Measured using $\Lambda_c\ell^-$ and $\Lambda\ell^+\ell^-$.

⁶ Measured using the excess of $\Lambda\ell^-$, lepton impact parameter.

⁷ Measured using $\Lambda_c\ell^-$.

⁸ This ABREU 99w result is the combined result of the $\Lambda\ell^-$, $p\ell^-$, and excess $\Lambda\mu^-$ impact parameter measurements.

⁹ ABREU 93F superseded by ABREU 96D.

¹⁰ AKERS 93 superseded by AKERS 96.

¹¹ BUSKULIC 92I superseded by BUSKULIC 95L.

b -baryon ADMIXTURE DECAY MODES ($\Lambda_b, \Xi_b, \Sigma_b, \Omega_b$)

These branching fractions are actually an average over weakly decaying b -baryons weighted by their production rates in Z decay (or high-energy $p\bar{p}$), branching ratios, and detection efficiencies. They scale with the LEP b -baryon production fraction $B(b \rightarrow b\text{-baryon})$ and are evaluated for our value $B(b \rightarrow b\text{-baryon}) = (9.2 \pm 1.8)\%$.

The branching fractions $B(b\text{-baryon} \rightarrow \Lambda\ell^-\bar{\nu}_\ell\text{anything})$ and $B(\Lambda_b^0 \rightarrow \Lambda_c^+\ell^-\bar{\nu}_\ell\text{anything})$ are not pure measurements because the underlying measured products of these with $B(b \rightarrow b\text{-baryon})$ were used to determine $B(b \rightarrow b\text{-baryon})$, as described in the note "Production and Decay of b -Flavored Hadrons."

For inclusive branching fractions, e.g., $B \rightarrow D^\pm\text{anything}$, the values usually are multiplicities, not branching fractions. They can be greater than one.

Mode	Fraction (Γ_i/Γ)
Γ_1 $p\mu^-\bar{\nu}$ anything	$(5.3 \pm \frac{2.3}{2.0})\%$
Γ_2 $p\ell\bar{\nu}_\ell$ anything	$(5.1 \pm 1.4)\%$
Γ_3 p anything	$(64 \pm 23)\%$
Γ_4 $\Lambda\ell^-\bar{\nu}_\ell$ anything	$(3.5 \pm 0.8)\%$
Γ_5 $\Lambda\ell^+\nu_\ell$ anything	
Γ_6 Λ anything	
Γ_7 $\Lambda_c^+\ell^-\bar{\nu}_\ell$ anything	
Γ_8 $\Lambda/\bar{\Lambda}$ anything	$(36 \pm 9)\%$
Γ_9 $\Xi^-\ell^-\bar{\nu}_\ell$ anything	$(6.0 \pm 1.8) \times 10^{-3}$

b -baryon ADMIXTURE ($\Lambda_b, \Xi_b, \Sigma_b, \Omega_b$) BRANCHING RATIOS

$\Gamma(p\mu^-\bar{\nu}\text{anything})/\Gamma_{\text{total}}$		Γ_1/Γ	
VALUE	EVTS	DOCUMENT ID	TECN COMMENT
$0.053 \pm \frac{0.020}{0.017} \pm 0.011$	125	¹² ABREU	95s DLPH $e^+e^- \rightarrow Z$

¹² ABREU 95s reports $[B(b\text{-baryon} \rightarrow p\mu^-\bar{\nu}\text{anything})] \times [B(\bar{b} \rightarrow b\text{-baryon})] = 0.0049 \pm 0.0011 \pm \frac{0.0015}{0.0011}$. We divide by our best value $B(\bar{b} \rightarrow b\text{-baryon}) = (9.2 \pm 1.9) \times 10^{-2}$. Our first error is their experiment's error and our second error is the systematic error from using our best value.

$\Gamma(p\ell\bar{\nu}_\ell\text{anything})/\Gamma_{\text{total}}$		Γ_2/Γ	
VALUE	DOCUMENT ID	TECN	COMMENT
$0.051 \pm 0.009 \pm 0.011$	¹³ BARATE	98V	ALEP $e^+e^- \rightarrow Z$

¹³ BARATE 98V reports $[B(b\text{-baryon} \rightarrow p\ell\bar{\nu}_\ell\text{anything})] \times [B(\bar{b} \rightarrow b\text{-baryon})] = (4.72 \pm 0.66 \pm 0.44) \times 10^{-3}$. We divide by our best value $B(\bar{b} \rightarrow b\text{-baryon}) = (9.2 \pm 1.9) \times 10^{-2}$. Our first error is their experiment's error and our second error is the systematic error from using our best value.

$\Gamma(p\ell\bar{\nu}_\ell\text{anything})/\Gamma(p\text{anything})$		Γ_2/Γ_3	
VALUE	DOCUMENT ID	TECN	COMMENT
$0.080 \pm 0.012 \pm 0.014$	BARATE	98V	ALEP $e^+e^- \rightarrow Z$

$\Gamma(\Lambda\ell^-\bar{\nu}_\ell\text{anything})/\Gamma_{\text{total}}$		Γ_4/Γ	
--	--	-------------------	--

The values and averages in this section serve only to show what values result if one assumes our $B(b \rightarrow b\text{-baryon})$. They cannot be thought of as measurements since the underlying product branching fractions were also used to determine $B(b \rightarrow b\text{-baryon})$ as described in the note on "Production and Decay of b -Flavored Hadrons."

VALUE	EVTS	DOCUMENT ID	TECN	COMMENT
0.035 ± 0.008 OUR AVERAGE				
$0.035 \pm 0.005 \pm 0.007$		¹⁴ BARATE	98D	ALEP $e^+e^- \rightarrow Z$
$0.032 \pm 0.004 \pm 0.007$		¹⁵ AKERS	96	OPAL Excess of $\Lambda\ell^-$ over $\Lambda\ell^+$
$0.033 \pm 0.008 \pm 0.007$	262	¹⁶ ABREU	95s	DLPH Excess of $\Lambda\ell^-$ over $\Lambda\ell^+$
$0.066 \pm 0.013 \pm 0.014$	290	¹⁷ BUSKULIC	95L	ALEP Excess of $\Lambda\ell^-$ over $\Lambda\ell^+$
••• We do not use the following data for averages, fits, limits, etc. •••				
seen	157	¹⁸ AKERS	93	OPAL Excess of $\Lambda\ell^-$ over $\Lambda\ell^+$
$0.076 \pm 0.022 \pm 0.016$	101	¹⁹ BUSKULIC	92I	ALEP Excess of $\Lambda\ell^-$ over $\Lambda\ell^+$

¹⁴ BARATE 98D reports $[B(b\text{-baryon} \rightarrow \Lambda\ell^-\bar{\nu}_\ell\text{anything})] \times [B(\bar{b} \rightarrow b\text{-baryon})] = 0.00326 \pm 0.00016 \pm 0.00039$. We divide by our best value $B(\bar{b} \rightarrow b\text{-baryon}) = (9.2 \pm 1.9) \times 10^{-2}$. Our first error is their experiment's error and our second error is the systematic error from using our best value. Measured using the excess of $\Lambda\ell^-$, lepton impact parameter.

¹⁵ AKERS 96 reports $[B(b\text{-baryon} \rightarrow \Lambda\ell^-\bar{\nu}_\ell\text{anything})] \times [B(\bar{b} \rightarrow b\text{-baryon})] = 0.00291 \pm 0.00023 \pm 0.00025$. We divide by our best value $B(\bar{b} \rightarrow b\text{-baryon}) = (9.2 \pm 1.9) \times 10^{-2}$. Our first error is their experiment's error and our second error is the systematic error from using our best value.

¹⁶ ABREU 95s reports $[B(b\text{-baryon} \rightarrow \Lambda\ell^-\bar{\nu}_\ell\text{anything})] \times [B(\bar{b} \rightarrow b\text{-baryon})] = 0.0030 \pm 0.0006 \pm 0.0004$. We divide by our best value $B(\bar{b} \rightarrow b\text{-baryon}) = (9.2 \pm 1.9) \times 10^{-2}$. Our first error is their experiment's error and our second error is the systematic error from using our best value.

¹⁷ BUSKULIC 95L reports $[B(b\text{-baryon} \rightarrow \Lambda\ell^-\bar{\nu}_\ell\text{anything})] \times [B(\bar{b} \rightarrow b\text{-baryon})] = 0.0061 \pm 0.0006 \pm 0.0010$. We divide by our best value $B(\bar{b} \rightarrow b\text{-baryon}) = (9.2 \pm 1.9) \times 10^{-2}$. Our first error is their experiment's error and our second error is the systematic error from using our best value.

¹⁸ AKERS 93 superseded by AKERS 96.

¹⁹ BUSKULIC 92I reports $[B(b\text{-baryon} \rightarrow \Lambda\ell^-\bar{\nu}_\ell\text{anything})] \times [B(\bar{b} \rightarrow b\text{-baryon})] = 0.0070 \pm 0.0010 \pm 0.0018$. We divide by our best value $B(\bar{b} \rightarrow b\text{-baryon}) = (9.2 \pm 1.9) \times 10^{-2}$. Our first error is their experiment's error and our second error is the systematic error from using our best value. Superseded by BUSKULIC 95L.

$\Gamma(\Lambda\ell^+\nu_\ell\text{anything})/\Gamma(\Lambda\text{anything})$		Γ_5/Γ_6	
VALUE	DOCUMENT ID	TECN	COMMENT
$0.080 \pm 0.012 \pm 0.008$	ABBIENDI	99L	OPAL $e^+e^- \rightarrow Z$
••• We do not use the following data for averages, fits, limits, etc. •••			
$0.070 \pm 0.012 \pm 0.007$	ACKERSTAFF	97N	OPAL Repl. by ABBI- ENDI 99L

$\Gamma(\Lambda/\bar{\Lambda}\text{anything})/\Gamma_{\text{total}}$		Γ_8/Γ	
VALUE	DOCUMENT ID	TECN	COMMENT
0.36 ± 0.09 OUR AVERAGE			
$0.38 \pm 0.05 \pm 0.08$	²⁰ ABBIENDI	99L	OPAL $e^+e^- \rightarrow Z$
$0.24 \pm \frac{0.13}{0.08} \pm 0.05$	²¹ ABREU	95c	DLPH $e^+e^- \rightarrow Z$

••• We do not use the following data for averages, fits, limits, etc. •••

$0.43 \pm 0.06 \pm 0.09$ ²²ACKERSTAFF 97N OPAL Repl. by ABBI-
ENDI 99L

²⁰ ABBIENDI 99L reports $[B(b\text{-baryon} \rightarrow \Lambda/\bar{\Lambda}\text{anything})] \times [B(\bar{b} \rightarrow b\text{-baryon})] = 0.035 \pm 0.0032 \pm 0.0035$. We divide by our best value $B(\bar{b} \rightarrow b\text{-baryon}) = (9.2 \pm 1.9) \times 10^{-2}$. Our first error is their experiment's error and our second error is the systematic error from using our best value.

²¹ ABREU 95c reports $0.28 \pm \frac{0.17}{0.12}$ for $B(\bar{b} \rightarrow b\text{-baryon}) = 0.08 \pm 0.02$. We rescale to our best value $B(\bar{b} \rightarrow b\text{-baryon}) = (9.2 \pm 1.9) \times 10^{-2}$. Our first error is their experiment's error and our second error is the systematic error from using our best value.

²² ACKERSTAFF 97N reports $[B(b\text{-baryon} \rightarrow \Lambda/\bar{\Lambda}\text{anything})] \times [B(\bar{b} \rightarrow b\text{-baryon})] = 0.0393 \pm 0.0046 \pm 0.0037$. We divide by our best value $B(\bar{b} \rightarrow b\text{-baryon}) = (9.2 \pm 1.9) \times 10^{-2}$. Our first error is their experiment's error and our second error is the systematic error from using our best value.

$\Gamma(\Xi^-\ell^-\bar{\nu}_\ell\text{anything})/\Gamma_{\text{total}}$		Γ_9/Γ	
VALUE	DOCUMENT ID	TECN	COMMENT
0.0060 ± 0.0018 OUR AVERAGE			
$0.0059 \pm 0.0015 \pm 0.0012$	²³ BUSKULIC	96T	ALEP Excess $\Xi^-\ell^-$ over $\Xi^-\ell^+$
$0.0064 \pm 0.0025 \pm 0.0013$	²⁴ ABREU	95v	DLPH Excess $\Xi^-\ell^-$ over $\Xi^-\ell^+$

²³ BUSKULIC 96T reports $[B(b\text{-baryon} \rightarrow \Xi^-\ell^-\bar{\nu}_\ell\text{anything})] \times [B(\bar{b} \rightarrow b\text{-baryon})] = 0.00054 \pm 0.00011 \pm 0.00008$. We divide by our best value $B(\bar{b} \rightarrow b\text{-baryon}) = (9.2 \pm 1.9) \times 10^{-2}$. Our first error is their experiment's error and our second error is the systematic error from using our best value.

²⁴ ABREU 95v reports $[B(b\text{-baryon} \rightarrow \Xi^-\ell^-\bar{\nu}_\ell\text{anything})] \times [B(\bar{b} \rightarrow b\text{-baryon})] = 0.00059 \pm 0.00021 \pm 0.0001$. We divide by our best value $B(\bar{b} \rightarrow b\text{-baryon}) = (9.2 \pm 1.9) \times 10^{-2}$. Our first error is their experiment's error and our second error is the systematic error from using our best value.

b -baryon ADMIXTURE ($\Lambda_b, \Xi_b, \Sigma_b, \Omega_b$) REFERENCES

ABAZOV	07S	PRL 99 142001	V.M. Abazov et al.	(D0 Collab.)
ABAZOV	07U	PRL 99 182001	V.M. Abazov et al.	(D0 Collab.)
ABULENCIA	07A	PRL 98 122001	A. Abulencia et al.	(FNAL CDF Collab.)
ABAZOV	05C	PRL 94 102001	V.M. Abazov et al.	(D0 Collab.)
ABBIENDI	99L	EPJ C9 1	G. Abbiendi et al.	(OPAL Collab.)
ABREU	99W	EPJ C10 185	P. Abreu et al.	(DELPHI Collab.)
ACKERSTAFF	98G	PL B426 161	K. Ackerstaff et al.	(OPAL Collab.)
BARATE	98D	EPJ C2 197	R. Barate et al.	(ALEPH Collab.)
BARATE	98V	EPJ C5 205	R. Barate et al.	(ALEPH Collab.)
ACKERSTAFF	97N	ZPHY C74 423	K. Ackerstaff et al.	(OPAL Collab.)
ABE	96M	PRL 77 1439	F. Abe et al.	(CDF Collab.)

Baryon Particle Listings

 b -baryon ADMIXTURE ($\Lambda_b, \Xi_b, \Sigma_b, \Omega_b$)

ABREU	96D	ZPHY C71 199	P. Abreu <i>et al.</i>	(DELPHI Collab.)	ABREU	95V	ZPHY C68 541	P. Abreu <i>et al.</i>	(DELPHI Collab.)
AKERS	96	ZPHY C69 195	R. Akers <i>et al.</i>	(OPAL Collab.)	BUSKULIC	95L	PL B357 685	D. Buskulic <i>et al.</i>	(ALEPH Collab.)
BUSKULIC	96T	PL B384 449	D. Buskulic <i>et al.</i>	(ALEPH Collab.)	ABREU	93F	PL B311 379	P. Abreu <i>et al.</i>	(DELPHI Collab.)
ABREU	95C	PL B347 447	P. Abreu <i>et al.</i>	(DELPHI Collab.)	AKERS	93	PL B316 435	R. Akers <i>et al.</i>	(OPAL Collab.)
ABREU	95S	ZPHY C68 375	P. Abreu <i>et al.</i>	(DELPHI Collab.)	BUSKULIC	92I	PL B297 449	D. Buskulic <i>et al.</i>	(ALEPH Collab.)

MISCELLANEOUS SEARCHES

Magnetic Monopole Searches	1209
Supersymmetric Particle Searches	1211
Technicolor	1258
Quark and Lepton Compositeness	1265
Extra Dimensions	1272
WIMPs and Other Particle Searches	1282

Notes in the Search Listings

Magnetic Monopole Searches	1209
Supersymmetry	1211
I. Theory (rev.)	1211
II. Experiment (rev.)	1228
Dynamical Electroweak Symmetry Breaking (rev.)	1258
Searches for Quark and Lepton Compositeness	1265
Extra Dimensions (rev.)	1272
WIMPs and Other Particle Searches	1282

SEARCHES IN OTHER SECTIONS

Higgs Bosons — H^0 and H^\pm	414
Heavy Bosons Other than Higgs Bosons	443
Leptoquarks	452
Axions (A^0) and Other Very Light Bosons	459
Heavy Charged Lepton Searches	516
Double- β Decay	525
Heavy Neutral Leptons, Searches for	545
b' (Fourth Generation) Quark	576
Free Quark Searches	577





**SEARCHES FOR
MONOPOLES,
SUPERSYMMETRY,
TECHNICOLOR,
COMPOSITENESS,
EXTRA DIMENSIONS, etc.**

Magnetic Monopole Searches

MAGNETIC MONOPOLE SEARCHES

Revised December 1997 by D.E. Groom (LBNL).

“At the present time (1975) there is no experimental evidence for the existence of magnetic charges or monopoles, but chiefly because of an early, brilliant theoretical argument by Dirac, the search for monopoles is renewed whenever a new energy region is opened up in high energy physics or a new source of matter, such as rocks from the moon, becomes available [1].” Dirac argued that a monopole anywhere in the universe results in electric charge quantization everywhere, and leads to the prediction of a least magnetic charge $g = e/2\alpha$, the Dirac charge [2]. Recently monopoles have become indispensable in many gauge theories, which endow them with a variety of extraordinarily large masses. The discovery by a candidate event in a single superconducting loop in 1982 [6] stimulated an enormous experimental effort to search for supermassive magnetic monopoles [3,4,5].

Monopole detectors have predominantly used either induction or ionization. Induction experiments measure the monopole magnetic charge and are independent of monopole electric charge, mass, and velocity. Monopole candidate events in single semiconductor loops [6,7] have been detected by this method, but no two-loop coincidence has been observed. Ionization experiments rely on a magnetic charge producing more ionization than an electrical charge with the same velocity. In the case of supermassive monopoles, time-of-flight measurements indicating $v \ll c$ has also been a frequently sought signature.

Cosmic rays are the most likely source of massive monopoles, since accelerator energies are insufficient to produce them. Evidence for such monopoles may also be obtained from astrophysical observations.

Jackson’s 1975 assessment remains true. The search is somewhat abated by the lack of success in the 1980’s and the decrease of interest in grand unified gauge theories.

References

1. J. D. Jackson, *Classical Electrodynamics*, 2nd edition (John Wiley & Sons, New York, 1975).
2. P.A.M. Dirac, Proc. Royal Soc. London **A133**, 60 (1931).
3. J. Preskill, Ann. Rev. Nucl. and Part. Sci. **34**, 461 (1984).
4. G. Giacomelli, La Rivista del Nuovo Cimento **7**, N. 12, 1 (1984).
5. Phys. Rep. **140**, 323 (1986).

6. B. Cabrera, Phys. Rev. Lett. **48**, 1378 (1982).
7. A.D. Caplin *et al.*, Nature **321**, 402 (1986).

Monopole Production Cross Section — Accelerator Searches

X-SECT (cm ²)	MASS (GeV)	CHG	ENERGY (GeV)	BEAM	DOCUMENT ID	TECN
<0.2E-36	200-700	1	1960	p \bar{p}	1 ABULENCIA	06K CNTR
< 2.E-36		1	300	e ⁺ p	2,3 AKTAS	05A INDU
< 0.2 E-36		2	300	e ⁺ p	2,3 AKTAS	05A INDU
< 0.09E-36		3	300	e ⁺ p	2,3 AKTAS	05A INDU
< 0.05E-36		≥ 6	300	e ⁺ p	2,3 AKTAS	05A INDU
< 2.E-36		1	300	e ⁺ p	2,4 AKTAS	05A INDU
< 0.2E-36		2	300	e ⁺ p	2,4 AKTAS	05A INDU
< 0.07E-36		3	300	e ⁺ p	2,4 AKTAS	05A INDU
< 0.06E-36		≥ 6	300	e ⁺ p	2,4 AKTAS	05A INDU
< 0.6E-36	>265	1	1800	p \bar{p}	5 KALBFLEISCH 04	INDU
< 0.2E-36	>355	2	1800	p \bar{p}	5 KALBFLEISCH 04	INDU
< 0.07E-36	>410	3	1800	p \bar{p}	5 KALBFLEISCH 04	INDU
< 0.2E-36	>375	6	1800	p \bar{p}	5 KALBFLEISCH 04	INDU
< 0.7E-36	>295	1	1800	p \bar{p}	6,7 KALBFLEISCH 00	INDU
< 7.8E-36	>260	2	1800	p \bar{p}	6,7 KALBFLEISCH 00	INDU
< 2.3E-36	>325	3	1800	p \bar{p}	6,8 KALBFLEISCH 00	INDU
< 0.11E-36	>420	6	1800	p \bar{p}	6,8 KALBFLEISCH 00	INDU
<0.65E-33	<3.3	≥ 2	11A	197Au	9 HE	97
<1.90E-33	<8.1	≥ 2	160A	208Pb	9 HE	97
<3.E-37	<45.0	1.0	88-94	e ⁺ e ⁻	PINFOLD	93 PLAS
<3.E-37	<41.6	2.0	88-94	e ⁺ e ⁻	PINFOLD	93 PLAS
<7.E-35	<44.9	0.2-1.0	89-93	e ⁺ e ⁻	KINOSHITA	92 PLAS
<2.E-34	<850	≥ 0.5	1800	p \bar{p}	BERTANI	90 PLAS
<1.2E-33	<800	≥ 1	1800	p \bar{p}	PRICE	90 PLAS
<1.E-37	<29	1	50-61	e ⁺ e ⁻	KINOSHITA	89 PLAS
<1.E-37	<18	2	50-61	e ⁺ e ⁻	KINOSHITA	89 PLAS
<1.E-38	<17	<1	35	e ⁺ e ⁻	BRAUNSCH...	88B CNTR
<8.E-37	<24	1	50-52	e ⁺ e ⁻	KINOSHITA	88 PLAS
<1.3E-35	<22	2	50-52	e ⁺ e ⁻	KINOSHITA	88 PLAS
<9.E-37	<4	<0.15	10.6	e ⁺ e ⁻	GENTILE	87 CLEO
<3.E-32	<800	≥ 1	1800	p \bar{p}	PRICE	87 PLAS
<3.E-38	<3	<3	29	e ⁺ e ⁻	FRYBERGER	84 PLAS
<1.E-31	<10	1,3	540	p \bar{p}	AUBERT	83B PLAS
<4.E-38	<10	<6	34	e ⁺ e ⁻	MUSSET	83 PLAS
<8.E-36	<20	<2	52	p \bar{p}	10 DELL	82 CNTR
<9.E-37	<30	<3	29	e ⁺ e ⁻	KINOSHITA	82 PLAS
<1.E-37	<20	<24	63	p \bar{p}	CARRIGAN	78 CNTR
<1.E-37	<30	<3	56	p \bar{p}	HOFFMANN	78 PLAS
			62	p \bar{p}	10 DELL	76 SPRK
<4.E-33			300	p	10 STEVENS	76B SPRK
<1.E-40	<5	<2	70	p	11 ZRELOV	76 CNTR
<2.E-30			300	n	10 BURKE	75 OSPK
<1.E-38			8	ν	12 CARRIGAN	75 HLBC
<5.E-43	<12	<10	400	p	EBERHARD	75B INDU
<2.E-36	<30	<3	60	p \bar{p}	GIACOMELLI	75 PLAS
<5.E-42	<13	<24	400	p	CARRIGAN	74 CNTR
<6.E-42	<12	<24	300	p	CARRIGAN	73 CNTR
<2.E-36		1	0.001	γ	11 BARTLETT	72 CNTR
<1.E-41	<5	<2	70	p	GUREVICH	72 EMUL
<1.E-40	<3	<2	28	p	AMALDI	63 EMUL
<2.E-40	<3	<2	30	p	PURCELL	63 CNTR
<1.E-35	<3	<4	28	p	FIDECARO	61 CNTR
<2.E-35	<1	1	6	p	BRADNER	59 EMUL

- 1 ABULENCIA 06K searches for high-ionizing signals in CDF central outer tracker and time-of-flight detector. For Drell-Yan $M\bar{M}$ production, the cross section limit implies $M > 360$ GeV at 95% CL.
- 2 AKTAS 05A model-dependent limits as a function of monopole mass shown for arbitrary mass of 60 GeV. Based on search for stopped monopoles in the H1 A1 beam pipe.
- 3 AKTAS 05A limits with assumed elastic spin 0 monopole pair production.
- 4 AKTAS 05A limits with assumed inelastic spin 1/2 monopole pair production.
- 5 KALBFLEISCH 04 reports searches for stopped magnetic monopoles in Be, Al, and Pb samples obtained from discarded material from the upgrading of DØ and CDF. A large-aperture warm-bore cryogenic detector was used. The approach was an extension of the methods of KALBFLEISCH 00. Cross section results moderately model dependent; interpretation as a mass lower limit depends on possibly invalid perturbation expansion.
- 6 KALBFLEISCH 00 used an induction method to search for stopped monopoles in pieces of the DØ (FNAL) beryllium beam pipe and in extensions to the drift chamber aluminum support cylinder. Results are model dependent.
- 7 KALBFLEISCH 00 result is for aluminum.
- 8 KALBFLEISCH 00 result is for beryllium.
- 9 HE 97 used a lead target and barium phosphate glass detectors. Cross-section limits are well below those predicted via the Drell-Yan mechanism.
- 10 Multiphoton events.
- 11 Cherenkov radiation polarization.
- 12 Re-examines CERN neutrino experiments.

Searches Particle Listings

Magnetic Monopole Searches

Monopole Production — Other Accelerator Searches

MASS (GeV)	CHG (g)	SPIN	ENERGY (GeV)	BEAM	DOCUMENT ID	TECN
> 610	≥ 1	0	1800	p \bar{p}	13 ABBOTT 98k	D0
> 870	≥ 1	1/2	1800	p \bar{p}	13 ABBOTT 98k	D0
>1580	≥ 1	1	1800	p \bar{p}	13 ABBOTT 98k	D0
> 510			88-94	e ⁺ e ⁻	14 ACCIARRI 95c	L3

¹³ABBOTT 98k search for heavy pointlike Dirac monopoles via central production of a pair of photons with high transverse energies.

¹⁴ACCIARRI 95c finds a limit $B(Z \rightarrow \gamma\gamma) < 0.8 \times 10^{-5}$ (which is possible via a monopole loop) at 95% CL and sets the mass limit via a cross section model.

Monopole Flux — Cosmic Ray Searches

"Caty" in the charge column indicates a search for monopole-catalyzed nucleon decay. The absence of an entry usually means a track-etch experiment.

FLUX (cm ⁻² sr ⁻¹ s ⁻¹)	MASS (GeV)	CHG (g)	COMMENTS ($\beta = v/c$)	EVTS	DOCUMENT ID	TECN
<1.4E-16		1	1.1E-4 < β < 1	0	15 AMBROSIO 02b	MCRO
<3E-16		Caty	1.1E-4 < β < 5E-3	0	16 AMBROSIO 02c	MCRO
<1.5E-15		1	5E-3 < β < 0.99	0	17 AMBROSIO 02b	MCRO
<1E-15		1	1.1 × 10 ⁻⁴ -0.1	0	18 AMBROSIO 97	MCRO
<5.6E-15		1	(0.18-3.0)E-3	0	19 AHLEN 94	MCRO
<2.7E-15		Caty	$\beta \sim 1 \times 10^{-3}$	0	20 BECKER-SZ...	IMB
<8.7E-15		1	>2.E-3	0	21 THRON 92	SOUND
<4.4E-12		1	all β	0	22 GARDNER 91	INDU
<7.2E-13		1	all β	0	23 HUBER 91	INDU
<3.7E-15	>E12	1	$\beta=1.E-4$	0	21 ORITO 91	PLAS
<3.2E-16	>E10	1	$\beta > 0.05$	0	21 ORITO 91	PLAS
<3.2E-16	>E10-E12	2,3		0	21 ORITO 91	PLAS
<3.8E-13		1	all β	0	20 BERMON 90	INDU
<5E-16		Caty	$\beta < 1.E-3$	0	20 BEZRUKOV 90	CHER
<1.8E-14		1	$\beta > 1.1E-4$	0	22 BUCKLAND 90	HEPT
<1E-18		1	3.E-4 < β < 1.5E-3	0	23 GHOSH 90	MICA
<7.2E-13		1	all β	0	20 HUBER 90	INDU
<5E-12	>E7	1	3.E-4 < β < 5E-3	0	20 BARISH 87	CNTR
<1.E-13		Caty	1.E-5 < β < 1	0	20 BARTELT 87	SOUND
<1.E-10		1	all β	0	20 EBISU 87	INDU
<2.E-13		1	1.E-4 < β < 6.E-4	0	20 MASEK 87	HEPT
<2.E-14		1	4.E-5 < β < 2.E-4	0	20 NAKAMURA 87	PLAS
<2.E-14		1	1.E-3 < β < 1	0	20 NAKAMURA 87	PLAS
<5.E-14		1	9.E-4 < β < 1.E-2	0	20 SHEP KO 87	CNTR
<2.E-13		1	4.E-4 < β < 1	0	20 TSUKAMOTO 87	CNTR
<5.E-14		1	all β	1	24 CAPLIN 86	INDU
<5.E-12		1		0	20 CROMAR 86	INDU
<1.E-13		1	7.E-4 < β	0	20 HARA 86	CNTR
<7.E-11		1	all β	0	20 INCANDELA 86	INDU
<1.E-18		1	4.E-4 < β < 1.E-3	0	23 PRICE 86	MICA
<5.E-12		1		0	20 BERMON 85	INDU
<6.E-12		1		0	20 CAPLIN 85	INDU
<6.E-10		1		0	20 EBISU 85	INDU
<3.E-15		Caty	5.E-5 < $\beta \leq 1.E-3$	0	20 KAJITA 85	KAMI
<2.E-21		Caty	$\beta < 1.E-3$	0	20,25 KAJITA 85	KAMI
<3.E-15		Caty	1.E-3 < β < 1.E-1	0	20 PARK 85b	CNTR
<5.E-12		1	1.E-4 < β < 1	0	20 BATTISTONI 84	NUSX
<7.E-12		1		0	20 INCANDELA 84	INDU
<7.E-13		1	3.E-4 < β	0	22 KAJINO 84	CNTR
<2.E-12		1	3.E-4 < β < 1.E-1	0	22 KAJINO 84b	CNTR
<6.E-13		1	5.E-4 < β < 1	0	20 KAWAGOE 84	CNTR
<2.E-14		1	1.E-3 < β	0	20 KRISHNA... 84	CNTR
<4.E-13		1	6.E-4 < β < 2.E-3	0	20 LISS 84	CNTR
<1.E-16		1	3.E-4 < β < 1.E-3	0	23 PRICE 84	MICA
<1.E-13		1	1.E-4 < β	0	20 PRICE 84b	PLAS
<4.E-13		1	6.E-4 < β < 2.E-3	0	20 TARLE 84	CNTR
<4.E-13		1	1.E-2 < β < 1.E-3	0	26 ANDERSON 7	EMUL
<1.E-12		1	7.E-3 < β < 1	0	20 BARTELT 83b	CNTR
<3.E-13		1	1.E-3 < β < 4.E-1	0	20 BARWICK 83	PLAS
<3.E-12		Caty	5.E-4 < β < 5.E-2	0	20 BONARELLI 83	CNTR
<4.E-11		1		0	20 BOSETTI 83	CNTR
<5.E-15		1	1.E-2 < β < 1	0	20 CABRERA 83	INDU
<8.E-15		Caty	1.E-4 < β < 1.E-1	0	20 DOKE 83	PLAS
<5.E-12		1	1.E-4 < β < 3.E-2	0	20 ERREDE 83	IMB
<2.E-12		1	6.E-4 < β < 1	0	20 GROOM 83	CNTR
<1.E-13		1	$\beta=3.E-3$	0	20 MASHIMO 83	CNTR
<2.E-12		1	7.E-3 < β < 6.E-1	0	20 ALEXEYEV 82	CNTR
6.E-10		1	all β	1	20 BONARELLI 82	CNTR
<2.E-11		1	1.E-2 < β < 1.E-1	0	27 CABRERA 82	INDU
<2.E-15		concentrator		0	20 MASHIMO 82	CNTR
<1.E-13	>1	1	1.E-3 < β	0	20 BARTLETT 81	PLAS
<5.E-11	<E17	1	3.E-4 < β < 1.E-3	0	20 KINOSHITA 81b	PLAS
<2.E-11		concentrator		0	20 ULLMAN 81	CNTR
1.E-1	>200	2		1	20 BARTLETT 78	PLAS
<2.E-13	>2	>2		1	28 PRICE 75	PLAS
<1.E-19	>2	obsidian, mica		0	20 FLEISCHER 71	PLAS
<5.E-15	<15	<3	concentrator	0	20 FLEISCHER 69c	PLAS
<2.E-11		<1-3	concentrator	0	20 CARITHERS 66	ELEC
				0	20 MALKUS 51	EMUL

¹⁵AMBROSIO 02b direct search final result for $m \geq 10^{17}$ GeV, based upon 4.2 to 9.5 years of running, depending upon the subsystem. Limit with CR39 track-etch detector extends the limit from $\beta=4 \times 10^{-5}$ (3.1×10^{-16} cm⁻²sr⁻¹s⁻¹) to $\beta=1 \times 10^{-4}$ (2.1×10^{-16} cm⁻²sr⁻¹s⁻¹). Limit curve in paper is piecewise continuous due to different detection techniques for different β ranges.

¹⁶AMBROSIO 02c limit for catalysis of nucleon decay with catalysis cross section of ≈ 1 mb. The flux limit increases by ~ 3 at the higher β limit, and increases to 1×10^{-14} cm⁻²sr⁻¹s⁻¹ if the catalysis cross section is 0.01 mb. Based upon 71193 hr of data with the streamer detector, with an acceptance of 4250 m²sr.

¹⁷AMBROSIO 02b result for "more than two years of data." Ionization search using several subsystems. Limit curve as a function of β not given. Included in AMBROSIO 02b.

¹⁸AMBROSIO 97 global MACRO 90%CL is 0.78×10^{-15} at $\beta=1.1 \times 10^{-4}$, goes through a minimum at 0.61×10^{-15} near $\beta=(1.1-2.7) \times 10^{-3}$, then rises to 0.84×10^{-15} at $\beta=0.1$. The global limit in this region is below the Parker bound at 10^{-15} . Less stringent limits are established for $4 \times 10^{-5} < \beta < 1 \times 10^{-4}$. Limits set by various triggers and different subdetectors are given in the paper. All limits assume a catalysis cross section smaller than a few mb.

¹⁹AHLEN 94 limit for dyons extends down to $\beta=0.9E-4$ and a limit of $1.3E-14$ extends to $\beta=0.8E-4$. Also see comment by PRICE 94 and reply of BARISH 94. One loophole in the AHLEN 94 result is that in the case of monopoles catalyzing nucleon decay, relativistic particles could veto the events. See AMBROSIO 97 for additional results.

²⁰Catalysis of nucleon decay; sensitive to assumed catalysis cross section.

²¹ORITO 91 limits are functions of velocity. Lowest limits are given here.

²²Used DKMPR mechanism and Penning effect.

²³Assumes monopole attaches fermion nucleus.

²⁴Limit from combining data of CAPLIN 86, BERMON 85, INCANDELA 84, and CABRERA 83. For a discussion of controversy about CAPLIN 86 observed event, see GUY 87. Also see SCHOUTEN 87.

²⁵Based on lack of high-energy solar neutrinos from catalysis in the sun.

²⁶Anomalous long-range α (⁴He) tracks.

²⁷CABRERA 82 candidate event has single Dirac charge within $\pm 5\%$.

²⁸ALVAREZ 75, FLEISCHER 75, and FRIEDLANDER 75 explain as fragmenting nucleus. EBERHARD 75 and ROSS 76 discuss conflict with other experiments. HAGSTROM 77 reinterprets as antinucleus. PRICE 78 reassesses.

Monopole Flux — Astrophysics

FLUX (cm ⁻² sr ⁻¹ s ⁻¹)	MASS (GeV)	CHG (g)	COMMENTS ($\beta = v/c$)	EVTS	DOCUMENT ID	TECN
<1.3E-20			faint white dwarf		29 FREESE 99	ASTR
<1.E-16	E17	1	galactic field	0	30 ADAMS 93	COSM
<1.E-23			Jovian planets		29 ARAFUNE 85	ASTR
<1.E-16	E15		solar trapping	0	BRACCI 85b	ASTR
<1.E-18		1		0	29 HARVEY 84	COSM
<3.E-23			neutron stars		KOLB 84	ASTR
<7.E-22			pulsars	0	29 FREESE 83b	ASTR
<1.E-18	<E18	1	intergalactic field	0	29 REPHAELI 83	COSM
<1.E-23			neutron stars	0	29 DIMOPOUL... 82	COSM
<5.E-22			neutron stars	0	29 KOLB 82	COSM
<5.E-15	>E21		galactic halo		SALPETER 82	COSM
<1.E-12	E19	1	$\beta=3.E-3$	0	31 TURNER 82	COSM
<1.E-16		1	galactic field	0	PARKER 70	COSM

²⁹Catalysis of nucleon decay.

³⁰ADAMS 93 limit based on "survival and growth of a small galactic seed field" is 10^{-16} ($m/10^{17}$ GeV) cm⁻²sr⁻¹s⁻¹. Above 10^{17} GeV, limit 10^{-16} (10^{17} GeV/m) cm⁻²s⁻¹sr⁻¹ (from requirement that monopole density does not overclose the universe) is more stringent.

³¹Re-evaluates PARKER 70 limit for GUT monopoles.

Monopole Density — Matter Searches

DENSITY	CHG (g)	MATERIAL	EVTS	DOCUMENT ID	TECN
<6.9E-6/gram	>1/3	Meteorites and other	0	JEON 95	INDU
<2.E-7/gram	>0.6	Fe ore	0	32 EBISU 87	INDU
<4.6E-6/gram	>0.5	deep schist	0	KOVALIK 86	INDU
<1.6E-6/gram	>0.5	manganese nodules	0	33 KOVALIK 86	INDU
<1.3E-6/gram	>0.5	seawater	0	KOVALIK 86	INDU
>1.E+14/gram	>1/3	iron aerosols	>1	MIKHAILOV 83	SPEC
<6.E-4/gram		air, seawater	0	CARRIGAN 76	CNTR
<5.E-1/gram	>0.04	11 materials	0	CABRERA 75	INDU
<2.E-4/gram	>0.05	moon rock	0	ROSS 73	INDU
<6.E-7/gram	<140	seawater	0	KOLM 71	CNTR
<1.E-2/gram	<120	manganese nodules	0	FLEISCHER 69	PLAS
<1.E-4/gram	>0	manganese	0	FLEISCHER 69b	PLAS
<2.E-3/gram	<1-3	magnetite, meteor	0	GOTO 63	EMUL
<2.E-2/gram		meteorite	0	PETUKHOV 63	CNTR

³²Mass $1 \times 10^{14}-1 \times 10^{17}$ GeV.

³³KOVALIK 86 examined 498 kg of schist from two sites which exhibited clear minearalogical evidence of having been buried at least 20 km deep and held below the Curie temperature.

Monopole Density — Astrophysics

DENSITY	CHG (g)	MATERIAL	EVTS	DOCUMENT ID	TECN
<1.E-9/gram	1	sun, catalysis	0	34 ARAFUNE 83	COSM
<6.E-33/nuclei	1	moon wake	0	SCHATTEN 83	ELEC
<2.E-28/nuclei		earth heat	0	CARRIGAN 80	COSM
<2.E-4/prot		42cm absorption	0	BRODERICK 79	COSM
<2.E-13/m ³		moon wake	0	SCHATTEN 70	ELEC

³⁴Catalysis of nucleon decay.

REFERENCES FOR Magnetic Monopole Searches

ABULENCIA 06K PRL 96 201801 A. Abulencia et al. (CDF Collab.)
AKTAS 05A EPJ C41 133 G.R. Kalbfeisch et al. (HI Collab.)
KALBFLEISCH 04 PR D69 052002 G.R. Kalbfeisch et al. (OKLA)
AMBROSIO 02B EPJ C25 511 M. Ambrosio et al. (MACRO Collab.)
AMBROSIO 02C EPJ C26 163 M. Ambrosio et al. (MACRO Collab.)
AMBROSIO 02D ASP 18 27 M. Ambrosio et al. (MACRO Collab.)
KALBFLEISCH 00 PRL 85 5292 G.R. Kalbfeisch et al.
FRESE 99 PR D59 063007 K. Freese, E. Krasteva
ABBOTT 98K PRL 81 524 B. Abbott et al. (D0 Collab.)
AMBROSIO 97 PL B406 249 M. Ambrosio et al. (MACRO Collab.)
HE 97 PRL 79 3134 Y.D. He (UCB)
ACCIARRI 95C PL B345 609 M. Acciari et al. (L3 Collab.)
JEON 95 PRL 75 1443 H. Jeon, M.J. Longo (MICH)
Also PRL 76 159 (erratum)
AHLN 94 PRL 72 608 S.P. Ahlen et al. (MACRO Collab.)
BARISH 94 PRL 73 1306 B.C. Barish, G. Giacomelli, J.T. Hong (CIT+)
BECKER-SZ... 94 PR D49 2169 R.A. Becker-Szendy et al. (IMB Collab.)
PRICE 94 PRL 73 1305 P.B. Price (UCB)
ADAMS 93 PRL 70 2511 F.C. Adams et al. (MICH, FNAL)
PINFOLD 93 PL B316 407 J.L. Pinfold et al. (ALBE, HARV, MONT+)
KINOSHITA 92 PR D46 R081 K. Kinoshita et al. (HARV, BGNA, REHO)
THRON 92 PR D46 4846 J.L. Thron et al. (SUDAN-2 Collab.)
GARDNER 91 PR D44 622 R.D. Gardner et al. (STAN)
HUBER 91 PR D44 636 M.E. Huber et al. (STAN)
ORIO 91 PRL 66 1951 S. Orlio et al. (ICEPP, WASC, NIHO, ICRR)
BERMON 90 PRL 64 839 S. Bermon et al. (IBM, BNL)
BERTANI 90 EPL 12 613 M. Bertani et al. (BGNA, INFN)
BEZRUKOV 90 SJNP 52 54 L.B. Bezrukov et al. (INRM)
Translated from YAF 52 86.
BUCKLAND 90 PR D41 2726 K.N. Buckland et al. (UCSD)
GHOSH 90 EPL 12 254 D.C. Ghosh, S. Chatterjee (IADA)
HUBER 90 PRL 64 835 M.E. Huber et al. (STAN)
PRICE 90 PRL 65 149 P.B. Price, J. Guir, K. Kinoshita (UCB, HARV)
KINOSHITA 89 PL B228 543 K. Kinoshita et al. (HARV, TISA, KEK+)
BRAUNSCH... 88B ZPHY C38 543 R. Braunschweig et al. (TASSO Collab.)
KINOSHITA 88 PRL 60 1610 K. Kinoshita et al. (HARV, TISA, KEK+)
BARISH 87 PR D36 2641 B.C. Barish, G. Liu, C. Lane (CIT)
BARTELT 87 PR D36 1990 J.E. Bartelt et al. (Soudan Collab.)
Also PR D40 1701 (erratum)
EBISU 87 PR D36 3359 T. Ebisu, T. Watanabe (KOBÉ)
Also JPG 11 803 T. Ebisu, T. Watanabe (KOBÉ)
GENTILE 87 PR D35 1081 T. Gentile et al. (CLEO Collab.)
GUY 87 NAT 325 463 J. Guy (LOIC)
MASEK 87 PR D35 2758 G.E. Masek et al. (UCSD)
NAKAMURA 87 PL B183 395 S. Nakamura et al. (INUS, WASC, NIHO)
PRICE 87 PRL 59 2523 P.B. Price, R. Guoxiao, K. Kinoshita (UCB, HARV)
SCHOUTEN 87 JPE 20 850 J.C. Schouten et al. (LOIC)
SHEPKO 87 PR D35 2917 M.J. Shepko et al. (TAMU)
TSUKAMOTO 87 EPL 3 39 T. Tsukamoto et al. (ICRR)
CAPLIN 86 NAT 321 402 A.D. Caplin et al. (LOIC)
Also JPE 20 850 J.C. Schouten et al. (LOIC)
GROMAR 86 PR D36 2561 J.M. Gromar, A.F. Clark, F.R. Fickett (IBSB)
HARA 86 PRL 56 553 T. Hara et al. (ICRR, KYOT, KEK, KOBÉ+)
INCANDELA 86 PR D34 2637 J. Incandela et al. (CHIC, FNAL, MICH)
KOVALIK 86 PR A33 1183 J.M. Kovalik, J.L. Kirschvink (CIT)
PRICE 86 PRL 56 1226 P.B. Price, M.H. Salamon (UCB)
ARAFUNE 85 PR D32 2586 J. Arafune, M. Fukugita, S. Yanagita (ICRR, KYOTU+)
BERMON 85 PRL 55 1850 S. Bermon et al. (IBM)
BRACCI 85B NP B258 726 L. Bracci, G. Fiorentini, G. Mezzorani (PISA+)
Also LNC 42 123 L. Bracci, G. Fiorentini (PISA)
CAPLIN 85 NAT 317 234 A.D. Caplin et al. (LOIC)
EBISU 85 JPG 11 803 T. Ebisu, T. Watanabe (KOBÉ)
KAJITA 85B JPSJ 54 4065 T. Kajita et al. (ICRR, KEK, MIIG)
PARK 85B NP B252 261 H.S. Park et al. (IMB Collab.)
BATTISTONI 84 PL 133B 454 G. Battistoni et al. (NUSEX Collab.)
FRYBERGER 84 PR D29 1524 D. Fryberger et al. (SLAC, UCB)
HARVEY 84 NP B236 255 J.A. Harvey (PRIN)
INCANDELA 84 PRL 53 2067 J. Incandela et al. (CHIC, FNAL, MICH)
KAJINO 84 PRL 52 1373 F. Kajino et al. (ICRR)
KAJINO 84B JPG 10 447 F. Kajino et al. (ICRR)
KAWAGOE 84 LNC 41 315 K. Kawagoe et al. (TOKY)
KOLB 84 APJ 286 702 E.W. Kolb, M.S. Turner (FNAL, CHIC)
KRISHNA... 84 PL 142B 99 M.R. Krishnaswamy et al. (TATA, OSKC+)
LISS 84 PR D30 804 T.M. Liss, S.P. Ahlen, G. Tarle (UCB, IND+)
PRICE 84 PRL 52 1245 P.B. Price et al. (ROMA, UCB, IND+)
PRICE 84B PL 140B 112 P.B. Price (CERN)
TARLE 84 PRL 52 90 G. Tarle, S.P. Ahlen, T.M. Liss (UCB, MICH+)
ANDERSON 83 PR D28 2308 S.N. Anderson et al. (WASH)
ARAFUNE 83 PL 133B 380 J. Arafune, M. Fukugita (ICRR, KYOTU)
AUBERT 83B PL 120B 465 B. Aubert et al. (CERN, LAPP)
BARTELT 83B PRL 50 655 J.E. Bartelt et al. (MINN, ANL)
BARWICK 83 PR D28 2338 S.W. Barwick, K. Kinoshita, P.B. Price (UCB)
BONARELLI 83 PL 126B 137 R. Bonarelli, P. Capiluppi, I. d'Antone (BGNA)
BOSETTI 83 PL 133B 265 P.C. Bosetti et al. (AA3, HAWA, TOKY)
CABRERA 83 PRL 51 1333 B. Cabrera et al. (STAN)
DOKE 83 PR D29B 370 T. Doke et al. (WASU, RIKK, TTAM, RIKEN)
ERREDE 83 PRL 51 245 S.M. Errede et al. (IMB Collab.)
FRESE 83B PRL 51 1625 K. Freese, M.S. Turner, D.N. Schramm (CHIC)
GROOM 83 PRL 50 573 D.E. Groom et al. (UTAH, STAN)
MASHIMO 83 PL 128B 327 T. Mashimo et al. (ICEPP)
MIKHAILOV 83 PL 130B 331 V.F. Mikhailov (KAZA)
MUSSET 83 PL 128B 333 P. Musset, M. Price, E. Lohrmann (CERN, HAMB)
REPHAEIL 83 PL 121B 115 Y. Rephaeli, M.S. Turner (CHIC)
SCHATTEN 83 PR D27 1525 K.H. Schatten (NASA)
ALEXEYEV 82 LNC 35 413 E.N. Alekseev et al. (INRM)
BONARELLI 82 PL 112B 100 R. Bonarelli et al. (BGNA)
CABRERA 82 PR 48 1378 B. Cabrera et al. (STAN)
DELL 82 NP B209 45 G.F. Dell et al. (BNL, ADEL, ROMA)
DIMOPOUL... 82 PL 119B 320 S. Dimopoulos, J. Preskill, F. Wilczek (HARV+)
KINOSHITA 82 PRL 48 77 K. Kinoshita, P.B. Price, D. Fryberger (UCB+)
KOLB 82 PRL 49 1373 E.W. Kolb, S.A. Colgate, J.A. Harvey (LASL, PRIN)
MASHIMO 82 PJSJ 51 3067 T. Mashimo, K. Kawagoe, M. Koshiba (INUS)
SALPETER 82 PRL 49 1114 E.E. Salpeter, S.L. Shapiro, I. Wasserman (CORN)
TURNER 82 PR D26 1296 M.S. Turner, E.N. Parker, T.J. Bogdan (CHIC)
BARTELT 81 PR D24 612 D.F. Bartelt et al. (COLO, GESC)
KINOSHITA 81B PR D24 1707 K. Kinoshita, P.B. Price (UCB)
ULLMAN 81 PRL 47 209 J.D. Ullman (LEHM, BNL)
CARRIGAN 80 NAT 288 348 T.A. Carrigan (FNAL)
BRODERICK 79 PR D19 1046 J.J. Broderick et al. (VPI)
BARTELT 78 PR D18 2253 D.F. Bartelt, D. Soo, M.G. White (COLO, PRIN)
CARRIGAN 78 PR D17 1754 R.A. Carrigan, B.P. Strauss, G. Giacomelli (FNAL+)
HOFFMANN 78 LNC 23 357 H. Hoffmann et al. (CERN, ROMA)
PRICE 78 PR D18 1382 P.B. Price et al. (UCB, HOUS)
HAGSTROM 77 PRL 38 729 R. Hagstrom (LBL)
CARRIGAN 76 PR D13 1823 R.A. Carrigan, F.A. Nezrick, B.P. Strauss (FNAL)
DELL 76 LNC 15 269 G.F. Dell et al. (CERN, BNL, ROMA, ADEL)
ROSS 76 LBL-4665 R.R. Ross (LBL)
STEVENS 76B PR D14 2207 D.M. Stevens et al. (VPI, BNL)

ZRELOV 76 CZJP B26 1306 V.P. Zrelov et al. (JINR)
ALVAREZ 75 LBL-4260 L.W. Alvarez (LBL)
BURKE 75 PL 60B 113 D.L. Burke et al. (MICH)
CABRERA 75 Thesis R.A. Carrigan, F.A. Nezrick (STAN)
CARRIGAN 75 NP B91 279 B. Cabrera, F.A. Nezrick (FNAL)
Also PR D3 56 R.A. Carrigan, F.A. Nezrick (FNAL)
EBERHARD 75 PR D11 3099 P.H. Eberhard et al. (LBL, MPIM)
EBERHARD 75B LBL-4289 P.H. Eberhard (LBL)
FLEISCHER 75 PRL 35 1412 R.L. Fleischer, R.N.F. Walker (GESC, WUSL)
FRIEDLANDER 75 PRL 35 1167 M.W. Friedlander (WUSL)
GIACOMELLI 75 NC 28A 21 G. Giacomelli et al. (BGNA, CERN, SACL+)
PRICE 75 PRL 35 487 P.B. Price et al. (UCB, HOUS)
CARRIGAN 74 PR D10 3867 R.A. Carrigan, F.A. Nezrick, B.P. Strauss (FNAL)
CARRIGAN 73 PR D8 3717 R.A. Carrigan, F.A. Nezrick, B.P. Strauss (FNAL)
ROSS 73 PR D8 698 R.R. Ross et al. (LBL, SLAC)
Also PR D4 3260 P.H. Eberhard et al. (LBL, SLAC)
Also SCI 167 701 L.W. Alvarez et al. (LBL, SLAC)
BARTELT 72 PR D6 1817 D.F. Bartelt, M.D. Lahana (COLO)
GUREVICH 72 PL 38B 549 I.I. Gurevich et al. (KIAE, NOVO, SERP)
Also JETP 34 917 L.M. Barikov, I.I. Gurevich, M.S. Zolotarev (KIAE+)
Translated from ZETF 61 1721.
Also PL 31B 394 I.I. Gurevich et al. (KIAE, NOVO, SERP)
FLEISCHER 71 PR D4 24 R.L. Fleischer et al. (GESC)
KOLM 71 PR D4 1285 H.H. Kolm, F. Villa, A. Odian (MIT, SLAC)
PARKER 70 APJ 160 383 E.N. Parker (CHIC)
SCHATTEN 70 PR D1 2245 K.H. Schatten (NASA)
FLEISCHER 69 PR 177 2029 R.L. Fleischer et al. (GESC, FSU)
FLEISCHER 69B PR 184 1393 R.L. Fleischer et al. (GESC, UNCS, GSCO)
FLEISCHER 69C PR 184 1398 R.L. Fleischer, P.B. Price, R.T. Woods (GESC)
Also JAP 41 958 R.L. Fleischer et al. (GESC)
CARITHERS 66 PR 149 1070 W.C.J. Carithers, R.J. Stefanski, R.K. Adair
AMALDI 63 NC 28 773 E. Amaldi et al. (ROMA, UCSD, CERN)
GOTO 63 PR 132 387 E. Goto, H.H. Kolm, K.W. Ford (TOKY, MIT, BRAN)
PETUKHOV 63 NP 49 87 V.A. Petukhov, M.N. Yakimenko (LEAD)
PURCELL 63 PR 129 2326 E.M. Purcell et al. (HARV, BNL)
FIDECARO 61 NC 22 657 M. Fidecaro, G. Finocchiaro, G. Giacomelli (CERN)
BRADNER 59 PR 114 603 H. Bradner, W.M. Isbell (LBL)
MALKUS 51 PR 83 899 W.V.R. Malkus (CHIC)

OTHER RELATED PAPERS

GROOM 86 PRPL 140 323 D.E. Groom (UTAH)
Review

Supersymmetric Particle Searches

SUPERSYMMETRY, PART I (THEORY)

Revised October 2007 by Howard E. Haber (UC Santa Cruz).

I.1. Introduction: Supersymmetry (SUSY) is a generalization of the space-time symmetries of quantum field theory that transforms fermions into bosons and vice versa. The existence of such a non-trivial extension of the Poincaré symmetry of ordinary quantum field theory was initially surprising, and its form is highly constrained by theoretical principles [1]. Supersymmetry also provides a framework for the unification of particle physics and gravity [2-5], which is governed by the Planck energy scale, $M_P \approx 10^{19}$ GeV (where the gravitational interactions become comparable in magnitude to the gauge interactions). In particular, it is possible that supersymmetry will ultimately explain the origin of the large hierarchy of energy scales from the W and Z masses to the Planck scale [6-10]. This is the so-called *gauge hierarchy*. The stability of the gauge hierarchy in the presence of radiative quantum corrections is not possible to maintain in the Standard Model, but can be maintained in supersymmetric theories.

If supersymmetry were an exact symmetry of nature, then particles and their superpartners (which differ in spin by half a unit) would be degenerate in mass. Since superpartners have not (yet) been observed, supersymmetry must be a broken symmetry. Nevertheless, the stability of the gauge hierarchy can still be maintained if the supersymmetry breaking is *soft* [11,12], and the corresponding supersymmetry-breaking mass parameters are no larger than a few TeV. In particular, soft-supersymmetry-breaking terms are non-supersymmetric terms in the Lagrangian that are either linear, quadratic, or cubic in the fields, with some restrictions elucidated in Ref. 11. The

Searches Particle Listings

Supersymmetric Particle Searches

impact of such terms becomes negligible at energy scales much larger than the size of the supersymmetry-breaking masses. The most interesting theories of this type are theories of “low-energy” (or “weak-scale”) supersymmetry, where the effective scale of supersymmetry breaking is tied to the scale of electroweak symmetry breaking [7–10]. The latter is characterized by the Standard Model Higgs vacuum expectation value, $v = 246$ GeV.

Although there are no unambiguous experimental results (at present) that require the existence of new physics at the TeV-scale, expectations of the latter are primarily based on three theoretical arguments. First, a *natural* explanation (*i.e.*, one that is stable with respect to quantum corrections) of the gauge hierarchy demands new physics at the TeV-scale [10]. Second, the unification of the three gauge couplings at a very high energy close to the Planck scale does not occur in the Standard Model. However, unification can be achieved with the addition of new physics that can modify the way gauge couplings run above the electroweak scale. A simple example of successful unification arises in the minimal supersymmetric extension of the Standard Model, where supersymmetric masses lie below a few TeV [13]. Third, the existence of dark matter, which makes up approximately one quarter of the energy density of the universe, cannot be explained within the Standard Model of particle physics [14]. It is tempting to attribute the dark matter to the existence of a neutral stable thermal relic (*i.e.*, a particle that was in thermal equilibrium with all other fundamental particles in the early universe at temperatures above the particle mass). Remarkably, the existence of such a particle could yield the observed density of dark matter if its mass and interaction rate were governed by new physics associated with the TeV-scale. The lightest supersymmetric particle is a promising (although not the unique) candidate for the dark matter [15].

Low-energy supersymmetry has traditionally been motivated by the three theoretical arguments just presented. More recently, some theorists [16,17] have argued that the explanation for the gauge hierarchy could lie elsewhere, in which case the effective TeV-scale theory would appear to be highly *unnatural*. Nevertheless, even without the naturalness argument, supersymmetry is expected to be a necessary ingredient of the ultimate theory at the Planck scale that unifies gravity with the other fundamental forces. Moreover, one can imagine that some remnant of supersymmetry does survive down to the TeV-scale. For example, in models of *split-supersymmetry* [17,18], some fraction of the supersymmetric spectrum remains light enough (with masses near the TeV scale) to provide successful gauge-coupling unification and a viable dark-matter candidate. If experimentation at future colliders uncovers evidence for (any remnant of) supersymmetry at low energies, this would have a profound effect on the study of TeV-scale physics, and the development of a more fundamental theory of mass and symmetry-breaking phenomena in particle physics.

I.2. Structure of the MSSM: The minimal supersymmetric extension of the Standard Model (MSSM) consists of taking the fields of the two-Higgs-doublet extension of the Standard Model and adding the corresponding supersymmetric partners [19,20]. The corresponding field content of the MSSM and their gauge quantum numbers are shown in Table 1. The electric charge $Q = T_3 + \frac{1}{2}Y$ is determined in terms of the third component of the weak isospin (T_3) and the U(1) hypercharge (Y).

Table 1: The fields of the MSSM and their SU(3)×SU(2)×U(1) quantum numbers are listed. Only one generation of quarks and leptons is exhibited. For each lepton, quark, and Higgs super-multiplet, there is a corresponding anti-particle multiplet of charge-conjugated fermions and their associated scalar partners.

Field Content of the MSSM					
Super-Multiplets	Boson Fields	Fermionic Partners	SU(3)	SU(2)	U(1)
gluon/gluino	g	\tilde{g}	8	0	0
gauge/	W^\pm, W^0	$\tilde{W}^\pm, \tilde{W}^0$	1	3	0
gaugino	B	\tilde{B}	1	1	0
slepton/	$(\tilde{\nu}, \tilde{e}^-)_L$	$(\nu, e^-)_L$	1	2	-1
lepton	\tilde{e}_R^-	e_R^-	1	1	-2
squark/	$(\tilde{u}_L, \tilde{d}_L)$	$(u, d)_L$	3	2	1/3
quark	\tilde{u}_R	u_R	3	1	4/3
	\tilde{d}_R	d_R	3	1	-2/3
Higgs/	(H_d^0, H_d^-)	$(\tilde{H}_d^0, \tilde{H}_d^-)$	1	2	-1
higgsino	(H_u^+, H_u^0)	$(\tilde{H}_u^+, \tilde{H}_u^0)$	1	2	1

The gauge super-multiplets consist of the gluons and their *gluino* fermionic superpartners, and the SU(2)×U(1) gauge bosons and their *gaugino* fermionic superpartners. The Higgs multiplets consist of two complex doublets of Higgs fields, their *higgsino* fermionic superpartners, and the corresponding antiparticle fields. The matter super-multiplets consist of three generations of left-handed and right-handed quarks and lepton fields, their scalar superpartners (squark and slepton fields), and the corresponding antiparticle fields. The enlarged Higgs sector of the MSSM constitutes the minimal structure needed to guarantee the cancellation of anomalies from the introduction of the higgsino superpartners. Moreover, without a second Higgs doublet, one cannot generate mass for both “up”-type and “down”-type quarks (and charged leptons) in a way consistent with the supersymmetry [21–23].

A general supersymmetric Lagrangian is determined by three functions of the superfields (composed of the fields of the super-multiplets): the superpotential, the Kähler potential, and the gauge kinetic-energy function [5]. For *renormalizable* globally supersymmetric theories, minimal forms for the latter two functions are required in order to generate minimal (canonical) kinetic energy terms for all the fields. A renormalizable superpotential, which is at most cubic in the superfields, yields supersymmetric Yukawa couplings and mass terms. A combination of gauge invariance and supersymmetry

produces couplings of gaugino fields to matter (or Higgs) fields and their corresponding superpartners. The (renormalizable) MSSM Lagrangian is then constructed by including all possible supersymmetric interaction terms (of dimension four or less) that satisfy $SU(3)\times SU(2)\times U(1)$ gauge invariance and $B-L$ conservation (B = baryon number and L = lepton number). Finally, the most general soft-supersymmetry-breaking terms are added [11,12,24]. To generate nonzero neutrino masses, extra structure is needed as discussed in section I.8.

I.2.1. Constraints on supersymmetric parameters: If supersymmetry is associated with the origin of the electroweak scale, then the mass parameters introduced by the soft-supersymmetry-breaking must be generally on the order of 1 TeV or below [25] (although models have been proposed in which some supersymmetric particle masses can be larger, in the range of 1–10 TeV [26]). Some lower bounds on these parameters exist due to the absence of supersymmetric-particle production at current accelerators [27]. Additional constraints arise from limits on the contributions of virtual supersymmetric particle exchange to a variety of Standard Model processes [28,29].

For example, the Standard Model global fit to precision electroweak data is quite good [30]. If all supersymmetric particle masses are significantly heavier than m_Z (in practice, masses greater than 300 GeV are sufficient [31]), then the effects of the supersymmetric particles decouple in loop corrections to electroweak observables [32]. In this case, the Standard Model global fit to precision data, and the corresponding MSSM fit yield similar results. On the other hand, regions of parameter space with light supersymmetric particle masses (just above the present day experimental limits) can in some cases generate significant one-loop corrections, resulting in a slight improvement or worsening of the overall global fit to the electroweak data, depending on the choice of the MSSM parameters [33]. Thus, the precision electroweak data provide some constraints on the magnitude of the soft-supersymmetry-breaking terms.

There are a number of other low-energy measurements that are especially sensitive to the effects of new physics through virtual loops. For example, the virtual exchange of supersymmetric particles can contribute to the muon anomalous magnetic moment, $a_\mu \equiv \frac{1}{2}(g-2)_\mu$ [34], and to the inclusive decay rate for $b \rightarrow s\gamma$. The Standard Model prediction for a_μ exhibits a 3.4σ deviation from the experimentally observed value [35]. Less significant is the slight discrepancy (roughly one standard deviation) between the Standard Model prediction for $\Gamma(b \rightarrow s\gamma)$ and the experimentally observed rate [36]. In both cases, supersymmetric corrections can contribute an observable shift from the Standard Model prediction in some regions of the MSSM parameter space [37–38]. The absence of a *significant* deviation in these and other B -physics observables from their Standard Model predictions places interesting constraints on the low-energy supersymmetry parameters [39].

There is some tension between the expectation that supersymmetry-breaking is associated with the electroweak symmetry-breaking scale and the non-observation of supersymmetric particles in present day collider experiments [40]. In particular, the experimental lower bound on squark and gluino masses is already three to four times larger than the masses of the W and Z bosons [27]. The non-observation at LEP [41] of the Higgs boson [whose mass depends indirectly on the top-squark mass via radiative corrections, cf. Eq. (11)] adds to this tension [42]. The separation of scales that govern electroweak symmetry and supersymmetry breaking is an example of the *little hierarchy problem* [43]. It appears that the Higgs vacuum expectation value must be fine-tuned at the percent level in the MSSM, although one can imagine model extensions in which the degree of fine-tuning is relaxed [44].

I.2.2. R-Parity and the lightest supersymmetric particle: As a consequence of $B-L$ invariance, the MSSM possesses a multiplicative R-parity invariance, where $R = (-1)^{3(B-L)+2S}$ for a particle of spin S [45]. Note that this implies that all the ordinary Standard Model particles have even R parity, whereas the corresponding supersymmetric partners have odd R parity. The conservation of R parity in scattering and decay processes has a crucial impact on supersymmetric phenomenology. For example, starting from an initial state involving ordinary (R-even) particles, it follows that supersymmetric particles must be produced in pairs. In general, these particles are highly unstable and decay into lighter states. However, R-parity invariance also implies that the lightest supersymmetric particle (LSP) is absolutely stable, and must eventually be produced at the end of a decay chain initiated by the decay of a heavy unstable supersymmetric particle.

In order to be consistent with cosmological constraints, a stable LSP is almost certainly electrically and color neutral [46]. (There are some model circumstances in which a colored gluino LSP is allowed [47], but we do not consider this possibility further here.) Consequently, the LSP in an R-parity-conserving theory is weakly interacting with ordinary matter, *i.e.*, it behaves like a stable heavy neutrino and will escape collider detectors without being directly observed. Thus, the canonical signature for conventional R-parity-conserving supersymmetric theories is missing (transverse) energy, due to the escape of the LSP. Moreover, the LSP is a prime candidate for *cold dark matter* [15], an important component of the non-baryonic dark matter that is required in many models of cosmology and galaxy formation [48]. Further aspects of dark matter can be found in Ref. 49.

I.2.3. The goldstino and gravitino: In the MSSM, supersymmetry breaking is accomplished by including the most general renormalizable soft-supersymmetry-breaking terms consistent with the $SU(3)\times SU(2)\times U(1)$ gauge symmetry and R-parity invariance. These terms parameterize our ignorance of the fundamental mechanism of supersymmetry breaking. If supersymmetry breaking occurs spontaneously, then a massless Goldstone fermion called the *goldstino* ($\tilde{G}_{1/2}$) must exist. The

Searches Particle Listings

Supersymmetric Particle Searches

goldstino would then be the LSP, and could play an important role in supersymmetric phenomenology [50]. However, the goldstino degrees of freedom are physical only in models of spontaneously-broken global supersymmetry. If supersymmetry is a local symmetry, then the theory must incorporate gravity; the resulting theory is called supergravity [51]. In models of spontaneously-broken supergravity, the goldstino is “absorbed” by the *gravitino* (\tilde{G}) [sometimes called $\tilde{g}_{3/2}$ in the older literature], the spin-3/2 superpartner of the graviton [52]. By this super-Higgs mechanism, the goldstino is removed from the physical spectrum and the gravitino acquires a mass ($m_{3/2}$). In processes with center-of-mass energy $E \gg m_{3/2}$, the goldstino–gravitino equivalence theorem [53] states that the interactions of the helicity $\pm\frac{1}{2}$ gravitino (whose properties approximate those of the goldstino) dominate those of the helicity $\pm\frac{3}{2}$ gravitino.

I.2.4. Hidden sectors and the structure of supersymmetry breaking [24]: It is very difficult (perhaps impossible) to construct a realistic model of spontaneously-broken low-energy supersymmetry where the supersymmetry breaking arises solely as a consequence of the interactions of the particles of the MSSM. A more viable scheme posits a theory consisting of at least two distinct sectors: a *hidden* sector consisting of particles that are completely neutral with respect to the Standard Model gauge group, and a *visible* sector consisting of the particles of the MSSM. There are no renormalizable tree-level interactions between particles of the visible and hidden sectors. Supersymmetry breaking is assumed to occur in the hidden sector, and to then be transmitted to the MSSM by some mechanism (often involving the mediation by particles that comprise an additional *messenger* sector). Two theoretical scenarios have been examined in detail: gravity-mediated and gauge-mediated supersymmetry breaking.

Supergravity models provide a natural mechanism for transmitting the supersymmetry breaking of the hidden sector to the particle spectrum of the MSSM. In models of *gravity-mediated* supersymmetry breaking, gravity is the messenger of supersymmetry breaking [54–56]. More precisely, supersymmetry breaking is mediated by effects of gravitational strength (suppressed by inverse powers of the Planck mass). In this scenario, the gravitino mass is of order the electroweak-symmetry-breaking scale, while its couplings are roughly gravitational in strength [2,57]. Such a gravitino typically plays no role in supersymmetric phenomenology at colliders (except perhaps indirectly in the case where the gravitino is the LSP [58]).

In *gauge-mediated* supersymmetry breaking, supersymmetry breaking is transmitted to the MSSM via gauge forces. A typical structure of such models involves a hidden sector where supersymmetry is broken, a messenger sector consisting of particles (messengers) with $SU(3) \times SU(2) \times U(1)$ quantum numbers, and the visible sector consisting of the fields of the MSSM [59,60,61]. The direct coupling of the messengers to

the hidden sector generates a supersymmetry-breaking spectrum in the messenger sector. Finally, supersymmetry breaking is transmitted to the MSSM via the virtual exchange of the messengers. If this approach is extended to incorporate gravitational phenomena, then supergravity effects will also contribute to supersymmetry breaking. However, in models of gauge-mediated supersymmetry breaking, the model parameters are chosen in such a way that the virtual exchange of the messengers dominates the effects of the direct gravitational interactions between the hidden and visible sectors. Consequently, the gravitino mass is typically in the eV to keV range, in which case \tilde{G} is the LSP. The couplings of the helicity $\pm\frac{1}{2}$ components of \tilde{G} to the particles of the MSSM (which approximate those of the goldstino, cf. Section I.2.3) are significantly stronger than gravitational strength and amenable to experimental collider analyses.

I.2.5. Supersymmetry and extra dimensions: During the last decade, new approaches to supersymmetry breaking have been proposed, based on theories in which the number of space dimensions is greater than three. This is not a new idea—consistent superstring theories are formulated in ten spacetime dimensions, and the associated M -theory is based in eleven spacetime dimensions [62]. Nevertheless, in all approaches considered above, the string scale and the inverse size of the extra dimensions are assumed to be at or near the Planck scale, below which an effective four-spacetime-dimensional broken supersymmetric field theory emerges. More recently, a number of supersymmetry-breaking mechanisms have been proposed that are inherently extra-dimensional [63]. The size of the extra dimensions can be significantly larger than M_{P}^{-1} ; in some cases on the order of $(\text{TeV})^{-1}$ or even larger [64,65]. For example, in one approach, the fields of the MSSM live on some brane (a lower-dimensional manifold embedded in a higher-dimensional spacetime), while the sector of the theory that breaks supersymmetry lives on a second-separated brane. Two examples of this approach are anomaly-mediated supersymmetry breaking of Ref. 66, and gaugino-mediated supersymmetry breaking of Ref. 67; in both cases supersymmetry breaking is transmitted through fields that live in the bulk (the higher-dimensional space between the two branes). This setup has some features in common with both gravity-mediated and gauge-mediated supersymmetry breaking (*e.g.*, a hidden and visible sector and messengers).

Alternatively, one can consider a higher-dimensional theory that is compactified to four spacetime dimensions. In this approach, supersymmetry is broken by boundary conditions on the compactified space that distinguish between fermions and bosons. This is the so-called Scherk-Schwarz mechanism [68]. The phenomenology of such models can be strikingly different from that of the usual MSSM [69]. All these extra-dimensional ideas clearly deserve further investigation, although they will not be discussed further here.

I.2.6. Split-supersymmetry: If supersymmetry is not connected with the origin of the electroweak scale, string theory suggests that supersymmetry still plays a significant role in Planck-scale physics. However, it may still be possible that some remnant of the superparticle spectrum survives down to the TeV-scale or below. This is the idea of split-supersymmetry [17], in which supersymmetric scalar partners of the quarks and leptons are significantly heavier (perhaps by many orders of magnitude) than 1 TeV, whereas the fermionic partners of the gauge and Higgs bosons have masses on the order of 1 TeV or below (presumably protected by some chiral symmetry). With the exception of a single light neutral scalar whose properties are indistinguishable from those of the Standard Model Higgs boson, all other Higgs bosons are also taken to be very heavy.

The supersymmetry breaking required to produce such a scenario would destabilize the gauge hierarchy. In particular, split-supersymmetry cannot provide a natural explanation for the existence of the light Standard-Model-like Higgs boson, whose mass lies orders below the mass scale of the heavy scalars. Nevertheless, models of split-supersymmetry can account for the dark matter (which is assumed to be the LSP) and gauge coupling unification. Thus, there is some motivation for pursuing the phenomenology of such approaches [18]. One notable difference from the usual MSSM phenomenology is the existence of a long-lived gluino [70].

I.3. Parameters of the MSSM: The parameters of the MSSM are conveniently described by considering separately the supersymmetry-conserving sector and the supersymmetry-breaking sector. A careful discussion of the conventions used in defining the tree-level MSSM parameters can be found in Ref. 71. (Additional fields and parameters must be introduced if one wishes to account for non-zero neutrino masses. We shall not pursue this here; see section I.8 for a discussion of supersymmetric approaches that incorporate neutrino masses.) For simplicity, consider first the case of one generation of quarks, leptons, and their scalar superpartners.

I.3.1. The supersymmetric-conserving parameters:

The parameters of the supersymmetry-conserving sector consist of: (i) gauge couplings: g_s , g , and g' , corresponding to the Standard Model gauge group $SU(3) \times SU(2) \times U(1)$ respectively; (ii) a supersymmetry-conserving higgsino mass parameter μ ; and (iii) Higgs-fermion Yukawa coupling constants: λ_u , λ_d , and λ_e (corresponding to the coupling of one generation of left- and right-handed quarks and leptons, and their superpartners to the Higgs bosons and higgsinos). Because there is no right-handed neutrino (and its superpartner) in the MSSM as defined here, one cannot introduce a Yukawa coupling λ_ν .

I.3.2. The supersymmetric-breaking parameters:

The supersymmetry-breaking sector contains the following set of parameters: (i) gaugino Majorana masses M_3 , M_2 , and M_1 associated with the $SU(3)$, $SU(2)$, and $U(1)$ subgroups of the Standard Model; (ii) five scalar squared-mass parameters for the

squarks and sleptons, M_Q^2 , M_U^2 , M_D^2 , M_L^2 , and M_E^2 [corresponding to the five electroweak gauge multiplets, *i.e.*, superpartners of $(u, d)_L$, u_L^c , d_L^c , $(\nu, e^-)_L$, and e_L^c , where the superscript c indicates a charge-conjugated fermion]; and (iii) Higgs-squark-squark and Higgs-slepton-slepton trilinear interaction terms, with coefficients $\lambda_u A_U$, $\lambda_d A_D$, and $\lambda_e A_E$ (which define the so-called “ A -parameters”). It is traditional to factor out the Yukawa couplings in the definition of the A -parameters (originally motivated by a simple class of gravity-mediated supersymmetry-breaking models [2,4]). If the A -parameters defined in this way are parametrically of the same order (or smaller) as compared to other supersymmetry-breaking mass parameters, then only the A -parameters of the third generation will be phenomenologically relevant.

Finally, we add: (iv) three scalar squared-mass parameters—two of which (m_1^2 and m_2^2) contribute to the diagonal Higgs squared-masses, given by $m_1^2 + |\mu|^2$ and $m_2^2 + |\mu|^2$, and a third which contributes to the off-diagonal Higgs squared-mass term, $m_{12}^2 \equiv B\mu$ (which defines the “ B -parameter”). The breaking of the electroweak symmetry $SU(2) \times U(1)$ to $U(1)_{EM}$ is only possible after introducing the supersymmetry-breaking Higgs squared-mass parameters. Minimizing the resulting Higgs scalar potential, these three squared-mass parameters can be re-expressed in terms of the two Higgs vacuum expectation values, v_d and v_u (also called v_1 and v_2 , respectively, in the literature), and one physical Higgs mass. Here, v_d [v_u] is the vacuum expectation value of the neutral component of the Higgs field H_d [H_u] that couples exclusively to down-type (up-type) quarks and leptons. Note that $v_d^2 + v_u^2 = 4m_W^2/g^2 = (246 \text{ GeV})^2$ is fixed by the W mass and the gauge coupling, whereas the ratio

$$\tan \beta = v_u/v_d \quad (1)$$

is a free parameter of the model. By convention, the Higgs field phases are chosen such that $0 \leq \beta \leq \pi/2$.

Note that supersymmetry-breaking mass terms for the fermionic superpartners of scalar fields and non-holomorphic trilinear scalar interactions (*i.e.*, interactions that mix scalar fields and their complex conjugates) have not been included above in the soft-supersymmetry-breaking sector. These terms can potentially destabilize the gauge hierarchy [11] in models with a gauge-singlet superfield. The latter is not present in the MSSM; hence as noted in Ref. [12], these so-called non-standard soft-supersymmetry-breaking terms are benign. However, the coefficients of these terms (which have dimensions of mass) are expected to be significantly suppressed compared to the TeV-scale in a fundamental theory of supersymmetry-breaking. Consequently, we follow the usual approach and omit these terms from further consideration.

I.3.3. MSSM-124: The total number of degrees of freedom of the MSSM is quite large, primarily due to the parameters of the soft-supersymmetry-breaking sector. In particular, in the case of three generations of quarks, leptons, and their

Searches Particle Listings

Supersymmetric Particle Searches

superpartners, M_Q^2 , M_U^2 , M_D^2 , M_L^2 , and M_E^2 are hermitian 3×3 matrices, and A_U , A_D , and A_E are complex 3×3 matrices. In addition, M_1 , M_2 , M_3 , B , and μ are, in general, complex. Finally, as in the Standard Model, the Higgs-fermion Yukawa couplings, λ_f ($f = u, d$, and e), are complex 3×3 matrices that are related to the quark and lepton mass matrices via: $M_f = \lambda_f v_f / \sqrt{2}$, where $v_e \equiv v_d$ [with v_u and v_d as defined above Eq. (1)].

However, not all these parameters are physical. Some of the MSSM parameters can be eliminated by expressing interaction eigenstates in terms of the mass eigenstates, with an appropriate redefinition of the MSSM fields to remove unphysical degrees of freedom. The analysis of Ref. 72 shows that the MSSM possesses 124 independent parameters. Of these, 18 parameters correspond to Standard Model parameters (including the QCD vacuum angle θ_{QCD}), one corresponds to a Higgs sector parameter (the analogue of the Standard Model Higgs mass), and 105 are genuinely new parameters of the model. The latter include: five real parameters and three CP -violating phases in the gaugino/higgsino sector, 21 squark and slepton masses, 36 real mixing angles to define the squark and slepton mass eigenstates, and 40 CP -violating phases that can appear in squark and slepton interactions. The most general R-parity-conserving minimal supersymmetric extension of the Standard Model (without additional theoretical assumptions) will be denoted henceforth as MSSM-124 [73].

I.4. The supersymmetric-particle sector: Consider the sector of supersymmetric particles (*sparticles*) in the MSSM. The supersymmetric partners of the gauge and Higgs bosons are fermions, whose names are obtained by appending “ino” at the end of the corresponding Standard Model particle name. The gluino is the color-octet Majorana fermion partner of the gluon with mass $M_{\tilde{g}} = |M_3|$. The supersymmetric partners of the electroweak gauge and Higgs bosons (the gauginos and higgsinos) can mix. As a result, the physical states of definite mass are model-dependent linear combinations of the charged and neutral gauginos and higgsinos, called *charginos* and *neutralinos*, respectively. Like the gluino, the neutralinos are also Majorana fermions, which provide for some distinctive phenomenological signatures [74,75]. The supersymmetric partners of the quarks and leptons are spin-zero bosons: the *squarks*, charged *sleptons*, and *sneutrinos*, respectively. A complete set of Feynman rules for the sparticles of the MSSM can be found in Ref. 76.

I.4.1. The charginos and neutralinos: The mixing of the charged gauginos (\tilde{W}^\pm) and charged higgsinos (H_u^\pm and H_d^\pm) is described (at tree-level) by a 2×2 complex mass matrix [77–79]:

$$M_C \equiv \begin{pmatrix} M_2 & \frac{1}{\sqrt{2}} g v_u \\ \frac{1}{\sqrt{2}} g v_d & \mu \end{pmatrix}. \quad (2)$$

To determine the physical chargino states and their masses, one must perform a singular value decomposition [80] of the complex matrix M_C :

$$U^* M_C V^{-1} = \text{diag}(M_{\tilde{\chi}_1^\pm}, M_{\tilde{\chi}_2^\pm}), \quad (3)$$

where U and V are unitary matrices, and the right-hand side of Eq. (3) is the diagonal matrix of (non-negative) chargino masses. The physical chargino states are denoted by $\tilde{\chi}_1^\pm$ and $\tilde{\chi}_2^\pm$. These are linear combinations of the charged gaugino and higgsino states determined by the matrix elements of U and V [77–79]. The chargino masses correspond to the *singular values* [80] of M_C , *i.e.*, the positive square roots of the eigenvalues of $M_C^\dagger M_C$:

$$M_{\tilde{\chi}_1^\pm, \tilde{\chi}_2^\pm}^2 = \frac{1}{2} \left\{ |\mu|^2 + |M_2|^2 + 2m_W^2 \mp \left[(|\mu|^2 + |M_2|^2 + 2m_W^2)^2 - 4|\mu|^2 |M_2|^2 - 4m_W^4 \sin^2 2\beta + 8m_W^2 \sin 2\beta \text{Re}(\mu M_2) \right]^{1/2} \right\}, \quad (4)$$

where the states are ordered such that $M_{\tilde{\chi}_1^\pm} \leq M_{\tilde{\chi}_2^\pm}$. It is convenient to choose a convention where $\tan \beta$ and M_2 are real and positive. Note that the relative phase of M_2 and μ is meaningful. (If CP -violating effects are neglected, then μ can be chosen real but may be either positive or negative.) The sign of μ is convention-dependent; the reader is warned that both sign conventions appear in the literature. The sign convention for μ in Eq. (2) is used by the LEP collaborations [27] in their plots of exclusion contours in the M_2 vs. μ plane derived from the non-observation of $e^+ e^- \rightarrow \tilde{\chi}_1^+ \tilde{\chi}_1^-$.

The mixing of the neutral gauginos (\tilde{B} and \tilde{W}^0) and neutral higgsinos (\tilde{H}_d^0 and \tilde{H}_u^0) is described (at tree-level) by a 4×4 complex symmetric mass matrix [77,78,81,82]:

$$M_N \equiv \begin{pmatrix} M_1 & 0 & -\frac{1}{2} g' v_d & \frac{1}{2} g' v_u \\ 0 & M_2 & \frac{1}{2} g v_d & -\frac{1}{2} g v_u \\ -\frac{1}{2} g' v_d & \frac{1}{2} g v_d & 0 & -\mu \\ \frac{1}{2} g' v_u & -\frac{1}{2} g v_u & -\mu & 0 \end{pmatrix}. \quad (5)$$

To determine the physical neutralino states and their masses, one must perform a Takagi-diagonalization [80,83,84] of the complex symmetric matrix M_N :

$$W^T M_N W = \text{diag}(M_{\tilde{\chi}_1^0}, M_{\tilde{\chi}_2^0}, M_{\tilde{\chi}_3^0}, M_{\tilde{\chi}_4^0}), \quad (6)$$

where W is a unitary matrix and the right-hand side of Eq. (6) is the diagonal matrix of (non-negative) neutralino masses. The physical neutralino states are denoted by $\tilde{\chi}_i^0$ ($i = 1, \dots, 4$), where the states are ordered such that $M_{\tilde{\chi}_1^0} \leq M_{\tilde{\chi}_2^0} \leq M_{\tilde{\chi}_3^0} \leq M_{\tilde{\chi}_4^0}$. The $\tilde{\chi}_i^0$ are the linear combinations of the neutral gaugino and higgsino states determined by the matrix elements of W (in Ref. 77, $W = N^{-1}$). The neutralino masses correspond to the singular values of M_N (*i.e.*, the positive square roots of the eigenvalues of $M_N^\dagger M_N$). Exact formulae for these masses can be found in Refs. [81] and [85]. A numerical algorithm for determining the mixing matrix W has been given by Ref. 86.

If a chargino or neutralino state approximates a particular gaugino or higgsino state, it is convenient to employ the

corresponding nomenclature. Specifically, if M_1 and M_2 are small compared to m_Z and $|\mu|$, then the lightest neutralino $\tilde{\chi}_1^0$ would be nearly a pure *photino*, $\tilde{\gamma}$, the supersymmetric partner of the photon. If M_1 and m_Z are small compared to M_2 and $|\mu|$, then the lightest neutralino would be nearly a pure *bin*o, \tilde{B} , the supersymmetric partner of the weak hypercharge gauge boson. If M_2 and m_Z are small compared to M_1 and $|\mu|$, then the lightest chargino pair and neutralino would constitute a triplet of roughly mass-degenerate pure *wino*s, \tilde{W}^\pm , and \tilde{W}_3^0 , the supersymmetric partners of the weak SU(2) gauge bosons. Finally, if $|\mu|$ and m_Z are small compared to M_1 and M_2 , then the lightest neutralino would be nearly a pure *higgsino*. Each of the above cases leads to a strikingly different phenomenology.

I.4.2. The squarks, sleptons and sneutrinos: For a given fermion f , there are two supersymmetric partners, \tilde{f}_L and \tilde{f}_R , which are scalar partners of the corresponding left- and right-handed fermion. (There is no $\tilde{\nu}_R$ in the MSSM.) However, in general, \tilde{f}_L and \tilde{f}_R are not mass eigenstates, since there is \tilde{f}_L - \tilde{f}_R mixing. For three generations of squarks, one must in general diagonalize 6×6 matrices corresponding to the basis $(\tilde{q}_{iL}, \tilde{q}_{iR})$, where $i = 1, 2, 3$ are the generation labels. For simplicity, only the one-generation case is illustrated in detail below (using the notation of the third family). In this case, the tree-level squark squared-mass matrix is given by [87]

$$M_F^2 = \begin{pmatrix} M_Q^2 + m_q^2 + L_q & m_q X_q^* \\ m_q X_q & M_R^2 + m_q^2 + R_q \end{pmatrix}, \quad (7)$$

where

$$X_q \equiv A_q - \mu^* (\cot \beta)^{2T_{3q}}, \quad (8)$$

and $T_{3q} = \frac{1}{2} [-\frac{1}{2}]$ for $q = t [b]$. The diagonal squared masses are governed by soft-supersymmetry-breaking squared masses M_Q^2 and $M_R^2 \equiv M_U^2 [M_D^2]$ for $q = t [b]$, the corresponding quark masses $m_t [m_b]$, and electroweak correction terms:

$$\begin{aligned} L_q &\equiv (T_{3q} - e_q \sin^2 \theta_W) m_Z^2 \cos 2\beta, \\ R_q &\equiv e_q \sin^2 \theta_W m_Z^2 \cos 2\beta, \end{aligned} \quad (9)$$

where $e_q = \frac{2}{3} [-\frac{1}{3}]$ for $q = t [b]$. The off-diagonal squared squark masses are proportional to the corresponding quark masses and depend on $\tan \beta$ [Eq. (1)], the soft-supersymmetry-breaking A -parameters and the higgsino mass parameter μ . The signs of the A and μ parameters are convention-dependent; other choices appear frequently in the literature. Due to the appearance of the *quark* mass in the off-diagonal element of the squark squared-mass matrix, one expects the \tilde{q}_L - \tilde{q}_R mixing to be small, with the possible exception of the third generation, where mixing can be enhanced by factors of m_t and $m_b \tan \beta$.

In the case of third generation \tilde{q}_L - \tilde{q}_R mixing, the mass eigenstates (usually denoted by \tilde{q}_1 and \tilde{q}_2 , with $m_{\tilde{q}_1} < m_{\tilde{q}_2}$) are determined by diagonalizing the 2×2 matrix M_F^2 given by

Eq. (7). The corresponding squared masses and mixing angle are given by [87]:

$$\begin{aligned} m_{\tilde{q}_{1,2}}^2 &= \frac{1}{2} \left[\text{Tr } M_F^2 \pm \sqrt{(\text{Tr } M_F^2)^2 - 4 \det M_F^2} \right], \\ \sin 2\theta_{\tilde{q}} &= \frac{2m_q |X_q|}{m_{\tilde{q}_2}^2 - m_{\tilde{q}_1}^2}. \end{aligned} \quad (10)$$

The one-generation results above also apply to the charged sleptons, with the obvious substitutions: $q \rightarrow \tau$ with $T_{3\tau} = -\frac{1}{2}$ and $e_\tau = -1$, and the replacement of the supersymmetry-breaking parameters: $M_Q^2 \rightarrow M_L^2$, $M_U^2 \rightarrow M_E^2$, and $A_q \rightarrow A_\tau$. For the neutral sleptons, $\tilde{\nu}_R$ does not exist in the MSSM, so $\tilde{\nu}_L$ is a mass eigenstate.

In the case of three generations, the supersymmetry-breaking scalar-squared masses $[M_Q^2, M_U^2, M_D^2, M_L^2, \text{ and } M_E^2]$ and the A -parameters that parameterize the Higgs couplings to up- and down-type squarks and charged sleptons (henceforth denoted by A_U, A_D , and A_E , respectively) are now 3×3 matrices as noted in Section I.3. The diagonalization of the 6×6 squark mass matrices yields \tilde{f}_L - \tilde{f}_R mixing (for $i \neq j$). In practice, since the \tilde{f}_L - \tilde{f}_R mixing is appreciable only for the third generation, this additional complication can usually be neglected.

Radiative loop corrections will modify all tree-level results for masses quoted in this section. These corrections must be included in any precision study of supersymmetric phenomenology [88]. Beyond tree level, the definition of the supersymmetric parameters becomes convention-dependent. For example, one can define physical couplings or running couplings, which differ beyond the tree level. This provides a challenge to any effort that attempts to extract supersymmetric parameters from data. The supersymmetric parameter analysis (SPA) project proposes a set of conventions [89] based on a consistent set of conventions and input parameters. This work employs a consistent dimensional reduction scheme for the regularization of higher-order loop corrections in supersymmetric theories recently advocated in Ref. 90. Ultimately, these efforts will facilitate the reconstruction of the fundamental supersymmetric theory (and its breaking mechanism) from high-precision studies of supersymmetric phenomena at future colliders.

I.5. The Higgs sector of the MSSM: Next, consider the MSSM Higgs sector [22,23,91]. Despite the large number of potential CP -violating phases among the MSSM-124 parameters, the tree-level MSSM Higgs sector is automatically CP -conserving. That is, unphysical phases can be absorbed into the definition of the Higgs fields such that $\tan \beta$ is a real parameter (conventionally chosen to be positive). Consequently, the physical neutral Higgs scalars are CP eigenstates. The MSSM Higgs sector contains five physical spin-zero particles: a charged Higgs boson pair (H^\pm), two CP -even neutral Higgs bosons (denoted by h^0 and H^0 where $m_h \leq m_H$), and one CP -odd neutral Higgs boson (A^0).

Searches Particle Listings

Supersymmetric Particle Searches

I.5.1 The Tree-level MSSM Higgs sector: The properties of the Higgs sector are determined by the Higgs potential, which is made up of quadratic terms [whose squared-mass coefficients were specified above in Eq. (1)] and quartic interaction terms governed by dimensionless couplings. The quartic interaction terms are manifestly supersymmetric at tree level (although these are modified by supersymmetry-breaking effects at the loop level). In general, the quartic couplings arise from two sources: (i) the supersymmetric generalization of the scalar potential (the so-called “ F -terms”), and (ii) interaction terms related by supersymmetry to the coupling of the scalar fields and the gauge fields, whose coefficients are proportional to the corresponding gauge couplings (the so-called “ D -terms”). In the MSSM, F -term contributions to the quartic couplings are absent (although such terms may be present in extensions of the MSSM, *e.g.*, models with Higgs singlets). As a result, the strengths of the MSSM quartic Higgs interactions are fixed in terms of the gauge couplings. Due to the resulting constraint on the form of the two-Higgs-doublet scalar potential, all the tree-level MSSM Higgs-sector parameters depend only on two quantities: $\tan\beta$ [defined in Eq. (1)] and one Higgs mass usually taken to be m_A . From these two quantities, one can predict the values of the remaining Higgs boson masses, an angle α (which measures the component of the original $Y = \pm 1$ Higgs doublet states in the physical CP -even neutral scalars), and the Higgs boson self-couplings.

I.5.2 The radiatively-corrected MSSM Higgs sector: When radiative corrections are incorporated, additional parameters of the supersymmetric model enter via virtual loops. The impact of these corrections can be significant [92]. For example, the tree-level MSSM-124 prediction for the upper bound of the lightest CP -even Higgs mass, $m_h \leq m_Z |\cos 2\beta| \leq m_Z$ [22,23], can be substantially modified when radiative corrections are included. The qualitative behavior of these radiative corrections can be most easily seen in the large top-squark mass limit, where in addition, both the splitting of the two diagonal entries and the two off-diagonal entries of the top-squark squared-mass matrix [Eq. (7)] are small in comparison to the average of the two top-squark squared masses, $M_S^2 \equiv \frac{1}{2}(M_{t_1}^2 + M_{t_2}^2)$. In this case (assuming $m_A > m_Z$), the predicted upper bound for m_h (which reaches its maximum at large $\tan\beta$) is approximately given by

$$m_h^2 \lesssim m_Z^2 + \frac{3g^2 m_t^4}{8\pi^2 m_W^2} \left\{ \ln(M_S^2/m_t^2) + \frac{X_t^2}{M_S^2} \left(1 - \frac{X_t^2}{12M_S^2} \right) \right\}, \quad (11)$$

where $X_t \equiv A_t - \mu \cot\beta$ is the top-squark mixing factor [see Eq. (7)]. A more complete treatment of the radiative corrections [93] shows that Eq. (11) somewhat overestimates the true upper bound of m_h . These more refined computations, which incorporate renormalization group improvement and the leading two-loop contributions, yield $m_h \lesssim 135$ GeV (with an accuracy of a few GeV) for $m_t = 175$ GeV and $M_S \lesssim 2$ TeV [93]. This Higgs-mass upper bound can be relaxed somewhat in non-minimal extensions of the MSSM, as noted in Section I.9.

In addition, one-loop radiative corrections can introduce CP -violating effects in the Higgs sector, which depend on some of the CP -violating phases among the MSSM-124 parameters [94]. Although these effects are more model-dependent, they can have a non-trivial impact on the Higgs searches at future colliders. A summary of the current MSSM Higgs mass limits can be found in Ref. 41.

I.6. Restricting the MSSM parameter freedom: In Sections I.4 and I.5, we surveyed the parameters that comprise the MSSM-124. However, in its most general form, the MSSM-124 is not a phenomenologically-viable theory over most of its parameter space. This conclusion follows from the observation that a generic point in the MSSM-124 parameter space exhibits: (i) no conservation of the separate lepton numbers L_e , L_μ , and L_τ ; (ii) unsuppressed flavor-changing neutral currents (FCNC’s); and (iii) new sources of CP violation that are inconsistent with the experimental bounds.

For example, the MSSM contains many new sources of CP violation [95]. In particular, some combinations of the complex phases of the gaugino-mass parameters, the A parameters, and μ must be less than on the order of 10^{-2} – 10^{-3} (for a supersymmetry-breaking scale of 100 GeV) to avoid generating electric dipole moments for the neutron, electron, and atoms in conflict with observed data [96–98]. The non-observation of FCNC’s [28,29] places additional strong constraints on the off-diagonal matrix elements of the squark and slepton soft-supersymmetry-breaking squared masses and A -parameters (see Section I.3.3). As a result of the phenomenological deficiencies listed above, almost the entire MSSM-124 parameter space is ruled out! This theory is viable only at very special “exceptional” regions of the full parameter space.

The MSSM-124 is also theoretically incomplete as it provides no explanation for the origin of the supersymmetry-breaking parameters (and in particular, why these parameters should conform to the exceptional points of the parameter space mentioned above). Moreover, there is no understanding of the choice of parameters that leads to the breaking of the electroweak symmetry. What is needed ultimately is a fundamental theory of supersymmetry breaking (depending on far fewer than 124 parameters), which would provide a rationale for a set of soft-supersymmetry-breaking terms that would be consistent with all phenomenological constraints.

I.6.1. Bottom-up approach for constraining the parameters of the MSSM: In the absence of a fundamental theory of supersymmetry breaking, there are two general approaches for reducing the parameter freedom of MSSM-124. In the low-energy approach, an attempt is made to elucidate the nature of the exceptional points in the MSSM-124 parameter space that are phenomenologically viable. Consider two possible scenarios (under the assumption that squark and slepton masses are not significantly larger than the scale of electroweak symmetry breaking). First, one can assume that $M_{\tilde{Q}}^2$, $M_{\tilde{U}}^2$, $M_{\tilde{D}}^2$, $M_{\tilde{L}}^2$, $M_{\tilde{E}}^2$, and A_U , A_D , A_E are generation-independent (horizontal

universality [8,72,99]). Alternatively, one can simply require that all the aforementioned matrices are flavor diagonal in a basis where the quark and lepton mass matrices are diagonal (flavor alignment [100]). In either case, L_e , L_μ , and L_τ are separately conserved, while tree-level FCNC's are automatically absent. In both cases, the number of free parameters characterizing the MSSM is substantially less than 124, although there is no firm fundamental theoretical basis for either scenario. Recently, it has been argued that flavor alignment scenarios are disfavored [101] in light of the recent observation of $D^0-\bar{D}^0$ mixing [102]. Thus, if squarks are discovered with masses below about 1–2 TeV, then one would expect the first two generations of squarks to be highly degenerate in mass.

I.6.2. Top-down approach for constraining the parameters of the MSSM: In the high-energy approach, one imposes a particular structure on the soft-supersymmetry-breaking terms at a common high-energy scale (such as the Planck scale, M_P). Using the renormalization group equations, one can then derive the low-energy MSSM parameters relevant for collider physics. The initial conditions (at the appropriate high-energy scale) for the renormalization group equations depend on the mechanism by which supersymmetry breaking is communicated to the effective low energy theory. Examples of this scenario are provided by models of gravity-mediated and gauge-mediated supersymmetry breaking (see Section I.2). One bonus of such an approach is that one of the diagonal Higgs squared-mass parameters is typically driven negative by renormalization group evolution [103]. Thus, electroweak symmetry breaking is generated radiatively, and the resulting electroweak symmetry-breaking scale is intimately tied to the scale of low-energy supersymmetry breaking.

One prediction of the high-energy approach that arises in most grand unified supergravity models and gauge-mediated supersymmetry-breaking models is the unification of the (tree-level) gaugino mass parameters at some high-energy scale M_X :

$$M_1(M_X) = M_2(M_X) = M_3(M_X) = m_{1/2}. \quad (12)$$

Consequently, the effective low-energy gaugino mass parameters (at the electroweak scale) are related:

$$M_3 = (g_s^2/g^2)M_2, \quad M_1 = (5g'^2/3g^2)M_2 \simeq 0.5M_2. \quad (13)$$

In this case, the chargino and neutralino masses and mixing angles depend only on three unknown parameters: the gluino mass, μ , and $\tan\beta$. If in addition $|\mu| \gg M_1 \gtrsim m_Z$, then the lightest neutralino is nearly a pure bino, an assumption often made in supersymmetric particle searches at colliders.

Given the initial condition for gaugino masses [e.g., Eq. (13) or Eq. (14) below], the prediction of the low-energy gaugino mass parameters is robust. In contrast, the renormalization group evolution of the scalar masses may depend strongly on the unknown fundamental supersymmetry-breaking dynamics [104]. Such effects have generally been ignored (or assumed to have negligible effect) in the prediction of low-energy scalar masses in the literature.

I.6.3. Anomaly-mediated supersymmetry-breaking:

In some supergravity models, tree-level masses for the gauginos are absent. The gaugino mass parameters arise at one-loop and do not satisfy Eq. (13). In this case, one finds a model-independent contribution to the gaugino mass whose origin can be traced to the super-conformal (super-Weyl) anomaly, which is common to all supergravity models [66]. This approach is called *anomaly-mediated* supersymmetry breaking (AMSB). Eq. (13) is then replaced (in the one-loop approximation) by:

$$M_i \simeq \frac{b_i g_i^2}{16\pi^2} m_{3/2}, \quad (14)$$

where $m_{3/2}$ is the gravitino mass (assumed to be on the order of 1 TeV), and b_i are the coefficients of the MSSM gauge beta-functions corresponding to the corresponding U(1), SU(2), and SU(3) gauge groups: $(b_1, b_2, b_3) = (\frac{33}{5}, 1, -3)$. Eq. (14) yields $M_1 \simeq 2.8M_2$ and $M_3 \simeq -8.3M_2$, which implies that the lightest chargino pair and neutralino comprise a nearly mass-degenerate triplet of winos, $\widetilde{W}^\pm, \widetilde{W}^0$ (c.f. Table 1), over most of the MSSM parameter space. (For example, if $|\mu| \gg m_Z$, then Eq. (14) implies that $M_{\widetilde{\chi}_1^\pm} \simeq M_{\widetilde{\chi}_1^0} \simeq M_2$ [105].) The corresponding supersymmetric phenomenology differs significantly from the standard phenomenology based on Eq. (13), and is explored in detail in Ref. 106. Anomaly-mediated supersymmetry breaking also generates (approximate) flavor-diagonal squark and slepton mass matrices. However, this yields negative squared-mass contributions for the sleptons in the MSSM. It may be possible to cure this fatal flaw in approaches beyond the minimal supersymmetric model [107]. Alternatively, one may conclude that anomaly-mediation is not the sole source of supersymmetry-breaking in the slepton sector.

I.7. The constrained MSSMs: mSUGRA, GMSB, and SGUTs:

One way to guarantee the absence of significant FCNC's mediated by virtual supersymmetric particle exchange is to posit that the diagonal soft-supersymmetry-breaking scalar squared masses are universal at some energy scale. In this Section, we examine a number of top-down theoretical frameworks that constrain the parameters of the general MSSM. These frameworks provide predictions for the low-energy supersymmetric particle spectrum as a function of their input parameters. Of course, any of the theoretical assumptions described in this Section could be wrong and must eventually be tested experimentally. In practice, one anticipates that the measurements of low-energy supersymmetric parameters may eventually provide sufficient information to determine the organizing principle governing supersymmetry breaking and yield significant constraints on the values of the fundamental (high-energy) supersymmetric parameters [108].

I.7.1. The minimal supergravity (mSUGRA) model:

In the *minimal* supergravity (mSUGRA) framework [2–4], a form of the Kähler potential is employed that yields minimal kinetic energy terms for the MSSM fields [109]. As a result, the soft-supersymmetry-breaking parameters at the Planck scale take a particularly simple form in which the scalar

Searches Particle Listings

Supersymmetric Particle Searches

squared masses and the A -parameters are flavor-diagonal and universal [55]:

$$\begin{aligned} M_Q^2(M_P) &= M_U^2(M_P) = M_D^2(M_P) = m_0^2 \mathbf{1}, \\ M_L^2(M_P) &= M_E^2(M_P) = m_0^2 \mathbf{1}, \\ m_{\tilde{1}}^2(M_P) &= m_{\tilde{2}}^2(M_P) = m_0^2, \\ A_U(M_P) &= A_D(M_P) = A_E(M_P) = A_0 \mathbf{1}, \end{aligned} \quad (15)$$

where $\mathbf{1}$ is a 3×3 identity matrix in generation space. Renormalization group evolution is then used to derive the values of the supersymmetric parameters at the low-energy (electroweak) scale. For example, to compute squark masses, one must use the *low-energy* values for M_Q^2 , M_U^2 , and M_D^2 in Eq. (7). Through the renormalization group running with boundary conditions specified in Eq. (13) and Eq. (15), one can show that the low-energy values of M_Q^2 , M_U^2 , and M_D^2 depend primarily on m_0^2 and $m_{1/2}^2$. A number of useful approximate analytic expressions for superpartner masses in terms of the mSUGRA parameters can be found in Ref. 110.

In the mSUGRA approach, the MSSM-124 parameter freedom has been significantly reduced. Typical mSUGRA models give low-energy values for the scalar mass parameters that satisfy $M_{\tilde{L}} \lesssim M_{\tilde{E}} < M_{\tilde{Q}} \approx M_{\tilde{U}} \approx M_{\tilde{D}}$, with the squark mass parameters somewhere between a factor of 1–3 larger than the slepton mass parameters (*e.g.*, see Ref. 110). More precisely, the low-energy values of the squark mass parameters of the first two generations are roughly degenerate, while $M_{\tilde{Q}_3}$ and $M_{\tilde{U}_3}$ are typically reduced by a factor of 1–3 from the values of the first- and second-generation squark mass parameters, because of renormalization effects due to the heavy top-quark mass.

As a result, one typically finds that four flavors of squarks (with two squark eigenstates per flavor) and \tilde{b}_R are nearly mass-degenerate. The \tilde{b}_L mass and the diagonal \tilde{t}_L and \tilde{t}_R masses are reduced compared to the common squark mass of the first two generations. In addition, there are six flavors of nearly mass-degenerate sleptons (with two slepton eigenstates per flavor for the charged sleptons and one per flavor for the sneutrinos); the sleptons are expected to be somewhat lighter than the mass-degenerate squarks. Finally, third-generation squark masses and tau-slepton masses are sensitive to the strength of the respective \tilde{f}_L – \tilde{f}_R mixing, as discussed below Eq. (7). If $\tan\beta \gg 1$, then the pattern of third-generation squark masses is somewhat altered, as discussed in Ref. 111.

In mSUGRA models, the LSP is typically the lightest neutralino, $\tilde{\chi}_1^0$, which is dominated by its bino component. In particular, one can reject those mSUGRA parameter regimes in which the LSP is a chargino or the $\tilde{\tau}_1$ (the lightest scalar superpartner of the τ -lepton). In general, if one imposes the constraints of supersymmetric particle searches and those of cosmology (say, by requiring the LSP to be a suitable dark matter candidate), one obtains significant restrictions to the mSUGRA parameter space [39,112].

One can count the number of independent parameters in the mSUGRA framework. In addition to 18 Standard Model parameters (excluding the Higgs mass), one must specify m_0 , $m_{1/2}$, A_0 , the Planck-scale values for μ and B -parameters (denoted by μ_0 and B_0), and the gravitino mass $m_{3/2}$. Without additional model assumptions, $m_{3/2}$ is independent of the parameters that govern the mass spectrum of the superpartners of the Standard Model [55]. In principle, A_0 , B_0 , μ_0 , and $m_{3/2}$ can be complex, although in the mSUGRA approach, these parameters are taken (arbitrarily) to be real. In the early literature, additional conditions were obtained by assuming a simplifying form for the hidden sector that provides the fundamental source of supersymmetry breaking. Two additional relations emerged among the mSUGRA parameters [109]: $B_0 = A_0 - m_0$ and $m_{3/2} = m_0$. Although these relations characterize a theory that was called minimal supergravity when first proposed, it is now more common to omit these extra constraints in defining the mSUGRA model. To accommodate this prevailing convention, we propose that the more constrained mSUGRA models, in which additional parameter relations are imposed, shall be designated as *more* minimal supergravity (mmSUGRA) models. Detailed studies of the phenomenology of various mmSUGRA models have been presented in Ref. 113.

As previously noted, renormalization group evolution is used to compute the low-energy values of the mSUGRA parameters, which then fixes all the parameters of the low-energy MSSM. In particular, the two Higgs vacuum expectation values (or equivalently, m_Z and $\tan\beta$) can be expressed as a function of the Planck-scale supergravity parameters. The simplest procedure is to remove μ_0 and B_0 in favor of m_Z and $\tan\beta$ [the sign of μ_0 , denoted $\text{sgn}(\mu_0)$ below, is not fixed in this process]. In this case, the MSSM spectrum and its interaction strengths are determined by five parameters:

$$m_0, A_0, m_{1/2}, \tan\beta, \text{ and } \text{sgn}(\mu_0), \quad (16)$$

in addition to the 18 parameters of the Standard Model. However, the mSUGRA approach is probably too simplistic. Theoretical considerations suggest that the universality of Planck-scale soft-supersymmetry-breaking parameters is not generic [114]. In particular, effective operators at the Planck scale exist that do not respect flavor universality, and it is difficult to find a theoretical principle that would forbid them.

In order to facilitate studies of supersymmetric phenomenology at colliders, it has been a valuable exercise to compile a set of benchmark supersymmetric parameters, from which supersymmetric spectra and couplings can be derived [115]. A compilation of benchmark mSUGRA points consistent with present data from particle physics and cosmology can be found in Ref. 116. One particular well-studied benchmark points, the so-called SPS 1a' reference point [89] (this is a slight modification of the SPS 1a point of Ref. 115, which incorporates the latest constraints from collider data and cosmology) has been especially useful in experimental studies of supersymmetric phenomena at future colliders. In Figure 1, the supersymmetric

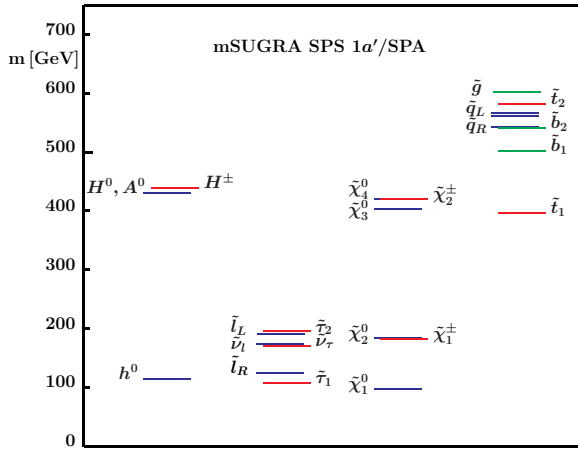


Figure 1: Mass spectrum of supersymmetric particles and Higgs bosons for the mSUGRA reference point SPS 1a'. The masses of the first and second generation squarks, sleptons, and sneutrinos are denoted collectively by \tilde{q} , $\tilde{\ell}$ and $\tilde{\nu}_\ell$, respectively. Taken from Ref. 89.

particle spectrum for the SPS 1a' reference point is exhibited. However, it is important to keep in mind that even within the mSUGRA framework, the resulting supersymmetric theory and its attendant phenomenology can be quite different from the SPS 1a' reference point.

I.7.2. Gauge-mediated supersymmetry breaking: In contrast to models of gravity-mediated supersymmetry breaking, the universality of the fundamental soft-supersymmetry-breaking squark and slepton squared-mass parameters is guaranteed in gauge-mediated supersymmetry breaking because the supersymmetry breaking is communicated to the sector of MSSM fields via gauge interactions [60,61]. In the minimal gauge-mediated supersymmetry-breaking (GMSB) approach, there is one effective mass scale, Λ , that determines all low-energy scalar and gaugino mass parameters through loop effects (while the resulting A parameters are suppressed). In order that the resulting superpartner masses be on the order of 1 TeV or less, one must have $\Lambda \sim 100$ TeV. The origin of the μ and B -parameters is quite model-dependent, and lies somewhat outside the ansatz of gauge-mediated supersymmetry breaking. The simplest models of this type are even more restrictive than mSUGRA, with two fewer degrees of freedom. Benchmark reference points for GMSB models have been proposed in Ref. 115 to facilitate collider studies.

The minimal GMSB is not a fully realized model. The sector of supersymmetry-breaking dynamics can be very complex, and no complete model of gauge-mediated supersymmetry yet exists that is both simple and compelling. However, recent advances in the theory of dynamical supersymmetry breaking (which exploit the existence of metastable supersymmetry-breaking vacua in broad classes of models [117]) have generated new ideas and opportunities for model building. As a result, simpler models of successful gauge mediation of supersymmetry

breaking have been achieved with the potential for overcoming a number of long-standing theoretical challenges [118].

It was noted in Section I.2 that the gravitino is the LSP in GMSB models. Thus, in such models, the next-to-lightest supersymmetric particle (NLSP) plays a crucial role in the phenomenology of supersymmetric particle production and decay. Note that unlike the LSP, the NLSP can be charged. In GMSB models, the most likely candidates for the NLSP are $\tilde{\chi}_1^\pm$ and $\tilde{\tau}_R^\pm$. The NLSP will decay into its superpartner plus a gravitino (e.g., $\tilde{\chi}_1^0 \rightarrow \gamma\tilde{G}$, $\tilde{\chi}_1^\pm \rightarrow Z\tilde{G}$, or $\tilde{\tau}_R^\pm \rightarrow \tau^\pm\tilde{G}$), with lifetimes and branching ratios that depend on the model parameters.

Different choices for the identity of the NLSP and its decay rate lead to a variety of distinctive supersymmetric phenomenologies [61,119]. For example, a long-lived $\tilde{\chi}_1^0$ -NLSP that decays outside collider detectors leads to supersymmetric decay chains with missing energy in association with leptons and/or hadronic jets (this case is indistinguishable from the standard phenomenology of the $\tilde{\chi}_1^0$ -LSP). On the other hand, if $\tilde{\chi}_1^0 \rightarrow \gamma\tilde{G}$ is the dominant decay mode, and the decay occurs inside the detector, then nearly *all* supersymmetric particle decay chains would contain a photon. In contrast, in the case of a $\tilde{\tau}_R^\pm$ -NLSP, the $\tilde{\tau}_R^\pm$ would either be long-lived or would decay inside the detector into a τ -lepton plus missing energy.

I.7.3. Supersymmetric grand unification: Finally, grand unification [120] can impose additional constraints on the MSSM parameters. As emphasized in Section I.1, it is striking that the $SU(3)\times SU(2)\times U(1)$ gauge couplings unify in models of supersymmetric grand unified theories (SGUTs) [8,17,121,122] with (some of) the supersymmetry-breaking parameters on the order of 1 TeV or below. Gauge coupling unification, which takes place at an energy scale on the order of 10^{16} GeV, is quite robust [123]. For example, successful unification depends weakly on the details of the theory at the unification scale. In particular, given the low-energy values of the electroweak couplings $g(m_Z)$ and $g'(m_Z)$, one can predict $\alpha_s(m_Z)$ by using the MSSM renormalization group equations to extrapolate to higher energies, and by imposing the unification condition on the three gauge couplings at some high-energy scale, M_X . This procedure, which fixes M_X , can be successful (*i.e.*, three running couplings will meet at a single point) only for a unique value of $\alpha_s(m_Z)$. The extrapolation depends somewhat on the low-energy supersymmetric spectrum (so-called low-energy ‘‘threshold effects’’), and on the SGUT spectrum (high-energy threshold effects), which can somewhat alter the evolution of couplings. A comparison of data with the expectations of SGUTs shows that the measured value of $\alpha_s(m_Z)$ is in good agreement with the predictions of supersymmetric grand unification for a reasonable choice of supersymmetric threshold corrections [124].

Additional SGUT predictions arise through the unification of the Higgs-fermion Yukawa couplings (λ_f). There is some evidence that $\lambda_b = \lambda_\tau$ is consistent with observed low-energy data [125], and an intriguing possibility that $\lambda_b = \lambda_\tau = \lambda_t$ may be phenomenologically viable [111,126] in the parameter regime

Searches Particle Listings

Supersymmetric Particle Searches

where $\tan\beta \simeq m_t/m_b$. Finally, grand unification imposes constraints on the soft-supersymmetry-breaking parameters. For example, gaugino-mass unification leads to the relations given by Eq. (13). Diagonal squark and slepton soft-supersymmetry-breaking scalar masses may also be unified, which is analogous to the unification of Higgs-fermion Yukawa couplings.

1.8. Massive neutrinos in low-energy supersymmetry:

With the overwhelming evidence for neutrino masses and mixing [127,128], it is clear that any viable supersymmetric model of fundamental particles must incorporate some form of L -violation in the low-energy theory [129]. This requires an extension of the MSSM, which (as in the case of the minimal Standard Model) contains three generations of massless neutrinos. To construct a supersymmetric model with massive neutrinos, one can follow one of two different approaches.

1.8.1. The supersymmetric seesaw: In the first approach, one starts with an extended version of the Standard Model, which incorporates new structure that yields nonzero neutrino masses. Following the procedures of Sections I.2 and I.3, one then formulates a supersymmetric version of this extended Standard Model. For example, neutrino masses can be incorporated into the Standard Model by introducing an $SU(3)\times SU(2)\times U(1)$ singlet right-handed neutrino (ν_R) and a super-heavy Majorana mass (typically on the order of a grand unified mass) for the ν_R . In addition, one must also include a standard Yukawa coupling between the lepton doublet, the Higgs doublet, and ν_R . The Higgs vacuum expectation value then induces an off-diagonal ν_L - ν_R mass on the order of the electroweak scale. Diagonalizing the neutrino mass matrix (in the three-generation model) yields three superheavy neutrino states, and three very light neutrino states that are identified as the light neutrino states observed in nature. This is the seesaw mechanism [130]. The supersymmetric generalization of the seesaw model of neutrino masses is now easily constructed [131,132].

In the seesaw-extended Standard Model, lepton number is broken due to the presence of $\Delta L = 2$ terms in the Lagrangian (which include the Majorana mass terms for the light and superheavy neutrinos). Consequently, the seesaw-extended MSSM conserves R-parity. The supersymmetric analogue of the Majorana neutrino mass term in the sneutrino sector leads to sneutrino-antisneutrino mixing phenomena [132,133].

1.8.2. R-parity-violating supersymmetry: A second approach to incorporating massive neutrinos in supersymmetric models is to retain the minimal particle content of the MSSM but remove the assumption of R-parity invariance [134]. The most general R-parity-violating (RPV) theory involving the MSSM spectrum introduces many new parameters to both the supersymmetry-conserving and the supersymmetry-breaking sectors. Each new interaction term violates either B or L conservation. For example, consider new scalar-fermion Yukawa couplings derived from the following interactions:

$$(\lambda_L)_{pmn}\widehat{L}_p\widehat{L}_m\widehat{E}_n^c+(\lambda'_L)_{pmn}\widehat{L}_p\widehat{Q}_m\widehat{D}_n^c+(\lambda_B)_{pmn}\widehat{U}_p\widehat{D}_m^c\widehat{D}_n^c, \quad (17)$$

where p , m , and n are generation indices, and gauge group indices are suppressed. In the notation above, \widehat{Q} , \widehat{U}^c , \widehat{D}^c , \widehat{L} , and \widehat{E}^c respectively represent $(u, d)_L$, u_L^c , d_L^c , $(\nu, e^-)_L$, and e_L^c and the corresponding superpartners. The Yukawa interactions are obtained from Eq. (17) by taking all possible combinations involving two fermions and one scalar superpartner. Note that the term in Eq. (17) proportional to λ_B violates B , while the other two terms violate L . Even if all the terms of Eq. (17) are absent, there is one more possible supersymmetric source of R-parity violation. In the notation of Eq. (17), one can add a term of the form $(\mu_L)_p\widehat{H}_u\widehat{L}_p$, where \widehat{H}_u represents the $Y = 1$ Higgs doublet and its higgsino superpartner. This term is the RPV generalization of the supersymmetry-conserving Higgs mass parameter μ of the MSSM, in which the $Y = -1$ Higgs/higgsino super-multiplet \widehat{H}_d is replaced by the slepton/lepton super-multiplet \widehat{L}_p . The RPV-parameters $(\mu_L)_p$ also violate L .

Phenomenological constraints derived from data on various low-energy B - and L -violating processes can be used to establish limits on each of the coefficients $(\lambda_L)_{pmn}$, $(\lambda'_L)_{pmn}$, and $(\lambda_B)_{pmn}$ taken one at a time [134,135]. If more than one coefficient is simultaneously non-zero, then the limits are, in general, more complicated [136]. All possible RPV terms cannot be simultaneously present and unsuppressed; otherwise the proton decay rate would be many orders of magnitude larger than the present experimental bound. One way to avoid proton decay is to impose B or L invariance (either one alone would suffice). Otherwise, one must accept the requirement that certain RPV coefficients must be extremely suppressed.

One particularly interesting class of RPV models is one in which B is conserved, but L is violated. It is possible to enforce baryon number conservation, while allowing for lepton-number-violating interactions by imposing a discrete \mathbf{Z}_3 baryon *triality* symmetry on the low-energy theory [137], in place of the standard \mathbf{Z}_2 R-parity. Since the distinction between the Higgs and matter super-multiplets is lost in RPV models, R-parity violation permits the mixing of sleptons and Higgs bosons, the mixing of neutrinos and neutralinos, and the mixing of charged leptons and charginos, leading to more complicated mass matrices and mass eigenstates than in the MSSM.

The supersymmetric phenomenology of the RPV models exhibits features that are quite distinct from that of the MSSM [134]. The LSP is no longer stable, which implies that not all supersymmetric decay chains must yield missing-energy events at colliders. Nevertheless, the loss of the missing-energy signature is often compensated by other striking signals (which depend on which R-parity-violating parameters are dominant). For example, supersymmetric particles in RPV models can be singly produced (in contrast to R-parity-conserving models where supersymmetric particles must be produced in pairs). The phenomenology of pair-produced supersymmetric particles is also modified in RPV models due to new decay chains not present in R-parity-conserving supersymmetry [134].

In RPV models with lepton number violation (these include low-energy supersymmetry models with baryon triality mentioned above), both $\Delta L=1$ and $\Delta L=2$ phenomena are allowed, leading to neutrino masses and mixing [138], neutrinoless double-beta decay [139], sneutrino-antisneutrino mixing [140], s-channel resonant production of sneutrinos in e^+e^- collisions [141] and charged sleptons in $p\bar{p}$ and pp collisions [142]. For example, Ref. 143 demonstrates how one can fit both the solar and atmospheric neutrino data in an RPV model where μ_L provides the dominant source of R-parity violation.

I.9. Other non-minimal extensions of the MSSM: Extensions of the MSSM have been proposed to solve a variety of theoretical problems. One such problem involves the μ parameter of the MSSM. Although μ is a supersymmetric-preserving parameter, it must be of order the supersymmetry-breaking scale to yield a consistent supersymmetric phenomenology. In the MSSM, one must devise a theoretical mechanism to guarantee that the magnitude of μ is not larger than the TeV-scale (e.g., in gravity-mediated supersymmetry, the Giudice-Masiero mechanism of Ref. 144 is the most cited explanation).

In extensions of the MSSM, new compelling solutions to the so-called μ -problem are possible. For example, one can replace μ by the vacuum expectation value of a new $SU(3)\times SU(2)\times U(1)$ singlet scalar field. In such a model, the Higgs sector of the MSSM is enlarged (and the corresponding fermionic higgsino superpartner is added). This is the so-called NMSSM (here, NM stands for non-minimal) [145]. There are some advantages to extending the model further by adding an additional $U(1)$ broken gauge symmetry [146] (which yields the USSM [84]).

Non-minimal extensions of the MSSM involving additional matter and/or Higgs super-multiplets can also yield a less restrictive bound on the mass of the lightest Higgs boson (as compared to the bound quoted in Section I.5.2). For example, MSSM-extended models consistent with gauge coupling unification can be constructed in which the upper limit on the lightest Higgs boson mass can be as high as 200–300 GeV [147] (a similar relaxation of the Higgs mass bound occurs in split supersymmetry [148] and extra-dimensional scenarios [149]).

Other MSSM extensions considered in the literature include an enlarged electroweak gauge group beyond $SU(2)\times U(1)$ [150]; and/or the addition of new, possibly exotic, matter super-multiplets (e.g., new $U(1)$ gauge groups and a vector-like color triplet with electric charge $\frac{1}{3}e$ that appear as low-energy remnants in E_6 grand unification models [151]). A possible theoretical motivation for such new structures arises from the study of phenomenologically viable string theory ground states [152].

References

- R. Haag, J.T. Lopuszanski, and M. Sohnius, Nucl. Phys. **B88**, 257 (1975); S.R. Coleman and J. Mandula, Phys. Rev. **159** (1967) 1251.
- H.P. Nilles, Phys. Reports **110**, 1 (1984).
- P. Nath, R. Arnowitt, and A.H. Chamseddine, *Applied $N=1$ Supergravity* (World Scientific, Singapore, 1984).
- S.P. Martin, in *Perspectives on Supersymmetry*, edited by G.L. Kane (World Scientific, Singapore, 1998) pp. 1–98; and a longer archive version in hep-ph/9709356.
- S. Weinberg, *The Quantum Theory of Fields, Volume III: Supersymmetry* (Cambridge University Press, Cambridge, UK, 2000); P. Binétruy, *Supersymmetry: Theory, Experiment, and Cosmology* (Oxford University Press, Oxford, UK, 2006).
- L. Maiani, in *Vector bosons and Higgs bosons in the Salam-Weinberg theory of weak and electromagnetic interactions, Proceedings of the 11th GIF Summer School on Particle Physics*, Gif-sur-Yvette, France, 3–7 September, 1979, edited by M. Davier *et al.*, (IN2P3, Paris, 1980) pp. 1–52.
- E. Witten, Nucl. Phys. **B188**, 513 (1981).
- S. Dimopoulos and H. Georgi, Nucl. Phys. **B193**, 150 (1981).
- N. Sakai, Z. Phys. **C11**, 153 (1981); R.K. Kaul, Phys. Lett. **109B**, 19 (1982).
- L. Susskind, Phys. Reports **104**, 181 (1984).
- L. Girardello and M. Grisaru, Nucl. Phys. **B194**, 65 (1982).
- L.J. Hall and L. Randall, Phys. Rev. Lett. **65**, 2939 (1990); I. Jack and D.R.T. Jones, Phys. Lett. **B457**, 101 (1999).
- For a review, see N. Polonsky, *Supersymmetry: Structure and phenomena. Extensions of the standard model*, Lect. Notes Phys. **M68**, 1 (2001).
- G. Bertone, D. Hooper, and J. Silk, Phys. Reports **405**, 279 (2005).
- G. Jungman, M. Kamionkowski, and K. Griest, Phys. Reports **267**, 195 (1996).
- V. Agrawal *et al.*, Phys. Rev. **D57**, 5480 (1998).
- N. Arkani-Hamed and S. Dimopoulos, JHEP **0506**, 073 (2005); G.F. Giudice and A. Romanino, Nucl. Phys. **B699**, 65 (2004) [erratum: **B706**, 65 (2005)].
- N. Arkani-Hamed *et al.*, Nucl. Phys. **B709**, 3 (2005); W. Kilian *et al.*, Eur. Phys. J. **C39**, 229 (2005).
- H.E. Haber and G.L. Kane, Phys. Reports **117**, 75 (1985).
- M. Drees, R. Godbole, and P. Roy, *Theory and Phenomenology of Sparticles* (World Scientific, Singapore, 2005); H. Baer and X. Tata, *Weak scale supersymmetry: from superfields to scattering events* (Cambridge University Press, Cambridge, UK, 2006); I.J.R. Aitchison, *Supersymmetry in particle physics: an elementary introduction* (Cambridge University Press, Cambridge, UK, 2007).
- P. Fayet, Nucl. Phys. **B78**, 14 (1974); *ibid.*, **B90**, 104 (1975).
- K. Inoue *et al.*, Prog. Theor. Phys. **67**, 1889 (1982) [erratum: **70**, 330 (1983)]; *ibid.*, **71**, 413 (1984); R. Flores and M. Sher, Ann. Phys. (NY) **148**, 95 (1983).
- J.F. Gunion and H.E. Haber, Nucl. Phys. **B272**, 1 (1986) [erratum: **B402**, 567 (1993)].
- For an overview of the theory and models of the soft-supersymmetry-breaking Lagrangian, see D.J.H. Chung *et al.*, Phys. Reports **407**, 1 (2005).

Searches Particle Listings

Supersymmetric Particle Searches

25. See, *e.g.*, R. Barbieri and G.F. Giudice, Nucl. Phys. **B305**, 63 (1988);
G.W. Anderson and D.J. Castano, Phys. Lett. **B347**, 300 (1995); Phys. Rev. **D52**, 1693 (1995); Phys. Rev. **D53**, 2403 (1996);
J.L. Feng, K.T. Matchev, and T. Moroi, Phys. Rev. **D61**, 075005 (2000);
P. Athron and D.J. Miller, Phys. Rev. **D76**, 075010 (2007).
26. S. Dimopoulos and G.F. Giudice, Phys. Lett. **B357**, 573 (1995);
A. Pomarol and D. Tommasini, Nucl. Phys. **B466**, 3 (1996);
A.G. Cohen, D.B. Kaplan, and A.E. Nelson, Phys. Lett. **B388**, 588 (1996);
J.L. Feng, K.T. Matchev, and T. Moroi, Phys. Rev. Lett. **84**, 2322 (2000).
27. L. Pape and D. Treille, Prog. Part. Nucl. Phys. **69**, 63 (2006);
J.-F. Grivaz, “Supersymmetry Part II (Experiment),” immediately following, in the section on Reviews, Tables, and Plots in this *Review*. See also *Particle Listings: Other Searches—Supersymmetric Particles* in this *Review*.
28. See, *e.g.*, F. Gabbiani *et al.*, Nucl. Phys. **B477**, 321 (1996);
A. Masiero, and O. Vives, New J. Phys. **4**, 4.1 (2002).
29. For a recent review and references to the original literature, see: M.J. Ramsey-Musolf and S. Su, Phys. Reports **456**, 1 (2008).
30. J. Erler and P. Langacker, “Electroweak Model and Constraints on New Physics,” in the section on Reviews, Tables, and Plots in this *Review*;
J. Alcaraz *et al.* [The LEP Collaborations ALEPH, DELPHI, L3, OPAL, and the LEP Electroweak Working Group], arXiv:0712.0929 [hep-ex] (6 December 2007).
31. P.H. Chankowski and S. Pokorski, in *Perspectives on Supersymmetry*, edited by G.L. Kane (World Scientific, Singapore, 1998) pp. 402–422.
32. A. Dobado, M.J. Herrero, and S. Penaranda, Eur. Phys. J. **C7**, 313 (1999); **C12**, 673 (2000); **C17**, 487 (2000).
33. J. Erler and D.M. Pierce, Nucl. Phys. **B526**, 53 (1998);
G. Altarelli *et al.*, JHEP **0106**, 018 (2001);
J.R. Ellis *et al.*, JHEP **0502**, 013 (2005); **0605**, 005 (2006).
34. For a review, see D. Stockinger, J. Phys. **G34**, R45 (2007).
35. A. Höcker and W. Marciano, “The Muon Anomalous Magnetic Moment,” in this *Review*;
J.P. Miller, E. de Rafael, and B.L. Roberts, Rept. Prog. Phys. **70**, 795 (2007);
S. Eidelman, Acta Phys. Polon. **38**, 3015 (2007);
F. Jegerlehner, Acta Phys. Polon. **38**, 3021 (2007).
36. M. Misiak *et al.*, Phys. Rev. Lett. **98**, 022002 (2007);
T. Becher and M. Neubert, Phys. Rev. Lett. **98**, 022003 (2007).
37. See, *e.g.*, M. Ciuchini *et al.*, Phys. Rev. **D67**, 075016 (2003);
T. Hurth, Rev. Mod. Phys. **75**, 1159 (2003).
38. U. Chattopadhyay and P. Nath, Phys. Rev. **D66**, 093001 (2002);
S.P. Martin and J.D. Wells, Phys. Rev. **D67**, 015002 (2003).
39. J.R. Ellis *et al.*, Phys. Lett. **B653**, 292 (2007);
J.R. Ellis *et al.*, JHEP **0708**, 083 (2007).
40. L. Giusti, A. Romanino, and A. Strumia, Nucl. Phys. **B550**, 3 (1999);
R. Barbieri and A. Strumia, Talk given at 4th Rencontres du Vietnam: International Conference on Physics at Extreme Energies (Particle Physics and Astrophysics), Hanoi, Vietnam, 19-25 July 2000, hep-ph/0007265.
41. A summary of the MSSM Higgs mass limits can be found in G. Bernardi, M. Carena, and T. Junk, “Searches for Higgs Bosons,” in “Particle Listings—Gauge and Higgs bosons” in this *Review*.
42. J.A. Casas, J.R. Espinosa, and I. Hidalgo, JHEP **0401**, 008 (2004);
P. Batra *et al.*, JHEP **0406**, 032 (2004);
R. Harnik *et al.*, Phys. Rev. **D70**, 015002 (2004);
A. Birkedal, Z. Chacko, and M.K. Gaillard, JHEP **0410**, 036 (2004).
43. H.C. Cheng and I. Low, JHEP **0309**, 051 (2003); **0408**, 061 (2004).
44. See, *e.g.*, R. Kitano and Y. Nomura, Phys. Rev. **D73**, 095004 (2006), and references contained therein.
45. P. Fayet, Phys. Lett. **69B**, 489 (1977);
G. Farrar and P. Fayet, Phys. Lett. **76B**, 575 (1978).
46. J. Ellis *et al.*, Nucl. Phys. **B238**, 453 (1984).
47. S. Raby, Phys. Lett. **B422**, 158 (1998);
S. Raby and K. Tobe, Nucl. Phys. **B539**, 3 (1999);
A. Mafi and S. Raby, Phys. Rev. **D62**, 035003 (2000).
48. A.R. Liddle and D.H. Lyth, Phys. Reports **213**, 1 (1993).
49. M. Drees and G. Gerbier, “Dark Matter,” in the section on Reviews, Tables, and Plots in this *Review*.
50. P. Fayet, Phys. Lett. **84B**, 421 (1979); Phys. Lett. **86B**, 272 (1979).
51. P. van Nieuwenhuizen, Phys. Reports **68**, 189 (1981).
52. S. Deser and B. Zumino, Phys. Rev. Lett. **38**, 1433 (1977);
E. Cremmer *et al.*, Phys. Lett. **79B**, 231 (1978).
53. R. Casalbuoni *et al.*, Phys. Lett. **B215**, 313 (1988); Phys. Rev. **D39**, 2281 (1989);
A.L. Maroto and J.R. Pelaez, Phys. Rev. **D62**, 023518 (2000).
54. A.H. Chamseddine, R. Arnowitt, and P. Nath, Phys. Rev. Lett. **49**, 970 (1982);
R. Barbieri, S. Ferrara, and C.A. Savoy, Phys. Lett. **119B**, 343 (1982);
H.-P. Nilles, M. Srednicki, and D. Wyler, Phys. Lett. **120B**, 346 (1983); **124B**, 337 (1983) 337;
E. Cremmer, P. Fayet, and L. Girardello, Phys. Lett. **122B**, 41 (1983);
L. Ibáñez, Nucl. Phys. **B218**, 514 (1982);
L. Alvarez-Gaumé, J. Polchinski, and M.B. Wise, Nucl. Phys. **B221**, 495 (1983).
55. L.J. Hall, J. Lykken, and S. Weinberg, Phys. Rev. **D27**, 2359 (1983).
56. S.K. Soni and H.A. Weldon, Phys. Lett. **126B**, 215 (1983);
Y. Kawamura, H. Murayama, and M. Yamaguchi, Phys. Rev. **D51**, 1337 (1995).
57. A.B. Lahanas and D.V. Nanopoulos, Phys. Reports **145**, 1 (1987).

58. J.L. Feng, A. Rajaraman, and F. Takayama, *Phys. Rev. Lett.* **91**, 011302 (2003); *Phys. Rev.* **D68**, 063504 (2003); *Gen. Rel. Grav.* **36**, 2575 (2004).
59. M. Dine, W. Fischler, and M. Srednicki, *Nucl. Phys.* **B189**, 575 (1981); S. Dimopoulos and S. Raby, *Nucl. Phys.* **B192**, 353 (1982); **B219**, 479 (1983); M. Dine and W. Fischler, *Phys. Lett.* **110B**, 227 (1982); C. Nappi and B. Ovrut, *Phys. Lett.* **113B**, 175 (1982); L. Alvarez-Gaumé, M. Claudson, and M. Wise, *Nucl. Phys.* **B207**, 96 (1982).
60. M. Dine and A.E. Nelson, *Phys. Rev.* **D48**, 1277 (1993); M. Dine, A.E. Nelson, and Y. Shirman, *Phys. Rev.* **D51**, 1362 (1995); M. Dine *et al.*, *Phys. Rev.* **D53**, 2658 (1996).
61. G.F. Giudice and R. Rattazzi, *Phys. Reports* **322**, 419 (1999).
62. J. Polchinski, *String Theory, Volumes I and II* (Cambridge University Press, Cambridge, UK, 1998).
63. Pedagogical lectures describing such mechanisms can be found in: M. Quiros, in *Particle Physics and Cosmology: The Quest for Physics Beyond the Standard Model(s), Proceedings of the 2002 Theoretical Advanced Study Institute in Elementary Particle Physics (TASI 2002)*, edited by H.E. Haber and A.E. Nelson (World Scientific, Singapore, 2004) pp. 549–601; C. Csaki, in *ibid.*, pp. 605–698.
64. See, *e.g.*, G.F. Giudice and J.D. Wells, “Extra Dimensions,” in the section on Reviews, Tables, and Plots in this *Review*.
65. These ideas are reviewed in: V.A. Rubakov, *Phys. Usp.* **44**, 871 (2001); J. Hewett and M. Spiropulu, *Ann. Rev. Nucl. Part. Sci.* **52**, 397 (2002).
66. L. Randall and R. Sundrum, *Nucl. Phys.* **B557**, 79 (1999).
67. Z. Chacko, M.A. Luty, and E. Ponton, *JHEP* **0007**, 036 (2000); D.E. Kaplan, G.D. Kribs, and M. Schmaltz, *Phys. Rev.* **D62**, 035010 (2000); Z. Chacko *et al.*, *JHEP* **0001**, 003 (2000).
68. J. Scherk and J.H. Schwarz, *Phys. Lett.* **82B**, 60 (1979); *Nucl. Phys.* **B153**, 61 (1979).
69. See, *e.g.*, R. Barbieri, L.J. Hall, and Y. Nomura, *Phys. Rev.* **D66**, 045025 (2002); *Nucl. Phys.* **B624**, 63 (2002).
70. K. Cheung and W. Y. Keung, *Phys. Rev.* **D71**, 015015 (2005); P. Gambino, G.F. Giudice, and P. Slavich, *Nucl. Phys.* **B726**, 35 (2005).
71. H.E. Haber, in *Recent Directions in Particle Theory, Proceedings of the 1992 Theoretical Advanced Study Institute in Particle Physics*, edited by J. Harvey and J. Polchinski (World Scientific, Singapore, 1993) pp. 589–686.
72. S. Dimopoulos and D. Sutter, *Nucl. Phys.* **B452**, 496 (1995); D.W. Sutter, Stanford Ph. D. thesis, [hep-ph/9704390](#).
73. H.E. Haber, *Nucl. Phys. B (Proc. Suppl.)* **62A-C**, 469 (1998).
74. R.M. Barnett, J.F. Gunion, and H.E. Haber, *Phys. Lett.* **B315**, 349 (1993); H. Baer, X. Tata, and J. Woodside, *Phys. Rev.* **D41**, 906 (1990).
75. S.M. Bilenky, E.Kh. Khristova, and N.P. Nedelcheva, *Phys. Lett.* **B161**, 397 (1985); *Bulg. J. Phys.* **13**, 283 (1986); G. Moortgat-Pick and H. Fraas, *Eur. Phys. J.* **C25**, 189 (2002).
76. J. Rosiek, *Phys. Rev.* **D41**, 3464 (1990) [erratum: [hep-ph/9511250](#)]. The most recent corrected version of this manuscript can be found on the author’s webpage, [www.fuw.edu.pl/~rosiek/physics/prd41.html](#).
77. For further details, see *e.g.*, Appendix C of Ref. 19 and Appendix A of Ref. 23.
78. J.L. Kneur and G. Moultaka, *Phys. Rev.* **D59**, 015005 (1999).
79. S.Y. Choi *et al.*, *Eur. Phys. J.* **C14**, 535 (2000).
80. R.A. Horn and C.R. Johnson, *Matrix Analysis*, (Cambridge University Press, Cambridge, UK, 1985).
81. S.Y. Choi *et al.*, *Eur. Phys. J.* **C22**, 563 (2001); **C23**, 769 (2002).
82. G.J. Gounaris, C. Le Mouel, and P.I. Porfyriadis, *Phys. Rev.* **D65**, 035002 (2002); G.J. Gounaris and C. Le Mouel, *Phys. Rev.* **D66**, 055007 (2002).
83. T. Takagi, *Japan J. Math.* **1**, 83 (1925).
84. S.Y. Choi *et al.*, *Nucl. Phys.* **B778**, 85 (2007).
85. M.M. El Kheishen, A.A. Aboshousha, and A.A. Shafik, *Phys. Rev.* **D45**, 4345 (1992); M. Guchait, *Z. Phys.* **C57**, 157 (1993) [erratum: **C61**, 178 (1994)].
86. T. Hahn, preprint MPP-2006-85, [physics/0607103](#).
87. J. Ellis and S. Rudaz, *Phys. Lett.* **128B**, 248 (1983); F. Browning, D. Chang, and W.Y. Keung, *Phys. Rev.* **D64**, 015010 (2001); A. Bartl *et al.*, *Phys. Lett.* **B573**, 153 (2003); *Phys. Rev.* **D70**, 035003 (2004).
88. D.M. Pierce *et al.*, *Nucl. Phys.* **B491**, 3 (1997).
89. J.A. Aguilar-Saavedra *et al.*, *Eur. Phys. J.* **C46**, 43 (2006).
90. D. Stockinger, *JHEP* **0503**, 076 (2005); *Nucl. Phys. B (Proc. Suppl.)* **160**, 250 (2006).
91. J.F. Gunion *et al.*, *The Higgs Hunter’s Guide* (Perseus Publishing, Cambridge, MA, 1990); M. Carena and H.E. Haber, *Prog. Part. Nucl. Phys.* **50**, 63 (2003); A. Djouadi, *Phys. Reports* **459**, 1 (2008).
92. H.E. Haber and R. Hempfling, *Phys. Rev. Lett.* **66**, 1815 (1991); Y. Okada, M. Yamaguchi, and T. Yanagida, *Prog. Theor. Phys.* **85**, 1 (1991); J. Ellis, G. Ridolfi, and F. Zwirner, *Phys. Lett.* **B257**, 83 (1991).
93. See, *e.g.*, G. Degrassi *et al.*, *Eur. Phys. J.* **C28**, 133 (2003); B.C. Allanach *et al.*, *JHEP* **0409**, 044 (2004); S.P. Martin, *Phys. Rev.* **D75**, 055005 (2007).
94. A. Pilaftsis and C.E.M. Wagner, *Nucl. Phys.* **B553**, 3 (1999); D.A. Demir, *Phys. Rev.* **D60**, 055006 (1999); S.Y. Choi, M. Drees, and J.S. Lee, *Phys. Lett.* **B481**, 57 (2000); M. Carena *et al.*, *Nucl. Phys.* **B586**, 92 (2000); *Phys. Lett.* **B495**, 155 (2000); *Nucl. Phys.* **B625**, 345 (2002);

Searches Particle Listings

Supersymmetric Particle Searches

- M. Frank *et al.*, JHEP **0702**, 047 (2007);
S. Heinemeyer *et al.*, Phys. Lett. **B652**, 300 (2007).
95. S. Khalil, Int. J. Mod. Phys. **A18**, 1697 (2003).
96. W. Fischler, S. Paban, and S. Thomas, Phys. Lett. **B289**, 373 (1992);
S.M. Barr, Int. J. Mod. Phys. **A8**, 209 (1993);
T. Ibrahim and P. Nath, Phys. Rev. **D58**, 111301 (1998) [erratum: **D60**, 099902 (1999)];
M. Brhlik, G.J. Good, and G.L. Kane, Phys. Rev. **D59**, 115004 (1999);
V.D. Barger *et al.*, Phys. Rev. **D64**, 056007 (2001);
S. Abel, S. Khalil, and O. Lebedev, Nucl. Phys. **B606**, 151 (2001);
K.A. Olive *et al.*, Phys. Rev. **D72**, 075001 (2005);
G.F. Giudice and A. Romanino, Phys. Lett. **B634**, 307 (2006).
97. A. Masiero and L. Silvestrini, in *Perspectives on Supersymmetry*, edited by G.L. Kane (World Scientific, Singapore, 1998) pp. 423–441.
98. M. Pospelov and A. Ritz, Annals Phys. **318**, 119 (2005).
99. H. Georgi, Phys. Lett. **169B**, 231 (1986);
L.J. Hall, V.A. Kostelecky, and S. Raby, Nucl. Phys. **B267**, 415 (1986).
100. Y. Nir and N. Seiberg, Phys. Lett. **B309**, 337 (1993);
S. Dimopoulos, G.F. Giudice, and N. Tetradis, Nucl. Phys. **B454**, 59 (1995);
G.F. Giudice *et al.*, JHEP **12**, 027 (1998);
J.L. Feng and T. Moroi, Phys. Rev. **D61**, 095004 (2000);
Y. Nir and G. Raz, Phys. Rev. **D66**, 035007 (2002).
101. M. Ciuchini *et al.*, Phys. Lett. **B655**, 162 (2007);
Y. Nir, JHEP **0705**, 102 (2007); and in Lectures given at 2nd Joint Fermilab-CERN Hadron Collider Physics Summer School, CERN, Geneva, Switzerland, 6–15 June 2007, arXiv:0708.1872 [hep-ph].
102. B. Aubert *et al.* [BABAR Collaboration], Phys. Rev. Lett. **98**, 211802 (2007);
M. Staric *et al.* [Belle Collaboration], Phys. Rev. Lett. **98**, 211803 (2007).
103. L.E. Ibáñez and G.G. Ross, Phys. Lett. **B110**, 215 (1982).
104. A.G. Cohen, T.S. Roy, and M. Schmaltz, JHEP **0702**, 027 (2007).
105. J.F. Gunion and H.E. Haber, Phys. Rev. **D37**, 2515 (1988);
S.Y. Choi, M. Drees, and B. Gaissmaier, Phys. Rev. **D70**, 014010 (2004).
106. J.L. Feng *et al.*, Phys. Rev. Lett. **83**, 1731 (1999);
T. Gherghetta, G.F. Giudice, and J.D. Wells, Nucl. Phys. **B559**, 27 (1999);
J.F. Gunion and S. Mrenna, Phys. Rev. **D62**, 015002 (2000).
107. For a number of recent attempts to resolve the tachyonic slepton problem, see *e.g.*, I. Jack, D.R.T. Jones, and R. Wild, Phys. Lett. **B535**, 193 (2002);
B. Murakami and J.D. Wells, Phys. Rev. **D68**, 035006 (2003);
R. Kitano, G.D. Kribs, and H. Murayama, Phys. Rev. **D70**, 035001 (2004);
R. Hodgson *et al.*, Nucl. Phys. **B728**, 192 (2005);
D.R.T. Jones and G.G. Ross, Phys. Lett. **B642**, 540 (2006).
108. R. Lafaye *et al.*, Eur. Phys. J. **C54**, 617 (2008);
G.L. Kane *et al.*, Phys. Rev. **D75**, 115018 (2007);
P. Bechtle *et al.*, Eur. Phys. J. **C46**, 533 (2006);
B.C. Allanach, D. Grellscheid, and F. Quevedo, JHEP **0407**, 069 (2004);
G.A. Blair, W. Porod, and P.M. Zerwas, Eur. Phys. J. **C27**, 263 (2003).
109. See, *e.g.*, A. Brignole, L.E. Ibanez, and C. Munoz, in *Perspectives on Supersymmetry*, edited by G.L. Kane (World Scientific, Singapore, 1998) pp. 125–148.
110. M. Drees and S.P. Martin, in *Electroweak Symmetry Breaking and New Physics at the TeV Scale*, edited by T. Barklow *et al.* (World Scientific, Singapore, 1996) pp. 146–215.
111. M. Carena *et al.*, Nucl. Phys. **B426**, 269 (1994).
112. B.C. Allanach and C.G. Lester, Phys. Rev. **D73**, 015013 (2006);
J.R. Ellis *et al.*, Phys. Lett. **B565**, 176 (2003); Phys. Rev. **D69**, 095004 (2004);
H. Baer and C. Balazs, JCAP **0305**, 006 (2003).
113. J.R. Ellis *et al.*, Phys. Lett. **B573**, 162 (2003); Phys. Rev. **D70**, 055005 (2004).
114. L.E. Ibáñez and D. Lüst, Nucl. Phys. **B382**, 305 (1992);
B. de Carlos, J.A. Casas, and C. Munoz, Phys. Lett. **B299**, 234 (1993);
V. Kaplunovsky and J. Louis, Phys. Lett. **B306**, 269 (1993);
A. Brignole, L.E. Ibáñez, and C. Munoz, Nucl. Phys. **B422**, 125 (1994) [erratum: **B436**, 747 (1995)].
115. B.C. Allanach *et al.*, Eur. Phys. J. **C25**, 113 (2002).
116. M. Battaglia *et al.*, Eur. Phys. J. **C33**, 273 (2004).
117. K. Intriligator, N. Seiberg, and D. Shih, JHEP **0604**, 021 (2006); **0707**, 017 (2007).
118. See, *e.g.*, M. Dine, J.L. Feng, and E. Silverstein, Phys. Rev. **D74**, 095012 (2006);
H. Murayama and Y. Nomura, Phys. Rev. Lett. **98**, 151803 (2007); Phys. Rev. **D75**, 095011 (2007);
R. Kitano, H. Ooguri, and Y. Ookouchi, Phys. Rev. **D75**, 045022 (2007);
A. Delgado, G.F. Giudice, and P. Slavich, Phys. Lett. **B653**, 424 (2007);
O. Aharony and N. Seiberg, JHEP **0702**, 054 (2007);
C. Sasaki, Y. Shirman and J. Terning, JHEP **0705**, 099 (2007);
N. Haba and N. Maru, Phys. Rev. **D76**, 115019 (2007).
119. For a review and guide to the literature, see J.F. Gunion and H.E. Haber, in *Perspectives on Supersymmetry*, edited by G.L. Kane (World Scientific, Singapore, 1998) pp. 235–255.
120. S. Raby, “Grand Unified Theories,” in the section on Reviews, Tables, and Plots in this *Review*.
121. M.B. Einhorn and D.R.T. Jones, Nucl. Phys. **B196**, 475 (1982).
122. For a review, see R.N. Mohapatra, in *Particle Physics 1999*, ICTP Summer School in Particle Physics, Trieste, Italy, 21 June–9 July, 1999, edited by G. Senjanovic and A.Yu. Smirnov (World Scientific, Singapore, 2000) pp. 336–394;
W.J. Marciano and G. Senjanovic, Phys. Rev. **D25**, 3092 (1982).
123. D.M. Ghilencea and G.G. Ross, Nucl. Phys. **B606**, 101 (2001).
124. S. Pokorski, Acta Phys. Polon. **B30**, 1759 (1999).

See key on page 373

Searches Particle Listings Supersymmetric Particle Searches

-
125. H. Arason *et al.*, Phys. Rev. Lett. **67**, 2933 (1991);
Phys. Rev. **D46**, 3945 (1992);
V. Barger, M.S. Berger, and P. Ohmann, Phys. Rev.
D47, 1093 (1993);
M. Carena, S. Pokorski, and C.E.M. Wagner, Nucl. Phys.
B406, 59 (1993);
P. Langacker and N. Polonsky, Phys. Rev. **D49**, 1454
(1994).
126. M. Olechowski and S. Pokorski, Phys. Lett. **B214**, 393
(1988);
B. Ananthanarayan, G. Lazarides, and Q. Shafi, Phys.
Rev. **D44**, 1613 (1991);
S. Dimopoulos, L.J. Hall, and S. Raby, Phys. Rev. Lett.
68, 1984 (1992);
L.J. Hall, R. Rattazzi, and U. Sarid, Phys. Rev. **D50**,
7048 (1994);
R. Rattazzi and U. Sarid, Phys. Rev. **D53**, 1553 (1996).
127. For a review of the current status of neutrino masses
and mixing, see: M.C. Gonzalez-Garcia and M. Maltoni,
Phys. Reports **460**, 1 (2008);
A. Strumia and F. Vissani, hep-ph/0606054.
128. See the section on neutrinos in “Particle Listings—
Leptons” in this *Review*.
129. For a recent review of neutrino masses in supersymmetry,
see B. Mukhopadhyaya, Proc. Indian National Science
Academy **A70**, 239 (2004).
130. P. Minkowski, Phys. Lett. **67B**, 421 (1977);
M. Gell-Mann, P. Ramond, and R. Slansky, in *Supergrav-*
ity, edited by D. Freedman and P. van Nieuwenhuizen
(North Holland, Amsterdam, 1979) p. 315;
T. Yanagida, in *Proceedings of the Workshop on Unvied*
Theory and Baryon Number in the Universe, edited by
O. Sawada and A. Sugamoto (KEK, Tsukuba, Japan,
1979);
R. Mohapatra and G. Senjanovic, Phys. Rev. Lett. **44**,
912 (1980); Phys. Rev. **D23**, 165 (1981).
131. J. Hisano *et al.*, Phys. Lett. **B357**, 579 (1995);
J. Hisano *et al.*, Phys. Rev. **D53**, 2442 (1996);
J.A. Casas and A. Ibarra, Nucl. Phys. **B618**, 171 (2001);
J. Ellis *et al.*, Phys. Rev. **D66**, 115013 (2002);
A. Masiero, S.K. Vempati, and O. Vives, New J. Phys. **6**,
202 (2004);
E. Arganda *et al.*, Phys. Rev. **D71**, 035011 (2005);
Phys. Rev. Lett. **97**, 181801 (2006);
J.R. Ellis and O. Lebedev, Phys. Lett. **B653**, 411 (2007).
132. Y. Grossman and H.E. Haber, Phys. Rev. Lett. **78**, 3438
(1997);
A. Dedes, H.E. Haber, and J. Rosiek, JHEP **0711**, 059
(2007).
133. M. Hirsch, H.V. Klapdor-Kleingrothaus, and S.G. Ko-
valenko, Phys. Lett. **B398**, 311 (1997);
L.J. Hall, T. Moroi, and H. Murayama, Phys. Lett. **B424**,
305 (1998);
K. Choi, K. Hwang, and W.Y. Song, Phys. Rev. Lett.
88, 141801 (2002);
T. Honkavaara, K. Huitu, and S. Roy, Phys. Rev. **D73**,
055011 (2006).
134. For a recent review and references to the original liter-
ature, see M. Chemtob, Prog. Part. Nucl. Phys. **54**, 71
(2005);
R. Barbier *et al.*, Phys. Reports **420**, 1 (2005).
135. H. Dreiner, in *Perspectives on Supersymmetry*, edited by
G.L. Kane (World Scientific, Singapore, 1998) pp. 462–
479.
136. B.C. Allanach, A. Dedes, and H.K. Dreiner, Phys. Rev.
D60, 075014 (1999).
137. L.E. Ibáñez and G.G. Ross, Nucl. Phys. **B368**, 3 (1992);
L.E. Ibáñez, Nucl. Phys. **B398**, 301 (1993).
138. For a review, see J.C. Romao, Nucl. Phys. Proc. Suppl.
81, 231 (2000).
139. R.N. Mohapatra, Phys. Rev. **D34**, 3457 (1986);
K.S. Babu and R.N. Mohapatra, Phys. Rev. Lett. **75**,
2276 (1995);
M. Hirsch, H.V. Klapdor-Kleingrothaus, and S.G. Ko-
valenko, Phys. Rev. Lett. **75**, 17 (1995); Phys. Rev. **D53**,
1329 (1996).
140. Y. Grossman and H.E. Haber, Phys. Rev. **D59**, 093008
(1999).
141. S. Dimopoulos and L.J. Hall, Phys. Lett. **B207**, 210
(1988);
J. Kalinowski *et al.*, Phys. Lett. **B406**, 314 (1997);
J. Erler, J.L. Feng, and N. Polonsky, Phys. Rev. Lett.
78, 3063 (1997).
142. H.K. Dreiner, P. Richardson, and M.H. Seymour, Phys.
Rev. **D63**, 055008 (2001).
143. See, *e.g.*, M. Hirsch *et al.*, Phys. Rev. **D62**, 113008 (2000)
[erratum: **D65**, 119901 (2002)];
A. Abada, G. Bhattacharyya, and M. Losada, Phys. Rev.
D66, 071701 (2002);
M.A. Diaz *et al.*, Phys. Rev. **D68**, 013009 (2003);
M. Hirsch and J.W.F. Valle, New J. Phys. **6**, 76 (2004).
144. G.F. Giudice and A. Masiero, Phys. Lett. **B206**, 480
(1988).
145. See, *e.g.*, U. Ellwanger, M. Rausch de Traubenberg, and
C.A. Savoy, Nucl. Phys. **B492**, 21 (1997);
U. Ellwanger and C. Hugonie, Eur. J. Phys. **C25**, 297
(2002), and references contained therein.
146. M. Cvetič *et al.*, Phys. Rev. **D56**, 2861 (1997) [erratum:
D58, 119905 (1998)].
147. J.R. Espinosa and M. Quiros, Phys. Rev. Lett. **81**, 516
(1998);
P. Batra *et al.*, JHEP **0402**, 043 (2004);
K.S. Babu, I. Gogoladze, and C. Kolda, hep-ph/0410085;
R. Barbieri *et al.*, Phys. Rev. **D75**, 035007 (2007).
148. R. Mahbubani, hep-ph/0408096.
149. A. Birkedal, Z. Chacko, and Y. Nomura, Phys. Rev. **D71**,
015006 (2005).
150. J.L. Hewett and T.G. Rizzo, Phys. Reports **183**, 193
(1989).
151. S.F. King, S. Moretti, and R. Nevzorov, Phys. Lett.
B634, 278 (2006); Phys. Rev. **D73**, 035009 (2006).
152. M. Cvetič and P. Langacker, Mod. Phys. Lett. **A11**, 1247
(1996);
K.R. Dienes, Phys. Reports **287**, 447 (1997).
-

Searches Particle Listings

Supersymmetric Particle Searches

SUPERSYMMETRY, PART II (EXPERIMENT)

Revised August, 2007 by J.-F. Grivaz (LAL - Orsay)

II.1. Introduction: Low energy supersymmetry (SUSY) is probably the most extensively studied among the theories beyond the standard model (SM). Reasons are its success in solving some of the deficiencies of the SM, such as the stabilization of the Higgs boson mass or gauge coupling unification, while not being in contradiction with the precision electroweak measurements. If unbroken, SUSY would predict the existence of partners of the SM particles, differing by half a unit of spin but otherwise sharing the same properties. Since no such particles have been observed with the same mass as their SM counterpart, SUSY is a broken symmetry. With an appropriate choice of SUSY breaking terms, denoted “soft,” and with superpartner masses at the TeV scale, the good properties of SUSY, such as those mentioned above, however remain preserved.

SUSY and SM particles are distinguished by a multiplicative quantum number, R -parity, with $R = (-1)^{3(B-L)+2S}$ where B and L are the baryon and lepton numbers, and S is the spin. If R -parity is violated, the exchange of SUSY particles may lead to an unacceptably fast proton decay. It is therefore commonly assumed that R -parity is conserved. As a consequence, SUSY particles are produced in pairs, and a SUSY particle decays (possibly via a cascade) into SM particles accompanied by the lightest SUSY particle (LSP) which is stable. Cosmological constraints require that the LSP be neutral and colorless.

The first part of this review, by H.E. Haber, provides details of the theoretical aspects of supersymmetry, of the various SUSY breaking schemes, and of the structure of the minimal supersymmetric extension of the standard model (MSSM), as well as an extensive set of references. The same notations and terminology are used in the following.

As will unfortunately appear in this review, no evidence for SUSY particle production has been found up to now. The search results are therefore presented in terms of production cross section upper limits or of mass lower limits. In the following, all such limits are given at the 95% confidence level.

II.2. SUSY models: In the MSSM, every degree of freedom of the SM is balanced by a new one differing by half-a-unit of spin. There are, for instance, two scalar-quark weak eigenstates \tilde{q}_L and \tilde{q}_R , associated with the left and right chirality states of a given quark flavor. Two Higgs doublets are, however, needed, in contrast to the minimal standard model, in order to give masses to both up-type and down-type quarks, with vacuum expectation values v_2 and v_1 , the ratio of which is denoted $\tan\beta$. The SUSY partner weak eigenstates of the W^\pm and charged Higgs bosons mix to form the two chargino mass eigenstates $\tilde{\chi}_i^\pm$ ($i = 1, 2$). Similarly, there are four neutralinos $\tilde{\chi}_i^0$ ($i = 1, 4$) associated to the B , W^0 and neutral Higgs bosons. Full details are given in H.E. Haber’s review.

The main phenomenological features of SUSY models arise from the choice of mechanism for SUSY breaking mediation,

and of the soft SUSY breaking terms. There are more than one hundred such terms in the MSSM, and simplifying assumptions are necessary to bring this number to a more manageable level. Requiring no additional source of flavor mixing and CP -violation than those present in the Cabibbo-Kobayashi-Maskawa matrix of the SM leaves only the gaugino mass terms M_1 , M_2 and M_3 associated with the three gauge groups of the SM, mass terms for the various slepton and squark fields, *e.g.*, $m_{\tilde{t}_R}$, and trilinear Higgs-squark-squark and Higgs-slepton-slepton couplings such as A_t . The model is then fully specified with the addition of $\tan\beta$, of the supersymmetric Higgs mixing mass term μ , and of the mass of the CP -odd Higgs boson m_A .

By far the most widely studied models involve mediation by gravitational forces. In these supergravity models, the gravitino plays essentially no rôle in the phenomenology, unless it is the LSP. This possibility, which has not been addressed by experimental searches at colliders up to now except in terms of future prospects, is not considered in this review. In the minimal model of supergravity (mSUGRA), the number of free parameters is reduced to five: a universal gaugino mass $m_{1/2}$, a universal scalar mass m_0 , and a universal trilinear coupling A_0 , all defined at the scale of grand unification (GUT), $\tan\beta$, and the sign of μ . The low energy parameters are obtained using the renormalization group equations (RGEs), which in particular fix the absolute value of μ through the requirement of electroweak symmetry breaking at the appropriate scale. In most of the mSUGRA parameter space, the LSP, required to be neutral and colorless, turns out to be the lightest neutralino, $\tilde{\chi}_1^0$. For appropriate mSUGRA parameter choices and imposing R -parity conservation, this neutralino LSP has the right properties to form the dark matter of the universe. A slightly less constrained model has also been used, primarily at LEP, where μ and m_A are kept free. In such an approach, the mass parameters in the Higgs sector are not related to the universal sfermion mass m_0 , where “sfermion” stands for squark and slepton.

In contrast, the LSP is a very light gravitino \tilde{G} in models with gauge mediated SUSY breaking (GMSB). The phenomenology depends on the nature of the next-to-lightest SUSY particle (NLSP), typically the lightest neutralino or the lightest stau, and on its lifetime. Another mediation mechanism which has been considered is via the super-conformal anomaly (AMSB, for anomaly mediation SUSY breaking). In such models, the LSP is a wino \tilde{W}^0 , with a small mass splitting with the lightest chargino, so that the lifetime of that chargino may become phenomenologically relevant, possibly long enough for the chargino to behave like a stable charged particle. More recently, a model called “split SUSY,” which does not aim at solving the hierarchy problem, sets all scalar quark and lepton masses at a very high scale, such as the GUT scale, while keeping the gauginos at the TeV scale. As a result, the gluino, whose decay is mediated by squark exchange, becomes long-lived, which leads to unusual signatures.

II.3. Search strategies: Indirect constraints on SUSY particles can be obtained from cosmological considerations, primarily from the relic dark-matter density [1], from measurements of, or limits on, rare decays, mostly of B mesons [2], or from the anomalous magnetic moment of the muon [3]. These topics are not within the scope of this review. The most significant direct constraints on SUSY particles have been obtained at LEP and at the Tevatron. The large e^+e^- collider, LEP, was in operation at CERN from 1989 to 2000, first at and near the mass of the Z boson, 91.2 GeV, and progressively up to a center-of-mass energy of 209 GeV. Four detectors, ALEPH, DELPHI, L3 and OPAL, each collected a total of about 1 fb^{-1} of data. The Tevatron is a $p\bar{p}$ collider located at Fermilab. After a first run at a center-of-mass energy of 1.8 TeV, which ended in 1996, and during which the CDF and DØ detectors collected about 110 pb^{-1} of data each, both the accelerator complex and the detectors were substantially upgraded for Run II, which began in 2001. The center-of-mass energy was raised to 1.96 TeV, and the instantaneous luminosity reached the level of $2.8 \cdot 10^{32} \text{ cm}^{-2} \text{ s}^{-1}$ in the winter of 2007. By August 2007, about 3 fb^{-1} had been accumulated by each experiment.

The “canonical” SUSY scenario is an mSUGRA-inspired MSSM with R -parity conservation and a neutralino LSP. Since such an LSP is stable and weakly interacting, pair production of SUSY particles will lead to missing energy and momentum carried away by the LSPs resulting from the produced SUSY particle decays. In scenarios other than the canonical one, the expected SUSY signatures may exhibit some additional, or even different features. In GMSB with a neutralino NLSP, for instance, photons are expected in addition to the missing energy carried away by the gravitino LSPs, arising from $\tilde{\chi}_1^0 \rightarrow \gamma\tilde{G}$ decays. But in GMSB again, a stau NLSP might have a lifetime long enough to appear stable in the detector and therefore not to give rise to missing energy. If R -parity is not conserved, the LSP will decay into SM particles; increased lepton or jet multiplicities are hence expected, but missing energy will arise only from possible final state neutrinos.

In e^+e^- collisions, the missing energy can be directly inferred as $\sqrt{s}-E$, from the center-of-mass energy \sqrt{s} , and from the total energy E of the visible final state products. Similarly, the missing momentum is the opposite of the total momentum of those products. The situation is different in $p\bar{p}$ collisions where the center-of-mass energy of the colliding partons is not known. Only its probability density can be determined, by making use of universal parton distribution functions (PDFs) obtained from fits to a large set of experimental data, most prominently the proton structure functions measured at HERA. Since most of the beam remnants escape undetected in the beam pipe, only conservation of momentum in the plane transverse to the beam direction can be used, and canonical SUSY signals will be searched for in events exhibiting large missing *transverse* energy \cancel{E}_T .

All SUSY particles, except for the gluino, are produced in a democratic way in e^+e^- collisions via electroweak interactions.

The search is therefore naturally directed toward the lightest ones, typically the NLSP, and the results are interpreted in a fairly model-independent way. Further specifying the model, various search results can be combined to obtain constraints on the model parameters. In $p\bar{p}$ collisions, the most copiously produced SUSY particles are expected to be the colored ones, namely squarks and gluinos. The pattern of lighter SUSY particles, however, plays a rôle in the interpretation of the search results, as it has an impact on the squark and gluino decay chains. A model, typically mSUGRA, is therefore needed to translate the search results into constraints on physically relevant quantities. As will be discussed later, the searches for squarks and gluinos in the canonical scenario suffer from large backgrounds, which renders competitive the searches for electroweak gauginos, in spite of lower production cross sections, for parameter configurations such that multileptonic final states arising from the gaugino decays are enhanced. Searches in scenarios other than the canonical one call for specific strategies relying, for instance, on the observation of additional photons or stable particles.

II.4. Searches at LEP in the canonical scenario: At LEP, the production of SUSY particles via electroweak interactions is only suppressed, compared to similar SM processes, by the phase space reduction near the kinematic limit. This suppression is stronger for scalars (sleptons and squarks) than for charginos. In general, for a given process, only data collected at the highest LEP energies are relevant for the ultimate mass limits obtained, but it may happen for some specific processes that the cross section is strongly reduced by mixing effects, *e.g.*, for neutralinos with a small higgsino component, in which case the large integrated luminosity collected at lower energies provides additional sensitivity.

Sleptons: The simplest case is that of smuon pair production, which proceeds only via s -channel Z/γ^* exchange. In models with slepton and gaugino mass unification, the $\tilde{\mu}_R$ is expected to be lighter than the $\tilde{\mu}_L$. The search results are therefore interpreted under this assumption, which is conservative since the $\tilde{\mu}_R$ coupling to the Z is smaller than that of the $\tilde{\mu}_L$. Only one parameter is necessary to calculate the production cross section, the smuon mass $m_{\tilde{\mu}_R}$. If the $\tilde{\mu}_R$ is the NLSP, its only decay mode is $\tilde{\mu}_R \rightarrow \mu\tilde{\chi}_1^0$, and its pair production therefore leads to a distinct final state consisting of two acoplanar muons with missing energy. (“Acoplanar” means that the difference in azimuth between the two muons is smaller than 180° , *i.e.*, the two muons are not back-to-back when projected onto a plane perpendicular to the beam axis.) The only significant background comes from $e^+e^- \rightarrow W^+W^- \rightarrow \mu^+\nu\mu^-\bar{\nu}$, which is well under control. The selection efficiency is very high, except when the $\tilde{\mu}_R-\tilde{\chi}_1^0$ mass difference is small, in which case the muons carry little momentum. A second parameter, the LSP mass $m_{\tilde{\chi}_1^0}$ is therefore needed to interpret the search results, as shown in Fig. 1 for the combination of the four LEP experiments [4]. In models with gaugino mass unification, it

Searches Particle Listings

Supersymmetric Particle Searches

is expected that the second lightest neutralino $\tilde{\chi}_2^0$ will have a mass roughly twice that of the LSP, in which case the $\tilde{\mu}_R \rightarrow \mu\tilde{\chi}_2^0$ decay can compete with the direct decay into $\mu\tilde{\chi}_1^0$ for small $\tilde{\chi}_1^0$ masses. The impact of this effective efficiency reduction can be seen in Fig. 1, for $\mu = -200$ GeV and $\tan\beta = 1.5$. Altogether, smuon masses below 95 to 99 GeV, depending on the $\tilde{\chi}_1^0$ mass, are excluded as long as the $\tilde{\mu}_R - \tilde{\chi}_1^0$ mass difference is larger than 5 GeV.

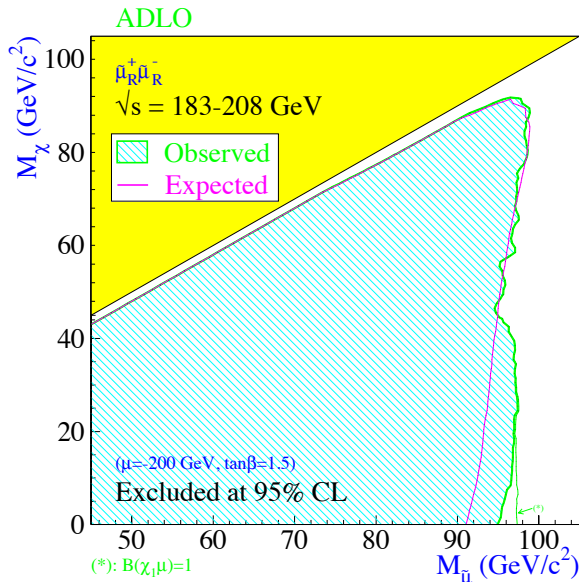


Figure 1: Region in the $(m_{\tilde{\mu}_R}, m_{\tilde{\chi}_1^0})$ plane excluded by the searches for smuons at LEP. Color version at end of book.

The case of staus is similar, except for the fact that the final taus further decay, and that the ultimate decay products are softer than the muons in the smuon case. The selection efficiency is therefore lower. An additional complication comes from the L - R mixing, which is expected to be non-negligible for large values of $\tan\beta$, and can reduce the coupling of the lightest stau to the Z . In the worst case where the stau does not couple to the Z , stau masses smaller than 86 to 95 GeV are excluded, depending on $m_{\tilde{\chi}_1^0}$, as long as the stau- $\tilde{\chi}_1^0$ mass difference is larger than 7 GeV [4].

For selectrons as for smuons, L - R mixing is expected to be negligible. But pair production receives an additional contribution from t -channel neutralino exchange, which tends to increase the production cross section. For $\mu = -200$ GeV and $\tan\beta = 1.5$, the \tilde{e}_R mass lower limit is 100 GeV for $m_{\tilde{\chi}_1^0} < 85$ GeV [4]. Furthermore, the t -channel exchange allows for associated $\tilde{e}_L\tilde{e}_R$ production. Assuming slepton and gaugino mass unification at the GUT scale, the \tilde{e}_L and \tilde{e}_R masses are related, with the former heavier by a few GeV. Associated production gives the viable signal of a single energetic electron in the case where the $\tilde{e}_R - \tilde{\chi}_1^0$ mass difference is too small

to observe \tilde{e}_R pair production. This allows a lower limit of 73 GeV to be set on $m_{\tilde{e}_R}$, independent of the $\tilde{\chi}_1^0$ mass [5].

Indirect limits on the sneutrino mass can be derived from the slepton mass limits if slepton and gaugino mass unification is assumed. More generally, a $\tilde{\nu}$ LSP or NLSP mass limit of 45 GeV can be deduced from the measurement of the invisible Z width [6], for three mass degenerate sneutrinos.

Charginos and neutralinos: The masses and field content in the chargino sector depend on only three parameters: M_2 , μ and $\tan\beta$. The masses and field content in the neutralino sector depend on those same parameters, and, in addition, on M_1 . The latter is, however, related to M_2 assuming gaugino mass unification: $M_1 = (5/3)\tan^2\theta_W M_2 \sim 0.5M_2$. This assumption is made for the results presented below, unless explicitly specified. Traditionally, three regions are distinguished: “gaugino” if $M_2 \ll |\mu|$, “higgsino” if $|\mu| \ll M_2$, and mixed if M_2 and $|\mu|$ have similar values. In the gaugino region, the lighter chargino and second lightest neutralino masses are close to M_2 , the mass of the lightest neutralino is close to M_1 , while the heavier chargino and neutralinos all have masses close to $|\mu|$; this is the typical configuration encountered in mSUGRA. In the higgsino region, all chargino and neutralino masses are close to $|\mu|$, so that the mass splitting between the lightest chargino and neutralino tends to be small. In the following, “chargino” will stand for “lighter chargino.”

Chargino pair production proceeds via s -channel Z/γ^* and t -channel $\tilde{\nu}_e$ exchanges, with destructive interference. For chargino masses accessible at LEP energies, the decays are mediated by virtual W ($\tilde{\chi}^\pm \rightarrow W^{*\pm}\tilde{\chi}_1^0 \rightarrow f\bar{f}'\tilde{\chi}_1^0$) and sfermion ($\tilde{\chi}^\pm \rightarrow \tilde{f}^*f' \rightarrow f\bar{f}'\tilde{\chi}_1^0$) exchange. Two-body decays such as $\tilde{\chi}^\pm \rightarrow \ell^\pm\tilde{\nu}$ are occasionally kinematically allowed, in which case they are dominant. Similarly, neutralino pair or associated production proceeds via s -channel Z and t -channel \tilde{e} exchange, and $\tilde{\chi}_2^0$ decays are mediated by virtual Z and sfermion exchange. Here also, two-body decays such as $\tilde{\chi}_2^0 \rightarrow \nu\tilde{\nu}$ may have to be considered.

First, the case of heavy sfermions is addressed. Only s -channel exchange contributes to gaugino production, and the decays proceed via gauge boson exchange. For chargino pair production, the final states are therefore the same as those arising from W pairs, but for the addition of two LSPs. Selections have been designed for all-hadronic ($q\bar{q}'q\bar{q}'\tilde{\chi}_1^0\tilde{\chi}_1^0$), mixed ($q\bar{q}'\ell\nu\tilde{\chi}_1^0\tilde{\chi}_1^0$) and fully leptonic ($\ell\nu\ell\nu\tilde{\chi}_1^0\tilde{\chi}_1^0$) topologies. No excess over SM backgrounds, of which the largest comes from W pair production, was observed. A scan over M_2 , μ , and $\tan\beta$ provided a robust chargino mass lower limit of 103 GeV for sneutrino masses larger than 200 GeV [7], except for unnaturally large values of M_2 ($> \sim 1$ TeV), in the so-called “deep higgsino” region, where the $\tilde{\chi}^\pm - \tilde{\chi}_1^0$ mass splitting is very small.

This limit is degraded for lower sneutrino masses for two reasons. First, the production cross section is reduced by the negative interference between the s - and t -channel exchanges.

Second, two-body decays open up, which may reduce the selection efficiency. This is the case in particular in the so-called “corridor” where $m_{\tilde{\chi}^\pm} - m_{\tilde{\nu}}$ is smaller than a few GeV, so that the lepton from the $\tilde{\chi}^\pm \rightarrow \ell\tilde{\nu}$ decay is hardly visible. Neutralino associated production ($e^+e^- \rightarrow \tilde{\chi}_1^0\tilde{\chi}_2^0$), for which the interference tends to be positive, can be used to mitigate those effects, and searches for acoplanar jets or leptons from $\tilde{\chi}_2^0 \rightarrow f\bar{f}\tilde{\chi}_1^0$ were devised, which did not reveal any excess over SM backgrounds. Chargino and neutralino production and decays now depend, however, on the detailed sfermion spectrum. To interpret the search results, squark and slepton mass unification is therefore also assumed, so that the relevant phenomenology can be described with the addition of the single m_0 parameter. At this point, the results of neutralino searches can be combined with those for charginos into exclusion domains in the (M_2, μ) plane for selected values of $\tan\beta$ and m_0 .

The searches for neutralinos, however, lose their sensitivity when the two-body decay $\tilde{\chi}_2^0 \rightarrow \nu\tilde{\nu}$ opens up, which leads to an invisible final state. Slepton mass lower limits can provide useful constraints in that configuration. The reason is that the slepton and gaugino masses are related by the RGEs as $m_{\tilde{\ell}_R}^2 \simeq m_0^2 + 0.22M_2^2 - \sin^2\theta_W m_Z^2 \cos 2\beta$. For given values of $\tan\beta$ and m_0 , a lower limit on $m_{\tilde{\ell}_R}$ can therefore be translated into a lower limit on M_2 . In the end, the chargino mass lower limit obtained in the simple case of heavy sfermions is only moderately degraded.

As indicated above, the chargino searches lose their sensitivity in the deep-higgsino region, because of too small a $\tilde{\chi}^\pm - \tilde{\chi}_1^0$ mass difference. In the most extreme case, the chargino becomes long-lived. Dedicated searches for charged massive stable particles were designed, which take advantage of the higher ionization of such particles. In less extreme cases, the soft final state products resemble those resulting from “two-photon” interactions. In such interactions, the beam electrons radiate quasi-real photons whose collision produces a low mass system, while the incoming electrons escape undetected in the beam pipe. Chargino pair production can however be disentangled from that background when “tagged” by an energetic photon from initial state radiation ($e^+e^- \rightarrow \gamma\tilde{\chi}^+\tilde{\chi}^-$).

These various techniques allowed charginos with masses smaller than 92 GeV to be excluded in the canonical scenario with gaugino and sfermion mass unification [8].

The lightest neutralino: If the gaugino mass unification assumption is not made, there is no general mass limit from e^+e^- collisions for the lightest neutralino. A very light photino-like neutralino decouples from the Z , so that it cannot be pair produced via s -channel Z exchange, and production via t -channel selectron exchange can be rendered negligible for sufficiently heavy selectrons.

With the assumption of gaugino mass unification, on the other hand, indirect mass limits can be derived, mostly from chargino pair production. In the case of heavy sfermions, the limit is 52 GeV at large $\tan\beta$, somewhat lower otherwise. If

sfermions are allowed to be light, sfermion mass unification is used and the limit at large $\tan\beta$ becomes 47 GeV. It is set by slepton searches in the corridor.

Higgs boson searches at LEP provide additional constraints at low $\tan\beta$. The analysis is rather involved, but can be summarized (and simplified) as follows. The mass of the lightest Higgs boson in the MSSM receives radiative corrections due to the splitting between the top and stop masses. The stop mass depends on m_0 and M_3 , the latter being related by unification to M_2 . For given values of m_0 and $\tan\beta$, the mass lower limit on the Higgs boson translates into a lower limit on M_3 , hence on M_2 . These constraints are most effective at low m_0 and $\tan\beta$, where those from chargino searches are weakest.

The combination of chargino, slepton and Higgs boson searches provides the lower limit on $m_{\tilde{\chi}_1^0}$ as a function of $\tan\beta$ displayed in Fig. 2 [9]. The “absolute” lower limit is 47 GeV, obtained at large $\tan\beta$. In the more constrained mSUGRA scenario, where in particular μ is no longer a free parameter, a slightly tighter limit of 50 GeV is derived [10].

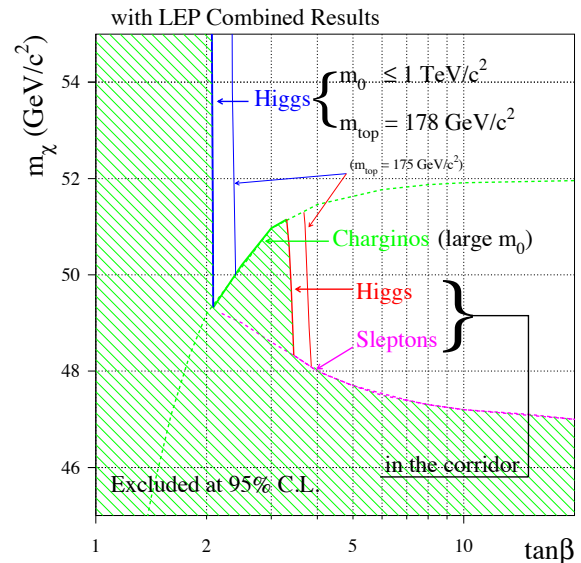


Figure 2: Lower mass limit for the lightest neutralino as a function of $\tan\beta$, inferred in the conventional scenario from searches at LEP for charginos, sleptons, and neutral Higgs bosons. Color version at end of book.

Squarks: As will be seen later, the mass reach for squarks at the Tevatron extends well beyond the masses accessible at LEP. There are, however, configurations for which the Tevatron searches are not efficient, and for which useful information is still provided by LEP. This is particularly relevant in the stop sector because the lighter of the two mass eigenstates (hereafter simply denoted “stop” or \tilde{t}) may be substantially less massive than all other squarks. One reason is that, if squark masses are unified at the GUT scale, $m_{\tilde{t}_R}$ is driven at the electroweak scale to lower values than the other squark mass terms by the large

Searches Particle Listings

Supersymmetric Particle Searches

top Yukawa coupling. Another reason is that the off-diagonal terms of the stop squared-mass matrix, which are proportional to m_t , are much larger than for the other squark species.

At LEP energies, given the chargino mass limit which effectively forbids $\tilde{t} \rightarrow b\tilde{\chi}^+$, and as long as $m_{\tilde{t}} < m_W + m_b + m_{\tilde{\chi}_1^0}$, the main stop decay mode is expected to be $\tilde{t} \rightarrow c\tilde{\chi}_1^0$, which proceeds via flavor-changing loops. The stop lifetime may therefore be long enough to compete with the hadronization time, a feature which has been included in the simulation programs. The final state arising from stop pair production followed by $\tilde{t} \rightarrow c\tilde{\chi}_1^0$ is a pair of acoplanar jets with missing energy. The mass limit obtained depends slightly on the amount of L - R mixing. In the worst case where the stop does not couple to the Z , stop masses from 96 to 99 GeV, depending on the $\tilde{\chi}_1^0$ mass, are excluded as long as $m_{\tilde{t}} - m_{\tilde{\chi}_1^0} - m_c > 5$ GeV [11]. Dedicated searches were performed in addition to cope with smaller mass differences. In particular, the creation of long-lived R -hadrons in the stop hadronization process was taken into account, as well as the specific interactions of those R -hadrons in the detector material. (R -hadrons are color-neutral exotic bound states, *e.g.*, formed from a squark and an antiquark.) In the end, a mass lower limit of 63 GeV was set for the top squark, irrespective of $m_{\tilde{t}} - m_{\tilde{\chi}_1^0}$ [12].

It has been pointed out that, for specific choices of parameters, the four-body decay mode $\tilde{t} \rightarrow bff'\tilde{\chi}_1^0$ could compete with $\tilde{t} \rightarrow c\tilde{\chi}_1^0$ [13]. A set of selections was designed to address this possibility, and the 63 GeV mass limit was found to hold, independent of the proportions of four-body and two-body decay modes [12]. Finally, if sneutrinos are sufficiently light for the $\tilde{t} \rightarrow b\tilde{l}\tilde{\nu}$ three-body decay mode to be kinematically allowed, in which case it will be dominant, a stop mass lower limit of 96 GeV was obtained for sneutrino masses smaller than 86 GeV [11].

The lightest sbottom mass eigenstate, \tilde{b} , could also be light for large values of $\tan\beta$, which enhance the off-diagonal terms of the sbottom squared-mass matrix. The situation is simpler than for the stop because the $\tilde{b} \rightarrow b\tilde{\chi}_1^0$ tree-level decay mode is expected to be dominant. Searches for acoplanar b -flavored jets were performed, leading to mass lower limits of about 95 GeV for a vanishing coupling of the sbottom to the Z [11].

II.5. Searches at LEP in non-canonical scenarios:

SUSY scenarios beyond the canonical one were also extensively studied at LEP.

GMSB: The phenomenology of GMSB, with an ultra-light gravitino LSP, depends essentially on the nature of the NLSP and on its lifetime.

In the case of a neutralino NLSP, the $\tilde{\chi}_1^0 \rightarrow \gamma\tilde{G}$ decay mode is expected to be dominant in the mass range accessible at LEP. The production of a pair of $\tilde{\chi}_1^0$ with short lifetime would therefore lead to acoplanar photons with missing energy. No excess was observed above the background from $e^+e^- \rightarrow (Z^*) \rightarrow \nu\bar{\nu}\gamma\gamma$ [14]. In typical GMSB models, the neutralino NLSP is bino-like. Pair production is thus mediated

by t -channel selectron exchange. An exclusion domain in the $(m_{\tilde{e}_R}, m_{\tilde{\chi}_1^0})$ plane was therefore derived. The highest $\tilde{\chi}_1^0$ mass excluded is 102 GeV for light selectrons, and the interpretation of an anomalous $ee\gamma\gamma+\cancel{E}_T$ event observed by CDF in Run I of the Tevatron [15] in terms of pair production of selectrons with $\tilde{e} \rightarrow e\tilde{\chi}_1^0 \rightarrow e\gamma\tilde{G}$ is excluded. For non-prompt decays, searches for photons which do not point back to the primary vertex were performed, while long neutralino lifetimes lead to a phenomenology similar to that of the canonical scenario. Combinations of the results of these and a number of other searches in various topologies expected within a minimal GMSB framework were performed, leading to an absolute neutralino NLSP mass limit of 54 GeV [16].

The other generic NLSP candidate in GMSB is a scalar tau, for some parameter configurations almost mass degenerate with \tilde{e}_R and $\tilde{\mu}_R$. A stau NLSP decays according to $\tilde{\tau} \rightarrow \tau\tilde{G}$. For prompt decays, this is similar to a stau NLSP with a light $\tilde{\chi}_1^0$ in the canonical scenario. For long lifetimes, the stau will appear as a highly ionizing charged particle, for which searches have been designed as discussed for charginos in the deep-higgsino region. For intermediate lifetimes, dedicated selections for in-flight decays along charged particle tracks were devised. A combination of all these searches excluded a stau NLSP with mass below 87 GeV, irrespective of its lifetime [17].

AMSB: With a wino LSP, the mass difference between the chargino and the LSP is expected to be small, leading to topologies identical to those encountered in the deep higgsino region of the canonical scenario. The chargino mass lower limit of 92 GeV [8] also holds in the AMSB framework for large sfermion masses.

A gluino LSP: The possibility that the LSP be a light gluino has also been considered. Gluinos cannot be produced directly by e^+e^- annihilation, but they could be produced by gluon splitting, for instance in $e^+e^- \rightarrow Z \rightarrow q\bar{q}g^* \rightarrow q\bar{q}g\tilde{g}$, or in the decays of pair-produced squarks. Such gluinos would then hadronize into long-lived R -hadrons. Dedicated searches were performed [18], leading to the exclusion of a gluino LSP with mass smaller than 27 GeV.

R -parity violation: If R -parity is allowed to be violated, new terms appear in the superpotential, that do not conserve the lepton or baryon number: $\lambda_{ijk}L_iL_j\bar{E}_k$, $\lambda'_{ijk}L_iQ_j\bar{D}_k$, $\lambda''_{ijk}\bar{U}_i\bar{D}_j\bar{D}_k$, where L and Q are lepton and quark doublet superfields, E , D and U are lepton and quark singlet superfields, and i , j and k are generation indices. These terms induce new couplings such that the LSP can decay to SM particles. For instance, a neutralino LSP could decay according to $\tilde{\chi}_1^0 \rightarrow e\mu\nu$ via a λ type coupling. With a λ'' coupling, a $\tilde{\chi}_1^0$ decay would lead to three hadronic jets. Since the simultaneous presence of different coupling types is strongly constrained, for instance by the lower limit on the proton lifetime, the assumption was made that only one of the R -parity violating couplings is non-vanishing. It was also assumed that this coupling is sufficiently large for

the R -parity violating decays to take place close to the e^+e^- collision point ($< \sim 1$ cm) so that lifetime issues can be ignored.

Even with these simplifying assumptions, the number of possible final states arising from SUSY particle pair production is considerable. Nevertheless, all were considered at LEP, ranging from four leptons with missing energy for a λ coupling and $\tilde{\chi}_1^0$ pair production, now a process leaving a visible signature, to ten jets for a λ' coupling and chargino pair production with $\tilde{\chi}^\pm \rightarrow q\bar{q}'\tilde{\chi}_1^0$. In the end, limits at least as constraining as in the canonical scenario were obtained [19].

Single production of a SUSY particle may also take place when R -parity is violated, with a production cross section now depending on the value of the λ coupling involved. The possibility of single, possibly resonant sneutrino production was investigated [20], and, in the absence of any signal, sneutrino mass lower limits extending almost to the full center-of-mass energy were established for sufficiently large values of the coupling.

II.6. Searches at HERA: The HERA $e^\pm p$ collider at DESY terminated its operation at the end of June 2007, after having delivered an integrated luminosity of ~ 0.5 fb $^{-1}$ at a center-of-mass energy of 320 GeV to each of the H1 and ZEUS experiments. Since ep collisions do not involve annihilation processes, only R -parity violating resonant production of squarks could be investigated with good sensitivity. The production proceeds via a λ'_{1j1} or λ'_{11k} coupling, with a cross section depending on the value of the R -parity violating coupling involved. The produced squark can decay either directly with R -parity violation, or indirectly via a cascade leading to the LSP which in turn decays to SM particles (two jets and a neutrino or a charged lepton). Selections for these various topologies were combined to lead, within some mild model assumptions, to squark mass lower limits as high as 275 GeV for a λ' coupling of electromagnetic strength, *i.e.*, equal to 0.3 [21]. These results should be improved once the full HERA integrated luminosity is analyzed.

II.7. Searches at the Tevatron: Because of the much higher center-of-mass energy, the mass reach of the Tevatron for SUSY particles is expected to largely exceed the one achieved at LEP. In $p\bar{p}$ collisions, however, the effective parton-parton center-of-mass energy $\sqrt{\hat{s}}$ is only a fraction $\sqrt{x_1x_2}$ of the total center-of-mass energy \sqrt{s} , where x_1 and x_2 are the fractions of the p and \bar{p} momenta carried by the colliding partons. Because of the rapid decrease of the PDFs as a function of x , probing high $\sqrt{\hat{s}}$ values implies accumulating correspondingly large integrated luminosities.

Compared to the situation at LEP, the searches for SUSY in $p\bar{p}$ collisions are further complicated by the huge disparity between the cross sections of the processes of interest, currently of order 0.1 pb, and those of the SM backgrounds, *e.g.*, ~ 80 mb for the total inelastic cross section. Even for final states involving leptons, one has to cope with the $W \rightarrow \ell\nu$ and $Z \rightarrow \ell\ell$ backgrounds, with cross sections as large as ~ 2.6 nb and ~ 240 pb, respectively, per lepton flavor.

In the following, all results presented were obtained during Run II of the Tevatron collider, as they supersede those from Run I due to the higher center-of-mass energy and to integrated luminosities already up to a factor twenty larger.

Squarks and gluinos: Colored SUSY particles are expected to be the most copiously produced in $p\bar{p}$ collisions. If $m_{\tilde{q}} \ll m_{\tilde{g}}$, $\tilde{q}\tilde{q}$ and, to a lesser extent, $\tilde{q}\tilde{q}$ pair productions are the dominant processes, and the search is performed in the $\tilde{q} \rightarrow q\tilde{\chi}_1^0$ decay channel, which leads to a final state consisting of a pair of acoplanar jets. If $m_{\tilde{g}} \ll m_{\tilde{q}}$, gluino pair production dominates, and the decay channel considered is $\tilde{g} \rightarrow \tilde{q}^* \tilde{q} \rightarrow q\bar{q}\tilde{\chi}_1^0$, leading to a four-jet final state with \cancel{E}_T . Finally, if squark and gluino masses are similar, three-jet final states are expected to arise from $\tilde{q}\tilde{g}$ associated production. Soft jets from initial and final state radiation may increase these jet multiplicities. Cascade decays such as $\tilde{q} \rightarrow \tilde{\chi}^\pm q' \rightarrow \ell\nu q'\tilde{\chi}_1^0$, however, complicate the picture, and a specific model has to be used to assess their impact. This is why both CDF and DØ revert to the mSUGRA framework to interpret their search results, in which case the ten SUSY partners of the five light quark flavors can be considered mass degenerate for practical purposes.

Backgrounds to squark and gluino production arise from two types of sources: those with real \cancel{E}_T , such as ($W \rightarrow \ell\nu$)+jets, and those with fake \cancel{E}_T from jet energy mismeasurements in standard multijet events produced by strong interaction. In the following, these backgrounds are denoted SM and QCD, respectively. Selection criteria were designed for each of the three relative mass configurations listed above, with at least two, at least three and at least four energetic jets, and with large \cancel{E}_T . Backgrounds of the SM type are largely suppressed by vetoes on isolated leptons, except for ($Z \rightarrow \nu\nu$)+jets, which is irreducible, and the remaining contribution is determined from Monte Carlo simulations. In the QCD background, the distribution of missing transverse energy from jet mismeasurements peaks strongly at low values but, because of the huge multijet production cross section, significant contributions remain even at large \cancel{E}_T . A substantial reduction is obtained, however, by requiring that the \cancel{E}_T direction point away from the jets. While CDF estimates the remaining contribution from Monte Carlo simulations calibrated on control samples, DØ applies tighter selection criteria so that the QCD background is brought to a negligible level.

In the end, no excess was observed above expected backgrounds in the various selections, which translates into excluded domains in the $(m_{\tilde{g}}, m_{\tilde{q}})$ plane. Taking into account the large theoretical uncertainties on the signal production cross sections arising from the choice of PDFs, and of renormalization and factorization scales, lower limits of 325 and 241 GeV were published by DØ [22] for the squark and gluino masses, respectively, based on an integrated luminosity of 310 pb $^{-1}$. Along the $m_{\tilde{g}} = m_{\tilde{q}}$ line, the limit is 337 GeV. These results, derived for $\tan\beta = 3$, $A_0 = 0$, and $\mu < 0$, are valid for a large class of parameter sets at low $\tan\beta$. A preliminary result from DØ [23], based on

Searches Particle Listings

Supersymmetric Particle Searches

an integrated luminosity of $\sim 1 \text{ fb}^{-1}$, excludes $m_{\tilde{g}} < 375 \text{ GeV}$, $m_{\tilde{g}} < 289 \text{ GeV}$, and $(m_{\tilde{g}} = m_{\tilde{q}}) < 383 \text{ GeV}$, as shown in Fig. 3. Similar preliminary results were obtained by the CDF collaboration, based on an integrated luminosity of 1.4 fb^{-1} [24]. Within the mSUGRA framework, these limits can be compared with those from slepton and chargino searches in e^+e^- collisions, as shown for $D\tilde{O}$ in Fig. 3 and for CDF in Fig. 4. The domain in the parameter space excluded at LEP is extended for simultaneously low values of m_0 (below 250 GeV) and $m_{1/2}$ (below 160 GeV).

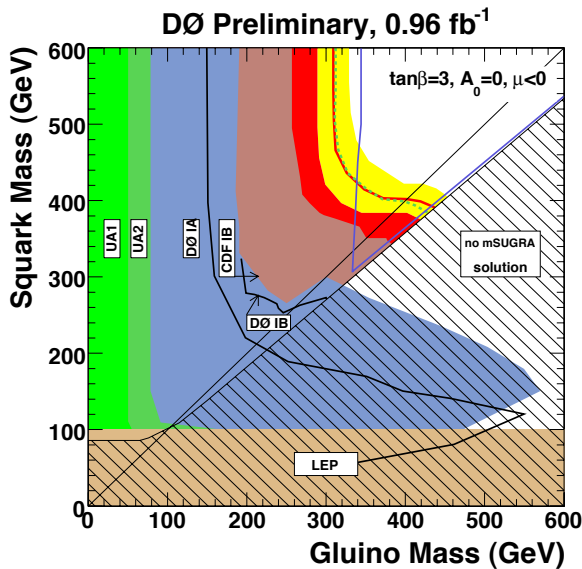


Figure 3: Region in the $(m_{\tilde{g}}, m_{\tilde{q}})$ plane excluded by $D\tilde{O}$ and by earlier experiments. The red curve corresponds to the nominal scale and PDF choices. The yellow band represents the uncertainty associated with these choices. The blue curves represent the indirect limits inferred from the LEP chargino and slepton searches. Color version at end of book.

For larger values of $\tan\beta$, mass hierarchies such as $m_{\tilde{q}_L} > m_{\tilde{e}} \sim m_{\tilde{\mu}} > m_{\tilde{\chi}^\pm} > m_{\tilde{\tau}}$ are not uncommon, for which squark pair production leads to final states involving jets, τ s, and \cancel{E}_T . A dedicated search for these topologies was performed by $D\tilde{O}$ [25], which provides additional sensitivity for squark searches at larger values of $\tan\beta$.

Stop and sbottom: As explained earlier, a stop mass eigenstate could be much lighter than the other squarks. Dedicated searches were therefore performed for stop pair production followed by $\tilde{t} \rightarrow c\tilde{\chi}_1^0$ decays. The final state is a pair of acoplanar charm jets with \cancel{E}_T . Compared to the previous case of generic squarks, the cross section is much smaller because only one squark species is produced. The mass range probed is, therefore, accordingly smaller. Consequently, the jets are softer and there is less \cancel{E}_T . A lifetime-based heavy-flavor tagging is used in the selection to mitigate the corresponding loss of sensitivity.

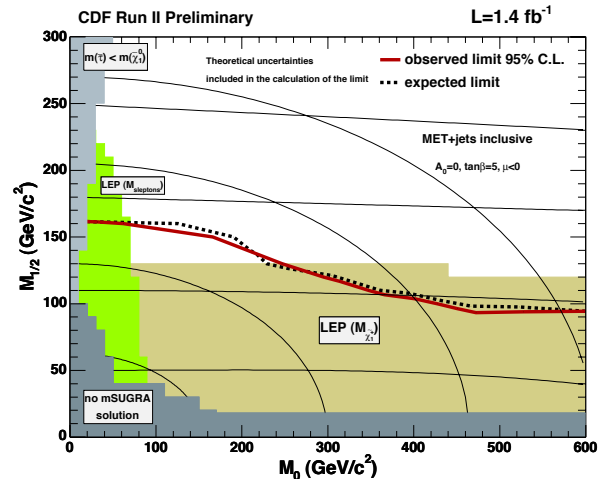


Figure 4: Region in the $(m_0, m_{1/2})$ plane excluded by CDF and by the LEP experiments. The nearly horizontal black lines are the iso-mass curves for gluinos corresponding to masses of 150, 300, 450 and 600 GeV. The other lines are iso-mass curves for squarks, corresponding to masses of 150, 300, 450 and 600 GeV. Color version at end of book.

The published CDF [26] and $D\tilde{O}$ [27] results, based on integrated luminosities of 295 and 360 pb^{-1} , respectively, exclude stop masses up to 134 GeV for $m_{\tilde{\chi}_1^0} = 48 \text{ GeV}$. A preliminary result from $D\tilde{O}$ [28], based on an integrated luminosity of $\sim 1 \text{ fb}^{-1}$, excludes $m_{\tilde{t}} < 149 \text{ GeV}$ for $m_{\tilde{\chi}_1^0} = 63 \text{ GeV}$, as shown in Fig. 5, with theoretical uncertainties taken into account as explained above. These stop searches at the Tevatron lose their sensitivity when the $\tilde{t} - \tilde{\chi}_1^0$ mass difference becomes smaller than $\sim 40 \text{ GeV}$, because of the \cancel{E}_T requirement applied to reduce the otherwise overwhelming QCD background, so that the LEP constraints remain relevant, although restricted to $m_{\tilde{t}} < 100 \text{ GeV}$.

Similar searches were performed for sbottom pair production [26,29], with $\tilde{b} \rightarrow b\tilde{\chi}_1^0$. The sensitivity extends to higher masses than in the stop case because heavy-flavor tagging is more efficient for b than for c jets. The lower \tilde{b} mass limit set by $D\tilde{O}$ reaches 222 GeV for $m_{\tilde{\chi}_1^0} < 60 \text{ GeV}$. The CDF collaboration investigated the configuration where gluinos are lighter than all squark species except for the sbottom, thus decaying according to $\tilde{g} \rightarrow b\tilde{b}$, followed by $\tilde{b} \rightarrow b\tilde{\chi}_1^0$. The final state consists of four b jets with \cancel{E}_T . Gluino and sbottom mass lower limits reaching 280 and 240 GeV , respectively, were obtained for $m_{\tilde{\chi}_1^0} = 60 \text{ GeV}$, based on an integrated luminosity of 156 pb^{-1} [30].

A search for stop pair production followed by $\tilde{t} \rightarrow b\ell\tilde{\nu}$ decays was also performed by $D\tilde{O}$, based on 400 pb^{-1} , to address the parameter configurations leading to light sneutrinos. Final states with two muons or with a muon and an electron together with b jets and \cancel{E}_T were investigated. The largest stop mass excluded is 186 GeV for a sneutrino mass of 71 GeV [31].

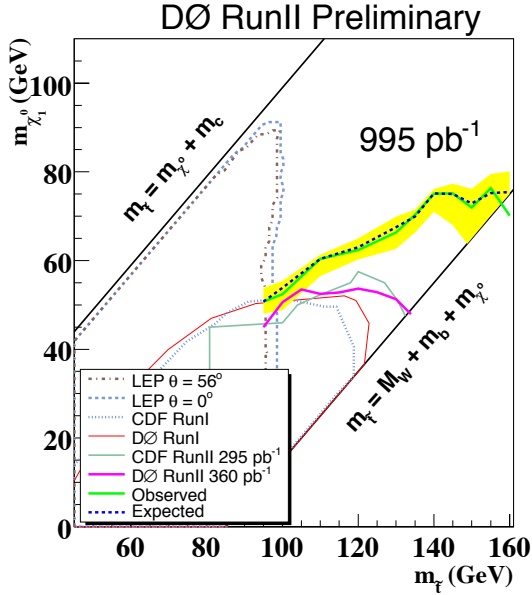


Figure 5: Region in the $(m_{\tilde{\chi}_1^0}, m_{\tilde{\chi}_1^\pm})$ plane excluded by DØ and by earlier experiments. The solid curve corresponds to the nominal scale and PDF choices. The yellow band represents the uncertainty associated with these choices. Color version at end of book.

Finally, the possibility of a stop stable on the scale of the time needed to escape the detector was considered by the CDF collaboration [32]. The resulting R -hadron would behave as a slow moving muon, and can be discriminated from the real muon background by comparing its momentum and its velocity, using a time-of-flight measurement. A preliminary mass lower limit of 250 GeV was obtained, based on an integrated luminosity of 1 fb^{-1} .

Charginos and neutralinos: Associated chargino-neutralino production, $p\bar{p} \rightarrow \tilde{\chi}_1^\pm \tilde{\chi}_2^0$, proceeds via s -channel W and t -channel squark exchange, with destructive interference. This process could provide a distinct trilepton+ \cancel{E}_T signal at the Tevatron if the branching ratios for leptonic decays ($\tilde{\chi}_1^\pm \rightarrow \ell^\pm \nu \tilde{\chi}_1^0$ and $\tilde{\chi}_2^0 \rightarrow \ell^+ \ell^- \tilde{\chi}_1^0$) are sufficiently large. Since these decays are mediated by virtual vector boson or sfermion exchange, this condition will be satisfied if sleptons are sufficiently light. The search is nevertheless challenging because the final state leptons carry little energy, and the production cross section is only a fraction of a picobarn.

In order to reduce the impact of lepton identification inefficiencies, and also to retain some sensitivity for final states involving τ s, only two leptons were required to be positively identified as electrons or muons, while for the third lepton only an isolated charged track requirement was imposed. In addition, searches were performed for same sign leptons since in that case SM backgrounds from Z/γ^* production are much smaller. Series of analysis criteria involving requirements on

the lepton and third track isolation, on the amount of \cancel{E}_T , and on the absence of energetic jets were applied.

No significant excess over SM background expectation was observed by DØ [33] or CDF [34], based on 320 pb^{-1} and 1.1 fb^{-1} , respectively. These results were interpreted within slightly modified versions of mSUGRA. In the case of CDF, m_0 was set equal to 70 GeV, while for DØ m_0 was adjusted for every value of $m_{1/2}$ such that the slepton masses are just above $m_{\tilde{\chi}_2^0}$ (this configuration is denoted “3l-max”). In practice, the CDF and DØ prescriptions favor two- and three-body decays, respectively. Both collaborations set $\tan\beta = 3$ and $\mu > 0$, and adjust A_0 so that there is no mixing in the stau sector. The chargino mass limit obtained by CDF under these conditions is 129 GeV. A recent update from DØ [35], based on 0.9 to 1.7 fb^{-1} , depending on the channel, provides a preliminary chargino mass lower limit of 145 GeV, as shown in Fig. 6. For large values of m_0 , the leptonic branching ratios are reduced, so that the current searches do not have sensitivity beyond the LEP limit of 103 GeV.

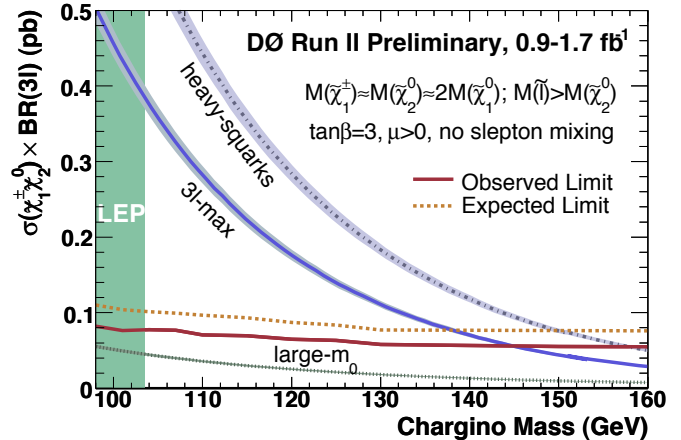


Figure 6: Upper limit from DØ on the product of cross section times branching ratio into three leptons for the associated $\tilde{\chi}_1^\pm \tilde{\chi}_2^0$ production at the Tevatron. The “3l-max” theoretical curve corresponds to the hypotheses detailed in the text. Color version at end of book.

R -parity violation: A whole new phenomenology opens up if R -parity is not assumed to be conserved. The searches can be divided into two classes.

First, R -parity conserving pair production of SUSY particles has been considered, with R -parity violation appearing only in the LSP decay at the end of the decay chains. The case of gaugino pair production, with a lepton-number violating coupling of the λ type in the neutralino LSP decay, has been extensively studied. Four charged leptons are expected in the final state, with flavors depending on the generation indices in the λ_{ijk} coupling, and there is also some \cancel{E}_T from the two neutrinos. Searches have been performed by CDF [36] and DØ [37] in the cases of λ_{121} and λ_{122} couplings, and by DØ

Searches Particle Listings

Supersymmetric Particle Searches

in the case of a λ_{133} coupling for which τ s appear in the final state. The chargino mass lower limits obtained by $D\mathcal{O}$ in the mSUGRA framework with $m_0 = 1$ TeV, $\tan\beta = 5$, and $\mu > 0$ are 231, 229, and 166 GeV for the λ_{121} , λ_{122} , and λ_{133} couplings, respectively, based on 360 pb^{-1} .

The CDF collaboration also searched for stop pair production, with $\tilde{t} \rightarrow b\tau$ decays mediated by a λ'_{333} coupling [38]. No such signal was observed in the topology where one τ decays into an electron or a muon and the other into hadrons, and a stop mass lower limit of 151 GeV was derived, based on 322 pb^{-1} .

The $D\mathcal{O}$ collaboration investigated the case of pair production of a neutralino LSP with a mass of a few GeV, followed by $\tilde{\chi}_1^0 \rightarrow \mu^+\mu^-\nu$ decays via a λ_{i22} coupling [39]. The values of the coupling considered were such that the $\tilde{\chi}_1^0$ is long-lived, and the search was therefore directed toward dimuon vertices displaced from the main interaction vertex. This search was motivated by anomalous dimuon events observed by the NuTeV collaboration in a neutrino experiment [40]. With no signal observed by $D\mathcal{O}$, such an explanation for those events has been ruled out.

Second, resonant slepton production could occur via a λ'_{i11} R -parity violating coupling. The case of a λ'_{211} coupling was considered by $D\mathcal{O}$ [41], with R -parity conserving decays of the resonantly produced slepton ($\tilde{\mu} \rightarrow \tilde{\chi}_i^0\mu$ and $\tilde{\nu}_\mu \rightarrow \tilde{\chi}^\pm\mu$). The violation of R -parity is again manifest in the decay of the neutralino LSP into a muon or a neutrino + two jets. No excess over background was observed, and an exclusion domain was placed in the $(m_{\tilde{\mu}}, \lambda'_{211})$ plane, the production cross section now depending on the value of λ'_{211} . For $\lambda'_{211} = 0.1$, a smuon mass lower limit of 363 GeV is obtained in mSUGRA with $\tan\beta = 5$, $A_0 = 0$ and $\mu < 0$, based on 380 pb^{-1} .

Resonant sneutrino production was also investigated by the CDF collaboration in the case where the sneutrino decays via a λ type coupling, hence different from the coupling involved in the production. The decay channels considered were ee , $\mu\mu$, $\tau\tau$ and $e\mu$. Sneutrino mass limits were derived, dependent on the product of the λ' and λ couplings considered [42].

Other non-canonical scenarios: As discussed earlier, a neutralino or stau NLSP is expected in GMSB. SUSY particle pair production, with cascade decays to a $\tilde{\chi}_1^0$ NLSP followed by $\tilde{\chi}_1^0 \rightarrow \gamma\tilde{G}$ has been investigated by both CDF and $D\mathcal{O}$ through inclusive searches for diphoton final states with large \cancel{E}_T . Backgrounds from photon misidentification or from fake \cancel{E}_T were determined from data, and no significant excess of events was observed. The two collaborations combined their published results [43], based on $200\text{--}260 \text{ pb}^{-1}$, to set a chargino mass lower limit of 209 GeV in a benchmark GMSB model known as the ‘‘Snowmass slope SPS 8’’ [44]. (This model has one parameter, the effective SUSY-breaking scale Λ , with $N_5 = 1$ messenger, a messenger mass of 2Λ , $\tan\beta = 15$ and $\mu > 0$.) A recent preliminary result from $D\mathcal{O}$, based on 1.1 fb^{-1} , increased the chargino mass limit to 231 GeV [45].

The additional possibility of non-prompt $\tilde{\chi}_1^0$ decays was considered by CDF, taking advantage of the timing information provided by their calorimeter [46]. No signal of delayed photons was observed in 570 pb^{-1} , and an excluded domain in the $(m_{\tilde{\chi}_1^0}, \tau_{\tilde{\chi}_1^0})$ plane was derived, where $\tau_{\tilde{\chi}_1^0}$ is the $\tilde{\chi}_1^0$ lifetime, extending out to 101 GeV for $\tau_{\tilde{\chi}_1^0} = 5 \text{ ns}$.

The case of a long-lived stau NLSP was also investigated. Pair production would resemble a pair of slow-moving muons. The timing information of their muon system was used by $D\mathcal{O}$, and no excess of such anomalously slow muons was observed in 390 pb^{-1} [47]. However, the sensitivity of the search is not yet sufficient to set a stau mass lower limit. Long-lived charginos as in AMSB would lead to the same signature. The larger production cross section allowed a preliminary lower limit of 174 GeV to be set on the mass of such long-lived gaugino-like charginos.

Within the recently proposed model of split SUSY, gluinos are expected to acquire a substantial lifetime. After hadronization into a R -hadron, such a long-lived gluino produced in a $p\bar{p}$ collision could come to rest in a calorimeter, and decay during a later bunch crossing than that during which it was produced [48]. The main decay mode is expected to be $\tilde{g} \rightarrow g\tilde{\chi}_1^0$, with some competition from $\tilde{g} \rightarrow q\bar{q}\tilde{\chi}_1^0$. Such a late gluino decay would appear as a jet not pointing toward the detector center in an otherwise empty event. Such a possibility was considered by the $D\mathcal{O}$ collaboration. The main backgrounds, coming from showering cosmic muons and from muons belonging to the beam halo, were estimated from data, and no excess of such a topology was observed. Based on an integrated luminosity of 410 pb^{-1} , limits were set on the mass of such a gluino, with some dependence on the lifetime, the decay branching ratio, the $\tilde{\chi}_1^0$ mass, and the probability for a neutral R -hadron to convert into a charged one in the calorimeter [49]. For instance, for a lifetime smaller than three hours, a neutralino mass of 50 GeV, a conversion cross section of 3 mb, and a 100% branching ratio into $g\tilde{\chi}_1^0$, a mass limit of 270 GeV was obtained.

II.8. Conclusion: The masses of SUSY particles other than the gluino and the LSP have been constrained at LEP to be larger than ~ 100 GeV, essentially independent of any specific model. Within the MSSM with unification of gaugino and sfermion masses, an indirect lower limit of 47 GeV has been set by the LEP experiments for the mass of a neutralino LSP. The mass reach at the Tevatron is much larger than at LEP, but the results need to be interpreted in the context of specific models. Based on an integrated luminosity of 1 fb^{-1} , the current squark and gluino mass lower limits are 375 and 289 GeV, respectively, within the mSUGRA framework at low $\tan\beta$. It is expected that $6\text{--}7 \text{ fb}^{-1}$ will be accumulated at the Tevatron by 2009, and that the LHC will begin operation in the course of 2008, which will open a whole new window for SUSY searches.

References

1. M. Drees and G. Gerbier, *Dark matter*, in this volume of The Review of Particle Physics.

2. Y. Kwon and G. Punzi, *Production and decay of b-flavored hadrons*, in this volume of The Review of Particle Physics.
3. A. Höcker and W.J. Marciano, *The muon anomalous moment*, in this volume of The Review of Particle Physics.
4. LEPSUSYWG, ALEPH, DELPHI, L3 and OPAL experiments, note LEPSUSYWG/04-01.1, <http://lepsusy.web.cern.ch/lepsusy/Welcome.html>.
5. ALEPH Coll., Phys. Lett. **B544**, 73 (2002); L3 Coll., Phys. Lett. **B580**, 37 (2004).
6. The ALEPH, DELPHI, L3, OPAL, SLD Collaborations, the LEP Electroweak Working Group, the SLD Electroweak and Heavy Flavours Groups, Phys. Reports **427**, 257 (2006).
7. LEPSUSYWG, *ibid.*, note LEPSUSYWG/01-03.1.
8. LEPSUSYWG, *ibid.*, note LEPSUSYWG/02-04.1.
9. LEPSUSYWG, *ibid.*, note LEPSUSYWG/04-07.1.
10. LEPSUSYWG, *ibid.*, note LEPSUSYWG/02-06.2.
11. LEPSUSYWG, *ibid.*, note LEPSUSYWG/04-02.1.
12. ALEPH Coll., Phys. Lett. **B537**, 5 (2002).
13. C. Boehm, A. Djouadi, and Y. Mambrini, Phys. Rev. **D61**, 095006 (2000).
14. LEPSUSYWG, *ibid.*, note LEPSUSYWG/04-09.1.
15. CDF Coll., Phys. Rev. **D59**, 092002 (1999).
16. ALEPH Coll., Eur. Phys. J. **C25**, 339 (2002); OPAL Coll., Eur. Phys. J. **C46**, 307 (2006).
17. LEPSUSYWG, *ibid.*, note LEPSUSYWG/02-09.2.
18. ALEPH Coll., Eur. Phys. J. **C31**, 327 (2003); DELPHI Coll., Eur. Phys. J. **C26**, 505 (2003).
19. LEPSUSYWG, *ibid.*, note LEPSUSYWG/02-10.1; ALEPH Coll., Eur. Phys. J. **C31**, 1 (2003); DELPHI Coll., Eur. Phys. J. **C36**, 1 (2004); L3 Coll., Phys. Lett. **B524**, 65 (2002); OPAL Coll., Eur. Phys. J. **C33**, 149 (2004).
20. ALEPH Coll., Eur. Phys. J. **C19**, 415 (2001) and Eur. Phys. J. **C25**, 1 (2002); DELPHI Coll., Eur. Phys. J. **C28**, 15 (2003); L3 Coll., Phys. Lett. **B414**, 373 (1997); OPAL Coll., Eur. Phys. J. **C13**, 553 (2000).
21. H1 Coll., Phys. Lett. **B599**, 159 (2004); H1 Coll., Eur. Phys. J. **C36**, 425 (2004); ZEUS Coll., Eur. Phys. J. **C50**, 269 (2007).
22. DØ Coll., Phys. Lett. **B638**, 119 (2006).
23. DØ Coll., *Search for squarks and gluinos in events with jets and missing transverse energy with the DØ detector using 1 fb⁻¹ of Run IIa data*, DØ-Note 5312-CONF.
24. CDF Coll., *Search for Squark/Gluino Production in MET+ jets Final State (1.4 fb⁻¹ analysis)*, http://www-cdf.fnal.gov/physics/exotic/r2a/20070809.squark_gluino/public.html.
25. DØ Coll., *Search for squark production in events with jets, hadronically decaying taus and missing transverse energy with the DØ detector at √s = 1.96 TeV in the Run IIa data*, DØ-Note 5468-CONF.
26. CDF Coll., Phys. Rev. **D76**, 072010 (2007).
27. DØ Coll., Phys. Lett. **B645**, 119 (2007).
28. DØ Coll., *Search for the pair production of scalar top quarks in acoplanar charm jet + missing transverse energy final state in p̄p collisions at √s = 1.96 TeV*, DØ-Note 5436-CONF.
29. DØ Coll., Phys. Rev. Lett. **97**, 171806 (2006).
30. CDF Coll., Phys. Rev. Lett. **96**, 171802 (2006).
31. DØ Coll., *Search for the lightest scalar top quark in events with two leptons in p̄p collisions at √s = 1.96 TeV*, submitted to Phys. Lett. **B**, arXiv:0707.2864v1[hep-ex].
32. CDF Coll., *Search for charged, massive stable particles*, CDF-Note 8701.
33. DØ Coll., Phys. Rev. Lett. **95**, 151805 (2005).
34. CDF Coll., Phys. Rev. Lett. **98**, 221803 (2007) and *Search for chargino-neutralino production in p̄p collisions at √s = 1.96 TeV*, accepted for publication in Phys. Rev. Lett., arXiv:0707.2362v1[hep-ex].
35. DØ Coll., *Search for the Associated Production of Chargino and Neutralino in Final States with Two Electrons and an Additional Lepton*, DØ-Note 5464-CONF.
36. CDF Coll., Phys. Rev. Lett. **98**, 131804 (2007).
37. DØ Coll., Phys. Lett. **B638**, 441 (2006).
38. CDF Coll., *Search for Pair Production of Scalar Top Quarks Decaying to a τ Lepton and a b Quark*, CDF-Note 7835.
39. DØ Coll., Phys. Rev. Lett. **97**, 161802 (2006).
40. NuTeV Coll., Phys. Rev. Lett. **87**, 041801 (2001).
41. DØ Coll., Phys. Rev. Lett. **97**, 111801 (2006).
42. CDF Coll., Phys. Rev. Lett. **95**, 252001 (2005); CDF Coll., Phys. Rev. Lett. **95**, 131801 (2005); CDF Coll., Phys. Rev. Lett. **96**, 211802 (2006).
43. V. Buescher *et al.*, for the CDF and DØ Collaborations, *Combination of CDF and DØ Limits on a Gauge Mediated SUSY Model Using Diphoton and Missing Transverse Energy Channel*, arXiv:hep-ex/0504004v1.
44. B.C. Allanach *et al.*, Eur. Phys. J. **C25**, 113 (2002).
45. DØ Coll., *Search for GMSB in diphoton final states by DØ at √s = 1.96 TeV*, DØ-Note 5427-CONF.
46. CDF Coll., Phys. Rev. Lett. **99**, 121801 (2007).
47. DØ Coll., *A Search for Charged Massive Stable Particles at DØ*, DØ-Note 4746-CONF.
48. A. Arvanitaki *et al.*, *Stopping Gluinos*, arXiv:hep-ph/0506242v2.
49. DØ Coll., Phys. Rev. Lett. **99**, 131801 (2007).

SUPERSYMMETRIC MODEL ASSUMPTIONS

The exclusion of particle masses within a mass range (m_1, m_2) will be denoted with the notation "none $m_1 - m_2$ " in the VALUE column of the following Listings.

Most of the results shown below, unless stated otherwise, are based on the Minimal Supersymmetric Standard Model (MSSM), as described in the Note on Supersymmetry. Unless otherwise indicated, this includes the assumption of common gaugino and scalar masses at the scale of Grand Unification (GUT), and use of the resulting relations in the spectrum and decay branching ratios. It is also assumed that R -parity (R) is conserved. Unless otherwise indicated, the results also assume that:

- 1) The $\tilde{\chi}_1^0$ is the lightest supersymmetric particle (LSP)
- 2) $m_{\tilde{f}_L} = m_{\tilde{f}_R}$, where $\tilde{f}_{L,R}$ refer to the scalar partners of left- and right-handed fermions.

Limits involving different assumptions are identified in the Comments or in the Footnotes. We summarize here the notations used in this Chapter to characterize some of the most

Searches Particle Listings

Supersymmetric Particle Searches

common deviations from the MSSM (for further details, see the Note on Supersymmetry).

Theories with R -parity violation (\mathcal{R}) are characterized by a superpotential of the form: $\lambda_{ijk} L_i L_j e_k^c + \lambda'_{ijk} L_i Q_j d_k^c + \lambda''_{ijk} u_i^c d_j^c d_k^c$, where i, j, k are generation indices. The presence of any of these couplings is often identified in the following by the symbols $L\bar{L}\bar{E}$, $LQ\bar{D}$, and $\bar{U}\bar{D}\bar{D}$. Mass limits in the presence of \mathcal{R} will often refer to “direct” and “indirect” decays. Direct refers to \mathcal{R} decays of the particle in consideration. Indirect refers to cases where \mathcal{R} appears in the decays of the LSP.

In several models, most notably in theories with so-called Gauge Mediated Supersymmetry Breaking (GMSB), the gravitino (\tilde{G}) is the LSP. It is usually much lighter than any other massive particle in the spectrum, and $m_{\tilde{G}}$ is then neglected in all decay processes involving gravitinos. In these scenarios, particles other than the neutralino are sometimes considered as the next-to-lightest supersymmetric particle (NLSP), and are assumed to decay to their even- R partner plus \tilde{G} . If the lifetime is short enough for the decay to take place within the detector, \tilde{G} is assumed to be undetected and to give rise to missing energy (\cancel{E}) or missing transverse energy (\cancel{E}_T) signatures.

When needed, specific assumptions on the eigenstate content of $\tilde{\chi}^0$ and $\tilde{\chi}^\pm$ states are indicated, using the notation $\tilde{\gamma}$ (photino), \tilde{H} (higgsino), \tilde{W} (wino), and \tilde{Z} (zino) to signal that the limit of pure states was used. The terms gaugino is also used, to generically indicate wino-like charginos and zino-like neutralinos.

$\tilde{\chi}_1^0$ (Lightest Neutralino) MASS LIMIT

$\tilde{\chi}_1^0$ is often assumed to be the lightest supersymmetric particle (LSP). See also the $\tilde{\chi}_2^0, \tilde{\chi}_3^0, \tilde{\chi}_4^0$ section below.

We have divided the $\tilde{\chi}_1^0$ listings below into five sections:

- 1) Accelerator limits for stable $\tilde{\chi}_1^0$,
- 2) Bounds on $\tilde{\chi}_1^0$ from dark matter searches,
- 3) Bounds on $\tilde{\chi}_1^0$ elastic cross sections from dark matter searches,
- 4) Other bounds on $\tilde{\chi}_1^0$ from astrophysics and cosmology, and
- 5) Bounds on unstable $\tilde{\chi}_1^0$.

Accelerator limits for stable $\tilde{\chi}_1^0$

Unless otherwise stated, results in this section assume spectra, production rates, decay modes, and branching ratios as evaluated in the MSSM, with gaugino and sfermion mass unification at the GUT scale. These papers generally study production of $\tilde{\chi}_i^+ \tilde{\chi}_j^0$ ($i \geq 1, j \geq 2$), $\tilde{\chi}_1^+ \tilde{\chi}_1^-$, and (in the case of hadronic collisions) $\tilde{\chi}_1^+ \tilde{\chi}_2^0$ pairs. The mass limits on $\tilde{\chi}_1^0$ are either direct, or follow indirectly from the constraints set by the non-observation of $\tilde{\chi}_1^\pm$ and $\tilde{\chi}_2^0$ states on the gaugino and higgsino MSSM parameters M_2 and μ . In some cases, information is used from the nonobservation of slepton decays.

Obsolete limits obtained from $e^+ e^-$ collisions up to $\sqrt{s}=184$ GeV have been removed from this compilation and can be found in the 2000 Edition (The European Physical Journal **C15** 1 (2000)) of this Review. $\Delta m = m_{\tilde{\chi}_2^0} - m_{\tilde{\chi}_1^0}$.

VALUE (GeV)	CL%	DOCUMENT ID	TECN	COMMENT
>40	95	1 ABBIENDI 04H	OPAL	all $\tan\beta$, $\Delta m > 5$ GeV, $m_0 > 500$ GeV, $A_0 = 0$
>42.4	95	2 HEISTER 04	ALEP	all $\tan\beta$, all Δm , all m_0
>39.2	95	3 ABDALLAH 03M	DLPH	all $\tan\beta$, $m_{\tilde{\nu}} > 500$ GeV
>46	95	4 ABDALLAH 03M	DLPH	all $\tan\beta$, all Δm , all m_0
>32.5	95	5 ACCIARRI 00D	L3	$\tan\beta > 0.7$, $\Delta m > 3$ GeV, all m_0
• • • We do not use the following data for averages, fits, limits, etc. • • •				
		6 ABBOTT 98c	D0	$p\bar{p} \rightarrow \tilde{\chi}_1^\pm \tilde{\chi}_2^0$
>41	95	7 ABE 98J	CDF	$p\bar{p} \rightarrow \tilde{\chi}_1^\pm \tilde{\chi}_2^0$

1 ABBIENDI 04H search for charginos and neutralinos in events with acoplanar leptons+jets and multi-jet final states in the 192–209 GeV data, combined with the results on leptonic final states from ABBIENDI 04. The results hold for a scan over the parameter space covering the region $0 < M_2 < 5000$ GeV, $-1000 < \mu < 1000$ GeV and $\tan\beta$ from 1 to 40. This limit supersedes ABBIENDI 00H.

2 HEISTER 04 data collected up to 209 GeV. Updates earlier analysis of selectrons from HEISTER 02E, includes a new analysis of charginos and neutralinos decaying into stau and uses results on charginos with initial state radiation from HEISTER 02J. The limit is based on the direct search for charginos and neutralinos, the constraints from the slepton search and the Higgs mass limits from HEISTER 02 using a top mass of 175 GeV, interpreted in a framework with universal gaugino and sfermion masses. Assuming the mixing in the stau sector to be negligible, the limit improves to 43.1 GeV. Under the assumption of MSUGRA with unification of the Higgs and sfermion masses, the limit improves to 50 GeV, and reaches 53 GeV for $A_0 = 0$. These limits include and update the results of BARATE 01.

3 ABDALLAH 03M uses data from $\sqrt{s} = 192$ –208 GeV. A limit on the mass of $\tilde{\chi}_1^0$ is derived from direct searches for neutralinos combined with the chargino search. Neutralinos are searched in the production of $\tilde{\chi}_1^0 \tilde{\chi}_2^0, \tilde{\chi}_1^0 \tilde{\chi}_3^0$, as well as $\tilde{\chi}_2^0 \tilde{\chi}_3^0$ and $\tilde{\chi}_2^0 \tilde{\chi}_4^0$ giving rise to cascade decays, and $\tilde{\chi}_1^0 \tilde{\chi}_2^0$ and $\tilde{\chi}_1^0 \tilde{\chi}_3^0$, followed by the decay $\tilde{\chi}_2^0 \rightarrow \tilde{\tau} \tau$. The results hold for the parameter space defined by values of $M_2 < 1$ TeV, $|\mu| \leq 2$ TeV with the $\tilde{\chi}_1^0$ as LSP. The limit is obtained for $\tan\beta = 1$ and large m_0 , where $\tilde{\chi}_2^0 \tilde{\chi}_3^0$ and chargino pair production are important. If the constraint from Higgs searches is also imposed, the limit improves to 49.0 GeV in the M_h^{max} scenario with $m_t = 174.3$ GeV. These limits update the results of ABREU 00J.

4 ABDALLAH 03M uses data from $\sqrt{s} = 192$ –208 GeV. An indirect limit on the mass of $\tilde{\chi}_1^0$ is derived by constraining the MSSM parameter space by the results from direct searches for neutralinos (including cascade decays and $\tilde{\tau}\tau$ final states), for charginos (for all Δm_{\pm}) and for sleptons, stop and sbottom. The results hold for the full parameter space defined by values of $M_2 < 1$ TeV, $|\mu| \leq 2$ TeV with the $\tilde{\chi}_1^0$ as LSP. Constraints from the Higgs search in the M_h^{max} scenario assuming $m_t = 174.3$ GeV are included. The limit is obtained for $\tan\beta \geq 5$ when stau mixing leads to mass degeneracy between $\tilde{\tau}_1$ and $\tilde{\chi}_1^0$ and the limit is based on $\tilde{\chi}_2^0$ production followed by its decay to $\tilde{\tau}_1 \tau$. In the pathological scenario where m_0 and $|\mu|$ are large, so that the $\tilde{\chi}_2^0$ production cross section is negligible, and where there is mixing in the stau sector but not in stop nor sbottom, the limit is based on charginos with soft decay products and an ISR photon. The limit then degrades to 39 GeV. See Figs 40–42 for the dependence of the limit on $\tan\beta$ and $m_{\tilde{\nu}}$. These limits update the results of ABREU 00W.

5 ACCIARRI 00D data collected at $\sqrt{s}=189$ GeV. The results hold over the full parameter space defined by $0.7 \leq \tan\beta \leq 60$, $0 \leq M_2 \leq 2$ TeV, $m_0 \leq 500$ GeV, $|\mu| \leq 2$ TeV. The minimum mass limit is reached for $\tan\beta=1$ and large m_0 . The results of slepton searches from ACCIARRI 99W are used to help set constraints in the region of small m_0 . The limit improves to 48 GeV for $m_0 \gtrsim 200$ GeV and $\tan\beta \gtrsim 10$. See their Figs. 6–8 for the $\tan\beta$ and m_0 dependence of the limits. Updates ACCIARRI 98F.

6 ABBOTT 98c searches for trilepton final states ($\ell=e,\mu$). See footnote to ABBOTT 98c in the Chargino Section for details on the assumptions. Assuming a negligible decay rate of $\tilde{\chi}_1^\pm$ and $\tilde{\chi}_2^0$ to quarks, they obtain $m_{\tilde{\chi}_2^0} \gtrsim 51$ GeV.

7 ABE 98J searches for trilepton final states ($\ell=e,\mu$). See footnote to ABE 98J in the Chargino Section for details on the assumptions. The quoted result corresponds to the best limit within the selected range of parameters, obtained for $m_{\tilde{q}} > m_{\tilde{g}}$, $\tan\beta=2$, and $\mu = -600$ GeV.

Bounds on $\tilde{\chi}_1^0$ from dark matter searches

These papers generally exclude regions in the $M_2 - \mu$ parameter plane assuming that $\tilde{\chi}_1^0$ is the dominant form of dark matter in the galactic halo. These limits are based on the lack of detection in laboratory experiments or by the absence of a signal in underground neutrino detectors. The latter signal is expected if $\tilde{\chi}_1^0$ accumulates in the Sun or the Earth and annihilates into high-energy $\nu\bar{\nu}$ s.

VALUE	DOCUMENT ID	TECN
• • •	We do not use the following data for averages, fits, limits, etc. • • •	
	1 ACHTERBERG 06	AMND
	2 ACKERMANN 06	AMND
	3 DEBOER 06	RVUE
	4 DESAI 04	SKAM
	4 AMBROSIO 99	MCRO
	5 LOSECCO 95	RVUE
	6 MORI 93	KAMI
	7 BOTTINO 92	COSM
	8 BOTTINO 91	RVUE
	9 GELMINI 91	COSM
	10 KAMIONKOW.91	RVUE
	11 MORI 91B	KAMI
none 4–15 GeV	12 OLIVE 88	COSM

1 ACHTERBERG 06 is based on data collected during 421.9 effective days with the AMANDA detector. They looked for interactions of ν_{μ} s from the centre of the Earth over a background of atmospheric neutrinos and set 90 % CL limits on the muon flux. Their limit is compared with the muon flux expected from neutralino annihilations into $W^+ W^-$ and $b\bar{b}$ at the centre of the Earth for MSSM parameters compatible with the relic dark matter density, see their Fig. 7.

2 ACKERMANN 06 is based on data collected during 143.7 days with the AMANDA-II detector. They looked for interactions of ν_{μ} s from the Sun over a background of atmospheric neutrinos and set 90 % CL limits on the muon flux. Their limit is compared with the muon flux expected from neutralino annihilations into $W^+ W^-$ in the Sun for SUSY model parameters compatible with the relic dark matter density, see their Fig. 3.

- ³ DEBOER 06 interpret an excess of diffuse Galactic gamma rays observed with the EGRET satellite as originating from π^0 decays from the annihilation of neutralinos into quark jets. They analyze the corresponding parameter space in a supergravity inspired MSSM model with radiative electroweak symmetry breaking, see their Fig. 3 for the preferred region in the $(m_0, m_{1/2})$ plane of a scenario with large $\tan\beta$.
- ⁴ AMBROSIO 99 and DESAI 04 set new neutrino flux limits which can be used to limit the parameter space in supersymmetric models based on neutralino annihilation in the Sun and the Earth.
- ⁵ LOSECCO 95 reanalyzed the IMB data and places lower limit on $m_{\tilde{\chi}_1^0}$ of 18 GeV if the LSP is a photino and 10 GeV if the LSP is a higgsino based on LSP annihilation in the sun producing high-energy neutrinos and the limits on neutrino fluxes from the IMB detector.
- ⁶ MORI 93 excludes some region in $M_2-\mu$ parameter space depending on $\tan\beta$ and lightest scalar Higgs mass for neutralino dark matter $m_{\tilde{\chi}_1^0} > m_W$, using limits on upgoing muons produced by energetic neutrinos from neutralino annihilation in the Sun and the Earth.
- ⁷ BOTTINO 92 excludes some region $M_2-\mu$ parameter space assuming that the lightest neutralino is the dark matter, using upgoing muons at Kamiokande, direct searches by Ge detectors, and by LEP experiments. The analysis includes top radiative corrections on Higgs parameters and employs two different hypotheses for nucleon-Higgs coupling. Effects of rescaling in the local neutralino density according to the neutralino relic abundance are taken into account.
- ⁸ BOTTINO 91 excluded a region in $M_2-\mu$ plane using upgoing muon data from Kamioka experiment, assuming that the dark matter surrounding us is composed of neutralinos and that the Higgs boson is not too heavy.
- ⁹ GELMINI 91 exclude a region in $M_2-\mu$ plane using dark matter searches.
- ¹⁰ KAMIONKOWSKI 91 excludes a region in the $M_2-\mu$ plane using IMB limit on upgoing muons originated by energetic neutrinos from neutralino annihilation in the sun, assuming that the dark matter is composed of neutralinos and that $m_{H_1^0} \lesssim 50$ GeV. See Fig. 8 in the paper.
- ¹¹ MORI 91B exclude a part of the region in the $M_2-\mu$ plane with $m_{\tilde{\chi}_1^0} \lesssim 80$ GeV using a limit on upgoing muons originated by energetic neutrinos from neutralino annihilation in the earth, assuming that the dark matter surrounding us is composed of neutralinos and that $m_{H_1^0} \lesssim 80$ GeV.
- ¹² OLIVE 88 result assumes that photinos make up the dark matter in the galactic halo. Limit is based on annihilations in the sun and is due to an absence of high energy neutrinos detected in underground experiments. The limit is model dependent.

$\tilde{\chi}_1^0-p$ elastic cross section

Experimental results on the $\tilde{\chi}_1^0-p$ elastic cross section are evaluated at $m_{\tilde{\chi}_1^0}=100$ GeV. The experimental results on the cross section are often mass dependent. Therefore, the mass and cross section results are also given where the limit is strongest, when appropriate. Results are quoted separately for spin-dependent interactions (based on an effective 4-Fermi Lagrangian of the form $\overline{\chi}\gamma^\mu\gamma^5\chi\overline{p}\gamma_\mu\gamma^5q$) and spin-independent interactions ($\overline{\chi}\chi\overline{p}q$). For calculational details see GRIEST 88b, ELLIS 88b, BARBIERI 89c, DREES 93b, ARNOWITT 96, BERGSTROM 96, and BAER 97 in addition to the theory papers listed in the Tables. For a description of the theoretical assumptions and experimental techniques underlying most of the listed papers, see the review on "Dark matter" in this "Review of Particle Physics," and references therein. Most of the following papers use galactic halo and nuclear interaction assumptions from (LEWIN 96).

Spin-dependent interactions

VALUE (pb)	CL%	DOCUMENT ID	TECN	COMMENT
••• We do not use the following data for averages, fits, limits, etc. •••				
< 15	90	1 ALNER	07 ZEP2	Xe
< 0.17	90	2 LEE	07A KIMS	Csl
< 5		3 AKERIB	06 CDMS	Ge
< 2		4 SHIMIZU	06A CNTR	CaF ₂
< 0.4		5 ALNER	05 NAIA	Nal Spin Dep.
< 2		6 BARNABE-HE.	05 PICA	C
< 1.4		7 GIRARD	05 SMPL	F, Cl
< 4		8 KLAPDOR-K...	05 HDMS	Ge
2×10^{-11} to 1×10^{-4}		9 ELLIS	04 THEO	$\mu > 0$
< 16		10 GIULIANI	04 SIMP	F
< 0.8		11 AHMED	03 NAIA	Nal Spin Dep.
< 40		12 TAKEDA	03 BOLO	NaF Spin Dep.
< 10		13 ANGLOHER	02 CRES	Sapphire
8×10^{-7} to 2×10^{-5}		14 ELLIS	01c THEO	$\tan\beta \leq 10$
< 3.8		15 BERNABE	00D DAMA	Xe
< 15		16 COLLAR	00 SMPL	F
< 0.8		17 SPOONER	00 UKDM	Nal
< 4.8		17 BELLI	99c DAMA	F
< 100		18 OOTANI	99 BOLO	LIF
< 0.6		18 BERNABE	98c DAMA	Xe
< 5		17 BERNABE	97 DAMA	F

- ¹ The strongest upper limit is 14 pb and occurs at $m_\chi \approx 65$ GeV. The limit on the neutron spin-dependent cross section is 0.08 pb at $m_\chi = 100$ GeV and the strongest limit for scattering on neutrons is 0.07 pb at $m_\chi = 65$ GeV.
- ² The limit on the neutron spin-dependent cross section is 6 pb at $m_\chi = 100$ GeV.
- ³ The strongest upper limit is 4 pb and occurs at $m_\chi \approx 60$ GeV. The limit on the neutron spin-dependent elastic cross section is 0.07 pb.
- ⁴ The strongest upper limit is 1.2 pb and occurs at $m_\chi \approx 40$ GeV. The limit on the neutron spin-dependent cross section is 35 pb.
- ⁵ The strongest upper limit is 0.35 pb and occurs at $m_\chi \approx 60$ GeV.

- ⁶ The strongest upper limit is 1.2 pb and occurs $m_\chi \approx 30$ GeV.
- ⁷ The strongest upper limit is 1.2 pb and occurs $m_\chi \approx 40$ GeV.
- ⁸ Limit applies to neutron elastic cross section.
- ⁹ ELLIS 04 calculates the χp elastic scattering cross section in the framework of $N=1$ supergravity models with radiative breaking of the electroweak gauge symmetry, but without universal scalar masses. In the case of universal squark and slepton masses, but non-universal Higgs masses, the limit becomes 2×10^{-4} , see ELLIS 03e.
- ¹⁰ The strongest upper limit is 10 pb and occurs at $m_\chi \approx 30$ GeV.
- ¹¹ The strongest upper limit is 0.75 pb and occurs at $m_\chi \approx 70$ GeV.
- ¹² The strongest upper limit is 30 pb and occurs at $m_\chi \approx 20$ GeV.
- ¹³ The strongest upper limit is 8 pb and occurs at $m_\chi \approx 30$ GeV.
- ¹⁴ ELLIS 01c calculates the $\chi-p$ elastic scattering cross section in the framework of $N=1$ supergravity models with radiative breaking of the electroweak gauge symmetry. In models with nonuniversal Higgs masses, the upper limit to the cross section is 6×10^{-4} .
- ¹⁵ The strongest upper limit is 3 pb and occurs at $m_\chi \approx 60$ GeV. The limits are for inelastic scattering $\chi^0 + 129\text{Xe} \rightarrow \chi^0 + 129\text{Xe}^* (39.58 \text{ keV})$.
- ¹⁶ The strongest upper limit is 9 pb and occurs at $m_\chi \approx 30$ GeV.
- ¹⁷ The strongest upper limit is 4.4 pb and occurs at $m_\chi \approx 60$ GeV.
- ¹⁸ The strongest upper limit is about 35 pb and occurs at $m_\chi \approx 15$ GeV.

Spin-independent interactions

VALUE (pb)	CL%	DOCUMENT ID	TECN	COMMENT
••• We do not use the following data for averages, fits, limits, etc. •••				
$< 8.8 \times 10^{-8}$	90	1 ANGLE	08 XE10	Xe
$< 7.5 \times 10^{-7}$	90	2 ALNER	07A ZEP2	Xe
$< 22 \times 10^{-7}$	90	3 LEE	07A KIMS	Csl
$< 2 \times 10^{-7}$		4 AKERIB	06A CDMS	Ge
$< 90 \times 10^{-7}$		5 LEE	06 KIMS	Csl
$< 5 \times 10^{-7}$		6 AKERIB	05 CDMS	Ge
$< 90 \times 10^{-7}$		ALNER	05 NAIA	Nal Spin Indep.
$< 12 \times 10^{-7}$		7 ALNER	05A ZEPL	
$< 20 \times 10^{-7}$		8 ANGLOHER	05 CRES	CaWO ₄
$< 14 \times 10^{-7}$		SANGLARD	05 EDEL	Ge
$< 4 \times 10^{-7}$		9 AKERIB	04 CDMS	Ge
2×10^{-11} to 8×10^{-6}	10,11	ELLIS	04 THEO	$\mu > 0$
$< 5 \times 10^{-8}$		12 PIERCE	04A THEO	
$< 2 \times 10^{-5}$		13 AHMED	03 NAIA	Nal Spin Indep.
$< 3 \times 10^{-6}$		14 AKERIB	03 CDMS	Ge
2×10^{-13} to 2×10^{-7}		15 BAER	03A THEO	
$< 1.4 \times 10^{-5}$		16 KLAPDOR-K...	03 HDMS	Ge
$< 6 \times 10^{-6}$		17 ABRAMS	02 CDMS	Ge
$< 1.4 \times 10^{-6}$		18 BENOIT	02 EDEL	Ge
1×10^{-12} to 7×10^{-6}		10 KIM	02B THEO	
$< 3 \times 10^{-5}$		19 MORALES	02B CSME	Ge
$< 1 \times 10^{-5}$		20 MORALES	02c IGEX	Ge
$< 1 \times 10^{-6}$		BALTZ	01 THEO	
$< 3 \times 10^{-5}$		21 BAUDIS	01 HDMS	Ge
$< 4.5 \times 10^{-6}$		BENOIT	01 EDEL	Ge
$< 7 \times 10^{-6}$		22 BOTTINO	01 THEO	
$< 1 \times 10^{-8}$		23 CORSETTI	01 THEO	$\tan\beta \leq 25$
5×10^{-10} to 1.5×10^{-8}		24 ELLIS	01c THEO	$\tan\beta \leq 10$
$< 4 \times 10^{-6}$		23 GOMEZ	01 THEO	
2×10^{-10} to 1×10^{-7}		23 LAHANAS	01 THEO	
$< 3 \times 10^{-6}$		ABUSAIDI	00 CDMS	Ge, Si
$< 6 \times 10^{-7}$		25 ACCOMANDO	00 THEO	
		26 BERNABE	00 DAMA	Nal
		27 FENG	00 THEO	$\tan\beta=10$
2.5×10^{-9} to 3.5×10^{-8}		MORALES	00 IGEX	Ge
$< 1.5 \times 10^{-5}$		SPOONER	00 UKDM	Nal
$< 4 \times 10^{-5}$		BAUDIS	99 HDMO	⁷⁶ Ge
$< 7 \times 10^{-6}$		28 BERNABE	99 DAMA	Nal
		29 BERNABE	98 DAMA	Nal
$< 7 \times 10^{-6}$		BERNABE	98c DAMA	Xe

- ¹ The strongest upper limit is 4.5×10^{-8} pb and occurs at $m_\chi \approx 30$ GeV.
- ² The strongest upper limit is 6.6×10^{-7} pb and occurs at $m_\chi \approx 65$ GeV.
- ³ The strongest upper limit is 19×10^{-7} pb and occurs at $m_\chi \approx 65$ GeV. Supersedes LEE 06.
- ⁴ AKERIB 06A updates the results of AKERIB 05. The strongest upper limit is 1.6×10^{-7} pb and occurs at $m_\chi \approx 60$ GeV.
- ⁵ The strongest upper limit is 8×10^{-6} pb and occurs at $m_\chi \approx 70$ GeV.
- ⁶ AKERIB 05 is incompatible with the DAMA most likely value. The strongest upper limit is 4×10^{-7} pb and occurs at $m_\chi \approx 60$ GeV.
- ⁷ The strongest upper limit is also close to 1.0×10^{-6} pb and occurs at $m_\chi \approx 70$ GeV. BENOIT 06 claim that the discrimination power of ZEPLIN-I measurement (ALNER 05A) is not reliable enough to obtain a limit better than 1×10^{-3} pb. However, SMITH 06 do not agree with the criticisms of BENOIT 06.
- ⁸ The strongest upper limit is also close to 1.4×10^{-6} pb and occurs at $m_\chi \approx 70$ GeV.
- ⁹ AKERIB 04 is incompatible with BERNABE 00 most likely value, under the assumption of standard WIMP-halo interactions. The strongest upper limit is 4×10^{-7} pb and occurs at $m_\chi \approx 60$ GeV.
- ¹⁰ KIM 02 and ELLIS 04 calculate the χp elastic scattering cross section in the framework of $N=1$ supergravity models with radiative breaking of the electroweak gauge symmetry, but without universal scalar masses.

Searches Particle Listings

Supersymmetric Particle Searches

- ¹¹ In the case of universal squark and slepton masses, but non-universal Higgs masses, the limit becomes 2×10^{-6} (2×10^{-11} when constraint from the BNL $g-2$ experiment are included), see ELLIS 03E. ELLIS 05 display the sensitivity of the elastic scattering cross section to the π -Nucleon Σ term.
- ¹² PIERCE 04A calculates the χ - p elastic scattering cross section in the framework of models with very heavy scalar masses. See Fig. 2 of the paper.
- ¹³ The strongest upper limit is 1.8×10^{-5} pb and occurs at $m_\chi \approx 80$ GeV.
- ¹⁴ Under the assumption of standard WIMP-halo interactions, Akerib 03 is incompatible with BERNABEI 00 most likely value at the 99.98% CL. See Fig. 4.
- ¹⁵ BAER 03A calculates the χ - p elastic scattering cross section in several models including the framework of $N=1$ supergravity models with radiative breaking of the electroweak gauge symmetry.
- ¹⁶ The strongest upper limit is 7×10^{-6} pb and occurs at $m_\chi \approx 30$ GeV.
- ¹⁷ ABRAMS 02 is incompatible with the DAMA most likely value at the 99.9% CL. The strongest upper limit is 3×10^{-6} pb and occurs at $m_\chi \approx 30$ GeV.
- ¹⁸ BENOIT 02 excludes the central result of DAMA at the 99.8% CL.
- ¹⁹ The strongest upper limit is 2×10^{-5} pb and occurs at $m_\chi \approx 40$ GeV.
- ²⁰ The strongest upper limit is 7×10^{-6} pb and occurs at $m_\chi \approx 46$ GeV.
- ²¹ The strongest upper limit is 1.8×10^{-5} pb and occurs at $m_\chi \approx 32$ GeV
- ²² BOTTINO 01 calculates the χ - p elastic scattering cross section in the framework of the following supersymmetric models: $N=1$ supergravity with the radiative breaking of the electroweak gauge symmetry, $N=1$ supergravity with nonuniversal scalar masses and an effective MSSM model at the electroweak scale.
- ²³ Calculates the χ - p elastic scattering cross section in the framework of $N=1$ supergravity models with radiative breaking of the electroweak gauge symmetry.
- ²⁴ ELLIS 01c calculates the χ - p elastic scattering cross section in the framework of $N=1$ supergravity models with radiative breaking of the electroweak gauge symmetry. ELLIS 02b find a range 2×10^{-8} – 1.5×10^{-7} at $\tan\beta=50$. In models with nonuniversal Higgs masses, the upper limit to the cross section is 4×10^{-7} .
- ²⁵ ACCOMANDO 00 calculate the χ - p elastic scattering cross section in the framework of minimal $N=1$ supergravity models with radiative breaking of the electroweak gauge symmetry. The limit is relaxed by at least an order of magnitude when models with nonuniversal scalar masses are considered. A subset of the authors in ARNOWITT 02 updated the limit to $< 9 \times 10^{-8}$ ($\tan\beta < 55$).
- ²⁶ BERNABEI 00 search for annual modulation of the WIMP signal. The data favor the hypothesis of annual modulation at 4σ and are consistent, for a particular model framework quoted there, with $m_{\chi^0} = 44^{+12}_{-9}$ GeV and a spin-independent χ^0 -proton cross section of $(5.4 \pm 1.0) \times 10^{-6}$ pb. See also BERNABEI 01 and BERNABEI 00c.
- ²⁷ FENG 00 calculate the χ - p elastic scattering cross section in the framework of $N=1$ supergravity models with radiative breaking of the electroweak gauge symmetry with a particular emphasis on focus point models. At $\tan\beta=50$, the range is 8×10^{-8} – 4×10^{-7} .
- ²⁸ BERNABEI 99 search for annual modulation of the WIMP signal. The data favor the hypothesis of annual modulation at 99.6%CL and are consistent, for the particular model framework considered there, with $m_{\chi^0} = 59^{+17}_{-14}$ GeV and spin-independent χ^0 -proton cross section of $(7.0^{+0.4}_{-1.2}) \times 10^{-6}$ pb (1 σ errors).
- ²⁹ BERNABEI 98 search for annual modulation of the WIMP signal. The data are consistent, for the particular model framework considered there, with $m_{\chi^0} = 59^{+36}_{-19}$ GeV and spin-independent χ^0 -proton cross section of $(1.0^{+0.1}_{-0.4}) \times 10^{-5}$ pb (1 σ errors).

Other bounds on $\tilde{\chi}_1^0$ from astrophysics and cosmology

Most of these papers generally exclude regions in the $M_2 - \mu$ parameter plane by requiring that the $\tilde{\chi}_1^0$ contribution to the overall cosmological density is less than some maximal value to avoid overclosure of the Universe. Those not based on the cosmological density are indicated. Many of these papers also include LEP and/or other bounds.

VALUE	DOCUMENT ID	TECN	COMMENT
>46 GeV	¹ ELLIS 00	RVUE	
• • • We do not use the following data for averages, fits, limits, etc. • • •			
> 6 GeV	^{2,3} BELANGER 04	THEO	
	⁴ ELLIS 04B	COSM	
	⁵ PIERCE 04A	COSM	
	⁶ BAER 03	COSM	
> 6 GeV	² BOTTINO 03	COSM	
	⁶ CHATTOPAD...03	COSM	
	⁷ ELLIS 03	COSM	
	⁸ ELLIS 03B	COSM	
	⁶ ELLIS 03C	COSM	
> 18 GeV	² HOOPER 03	COSM	$\Omega_\chi = 0.05-0.3$
	⁶ LAHANAS 03	COSM	
	⁹ BAER 02	COSM	
	¹⁰ ELLIS 02	COSM	
	¹¹ LAHANAS 02	COSM	
	¹² BARGER 01c	COSM	
	⁹ DJOUADI 01	COSM	
	¹³ ELLIS 01B	COSM	
	⁹ ROSZKOWSKI 01	COSM	
	⁷ BOEHM 00B	COSM	
	¹⁴ FENG 00	COSM	
	¹⁵ LAHANAS 00	COSM	
< 600 GeV	¹⁶ ELLIS 98B	COSM	
	¹⁷ EDSJO 97	COSM	Co-annihilation
	¹⁸ BAER 96	COSM	
	¹⁹ BEREZINSKY 95	COSM	

	²⁰ FALK 95	COSM	CP-violating phases
	²¹ DREES 93	COSM	Minimal supergravity
	²² FALK 93	COSM	Sfermion mixing
	²¹ KELLEY 93	COSM	Minimal supergravity
	²³ MIZUTA 93	COSM	Co-annihilation
	²⁴ LOPEZ 92	COSM	Minimal supergravity, $m_0=A=0$
	²⁵ MCDONALD 92	COSM	
	²⁶ GRIEST 91	COSM	
	²⁷ NOJIRI 91	COSM	Minimal supergravity
	²⁸ OLIVE 91	COSM	
	²⁹ ROSZKOWSKI 91	COSM	
	³⁰ GRIEST 90	COSM	
	²⁸ OLIVE 89	COSM	
none 100 eV – 15 GeV	SREDNICKI 88	COSM	$\tilde{\gamma}; m_{\tilde{f}}=100$ GeV
none 100 eV–5 GeV	ELLIS 84	COSM	$\tilde{\gamma};$ for $m_{\tilde{f}}=100$ GeV
	GOLDBERG 83	COSM	$\tilde{\gamma}$
	³¹ KRAUSS 83	COSM	$\tilde{\gamma}$
	VYSOTSKII 83	COSM	$\tilde{\gamma}$

- ¹ ELLIS 00 updates ELLIS 98. Uses LEP e^+e^- data at $\sqrt{s}=202$ and 204 GeV to improve bound on neutralino mass to 51 GeV when scalar mass universality is assumed and 46 GeV when Higgs mass universality is relaxed. Limits on $\tan\beta$ improve to > 2.7 ($\mu > 0$), > 2.2 ($\mu < 0$) when scalar mass universality is assumed and > 1.9 (both signs of μ) when Higgs mass universality is relaxed.
- ² HOOPER 03, BOTTINO 03 (see also BOTTINO 03A and BOTTINO 04), and BELANGER 04 do not assume gaugino or scalar mass unification.
- ³ Limit assumes a pseudo scalar mass < 200 GeV. For larger pseudo scalar masses, $m_\chi > 18(29)$ GeV for $\tan\beta = 50(10)$. Bounds from WMAP, $(g-2)_\mu$, $b \rightarrow s\gamma$, LEP.
- ⁴ ELLIS 04b places constraints on the SUSY parameter space in the framework of $N=1$ supergravity models with radiative breaking of the electroweak gauge symmetry including supersymmetry breaking relations between A and B parameters. See also ELLIS 03d.
- ⁵ PIERCE 04A places constraints on the SUSY parameter space in the framework of models with very heavy scalar masses.
- ⁶ BAER 03, CHATTOPADHYAY 03, ELLIS 03c and LAHANAS 03 place constraints on the SUSY parameter space in the framework of $N=1$ supergravity models with radiative breaking of the electroweak gauge symmetry based on WMAP results for the cold dark matter density.
- ⁷ BOEHM 00b and ELLIS 03 place constraints on the SUSY parameter space in the framework of minimal $N=1$ supergravity models with radiative breaking of the electroweak gauge symmetry. Includes the effect of χ - \tilde{t} co-annihilations.
- ⁸ BEREZINSKY 95 and ELLIS 03b places constraints on the SUSY parameter space in the framework of $N=1$ supergravity models with radiative breaking of the electroweak gauge symmetry but non-Universal Higgs masses.
- ⁹ DJOUADI 01, ROSZKOWSKI 01, and BAER 02 place constraints on the SUSY parameter space in the framework of minimal $N=1$ supergravity models with radiative breaking of the electroweak gauge symmetry.
- ¹⁰ ELLIS 02 places constraints on the soft supersymmetry breaking masses in the framework of minimal $N=1$ supergravity models with radiative breaking of the electroweak gauge symmetry.
- ¹¹ LAHANAS 02 places constraints on the SUSY parameter space in the framework of minimal $N=1$ supergravity models with radiative breaking of the electroweak gauge symmetry. Focuses on the role of pseudo-scalar Higgs exchange.
- ¹² BARGER 01c use the cosmic relic density inferred from recent CMB measurements to constrain the parameter space in the framework of minimal $N=1$ supergravity models with radiative breaking of the electroweak gauge symmetry.
- ¹³ ELLIS 01B places constraints on the SUSY parameter space in the framework of minimal $N=1$ supergravity models with radiative breaking of the electroweak gauge symmetry. Focuses on models with large $\tan\beta$.
- ¹⁴ FENG 00 explores cosmologically allowed regions of MSSM parameter space with multi-TeV masses.
- ¹⁵ LAHANAS 00 use the new cosmological data which favor a cosmological constant and its implications on the relic density to constrain the parameter space in the framework of minimal $N=1$ supergravity models with radiative breaking of the electroweak gauge symmetry.
- ¹⁶ ELLIS 98B assumes a universal scalar mass and radiative supersymmetry breaking with universal gaugino masses. The upper limit to the LSP mass is increased due to the inclusion of $\chi - \tilde{\tau}_R$ coannihilations.
- ¹⁷ EDSJO 97 included all coannihilation processes between neutralinos and charginos for any neutralino mass and composition.
- ¹⁸ Notes the location of the neutralino Z resonance and h resonance annihilation corridors in minimal supergravity models with radiative electroweak breaking.
- ¹⁹ BEREZINSKY 95 and ELLIS 02c places constraints on the SUSY parameter space in the framework of $N=1$ supergravity models with radiative breaking of the electroweak gauge symmetry but non-Universal Higgs masses.
- ²⁰ Mass of the bino (=LSP) is limited to $m_{\tilde{B}} \lesssim 350$ GeV for $m_t = 174$ GeV.
- ²¹ DREES 93, KELLEY 93 compute the cosmic relic density of the LSP in the framework of minimal $N=1$ supergravity models with radiative breaking of the electroweak gauge symmetry.
- ²² FALK 93 relax the upper limit to the LSP mass by considering sfermion mixing in the MSSM.
- ²³ MIZUTA 93 include coannihilations to compute the relic density of Higgsino dark matter.
- ²⁴ LOPEZ 92 calculate the relic LSP density in a minimal SUSY GUT model.
- ²⁵ MCDONALD 92 calculate the relic LSP density in the MSSM including exact tree-level annihilation cross sections for all two-body final states.
- ²⁶ GRIEST 91 improve relic density calculations to account for coannihilations, pole effects, and threshold effects.
- ²⁷ NOJIRI 91 uses minimal supergravity mass relations between squarks and sleptons to narrow cosmologically allowed parameter space.
- ²⁸ Mass of the bino (=LSP) is limited to $m_{\tilde{B}} \lesssim 350$ GeV for $m_t \leq 200$ GeV. Mass of the higgsino (=LSP) is limited to $m_{\tilde{H}} \lesssim 1$ TeV for $m_t \leq 200$ GeV.
- ²⁹ ROSZKOWSKI 91 calculates LSP relic density in mixed gaugino/higgsino region.

See key on page 373

Searches Particle Listings

Supersymmetric Particle Searches

³⁰ Mass of the bino (=LSP) is limited to $m_{\tilde{B}} \lesssim 550$ GeV. Mass of the higgsino (=LSP) is limited to $m_{\tilde{H}} \lesssim 3.2$ TeV.

³¹ KRAUSS 83 finds $m_{\tilde{\gamma}}$ not 30 eV to 2.5 GeV. KRAUSS 83 takes into account the gravitino decay. Find that limits depend strongly on reheated temperature. For example a new allowed region $m_{\tilde{\gamma}} = 4\text{--}20$ MeV exists if $m_{\text{gravitino}} < 40$ TeV. See figure 2.

Unstable $\tilde{\chi}_1^0$ (Lightest Neutralino) MASS LIMIT

Unless otherwise stated, results in this section assume spectra and production rates as evaluated in the MSSM. Unless otherwise stated, the goldstino or gravitino mass $m_{\tilde{G}}$ is assumed to be negligible relative to all other masses. In the following, \tilde{G} is assumed to be undetected and to give rise to a missing energy (\cancel{E}) signature.

VALUE (GeV)	CL%	DOCUMENT ID	TECN	COMMENT
>125	95	¹ ABAZOV	08F D0	$p\bar{p} \rightarrow \tilde{\chi}\tilde{\chi}, \tilde{\chi}=\tilde{\chi}_2^0, \tilde{\chi}_1^\pm, \tilde{\chi}_1^0 \rightarrow \gamma\tilde{G}$, GMSB
		² ABULENCIA	07H CDF	$R, L\tilde{L}\tilde{E}$
		³ ABULENCIA	07P CDF	$\tilde{\chi}_1^0 \rightarrow \gamma\tilde{G}$, GMSB
		⁴ ABAZOV	06D D0	$R, L\tilde{L}\tilde{E}$
		⁵ ABAZOV	06P D0	R, λ_{122}
> 96.8	95	⁶ ABBIENDI	06B OPAL	$e^+e^- \rightarrow \tilde{B}\tilde{B}, (\tilde{B} \rightarrow \tilde{G}\gamma)$
>108	95	⁷ ABAZOV	05A D0	Superseded by ABAZOV 08F
		⁸ ABDALLAH	05B DLPH	$e^+e^- \rightarrow \tilde{G}\tilde{\chi}_1^0, (\tilde{\chi}_1^0 \rightarrow \tilde{G}\gamma)$
> 96	95	⁹ ABDALLAH	05B DLPH	$e^+e^- \rightarrow \tilde{B}\tilde{B}, (\tilde{B} \rightarrow \tilde{G}\gamma)$
> 93	95	¹⁰ ACOSTA	05E CDF	$p\bar{p} \rightarrow \tilde{\chi}\tilde{\chi}, \tilde{\chi}=\tilde{\chi}_2^0, \tilde{\chi}_1^\pm, \tilde{\chi}_1^0 \rightarrow \gamma\tilde{G}$, GMSB
		¹¹ AKTAS	05 H1	$e^\pm p \rightarrow q\tilde{\chi}_1^0, \tilde{\chi}_1^0 \rightarrow \gamma\tilde{G}$, GMSB+ R, L, Q, \bar{D}
		¹² ABBIENDI	04N OPAL	$e^+e^- \rightarrow \gamma\gamma\cancel{E}$
> 66	95	^{13,14} ABDALLAH	04H DLPH	AMS $B, \mu > 0$
> 38.0	95	^{15,16} ABDALLAH	04M DLPH	$R(\overline{U}\overline{D}\overline{D})$
		¹⁷ ACHARD	04E L3	$e^+e^- \rightarrow \tilde{G}\tilde{\chi}_1^0, \tilde{\chi}_1^0 \rightarrow \tilde{G}\gamma$
> 99.5	95	¹⁸ ACHARD	04E L3	$e^+e^- \rightarrow \tilde{B}\tilde{B}, (\tilde{B} \rightarrow \tilde{G}\gamma)$
> 89	95	¹⁹ ABDALLAH	03D DLPH	$e^+e^- \rightarrow \tilde{\chi}_1^0\tilde{\chi}_1^0$, GMSB, $m(\tilde{G}) < 1\text{eV}$
		²⁰ HEISTER	03C ALEP	$e^+e^- \rightarrow \tilde{B}\tilde{B}, (\tilde{B} \rightarrow \tilde{G}\gamma)$
		²¹ HEISTER	03C ALEP	$e^+e^- \rightarrow \tilde{G}\tilde{\chi}_1^0, (\tilde{\chi}_1^0 \rightarrow \tilde{G}\gamma)$
> 39.9	95	²² ACHARD	02 L3	R, MSUGRA
> 92	95	²³ HEISTER	02R ALEP	short lifetime
> 54	95	²³ HEISTER	02R ALEP	any lifetime
> 85	95	²⁴ ABBIENDI	01 OPAL	$e^+e^- \rightarrow \tilde{\chi}_1^0\tilde{\chi}_1^0$, GMSB, $\tan\beta=2$
> 76	95	²⁴ ABBIENDI	01 OPAL	$e^+e^- \rightarrow \tilde{\chi}_1^0\tilde{\chi}_1^0$, GMSB, $\tan\beta=20$
> 32.5	95	²⁵ ACCIARRI	01 L3	R , all $m_0, 0.7 \leq \tan\beta \leq 40$
		²⁶ ADAMS	01 NTEV	$\tilde{\chi}^0 \rightarrow \mu\mu\nu, R, L\tilde{L}\tilde{E}$
> 29	95	²⁷ ABBIENDI	99T OPAL	$e^+e^- \rightarrow \tilde{\chi}_1^0\tilde{\chi}_1^0, R, m_0=500$ GeV, $\tan\beta > 1.2$
> 88.2	95	²⁸ ACCIARRI	99R L3	Superseded by ACHARD 04E
> 29	95	²⁹ ACCIARRI	99R L3	Superseded by ACHARD 04E
		³⁰ BARATE	99E ALEP	$R, L, Q, \bar{D}, \tan\beta=1.41, m_0=500$ GeV
		³¹ ABREU	98 DLPH	$e^+e^- \rightarrow \tilde{\chi}_1^0\tilde{\chi}_1^0, (\tilde{\chi}_1^0 \rightarrow \gamma\tilde{G})$
> 23	95	³² BARATE	98S ALEP	$R, L\tilde{L}\tilde{E}$
		³³ ELLIS	97 THEO	$e^+e^- \rightarrow \tilde{\chi}_1^0\tilde{\chi}_1^0, \tilde{\chi}_1^0 \rightarrow \gamma\tilde{G}$
		³⁴ CABIBBO	81 COSM	

¹ ABAZOV 08F looked in 1.1 fb^{-1} of $p\bar{p}$ collisions at $\sqrt{s} = 1.96$ TeV for diphoton events with large \cancel{E}_T . They may originate from the production of $\tilde{\chi}^\pm$ in pairs or associated to a $\tilde{\chi}_1^0$, decaying to a $\tilde{\chi}_1^0$ which itself decays promptly in GMSB to $\tilde{\chi}_1^0 \rightarrow \gamma\tilde{G}$. No significant excess was found compared to the background expectation. A limit is derived on the masses of SUSY particles in the GMSB framework for $M = 2\Lambda, N = 1, \tan\beta = 15$ and $\mu > 0$, see Figure 2. It also excludes $\Lambda < 91.5$ TeV. Supersedes the results of ABAZOV 05A.

² ABULENCIA 07H searched in 346 pb^{-1} of $p\bar{p}$ collisions at $\sqrt{s} = 1.96$ TeV for events with at least three leptons (e or μ) from the decay of $\tilde{\chi}_1^0$ via $L\tilde{L}\tilde{E}$ couplings. The results are consistent with the hypothesis of no signal. Upper limits on the cross-section are extracted and a limit is derived in the framework of mSUGRA on the masses of $\tilde{\chi}_1^0$ and $\tilde{\chi}_1^\pm$, see e.g. their Fig. 3 and Tab. II.

³ ABULENCIA 07P searched in 570 pb^{-1} of $p\bar{p}$ collisions at $\sqrt{s} = 1.96$ TeV for events that contain a time-delayed photon, at least one jet, and large \cancel{E}_T . The time-of-arrival is measured for each electromagnetic tower with a resolution of 0.64 ns (if the correct vertex is used). The number of observed events in the signal region is consistent with the background estimation. An upper limit on the cross section is derived as a function of the $\tilde{\chi}_1^0$ mass and lifetime, shown in their Fig. 2. The comparison with the NLO cross section for GMSB yields the exclusion of the $\tilde{\chi}_1^0$ mass as a function of its lifetime, see Fig. 3.

⁴ ABAZOV 06D looked in 360 pb^{-1} of $p\bar{p}$ collisions at $\sqrt{s} = 1.96$ TeV for events with three leptons originating from the pair production of charginos and neutralinos, followed by R decays mediated by $L\tilde{L}\tilde{E}$ couplings. One coupling is assumed to be dominant at a time. No significant excess was found compared to the background expectation in the $e\ell, \mu\mu\ell$ nor $e\tau$ ($\ell = e, \mu$) final states. Upper limits on the cross-section are extracted in a specific MSUGRA model and a MSSM model without unification of M_1 and M_2 at the GUT scale. A limit is derived on the masses of charginos and neutralinos for both scenarios assuming λ_{ijk} couplings such that the decay length is less than 1 cm, see their Table III and Fig. 4.

⁵ ABAZOV 06P looked in 380 pb^{-1} of $p\bar{p}$ collisions at $\sqrt{s} = 1.96$ TeV for events with at least 2 opposite sign isolated muons which might arise from the decays of neutralinos into $\mu\mu\nu$ via R couplings $L\tilde{L}\tilde{E}$. No events are observed in the decay region defined by a radius between 5 and 20 cm, in agreement with the SM expectation. Limits are set on the cross-section times branching ratio as a function of lifetime, shown in their Fig. 3. This limit excludes the SUSY interpretation of the NuTeV excess of dimuon events reported in ADAMS 01.

⁶ ABBIENDI 06B use 600 pb^{-1} of data from $\sqrt{s} = 189\text{--}209$ GeV. They look for events with diphotons + \cancel{E} final states originating from prompt decays of pair-produced neutralinos in a GMSB scenario with $\tilde{\chi}_1^0$ NLSP. Limits on the cross-section are computed as a function of $m(\tilde{\chi}_1^0)$, see their Fig. 14. The limit on the $\tilde{\chi}_1^0$ mass is for a pure Bino state assuming a prompt decay, with lifetimes up to 10^{-9} s. Supersedes the results of ABBIENDI 04N.

⁷ ABAZOV 05A looked in 263 pb^{-1} of $p\bar{p}$ collisions at $\sqrt{s} = 1.96$ TeV for diphoton events with large \cancel{E}_T . They may originate from the production of $\tilde{\chi}^\pm$ in pairs or associated to a $\tilde{\chi}_2^0$, decaying to a $\tilde{\chi}_1^0$ which itself decays promptly in GMSB to $\tilde{\chi}_1^0 \rightarrow \gamma\tilde{G}$. No significant excess was found at large \cancel{E}_T compared to the background expectation. A limit is derived on the masses of SUSY particles in the GMSB framework for $M = 2\Lambda, N = 1, \tan\beta = 15$ and $\mu > 0$, see Figure 2. It also excludes $\Lambda < 79.6$ TeV. Very similar results are obtained for different choices of parameters, see their Table 2. Supersedes the results of ABBOTT 98.

⁸ ABDALLAH 05B use data from $\sqrt{s} = 180\text{--}209$ GeV. They look for events with single photons + \cancel{E} final states. Limits are computed in the plane $(m(\tilde{G}), m(\tilde{\chi}_1^0))$, shown in their Fig. 9b for a pure Bino state in the GMSB framework and in Fig. 9c for a no-scale supergravity model. Supersedes the results of ABREU 00Z.

⁹ ABDALLAH 05B use data from $\sqrt{s} = 130\text{--}209$ GeV. They look for events with diphotons + \cancel{E} final states and single photons not pointing to the vertex, expected in GMSB when the $\tilde{\chi}_1^0$ is the NLSP. Limits are computed in the plane $(m(\tilde{G}), m(\tilde{\chi}_1^0))$, see their Fig. 10. The lower limit is derived on the $\tilde{\chi}_1^0$ mass for a pure Bino state assuming a prompt decay and $m_{\tilde{e}_R} = m_{\tilde{e}_L} = 2 m_{\tilde{\tau}_0}$. It improves to 100 GeV for $m_{\tilde{e}_R} = m_{\tilde{e}_L} = 1.1 m_{\tilde{\tau}_0}$ and

the limit in the plane $(m(\tilde{\chi}_1^0), m(\tilde{e}_R))$ is shown in Fig. 10b. For long-lived neutralinos, cross-section limits are displayed in their Fig 11. Supersedes the results of ABREU 00Z.

¹⁰ ACOSTA 05E looked in 202 pb^{-1} of $p\bar{p}$ collisions at $\sqrt{s} = 1.96$ TeV for diphoton events with large \cancel{E}_T . They may originate from the production of $\tilde{\chi}^\pm$ in pairs or associated to a $\tilde{\chi}_2^0$, decaying to a $\tilde{\chi}_1^0$ which itself decays promptly in GMSB to $\tilde{\chi}_1^0 \rightarrow \gamma\tilde{G}$. No events are selected at large \cancel{E}_T compared to the background expectation. A limit is derived on the masses of SUSY particles in the GMSB framework for $M = 2\Lambda, N = 1, \tan\beta = 15$ and $\mu > 0$, see Figure 2. It also excludes $\Lambda < 69$ TeV. Supersedes the results of ABE 99i.

¹¹ AKTAS 05 data collected at 319 GeV with 64.3 pb^{-1} of e^+p and 13.5 pb^{-1} of $e-p$. They look for R resonant $\tilde{\chi}_1^0$ production via t -channel exchange of a \tilde{e} , followed by prompt GMSB decay of the $\tilde{\chi}_1^0$ to $\gamma\tilde{G}$. Upper limits at 95% on the cross section are derived, see their Figure 4, and compared to two example scenarios. In Figure 5, they display 95% exclusion limits in the plane of $M(\tilde{\chi}_1^0)$ versus $M(\tilde{e}_L) - M(\tilde{\chi}_1^0)$ for the two scenarios and several values of the χ' Yukawa coupling.

¹² ABBIENDI 04N use data from $\sqrt{s} = 189\text{--}209$ GeV, setting limits on $\sigma(e^+e^- \rightarrow X X) \times B^2(X \rightarrow Y \gamma)$, with Y invisible (see their Fig. 4). Limits on $\tilde{\chi}_1^0$ masses for a specific model are given. Supersedes the results of ABBIENDI, G 00D.

¹³ ABDALLAH 04H use data from LEP 1 and $\sqrt{s} = 192\text{--}208$ GeV. They re-use results or re-analyze the data from ABDALLAH 03M to put limits on the parameter space of anomaly-mediated supersymmetry breaking (AMS B), which is scanned in the region $1 < m_{3/2} < 50$ TeV, $0 < m_0 < 1000$ GeV, $1.5 < \tan\beta < 35$, both signs of μ . The constraints are obtained from the searches for mass degenerate chargino and neutralino, for SM-like and invisible Higgs, for leptonically decaying charginos and from the limit on non-SM Z width of 3.2 MeV. The limit is for $m_t = 174.3$ GeV (see Table 2 for other m_t values).

¹⁴ The limit improves to 73 GeV for $\mu < 0$.

¹⁵ ABDALLAH 04M use data from $\sqrt{s} = 192\text{--}208$ GeV to derive limits on sparticle masses under the assumption of R with $L\tilde{L}\tilde{E}$ or $\overline{U}\overline{D}\overline{D}$ couplings. The results are valid in the ranges $90 < m_0 < 500$ GeV, $0.7 < \tan\beta < 30$, $-200 < \mu < 200$ GeV, $0 < M_2 < 400$ GeV. Supersedes the result of ABREU 01D and ABREU 00U.

¹⁶ The limit improves to 39.5 GeV for $L\tilde{L}\tilde{E}$ couplings.

¹⁷ ACHARD 04E use data from $\sqrt{s} = 189\text{--}209$ GeV. They look for events with single photons + \cancel{E} final states. Limits are computed in the plane $(m(\tilde{G}), m(\tilde{\chi}_1^0))$, shown in their Fig. 8c for a no-scale supergravity model, excluding, e.g., Gravitino masses below 10^{-5} eV for neutralino masses below 172 GeV. Supersedes the results of ACCIARRI 99R.

¹⁸ ACHARD 04E use data from $\sqrt{s} = 189\text{--}209$ GeV. They look for events with diphotons + \cancel{E} final states. Limits are computed in the plane $(m(\tilde{\chi}_1^0), m(\tilde{e}_R))$, see their Fig. 8d. The limit on the $\tilde{\chi}_1^0$ mass is for a pure Bino state assuming a prompt decay, with $m_{\tilde{e}_L} = 1.1 m_{\tilde{\tau}_0}$ and $m_{\tilde{e}_R} = 2.5 m_{\tilde{\tau}_0}$. Supersedes the results of ACCIARRI 99R.

¹⁹ ABDALLAH 03D use data from $\sqrt{s} = 161\text{--}208$ GeV. They look for 4-tau + \cancel{E} final states, expected in GMSB when the $\tilde{\tau}_1$ is the NLSP, and 4-lepton + \cancel{E} final states, expected in the co-NLSP scenario, and assuming a short-lived $\tilde{\chi}_1^0$ ($m(\tilde{G}) < 1$ eV). Limits are computed in the plane $(m(\tilde{\tau}_1), m(\tilde{\chi}_1^0))$ from a scan of the GMSB parameters space, after combining these results with the search for slepton pair production from the same paper to cover prompt decays and for the case of $\tilde{\chi}_1^0$ NLSP from ABREU 00Z. The limit above is reached for a single generation of messengers and when the $\tilde{\tau}_1$ is the NLSP. Stronger limits are obtained when more messenger generations are assumed or when the other sleptons are co-NLSP, see their Fig. 10. Supersedes the results of ABREU 01G.

²⁰ HEISTER 03C use the data from $\sqrt{s} = 189\text{--}209$ GeV to search for $\gamma\cancel{E}_T$ final states with non-pointing photons and $\gamma\gamma\cancel{E}_T$ events. Interpreted in the framework of Minimal GMSB, a lower bound on the $\tilde{\chi}_1^0$ mass is obtained as function of its lifetime. For a laboratory lifetime of less than 3 ns, the limit at 95% CL is 98.8 GeV. For other lifetimes, see their Fig. 5. These results are interpreted in a more general GMSB framework in HEISTER 02R.

²¹ HEISTER 03C use the data from $\sqrt{s} = 189\text{--}209$ GeV to search for $\gamma\cancel{E}_T$ final states. They obtained an upper bound on the cross section for the process $e^+e^- \rightarrow \tilde{G}\tilde{\chi}_1^0$, followed by the prompt decay $\tilde{\chi}_1^0 \rightarrow \gamma\tilde{G}$, shown in their Fig. 4. These results supersede BARATE 98H.

Searches Particle Listings

Supersymmetric Particle Searches

- 22** ACHARD 02 searches for the production of sparticles in the case of \tilde{R} prompt decays with $L\tilde{L}\tilde{E}$ or $U\tilde{D}\tilde{D}$ couplings at $\sqrt{s}=189\text{--}208$ GeV. The search is performed for direct and indirect decays, assuming one coupling at the time to be nonzero. The MSUGRA limit results from a scan over the MSSM parameter space with the assumption of gaugino and scalar mass unification at the GUT scale, imposing simultaneously the exclusions from neutralino, chargino, sleptons, and squarks analyses. The limit holds for $U\tilde{D}\tilde{D}$ couplings and increases to 40.2 GeV for $L\tilde{L}\tilde{E}$ couplings. For L3 limits from $LQ\tilde{D}$ couplings, see ACCIARRI 01.
- 23** HEISTER 02R search for signals of GMSB in the 189–209 GeV data. For the $\tilde{\chi}_1^0$ NLSP scenario, they looked for topologies consisting of $\gamma\gamma\tilde{E}$ or a single γ not pointing to the interaction vertex. For the $\tilde{\ell}$ NLSP case, the topologies consist of $\ell\tilde{L}\tilde{E}$ or $4\ell\tilde{E}$ (from $\tilde{\chi}_1^0\tilde{\chi}_1^0$ production), including leptons with large impact parameters, kinks, or stable particles. Limits are derived from a scan over the GMSB parameters (see their Table 5 for the ranges). The limits are valid whichever is the NLSP. The absolute mass bound on the $\tilde{\chi}_1^0$ for any lifetime includes indirect limits from the chargino search, and from the slepton search HEISTER 02E performed within the MSUGRA framework. A bound for any NLSP and any lifetime of 77 GeV has also been derived by using the constraints from the neutral Higgs search in HEISTER 02. Limits on the universal SUSY mass scale Λ are also derived in the paper. Supersedes the results from BARATE 00G.
- 24** ABBIENDI 01 looked for final states with $\gamma\gamma\tilde{E}$, $\ell\tilde{L}\tilde{E}$, with possibly additional activity and four leptons + \tilde{E} to search for prompt decays of $\tilde{\chi}_1^0$ or $\tilde{\ell}_1$ in GMSB. They derive limits in the plane $(m_{\tilde{\chi}_1^0}, m_{\tilde{\ell}_1})$, see Fig. 6, allowing either the $\tilde{\chi}_1^0$ or a $\tilde{\ell}_1$ to be the NLSP. Two scenarios are considered: $\tan\beta=2$ with the 3 sleptons degenerate in mass and $\tan\beta=20$ where the $\tilde{\tau}_1$ is lighter than the other sleptons. Data taken at $\sqrt{s}=189$ GeV.
- 25** ACCIARRI 01 searches for multi-lepton and/or multi-jet final states from \tilde{R} prompt decays with $L\tilde{L}\tilde{E}$, $LQ\tilde{D}$, or $U\tilde{D}\tilde{D}$ couplings at $\sqrt{s}=189$ GeV. The search is performed for direct and indirect decays of neutralinos, charginos, and scalar leptons, with the $\tilde{\chi}_1^0$ or a $\tilde{\ell}$ as LSP and assuming one coupling to be nonzero at a time. Mass limits are derived using simultaneously the constraints from the neutralino, chargino, and slepton analyses; and the Z^0 width measurements from ACCIARRI 00C in a scan of the parameter space assuming MSUGRA with gaugino and scalar mass universality. Updates and supersedes the results from ACCIARRI 99I.
- 26** ADAMS 01 looked for neutral particles with mass > 2.2 GeV, produced by 900 GeV protons incident on a Beryllium oxide target and decaying through weak interactions into $\mu\mu$, μe , or $\mu\pi$ final states in the decay channel of the NuTeV detector (E815) at Fermilab. The number of observed events is $3\mu\mu$, $0\mu e$, and $0\mu\pi$ with an expected background of 0.069 ± 0.010 , 0.13 ± 0.02 , and 0.14 ± 0.02 , respectively. The $\mu\mu$ events are consistent with the \tilde{R} decay of a neutralino with mass around 5 GeV. However, they share several aspects with ν -interaction backgrounds. An upper limit on the differential production cross section of neutralinos in pp interactions as function of the decay length is given in Fig. 3.
- 27** ABBIENDI 99T searches for the production of neutralinos in the case of R -parity violation with $L\tilde{L}\tilde{E}$, $LQ\tilde{D}$, or $U\tilde{D}\tilde{D}$ couplings using data from $\sqrt{s}=183$ GeV. They investigate topologies with multiple leptons, jets plus leptons, or multiple jets, assuming one coupling at the time to be non-zero and giving rise to direct or indirect decays. Mixed decays (where one particle has a direct, the other an indirect decay) are also considered for the $U\tilde{D}\tilde{D}$ couplings. Upper limits on the cross section are derived which, combined with the constraint from the Z^0 width, allow to exclude regions in the M_2 versus μ plane for any coupling. Limits on the neutralino mass are obtained for non-zero $L\tilde{L}\tilde{E}$ couplings $> 10^{-5}$. The limit disappears for $\tan\beta < 1.2$ and it improves to 50 GeV for $\tan\beta > 20$.
- 28** ACCIARRI 99R searches for $\gamma\tilde{E}$ final states using data from $\sqrt{s}=189$ GeV. From limits on cross section times branching ratio, mass limits are derived in a no-scale SUGRA model, see their Fig. 5. Supersedes the results of ACCIARRI 98V.
- 29** ACCIARRI 99R searches for $\gamma\tilde{E}$ final states using data from $\sqrt{s}=189$ GeV. From a scan over the GMSB parameter space, a limit on the mass is derived under the assumption that the neutralino is the NLSP. Supersedes the results of ACCIARRI 98V.
- 30** BARATE 99E looked for the decay of gauginos via R -violating couplings $LQ\tilde{D}$. The bound is significantly reduced for smaller values of m_0 . Data collected at $\sqrt{s}=130\text{--}172$ GeV.
- 31** ABREU 98 uses data at $\sqrt{s}=161$ and 172 GeV. Upper bounds on $\gamma\tilde{E}$ cross section are obtained. Similar limits on \tilde{E} are also given, relevant for $e^+e^- \rightarrow \tilde{\chi}_1^0\tilde{G}$ production.
- 32** BARATE 98S looked for the decay of gauginos via R -violating coupling $L\tilde{L}\tilde{E}$. The bound improves to 25 GeV if the chargino decays into neutralino which further decays into lepton pairs. Data collected at $\sqrt{s}=130\text{--}172$ GeV.
- 33** ELLIS 97 reanalyzed the LEP2 ($\sqrt{s}=161$ GeV) limits of $\sigma(\gamma\gamma+E_{\text{miss}}) < 0.2$ pb to exclude $m_{\tilde{\chi}_1^0} < 63$ GeV if $m_{\tilde{\ell}_L} = m_{\tilde{\ell}_R} < 150$ GeV and $\tilde{\chi}_1^0$ decays to $\gamma\tilde{G}$ inside detector.
- 34** CABIBBO 81 consider $\tilde{\gamma} \rightarrow \gamma + \text{goldstino}$. Photino must be either light enough (< 30 eV) to satisfy cosmology bound, or heavy enough (> 0.3 MeV) to have disappeared at early universe.

$\tilde{\chi}_2^0, \tilde{\chi}_3^0, \tilde{\chi}_4^0$ (Neutralinos) MASS LIMITS

Neutralinos are unknown mixtures of photinos, z-inos, and neutral higgsinos (the supersymmetric partners of photons and of Z and Higgs bosons). The limits here apply only to $\tilde{\chi}_2^0, \tilde{\chi}_3^0$, and $\tilde{\chi}_4^0$. $\tilde{\chi}_1^0$ is the lightest supersymmetric particle (LSP); see $\tilde{\chi}_1^0$ Mass Limits. It is not possible to quote rigorous mass limits because they are extremely model dependent; i.e. they depend on branching ratios of various $\tilde{\chi}_i^0$ decay modes, on the masses of decay products ($\tilde{e}, \tilde{\gamma}, \tilde{q}, \tilde{g}$), and on the \tilde{e} mass exchanged in $e^+e^- \rightarrow \tilde{\chi}_i^0\tilde{X}_j^0$. Limits arise either from direct searches, or from the MSSM constraints set on the gaugino and higgsino mass parameters M_2 and μ through searches for lighter charginos and neutralinos. Often limits are given as contour plots in the $m_{\tilde{\chi}_i^0} - m_{\tilde{e}}$ plane vs other parameters. When specific assumptions are made, e.g. the neutralino is a pure photino ($\tilde{\gamma}$), pure z-ino (\tilde{Z}), or pure neutral higgsino (\tilde{H}^0), the neutralinos will be labelled as such.

Limits obtained from e^+e^- collisions at energies up to 136 GeV, as well as other limits from different techniques, are now superseded and have not been included in this compilation. They can be found in the 1998 Edition (The European Physical Journal C 3 1 (1998)) of this Review. $\Delta m = m_{\tilde{\chi}_2^0} - m_{\tilde{\chi}_1^0}$.

VALUE (GeV)	CL%	DOCUMENT ID	TECN	COMMENT
> 78	95	1 ABBIENDI	04H OPAL	$\tilde{\chi}_2^0$, all $\tan\beta$, $\Delta m > 5$ GeV, $m_0 > 500$ GeV, $A_0 = 0$
> 62.4	95	2 ABREU	00W DLPH	$\tilde{\chi}_2^0$, $1 \leq \tan\beta \leq 40$, all Δm , all m_0
> 99.9	95	2 ABREU	00W DLPH	$\tilde{\chi}_3^0$, $1 \leq \tan\beta \leq 40$, all Δm , all m_0
> 116.0	95	2 ABREU	00W DLPH	$\tilde{\chi}_4^0$, $1 \leq \tan\beta \leq 40$, all Δm , all m_0
• • • We do not use the following data for averages, fits, limits, etc. • • •				
		3 ABULENCIA	07N CDF	$p\bar{p} \rightarrow \tilde{\chi}_1^\pm \tilde{\chi}_2^0$
		4 ABDALLAH	05B DLPH	$e^+e^- \rightarrow \tilde{\chi}_2^0\tilde{\chi}_1^0$, ($\tilde{\chi}_2^0 \rightarrow \tilde{\chi}_1^0\gamma$)
		5 ACHARD	04E L3	$e^+e^- \rightarrow \tilde{\chi}_2^0\tilde{\chi}_1^0$, ($\tilde{\chi}_2^0 \rightarrow \tilde{\chi}_1^0\gamma$)
> 80.0	95	6 ACHARD	02 L3	$\tilde{\chi}_2^0, \tilde{R}$, MSUGRA
> 107.2	95	6 ACHARD	02 L3	$\tilde{\chi}_3^0, \tilde{R}$, MSUGRA
		7 ABREU	01B DLPH	$e^+e^- \rightarrow \tilde{\chi}_i^0\tilde{\chi}_j^0$
> 68.0	95	8 ACCIARRI	01 L3	$\tilde{\chi}_2^0, \tilde{R}$, all m_0 , $0.7 \leq \tan\beta \leq 40$
> 99.0	95	8 ACCIARRI	01 L3	$\tilde{\chi}_3^0, \tilde{R}$, all m_0 , $0.7 \leq \tan\beta \leq 40$
> 50	95	9 ABREU	00U DLPH	$\tilde{\chi}_2^0, \tilde{R}$ ($L\tilde{L}\tilde{E}$), all Δm , $1 \leq \tan\beta \leq 30$
		10 ABBIENDI	99F OPAL	$e^+e^- \rightarrow \tilde{\chi}_2^0\tilde{\chi}_1^0$ ($\tilde{\chi}_2^0 \rightarrow \gamma\tilde{\chi}_1^0$)
		11 ABBIENDI	99F OPAL	$e^+e^- \rightarrow \tilde{\chi}_2^0\tilde{\chi}_1^0$ ($\tilde{\chi}_2^0 \rightarrow \gamma\tilde{\chi}_1^0$)
		12 ABBOTT	98C D0	$p\bar{p} \rightarrow \tilde{\chi}_1^\pm \tilde{\chi}_2^0$
> 82.2	95	13 ABE	98J CDF	$p\bar{p} \rightarrow \tilde{\chi}_1^\pm \tilde{\chi}_2^0$
> 92	95	14 ACCIARRI	98F L3	H_1^0 , $\tan\beta=1.41$, $M_2 < 500$ GeV
		15 ACCIARRI	98V L3	$e^+e^- \rightarrow \tilde{\chi}_2^0\tilde{\chi}_{1,2}^0$ ($\tilde{\chi}_2^0 \rightarrow \gamma\tilde{\chi}_1^0$)
> 53	95	16 BARATE	98H ALEP	$e^+e^- \rightarrow \tilde{\gamma}\tilde{\gamma}$ ($\tilde{\gamma} \rightarrow \gamma\tilde{H}^0$)
> 74	95	17 BARATE	98J ALEP	$e^+e^- \rightarrow \tilde{\gamma}\tilde{\gamma}$ ($\tilde{\gamma} \rightarrow \gamma\tilde{H}^0$)
		18 ABACHI	96 D0	$p\bar{p} \rightarrow \tilde{\chi}_1^\pm \tilde{\chi}_2^0$
		19 ABE	96K CDF	$p\bar{p} \rightarrow \tilde{\chi}_1^\pm \tilde{\chi}_2^0$

1 ABBIENDI 04H search for charginos and neutralinos in events with acoplanar leptons+jets and multi-jet final states in the 192–209 GeV data, combined with the results on leptonic final states from ABBIENDI 04. The results hold for a scan over the parameter space covering the region $0 < M_2 < 5000$ GeV, $-1000 < \mu < 1000$ GeV and $\tan\beta$ from 1 to 40. This limit supersedes ABBIENDI 00H.

2 ABREU 00W combines data collected at $\sqrt{s}=189$ GeV with results from lower energies. The mass limit is obtained by constraining the MSSM parameter space with gaugino and sfermion mass universality at the GUT scale, using the results of negative direct searches for neutralinos (including cascade decays and $\tilde{\tau}\tilde{\tau}$ final states) from ABREU 01, for charginos from ABREU 00J and ABREU 00T (for all Δm_\pm), and for charged sleptons from ABREU 01B. The results hold for the full parameter space defined by all values of M_2 and $|\mu| \leq 2$ TeV with the $\tilde{\chi}_1^0$ as LSP.

3 ABULENCIA 07N searched in 1 fb^{-1} of $p\bar{p}$ collisions at $\sqrt{s} = 1.96$ TeV for events with two same sign leptons (e or μ) from the decay of $\tilde{\chi}_1^\pm \tilde{\chi}_2^0 X$ and large \cancel{E}_T . A slight excess of 13 events is observed over a SM background expectation of 7.8 ± 1.1 . However, the kinematic distributions do not show any anomalous deviation from expectations in any particular region of parameter space.

4 ABDALLAH 05B use data from $\sqrt{s} = 130\text{--}209$ GeV, looking for events with diphotons + \tilde{E} . Limits on the cross-section are computed in the plane $(m(\tilde{\chi}_2^0), m(\tilde{\chi}_1^0))$, see Fig. 12. Supersedes the results of ABREU 00Z.

5 ACHARD 04E use data from $\sqrt{s} = 189\text{--}209$ GeV, looking for events with diphotons + \tilde{E} . Limits are computed in the plane $(m(\tilde{\chi}_2^0), m(\tilde{e}_R))$, for $\Delta m > 10$ GeV, see Fig. 7. Supersedes the results of ACCIARRI 99R.

6 ACHARD 02 searches for the production of sparticles in the case of \tilde{R} prompt decays with $L\tilde{L}\tilde{E}$ or $U\tilde{D}\tilde{D}$ couplings at $\sqrt{s}=189\text{--}208$ GeV. The search is performed for direct and indirect decays, assuming one coupling at the time to be nonzero. The MSUGRA limit results from a scan over the MSSM parameter space with the assumption of gaugino and scalar mass unification at the GUT scale, imposing simultaneously the exclusions from neutralino, chargino, sleptons, and squarks analyses. The limit of $\tilde{\chi}_3^0$ holds for $U\tilde{D}\tilde{D}$ couplings and increases to 84.0 GeV for $L\tilde{L}\tilde{E}$ couplings. The same $\tilde{\chi}_3^0$ limit holds for both $L\tilde{L}\tilde{E}$ and $U\tilde{D}\tilde{D}$ couplings. For L3 limits from $LQ\tilde{D}$ couplings, see ACCIARRI 01.

7 ABREU 01B used data from $\sqrt{s}=189$ GeV to search for the production of $\tilde{\chi}_i^0\tilde{\chi}_j^0$. They looked for di-jet and di-lepton pairs with \cancel{E} for events from $\tilde{\chi}_i^0\tilde{\chi}_j^0$ with the decay $\tilde{\chi}_j^0 \rightarrow f\tilde{\chi}_1^0$; multi-jet and multi-lepton pairs with or without additional photons to cover the cascade decays $\tilde{\chi}_i^0 \rightarrow f\tilde{\chi}_2^0$, followed by $\tilde{\chi}_j^0 \rightarrow f\tilde{\chi}_1^0$ or $\tilde{\chi}_j^0 \rightarrow \gamma\tilde{\chi}_1^0$; multi-tau final states from $\tilde{\chi}_2^0 \rightarrow \tilde{\tau}\tilde{\tau}$ with $\tilde{\tau} \rightarrow \tau\tilde{\chi}_1^0$. See Figs. 9 and 10 for limits on the (μ, M_2) plane for $\tan\beta=1.0$ and different values of m_0 .

8 ACCIARRI 01 searches for multi-lepton and/or multi-jet final states from \tilde{R} prompt decays with $L\tilde{L}\tilde{E}$, $LQ\tilde{D}$, or $U\tilde{D}\tilde{D}$ couplings at $\sqrt{s}=189$ GeV. The search is performed for direct and indirect decays of neutralinos, charginos, and scalar leptons, with the $\tilde{\chi}_1^0$ or a $\tilde{\ell}$ as LSP and assuming one coupling to be nonzero at a time. Mass limits are derived using simultaneously the constraints from the neutralino, chargino, and slepton analyses; and the Z^0 width measurements from ACCIARRI 00C in a scan of the parameter space assuming MSUGRA with gaugino and scalar mass universality. Updates and supersedes the results from ACCIARRI 99I.

9 ABREU 00U searches for the production of charginos and neutralinos in the case of R -parity violation with $L\tilde{L}\tilde{E}$ couplings, using data from $\sqrt{s}=189$ GeV. They investigate topologies with multiple leptons or jets plus leptons, assuming one coupling to be nonzero at the time and giving rise to direct or indirect decays. Limits are obtained in the M_2 versus μ plane and a limit on the neutralino mass is derived from a scan over the parameters m_0 and $\tan\beta$.

See key on page 373

Searches Particle Listings

Supersymmetric Particle Searches

- 10** ABBIENDI 99F looked for $\gamma\bar{\ell}$ final states at $\sqrt{s}=183$ GeV. They obtained an upper bound on the cross section for the production $e^+e^- \rightarrow \tilde{\chi}_2^0\tilde{\chi}_1^0$ followed by the prompt decay $\tilde{\chi}_2^0 \rightarrow \gamma\tilde{\chi}_1^0$ of 0.075–0.80 pb in the region $m_{\tilde{\chi}_2^0} + m_{\tilde{\chi}_1^0} > m_Z$, $m_{\tilde{\chi}_2^0} = 91$ –183 GeV, and $\Delta m > 5$ GeV. See Fig. 7 for explicit limits in the $(m_{\tilde{\chi}_2^0}, m_{\tilde{\chi}_1^0})$ plane.
- 11** ABBIENDI 99F looked for $\gamma\gamma\bar{\ell}$ final states at $\sqrt{s}=183$ GeV. They obtained an upper bound on the cross section for the production $e^+e^- \rightarrow \tilde{\chi}_2^0\tilde{\chi}_2^0$ followed by the prompt decay $\tilde{\chi}_2^0 \rightarrow \gamma\tilde{\chi}_1^0$ of 0.08–0.37 pb for $m_{\tilde{\chi}_2^0} = 45$ –81.5 GeV, and $\Delta m > 5$ GeV. See Fig. 11 for explicit limits in the $(m_{\tilde{\chi}_2^0}, m_{\tilde{\chi}_1^0})$ plane.
- 12** ABBOTT 98C searches for trilepton final states ($\ell=e,\mu$). See footnote to ABBOTT 98C in the Chargino Section for details on the assumptions. Assuming a negligible decay rate of $\tilde{\chi}_1^\pm$ and $\tilde{\chi}_2^0$ to quarks, they obtain $m_{\tilde{\chi}_2^0} \gtrsim 103$ GeV.
- 13** ABE 98J searches for trilepton final states ($\ell=e,\mu$). See footnote to ABE 98J in the Chargino Section for details on the assumptions. The quoted result for $m_{\tilde{\chi}_2^0}$ corresponds to the best limit within the selected range of parameters, obtained for $m_{\tilde{q}} > m_{\tilde{g}}$, $\tan\beta=2$, and $\mu=-600$ GeV.
- 14** ACCIARRI 98F is obtained from direct searches in the $e^+e^- \rightarrow \tilde{\chi}_{1,2}^0\tilde{\chi}_2^0$ production channels, and indirectly from $\tilde{\chi}_1^\pm$ and $\tilde{\chi}_1^0$ searches within the MSSM. See footnote to ACCIARRI 98F in the Chargino Section for further details on the assumptions. Data taken at $\sqrt{s} = 130$ –172 GeV.
- 15** ACCIARRI 98V looked for $\gamma(\gamma)\bar{\ell}$ final states at $\sqrt{s}=183$ GeV. They obtained an upper bound on the cross section for the production $e^+e^- \rightarrow \tilde{\chi}_2^0\tilde{\chi}_{1,2}^0$ followed by the prompt decay $\tilde{\chi}_2^0 \rightarrow \gamma\tilde{\chi}_1^0$. See Figs. 4a and 6a for explicit limits in the $(m_{\tilde{\chi}_2^0}, m_{\tilde{\chi}_1^0})$ plane.
- 16** BARATE 98H looked for $\gamma\gamma\bar{\ell}$ final states at $\sqrt{s} = 161,172$ GeV. They obtained an upper bound on the cross section for the production $e^+e^- \rightarrow \tilde{\chi}_2^0\tilde{\chi}_2^0$ followed by the prompt decay $\tilde{\chi}_2^0 \rightarrow \gamma\tilde{\chi}_1^0$ of 0.4–0.8 pb for $m_{\tilde{\chi}_2^0} = 10$ –80 GeV. The bound above is for the specific case of $\tilde{\chi}_1^0 = \tilde{H}^0$ and $\tilde{\chi}_2^0 = \tilde{\gamma}$ and $m_{\tilde{e}_R} = 100$ GeV. See Fig. 6 and 7 for explicit limits in the $(\tilde{\chi}_2^0, \tilde{\chi}_1^0)$ plane and in the $(\tilde{\chi}_2^0, \tilde{e}_R)$ plane.
- 17** BARATE 98I looked for $\gamma\gamma\bar{\ell}$ final states at $\sqrt{s} = 161$ –183 GeV. They obtained an upper bound on the cross section for the production $e^+e^- \rightarrow \tilde{\chi}_2^0\tilde{\chi}_2^0$ followed by the prompt decay $\tilde{\chi}_2^0 \rightarrow \gamma\tilde{\chi}_1^0$ of 0.08–0.24 pb for $m_{\tilde{\chi}_2^0} < 91$ GeV. The bound above is for the specific case of $\tilde{\chi}_1^0 = \tilde{H}^0$ and $\tilde{\chi}_2^0 = \tilde{\gamma}$ and $m_{\tilde{e}_R} = 100$ GeV.
- 18** ABACHI 96 searches for 3-lepton final states. Efficiencies are calculated using mass relations and branching ratios in the Minimal Supergravity scenario. Results are presented as lower bounds on $\sigma(\tilde{\chi}_1^\pm\tilde{\chi}_2^0) \times \text{B}(\tilde{\chi}_1^\pm \rightarrow \ell\nu\ell\tilde{\chi}_1^0) \times \text{B}(\tilde{\chi}_2^0 \rightarrow \ell^+\ell^-\tilde{\chi}_1^0)$ as a function of $m_{\tilde{\chi}_1^0}$. Limits range from 3.1 pb ($m_{\tilde{\chi}_1^0} = 45$ GeV) to 0.6 pb ($m_{\tilde{\chi}_1^0} = 100$ GeV).
- 19** ABE 96K looked for trilepton events from chargino-neutralino production. They obtained lower bounds on $m_{\tilde{\chi}_2^0}$ as a function of μ . The lower bounds are in the 45–50 GeV range for gaugino-dominant $\tilde{\chi}_2^0$ with negative μ , if $\tan\beta < 10$. See paper for more details of the assumptions.

- > 75 95 ³ ABDALLAH 03M DLPH $\tilde{\chi}_1^\pm, \text{higgsino, all } \Delta m_+, m_{\tilde{\gamma}} > m_{\tilde{\chi}^\pm}$
- > 70 95 ³ ABDALLAH 03M DLPH $\tilde{\chi}_1^\pm, \text{ all } \Delta m_+, m_{\tilde{\gamma}} > 500 \text{ GeV}, M_2 \leq 2M_1 \leq 10M_2$
- > **94** 95 ⁴ ABDALLAH 03M DLPH $\tilde{\chi}_1^\pm, \tan\beta \leq 40, \Delta m_+ > 3 \text{ GeV, all } m_0$
- > 88 95 ⁵ HEISTER 02J ALEP $\tilde{\chi}_1^\pm, \text{ all } \Delta m_+, \text{ large } m_0$
- > 67.7 95 ⁶ ACCIARRI 00D L3 $\tan\beta > 0.7, \text{ all } \Delta m_+, \text{ all } m_0$
- > 69.4 95 ⁷ ACCIARRI 00K L3 $e^+e^- \rightarrow \tilde{\chi}^\pm\tilde{\chi}^\mp, \text{ all } \Delta m_+, \text{ heavy scalars}$
- • • We do not use the following data for averages, fits, limits, etc. • • •
- >229 95 ⁸ AALTONEN 08L CDF $p\bar{p} \rightarrow \tilde{\chi}_1^\pm\tilde{\chi}_2^0$
- ⁹ ABAZOV 08F D0 $p\bar{p} \rightarrow \tilde{\chi}\tilde{\chi}, \tilde{\chi}=\tilde{\chi}_2^0, \tilde{\chi}_1^\pm, \tilde{\chi}_1^0 \rightarrow \gamma\tilde{G}, \text{ GMSB}$
- ¹⁰ AALTONEN 07J CDF $p\bar{p} \rightarrow \tilde{\chi}_1^\pm\tilde{\chi}_2^0$
- ¹¹ ABULENCIA 07H CDF $R, \text{ LLE}$
- ¹² ABULENCIA 07N CDF $p\bar{p} \rightarrow \tilde{\chi}_1^\pm\tilde{\chi}_2^0$
- ¹³ ABAZOV 06D D0 $R, \text{ LLE}$
- >195 95 ¹⁴ ABAZOV 05A D0 $p\bar{p} \rightarrow \tilde{\chi}\tilde{\chi}, \tilde{\chi}=\tilde{\chi}_2^0, \tilde{\chi}_1^\pm, \tilde{\chi}_1^0 \rightarrow \gamma\tilde{G}, \text{ GMSB}$
- >117 95 ¹⁵ ABAZOV 05U D0 $p\bar{p} \rightarrow \tilde{\chi}_1^\pm\tilde{\chi}_2^0$
- >167 95 ¹⁶ ACOSTA 05E CDF $p\bar{p} \rightarrow \tilde{\chi}\tilde{\chi}, \tilde{\chi}=\tilde{\chi}_2^0, \tilde{\chi}_1^\pm, \tilde{\chi}_1^0 \rightarrow \gamma\tilde{G}, \text{ GMSB}$
- > 66 95 ^{17,18} ABDALLAH 04H DLPH AMSB, $\mu > 0$
- >102.5 95 ^{19,20} ABDALLAH 04M DLPH $R(\overline{U}\overline{D})$
- >100 ²¹ ABDALLAH 03D DLPH $e^+e^- \rightarrow \tilde{\chi}_1^\pm\tilde{\chi}_1^\mp (\tilde{\chi}_1^\pm \rightarrow \tilde{\tau}_1\nu_\tau, \tilde{\tau}_1 \rightarrow \tau\tilde{G})$
- >103 95 ²² HEISTER 03G ALEP R decays, $m_0 > 500 \text{ GeV}$
- >102.7 95 ²³ ACHARD 02 L3 $R, \text{ MSUGRA}$
- ²⁴ GHODBANE 02 THEO
- > 94.3 95 ²⁵ ABREU 01C DLPH $\tilde{\chi}^\pm \rightarrow \tau J$
- > 93.8 95 ²⁶ ACCIARRI 01 L3 $R, \text{ all } m_0, 0.7 \leq \tan\beta \leq 40$
- >100 95 ²⁷ BARATE 01B ALEP R decays, $m_0 > 500 \text{ GeV}$
- > 91.8 95 ²⁸ ABREU 00V DLPH $e^+e^- \rightarrow \tilde{\chi}_1^\pm\tilde{\chi}_1^\pm (\tilde{\chi}_1^\pm \rightarrow \tilde{\tau}_1\nu_\tau, \tilde{\tau}_1 \rightarrow \tau\tilde{G})$
- ²⁹ CHO 00B THEO EW analysis
- > 76 95 ³⁰ ABBIENDI 99T OPAL $R, m_0=500 \text{ GeV}$
- > 51 95 ³¹ MALTONI 99B THEO EW analysis, $\Delta m_+ \sim 1 \text{ GeV}$
- > 81.5 95 ³² ABE 98J CDF $p\bar{p} \rightarrow \tilde{\ell}^\pm\tilde{\chi}_2^0$
- ³³ ACKERSTAFF 98K OPAL $\tilde{\chi}^+ \rightarrow \ell^+\bar{\ell}$
- ³⁴ ACKERSTAFF 98L OPAL $\Delta m_+ > 3 \text{ GeV}, \Delta m_\nu > 2 \text{ GeV}$
- ³⁵ ACKERSTAFF 98V OPAL light gluino
- ³⁶ CARENA 97 THEO $g_\mu = 2$
- ³⁷ KALINOWSKI 97 THEO $W \rightarrow \tilde{\chi}_1^\pm\tilde{\chi}_1^0$
- ³⁸ ABE 96K CDF $p\bar{p} \rightarrow \tilde{\chi}_1^\pm\tilde{\chi}_2^0$

$\tilde{\chi}_1^\pm, \tilde{\chi}_2^0$ (Charginos) MASS LIMITS

Charginos are unknown mixtures of w -inos and charged higgsinos (the supersymmetric partners of W and Higgs bosons). A lower mass limit for the lightest chargino ($\tilde{\chi}_1^\pm$) of approximately 45 GeV, independent of the field composition and of the decay mode, has been obtained by the LEP experiments from the analysis of the Z width and decays. These results, as well as other now superseded limits from e^+e^- collisions at energies below 136 GeV, and from hadronic collisions, can be found in the 1998 Edition (The European Physical Journal **C3** 1 (1998)) of this Review.

Unless otherwise stated, results in this section assume spectra, production rates, decay modes and branching ratios as evaluated in the MSSM, with gaugino and sfermion mass unification at the GUT scale. These papers generally study production of $\tilde{\chi}_1^0\tilde{\chi}_2^0$, $\tilde{\chi}_1^\pm\tilde{\chi}_1^\mp$ and (in the case of hadronic collisions) $\tilde{\chi}_1^\pm\tilde{\chi}_2^0$ pairs, including the effects of cascade decays. The mass limits on $\tilde{\chi}_1^\pm$ are either direct, or follow indirectly from the constraints set by the non-observation of $\tilde{\chi}_2^0$ states on the gaugino and higgsino MSSM parameters M_2 and μ . For generic values of the MSSM parameters, limits from high-energy e^+e^- collisions coincide with the highest value of the mass allowed by phase-space, namely $m_{\tilde{\chi}_1^\pm} \lesssim \sqrt{s}/2$. At the time of this writing, preliminary and unpublished results from the 2000 run of LEP2 at \sqrt{s} up to ≈ 209 GeV give therefore a lower mass limit of approximately 104 GeV valid for general MSSM models. The limits become however weaker in special regions of the MSSM parameter space where the detection efficiencies or production cross sections are suppressed. For example, this may happen when: (i) the mass differences $\Delta m_+ = m_{\tilde{\chi}_1^\pm} - m_{\tilde{\chi}_1^0}$ or $\Delta m_\nu = m_{\tilde{\chi}_1^\pm} - m_{\tilde{\nu}}$ are very small, and the detection efficiency is reduced; (ii) the electron sneutrino mass is small, and the $\tilde{\chi}_1^\pm$ production rate is suppressed due to a destructive interference between s and t channel exchange diagrams. The regions of MSSM parameter space where the following limits are valid are indicated in the comment lines or in the footnotes.

VALUE (GeV)	CL%	DOCUMENT ID	TECN	COMMENT
>101	95	¹ ABBIENDI 04H	OPAL	all $\tan\beta, \Delta m_+ > 5 \text{ GeV}, m_0 > 500 \text{ GeV}, A_0 = 0$
> 89		² ABBIENDI 03H	OPAL	$0.5 \leq \Delta m_+ \leq 5 \text{ GeV}, \text{ higgsino-like}, \tan\beta=1.5$
> 97.1	95	³ ABDALLAH 03M	DLPH	$\tilde{\chi}_1^\pm, \Delta m_+ \geq 3 \text{ GeV}, m_{\tilde{\nu}} > m_{\tilde{\chi}^\pm}$

¹ ABBIENDI 04H search for charginos and neutralinos in events with acoplanar leptons+jets and multi-jet final states in the 192–209 GeV data, combined with the results on leptonic final states from ABBIENDI 04. The results hold for a scan over the parameter space covering the region $0 < M_2 < 5000 \text{ GeV}, -1000 < \mu < 1000 \text{ GeV}$ and $\tan\beta$ from 1 to 40. This limit supersedes ABBIENDI 00H.

² ABBIENDI 03H used e^+e^- data at $\sqrt{s} = 188$ –209 GeV to search for chargino pair production in the case of small Δm_+ . They select events with an energetic photon, large E and little hadronic or leptonic activity. The bound applies to higgsino-like charginos with zero lifetime and a 100% branching ratio $\tilde{\chi}_1^\pm \rightarrow \tilde{\chi}_1^0 W^\pm$. The mass limit for gaugino-like charginos, in case of non-universal gaugino masses, is of 92 GeV for $m_{\tilde{\nu}} = 1000 \text{ GeV}$ and is lowered to 74 GeV for $m_{\tilde{\nu}} \geq 100 \text{ GeV}$. Limits in the plane $(m_{\tilde{\chi}_1^\pm}, \Delta m_+)$ are shown in Fig. 7. Exclusion regions are also derived for the AMSB scenario in the $(m_{3/2}, \tan\beta)$ plane, see their Fig. 9.

³ ABDALLAH 03M searches for the production of charginos using data from $\sqrt{s} = 192$ to 208 GeV to investigate topologies with multiple leptons, jets plus leptons, multi-jets, or isolated photons. The first limit holds for $\tan\beta \geq 1$ and is obtained at $\Delta m_+ = 3 \text{ GeV}$ in the higgsino region. For $\Delta m_+ \geq 10$ (5) GeV and large m_0 , the limit improves to 102.7 (101.7) GeV. For the region of small Δm_+ , all data from $\sqrt{s} = 130$ to 208 GeV are used to investigate final states with heavy stable charged particles, decay vertices inside the detector and soft topologies with a photon from initial state radiation. The second limit is obtained in the higgsino region, assuming gaugino mass universality at the GUT scale and $1 < \tan\beta < 50$. For the case of non-universality of gaugino masses, the parameter space is scanned in the domain $1 < \tan\beta < 50$ and, for $\Delta m_+ < 3 \text{ GeV}$, for values of M_1, M_2 and μ such that $M_2 \leq 2M_1 \leq 10M_2$ and $|\mu| \geq M_2$. The third limit is obtained in the gaugino region. See Fig. 36 for the dependence of the low Δm_+ limits on Δm_+ . These limits include and update the results of ABREU 00J and ABREU 00T.

⁴ ABDALLAH 03M uses data from $\sqrt{s} = 192$ –208 GeV to obtain limits in the framework of the MSSM with gaugino and sfermion mass universality at the GUT scale. An indirect limit on the mass of charginos is derived by constraining the MSSM parameter space by the results from direct searches for neutralinos (including cascade decays), for charginos and for sleptons. These limits are valid for values of $M_2 < 1 \text{ TeV}, |\mu| \leq 2 \text{ TeV}$ with the $\tilde{\chi}_1^0$ as LSP. Constraints from the Higgs search in the $M_{H_u}^{max}$ scenario assuming $m_t = 174.3 \text{ GeV}$ are included. The quoted limit applies if there is no mixing in the third family or when $m_{\tilde{\tau}_1} - m_{\tilde{\chi}_1^0} > 6 \text{ GeV}$. If mixing is included the limit degrades to 90 GeV. See Fig. 43 for the mass limits as a function of $\tan\beta$. These limits update the results of ABREU 00W.

⁵ HEISTER 02J search for chargino production with small Δm_+ in final states with a hard isolated initial state radiation photon and few low-momentum particles, using 189–208 GeV data. This search is sensitive in the intermediate Δm_+ region. Combined with

Searches Particle Listings

Supersymmetric Particle Searches

- searches for \tilde{E} topologies and for stable charged particles, the above bound is obtained for m_0 larger than few hundred GeV, $1 < \tan\beta < 300$ and holds for any chargino field contents. For light scalars, the general limit reduces to the one from the Z^0 , but under the assumption of gaugino and sfermion mass unification the above bound is recovered. See Figs. 4–6 for the more general dependence of the limits on Δm_{\pm} . Updates BARATE 98x.
- 6 ACCIARRI 00D data collected at $\sqrt{s}=189$ GeV. The results hold over the full parameter space defined by $0.7 \leq \tan\beta \leq 60$, $0 \leq M_2 \leq 2$ TeV, $|\mu| \leq 2$ TeV $m_0 \leq 500$ GeV. The results of slepton searches from ACCIARRI 99W are used to help set constraints in the region of small m_0 . See their Figs. 5 for the $\tan\beta$ and M_2 dependence on the limits. See the text for the impact of a large $B(\tilde{\chi}^{\pm} \rightarrow \tau\tilde{\nu}_{\tau})$ on the result. The region of small Δm_{\pm} is excluded by the analysis of ACCIARRI 00K. Updates ACCIARRI 98f.
- 7 ACCIARRI 00k searches for the production of charginos with small Δm_{\pm} using data from $\sqrt{s}=189$ GeV. They investigate soft final states with a photon from initial state radiation. The results are combined with the limits on prompt decays from ACCIARRI 00b and from heavy stable charged particles from ACCIARRI 99l (see Heavy Charged Lepton Searches). The production and decay branching ratios are evaluated within the MSSM, assuming heavy sfermions. The parameter space is scanned in the domain $1 < \tan\beta < 50$, $0.3 < M_1/M_2 < 50$, and $0 < |\mu| < 2$ TeV. The limit is obtained in the higgsino region and improves to 78.6 GeV for gaugino-like charginos. The limit is unchanged for light scalar quarks. For light $\tilde{\tau}$ or $\tilde{\nu}_{\tau}$, the limit is unchanged in the gaugino-like region and is lowered by 0.8 GeV in the higgsino-like case. For light $\tilde{\mu}$ or $\tilde{\nu}_{\mu}$, the limit is unchanged in the higgsino-like region and is lowered by 0.9 GeV in the gaugino-like region. No direct mass limits are obtained for light \tilde{e} or $\tilde{\nu}_{e}$.
- 8 AALTONEN 08L searched in 0.7 to 1.0 fb^{-1} of $p\bar{p}$ collisions at $\sqrt{s} = 1.96$ TeV for events with one high- p_T electron or muon and two additional leptons (e or μ) from the decay of $\tilde{\chi}_1^{\pm} \tilde{\chi}_2^0 X$. The selected number of events is consistent with the SM background expectation. The data are used to constrain the cross section times branching ratio as a function of the $\tilde{\chi}_1^{\pm}$ mass. The results are compared to three MSSM scenarios. An exclusion on chargino and neutralino production is only obtained in a scenario of no mixing between sleptons, yielding nearly equal branching ratios to all three lepton flavors. It amounts to $m_{\tilde{\chi}_1^{\pm}} > 151$ GeV, while the analysis is not sensitive to chargino masses below about 110 GeV. The analyses have been combined with the analyses of AALTONEN 07J and ABULENCIA 07N. The observed limits for the combination are less stringent than the one obtained for the high- p_T analysis due to slight excesses in the other channels.
- 9 ABAZOV 08f looked in 1.1 fb^{-1} of $p\bar{p}$ collisions at $\sqrt{s} = 1.96$ TeV for diphoton events with large E_T . They may originate from the production of $\tilde{\chi}^{\pm}$ in pairs or associated to a $\tilde{\chi}_2^0$, decaying to a $\tilde{\chi}_1^0$ which itself decays promptly in GMSB to $\tilde{\chi}_1^0 \rightarrow \gamma\tilde{G}$. No significant excess was found compared to the background expectation. A limit is derived on the masses of SUSY particles in the GMSB framework for $M = 2\Lambda$, $N = 1$, $\tan\beta = 15$ and $\mu > 0$, see Figure 2. It also excludes $\Lambda < 91.5$ TeV. Supersedes the results of ABAZOV 05a.
- 10 AALTONEN 07J searched in 0.7 to 1.1 fb^{-1} of $p\bar{p}$ collisions at $\sqrt{s} = 1.96$ TeV for events with either two same sign leptons (e or μ) or trileptons from the decay of $\tilde{\chi}_1^{\pm} \tilde{\chi}_2^0 X$ and large E_T . The selected number of events is consistent with the SM background expectation. The data are used to constrain the cross section times branching ratio as a function of the $\tilde{\chi}_1^{\pm}$ mass. The results, shown in their Fig. 2, are compared to several MSSM scenarios. The strongest exclusion is in the case of no mixing between sleptons, yielding nearly equal branching ratios to all three lepton flavors, and amounting to $m_{\tilde{\chi}_1^{\pm}} > 129$ GeV. This analysis includes the same sign dilepton analysis of ABULENCIA 07N.
- 11 ABULENCIA 07H searched in 346 pb^{-1} of $p\bar{p}$ collisions at $\sqrt{s} = 1.96$ TeV for events with at least three leptons (e or μ) from the decay of $\tilde{\chi}_1^0$ via $L\tilde{E}$ couplings. The results are consistent with the hypothesis of no signal. Upper limits on the cross-section are extracted and a limit is derived in the framework of mSUGRA on the masses of $\tilde{\chi}_1^0$ and $\tilde{\chi}_1^{\pm}$, see e.g. their Fig. 3 and Tab. II.
- 12 ABULENCIA 07N searched in 1 fb^{-1} of $p\bar{p}$ collisions at $\sqrt{s} = 1.96$ TeV for events with two same sign leptons (e or μ) from the decay of $\tilde{\chi}_1^{\pm} \tilde{\chi}_2^0 X$ and large E_T . A slight excess of 13 events is observed over a SM background expectation of 7.8 ± 1.1 . However, the kinematic distributions do not show any anomalous deviation from expectations in any particular region of parameter space.
- 13 ABAZOV 06D looked in 360 pb^{-1} of $p\bar{p}$ collisions at $\sqrt{s} = 1.96$ TeV for events with three leptons originating from the pair production of charginos and neutralinos, followed by R decays mediated by $L\tilde{E}$ couplings. One coupling is assumed to be dominant at a time. No significant excess was found compared to the background expectation in the $e\bar{e}\ell$, $\mu\bar{\mu}\ell$ nor $e\bar{e}\tau$ ($\ell = e, \mu$) final states. Upper limits on the cross-section are extracted in a specific MSUGRA model and a MSSM model without unification of M_1 and M_2 at the GUT scale. A limit is derived on the masses of charginos and neutralinos for both scenarios assuming λ_{ijk} couplings such that the decay length is less than 1 cm, see their Table III and Fig. 4.
- 14 ABAZOV 05A looked in 263 pb^{-1} of $p\bar{p}$ collisions at $\sqrt{s} = 1.96$ TeV for diphoton events with large E_T . They may originate from the production of $\tilde{\chi}^{\pm}$ in pairs or associated to a $\tilde{\chi}_2^0$, decaying to a $\tilde{\chi}_1^0$ which itself decays promptly in GMSB to $\tilde{\chi}_1^0 \rightarrow \gamma\tilde{G}$. No significant excess was found at large E_T compared to the background expectation. A limit is derived on the masses of SUSY particles in the GMSB framework for $M = 2\Lambda$, $N = 1$, $\tan\beta = 15$ and $\mu > 0$, see Figure 2. It also excludes $\Lambda < 79.6$ TeV. Very similar results are obtained for different choices of parameters, see their Table 2. Supersedes the results of ABBOTT 98.
- 15 ABAZOV 05U looked in 320 pb^{-1} of $p\bar{p}$ collisions at $\sqrt{s} = 1.96$ TeV for events with large E_T , no jets and three leptons (e, μ, τ) of which at least two are e or μ . No significant excess was found at large E_T compared to the background expectation. A limit is derived on the cross section times branching ratio to 3 leptons, see their Figures 2 and 3. The mass limit assumes gaugino mass universality, three degenerate sleptons and “maximally enhanced” leptonic branching fraction, i.e. a decay dominated by a slepton rather than W/Z . If, in addition, squarks are heavy, the limit improves to 132 GeV. Supersedes the results of ABBOTT 98c.
- 16 ACOSTA 05e looked in 202 pb^{-1} of $p\bar{p}$ collisions at $\sqrt{s}=1.96$ TeV for diphoton events with large E_T . They may originate from the production of $\tilde{\chi}^{\pm}$ in pairs or associated to a $\tilde{\chi}_2^0$, decaying to a $\tilde{\chi}_1^0$ which itself decays promptly in GMSB to $\gamma\tilde{G}$. No events are selected at large E_T compared to the background expectation. A limit is derived on the masses of SUSY particles in the GMSB framework for $M = 2\Lambda$, $N = 1$, $\tan\beta = 15$ and $\mu > 0$, see Figure 2. It also excludes $\Lambda < 69$ TeV. Supersedes the results of ABE 99l.
- 17 ABDALLAH 04H use data from LEP 1 and $\sqrt{s} = 192$ –208 GeV. They re-use results or re-analyze the data from ABDALLAH 03M to put limits on the parameter space of anomaly-mediated supersymmetry breaking (AMSB), which is scanned in the region $1 < m_{3/2} < 50$ TeV, $0 < m_0 < 1000$ GeV, $1.5 < \tan\beta < 35$, both signs of μ . The constraints are obtained from the searches for mass degenerate chargino and neutralino, for SM-like and invisible Higgs, for leptonically decaying charginos and from the limit on non-SM Z width of 3.2 MeV. The limit is for $m_t = 174.3$ GeV (see Table 2 for other m_t values).
- 18 The limit improves to 73 GeV for $\mu < 0$.
- 19 ABDALLAH 04M use data from $\sqrt{s} = 192$ –208 GeV to derive limits on sparticle masses under the assumption of R with $L\tilde{E}$ or $\tilde{U}\tilde{D}\tilde{D}$ couplings. The results are valid in the ranges $90 < m_0 < 500$ GeV, $0.7 < \tan\beta < 30$, $-200 < \mu < 200$ GeV, $0 < M_2 < 400$ GeV. Supersedes the result of ABREU 01D and ABREU 00U.
- 20 The limit improves to 103 GeV for $L\tilde{E}$ couplings.
- 21 ABDALLAH 03D use data from $\sqrt{s} = 183$ –208 GeV. They look for final states with two acoplanar leptons, expected in GMSB when the $\tilde{\tau}_1$ is the NLSP and assuming a short-lived $\tilde{\chi}_1^{\pm}$. Limits are obtained in the plane $(m(\tilde{\tau}), m(\tilde{\chi}_1^{\pm}))$ for different domains of $m(\tilde{G})$, after combining these results with the search for slepton pair production from the same paper. The limit above is valid if the $\tilde{\tau}_1$ is the NLSP for all values of $m(\tilde{G})$ provided $m(\tilde{\chi}_1^{\pm}) - m(\tilde{\tau}_1) \geq 0.3$ GeV. For larger $m(\tilde{G}) > 100$ eV the limit improves to 102 GeV, see their Fig. 11. In the co-NLSP scenario, the limits are 96 and 102 GeV for all $m(\tilde{G})$ and $m(\tilde{G}) > 100$ eV, respectively. Supersedes the results of ABREU 01G.
- 22 HEISTER 03G searches for the production of charginos prompt decays. In the case of R prompt decays with $L\tilde{E}$, $L\tilde{Q}\tilde{D}$ or $\tilde{U}\tilde{D}\tilde{D}$ couplings at $\sqrt{s}=189$ –209 GeV. The search is performed for indirect decays, assuming one coupling at a time to be non-zero. The limit holds for $\tan\beta=1.41$. Excluded regions in the (μ, M_2) plane are shown in their Fig. 3.
- 23 ACHARD 02 searches for the production of sparticles in the case of R prompt decays with $L\tilde{E}$ or $\tilde{U}\tilde{D}\tilde{D}$ couplings at $\sqrt{s}=189$ –208 GeV. The search is performed for direct and indirect decays, assuming one coupling at the time to be nonzero. The MSUGRA limit results from a scan over the MSSM parameter space with the assumption of gaugino and scalar mass unification at the GUT scale, imposing simultaneously the exclusions from neutralino, chargino, sleptons, and squarks analyses. The limit of $\tilde{\chi}_1^{\pm}$ holds for $\tilde{U}\tilde{D}\tilde{D}$ couplings and increases to 103.0 GeV for $L\tilde{E}$ couplings. For L3 limits from $L\tilde{Q}\tilde{D}$ couplings, see ACCIARRI 01.
- 24 GHODBANE 02 reanalyzes DELPHI data at $\sqrt{s}=189$ GeV in the presence of complex phases for the MSSM parameters.
- 25 ABREU 01C looked for τ pairs with \tilde{E} at $\sqrt{s}=183$ –189 GeV to search for the associated production of charginos, followed by the decay $\tilde{\chi}^{\pm} \rightarrow \tau J$, J being an invisible massless particle. See Fig. 6 for the regions excluded in the (μ, M_2) plane.
- 26 ACCIARRI 01 searches for multi-lepton and/or multi-jet final states from R prompt decays with $L\tilde{E}$, $L\tilde{Q}\tilde{D}$, or $\tilde{U}\tilde{D}\tilde{D}$ couplings at $\sqrt{s}=189$ GeV. The search is performed for direct and indirect decays of neutralinos, charginos, and scalar leptons, with the $\tilde{\chi}_1^0$ or a $\tilde{\ell}$ as LSP and assuming one coupling to be nonzero at a time. Mass limits are derived using simultaneously the constraints from the neutralino, chargino, and slepton analyses; and the Z^0 width measurements from ACCIARRI 00c in a scan of the parameter space assuming MSUGRA with gaugino and scalar mass universality. Updates and supersedes the results from ACCIARRI 99l.
- 27 BARATE 01B searches for the production of charginos in the case of R prompt decays with $L\tilde{E}$, $L\tilde{Q}\tilde{D}$, or $\tilde{U}\tilde{D}\tilde{D}$ couplings at $\sqrt{s}=189$ –202 GeV. The search is performed for indirect decays, assuming one coupling at a time to be nonzero. Updates BARATE 00H.
- 28 ABREU 00V use data from $\sqrt{s} = 183$ –189 GeV. They look for final states with two acoplanar leptons, expected in GMSB when the $\tilde{\tau}_1$ is the NLSP and assuming a short-lived $\tilde{\chi}_1^{\pm}$. Limits are obtained in the plane $(m(\tilde{\tau}), m(\tilde{\chi}_1^{\pm}))$ for different domains of $m(\tilde{G})$, after combining these results with the search for slepton pair production in the SUGRA framework from ABREU 01 to cover prompt decays and on stable particle searches from ABREU 00Q. The limit above is valid for all values of $m(\tilde{G})$.
- 29 CHO 00B studied constraints on the MSSM spectrum from precision EW observables. Global fits favour charginos with masses at the lower bounds allowed by direct searches. Allowing for variations of the squark and slepton masses does not improve the fits.
- 30 ABBIENDI 99T searches for the production of neutralinos in the case of R -parity violation with $L\tilde{E}$, $L\tilde{Q}\tilde{D}$, or $\tilde{U}\tilde{D}\tilde{D}$ couplings using data from $\sqrt{s}=183$ GeV. They investigate topologies with multiple leptons, jets plus leptons, or multiple jets, assuming one coupling at the time to be non-zero and giving rise to direct or indirect decays. Mixed decays (where one particle has a direct, the other an indirect decay) are also considered for the $\tilde{U}\tilde{D}\tilde{D}$ couplings. Upper limits on the cross section are derived which, combined with the constraint from the Z^0 width, allow to exclude regions in the M_2 versus μ plane for any coupling. Limits on the chargino mass are obtained for non-zero $L\tilde{E}$ couplings $> 10^{-5}$ and assuming decays via a W^* .
- 31 MALTONI 99B studied the effect of light chargino-neutralino to the electroweak precision data with a particular focus on the case where they are nearly degenerate ($\Delta m_{\pm} \sim 1$ GeV) which is difficult to exclude from direct collider searches. The quoted limit is for higgsino-like case while the bound improves to 56 GeV for wino-like case. The values of the limits presented here are obtained in an update to MALTONI 99B, as described in MALTONI 00.
- 32 ABE 98J searches for trilepton final states ($\ell=e, \mu$). Efficiencies are calculated using mass relations in the Minimal Supergravity scenario, exploring the domain of parameter space defined by $1.1 < \tan\beta < 8$, $-1000 < \mu(\text{GeV}) < -200$, and $m_{\tilde{q}}/m_{\tilde{g}}=1-2$. In this region $m_{\tilde{\chi}_1^{\pm}} \sim m_{\tilde{\chi}_2^0}$ and $m_{\tilde{\chi}_1^{\pm}} \sim 2m_{\tilde{\chi}_1^0}$. Results are presented in Fig. 1 as upper bounds on $\sigma(p\bar{p} \rightarrow \tilde{\chi}_1^{\pm} \tilde{\chi}_2^0) \times B(3\ell)$. Limits range from 0.8 pb ($m_{\tilde{\chi}_1^{\pm}}=50$ GeV) to 0.23 pb ($m_{\tilde{\chi}_1^{\pm}}=100$ GeV) at 95%CL. The gaugino mass unification hypothesis and the assumed mass relation between squarks and gluinos define the value of the leptonic branching ratios. The quoted result corresponds to the best limit within the selected range of parameters, obtained for $m_{\tilde{q}} > m_{\tilde{g}}$, $\tan\beta=2$, and $\mu=-600$ GeV. Mass limits for different values of $\tan\beta$ and μ are given in Fig. 2.
- 33 ACKERSTAFF 98K looked for dilepton+ \tilde{E} final states at $\sqrt{s}=130$ –172 GeV. Limits on $\sigma(e^+e^- \rightarrow \tilde{\chi}_1^{\pm} \tilde{\chi}_1^{\mp}) \times B^2(\ell)$, with $B(\ell)=B(\chi^+ \rightarrow \ell^+ \nu_{\ell} \chi_1^0)$ ($B(\ell)=B(\chi^+ \rightarrow \ell^+ \tilde{\nu}_{\ell})$), are given in Fig. 16 (Fig. 17).
- 34 ACKERSTAFF 98L limit is obtained for $0 < M_2 < 1500$, $|\mu| < 500$ and $\tan\beta > 1$, but remains valid outside this domain. The dependence on the trilinear-coupling parameter A is studied, and found negligible. The limit holds for the smallest value of m_0 consistent

with scalar lepton constraints (ACKERSTAFF 97h) and for all values of m_0 where the condition $\Delta m_{\tilde{\nu}} > 2.0$ GeV is satisfied. $\Delta m_{\nu} > 10$ GeV if $\tilde{\chi}^{\pm} \rightarrow \ell \tilde{\nu}_{\ell}$. The limit improves to 84.5 GeV for $m_0=1$ TeV. Data taken at $\sqrt{s}=130-172$ GeV.

³⁵ ACKERSTAFF 98v excludes the light gluino with universal gaugino mass where charginos, neutralinos decay as $\tilde{\chi}_1^{\pm}, \tilde{\chi}_2^0 \rightarrow q \bar{q} \tilde{g}$ from total hadronic cross sections at $\sqrt{s}=130-172$ GeV. See paper for the case of nonuniversal gaugino mass.

³⁶ CARENA 97 studied the constraints on chargino and sneutrino masses from muon $g-2$. The bound can be important for large $\tan\beta$.

³⁷ KALINOWSKI 97 studies the constraints on the chargino-neutralino parameter space from limits on $\Gamma(W \rightarrow \tilde{\chi}_1^{\pm} \tilde{\chi}_1^0)$ achievable at LEP2. This is relevant when $\tilde{\chi}_1^{\pm}$ is "invisible," i.e., if $\tilde{\chi}_1^{\pm}$ dominantly decays into $\tilde{\nu}_{\ell} \ell^{\pm}$ with little energy for the lepton. Small otherwise allowed regions could be excluded.

³⁸ ABE 96k looked for trilepton events from chargino-neutralino production. The bound on $m_{\tilde{\chi}_1^{\pm}}$ can reach up to 47 GeV for specific choices of parameters. The limits on the combined production cross section times 3-lepton branching ratios range between 1.4 and 0.4 pb, for $45 < m_{\tilde{\chi}_1^{\pm}} < 100$. See the paper for more details on the parameter dependence of the results.

Long-lived $\tilde{\chi}^{\pm}$ (Chargino) MASS LIMITS

Limits on charginos which leave the detector before decaying.

VALUE (GeV)	CL%	DOCUMENT ID	TECN	COMMENT
>102	95	¹ ABBIENDI	03L OPAL	$m_{\tilde{\nu}} > 500$ GeV
none 2-93.0	95	² ABREU	00T DLPH	H^{\pm} or $m_{\tilde{\nu}} > m_{\tilde{\chi}^{\pm}}$

- • • We do not use the following data for averages, fits, limits, etc. • • •

VALUE (GeV)	CL%	DOCUMENT ID	TECN	COMMENT
> 83	95	³ BARATE	97k ALEP	
> 28.2	95	ADACHI	90c TOPZ	

¹ ABBIENDI 03L used e^+e^- data at $\sqrt{s} = 130-209$ GeV to select events with two high momentum tracks with anomalous dE/dx . The excluded cross section is compared to the theoretical expectation as a function of the heavy particle mass in their Fig. 3. The bounds are valid for colorless fermions with lifetime longer than 10^{-6} s. Supersedes the results from ACKERSTAFF 98p.

² ABREU 00T searches for the production of heavy stable charged particles, identified by their ionization or Cherenkov radiation, using data from $\sqrt{s} = 130$ to 189 GeV. These limits include and update the results of ABREU 98p.

³ BARATE 97k uses e^+e^- data collected at $\sqrt{s} = 130-172$ GeV. Limit valid for $\tan\beta = \sqrt{2}$ and $m_{\tilde{\nu}} > 100$ GeV. The limit improves to 86 GeV for $m_{\tilde{\nu}} > 250$ GeV.

$\tilde{\nu}$ (Sneutrino) MASS LIMIT

The limits may depend on the number, $N(\tilde{\nu})$, of sneutrinos assumed to be degenerate in mass. Only $\tilde{\nu}_L$ (not $\tilde{\nu}_R$) is assumed to exist. It is possible that $\tilde{\nu}$ could be the lightest supersymmetric particle (LSP).

We report here, but do not include in the Listings, the limits obtained from the final, but unpublished, fit of the final results obtained by the LEP Collaborations on the invisible width of the Z boson ($\Delta\Gamma_{inv.} < 2.0$ MeV, LEP 03): $m_{\tilde{\nu}} > 43.7$ GeV ($N(\tilde{\nu})=1$) and $m_{\tilde{\nu}} > 44.7$ GeV ($N(\tilde{\nu})=3$).

VALUE (GeV)	CL%	DOCUMENT ID	TECN	COMMENT
> 94	95	¹ ABDALLAH	03M DLPH	$1 \leq \tan\beta \leq 40$, $m_{\tilde{e}_R} - m_{\tilde{\chi}_1^0} > 10$ GeV
> 84	95	² HEISTER	02N ALEP	$\tilde{\nu}_e$, any Δm
> 37.1	95	³ ADRIANI	93M L3	$\Gamma(Z \rightarrow \text{invisible}); N(\tilde{\nu})=1$
> 41	95	⁴ DECAMP	92 ALEP	$\Gamma(Z \rightarrow \text{invisible}); N(\tilde{\nu})=3$
> 36	95	ABREU	91F DLPH	$\Gamma(Z \rightarrow \text{invisible}); N(\tilde{\nu})=1$
> 31.2	95	⁵ ALEXANDER	91F OPAL	$\Gamma(Z \rightarrow \text{invisible}); N(\tilde{\nu})=1$

- • • We do not use the following data for averages, fits, limits, etc. • • •

VALUE (GeV)	CL%	DOCUMENT ID	TECN	COMMENT
> 95	95	⁶ SCHAEEL	07A ALEP	$\tilde{\nu}_{\mu,\tau}, \tilde{R}, (s+t)$ -channel
> 98	95	⁷ ABAZOV	06I D0	$\tilde{R}, \lambda_{211}^I$
> 85	95	⁸ ABDALLAH	06C DLPH	$\tilde{\nu}_{\ell}, \tilde{R}, (s+t)$ -channel
> 85	95	⁹ ABULENCIA	06M CDF	$\tilde{\nu}_{\tau}, \tilde{R}$
> 85	95	¹⁰ ABULENCIA	05A CDF	$p\bar{p} \rightarrow \tilde{\nu} \rightarrow ee, \mu\mu, \tilde{R} LQ\bar{D}$
> 85	95	¹¹ ACOSTA	05R CDF	$p\bar{p} \rightarrow \tilde{\nu} \rightarrow \tau\tau, \tilde{R} LQ\bar{D}$
> 85	95	¹² ABBIENDI	04F OPAL	$\tilde{R}, \tilde{\nu}_{e,\mu,\tau}$
> 95	95	^{13,14} ABDALLAH	04H DLPH	AMSB, $\mu > 0$
> 98	95	¹⁵ ABDALLAH	04M DLPH	$R(LLE), \tilde{\nu}_{\mu}, \text{indirect}, \Delta m > 5$ GeV
> 85	95	¹⁵ ABDALLAH	04M DLPH	$R(LLE), \tilde{\nu}_{\mu}, \text{indirect}, \Delta m > 5$ GeV
> 85	95	¹⁵ ABDALLAH	04M DLPH	$R(LLE), \tilde{\nu}_{\mu}, \text{indirect}, \Delta m > 5$ GeV
> 85	95	¹⁶ ABDALLAH	03F DLPH	$\tilde{\nu}_{\mu,\tau}, \tilde{R} LLE$ decays
> 85	95	¹⁷ ACOSTA	03E CDF	$\tilde{\nu}, \tilde{R}, LQ\bar{D}$ production and LLE decays
> 88	95	¹⁸ HEISTER	03G ALEP	$\tilde{\nu}_e, \tilde{R}$ decays, $\mu = -200$ GeV, $\tan\beta=2$
> 65	95	¹⁸ HEISTER	03G ALEP	$\tilde{\nu}_{\mu,\tau}, \tilde{R}$ decays
> 95	95	¹⁹ ABAZOV	02H D0	$\tilde{R}, \lambda_{211}^I$
> 95	95	²⁰ ACHARD	02 L3	$\tilde{\nu}_e, \tilde{R}$ decays, $\mu = -200$ GeV, $\tan\beta = \sqrt{2}$
> 65	95	²⁰ ACHARD	02 L3	$\tilde{\nu}_{\mu,\tau}, \tilde{R}$ decays
> 149	95	²⁰ ACHARD	02 L3	$\tilde{\nu}, \tilde{R}$ decays, MSUGRA
> 149	95	²¹ HEISTER	02F ALEP	$e\gamma \rightarrow \tilde{\nu}_{\mu,\tau} \ell_k, \tilde{R} LLE$
none 100-264	95	²² ABBIENDI	00R OPAL	$\tilde{\nu}_{\mu,\tau}, \tilde{R}, (s+t)$ -channel
none 100-200	95	²³ ABBIENDI	00R OPAL	$\tilde{\nu}_{\tau}, \tilde{R}, s$ -channel

24	ABREU	00s	DLPH	$\tilde{\nu}_{\ell}, \tilde{R}, (s+t)$ -channel
25	ACCIARRI	00P	L3	$\tilde{\nu}_{\mu,\tau}, \tilde{R}, s$ -channel
26	BARATE	00i	ALEP	Superseded by SCHAEEL 07A
27	BARATE	00i	ALEP	Superseded by SCHAEEL 07A
28	ABBIENDI	99	OPAL	$\tilde{\nu}_e, \tilde{R}, t$ -channel
29	ACCIARRI	97U	L3	$\tilde{\nu}_{\tau}, \tilde{R}, s$ -channel
29	ACCIARRI	97U	L3	$\tilde{\nu}_{\tau}, \tilde{R}, s$ -channel
30	CARENA	97	THEO	$g_{\mu} - 2$
> 46.0	95	³¹ BUSKULIC	95E ALEP	$N(\tilde{\nu})=1, \tilde{\nu} \rightarrow \nu\nu \ell\bar{\ell}$
none 20-25000	95	³² BECK	94A COSM	Stable $\tilde{\nu}$, dark matter
<600	94	³³ FALK	94A COSM	$\tilde{\nu}$ LSP, cosmic abundance
none 3-90	90	³⁴ SATO	91 KAMI	Stable $\tilde{\nu}_e$ or $\tilde{\nu}_{\mu}$, dark matter
none 4-90	90	³⁴ SATO	91 KAMI	Stable $\tilde{\nu}_{\tau}$, dark matter

- ¹ ABDALLAH 03M uses data from $\sqrt{s} = 192-208$ GeV to obtain limits in the framework of the MSSM with gaugino and sfermion mass universality at the GUT scale. An indirect limit on the mass is derived by constraining the MSSM parameter space by the results from direct searches for neutralinos (including cascade decays) and for sleptons. These limits are valid for values of $M_2 < 1$ TeV, $|\mu| \leq 1$ TeV with the $\tilde{\chi}_1^0$ as LSP. The quoted limit is obtained when there is no mixing in the third family. See Fig. 43 for the mass limits as a function of $\tan\beta$. These limits update the results of ABREU 00w.
- ² HEISTER 02N derives a bound on $m_{\tilde{\nu}_e}$ by exploiting the mass relation between the $\tilde{\nu}_e$ and \tilde{e} , based on the assumption of universal GUT scale gaugino and scalar masses $m_{1/2}$ and m_0 and the search described in the \tilde{e} section. In the MSUGRA framework with radiative electroweak symmetry breaking, the limit improves to $m_{\tilde{\nu}_e} > 130$ GeV, assuming a trilinear coupling $A_0=0$ at the GUT scale. See Figs. 5 and 7 for the dependence of the limits on $\tan\beta$.
- ³ ADRIANI 93M limit from $\Delta\Gamma(Z)(\text{invisible}) < 16.2$ MeV.
- ⁴ DECAMP 92 limit is from $\Gamma(\text{invisible})/\Gamma(\ell\ell) = 5.91 \pm 0.15$ ($N_{\nu} = 2.97 \pm 0.07$).
- ⁵ ALEXANDER 91F limit is for one species of $\tilde{\nu}$ and is derived from $\Gamma(\text{invisible, new})/\Gamma(\ell\ell) < 0.38$.
- ⁶ SCHAEEL 07A searches for the s- or t-channel exchange of sneutrinos in the case of \tilde{R} with LLE couplings by studying di-lepton production at $\sqrt{s} = 189-209$ GeV. Limits are obtained on the couplings as a function of the $\tilde{\nu}$ mass, see their Figs. 22-24. The results of this analysis are combined with BARATE 00i.
- ⁷ ABAZOV 06I looked in 380 pb^{-1} of $p\bar{p}$ collisions at $\sqrt{s} = 1.96$ TeV for events with at least 2 muons and 2 jets for s-channel production of $\tilde{\mu}$ or $\tilde{\nu}$ and subsequent decay via \tilde{R} couplings $LQ\bar{D}$. The data are in agreement with the SM expectation. They set limits on resonant slepton production and derive exclusion contours on λ_{211}^I in the mass plane of $\tilde{\ell}$ versus $\tilde{\chi}_1^0$ assuming a MSUGRA model with $\tan\beta = 5$, $\mu < 0$ and $A_0 = 0$, see their Fig. 3. For $\lambda_{211}^I \geq 0.09$ slepton masses up to 358 GeV are excluded. Supersedes the results of ABAZOV 02h.
- ⁸ ABDALLAH 06c searches for anomalies in the production cross sections and forward-backward asymmetries of the $\ell^+ \ell^- (\gamma)$ final states ($\ell = e, \mu, \tau$) from 675 pb^{-1} of e^+e^- data at $\sqrt{s}=130-207$ GeV. Limits are set on the s- and t-channel exchange of sneutrinos in the presence of \tilde{R} with λLLE couplings. For points between the energies at which data were taken, information is obtained from events in which a photon was radiated. Exclusion limits in the $(\lambda, m_{\tilde{\nu}})$ plane are given in Fig. 16. These limits include and update the results of ABREU 00s.
- ⁹ ABULENCIA 06M searched in 344 pb^{-1} of $p\bar{p}$ collisions at $\sqrt{s} = 1.96$ TeV for an excess of events with oppositely charged $e\mu$ pairs. They might be expected in a SUSY model with \tilde{R} where a sneutrino is produced by $LQ\bar{D}$ couplings and decays via LLE couplings, focusing on $\tilde{\nu}_{\tau}$, hence on the λ_{311}^I and λ_{132} constants. No significant excess was found compared to the background expectation. Upper limits on the cross-section times branching ratio are extracted and exclusion regions determined for the $\tilde{\nu}_{\tau}$ mass as a function of both couplings, see their Fig. 3. As an indication, $\tilde{\nu}_{\tau}$ masses are excluded up to 300 GeV for $\lambda_{311}^I \geq 0.01$ and $\lambda_{132} \geq 0.02$.
- ¹⁰ ABULENCIA 05A looked in $\sim 200 \text{ pb}^{-1}$ of $p\bar{p}$ collisions at $\sqrt{s} = 1.96$ TeV for dimuon and dilepton events. They may originate from the \tilde{R} production of a sneutrino decaying to dileptons. No significant excess rate was found compared to the background expectation. A limit is derived on the cross section times branching ratio, B , of $\tilde{\nu} \rightarrow e\mu, \mu\mu$ of 25 fb at high mass, see their Figure 2. Sneutrino masses are excluded at 95% CL below 680, 620, 460 GeV ($e\mu$ channel) and 665, 590, 450 GeV ($\mu\mu$ channel) for a λ' coupling and branching ratio such that $\lambda'^2 B = 0.01, 0.005, 0.001$, respectively.
- ¹¹ ACOSTA 05R looked in 195 pb^{-1} of $p\bar{p}$ collisions at $\sqrt{s} = 1.96$ TeV for ditau events with one identified hadronic tau decay and one other tau decay. They may originate from the \tilde{R} production of a sneutrino decaying to $\tau\tau$. No significant excess rate was found compared to the background expectation, dominated by Drell-Yan. A limit is derived on the cross section times branching ratio, B , of $\tilde{\nu} \rightarrow \tau\tau$, see their Figure 3. Sneutrino masses below 377 GeV are excluded at 95% CL for a λ' coupling to $d\bar{d}$ and branching ratio such that $\lambda'^2 B = 0.01$.
- ¹² ABBIENDI 04F use data from $\sqrt{s} = 189-209$ GeV. They derive limits on sparticle masses under the assumption of \tilde{R} with LLE or $LQ\bar{D}$ couplings. The results are valid for $\tan\beta = 1.5, \mu = -200$ GeV, and a BR for the decay given by CMSSM, assuming no sensitivity to other decays. Limits are quoted for $m_{\tilde{\chi}_1^0} = 60$ GeV and degrade for low-mass $\tilde{\chi}_1^0$. For $\tilde{\nu}_e$ the direct (indirect) limits with LLE couplings are 89 (95) GeV and with $LQ\bar{D}$ they are 89 (88) GeV. For $\tilde{\nu}_{\mu,\tau}$ the direct (indirect) limits with LLE couplings are 79 (81) GeV and with $LQ\bar{D}$ they are 74 (no limit) GeV. Supersedes the results of ABBIENDI 00.
- ¹³ ABDALLAH 04H use data from LEP 1 and $\sqrt{s} = 192-208$ GeV. They re-use results or re-analyze the data from ABDALLAH 03M to put limits on the parameter space of anomaly-mediated supersymmetry breaking (AMSB), which is scanned in the region $1 < m_{3/2} < 50$ TeV, $0 < m_0 < 1000$ GeV, $1.5 < \tan\beta < 35$, both signs of μ . The constraints are obtained from the searches for mass degenerate chargino and neutralino, for SM-like and invisible Higgs, for leptonically decaying charginos and from the limit on non-SM Z width of 3.2 MeV. The limit is for $m_t = 174.3$ GeV (see Table 2 for other m_t values).
- ¹⁴ The limit improves to 114 GeV for $\mu < 0$.
- ¹⁵ ABDALLAH 04M use data from $\sqrt{s} = 189-208$ GeV. The results are valid for $\mu = -200$ GeV, $\tan\beta = 1.5, \Delta m > 5$ GeV and assuming a BR of 1 for the given decay. The limit quoted is for indirect decays using the neutralino constraint of 39.5 GeV, also derived in ABDALLAH 04M. For indirect decays the limit on $\tilde{\nu}_e$ decreases to 96 GeV

Searches Particle Listings

Supersymmetric Particle Searches

- if the constraint from the neutralino is not used and for direct decays it remains 96 GeV. For indirect decays the limit on $\tilde{\nu}_\mu$ decreases to 82 GeV if the constraint from the neutralino is not used and to 83 GeV for direct decays. For indirect decays the limit on $\tilde{\nu}_\tau$ decreases to 82 GeV if the constraint from the neutralino is not used and improves to 91 GeV for direct decays. Supersedes the results of ABREU 00U.
- 16 ABDALLAH 03F looked for events of the type $e^+e^- \rightarrow \tilde{\nu} \rightarrow \tilde{\chi}^0 \nu, \tilde{\chi}^\pm \ell \bar{\nu}$ followed by R decays of the $\tilde{\chi}^0$ via λ_{1j1} ($j = 2, 3$) couplings in the data at $\sqrt{s} = 183\text{--}208$ GeV. From a scan over the SUGRA parameters, they derive upper limits on the λ_{1j1} couplings as a function of the sneutrino mass, see their Figs. 5–8.
- 17 ACOSTA 03E search for $e\mu, e\tau$ and $\mu\tau$ final states, and sets limits on the product of production cross-section and decay branching ratio for a $\tilde{\nu}$ in RPV models (see Fig. 3).
- 18 HEISTER 03G searches for the production of sneutrinos in the case of R prompt decays with $L\bar{L}E, LQ\bar{D}$ or $U\bar{D}D$ couplings at $\sqrt{s} = 189\text{--}209$ GeV. The search is performed for direct and indirect decays, assuming one coupling at a time to be non-zero. The limit holds for indirect $\tilde{\nu}$ decays via $U\bar{D}D$ couplings and $\Delta m > 10$ GeV. Stronger limits are reached for $(\tilde{\nu}_e, \tilde{\nu}_{\mu,\tau})$ for $L\bar{L}E$ direct (100,90) GeV or indirect (98,89) GeV and for $LQ\bar{D}$ direct (–79) GeV or indirect (91,78) GeV couplings. For $L\bar{L}E$ indirect decays, use is made of the bound $m(\tilde{\chi}_1^0) > 23$ GeV from BARATE 98s. Supersedes the results from BARATE 01b.
- 19 ABAZOV 02H looked in 94 pb^{-1} of $p\bar{p}$ collisions at $\sqrt{s}=1.8$ TeV for events with at least 2 muons and 2 jets for s -channel production of $\tilde{\mu}$ or $\tilde{\nu}$ and subsequent decay via R couplings $LQ\bar{D}$. A scan over the MSUGRA parameters is performed to exclude regions of the $(m_0, m_{1/2})$ plane, examples being shown in Fig. 2.
- 20 ACHARD 02 searches for the associated production of sneutrinos in the case of R prompt decays with $L\bar{L}E$ or $U\bar{D}D$ couplings at $\sqrt{s}=189\text{--}208$ GeV. The search is performed for direct and indirect decays, assuming one coupling at a time to be nonzero. The limit holds for direct decays via $L\bar{L}E$ couplings. Stronger limits are reached for $(\tilde{\nu}_e, \tilde{\nu}_{\mu,\tau})$ for $L\bar{L}E$ indirect (99,78) GeV and for $U\bar{D}D$ direct or indirect (99,70) GeV decays. The MSUGRA limit results from a scan over the MSSM parameter space with the assumption of gaugino and scalar mass unification at the GUT scale, imposing simultaneously the exclusions from neutralino, chargino, sleptons, and squarks analyses. The limit holds for $U\bar{D}D$ couplings and increases to 152.7 GeV for $L\bar{L}E$ couplings.
- 21 HEISTER 02F searched for single sneutrino production via $e\gamma \rightarrow \tilde{\nu}_j \ell_k$ mediated by R $L\bar{L}E$ couplings, decaying directly or indirectly via a $\tilde{\chi}_1^0$ and assuming a single coupling to be nonzero at a time. Final states with three leptons and possible \cancel{E}_T due to neutrinos were selected in the 189–209 GeV data. Limits on the couplings λ_{1j1} as a function of the sneutrino mass are shown in Figs. 10–14. The couplings λ_{232} and λ_{233} are not accessible and λ_{121} and λ_{131} are measured with better accuracy in sneutrino resonant production. For all tested couplings, except λ_{133} , the limits are significantly improved compared to the low-energy limits.
- 22 ABBIENDI 00R studied the effect of s - and t -channel τ or μ sneutrino exchange in $e^+e^- \rightarrow e^+e^-$ at $\sqrt{s}=130\text{--}189$ GeV, via the R -parity violating coupling $\lambda_{1j1} L_j L_i e_1^c$ ($i=2$ or 3). The limits quoted here hold for $\lambda_{1j1} > 0.13$, and supersede the results of ABBIENDI 99. See Fig. 11 for limits on $m_{\tilde{\nu}}$ versus coupling.
- 23 ABBIENDI 00R studied the effect of s -channel τ sneutrino exchange in $e^+e^- \rightarrow \mu^+\mu^-$ at $\sqrt{s}=130\text{--}189$ GeV, in presence of the R -parity violating couplings $\lambda_{1j1} L_j L_i e_1^c$ ($i=1$ and 2), with $\lambda_{131}=\lambda_{232}$. The limits quoted here hold for $\lambda_{131} > 0.09$, and supersede the results of ABBIENDI 99. See Fig. 12 for limits on $m_{\tilde{\nu}}$ versus coupling.
- 24 ABREU 00s searches for anomalies in the production cross sections and forward-backward asymmetries of the $\ell^+\ell^-(\gamma)$ final states ($\ell=e,\mu,\tau$) from e^+e^- collisions at $\sqrt{s}=130\text{--}189$ GeV. Limits are set on the s - and t -channel exchange of sneutrinos in the presence of R with $L\bar{L}E$ couplings. For points between the energies at which data were taken, information is obtained from events in which a photon was radiated. Exclusion limits in the $(\lambda, m_{\tilde{\nu}})$ plane are given in Fig. 5. These limits include and update the results of ABREU 99a.
- 25 ACCIARRI 00P use the dilepton total cross sections and asymmetries at $\sqrt{s}=m_Z$ and $\sqrt{s}=130\text{--}189$ GeV data to set limits on the effect of R $L\bar{L}E$ couplings giving rise to μ or τ sneutrino exchange. See their Fig. 5 for limits on the sneutrino mass versus couplings.
- 26 BARATE 00I studied the effect of s -channel and t -channel τ or μ sneutrino exchange in $e^+e^- \rightarrow e^+e^-$ at $\sqrt{s}=130\text{--}183$ GeV, via the R -parity violating coupling $\lambda_{1j1} L_j L_i e_1^c$ ($i=2$ or 3). The limits quoted here hold for $\lambda_{1j1} > 0.1$. See their Fig. 15 for limits as a function of the coupling.
- 27 BARATE 00I studied the effect of s -channel τ sneutrino exchange in $e^+e^- \rightarrow \mu^+\mu^-$ at $\sqrt{s}=130\text{--}183$ GeV, in presence of the R -parity violating coupling $\lambda_{1j1} L_j L_i e_1^c$ ($i=1$ and 2). The limits quoted here hold for $\sqrt{|\lambda_{131}\lambda_{232}|} > 0.2$. See their Fig. 16 for limits as a function of the coupling.
- 28 ABBIENDI 99 studied the effect of t -channel electron sneutrino exchange in $e^+e^- \rightarrow \tau^+\tau^-$ at $\sqrt{s}=130\text{--}183$ GeV, in presence of the R -parity violating couplings $\lambda_{1j1} L_j L_i e_1^c$. The limits quoted here hold for $\lambda_{131} > 0.6$.
- 29 ACCIARRI 97U studied the effect of the s -channel tau-sneutrino exchange in $e^+e^- \rightarrow e^+e^-$ at $\sqrt{s}=m_Z$ and $\sqrt{s}=130\text{--}172$ GeV, via the R -parity violating coupling $\lambda_{1j1} L_j L_i e_1^c$. The limits quoted here hold for $\lambda_{131} > 0.05$. Similar limits were studied in $e^+e^- \rightarrow \mu^+\mu^-$ together with $\lambda_{232}L_2L_3e_2^c$ coupling.
- 30 CARENA 97 studied the constraints on chargino and sneutrino masses from muon $g-2$. The bound can be important for large $\tan\beta$.
- 31 BUSKULIC 95E looked for $Z \rightarrow \tilde{\nu}\tilde{\nu}^*$, where $\tilde{\nu} \rightarrow \nu\chi_1^0$ and χ_1^0 decays via R -parity violating interactions into two leptons and a neutrino.
- 32 BECK 94 limit can be inferred from limit on Dirac neutrino using $\sigma(\tilde{\nu}) = 4\sigma(\nu)$. Also private communication with H.V. Klapdor-Kleingrothaus.
- 33 FALK 94 puts an upper bound on $m_{\tilde{\nu}}$ when $\tilde{\nu}$ is LSP by requiring its relic density does not overclose the Universe.
- 34 SATO 91 search for high-energy neutrinos from the sun produced by annihilation of sneutrinos in the sun. Sneutrinos are assumed to be stable and to constitute dark matter in our galaxy. SATO 91 follow the analysis of NG 87, OLIVE 88, and GAISSER 86.

CHARGED SLEPTONS

This section contains limits on charged scalar leptons ($\tilde{\ell}$, with $\ell=e,\mu,\tau$). Studies of width and decays of the Z boson (use is made here of $\Delta\Gamma_{\text{inv}} < 2.0$ MeV, LEP 00) conclusively rule out $m_{\tilde{\ell}_R}^- < 40$ GeV (41

GeV for $\tilde{\ell}_L$), independently of decay modes, for each individual slepton. The limits improve to 43 GeV (43.5 GeV for $\tilde{\ell}_L$) assuming all 3 flavors to be degenerate. Limits on higher mass sleptons depend on model assumptions and on the mass splitting $\Delta m = m_{\tilde{\ell}} - m_{\tilde{\chi}_1^0}$. The mass and composition

of $\tilde{\chi}_1^0$ may affect the slepton production rate in e^+e^- collisions through t -channel exchange diagrams. Production rates are also affected by the potentially large mixing angle of the lightest mass eigenstate $\tilde{\ell}_1 = \tilde{\ell}_R \sin\theta_{\tilde{\ell}} + \tilde{\ell}_L \cos\theta_{\tilde{\ell}}$. It is generally assumed that only $\tilde{\tau}$ may have significant mixing. The coupling to the Z vanishes for $\theta_{\tilde{\ell}}=0.82$. In the high-energy limit of e^+e^- collisions the interference between γ and Z exchange leads to a minimal cross section for $\theta_{\tilde{\ell}}=0.91$, a value which is sometimes used in the following entries relative to data taken at LEP2. When limits on $m_{\tilde{\ell}_R}$ are quoted, it is understood that limits on $m_{\tilde{\ell}_L}$ are usually at least as strong.

Possibly open decays involving gauginos other than $\tilde{\chi}_1^0$ will affect the detection efficiencies. Unless otherwise stated, the limits presented here result from the study of $\tilde{\ell}^+\tilde{\ell}^-$ production, with production rates and decay properties derived from the MSSM. Limits made obsolete by the recent analyses of e^+e^- collisions at high energies can be found in previous Editions of this Review.

For decays with final state gravitinos (\tilde{G}), $m_{\tilde{G}}$ is assumed to be negligible relative to all other masses.

\tilde{e} (Selectron) MASS LIMIT

VALUE (GeV)	CL%	DOCUMENT ID	TECN	COMMENT
> 97.5		1 ABBIENDI	04 OPAL	$\tilde{e}_R, \Delta m > 11$ GeV, $ \mu > 100$ GeV, $\tan\beta=1.5$
> 94.4		2 ACHARD	04 L3	$\tilde{e}_R, \Delta m > 10$ GeV, $ \mu > 200$ GeV, $\tan\beta \geq 2$
> 71.3		2 ACHARD	04 L3	\tilde{e}_R , all Δm
none 30–94	95	3 ABDALLAH	03M DLPH	$\Delta m > 15$ GeV, $\tilde{e}_R^+ \tilde{e}_R^-$
> 94	95	4 ABDALLAH	03M DLPH	$\tilde{e}_R, 1 \leq \tan\beta \leq 40$, $\Delta m > 10$ GeV
> 95	95	5 HEISTER	02E ALEP	$\Delta m > 15$ GeV, $\tilde{e}_R^+ \tilde{e}_R^-$
> 73	95	6 HEISTER	02N ALEP	\tilde{e}_R , any Δm
> 107	95	6 HEISTER	02N ALEP	\tilde{e}_L , any Δm
••• We do not use the following data for averages, fits, limits, etc. •••				
> 89	95	7 ABBIENDI	04F OPAL	\tilde{R}, \tilde{e}_L
> 92	95	8 ABDALLAH	04M DLPH	\tilde{R}, \tilde{e}_R , indirect, $\Delta m > 5$ GeV
> 93	95	9 HEISTER	03G ALEP	\tilde{e}_R, R decays, $\mu = -200$ GeV, $\tan\beta=2$
> 69	95	10 ACHARD	02 L3	\tilde{e}_R, R decays, $\mu = -200$ GeV, $\tan\beta=\sqrt{2}$
> 92	95	11 BARATE	01 ALEP	$\Delta m > 10$ GeV, $\tilde{e}_R^+ \tilde{e}_R^-$
> 77	95	12 ABBIENDI	00J OPAL	$\Delta m > 5$ GeV, $\tilde{e}_R^+ \tilde{e}_R^-$
> 83	95	13 ABREU	00U DLPH	Superseded by ABDALLAH 04M
> 87	95	14 ABREU	00V DLPH	$\tilde{e}_R \tilde{e}_R$ ($\tilde{e}_R \rightarrow e\tilde{G}$), $m_{\tilde{G}} > 10$ eV
> 85	95	15 BARATE	00G ALEP	$\tilde{\ell}_R \rightarrow \ell\tilde{G}$, any $\tau(\tilde{\ell}_R)$
> 29.5	95	16 ACCIARRI	99J L3	\tilde{e}_R, R , $\tan\beta \geq 2$
> 56	95	17 ACCIARRI	98F L3	$\Delta m > 5$ GeV, $\tilde{e}_R^+ \tilde{e}_R^-$, $\tan\beta \geq 1.41$
> 77	95	18 BARATE	98K ALEP	Any Δm , $\tilde{e}_R^+ \tilde{e}_R^-$, $\tilde{e}_R \rightarrow e\gamma\tilde{G}$
> 77	95	19 BREITWEG	98 ZEUS	$m_{\tilde{q}}=m_{\tilde{e}}$, $m(\tilde{\chi}_1^0)=40$ GeV
> 63	95	20 AID	96c H1	$m_{\tilde{q}}=m_{\tilde{e}}$, $m_{\tilde{\chi}_1^0}=35$ GeV

- 1 ABBIENDI 04 search for $\tilde{e}_R \tilde{e}_R$ production in acoplanar di-electron final states in the 183–208 GeV data. See Fig. 13 for the dependence of the limits on $m_{\tilde{\chi}_1^0}$ and for the limit at $\tan\beta=35$. This limit supersedes ABBIENDI 00G.
- 2 ACHARD 04 search for $\tilde{e}_R \tilde{e}_L$ and $\tilde{e}_R \tilde{e}_R$ production in single- and acoplanar di-electron final states in the 192–209 GeV data. Absolute limits on $m_{\tilde{e}_R}$ are derived from a scan over the MSSM parameter space with universal GUT scale gaugino and scalar masses $m_{1/2}$ and m_0 , $1 \leq \tan\beta \leq 60$ and $-2 \leq \mu \leq 2$ TeV. See Fig. 4 for the dependence of the limits on $m_{\tilde{\chi}_1^0}$. This limit supersedes ACCIARRI 99W.
- 3 ABDALLAH 03M looked for acoplanar dielectron + \cancel{E} final states at $\sqrt{s} = 189\text{--}208$ GeV. The limit assumes $\mu = -200$ GeV and $\tan\beta=1.5$ in the calculation of the production cross section and $B(\tilde{e} \rightarrow e\tilde{\chi}_1^0)$. See Fig. 15 for limits in the $(m_{\tilde{e}_R}, m_{\tilde{\chi}_1^0})$ plane. These limits include and update the results of ABREU 01
- 4 ABDALLAH 03M uses data from $\sqrt{s} = 192\text{--}208$ GeV to obtain limits in the framework of the MSSM with gaugino and sfermion mass universality at the GUT scale. An indirect limit on the mass is derived by constraining the MSSM parameter space by the results from direct searches for neutralinos (including cascade decays) and for sleptons. These limits are valid for values of $M_2 < 1$ TeV, $|\mu| \leq 1$ TeV with the $\tilde{\chi}_1^0$ as LSP. The quoted limit is obtained when there is no mixing in the third family. See Fig. 43 for the mass limits as a function of $\tan\beta$. These limits update the results of ABREU 00W.
- 5 HEISTER 02E looked for acoplanar dielectron + \cancel{E}_T final states from e^+e^- interactions between 183 and 209 GeV. The mass limit assumes $\mu < -200$ GeV and $\tan\beta=2$ for the production cross section and $B(\tilde{e} \rightarrow e\tilde{\chi}_1^0)=1$. See their Fig. 4 for the dependence of the limit on Δm . These limits include and update the results of BARATE 01.

See key on page 373

Searches Particle Listings

Supersymmetric Particle Searches

- ⁶ HEISTER 02n search for $\tilde{e}_L \tilde{e}_L$ and $\tilde{e}_R \tilde{e}_R$ production in single- and acoplanar di-electron final states in the 183–208 GeV data. Absolute limits on $m_{\tilde{e}_R}$ are derived from a scan over the MSSM parameter space with universal GUT scale gaugino and scalar masses $m_{1/2}$ and m_0 , $1 \leq \tan\beta \leq 50$ and $-10 \leq \mu \leq 10$ TeV. The region of small $|\mu|$, where cascade decays are important, is covered by a search for $\tilde{\chi}_1^0 \tilde{\chi}_3^0$ in final states with leptons and possibly photons. Limits on $m_{\tilde{e}_L}$ are derived by exploiting the mass relation between the \tilde{e}_L and \tilde{e}_R , based on universal m_0 and $m_{1/2}$. When the constraint from the mass limit of the lightest Higgs from HEISTER 02 is included, the bounds improve to $m_{\tilde{e}_R} > 77(75)$ GeV and $m_{\tilde{e}_L} > 115(115)$ GeV for a top mass of 175(180) GeV. In the MSUGRA framework with radiative electroweak symmetry breaking, the limits improve further to $m_{\tilde{e}_R} > 95$ GeV and $m_{\tilde{e}_L} > 152$ GeV, assuming a trilinear coupling $A_0=0$ at the GUT scale. See Figs. 4, 5, 7 for the dependence of the limits on $\tan\beta$.
- ⁷ ABBIENDI 04F use data from $\sqrt{s}=189$ –209 GeV. They derive limits on sparticle masses under the assumption of \tilde{R} with $LL\bar{E}$ or $LQ\bar{D}$ couplings. The results are valid for $\tan\beta=1.5$, $\mu=-200$ GeV, with, in addition, $\Delta m > 5$ GeV for indirect decays via $LQ\bar{D}$. The limit quoted applies to direct decays via $LL\bar{E}$ or $LQ\bar{D}$ couplings. For indirect decays, the limits on the \tilde{e}_R mass are respectively 99 and 92 GeV for $LL\bar{E}$ and $LQ\bar{D}$ couplings and $m_{\tilde{\chi}_1^0}=10$ GeV and degrade slightly for larger $\tilde{\chi}_1^0$ mass. Supersedes the results of ABBIENDI 00.
- ⁸ ABDALLAH 04M use data from $\sqrt{s}=192$ –208 GeV to derive limits on sparticle masses under the assumption of \tilde{R} with $LL\bar{E}$ or UDD couplings. The results are valid for $\mu=-200$ GeV, $\tan\beta=1.5$, $\Delta m > 5$ GeV and assuming a BR of 1 for the given decay. The limit quoted is for indirect UDD decays using the neutralino constraint of 39.5 GeV for $LL\bar{E}$ and of 38.0 GeV for UDD couplings, also derived in ABDALLAH 04M. For indirect decays via $LL\bar{E}$ the limit improves to 95 GeV if the constraint from the neutralino is used and to 94 GeV if it is not used. For indirect decays via UDD couplings it remains unchanged when the neutralino constraint is not used. Supersedes the result of ABREU 00u.
- ⁹ HEISTER 03G searches for the production of selectrons in the case of \tilde{R} prompt decays with $LL\bar{E}$, $LQ\bar{D}$ or UDD couplings at $\sqrt{s}=189$ –209 GeV. The search is performed for direct and indirect decays, assuming one coupling at a time to be non-zero. The limit holds for indirect decays mediated by $LQ\bar{D}$ couplings with $\Delta m > 10$ GeV. Limits are also given for $LL\bar{E}$ direct ($m_{\tilde{e}_R} > 96$ GeV) and indirect decays ($m_{\tilde{e}_R} > 94$ GeV for $m(\tilde{\chi}_1^0) > 23$ GeV from BARATE 98s) and for UDD indirect decays ($m_{\tilde{e}_R} > 94$ GeV with $\Delta m > 10$ GeV). Supersedes the results from BARATE 01b.
- ¹⁰ ACHARD 02 searches for the production of selectrons in the case of \tilde{R} prompt decays with $LL\bar{E}$ or UDD couplings at $\sqrt{s}=189$ –208 GeV. The search is performed for direct and indirect decays, assuming one coupling at a time to be non-zero. The limit holds for direct decays via $LL\bar{E}$ couplings. Stronger limits are reached for $LL\bar{E}$ indirect (79 GeV) and for UDD direct or indirect (96 GeV) decays.
- ¹¹ BARATE 01 looked for acoplanar dielectron + \cancel{E}_T final states at 189 to 202 GeV. The limit assumes $\mu=-200$ GeV and $\tan\beta=2$ for the production cross section and 100% branching ratio for $\tilde{e} \rightarrow e\tilde{\chi}_1^0$. See their Fig. 1 for the dependence of the limit on Δm . These limits include and update the results of BARATE 99q.
- ¹² ABBIENDI 00j looked for acoplanar dielectron + \cancel{E}_T final states at $\sqrt{s}=161$ –183 GeV. The limit assumes $\mu < -100$ GeV and $\tan\beta=1.5$ for the production cross section and decay branching ratios, evaluated within the MSSM, and zero efficiency for decays other than $\tilde{e} \rightarrow e\tilde{\chi}_1^0$. See their Fig. 12 for the dependence of the limit on Δm and $\tan\beta$.
- ¹³ ABREU 00u studies decays induced by R-parity violating $LL\bar{E}$ couplings, using data from $\sqrt{s}=189$ GeV. They investigate topologies with multiple leptons, assuming one coupling at a time to be non-zero and giving rise to indirect decays. The limits assume a neutralino mass limit of 30 GeV, also derived in ABREU 00u. Updates ABREU 00i.
- ¹⁴ ABREU 00v use data from $\sqrt{s}=130$ –189 GeV to search for tracks with large impact parameter or visible decay vertices. Limits are obtained as a function of $m_{\tilde{G}}$, from a scan of the GMSB parameters space, after combining these results with the search for slepton pair production in the SUGRA framework from ABREU 01 to cover prompt decays and on stable particle searches from ABREU 00q. For limits at different $m_{\tilde{G}}$, see their Fig. 12.
- ¹⁵ BARATE 00g combines the search for acoplanar dileptons, leptons with large impact parameters, kinks, and stable heavy-charged tracks, assuming 3 flavors of degenerate sleptons, produced in the channel. Data collected at $\sqrt{s}=189$ GeV.
- ¹⁶ ACCIARRI 99i establish indirect limits on $m_{\tilde{e}_R}$ from the regions excluded in the M_2 versus m_0 plane by their chargino and neutralino searches at $\sqrt{s}=130$ –183 GeV. The situations where the $\tilde{\chi}_1^0$ is the LSP (indirect decays) and where a \tilde{e} is the LSP (direct decays) were both considered. The weakest limit, quoted above, comes from direct decays with UDD couplings; $LL\bar{E}$ couplings or indirect decays lead to a stronger limit.
- ¹⁷ ACCIARRI 98f looked for acoplanar dielectron+ \cancel{E}_T final states at $\sqrt{s}=130$ –172 GeV. The limit assumes $\mu=-200$ GeV, and zero efficiency for decays other than $\tilde{e}_R \rightarrow e\tilde{\chi}_1^0$. See their Fig. 6 for the dependence of the limit on Δm .
- ¹⁸ BARATE 98k looked for $e^+e^- \gamma\gamma + \cancel{E}$ final states at $\sqrt{s}=161$ –184 GeV. The limit assumes $\mu=-200$ GeV and $\tan\beta=2$ for the evaluation of the production cross section. See Fig. 4 for limits on the $(m_{\tilde{e}_R}, m_{\tilde{\chi}_1^0})$ plane and for the effect of cascade decays.
- ¹⁹ BREITWEG 98 used positron+jet events with missing energy and momentum to look for $e^+q \rightarrow \tilde{e}q$ via gaugino-like neutralino exchange with decays into $(e\tilde{\chi}_1^0)(q\tilde{\chi}_1^0)$. See paper for dependences in $m(\tilde{q})$, $m(\tilde{\chi}_1^0)$.
- ²⁰ AID 96c used positron+jet events with missing energy and momentum to look for $e^+q \rightarrow \tilde{e}q$ via neutralino exchange with decays into $(e\tilde{\chi}_1^0)(q\tilde{\chi}_1^0)$. See the paper for dependences on $m_{\tilde{q}}$, $m_{\tilde{\chi}_1^0}$.

$\tilde{\mu}$ (Smuon) MASS LIMIT

VALUE (GeV)	CL%	DOCUMENT ID	TECN	COMMENT
>91.0		¹ ABBIENDI 04	OPAL	$\Delta m > 3$ GeV, $\tilde{\mu}_R^+ \tilde{\mu}_R^-$, $ \mu > 100$ GeV, $\tan\beta=1.5$
>86.7		² ACHARD 04	L3	$\Delta m > 10$ GeV, $\tilde{\mu}_R^+ \tilde{\mu}_R^-$, $ \mu > 200$ GeV, $\tan\beta \geq 2$
none 30–88	95	³ ABDALLAH 03M	DLPH	$\Delta m > 5$ GeV, $\tilde{\mu}_R^+ \tilde{\mu}_R^-$
>94	95	⁴ ABDALLAH 03M	DLPH	$\tilde{\mu}_R, 1 \leq \tan\beta \leq 40$, $\Delta m > 10$ GeV
>88	95	⁵ HEISTER 02E	ALEP	$\Delta m > 15$ GeV, $\tilde{\mu}_R^+ \tilde{\mu}_R^-$

• • • We do not use the following data for averages, fits, limits, etc. • • •

		⁶ ABAZOV 06i	D0	$\tilde{R}, \lambda_{211}^0$
>74	95	⁷ ABBIENDI 04F	OPAL	$\tilde{R}, \tilde{\mu}_L$
>87	95	⁸ ABDALLAH 04M	DLPH	$\tilde{R}, \tilde{\mu}_R$, indirect, $\Delta m > 5$ GeV
>81	95	⁹ HEISTER 03G	ALEP	$\tilde{\mu}_L, \tilde{R}$ decays
		¹⁰ ABAZOV 02H	D0	$\tilde{R}, \lambda_{211}^0$
>61	95	¹¹ ACHARD 02	L3	$\tilde{\mu}_R, \tilde{R}$ decays
>85	95	¹² BARATE 01	ALEP	$\Delta m > 10$ GeV, $\tilde{\mu}_R^+ \tilde{\mu}_R^-$
>65	95	¹³ ABBIENDI 00j	OPAL	$\Delta m > 2$ GeV, $\tilde{\mu}_R^+ \tilde{\mu}_R^-$
>80	95	¹⁴ ABREU 00v	DLPH	$\tilde{\mu}_R \tilde{\mu}_R$ ($\tilde{\mu}_R \rightarrow \mu\tilde{G}$), $m_{\tilde{G}} > 8$ eV
>77	95	¹⁵ BARATE 98k	ALEP	Any Δm , $\tilde{\mu}_R^+ \tilde{\mu}_R^-$, $\tilde{\mu}_R \rightarrow \mu\tilde{G}$

¹ ABBIENDI 04 search for $\tilde{\mu}_R \tilde{\mu}_R$ production in acoplanar di-muon final states in the 183–208 GeV data. See Fig. 14 for the dependence of the limits on $m_{\tilde{\chi}_1^0}$ and for the limit at $\tan\beta=35$. Under the assumption of 100% branching ratio for $\tilde{\mu}_R \rightarrow \mu\tilde{\chi}_1^0$, the limit improves to 94.0 GeV for $\Delta m > 4$ GeV. See Fig. 11 for the dependence of the limits on $m_{\tilde{\chi}_1^0}$ at several values of the branching ratio. This limit supersedes ABBIENDI 00g.

² ACHARD 04 search for $\tilde{\mu}_R \tilde{\mu}_R$ production in acoplanar di-muon final states in the 192–209 GeV data. Limits on $m_{\tilde{\mu}_R}$ are derived from a scan over the MSSM parameter space with universal GUT scale gaugino and scalar masses $m_{1/2}$ and m_0 , $1 \leq \tan\beta \leq 60$ and $-2 \leq \mu \leq 2$ TeV. See Fig. 4 for the dependence of the limits on $m_{\tilde{\chi}_1^0}$. This limit supersedes ACCIARRI 99w.

³ ABDALLAH 03M looked for acoplanar dimuon + \cancel{E} final states at $\sqrt{s}=189$ –208 GeV. The limit assumes $B(\tilde{\mu} \rightarrow \mu\tilde{\chi}_1^0) = 100\%$. See Fig. 16 for limits on the $(m_{\tilde{\mu}_R}, m_{\tilde{\chi}_1^0})$ plane. These limits include and update the results of ABREU 01.

⁴ ABDALLAH 03M uses data from $\sqrt{s}=192$ –208 GeV to obtain limits in the framework of the MSSM with gaugino and sfermion mass universality at the GUT scale. An indirect limit on the mass is derived by constraining the MSSM parameter space by the results from direct searches for neutralinos (including cascade decays) and for sleptons. These limits are valid for values of $M_2 < 1$ TeV, $|\mu| \leq 1$ TeV with the $\tilde{\chi}_1^0$ as LSP. The quoted limit is obtained when there is no mixing in the third family. See Fig. 43 for the mass limits as a function of $\tan\beta$. These limits update the results of ABREU 00w.

⁵ HEISTER 02E looked for acoplanar dimuon + \cancel{E}_T final states from e^+e^- interactions between 183 and 209 GeV. The mass limit assumes $B(\tilde{\mu} \rightarrow \mu\tilde{\chi}_1^0)=1$. See their Fig. 4 for the dependence of the limit on Δm . These limits include and update the results of BARATE 01.

⁶ ABAZOV 06i looked in 380 pb^{-1} of $p\bar{p}$ collisions at $\sqrt{s}=1.96$ TeV for events with at least 2 muons and 2 jets for s-channel production of $\tilde{\mu}$ or $\tilde{\nu}$ and subsequent decay via \tilde{R} couplings $LQ\bar{D}$. The data are in agreement with the SM expectation. They set limits on resonant slepton production and derive exclusion contours on λ_{211}^0 in the mass plane of \tilde{e} versus $\tilde{\chi}_1^0$ assuming a MSUGRA model with $\tan\beta=5$, $\mu < 0$ and $A_0=0$, see their Fig. 3. For $\lambda_{211}^0 \geq 0.09$ slepton masses up to 358 GeV are excluded. Supersedes the results of ABAZOV 02H.

⁷ ABBIENDI 04F use data from $\sqrt{s}=189$ –209 GeV. They derive limits on sparticle masses under the assumption of \tilde{R} with $LL\bar{E}$ or $LQ\bar{D}$ couplings. The results are valid for $\tan\beta=1.5$, $\mu=-200$ GeV, with, in addition, $\Delta m > 5$ GeV for indirect decays via $LQ\bar{D}$. The limit quoted applies to direct decays with $LL\bar{E}$ couplings and improves to 75 GeV for $LQ\bar{D}$ couplings. The limits on the $\tilde{\mu}_R$ mass for indirect decays are respectively 94 and 87 GeV for $LL\bar{E}$ and $LQ\bar{D}$ couplings and $m_{\tilde{\chi}_1^0}=10$ GeV. Supersedes the results of ABBIENDI 00.

⁸ ABDALLAH 04M use data from $\sqrt{s}=192$ –208 GeV to derive limits on sparticle masses under the assumption of \tilde{R} with $LL\bar{E}$ or UDD couplings. The results are valid for $\mu=-200$ GeV, $\tan\beta=1.5$, $\Delta m > 5$ GeV and assuming a BR of 1 for the given decay. The limit quoted is for indirect UDD decays using the neutralino constraint of 39.5 GeV for $LL\bar{E}$ and of 38.0 GeV for UDD couplings, also derived in ABDALLAH 04M. For indirect decays via $LL\bar{E}$ the limit improves to 90 GeV if the constraint from the neutralino is used and remains at 87 GeV if it is not used. For indirect decays via UDD couplings it degrades to 85 GeV when the neutralino constraint is not used. Supersedes the result of ABREU 00u.

⁹ HEISTER 03G searches for the production of smuons in the case of \tilde{R} prompt decays with $LL\bar{E}$, $LQ\bar{D}$ or UDD couplings at $\sqrt{s}=189$ –209 GeV. The search is performed for direct and indirect decays, assuming one coupling at a time to be non-zero. The limit holds for direct decays mediated by $R LQ\bar{D}$ couplings and improves to 90 GeV for indirect decays (for $\Delta m > 10$ GeV). Limits are also given for $LL\bar{E}$ direct ($m_{\tilde{\mu}_R} > 87$ GeV) and indirect decays ($m_{\tilde{\mu}_R} > 96$ GeV for $m(\tilde{\chi}_1^0) > 23$ GeV from BARATE 98s) and for UDD indirect decays ($m_{\tilde{\mu}_R} > 85$ GeV for $\Delta m > 10$ GeV). Supersedes the results from BARATE 01b.

¹⁰ ABAZOV 02H looked in 94 pb^{-1} of $p\bar{p}$ collisions at $\sqrt{s}=1.8$ TeV for events with at least 2 muons and 2 jets for s-channel production of $\tilde{\mu}$ or $\tilde{\nu}$ and subsequent decay via \tilde{R} couplings $LQ\bar{D}$. A scan over the MSUGRA parameters is performed to exclude regions of the $(m_0, m_{1/2})$ plane, examples being shown in Fig. 2.

¹¹ ACHARD 02 searches for the production of smuons in the case of \tilde{R} prompt decays with $LL\bar{E}$ or UDD couplings at $\sqrt{s}=189$ –208 GeV. The search is performed for direct and indirect decays, assuming one coupling at a time to be non-zero. The limit holds for direct decays via $LL\bar{E}$ couplings. Stronger limits are reached for $LL\bar{E}$ indirect (87 GeV) and for UDD direct or indirect (86 GeV) decays.

¹² BARATE 01 looked for acoplanar dimuon + \cancel{E}_T final states at 189 to 202 GeV. The limit assumes 100% branching ratio for $\tilde{\mu} \rightarrow \mu\tilde{\chi}_1^0$. See their Fig. 1 for the dependence of the limit on Δm . These limits include and update the results of BARATE 99q.

¹³ ABBIENDI 00j looked for acoplanar dimuon + \cancel{E}_T final states at $\sqrt{s}=161$ –183 GeV. The limit assumes $B(\tilde{\mu} \rightarrow \mu\tilde{\chi}_1^0)=1$. Using decay branching ratios derived from the MSSM, a lower limit of 65 GeV is obtained for $\mu < -100$ GeV and $\tan\beta=1.5$. See their Figs. 10 and 13 for the dependence of the limit on the branching ratio and on Δm .

¹⁴ ABREU 00v use data from $\sqrt{s}=130$ –189 GeV to search for tracks with large impact parameter or visible decay vertices. Limits are obtained as function of $m_{\tilde{G}}$, after combining these results with the search for slepton pair production in the SUGRA framework from ABREU 01 to cover prompt decays and on stable particle searches from ABREU 00q. For limits at different $m_{\tilde{G}}$, see their Fig. 12.

Searches Particle Listings

Supersymmetric Particle Searches

¹⁵ BARATE 98k looked for $\mu^+ \mu^- \gamma \gamma + \cancel{E}$ final states at $\sqrt{s}=161\text{--}184$ GeV. See Fig. 4 for limits on the $(m_{\tilde{\mu}_R}, m_{\tilde{\chi}_1^0})$ plane and for the effect of cascade decays.

$\tilde{\tau}$ (Stau) MASS LIMIT

VALUE (GeV)	CL%	DOCUMENT ID	TECN	COMMENT
>85.2		¹ ABBIENDI 04	OPAL	$\Delta m > 6$ GeV, $\theta_\tau = \pi/2$, $ \mu > 100$ GeV, $\tan\beta = 1.5$
>78.3		² ACHARD 04	L3	$\Delta m > 15$ GeV, $\theta_\tau = \pi/2$, $ \mu > 200$ GeV, $\tan\beta \geq 2$
>81.9	95	³ ABDALLAH 03M	DLPH	$\Delta m > 15$ GeV, all θ_τ
none $m_{\tilde{\tau}} - 26.3$	95	³ ABDALLAH 03M	DLPH	$\Delta m > m_{\tilde{\tau}}$, all θ_τ
>79	95	⁴ HEISTER 02E	ALEP	$\Delta m > 15$ GeV, $\theta_\tau = \pi/2$
>76	95	⁴ HEISTER 02E	ALEP	$\Delta m > 15$ GeV, $\theta_\tau = 0.91$
• • • We do not use the following data for averages, fits, limits, etc. • • •				
>87.4	95	⁵ ABBIENDI 06B	OPAL	$\tilde{\tau}_R \rightarrow \tau \tilde{G}$, all $\tau(\tilde{\tau}_R)$
>74	95	⁶ ABBIENDI 04F	OPAL	$\tilde{R}, \tilde{\tau}_1$
>68	95	^{7,8} ABDALLAH 04H	DLPH	AMSB, $\mu > 0$
>90	95	⁹ ABDALLAH 04M	DLPH	$\tilde{R}, \tilde{\tau}_R$, indirect, $\Delta m > 5$ GeV
>82.5	10	¹⁰ ABDALLAH 03D	DLPH	$\tilde{\tau}_R \rightarrow \tau \tilde{G}$, all $\tau(\tilde{\tau}_R)$
>70	95	¹¹ HEISTER 03G	ALEP	$\tilde{\tau}_R, \tilde{R}$ decay
>61	95	¹² ACHARD 02	L3	$\tilde{\tau}_R, \tilde{R}$ decays
>77	95	¹³ HEISTER 02R	ALEP	τ_1 , any lifetime
>70	95	¹⁴ BARATE 01	ALEP	$\Delta m > 10$ GeV, $\theta_\tau = \pi/2$
>68	95	¹⁴ BARATE 01	ALEP	$\Delta m > 10$ GeV, $\theta_\tau = 0.91$
>64	95	¹⁵ ABBIENDI 00J	OPAL	$\Delta m > 10$ GeV, $\tilde{\tau}_R^+ \tilde{\tau}_R^-$
>84	95	¹⁶ ABREU 00V	DLPH	$\tilde{\tau}_R \tilde{\ell}_R$ ($\tilde{\ell}_R \rightarrow \ell \tilde{G}$), $m_{\tilde{G}} > 9$ eV
>73	95	¹⁷ ABREU 00V	DLPH	$\tilde{\tau}_1 \tilde{\tau}_1$ ($\tilde{\tau}_1 \rightarrow \tau \tilde{G}$), all $\tau(\tilde{\tau}_1)$
>52		¹⁸ BARATE 98k	ALEP	Any $\Delta m, \theta_\tau = \pi/2, \tilde{\tau}_R \rightarrow \tau \gamma \tilde{G}$

¹ ABBIENDI 04 search for $\tilde{\tau}\tilde{\tau}$ production in acoplanar di-tau final states in the 183–208 GeV data. See Fig. 15 for the dependence of the limits on $m_{\tilde{\chi}_1^0}$ and for the limit at $\tan\beta=35$. Under the assumption of 100% branching ratio for $\tilde{\tau}_R \rightarrow \tau \tilde{\chi}_1^0$, the limit improves to 89.8 GeV for $\Delta m > 8$ GeV. See Fig. 12 for the dependence of the limits on $m_{\tilde{G}}$ at several values of the branching ratio and for their dependence on θ_τ . This limit supersedes ABBIENDI 00G.

² ACHARD 04 search for $\tilde{\tau}\tilde{\tau}$ production in acoplanar di-tau final states in the 192–209 GeV data. Limits on $m_{\tilde{\tau}_R}$ are derived from a scan over the MSSM parameter space with universal GUT scale gaugino and scalar masses $m_{1/2}$ and m_0 , $1 \leq \tan\beta \leq 60$ and $-2 \leq \mu \leq 2$ TeV. See Fig. 4 for the dependence of the limits on $m_{\tilde{\chi}_1^0}$.

³ ABDALLAH 03M looked for acoplanar $\tilde{\tau}\tilde{\tau}$ final states at $\sqrt{s}=130\text{--}208$ GeV. A dedicated search was made for low mass $\tilde{\tau}$ s decoupling from the Z^0 . The limit assumes $B(\tilde{\tau} \rightarrow \tau \tilde{\chi}_1^0) = 100\%$. See Fig. 20 for limits on the $(m_{\tilde{\tau}}, m_{\tilde{\chi}_1^0})$ plane and as function

of the $\tilde{\chi}_1^0$ mass and of the branching ratio. The limit in the low-mass region improves to 29.6 and 31.1 GeV for $\tilde{\tau}_R$ and $\tilde{\tau}_1$, respectively, at $\Delta m > m_{\tilde{\tau}}$. The limit in the high-mass region improves to 84.7 GeV for $\tilde{\tau}_R$ and $\Delta m > 15$ GeV. These limits include and update the results of ABREU 01.

⁴ HEISTER 02E looked for acoplanar ditau + \cancel{E}_T final states from e^+e^- interactions between 183 and 209 GeV. The mass limit assumes $B(\tilde{\tau} \rightarrow \tau \tilde{\chi}_1^0) = 1$. See their Fig. 4 for the dependence of the limit on Δm . These limits include and update the results of BARATE 01.

⁵ ABBIENDI 06B use 600 pb^{-1} of data from $\sqrt{s}=189\text{--}209$ GeV. They look for events from pair-produced staus in a GMSB scenario with $\tilde{\tau}$ NLSP including prompt $\tilde{\tau}$ decays to ditaus + \cancel{E} final states, large impact parameters, kinked tracks and heavy stable charged particles. Limits on the cross-section are computed as a function of $m(\tilde{\tau})$ and the lifetime, see their Fig. 7. The limit is compared to the $\sigma \cdot BR^2$ from a scan over the GMSB parameter space.

⁶ ABBIENDI 04F use data from $\sqrt{s}=189\text{--}209$ GeV. They derive limits on sparticle masses under the assumption of \tilde{R} with $LL\bar{E}$ or $LQ\bar{D}$ couplings. The results are valid for $\tan\beta = 1.5$, $\mu = -200$ GeV, with, in addition, $\Delta m > 5$ GeV for indirect decays via $LQ\bar{D}$. The limit quoted applies to direct decays with $LL\bar{E}$ couplings and improves to 75 GeV for $LQ\bar{D}$ couplings. The limit on the $\tilde{\tau}_R$ mass for indirect decays is 92 GeV for $LL\bar{E}$ couplings at $m_{\tilde{G}} = 10$ GeV and no exclusion is obtained for $LQ\bar{D}$ couplings. Supersedes the results of ABBIENDI 00.

⁷ ABDALLAH 04H use data from LEP 1 and $\sqrt{s}=192\text{--}208$ GeV. They re-use results or re-analyze the data from ABDALLAH 03M to put limits on the parameter space of anomaly-mediated supersymmetry breaking (AMSB), which is scanned in the region $1 < m_{3/2} < 50$ TeV, $0 < m_0 < 1000$ GeV, $1.5 < \tan\beta < 35$, both signs of μ . The constraints are obtained from the searches for mass degenerate chargino and neutralino, for SM-like and invisible Higgs, for leptonically decaying charginos and from the limit on non-SM Z width of 3.2 MeV. The limit is for $m_t = 174.3$ GeV (see Table 2 for other m_t values).

⁸ The limit improves to 75 GeV for $\mu < 0$.

⁹ ABDALLAH 04M use data from $\sqrt{s}=192\text{--}208$ GeV to derive limits on sparticle masses under the assumption of \tilde{R} with $LL\bar{E}$ couplings. The results are valid for $\mu = -200$ GeV, $\tan\beta = 1.5$, $\Delta m > 5$ GeV and assuming a BR of 1 for the given decay. The limit quoted is for indirect decays using the neutralino constraint of 39.5 GeV, also derived in ABDALLAH 04M. For indirect decays via $LL\bar{E}$ the limit decreases to 86 GeV if the constraint from the neutralino is not used. Supersedes the result of ABREU 00.

¹⁰ ABDALLAH 03D use data from $\sqrt{s}=130\text{--}208$ GeV to search for tracks with large impact parameter or visible decay vertices and for heavy charged stable particles. Limits are obtained as function of $m(\tilde{G})$, after combining these results with the search for slepton pair production in the SUGRA framework from ABDALLAH 03M to cover prompt decays. The above limit is reached for the stau decaying promptly, $m(\tilde{G}) < 6$ eV, and is computed for stau mixing yielding the minimal cross section. Stronger limits are obtained for longer lifetimes. See their Fig. 9. Supersedes the results of ABREU 01G.

¹¹ HEISTER 03G searches for the production of stau in the case of \tilde{R} prompt decays with $LL\bar{E}$, $LQ\bar{D}$ or $U\bar{D}\bar{D}$ couplings at $\sqrt{s}=189\text{--}209$ GeV. The search is performed for direct and indirect decays, assuming one coupling at a time to be non-zero. The limit holds for

indirect decays mediated by \tilde{R} $U\bar{D}\bar{D}$ couplings with $\Delta m > 10$ GeV. Limits are also given for $LL\bar{E}$ direct ($m_{\tilde{\tau}_R} > 87$ GeV) and indirect decays ($m_{\tilde{\tau}_R} > 95$ GeV for $m(\tilde{\chi}_1^0) > 23$ GeV from BARATE 98s) and for $LQ\bar{D}$ indirect decays ($m_{\tilde{\tau}_R} > 76$ GeV). Supersedes the results from BARATE 01B.

¹² ACHARD 02 searches for the production of staus in the case of \tilde{R} prompt decays with $LL\bar{E}$ or $U\bar{D}\bar{D}$ couplings at $\sqrt{s}=189\text{--}208$ GeV. The search is performed for direct and indirect decays, assuming one coupling at the time to be nonzero. The limit holds for direct decays via $LL\bar{E}$ couplings. Stronger limits are reached for $LL\bar{E}$ indirect (86 GeV) and for $U\bar{D}\bar{D}$ direct or indirect (75 GeV) decays.

¹³ HEISTER 02R search for signals of GMSB in the 189–209 GeV data. For the $\tilde{\chi}_1^0$ NLSP scenario, they looked for topologies consisting of $\gamma\gamma\cancel{E}$ or a single γ not pointing to the interaction vertex. For the \tilde{L} NLSP case, the topologies consist of $\ell\ell\cancel{E}$, including leptons with large impact parameters, kinks, or stable particles. Limits are derived from a scan over the GMSB parameters (see their Table 5 for the ranges). The limit remains valid whichever is the NLSP. The absolute mass bound on the $\tilde{\chi}_1^0$ for any lifetime includes indirect limits from the slepton search HEISTER 02E performed within the MSUGRA framework. A bound for any NLSP and any lifetime of 77 GeV has also been derived by using the constraints from the neutral Higgs search in HEISTER 02. In the co-NLSP scenario, limits $m_{\tilde{\tau}_R} > 83$ GeV (neglecting t-channel exchange) and $m_{\tilde{\mu}_R} > 88$ GeV are obtained independent of the lifetime. Supersedes the results from BARATE 00G.

¹⁴ BARATE 01 looked for acoplanar ditau + \cancel{E}_T final states at 189 to 202 GeV. A slight excess (with 1.2% probability) of events is observed relative to the expected SM background. The limit assumes 100% branching ratio for $\tilde{\tau} \rightarrow \tau \tilde{\chi}_1^0$. See their Fig. 1 for the dependence of the limit on Δm . These limits include and update the results of BARATE 99G.

¹⁵ ABBIENDI 00J looked for acoplanar ditau + \cancel{E}_T final states at $\sqrt{s}=161\text{--}183$ GeV. The limit assumes $B(\tilde{\tau} \rightarrow \tau \tilde{\chi}_1^0) = 1$. Using decay branching ratios derived from the MSSM, a lower limit of 60 GeV at $\Delta m > 9$ GeV is obtained for $\mu < -100$ GeV and $\tan\beta = 1.5$. See their Figs. 11 and 14 for the dependence of the limit on the branching ratio and on Δm .

¹⁶ ABREU 00v use data from $\sqrt{s}=130\text{--}189$ GeV to search for tracks with large impact parameter or visible decay vertices. Limits are obtained as function of $m_{\tilde{G}}$, after combining these results with the search for slepton pair production in the SUGRA framework from ABREU 01 to cover prompt decays and on stable particle searches from ABREU 00Q. The above limit assumes the degeneracy of stau and smuon. For limits at different $m_{\tilde{G}}$, see their Fig. 12.

¹⁷ ABREU 00v use data from $\sqrt{s}=130\text{--}189$ GeV to search for tracks with large impact parameter or visible decay vertices. Limits are obtained as function of $m_{\tilde{G}}$, after combining these results with the search for slepton pair production in the SUGRA framework from ABREU 01 to cover prompt decays and on stable particle searches from ABREU 00Q. The above limit is reached for the stau mixing yielding the minimal cross section and decaying promptly. Stronger limits are obtained for longer lifetimes or for $\tilde{\tau}_R$; see their Fig. 11. For $10 \leq m_{\tilde{G}} \leq 310$ eV, the whole range $2 \leq m_{\tilde{\tau}_1} \leq 80$ GeV is excluded. Supersedes the results of ABREU 99c and ABREU 99f.

¹⁸ BARATE 98k looked for $\tau^+ \tau^- \gamma \gamma + \cancel{E}$ final states at $\sqrt{s}=161\text{--}184$ GeV. See Fig. 4 for limits on the $(m_{\tilde{\tau}_R}, m_{\tilde{\chi}_1^0})$ plane and for the effect of cascade decays.

Degenerate Charged Sleptons

Unless stated otherwise in the comment lines or in the footnotes, the following limits assume 3 families of degenerate charged sleptons.

VALUE (GeV)	CL%	DOCUMENT ID	TECN	COMMENT
>93	95	¹ BARATE 01	ALEP	$\Delta m > 10$ GeV, $\tilde{\ell}_R^+ \tilde{\ell}_R^-$
>70	95	¹ BARATE 01	ALEP	all $\Delta m, \tilde{\ell}_R^+ \tilde{\ell}_R^-$
• • • We do not use the following data for averages, fits, limits, etc. • • •				
>91.9	95	² ABBIENDI 06B	OPAL	$\tilde{\tau}_R \rightarrow \ell \tilde{G}$, all $\ell(\tilde{\ell}_R)$
>88	95	³ ABDALLAH 03D	DLPH	$\tilde{\ell}_R \rightarrow \ell \tilde{G}$, all $\ell(\tilde{\ell}_R)$
>82.7	95	⁴ ACHARD 02	L3	$\tilde{\ell}_R, \tilde{R}$ decays, MSUGRA
>83	95	⁵ ABBIENDI 01	OPAL	$e^+ e^- \rightarrow \tilde{\ell}_1 \tilde{\ell}_1$, GMSB, $\tan\beta = 2$
		⁶ ABREU 01	DLPH	$\tilde{\ell} \rightarrow \ell \tilde{\chi}_2^0, \tilde{\chi}_2^0 \rightarrow \gamma \tilde{\chi}_1^0$, $\ell = e, \mu$
>68.8	95	⁷ ACCIARRI 01	L3	$\tilde{\ell}_R, \tilde{R}$, $0.7 \leq \tan\beta \leq 40$
>84	95	^{8,9} ABREU 00V	DLPH	$\tilde{\ell}_R \tilde{\ell}_R$ ($\tilde{\ell}_R \rightarrow \ell \tilde{G}$), $m_{\tilde{G}} > 9$ eV

¹ BARATE 01 looked for acoplanar dilepton + \cancel{E}_T and single electron (for $\tilde{\ell}_R \tilde{\ell}_L$) final states at 189 to 202 GeV. The limit assumes $\mu = -200$ GeV and $\tan\beta = 2$ for the production cross section and decay branching ratios, evaluated within the MSSM, and zero efficiency for decays other than $\tilde{\ell} \rightarrow \ell \tilde{\chi}_1^0$. The slepton masses are determined from the GUT relations without stau mixing. See their Fig. 1 for the dependence of the limit on Δm .

² ABBIENDI 06B use 600 pb^{-1} of data from $\sqrt{s}=189\text{--}209$ GeV. They look for events from pair-produced staus in a GMSB scenario with $\tilde{\tau}$ NLSP including prompt $\tilde{\tau}$ decays to dileptons + \cancel{E} final states, large impact parameters, kinked tracks and heavy stable charged particles. Limits on the cross-section are computed as a function of $m(\tilde{\ell})$ and the lifetime, see their Fig. 7. The limit is compared to the $\sigma \cdot BR^2$ from a scan over the GMSB parameter space. The highest mass limit is reached for $\tilde{\mu}_R$, from which the quoted mass limit is derived by subtracting $m_{\tilde{\tau}}$.

³ ABDALLAH 03D use data from $\sqrt{s}=130\text{--}208$ GeV to search for tracks with large impact parameter or visible decay vertices and for heavy charged stable particles. Limits are obtained as function of $m(\tilde{G})$, after combining these results with the search for slepton pair production in the SUGRA framework from ABDALLAH 03M to cover prompt decays. The above limit is reached for prompt decays and assumes the degeneracy of the sleptons. For limits at different $m(\tilde{G})$, see their Fig. 9. Supersedes the results of ABREU 01G.

⁴ ACHARD 02 searches for the production of sparticles in the case of \tilde{R} prompt decays with $LL\bar{E}$ or $U\bar{D}\bar{D}$ couplings at $\sqrt{s}=189\text{--}208$ GeV. The search is performed for direct and indirect decays, assuming one coupling at the time to be nonzero. The MSUGRA limit results from a scan over the MSSM parameter space with the assumption of gaugino and scalar mass unification at the GUT scale and no mixing in the slepton sector, imposing simultaneously the exclusions from neutralino, chargino, sleptons, and squarks analyses. The limit holds for $LL\bar{E}$ couplings and increases to 88.7 GeV for $U\bar{D}\bar{D}$ couplings. For L3 limits from $LQ\bar{D}$ couplings, see ACCIARRI 01.

See key on page 373

Searches Particle Listings

Supersymmetric Particle Searches

⁵ ABBIENDI 01 looked for final states with $\gamma\gamma\mathbb{E}$, $\ell\ell\mathbb{E}$, with possibly additional activity and four leptons + \mathbb{E} to search for prompt decays of $\tilde{\chi}_1^0$ or $\tilde{\ell}_1$ in GMSB. They derive limits in the plane ($m_{\tilde{\chi}_1^0}, m_{\tilde{\tau}_1}$), see Fig. 6, allowing either the $\tilde{\chi}_1^0$ or a $\tilde{\ell}_1$ to be the NLSP.

Two scenarios are considered: $\tan\beta=2$ with the 3 sleptons degenerate in mass and $\tan\beta=20$ where the $\tilde{\tau}_1$ is lighter than the other sleptons. Data taken at $\sqrt{s}=189$ GeV. For $\tan\beta=20$, the obtained limits are $m_{\tilde{\tau}_1} > 69$ GeV and $m_{\tilde{e}_1}, \tilde{\mu}_1 > 88$ GeV.

⁶ ABREU 01 looked for acoplanar dilepton + diphoton + \mathbb{E} final states from $\tilde{\ell}$ cascade decays at $\sqrt{s}=130$ –189 GeV. See Fig. 9 for limits on the (μ, M_2) plane for $m_{\tilde{\ell}}=80$ GeV, $\tan\beta=1.0$, and assuming degeneracy of $\tilde{\mu}$ and \tilde{e} .

⁷ ACCIARRI 01 searches for multi-lepton and/or multi-jet final states from \mathbb{R} prompt decays with $LL\mathbb{E}$, $LQ\mathbb{D}$, or UDD couplings at $\sqrt{s}=189$ GeV. The search is performed for direct and indirect decays of neutralinos, charginos, and scalar leptons, with the $\tilde{\chi}_1^0$ or a $\tilde{\ell}$ as LSP and assuming one coupling to be nonzero at a time. Mass limits are derived using simultaneously the constraints from the neutralino, chargino, and slepton analyses; and the Z^0 width measurements from ACCIARRI 00c in a scan of the parameter space assuming MSUGRA with gaugino and scalar mass universality. Updates and supersedes the results from ACCIARRI 99i.

⁸ ABREU 00v use data from $\sqrt{s}=130$ –189 GeV to search for tracks with large impact parameter or visible decay vertices. Limits are obtained as function of $m_{\tilde{G}}$, after combining these results with the search for slepton pair production in the SUGRA framework from ABREU 01 to cover prompt decays and on stable particle searches from ABREU 00q. For limits at different $m_{\tilde{G}}$, see their Fig. 12.

⁹ The above limit assumes the degeneracy of stau and smuon.

Long-lived $\tilde{\ell}$ (Slepton) MASS LIMIT

Limits on scalar leptons which leave detector before decaying. Limits from Z decays are independent of lepton flavor. Limits from continuum e^+e^- annihilation are also independent of flavor for smuons and staus. Selection limits from e^+e^- collisions in the continuum depend on MSSM parameters because of the additional neutralino exchange contribution.

VALUE (GeV)	CL%	DOCUMENT ID	TECN	COMMENT
>98	95	1 ABBIENDI	03L OPAL	$\tilde{\mu}_R, \tilde{\tau}_R$
none 2–87.5		2 ABREU	00q DLPH	$\tilde{\mu}_R, \tilde{\tau}_R$
>81.2	95	3 ACCIARRI	99H L3	$\tilde{\mu}_R, \tilde{\tau}_R$
>81	95	4 BARATE	98K ALEP	$\tilde{\mu}_R, \tilde{\tau}_R$

¹ ABBIENDI 03L used e^+e^- data at $\sqrt{s}=130$ –209 GeV to select events with two high momentum tracks with anomalous dE/dx . The excluded cross section is compared to the theoretical expectation as a function of the heavy particle mass in their Fig. 3. The limit improves to 98.5 GeV for $\tilde{\mu}_L$ and $\tilde{\tau}_L$. The bounds are valid for colorless spin 0 particles with lifetimes longer than 10^{-6} s. Supersedes the results from ACKERSTAFF 98P.

² ABREU 00q searches for the production of pairs of heavy, charged stable particles in e^+e^- annihilation at $\sqrt{s}=130$ –189 GeV. The upper bound improves to 88 GeV for $\tilde{\mu}_L, \tilde{\tau}_L$. These limits include and update the results of ABREU 98P.

³ ACCIARRI 99H searched for production of pairs of back-to-back heavy charged particles at $\sqrt{s}=130$ –183 GeV. The upper bound improves to 82.2 GeV for $\tilde{\mu}_L, \tilde{\tau}_L$.

⁴ The BARATE 98K mass limit improves to 82 GeV for $\tilde{\mu}_L, \tilde{\tau}_L$. Data collected at $\sqrt{s}=161$ –184 GeV.

\tilde{q} (Squark) MASS LIMIT

For $m_{\tilde{q}} > 60$ –70 GeV, it is expected that squarks would undergo a cascade decay via a number of neutralinos and/or charginos rather than undergo a direct decay to photinos as assumed by some papers. Limits obtained when direct decay is assumed are usually higher than limits when cascade decays are included.

Limits from e^+e^- collisions depend on the mixing angle of the lightest mass eigenstate $\tilde{q}_1 = \tilde{q}_R \sin\theta_q + \tilde{q}_L \cos\theta_q$. It is usually assumed that only the sbottom and stop squarks have non-trivial mixing angles (see the stop and sbottom sections). Here, unless otherwise noted, squarks are always taken to be either left/right degenerate, or purely of left or right type. Data from Z decays have set squark mass limits above 40 GeV, in the case of $\tilde{q} \rightarrow q\tilde{\chi}_1^0$ decays if $\Delta m = m_{\tilde{q}} - m_{\tilde{\chi}_1^0} \gtrsim 5$ GeV. For smaller values of Δm , current constraints on the invisible width of the Z ($\Delta\Gamma_{\text{inv}} < 2.0$ MeV, LEP 00) exclude $m_{\tilde{u}_{L,R}} < 44$ GeV, $m_{\tilde{d}_R} < 33$ GeV, $m_{\tilde{d}_L} < 44$ GeV and, assuming all squarks degenerate, $m_{\tilde{q}} < 45$ GeV.

Limits made obsolete by the most recent analyses of e^+e^- , $p\bar{p}$, and ep collisions can be found in previous Editions of this Review.

VALUE (GeV)	CL%	DOCUMENT ID	TECN	COMMENT
>379	95	1 ABAZOV	08G D0	jets+ \mathbb{E}_T , $\tan\beta=3, \mu<0, A_0=0$, any $m_{\tilde{g}}$
> 99.5		2 ACHARD	04 L3	$\Delta m > 10$ GeV, $e^+e^- \rightarrow \tilde{q}_{L,R}\tilde{q}_{L,R}$
> 97		2 ACHARD	04 L3	$\Delta m > 10$ GeV, $e^+e^- \rightarrow \tilde{q}_R\tilde{q}_R$
>138	95	3 ABBOTT	01D D0	$\ell\ell$ +jets+ \mathbb{E}_T , $\tan\beta < 10, m_0 < 300$ GeV, $\mu < 0, A_0=0$
>255	95	3 ABBOTT	01D D0	$\tan\beta=2, m_{\tilde{g}}=m_{\tilde{q}}, \mu < 0, A_0=0, \ell\ell$ +jets+ \mathbb{E}_T
> 97	95	4 BARATE	01 ALEP	$e^+e^- \rightarrow \tilde{q}\tilde{q}, \Delta m > 6$ GeV
>224	95	5 ABE	96D CDF	$m_{\tilde{g}} \leq m_{\tilde{q}}$; with cascade decays, $\ell\ell$ +jets+ \mathbb{E}_T

• • • We do not use the following data for averages, fits, limits, etc. • • •

>490	95	6 SCHAEEL	07A ALEP	$\tilde{d}_R, \mathbb{R}, \lambda=0.3$
>544	95	6 SCHAEEL	07A ALEP	$\tilde{s}_R, \mathbb{R}, \lambda=0.3$
>325	95	7 ABAZOV	06c D0	jets+ \mathbb{E}_T , $\tan\beta=3, \mu<0, A_0=0$, any $m_{\tilde{g}}$
>273	95	8 CHEKANOV	05A ZEUS	$\tilde{q} \rightarrow \mu q, \mathbb{R}, LQ\mathbb{D}, \lambda=0.3$
>270	95	8 CHEKANOV	05A ZEUS	$\tilde{q} \rightarrow \tau q, \mathbb{R}, LQ\mathbb{D}, \lambda=0.3$
>275		9 AKTAS	04D H1	$e^\pm p \rightarrow \tilde{u}_L, \mathbb{R}, LQ\mathbb{D}$
>280		9 AKTAS	04D H1	$e^\pm p \rightarrow \tilde{d}_R, \mathbb{R}, LQ\mathbb{D}$
		10 ADLOFF	03 H1	$e^\pm p \rightarrow \tilde{q}, \mathbb{R}, LQ\mathbb{D}$
>276	95	11 CHEKANOV	03B ZEUS	$\tilde{d} \rightarrow e^- u, \nu d, \mathbb{R}, LQ\mathbb{D}, \lambda > 0.1$
>260	95	11 CHEKANOV	03B ZEUS	$\tilde{u} \rightarrow e^+ d, \mathbb{R}, LQ\mathbb{D}, \lambda > 0.1$
> 82.5	95	12 HEISTER	03G ALEP	\tilde{u}_R, \mathbb{R} decay
> 77	95	12 HEISTER	03G ALEP	\tilde{d}_R, \mathbb{R} decay
>240	95	13 ABAZOV	02F D0	$\tilde{q}, \mathbb{R}, \lambda'_{jk}$ indirect decays, $\tan\beta=2$, any $m_{\tilde{g}}$
>265	95	13 ABAZOV	02F D0	$\tilde{q}, \mathbb{R}, \lambda'_{jk}$ indirect decays, $\tan\beta=2, m_{\tilde{q}}=m_{\tilde{g}}$
none 80–121	95	14 ABAZOV	02G D0	$p\bar{p} \rightarrow \tilde{g}\tilde{g}, \tilde{g}\tilde{q}$
none 80–158	95	15 ABBIENDI	02 OPAL	$e\gamma \rightarrow \tilde{u}_L, \mathbb{R}, LQ\mathbb{D}, \lambda=0.3$
none 80–185	95	15 ABBIENDI	02 OPAL	$e\gamma \rightarrow \tilde{d}_R, \mathbb{R}, LQ\mathbb{D}, \lambda=0.3$
none 80–196	95	16 ABBIENDI	02B OPAL	$e\gamma \rightarrow \tilde{u}_L, \mathbb{R}, LQ\mathbb{D}, \lambda=0.3$
> 79	95	16 ABBIENDI	02B OPAL	$e\gamma \rightarrow \tilde{d}_R, \mathbb{R}, LQ\mathbb{D}, \lambda=0.3$
> 55	95	17 ACHARD	02 L3	\tilde{u}_R, \mathbb{R} decays
> 55	95	17 ACHARD	02 L3	\tilde{d}_R, \mathbb{R} decays
>263	95	18 CHEKANOV	02 ZEUS	$\tilde{u}_L \rightarrow \mu q, \mathbb{R}, LQ\mathbb{D}, \lambda=0.3$
>258	95	18 CHEKANOV	02 ZEUS	$\tilde{u}_L \rightarrow \tau q, \mathbb{R}, LQ\mathbb{D}, \lambda=0.3$
> 82	95	19 BARATE	01B ALEP	\tilde{u}_R, \mathbb{R} decays
> 68	95	19 BARATE	01B ALEP	\tilde{d}_R, \mathbb{R} decays
none 150–204	95	20 BREITWEG	01 ZEUS	$e^+p \rightarrow \tilde{d}_R, \mathbb{R}, LQ\mathbb{D}, \lambda=0.3$
>200	95	21 ABBOTT	00c D0	$\tilde{u}_L, \mathbb{R}, \lambda'_{jk}$ decays
>180	95	21 ABBOTT	00c D0	$\tilde{d}_R, \mathbb{R}, \lambda'_{jk}$ decays
>390	95	22 ACCIARRI	00P L3	$e^+e^- \rightarrow q\tilde{q}, \mathbb{R}, \lambda=0.3$
>148	95	23 AFFOLDER	00K CDF	$\tilde{d}_L, \mathbb{R}, \lambda'_{ij3}$ decays
>200	95	24 BARATE	00I ALEP	Superseded by SCHAEEL 07A
none 150–269	95	25 BREITWEG	00E ZEUS	$e^+p \rightarrow \tilde{u}_L, \mathbb{R}, LQ\mathbb{D}, \lambda=0.3$
>240	95	26 ABBOTT	99 D0	$\tilde{q} \rightarrow \tilde{\chi}_1^0 X \rightarrow \tilde{\chi}_1^0 \gamma X$, $m_{\tilde{\chi}_2^0} - m_{\tilde{\chi}_1^0} > 20$ GeV
>320	95	26 ABBOTT	99 D0	$\tilde{q} \rightarrow \tilde{\chi}_1^0 X \rightarrow \tilde{G} \gamma X$
>243	95	27 ABBOTT	99K D0	any $m_{\tilde{g}}, \mathbb{R}, \tan\beta=2, \mu < 0$
>250	95	28 ABBOTT	99L D0	$\tan\beta=2, \mu < 0, A_0=0$, jets+ \mathbb{E}_T
>200	95	29 ABE	99M CDF	$p\bar{p} \rightarrow \tilde{q}\tilde{q}, \mathbb{R}$
none 80–134	95	30 ABREU	99G DLPH	$e\gamma \rightarrow \tilde{u}_L, \mathbb{R}, LQ\mathbb{D}, \lambda=0.3$
none 80–161	95	30 ABREU	99G DLPH	$e\gamma \rightarrow \tilde{d}_R, \mathbb{R}, LQ\mathbb{D}, \lambda=0.3$
>225	95	31 ABBOTT	98E D0	$\tilde{u}_L, \mathbb{R}, \lambda'_{ijk}$ decays
>204	95	31 ABBOTT	98E D0	$\tilde{d}_R, \mathbb{R}, \lambda'_{ijk}$ decays
> 79	95	31 ABBOTT	98E D0	$\tilde{d}_L, \mathbb{R}, \lambda'_{ijk}$ decays
>202	95	32 ABE	98S CDF	$\tilde{u}_L, \mathbb{R}, \lambda'_{2jk}$ decays
>160	95	32 ABE	98S CDF	$\tilde{d}_R, \mathbb{R}, \lambda'_{2jk}$ decays
>140	95	33 ACKERSTAFF	98V OPAL	$e^+e^- \rightarrow q\tilde{q}, \mathbb{R}, \lambda=0.3$
> 77	95	34 BREITWEG	98 ZEUS	$m_{\tilde{q}}=m_{\tilde{e}}, m(\tilde{\chi}_1^0)=40$ GeV
>216	95	35 DATTA	97 THEO	$\tilde{\nu}$'s lighter than $\tilde{\chi}_1^\pm, \tilde{\chi}_2^0$
none 130–573	95	36 DERRICK	97 ZEUS	$e\bar{p} \rightarrow \tilde{q}, \tilde{q} \rightarrow \mu j$ or $\tau j, \mathbb{R}$
none 190–650	95	37 HEWETT	97 THEO	$e\bar{p} \rightarrow \tilde{q}, \tilde{q} \rightarrow q\tilde{g}$, with a light gluino
> 63	95	38 TEREKHOV	97 THEO	$q\bar{g} \rightarrow q\tilde{g}, \tilde{q} \rightarrow q\tilde{g}$, with a light gluino
none 330–400	95	39 AID	96C H1	$m_{\tilde{q}}=m_{\tilde{e}}, m_{\tilde{d}_0}=35$ GeV
>176	95	40 TEREKHOV	96 THEO	$u\bar{g} \rightarrow \tilde{u}\tilde{g}, \tilde{u} \rightarrow \tilde{u}\tilde{g}$ with a light gluino
> 90	90	41 ABACHI	95C D0	Any $m_{\tilde{g}} < 300$ GeV; with cascade decays
>100		42 ABE	95T CDF	$\tilde{q} \rightarrow \tilde{\chi}_2^0 \rightarrow \tilde{\chi}_1^0 \gamma$
		43 ABE	92L CDF	Any $m_{\tilde{g}} < 410$ GeV; with cascade decay
		44 ROY	92 RVUE	$p\bar{p} \rightarrow \tilde{q}\tilde{q}, \mathbb{R}$
		45 NOJIRI	91 COSM	

¹ ABAZOV 08G looked in 2.1 fb⁻¹ of $p\bar{p}$ collisions at $\sqrt{s}=1.96$ TeV for events with acoplanar jets or multijets with large \mathbb{E}_T . No significant excess was found compared to the background expectation. A limit is derived on the masses of squarks and gluinos for specific MSUGRA parameter values, see Figure 3. Similar results would be obtained for a large class of parameter sets. Supersedes the results of ABAZOV 06c.

² ACHARD 04 search for the production of $\tilde{q}\tilde{q}$ of the first two generations in acoplanar di-jet final states in the 192–209 GeV data. Degeneracy of the squark masses is assumed either for both left and right squarks or for right squarks only, as well as $B(\tilde{q} \rightarrow q\tilde{\chi}_1^0) = 1$. See Fig. 7 for the dependence of the limits on $m_{\tilde{d}_0}$. This limit supersedes ACCIARRI 99v.

³ ABBOTT 01D looked in ~ 108 pb⁻¹ of $p\bar{p}$ collisions at $\sqrt{s}=1.8$ TeV for events with e, μ, ν , or e, μ accompanied by at least 2 jets and \mathbb{E}_T . Excluded regions are obtained in the MSUGRA framework from a scan over the parameters $0 < m_0 < 300$ GeV, $10 < m_{1/2} < 110$ GeV, and $1.2 < \tan\beta < 10$.

Searches Particle Listings

Supersymmetric Particle Searches

- ⁴ BARATE 01 looked for acoplanar dijets + \cancel{E}_T final states at 189 to 202 GeV. The limit assumes $B(\bar{q} \rightarrow q\tilde{\chi}_1^0)=1$, with $\Delta m = m_{\tilde{q}} - m_{\tilde{\chi}_1^0}$. It applies to $\tan\beta=4$, $\mu=-400$ GeV. See their Fig. 2 for the exclusion in the $(m_{\tilde{q}}, m_{\tilde{g}})$ plane. These limits include and update the results of BARATE 99Q.
- ⁵ ABE 96b searched for production of gluinos and five degenerate squarks in final states containing a pair of leptons, two jets, and missing E_T . The two leptons arise from the semileptonic decays of charginos produced in the cascade decays. The limit is derived for fixed $\tan\beta = 4.0$, $\mu = -400$ GeV, and $m_{H^\pm} = 500$ GeV, and with the cascade decays of the squarks and gluinos calculated within the framework of the Minimal Supergravity scenario.
- ⁶ SCHAE 07A studied the effect on hadronic cross sections and charge asymmetries of t -channel down-type squark exchange via R -parity violating couplings $LQ\bar{D}$ at $\sqrt{s} = 189$ –209 GeV. The limit here refers to the case $j = 1, 2$ and holds for λ'_{1jk} of electromagnetic strength. The results of this analysis are combined with BARATE 00I.
- ⁷ ABZOV 06c looked in 310 pb^{-1} of $p\bar{p}$ collisions at $\sqrt{s} = 1.96$ TeV for events with acoplanar jets or multijets with large \cancel{E}_T . No significant excess was found compared to the background expectation. A limit is derived on the masses of squarks and gluinos for specific MSUGRA parameter values, see Figure 3. Similar results would be obtained for a large class of parameter sets. Supersedes the results of ABBOTT 99L.
- ⁸ CHEKANOV 05A search for lepton flavor violating processes $e^\pm p \rightarrow \ell X$, where $\ell = \mu$ or τ with high p_T , in 130 pb^{-1} at 300 and 318 GeV. Such final states may originate from LQD couplings with simultaneously non-zero λ'_{1jk} and λ'_{ijk} ($i=2$ or 3). The quoted mass bounds hold for a u -type squark, assume a λ' of electromagnetic strength and contributions from only direct squark decays. For d -type squarks the bounds are strengthened to 278 and 275 GeV for the μ and τ final states, respectively. Supersedes the results of CHEKANOV 02.
- ⁹ AKTAS 04b looked in 77.8 pb^{-1} of $e^\pm p$ collisions at $\sqrt{s} = 319$ GeV for resonant production of \bar{q} by R -parity violating $LQ\bar{D}$ couplings assuming that one of the λ' couplings dominates over all others. They consider final states with or without leptons and/or jets and/or \cancel{p}_T resulting from direct and indirect decays. They combine the channels to derive limits on λ'_{1j1} and λ'_{11k} as a function of the squark mass, see their Figs. 8 and 9, from a scan over the parameters $70 < M_2 < 350$ GeV, $-300 < \mu < 300$ GeV, $\tan\beta = 6$, for a fixed mass of 90 GeV for degenerate sleptons and an LSP mass > 30 GeV. The quoted limits refer to $\lambda' = 0.3$, with $U=u,c,t$ and $D=d,s,b$. Supersedes the results of ADLOFF 01b.
- ¹⁰ ADLOFF 03 looked for the s -channel production of squarks via R $LQ\bar{D}$ couplings in 117.2 pb^{-1} of e^+p data at $\sqrt{s} = 301$ and 319 GeV and of e^-p data at $\sqrt{s} = 319$ GeV. The comparison of the data with the SM differential cross section allows limits to be set on couplings for processes mediated through contact interactions. They obtain lower bounds on the value of $m_{\tilde{q}}/\lambda'$ of 710 GeV for the process $e^+ \bar{u} \rightarrow \bar{d}^k$ (and charge conjugate), mediated by λ'_{11k} , and of 430 GeV for the process $e^+ d \rightarrow \bar{u}^j$ (and charge conjugate), mediated by λ'_{1j1} .
- ¹¹ CHEKANOV 03b used 131.5 pb^{-1} of e^+p and e^-p data taken at 300 and 318 GeV to look for narrow resonances in the $e q$ or νq final states. Such final states may originate from $LQ\bar{D}$ couplings with non-zero λ'_{1j1} (leading to \bar{u}_j) or λ'_{11k} (leading to \bar{d}_k). See their Fig. 8 and explanations in the text for limits. The quoted mass bound assumes that only direct squark decays contribute.
- ¹² HEISTER 03g searches for the production of squarks in the case of R prompt decays with $U\bar{D}\bar{D}$ direct couplings at $\sqrt{s} = 189$ –209 GeV.
- ¹³ ABZOV 02f looked in 77.5 pb^{-1} of $p\bar{p}$ collisions at 1.8 TeV for events with $\geq 2\mu + \geq 4$ jets, originating from associated production of squarks followed by an indirect R decay (of the $\tilde{\chi}_1^0$) via $LQ\bar{D}$ couplings of the type λ'_{2jk} where $j=1,2$ and $k=1,2,3$. Bounds are obtained in the MSUGRA scenario by a scan in the range $0 \leq M_0 \leq 400$ GeV, $60 \leq m_{1/2} \leq 120$ GeV for fixed values $A_0=0$, $\mu < 0$, and $\tan\beta=2$ or 6 . The bounds are weaker for $\tan\beta=6$. See Figs. 2,3 for the exclusion contours in $m_{1/2}$ versus m_0 for $\tan\beta=2$ and 6 , respectively.
- ¹⁴ ABZOV 02g search for associated production of gluinos and squarks in 92.7 pb^{-1} of $p\bar{p}$ collisions at $\sqrt{s}=1.8$ TeV, using events with one electron, ≥ 4 jets, and large \cancel{E}_T . The results are compared to a MSUGRA scenario with $\mu < 0$, $A_0=0$, and $\tan\beta=3$ and allow to exclude a region of the $(m_0, m_{1/2})$ shown in Fig. 11.
- ¹⁵ ABBIENDI 02 looked for events with an electron or neutrino and a jet in e^+e^- at 189 GeV. Squarks (or leptoquarks) could originate from a $LQ\bar{D}$ coupling of an electron with a quark from the fluctuation of a virtual photon. Limits on the couplings λ'_{1jk} as a function of the squark mass are shown in Figs. 8–9, assuming that only direct squark decays contribute.
- ¹⁶ ABBIENDI 02b looked for events with an electron or neutrino and a jet in e^+e^- at 189–209 GeV. Squarks (or leptoquarks) could originate from a $LQ\bar{D}$ coupling of an electron with a quark from the fluctuation of a virtual photon. Limits on the couplings λ'_{1jk} as a function of the squark mass are shown in Fig. 4, assuming that only direct squark decays contribute. The quoted limits are read off from Fig. 4. Supersedes the results of ABBIENDI 02.
- ¹⁷ ACHARD 02 searches for the production of squarks in the case of R prompt decays with $U\bar{D}\bar{D}$ couplings at $\sqrt{s}=189$ –208 GeV. The search is performed for direct and indirect decays, assuming one coupling at the time to be nonzero. The limit holds for indirect decays. Stronger limits are reached for (\bar{u}_R, \bar{d}_R) direct (80,56) GeV and (\bar{u}_L, \bar{d}_L) direct or indirect (87,86) GeV decays.
- ¹⁸ CHEKANOV 02 search for lepton flavor violating processes $e^+p \rightarrow \ell X$, where $\ell = \mu$ or τ with high p_T , in 47.7 pb^{-1} of e^+p collisions at 300 GeV. Such final states may originate from $LQ\bar{D}$ couplings with simultaneously nonzero λ'_{1jk} and λ'_{ijk} ($i=2$ or 3). The quoted mass bound assumes that only direct squark decays contribute.
- ¹⁹ BARATE 01b searches for the production of squarks in the case of R prompt decays with LLE indirect or $U\bar{D}\bar{D}$ direct couplings at $\sqrt{s}=189$ –202 GeV. The limit holds for direct decays mediated by R $U\bar{D}\bar{D}$ couplings. Limits are also given for LLE indirect decays ($m_{\tilde{u}_R} > 90$ GeV and $m_{\tilde{d}_R} > 89$ GeV). Supersedes the results from BARATE 00H.
- ²⁰ BREITWEG 01 searches for squark production in 47.7 pb^{-1} of e^+p collisions, mediated by R couplings $LQ\bar{D}$ and leading to final states with $\bar{\nu}$ and ≥ 1 jet, complementing the e^+X final states of BREITWEG 00E. Limits are derived on $\lambda'\sqrt{\beta}$, where β is the branching fraction of the squarks into $e^+q+\cancel{p}q$, as function of the squark mass, see their Fig. 15. The quoted mass limit assumes that only direct squark decays contribute.
- ²¹ ABBOTT 00c searched in $\sim 94 \text{ pb}^{-1}$ of $p\bar{p}$ collisions for events with $\mu\mu$ +jets, originating from associated production of leptoquarks. The results can be interpreted as limits on production of squarks followed by direct R decay via $\lambda'_{2jk}L_2Q_jd_k^c$ couplings. Bounds are obtained on the cross section for branching ratios of 1 and of 1/2, see their Fig. 4. The former yields the limit on the \bar{u}_L . The latter is combined with the bound of ABBOTT 99J from the $\mu\nu$ +jets channel and of ABBOTT 98E and ABBOTT 98J from the $\nu\nu$ +jets channel to yield the limit on \bar{d}_R .
- ²² ACCIARRI 00P studied the effect on hadronic cross sections of t -channel down-type squark exchange via R -parity violating coupling $\lambda'_{1jk}L_1Q_jd_k^c$. The limit here refers to the case $j=1,2$, and holds for $\lambda'_{1jk}=0.3$. Data collected at $\sqrt{s}=130$ –189 GeV, superseding the results of ACCIARRI 98J.
- ²³ AFFOLDER 00k searched in $\sim 88 \text{ pb}^{-1}$ of $p\bar{p}$ collisions for events with 2–3 jets, at least one being b -tagged, large \cancel{E}_T , and no high p_T leptons. Such $\nu\nu$ + b -jets events would originate from associated production of squarks followed by direct R decay via $\lambda'_{1j3}L_1Q_jd_3^c$ couplings. Bounds are obtained on the production cross section assuming zero branching ratio to charged leptons.
- ²⁴ BARATE 00i studied the effect on hadronic cross sections and charge asymmetries of t -channel down-type squark exchange via R -parity violating coupling $\lambda'_{1jk}L_1Q_jd_k^c$. The limit here refers to the case $j=1,2$, and holds for $\lambda'_{1jk}=0.3$. A 50 GeV limit is found for up-type squarks with $k=3$. Data collected at $\sqrt{s}=130$ –183 GeV.
- ²⁵ BREITWEG 00e searches for squark exchange in e^+p collisions, mediated by R couplings $LQ\bar{D}$ and leading to final states with an identified e^+ and ≥ 1 jet. The limit applies to up-type squarks of all generations, and assumes $B(\bar{q} \rightarrow qe)=1$.
- ²⁶ ABBOTT 99 searched for $\gamma\cancel{E}_T + \geq 2$ jet final states, and set limits on $\sigma(p\bar{p} \rightarrow \bar{q}+X) \cdot B(\bar{q} \rightarrow \gamma\cancel{E}_T+X)$. The quoted limits correspond to $m_{\tilde{g}} \geq m_{\tilde{q}}$, with $B(\tilde{\chi}_2^0 \rightarrow \tilde{\chi}_1^0\gamma)=1$ and $B(\tilde{\chi}_1^0 \rightarrow \tilde{G}\gamma)=1$, respectively. They improve to 310 GeV (360 GeV in the case of $\gamma\tilde{G}$ decay) for $m_{\tilde{g}}=m_{\tilde{q}}$.
- ²⁷ ABBOTT 99k uses events with an electron pair and four jets to search for the decay of the $\tilde{\chi}_1^0$ LSP via R $LQ\bar{D}$ couplings. The particle spectrum and decay branching ratios are taken in the framework of minimal supergravity. An excluded region at 95% CL is obtained in the $(m_0, m_{1/2})$ plane under the assumption that $A_0=0$, $\mu < 0$, $\tan\beta=2$ and any one of the couplings $\lambda'_{1jk} > 10^{-3}$ ($j=1,2$ and $k=1,2,3$) and from which the above limit is computed. For equal mass squarks and gluinos, the corresponding limit is 277 GeV. The results are essentially independent of A_0 , but the limit deteriorates rapidly with increasing $\tan\beta$ or $\mu > 0$.
- ²⁸ ABBOTT 99l consider events with three or more jets and large \cancel{E}_T . Spectra and decay rates are evaluated in the framework of minimal Supergravity, assuming five flavors of degenerate squarks, and scanning the space of the universal gaugino ($m_{1/2}$) and scalar (m_0) masses. See their Figs. 2–3 for the dependence of the limit on the relative value of $m_{\tilde{q}}$ and $m_{\tilde{g}}$.
- ²⁹ ABE 99m looked in 107 pb^{-1} of $p\bar{p}$ collisions at $\sqrt{s}=1.8$ TeV for events with like sign dielectrons and two or more jets from the sequential decays $\bar{q} \rightarrow q\tilde{\chi}_1^0$ and $\tilde{\chi}_1^0 \rightarrow e q\bar{q}'$, assuming R coupling $L_1Q_jd_k^c$, with $j=2,3$ and $k=1,2,3$. They assume five degenerate squark flavors, $B(\bar{q} \rightarrow q\tilde{\chi}_1^0)=1$, $B(\tilde{\chi}_1^0 \rightarrow e q\bar{q}')=0.25$ for both e^+ and e^- , and $m_{\tilde{g}} \geq 200$ GeV. The limit is obtained for $m_{\tilde{\chi}_1^0} \geq m_{\tilde{q}}/2$ and improves for heavier gluinos or heavier $\tilde{\chi}_1^0$.
- ³⁰ ABREU 99g looked for events with an electron or neutrino and a jet in e^+e^- at 183 GeV. Squarks (or leptoquarks) could originate from a $LQ\bar{D}$ coupling of an electron with a quark from the fluctuation of a virtual photon. Limits on the couplings λ'_{1jk} as a function of the squark mass are shown in Fig. 4, assuming that only direct squark decays contribute.
- ³¹ ABBOTT 98E searched in $\sim 115 \text{ pb}^{-1}$ of $p\bar{p}$ collisions for events with $e\nu$ +jets, originating from associated production of squarks followed by direct R decay via $\lambda'_{1jk}L_1Q_jd_k^c$ couplings. Bounds are obtained by combining these results with the previous bound of ABBOTT 97B from the ee +jets channel and with a reinterpretation of ABACHI 96b $\nu\nu$ +jets channel.
- ³² ABE 98s looked in $\sim 110 \text{ pb}^{-1}$ of $p\bar{p}$ collisions at $\sqrt{s}=1.8$ TeV for events with $\mu\mu$ +jets originating from associated production of squarks followed by direct R decay via $\lambda'_{2jk}L_2Q_jd_k^c$ couplings. Bounds are obtained on the production cross section times the square of the branching ratio, see Fig. 2. Mass limits result from the comparison with theoretical cross sections and branching ratio equal to 1 for \bar{u}_L and 1/2 for \bar{d}_R .
- ³³ ACKERSTAFF 98v and ACCIARRI 98j studied the interference of t -channel squark (\bar{d}_R) exchange via R -parity violating $\lambda'_{1jk}L_1Q_jd_k^c$ coupling in $e^+e^- \rightarrow q\bar{q}$. The limit is for $\lambda'_{1jk}=0.3$. See paper for related limits on \bar{u}_L exchange. Data collected at $\sqrt{s}=130$ –172 GeV.
- ³⁴ BREITWEG 98 used positron+jet events with missing energy and momentum to look for $e^+q \rightarrow \bar{e}q$ via gaugino-like neutralino exchange with decays into $(e\tilde{\chi}_1^0)(q\tilde{\chi}_1^0)$. See paper for dependences in $m_{\tilde{e}}, m_{\tilde{\chi}_1^0}$.
- ³⁵ DATTA 97 argues that the squark mass bound by ABACHI 95c can be weakened by 10–20 GeV if one relaxes the assumption of the universal scalar mass at the GUT-scale so that the $\tilde{\chi}_1^\pm, \tilde{\chi}_2^0$ in the squark cascade decays have dominant and invisible decays to $\bar{\nu}$.
- ³⁶ DERRICK 97 looked for lepton-number violating final states via R -parity violating couplings $\lambda'_{1jk}L_1Q_jd_k$. When $\lambda'_{11k}\lambda'_{ijk} \neq 0$, the process $e\nu \rightarrow \bar{d}_k^* \rightarrow \ell_i\nu_j$ is possible. When $\lambda'_{1j1}\lambda'_{ijk} \neq 0$, the process $e\bar{d} \rightarrow \bar{u}_j^* \rightarrow \ell_i\bar{d}_k$ is possible. 100% branching fraction $\bar{q} \rightarrow \ell j$ is assumed. The limit quoted here corresponds to $\bar{t} \rightarrow \tau q$ decay, with $\lambda'=0.3$. For different channels, limits are slightly better. See Table 6 in their paper.
- ³⁷ HEWETT 97 reanalyzed the limits on possible resonances in di-jet mode ($\bar{q} \rightarrow q\bar{g}$) from ALITTI 93 quoted in "Limits for Excited q (q^*) from Single Production," ABE 96

- in "SCALE LIMITS for Contact Interactions: $\Lambda(qqqq)$," and unpublished CDF, DØ bounds. The bound applies to the gluino mass of 5 GeV, and improves for lighter gluino. The analysis has gluinos in parton distribution function.
- 38 TEREKHOV 97 improved the analysis of TEREKHOV 96 by including di-jet angular distributions in the analysis.
- 39 AID 96c used positron+jet events with missing energy and momentum to look for $e^+q \rightarrow \bar{e}q$ via neutralino exchange with decays into $(e\tilde{\chi}_1^0)(q\tilde{\chi}_1^0)$. See the paper for dependences on $m_{\tilde{e}}, m_{\tilde{\chi}_1^0}$.
- 40 TEREKHOV 96 reanalyzed the limits on possible resonances in di-jet mode ($\bar{u} \rightarrow u\tilde{g}$) from ABE 95N quoted in "MASS LIMITS for g_A (axigluon)." The bound applies only to the case with a light gluino.
- 41 ABACHI 95c assume five degenerate squark flavors with $m_{\tilde{q}_L} = m_{\tilde{q}_R}$. Sleptons are assumed to be heavier than squarks. The limits are derived for fixed $\tan\beta = 2.0$, $\mu = -250$ GeV, and $m_{H^\pm} = 500$ GeV, and with the cascade decays of the squarks and gluinos calculated within the framework of the Minimal Supergravity scenario. The bounds are weakly sensitive to the three fixed parameters for a large fraction of parameter space. No limit is given for $m_{\text{gluino}} > 547$ GeV.
- 42 ABE 95T looked for a cascade decay of five degenerate squarks into $\tilde{\chi}_2^0$ which further decays into $\tilde{\chi}_1^0$ and a photon. No signal is observed. Limits vary widely depending on the choice of parameters. For $\mu = -40$ GeV, $\tan\beta = 1.5$, and heavy gluinos, the range $50 < m_{\tilde{q}} \text{ (GeV)} < 110$ is excluded at 90% CL. See the paper for details.
- 43 ABE 92L assume five degenerate squark flavors and $m_{\tilde{q}_L} = m_{\tilde{q}_R}$. ABE 92L includes the effect of cascade decay, for a particular choice of parameters, $\mu = -250$ GeV, $\tan\beta = 2$. Results are weakly sensitive to these parameters over much of parameter space. No limit for $m_{\tilde{q}} \leq 50$ GeV (but other experiments rule out that region). Limits are 10–20 GeV higher if $B(\tilde{q} \rightarrow q\tilde{\gamma}) = 1$. Limit assumes GUT relations between gaugino masses and the gauge coupling; in particular that for $|\mu|$ not small, $m_{\tilde{\chi}_1^0} \approx m_{\tilde{g}}/6$. This last relation implies that as $m_{\tilde{g}}$ increases, the mass of $\tilde{\chi}_1^0$ will eventually exceed $m_{\tilde{q}}$ so that no decay is possible. Even before that occurs, the signal will disappear; in particular no bounds can be obtained for $m_{\tilde{g}} > 410$ GeV, $m_{H^\pm} = 500$ GeV.
- 44 ROY 92 reanalyzed CDF limits on di-lepton events to obtain limits on squark production in R -parity violating models. The 100% decay $\tilde{q} \rightarrow q\tilde{\chi}$ where $\tilde{\chi}$ is the LSP, and the LSP decays either into $\ell q\bar{q}$ or $\ell\ell\bar{\nu}$ is assumed.
- 45 NOJIRI 91 argues that a heavy squark should be nearly degenerate with the gluino in minimal supergravity not to overclose the universe.

Long-lived \tilde{q} (Squark) MASS LIMIT

The following are bounds on long-lived scalar quarks, assumed to hadronise into hadrons with lifetime long enough to escape the detector prior to a possible decay. Limits may depend on the mixing angle of mass eigenstates: $\tilde{q}_1 = \tilde{q}_L \cos\theta_q + \tilde{q}_R \sin\theta_q$. The coupling to the Z^0 boson vanishes for up-type squarks when $\theta_u = 0.98$, and for down type squarks when $\theta_d = 1.17$.

VALUE (GeV)	CL%	DOCUMENT ID	TECN	COMMENT
••• We do not use the following data for averages, fits, limits, etc. •••				
>95	95	1 HEISTER	03H ALEP	\bar{u}
>92	95	1 HEISTER	03H ALEP	\bar{d}
none 2–85	95	2 ABREU	98P DLPH	\bar{u}_L
none 2–81	95	2 ABREU	98P DLPH	\bar{u}_R
none 2–80	95	2 ABREU	98P DLPH	$\bar{u}, \theta_u = 0.98$
none 2–83	95	2 ABREU	98P DLPH	\bar{d}_L
none 5–40	95	2 ABREU	98P DLPH	\bar{d}_R
none 5–38	95	2 ABREU	98P DLPH	$\bar{d}, \theta_d = 1.17$

- 1 HEISTER 03H use e^+e^- data at and around the Z^0 peak to look for hadronizing stable squarks. Combining their results on searches for charged and neutral R -hadrons with JANOT 03, a lower limit of 15.7 GeV on the mass is obtained. Combining this further with the results of searches for tracks with anomalous ionization in data from 183 to 208 GeV yields the quoted bounds.
- 2 ABREU 98P assumes that 40% of the squarks will hadronise into a charged hadron, and 60% into a neutral hadron which deposits most of its energy in hadron calorimeter. Data collected at $\sqrt{s} = 130\text{--}183$ GeV.

\tilde{b} (Sbottom) MASS LIMIT

Limits in e^+e^- depend on the mixing angle of the mass eigenstate $\tilde{b}_1 = \tilde{b}_L \cos\theta_b + \tilde{b}_R \sin\theta_b$. Coupling to the Z vanishes for $\theta_b \sim 1.17$. As a consequence, no absolute constraint in the mass region $\lesssim 40$ GeV is available in the literature at this time from e^+e^- collisions. In the Listings below, we use $\Delta m = m_{\tilde{b}_1} - m_{\tilde{\chi}_1^0}$.

VALUE (GeV)	CL%	DOCUMENT ID	TECN	COMMENT
>193	95	1 AALTONEN	07E CDF	$\tilde{b}_1 \rightarrow b\tilde{\chi}_1^0, m_{\tilde{\chi}_1^0} = 40$ GeV
none 35–222	95	2 ABAZOV	06R D0	$\tilde{b} \rightarrow b\tilde{\chi}_1^0, m_{\tilde{\chi}_1^0} = 50$ GeV
>220	95	3 ABULENCIA	06I CDF	$\tilde{g} \rightarrow \tilde{b}b, \Delta m > 6$ GeV, $\tilde{b}_1 \rightarrow b\tilde{\chi}_1^0, m_{\tilde{g}} < 270$ GeV
> 95		4 ACHARD	04 L3	$\tilde{b} \rightarrow b\tilde{\chi}_1^0, \theta_b = 0, \Delta m > 15\text{--}25$ GeV
> 81		4 ACHARD	04 L3	$\tilde{b} \rightarrow b\tilde{\chi}_1^0, \text{all } \theta_b, \Delta m > 15\text{--}25$ GeV
> 7.5	95	5 JANOT	04 THEO	unstable $\tilde{b}_1, e^+e^- \rightarrow$ hadrons
> 93	95	6 ABDALLAH	03M DLPH	$\tilde{b} \rightarrow b\tilde{\chi}_1^0, \theta_b = 0, \Delta m > 7$ GeV
> 76	95	6 ABDALLAH	03M DLPH	$\tilde{b} \rightarrow b\tilde{\chi}_1^0, \text{all } \theta_b, \Delta m > 7$ GeV
> 85.1	95	7 ABBIENDI	02H OPAL	$\tilde{b} \rightarrow b\tilde{\chi}_1^0, \text{all } \theta_b, \Delta m > 10$ GeV,
> 89	95	8 HEISTER	02K ALEP	CDF $\tilde{b} \rightarrow b\tilde{\chi}_1^0, \text{all } \theta_b, \Delta m > 8$ GeV,
none 3.5–4.5	95	9 SAVINOV	01 CLEO	CDF \tilde{B} meson
none 80–145		10 AFFOLDER	00D CDF	$\tilde{b} \rightarrow b\tilde{\chi}_1^0, m_{\tilde{\chi}_1^0} < 50$ GeV

••• We do not use the following data for averages, fits, limits, etc. •••				
> 78	95	11 ABDALLAH	04M DLPH	\tilde{R}, \tilde{b}_L , indirect, $\Delta m > 5$ GeV
none 50–82	95	12 ABDALLAH	03C DLPH	$\tilde{b} \rightarrow b\tilde{g}$, stable \tilde{g} , all θ_b , $\Delta m > 10$ GeV
		13 BERGER	03 THEO	
> 71.5	95	14 HEISTER	03G ALEP	\tilde{b}_L, R decay
> 27.4	95	15 HEISTER	03H ALEP	$\tilde{b} \rightarrow b\tilde{g}$, stable \tilde{g} or \tilde{b}
> 48	95	16 ACHARD	02 L3	\tilde{b}_1, R decays
		17 BAEK	02 THEO	
		18 BECHER	02 THEO	
		19 CHEUNG	02B THEO	
		20 CHO	02 THEO	
		21 BERGER	01 THEO	$p\bar{p} \rightarrow X+b$ -quark
none 52–115	95	22 ABBOTT	99F D0	$\tilde{b} \rightarrow b\tilde{\chi}_1^0, m_{\tilde{\chi}_1^0} < 20$ GeV

- 1 AALTONEN 07E searched in 295 pb^{-1} of $p\bar{p}$ collisions at $\sqrt{s} = 1.96$ TeV for multijet events with large E_T . They request at least one heavy flavor-tagged jet and no identified leptons. The branching ratio $\tilde{b}_1 \rightarrow b\tilde{\chi}_1^0$ is assumed to be 100%. No significant excess was found compared to the background expectation. Upper limits on the cross-section are extracted and a limit is derived on the masses of sbottom versus $\tilde{\chi}_1^0$, see their Fig. 5.
- 2 ABAZOV 06R looked in 310 pb^{-1} of $p\bar{p}$ collisions at $\sqrt{s} = 1.96$ TeV for events with 2 or 3 jets and large E_T with at least 1 b -tagged jet and a veto against isolated leptons. No excess is observed relative to the SM background expectations. Limits are set on the sbottom pair production cross-section under the assumption that the only decay mode is into $b\tilde{\chi}_1^0$. Exclusion contours are derived in the plane of sbottom versus neutralino masses, shown in their Fig. 2. The observed limit is more constraining than the expected one due to a lack of events corresponding to large sbottom masses. Supersedes the results of ABBOTT 99f.
- 3 ABULENCIA 06i searched in 156 pb^{-1} of $p\bar{p}$ collisions at $\sqrt{s} = 1.96$ TeV for multijet events with large E_T . They request at least 2 b -tagged jets and no isolated leptons. They investigate the production of gluinos decaying into $\tilde{b}_1 b$ followed by $\tilde{b}_1 \rightarrow b\tilde{\chi}_1^0$. Both branching fractions are assumed to be 100% and the LSP mass to be 60 GeV. No significant excess was found compared to the background expectation. Upper limits on the cross-section are extracted and a limit is derived on the masses of sbottom and gluinos, see their Fig. 3.
- 4 ACHARD 04 search for the production of $\tilde{b}\tilde{b}$ in acoplanar b -tagged di-jet final states in the 192–209 GeV data. See Fig. 6 for the dependence of the limits on $m_{\tilde{\chi}_1^0}$. This limit supersedes ACCIARRI 99v.
- 5 JANOT 04 reanalyzes $e^+e^- \rightarrow$ hadrons total cross section data with $\sqrt{s} = 20\text{--}209$ GeV from PEP, PETRA, TRISTAN, SLC, and LEP and constrains the mass of \tilde{b}_1 assuming it decays quickly to hadrons.
- 6 ABDALLAH 03M looked for \tilde{b} pair production in events with acoplanar jets and E at $\sqrt{s} = 189\text{--}208$ GeV. The limit improves to 87 (98) GeV for all θ_b ($\theta_b = 0$) for $\Delta m > 10$ GeV. See Fig. 24 and Table 11 for other choices of Δm . These limits include and update the results of ABREU, P 00d.
- 7 ABBIENDI 02H search for events with two acoplanar jets and p_T in the 161–209 GeV data. The limit assumes 100% branching ratio and uses the exclusion at large Δm from CDF (AFFOLDER 00d). For $\theta_b = 0$, the bound improves to > 96.9 GeV. See Fig. 4 and Table 6 for the more general dependence on the limits on Δm . These results supersede ABBIENDI 99m.
- 8 HEISTER 02k search for bottom squarks in final states with acoplanar jets with b tagging, using 183–209 GeV data. The mass bound uses the CDF results from AFFOLDER 00d. See Fig. 5 for the more general dependence of the limits on Δm . Updates BARATE 01.
- 9 SAVINOV 01 use data taken at $\sqrt{s} = 10.52$ GeV, below the $B\bar{B}$ threshold. They look for events with a pair of leptons with opposite charge and a fully reconstructed hadronic D or D^* decay. These could originate from production of a light-sbottom hadron followed by $\tilde{B} \rightarrow D^{(*)}e^- \bar{\nu}$, in case the $\bar{\nu}$ is the LSP, or $\tilde{B} \rightarrow D^{(*)}\pi\ell^-$, in case of R . The mass range $3.5 \leq M(\tilde{B}) \leq 4.5$ GeV was explored, assuming 100% branching ratio for either of the decays. In the $\bar{\nu}$ LSP scenario, the limit holds only for $M(\bar{\nu})$ less than about 1 GeV and for the D^* decays it is reduced to the range 3.9–4.5 GeV. For the R decay, the whole range is excluded.
- 10 AFFOLDER 00d search for final states with 2 or 3 jets and E_T , one jet with a b tag. See their Fig. 3 for the mass exclusion in the $m_{\tilde{b}_1} - m_{\tilde{\chi}_1^0}$ plane.
- 11 ABDALLAH 04M use data from $\sqrt{s} = 192\text{--}208$ GeV to derive limits on sparticle masses under the assumption of R with $\tilde{U}\tilde{D}\tilde{D}$ couplings. The results are valid for $\mu = -200$ GeV, $\tan\beta = 1.5$, $\Delta m > 5$ GeV and assuming a BR of 1 for the given decay. The limit quoted is for indirect $\tilde{U}\tilde{D}\tilde{D}$ decays using the neutralino constraint of 38.0 GeV, also derived in ABDALLAH 04M, and assumes no mixing. For indirect decays it remains at 78 GeV when the neutralino constraint is not used. Supersedes the result of ABREU 01d.
- 12 ABDALLAH 03c looked for events of the type $q\bar{q}R^\pm R^\pm, q\bar{q}R^\pm R^0, \text{ or } q\bar{q}R^0 R^0$ in e^+e^- interactions at $\sqrt{s} = 189\text{--}208$ GeV. The R^\pm bound states are identified by anomalous dE/dx in the tracking chambers and the R^0 by missing energy due to their reduced energy loss in the calorimeters. Excluded mass regions in the $(m(\tilde{b}), m(\tilde{g}))$ plane for $m(\tilde{g}) > 2$ GeV are obtained for several values of the probability for the gluino to fragment into R^\pm or R^0 , as shown in their Fig. 19. The limit improves to 94 GeV for $\theta_b = 0$.
- 13 BERGER 03 studies the constraints on a \tilde{b}_1 with mass in the 2.2–5.5 GeV region coming from radiative decays of $\Upsilon(nS)$ into sbottomonium. The constraints apply only if \tilde{b}_1 lives long enough to permit formation of the sbottomonium bound state. A small region of mass in the $m_{\tilde{b}_1} - m_{\tilde{g}}$ plane survives current experimental constraints from CLEO.
- 14 HEISTER 03g searches for the production of \tilde{b} pairs in the case of R prompt decays with $L\bar{L}E, LQ\bar{D}$ or $U\bar{D}\bar{D}$ couplings at $\sqrt{s} = 189\text{--}209$ GeV. The limit holds for indirect decays mediated by R $\tilde{U}\tilde{D}\bar{D}$ couplings. It improves to 90 GeV for indirect decays mediated by R $L\bar{L}E$ couplings and to 80 GeV for indirect decays mediated by R $LQ\bar{D}$ couplings. Supersedes the results from BARATE 01b.
- 15 HEISTER 03h use their results on bounds on stable squarks, on stable gluinos and on squarks decaying to a stable gluino from the same paper to derive a mass limit on \tilde{b} , see their Fig. 13. The limit for a long-lived \tilde{b}_1 is 92 GeV.
- 16 ACHARD 02 searches for the production of squarks in the case of R prompt decays with $\tilde{U}\tilde{D}\bar{D}$ couplings at $\sqrt{s} = 189\text{--}208$ GeV. The search is performed for direct and indirect

Searches Particle Listings

Supersymmetric Particle Searches

- decays, assuming one coupling at the time to be nonzero. The limit is computed for the minimal cross section and holds for indirect decays and reaches 55 GeV for direct decays.
- ¹⁷BAEK 02 studies the constraints on a \tilde{b}_1 with mass in the 2.2–5.5 GeV region coming from precision measurements of Z^0 decays. It is noted that CP -violating couplings in the MSSM parameters relax the strong constraints otherwise derived from CP conservation.
- ¹⁸BECHER 02 studies the constraints on a \tilde{b}_1 with mass in the 2.2–5.5 GeV region coming from radiative B meson decays, and sets limits on the off-diagonal flavor-changing couplings $q b \tilde{g}$ ($q=d,s$).
- ¹⁹CHEUNG 02b studies the constraints on a \tilde{b}_1 with mass in the 2.2–5.5 GeV region and a gluino in the mass range 12–16 GeV, using precision measurements of Z^0 decays and e^+e^- annihilations at LEP2. Few detectable events are predicted in the LEP2 data for the model proposed by BERGER 01.
- ²⁰CHO 02 studies the constraints on a \tilde{b}_1 with mass in the 2.2–5.5 GeV region coming from precision measurements of Z^0 decays. Strong constraints are obtained for CP -conserving MSSM couplings.
- ²¹BERGER 01 reanalyzed interpretation of Tevatron data on bottom-quark production. Argues that pair production of light gluinos ($m \sim 12$ –16 GeV) with subsequent 2-body decay into a light sbottom ($m \sim 2$ –5.5 GeV) and bottom can reconcile Tevatron data with predictions of perturbative QCD for the bottom production rate. The sbottom must either decay hadronically via a R -parity- and B -violating interaction, or be long-lived. Constraints on the mass spectrum are derived from the measurements of time-averaged $B^0\text{-}\bar{B}^0$ mixing.
- ²²ABBOTT 99f looked for events with two jets, with or without an associated muon from b decay, and \cancel{E}_T . See Fig. 2 for the dependence of the limit on $m_{\tilde{\chi}_1^0}$. No limit for $m_{\tilde{\chi}_1^0} > 47$ GeV.

$\tilde{\tau}$ (Stop) MASS LIMIT

Limits depend on the decay mode. In e^+e^- collisions they also depend on the mixing angle of the mass eigenstate $\tilde{t}_1 = \tilde{t}_L \cos\theta_t + \tilde{t}_R \sin\theta_t$. The coupling to the Z vanishes when $\theta_t = 0.98$. In the Listings below, we use $\Delta m \equiv m_{\tilde{t}_1} - m_{\tilde{\chi}_1^0}$ or $\Delta m \equiv m_{\tilde{t}_1} - m_{\tilde{\nu}}$, depending on relevant decay mode. See also bounds in “ \tilde{q} (Squark) MASS LIMIT.” Limits made obsolete by the most recent analyses of e^+e^- and $p\bar{p}$ collisions can be found in previous Editions of this Review.

VALUE (GeV)	CL%	DOCUMENT ID	TECN	COMMENT
>176	95	¹ ABAZOV 08	D0	$\tilde{\tau} \rightarrow b\tilde{\nu}, m_{\tilde{\nu}}=60$ GeV
none 80–134	95	² ABAZOV 07b	D0	$\tilde{\tau} \rightarrow c\tilde{\chi}_1^0, m_{\tilde{\chi}_1^0} < 48$ GeV
none 80–120	95	³ ABAZOV 04	D0	$\tilde{\tau} \rightarrow b\ell\nu\tilde{\chi}_1^0, m_{\tilde{\chi}_1^0}=50$ GeV
> 90		⁴ ACHARD 04	L3	$\tilde{\tau} \rightarrow c\tilde{\chi}_1^0$, all θ_t , $\Delta m > 15$ –25 GeV
> 93		⁴ ACHARD 04	L3	$\tilde{\tau} \rightarrow b\tilde{\nu}$, all θ_t , $\Delta m > 15$ GeV
> 88		⁴ ACHARD 04	L3	$\tilde{\tau} \rightarrow b\tau\tilde{\nu}$, all $\theta_t, \Delta m > 15$ GeV
> 75	95	⁵ ABDALLAH 03M	DLPH	$\tilde{\tau} \rightarrow c\tilde{\chi}_1^0, \theta_t=0$, $\Delta m > 2$ GeV
> 71	95	⁵ ABDALLAH 03M	DLPH	$\tilde{\tau} \rightarrow c\tilde{\chi}_1^0$, all θ_t , $\Delta m > 2$ GeV
> 96	95	⁵ ABDALLAH 03M	DLPH	$\tilde{\tau} \rightarrow c\tilde{\chi}_1^0, \theta_t=0, \Delta m > 10$ GeV
> 92	95	⁵ ABDALLAH 03M	DLPH	$\tilde{\tau} \rightarrow c\tilde{\chi}_1^0$, all $\theta_t, \Delta m > 10$ GeV
none 80–131	95	⁶ ACOSTA 03c	CDF	$\tilde{\tau} \rightarrow b\tilde{\nu}, m_{\tilde{\nu}}=63$ GeV
>144	95	⁷ ABAZOV 02c	D0	$\tilde{\tau} \rightarrow b\tilde{\nu}, m_{\tilde{\nu}}=45$ GeV
> 95.7	95	⁸ ABBIENDI 02H	OPAL	$c\tilde{\chi}_1^0$, all $\theta_t, \Delta m > 10$ GeV
> 92.6	95	⁸ ABBIENDI 02H	OPAL	$b\tilde{\nu}$, all $\theta_t, \Delta m > 10$ GeV
> 91.5	95	⁸ ABBIENDI 02H	OPAL	$b\tau\tilde{\nu}$, all $\theta_t, \Delta m > 10$ GeV
> 63	95	⁹ HEISTER 02k	ALEP	any decay, any lifetime, all θ_t
> 92	95	⁹ HEISTER 02k	ALEP	$\tilde{\tau} \rightarrow c\tilde{\chi}_1^0$, all $\theta_t, \Delta m > 8$ GeV, CDF
> 97	95	⁹ HEISTER 02k	ALEP	$\tilde{\tau} \rightarrow b\tilde{\nu}$, all $\theta_t, \Delta m > 8$ GeV, DØ
> 78	95	⁹ HEISTER 02k	ALEP	$\tilde{\tau} \rightarrow b\tilde{\chi}_1^0 W^*$, all $\theta_t, \Delta m > 8$ GeV
• • • We do not use the following data for averages, fits, limits, etc. • • •				
>132		¹⁰ AALTONEN 07e	CDF	$\tilde{\tau}_1 \rightarrow c\tilde{\chi}_1^0, m_{\tilde{\chi}_1^0}=48$ GeV
> 77	95	¹¹ CHEKANOV 07	ZEUS	$e^+p \rightarrow \tilde{t}_1, R, LQ\bar{D}$
> 77	95	¹² ABBIENDI 04f	OPAL	R , direct, all $\theta_t, \Delta m > 5$ GeV
>122	95	¹³ ABDALLAH 04M	DLPH	R , indirect, all $\theta_t, \Delta m > 5$ GeV
>122	95	¹⁴ ACOSTA 04b	CDF	R , direct, all θ_t
> 74.5		¹⁵ AKTAS 04b	H1	R, \tilde{t}_1
		¹⁶ DAS 04	THEO	$\tilde{\tau}\tilde{\tau} \rightarrow b\ell\nu\chi^0\bar{b}q\bar{q}'\chi^0, m_{\tilde{\chi}_1^0} = 15$ GeV, no $\tilde{\tau} \rightarrow c\tilde{\chi}_1^0$
none 50–87	95	¹⁷ ABDALLAH 03c	DLPH	$\tilde{\tau} \rightarrow c\tilde{g}$, stable \tilde{g} , all $\theta_t, \Delta m > 10$ GeV
> 71.5	95	¹⁸ CHAKRAB... 03	THEO	$p\bar{p} \rightarrow \tilde{t}\tilde{t}^*$, RPV
> 80	95	¹⁹ HEISTER 03g	ALEP	\tilde{t}_1, R decay
> 77	95	²⁰ HEISTER 03h	ALEP	$\tilde{\tau} \rightarrow c\tilde{g}$, stable \tilde{g} or \tilde{t} , all θ_t , all Δm
> 61	95	²¹ ACHARD 02	L3	\tilde{t}_1, R decays
none 68–119	95	²² AFFOLDER 01b	CDF	$\tilde{t} \rightarrow \tilde{t}_1^0$
none 84–120	95	²³ ABREU 00i	DLPH	$R(LL\bar{E}), \theta_t=0.98, \Delta m > 4$ GeV
		²⁴ AFFOLDER 00d	CDF	$\tilde{\tau} \rightarrow c\tilde{\chi}_1^0, m_{\tilde{\chi}_1^0} < 40$ GeV
		²⁵ AFFOLDER 00g	CDF	$\tilde{\tau}_1 \rightarrow b\tilde{\nu}, m_{\tilde{\nu}} < 45$

> 59	95	²⁶ BARATE 00p	ALEP	Repl. by HEISTER 02k
>120	95	²⁷ ABE 99m	CDF	$p\bar{p} \rightarrow \tilde{t}_1\tilde{t}_1, R$
none 61–91	95	²⁸ ABACHI 96b	D0	$\tilde{\tau} \rightarrow c\tilde{\chi}_1^0, m_{\tilde{\chi}_1^0} < 30$ GeV
none 9–24.4	95	²⁹ AID 96	H1	$e p \rightarrow \tilde{t}\tilde{t}, R$ decays
>138	95	³⁰ AID 96	H1	$e p \rightarrow \tilde{t}, R, \lambda\cos\theta_t > 0.03$
> 45		³¹ CHO 96	RVUE	$B^0\text{-}\bar{B}^0$ and $\epsilon, \theta_t=0.98, \tan\beta < 2$
none 11–41	95	³² BUSKULIC 95e	ALEP	$R(LL\bar{E}), \theta_t=0.98$
none 6.0–41.2	95	AKERS 94k	OPAL	$\tilde{\tau} \rightarrow c\tilde{\chi}_1^0, \theta_t=0, \Delta m > 2$ GeV
none 5.0–46.0	95	AKERS 94k	OPAL	$\tilde{\tau} \rightarrow c\tilde{\chi}_1^0, \theta_t=0, \Delta m > 5$ GeV
none 11.2–25.5	95	AKERS 94k	OPAL	$\tilde{\tau} \rightarrow c\tilde{\chi}_1^0, \theta_t=0.98, \Delta m > 2$ GeV
none 7.9–41.2	95	AKERS 94k	OPAL	$\tilde{\tau} \rightarrow c\tilde{\chi}_1^0, \theta_t=0.98, \Delta m > 5$ GeV
none 7.6–28.0	95	³³ SHIRAI 94	VNS	$\tilde{\tau} \rightarrow c\tilde{\chi}_1^0$, any $\theta_t, \Delta m > 10$ GeV
none 10–20	95	³³ SHIRAI 94	VNS	$\tilde{\tau} \rightarrow c\tilde{\chi}_1^0$, any $\theta_t, \Delta m > 2.5$ GeV

¹ABAZOV 08 looked at approximately 400 pb⁻¹ of $p\bar{p}$ collisions at $\sqrt{s} = 1.96$ TeV for events with $b\bar{b}\ell\ell'\cancel{E}_T$ with $\ell\ell' = e^+\mu^\mp$ or $\ell\ell' = \mu^+\mu^-$, originating from associated production $\tilde{t}\tilde{t}$. Branching ratios are assumed to be 100% for both $\tilde{\chi}_1^+ \rightarrow \ell\nu$ and $\tilde{\nu} \rightarrow \nu\tilde{\chi}_1^0$. No evidence for an excess over the SM expectation is observed. The excluded region is shown in a plane of $m_{\tilde{\nu}}$ versus $m_{\tilde{\tau}}$, see their Fig. 3.

²ABAZOV 07b looked in 360 pb⁻¹ of $p\bar{p}$ collisions at $\sqrt{s} = 1.96$ TeV for events with a pair of acoplanar heavy-flavor jets with \cancel{E}_T . No excess is observed relative to the SM background expectations. Limits are set on the production of \tilde{t}_1 under the assumption that the only decay mode is into $c\tilde{\chi}_1^0$, see their Fig. 4 for the limit in the $(m_{\tilde{\tau}}, m_{\tilde{\chi}_1^0})$ plane. No limit can be obtained for $m_{\tilde{\chi}_1^0} > 54$ GeV. Supersedes the results of ABAZOV 04b.

³ABAZOV 04 looked at 108.3pb⁻¹ of $p\bar{p}$ collisions at $\sqrt{s} = 1.8$ TeV for events with $e+\mu+\cancel{E}_T$ as signature for the 3- and 4-body decays of stop into $b\ell\nu\tilde{\chi}_1^0$ final states. For the $b\ell\nu$ channel they use the results from ABAZOV 02c. No significant excess is observed compared to the Standard Model expectation and limits are derived on the mass of \tilde{t}_1 for the 3- and 4-body decays in the $(m_{\tilde{\tau}}, m_{\tilde{\chi}_1^0})$ plane, see their Figure 4.

⁴ACHARD 04 search in the 192–209 GeV data for the production of $\tilde{t}\tilde{t}$ in acoplanar di-jet final states and, in case of $b\ell\nu$ ($b\tau\nu$) final states, two leptons (taus). The limits for $\theta_t=0$ improve to 95, 96 and 93 GeV, respectively. All limits assume 100% branching ratio for the respective decay modes. See Fig. 6 for the dependence of the limits on $m_{\tilde{\chi}_1^0}$.

These limits supersede ACCIARRI 99v.

⁵ABDALLAH 03m looked for $\tilde{\tau}$ pair production in events with acoplanar jets and \cancel{E}_T at $\sqrt{s} = 189$ –208 GeV. See Fig. 23 and Table 11 for other choices of Δm . These limits include and update the results of ABREU, P 00b.

⁶ACOSTA 03c searched in 107 pb⁻¹ of $p\bar{p}$ collisions at $\sqrt{s}=1.8$ TeV for pair production of $\tilde{\tau}$ followed by the decay $\tilde{\tau} \rightarrow b\ell\nu$. They looked for events with two isolated leptons (e or μ), at least one jet and \cancel{E}_T . The excluded mass range is reduced for larger $m_{\tilde{\nu}}$, and no limit is set for $m_{\tilde{\nu}} > 88.4$ GeV (see Fig. 2).

⁷ABAZOV 02c looked in 108.3pb⁻¹ of $p\bar{p}$ collisions at $\sqrt{s}=1.8$ TeV for events with $e\mu\cancel{E}_T$, originating from associated production $\tilde{t}\tilde{t}$. Branching ratios are assumed to be 100%. The bound for the $b\ell\nu$ decay weakens for large $\tilde{\nu}$ mass (see Fig. 3), and no limit is set when $m_{\tilde{\nu}} > 85$ GeV. See Fig. 4 for the limits in case of decays to a real $\tilde{\chi}_1^\pm$, followed by $\tilde{\chi}_1^\pm \rightarrow \ell\nu$, as a function of $m_{\tilde{\chi}_1^\pm}$.

⁸ABBIENDI 02h looked for events with two acoplanar jets, \cancel{E}_T , and, in the case of $b\ell\nu$ final states, two leptons, in the 161–209 GeV data. The bound for $c\tilde{\chi}_1^0$ applies to the region where $\Delta m < m_W + m_b$, else the decay $\tilde{t}_1 \rightarrow b\tilde{\chi}_1^0 W^+$ becomes dominant. The limit for $b\ell\nu$ assumes equal branching ratios for the three lepton flavors and for $b\tau\nu$ 100% for this channel. For $\theta_t=0$, the bounds improve to > 97.6 GeV ($c\tilde{\chi}_1^0$), > 96.0 GeV ($b\ell\nu$), and > 95.5 ($b\tau\nu$). See Figs. 5–6 and Table 5 for the more general dependence of the limits on Δm . These results supersede ABBIENDI 99m.

⁹HEISTER 02k search for top squarks in final states with jets (with/without b tagging or leptons) or long-lived hadrons, using 183–209 GeV data. The absolute mass bound is obtained by varying the branching ratio of $\tilde{\tau} \rightarrow c\tilde{\chi}_1^0$ and the lepton fraction in $\tilde{\tau} \rightarrow b\tilde{\chi}_1^0 \ell\ell'$ decays. The mass bound for $\tilde{\tau} \rightarrow c\tilde{\chi}_1^0$ uses the CDF results from AFFOLDER 00b and for $\tilde{\tau} \rightarrow b\ell\nu$ the DØ results from ABAZOV 02c. See Figs. 2–5 for the more general dependence of the limits on Δm . Updates BARATE 01 and BARATE 00p.

¹⁰AALTONEN 07e searched in 295 pb⁻¹ of $p\bar{p}$ collisions at $\sqrt{s} = 1.96$ TeV for multijet events with large \cancel{E}_T . They request at least one heavy flavor-tagged jet and no identified leptons. The branching ratio $\tilde{t}_1 \rightarrow c\tilde{\chi}_1^0$ is assumed to be 100%. No significant excess was found compared to the background expectation. Upper limits on the cross-section are extracted and a limit is derived on the masses of stop versus $\tilde{\chi}_1^0$, see their Fig. 4.

¹¹CHEKANOV 07 search for the $LQ\bar{D}$ R -parity violating process $e^+p \rightarrow \tilde{t}_1$ in 65 pb⁻¹ at 318 GeV. Final states may originate from $LQ\bar{D}$ couplings $\tilde{t} \rightarrow e^+d$ and from the R -parity conserving decay $\tilde{t} \rightarrow \tilde{\chi}^+b$, giving rise to $e + \text{jet}, e + \text{multi-jet},$ and $\nu + \text{multi-jet}$. The excluded region in an MSSM scenario is presented for λ'_{31} as a function of the stop mass in Fig. 6. Other excluded regions in a more restricted mSUGRA model are shown in Fig. 7 and 8.

¹²ABBIENDI 04f use data from $\sqrt{s} = 189$ –209 GeV. They derive limits on the stop mass under the assumption of R with $LQ\bar{D}$ or $U\bar{D}\bar{D}$ couplings. The limit quoted applies to direct decays with $U\bar{D}\bar{D}$ couplings when the stop decouples from the Z^0 and improves to 88 GeV for $\theta_t = 0$. For $LQ\bar{D}$ couplings, the limit improves to 98 (100) GeV for λ'_{13k} or λ'_{23k} couplings and all θ_t ($\theta_t = 0$). For λ'_{33k} couplings it is 96 (98) GeV for all θ_t ($\theta_t = 0$). Supersedes the results of ABBIENDI 00.

- 13 ABDALLAH 04M use data from $\sqrt{s}=192\text{--}208$ GeV to derive limits on sparticle masses under the assumption of R with $LL\bar{E}$ or UDD couplings. The results are valid for $\mu = -200$ GeV, $\tan\beta = 1.5$, $\Delta m > 5$ GeV and assuming a BR of 1 for the given decay. The limit quoted is for decoupling of the stop from the Z^0 and indirect UDD decays using the neutralino constraint of 39.5 GeV for $LL\bar{E}$ and of 38.0 GeV for UDD couplings, also derived in ABDALLAH 04M. For no mixing (decoupling) and indirect decays via $LL\bar{E}$ the limit improves to 92 (87) GeV if the constraint from the neutralino is used and to 88 (81) GeV if it is not used. For indirect decays via UDD couplings it improves to 87 GeV for no mixing and using the constraint from the neutralino, whereas it becomes 81 GeV (67) GeV for no mixing (decoupling) if the neutralino constraint is not used. Supersedes the result of ABREU 01D.
- 14 ACOSTA 04B looked in 106 pb^{-1} of $p\bar{p}$ collisions at $\sqrt{s}=1.8$ TeV for R -parity violating decays of \tilde{t}_1 with $LQ\bar{D}$ couplings. They search for events of the type $\tilde{t}_1 \tilde{t}_1 \rightarrow \ell \tau_H jj$ where $\ell = e, \mu$ originates from a leptonic τ decay and τ_H represents a hadronic decay of τ . They derive limits on the stop mass for direct decays after combining the results from e and μ and under the assumption that $BR = 1$ for the decay to τ .
- 15 AKTAS 04B looked in 106 pb^{-1} of e^+e^- collisions at $\sqrt{s}=319$ GeV and 301 GeV for resonant production of \tilde{t}_1 by R -parity violating $LQ\bar{D}$ couplings with λ'_{131} , others being zero. They consider the decays $\tilde{t}_1 \rightarrow e^+d$ and $\tilde{t}_1 \rightarrow Wb$ followed by $b \rightarrow \bar{\nu}_e d$ and assume gauginos too heavy to participate in the decays. They combine the channels $j\ell\bar{\nu}_T, j\mu\bar{\nu}_T, jj\bar{\nu}_T$ to derive limits in the plane $(m_{\tilde{t}_1}, \lambda'_{131})$, see their Fig. 5.
- 16 DAS 04 reanalyzes AFFOLDER 00G data and obtains constraints on $m_{\tilde{t}_1}$ as a function of $B(\tilde{t} \rightarrow b\ell\nu\chi^0) \times B(\tilde{t} \rightarrow b\bar{q}'\chi^0)$, $B(\tilde{t} \rightarrow c\chi^0)$ and m_{χ^0} . Bound weakens for larger $B(\tilde{t} \rightarrow c\chi^0)$ and m_{χ^0} .
- 17 ABDALLAH 03C looked for events of the type $q\bar{q}R^\pm R^\pm$, $q\bar{q}R^\pm R^0$ or $q\bar{q}R^0 R^0$ in e^+e^- interactions at $\sqrt{s}=189\text{--}208$ GeV. The R^\pm bound states are identified by anomalous dE/dx in the tracking chambers and the R^0 by missing energy, due to their reduced energy loss in the calorimeters. Excluded mass regions in the $(m(\tilde{t}), m(\tilde{g}))$ plane for $m(\tilde{g}) > 2$ GeV are obtained for several values of the probability for the gluino to fragment into R^\pm or R^0 , as shown in their Fig. 18. The limit improves to 90 GeV for $\theta_t = 0$.
- 18 Theoretical analysis of $e^+e^- + 2$ jet final states from the RPV decay of $\tilde{t}\tilde{t}^*$ pairs produced in $p\bar{p}$ collisions at $\sqrt{s}=1.8$ TeV. 95%CL limits of 220 (165) GeV are derived for $B(\tilde{t} \rightarrow e q) = 1$ (0.5).
- 19 HEISTER 03G searches for the production of \tilde{t} pairs in the case of R prompt decays with $LL\bar{E}$, $LQ\bar{D}$ or UDD couplings at $\sqrt{s}=189\text{--}209$ GeV. The limit holds for indirect decays mediated by R UDD couplings. It improves to 91 GeV for indirect decays mediated by R $LL\bar{E}$ couplings, to 97 GeV for direct (assuming $B(\tilde{t}_1 \rightarrow q\tau) = 100\%$) and to 85 GeV for indirect decays mediated by R $LQ\bar{D}$ couplings. Supersedes the results from BARATE 01B.
- 20 HEISTER 03H use e^+e^- data from 183–208 GeV to look for the production of stop decaying into a c quark and a stable gluino hadronizing into charged or neutral R -hadrons. Combining these results with bounds on stable squarks and on a stable gluino LSP from the same paper yields the quoted limit. See their Fig. 13 for the dependence of the mass limit on the gluino mass and on θ_t .
- 21 ACHARD 02 searches for the production of squarks in the case of R prompt decays with UDD couplings at $\sqrt{s}=189\text{--}208$ GeV. The search is performed for direct and indirect decays, assuming one coupling at the time to be nonzero. The limit is computed for the minimal cross section and holds for both direct and indirect decays.
- 22 AFFOLDER 01B searches for decays of the top quark into stop and LSP, in $t\bar{t}$ events. Limits on the stop mass as a function of the LSP mass and of the decay branching ratio are shown in Fig. 3. They exclude branching ratios in excess of 45% for SLP masses up to 40 GeV.
- 23 ABREU 00I searches for the production of stop in the case of R -parity violation with $LL\bar{E}$ couplings, for which only indirect decays are allowed. They investigate topologies with jets plus leptons in data from $\sqrt{s}=183$ GeV. The lower bound on the stop mass assumes a neutralino mass limit of 27 GeV, also derived in ABREU 00I.
- 24 AFFOLDER 00D search for final states with 2 or 3 jets and E_T , one jet with a c tag. See their Fig. 2 for the mass exclusion in the $(m_{\tilde{t}_1}, m_{\chi^0_1})$ plane. The maximum excluded $m_{\tilde{t}_1}$ value is 119 GeV, for $m_{\chi^0_1} = 40$ GeV.
- 25 AFFOLDER 00G searches for $\tilde{t}_1 \tilde{t}_1^*$ production, with $\tilde{t}_1 \rightarrow b\ell\bar{\nu}$, leading to topologies with ≥ 1 isolated lepton (e or μ), E_T , and ≥ 2 jets with ≥ 1 tagged as b quark by a secondary vertex. See Fig. 4 for the excluded mass range as a function of $m_{\tilde{\nu}}$. Cross-section limits for $\tilde{t}_1 \tilde{t}_1^*$, with $\tilde{t}_1 \rightarrow b\chi_{1,2}^\pm$ ($\chi_{1,2}^\pm \rightarrow \ell^\pm \nu\chi_{1,2}^0$), are given in Fig. 2.
- 26 BARATE 00P use data from $\sqrt{s}=189\text{--}202$ GeV to explore the region of small mass difference between the stop and the neutralino by searching heavy stable charged particles or tracks with large impact parameters. For prompt decays, they make use of acoplanar jets from BARATE 99q, updated up to 202 GeV. The limit is reached for $\Delta m=1.6$ GeV and a decay length of 1 cm. If the MSSM relation between the decay width and Δm is used, the limit improves to 63 GeV. It is set for $\Delta m=1.9$ GeV, $\tan\beta=2.6$, and $\theta_t=0.98$, and large negative μ .
- 27 ABE 99M looked in 107 pb^{-1} of $p\bar{p}$ collisions at $\sqrt{s}=1.8$ TeV for events with like sign dielectrons and two or more jets from the sequential decays $\tilde{q} \rightarrow q\bar{\chi}_2^0$ and $\bar{\chi}_2^0 \rightarrow e q\bar{q}'$, assuming R coupling $L_1 Q_j D_k^c$, with $j=2,3$ and $k=1,2,3$. They assume $B(\tilde{t}_1 \rightarrow c\chi_1^0)=1$, $B(\bar{\chi}_1^0 \rightarrow e q\bar{q}')=0.25$ for both e^+ and e^- , and $m_{\chi_1^0} \geq m_{\tilde{t}_1}/2$. The limit improves for heavier $\bar{\chi}_1^0$.
- 28 ABACHI 96B searches for final states with 2 jets and missing E_T . Limits on $m_{\tilde{t}_1}$ are given as a function of $m_{\chi_1^0}$. See Fig. 4 for details.
- 29 AID 96 considers photoproduction of $\tilde{t}\tilde{t}^*$ pairs, with 100% R -parity violating decays of \tilde{t} to eq , with $q=d, s$, or b quarks.
- 30 AID 96 considers production and decay of \tilde{t} via the R -parity violating coupling $\lambda' L_1 Q_3 d_3^c$.
- 31 CHO 96 studied the consistency among the $B^0\text{--}\bar{B}^0$ mixing, ϵ in $K^0\text{--}\bar{K}^0$ mixing, and the measurements of V_{cb} , V_{ub}/V_{cb} . For the range $25.5\text{ GeV} < m_{\tilde{t}_1} < m_Z/2$ left by AKERS 94K for $\theta_t = 0.98$, and within the allowed range in $M_2\text{--}\mu$ parameter space from

chargino, neutralino searches by ACCIARRI 95E, they found the scalar top contribution to $B^0\text{--}\bar{B}^0$ mixing and ϵ to be too large if $\tan\beta < 2$. For more on their assumptions, see the paper and their reference 10.

- 32 BUSKULIC 95E looked for $Z \rightarrow \tilde{t}\tilde{t}^*$, where $\tilde{t} \rightarrow c\chi_1^0$ and χ_1^0 decays via R -parity violating interactions into two leptons and a neutrino.

- 33 SHIRAI 94 bound assumes the cross section without the s -channel Z -exchange and the QCD correction, underestimating the cross section up to 20% and 30%, respectively. They assume $m_c=1.5$ GeV.

Heavy \tilde{g} (Gluino) MASS LIMIT

For $m_{\tilde{g}} > 60\text{--}70$ GeV, it is expected that gluinos would undergo a cascade decay via a number of neutralinos and/or charginos rather than undergo a direct decay to photinos as assumed by some papers. Limits obtained when direct decay is assumed are usually higher than limits when cascade decays are included. Limits made obsolete by the most recent analyses of $p\bar{p}$ collisions can be found in previous Editions of this Review.

VALUE (GeV)	CL%	DOCUMENT ID	TECN	COMMENT
>308	95	1 ABAZOV	08G D0	jets+ E_T , $\tan\beta=3$, $\mu < 0$, $A_0=0$, any $m_{\tilde{q}}$
>390	95	1 ABAZOV	08G D0	jets+ E_T , $\tan\beta=3$, $\mu < 0$, $A_0=0$, $m_{\tilde{q}}=m_{\tilde{g}}$
>270	95	2 ABULENCIA	06I CDF	$\tilde{g} \rightarrow \tilde{b}b$, $\Delta m > 6$ GeV, $\tilde{b}_1 \rightarrow b\bar{\chi}_1^0$, $m_{\tilde{b}_1} < 220$ GeV
>195	95	3 AFFOLDER	02 CDF	Jets+ E_T , any $m_{\tilde{q}}$
>300	95	3 AFFOLDER	02 CDF	Jets+ E_T , $m_{\tilde{q}}=m_{\tilde{g}}$
>129	95	4 ABBOTT	01D D0	$\ell\ell$ +jets+ E_T , $\tan\beta < 10$, $m_0 < 300$ GeV, $\mu < 0$, $A_0=0$
>175	95	4 ABBOTT	01D D0	$\ell\ell$ +jets+ E_T , $\tan\beta=2$, large m_0 , $\mu < 0$, $A_0=0$
>255	95	4 ABBOTT	01D D0	$\ell\ell$ +jets+ E_T , $\tan\beta=2$, $m_{\tilde{g}}=m_{\tilde{q}}$, $\mu < 0$, $A_0=0$
>168	95	5 AFFOLDER	01J CDF	$\ell\ell$ +Jets+ E_T , $\tan\beta=2$, $\mu = -800$ GeV, $m_{\tilde{q}} \gg m_{\tilde{g}}$
>221	95	5 AFFOLDER	01J CDF	$\ell\ell$ +Jets+ E_T , $\tan\beta=2$, $\mu = -800$ GeV, $m_{\tilde{q}}=m_{\tilde{g}}$
>190	95	6 ABBOTT	99L D0	Jets+ E_T , $\tan\beta=2$, $\mu < 0$, $A_0=0$
>260	95	6 ABBOTT	99L D0	Jets+ E_T , $m_{\tilde{g}}=m_{\tilde{q}}$
••• We do not use the following data for averages, fits, limits, etc. •••				
>241	95	7 ABAZOV	06c D0	jets+ E_T , $\tan\beta=3$, $\mu < 0$, $A_0=0$, any $m_{\tilde{q}}$
>337	95	7 ABAZOV	06c D0	jets+ E_T , $\tan\beta=3$, $\mu < 0$, $A_0=0$, $m_{\tilde{q}}=m_{\tilde{g}}$
>224	95	8 ABAZOV	02F D0	$R \lambda'_{2jk}$ indirect decays, $\tan\beta=2$, any $m_{\tilde{q}}$
>265	95	8 ABAZOV	02F D0	$R \lambda'_{2jk}$ indirect decays, $\tan\beta=2$, $m_{\tilde{q}}=m_{\tilde{g}}$
		9 ABAZOV	02G D0	$p\bar{p} \rightarrow \tilde{g}\tilde{g}, \tilde{g}\tilde{q}$
		10 CHEUNG	02B THEO	
		11 BERGER	01 THEO	$p\bar{p} \rightarrow X+b$ quark
>240	95	12 ABBOTT	99 D0	$\tilde{g} \rightarrow \bar{\chi}_2^0 X \rightarrow \bar{\chi}_1^0 \gamma X$, $m_{\tilde{g}} - m_{\chi_1^0} > 20$ GeV
>320	95	12 ABBOTT	99 D0	$\tilde{g} \rightarrow \bar{\chi}_1^0 X \rightarrow \bar{G} \gamma X$
>227	95	13 ABBOTT	99K D0	any $m_{\tilde{q}}$, R , $\tan\beta=2$, $\mu < 0$
>212	95	14 ABACHI	95c D0	$m_{\tilde{g}} \geq m_{\tilde{q}}$; with cascade decays
>144	95	14 ABACHI	95c D0	Any $m_{\tilde{q}}$; with cascade decays
		15 ABE	95T CDF	$\tilde{g} \rightarrow \bar{\chi}_2^0 \rightarrow \bar{\chi}_1^0 \gamma$
		16 HEBBEKER	93 RVUE	e^+e^- jet analyses
>218	90	17 ABE	92L CDF	$m_{\tilde{q}} \leq m_{\tilde{g}}$; with cascade decay
>100		18 ROY	92 RVUE	$p\bar{p} \rightarrow \tilde{g}\tilde{g}; R$
		19 NOJIRI	91 COSM	
none 4–53	90	20 ALBAJAR	87D UA1	Any $m_{\tilde{q}} > m_{\tilde{g}}$
none 4–75	90	20 ALBAJAR	87D UA1	$m_{\tilde{q}} = m_{\tilde{g}}$
none 16–58	90	21 ANSARI	87D UA2	$m_{\tilde{q}} \lesssim 100$ GeV

- 1 ABAZOV 08G looked in 2.1 fb^{-1} of $p\bar{p}$ collisions at $\sqrt{s}=1.96$ TeV for events with acoplanar jets or multijets with large E_T . No significant excess was found compared to the background expectation. A limit is derived on the masses of squarks and gluinos for specific MSUGRA parameter values, see Figure 3. Similar results would be obtained for a large class of parameter sets. Supersedes the results of ABAZOV 06c.

- 2 ABULENCIA 06I searched in 156 pb^{-1} of $p\bar{p}$ collisions at $\sqrt{s}=1.96$ TeV for multijet events with large E_T . They request at least 2 b -tagged jets and no isolated leptons. They investigate the production of gluinos decaying into $b_1 b$ followed by $\tilde{b}_1 \rightarrow b\bar{\chi}_1^0$. Both branching fractions are assumed to be 100% and the LSP mass to be 60 GeV. No significant excess was found compared to the background expectation. Upper limits on the cross-section are extracted and a limit is derived on the masses of sbottom and gluinos, see their Fig. 3.

- 3 AFFOLDER 02 searched in $\sim 84\text{ pb}^{-1}$ of $p\bar{p}$ collisions for events with ≥ 3 jets and E_T , arising from the production of gluinos and/or squarks. Limits are derived by scanning the parameter space, for $m_{\tilde{q}} \geq m_{\tilde{g}}$ in the framework of minimal Supergravity, assuming five flavors of degenerate squarks, and for $m_{\tilde{q}} < m_{\tilde{g}}$ in the framework of constrained MSSM,

Searches Particle Listings

Supersymmetric Particle Searches

Reference	Search Description	Value	CL%	Document ID	TECN	Comment
	assuming conservatively four flavors of degenerate squarks. See Fig. 3 for the variation of the limit as function of the squark mass. Supersedes the results of ABE 97K.					
4 ABBOTT 01D	looked in $\sim 108 \text{ pb}^{-1}$ of $p\bar{p}$ collisions at $\sqrt{s}=1.8 \text{ TeV}$ for events with $e, \mu, \mu, \text{ or } e\mu$ accompanied by at least 2 jets and \cancel{E}_T . Excluded regions are obtained in the MSUGRA framework from a scan over the parameters $0 < m_0 < 300 \text{ GeV}, 10 < m_{1/2} < 110 \text{ GeV}$, and $1.2 < \tan\beta < 10$.	> 12 none 2-18 > 5				
5 AFFOLDER 01J	searched in $\sim 106 \text{ pb}^{-1}$ of $p\bar{p}$ collisions for events with 2like-sign leptons (e or μ), ≥ 2 jets and \cancel{E}_T , expected to arise from the production of gluinos and/or squarks with cascade decays into $\tilde{\chi}^{\pm}$ or $\tilde{\chi}_2^0$. Spectra and decay rates are evaluated in the framework of minimal Supergravity, assuming five flavors of degenerate squarks and a pseudoscalar Higgs mass $m_A=500 \text{ GeV}$. The limits are derived for $\tan\beta=2, \mu=-800 \text{ GeV}$, and scanning over $m_{\tilde{g}}$ and $m_{\tilde{q}}$. See Fig. 2 for the variation of the limit as function of the squark mass. These limits supersede the results of ABE 96D.	> 26.9 > 6.3				
6 ABBOTT 99L	consider events with three or more jets and large \cancel{E}_T . Spectra and decay rates are evaluated in the framework of minimal Supergravity, assuming five flavors of degenerate squarks, and scanning the space of the universal gaugino ($m_{1/2}$) and scalar (m_0) masses. See their Figs. 2-3 for the dependence of the limit on the relative value of $m_{\tilde{q}}$ and $m_{\tilde{g}}$.					
7 ABAZOV 06c	looked in 310 pb^{-1} of $p\bar{p}$ collisions at $\sqrt{s}=1.96 \text{ TeV}$ for events with acoplanar jets or multijets with large \cancel{E}_T . No significant excess was found compared to the background expectation. A limit is derived on the masses of squarks and gluinos for specific MSUGRA parameter values, see Figure 3. Similar results would be obtained for a large class of parameter sets. Supersedes the results of ABBOTT 99L.	> 6.3 > 5 > 1.5				
8 ABAZOV 02f	looked in 77.5 pb^{-1} of $p\bar{p}$ collisions at 1.8 TeV for events with $\geq 2\mu + \geq 4$ jets, originating from associated production of squarks followed by an indirect R decay (of the $\tilde{\chi}_1^0$) via $LQ\bar{D}$ couplings of the type λ'_{jlk} where $j=1,2$ and $k=1,2,3$. Bounds are obtained in the MSUGRA scenario by a scan in the range $0 \leq M_0 \leq 400 \text{ GeV}, 60 \leq m_{1/2} \leq 120 \text{ GeV}$ for fixed values $A_0=0, \mu < 0$, and $\tan\beta=2$ or 6 . The bounds are weaker for $\tan\beta=6$. See Figs. 2,3 for the exclusion contours in $m_{1/2}$ versus m_0 for $\tan\beta=2$ and 6 , respectively.	none 1.5-3.5 not 3-5 ≈ 4				
9 ABAZOV 02g	search for associated production of gluinos and squarks in 92.7 pb^{-1} of $p\bar{p}$ collisions at $\sqrt{s}=1.8 \text{ TeV}$, using events with one electron, ≥ 4 jets, and large \cancel{E}_T . The results are compared to a R -parity scenario with $\mu < 0, A_0=0$, and $\tan\beta=3$ and allow to exclude a region of the $(m_0, m_{1/2})$ shown in Fig. 11.	none 1.9-13.6				
10 CHEUNG 02b	studies the constraints on a \tilde{b}_1 with mass in the $2.2\text{--}5.5 \text{ GeV}$ region and a gluino in the mass range $12\text{--}16 \text{ GeV}$, using precision measurements of Z^0 decays and e^+e^- annihilations at LEP2. Few detectable events are predicted in the LEP2 data for the model proposed by BERGER 01.	< 0.7 none 1.5-3.5 not 3-5 ≈ 4				
11 BERGER 01	reanalyzed interpretation of Tevatron data on bottom-quark production. Argues that pair production of light gluinos ($m \sim 12\text{--}16 \text{ GeV}$) with subsequent 2-body decay into a light sbottom ($m \sim 2\text{--}5.5 \text{ GeV}$) and bottom can reconcile Tevatron data with predictions of perturbative QCD for the bottom production rate. The sbottom must either decay hadronically via a R -parity- and B -violating interaction, or be long-lived.	> 1				
12 ABBOTT 99	searched for $\gamma\cancel{E}_T + \geq 2$ jet final states, and set limits on $\sigma(p\bar{p} \rightarrow \tilde{g} + X) \cdot \text{B}(\tilde{g} \rightarrow \gamma\cancel{E}_T X)$. The quoted limits correspond to $m_{\tilde{g}} \geq m_{\tilde{q}}$, with $\text{B}(\tilde{\chi}_2^0 \rightarrow \tilde{\chi}_1^0 \gamma)=1$ and $\text{B}(\tilde{\chi}_1^0 \rightarrow \tilde{G} \gamma)=1$, respectively. They improve to 310 GeV (360 GeV) in the case of $\gamma\tilde{G}$ decay for $m_{\tilde{g}}=m_{\tilde{q}}$.	> 3.8 > 3.2 none 0.6-2.2 none 1-4.5 none 1-4 none 3-5 none				
13 ABBOTT 99k	uses events with an electron pair and four jets to search for the decay of the $\tilde{\chi}_1^0$ LSP via $R L Q \bar{D}$ couplings. The particle spectrum and decay branching ratios are taken in the framework of minimal supergravity. An excluded region at 95% CL is obtained in the $(m_0, m_{1/2})$ plane under the assumption that $A_0=0, \mu < 0, \tan\beta=2$ and any one of the couplings $\lambda'_{jlk} > 10^{-3}$ ($j=1,2$ and $k=1,2,3$) and from which the above limit is computed. For equal mass squarks and gluinos, the corresponding limit is 277 GeV . The results are essentially independent of A_0 , but the limit deteriorates rapidly with increasing $\tan\beta$ or $\mu > 0$.	none 0.5-2 none 0.5-4 none 0.5-3 none 2-4 none 1-2.5 none 0.5-4.1 > 1 $> 1-2$				
14 ABACHI 95c	assume five degenerate squark flavors with $m_{\tilde{q}_L} = m_{\tilde{q}_R}$. Sleptons are assumed to be heavier than squarks. The limits are derived for fixed $\tan\beta = 2.0, \mu = -250 \text{ GeV}$, and $m_{H^+} = 500 \text{ GeV}$, and with the cascade decays of the squarks and gluinos calculated within the framework of the Minimal Supergravity scenario. The bounds are weakly sensitive to the three fixed parameters for a large fraction of parameter space.	> 2 $> 2-3$ $> 1.5-2$				
15 ABE 95T	looked for a cascade decay of gluino into $\tilde{\chi}_2^0$ which further decays into $\tilde{\chi}_1^0$ and a photon. No signal is observed. Limits vary widely depending on the choice of parameters. For $\mu = -40 \text{ GeV}$, $\tan\beta = 1.5$, and heavy squarks, the range $50 < m_{\tilde{g}} (\text{GeV}) < 140$ is excluded at 90% CL. See the paper for details.					
16 HEBBEKER 93	combined jet analyses at various e^+e^- colliders. The 4-jet analyses at TRISTAN/LEP and the measured α_s at PEP/PETRA/TRISTAN/LEP are used. A constraint on effective number of quarks $N=6.3 \pm 1.1$ is obtained, which is compared to that with a light gluino, $N=8$.					
17 ABE 92L	bounds are based on similar assumptions as ABACHI 95c. Not sensitive to $m_{\text{gluino}} < 40 \text{ GeV}$ (but other experiments rule out that region).					
18 ROY 92	reanalyzed CDF limits on di-lepton events to obtain limits on gluino production in R -parity violating models. The 100% decay $\tilde{g} \rightarrow q\bar{q}\tilde{\chi}$ where $\tilde{\chi}$ is the LSP, and the LSP decays either into $\ell q \bar{d}$ or $\ell \ell \bar{e}$ is assumed.					
19 NOJIRI 91	argues that a heavy gluino should be nearly degenerate with squarks in minimal supergravity not to overclose the universe.					
20	The limits of ALBAJAR 87D are from $p\bar{p} \rightarrow \tilde{g}\tilde{g}X$ ($\tilde{g} \rightarrow q\bar{q}\tilde{\chi}$) and assume $m_{\tilde{q}} > m_{\tilde{g}}$. These limits apply for $m_{\tilde{\chi}} \lesssim 20 \text{ GeV}$ and $\tau(\tilde{g}) < 10^{-10} \text{ s}$.					
21	The limit of ANSARI 87D assumes $m_{\tilde{q}} > m_{\tilde{g}}$ and $m_{\tilde{\chi}} \approx 0$.					
1 ABAZOV 07L	looked in approximately 410 pb^{-1} of $p\bar{p}$ collisions at $\sqrt{s}=1.96 \text{ TeV}$ for events with a long-lived gluino from split supersymmetry, decaying after stopping in the detector into $g\tilde{\chi}_1^0$ with lifetimes from $30 \mu\text{s}$ to 100 h . The signal signature is a largely empty event with a single large transverse energy deposit in the calorimeter. The main background is due to cosmic muons interacting in the calorimeter. The data agree with the estimated background and allow the authors to estimate a limit on the rate of an out-of-time monojet signal of a given energy. Assuming the branching ratios $\tilde{g} \rightarrow g\tilde{\chi}_1^0$ to be 100% the results can be translated to limits on the gluino cross section versus the gluino mass for fixed $\tilde{\chi}_1^0$ mass. After comparing to the expected gluino cross sections, the excluded region of gluino masses can be obtained, see examples in their Fig. 3.					
2 BERGER 05	include the light gluino in proton PDF and perform global analysis of hadronic data. Effects on the running of α_s also included. Strong dependency on $\alpha_s(m_Z)$. Bound quoted for $\alpha_s(m_Z) = 0.118$.					
3 ABDALLAH 03c	looked for events of the type $q\bar{q}R \pm R^{\pm}, q\bar{q}R^{\pm}R^0$ or $q\bar{q}R^0R^0$ in e^+e^- interactions at 91.2 GeV collected in 1994. The R^{\pm} bound states are identified by anomalous dE/dx in the tracking chambers and the R^0 by missing energy, due to their reduced energy loss in the calorimeters. The upper value of the excluded range depends on the probability for the gluino to fragment into R^{\pm} or R^0 , see their Fig. 17. It improves to 23 GeV for 100% fragmentation to R^{\pm} .					
4 ABDALLAH 03g	use e^+e^- data at and around the Z^0 peak, above the Z^0 up to $\sqrt{s}=202 \text{ GeV}$ and events from radiative return to cover the low energy region. They perform a direct measurement of the QCD beta-function from the means of fully inclusive event observables. Compared to the energy range, gluinos below 5 GeV can be considered massless and are firmly excluded by the measurement.					
5 HEISTER 03	use e^+e^- data from 1994 and 1995 at and around the Z^0 peak to measure the 4-jet rate and angular correlations. The comparison with QCD NLO calculations allow $\alpha_s(M_Z)$ and the color factor ratios to be extracted and the results are in agreement with the expectations from QCD. The inclusion of a massless gluino in the beta functions yields $T_R / C_F = 0.15 \pm 0.06 \pm 0.06$ (expectation is $T_R / C_F = 3/8$), excluding a massless gluino at more than 95% CL. As no NLO calculations are available for massive gluinos, the earlier LO results from BARATE 97L for massive gluinos remain valid.					
6 HEISTER 03H	use e^+e^- data at and around the Z^0 peak to look for stable gluinos hadronizing into charged or neutral R-hadrons with arbitrary branching ratios. Combining these results with bounds on the Z^0 hadronic width from electroweak measurements (JANOT 03) to cover the low mass region the quoted lower limit on the mass of a long-lived gluino is obtained.					

Long-lived/light \tilde{g} (Gluino) MASS LIMIT

Limits on light gluinos ($m_{\tilde{g}} < 5 \text{ GeV}$), or gluinos which leave the detector before decaying.

VALUE (GeV)	CL%	DOCUMENT ID	TECN	COMMENT
•••	•••	•••	•••	••• We do not use the following data for averages, fits, limits, etc. •••

- 7 JANOT 03 excludes a light gluino from the upper limit on an additional contribution to the Z hadronic width. At higher confidence levels, $m_{\tilde{g}} > 5.3(4.2)$ GeV at $3\sigma(5\sigma)$ level.
- 8 MAFI 00 reanalyzed CDF data assuming a stable heavy gluino as the LSP, with model for R-hadron-nucleon scattering. Gluino masses between 35 GeV and 115 GeV are excluded based on the CDF Run I data. Combined with the analysis of BAER 99, this allows a LSP gluino mass between 25 and 35 GeV if the probability of fragmentation into charged R-hadron $P > 1/2$. The cosmological exclusion of such a gluino LSP are assumed to be avoided as in BAER 99. Gluino could be NLSP with $\tau_{\tilde{g}} \sim 100$ yrs, and decay to gluon gravitino.
- 9 ALAVI-HARATI 99E looked for R^0 bound states, yielding $\pi^+\pi^-$ or π^0 in the final state. The experiment is sensitive to values of $\Delta m = m_{R^0} - m_{\tilde{g}}$ larger than 280 MeV and 140 MeV for the two decay modes, respectively, and to R^0 mass and lifetime in the ranges 0.8–5 GeV and 10^{-10} – 10^{-3} s. The limits obtained depend on $B(R^0 \rightarrow \pi^+\pi^- \text{ photino})$ and $B(R^0 \rightarrow \pi^0 \text{ photino})$ on the value of $m_{R^0}/m_{\tilde{g}}$, and on the ratio of production rates $\sigma(R^0)/\sigma(K_L^0)$. See Figures in the paper for the excluded R^0 production rates as a function of Δm , R^0 mass and lifetime. Using the production rates expected from perturbative QCD, and assuming dominance of the above decay channels over the suitable phase space, R^0 masses in the range 0.8–5 GeV are excluded at 90%CL for a large fraction of the sensitive lifetime region. ALAVI-HARATI 99E updates and supersedes the results of ADA MS 97b.
- 10 BAER 99 set constraints on the existence of stable \tilde{g} hadrons, in the mass range $m_{\tilde{g}} > 3$ GeV. They argue that strong-interaction effects in the low-energy annihilation rates could leave small enough relic densities to evade cosmological constraints up to $m_{\tilde{g}} < 10$ TeV. They consider $\text{jet} + \cancel{E}_T$ as well as heavy-ionizing charged-particle signatures from production of stable \tilde{g} hadrons at LEP and Tevatron, developing modes for the energy loss of \tilde{g} hadrons inside the detectors. Results are obtained as a function of the fragmentation probability P of the \tilde{g} into a charged hadron. For $P < 1/2$, and for various energy-loss models, OPAL and CDF data exclude gluinos in the $3 < m_{\tilde{g}}(\text{GeV}) < 130$ mass range. For $P > 1/2$, gluinos are excluded in the mass ranges $3 < m_{\tilde{g}}(\text{GeV}) < 23$ and $50 < m_{\tilde{g}}(\text{GeV}) < 200$.
- 11 FANTI 99 looked for R^0 bound states yielding high $P_T \eta \rightarrow 3\pi^0$ decays. The experiment is sensitive to a region of R^0 mass and lifetime in the ranges of 1–5 GeV and 10^{-10} – 10^{-3} s. The limits obtained depend on $B(R^0 \rightarrow \eta\gamma)$, on the value of $m_{R^0}/m_{\tilde{g}}$, and on the ratio of production rates $\sigma(R^0)/\sigma(K_L^0)$. See Fig. 6–7 for the excluded production rates as a function of R^0 mass and lifetime.
- 12 ACKERSTAFF 98v excludes the light gluino with universal gaugino mass where charginos, neutralinos decay as $\tilde{\chi}_1^\pm, \tilde{\chi}_2^0 \rightarrow q\tilde{q}\tilde{g}$ from total hadronic cross sections at $\sqrt{s}=130$ –172 GeV. See paper for the case of nonuniversal gaugino mass.
- 13 ADA MS 97b looked for $\rho^0 \rightarrow \pi^+\pi^-$ as a signature of $R^0=(\tilde{g}\tilde{g})$ bound states. The experiment is sensitive to an R^0 mass range of 1.2–4.5 GeV and to a lifetime range of 10^{-10} – 10^{-3} sec. Precise limits depend on the assumed value of $m_{R^0}/m_{\tilde{g}}$. See Fig. 7 for the excluded mass and lifetime region.
- 14 ALBUQUERQUE 97 looked for weakly decaying baryon-like states which contain a light gluino, following the suggestions in FARRAR 96. See their Table 1 for limits on the production fraction. These limits exclude gluino masses in the range 100–600 MeV for the predicted lifetimes (FARRAR 96) and production rates, which are assumed to be comparable to those of strange or charmed baryons.
- 15 BARATE 97L studied the QCD color factors from four-jet angular correlations and the differential two-jet rate in Z decay. Limit obtained from the determination of $n_f = 4.24 \pm 0.29 \pm 1.15$, assuming $T_F/C_F=3/8$ and $C_A/C_F=9/4$.
- 16 CSIKOR 97 combined the α_s from $\sigma(e^+e^- \rightarrow \text{hadron})$, τ decay, and jet analysis in Z decay. They exclude a light gluino below 5 GeV at more than 99.7%CL.
- 17 DEGOUVEA 97 reanalyzed AKERS 95A data on Z decay into four jets to place constraints on a light stable gluino. The mass limit corresponds to the pole mass of 2.8 GeV. The analysis, however, is limited to the leading-order QCD calculation.
- 18 FARRAR 96 studied the possible $R^0=(\tilde{g}\tilde{g})$ component in Fermilab E799 experiment and used its bound $B(K_L^0 \rightarrow \pi^0\nu\bar{\nu}) \leq 5.8 \times 10^{-5}$ to place constraints on the combination of R^0 production cross section and its lifetime.
- 19 AKERS 95R looked for Z decay into $q\tilde{q}\tilde{g}\tilde{g}$, by searching for charged particles with dE/dx consistent with \tilde{g} fragmentation into a state $(\tilde{g}q\tilde{q})^\pm$ with lifetime $\tau > 10^{-7}$ sec. The fragmentation probability into a charged state is assumed to be 25%.
- 20 CLAVELLI 95 updates the analysis of CLAVELLI 93, based on a comparison of the hadronic widths of charmonium and bottomonium S-wave states. The analysis includes a parametrization of relativistic corrections. Claims that the presence of a light gluino improves agreement with the data by slowing down the running of α_s .
- 21 CAKIR 94 reanalyzed TUTS 87 and later unpublished data from CUSB to exclude pseudo-scalar gluinonium $\eta_{\tilde{g}}(\tilde{g}\tilde{g})$ of mass below 7 GeV. It was argued, however, that the perturbative QCD calculation of the branching fraction $\Upsilon \rightarrow \eta_{\tilde{g}}\gamma$ is unreliable for $m_{\eta_{\tilde{g}}} < 3$ GeV. The gluino mass is defined by $m_{\tilde{g}}=(m_{\eta_{\tilde{g}}})/2$. The limit holds for any gluino lifetime.
- 22 LOPEZ 93c uses combined restraint from the radiative symmetry breaking scenario within the minimal supergravity model, and the LEP bounds on the (M_2, μ) plane. Claims that the light gluino window is strongly disfavored.
- 23 CLAVELLI 92 claims that a light gluino mass around 4 GeV should exist to explain the discrepancy between α_s at LEP and at quarkonia (Υ), since a light gluino slows the running of the QCD coupling.
- 24 ANTONIADIS 91 argue that possible light gluinos (< 5 GeV) contradict the observed running of α_s between 5 GeV and m_Z . The significance is less than 2 s.d.
- 25 ANTONIADIS 91 interpret the search for missing energy events in 450 GeV/c pN collisions, AKESSON 91, in terms of light gluinos.
- 26 NAKAMURA 89 searched for a long-lived ($\tau \gtrsim 10^{-7}$ s) charge-(± 2) particle with mass $\lesssim 1.6$ GeV in proton-Pt interactions at 12 GeV and found that the yield is less than 10^{-8} times that of the pion. This excludes $R\text{-}\Delta^{++}$ (a $\tilde{g}uuu$ state) lighter than 1.6 GeV.
- 27 The limits assume $m_{\tilde{q}} = 100$ GeV. See their figure 3 for limits vs. $m_{\tilde{q}}$.
- 28 The gluino mass is defined by half the bound $\tilde{g}\tilde{g}$ mass. If zero gluino mass gives a $\tilde{g}\tilde{g}$ of mass about 1 GeV as suggested by various glueball mass estimates, then the low-mass bound can be replaced by zero. The high-mass bound is obtained by comparing the data with nonrelativistic potential-model estimates.
- 29 ALBRECHT 86c search for secondary decay vertices from $\chi_{b1}(1P) \rightarrow \tilde{g}\tilde{g}\tilde{g}$ where \tilde{g} 's make long-lived hadrons. See their figure 4 for excluded region in the $m_{\tilde{g}} - m_{\tilde{q}}$ and $m_{\tilde{g}} - m_{\tilde{q}}$ plane. The lower $m_{\tilde{g}}$ region below ~ 2 GeV may be sensitive to fragmentation effects. Remark that the \tilde{g} -hadron mass is expected to be ~ 1 GeV (glueball mass) in the zero \tilde{g} mass limit.
- 30 BADIER 86 looked for secondary decay vertices from long-lived \tilde{g} -hadrons produced at 300 GeV π^- beam dump. The quoted bound assumes \tilde{g} -hadron nucleon total cross section of $10\mu\text{b}$. See their figure 7 for excluded region in the $m_{\tilde{g}} - m_{\tilde{q}}$ plane for several assumed total cross-section values.
- 31 BARNETT 86 rule out light gluinos ($m = 3$ –5 GeV) by calculating the monojet rate from gluino gluino gluon events (and from gluino gluino events) and by using UA1 data from $p\bar{p}$ collisions at CERN.
- 32 VOLOSHIN 86 rules out stable gluino based on the cosmological argument that predicts too much hydrogen consisting of the charged stable hadron $\tilde{g}uud$. Quasi-stable ($\tau > 1 \times 10^{-7}$ s) light gluino of $m_{\tilde{g}} < 3$ GeV is also ruled out by nonobservation of the stable charged particles, $\tilde{g}uud$, in high energy hadron collisions.
- 33 COOPER-SARKAR 85b is BEBC beam-dump. Gluinos decaying in dump would yield $\tilde{\gamma}$'s in the detector giving neutral-current-like interactions. For $m_{\tilde{q}} > 330$ GeV, no limit is set.
- 34 DAWSON 85 first limit from neutral particle search. Second limit based on FNAL beam dump experiment.
- 35 FARRAR 85 points out that BALL 84 analysis applies only if the \tilde{g} 's decay before interacting, i.e. $m_{\tilde{q}} < 80m_{\tilde{g}}^{1.5}$. FARRAR 85 finds $m_{\tilde{g}} < 0.5$ not excluded for $m_{\tilde{q}} = 30$ –1000 GeV and $m_{\tilde{g}} < 1.0$ not excluded for $m_{\tilde{q}} = 100$ –500 GeV by BALL 84 experiment.
- 36 GOLDMAN 85 use nonobservation of a pseudoscalar $\tilde{g}\tilde{g}$ bound state in radiative ψ decay.
- 37 HABER 85 is based on survey of all previous searches sensitive to low mass \tilde{g} 's. Limit makes assumptions regarding the lifetime and electric charge of the lightest supersymmetric particle.
- 38 BALL 84 is FNAL beam dump experiment. Observed no interactions of $\tilde{\gamma}$ in the calorimeter, where $\tilde{\gamma}$'s are expected to come from pair-produced \tilde{g} 's. Search for long-lived $\tilde{\gamma}$ interacting in calorimeter 56m from target. Limit is for $m_{\tilde{q}} = 40$ GeV and production cross section proportional to $A^{0.72}$. BALL 84 find no \tilde{g} allowed below 4.1 GeV at CL = 90%. Their figure 1 shows dependence on $m_{\tilde{q}}$ and A. See also KANE 82.
- 39 BRICK 84 reanalyzed FNAL 147 GeV HBC data for $R\text{-}\Delta(1232)^{++}$ with $\tau > 10^{-9}$ s and $p_{\text{lab}} > 2$ GeV. Set CL = 90% upper limits 6.1, 4.4, and 29 microbarns in $p\bar{p}$, $\pi^+\pi^-$, K^+p collisions respectively. $R\text{-}\Delta^{++}$ is defined as being \tilde{g} and 3 up quarks. If mass = 1.2–1.5 GeV, then limits may be lower than theory predictions.
- 40 FARRAR 84 argues that $m_{\tilde{g}} < 100$ MeV is not ruled out if the lightest R-hadrons are long-lived. A long lifetime would occur if R-hadrons are lighter than $\tilde{\gamma}$'s or if $m_{\tilde{q}} > 100$ GeV.
- 41 BERGSMAN 83c is reanalysis of CERN-SPS beam-dump data. See their figure 1.
- 42 CHANOWITZ 83 find in bag-model that charged s-hadron exists which is stable against strong decay if $m_{\tilde{g}} < 1$ GeV. This is important since tracks from decay of neutral s-hadron cannot be reconstructed to primary vertex because of missed $\tilde{\gamma}$. Charged s-hadron leaves track from vertex.
- 43 KANE 82 inferred above \tilde{g} mass limit from retroactive analysis of hadronic collision and beam dump experiments. Limits valid if \tilde{g} decays inside detector.

LIGHT \tilde{G} (Gravitino) MASS LIMITS FROM COLLIDER EXPERIMENTS

The following are bounds on light ($\ll 1$ eV) gravitino indirectly inferred from its coupling to matter suppressed by the gravitino decay constant.

Unless otherwise stated, all limits assume that other supersymmetric particles besides the gravitino are too heavy to be produced. The gravitino is assumed to be undetected and to give rise to a missing energy (\cancel{E}) signature.

VALUE (eV)	CL%	DOCUMENT ID	TECN	COMMENT
• • • We do not use the following data for averages, fits, limits, etc. • • •				
$> 1.09 \times 10^{-5}$	95	1 ABDALLAH	05B DLPH	$e^+e^- \rightarrow \tilde{G}\tilde{G}\gamma$
$> 1.35 \times 10^{-5}$	95	2 ACHARD	04E L3	$e^+e^- \rightarrow \tilde{G}\tilde{G}\gamma$
$> 1.3 \times 10^{-5}$		3 HEISTER	03C ALEP	$e^+e^- \rightarrow \tilde{G}\tilde{G}\gamma$
$> 11.7 \times 10^{-6}$	95	4 ACOSTA	02H CDF	
$> 8.7 \times 10^{-6}$	95	5 ABBIENDI,G	00D OPAL	$e^+e^- \rightarrow \tilde{G}\tilde{G}\gamma$
$> 10.0 \times 10^{-6}$	95	6 ABREU	00Z DLPH	Superseded by ABDALLAH 05B
$> 11 \times 10^{-6}$	95	7 AFFOLDER	03J CDF	$p\bar{p} \rightarrow \tilde{G}\tilde{G} + \text{jet}$
$> 8.9 \times 10^{-6}$	95	6 ACCIARRI	99R L3	Superseded by ACHARD 04E
$> 7.9 \times 10^{-6}$	95	8 ACCIARRI	98J L3	$e^+e^- \rightarrow \tilde{G}\tilde{G}\gamma$
$> 8.3 \times 10^{-6}$	95	8 BARATE	98J ALEP	$e^+e^- \rightarrow \tilde{G}\tilde{G}\gamma$

- 1 ABDALLAH 05B use data from $\sqrt{s} = 180$ –208 GeV. They look for events with a single photon + \cancel{E} final states from which a cross section limit of $\sigma < 0.18$ pb at 208 GeV is obtained, allowing a limit on the mass to be set. Supersedes the results of ABREU 00Z.
- 2 ACHARD 04E use data from $\sqrt{s} = 189$ –209 GeV. They look for events with a single photon + \cancel{E} final states from which a limit on the Gravitino mass is set corresponding to $\sqrt{F} > 238$ GeV. Supersedes the results of ACCIARRI 99R.
- 3 HEISTER 03C use the data from $\sqrt{s} = 189$ –209 GeV to search for $\gamma\cancel{E}_T$ final states.
- 4 ACOSTA 02H looked in 87 pb $^{-1}$ of $p\bar{p}$ collisions at $\sqrt{s}=1.8$ TeV for events with a high- E_T photon and \cancel{E}_T . They compared the data with a GMSB model where the final state could arise from $q\tilde{q} \rightarrow \tilde{G}\tilde{G}\gamma$. Since the cross section for this process scales as $1/|F|^4$, a limit at 95% CL is derived on $|F|^{1/2} > 221$ GeV. A model independent limit for the above topology is also given in the paper.
- 5 ABBIENDI,G 00D searches for $\gamma\tilde{E}$ final states from $\sqrt{s}=189$ GeV.
- 6 ABREU 00Z, ACCIARRI 99R search for $\gamma\tilde{E}$ final states using data from $\sqrt{s}=189$ GeV.
- 7 AFFOLDER 00J searches for final states with an energetic jet (from quark or gluon) and large \cancel{E}_T from undetected gravitinos.

Searches Particle Listings

Supersymmetric Particle Searches

⁸ Searches for $\gamma\cancel{E}_T$ final states at $\sqrt{s}=183$ GeV.

Supersymmetry Miscellaneous Results

Results that do not appear under other headings or that make nonminimal assumptions.

VALUE	DOCUMENT ID	TECN	COMMENT
• • •	We do not use the following data for averages, fits, limits, etc. • • •		
1	ABULENCIA 06P	CDF	$\ell\gamma\cancel{E}_T, \ell\ell\gamma, \text{GMSB}$
2	ACOSTA 04E	CDF	
3	TCHIKILEV 04	ISTR	$K^- \rightarrow \pi^- \pi^0 P$
4	AFFOLDER 02D	CDF	$p\bar{p} \rightarrow \gamma b (\cancel{E}_T)$
5	AFFOLDER 01H	CDF	$p\bar{p} \rightarrow \gamma\gamma X$
6	ABBOTT 00G	D0	$p\bar{p} \rightarrow 3\ell + \cancel{E}_T, R, LL\bar{E}$
7	ABREU,P	00C	DLPH $e^+e^- \rightarrow \gamma + S/P$
8	ABACHI 97	D0	$\gamma\gamma X$
9	BARBER 84B	RVUE	
10	HOFFMAN 83	CNTR	$\pi p \rightarrow n(e^+e^-)$

¹ ABULENCIA 06P searched in 305 pb^{-1} of $p\bar{p}$ collisions at $\sqrt{s} = 1.96$ TeV for an excess of events with $\ell\gamma\cancel{E}_T$ and $\ell\ell\gamma$ ($\ell = e, \mu$). No significant excess was found compared to the background expectation. No events are found such as the $e\gamma\gamma\cancel{E}_T$ event observed in ABE 99i.

² ACOSTA 04E looked in 107 pb^{-1} of $p\bar{p}$ collisions at $\sqrt{s} = 1.8$ TeV for events with two same sign leptons without selection of other objects nor \cancel{E}_T . No significant excess is observed compared to the Standard Model expectation and constraints are derived on the parameter space of MSUGRA models, see Figure 4.

³ Looked for the scalar partner of a goldstino in decays $K^- \rightarrow \pi^- \pi^0 P$ from a 25 GeV K^- beam produced at the IHEP 70 GeV proton synchrotron. The goldstino is assumed to be sufficiently long-lived to be invisible. A 90% CL upper limit on the decay branching ratio is set at $\sim 9.0 \times 10^{-6}$ for a goldstino mass range from 0 to 200 MeV, excluding the interval near $m(\pi^0)$, where the limit is $\sim 3.5 \times 10^{-5}$.

⁴ AFFOLDER 02D looked in 85 pb^{-1} of $p\bar{p}$ collisions at $\sqrt{s}=1.8$ TeV for events with a high- E_T photon, and a b -tagged jet with or without \cancel{E}_T . They compared the data with models where the final state could arise from cascade decays of gluinos and/or squarks into $\tilde{\chi}^\pm$ and $\tilde{\chi}_2^0$ or direct associated production of $\tilde{\chi}_2^0 \tilde{\chi}_2^\pm$, followed by $\tilde{\chi}_2^0 \rightarrow \gamma\tilde{\chi}_1^0$ or a GMSB model where $\tilde{\chi}_1^0 \rightarrow \gamma\tilde{G}$. It is concluded that the experimental sensitivity is insufficient to detect the associated production or the GMSB model, but some sensitivity may exist to the cascade decays. A model independent limit for the above topology is also given in the paper.

⁵ AFFOLDER 01H searches for $p\bar{p} \rightarrow \gamma\gamma X$ events, where the di-photon system originates from goldstino production, in 100 pb^{-1} of data. Upper limits on the cross section times branching ratio are shown as function of the di-photon mass >70 GeV in Fig. 5. Excluded regions are derived in the plane of the goldstino mass versus the supersymmetry breaking scale for two representative sets of parameter values, as shown in Figs. 6 and 7.

⁶ ABBOTT 00G searches for trilepton final states ($\ell=e,\mu$) with \cancel{E}_T from the indirect decay of gauginos via $LL\bar{E}$ couplings. Efficiencies are computed for all possible production and decay modes of SUSY particles in the framework of the Minimal Supergravity scenario. See Figs. 1-4 for excluded regions in the $m_{1/2}$ versus m_0 plane.

⁷ ABREU,P 00C look for the CP -even (S) and CP -odd (P) scalar partners of the goldstino, expected to be produced in association with a photon. The S/P decay into two photons or into two gluons and both the tri-photon and the photon + two jets topologies are investigated. Upper limits on the production cross section are shown in Fig. 5 and the excluded regions in Fig. 6. Data collected at $\sqrt{s}=189-202$ GeV.

⁸ ABACHI 97 searched for $p\bar{p} \rightarrow \gamma\gamma\cancel{E}_T + X$ as supersymmetry signature. It can be caused by selectron, sneutrino, or neutralino production with a radiative decay of their decay products. They placed limits on cross sections.

⁹ BARBER 84B consider that $\tilde{\mu}$ and \tilde{e} may mix leading to $\mu \rightarrow e\tilde{\gamma}\tilde{\gamma}$. They discuss mass-mixing limits from decay dist. asym. in LBL-TRIUMF data and e^+ polarization in SIN data.

¹⁰ HOFFMAN 83 set CL = 90% limit $d\sigma/dt \text{ B}(e^+e^-) < 3.5 \times 10^{-32} \text{ cm}^2/\text{GeV}^2$ for spin-1 partner of Goldstone fermions with $140 < m < 160$ MeV decaying $\rightarrow e^+e^- \text{ pair}$.

ABAZOV 05A	PRL 94 041801	V.M. Abazov et al.	(D0 Collab.)
ABAZOV 05B	PRL 95 151805	V.M. Abazov et al.	(D0 Collab.)
ABDALLAH 05U	EPJ C38 395	J. Abdallah et al.	(DELPHI Collab.)
ABULENCIA 05A	PRL 95 252001	A. Abulencia et al.	(CDF Collab.)
ACOSTA 05E	PR D71 031104R	D. Acosta et al.	(CDF Collab.)
ACOSTA 05R	PRL 95 131801	D. Acosta et al.	(CDF Collab.)
AKERIB 05	PR D72 052009	D.S. Akerib et al.	(CDMS Collab.)
AKTAS 05	PL B616 31	A. Aktas et al.	(HI Collab.)
ALNER 05	PL B616 37	G.J. Alner et al.	(UK Dark Matter Collab.)
ALNER 05A	ASP 23 444	G.J. Alner et al.	(UK Dark Matter Collab.)
ANGLOHER 05	ASP 23 325	G. Angloher et al.	(CREST-II Collab.)
BARNABE-HE... 05	PL B624 186	M. Barnabe-Heider et al.	(PICASSO Collab.)
BERGER 05	PR D71 014007	E.L. Berger et al.	
CHEKANOV 05A	EPJ C44 463	S. Chekanov et al.	(ZEUS Collab.)
ELLIS 05	PR D71 095007	J. Ellis et al.	
GIRARD 05	PL B621 233	T.A. Girard et al.	(SIMPLE Collab.)
KLAPDOR-K... 05	PL B609 226	H.V. Klapdor-Kleingrothaus, I.V. Krivosheina, C. Tomei	
SANGLARD 05	PR D71 122002	V. Sanglard et al.	(EDELWEISS Collab.)
ABAZOV 04	PL B581 147	V.M. Abazov et al.	(D0 Collab.)
ABAZOV 04B	PRL 93 011801	V.M. Abazov et al.	(D0 Collab.)
ABBIENDI 04	EPJ C32 453	G. Abbiendi et al.	(OPAL Collab.)
ABBIENDI 04F	EPJ C33 149	G. Abbiendi et al.	(OPAL Collab.)
ABBIENDI 04H	EPJ C35 1	G. Abbiendi et al.	(OPAL Collab.)
ABBIENDI 04N	PL B602 167	G. Abbiendi et al.	(OPAL Collab.)
ABDALLAH 04H	EPJ C34 145	J. Abdallah et al.	(DELPHI Collab.)
ABDALLAH 04M	EPJ C36 1	J. Abdallah et al.	(DELPHI Collab.)
Also	EPJ C37 129 (erratum)	J. Abdallah et al.	(DELPHI Collab.)
ACHARD 04	PL B580 37	P. Achard et al.	(L3 Collab.)
ACHARD 04E	PL B587 16	P. Achard et al.	(L3 Collab.)
ACOSTA 04B	PRL 92 051803	D. Acosta et al.	(CDF Collab.)
ACOSTA 04E	PRL 93 051802	D. Acosta et al.	(CDF Collab.)
AKERIB 04	PRL 93 211301	D. Akerib et al.	(CDMSII Collab.)
AKTAS 04B	PL B599 159	A. Aktas et al.	(HI Collab.)
AKTAS 04D	EPJ C36 425	A. Aktas et al.	(HI Collab.)
BELANGER 04	JHEP 0403 012	G. Belanger et al.	
BOTTINO 04	PR D69 037302	A. Bottino et al.	
DAS 04	PL B596 293	S.P. Das, A. Datta, M. Maity	(Super-Kamiokande Collab.)
DESAI 04	PR D70 083523	S. Desai et al.	
ELLIS 04	PR D69 015005	J. Ellis et al.	
ELLIS 04B	PR D70 055005	J. Ellis et al.	
GIULIANI 04	PL B588 151	F. Giuliani, T.A. Girard	
HEISTER 04	PL B583 247	A. Heister et al.	(ALEPH Collab.)
JANOT 04	PL B594 23	P. Janot	
PIERCE 04A	PR D70 075006	A. Pierce	
TCHIKILEV 04	PL B602 149	O.G. Tchikilev et al.	(ISTRA+ Collab.)
ABBIENDI 03H	EPJ C29 479	G. Abbiendi et al.	(OPAL Collab.)
ABBIENDI 03L	PL B572 8	G. Abbiendi et al.	(OPAL Collab.)
ABDALLAH 03C	EPJ C26 505	J. Abdallah et al.	(DELPHI Collab.)
ABDALLAH 03D	EPJ C27 153	J. Abdallah et al.	(DELPHI Collab.)
ABDALLAH 03F	EPJ C28 15	J. Abdallah et al.	(DELPHI Collab.)
ABDALLAH 03G	EPJ C29 285	J. Abdallah et al.	(DELPHI Collab.)
ABDALLAH 03M	EPJ C31 421	J. Abdallah et al.	(DELPHI Collab.)
ACOSTA 03C	PRL 90 251801	D. Acosta et al.	(CDF Collab.)
ACOSTA 03E	PRL 91 171602	D. Acosta et al.	(CDF Collab.)
ADLOFF 03	PL B568 35	C. Adloff et al.	(HI Collab.)
AHMED 03	ASP 19 691	B. Ahmed et al.	(UK Dark Matter Collab.)
AKERIB 03	PR D68 082002	D. Akerib et al.	(CDMS Collab.)
BAER 03	JCAP 0305 006	H. Baer, C. Balazs	
BAER 03A	JCAP 0309 007	H. Baer et al.	
BERGER 03	PL B552 223	E. Berger et al.	
BOTTINO 03	PR D68 043506	A. Bottino et al.	
BOTTINO 03A	PR D67 063519	A. Bottino, N. Fornengo, S. Scopel	
CHAKRAB... 03	PR D68 015005	S. Chakrabarti, M. Guchait, N.K. Mondal	
CHATTOPAD... 03	PR D68 035005	U. Chattopadhyay, A. Corsetti, P. Nath	
CHEKANOV 03B	PR D68 052004	S. Chekanov et al.	(ZEUS Collab.)
ELLIS 03	ASP 18 395	J. Ellis, K.A. Olive, Y. Santoso	
ELLIS 03B	NP B652 259	J. Ellis et al.	
ELLIS 03C	PL B565 176	J. Ellis et al.	
ELLIS 03D	PL B573 162	J. Ellis et al.	
ELLIS 03E	PR D67 123502	J. Ellis et al.	
HEISTER 03	EPJ C27 1	A. Heister et al.	(ALEPH Collab.)
HEISTER 03C	EPJ C28 1	A. Heister et al.	(ALEPH Collab.)
HEISTER 03G	EPJ C31 1	A. Heister et al.	(ALEPH Collab.)
HEISTER 03H	EPJ C31 327	A. Heister et al.	(ALEPH Collab.)
HOOPER 03	PL B562 18	D. Hooper, T. Plehn	
JANOT 03	PL B564 183	P. Janot	
KLAPDOR-K... 03	ASP 18 525	H.V. Klapdor-Kleingrothaus et al.	
LAHANAS 03	PL B568 55	A. Lahanas, D. Nanopoulos	
LEP 03	SLAC-R-701, LEPWWG/2003-02		(LEP Collabs.)

REFERENCES FOR Supersymmetric Particle Searches

AALTONEN 06L	PR D77 052002	T. Aaltonen et al.	(CDF Collab.)
ABAZOV 08	PL B659 500	V.M. Abazov et al.	(D0 Collab.)
ABAZOV 08F	PL B659 856	V.M. Abazov et al.	(D0 Collab.)
ABAZOV 08G	PL B660 449	V.M. Abazov et al.	(D0 Collab.)
ANGLE 08	PRL 100 021303	J. Angle et al.	(XENON10 Collab.)
AALTONEN 07E	PR D76 072010	T. Aaltonen et al.	(CDF Collab.)
AALTONEN 07J	PRL 99 191806	T. Aaltonen et al.	(CDF Collab.)
ABAZOV 07B	PL B645 119	V.M. Abazov et al.	(D0 Collab.)
ABAZOV 07L	PRL 99 131801	V.M. Abazov et al.	(D0 Collab.)
ABULENCIA 07H	PRL 98 131804	A. Abulencia et al.	(CDF Collab.)
ABULENCIA 07N	PRL 98 221803	A. Abulencia et al.	(CDF Collab.)
ABULENCIA 07P	PRL 99 121801	A. Abulencia et al.	(CDF Collab.)
ALNER 07	PL B653 161	G.J. Alner et al.	(ZEPLIN-II Collab.)
ALNER 07A	ASP 28 287	G.J. Alner et al.	(ZEPLIN-II Collab.)
CHEKANOV 07	EPJ C50 269	S. Chekanov et al.	(ZEUS Collab.)
LEE 07A	PRL 99 091301	H.S. Lee et al.	(KIMS Collab.)
SCHAEF 07A	EPJ C49 411	S. Schaefer et al.	(ALEPH Collab.)
ABAZOV 06C	PL B638 119	V.M. Abazov et al.	(D0 Collab.)
ABAZOV 06D	PL B638 441	V.M. Abazov et al.	(D0 Collab.)
ABAZOV 06I	PRL 97 111801	V.M. Abazov et al.	(D0 Collab.)
ABAZOV 06P	PRL 97 161802	V.M. Abazov et al.	(D0 Collab.)
ABAZOV 06R	PRL 97 171806	V.M. Abazov et al.	(D0 Collab.)
ABBIENDI 06B	EPJ C46 307	G. Abbiendi et al.	(OPAL Collab.)
ABDALLAH 06C	EPJ C45 589	J. Abdallah et al.	(DELPHI Collab.)
ABULENCIA 06I	PRL 96 171802	A. Abulencia et al.	(CDF Collab.)
ABULENCIA 06M	PRL 96 211802	A. Abulencia et al.	(CDF Collab.)
ABULENCIA 06P	PRL 97 031801	A. Abulencia et al.	(CDF Collab.)
ACHTERBERG 06	ASP 26 129	A. Achterberg et al.	(AMANDA Collab.)
ACKERMANN 06	ASP 24 459	M. Ackermann et al.	(AMANDA Collab.)
AKERIB 06	PR D73 011102R	D.S. Akerib et al.	(CDMS Collab.)
AKERIB 06A	PRL 96 011302	D.S. Akerib et al.	(CDMS Collab.)
BEENOIT 06	PL B637 156	A. Benoit et al.	
DEBOER 06	PL B636 13	W. de Boer et al.	
LEE 06	PL B633 201	H.S. Lee et al.	(KIMS Collab.)
SHIMIZU 06A	PL B633 195	Y. Shimizu et al.	
SMITH 06	PL B642 567	N.J.T. Smith, A.S. Murphy, T.J. Sumner	

TAKEDA 03	PL B572 145	A. Takeda et al.	
ABAZOV 02C	PRL 88 171802	V.M. Abazov et al.	(D0 Collab.)
ABAZOV 02F	PRL 89 171801	V.M. Abazov et al.	(D0 Collab.)
ABAZOV 02G	PR D66 112001	V.M. Abazov et al.	(D0 Collab.)
ABAZOV 02H	PRL 89 261801	V.M. Abazov et al.	(D0 Collab.)
ABBIENDI 02B	EPJ C23 1	G. Abbiendi et al.	(OPAL Collab.)
ABBIENDI 02H	PL B526 233	G. Abbiendi et al.	(OPAL Collab.)
ABBIENDI 02H	PL B545 272	G. Abbiendi et al.	(OPAL Collab.)
Also	PL B548 258 (erratum)	G. Abbiendi et al.	(OPAL Collab.)
ABRAMS 02	PR D66 122003	D. Abrams et al.	(CDMS Collab.)
ACHARD 02	PL B524 65	P. Achard et al.	(L3 Collab.)
ACOSTA 02H	PRL 89 281801	D. Acosta et al.	(CDF Collab.)
AFFOLDER 02	PRL 88 041801	T. Affolder et al.	(CDF Collab.)
AFFOLDER 02D	PR D65 052006	T. Affolder et al.	(CDF Collab.)
ANGLOHER 02	ASP 18 43	G. Angloher et al.	(CREST Collab.)
ARNOWITT 02	hep-ph/0211417	R. Arnowitt, B. Dutta	
BAEK 02	PL B541 161	S. BaeK	
BAER 02	JHEP 0207 050	H. Baer et al.	
BECHER 02	PL B540 278	T. Becher et al.	
BENOIT 02	PL B545 43	A. Benoit et al.	(EDELWEISS Collab.)
CHEKANOV 02	PR D65 092004	S. Chekanov et al.	(ZEUS Collab.)
CHEUNG 02B	PRL 89 221801	K. Cheung, W.-Y. Keung	
CHO 02	PRL 89 091801	G.-C. Cho	
ELLIS 02	PL B525 308	J. Ellis, D.V. Nanopoulos, K.A. Olive	
ELLIS 02B	PL B532 318	J. Ellis, A. Ferstl, K.A. Olive	
ELLIS 02C	PL B539 107	J. Ellis, K.A. Olive, Y. Santoso	
GHOODBANE 02	NP B647 190	N. Ghodbane et al.	
HEISTER 02	PL B526 191	A. Heister et al.	(ALEPH Collab.)
HEISTER 02E	PL B526 206	A. Heister et al.	(ALEPH Collab.)
HEISTER 02F	EPJ C25 1	A. Heister et al.	(ALEPH Collab.)
HEISTER 02J	PL B533 223	A. Heister et al.	(ALEPH Collab.)
HEISTER 02K	PL B537 5	A. Heister et al.	(ALEPH Collab.)
HEISTER 02L	PL B544 73	A. Heister et al.	(ALEPH Collab.)
HEISTER 02R	EPJ C25 339	A. Heister et al.	(ALEPH Collab.)
KIM 02	PL B527 18	H.B. Kim et al.	
KIM 02B	JHEP 0212 034	Y.G. Kim et al.	
LAHANAS 02	EPJ C23 185	A. Lahanas, V.C. Spanos	
MORALES 02B	ASP 16 325	A. Morales et al.	(COSME Collab.)
MORALES 02C	PL B532 8	A. Morales et al.	(ICEX Collab.)
ABBIENDI 01	PL B501 12	G. Abbiendi et al.	(OPAL Collab.)
ABBOTT 01D	PR D63 091102	B. Abbott et al.	(D0 Collab.)
ABREU 01	EPJ C19 29	P. Abreu et al.	(DELPHI Collab.)

Searches Particle Listings

Supersymmetric Particle Searches

ABREU	01B	EPJ C19 201	P. Abreu et al.	(DELPHI Collab.)	ACKERSTAFF	98L	EPJ C2 213	K. Ackerstaff et al.	(OPAL Collab.)
ABREU	01C	PL B502 24	P. Abreu et al.	(DELPHI Collab.)	ACKERSTAFF	98P	PL B433 195	K. Ackerstaff et al.	(OPAL Collab.)
ABREU	01D	PL B500 22	P. Abreu et al.	(DELPHI Collab.)	ACKERSTAFF	98V	EPJ C2 441	K. Ackerstaff et al.	(OPAL Collab.)
ABREU	01G	PL B503 34	P. Abreu et al.	(DELPHI Collab.)	BARATE	98H	PL B420 127	R. Barate et al.	(ALEPH Collab.)
ACCIARRI	01	EPJ C19 397	M. Acciari et al.	(L3 Collab.)	BARATE	98J	PL B429 201	R. Barate et al.	(ALEPH Collab.)
ADAMS	01	PRL 87 041801	T. Adams et al.	(NuTeV Collab.)	BARATE	98K	PL B433 176	R. Barate et al.	(ALEPH Collab.)
ADLOFF	01B	EPJ C20 639	C. Adloff et al.	(HI Collab.)	BARATE	98S	EPJ C4 433	R. Barate et al.	(ALEPH Collab.)
AFFOLDER	01B	PR D63 091101	T. Affolder et al.	(CDF Collab.)	BARATE	98X	EPJ C2 417	R. Barate et al.	(ALEPH Collab.)
AFFOLDER	01H	PR D64 092002	T. Affolder et al.	(CDF Collab.)	BERNABEI	98	PL B424 195	R. Bernabei et al.	(DAMA Collab.)
AFFOLDER	01J	PRL 87 251803	T. Affolder et al.	(CDF Collab.)	BERNABEI	98C	PL B436 379	R. Bernabei et al.	(DAMA Collab.)
BALTZ	01	PRL 86 5004	E. Baltz, P. Gondolo		BREITWEG	98	PL B434 214	J. Breitweg et al.	(ZEUS Collab.)
BARATE	01	PL B499 67	R. Barate et al.	(ALEPH Collab.)	ELLIS	98	PR D58 095002	J. Ellis et al.	
BARATE	01B	EPJ C19 415	R. Barate et al.	(ALEPH Collab.)	ELLIS	98B	PL B444 367	J. Ellis, T. Falk, K. Olive	
BARGER	01C	PL B518 117	V. Barger, C. Kao		PDG	98	EPJ C3 1	C. Caso et al.	
BAUDIS	01	PR D63 022001	L. Baudis et al.	(Heidelberg-Moscow Collab.)	ABACHI	97	PRL 78 2070	S. Abachi et al.	(DO Collab.)
BENOIT	01	PL B513 15	A. Benoit et al.	(EDELWEISS Collab.)	ABBOTT	97B	PRL 79 4321	B. Abbott et al.	(DO Collab.)
BERGER	01	PRL 86 4231	E. Berger et al.		ABE	97U	PR D56 R1357	F. Abe et al.	(CDF Collab.)
BERNABEI	01	PL B509 197	R. Bernabei et al.	(DAMA Collab.)	ACCIARRI	97K	PL B414 373	M. Acciari et al.	(L3 Collab.)
BOTTINO	01	PR D63 125003	A. Bottino et al.		ACKERSTAFF	97H	PL B396 301	K. Ackerstaff et al.	(OPAL Collab.)
BREITWEG	01	PR D63 052002	J. Breitweg et al.	(ZEUS Collab.)	ADAMS	97B	PRL 79 4083	J. Adams et al.	(FNAL KTeV Collab.)
CORSETTI	01	PR D64 125010	A. Corsetti, P. Nath		ALBUQUERQUE...	97	PRL 78 3252	L.F. Albuquerque et al.	(FNAL E761 Collab.)
DJOUADI	01	JHEP 0108 055	A. Djouadi, M. Drees, J.L. Kneur		BAER	97	PR D57 567	H. Baer, M. Brhlik	
ELLIS	01B	PL B510 236	J. Ellis et al.		BARATE	97K	PL B405 379	R. Barate et al.	(ALEPH Collab.)
ELLIS	01C	PR D63 065016	J. Ellis, A. Ferstl, K.A. Olive		BARATE	97L	ZPHY C76 1	R. Barate et al.	(ALEPH Collab.)
GOMEZ	01	PL B512 252	M.E. Gomez, J.D. Vergados		BERNABEI	97	ASP 7 73	R. Bernabei et al.	(DAMA Collab.)
LAHANAS	01	PL B518 94	A. Lahanas, D.V. Nanopoulos, V. Spanos		CARENA	97	PL B390 234	M. Carena, G.F. Giudice, C.E.M. Wagner	
ROSKOWSKI	01	JHEP 0108 024	L. Roszkowski, R. Ruiz de Austri, T. Nihei		CSIKOR	97	PRL 78 4335	F. Csikor, Z. Fodor	(EOTV, CERN)
SAVINOV	01	PR D63 051101	V. Savinov et al.	(CLEO Collab.)	DATTA	97	PL B395 54	A. Datta, M. Guchait, N. Parua	(ICTP, TATA)
ABBIENDI	00	EPJ C12 1	G. Abbiendi et al.	(OPAL Collab.)	DEGOUVEA	97	PL B400 117	A. de Gouvea, H. Murayama	(ZEUS Collab.)
ABBIENDI	00G	EPJ C14 51	G. Abbiendi et al.	(OPAL Collab.)	DERRICK	97	ZPHY C73 613	M. Derrick et al.	(ZEUS Collab.)
ABBIENDI	00H	EPJ C14 187	G. Abbiendi et al.	(OPAL Collab.)	EDSJO	97	PR D56 1879	J. Edsjo, P. Gondolo	(L3 Collab.)
Also		EPJ C16 707 (erratum)	G. Abbiendi et al.	(OPAL Collab.)	ELLIS	97	PL B394 354	J. Ellis, J.L. Lopez, D.V. Nanopoulos	
ABBIENDI	00J	EPJ C12 551	G. Abbiendi et al.	(OPAL Collab.)	HEWETT	97	PR D56 5703	J.L. Hewett, T.G. Rizzo, M.A. Doncheski	
ABBIENDI	00R	EPJ C13 553	G. Abbiendi et al.	(OPAL Collab.)	KALINOWSKI	97	PL B400 112	J. Kalinowski, P. Zerwas	
ABBIENDI,G	00D	EPJ C18 253	G. Abbiendi et al.	(OPAL Collab.)	TEREKHOV	97	PL B412 86	I. Terekhov	(ALAT)
ABBOTT	00C	PRL 84 2088	G. Abbott et al.	(DO Collab.)	ABACHI	96	PRL 76 2228	S. Abachi et al.	(DO Collab.)
ABBOTT	00G	PR D62 071701R	B. Abbott et al.	(DO Collab.)	ABACHI	96B	PRL 76 2222	S. Abachi et al.	(DO Collab.)
ABREU	001	EPJ C13 591	P. Abreu et al.	(DELPHI Collab.)	ABE	96	PRL 77 438	F. Abe et al.	(CDF Collab.)
ABREU	00J	PL B479 129	P. Abreu et al.	(DELPHI Collab.)	ABE	96D	PRL 76 2006	F. Abe et al.	(CDF Collab.)
ABREU	00Q	PL B478 65	P. Abreu et al.	(DELPHI Collab.)	ABE	96K	PRL 76 4307	F. Abe et al.	(CDF Collab.)
ABREU	00S	PL B485 45	P. Abreu et al.	(DELPHI Collab.)	AID	96	ZPHY C71 211	S. Aid et al.	(HI Collab.)
ABREU	00P	PL B485 95	P. Abreu et al.	(DELPHI Collab.)	AID	96C	PL B330 109	S. Aid et al.	(HI Collab.)
ABREU	00U	PL B487 36	P. Abreu et al.	(DELPHI Collab.)	ARNOWITT	96	PR D54 2374	R. Arnowitt, P. Nath	
ABREU	00V	EPJ C16 211	P. Abreu et al.	(DELPHI Collab.)	BAER	96	PR D53 597	H. Baer, M. Brhlik	
ABREU	00W	PL B489 38	P. Abreu et al.	(DELPHI Collab.)	BERGSTROM	96	ASP 5 263	L. Bergstrom, P. Gondolo	
ABREU	00Z	EPJ C17 53	P. Abreu et al.	(DELPHI Collab.)	CHO	96	PL B372 101	G.C. Cho, Y. Kizukuri, N. Oshimo	(TOKAH, OCH)
ABREU,P	00C	PL B494 203	P. Abreu et al.	(DELPHI Collab.)	FARRAR	96	PRL 76 4111	G.R. Farrar	(RUTG)
ABREU,P	00D	PL B496 59	P. Abreu et al.	(DELPHI Collab.)	LEWIN	96	ASP 6 87	J.D. Lewin, P.F. Smith	
ABUSAJID	00	PRL 84 5699	R. Abusajid et al.	(CDMS Collab.)	TEREKHOV	96	PL B385 139	I. Terekhov, L. Clavelli	(ALAT)
ACCIARRI	00C	EPJ C16 1	M. Acciari et al.	(L3 Collab.)	ABACHI	95C	PRL 75 618	S. Abachi et al.	(DO Collab.)
ACCIARRI	00D	PL B472 420	M. Acciari et al.	(L3 Collab.)	ABE	95N	PRL 74 3538	F. Abe et al.	(CDF Collab.)
ACCIARRI	00K	PL B482 31	M. Acciari et al.	(L3 Collab.)	ABE	95T	PRL 75 613	F. Abe et al.	(CDF Collab.)
ACCIARRI	00P	PR B489 81	M. Acciari et al.	(L3 Collab.)	ACCIARRI	95E	PL B350 109	M. Acciari et al.	(L3 Collab.)
ACCOMANDO	00	NP B585 124	E. Accomando et al.		AKERS	95A	ZPHY C65 367	R. Akers et al.	(OPAL Collab.)
AFFOLDER	00D	PRL 84 5704	T. Affolder et al.	(CDF Collab.)	AKERS	95R	ZPHY C67 203	R. Akers et al.	(OPAL Collab.)
AFFOLDER	00G	PRL 84 5273	T. Affolder et al.	(CDF Collab.)	BEREZINSKY	95	ASP 5 1	V. Berezhinsky et al.	
AFFOLDER	00J	PRL 85 1378	T. Affolder et al.	(CDF Collab.)	BUSKULIC	95E	PL B349 238	D. Buskulic et al.	(ALEPH Collab.)
AFFOLDER	00K	PRL 85 2056	T. Affolder et al.	(CDF Collab.)	CLAVELLI	95	PR D51 1117	L. Clavelli, P.W. Coulter	(ALAT)
BARATE	00G	EPJ C16 71	R. Barate et al.	(ALEPH Collab.)	FALK	95	PL B354 99	T. Falk, K.A. Olive, M. Srednicki	(MINN, UCSB)
BARATE	00H	EPJ C13 29	R. Barate et al.	(ALEPH Collab.)	LOSECCO	95	PL B342 392	J.M. Losecco	(NDAM)
BARATE	00I	EPJ C12 183	R. Barate et al.	(ALEPH Collab.)	AKERS	94K	PL B337 207	R. Akers et al.	(OPAL Collab.)
BARATE	00P	PL B488 234	R. Barate et al.	(ALEPH Collab.)	BECK	94	PL B336 141	M. Beck et al.	(MPHI, KIAE, SASSO)
BERNABEI	00	PL B480 23	R. Bernabei et al.	(DAMA Collab.)	CAKIR	94	PR D50 3268	M.B. Cakir, G.R. Farrar	(RUTG)
BERNABEI	00C	EPJ C18 283	R. Bernabei et al.	(DAMA Collab.)	FALK	94	PL B339 248	T. Falk, K.A. Olive, M. Srednicki	(UCSB, MINN)
BERNABEI	00D	NJP 2 15	R. Bernabei et al.	(DAMA Collab.)	SHIRAI	94	PRL 72 3313	J. Shirai et al.	(VENUS Collab.)
BOEHM	00B	PR D62 035012	C. Boehm, A. Djouadi, M. Drees		ADRIANI	93M	PRPL 236 1	O. Adriani et al.	(L3 Collab.)
BREITWEG	00E	EPJ C16 253	J. Breitweg et al.	(ZEUS Collab.)	ALITTI	93	NP B400 3	J. Alitti et al.	(UA2 Collab.)
CHO	00B	NP B574 623	G.-C. Cho, K. Hagiwara		CLAVELLI	93	PR D47 1973	L. Clavelli, P.W. Coulter, K.J. Yuan	(ALAT)
COLLAR	00	PRL 85 3083	J.J. Collar et al.	(SIMPLE Collab.)	DREES	93	PR D47 376	M. Drees, M.M. Nojiri	(DESY, SLAC)
ELLIS	00	PR D62 075010	J. Ellis et al.		DREES	93B	PR D48 3483	M. Drees, M.M. Nojiri	
FENG	00	PL B482 388	J.L. Feng, K.T. Matchev, F. Wilczek		FALK	93	PL B318 354	T. Falk et al.	(UCB, UCSB, MINN)
LAHANAS	00	PR D62 023515	A. Lahanas, D.V. Nanopoulos, V.C. Spanos		HEBBEKER	93	ZPHY C60 63	T. Hebbeker	(ALAT)
LEP	00	CERN-EP-2000-016	LEP Collabs. (ALEPH, DELPHI, L3, OPAL, SLD+)		KELLEY	93	PR D47 2461	S. Kelley et al.	(CERN)
MAFI	00	PR D62 035003	A. Mafi, S. Raby		LOPEZ	93C	PL B313 241	J.L. Lopez, D.V. Nanopoulos, X. Wang	(TAMU, HARC+)
MALTONI	00	PL B476 107	M. Maltoni et al.		MIZUTA	93	PL B298 120	S. Mizuta, M. Yamaguchi	(TOFO)
MORALES	00	PL B489 268	A. Morales et al.	(IGEX Collab.)	MORI	93	PL B388 5505	M. Mori et al.	(KEK, NIIG, TOKY, TOKA+)
PDG	00	EPJ C15 1	D.E. Groom et al.		ABE	92L	PRL 69 3439	F. Abe et al.	(CDF Collab.)
SPOONER	00	PL B473 330	N.J.C. Spooner et al.	(UK Dark Matter Col.)	BOTTINO	92	MPL A7 733	A. Bottino et al.	(TORI, ZARA)
ABBIENDI	99	EPJ C6 1	G. Abbiendi et al.	(OPAL Collab.)	Also	92	PL B265 57	A. Bottino et al.	(TORI, INFN)
ABBIENDI	99F	EPJ C8 23	G. Abbiendi et al.	(OPAL Collab.)	CLAVELLI	92	PR D46 2112	L. Clavelli	(ALAT)
ABBIENDI	99M	PL B456 95	G. Abbiendi et al.	(OPAL Collab.)	DECAMP	92	PRPL 216 253	D. Decamp et al.	(ALEPH Collab.)
ABBIENDI	99T	EPJ C11 619	G. Abbiendi et al.	(OPAL Collab.)	LOPEZ	92	NP B370 445	J.L. Lopez, D.V. Nanopoulos, K.J. Yuan	(TAMU)
ABBOTT	99	PRL 82 29	B. Abbott et al.	(DO Collab.)	MCDONALD	92	PL B283 80	J. McDonald, K.A. Olive, M. Srednicki	(LSB+)
ABBOTT	99F	PR D60 031101	B. Abbott et al.	(DO Collab.)	ROY	92	PL B283 270	D.P. Roy	(CERN)
ABBOTT	99J	PRL 83 2896	B. Abbott et al.	(DO Collab.)	ABREU	91F	NP B367 511	P. Abreu et al.	(DELPHI Collab.)
ABBOTT	99K	PRL 83 4476	B. Abbott et al.	(DO Collab.)	AKESSON	91	ZPHY C52 219	T. Akesson et al.	(HELIOS Collab.)
ABBOTT	99L	PRL 83 4937	B. Abbott et al.	(DO Collab.)	ALEXANDER	91F	ZPHY C52 175	G. Alexander et al.	(OPAL Collab.)
ABE	99I	PR D59 092002	F. Abe et al.	(CDF Collab.)	ANTONIADIS	91	PL B262 109	I. Antoniadis, J. Ellis, D.V. Nanopoulos	(EPOL+)
ABE	99M	PRL 83 2133	F. Abe et al.	(CDF Collab.)	BOTTINO	91	PL B265 57	A. Bottino et al.	(TORI, INFN)
ABREU	99A	EPJ C11 383	P. Abreu et al.	(DELPHI Collab.)	GELMINI	91	NP B351 623	G.B. Gelmini, P. Gondolo, E. Roulet	(UCLA, TRST)
ABREU	99C	EPJ C6 385	P. Abreu et al.	(DELPHI Collab.)	GRIEST	91	PR D43 3191	K. Griest, D. Seckel	
ABREU	99F	EPJ C7 595	P. Abreu et al.	(DELPHI Collab.)	KAMIONKOWSKI...	91	PR D44 3021	M. Kamionkowski	(CHIC, FNAL)
ABREU	99G	PL B446 62	P. Abreu et al.	(DELPHI Collab.)	MORI	91B	PL B270 89	M. Mori et al.	(Kamioke Collab.)
ACCIARRI	99H	PL B456 283	M. Acciari et al.	(L3 Collab.)	NOJIRI	91	PL B261 76	M.M. Nojiri	(KEK)
ACCIARRI	99I	PL B459 354	M. Acciari et al.	(L3 Collab.)	OLIVE	91	NP B385 208	K.A. Olive, M. Srednicki	(MINN, UCSB)
ACCIARRI	99J	PL B462 354	M. Acciari et al.	(L3 Collab.)	ROSKOWSKI	91	PL B262 59	L. Roszkowski	(CERN)
ACCIARRI	99L	PL B470 268	M. Acciari et al.	(L3 Collab.)	SATO	91	PR D44 2220	N. Sato et al.	(Kamioke Collab.)
ACCIARRI	99V	PL B471 306	M. Acciari et al.	(L3 Collab.)	ADACHI	90C	PL B244 352	I. Adachi et al.	(TOPAZ Collab.)
ACCIARRI	99W	PL B471 280	M. Acciari et al.	(L3 Collab.)	GRIEST	90	PR D41 3565	K. Griest, M. Kamionkowski, M.S. Turner	(UCB+)
ALAVI-HARATI	99E	PRL 83 2128	A. Alavi-Harati et al.	(FNAL KTeV Collab.)	BARBIERI	89C	NP B313 725	R. Barbieri, M. Frigeni, G. Giudice	
AMBROSIO	99	PR D60 082002	M. Ambrosio et al.	(Macro Collab.)	NAKAMURA	89	PR D39 1261	T.T. Nakamura et al.	(KYOT, TMT C)
BAER	99	PR D59 075002	H. Baer, K. Cheung, J.F. Guion		OLIVE	89	PL B230 78	K.A. Olive, M. Srednicki	(MINN, UCSB)
BARATE	99E	EPJ C7 383	R. Barate et al.	(ALEPH Collab.)	ELLIS	88D	NP B307 883	J. Ellis, R. Flores	
BARATE	99Q	PL B469 303	R. Barate et al.	(ALEPH Collab.)	GRIEST	88B	PR D38 2357	K. Griest	
BAUDIS	99	PR D59 022001	L. Baudis et al.	(Heidelberg-Moscow Collab.)	OLIVE	88	PL B205 553	K.A. Olive, M. Srednicki	(MINN, UCSB)
BELLI	99C	NP B563 97	P. Belli et al.	(DAMA Collab.)	SREDNICKI	88	NP B310 693	M. Srednicki, R. Watkins, K.A. Olive	(MINN, UCSB)
BERNABEI	99	PL B450 448	R. Bernabei et al.	(DAMA Collab.)	ALBAJAR	87D	PL B198 261	C. Albajar et al.	(UA1 Collab.)
FANTI	99	PL B446 117	F. Fanti et al.	(DAMA Collab.)	ANSARI	87D	PL B195 613	R. Ansari et al.	(UA2 Collab.)
MALTONI	99B	PL B463 230	E. Maltoni, M.I. Vyssotsky	(CERN NA48 Collab.)	ARNOLD	87	PL B186 435	R.G. Arnold et al.	(BRUX, DIUC, LOUC+)
OOTANI	99	PL B461 371	W. Ootani et al.		NG	87	PL B188 138	K.W. Ng, K.A. Olive, M. Srednicki	(MINN, UCSB)
ABBOTT	98	PRL 80 442	B. Abbott et al.	(DO Collab.)	TUTS	87	PL B186 233	P.M. Tuts et al.	(CUSB Collab.)
ABBOTT	98C	PRL 80 1591	B. Abbott et al.	(DO Collab.)	ALBRECHT	86C	PL 167B 360	H. Albrecht et al.	(ARGUS Collab.)
ABBOTT	98E	PRL 80 2051	B. Abbott et al.	(DO Collab.)	BADIER	86	ZPHY C31 21	J. Badier et al.	(NA3 Collab.)
ABBOTT	98J	PRL 81 38	B. Abbott et al.	(DO Collab.)	BARNETT	86	NP B267 625	R.M. Barnett, H.E. Haber, G.L. Kane	(LBL, UCS+)
ABE	98J	PRL 80 5275	F. Abe et al.	(CDF Collab.)	GAISSER	86	PR D34 2206	T.K. Gaisser, G. Steigman, S. Tilav	(BART, DELA)
ABE	98S	PRL 81 4806	F. Abe et al.	(CDF Collab.)	VOLOSHIN	86	SJNP 43 495	M.B. Voloshin, L.B. Okun	(ITEP)
ABREU	98	EPJ C1 1	P. Abreu et al.	(DELPHI Collab.)					
ABREU	98P	PL B444 491	P. Abreu et al.	(DELPHI Collab.)					

Searches Particle Listings

Supersymmetric Particle Searches, Technicolor

COOPER...	85B	PL 160B 212	A.M. Cooper-Sarkar <i>et al.</i>	(WA66 Collab.)
DAWSON	85	PR D31 1581	S. Dawson, E. Eichten, C. Quigg	(LBL, FNAL)
FARRAR	85	PRL 55 895	G.R. Farrar	(RUTG)
GOLDMAN	85	Physica 15D 181	T. Goldman, H.E. Haber	(LANL, UCSC)
HABER	85	PRPL 117 75	H.E. Haber, G.L. Kane	(UCSC, MICH)
BALL	84	PRL 53 1314	R.C. Ball <i>et al.</i>	(MICH, FIRZ, OSU, FNAL+)
BARBER	84B	PL 139B 427	J.S. Barber, R.E. Shrock	(STON)
BRICK	84	PR D30 1134	D.H. Brick <i>et al.</i>	(BROW, CAVE, IIT+)
ELLIS	84	NP B238 453	J. Ellis <i>et al.</i>	(CERN)
FARRAR	84	PRL 53 1029	G.R. Farrar	(RUTG)
BERGSMIA	83C	PL 121B 429	F. Bergsma <i>et al.</i>	(CHARM Collab.)
CHANOWITZ	83	PL 126B 225	M.S. Chanowitz, S. Sharpe	(UCB, LBL)
GOLDBERG	83	PRL 50 1419	H. Goldberg	(NEAS)
HOFFMAN	83	PR D28 660	C.M. Hoffman <i>et al.</i>	(LANL, ARZS)
KRAUSS	83	NP B227 556	L.M. Krauss	(HARV)
VYSOTSKII	83	SJNP 37 948	M.I. Vysotsky	(ITEP)
		Translated from YAF 37 1597		
KANE	82	PL 112B 227	G.L. Kane, J.P. Leveille	(MICH)
CABIBBO	81	PL 105B 155	N. Cabibbo, G.R. Farrar, L. Maiani	(ROMA, RUTG)
FARRAR	78	PL 76B 575	G.R. Farrar, P. Fayet	(CIT)
Also		PL 79B 442	G.R. Farrar, P. Fayet	(CIT)

Technicolor

DYNAMICAL ELECTROWEAK SYMMETRY BREAKING

Revised August 2007 by R.S. Chivukula (Michigan State University), M. Narain (Brown University), and J. Womersley (STFC, Rutherford Appleton Laboratory).

In theories of dynamical electroweak symmetry breaking, the electroweak interactions are broken to electromagnetism by the vacuum expectation value of a fermion bilinear. These theories may thereby avoid the introduction of fundamental scalar particles, of which we have no examples in nature. In this note, we review the status of experimental searches for the particles predicted in technicolor, topcolor, and related models. The limits from these searches are summarized in Table 1.

I. Technicolor

The earliest models [1,2] of dynamical electroweak symmetry breaking [3] include a new asymptotically free non-abelian gauge theory (“technicolor”) and additional massless fermions (“technifermions” transforming under a vectorial representation of the gauge group) which feel this new force. The global chiral symmetry of the fermions is spontaneously broken by the formation of a technifermion condensate, just as the approximate chiral $SU(2) \times SU(2)$ symmetry in QCD is broken down to $SU(2)$ isospin by the formation of a quark condensate. If the quantum numbers of the technifermions are chosen correctly (*e.g.*, by choosing technifermions in the fundamental representation of an $SU(N)$ technicolor gauge group, with the left-handed technifermions being weak doublets and the right-handed ones weak singlets), this condensate can break the electroweak interactions down to electromagnetism.

The breaking of the global chiral symmetries implies the existence of Goldstone bosons, the “technipions” (π_T). Through the Higgs mechanism, three of the Goldstone bosons become the longitudinal components of the W and Z , and the weak gauge bosons acquire a mass proportional to the technipion decay constant (the analog of f_π in QCD). The quantum numbers and masses of any remaining technipions are model-dependent. There may be technipions which are colored (octets and triplets), as well as those carrying electroweak quantum numbers, and some color-singlet technipions are too light [4,3] unless additional sources of chiral-symmetry breaking are introduced. The next lightest technicolor resonances are expected to

Table 1: Summary of the mass limits. Symbols are defined in the text.

Process	Excluded mass range	Decay channels Ref.
$p\bar{p} \rightarrow \rho_T \rightarrow W\pi_T$	$170 < m_{\rho_T} < 215$ GeV and $80 < m_{\pi_T} < 115$ GeV for $M_V = 500$ GeV	$\rho_T \rightarrow W\pi_T$ [18] $\pi_T^0 \rightarrow b\bar{b}$ $\pi_T^\pm \rightarrow b\bar{c}$
$p\bar{p} \rightarrow \omega_T \rightarrow \gamma\pi_T$	$140 < m_{\omega_T} < 290$ GeV for $m_{\pi_T} \approx m_{\omega_T}/3$ and $M_T = 100$ GeV	$\omega_T \rightarrow \gamma\pi_T$ [19] $\pi_T^0 \rightarrow b\bar{b}$ $\pi_T^\pm \rightarrow b\bar{c}$
$p\bar{p} \rightarrow \omega_T/\rho_T$	$m_{\omega_T} = m_{\rho_T} < 203$ GeV for $m_{\omega_T} < m_{\pi_T} + m_W$ or $M_T > 200$ GeV $m_{\omega_T} = m_{\rho_T} < 280$ GeV for $m_{\omega_T} < m_{\pi_T} + m_W$ or $M_T > 500$ GeV	$\omega_T/\rho_T \rightarrow \ell^+\ell^-$ [20] $\omega_T/\rho_T \rightarrow \ell^+\ell^-$ [21]
$e^+e^- \rightarrow \omega_T/\rho_T$	$90 < m_{\rho_T} < 206.7$ GeV $m_{\pi_T} < 79.8$ GeV	$\rho_T \rightarrow WW$, [22] $W\pi_T$, $\pi_T\pi_T$, $\gamma\pi_T$, hadrons
$p\bar{p} \rightarrow \rho_{T8}$	$260 < m_{\rho_{T8}} < 480$ GeV	$\rho_{T8} \rightarrow q\bar{q}, gg$ [24]
$p\bar{p} \rightarrow \rho_{T8}$ $\rightarrow \pi_{LQ}\pi_{LQ}$	$m_{\rho_{T8}} < 510$ GeV $m_{\rho_{T8}} < 600$ GeV $m_{\rho_{T8}} < 465$ GeV	$\pi_{LQ} \rightarrow c\nu$ [27] $\pi_{LQ} \rightarrow b\nu$ [27] $\pi_{LQ} \rightarrow \tau q$ [26]
$p\bar{p} \rightarrow g_t$	$0.3 < m_{g_t} < 0.6$ TeV for $0.3m_{g_t} < \Gamma < 0.7m_{g_t}$	$g_t \rightarrow b\bar{b}$ [32]
$p\bar{p} \rightarrow Z'$	$m_{Z'} < 480$ GeV for $\Gamma = 0.012m_{Z'}$ $m_{Z'} < 780$ GeV for $\Gamma = 0.04m_{Z'}$	$Z' \rightarrow t\bar{t}$ [33]

be the analogs of the vector mesons in QCD. The technivector mesons can also have color and electroweak quantum numbers and, for a theory with a small number of technifermions, are expected to have a mass in the TeV range [5].

While technicolor chiral symmetry breaking can give mass to the W and Z particles, additional interactions must be introduced to produce the masses of the standard model fermions. The most thoroughly studied mechanism for this invokes “extended technicolor” (ETC) gauge interactions [4,6]. In ETC, technicolor and flavor are embedded into a larger gauge group, which is broken at a sequence of mass scales down to the residual, exact technicolor gauge symmetry. The massive gauge bosons associated with this breaking mediate transitions between quarks/leptons and technifermions, giving rise to the couplings necessary to produce fermion masses. The ETC gauge bosons also mediate transitions among technifermions themselves, leading to interactions which can explicitly break unwanted chiral symmetries and raise the masses of any light technipions. The ETC interactions connecting technifermions to quarks/leptons also mediate technipion decays to ordinary fermion pairs. Since these interactions are responsible for fermion masses, one generally expects technipions to decay to the heaviest fermions kinematically allowed (though this need not hold in all models).

In addition to quark masses, ETC interactions must also give rise to quark mixing. One expects, therefore, that there are ETC interactions coupling quarks of the same charge from different generations. A stringent limit on these flavor-changing neutral current interactions comes from $K^0-\bar{K}^0$ mixing [4]. These force the scale of ETC breaking and the corresponding ETC gauge boson masses to be in the 100-1000 TeV range (at least insofar as ETC interactions of first two generations are concerned). To obtain quark and technipion masses that are large enough then requires an enhancement of the technifermion condensate over that expected naively by scaling from QCD. Such an enhancement can occur if the technicolor gauge coupling runs very slowly, or “walks” [7]. Some theories of walking technicolor incorporate many technifermions, implying that the technicolor scale and, in particular, the technivector mesons may be much lighter than 1 TeV [3,8]. It should also be noted that there is no reliable calculation of electroweak parameters in a walking technicolor theory, and the values of precisely measured electroweak quantities [9] cannot directly be used to constrain the models. Recently, progress has been made in constructing a complete theory of fermion masses (including neutrino masses) in the context of extended technicolor [10].

In existing colliders, technivector mesons are dominantly produced when an off-shell standard model gauge boson “resonates” into a technivector meson with the same quantum numbers [11]. The technivector mesons may then decay, in analogy with $\rho \rightarrow \pi\pi$, to pairs of technipions. However, in walking technicolor the technipion masses may be increased to the point that the decay of a technirho to pairs of technipions is kinematically forbidden [8]. In this case the decay to a technipion and a longitudinally polarized weak boson (an “eaten” Goldstone boson) may be preferred, and the technivector meson would be very narrow. Alternatively, the technivector may also decay, in analogy with the decay $\rho \rightarrow \pi\gamma$, to a technipion plus a photon, gluon, or transversely polarized weak gauge boson. Finally, in analogy with the decay $\rho \rightarrow e^+e^-$, the technivector meson may resonate back to an off-shell gluon or electroweak gauge boson, leading to a decay into a pair of leptons, quarks, or gluons.

When comparing the various results presented in this review, one should be aware that the more recent analyses [17,18,20,22] make use of newer calculations [12] of technihadron production and decay, as implemented in PYTHIA [13] version 6.126 and higher [14]. The results obtained with older cross section calculations are not generally directly comparable, and have only been listed in Table 1 when newer results are not available.

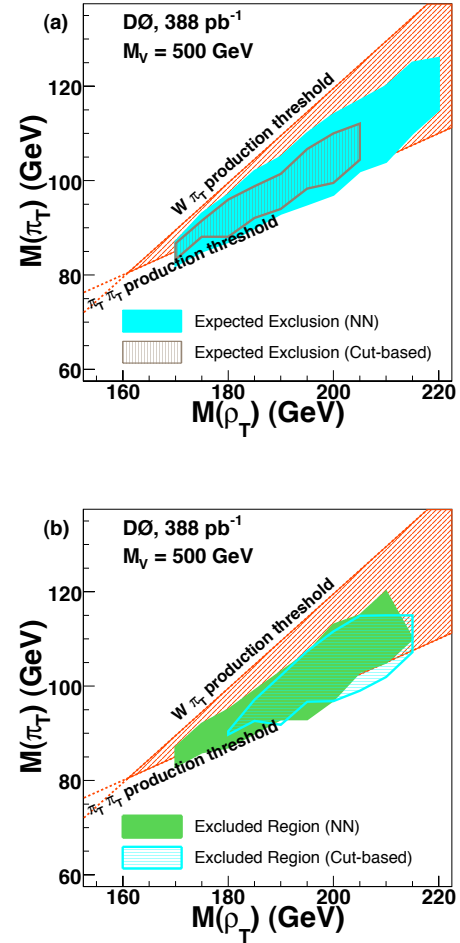


Figure 1: Search for a light technirho decaying to W^\pm and a π_T , and in which the π_T decays to two jets including at least one b quark [18]. Expected region of exclusion (a) and excluded region (b) at the 95% C.L. in the $M(\rho_T), M(\pi_T)$ plane for $\rho_T \rightarrow W\pi_T \rightarrow e\nu b\bar{b}(\bar{c})$ production with $M_V = 500$ GeV. Kinematic thresholds from $W\pi_T$ and $\pi_T\pi_T$ are shown on the figures. Color version at end of book.

If the dominant decay mode of the technirho is $W_L\pi_T$, promising signal channels [15] are $\rho_T^\pm \rightarrow W^\pm\pi_T^0$ and $\rho_T^0 \rightarrow W^\pm\pi_T^\mp$. If we assume that the technipions decay to $b\bar{b}$ (neutral) and $b\bar{c}$ (charged), then both channels yield a signal of $W(\ell\nu) + 2$ jets, with one or more heavy flavor tags. The CDF collaboration carried out a search in this final state [16] based on Run I data and using PYTHIA version 6.1 for the signal simulation. Using 162 pb^{-1} of data from Run II, CDF [17] has shown a preliminary update of this analysis. The DØ [18] collaboration recently published an analysis based on 388 pb^{-1} of data from Run II and PYTHIA 6.22. The searches are sensitive to $\sigma \cdot B \gtrsim 4 \text{ pb}$ and DØ finds mass combinations up to $m_{\rho_T} = 215 \text{ GeV}$, $m_{\pi_T} = 115 \text{ GeV}$ to be excluded for certain values of the model parameters. The expected sensitivity and the region excluded at 95% C.L. by the DØ analysis for

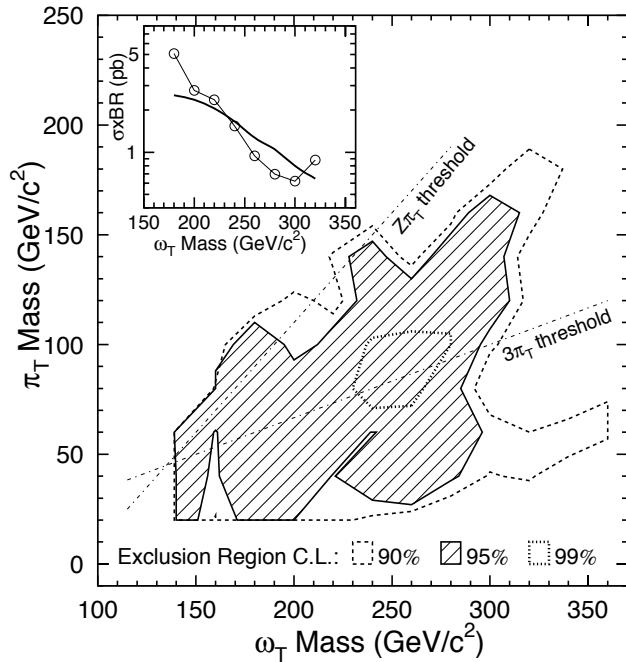


Figure 2: 95% CL exclusion region [19] for a light technirho decaying to γ and a π_T , and in which the π_T decays to two jets, including at least one b quark. (Inset: cross section limit for $m_{\pi_T} = 120$ GeV.)

$M_V = 500$ GeV is shown in Fig. 1. For $M_V = 100$ GeV, only a small region around $M(\rho_T) = 190$ GeV and $M(\pi_T) = 95$ GeV can be excluded. For an integrated luminosity of 2 fb^{-1} , the 5σ discovery reach is expected to extend to $m_{\rho_T} = 210$ GeV and $m_{\pi_T} = 110$ GeV, while the 95% exclusion sensitivity will extend to $m_{\rho_T} = 250$ GeV and $m_{\pi_T} = 145$ GeV.

CDF also searched [19] in Run I for the process $\omega_T^0 \rightarrow \gamma\pi_T^0$, yielding a signal of a hard photon plus two jets, with one or more heavy flavor tags. The sensitivity to $\sigma \cdot B$ is of order 1 pb. The excluded region is shown in Fig. 2 and is roughly $140 < m_{\omega_T} < 290$ GeV at the 95% level, for $m_{\pi_T} \approx m_{\omega_T}/3$. The analysis assumes four technicolors, $Q_D = Q_U - 1 = \frac{1}{3}$ and $M_T = 100 \text{ GeV}/c^2$. Here Q_U and Q_D are the charges of the lightest technifermion doublet, and M_T is a dimensional parameter, of order $100 \text{ GeV}/c^2$, which controls the rate of $\rho_T, \omega_T \rightarrow \gamma\pi_T$.

The DØ experiment has searched [20] for low-scale technicolor resonances ρ_T and ω_T decaying to dileptons, using an inclusive e^+e^- sample from Run I. In the search, the ρ_T and ω_T are assumed to be degenerate in mass. The absence of structure in the dilepton invariant mass distribution is then used to set limits. Masses $m_{\rho_T} = m_{\omega_T} \lesssim 200$ GeV are excluded, provided either $m_{\rho_T} < m_{\pi_T} + m_W$, or $M_T > 200$ GeV (as shown in Fig. 3). The CDF experiment also performed a similar search with 200 pb^{-1} of Run II data, and excluded equal

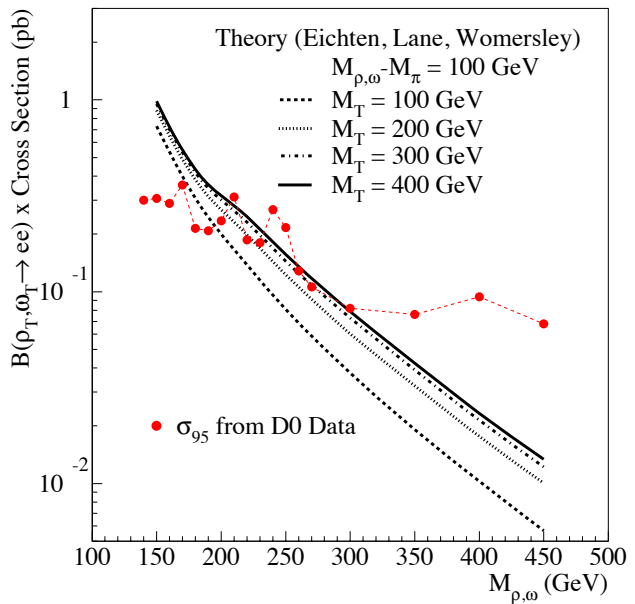


Figure 3: 95% CL cross-section limit [20] for a light technirho and a light technipion decaying to l^+l^- .

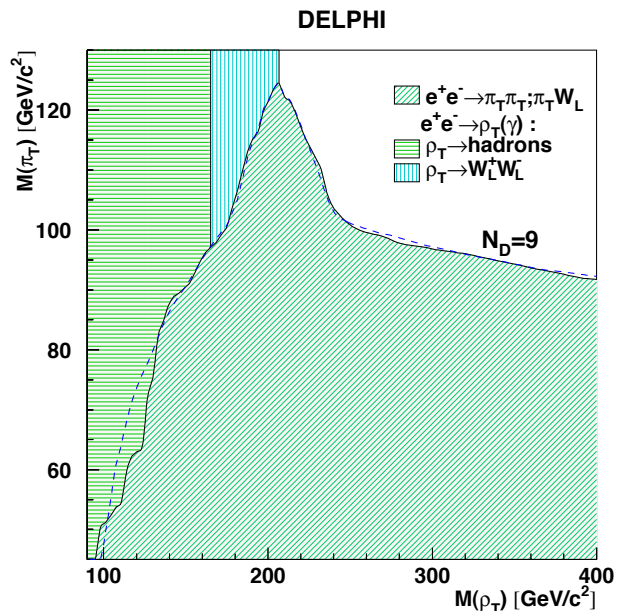


Figure 4: 95% CL exclusion region [22] in the technirho-technipion mass plane obtained from searches by the DELPHI collaboration at LEP 2, for nine technifermion doublets. The dashed line shows the expected limit for the 4-jet analysis.

$m_{\rho_T} = m_{\omega_T}$ masses below 280 GeV for $M_V = 500$ GeV and

$m_{\rho_T} < m_{\pi_T} + m_W$ at 95% C.L. [21]. With 2 fb^{-1} of data, the sensitivity will extend to $m_{\rho_T} = m_{\omega_T} \approx 500 \text{ GeV}$.

DELPHI [22] has reported a search for technicolor production in 452 pb^{-1} of e^+e^- data taken between 192 and 208 GeV. The analysis combines searches for $e^+e^- \rightarrow \rho_T(\gamma)$ with $\rho_T \rightarrow W_L W_L$, $\rho_T \rightarrow \text{hadrons}$ ($\pi_T \pi_T$ or $q\bar{q}$), $\rho_T \rightarrow \pi_T \gamma$, and $e^+e^- \rightarrow \rho_T^* \rightarrow W_L \pi_T$ or $\pi_T \pi_T$. Technirho masses in the range $90 < m_{\rho_T} < 206.7 \text{ GeV}$ are excluded, while technipion masses $m_{\pi_T} < 79.8 \text{ GeV}$ are ruled out independent of the parameters of the technicolor model.

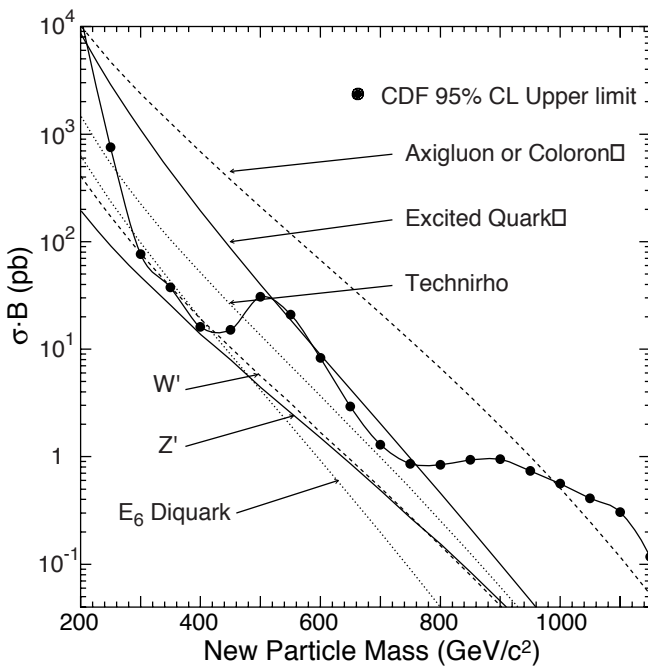


Figure 5: 95% CL Cross-section limits [24] for a technirho decaying to two jets at the Tevatron.

Searches have also been carried out at the Tevatron for colored technihadron resonances [23,24]. CDF has used a search for structure in the dijet invariant mass spectrum to set limits on a color-octet technirho ρ_{T8} produced by an off-shell gluon, and decaying to two real quarks or gluons. As shown in Fig. 5, masses $260 < m_{\rho_{T8}} < 480 \text{ GeV}$ are excluded; in Run II the limits will improve to cover the whole mass range up to about 0.8 TeV [25].

The CDF second- and third-generation leptoquark searches (see Refs. [26,27]) have also been interpreted in terms of the complementary ρ_{T8} decay mode: $p\bar{p} \rightarrow \rho_{T8} \rightarrow \pi_{LQ} \pi_{LQ}$. Here π_{LQ} denotes a color-triplet technipion carrying both color and lepton number, assumed to decay to $b\nu$ or $c\nu$ [27], or to a τ plus a quark [26]. The searches exclude technirho masses $m_{\rho_{T8}}$ less than 510 GeV ($\pi_{LQ} \rightarrow c\nu$), 600 GeV ($\pi_{LQ} \rightarrow b\nu$), and 465 GeV ($\pi_{LQ} \rightarrow \tau q$) for technipion masses up to $m_{\rho_{T8}}/2$.

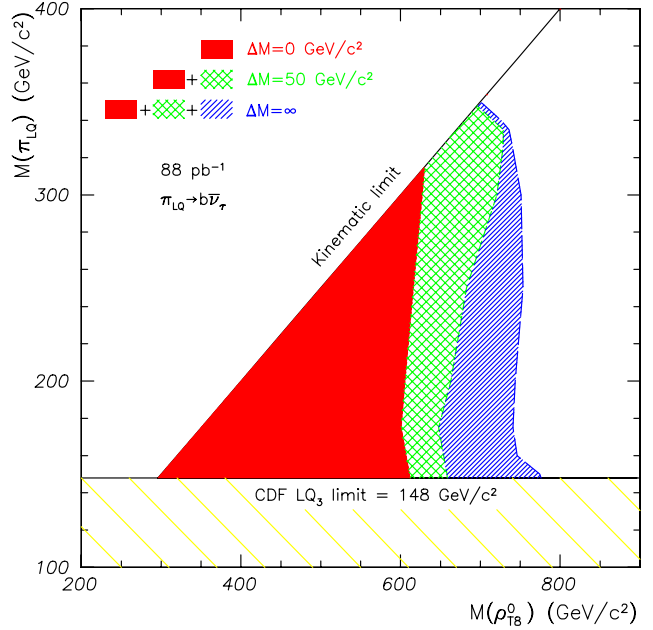


Figure 6: 95% CL exclusion region [27] in the technirho-technipion mass plane for pair produced technipions, with leptoquark couplings, decaying to $b\nu$.

Figure 6 shows the $\pi_{LQ} \rightarrow b\nu$ exclusion region. (Leptoquark masses $m_{\pi_{LQ}}$ less than 123 GeV ($c\nu$), 148 GeV ($b\nu$), and 99 GeV (τq) are already ruled out by standard continuum-production leptoquark searches).

Recently, it has been demonstrated that there is substantial uncertainty in the theoretical estimate of the ρ_{T8} production cross section at the Tevatron and that the cross section may be as much as an order of magnitude lower than the naive vector meson dominance estimate [28]. To establish the range of allowed masses, these limits will need to be redone with a reduced theoretical cross section.

II. Top Condensate, Higgsless, and Related Models

The top quark is much heavier than other fermions and must be more strongly coupled to the symmetry-breaking sector. It is natural to consider whether some or all of electroweak-symmetry breaking is due to a condensate of top quarks [3,29]. Top quark condensation alone, without additional fermions, seems to produce a top quark mass larger [30] than observed experimentally, and is therefore not favored. Topcolor-assisted technicolor [31] combines technicolor and top condensation. In addition to technicolor, which provides the bulk of electroweak symmetry breaking, top condensation and the top quark mass arise predominantly from “topcolor,” a new QCD-like interaction which couples strongly to the third generation of quarks. An additional, strong, U(1) interaction (giving rise to a topcolor Z') precludes the formation of a b -quark condensate.

Searches Particle Listings

Technicolor

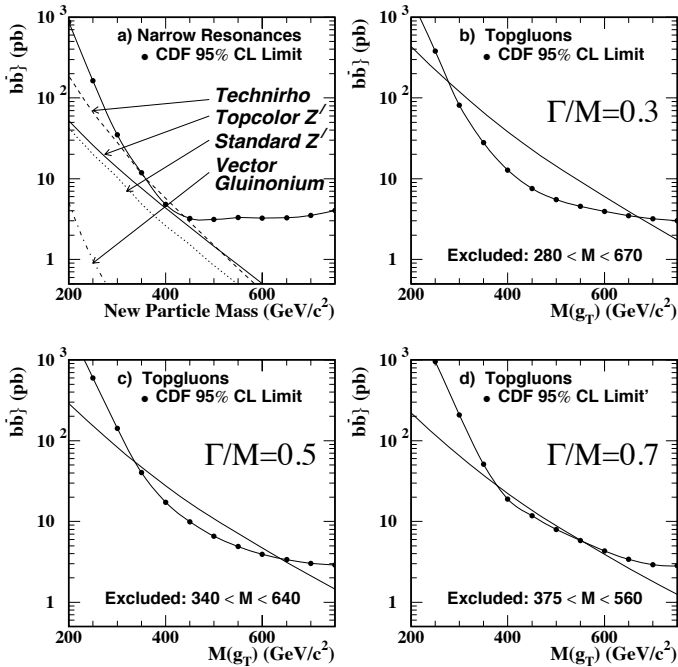


Figure 7: Tevatron limits [32] on new particles decaying to $b\bar{b}$: narrow resonances and topgluons for various widths.

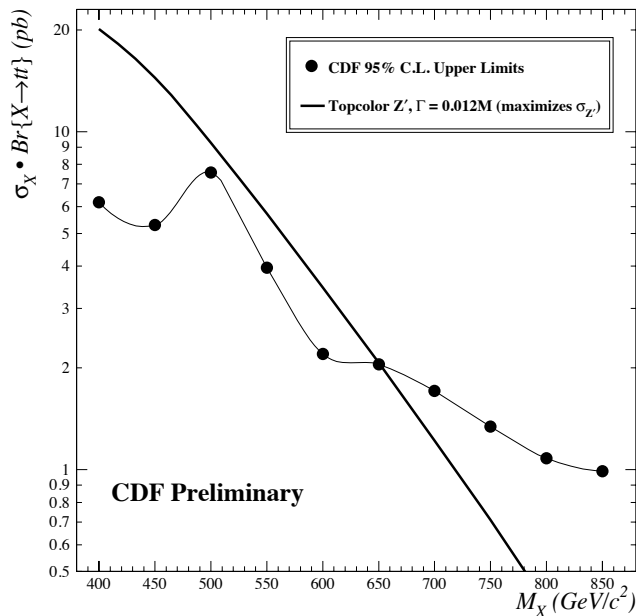


Figure 8: Cross-section limits for a narrow resonance decaying to $t\bar{t}$ [33] and expected cross section for a leptophobic topcolor Z' boson.

CDF has searched [32] for the “topgluon,” a massive color-octet vector which couples preferentially to the third generation, in the mode $p\bar{p} \rightarrow g_t \rightarrow b\bar{b}$. The results are shown in Fig. 7.

Topgluon masses from approximately 0.3 to 0.6 TeV are excluded at 95% confidence level, for topgluon widths in the range $0.3m_{g_t} < \Gamma < 0.7m_{g_t}$. Results have also been reported by CDF [33] on a search for narrow resonances in the $t\bar{t}$ invariant mass distribution. The cross section limit is shown in Fig. 8 and excludes a leptophobic topcolor Z' with masses less than 480 (780) GeV/c^2 , for the case where its width $\Gamma = 0.012(0.04)m_{Z'}$. (DØ has carried out a similar search, with greater sensitivity [34], but has not derived comparable Z' mass limits.) A broad topgluon could also be detected in the same final state, though no results are yet available. In Run II, the Tevatron [25] should be sensitive to topgluon and topcolor Z' masses up to of order 1 TeV in $b\bar{b}$ and $t\bar{t}$ final states. A detailed theoretical analysis of $B-\bar{B}$ mixing and light quark mass generation in top-color-assisted technicolor shows that, at least in some models, the topgluon and Z' boson masses must be greater than about 5 TeV [35].

The top quark seesaw model of electroweak symmetry breaking [36] is a variant of the original top condensate idea which reconciles top condensation with a lighter top quark mass. Such a model can easily be consistent with precision electroweak tests, either because the spectrum includes a light composite Higgs [37], or because additional interactions allow for a heavier Higgs [38]. Such theories may arise naturally from gauge fields propagating in compact extra spatial dimensions [39].

A variant of topcolor-assisted technicolor is flavor-universal, in which the topcolor $SU(3)$ gauge bosons, called colorons, couple equally to all quarks [40]. Flavor-universal versions of the seesaw model [41] incorporating a gauged flavor symmetry are also possible. In these models *all* left-handed quarks (and possibly leptons as well) participate in electroweak-symmetry-breaking condensates with separate (one for each flavor) right-handed weak singlets, and the different fermion masses arise by adjusting the parameters which control the mixing of each fermion with the corresponding condensate.

A prediction of these flavor-universal models is the existence of new heavy gauge bosons, coupling to color or flavor, at relatively low mass scales. The absence of an excess of high- E_T jets in DØ data [42] has been used to constrain strongly coupled flavor-universal colorons (massive color-octet bosons coupling to all quarks). A mass limit of between 0.8 and 3.5 TeV is set [43] depending on the coloron-gluon mixing angle. Precision electroweak measurements constrain [44] the masses of these new gauge bosons to be greater than 1–3 TeV in a variety of models, for strong couplings.

A new class [45] of composite Higgs model [46], dubbed “Little Higgs Theory,” has been developed which gives rise to naturally light Higgs bosons without supersymmetry [47]. Inspired by discretized versions of higher-dimensional gauge theory [48], these models are based on the chiral symmetries of “theory space.” The models involve extended gauge groups and novel gauge symmetry-breaking patterns [49]. The new chiral symmetries prevent large corrections to the Higgs boson mass, and allow the scale (Λ) of the underlying strong dynamics

giving rise to the composite particles to be as large as 10 TeV. These models typically require new gauge bosons and fermions, and possibly additional composite scalars beyond the Higgs, in the TeV mass range [50].

Finally, “Higgsless” models [51] provide electroweak symmetry breaking, including unitarization of the scattering of longitudinal W and Z bosons, without employing a scalar Higgs boson. The most extensively studied models [52] are based on a five-dimensional $SU(2) \times SU(2) \times U(1)$ gauge theory in a slice of Anti-deSitter space, and electroweak symmetry breaking is encoded in the boundary conditions of the gauge fields. Using the AdS/CFT correspondence [53], these theories may be viewed as “dual” descriptions of walking technicolor theories [7]. In addition to a massless photon and near-standard W and Z bosons, the spectrum includes an infinite tower of additional massive vector bosons (the higher Kaluza-Klein or KK excitations), whose exchange is responsible for unitarizing longitudinal W and Z boson scattering [54]. Using deconstruction, it has been shown [55] that a Higgsless model whose fermions are localized (*i.e.*, derive their electroweak properties from a single site on the deconstructed lattice) cannot simultaneously satisfy unitarity bounds and precision electroweak constraints.

It has recently been proposed [56] that the size of corrections to electroweak processes in Higgsless models may be reduced by considering delocalized fermions, *i.e.*, considering the effect of the distribution of the wavefunctions of ordinary fermions in the fifth dimension (corresponding, in the deconstruction language, to allowing the fermions to derive their electroweak properties from several sites on the lattice). It has been shown [57] that, in an arbitrary Higgsless model, if the probability distribution of the delocalized fermions is related to the W wavefunction (a condition called “ideal” delocalization), then deviations in precision electroweak parameters are minimized. Phenomenological limits on delocalized Higgsless models may be derived [58] from limits on the deviation of the triple-gauge boson (WWZ) vertices from the standard model, and current constraints allow for the lightest KK resonances (which tend to be fermiophobic in the case of ideal fermion delocalization) to have masses of only a few hundred GeV. Such resonances would have to be studied using WW scattering [59].

Acknowledgments

We thank Tom Appelquist, Bogdan Dobrescu, Emilian Dudas, Robert Harris, Chris Hill, Greg Landsberg, Kenneth Lane, Bob Shrock, Elizabeth Simmons, and John Terning for help in the preparation of this article. *This work was supported in part by the Department of Energy under grant DE-FG02-91ER40676 and by the National Science Foundation under grant PHY-0354226.*

References

1. S. Weinberg, Phys. Rev. **D19**, 1277 (1979).
2. L. Susskind, Phys. Rev. **D20**, 2619 (1979).
3. For a recent reviews, see K. Lane, hep-ph/0202255; C.T. Hill, E.H. Simmons, Phys. Rept. **381**, 235 (2003); R. Shrock, hep-ph/0703050.
4. E. Eichten and K. Lane, Phys. Lett. **90B**, 125 (1980).
5. S. Dimopoulos, S. Raby, and G.L. Kane, Nucl. Phys. **B182**, 77 (1981).
6. S. Dimopoulos and L. Susskind, Nucl. Phys. **B155**, 237 (1979).
7. B. Holdom, Phys. Rev. **D24**, 1441 (1981) and Phys. Lett. **150B**, 301 (1985); K. Yamawaki, M. Bando, and K. Matumoto, Phys. Rev. Lett. **56**, 1335 (1986); T.W. Appelquist, D. Karabali, and L.C.R. Wijewardhana, Phys. Rev. Lett. **57**, 957 (1986); T. Appelquist and L.C.R. Wijewardhana, Phys. Rev. **D35**, 774 (1987) and Phys. Rev. **D36**, 568 (1987).
8. E. Eichten and K. Lane, Phys. Lett. **B222**, 274 (1989).
9. J. Erler and P. Langacker, “Electroweak Model and Constraints on New Physics,” in the section on Reviews, Tables, and Plots in this *Review*.
10. T.W. Appelquist and R. Shrock, Phys. Lett. **B548**, 204 (2002) and Phys. Rev. Lett. **90**, 201801 (2003); T.W. Appelquist, M. Piai, and R. Shrock, Phys. Rev. **D69**, 015002 (2004); T. Appelquist *et al.*, Phys. Rev. **D70**, 093010 (2004).
11. E. Eichten *et al.*, Rev. Mod. Phys. **56**, 579 (1984) and Phys. Rev. **D34**, 1547 (1986).
12. K. Lane, Phys. Rev. **D60**, 075007 (1999).
13. T. Sjostrand, Comp. Phys. Comm. **82**, 74 (1994).
14. S. Mrenna, Technihadron production and decay at LEP2, Phys. Lett. **B461**, 352 (1999).
15. E. Eichten, K. Lane, and J. Womersley, Phys. Lett. **B405**, 305 (1997).
16. CDF Collaboration (T. Affolder *et al.*), Phys. Rev. Lett. **84**, 1110 (2000).
17. CDF Collaboration, “Search for New Particle $X \rightarrow b\bar{b}$ Produced in Association with W^\pm Bosons at $\sqrt{s} = 1.96$ TeV,” CDF/PUB/EXOTIC/PUBLIC 7126, July 2004.
18. $D\bar{0}$ Collaboration (V.M. Abazov *et al.*), Phys. Rev. **98**, 221801 (2007).
19. CDF Collaboration (F. Abe *et al.*), Phys. Rev. Lett. **83**, 3124 (1999).
20. $D\bar{0}$ Collaboration (V.M. Abazov *et al.*), Phys. Rev. Lett. **87**, 061802 (2001).
21. CDF Collaboration (A. Abulencia *et al.*), Phys. Rev. Lett. **95**, 252001 (2005).
22. DELPHI Collaboration (J. Abdallah *et al.*), Eur. Phys. J. **C22**, 17 (2001).
23. K. Lane and M.V. Ramana, Phys. Rev. **D44**, 2678 (1991).
24. CDF Collaboration (F. Abe *et al.*), Phys. Rev. **D55**, R5263 (1997).
25. K. Cheung and R.M. Harris, hep-ph/9610382.
26. CDF Collaboration (F. Abe *et al.*), Phys. Rev. Lett. **82**, 3206 (1999).
27. CDF Collaboration (T. Affolder *et al.*), Phys. Rev. Lett. **85**, 2056 (2000).
28. A. Zerwekh and R. Rosenfeld, Phys. Lett. **B503**, 325 (2001); R.S. Chivukula, *et al.*, Boston Univ. preprint BUHEP-01-19.

Searches Particle Listings

Technicolor

29. V.A. Miransky, M. Tanabashi, and K. Yamawaki, Phys. Lett. **221B**, 177 (1989), and Mod. Phys. Lett. **4**, 1043 (1989);
Y. Nambu, EFI-89-08 (1989);
W.J. Marciano, Phys. Rev. Lett. **62**, 2793 (1989).
30. W.A. Bardeen, C.T. Hill, and M. Lindner, Phys. Rev. **D41**, 1647 (1990).
31. C.T. Hill, Phys. Lett. **B345**, 483 (1995);
see also Phys. Lett. **266B**, 419 (1991).
32. CDF Collaboration (F. Abe *et al.*), Phys. Rev. Lett. **82**, 2038 (1999).
33. CDF Collaboration (F. Affolder *et al.*), Phys. Rev. Lett. **85**, 2062 (2000).
34. D0 Collaboration (V. Abazov *et al.*), Phys. Rev. Lett. **87**, 231801 (2001).
35. G. Burdman *et al.*, Phys. Lett. **B514**, 41 (2001).
36. B.A. Dobrescu and C.T. Hill, Phys. Rev. Lett. **81**, 2634 (1998).
37. R.S. Chivukula *et al.*, Phys. Rev. **D59**, 075003 (1999).
38. H. Collins, A. Grant, and H. Georgi, Phys. Rev. **D61**, 055002 (2000).
39. B.A. Dobrescu, Phys. Lett. **B461**, 99 (1999);
H.-C. Cheng, *et al.*, Nucl. Phys. **B589**, 249 (2000).
40. E.H. Simmons, Nucl. Phys. **B324**, 315 (1989).
41. G. Burdman and N. Evans, Phys. Rev. **D59**, 115005 (1999).
42. DØ Collaboration (B. Abbott *et al.*), Phys. Rev. Lett. **82**, 2457 (1999).
43. I. Bertram and E.H. Simmons, Phys. Lett. **B443**, 347 (1998).
44. G. Burdman, R.S. Chivukula, and N. Evans, Phys. Rev. **D61**, 035009 (2000).
45. N. Arkani-Hamed, A. G. Cohen and H. Georgi, Phys. Lett. **B513**, 232 (2001).
46. D.B. Kaplan and H. Georgi, Phys. Lett. **B136**, 183 (1984) and Phys. Lett. **B145**, 216 (1984);
T. Banks, Nucl. Phys. **B243**, 123 (1984);
D.B. Kaplan, H. Georgi, and S. Dimopoulos, Phys. Lett. **B136**, 187 (1984);
M.J. Dugan, H. Georgi, and D.B. Kaplan, Nucl. Phys. **B254**, 299 (1985).
47. See also review by P. Igo-Kemenes, "Searches for Higgs Bosons," in the Boson Listings in this *Review*.
48. N. Arkani-Hamed, A. G. Cohen, and H. Georgi, Phys. Rev. **D86**, 4757 (2001);
H. C. Cheng, C. T. Hill, and J. Wang, Phys. Rev. **D64**, 095003 (2001).
49. M Schmaltz and D. Tucker-Smith, Ann. Rev. Nucl. Part. Sci. **55**, 229 (2005).
50. C. Csaki *et al.*, Phys. Rev. **D67**, 115002 (2003);
J. Hewett, F. Petriello, and T. Rizzo, JHEP **310**, 062 (2003);
T. Han *et al.*, Phys. Rev. **D67**, 095004 (2003) Z. Han and W. Skba, Phys. Rev. **D72**, 035005 (2005).
51. C. Csaki *et al.*, Phys. Rev. **D69**, 055006 (2003).
52. K. Agashe *et al.*, JHEP **0308**, 050 (2003);
C. Csaki *et al.*, Phys. Rev. Lett. **92**, 101802 (2004).
53. J. Maldacena, Adv. Theor. Math. Phys. **2**, 231 (1998).
54. R. S. Chivukula, D. Dicus, and H.-J. He, Phys. Lett. **B525**, 175 (2002).

55. R. S. Chivukula *et al.*, Phys. Rev. **D71**, 035007 (2005).
56. G. Cacciapaglia *et al.*, Phys. Rev. **D71**, 035015 (2005);
R. Foadi, S. Gopalkrishna, and C. Schmidt, Phys. Lett. **B606**, 157 (2005);
G. Cacciapaglia *et al.*, Phys. Rev. **D72**, 095018 (2005).
57. R. S. Chivukula *et al.*, Phys. Rev. **D72**, 015008 (2005).
58. R. S. Chivukula *et al.*, Phys. Rev. **D72**, 075012 (2005).
59. A. Birkedal, K. Matchev, and M. Perelstein, Phys. Rev. Lett. **94**, 191803 (2005);
H.-J. He, *et. al.*, arXiv:0708.2588.

**MASS LIMITS for Resonances
in Models of Dynamical Electroweak Symmetry Breaking**

VALUE (GeV)	CL%	DOCUMENT ID	TECN	COMMENT
••• We do not use the following data for averages, fits, limits, etc. •••				
>280	95	1 ABAZOV 07I	D0	$\rho\bar{P} \rightarrow \rho_T/\omega_T \rightarrow W\pi_T$
		2 ABULENCIA 05A	CDF	$\rho_T \rightarrow e^+e^-, \mu^+\mu^-$
		3 CHEKANOV 02B	ZEUS	color octet techni- π
>207	95	4 ABAZOV 01B	D0	$\rho_T \rightarrow e^+e^-$
none 90-206.7	95	5 ABDALLAH 01	DLPH	$e^+e^- \rightarrow \rho_T$
		6 AFFOLDER 00F	CDF	color-singlet techni- ρ , $\rho_T \rightarrow W\pi_T, 2\pi_T$
>600	95	7 AFFOLDER 00K	CDF	color-octet techni- ρ , $\rho_{T8} \rightarrow 2\pi_{LQ}$
>480	95	8 AFFOLDER 00L	CDF	top-color Z'
none 350-440	95	9 ABE 99F	CDF	color-octet techni- ρ , $\rho_{T8} \rightarrow \bar{b}b$
>465	95	10 ABE 99H	CDF	color-octet techni- ρ , $\rho_{T8} \rightarrow 2\pi_{LQ}$
none 260-480	95	11 ABE 99N	CDF	techni- ω , $\omega_T \rightarrow \gamma\bar{b}b$
		12 ABE 97G	CDF	color-octet techni- ρ , $\rho_{T8} \rightarrow 2\text{jets}$

- 1 ABAZOV 07I search for the vector techni-resonances (ρ_T, ω_T) decaying into $W\pi_T$ with $W \rightarrow e\nu$ and $\pi_T \rightarrow b\bar{b}$ or $b\bar{c}$. See their Fig. 2 for the exclusion plot in the $M_{\pi_T}-M_{\rho_T}$ plane.
- 2 ABULENCIA 05A search for resonances decaying to electron or muon pairs in $p\bar{p}$ collisions. at $\sqrt{s} = 1.96$ TeV. The limit assumes Technicolor-scale mass parameters $M_V = M_A = 500$ GeV.
- 3 CHEKANOV 02B search for color octet techni- π P decaying into dijets in ep collisions. See their Fig. 5 for the limit on $\sigma(ep \rightarrow ePX) \cdot B(P \rightarrow 2j)$.
- 4 ABAZOV 01B searches for vector techni-resonances (ρ_T, ω_T) decaying to e^+e^- . The limit assumes $M_{\rho_T} = M_{\omega_T} < M_{\pi_T} + M_W$.
- 5 The limit is independent of the π_T mass. See their Fig. 9 and Fig. 10 for the exclusion plot in the $M_{\rho_T}-M_{\pi_T}$ plane. ABDALLAH 01 limit on the techni-pion mass is $M_{\pi_T} > 79.8$ GeV for $N_D=2$, assuming its point-like coupling to gauge bosons.
- 6 AFFOLDER 00F search for ρ_T decaying into $W\pi_T$ or $\pi_T\pi_T$ with $W \rightarrow \ell\nu$ and $\pi_T \rightarrow \bar{b}b, \bar{b}c$. See Fig. 1 in the above Note on "Dynamical Electroweak Symmetry Breaking" for the exclusion plot in the $M_{\rho_T}-M_{\pi_T}$ plane.
- 7 AFFOLDER 00K search for the ρ_{T8} decaying into $\pi_{LQ}\pi_{LQ}$ with $\pi_{LQ} \rightarrow b\nu$. For $\pi_{LQ} \rightarrow c\nu$, the limit is $M_{\rho_{T8}} > 510$ GeV. See their Fig. 2 and Fig. 3 for the exclusion plot in the $M_{\rho_{T8}}-M_{\pi_{LQ}}$ plane.
- 8 AFFOLDER 00L search for top-color Z'_{top} decaying into $\bar{t}t$. The quoted limit is for Z'_{top} with decay width $\Gamma=0.012 M_{Z'}$. For $\Gamma=0.04 M_{Z'}$, the limit becomes 780 GeV.
- 9 ABE 99F search for a new particle X decaying into $b\bar{b}$ in $p\bar{p}$ collisions at $E_{\text{cm}} = 1.8$ TeV. See Fig. 7 in the above Note on "Dynamical Electroweak Symmetry Breaking" for the upper limit on $\sigma(p\bar{p} \rightarrow X) \times B(X \rightarrow b\bar{b})$. ABE 99F also exclude top gluons of width $\Gamma=0.3M$ in the mass interval $280 < M < 670$ GeV, of width $\Gamma=0.5M$ in the mass interval $340 < M < 640$ GeV, and of width $\Gamma=0.7M$ in the mass interval $375 < M < 560$ GeV.
- 10 ABE 99H search for the color-octet techni- ρ decaying into a pair of color-triplet technipions which subsequently decay into $\tau+$ jet. See Fig. 6 in the above Note on "Dynamical Electroweak Symmetry Breaking" for the exclusion plot in the $M_{\rho_{T8}}-M_{\pi_{LQ}}$ plane.
- 11 ABE 99N search for the techni- ω decaying into $\gamma\pi_T$. The technipion is assumed to decay $\pi_T \rightarrow b\bar{b}$. See Fig. 2 in the above Note on "Dynamical Electroweak Symmetry Breaking" for the exclusion plot in the $M_{\omega_T}-M_{\pi_T}$ plane.
- 12 ABE 97G search for a new particle X decaying into dijets in $p\bar{p}$ collisions at $E_{\text{cm}} = 1.8$ TeV. See Fig. 5 in the above Note on "Dynamical Electroweak Symmetry Breaking" for the upper limit on $\sigma(p\bar{p} \rightarrow X) \times B(X \rightarrow 2j)$.

REFERENCES FOR Technicolor

ABAZOV	07I	PRL 98 221801	V.M. Abazov <i>et al.</i>	(D0 Collab.)
ABULENCIA	05A	PRL 95 252001	A. Abulencia <i>et al.</i>	(CDF Collab.)
CHEKANOV	02B	PL B531 9	S. Chekanov <i>et al.</i>	(ZEUS Collab.)
ABAZOV	01B	PRL 87 061802	V.M. Abazov <i>et al.</i>	(D0 Collab.)
ABDALLAH	01	EPJ C22 17	J. Abdallah <i>et al.</i>	(DELPHI Collab.)
AFFOLDER	00F	PRL 84 1110	T. Affolder <i>et al.</i>	(CDF Collab.)
AFFOLDER	00K	PRL 85 2056	T. Affolder <i>et al.</i>	(CDF Collab.)
AFFOLDER	00L	PRL 85 2062	T. Affolder <i>et al.</i>	(CDF Collab.)
ABE	99F	PRL 82 2038	F. Abe <i>et al.</i>	(CDF Collab.)
ABE	99H	PRL 82 3206	F. Abe <i>et al.</i>	(CDF Collab.)
ABE	99N	PRL 83 3124	F. Abe <i>et al.</i>	(CDF Collab.)
ABE	97G	PR D55 R5263	F. Abe <i>et al.</i>	(CDF Collab.)

Quark and Lepton Compositeness, Searches for

SEARCHES FOR QUARK AND LEPTON COMPOSITENESS

Revised 2001 by K. Hagiwara (KEK), and K. Hikasa and M. Tanabashi (Tohoku University).

If quarks and leptons are made of constituents, then at the scale of constituent binding energies, there should appear new interactions among quarks and leptons. At energies much below the compositeness scale (Λ), these interactions are suppressed by inverse powers of Λ . The dominant effect should come from the lowest dimensional interactions with four fermions (contact terms), whose most general chirally invariant form reads [1]

$$L = \frac{g^2}{2\Lambda^2} \left[\eta_{LL} \bar{\psi}_L \gamma_\mu \psi_L \bar{\psi}_L \gamma^\mu \psi_L + \eta_{RR} \bar{\psi}_R \gamma_\mu \psi_R \bar{\psi}_R \gamma^\mu \psi_R + 2\eta_{LR} \bar{\psi}_L \gamma_\mu \psi_L \bar{\psi}_R \gamma^\mu \psi_R \right]. \quad (1)$$

Chiral invariance provides a natural explanation why quark and lepton masses are much smaller than their inverse size Λ . We may determine the scale Λ unambiguously by using the above form of the effective interactions; the conventional method [1] is to fix its scale by setting $g^2/4\pi = g^2(\Lambda)/4\pi = 1$ for the new strong interaction coupling and by setting the largest magnitude of the coefficients $\eta_{\alpha\beta}$ to be unity. In the following, we denote

$$\begin{aligned} \Lambda &= \Lambda_{LL}^\pm \text{ for } (\eta_{LL}, \eta_{RR}, \eta_{LR}) = (\pm 1, 0, 0), \\ \Lambda &= \Lambda_{RR}^\pm \text{ for } (\eta_{LL}, \eta_{RR}, \eta_{LR}) = (0, \pm 1, 0), \\ \Lambda &= \Lambda_{VV}^\pm \text{ for } (\eta_{LL}, \eta_{RR}, \eta_{LR}) = (\pm 1, \pm 1, \pm 1), \\ \Lambda &= \Lambda_{AA}^\pm \text{ for } (\eta_{LL}, \eta_{RR}, \eta_{LR}) = (\pm 1, \pm 1, \mp 1), \end{aligned} \quad (2)$$

as typical examples. Such interactions can arise by constituent interchange (when the fermions have common constituents, *e.g.*, for $ee \rightarrow ee$) and/or by exchange of the binding quanta (when ever binding quanta couple to constituents of both particles).

Another typical consequence of compositeness is the appearance of excited leptons and quarks (ℓ^* and q^*). Phenomenologically, an excited lepton is defined to be a heavy lepton which shares leptonic quantum number with one of the existing leptons (an excited quark is defined similarly). For example, an excited electron e^* is characterized by a nonzero transition-magnetic coupling with electrons. Smallness of the lepton mass and the success of QED prediction for $g-2$ suggest chirality conservation, *i.e.*, an excited lepton should not couple to both left- and right-handed components of the corresponding lepton.

Excited leptons may be classified by $SU(2) \times U(1)$ quantum numbers. Typical examples are:

1. Sequential type

$$\begin{pmatrix} \nu^* \\ \ell^* \end{pmatrix}_L, \quad [\nu_R^*], \quad \ell_R^*.$$

ν_R^* is necessary unless ν^* has a Majorana mass.

2. Mirror type

$$[\nu_R^*], \quad \ell_L^*, \quad \begin{pmatrix} \nu^* \\ \ell^* \end{pmatrix}_R.$$

3. Homodoublet type

$$\begin{pmatrix} \nu^* \\ \ell^* \end{pmatrix}_L, \quad \begin{pmatrix} \nu^* \\ \ell^* \end{pmatrix}_R.$$

Similar classification can be made for excited quarks.

Excited fermions can be pair produced via their gauge couplings. The couplings of excited leptons with Z are listed in the following table (for notation see Eq. (1) in ‘‘Standard Model of Electroweak Interactions’’):

	Sequential type	Mirror type	Homodoublet type
V^{ℓ^*}	$-\frac{1}{2} + 2 \sin^2 \theta_W$	$-\frac{1}{2} + 2 \sin^2 \theta_W$	$-1 + 2 \sin^2 \theta_W$
A^{ℓ^*}	$-\frac{1}{2}$	$+\frac{1}{2}$	0
$V^{\nu_D^*}$	$+\frac{1}{2}$	$+\frac{1}{2}$	+1
$A^{\nu_D^*}$	$+\frac{1}{2}$	$-\frac{1}{2}$	0
$V^{\nu_M^*}$	0	0	—
$A^{\nu_M^*}$	+1	-1	—

Here ν_D^* (ν_M^*) stands for Dirac (Majorana) excited neutrino. The corresponding couplings of excited quarks can be easily obtained. Although form factor effects can be present for the gauge couplings at $q^2 \neq 0$, they are usually neglected.

In addition, transition magnetic type couplings with a gauge boson are expected. These couplings can be generally parameterized as follows:

$$\begin{aligned} \mathcal{L} &= \frac{\lambda_\gamma^{(f^*)}}{2m_{f^*}} e \bar{f}^* \sigma^{\mu\nu} (\eta_L \frac{1-\gamma_5}{2} + \eta_R \frac{1+\gamma_5}{2}) f F_{\mu\nu} \\ &+ \frac{\lambda_Z^{(f^*)}}{2m_{f^*}} e \bar{f}^* \sigma^{\mu\nu} (\eta_L \frac{1-\gamma_5}{2} + \eta_R \frac{1+\gamma_5}{2}) f Z_{\mu\nu} \\ &+ \frac{\lambda_W^{(\ell^*)}}{2m_{\ell^*}} g \bar{\ell}^* \sigma^{\mu\nu} \frac{1-\gamma_5}{2} \nu W_{\mu\nu} \\ &+ \frac{\lambda_W^{(\nu^*)}}{2m_{\nu^*}} g \bar{\nu}^* \sigma^{\mu\nu} (\eta_L \frac{1-\gamma_5}{2} + \eta_R \frac{1+\gamma_5}{2}) \ell W_{\mu\nu}^\dagger \\ &+ \text{h.c.}, \end{aligned} \quad (3)$$

where $g = e/\sin \theta_W$, $F_{\mu\nu} = \partial_\mu A_\nu - \partial_\nu A_\mu$ is the photon field strength, $Z_{\mu\nu} = \partial_\mu Z_\nu - \partial_\nu Z_\mu$, *etc.* The normalization of the coupling is chosen such that

$$\max(|\eta_L|, |\eta_R|) = 1.$$

Chirality conservation requires

$$\eta_L \eta_R = 0. \quad (4)$$

Searches Particle Listings

Quark and Lepton Compositeness

Some experimental analyses assume the relation $\eta_L = \eta_R = 1$, which violates chiral symmetry. We encode the results of such analyses if the crucial part of the cross section is proportional to the factor $\eta_L^2 + \eta_R^2$ and the limits can be reinterpreted as those for chirality conserving cases $(\eta_L, \eta_R) = (1, 0)$ or $(0, 1)$ after rescaling λ .

These couplings in Eq. (3) can arise from $SU(2) \times U(1)$ -invariant higher-dimensional interactions. A well-studied model is the interaction of homodoublet type ℓ^* with the Lagrangian [2,3]

$$\mathcal{L} = \frac{1}{2\Lambda} \bar{L}^* \sigma^{\mu\nu} (g f \frac{\tau^a}{2} W_{\mu\nu}^a + g' f' Y B_{\mu\nu}) \frac{1-\gamma_5}{2} L + \text{h.c.}, \quad (5)$$

where L denotes the lepton doublet (ν, ℓ) , Λ is the compositeness scale, g, g' are $SU(2)$ and $U(1)_Y$ gauge couplings, and $W_{\mu\nu}^a$ and $B_{\mu\nu}$ are the field strengths for $SU(2)$ and $U(1)_Y$ gauge fields. The same interaction occurs for mirror-type excited leptons. For sequential-type excited leptons, the ℓ^* and ν^* couplings become unrelated, and the couplings receive the extra suppression of $(250 \text{ GeV})/\Lambda$ or m_{L^*}/Λ . In any case, these couplings satisfy the relation

$$\lambda_W = -\sqrt{2} \sin^2 \theta_W (\lambda_Z \cot \theta_W + \lambda_\gamma). \quad (6)$$

Additional coupling with gluons is possible for excited quarks:

$$\mathcal{L} = \frac{1}{2\Lambda} \bar{Q}^* \sigma^{\mu\nu} (g_s f_s \frac{\lambda^a}{2} G_{\mu\nu}^a + g f \frac{\tau^a}{2} W_{\mu\nu}^a + g' f' Y B_{\mu\nu}) \times \frac{1-\gamma_5}{2} Q + \text{h.c.}, \quad (7)$$

where Q denotes a quark doublet, g_s is the QCD gauge coupling, and $G_{\mu\nu}^a$ the gluon field strength.

It should be noted that the electromagnetic radiative decay of $\ell^*(\nu^*)$ is forbidden if $f = -f'$ ($f = f'$). These two possibilities ($f = f'$ and $f = -f'$) are investigated in many analyses of the LEP experiments above the Z pole.

Several different conventions are used by LEP experiments on Z pole to express the transition magnetic couplings. To facilitate comparison, we re-express these in terms of λ_Z and λ_γ using the following relations and taking $\sin^2 \theta_W = 0.23$. We assume chiral couplings, *i.e.*, $|c| = |d|$ in the notation of Ref. 2.

1. ALEPH (charged lepton and neutrino)

$$\lambda_Z^{\text{ALEPH}} = \frac{1}{2} \lambda_Z \quad (1990 \text{ papers}) \quad (8a)$$

$$\frac{2c}{\Lambda} = \frac{\lambda_Z}{m_{\ell^*} [\text{or } m_{\nu^*}]} \quad (\text{for } |c| = |d|) \quad (8b)$$

2. ALEPH (quark)

$$\lambda_u^{\text{ALEPH}} = \frac{\sin \theta_W \cos \theta_W}{\sqrt{\frac{1}{4} - \frac{2}{3} \sin^2 \theta_W + \frac{8}{9} \sin^4 \theta_W}} \lambda_Z = 1.11 \lambda_Z \quad (9)$$

3. L3 and DELPHI (charged lepton)

$$\lambda^{\text{L3}} = \lambda_Z^{\text{DELPHI}} = -\frac{\sqrt{2}}{\cot \theta_W - \tan \theta_W} \lambda_Z = -1.10 \lambda_Z \quad (10)$$

4. L3 (neutrino)

$$f_Z^{\text{L3}} = \sqrt{2} \lambda_Z \quad (11)$$

5. OPAL (charged lepton)

$$\frac{f^{\text{OPAL}}}{\Lambda} = -\frac{2}{\cot \theta_W - \tan \theta_W} \frac{\lambda_Z}{m_{\ell^*}} = -1.56 \frac{\lambda_Z}{m_{\ell^*}} \quad (12)$$

6. OPAL (quark)

$$\frac{f^{\text{OPAL}} c}{\Lambda} = \frac{\lambda_Z}{2m_{q^*}} \quad (\text{for } |c| = |d|) \quad (13)$$

7. DELPHI (charged lepton)

$$\lambda_\gamma^{\text{DELPHI}} = -\frac{1}{\sqrt{2}} \lambda_\gamma \quad (14)$$

If leptons are made of color triplet and antitriplet constituents, we may expect their color-octet partners. Transitions between the octet leptons (ℓ_8) and the ordinary lepton (ℓ) may take place via the dimension-five interactions

$$\mathcal{L} = \frac{1}{2\Lambda} \sum_\ell \left\{ \bar{\ell}_8^\alpha g_S F_{\mu\nu}^\alpha \sigma^{\mu\nu} (\eta_L \ell_L + \eta_R \ell_R) + \text{h.c.} \right\} \quad (15)$$

where the summation is over charged leptons and neutrinos. The leptonic chiral invariance implies $\eta_L \eta_R = 0$ as before.

References

1. E.J. Eichten, K.D. Lane, and M.E. Peskin, Phys. Rev. Lett. **50**, 811 (1983).
2. K. Hagiwara, S. Komamiya, and D. Zeppenfeld, Z. Phys. **C29**, 115 (1985).
3. N. Cabibbo, L. Maiani, and Y. Srivastava, Phys. Lett. **139B**, 459 (1984).

SCALE LIMITS for Contact Interactions: $\Lambda(eeee)$

Limits are for Λ_{LL}^\pm only. For other cases, see each reference.

$\Lambda_{LL}^+(\text{TeV})$	$\Lambda_{LL}^-(\text{TeV})$	CL%	DOCUMENT ID	TECN	COMMENT
>8.3	>10.3	95	1 BOURILKOV 01	RVUE	$E_{\text{cm}} = 192\text{--}208 \text{ GeV}$
••• We do not use the following data for averages, fits, limits, etc. •••					
>4.5	>7.0	95	2 SCHAEEL 07A	ALEP	$E_{\text{cm}} = 189\text{--}209 \text{ GeV}$
>5.3	>6.8	95	ABDALLAH 06c	DLPH	$E_{\text{cm}} = 130\text{--}207 \text{ GeV}$
>4.7	>6.1	95	3 ABBIENDI 04g	OPAL	$E_{\text{cm}} = 130\text{--}207 \text{ GeV}$
>3.8	>5.6	95	ABBIENDI 00R	OPAL	$E_{\text{cm}} = 189 \text{ GeV}$
>4.4	>5.4	95	ABREU 00s	DLPH	$E_{\text{cm}} = 183\text{--}189 \text{ GeV}$
>4.3	>4.9	95	ACCIARRI 00P	L3	$E_{\text{cm}} = 130\text{--}189 \text{ GeV}$
>3.5	>3.2	95	BARATE 00i	ALEP	Superseded by SCHAEEL 07A
>6.0	>7.7	95	4 BOURILKOV 00	RVUE	$E_{\text{cm}} = 183\text{--}189 \text{ GeV}$
>3.1	>3.8	95	ABBIENDI 99	OPAL	$E_{\text{cm}} = 130\text{--}136, 161\text{--}172, 183 \text{ GeV}$
>2.2	>2.8	95	ABREU 99A	DLPH	$E_{\text{cm}} = 130\text{--}172 \text{ GeV}$
>2.7	>2.4	95	ACCIARRI 98i	L3	$E_{\text{cm}} = 130\text{--}172 \text{ GeV}$
>3.0	>2.5	95	ACKERSTAFF 98v	OPAL	$E_{\text{cm}} = 130\text{--}172 \text{ GeV}$

¹A combined analysis of the data from ALEPH, DELPHI, L3, and OPAL.

²SCHAEEL 07A limits are from $R_c, Q_{FB}^{\text{depl}}$, and hadronic cross section measurements.

³ABBIENDI 04g limits are from $e^+ e^- \rightarrow e^+ e^-$ cross section at $\sqrt{s} = 130\text{--}207 \text{ GeV}$.

⁴A combined analysis of the data from ALEPH, L3, and OPAL.

SCALE LIMITS for Contact Interactions: $\Lambda(e\mu\mu\mu)$

Limits are for Λ_{LL}^\pm only. For other cases, see each reference.

$\Lambda_{LL}^+(\text{TeV})$	$\Lambda_{LL}^-(\text{TeV})$	CL%	DOCUMENT ID	TECN	COMMENT
>6.6	>9.5	95	5 SCHAEEL 07A	ALEP	$E_{\text{cm}} = 189\text{--}209 \text{ GeV}$
>8.5	>3.8	95	ACCIARRI 00P	L3	$E_{\text{cm}} = 130\text{--}189 \text{ GeV}$

• • • We do not use the following data for averages, fits, limits, etc. • • •

>	>	95							
>7.3	>7.6	95	ABDALLAH	06c	DLPH	$E_{cm} = 130\text{--}207$ GeV			
>8.1	>7.3	95	6 ABBIENDI	04g	OPAL	$E_{cm} = 130\text{--}207$ GeV			
>7.3	>4.6	95	ABBIENDI	00r	OPAL	$E_{cm} = 189$ GeV			
>6.6	>6.3	95	ABREU	00s	DLPH	$E_{cm} = 183\text{--}189$ GeV			
>4.0	>4.7	95	BARATE	00i	ALEP	Superseded by SCHAEEL 07A			
>4.5	>4.3	95	ABBIENDI	99	OPAL	$E_{cm} = 130\text{--}136, 161\text{--}172, 183$ GeV			
>3.4	>2.7	95	ABREU	99a	DLPH	$E_{cm} = 130\text{--}172$ GeV			
>3.6	>2.4	95	ACCIARRI	98j	L3	$E_{cm} = 130\text{--}172$ GeV			
>2.9	>3.4	95	ACKERSTAFF	98v	OPAL	$E_{cm} = 130\text{--}172$ GeV			
>3.1	>2.0	95	MIURA	98	VNS	$E_{cm} = 57.77$ GeV			

⁵ SCHAEEL 07A limits are from R_c, Q_{FB}^{depl} , and hadronic cross section measurements.
⁶ ABBIENDI 04G limits are from $e^+e^- \rightarrow \mu\mu$ cross section at $\sqrt{s} = 130\text{--}207$ GeV.

SCALE LIMITS for Contact Interactions: $\Lambda(ee\tau)$

Limits are for Λ_{LL}^\pm only. For other cases, see each reference.

$\Lambda_{LL}^+(TeV)$	$\Lambda_{LL}^-(TeV)$	CL%	DOCUMENT ID	TECN	COMMENT
>7.9	>5.8	95	7 SCHAEEL	07A	ALEP $E_{cm} = 189\text{--}209$ GeV
>7.9	>4.6	95	ABDALLAH	06c	DLPH $E_{cm} = 130\text{--}207$ GeV
>4.9	>7.2	95	8 ABBIENDI	04g	OPAL $E_{cm} = 130\text{--}207$ GeV

• • • We do not use the following data for averages, fits, limits, etc. • • •

>3.9	>6.5	95	ABBIENDI	00r	OPAL $E_{cm} = 189$ GeV
>5.2	>5.4	95	ABREU	00s	DLPH $E_{cm} = 183\text{--}189$ GeV
>5.4	>4.7	95	ACCIARRI	00p	L3 $E_{cm} = 130\text{--}189$ GeV
>3.9	>3.7	95	BARATE	00i	ALEP Superseded by SCHAEEL 07A
>3.8	>4.0	95	ABBIENDI	99	OPAL $E_{cm} = 130\text{--}136, 161\text{--}172, 183$ GeV
>2.8	>2.6	95	ABREU	99a	DLPH $E_{cm} = 130\text{--}172$ GeV
>2.4	>2.8	95	ACCIARRI	98j	L3 $E_{cm} = 130\text{--}172$ GeV
>2.3	>3.7	95	ACKERSTAFF	98v	OPAL $E_{cm} = 130\text{--}172$ GeV

⁷ SCHAEEL 07A limits are from R_c, Q_{FB}^{depl} , and hadronic cross section measurements.
⁸ ABBIENDI 04G limits are from $e^+e^- \rightarrow \tau\tau$ cross section at $\sqrt{s} = 130\text{--}207$ GeV.

SCALE LIMITS for Contact Interactions: $\Lambda(e\ell\ell\ell)$

Lepton universality assumed. Limits are for Λ_{LL}^\pm only. For other cases, see each reference.

$\Lambda_{LL}^+(TeV)$	$\Lambda_{LL}^-(TeV)$	CL%	DOCUMENT ID	TECN	COMMENT
>7.9	> 10.3	95	9 SCHAEEL	07A	ALEP $E_{cm} = 189\text{--}209$ GeV
>9.1	>8.2	95	ABDALLAH	06c	DLPH $E_{cm} = 130\text{--}207$ GeV

• • • We do not use the following data for averages, fits, limits, etc. • • •

>7.7	>9.5	95	10 ABBIENDI	04g	OPAL $E_{cm} = 130\text{--}207$ GeV
			11 BABICH	03	RVUE
>6.4	>7.2	95	ABBIENDI	00r	OPAL $E_{cm} = 189$ GeV
>7.3	>7.8	95	ABREU	00s	DLPH $E_{cm} = 183\text{--}189$ GeV
>9.0	>5.2	95	ACCIARRI	00p	L3 $E_{cm} = 130\text{--}189$ GeV
>5.3	>5.5	95	BARATE	00i	ALEP Superseded by SCHAEEL 07A
>5.2	>5.3	95	ABBIENDI	99	OPAL $E_{cm} = 130\text{--}136, 161\text{--}172, 183$ GeV
>4.4	>4.2	95	ABREU	99a	DLPH $E_{cm} = 130\text{--}172$ GeV
>4.0	>3.1	95	12 ACCIARRI	98j	L3 $E_{cm} = 130\text{--}172$ GeV
>3.4	>4.4	95	ACKERSTAFF	98v	OPAL $E_{cm} = 130\text{--}172$ GeV

⁹ SCHAEEL 07A limits are from R_c, Q_{FB}^{depl} , and hadronic cross section measurements.
¹⁰ ABBIENDI 04G limits are from $e^+e^- \rightarrow \ell^+\ell^-$ cross section at $\sqrt{s} = 130\text{--}207$ GeV.
¹¹ BABICH 03 obtain a bound $-0.175 \text{ TeV}^{-2} < 1/\Lambda_{LL}^2 < 0.095 \text{ TeV}^{-2}$ (95%CL) in a model independent analysis allowing all of $\Lambda_{LL}, \Lambda_{LR}, \Lambda_{RL}, \Lambda_{RR}$ to coexist.
¹² From $e^+e^- \rightarrow e^+e^-, \mu^+\mu^-, \text{ and } \tau^+\tau^-$.

SCALE LIMITS for Contact Interactions: $\Lambda(ee\tau\tau)$

Limits are for Λ_{LL}^\pm only. For other cases, see each reference.

$\Lambda_{LL}^+(TeV)$	$\Lambda_{LL}^-(TeV)$	CL%	DOCUMENT ID	TECN	COMMENT
> 9.4	>5.6	95	13 SCHAEEL	07A	ALEP (<i>eecc</i>)
> 9.4	>4.9	95	14 SCHAEEL	07A	ALEP (<i>eebb</i>)
>23.3	>12.5	95	15 CHEUNG	01B	RVUE (<i>eeuu</i>)
>11.1	>26.4	95	15 CHEUNG	01B	RVUE (<i>eedd</i>)

• • • We do not use the following data for averages, fits, limits, etc. • • •

>12.9	>7.2	95	16 SCHAEEL	07A	ALEP (<i>eeqq</i>)
> 3.7	>5.9	95	17 ABULENCIA	06L	CDF (<i>eeqq</i>)
> 8.2	>3.7	95	18 ABBIENDI	04G	OPAL (<i>eeqq</i>)
> 5.9	>9.1	95	18 ABBIENDI	04G	OPAL (<i>eeuu</i>)
> 8.6	>5.5	95	18 ABBIENDI	04G	OPAL (<i>eedd</i>)
> 2.7	>1.7	95	CHEKANOV	04B	ZEUS (<i>eeqq</i>)
> 2.8	>1.6	95	19 ADLOFF	03	H1 (<i>eeqq</i>)
> 2.7	>2.7	95	20 ACHARD	02j	L3 (<i>eecc</i>)
> 5.5	>3.1	95	21 ABBIENDI	00R	OPAL (<i>eeqq</i>)
> 4.9	>6.1	95	21 ABBIENDI	00R	OPAL (<i>eeuu</i>)
> 5.7	>4.5	95	21 ABBIENDI	00R	OPAL (<i>eedd</i>)
> 4.2	>2.8	95	22 ACCIARRI	00P	L3 (<i>eeqq</i>)
> 2.4	>1.3	95	23 ADLOFF	00	H1 (<i>eeqq</i>)
> 5.4	>6.2	95	24 BARATE	00i	ALEP Superseded by SCHAEEL 07A

> 5.6	>4.9	95	25 BARATE	00i	ALEP Superseded by SCHAEEL 07A
> 4.4	>2.8	95	26 BREITWEG	00B	ZEUS
> 4.0	>4.8	95	27 ABBIENDI	99	OPAL (<i>eeqq</i>)
> 3.3	>4.2	95	28 ABBIENDI	99	OPAL (<i>eebb</i>)
> 2.4	>2.8	95	29 ABBOTT	99D	D0 (<i>eeqq</i>)
> 4.4	>3.9	95	30 ABREU	99A	DLPH (<i>eeqq</i>) (<i>d</i> or <i>s</i> quark)
> 1.0	>2.4	95	30 ABREU	99A	DLPH (<i>eebb</i>)
> 1.0	>2.1	95	30 ABREU	99A	DLPH (<i>eeuu</i>)
> 4.0	>3.4	95	30 ABREU	99A	DLPH (<i>eecc</i>)
> 4.3	>5.6	95	31 ZARNECKI	99	RVUE (<i>eedd</i>)
> 3.0	>2.1	95	31 ZARNECKI	99	RVUE (<i>eeuu</i>)
> 3.4	>2.2	95	32 ACCIARRI	98J	L3 (<i>eeqq</i>)
> 4.0	>2.8	95	33 ACKERSTAFF	98V	OPAL (<i>eeqq</i>)
> 9.3	>12.0	95	34 ACKERSTAFF	98V	OPAL (<i>eebb</i>)
> 8.8	>11.9	95	35 BARGER	98E	RVUE (<i>eeuu</i>)
			35 BARGER	98E	RVUE (<i>eedd</i>)

¹³ SCHAEEL 07A limits are from R_c, Q_{FB}^{depl} , and hadronic cross section measurements.
¹⁴ SCHAEEL 07A limits are from R_b, A_{FB}^b .
¹⁵ CHEUNG 01B is an update of BARGER 98E.
¹⁶ SCHAEEL 07A limit assumes quark flavor universality of the contact interactions.
¹⁷ ABULENCIA 06L limits are from $p\bar{p}$ collisions at $\sqrt{s} = 1.96$ TeV.
¹⁸ ABBIENDI 04G limits are from $e^+e^- \rightarrow q\bar{q}$ cross section at $\sqrt{s} = 130\text{--}207$ GeV.
¹⁹ ADLOFF 03 limits are from the $d\sigma/dQ^2$ measurement of $e^\pm p \rightarrow e^\pm X$.
²⁰ ACHARD 02j limit is from the bound on the $e^+e^- \rightarrow t\bar{t}$ cross section. $\Lambda_{LL} = \Lambda_{LR} = \Lambda_{RL} = \Lambda_{RR}$ and $m_t = 175$ GeV are assumed.
²¹ ABBIENDI 00R limits are from $e^+e^- \rightarrow q\bar{q}$ cross section at $\sqrt{s} = 130\text{--}189$ GeV.
²² ACCIARRI 00P limit is from $e^+e^- \rightarrow q\bar{q}$ cross section at $\sqrt{s} = 130\text{--}189$ GeV.
²³ ADLOFF 00 limits are from the Q^2 spectrum measurement of $e^+p \rightarrow e^+X$.
²⁴ BARATE 00i limits are from $e^+e^- \rightarrow q\bar{q}$ cross section and jet-charge asymmetry at $130\text{--}183$ GeV.
²⁵ BARATE 00i limits are from R_b and jet-charge asymmetry at $130\text{--}183$ GeV.
²⁶ BREITWEG 00B limits are from Q^2 spectrum measurement of e^+p collisions. See their Table 3 for the limits of various models.
²⁷ ABBIENDI 99 limits are from $e^+e^- \rightarrow q\bar{q}$ cross section at $130\text{--}136, 161\text{--}172, 183$ GeV.
²⁸ ABBIENDI 99 limits are from R_b at $130\text{--}136, 161\text{--}172, 183$ GeV.
²⁹ ABBOTT 99D limits are from e^+e^- mass distribution in $p\bar{p} \rightarrow e^+e^-X$ at $E_{cm} = 1.8$ TeV.
³⁰ ABREU 99A limits are from flavor-tagged $e^+e^- \rightarrow q\bar{q}$ cross section at $130\text{--}172$ GeV.
³¹ ZARNECKI 99 use data from HERA, LEP, Tevatron, and various low-energy experiments.
³² ACCIARRI 98J limits are from $e^+e^- \rightarrow q\bar{q}$ cross section at $E_{cm} = 130\text{--}172$ GeV.
³³ ACKERSTAFF 98V limits are from $e^+e^- \rightarrow q\bar{q}$ at $E_{cm} = 130\text{--}172$ GeV.
³⁴ ACKERSTAFF 98V limits are from R_b measurements at $E_{cm} = 130\text{--}172$ GeV.
³⁵ BARGER 98E use data from HERA, LEP, Tevatron, and various low-energy experiments.

SCALE LIMITS for Contact Interactions: $\Lambda(\mu\mu q\bar{q})$

$\Lambda_{LL}^+(TeV)$	$\Lambda_{LL}^-(TeV)$	CL%	DOCUMENT ID	TECN	COMMENT
> 2.9	> 4.2	95	36 ABE	97T	CDF ($\mu\mu q\bar{q}$) (isosinglet)

• • • We do not use the following data for averages, fits, limits, etc. • • •

>1.4	>1.6	95	ABE	92B	CDF ($\mu\mu q\bar{q}$) (isosinglet)
------	------	----	-----	-----	--

³⁶ ABE 97T limits are from $\mu^+\mu^-$ mass distribution in $p\bar{p} \rightarrow \mu^+\mu^-X$ at $E_{cm} = 1.8$ TeV.

SCALE LIMITS for Contact Interactions: $\Lambda(\ell\nu\ell\nu)$

VALUE (TeV)	CL%	DOCUMENT ID	TECN	COMMENT
>3.10	90	37 JODIDIO	86	SPEC $\Lambda_{LR}^\pm(\nu_\mu\nu_e\mu e)$

• • • We do not use the following data for averages, fits, limits, etc. • • •

>3.8		38 DIAZCRUZ	94	RVUE $\Lambda_{LL}^\pm(\tau\nu_\tau\nu_e)$
>8.1		38 DIAZCRUZ	94	RVUE $\Lambda_{LL}^\pm(\tau\nu_\tau\nu_e)$
>4.1		39 DIAZCRUZ	94	RVUE $\Lambda_{LL}^\pm(\tau\nu_\tau\nu_\mu)$
>6.5		39 DIAZCRUZ	94	RVUE $\Lambda_{LL}^\pm(\tau\nu_\tau\nu_\mu)$

³⁷ JODIDIO 86 limit is from $\mu^+ \rightarrow \bar{\nu}_\mu e^+ \nu_e$. Chirality invariant interactions $L = (g^2/\Lambda^2) [\eta_{LL} (\bar{\nu}_\mu \gamma^\alpha \mu_L) (\bar{e}_L \gamma_\alpha \nu_e L) + \eta_{LR} (\bar{\nu}_\mu \gamma^\alpha \nu_e L) (\bar{e}_R \gamma_\alpha \mu_R)]$ with $g^2/4\pi = 1$ and $(\eta_{LL}, \eta_{LR}) = (0, \pm 1)$ are taken. No limits are given for Λ_{LL}^\pm with $(\eta_{LL}, \eta_{LR}) = (\pm 1, 0)$. For more general constraints with right-handed neutrinos and chirality nonconserving contact interactions, see their text.
³⁸ DIAZCRUZ 94 limits are from $\Gamma(\tau \rightarrow e\nu\nu)$ and assume flavor-dependent contact interactions with $\Lambda(\tau\nu_\tau\nu_e) \ll \Lambda(\mu\nu_\mu\nu_e)$.
³⁹ DIAZCRUZ 94 limits are from $\Gamma(\tau \rightarrow \mu\nu\nu)$ and assume flavor-dependent contact interactions with $\Lambda(\tau\nu_\tau\nu_\mu) \ll \Lambda(\mu\nu_\mu\nu_e)$.

SCALE LIMITS for Contact Interactions: $\Lambda(e\nu q\bar{q})$

VALUE (TeV)	CL%	DOCUMENT ID	TECN	
>2.81	95	40 AFFOLDER	01i	CDF

Searches Particle Listings

Quark and Lepton Compositeness

⁴⁰ AFFOLDER 00i bound is for a scalar interaction $\bar{q}_R q_L \bar{\nu}_R \nu_L$.

SCALE LIMITS for Contact Interactions: $\Lambda(qqqq)$

Limits are for Λ_{LL}^{\pm} with color-singlet isoscalar exchanges among u_L 's and d_L 's only, unless otherwise noted. See EICHTEN 84 for details.

VALUE (TeV)	CL%	DOCUMENT ID	TECN	COMMENT
>2.7	95	41 ABBOTT	99c D0	$p\bar{p} \rightarrow$ dijet mass. Λ_{LL}^+
>2.0	95	42 ABBOTT	00E D0	H_T distribution; Λ_{LL}^+
>2.1	95	43 ABBOTT	98G D0	$p\bar{p} \rightarrow$ dijet angl. Λ_{LL}^+
		44 BERTRAM	98 RVUE	$p\bar{p} \rightarrow$ dijet mass

⁴¹ The quoted limit is from inclusive dijet mass spectrum in $p\bar{p}$ collisions at $E_{cm}=1.8$ TeV. ABBOTT 99c also obtain $\Lambda_{LL}^+ > 2.4$ TeV. All quarks are assumed composite.

⁴² The quoted limit for ABBOTT 00E is from H_T distribution in $p\bar{p}$ collisions at $E_{cm}=1.8$ TeV. CTEQ4M PDF and $\mu=E^{0.3x}$ are assumed. For limits with different assumptions, see their Tables 2 and 3. All quarks are assumed composite.

⁴³ ABBOTT 98G limit is from dijet angular distribution in $p\bar{p}$ collisions at $E_{cm}=1.8$ TeV. All quarks are assumed composite.

⁴⁴ BERTRAM 98 obtain limit on the scale of color-octet axial-vector flavor-universal contact interactions: $\Lambda_{A8} > 2.1$ TeV. They also obtain a limit $\Lambda_{V8} > 2.4$ TeV on a color-octet flavor-universal vectorial contact interaction.

SCALE LIMITS for Contact Interactions: $\Lambda(\nu\nu qq)$

Limits are for Λ_{LL}^{\pm} only. For other cases, see each reference.

Λ_{LL}^+ (TeV)	Λ_{LL}^- (TeV)	CL%	DOCUMENT ID	TECN	COMMENT
>5.0	>5.4	95	45 MCFARLAND	98 CCFR	νN scattering

⁴⁵ MCFARLAND 98 assumed a flavor universal interaction. Neutrinos were mostly of muon type.

MASS LIMITS for Excited e^*

Most e^+e^- experiments assume one-photon or Z exchange. The limits from some e^+e^- experiments which depend on λ have assumed transition couplings which are chirality violating ($\eta_L = \eta_R$). However they can be interpreted as limits for chirality-conserving interactions after multiplying the coupling value λ by $\sqrt{2}$; see Note.

Excited leptons have the same quantum numbers as other ortho-leptons. See also the searches for ortho-leptons in the "Searches for Heavy Leptons" section.

Limits for Excited e^* from Pair Production

These limits are obtained from $e^+e^- \rightarrow e^*e^{*-}$ and thus rely only on the (electroweak) charge of e^* . Form factor effects are ignored unless noted. For the case of limits from Z decay, the e^* coupling is assumed to be of sequential type. Possible t channel contribution from transition magnetic coupling is neglected. All limits assume a dominant $e^* \rightarrow e\gamma$ decay except the limits from $\Gamma(Z)$.

For limits prior to 1987, see our 1992 edition (Physical Review D45 S1 (1992)).

VALUE (GeV)	CL%	DOCUMENT ID	TECN	COMMENT
>103.2	95	46 ABBIENDI	02G OPAL	$e^+e^- \rightarrow e^*e^*$ Homodoublet type
>102.8	95	47 ACHARD	03B L3	$e^+e^- \rightarrow e^*e^*$ Homodoublet type
>100.0	95	48 ACCIARRI	01D L3	$e^+e^- \rightarrow e^*e^*$ Homodoublet type
> 91.3	95	49 ABBIENDI	00I OPAL	$e^+e^- \rightarrow e^*e^*$ Homodoublet type
> 94.2	95	50 ACCIARRI	00E L3	$e^+e^- \rightarrow e^*e^*$ Homodoublet type
> 90.7	95	51 ABREU	99O DLPH	Homodoublet type
> 85.0	95	52 ACKERSTAFF	98C OPAL	$e^+e^- \rightarrow e^*e^*$ Homodoublet type
> 79.6	95	53 BARATE	98U ALEP	$Z \rightarrow e^*e^*$
		54,55 ABREU	97B DLPH	$e^+e^- \rightarrow e^*e^*$ Homodoublet type
> 77.9	95	54,56 ABREU	97B DLPH	$e^+e^- \rightarrow e^*e^*$ Sequential type
> 79.7	95	54 ACCIARRI	97G L3	$e^+e^- \rightarrow e^*e^*$ Sequential type

- ⁴⁶ From e^+e^- collisions at $\sqrt{s}=183-209$ GeV. $f=f'$ is assumed.
- ⁴⁷ From e^+e^- collisions at $\sqrt{s}=189-209$ GeV. $f=f'$ is assumed. ACHARD 03b also obtain limit for $f=-f'$: $m_{e^*} > 96.6$ GeV.
- ⁴⁸ From e^+e^- collisions at $\sqrt{s}=192-202$ GeV. $f=f'$ is assumed. ACCIARRI 01D also obtain limit for $f=-f'$: $m_{e^*} > 93.4$ GeV.
- ⁴⁹ From e^+e^- collisions at $\sqrt{s}=161-183$ GeV. $f=f'$ is assumed. ABBIENDI 00i also obtain limit for $f=-f'$ ($e^* \rightarrow \nu W$): $m_{e^*} > 86.0$ GeV.
- ⁵⁰ From e^+e^- collisions at $\sqrt{s}=189$ GeV. $f=f'$ is assumed. ACCIARRI 00E also obtain limit for $f=-f'$ ($e^* \rightarrow \nu W$): $m_{e^*} > 92.6$ GeV.
- ⁵¹ From e^+e^- collisions at $\sqrt{s}=183$ GeV. $f=f'$ is assumed. ABREU 99O also obtain limit for $f=-f'$ ($e^* \rightarrow \nu W$): $m_{e^*} > 81.3$ GeV.

⁵² From e^+e^- collisions at $\sqrt{s}=170-172$ GeV. ACKERSTAFF 98c also obtain limit from $e^* \rightarrow \nu W$ decay mode: $m_{e^*} > 81.3$ GeV.

⁵³ BARATE 98u obtain limits on the form factor. See their Fig. 14 for limits in mass-form factor plane.

⁵⁴ From e^+e^- collisions at $\sqrt{s}=161$ GeV.

⁵⁵ ABREU 97B also obtain limit from charged current decay mode $e^* \rightarrow \nu W$, $m_{e^*} > 70.9$ GeV.

⁵⁶ ABREU 97B also obtain limit from charged current decay mode $e^* \rightarrow \nu W$, $m_{e^*} > 44.6$ GeV.

Limits for Excited e^* from Single Production

These limits are from $e^+e^- \rightarrow e^*e$, $W \rightarrow e^*\nu$, or $ep \rightarrow e^*X$ and depend on transition magnetic coupling between e and e^* . All limits assume $e^* \rightarrow e\gamma$ decay except as noted. Limits from LEP, UA2, and H1 are for chiral coupling, whereas all other limits are for nonchiral coupling, $\eta_L = \eta_R = 1$. In most papers, the limit is expressed in the form of an excluded region in the $\lambda-m_{e^*}$ plane. See the original papers.

For limits prior to 1987, see our 1992 edition (Physical Review D45 S1 (1992)).

VALUE (GeV)	CL%	DOCUMENT ID	TECN	COMMENT
>255	95	57 ADLOFF	02B H1	$e\gamma \rightarrow e^*X$
>209	95	58 ACOSTA	05B CDF	$p\bar{p} \rightarrow e^*X$
>206	95	59 ACHARD	03B L3	$e^+e^- \rightarrow ee^*$
>208	95	60 ABBIENDI	02G OPAL	$e^+e^- \rightarrow ee^*$
>228	95	61 CHEKANOV	02D ZEUS	$e\gamma \rightarrow e^*X$
>202		62 ACCIARRI	01D L3	$e^+e^- \rightarrow ee^*$
		63 ABBIENDI	00I OPAL	$e^+e^- \rightarrow ee^*$
		64 ACCIARRI	00E L3	$e^+e^- \rightarrow ee^*$
>223	95	65 ADLOFF	00E H1	$e\gamma \rightarrow e^*X$
		66 ABREU	99O DLPH	$e^+e^- \rightarrow ee^*$
none 20-170	95	67 ACCIARRI	98T L3	$e\gamma \rightarrow e^* \rightarrow e\gamma$
		68 ACKERSTAFF	98C OPAL	$e^+e^- \rightarrow ee^*$
		69 BARATE	98U ALEP	$e^+e^- \rightarrow ee^*$
		70,71 ABREU	97B DLPH	$e^+e^- \rightarrow ee^*$
		70,72 ACCIARRI	97G L3	$e^+e^- \rightarrow ee^*$
		73 ACKERSTAFF	97 OPAL	$e^+e^- \rightarrow ee^*$
		74 ADLOFF	97 H1	Lepton-flavor violation
none 30-200	95	75 BREITWEG	97C ZEUS	$e\gamma \rightarrow e^*X$

⁵⁷ ADLOFF 02b search for single e^* production in ep collisions with the decays $e^* \rightarrow e\gamma$, eZ , νW . $f=f'=\Lambda/m_{e^*}$ is assumed for the e^* coupling. See their Fig. 3 for the exclusion plot in the mass-coupling plane.

⁵⁸ ACOSTA 05b search for single e^* production in $p\bar{p}$ collisions with the decays $e^* \rightarrow e\gamma$. $f=f'=\Lambda/m_{e^*}$ is assumed for the e^* coupling. See their Fig.3 for the exclusion limit in the mass-coupling plane.

⁵⁹ ACHARD 03b result is from e^+e^- collisions at $\sqrt{s}=189-209$ GeV. See their Fig. 4 for the exclusion plot in the mass-coupling plane.

⁶⁰ ABBIENDI 02G result is from e^+e^- collisions at $\sqrt{s}=183-209$ GeV. $f=f'=\Lambda/m_{e^*}$ is assumed for e^* coupling. See their Fig. 4c for the exclusion limit in the mass-coupling plane.

⁶¹ CHEKANOV 02D search for single e^* production in ep collisions with the decays $e^* \rightarrow e\gamma$, eZ , νW . $f=f'=\Lambda/m_{e^*}$ is assumed for the e^* coupling. See their Fig. 5a for the exclusion plot in the mass-coupling plane.

⁶² ACCIARRI 01D result is from e^+e^- collisions at $\sqrt{s}=192-202$ GeV. $f=f'=\Lambda/m_{e^*}$ is assumed for the e^* coupling. See their Fig. 4 for limits in the mass-coupling plane.

⁶³ ABBIENDI 00i result is from e^+e^- collisions at $\sqrt{s}=161-183$ GeV. See their Fig. 7 for limits in mass-coupling plane.

⁶⁴ ACCIARRI 00E result is from e^+e^- collisions at $\sqrt{s}=189$ GeV. See their Fig. 3 for limits in mass-coupling plane.

⁶⁵ ADLOFF 00E search for single e^* production in ep collisions with the decays $e^* \rightarrow e\gamma$, eZ , νW . $f=f'=\Lambda/m_{e^*}$ is assumed for the e^* coupling. See their Fig. 9 for the exclusion plot in the mass-coupling plane.

⁶⁶ ABREU 99O result is from e^+e^- collisions at $\sqrt{s}=183$ GeV. See their Figs. 4 and 5 for the exclusion limit in the mass-coupling plane.

⁶⁷ ACCIARRI 98T search for single e^* production in quasi-real Compton scattering. The limit is for $|\lambda| > 1.0 \times 10^{-1}$ and non-chiral coupling of e^* . See their Fig. 7 for the exclusion plot in the mass-coupling plane.

⁶⁸ ACKERSTAFF 98c from e^+e^- collisions at $\sqrt{s}=170-172$ GeV. See their Fig. 11 for the exclusion limit in the mass-coupling plane.

⁶⁹ BARATE 98u is from e^+e^- collision at $\sqrt{s}=M_Z$. See their Fig. 12 for limits in mass-coupling plane

⁷⁰ From e^+e^- collisions at $\sqrt{s}=161$ GeV.

⁷¹ See Fig. 4a and Fig. 5a of ABREU 97B for the exclusion limit in the mass-coupling plane.

⁷² See Fig. 2 and Fig. 3 of ACCIARRI 97G for the exclusion limit in the mass-coupling plane.

⁷³ ACKERSTAFF 97 result is from e^+e^- collisions at $\sqrt{s}=161$ GeV. See their Fig. 3 for the exclusion limit in the mass-coupling plane.

⁷⁴ ADLOFF 97 search for single e^* production in ep collisions with the decays $e^* \rightarrow e\gamma$, eZ , νW . See their Fig. 4 for the rejection limits on the product of the production cross section and the branching ratio into a specific decay channel.

⁷⁵ BREITWEG 97c search for single e^* production in ep collisions with the decays $e^* \rightarrow e\gamma$, eZ , νW . $f=f'=2\Lambda/m_{e^*}$ is assumed for the e^* coupling. See their Fig. 9 for the exclusion plot in the mass-coupling plane.

Limits for Excited e (e*) from e+e- -> gamma gamma

These limits are derived from indirect effects due to e* exchange in the t channel and depend on transition magnetic coupling between e and e*. All limits are for lambda_gamma = 1. All limits except ABE 89j and ACHARD 02D are for nonchiral coupling with eta_L = eta_R = 1. We choose the chiral coupling limit as the best limit and list it in the Summary Table.

For limits prior to 1987, see our 1992 edition (Physical Review **D45** S1 (1992)).

VALUE (GeV)	CL%	DOCUMENT ID	TECN	COMMENT
>310	95	ACHARD 02D	L3	sqrt(s)=192-209 GeV
••• We do not use the following data for averages, fits, limits, etc. •••				
>356	95	⁷⁶ ABDALLAH 04N	DLPH	sqrt(s)=161-208 GeV
>311	95	ABREU 00A	DLPH	sqrt(s)=189-202 GeV
>283	95	⁷⁷ ACCIARRI 00G	L3	sqrt(s)=183-189 GeV
>306	95	ABBIENDI 99P	OPAL	sqrt(s)=189 GeV
>231	95	ABREU 98J	DLPH	sqrt(s)=130-183 GeV
>194	95	ACKERSTAFF 98	OPAL	sqrt(s)=130-172 GeV
>227	95	ACKER...K... 98B	OPAL	sqrt(s)=183 GeV
>250	95	BARATE 98J	ALEP	sqrt(s)=183 GeV
>160	95	⁷⁸ BARATE 98U	ALEP	

⁷⁶ ABDALLAH 04N also obtain a limit on the excited electron mass with e* chiral coupling, m_e* > 295 GeV at 95% CL.

⁷⁷ ACCIARRI 00G also obtain a limit on e* with chiral coupling, m_e* > 213 GeV.

⁷⁸ BARATE 98U is from e+e- collision at sqrt(s)=M_Z. See their Fig. 5 for limits in mass-coupling plane

Indirect Limits for Excited e (e*)

These limits make use of loop effects involving e* and are therefore subject to theoretical uncertainty.

VALUE (GeV)	DOCUMENT ID	TECN	COMMENT
••• We do not use the following data for averages, fits, limits, etc. •••			
	⁷⁹ DORENBOS... 89	CHRM	nu_mu e -> nu_mu e and nu_mu e -> nu_mu e
	⁸⁰ GRIFOLS 86	THEO	nu_mu e -> nu_mu e
	⁸¹ RENARD 82	THEO	g-2 of electron

⁷⁹ DORENBOSCH 89 obtain the limit lambda_cut^2/m^2 < 2.6 (95% CL), where lambda_cut is the cutoff scale, based on the one-loop calculation by GRIFOLS 86. If one assumes that lambda_cut = 1 TeV and lambda_gamma = 1, one obtains m_e* > 620 GeV. However, one generally expects lambda_gamma approx m_e*/lambda_cut in composite models.

⁸⁰ GRIFOLS 86 uses nu_mu e -> nu_mu e and nu_mu e -> nu_mu e data from CHARM Collaboration to derive mass limits which depend on the scale of compositeness.

⁸¹ RENARD 82 derived from g-2 data limits on mass and couplings of e* and mu*. See figures 2 and 3 of the paper.

MASS LIMITS for Excited mu (mu*)

Limits for Excited mu (mu*) from Pair Production

These limits are obtained from e+e- -> mu*+mu*- and thus rely only on the (electroweak) charge of mu*. Form factor effects are ignored unless noted. For the case of limits from Z decay, the mu* coupling is assumed to be of sequential type. All limits assume a dominant mu* -> mu gamma decay except the limits from Gamma(Z).

For limits prior to 1987, see our 1992 edition (Physical Review **D45** S1 (1992)).

VALUE (GeV)	CL%	DOCUMENT ID	TECN	COMMENT
>103.2	95	⁸² ABBIENDI 02G	OPAL	e+e- -> mu*mu* Homodoublet type
••• We do not use the following data for averages, fits, limits, etc. •••				
>102.8	95	⁸³ ACHARD 03B	L3	e+e- -> mu*mu* Homodoublet type
>100.2	95	⁸⁴ ACCIARRI 01D	L3	e+e- -> mu*mu* Homodoublet type
> 91.3	95	⁸⁵ ABBIENDI 00I	OPAL	e+e- -> mu*mu* Homodoublet type
> 94.2	95	⁸⁶ ACCIARRI 00E	L3	e+e- -> mu*mu* Homodoublet type
> 90.7	95	⁸⁷ ABREU 99O	DLPH	Homodoublet type
> 85.3	95	⁸⁸ ACKERSTAFF 98C	OPAL	e+e- -> mu*mu* Homodoublet type
> 79.6	95	^{89,91} BARATE 98U	ALEP	Z -> mu*mu*
> 78.4	95	^{90,92} ABREU 97B	DLPH	e+e- -> mu*mu* Sequential type
> 79.9	95	⁹⁰ ACCIARRI 97G	L3	e+e- -> mu*mu* Sequential type

⁸² From e+e- collisions at sqrt(s)=183-209 GeV. f=f' is assumed.

⁸³ From e+e- collisions at sqrt(s)=189-209 GeV. f=f' is assumed. ACHARD 03B also obtain limit for f=-f': m_mu* > 96.6 GeV.

⁸⁴ From e+e- collisions at sqrt(s)=192-202 GeV. f=f' is assumed. ACCIARRI 01D also obtain limit for f=-f': m_mu* > 93.4 GeV.

⁸⁵ From e+e- collisions at sqrt(s)=161-183 GeV. f=f' is assumed. ABBIENDI 00I also obtain limit for f=-f' (mu* -> nu W): m_mu* > 86.0 GeV.

⁸⁶ From e+e- collisions at sqrt(s)=189 GeV. f=f' is assumed. ACCIARRI 00E also obtain limit for f=-f' (mu* -> nu W): m_mu* > 92.6 GeV.

⁸⁷ From e+e- collisions at sqrt(s)=183 GeV. f=f' is assumed. ABREU 99O also obtain limit for f=-f' (mu* -> nu W): m_mu* > 81.3 GeV.

⁸⁸ From e+e- collisions at sqrt(s)=170-172 GeV. ACKERSTAFF 98C also obtain limit from mu* -> nu W decay mode; m_mu* > 81.3 GeV.

⁸⁹ BARATE 98U obtain limits on the form factor. See their Fig. 14 for limits in mass-form factor plane.

⁹⁰ From e+e- collisions at sqrt(s)=161 GeV.

⁹¹ ABREU 97B also obtain limit from charged current decay mode mu* -> nu W, m_mu* > 70.9 GeV.

⁹² ABREU 97B also obtain limit from charged current decay mode mu* -> nu W, m_mu* > 44.6 GeV.

Limits for Excited mu (mu*) from Single Production

These limits are from e+e- -> mu* mu and depend on transition magnetic coupling between mu and mu*. All limits assume mu* -> mu gamma decay. Limits from LEP are for chiral coupling, whereas all other limits are for nonchiral coupling, eta_L = eta_R = 1. In most papers, the limit is expressed in the form of an excluded region in the lambda-mu* plane. See the original papers.

For limits prior to 1987, see our 1992 edition (Physical Review **D45** S1 (1992)).

VALUE (GeV)	CL%	DOCUMENT ID	TECN	COMMENT
>221	95	⁹³ ABULENCIA,A 06B	CDF	p p -> mu mu*, mu* -> mu gamma
••• We do not use the following data for averages, fits, limits, etc. •••				
>180	95	⁹⁴ ABAZOV 06E	D0	p p -> mu mu*
>190	95	⁹⁵ ACHARD 03B	L3	e+e- -> mu mu*
>178	95	⁹⁶ ABBIENDI 02G	OPAL	e+e- -> mu mu*
		⁹⁷ ACCIARRI 01D	L3	e+e- -> mu mu*
		⁹⁸ ABBIENDI 00I	OPAL	e+e- -> mu mu*
		⁹⁹ ACCIARRI 00E	L3	e+e- -> mu mu*
		¹⁰⁰ ABREU 99O	DLPH	e+e- -> mu mu*
		¹⁰¹ ACKERSTAFF 98C	OPAL	e+e- -> mu mu*
		¹⁰² BARATE 98U	ALEP	Z -> mu mu*

⁹³ f = f' = Lambda/m_mu* is assumed for the mu* coupling. See their Fig.4 for the exclusion limit in the mass-coupling plane. ABULENCIA,A 06B also obtain m_mu* limit in the contact interaction model with Lambda = m_mu*, m_mu* > 696 GeV.

⁹⁴ ABAZOV 06E assume mu mu* production via four-fermion contact interaction (4pi/Lambda^2)(q_L gamma mu q_L)(l_R gamma mu l_R). The obtained limit is m_mu* > 618 GeV (m_mu* > 688 GeV) for Lambda = 1 TeV (Lambda = m_mu*).

⁹⁵ ACHARD 03B result is from e+e- collisions at sqrt(s)=189-209 GeV. f=f'=Lambda/m_mu* is assumed. See their Fig. 4 for the exclusion plot in the mass-coupling plane.

⁹⁶ ABBIENDI 02G result is from e+e- collisions at sqrt(s)=183-209 GeV. f=f'=Lambda/m_mu* is assumed for mu* coupling. See their Fig. 4c for the exclusion limit in the mass-coupling plane.

⁹⁷ ACCIARRI 01D result is from e+e- collisions at sqrt(s)=192-202 GeV. f=f'=Lambda/m_mu* is assumed for the mu* coupling. See their Fig. 4 for limits in the mass-coupling plane.

⁹⁸ ABBIENDI 00I result is from e+e- collisions at sqrt(s)=161-183 GeV. See their Fig. 7 for limits in mass-coupling plane.

⁹⁹ ACCIARRI 00E result is from e+e- collisions at sqrt(s)=189 GeV. See their Fig. 3 for limits in mass-coupling plane.

¹⁰⁰ ABREU 99O result is from e+e- collisions at sqrt(s)=183 GeV. See their Figs. 4 and 5 for the exclusion limit in the mass-coupling plane.

¹⁰¹ ACKERSTAFF 98C result is from e+e- collisions at sqrt(s)=170-172 GeV. See their Fig. 11 for the exclusion limit in the mass-coupling plane.

¹⁰² BARATE 98U obtain limits on the Z mu mu* coupling. See their Fig. 12 for limits in mass-coupling plane

Indirect Limits for Excited mu (mu*)

These limits make use of loop effects involving mu* and are therefore subject to theoretical uncertainty.

VALUE (GeV)	DOCUMENT ID	TECN	COMMENT
••• We do not use the following data for averages, fits, limits, etc. •••			
	¹⁰³ RENARD 82	THEO	g-2 of muon
¹⁰³ RENARD 82			derived from g-2 data limits on mass and couplings of e* and mu*. See figures 2 and 3 of the paper.

MASS LIMITS for Excited tau (tau*)

Limits for Excited tau (tau*) from Pair Production

These limits are obtained from e+e- -> tau*+tau*- and thus rely only on the (electroweak) charge of tau*. Form factor effects are ignored unless noted. For the case of limits from Z decay, the tau* coupling is assumed to be of sequential type. All limits assume a dominant tau* -> tau gamma decay except the limits from Gamma(Z).

For limits prior to 1987, see our 1992 edition (Physical Review **D45** S1 (1992)).

VALUE (GeV)	CL%	DOCUMENT ID	TECN	COMMENT
>103.2	95	¹⁰⁴ ABBIENDI 02G	OPAL	e+e- -> tau*tau* Homodoublet type

Searches Particle Listings

Quark and Lepton Compositeness

• • • We do not use the following data for averages, fits, limits, etc. • • •

>102.8	95	105	ACHARD	03B L3	$e^+e^- \rightarrow \tau^*\tau^*$ Homodoublet type
> 99.8	95	106	ACCIARRI	01D L3	$e^+e^- \rightarrow \tau^*\tau^*$ Homodoublet type
> 91.2	95	107	ABBIENDI	00I OPAL	$e^+e^- \rightarrow \tau^*\tau^*$ Homodoublet type
> 94.2	95	108	ACCIARRI	00E L3	$e^+e^- \rightarrow \tau^*\tau^*$ Homodoublet type
> 89.7	95	109	ABREU	99O DLPH	Homodoublet type
> 84.6	95	110	ACKERSTAFF	98C OPAL	$e^+e^- \rightarrow \tau^*\tau^*$ Homodoublet type
> 79.4	95	111,113	BARATE	98U ALEP	$Z \rightarrow \tau^*\tau^*$
> 77.4	95	112,114	ABREU	97B DLPH	$e^+e^- \rightarrow \tau^*\tau^*$ Sequential type
> 79.3	95	112	ACCIARRI	97G L3	$e^+e^- \rightarrow \tau^*\tau^*$ Sequential type
104 From e^+e^- collisions at $\sqrt{s} = 183-209$ GeV. $f = f'$ is assumed.					
105 From e^+e^- collisions at $\sqrt{s} = 189-209$ GeV. $f = f'$ is assumed. ACHARD 03B also obtain limit for $f = -f'$: $m_{\tau^*} > 96.6$ GeV.					
106 From e^+e^- collisions at $\sqrt{s} = 192-202$ GeV. $f = f'$ is assumed. ACCIARRI 01D also obtain limit for $f = -f'$: $m_{\tau^*} > 93.4$ GeV.					
107 From e^+e^- collisions at $\sqrt{s} = 161-183$ GeV. $f = f'$ is assumed. ABBIENDI 00I also obtain limit for $f = -f'$ ($\tau^* \rightarrow \nu W$): $m_{\tau^*} > 86.0$ GeV.					
108 From e^+e^- collisions at $\sqrt{s} = 189$ GeV. $f = f'$ is assumed. ACCIARRI 00E also obtain limit for $f = -f'$ ($\tau^* \rightarrow \nu W$): $m_{\tau^*} > 92.6$ GeV.					
109 From e^+e^- collisions at $\sqrt{s} = 183$ GeV. $f = f'$ is assumed. ABREU 99O also obtain limit for $f = -f'$ ($\tau^* \rightarrow \nu W$): $m_{\tau^*} > 81.3$ GeV.					
110 From e^+e^- collisions at $\sqrt{s} = 170-172$ GeV. ACKERSTAFF 98C also obtain limit from $\tau^* \rightarrow \nu W$ decay mode: $m_{\tau^*} > 81.3$ GeV.					
111 BARATE 98U obtain limits on the form factor. See their Fig. 14 for limits in mass-form factor plane.					
112 From e^+e^- collisions at $\sqrt{s} = 161$ GeV.					
113 ABREU 97B also obtain limit from charged current decay mode $\tau^* \rightarrow \nu W$, $m_{\tau^*} > 70.9$ GeV.					
114 ABREU 97B also obtain limit from charged current decay mode $\tau^* \rightarrow \nu W$, $m_{\tau^*} > 44.6$ GeV.					

Limits for Excited τ (τ^*) from Single Production

These limits are from $e^+e^- \rightarrow \tau^*\tau$ and depend on transition magnetic coupling between τ and τ^* . All limits assume $\tau^* \rightarrow \tau\gamma$ decay. Limits from LEP are for chiral coupling, whereas all other limits are for nonchiral coupling, $\eta_L = \eta_R = 1$. In most papers, the limit is expressed in the form of an excluded region in the $\lambda - m_{\tau^*}$ plane. See the original papers.

VALUE (GeV)	CL%	DOCUMENT ID	TECN	COMMENT
>185	95	115	ABBIENDI	02G OPAL $e^+e^- \rightarrow \tau\tau^*$
• • • We do not use the following data for averages, fits, limits, etc. • • •				
>180	95	116	ACHARD	03B L3 $e^+e^- \rightarrow \tau\tau^*$
>173	95	117	ACCIARRI	01D L3 $e^+e^- \rightarrow \tau\tau^*$
		118	ABBIENDI	00I OPAL $e^+e^- \rightarrow \tau\tau^*$
		119	ACCIARRI	00E L3 $e^+e^- \rightarrow \tau\tau^*$
		120	ABREU	99O DLPH $e^+e^- \rightarrow \tau\tau^*$
		121	ACKERSTAFF	98C OPAL $e^+e^- \rightarrow \tau\tau^*$
		122	BARATE	98U ALEP $Z \rightarrow \tau\tau^*$

- 115 ABBIENDI 02G result is from e^+e^- collisions at $\sqrt{s} = 183-209$ GeV. $f = f' = \Lambda/m_{\tau^*}$ is assumed for τ^* coupling. See their Fig. 4c for the exclusion limit in the mass-coupling plane.
- 116 ACHARD 03B result is from e^+e^- collisions at $\sqrt{s} = 189-209$ GeV. $f = f' = \Lambda/m_{\tau^*}$ is assumed. See their Fig. 4 for the exclusion plot in the mass-coupling plane.
- 117 ACCIARRI 01D result is from e^+e^- collisions at $\sqrt{s} = 192-202$ GeV. $f = f' = \Lambda/m_{\tau^*}$ is assumed for the τ^* coupling. See their Fig. 4 for limits in the mass-coupling plane.
- 118 ABBIENDI 00I result is from e^+e^- collisions at $\sqrt{s} = 161-183$ GeV. See their Fig. 7 for limits in mass-coupling plane.
- 119 ACCIARRI 00E result is from e^+e^- collisions at $\sqrt{s} = 189$ GeV. See their Fig. 3 for limits in mass-coupling plane.
- 120 ABREU 99O result is from e^+e^- collisions at $\sqrt{s} = 183$ GeV. See their Figs. 4 and 5 for the exclusion limit in the mass-coupling plane.
- 121 ACKERSTAFF 98C from e^+e^- collisions at $\sqrt{s} = 170-172$ GeV. See their Fig. 11 for the exclusion limit in the mass-coupling plane.
- 122 BARATE 98U obtain limits on the $Z\tau\tau^*$ coupling. See their Fig. 12 for limits in mass-coupling plane

MASS LIMITS for Excited Neutrino (ν^*)

Limits for Excited ν (ν^*) from Pair Production

These limits are obtained from $e^+e^- \rightarrow \nu^*\nu^*$ and thus rely only on the (electroweak) charge of ν^* . Form factor effects are ignored unless noted. The ν^* coupling is assumed to be of sequential type unless otherwise noted. All limits assume a dominant $\nu^* \rightarrow \nu\gamma$ decay except the limits from $\Gamma(Z)$.

VALUE (GeV)	CL%	DOCUMENT ID	TECN	COMMENT
>102.6	95	123	ACHARD	03B L3 $e^+e^- \rightarrow \nu^*\nu^*$ Homodoublet type

• • • We do not use the following data for averages, fits, limits, etc. • • •

> 99.4	95	124	ABBIENDI	04N OPAL	
> 91.2	95	125	ACCIARRI	01D L3	$e^+e^- \rightarrow \nu^*\nu^*$ Homodoublet type
> 91.2	95	126	ABBIENDI	00I OPAL	$e^+e^- \rightarrow \nu^*\nu^*$ Homodoublet type
> 94.1	95	127	ABBIENDI,G	00D OPAL	
> 94.1	95	128	ACCIARRI	00E L3	$e^+e^- \rightarrow \nu^*\nu^*$ Homodoublet type
> 90.0	95	129	ABBIENDI	99F OPAL	
> 84.9	95	130	ABREU	99O DLPH	Homodoublet type
> 84.9	95	131	ACKERSTAFF	98C OPAL	$e^+e^- \rightarrow \nu^*\nu^*$ Homodoublet type
> 77.6	95	132	BARATE	98U ALEP	$Z \rightarrow \nu^*\nu^*$
> 77.6	95	133,134	ABREU	97B DLPH	$e^+e^- \rightarrow \nu^*\nu^*$ Homodoublet type
> 64.4	95	133,135	ABREU	97B DLPH	$e^+e^- \rightarrow \nu^*\nu^*$ Sequential type
> 71.2	95	133,136	ACCIARRI	97G L3	$e^+e^- \rightarrow \nu^*\nu^*$ Sequential type
123 From e^+e^- collisions at $\sqrt{s} = 189-209$ GeV. $f = -f'$ is assumed. ACHARD 03B also obtain limit for $f = f'$: $m_{\nu_e^*} > 101.7$ GeV, $m_{\nu_\mu^*} > 101.8$ GeV, and $m_{\nu_\tau^*} > 92.9$ GeV. See their Fig. 4 for the exclusion plot in the mass-coupling plane.					
124 From e^+e^- collisions at $\sqrt{s} = 192-209$ GeV, ABBIENDI 04N obtain limit on $\sigma(e^+e^- \rightarrow \nu^*\nu^*) B^2(\nu^* \rightarrow \nu\gamma)$. See their Fig. 2. The limit ranges from 20 to 45 fb for $m_{\nu_e^*} > 45$ GeV.					
125 From e^+e^- collisions at $\sqrt{s} = 192-202$ GeV. $f = f'$ is assumed. ACCIARRI 01D also obtain limit for $f = -f'$: $m_{\nu_e^*} > 99.1$ GeV, $m_{\nu_\mu^*} > 99.3$ GeV, $m_{\nu_\tau^*} > 90.5$ GeV.					
126 From e^+e^- collisions at $\sqrt{s} = 161-183$ GeV. $f = -f'$ (photonic decay) is assumed. ABBIENDI 00I also obtain limit for $f = f'$ ($\nu^* \rightarrow \ell W$): $m_{\nu_e^*} > 91.1$ GeV, $m_{\nu_\mu^*} > 91.1$ GeV, $m_{\nu_\tau^*} > 83.1$ GeV.					
127 From e^+e^- collisions at $\sqrt{s} = 189$ GeV. ABBIENDI,G 00D obtain limit on $\sigma(e^+e^- \rightarrow \nu^*\nu^*) B(\nu^* \rightarrow \nu\gamma)^2$. See their Fig. 14. The limit ranges from 50 to 80 fb for $\sqrt{s}/2 = 95$ GeV $> m_{\nu_e^*} > 45$ GeV.					
128 From e^+e^- collisions at $\sqrt{s} = 189$ GeV. $f = -f'$ (photonic decay) is assumed. ACCIARRI 00E also obtain limit for $f = f'$ ($\nu^* \rightarrow \ell W$): $m_{\nu_e^*} > 93.9$ GeV, $m_{\nu_\mu^*} > 94.0$ GeV, $m_{\nu_\tau^*} > 91.5$ GeV.					
129 From e^+e^- collisions at $\sqrt{s} = 130-183$ GeV, ABBIENDI 99F obtain limit on $\sigma(e^+e^- \rightarrow \nu^*\nu^*) B(\nu^* \rightarrow \nu\gamma)^2$. See their Fig. 13. The limit ranges from 0.094 to 0.14 pb for $\sqrt{s}/2 > m_{\nu_e^*} > 45$ GeV.					
130 From e^+e^- collisions at $\sqrt{s} = 183$ GeV. $f = -f'$ is assumed. ABREU 99O also obtain limit for $f = f'$: $m_{\nu_e^*} > 87.3$ GeV, $m_{\nu_\mu^*} > 88.0$ GeV, $m_{\nu_\tau^*} > 81.0$ GeV.					
131 From e^+e^- collisions at $\sqrt{s} = 170-172$ GeV. ACKERSTAFF 98C also obtain limit from charged decay modes: $m_{\nu_e^*} > 84.1$ GeV, $m_{\nu_\mu^*} > 83.9$ GeV, and $m_{\nu_\tau^*} > 79.4$ GeV.					
132 BARATE 98U obtain limits on the form factor. See their Fig. 14 for limits in mass-form factor plane.					
133 From e^+e^- collisions at $\sqrt{s} = 161$ GeV.					
134 ABREU 97B also obtain limits from charged current decay modes, $m_{\nu_e^*} > 56.4$ GeV.					
135 ABREU 97B also obtain limits from charged current decay modes, $m_{\nu_e^*} > 44.9$ GeV.					
136 ACCIARRI 97G also obtain limits from charged current decay mode $\nu_e^* \rightarrow eW$, $m_{\nu_e^*} > 64.5$ GeV.					

Limits for Excited ν (ν^*) from Single Production

These limits are from $e^+e^- \rightarrow \nu^*\nu^*$, $Z \rightarrow \nu^*\nu^*$, or $e p \rightarrow \nu^* X$ and depend on transition magnetic coupling between ν/e and ν^* . Assumptions about ν^* decay mode are given in footnotes.

VALUE (GeV)	CL%	DOCUMENT ID	TECN	COMMENT
>190	95	137	ACHARD	03B L3 $e^+e^- \rightarrow \nu\nu^*$
• • • We do not use the following data for averages, fits, limits, etc. • • •				
none 50-150	95	138	ADLOFF	02 H1 $e p \rightarrow \nu^* X$
>158	95	139	CHEKANOV	02D ZEUS $e p \rightarrow \nu^* X$
>171	95	140	ACCIARRI	01D L3 $e^+e^- \rightarrow \nu\nu^*$
		141	ABBIENDI	00I OPAL $e^+e^- \rightarrow \nu\nu^*$
		142	ABBIENDI,G	00D OPAL
		143	ACCIARRI	00E L3 $e^+e^- \rightarrow \nu\nu^*$
>114	95	144	ADLOFF	00E H1 $e p \rightarrow \nu^* X$
		145	ABBIENDI	99F OPAL
		146	ABREU	99O DLPH $e^+e^- \rightarrow \nu\nu^*$
		147	ACKERSTAFF	98C OPAL $e^+e^- \rightarrow \nu^*\nu^*$ Homodoublet type
		148	BARATE	98U ALEP $Z \rightarrow \nu\nu^*$

- 137 ACHARD 03B result is from e^+e^- collisions at $\sqrt{s} = 189-209$ GeV. The quoted limit is for ν_e^* . $f = -f' = \Lambda/m_{\nu_e^*}$ is assumed. See their Fig. 4 for the exclusion plot in the mass-coupling plane.
- 138 ADLOFF 02 search for single ν^* production in $e p$ collisions with the decays $\nu^* \rightarrow \nu\gamma$, νZ , eW . The quoted limit assumes $f = -f' = \Lambda/m_{\nu_e^*}$. See their Fig. 1 for the exclusion plots in the mass-coupling plane.
- 139 CHEKANOV 02D search for single ν^* production in $e p$ collisions with the decays $\nu^* \rightarrow \nu\gamma$, νZ , eW . $f = -f' = \Lambda/m_{\nu_e^*}$ is assumed for the e^* coupling. CHEKANOV 02D also obtain limit for $f = f' = \Lambda/m_{\nu_e^*}$: $m_{\nu_e^*} > 135$ GeV. See their Fig. 5c and Fig. 5d for the exclusion plot in the mass-coupling plane.

- 140 ACCIARRI 01D search for $\nu\nu^*$ production in e^+e^- collisions at $\sqrt{s} = 192\text{--}202$ GeV with decays $\nu^* \rightarrow \nu\gamma, \nu^* \rightarrow eW$. $f = f' = \Lambda/m_{\nu^*}$ is assumed for the ν^* coupling. See their Fig. 4 for limits in the mass-coupling plane.
- 141 ABBIENDI 00I result is from e^+e^- collisions at $\sqrt{s}=161\text{--}183$ GeV. See their Fig. 7 for limits in mass-coupling plane.
- 142 From e^+e^- collisions at $\sqrt{s} = 189$ GeV. ABBIENDI,G 00D obtain limit on $\sigma(e^+e^- \rightarrow \nu^*\nu^*)B(\nu^* \rightarrow \nu\gamma)^2$. See their Fig. 11.
- 143 ACCIARRI 00E result is from e^+e^- collisions at $\sqrt{s}=189$ GeV. See their Fig. 3 for limits in mass-coupling plane.
- 144 ADLOFF 00E search for single ν^* production in ep collisions with the decays $\nu^* \rightarrow \nu\gamma, \nu Z, eW$. The quoted limit assumes $f = f' = \Lambda/m_{\nu^*}$. See their Fig. 10 for the exclusion plot in the mass-coupling plane.
- 145 From e^+e^- collisions at $\sqrt{s} = 130\text{--}183$ GeV, ABBIENDI 99F obtain limit on $\sigma(e^+e^- \rightarrow \nu\nu^*)B(\nu^* \rightarrow \nu\gamma)$. See their Fig. 8.
- 146 ABREU 99O result is from e^+e^- collisions at $\sqrt{s} = 183$ GeV. See their Figs. 4 and 5 for the exclusion limit in the mass-coupling plane.
- 147 ACKERSTAFF 98C from e^+e^- collisions at $\sqrt{s}=170\text{--}172$ GeV. See their Fig. 11 for the exclusion limit in the mass-coupling plane.
- 148 BARATE 98U obtain limits on the $Z\nu\nu^*$ coupling. See their Fig. 13 for limits in mass-coupling plane

MASS LIMITS for Excited $q (q^*)$

Limits for Excited $q (q^*)$ from Pair Production

These limits are obtained from $e^+e^- \rightarrow q^*\bar{q}^*$ and thus rely only on the (electroweak) charge of the q^* . Form factor effects are ignored unless noted. Assumptions about the q^* decay are given in the comments and footnotes.

VALUE (GeV)	CL%	DOCUMENT ID	TECN	COMMENT
>45.6	95	149 ADRIANI	93M L3	u or d type, $Z \rightarrow q^*q^*$
• • • We do not use the following data for averages, fits, limits, etc. • • •				
		150 BARATE	98U ALEP	$Z \rightarrow q^*q^*$
		151 ADRIANI	92F L3	$Z \rightarrow q^*q^*$
>41.7	95	152 BARDADIN...	92 RVUE	u -type, $\Gamma(Z)$
>44.7	95	152 BARDADIN...	92 RVUE	d -type, $\Gamma(Z)$
>40.6	95	153 DECAMP	92 ALEP	u -type, $\Gamma(Z)$
>44.2	95	153 DECAMP	92 ALEP	d -type, $\Gamma(Z)$
>45	95	154 DECAMP	92 ALEP	u or d type,
		153 ABREU	91F DLPH	$Z \rightarrow q^*q^*$
>45	95	153 ABREU	91F DLPH	u -type, $\Gamma(Z)$
		153 ABREU	91F DLPH	d -type, $\Gamma(Z)$
149 ADRIANI 93M limit is valid for $B(q^* \rightarrow qg) > 0.25$ (0.17) for up (down) type.				
150 BARATE 98U obtain limits on the form factor. See their Fig. 16 for limits in mass-form factor plane.				
151 ADRIANI 92F search for $Z \rightarrow q^*\bar{q}^*$ followed with $q^* \rightarrow q\gamma$ decays and give the limit $\sigma_Z \cdot B(Z \rightarrow q^*\bar{q}^*) \cdot B^2(q^* \rightarrow q\gamma) < 2$ pb at 95%CL. Assuming five flavors of degenerate q^* of homodoublet type, $B(q^* \rightarrow q\gamma) < 4\%$ is obtained for $m_{q^*} < 45$ GeV.				
152 BARDADIN-OTWINOWSKA 92 limit based on $\Delta\Gamma(Z) < 36$ MeV.				
153 These limits are independent of decay modes.				
154 Limit is for $B(q^* \rightarrow qg) + B(q^* \rightarrow q\gamma) = 1$.				

Limits for Excited $q (q^*)$ from Single Production

These limits are from $e^+e^- \rightarrow q^*\bar{q}^*$ or $p\bar{p} \rightarrow q^*X$ and depend on transition magnetic couplings between q and q^* . Assumptions about q^* decay mode are given in the footnotes and comments.

VALUE (GeV)	CL%	DOCUMENT ID	TECN	COMMENT
>775	95	155 ABAZOV	04C D0	$p\bar{p} \rightarrow q^*X, q^* \rightarrow qg$
none 200–520 and 580–760	95	156 ABE	97G CDF	$p\bar{p} \rightarrow q^*X, q^* \rightarrow 2$ jets
none 80–570	95	157 ABE	95N CDF	$p\bar{p} \rightarrow q^*X, q^* \rightarrow qg, q\gamma, qW$
• • • We do not use the following data for averages, fits, limits, etc. • • •				
>510	95	158 ABAZOV	06F D0	$p\bar{p} \rightarrow q^*X, q^* \rightarrow qZ$
>205	95	159 CHEKANOV	02D ZEUS	$ep \rightarrow q^*X$
>188	95	160 ADLOFF	00E H1	$ep \rightarrow q^*X$
		161 ABREU	99O DLPH	$e^+e^- \rightarrow qq^*$
		162 BARATE	98U ALEP	$Z \rightarrow qq^*$
155 ABAZOV 04C assume $f_s = f = f' = \Lambda/m_{q^*}$.				
156 ABE 97G search for new particle decaying to dijets.				
157 ABE 95N assume a degenerate u^* and d^* with $f_s = f = f' = \Lambda/m_{q^*}$. See their Fig. 4 for the excluded region in $m_{q^*} - f$ plane.				
158 ABAZOV 06F assume q^* production via qg fusion and via contact interactions. The quoted limit is for $\Lambda = m_{q^*}$.				
159 CHEKANOV 02D search for single q^* production in ep collisions with the decays $q^* \rightarrow q\gamma, qZ, qW$. $f_s = 0$ and $f = f' = \Lambda/m_{q^*}$ is assumed for the q^* coupling. See their Fig. 5b for the exclusion plot in the mass-coupling plane.				
160 ADLOFF 00E search for single q^* production in ep collisions with the decays $q^* \rightarrow q\gamma, qZ, qW$. $f_s = 0$ and $f = f' = \Lambda/m_{q^*}$ is assumed for the q^* coupling. See their Fig. 11 for the exclusion plot in the mass-coupling plane.				
161 ABREU 99O result is from e^+e^- collisions at $\sqrt{s} = 183$ GeV. See their Fig. 6 for the exclusion limit in the mass-coupling plane.				
162 BARATE 98U obtain limits on the Zqq^* coupling. See their Fig. 16 for limits in mass-coupling plane				

MASS LIMITS for Color Sextet Quarks (q_6)

VALUE (GeV)	CL%	DOCUMENT ID	TECN	COMMENT
>84	95	163 ABE	89D CDF	$p\bar{p} \rightarrow q_6\bar{q}_6$

163 ABE 89D look for pair production of unit-charged particles which leave the detector before decaying. In the above limit the color sextet quark is assumed to fragment into a unit-charged or neutral hadron with equal probability and to have long enough lifetime not to decay within the detector. A limit of 121 GeV is obtained for a color decuplet.

MASS LIMITS for Color Octet Charged Leptons (ℓ_8)

VALUE (GeV)	CL%	DOCUMENT ID	TECN	COMMENT
>86	95	164 ABE	89D CDF	Stable ℓ_8 : $p\bar{p} \rightarrow \ell_8\bar{\ell}_8$
• • • We do not use the following data for averages, fits, limits, etc. • • •				
		165 ABT	93 H1	$e_8: ep \rightarrow e_8X$
none 3.0–30.3	95	166 KIM	90 AMY	$e_8: e^+e^- \rightarrow ee +$ jets
none 3.5–30.3	95	166 KIM	90 AMY	$\mu_8: e^+e^- \rightarrow \mu\mu +$ jets
		167 KIM	90 AMY	$e_8: e^+e^- \rightarrow gg; R$
164 ABE 89D look for pair production of unit-charged particles which leave the detector before decaying. In the above limit the color octet lepton is assumed to fragment into a unit-charged or neutral hadron with equal probability and to have long enough lifetime not to decay within the detector. The limit improves to 99 GeV if it always fragments into a unit-charged hadron.				
165 ABT 93 search for e_8 production via e -gluon fusion in ep collisions with $e_8 \rightarrow eg$. See their Fig. 3 for exclusion plot in the $m_{e_8}-\Lambda$ plane for $m_{e_8} = 35\text{--}220$ GeV.				
166 KIM 90 is at $E_{cm} = 50\text{--}60.8$ GeV. The same assumptions as in BARTELL 87B are used.				
167 KIM 90 result $(m_{e_8}\Lambda_M)^{1/2} > 178.4$ GeV (95%CL, $\alpha_s = 0.16$ used) is subject to the same restriction as for BARTELL 85K.				

MASS LIMITS for Color Octet Neutrinos (ν_8)

VALUE (GeV)	CL%	DOCUMENT ID	TECN	COMMENT
>110	90	168 BARGER	89 RVUE	$\nu_8: p\bar{p} \rightarrow \nu_8\bar{\nu}_8$
• • • We do not use the following data for averages, fits, limits, etc. • • •				
none 3.8–29.8	95	169 KIM	90 AMY	$\nu_8: e^+e^- \rightarrow$ acoplanar jets
none 9–21.9	95	170 BARTELL	87B JADE	$\nu_8: e^+e^- \rightarrow$ acoplanar jets
168 BARGER 89 used ABE 89B limit for events with large missing transverse momentum. Two-body decay $\nu_8 \rightarrow \nu g$ is assumed.				
169 KIM 90 is at $E_{cm} = 50\text{--}60.8$ GeV. The same assumptions as in BARTELL 87B are used.				
170 BARTELL 87B is at $E_{cm} = 46.3\text{--}46.78$ GeV. The limit assumes the ν_8 pair production cross section to be eight times larger than that of the corresponding heavy neutrino pair production. This assumption is not valid in general for the weak couplings, and the limit can be sensitive to its $SU(2)_L \times U(1)_Y$ quantum numbers.				

MASS LIMITS for W_8 (Color Octet W Boson)

VALUE (GeV)	DOCUMENT ID	TECN	COMMENT
• • • We do not use the following data for averages, fits, limits, etc. • • •			
	171 ALBAJAR	89 UA1	$p\bar{p} \rightarrow W_8X, W_8 \rightarrow Wg$
171 ALBAJAR 89 give $\sigma(W_8 \rightarrow W + \text{jet})/\sigma(W) < 0.019$ (90% CL) for $m_{W_8} > 220$ GeV.			

REFERENCES FOR Searches for Quark and Lepton Compositeness

SCHAEL 07A EPJ C49 411	S. Schael et al.	(ALEPH Collab.)
ABAZOV 06E PR D73 111102R	V.M. Abazov et al.	(D0 Collab.)
ABAZOV 06F PR D74 011104R	V.M. Abazov et al.	(D0 Collab.)
ABDALLAH 06C EPJ C45 589	J. Abdallah et al.	(DELPHI Collab.)
ABULENCIA 06L PRL 96 21801	A. Abulencia et al.	(CDF Collab.)
ABULENCIA,A 06B PRL 97 191802	A. Abulencia et al.	(CDF Collab.)
ACOSTA 05B PRL 94 101802	D. Acosta et al.	(CDF Collab.)
ABAZOV 04C PR D69 111101R	V.M. Abazov et al.	(D0 Collab.)
ABBIENDI 04G EPJ C33 173	G. Abbiendi et al.	(OPAL Collab.)
ABBIENDI 04N PL B602 167	G. Abbiendi et al.	(OPAL Collab.)
ABDALLAH 04N EPJ C37 405	J. Abdallah et al.	(DELPHI Collab.)
CHEKANOV 04B PL B591 23	S. Chekanov et al.	(ZEUS Collab.)
ACHARD 03B PL B568 23	P. Achard et al.	(L3 Collab.)
ADLOFF 03 PL B568 38	C. Adloff et al.	(H1 Collab.)
BABICH 02G EPJ C29 103	A.A. Babich et al.	(OPAL Collab.)
ABBIENDI 02G EPJ B544 57	G. Abbiendi et al.	(L3 Collab.)
ACHARD 02D PL B531 28	P. Achard et al.	(L3 Collab.)
P. Achard et al.		
ACHARD 02J PL B549 290	P. Achard et al.	(L3 Collab.)
ADLOFF 02 PL B525 9	C. Adloff et al.	(H1 Collab.)
ADLOFF 02B PL B548 35	C. Adloff et al.	(H1 Collab.)
CHEKANOV 02D PL B549 32	S. Chekanov et al.	(ZEUS Collab.)
ACCIARRI 01D PL B502 37	M. Acciarri et al.	(L3 Collab.)
AFFOLDER 01I PRL 87 231803	T. Affolder et al.	(CDF Collab.)
BOURLIKOV 01 PR D64 071701	D. Bourlikov	
CHEUNG 01B PL B517 167	K. Cheung	
ABBIENDI 00I EPJ C14 73	G. Abbiendi et al.	(OPAL Collab.)
ABBIENDI 00R EPJ C13 553	G. Abbiendi et al.	(OPAL Collab.)
ABBIENDI,G 00D EPJ C18 253	G. Abbiendi et al.	(OPAL Collab.)
ABBOTT 00E PR D62 031101	B. Abbott et al.	(D0 Collab.)
ABREU 00A PL B491 67	P. Abreu et al.	(DELPHI Collab.)
ABREU 00S PL B485 45	P. Abreu et al.	(DELPHI Collab.)
ACCIARRI 00E PL B473 177	M. Acciarri et al.	(L3 Collab.)
ACCIARRI 00G PL B475 198	M. Acciarri et al.	(L3 Collab.)
ACCIARRI 00P PL B489 81	M. Acciarri et al.	(L3 Collab.)
ADLOFF 00 PL B479 358	C. Adloff et al.	(H1 Collab.)
ADLOFF 00E EPJ C17 567	C. Adloff et al.	(H1 Collab.)
AFFOLDER 00I PR D62 012004	T. Affolder et al.	(CDF Collab.)
BARATE 00I EPJ C12 183	R. Barate et al.	(ALEPH Collab.)

Searches Particle Listings

Quark and Lepton Compositeness, Extra Dimensions

BOURLIKOV	00	PR D62 076005	D. Bourlikov	
BREITWEG	00B	EPJ C14 239	J. Breitweg <i>et al.</i>	(ZEUS Collab.)
ABBIENDI	99	EPJ C6 1	G. Abbiendi <i>et al.</i>	(OPAL Collab.)
ABBIENDI	99F	EPJ C8 23	G. Abbiendi <i>et al.</i>	(OPAL Collab.)
ABBIENDI	99P	PL B465 303	G. Abbiendi <i>et al.</i>	(OPAL Collab.)
ABBOTT	99C	PRL 82 2457	B. Abbott <i>et al.</i>	(D0 Collab.)
ABBOTT	99D	PRL 82 4769	B. Abbott <i>et al.</i>	(D0 Collab.)
ABREU	99A	EPJ C11 383	P. Abreu <i>et al.</i>	(DELPHI Collab.)
ABREU	99O	EPJ C8 41	P. Abreu <i>et al.</i>	(DELPHI Collab.)
ZARNECKI	99	EPJ C11 539	A.F. Zarnecki	
ABBOTT	98G	PRL 80 666	B. Abbott <i>et al.</i>	(D0 Collab.)
ABREU	98J	PL B433 429	P. Abreu <i>et al.</i>	(DELPHI Collab.)
ACCIARRI	98J	PL B433 163	M. Acciari <i>et al.</i>	(L3 Collab.)
ACCIARRI	98T	PL B439 183	M. Acciari <i>et al.</i>	(L3 Collab.)
ACKERSTAFF	98	EPJ C1 21	K. Ackerstaff <i>et al.</i>	(OPAL Collab.)
ACKERSTAFF	98C	EPJ C1 45	K. Ackerstaff <i>et al.</i>	(OPAL Collab.)
ACKERSTAFF	98V	EPJ C2 441	K. Ackerstaff <i>et al.</i>	(OPAL Collab.)
ACKER...K...	98B	PL B438 379	K. Ackerstaff <i>et al.</i>	(OPAL Collab.)
BARATE	98J	PL B429 201	R. Barate <i>et al.</i>	(ALEPH Collab.)
BARATE	98U	EPJ C4 571	R. Barate <i>et al.</i>	(ALEPH Collab.)
BARGER	98E	PR D57 391	V. Barger <i>et al.</i>	
BERTRAM	98	PL B443 347	I. Bertram, E.H. Simmons	
McFARLAND	98	EPJ C1 509	K.S. McFarland <i>et al.</i>	(CCFR/NuTeV Collab.)
MIURA	98	PR D57 5345	M. Miura <i>et al.</i>	(VENUS Collab.)
ABE	97G	PR D55 R5263	F. Abe <i>et al.</i>	(CDF Collab.)
ABE	97T	PRL 79 2198	F. Abe <i>et al.</i>	(CDF Collab.)
ABREU	97B	PL B393 245	P. Abreu <i>et al.</i>	(DELPHI Collab.)
ACCIARRI	97G	PL B401 139	M. Acciari <i>et al.</i>	(L3 Collab.)
ACKERSTAFF	97	PL B391 197	K. Ackerstaff <i>et al.</i>	(OPAL Collab.)
ADLOFF	97	NP B463 44	C. Adloff <i>et al.</i>	(HI Collab.)
BREITWEG	97C	ZPHY C76 631	J. Breitweg <i>et al.</i>	(ZEUS Collab.)
ABE	95N	PRL 74 3538	F. Abe <i>et al.</i>	(CDF Collab.)
DIAZCRUZ	94	PR D49 R2149	J.L. Diaz Cruz, O.A. Sampayo	(CINV Collab.)
ABT	93	NP B396 3	I. Abt <i>et al.</i>	(H1 Collab.)
ADRIANI	93M	PRPL 236 1	O. Adriani <i>et al.</i>	(L3 Collab.)
ABE	92B	PRL 68 1463	F. Abe <i>et al.</i>	(CDF Collab.)
ADRIANI	92F	PL B292 472	O. Adriani <i>et al.</i>	(L3 Collab.)
BARADIN...	92	ZPHY C55 163	M. Baradin-Otwinowska	(CLER Collab.)
DECAMP	92	PRPL 216 253	D. Decamp <i>et al.</i>	(ALEPH Collab.)
PDG	92	PR D45 51	K. Hikasa <i>et al.</i>	(KEK, LBL, BOST+ Collab.)
ABREU	91F	NP B367 511	P. Abreu <i>et al.</i>	(DELPHI Collab.)
KIM	90	PL B240 243	G.M. Kim <i>et al.</i>	(AMY Collab.)
ABE	89B	PRL 62 1825	F. Abe <i>et al.</i>	(CDF Collab.)
ABE	89D	PRL 63 1447	F. Abe <i>et al.</i>	(CDF Collab.)
ABE	89J	ZPHY C45 175	K. Abe <i>et al.</i>	(VENUS Collab.)
ALBAJAR	89	ZPHY C44 15	C. Albajar <i>et al.</i>	(UA1 Collab.)
BARGER	89	PL B220 464	V. Barger <i>et al.</i>	(WIS C, KEK Collab.)
DORENBOS...	89	ZPHY C41 567	J. Dorenbosch <i>et al.</i>	(CHARM Collab.)
BARTEL	87B	ZPHY C36 15	W. Bartel <i>et al.</i>	(JADE Collab.)
GRIFOLS	86	PL 168B 264	J.A. Grifols, S. Peris	(BARC Collab.)
JODIDIO	86	PR D34 1967	A. Jodidio <i>et al.</i>	(LBL, NWES, TRIU Collab.)
Also		PR D37 237 (erratum)	A. Jodidio <i>et al.</i>	(LBL, NWES, TRIU Collab.)
BARTEL	85K	PL 160B 337	W. Bartel <i>et al.</i>	(JADE Collab.)
EICHTEN	84	RMP 56 579	E. Eichten <i>et al.</i>	(FNAL, LBL, OSU Collab.)
RENARD	82	PL 116B 264	F.M. Renard	(CERN Collab.)

Extra Dimensions

For explanation of terms used and discussion of significant model dependence of following limits, see the "Extra Dimensions" review. Footnotes describe originally quoted limit. n indicates the number of extra dimensions.

Limits not encoded here are summarized in the "Extra Dimensions" review.

EXTRA DIMENSIONS

Updated Sept. 2007 by G.F. Giudice (CERN) and J.D. Wells (MCTP/Michigan).

I Introduction

The idea of using extra spatial dimensions to unify different forces started in 1914 with Nordstöm, who proposed a 5-dimensional vector theory to simultaneously describe electromagnetism and a scalar version of gravity. After the invention of general relativity, in 1919 Kaluza noticed that the 5-dimensional generalization of Einstein theory can simultaneously describe gravitational and electromagnetic interactions. The role of gauge invariance and the physical meaning of the compactification of extra dimensions was elucidated by Klein. However, the Kaluza-Klein (KK) theory failed in its original purpose because of internal inconsistencies and was essentially abandoned until the advent of supergravity in the late 1970's. Higher-dimensional theories were reintroduced in physics to exploit the special properties that supergravity and superstring theories possess for particular values of spacetime dimensions. More recently it was realized [1,2] that extra dimensions with

a fundamental scale of order TeV^{-1} could address the $M_W - M_{\text{Pl}}$ hierarchy problem and therefore have direct implications for collider experiments. Here we will review [3] the proposed scenarios with experimentally accessible extra dimensions.

II Gravity in Flat Extra Dimensions

II.1 Theoretical Setup

Following Ref. 1, let us consider a D -dimensional spacetime with $D = 4 + \delta$, where δ is the number of extra spatial dimensions. The space is factorized into $R^4 \times M_\delta$ (meaning that the 4-dimensional part of the metric does not depend on extra-dimensional coordinates), where M_δ is a δ -dimensional compact space with finite volume V_δ . For concreteness, we will consider a δ -dimensional torus of radius R , for which $V_\delta = (2\pi R)^\delta$. Standard Model (SM) fields are assumed to be localized on a $(3+1)$ -dimensional subspace. This assumption can be realized in field theory, but it is most natural [4] in the setting of string theory, where gauge and matter fields can be confined to live on "branes" (for a review see Ref. 5). On the other hand, gravity, which according to general relativity is described by the spacetime geometry, extends to all D dimensions. The Einstein action takes the form

$$S_E = \frac{\bar{M}_D^{2+\delta}}{2} \int d^4x d^\delta y \sqrt{-\det g} \mathcal{R}(g), \quad (1)$$

where x and y describe ordinary and extra coordinates, respectively. The metric g , the scalar curvature \mathcal{R} , and the reduced Planck mass \bar{M}_D refer to the D -dimensional theory. The effective action for the 4-dimensional graviton is obtained by restricting the metric indices to 4 dimensions and by performing the integral in y . Because of the above-mentioned factorization hypothesis, the integral in y reduces to the volume V_δ , and therefore the 4-dimensional reduced Planck mass is given by

$$\bar{M}_{\text{Pl}}^2 = \bar{M}_D^{2+\delta} V_\delta = \bar{M}_D^{2+\delta} (2\pi R)^\delta, \quad (2)$$

where $\bar{M}_{\text{Pl}} = M_{\text{Pl}}/\sqrt{8\pi} = 2.4 \times 10^{18}$ GeV. The same formula can be obtained from Gauss's law in extra dimensions [6]. Following ref. [7], we will consider $M_D = (2\pi)^\delta/(2+\delta)\bar{M}_D$ as the fundamental D -dimensional Planck mass.

The key assumption of Ref. 1 is that the hierarchy problem is solved because the truly fundamental scale of gravity M_D (and therefore the ultraviolet cut-off of field theory) lies around the TeV region. From Eq. (2) it follows that the correct value of \bar{M}_{Pl} can be obtained with a large value of $R M_D$. The inverse compactification radius is therefore given by

$$R^{-1} = M_D (M_D/\bar{M}_{\text{Pl}})^{2/\delta}, \quad (3)$$

which corresponds to 4×10^{-4} eV, 20 keV, 7 MeV for $M_D = 1$ TeV and $\delta = 2, 4, 6$, respectively. In this framework, gravity is weak because it is diluted in a large space ($R \gg M_D^{-1}$). Of course, a complete solution of the hierarchy problem would require a dynamical explanation for the radius stabilization at a large value.

A D -dimensional bosonic field can be expanded in Fourier modes in the extra coordinates

$$\phi(x, y) = \sum_{\vec{n}} \frac{\varphi^{(\vec{n})}(x)}{\sqrt{V_\delta}} \exp\left(i \frac{\vec{n} \cdot \vec{y}}{R}\right). \quad (4)$$

The sum is discrete because of the finite size of the compactified space. The fields $\varphi^{(\vec{n})}$ are called the n^{th} KK excitations (or modes) of ϕ , and correspond to particles propagating in 4 dimensions with masses $m_{(\vec{n})}^2 = |\vec{n}|^2/R^2 + m_0^2$, where m_0 is the mass of the zero mode. The D -dimensional graviton can then be recast as a tower of KK states with increasing mass. However, since R^{-1} in Eq. (3) is smaller than the typical energy resolution in collider experiments, the mass distribution of KK gravitons is practically continuous.

Although each KK graviton has a purely gravitational coupling suppressed by $\overline{M}_{\text{Pl}}^{-1}$, inclusive processes in which we sum over the large number of available gravitons have cross sections suppressed only by powers of M_D . Indeed, for scatterings with typical energy E , we expect $\sigma \sim E^\delta/M_D^{2+\delta}$, as evident from power-counting in D dimensions. Processes involving gravitons are therefore detectable in collider experiments if M_D is in the TeV region.

The astrophysical considerations described in Sec. II.6 set very stringent bounds on M_D for $\delta < 4$, in some cases even ruling out the possibility of observing any signal at the LHC. However, these bounds disappear if there are no KK gravitons lighter than about 100 MeV. Variations of the original model exist [8,9] in which the light KK gravitons receive small extra contributions to their masses, sufficient to evade the astrophysical bounds. Notice that collider experiments are nearly insensitive to such modifications of the infrared part of the KK graviton spectrum, since they mostly probe the heavy graviton modes. Therefore, in the context of these variations, it is important to test at colliders extra-dimensional gravity also for low values of δ , and even for $\delta = 1$ [9]. In addition to these direct experimental constraints, the proposal of gravity in flat extra dimensions has dramatic cosmological consequences and requires a rethinking of the thermal history of the universe for temperatures as low as the MeV scale.

II.2 Collider Signals in Linearized Gravity

By making a derivative expansion of Einstein gravity, one can construct an effective theory describing KK graviton interactions, which is valid for energies much smaller than M_D [7,10,11]. With the aid of this effective theory, it is possible to make predictions for graviton-emission processes at colliders. Since the produced gravitons interact with matter only with rates suppressed by inverse powers of \overline{M}_{Pl} , they will remain undetected leaving a “missing-energy” signature. Extra-dimensional gravitons have been searched for in the processes $e^+e^- \rightarrow \gamma + \cancel{E}$ and $e^+e^- \rightarrow Z + \cancel{E}$ at LEP, and $p\bar{p} \rightarrow \text{jet} + \cancel{E}_T$ and $p\bar{p} \rightarrow \gamma + \cancel{E}_T$ at the Tevatron. The combined LEP 95% CL limits are [12] $M_D > 1.60, 1.20, 0.94, 0.77, 0.66$ TeV for $\delta = 2, \dots, 6$ respectively. Experiments at the LHC will improve the sensitivity. However, the theoretical predictions for

the graviton-emission rates should be applied with care to hadron machines. The effective theory results are valid only for center-of-mass energy of the parton collision much smaller than M_D .

The effective theory under consideration also contains the full set of higher-dimensional operators, whose coefficients are, however, not calculable, because they depend on the ultraviolet properties of gravity. This is in contrast with graviton emission, which is a calculable process within the effective theory because it is linked to the infrared properties of gravity. The higher-dimensional operators are the analogue of the contact interactions described in ref. [13]. Of particular interest is the dimension-8 operator mediated by tree-level graviton exchange [7,11,14]

$$\mathcal{L}_{\text{int}} = \pm \frac{4\pi}{A_T^4} \mathcal{T}, \quad \mathcal{T} = \frac{1}{2} \left(T_{\mu\nu} T^{\mu\nu} - \frac{1}{\delta+2} T_\mu^\mu T_\nu^\nu \right), \quad (5)$$

where $T_{\mu\nu}$ is the energy momentum tensor. (There exist several alternate definitions in the literature for the cutoff in Eq. (5) including M_{TT} used in the Listings, where $M_{TT}^4 = (2/\pi)A_T^4$.) This operator gives anomalous contributions to many high-energy processes. The 95% CL limit from Bhabha scattering and diphoton production at LEP is [15] $A_T > 1.29$ (1.12) TeV for constructive (destructive) interference, corresponding to the \pm signs in Eq. (5). The analogous limit from Drell-Yan and diphotons at Tevatron is [16] $A_T > 1.43$ (1.27) TeV.

Graviton loops can be even more important than tree-level exchange, because they can generate operators of dimension lower than 8. For simple graviton loops, there is only one dimension-6 operator that can be generated (excluding Higgs fields in the external legs) [18,19],

$$\mathcal{L}_{\text{int}} = \pm \frac{4\pi}{A_T^2} \mathcal{Y}, \quad \mathcal{Y} = \frac{1}{2} \left(\sum_{f=q,\ell} \bar{f} \gamma_\mu \gamma_5 f \right)^2. \quad (6)$$

Here the sum extends over all quarks and leptons in the theory. The 95% CL combined LEP limit [20] from lepton-pair processes is $A_T > 17.2$ (15.1) TeV for constructive (destructive) interference, and $A_T > 15.3$ (11.5) TeV is obtained from $b\bar{b}$ production. Limits from graviton emission and effective operators cannot be compared in a model-independent way, unless one introduces some well-defined cutoff procedure (see, *e.g.*, Ref. 19).

II.3 The Transplanckian Regime

The use of linearized Einstein gravity, discussed in Sec. II.2, is valid for processes with typical center-of-mass energy $\sqrt{s} \ll M_D$. The physics at $\sqrt{s} \sim M_D$ can be described only with knowledge of the underlying quantum-gravity theory. Toy models have been used to mimic possible effects of string theory at colliders [21]. Once we access the transplanckian region $\sqrt{s} \gg M_D$, a semiclassical description of the scattering process becomes adequate. Indeed, in the transplanckian limit, the

Searches Particle Listings

Extra Dimensions

Schwarzschild radius for a colliding system with center-of-mass energy \sqrt{s} in $D = 4 + \delta$ dimensions,

$$R_S = \left[\frac{2^\delta \pi^{(\delta-3)/2}}{\delta+2} \Gamma\left(\frac{\delta+3}{2}\right) \frac{\sqrt{s}}{M_D^{\delta+2}} \right]^{1/(\delta+1)}, \quad (7)$$

is larger than the D -dimensional Planck length M_D^{-1} . Therefore, quantum-gravity effects are subleading with respect to classical gravitational effects (described by R_S).

If the impact parameter b of the process satisfies $b \gg R_S$, the transplanckian collision is determined by linear semiclassical gravitational scattering. The corresponding cross sections have been computed [22] in the eikonal approximation, valid in the limit of small deflection angle. The collider signal at the LHC is a dijet final state, with features characteristic of gravity in extra dimensions.

When $b < R_S$, we expect gravitational collapse and black-hole formation [23,24] (see Ref. 25 and references therein). The black-hole production cross section is estimated to be of order the geometric area $\sigma \sim \pi R_S^2$. This estimate has large uncertainties due, for instance, to the unknown amount of gravitational radiation emitted during collapse. Nevertheless, for M_D close to the weak scale, the black-hole production rate at the LHC is large. For example, the production cross section of 6 TeV black holes is about 10 pb, for $M_D = 1.5$ TeV. The produced black-hole emits thermal radiation with Hawking temperature $T_H = (\delta+1)/(4\pi R_S)$ until it reaches the Planck phase (where quantum-gravity effects become important). A black hole of initial mass M_{BH} completely evaporates with lifetime $\tau \sim M_{BH}^{(\delta+3)/(\delta+1)}/M_D^{2(\delta+2)/(\delta+1)}$, which typically is 10^{-26} – 10^{-27} s for $M_D = 1$ TeV. The black hole can be easily detected because it emits a significant fraction of visible (*i.e.*, non-gravitational) radiation, although the precise amount is not known in the general case of D dimensions. Computations exist [26] for the grey-body factors, which describe the distortion of the emitted radiation from pure black-body caused by the strong gravitational background field.

To trust the semiclassical approximation, the typical energy of the process has to be much larger than M_D . Given the present constraints on extra-dimensional gravity, it is clear that the maximum energy available at the LHC allows, at best, to only marginally access the transplanckian region. If gravitational scattering and black-hole production are observed at the LHC, it is likely that significant quantum-gravity (or string-theory) corrections will affect the semiclassical calculations or estimates. In the context of string theory, it is possible that the production of string-balls [27] dominates over black holes.

If M_D is around the TeV scale, transplanckian collisions would regularly occur in the interaction of high-energy cosmic rays with the earth's atmosphere and could be observed in present and future cosmic ray experiments [28,29].

II.4 Graviscalars

After compactification, the D -dimensional graviton contains KK towers of spin-2 gravitational states (as discussed above),

of spin-1 “graviphoton” states, and of spin-0 “graviscalar” states. In most processes, the graviphotons and graviscalars are much less important than their spin-2 counterparts. A single graviscalar tower is coupled to SM fields through the trace of the energy momentum tensor. The resulting coupling is, however, very weak for SM particles with small masses.

Perhaps the most accessible probe of the graviscalars would be through their allowed mixing with the Higgs boson [30] in the induced curvature-Higgs term of the 4-dimensional action. This can be recast as a contribution to the decay width of the SM Higgs boson into an invisible channel. Although the invisible branching fraction is a free parameter of the theory, it is more likely to be important when the SM Higgs boson width is particularly narrow ($m_H \lesssim 140$ GeV). The collider phenomenology of invisibly decaying Higgs bosons investigated in the literature is applicable here (see Ref. 31 and references therein).

II.5 Tests of the Gravitational Force Law

The theoretical developments in gravity with large extra dimensions have further stimulated interest in experiments looking for possible deviations from the gravitational inverse-square law (for a review, see Ref. 32). Such deviations are usually parametrized by a modified Newtonian potential of the form

$$V(r) = -G_N \frac{m_1 m_2}{r} [1 + \alpha \exp(-r/\lambda)]. \quad (8)$$

The experimental limits on the parameters α and λ are summarized in Fig. 1, taken from Ref. [33].

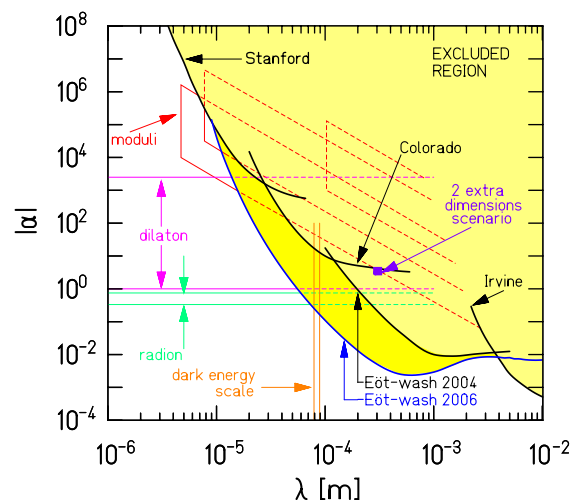


Figure 1: Experimental limits on α and λ of Eq. (8), which parametrize deviations from Newton’s law. From Ref. [33].

For gravity with δ extra dimensions, in the case of toroidal compactifications, the parameter α is given by $\alpha = 8 \delta/3$ and λ is the Compton wavelength of the first graviton Kaluza-Klein mode, equal to the radius R . From the results shown in Fig. 1, one finds $R < 37$ (44) μm at 95% CL for $\delta = 2$ (1)

which, using Eq. (3), becomes $M_D > 3.6$ TeV for $\delta = 2$. This bound is weaker than the astrophysical bounds discussed in Sec. II.6, which actually exclude the occurrence of any visible signal in planned tests of Newton's law. However, in the context of higher-dimensional theories, other particles like light gauge bosons, moduli or radions could mediate detectable modifications of Newton's law, without running up against the astrophysical limits.

II.6 Astrophysical Bounds

Because of the existence of the light and weakly-coupled KK gravitons, gravity in extra dimensions is strongly constrained by several astrophysical considerations (see Ref. [34] and references therein). The requirement that KK gravitons do not carry away more than half of the energy emitted by the supernova SN1987A gives the bounds [35] $M_D > 14$ (1.6) TeV for $\delta = 2$ (3). KK gravitons produced by all supernovae in the universe lead to a diffuse γ ray background generated by graviton decays into photons. Measurements by the EGRET satellite imply [36] $M_D > 38$ (4.1) TeV for $\delta = 2$ (3). Most of the KK gravitons emitted by supernova remnants and neutron stars are gravitationally trapped. The gravitons forming this halo occasionally decay, emitting photons. Limits on γ rays from neutron-star sources imply [34] $M_D > 200$ (16) TeV for $\delta = 2$ (3). The decay products of the gravitons forming the halo can hit the surface of the neutron star, providing a heat source. The low measured luminosities of some pulsars imply [34] $M_D > 750$ (35) TeV for $\delta = 2$ (3). These bounds are valid only if the graviton KK mass spectrum below about 100 MeV is not modified by distortions of the compactification space (see Sec. II.1).

III Gravity in Warped Extra Dimensions

III.1 Theoretical Setup

In the proposal of Ref. 2, the M_W - M_{Pl} hierarchy is explained using an extra-dimensional analogy of the classical gravitational redshift in curved space, as we illustrate below. The setup consists of a 5-dimensional space in which the fifth dimension is compactified on S^1/Z_2 , *i.e.*, a circle projected into a segment by identifying points of the circle opposite with respect to a given diameter. Each end-point of the segment (the "fixed-points" of the orbifold projection) is the location of a 3-dimensional brane. The two branes have equal but opposite tensions. We will refer to the negative-tension brane as the infrared (IR) brane, where SM fields are assumed to be localized, and the positive-tension brane as the ultraviolet (UV) brane. The bulk cosmological constant is fine-tuned such that the effective cosmological constant in the 3-dimensional space exactly cancels.

The solution of the Einstein equation in vacuum gives the metric corresponding to the line element

$$ds^2 = \exp(-2k|y|) \eta_{\mu\nu} dx^\mu dx^\nu - dy^2. \quad (9)$$

Here y is the 5th coordinate, with the UV and IR branes located at $y = 0$ and $y = \pi R$, respectively; R is the compactification

radius and k is the AdS curvature. The 4-dimensional metric in Eq. (9) is modified with respect to the flat Minkowski metric $\eta_{\mu\nu}$ by the factor $\exp(-2k|y|)$. This shows that the 5-dimensional space is not factorized, meaning that the 4-dimensional metric depends on the extra-dimensional coordinate y . This feature is key to the desired effect.

As is known from general relativity, the energy of a particle travelling through a gravitational field is redshifted by an amount proportional to $|g_{00}|^{-1/2}$, where g_{00} is the time-component of the metric. Analogously, energies (or masses) viewed on the IR brane ($y = \pi R$) are red-shifted with respect to their values at the UV brane ($y = 0$) by an amount equal to the warp factor $\exp(-\pi k R)$, as shown by Eq. (9):

$$m_{IR} = m_{UV} \exp(-\pi k R). \quad (10)$$

A mass $m_{UV} \sim \mathcal{O}(\overline{M}_{\text{Pl}})$ on the UV brane corresponds to a mass on the IR brane with a value $m_{IR} \sim \mathcal{O}(M_W)$, if $R \simeq 12k^{-1}$. A radius moderately larger than the fundamental scale k is therefore sufficient to reproduce the large hierarchy between the Planck and Fermi scales. A simple and elegant mechanism to stabilize the radius exists [38], by adding a scalar particle with a bulk mass and different potential terms on the two branes.

The effective theory describing the interaction of the KK modes of the graviton is characterized by two mass parameters, which we take to be m_1 and Λ_π . Both are a warp-factor smaller than the UV scale, and therefore they are naturally of order the weak scale. The parameter m_1 is the mass of the first KK graviton mode, from which the mass m_n of the generic n^{th} mode is determined,

$$m_n = \frac{x_n}{x_1} m_1. \quad (11)$$

Here x_n is the n^{th} root of the Bessel function J_1 ($x_1 = 3.83$, $x_2 = 7.02$ and, for large n , $x_n = (n + 1/4)\pi$). The parameter Λ_π determines the strength of the coupling of the KK gravitons $h_{\mu\nu}^{(n)}$ with the energy momentum tensor $T_{\mu\nu}$,

$$\mathcal{L} = -\frac{T^{\mu\nu}}{\overline{M}_{\text{Pl}}} h_{\mu\nu}^{(0)} - \frac{T^{\mu\nu}}{\Lambda_\pi} \sum_{n=1}^{\infty} h_{\mu\nu}^{(n)}. \quad (12)$$

In the approach discussed in Sec. II.1, M_{Pl} appears to us much larger than the weak scale because gravity is diluted in a large space. In the approach described in this section, the explanation lies instead in the non-trivial configuration of the gravitational field: the zero-mode graviton wavefunction is peaked around the UV brane and it has an exponentially small overlap with the IR brane where we live. The extra dimensions discussed in Sec. II.1 are large and "nearly flat;" the graviton excitations are very weakly coupled and have a mass gap that is negligibly small in collider experiments. Here, instead, the gravitons have a mass gap of \sim TeV size and become strongly-coupled at the weak scale.

III.2 Collider Signals

The KK excitations of the graviton, possibly being of order the TeV scale, are subject to experimental discovery at high-energy colliders. As discussed above, KK graviton production

Searches Particle Listings

Extra Dimensions

cross-sections and decay widths are set by the first KK mass m_1 and the graviton-matter interaction scale Λ_π . Some studies use m_1 and k as the independent parameters, and so it is helpful to keep in mind that the relationships between all of these parameters are

$$\frac{m_n}{\Lambda_\pi} = \frac{kx_n}{\overline{M}_{\text{Pl}}}, \quad \Lambda_\pi = \overline{M}_{\text{Pl}} \exp(-\pi kR), \quad (13)$$

where again x_n are the zeros of the J_1 Bessel function. Resonant and on-shell production of the n^{th} KK gravitons leads to characteristic peaks in the dilepton and diphoton invariant-mass spectra and it is probed at colliders for $\sqrt{s} \geq m_n$. Current limits from dimuon, dielectron, and diphoton channels at CDF and $D\bar{O}$ give the 95% CL limits $\Lambda_\pi > 4.3(2.6)$ TeV for $m_1 = 500(700)$ GeV [16,17].

Contact interactions arising from integrating out heavy KK modes of the graviton generate the dimension-8 operator \mathcal{T} , analogous to the one in Eq. (5) in the flat extra dimensions case. Although searches for effects of these non-renormalizable operators cannot confirm directly the existence of a heavy spin-2 state, they nevertheless provide a good probe of the model [39,40].

Searches for direct production of KK excitations of the graviton and contact interactions induced by gravity in compact extra-dimensional warped space will continue at the LHC. With the large increase in energy, one expects prime regions of the parameter space up to $m_n, \Lambda_\pi \sim 10$ TeV [39] to be probed.

If SM states are in the AdS bulk, KK graviton phenomenology becomes much more model dependent. Present limits and future collider probes of the masses and interaction strengths of the KK gravitons to matter fields are significantly reduced [41] in some circumstances, and each specific model of SM fields in the AdS bulk should be analyzed on a case-by-case basis.

For warped metrics, black-hole production is analogous to the case discussed in Sec. II.3, as long the radius of the black hole is smaller than the AdS radius $1/k$, when the space is effectively flat. For heavier black holes, the production cross section is expected to grow with energy only as $\log^2 E$, saturating the Froissart bound [37].

III.3 The Radion

The size of the warped extra-dimensional space is controlled by the value of the radion, a scalar field corresponding to an overall dilatation of the extra coordinates. Stabilizing the radion is required for a viable theory, and known stabilization mechanisms often imply that the radion is less massive than the KK excitations of the graviton [38], thus making it perhaps the lightest beyond-the-SM particle in this scenario.

The coupling of the radion r to matter is $\mathcal{L} = -rT/\Lambda_\varphi$, where T is the trace of the energy momentum tensor and $\Lambda_\varphi = \sqrt{24}\Lambda_\pi$ is expected to be near the weak scale. The relative couplings of r to the SM fields are similar to, but not exactly the same as, those of the Higgs boson. The partial widths are generally smaller by a factor of v/Λ_φ compared to SM Higgs decay widths, where $v = 246$ GeV is the vacuum

expectation value of the SM Higgs doublet. On the other hand, the trace anomaly that arises in the SM gauge groups by virtue of quantum effects enhances the couplings of the radion to gluons and photons over the naive v/Λ_φ rescaling of the Higgs couplings to these same particles. Thus, for example, one finds that the radion's large coupling to gluons [30,43] enables a sizeable $gg \rightarrow r$ cross section even for Λ_φ large compared to m_W .

Another subtlety of the radion is its ability to mix with the Higgs boson through the curvature-scalar interaction [30],

$$S_{mix} = -\xi \int d^4x \sqrt{-\det g_{\text{ind}}} R(g_{\text{ind}}) H^+ H, \quad (14)$$

where g_{ind} is the four-dimensional induced metric. With $\xi \neq 0$, there is neither a pure Higgs boson nor pure radion mass eigenstate. Mixing between states enables decays of the heavier eigenstate into lighter eigenstates if kinematically allowed. Overall, the production cross sections, widths and relative branching fractions can all be affected significantly by the value of the mixing parameter ξ [30,42,43,44]. Despite the various permutations of couplings and branching fractions that the radion and the Higgs-radion mixed states can have into SM particles, the search strategies for these particles at high-energy colliders are similar to those of the SM Higgs boson.

IV Standard Model Fields in Flat Extra Dimensions

IV.1 TeV-Scale Compactification

Not only gravity, but also SM fields could live in an experimentally accessible higher-dimensional space [45]. This hypothesis could lead to unification of gauge couplings at a low scale [46]. In contrast with gravity, these extra dimensions must be at least as small as about TeV^{-1} in order to avoid incompatibility with experiment. The canonical extra-dimensional space of this type is a 5th dimension compactified on the interval S^1/Z_2 , where again the radius of the S^1 is denoted R , and the Z_2 symmetry identifies $y \leftrightarrow -y$ of the extra-dimensional coordinate. The two fixed points $y = 0$ and $y = \pi R$ define the end-points of the compactification interval.

Let us first consider the case in which gauge fields live in extra dimensions, while matter and Higgs fields are confined to a 3-brane. The masses M_n of the gauge-boson KK excitations are related to the masses M_0 of the zero-mode normal gauge bosons by

$$M_n^2 = M_0^2 + \frac{n^2}{R^2}. \quad (15)$$

The KK excitations of the vector bosons have couplings to matter a factor of $\sqrt{2}$ larger than the zero modes ($g_n = \sqrt{2}g$). Therefore, if the first KK excitation is $\sim \text{TeV}$, tree-level virtual effects of the KK gauge bosons can have a significant effect on precision electroweak observables and high-energy processes such as $e^+e^- \rightarrow f\bar{f}$. In this theory one expects that observables will be shifted with respect to their SM value by a fractional amount proportional to [47]

$$V = 2 \sum_n \left(\frac{g_n^2}{g^2} \right) \frac{M_Z^2 R^2}{n^2} \sim \frac{2}{3} \pi^2 M_Z^2 R^2. \quad (16)$$

More complicated compactifications lead to more complicated representations of V . A global fit to all relevant observables, including precision electroweak data, Tevatron, HERA and LEP2 results, shows that $R^{-1} \gtrsim 6.8$ TeV is required [48,49]. The LHC with 100 fb^{-1} integrated luminosity would be able to search nearly as high as $R^{-1} \sim 16$ TeV [48].

Fermions can also be promoted to live in the extra dimensions. Although fermions are vector-like in 5-dimension, chiral states in 4-dimensions can be obtained by using the Z_2 symmetry of the orbifold. An interesting possibility to explain the observed spectrum of quark and lepton masses is to assume that different fermions are localized in different points of the extra dimension. Their different overlap with the Higgs wavefunction can generate a hierarchical structure of Yukawa couplings [50], although there are strong bounds on the non-universal couplings of fermions to the KK gauge bosons from flavor-violating processes [51].

The case in which all SM particles uniformly propagate in the bulk of an extra-dimensional space is referred to as Universal Extra Dimensions (UED) [52]. The absence of a reference brane that breaks translation invariance in the extra dimensional direction implies extra-dimensional momentum conservation. After compactification and after inclusion of boundary terms at the fixed points, the conservation law preserves only a discrete Z_2 parity (called KK-parity). The KK-parity of the n^{th} KK mode of each particle is $(-1)^n$. Thus, in UED, the first KK excitations can only be pair-produced and their virtual effect comes only from loop corrections. Therefore the ability to search for and constrain parameter space is diminished. The result is that for one extra dimension the limit on R^{-1} is between 300 and 500 GeV depending on the Higgs mass [53].

Because of KK-parity conservation, the lightest KK state is stable. Thus, one interesting consequence of UED is the possibility of the lightest KK state comprising the dark matter. After including radiative corrections [54], it is found that the lightest KK state is the first excitation of the hypercharge gauge boson $B^{(1)}$. It can constitute the cold dark matter of the universe if its mass is approximately 600 GeV [55], well above current collider limits. The LHC should be able to probe UED up to $R^{-1} \sim 1.5$ TeV [56], and thus possibly confirm the UED dark matter scenario.

An interesting and ambitious approach is to use extra dimensions to explain the hierarchy problem through Higgs-gauge unification [57]. The SM Higgs doublet is interpreted as the extra-dimensional component of an extended gauge symmetry acting in more than four dimensions, and the weak scale is protected by the extra-dimensional gauge symmetry. There are several obstacles to make this proposal fully realistic, but ongoing research is trying to overcome them.

IV.2 Grand Unification in Extra Dimensions

Extra dimensions offer a simple and elegant way to break GUT symmetries [58] by appropriate field boundary conditions in compactifications on orbifolds. In this case the size of the

relevant extra dimensions is much smaller than what has been considered so far, with compactification radii that are typically $\mathcal{O}(M_{\text{GUT}})$. This approach has several attractive features (for a review, see Ref. 59). The doublet-triplet splitting problem [60] is solved by projecting out the unwanted light Higgs triplet in the compactification. In the same way, one can eliminate the dangerous supersymmetric $d = 5$ proton-decay operators, or even forbid proton decay [61]. However, the prospects for proton-decay searches are not necessarily bleak. Because of the effect of the KK modes, the unification scale can be lowered to 10^{14} – 10^{15} GeV, enhancing the effect of $d = 6$ operators. The prediction for the proton lifetime is model-dependent.

V Standard Model Fields in Warped Extra Dimensions

V.1 Extra Dimensions and Strong Dynamics at the Weak Scale

In the original warped model of Ref. 2, all SM fields are confined on the IR brane, although to solve the hierarchy problem it is sufficient that only the Higgs field lives on the brane. The variation in which SM fermions and gauge bosons are bulk fields is interesting because it links warped extra dimensions to technicolor-like models with strong dynamics at the weak scale. This connection comes from the AdS/CFT correspondence [62], which relates the properties of AdS₅, 5-dimensional gravity with negative cosmological constant, to a strongly-coupled 4-dimensional conformal field theory (CFT). In the correspondence, the motion along the 5th dimension is interpreted as the renormalization-group flow of the 4-dimensional theory, with the UV brane playing the role of the Planck-mass cutoff and the IR brane as the breaking of the conformal invariance. Local gauge symmetries acting on the bulk of AdS₅ correspond to global symmetries of the 4-dimensional theory. The original warped model of Ref. 2 is then reinterpreted as an “almost CFT,” whose couplings run very slowly with the renormalization scale until the TeV scale is reached, where the theory develops a mass gap. In the variation in which SM fields, other than the Higgs, are promoted to the bulk, these fields correspond to elementary particles coupled to the CFT. Around the TeV scale the theory becomes strongly-interacting, producing a composite Higgs, which breaks electroweak symmetry. Notice the similarity with walking technicolor [63].

The most basic version of this theory is in conflict with electroweak precision measurements. To reduce the contribution to the ρ parameter, it is necessary to introduce an approximate global symmetry, a custodial $SU(2)$ under which the generators of $SU(2)_L$ transform as a triplet. Using the AdS/CFT correspondence, this requires the extension of the electroweak gauge symmetry to $SU(2)_L \times SU(2)_R \times U(1)$ in the bulk of the 5-dimensional theory [64]. Models along these lines have been constructed. The composite Higgs can be lighter than the strongly-interacting scale in models in which it is a pseudo-Goldstone boson [65]. Nevertheless, electroweak data provide strong constraints on such models.

Searches Particle Listings

Extra Dimensions

When SM fermions are promoted to 5 dimensions, they become non-chiral and can acquire a bulk mass. The fermions are localized in different positions along the 5th dimension, with an exponential dependence on the value of the bulk mass (in units of the AdS curvature). Since the masses of the ordinary zero-mode SM fermions depend on their wavefunction overlap with the Higgs (localized on the IR brane), large hierarchies in the mass spectrum of quarks and leptons can be obtained from order-unity variations of the bulk masses [66]. This mechanism can potentially explain the fermion mass pattern, and it can lead to new effects in flavor-changing processes, especially those involving the third-generation quarks [67]. The smallness of neutrino masses can also be explained, if right-handed neutrinos propagate in the bulk [68].

V.2 Higgsless Models

Extra dimensions offer new possibilities for breaking gauge symmetries. Even in the absence of physical scalars, electroweak symmetry can be broken by field boundary conditions on compactified spaces. The lightest KK modes of the gauge bosons corresponding to broken generators acquire masses equal to R^{-1} , the inverse of the compactification radius, now to be identified with M_W . In the ordinary 4-dimensional case, the SM without a Higgs boson violates unitarity at energies $E \sim 4\pi M_W/g \sim 1$ TeV. On the other hand, in extra dimensions, the breaking of unitarity in the longitudinal- W scattering amplitudes is delayed because of the contribution of the heavy KK gauge-boson modes [69]. The largest effect is obtained for one extra dimension, where the violation of unitarity occurs around $E \sim 12\pi^2 M_W/g \sim 10$ TeV. This is conceivably a large enough scale to render the strong dynamics, which is eventually responsible for unitarization, invisible to the processes measured by LEP experiments.

These Higgsless models, in their minimal version, are inconsistent with observations, because they predict new W gauge bosons with masses nM_W (with $n \geq 2$ integers) [70]. However, warping the 5th dimension has a double advantage [71]. The excited KK modes of the gauge bosons can all have masses in the TeV range, making them compatible with present collider limits. Also, by enlarging the bulk gauge symmetry to $SU(2)_L \times SU(2)_R \times U(1)$, one can obtain an approximate custodial symmetry, as described above, to tame tree-level corrections to ρ . If quarks and leptons are extended to the bulk, they can obtain masses through the electroweak-breaking effect on the boundaries. However at present, there is no model that reproduces the top quark mass and is totally consistent with electroweak data [72].

VI. Supersymmetry in Extra Dimensions

Extra dimensions have a natural home within string theory. Similarly, string theory and supersymmetry are closely connected, as the latter is implied by the former in most constructions. Coexistence between extra dimensions and supersymmetry is often considered a starting point for string model

building. From a low-energy model-building point of view, perhaps the most compelling reason to introduce extra dimensions with supersymmetry lies in the mechanism of supersymmetry breaking.

When the field periodic boundary conditions on the compactified space are twisted using an R -symmetry, different zero modes for bosons and fermions are projected out and supersymmetry is broken. This is known as the Scherk-Schwarz mechanism of supersymmetry breaking [73]. In the simplest approach [74], a 5th dimension with $R^{-1} \sim 1$ TeV is introduced in which the non-chiral matter (gauge and Higgs multiplets) live. The chiral matter (quark and lepton multiplets) live on the three-dimensional spatial boundary. S^1/Z_2 compactification of the 5th dimension, which simultaneously employs the Scherk-Schwarz mechanism, generates masses for the bulk fields (gauginos and higgsinos) of order R^{-1} . Boundary states (squarks and sleptons) get mass from loop corrections, and are parametrically smaller in value. The right-handed slepton is expected to be the lightest supersymmetric particle (LSP), which being charged is not a good dark matter candidate. Thus, this theory likely requires R -parity violation in order to allow this charged LSP to decay and not cause cosmological problems.

By allowing all supersymmetric fields to propagate in the bulk of a $S_1/Z_2 \times Z'_2$ compactified space, it is possible to construct a model [75] taking advantage of the nonlocal breaking of supersymmetry. In this case, there are no quadratic divergences (except for a Fayet-Iliopoulos term [76]) and the Higgs mass is calculable. In the low-energy effective theory there is a single Higgs doublet, two superpartners for each SM particle, and the stop is the LSP, requiring a small amount of R -parity breaking.

Supersymmetry in warped space is also an interesting possibility. Again, one can consider [77] the case of chiral fields confined to our ordinary 3+1 dimensions, and gravity and gauge fields living in the 5-dimensional bulk space. Rather than being TeV^{-1} size, the 5th dimension is strongly warped to generate the supersymmetry-breaking scale. In this case, the tree-level mass of the gravitino is $\sim 10^{-3}$ eV and the masses of the gauginos are $\sim \text{TeV}$. The sleptons and squarks get mass at one loop from gauge interactions and thus are diagonal in flavor space, creating no additional FCNC problems. It has also been proposed [78] that an approximately supersymmetric Higgs sector confined on the IR brane could coexist with non-supersymmetric SM fields propagating in the bulk of the warped space.

In conclusion, we should reiterate that an important general consequence of extra dimensional theories is retained in supersymmetric extensions: KK excitations of the graviton and/or gauge fields are likely to be accessible at the LHC if the scale of compactification is directly related to solving the hierarchy problem. Any given extra-dimensional theory has many aspects to it, but the KK excitation spectrum is the most generic and most robust aspect of the idea to test in experiments.

References

1. N. Arkani-Hamed *et al.*, Phys. Lett. **B429**, 263 (1998).
2. L. Randall and R. Sundrum, Phys. Rev. Lett. **83**, 3370 (1999).
3. For other reviews, see V. A. Rubakov, Phys. Usp. **44**, 871 (2001);
J. Hewett and M. Spiropulu, Ann. Rev. Nucl. and Part. Sci. **52**, 397 (2002);
R. Rattazzi, *Proc. of Cargese School of Particle Physics and Cosmology*, Corsica, France, 4-16 Aug 2003;
C. Csaki, hep-ph/0404096;
R. Sundrum, hep-th/0508134.
4. I. Antoniadis *et al.*, Phys. Lett. **B436**, 257 (1998).
5. J. Polchinski, "Lectures on D-branes," hep-th/9611050.
6. N. Arkani-Hamed *et al.*, Phys. Rev. **D59**, 086004 (1999).
7. G. F. Giudice *et al.*, Nucl. Phys. **B544**, 3 (1999).
8. N. Kaloper *et al.*, Phys. Rev. Lett. **85**, 928 (2000);
K. R. Dienes, Phys. Rev. Lett. **88**, 011601 (2002).
9. G. F. Giudice *et al.*, Nucl. Phys. **B706**, 455 (2005).
10. E. A. Mirabelli *et al.*, Phys. Rev. Lett. **82**, 2236 (1999).
11. T. Han *et al.*, Phys. Rev. **D59**, 105006 (1999).
12. LEP Exotica Working Group, LEP Exotica WG 2004-03.
13. K. Hagiwara *et al.*, "Searches for Quark and Lepton Compositeness," in this *Review*.
14. J. L. Hewett, Phys. Rev. Lett. **82**, 4765 (1999).
15. D. Bourilkov, hep-ex/0103039.
16. G. Landsberg, [D0 and CDF Collaboration], hep-ex/0412028.
17. V. M. Abazov *et al.*, [D0 Collaboration], Phys. Rev. Lett. **95**, 091801 (2005).
18. R. Contino *et al.*, JHEP **106**, 005 (2001).
19. G. F. Giudice and A. Strumia, Nucl. Phys. **B663**, 377 (2003).
20. LEP Working Group LEP2FF/02-03.
21. E. Dudas and J. Mourad, Nucl. Phys. **B575**, 3 (2000);
S. Cullen *et al.*, Phys. Rev. **D62**, 055012 (2000);
P. Burikham *et al.*, Phys. Rev. **D71**, 016005 (2005);
[Erratum-*ibid.*, **71**, 019905 (2005)].
22. G. F. Giudice *et al.*, Nucl. Phys. **B630**, 293 (2002).
23. S. B. Giddings and S. Thomas, Phys. Rev. **D65**, 056010 (2002).
24. S. Dimopoulos and G. Landsberg, Phys. Rev. Lett. **87**, 161602 (2001).
25. P. Kanti, Int. J. Mod. Phys. **A19**, 4899 (2004).
26. P. Kanti and J. March-Russell, Phys. Rev. **D66**, 024023 (2002);
Phys. Rev. **D67**, 104019 (2003).
27. S. Dimopoulos and R. Emparan, Phys. Lett. **B526**, 393 (2002).
28. J. L. Feng and A. D. Shapere, Phys. Rev. Lett. **88**, 021303 (2002).
29. R. Emparan *et al.*, Phys. Rev. **D65**, 064023 (2002).
30. G. F. Giudice *et al.*, Nucl. Phys. **B595**, 250 (2001).
31. D. Dominici, hep-ph/0503216.
32. E. G. Adelberger *et al.*, Ann. Rev. Nucl. and Part. Sci. **53**, 77 (2003).
33. D. J. Kapner *et al.*, Phys. Rev. Lett. **98**, 021101 (2007).
34. S. Hannestad and G. G. Raffelt, Phys. Rev. Lett. **88**, 071301 (2002).
35. C. Hanhart *et al.*, Phys. Lett. **B509**, 1 (2002).
36. S. Hannestad and G. Raffelt, Phys. Rev. Lett. **87**, 051301 (2001).
37. S. B. Giddings, Phys. Rev. **D67**, 126001 (2003).
38. W. D. Goldberger and M. B. Wise, Phys. Rev. Lett. **83**, 4922 (1999).
39. H. Davoudiasl *et al.*, Phys. Rev. Lett. **84**, 2080 (2000).
40. K. Cheung, hep-ph/0409028.
41. H. Davoudiasl *et al.*, Phys. Rev. **D63**, 075004 (2001).
42. C. Csaki *et al.*, Phys. Rev. **D63**, 065002 (2001).
43. D. Dominici *et al.*, Nucl. Phys. **B671**, 243 (2003).
44. K. Cheung *et al.*, Phys. Rev. **D69**, 075011 (2004).
45. I. Antoniadis, Phys. Lett. **B246**, 377 (1990).
46. K. R. Dienes *et al.*, Phys. Lett. **B436**, 55 (1998);
K. R. Dienes *et al.*, Nucl. Phys. **B537**, 47 (1999).
47. T. G. Rizzo and J. D. Wells, Phys. Rev. **D61**, 016007 (2000).
48. K. Cheung and G. Landsberg, Phys. Rev. **D65**, 076003 (2002).
49. R. Barbieri *et al.*, Nucl. Phys. **B703**, 127 (2004).
50. N. Arkani-Hamed and M. Schmaltz, Phys. Rev. **D61**, 033005 (2000).
51. A. Delgado *et al.*, JHEP **0001**, 030 (2000).
52. T. Appelquist *et al.*, Phys. Rev. **D64**, 035002 (2001).
53. T. Appelquist and H. U. Yee, Phys. Rev. **D67**, 055002 (2003).
54. H. C. Cheng *et al.*, Phys. Rev. **D66**, 036005 (2002).
55. G. Servant and T. M. P. Tait, Nucl. Phys. **B650**, 391 (2003);
F. Burnell and G. D. Kribs, hep-ph/0509118;
K. Kong and K. T. Matchev, hep-ph/0509119.
56. H. C. Cheng *et al.*, Phys. Rev. **D66**, 056006 (2002).
57. N. S. Manton, Nucl. Phys. **B158**, 141 (1979).
58. Y. Kawamura, Prog. Theor. Phys. **105**, 999 (2001).
59. L. J. Hall and Y. Nomura, Annals Phys. **306**, 132 (2003).
60. S. Raby, "Grand Unified Theories," in this *Review*.
61. G. Altarelli and F. Feruglio, Phys. Lett. **B5111**, 257 (2001);
L. J. Hall and Y. Nomura, Phys. Rev. **D64**, 055003 (2001).
62. J. M. Maldacena, Adv. Theor. Math. Phys. **2**, 231 (1998) [Int. J. Theor. Phys. **38**, 1113 (1999)].
63. R.S. Chivukula *et al.*, "Technicolor," in this *Review*.
64. K. Agashe *et al.*, JHEP **0308**, 050 (2003).
65. K. Agashe *et al.*, Nucl. Phys. **B719**, 165 (2005).
66. T. Gherghetta and A. Pomarol, Nucl. Phys. **B586**, 141 (2000);
S. J. Huber and Q. Shafi, Phys. Lett. **B498**, 256 (2001).
67. K. Agashe *et al.*, Phys. Rev. **D71**, 016002 (2005).
68. Y. Grossman and M. Neubert, Phys. Lett. **B474**, 361 (2000).
69. R. S. Chivukula *et al.*, Phys. Lett. **B525**, 175 (2002).
70. C. Csaki *et al.*, Phys. Rev. **D69**, 055006 (2004).
71. C. Csaki *et al.*, Phys. Rev. Lett. **92**, 101802 (2004).
72. R. Barbieri *et al.*, Phys. Lett. **B591**, 141 (2004);
G. Cacciapaglia *et al.*, Phys. Rev. **D70**, 075014 (2004).

Searches Particle Listings

Extra Dimensions

73. J. Scherk and J. H. Schwarz, Phys. Lett. **B82**, 60 (1979).
 74. A. Pomarol and M. Quiros, Phys. Lett. **B438**, 255 (1998);
 A. Delgado *et al.*, Phys. Rev. **D60**, 095008 (1999).
 75. R. Barbieri *et al.*, Phys. Rev. **D63**, 105007 (2001).
 76. D. M. Ghilencea *et al.*, Nucl. Phys. **B619**, 385 (2001).
 77. T. Gherghetta and A. Pomarol, Nucl. Phys. **B602**, 3
 (2001).
 78. T. Gherghetta and A. Pomarol, Phys. Rev. **D67**, 085018
 (2003).

Limits on R from Deviations in Gravitational Force Law

This section includes limits on the size of extra dimensions from deviations in the Newtonian ($1/r^2$) gravitational force law at short distances. Deviations are parametrized by a gravitational potential of the form $V = -(G m m'/r) [1 + \alpha \exp(-r/R)]$. For δ toroidal extra dimensions of equal size, $\alpha = 8\delta/3$. Quoted bounds are for $\delta = 2$ unless otherwise noted.

VALUE (μm)	CL%	DOCUMENT ID	COMMENT
••• We do not use the following data for averages, fits, limits, etc. •••			
< 30	95	1 DECCA 07A	Torsion pendulum
< 47	95	2 KAPNER 07	Torsion pendulum
< 130	95	3 TU 07	Torsion pendulum
< 200	95	4 SMULLIN 05	Microcantilever
< 190	95	5 HOYLE 04	Torsion pendulum
		6 CHIAVERINI 03	Microcantilever
		7 LONG 03	Microcantilever
		8 HOYLE 01	Torsion pendulum
		9 HOSKINS 85	Torsion pendulum

- ¹ DECCA 07A search for new forces and obtain bounds in the region with strengths $|\alpha| \approx 10^{13}-10^{18}$ and length scales $R = 20-86$ nm. See their Fig. 6. This bound does not place limits on the size of extra flat dimensions.
² KAPNER 07 search for new forces, probing a range of $\alpha \approx 10^{-3}-10^5$ and length scales $R \approx 10-1000$ μm . For $\delta = 1$ the bound on R is 44 μm . For $\delta = 2$, the bound is expressed in terms of M_* , here translated to a bound on the radius. See their Fig. 6 for details on the bound.
³ TU 07 search for new forces probing a range of $|\alpha| \approx 10^{-1}-10^5$ and length scales $R \approx 20-1000$ μm . For $\delta = 1$ the bound on R is 53 μm . See their Fig. 3 for details on the bound.
⁴ SMULLIN 05 search for new forces, and obtain bounds in the region with strengths $\alpha \approx 10^3-10^8$ and length scales $R = 6-20$ μm . See their Figs. 1 and 16 for details on this work. This work does not place limits on the size of extra flat dimensions.
⁵ HOYLE 04 search for new forces, probing α down to 10^{-2} and distances down to 10 μm . Quoted bound on R is for $\delta = 2$. For $\delta = 1$, bound goes to 160 μm . See their Fig. 34 for details on the bound.
⁶ CHIAVERINI 03 search for new forces, probing α above 10^4 and λ down to 3 μm , finding no signal. See their Fig. 4 for details on the bound. This bound does not place limits on the size of extra flat dimensions.
⁷ LONG 03 search for new forces, probing α down to 3, and distances down to about 10 μm . See their Fig. 4 for details on the bound.
⁸ HOYLE 01 search for new forces, probing α down to 10^{-2} and distances down to 20 μm . See their Fig. 4 for details on the bound. The quoted bound is for $\alpha \geq 3$.
⁹ HOSKINS 85 search for new forces, probing distances down to 4 mm. See their Fig. 13 for details on the bound. This bound does not place limits on the size of extra flat dimensions.

Limits on R from On-Shell Production of Gravitons: $\delta = 2$

This section includes limits on on-shell production of gravitons in collider and astrophysical processes. Bounds quoted are on R , the assumed common radius of the flat extra dimensions, for $\delta = 2$ extra dimensions. Studies often quote bounds in terms of derived parameter; experiments are actually sensitive to the masses of the KK gravitons: $m_{\vec{n}} = |\vec{n}|/R$. See the Review on "Extra Dimensions" for details. Bounds are given in μm for $\delta=2$.

VALUE (μm)	CL%	DOCUMENT ID	TECN	COMMENT
••• We do not use the following data for averages, fits, limits, etc. •••				
< 350	95	10 ABULENCIA,A 06	06 CDF	$p\bar{p} \rightarrow jG$
< 270	95	11 ABDALLAH 05B	05B DLPH	$e^+e^- \rightarrow \gamma G$
< 210	95	12 ACHARD 04E	04E L3	$e^+e^- \rightarrow \gamma G$
< 480	95	13 ACOSTA 04C	04C CDF	$\bar{p}p \rightarrow jG$
< 0.00038	95	14 CASSE 04	04	Neutron star γ sources
< 610	95	15 ABAZOV 03	03 D0	$\bar{p}p \rightarrow jG$
< 0.96	95	16 HANNESTAD 03	03	Supernova cooling
< 0.096	95	17 HANNESTAD 03	03	Diffuse γ background
< 0.051	95	18 HANNESTAD 03	03	Neutron star γ sources
< 0.00016	95	19 HANNESTAD 03	03	Neutron star heating
< 300	95	20 HEISTER 03C	03C ALEP	$e^+e^- \rightarrow \gamma G$
		21 FAIRBAIRN 01	01	Cosmology
		22 HANHART 01	01	Supernova cooling
		23 CASSISI 00	00	Red giants
< 0.66	95	24 ACCIARRI 99s	99s L3	$e^+e^- \rightarrow ZG$
< 1300	95			

Limits on R from On-Shell Production of Gravitons: $\delta \geq 3$

This section includes limits similar to those in the previous section, but for $\delta = 3$ extra dimensions. Bounds are given in nm for $\delta = 3$. Entries are also shown for papers examining models with $\delta > 3$.

VALUE (nm)	CL%	DOCUMENT ID	TECN	COMMENT
••• We do not use the following data for averages, fits, limits, etc. •••				
< 3.6	95	10 ABULENCIA,A 06	06 CDF	$p\bar{p} \rightarrow jG$
< 3.5	95	11 ABDALLAH 05B	05B DLPH	$e^+e^- \rightarrow \gamma G$
< 2.9	95	12 ACHARD 04E	04E L3	$e^+e^- \rightarrow \gamma G$
		13 ACOSTA 04C	04C CDF	$\bar{p}p \rightarrow jG$
< 0.0042	95	14 CASSE 04	04	Neutron star γ sources
< 6.1	95	15 ABAZOV 03	03 D0	$\bar{p}p \rightarrow jG$
< 1.14	95	16 HANNESTAD 03	03	Supernova cooling
< 0.025	95	17 HANNESTAD 03	03	Diffuse γ background
< 0.11	95	18 HANNESTAD 03	03	Neutron star γ sources
< 0.0026	95	19 HANNESTAD 03	03	Neutron star heating
< 3.9	95	20 HEISTER 03C	03C ALEP	$e^+e^- \rightarrow \gamma G$
		21 FAIRBAIRN 01	01	Cosmology
< 0.8	95	22 HANHART 01	01	Supernova cooling
		23 CASSISI 00	00	Red giants
< 18	95	24 ACCIARRI 99s	99s L3	$e^+e^- \rightarrow ZG$

- ¹⁰ ABULENCIA,A 06 search for $p\bar{p} \rightarrow jG$ using 368 pb^{-1} of data at $\sqrt{s} = 1.96$ TeV. See their Table II for bounds for all $\delta \leq 6$.
¹¹ ABDALLAH 05B search for $e^+e^- \rightarrow \gamma G$ at $\sqrt{s} = 180-209$ GeV to place bounds on the size of extra dimensions and the fundamental scale. Limits for all $\delta \leq 6$ are given in their Table 6. These limits supersede those in ABREU 00Z.
¹² ACHARD 04E search for $e^+e^- \rightarrow \gamma G$ at $\sqrt{s} = 189-209$ GeV to place bounds on the size of extra dimensions and the fundamental scale. See their Table 8 for limits with $\delta \leq 8$. These limits supersede those in ACCIARRI 99R.
¹³ ACOSTA 04C search for $\bar{p}p \rightarrow jG$ at $\sqrt{s} = 1.8$ TeV to place bounds on the size of extra dimensions and the fundamental scale. See their paper for bounds on $\delta = 4, 6$.
¹⁴ CASSE 04 obtain a limit on R from the gamma-ray emission of point γ sources that arises from the photon decay of gravitons around newly born neutron stars, applying the technique of HANNESTAD 03 to neutron stars in the galactic bulge. Limits for all $\delta \leq 7$ are given in their Table I.
¹⁵ ABAZOV 03 search for $p\bar{p} \rightarrow jG$ at $\sqrt{s} = 1.8$ TeV to place bounds on M_D for 2 to 7 extra dimensions, from which these bounds on R are derived. See their paper for bounds on intermediate values of δ . We quote results without the approximate NLO scaling introduced in the paper.
¹⁶ HANNESTAD 03 obtain a limit on R from graviton cooling of supernova SN1987a. Limits for all $\delta \leq 7$ are given in their Tables V and VI.
¹⁷ HANNESTAD 03 obtain a limit on R from gravitons emitted in supernovae and which subsequently decay, contaminating the diffuse cosmic γ background. Limits for all $\delta \leq 7$ are given in their Tables V and VI. These limits supersede those in HANNESTAD 02.
¹⁸ HANNESTAD 03 obtain a limit on R from gravitons emitted in two recent supernovae and which subsequently decay, creating point γ sources. Limits for all $\delta \leq 7$ are given in their Tables V and VI. These limits are corrected in the published erratum.
¹⁹ HANNESTAD 03 obtain a limit on R from the heating of old neutron stars by the surrounding cloud of trapped KK gravitons. Limits for all $\delta \leq 7$ are given in their Tables V and VI. These limits supersede those in HANNESTAD 02.
²⁰ HEISTER 03C use the process $e^+e^- \rightarrow \gamma G$ at $\sqrt{s} = 189-209$ GeV to place bounds on the size of extra dimensions and the scale of gravity. See their Table 4 for limits with $\delta \leq 6$ for derived limits on M_D .
²¹ FAIRBAIRN 01 obtains bounds on R from over production of KK gravitons in the early universe. Bounds are quoted in paper in terms of fundamental scale of gravity. Bounds depend strongly on temperature of QCD phase transition and range from $R < 0.13$ μm to 0.001 μm for $\delta=2$; bounds for $\delta=3,4$ can be derived from Table 1 in the paper.
²² HANHART 01 obtain bounds on R from limits on graviton cooling of supernova SN 1987a using numerical simulations of proto-neutron star neutrino emission.
²³ CASSISI 00 obtain rough bounds on M_D (and thus R) from red giant cooling for $\delta=2,3$. See their paper for details.
²⁴ ACCIARRI 99s search for $e^+e^- \rightarrow ZG$ at $\sqrt{s} = 189$ GeV. Limits on the gravity scale are found in their Table 2, for $\delta \leq 4$.

Mass Limits on M_{TT}

This section includes limits on the cut-off mass scale, M_{TT} , of dimension-8 operators from KK graviton exchange in models of large extra dimensions. Ambiguities in the UV-divergent summation are absorbed into the parameter λ , which is taken to be $\lambda = \pm 1$ in the following analyses. Bounds for $\lambda = -1$ are shown in parenthesis after the bound for $\lambda = +1$, if appropriate. Different papers use slightly different definitions of the mass scale. The definition used here is related to another popular convention by $M_{TT}^2 = (2/\pi) \Lambda_{T,1}^2$, as discussed in the above Review on "Extra Dimensions."

VALUE (TeV)	CL%	DOCUMENT ID	TECN	COMMENT
••• We do not use the following data for averages, fits, limits, etc. •••				
> 1.1 (> 1.0)	95	25 SCHAEEL 07A	07A ALEP	$e^+e^- \rightarrow e^+e^-$
> 0.898 (> 0.998)	95	26 ABDALLAH 06C	06C DLPH	$e^+e^- \rightarrow \ell^+\ell^-$
> 0.853 (> 0.939)	95	27 GERDES 06	06	$p\bar{p} \rightarrow e^+e^-, \gamma\gamma$
> 0.96 (> 0.93)	95	28 ABAZOV 05V	05V D0	$p\bar{p} \rightarrow \mu^+\mu^-$
> 0.78 (> 0.79)	95	29 CHEKANOV 04B	04B ZEUS	$e^\pm p \rightarrow e^\pm X$
> 0.805 (> 0.956)	95	30 ABBIENDI 03D	03D OPAL	$e^+e^- \rightarrow \gamma\gamma$
> 0.7 (> 0.7)	95	31 ACHARD 03D	03D L3	$e^+e^- \rightarrow ZZ$
> 0.82 (> 0.78)	95	32 ADLOFF 03	03 H1	$e^\pm p \rightarrow e^\pm X$
> 1.28 (> 1.25)	95	33 GIUDICE 03	03 RVUE	
> 20.6 (> 15.7)	95	34 GIUDICE 03	03 RVUE	Dim-6 operators
> 0.80 (> 0.85)	95	35 HEISTER 03C	03C ALEP	$e^+e^- \rightarrow \gamma\gamma$
> 0.84 (> 0.99)	95	36 ACHARD 02D	02D L3	$e^+e^- \rightarrow \gamma\gamma$
> 1.2 (> 1.1)	95	37 ABBOTT 01	01 D0	$p\bar{p} \rightarrow e^+e^-, \gamma\gamma$
> 0.60 (> 0.63)	95	38 ABBIENDI 00R	00R OPAL	$e^+e^- \rightarrow \mu^+\mu^-$

> 0.63 (> 0.50)	95	38	ABBIENDI	00R	OPAL	$e^+e^- \rightarrow \tau^+\tau^-$
> 0.68 (> 0.61)	95	38	ABBIENDI	00R	OPAL	$e^+e^- \rightarrow \mu^+\mu^-, \tau^+\tau^-$
> 0.680 (> 0.542)	95	40	ABREU	00A	DLPH	$e^+e^- \rightarrow \gamma\gamma$
> 15–28	99.7	41	CHANG	00B	RVUE	Electroweak
> 0.98	95	42	CHEUNG	00	RVUE	$e^+e^- \rightarrow \gamma\gamma$
> 0.29–0.38	95	43	GRAESSER	00	RVUE	$(g-2)_\mu$
> 0.50–1.1	95	44	HAN	00	RVUE	Electroweak
> 2.0 (> 2.0)	95	45	MATHEWS	00	RVUE	$\bar{p}p \rightarrow jj$
> 1.0 (> 1.1)	95	46	MELE	00	RVUE	$e^+e^- \rightarrow VV$
		47	ABBIENDI	99P	OPAL	
		48	ACCIARRI	99M	L3	
		49	ACCIARRI	99S	L3	
> 1.412 (> 1.077)	95	50	BOURLIKOV	99		$e^+e^- \rightarrow e^+e^-$

25 SCHAEL 07A use e^+e^- collisions at $\sqrt{s} = 189\text{--}209$ GeV to place lower limits on Λ_T , here converted to limits on M_{TT} .

26 ABDALLAH 06C use e^+e^- collisions at $\sqrt{s} \sim 130\text{--}207$ GeV to place lower limits on M_{TT} , which is equivalent to their definition of M_S . Bound shown includes all possible final state leptons, $\ell = e, \mu, \tau$. Bounds on individual leptonic final states can be found in their Table 31.

27 GERDES 06 use 100 to 110 pb^{-1} of data from $p\bar{p}$ collisions at $\sqrt{s} = 1.8$ TeV, as recorded by the CDF Collaboration during Run I of the Tevatron. Bound shown includes a K -factor of 1.3. Bounds on individual e^+e^- and $\gamma\gamma$ final states are found in their Table 1.

28 ABAZOV 05V use 246 pb^{-1} of data from $p\bar{p}$ collisions at $\sqrt{s} = 1.96$ TeV to search for deviations in the differential cross section to $\mu^+\mu^-$ from graviton exchange.

29 CHEKANOV 04B search for deviations in the differential cross section of $e^\pm p \rightarrow e^\pm X$ with 130 pb^{-1} of combined data and Q^2 values up to 40,000 GeV^2 to place a bound on M_{TT} .

30 ABBIENDI 03D use e^+e^- collisions at $\sqrt{s}=181\text{--}209$ GeV to place bounds on the ultraviolet scale M_{TT} , which is equivalent to their definition of M_S .

31 ACHARD 03D look for deviations in the cross section for $e^+e^- \rightarrow ZZ$ from $\sqrt{s} = 200\text{--}209$ GeV to place a bound on M_{TT} .

32 ADLOFF 03 search for deviations in the differential cross section of $e^\pm p \rightarrow e^\pm X$ at $\sqrt{s}=301$ and 319 GeV to place bounds on M_{TT} .

33 GIUDICE 03 review existing experimental bounds on M_{TT} and derive a combined limit.

34 GIUDICE 03 place bounds on Λ_6 , the coefficient of the gravitationally-induced dimension-6 operator $(2\pi\lambda/\Lambda_6^2)(\sum \bar{T}_i\gamma_\mu\gamma^5\eta)(\sum \bar{T}_j\mu\gamma^5\eta)$, using data from a variety of experiments. Results are quoted for $\lambda=\pm 1$ and are independent of δ .

35 HEISTER 03C use e^+e^- collisions at $\sqrt{s}=189\text{--}209$ GeV to place bounds on the scale of dim-8 gravitational interactions. Their M_S^\pm is equivalent to our M_{TT} with $\lambda=\pm 1$.

36 ACHARD 02 search for s -channel graviton exchange effects in $e^+e^- \rightarrow \gamma\gamma$ at $E_{\text{cm}} = 192\text{--}209$ GeV.

37 ABBOTT 01 search for variations in differential cross sections to e^+e^- and $\gamma\gamma$ final states at the Tevatron.

38 ABBIENDI 00R uses e^+e^- collisions at $\sqrt{s}=189$ GeV.

39 ABREU 00A search for s -channel graviton exchange effects in $e^+e^- \rightarrow \gamma\gamma$ at $E_{\text{cm}} = 189\text{--}202$ GeV.

40 ABREU 00S uses e^+e^- collisions at $\sqrt{s}=183$ and 189 GeV. Bounds on μ and τ individual final states given in paper.

41 CHANG 00B derive 3σ limit on M_{TT} of (28,19,15) TeV for $\delta=(2,4,6)$ respectively assuming the presence of a torsional coupling in the gravitational action. Highly model dependent.

42 CHEUNG 00 obtains limits from anomalous diphoton production at OPAL due to graviton exchange. Original limit for $\delta=4$. However, unknown UV theory renders δ dependence unreliable. Original paper works in HLZ convention.

43 GRAESSER 00 obtains a bound from graviton contributions to $g-2$ of the muon through loops of 0.29 TeV for $\delta=2$ and 0.38 TeV for $\delta=4,6$. Limits scale as $\lambda^{1/2}$. However calculational scheme not well-defined without specification of high-scale theory. See the "Extra Dimensions Review."

44 HAN 00 calculates corrections to gauge boson self-energies from KK graviton loops and constrain them using S and T . Bounds on M_{TT} range from 0.5 TeV ($\delta=6$) to 1.1 TeV ($\delta=2$); see text. Limits have strong dependence, $\lambda^{\delta+2}$, on unknown λ coefficient.

45 MATHEWS 00 search for evidence of graviton exchange in CDF and DØ dijet production data. See their Table 2 for slightly stronger δ -dependent bounds. Limits expressed in terms of $\bar{M}_S^4 = M_{TT}^4/8$.

46 MELE 00 obtains bound from KK graviton contributions to $e^+e^- \rightarrow VV$ ($V=\gamma, W, Z$) at LEP. Authors use Hewett conventions.

47 ABBIENDI 99P search for s -channel graviton exchange effects in $e^+e^- \rightarrow \gamma\gamma$ at $E_{\text{cm}}=189$ GeV. The limits $G_\pm > 660$ GeV and $G_\pm > 634$ GeV are obtained from combined $E_{\text{cm}}=183$ and 189 GeV data, where G_\pm is a scale related to the fundamental gravity scale.

48 ACCIARRI 99M search for the reaction $e^+e^- \rightarrow \gamma G$ and s -channel graviton exchange effects in $e^+e^- \rightarrow \gamma\gamma, W^+W^-, ZZ, e^+e^-, \mu^+\mu^-, \tau^+\tau^-, q\bar{q}$ at $E_{\text{cm}}=183$ GeV. Limits on the gravity scale are listed in their Tables 1 and 2.

49 ACCIARRI 99S search for the reaction $e^+e^- \rightarrow ZG$ and s -channel graviton exchange effects in $e^+e^- \rightarrow \gamma\gamma, W^+W^-, ZZ, e^+e^-, \mu^+\mu^-, \tau^+\tau^-, q\bar{q}$ at $E_{\text{cm}}=189$ GeV. Limits on the gravity scale are listed in their Tables 1 and 2.

50 BOURLIKOV 99 performs global analysis of LEP data on e^+e^- collisions at $\sqrt{s}=183$ and 189 GeV. Bound is on Λ_T .

Direct Limits on Gravitational or String Mass Scale

This section includes limits on the fundamental gravitational scale and/or the string scale from processes which depend directly on one or the other of these scales.

VALUE (TeV)	DOCUMENT ID	TECN	COMMENT
> 1–2	51	ANCHORDOQ.02B	RVUE Cosmic Rays
> 0.49	52	ACCIARRI	00P L3 $e^+e^- \rightarrow e^+e^-$

- 51 ANCHORDOQUI 02B derive bound on M_D from non-observation of black hole production in high-energy cosmic rays. Bound is stronger for larger δ , but depends sensitively on threshold for black hole production.
- 52 ACCIARRI 00P uses e^+e^- collisions at $\sqrt{s}=183$ and 189 GeV. Bound on string scale M_S from massive string modes. M_S is defined in hep-ph/0001166 by $M_S(1/\pi)^{1/8}\alpha^{-1/4} = M$ where $(4\pi G)^{-1} = M^{n+2}R^n$.

Limits on $1/R = M_c$

This section includes limits on $1/R = M_c$, the compactification scale in models with TeV extra dimensions, due to exchange of Standard Model KK excitations. Bounds assume fermions are not in the bulk, unless stated otherwise. See the "Extra Dimensions" review for discussion of model dependence.

VALUE (TeV)	CL%	DOCUMENT ID	TECN	COMMENT
> 0.6	95	53	HAISCH	07 RVUE $\bar{B} \rightarrow X_S \gamma$
> 0.6	90	54	GOGOLADZE	06 RVUE Electroweak
> 3.3	95	55	CORNET	00 RVUE Electroweak
> 3.3–3.8	95	56	RIZZO	00 RVUE Electroweak

• • • We do not use the following data for averages, fits, limits, etc. • • •

53 HAISCH 07 use inclusive \bar{B} -meson decays to place a Higgs mass independent bound on the compactification scale $1/R$ in the minimal universal extra dimension model.

54 GOGOLADZE 06 use electroweak precision observables to place a lower bound on the compactification scale in models with universal extra dimensions. Bound assumes a 115 GeV Higgs mass. See their Fig. 3 for the bound as a function of the Higgs mass.

55 CORNET 00 translates a bound on the coefficient of the 4-fermion operator $(\bar{\ell}\gamma_\mu\tau^\alpha\ell)(\bar{\ell}\gamma^\mu\tau^\alpha\ell)$ derived by Hagiwara and Matsumoto into a limit on the mass scale of KK W bosons.

56 RIZZO 00 obtains limits from global electroweak fits in models with a Higgs in the bulk (3.8 TeV) or on the standard brane (3.3 TeV).

Limits on Kaluza-Klein Gravitons in Warped Extra Dimensions

This section places limits on the mass of the first Kaluza-Klein (KK) excitation of the graviton in the warped extra dimension model of Randall and Sundrum. Experimental bounds depend strongly on the warp parameter, k . See the "Extra Dimensions" review for a full discussion.

VALUE	DOCUMENT ID	TECN	COMMENT
• • • We do not use the following data for averages, fits, limits, etc. • • •			
	57	AALTONEN	07G CDF $p\bar{p} \rightarrow G \rightarrow \gamma\gamma$
	58	AALTONEN	07H CDF $p\bar{p} \rightarrow G \rightarrow e\bar{e}$
	59	ABAZOV	05N DØ $p\bar{p} \rightarrow G \rightarrow \ell\ell, \gamma\gamma$
	60	ABULENCIA	05A CDF $p\bar{p} \rightarrow G \rightarrow \ell\bar{\ell}$

57 AALTONEN 07G use $p\bar{p}$ collisions at 1.96 TeV to search for KK gravitons in warped extra dimensions. They search for graviton resonances decaying to photons using 1.2 fb^{-1} of data. For warp parameter values of $k/\bar{M}_P = 0.1, 0.05,$ and 0.01 the bounds on the graviton mass are 850, 694, and 230 GeV, respectively. See their Fig. 3 for more details.

58 AALTONEN 07H use $p\bar{p}$ collisions at 1.96 TeV to search for KK gravitons in warped extra dimensions. They search for graviton resonances decaying to electrons using 1.3 fb^{-1} of data. For a warp parameter value of $k/\bar{M}_P = 0.1$ the bound on the graviton mass is 807 GeV. See their Fig. 4 for more details. A combined analysis with the diphoton data of AALTONEN 07G yields for $k/\bar{M}_P = 0.1$ a graviton mass lower bound of 889 GeV.

59 ABAZOV 05N use $p\bar{p}$ collisions at 1.96 TeV to search for KK gravitons in warped extra dimensions. They search for graviton resonances decaying to muons, electrons or photons, using 260 pb^{-1} of data. For warp parameter values of $k/\bar{M}_P = 0.1, 0.05,$ and $0.01,$ the bounds on the graviton mass are 785, 650 and 250 GeV respectively. See their Fig. 3 for more details.

60 ABULENCIA 05A use $p\bar{p}$ collisions at 1.96 TeV to search for KK gravitons in warped extra dimensions. They search for graviton resonances decaying to muons or electrons, using 200 pb^{-1} of data. For warp parameter values of $k/\bar{M}_P = 0.1, 0.05,$ and $0.01,$ the bounds on the graviton mass are 710, 510 and 170 GeV respectively.

Limits on Mass of Radion

This section includes limits on mass of radion, usually in context of Randall-Sundrum models. See the "Extra Dimension Review" for discussion of model dependence.

VALUE (GeV)	DOCUMENT ID	TECN	COMMENT
• • • We do not use the following data for averages, fits, limits, etc. • • •			
> 35	61	ABBIENDI	05 OPAL $e^+e^- \rightarrow Z$ radion
> 120	62	MAHANTA	00 Z \rightarrow radion $\ell\bar{\ell}$
	63	MAHANTA	00B $p\bar{p} \rightarrow$ radion $\rightarrow \gamma\gamma$

61 ABBIENDI 05 use e^+e^- collisions at $\sqrt{s} = 91$ GeV and $\sqrt{s} = 189\text{--}209$ GeV to place bounds on the radion mass in the RS model. See their Fig. 5 for bounds that depend on the radion-Higgs mixing parameter ξ and on $\Lambda_{WV} = \Lambda_\phi/\sqrt{6}$. No parameter-independent bound is obtained.

62 MAHANTA 00 obtain bound on radion mass in the RS model. Bound is from Higgs boson search at LEP I.

63 MAHANTA 00B uses $p\bar{p}$ collisions at $\sqrt{s} = 1.8$ TeV; production via gluon-gluon fusion. Authors assume a radion vacuum expectation value of 1 TeV.

Searches Particle Listings

Extra Dimensions, WIMPs and Other Particle Searches

REFERENCES FOR Extra Dimensions

AALTONEN	07G	PRL 99 171801	T. Aaltonen <i>et al.</i>	(CDF Collab.)
AALTONEN	07H	PRL 99 171802	T. Aaltonen <i>et al.</i>	(CDF Collab.)
DECCA	07A	EPJ C51 963	R.S. Decca <i>et al.</i>	
HAISCH	07	PR D76 034014	U. Haisch, A. Weiler	
KAPNER	07	PRL 98 021101	D.J. Kapner <i>et al.</i>	(ALEPH Collab.)
SCHAEF	07A	EPJ C49 411	S. Schaefer <i>et al.</i>	(ALEPH Collab.)
TU	07	PRL 99 201101	L.-C. Tu <i>et al.</i>	(DELPHI Collab.)
ABDALLAH	06C	EPJ C95 509	J. Abdallah <i>et al.</i>	(CDF Collab.)
ABULENCIA,A	06	PRL 97 171802	A. Abulencia <i>et al.</i>	(CDF Collab.)
GERDES	06	PR D73 112008	D. Gerdes <i>et al.</i>	
GOGOLADZE	06	PR D74 093012	I. Gogoladze, C. Macesanu	
ABAZOV	05N	PRL 95 091801	V.M. Abazov <i>et al.</i>	(DO Collab.)
ABAZOV	05V	PRL 95 161602	V.M. Abazov <i>et al.</i>	(DO Collab.)
ABBIENDI	05	PL B609 20	G. Abbiendi <i>et al.</i>	(OPAL Collab.)
ABDALLAH	05B	EPJ C38 395	J. Abdallah <i>et al.</i>	(DELPHI Collab.)
ABULENCIA	05A	PRL 95 252001	A. Abulencia <i>et al.</i>	(CDF Collab.)
SMULLIN	05	PR D72 122001	S.J. Smullin <i>et al.</i>	
ACHARD	04E	PL B587 16	P. Achard <i>et al.</i>	(L3 Collab.)
ACOSTA	04C	PRL 92 121802	D. Acosta <i>et al.</i>	(CDF Collab.)
CASSE	04	PRL 92 111102	M. Casse <i>et al.</i>	
CHEKANOV	04B	PL B591 23	S. Chekanov <i>et al.</i>	(ZEUS Collab.)
HOYLE	04	PR D70 042004	C.D. Hoyle <i>et al.</i>	(WASH Collab.)
ABAZOV	03	PRL 90 251802	V.M. Abazov <i>et al.</i>	(DO Collab.)
ABBIENDI	03D	EPJ C26 331	G. Abbiendi <i>et al.</i>	(OPAL Collab.)
ACHARD	03D	PL B572 133	P. Achard <i>et al.</i>	(L3 Collab.)
ADLOFF	03	PL B568 35	C. Adloff <i>et al.</i>	(H1 Collab.)
CHIAVERINI	03	PRL 90 151101	J. Chiaverini <i>et al.</i>	
GIUDICE	03	NP B663 377	G.F. Giudice, A. Strumia	
HANNESSTAD	03	PR D67 125008	S. Hannestad, G.G. Raffelt	
Also		PR D69 029901(erratum)	S. Hannestad, G.G. Raffelt	
HEISTER	03C	EPJ C28 1	A. Heister <i>et al.</i>	(ALEPH Collab.)
LONG	03	Nature 421 922	J.C. Long <i>et al.</i>	
ACHARD	02	PL B524 65	P. Achard <i>et al.</i>	(L3 Collab.)
ACHARD	02D	PL B531 28	P. Achard <i>et al.</i>	(L3 Collab.)
ANCHORDOQI	02B	PR D66 103002	L. Anchordoqui <i>et al.</i>	
HANNESSTAD	02	PRL 88 071301	S. Hannestad, G. Raffelt	
ABBOTT	01	PRL 86 1156	B. Abbott <i>et al.</i>	(DO Collab.)
FAIRBAIRN	01	PL B508 335	M. Fairbairn	
HANHART	01	PL B509 1	C. Hanhart <i>et al.</i>	
HOYLE	01	PRL 86 1418	C.D. Hoyle <i>et al.</i>	
ABBIENDI	00R	EPJ C13 353	G. Abbiendi <i>et al.</i>	(OPAL Collab.)
ABREU	00A	PL B491 87	P. Abreu <i>et al.</i>	(DELPHI Collab.)
ABREU	00S	PL B485 45	P. Abreu <i>et al.</i>	(DELPHI Collab.)
ABREU	00Z	EPJ C17 53	P. Abreu <i>et al.</i>	(DELPHI Collab.)
ACCIARRI	00P	PL B489 81	M. Acciari <i>et al.</i>	(L3 Collab.)
CASSISI	00	PL B481 323	S. Cassisi <i>et al.</i>	
CHANG	00B	PRL 85 3765	L.N. Chang <i>et al.</i>	
CHEUNG	00	PR D61 015005	K. Cheung	
CORNET	00	PR D61 037701	F. Cornet, M. Relano, J. Rico	
GRAESSER	00	PR D61 074019	M.L. Graesser	
HAN	00	PR D62 125018	T. Han, D. Marfatia, R.-J. Zhang	
MAHANTA	00	PL B480 176	U. Mahanta, S. Raksit	
MAHANTA	00B	PL B483 196	U. Mahanta, A. Datta	
MATHEWS	00	JHEP 0007 008	P. Mathews, S. Raychaudhuri, K. Sridhar	
MELE	00	PR D61 117901	S. Mele, E. Sanchez	
RIZZO	00	PR D61 016007	T.G. Rizzo, J.D. Wells	
ABBIENDI	99P	PL B465 303	G. Abbiendi <i>et al.</i>	(OPAL Collab.)
ACCIARRI	99M	PL B464 135	M. Acciari <i>et al.</i>	(L3 Collab.)
ACCIARRI	99R	PL B470 268	M. Acciari <i>et al.</i>	(L3 Collab.)
ACCIARRI	99S	PL B470 281	M. Acciari <i>et al.</i>	(L3 Collab.)
BOURLIKOV	99	JHEP 9908 006	D. Bourlikov	
HOSKINS	85	PR D32 3084	J.K. Hoskins <i>et al.</i>	

We omit papers on CHAMP's, millicharged particles, and other exotic particles. We no longer list for limits on tachyons and centauros. See our 1994 edition for these limits.

GALACTIC WIMP SEARCHES

Cross-Section Limits for Dark Matter Particles (X^0) on Nuclei

These limits are for weakly-interacting stable particles that may constitute the invisible mass in the galaxy. Unless otherwise noted, a local mass density of $0.3 \text{ GeV}/\text{cm}^3$ is assumed; see each paper for velocity distribution assumptions. In the papers the limit is given as a function of the X^0 mass. Here we list limits only for typical mass values of 20 GeV, 100 GeV, and 1 TeV. Specific limits on supersymmetric dark matter particles may be found in the Symmetry section.

For $m_{X^0} = 20 \text{ GeV}$

VALUE (nb)	CL%	DOCUMENT ID	TECN	COMMENT
•••				We do not use the following data for averages, fits, limits, etc. •••
		1 ALNER 07	ZEP2	Xe
		2 LEE 07A	KIMS	Csl
		3 AKERIB 06	CDMS	^{73}Ge , ^{29}Si
		4 SHIMIZU 06A	CNTR	F (CaF_2)
		5 ALNER 05	NAIA	NaI
		6 BARNABE-HE.05	PICA	F (C_4F_{10})
		7 BENOIT 05	EDEL	^{73}Ge
		8 GIRARD 05	SMPL	F (C_2ClF_5)
		9 KLAPDOR-K...05	HDMS	^{73}Ge (enriched)
		10 MIUCHI 03	BOLO	LiF
		11 TAKEDA 03	BOLO	NaF
		12 ANGLOHER 02	CRES	Al
		13 BENOIT 00	EDEL	Ge
		14 KLIMENKO 98	CNTR	^{73}Ge , incl.
		ALESSAND... 96	CNTR	O
		ALESSAND... 96	CNTR	Te
		15 BELLI 96	CNTR	^{129}Xe , incl.
		16 BELLI 96C	CNTR	^{129}Xe
		17 BERNABE 96	CNTR	Na
		17 BERNABE 96	CNTR	I
		18 SARSA 96	CNTR	Na
		19 SMITH 96	CNTR	Na
		20 GARCIA 95	CNTR	Natural Ge
		QUENBY 95	CNTR	Na
		21 SNOWDEN... 95	MICA	^{16}O
		21 SNOWDEN... 95	MICA	^{39}K
		BACCI 92	CNTR	Na
		22 REUSSER 91	CNTR	Natural Ge
		CALDWELL 88	CNTR	Natural Ge
< 0.08	90			
< 0.04	95			
< 0.8				
< 6				
< 0.02	90			
< 0.004	90			
< 0.3	90			
< 0.2	95			
< 0.015	90			
< 0.05	95			
< 0.1	95			
< 90	90			
< 4 $\times 10^3$	90			
< 0.7	90			
< 0.12	90			
< 0.06	95			

WIMPs and Other Particles Searches for

OMITTED FROM SUMMARY TABLE

WIMPS AND OTHER PARTICLE SEARCHES

Revised March 2002 by K. Hikasa (Tohoku University).

We collect here those searches which do not appear in any of the above search categories. These are listed in the following order:

1. Galactic WIMP (weakly-interacting massive particle) searches
2. Concentration of stable particles in matter
3. Limits on neutral particle production at accelerators
4. Limits on jet-jet resonance in hadron collisions
5. Limits on charged particles in e^+e^- collisions
6. Limits on charged particles in hadron reactions
7. Limits on charged particles in cosmic rays

Note that searches appear in separate sections elsewhere for Higgs bosons (and technipions), other heavy bosons (including W_R , W' , Z' , leptoquarks, axiglons), axions (including pseudo-Goldstone bosons, Majorons, familons), heavy leptons, heavy neutrinos, free quarks, monopoles, supersymmetric particles, and compositeness. We include specific WIMP searches in the appropriate sections when they yield limits on hypothetical particles such as supersymmetric particles, axions, massive neutrinos, monopoles, *etc.*

- 1 ALNER 07 give $\sigma < 100$ (0.5) pb (90% CL) for spin-dependent X^0 -proton (neutron) cross section.
- 2 LEE 07A give $\sigma < 1$ (25) pb (90% CL) for spin-dependent X^0 -proton (neutron) cross section.
- 3 AKERIB 06 give $\sigma < 20$ (0.3) pb (90% CL) for spin-dependent X^0 -proton (neutron) cross section. See also AKERIB 05.
- 4 SHIMIZU 06A give $\sigma < 2$ (30) pb (90% CL) for spin-dependent X^0 -proton (neutron) cross section.
- 5 ALNER 05 give $\sigma < 0.5$ (60) pb (90% CL) for spin-dependent X^0 -proton (neutron) cross section.
- 6 BARNABE-HEIDER 05 give $\sigma < 1.5$ (20) pb (90% CL) for spin-dependent X^0 -proton (neutron) cross section.
- 7 BENOIT 05 give $\sigma < 10$ pb (90% CL) for spin-dependent X^0 -neutron cross section.
- 8 GIRARD 05 give $\sigma < 1.5$ pb (90% CL) for spin-dependent X^0 -proton cross section.
- 9 KLAPDOR-KLEINGROTHAUS 05 give $\sigma < 4$ pb (90% CL) for spin-dependent X^0 -neutron cross section.
- 10 MIUCHI 03 give model-independent limit $\sigma < 35$ pb (90% CL) for spin-dependent X^0 -proton cross section.
- 11 TAKEDA 03 give model-independent limit $\sigma < 0.03$ (0.6) nb (90% CL) for spin-dependent X^0 -proton (neutron) cross section.
- 12 ANGLOHER 02 limit is for spin-dependent WIMP-Aluminum cross section.
- 13 BENOIT 00 find four event categories in Ge detectors and suggest that low-energy surface nuclear recoils can explain anomalous events reported by UKDMC and Saclay NaI experiments.
- 14 KLIMENKO 98 limit is for inelastic scattering $X^0 \text{ } ^{73}\text{Ge} \rightarrow X^0 \text{ } ^{73}\text{Ge}^*$ (13.26 keV).
- 15 BELLI 96 limit for inelastic scattering $X^0 \text{ } ^{129}\text{Xe} \rightarrow X^0 \text{ } ^{129}\text{Xe}^*$ (39.58 keV).
- 16 BELLI 96C use background subtraction and obtain $\sigma < 150$ pb (< 1.5 fb) (90% CL) for spin-dependent (independent) X^0 -proton cross section. The confidence level is from R. Bernabei, private communication, May 20, 1999.
- 17 BERNABE 96 use pulse shape discrimination to enhance the possible signal. The limit here is from R. Bernabei, private communication, September 19, 1997.
- 18 SARSA 96 search for annual modulation of WIMP signal. See SARSA 97 for details of the analysis. The limit here is from M.L. Sarsa, private communication, May 26, 1997.
- 19 SMITH 96 use pulse shape discrimination to enhance the possible signal. A dark matter density of 0.4 GeV cm^{-3} is assumed.
- 20 GARCIA 95 limit is from the event rate. A weaker limit is obtained from searches for diurnal and annual modulation.
- 21 SNOWDEN-IFTT 95 look for recoil tracks in an ancient mica crystal. Similar limits are also given for ^{27}Al and ^{28}Si . See COLLAR 96 and SNOWDEN-IFTT 96 for discussion on potential backgrounds.
- 22 REUSSER 91 limit here is changed from published (0.04) after reanalysis by authors. J.L. Vuilleumier, private communication, March 29, 1996.

See key on page 373

Searches Particle Listings

WIMPs and Other Particle Searches

For $m_{\chi^0} = 100 \text{ GeV}$

VALUE (nb)	CL%	DOCUMENT ID	TECN	COMMENT
• • • We do not use the following data for averages, fits, limits, etc. • • •				
		23 ALNER 07	ZEP2	Xe
		24 LEE 07A	KIMS	CsI
		25 MIUCHI 07	CNTR	F (CF ₄)
		26 AKERIB 06	CDMS	⁷³ Ge, ²⁹ Si
		27 SHIMIZU 06A	CNTR	F (CaF ₂)
		28 ALNER 05	NAIA	NaI
		29 BARNABE-HE.05	PICA	F (C ₄ F ₁₀)
		30 BENOIT 05	EDEL	⁷³ Ge
		31 GIRARD 05	SMPL	F (C ₂ ClF ₅)
		32 GIULIANI 05	RVUE	
		33 GIULIANI 05A	RVUE	
		34 KLAPDOR-K... 05	HDMS	⁷³ Ge (enriched)
		35 GIULIANI 04	RVUE	
		36 GIULIANI 04A	RVUE	
		37 MIUCHI 03	BOLO	LIF
		38 MIUCHI 03	BOLO	LIF
		39 TAKEDA 03	BOLO	NaF
< 0.3	90	40 ANGLOHER 02	CRES	Al
		41 BELLI 02	RVUE	
		42 BERNABEI 02c	DAMA	
		43 GREEN 02	RVUE	
		44 ULLIO 01	RVUE	
		45 BENOIT 00	EDEL	Ge
< 0.004	90	46 BERNABEI 00d		¹²⁹ Xe, incl.
		47 AMBROSIO 99	MCRO	
		48 BRHLIK 99	RVUE	
< 0.008	95	49 KLIMENKO 98	CNTR	⁷³ Ge, incl.
< 0.08	95	50 KLIMENKO 98	CNTR	⁷³ Ge, incl.
< 4		ALESSAND...	CNTR	O
< 25		ALESSAND...	CNTR	Te
< 0.006	90	51 BELLI 96	CNTR	¹²⁹ Xe, incl.
		52 BELLI 96c	CNTR	¹²⁹ Xe
< 0.001	90	53 BERNABEI 96	CNTR	Na
< 0.3	90	53 BERNABEI 96	CNTR	I
< 0.7	95	54 SARSA 96	CNTR	Na
< 0.03	90	55 SMITH 96	CNTR	Na
< 0.8	90	55 SMITH 96	CNTR	I
< 0.35	95	56 GARCIA 95	CNTR	Natural Ge
< 0.6	95	QUENBY 95	CNTR	Na
< 3	95	QUENBY 95	CNTR	I
< 1.5 × 10 ²	90	57 SNOWDEN... 95	MICA	¹⁶ O
< 4 × 10 ²	90	57 SNOWDEN... 95	MICA	³⁹ K
< 0.08	90	58 BECK 94	CNTR	⁷⁶ Ge
< 2.5	90	BACCI 92	CNTR	Na
< 3	90	BACCI 92	CNTR	I
< 0.9	90	59 REUSSER 91	CNTR	Natural Ge
< 0.7	95	CALDWELL 88	CNTR	Natural Ge
23 ALNER 07	give $\sigma < 15$ (0.08) pb (90% CL) for spin-dependent X^0 -proton (neutron) cross section.			
24 LEE 07A	give $\sigma < 0.2$ (6) pb (90% CL) for spin-dependent X^0 -proton (neutron) cross section.			
25 MIUCHI 07	give $\sigma < 1 \times 10^4$ pb (90% CL) for spin-dependent X^0 -proton cross section with a direction-sensitive detector.			
26 AKERIB 06	give $\sigma < 5$ (0.07) pb (90% CL) for spin-dependent X^0 -proton (neutron) cross section. See also AKERIB 05.			
27 SHIMIZU 06A	give $\sigma < 2$ (30) pb (90% CL) for spin-dependent X^0 -proton (neutron) cross section.			
28 ALNER 05	give $\sigma < 0.3$ (10) pb (90% CL) for spin-dependent X^0 -proton (neutron) cross section.			
29 BARNABE-HEIDER 05	give $\sigma < 2$ (30) pb (90% CL) for spin-dependent X^0 -proton (neutron) cross section.			
30 BENOIT 05	give $\sigma < 100$ (0.7) pb (90% CL) for spin-dependent X^0 -proton (neutron) cross section.			
31 GIRARD 05	give $\sigma < 1.5$ pb (90% CL) for spin-dependent X^0 -proton cross section.			
32 GIULIANI 05	analyzes the spin-independent X^0 -nucleon cross section limits with both isoscalar and isovector couplings. See Figs. 3 and 4 for limits on the couplings.			
33 GIULIANI 05A	analyze available data and give combined limits $\sigma < 0.7$ (0.2) pb for spin-dependent X^0 -proton (neutron) cross section.			
34 KLAPDOR-KLEINGROTHAUS 05	give $\sigma < 1.5$ pb (90% CL) for spin-dependent X^0 -neutron cross section.			
35 GIULIANI 04	reanalyze COLLAR 00 data and give limits for spin-dependent X^0 -proton and neutron couplings.			
36 GIULIANI 04A	gives limits for spin-dependent X^0 -proton and neutron couplings from existing data.			
37 MIUCHI 03	give model-independent limit for spin-dependent X^0 -proton and neutron cross sections. See their Fig. 5.			
38 MIUCHI 03	give model-independent limit $\sigma < 35$ pb (90% CL) for spin-dependent X^0 -proton cross section.			
39 TAKEDA 03	give model-independent limit $\sigma < 0.04$ (0.8) nb (90% CL) for spin-dependent X^0 -proton (neutron) cross section.			
40 ANGLOHER 02	limit is for spin-dependent WIMP-Aluminum cross section.			
41 BELLI 02	discuss dependence of the extracted WIMP cross section on the assumptions of the galactic halo structure.			
42 BERNABEI 02c	analyze the DAMA data in the scenario in which X^0 scatters into a slightly heavier state as discussed by SMITH 01.			

- 43 GREEN 02 discusses dependence of extracted WIMP cross section limits on the assumptions of the galactic halo structure.
- 44 ULLIO 01 discuss the possibility that the BERNABEI 99 signal is due to spin-dependent WIMP coupling.
- 45 BENOIT 00 find four event categories in Ge detectors and suggest that low-energy surface nuclear recoils can explain anomalous events reported by UKDMC and Saclay NaI experiments.
- 46 BERNABEI 00d limit is for inelastic scattering $X^0 129\text{Xe} \rightarrow X^0 129\text{Xe}^*$ (39.58 keV).
- 47 AMBROSIO 99 search for upgoing muon events induced by neutrinos originating from WIMP annihilations in the Sun and Earth.
- 48 BRHLIK 99 discuss the effect of astrophysical uncertainties on the WIMP interpretation of the BERNABEI 99 signal.
- 49 KLIMENKO 98 limit is for inelastic scattering $X^0 73\text{Ge} \rightarrow X^0 73\text{Ge}^*$ (13.26 keV).
- 50 KLIMENKO 98 limit is for inelastic scattering $X^0 73\text{Ge} \rightarrow X^0 73\text{Ge}^*$ (66.73 keV).
- 51 BELLI 96 limit for inelastic scattering $X^0 129\text{Xe} \rightarrow X^0 129\text{Xe}^*$ (39.58 keV).
- 52 BELLI 96c use background subtraction and obtain $\sigma < 0.35$ pb (< 0.15 fb) (90% CL) for spin-dependent (independent) X^0 -proton cross section. The confidence level is from R. Bernabei, private communication, May 20, 1999.
- 53 BERNABEI 96 use pulse shape discrimination to enhance the possible signal. The limit here is from R. Bernabei, private communication, September 19, 1997.
- 54 SARSA 96 search for annual modulation of WIMP signal. See SARSA 97 for details of the analysis. The limit here is from M.L. Sarsa, private communication, May 26, 1997.
- 55 SMITH 96 use pulse shape discrimination to enhance the possible signal. A dark matter density of 0.4 GeV cm^{-3} is assumed.
- 56 GARCIA 95 limit is from the event rate. A weaker limit is obtained from searches for diurnal and annual modulation.
- 57 SNOWDEN-IFFT 95 look for recoil tracks in an ancient mica crystal. Similar limits are also given for ²⁷Al and ²⁸Si. See COLLAR 96 and SNOWDEN-IFFT 96 for discussion on potential backgrounds.
- 58 BECK 94 uses enriched ⁷⁶Ge (86% purity).
- 59 REUSSER 91 limit here is changed from published (0.3) after reanalysis by authors. J.L. Vuilleumier, private communication, March 29, 1996.

For $m_{\chi^0} = 1 \text{ TeV}$

VALUE (nb)	CL%	DOCUMENT ID	TECN	COMMENT
• • • We do not use the following data for averages, fits, limits, etc. • • •				
		60 ALNER 07	ZEP2	Xe
		61 LEE 07A	KIMS	CsI
		62 MIUCHI 07	CNTR	F (CF ₄)
		63 AKERIB 06	CDMS	⁷³ Ge, ²⁹ Si
		64 ALNER 05	NAIA	NaI
		65 BARNABE-HE.05	PICA	F (C ₄ F ₁₀)
		66 BENOIT 05	EDEL	⁷³ Ge
		67 GIRARD 05	SMPL	F (C ₂ ClF ₅)
		68 KLAPDOR-K... 05	HDMS	⁷³ Ge (enriched)
		69 MIUCHI 03	BOLO	LIF
		70 TAKEDA 03	BOLO	NaF
< 3	90	71 ANGLOHER 02	CRES	Al
		72 BENOIT 00	EDEL	Ge
		73 BERNABEI 99d	CNTR	SIMP
		74 DERBIN 99	CNTR	SIMP
< 0.06	95	75 KLIMENKO 98	CNTR	⁷³ Ge, incl.
< 0.4	95	76 KLIMENKO 98	CNTR	⁷³ Ge, incl.
< 40		ALESSAND...	CNTR	O
< 700		ALESSAND...	CNTR	Te
< 0.05	90	77 BELLI 96	CNTR	¹²⁹ Xe, incl.
< 1.5	90	78 BELLI 96	CNTR	¹²⁹ Xe, incl.
		79 BELLI 96c	CNTR	¹²⁹ Xe
< 0.01	90	80 BERNABEI 96	CNTR	Na
< 9	90	80 BERNABEI 96	CNTR	I
< 7	95	81 SARSA 96	CNTR	Na
< 0.3	90	82 SMITH 96	CNTR	Na
< 6	90	82 SMITH 96	CNTR	I
< 6	95	83 GARCIA 95	CNTR	Natural Ge
< 8	95	QUENBY 95	CNTR	Na
< 50	95	QUENBY 95	CNTR	I
< 7 × 10 ²	90	84 SNOWDEN... 95	MICA	¹⁶ O
< 1 × 10 ³	90	84 SNOWDEN... 95	MICA	³⁹ K
< 0.8	90	85 BECK 94	CNTR	⁷⁶ Ge
< 30	90	BACCI 92	CNTR	Na
< 30	90	BACCI 92	CNTR	I
< 15	90	86 REUSSER 91	CNTR	Natural Ge
< 6	95	CALDWELL 88	CNTR	Natural Ge
60 ALNER 07	give $\sigma < 100$ (0.6) pb (90% CL) for spin-dependent X^0 -proton (neutron) cross section.			
61 LEE 07A	give $\sigma < 0.8$ (30) pb (90% CL) for spin-dependent X^0 -proton (neutron) cross section.			
62 MIUCHI 07	give $\sigma < 4 \times 10^4$ pb (90% CL) for spin-dependent X^0 -proton cross section with a direction-sensitive detector.			
63 AKERIB 06	give $\sigma < 30$ (0.5) pb (90% CL) for spin-dependent X^0 -proton (neutron) cross section. See also AKERIB 05.			
64 ALNER 05	give $\sigma < 1.5$ (40) pb (90% CL) for spin-dependent X^0 -proton (neutron) cross section.			
65 BARNABE-HEIDER 05	give $\sigma < 15$ (200) pb (90% CL) for spin-dependent X^0 -proton (neutron) cross section.			
66 BENOIT 05	give $\sigma < 600$ (4) pb (90% CL) for spin-dependent X^0 -proton (neutron) cross section.			
67 GIRARD 05	give $\sigma < 10$ pb (90% CL) for spin-dependent X^0 -proton cross section.			
68 KLAPDOR-KLEINGROTHAUS 05	give $\sigma < 10$ pb (90% CL) for spin-dependent X^0 -neutron cross section.			

Searches Particle Listings

WIMPs and Other Particle Searches

- 69 MIUCHI 03 give model-independent limit $\sigma < 260$ pb (90% CL) for spin-dependent X^0 -proton cross section.
- 70 TAKEDA 03 give model-independent limit $\sigma < 0.15$ (4) nb (90% CL) for spin-dependent X^0 -proton (neutron) cross section.
- 71 ANGLÖHER 02 limit is for spin-dependent WIMP-Aluminum cross section.
- 72 BENOIT 00 find four event categories in Ge detectors and suggest that low-energy surface nuclear recoils can explain anomalous events reported by UKDMC and Saclay Nal experiments.
- 73 BERNABEI 99b search for SIMPs (Strongly Interacting Massive Particles) in the mass range 10^3 – 10^{16} GeV. See their Fig. 3 for cross-section limits.
- 74 DERBIN 99 search for SIMPs (Strongly Interacting Massive Particles) in the mass range 10^2 – 10^{14} GeV. See their Fig. 3 for cross-section limits.
- 75 KLIMENKO 98 limit is for inelastic scattering $X^0 \text{ } ^{73}\text{Ge} \rightarrow X^0 \text{ } ^{73}\text{Ge}^*$ (13.26 keV).
- 76 KLIMENKO 98 limit is for inelastic scattering $X^0 \text{ } ^{73}\text{Ge} \rightarrow X^0 \text{ } ^{73}\text{Ge}^*$ (66.73 keV).
- 77 BELLI 96 limit for inelastic scattering $X^0 \text{ } ^{129}\text{Xe} \rightarrow X^0 \text{ } ^{129}\text{Xe}^*$ (39.58 keV).
- 78 BELLI 96 limit for inelastic scattering $X^0 \text{ } ^{129}\text{Xe} \rightarrow X^0 \text{ } ^{129}\text{Xe}^*$ (236.14 keV).
- 79 BELLI 96c use background subtraction and obtain $\sigma < 0.7$ pb (< 0.7 fb) (90% CL) for spin-dependent (independent) X^0 -proton cross section. The confidence level is from R. Bernabei, private communication, May 20, 1999.
- 80 BERNABEI 96 use pulse shape discrimination to enhance the possible signal. The limit here is from R. Bernabei, private communication, September 19, 1997.
- 81 SARSA 96 search for annual modulation of WIMP signal. See SARSA 97 for details of the analysis. The limit here is from M.L. Sarsa, private communication, May 26, 1997.
- 82 SMITH 96 use pulse shape discrimination to enhance the possible signal. A dark matter density of 0.4 GeV cm^{-3} is assumed.
- 83 GARCIA 95 limit is from the event rate. A weaker limit is obtained from searches for diurnal and annual modulation.
- 84 SNOWDEN-IFFT 95 look for recoil tracks in an ancient mica crystal. Similar limits are also given for ^{27}Al and ^{28}Si . See COLLAR 96 and SNOWDEN-IFFT 96 for discussion on potential backgrounds.
- 85 BECK 94 uses enriched ^{76}Ge (86% purity).
- 86 REUSSER 91 limit here is changed from published (5) after reanalysis by authors. J.L. Vuilleumier, private communication, March 29, 1996.

CONCENTRATION OF STABLE PARTICLES IN MATTER

Concentration of Heavy (Charge + 1) Stable Particles in Matter

VALUE	CL%	DOCUMENT ID	TECN	COMMENT
• • • We do not use the following data for averages, fits, limits, etc. • • •				
$< 4 \times 10^{-17}$	95	87 YAMAGATA	93	SPEC Deep sea water, $M=5$ – $1600 m_p$
$< 6 \times 10^{-15}$	95	88 VERKERK	92	SPEC Water, $M=10^5$ to 3×10^7 GeV
$< 7 \times 10^{-15}$	95	88 VERKERK	92	SPEC Water, $M=10^4$, 6×10^7 GeV
$< 9 \times 10^{-15}$	95	88 VERKERK	92	SPEC Water, $M=10^8$ GeV
$< 3 \times 10^{-23}$	90	89 HEMMICK	90	SPEC Water, $M=1000 m_p$
$< 2 \times 10^{-21}$	90	89 HEMMICK	90	SPEC Water, $M=5000 m_p$
$< 3 \times 10^{-20}$	90	89 HEMMICK	90	SPEC Water, $M=10000 m_p$
$< 1. \times 10^{-29}$		SMITH	82B	SPEC Water, $M=30$ – $400 m_p$
$< 2. \times 10^{-28}$		SMITH	82B	SPEC Water, $M=12$ – $1000 m_p$
$< 1. \times 10^{-14}$		SMITH	82B	SPEC Water, $M > 1000 m_p$
$< (0.2\text{--}1.) \times 10^{-21}$		SMITH	79	SPEC Water, $M=6$ – $350 m_p$
87 YAMAGATA 93 used deep sea water at 4000 m since the concentration is enhanced in deep sea due to gravity.				
88 VERKERK 92 looked for heavy isotopes in sea water and put a bound on concentration of stable charged massive particle in sea water. The above bound can be translated into a bound on charged dark matter particle (5×10^6 GeV), assuming the local density, $\rho=0.3 \text{ GeV/cm}^3$, and the mean velocity (v)=300 km/s.				
89 See HEMMICK 90 Fig. 7 for other masses 100–10000 m_p .				

Concentration of Heavy Stable Particles Bound to Nuclei

VALUE	CL%	DOCUMENT ID	TECN	COMMENT
• • • We do not use the following data for averages, fits, limits, etc. • • •				
$< 1.2 \times 10^{-11}$	95	90 JAVORSEK	01	SPEC Au, $M=3$ GeV
$< 6.9 \times 10^{-10}$	95	90 JAVORSEK	01	SPEC Au, $M=144$ GeV
$< 1 \times 10^{-11}$	95	91 JAVORSEK	01B	SPEC Au, $M=188$ GeV
$< 1 \times 10^{-8}$	95	91 JAVORSEK	01B	SPEC Au, $M=1669$ GeV
$< 6 \times 10^{-9}$	95	91 JAVORSEK	01B	SPEC Fe, $M=188$ GeV
$< 1 \times 10^{-8}$	95	91 JAVORSEK	01B	SPEC Fe, $M=647$ GeV
$< 4 \times 10^{-20}$	90	92 HEMMICK	90	SPEC C, $M=100 m_p$
$< 8 \times 10^{-20}$	90	92 HEMMICK	90	SPEC C, $M=1000 m_p$
$< 2 \times 10^{-16}$	90	92 HEMMICK	90	SPEC C, $M=10000 m_p$
$< 6 \times 10^{-13}$	90	92 HEMMICK	90	SPEC Li, $M=1000 m_p$
$< 1 \times 10^{-11}$	90	92 HEMMICK	90	SPEC Be, $M=1000 m_p$
$< 6 \times 10^{-14}$	90	92 HEMMICK	90	SPEC B, $M=1000 m_p$
$< 4 \times 10^{-17}$	90	92 HEMMICK	90	SPEC O, $M=1000 m_p$
$< 4 \times 10^{-15}$	90	92 HEMMICK	90	SPEC F, $M=1000 m_p$
$< 1.5 \times 10^{-13}$ /nucleon	68	93 NORMAN	89	SPEC $^{206}\text{Pb} X^-$
$< 1.2 \times 10^{-12}$ /nucleon	68	93 NORMAN	87	SPEC $^{56,58}\text{Fe} X^-$

- 90 JAVORSEK 01 search for (neutral) SIMPs (strongly interacting massive particles) bound to Au nuclei. Here M is the effective SIMP mass.
- 91 JAVORSEK 01b search for (neutral) SIMPs (strongly interacting massive particles) bound to Au and Fe nuclei from various origins with exposures on the earth's surface, in a satellite, heavy ion collisions, etc. Here M is the mass of the anomalous nucleus. See also JAVORSEK 02.
- 92 See HEMMICK 90 Fig. 7 for other masses 100–10000 m_p .
- 93 Bound valid up to $m_{X^-} \sim 100$ TeV.

LIMITS ON NEUTRAL PARTICLE PRODUCTION

Production Cross Section of Radiatively-Decaying Neutral Particle

VALUE (pb)	CL%	DOCUMENT ID	TECN	COMMENT
• • • We do not use the following data for averages, fits, limits, etc. • • •				
$< (0.043\text{--}0.17)$	95	94 ABBIENDI	00D	OPAL $e^+e^- \rightarrow X^0 \gamma^0$, $X^0 \rightarrow \gamma^0 \gamma^0$
$< (0.05\text{--}0.8)$	95	95 ABBIENDI	00D	OPAL $e^+e^- \rightarrow X^0 X^0$, $X^0 \rightarrow \gamma^0 \gamma^0$
$< (2.5\text{--}0.5)$	95	96 ACKERSTAFF	97B	OPAL $e^+e^- \rightarrow X^0 \gamma^0$, $X^0 \rightarrow \gamma^0 \gamma^0$
$< (1.6\text{--}0.9)$	95	97 ACKERSTAFF	97B	OPAL $e^+e^- \rightarrow X^0 X^0$, $X^0 \rightarrow \gamma^0 \gamma^0$
94 ABBIENDI 00D associated production limit is for $m_{X^0} = 90$ – 188 GeV, $m_{\gamma^0} = 0$ at $E_{cm} = 189$ GeV. See also their Fig. 9.				
95 ABBIENDI 00D pair production limit is for $m_{X^0} = 45$ – 94 GeV, $m_{\gamma^0} = 0$ at $E_{cm} = 189$ GeV. See also their Fig. 12.				
96 ACKERSTAFF 97B associated production limit is for $m_{X^0} = 80$ – 160 GeV, $m_{\gamma^0} = 0$ from 10.0 pb^{-1} at $E_{cm} = 161$ GeV. See their Fig. 3(a).				
97 ACKERSTAFF 97B pair production limit is for $m_{X^0} = 40$ – 80 GeV, $m_{\gamma^0} = 0$ from 10.0 pb^{-1} at $E_{cm} = 161$ GeV. See their Fig. 3(b).				

Heavy Particle Production Cross Section

VALUE (cm ² /N)	CL%	EVTS	DOCUMENT ID	TECN	COMMENT
• • • We do not use the following data for averages, fits, limits, etc. • • •					
< 10 – 36 – 10 – 33	90		98 ADAMS	97B	KTEV $m = 1.2$ – 5 GeV
$< (4\text{--}0.3) \times 10$ – 31	95		99 GALLAS	95	TOF $m = 0.5$ – 20 GeV
$< 2 \times 10$ – 36	90	0	100 AKESSON	91	CNTR $m = 0$ – 5 GeV
$< 2.5 \times 10$ – 35	90	0	101 BADIER	86	BDMP $\tau = (0.05\text{--}1.) \times 10$ – 8 s
		0	102 GUSTAFSON	76	CNTR $\tau > 10$ – 7 s
98 ADAMS 97B search for a hadron-like neutral particle produced in pN interactions, which decays into a ρ^0 and a weakly interacting massive particle. Upper limits are given for the ratio to K_S production for the mass range 1.2–5 GeV and lifetime 10 – 9 – 10 – 4 s. See also our Light Gluino Section.					
99 GALLAS 95 limit is for a weakly interacting neutral particle produced in 800 GeV c/pN interactions decaying with a lifetime of 10 – 4 – 10 – 8 s. See their Figs. 8 and 9. Similar limits are obtained for a stable particle with interaction cross section 10 – 29 – 10 – 33 cm ² . See Fig. 10.					
100 AKESSON 91 limit is from weakly interacting neutral long-lived particles produced in pN reaction at 450 GeV/c performed at CERN SPS. Bourquin-Gaillard formula is used as the production model. The above limit is for $\tau > 10$ – 7 s. For $\tau > 10$ – 9 s, $\sigma < 10$ – 30 cm ² /nucleon is obtained.					
101 BADIER 86 looked for long-lived particles at 300 GeV π^- beam dump. The limit applies for nonstrongly interacting neutral or charged particles with mass > 2 GeV. The limit applies for particle modes, $\mu^+\pi^-$, $\mu^+\mu^-$, $\pi^+\pi^-X$, $\pi^+\pi^-\pi^\pm$ etc. See their figure 5 for the contours of limits in the mass- τ plane for each mode.					
102 GUSTAFSON 76 is a 300 GeV FNAL experiment looking for heavy ($m > 2$ GeV) long-lived neutral hadrons in the M4 neutral beam. The above typical value is for $m = 3$ GeV and assumes an interaction cross section of 1 mb. Values as a function of mass and interaction cross section are given in figure 2.					

Production of New Penetrating Non- ν Like States in Beam Dump

VALUE	DOCUMENT ID	TECN	COMMENT
• • • We do not use the following data for averages, fits, limits, etc. • • •			
	103 LOSECCO	81	CALO 28 GeV protons
103 No excess neutral-current events leads to $\sigma(\text{production}) \times \sigma(\text{interaction}) \times \text{acceptance} < 2.26 \times 10$ – 71 cm ⁴ /nucleon ² (CL = 90%) for light neutrals. Acceptance depends on models (0.1 to $4. \times 10$ – 4).			

LIMITS ON JET-JET RESONANCES

Heavy Particle Production Cross Section in $p\bar{p}$

Units(pb)	CL%	Mass(GeV)	DOCUMENT ID	TECN	COMMENT
• • • We do not use the following data for averages, fits, limits, etc. • • •					
			104 ABE	99F	CDF 1.8 TeV $p\bar{p} \rightarrow b\bar{b} + \text{anything}$
< 2603	95	200	105 ABE	97G	CDF 1.8 TeV $p\bar{p} \rightarrow 2$ jets
< 44	95	400	106 ABE	93G	CDF 1.8 TeV $p\bar{p} \rightarrow 2$ jets
< 7	95	600	106 ABE	93G	CDF 1.8 TeV $p\bar{p} \rightarrow 2$ jets

See key on page 373

Searches Particle Listings

WIMPs and Other Particle Searches

- 104 ABE 99F search for narrow $b\bar{b}$ resonances in $p\bar{p}$ collisions at $E_{cm}=1.8$ TeV. Limits on $\sigma(p\bar{p} \rightarrow X + \text{anything}) \times B(X \rightarrow b\bar{b})$ in the range $3-10^3$ pb (95%CL) are given for $m_X=200-750$ GeV. See their Table I.
- 105 ABE 97G search for narrow dijet resonances in $p\bar{p}$ collisions with 106 pb^{-1} of data at $E_{cm}=1.8$ TeV. Limits on $\sigma(p\bar{p} \rightarrow X + \text{anything}) \times B(X \rightarrow jj)$ in the range 10^4-10^{-1} pb (95%CL) are given for dijet mass $m=200-1150$ GeV with both jets having $|\eta| < 2.0$ and the dijet system having $|\cos\theta^*| < 0.67$. See their Table I for the list of limits. Supersedes ABE 93G.
- 106 ABE 93G gives cross section times branching ratio into light (d, u, s, c, b) quarks for $\Gamma = 0.02 M$. Their Table II gives limits for $M = 200-900$ GeV and $\Gamma = (0.02-0.2) M$.

LIMITS ON CHARGED PARTICLES IN e^+e^-

Heavy Particle Production Cross Section in e^+e^-

Ratio to $\sigma(e^+e^- \rightarrow \mu^+\mu^-)$ unless noted. See also entries in Free Quark Search and Magnetic Monopole Searches.

VALUE	CL%	EVTS	DOCUMENT ID	TECN	COMMENT
• • • We do not use the following data for averages, fits, limits, etc. • • •					
			107 ACKERSTAFF 98P	OPAL	$Q=1,2/3, m=45-89.5$ GeV
			108 ABREU 97D	DLPH	$Q=1,2/3, m=45-84$ GeV
$<2 \times 10^{-5}$	95		109 BARATE 97K	ALEP	$Q=1, m=45-85$ GeV
$<1 \times 10^{-5}$	95		110 AKERS 95R	OPAL	$Q=1, m=5-45$ GeV
$<2 \times 10^{-3}$	90		111 BUSKULIC 93C	ALEP	$Q=1, m=32-72$ GeV
$<(10^{-2}-1)$	95		112 ADACHI 90C	TOPZ	$Q=1, m=1-16, 18-27$ GeV
$<7 \times 10^{-2}$	90		113 ADACHI 90E	TOPZ	$Q=1, m=5-25$ GeV
$<1.6 \times 10^{-2}$	95	0	114 KINOSHITA 82	PLAS	$Q=3-180, m < 14.5$ GeV
$<5.0 \times 10^{-2}$	90	0	115 BARTEL 80	JADE	$Q=(3,4,5)/3$ 2-12 GeV

- 107 ACKERSTAFF 98P search for pair production of long-lived charged particles at E_{cm} between 130 and 183 GeV and give limits $\sigma < (0.05-0.2)$ pb (95%CL) for spin-0 and spin-1/2 particles with $m=45-89.5$ GeV, charge 1 and 2/3. The limit is translated to the cross section at $E_{cm}=183$ GeV with the s dependence described in the paper. See their Figs. 2-4.
- 108 ABREU 97D search for pair production of long-lived particles and give limits $\sigma < (0.4-2.3)$ pb (95%CL) for various center-of-mass energies $E_{cm}=130-136, 161,$ and 172 GeV, assuming an almost flat production distribution in $\cos\theta$.
- 109 BARATE 97K search for pair production of long-lived charged particles at $E_{cm}=130, 136, 161,$ and 172 GeV and give limits $\sigma < (0.2-0.4)$ pb (95%CL) for spin-0 and spin-1/2 particles with $m=45-85$ GeV. The limit is translated to the cross section at $E_{cm}=172$ GeV with the E_{cm} dependence described in the paper. See their Figs. 2 and 3 for limits on $J=1/2$ and $J=0$ cases.
- 110 AKERS 95R is a CERN-LEP experiment with $W_{cm} \sim m_Z$. The limit is for the production of a stable particle in multihadron events normalized to $\sigma(e^+e^- \rightarrow \text{hadrons})$. Constant phase space distribution is assumed. See their Fig. 3 for bounds for $Q = \pm 2/3, \pm 4/3$.
- 111 BUSKULIC 93C is a CERN-LEP experiment with $W_{cm} = m_Z$. The limit is for a pair or single production of heavy particles with unusual ionization loss in TPC. See their Fig. 5 and Table 1.
- 112 ADACHI 90C is a KEK-TRISTAN experiment with $W_{cm} = 52-60$ GeV. The limit is for pair production of a scalar or spin-1/2 particle. See Figs. 3 and 4.
- 113 ADACHI 90E is KEK-TRISTAN experiment with $W_{cm} = 52-61.4$ GeV. The above limit is for inclusive production cross section normalized to $\sigma(e^+e^- \rightarrow \mu^+\mu^-) \cdot \beta(3-\beta^2)/2$, where $\beta = (1 - 4m^2/W_{cm}^2)^{1/2}$. See the paper for the assumption about the production mechanism.
- 114 KINOSHITA 82 is SLAC PEP experiment at $W_{cm} = 29$ GeV using lexan and ^{39}Cr plastic sheets sensitive to highly ionizing particles.
- 115 BARTEL 80 is DESY-PETRA experiment with $W_{cm} = 27-35$ GeV. Above limit is for inclusive pair production and ranges between $1. \times 10^{-1}$ and $1. \times 10^{-2}$ depending on branching and production momentum distributions. (See their figures 9, 10, 11).

Branching Fraction of Z^0 to a Pair of Stable Charged Heavy Fermions

VALUE	CL%	DOCUMENT ID	TECN	COMMENT
• • • We do not use the following data for averages, fits, limits, etc. • • •				
$<5 \times 10^{-6}$	95	116 AKERS 95R	OPAL	$m=40.4-45.6$ GeV
$<1 \times 10^{-3}$	95	AKRAWY 90O	OPAL	$m=29-40$ GeV

116 AKERS 95R give the 95% CL limit $\sigma(X\bar{X})/\sigma(\mu\mu) < 1.8 \times 10^{-4}$ for the pair production of singly- or doubly-charged stable particles. The limit applies for the mass range 40.4-45.6 GeV for X^\pm and < 45.6 GeV for $X^{\pm\pm}$. See the paper for bounds for $Q = \pm 2/3, \pm 4/3$.

LIMITS ON CHARGED PARTICLES IN HADRONIC REACTIONS

Heavy Particle Production Cross Section

VALUE (nb)	CL%	EVTS	DOCUMENT ID	TECN	COMMENT
• • • We do not use the following data for averages, fits, limits, etc. • • •					
<0.19	95		117 AKTAS 04C	H1	$m=3-10$ GeV
<0.05	95		118 ABE 92J	CDF	$m=50-200$ GeV
$<10^{-3}$			119 CARROLL 78	SPEC	$m=2-2.5$ GeV
<100	0		120 LEIPUNER 73	CNTR	$m=3-11$ GeV

117 AKTAS 04C look for charged particle photoproduction at HERA with mean c.m. energy of 200 GeV.

118 ABE 92J look for pair production of unit-charged particles which leave detector before decaying. Limit shown here is for $m=50$ GeV. See their Fig. 5 for different charges and stronger limits for higher mass.

119 CARROLL 78 look for neutral, $S = -2$ dihyperon resonance in $pp \rightarrow 2K^+X$. Cross section varies within above limits over mass range and $p_{T,ab} = 5.1-5.9$ GeV/c.

120 LEIPUNER 73 is an NAL 300 GeV p experiment. Would have detected particles with lifetime greater than 200 ns.

Heavy Particle Production Differential Cross Section

VALUE ($\text{cm}^2\text{sr}^{-1}\text{GeV}^{-1}$)	CL%	EVTS	DOCUMENT ID	TECN	CHG	COMMENT
• • • We do not use the following data for averages, fits, limits, etc. • • •						
$<2.6 \times 10^{-36}$	90	0	121 BALDIN	76	CNTR	$Q=1, m=2.1-9.4$ GeV
$<2.2 \times 10^{-33}$	90	0	122 ALBROW	75	SPEC	$Q=\pm 1, m=4-15$ GeV
$<1.1 \times 10^{-33}$	90	0	122 ALBROW	75	SPEC	$Q=\pm 2, m=6-27$ GeV
$<8. \times 10^{-35}$	90	0	123 JOVANOVI...	75	CNTR	$m=15-26$ GeV
$<1.5 \times 10^{-34}$	90	0	123 JOVANOVI...	75	CNTR	$Q=\pm 2, m=3-10$ GeV
$<6. \times 10^{-35}$	90	0	123 JOVANOVI...	75	CNTR	$Q=\pm 2, m=10-26$ GeV
$<1. \times 10^{-31}$	90	0	124 APPEL	74	CNTR	$m=3.2-7.2$ GeV
$<5.8 \times 10^{-34}$	90	0	125 ALPER	73	SPEC	$m=1.5-24$ GeV
$<1.2 \times 10^{-35}$	90	0	126 ANTIPOV	71B	CNTR	$Q=-, m=2.2-2.8$
$<2.4 \times 10^{-35}$	90	0	127 ANTIPOV	71C	CNTR	$Q=-, m=1.2-1.7, 2.1-4$
$<2.4 \times 10^{-35}$	90	0	BINON	69	CNTR	$Q=-, m=1-1.8$ GeV
$<1.5 \times 10^{-36}$	0		128 DORFAN	65	CNTR	Be target $m=3-7$ GeV
$<3.0 \times 10^{-36}$	0		128 DORFAN	65	CNTR	Fe target $m=3-7$ GeV

- 121 BALDIN 76 is a 70 GeV Serpukhov experiment. Value is per Al nucleus at $\theta = 0$. For other charges in range -0.5 to -3.0 , CL = 90% limit is $(2.6 \times 10^{-36})/|(charge)|$ for mass range $(2.1-9.4 \text{ GeV}) \times |(charge)|$. Assumes stable particle interacting with matter as do antiprotons.
- 122 ALBROW 75 is a CERN ISR experiment with $E_{cm} = 53$ GeV. $\theta = 40$ mr. See figure 5 for mass ranges up to 35 GeV.
- 123 JOVANOVI 75 is a CERN ISR 26+26 and 15+15 GeV pp experiment. Figure 4 covers ranges $Q = 1/3$ to 2 and $m = 3$ to 26 GeV. Value is per GeV momentum.
- 124 APPEL 74 is NAL 300 GeV pW experiment. Studies forward production of heavy (up to 24 GeV) charged particles with momenta 24-200 GeV ($-charge$) and 40-150 GeV ($+charge$). Above typical value is for 75 GeV and is per GeV momentum per nucleon.
- 125 ALPER 73 is CERN ISR 26+26 GeV pp experiment. $p > 0.9$ GeV, $0.2 < \beta < 0.65$.
- 126 ANTIPOV 71B is from same 70 GeV p experiment as ANTIPOV 71C and BINON 69.
- 127 ANTIPOV 71C limit inferred from flux ratio. 70 GeV p experiment.
- 128 DORFAN 65 is a 30 GeV/c p experiment at BNL. Units are per GeV momentum per nucleus.

Long-Lived Heavy Particle Invariant Cross Section

VALUE ($\text{cm}^2/\text{GeV}^2/N$)	CL%	DOCUMENT ID	TECN	CHG	COMMENT
• • • We do not use the following data for averages, fits, limits, etc. • • •					
$<5-700 \times 10^{-35}$	90	129 BERNSTEIN 88	CNTR		
$<5-700 \times 10^{-37}$	90	129 BERNSTEIN 88	CNTR		
$<2.5 \times 10^{-36}$	90	130 THRON	85	CNTR	$Q=1, m=4-12$ GeV
$<1. \times 10^{-35}$	90	130 THRON	85	CNTR	$Q=1, m=4-12$ GeV
$<6. \times 10^{-33}$	90	131 ARMITAGE 79	SPEC		$m=1.87$ GeV
$<1.5 \times 10^{-33}$	90	131 ARMITAGE 79	SPEC		$m=1.5-3.0$ GeV
		132 BOZZOLI 79	CNTR	\pm	$Q = (2/3, 1, 4/3, 2)$
$<1.1 \times 10^{-37}$	90	133 CUTTS 78	CNTR		$m=4-10$ GeV
$<3.0 \times 10^{-37}$	90	134 VIDAL 78	CNTR		$m=4.5-6$ GeV

129 BERNSTEIN 88 limits apply at $x = 0.2$ and $p_T = 0$. Mass and lifetime dependence of limits are shown in the regions: $m = 1.5-7.5$ GeV and $\tau = 10^{-8}-2 \times 10^{-6}$ s. First number is for hadrons; second is for weakly interacting particles.

130 THRON 85 is FNAL 400 GeV proton experiment. Mass determined from measured velocity and momentum. Limits are for $\tau > 3 \times 10^{-9}$ s.

131 ARMITAGE 79 is CERN-ISR experiment at $E_{cm} = 53$ GeV. Value is for $x = 0.1$ and $p_T = 0.15$. Observed particles at $m = 1.87$ GeV are found all consistent with being antideuteron.

132 BOZZOLI 79 is CERN-SPS 200 GeV pN experiment. Looks for particle with τ larger than 10^{-8} s. See their figure 11-18 for production cross-section upper limits vs mass.

133 CUTTS 78 is $p\text{Be}$ experiment at FNAL sensitive to particles of $\tau > 5 \times 10^{-8}$ s. Value is for $-0.3 < x < 0$ and $p_T = 0.175$.

134 VIDAL 78 is FNAL 400 GeV proton experiment. Value is for $x = 0$ and $p_T = 0$. Puts lifetime limit of $< 5 \times 10^{-8}$ s on particle in this mass range.

Long-Lived Heavy Particle Production

$\sigma(\text{Heavy Particle}) / \sigma(\pi)$

VALUE	EVTS	DOCUMENT ID	TECN	CHG	COMMENT
• • • We do not use the following data for averages, fits, limits, etc. • • •					
$<10^{-8}$		135 NAKAMURA 89	SPEC	\pm	$Q = (-5/3, \pm 2)$
	0	136 BUSSIÈRE 80	CNTR	\pm	$Q = (2/3, 1, 4/3, 2)$

135 NAKAMURA 89 is KEK experiment with 12 GeV protons on Pt target. The limit applies for mass $\lesssim 1.6$ GeV and lifetime $\gtrsim 10^{-7}$ s.

136 BUSSIÈRE 80 is CERN-SPS experiment with 200-240 GeV protons on Be and Al target. See their figures 6 and 7 for cross-section ratio vs mass.

Production and Capture of Long-Lived Massive Particles

VALUE (10^{-36} cm^2)	EVTS	DOCUMENT ID	TECN	COMMENT
• • • We do not use the following data for averages, fits, limits, etc. • • •				
<20 to 800	0	137 ALEKSEEV 76	ELEC	$\tau=5$ ms to 1 day
<200 to 2000	0	137 ALEKSEEV 76B	ELEC	$\tau=100$ ms to 1 day
<1.4 to 9	0	138 FRANKEL 75	CNTR	$\tau=50$ ms to 10 hours
<0.1 to 9	0	139 FRANKEL 74	CNTR	$\tau=1$ to 1000 hours

Searches Particle Listings

WIMPs and Other Particle Searches

- 137 ALEKSEEV 76 and ALEKSEEV 76B are 61–70 GeV p Serpukhov experiment. Cross section is per Pb nucleus.
 138 FRANKEL 75 is extension of FRANKEL 74.
 139 FRANKEL 74 looks for particles produced in thick Al targets by 300–400 GeV/c protons.

Long-Lived Particle Search at Hadron Collisions

Limits are for cross section times branching ratio.

VALUE ($\text{fb}/\text{nucleon}$)	CL%	EVTS	DOCUMENT ID	TECN	COMMENT
• • • We do not use the following data for averages, fits, limits, etc. • • •					
<2	90	0	140 BADIER	86	BDMP $\tau = (0.05\text{--}1.) \times 10^{-8}\text{s}$
140			BADIER 86		looked for long-lived particles at 300 GeV π^- beam dump. The limit applies for nonstrongly interacting neutral or charged particles with mass >2 GeV. The limit applies for particle modes, $\mu^+\pi^-, \mu^+\mu^-, \pi^+\pi^-X, \pi^+\pi^-\pi^\pm$ etc. See their figure 5 for the contours of limits in the mass- τ plane for each mode.

Long-Lived Heavy Particle Cross Section

VALUE (pb/sr)	CL%	DOCUMENT ID	TECN	COMMENT
• • • We do not use the following data for averages, fits, limits, etc. • • •				
<34	95	141 RAM	94	SPEC $1015 < m_{X^{++}} < 1085$ MeV
<75	95	141 RAM	94	SPEC $920 < m_{X^{++}} < 1025$ MeV
141			RAM 94	search for a long-lived doubly-charged fermion X^{++} with mass between m_N and $m_N + m_\pi$ and baryon number +1 in the reaction $pp \rightarrow X^{++}n$. No candidate is found. The limit is for the cross section at 15° scattering angle at 460 MeV incident energy and applies for $\tau(X^{++}) \gg 0.1 \mu\text{s}$.

LIMITS ON CHARGED PARTICLES IN COSMIC RAYS

Heavy Particle Flux in Cosmic Rays

VALUE ($\text{cm}^{-2}\text{sr}^{-1}\text{s}^{-1}$)	CL%	EVTS	DOCUMENT ID	TECN	CHG	COMMENT
• • • We do not use the following data for averages, fits, limits, etc. • • •						
$\sim 6 \times 10^{-9}$		2	142 SAITO	90		$Q \approx 14, m \approx 370m_p$
< 1.4 $\times 10^{-12}$	90	0	143 MINCER	85	CALO	$m \geq 1 \text{ TeV}$
			144 SAKUYAMA	83B	PLAS	$m \sim 1 \text{ TeV}$
< 1.7 $\times 10^{-11}$	99	0	145 BHAT	82	CC	
< 1. $\times 10^{-9}$	90	0	146 MARINI	82	CNTR \pm	$Q = 1, m \sim 4.5m_p$
2. $\times 10^{-9}$		3	147 YOCK	81	SPRK \pm	$Q = 1, m \sim 4.5m_p$
		3	147 YOCK	81	SPRK	Fractionally charged
3.0 $\times 10^{-9}$		3	148 YOCK	80	SPRK	$m \sim 4.5 m_p$
$(4 \pm 1) \times 10^{-11}$		3	GOODMAN	79	ELEC	$m \geq 5 \text{ GeV}$
< 1.3 $\times 10^{-9}$	90	0	149 BHAT	78	CNTR \pm	$m > 1 \text{ GeV}$
< 1.0 $\times 10^{-9}$	0	0	BRIATORE	76	ELEC	
< 7. $\times 10^{-10}$	90	0	YOCK	75	ELEC \pm	$Q > 7e$ or $< -7e$
> 6. $\times 10^{-9}$		5	150 YOCK	74	CNTR	$m > 6 \text{ GeV}$
< 3.0 $\times 10^{-8}$	0	0	DARDO	72	CNTR	
< 1.5 $\times 10^{-9}$	0	0	TONWAR	72	CNTR	$m > 10 \text{ GeV}$
< 3.0 $\times 10^{-10}$	0	0	BJORNBOE	68	CNTR	$m > 5 \text{ GeV}$
< 5.0 $\times 10^{-11}$	90	0	JONES	67	ELEC	$m = 5\text{--}15 \text{ GeV}$

- 142 SAITO 90 candidates carry about 450 MeV/nucleon. Cannot be accounted for by conventional backgrounds. Consistent with strange quark matter hypothesis.
 143 MINCER 85 is high statistics study of calorimeter signals delayed by 20–200 ns. Collaboration with AGS beam shows they can be accounted for by rare fluctuations in signals from low-energy hadrons in the shower. Claim that previous delayed signals including BJORNBOE 68, DARDO 72, BHAT 82, SAKUYAMA 83B below may be due to this fake effect.
 144 SAKUYAMA 83B analyzed 6000 extended air shower events. Increase of delayed particles and change of lateral distribution above 10^{17} eV may indicate production of very heavy parent at top of atmosphere.
 145 BHAT 82 observed 12 events with delay $> 2. \times 10^{-8}$ s and with more than 40 particles. 1 eV has good hadron shower. However all events are delayed in only one of two detectors in cloud chamber, and could not be due to strongly interacting massive particle.
 146 MARINI 82 applied PEP-counter for TOF. Above limit is for velocity = 0.54 of light. Limit is inconsistent with YOCK 80 YOCK 81 events if isotropic dependence on zenith angle is assumed.
 147 YOCK 81 saw another 3 events with $Q = \pm 1$ and m about $4.5m_p$ as well as 2 events with $m > 5.3m_p, Q = \pm 0.75 \pm 0.05$ and $m > 2.8m_p, Q = \pm 0.70 \pm 0.05$ and 1 event with $m = (9.3 \pm 3.)m_p, Q = \pm 0.89 \pm 0.06$ as possible heavy candidates.
 148 YOCK 80 events are with charge exactly or approximately equal to unity.
 149 BHAT 78 is at Kolar gold fields. Limit is for $\tau > 10^{-6}$ s.
 150 YOCK 74 events could be tritons.

Superheavy Particle (Quark Matter) Flux in Cosmic Rays

VALUE ($\text{cm}^{-2}\text{sr}^{-1}\text{s}^{-1}$)	CL%	EVTS	DOCUMENT ID	TECN	COMMENT
• • • We do not use the following data for averages, fits, limits, etc. • • •					
<5 $\times 10^{-16}$	90		151 AMBROSIO	00B	MCRO $m > 5 \times 10^{14} \text{ GeV}$
<1.8 $\times 10^{-12}$	90		152 ASTONE	93	CNTR $m \geq 1.5 \times 10^{-13} \text{ gram}$
<1.1 $\times 10^{-14}$	90		153 AHLEN	92	MCRO $10^{-10} < m < 0.1 \text{ gram}$
<2.2 $\times 10^{-14}$	90	0	154 NAKAMURA	91	PLAS $m > 10^{11} \text{ GeV}$
<6.4 $\times 10^{-16}$	90	0	155 ORITO	91	PLAS $m > 10^{12} \text{ GeV}$

- <2.0 $\times 10^{-11}$ 90 156 LIU 88 BOLO $m > 1.5 \times 10^{-13} \text{ gram}$
 <4.7 $\times 10^{-12}$ 90 157 BARISH 87 CNTR $1.4 \times 10^8 < m < 10^{12} \text{ GeV}$
 <3.2 $\times 10^{-11}$ 90 0 158 NAKAMURA 85 CNTR $m > 1.5 \times 10^{-13} \text{ gram}$
 <3.5 $\times 10^{-11}$ 90 0 159 ULLMAN 81 CNTR Planck-mass 10^{13} GeV
 <7. $\times 10^{-11}$ 90 0 159 ULLMAN 81 CNTR $m \leq 10^{16} \text{ GeV}$
 151 AMBROSIO 00B searched for quark matter ("nuclearites") in the velocity range $(10^{-5}\text{--}1)$ c. The listed limit is for 2×10^{-3} c.
 152 ASTONE 93 searched for quark matter ("nuclearites") in the velocity range $(10^{-3}\text{--}1)$ c. Their Table 1 gives a compilation of searches for nuclearites.
 153 AHLEN 92 searched for quark matter ("nuclearites"). The bound applies to velocity $< 2.5 \times 10^{-3}$ c. See their Fig. 3 for other velocity/c and heavier mass range.
 154 NAKAMURA 91 searched for quark matter in the velocity range $(4 \times 10^{-5}\text{--}1)$ c.
 155 ORITO 91 searched for quark matter. The limit is for the velocity range $(10^{-4}\text{--}10^{-3})$ c.
 156 LIU 88 searched for quark matter ("nuclearites") in the velocity range $(2.5 \times 10^{-3}\text{--}1)$ c. A less stringent limit of 5.8×10^{-11} applies for $(1\text{--}2.5) \times 10^{-3}$ c.
 157 BARISH 87 searched for quark matter ("nuclearites") in the velocity range $(2.7 \times 10^{-4}\text{--}5 \times 10^{-3})$ c.
 158 NAKAMURA 85 at KEK searched for quark-matter. These might be lumps of strange quark matter with roughly equal numbers of u, d, s quarks. These lumps or nuclearites were assumed to have velocity of $(10^{-4}\text{--}10^{-3})$ c.
 159 ULLMAN 81 is sensitive for heavy slow singly charge particle reaching earth with vertical velocity 100–350 km/s.

Highly Ionizing Particle Flux

VALUE ($\text{m}^{-2}\text{yr}^{-1}$)	CL%	EVTS	DOCUMENT ID	TECN	COMMENT
• • • We do not use the following data for averages, fits, limits, etc. • • •					
<0.4	95	0	KINOSHITA	81B	PLAS Z/β 30–100

REFERENCES FOR SEARCHES FOR WIMPS AND OTHER PARTICLES

ALNER 07	PL B653 161	G.J. Alner et al.	(ZEPLIN-II Collab.)
LEE 07A	PRL 99 091301	H.S. Lee et al.	(KIMS Collab.)
MUICHI 07	PL B654 58	K. Miuchi et al.	
AKERIB 06	PR D73 01102R	D.S. Akerib et al.	(CDMS Collab.)
SHIMIZU 06A	PL B633 195	Y. Shimizu et al.	
AKERIB 05	PR D72 052009	D.S. Akerib et al.	(CDMS Collab.)
ALNER 05	PL B616 17	G.J. Alner et al.	(UK Dark Matter Collab.)
BARNABE-HE... 05	PL B624 186	M. Barnabe-Heider et al.	(PICASSO Collab.)
BERNOIT 05	PL B616 25	A. Benoit et al.	(EDELWEISS Collab.)
GIRARD 05	PL B621 233	T.A. Girard et al.	(SIMPLE Collab.)
GIULIANI 05	PRL 95 101301	F. Giuliani	
GIULIANI 05A	PR D71 123503	F. Giuliani, T.A. Girard	
KLAPDOR-K... 05	PL B609 226	H.V. Klapdor-Kleingrothaus, I.V. Krivosheina, C. Tomei	
AKTAS 04C	EPJ C36 413	A. Aktas et al.	(HI Collab.)
GIULIANI 04	PL B588 151	F. Giuliani, T.A. Girard	
GIULIANI 04A	PRL 93 161301	F. Giuliani	
MUICHI 03	ASP 19 135	K. Miuchi et al.	
TAKEDA 03	PL B572 145	A. Takeda et al.	
ANGLOHER 02	ASP 18 43	G. Angloher et al.	(CRESS T Collab.)
BELLI 02	PR D66 043503	P. Belli et al.	
BERNABE 02C	EPJ C23 61	R. Bernabei et al.	(DAMA Collab.)
GREEN 02	PR D66 083003	A.M. Green	
JAVORSK 02	PR D65 072003	D. Javorsk II et al.	
JAVORSK 01	PR D64 012005	D. Javorsk II et al.	
JAVORSK 01B	PRL 87 231804	D. Javorsk II et al.	
SMITH 01	PR D64 043502	D. Smith, W. Weimer	
ULLIO 01	JHEP 0107 044	P. Ullio, M. Kamionkowski, P. Vogel	
ABBIENDI 00D	EPJ C13 197	G. Abbiendi et al.	(OPAL Collab.)
AMBROSIO 00B	EPJ C13 453	M. Ambrosio et al.	(MACRO Collab.)
BERNOIT 00	PL B479 8	A. Benoit et al.	(EDELWEISS Collab.)
BERNABE 00D	NJP 2 15	R. Bernabei et al.	(DAMA Collab.)
COLLAR 00	PRL 85 3083	J.I. Collar et al.	(SIMPLE Collab.)
ABE 99F	PRL 82 2038	F. Abe et al.	(CDF Collab.)
AMBROSIO 99	PR D60 082002	M. Ambrosio et al.	(Macro Collab.)
BERNABE 99	PL B450 448	R. Bernabei et al.	(DAMA Collab.)
BERNABE 99D	PRL 83 4918	R. Bernabei et al.	(DAMA Collab.)
BRHLK 99	PL B464 303	M. Brhlk, L. Roszkowski	
DERBIN 99	PAN 62 1886	A.V. Derbin et al.	
Translated from YAF 62 2034.			
ACKERSTAFF 98P	PL B433 195	K. Akerstaff et al.	(OPAL Collab.)
KLIMENKO 98	JETPL 67 875	A.A. Klimenko et al.	
Translated from ZETFP 67 835.			
ABE 97G	PR D55 R5263	F. Abe et al.	(CDF Collab.)
ABREU 97D	PL B396 315	P. Abreu et al.	(DELPHI Collab.)
ACKERSTAFF 97B	PL B391 210	K. Akerstaff et al.	(OPAL Collab.)
ADAMS 97B	PRL 79 4083	J. Adams et al.	(FNAL KTeV Collab.)
BARATE 97K	PL B405 379	R. Barate et al.	(ALEPH Collab.)
SARSA 97	PR D56 1856	M.L. Sarsa et al.	(ZARA Collab.)
ALESSAND... 96	PL B384 316	A. Alessandrello et al.	(MILA, MILAI, SASSO Collab.)
BELLI 96	PL B387 222	P. Belli et al.	(DAMA Collab.)
Also 96	PL B389 783 (erratum)	P. Belli et al.	(DAMA Collab.)
BELLI 96C	NC 19C 537	P. Belli et al.	(DAMA Collab.)
BERNABE 96	PL B389 757	R. Bernabei et al.	(DAMA Collab.)
COLLAR 96	PRL 76 331	J.I. Collar	(SUC Collab.)
SARSA 96	PL B386 458	M.L. Sarsa et al.	(ZARA Collab.)
Also 96	PR D56 1856	M.L. Sarsa et al.	(ZARA Collab.)
SMITH 96	PL B379 299	P.F. Smith et al.	(RAL, SHEF, LOIC+) Collab.
SNOWDEN... 96	PRL 76 332	D.P. Snowden-Ifft, E.S. Freeman, P.B. Price	(UCB Collab.)
AKERS 95R	ZPHY C67 203	R. Akers et al.	(OPAL Collab.)
GALLAS 95	PR D52 6	E. Gallas et al.	(MSU, FNAL, MIT, FLOR Collab.)
GARCIA 95	PR D51 1458	E. Garcia et al.	(ZARA, SUC, PNL Collab.)
QUENBY 95	PL B351 70	J.J. Quenby et al.	(LOIC, RAL, SHEF+) Collab.
SNOWDEN... 95	PRL 74 4133	D.P. Snowden-Ifft, E.S. Freeman, P.B. Price	(UCB Collab.)
Also 95	PRL 76 331	J.I. Collar	(SUC Collab.)
Also 95	PRL 76 332	D.P. Snowden-Ifft, E.S. Freeman, P.B. Price	(UCB Collab.)
BECK 94	PL B336 141	M. Beck et al.	(MPH, KIAE, SASSO Collab.)
RAM 94	PR D49 3120	S. Ram et al.	(TELA, TRIU Collab.)
ABE 93G	PRL 71 2542	F. Abe et al.	(CDF Collab.)
ASTONE 93	PR D47 4770	P. Astone et al.	(ROMA, ROMAI, CATA, FRAS Collab.)
BUSKULIC 93C	PL B303 198	D. Buskulic et al.	(ALEPH Collab.)
YAMAGATA 93	PR D47 1231	T. Yamagata, Y. Takamori, H. Utsunomiya	(KONAN Collab.)
ABE 92J	PR D46 R1889	F. Abe et al.	(CDF Collab.)
AHLEN 92	PRL 69 1860	S.P. Ahlen et al.	(MACRO Collab.)
BACCI 92	PL B293 460	C. Bacci et al.	(Beijing-Roma-Saclay Collab.)
VERKERK 92	PRL 68 1116	P. Verkerk et al.	(ENSP, SACL, PAST Collab.)
AKESSON 91	ZPHY C52 219	T. Akesson et al.	(HELIOS Collab.)

See key on page 373

Searches Particle Listings

WIMPs and Other Particle Searches

NAKAMURA	91	PL B263 529	S. Nakamura <i>et al.</i>		ARMITAGE	79	NP B150 87	J.C.M. Armitage <i>et al.</i>	(CERN, DARE, FOM+)
ORITO	91	PRL 66 1951	S. Orito <i>et al.</i>	(ICEPP, WASCR, NIHO, ICRR)	BOZZOLI	79	NP B159 363	W. Bozzoli <i>et al.</i>	(BGNA, LAPP, SACL+)
REUSSER	91	PL B255 143	D. Reusser <i>et al.</i>	(NEUC, CIT, PSI)	GOODMAN	79	PR D19 2572	J.A. Goodman <i>et al.</i>	(UMD)
ADACHI	90C	PL B244 352	I. Adachi <i>et al.</i>	(TOPAZ Collab.)	SMITH	79	NP B149 525	P.F. Smith, J.R.J. Bennett	(RHEL)
ADACHI	90E	PL B249 336	I. Adachi <i>et al.</i>	(TOPAZ Collab.)	BHAT	78	PRAM 10 115	P.N. Bhat, P.V. Ramana Murthy	(TATA)
AKRAWY	90O	PL B252 290	M.Z. Akrawy <i>et al.</i>	(OPAL Collab.)	CARROLL	78	PRL 41 777	A.S. Carroll <i>et al.</i>	(BNL, PRIN)
HENMICK	90	PR D41 2074	T.K. Hemmick <i>et al.</i>	(ROCH, MICH, OHIO+)	CUTTS	78	PRL 41 363	D. Cutts <i>et al.</i>	(BROW, FNAL, ILL, BARI+)
SAITO	90	PRL 65 2094	T. Saito <i>et al.</i>	(ICRR, KOBE)	VIDAL	78	PL 77B 344	R.A. Vidal <i>et al.</i>	(COLU, FNAL, STON+)
NAKAMURA	89	PR D39 1261	T.T. Nakamura <i>et al.</i>	(KYOT, TMTCC)	ALEKSEEV	76	SJNP 22 531	G.D. Alekseev <i>et al.</i>	(JINR)
NORMAN	89	PR D39 2499	E.B. Norman <i>et al.</i>	(LBL)	ALEKSEEV	76B	Translated from YAF 22 1021. SJNP 23 633	G.D. Alekseev <i>et al.</i>	(JINR)
BERNSTEIN	88	PR D37 3103	R.M. Bernstein <i>et al.</i>	(STAN, WISC)	BALDIN	76	SJNP 22 264	B.Y. Baldin <i>et al.</i>	(JINR)
CALDWELL	88	PRL 61 510	D.O. Caldwell <i>et al.</i>	(UCSB, UCB, LBL)	BRIATORE	76	NC 31A 555	L. Briatore <i>et al.</i>	(LCGT, FRAS, FREIB)
LIU	88	PRL 61 271	G. Liu, B. Barish		GUSTAFSON	76	PRL 37 474	H.R. Gustafson <i>et al.</i>	(MICH)
BARISH	87	PR D36 2641	B.C. Barish, G. Liu, C. Lane	(CIT)	ALBROW	75	NP B97 189	M.G. Albrow <i>et al.</i>	(CERN, DARE, FOM+)
NORMAN	87	PRL 58 1403	E.B. Norman, S.B. Gazes, D.A. Bennett	(LBL)	FRANKEL	75	PR D12 2561	S. Frankel <i>et al.</i>	(PENN, FNAL)
BADIER	86	ZPHY C31 21	J. Badier <i>et al.</i>	(NA3 Collab.)	JOVANOV...	75	PL 56B 105	J.V. Jovanovich <i>et al.</i>	(MANI, AACH, CERN+)
MINCER	85	PR D32 541	A. Mincer <i>et al.</i>	(UMD, GMAS, NSF)	YOCK	75	NP B86 216	P.C.M. Yock	(AUCK, SLAC)
NAKAMURA	85	PL 161B 417	K. Nakamura <i>et al.</i>	(KEK, INUS)	APPEL	74	PRL 32 428	J.A. Appel <i>et al.</i>	(COLU, FNAL)
THRON	85	PR D31 451	J.L. Thron <i>et al.</i>	(YALE, FNAL, IOWA)	FRANKEL	74	PR D9 1932	S. Frankel <i>et al.</i>	(PENN, FNAL)
SAKUYAMA	83B	LNC 37 17	H. Sakuyama, N. Suzuki	(MEIS)	YOCK	74	NP B76 175	P.C.M. Yock	(AUCK)
Also		LNC 36 389	H. Sakuyama, K. Watanabe	(MEIS)	ALPER	73	PL 46B 265	B. Alper <i>et al.</i>	(CERN, LVP, LUND, BOHR+)
Also		NC 78A 147	H. Sakuyama, K. Watanabe	(MEIS)	LEIPUNER	73	PRL 31 1226	L.B. Leipuner <i>et al.</i>	(BNL, YALE)
Also		NC 6C 371	H. Sakuyama, K. Watanabe	(MEIS)	DARDO	72	NC 9A 319	M. Dardo <i>et al.</i>	(TORI)
BHAT	82	PR D25 2820	P.N. Bhat <i>et al.</i>	(TATA)	TONWAR	72	JPA 5 569	S.C. Tonwar, S. Naranan, B.V. Sreekantan	(TATA)
KINOSHITA	82	PRL 48 77	K. Kinoshita, P.B. Price, D. Fryberger	(UCB+)	ANTIPOV	71B	NP B31 235	Y.M. Antipov <i>et al.</i>	(SERP)
MARINI	82	PR D26 1777	A. Marini <i>et al.</i>	(FRAS, LBL, NWES, STAN+)	ANTIPOV	71C	PL 34B 164	Y.M. Antipov <i>et al.</i>	(SERP)
SMITH	82B	NP B206 333	P.F. Smith <i>et al.</i>	(RAL)	BINON	69	PL 30B 510	F.G. Binon <i>et al.</i>	(SERP)
KINOSHITA	81B	PR D24 1707	K. Kinoshita, P.B. Price	(UCB)	BJORNBOE	68	NC B53 241	J. Bjornboe <i>et al.</i>	(BOHR, TATA, BERN+)
LOSECCO	81	PL 102B 209	J.M. LoSecco <i>et al.</i>	(MICH, PENN, BNL)	JONES	67	PR 164 1584	L.W. Jones	(MICH, WISC, LBL, UCLA, MINN+)
ULLMAN	81	PRL 47 289	J.D. Ullman	(LEHM, BNL)	DORFAN	65	PRL 14 999	D.E. Dorfan <i>et al.</i>	(COLU)
YOCK	81	PR D23 1207	P.C.M. Yock	(AUCK)					
BARTEL	80	ZPHY C6 295	W. Bartel <i>et al.</i>	(JADE Collab.)					
BUSSIERE	80	NP B174 1	A. Bussiere <i>et al.</i>	(BGNA, SACL, LAPP)					
YOCK	80	PR D22 61	P.C.M. Yock	(AUCK)					

INDEX

- A*, *a* meson resonances
- A*(1680) or [*now called* π_2 (1670)] **42**, 664
 - A*(2100) [*now called* π_2 (2100)] 688
 - a*₀(980) [*was* δ (980)] **39**, 615
 - a*₀(1450) 648
 - a*₁(1260) [*was* *A*₁(1270) or *A*₁] **40**, 625
 - a*₁(1260), note on
 - a*₁(1640) 661
 - a*₂(1320) [*was* *A*₂(1320)] **40**, 634
 - a*₂(1700) 674
 - A*₃ [*now called* π_2 (1670)] **42**, 664
 - a*₄(2040) [*was* δ_4 (2040)] 685
 - a*₆(2450) [*was* δ_6 (2450)] 696
- Abbreviations used in Particle Listings 374
- Accelerator-induced radioactivity 313
- Accelerator parameters (colliders) 264
- Accelerator physics of colliders 261
- Acceptance-rejection method in Monte Carlo 330
- Accessing the high-energy physics databases 21
- Activity, unit of, for radioactivity 312
- Age of the universe 104, 219
- Air showers (cosmic ray) 258
- Algorithms for Monte Carlo 331
- α_s , QCD coupling constant 103, 116
- Amplitudes, Lorentz invariant 340
- Angular-diameter distance, d_A 219
- Anisotropy of cosmic microwave background radiation (CBR) 236, 246
- Anomalous *W/Z* Quartic Couplings 392
- Anomalous $ZZ\gamma$, $Z\gamma\gamma$, and ZZV couplings 411
- Argand diagram, definition 343
- Astronomical unit 104
- Astrophysics 217, 241
- Asymmetries of *Z*-boson decay 394
- Asymmetry formulae in Standard Model 128
- Atmospheric cosmic rays 255
- Atmospheric pressure 103
- Atomic and nuclear properties of materials 110
- Atomic mass unit 103
- Atomic weights of elements 107
- Attenuation length for photons 275
- Authors and consultants 13
- Average hadron multiplicities in e^+e^- annihilation events 355
- Averaging of data 16
- Avogadro number 103
- Axial vector couplings, g_V , g_A vector 125
- Axions as dark matter 217, 242
- Axion searches **32**, 459
 - Axion searches, note on 459
- b*-baryon ADMIXTURE (A_b , Ξ_b , Σ_b , Ω_b) **89**, 1204
- b*-flavored hadrons, production and decay of, note on 833
- b*-hadron mixing and production fractions, note on 919
- b*₁(1235) [*was* *B*(1235)] **40**, 624
- b* (quarks) **37**, 562
- b*-quark fragmentation 207
- b'* quark (*4th* generation), searches for, **37**, 576
- b* \bar{b} mesons **71**, 1042
 - B^0 - \bar{B}^0 mixing, note on 914
- B* decay, *CP* violation in 153
- B* decays, hadronic, note on 838
- B* decays, rare, note on 838
- B*, bottom mesons
- Bottom mesons, HFAG activities 842
 - B* (bottom meson) **53**, 833
 - B^\pm (bottom meson) **54**, 842
 - B^0 , \bar{B}^0 (bottom meson) **58**, 878
 - B^\pm/B^0 ADMIXTURE **62**, 932
 - $B^\pm/B^0/B_s^0/b$ -baryon ADMIXTURE **64**, 945
 - B^* **65**, 966
 - B_{sJ}^* (5732) 966
 - B_c^\pm 976
 - B_d mixing studies, note on 917
 - B_s^0 **65**, 968
 - B_s mixing studies, note on 917
 - B_s^* 974
 - B_{sJ}^* (5850) 975
 - b* \bar{b} mesons **71**, 1042
- Baryogenesis 222
- Baryon decay parameters, note on 1071
- Baryon magnetic moments, note on 1126
- Baryon number conservation 93
- Baryon resonances, SU(3) classification of 175
- Baryonium candidates 698
- Baryons **77**, 1061
 - Bottom (beauty) baryons **89**, 1202
 - Cascade baryons (Ξ baryons) **84**, 1166
 - Charmed baryons **85**, 1182
 - Dibaryons
 - (see p. VIII.118 in our 1992 edition, Phys. Rev. **D45**, Part II)
 - Exotic baryons (formerly Z^* resonances) , 1124
 - Pentaquarks 1124
 - Hyperon baryons (Λ baryons) **81**, 1126
 - Hyperon baryons (Σ baryons) **82**, 1142
 - Nucleon resonances (Δ resonances) **80**, 1104
 - Nucleon resonances (N resonances) **78**, 1076
 - Nucleons **77**, 1061
 - Ω baryons **85**, 1179

- Baryons in quark model 175
- Baryons, stable **77**, 1061
(see entries for p , n , Λ , Σ , Ξ , Ω , Λ_c , Ξ_c , Ω_c , Λ_b , and Ξ_b)
- Bayes' theorem 316
- Bayesian statistics 324
- Beam-beam tune shift in colliders 263
- Beam dynamics 261
- Beam momentum, c.m. energy and momentum vs 340
- Beauty – see Bottom
- Becquerel, unit of radioactivity 312
- BEPC (China) collider parameters 264
- BEPC-II (China) collider parameters 264
- β decay, neutrinoless double, search for 525
- β -rays, from radioactive sources 315
- Betatron oscillations 261
- Bethe-Bloch equation 268
- Bias of an estimator 320
- Big-bang cosmology 217
- Binary pulsars 213
- Binomial distribution 318
- Binomial distribution, Monte Carlo algorithm for 331
- Binomial distribution, table of 318
- Biological damage from radiation 312
- Birks' law 285
- Black holes 1272
- Bohr magneton 103
- Bohr radius 103
- Boiling points of cryogenic gases 110
- Boltzmann constant 103
- Booklet, Particle Physics, how to get 13
- Bosons **31**, 385
(see individual entries for γ , W , Z , g , Axions, graviton, Higgs)
- Bottom baryons (Λ_b^0 , Ξ_b) **89**, 1202
- Bottom, B^0 - \bar{B}^0 mixing, note on 914
- Bottom-changing neutral currents, tests for 93
- Bottom, charmed meson **66**, 976
- Bottom mesons (B , B^* , B_s , B_s^* , B_c^\pm) **53**, 833
Bottom mesons, note on HFAG activities 842
- Bottom quark (b) **37**, 562
- Bottom, strange mesons **65**, 968
- Bottomonium system, level diagram 1042
- Bragg additivity 271
- Branes 1272
- Breit-Wigner
distribution, Monte Carlo algorithm for 331
resonance, definition 343
vs pole parameters of N and Δ Resonances 1075
- Bremsstrahlung by electrons 273
- Bulletin boards 22
- C (charge conjugation), tests of conservation 93
- c (quark) **37**, 561
- $c\bar{c}$ Region in e^+e^- Collisions, plot of 359
- c -quark fragmentation 207
- $c\bar{c}$ mesons **66**, 977
- Cabibbo-Kobayashi-Maskawa mixing in B decay, note on 914
- Calorimetry 303
- Cascade baryons (Ξ baryons) **84**, 1166
- CBR—Cosmic background radiation (see CMB) 246
- Central limit theorem 318
- Cepheid variable stars 235
- CESR (Cornell) collider parameters 265
- CESR-C (Cornell) collider parameters 265
- Change of random variables 317
- Characteristic functions 317
- Charge conjugation (C) conservation 93
- Charge conservation 93
- Charge conservation and the Pauli exclusion principle, note on
(see p. VI.10 in our 1992 edition, Phys. Rev. **D45**)
- Chargino searches 1243
- Charm-changing neutral currents, tests for 93
- Charm Dalitz analyses, note on 774
- Charm quark (c) **37**, 561
- Charmed baryons (Λ_c^+ , Σ_c , Ξ_c , Ω_c^0) **85**, 1184
- Charmed, bottom meson (B_c^\pm) **66**, 976
- Charmed mesons (D , D^* , D_J) **47**, 766
- Charmed, strange mesons [D_s , D_s^* , D_{sJ}] **52**, 816
- Charmonium system, level diagram 977
- Cherenkov detectors 289
- Cherenkov radiation 278
- χ^2 distribution 319
- χ^2 distribution, Monte Carlo algorithm for 331
- χ^2 distribution, table of 318
- χ_b and χ_c mesons
 $\chi_{b0}(1P)$ **72**, 1046
 $\chi_{b0}(2P)$ **72**, 1049
 $\chi_{b1}(1P)$ **72**, 1047
 $\chi_{b1}(2P)$ **72**, 1050
 $\chi_{b2}(1P)$ **72**, 1047
 $\chi_{b2}(2P)$ **72**, 1051
 $\chi_{c0}(1P)$ **68**, 999
 $\chi_{c1}(1P)$ **68**, 1005
 $\chi_{c2}(1P)$ **68**, 1008
- $\chi_{c0,1,2}$ and $\psi(2S)$, branching ratios, note on 997
- CKM mixing elements in B decay, note on 914
- Clebsch-Gordan coefficients 337

c.m. energy and momentum vs beam momentum	340	Coupling unification	180
CMB–Cosmic microwave background	223, 246, 236	Couplings, anomalous W/Z Quartic	392
Collaboration databases	21	Couplings, anomalous $ZZ\gamma$, $Z\gamma\gamma$, and ZZV	411
Collider parameters	264	Couplings for photon, W , Z	125
Colliders, accelerator physics of	261	Couplings, note on the extraction of triple-gauge	389
Color octet leptons	92 , 1271	Covariance, definition	317
Color sextet quarks	92 , 1271	Coverage	325
Compensating calorimeters	304	CP , tests of conservation	93
Compositeness, quark and lepton, searches	91 , 1265	CP violation	
Compositeness, quark and lepton, searches, note on	1265	in B decay	153
Composition of the Universe	228	in K_L^0 decay	153
Compton wavelength, electron	103	in K_L^0 decays, note on	741
Concordance cosmology	233	in $K_S^0 \rightarrow 3\pi$ decays, note on	727
Conditional probability density function	317	overview	153
Conference databases	21	CPT Invariance tests in neutral kaon decay	721
Confidence intervals	324	CPT , tests of conservation	93
Confidence intervals, frequentist	325	Critical density in cosmology	104, 217
Confidence intervals, Poisson	327	Critical energy, electrons	274
Conservation laws	93	Critical energy, muons	277
Consistency of an estimator	320	Cross sections and related quantities, plots of	353
Cosmic microwave background	236	e^+e^- annihilation cross section near M_Z	360
Constrained fits, procedures for	17	Fragmentation functions	202
Consultants	14	gamma production in $p\bar{p}$ interactions	353
Conversion probability for photons to e^+e^-	275	Jet production in pp and $\bar{p}p$ interactions	353
Correlation coefficient, definition	317	νN and $\bar{\nu} N$ c.c. total cross section	361
Cosmic background radiation (CBR) temperature	104	Nucleon structure functions	194
Cosmic ray(s)	254	Pseudorapidity distributions	354
air showers	258	W and Z differential cross section	354
ankle	259	Cross sections, Regge theory fits to total, table	362
at surface of earth	255	Cross sections, relations for	342, 345
background in counters	312	Cryogenic gases, boiling points	110
composition	254	Cumulative distribution function, definition	316
fluxes	255	Curie, unit of radioactivity	312
in atmosphere	255, 258	d (quark)	37 , 558
knee	259	d functions	337
primary spectra	254	D^0 – \bar{D}^0 mixing, note on	783
secondary neutrinos	257	D -meson, Dalitz analyses, note on	774
underground	256	D mesons	
Cosmological constant Λ	104, 217, 232	D^\pm	47 , 766
Cosmological density parameter, Ω	218	D^0 , \bar{D}^0	48 , 783
Cosmological equation of state	218	$D_1(2420)^0$	51 , 812
Cosmological mass density parameter	218	$D_1(2420)^\pm$	813
Cosmological mass density parameter of vacuum (dark energy)	218	$D^*(2007)^0$	51 , 810
Cosmological parameters	232, 233	$D^*(2010)^\pm$	51 , 811
Cosmology	217, 232, 241	$D^*(2640)^\pm$	815
Coulomb scattering through small angles, multiple	271	$D_2^*(2460)^0$	52 , 814
Coupling between matter and gravity	212	$D_2^*(2460)^\pm$	52 , 815
Coupling constant in QCD	103, 116		

Greek letters are alphabetized by their English-language spelling. Bold page numbers signify entries in the Particle Properties Summary Tables.

- D_s^\pm [*was* F^\pm] **52**, 816
 $D_s^{*\pm}$ [*was* $F^{*\pm}$] **53**, 827
 $D_{s1}(2536)^\pm$ **53**, 830
 $D_{s2}(2573)^\pm$ **53**, 831
 D_s^+ Decay constant, note on 818
Dalitz analyses, D -meson, note on 774
Dalitz plot, relations for 341
Damage, biological, from radiation 312
DAΦNE (Frascati) collider parameters 264
Dark energy 218, 234
Dark energy equation of state parameter w 235
Dark energy parameter, Ω_N 218
Dark matter 225, 241, 233, 234
Dark matter limits:
 Neutralinos mass limits 1242
 Sneutrino mass limits 1245
Dark matter, nonbaryonic 241
Data, averaging and fitting procedures 16
Data, selection and treatment 15
Databases, availability online 21
Databases, high-energy physics 21
Databases, particle physics 21
Day, sidereal 104
 dE/dx 268
Decay amplitudes (for hyperon decays)
 (see p. 286 in our 1982 edition, Phys. Lett. **111B**)
Decay constant, D_s^+ , note on 818
Decay constants of charged pseudoscalar mesons, note on
Decays, kinematics and phase space for 340
Deceleration parameter, q_0 218
Deep-inelastic scattering 117, 188
Definitions for abbreviations used in Particle Listings 374
 δ -rays 270
 $\delta(980)$ [*now called* $a_0(980)$] **39**, 615
 $\delta_4(2040)$ [*now called* $a_4(2040)$] 685
 $\delta_6(2450)$ [*now called* $a_6(2450)$] 696
 Δ resonances (see also N and Δ resonances) **80**, 1104
 $\Delta B = 1$, weak-neutral currents, tests for 93
 $\Delta B = 2$, tests for 93
 $\Delta C = 1$, weak-neutral currents, tests for 93
 $\Delta C = 2$, tests for 93
 $\Delta I = 1/2$ rule for hyperon decays, test of
 (see p. 286 in our 1982 edition, Phys. Lett. **111B**)
 $\Delta S = 1$, weak-neutral currents, tests for 93
 $\Delta S = 2$, tests for 93
 $\Delta S = \Delta Q$ rule in K^0 decay, note on 747
 $\Delta S = \Delta Q$, tests of 93
 $\Delta T = 1$, weak-neutral currents, tests for 93
Density effect in energy loss rate 269
Density of materials, table 110
Density of matter, critical 104
Density of matter, local 104
Density parameter of the universe, Ω_0 104
Detector parameters 281
Deuteron mass 103
Deuteron structure function 195, 196
Dibaryons
 (see p. VIII.118 in our 1992 edition, Phys. Rev. **D45**, Part II)
Dielectric constant of gaseous elements, table 111
Dielectric suppression of bremsstrahlung 276
DIEHARD 330
Differential Cherenkov detectors 290
Diffractive events, QCD in 121
Dimensions, extra **92**, 1272
Directories, online, people, and organizations 22
Disk density 104
Distance-redshift relation 217, 232
Dose, radioactivity, unit of absorbed 312
Dose rate from gamma ray sources 314
Double- β Decay 525
 Double- β Decay, Limits from Neutrinoless, note on 525
Double- β decay, neutrinoless, search for 525
Durham databases 21
Dynamical electroweak symmetry breaking 1258
 e (electron) **34**, 479
 e (natural log base) 103
 Charge conservation and the Pauli exclusion principle, note on
 (see p. VI.10 in our 1992 edition, Phys. Rev. **D45**)
 e^+e^- average multiplicity, plot of 357
 ep collisions, jet rates 121
 $E(1420)$ [*now called* $f_1(1420)$] **41**, 645
Earth equatorial radius 104
Earth mass 104
Education databases 25
Efficiency of an estimator 320
Electric charge (Q) conservation 93
Electrical resistivity of elements, table 111
Electromagnetic
 calorimeters 304
 interactions of N and Δ baryons (review) 1076
 penguin decays, note on 839
 relations 112
 shower detectors, energy resolution 304
 showers, lateral distribution 277
 showers, longitudinal distribution 276

Electron	34 , 479	$\eta_b(1S)$	1043
and photon interactions in matter	272	$\eta_c(1S)$	66 , 977
charge	103	$\eta_c(2S)$	1013
critical energy	274	Excitation energy	268
cyclotron frequency/field	103	Excited lepton searches	91 , 1268
mass	103, 34	Exotic baryons (formerly Z^* resonances)	1124
radius, classical	103	Pentaquarks	1124
volt	103	(see p. VIII.58 in our 1992 edition, Phys. Rev. D45 , Part II)	
Electronic structure of the elements	108	Exotic meson resonances	1057
Electroweak analyses of new physics	136	Expansion of the Universe	218
Electroweak interactions, Standard Model of	125	Expectation value, definition	316
Elements, electronic structure of	108	Experiment databases	21
Elements, ionization energies of	108	Experimental issues in $B^0-\bar{B}^0$ mixing, note on	915
Elements, periodic table of	107	Experimental tests of gravitational theory	212
Energy and momentum (c.m.) vs beam momentum	340	Exposure, radioactivity, unit of	312
Energy density / Boltzmann constant	104	Extensions to the cosmological standard model	234
Energy density of CBR	104	Extra Dimensions	92 , 1272
Energy density of relativistic particles	104	$f_{D^+}, f_{D_s^+}, f_{K^-}, f_{\pi^-}$ decay constants	818
Energy loss		F, f meson resonances	
by electrons	273	F^\pm [<i>now called</i> D_s^\pm]	52 , 816
(fractional) for electrons and positrons in lead	272	$F^{*\pm}$ [<i>now called</i> $D_s^{*\pm}$]	53 , 827
rate for charged particles	268	$f_0(600)$ [<i>was</i> $\epsilon(1200)$]	38 , 594
rate for muons at high energies	277	$f_0(980)$ [<i>was</i> $S(975)$ or S^*]	39 , 613
rate, form factor corrections	268	$f_0(1370)$	41 , 637
rate in compounds	271	$f_0(1500)$	41 , 652
rate, restricted	270	$f_0(1710)$ [<i>was</i> $\theta(1690)$]	43 , 675
Entropy density	222	$f_0(2020)$	685
Entropy density / Boltzmann constant	104	$f_0(2100)$	688
Eprints	23	$f_0(2200)$	691
$\epsilon(1200)$ [<i>now called</i> $f_0(600)$]	38 , 594	$f_1(1285)$	40 , 630
$\epsilon(2150)$ [<i>now called</i> $f_2(2150)$]	688	$f_1(1420)$ [<i>was</i> $E(1420)$]	41 , 645
$\epsilon(2300)$ [<i>now called</i> $f_4(2300)$]	694	$f_1(1420)$, note on	641
ϵ (permittivity)	103, 111, 112	$f_1(1510)$	655
ϵ_0 (permittivity of free space)	103, 112	$f_1(1510)$, note on	641
$\hat{\epsilon}_1, \hat{\epsilon}_2, \hat{\epsilon}_3$ electroweak variables	137–138	$f_2(1270)$	40 , 627
Error function	318	$f_2(1430)$	648
Error procedure for masses and widths of meson resonances	751	$f_2(1565)$	658
Errors, treatment of	16	$f_2(1640)$	661
Estimator	320	$f_2(1810)$	679
η meson	38 , 589	$f_2(1910)$	682
$\eta(1295)$	40 , 632	$f_2(1950)$	683
$\eta(1405)$ [<i>was</i> $\iota(1440)$]	41 , 641	$f_2(2010)$ [<i>was</i> $g_T(2010)$]	43 , 685
$\eta(1440)$, note on	641	$f_2(2150)$ [<i>was</i> $\epsilon(2150)$]	688
$\eta(1760)$	678	$f_2(2300)$ [<i>was</i> $g_T'(2300)$]	43 , 694
$\eta(2225)$	693	$f_2(2340)$ [<i>was</i> $g_T'(2340)$]	43 , 695
$\eta_2(1645)$	662	$f_2'(1525)$ [<i>was</i> $f'(1525)$]	41 , 655
$\eta_2(1870)$	681	$f_4(2050)$ [<i>was</i> $h(2030)$]	43 , 686
$\eta'(958)$	39 , 610		

$f_4(2300)$ [<i>was</i> $\epsilon(2300)$]	694	Gamma distribution, table of	318
$f_6(2510)$ [<i>was</i> $r(2510)$]	697	Gas-filled detectors	292
$f_J(2220)$ [<i>was</i> $\xi(2220)$]	692	Gauge bosons	31 , 385 (see individual entries for γ , W , Z , g , Axions, graviton, Higgs)
F_2 structure function, plots	194	Gauge couplings	125
Familon searches	472	Gaussian confidence intervals	326
Fermi coupling constant	103	Gaussian confidence intervals close to physical boundary	328
Fermi plateau	270	Gaussian distribution, Monte Carlo algorithm for	331
Feynman's x variable	342	Gaussian distribution, Multivariate	319
Field equations, electromagnetic	112	Gaussian ellipsoid	319
Fine structure constant	103	Gluino searches	91 , 1253
Fit to Z electroweak measurements	393	gluon, g	31 , 385
Fits to data	16	Gluon fragmentation	204
Flatness of Universe	104	Gluonium candidates	1057
Flavor-changing neutral currents, tests for	93	Goldstone boson searches	472
Fly's Eye	259	Grand unified theories	180
Forbidden states in quark model	114	Gravitational	
Force, Lorentz	112	acceleration g	103
Form factors, $K_{\ell 3}$, note on	717	constant G_N	103, 104
Form factors, $\pi \rightarrow \ell\nu\gamma$ and $K \rightarrow \ell\nu\gamma$, note on	584	field in the strong field regime, dynamical tests	213
Fourth generation (b') searches	37 , 576	field in the weak field regime, dynamical tests	213
Fractional energy loss for electrons and positrons in lead	272	lensing	224, 238
Fragmentation functions	202	radiation	214
Fragmentation functions, scaling violations in	120	theory, experimental tests of	212
Fragmentation, gluon	204	graviton	385
Fragmentation, heavy-quark	207	Gravitons	1272
Fragmentation in e^+e^- annihilation	202	Gravity in extra dimensions	1272
Fragmentation, longitudinal	203	Gray, unit of absorbed dose of radiation	312
Fragmentation models	205	GUTs	180
Free quark searches	37 , 577	$h(2030)$ [<i>now called</i> $f_4(2050)$]	43 , 686
Frequentist statistics	325	$h_1(1170)$ [<i>was</i> $H(1190)$]	40 , 623
Friedmann-Lemaître equations	217	$h_1(1380)$	640
Further States	698	$h_1(1595)$	660
g (gluon)	31 , 385	$h_c(1P)$	1008
$g(1690)$ [<i>now called</i> $\rho_3(1690)$]	42 , 667	Hadron (average) multiplicities in e^+e^- annihilation events	355
$g_T(2010)$ [<i>now called</i> $f_2(2010)$]	43 , 685	Hadronic	
$g'_T(2300)$ [<i>now called</i> $f_2(2300)$]	43 , 694	calorimeters	304
$g''_T(2340)$ [<i>now called</i> $f_2(2340)$]	43 , 695	flavor conservation	93
g_V, g_A vector, axial vector couplings	125	shower detectors	304
Galaxy clustering	237	Half-lives of commonly used radioactive nuclides	315
Galaxy power spectrum	237	Halo density	104
γ (Euler constant)	103	Harrison-Zel'dovich effect	232
γ (photon)	31 , 385	Heavy boson searches	32 , 443
γp and γd cross sections, plots of	369	Heavy lepton searches	36 , 516
gamma production in $p\bar{p}$ interactions	353	Heavy-Neutral Leptons, Searches for	36 , 545
γ -rays, from radioactive sources	315	Heavy particle searches	1285
Gamma distribution	319	Heavy physics from precision experiments	136, 136
Gamma distribution, Monte Carlo algorithm for	331		

Heavy-quark fragmentation	207	K^+p , K^+n , and K^+d cross sections, plots of	368
Heavy-quarkonium decay, QCD in	119	K^-p , K^-n , and K^-d cross sections, plots of	367
HERA (DESY) collider parameters	266	K stable mesons (see meson resonances below)	
Hierarchy problem	1211 , 1272	K^\pm	43 , 704
Higgs boson in Standard Model	125, 135, 414	K^0 , \bar{K}^0	44 , 721
Higgs boson mass in electroweak analyses	135–137	K_L^0	45 , 728
Higgs, M_H , constraints on	135–137	K_S^0	44 , 725
Higgs production in e^+e^- annihilation, cross-section formula	347	K stable mesons, notes therein	
Higgs searches	32 , 414	K_L^0 CP -violation parameters, fits for, note on	741
Higgs searches, note on	414	K decay, CPT invariance tests in neutral	721
High-energy hadron collisions, QCD in	118	K^0 decay, note on $\Delta S = \Delta Q$ rule in	747
History of measurements, discussion	18	K_L^0 decay, CP violation in	153
Hubble constant (expansion rate)	104	$K_{\ell 3}$ form factors, note on	717
Hubble constant H_0	232	K^\pm mass, note on	704
Hubble expansion	218	K rare decay, note on	706
Hyperon baryons (see Λ and Σ baryons)	81 , 1126	$K \rightarrow \ell\nu\gamma$ form factors, note on	584
Hyperon decays, nonleptonic decay amplitudes		$K \rightarrow 3\pi$ Dalitz plot parameters, note on	715
(see p. 286 in our 1982 edition, Phys. Lett. 111B)		$K_S^0 \rightarrow 3\pi$ decay, note on CP violation in	727
Hyperon decays, test of $\Delta I = 1/2$ rule for		K, K^* meson resonances	
(see p. 286 in our 1982 edition, Phys. Lett. 111B)		$K(1460)$ [<i>was</i> $K(1400)$]	758
Hyperon radiative decays, note on	1167	$K(1630)$	759
ID particle codes for Monte Carlos	333	$K(1830)$	762
Ideograms, criteria for presentation	17	$K(3100)$	765
Illustrative key to the Particle Listings	373	$K^*(892)$	46 , 750
Impedance, relations for	113	$K^*(892)$ mass and mass differences, note on	751
Importance sampling in Monte Carlo calculations	330	$K^*(1410)$	46 , 755
Inclusive hadronic reactions	347	$K^*(1680)$ [<i>was</i> $K^*(1790)$]	46 , 759
Inclusive reactions, kinematics for	342	$K_0^*(1430)$ [<i>was</i> $\kappa(1350)$]	46 , 755
Inconsistent data, treatment of	17	$K_0^*(1950)$	762
Independence of random variables	317	$K_1(1270)$ [<i>was</i> $Q(1280)$ or Q_1]	46 , 752
Inflation of early universe	222, 232	$K_1(1400)$ [<i>was</i> $Q(1400)$ or Q_2]	46 , 754
Information horizon	220	$K_1(1650)$	759
Inorganic scintillators	286	$K_2(1580)$ [<i>was</i> $L(1580)$]	758
Inorganic scintillator parameters	285	$K_2(1770)$ [<i>was</i> $L(1770)$]	46 , 760
International System (SI) units	106	$K_2(1820)$	47 , 762
INTERNET address for comments	13	$K_2(2250)$ [<i>was</i> $K(2250)$]	764
Introduction	13	$K_2^*(1430)$ [<i>was</i> $K^*(1430)$]	46 , 756
Inverse transform method in Monte Carlo	330	$K_2^*(1980)$	763
Ionization energies of the elements	108	$K_3(2320)$ [<i>was</i> $K(2320)$]	764
Ionization energy loss at minimum, table	110	$K_3^*(1780)$ [<i>was</i> $K^*(1780)$]	46 , 760
Ionization yields for charged particles	271	$K_4(2500)$ [<i>was</i> $K(2500)$]	764
$\iota(1440)$ [<i>now called</i> $\eta(1405)$]	41 , 641	$K_4^*(2045)$ [<i>was</i> $K^*(2060)$]	47 , 763
Jansky	104	$K_5^*(2380)$	764
Jet production in pp and $\bar{p}p$ interactions, plot of	353	$K_{\ell 3}$ form factors, note on	717
Jet rates in ep collisions	121	Kaluza-Klein states	1272
Journals	23	Kaon (see also K)	43 , 704
$J/\psi(1S)$ or $\psi(1S)$	66 , 981	Kaon decay, CPT invariance tests in neutral	721
		Kaon rare decay, note on	706

- $\kappa(1350)$ [*now called* $K_0^*(1430)$] **46**, 755
- KEKB collider parameters 265
- Key to the Particle Listings 373
- Kinematics, decays, and scattering 340
- Knock-on electrons, energetic 270
- Kobayashi-Maskawa (Cabibbo-) mixing matrix 145
- $L(1580)$ [*now called* $K_2(1580)$] 758
- $L(1770)$ [*now called* $K_2(1770)$] **46**, 760
- Lagrangian, QCD 116
- Lagrangian, standard electroweak 125
- Λ , cosmological constant 104, 217, 232
- Λ CDM (cold dark matter with dark energy) 233
- Λ , QCD parameter 116
- Λ **81**, 1126
- Λ and Σ baryons **81**, 1126
- Listings, Λ baryons 1126
- Listings, Σ baryons 1142
- Status of (review) 1129
- Λp cross section, plot of 369
- Λ_b^0 1202
- Λ_c^+ **85**, 1184
- Λ_c^+ branching fractions, note on 1185
- $\Lambda_c(2595)^+$ **86**, 1190
- $\Lambda_c(2625)^+$ **86**, 1191
- $\Lambda_c(2765)^+$ 1191
- $\Lambda_c(2880)^+$ 1192
- Lagged-Fibonacci-based random number generator 330
- Landau-Pomeranchuk-Migdal (LPM) effect 275
- Large-scale structure of the Universe 225
- Lattice QCD 121
- Least squares 321
- Least squares with nonindependent data 321
- LEP (CERN) collider parameters 265
- Lepton conservation, tests of 93
- Lepton family number conservation 93
- Lepton (heavy) searches **36**, 516
- Lepton mixing, neutrinos (massive) and, search for **36**, 530
- Lepton, quark compositeness searches **91**, 1265
- Lepton, quark substructure searches **91**, 1265
- Leptons **34**, 479
- (see individual entries for e , μ , τ , and neutrino properties)
- Leptons, weak interactions of quarks and 125, 136
- Leptoquark quantum numbers, note on 452
- Leptoquark searches 455
- Lethal dose from penetrating ionizing radiation 312
- LHC (CERN) collider parameters 266
- Libraries, HEP 22
- Lifetimes of b -flavored hadrons, note on 833
- Light boson searches 459
- Light neutrino types, number of **36**, 523
- Light neutrino types from collider expts., number of, note on 523
- Light, speed of 103
- Light year 104
- Lineshape of Z boson 393
- Liquid ionization chambers, free electron drift velocity 306
- Listings, Full, keys to reading 373
- Local group velocity relative to CBR 104
- Longitudinal fragmentation 203
- Longitudinal structure function, plots of 199
- Lorentz force 112
- Lorentz invariant amplitudes 340
- Lorentz transformations of four-vectors 340
- Low-noise electronics 301
- Luminosity conversion 104
- Luminosity distance d_L 219
- Luminosity in colliders 261
- Luminosity lifetime 263
- Ly α forest 223
- Magnetic moments, baryon, note on 1126
- Magnetic monopoles 180
- Magnetic monopole searches **91**, 1209
- Magnetic monopole searches, note on 1209
- Majoron searches 472
- Mandelstam variables 342
- Marginal probability density function 317
- Mass attenuation coefficient for photons 275
- Mass density parameter, Ω_m 233, 238
- Massive neutrinos and lepton mixing, search for **36**, 530
- Materials, atomic and nuclear properties of 110
- Matter, passage of particles through 267
- Maximum energy transfer to e^- 268
- Maximum likelihood 321
- Maxwell equations 112
- Mean energy loss rate in H_2 liquid, He gas, C, Al, Fe, Sn, and
- Pb, plots 268
- Mean excitation energy 268
- Mean range in H_2 liquid, He gas, C, Fe, Pb, plots 268
- Median, definition 317
- Meson multiplets in quark model 172
- Mesons **38**, 583
- $b\bar{b}$ mesons **71**, 1042
- Bottom, charmed mesons **66**, 976
- Bottom mesons **53**, 833
- Bottom, strange mesons **65**, 968

$c\bar{c}$ mesons	66 , 977	critical energy	277
Charmed, bottom meson	66 , 976	anomalous magnetic moment, note on	481
Charmed mesons	66 , 977	decay parameters, note on	485
Charmed, strange mesons	52 , 816	energy loss rate at high energies	277
Exotic mesons	1057	g-2	481
Nonstrange mesons	38 , 583	range/energy in rock	256
Strange mesons	43 , 704	MWPC, Multi-wire proportional chamber	294
Mesons, stable	38 , 583	M_W	103, 126, 133
(see individual entries for π , η , K , D , D_s , B , and B_s)		M_Z	103, 126, 133
Metric prefixes, commonly used	106	n (neutron)	78 , 1069
Michel parameter ρ	34 , 512	n -body differential cross sections	342
Microwave background	223	n -body phase space	340
Minimal subtraction scheme in QCD	116	$n - \bar{n}$ oscillations	1071
Minimum ionization	268	N and Δ resonances	78 , 1075
Minimum ionization loss, table	110	Breit-Wigner vs pole parameters of	1075
MIP (minimum ionizing particle)	268	Electromagnetic interactions (review)	1076
Mistag probabilities in $B^0-\bar{B}^0$ mixing, note on	916	Listings, Δ resonances	1104
Mixing angle, weak ($\sin^2 \theta_W$)	103, 125, 134	Listings, N resonances	1075
Mixing, $B^0-\bar{B}^0$, note on	914	Status of (review)	1075
Mixing, $D^0-\bar{D}^0$, note on	783	N^* resonances (see N and Δ resonances)	78 , 1075
Mixing studies, B_d , note on	917	Names, hadrons	15, 114
Mixing studies, B_s , note on	917	Neutral-current parameters, standard model expressions for	128
Molar volume	103	Neutral-current parameters, values for	136
Molière radius	277	Neutralino as dark matter	217
Momenta, measurement of, in a magnetic field	308	Neutralino searches	1242
Momentum — c.m. energy and momentum		Neutrino(s)	34 , 479
vs beam momentum	340	from cosmic rays	257
Momentum transfer, minimum and maximum	340	mass, cosmological limit	237
Monopole searches	91 , 1209	mass, mixing, and flavor change, note on	163
Monopole searches, note on	1209	masses	180
Monte Carlo particle numbering scheme	333	(massive) and lepton mixing, search for	36 , 530
Monte Carlo techniques	330	mixing	36 , 530
$\overline{\text{MS}}$ renormalization scheme (QCD)	116	oscillation searches	36 , 530
$\overline{\text{MS}}$ renormalization scheme (Standard Model)	125	properties	36 , 517
μ (muon)	34 , 480	solar, review	531
$\mu \rightarrow e$ conversion	484	types (light), number of	36 , 523
μ_0 (permeability of free space)	103, 112	types (light) from collider experiments, number of, note on	523
Multibody decay kinematics	342	Neutrinoless double- β decay, search for	525
Multiple Coulomb scattering through small angles	271	Neutrino mass density parameter, Ω_ν	232
Multiplets, meson in quark model	172	Neutron	78 , 1069
Multiplets, SU(n)	339	Neutrons at accelerators	312
Multiplicities, average in e^+e^- interactions, table of	355	Neutrons, from radioactive sources	315
Multiplicity, average in e^+e^- interactions, plot of	357	New physics from electroweak analyses	136–137
Multiplicity, average in pp and $\bar{p}p$ interactions, plot of	357	Newtonian gravitational constant G_N	104
Multivariate Gaussian distribution	319	Nomenclature for hadrons	15, 114
Multivariate Gaussian distribution, table of	318	Nonbaryonic dark matter	228
Multi-wire proportional chamber (MWPC)	294	Non- $q\bar{q}$ candidates	1057
Muon	34 , 480		

- Normal distribution 318
- Normal distribution, table of 318
- Neutrino Mixing **36**, 530
- Neutrino Properties **36**, 517
- νN and $\bar{\nu} N$ cross sections, plot of
(see p. III.75 in our 1992 edition, Phys. Rev. **D45**, Part II)
- Nuclear collision length, table 110
- Nuclear interaction length, table 110
- Nuclear magneton 103
- Nuclear (and atomic) properties of materials 110
- Nucleon decay 180
- Nucleon resonances (see N and Δ resonances) **78**, 1075
- Nucleon structure functions, plots of 194
- Nuclides, radioactive, commonly used 315
- Number density of baryons 104
- Number density of CBR photons 104
- Numbering scheme for particles in Monte Carlos 333
- Occupational radiation dose, U.S. maximum permissible 312
- Omega baryons (Ω baryons) **85**, 1179
- Ω^- resonances 1180
- Ω^- **85**, 1179
- Ω_c^0 1200
- Ω , cosmological density parameter 218
- Ω_b , baryon mass density 238
- Ω_{dm} , dark matter density 233, 234
- Ω_i , density parameter for i th matter constituent 232
- Ω_Λ , scaled cosmological constant 104, 218
- Ω_m , mass density parameter 104, 218, 233, 238
- Ω_ν , neutrino mass density parameter 232
- $\Omega_m + \Omega_\Lambda$ 104
- Ω_{tot} , total energy density of Universe 104, 237
- Ω_Q , quintessence (dark) energy density 235, 235
- Ω_v , vacuum energy parameter 218
- $\omega(782)$ **39**, 605
- $\omega(1420)$ **41**, 647
- $\omega(1650)$ **42**, 662
- $\omega_3(1670)$ **42**, 663
- Opposite-side tag in $B^0-\bar{B}^0$ mixing, note on 916
- Optical theorem 343
- Organic scintillators 285
- Organization of Particle Listings and Summary Tables 13
- Oscillation analyses in $B^0-\bar{B}^0$ mixing, note on 915
- Oscillation parameters, three-flavor, note 540
- Oscillations, betatron 261
- Oscillations, synchrotron 262
- Other particle searches 1282
- Other particle searches, note on 1282
- P (parity), tests of conservation 93
- p (proton) **77**, 1061
- $pp, \bar{p}p$ average multiplicity, plot of 357
- pp jet production 353
- pp, pn , and pd cross sections, plots of 364, 365
- $\bar{p}p$
- average multiplicity, plot of 357
- gamma production 353
- jet production 353
- $\bar{p}n$, and $\bar{p}d$ cross sections, plots of 364, 365
- pseudorapidity 354
- Parameter estimation 320
- Parity of $q\bar{q}$ states 172
- Parsec 104
- Partial-wave expansion of scattering amplitude 343
- Particle detectors 281
- Particle ID numbers for Monte Carlos 333
- Particle Listings, key to reading 373
- Particle Listings, organization of 13
- Particle nomenclature 15, 114
- Particle Physics Booklet, how to get 13
- Particle symbol style conventions 114
- Parton distributions 191
- Passage of particles through matter 267
- Pauli exclusion principle, charge conservation, note on
(see p. VI.10 in our 1992 edition, Phys. Rev. **D45**)
- Penguin decays, electromagnetic, note on 839
- PEP-II (SLAC) collider parameters 265
- Periodic table of the elements 107
- Permeability μ_0 of free space 103, 112
- Permittivity ϵ_0 of free space 103, 112
- Perturbative QCD in e^+e^- collisions 119
- Phase space, Lorentz invariant 340
- Phase space, relations for 340
- Phase stability in circular machines 262
- $\phi(1020)$ **39**, 618
- $\phi(1680)$ **42**, 666
- $\phi_3(1850)$ [*was* $X(1850)$] **43**, 681
- Photino searches 1238
- Photon **31**, 385
- and electron interactions with matter 272
- attenuation length 275
- collection efficiency, scintillators 285
- coupling 125
- cross section in carbon and lead, contributions to 274
- pair production cross section 274
- Photon structure functions 121
- to e^+e^- conversion probability 275

total cross sections (C and Pb)	274	$X(3945)$	1037
Physical constants, table of	103	$\psi(4040)$	70 , 1038
Physical region, for confidence intervals	328	$\psi(4160)$	71 , 1039
π , value of	103	$\psi(4415)$	71 , 1041
$\pi^\pm p$ and $\pi^\pm d$ cross sections, plots of	366	Pulsars, binary	213
$\pi \rightarrow \ell\nu\gamma$ form factors, note on	584	$Q(1280)$ or Q_1 [<i>now called</i> $K_1(1270)$]	46 , 752
π mesons		$Q(1400)$ or Q_2 [<i>now called</i> $K_1(1400)$]	46 , 754
π^\pm	38 , 583	QCD	116
π^0	38 , 587	in diffractive events	121
$\pi(1300)$	40 , 633	in ep collisions	121
$\pi(1800)$	678	in heavy-quarkonium decay	119
$\pi_1(1400)$	640	in high-energy hadron collisions	118
$\pi_1(1600)$	660	in Lattice	121
$\pi_2(1670)$ [<i>was</i> $A(1680)$ or A_3]	42 , 664	and structure functions	189
$\pi_2(2100)$ [<i>was</i> $A(2100)$]	688	in τ decays	117
Pion	38 , 583	perturbative in e^+e^- collisions	119
Planck constant	103	Quality factor for biological damage due to radiation	312
Planck mass	104	Quintessence (general dark energy of Universe)	235, 235
Plasma energy	267	Quantum mechanics in $B^0-\bar{B}^0$ mixing, note on	914
Plastic scintillators	285	Quantum numbers in quark model	172
Poisson distribution	318	Quarks	37 , 551
Poisson distribution, Monte Carlo algorithm for	331	and lepton compositeness searches	91 , 1265
Poisson distribution, table of	318	and lepton substructure searches	91 , 1265
Potentials, electromagnetic	112	current masses of	125, 551
PPDS databases	21	fragmentation in e^+e^- annihilation, heavy	207
Precision experiments, heavy physics	134, 136	and leptons, weak interactions of	125, 136
Prefixes, metric, commonly used	106	mass, note on	551
Preprints, electronic	23	model	172
Primary spectra, cosmic rays	254	model assignments	172
Probability	316	model, dynamical ingredients	177
Probability density function, definition	316	properties of	172
Production and spectroscopy of b -flavored hadrons, note on	834	Quark searches, free	37 , 577
Propagation of errors	322	Quark searches, note on	577
Properties (atomic and nuclear) of materials	110	Quarkonium (heavy) decay, QCD in	119
Proton (see p)	77 , 1061	R function, e^+e^- collisions, plot of	358
Proton cyclotron frequency/field	103	$r(2510)$ [<i>now called</i> $f_6(2510)$]	697
Proton decay	180	Rad, unit of absorbed dose of radiation	312
Proton mass	77 , 103	Radiation	
Proton structure function	188	biological damage from chronic exposure	312
Proton structure function, plots	194, 197	Cherenkov	278
Pseudorapidity distribution in $\bar{p}p$ interactions, plot of	354	damage in Silicon detectors	301
Pseudorapidity η , defined	342	-dominated epoch	221
Pseudoscalar mesons, decay constants of charged, note on	818	gravitational	214
ψ mesons		length	272
$\psi(1S) = J/\psi(1S)$	66 , 981	length, approximate algorithm	273
$\psi(2S)$	69 , 1014	length of materials, table	110
$\psi(2S)$ and $\chi_{c0,1,1}$, branching ratios, note on	997	lethal dose from	312
$\psi(3770)$	70 , 1026		

- long-term risk 312
 weighting factor 312
 Radiative corrections in Standard Model 125
 Radiative decays, hyperons, note on 1167
 Radiative loss by muons 277
 Radioactive sources, commonly used 315
 Radioactivity
 and radiation protection 312
 at accelerators 313
 natural annual background 312
 unit of absorbed dose 312
 unit of activity 312
 unit of exposure 312
 Radon, as component of natural background radioactivity 312
 Random angle, Monte Carlo algorithm for sine and cosine of . . . 331
 Random number generators 330
 RANLUX 330
 Rapidity 342
 Rare B decays, note on 838
 Redshift 217
 Refractive index of materials, table 110
 Regge theory fits to total cross sections, table 362
 Re-ionization of the Universe 237
 Relativistic kinematics 340
 Relativistic rise 269
 Relativistic transformation of electromagnetic fields 112
 Rem, roentgen equivalent for man 312
 Renormalization in Standard Model 125
 Renormalization schemes in QCD 116
 Representations, $SU(n)$ 339
 Resistive plate chambers 299
 Resistivity, electrical, of elements, table 111
 Resistivity of metals 113
 Resistivity, relations for 113
 Resonance, Breit-Wigner form and Argand plot for 343
 Resonances (see Mesons and Baryons)
 Restricted energy loss rate, charged particles 270
 RHIC (Brookhaven) collider parameters 266
 ρ mesons
 $\rho(770)$ **39**, 599
 $\rho(770)$, note on 599
 $\rho(1450)$ **41**, 649
 $\rho(1450)$ and $\rho(1770)$, note on 670
 $\rho(1700)$ **42**, 670
 $\rho(1900)$ 682
 $\rho(2150)$ 690
 $\rho_3(1690)$ [*was* $g(1690)$] **42**, 667
 $\rho_3(1990)$ 684
 $\rho_3(2250)$ 693
 $\rho_5(2350)$ 696
 ρ parameter of electroweak interactions 136
 ρ parameter in electroweak analyses (Standard Model) 136
 ρ_c , critical density 104
 Ring-Imaging Cherenkov detectors 290
 Robertson-Walker metric 217
 Robustness of an estimator 320
 Roentgen, measure of X or γ radiation intensity 312
 RPC (Resistive Plate Chambers) 299
 Rounding errors, treatment of 18
 Rydberg energy 103
 s (quark) **37**, 558
 S, T, U electroweak variables 137, 138
 $S = +1$ baryons (formerly Z^* baryons) 1124
 Pentaquarks 1124
 (see p. VIII.58 in our 1992 edition, Phys. Rev. **D45**, Part II)
 $S(975)$ or S^* [*now called* $f_0(980)$] **39**, 613
 S -matrix approach to Z lineshape 393
 S -matrix for two-body scattering 340
 Sachs-Wolfe effect 236
 Same-side tag in $B^0-\bar{B}^0$ mixing, note on 916
 Scalar mesons, note on 594
 Scale factor, definition of 16
 Scaled cosmological constant, Ω_Λ 104, 218
 Scaled Hubble constant 104, 218
 Scaling violations in fragmentation functions 120, 202
 Schwarzschild radius of the Earth 104
 Schwarzschild radius of the Sun 104
 Scintillator parameters 285
 Sea-level cosmic ray fluxes 254
 Searches:
 Axion searches **32**, 459
 Baryonium candidates 698
 Chargino searches 1243
 Color octet leptons **92**, 1271
 Color sextet quarks **92**, 1271
 Compositeness, quark and lepton, searches **91**, 1265
 Excited lepton searches **91**, 1268
 Familon searches 472
 Fourth generation (b') searches **37**, 576
 Free quark searches **37**, 577
 Gluino searches **91**, 1253
 Gluonium candidates 1057
 Goldstone boson searches 472
 Heavy boson searches **32**, 443
 Heavy lepton searches **36**, 516

Heavy particle searches	1285	Σ^+	82 , 1142
Higgs searches	32 , 414	Σ^0	83 , 1144
Lepton (heavy) searches	36 , 516	Σ^-	83 , 1145
Lepton mixing, neutrinos (massive) and, search for	36 , 530	$\Sigma(1670)$, note on	1152
Lepton, quark compositeness searches	91 , 1265	$\Sigma_c(2455)$	87 , 1192
Lepton, quark substructure searches	91 , 1265	$\Sigma_c(2520)$	1193
Leptoquark searches	455	Silicon detectors, radiation damage	301
Light boson searches	32 , 459	Silicon particle detectors	300
Light neutrino types, number of	36 , 523	Silicon photodiodes	300
Magnetic monopole searches	91 , 1209	Silicon strip detectors	300
Majoron searches	472	$\sin^2 \theta_W$, weak-mixing angle	103, 125, 134
Massive neutrinos and lepton mixing, searches	36 , 530	SLC (SLAC) collider parameters	265
Monopole searches	91 , 1209	Slepton searches	1245
Neutralino searches	1242	Sloan Digital Sky Survey (SDSS)	237
Neutrino oscillation searches	36 , 530	Sneutrino searches	1245
Neutrino, solar, experiments	531	Software directories	28
Neutrino types, number of	36 , 523	Solar	
Neutrinoless double- β decay searches	525	equatorial radius	104
Neutrinos (massive) and lepton mixing, search for	36 , 530	luminosity	104
Non- $q\bar{q}$ candidates	1057	mass	104
Other particle searches	1282	ν experiments	531
Photino searches	1238	radius in galaxy	104
Quark and lepton compositeness searches	91 , 1265	velocity in galaxy	104
Quark and lepton substructure searches	91 , 1265	velocity with respect to CBR	104
Quark searches, free	37 , 577	Solar Neutrinos, note on	531
Slepton searches	1245	Solenoidal collider detector magnets	307
Sneutrino searches	1245	Sources, radioactive, commonly used	315
Squark searches	1249	Specific heats of elements, table	111
Solar ν experiments	531	Spectroscopy of b -flavored hadrons, note on	834
Substructure, quark and lepton, searches	91 , 1265	Speed of light	104
Supersymmetric partner searches	91 , 1211	Spherical harmonics	337
Technicolor, review of	1258	Spin-dependent structure functions	200
Techniparticle searches	91 , 1258	SPIRES database	23
Technipion searches	32 , 441	$Spp\bar{p}S$ (CERN) collider parameters	266
Vector meson candidates	698	Squark searches	1249
W' searches, note on	443	Standard cosmological model	233
Weak gauge boson searches	32 , 443	Standard Model of electroweak interactions	125
Z' searches, note on	446	Standard Model predictions in $B^0-\bar{B}^0$ mixing, note on	915
Selection and treatment of data	15	Standard particle numbering for Monte Carlos	333
Shower detector energy resolution	304	Statistical procedures	16
Showers, electromagnetic, lateral distribution of	277	Statistical significance in $B^0-\bar{B}^0$ mixing, note on	916
Showers, electromagnetic, longitudinal distribution of	276	Statistics	320
SI units, complete set	106	Stefan-Boltzmann constant	103
Sidereal day	104	Stopping power	268
Sidereal year	104	Stopping power for heavy-charged projectiles	268
Sievert, unit of radiation dose equivalent	312	Strange baryons	81 , 1126
σ, R function, e^+e^- collisions, plot of	358	Strange, bottom meson	65 , 968
Σ baryons (see also Λ and Σ baryons)	82 , 1142	Strange, charmed mesons	52 , 816

Greek letters are alphabetized by their English-language spelling. Bold page numbers signify entries in the Particle Properties Summary Tables.

- Strange mesons **43**, 704
- Strange quark (s) **37**, 558
- Strangeness-changing neutral currents, tests for 93
- Strong coupling constant in QCD 103, 116
- Structure functions 188
- photon 121
- Student's t distribution 319
- Student's t distribution, Monte Carlo algorithm for 331
- Student's t distribution, table of 318
- SU(2) \times U(1) 125
- SU(3) classification of baryon resonances 175
- SU(3), generators of transformations 338
- SU(3) isoscalar factors 338
- SU(3) multiplets (representations) 175
- SU(3) representation matrices 338
- SU(6) multiplets 176
- SU(n) multiplets 339
- Substructure, quark and lepton, searches **91**, 1265
- Substructure, quark and lepton, searches, note on 1265
- Summary Tables, organization of 13
- Sunyaev-Zel'dovich effect 232
- Superconducting solenoidal magnet 307
- Supernovae, Type Ia and Type II supernovae 235
- Supersymmetric partner searches **91**, 1211
- Supersymmetry, electroweak analyses of 137
- Superweak model of CP violation 741
- Survival probability, relations for 340
- Symmetry breaking 180, 125
- Synchrotron oscillation 262
- Synchrotron radiation 113
- Synchrotron radiation in accelerators 262
- Systematic errors, treatment of 16
- t (quark) **37**, 563
- T (time reversal), tests of conservation 93
- Tags in B^0 - \bar{B}^0 mixing, note on 916
- τ decays, QCD in 117
- τ lepton **34**, 489
- τ branching fractions, note on 493
- τ -decay parameters, note on 511
- τ polarization in Z decay 394
- Technicolor, electroweak analyses of 137
- Technicolor, review of 1258
- Techniparticle searches **91**, 1258
- Technipion searches **32**, 441
- Temperature of CBR 104
- TEVATRON (Fermilab) collider parameters 266
- Thermal conductivity of elements, table 111
- Thermal expansion coefficients of elements, table 111
- Thermal history of the Universe 220
- $\theta(1690)$ [*now called* $f_0(1710)$] **43**, 675
- θ_W , weak-mixing angle 103, 125, 135
- Thomson cross section 103
- Three-body decay kinematics 341
- Three-body phase space 340
- Threshold Cherenkov detectors 289
- Time-projection chambers (TPC) 297
- Top-changing neutral currents, tests for 93
- Top quark (t) **37**, 563
- Top quark, note on 563
- Top quark mass from electroweak analyses 134
- Top quark, m_t , constraints on 134–136
- Toroidal collider detector magnets 308
- Total cross sections, table of fit parameters 362
- Total cross sections, summary plot 363
- Total energy density of Universe, Ω_{tot} 237
- Total lepton number conservation 93
- TPC, Time-projection chambers 297
- Tracking Cherenkov detectors (underground) 290
- Transformation of electromagnetic fields, relativistic 112
- Transition radiation 278
- Transition radiation detectors (TRD) 298
- Triangles, unitarity, note on 145
- Triple gauge couplings, note on the extraction of 389
- Tropical year 104
- Two-body decay kinematics 340
- Two-body differential cross sections 340
- Two-body partial decay rate 340
- Two-body scattering kinematics 340
- Two-photon processes in e^+e^- annihilation 345
- Tune shift in colliders 263
- u (quark) **37**, 557
- Ultra-high-energy cosmic rays 259
- Underground Cherenkov detectors 290
- Underground cosmic rays 256
- Unified atomic mass unit 103
- Unified theories, grand 180
- Uniform distribution, table of 318
- Units and conversion factors 103
- Units, electromagnetic 112
- Units, SI, complete set 106
- Universe
- age of 104, 217, 219, 239
- baryon density of 104, 228
- composition 219, 228

- cosmological properties of 217
- cosmological structure 221
- critical density of 104
- curvature of 218
- density fluctuations 224
- density parameter of 104
- entropy density 222
- (Hubble) expansion of 217, 232
- large-scale structure of 219, 225
- mass-energy 241
- Universe (cont.)
- matter-dominated 223
- phase transitions 222
- radiation content at early times 221
- thermodynamic equilibrium 221
- thermal history of 220
- Υ states, width determinations of, note on 1042
- $\Upsilon(1S)$ **71**, 1043
- $\Upsilon(2S)$ **72**, 1047
- $\Upsilon(3S)$ **72**, 1051
- $\Upsilon(4S)$ **72**, 1054
- $\Upsilon(10860)$ **73**, 1055
- $\Upsilon(11020)$ **73**, 1056
- V_{cb} and V_{ub} CKM Matrix Elements 951
- V_{cb} and V_{ub} determination of, note on 951
- V_{ud} , V_{us} determination of, note on 733
- V_{ud} , V_{us} , V_{ub} , V_{cd} , V_{cs} , V_{cb} , V_{td} , V_{ts} , V_{tb} 145
- Vacuum energy parameter, Ω_v 218
- Variance, definition 316
- Vector meson candidates 698
- VEPP-2000 (Novosibirsk) collider parameters 264
- VEPP-4m (Novosibirsk) collider parameters 264
- W (gauge boson) **31**, 386
- W -boson mass, note on 386
- W boson, mass, width, branching ratios,
- and coupling to fermions **31**, 103, 126, 134, 134
- W^\pm : Triple gauge couplings, note on the extraction of 389
- W and Z differential cross section 354
- w , dark energy equation of state parameter 218, 235
- W' searches, note on 443
- WMAP, NASA's Wilkinson Microwave Anisotropy Probe 236
- Weak boson searches **32**, 443
- Weak interactions of quarks and leptons 125, 136
- Weak-mixing angle ($\sin^2 \theta_W$) 103, 125, 136
- Weak neutral currents, tests for ($\Delta B = 1$, $\Delta C = 1$, $\Delta S = 1$, $\Delta T = 1$) 93
- Weinberg angle ($\sin^2 \theta_W$) 103, 125
- Width determinations of Υ states, note on 1042
- Width of W and Z bosons 134
- Wien displacement law constant 103
- WIMPs (also see dark matter limits) 242
- WIMPs and other particle searches, note on 1282
- World-Wide Web information 21
- xF_3 structure function, plots of 198
- x variable (of Feynman's) 342
- X mesons
- $X(1850)$ [*now called* $\phi_3(1850)$] **43**, 681
- Ξ baryons **84**, 1166
- Ξ resonances, note on 1171
- Ξ^0 **84**, 1166
- Ξ^- **84**, 1168
- Ξ_b^0, Ξ_b^- 1204
- Ξ_c^+ **87**, 1194
- Ξ_c^0 **87**, 1196
- $\Xi_c'^+$ **88**, 1197
- $\Xi_c'^0$ **88**, 1197
- $\Xi_c(2645)$ **88**, 1197
- $\Xi_c(2790)$ **88**, 1198
- $\Xi_c(2815)$ **88**, 1198
- $\xi(2220)$ [*now called* $f_J(2220)$] 692
- Year, sidereal 104
- Year, tropical 104
- Young diagrams (tableaux) 339
- Young's modulus of solid elements, table 111
- Yukawa coupling unification 180
- Z : Anomalous $ZZ\gamma$, $Z\gamma\gamma$, and ZZV couplings 411
- Z (gauge boson) **31**, 393
- Z boson, note on 393
- Z boson, mass, width, branching ratios,
- and coupling to fermions **31**, 103, 126, 134, 134, 446
- Z decay to heavy flavors 396
- Z width, plot 360
- Z' searches, note on 446
- Z^* resonances (KN system) , 1124
- Pentaquarks 1124

COLOR FIGURES

Electroweak model and constraints on new physics (Figure 10.1)	1309
Electroweak model and constraints on new physics (Figure 10.2)	1309
Electroweak model and constraints on new physics (Figure 10.3)	1310
Electroweak model and constraints on new physics (Figure 10.4)	1310
CKM quark-mixing matrix (Figure 11.2)	1311
CP violation in meson decays (Figure 12.3)	1311
Neutrino mixing (Figure 13.1)	1312
Neutrino mixing (Figure 13.3)	1312
Neutrino mixing (Figure 13.4)	1313
Structure functions (Figure 16.3)	1314
Structure functions (Figure 16.4)	1314
Big-Bang cosmology (Figure 19.2)	1315
Big-Bang cosmology (Figure 19.5)	1315
Big-Bang nucleosynthesis (Figure 20.1)	1316
The Cosmological Parameters (Figure 21.1)	1316
Cosmic microwave background (Figure 23.2)	1317
Cosmic microwave background (Figure 23.3)	1317
Cosmic microwave background (Figure 23.4)	1318
Cosmic Rays (Figure 24.1)	1318
Cosmic Rays (Figure 24.9)	1319
Cosmic Rays (Figure 24.10)	1319
Jet Production in pp and $\bar{p}p$ Interactions (Figure 40.1)	1320
Direct γ Production in $\bar{p}p$ Interactions (Figure 40.2)	1320
Plots of cross sections and related quantities (Figure 40.6)	1321
Plots of cross sections and related quantities (Figure 40.7)	1322
Plots of cross sections and related quantities (Figure 40.10)	1323
The Mass of the W boson (Figure 1)	1324
The Mass of the W boson (Figure 2)	1324
Searches for Higgs Bosons (Figure 1)	1325
Searches for Higgs Bosons (Figure 2)	1325
Searches for Higgs Bosons (Figure 5)	1326
Searches for Higgs Bosons (Figure 6)	1326
Searches for Higgs Bosons (Figure 7)	1327
Searches for Higgs Bosons (Figure 8)	1327
Searches for Higgs Bosons (Figure 9)	1328
Searches for Higgs Bosons (Figure 10)	1328
Searches for Higgs Bosons (Figure 11)	1329
Searches for Higgs Bosons (Figure 12)	1329
Leptoquarks (Figure 1)	1330
Axions (Figure 4)	1330
Solar neutrinos Review (Figure 2)	1331
Solar neutrinos Review (Figure 3)	1331
CP Violation in K_L Decays (Figure 1)	1332
CP Violation in K_L Decays (Figure 2)	1332
$D^0-\bar{D}^0$ Mixing (Figure 1)	1333
$D^0-\bar{D}^0$ Mixing (Figure 2)	1333
$B^0-\bar{B}^0$ Mixing (Figure 2)	1334
V_{cb} and V_{ub} CKM Matrix Elements (Figure 1)	1334
V_{cb} and V_{ub} CKM Matrix Elements (Figure 2)	1335
V_{cb} and V_{ub} CKM Matrix Elements (Figure 3)	1335
Supersymmetry, Part II (Experiment, Figure 1)	1336
Supersymmetry, Part II (Experiment, Figure 2)	1336
Supersymmetry, Part II (Experiment, Figure 3)	1337
Supersymmetry, Part II (Experiment, Figure 4)	1337
Supersymmetry, Part II (Experiment, Figure 5)	1338
Supersymmetry, Part II (Experiment, Figure 6)	1338
Dynamical Electroweak Symmetry Breaking (Figure 1)	1339

Electroweak model and constraints on new physics (p.131)

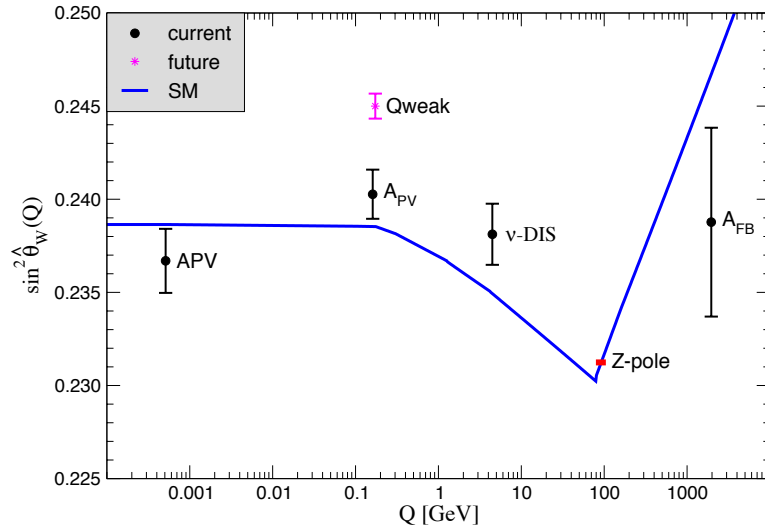


Figure 10.1: Scale dependence of the weak mixing angle defined in the $\overline{\text{MS}}$ scheme [146]. The minimum of the curve corresponds to $Q = M_W$, below which we switch to an effective theory with the W^\pm bosons integrated out, and where the β -function for the weak mixing angle changes sign. At the location of the W boson mass and each fermion mass, there are also discontinuities arising from scheme dependent matching terms which are necessary to ensure that the various effective field theories within a given loop order describe the same physics. However, in the $\overline{\text{MS}}$ scheme these are very small numerically and barely visible in the figure provided one decouples quarks at $Q = \hat{m}_q(\hat{m}_q)$. The width of the curve reflects the theory uncertainty from strong interaction effects which is at the level of $\pm 7 \times 10^{-5}$ [146].

Electroweak model and constraints on new physics (p.136)

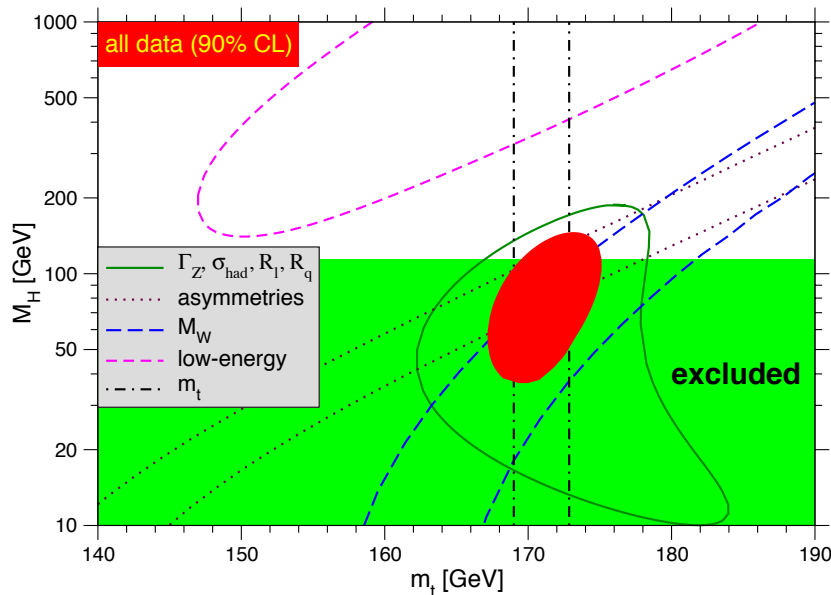


Figure 10.2: One-standard-deviation (39.35%) uncertainties in M_H as a function of m_t for various inputs, and the 90% CL region ($\Delta\chi^2 = 4.605$) allowed by all data. $\alpha_s(M_Z) = 0.120$ is assumed except for the fits including the Z lineshape data. The 95% direct lower limit from LEP 2 is also shown.

Electroweak model and constraints on new physics (p.136)

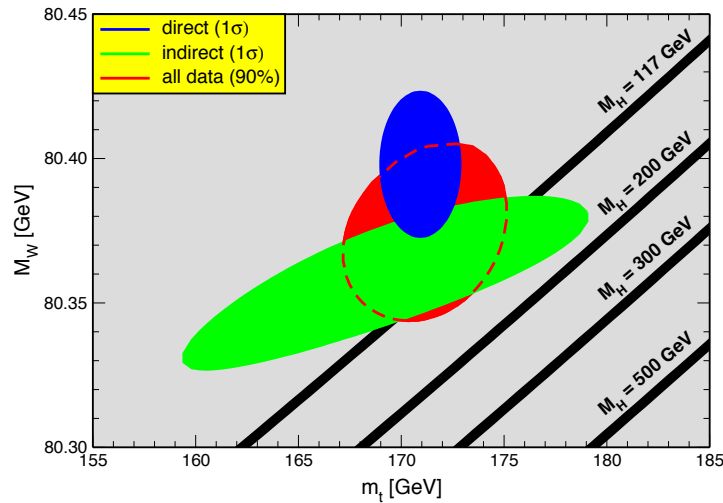


Figure 10.3: One-standard-deviation (39.35%) region in M_W as a function of m_t for the direct and indirect data, and the 90% CL region ($\Delta\chi^2 = 4.605$) allowed by all data. The SM prediction as a function of M_H is also indicated. The widths of the M_H bands reflect the theoretical uncertainty from $\alpha(M_Z)$.

Electroweak model and constraints on new physics (p.138)

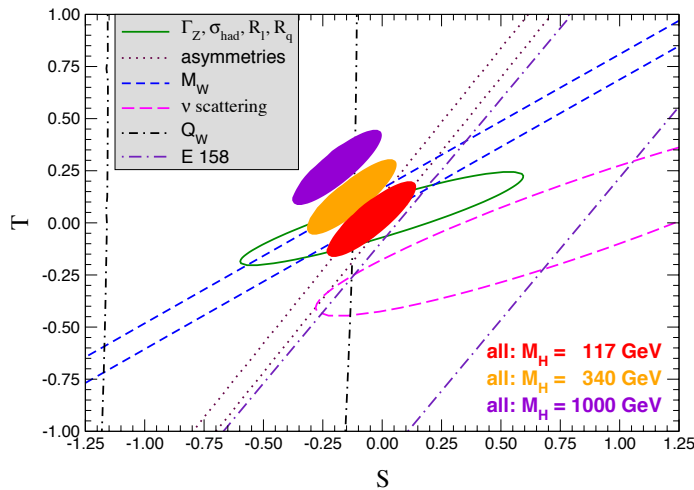


Figure 10.4: 1σ constraints (39.35 %) on S and T from various inputs combined with M_Z . S and T represent the contributions of new physics only. (Uncertainties from m_t are included in the errors.) The contours assume $M_H = 117$ GeV except for the central and upper 90% CL contours allowed by all data, which are for $M_H = 340$ GeV and 1000 GeV, respectively. Data sets not involving M_W are insensitive to U . Due to higher order effects, however, $U = 0$ has to be assumed in all fits. α_s is constrained using the τ lifetime as additional input in all fits.

CKM quark-mixing matrix (p.149)

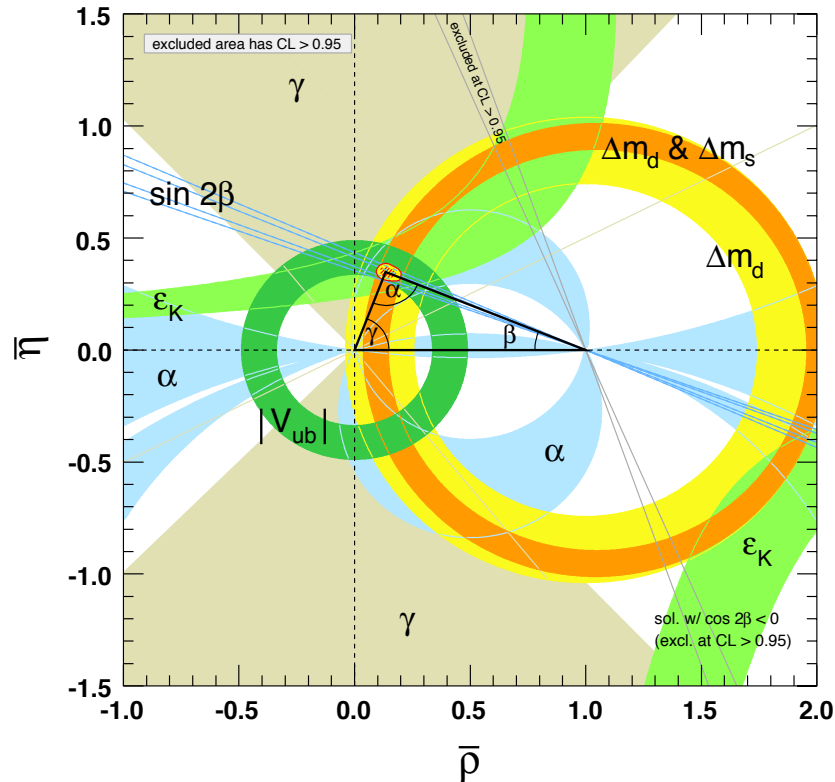


Figure 11.2: Constraints on the $\bar{\rho}, \bar{\eta}$ plane. The shaded areas have 95% CL.

CP violation in meson decays (p.160)

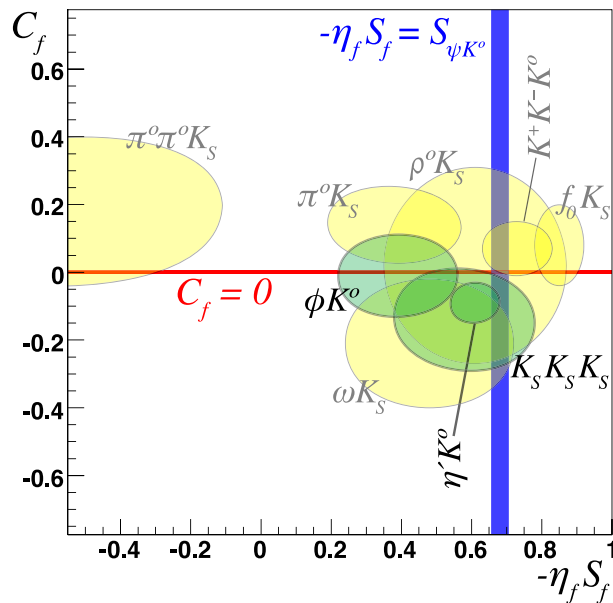


Figure 12.3: Summary of the results [20] of time-dependent analyses of $b \rightarrow q\bar{q}s$ decays, which are potentially sensitive to new physics. Subdominant corrections are expected to be smallest for the modes shown in green (darker). Results for final states including K^0 mesons combine CP -conjugate K_S and K_L measurements. The final state $K^+K^-K^0$ is not a CP eigenstate; the mixture of CP -even and CP -odd components is taken into account in obtaining an effective value for $\eta_f S_f$. Correlations between C_f and S_f are included when available.

Neutrino mixing (p.165)

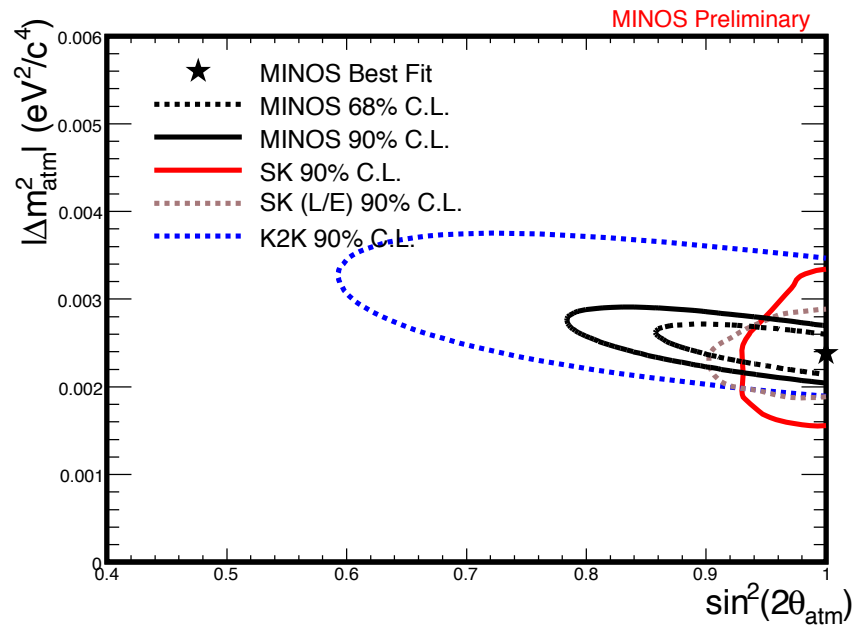


Figure 13.1: The region of the atmospheric oscillation parameters Δm_{atm}^2 and $\sin^2 2\theta_{\text{atm}}$ allowed by the SK, K2K, and MINOS data. The results of two different analyses of the SK (“Super K”) data are shown [21].

Neutrino mixing (p.167)

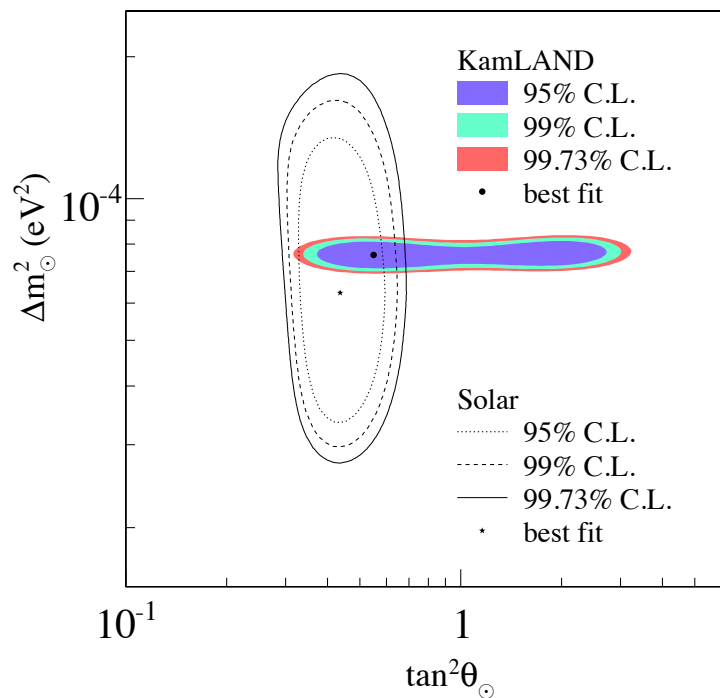


Figure 13.3: Regions allowed by the “solar” neutrino oscillation parameters by KamLAND and by solar neutrino experiments [28].

Neutrino mixing (p.167)

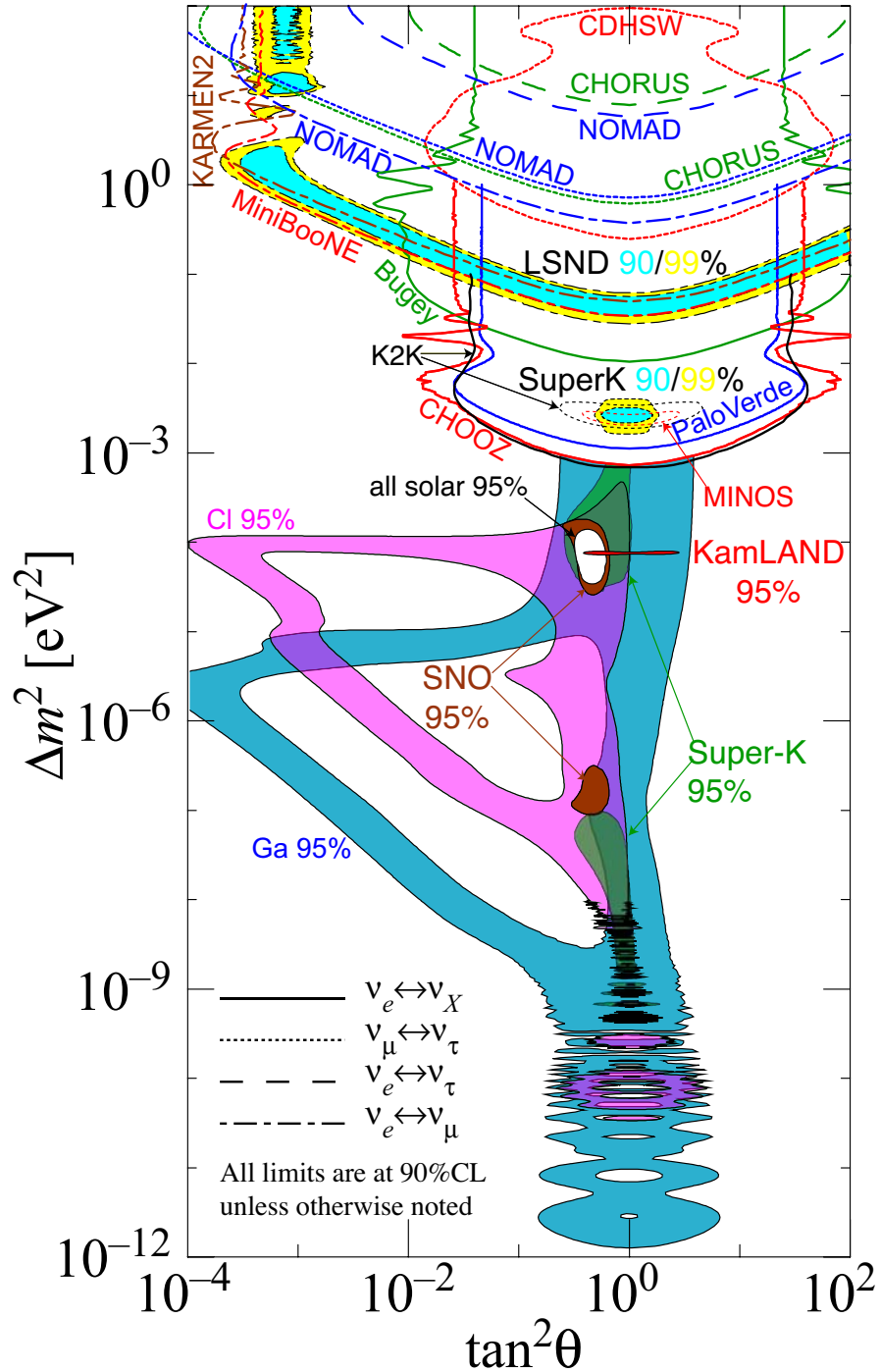


Figure 13.4: The regions of squared-mass splitting and mixing angle favored or excluded by various experiments. This figure was contributed by H. Murayama (University of California, Berkeley). References to the data used in the figure can be found at <http://hitoshi.berkeley.edu/neutrino/>.

Structure functions (p.191)

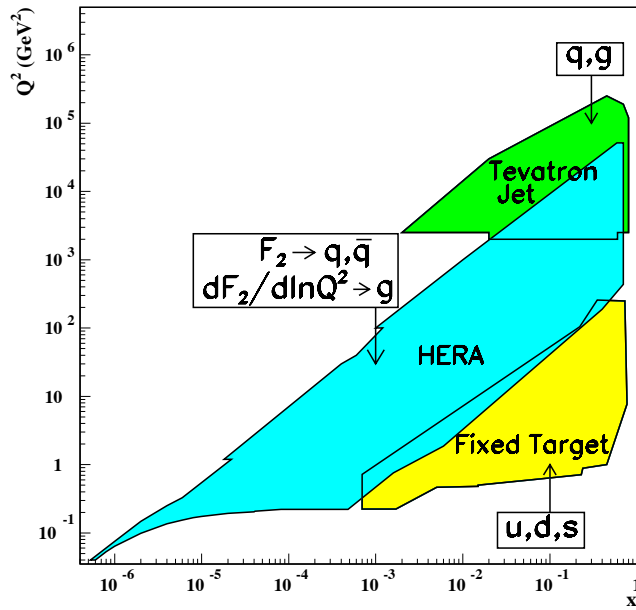


Figure 16.3: Kinematic domains in x and Q^2 probed by fixed-target and collider experiments, shown together with the important constraints they make on the various parton distributions.

Structure functions (p.191)

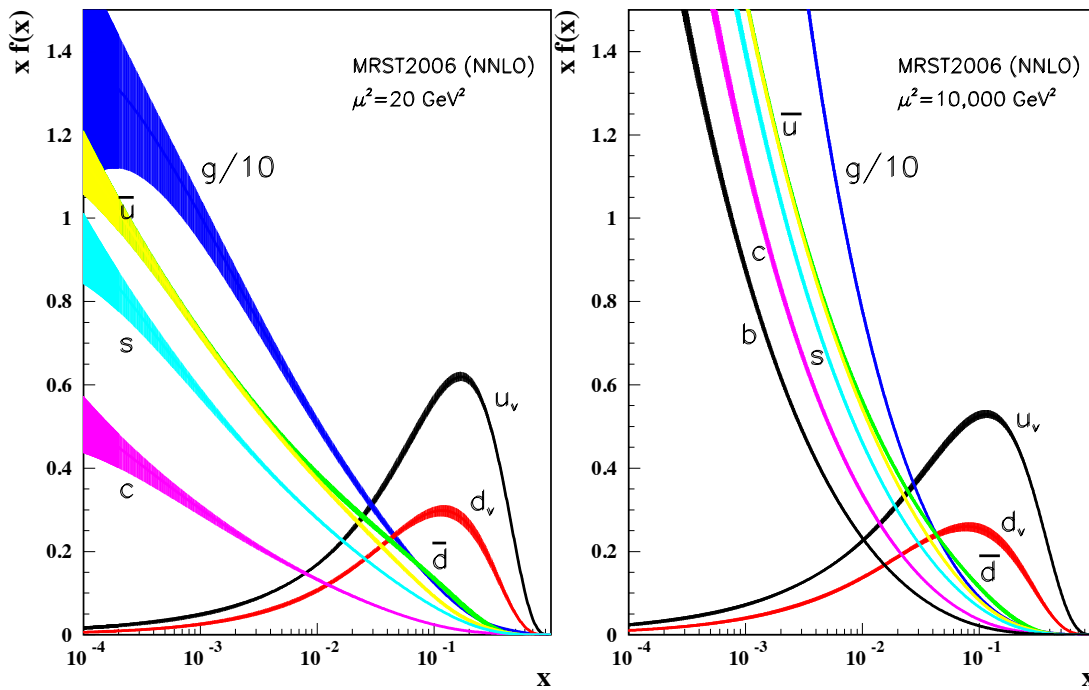


Figure 16.4: Distributions of x times the unpolarized parton distributions $f(x)$ (where $f = u_v, d_v, \bar{u}, \bar{d}, s, c, b, g$) and their associated uncertainties using the NNLO MRST2006 parameterization [13] at a scale $\mu^2 = 20 \text{ GeV}^2$ and $\mu^2 = 10,000 \text{ GeV}^2$.

Big-Bang cosmology (p.220)

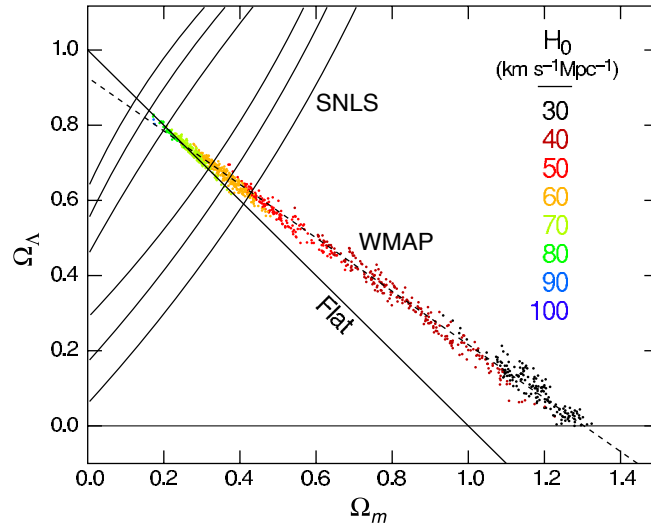


Figure 19.2: Likelihood-based probability densities on the plane Ω_Λ (*i.e.*, Ω_v assuming $w = -1$) vs Ω_m . The colored Monte-Carlo points derive from WMAP [22] and show that the CMB alone requires a flat universe $\Omega_v + \Omega_m \simeq 1$ if the Hubble constant is not too high. The SNe Ia results [28] very nearly constrain the orthogonal combination $\Omega_v - \Omega_m$. The intersection of these constraints is the most direct (but far from the only) piece of evidence favoring a flat model with $\Omega_m \simeq 0.25$.

Big-Bang cosmology (p.226)

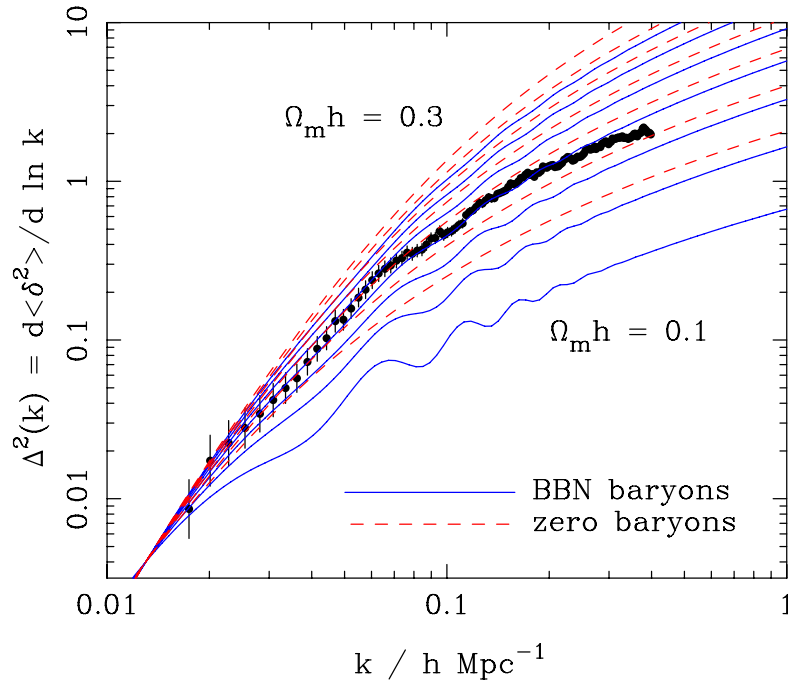


Figure 19.5: The galaxy power spectrum from the 2dFGRS, shown in dimensionless form, $\Delta^2(k) \propto k^3 P(k)$. The solid points with error bars show the power estimate. The window function correlates the results at different k values, and also distorts the large-scale shape of the power spectrum. An approximate correction for the latter effect has been applied. The solid and dashed lines show various CDM models, all assuming $n = 1$. For the case with non-negligible baryon content, a big-bang nucleosynthesis value of $\Omega_b h^2 = 0.02$ is assumed, together with $h = 0.7$. A good fit is clearly obtained for $\Omega_m h \simeq 0.2$.

Big-Bang nucleosynthesis (p.228)

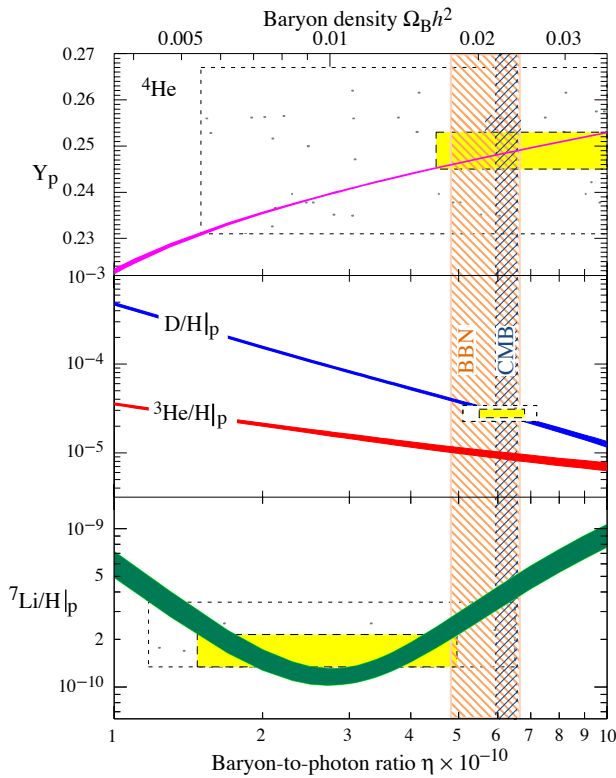


Figure 20.1: The abundances of ${}^4\text{He}$, D, ${}^3\text{He}$, and ${}^7\text{Li}$ as predicted by the standard model of big-bang nucleosynthesis — the bands show the 95% CL range. Boxes indicate the observed light element abundances (smaller boxes: $\pm 2\sigma$ statistical errors; larger boxes: $\pm 2\sigma$ statistical *and* systematic errors). The narrow vertical band indicates the CMB measure of the cosmic baryon density, while the wider band indicates the BBN concordance range (both at 95% CL).

The Cosmological Parameters (p.236)

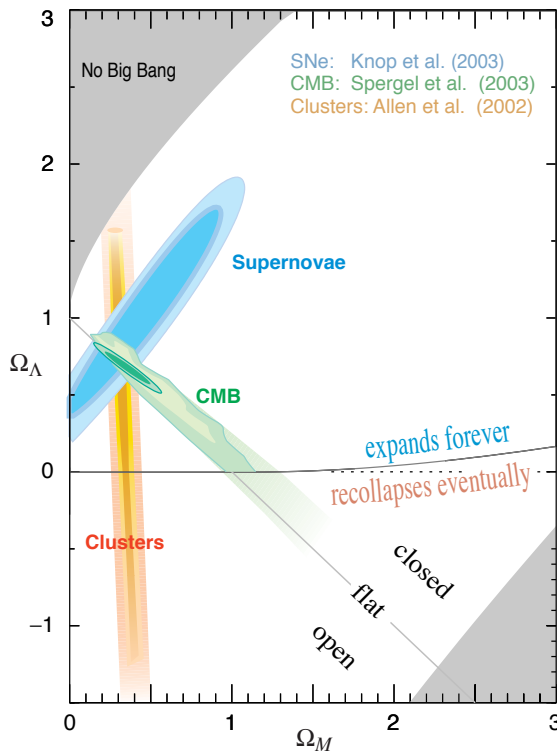


Figure 21.1: This shows the preferred region in the Ω_m - Ω_Λ plane from the compilation of supernovae data in Ref. 18, and also the complementary results coming from some other observations. [Courtesy of the Supernova Cosmology Project.]

Cosmic microwave background (p.249)

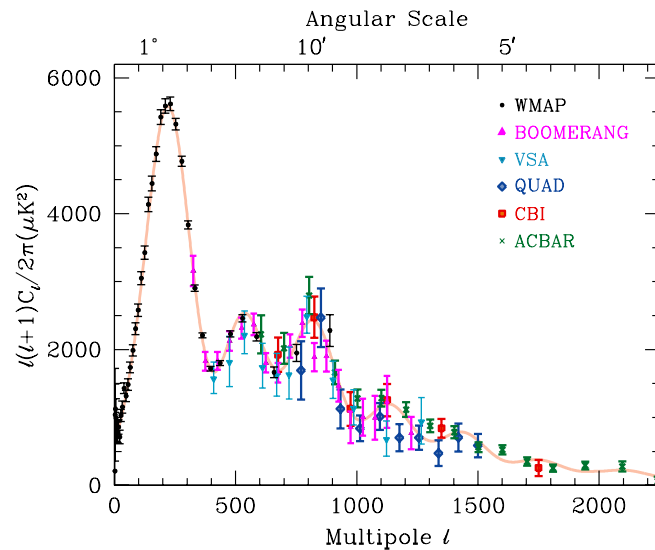


Figure 23.2: Band-power estimates from the WMAP, BOOMERANG, VSA, QUAD, CBI, and ACBAR experiments. Some of the low- ℓ and high- ℓ band-powers which have large error bars have been omitted. Note also that the widths of the ℓ -bands varies between experiments and have not been plotted. This figure represent only a selection of available experimental results, with some other data-sets being of similar quality. The multipole axis here is linear, so the Sachs-Wolfe plateau is hard to see. However, the acoustic peaks and damping region are very clearly observed, with no need for a theoretical curve to guide the eye.

Cosmic microwave background (p.249)

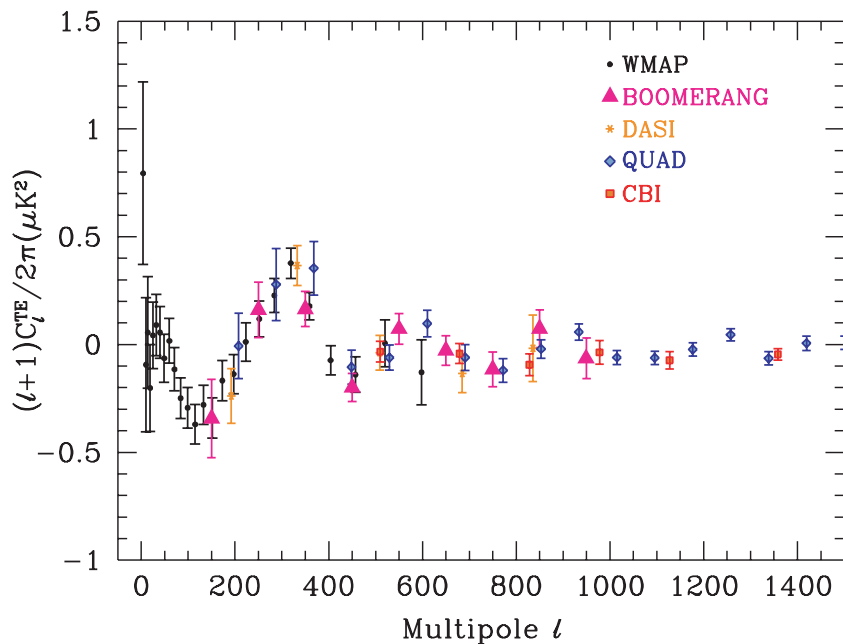


Figure 23.3: Cross power spectrum of the temperature anisotropies and E-mode polarization signal from WMAP [45], together with estimates from BOOMERANG, DASI, QUAD and CBI, which extend to higher ℓ . Note that the BOOMERANG bands are wider in ℓ than those of WMAP, while those of DASI are almost as wide as the features in the power spectrum. Also note that the y -axis here is not multiplied by the additional ℓ , which helps to show both the large and small angular scale features.

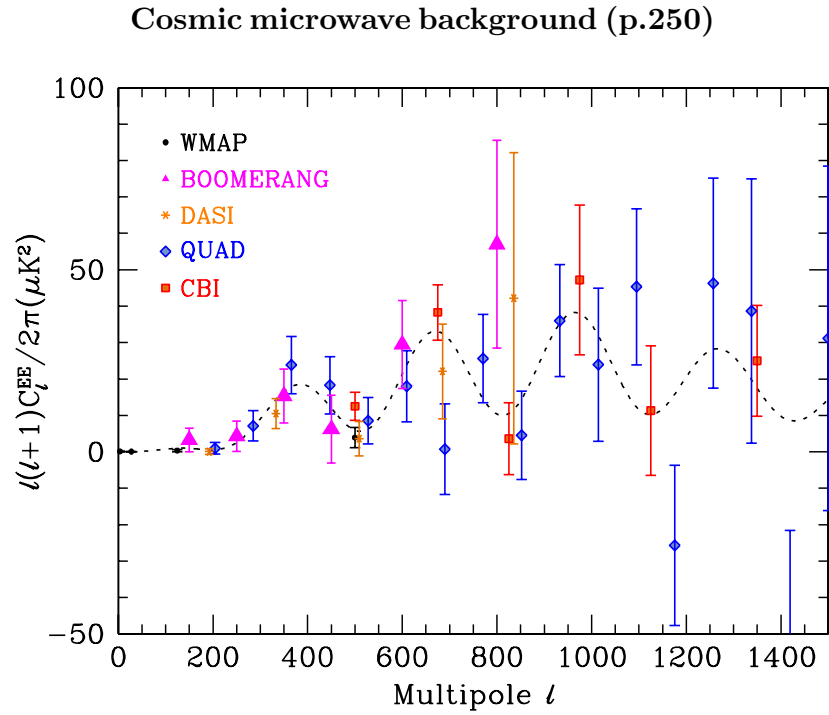


Figure 23.4: Power spectrum of E-mode polarization from several different experiments, plotted along with the theoretical model using parameters which fit the *WMAP* temperature and polarization data.

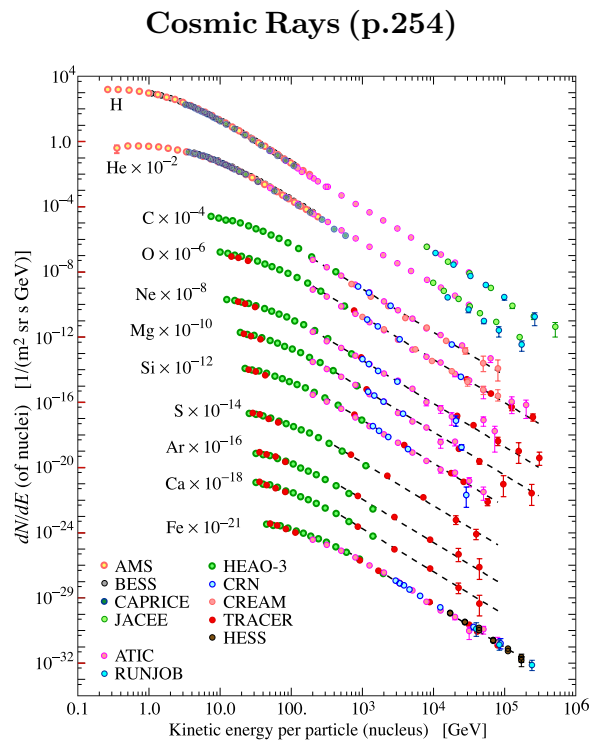


Figure 24.1: Major components of the primary cosmic radiation from Refs. [1–12]. The figure was created by P. Boyle and D. Muller.

Cosmic Rays (p.259)

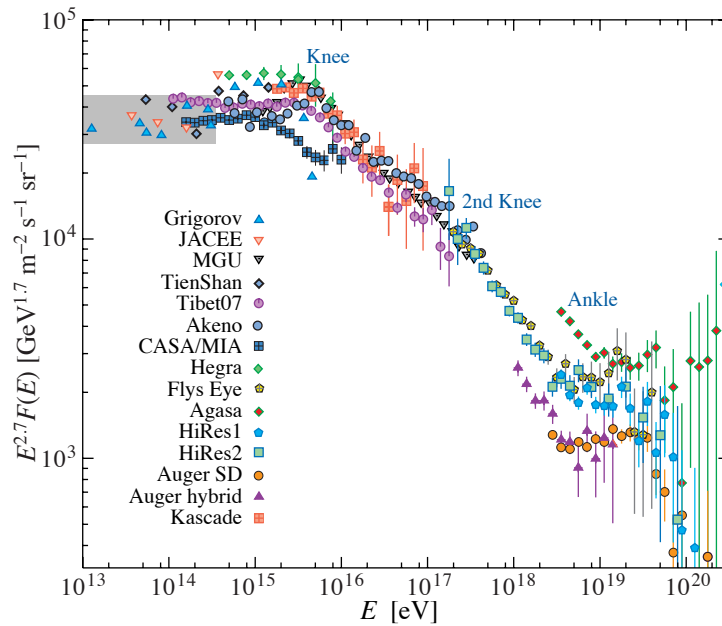


Figure 24.9: The all-particle spectrum from air shower measurements. The shaded area shows the range of the direct cosmic ray spectrum measurements.

Cosmic Rays (p.259)

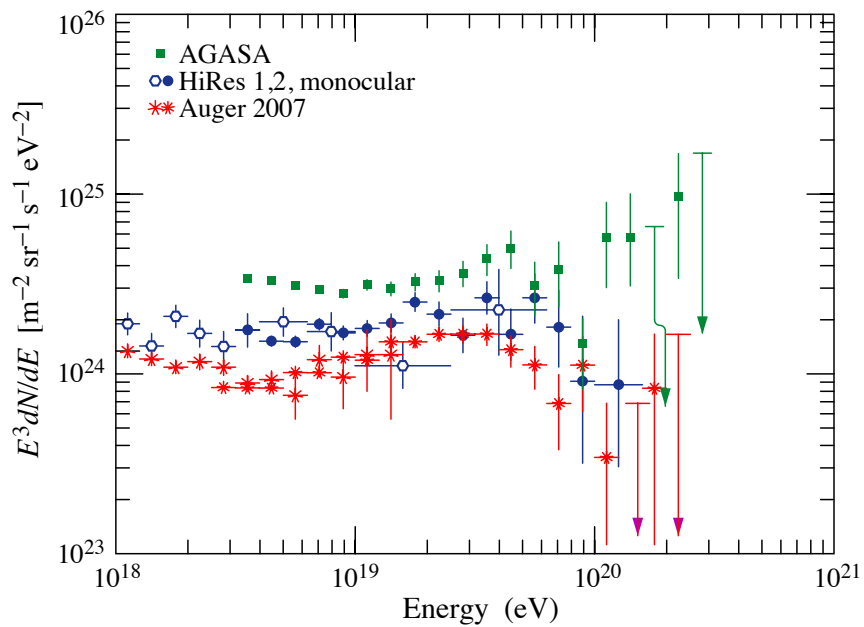


Figure 24.10: Expanded view of the highest energy portion of the cosmic-ray spectrum. ■ [87] (AGASA), ● [88] (HiRes1,2 monocular), * [89], [90] (Auger).

Jet Production in pp and $\bar{p}p$ Interactions (p.353)

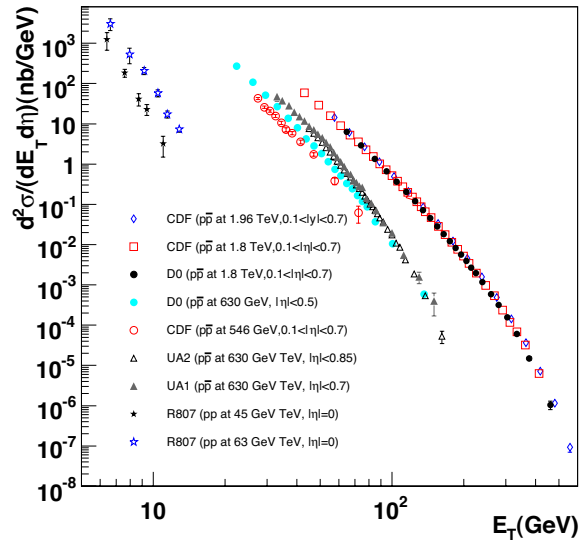


Figure 40.1: Inclusive differential jet cross sections plotted as a function of the jet transverse energy. The CDF and D0 measurements use a cone algorithm of radius 0.7 for all results shown except for the CDF measurement at 1.96 TeV which uses a k_T algorithm with a D parameter of 0.7. The cone/ k_T results should be similar if $R_{cone} = D$. UA1 (UA2) uses a non-iterative cone algorithm with a radius of 1.0 (1.3). Recent NLO QCD predictions (such as CTEQ6M) provide a good description of the CDF and D0 jet cross sections, Rept. on Prog. in Phys. **70**, 89 (2007). Comparisons with the older cross sections are more difficult due to the nature of the jet algorithms used. **CDF**: Phys. Rev. **D75**, 092006 (2007), Phys. Rev. **D64**, 032001 (2001), Phys. Rev. Lett. **70**, 1376 (1993); **D0**: Phys. Rev. **D64**, 032003 (2001); **UA2**: Phys. Lett. **B257**, 232 (1991); **UA1**: Phys. Lett. **B172**, 461 (1986); **R807**: Phys. Lett. **B123**, 133 (1983). (Courtesy of J. Huston, Michigan State University, 2007)

Direct γ Production in $\bar{p}p$ Interactions (p.353)

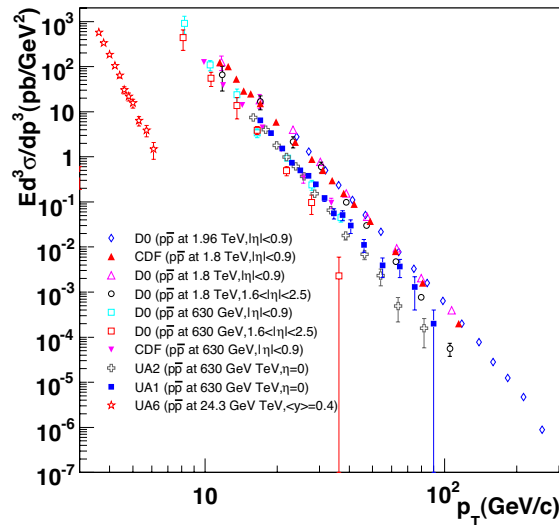


Figure 40.2: Isolated photon cross sections plotted as a function of the photon transverse momentum. The errors are either statistical only (CDF, D0 (1.96 TeV), UA1, UA2, UA6) or uncorrelated (D0 1.8 TeV, 630 GeV). The data are generally in good agreement with NLO QCD predictions, albeit with a tendency for the data to be above (below) the theory for lower (large) transverse momenta, Phys. Rev. **D59**, 074007 (1999). **D0**: Phys. Lett. **B639**, 151 (2006), Phys. Rev. Lett. **87**, 251805 (2001); **CDF**: Phys. Rev. **D65**, 112003 (2002); **UA6**: Phys. Lett. **B206**, 163 (1988); **UA1**: Phys. Lett. **B209**, 385 (1988); **UA2**: Phys. Lett. **B288**, 386 (1992). (Courtesy of J. Huston, Michigan State University, 2007)

Plots of cross sections and related quantities (p.358)

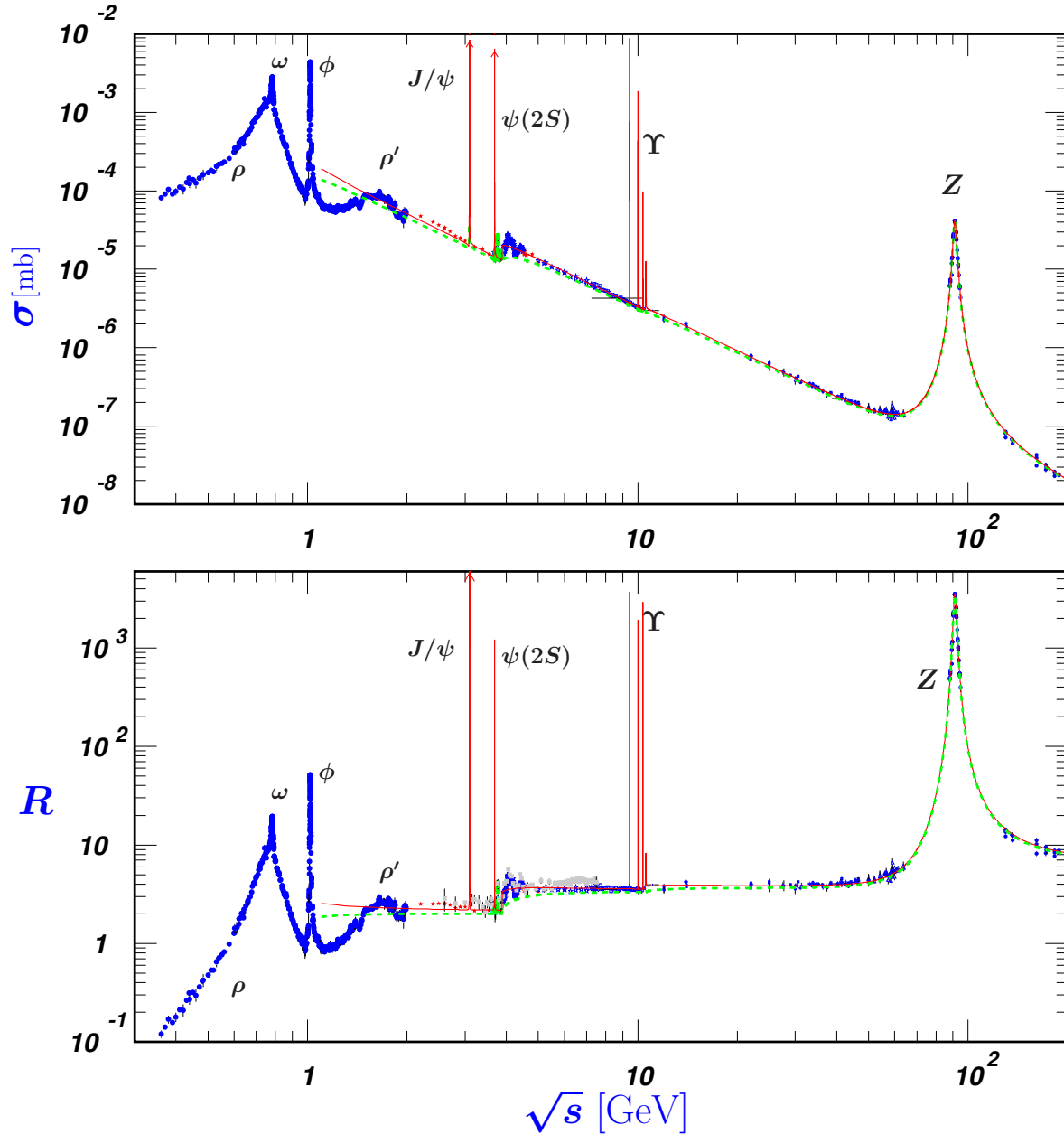
 σ and R in e^+e^- Collisions

Figure 40.6: World data on the total cross section of $e^+e^- \rightarrow \text{hadrons}$ and the ratio $R(s) = \sigma(e^+e^- \rightarrow \text{hadrons}, s) / \sigma(e^+e^- \rightarrow \mu^+\mu^-, s)$. $\sigma(e^+e^- \rightarrow \text{hadrons}, s)$ is the experimental cross section corrected for initial state radiation and electron-positron vertex loops, $\sigma(e^+e^- \rightarrow \mu^+\mu^-, s) = 4\pi\alpha^2(s)/3s$. Data errors are total below 2 GeV and statistical above 2 GeV. The curves are an educative guide: the broken one (green) is a naive quark-parton model prediction, and the solid one (red) is 3-loop pQCD prediction (see “Quantum Chromodynamics” section of this *Review*, Eq. (9.12) or, for more details, K. G. Chetyrkin *et al.*, Nucl. Phys. **B586**, 56 (2000) (Erratum *ibid.* **B634**, 413 (2002)). Breit-Wigner parameterizations of J/ψ , $\psi(2S)$, and $\Upsilon(nS)$, $n = 1, 2, 3, 4$ are also shown. The full list of references to the original data and the details of the R ratio extraction from them can be found in [arXiv:hep-ph/0312114]. Corresponding computer-readable data files are available at <http://pdg.lbl.gov/current/xsect/>. (Courtesy of the COMPAS (Protvino) and HEPDATA (Durham) Groups, August 2007. Corrections by P. Janot (CERN) and M. Schmitt (Northwestern U.)

Plots of cross sections and related quantities (p.359)

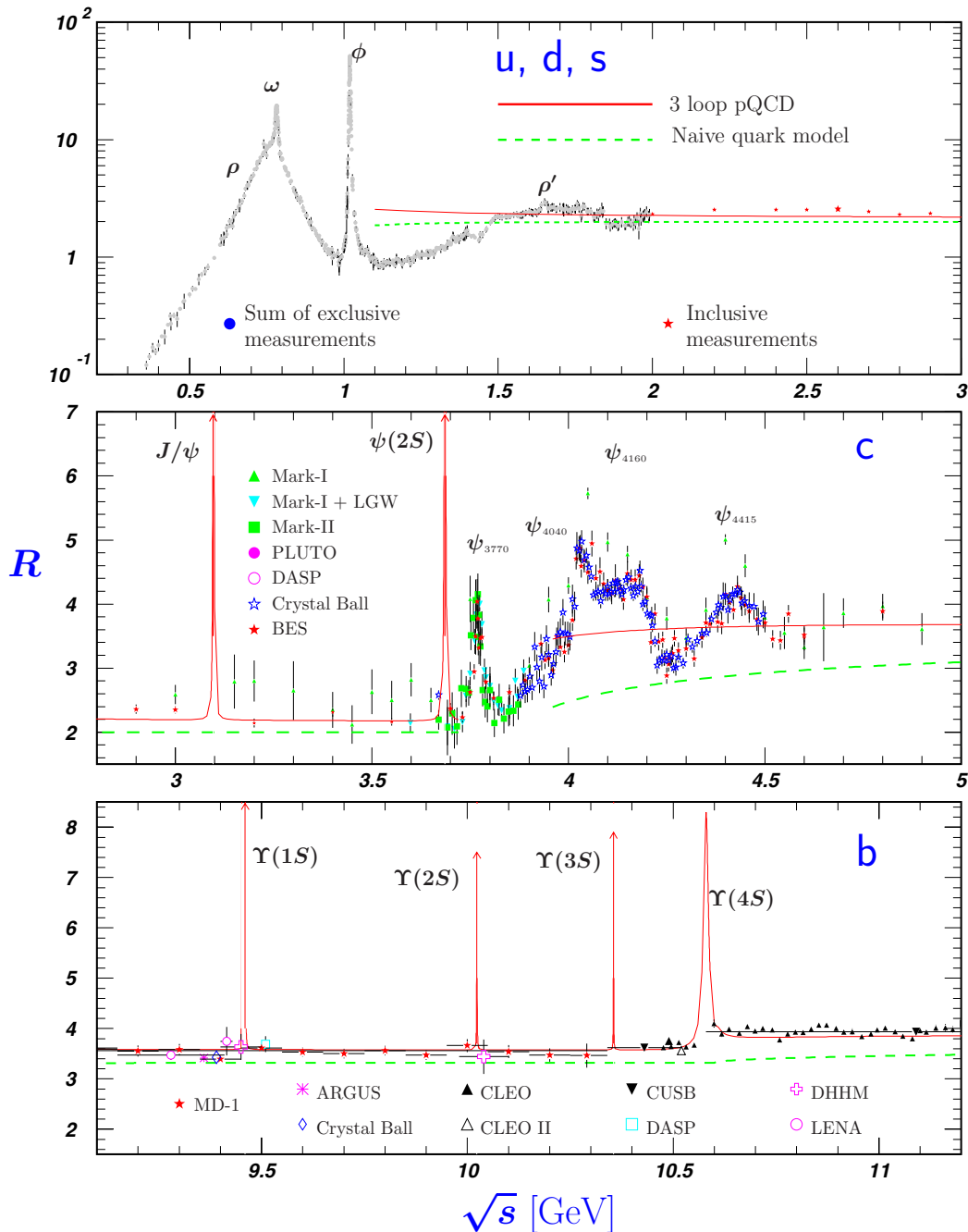
 R in Light-Flavor, Charm, and Beauty Threshold Regions

Figure 40.7: R in the light-flavor, charm, and beauty threshold regions. Data errors are total below 2 GeV and statistical above 2 GeV. The curves are the same as in Fig. 40.6. **Note:** CLEO data above $\Upsilon(4S)$ were not fully corrected for radiative effects, and we retain them on the plot only for illustrative purposes with a normalization factor of 0.8. The full list of references to the original data and the details of the R ratio extraction from them can be found in [arXiv:hep-ph/0312114]. The computer-readable data are available at <http://pdg.lbl.gov/current/xsect/>. (Courtesy of the COMPAS (Protvino) and HEPDATA (Durham) Groups, August 2007)

Plots of cross sections and related quantities (p.363)

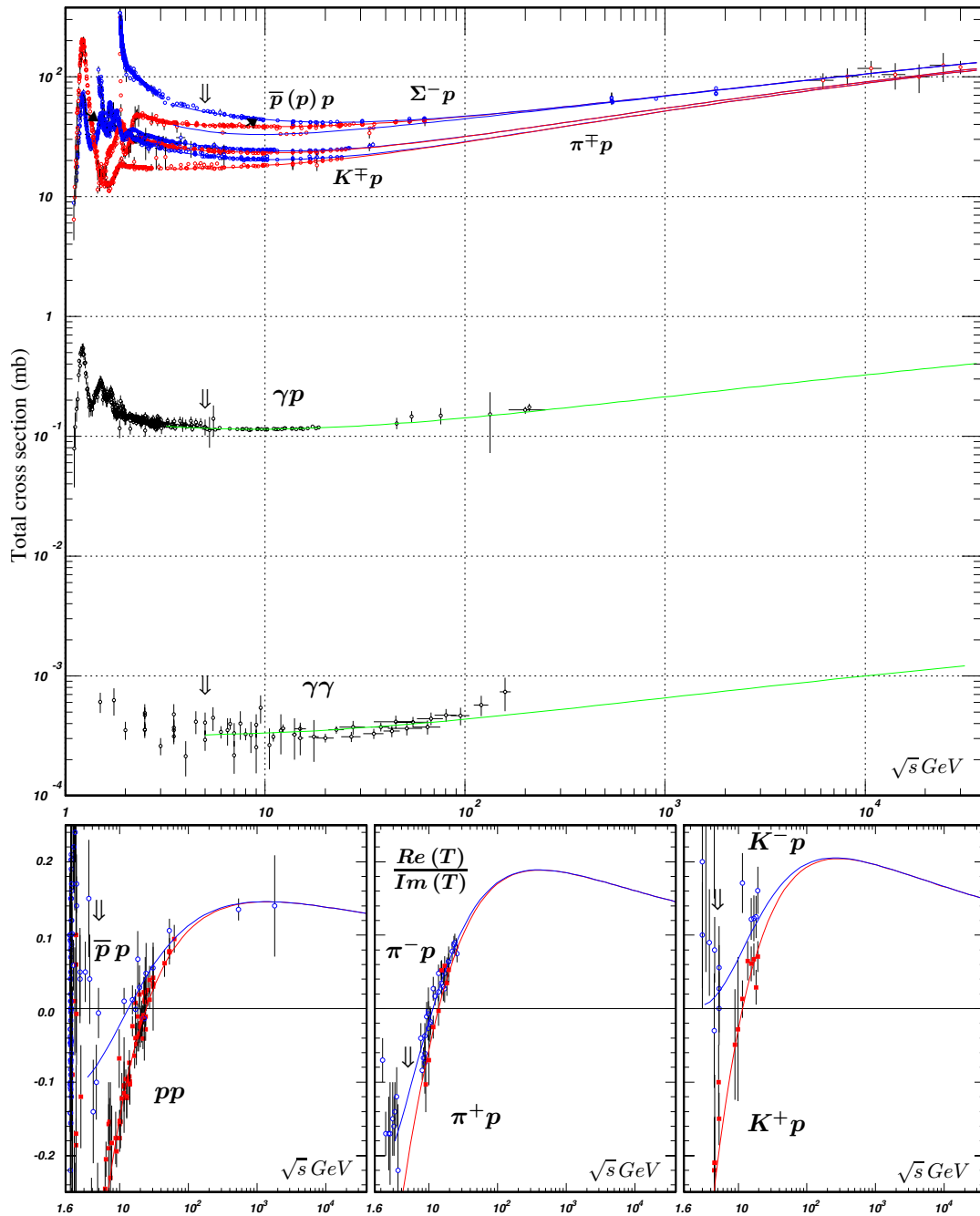
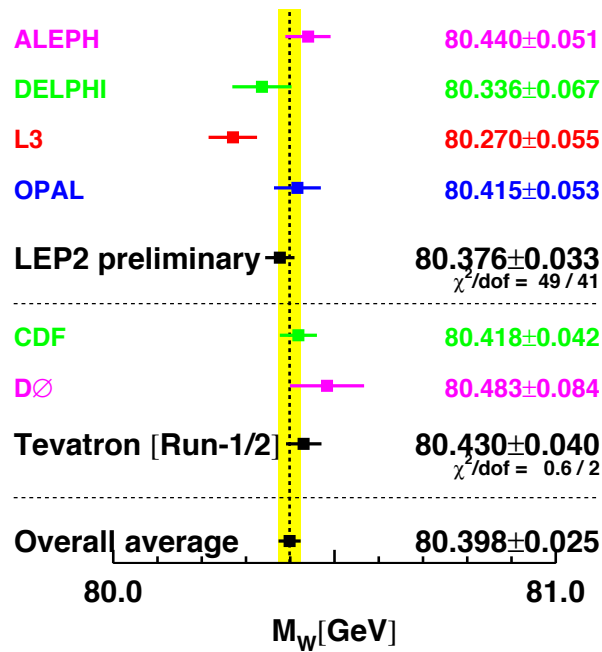
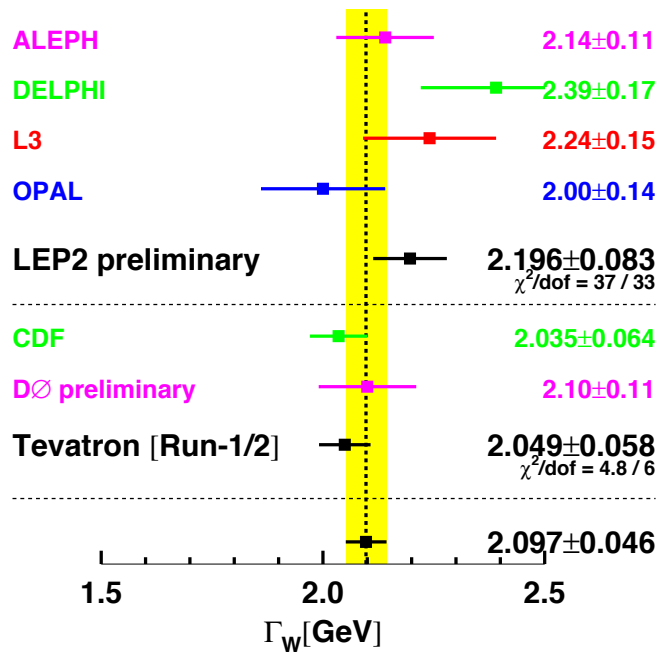
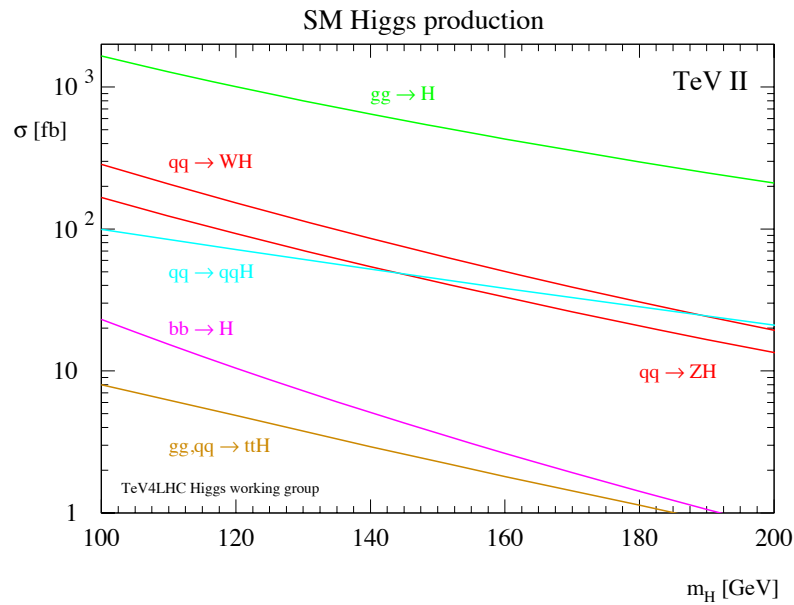


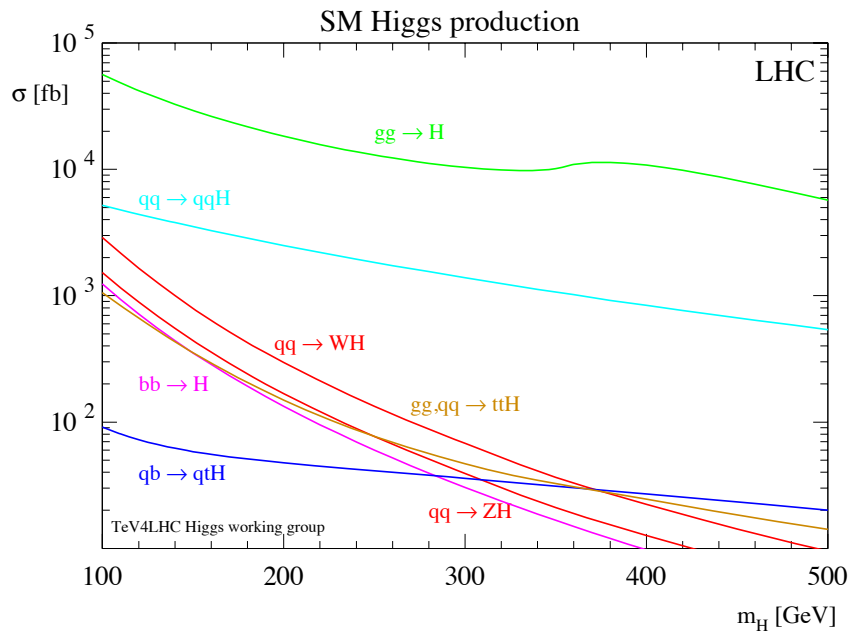
Figure 40.10: Summary of hadronic, γp , and $\gamma\gamma$ total cross sections, and ratio of the real to imaginary parts of the forward hadronic amplitudes. Corresponding computer-readable data files may be found at <http://pdg.lbl.gov/current/xsect/>. (Courtesy of the COMPAS group, IHEP, Protvino, August 2005)

The Mass and Width of the W boson (p.386)Figure 1: Measurements of the W -boson mass by the LEP and Tevatron experiments.The Mass and Width of the W boson (p.386)Figure 2: Measurements of the W -boson width by the LEP and Tevatron experiments.

Searches for Higgs Bosons (p.416)

Figure 1: SM Higgs production cross sections for $p\bar{p}$ collisions at 1.96 TeV [26].

Searches for Higgs Bosons (p.416)

Figure 2: SM Higgs production cross sections for pp collisions at 14 TeV [26].

Searches for Higgs Bosons (p.417)

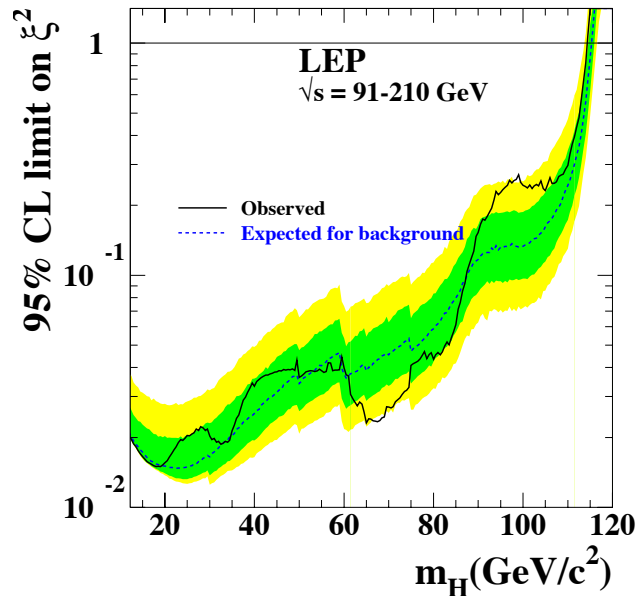


Figure 5: The 95% confidence level upper bound on the ratio $\xi^2 = (g_{HZZ}/g_{HZZ}^{\text{SM}})^2$ [15]. The solid line indicates the observed limit, and the dashed line indicates the median limit expected in the absence of a Higgs boson signal. The dark and light shaded bands around the expected limit line correspond to the 68% and 95% probability bands, indicating the range of statistical fluctuations of the expected outcomes. The horizontal line corresponds to the Standard Model coupling. Standard Model Higgs boson decay branching fractions are assumed.

Searches for Higgs Bosons (p.419)

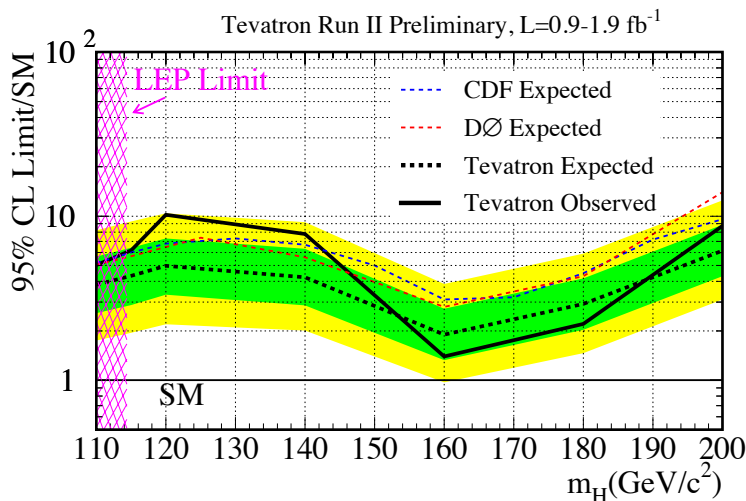


Figure 6: Upper bound on the SM Higgs boson cross section obtained by combining CDF and $D\bar{0}$ search results, as a function of the mass of the Higgs boson sought. The limits are shown as a multiple of the SM cross section. The ratios of different production and decay modes are assumed to be as predicted by the SM. The solid curve shows the observed upper bound, the dashed black curve shows the median expected upper bound assuming no signal is present, and the colored bands show the 68% and 95% probability bands around the expected upper bound. The CDF and $D\bar{0}$ combined expected limits are also shown separately. See Ref. 59 for details and status of these results.

Searches for Higgs Bosons (p.423)

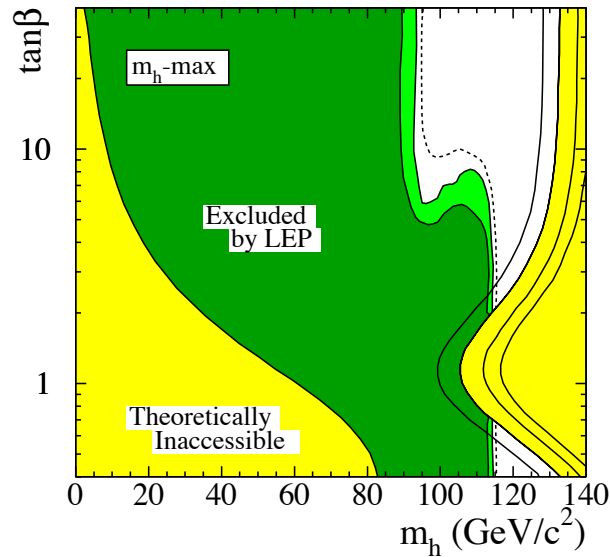


Figure 7: The MSSM exclusion contours, at 95% C.L. (light-green) and 99.7% CL (dark-green), obtained by LEP for the *CPC* m_h -max benchmark scenario, with $m_t = 174.3$ GeV. The figure shows the excluded and theoretically inaccessible regions in the $(m_h, \tan\beta)$ projection. The upper edge of the theoretically allowed region is sensitive to the top quark mass; it is indicated, from left to right, for $m_t = 169.3, 174.3, 179.3$ and 183.0 GeV. The dashed lines indicate the boundaries of the regions which are expected to be excluded on the basis of Monte Carlo simulations with no signal (from Ref. 16).

Searches for Higgs Bosons (p.424)

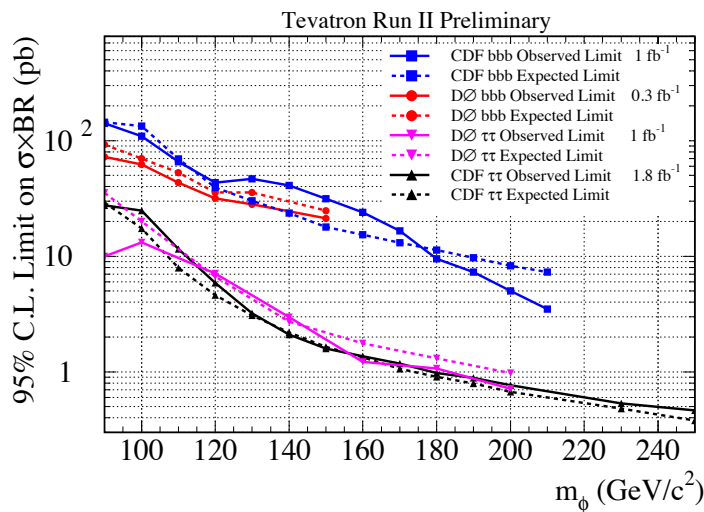


Figure 8: The 95% C.L. limits on the production cross section times the relevant decay branching ratios for the Tevatron searches for $\phi \rightarrow b\bar{b}$ and $\phi \rightarrow \tau^+\tau^-$. The observed limits are indicated with solid lines, and the expected limits are indicated with dashed lines. The limits are to be compared with the sum of signal predictions for Higgs boson with similar masses. The decay widths of the Higgs bosons are assumed to be much smaller than the experimental resolution.

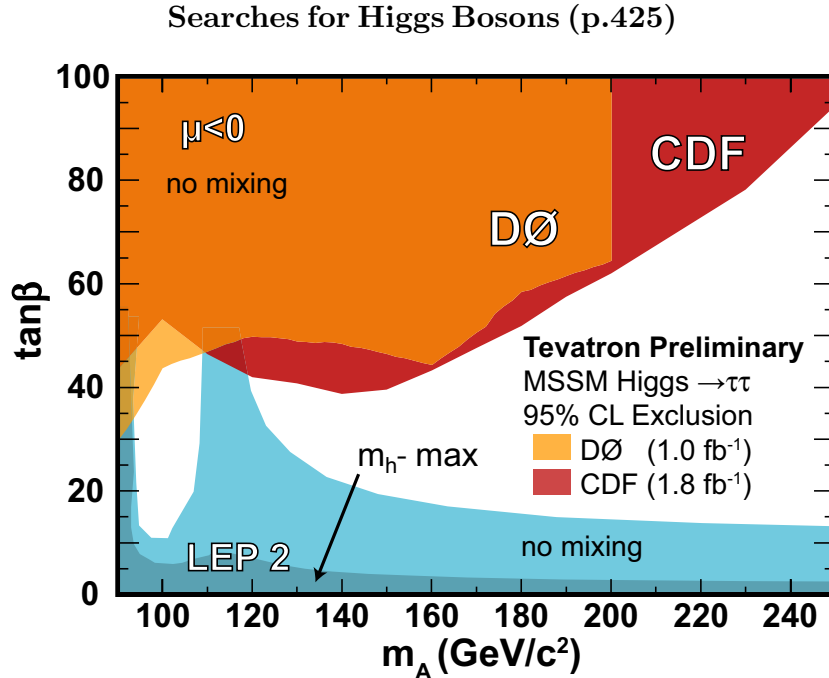


Figure 9: The 95% C.L. MSSM exclusion contours obtained by CDF and DØ in the $H \rightarrow \tau^+\tau^-$ searches in the *no-mixing* benchmark scenario with $\mu = -200$ GeV, projected onto the $(m_A, \tan\beta)$ plane [118,119]. The Tevatron limits for the m_h -max scenario are nearly the same as in the *no-mixing* scenario. Also shown are the regions excluded by LEP searches [16], separately for the m_h -max scenario (darker shading) and the *no-mixing* scenario, (lighter shading). The LEP limits are shown for a top quark mass of 174.3 GeV (the Tevatron results are not sensitive to the precise value of the top mass).

Searches for Higgs Bosons (p.427)

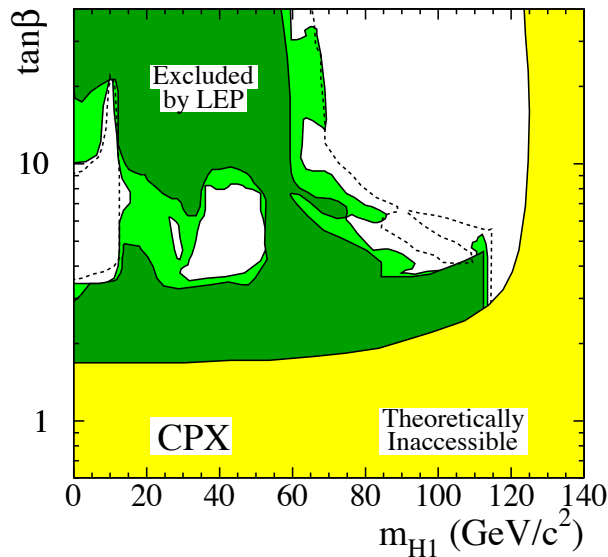


Figure 10: The MSSM exclusion contours, at 95% C.L. (light-green) and 99.7% CL (dark-green), obtained by LEP for a *CPV* scenario, called CPX, specified by $|A_t| = |A_b| = 1000$ GeV, $\phi_A = \phi_{m_{\tilde{g}}} = \pi/2$, $\mu = 2$ TeV, $M_{\text{SUSY}} = 500$ GeV [16]. Here, $m_t = 174.3$ GeV. The figure shows the excluded and theoretically inaccessible regions in the $(m_{H_1}, \tan\beta)$ projection. The dashed lines indicate the boundaries of the regions which are expected to be excluded on the basis of simulations with no signal.

Searches for Higgs Bosons (p.428)

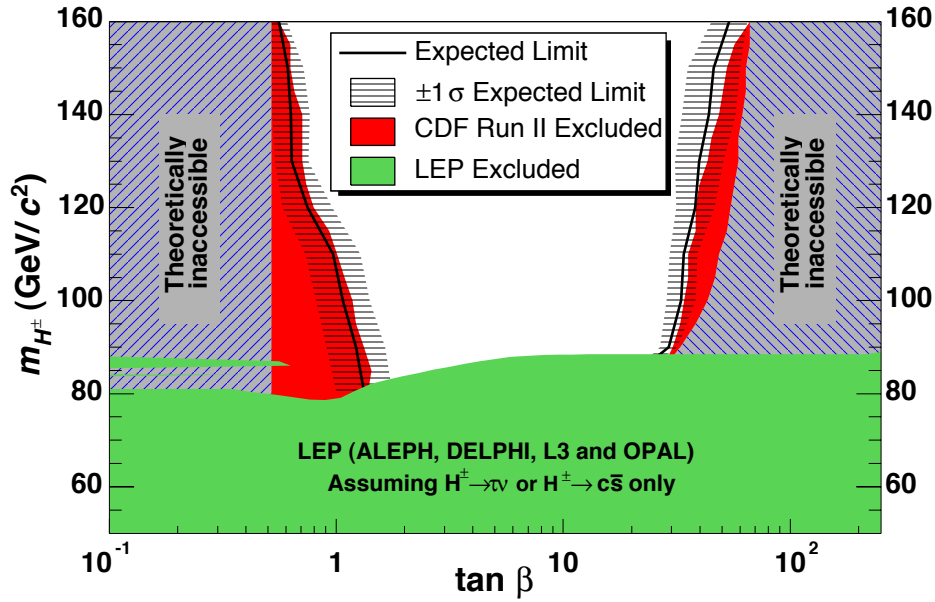


Figure 11: Summary of the 95% C.L. exclusions in the $(m_{H^\pm}, \tan \beta)$ plane obtained by LEP [158] and CDF [177]. The benchmark scenario parameters used to interpret the CDF results are very close to those of the m_h^{\max} scenario, and m_t is assumed to be 175 GeV. The full lines indicate the median limits expected in the absence of a H^\pm signal, and the horizontal hatching represents the $\pm 1\sigma$ bands about this expectation.

Searches for Higgs Bosons (p.429)

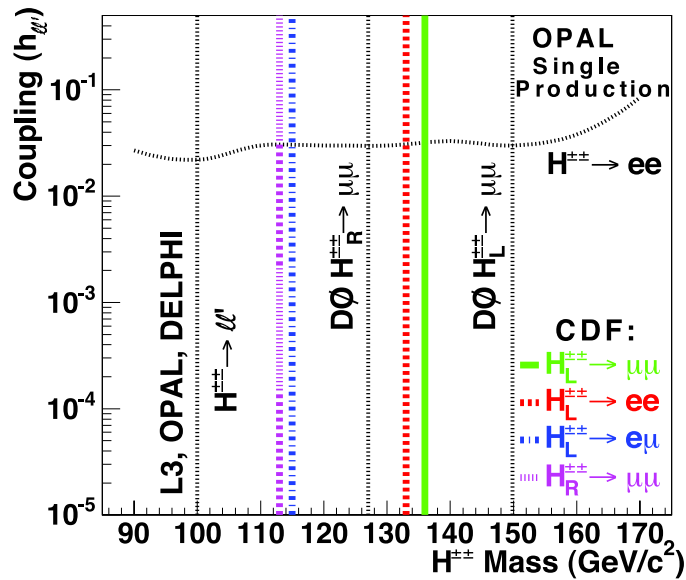


Figure 12: The 95% C.L. exclusion limits on the masses and couplings to leptons of right- and left-handed doubly-charged Higgs bosons, obtained by LEP and Tevatron experiments (from Ref. 185).

Leptoquarks (p.454)

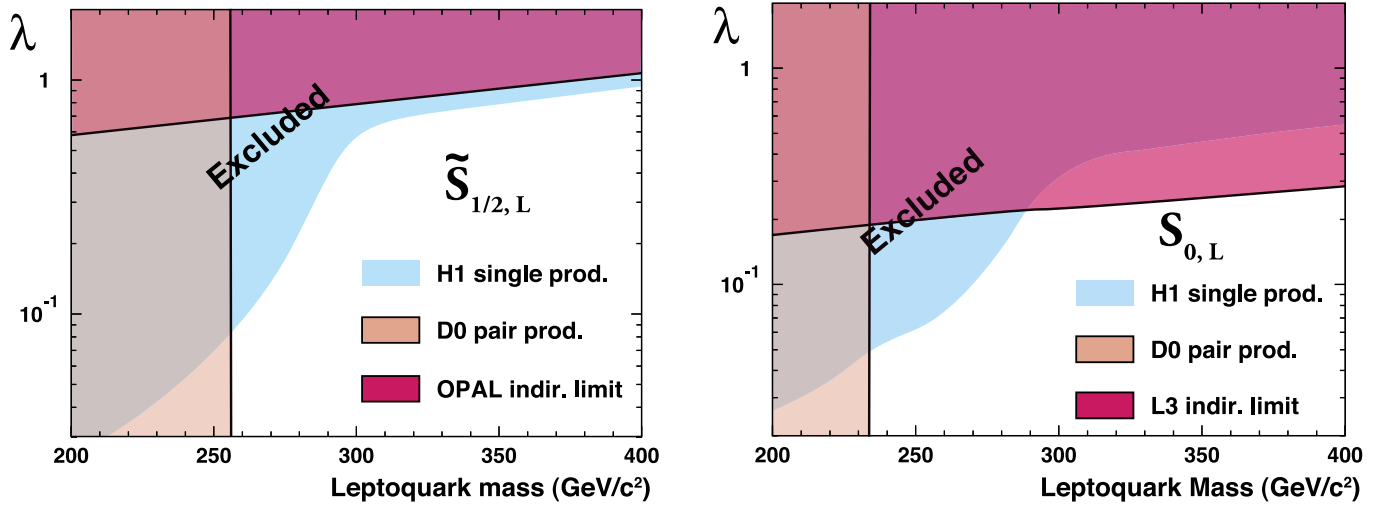


Figure 1: Limits on two typical first-generation scalar leptoquark states in the mass-coupling plane. The upper figure is for a weak-isodoublet, weak-hypercharge $7/6$, $3B + L = 0$ leptoquark state, while the lower figure for a weak-isosinglet, weak-hypercharge $-1/3$, $3B + L = 2$ state.

Axions (p.466)

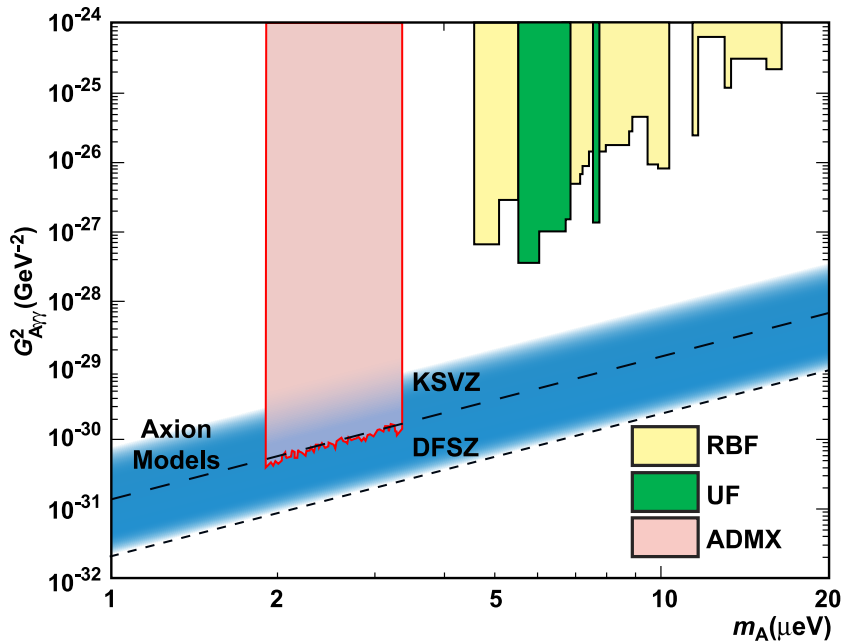


Figure 4: Exclusion region reported from the microwave cavity experiments RBF and UF [75] and ADMX [76]. A local dark-matter density of 450 MeV cm^{-3} is assumed.

Solar Neutrinos Review (p.535)

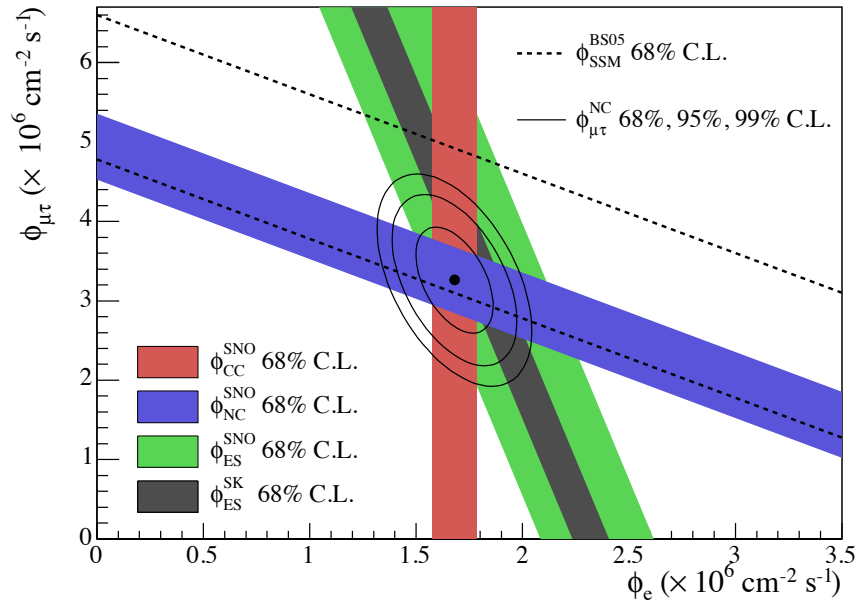


Figure 2: Fluxes of ${}^8\text{B}$ solar neutrinos, $\phi(\nu_e)$, and $\phi(\nu_\mu \text{ or } \tau)$, deduced from the SNO's charged-current (CC), ν_e elastic scattering (ES), and neutral-current (NC) results for the salt phase measurement [11]. The Super-Kamiokande ES flux is from Ref. [36]. The BS05(OP) standard solar model prediction [13] is also shown. The bands represent the 1σ error. The contours show the 68%, 95%, and 99% joint probability for $\phi(\nu_e)$ and $\phi(\nu_\mu \text{ or } \tau)$. This figure is taken from Ref. 11.

Solar Neutrinos Review (p.536)

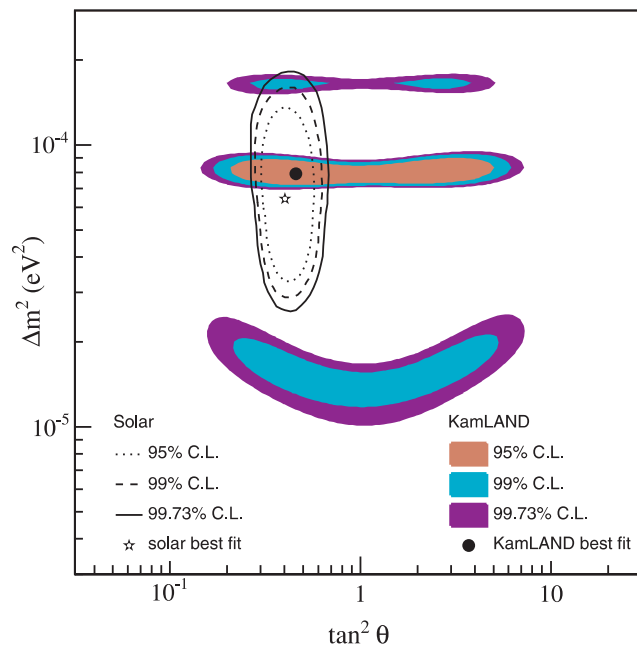


Figure 3: Allowed regions of neutrino-oscillation parameters from the KamLAND 766 ton-yr exposure $\bar{\nu}_e$ data [10]. The LMA region from solar-neutrino experiments [9] is also shown. This figure is taken from Ref. [10].

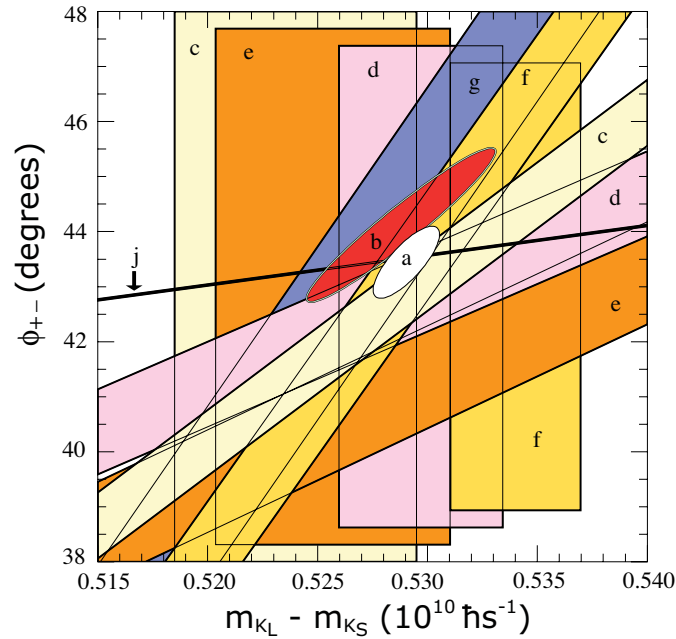
CP Violation in K_L Decays (p.742)

Figure 1: ϕ_{+-} vs Δm for experiments which do not assume CPT invariance. Δm measurements appear as vertical bands spanning $\Delta m \pm 1\sigma$, cut near the top and bottom to aid the eye. Most ϕ_{+-} measurements appear as diagonal bands spanning $\phi_{+-} \pm \sigma_\phi$. Data are labeled by letters: “b”–FNAL KTeV, “c”–CERN CPLEAR, “d”–FNAL E773, “e”–FNAL E731, “f”–CERN, “g”–CERN NA31, and are cited in Table 1. The narrow band “j” shows ϕ_{SW} . The ellipse “a” shows the $\chi^2 = 1$ contour of the fit result.

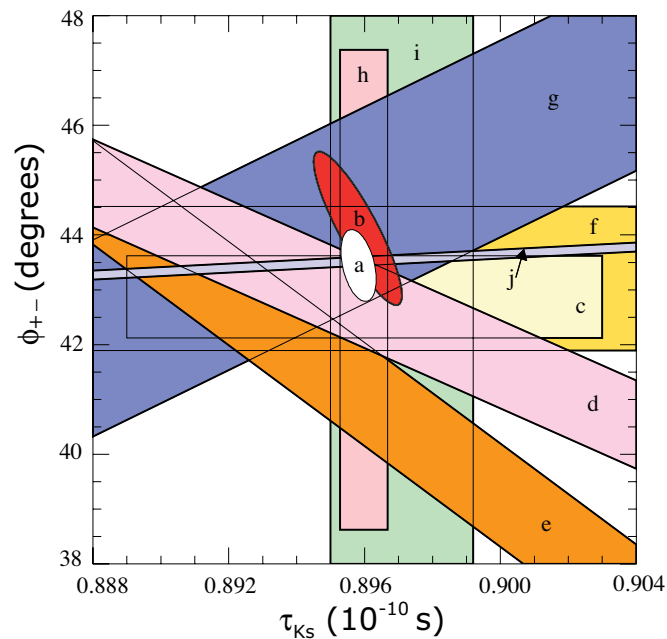
CP Violation in K_L Decays (p.743)

Figure 2: ϕ_{+-} vs τ_S . τ_S measurements appear as vertical bands spanning $\tau_S \pm 1\sigma$, some of which are cut near the top and bottom to aid the eye. Most ϕ_{+-} measurements appear as diagonal or horizontal bands spanning $\phi_{+-} \pm \sigma_\phi$. Data are labeled by letters: “b”–FNAL KTeV, “c”–CERN CPLEAR, “d”–FNAL E773, “e”–FNAL E731, “f”–CERN, “g”–CERN NA31, “h”–CERN NA48, “i”–CERN NA31, and are cited in Table 1. The narrow band “j” shows ϕ_{SW} . The ellipse “a” shows the fit result’s $\chi^2 = 1$ contour.

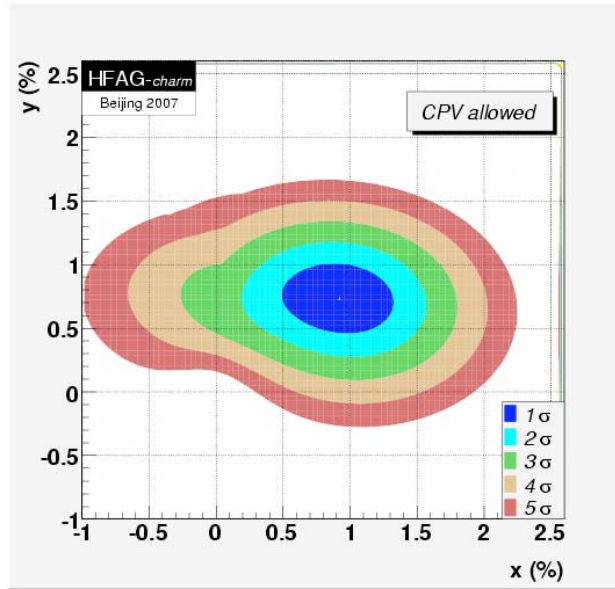
$D^0-\bar{D}^0$ Mixing (p.788)

Figure 1: Two-dimensional 1σ - 5σ contours for (x, y) from measurements of $D^0 \rightarrow K^+\ell\nu$, h^+h^- , $K^+\pi^-$, $K^+\pi^-\pi^0$, $K^+\pi^-\pi^+\pi^-$, and $K_S^0\pi^+\pi^-$ decays, and double-tagged branching fractions measured at the $\psi(3770)$ resonance (from HFAG [10]).

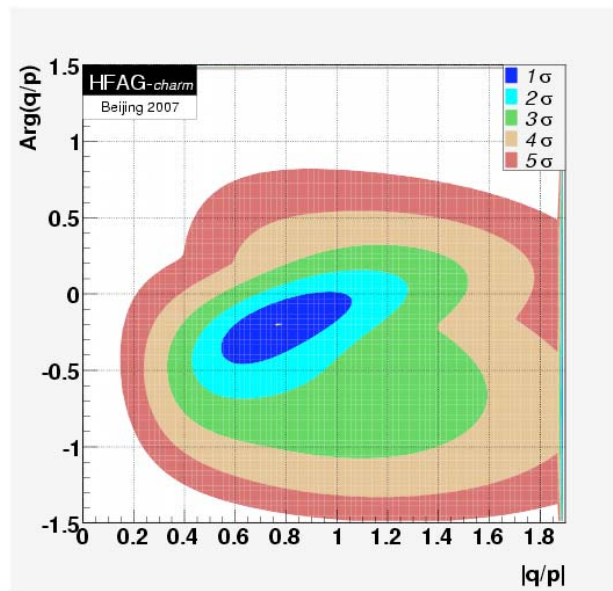
 $D^0-\bar{D}^0$ Mixing (p.789)

Figure 2: Two-dimensional 1σ - 5σ contours for $(|q/p|, \text{Arg}(q/p))$ from measurements of $D^0 \rightarrow K^+\ell\nu$, h^+h^- , $K^+\pi^-$, $K^+\pi^-\pi^0$, $K^+\pi^-\pi^+\pi^-$, and $K_S^0\pi^+\pi^-$ decays, and double-tagged branching fractions measured at the $\psi(3770)$ resonance (from HFAG [10]).

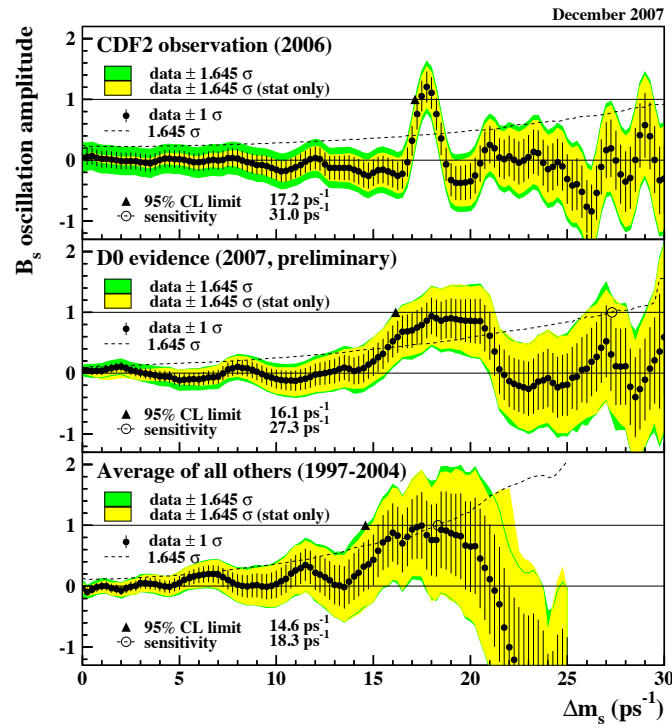
$B^0-\bar{B}^0$ Mixing (p.918)

Figure 2: Combined measurements of the B_s^0 oscillation amplitude as a function of Δm_s . Top: CDF result based on Run II data, published in 2006 [19]. Middle: Average of all preliminary $D\bar{O}$ results available at the end of 2007 [21]. Bottom: Average of all other results (mainly from LEP and SLD) published between 1997 and 2004. All measurements are dominated by statistical uncertainties. Neighboring points are statistically correlated.

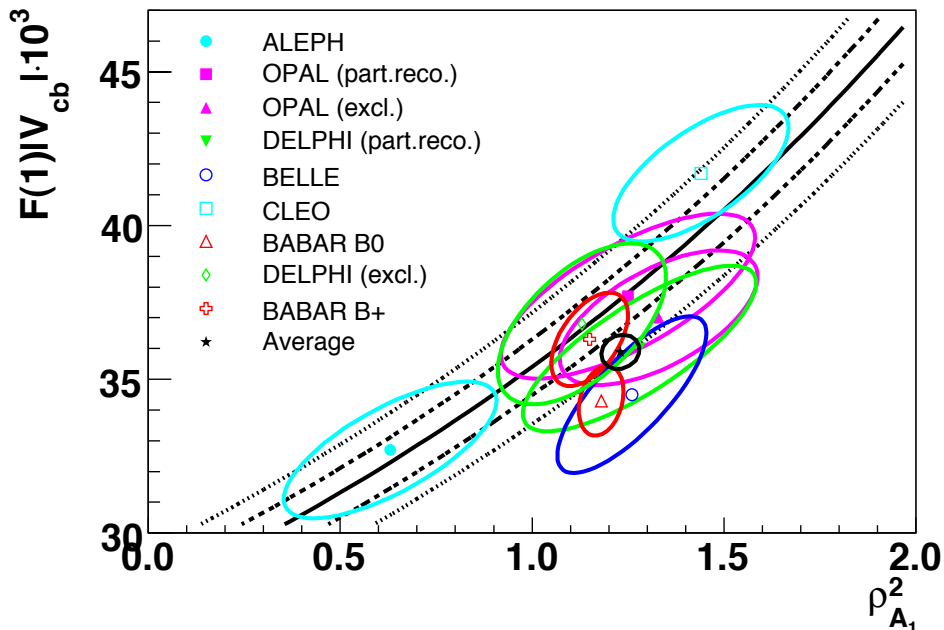
 V_{cb} and V_{cb} CKM Matrix Elements (p.953)

Figure 1: Measurements of $|V_{cb}|\mathcal{F}(1)$ vs. $\rho_{A_1}^2$ are shown as $\Delta\chi^2 = 1$ ellipses. The curves (central value, $\pm 1\sigma$ and $\pm 2\sigma$) correspond to the measurement of the total rate $\Gamma(\bar{B} \rightarrow D^* \ell \bar{\nu}_\ell)$ from Ref. 22.

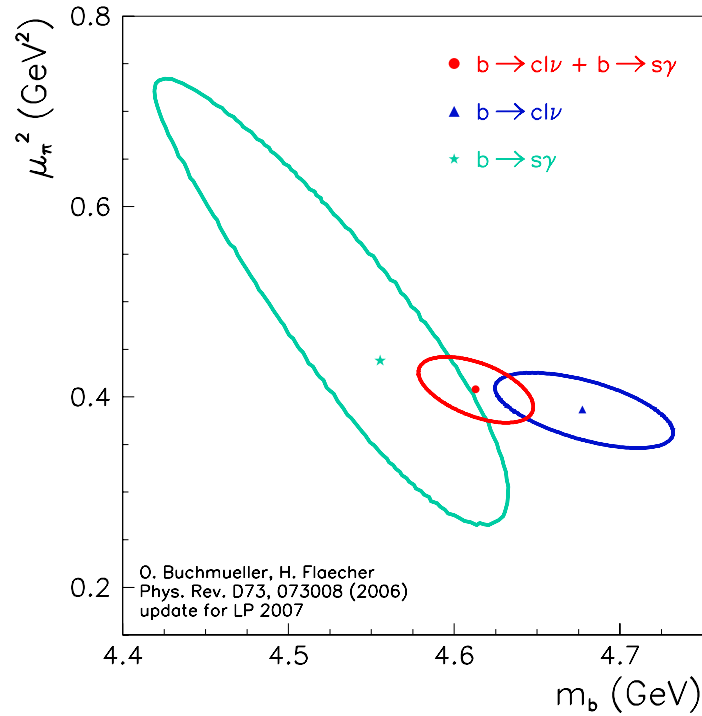
V_{cb} and V_{ub} CKM Matrix Elements (p.959)

Figure 2: Fit results from global moment fits in the kinetic scheme [58]. The $\Delta\chi^2 = 1$ curves for separate fits to $\overline{B} \rightarrow X_s \gamma$ moments and $\overline{B} \rightarrow X_c \ell \overline{\nu}_\ell$ moments are shown along with the combined fit.

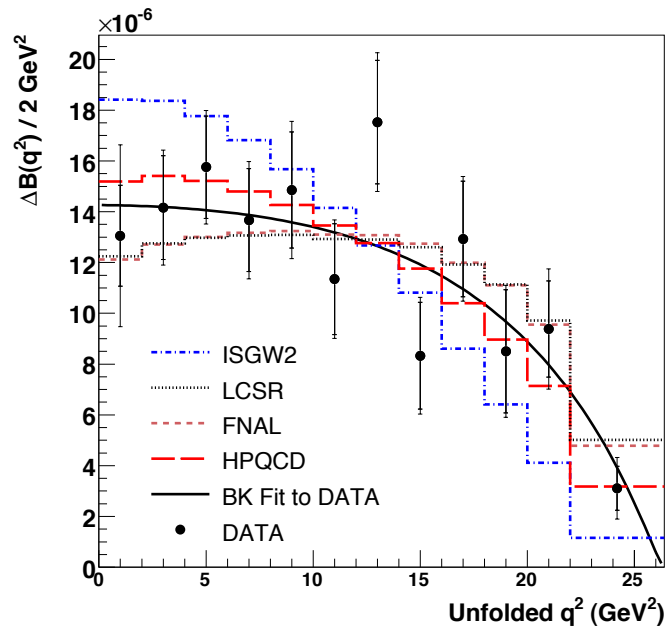
 V_{cb} and V_{ub} CKM Matrix Elements (p.962)

Figure 3: The differential branching fraction versus q^2 from BaBar [126] with several theoretical predictions overlaid.

Supersymmetry, Part II (Experiment) (p.1230)

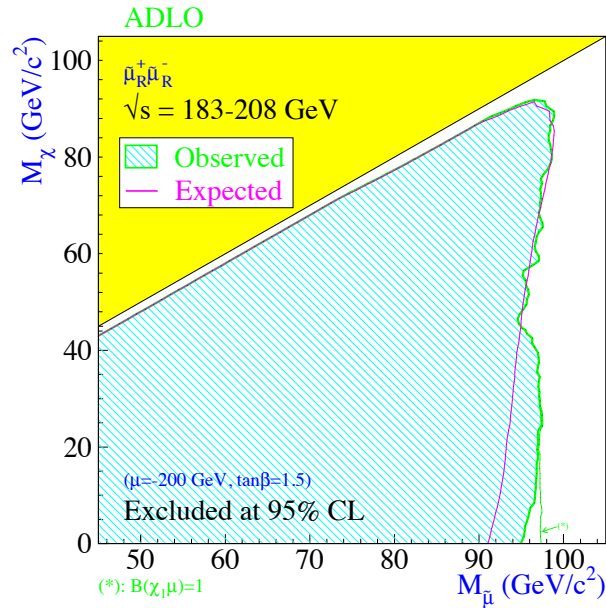


Figure 1: Region in the $(m_{\tilde{\mu}_R}, m_{\tilde{\chi}_1^0})$ plane excluded by the searches for smuons at LEP.

Supersymmetry, Part II (Experiment) (p.1231)

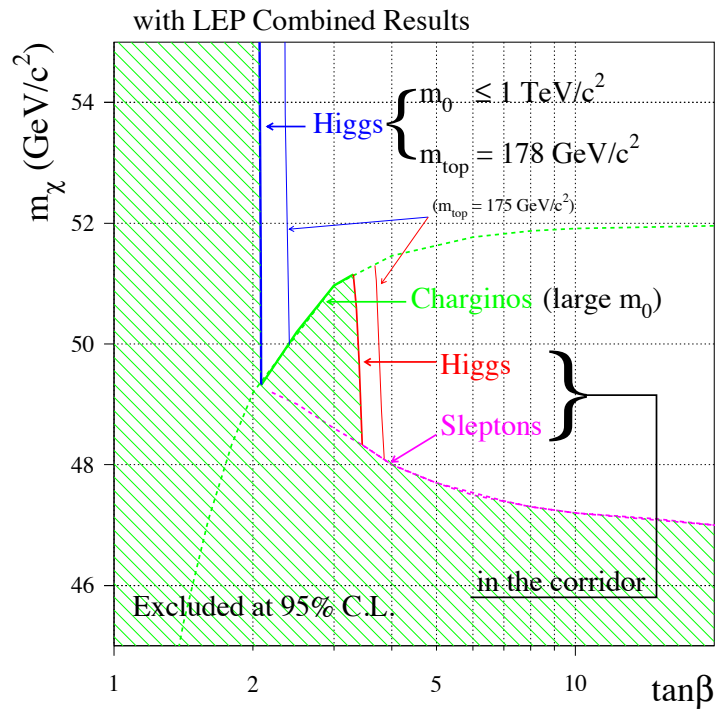


Figure 2: Lower mass limit for the lightest neutralino as a function of $\tan\beta$, inferred in the conventional scenario from searches at LEP for charginos, sleptons, and neutral Higgs bosons.

Supersymmetry, Part II (Experiment) (p.1234)

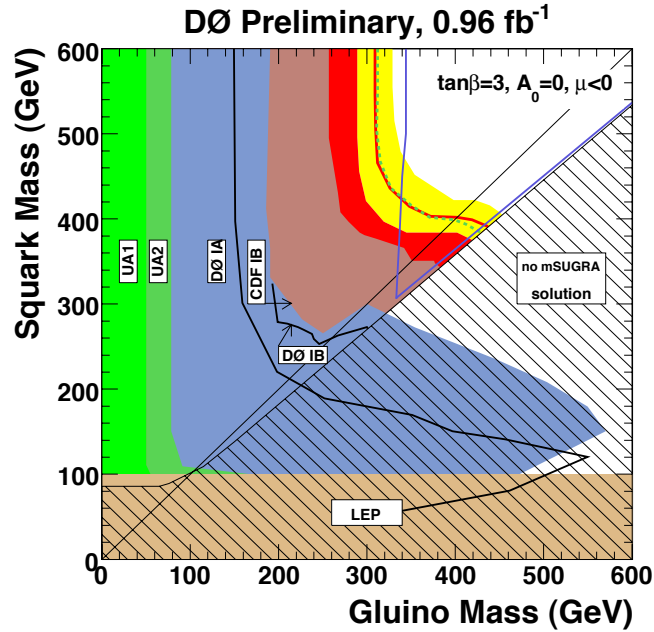


Figure 3: Region in the $(m_{\tilde{g}}, m_{\tilde{q}}$) plane excluded by DØ and by earlier experiments. The red curve corresponds to the nominal scale and PDF choices. The yellow band represents the uncertainty associated with these choices. The blue curves represent the indirect limits inferred from the LEP chargino and slepton searches.

Supersymmetry, Part II (Experiment) (p.1234)

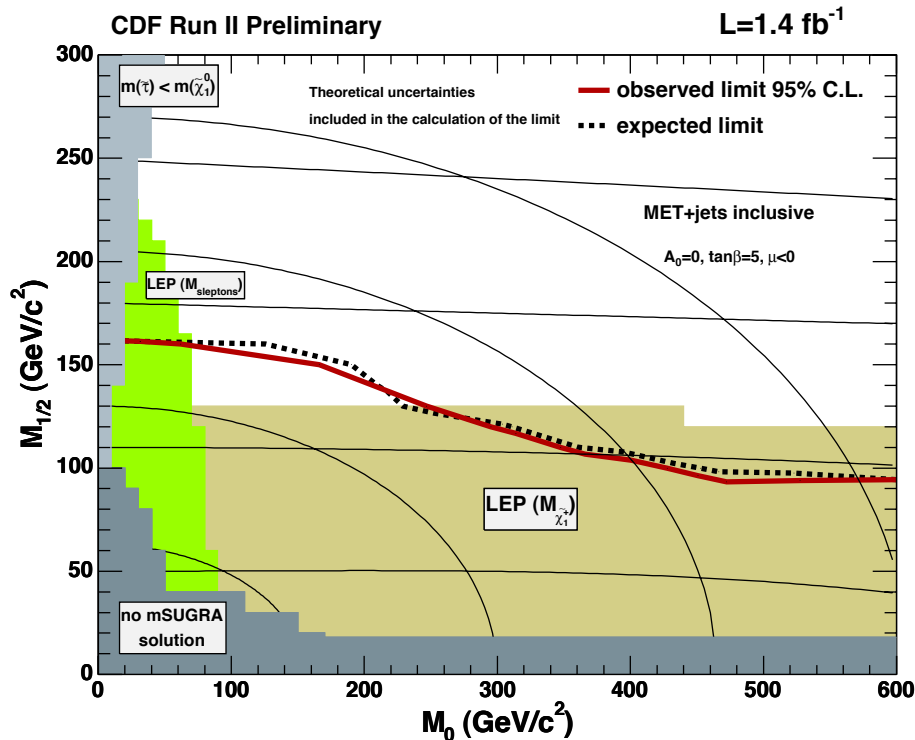


Figure 4: Region in the $(m_0, m_{1/2})$ plane excluded by CDF and by the LEP experiments. The nearly horizontal black lines are the iso-mass curves for gluinos corresponding to masses of 150, 300, 450 and 600 GeV. The other lines are iso-mass curves for squarks, corresponding to masses of 150, 300, 450 and 600 GeV.

Supersymmetry, Part II (Experiment) (p.1235)

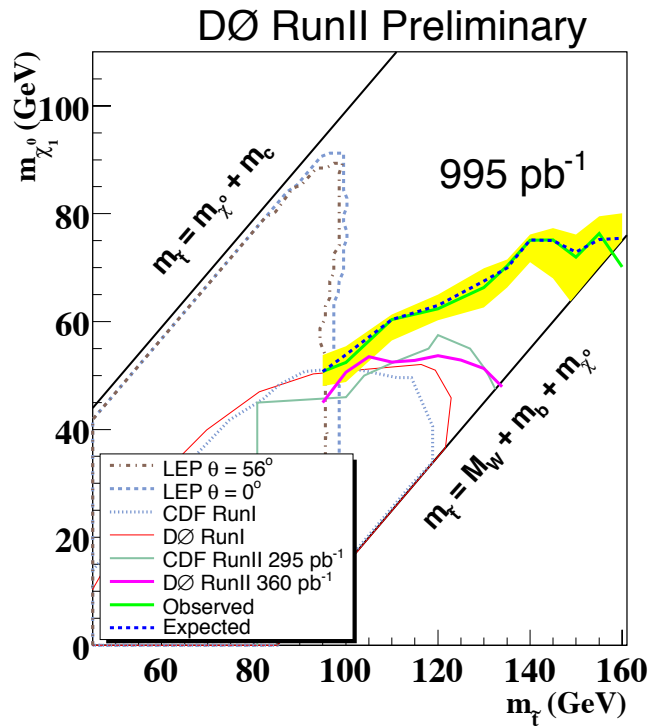


Figure 5: Region in the $(m_{\tilde{t}}, m_{\tilde{\chi}_1^0})$ plane excluded by DØ and by earlier experiments. The solid curve corresponds to the nominal scale and PDF choices. The yellow band represents the uncertainty associated with these choices.

Supersymmetry, Part II (Experiment) (p.1235)

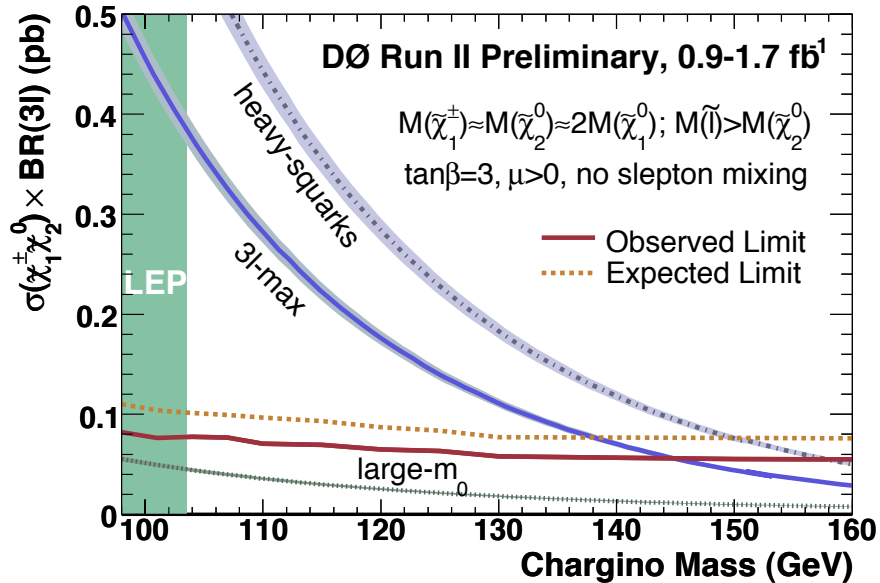


Figure 6: Upper limit from DØ on the product of cross section times branching ratio into three leptons for the associated $\tilde{\chi}_1^\pm \tilde{\chi}_2^0$ production at the Tevatron. The “3l-max” theoretical curve corresponds to the hypotheses detailed in the text.

Dynamical Electroweak Symmetry Breaking (p.1259)

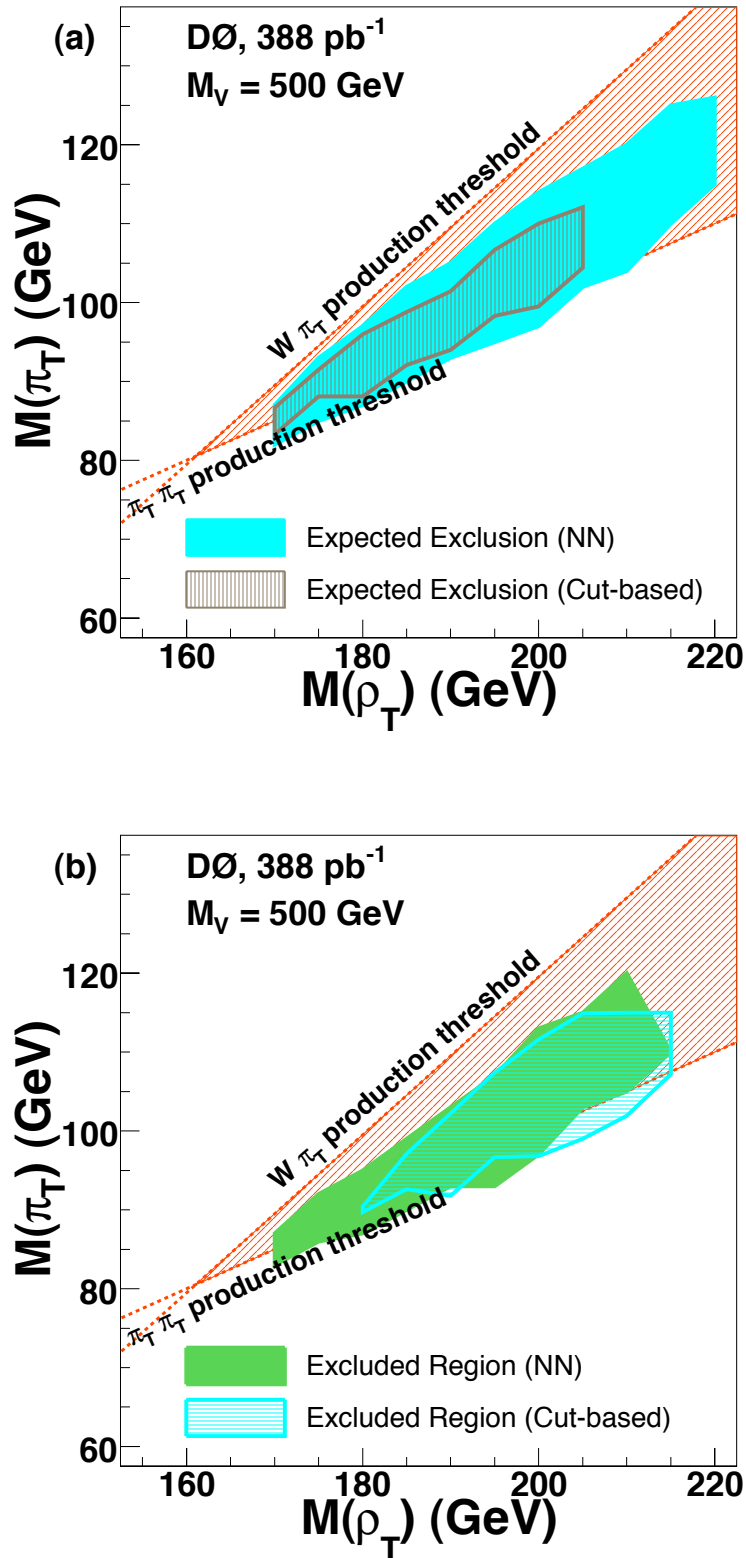


Figure 1: Search for a light technirho decaying to W^\pm and a π_T , and in which the π_T decays to two jets including at least one b quark [18]. Expected region of exclusion (a) and excluded region (b) at the 95% C.L. in the $M(\rho_T), M(\pi_T)$ plane for $\rho_T \rightarrow W\pi_T \rightarrow e\nu b\bar{b}(\bar{c})$ production with $M_V = 500 \text{ GeV}$. Kinematic thresholds from $W\pi_T$ and $\pi_T\pi_T$ are shown on the figures.

